nature

Vol 286 No 5768 3 July 1980 £1.00 $2.25

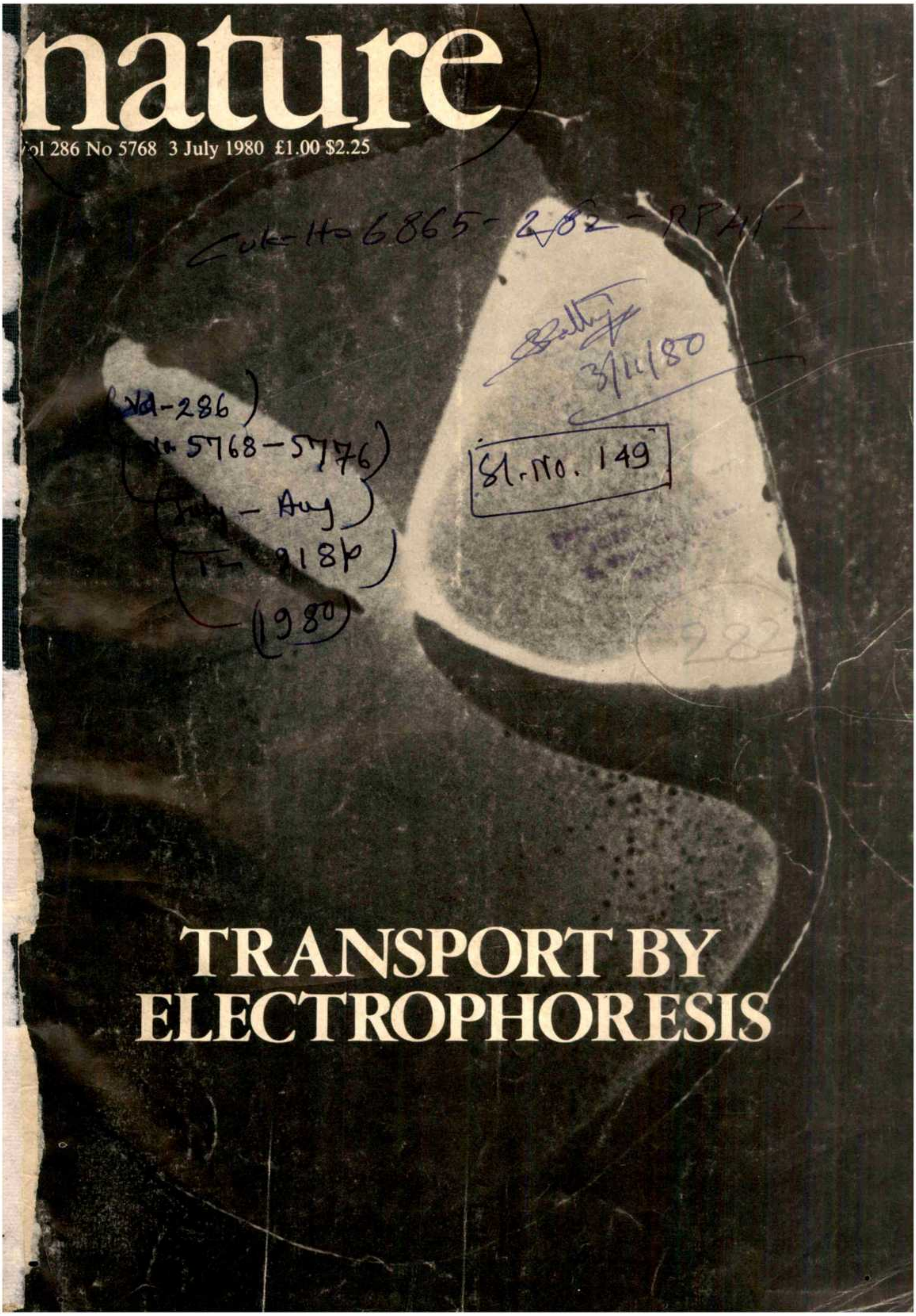

TRANSPORT BY ELECTROPHORESIS

Cuk-H0 6865-2/82-RPA12

Vol-286

No. 5768-5776

July - Aug

T- 918P

1980

3/11/80

Sl. No. 149

222

ICE COLD IN THE MORNING

IF YOU WILL PHONE TODAY
THEY WILL BE IN YOUR
LABORATORY IN THE MORNING

ALL THE FOLLOWING ARE IMMEDIATELY AVAILABLE

RESTRICTION ENDONUCLEASES

- Acc I
- Alu I
- Ava I
- Ava II
- Avr II
- Bal I
- Bam HI
- Bbv I
- Bcl I
- Bgl I
- Bgl II
- BstE II
- BstN I
- Dde I
- Eco RI
- Fnu4 HI
- Fnu DII
- Hae II
- Hae III
- Hga I
- HgiA I
- Hha I
- Hinc II
- Hind III
- Hinf I
- Hpa I
- Hpa II
- Hph I
- Kpn I
- Mbo I
- Mbo II
- Mnl I
- Msp I (Hpa II)
- Mst I
- Mst II
- PaeR7 I
- Pst I
- Pvu I
- Pvu II
- Rsa I
- Sac I
- Sac II
- Sal I
- Sau3A I
- Sau96 I
- Sma I
- Taq I
- Xba I
- Xho I
- Xma I
- Xma III

ENZYMES

- T4 DNA Ligase
- T4 RNA Ligase
- DNA Ligase (E.coli, DPN)
- Polynucleotide Kinase
- DNA Polymerase I (E.coli)
- Polynucleotide Kinase concentrated
- DNA PolymeraseI— Large Fragment (E.coli)
- RNA Polymerase (Holoenzyme, E. coli)
- Exonuclease III
- Lambda Exonuclease
- Eco RI Methylase

NUCLEIC ACIDS

- Lambda DNA
- Lambda DNA (N^6— methyladenine-free)
- ΦX174RFI DNA
- ΦX174RF II DNA
- ΦX174Virion DNA
- ΦX174 RF DNA-Hinc II Digest
- ΦX174 RF DNA-Hpa I Digest
- ΦX174 RF DNA-Hae III Digest
- ΦX174 RF DNA-Xho I Digest
- Lambda DNA-Hind III Digest

Quality products from

NEW ENGLAND
BioLabs INC.

CP Laboratories Limited
P.O. Box 22 Bishop's Stortford,
Herts. England
Telephone (0279) 53734 Telex 817509

Circle No. 19 on Reader Enquiry Card.

nature

Volume 286 No.5768 3 July 1980

282

[illegible] SCIENCE COLLEGE [illegible] CALCUTTA

NEWS

Venice, energy, Brandt and politicians 1
Why bother with examinations? 2
New Basel director changes direction
Sitting-in in Spanish labs
Correction 3
High-energy physics: LEP leaps ahead
Radioactive waste: polite debate
Russian language: Finns struggling 4
Experimental animals: lab invaded
Whaling quotas: more wrangling 5
Big science: German doubts
Genetic manipulation: Soviet claim 6
Dioxin: ASTMS says no
Arctic voyage: Swedes set out 7
Correspondence: Arthur Frank (William Reid); Book prices again (Robert Campbell, P.V.E. McClintock); Parkinson extended (J.C. Thorpe); Ethnographic DNA (A. Harris); Conversion courses (L.R.B. Elton) 8

NEWS AND VIEWS

Cell cycle control: Paul Nurse compares deterministic and probabilistic models 9
Can comets become asteroids?: David W. Hughes examines the evidence 10
The strong coupling constant is measured: Mary K. Gaillard on the quark-gluon interaction 11
Extra-pituitary actions of LHRH: Richard M. Sharpe describes how endocrinological dogma is being challenged 12
How does the mantle move: Geoffrey F. Davies reports a recent conference 14
MHC restriction, self-tolerance and the thymus: Jonathan Howard examines some properties of T cells of the immune system 15

ARTICLES

B. Dupré and C.J. Allègre — **Pb-Sr-Nd isotopic correlation and the chemistry of the North Atlantic mantle** 17
J.C. Liddicoat, N.D. Opdyke and G.I. Smith — **Palaeomagnetic polarity in a 930-m core from Searles Valley, California** 22
T. Ebendal, L. Olson, A. Seiger and K.-O. Hedlund — **Nerve growth factors in the rat iris** 25
K.R. Dumbell and L.C. Archard — **Comparison of white pock (h) mutants of monkeypox virus with parental monkeypox and with variola-like viruses isolated from animals** 29
C. Abad-Zapatero, S.S. Abdel-Meguid, J.E. Johnson, A.G.W. Leslie, I. Rayment, M.G. Rossmann, D. Suck and T. Tsukihara — **Structure of southern bean mosaic virus at 2.8 Å resolution** 33

LETTERS

E.P.T. Liang — **Cosmic X-ray background and intergalactic gas accretion onto intergalactic collapsed objects** 39
W.-H. Ip — **Discontinuities in the jovian plasma disk of sulphur and oxygen ions** 40
M. Ando, Y. Ishikawa and H. Wada — **S-wave anisotropy in the upper mantle under a volcanic area in Japan** 43
H.E. Huppert and R.S.J. Sparks — **Restrictions on the compositions of mid-ocean ridge basalts: a fluid dynamical investigation** 46
T.L. Vallier, K.E. Windom, K.E. Seifert and J. Thiede — **Volcanic rocks cored on Hess Rise, western Pacific Ocean** 48
D.E. Ingmanson and M.J. Dowler — **Unique amino acid composition of Red Sea brine** 51

Contents continued overleaf

Cover: A fluorescence micrograph of an ovarian moth follicle showing three nurse cells, the oocyte and two of the intercellular bridges that connect these cells. Evidence that electrical forces prevent a fluorescein-labelled protein in the nurse cells from crossing the bridges into the oocyte is presented on page 84.

Published weekly ISSN 0028-0836
Registered as a newspaper at the British Post Office
and the United States Post Office

0028-0836/80/27000C-02$01.00

ames

Two instruments with a difference you'll want to pocket

COMPUR M1000
Miniphotometer Set*

pocket miniphotometer for Haemoglobin estimation and Erythrocyte count.

COMPUR M1100
Minicentrifuge*

provides rapid haematocrit value and plasma separation.

* Trademark

Manufactured by Compur-Electronic GmbH, Germany
(a company of Bayer AG and Carl Zeiss)
Distributed by:

Ames Division MILES

Miles Laboratories Limited
PO Box 37, Stoke Court, Stoke Poges, Slough SL2 4LY
Telephone Farnham Common 5151 or 2151

I would be interested in obtaining further information and/or a demonstration of Compur instrumentation.
Please ask your representative to contact.

Name ____________________

Address ____________________

Telephone No. ____________________

N.I.

Circle No. 22 on Reader Enquiry Card.

~~R511~~ R412

LETTERS

C.F. Nordin Jr, R.H. Meade, W.F. Curtis, N.J. Bósio and P.M.B. Landim — **Size distribution of Amazon River bed sediment** 52

R.A.J. Taylor — **A family of regression equations describing the density distribution of dispersing organisms** 53

L. Greenwald, P.D. Ward and O.E. Greenwald — **Cameral liquid transport and buoyancy control in chambered nautilus (*Nautilus macromphalus*)** 55

M. Rothschild J.W. Fairbairn — **Ovipositing butterfly (*Pieris brassicae* L.) distinguishes between aqueous extracts of two strains of *Cannabis sativa* L. and THC and CBD** 56

J.D. Mollon and P.G. Polden — **A curiosity of light adaptation** 59

R.D. Freeman — **Visual acuity is better for letters in rows than in columns** 62

M. Cynader and L. Harris — **Eye movement in strabismic cats** 64

P. Vandervorst and A. Ghysen — **Genetic control of sensory connections in *Drosophila*** 65

K.M. Kendrick and R.F. Drewett — **Testosterone-sensitive neurones respond to oestradiol but not to dihydrotestosterone** 67

R.P. Kline, I. Cohen, R. Falk and J. Kupersmith — **Activity-dependent extracellular K^+ fluctuations in canine Purkinje fibres** 68

B. Sakmann, J. Patlak and E. Neher — **Single acetylcholine-activated channels show burst-kinetics in presence of desensitizing concentrations of agonist** 71

C.J. Pycock, R.W. Kerwin and C.J. Carter — **Effect of lesion of cortical dopamine terminals on subcortical dopamine receptors in rats** 74

L.A. Culp — **Behavioural variants of rat neuroblastoma cells** 77

A.H. Gordon, P. D'Arcy Hart and M.R. Young — **Ammonia inhibits phagosome-lysosome fusion in macrophages** 79

A.L. Koch — **Does the variability of the cell cycle result from one or many chance events?** 80

D. Owerbach, G.I. Bell, W.J. Rutter and T.B. Shows — **The insulin gene is located on chromosome 11 in humans** 82

R.I. Woodruff and W.H. Telfer — **Electrophoresis of proteins in intercellular bridges** 84

BOOK REVIEWS

Kenneth Mellanby — **The Common Ground: A Place for Nature in Britain's Future? (Richard Mabey)** 87

J.D. Barrow — **White Dwarfs, Black Holes: An Introduction to Relativistic Astrophysics (R. Sexl and H. Sexl)** 88

John Yarwood — **Vacuum Physics and Technology (G.L. Weissler and R.W. Carlson, editors)** 89

G.P. Lewis — **Chemical Messengers of the Inflammatory Process (J.C. Houck, editor)** 89

Hans Kruuk — **Serengeti: Dynamics of an Ecosystem (A.R.E. Sinclair and M. Norton-Griffiths, editors)** 90

H.W. Kroto — **Modern Aspects of Microwave Spectroscopy (G.W. Chantry, editor)** 91

M.W. Moncrieff — **Weather Modification (G. Breuer)** 91

Maurice Smith — **The Laboratory Rat. Vol. 1, Biology and Diseases (H.J. Baker, J. Russell Lindsay and S.H. Weisbroth, editors)** 92

Barry Cross — **Oxford Reviews of Reproductive Biology. Vol. 1, 1979 (C.A. Finn, editor)** 92

MISCELLANY

100 years ago 13
Books received 93
Announcements 94
New on the market xiii
Classified advertising xv

Cell at Half Price

One of the indispensable journals of modern biology, Cell is now available at a greatly reduced rate to individual subscribers. Why not join the many others who have taken advantage of this offer to gain immediate access to the seminal research papers published in Cell without waiting in turn for library copies? (It can be a long wait; Cell is famous—perhaps infamous—for its unavailability in the library due to excess demand.)

An international journal edited from MIT and England, Cell is published as 13 issues per year, containing the work of leading institutions in molecular biology, cell biology, virology, genetics, developmental biology and immunology. The range of subjects contained in Cell is too great to list, but papers of critical importance have already been published this year on the topics listed opposite. With all this, plus reviews of rapidly developing topics and critical book reviews, can you afford to miss a personal subscription to Cell?

A personal subscription may be taken for $85 per year (compared with the usual rate of $185). The only restrictions are that payment should be made direct to the publisher by a personal check (no invoice or receipt can be sent), and the subscriber should certify that the copies are for his personal use only. The more personal subscriptions taken, the lower the price in future years—so help us and help yourself. A subscription to start the eighties can be obtained with the form below.

Cell in the Eighties

- location of promoters in the middle of genes
- switching in the splicing pathway for immunoglobulin production
- presence of circular RNA in yeast mitochondria
- role of RNA in splicing
- discovery of new embryonic and pseudo-globin genes
- roles of new classes of enzymes in translocation and catenation of DNA
- cis dominant locus responsible for plasmid partitioning
- translocation specificities of Tn elements
- new loci involved in lambda integration
- initiation of DNA synthesis at non-origins
- action of src protein
- phenotypic control of SV40 gene expression
- mechanism of SV40 integration
- RNA virus expression and cell phenotype
- sequences of flu hemagglutinin genes
- dependence of poliovirus replicase on host protein
- association of DNA methylation with cell differentiation
- role of phorbol esters in differentiation
- fibronectin and cell growth
- nature of mouse t antigens
- segregation of developmental potential of nematodes
- role of the fv2 locus in erythropoiesis
- fate of the nuclear lamina in mitosis
- identification of cell-cell adhesion glycoprotein
- control of RNA virus expression by adjacent cellular DNA
- differences in dye binding of normal and leukemic cells
- colchicine-resistant mutants of tubulin
- recycling of cell surface receptors
- inclusion of LDL receptors in coated vesicles

Cell Discount Order Form

To: The Journals Department
The MIT Press
28 Carleton Street
Cambridge, Massachusetts 02142
USA

I should like to subscribe to Cell for 1980 and I enclose a personal check for $85. (Overseas subscribers please add $10 for postage.) The subscription is solely for my personal use.

Name ____________________

Address ____________________

N1

Circle No. 04 on Reader Enquiry Card.

nature

Volume 286 No.5769 10 July 1980

Pure Chemistry Library
SCIENCE COLLEGE
92, Upper Circular Road
CALCUTTA

NEWS

Progress on chemical weapons treaty 95
Two views on technological change 96
Red faces (and hot tempers) on 2,4,5-T
Supreme Court reprieves benzene 97
Soviet environment: Spending more 98
Biotechnology: France now
University industry: Surrey consults 99
Chemical weapons: Congress agrees
British farming: Science on show
Fusion: Studied design 100
US fusion: Middle course?
New NSF director 101
Albanian science: Isolated still
Correspondence: Cruel Malthus (Harry Grundfest); Nuclear protest (Brian Cummins, Alan Beard, Dave Smith). 102

NEWS AND VIEWS

Geothermal energy: S.W. Richardson and A.A.L. White compare district heating and electricity generation options 103
Changes in length-of-day: Kurt Lambeck discusses fluctuations caused by atmospheric circulation 104
Neurological mutants affecting myelination: Richard P. Bunge looks at murine models of human neural disorders 106
Timing in embryological development: Michael H.L. Snow and Patrick P.L. Tam review 'clock' models 107
Cree-Ojibwa hunting and the hare-lynx cycle: Robert M. May on cyclic variations of animal numbers 108
Primary productivity in the sea: Richard W. Epplay reports a recent conference 109
Interferon nomenclature: Proposals from an international committee 110

ARTICLES

L.A. Bursill, E.A. Lodge and J.M. Thomas — **Zeolitic structures as revealed by high-resolution electron microscopy** 111
R. Hide, N.T. Birch, L.V. Morrison, D.J. Shea and A.A. White — **Atmospheric angular momentum fluctuations and changes in the length of the day** 114
M. Tatsumoto and T. Shimamura — **Evidence for live ^{247}Cm in the early Solar System** 118
L. Bossi and J.R. Roth — **The influence of codon context on genetic code translation** 123
R. Dixon, R.R. Eady, G.Espin, S. Hill, M. Iaccarino, D. Kahn and M. Merrick — **Analysis of regulation of *Klebsiella pneumoniae* nitrogen fixation (*nif*) gene cluster with gene fusions** 128

LETTERS

P.D. Feldman, H.A. Weaver, M.C. Festou, M.F.A'Hearn, W.M. Jackson, B. Donn, J. Rahe, A.M. Smith and P. Benvenuti — **IUE observations of the UV spectrum of comet Bradfield** 132
A. Dekel, M. Lecar and J. Shaham — **Tidal effects on the mass profile of galactic haloes** 135
W.H. Kegel and D.A. Varshalovich — **Interpretation of type I OH maser sources** 136
D. Elmore, H.E. Gove, R. Ferraro, L.R. Kilius, H.W. Lee, K.H. Chang, R.P. Beukens, A.E. Litherland, C.J. Russo, K.H. Purser, M.T. Murrell and R.C. Finkel — **Determination of ^{129}I using tandem accelerator mass spectrometry** 138
Th. Armbruster and F.D. Bloss — **Channel CO_2 in cordierites** 140
G. King — **A fault plane solution for the Carlisle earthquake, 26 December 1979** 142

Contents continued overleaf

Cover: False colour image of comet Bradfield (1979*l*) taken on 10 January 1980 by the Fine Error Sensor of the IUE satellite observatory. The field is 16′ × 16′. Comet Bradfield was observed by IUE several times between 10 January and 3 March 1980 corresponding to a range of heliocentric distance from 0.71 to 1.53 AU. These observations are discussed on page 132. NASA photo.

Nature® published weekly ISSN 0028-0836
Registered as a newspaper at the British Post Office and the United States Post Office

0028-0836/80/28000C-02$01.00

5 New Nucleases Ready For Use

No.	Product	Quantity	Price
0584	NUCLEASE, Micrococcal See P-L Analects 6 (1) 1978 for use in mRNA removal.	15 Kilounits	$56.00
0912	NUCLEASE, Mung Bean Sprouts SINGLE STRAND SPECIFIC This highly purified enzyme available only from P-L Biochemicals.	5000 units	$45.00*
0852	NUCLEASE P_1 (*Penicillium citrinum*) >600 units/mg. Produces 5'mononucleotides from RNA and DNA.	1 mg.	$40.00
0920	NUCLEASE S_1 (*Aspergillus oryzae*) >200,000 units/mg protein. SINGLE STRAND SPECIFIC.	50 Kilounits	$37.50*
0924	RIBONUCLEASE Phy I Free of RNase II and acid phosphatase.	15 units	$57.50*

**Insulated container and refrigerant charge $10 00*

Call or write for complete information.

excellence in biochemistry
P-L biochemicals, inc.
1037 WEST McKINLEY AVENUE, MILWAUKEE, WIS 53205
® (414) 271-0667, Telex 26881

mRNA Termini (caps)

Name	Cat. No.	5 units	5x5 units
$m^7G(5')ppp(5')Cm$	4607	$40.00	$160.00
$m^7G(5')ppp(5')Um$	4609	40.00	160.00
$m^7G(5')ppp(5')Am$	4633	40.00	160.00
$m^7G(5')ppp(5')Gm$	4631	40.00	160.00
$m^7G(5')ppp(5')N^6mAm$	4611	50.00	200.00

Or their precursors

Name	Cat. No.	5 units	5x5 units
$m^7G(5')ppp(5')A$	4637	$35.00	$150.00
$m^7G(5')ppp(5')G$	4635	35.00	150.00
$G(5')ppp(5')Am$	4641	30.00	125.00
$G(5')ppp(5')Gm$	4639	30.00	125.00
$G(5')ppp(5')A$	4645	25.00	100.00
$G(5')ppp(5')G$	4643	25 units	40.00

We have them all in stock for immediate delivery.

excellence in biochemistry
P-L biochemicals, inc.
1037 WEST McKINLEY AVENUE, MILWAUKEE, WIS 53205
® Call 414/347-7442 TWX 910-262-1111

Circle No. 01 on Reader Enquiry Card.

M

Introduction to NUCLEAR REACTIONS

G. R. SATCHLER

– Research staff member, Oak Ridge National Laboratory, Tennessee.

Spring 1980; £25; 336pp; ISBN 0 333 25907 6.

Contents include – Some Background; Introduction to Nuclear Reactions; Elementary Scattering Theory; Models of Nuclear Reactions.

This book presents a summary of our present understanding of the Scattering and Reactions that occur in collisions between nuclei and is an introduction to the theoretical formalisms used to describe them. It is aimed primarily at readers in the undergraduate and beginning graduate student level but many others will also find it useful. The specialist from another field will find that this book is excellent background reading and the established nuclear physicist will find reading it to be helpful in refreshing the memory about areas in which he or she is not currently working.

For further details contact Francis Roach, Scientific and Medical Division, Macmillan Publishers Limited, Houndmills, Basingstoke, Hampshire, RG21 2XS.

LETTERS

C. Frohlich, J G. Caldwell, A. Malahoff, G V. Latham and J. Lawton	**Ocean bottom seismograph measurements in the Central Aleutians**	144
S.V. Margolis and Y. Herman	**Northern Hemisphere sea-ice and glacial development in the late Cenozoic**	145
J.L. Gittleman and P.H. Harvey	**Why are distasteful prey not cryptic?**	149
H. Simon, B. Scatton and M. Le Moal	**Dopaminergic A10 neurones are involved in cognitive functions**	150
S Hansen, E.J. Stanfield and B.J Everitt	**The role of ventral bundle noradrenergic neurones in sensory components of sexual behaviour and coitus-induced pseudopregnancy**	152
K.J Smith and W I McDonald	**Spontaneous and mechanically evoked activity due to central demyelinating lesion**	154
T L Yaksh, T M Jessell, R Gamse, A.W. Mudge and S E. Leeman	**Intrathecal morphine inhibits substance P release from mammalian spinal cord *in vivo***	155
M. Schachter, P. Bédard, A.G Debono, P. Jenner, C.D Marsden, P Price, J.D. Parkes, J Keenan, B. Smith, J. Rosenthaler, R Horowski and R. Dorow	**The role of D-1 and D-2 receptors**	157
E A. Woodcock and C.I. Johnston	**α-Adrenergic receptors modulate β-receptor affinity in rat kidney membranes**	159
L.B Hersh, T.E. Smith and J F McKelvy	**Cleavage of endorphins to des-Tyr endorphins by homogeneous bovine brain aminopeptidase**	160
J. Pouysségur, Y. Jacques and M. Lazdunski	**Identification of a tetrodotoxin-sensitive Na$^+$ channel in a variety of fibroblast lines**	162
M.R Szewczuk and R J. Campbell	**Loss of immune competence with age may be due to auto-anti-idiotypic antibody regulation**	164
P. Guglielmi, J -L. Preud'homme and G. Flandrin	**Phenotypic changes of phytohaemagglutinin-stimulated hairy cells**	166
D J. Kemp, A. Wilson, A.W. Harris and K. Shortman	**The immunoglobulin μ constant region gene is expressed in mouse thymocytes**	168
H. Schnell, M. Steinmetz, H G Zachau and I. Schechter	**An unusual translocation of immunoglobulin gene segments in variants of the mouse myeloma MPC11**	170
R C Jackson, P. Walter and G Blobel	**Secretion requires a cytoplasmically disposed sulphydryl of the RER membrane**	174
J. Cairns	**Efficiency of the adaptive response of *Escherichia coli* to alkylating agents**	176
T.W Nilsen, D.L. Wood and C Baglioni	**Virus-specific effects of interferon in embryonal carcinoma cells**	178
M Saveria Campo, M.H. Moar, W.F.H. Jarrett and H.M Laird	**A new papillomavirus associated with alimentary cancer in cattle**	180
E.H. Radany and E.C. Friedberg	**A pyrimidine dimer-DNA glycosylase activity associated with the *v* gene product of bacteriophage T4**	182
J. Campisi and C.J. Scandella	**Calcium-induced decrease in membrane fluidity of sea urchin egg cortex after fertilization**	185

BOOK REVIEWS

R.W. Burkhardt	**Lamarck ou le Mythe du Précurseur (M. Barthélemy-Madaule)**	187
Peter D. Moore	**Flora Europaea, Vol. 5 (T.G. Tutin, B.H. Heywood, N.A. Burges *et al.*, editors). Flora Palaestina, Part 3 (N. Feinbrun-Dothan)**	188
D.J. Gunn	**Porous Media (F.A.L. Dullien)**	189
Colin Blake	**Teaching Aids for Macromolecular Structure (compiled by Richard J. Feldmann and David H. Bing)**	189
M.A. Moore	**Scaling Concepts in Polymer Physics (Pierre-Gilles de Gennes)**	190
Michael Berry	**Bifurcation Theory and Applications in Scientific Disciplines (O. Gurel and O.E. Rössler, editors)**	191
M.H. Martin	**The Chemistry, Biochemistry and Biology of Cadmium (M. Webb, editor)**	191

MISCELLANY

100 years ago	106
Books received	192
New on the market	xiii
Classified advertising	xv

Getting down to the finer details of microelectronics

As a leading manufacturer, and user, of microelectronic technology, Philips is constantly searching for techniques that will improve the production process, or the product, or – ideally – both. This objective has now been achieved with the development of the 'Beamwriter' vector scan lithography system. In fact, it's the only production-oriented vector scan electron beam writing system available in the world.

Compared to conventional optical lithography techniques, vector scanning produces significant savings in the time taken to produce a set of masks or reticles; hours instead of days. It is also much more efficient than the raster scan E-beam method because the writing beam is directed only to points where exposure is required. The Beamwriter also generates an exposure dosage twenty times greater than other

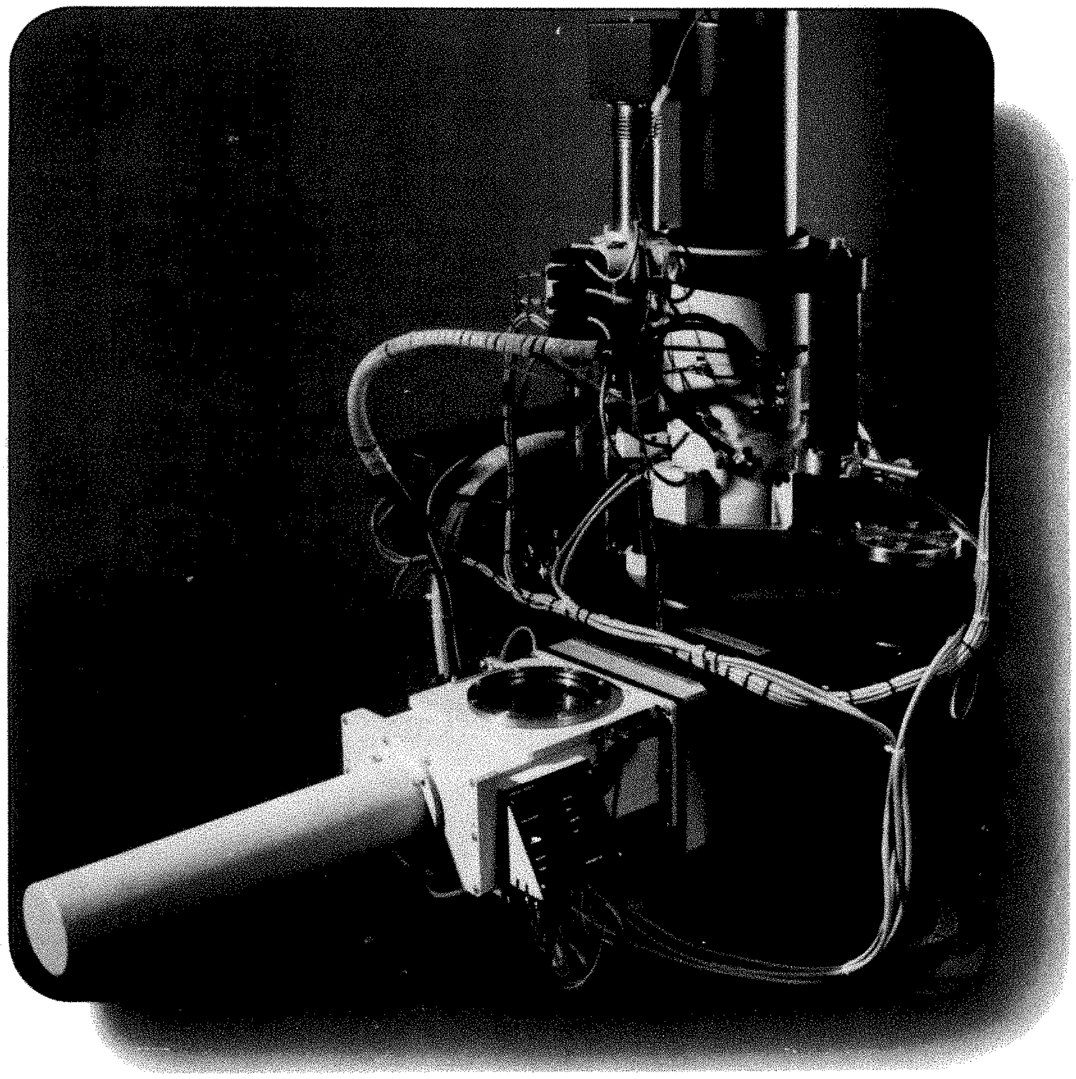

Circle No. 20 on Reader Enquiry Card.

PHILIPS

nature

Volume 286 No.5770 17 July 1980

Pure Chemistry Library
SCIENCE COLLEGE
[illegible] Upper Circular Road
CALCUTTA

NEWS

What to do about new herbicides 193
Nato, France and the neutron bomb 194
Congress supports technology centres 195
Carnesale for NRC chairman 195
Policy analysis — UK adventure? 196
Teaching companies — Victims of success? 196
Technological forecasting — Rush programme 197
Soviet energy — No shortage? 197
Technological change — Worry about jobs 198
Thermonuclear fusion — Soviets bid half 198
Laboratory merger — Harwell again 199
Siberian science — Marchuk on top 199
Correspondence: Biko's doctors (Phillip V. Tobias); Russian continues (Alan Wood); Dioxin disclaimer (K.D. Crow) 200

NEWS AND VIEWS

Tectonics of the Northwest European Continental shelf: P.E. Kent reports a recent conference 201
Genetic recombination: John Rosamond on high-frequency recombination 'hotspots' 202
The structure of zeolites: L.V.C. Rees comments on the first electron microscope pictures 204
Epidermal growth factor and mitogenesis: Colin R. Hopkins traces a hormone-target cell interaction 205
The fenlands: Peter Moore explains why the fenlands are sinking 206
Cometary science: M.K. Wallis on the first results from the International Ultraviolet Explorer satellite 207
Natural Killer cells: Rod Langman on tumours and natural killer activity 208

ARTICLES

H. Bougault and M. Treuil **Mid-Atlantic Ridge: zero-age geochemical variations between Azores and 22°N** 209
W.W. Shilts **Flow patterns in the central North American ice sheet** 213
P. van de Putte, S. Cramer and M. Giphart-Gassler **Invertible DNA determines host specificity of bacteriophage Mu** 218
E.F. Vanin, G.I. Goldberg, P.W. Tucker and O. Smithies **A mouse α-globin-related pseudogene lacking intervening sequences** 222
K. Nakashima, E. Darzynkiewicz and A.J. Shatkin **Proximity of mRNA5′-end and 18S rRNA in eukaryotic initiation complexes** 226
C.J. Barnstable **Monoclonal antibodies which recognize different cell types in the rat retina** 231

LETTERS

O.L. Vaisberg, D.S. Intriligator and V.N. Smirnov **Pressure balance and pressure distribution along the dayside ionopause of Venus** 235
M. Torbett and R. Smoluchowski **Hydromagnetic dynamo in the cores of Uranus and Neptune** 237
W.A. Coles, B.J. Rickett, V.H. Rumsey, J.J. Kaufman, D.G. Turley, S. Ananthakrishnan, J.W. Armstrong, J.K. Harmons, S.L. Scott and D.G. Sime **Solar cycle changes in the polar solar wind** 239
A.C. Fraser-Smith and O.G. Villard Jr **Peninsula method of ULF signal generation** 242

Contents continued overleaf

Cover: The solar corona as viewed by the NASA Solar Maximum Mission. Solar cycle variations of the Sun's polar wind are reported on page 239.

M
© 1980 Macmillan Journals Ltd
Nature® published weekly ISSN 0028-0836
Registered as a newspaper at the British Post Office and the United States Post Office

0028-0836/80/29000C-03$01.00

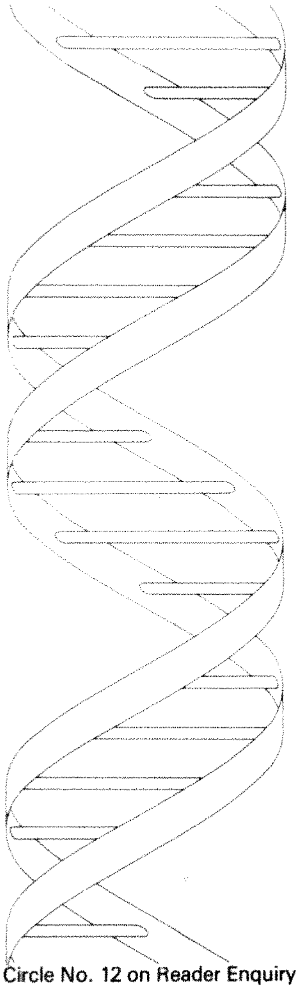

Fast, convenient, safe

^{32}P-nucleotides — straight from the bottle

You can add our [α-^{32}P]dNTP's or [γ-^{32}P]ATP's in stabilized aqueous solution* at 10mCi/ml directly to your reaction mixture in most cases. Elimination of the evaporation step

- saves time
- minimizes handling
- reduces possibility of decomposition or spillage

Extensive trials have shown that you can expect the same high stability and performance from these products as you obtain from the solutions in 50% aqueous ethanol that make us the world's leading supplier.

Call Amersham or your local distributor for a brochure and despatch schedule.

*Patent applied for

The Radiochemical Centre
Amersham

Full information is available on request.
The Radiochemical Centre Limited, Amersham,
England. Telephone: 024-04-4444.
In the U.S.A. and Canada: Amersham Corporation,
Illinois 60005. Telephone: 312-364-7100
and 800/323-9750 (Tollfree).
In W. Germany: Amersham Buchler GmbH & Co KG,
Braunschweig. Telephone: 05307-4691.

Circle No. 12 on Reader Enquiry Card.

ANIMAL ACTIVITY METER

FOR RODENTS, FISH OR INSECTS

MEASURES TRAVELED DISTANCE, PLOTS PATTERN OF MOVEMENTS.

Measures Animal Respiration and Tremors

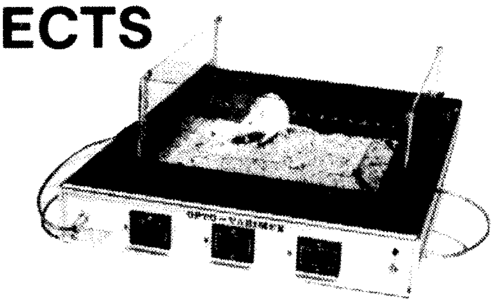

★ Measures horizontal activity by interruption of invisible infrared beams criss-crossing animal cage 1" above the bottom.
★ Measures rearing and jumping activity by means of two adjustable light curtains.
★ Plots pattern of animal movements on X-Y chart recorder by decoding position of animal from interrupted IR beams.
★ *Completely* insensitive to urine bedding or feces as IR beams cross the cage 1" above bottom.
★ Large 15" x 15" transparent plastic cage—not attached to the instrument.
★ Measures tremors and respiration by proximity sensor.

for more information call or write:

COLUMBUS INSTRUMENTS

950 NORTH HAGUE AVENUE
COLUMBUS, OHIO 43204 U.S.A.
PHONE (614) 488-6176

Circle No. 03 on Reader Enquiry Card.

LETTERS

C.E. Roos, J. Marraffino, S. Reucroft, J. Waters, M.S. Webster, E.G.H. Williams A. Manz, R. Settles and G. Wolf **Σ^+ lifetimes and longitudinal acceleration** 244

D. Walton **Time-temperature relations in the magnetization of assemblies of single domain grains** 245

A.E. Milodowski and D.J. Morgan **Identification and estimation of carbonate minerals at low levels by evolved CO_2 analysis** 248

J. Chappell **Coral morphology, diversity and reef growth** 249

M.B. Hart **A water depth model for the evolution of the planktonic Foraminiferida** 252

T.-F. Ho, A.R. McIntosh and J.R. Bolton **Intramolecular photochemical electron transfer in a linked porphyrin-quinone molecule as a model for the primary step of photosynthesis** 254

C.R. Somerville and W.L. Ogren **Inhibition of photosynthesis in *Arabidopsis* mutants lacking leaf glutamate synthase activity** 257

T. Boller and H. Kende **Regulation of wound ethylene synthesis in plants** 259

P. Handford **Heterozygosity at enzyme loci and morphological variation** 261

H. Endo, M. Kiyoki, K. Kawashima, T. Naruchi and Y. Hashimoto **Vitamin D_3 metabolites and PTH synergistically stimulate bone formation of chick embryonic femur *in vitro*** 262

A.W. Ford-Hutchinson, M.A. Bray, M.V. Doig, M.E. Shipley and M.J.H. Smith **Leukotriene B, a potent chemokinetic and aggregating substance released from polymorphonuclear leukocytes** 264

A.K. Fowler, C.D. Reed and D.J. Giron **Identification of an interferon in murine placentas** 266

P.J. Shearman, W.M. Gallatin and B.M. Longenecker **Detection of a cell-surface antigen correlated with organ-specific metastasis** 267

Z. Eshhar, R.N. Apte, I. Löwy, Y. Ben-Neriah, D. Givol and E. Mozes **T-cell hybridoma bearing heavy chain variable region determinants producing (T,G)-A-L-specific helper factor** 270

J. Silver, S.L. Swain and J.J. Hubert **Small subunit of I-A subregion antigens determines the allospecificity recognized by a monoclonal antibody** 272

S.L. Brooks, N.J. Rothwell, M.J. Stock, A.E. Goodbody and P. Trayhurn **Increased proton conductance pathway in brown adipose tissue mitochondria of rats exhibiting diet-induced thermogenesis** 274

P.F. Baker and A. Carruthers **Insulin stimulates sugar transport in giant muscle fibres of the barnacle** 276

V. Herzberg, J.M. Boughter, S. Carlisle and D.E. Hill **Evidence for two insulin receptor populations on human erythrocytes** 279

A.R. Chipperfield **An effect of chloride on (Na + K) co-transport in human red blood cells** 281

G. Klages, H. Emmerich and M.G. Peter **High-affinity binding sites for juvenile integument of hormone I in the larval *Drosophila hydei*** 282

W. Sieghart and M. Karobath **Molecular heterogeneity of benzodiazepine receptors** 285

P. Laduron **Axoplasmic transport of muscarinic receptors** 287

J.A. Angus and P.I. Korner **Evidence against presynaptic α-adrenoreceptor modulation of cardiac sympathetic transmission** 288

A. Trautmann and A. Feltz **Open time of channels activated by binding of two distinct agonists** 291

H. Stadler and H.H. Füldner **Proton NMR detection of acetylcholine status in synaptic vesicles** 293

M. Karin, R.D. Andersen, E. Slater, K. Smith and H.R. Herschman **Metallothionein mRNA induction in HeLa cells in response to zinc or dexamethasone is a primary induction response** 295

R. Goldbach, G. Rezelman and A. van Kammen **Independent replication and expression of B-component RNA of cowpea mosaic virus** 297

B.L. Trus and K.A. Piez **Compressed microfibril models of the native collagen fibril** 300

P.C. Weber, R.G. Bartsch, M.A. Cusanovich, R.C. Hamlin, A. Howard, S.R. Jordan, M.D. Kamen, T.E. Meyer, D.W. Weatherford, N.H. Xuong and F.R. Salemme **Structure of cytochrome c': a dimeric, high-spin haem protein** 302

S.H. Northrup, M.R. Pear, J.A. McCammon and M. Karplus **Molecular dynamics of ferrocytochrome *c*** 304

MATTERS ARISING

J.G. Kirk **Cometary evidence against the solar companion** 306

D. Wilkins **Reply to Kirk** 306

I.W.A. Browne **Redshifts and distances** 307

G. Burbidge **Reply to Browne** 307

A.T.V. Rothstein **The Lizard complex as an ophiolite** 307

G.A. Kirby **Reply to Rothstein** 307

J. Novotny and A. Vitek **Evolution of bacterial cytochromes c_2** 308

G.C.K. Roberts, J. Feeny, B. Birdsall, P. Charlton and D. Young **Methotrexate binding to dihydrofolate reductase** 309

G.E. Williams **Effects of the Earth's rotation rate on climate** 309

B.G. Hunt **Reply to Williams** 310

S. Smith **Analysis of host specificity of temperate and tropical animals** 310

R.A. Beaver **Reply to Smith** 310

SOLAR RADIATION MEASURING INSTRUMENTS & SYSTEMS

EKO, having 50 years' experience in manufacturing meteorological instruments, offer various and precise radiation instruments and systems. Consultation and instrumentation for special measuring requirements are available.

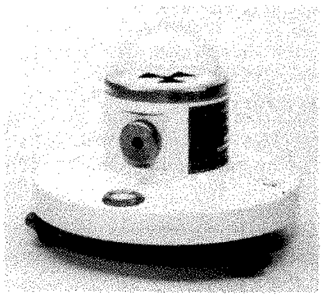

Neo Pyranometer
MS-42

Serves for precise and stable measurement of global radiation from sun and sky. The detector is thermopile with the black hot-junction receivers and the white cold-junction receivers.
Secular fluctuations are free.

Measures with high accuracy sun and sky radiation in defined wavelength bands. Delivered with a polished hemisphere of a quartz glass in the inside and a filter in the outside which can readily be replaced by other filter (cut-off filters WG-305, GG-395, RG-695 available).

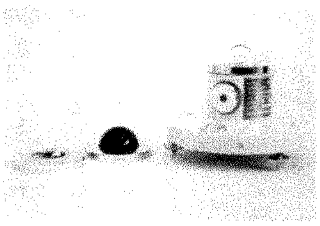

Precision Spectral Pyranometer
MS-800

Measures precisely and continuously the intensity of direct solar radiation. The opening angle, slope angle and limit angle of Pyrheliometer tube (permanently mounted on a power driven equatorial mount) are according to WMO recommendation (opening angle 3.98°).

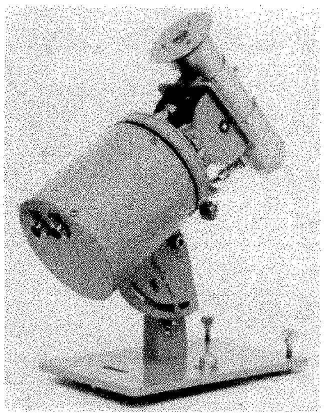

Pyrheliometer
MS-52

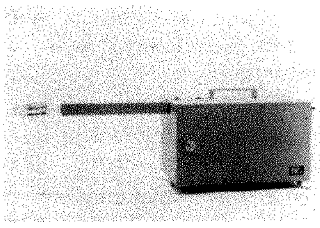

Net Radiometer
CN-II

Newly designed net radiometer having characteristics of both wind through type and wind protection type. Wind through system protects polyethylene hemispheres against frost and homoginizes the temperature of the hemispheres. The built-in fan and dryer keep the shapes of upper and down hemispheres round constantly and prevents them from freezing.

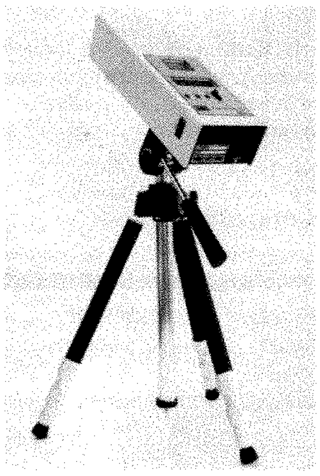

Sunphotometer
MS-120

Latest new development based on WMO recommendation for measurement of atmospheric turbidity, eliminating disadvantages of same measurement with pyrheliometer with broad band filters or traditional sunphotometer in respects of accuracy and handling.
MS-120 has high spectral purity and stability against temperature fluctuation.

Connectable to all kinds of mV output type detector such as solarimeter, thermometer, radiometer, anemometer, hygrometer and other instruments of meteorological and engineering fields. Minus signals can also be integrated. By using with multi-points recorder, the integrated and the time dependent values are recorded on a same chart.

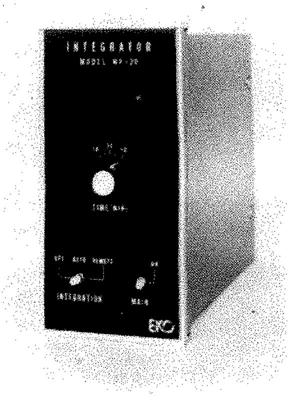

Analogue Integrator
MP-20

OTHER AVAILABLE SENSORS

- Tube Type Solarimeter
- Pyranometer + Shadow Band Stand (for measuring diffuse sky radiation)
- Various Heat Flow Measuring Sensors
- Alhedometers
- Dew Detector

RECORDERS & INTEGRATORS

- Electronic Self-Balancing Recorders
- DC Mini-Recorders
- Digital Integrator
- DC Portable Integrator
- Data Logger

For details please contact:

EKO INSTRUMENTS TRADING CO., LTD.

21-8, Hatagaya 1-chome,
Shibuya-ku, Tokyo
151 Japan

Telephone	**03-469-4511 Tokyo**
Telex	**J25364 EKOTRA**
Cable Address	**EKOTRA TOKYO**

Circle No. 32 on Reader Enquiry Card.

BOOK REVIEWS

C.A. Russell	**The Papers of Joseph Henry. Vol. 3. (N. Reingold, editor)**	311
G.T. Bath	**Introduction to Advanced Astrophysics (V. Kourganoff)**	312
George Fink	**Hormones and Evolution (E.J.W. Barrington, editor)**	313
A.J. Munro	**Selected Methods in Cellular Immunology (Barbara B. Mishell and Stanley M. Shiigi, editors)**	314
Barry Cox	**Mesozoic Mammals: The First Two-Thirds of Mammalian History (J.A. Lillegraven *et al.*, editors)**	314
C.J. Gilmore	**Theory and Practice of Direct Methods in Crystallography (M.F.C. Ladd and R.A. Palmer, editors)**	315
D.H. Watson	**Introduction to Virology (K.M. Smith and D.A. Ritchie)**	316
R.J. Bickerton	**Plasma Physics for Nuclear Fusion (K. Miyamoto)**	316

MISCELLANY

100 years ago	203
Books received	317
Product review, Astronomy and Meteorology	xiii
Classified advertising	xix

Nature manuscripts

The Articles and Biological Letters in this issue are the last to be seriously affected by an industrial dispute that has been delaying the typesetting of manuscripts in the past 3 months.

GUIDE TO AUTHORS

- Review articles should be aimed at a relatively wide readership. Many reviews are invited, but submitted articles may also be accepted; it is advisable to consult us before writing a review article.
- Articles may be up to 3,000 words long with at most six displayed items (figures and tables); they are reports of major research developments.
- Letters are brief reports of original research of unusual and wide interest, not in general longer than 1,000 words; they have at most three or four displayed items.
- 'Matters Arising' permits short discussion (up to 300 words) of papers that have recently appeared in *Nature*.

Articles should be accompanied by an abstract of not more than fifty words. Letters should begin with a paragraph giving the background and main conclusion in terms intelligible to as wide a readership as possible.

Manuscripts may be submitted either to London or New York. Three typed copies should be submitted, each including lettered copies of figures. Typing (including references) should be double spaced. The title should be brief and informative. Pages should be numbered. References, tables and figure legends should start on separate pages. Experimental detail vital to the paper yet which would interrupt the narrative is best placed in the figure legends. Units should be identified in the margin on their first appearance. Equations should occupy single lines if possible: exp(a) is preferred to e^a if 'a' is more than one character.

References are indicated by superscripts in the text. See any contemporary *Nature* for style, but note:

(i) only one reference number need be used if the reference is to several papers by identical authors.

(ii) first and last pages of references should be cited.

Abbreviations should follow the *World List of Scientific Periodicals*, fourth edn (Butterworth, 1963-65). Symposia are often difficult to refer to and only published or soon-to-be-published volumes should be mentioned in references. Their publisher and place of publication should be clearly indicated 'Personal communication' and 'unpublished' should be incorporated in text.

Artwork should be sent with the manuscript and clearly marked with author's name and the figure number. Line drawings should be either photographic prints or in Indian ink on heavy cartridge paper, tracing paper or similar materials. Most figures are reduced to one column width so originals should be about as wide as a page of *Nature*. To enable figures, particularly maps, to be edited in the same style as the text, they should contain only essential material. Ideally, an unlettered original and three lettered copies should be provided; labelling on halftones should, if possible, be avoided entirely. Magnifications quoted should be for the figures as submitted. We are always glad to see artwork for possible use on the cover, but cannot guarantee its return.

In order to save on postal expenses we return only the top copy and artwork of manuscripts that we cannot publish.

Nature's publishing policy is outlined in **258**, 1 (1975) and **264**, v, 11 Nov. (1976).

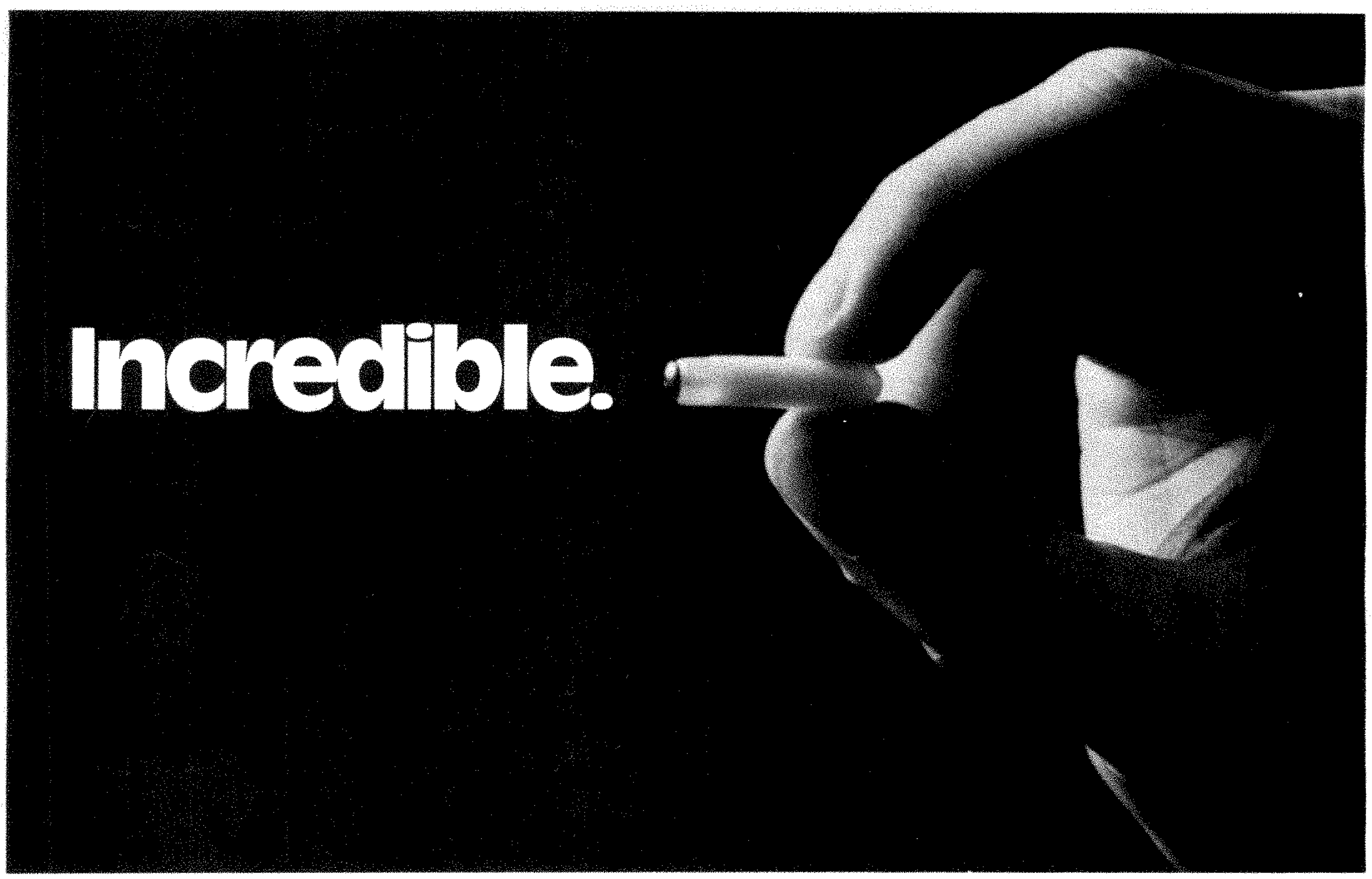

This tiny, completely self-contained pump provides continuous, unattended delivery of test solutions for one or two weeks.

It's called the Alzet® osmotic minipump.

It is a self-contained pump that is implanted subcutaneously in animals as small as mice or rats and that delivers your test solution to the animal at a controlled, continuous rate of 1µl/hr for one week, or .5µl/hr for two weeks.

And, while the Alzet® osmotic minipump frees you and your staff from the burden of dosing the animal several times a day, it can free the animal from the trauma of multiple injections.

With this pump, you can expect to produce sustained biological effects, more reproducible than with injections. The animals are unrestrained and do not undergo the continual stress of being externally catheterized.

The Alzet® osmotic minipump is ideal for compounds with short half-lives, since its constant infusion maintains steady state plasma levels of the agents. And the constant, continuous delivery assures you that there are no missed or late doses.

Steady state biological effects in unrestrained animals . . . that's what the incredible Alzet® osmotic minipump can offer you.

For technical information, call 415/494-5323. To order, call 800/227-9953 or write to Alza, Dept. Y, 950 Page Mill Road, Palo Alto, California 94304.

alzet®
OSMOTIC MINIPUMP

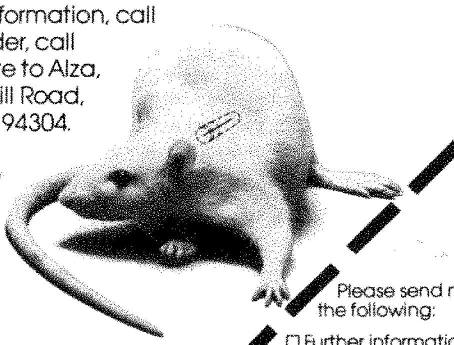

Please send me the following:

☐ Further information on the Alzet® osmotic minipump

☐ Ordering information

Name ____________________

Institution ____________________

Address ____________________

City ____________________ State ________ Zip ____________

© 1979 Alza Corp.

Circle No. 04 on Reader Enquiry Card.

nature

Volume 286 No.5771 24 July 1980

NEWS

Should academics make money outside? 319
Reviving (in the US) an old British recipe 320
British biotechnology boat comes home 321
Supreme Court stirs up more fear 321
Biotechnology: European setback 322
Yugoslav academics: no liberalization 322
Scientists' pay: UK rumpus 323
Long-standing pay dispute continues 323
US science budget: stability ahead? 324
US scientific unemployment 324
Indian space: One up so far 324
Nuclear explosions: no alarm 325
Nuclear power: ore running out? 325
Correspondence: Geothermal electricity generation (J.D. Garnish); Banking DNA sequences (M.O. Dayhoff *et al.*) 326

NEWS AND VIEWS

Just so stories and cautionary tales: Robert M. May and Miranda Robertson on the evolution of social behaviour 327
Malignant transformation: Thomas Langan on the role of a unique class of protein kinases 329
Repressor represses cro represses repressor: Mark E. Furth on a developmental switch in λ phage 330
The problem of defining a substorm: S.W.H. Cowley on auroras and magnetic storms 332
Radar measurements of estuarine currents and tides: E.D.R. Shearman on a new remote sensing system 333

ARTICLES

C.J. Allègre and D. Ben Othman **Nd–Sr isotopic relationship in granitoid rocks and continental crust development: a chemical approach to orogenesis** 335
B.L. Weaver and J. Tarney **Continental crust composition and nature of the lower crust: constraints from mantle Nd–Sr isotope correlation** 342
N.H. Woo, B.A. Roe and A. Rich **Three-dimensional structure of *Escherichia coli* initiator tRNA$^{\mathrm{Met}}_{\mathrm{f}}$** 346
P.J. Farabaugh and G.R. Fink **Insertion of the eukaryotic transposable element Ty*1* creates a 5-base pair duplication** 352
F. Moreno, A.V. Fowler, M. Hall, T.J. Silhavy, I. Zabin and M. Schwartz **A signal sequence is not sufficient to lead β-galactosidase out of the cytoplasm** 356

LETTERS

C.J. Hogan **Spontaneous production of cosmological fluctuations** 360
G.E. Hunt, A.O. Pickersgill, P.B. James and G. Johnson **Some diurnal properties of clouds over the martian volcanoes** 362
F. Winterberg **Black-body radiation as an inertial confinement fusion driver** 364
J.A. Halbleib, P.A. Miller, L.P. Mix and T.P. Wright **Overlap of intense charged particle beams for intertial confinement fusion** 366
C.K.N. Patel, E.T. Nelson and R.J. Kerl **Opto-acoustic study of weak optical absorption of liquid methane** 368
M.P. Aronson and H.M. Princen **Contact angles associated with thin liquid films in emulsions** 370
A.R. Rennie and D. Tabor **Hydrostatic pressure and long-chain organic molecule diffusion through a polymer matrix** 372
J.A. Pyle and R.G. Derwent **Possible ozone reductions and UV changes at the Earth's surface** 373

Contents continued overleaf

Cover: Photograph of 12 electron beams from a common accelerator source incident on a target. Such a particle beam arrangement appears promising for future inertial confinement fusion devices. This is discussed further on page 366.

Nature® published weekly ISSN 0028-0836
Registered as a newspaper at the British Post Office and the United States Post Office

0028-0836/80/30000C-02$01.00

Fast, convenient, safe
^{32}P-nucleotides — straight from the bottle

You can add our [α-^{32}P]dNTP's or [γ-^{32}P]ATP's in stabilized aqueous solution* at 10mCi/ml directly to your reaction mixture in most cases. Elimination of the evaporation step

- saves time
- minimizes handling
- reduces possibility of decomposition or spillage

Extensive trials have shown that you can expect the same high stability and performance from these products as you obtain from the solutions in 50% aqueous ethanol that make us the world's leading supplier.

Call Amersham or your local distributor for a brochure and despatch schedule.

*Patent applied for

The Radiochemical Centre
Amersham

Full information is available on request.
The Radiochemical Centre Limited, Amersham,
England. Telephone: 024-04-4444.
In the U.S.A. and Canada: Amersham Corporation,
Illinois 60005. Telephone: 312-364-7100
and 800/323-9750 (Tollfree).
In W. Germany: Amersham Buchler GmbH & Co KG,
Braunschweig. Telephone: 05307-4691.

Circle No. 05 on Reader Enquiry Card.

British Journal of
CLINICAL PHARMACOLOGY

ESSENTIAL INFORMATION AT YOUR FINGERTIPS. EVERY MONTH!

Published monthly on behalf of the British Pharmacological Society, *British Journal of Clinical Pharmacology* is as fast-moving as the area of science it examines:

Bridging the gap between medical professions, clinical research and the pharmaceutical industry.

Containing papers and reports on all aspects of drug action in man, in both health and disease.

Providing free copies of the proceedings of selected symposia on new methods, new drugs and new approaches to treatment, to all subscribers.

To keep up-to-date in this fast-moving area of science why not join the ever-increasing number of clinical pharmacologists all over the world who rely on the *British Journal of Clinical Pharmacology* as their professional journal.

ANNUAL SUBSCRIPTIONS
UK £59.50
USA/Canada US$195 USA/Canada (surface) US$150
Rest of the world £82 Rest of the world (surface) £70

Orders should be accompanied by remittance, cheques made payable to Macmillan Journals Ltd: Subscription Department, Brunel Road, Basingstoke, Hampshire, RG21 2XS, England.

Sample copies are also available from the same address.

T. Turunen, P.S. Cannon and M.J. Rycroft	**ELF radio signals in the auroral ionosphere generated by non-linear demodulation of LF and/or MF transmissions**	375
D.G. King-Hele, C.J. Brookes and G.E. Cook	**The pear-shaped section of the Earth**	377
D.E. Sugden and C.M. Clapperton	**West Antarctic ice sheet fluctuations in the Antarctic Peninsula area**	378
S. Conway Morris and W.H. Fritz	**Shelly microfossils near the Precambrian–Cambrian boundary, Mackenzie Mountains, northwestern Canada**	381
R.P. Blakemore, R.B. Frankel and Ad. J. Kalmijn	**South-seeking magnetotactic bacteria in the Southern Hemisphere**	384
M.H. Day and E.H. Wickens	**Laetoli Pliocene hominid footprints and bipedalism**	385
P. Jaisson	**Environmental preference induced experimentally in ants (Hymenoptera: Formicidae)**	388
W.R. Levick and L.N. Thibos	**Orientation bias of cat retinal ganglion cells**	389
D. Johnston, J.J. Hablitz and W.A. Wilson	**Voltage clamp discloses slow inward current in hippocampal burst-firing neurones**	391
E. Kaplan and R.B. Barlow Jr	**Circadian clock in *Limulus* brain increases response and decreases noise of retinal photoreceptors**	393
S. Yoshikami, J.S. George and W.A. Hagins	**Light-induced calcium fluxes from outer segment layer of vertebrate retinas**	395
L.R. Pease and W.H. Murphy	**Co-infection by lactic dehydrogenase virus and C-type retrovirus elicits neurological disease**	398
R. Gaynor, R. Irie, D. Morton and H.R. Herschman	**S100 protein is present in cultured human malignant melanomas**	400
P. Barazzone, J.-L. Carpentier, P. Gorden, E. Van Obberghen and L. Orci	**Polar redistribution of ^{125}I-labelled insulin on the plasma membrane of cultured human lymphocytes**	401
G.W. Stewart, J.C. Ellory and R.A. Klein	**Increased human red cell cation passive permeability below 12°C**	403
D.L. Cook, W.E. Crill and D. Porte Jr	**Plateau potentials in pancreatic islet cells are voltage-dependent action potentials**	404
J.P. Pandey, E. Tung, S. Mathur, K.K. Namboodiri, A.C. Wang, H.H. Fudenberg, W.A. Blattner, R.C. Elston and C.G. Hames	**Linkage relationship between variable and constant region allotypic determinants of human immunoglobulin heavy chains**	406
J.M. Malpica and J.M. Vassallo	**A test for the selective origin of environmentally correlated allozyme patterns**	407
F.H. Reynolds Jr, W.J.M. Van de Ven and J.R. Stephenson	**Feline sarcoma virus polyprotein P115 binds a host phosphoprotein in transformed cells**	409
M.C. Maw and A.J. Rowe	**Fraying of A-filaments into three subfilaments**	412
J. Gafner and P. Philippsen	**The yeast transposon Ty*1* generates duplications of target DNA on insertion**	414
A. Goldfarb and V. Daniel	**Transcriptional control of two gene subclusters in the tRNA operon of bacteriophage T4**	418
T.I. Bonner, R. Heinemann and G.J. Todaro	**Evolution of DNA sequences has been retarded in Malagasy primates**	420
M. Charlier, J.C. Maurizot and G. Zaccai	**Neutron scattering studies of *lac* repressor**	423
G. Cevc, P. Cevc, M. Schara and U. Skalerič	**The caries resistance of human teeth is determined by the spatial arrangement of hydroxyapatite microcrystals in the enamel**	425

BOOK REVIEWS

Vera Rich	**It Seems I Am a Jew (Grigori Freiman)**	427
C.J. Batty	**Exotic Atoms '79: Fundamental Interactions and Structure of Matter (Kenneth Crowe *et al.*, editors)**	428
Melody Siegler	**Insect Neurophysiological Techniques (T.A. Miller)**	428
Ian Dawes	**Developmental Biology of Prokaryotes (J.H. Parish, editor)**	429
Talbot H. Waterman	**The Ecology of Vision (J.N. Lythgoe)**	429
Richard Lynn	**Brain and Personality (Graham E. Powell)**	430

MISCELLANY

100 years ago	328
Author index	vii
Books received	xii
Classified advertising	xvi

Pure Chemistry Library
SCIENCE COLLEGE
Upper Circular Road
Calcutta

***Nature* Indexes:** This week *Nature* includes an Author Index to volume 285, covering May and June 1980. Previous Author Indexes this year appeared in the issues of 20 March (for vol. 283) and 22 May (vol. 284).

Preston Publications, Inc.
offers
the following:

for Chromatographers;

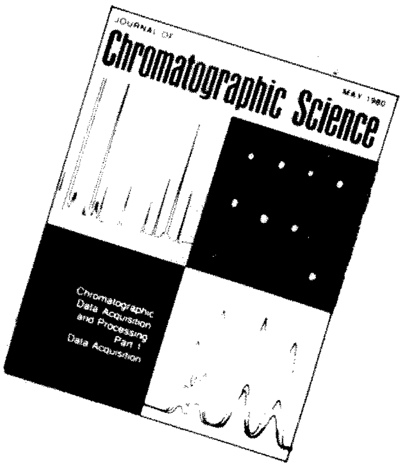
Journal of
Chromatographic Science
May 1980
Chromatographic Data Acquisition and Processing Part I Data Acquisition

for toxicologists,

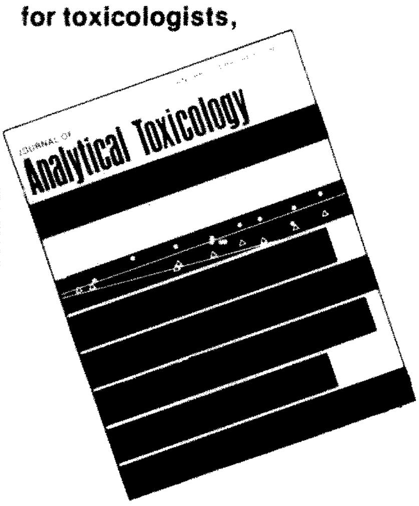

and
for the photographer...

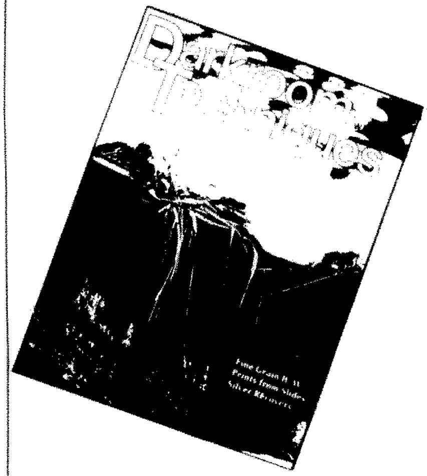

For more information about our publications write:

Preston Publications, Inc.
6366 Gross Point Road
Niles, Illinois 60648

Circle No. 11 on Reader Enquiry Card.

text books from MACMILLAN PRESS

FROM DNA TO PROTEIN: The Transfer of Genetic Information
MARIA SZEKELY

This is the first textbook which discusses gene structure on the basis of recent discoveries of overlapping and split genes and which genetic information can be encoded into the genetic material and how it can be transferred to other materials.
A perfectly up-to-date account of our present knowledge of the structure and expression of genes in prokaryotic and eukaryotic organisms and the only available text showing the correlation between the structure and function of nucleic acids.
March, £18.00, 0 333 21836 1
£9.95, 0 333 21828 8

HUMAN REPRODUCTION AND DEVELOPMENTAL BIOLOGY
D. J. BEGLEY, J. A. FIRTH and J. R. S. HOULT

An integrated approach to describe the cellular and physiological processes of human reproduction and embryological development in relation to their underlying mechanisms and to their practical applications in medicine. The book combines anatomy, biochemistry, physiology and pharmacology, making it more suitable for modern preclinical and human biology courses.
February, £20.00, 0 333 23423 5
£9.95, 0 333 23424 3

GYNAECOLOGICAL CYTOLOGY
MATHILDE E. BOON and METTE LISE TABBERS-BOUMEESTER

Dr Boon and Dr Tabbers-Boumeester have, over the past ten years, developed the course in diagnostic cytology which was first given in Leiden in 1969.
In this volume they present their insight into both the study of diagnostic cytology, and into the teaching of this increasingly important subject. To illustrate the modern concepts of cytopathology, examples of more advanced approaches are included: as well as scanning and electron microscopy there are details of DNA measurements, morphometry and immunopathology.
June, £25.00, 0 333 26117 8
£14.00, 0 333 26118 6

Macmillan Press books are available from leading booksellers
If you have difficulty obtaining these titles please write to Tony Watson, Macmillan Retail Ltd, Houndmills, Basingstoke, Hants, enclosing purchase price + 70p (p&p).

Circle No. 111 on Reader Enquiry Card.

M MACMILLAN PRESS

M

© 1980 Macmillan Journals Ltd
Nature® is published weekly
ISSN 0028-0836
Registered as a newspaper at the British Post Office

London
4 Little Essex Street, WC2R 3LF
Telephone: (01) 836 6633 Telex: 262024
Telegrams: Phusis London WC2R 3LF

Editor: John Maddox
Deputy Editor: Peter Newmark
Editorial Staff
Alun Anderson
Philip Campbell
Isobel Collins
Konrad Guettler
Tim Lincoln
Mary Lindley
Naomi Molson
Sara Nash
Judy Redfearn
Miranda Robertson
Robert Walgate
Charles Wenz
Jonathan Wolfe
Publishing Director: Christopher Paterson
Marketing Director: Ray Barker

New York
15 East 26 Street, New York, NY 10010
Telephone: (212) 689 5900 Telex: 668497
Robert Ubell (American Publisher) and Sheila Kane

Washington News Bureau
801 National Press Building, DC 20045
Telephone: (202) 737 2355 Telex: 64280
David Dickson (Washington News Editor)

International Advertising Manager:
Richard Webb (London) (01) 240 2044

USA Advertising Manager
Henry Dale (New York) (212) 689 5900

Classified Advertising:
4 Little Essex Street, WC2R 3LF
Telephone: (01) 240 1101

Classified(USA)
Terence Miller, Suite 832, 50 Rockefeller Plaza, New York, NY 10020—(212) 765 5758

Display and Classified(Canada)
Peter Drake, 32 Front Street West, 201 Toronto, Ontario M5J 1C5
(416) 364 1623

Advertising Representatives in USA
Display
Nature New York Office—(212) 689 5900
Media Group, Inc. (Dallas)—(214) 631 4480
Didier & Broderick, Inc. (Chicago)—(312) 498 4520
Jobson/Jordan/Harrison/Schulz, Inc. (San Francisco) (415) 392 6794 (Los Angeles & Pasadena) (213) 796 9200
Daniel Adams Associates, Inc. Philadelphia—(215) 353 6191
CEL Associates (Boston)—(617) 383 6136
Brinker & Brinker (Fort Lauderdale) (305) 771 0064

German Advertising Representative
E. Meckelburg, 6450 Hanau 1, Jahnstrasse 15, West Germany Tel:— (49) 61 8115343

Japanese Advertising Representative
Orient Echo Inc.
11th Fl, Sankyo Bldg. 7-12, Tsukiji 2-Chome, Chuo-Ku, Tokyo, Japan, Tel: 541-4923.

Annual Subscription including Index

UK		£55
USA & Canada		US$135
Belgium	Airspeed	BF4900
West Germany	Airspeed	DM300
Holland	Airspeed	G325
Switzerland	Airspeed	SF265
Rest of World	Surface	£70
	Airmail	£95

Single copy (post-paid); UK, £1.20; USA & Canada, US$3.50 (surface), US$5.00 (air); Rest of World, £1.15 (surface), £2 (air).

Orders (with remittance) to:
Macmillan Journals Ltd, Brunel Road, Basingstoke, Hants RG21 2XS.
Telephone: Basingstoke (0256) 29242

Nature is published weekly, except the last week in December, by Macmillan Journals Ltd. Second-class postage paid at New York, NY 10010 and at additional mailing offices.
US Postmaster, please send form 3579 to: *Nature*, 15 East 26 Street, New York, NY 10010.

Vol. 286 No. 5771 24 July 1980

nature

Volume 286 No.5772 31 July 1980

NEWS

Public monopoly and private enterprise 431
Subject in search of discipline? 432
Proliferation a test of nerve in Congress 433
Plagiarism strikes again 433
US budgets: end in sight? 434
International laboratory: Danes turn soft 434
Scientific instruments: *Nature* spin-off 435
High-energy physics: trouble ahead 435
Dead Sea: coming to life 436
Biogenetic hormones: insulin trial 436
Environmental protection: Bulgaria ahead 437
One journal disowns plagiarism 437
Correspondence: Biologists mis-cite (R.F. Burton); Chemical warfare (J.H. Humphrey); Budapest disclaimer (Gyorgy Paris); Adjectival concerns (Peter Rastall); Unsplit infinitives (Editor, *Nature*) 438

NEWS AND VIEWS

Solar size variation: David W. Hughes looks at the evidence for a shrinking Sun 439
Structure of bacteriophage Pf1: R.A. Crowther describes a new model for the protein coat 440
Plant opportunists: Peter D. Moore looks at adaptability in weeds 441
Iron-sulphur proteins: R. Cammack on the discovery of new type of iron-sulphur cluster 442
Two-nucleon transfer reactions: P.E.Hodgson describes a new method of interpretation 443
Evolution and gaps in the fossil record: Mark Ridley examines Eldredge and Gould's model 444
Earthquake prediction: David W. Simpson reports a recent international meeting 445
Insect diapause: A.D. Lees on diapause change in introduced insects 446

REVIEW ARTICLE

H.R. Morris **Biomolecular structure determination by mass spectrometry** 447

ARTICLES

H. Gadasi & E.D. Korn **Evidence for differential intracellular localization of the *Acanthamoeba* myosin isoenzymes** 452
R.L. Heimark, K. Kurachi, K. Fujikawa & E.W. Davie **Surface activation of blood coagulation, fibrinolysis and kinin formation** 456
I.C. Eperon, S. Anderson & D.P. Nierlich **Distinctive sequence of human mitochondrial ribosomal RNA genes** 460

LETTERS

M.R.S. Hawkins **Discovery of a very distant supernova** 467
D.R. Lepine, D.A. Bryant & D.S. Hall **A 2.2-Hz modulation of auroral electrons imposed at the geomagnetic equator** 469
G.E. Thompson, K. Shimizu & G.C. Wood **Observation of flaws in anodic films on aluminium** 471
J.R. Walker & C.R.A. Catlow **The structure and energetics of the conduction plane in $\mathrm{Na}\beta\mathrm{Al_2O_3}$** 473
T. Kawai & T. Sakata **Conversion of carbohydrate into hydrogen fuel by a photocatalytic process** 474
R. Batiza, R.L. Larson, S.O. Schlanger, S.A. Shcheka & H. Tokuyama **Trace element abundances in basalts of Nauru Basin** 476

Contents continued overleaf

Cover: The original mass spectrograph (now in the Science Museum, London) designed by F.W. Aston and described in the *Philosophical Magazine* for December 1919 (drawing by Satoshi Kitamura) together with the first mass spectrum of slow reacting substance of anaphylaxis and its structure determined from this spectrum and associated data. This is discussed further on page 447.

Nature® published weekly ISSN 0028-0836
Registered as a newspaper at the British Post Office and the United States Post Office

0028-0836/80/31000C-02$01.00

New Products

Our range is always growing . . .

Amersham supplies radiochemicals for all aspects of biochemical research.

Some recent additions are

Deoxy[1′,2′,5-^{3}H]cytidine 5′-triphosphate	50-70Ci/mmol	TRK.625
[1,2,4,6,7-^{3}H]Dexamethazone	70-110Ci/mmol	TRK.645
l-[4,6,*propyl*-^{3}H]Dihydroalprenolol	70-110Ci/mmol	TRK.649
[^{14}C]Methyltriphenylphosphonium iodide	1-10mCi/mmol	CFA.640
L-[2,3,4,5,6-^{3}H]Phenylalanine	100-130Ci/mmol	TRK.648
L-α-Phosphatidylcholine, di[1-^{14}C]stearoyl	80-120mCi/mmol	CFA.649
Protein A, *N*-[*propionyl*-^{3}H]propionylated	40-80Ci/mmol	TRK.653

A full list of additions to our current catalogue is available on request.

The Radiochemical Centre Amersham

Full information is available on request.
The Radiochemical Centre Limited, Amersham, England. Telephone: 024-04-4444.
In the U.S.A. and Canada:
Amersham Corporation, Illinois 60005.
Telephone: 312-364-7100 and 800/323-9750 (Tollfree).
In W. Germany:
Amersham Buchler GmbH & Co KG, Braunschweig. Telephone: 05307-4691.

Circle No. 03 on Reader Enquiry Card.

---

nature

is Available in MICROFORM

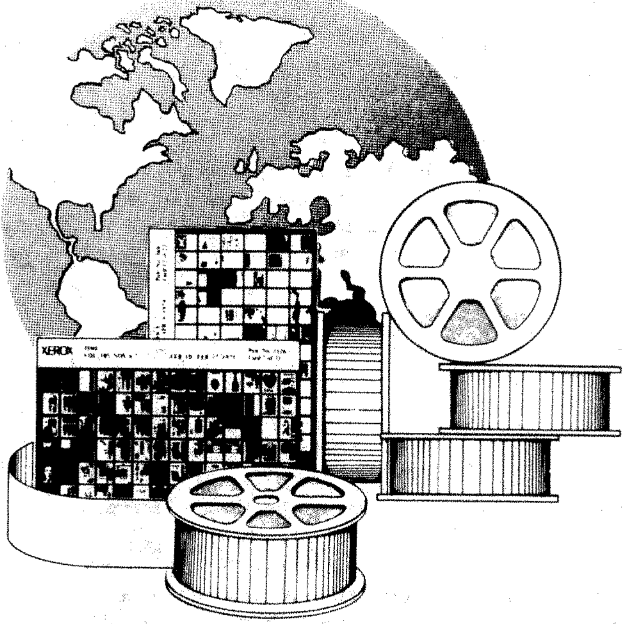

FOR INFORMATION,
WRITE:

University Microfilms International

300 North Zeeb Road
Ann Arbor, Mich. 48106
U.S.A.

18 Bedford Row
London, WC1R 4EJ
England

J.-C. Duplessy, J. Moyes & C. Pujol **Deep water formation in the North Atlantic Ocean during the last ice age** 479

D.J. Carlson & L.M. Mayer **Enrichment of dissolved phenolic material in the surface microlayer of coastal waters** 482

D.R. Prothero & R. Estes **Late Jurassic lizards from Como Bluff, Wyoming and their palaeobiogeographic significance** 484

O. Rieppel **Green anole in Dominican amber** 486

J.M. Pettitt, C.A. McConchie, S.C. Ducker & R.B. Knox **Unique adaptations for submarine pollination in seagrasses** 487

S.L. Goldson & R.M. Emberson **Relict diapause in an introduced weevil in New Zealand** 489

D.C. Kaushal, R. Carter, L.H. Miller & G. Krishna **Gametocytogenesis by malaria parasites in continuous culture** 490

D. Forman & J.M.W. Slack **Determination and cellular commitment in the embryonic amphibian mesoderm** 492

I. Orchard & B.G. Loughton **A hypolipaemic factor from the corpus cardiacum of locusts** 494

J.C. Rothwell, M.M. Traub & C.D. Marsden **Influence of voluntary intent on the human long-latency stretch reflex** 496

M.F. Johnston, S.A. Simon & F. Ramón **Interaction of anaesthetics with electrical synapses** 498

S.G. Cull-Candy, R. Miledi & O.D. Uchitel **Diffusion of acetylcholine in the synaptic cleft of normal and myasthenia gravis human endplates** 500

F.L. Harrison & C.J. Chesterton **Erythroid developmental agglutinin is a protein lectin mediating specific cell-cell adhesion between differentiating rabbit erythroblasts** 502

J. Blomberg, F.H. Reynolds Jr, W.J.M. Van de Ven & J.R. Stephenson **Abelson murine leukaemia virus transformation involves loss of epidermal growth factor-binding sites** 504

T.J. Schmidt, J.M. Harmon & E.B. Thompson **'Activation-labile' glucocorticoid-receptor complexes of a steroid-resistant variant of CEM-C7 human lymphoid cells** 507

B.M. Sutherland & S.G. Hausrath **Insertion of *E.coli* photoreactivating enzyme into V79 hamster cells** 510

W.F. Rall, D.S. Reid & J. Farrant **Innocuous biological freezing during warming** 511

G. Goldberger & H.R. Colten **Precursor complement protein (pro-C4) is converted *in vitro* to native C4 by plasmin** 514

F. Vyskočil, J. Teisinger & H. Dlouhá **A specific enzyme is not necessary for vanadate-induced oxidation of NADH** 516

S.R. Heidemann & J.R. McIntosh **Visualization of the structural polarity of microtubules** 517

P.R. Shewry, J.-C. Autran, C.C. Nimmo, E.J.-L. Lew & D.D. Kasarda **N-terminal amino acid sequence homology of storage protein components from barley and a diploid wheat** 520

K. Fukuyama, T. Hase, S. Matsumoto, T. Tsukihara, Y. Katsube, N. Tanaka, M. Kakudo, K. Wada & H. Matsubara **Structure of *S. platensis* [2Fe-2S] ferredoxin and evolution of chloroplast-type ferredoxins** 522

B. Marshall & S.B. Levy **Prevalence of amber suppressor-containing coliforms in the natural environment** 524

C.J. Thompson, J.M. Ward & D.A. Hopwood **DNA cloning in *Streptomyces*: resistance genes from antibiotic-producing species** 525

J.E. Suarez & K.F. Chater **DNA cloning in *Streptomyces*: a bifunctional replicon comprising pBR322 inserted into a *Streptomyces* phage** 527

H.J. Edenberg **Novobiocin inhibition of simian virus 40 DNA replication** 529

P.R. Chakraborty, N. Ruiz-Opazo, D. Shouval & D.A. Shafritz **Identification of integrated hepatitis B virus DNA and expression of viral RNA in an HBsAg-producing human hepatocellular carcinoma cell line** 531

C. Brechot, C. Pourcel, A. Louise, B. Rain & P. Tiollais **Presence of integrated hepatitis B virus DNA sequences in cellular DNA of human hepatocellular carcinoma** 533

J.C. Edman, P. Gray, P. Valenzuela, L.B. Rall & W.J. Rutter **Integration of hepatitis B virus sequences and their expression in a human hepatoma cell** 535

S.H. Orkin & A. Michelson **Partial deletion of the α-globin structural gene in human α-thalassaemia** 538

BOOK REVIEWS

A.H. Bunting **Science and Colonial Expansion: The Role of the British Royal Botanic Gardens (L.H. Brockway)** 541

Michael Berry **Works on the Foundations of Statistical Physics (N.S. Krylov)** 542

Martin R. Hartley and R. John Ellis **Nucleic Acids in Plants (T.C. Hall and J.W. Davies)** 542

M.W. Roberts **Palladium Catalyzed Oxidation of Hydrocarbons (P.M. Henry)** 543

R.J.G. Savage **Splendid Isolation: The Curious History of South American Mammals (G.G. Simpson)** 543

David E. Pegg **Low Temperature Preservation in Medicine and Biology (M.J. Ashwood-Smith and J. Farrant, editors)** 544

MISCELLANY

100 years ago **443**

Errata **540**

Product review, mass spectrometry and spectrophotometers **ix**

Announcements **xiii**

Classified advertising **xiv**

text books from MACMILLAN PRESS

FROM DNA TO PROTEIN: The Transfer of Genetic Information
MARIA SZEKELY

This is the first textbook which discusses gene structure on the basis of recent discoveries of overlapping and split genes and which genetic information can be encoded into the genetic material and how it can be transferred to other materials.
A perfectly up-to-date account of our present knowledge of the structure and expression of genes in prokaryotic and eukaryotic organisms and the only available text showing the correlation between the structure and function of nucleic acids.
March, £18.00, 0 333 21836 1
£9.95, 0 333 21828 8

HUMAN REPRODUCTION AND DEVELOPMENTAL BIOLOGY
D. J. BEGLEY, J. A. FIRTH and J. R. S. HOULT

An integrated approach to describe the cellular and physiological processes of human reproduction and embryological development in relation to their underlying mechanisms and to their practical applications in medicine. The book combines anatomy, biochemistry, physiology and pharmacology, making it more suitable for modern preclinical and human biology courses.
February, £20.00, 0 333 23423 5
£9.95, 0 333 23424 3

GYNAECOLOGICAL CYTOLOGY
MATHILDE E. BOON and METTE LISE TABBERS-BOUMEESTER

Dr Boon and Dr Tabbers-Boumeester have, over the past ten years, developed the course in diagnostic cytology which was first given in Leiden in 1969.
In this volume they present their insight into both the study of diagnostic cytology, and into the teaching of this increasingly important subject. To illustrate the modern concepts of cytopathology, examples of more advanced approaches are included: as well as scanning and electron microscopy there are details of DNA measurements, morphometry and immunopathology.
June, £25.00, 0 333 26117 8
£14.00, 0 333 26118 6

Macmillan Press books are available from leading booksellers
If you have difficulty obtaining these titles please write to Tony Watson, Macmillan Retail Ltd, Houndmills, Basingstoke, Hants, enclosing purchase price + 70p (p&p).

M MACMILLAN PRESS

Essential information at your fingertips

Every month!

The British Journal of Clinical Pharmacology is the leading authoritative journal presenting results of clinical pharmacological research.
Published monthly on behalf of the British Pharmacological Society the journal:
★ Bridges the gap between medical professions, clinical research and the Pharmaceutical industry.
★ Contains papers and reports on all aspects of drug action in man, in both health and disease.
★ Prints letters and short communications which allow immediate discussion of urgent observations.
Subscribers to British Journal of Clinical Pharmacology receive, free of charge, the proceedings of selected symposia on new methods, new drugs, and new approaches to treatment. Some past symposia have been on narcotic antagonists and antagonist analgesics, labetalol, clobazam mianserin, temazepam and the relationship between angina pectoris and hypertension.
Why not join the growing number of clinical pharmacologists, clinicians and others who rely on the British Journal of Clinical Pharmacology as their information medium.

For a sample copy write to: Frances Roach, Scientific & Medical Division, Macmillan Publishers Ltd., Houndmills, Basingstoke, Hampshire, RG21 2XS.

M

© 1980 Macmillan Journals Ltd
Nature® is published weekly
ISSN 0028-0836
Registered as a newspaper at the
British Post Office

London
4 Little Essex Street, WC2R 3LF
Telephone: (01) 836 6633 Telex: 262024
Telegrams: Phusis London WC2R 3LF

Editor: John Maddox
Deputy Editor: Peter Newmark
Editorial Staff
Alun Anderson Naomi Molson
Philip Campbell Sara Nash
Isobel Collins Judy Redfearn
Konrad Guettler Miranda Robertson
Tim Lincoln Robert Walgate
Mary Lindley Charles Wenz
Jonathan Wolfe
Publishing Director: Christopher Paterson
Marketing Director: Ray Barker

New York
15 East 26 Street, New York, NY 10010
Telephone: (212) 689 5900 Telex: 668497
Robert Ubell (American Publisher)
and Sheila Kane

Washington News Bureau
801 National Press Building, DC 20045
Telephone: (202) 737 2355 Telex: 64280
David Dickson (Washington News Editor)

International Advertising Manager:
Richard Webb (London) (01) 240 2044

USA Advertising Manager
Henry Dale (New York) (212) 689 5900

Classified Advertising:
4 Little Essex Street, WC2R 3LF
Telephone: (01) 240 1101
Classified(USA)
Terence Miller, Suite 832, 50 Rockefeller Plaza,
New York, NY 10020—(212) 765 5758
Display and Classified(Canada)
Peter Drake, 32 Front Street West,
201 Toronto, Ontario M5J IC5
(416) 364 1623

Advertising Representatives in USA
Display
Nature New York Office—(212) 689 5900
Media Group, Inc. (Dallas)—(214) 631 4480
Didier & Broderick, Inc. (Chicago)—
(312) 498 4520
Jobson/Jordan/Harrison/Schulz, Inc.
(San Francisco) (415) 392 6794 (Los Angeles
& Pasadena) (213) 796 9200
Daniel Adams Associates, Inc.
Philadelphia—(215) 353 6191
CEL Associates (Boston)—(617) 383 6136
Brinker & Brinker (Fort Lauderdale)
(305) 771 0064
German Advertising Representative
E. Meckelburg, 6450 Hanau 1, Jahnstrasse 15,
West Germany Tel:— (49) 61 8115343
Japanese Advertising Representative
Orient Echo Inc.
11th Fl, Sankyo Bldg. 7-12, Tsukiji 2-Chome,
Chuo-Ku, Tokyo, Japan, Tel: 541-4923.
Annual Subscription including Index

UK		£55
USA & Canada		US$135
Belgium	Airspeed	BF4900
West Germany	Airspeed	DM300
Holland	Airspeed	G325
Switzerland	Airspeed	SF265
Rest of World	Surface	£70
	Airmail	£95

Single copy (post-paid); UK, £1.20; USA & Canada, US$3.50 (surface), US$5.00 (air); Rest of World, £1.15 (surface), £2 (air).

Orders (with remittance) to:
Macmillan Journals Ltd, Brunel Road,
Basingstoke, Hants RG21 2XS.
Telephone: Basingstoke (0256) 29242

Nature is published weekly, except the last week in December, by Macmillan Journals Ltd. Second-class postage paid at New York, NY 10010 and at additional mailing offices.
US Postmaster, please send form 3579 to:
Nature, 15 East 26 Street, New York, NY 10010.

Vol. 286 No. 5772 31 July 1980

nature

Volume 286 No.5773 7 August 1980

NEWS

Towards a more competent Civil Service 545
Radiation standards not yet for changing 546
Congress turns sour on technology fund 547
Compromise for Finniston? 547
European biotechnology: EEC proposals 548
IWC whaling quotas: politics wins out 548
More Soviet psychiatry: Physicist held 549
Neuroscience: Snyder's pad 550
Byelorussian graduates: Missing out 550
Radiation risks: Twice lucky? 550
Calculations and measurements 551
Alternative energy: Europe stirs 552
Alternative technology: Water-mills again 552

NEWS AND VIEWS

Pre-Pleistocene climates: Samuel M. Savin explains attempts to reconstruct climatic history 553
Towards a submarine hydrology: Marcus G. Langseth reports a recent conference 554
Membrane protein distributors: M. J. Geisow on the function of coated vesicles 555
Adhesion of pathogenic microorganisms: Mary Lindley describes the link between adhesion and pathogenicity 556
Virus crystallography comes of age: Stephen C. Harrison compares new models of virus structure 558
Open-ended fusion systems: R. F. Post reports a recent nuclear fusion conference 559

REVIEW ARTICLE

I.J. Higgins, D.J. Best and R.C. Hammond **New findings in methane-utilizing bacteria highlight their importance in the biosphere and their commercial potential** 561

ARTICLES

R.A. Wiebe **Anorthositic magmas and the origin of proterozoic anorthosite massifs** 564
H. Drew, T. Takano, S. Tanaka, K. Itakura and R.E. Dickerson **High-salt d(CpGpCpG), a left-handed Z′ DNA double helix** 567
D. Rhodes and A. Klug **Helical periodicity of DNA determined by enzyme digestion** 573

LETTERS

J.G. Robertson **The complex radio galaxy 4C47.51 (1919 + 479)** 579
R.D. Chapman **IUE observations of the atmospheric eclipsing binary system ξ Aurigae** 580
M.A. Hapgood **IR observation of a persistent meteor train** 582
A.F. Janzen and M. Seibert **Photoelectrochemical conversion using reaction-centre electrodes** 584
P.F. Barron, M.A. Wilson, J.F. Stephens, B.A. Cornell and K.R. Tate **Cross-polarization ^{13}C NMR spectroscopy of whole soils** 585
G. McTainsh **Harmattan dust deposition in northern Nigeria** 587
W.-C. Wang and N.D. Sze **Coupled effects of atmospheric N_2O and O_3 on the Earth's climate** 589

Contents continued overleaf

Cover: Photomicrograph of supracrustal rocks from southern Africa. A mineralogical study of the parameters for the high-grade metamorphism of these early Archaeon rocks is presented on page 596.

Nature® published weekly ISSN 0028-0836
Registered as a newspaper at the British Post Office
and the United States Post Office

0028-0836/80/32000C-02$01.00

Wiley NEW YORK · CHICHESTER
BRISBANE · TORONTO

Biochemical Applications of Mass Spectrometry, First Supplementary Volume
by **G.R. Waller** and **O.C. Dermer**, *both of Oklahoma State University, Stillwater*

Providing a comprehensive, up-to-date treatment of the areas of biochemical and biological knowledge elucidated by mass spectrometry, the book discusses methods and results. It is a supplement to the standard work, published in 1972, covering instrumentation, interpretation of spectra, and application.

July 1980 — 1300 pages
0471 03810 5 — $187.50/£81.75

Potential Energy Surfaces
edited by **K.P. Lawley**, *Department of Chemistry, Edinburgh University*

In this volume of essays, the major aspects of molecular collisions are examined from the point of view of the potential surface. The concept of a potential energy surface underlies the whole field of inelastic and reactive collisions between molecules. Such topics as the quenching of excited atoms, the cooling of molecules in interstellar space, chemi-ionisation and the relaxation of molecular orientation in liquids are all unified by the idea of a multi-dimensional potential.

Rapid advances in spectroscopy and beam scattering now enable some aspects of these surfaces to be reliably parameterized. Our knowledge about such topics as angle dependent potentials, vibronic coupling and branching ratios in simple atomic reactions is summarised by the various authors.

Series: *Advances in Chemical Physics, Volume 42* edited by **I. Prigogine** and **S.A. Rice**

April 1980 — 618 pages
0471 27633 2 — $78.40/£27.00

Advances in Chemical Physics Vol. 41
edited by **I. Prigogine**, *University of Brussels,*
and **S.A. Rice**, *University of Chicago*

This volume reports, interprets, and evaluates progress in this field. Topics, chosen by the editors for their timeliness, have been treated comprehensively, without limitation of space, by the authors all of whom are experts in the field.

June 1980 — 552 pages
0471 05742 8 — $59.40/£25.95

Basic Chemical Kinetics
by **H. Eyring**, *University of Utah,*
S.H. Lin, *Arizona State University,*
and **S.M. Lin**, *National Chung-Shan Institute of Sciences*

This presents, in an elementary and self-contained manner, both classical and quantal treatments of chemical kinetics for comparison. Two chapters are devoted to elementary processes in photochemistry, photophysics, and photobiology. References are provided where derivations were too long to include and problems help clarify the material covered.

May 1980 — 504 pages
0471 05496 8 — $43.75/£19.15

Cell Biology
by **P. Sheeler** and **D.E. Bianchi**, *both of California State University, Northridge*

A modern interpretation of the structure, biochemistry, and function of cells, their organelles, and other constituents. The generalized microanatomical structure of cells characterizing their organelles and their primary functions; chemistry of cells; principles for modern, experimental study; and the major structural and functional elements of the cell are all covered.

July 1980 — 596 pages
0471 78220 3 — $26.50/£11.50

Diseases of Marine Animals Vol. 1:
General Aspects, Protozoa to Gastropoda
edited by **O. Kinne**, *Biologische Anstalt Helgoland (Zentrale), W. Germany*

A comprehensive and critical review of all essential information available to date on the biotic diseases, proliferative disorders and structural abnormalities of marine animals. Produced after a decade of careful literature research, this four-volume treatise brings together, for the first time, a host of data scattered over a wide array of scientific journals and books.

Topical emphasis is placed on a detailed documentation of the types and causes of the diseases of marine animals (from the Protozoa via the Invertebrata to the Aves and Mammalia), the significance of disease as an ecological and evolutionary phenomenon, and the importance of disease for organismic performance, with a special view on experimental ecology and aquaculture.

March 1980 — 482 pages
0471 99584 3 — $73.15/£25.00

Biological Principles with Human Perspectives
by **G.E. Nelson, Jr.**, *University of South Florida*

An innovative introduction to basic biological concepts that uses the human organism extensively to exemplify major points and concepts. Topics covered include: cell structure and function, energy acquisition and use (nutrition), control systems, homeostasis, nature of the gene, human genetics and evolution, and basic ecology.

May 1980 — 442 pages
0471 02194 6 — $20.50/£8.15

Hydrobiology — A Text for Engineers and Scientists
by **D. Uhlmann**, *Professor of Hydrobiology, Technical University, Dresden*
Translated from the German by **M.F. Standen, P.J. Wilkinson** and **J. Wilkinson**

This introduction to the biology of fresh waters and water installations is intended to provide both engineers already working in the field of water economy and future engineers with a knowledge of fundamental biological principles.

March 1980 — 314 pages
0471 99557 6 — $45.10/£15.00

Co-published with Veb Gustav Fischer Verlag.

John Wiley & Sons Limited
Baffins Lane · Chichester · Sussex PO19 1UD · England

Circle No. 08 on Reader Enquiry Card.

P.L. Hancock and A.A. Barka **Plio-Pleistocene reversal of displacement on the North Anatolian fault zone** 591

M.A. Lanphere, K.L. Cameron and M. Cameron **Sr isotopic geochemistry of voluminous rhyolitic ignimbrites and related rocks, Batopilas area, western Mexico** 594

P.C. Horrocks **Ancient Archaean supracrustal rocks from the Limpopo Mobile Belt** 596

J. Boardman **Evidence for pre-Devensian glaciation in the northeastern Lake District** 599

E. Gosling **Gene frequency changes and adaptation in marine cockles** 601

J. Hardie **Juvenile hormone mimics photoperiodic apterization of the alate gynopara of aphid, *Aphis fabae*** 602

W.M. Carroll, B.S. Jay, W.I. McDonald and A.M. Halliday **Two distinct patterns of visual evoked response asymmetry in human albinism** 604

M. Nielsen and C. Bræstrup **Ethyl β-carboline-3-carboxylate shows differential benzodiazepine receptor interaction** 606

P.L. Mobley and F. Sulser **Adrenal corticoids regulate sensitivity of noradrenaline receptor coupled adenylate cyclase in brain** 608

T. Horsburgh, P. Wood and L. Brent **Suppression of *in vitro* lymphocyte reactivity by cyclosporin A: existence of a population of drug-resistant cytotoxic lymphocytes** 609

J.T. Rosenbaum, H.O. McDevitt, R.B. Guss and P.R. Egbert **Endotoxin-induced uveitis in rats as a model for human disease** 611

P. Seth and N. Balachandran **Elution of herpes simplex virus-specific cytotoxic antibodies from squamous cell carcinoma of uterine cervix** 613

R. Anand and R. Steeves **How many types of erythroleukaemia are induced by retroviruses in mice?** 615

J. Pawelek, A. Körner, A. Bergstrom and J. Bologna **New regulators of melanin biosynthesis and the autodestruction of melanoma cells** 617

D.R. Senger, D.F. Wirth and R.O. Hynes **Transformation-specific secreted phosphoproteins** 619

C. Steinemann and R.W. Parish **Evidence that a developmentally regulated glycoprotein is target of adhesion-blocking Fab in reaggregating *Dictyostelium*** 621

J. Jolles, H. Zwiers, C.J. van Dongen, P. Schotman, K.W.A. Wirtz and W.H. Gispen **Modulation of brain polyphosphoinositide metabolism by ACTH-sensitive protein phosphorylation** 623

A.H. Bretag, S.R. Dawe and A.G. Moskwa **Chemically induced myotonia in amphibia** 625

R.M. Simmons and A.G. Szent-Györgyi **Control of tension development in scallop muscle fibres with foreign regulatory light chains** 626

R. Kamiya, S. Asakura and S. Yamaguchi **Formation of helical filaments by copolymerization of two types of 'straight' flagellins** 628

D.J. States, C.M. Dobson, M. Karplus and T.E. Creighton **A conformational isomer of bovine pancreatic trypsin inhibitor protein produced by refolding** 630

F.E. Cohen, M.J.E. Sternberg, D.C. Phillips, I.D. Kuntz and P.A. Kollman **A diffusion-collision-adhesion model for the kinetics of myoglobin refolding** 632

P. Gruss and G. Khoury **Rescue of a splicing defective mutant by insertion of an heterologous intron** 634

C.J. Benham **Theoretical analysis of transitions between B- and Z-conformations in torsionally stressed DNA** 637

U.B. Kaupp, P.P.M. Schnetkamp and W. Junge **Metarhodopsin I/metarhodopsin II transition triggers light-induced change in calcium binding at rod disk membranes** 638

S. Devarajan, C.M.K. Nair, K.R.K. Easwaran and M. Vijayan **A novel conformation of valinomycin in its barium complex** 640

H. Wynberg, E.W. Meijer, J.C. Hummelen, H.P.J.M. Dekkers, P.H. Schippers and A.D. Carlson **Circular polarization observed in bioluminescence** 641

BOOK REVIEWS

Ian Smart **Nuclear Nonproliferation: The Spent Fuel Problem (Frederick C. Williams and David A. Deese, editors)** 643

John Ebling **The Human Biology of Circumpolar Populations (F.A. Milan, editor)** 644

R.J. Roberts **Diseases of Marine Animals. Vol. 1. (O. Kinne, editor)** 644

J.L. Martin **Quantum Mechanics (A. Böhm)** 645

R.D. Martin **Evolutionary History of the Primates (Frederick S. Szalay and Eric Delson)** 645

A.R. Katritzky **The Conformational Analysis of Heterocyclic Compounds (Frank Riddell)** 646

A.J. Leggett **Physics Reviews Vol. 1. (I.M. Khalatnikov, editor)** 646

MISCELLANY

100 years ago 560

Classified advertising ix

Molecular Biology Enzymes For Synthesis

0881 RNA LIGASE (T_4 inf. *E. coli*)
RNase and DNase FREE
Applications of this product to DNA synthesis and modifications are featured in P-L Analects 7 (2) April 1979. Minimum 1000 units/mg protein.
40 μg ..... $90.00* 200 μg. $390.00*

0880 RNA LIGASE (T_4 inf. *E. coli*)
For synthesis of oligonucleotide with specified 3′ terminus and other applications, see P-L Analects 6 (2) April 1978.
New Lower Price .... 150 units $60.00*

0872 DNA LIGASE (NAD, *E. coli*)
λ lysogenic system
New technology permits 90% lower price.
New Lower Price .... 2500 units $50.00*

0916 RNA POLYMERASE (*E. coli*)
This new product with a specific activity >800 units/mg is nuclease free.
New Low Price .... 80 units .... $ 60.00*
400 units $240.00*

0870 DNA LIGASE (T_4 inf. *E. coli*)
New process yields quality product at reduced price.
25 Weiss units (500 P-L units) $55.00*

**Insulated container and refrigerant charge $10.00.*

Call or write for complete information.

excellence in biochemistry
P.L biochemicals, inc.
1037 WEST McKINLEY AVENUE, MILWAUKEE, WIS. 53205
® **Call 414/347-7442 TWX 910-262-1111**

2′,3′-Dideoxynucleoside 5′-Triphosphates

DNA Sequencing Reagents (Chain—Terminators)

4831 2′, 3′-Dideoxythymidine 5′-Triphosphate
Pkg. Sizes and Prices:
5 mg ...... $40.00 25 mg $175.00

4823 2′, 3′-Dideoxycytidine 5′-Triphosphate
Pkg. Sizes and Prices:
4 μmoles ... $60.00 5x4 μmoles ... $275.00

4819 2′, 3′-Dideoxyadenosine 5′-Triphosphate
Pkg. Sizes and Prices:
4 μmoles ... $60.00 5x4 μmoles ... $275.00

4817 2′, 3′-Dideoxyguanosine 5′-Triphosphate
Pkg. Sizes and Prices:
4 μmoles ... $60.00 5x4 μmoles ... $275.00

4865 Dideoxynucleoside Triphosphate Kit
One micromole of each of the four dideoxynucleoside triphosphates **1 Kit ... $80.00**

Available from stock

excellence in biochemistry
P.L biochemicals, inc.
1037 WEST McKINLEY AVENUE, MILWAUKEE, WIS. 53205
® **Call 414/347-7442 TWX 910-262-1111**

Circle No. 02 on Reader Enquiry Card.

M

©1980 Macmillan Journals Ltd
Nature® is published weekly
ISSN 0028-0836
Registered as a newspaper at the British Post Office

London
4 Little Essex Street, WC2R 3LF
Telephone: (01) 836 6633 Telex: 262024
Telegrams: Phusis London WC2R 3LF

Editor: John Maddox
Deputy Editor: Peter Newmark

Editorial Staff
Alun Anderson Naomi Molson
Philip Campbell Sara Nash
Isobel Collins Judy Redfearn
Konrad Guettler Miranda Robertson
Tim Lincoln Robert Walgate
Mary Lindley Charles Wenz
Jonathan Wolfe
Publishing Director: Christopher Paterson
Marketing Director: Ray Barker

New York
15 East 26 Street, New York, NY 10010
Telephone: (212) 689 5900 Telex: 668497
Robert Ubell (American Publisher) and Sheila Kane

Washington News Bureau
801 National Press Building, DC 20045
Telephone: (202) 737 2355 Telex: 64280
David Dickson (Washington News Editor)

International Advertising Manager:
Richard Webb (London) (01) 240 2044

USA Advertising Manager
Henry Dale (New York) (212) 689 5900

Classified Advertising:
4 Little Essex Street, WC2R 3LF
Telephone: (01) 240 1101

Classified(USA)
Terence Miller, Suite 832, 50 Rockefeller Plaza, New York, NY 10020—(212) 765 5758

Display and Classified(Canada)
Peter Drake, 32 Front Street West, 201 Toronto, Ontario M5J 1C5
(416) 364 1623

Advertising Representatives in USA
Display
Nature New York Office—(212) 689 5900
Media Group, Inc. (Dallas)—(214) 631 4480
Didier & Broderick, Inc. (Chicago)—(312) 498 4520
Jobson/Jordan/Harrison/Schulz, Inc. (San Francisco) (415) 392 6794 (Los Angeles & Pasadena) (213) 796 9200
Daniel Adams Associates, Inc. Philadelphia—(215) 353 6191
CEL Associates (Boston)—(617) 383 6136
Brinker & Brinker (Fort Lauderdale) (305) 771 0064

German Advertising Representative
E. Meckelburg, 6450 Hanau 1, Jahnstrasse 15, West Germany Tel:— (49) 61 8115343

Japanese Advertising Representative
Orient Echo Inc.
11th Fl, Sankyo Bldg. 7-12, Tsukiji 2-Chome, Chuo-Ku, Tokyo, Japan, Tel: 541-4923.

Annual Subscription including Index

UK		£55
USA & Canada		US$135
Belgium	Airspeed	BF4900
West Germany	Airspeed	DM300
Holland	Airspeed	G325
Switzerland	Airspeed	SF265
Rest of World	Surface	£70
	Airmail	£95

Single copy (post-paid); UK, £1.20; USA & Canada, US$3.50 (surface), US$5.00 (air); Rest of World, £1.15 (surface), £2 (air).

Orders (with remittance) to:
Macmillan Journals Ltd, Brunel Road, Basingstoke, Hants RG21 2XS.
Telephone: Basingstoke (0256) 29242

Nature is published weekly, except the last week in December, by Macmillan Journals Ltd. Second-class postage paid at New York, NY 10010 and at additional mailing offices. US Postmaster, please send form 3579 to: *Nature*, 15 East 26 Street, New York, NY 10010.

Vol.286 No.5773 7 August 1980

nature

Volume 286 No.5774 14 August 1980

Pure Chemistry Library
SCIENCE COLLEGE
92 Upper Circular Road
CALCUTTA

NEWS

Open season for nuclear diplomatists 647
Putting Finniston's cart before the horse 648
Another violation of NIH guidelines 649
Small beer for scientists 649
Nuclear Iraq: Perrin protests 650
Remote sensing: Going private? 650
Lords committee: Dumping ahead 651
Energy alternatives: German plans 651
Pesticide safety: No numbers 652
Drift of change: Russian plate tectonics 652
Vietnam in space: Queue-jumping 653
Shuttle for orbit 653
Airport noise: London's out 653
Polish water: Much and little 654

NEWS AND VIEWS

The cooling Earth: Henry N. Pollack examines the source of the Earth's heat flow 655
The collagen gene family: Ellen Solomon reports on a recent meeting 656
Assembly of immunoglobulin genes: H.V. Molgaard on heavy chain gene rearrangement and deletion 657
Marine bioluminescence: Frank McCapra and Russell Hart look at the origins of the luciferins 660
Particle detectors: David J. Miller on detectors for the new large electron-positron machine 661

REVIEW ARTICLE

N.M. Le Douarin **The ontogeny of the neural crest in avian embryo chimaeras** 663

ARTICLES

W. Dunnick, T.H. Rabbitts and C. Milstein **An immunoglobulin deletion mutant with implications for the heavy-chain switch and RNA splicing** 669
H. Sakano, R. Maki, Y. Kurosawa, W. Roeder and S. Tonegawa **Two types of somatic recombination are necessary for the generation of complete immunoglobulin heavy-chain genes** 676
J.C. Fiddes and H.M. Goodman **The cDNA for the β-subunit of human chorionic gonadotropin suggests evolution of a gene by readthrough into the 3′-untranslated region** 684

Pure Chemistry Library
SCIENCE COLLEGE
92 Upper Circular Road
CALCUTTA

LETTERS

S. Sato, K. Kawara, Y. Kobayashi, T. Maihara, H. Okuda and J. Jugaku **No IR burst from the X-ray rapid burster MXB1730–335** 688
A.B. Giles, A.R. King, R.F. Jameson, M.R. Sherrington, J.H. Hough, J.A. Bailey and E.C. Cunningham **The IR variability of SS433** 689
G.S. Cargill III **Ultrasonic imaging in scanning electron microscopy** 691
Y. Osada, M. Hashidzume, E. Tsuchida and A.T. Bell **Polymerization of phosphazene crystal by plasma-exposure** 693
J.R. Maxwell, A.S. Mackenzie and J.K. Volkman **Configuration at C-24 in steranes and sterols** 694

Contents continued overleaf

Cover. Differentiating quail neural crest cells are revealed in a chick-quail chimaera. A formol-induced fluorescence technique is used for cytochemical detection of catecholamine (left) and Feulgen staining is used to reveal a distinctive heterochromatin DNA marker (right). The migration of developing nerve cells is reviewed on p.663.

Nature® published weekly ISSN 0028-0836
Registered as a newspaper at the British Post Office and the United States Post Office

0028-0836/80/33000C-03$01.00

The 3 R's of focusing

Rapid Reliable Resolution

Pharmalyte™

The basis of good results.

Pharmacia Fine Chemicals AB
Box 175
S-751 04 Uppsala 1
Sweden

Pharmacia Fine Chemicals

Circle No. 39 on Reader Enquiry Card.

LETTERS

G. Guérin and G. Valladas **Thermoluminescence dating of volcanic plagioclases** 697

M. Idnurm and P.J. Cook **Palaeomagnetism of beach ridges in South Australia and the Milankovitch theory of ice ages** 699

C.J. Heusser, L.E. Heusser and S.S. Streeter **Quaternary temperatures and precipitation for the north-west coast of North America** 702

J.E. Harms, D.J. Milton, J. Ferguson, D.J. Gilbert, W.K. Harris and B. Goleby **Goat Paddock cryptoexplosion crater, Western Australia** 704

R. Anderton **Did Iapetus start to open during the Cambrian?** 706

E. Jagoutz, R.W. Carlson and G.W. Lugmair **Equilibrated Nd–unequilibrated Sr isotopes in mantle zenoliths** 708

P. Moesta and H. Grisebach **Effects of biotic and abiotic elicitors on phytoalexin metabolism in soybean** 710

S. Fridman-Cohen and M.P. Pener **Precocenes induce effect of juvenile hormone excess in *Locusta migratoria*** 711

H. van Dijk, F.M.A. Hofhuis, E.M.J.J. Berns, C. van der Meer and J.M. Willers **Killed *Listeria monocytogenes* vaccine is protective in C3H/HeJ mice without addition of adjuvants** 713

P.A. Jacobs, C.M. Wilson, J.A. Sprenkle, N.B. Rosenshein and B.R. Migeon **Mechanism of origin of complete hydatidiform moles** 714

J.F. Nicolas, J. Gaillard, H. Jakob and F. Jacob **Bone-forming cell line derived from embryonal carcinoma cells** 716

K.K. Sethi, I. Stroehmann and H. Brandis **Human T-cell cultures from virus- sensitized donors can mediate virus-specific and HLA-restricted cell lysis** 718

D.A. Cunliffe and K.O. Cox **IgM-autoantibodies against isologous erythrocytes also react with isologous IgG(Fc)** 720

N. Mazurek, G. Berger and I. Pecht **A binding site on mast cells and basophils for the anti-allergic drug cromolyn** 722

R.J. Walter, R.D. Berlin and J.M. Oliver **Asymmetric Fc receptor distribution on human PMN oriented in a chemotactic gradient** 724

D.L. Weinbaum, J.A. Sullivan and G.L. Mandell **Receptors for concanavalin A cluster at the front of polarized neutrophils** 725

J.R. Pfeiffer, J.M. Oliver and R.D. Berlin **Topographical distribution of coated pits** 727

J. Schlessinger, E. Van Obberghen and C.R. Kahn **Insulin and antibodies against insulin receptor cap on the membrane of cultured human lymphocytes** 729

R.G. Whalen and S.M. Sell **Myosin from fetal hearts contains the skeletal muscle embryonic light chain** 731

C.D. Toran-Allerand **Coexistence of α-fetoprotein, albumin and transferrin immunoreactivity in neurones of in neurones of the developing mouse brain** 733

K.R. Jessen and R. Mirsky **Glial cells in the enteric nervous system contain glial fibrillary acidic protein** 736

D.P. Richman, C.M. Gomez, P.W. Berman, S.A. Burres, F.W. Fitch and B.G.W. Arnason **Monoclonal anti-acetylcholine receptor antibodies can cause experimental myasthenia** 738

S. Matsuura, M. Ohashi, H.C. Chen, R.C. Shownkeen, A. Stockell Hartree, L.E. Reichert Jr, V.C. Stevens and J.E. Powell **Physicochemical and immunological characterization of an HCG-like substance from human pituitary glands** 740

Contents continued overleaf

GUIDE TO AUTHORS

- Review articles should be aimed at a relatively wide readership. Many reviews are invited, but submitted articles may also be accepted; it is advisable to consult us before writing a review article.
- Articles may be up to 3,000 words long with at most six displayed items (figures and tables); they are reports of major research developments.
- Letters are brief reports of original research of unusual and wide interest, not in general longer than 1,000 words; they have at most three or four displayed items.
- 'Matters Arising' permits short discussion (up to 300 words) of papers that have recently appeared in *Nature*.

Articles should be accompanied by an abstract of not more than fifty words. Letters should begin with a paragraph giving the background and main conclusion in terms intelligible to as wide a readership as possible.

Manuscripts may be submitted either to London or New York. Three typed copies should be submitted, each including lettered copies of figures. Typing (including references) should be double spaced. The title should be brief and informative. Pages should be numbered. References, tables and figure legends should start on separate pages. Experimental detail vital to the paper yet which would interrupt the narrative is best placed in the figure legends. Units should be identified in the margin on their first appearance. Equations should occupy single lines if possible: exp(a) is preferred to e^a if 'a' is more than one character.

References are indicated by superscripts in the text. See any contemporary *Nature* for style, but note:

(i) only one reference number need be used if the reference is to several papers by identical authors.

(ii) first and last pages of references should be cited.

Abbreviations should follow the *World List of Scientific Periodicals*, fourth edn (Butterworth, 1963-65). Symposia are often difficult to refer to and only published or soon-to-be-published volumes should be mentioned in references. Their publisher and place of publication should be clearly indicated 'Personal communication' and 'unpublished' should be incorporated in text.

Artwork should be sent with the manuscript and clearly marked with author's name and the figure number. Line drawings should be either photographic prints or in Indian ink on heavy cartridge paper, tracing paper or similar materials. Most figures are reduced to one column width so originals should be about as wide as a page of *Nature*. To enable figures, particularly maps, to be edited in the same style as the text, they should contain only essential material. Ideally, an unlettered original and three lettered copies should be provided; labelling on halftones should, if possible, be avoided entirely. Magnifications quoted should be for the figures as submitted. We are always glad to see artwork for possible use on the cover, but cannot guarantee its return.

In order to save on postal expenses we return only the top copy and artwork of manuscripts that we cannot publish.

Nature's publishing policy is outlined in **258**, 1 (1975) and **264**, v, 11 Nov. (1976).

LEITZ-WILD
MICRO 80

A welcome awaits you at stand No. 8. And a welcome sight . . . the largest display ever seen in the U.K. of Light Microscopes for all purposes, Preparation Equipment, Balances, Image Analysis, TAS and ASM, and TV Microscopy.

Leitz — Microscopes, Image Analysis (especially TAS — for the first time in the U.K.).

WILD HEERBRUGG — Photomacroscopes, Stereo Microscopes, Automatic Cameras.

PRESI — Metallurgical Preparation Machines and software for preparation of metal specimens.

PRECISA — A new range of Balances.

STAND 8 E. LEITZ (Instruments) Ltd., 48 Park Street, Luton, LU1 3HP

Circle No. 26 on Reader Enquiry Card.

MATTERS ARISING

G.J. Dockray and R.A. Gregory — **Does the C-terminal tetrapeptide of gastrin and CCK exist as an entity?** 742
J.F. Rehfeld, L.-I. Larsson, N.R. Goltermann, T.W. Schwartz, J.J. Holst, S.L. Jensen and J.S. Morley — **Reply to Dockray and Gregory** 742

BOOK REVIEWS

Steve Blinkhorn — **Bias in Mental Testing (Arthur R. Jensen)** 743
Bernard Pagel — **An Introduction to Nuclear Astrophysics (Jean Audouze and Sylvie Vauclair)** 744
Athel Cornish-Bowden — **Enzymes. Third edition. (Malcolm Dixon and Edwin C. Webb)** 745
Alan Isaacs — **Longman Dictionary of Scientific Usage (A. Godman and E.M.F. Payne)** 745
B.S. Cox — **Viruses and Plasmids in Fungi (Paul A. Lemke, editor)** 746
Kurt Hirschhorn — **Genetic Disorders among the Jewish People (R.M. Goodman)** 746

MISCELLANY

100 years ago **662**
New products: Microscopy **xxv**
New on the market **xliv**
Classified advertising **xlv**

KEEP ABREAST OF THE LATEST DEVELOPMENTS IN ANAESTHESIA, INTENSIVE CARE AND THE ASSOCIATED BASIC SCIENCES BY SUBSCRIBING TO

BRITISH JOURNAL OF
ANÆSTHESIA

British Journal of Anaesthesia has consistently been the leading independent journal in anaesthesia, enjoying contributions from and readership in almost every country.

Published monthly, the journal offers:

Sections on laboratory investigations, clinical research, case reports and information on apparatus.
A correspondence section with short communications on current matters of professional interest.
Authoritative book reviews.
Twice yearly Postgraduate Educational Issues on both clinical and basic science themes.

ANNUAL SUBSCRIPTION
UK £22.50
USA & Canada US$54
Rest of the World £27.50

Orders should be accompanied by remittance, cheques made payable to Macmillan Journals Ltd.
Subscription Department, Brunel Road, Basingstoke, Hampshire, RG21 2XS, England.
Sample copies are also available from the same address.

Remembering mnemonic codes can give you a headache...

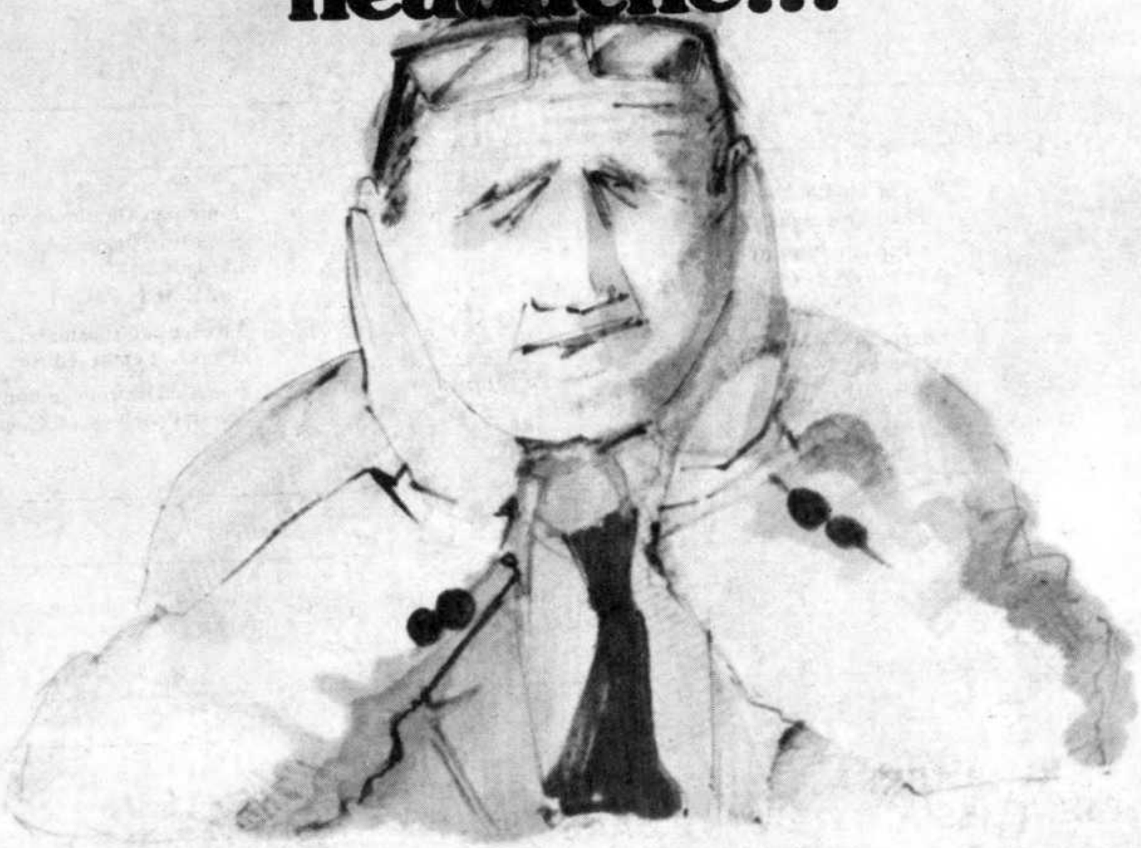

Let the EDAX 9100 remember them instead

When it comes down to Energy-Dispersive X-Ray analysis machines you must look for the one which gives *you* the least problems. With the EDAX 9100, we have designed a machine to work for you—not vice-versa. Within its compact modular construction you have a self contained operator-programmable computer with a 4000 channel memory store. The clear display gives you not only more information at a glance, visual plus numerical results on the screen, but a choice of methods in localising inhomogenious areas. Once found, our special dynastatic display feature will give you element comparison in just 5 seconds.

And when it comes to detection, Sodium right through to Plutonium are our standard range, or if you want to detect down to *Carbon*—then we can do that too—with our ECON detector.

Last but not least—the mnemonic headache. The EDAX 9100 has a unique keyboard/display which asks you which direction you wish to take your analysis—without you having to remember anything, with of course the facility to store information at any step either on floppy disc or printed on hard copy.

Perhaps the sort of thing you might rely on from the Worlds largest supplier.

ECON Detector

THE EDAX 9100

EDAX

EDAX UK Limited,
Arden House,
West Street,
Leighton Buzzard,
Beds. LU7 7ND,
Tel: (0525) 371215
Telex: 825298

Circle No. 23 on Reader Enquiry Card.

nature

Volume 286 No.5775 21 August 1980

NEWS

Directive 59 and European defence 747

What price the price of crude petroleum? 748

Columbia and Yale at odds about Felig 749

School computing: Money to spend 750

Soviet environment: Old hands back 750

Frogs to eat 750

Interferon production: Japan now 751

Occupational safety: Cuts ahead 751

Graduate students: Places sought 751

NPT review conference: Smooth start 752

Windmill power: UK gets wind 752

Nuclear generation costs compared 753

Correspondence — Nuclear power debate (L. E. J. Roberts) — International Geological Congress (S. J. Wakefield) — 2,4,5-T (Clive Jenkins) — Reference misciting (Paul Harvey, Jon Seger) — Distance measurement (Paul Mohr) — More on filters (Takeshi Uozumi). 754

NEWS AND VIEWS

Neutrino weight watching: A. De Rújula and S. L. Glashow examine evidence for non-zero neutrino masses 755

Esoteric DNA?: Mervyn J. Turner and John S. Cordingley on kinetoplast DNA 756

Can genes choose habitats?: J.S. Jones looks at how genetic variation might be maintained 757

Switching on the muscle genes: Harriet Harris on the control of gene expression 758

Multiphoton ionization interference effects: Peter Knight explains the differences between results and theory 759

Regeneration: J.M.W. Slack on the source of cells for planarian and amphibian limb regeneration 760

A glacial relict mollusc: B. Coles and B. Colville describe a mollusc thought extinct in Britain 761

Sign, symbol and syntax in the language of apes: Brendan O. McGonigle on the "ape language" controversy 761

REVIEW ARTICLE

R.A. Laskey and W.C. Earnshaw **Nucleosome assembly** 763

ARTICLES

P.J. MacGeehan and W.H. MacLean **An Archaean sub-seafloor geothermal system, 'calc-alkali' trends, and massive sulphide genesis** 767

M. Verhoeyen, R. Fang, W.Min Jou, R. Devos, D. Huylebroeck, E. Saman and W. Fiers **Antigenic drift between the haemagglutinin of the Hong Kong influenza strains A/Aichi/2/68 and A/Victoria/3/75** 771

E. Choi, M. Kuehl and R. Wall **RNA splicing generates a variant light chain from an aberrantly rearranged κ gene** 776

J.G. Seidman and P. Leder **A mutant immunoglobulin light chain is formed by aberrant DNA- and RNA-splicing events** 779

LETTERS

W.D. Evans, R.W. Klebesadel, J.G. Laros, J. Terrell and S.R. Kane **γ-Ray burst observations from the UCB/LASL experiment on ISEE-3** 784

R.E. Rothschild, D.E. Gruber, F.K. Knight, P.L. Nolan, Y. Soong, A.M. Levine, F.A. Primini, W.A. Wheaton and W.H.G. Lewin **A high sensitivity determination of the hard X-ray spectrum of Sco X-1** 786

M.N Rao and T.R. Venkatesan **Solar-flare produced ^{3}He in lunar samples** 788

D.R. Bates and P.C. Ojha **Excitation of the Na D-doublet of the nightglow** 790

R.M. Harrison and D.P.H. Laxen **Physicochemical speciation of lead in drinking water** 791

Contents continued overleaf

Cover: Fruiting body of the slime mould *Polysphondylium pallidum*. The spacing between branches is regular and is shown, on page 806, to be independent of the number of cells in the stalk.

M

© 1980 Macmillan Journals Ltd
Nature® published weekly ISSN 0028-0836
Registered as a newspaper at the British Post Office
and the United States Post Office

0028-0836/80/34000C-02$01.00

New Products

Our range is always growing...

Amersham supplies radiochemicals for all aspects of biochemical research.

Some recent additions are

Deoxy[1',2',5-^{3}H]cytidine 5'-triphosphate	50-70Ci/mmol	TRK.625
[1,2,4,6,7-^{3}H]Dexamethazone	70-110Ci/mmol	TRK.645
l-[4,6,*propyl*-^{3}H]Dihydroalprenolol	70-110Ci/mmol	TRK.649
[^{14}C]Methyltriphenylphosphonium iodide	1-10mCi/mmol	CFA.640
L-[2,3,4,5,6-^{3}H]Phenylalanine	100-130Ci/mmol	TRK.648
L-α-Phosphatidylcholine, di[1-^{14}C]stearoyl	80-120mCi/mmol	CFA.649
Protein A, *N*-[*propionyl*-^{3}H]propionylated	40-80Ci/mmol	TRK.653

A full list of additions to our current catalogue is available on request.

The Radiochemical Centre Amersham

Full information is available on request.
The Radiochemical Centre Limited, Amersham, England. Telephone: 024-04-4444.
In the U.S.A. and Canada:
Amersham Corporation, Illinois 60005.
Telephone: 312-364-7100 and 800/323-9750(Tollfree).
In W. Germany:
Amersham Buchler GmbH & Co KG, Braunschweig. Telephone: 05307-4691.

Circle No. 06 on Reader Enquiry Card.

BIOSIS

BIOSIS

NOTICE
To Zoologists, Librarians and Users of
ZOOLOGICAL RECORD
A Publication of the Zoological Society of London
from
BIOSCIENCES INFORMATION SERVICE
PHILADELPHIA, PA. • USA

On March 12, 1980 an agreement was signed between the Zoological Society of London and BioSciences Information Service (BIOSIS) which provides that BIOSIS assume publication of Zoological Record effective with Volume 115.

1. Under the agreement the editorial policies which have made **Zoological Record** the world's leading authority in zoological bibliography will be continued and the standard of quality of the publication maintained.

2. To assure a smooth transition, all processing of orders and delivery of publications for Volume 114 will be handled by the Zoological Society of London. It is expected that initial order processing will be completed for Volume 114 by January, 1981.

3. Order processing for Volume 115 will be initiated by BIOSIS on or about July 1, 1981. Complete delivery of all sections of Volume 115 is planned to be accomplished in 1981.

4. New computing equipment has been ordered for **Zoological Record.** It is expected that accelerated processing and delivery of **Zoological Record** will be accomplished in 1981.

For information pertaining to Volume 114 and earlier volumes please contact: Zoological Society of London, Regent's Park, London NW1 4 RY, England. Phone: 01-722-3333.

For information pertaining to Volume 115 please contact: User Services Department, BIOSIS, 2100 Arch St., Philadelphia, PA, USA 19103. Telex: 831-739 Phone 215/568-4016 or 800/523-4806 (USA only).

Circle No. 01 on Reader Enquiry Card.

LETTERS

S.A. Penkett, N.J.D. Prosser, R.A. Rasmussen and M.A.K. Khalil — **Measurements of $CHFCl_2$ in background tropospheric air** 793

P.W. Dunwiddie and V.C. LaMarche Jr — **A climatically responsive tree-ring record from *Widdringtonia cedarbergensis*, Cape Province, South Africa** 796

S.G. Wakeham, J.W. Farrington, R.B. Gagosian, C. Lee, H. DeBaar, G.E. Nigrelli, B.W. Tripp, S.O. Smith and N.M. Frew — **Organic matter fluxes from sediment traps in the equatorial Atlantic Ocean** 798

F. Surlyk, J.M. Hurst and M. Bjerreskov — **First age-diagnostic fossils from the central part of the North Greenland foldbelt** 800

M. Maden — **Structure of supernumerary limbs** 803

F.W. Spiegel and E.C. Cox — **A one-dimensional pattern in the cellular slime mould *Polysphondylium pallidum*** 806

F.V. Schaefer, R.P. Custer and S. Sorof — **Induction of abnormal development and differentiation in cultured mammary glands by cyclic adenine nucleotide and prostaglandins** 807

M.R. Hanley, B.E.B. Sandberg, C.M. Lee, L.L. Iversen, D.E. Brundish and R. Wade — **Specific binding of ^3H-substance P to rat brain membranes** 810

N. Parvizi and F. Ellendorff — **β-Endorphin alters luteinizing hormone secretion via the amygdala but not the hypothalamus** 812

C.-F. Wu and B. Ganetzky — **Genetic alteration of nerve membrane excitability in temperature-sensitive paralytic mutants of *Drosophila melanogaster*** 814

D. Tillotson and A.L.F. Gorman — **Non-uniform Ca^{2+} buffer distribution in a nerve cell body** 816

V.K. Sharma, L.A. Pottick and S.P. Banerjee — **Ouabain stimulation of noradrenaline transport in guinea pig heart** 817

S.E. Harding and J. Halliday — **Removal of sialic acid from cardiac sarcolemma does not affect contractile function in electrically stimulated guinea pig left atria** 819

D. Brandenburg, C. Diaconescu, D. Saunders and P. Thamm — **Covalent linking of photoreactive insulin to adipocytes produces a prolonged signal** 821

R. Horuk, T.L. Blundell, N.R. Lazarus, R.W.J. Neville, D. Stone and A. Wollmer — **A monomeric insulin from the procupine (*Hystrix cristata*), an Old World hystricomorph** 822

M. Leijonmarck, S. Eriksson and A. Liljas — **Crystal structure of ribosomal component at 2.6 Å resolution** 824

BOOK REVIEWS

Rudolf Peierls — **Robert Oppenheimer: Letters and Recollections (Alice Kimball Smith and Charles Weiner, editors)** 827

J. Veverka — **The Planet Pluto (A.J. Whyte)** 828

Alan Robertson — **Mathematical Population Genetics (W.J. Ewens)** 829

Hamish Anderson — **Peat: Industrial Chemistry and Technology (Charles H. Fuchsman)** 829

R.H. Pain — **Hydrophobic Interactions (A. Ben-Naim)** 830

MISCELLANY

100 years ago 762

New on the market xi

Classified advertising xiii

GUIDE TO AUTHORS

- Review articles should be aimed at a relatively wide readership. Many reviews are invited, but submitted articles may also be accepted; it is advisable to consult us before writing a review article.
- Articles may be up to 3,000 words long with at most six displayed items (figures and tables); they are reports of major research developments.
- Letters are brief reports of original research of unusual and wide interest, not in general longer than 1,000 words; they have at most three or four displayed items.
- 'Matters Arising' permits short discussion (up to 300 words) of papers that have recently appeared in *Nature*.

Articles should be accompanied by an abstract of not more than fifty words. Letters should begin with a paragraph giving the background and main conclusion in terms intelligible to as wide a readership as possible.

Manuscripts may be submitted either to London or New York. Three typed copies should be submitted, each including lettered copies of figures. Typing (including references) should be double spaced. The title should be brief and informative. Pages should be numbered. References, tables and figure legends should start on separate pages. Experimental detail vital to the paper yet which would interrupt the narrative is best placed in the figure legends. Units should be identified in the margin on their first appearance. Equations should occupy single lines if possible: exp (a) is preferred to e^a if 'a' is more than one character.

References are indicated by superscripts in the text. See any contemporary *Nature* for style, but note:

(i) only one reference number need be used if the reference is to several papers by identical authors.

(ii) first and last pages of references should be cited.

Abbreviations should follow the *World List of Scientific Periodicals*, fourth edn (Butterworth, 1963-65). Symposia are often difficult to refer to and only published or soon-to-be-published volumes should be mentioned in references. Their publisher and place of publication should be clearly indicated 'Personal communication' and 'unpublished' should be incorporated in text.

Artwork should be sent with the manuscript and clearly marked with author's name and the figure number. Line drawings should be either photographic prints or in Indian ink on heavy cartridge paper, tracing paper or similar materials. Most figures are reduced to one column width so originals should be about as wide as a page of *Nature*. To enable figures, particularly maps, to be edited in the same style as the text, they should contain only essential material. ideally, an unlettered original and three lettered copies should be provided; labelling on halftones should, if possible, be avoided entirely. Magnifications quoted should be for the figures as submitted. We are always glad to see artwork for possible use on the cover, but cannot guarantee its return.

In order to save on postal expenses we return only the top copy and artwork of manuscripts that we cannot publish.

Nature's publishing policy is outlined in **258**, 1 (1975) and **264**, v, 11 Nov. (1976).

PHLS

Centre for Applied Microbiology
and Research

Bacterial
Cell Pastes

Escherichia coli MRE 600
The original ribonuclease free strain, buffer washed.
(Minimum quantity 3kg – £420)

Bacillus stearothermophilus NCA 1503
Grown at 60°C the source of many thermostable enzymes.
(Minimum quantity 1·5kg – £480)

Escherichia coli RY 13
Contains restriction endonuclease Eco RI and Eco RI¹.
(Minimum quantity 3kg – £420)

Thermus aquaticus YT-1
Grown at 70°C, the source of thermostable enzymes including restriction endonuclease Taq YI.
(Minimum quantity 0·5kg – £400)

Escherichia coli B
A source of ribosomes, DNA polymerase I, RNA polymerase, DNA ligase and exonuclease III.
(Minimum quantity 3kg – £420)

Micrococcus lysodeikticus NCTC 2665
A source of catalase.
(Minimum quantity 3kg – £420)

All these products can be supplied to overseas customers. 48 other types of cell paste are also available.

The listed products are offered at the quoted sterling prices, subject to availability. Prices include packing in dry ice, and delivery on UK orders, which are subject to VAT at ruling rates. Overseas orders are subject to transport charges at cost. For listed items please send your official order to:

Microbial Products Development
& Production Laboratory, PHLS.
Centre for Applied Microbiology and Research,
Porton, Salisbury, SP4 0JG, Wiltshire, UK.

Circle No 08 on Reader Enquiry Card.

M

© 1980 Macmillan Journals Ltd
Nature® is published weekly
ISSN 0028-0836
Registered as a newspaper at the
British Post Office

London
4 Little Essex Street, WC2R 3LF
Telephone: (01) 836 6633 Telex: 262024
Telegrams: Phusis London WC2R 3LF

Editor: John Maddox
Deputy Editor: Peter Newmark

Editorial Staff
Alun Anderson Naomi Molson
Philip Campbell Sara Nash
Isobel Collins Judy Redfearn
Konrad Guettler Miranda Robertson
Tim Lincoln Robert Walgate
Mary Lindley Charles Wenz
Jonathan Wolfe
Publishing Director: Christopher Paterson
Marketing Director: Ray Barker

New York
15 East 26 Street, New York, NY 10010
Telephone: (212) 689 5900 Telex: 668497
Robert Ubell (American Publisher)
and Sheila Kane

Washington News Bureau
801 National Press Building, DC 20045
Telephone: (202) 737 2355 Telex: 64280
David Dickson (Washington News Editor)

International Advertising Manager:
Richard Webb (London) (01) 240 2044

USA Advertising Manager
Henry Dale (New York) (212) 689 5900

Classified Advertising:
4 Little Essex Street, WC2R 3LF
Telephone: (01) 240 1101

Classified(USA)
Terence Miller, Suite 832, 50 Rockefeller Plaza,
New York, NY 10020—(212) 765 5758

Display and Classified(Canada)
Peter Drake, 32 Front Street West,
201 Toronto, Ontario M5J IC5
(416) 364 1623

Advertising Representatives in USA
Display
Nature New York Office—(212) 689 5900
Media Group, Inc. (Dallas)—(214) 631 4480
Didier & Broderick, Inc. (Chicago)—
(312) 498 4520
Jobson/Jordan/Harrison/Schulz, Inc
(San Francisco) (415) 392 6794 (Los Angeles
& Pasadena) (213) 796 9200
Daniel Adams Associates, Inc
Philadelphia—(215) 353 6191
CEL Associates (Boston)—(617) 383 6136
Brinker & Brinker (Fort Lauderdale)
(305) 771 0064

German Advertising Representative
E Meckelburg, 6450 Hanau 1, Jahnstrasse 15,
West Germany Tel:— (49) 61 8115343

Japanese Advertising Representative
Orient Echo Inc.
11th Fl, Sankyo Bldg. 7-12, Tsukiji 2-Chome,
Chuo-Ku, Tokyo, Japan, Tel: 541-4923.

Annual Subscription including Index

UK		£55
USA & Canada		US$135
Belgium	Airspeed	BF4900
West Germany	Airspeed	DM300
Holland	Airspeed	G325
Switzerland	Airspeed	SF265
Rest of World	Surface	£70
	Airmail	£95

Single copy (post-paid), UK, £1 20; USA & Canada, US$3 50 (surface), US$5.00 (air), Rest of World, £1.15 (surface), £2 (air).

Orders (with remittance) to:
Macmillan Journals Ltd, Brunel Road,
Basingstoke, Hants RG21 2XS.
Telephone. Basingstoke (0256) 29242

Nature is published weekly, except the last week
in December, by Macmillan Journals Ltd
Second-class postage paid at New York, NY
10010 and at additional mailing offices.
US Postmaster, please send form 3579 to:
Nature, 15 East 26 Street, New York, NY 10010.

Vol. 286 No. 5775 21 August 1980

nature

Volume 286 No.5776 28 August 1980

[illegible] Library
[illegible] COLLEGE.
Upper Circular Road
CALCUTTA

NEWS

Plagiarism, piracy and principles 831
Pesticides in developing countries 832
Uranium exposure limits in dispute 833
High-altitude research: Reflated hopes 833
Nuclear reactors: Czech closure 834
Space telescope: Edinburgh's bid 834
German workforce: Ten years on 835
Environmental carcinogens: Nitrite safe? 835
Energy conservation: UK forecasts 836
Soviet space: Salyut women 836

NEWS AND VIEWS

Lamarckist revival in immunology: R.B. Taylor on new evidence that acquired characteristics can be inherited 837
Solar luminosity variations: Ronald L. Gilliland examines models of the solar convection zone 838
Devonian trilobites: R.A. Fortey on new finds from Bolivia 839
Pseudogenes: Nick Proudfoot describes 'dead' genes in the globin family 840
Volcanic ash southern style: Ian Smalley on New Zealand's colossal volcanic eruptions 841
Drug resistance in herpes simplex: H.J. Field and G.K. Darby describe anti-viral drug resistance strategies 842
Primeval galaxies and the X-ray background: Beatrice M. Tinsley on the search for primeval galaxies 842
Noisy chaos: N. MacDonald on mathematical models with 'chaotic' solutions 843
Cystic fibrosis: Leighton Dann reports a recent conference 844

ARTICLES

E. Marban, T.J. Rink, R.W. Tsien and R.Y. Tsien **Free calcium in heart muscle at rest and during contraction measured with Ca^{2+}-sensitive microelectrodes** 845
Y. Yaoita and T. Honjo **Deletion of immunoglobulin heavy chain genes from expressed allelic chromosome** 850
C. Wu **The 5′ ends of *Drosophila* heat shock genes in chromatin are hypersensitive to DNase I** 854
J.L. Hartley and J.E. Donelson **Nucleotide sequence of the yeast plasmid** 860
J. Hindley **Addendum** 865

LETTERS

P.E. Greenfield, B.F. Burke and D.H. Roberts **The double quasar 0957 + 561 as a gravitational lens: further VLA observations** 865
P. Fraundorf, R.I. Patel, J. Shirck, R.M Walker and J.J. Freeman **Optical spectroscopy of interplanetary dust collected in the Earth's stratosphere** 866
M. Stuiver **Solar variability and climatic change during the current millennium** 868
H.L. Garfinkel and L.B. Brubaker **Modern climate–tree-growth relationships and climatic reconstruction in sub-Arctic Alaska** 872
S. Crampin, R. Evans, B. Üçer, M. Doyle, J.P. Davis, G.V. Yegorkina and A. Miller **Observations of dilatancy-induced polarization anomalies and earthquake prediction** 874
W.J. Jenkins and P.B. Rhines **Tritium in the deep North Atlantic Ocean** 877
D.Z. Piper and B. Fowler **New constraint on the maintenance of Mn nodules at the sediment surface** 880
S. Matsu'ura and N. Ueta **Fraction dependent variation of aspartic acid racemization age of fossil bone** 883

Contents continued overleaf

Cover: The ramifications of a cat retinal ganglion cell are revealed by injection of horseradish peroxidase. The results described on page 899 show that single fibres send branches to many areas of the thalamus and midbrain.

M
© 1980 Macmillan Journals Ltd

Nature® published weekly ISSN 0028-0836
Registered as a newspaper at the British Post Office and the United States Post Office

0028-0836/80/35000C-02$01.00

M

IMMUNODEFICIENT ANIMALS IN CANCER RESEARCH

Edited by Stephen Sparrow, Pathologist at the Medical Research Council's Laboratory Animals Centre.

1980; £20.00; 208pp; ISBN 0 333 275500

CONTENTS

Immunodeficient Animals-A. J. S. Davies; Inherited immunological defects in laboratory animals -M. F. W. Festing; The importance of disease in immunodeficient mice and rats-S. Sparrow; Pathological observations on nude mice -J. P. O'Sullivan; Morphology of non-lymphatic cells in the lymph node of the nude mouse-P. Groscurth; Some aspects of immunology in the nude rat-D. I. Pritchard & R. P. Eady; Comparison of the growth of xenografts in various kinds of immunodeficient mice-S. I. Detre; Hetero-transplantation of human malignant tumours to athymic nude mice -C. O. Povelsen, M. Spang-Thomsen, J. Rygaard & J. Visfeldt; Tumour transplantation in nude rats and mice -J. C. Salomon, N. Lynch, J. Prin, V. Lascaux & A. Galinha; Transplantation of canine tumours into immunosuppressed dogs and nude mice-L. N. Owen; Human tumour xenografts in athymic nude mice: non-specific host rejection responses-R. W. Baldwin & M. V. Pimm; A prospective test for human tumour rejection antigens-M. Moore; Metastasis of human tumours implanted in immunodeficient mice -A. J. Garrett, D. Bishop, D. E. Reeson & S. Marsden; Metastatic behaviour of human colon carcinoma in nude mice-B. Sordat & E. Bogenmann; Lewis lung tumour growth and metastases in nude mice -J. C. Salomon, N. Lynch & J. Prin; Tumour metastasis in thymectomised and athymic rats -S. A. Eccles; The therapeutic response of human tumour xenografts-G. G. Steel, V. D. Courtenay, T. A. Phelps & M. J. Peckham; Cytofluorometric analysis of tumours in nude mice -P. Sordillo, H. Hansen, L. Helson & C. Helson; Identification and separation of mouse and human components of heterotransplanted human tumours-H. M. Warenius; Viral contaminants of xenografts-R. A. Weiss; The potential role of xenografts in the investigation of the clonal structure of human tumours-M. J. Peckham, P. J. Selby & G. G. Steel.

This book brings together for the first time a variety of animal models in cancer research, from the simple immunodeficient foetus to the complex genetic manipulation needed to produce the 'Lasat' mouse deficient in both thymus and spleen.
This is the first book to deal with this aspect of cancer research in such detail and it will be valuable reading for all those involved in cancer and immunological research. It will also be an important reference for students undertaking courses in Cancer Studies or Immunology.

For further details contact Ms Frances Roach, Scientific and Medical Division, Macmillan Publishers Limited, Houndmills, Basingstoke, Hampshire RG21 2XS.

LETTERS

J.W. Kloepper, J. Leong, M. Teintze and M.N. Schroth — **Enhanced plant growth by siderophores produced by plant growth-promoting rhizobacteria** 885

J.A. Ruben and A.F. Bennett — **Antiquity of the vertebrate pattern of activity metabolism and its possible relation to vertebrate origins** 886

M.B. Omary, I.S. Trowbridge and J. Minowada — **Human cell-surface glycoprotein with unusual properties** 888

J.E. Meats, M.B. McGuire and R.G.G. Russell — **Human synovium releases a factor which stimulates chondrocyte production of PGE and plasminogen activator** 891

P. Charnay, M. Gervais, A. Louise, F. Galibert and P. Tiollais — **Biosynthesis of hepatitis B virus surface antigen in *Escherichia coli*** 893

E.A.J. Wolters and R. Benner — **Different target antigens for T-cell subsets acting synergistically *in vivo*** 895

A. Forster, M. Hobart, H. Hengartner and T.H. Rabbitts — **An immunoglobulin heavy-chain gene is altered in two T-cell clones** 897

D.B. Bowling and C.R. Michael — **Projection patterns of single physiologically characterized optic tract fibres in cat** 899

F. Gonon, M. Buda, R. Cespuglio, M. Jouvet and J.-F. Pujol — ***In vivo* electrochemical detection of catechols in the neostriatum of anaesthetized rats: dopamine or DOPAC?** 902

R.J. Marchmont and M.D. Houslay — **Insulin triggers cyclic AMP-dependent activation and phosphorylation of a plasma membrane cyclic AMP phosphodiesterase** 904

A. Horvat — **Stimulation of RNA synthesis in isolated nuclei by an insulin-induced factor in liver** 906

L. Graf, H. Kössel and E. Stutz — **Sequencing of 16S–23S spacer in a ribosomal RNA operon of *Euglena gracilis* chloroplast DNA reveals two tRNA genes** 908

MATTERS ARISING

B.M. Tinsley — **The rhenium–osmium age of the Galaxy** 911

M.J. Aitken and J. Huxtable — **Accuracy of thermoluminescence dates** 911

Y. Liritzis — **Reply to Aitken and Huxtable** 911

R.V. Fisher, A.L. Smith, J.V. Wright and M.J. Roobol — **Ignimbrite veneer deposits or pyroclastic surge deposits?** 912

G.P.L. Walker, R.F. Heming and C.J.N. Wilson — **Reply to Fisher *et al.*** 912

BOOK REVIEWS

William S. Beck — **Blood, Pure and Eloquent: A Story of Discovery, of People, and of Ideas (M.M. Wintrobe, editor)** 913

P.W. Hawkes — **Holography and Coherent Optics (L.M. Soroko)** 914

John M. Deag — **Baboon Mothers and Infants (Jeanne Altmann)** 914

Karl-Erik Falk — **ESR and NMR of Paramagnetic Species in Biological and Related Systems (I. Bertini and R.S. Drago, editors)** 915

MISCELLANY

Erratum 910

Books received 916

New on the market xi

Classified advertising xiv

GUIDE TO AUTHORS

- Review articles should be aimed at a relatively wide readership. Many reviews are invited, but submitted articles may also be accepted; it is advisable to consult us before writing a review article.
- Articles may be up to 3,000 words long with at most six displayed items (figures and tables); they are reports of major research developments.
- Letters are brief reports of original research of unusual and wide interest, not in general longer than 1,000 words; they have at most three or four displayed items.
- 'Matters Arising' permits short discussion (up to 300 words) of papers that have recently appeared in *Nature*.

Articles should be accompanied by an abstract of not more than fifty words. Letters should begin with a paragraph giving the background and main conclusion in terms intelligible to as wide a readership as possible.

Manuscripts may be submitted either to London or New York. Three typed copies should be submitted, each including lettered copies of figures. Typing (including references) should be double spaced. The title should be brief and informative. Pages should be numbered. References, tables and figure legends should start on separate pages. Experimental detail vital to the paper yet which would interrupt the narrative is best placed in the figure legends. Units should be identified in the margin on their first appearance. Equations should occupy single lines if possible: exp (a) is preferred to e^a if 'a' is more than one character.

References are indicated by superscripts in the text. See any contemporary *Nature* for style, but note:

(i) only one reference number need be used if the reference is to several papers by identical authors.

(ii) first and last pages of references should be cited.

Abbreviations should follow the *World List of Scientific Periodicals*, fourth edn (Butterworth, 1963-65). Symposia are often difficult to refer to and only published or soon-to-be-published volumes should be mentioned in references. Their publisher and place of publication should be clearly indicated 'Personal communication' and 'unpublished' should be incorporated in text.

Artwork should be sent with the manuscript and clearly marked with author's name and the figure number. Line drawings should be either photographic prints or in Indian ink on heavy cartridge paper, tracing paper or similar materials. Most figures are reduced to one column width so originals should be about as wide as a page of *Nature*. To enable figures, particularly maps, to be edited in the same style as the text, they should contain only essential material. ideally, an unlettered original and three lettered copies should be provided; labelling on halftones should, if possible, be avoided entirely. Magnifications quoted should be for the figures as submitted. We are always glad to see artwork for possible use on the cover, but cannot guarantee its return.

In order to save on postal expenses we return *only the top copy* and artwork of manuscripts that we cannot publish.

Nature's publishing policy is outlined in **258**, 1 (1975) and **264**, v, 11 Nov. (1976).

M

Introduction
to
NUCLEAR
REACTIONS

G. R. SATCHLER

– Research staff member,
Oak Ridge National
Laboratory, Tennessee.

Spring 1980; £25; 336pp;
ISBN 0 333 25907 6.

Contents include – Some Background; Introduction to Nuclear Reactions; Elementary Scattering Theory; Models of Nuclear Reactions.

This book presents a summary of our present understanding of the Scattering and Reactions that occur in collisions between nuclei and is an introduction to the theoretical formalisms used to describe them. It is aimed primarily at readers in the undergraduate and beginning graduate student level but many others will also find it useful. The specialist from another field will find that this book is excellent background reading and the established nuclear physicist will find reading it to be helpful in refreshing the memory about areas in which he or she is not currently working.

For further details contact Frances Roach, Scientific and Medical Division, Macmillan Publishers Limited, Houndmills, Basingstoke, Hampshire, RG21 2XS.

M

© 1980 Macmillan Journals Ltd
Nature® is published weekly
ISSN 0028-0836
Registered as a newspaper at the
British Post Office

London
4 Little Essex Street, WC2R 3LF
Telephone: (01) 836 6633 Telex: 262024
Telegrams: Phusis London WC2R 3LF

Editor: John Maddox
Deputy Editor: Peter Newmark

Editorial Staff
Alun Anderson Naomi Molson
Philip Campbell Sara Nash
Isobel Collins Judy Redfearn
Konrad Guettler Miranda Robertson
Tim Lincoln Robert Walgate
Mary Lindley Charles Wenz
Jonathan Wolfe
Publishing Director: Christopher Paterson
Marketing Director: Ray Barker

New York
15 East 26 Street, New York, NY 10010
Telephone: (212) 689 5900 Telex: 668497

Robert Ubell (American Publisher)
and Sheila Kane

Washington News Bureau
801 National Press Building, DC 20045
Telephone: (202) 737 2355 Telex: 64280
David Dickson (Washington News Editor)

International Advertising Manager:
Richard Webb (London) (01) 240 2044

USA Advertising Manager
Henry Dale (New York) (212) 689 5900

Classified Advertising:
4 Little Essex Street, WC2R 3LF
Telephone: (01) 240 1101
Classified(USA)
Terence Miller, Suite 832, 50 Rockefeller Plaza,
New York, NY 10020—(212) 765 5758
Display and Classified(Canada)
Peter Drake, 32 Front Street West,
201 Toronto, Ontario M5J IC5
(416) 364 1623

Advertising Representatives in USA
Display
Nature New York Office—(212) 689 5900

Media Group, Inc. (Dallas)—(214) 631 4480
Didier & Broderick, Inc. (Chicago)—
(312) 498 4520

Jobson/Jordan/Harrison/Schulz, Inc.
(San Francisco) (415) 392 6794 (Los Angeles
& Pasadena) (213) 796 9200
Daniel Adams Associates, Inc.
Philadelphia—(215) 353 6191

CEL Associates (Boston)—(617) 383 6136
Brinker & Brinker (Fort Lauderdale)
(305) 771 0064

German Advertising Representative
E. Meckelburg, 6450 Hanau 1, Jahnstrasse 15,
West Germany Tel:— (49) 61 8115343

Japanese Advertising Representative
Orient Echo Inc.
11th Fl, Sankyo Bldg. 7-12, Tsukiji 2-Chome,
Chuo-Ku, Tokyo, Japan, Tel: 541-4923.

Annual Subscription including Index

UK		£55
USA & Canada		US$135
Belgium	Airspeed	BF4900
West Germany	Airspeed	DM300
Holland	Airspeed	G325
Switzerland	Airspeed	SF265
Rest of World	Surface	£70
	Airmail	£95

Single copy (post-paid); UK, £1.20; USA & Canada, US$3.50 (surface), US$5.00 (air); Rest of World, £1.15 (surface), £2 (air).

Orders (with remittance) to:
Macmillan Journals Ltd, Brunel Road,
Basingstoke, Hants RG21 2XS.
Telephone: Basingstoke (0256) 29242

Nature is published weekly, except the last week
in December, by Macmillan Journals Ltd.
Second-class postage paid at New York, NY
10010 and at additional mailing offices.
US Postmaster, please send form 3579 to:
Nature, 15 East 26 Street, New York, NY 10010.

Vol. 286 No. 5776 28 August 1980

nature

3 July 1980

Venice, Energy, Brandt and politicians

Meetings of political leaders such as that which ended in Venice on 23 June are always risky for the participants. The chief risk is simply that they fail to agree on whatever it is they have chosen to talk about, the final communique says little more than that a meeting has taken place and doubts are cast on the value of high-level consultation as such. The seven Western politicians gathered in Venice have avoided that risk. Their parting communique was at once more detailed and more constructive than for many a year. It remains to be seen, however, whether they will be able to avoid the second hazard that faces summit-goers — that having agreed on something they go back home and discover there is nothing they can do to put flesh on the bones of what they have agreed. The chances of that happening are, unfortunately, all too real. It has, after all, taken a full seven years for the heads of government to come to the belated recognition, embodied in their communique from Venice, that something must be done about the price of oil.

The argument is familiar. Increasing OPEC prices have brought about the curious blend of inflation and deflation from which the industrialized nations of the West are suffering. It has also jeopardized the future of the developing countries, which must keep on borrowing from abroad in circumstances which must throw doubt on their capacity ever to repay their debts, and which certainly diminish the chances that they will be able again to move forward socially and economically. So, the Venice communique has it, the industrialized West must diminish its own dependence on OPEC oil, must aim at making its own industry more productive and must not be seduced by the blandishments of those who argue, on narrow national grounds, for more constraints on international trade. In short, the major industrialized states appear belatedly to have recognized where their true economic interests lie, and have also made more than a passing acknowledgement of the still more serious problems of the developing countries, most recently and cogently described by the Brandt Commission (*Nature*, 21 February). So far, so good.

But why have the industrialized states not had the gumption to say all this before? That is a natural question to ask. In other less exalted contexts, in the Council of the International Energy Agency and the OECD for example, bits and pieces of the problem have been tackled. Why have the heads of government been so slow off the mark? The explication is not wholly creditable. It is only in the past year or so that all the governments represented in Venice have found themselves companions in misfortune. Both West Germany and Japan have found it possible for most of the past seven years to import oil and to pay the bills for it like men, without having to resort to their currency printing presses. It is also true that, during most of that time, several of the governments represented at Venice have been following economic policies that would have allowed inflation to bounce along at an alarming rate even if the price of oil had remained just a few dollars a barrel. The American, British and Italian governments have been the chief offenders. Readers of their communique from Venice must be forgiven the suspicion that some of the fine words are not backed by sufficient resolution. Some OPEC governments will complain, with justice, that the price of oil is being made a scapegoat for deeper ills.

The same kind of scepticism will attach to what the communique says about the steps the governments have agreed upon to lessen their dependence on OPEC oil. As these things go, the Venice document is unusually specific, replete with words such as "base-load". Plainly the world's leaders have been got at by their technical people, which no doubt is why the civil servants of the West are convinced that Venice was a "success". And, of course, it is sensible enough that the West should forswear oil-burning power stations, thereby avoiding extra demand for imported oil for the following quarter of a century. But did anybody in Venice think of asking Mrs Thatcher, the British Prime Minister, why the British nationalized utility, the Central Electricity Generating Board, is still trying to complete the oil-fired power station on the Isle of Grain (on the south bank of the Thames estuary) when the workforce of laggers (men who wrap insulation around pipes) has refused to work except at salaries which offend other workers (and their unions) on the site? The Venice declaration is also full of promises that there will be incentives, "where necessary" including fiscal incentives, to encourage the exploration for oil. Why, then, is the deregulation of United States oil prices not yet complete? Why has the British government just put up the tax on oil production in the North Sea? Why has the search for a way of taxing the "windfall profits" of the oil companies become the equivalent in the 1980s of the spate of legislation against "monopolies" in the 1920s?

The politicans at Venice can only blame themselves if some of their other specific declarations on energy policy provoke the same kind of disbelief. For the medium term, the declaration says, nuclear power, coal and conservation must bear the burden of helping to slacken external oil dependence. This, of course, has been clear for a decade. The trouble is that the governments at Venice have also known this to be the truth, but have mostly failed to make progress. The British government has only just emerged from what has been essentially a moratorium on decisions about nuclear power. (One ironical consequence is that British Nuclear Fuels Limited, which had wanted to build a prototype of a plant to vitrify nuclear waste as long ago as 1974, is now having to think of using a French process instead — see page 5.) In the United States, the Nuclear Regulatory Commission limps along with a stand-by chairman whose successor, soon to be appointed, is likely to be replaced again when the Administration changes. United States coal production, which President Nixon promised would reach 800 million tons a year at least by 1980, remains only 600 million tons a year, largely because of the endless troubles about strip-mining projects. In Britain, the National Coal Board still waits to know (after a public inquiry on the subject) whether it will be allowed to exploit a profitable reserve of coal in the Vale of Belvoir. But these, alas, are only some of the ways in which performance has fallen behind precept in energy policy. What is to be done?

Some intolerant souls, offended by this contrast, have been saying that the Venice governments should take the bull by the horns and ram what are undoubtedly sensible policies down the throats of their people. Quite apart from being a recipe for electoral disaster, such a course would risk throwing away the baby with the bathwater. The reason why it is important that the West should be freed from its dependence on OPEC oil is that money inflation is destroying valuable social institutions (educational systems, health care services, charitable institutions) while the accompanying deflation is hampering innovation. It would not however be acceptable that for the sake of being liberated from these economic shackles, people in supposedly democratic countries should be told from on high what to do and then required to put up with the consequences. Would the game then be worth the candle? Do not even self-styled and usually unqualified ecologists deserve a hearing? On nuclear power, there

0028-0836/80/270001-02$01.00

are special reasons why the professional community has a special role to play in ridding the nuclear wrangle — it is not an honest debate — of mumbo jumbo. Here and elsewhere, however, the responsibility for getting things done lies also with governments. If higher (or even higher) energy taxes are thought necessary, it is for them to persuade their voters that the benefits will be worthwhile — the chance to remain citizens of progressive yet dynamic communities. If strip mines, or ordinary coal mines, or nuclear power plants, are necessary, governments have a duty to make sure that their people know what are the stakes — the avoidance of economic debacle, to put it at its mildest; at the other end of the spectrum, the avoidance of the much more serious trouble there would be bound to be if, say, Saudi Arabia were unable to produce 11 million barrels of oil each single day.

Telling it like it is is unfortunately unfashionable. Signing communiques is easier. So too is making promises for the long term that become confused in voters' minds with solutions to immediate problems. President Carter's promise two years ago that 20 per cent of American energy production would come from the sun by the end of the century is of this kind. For the industrialized West, the question is not that of what the energy mix will be in the year 2000 but how to get from here to there. Implicitly, that is what the heads of government at Venice said. They had better now tell their people even if, as a result, they suffer the traditional fate of the bearers of bad tidings. They might make their message more palatable by seeking more imaginative ways out of their present fix — by counterbalancing the rigged OPEC market in oil with their own free market (*Nature*, 12 May). This week, for what it is worth, the spot price at Rotterdam has fallen below that charged by some OPEC countries, which can only suggest that the price would fall even more quickly if the market were assured of a regular share of the West's own oil production.

Happily, however, Venice was not entirely a recitation of familiar platitudes. Habitually, the industrialized West has collectively been shy of saying much about it obligation to the developing countries of the world for fear of giving too many hostages to fortune. At Venice, they broke cautiously with precedent and even went as far as to "welcome" the report of the Brandt Commission, promising to "study" its recommendations. They also undertook not to organize their policies on international trade in ways that would be harmful to the non-oil developing countries. That is as it should be, although it is doubtful whether the Venice signatories appreciate the magnitude of their undertaking; it implies nothing less than recreation of their industrial base at a time of perhaps indefinite recession. Such magnanimity will not come easily to the unemployed shoe-workers of New England or the unemployed workers of the British steel and motor car industries. Nor is there much hope that the industrialized West can share this burden with other states.

Why bother with school examinations?

LIKE Stratford-upon-Avon, the Changing of the Guard and the game of cricket, the British examination system is one of those characteristically British phenomena which the rest of the world knows it will never understand. Increasingly, the British are in the same plight. Now that the examinations season is at an end, when only the most diligent of those who have survived their recent trauma have begun preparing for the next, and when many of those responsible for assessing the gigantic paper output of the examination system have withdrawn temporarily from the real world, it may be safe to raise the question whether the system as a whole is worth preserving. The answer is not simple. Plainly the system cannot be entirely swept away but it is equally unthinkable that it should be preserved in its present form.

The rules of the game are worth a little effort to understand, if only for the light that understanding may throw on what must surely be one of the most pathetic of human frailties — the belief that ordinary men and women in some stratum of the academic profession can reduce any other person's quality to a number of some kind, usually between zero and 100. One of the curiosities of the recent proliferation of examinations in Britain is that in the 1950s the country was riven into the camps of those who passionately held that it is possible by means of an examination to tell at the age of eleven whether a child should have an academic or grammar school education, and the camp of those who considered the eleven-plus examination to be unjust. In the end, the abolitionists more or less won the day, comprehensive schools were invented and for a time preoccupation with school examinations seemed to have been stilled.

Alas, the wish to examine and to be examined has since reasserted itself with a vengeance. Increasing numbers of no doubt fond parents now subject their sons and daughters, often at the age of seven or eight, to the competitive examinations put up as hurdles by the fee-paying schools, knowing that their offspring will thereafter be graded once a year either by means of a number or, more elegantly, by a letter from the Greek alphabet, with pluses or minuses appended. For most British children, the first external yardstick comes at about 16, the age of O (which stands for "Ordinary") level, or alternatively of "CSE" (which stands for Certificate of Secondary Education). The word that echoes around the corridors of secondary education is that you cannot get a job unless you do reasonably well in one or other.

In ancient days (but even now in Scotland) there used to be an examination called "School Certificate" devised at least in part to meet the entrance requirements of universities. Since entry to universities was in question, universities came to dominate the committees which administered these examinations. Knowing that not every university could run its own examinations board, the universities grouped themselves into consortia, of which there at present nine, and which now administer the O-level examinations and the A (for "Advanced") equivalents, literally used by most universities as a way of telling which students should be given a chance to study something serious.

The problems of the sixteen-plus examination are unfortunately minor compared with those which crop up two years later. The rules of the game, in Britain, are that those wishing to find themselves a place in a university are required not merely to jump the hurdle of the O-level examinations but of A-level as well. They are, for practical purposes, required to elect two years in advance for what they will take an interest in at university, and then to prove (with the help of the school-teachers who happen to be around) that they can perform. Many youngsters rebel at choosing, but eventually are forced to toe the line. Others, no doubt, give up, or worse still find they have chosen wrongly. In all secondary schools, teaching A-level students is regarded as the pinacle of academic life (and in many schools it is quite remarkable how successfully the image of specialist can be created at sixteen or seventeen).

If the charge against this part of the British educational system were merely that it is farcical, it might be allowed to continue. The truth is that it is actively harmful. It ensures that young people are too narrowly prepared for the academic life, and frequently have been forced at an early age to choose the wrong disciplines to follow. In justice, and in the national interest of the British, it would be better if A-level were to be abolished. Since, however, that will not happen overnight, it would serve the same purpose if A-level were to be subverted. The way in which this might be done is easy to identify. If only universities were once again to take responsibility for their student entry, and were to select say ten per cent of intending students by some quite different method — a scholastic aptitude test, an interview or some other indicator of performance — the result would be that lots of bright young people would be found to prefer that route. If selection for the people not taking A-level were a year earlier than for the rest, but if university courses were a year longer for the early ten per cent, there would at least be a chance to tell which way was the best. Is it not time that this was tried?

0028-0836/80/270002-01$01.00

New Basel director changes direction

The Basel Institute for Immunology, founded in 1971 by Hoffman-La Roche, the Swiss pharmaceutical manufacturer, is soon to have a new director, the 44-year-old chemist and geneticist Fritz Melchers. Dr Melchers, already a member of the institute, will take up his appointment with effect from 1 October.

Melchers will succeed Dr Niels Jerne, the first director, who has helped to give the institute its now outstanding reputation in basic immunology. During his tenure of the post, Jerne has also fought strongly for the independence of the institute from the company which finances it, insisting on the freedom of the members of the institute (who have no other titles) to pursue whatever research appears appropriate, to publish in the scientific literature and to pay no more attention than they wish to the research interests of their parent company.

Inevitably there is now some concern that the old arm's length policy will be changed. Melchers agreed on the telephone last week that his policy may be "more friendly" than that of Dr Jerne. The new director says, however, that he intends to maintain the role of the institute as a centre for fundamental research in immunology, cell biology and molecular genetics. Applied work will have no place at the institute, he says, and researchers will be completely free to publish their results.

Melchers says that he would not have taken the job unless these conditions had been satisfied. The future of the institute has also been underwritten by the company "for a considerable period". The implication is that the integrity of the research programme will not be compromised by short-term money problems.

The institute has a small tenured staff, but provides facilities for a much larger number of visiting scientists. It was originally set up by Roche for a limited period of ten years, although Jerne has said that Roche told him it would keep the institute going "so long as the Western world did not change drastically". Jerne took this to mean that the laboratory would continue at least as long as the world took Valium, one of the company's most successful products.

Some change in the relationship between the institute and the company is nevertheless on the cards. Melchers said last week, for example, that the role of the scientific board of the institute, as well as the mechanism for providing scientific advice to Roche, are under consideration. The function of the board has been to advise the company on the scientific work of the institute and "all matters relevant thereto". Melchers said last week that "we want a board of independent scientists who will help in the exchange of ideas with the firm while maintaining the scientific integrity of the institute". The company, he said, "has a growing interest in molecular biology and its applications", and correctly feels that the subject should be part of its research effort. Roche, said Melchers, spends a lot of money on the institute and deserves some return from it.

This does not imply that the institute will become a wing of Hoffman-La Roche research, however, Melchers says, but rather that communications between the institute and the company should be improved. He cites the setting up of a hybridoma research group at Roche with the institute's help as an example of the improved communications he has in mind.

One present member of the board, Avrion Mitchison of University College, London, greeted Melcher's appointment with delight. "He is an able scientist, decisive, and can deal with the company."

Robert Walgate

Sitting-in in Spanish labs

DEMONSTRATIONS of scientists are uncommon events, even in Spain. On 27 May, however, more than five hundred scientists of the research centres of the CSIC (*Consejo Superior de Investigaciones Científicas*) marched through the streets of Madrid to the Ministry of Universities and Research in one of the most spectacular events in three weeks of protest by Spanish researchers.

Hopes of a change in government policy towards science were aroused by the establishment of a democratic regime in Spain. The experience of the past three years has, however, been disappointing, despite some beneficial changes in the structure of the CSIC and universities.

It now seems that the creation of the Ministry for Universities and Research has not brought the benefits expected. In fact, the 1980 budget for research has increased by only 7.2 per cent, a figure far below the inflation rate. As a consequence, financial support for research has decreased in real terms compared even with the past level.

Thus the budget for one of the main sources of grants, *Fondo Nacional de Ayuda a la Investigación* (FNAI), was withheld for more than a year and afterwards fixed at only 2,500 million pesetas ($35 million), one-eighth of the applications.

This may be too late to avoid the interruption of the research in certain cases. At the same time, another important source of support for research — the programme for predoctoral fellowships — has been cut by a half. This means that an average university may receive fewer than 30 fellowships — and this at a time when unemployment among young graduates is reaching dramatic proportions.

To add to these uncertainties, the abolition of the CSIC has been considered within the government and publicly discussed. A new Universities Bill (*Ley de Autonomía Universitaria*) has been presented unchanged to parliament in spite of criticism from many sections of the scientific and university communities.

Against this background, the staff of the Institute of Astrophysics and the Experimental Station of El Zaidín in Granada recently decided to sit in as a protest against "the chaotic situation existing in the CSIC". A manifesto was issued denouncing the worsening condition of Spanish research and proclaiming that the trouble stemmed from the absence of a coherent science policy, the inadequacy of the funding for research and the low salaries and lack of promotion for scientists and technicians. Shortly afterwards, a meeting was held in Madrid by scientists and technicians and that was followed by the demonstration ending at the Ministry for Universities and Research with the reception of a delegation by the minister.

On 2 June, the minister attended the first session in Madrid of a National Congress on Science Policy after a request by the Association of Research Personnel, which consists mainly of CSIC workers. In his speech, the minister acknowledged the absence of a science policy in Spain and conceded that the present situation was caused by the low level of funding.

The day the Congress on Science Policy ended, the Ministry of Universities and Research issued a statement promising that the CSIC will not be dismantled but radically reorganized. In another statement, the ministry announced the publication of a White Paper on research and a Three-Year Plan for research. The publication of a White Paper was said to be imminent in August 1979, and a Three-Year Plan has already been promised for more than three years.

Pedro Puigdoménech

Correction

The report on 26 June of the views of the Astronomy II Committee of the Science Research Council appears to be substantially incorrect. The committee did not decide to ignore SRC policy on the appointment of postdoctoral fellows; did not offer advice to senior researchers on how best to deal with short-term appointments; and did not empower the Royal Astronomical Society to act on its behalf. The position appears to be that the Astronomy II committee did discuss the problems of short-term appointments but postponed a full-scale discussion until a meeting in October. We regret the error.

Editor, *Nature*

0028-0836/80/270003-01$01.00

High-energy physics

LEP leaps ahead

The European Centre for Nuclear Research (CERN) last week made a firm proposal to its 12 member states for a new accelerator to be built in the 1980s. The machine, called LEP, is a 30 km circumference ring for accelerating, storing and colliding very high energy beams of electrons. The proposal already bears the mark of CERN's firebrand director-general-designate, German Professor Herwig Schopper: LEP is now cheaper than in any former design — 900 million Swiss francs (£235 million) compared with 1100 million Swiss francs (£280 million).

The scientific case for LEP is considered by high-energy physicists to be outstanding, better than that for any accelerator since the early 1950s, when the Lawrence cyclotron was built to create what was then thought to be the quantum of the nuclear force-field — the pion. LEP, it is hoped, would produce the intermediate vector bosons, the Z^0 and the W^+ and W^-, the predicted quanta of the Salam-Weinberg unified theory of the weak and electromagnetic interactions. Testing this theory is now recognized to be crucial. Success will give confidence to more ambitious attempts to construct unified field theories. Failure, however, would also be suggestive.

CERN's proposal is strictly for "LEP phase 1", which involves building a tunnel so large that ultimately beams of 130 GeV could be retained (more than enough to create $W^+ — W^-$ pairs), while cutting back on accelerating cavities (which inject the energy into the beam). The result is that LEP phase 1 would reach 50 GeV per beam, enough to make the Z^0 and make the initial tests of the Salam-Weinberg theory.

LEP phase 1 also cuts back on experimental facilities: only four of the possible eight experimental halls would be equipped. And it proposes a new injection system, which makes use of existing accelerators at CERN and eliminates the need for a large electron synchrotron, which would have been the biggest in the world, merely to inject electrons into LEP. In contrast, the intersecting storage rings, one of CERN's greatest technical successes, will not now be needed for the electrons and will be devoted to experiments outside subnuclear physics.

Professor Schopper, who is at present director of the German electron physics laboratory DESY near Hamburg, said this week that it was most important that the CERN Council had recommended that LEP be built out of CERN's running budget rather than as a separate programme. A director has been appointed to act as LEP project leader, as soon as governments give approval; this is Dr Emilio Picasso, a prominent Italian physicist at CERN. The project leader, said Schopper, would be able to organize and draw on talent throughout CERN, for short and long periods, avoiding the career problems and inflexibility that would come with a new "LEP division". "We will bring the work to the people", he said.

The CERN Council has adopted a "firm" budget for 1981 of 596 million Swiss francs (£156 million), but this includes no provision for the construction of LEP. Schopper will propose a running budget which will include LEP in six months' time: he expects it to be a little larger than the 1981 budget "but we are only talking of a per cent or two". CERN staff are now working on reducing the cost of individual LEP components. The level of the budget will determine not whether, but how fast, LEP can be built.

●CERN's 25-metre-square antiproton accumulator is to receive its first particles in the next few days — less than two years after the ground was first broken. The accumulator will be tested with protons, but the intention is to use it to reduce or "cool" the transverse motions of antiprotons created in proton-target collisions. The antiprotons, a few per collision, will be accumulated and then injected into the 400 GeV super proton synchrotron countercurrent to the SPS proton beam.

Robert Walgate

Radioactive waste

Polite debate

A first attempt by the UK National Radiological Protection Board and the British Association for the Advancement of Science to stimulate public discussion on the problems of radioactive waste management was a damp squib. A meeting they organized on 18 May, attended by interested parties in the nuclear industry, government agencies and the anti-nuclear groups, did little to uncover the detailed technical problems.

Part of the reason for the low key in which the meeting was conducted appears to have been the decision of the British authorities that, even with the new nuclear programme, fresh arrangements for long-term disposal will not be needed until the end of the century.

Both intermediate and high-level waste have been stored at Windscale for 25 years and could sit there for many more without the authorities becoming unduly bothered. If anything, the intermediate waste is a more urgent problem — it accumulates fairly rapidly and storage facilities are costly. High-level waste disposal is nevertheless receiving most attention. Out of a total waste management research budget of £25 million, the UK expects to spend more than £10 million this year on one method of treating high-level waste: the HARVEST vitrification process which has been under development by the UK Atomic Energy Authority since the late 1950s. The British government plans a prototype vitrification plant operating at Windscale by 1990 if the go-ahead for the plant can be given some time this year.

The decision for British Nuclear Fuels, which runs Windscale, will not be easy, however; it will have to choose between its own HARVEST process and the French equivalent (AVM) which has been operating commercially since 1978. Officials are keen to point out that a decision to opt for AVM would not mean the end of HARVEST, which should be kept going to keep later options open.

The government plans to start producing vitrified high-level waste by the early 1990s for several years' storage and then final disposal in some sort of demonstration facility at the end of the century. There are three options for final disposal — on or under the ocean bed or in deep geological structures.

The Radioactive Waste Advisory Committee, a group of independent advisers, recommended in its first annual report, published earlier this year, that research on the first two options should be increased.

The most promising option seems to be disposal in deep geological structures . The government programme of test-drilling in various rock formations throughout the country, however, has excited considerable public opposition. The UK Atomic Energy Authority, which started the programme now under the aegis of the Department of the Environment, has so far been able to drill boreholes at only one site in Scotland.

Planning permission for three others has been refused and the authority is awaiting the results of appeals. The Institute of Geological Sciences is now making preliminary surveys of about fifteen other sites for the Department of the Environment in the hope of drilling at some of them fairly soon.

Judy Redfearn

Russian language

Finns struggling

Recent cutbacks in university Russian departments, the falling off in the numbers of school-children sitting for Russian Advanced-level examinations in secondary schools and the virtually overnight decision to close down the Russian department of the University of Lancaster have caused considerable concern in British academic circles. Very different, one might think, the situation in Finland, where a recent report of the Ministry of Education urged substantial increases in the teaching of Russian.

According to a memorandum submitted last month to the Minister of Education, Paer Stenbaeck, at least one group of students is however at risk. The memorandum, drawn up jointly by the Finland-USSR Society and the Fund for the Promotion of the Study of the Russian language claims that a "worsening" of the position of Russian language teaching in Finnish secondary schools could be a

0028-0836/80/270004-02$01.00

serious handicap to university students reading mathematics and science.

The report sets a target that 30 per cent of the active population (people between 20 and 63) should have a knowledge of Russian — thus giving Russian, for the first time, parity with German in importance as a means of international communication.

Language study in Finnish schools is complicated by the existence of two national languages — Finnish and Swedish — one of which has virtually no use and the other only limited use as a means of international communication.

According to the new proposals, all school-children must learn one foreign language (at present this is usually English) and the "other national language" (Swedish for Finnish-speakers and conversely). Study of a third language is optional, and introduced in the eighth class (15 plus).

According to the 1977 figures, some 0.2 per cent of school-children learn Russian as their first language and 6.2 per cent as their third language. The committee's recommendation of a 30 per cent Russian-speaking "active population" seems, therefore, an improvement. Their recommendations, however, refer to the whole range of language teaching — including, for example, business and secretarial courses. The "pro-Russian" lobby maintains that the school timetable is now so overburdened that few science-orientated students will be able to fit in a third optional language and will, accordingly, have no access to Russian scientific literature.

To the present generation of Finnish scientists, however, a lack of knowledge of Russian seems no particular burden. They use the cover-to-cover English-language translations of Soviet journals, and have little need, they say, for spoken Russian as a medium of scientific communication.

Vera Rich

Experimental animals

Lab invaded

The UK Agricultural Research Council's Institute of Animal Physiology at Babraham, near Cambridge, has lived under threat of physical attack by anti-vivisectionists for several years. Last weekend the expected happened when a group of demonstrators forced their way into administrative buildings and laboratories housing animals. One object of the invasion was apparently to photograph animals in the laboratory.

The cost of the damage is small — no scientific experiments were tampered with. Preliminary estimates put it at a few hundred pounds. But, says the ARC statement, the noise of the break-in and the flashing bulbs of cameras must have caused alarm to the animals, which are accustomed to good treatment.

After some reports in the press earlier this week, the ARC also said that neither "outsize" goats nor crossbreeds between goats and horses are kept at Babraham. Some demonstrators questioned on the site were apparently under the misapprehension that toxicity tests with cosmetics and cigarettes were being carried out.

The Institute of Animal Physiology has been a focus for the anti-vivisectionists for some time. The institute has pointed out before that all experiments done there are subject to licensing by the Home Office and are not exceptional in that similar experiments take place in other laboratories.

Judy Redfearn

Whaling quotas

More wrangling

The 1980 general meeting of the International Whaling Commission at Brighton on 21-26 July will have on its agenda a call for a total moratorium on whaling. This is the third time that the issue has been raised; on previous occasions, however (1972 and 1979), the motion was amended to one for selective moratoria. This year, the proposal for a total moratorium is tabled, *inter alia,* by France, the Netherlands and the United States, and is felt to have an even chance of success.

As in previous years, defeat or amendment of the motion would probably result not from a change of heart by the pro-moratorium lobby but from a feeling that adoption of such a motion would push anti-moratorium countries out of the convention and therefore beyond international control.

The way in which the argument at Brighton is likely to go can be told from what opponents of a total moratorium are saying in advance. One of the strongest opponents of a total moratorium, the Soviet Union, recently made its position clear in an English-language broadcast on Moscow radio. Calls for a total moratorium, said commentator Boris Belitskii, have no ecological basis, but are based on emotional attitudes encouraged in some quarters for political reasons.

The English-language broadcast added that in the case of really endangered species and in certain limited areas the Soviet Union has cut back its whaling considerably. (In the case of the baleen whales of the Sea of Okhotsk, a 2-year total ban has restored the population from the verge of extinction.) The broadcast went on to say that, over the past few years, the Soviet Union has closed down on-shore whaling factories and has disbanded the whaling fleet based on the Baltic port of Kaliningrad, dispersing the ships to marine and ichthyological research.

At present, Soviet whaling operation are said to be based on Vladivostok, and the two flotillas, with mother ships *Sovetskaya Rossiya* and *Sovetskaya Ukraina,* carry the necessary international observers as well as Soviet marine ecologists.

Rhetoric apart, the Soviet Union and other anti-moratorium countries such as Japan appear to have a certain case: they joined, they say, a "whaling" commission (to control and maintain the industry) not an "anti-whaling" commission.

There has been considerable speculation that, should the pro-moratorium advocates carry the day at Brighton, the Soviet Union and Japan might set up a rival commission of their own. Already the two countries have had some bilateral cooperation over quotas.

When, last year, the Soviet Union accepted the IWC's decision for a partial moratorium, in which fishing from factory ships would be confined to minke whales, it implemented this decision by ceding to Japan its North Pacific quota of 230 bryde whales in return for 300 of the less valuable minke whales from Japan's quota in the Antarctic.

Vera Rich

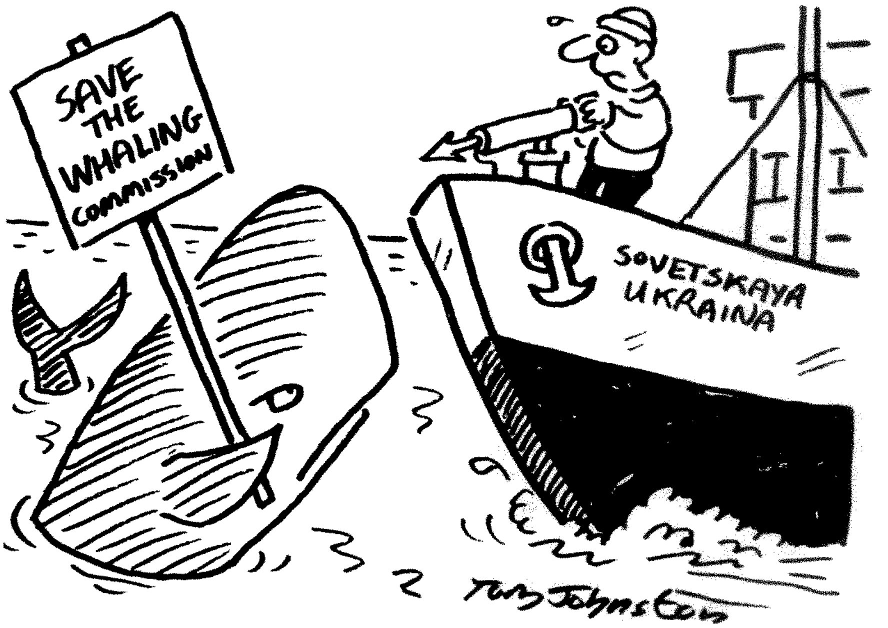

Big science

German doubts

WEST Germany is in the process of reviewing ten major scientific projects which would cost more than £500 million if all were funded now. They range from a continental deep drilling project which would reach the Mohorovic discontinuity at a cost of £30-75 million per hole to the possible commitment to the European proposal to build a large electron-positron ring (LEP) at CERN, Geneva at an estimated cost to Germany of £90 million.

The German research ministry, the BMFT, has set up an *ad hoc* committee of seven distinguished scientists and one journalist (to give "the people's view") which has already begun taking evidence. The cases have been heard for LEP, HERA (an electron-proton ring proposed for the DESY laboratory near Hamburg) and a relativistic heavy ion accelerator (10 GeV per nucleon) for the nuclear laboratory GSI at Darmstadt.

The chairman of the committee, Professor Klaus Pinkau of the Max-Planck-Institute für Physik und Astrophysik, Munich, said last week that he would make "a brave attempt" to finish all the hearings before August; the committee's views are not requested before mid-1981, but the sooner they are received by the new government after the October 1980 general elections, the more likely they are to affect policy, Pinkau believes.

It is not possible, says Pinkau, to make a linear list of priorities through the projects; rather the committee must "model a research landscape". The committee has been given no financial guidelines, so that it will be "a piece of artistry" to work out what the government can afford. Pinkau sees the committee as one lying between scientists and government rather than a part of government: it will make judgements among the projects on their merits, and then turn around and plead with government on behalf of those it supports.

Despite the strength of the German economy and the scale of the package of proposals now being reviewed, financial pressures are now making themselves felt. Recently, the minister for universities, Dr J Schmude, said in a speech at the Deutches Forschungs Gemeinschaft (which funds most German university research) that scientists would have to be prepared to spend less. The national budget is being pressed by the world recession, the increasing defence budget and an increased contribution to the European Community budget to offset Britain's soon-to-be-reduced subscription as negotiated by Mrs Margaret Thatcher. "Research won't be exempted" from the cuts to come, said Pinkau.

One result will probably be that the biggest projects on the list will not be funded simultaneously. And the most direct conflict now seems to be between HERA (for Hamburg) and the relativistic heavy ion accelerator (for Darmstadt). LEP is an international project which would be paid for if the current budget for CERN at Geneva can be maintained at something like its present level. Germany has said that, on terms like these, it will not object.

HERA (electron-proton) and GSI (relativistic nuclei) are, however, both national projects in closely adjacent fields. HERA would probe the structure of the proton and the quark, and the GSI device would create, for example, regions of extreme nuclear density which in principle could simulate neutron star conditions (although it would be difficult to extract the relevant information from the experiments). And, said Pinkau cryptically, "one should be aware that DESY", where HERA would go "is an internationally important laboratory". **Robert Walgate**

Major projects under review

	Cost (million DM)*	Timescale (yr)	Proposer
Spallation neutron source	400-570	8-15	Karlsruhe and Julich
BER II reactor improvement	47	2	Hahn-Meitner Inst., Berlin
Relativistic heavy ion accelerator	190	6	Darmstadt
Superconducting nuclear cyclotron, 250-300 MeV per nucleon	a) 44 b) 33	4-6	a) Julich b) Technical Univ., Munich
Ion beam fusion accelerator	100	5	Karlsruhe; *proposal withdrawn*
LEP	350 (for Germany)	6-8	CERN, Geneva
HERA	600	7	DESY, Hamburg
European synchrotron radiation source	100-230	5	European Science Foundation
Research vessel	75	2	DFG; to replace 'Meteor'
Continental deep drilling	120-300	1-5	DFG; price is per hole

* £1 sterling = 4.14 DM

Genetic manipulation

Soviet claims

On at least two occasions in the past month, the foreign services of Moscow Radio have put forward the startling claim that a team of geneticists at the Institute of Genetics and Cytology of the Byelorussian Academy of Sciences in Minsk have succeeded in manipulating the symbiotic bacteria of cereals to yield nitrogen-fixing properties.

The claimed success is surprising, especially because Minsk has no particular renown as a centre for genetic engineering, and even the most prestigious of the Comecon molecular biological establishments — Szeged — admits that its own work in this field still has a very long way to go. There is, however, a possibility that the reported discovery was not made at Minsk at all.

Indeed, the claim seems to be based on a paper by a team headed by M.A. Troicki entitled "Nitrogen fixing activity of hybrids between *Bacillus oligonitrophilus* and *E. coli*" (*Viesci Akademii Navuk BSSR, Serija Bijalahicnych navuk,* **3,** 1980). This describes a fairly routine procedure — nitrogen-fixing hybrids of *E. coli* with soil bacteria were produced at the University of Sussex nitrogen fixation unit as early as 1972, and the only novelty seems to be the use of *B. oligonitrophilus*, a name unknown to Western taxonomy, but which Troicki *et al.* state that they themselves isolated from the soil.

The authors themselves claim merely to have demonstrated the possibility of transferring nitrogen fixation genes from *B. oligonitrophilus* to *E. coli*, although the fact that their paper was published in Russian, whereas previous papers had appeared in Byelorussian, may suggest that they felt it merited All-Union rather than local attention.

Why, then, did TASS make such inflated claims? It is possible that the TASS science commentators simply misunderstood the paper, though it is difficult to see how they could do so, since Troicki's team does not mention cereal crops at all — the work reported relates to nitrogen fixation *in vitro*. It is not impossible, however, that the claim, coming at this particular time, has political overtones.

The first announcement was made on 25 May. The following day, *Pravda* published a major article on the Warsaw conference of the Warsaw Pact states entitled "Disarmament: Real Measures are Possible". Ostensibly an appeal for military detente, it contained claims that the United Kingdom and the United States are stepping up work on bacteriological weapons. In particular, said *Pravda*, the United States is working on "ethnic viruses" — bacteriological weapons which would selectively attack members of particular races or ethnic groups.

The case is cited of a black American, Eli

0028-0836/80/270007-02$01.00

Mayji, who allegedly developed a throat tumour after working as a guard at a secret US naval installation at West Oakland, where, it was alleged, Rift Valley Fever, which causes inflammation and malignant tumours, was used as a basis for an "ethnic" weapon.

Such allegations are not entirely new. Reports of alleged research on an "ethnic bomb" and other bacteriological weapons were put out by Soviet radio in 1978 (apparently in connection with the Robert Toth affair) and again earlier this year, to counter Western intelligence reports of a fatal epidemic in April 1979 emanating from a Soviet military bacteriological research station outside Sverdlovsk. (Soviet official sources said the incident was a natural outbreak of anthrax.)

Hitherto, the specific bugbear of a US "ethnic" killer has been restricted to transmissions on "Radio Peace and Progress", the Soviet service beamed to the Third World. The appearance of such charges in *Pravda*, the leading Party newspaper, is a new departure.

Vera Rich

Dioxin

ASTMS says no

The UK Health and Safety Executive came in for some sharp criticism last week from the Association of Scientific, Technical and Managerial Staffs (ASTMS). The union, with a strong following among scientists, accused the HSE of being "sluggish and ineffective" in its handling of the case of workers exposed to dioxin during an explosion at the Derbyshire plant of the Coalite and Chemical Products Company in 1968 (*Nature*, 6 March).

In 1976, after a similar accident at Seveso, Italy, the Employment Medical Advisory Service of the HSE persuaded the Coalite company to carry out studies of the workers exposed in the accident. Full reports of those studies, however, were not released to the HSE until last April in spite of several previous requests from the medical advisory service for all the information available.

In its document "Report on Coalite Chemicals", published last week, ASTMS criticizes the advisory service for not pressing harder for the earlier release of the studies. Results published in *The Lancet* early last year, it says, were sufficiently at variance with a summary of the studies released by the company to have persuaded the HSE to invoke its powers to secure the information. The HSE, however, says that increasing its pressure on the company would almost certainly have involved a lengthy legal case. Since manufacture of 2,4,5–T, of which dioxin is a contaminant, had already stopped at Coalite — indeed everywhere in the UK — the HSE did not consider release of the reports as its first priority, preferring instead to concentrate on current hazards.

The ASTMS document is also critical of the way in which Coalite conducted the studies. There was no properly matched control and not all the exposed workers were included, which means, says ASTMS, that little weight can be attached to the interpretation of the results.

The HSE is a little peeved that ASTMS appears to put the blame for these inadequacies on its shoulders, holding that Coalite must be held responsible. Both ASTMS and the HSE are agreed, however, that further studies need to be done. ASTMS is suggesting that they be carried out independently of Coalite and the advisory service under a joint union-steering committee. The advisory service is however persuading Coalite to re-do the studies, this time under tighter control.

Another specific point which ASTMS takes up is the lack of union participation at two key meetings. One was held last November to discuss the occurrence of chloracne, the disfiguring skin disease caused by dioxin and some other related chemicals, at three companies — Coalite, Stavely Chemicals and Monsanto in South Wales. According to ASTMS, the TUC medical adviser had pressed for union involvement in this meeting throughout 1979, but after some delay the HSE group finally decided that the meeting should be for "doctors only". The second meeting was held on 1 May between the advisory service and the Coalite workforce and management to discuss the preliminary assessment of the studies. ASTMS complains that the first it knew of the meeting was from that day's *Nature*.

All in all, ASTMS now says it has lost confidence in the HSE to make sure that sensible studies on workers are carried out. It asks that the HSE should compile a full report for the unions of the extent of recent contact with chloracnegenic chemicals, that the TUC and the HSE should draw up guidelines for union involvement in future studies of workers and that they should discuss what to do now about Coalite.

In the midst of these specific criticisms, the ASTMS document says that it is important not to lose sight of the most important issue, that of the inherent dangers of dioxin and the herbicide 2,4,5–T. It has now joined the growing group of unions calling for a complete ban on import into and use of the chemical in the UK. The most important thing, says Clive Jenkins, president of ASTMS, is to "get rid of the stuff".

Judy Redfearn

Arctic voyage

Swedes set out

Stockholm

The Swedish icebreaker "Ymer" sailed for the Arctic on 24 June on an expedition which has been delayed for more than a year because of Russian sensitivities about the strategic importance of the Arctic Ocean. When the ship left last week, it carried a team of biologists; it will return later in the summer to pick up a group of earth scientists.

The expedition was originally planned to celebrate the centenary of the first circumnavigation in 1897 of Europe and Asia by the Swedish explorer Adolf Erik Nordenskiöld, who began his voyage by sailing from the Atlantic to the Pacific along the Siberian coast, through the Northwest Passage. The original plan had been to retrace this route as far as the Bering Strait, and then to circumnavigate the Arctic Ocean.

Permission was asked of the Russian authorities to sail along the Siberian coast and to take sediment cores from the continental shelf there. Although the Swedish Prime Minister Fälldin took up the matter with Mr Kosygin, the Russians never replied. Reconciling themselves to Russian views about the strategic importance of the area, the Swedes changed their route.

Under the revised plan, the "Ymer" will sail through the northern Barents Sea, the deep ocean north and northeast of Spitsbergen, the sea between Spitsbergen and Greenland and the waters off northern Greenland, some never sailed before. The research is being financed by the Natural Sciences Research Council, and will involve about 80 scientists from eight countries.

One of the chief objectives will be to tell to what extent the Arctic is polluted. An increase of the lead content of Greenland snow and ferns has been recorded after the introduction of high octane petrol in the USA; but the origins and extent of other pollutants (aerosols, gases and particles) in the Arctic atmosphere, are not known. Atmospheric pollution may however affect the delicate radiation balance of the Arctic, which could in turn affect climate in neighbouring latitudes.

The expedition also plans to investigate the cooling during the Arctic summer of the lower atmosphere under the influence of the ice-pack. The formation of stratus clouds is thought to influence radiation balance and thus the climate.

The Arctic climate is also affected by the movement of huge bodies of water. Large amounts of warm, salty Atlantic water flow north along the west coast of Spitsbergen to the Arctic Ocean, while a mass of cold and less saline Arctic water flows south along the east coast of Greenland. Oceanographers with the expedition will collect information on temperature, salinity and currents down to great depths. They will be able to trace water movements in the Arctic basin by measuring concentrations of radioactive pollutants from the reprocessing plant at Windscale in the UK.

The expedition hopes to be able to determine the extent of the Quaternary ice sheet in the European Arctic. From earlier expeditions to the area, glaciologists think that an earlier Arctic ice sheet reached the Barents Sea, but they have not yet been able to tell whether it was ever joined to the Scandinavian ice sheet.

Wendy Barnaby

0028-0836/80/270007-01$01.00

CORRESPONDENCE

Mr Arthur Frank

Sir, — The implications in Judy Redfearn's article (29 May) must not be allowed to pass unchallenged. I cannot speak for other directors but I trust that you will correct some of the misconceptions in the piece insofar as they may be thought to apply to Mr Frank's relations with the National Army Museum.

Three years ago he presented 80 optical and other instruments used by the British Army. They came free of any charges or conditions. This year the museum again benefited from Mr Frank's generosity when we received another 33 instruments. The second series came with the painless condition that they are on loan until such time as they can be put on display. They will then become the inalienable property of the museum, an invaluable addition to a section of the museum's collections which was extremely weak.

The caption "Arthur Frank with his instruments: gift horse or salesman?" is as unjust as it is clumsy. It is misleading, offensive and unworthy of a journal of the standing rightly enjoyed by *Nature*.

Yours faithfully

William Reid

National Army Museum,
London SW3, UK

Book prices again

Sir,— Dr Brindley (12 June) points out that paperbacks are published, on the average, at less than half the selling price of the cloth edition of the same title. He suggests that publishers of scientific books should make paperbacks more widely available to increase sales and perhaps profits.

The actual difference in cost between producing a paperback and cloth edition is about 65p for a book of 300 pages. What most publishers do is to subsidise the paperback edition by overpricing the cloth edition; this also happens in the pricing of journals where libraries have to pay an inflated rate which subsidises the cost of supplying copies to members. It should be understood, therefore, that where there is a dual edition the paperback is made available to individuals at an artificially low price at the expense of libraries. There is a strong feeling among publishers that this is just as most libraries are still allowing widespread photocopying which must reduce sales.

Yours faithfully,

Robert Campbell

Blackwell Scientific Publications Ltd.,
Oxford, UK

Sir, — The comparison of typical paperback and hardback book prices tabulated by G W Brindley (12 June) is illuminating, but I could hardly disagree more strongly with the conclusion which he draws from these data. The fact that paperback editions are usually much cheaper does not necessarily imply that it would be in the public interest for them to be made yet more widely available. It would surely be infinitely preferable to persuade publishers to adopt a pricing policy which honestly reflected the difference in unit costs (*ca* £1-£3) of the two types of binding.

An alternative way of looking at G W Brindley's figures is to work out, in each case, the publisher's pretended costs incurred in providing hard covers as opposed to paper: the booby prize clearly falls to Elsevier, who seek to extort from the unfortunate purchaser an astounding $45.75, merely for putting covers on their *Practical methods in electron microscopy*, followed by U California Press who price the covers of *Mezozoic mammals* at an almost equally surprising £15.25. It is admittedly unfair to make this sort of comparison without taking proper account of the comparative length, page size, quality and so on of the books in question; but this hardly alters the central conclusion, which is that the alleged cost of hard covers bears remarkably little relation to reality.

The explanation, one is told, lies in the publishers' naive belief that libraries will always purchase hardback editions, virtually regardless of cost, so that profits can supposedly be maximised by raising the hardback prices to increasingly absurd levels. The ordinary reader is then offered an edition identical in every respect except that it is bound between paper covers and carries a rather more realistic price tag. The fact that he or she would often prefer to pay an extra pound or so in order to gain the durability and convenience provided by a hard cover, is conveniently ignored.

There appears to be little justification for this abominable practice, which is a continuing source of despair for bibliophiles and of frustration for practising scientists. It is surely high time that it was brought to an end. Is there really no hope of persuading publishers to move back towards a pricing policy showing some degree of sensitivity towards the interests of ordinary book buyers?

Yours faithfully

P V E McClintock

Physics Department
University of Lancaster, UK

Parkinson extended

Sir, — In his letter "Expanding on Parkinson's law" R. Moss produces the relations $I_{ai} = W^2/A + A$ where I_{ai} is the workload of a single administrator, W is the number of productive workers and A the number of administrators, for the most advanced state of any organisation. He then suggests that this relationship will lead to a limiting ratio of one administrator for each productive worker. Under some conditions, however, the relationship gives rise to a bureaucracy which expands without limit.

The workload of a single administrator, I_{ai}, falls to $2W$ as $A \rightarrow W$ and increases thereafter. If the objective of the chief administrator is to minimise I_{ai} the number of administrators will tend to W, but this will not be the case if instead the chief administrator seeks to increase the number of administrators until some aspiration level O is reached. If O is greater than $2W$, recruitment will slow down before the Moss ratio is reached. If, on the other hand, O is less than $2W$, the individual workload of an administrator will never reach the aspiration level, no matter how many administrators are employed, and recruitment will proceed at an ever more furious pace as more administrators are needed to meet the demands of an ever-increasing workload. Even if the chief administrator does attempt to minimise individual workloads, should the number of administrators ever exceed the number of productive workers the chief administrator will find himself appointing still more administrators in an attempt to regain his previous workloads.

The Moss ratio can thus be envisaged not as a limit on the number of administrators but as an event horizon beyond which a bureaucracy is doomed to expand ever more rapidly in an attempt to cope with the ever-increasing flow of minutes and memoranda generated within its own bounds. Ultimately it is unable to cope even with that function and becomes a veritable black hole of forms and minutes.

Yours faithfully

J.C. Thorpe

Physics Department,
Manchester Polytechnic,
Manchester, UK.

Ethnographic DNA

Sir— Several of the articles in your issue of 26 June note that both confusion and entertainment can be had by considering DNA as selfish, ignorant or, indeed, both. Perhaps these terms are not so much anthromorphic as ethological. Competing DNA molecules are, after all, made up of four main nucleotides, the deoxyribonucleotides of that famous intratribal totem sub-group A,T,C and G. We know from previous analysis of intra-tribal totem preferences that totem clan A is matched by totem clan T, and so is totem clan G with C. Commonly called base-pairing, it is of course fully understood that neither a moral imputation is implied by base, nor sexual by pairing.

We have yet to learn what resources competing DNA molecules had thermodynamically to writhe over, but it may very well be that the totems of A,T,C and G hold secrets. For example, codons with their middle base T preferentially code amino acids with polar side chains, while those with A as centre base in the triplet preferentially code non-polar side-chain amino acids. There appears litle bias towards polar or non-polar by codons with C or G as the triplet centre[1]. Closer inspection reveals that A is replete with two amino groups and T with two hydroxy groups on the base nucleus; G has an amino and a hydroxy, so does C. As Kipling noted, there are 99 ways of making tribal lays — but in this tribe why should a totem of $-NH_2$ mean non polar coding, and -OH polar? What happens to totem loyalties when $-NH_2$ and -OH are paired, in C and G? The strong totem preference is annulled — are we seeing cultural impoverishment by mere group composition?

Since it appears that we have no answers to these questions at the anthropomorphic, ethological or any other level, it may be salutary to recall that molecular biology is about molecules — not selfish this or that. If this trend continues we can expect to see defrocked DNA and rampant tRNA.

Yours faithfully

Anthony Harris

34 Avenue Gardens,
London W3

---

[1] Wolfenden, R.V; Cullis, P.M. & Southgate, C.C.F. *Science*, **206**, 575 (1979).

Conversion courses

Sir, — My attention has been drawn to the reference in Robert Walgate's article on Dr Shallis (7 February) to our conversion course from arts to sciences and to the fact that it has closed. Sadly this is true; it closed seven years ago for lack of applicants. Not all our students were as successful as Mike Shallis, but a number are now active as scientists. We demonstrated that with motivated students it was possible and not too difficult to effect such a conversion, and we gained experience in the ways of doing it and the pitfalls to avoid. Although the course has closed, the experience is still there and available to anyone who wishes to start such a course again. There is surely need for it as long as our schools force children into choices at an age too early for them to know their minds.

Yours faithfully

L R B Elton

University of Surrey,
Guildford, UK

NEWS AND VIEWS

Cell cycle control — both deterministic and probabilistic?

from Paul Nurse

ONE of the basic questions of cell biology is what determines the rate at which cells undergo division. Currently there are two models of cell cycle control which provide answers to this question. The first is the deterministic growth controlled model which developed mainly from experiments with microbial cells, and the second is the transition probability model which developed to explain the behaviour of mammalian cells.

The basic postulate of the growth controlled model is that the rate of division is determined by the rate of growth of the cell[1]. Some cell cycle event cannot take place until the cell has attained a critical cell size, and as a consequence the rate at which cells grow to that size determines the rate at which they divide. The model very simply explains why in steady state populations of exponentially growing cells, size at division remains constant and the rate of division parallels the rate of increase in cell mass. It is further supported by observations that the occurrence of certain cell cycle events, such as the initiation of DNA replication in *Escherichia coli*[2], traverse of 'start' as marked by bud emergence in budding yeast[3], and cell division in fission yeast[4], are well correlated with the attainment of a particular cell size.

In the original form of the Smith and Martin transition probability model, the cell cycle is composed of an A-state and B-phase[5]. In the A-state the cell does not progress towards division but it has a constant transition probability of entering the B-phase. The B-phase is made up of most of the conventional cell cycle and is completed in a constant period of time. Therefore the rate of division is determined by the time a cell takes to undergo the random or probabilistic transition from the A-state and to the complete the constant time period in the B-phase. The main evidence in favour of the model is that the distribution of cell cycle times includes an exponential component which reflects the probabilistic transition from the A-state. This evidence is particularly strong if it is assumed that the B-phase is identical for sister cells, since the differences in cell cycle times between sister cells can be described solely in terms of an exponential[6]. The deterministic or growth controlled model cannot easily explain such a distribution[7], although with further assumptions it can do so (for example see reference 8).

Brooks *et al.*[9] have recently modified the transition probability model to account for the identical B-phase in sister cells, and to deal with the behaviour of cells stimulated from quiescence. In the modified model, cells begin their progress towards division by a random transition from a Q-state to commence a process L. This process takes a constant time period to be completed after which the cell enters the A-state. Exit from the A-state is at random and leads to DNA replication and subsequently cell division, and, in addition, to entry into the next Q-state. In the modified model the time take to complete the two random transitions and constant time period of the sequence Q→L→A determines the rate of cell division. The model explains why the differences in cell cycle times between sister cells can be described solely in terms of an exponential since the Q→L part of the sequence occurs in the mother cell and thus is common to the two sister cells. Consequently the differences between sister cell cycle times are due solely to the random A-transition which results in the exponential distribution. The B-phase does not feature in the modified model, but its duration is equivalent to the Q→L sequence accounting for the identical B-phases of sister cells. The modified model also explains why there were two points of control in stimulated quiescent 3T3 cells[10], since one control was acting at the Q-state transition and the other at the A-state transition. Brooks *et al.*[9] have also suggested that the behaviour of the mitotic centres organising the spindle poles could act as an analogue of the Q→L→A sequence[9]. The initiation of duplication of the centres could correspond to the Q-state transition, their maturation to the L-process, and their separation to the A-state transition. This suggestion is interesting, since centrioles are likely to provide a convenient marker for the behaviour of the less tangible mitotic centres[9], and centrioles or their equivalents have been implicated in cell cycle control of both 3T3 cells[11] and budding yeast cells[12].

Paul Nurse is in the School of Biological Sciences, University of Sussex, UK.

The modified transition probability model is an advance on the original form of the model but suffers from one or two difficulties. In rat hepatoma cells van Wijk *et al.*[13] have found that most of the variability in cell cycle times between sister cells is due to variability in the duration of G_2. This is difficult to reconcile with the A-state transition occurring before S-phase. In addition, the duration of the B-phase (equivalent to the Q→L sequence) is more similar for cells of rat hepatoma which share a common grandmother (cousins), than for unrelated cells[14]. The modified transition probability model predicts that sister cells should have identical B-phases, but that cousin cells should be as dissimilar as any pair of unrelated cells within the population. Finally, centriolar behaviour may not be such a good analogue of the Q→L→A sequence, since the model predicts that quiescent cells in the Q-state should only have a single centriole, whereas Tucker and Pardee[11] have shown that 3T3 cells in such a state have a pair of centrioles.

The deterministic growth controlled model and the transition probability model give apparently different answers to the question of what determines the rate at which cells divide. One explanation for this may be that the cell cycle controls are quite different for microbial and mammalian cells. However, some experiments suggest that this may not be the case. The rate of bud emergence has been followed in cells of

0028-0836/80/270009-02$01.00

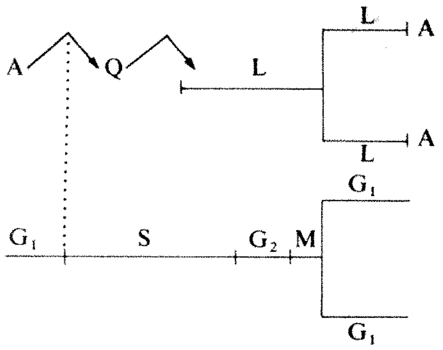

After an indeterminate period of time in the A state, a cell makes the transition to the Q state and at the same time starts synthesizing DNA (S phase). The cell remains in Q for an indeterminate period before making the transition to L. If the transition occurs during S (as shown here) or G_2, the L state, which has a fixed time span, will last until after mitosis (M) and division. Therefore both sister cells will start their own A state simultaneously.

budding yeast that have been released from a block at 'start'[13]. The distribution of times to bud-emergence within the population includes an exponential component as would be expected from the transition probability model. To explain this observation and the cell size correlation with bud-emergence mentioned above, Shilo *et al.*[15] suggested that traverse of 'start' requires growth of the cell to a critical size followed by a random transition which 'started' the cell cycle. A rather similar conclusion has been arrived at by Shields *et al.*[16] from investigations of the role of cell size on cell cycle time in mouse fibroblasts. Quiescent small cells take longer to enter S-phase than do large ones, and cells born of small mother cells have longer cell cycle times than those derived from larger mothers. The distributions of the times required before S-phase and cell division took place were found to include exponential components. The authors proposed that cell size affects the length of the B-phase acting before G_1, and within the framework of the modified transition probability model, that cell size affects the length of the L-process[7]. These experiments are suggestive that there is a size related element and a probabilistic element in the cell cycle control of both microbial and mammalian cells. Therefore it is possible that the deterministic and probabilistic models are describing different aspects of a single cell cycle control. In microbial cells the probabilistic transition occurs very rapidly, and the deterministic size element is more important in controlling the rate of division. In mammalian cells the probabilistic transition is much slower, and the deterministic size element is of less importance in controlling the rate of division.

In this context it is of interest that some mechanisms for monitoring cell size and controlling the cell cycle include both deterministic and probabilistic elements[17]. For example, in one mechanism a structure is built up at a rate proportional to the size of the cell. Smaller cells will build up the structure slower than larger ones and consequently cells will tend to complete the structure at the same cell size. This is the deterministic size related element of the mechanism. Once completed, the structure then has to interact with some site within the cell to become active. Since there is only a single copy of the structure its interaction with the site will be a random process and forms the probabilistic element in the control. If the building of the structure takes a long time then the control will appear deterministic and size related as in microbial cells, and if the interaction between the structure and site takes a long time then the control will appear probabilistic as in mammalian cells.

The possibility that the deterministic and probabilistic models describe different aspects of a single cell cycle control common to both microbial and mammalian cells, and that both aspects are important for determining the rate of division is at present based on few experiments. What is required are more kinetic investigations of the distributions of cell cycle times coupled with measurements of cell size. It would also be of interest to follow the behaviour of centrioles or their equivalent in the same experiments, to see if a firmer link can be established between these structures and the more abstract elements of the cell cycle control models. □

---

1. Koch, A.L. & Schaechter, M. *J. Gen. Micro.* **29**, 435 (1962).
2. Donachie, W.D. *Nature* **219**, 1077 (1968).
3. Johnston, G., Pringle, S. & Hartwell, L. *Expl. Cell. Res.* **105**, 79 (1977).
4. Fantes, P. *J. Cell Sci.* **24**, 51 (1977). Miyata, H., Miyata, M. & Ito, M. *Cell Structure & Function* **3**, 39 (1973).
5. Smith, J.A. & Martin, L. *Proc. natn. Acad. Sci. U.S.A.* **70**, 1263 (1973).
6. Minor, P.S. & Smith, J.A. *Nature* **248**, 241 (1974).
7. Brooks, R.F. In *Cell Cycle, (C.U.P. in the press).*
8. Koch, A.L. *Nature* **85**, 80 (1980).
9. Brooks, R.F. *Nature* **260**, 248 (1976).
10. Brooks, R.F. *Nature* **260**, 248 (1976).
11. Tucker, R.W. & Pardee, A.B. *Cell* **17**, 527 (1979).
12. Byers, B. & Goetsch, L. *J. Bact.* **124**, 511 (1975).
13. van Wijk, R., van de Poll, K., Amesz, W. & Geilenkirchen, W. *Expl. Cell. Res.* **109**, 371 (1977).
14. van Wijk R. & van de Poll, K. *Cell Tis. Kinet.* **12**, 659 (1979).
15. Shilo, B., Shilo, V. & Simchen, G. *Nature* **264**, 767 (1976).
16. Shields, R., Brooks, R.F., Riddle, P.N., Capellaro, D.F. & Delia, D. *Cell* **15**, 469 (1978).
17. Fantes, P. & Nurse, P. In *Cell Cycle* (C.U.P. in the press).

Can comets become asteroids?

from David W. Hughes

COMETARY nuclei, kilometric sized dirty snowballs, obviously evolve as the comets age. At each perihelion passage the nucleus will lose about a metre or so of dust and ice, producing the coma and the tail and also a large collection of meteoroids which feed the meteor stream. This process can continue until the nucleus has completely disintegrated into gas and dust but there are other possibilities. The nucleus could disrupt into a number of boulders which quickly outgas. The core of the nucleus could be slightly more compact than the outer regions and could remain when all the ice has sublimated. Or an insulating crust could develop which reduces the heat flow in towards the centre of the nucleus and thus stops the sublimation and the loss of volatiles. The last two possibilities lead to an apparent transformation of the comet into an asteroid. The Solar System would then contain active comets, asteroids and a third class of objects, extinct cometary nuclei which looks like asteroids but have the orbits of comets.

The problems of this evolutionary transformation have been discussed recently in two papers published in *The Moon and the Planets*. These are by Ľubor Kresák of the Astronomical Institute of the Slovak Academy of Science, Bratislava (**22**, 83; 1980) and H. Rickman, Astronomical Observatory, Uppsala, Sweden and C. Froeschlé, The Nice Observatory, France (**22**, 125; 1980).

Kresák stresses the role of Jupiter. The mean of the asteroidal orbits has the same eccentricity and orientation as the orbit of Jupiter. Also there is a spherical region around Jupiter of at least 1 AU in radius which is completely void of asteroids. The system of short period comets on the other hand is aligned with the line of apsides of the jovian orbit and the immediate environment of Jupiter is filled with an overabundance of comets some of which even become jovian satellites for a time. Added to this fundamental difference in orbital characteristics is the problem of observational selection. In the case of comets we are dealing with a class of objects which have a potential lifetime very much shorter than the age of the Solar System. So the comets that *are* observed today are either the last, abnormally long lived survivors of a much more abundant original population or they must be a late generation of an evolutionary sequence.

The first of these hypotheses is unlikely. The second implies that we are observing an evolved state of equilibrium between source and sink and consequentially short lived objects are underrepresented.

It would also be very presumptious of us to believe that all the types of asteroids and comets have been discovered. For example, asteroids were known for over a century before the Trojans (which follow Jupiter's orbit and have a mean elongation of 60° ahead and behind Jupiter) and the Apollo's (perihelian distance less than 1 AU) were

---

David W. Hughes is in the Department of Physics, University of Sheffield.

0028-0836/80/270010-02$01.00

discovered. In the last few years certain new classes of objects have been found, one with inclinations over 60°, another with periods less than a year. Chiron (asteroid number 2060) has an orbit between the orbits of Saturn and Uranus and considering the immense effect of distance dependent observational selection it is difficult to tell how many others there are in Chiron's class. One asteroid 1978 SB has been found to have an orbit similar to that of Comet Encke.

Observational bias is even stronger for comets because the brightness decreases drastically with heliocentric distance. Comets can only be seen if they get close enough to the Sun to display outgassing phenomena and to do this they have to get to within 0.0001 of the radius of the distant cometary reservoir known as the Oort cloud. Even considering temporal variations it is interesting to note that dependable astronomical observations have only been going on for about one ten-thousandth the average revolution period of a 'new' comet. At best we can only have seen 0.00001% of the whole comet population. A great number of long period comets must exist with perihelia beyond the orbit of Jupiter. Only five have been discovered so far, the first in 1974.

Even bearing these problems in mind Kresák concludes that very few of the asteroids could have been comets and none have been definitely identified as such. There are only two possible paths between the two orbital classes. Both require a complicated sequence of planetary capture by Jupiter or Saturn followed by strong non-gravitational forces to vary the aphelion distance thus pulling the comet away from Jupiter or Saturn into a more stable orbit undisturbed by planetary encounters. On attaining this stable orbit the non-gravitational forces have to cease.

The possible (even if non probable) ex-comets among the asteroids are Chiron, Hidalgo, Thule, members of the Trojan, Hilda and Grigua groups and the Apollo and Amor objects (the Amor's have perihelia between the orbits of Earth and Mars).

Rickman and Froeschlé specifically discuss the possible cometary contribution to the Apollo-Amor population. In 1963 Öpik suggested (*Adv. Astron. Astrophys.*, **2**, 219) that the perturbations of Mars on the inner boundary of the asteroid belt were too weak to account for the observed numbers of Apollo and Amor asteroids. A cometary origin was thus proposed for most of them. Rickman and Froeschlé consider the steady state where all the Jupiter family of comets (aphelion distances between 4 and 8 AU) is a possible source, this family being fed by capture and depleted by deactivation. The deactivated comets are also in a steady state, their loss mechanism being expulsion from the inner solar system by Jovian perturbation. The number of Mars crossing deactivated comets is estimated by means of a Monte Carlo simulation of the orbital evolution of the Jupiter family under the influence of Jovian pertubations.

The authors conclude that no more than five percent of the short period comets can develop orbitally into Apollo-Amor asteroids after loosing their activity. Also no more than five percent of the nuclei of comets can contain sizeable asteroidal cores.

So even bearing in mind the problems of observational selection it seems that comets are comets and asteroids are asteroids. Even though it is possible in rare cases to perturb a comet's orbit into an orbit similar to that of an asteroid, there are no obvious dead comets amongst the asteroid population. This seems to favour the hypothesis that comets do not have asteroidal cores and decay completely into meteor streams. □

The strong coupling constant is measured

from Mary K. Gaillard

THE initial evidence for hard gluon radiation by quarks came from the high energy electron-positron annihilation data of PETRA (*Nature* **281**, 104; 1979). The continued accumulation of data has permitted quantitative measurements of this process, thus providing a direct determination of the strong coupling constant. In analogy with electric charge (which determines the interaction between electrons and photons), this constant determines the interaction between quarks and gluons.

According to the widely accepted quantum chromodynamic (QCD) theory of the strong forces, the dominant mechanism for hadron production is via quark-antiquark pair creation (Fig. 1a):

$$e^+e^- \rightarrow \text{virtual photon } (\gamma) \rightarrow \bar{q}q$$

However since quarks carry color charge they can radiate gluons, i.e. quanta of the color field. This is completely analogous to the well established quantum electrodynamic (QED) theory of electromagnetic forces where, e.g., the primary mechanism for μ-pair production

$$e^+e^- \rightarrow \text{virtual photon} \rightarrow \mu^+\mu^-$$

is dressed by photon radiation. The difference is that while photons and leptons can be detected in the laboratory, quarks and gluons materialize as clusters ('jets') of hadrons, and sophisticated analyses must be performed in order to uncover the elementary QCD processes underlying what is actually observed.

The dominant component of gluon (or photon) radiation is soft or collinear with the quarks and its effects are submerged by the (so far) uncalculable angular spread inherent to the confinement mechanism governing the conversion of a quark or gluon into a jet of hadrons. Therefore most events should appear as two back-to-back jets (Fig. 1b), and this is indeed what was inferred from analyses of event configurations at SLAC several years ago, and directly observed more recently at PETRA where the higher energies produced jets sufficiently collimated to be recognized as such at a glance. Again there is an analogy with QED, where the dominant, very soft or collinear, component of photon radiation escapes detection through an inherent limit on measurement precision — except that for QCD the limiting precision is furnished by the dynamical effects of confinement.

However, sometimes in QED hard, large angle photons are emitted, but with emission rates suppressed by a factor of the fine structure constant $\alpha = e^2/4\pi$ for each such photon. In the same way, hard large angle gluons should be radiated by quarks with a suppression factor per gluon given by the strong coupling constant $\alpha_s = g_s^2/4\pi$, which is believed to be smaller than one. Therefore one expects some fraction of events to appear as three distinct jets of hadrons, a smaller fraction as four jets, and so on. Only at very high energies where jets are highly collimated can one hope to seperate visually the clusters of hadrons in a multi-jet event, and the first three jet event, presented by the TASSO collaboration at the Bergen neutrino conference in June 1979, was obtained at a center-of-mass energy of about 30 GeV. A statistically significant sample of three jet events was presented by the TASSO group at the EPS conference in Geneva. By the Fermilab conference in August, the PLUTO and JADE groups had collected samples of three jet events where neutral as well as charged hadrons were measured, and the MARK J group also presented evidence for gluon radiation.

The relative production rate for three jet events provides a direct measure of the strong coupling constant α_s. Previous determinations of α_s were based primarily on the analysis of highly inelastic lepton-nucleon interactions where the dependence of observed phenomena on the strong coupling constant is considerably more

Mary K. Gaillard is in the Laboratoire d'Annecy le-Vieux de Physique des Particules, France.

0028-0836/80/270011-02$01.00

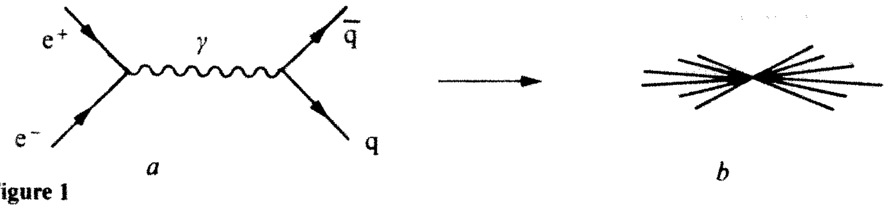

Figure 1

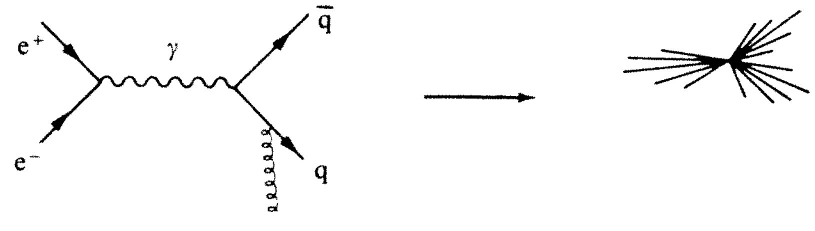

Figure 2

subtle. The method has been somewhat controversial as it requires measurements over a large energy range, including lower energies where the interpretation of the theory is somewhat problematic. On the other hand, a measurement of the rate for radiation of hard wide angle gluons at high energies is in principle straightforward and its interpretation is intuitively simple. However, a meaningful measurement of α_s requires substantial statistics, and since gluon (like photon) radiation prefers collinearity, even large angle radiation will most often produce events intermediate between Figs 1b and 2b, with two jets merged to form a single broadened jet.

The first task of the experimenters was to convince themselves that the collection of phenomena characterizing deviations from the two jet process of Fig. 1 could indeed be attributed to hard gluon radiation. There are various tests of this hypothesis, among them: a) the rate of jet broadening with increasing center-of-mass energy; b) coplanarity (up to the limited jet spread due to confinement effects) of the final state hadrons which are supposed to arise from a primitive 3-quanta final state; c) asymmetric jet broadening — since the dominant deviation from two jet events is a single hard gluon emission, only one quark jet, the one with an accompanying gluon, should appear broadened. All four groups from PETRA presented analyses supporting these features at the Fermilab conference in August.

Since then more data has been taken, providing sufficient statistics for the first quantitative analyses published by the MARK J and JADE groups. The analysis of the MARK J group, based on the angular pattern of energy flow, rather than on an event by event reconstruction of jets, showed a statistically significant excess of oblate planar events which, when projected on the event plane and oriented so as to align the axes of maximum energy flow, displayed a three lobed structure which reproduced the "antenna pattern" expected from single hard gluon radiation. From the size of the effect they reported the first evaluation of α_s based on gluon radiation. This was soon followed by a value quoted by the JADE group based on detailed analysis of event shapes. More recently the TASSO group has extracted a value for α_s from a careful study of event topologies including various checks that their result is insensitive to the uncalculable confinement effects. The result of these analyses are consistent within their estimated errors of 20% or so and yield a value for α_s of about 1/5.

What does this number mean? Even without the complications of confinement effects which arise in QCD, one never really measures a fixed coupling constant, but rather the effective strength of some coupling among field quanta of specified energy and momenta. One then extracts a momentum dependent effective coupling; the momentum dependence reflects the effects of a higher order 'dressing' of the coupling through the exchange of virtual quanta. In QED these effects are tiny because the coupling is very weak, but in QCD they are appreciable, albeit calculable. A value $\alpha_s \simeq 0.2$ for processes characterized by the PETRA energies where gluon radiation has been measured is quite consistent with expectations based on analyses of lepton-nucleon interactions mentioned earlier. More theoretical work, specifically addressed to higher order effects in electron-positron annihilation into hadrons, as well as more experimental work, allowing a determination of the momentum dependence of hard gluon radiation, are still needed for precision tests of the theory. Further studies are also needed to pin down the spin of the gluon and to measure the self-coupling of three gluons, a predicted feature of QCD which has no analogue in QED. ☐

Extra-pituitary actions of LHRH and its agonists

from Richard M. Sharpe

SINCE the origination of the concept of hypothalamic control of the anterior pituitary gland, it has been an accepted dogma of endocrinology that the releasing factors from the hypothalamus act solely on the pituitary to regulate the release of the appropriate trophic hormone. The vast number of animal experiments and clinical studies with LHRH since its structural characterization 9 years ago, have consolidated this belief. Now, a spate of recent results appears to have demolished this idea by demonstrating extra-pituitary inhibitory effects of LHRH or its agonistic analogues. The latter are considerably more potent *in vivo* that native LHRH, principally because of their resistance to enzymatic breakdown (Clayton *et al. Endocrinology* **104**, 1484; 1979), and this has been an important factor in permitting the demonstration of peripheral sites of LHRH action.

There have been numerous reports in the last 3 years demonstrating inhibitory effects of LHRH and its agonists on gonadal growth and function in intact animals, and LHRH agonists have exciting potential as new contraceptive methods in women, as luteolytic agents (Casper & Yen *Science* **205**, 408; 1979; Lemay *et al. Fertil. Steril.* **32**, 646; 1979) or, more probably, as inhibitors of ovulation (Bergquist *et al., Lancet*, **ii**, 215; 1979). As it was already established that similar 'down-regulatory' effects could be achieved by overstimulation of the gonads with exogenous gonadotrophins (see Catt *et al. Nature* **280**, 109; 1979), it was thought logical that LHRH and its agonists exerted their inhibitory effects via the pituitary.

But in fact, there was already published evidence to show that LHRH agonists could have extra-pituitary effects, as Rippel and Johnson (*Proc. Soc. Exp. Biol. Med.* **152**, 432, 1976) had reported inhibition by an LHRH agonist of human chorionic gonadotrophin (hCG)-induced ovarian and uterine weight gain in hypophysectomized rats. This brief challenge to one of the bastions of endocrinological thinking seems to have gone largely unnoticed. But in 1979 the walls began to crumble when Hsueh and Erickson demonstrated inhibition by LHRH of the follicle-stimulating hormone (FSH)-induced increase in oestrogen and progesterone secretion by rat ovarian granulosa cells *in vitro* (*Science* **204**, 854, 1979), and followed this with a similar report concerning the male (*Nature* **281**, 66; 1979). In this they showed that concomitant treatment of hypophysectomized immature male rats with FSH and

---

Richard M. Sharpe is a Research Scientist in the MRC Reproductive Biology Unit, Edinburgh.

0028-0836/80/270012-03$01.00

LHRH agonist prevented the increases in testicular weight, LH-receptor numbers and steroidogenic responsiveness induced by the FSH treatment alone.

Confirmation of the extra-pituitary actions of LHRH and its agonists has been readily forthcoming. Ying and Guillemin (*Nature* **280**, 593; 1979) demonstrated a dose-dependent inhibitory effect of an LHRH agonist on gonadotrophin-induced ovarian weight gain in hypophysectomized female rats and also prevented ovulation, findings which a smaller study by Mayar *et al.* (*Proc. Soc. Exp. Biol. Med.* **161**, 216; 1979) confirmed. A preliminary report also suggests that LHRH agonists may directly influence ovum development following induction of super-ovulation (Erickson & Hsueh, *U.S.A. Soc. Gynec. Invest.* Abstract 371; 1980). In the male, Arimura and colleagues have shown that treatment with an LHRH agonist can reduce LH-receptor numbers in the testes of both immature and adult hypophysectomized rats (*Biochem. Biophys. Res. Commun.* **90**, 687; 1979). Outside of the gonads, inhibition by LHRH of progesterone production by human placental tissue *in vitro* has been reported (Wilson & Jawad *Fertil Steril.* **33**, 91; 1980), and preliminary work in baboons by McRae, Vickery and Stevens (*Endocrinology* Supp. in the press), suggests that LHRH agonists can suppress chorionic gonadotrophin secretion by the placenta. However, such effects may not be straightforward, as LHRH agonists do not impair the placental secretion of hCG and progesterone *in vivo* in women (Casper *et al. Proc. of P.A.R.F.R. Workshop on Fertility Regulation* Harper & Row; 1980). Gonadal or placental effects of LHRH are presumably important in explaining the local abortifacient action of LHRH on the pregnant rat uterus (Jones *Contraception* **20**, 569; 1979) and the termination by LHRH of pregnancy in rats hypophysectomized on day 12 (Bex & Corbin *61st. Endocr. Soc. Meeting, U.S.A.* Abstract 435; 1979).

The two most impressive aspects of the above findings are, firstly, that all but one of the extra-pituitary effects of LHRH and its agonists are inhibitory and, secondly, that the effects (particularly those on the gonads) are almost identical to those reported following similar treatment of intact animals. This raises the question as to whether all of the inhibitory effects of LHRH agonists in intact animals, including the contraceptive effects in women, are the result of extra-pituitary action? Although any answer must at this stage be qualified, the weight of evidence suggests this is not the case. To obtain the direct gonadal effects reported above, the investigators have used doses of LHRH agonists at least 10-times and, in most cases, over 1,000-times greater than those used in intact animals. Moreover, the direct effects reported have often been the inhibition of rather specialised changes which may not be directly relevant to the intact adult animal. Thus the acute steroidogenic responsiveness *in vitro* of Leydig cells from untreated rats is unaffected by LHRH or its agonists (Badger *et al. Endocrinology* **106**, 1149; 1980), although Clayton and colleagues (*Nature* **282**, 90; 1980) found a small decrease in the sensitivity of rat luteal cells to hCG-stimulation *in vitro* in the presence of 10^{-7}M LHRH agonist.

However, there is the very real possibility that some proportion of the inhibitory effects of LHRH and its agonists in intact animals is the result of extra-pituitary action. Indeed, the recent demonstration of specific, high affinity ($K_A = 10^9 M^{-1}$) receptors for LHRH and its agonists on luteal cells in the ovary (see last ref. above), and on Leydig cells in the testis (Labrie *et al. Int. J. Fertil.* in the press; Sharpe & Fraser *Biochem. biophys. Res. Commun.* in the press), must mean that LHRH has some role to play at the gonadal level, particularly as these receptors have almost identical properties to LHRH receptors in the pituitary (see Clayton *et al. Endocrinology* **105**, 1369; 1979). There is also persuasive evidence that the direct effects of LHRH agonists on the gonads are mediated through such receptors, as Hsueh and Erickson (*Life Sci.* **25**, 1223; 1979) have shown that the inhibitory effects of LHRH agonists *in vitro* can be prevented in a dose-dependent manner by a structurally similar, but antagonistic, analogue of LHRH. There is also immunohistochemical evidence for LHRH receptors in mouse adrenal cells (Bernardo *et al. J. Histochem. Cytochem.* **26**, 613; 1978).

Because of the specialized portal blood system, which transports LHRH from the hypothalamus to the pituitary, and because of the rapid degradation of LHRH, it seems certain that LHRH secreted from hypothalamic neurones can never reach peripheral tissues in effective concentrations. Are there, therefore, extra-hypothalamic sites of LHRH production? Two pieces of information suggest that there are. First, there is some evidence for the placental production of LHRH (Khodr & Siler-Khodr *Science* **207**, 315; 1980), and secondly, Guillemin and colleagues

---

NATURE

100 years ago

The *Times* Geneva correspondent writes under date June 20 that a remarkable electrical phenomenon occured at Clarens on the afternoon of Thursday last. Heavy masses of rain-cloud hid from view the mountains which separate Fribourg from Montreux, but their summits were from time to time lit up by vivid flashes of lightning, and a heavy thunderstorm seemed to be raging in the valleys of the Avants and the Alliaz. No rain was falling near the lake, and the storm still appeared far off, when a tremendous peal of thunder shook the houses of Clarens and Tavel to their foundations. At the same instant a magnificent cherry-tree near the cemetery, measuring a metre in circumference, was struck by lightning. Some people who were working in a vineyard hard by saw the electric "fluid" play about a little girl who had been gathering cherries and was already 30 paces from the tree. She was literally folded in a sheet of fire. The vine-dressers fled in terror from the spot. In the cemetery six persons, separated into three groups, none of them within 250 paces of the cherry-tree, were enveloped in a luminous cloud. They felt as if they were being struck in the face with hailstones of fine gravel, and when they touched each other sparks of electricty passed from their finger-ends. At the same time a column of fire was seen to descend in the direction of Chatelard, and it is averred that the electric fluid could be distinctly heard as it ran from point to point of the iron railing of a vault in the cemetery. The strangest part of the story is that neither the little girl, the people in the cemetery, nor the vine-dressers appear to have been hurt; the only inconvenience complained of being an unpleasant sensation in the joints, as if they had been violently twisted, a sensation which was felt with more or less acuteness for a few hours after. The explanation of this phenomenon is probably to be found in Prof. Colladon's theory of the way in which lightning descends, as described in Nature, vol. xxii. p.65. The Professor contends that it falls in a shower, not in a perpendicular flash, and that it runs along branches of trees until it is all gathered in the trunk, which is bursts or tears open in its effort to reach the ground. In the instance in question the trunk of the cherry-tree is as completely shivered as if it had been exploded by a charge of dynamite.

Amongst the peculiar institutions of Paris are the street astronomers, who exhibit through their telescopes the moon, sun-spots, comets' tails, and other celestial objects, according to circumstances. Their charges vary from 1*d*. in the suburbs to 5*d*. on the Place de la Concorde or the Place Vendôme, where the instruments are not unworthy of a regular observatory. At the last monthly meeting of the scientific journalists M. Flammarion read an address sent to him by the corporation of these itinerant teachers of the marvels of the heavens. They state that from the beginning of the publication of the "Astronomie Populaire" the number of their customers has more than doubled.
from *Nature* **22**, 1 July, 1980.

0028-0836/80/270013-01$01.00

(*Comptes Rendus* **D289**, 943; 1979; *Endocrinology* **106**, 114A; 1980) have identified a substance which is immunologically distinct from LHRH but has LHRH-like biological activity and is secreted by ovarian granulosa cell cultures and is present *in vivo* in follicular fluid.

The endocrine dogma concerning LHRH-like biological activity and is hypothalamic LHRH-producing neurones as unique and to view the portal blood supply as an insurance that LHRH reaches the pituitary without dilution in the peripheral circulation. The same was originally thought for somatostatin, which is also produced by hypothalamic neurones and acts on the pituitary, but is now known to be produced in the gut and elsewhere. It is therefore not too wild a speculation to consider LHRH as a 'transmitter' produced by nerve endings or other cells in the gonads or elsewhere. Certainly, if one accepts this possibility then the role of the portal blood system and the rapid degradation of LHRH by the pituitary can be viewed not only as an efficient local transport system, but also as a means of preventing hypothalamic LHRH from reaching peripheral target tissues.

It seems appropriate to end on another note of speculation. Before the advent of the enzymically-resistant LHRH agonists, binding studies with LHRH were plagued by hormone degradation problems, but there were at least two reports of extra-pituitary binding sites specific for LHRH (Marshall *et al. Clin. Endocr.* **5**, 671; 1976 and Heber *et al. Amer. J. Physiol.* **235**, E227; 1978), which were dismissed as unimportant because of their low affinity ($K_A = 10^5 M^{-1}$). These sites included the ovary and testis, which we now know to contain high affinity receptors for LHRH. Can we therefore expect that the other tissues identified (liver, spleen, renal cortex, cerebral cortex, lung) will also prove to have high affinity receptors for LHRH and its agonists? □

How does the mantle move?

from Geoffrey F. Davies

WHEN the kinematic theory of plate tectonics was developed over a decade ago, two kinds of questions were posed. The first kind concerned the implications of moving plates of lithosphere for geological processes and for the interpretation of the geological record. The second kind of question concerned the involvement of the underlying mantle and the dynamics of the plate mantle system: how much of the mantle is involved, what is the pattern of flow in the mantle, and which of several possible types of driving buoyancy forces are dominant? Although many parts of the system are now more clearly understood, the way in which they fit together into a working machine is still unclear. This is only partly because of the inaccessibility of the mantle to direct observation: it is also because of the extremes of mechanical and thermal states in the plate-mantle system, which pose a considerable challenge to would-be modelers of the system. Some of the current attempts being made to understand the system were illustrated by papers presented at a recent conference*.

It is usually presumed that the plates and underlying mantle comprise a thermally convecting system driven by the earth's internal radiogenic heat, but mantle convection is very different from the more familiar examples of convection in the atmosphere or laboratory. This is because the mantle has a very high Prandtl number (so that viscous forces dominate over inertial forces) and its rheology is complex. The stress-strain rate relation of mantle minerals is strongly dependent on temperature, and is strongly non-linear at high stresses; also, high stress at low temperatures can cause fracturing which will be observed as earthquakes. The Rayleigh number of the mantle is variously estimated to be between one million and one thousand million, which implies that temperature gradients are very large, notably near the top boundary. Combining the steep temperature gradient near the earth's surface with the temperature dependence of the rheology, one gets a picture of the lithosphere as a thermal boundary layer which is also a mechanical boundary layer: cold and therefore stronger, but also brittle. This rapid variation of temperature and mechanical properties in the lithosphere is an obstacle to finite-difference numerical modeling, since a prohibitive number of grid points is required. Also, the rheology of this lithosphere is not easily characterized in a manageable way. For example, simply increasing the viscosity in the lithosphere works for those parts of plates away from plate boundaries, but not near subduction zones, since brittle or quasi-plastic yielding may allow the large deformations associated with bending and subducting the lithosphere to occur at much lower stresses than would be predicted by a viscous rheology. Much of the recent work on plate-mantle dynamics has focussed on the lithosphere, either exploring and characterizing its rheology, or taking advantage of the order it imposes by being rigid most of the time.

The rheology of the lithosphere can be studied by using the constraints of bathymetric, gravity and geoid anomalies near subduction zones and volcanic seamounts. Models have evolved through simple elastic and viscous lithospheres to composites involving elastic-perfectly plastic or more complex rheologies. J. H. Bodine and A. B. Watts of Columbia University presented results showing that the current subsidence of Hawaii relative to Oahu at the rate of 4.1 mm per yr can be explained as a delayed response of the lithosphere to the load imposed by Kohala volcano on Hawaii, which was active until about 0.4 Myr ago. In their model, the initial response of the lithosphere is that of a thick elastic layer, but on longer time scales (a million years or more) the lower, hotter part of the lithosphere deforms, allowing stress relaxation. The result is that after a million years or so the effective elastic thickness of the lithosphere is two or three times less than the initial affective thickness. A. Cazenave and B. Lago of Toulouse presented results of analogous models incorporating plastic or semi-empirical rheologies, and they predict that the relaxation time of the lithosphere is about five percent of the age of the lithosphere at the time it was loaded. A. B. Watts reviewed analyses of gravity and bathymetric anomalies by himself and his colleagues showing that the long-term effective elastic thickness of the lithosphere is a strong function of the age of the lithosphere at the time of loading. The results are consistent with the elastic thickness being proportional to the square-root of age, as is predicted by a simple cooling half-space model of the lithosphere. The same conclusion was reached by analysis of geoid anomalies derived from the GEOS 3 and SEASAT radar altimeters (M. C. Roufousse, Smithsonian Astrophysical Observatory, Cambridge).

Although the lithosphere is difficult to incorporate into mantle convection models, its role as a rigid mechanical and thermal boundary layer has been exploited in several ways. P. Olson of Johns Hopkins University presented a generalization to spherical geometry of a boundary layer theory first applied to the mantle (Turcotte & Oxburgh *J. Fluid. Mech.* **28**, 29; 1967). Such a theory is ideally valid in the limit of high Rayleigh number, when the interior of the fluid is nearly isothermal and temperature gradients are concentrated in thin thermal boundary layers. Olson concluded that realistic surface velocities of several centimeters per year could be attained if convection was allowed to extend throughout the mantle (down to about half of the earth's radius), but could not if convection was confined to the upper 700 km of the mantle. However, Olson's models did not include a realistic lithosphere rheology, so this conclusion should probably be regarded as tentative at this stage.

Olson and several other speakers were concerned with testing a semi-empirical relation, based on laboratory and numerical experiments and on boundary layer theory, which states that the Nusselt number is proporational to the Rayleigh number to a small power, usually between

Geoffrey F. Davies is in the Department of Earth & Planetary Sciences and McDonnell Center for Space Sciences, Washington University, St. Louis, Missouri.

---

*The joint Spring Meeting of the American Geophysical Union and several Canadian Geophysical Societies was held in Toronto.

0028-0836/80/270014-02$01.00

one-fifth and one-third. The Nusselt number measures the efficiency of convective heat transport, and the relation has been applied to calculating thermal histories of planets (eg. Sharpe & Peltier *Geophys. J. R. astr. Soc.* **39**, 171; 1979; Reynolds & Cassen *Geophys. Res. Lett.* **6**, 121; 1979). E. R. Ivins and R. J. Phillips of the Jet Propulsion Laboratory, Pasadena, reported on numerical models with temperature-dependent viscosity in which the Nusselt number was systematically lower than in analogous constant viscosity cases. Again, their results may have been affected by an oversimplified lithospheric rheology, which did not include any stress dependence. E. M. Parmentier and J. Morgan, III of Brown University reported on numerical models which did include a moderately stress-dependent rheology. Their results implied that an initially hot, radioactively heated planet would approach a steady state about twice as fast as in the case of a stress-independent rheology, presumably because the larger buoyancy forces associated with higher temperatures would see a lower effective viscosity.

R. A. Lux and I. S. Sacks of the Carnegie Institution of Washington were concerned with the bottom boundary of the mantle, where seismologists have long suspected a layer of irregularities one or two hundred kilometers thick. If there is significant heat flow from the core, then one would expect a boundary layer at the bottom of the mantle complementary to the lithosphere at the top: the bottom layer would have higher temperatures and lower viscosities. One might further expect such a layer to be subject to strong Rayleigh-Taylor instabilities, which might then be the source of the seismic heterogeneities. Lux and Sacks presented results of numerical models which showed that the lower viscosities in the boundary layer allow faster horizontal flow, and the resulting larger velocity gradients actually stabilize the layer, at least in their two-dimensional models. If the instability occurred, it would have to be in the form of rolls or sheets aligned with the flow.

The usefulness and versatility of the rigid boundary layer concept of plates was further illustrated by R. J. O'Connell of Harvard University and B. H. Hager of the State University of New York at Stony Brook, who used it to investigate the chemical stratification of the mantle and the effect of plate motions on sea level. In a joint paper, O'Connell and Hager noted that the migration velocities of ridges and trenches are not negligible compared with expected mantle flow velocities. A consequence is that as trenches and ridges sweep around the globe, upper mantle material may be sampled more often than lower mantle material: roughly speaking, material recently subducted at a trench may be pulled back up by a passing ridge before it sinks to great depth. Thus a purely kinematic aspect of the plate-mantle system may give rise to a chemical gradation of the mantle, in which the shallower mantle is, on average, more strongly depleted in the incompatible elements which accumulate in continental crust.

Hager gave a new twist to an old problem by suggesting that changes in sea level relative to continents depend mainly on whether subducted lithosphere descends under continent or under ocean. Both the thermal contraction associated with the cold lithosphere and the deviatoric stresses transmitted from a sinking plate to the surface tend to lower the earth's surface above the plate. Thus subduction under continent would result in transgression and subduction under ocean would lead to regression. Hager estimated that the magnitude of this effect is considerably larger than that produced by changes in the volume of ridge systems (and hence of ocean basin volumes) resulting from changes in plate velocities. □

MHC restriction, self-tolerance and the thymus

from Jonathan Howard

THE phrase 'MHC restriction' was originally coined to describe a property of cytotoxic T lymphocytes, cells of the specific immune system which kill virus infected cells by a process involving direct membrane contact between the two cells. Specific receptors on the cytotoxic cell surface recognize and bind to virus-specific antigens on the membrane of the infected target cell. By an unknown mechanism this close contact results in lysis of the target. Oddly, however, the virus-specific antigens are not sufficient for the binding of cytotoxic cells: membrane molecules specified by the major histocompatibility complex (MHC) of the target cell are involved in the binding so intimately that they may be regarded as forming a component of the antigens recognized. In practice what this means is that cytotoxic T cells of a mouse of MHC type A, immunized with some virus X, will kill X-infected targets of MHC type A but not otherwise identical X-infected targets of MHC type B. That cytotoxic T cells recognize foreign antigens only in association with specific MHC antigens is the basic fact of MHC restriction. One can rationalize the involvement of membrane bound MHC molecules in this interaction by arguing that their presence in close association with virus specific molecules enables cytotoxic T cells to identify and kill virus infected cells while ignoring an excess of free virus.

Since its first clear definition in 1974, MHC restriction has become recognized as a fundamental feature of antigen recognition by many (if not all) classes of T cell and seems to be a corollary of the fact that specific T cell activities are probably mediated, like target cell killing, by cell-cell contact. Other examples of such activities are T cell induction by exogenous antigen, involving MHC molecules on antigen presenting cell surfaces at the beginning of an immune response, and T cell help for antibody production by B cells, this latter activity probably being mediated through MHC molecules presented to T-helper cells by the B cell surface.

A key question is, where and when is the dual specificity of the observed response established? At what point is the discrimination between different MHC molecules and different foreign antigens made? Until relatively recently it would have been a good bet that the critical stage for both discriminations was at the first encounter of a mature T cell with foreign antigen X. At this stage X is undoubtedly presented to the immune system by a specialized presenting cell which, in addition to trapping antigen, also carries MHC allelic products. If X and an MHC product are recognized together in some association by a subset of T cells, for example killer cell precursors carrying a receptor of the appropriate specificity, then the killer cells that are activated will kill only those targets which similarly express both the 'right' MHC allele and the 'right' X. Evidence in favour of this idea came from studies on the properties of T cells from F_1 hybrids between two strains carrying different MHC alleles, A and B. It was found that such animals carried two separate T cell populations, one able to recognize $X+A$ and the other $X+B$. Normally both populations were immunized by X, but if X was experimentally presented to $(A \times B)F_1$ T cells on cells of homozygous A origin, for example, only the $A+X$ reactive subset was activated.

Of course in all such simple MHC restriction experiments another class of recognition process could be imagined where T cell activation required that MHC antigens on the reactive cell should 'match' MHC antigens on the antigen presenting cell or

---

Jonathan Howard is in the Department of Immunology, Institute of Animal Physiology, Babraham, Cambridge.

target. Such a like-like requirement amounting to self-recognition could be excluded by experiments in radiation chimaeras. Irradiated $(A \times B)F_1$ recipients were reconstituted with a mixture of marrow cells or foetal liver of homozygous A and B origins. T cells of A type grown up in such chimaeras could collaborate with B cells of B type for the production of antibody. Related experiments with cytotoxic T cells have also been done successfully. These results are perfectly compatible with the idea that the specificity of H-2 restriction is laid down at the moment of antigen presentation. If, therefore, 'self' recognition is involved in MHC restriction, T cells must 'learn' the MHC type of self during their ontogeny: self does not necessarily coincide with the MHC carried by the T cells themselves.

The idea that T cells in some way learn a range of possible MHC restrictions during their ontogeny before meeting antigens is now widely accepted (see *Nature* **272**, 11; 1978). T cells differentiate from their precursors in the thymus gland and experiments by Bevan[1], Zinkernagel[2] and others gave results which suggested that some learning of MHC restriction specificity occurs during this maturation. Chimaeras were established in which the thymus was of MHC type A while the differentiating T cells were of F_1 type $A \times B$. When T cells from such $A \times B \to A$ chimaeras were immunized with a variety of antigens on $A \times B$ presenting cells the resultant immune response showed a marked bias towards restriction by the thymus H-2 type A. The unique capacity of the thymus to determine the restriction bias was demonstrated by experiments using thymus grafts[4,5,6].

A great deal of emphasis has been laid on this thymic 'bias'. It seems likely, however, that the results may have been greatly overinterpreted. If thymus learning of an MHC restriction repertoire were absolute, a T cell population restricted to MHC type B should never be found in animals in which $A \times B$ T cells had differentiated in an A thymus. In fact, however, some responses restricted to the B haplotype, albeit relatively weak, are often found [5,7], and immunization of such animals with antigens presented on cells of B type seems preferentially to immunize this B-restricted reportoire to give substantial responses[8]. There is a thymic MHC restriction bias, and it clearly requires an explanation. Nevertheless it is only a bias, and can be overriden by appropriate immunization.

Another class of experiment says even more clearly that 'learning' in the thymus cannot alone be responsible for determining the range of MHC restriction. These experiments involve analysis of the immunological reactivity of cells from normal A donors. The question is whether in any circumstances these cells can produce an MHC-restricted response to an antigen presented on cells carrying only MHC type B. Such experiments are complicated by the fact that cells carrying MHC type B are strongly antigenic to normal T cells of A origin by virtue of the MHC incompatibility itself. This alloreactivity can, however, be removed from normal A T cell populations experimentally by a process resembling filtration. Cells from normal A donors are injected into the blood of irradiated $A \times B$ or B recipients. Alloreactive T cells from the donor are retained in the tissues of the recipient while cells unable to recognize the B alloantigens pass through the host tissues into the lymphatics from which they can be collected. Such 'negatively selected' populations can now be tested for their ability to recognize a foreign antigen X presented on cells of MHC type B in the absence of an alloreaction directed against the B alloantigens themselves. These experiments often, but not always, produce substantial responses restricted by B[9–12]. When they do, they demonstrate clearly that the MHC type of the thymus does not necessarily predict the MHC restriction repertoire of the T cells derived from it. In negative selection experiments the 'wrong' MHC type is not encountered by the responsive population at all during ontogeny, yet after appropriate antigen presentation a repertoire can be found for a response restricted by this MHC type.

What then, is the explanation for the thymic bias in chimaera experiments? For the time being this question must remain open. There is, however, some evidence to support the idea that the thymic bias may be maintained in chimaeras by suppression[13,14], probably acting on the repertoire at a peripheral rather than thymic level. It is as if responses to antigens presented by the non-thymic MHC type were actively inhibited. It is tempting to associate this kind of explanation for the thymic bias with the problems faced by $A \times B \to A$ chimaeras in the acquisition of self tolerance to their MHC alloantigens. One specialised function often proposed for the thymus is as a place in which autoreactive T cells generated by some process of repertoire diversification are eliminated. If this elimination is normally mediated by contact with antigens on the non-lymphoid cells of the thymus, $A \times B$ T cells differentiating in an A thymus cannot acquire tolerance of their own B MHC antigens in the normal way. It has been shown in both mice and rats that very profound tolerance to MHC antigens absent from the fixed cells of the thymus, (as in neonatal A strain animals injected with $A \times B$ marrow at birth) may be mediated by specific suppressor cells[15,16]. There is no demonstrated mechanism by which such suppressor cells work, but the effect is to prevent expansion of the anti-B reactive repertoire and the animal is effectively tolerant of B. The extension of these findings to $A \times B \to A$ chimaeras required for an explanation of the restriction bias towards A is to argue that the animals maintain a suppression of the alloreactive anti-B repertoire, and this suppression also includes exogenous antigens presented in association with the B allelic product. It would be of considerable interest to know whether supressor cells from an A type donor made neonatally tolerant of B at birth can influence the restriction repertoire of an $A \times B$ recipient to mimic the thymic MHC restriction bias of an $A \times B \to A$ chimaera.

An extension of this argument is that in a normal A type animal there is no biological need for suppression of reactions restricted by MHC-type B. After removal of alloreactivity against B by filtration, as described above, A type T cell populations may therefore retain a repertoire able to recognize an antigen restricted by B more easily than do T cells from $A \times B \to A$ chimaeras. In experiments involving Vaccinia virus in mice Doherty and Bennick have demonstrated this effect quite clearly[17]. MHC type A T cells negatively selected and unreactive against B alloantigens can produce a good primary anti-Vaccinia virus response restricted by MHC type B, while cells from an $A \times B \to A$ chimaera do not. One can argue that in this case the postulated suppression of reactivity to B and B-associated antigens in the chimaera is more 'inclusive' than the depletion of reactivity to B by negative selection.

It is obviously time to re-evaluate the thymus learning experiments. Clearly something special happens in the thymus: the question is, what? I can think of three clearly distinct functions for the organ, firstly, the functional differentiation of T cells from immunologically incompetent precursors; secondly, the distribution of a diverse repertoire among separate clones of cells by repeated cell division; and thirdly, the elimination of autoreactive cells from that repertoire to induce self tolerance. Only the third process involves specific interference with the response repertoire. Although there may not be a fully consistent argument available, it is tempting to attribute the normal MHC restriction behaviour of T cells to the specificity of normal self tolerance induction in the thymus, and abnormal MHC restriction behaviour in $A \times B \to A$ chimaeras to an abnormal mechanism of induction of self tolerance in a non-thymic site. □

---

1. Bevan, M.J. *Nature* **269**, 417 (1977).
2. Zinkernagel, R.M. *et al. J. Exp. Med.* **147**, 882 (1978).
3. Howard, J.C. *Nature* **272**, 11 (1978).
4. Zinkernagel, R.M. *et al. Nature* **271**, 251 (1978).
5. Bevan, M.J. & Fink, P.J. *Immunol. Revs.* **42**, 3 (1978).
6. Waldmann, H. *et al. Nature* **274**, 166 (1978).
7. Blanden, R.V. & Andrew, M.E. *J. Exp. Med.* **149**, 535 (1979).
8. Matzinger, P. & Waterfield, J.D. *Nature* **285**, xxx (1978).
9. Wilson, D.B. *et al. J. Exp. Med.* **146**, 361 (1977).
10. Bennink, J.R. & Doherty, P.C. *J. Exp. Med.* **148**, 128 (1978).
11. Doherty, P.C. & Bennink, J.R. *J. Exp. Med.* **149**, 150 (1979).
12. Thomas, D.W. & Shevach, E.M. *Proc. natn. Acad. Sci. U.S.A.* **74**, 2104 (1977).
13. Blanden, R.V. & Ada, G.L. *Scand. J. Immunol.* **7**, 181 (1978).
14. Smith, F.I. & Miller, J.F.A.P. *J. Exp. Med.* **151**, 246 (1980).
15. Roser, B.J. & Dorsch, S. *Immunol. Revs.* **46**, 55 (1979).
16. Gorczynski, R.M. & MacRae, S. *J. Immunol.* **122**, 747 (1979).
17. Doherty, P.C. & Bennick, J. *J. Exp. Med.* **150**, 1187 (1979).

ARTICLES

Pb–Sr–Nd isotopic correlation and the chemistry of the North Atlantic mantle

Bernard Dupré & Claude J. Allègre

Laboratoire de Géochimie et Cosmochimie, Institut de Physique du Globe et Départment des Sciences de la Terre, Universités Paris VI et VII,
4 Place Jussieu, 75230 Paris Cedex 05, France

The Pb, Sr, Nd isotopic composition in North Atlantic mid-oceanic ridge basalts has been measured. A positive correlation is found between Sr and Pb and a negative one between Nd and Sr. There is also a negative correlation between Hf/Th or Ta/Th and isotopic ratios such as $^{87}Sr/^{86}Sr$ *or* $^{206}Pb/^{204}Pb$*. Using the data for oceanic island basalts with these coherent geochemical characteristics we discuss the origin of chemical variations in the North Atlantic mantle and the problem of the mantle geochemistry.*

SINCE the discovery of the variation of Nd isotopes in the terrestrial mantle[1], it has been argued that this variation seems to be anticorrelated with Sr isotopes but not with Pb isotopes. This problem is well expressed by the Sr–Pb isotope 'non-correlation' plot established by Sun and Hanson[2,3]. Thus Pb isotopes do not apparently follow the same logic as Nd and Sr isotopes in the mantle geochemistry and have been one of the problems in understanding mantle evolution. We have tried to clarify this problem by careful study of a restricted area and then by applying the results to other parts of the world. We also include a discussion of trace elements.

We have analysed tholeiites from 15 different sites of the Mid-Atlantic Ridge. Their locations are indicated on Fig. 1. The FAMOUS area has been studied in detail, and our results will be published elsewhere. We give here only mean or key samples from this area. We have measured Pb and Sr isotopic compositions on the same sample in each case with special treatment for Sr to minimize seawater exchanges. The positions, results and error limits are given in Table 1.

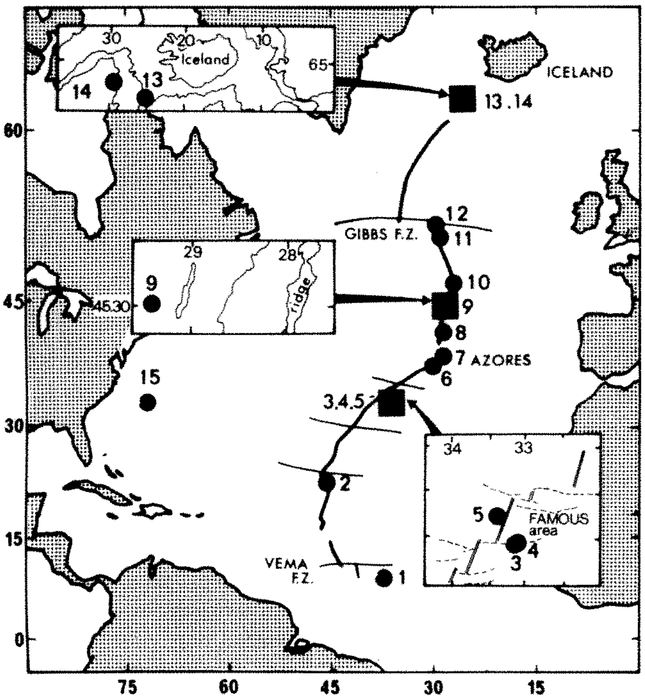

Fig. 1 Situation of the North Atlantic MORB samples.

Isotopic results

For the North Atlantic ocean, the expected inverse correlation between the Sr and Nd isotopic compositions is observed (see refs 1, 4, 5 and Fig. 2*c*). Comparison of the $^{206}Pb/^{204}Pb$ with $^{207}Pb/^{204}Pb$ and $^{206}Pb/^{204}Pb$ with $^{208}Pb/^{204}Pb$ diagrams give quite good correlations as was suggested by Tastumoto's work[6] on Pb isotopes in oceanic ridge basalts (Fig. 2*a*).

In contrast, the direct correlation between the Pb isotopes and the Sr isotopes is less expected (Fig. 2*b*). An inverse correlation between Nd and Pb isotopes is, of course, also obtained. Such an observation is true for $^{206}Pb/^{204}Pb$ as well as for the other Pb isotopic ratios. Note that one sample[10] is slightly out of correlation. When Sr isotopes were analysed for this sample by White and Schilling[7] without any treatment (leaching or diopside separation) a $^{87}Sr/^{86}Sr$ ratio of 0.70347 was obtained. Leaching lowers their value and as our leaching was incomplete our value may still be slightly too high, in which case the correlation could become perfect.

To appreciate this result one must remember that the Pb system on one hand and the Nd–Sr system on the other have been generally considered as being decoupled. This follows from Sun and Hanson's[2] plot in which a large cloud of points is observed rather than the line in the Nd–Sr diagram. We have then, for the first time, a coupling between Sr and Pb isotopes on mid-oceanic ridge basalts (MORB), which is exactly opposite to what has been claimed by Vidal and Dosso[8]. These remarkable regularities, also obtained by Cohen *et al.*[9] but on samples from more dispersed geographical areas in different oceans, are the basis of our following discussion.

Assuming that the present day Nd isotopic composition of the closed mantle is equal to that of achondrites and chondrites, the corresponding values of $^{87}Sr/^{86}Sr$ and Rb/Sr ratios can be deduced from the correlation diagram of Nd–Sr. These values are 0.70475 and 0.03 (ref. 10) with large errors. Using the same procedure for the Pb isotopes with our Sr–Pb isotope correlation, where we have more data. We obtain the following values:

$$^{206}Pb/^{204}Pb = 21.3\text{–}22$$

$$^{207}Pb/^{204}Pb = 15.78\text{–}15.90$$

$$^{208}Pb/^{204}Pb = 41.5\text{–}42.3$$

These values are called the 'planetary lead Atlantic' values (PLA) because they correspond to the planetary Sr in the correlation diagrams. Application of these values to the classical $^{206}Pb/^{204}Pb$, $^{207}Pb/^{204}Pb$ diagram reveals immediately that the

0028–0836/80/270017–06$01.00

Table 1 Location and Sr and Pb isotopic composition of the samples studied

Samples	Geographical coordinates	$^{206}Pb/^{204}Pb$	$^{207}Pb/^{204}Pb$	$^{208}Pb/^{204}Pb$	$^{87}Sr/^{86}Sr$	
AD5.5	9°39′N 40° 27′W	18.709	15.508	38.16		1
		18.670	15.496	38.12	0.70270	
		0.015	0.017	0.05	0.00004	
Leg 45						2
395A 33–2	22°N	18.279	15.467	37.65	0.70233	
9–13		0.014	0.016	0.05		
9–13	Leaching for lead	18.203	15.469	37.61		
		0.014	0.016	0.05		
395A 49–2						
13–17	22°N	18.211	15.476	37.62		
		0.019	0.020	0.06		
Leg 49 hole						3
413	36°32.6′N 33°10.5′W	18.706	15.524	38.41		
	2,608 m	0.025	0.022	0.07		
Leg 49 hole						4
412 7 2–5	36°33 74′N 33°09 96′W	18.965	15.555	38.52		
	2,609 m	0.012	0.015	0.05		
hole						
412 11 32–35	36°33 74′N 33°09 96′W	18.949	15.579	38.42	0.70299	
	2,609 m	0.015	0.017	0.05	0.00006	
Leg 49 hole						5
411 2 12–13	36°45 97′N 33°23 30′W	18.844	15.559	38.29		
	1,935 m	0.015	0.016	0.05		
DR 17	38°N 31°50′W	19.261	15.603	39.04	0.70307	6
		0.022	0.018	0.06	0.00008	
DR 24	39°N 30°W	19.444	15.587	38.98	0.70315	7
		0.018	0.018	0.06	0.00007	
TR 122 3D4	40°13 9′N 29°35.4′W	18.253	15.502	38.08	0.70299	8
	2,675 m	0.015	0.018	0.05	0.00009	
					0.70298	
					0.00007	
					strong leaching	
	Leaching for lead	18.381	15.515	38.19		
		0.024	0.024	0.07	0.70298	
					0.00007	
Leg 49 hole 410						9
41	45°30.51′N 29°28 56N	19.730	15.619	39.70	0.70346	
	2,975 m	0.018	0.019	0.06	0.00004	
55–60						
TR 138 1AD	46°31 6′N 27°29.1′W	18.355	15.483	38.51	0.70316	10
	2,400–2,550 m	0.017	0.021	0.07	0.00009	
	Leaching for lead	18.319	15.447	38.43		
		0.021	0.025	0.07		
TR 138 6D1	50°02 6′N 28°56.0′W	17.826	15.412	37.36		11
glass	3,360–3,380 m	0.021	0.021	0.065		
whole rock	50°02 6′N 28°56.0′W	17.798	15.420	37.33	0.70231	
	3,360–3,380 m	0.012	0.015	0.05	0.00006	
Gibbs Fracture						12
zone D1M	52°59 6′N 34°58 7′W	18.24	15.49	37.9		
	1,875 m	0.09	0.09	0.2		
Leg 49 hole						13
409 17 35–40	62°36 98′N 25°57 17′W	18.790	15.516	38.22	0.70299	
	832 m	0.015	0.016	0.05	0.00006	
Leg 49 hole						14
407 42 87–89	63°56 52′N 30°34 56′W	19.058	15.528	38.43		
	2,472 m	0.02	0.023	0.07		
Leg 52 Jurassic		18.559	15.488	37.76		15
15–3		0.018	0.020	0.06		
		18.483	15.506	37.79		
		0.015	0.016	0.05		

The values obtained by Tatsumoto[40] on AD 5.5. are reported; all the others are our results. Mattinson[41] measured Pb isotopes in some samples from the Leg 49 sites. We have obtained good agreement with his results. The Pb, Sr and Nd compositions have been measured using the techniques described respectively by Manhes *et al.*[25], Birck and C. J. A.[37] and Richard *et al.*[1] We have used the leaching technique on all samples for the Sr isotope compositions and also for some Pb measurements.

PLA values do not correspond to the closed system reference geochron (Fig. 2*a*), but are clearly in the so-called (*J*) field. This indicates that the U–Pb system has had an open system evolution through geological time. As, by definition, a planetary value should correspond to a closed system situation, the PLA values are certainly not planetary in the same way as Sr or Nd.

Relationship with trace elements

Trace elements are generally more difficult to handle than isotopic ratios because their concentrations are modified by magmatic processes (partial melting + fractional crystallization + other processes such as seawater interaction). Some elements are strongly enriched into the liquid during magmatic processes and are unmodified by interaction with seawater. Therefore their ratios can be considered representative of their mantle source. Such elements, called H elements by Treuil and Joron[11], are Hf, Ta, Th, La, Zr, Nb. We have a set of values for some of them in the North Atlantic published by Joron *et al.*[12] and Wood *et al.*[13,14]. Here we try to use only these elements, to avoid the secondary effects which would obscure the picture.

Sr and Pb isotopes have been compared with some H element ratios on Fig. 3*a*). Even if only five different sites can be used for

H elements, an inverse correlation is obtained between Sr or Pb isotopes and ratio like Hf/Th, La/Th, Ta/Th. The values obtained by Wood *et al.*[14] on samples from 63°N (site 13) seems anomalous as the ratios vary strongly within the site. If the Hf/Th, La/Th, Ta/Th ratios are considered which correspond to the $^{87}Sr/^{86}Sr$ planetary value a set of values is obtained which are very different from the chondritic values. For example Hf/Th corresponding to $^{87}Sr/^{86}Sr = 0.70475$ is about 1, while the chondritic value is about 10.

In a plot of Hf/Th versus Ta/Th where the ratios have the same denominator, mixing processes are represented by a straight line, as in the lead isotopes plot. The most remarkable observation (Fig. 3*b*) regarding the results for the North-Atlantic MORB is that they do not define simple straight lines. Therefore the variation for the North-Atlantic MORB source cannot be generated by a simple two-end member mixing process. Such a conclusion agrees with that of Langmuir *et al.*[16] which was obtained using different elements.

The 'regional' variations

A cross-section of regional variations along the ridge can be made from Iceland to the South. With our new Pb and Sr data which have been corrected for seawater contamination by a HCl leaching technique, we can draw two important conclusions from the regional variations which have been a source of confusion in the past.

(1) There is no clear correlation between bathymetry and isotopic ratios. Certainly some correlation occurs between the depth of the ridge and some trace element contents, especially for the incompatible ones, but this probably reflects a correlation between the bathymetry and the degree of partial melting rather than the composition of the mantle source. On the North-Atlantic scale, there is no clear correlation between bathymetry and isotopic ratios which would directly reflect the nature of the mantle source.

(2) The variation from Iceland to the South is not dominated by only two 'hot spots' (Iceland+Azores). Our Pb, Sr and Nd isotopic results reinforce those of White and Schilling[7] on Sr isotopic composition because Pb and Nd are not sensitive to alteration. The variations are such that if one wants to interpret the variations of isotopic ratios by a 'hot spot' model, a third hot spot must be added around 45°N and perhaps another around 9°N.

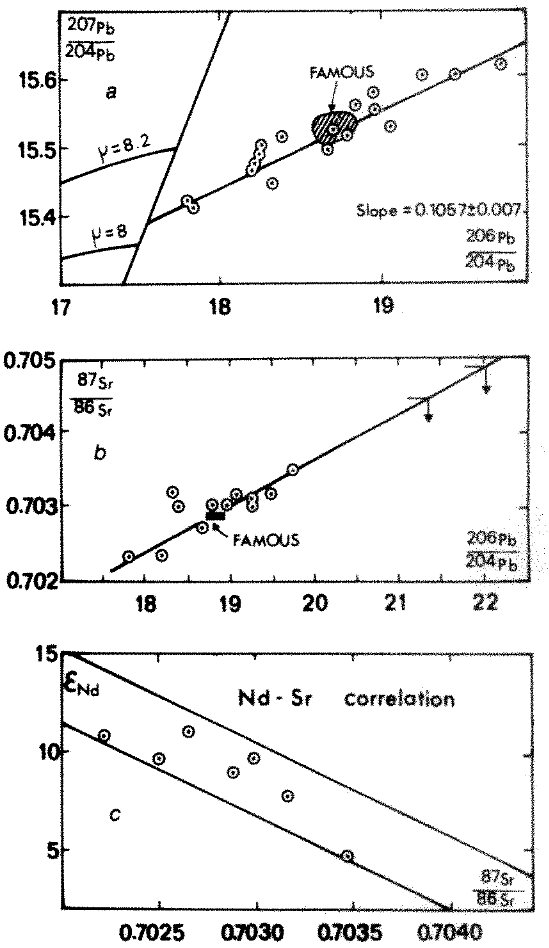

Fig. 2 Results for samples from North Atlantic tholeiites. *a*, $^{207}Pb/^{204}Pb$ versus $^{206}Pb/^{204}Pb$. The regression line has a slope of 0.1057±0.007. The model age is 1,720 Myr. *b*, Correlation $^{87}Sr/^{86}Sr$ versus $^{206}Pb/^{204}Pb$ for North Atlantic MORB. Lead isotopic Atlantic planetary values are determined from $^{87}Sr/^{86}Sr$ planetary value (0.70475). *c*, Nd–Sr isotopes correlation for the North Atlantic basalts. Data for MORB are from refs 1, 4, 5.

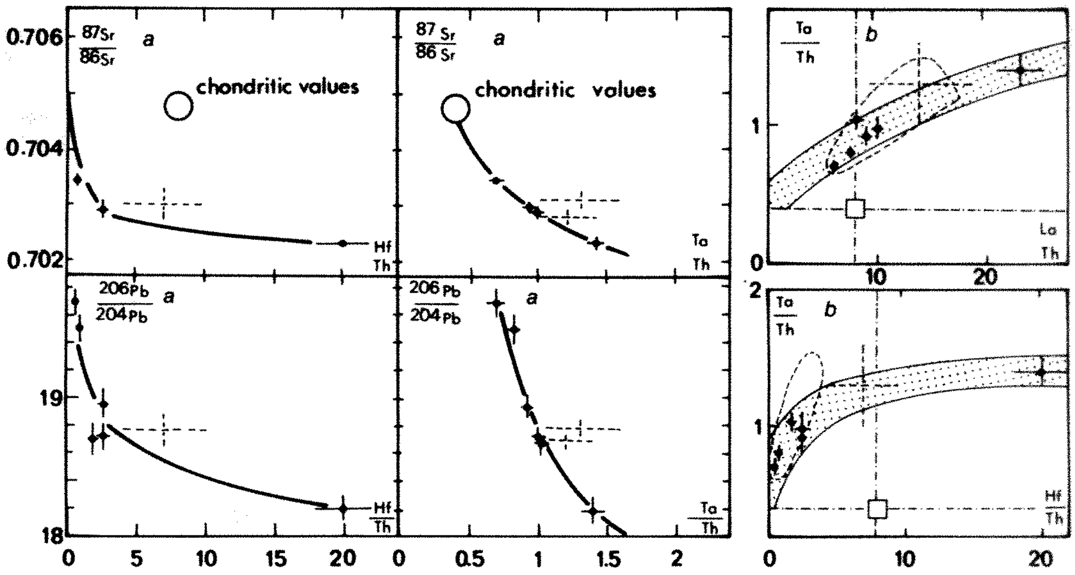

Fig. 3 *a*, $^{87}Sr/^{86}Sr$ versus $^{206}Pb/^{204}Pb$ versus HF/Th or La/Th trends for North Atlantic MORB. Data are from refs 12–14 and this paper (chondritic values are from refs 42, 43). The HF/Th and La/Th ratios are the mean value of these ratios for each site. The error of 0.1% for the isotopic ratios is taken as being equivalent to the dispersion observed on the FAMOUS site where many samples have been measured[38]. *b*, Ta/Th versus Hf/Th or La/Th trend for North Atlantic MORB. (Refs as in Fig. 4.) The dashed line area corresponds to oceanic islands domain (data from ref. 21).

Comparison of the North Atlantic MORB with other oceanic basalts

Only a few results have been obtained on the same samples for Pb-Sr-Nd isotopes (Fig. 4) using modern techniques and leaching or diopside separation to eliminate Sr seawater contamination. The only available results are those of Cohen *et al.*[9] on volcanic glasses and some of our unpublished results on Pacific and Indian oceans. Pb-Pb or Sr-Pb diagrams show a very good positive correlation which is identical with our Atlantic lines. Thus the values for Pb isotopes corresponding to the planetary strontium isotopic ratio are about the same as PLA. This being so the above anomaly should be considered a worldwide characteristic and not a local one.

We do not have measurements for some other oceans but preliminary data for the Pacific MORB seem to plot on the general trend in the Hf/Th Ta/Th) diagrams (H. Bougault, personal communication).

As Pb, Sr and Nd isotopes have been analysed in Icelandic samples[17-20]and in the Azores islands (see ref. 15 for Pb; refs 1, 22 for Sr and Nd) we can then try to place these samples with respect to MORB in the (Sr, Pb) isotope correlation diagram.

Iceland, Terceira, Corvo and Santa Maria are roughly in the correlation band. Other islands, like Faial or Sao Miguel are out of the trend. Sao Miguel is also outside the (Nd-Sr) main trend[22]. However, a more careful analysis shows that two populations of oceanic island basalts which do not follow the trend are older than the others. For instance, only the old part of the Sao Miguel island does not really follow the trend. All other islands, including the Canary Islands[24], plot around the main trend. Of course, this argument is rather statistical but the positive correlation including the North Atlantic islands is clear.

Although different isotopic ratios were often found in separate samples we will use the compilation of Sun[3] (Fig. 4). Such a compilation shows that the basalts from oceanic islands define a large band completely outside the MORB (Pb-Sr) or (Pb-Pb) correlations. In the (Pb-Sr) correlation diagram such a band can be even considered 'orthogonal' to the MORB's trend. In the (Pb-Pb) diagram, there is also a clear distinction between these two populations. Such a behaviour is in great contrast with the (Sr-Nd) diagram, which exhibits the correlation for both MORB and OIB.

We also want to emphasize another major difference. In the Sr-Nd diagram, the values observed for OIB can be interpreted as the result of a material derived from a planetary reservoir and contaminated by the MORB reservoir during its ascent. In contrast, for Pb isotopes, the OIB reservoir is clearly in the (*J*) type field, and thus corresponds to a largely open system (independent of any contamination by the MORB reservoir). Thus the OIB reservoir is certainly not the protected closed system proposed by Wasserburg and De Paolo[26].

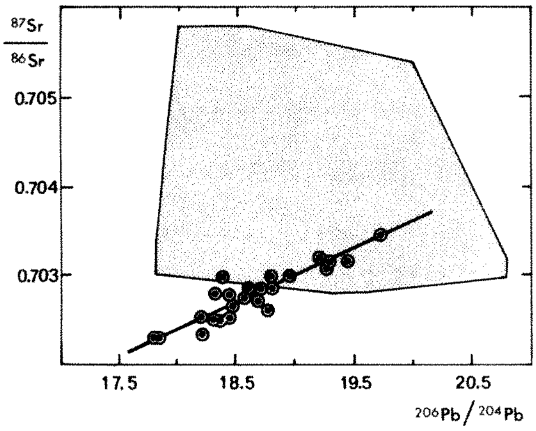

Fig. 4 $^{87}Sr/^{86}Sr$ versus $^{206}Pb/^{204}Pb$ for oceanic basalts. Oceanic island basalts do not seem to be correlated (dotted area from ref. 3) whereas MORB data define a positive correlation from our data and those of Cohen *et al.*[9].

We have plotted a large number of data concerning oceanic islands in (Hf/Th, Ta/Th) and (La/Th, Ta/Th) diagrams (Fig. 3*b*) which show that Ta/Th ratios from MORB and OIB, although distinct are very similar, and not too far from chondritic values. In contrast Hf/Th and Hf/Ta ratios are much lower in OIB than in MORB, and are very different from chondritic ratios. Unfortunately as Hf is less hygromagmatophile than Ta, Th and La (ref. 11) and because alkali basalts are created by small degrees of partial melting (with perhaps more or less fluid transfer and metasomatism), one does not know whether the Hf/Th and Hf/Ta ratios for OIB reflect that of their source or result from their formation processes. Thus we shall not include these ratios in the discussion of OIB sources.

Theoretical interpretations

The main result of the previous investigations is that we clearly have a coherent behaviour of the Rb-Sr, Sm-Nd, U-Th-Pb and Hf, Ta, Th, La systems for the North Atlantic province. This is the first demonstration of such a coherence with such detail. We will now try to explain the significance of these trends.

Models can be built in which the mantle heterogeneity is created by liquid-solid fractionation processes operating through geological time[27]. In this context, the inverse correlation between Nd and Sr isotopes, and the $^{87}Sr/^{86}Sr$ depletion compared with planetary values can be easily interpreted[27]. These observations can be understood if one remembers that Rb is enriched in liquid compared with Sr, and that Nd is enriched in liquid compared with Sr.

If the U-Th-Pb system is taken into account in this model, the positive correlation between Pb and Sr isotopes indicates that U and Th are more enriched in magmatic liquids than Pb. This conclusion agrees with the observations made in magmatic suites[28] and apparently solves the Pb paradox previously pointed out by C. J. A.[29]. However, as we have mentioned above, the problem with Pb is that the 'planetary values' determined from the correlations are not on the Pb-Pb closed system curve.

In the same way, the negative correlation between Hf/Th, Ta/Th, or La/Th and $^{87}Sr/^{86}Sr$ correspond to the fact that Hf, Ta or La are less enriched in magmatic liquids than Th. The slopes of the correlation lines in Hf/Th-Ta/Th and Hf/Th-La/Th diagrams indicate the degree of relative enrichment of Hf, Ta and La in the liquid. Then we can deduce the following increasing order of enrichment in the liquid: Hf < La < Ta < Th, which corresponds more or less to what can be established from the observation of the trace element fractionation in magmatic suites[11].

The preceding observations lead us to distinguish, on a worldwide scale, the existence of two reservoirs, one for MORB, one for OIB. Such a distinction was in fact made in the first isotopic measurements on MORB by Tatsumoto[6] and was subsequently adopted by others[2,30]. However, we feel that evidence presented here reinforces such an interpretation. Our description of these two reservoirs differs from the usual one. We do not consider here the subcontinental lithosphere which constitutes another reservoir, and this is discussed elsewhere[31].

The MORB reservoir is called the upper mantle, the OIB reservoir is considered to be the lower mantle. The OIB is probably partly contaminated by the MORB reservoir during ascent.

The upper mantle is isotopically extremely coherent but not homogeneous. The data for the Atlantic as well as the Pacific or Indian basalts (ref. 9 and our unpublished data) clearly indicate that variations may occur on regional scales. For trace elements, such variations are even more pronouned compared with the lower mantle. The variations observed in MORB are not the result of contamination by OIB as is usually claimed, but are created by the geodynamical system linked with the seafloor spreading which implies chemical fractionation. Imperfect homogenization results from convection. The basis of such processes which can be called 'chemical geodynamics' are discussed elsewhere[27,36].

Palit Chemistry Library
SCIENCE COLLEGE
92, Upper Circular Road
CALCUTTA

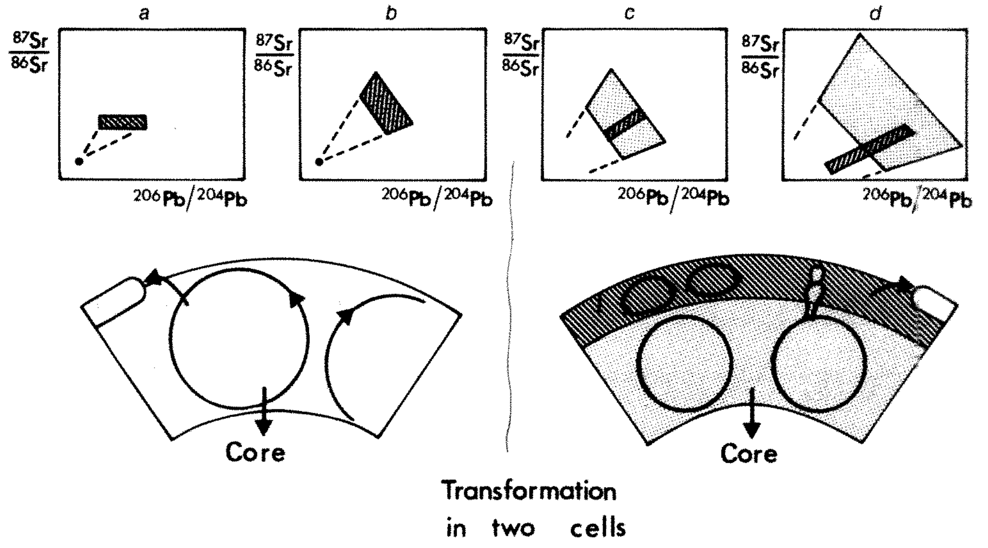

Fig. 5 *a*, Fractionation of U/Pb ratios in the early history of the Earth by core formation creates variations of Pb isotopic ratio only. *b*, The formation of the continental crust fractionates both Rb/Sr and U/Pb ratios, creating variation of Sr and Pb isotopic ratios. *c*, *d*, The transformation of the whole mantle into two independent cells leads to the creation of two types of reservoirs with distinct isotopic characters: relatively homogeneous and less radiogenic MORB reservoir compared with a heterogeneous and more radiogenic OIB reservoir.

The lower mantle is the source for OIB but is not an homogenized, uniform reservoir. It may be more uniform for Sr, Nd and H elements than the upper mantle, but strongly heterogeneous for Pb isotopes and then U/Pb ratios. This reservoir is not planetary for Pb isotopes, for some H elements, and probably also for Sr or Nd as has been shown for Sao Miguel[22]. This means that the reservoir has been fractionated in some way.

The different behaviour of Pb isotopes compared with Sr isotopes is illustrated by the lack of Pb–Sr correlation for OIB and by the planetary Atlantic values being in the *J*-field in the Pb–Pb diagram. There have been two interpretations for these features:

(1) An interaction between the core and the lower mantle has been admitted through geological times; Pb is buried in the core because it is chalcophilic and the core contains suphide. The rate of burying is assumed to decrease exponentially with time, with a time constant of 5,000 myr. This mechanism had been previously considered for a short period just after the differentiation of the Earth[32,33]. Vidal and Dosso[8] have also discussed this hypothesis but in their model, Rb was also buried; in such a case the Nd–Sr correlation would be destroyed, which does not occur. Although this long-term interaction has not been proposed by geochemists it agrees with the suggestion by Runcorn[34] of a continuous, but decaying with time, growth curve for the core.

(2) The alternative interpretation proposed by O'Nions *et al.*[35] allows a reinjection of sediments into the lower mantle. These sediments are H elements enriched by upwards migration within the continental crust. Reinjection rate decreases with time. However, the similarity of hygromagmatophile element ratios such as Ta/Th and La/Th for MORB and OIB does not favour such a model. Furthermore, this model would decouple Sr and Nd isotopes but not Pb and Sr as it is U and Rb simultaneous enrichment of the upper continental crust which is observed.

Note that a fundamental consequence of our observations is that the two reservoirs were connected at some time in the past.

The Pb isotopes systematic of MORB clearly show that the PLA values are anomalous. One way of explaining such anomalies is by assuming that the upper mantle exchanged with the core in the past. Some convection between upper mantle and core is needed. In the same way, H elements in the lower mantle should have been fractionated through time as their values are not chondritic. These elements have no chalcophile or siderophile character and the interaction with the core has no effect on them. The method of fractionating such elements is related to liquid–solid fractionation (or CO_2–magma fractionation?) or in other words to processes associated with the surface activity. This also leads to the conclusion that the two reservoirs were once linked.

Hence we conclude that convection cells affected the whole mantle during the Archaean and maybe even later. During that time seafloor spreading and continental crust differentiation occured at the same time as the core–mantle interaction. Later, the convection cells broke up and split in two cells, or continuously differentiated an upper mantle. The exact process for this mechanism remains unclear. In the lower cells, only the U–Pb system fractionated further, as probably did all other siderophile and chalcophile elements. The upper cells, probably of smaller dimension, are fractionated further through continental crust formation and vigorously stirred by advection. This creates the presently observed patterns of isotopic variations in MORB. And indeed, ~2,000 Myr are necessary to create the observed variation for Pb, Sr and Nd isotopes by such a process (Fig. 5). In which case a separated upper mantle would be an old phenomenon.

This study was supported by CNEXO. Some samples were given by Schilling, all the others were given by the COB. We thank D. Rousseau, M. Polvé, G. Manhes, O. Brévard and J. F. Minster for their help, and H. Bougault for discussions.

Received 10 December 1979, accepted 23 April 1980.

1. Richard, P., Shimizu, N. & Allègre, C. J. *Earth planet. Sci. Lett.* **31,** 269 (1976).
2. Sun, S. S. & Hanson, G. *Geology* **3,** 297 (1975a).
3. Sun, S. S. *Proc. R. Soc.* (in the press).
4. O'Nions, R. K., Hamilton, P. J. & Evensen, N. M. *Earth planet. Sci. Lett.* **34,** 12 (1977).
5. De Paolo, D. J. & Wasserburg, G. J. *Geophys. Res. Lett.* **3,** 743 (1976).
6. Tatsumoto, M. *Science* **153,** 1094 (1966).
7. White, W. M. & Schilling, J. G. *Geochim. cosmochim. Acta* **42,** 1501 (1978).
8. Vidal, P. & Dosso, L. *Geophys. Res. Lett.* **5,** 169 (1978).
9. Cohen, R. S., Evensen, N. M., Hamilton, P. J. & O'Nions, R. K. *Nature* **283,** 149 (1980).
10. Allègre, C. J., Ben Othman, D., Polvé, M. & Richard, P. *Phys. Earth planet. Sci. Inter.* **19,** 293 (1979).
11. Treuil, M. & Joron, J-L. *Soc. Ital. Miner. Petrol.* **31,** 125 (1975).
12. Joron, J-L., Bougault, H., Treuil, M. & Allègre, C. J. *Bull. Soc. geol. Fr.* **18,** 811 (1976).
13. Wood, D. A. *et al. Earth planet. Sci. Lett.* **42,** 77 (1979).
14. Wood, D. A. *et al. Init. Rep. DSDP* Leg **49,** 597 (1978).
15. Dupré, B., Hamelin, B., Allègre, C. J. & Manhes, G. *4th int. Conf. Geochron. Cosmochron. Isotope Geology* 103, (1978).
16. Langmuir, C. H., Vocke, R. D., Hanson, G. J. & Hart, S. R. *Earth planet. Sci. Lett.* **37,** 380 (1978).
17. Sun, S. S. & Jahn, *Nature* **255,** 527 (1975).
18. Hart, S. R., Schilling, J. G. & Powell, J. L. *Nature phys. Sci.* **246,** 104 (1973).
19. O'Nions, R. K. & Pankhurst, R. J. *J. Petrol.* **15,** 603 (1974).
20. Wood, D. A., Joron, J-L., Treuil, M., Norry, M. & Tarney, *J. Contr. Miner. Petrol.* **70,** 319 (1979).
21. Joron, J-L. & Treuil, M. *Bull. Soc. geol. Fr.* 1197 (1977).

~~R5H~~
R412

22. Hawkesworth, C. J., Norry, M. J., Roddick, J. C. & Vollmer, R. *Nature* **280**, 28 (1979).
23. Tatsumoto, M. *Earth planet. Sci. Lett.* **38**, 63 (1978).
24 Sun, S. S. thesis, Columbia Univ., New York, (1973).
25. Manhes, G., Minster, J.-F. & Allègre, C. J. *Earth planet. Sci. Lett.* **39**, 14 (1978).
26. Wasserburg, G. J. & De Paolo, D. J. *Proc. natn. Acad. Sci. U.S.A.* **76**, 3594 (1979).
27. Allègre, C. J., Brévart, O., Dupré, B. & Minster, J.-F. *Proc. R. Soc.* (in the press).
28. Hamelin, B., Dupré, B. & Allègre, C. J. (in preparation).
29. Allègre, C. J. *Earth planet. Sci. Lett.* **5**, 261 (1969).
30. Schilling, J. G. *Nature* **242**, 565 (1973).
31 Allègre, C. J., Dupré, B., Lambert, B. & Richard, P. *Earth planet. Sci. Lett.* (submitted).
32. Oversby, V. M. & Ringwood, A. E. *Nature* **234**, 463 (1971).
33. Volmer, R. *Nature* **270**, 144 (1977).
34. Runcorn, S. K. *Nature* **195**, 1248 (1962).
35. O'Nions, R. K., Evensen, N. M. & Hamilton, P. J. *J. geophys. Res.* **84**, 6091 (1979).
36. Allègre, C. J. *Mem. Soc. geol. Fr.* **10**, 1830 (1980).
37. Birck, J-L. & Allègre, C. J. *Earth planet. Sci. Lett.* **39**, 37 (1978).
38. White, W. M. *Yb. Carnegie Inst. Wash.* 325 (1979).
39. Sun, S. S., Tatsumoto, M. & Schilling, J. G. *Science* **190**, 143 (1975).
40. Tatsumoto, M. *Earth planet. Sci. Lett.* **38**, 63 (1978).
41. Mattinson, J. M. *Init. Rep. DSDP* Leg **49**, 721 (1978).
42. Ahrens, L. H. *Earth planet. Sci. Lett.* **10**, 1 (1970).
43. Nakamura, N. *Geochim. cosmochim. Acta* **38**, 757 (1974).

Palaeomagnetic polarity in a 930-m core from Searles Valley, California

Joseph C. Liddicoat & Neil D. Opdyke
Lamont-Doherty Geological Observatory, Columbia University, Palisades, New York 10964
George I. Smith
US Geological Survey, 345 Middlefield Road, Menlo Park, California 94025

Palaeomagnetic polarity to the base of the Mammoth subchron (3.15 Myr) has been determined in a core of lacustrine sediments from ancient Searles Lake. The magnetostratigraphy provides a chronological framework for palynological, tephrochronological and palaeoecological studies of the core. Five zones of inclination are found that are not in the polarity time scale of Mankinen and Dalrymple. Three of the zones may correlate with K–Ar-dated lava flows of that polarity elsewhere, and the other two may be new discoveries.

A 930-m, surface-to-bedrock core from Searles Valley, California (35°43'N, 242°40'E), has been used to study palaeoclimate in the western US[1]. The upper 695 m is sediment from Searles Lake, now dry; the remaining 235 m is arkose deposited by intermittent streams on an alluvial fan. The history of climate is in the Searles Lake deposits, the mineralogy and chemistry of which varied with the growth and recession of the lake[2]. The presence or absence of the lake closely mirrored changes in climate, for Searles Lake was near the terminus of a chain of lakes fed by runoff from the Sierra Nevada[3]. As such, Searles Lake was perennial and deep during wet (pluvial) periods; during dry (interpluvial) periods like the present, the lake shrunk to a playa or a salt flat.

A useful interpretation of palaeoclimate must be keyed to an accurate time base, which is also a requirement of corollary investigations (palynology, tephrochronology, palaeoecology), in progress, on the core. Radiocarbon dating of the upper ~50 m of valley fill is extensive [4–7], but radiometric dating of sediment beyond the range of ^{14}C has not been successful. The palaeomagnetic data reported here provide the necessary geochronology for the older portion of the core.

Searles Valley core

The core, called KM-3, was drilled in 1968 by the Kerr–McGee Chemical Corporation, which mines subsurface brines in Searles Valley, and in 1976, KM-3 was released to the US Geological Survey for scientific study. The core has a 9-cm diameter, and because of cracking during drying, is in pieces no longer than 50 cm each. However, some edges may be matched so that longer pieces can be reconstructed, some approaching 2 m in length.

Relatively thin, alternating layers of mud and salines make up the intervals between depths of 0–38, 69–228 and 291–403 m. Thick sections of deep-lake muds lie between depths of 38–69, 228–291 and 542–693 m. The interval between 403 and 542 m is brown sediment formed mostly in a playa lake[1]. (Conforming to accepted terminology[1,2], we use 'salines' for the evaporite minerals, and 'mud' as a general term for clay, silt, and marl that was moist and plastic when extruded as core; now dry, the clay and silt are claystone and siltstone, respectively.)

There are numerous tephra layers in the core, and a sequence of them in the interval 169.3–178.6 m may represent the Bishop Tuff (R. Hay, personal communication), a pyroclastic erupted in Long Valley (California) ~0.7 Myr ago[8,9]. A more positive identification of the tuff would provide an important time-line in the core, and this is in progress. Two other tephra layers lie near the bottom of the lacustrine section (684.0 and 690.9 m); if they too can be traced to their source and dated, another cross-check on the magnetostratigraphy will be available.

Sampling and laboratory procedures

Palaeomagnetic samples were taken at intervals of ~3 m or less in non-saline portions of the core below 100 m depth. Above 100 m, the core is not sufficiently intact to be reliable for palaeomagnetism. The large diameter of the core allowed us to take three specimens at each measured horizon. Each specimen was encased in a polythyrene box of 6.6 cm³, and the specimens from a horizon had the same relative azimuth.

For each subset of specimens, we partially demagnetized one specimen in stepwise increments to 300 Oe peak alternating fields or higher, and demagnetized the other two at the median destructive field. This was 200–300 Oe (Fig. 1) for about 80% of the specimens; for the remaining specimens (from saline-rich horizons), the median destructive field was 50–150 Oe. Within most subsets, and almost always below 400 m where the remanence is nearly 100-fold stronger than that of saline-rich zones, the grouping of magnetic vectors is good—the spread of values of inclination being commonly <5°. Samples taken at 581.0 and 619.8 m (brown mud deposited in a playa) were thermally demagnetized, and the directions were compared with those of the a.f. demagnetized specimens from those depths; in each case, there was no appreciable change in the magnetic vector (Fig. 1).

Magnetostratigraphy in Searles Valley

Interpretation of polarity change in KM-3 is most convincing if linked to one or more reliable markers in the Pleistocene. Although only tentatively identified in the core, the Bishop Tuff would serve as one such calibration point because it lies near the

0028–0836/80/270022–04$01.00

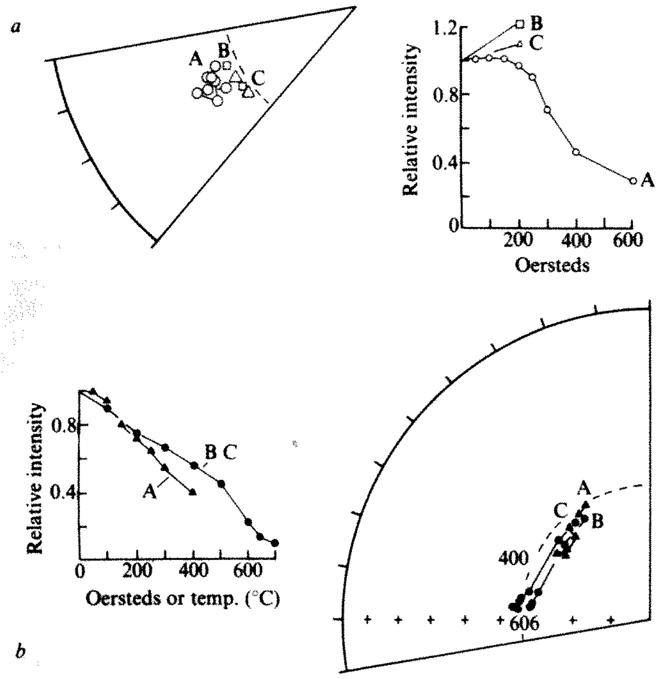

Fig. 1 Normalized a.f. and/or thermal demagnetization curves and equal-area plot of palaeomagnetic directions for: *a*, three specimens from 480.5 m (reversed polarity); and *b*, from 581.0 m (normal polarity). The azimuth of specimens within each horizon is the same, but different between horizons. In *b*, specimen A was a.f. demagnetized; specimens B and C were thermally demagnetized. The dashed line in the equal-area plot represents inclination of an axial dipole field (55°) for the site latitude; solid symbols are plotted on the lower hemisphere, open symbols on the upper.

Brunhes/Matuyama boundary[10]. Indeed, the youngest horizon of negative inclination is at 195.0 m, or $\sim$15 m below the zone of tephra layers that is thought to represent the Bishop Tuff. The nearest overlying horizon of positive inclination is at 174.9 m, so we interpret the Brunhes/Mayuyama boundary at 185.0 ± 10.0 m (Table 1). The underlying $\sim$320 m is predominantly of negative inclination (Fig. 2), which we assume to represent the Matuyama chron. Below that, the predominantly positive inclination is most probably the upper part of the Gauss chron.

Assuming that we have correctly identified the Brunhes/Matuyama and Matuyama/Gauss boundaries, it is then possible to plot age against depth to identify the zones of positive inclination within the Matuyama chron. From Fig. 3 it can be readily ascertained that the zones centred at $\sim$210 m, 390 m, 410 m, and 450 m correspond to the Jaramillo, Olduvai, and two-part Réunion subchrons, respectively. Further, the zones of negative inclination in the Gauss chron that are centred at about 630 m and 660 m would correlate to the Kaena and Mammoth subchrons, respectively (Table 1).

Note in Fig. 3 that there is a nearly linear relationship between the position of the polarity boundaries and the age assigned to them using the time scale of Mankinen and Dalrymple[11]. This is especially true for sediment below 400 m, where the lack of saline layers allows an approximation of uniform sedimentation rate. For those 295 m, spanning nearly 1.2 Myr, the average rate of sedimentation is $\sim$40 yr cm^{-1} (0.25 mm yr^{-1}). It is difficult to calculate sedimentation rates for other parts of the core because the time represented by saline layers can be either very long or short; salines initially accumulate more rapidly than mud, but this is countered by periods of almost no deposition when the lake becomes a seasonally flooded salt flat[2]. Nonetheless, the overall sedimentation rate to 695 m is $\sim$45 yr cm^{-1}, or only 10% slower than that of mud of the perennial lake.

Five zones of inclination in KM-3 are not in the standard polarity time scale proposed by Mankinen and Dalrymple[11]. Three of the zones may correspond to subchrons that have been proposed[12–14] but not universally accepted, while the other two could be new. These previously undetected short subchrons are not entirely surprising as their existence was predicted on the assumption that durations of polarity changes conform to a Poisson distribution[15]. The advantage of using lacustrine deposits such as in Searles Valley to search for short subchrons is that the sedimentation rate is at least 50-fold greater than in most deep-sea sediments, and is much less discontinuous than the eruption of lava flows. An obvious disadvantage is that part of the core might be inverted, accidentally either during initial recovery or some time during the intervening 8 yr of storage. As we were not present at the time of drilling, there is no guarantee that the top of the core was properly labelled on the drill rig or after splitting and storage; a realistic approach would be to assume that part of so long a core was inverted by human error. However, this probably did not occur during storage because we have compared the present core to Kerr-McGee's colour photographs of it taken at the time of recovery. When we removed samples, we photographed the potentially useful boxes of core, and those photographs have enabled us to check the orientation of back-up samples.

The question of inverted samples becomes critical when comparing measured zones of constant inclination to the generally accepted polarity time scale, or when detection of a new subchron is claimed. We examined notes made at the time of sampling to see if any of the unnamed short zones of inclination are restricted to a single core box or coring run, as these portions could be those most likely to be inverted. Three new zones of inclination were found restricted to single coring runs, and resampling of cores from adjacent runs showed that inversion of the core was probably not responsible for the zones. Additional checks included matching saw marks on the split side of the core to see if they were similar from piece to piece in a storage box, and determining whether the switch in inclination occurred between segments of core where the lithology suggested a discontinuity.

Matuyama chron

The zone of positive inclination that we interpret to be the Jaramillo subchron (0.90–0.97 Myr) lies between $\sim$205 and 220 m (Table 1). It includes four measured horizons and spans two boxes of core. The two horizons of negative inclination between the top of the zone and where we place the Brunhes/Matuyama boundary (Fig. 2) are also from two boxes of

Table 1 Location of polarity boundaries and unnamed zones of inclination in KM-3

Boundary	Depth (m)	Lithology
Brunhes–Matuyama	185.0 ± 10.0	Interbedded mud and salines
Matuyama–Jaramillo	204.9 ± 0.1	
Jaramillo–Matuyama	221.2 ± 10.6	
Matuyama–Unnamed zone (N3)	281.1 ± 0.4	Mud (deep lake)
Unnamed zone (N3)–Matuyama	287.7 ± 2.1	
Matuyama–Unnamed zone (N2)	322.3 ± 2.5	Interbedded mud and salines
Unnamed zone (N2)–Matuyama	330.2 ± 1.7	
Matuyama–Olduvai	378.5 ± 1.1	
Olduvai–Matuyama	398.9 ± 0.4	
Matuyama–Réunion*	408.3 ± 4.2	Mud (playa)
Réunion–Matuyama	424.7 ± 1.7	
Matuyama–Réunion	447.4 ± 1.6	
Réunion–Matuyama	456.0 ± 4.6	
Matuyama–Unnamed zone (N1)	516.5 ± 1.5	
Unnamed zone (N1)–Matuyama	519.8 ± 1.9	
Matuyama–Gauss	522.9 ± 1.2	
Gauss–Unnamed zone (R2)	569.3 ± 6.7	Mud (deep lake)
Unnamed zone (R2)–Gauss	580.8 ± 0.3	
Gauss–Unnamed zone (R1)	599.8 ± 0.6	
Unnamed zone (R1)–Gauss	603.3 ± 1.4	
Gauss–Kaena	616.2 ± 1.5	
Kaena–Gauss	643.1 ± 2.6	
Gauss–Mammoth	651.7 ± 2.2	
Mammoth–Gauss	683.9 ± 4.2	

* We assume the Réunion to be a multiple subchron[29,30].

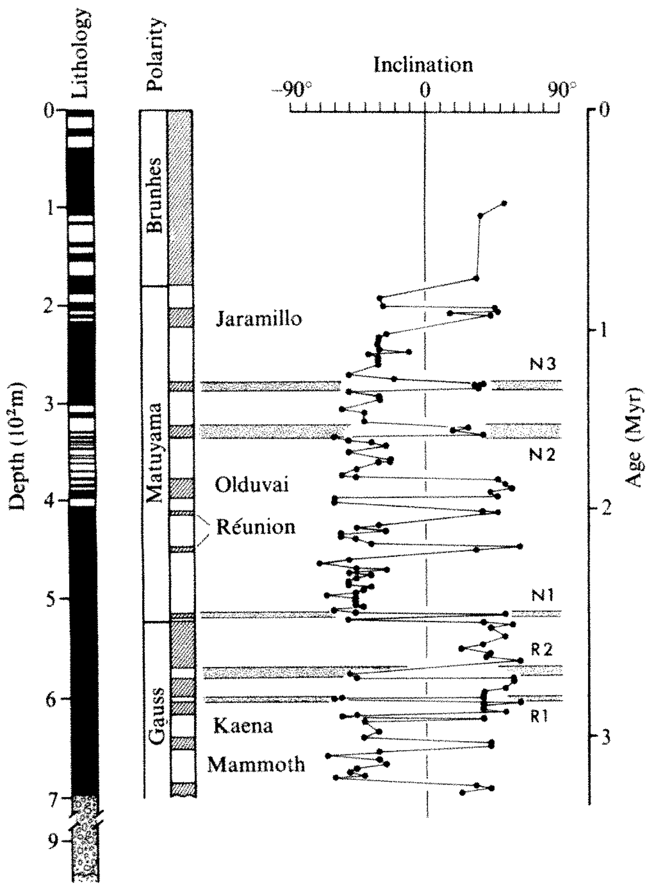

Fig. 2 Palaeomagnetic polarity in Searles Valley core KM-3. Shaded region highlights the unnamed zones of inclination, three in the Matuyama chron and two in the Gauss chron. In the lithological column: unshaded area, salines; black area, mud; spotted area, arkose. In the polarity column; hatched area, normal polarity; unshaded area, reversed polarity. Age is extrapolated from polarity boundaries in the time scale of Mankinen and Dalrymple[11], and by assuming a uniform sedimentation rate. Note that the time scale is not linear.

core, and the horizon of negative inclination below the zone is from another box. The switch from positive to negative inclination at the top of the zone occurs within one section of core pipe (each section is 10 m long), eliminating the possibility that the coring run was inverted or mislabelled at the time of recovery.

The other universally recognized subchron in the Matuyama chron is the Olduvai subchron (1.67–1.87 Myr); we place it between 379 and 399 m (Table 1). This portion of the core involves four measured horizons, one each from two different boxes of core and two from a third box. The third box also contains the horizon of negative inclination at the base of the subchron, and the two samples in that box are separated by ~0.3 m. Again, the change from positive to negative inclination occurs within one section of core pipe.

The two short zones of positive inclination below the Olduvai subchron we consider to be the multiple Réunion subchron (2.12–2.14 and 2.01–2.04 Myr)[16–18]. The older half occurs between 447 and 456 m (Table 1) and includes two measured horizons, one each from separate boxes of core that is little disturbed. The samples of negative inclination that bracket the zone are from two other boxes of core, and the switch in inclination is within a section of core. The younger half is between 408 and 424 m, and the two samples came from the same box of core. As is the case for the older part of the subchron, the horizons of negative inclination on either side came from different boxes of core. However, unlike the older part, the positive inclinations are all in one section of drill pipe that was obtained separately from the sections containing the horizons above and below; this raises the possibility of an inverted section of core.

Unnamed zones of inclination in the Matuyama chron

The palaeomagnetic record in KM-3 contains three other short segments of positive inclination that are not included in the Mankinen and Dalrymple time scale[11]. The youngest (N3; Fig. 2) is in deep-lake mud between 281 and 288 m (Table 1). The zone is found in two boxes of very good core from the same core run (the measured horizons above and below the zone are from different runs) and terminates 60 m below the start of the Jaramillo subchron; 54 of these 60 m are deep-lake mud. Using the 40 yr cm^{-1} accumulation rate cited above for the mud, this part of the core spans ~20,000 yr between 1.24 and 1.26 Myr ago. If no time is assigned to the 6 m of salines between the disappearance of the deep-water lake and onset of the Jaramillo subchron, this unnamed zone is dated 1.20–1.22 Myr.

Mankinen *et al.*[12] recently reviewed the evidence for a short subchron close to and preceding the Jaramillo subchron, and have identified one (Cobb Mountain subchron) in the volcanic units near Clear Lake, California. The K–Ar age given the Cobb Mountain subchron is 1.12 ± 0.02 Myr, so we cannot closely match the unnamed zone of inclination in KM-3 with that one, but given the uncertainty in sedimentation rate, the correlation is possible. It might also equate with the K–Ar-dated basalt of normal polarity in Madiera[19] and in the Lesser Antilles (Guadeloupe and St Vincent)[20] if the dates are accurate, and to a normally magnetized ash layer in the Osaka Group, Japan, having a fission-track age 1.1 ± 0.1 Myr (refs 21–23).

The zone of positive inclination near the middle of the Matuyama chron (N2; Fig. 2) may correlate with the controversial Gilsa subchron, whose existence has been affirmed and denied several times during the past decade[24]. The three measured horizons are in different boxes of core, and the samples used to bracket the zone are from two other boxes. Although the quality of that portion of the core is good, the horizons in question are from a single core run, and the opposite inclination on either side is from two other runs. Thus, we are concerned about whether the entire core run was mislabeled or inverted.

The oldest zone of positive inclination in the Matuyama chron (N1; Fig. 2) is near its beginning and might correspond to the 'X' subchron[14] that has been seen in some magnetic anomaly data; however, it may correlate to the short subchron observed in Icelandic lavas very close to the Matuyama/Gauss boundary[25]. The measured horizon is in part of the good core, and the switch in inclination occurs within one core run.

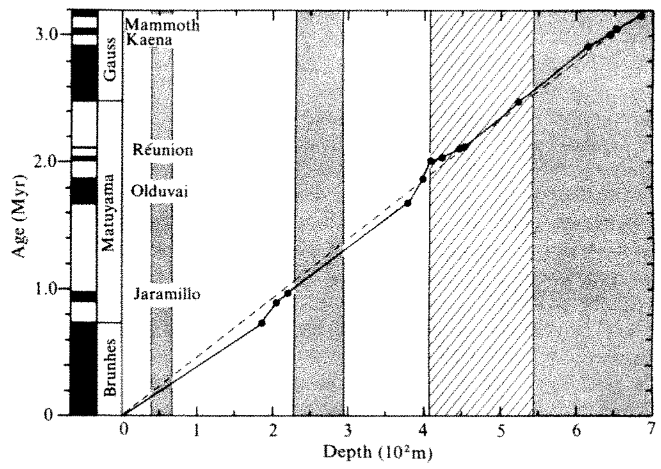

Fig. 3 Depth of interpreted polarity boundaries in KM-3 versus age in the polarity time scale[11]. Shaded area, mud deposited by a deep, perennial lake; hatched area, mud deposited by a playa lake[2]. Overall rate of sedimentation is ~45 cm yr^{-1} (dashed line); for the perennial lake, it is 40 cm yr^{-1}.

Gauss chron

We equate the two zones of negative inclination near the bottom of the lacustrine section with the Kaena subchron (2.92–3.01 Myr) and Mammoth subchron (3.05–3.15 Myr). Each represents at least five measured horizons, and they are in different boxes of core. The two horizons of positive inclination that separate the subchrons are also from separate boxes of core, and the switch of inclination occurs in one core run.

Unnamed zones of inclination in the Gauss chron

Reversed magnetozones occur in upper Gauss time in mud from a perennial, deep lake, the sediment type we believe to be the most reliable magnetic recorder in the core. Using estimated sedimentation rates again, the younger zone (R2; Fig. 2) spans ~40,000 yr, and the older one (R1; Fig. 2) perhaps 20,000 yr. Extrapolating from the Matuyama–Gauss boundary (2.48 Myr) (ref. 11) the ages for these zones are then 2.67–2.71 and 2.79–2.81 Myr, respectively. Some reversely magnetized K–Ar-dated basalt flows in this age range have been reported: two from Oahu in Hawaii[26], one in west Iceland[27] and one in St Vincent[20]. Thus, these may be real subchrons, but because of their brevity, they can only be clearly defined in a high sedimentation-rate environment such as Searles Lake. We must re-emphasize that the measured horizons defining both zones were found in single boxes of core (although the opposite polarity occurs in single core runs). For the younger of the two zones, there are two horizons of positive inclination and two of negative inclination, and the separation between the portion of the core where the inclination switches is 0.46 m, or slightly less than 1,000 yr using the assumed sedimentation rate for that part of the core. Three closely spaced horizons of good core define the older zone, and the horizon above and below are in different boxes of core and at least 2.2 m apart.

Conclusions

Based on the record of palaeomagnetic polarity in KM-3, the oldest lake deposits in Searles Valley formed ~3.2 Myr ago (Fig. 2). The timing of a changing climate that might have produced a permanent lake in that part of the Great Basin coincides with a general cooling in the Northern Hemisphere as seen in the $\delta^{18}O$ record in deep-sea core V28-179 (ref. 28). The sedimentary record is probably a result of the interplay of tectonics and climatic events[1].

Five unnamed zones of inclination are present in the core, and four involve two or more measured horizons. The three unnamed zones in the Matuyama chron may correspond to subchrons that have been proposed by others but are not universally accepted. The two unnamed zones in the Gauss chron occur in good-quality core, and the change from positive to negative inclination for both zones occurs in single, 10-m sections of core.

We thank D. A. McGee, chairman of Kerr-McGee Corporation, for permission to study this core, G. Moulton and C. Cowie for logistical support while obtaining samples, S. Liddicoat for field assistance, D. Lafferty for laboratory assistance, and R. Coe, R. Hay, C. Denham, E. Mankinen, S. Grommé, D. Champian, D. Kent, and G. Kukla for helpful comments. Funding was provided by the Climate Program of the US Geological Survey (contract 14-08-0001-18282). Lamont-Doherty Geological Observatory Contribution no. 2990.

Received 7 February; accepted 28 April 1980.

1. Smith, G. I., Barczak, V. J., Moulton, G. F. & Liddicoat, J. C. *U.S. Geol. Surv. Prof. Pap.* (in preparation).
2. Smith, G. I. *U.S. Geol. Surv. Prof. Pap. 1043*, 1–130 (1979).
3. Smith, G. I. in *Paleolimnology of Lake Biwa and the Japanese Pleistocene* Vol. 4 (ed. Horie, S.) 577–604 (1976).
4. Flint, R. F. & Gale, W. A. *Am. J. Sci.* **256,** 689–714 (1958).
5. Smith, G. I. *U.S. Geol. Surv. Prof. Pap. 450-C,* C65–C69 (1962).
6. Stuiver, M. *Am. J. Sci.* **262,** 377–392 (1964).
7. Stuiver, M. & Smith, G. I. in *U.S. Geol. Surv. Prof. Pap. 1043*, 68–75 (1979).
8. Dalrymple, G. B., Cox, A. & Doell, R. R. *Bull. geol. Soc. Am.* **76,** 665–673 (1965).
9. Izett, G. A. & Naeser, C. W. *Geology* **4,** 587–590 (1976).
10. Hillhouse, J. & Cox, A. *Earth planet. Sci. Lett.* **29,** 51–64 (1976).
11. Mankinen, E. A. & Dalrymple, G. B. *J. geophys. Res.* **84,** 615–626 (1979).
12. Mankinen, E. A., Donnelly, J. M. & Grommé, C. S. *Geology* **6,** 653–656 (1978).
13. Watkins, N. D., Kristjansson, L. & McDougall, I. *Earth planet. Sci. Lett.* **27,** 436–444 (1975).
14. Heirtzler, J. R., Dickson, G. O., Herron, E. M., Pitman, W. C. III & Le Pichon, X. *J. geophys. Res.* **73,** 2119–2136 (1968).
15. Cox, A. *J. geophys. Res.* **73,** 3247–3260 (1968).
16. Chamalaun, F. H. & McDougall, I. *Nature* **210,** 1212–1214 (1966).
17. McDougall, I. & Chamalaun, F. H. *Nature* **212,** 1415–1418 (1966).
18. McDougall, I. & Watkins, N. D. *Earth planet. Sci. Lett.* **19,** 443–452 (1973).
19. Watkins, N. D. & Abdel-Monem, A. *Bull. geol. Soc. Am.* **82,** 191–198 (1971).
20. Briden, J. C., Rex, D. C., Faller, A. M. & Tomblin, J. F. *Phil. Trans. R. Soc.* **291,** 485–528 (1979).
21. Nishimura, S. & Sasajima, S. *Chikyu Kagaku* (*Earth Sci.*) **24,** 222–224 (1970).
22. Maenaka, K. *Rock Magn. Paleogeophys.* **3,** 41–46 (1975).
23. Maenaka, K. *Geophys. Res. Lett.* **6,** 257–260 (1979).
24. McDougall, I. in *The Earth: Its Origin, Structure and Evolution* (ed. M. W. McElhinny) (Academic, London, 1979).
25. Kristjansson, L., Fridleifsson, I. B. & Watkins, N. D. *EOS* **59,** 270 (1978).
26. Doell, R. R. & Dalrymple, G. B. *Bull. geol. Soc. Am.* **84,** 1217–1242 (1973).
27. McDougall, I., Saemundsson, H., Johanesson, H., Watkins, N. D. & Kristjansson, L. *Bull. geol. Soc. Am.* **88,** 1–15 (1977).
28. Shackleton, N. J. & Opdyke, N. D. *Nature* **270,** 216–219 (1977).
29. Cox, A. *Science* **163,** 237–245 (1969).
30. Grommé, C. S. & Hay, R. L. *Earth planet. Sci. Lett.* **10,** 179–185 (1971).

Nerve growth factors in the rat iris

Ted Ebendal*, Lars Olson†, Åke Seiger† & Kjell-Olof Hedlund*

* Department of Zoology, Uppsala University, Box 561, S-751 22 Uppsala, Sweden
† Department of Histology, Karolinska Institutet, S-104 01 Stockholm, Sweden

Nerve growth factor (NGF) activity was not detected by bioassay in irides killed immediately after excision but NGF appeared within 24 h in living irides placed in culture or grafted to a host eye. Furthermore, sensory and, although less effective, sympathetic denervation of irides in situ *led within 10 days to the appearance of NGF activity. In addition, freezing and thawing released a parasympathetic neuronotrophic factor activity from irides.*

THE protein nerve growth factor (NGF)[1] has been suggested to mediate trophic influences to sympathetic and sensory neurones from innervated target organs[2]. However, little is known about the distribution of NGF in peripheral tissues to support this concept[3]. Except for some very rich sources of NGF (the male mouse submandibular gland[1], the guinea pig prostate[4]), mammalian tissues are normally inactive when tested as homogenates in the sensitive bioassay based on NGF-susceptible embryonic ganglia[3,5]. We now show that explants of the adult rat iris immediately killed by freezing do not contain NGF at levels detectable by bioassay but that NGF is readily detectable in irides killed by freezing within a day after transfer to a recon-

0028-0836/80/270025-04$01.00

stituted collagen gel[6] (compare refs 7, 8) or to the anterior eye chamber of another rat[9]. After re-innervation of the iris transplants, NGF was no longer detectable. Most compelling is the fact that the levels of NGF were also raised in irides *in situ* 10 days after sensory denervation and, although less prominent, 10 days after sympathetic denervation. Furthermore, evidence was obtained for the actions of a parasympathetic, non-NGF, trophic factor released from the rat iris after freezing and thawing. The results support a role for NGF as a signal initiating and directing regenerating sensory and sympathetic fibres in adult mammals and suggest that other trophic factors may fulfill a similar role in other fibre systems.

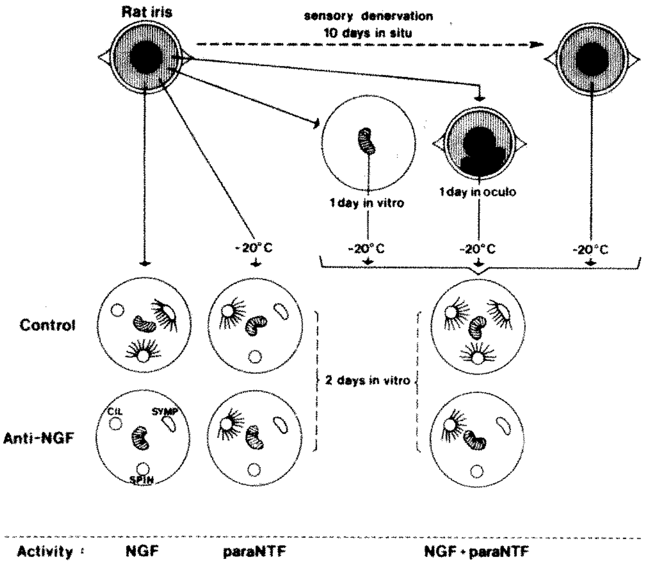

Fig. 1 Schematic representation of the experiments with rat irides and the resulting patterns of neurite growth responses in chick sympathetic (symp), spinal (spin) and ciliary (cil) ganglia. The results are interpreted as evoked by the actions of nerve growth factor (NGF), of a parasympathetic neuronotrophic factor (paraNTF) and of the simultaneous action of these two. Circles represent culture dishes. Irides were from normal rats (left) or from rats in which the trigeminal nerve had been lesioned (sensory denervation, right). For bioassay sympathetic, spinal and ciliary ganglia from 8- to 10-day-old chick embryos were placed surrounding a living or killed (by freezing to −20 °C) half-iris in an 0.3–0.5-mm thick collagen gel in a 35-mm plastic culture dish. The medium of the gel was Eagle's basal medium supplemented with 1% fetal calf serum, penicillin (100 units ml^{-1}) and streptomycin (100 $\mu\mathrm{g\,ml}^{-1}$). Parallel dishes received in addition 2–5 μl per ml of specific rabbit anti-mouse-βNGF antiserum[22], levels that readily blocked the activity of 1 biological unit (BU) of NGF. Cultures were incubated at 37 °C with 5% $\mathrm{CO_2}$ in water-saturated air for 2 days and then examined by phase-contrast microscopy.

Effects of culturing on NGF synthesis in the iris

To study the content of NGF, irides of adult Sprague–Dawley rats were excised aseptically and tested in a ganglionic bioassay (Fig. 1). The criterion for NGF activity is an induction of neurite outgrowth in the chick sympathetic and spinal ganglia, which in parallel dishes can be blocked by antiserum to NGF, combined with a lack of fibre response in the ciliary ganglion[6]. Three distinct patterns of neurite outgrowth responses were observed (Fig. 1). Living iris explants taken directly into co-culture with ganglia evoked neurite outgrowth in the sympathetic and spinal ganglia within 20–24 h. Outgrowths developed fully within 2 days (Table 1), were directed mainly towards the living iris explants and had fibre densities resembling those evoked by 0.8 to 1 biological units of NGF (BU)[1]. Anti-NGF nearly completely inhibited these outgrowths (Table 1, $P<0.01$). Thus it is evident that the living irides in culture release NGF. The ciliary ganglia showed nearly no nerve fibre outgrowth when combined with living iris tissue. In control cultures without irides all three types of ganglia failed to extend neurites[6] (Table 1).

To test whether NGF is present in freshly excised irides or whether it is synthesized *in vitro*, irides were killed by immediate freezing to −20 °C for 1 to 30 days and then thawed. No NGF activity was detected in such iris tissue in the bioassay (Figs 1, 2*a*): in sympathetic ganglia slightly more fibres extended than in controls ($P<0.05$) but anti-NGF did not significantly (by the *U*-test) reduce this outgrowth (Table 1). On the other hand, killed iris tissue significantly increased formation of neurite bundles in the ciliary ganglia (Fig. 2*b*; Table 1, $P<0.01$). This stimulation was not abolished by adding anti-NGF, although the antiserum sometimes slightly impaired the response in the ciliary ganglion in this and in the following culture combinations. These results suggest the existence in the iris of a parasympathetic neuronotrophic factor[2] (paraNTF), stimulating the cholinergic neurones of the ciliary ganglion, and being released only after disrupting cells by freezing and thawing. Furthermore, the results show that NGF is not present at detectable levels in the iris *in situ*, but that the iris begins to synthesize NGF when placed in culture.

Effects of freezing and transplantation

To rule out the possibility that the freezing–thawing itself destroys NGF activity in the iris, explanted irides were cultured for 1 day in order to accumulate NGF before being killed. Bioassay demonstrated the same level of NGF activity in these explants as in the living ones (Figs 1, 2*c*; Table 1). Moreover, the ciliary ganglia exhibited dense outgrowths of neurites not significantly different from those evoked by immediately killed irides (Table 1). Thus these cultures showed a pattern of neurite stimulation that evidently represents the combined activities of NGF and paraNTF (Fig. 1). Anti-NGF inhibited outgrowth of neurites in the sympathetic (Table 1; $P<0.01$) and spinal ganglia but did not affect outgrowth in ciliary ganglia.

Table 1 Relative density of neurite outgrowths in chick ganglia

			With irides killed after:				
	Without iris explants	With living iris explants	No special treatment	Culture *in vitro* (1 day)	Grafting *in oculo* (1 day)	Sympathetic denervation *in situ* (10 days)	Sensory denervation *in situ* (10 days)
Sympathetic ganglia							
without anti-NGF	0.0±0.0 (8)	1.0±0.0 (9)	0.3±0.1 (9)	1.0±0.0 (9)	1.0±0.0 (5)	0.6±0.1 (10)	0.9±0.0 (15)
with anti-NGF	0.0±0.0 (8)	0.1±0.0 (8)	0.2±0.1 (8)	0.4±0.1 (5)	0.4±0.1 (5)	0.3±0.1 (7)	0.3±0.1 (11)
Ciliary ganglia	0.0±0.0 (8)	0.1±0.1 (5)	0.7±0.0 (5)	0.8±0.1 (5)	0.8±0.1 (5)	0.8±0.0 (5)	0.7±0.1 (13)

Mean values ± s.e.m. are given. For each group 5 to 15 ganglia (number given in parentheses) were scored for density of outgrowing neurites after 2 days on a blind basis. The scores ranged from 0 (no neurites at all) to 1 (maximum density, fibre halo with circular outline). The scores for the two types of ganglia are not strictly comparable due to differences in neurite morphology. *P* values given in the text refer to rankings of the individual scores evaluated by the Mann–Whitney *U*-test.

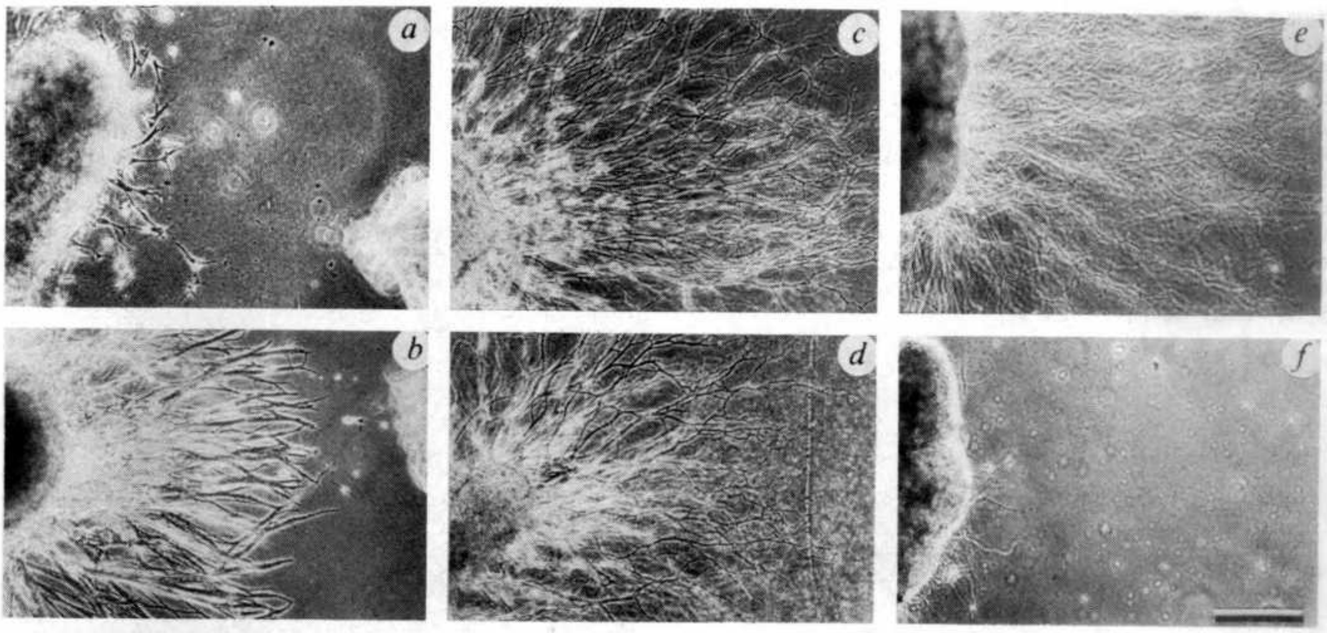

Fig. 2 *a*, Sympathetic ganglion (left) combined for 2 days in culture with rat iris (right) immediately killed after extirpation. No neurites emerge from the ganglion. *b*, Ciliary ganglion in the same conditions. In this parasympathetic ganglion extensive formation of thick neurite fascicles (identity controlled by the transmission electron microscope) is elicited by the killed iris explant. *c*, Sympathetic ganglion with dense fibre outgrowth elicited by an iris that had been cultured for 1 day and then frozen–thawed before being tested in the bioassay. *d*, Sympathetic ganglion combined with an iris transplanted to the anterior eye chamber of another rat for 1 day before being killed and tested. *e*, Extensive neurite formation in a sympathetic ganglion evoked by an iris killed 10 days after sensory denervation *in situ*. *f*, Inhibition by anti-βNGF of the neurite outgrowth in the foregoing combination. Phase contrast micrographs. Scale bar, 0.2 mm. See also ref. 13 for low-power darkfield micrographs of total outgrowths elicited by living irides.

To test whether NGF is produced in the iris only in *in vitro* conditions, the iris was either transplanted to the anterior eye chamber of another rat, rather than to a culture dish, or was left *in situ* but subjected either to sympathetic denervation by extirpation of the superior cervical ganglion or to sensory denervation by lesioning the trigeminal nerve[9] (Fig. 1). To prevent appearance of NGF during the subsequent bioassay the irides were killed by freezing before being combined with ganglia (Fig. 1).

After 1 day in the anterior eye chamber the transplanted iris contained the same amount of NGF as iris explants cultured *in vitro* for 1 day (Fig. 2*d*; Table 1). After 4, 7 and 11 days *in oculo* the same levels of NGF activity persisted but after 1 month, at which time the iris transplant had become at least sympathetically reinnervated by the host iris[10], NGF activity was no longer detectable. The responses evoked in the ciliary ganglia were the same as those elicited by the other frozen–thawed irides (Table 1).

Role of innervation in NGF synthesis

Experiments with irides denervated *in situ* show more clearly that the level of NGF is in some way related to the state of innervation. Irides taken for bioassay 10 days after sensory denervation consistently gave dense fibre outgrowths in sympathetic (Figs 1, 2*e*, Table 1; the increase over normal killed irides is significant, $P<0.01$) and spinal ganglia. The resulting outgrowth could be significantly reduced by anti-NGF (Figs 1, 2*f*, Table 1; $P<0.01$). Sympathetic denervation for 10 days resulted in a much less although significant ($P<0.05$) increase in fibre density in sympathetic ganglia (Table 1). That NGF is involved here also is indicated by the significant ($P<0.05$) reduction in fibre outgrowth by anti-NGF (Table 1). No NGF was detected 2 or 4 days after denervating the iris *in situ* nor was NGF found 1 month after denervation (at which time some reinnervation is likely to have taken place). Combined sensory and sympathetic denervations gave as high levels of NGF after 10 days as did sensory denervation. For the ciliary ganglia the denervations caused no further increase in fibre density above that evoked by normal killed irides (Table 1).

Sections of the ganglia cut for light microscopy at the end of bioassay add some information on the survival of neurones in response to the irides. In full agreement with the neurite outgrowth response the ciliary ganglion showed excellent neuronal survival after exposure to any iris that had been frozen–thawed (Fig. 3*a*; 19 ± 1 neurone profiles were found within an area of 0.01 mm^2; mean ± s.e.m. from sections of 5 ganglia) whereas living irides to a less ($P<0.01$) extent did promote survival of ciliary neurones (Fig. 3*b*; 5 ± 1 neurone profiles with living irides compared with 1 ± 0 neurone profiles in cultured control ganglia, $P<0.05$). The outcome for sympathetic ganglia was less expected: here the presence of iris tissue enhanced neuronal survival whether or not outgrowth of neurites occurred (Fig. 3*c*). The number of neurone profiles was thus 63 ± 4 with normal killed irides, which is not significantly different from the 71 ± 4 neurone profiles found with killed irides plus anti-NGF, whereas neuronal survival was significantly lower ($P<0.01$) in cultured control ganglia (Fig. 3*d*; 30 ± 3 neurone profiles). The enhancement may be due to an nonspecific, non-NGF, trophic influence on the neurones exerted by the presence of serum in the explanted irides: thus adding rat serum at 10% by volume resulted in 56 ± 5 neurone profiles. Rat serum, however, totally failed to induce neurite outgrowth in the sympathetic as well as the ciliary ganglia.

The present experiments show that the level of NGF may be raised in a mammalian tissue *in situ* by sensory or sympathetic denervation. The results thus favour the concept that a tissue after denervation during adulthood, and probably also during development, signals with NGF to initiate and attract growing or regrowing sympathetic and sensory nerve fibres[1,2]. This view is also supported by the finding that NGF content falls to undetectable levels concomitant with reinnervation of the iris grafts.

The appearance of NGF in the iris as a result of explantation, transplantation or denervation may be the result of an active

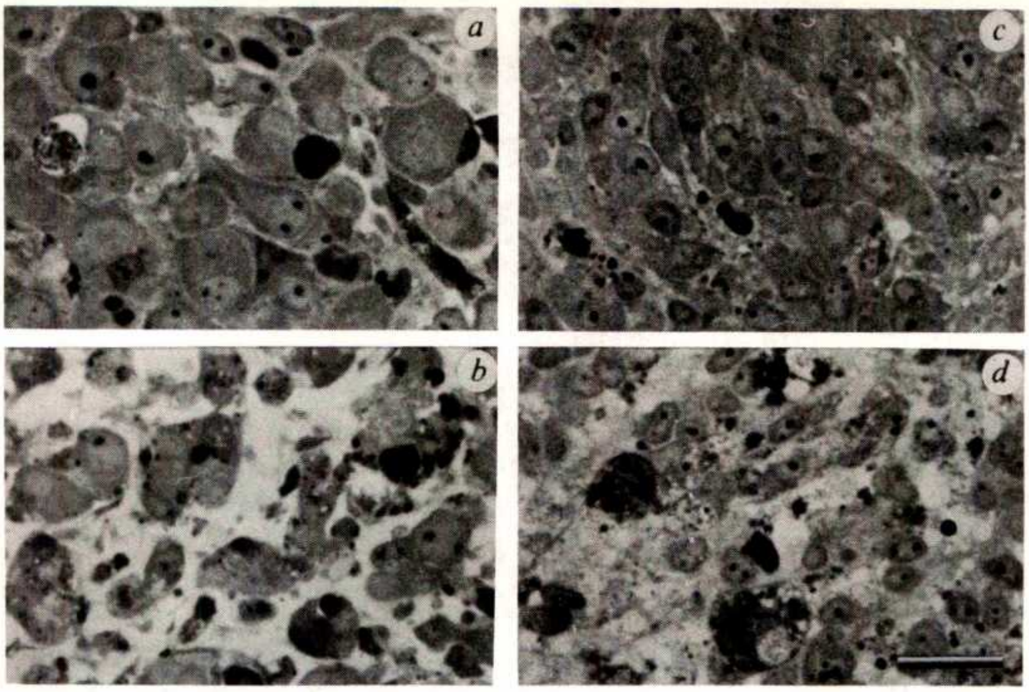

Fig. 3 *a*, Ciliary ganglion combined with a killed rat iris for 2 days in culture. A high neuronal survival is evident. *b*, Same but with a living iris explant. A massive death of neurones, also seen in control cultures, is not prevented by the living iris. *c*, Sympathetic ganglion cultured with an iris killed immediately after extirpation. Despite the addition of anti-βNGF and the fact that no or only few neurites extend from the ganglion (see Fig. 2*a*), a markedly good neuronal survival is induced by the iris tissue. *d*, Sympathetic control ganglion cultured without the presence of iris tissue. Only a few neurones survive in these conditions. For data on neurone survival, see text. Micrographs of toluidine blue-stained 2-μm sections of ganglia fixed in 1.5% glutaraldehyde plus 1.5% paraformaldehyde and embedded in Epon. Scale bar, 20 μm.

response of the iris to increase the production of the factor. Although less plausible, it may also be that the iris is normally drained of the NGF produced in it by retrograde axonal transport[11] to such an extent that the appearance of NGF after, for example, denervation represents an accumulation of the factor rather than an increased production.

The amounts of NGF released from the iris explants that induce a 0.8 to 1 BU response in chick ganglia (Fig. 2*c*, *d*, *e*) can be roughly calculated. The response was evoked only within a zone of about 2 mm around the approximately 5×1 mm half iris in the 0.3–0.5-mm thick gel. Thus the half iris spreads NGF to about 10–20 μl of the gel. If it is assumed[1] that 1 BU corresponds to 5 ng of NGF per ml and that the NGF is evenly distributed, this volume should contain about 40–80 pg. The wet weight of the half iris is about 0.5 mg and thus a reasonable amount of NGF released is of the order of 80–160 ng per g wet weight of cultured or denervated iris tissue. This value is slightly higher than that stated by Johnson *et al.*[8] measuring the release of NGF from irides to a culture medium by radioimmunoassay (RIA). Given the limits of detection of NGF activity for the present bioassay (0.03–0.06 BU)[6], and as we did not detect any NGF activity in initially killed irides, this tissue should release less than about 5–10 ng of NGF per g wet weight. Johnson *et al.*[8] stated that the iris initially contains 15–20 ng NGF per g as measured by RIA but this may be an overestimation due to their technique[12]. The present results thus show that the level of NGF is increased by at least one order of magnitude in the positive iris explants.

It is noteworthy that sensory denervation was a much more potent stimulus for the NGF increase *in situ* than sympathetic denervation (Table 1). One possible explanation for this difference may be that the lesioning technique used to obtain sensory denervation also damages a considerable proportion of the sympathetic axons to the iris. This may also explain why a combined sensory and sympathetic denervation was not found more effective in stimulating the production of NGF than was the trigeminal lesion alone. It is also of note that sensory denervation has been shown to cause massive ingrowth of central noradrenergic fibres into the iris from transplants of nucleus locus coeruleus (see ref. 9). Since this nucleus does not respond to NGF[13] the mechanism for this fibre stimulation is, however, unlikely to be a response to the increase in NGF demonstrated here.

A parasympathetic stimulation was evident by irides treated by freezing and thawing, indicating the presence in the iris of trophic factors besides NGF. Similar trophic factors have been found in rat cardiac and skeletal muscle[5,14]. Factors stimulating the ciliary ganglion have also recently been reported in the embryonic chick heart[6,15,16] and chick iris[17,18] as well as in culture medium conditioned by chick heart[19] and muscle cells[20].

Conclusions

Thus two nerve growth stimulating factors, one affecting sympathetic and sensory neurones and the other affecting parasympathetic neurones, were found in rat iris tissue. The present results provide the first demonstration that the level of NGF is raised in a tissue *in situ* as a result of denervation. Our data are in line with the demonstration that immunosympathectomy[1] is brought about by neutralizing endogenous NGF[21] and support the concept of NGF as a messenger between target organs and peripheral neurones in mammals.

This work was supported by the Swedish Medical and Natural Science Research Councils (grants 04X–03185 and B 2021–100, respectively), Magnus Bergvalls Stiftelse and Karolinska Institutets Fonder. We thank Miss Lena Hultgren, Mrs Annika Jordell-Kylberg and Mrs Stine Söderström for technical assistance.

Received 28 January; accepted 29 April 1980.

1. Levi-Montalcini, R. & Angeletti, P. U. *Physiol. Rev.* **48,** 534–569 (1968).
2. Varon, S. S. & Bunge, R. P. *A. Rev. Neurosci.* **1,** 327–361 (1978).
3. Harper, G. P. & Thoenen, H. *J. Neurochem.* **34,** 5–16 (1980).
4. Harper, G. P. *et al. Nature* **279,** 160–162 (1979).
5. Jacobson, C.-O., Ebendal, T., Hedlund, K.-O. & Norrgren, G. in *Control Mechanisms in Animal Cells—Specific Growth Factors* Vol. 1 (Raven, New York, 1980).
6. Ebendal, T. *Devl Biol.* **72,** 276–290 (1979).
7. Harper, G. P., Pearce, F. L. & Vernon, C. A. *Nature* **261,** 251–253 (1976).
8. Johnson, D. G., Silberstein, S. D., Hanbauer, I. & Kopin, I. J. *Neurochemistry* **19,** 2025–2029 (1972).
9. Olson, L., Seiger, Å. & Ålund, M. in *Formshaping Movements in Neurogenesis* (eds Jacobson, C.-O. & Ebendal, T.) 245–256 (Almqvist and Wiksell, Stockholm, 1978).
10. Olson, L. & Malmfors, T. *Acta physiol. scand.* Suppl. **348,** 1–112 (1970).
11. Stoeckel, K., Schwab, M. E. & Thoenen, H. *Brain Res.* **99,** 1–16 (1975).
12. Suda, K., Barde, Y. A. & Thoenen, H. *Proc. natn. Acad. Sci. U.S.A.* **75,** 4042–4046 (1978).
13. Olson, L., Ebendal, T. & Seiger, Å. *Devl Neurosci.* **2,** 160–176 (1979).
14. McLennan, I. S. & Hendry, I. A. *Neurosci. Lett.* **10,** 269–273 (1978).
15. Lindsay, R. M. & Tarbit, J. *Neurosci. Lett.* **12,** 195–200 (1979).
16. Ebendal, T., Belew, M., Jacobson, C.-O. & Porath, J. *Neurosci. Lett.* **14,** 91–95 (1979).
17. Adler, R., Landa, K. B., Manthorpe, M. & Varon, S. *Science* **204,** 1434–1436 (1979).
18. Manthorpe, M., Skaper, S., Adler, R., Landa, K. & Varon, S. *J. Neurochem.* **34,** 69–75 (1980).
19. Helfand, S. L., Riopelle, R. J. & Wessells, N. K. *Expl cell. Res.* **113,** 39–45 (1978).
20. Nishi, R. & Berg, D. K. *Nature* **277,** 232–234 (1979).
21. Banks, B. E. C., Carstairs, J. R. & Vernon, C. A. *Neuroscience* **4,** 1145–1155 (1979).
22. Anundi, H., Rask, L. & Peterson, P. A. in *Formshaping Movements in Neurogenesis* (eds Jacobson, C.-O. & Ebendal, T.) 213–216 (Almqvist and Wiksell, Stockholm, 1978).

Comparison of white pock (h) mutants of monkeypox virus with parental monkeypox and with variola-like viruses isolated from animals

K. R. Dumbell & L. C. Archard

Department of Virology, St Mary's Hospital Medical School, London W2 1PG, UK

Monkeypox mutants arising spontaneously or after serial, high multiplicity passage were characterized phenotypically and by restriction endonuclease mapping. Some resemble 'whitepox' and variola viruses in several of the markers tested but all are distinguishable phenotypically from these. None resembles 'whitepox' viruses in genome structure although near-terminal deletions or symmetrical, terminal rearrangements, relative to parental monkeypox, occurred. 'Whitepox' viruses isolated from animals closely resemble variola in both phenotype and genome structure.

THE last naturally occurring case of smallpox was in Somalia in 1977 and the WHO is satisfied that a human reservoir of this disease no longer exists. Attention is now focused on whether there exists any non-human reservoir of variola virus that might threaten the permanence of the eradication of smallpox. A few cases clinically resembling smallpox have occurred sporadically in villages or small towns in the rain forest belt of West Africa. These were caused, not by variola virus, but by another pox virus called monkeypox[1]. Monkeypox virus has shown no evidence of sustained transmission in man and seems not to be a serious public health problem[2].

Attempts to find the natural reservoir of monkeypox virus in West Africa have so far failed to provide any isolates of this virus from wild animals. Four pox viruses, however, which have been recovered from specimens of animals caught in Zaire, have proved indistinguishable from variola virus by biological tests in the laboratory. These four and two similar viruses isolated from monkeys imported into Holland from Malaysia have collectively been called the whitepox viruses. Their natural history is unknown, but there are two reports[3,4] that viruses with the laboratory phenotype of whitepox virus have been obtained from stocks of monkeypox virus, either from hamsters inoculated with monkeypox or by cloning on the chick chorioallantois (CAM).

The implication is that monkeypox virus, which does on rare occasions infect humans, can also produce, as a genetic variant, a virus which may have the same propensities as variola. It is clearly important to examine this question as closely as possible.

Restriction endonuclease cleavage sites were first mapped on a pox virus genome by Wittek *et al.*[5] and this technique has been used by Mackett and L.C.A.[6] to study the structure and relatedness of the genomes of several orthopoxviruses. Here we report the early results of an investigation of monkeypox variants, both by phenotype and by DNA analysis, to assess whether any such variants can be considered identical with whitepox viruses in all ascertainable respects.

Cloning technique

Stage 1: Material sampled from a single pock on the CAM was homogenized by manual shaking with sterile glass beads and 1 ml of 4 mM McIlvaine buffer, *p*H 7.4. The extract was then treated in an ultrasonic bath (Megasonic, 80 kc) for 1 min and centrifuged at 1,000g for 5 min. The supernatant was filtered through a Millipore filter, average pore size 650 μm, to remove most of the aggregates of virions. Filtration reduced the titre by about 90% and was assumed to leave a predominantly monodisperse suspension; suspensions were too dilute to check this by electron microscopy.

Stage 2: Dilutions were made immediately of the filtrate from stage 1 and were inoculated on the CAM and incubated for 64 h at 35 °C. A piece of membrane bearing a single pock was excised from a membrane having no other visible pock lesion, extracted as described above, and the extract inoculated on the CAM to produce stock virus. It was considered that two sequential 'clonings' resulted in a population which could be reasonably considered as the progeny of a single virion. Note that a 'clone' need not have invariant properties but might itself become genetically heterogeneous during multiple cycles of replication. Stability of biological properties was not taken as a criterion for the purity of a clone, although such constancy was found in practice for most of the clones studied.

Phenotypic characterization

Four markers were used in these experiments, each of which differentiated variola or whitepox from monkeypox. (1) Pock type. Monkeypox virus produces small, pink, haemorrhagic (h^+) pocks on the CAM at 35 °C. Variola or 'whitepox' viruses give small, non-ulcerated white (h) lesions. The 'white pock' character was used for the primary selection of the variants, so that the class of monkeypox variants described here all produce white pocks on the CAM, but are not necessarily whitepox viruses as defined above. (2) Ceiling temperature. Monkeypox virus, but not variola virus, will produce pocks on the CAM of eggs incubated at 39 °C (ref. 7). In the experiments described here ceiling temperature was tested in the CV-1 line of monkey kidney cells which supported the growth of all relevant viruses at 35 °C, but at 40 °C monkeypox virus (t^+) would grow and variola virus (t) would not. Note that embryonated eggs, being exothermic, maintain a temperature above the recorded temperature of the incubator[8] and that ceiling temperatures determined in cell cultures may therefore seem to be up to 1 °C higher than those measured on the CAM. (3) Haemagglutinin. Most strains of variola do not produce detectable haemagglutinin (HA) for

0028-0836/80/270029-04$01.00

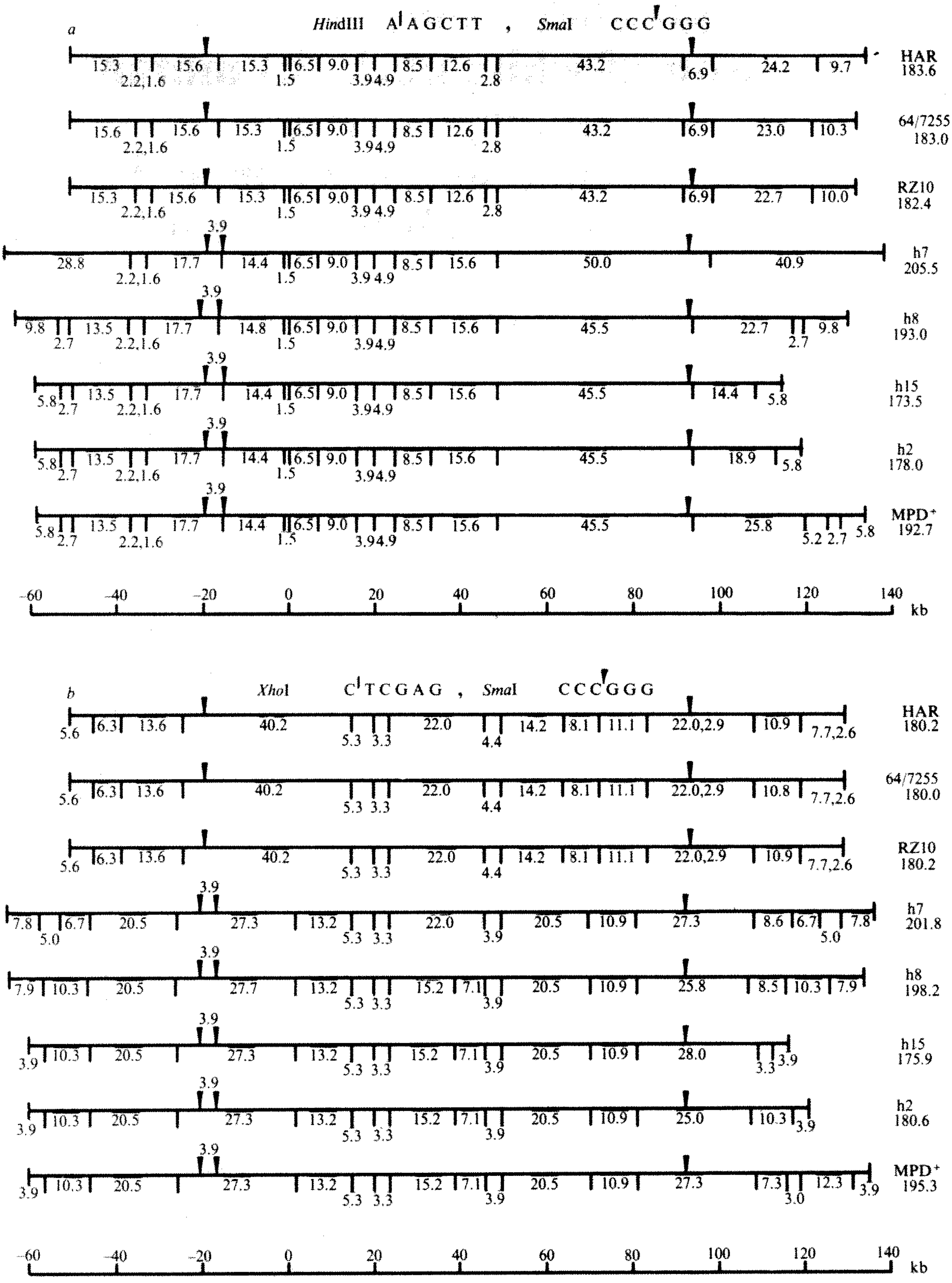

Fig. 1 Physical map locations of *Hin*dIII or *Sma*I restriction fragments (*a*) and *Xho*I or *Sma*I restriction fragments (*b*) of DNA from: variola Harvey (HAR), whitepox viruses 64/7255 and RZ10, monkeypox Copenhagen (MPD) and white pock mutants of MPD (h2, h7, h8, h15). Numbers indicate estimated sizes of individual fragments in kilobases (kb).

vaccinia-sensitive fowl erythrocytes when inoculated into RK13 cell cultures; monkeypox, on the other hand, makes large amounts of HA in RK13 cells[9] and some is produced by two of the whitepox viruses[10]. In our study, viruses were classed as HA producers in RK cells (rh$^+$) if 8 or more units were produced in standard HA titration[10]. (4) Growth in PEK cells. Marennikova *et al.*[11] reported that variola and whitepox viruses could be passed readily in a pig embryo kidney (PEK) cell line, but that monkeypox viruses were lost on passage. Ueda and K.R.D. (unpublished) confirmed that variola and vaccinia replicated to high titre in a line of pig kidney cells. Strains of monkeypox virus either did not replicate or reached only low titres in these cells and were classed as 'p'. Whitepox viruses all replicated in these cells to significant titre (p$^+$).

Isolation and phenotype of the h mutants

When the cloned wild-type monkeypox strain Copenhagen was inoculated on the CAM at approximately 50 pock forming units (PkFU) per membrane, less than 0.1% of the pocks were white. Two clones (h2, h15) were isolated.

The frequency of white pocks was significantly increased after passage of the wild stock on the CAM in high concentration. After four passes with an inoculum of $10^{6.0}$ PkFU, white pocks were present as 2–3% of the total and after six such passes, 50–60% of pocks were white. In a control series of eggs inoculated with 10^3 PkFU the frequency of white pocks remained at 0.2% after four and six passes. One clone (h3) was isolated after four passes at high concentration and seven (h4–h10) after the sixth such passage.

In subsequent experiments, two clones (h5 and h7) were re-passaged four times in high concentration and then recloned to give h5/1, h5/2, h7/1 and h7/3. Clone h7 was also recloned several times successively and stocks were made from the fifth and seventh reclonings (h7/c5, h7/c7). Another mutant (h16) was derived from a culture inoculated with parental monkeypox virus and incubated for 48 h in arginine-free medium, followed by a further 24 h in complete medium.

The phenotypes of all the h mutants are shown in Table 1. It will be seen that three clones (h2, h15, h6) are like the wild type except for the white pock character used in their selection. Five clones (h3, h4, h8, h9, h10) have one phenotypic change other than the white pock and two clones (h5, h7) resemble whitepox in three of the four markers used. Clones h5 and h7 did not change phenotype following passage in high concentration and recloning (clones h5/1, h5/2, h7/1, h7/3). None of the clones in this series had a lowered ceiling temperature, and this distinguishes them all from whitepox virus. However, a white pock mutant with a low ceiling temperature has been isolated from another strain of monkeypox and by using a different selection procedure. It is probable, therefore, that in an extended series, mutants would be found which were phenotypically like whitepox in all four characters used.

DNA analysis

Methods for virus growth and purification, extraction and cleavage of DNA and characterization of DNA restriction fragments were essentially as described previously[6,12].

Physical maps of cleavage sites were constructed mainly by hybridizations between restriction fragments generated from genomes of closely related viruses on the basis that, with the exception of terminal repetitions, fragments having sequence homology represent geographically equivalent regions of the genomes. Maps were also constructed by hybridizations between fragments cleaved from the same virus DNA by different restriction endonucleases. In some cases, physical maps of DNA from virus variants may be constructed from unequivocal interpretation of changes in the size of fragments generated by endonucleases *Hin*dIII, *Xho*I or *Sma*I and various double digests compared with those from wild-type DNA.

Comparative descriptions of the genomes of different orthopoxviruses and of changes between wild type and mutants are confusing when DNA fragments are labelled separately in order of size for each virus and for each restriction endonuclease. Additionally, it is impractical to measure from one end of the genome as most variation between and within orthopoxvirus types is found near the termini[6] and, even within a single strain of virus, variations are found in the length of the terminal fragments between one cloned line and another[13]. It was decided to select one arbitrary reference point in an internal region of the genome; we chose the site separating the contiguous *Hin*dIII fragments O and I in the original map of rabbitpox[5]. Fragments of similar size map in equivalent locations in all orthopoxvirus genomes for which *Hin*dIII maps have been constructed[6], and this region of the genomes is highly conserved. The reference point separates wild-type monkeypox *Hin*dIII fragments Q and I[6]. Locations of cleavage sites for particular endonucleases are defined as distances from the reference point measured in kilobases, with a positive sign if to the right and a negative sign if to the left. Sizes of genomes were derived by summation of restriction fragments sized by co-electrophoresis with digests of wild-type DNA. Physical maps were drawn to scale and the sizes of individual fragments indicated in kilobases (Fig. 1).

Physical maps of the cleavage sites for endonucleases *Hin*dIII, *Xho*I and *Sma*I in the genomes of two strains of variola and of three strains of wild-type monkeypox including Copenhagen (MPD) have been presented previously[6]. Physical maps for the same three endonucleases have been constructed from hybridization data and confirmed by double digestion for two of the whitepox viruses (64/7255 and RZ10) and are shown in Fig. 1. These are the first maps of whitepox viruses to be constructed, although electropherograms of endonuclease digests of whitepox DNA have been presented previously[14]. Viruses 64/7255 and RZ10 map very similarly to variola strain Harvey (HAR), preserving all characteristic internal cleavage sites but showing small variations in the size of the *Hin*dIII termini and of near-terminal *Hin*dIII or *Xho*I fragments mapping between 100 and 120 kilobases. The sizes of *Hin*dIII, *Xho*I or *Sma*I restriction fragments from the genomes of the other four whitepox viruses and of two whitepox-like viruses (Ham 8, Ham 9) isolated from hamsters[3] are similar to those presented here.

A general feature of orthopoxvirus genome structure is the presence of species-specific, terminal repetitions containing subsets of common sequences[6,15]. Because of this, the opposing terminal fragments from any particular genome cross-hybridize and either terminus will hybridize to both termini of the genome of another orthopoxvirus. A structural feature peculiar to variola and whitepox viruses is that the opposing termini fail to cross-hybridize. Additionally, the MPD/*Hin*dIII 2 molar terminal 5.8-kilobase fragment hybridizes specifically with only right-hand terminal fragments and the 2 molar MPD/*Hin*dIII 2.7-kilobase fragment with only left-hand terminal fragments of variola-like genomes. Such genome organization in relation to that of other orthopoxviruses may have resulted from non-symmetrical deletion of sequences within hypothetical repetitions or, from exchange of specific repetitive sequences between termini suggesting conjunction of the termini at some stage of replication.

Three sorts of genome have been obtained from the different white pock mutants of monkeypox (MPD). One (h16) has no change detectable by analysis with *Hin*dIII, *Xho*I or *Sma*I. White pock mutants of other monkeypox strains having a similar relationship to the respective parents have also been isolated. Second, the two spontaneous MPD white mutants (h2, h15) map with large deletions close to the right-hand terminus and another, not fully characterized, seems to be of the same class. The deleted sequences overlap partially and represent about 15 and 19 kilobases respectively. Variation at this locus is common in orthopoxvirus genome structure[6]. Third, white pock mutants isolated following high multiplicity passage (h3–h8, h10) show

Table 1 Phenotype of monkeypox virus and its 'h' mutants

Phenotype		Viruses
$h^+ t^+ rh^+ p$		Monkeypox, wild type
$t^+ rh^+ p$	h	h2, h6, h15
$t^+ rh^+$	$h \quad p^+$	h3, h4, h8, h9
$t^+ \quad p$	h rh	h10, h16
t^+	$h\ rh\ p^+$	h5, h7
t^+	$h\ rh\ p^+$	h5/1, h5/2, h7/1, h7/3, h7/c5, h7/c7
rh^+	$h\ t\ p^+$	64/7255, 64/7275 (whitepox viruses)
	$h\ t\ rh\ p^+$	Chimp 9, Mk7, RZ10, RZ38, (whitepox viruses)

Pocks: haemorrhagic, h^+; white, h. Growth in CV1 at 40 °C, t^+; no growth, t. Haemagglutinin in RK13 cells: titre ≥16, rh^+; <8, rh. Growth in PEK cells; good, p^+; none, p.

major and complex changes involving both termini of the genome symmetrically and smaller changes at some internal sites. Mutants h3–h7 and h10 are essentially similar and have genomes about 7–9 kilobases larger than that of the wild type. Assuming that symmetrical, near-terminal fragments generated by endonuclease *Xho*I result solely from cleavages within the terminal repetitive sequences, the repetition is then both larger than and divergent in sequence from that of the wild-type genome. A minimum estimate of the size of the parental repetition by summation of the symmetrical near-terminal fragments is 8.5 kilobases, whereas that for white mutants of this type is 19.5 kilobases and contains no sites for endonuclease *Hin*dIII. With the exception of h3, the genomes of these mutants have also lost a *Xho*I site in an internal, normally highly conserved region at the 38-kilobase position. A *Xho*I site at this locus, present in the genome of mutant h6 when isolated, was lost on subsequent recloning. Mutant h8 also shows extensive, symmetrical, near-terminal sequence rearrangements; the minimum size of the terminal repetition is 18 kilobases and the *Hin*dIII sites defining the MPD 2.7 kilobase fragment are retained. Mutant h8 is similar to h2 in some respects, showing a near-terminal deletion (3–4 kilobases) mapping to the right of the *Sma*I site located at 92 kilobases, and symmetrical, near-terminal sites for *Xho*I. Additionally, h8 has an apparent insertion, relative to the parental genome, of 0.4 kilobases mapping between −1.5 kilobases and the *Sma*I site at −15.5 kilobases. A similar small insertion is seen in the same region of the genome of mutant h5. Mutant h8 retains the internal *Xho*I site at the 38-kilobase position. The locations of *Sma*I sites, relative to those in wild-type DNA, are preserved in all the monkeypox mutants described.

The rearranged genome exemplified by mutant h7 is apparently a stable configuration as neither four further high multiplicity passages followed by recloning nor nine successive reclonings generated further changes detectable by restriction analysis with *Hin*dIII, *Xho*I or *Sma*I.

Although the genotypes of the spontaneous mutants h2 and h15 are readily recognizable as variants of wild-type monkeypox, the changes exhibited by, for example, mutants h7 and h8, seem to be as extensive as those distinguishing some orthopoxvirus species[6]. However, the genomes of these mutants remain readily distinguishable from those of variola and whitepox viruses.

Discussion

Monkeypox mutants. The objective of the present study was to characterize mutants of monkeypox virus, both phenotypically and by DNA analysis, and to assess how closely they might mimic whitepox or variola. The mutants were derived in different experimental conditions but each was selected initially from a white pock produced on the CAM.

Spontaneous white-pock mutants are relatively rare in monkeypox. The two which were obtained each had a genome substantially shorter than that of MPD due to deletion of DNA sequences near the right-hand terminus, together with some rearrangement of terminal sequences. The mutants obtained after high-multiplicity passage had more complex, symmetrical rearrangements of terminal sequences and the genomes were as big as or bigger than that of MPD. Smaller deletions of sequences were detected in some of them in approximately the same locus as the large deletions in the genomes of the spontaneous mutants. Although the numbers are small, it seems that particular experimental conditions affect the kind of mutant most likely to be selected. It is suggested that the spontaneous mutants may represent an early, and the high-multiplicity mutants a late stage in a process which can engender complex changes in genome structure during replication. This hypothesis is now being tested. Several phenotypically different mutants had genomes with maps similar to those shown for mutant h7. The genome of h7 seems to represent a stable configuration. The maps of h7 showed no detectable changes after further passages at high multiplicity and several reclonings. The symmetrical nature of the changes which occur at the two ends of the genome strongly suggest that the near-terminal configurations had been determined in the same process or that sequences from one end had been copied to the other. On either basis, the evidence supports the previously proposed[16,17] idea of transient circularization at some stage in the replication of orthopoxvirus DNA.

The mutants exhibited a variety of phenotypic changes but it was not expected that these could be correlated with the changes in the relatively crude restriction maps; indeed, one mutant (h16), with no changes detectable in the maps, had two changes in the phenotypic markers.

Whitepox and monkeypox. No phenotypic character has yet been described which distinguishes the group of whitepox viruses from variola. Consistent with this, the maps of the genomes of the whitepox viruses are closely similar to those of variola HAR, and they share with variola the failure of one terminus to cross-hybridize with the opposing terminal fragment. Although the present maps are too crude to prove identity, they add to the steadily growing evidence of the close relationship of whitepox to variola.

On the other hand, there are significant differences between the genomes of whitepox and monkeypox. Apart from the differences in near-terminal sequences, there are four cleavage-site differences within the conserved region of the genome. The *Sma*I site at −15 kilobases and the *Xho*I sites at 3 and 38 kilobases are present in monkeypox but not in variola or whitepox, whereas a *Hin*dIII site at 45 kilobases is present in variola and whitepox but not in monkeypox. Of these four sites, the only one found to be changed in some of the h mutants is the *Xho*I site at 38 kilobases. Even the two mutants (h5 and h7) which resemble whitepox in three of the four phenotypic markers have genomes which differ significantly from that of variola. On the other hand, there is evidence that different experimental conditions select for different kinds of complex mutations and some caution is necessary in forecasting what limits could be set to the possible variations in the monkeypox genome.

Our experiments have failed to generate any monkeypox mutants with genomes similar to those of the whitepox-like viruses described by Marennikova and Sheluchina[3]; however, the methods used in the generation of our mutants differ from those described by these authors.

A crucial question is whether variola virus possesses any DNA sequences unique to itself and which are missing from monkeypox (and even perhaps from whitepox), as rearrangements, however complex, could not be expected to create significant new information. This question cannot yet be answered, but several ways of approaching it are theoretically possible and one main reason for any continuing work with variola would be to obtain the answer.

We thank Drs R. Gispen, S. S. Marennikova and P. von Magnus for providing strains of whitepox viruses and monkeypox Copenhagen, and Mrs Ruth Reith for assistance. The work was supported by grants from the MRC and the WHO.

Received 9 April; accepted 14 May 1980.

1. Von Magnus, P., Andersen, E. K., Petersen, K. B. & Birch-Andersen, A. *Acta path. microb. scand.* **46,** 156–176 (1959).
2. Breman, J. G. *et al. Bull. Wld Hlth Org.* (in the press).
3. Marennikova, S. S. & Shelukhina, E. M. *Nature* **276,** 291–292 (1978).
4. Marennikova, S. S., Shelukhina, E. M., Maltseva, N. N. & Matsevich, G. R. *Intervirology* **11,** 333–340 (1979).
5. Wittek, R. *et al. J. Virol.* **23,** 669–678 (1977).
6. Mackett, M. & Archard, L. C. *J. gen. Virol.* **45,** 683–701 (1979).
7. Bedson, H. S. & Dumbell, K. R. *J. Hyg., Camb.* **59,** 457–469 (1961).
8. Siim, J. C. *Acta med. scand.* Suppl. **234,** 304–316 (1949).
9. Huq, F. thesis, Univ. London (1972).
10. Dumbell, K. R. *Lancet* **ii,** 585 (1974).
11. Marennikova, S. S., Gurvich, E. B. & Shelukhina, E. M. *Arch. ges. Virusforsch.* **33,** 201–210 (1971).
12. Archard, L. C. & Mackett, M. *J. gen. Virol.* **45,** 51–63 (1979).
13. Wittek, R., Müller, H. K., Menna, A. & Wyler, R. *FEBS Lett.* **90,** 41–46 (1978).
14. Esposito, J. J., Obijeski, J. F. & Nakano, J. H. *Virology* **89,** 53–66 (1978).
15. Wittek, R. *et al. J. Virol.* **28,** 171–181 (1978).
16. Archard, L. C. *J. gen. Virol.* **42,** 223–229 (1979).
17. McFadden, G. & Dales, S. *Cell* **18,** 101–108 (1979).

●

Pure Chemistry Library
SCIENCE COLLEGE
Upper Circular Road
CALCUTTA

Structure of southern bean mosaic virus at 2.8 Å resolution

Celerino Abad-Zapatero, Sherin S. Abdel-Meguid, John E. Johnson, Andrew G. W. Leslie*, Ivan Rayment†, Michael G. Rossmann, Dietrich Suck‡ & Tomitake Tsukihara§

Department of Biological Sciences, Purdue University, West Lafayette, Indiana 47907

X-ray diffraction studies reveal that the polypeptide chain of the southern bean mosaic virus protein subunit has a fold closely similar to the shell domain of tomato bushy stunt virus. The protruding domain of tomato bushy stunt virus is absent in southern bean mosaic virus. The tertiary structure observed in these viruses may be particularly suitable for the formation of the protein coat in small, spherical, RNA-containing, plant viruses.

SIMPLE plant viruses are composed of nucleic acid and a protein coat consisting of multiple copies of covalently identical subunits arranged in a symmetrical manner[1,2]. These viruses can be broadly categorized as rod-shaped, bacillus-shaped and spherical. The morphological classes can be subdivided into groups based on physical and biological properties such as stability, symmetry and strategy of replication[3,4]. High resolution X-ray structure determinations have been accomplished for the rod-shaped tobacco mosaic virus[5] (TMV) and its disk protein[6] as well as the spherical tomato bushy stunt virus[7] (TBSV). The contrasting structures of the proteins in these two viruses reveal differing requirements for assembly into a helical rod and icosahedral shell. Although TMV protein subunits consist primarily of four, roughly radial, α-helices, the two domains of TBSV are composed almost entirely of anti-parallel β-pleated sheet. A possible common feature in the two virus classes is the flexibility of the protein which interacts with the RNA. Although TMV is the only rod-shaped virus being studied at high resolution, several spherical plant viruses, representing different groups, are being investigated (ref. 8, and P. Argos and P. Colman, personal communications). We report here the structure determination of southern bean mosaic virus (SBMV) seen at 2.8 Å resolution. Although SBMV represents a group of viruses[9] with properties significantly different from those of the TBSV group, its viral envelope was found to possess a tertiary and quaternary structure closely similar to that of the TBSV shell (S) domains. It is proposed here and also by Argos[10] that other groups of small, spherical, RNA-containing, plant viruses may also be based on the same folding and assembly principles.

Structure determination

The high resolution structure of SBMV was determined using the rhombohedral type II SBMV crystals[11] with hexagonal axes of $a = 334.3$, $c = 757.5$ Å and a single particle in the unit cell. The R32 space group requires the particle to be situated on a site with 32 crystallographic symmetry, thus placing 10 icosahedral units within the crystallographic asymmetric unit (Fig. 1*a*).

Data for the native crystals and four heavy atom derivatives were collected using oscillation photography[12-15]. The X-ray source was an Elliott rotating anode generator, equipped with a 0.1-mm focal cup and a copper target. The Ni-filtered radiation was focused with two perpendicular mirrors[16]. Some details of the data collection are shown in Table 1*a*. In total, 2,022,187 useful intensities were measured which permitted the determination of phases for 275,966 independent reflections with the multiple isomorphous replacement method. This represented 71% of all possible reflections within the limiting 2.8-Å resolution sphere.

The analysis of the first heavy atom derivative was given previously[17] as were the results of a 5-Å resolution electron density map[18]. The heavy atom positions of four derivatives were found with difference electron density maps and refined by a least-squares procedure[19]. The final atomic parameters will be given elsewhere[20], but some statistics for the multiple isomorphous replacement phase determination are shown in Table 1*b*.

The final 'best' multiple isomorphous replacement (MIR) electron density map was averaged over the 10 different icosahedral units within one crystallographic asymmetric unit[21]. This map was originally used to solve the SBMV coat protein structure. One cycle of phase refinement using the molecular replacement method[22-24] has been completed which provided some improvement in the apparent resolution. For convenience and in accordance with general practice these maps will be referred to as having 2.8 Å resolution, even though the phasing and quality of data are less at high resolution than at low resolution. A more full account of the crystallographic work is reported elsewhere[20].

The averaged MIR electron density map was displayed in sections perpendicular to an icosahedral 2-fold axis. The quasi-3-fold axis relating the three subunits within the icosahedral unit was immediately obvious (Fig. 1*b*). The effect was particularly striking because this axis was nearly parallel to its neighbouring icosahedral 2-fold axis and, hence, perpendicular to the map sections. A similar situation pertains to TBSV[25]. The dominant feature in the SBMV map was a 'β-barrel' type structure (see ref. 26) in which the extended strands were well resolved from each other. A substantial portion of the polypeptide chain could be traced but some ambiguities remained in the connectivity of the strands at the end of the β-sheets. Five helices could be recognized and these determined the direction of the polypeptide. Certain features, in particular the amino-terminal arm, present in only the C subunit (Fig. 1*c*), were then seen to be similar to the TBSV structure. Superposition of the TBSV C_α co-ordinates onto the SBMV electron density map revealed a remarkable resemblance of the TBSV shell domain and the SBMV subunit. The TBSV co-ordinates had been referred to an icosahedral axial system and were used without change in radius on the SBMV map. This permitted an interpretation of all turns and bends on the original MIR map which was subsequently readily verified on the molecular replacement map. These results demonstrated the similarity not only of fold but also of the

---

Present addresses: * Biophysics Section, Blackett Laboratory, Imperial College of Science and Technology, Prince Consort Road, London SW7 2BZ, UK; † Structural Biology Laboratory, Rosenstiel Basic Medical Sciences Research Center, Brandeis University, Waltham, Massachusetts 02154; ‡ European Molecular Biology Laboratory, Postfach 10 22 09, 69 Heidelberg 1, FRG; § Department of Chemistry, Faculty of Engineering, Tottori University, Koyama-cho, Tottori 680, Japan.

0028-0836/80/270033-07$01.00

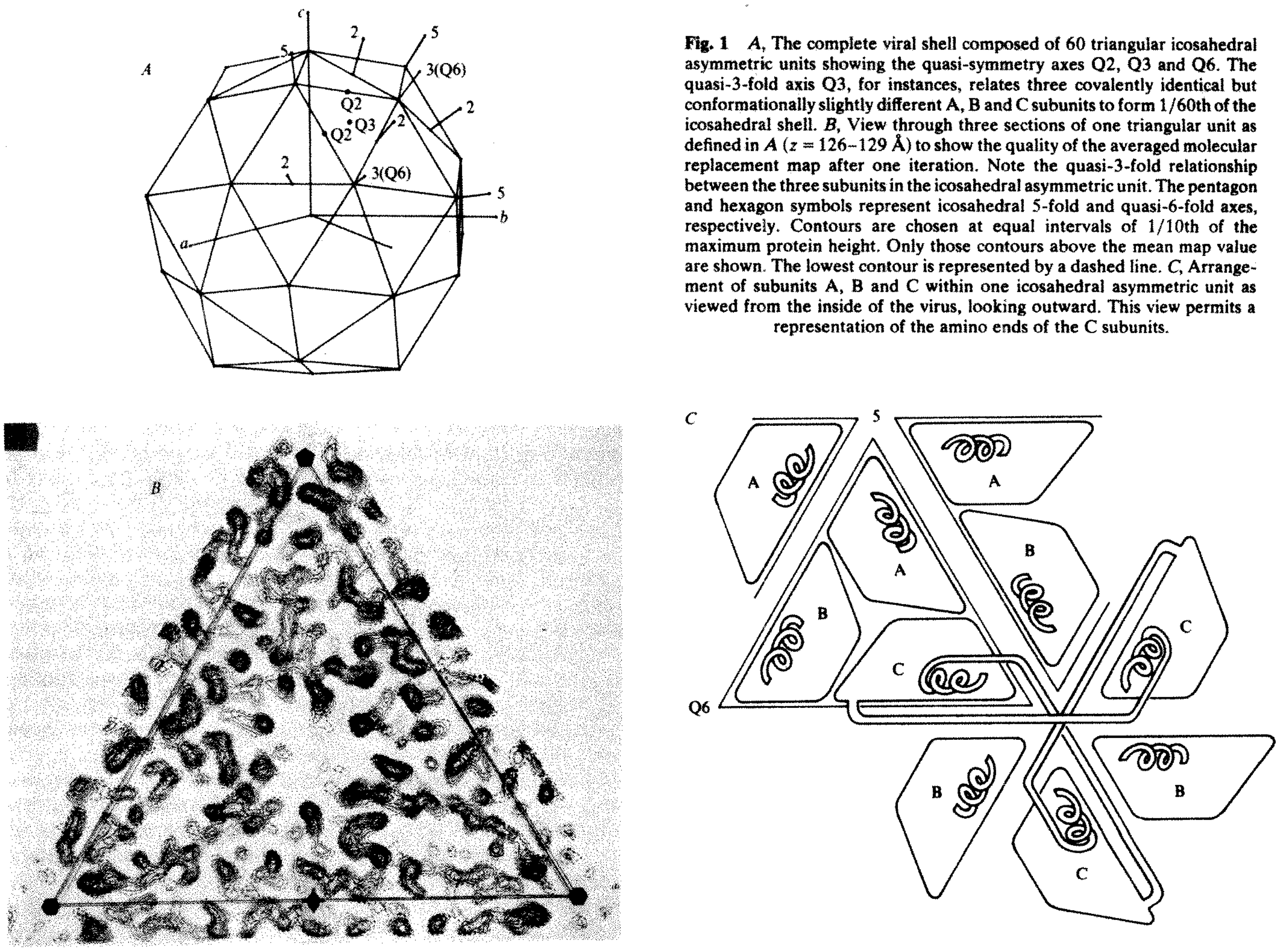

Fig. 1 *A*, The complete viral shell composed of 60 triangular icosahedral asymmetric units showing the quasi-symmetry axes Q2, Q3 and Q6. The quasi-3-fold axis Q3, for instances, relates three covalently identical but conformationally slightly different A, B and C subunits to form 1/60th of the icosahedral shell. *B*, View through three sections of one triangular unit as defined in *A* ($z = 126$–129 Å) to show the quality of the averaged molecular replacement map after one iteration. Note the quasi-3-fold relationship between the three subunits in the icosahedral asymmetric unit. The pentagon and hexagon symbols represent icosahedral 5-fold and quasi-6-fold axes, respectively. Contours are chosen at equal intervals of 1/10th of the maximum protein height. Only those contours above the mean map value are shown. The lowest contour is represented by a dashed line. *C*, Arrangement of subunits A, B and C within one icosahedral asymmetric unit as viewed from the inside of the virus, looking outward. This view permits a representation of the amino ends of the C subunits.

Table 1 Some data collection statistics (*a*) and multiple isomorphous replacement refinement parameters (*b*)

Compound	Resolution limit (Å)	Oscillation range	No. of reflections measured	No. of independent reflections	R^* (%)	Rejection criterion
a						
Native	2.8	0.5°	652,887	321,586	13.5	None
	3.5	1.0°	346,412	175,788	13.1	None
	2.8 combined		438,759	299,893	12.5	$F^2 < 1\sigma$
PHMBS	2.8	0.5°	633,954	318,227	15.6	None
	3.5	1.0°	357,937	178,606	12.2	None
	2.8 combined		430,717	289,234	11.3	$F^2 < 1\sigma$
$K_3(UO_2)F_5$	2.8	0.5°	631,979	320,184	16.5	None
	4.0	1.25°	188,711	100,739	14.5	None
	2.8 combined		358,606	280,857	14.4	$F^2 < 1\sigma$
K_2PtCl_4	3.5	1.0°	309,233	157,065	11.1	$F^2 < 1\sigma$
$AuCl_4$	3.5	1.0°	278,156	149,992	12.2	$F^2 < 1\sigma$

b									
Shell	1	2	3	4	5	6	7	8	Overall
Resolution (Å)	∞	22.2	11.1	7.4	5.6	4.4	3.7	3.2	2.8
Figures of merit:									
$<m>$	0.70	0.71	0.75	0.72	0.65	0.61	0.53	0.46	0.59
n	430	6228	15,963	30,853	42,879	64,440	69,530	45,643	275,966
R-factors†:									
PHMBS	31	28	25	33	33	37	44	61	42
$K_3(UO_2)F_5$	35	36	31	46	40	51	75	96	55
K_2PtCl_4	115	76	75	59	53	50	40	—	45
$AuCl_4$	41	50	58	49	52	47	52	—	53

PHMBS, *p*-hydroxymercuribenzoate sulphonate. $<m>$ is the mean figure of merit. n is the number of phased reflections in shell.

$$*R = \frac{\sum_h \sum_i |(F_{hi}^2 - \bar{F}_h^2)|}{\sum_h \sum_i \bar{F}_h^2} \times 100$$

where $\bar{F}_h^2$ is the mean of the i observations F_{hi}^2 on the reflection h.

$$\dagger R = \frac{\sum |[|F_{HV}| - |(F_V + f_H)|]|}{\sum |f_H|} \times 100$$

where F_{HV}, F_V, and f_H are the structure factors for the heavy atom derivative, the native virus crystals and the heavy atoms alone, respectively.

packing of protein subunits in the viral shells. Backbone models of the C subunits (see Fig. 1*b*) were built into a Richards optical comparator[27] with Kendrew-Watson model parts on a scale of 2 cm ≡ 1 Å. The co-ordinates of the SBMV backbone atoms were measured with a plumb line and checked for gross error. These have been deposited with the Protein Data Bank at Brookhaven National Laboratory[28].

The chain tracings of the C subunit, together with the corresponding structures of the quasi-3-fold-related A and B subunits, accounted for all the major features in the map. The internal boundary of the protein shell was well defined. Features of the electron density in the interior of the virus were lower and disconnected in the averaged maps, permitting no explicit recognition of nucleotides.

The 2.8-Å resolution map did not differ in substance from the earlier 5.0-Å map[18]; indeed, the electron density distributions were remarkably similar. The selection of the subunit boundaries had been essentially correct in the low resolution map. The feature referred to as a 'small lobe of the subunit' was now seen to be the extra protruding helix near the quasi-3-fold axis in SBMV (*vide infra*). The 'large helix-containing lobe' did not, in fact, contain helix but was related to the very obvious protrusions near the 5- and quasi-6-fold axes. The sheet near the 2-fold axes corresponded to one side of the β-barrel. The '26 distinct phosphate sites' seen at 5 Å resolution must now be regarded with some scepticism. Although these features within the RNA region remain in position, they are lower in density relative to the protein in the averaged isomorphous replacement map.

The protein shell and viral exterior

The SBMV subunit is primarily an eight-stranded anti-parallel β-barrel (Fig. 2). However, at least 66 residues at the amino end are not a part of the barrel, but form a partially ordered 'arm' in the interior of the virus. The protein shell of SBMV is about 35 Å thick, extending from around 110 Å to 145 Å radius. Each quasi-3-fold axis is 27 Å distant and parallel to its nearest icosahedral 2-fold axis. A careful analysis of the conformational differences between the three quasi-symmetrically related subunits A, B and C has not been completed. An initial examination of the electron density and position of equivalent heavy atoms[20] shows that the A subunits differ significantly from the B and C subunits at turns close to the 5-fold axes, where SBMV has insertions relative to TBSV. Other regions show less deviation, as was also the case in TBSV[7], where differences were less than 1 Å.

Figure 3 shows a superposition of the C_α coordinates for the S domain of TBSV and the SBMV subunits. Both structures are referred to the same icosahedral axial system. The r.m.s. difference in C_α coordinates is 2.7 Å over 182 residues, excluding those residues which are insertions or deletions in one or the other subunits. The extent of topological equivalence is almost as good as that between the α and β chains of horse haemoglobin and is certainly much better than that between the NAD-binding domains of lactate dehydrogenase and glyceraldehyde-3-phosphate dehydrogenase (Table 2).

Harrison (personal communication) has assigned a tentative amino acid numbering system to the TBSV C subunit which is shown in Figs 2 and 3, and shall also be used in SBMV. Some residues may have to be inserted or deleted pending the full amino acid sequence determination of TBSV and SBMV. The ordered amino-terminal arm of the TBSV C subunit runs from 1 to 32 followed by the S domain from 33 to 200. The TBSV P domain consists of the final 111 residues within the polypeptide chain. Major differences between the SBMV subunit and the TBSV S domain are (1) an extra α-helix (see following section), a feature which is ordered in all three quasi-equivalent subunits, (2) the organization of the β-annulus structure about the icosahedral 3-fold axes, (3) insertions of residues 49A and 177A, 177B, 177C, 177D near the quasi-6-fold and icosahedral 5-fold axes, (4) insertion of 17 residues between 155 and 160, replacing residues 156–159 near the quasi-3-fold axis, (5) deletion of residues 55–61 opposite the TBSV P domain on the viral exterior and replacement by residue 55A, (6) deletion of residue 104 at a subunit interface, (7) deletion of residue 114 and insertion of residue 118A at a different subunit interface near the viral surface, and (8) deletion of residue 130 and insertion of some residues at the protein–RNA interface.

The most dramatic alterations between TBSV and SBMV occur on the viral surface. The larger protruding P domains about the 2-fold axes in TBSV are replaced by the abbreviated protrusions around the quasi-3-fold axes in SBMV (Fig. 4*a*). The SBMV protrusions are formed by the insertion of a three-turn helix (155A to 155M) running tangential to the viral surface and a one-turn addition (155N–155Q) to the radial helix 160–164. The latter makes a 60° left-handed turn over a distance of 12 Å about the quasi-3-fold axis, thus forming a keratin-like structure[29] when taken in conjunction with its two neighbouring subunits. There is also a protrusion around the icosahedral 5-fold (Fig. 4*b*) and quasi-6-fold (Fig. 4*c*) axes in SBMV which is absent in TBSV. Both the trimer (Fig. 4*a*) and the pentamer (Fig. 4*b*) -hexamer (Fig. 4*c*) clustering in SBMV had been observed previously in a 22.5-Å resolution map[30]. The third major difference is the deletion of TBSV residues 55–61. These residues make an excursion, towards the TBSV P domain, out of the β-strand that runs between residues 52–62. They stabilize the orientation of the P domain in the C subunit, where the hinge between the domains is bent more acutely than in the A and B subunits. This function is not required in SBMV. The evolution of surface differences between TBSV and SBMV might be a recognition mechanism for altering host specificity by adapting to the properties of host or vector.

Both TBSV and SBMV require metal ions for assembly and stabilization of their protein shell. The function of calcium and magnesium ions has been extensively studied with respect to the properties of SBMV[31–34]. In the absence of metal ions and at alkaline *p*H these viruses swell by about 7% in radius. Wells and Sisler[35] have shown that swollen SBMV has only 2% of the infectivity of native SBMV. This could be due to the loss of integrity of the viral surface features or it might be the consequence of the ease with which the swollen virus can be degraded by nucleases and proteases. The positions of the metal ions in TBSV have been determined by Harrison *et al.* (ref. 7 and personal communication). There are significant conformational differences (Fig. 3) between TBSV and SBMV in the region (residues 113–120) of this site.

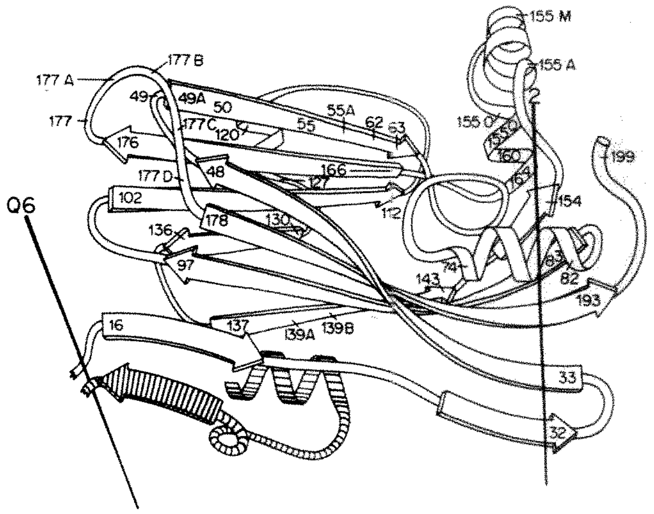

Fig. 2 Diagrammatic representation of the SBMV C subunit with its amino-terminal arm and α-helix. The latter is bound to the base of a subunit, possibly related by a 3-fold rotation. The very tentative amino acid numbering scheme is shown. Numbers such as 177A, 177B are insertions in SBMV relative to TBSV. Drawing by Jane Richardson.

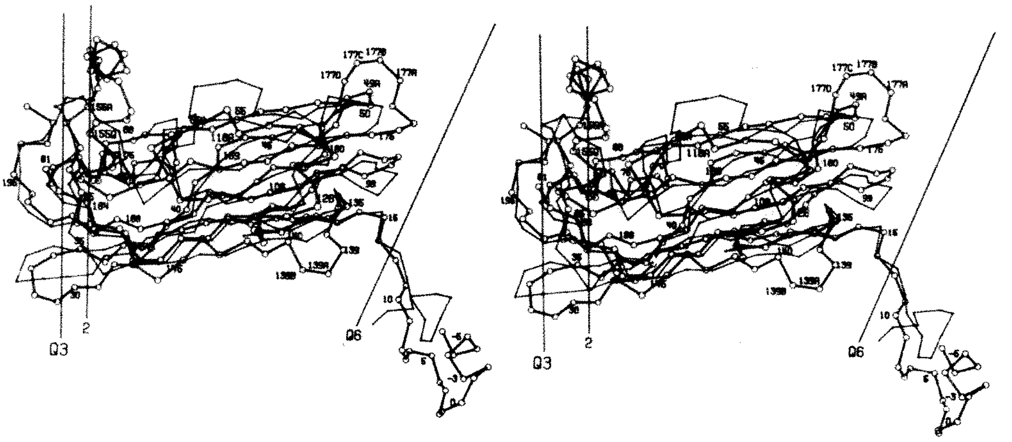

Fig. 3 Stereo diagram showing the C_α atoms in SBMV (large circles connected with thick bonds) superimposed on the TBSV shell domain (thin bonds). Both viruses are referred to the same icosahedral axial system. The amino acid numbering of SBMV is shown. It relates to a tentative system for TBSV.

The amino acid composition of SBMV has been determined by Tremaine[36], Ghabrial *et al.*[37] and Dietrich[38]. Dietrich has also partially determined the amino acid sequence of 15 tryptic and 2 cyanogen bromide fragments. Attempts to find the position of these peptides (the largest being 16 residues long) in the electron density map were only partially and tentatively successful.

The RNA–protein interface

The structure of SBMV as well as TBSV has the interesting feature of an 'amino-terminal arm' which is ordered only in the C subunits. It is positioned between quasi-6-fold-related C and B subunits and runs from a quasi-6-fold to an icosahedral 2-fold axis. Harrison *et al.*[7] point out that the space for this arm can only exist in the vicinity of an icosahedral 2-fold axis (the quasi-3-fold axes are parallel to the icosahedral 2-fold axes but make an acute angle with the quasi-2-fold axes). The differences of the arm structure are required to accommodate the quasi-symmetry of the $T = 3$ surface arrangement. The disordered arm in the A and B subunits must thus be closely associated with the RNA but in variable positions relative to the icosahedral coat. Chauvin *et al.*[39] have shown with neutron scattering of suitably matched solutions of TBSV with D_2O that the significant portion of this protein–RNA interaction is at a radius of less than 80 Å.

In the SBMV protein there is a structural feature situated between the base of the β-barrel and the RNA interior, consisting of an α-helix and extended polypeptide chain, that was not visible in the TBSV structure. This helix, interacting with the C subunit barrel, represents either the amino end of a neighbouring, 3-fold-related, C subunit (Fig. 2) or an insertion within the C subunit at position 139. The β-annulus structure around the quasi-6-fold axis in SBMV is a '2-way overlap', not a '3-way overlap' as in TBSV (Fig. 5*a*). The extra 'amino-terminal' helix and extended strand are clearly visible in the A, B and C subunits, but the β-annulus and amino-terminal arm (residues 8–32) are visible only in the C subunit (Fig. 5*b*). It is therefore possible that the extra 'amino-terminal' helix in subunits A (forming the pentamer cluster) or in the B subunits (forming the hexamer cluster with the C subunits) are associated with their own β-barrel rather than a neighbouring subunit.

Table 2 Quality of structural similarity between various proteins or protein domains

Comparison Molecule 1	Molecule 2	Equivalenced residues No.	r.m.s. distance (Å)	% of equivalenced residues Mol. 1	Mol. 2
TBSV(S)	SBMV	182	2.7	91.0	82.7
Hb(α)	Hb(β)	139	1.6	98.5	95.3
NAD domain LDH	NAD domain GAPDH	83	2.9	57.5	56.1
TBSV(S)	TBSV(P)	69	3.8	41.3	62.8

Abbreviations: LDH, lactate dehydrogenase; GAPDH, glyceraldehyde-3-phosphate dehydrogenase; Hb, haemoglobin. Equivalencing of residues is restricted to those in the same topological sequence[52].

There are a total of 220 ordered residues in the SBMV C subunit. An error of only a few residues might be expected in view of the close similarity in the placement of amino acids in homologous regions of SBMV and TBSV. The total number of residues in SBMV has been estimated to be between 260 and 270 (refs 36–38). Thus, the ordered SBMV C subunit lacks between 40 and 50 residues. A similar estimate by Harrison *et al.*[7] showed that there were probably around 50 disordered residues in the C subunit of TBSV, even without observing the extra 'amino-terminal' α-helix. The amino terminus of the extra α-helix in SBMV is buried by the β-annulus, leaving no room for any extension. It is therefore more likely that the missing polypeptide is inserted around residue 8, which has weak density and is accessible to the viral interior (Fig. 5*b*). Support for the occurrence and position of ordered and disordered protein segments comes from an analysis of heavy atom positions[20].

Sehgal has shown that swollen SBMV virions, produced by removal of calcium and magnesium, are susceptible to trypsin digestion[40], and Tremaine[41] has shown that the cleaved portion is strongly basic and consists of about 63 residues. The treated virus reassembles into particles of diameter 150–180 Å. Similar observations have been made for brome mosaic virus (BMV; ref. 42 and B. Verduin, personal communication), TBSV and turnip crinkle virus[43,44] and alfalfa mosaic virus[45] (AMV), with the cleaved fragment always being at the amino terminus. A β-annulus structure, near the amino terminus, and the insertion of the amino-terminal arm between subunits may thus be essential requirements for the formation of a hexamer cluster and hence in the construction of spherical viral coats with $T > 1$. If the amino-terminal segment is cleaved (including the β-annulus), only pentamer clusters can form, producing capsids similar to the satellite tobacco necrosis virus (STNV) with a diameter of around 190 Å.

The amino-terminal region of many spherical and bacillus-shaped plant virus coat proteins is often strongly basic (for example, SBMV, cowpea chlorotic mottle virus, BMV, AMV and STNV) and predicts as an α-helix where the amino acid sequence is known (see Argos[10]). In SBMV there are residues which form an α-helix binding to the base of the β-barrel at the protein–RNA interface. Thus, the side of the helix exposed to the RNA is likely to be basic and the other side hydrophobic. Indeed, the SBMV electron density shows that residue −3 (Fig. 3) is almost certainly arginine. These properties will make the amino-terminal region particularly susceptible to trypsin digestion once it has been sufficiently exposed[40].

There are on the average around 8 basic residues per subunit, where the amino-terminal arm sequence is known, providing a total of 1,440 positive charges within the RNA of the complete virus. As there are about 5,000 bases in the nucleic acid of SBMV, it follows that the amino termini together must contribute significantly towards the cancellation of charge within the virus and hence presumably are largely responsible for the RNA

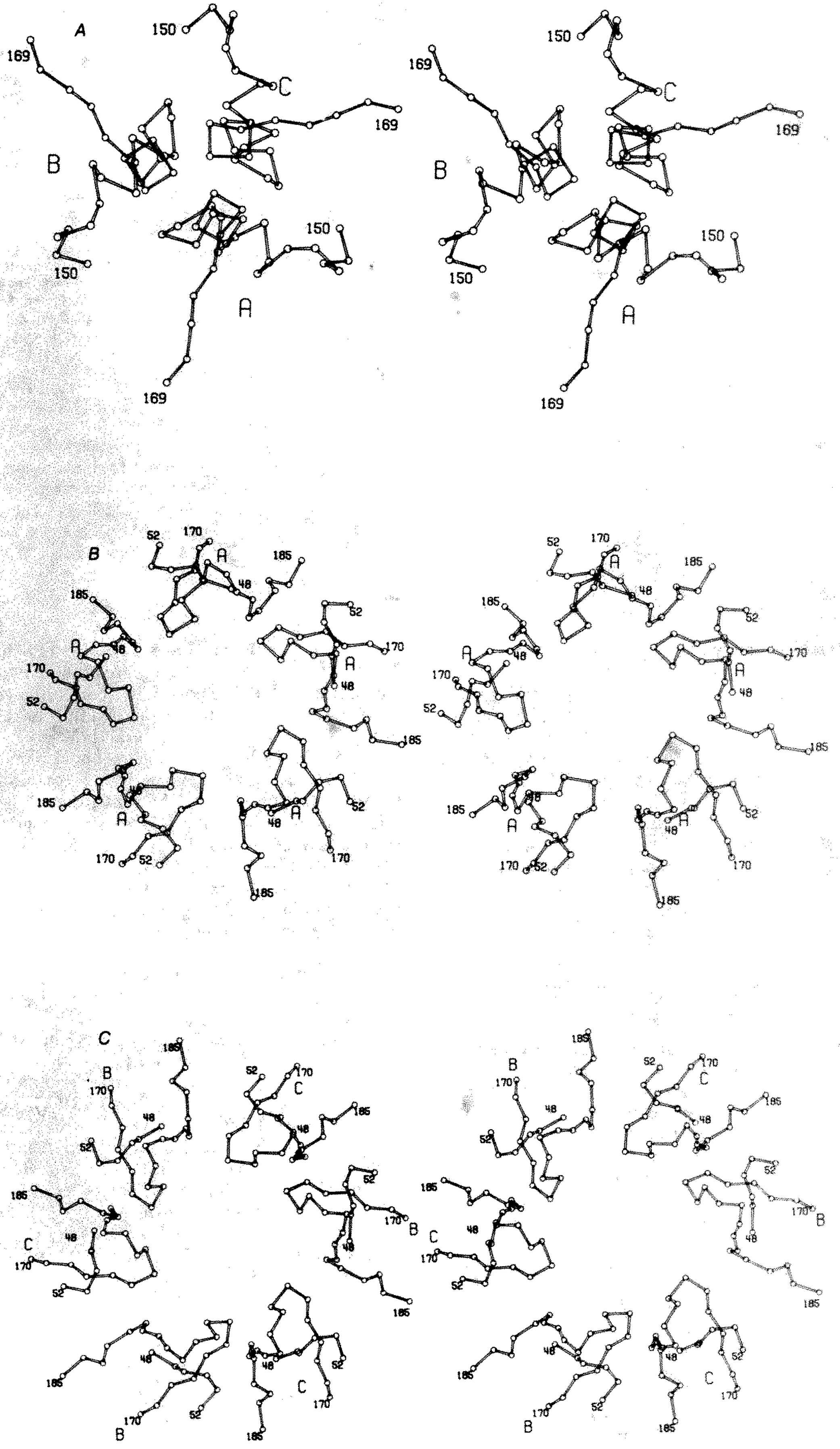

Fig. 4 Views of the viral exterior surface. *A*, Stereo diagram showing the protrusion around a quasi-3-fold axis produced by subunits A, B and C. The tangential α-helix occurs only in SBMV. The radial helix forms a keratin-like structure about the quasi-3-fold axis. *B*, Stereo diagram showing protrusion around an icosahedral 5-fold axis produced by adjacent A subunits. *C*, Stereo diagram showing protrusion around a quasi-6-fold axis produced by three C subunits separated by three B subunits.

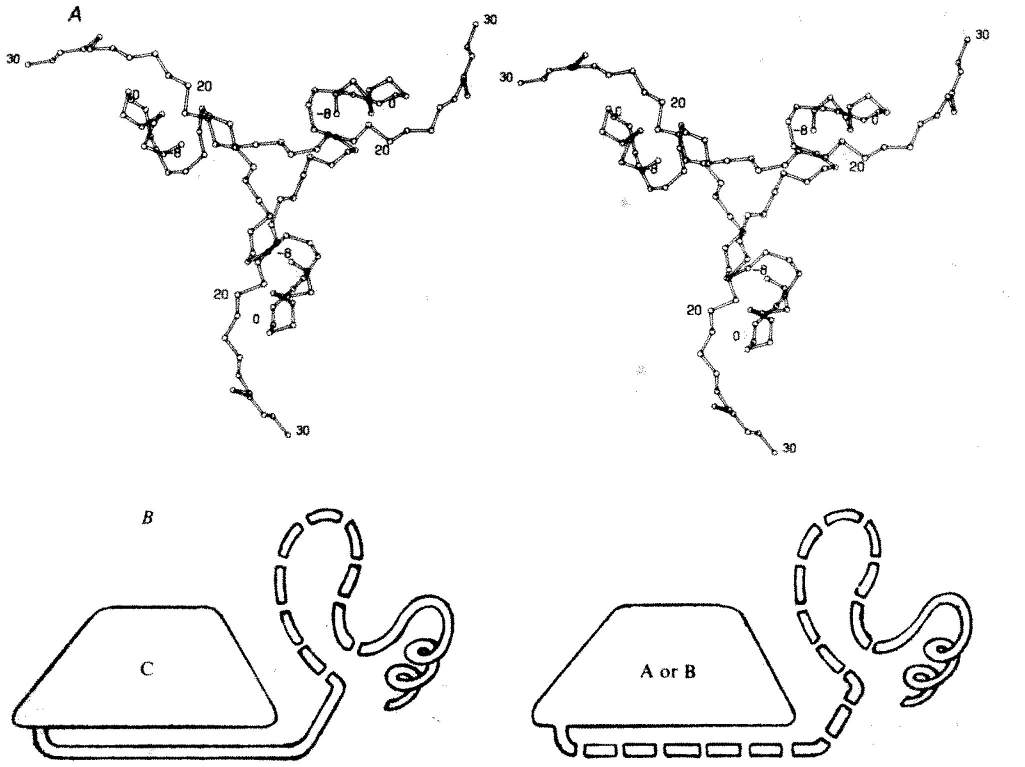

Fig. 5 *A*, Possible arrangement between C subunits in the vicinity of an icosahedral 3-fold axis which together form a 'β-annulus' structure. An alternative interpretation of the electron density places the amino-terminal helix as an insertion at position 139. *B*, Ordered and disordered (dashed) polypeptide in the A, B and C subunits of SBMV.

folding during viral assembly. The apparent tendency of α-helical formation with hydrophobic sides[10] suggests that the RNA backbones will have closely associated α-helical protein which form hydrophobic 'bundles'. These in turn can pack more easily within the virus by exclusion of water. A similar situation is encountered in the formation of α-helices when protamines associate with tRNA and also probably with DNA[46].

Histones H2A, H2B, H3 and H4, like viral coat proteins, also have basic amino-terminal ends which are not part of the ordered nucleosome structure. The H3 and H4 histones apparently undergo an ordering phenomenon by binding to the linker DNA[47–49]. The ordering of protein incurred by the binding of RNA to TMV, or the requirement of the random amino-terminal segments to assemble spherical viral RNA, is analogous.

The structure of other small, spherical, RNA-containing plant viruses

The most surprising aspect in the present report is the observation that, in spite of the obvious differences in physical characteristics, the structure of SBMV is closely related to that of TBSV. Argos[10] has shown that the amino acid sequence of some other viruses is consistent with a similar coat protein structure. Complementary arguments based on packing the SBMV shell protein are given here for the small $T=1$ STNV particle. Indeed, it has already been observed that trypsin-treated SBMV[40,41], turnip crinkle virus[43,44], AMV[45] and BMV[42] can form particles similar in diameter to STNV[50].

The overall dimensions of the SBMV subunit are given by a 35-Å thickness, a 27-Å separation between the quasi-3-fold and icosahedral 2-fold axes and a separation varying from 42 to 55 Å between the icosahedral 2-fold and quasi-6-fold axes. Similar measurements pertain to the thickness of the protein coat, the separation of the icosahedral 2-fold and 3-fold axes and the separation of the icosahedral 2-fold and 5-fold axes of the $T=1$ STNV particle, respectively[50]. Computer experiments in which pentamer clusters of SBMV A subunits are placed into a $T=1$ icosahedral lattice confirmed that the subunits pack without overlap when the external radius is 88 Å along the 3-fold axes. Furthermore, the general direction of the strands within the β-sheet of STNV runs between the 5-fold and 3-fold axes[50], consistent with the respective strand direction in SBMV.

The close similarity between SBMV and the S domain of TBSV strongly supports divergence of these two viruses from a common ancestor. The possibility of an earlier gene duplication from which the P and S domains of TBSV have evolved is also possible in light of their structural similarity[51]. The possibility that not only the coat protein genes but also much of the rest of the SBMV and TBSV genome have a common ancestry must therefore be considered. The similarities shown here and by Argos[10] between various groups of small spherical RNA viruses suggest that the β-barrel found in the SBMV subunit and TBSV S domain has been selected to comply with the functional needs of such viruses. The results of the structural studies of STNV[50], cowpea mosaic virus[8] and belladonna mottle virus (P. Argos, personal communication) will, therefore, be awaited with much interest.

This work has been possible only through the dedication of many people over a period of nine years. In particular we thank Mrs Mary Ann Wagner, Dr Ira Smiley, Dr Toshio Akimoto, Mr Joel White, Miss Karen Babos and Mrs Kumiko Tsukihara, also Dr Patrick Argos for stimulating discussions, Jane Richardson for producing the diagrammatic representation of SBMV, Dr Steve Harrison for supplying the TBSV C_α co-ordinates, Dr Saul Rosen, Mr John Steele and Dr Victor Abell for support in computations, Drs Richard Lister and Andrew Jackson for advice on the growth of SBMV, Mr Eric Henss, the late Mr Philip Hamilton and Sharon Wilder for technical assistance. The work was supported by NIH grant AI 11219, NSF grant PCM78-16584 and a grant from the Lilly Company. D.S. was supported by a Deutsche Forschungsgemeinschaft Postdoctoral Fellowship and S.S.A., J.E.J. and I.R. by NIH postdoctoral fellowships 1 F32 GM 07103, 6 F22 CA 00557 and 1 F32 AI 05600, respectively, during part of this work.

Received 18 January; accepted 23 April 1980.

1. Crick, F. H. C. & Watson, J. D. *Nature* **177,** 473–475 (1956).
2. Caspar, D. L. D. & Klug, A. *Cold Spring Harb. Symp. quant. Biol.* **27,** 1–24 (1962).
3. Fraenkel-Conrat, H. in *Comprehensive Virology* Vol. 1 (eds Fraenkel-Conrat, H. & Wagner, R. R.) 1–191 (Plenum, New York, 1974).
4. Commonwealth Mycological Institute and Association of Applied Biologists *Descriptions of Plant Viruses* (Commonwealth Mycological Institute, Surrey, 1970).
5. Stubbs, G., Warren, S. & Holmes, K. *Nature* **267,** 216–221 (1977).
6. Bloomer, A. C., Champness, J. N., Bricogne, G., Staden, R. & Klug, A. *Nature* **276,** 362–368 (1978).
7. Harrison, S. C., Olson, A. J., Schutt, C. E., Winkler, F. K. & Bricogne, G. *Nature* **276,** 368–373 (1978).
8. White, J. M. & Johnson, J. E. *Virology* **101,** 319–324 (1980).
9. Hull, R. *J. gen. Virol.* **36,** 289–295 (1977).

10. Argos, P. in *Proc. 7th Aharon Katzir-Katchalsky Conf.*, Rehovot (in the press).
11. Akimoto, T., Wagner, M. A., Johnson, J. E. & Rossmann, M. G. *J. ultrastruct. Res.* **53**, 306–318 (1975).
12. Arndt, U. W. & Wonacott, A. J. *The Rotation Method in Crystallography* (North-Holland, Amsterdam, 1977).
13. Rossmann, M. G. *J. appl. Crystallogr.* **12**, 225–238 (1979).
14. Rossmann, M. G., Leslie, A. G. W., Abdel-Meguid, S. S. & Tsukihara, T. *J. appl. Crystallogr.* **12**, 570–581 (1979).
15. Leslie, A. G. W. & Tsukihara, T. *J. appl. Crystallogr.* (in the press).
16. Harrison, S. C. *J. appl. Crystallogr.* **1**, 84–90 (1968).
17. Rayment, I., Johnson, J. E., Suck, D., Akimoto, T. & Rossmann, M. G. *Acta crystallogr.* **B34**, 567–578 (1978).
18. Suck, D., Rayment, I., Johnson, J. E. & Rossmann, M. G. *Virology* **85**, 187–197 (1978).
19. Rossmann, M. G. *Acta crystallogr.* **A32**, 774–777 (1976).
20. Abad-Zapatero, C. *et al. Acta crystallogr.* (submitted).
21. Johnson, J. E. *Acta crystallogr.* **B34**, 576–577 (1978).
22. Buehner, M., Ford, G. C., Moras, D., Olsen, K. W. & Rossmann, M. G. *J. molec. Biol.* **82**, 563–585 (1974).
23. Bricogne, G. *Acta crystallogr.* **A30**, 395–405 (1974).
24. Argos, P., Ford, G. C. & Rossmann, M. G. *Acta crystallogr.* **A31**, 499–506 (1975).
25. Winkler, F. K., Schutt, C. E., Harrison, S. C. & Bricogne, G. *Nature* **265**, 509–513 (1977).
26. Richardson, J. S. *Nature* **268**, 495–500 (1977).
27. Richards, F. M. *J. molec. Biol.* **37**, 225–230 (1968).
28. Bernstein, F. C. *et al. J. molec. Biol.* **112**, 535–542 (1977).
29. Dickerson, R. E. & Geis, I. *The Structure and Action of Proteins* (Harper & Row, New York, 1969).
30. Johnson, J. E., Akimoto, T., Suck, D., Rayment, I. & Rossmann, M. G. *Virology* **75**, 394–400 (1976).
31. Hsu, C. H., White, J. A. & Sehgal, O. P. *Virology* **81**, 471–475 (1977).
32. Sehgal, O. P. & Sinha, R. C. *Virology* **59**, 499–508 (1974).
33. Hull, R. *Virology* **89**, 418–422 (1978).
34. Rayment, I., Johnson, J. E. & Rossmann, M. G. *J. biol. Chem.* **254**, 5243–5245 (1979).
35. Wells, J. M. & Sisler, H. D. *Phytopathology* **58**, 1588–1592 (1968).
36. Tremaine, J. H. *Virology* **30**, 348–354 (1966).
37. Ghabrial, S. A., Shepherd, R. J. & Grogan, R. G. *Virology* **33**, 17–25 (1967).
38. Dietrich, J. B. thesis, Univ. Louis Pasteur de Strasbourg (1979).
39. Chauvin, C., Witz, J. & Jacrot, B. *J. molec. Biol.* **124**, 641–651 (1978).
40. Sehgal, O. P., Hsu, C. H., White, J. A. & Van, M. *Phytopath. Z.* **95**, 167–177 (1979).
41. Tremaine, J. H. & Ronald, W. P. *Virology* **91**, 164–172 (1978).
42. Pfeiffer, P. & Hirth, L. *FEBS Lett.* **56**, 144–148 (1975).
43. Leberman, R. & Finch, J. T. *J. molec. Biol.* **50**, 209–213 (1970).
44. Crowther, R. A. & Amos, L. A. *Cold Spring Harb. Symp. quant. Biol.* **36**, 489–494 (1972).
45. Bol, J. F., Kraal, B. & Brederode, F. Th. *Virology* **58**, 101–110 (1974).
46. Warrant, R. W. & Kim, S. H. *Nature* **271**, 130–135 (1978).
47. Thomas, J. O. *Int. Rev. Biochem.* **17**, 181–232 (1978).
48. Moss, T., Cary, P. D., Crane-Robinson, C. & Bradbury, E. M. *Biochemistry* **15**, 2261–2267 (1976).
49. Lilley, D. M. J., Howarth, O. W., Clark, V. M., Pardon, J. F. & Richards, B. M. *FEBS Lett.* **62**, 7–10 (1976).
50. Unge, T. *et al. Nature* **285**, 373–377 (1980).
51. Argos, P., Tsukihara, T. & Rossmann, M. G. *J. molec. Evolut.* (in the press).
52. Rossmann, M. G. & Argos, P. *J. molec. Biol.* **109**, 99–129 (1977).

LETTERS

Cosmic X-ray background and intergalactic gas accretion onto intergalactic collapsed objects

E. P. T. Liang

Institute of Theoretical Physics and Department of Applied Physics, Stanford University, Stanford, California 94305

The origin of the diffuse cosmic X-ray background (CXB) has become the subject of much speculation recently, with most theorists divided between the intergalactic hot gas bremstralung hypothesis and the QSO contribution theory. Stimulated by Sargent's recent argument about the existence of a cool, low density intergalactic gas, we investigate here the third possibility of its accretion onto intergalactic collapsed objects as the sources of the X-ray background. We conclude that if the CXB is hot thermal bremstralung (TB) from the accretion of Sargent type intergalactic gas onto intergalactic collapsed objects, a new class of faint ($L_x \lesssim 10^{41}$ erg s^{-1}) low mass ($M \sim 10^7$–$10^{10} M_\odot$) discrete X-ray sources must exist with no optical or IR images, some of which could be detected by the Einstein observatory.

HEAO 1 observations have established that the cosmic X-ray background spectrum (3–50 keV) is most naturally fit by TB with $kT = 45 \pm 5$ keV (ref. 1). Yet the hypothesis that it may be emission from a hot intergalactic gas (IGG) of Ω_0 (present mean density/closure density) $\sim 0.5(\langle\rho\rangle/\langle\rho^2\rangle^{1/2})$ faces severe difficulties, including the huge energy requirement, the destruction of H I clouds believed to be causing the quasar absorption lines, the Compton distortion of the microwave spectrum, and so on[2]. On the other hand, source counts by the Einstein observatory indicate that faint sources down to ~0.002 UFU (Uhuru flux unit) already make up 30–40% (at least in the 1–3 keV band) of the CXB. If the present number-flux relation $N(>S) = KS^{n(=1.5-1.8)}$ holds to much fainter S, then known discrete sources may easily account for all (or even exceed) the CXB intensity[3], consistent with the conjecture that contribution from known optical QSOs brighter than $B \simeq 20.3$ mag could account for essentially all of the CXB if L_x/L_{optical} remains large down to such magnitudes[4,5]. Reasonable as such estimates seem, they remain unverified extrapolations at present, not to mention the highly uncertain nature of QSO X-ray spectra. Hence it is still interesting to investigate alternative sources for at least a significant fraction of the CXB.

Recently, Sargent *et al.*[6] have proposed that the survival of the intergalactic H I absorption clouds favours the existence of an IGG with $\Omega \sim 0.1$ and $T \sim 10^5$ K at $Z \sim 2.5$, too cool to produce the CXB. However, its existence raises the question of whether the CXB might be produced by accretion onto an intergalactic population of collapsed objects whose existence could not be detected otherwise. Such a hypothesis has some merits as (1) accretion onto compact objects is the most efficient mechanism known in X-ray production; (2) the low IGG density makes high temperature TB favourable and leads to low X-ray luminosity objects difficult to resolve. Here we investigate the constraints on such a model. The dominant contribution comes from the present epoch ($Z < 3$). Our work, therefore, complements that of Carr[7] on pregalactic black holes ($Z > 10$).

A collapsed compact object of mass M moving with Mach number $\mathcal{M}$ in a fully ionized IGG of density ρ and temperature $T_4 10^4$ K (sound speed $c_s \sim 10^6\, T_4^{1/2}$) will accrete at the Bondi rate[8]

$$\dot{M} \simeq 10^{35}\,\mathrm{g\,s^{-1}} \left(\frac{M}{M_\odot}\right)^2 \rho T_4^{-3/2} \mu^{-3}; \quad \mu \equiv (1+\mathcal{M}^2)^{1/2} \qquad (1)$$

when the IGG turbulent velocity at distances $\gtrsim GM/c_s^2$ is small compared with keplerian orbital velocity, which we assume. The X-ray luminosity from accretion is

$$L_X = \varepsilon_X \dot{M} c^2 \simeq 10^{56}\,\mathrm{erg\,s^{-1}} \left(\frac{M}{M_\odot}\right)^2 \varepsilon_X \rho T_4^{-3/2} \mu^{-3} \qquad (2)$$

where ε_X, the X-ray energy conversion efficiency is assumed M-independent. For $T_4 > 1$ the dominant cooling of IGG is adiabatic[2]. Hence $T \propto (1+Z)^2$, $\rho \propto (1+Z)^3$ and L_X is epoch-independent provided ε_X is. For such non-evolving sources 80% of their contribution to the CXB comes from $Z \leqslant 1$ (ref. 9) and the volume emissivity needed to account for the observed CXB intensity is

$$\eta_X \simeq 6 \times 10^{-35}\,\mathrm{erg\,cm^{-3}\,s^{-1}}\,(1+Z)^3 \qquad (3)$$

If most of the CXB comes from sources of mass M and number density N then equating $\eta_X = NL_X$ we have

$$N_0 \left(\frac{M}{M_\odot}\right)^2 \varepsilon_X \rho_0 T_{04}^{-3/2} \mu_0^{-3} = 6 \times 10^{-91} \qquad (4)$$

where all quantities with subscript '0' refers to $Z = 0$. In the model by Sargent *et al.*[6], T drops faster than adiabatic after $Z \leqslant 2$ due to He-recombination cooling, leading to $T_0 \sim 10^3$ K (incomplete ionization) and contribution from $Z \leqslant 1$ greater than 80%. However, the uncertainties in other parameters are such that we can use equation (4) even in this case, lumping any correction into say, μ_0. Rewriting $N_0 M = \Omega_B 4.7 \times 10^{-30}$ g cm^{-3} and $\rho_0 = \Omega_0 4.7 \times 10^{-30}$ g cm^{-3}($H_0 = 50$ km s^{-1} Mpc^{-1}) gives

0028-0836/80/270039-02$01.00

$$\frac{M}{M_\odot} = 54\,q^{-1}; \qquad L_X = 1.2\times10^{30}\,\mathrm{erg\,s^{-1}}q^{-1}\Omega_B^{-1}$$

$$N_0 = 1.3\times10^{9}\,\mathrm{Mpc^{-3}}q\Omega_B \tag{5}$$

where $q \equiv \varepsilon_X\Omega_0\Omega_B T_{04}^{-3/2}\mu_0^{-3}$ is expected to be $\ll 1$. Hence such objects must be supermassive black holes. These constraints can be generalized to a power law mass spectrum of compact objects, say $\mathrm{d}N/\mathrm{d}M \propto M^{-\gamma}$ for $M_1 \leqslant M \leqslant M_2$. Then the mass constraint in equation (5) applies approximately to M_2 for $\gamma < 2$ or M_1 for $\gamma > 3$.

The strongest constraint on the parameters in equation (5) comes from the sources count and fluctuation limit. From Uhuru and Ariel 5 small scale fluctuations ($\delta I/I \leqslant 2.5\%$ at 0.004 sr beam width), Schwartz[9] already puts an upper limit on possible contribution of unknown classes of discrete sources to K (number of sources with $S > 1$ UFU per sr) < 10. The Einstein survey gives $K \simeq 7\pm3$ for all sources[3], most of which have optical images. In the preliminary Draco and Eridanus surveys, only three out of 43 sources have empty optical fields[3]. Hence it seems reasonable to put a conservative upper limit for the contribution of accreting intergalactic black holes to the source count

$$K_B \leqslant 2 \tag{6}$$

Future observations may further lower this limit. As most such contributions would come from $Z \leqslant 1$ we have (see ref. 9):

$$K_B \simeq 3.7\times10^{6} L_{X44}^{3/2} N_0;\ L_{X44} = L_X/10^{44}\,\mathrm{erg\,s^{-1}} \tag{7}$$

Combining equations (5), (6) and (7) we have:

$$\varepsilon_X^{1/2}\Omega_B \geqslant 3.2\times10^{-6}\Omega_0^{-1/2}T_{04}^{3/4}\mu_0^{3/2} \tag{8}$$

$$L_X \leqslant 1.2\times10^{41}\,\mathrm{erg\,s^{-1}} \tag{9}$$

$$M/M_\odot \leqslant 1.7\times10^{7}\,\varepsilon_X^{-1/2}\Omega_0^{-1/2}T_{04}^{3/4}\mu_0^{3/2} \tag{10}$$

$$N_0 \geqslant 1.3\times10^{-2}\,(\mathrm{Mpc})^{-3} \tag{11}$$

For the IGG proposed by Sargent *et al.*[6] with $\Omega_0 \sim 0.1$, $T_{04} \sim 1$ and $\mu_0 \sim 10$ we find $\Omega_B \geqslant 3\times10^{-4}\,\varepsilon_X^{-1/2}$ and $M \leqslant 2\times10^{9}\,M_\odot\varepsilon_X^{-1/2}$.

If the IGG contains even a minute amount of organized angular momentum, the accretion flow will turn into a disk near the black hole[10] where most of the X-ray is emitted, in which case ε_X could be high. The familiar disk model with optically thin TB emission has maximum temperature $T_e \sim 10(\dot{M}M_\odot/M)^{1/2}$ provided $10^7\,K \ll T_e \leqslant 10^9\,\mathrm{K}$ (ref. 11). If we set this to the observed CXB TB temperature we find (see equation (5))

$$\varepsilon_X\Omega_B \sim 10^{-7} \tag{12}$$

When equation (12) is combined with equations (8) and (5) we get the constraints

$$\varepsilon_X \leqslant 10^{-3}\,\Omega_0 T_{04}^{-3/2}\mu_0^{-3};\ \Omega_B \geqslant 10^{-4}\,\Omega_0^{-1}T_{04}^{3/2}\mu_0^{3}$$

$$\frac{M}{M_\odot} \sim 5\times10^{8}\,\Omega_0^{-1}T_{04}^{3/2}\mu_0^{3} \tag{13}$$

These numbers are uncertain to the extent the TB disk models are. Also, the requirement that the IGG is not depleted by accretion in a Hubble time demands $\varepsilon_X\Omega_B \geqslant 10^{-8}$. The above results are summarized in Fig. 1.

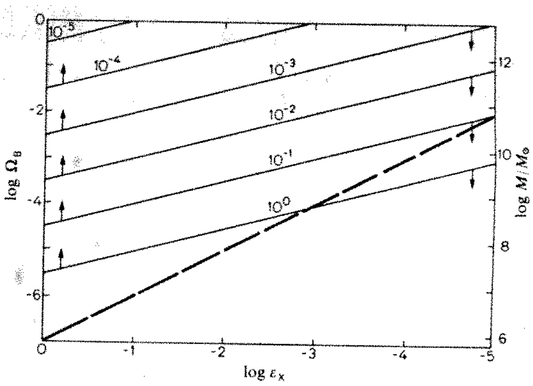

Fig. 1 Solid curves give the lower limit on Ω_B and upper limit on M as provided by the source count limit $K_B \leqslant 2$. The number on each curve labels the value of $\omega \equiv \Omega_0^{1/2}T_{04}^{-3/4}\mu_0^{-3/2}$ of the IGG (see equation (5)). The dashed curve represents the constraint on Ω_B for the TB disk model to give the observed CXB temperature. In this case M is independent of Ω_B or ε_X (see equation (13)).

We conclude that it is possible that much of the CXB is produced by the hot TB emission of Sargent type IGG accreting onto intergalactic black holes in the present epoch ($Z \leqslant 3$). This picture then predicts the existence of a new class of faint ($L_X \leqslant 10^{41}\,\mathrm{erg\,s^{-1}}$), numerous ($N_0 \geqslant 10^{-2}\,\mathrm{Mpc^{-3}}$) and low mass ($M \sim 10^{7}$–$10^{10}M_\odot$) discrete sources without optical or IR images. Gorenstein has pointed out that such objects may be separated from (optically) faint QSOs in the Einstein survey by studying the distribution of the lower limits to their L_X/L_{optical} ratio (P. Gorenstein, personal communication). Note that the bulk of such sources are fainter than the limit of the HR I of Einstein so their predicted $N \propto S^{-1.5}$ does not conflict with the observed steeper distribution. Note that these masses overlap with the mass corresponding to nonlinear density clumps ($\delta\rho/\rho \sim 1$) at decoupling as extrapolated from the present power law density correlation function[12,13]. Some of such clumps could (but need not) directly collapse into black holes without fragmenting into stellar systems at $Z \geqslant 10$ and their X-rays could have Compton-heated the denser IGG[7]. In such case the IGG would not evolve adiabatically and Carr finds that the direct contribution of accretion to the CXB at $Z = 10$ may also be significant[7].

I thank B. J. Carr for his pregalactic black hole results before publication, also D. Sciama, V. Petrosian and P. Gorenstein for helpful discussions.

Received 11 December 1979; accepted 24 April 1980.

1. Boldt, E. A. Preprint NASA TM-78106 (1978).
2. Field, G. B. & Perrenod, S. C. *Astrophys. J.* **215**, 717 (1977).
3. Giacconi, R. *et al. Astrophys. J. Lett.* (in the press).
4. Tananbaum, H. *et al. Astrophys. J. Lett.* (submitted).
5. Setti, G. & Woltjer, L. *Astr. Astrophys.* **76**, LI (1979).
6. Sargent, W. *et al. Astrophys. J.* (submitted).
7. Carr. B. J. *Mon. Not. R. astr. Soc.* **189**, 123 (1979).
8. Bondi, H. *Mon. Not. R. astr. Soc.* **112**, 195 (1952).
9. Schwarz, D. in *X-Ray Astronomy* (ed. Baity, W. A. & Peterson, L. E.) (Pergamon, Oxford, 1979).
10. Pringle, J., Rees, M. J. & Pacholczyk, A. G. *Astr. Astrophys.* **29**, 179 (1973).
11. Eardley, D. M., Lightman, A. P., Payne, D. G. & Shapiro, S. L. *Astrophys. J.* **224**, 53 (1978).
12. Gott, J. R. III & Rees, M. J. *Astr. Astrophys.* **45**, 415 (1975).
13. Peebles, P. J. E. *Astrophys. J. Lett.* **189**, 251 (1974).

Discontinuities in the jovian plasma disk of sulphur and oxygen ions

W.-H. Ip

Max-Planck-Institut für Aeronomie, D-3411 Katlenburg-Lindau 3, FRG

The process of local acceleration of the plasma cloud freshly ejected from Io into the jovian magnetosphere is considered here. A physical model previously employed to investigate the motion of artificial barium cloud, is used to estimate the time scale for such transient acceleration. In normal conditions, the new ions could be accelerated to full corotation within ~3 × 10^2s of injection. But the corresponding time scale might be increased 10-fold or so at the peaks of mass injection. In this way the observations of non-rigid corotation of the S^+ ions of sporadic nature may be understood. The temperature and ionization discontinuities in the Io torus as observed by the Voyager experiments is also considered. Here we propose that such a sharp transition is related to the coupling of the radial diffusion and heating plus cooling of the thermal plasma.

0028-0836/80/270040-04$01.00

Ground-based observations[1–6] indicate that the S^+ optical emissions of the jovian sulphur nebula at 6,717 and 6,730 Å usually have a very sharp cutoff at, or inside of, the orbit of Io at 6 R_J, whereas the inner boundary between 3 and 4 R_J has a diffuse appearance. At the same time, it has been established that the motion of the sulphur ions in this nebula is in corotation with the jovian magnetosphere[1]. Although these descriptions may be considered to represent the norm of the S^+ plasma disk, Mekler *et al.*[7] have recently presented evidence of occasional weak S^+ emission outside the orbit of Io. Particularly interesting are the velocities of the S^+ ions in this anomalous emission. Although the motion of the S^+ plasma inside of the sharp boundary was in rigid corotation, the corresponding motion in the outer emission was slower than would be expected for corotation. Such unusual phenomena may be caused by some disturbances in the jovian magnetosphere (for example, substorms), or simply related to the injection process of the sulphur ions from Io. [Note that evidence of non-rigid corotation (up to a few per cent) of the jovian magnetospheric plasma in the vicinity of the orbit of Io have been recently reported[8,9] on the basis of plasma wave and planetary radio astronomy experiments. These observations are presumably more representative of the quiescent state of the Io torus.]

A model formulated by Scholer[10] to study the motion of ionized barium cloud artificially released in the Earth's magnetosphere[11,12] will now be applied to the case of the Io torus of sulphur and oxygen ions. Although highly simplified, this treatment gives a reasonable approximation to the MHD transfer of angular momentum from Jupiter to the Io torus and the resultant heating of the ion cloud. This model together with considerations on the radial diffusion and cooling of the ion cloud, and the new information from the Voyager 1 and 2 observations of the jovian system[13–18], would allow us to interpret systematically the non-corotation events and several other related observations.

The geometry of the MHD coupling between the Io torus and the jovian ionosphere will first be represented by a two-dimensional system with both the ionosphere and the ion cloud idealized as flat slabs of finite vertical thickness and width in the y-direction, and the extension in the x-direction is supposed to be infinite, see Fig. 1. The planetary magnetic fields of uniform strength B are pointing in the z-direction. Furthermore, the magnetosphere between the ionosphere and the Io torus is assumed to have a plasma density of ρ, while the surface density of the torus is m_0 (in g cm^{-2}). The motion of the torus is then coupled to that of the ionosphere through the continuous transmissions and reflections of the Alfvén waves propagating between these two regions[19] with acceleration of the ion cloud as the end result.

More specifically, as the waves travel through the magnetosphere with the Alfvén speed $V_A = B/(4\pi\rho)^{1/2}$ there will be a polarization current j_p carried at the wave fronts[10,20–23]. As shown in Fig. 1*a*, the current will be closed in such a way that the $\mathbf{j} \times \mathbf{B}$ forces would decelerate the magnetospheric, or the ionospheric, plasma but accelerate the ion cloud. The total polarization current can be expressed as $I_p = \sum_A \mathbf{E}\uparrow$, where $\mathbf{E}\uparrow$ is the electric field applied at the (upward going) wave front and $\sum_A = c^2/4\pi V_A$ is the so-called wave conductivity of the magnetosphere. As the wave reaches the ionosphere with a height-integrated Pedersen conductivity $\sum$, an electric field $\mathbf{E}\downarrow$ will be reflected, whereas a conduction current $I_\perp = \sum(\mathbf{E}\uparrow - \mathbf{E}\downarrow)$ will be set up flowing across the magnetic field.

As the ionospheric conduction current must be equal to the total current in the magnetosphere, that is:

$$\textstyle\sum(\mathbf{E}\uparrow - \mathbf{E}\downarrow) = \sum_A(\mathbf{E}\uparrow + \mathbf{E}\downarrow) \qquad (1)$$

we have the following relationship between the incoming and reflected waves:

$$\mathbf{E}\downarrow = \left[\frac{1-X}{1+X}\right]E\uparrow \qquad (2)$$

with $X = \sum/\sum_A$. Thus, the reflection coefficient of the Alfvén waves at the ionospheric boundary is given by $\alpha = (1-X)/(1+X)$. From the same reasoning we can see that after a time $T_A = 2L/V_A$, which is the characteristic time for an Alfvén wave to travel back and forth between the ion cloud and the ionosphere, there will be another reflection, and so on. The acceleration of the ion cloud is, therefore, not just a function of the ratio between $\sum$ and $\sum_A$ but also time t. Another important factor in this dynamical problem is the distributed mass of the ion cloud. Assuming that the central slab is initially at rest (which is pertinent to the case when an ion cloud is just ejected from Io) and taking the inertia of the ion cloud into account, a general solution for the velocity of the cloud can be derived as was done by Scholer[10] for the barium cloud release experiments. In the present context we have

$$V(t) = V_0\{1 - \sum_{n=0} (-1)^n\alpha^n[\exp(-t_n/T_0)L_n(2t_n/T_0) + \alpha\exp(-t_{n+1}/T_0)L_n(2t_{n+1}/T_0)]\} \qquad (3)$$

Here $t_n = t - nT_A$, $T_0 = 2m_0V_A/B^2$, V_0 is the corotation speed, and the summation is carried out only for the Laguerre polynomials $L_n(t_n)$ with $t_n \geq 0$. The normalized velocity profiles for various combinations of T_0, T_A, and α are shown in Fig. 2.

Briefly, for $\sum \gg \sum_A$ and hence $\alpha \approx -1$, the MHD coupling between the ionosphere and the ion cloud is very strong, and in the case of small T_A/T_0 ratio the ion cloud will be accelerated to full corotation speed in just a few times of T_A. On the other hand, if $\sum \ll \sum_A$ and hence $\alpha \approx 1$, the motion of the ion cloud is only weakly coupled to the ionosphere by Alfvén waves. Acceleration of the ion cloud would be very slow. The inertia effect of the ion cloud can also be observed by examining the velocity profiles with different T_A/T_0 ratios but the same value of α.

To explore this result further we assume, for example, the magnetospheric plasma density to be ≈ 1 proton cm^{-2}, the surface number density n_s of the ion cloud just ejected from Io to be $\approx 2 \times 10^{12}$ ions cm^{-2}, and the length scale L to be $\approx 10R_J$; the

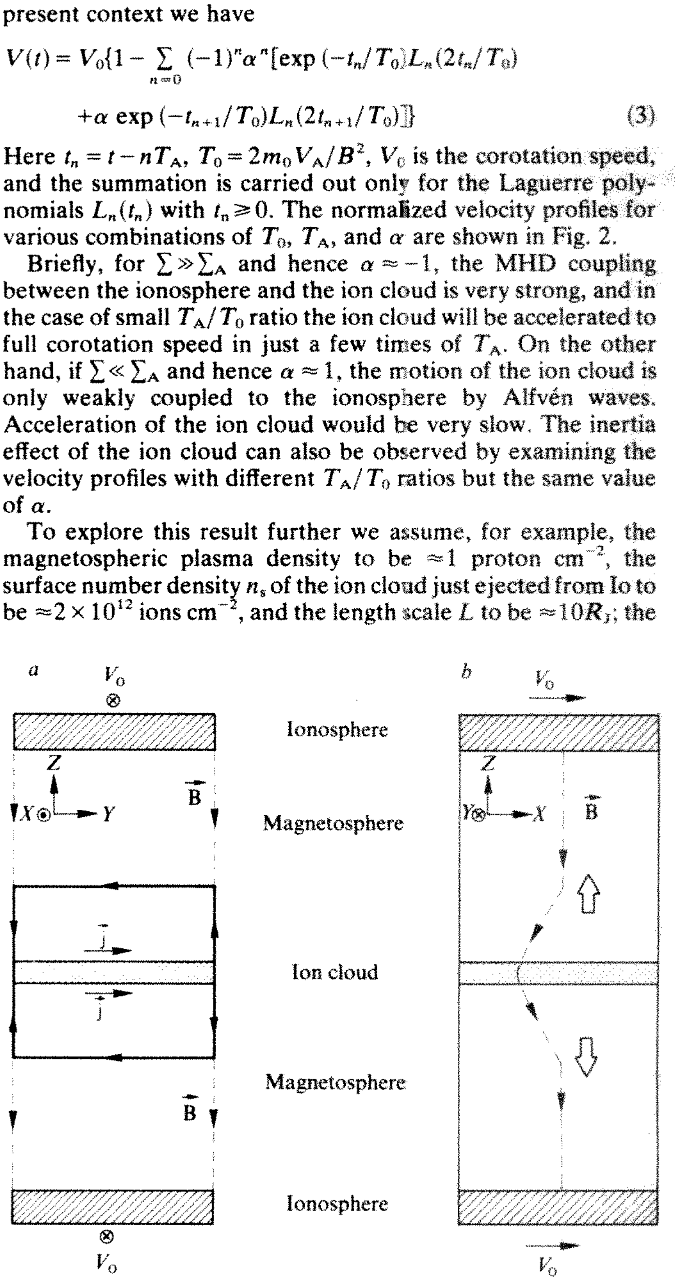

Fig. 1 *a*, A cross-section of the model in the Y–Z plane. The wave current system decelerating the magnetosphere and accelerating the ion cloud is sketched. As a result of the successive transmissions and reflections of these guided waves, a field-aligned current system will be established between the ionosphere and the Io cloud, similar to the current system detected in the vicinity of Io[21,40–43]. The auroral hiss observed on the inner edge of the torus at $L \approx 5.6$ R_J (ref. 43) is probably caused by the beaming of low energy electrons (10 eV–1 keV) associated with such current flows. *b*, A finite section of the model in the X–Z plane. The upward and downward propagations of the Alfvén waves are indicated.

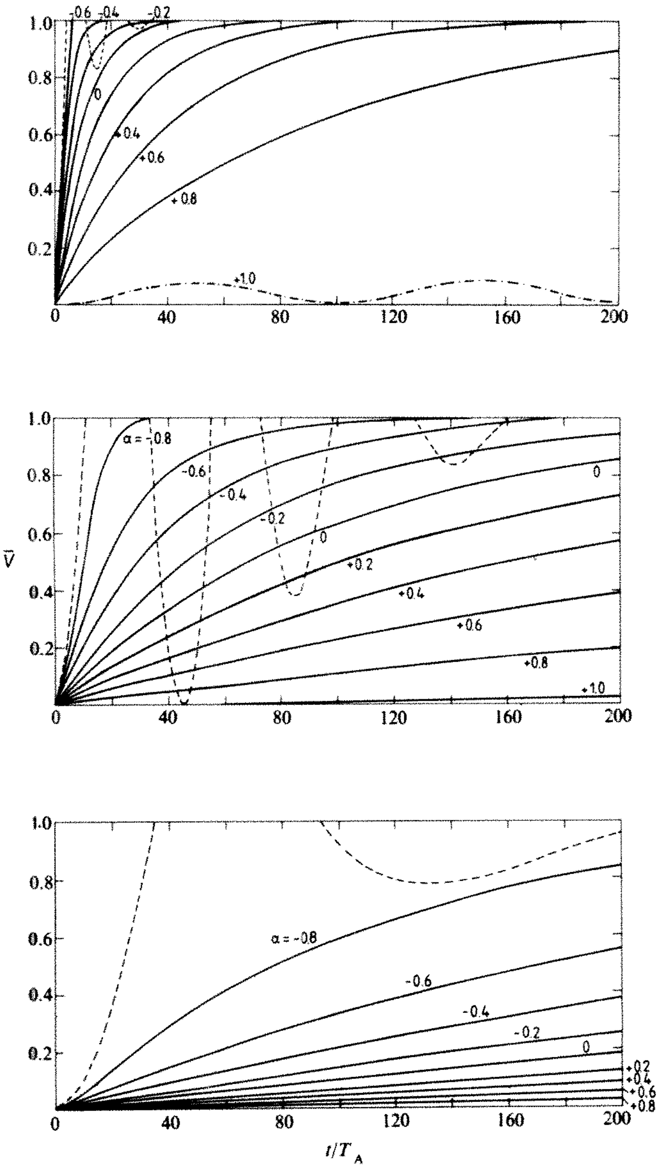

Fig. 2 Velocity profiles of the ion cloud (initially at rest) normalized to the corotation velocity V_0 for various values of the T_A/T_0 ratio and the reflection coefficients α. For $\alpha \leq -0.6, \Sigma \geq 4\Sigma_A$. If the plasma density in the magnetosphere is 1 proton cm^{-3}, and $B = 2\times10^3$ nT we have $\Sigma_A \geq 0.02$ S, consequently $\Sigma \geq 0.1$ S. In this MHD approximation, the ion cloud velocity oscillates before reaching the corotation velocity for $\alpha \to -1$ (see dashed lines). A more realistic description is for the ion cloud to be accelerated to the full speed without such overshoots. *a*, $T_A/T_0 = 10^{-1}$; *b*, $T_A/T_0 = 10^{-2}$; *c*, $T_A/T_0 = 10^{-3}$.

value of the ratio T_A/T_0 can then be approximated to be ≈ 0.1. (As the total ejection rate can be written as $\dot{N} \approx 2n_0R_sV_0$, $\dot{N} \approx 5\times10^{27}$ ions s^{-1} if $n_s \approx 2\times10^{12}$ and R_s is the radius of Io. This value is compatible with the production rate of the sulphur and oxygen ions as estimated by Broadfoot *et al.*[15].) As the S$^+$ nebula was generally observed to be in rigid corotation with the jovian magnetosphere, the characteristic time scale for the corresponding acceleration of the ion cloud probably is no more than a few times of T_A. Thus the α value may be taken to be ≤ -0.6, or $\Sigma/\Sigma_A \geq 4$, say. With $T_A \approx 30$ s and $V_0 = 57$ km s^{-1}, Fig. 2 shows that the ions picked up directly from the ionosphere/exosphere of Io will be accelerated to full corotation within 10 Io radii. This trail of slow moving ions may be interpreted as the wake of the satellite ionosphere[24–26]. (This picture would still hold qualitatively for the interaction of Io with the torus of dense hot plasma.)

Now, if the ejection rate $\dot{N}$ were occasionally increased by a factor of 10 or so (for example, at the maximum of volcanic activities if ionospheric loss is the dominant injection process), $T_A/T_0 \leq 0.01$ and the resulting acceleration time scale will be lengthened by a similar factor. Thus, after its first ejection from Io, the ion cloud would probably stay behind corotation for at least an hour, leaving an ion wake ~150° long. This non-corotation effect could persist even longer if the volcanic activity lasts more than a few hours. The large mass of the fresh S$^+$ and O$^+$ ions injected in these events, of course, would enable the non-rigid corotation behaviour to be discerned more easily, especially outside the nominal edge of the S II nebula.

If the non-corotation of the weak emission of S$^+$ ions observed outside the nominal outer edge[7] could be explained by the inertia effect of the MHD acceleration process plus the sporadic outbursts of the volcanic activities, how do we explain the simultaneous corotation of the S$^+$ ions observed in the inner region of stronger emission? And above all, why should there be a sharp discontinuity confining the S$^+$ emission within 6 R_J in the first place. These questions may be answered by referring to the Voyager observations of the Io torus. First, the EUV experiment[15] and the plasma experiments[16] have found that the bulk of the heavy ions is apparently in the form of S^{2+}, S^{3+}, and O^{2+} with thermal temperature $kT \approx 5$–50 eV. This hot ion torus—with its point of maximum number density approximately located at 5.8 R_J—has 5R_J as its inner boundary and 7–8 R_J the outer boundary. Second, a sharp drop in temperature from $kT \approx 10$ eV to 1 eV was found at 5.7 R_J by the plasma experiments[16]. Together with the temperature change, there is also an apparent change in the ionization state of the heavy ions from S^{2+}, O^{2+} to S$^+$ and O$^+$. Such stratification of the plasma temperature and ionization might be related to the balance between ionization equilibrium and thermal equilibrium as was found in the structures of planetary nebulae[27–29]. Note that the ions freshly created in the vicinity of Io can have kT as high as 260 eV for O$^+$ and 520 eV for S$^+$ (ref. 30) the maximum time scale for cooling of these new ions[31] can be calculated to be $t_c \leq 1.5\times10^5$s. In comparison, adopting a radial diffusion coefficient of 10^{-6} R_J^2 s^{-1} (ref. 32), the time scale for diffusion across a distance of 0.5 R_J at this region is $t_d \approx 7\times10^4$s. As $t_d \geq t_c$, the heating of the Io torus is then limited to a distance of less than 0.5 R_J around the orbit of Io. Although this may partly explain the sharp division between the hot and cold plasma at 5.7 R_J, issue could be raised about the absence of such discontinuity at 6.3 R_J or so. An explanation of such asymmetric behaviour may come from the additional heating effect beyond 6 R_J as a result of Landau damping of the ion cyclotron waves, for example (ref. 33 and C. K. Goertz, personal communication). We may argue that the energetic (S$^+$ and O$^+$) ions, which are responsible for generation of the ion cyclotron turbulence, would not be able to diffuse across Io due to its absorption effect; and this in turn would limit the plasma wave activities and hence plasma heating to radial distance >5.9 R_J.

The ionization state and thermal condition of the Io plasma disk is therefore determined by four inter-related time-dependent processes, namely: (1) the ejection rate; (2) the MHD acceleration; (3) the radial diffusion; and (4) the cooling and heating of the ion cloud. Not just the structure of the 'quiescent' S$^+$ nebula and the non-corotation of the anomalous emission during the 'disturbed' periods, but also the temperature and density discontinuities together with the apparent ionization stratification in the Io torus can be explained in this way.

While we have concentrated on the local and transient effect acceleration of the plasma just ejected from Io, clearly the time-averaged acceleration and transfer of angular momentum of the Io torus in a more global scale must be of the same vein. For a description of the non-rigid corotation of the jovian magnetospheric plasma at radial distances beyond 6R_J see refs 34–36. Alternative views on the asymmetric radial distribution of the thermal plasma[37,38] addressing the possibility of two different diffusion mechanisms at both sides of Io had also been proposed. The effect of such process on our hypothesis of the temperature and ionization discontinuity remains to be investigated. The recent report by Shemanski that an upper limit of 10^{27} ions s^{-1} may be derived for the ion source in the vicinity of Io is also problematic as it sets a stringent condition on the model of local mass pick up[25,26]. In any event, our primary result for the transient acceleration of the Io plasma cloud is by no means affected because, in principle, it is valid for both local (ionospheric scavenging) and more extended (ionization of the sputtered atoms) ion sources.

I thank Dr C. K. Goertz for useful discussions on the problem of magnetospheric propagation of the Alfvén waves.

Received 5 February; accepted 30 April 1980.

1. Kupo, I., Mekler, Yu. & Eviatar, A. *Astrophys. J. Lett.* **205,** L51 (1976).
2. Brown, R. A. *Astrophys. J. Lett.* **206,** L179 (1976).
3. Brown, R. A. *Astrophys. J. Lett.***224,** L97 (1978).
4. Mekler, Yu., Eviatar, A. & Kupo, I. *J. geophys. Res.* **82,** 2809 (1977).
5. Munch, H., Trauger, J. T. & Roesler, F. L. *Bull. Am. astr. Soc.* **9,** 465 (1977).
6. Pilcher, C. B. *Bull. Am. astr. Soc.* **10,** 579 (1978).
7. Mekler, Yu., Eviatar, A. & Siscoe, G. L. *Mon. Not. R. astr. Soc.* **189,** 15 (1979).
8. Kurth, W. S., Gurnett, D. A. & Scarf, F. L. *Geophys. Res. Lett.* **7,** 61 (1980).
9. Kaiser, M. L. & Desch, M. D. *NASA Tech. Mem.* 80626 (Goddard Space Flight Center, 1980).
10. Scholer, M. *Planet. Space Sci.* **18,** 977 (1970).
11. Biermann, L., Lüst, R., Lüst, Rh. & Schmidt, H. U. *Z. Astrophys.* **53,** 226 (1961).
12. Haerendel, G., Lüst, R. & Rieger, E. *Planet. Space Sci.* **15,** 1 (1967).
13. Smith, B. A. *et al. Science* **204,** 951 (1979).
14. Smith, B. A. *et al. Science* **206,** 927 (1979).
15. Broadfoot, A. L. *et al. Science* **204,** 979 (1979).
16. Bridge, H. S. *et al. Science* **204,** 987 (1979).
17. Scarf, F. L., Gurnett, D. A. & Kurth, W. S. *Science* **204,** 991 (1979).
18. *Nature* **280,** 725–806 (1979).
19. Kendall, P. C. *Astrophys. J.* **129,** 194 (1959).
20. Drell, S. D., Foley, H. M. & Ruderman, M. A. *J. geophys. Res.* **70,** 3131 (1965).
21. Neubauer, F. M. *J. geophys. Res.* **85,** 1171 (1980).
22. Maltsev, Yu. P., Leontyev, S. V. & Lyatsky, W. B. *Planet. Space Sci.* **22,** 1519 (1974).
23. Maltsev, Yu.P., Lyatsky, W. B. & Lyatskaya, A. M. *Planet. Space Sci.* **25,** 53 (1977).
24. Cloutier, P. A., Daniell, R. E. Jr, Dessler, A. J. & Hill, T. W. *Astrophys. Space Sci.* **55,** 93 (1978).
25. Ip, W.-H. & Axford, W. I. *Nature* **283,** 180 (1980).
26. Goertz, C. K. *J. geophys. Res.* (in the press).
27. Harrington, J. P. *Astrophys. J.* **152,** 943 (1968).
28. Harrington, J. P. *Astrophys. J.* **156,** 903 (1969).
29. Miller, J. S. *A. Rev. Astr. Astrophys.* **12,** 331 (1974).
30. Siscoe, G. L. & Chen, C. K. *Icarus* **31,** 1 (1978).
31. Spitzer, L. Jr *Physics of Fully Ionized Gases* 2nd edn, 135 (Interscience, New York, 1962).
32. Mogro-Campero, A. in *Jupiter* (ed. Gehrels, T.) 1190 (University of Arizona Press, 1976).
33. Eviatar, A., Mekler, Y. & Coroniti, F. V. *Astrophys. J.* **205,** 622 (1976).
34. Hill, T. W. *J. geophys. Res.* **84,** 6554 (1979).
35. Hill, T. W. *Science* **207,** 301 (1980).
36. McNutt, R. L. Jr, Belcher, J. W. Sullivan, J. D., Bagenal, F. & Bridge, H. S. *Nature* **280,** 803 (1979).
37. Froideraux, L. *Geophys. Res. Lett.* **7,** 33 (1980).
38. Richardson, J. D., Siscoe, G. L., Bagenal, F. & Sullivan, J. D. *Geophys. Res. Lett.* **7,** 37 (1980).
39. Shemanski, D. *3rd Conf. on the Jovian Magnetosphere*, Houston (1980).
40. Ness, N. F. *et al. Science* **204,** 982 (1979).
41. Piddington, J. H. & Drake, J. F. *Nature* **217,** 935 (1968).
42. Goldreich, P. & Lyndell Bell, D. *Astrophys. J.* **156,** 59 (1969).
43. Gurnett, D. A., Kurth, W. S. & Scarf, F. L. *Nature* **280,** 767 (1979).

S-wave anisotropy in the upper mantle under a volcanic area in Japan

Masataka Ando & Yuzo Ishikawa*

Disaster Prevention Research Institute, Kyoto University, Uji,
Kyoto 611, Japan

Hiroo Wada

Kamitakara Crustal Movement Observatory, Disaster Prevention
Research Institute, Kyoto University, Kamitakara,
Gifu 506-13, Japan

Most ultra-basic nodules that probably originated in the upper mantle have anisotropic petrofabric and elastic properties[1,2]. Within seismology, however, the Earth is generally assumed to be isotropic and this assumption is appropriate for most seismological studies. Thus, rocks can be considered isotropic on large scales although anisotropic on a scale of hand specimen[3]. This interpretation is questionable, however, in light of the increasing resolution of seismic observations. Many reliable reports on seismic anisotropies have been accumulating: for example, azimuthal anisotropy in P_n velocities in oceanic basins[4], and in the continent[5] and the back-arc basin[6], and an S-wave splitting of the SH and SV waves revealing an anisotropic structure as deep as 190 km (ref. 7). These suggest that some unsuccessful detections of the Earth's anisotropies may be due to lack of appropriate observations. We describe here the recent discovery of shear wave anisotropy in a volcanic area in Japan, which was revealed by an improvement in the seismographic observation systems.

Telemetery systems of the seismographic stations have recently been established by Kyoto and Nagoya Universities[8] (Fig. 1) in the Chubu area, Japan, beneath which the Pacific plate is subducting. This instrumental development improves the spatial coverage, timing accuracy and recording conditions of seismic observations. The Kamitakara Observatory of Kyoto University is located in the northern part of this area[9] (Fig. 1). Immediately beneath the observatory (Takayama area), at a depth of ~260 km (ref. 10) there are often deep earthquakes. These are very useful events for studies of structures within the wedge between the subducting plate and the Earth's surface in the island arc. As seismic ray paths from these events to the seismographic stations are almost vertical, the wave forms are quite simple because of little contamination of converted waves generated at conspicuous layer boundaries. The stations AMJ and KTJ of this observatory are equipped with the three-component seismographs and the station NRJ with a vertical component one only. The natural pendulum period T_0 is 1 s for both vertical and horizontal seismographs.

Figure 2*a* shows seismograms of one of those deep earthquakes (the earthquake 1 in Fig. 1 and Table 1) recorded at the Kamitakara Observatory. Because the P-wave arrives at the three stations within 0.2 s, the incidence angle is less than 5°. Remarkably, the horizontal seismograms show two distinct arrivals of the shear wave, a fast arrival for the NS component and a slower arrival for the EW one. The horizontal seismograms of three more earthquakes from the same area (earthquakes 2, 3 and 6 in Fig. 1 and Table 1) were examined. These seismograms showed the two different arrivals of the S-wave similar to that in Fig. 2*a*. Such differences in the arrival time of the S-wave between the two horizontal components would be caused by interference of converted waves, but for the present case this interpretation should be dismissed. No significant signal is in fact observed on the vertical component in Fig. 2*a*. A probable interpretation is that S-wave splitting is caused by anisotropy of the medium at intermediate locations between earthquake source and seismographic stations. The incident S-wave is generally resolved into two shear waves that travel along the same path with different velocities—a phenomenon known as acoustic 'double refraction'[11].

As the directions of horizontal seismographs, NS and EW, are not necessarily those of the principal axes of anisotropy, the two split shear waves are generally not resolved on the two horizontal seismograms. Figure 2*a* implies, however, that the directions of the principal axes of the anisotropy are rather close to NS and EW. To determine precise directions of the velocity axes, we synthesized the S-wave forms, by rotating the two orthogonal axes in a clockwise direction at an interval 15°, and projecting the observed S-wave particle motion onto the rotated axes. When a rotation angle θ from the north or east coincided with a principal axis, the two orthogonal S-waves became most widely separated. As shown in Fig. 2*b*, $\theta = 15°$ seems to provide the clearest separation for both records of AMJ and KTJ. The azimuth of maximum velocity, thus, is N15°E and the azimuth of minimum velocity is E15°S.

---

* Present address: Geophysical Research Institute, State Seismological Bureau, Peking, People's Republic of China.

0028–0836/80/270043–04$01.00

Table 1 A list of earthquakes used for this study and their anisotropic parameters

No.	Date (JST)	Depth (km)	KTJ			AMJ			KAJ			IMJ			TAK			ITD			TKC			INU			UGK		
			D	A_z	*Q*	*D*	A_z	*Q*	*D*	A_z	*Q*	*D*	A_z	*Q*	*D*	A_z	*Q*	*D*	A_z	*Q*	*D*	A_z	*Q*	*D*	A_z	*Q*	*D*	A_z	*Q*
	1977																												
1	25 Sep	260	0.8	15°	A	1.0	0°	A	0.0	0°	A																		
2	7 Oct	260	0.8	20°	A	0.3	0°	B																					
3	18 Nov	275	0.8	40°	A	0.9	15°	A																					
4	30 Nov	360	0.0	0°	A	0.0	0°	A																					
	1978																												
5	1 Feb	240	0.0	0°	B	0.0	0°	B																					
6	9 Mar	260	0.7	30°	A	0.5	15°	C																					
7	5 Apr	260										0.3	105°	B															
8	27 May	280	0.9	15°	A	?		C							0.8	15°	A	0.0	0°	A									
9	14 Jun	360	0.0	0°	B	0.0	0°	A							0.0	0°	A	0.0	0°	A	0.0	0°	B				0.0	0°	A
10	27 Jun	200	?			0.9	30°	B																					
11	3 Aug	230	0.0	0°	A	0.9	30°	B																					
12	14 Aug	280																0.3	90°	B				0.0	0°	B			

D, The arrival time difference between the two shear waves in s. A_z, The azimuth of the vibration with the maximum velocity in deg. *Q*, the quality of the data.

To constrain the size and location of the anisotropy, we collected more data which were recorded at neighbouring seismographic networks, the Hokuriku Observatory of Kyoto University (7 stations), and Nagoya University (10 stations) (Fig. 1). The seismographs of the Hokuriku Observatory are the same type as in the Kamitakara Observatory and the two-horizontal-component-observation was carried out at either KAJ or IMJ. In the large seismographic network of Nagoya University, two horizontal-component seismographs are installed at all the stations ($T_0 = 10$ s for both vertical and horizontal components). In each network, vertical seismograms were recorded continuously on paper, but horizontal seismograms were stored on only magnetic tapes when signal amplitudes exceeded a threshold value.

A clear split of the S-wave of earthquake 1 was also recorded on horizontal seismograms at TAK of Nagoya University, 20 km away from KTJ (Fig. 2*c*). The long-period nature of the seismographs of Nagoya University well suppresses short-period noises. The same procedure as described above was used to determine the anisotropic parameters for the Nagoya seismograms. The arrival time difference was 0.7 s, and the directions of the maximum and minimum velocity axes were N15°E and E15°S, respectively (Fig. 2*c*). The polarization angle of the S-wave's first motion corrected for the differential arrival is consistent with the P-wave's nodal plane solution. The consistency of the anisotropic parameters between the two independent networks is further evidence for the existence of the anisotropy under Takayama.

Twelve earthquakes were selected between September 1977 and October 1978; 28 ray paths were used (Table 1). Most of the earthquakes originated from the source 260 km beneath Takayama. To each S-wave signal, the same procedures represented in Fig. 2*b*, *c*, *d* were carried out. The azimuth of the principal axis of the maximum velocity from the north, the arrival time difference between the two S-wave components, and the quality of the data (A, B and C from high to low) are listed in Table 1. Data with quality C were not used for the estimation of the arrival time difference. To avoid corruption of S-wave form by converted waves, we restricted our study to emergence angles <20° at the hypocentre. Because each network has its own amplitude threshold for the start of magnetic tape recording and individual transmission-recording characteristics, the number of earthquakes available for this study differs among the networks. As the coverage of ray paths so far has been concentrated primarily under Takayama and its vicinity, we limit our discussion of anisotropy to that area.

The results are given in Table 1 and can be summarized as follows: (1) the S-wave splitting is observed at AMJ, KTJ and TAK for the earthquakes immediately beneath these stations, but not observed at ITD, TKC, IMJ and KAJ away from these stations; (2) the S-wave splitting is, on the other hand, not

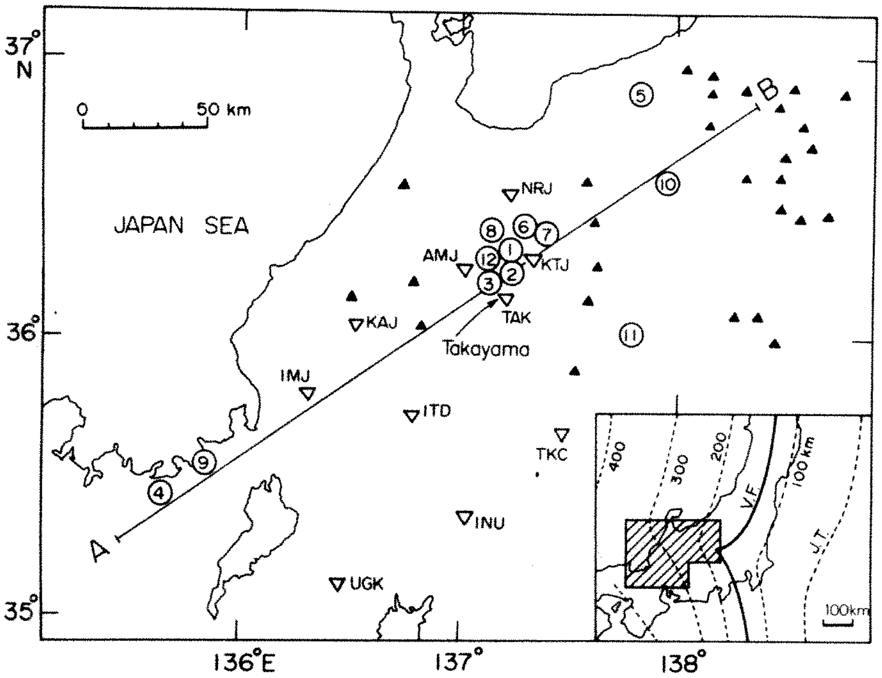

Fig. 1 Epicentres (○), seismographic stations (▽) and Quaternary volcanoes (▲) in the Chubu area, Japan. Numerals denote epicentres of the earthquakes corresponding to Table 1. Quaternary volcanoes are taken from Isshiki *et al.*[17]. The insert shows depths of earthquakes on the deep-focused seismic plane from Utsu[18], and the volcanic front which forms the trenchward bound active volcanism[16]. Line A–B refers to Fig. 3.

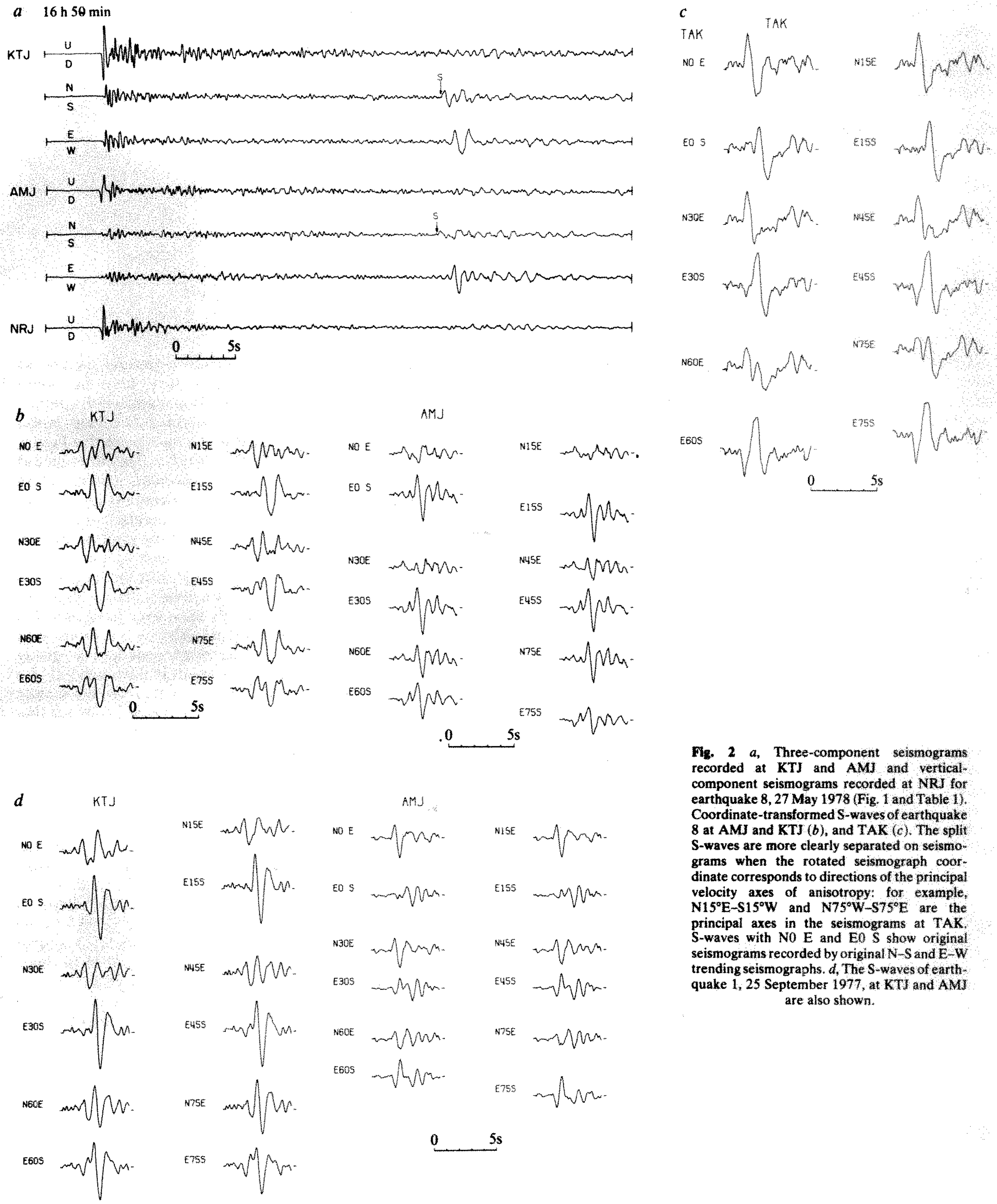

Fig. 2 *a*, Three-component seismograms recorded at KTJ and AMJ and vertical-component seismograms recorded at NRJ for earthquake 8, 27 May 1978 (Fig. 1 and Table 1). Coordinate-transformed S-waves of earthquake 8 at AMJ and KTJ (*b*), and TAK (*c*). The split S-waves are more clearly separated on seismograms when the rotated seismograph coordinate corresponds to directions of the principal velocity axes of anisotropy: for example, N15°E–S15°W and N75°W–S75°E are the principal axes in the seismograms at TAK. S-waves with N0 E and E0 S show original seismograms recorded by original N–S and E–W trending seismographs. *d*, The S-waves of earthquake 1, 25 September 1977, at KTJ and AMJ are also shown.

observed at AMJ, KTJ and TAK for deep earthquakes which occurred outside the Takayama area. These results suggest that the anisotropic medium is not distributed near the source or the receiver station, but rather at some intermediate location along the ray path as shown in Fig. 4. These arguments would be consistent with an anisotropic body ~50–100 km in both horizontal and vertical extents at depths ~100–200 km. The corresponding velocity difference between the two shear waves is ~2–4%. The travel times of the S-wave with the faster velocities associated with the splitting are identical to those of S-waves from the standard travel timetable of the Japan Meteorological Agency[12]. The travel times associated with the minimum velocities are thus delayed ~1 s relative to the standard time.

Preferred orientation of microcracks or liquid inclusion, or individual minerals may cause such an anisotropy of the S-wave[11,13-15]. At present, it is difficult to interpret the anisotropy. We, however, hypothesize that this anisotropy is related to a magma reservoir because AMJ, KTJ and TAK are located near volcanoes inside the volcanic front[16] (Fig. 1). It seems possible, therefore, that S-waves from the deep earthquakes pass through deep magma reservoirs beneath volcanoes (Fig. 3). If thin elliptical inclusions trending north–south exist within magma reservoirs, then a velocity anisotropy of S-waves could be caused with the maximum velocity axis NS.

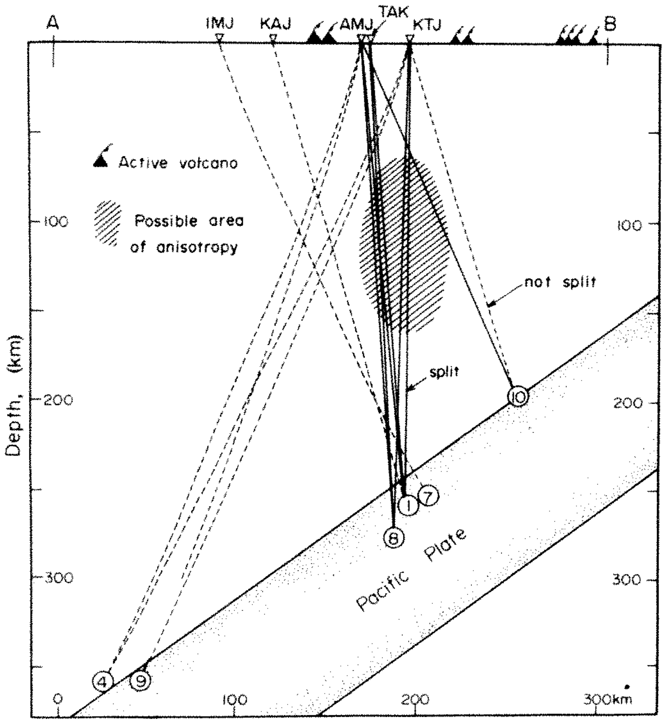

Fig. 3 S-wave ray paths for earthquakes 1, 4, 7, 8 and 10 projected on the plane A–B (Fig. 1). Solid rays denote those associated with the S-wave splitting (arrival time difference >0.4 s). A possible area of anisotropy is inferred from a combination of these ray paths.

We thank the Observation Center for Earthquake Prediction, Nagoya University and the Hokuriku Observatory of Kyoto University for providing the seismographic records and use of their facilities, and Professors K. Aki and S. Crampin, and Mr F. Yamazak for helpful comments.

Received 11 February; accepted 30 April 1980.

1. Kumazawa, M., Helmstaedt, H. & Masaki, K. *J. geophys. Res.* **76,** 1231–1247 (1971).
2. Christensen, N. I. *Bull. geol. Soc. Am.* **82,** 1681–1694 (1971).
3. Ewing, W. M., Jadetsky, W. S. & Press, F. *Elastic Waves in Layered Media* (McGraw-Hill, New York, 1957).
4. Morris, G. B., Raitt, R. W. & Shor, G. G. *J. geophys. Res.* **74,** 3095–3109 (1969).
5. Bamford, D. *Geophys J. R. astr. Soc.* **49,** 29–48 (1977).
6. Okada, H. *et al. J. Phys. Earth* **26,** Suppl. s491–s502 (1978).
7. Hirn, A. *Geophys. J. R. astr. Soc.* **49,** 49–58 (1977).
8. Suyehiro, S., Ichikawa, M. & Tsumura, K. *J. Phys. Earth* **25,** Suppl. s69–s78 (1977).
9. Kamitakara Crustal Movement Observatory and Research Section for Earthquake Prediction *Bull. Disaster Prev. Inst., Kyoto Univ.* **21,** 119–135 (1978).
10. Aoki, H. *J. Phys. Earth* **22,** 229–290 (1971).
11. Nur, A. & Simmons, G. *J. geophys. Res.* **74,** 6669–6674 (1969).
12. Ichikawa, M. & Mochizuki, E. *Pap. Meteor. Geophys. Jap. Meteor. Ag.* **22,** 229–290 (1971).
13. Birch, F. *J. geophys. Res.* **65,** 1083–1102 (1960); **66,** 2199–2224 (1961).
14. Christensen, N. L. & Ramananantoandro, *J. geophys. Res.* **76,** 4003–4010 (1971).
15. Todd, T., Simmons, G. & Baldridge, W. S. *Bull. seis. Soc. Am.* **63,** 2007–2020 (1973).
16. Matsuda, T., Nakamura, K. & Sugimura, A. *Tectonophysics* **4,** 349–366 (1967).
17. Isshiki, N., Matsui, K. & Ono, K. *Selected Bibliography of Japanese Volcanoes* (Japan Geological Survey, 1968).
18. Utsu, T. *Kagaku* (*Science*), *Tokyo* **44,** 739–746 (1944).

●

Restrictions on the compositions of mid-ocean ridge basalts: a fluid dynamical investigation

Herbert E. Huppert

Department of Applied Mathematics and Theoretical Physics,
University of Cambridge,

R. Stephen J. Sparks

Department of Earth Sciences, University of Cambridge,
Downing Place, Cambridge CB2 3EW, UK

The nature of the melts parental to mid-ocean ridge basalts has been vigorously debated. Opinions vary between those considering the parental magma to be magnesia-rich (picritic basalt) with 15–20% MgO and those arguing that the parental melts are compositionally related to the most primitive liquids erupted at mid-ocean ridges (MgO ~ 9–11%). This difference of between 5 and 11% in MgO content represents a temperature interval of 100–250 °C. The actual MgO content places constraints on the thermal conditions at the mantle source. The high-magnesia liquid theory is supported by melting experiments on mantle and basalt samples[1-3] and by petrological studies of ophiolite complexes[4]. However, this theory does not seem to be immediately consistent with the fact that no glasses or aphyric rocks of these compositions have ever been sampled from the sea floor. Indeed the most primitive glass compositions that occur as inclusions in olivine megacrysts and as glassy margins to pillow lavas have MgO contents in the range 9–11%. Models of generating low MgO partial melts from the mantle have been proposed. For example, Presnall *et al.*[5] consider that melting at cusps in the peridotite mantle solidus could generate such melts. We outline here a fluid dynamical model for a basaltic mid-ocean ridge magma chamber supplied by high-magnesia melt from the mantle. The model predicts that high-magnesia extrusives will not be erupted, that ultramafic cumulates should occur at the base of the oceanic crust, that lava compositions will be restricted to MgO contents < 10% and that magma mixing will be a common feature of sea-floor basalts[6].

Before presenting the model we emphasize a fundamental feature of the moderate to low pressure evolution of picritic to tholeiitic basalt by crystal fractionation[7]. Figure 1 shows the dependence of density of high-magnesia melts on MgO content as crystallization occurs, calculated by the method of Bottinga and Weill[8]. As an example, we use the estimate of Elthon[4] for the parent magma for the oceanic crust (MgO ~ 17·8%) and generate successive residual liquids by crystallization of olivine (Fo_{90}). As olivine crystallizes out the density of the residual liquid decreases despite the declining temperature. The residual liquid reaches the density minimum *A* and the liquid joins a cotectic (perhaps olivine-plagioclase or olivine–plagioclase–pyroxene). Subsequent crystallization, dominated by plagioclase and pyroxene, generates residual liquids of progressively increasing density, due to iron-enrichment accompanied by low degrees of silica enrichment. Similar relationships between density and composition have been documented from several suites of mid-ocean ridge basalts[7], although the exact position of the minimum point *A* may change slightly from case to case. The variation of magma density with composition is complicated by the effects of suspended crystals, but in general the effect of suspended crystals will accentuate the relationships shown in Fig. 1 (ref. 7) by increasing the magma density at a fixed temperature.

It is significant that the most primitive glasses yet recovered from the sea floor occupy the density minimum shown in Fig. 1 (9–11% MgO)[6,7,9,10]. Mid-ocean ridge basalts are all more

0028–0836/80/270046–03$01.00

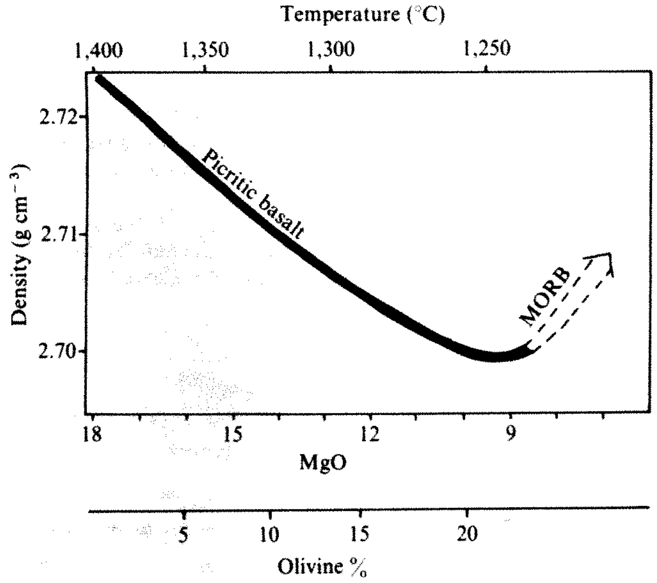

Fig. 1 Variation of melt density with MgO content in picritic liquids. The estimate of Elthon[4] is used as an example of the parental magma to the ocean crust with MgO ~ 17.8% and generated a succession of liquid compositions down to MgO = 10% by removal of forsterite (Fo_{90}). The approximate percentage of olivine removed in generating the successive liquids is indicated by the lower scale. Liquidus temperatures were estimated approximately from the experimental data of Krishnamurthy and Cox[17]. The density minimum at A is illustrated with the approximate trend of mid-ocean ridge basalt density with MgO content for MgO < 9% (after ref. 7).

evolved than this composition and show abundant evidence for mixing between evolved liquids and more primitive liquids (with MgO 9–11%)[6,9–11].

Figure 2 shows our model of a magma chamber containing typical mid-ocean ridge basalt into which a new influx of hot, but denser, picritic-basalt melt is intruded. The concept of an open-system magma chamber periodically replenished by new melt from depth[12] is now widely accepted as the most probable situation existing beneath the mid-ocean ridges, although the exact geometry and location of mid-ocean ridge magma chambers is still uncertain[13]. The temperature contrast between the two magmas may be 100–200 °C, depending largely on the MgO content of the picritic basalt. Investigations of an analogous system[14] where a hot salty layer of water underlies a cold freshwater layer indicates that the dense fluid will remain at the base of the chamber. Between the two layers there is a non-turbulent interface across which heat and salt are transferred by molecular rather than turbulent processes. Unless the densities of the two layers are virtually identical, no physical mixing occurs across the interface, although each layer convects vigorously. We suggest that this form of motion can also occur in magmas where the ratio of diffusivity of mass to that of heat is typically $< 10^{-5}$.

We have adapted the empirical and theoretical results of studies on the salt/water system to the picrite/basalt system in a magma chamber. A detailed treatment of the problem, which has several geological implications in addition to the situation described here, will be presented elsewhere. We summarize here the results pertinent to the problems of mid-ocean ridge magma genesis. Vigorous convection occurs in the two layers (Fig. 2*b*) and heat transfer through the interface between the two layers results in rapid cooling of the lower layer.

Our calculations indicate that the temperature of the lower layer as a function of time, $T(t)$, can be expressed as

$$T(t) = T(0) + \{[\Delta^{-7/3} + 7\,A(0.5 + r)t/3] - \Delta\}/(1 + 2r)$$

where $T(0)$ is the initial temperature, Δ is the initial temperature difference between the layers and r is the ratio of the thickness of the lower layer to that of the upper layer. The expression takes account of the heat of crystallization for olivine using a value of 200 cal g^{-1}. The constant A is dependent on the physical properties of the fluids.

$$A = 0.32(g\kappa^2\alpha^7/\nu)^{1/3}/(h\sigma^2)$$

where g is the gravitational acceleration, κ is the thermal diffusivity, α is the coefficient of thermal expansion, ν is the kinematic viscosity, h is the thickness of the lower layer and σ is the density contrast between the layers due to the difference in MgO contect divided by the mean density.

Typical values of the physical properties are: $\kappa = 10^{-6}\ \mathrm{m^2\,s^{-1}}$; $\alpha = 5\times10^{-5}\ \mathrm{K^{-1}}$; $\nu = 10^{-3}\ \mathrm{m^2\,s^{-1}}$; $\sigma = 2\times10^{-2}$. Figure 3 shows the cooling history of the lower layer for values of h between 3 and 300 m with an upper layer thickness of 4 km, an initial upper layer temperature of 1,255 °C and an initial lower layer temperature of 1,385 °C. We observe that the lower layer cools to thermal equilibrium with the upper layer in a time scale of a few months to a few years. The reason for the rapid cooling rates is the intense turbulent convection that occurs for large Rayleigh numbers[14]. Typically, the initial Rayleigh number of the lower layer exceeds 10^9.

Another consequence of the turbulently convecting flow regime is that olivines precipitated from the lower picrite layer will be kept in turbulent suspension throughout the cooling of the lower layer. In all plausible models we calculate that the mean turbulent velocities[15] are in the range 1–5 cm s^{-1}, whereas the free-fall velocities of olivine crystals of 1–5 mm diameter (typical dimensions in ultramafic cumulates and olivine–phyric lavas) in magnesia-rich liquids are in the range 10^{-2}–10^{-3} cm s^{-1}. The olivine settling rates only become comparable to the turbulent velocities when the temperature difference becomes small (< 1 °C).

The model predicts (Fig. 2) that the lower picritic basalt will not mix with the upper basalt layer and that it will cool rapidly in

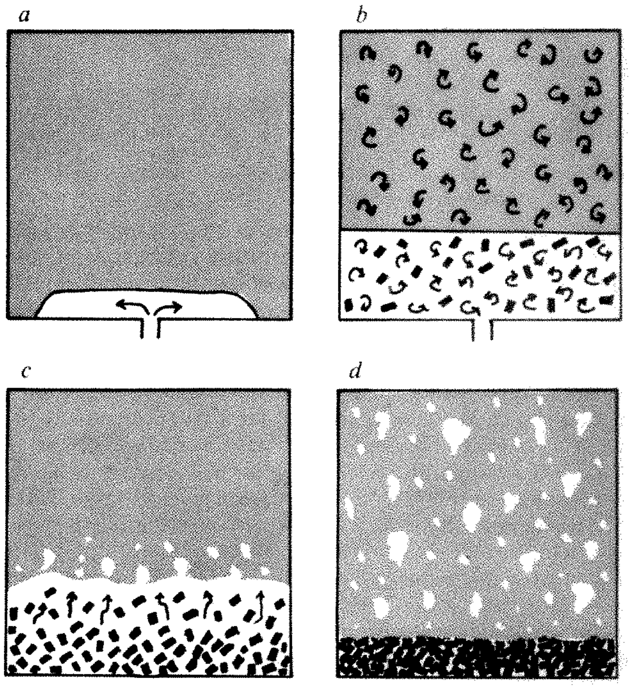

Fig. 2 Schematic model for the behaviour of a new influx of picritic melt into a MOR magma chamber (not to scale): *a*, intrusion of hot, dense picrite into reservoir of fractionating basalt; *b*, stable stratification into two layers which equilibrate thermally by turbulent convection with growth of olivine in lower layer; *c*, convection dies in lower layer at the end of cooling history allowing for olivine settling and separation of low density interstitial basaltic melt; *d*, Cumulate olivine layer formed at base of chamber as low density interstitial melt mixes convectively with heated upper layer.

a period of a few years at most. During its cooling to thermal equilibrium with the upper layer, the picrite will be highly turbulent and olivines precipitated from the liquid will remain in suspension until a late stage when the temperatures of the two layers are nearly equal. Provided that the upper layer is volumetrically large, the lower layer will transform into a mixture of suspended olivine in a basalt liquid. This basaltic liquid will be more primitive than the upper layer which has increased slightly in temperature. In many of our calculations, the residual liquid composition in the lower layer is estimated to occur near to the density minimum shown in Fig. 1. Note that the lower layer will in fact increase in bulk density as it crystallizes, as long as the olivines are kept in suspension. For example, the bulk density of liquid A plus 20% olivines in suspension is 2.82 g cm^{-3}. The dense lower layer remains in existence as long as the convection is sufficiently vigorous to suspend the olivine crystals.

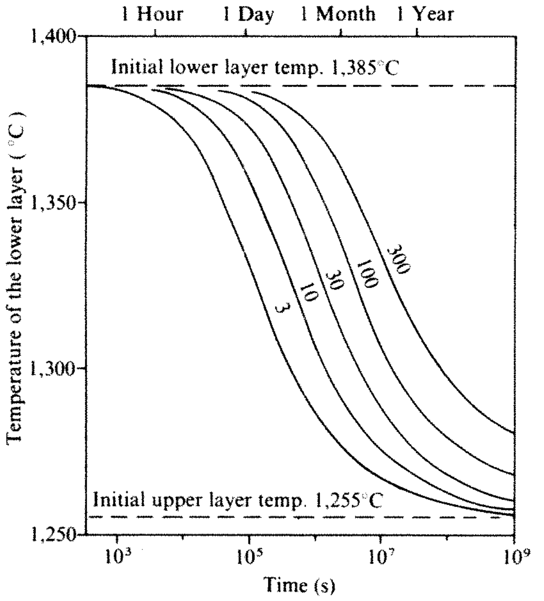

Fig. 3 Temperature of the lower layer as a function of time for various thicknesses (*h*) in metres of the lower layer for an upper layer 4 km thick.

Once convection has died down in the closing stages of cooling, theory[16] predicts a concentration gradient of olivines will be generated in the lower layer when the free-fall velocity and convective velocities become comparable (Fig. 2*c*). Only a slight concentration gradient is required to nullify completely the density instability caused by the slight temperature gradient at this late stage, leading to a transition to stable stratification of the lower layer. We predict that the layer will pass rapidly to a stage of *en masse* sedimentation of suspended olivine. A substantial amount of basaltic liquid will segregate as the olivines sediment (Fig. 2*c*). For example, if a picrite layer, 100 m thick, contained 18% MgO at 1,400 °C and the upper layer, 2,000 m thick, contained basalt with MgO = 9% at 1,250 °C, the lower layer would evolve to a suspension of 20% olivines in a basalt liquid at an equilibrium temperature of 1,264 °C and 10% MgO. Sedimentation of the olivine to a dense close-packed mode (60% olivine) would liberate ~80% of the remaining basaltic liquid, generating a cumulate layer 33 m thick (Fig. 2*d*). The olivines would be relatively uniform in composition as they have grown in conditions approximating equilibrium crystallization in the turbulent layer. Such features are found in the homogeneous olivine cumulates observed at the base of ophiolites. Further adcumulus growth (as is common in ultramafic cumulates) would drive out further basaltic liquid component.

Thermal equilibration between the two layers (Fig. 2) would require that the upper layer has increased in temperature. In many cases the upper layer would be more evolved and denser than the basalt liquid derived from the lower layer as illustrated in the example calculation above. We conclude that the basalt liquid squeezed out during olivine sedimentation in the lower layer will be buoyant in the upper layer and will mix with it convectively (Fig. 2*d*). In this way the compositions of basalts which can erupt at the surface are restricted in composition as they periodically become mixed with basalt close to the density minimum.

We thank G. M. Brown, C. H. Donaldson, D. P. MacKenzie, R. K. O'Nions, E. R. Oxburgh and J. S. Turner for helpful comments. Contribution no. 49 (Department of Earth Sciences, University of Cambridge).

Received 11 March; accepted 28 April 1980.

1. O'Hara, M. J. *Earth Sci. Rev.* **4,** 69 (1968).
2. Green, D. H., Hibberson, W. O. & Jaques, A. L. in *The Earth: its Origin, Structure and Evolution*, 265 (ed. McElhinny, E.) (1979).
3. Clarke, D. B. & O'Hara, M. J. *Earth planet. Sci. Lett.* **44,** 153 (1979).
4. Elthon, D. *Nature* **278,** 514 (1978).
5. Presnall, D. C., Dixon, J. R., O'Donnell, T. M. & Dixon, S. A. *J. Petrol.* **20,** 3 (1979).
6. Dungan, M. A. & Rhodes, J. M. *Contr. Miner. Petrol.* **67,** 417 (1978).
7. Sparks, R. S. J., Meyer, P. C. & Sigurdsson, H. *Earth planet. Sci. Lett.* **46,** 419 (1980).
8. Bottinga, Y. & Weill, D. F. *Am. J. Sci.* **269,** 169 (1970).
9. Donaldson, C. H. & Brown, R. W. *Earth planet. Sci. Lett.* **37,** 81 (1977).
10. Bryan, W. B. *J. Petrol.* **20,** 293 (1979).
11. Walker, D., Shibata, T. & DeLong, S. E. *Contr. Miner. Petrol.* **70,** 111 (1979).
12. O'Hara, M. J. *Nature* **266,** 503 (1977).
13. Nisbet, E. G. & Fowler, C. M. R. *Geophys. J. R. astr. Soc.* **54,** 631 (1978).
14. Turner, J. S. *Buoyancy Effects in Fluids* (Cambridge University Press, 1979); *A. Rev. Fluid Mech.* **6,** 37–56 (1974).
15. Townsend, A. A. *The Structure of Turbulent Shear Flow* (Cambridge University Press, 1976).
16. Batchelor, G. K. *2nd Austr. Conf. on Hydraulics and Fluid Mechanics* 19–41 (1965).
17. Krishnamurthy, P. & Cox, K. G. *Contr. Miner. Petrol.* **62,** 53 (1977).

Volcanic rocks cored on Hess Rise, western Pacific Ocean

T. L. Vallier*, K. E. Windom†, K. E. Seifert† & Jörn Thiede‡

* US Geological Survey, Menlo Park, California 94025
† Department of Earth Sciences, Iowa State University, Ames, Iowa 50011
‡ Institutt for Geologi, Universitet i Oslo, Norway

Large aseismic rises and plateaus in the western Pacific include the Ontong-Java Plateau, Magellan Rise, Shatsky Rise, Mid-Pacific Mountains, and Hess Rise. These are relatively old features that rise above surrounding sea floors as bathymetric highs. Thick sequences of carbonate sediments overlie, what are believed to be, Upper Jurassic and Lower Cretaceous volcanic pedestals. We discuss here petrological and tectonic implications of data from volcanic rocks cored on Hess Rise. The data suggest that Hess Rise originated at a spreading centre in the late early Cretaceous (Aptian–Albian stages). Subsequent off-ridge volcanism in the late Albian–early Cenomanian stages built a large archipelago of oceanic islands and seamounts composed, at least in part, of alkalic rocks. The volcanic platform subsided during its northward passage through the mid-Cretaceous equatorial zone. Faulting and uplift, and possibly volcanism, occurred in the latest Cretaceous (Campanian–Maastrichtian stages). Since then, Hess Rise continued its northward movement and subsidence. Volcanic rocks from holes drilled on Hess Rise during IPOD Leg 62 (Fig. 1) are briefly described here and we relate the petrological data to the origin and evolution of that rise. These are the first volcanic rocks reported from Hess Rise.

Hess Rise is a triangular-shaped bathymetric high that is bounded on the west by the Emperor Seamount chain, on the north-east by the Emperor Trough, and on the south by the Mendocino Fracture Zone. A clear sequence of magnetic anomalies has not been discovered on Hess Rise, but it is believed to lie entirely within the Cretaceous magnetic quiet

0028-0836/80/270048-03$01.00

zone and thereby is younger than early Aptian (~111 Myr old) in age. Our drilling results[1] and previous plate reconstructions[2,3] indicate that Hess Rise formed in Aptian or early Albian time south of the early Cretaceous palaeoequator and moved progressively northward as part of the Pacific Plate.

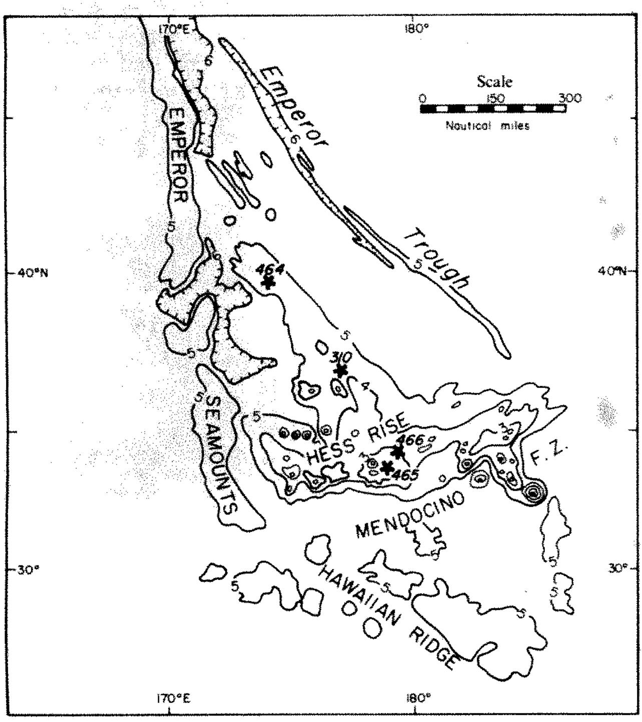

Fig. 1 Bathymetric chart of Hess Rise showing sites drilled and the major bathymetric features. Site 465 cores penetrated trachyte beneath upper Albian limestone and Site 466 cores contained alkali basalt clasts in Upper Cretaceous chalk. Site 464 cores penetrated altered tholeiitic basalt beneath lower Albian limestone. Site 310, drilled on DSDP Leg 32, did not penetrate igneous rocks. Contour intervals are in kilometres.

We recovered 16 cm of highly altered tholeiitic basalt from beneath Lower Albian (uppermost Lower Cretaceous) sediments at Site 464 on northern Hess Rise, 24 m of altered trachyte from beneath Upper Albian sediments at Site 465 on southern Hess Rise, and alkali basalt clasts in Upper Cretaceous (Campanian–Maastrichtian) sediments at Site 466 on southern Hess Rise. Petrological interpretations are based on the petrographical data from 68 thin sections, X-ray diffraction analyses of altered phases, whole-rock chemical analyses of 18 trachyte samples from Site 465 and three basalt samples from Site 464, and microprobe analyses of feldspar phenocrysts from Site 465 trachytes and clinopyroxene phenocrysts from Site 466 basalt clasts. The X-ray fluorescence and instrumental neutron activation analysis data for rocks from Sites 464 and 465 are given in Tables 1 and 2. Clinopyroxene data determined by microprobe analyses of basalt clasts from Site 466 are given in Table 3. Figures 2 and 3 are plots of rare earth element (REE) data.

The basalt from Site 464 is deeply altered as indicated by the high total water contents (7.12–8.05%), high K_2O contents, and abundant smectite minerals. The most convincing evidence that these are tholeiitic basalt, characteristic of mid-ocean ridge basalt (MORB), rather than alkalic basalt is the REE pattern (Fig. 2). The pattern is relatively flat at about 15 times the chondrite abundance and corresponds to a transitional type MORB[4]. In contrast, alkalic basalts show considerable light REE enrichment relative to heavy REE. Studies on the alteration of tholeiitic basalt by seawater[5–7] show that basalt increases in the amounts of H_2O^+, total Fe, K, and Ti and decreases in the abundances of Ca, Mg, and Si which are consistent with our results.

Table 1 Compositional ranges and averages of major and minor element oxides as determined by X-ray fluorescence, instrumental neutron activation analysis, and wet chemical techniques

	Trachyte (Site 465)		Basalt (Site 464)	
Oxide	Range	Average	Range	Average
SiO_2	58.07–60.81	59.66	45.58–46.75	46.16
TiO_2	0.99–1.07	1.03	1.72–1.75	1.74
Al_2O_3	18.40–19.08	18.78	15.69–16.14	15.92
Fe_2O_3*	2.37–3.59	2.97	6.27–6.49	6.38
FeO	0.14–1.00	0.56	6.46–7.16	6.81
MgO	0.31–2.08	1.03	7.82–7.89	7.85
CaO	1.94–3.40	2.31	3.91–4.72	4.32
Na_2O	4.68–5.46	5.12	3.08–3.38	3.23
K_2O	2.89–6.40	4.80	0.81–1.68	1.25
P_2O_5	0.28–0.46	0.36	0.09–0.10	0.09
MnO	0.015–0.060	0.034	0.25–0.29	0.27
H_2O^+	0.60–2.68	1.56	2.74–2.79	2.76
H_2O^-	0.64–3.98	1.84	4.33–5.31	4.82
CO_2	0.21–1.73	0.47	—	—

* Fe_2O_3 is total iron for Site 465 analyses only.

Site 465 data ($N = 18$) are from southern Hess Rise trachyte and Site 464 data ($N = 2$) are from northern Hess Rise basalt.

Subaerial eruption of trachyte flows at Site 465 is suggested by large (>5 mm diameter) vesicles, red iron oxide staining in some flow units, and the absence of glassy flow margins. The trachytic textures are defined by flow-alined feldspar laths and microlites in smectite-replaced glassy groundmasses. Plagioclase feldspar has a compositional range of An_{28} to An_{43} as determined by electron microprobe. Some plagioclase is completely replaced by potassium feldspar, possibly during a late-stage magmatic event.

Table 2 Trace element ranges and averages as determined by X-ray fluorescence and instrumental neutron activation analysis

	Trachyte (Site 465) (p.p.m.)		Basalt (Site 464) (p.p.m.)	
Element	Range	Average	Range	Average
La	75.1–89.1	82.5	4.8-5.1	5.0
Ce	156–187	171	12.8–13.6	13.2
Sm	8.9–11.7	10.5	3.1–3.5	3.2
Eu	2.9–3.2	3.0	1.17–1.25	1.20
Tb	1.0–1.6	1.3	0.66–0.69	0.68
Yb	1.8–4.4	2.9	2.37–2.96	2.27
Lu	0.3–0.7	0.5	0.32–0.42	0.36
Rb	15.3–66.5	33.6	— —	—
Ba	596–688	645	— —	—
Th	10.2–11.0	10.6	0.23–0.33	0.27
Hf	13.9–18.9	16.9	3.16–3.17	3.16
Ta	8.4–11.1	9.6	0.26–0.28	0.27
Zr	474–829	715	111–112	111
Sr	251–397	311	158–178	167
Co	8.5–22.6	16.2	38.6–50.3	45.3
Sc	2.1–3.2	2.7	55.0–55.8	55.3

For trachyte, $N = 18$; for basalt, $N = 3$.

Chemical data for trachyte samples from Site 465 (Tables 1 and 2) show that the oxides and elements have small ranges of values. Most data trends are consistent with either differentiation effects or high temperature alteration. For example, MgO decreases as K_2O increases and K_2O increases with SiO_2 as expected for differentiation. However, both K_2O and SiO_2 decrease as H_2O^+ increases and MgO increases as H_2O^+ increases. These data are consistent with effects caused by high-temperature alteration[8,9]. Rare earth data for the trachyte samples are plotted in Fig. 3. The REE patterns are consistent with patterns for differentiated alkalic rocks. The heavy REE, particularly Lu, also decreases with increasing H_2O^+. Despite their alteration, the trachytes from Hess Rise are chemically similar to trachytes from oceanic islands, particularly the Tristan da Cunha group[10], and are also similar to end members of differentiation trends discovered in rocks from other oceanic rises and plateaus[11–14].

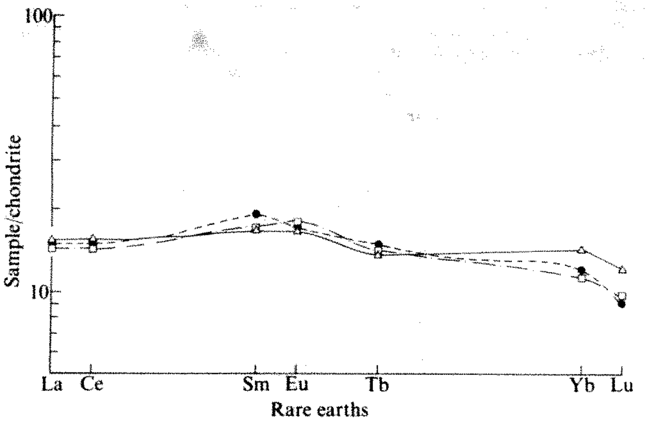

Fig. 2 Normalized plot of rare earth element abundance in basalt of Site 464. This plot is typical of tholeiitic basalt. △, 464-34-CC, 11 cm; ●, 464-34-CC, 19 cm; □, 464-34-CC, 22 cm.

Alkali basalt clasts were recovered from Upper Cretaceous (Campanian–Maastrichtian stages) sediments at Site 466. The rocks have phenocrysts of olivine (completely replaced), clinopyroxene, and plagioclase enclosed in altered glassy groundmasses. The alkalic nature of the rocks is suggested by the high calcium contents of clinopyroxene phenocrysts (Table 3). Plots of the molecular percentages En–Fs–Wo place the pyroxenes in the salite and high-calcium augite fields. Stratigraphic and petrological data from the clasts indicate that erosion of alkalic basalt islands occurred at least 25 Myr after the main volcanic pedestal had formed. It is apparent that some uplift and faulting took place in the late Cretaceous, but the reason for the tectonic activity is not known.

The age, as determined by overlying and associated biogenic sediment, and petrology of the volcanic rocks have important tectonic and petrological implications. Combined with our interpretations based on shipboard data[1] and recognition of plate-associated lateral and vertical movements[2,3], we can present some preliminary conclusions with regards to the geological history of Hess Rise.

Table 3 Clinopyroxene chemistry of two alkali basalt clasts in Upper Cretaceous sediment, Site 466, southern Hess Rise.

Oxide	1	2	3	4	5
SiO_2	50.57	51.09	48.17	49.97	48.16
TiO_2	0.89	0.91	1.41	0.88	1.25
Al_2O_3	3.14	3.39	5.76	4.32	5.50
Cr_2O_2	0.22	0.29	0.22	0.23	0.36
FeO	7.29	7.47	8.20	7.11	7.59
MnO	0.13	0.13	0.11	0.11	0.13
MgO	14.50	14.45	12.98	13.66	13.50
CaO	22.67	21.73	22.07	22.40	22.16
Na_2O	0.45	0.53	0.74	0.61	0.64
Total	99.86	99.99	99.66	99.29	99.29
Molecular percentage					
Wo	46.7	45.6	47.4	47.7	47.3
En	41.6	42.2	38.8	40.5	40.1
Fs	11.7	12.2	13.7	11.8	12.6

Column 1, Small phenocryst, Sample 1; 2, Phenocryst core, Sample 2; 3, Phenocryst edge, Sample 2; 4, Pyroxene lath, Sample 2; 5, Small phenocryst, Sample 2. Analyses were done by Florence Lee-Wong, US Geological Survey.

Hess Rise, at least in part, is a subsided oceanic volcanic archipelago that was buried by younger pelagic sediments. Active volcanic activity probably ended before late Albian time, although the presence of alkali basalt clasts in the Upper Cretaceous strata at Site 466 may indicate later volcanism. The age difference between oldest sediment cored at the northern (464) and southern (465) sites (early Albian and late Albian–Cenomanian respectively) is consistent with passage of the rise over a mantle hot spot, but this hypothesis needs additional testing.

The volcanic rocks we recovered from Hess Rise represent only the uppermost part of the pedestal; therefore, we do not know the nature of the underlying volcanic succession. Judging from studies of older parts of deeply eroded oceanic islands and seamounts, of rocks erupted from mid-ocean ridges, and of our data from sites on Hess Rise, we presume that the oldest volcanic rocks are tholeiitic basalt that were extruded at a spreading centre in Aptian or early Albian time. Younger intraplate, or off-ridge, volcanism commenced after the sea floor had migrated from the ridge axis and subsequently built a large archipelago. After volcanic activity ceased, the archipelago continued moving northward. Most of the archipelago had subsided beneath sea level by the time it crossed the biological high-productivity zone of the mid-Cretaceous equator[1]. Tectonic activity, probably mostly block faulting, raised parts of the old archipelago above sea level where subaerial erosion provided clasts that became incorporated in the Upper Cretaceous strata at Site 466. Synchronous volcanic activity may have occurred. Hess Rise continued to subside during the Cenozoic as it moved northward and is now a prominent bathymetric high in the western Pacific.

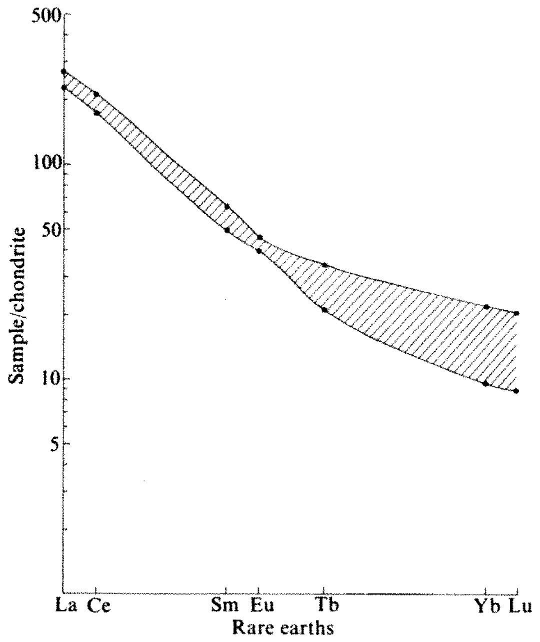

Fig. 3 Normalized plot of the total range of rare earth element abundance in Site 465 trachyte.

We thank Rodey Batiza and Florence Lee-Wong for helpful reviews. We thank the shipboard scientific staff on the Glomar Challenger for assistance during Leg 62 of the International Phase of Ocean Drilling.

Revised 10 March; accepted 2 May 1980.

1. Vallier, T. L. *et al. Geotimes* **24,** 24–26 (1979).
2. Lancelot, Y. & Larson, R. *Init. Rep. DSDP Leg* **32,** 925–940 (1975).
3. Lancelot, Y. *Mem. Soc. Geol. Fr.* **134,** (1978).
4. Sun, S. S. *et al. Earth Planet. Sci. Lett.* **44,** 119–138 (1979).
5. Hart, R. *Earth planet. Sci. Lett.* **9,** 269–279 (1970).
6. Andrews, A. J. *Can. J. Earth Sci.* **14,** 911–926 (1977).
7. Scarfe, C. M. & Smith, D. G. W. *Can. J. Earth Sci.* **14,** 903–910 (1977).
8. Humphries, S. E. & Thompson, G. *Geochim. cosmochim. Acta* **42,** 107–126 (1978).
9. Mottl, M. J. & Holland, H. D. *Geochim. cosmochim. Acta* **42,** 1103–1116 (1978).
10. Baker, P. E. *Ocean Basins and Margins* **1,** 493–553 (1973).
11. Natland, J. H. *Init. Rep. DSDP Leg* **33,** 749–788 (1976).
12. Batiza, R. *Mar. Geol.* **24,** 169–183 (1977).
13. Hekinian, R. *Contr. Miner. Petrol.* **43,** 125–147 (1974).
14. Fodor, R. V. *et al. Earth planet. Sci. Lett.* **35,** 225–233 (1977).

Unique amino acid composition of Red Sea brine

D. E. Ingmanson

Sea Grant, A-032, University of California, La Jolla, California 92093

M. J. Dowler

Natural Science Department, San Diego State University, San Diego, California 92182

The lack of evidence from terrestrial environments supporting the chemical evolution model has resulted in scientists looking elsewhere in the Solar System and in space for evidence. We have suggested that the Atlantis II Deep brine (21°22′N by 38°05′E) located in a submarine rift at the bottom of the Red Sea is a promising environment possibly containing terrestrial evidence for chemical evolution[1]. We have also reported finding a thiocyanate concentration of 2.4×10^{-5} M in the Atlantis II Deep brine[2]. We report here the discovery of an unusually large concentration of glycine in the Atlantis II Deep brine and virtually no other dissolved free amino acids. We further suggest four possible explanations for the unique amino acid composition of Red Sea brine. Our methods of location, sampling and storage of the brines have been discussed elsewhere[2].

Several investigators have analysed seawater and other saline solutions for their dissolved free amino acid composition[3-6]. Because in deep ocean waters the dissolved free amino acid concentration is extremely low[6], great care must be used in the sampling, storing and analysing the samples. Special precautions in our work included the following measures. All water used was double distilled in glassware. All glassware was acid (nitric acid/sulphuric acid, 1:2 by volume) washed and rinsed repeatedly with double distilled water. Before use, all inorganic compounds were heated at 450 °C for over 12 h to remove organic contaminants. Preparation of the reagents for chromatography entailed the following steps. Ammonium hydroxide was prepared by bubbling ammonia gas through acid-washed tubing, a water trap to remove any amino acids, and finally into water to produce 3 M NH_4OH. Hydrochloric acid reagent was made by two successive azeotropic distillations producing 6 M HCl.

Separation of the amino acids from the brine was accomplished by a liquid-exchange chromatography procedure using a copper–Chelex 100 (BIO-RAD) resin column and an ammonium–Chelex 100 column[4,6]. For column preparation and separation, these steps were followed in the order indicated:

(1) 25 ml of 3 M NH_4OH were passed through 10 ml of Cu^{2+}–Chelex 100;
(2) the column was rinsed with water until *p*H 9.8 was reached;
(3) 0.3 ml of 1 M NaOH was added to 10 ml of brine. The solution was brought up to 100 ml with water and poured onto the column;
(4) the column was flushed with water until Cl^- free as measured visually using $AgNO_3$ solution;
(5) amino acids were eluted with 25 ml of 1.5 M NH_4OH;
(6) 20 ml of 1.5 M NH_4OH were passed through 5 ml of NH_4^+–Chelex 100;
(7) the eluant amino acid solution was passed through the NH_4^+-Chelex 100 column to separate Cu^{2+} from the eluant;
(8) the column was chased with 5 ml 1.5 M NH_4OH;
(9) the sample was lyophilized. 2 ml of double glass distilled water was added, the solution was centrifuged, the supernatant removed and relyophilized.

Analysis was performed using a Beckman 121 MB amino acid analyser equipped with a model 126 data system. Samples were applied to a 0.28 × 20 cm column with Beckman AA-10 resin using a standard sodium citrate program (Beckman) with ninhydrin detection in a single column system.

Red Sea brine samples and several kinds of controls were all analysed for amino acids using identical procedures. The controls included many duplicates of 5 M NaCl synthetic brine, non-brine Red Sea water from a depth of 500 m, a solution of known amounts of amino acids, known contaminated solutions, the ammonium hydroxide reagent, the double glass distilled water and the hydrochloric acid used in preparing the resins. The synthetic brine and ammonium hydroxide revealed a glycine contamination level of <50 pmol per 10 ml. The water and acid were below the detection levels of the system. Recovery of known amino acids averaged ~50%. Known contaminated solutions showed a wide variety of amino acids.

The Atlantis II Deep brine samples yielded a mean glycine concentration of 1,090 nmol l^{-1} based on 11 analyses. About 10 nmol l^{-1} or less of serine was also detected. No other dissolved free amino acids were detected. The non-brine Red Sea sample showed a glycine concentration of ~122 nmol l^{-1}.

Previous reports of amino acids in deep ocean water suggest that a wide variety of dissolved free amino acids are present in most cases, but the total concentration levels are always below 100 nmol l^{-1} (ref. 6). Surface ocean water samples are reported to contain ~1,000 nmol l^{-1} with glycine comprising ~200 nmol l^{-1} (ref. 5).

How can the presence of high amounts of glycine and virtual absence of other amino acids be explained? As the glycine concentration is higher than that found in highly productive surface coastal waters, even though the brine is apparently sterile, an additional source must be sought. We suggest that one plausible source is an abiotic origin involving a Strecker synthesis of amino acids from aldehydes and cyanide. Because the methane content is known to be high, and formaldehyde is easily derived from methane, one can then explain the high glycine concentration. Why glycine is virtually the only amino acid found is unclear. Some investigators have invoked the properties of clays to explain unique amino acid distributions[8,9]. As relatively large volumes of samples are needed to check carbon isotope ratios, we have not yet determined the $^{12}C/^{13}C$ ratio which could shed light on the origin of the glycine. There are several other plausible explanations for our results. The most obvious is that there is biological contamination of the brines and/or our procedures. The Atlantis II brine has been reported sterile[7]. As the amino acid distribution of our control brine indicates no contamination and bacteriological assays done on water from the same sampler were negative (R. Cuhel, personal communication), we consider this explanation unlikely. Another explanation might involve chemical contamination of our sample. Glycine has been reported to bleed from or through Chelex 100[6]. If this were the explanation for our data, why were there such repeatable small amounts of glycine in the synthetic control brine? A third alternative is that the abundant bacteria above the Atlantis II brine decompose organisms and the amino acids leach into the brine where they accumulate. Perhaps there is some chemical compound in the brine that selectively removes all dissolved amino acids except glycine from the brine, or alters other amino acids to form glycine. However, there is no evidence to support this.

If amino acids are synthesized in geothermal systems, this might provide the nutrient base for some of the unique, highly productive regions surrounding deep-sea springs.

We have demonstrated the value of further exploration of Red Sea hot brines and especially the Atlantis II Deep brine from the perspective of chemical evolution. This should be done as soon as proposals have been made to mine commercially the rich heavy metal deposits in the sediment beneath the brines.[10].

We thank Drs David Ross, Leslie Orgel, Wylie Vale and Joachim Spiess for their assistance. We acknowledge financial support from NSF-OCE-76-10417, NSF-SP1-78-19097 and the San Diego State University Foundation.

Received 11 February; 30 April 1980.

1. Ingmanson, D. E. & Dowler, M. J. *Origins of Life* **8**, 221–224 (1977).
2. Dowler, M. J. & Ingmanson, D. E. *Nature* **279**, 51–52 (1979).

0028-0836/80/270051-02$01.00

3. Moore, S. & Stein, W. H. *J. biol. Chem.* **192,** 663–681 (1952).
4. Siegel, A. & Degens, E. T. *Science* **151,** 1098–1101 (1966).
5. Clark, M. E., Jackson, G. A. & North, W. J. *Limnol. Oceanogr.* **17,** 749–757 (1972).
6. Lee, C. & Bada, J. L. *Earth planet. Sci. Lett.* **26,** 61–68 (1975).
7. Watson, S. W. & Waterbury, J. B. in *Hot Brines and Recent Heavy Metal Deposits in the Red Sea,* 272–281 (eds Degens, E. T. & Ross, D. A.) (Springer, New York, 1969).
8. Degens, E. T. & Matheja, J. *J. Br. Interplanet. Soc.* **21,** 52–82 (1968).
9. Degens, E. T., Matheja, J. & Jackson, T. A. *Nature* **227,** 492 (1970).
10. Staff. *Sea Technol.* 67 (1979).

Size distribution of Amazon River bed sediment

Carl F. Nordin Jr*, Robert H. Meade*, William F. Curtis*, Nivaldo J. Bósio† & Paulo M. B. Landim†

* US Geological Survey, Denver, Colorado 80225
† Departamento de Geociências, Universidade Estadual Paulista, Rio Claro, Sao Paulo, Brazil

The first recorded observations of bed material of the Amazon River were made in 1843 by Lt William Lewis Herndon of the US Navy, when he travelled the river from its headwaters to its mouth, sounding its depths, and noting the nature of particles caught in a heavy grease smeared to the bottom of his sounding weight[1]. He reported the bed material of the river to be mostly sand and fine gravel. Oltman and Ames took samples at a few locations in 1963 and 1964, and reported the bed material at Óbidos, Brazil, to be fine sands, with median diameters ranging from 0.15 to 0.25 mm (ref. 2). We present here a summary of particle-size analyses of samples of streambed material collected from the Amazon River and its major tributaries along a reach of the river from Iquitos in Peru, ~3,500 km above Macapá, Brazil, to a point 220 km above Macapá[3].

The field work was done aboard RV Alpha Helix. Samples were collected with pipe dredges[3], or with a US BM-54 bed material sampler[4], dried aboard ship, and transported to the US Geological Survey laboratories in Denver, Colorado, for particle-size analysis by sieving, or by pipette–visual accumulation tube methods[5].

Herndon's observations were remarkably accurate; the bed of the Amazon is mostly fine sand. Many of our samples contained small percentages of fine gravel; these were especially prevalent at locations where there were local outcrops in the abutting terraces, or where conditions favoured hydraulic sorting; for example, on the outsides of bends, downstream from confluences with some of the major tributaries, where there are zones of high shearing both in the flow and at the bed with exceptionally high turbulence, or in very narrow sections with high velocities. Figure 1 shows a comparison of particle-size distributions of material collected in a deep hole just below the confluence of the Rio Negro and the Rio Solimões, and of material collected 131 km upstream and 74 km downstream of the confluence. The striking differences in size distribution are apparently due to hydraulic sorting at the confluence in combination with local outcrops of fine gravel in the Alter do Chão formation.

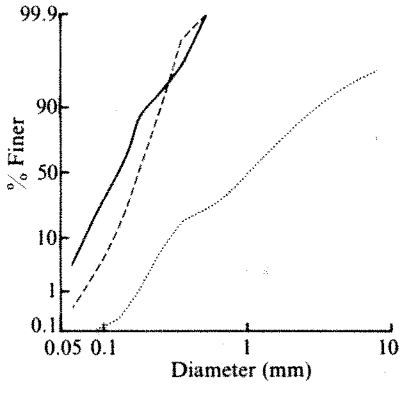

Fig. 1 Hydraulic sorting at the confluence of the Rio Negro and Rio Solimões results in the local deposits of gravel. The water depth was 54 m. Curves are coded as follows: ...., confluence of the Rio Negro and Rio Solimões; ----, Rio Amazonas, 74 km downstream of the confluence; ———, Rio Solimões, 131 km upstream of the confluence.

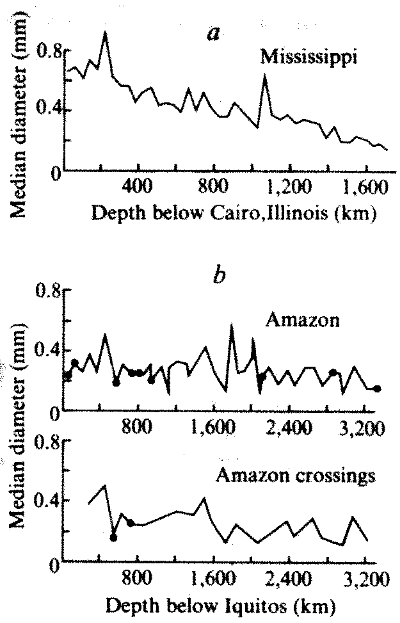

Fig. 2 Variation with distance of median particle size: *a*, for the Mississippi River; *b*, for the Amazon River. Median sizes shown for Mississippi are averages of sands (median diameters 0.06–2.00 mm) for 40-km reaches of river. Median sizes shown for Amazon are mostly individual samples; ●, average values where two or more samples were collected in a cross-section.

In most alluvial streams, bed material becomes finer and more uniform in a downstream direction. Figure 2*a*, for example, shows the trend of decreasing particle size for bed material of the Mississippi River along a 1,600-km reach below Cairo, Illinois[6]. The mean particle diameter along the reach is reduced from ~0.7 to 0.2 mm.

No such striking reduction in particle size was found for the Amazon River between Iquitos and Belem. A plot of the median diameters of bed materials from our 1977 samples against distance downstream from Iquitos, Fig. 2*b*, shows no significant trend. To eliminate the effects of local hydraulic sorting, we systematically collected some of our samples on the crossings between bends. When these data are plotted by themselves (Fig. 2*b*), a slight trend towards decreasing particle size is apparent.

At several cross-sections where we measured the suspended-sediment discharge[7,8], we collected five or more samples of the bed at equally spaced intervals across the sections. The average curves (Fig. 3) show no appreciable differences in particle-size distributions. Cross-channel variation in particle size at several cross-sections was at least as great as downstream variations encountered along the entire 3,300-km reach.

A sorting coefficient, σ, was computed for each sample:

$$\sigma = 1/2\left(\frac{d_{50}}{d_{16}}+\frac{d_{84}}{d_{50}}\right) \qquad (1)$$

where the subscript represents per cent finer. For example, d_{50} is the particle size for which 50% by weight is finer. Values of σ ranged from 1.18 to 2.59, with 70% of the values falling between 1.20 and 1.40. The highest value, 2.59, was for the

0028–0836/80/270052–02$01.00

sample taken at the confluence of the Rio Negro and Rio Solimões, the size distribution of which is shown in Fig. 1. When values of σ were plotted against distance, no significant trend was found. The bed material does not tend to become more uniform in the downstream direction, as it does in most other alluvial streams.

Although the median size and sorting coefficient of the sands on the bed of the Amazon mainstem are essentially constant in the 3,300-km reach we sampled, the composition of the sands in the same reach changes significantly. To the unaided eye, the sands collected near Iquitos appear darker than those collected farther down the river, because of a larger proportion of dark mineral grains and rock fragments. Heavy-mineral suites also differ.

Landim *et al.*[8] report that sands in the first 1,300 km or so downstream from Iquitos are rich in unstable minerals, such as hypersthene, augite and amphibole; these indicate a predominantly Andean source. Sands in the lower 2,000 km contain fewer unstable minerals and higher proportions of zircon and tourmaline. This change in mineral composition is unlikely to represent only the progressive decomposition of unstable Andean minerals during transport or during temporary storage in alluvial deposits, because such decomposition would be accompanied by attrition and a reduction in particle size along the channel. We hypothesize that the change in composition represents a combination of the decomposition of the Andean minerals and a dilution of that mainstem material by sands brought in by tributaries from the Precambrian shield areas north and south of the Amazon. Thus, any reduction in size of material from the Andean sources by attrition along the mainstem below Iquitos is offset by the addition of material from tributaries draining the Precambrian shield areas.

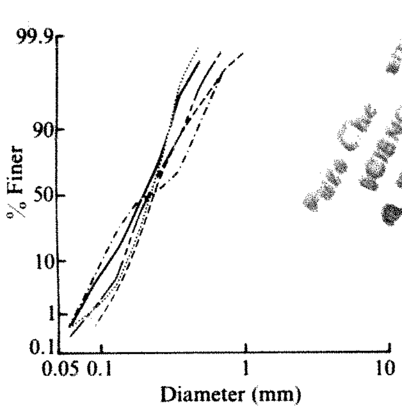

Fig. 3 Average particle-size distribution curves for cross-sections where five or more samples were collected. The curves are coded as follows: ————————, Rio Maranõn, 25 km below Iquitos; ----, Rio Solimões at São Paulo de Olivença, 757 km below Iquitos; ———, Rio Solimões near Santo Antonio do Içá, 909 km below Iquitos; ...., Rio Solimões at Manacapuru, 2,086 km below Iquitos; -·-·-·-·-, Rio Amazonas at Óbidos, 2,827 km below Iquitos.

Received 21 February; accepted 9 May 1980.

1. Herndon, W. L. *US Senate Executive Document* no. 36, 32nd Congress, 2nd Session (1853).
2. Oltman, R. E. *US Geol. Surv. Circ.* No. 552, 1–16 (1968).
3. Nordin, C. F. Jr *et al. US Geol. Surv. Open-File Rep.* 77-400, 1–19 (1977); 79-329, 1–23 (1979.
4. Inter-agency Committee on Water Resources, *Determination of Fluvial Sediment Discharge* Rep. no. 14, 1–151 (US Government Printing Office, Washington DC, 1963).
5. Guy, H. P. *Techniques of Water Resources Investigations of the US Geological Survey*, Book 5, Ch. C1, 1–58 (1969).
6. US Waterways Experiment Station Paper *17* 1–161 (Corps of Engineers, US Army, 1935).
7. Meade, R. H. *et al. US Geol. Surv. Open-File Rep.* 79-515, 1–41 (1979).
8. Meade, R. H. *et al. Nature* **278**, 161–163 (1979).
9. Landim, P. M. B. *et al. EOS* **59**, 227 (1978).

A family of regression equations describing the density distribution of dispersing organisms

R. A. J. Taylor

Department of Entomology, The Pennsylvania State University,
University Park, Pennsylvania 16802

I have previously shown[1] that some of the published regression equations for describing the decline of density of insects with distance from a centre of dispersal were each special cases of a more general equation:

$$N = \exp(a + bx^c) \tag{1}$$

where N is density at a distance x from a centre of dispersal and a, b, and c are parameters. Equation (1) is a good description of the dispersal of most insects so far investigated[1]. To describe any single set of data, a simpler expression can often be found to fit, but this approach will lead to as many theories of migration as there are equations. To describe all sets of data by a single generalized model may require greater complexity than equation (1), and more parameters. I present here such a generalization, which may lead to a unified theory.

The decline in density with distance is characteristically concave, being steep near the origin, and having a long tail, but more rarely the relationship is convex in form (for example, *Meligethes aeneus*[1,2]); permitting the exponent in equation (1) to vary enables both forms to be fitted by the same equation. But a problem with equation (1) is that as c approaches zero a singularity occurs which is difficult to interpret, leading as it does to $N = \exp(a+b) = $ a constant. When c approaches zero it is appropriate to adopt the logarithmic equation,

$$N = \exp(a + b \ln x). \tag{2}$$

The relationship between c and the residual variance after fitting equation (1) is a continuous function, except in the region of $c \sim 0$. As c approaches zero, equation (2) has been found to be a good fit for one set of data (*Glossina palpalis* and *G. tachinoides*[1,3]) of the eight previously examined, and the residual variance was the value which preserved the relationship between c and residual variance after fitting equation (1).

Early models used to describe dispersal have usually been derived from the normal distribution and are thus closely related to the diffusion equations of physics. In these models it is assumed that particles, or in this case, insects, separate at a constant velocity known as the coefficient of diffusion D, and for a given period. When applied to living organisms this assumes that their behaviour is fixed and is unaffected by the presence of others: an assumption with little justification[4].

The regression equation related to the diffusion equation is the so-called 'half-normal',

$$N = \exp(a + bx^2) \tag{3}$$

in which b is inversely proportional to the coefficient D. By assuming that D is proportional to x^{2-c}, equation (1) is obtained. With D proportional to distance x, the rate of diffusion must be inversely proportional to density, a relationship which can be interpreted biologically. A large number of animals released at a point are likely to interact with one another, changing their behaviour in a density-dependent fashion; high densities experienced during rearing or collection may lead to longer periods of activity. They also increase contacts between individuals which may, in turn, reduce the initial speed of movement away from the release

0028-0836/80/270053-03$01.00

Table 1 Parameter estimates

Species	Ref.	*a*	*b*	*c*	*d*	d.f.	r.m.s.	*F*-ratio
Drosophilia pseudoobscura	6	3.48	-0.03	0.83	-0.18	16	0.9376	356.41
Musca domestica	12	-4.22	51.59	-0.63	0.49	23	0.4483	31.95
Phormia regina	13	1.95	8×10^{-5}	-13.81	-0.61	15	4.4483	78.24
Lucilia sericata	14	2.90	-1.60	0.43	0.16	10	0.7456	20.93
*Glossina palpalis + tachinoides**	3	11.16	-3.72	1×10^{-3}	-0.99	14	1.2205	32.38
Erioischia brassica	15	3.80	-0.62	0.65	0.29	13	1.3192	96.86
Scolytus multistriatus	16	5.78	-2×10^{-12}	3.98	-0.59	6	9.2005	27.93
Meligethes aeneus	2	-17.94	1×10^{-4}	1.40	3.17	18	0.1360	50.56
Danaus plexippus	17	8.44	-4.25	0.14	0.64	4	4.9775	124.24
Larus argentatus	18	7.98	-1×10^{-5}	1.76	-0.68	4	9.7525	487.21
Larus novaehollandiae	19	2.69	-8×10^{-3}	1.99	-0.19	15	0.1257	673.50
Parus major	20	3.99	-2.40	0.47	2.00	13	0.4232	109.78
Turdus merula	21	7.80	-3.36	0.15	5×10^{-3}	4	6.7125	2128.72
Homo sapiens	22	3.17	-0.01	0.03	-0.93	12	2.8050	353.80
Peorian loess	10	2.66	-0.05	9×10^{-4}	-0.43	12	1.3775	125.71

Equation (5) fitted to dispersal data of 14 species, and also that of the deposition of Peorian loess in central North America. (Significance levels all less than 0.001.) The data are all of average numbers obtained at a distance from a point source except for the tsetse* data which are from a line source, and standardized for density (see ref. 23). The *Drosophila* data are of the combined data of Dobzhansky and Wright[1] as given in Wallace[24]. d.f. = degrees of freedom, r.m.s. = residual mean square.

point, thus decreasing the diffusion coefficient. As the number of contacts increases with the number released and a very large number of dispersing insects is needed to get sufficient recaptures for analysis, such experiments are likely to decrease the diffusion coefficient in the early stages of dispersal. Once an insect has left the central concentration, its diffusion coefficient may rise to some characteristic level determined by its earlier environmental history; the amount of interference required for a given effect is also likely to be a species characteristic.

This complex behaviour makes the diffusion process envisaged by Pearson[5] and Dobzhansky and Wright[6] seem unlikely; yet the prediction that the variance of distance flown should be linearly related to the time spent flying was apparently upheld by Dobzhansky and Wright's experiment[6]. Their discovery that the diffusion coefficient was constant only for a given experiment did not deter their faith in the model, but the fact that the coefficient varied between experiments[7] casts some doubt on the validity of the normal distribution as a basis for the model. With the potential for such varied behaviours in different species, it seems essential to increase the numbers of model parameters. While this may present problems in statistical estimation, it does make possible a rational search for behavioural interpretation that is not possible with the normal model[8].

The distribution from which equation (1) presents a form appropriate for regression analysis is a generalization of the Γ distribution (when $\gamma=0$), and which also includes the Weibull distribution ($\alpha=0$), and the half-normal ($a=\frac{1}{2}$, $c=2$, $\gamma=0$), and which has the probability density function[9],

$$p(x)=\frac{c(x-\gamma)^{c\alpha-1}}{\beta^{c\alpha}\Gamma(\alpha)}\exp\left(-\left[\frac{x-\gamma}{\beta}\right]^{c}\right). \qquad (4)$$

Equations (1) and (4) are related by ($\gamma=0$), ($\beta^{-c}=-b$), ($\alpha=1/c$), and ($c/\beta\Gamma(1/c)\equiv\exp(a)$). If the condition that ($\alpha=1/c$) is relaxed, a second term in x is obtained, and defining equivalent parameters gives,

$$N=\exp(a+bx^{c}+d\ln x) \qquad (5)$$

where ($\gamma=0$), ($\beta^{-c}=-b$), ($c\alpha=d+1$), and ($c/\beta^{c\alpha}\Gamma(\alpha)\equiv\exp(a)$). Equation (5) has equations (1) and (2) as special cases; equation (1) is obtained by setting $d=0$ and equation (2) when either b or $c=0$. In view of this relationship, the $\ln x$ term of equation (5) clearly becomes dominant as b or c approaches

Table 2 Residual SS after fitting equation

Species	Ref.	(3)	(2)	(1)	(5)	*F*-ratio
Drosophila pseudoobscura	6	160.92	86.07	15.81*	15.00	0.8650 NS
Musca domestica	12	31.43	18.81	10.35*	10.31	0.0914 NS
Phormia regina	13	167.06	121.23	79.02*	69.49	2.0571 NS
Lucilia sericata	14	13.19	11.32	7.46*	7.46	0.0080 NS
Glossina palpalis + tachinoides	3	25.65	17.09*	17.09	17.09	0.0004 NS
Erioischia brassica	15	18.62	20.40	17.17*	17.15	0.0171 NS
Scolytus multistriatus	16	232.17	81.78	64.77*	55.20	1.0040 NS
Meligethes aeneus	2	6.98	10.76	6.20*	2.45	27.5809 †
Danaus plexippus	17	144.79	69.86	21.43*	19.91	0.3052 NS
Larus argentatus	18	1330.52	302.43	48.53*	39.01	0.9763 NS
Larus novaehollandiae	19	4.61	27.89	1.92*	1.89	0.2625 NS
Parus major	20	17.71	84.59	16.66*	5.50	26.3686 †
Turdus merula	21	892.94	112.70	26.86*	26.85	0.0021 NS
Homo sapiens	22	525.40	33.65*	34.40	33.65	0.0005 NS
Peorian loess	10	22.21	16.53*	16.56	16.53	0.0018 NS

Residual sums of squares after fitting the four regression equations to the 15 sets of data.

*The *F*-ratio is the comparison of equation (5) with the next best fitting equation indicated by an asterisk.

†Significance shows that the somplete four-parameter equation is required for adequate description of the dispersal data ($P<0.001$). As expected, equation (5) has the minimum RSS for all data, but not necessarily the lowest mean square residual.

NS indicates no significant improvement in fit by using equation (5); SS = sums of squares. RSS = residual sums of squares.

zero, and shows why $N=\exp(a+b\ln x)$ is an appropriate alternative equation preserving the symmetry between c and residual variance. Thus the description of Morris' data of tsetse dispersal[3] is not qualitatively different from the other seven sets investigated in ref. 1.

Using literature data for several taxa, I attempted to determine the usefulness of these equations for description of animal dispersal from a point source. Table 1 shows the results of fitting equation (5) to data of 14 animal species and also, for comparison, one set of data of the aerial displacement by wind of grains of Peorian loess in central North America[10]. Table 1 shows that all the data fit the model well, and also that they can be separated into three types; two data sets have d comparatively large (*Meligethes* and *Parus*) suggesting that the fourth parameter has a large influence, and three sets in which c is small (*Glossina*, man and soil), supporting the logarithmic equation (2): of the remainder, approximately half have very small b but these coincide with large c.

To confirm that equations (1) and (2) are indeed special cases of equation (5) when b, c or d are small, all three equations were fitted to the data, with, for comparison, the 'half-normal' equation (3). Table 2 shows the residual sums of squares after fitting the four equations. The last column shows the F-ratio for improvement obtained by fitting equation (5) over the next best fitting equation, and equation (1) always fits better, usually significantly better than equation (3). Note that only man and the tsetse fly data conform to the same model as the soil. What features do man and tsetse have in common with air-blown soil? It has been suggested that all behaviour is the resultant of two opposing tendencies, to approach and to separate, and that the distributions we see of organisms in space are the sum of these two opposing behaviours[11]. The distribution of Peorian loess is probably also the result of characteristics of the grains which tend to promote or inhibit displacement by wind, for example, surface texture and mass. I do not suggest that the forces promoting displacement in animals are the same as for wind-blown soil, but that there are analogous forces acting in both cases.

Whatever those forces are, the same functional relation connecting them to the specific behaviour of the dispersing particle (soil, spores and seeds as well as actively moving animals) should apply. The equation presented here is a good candidate for such a function, even though at this stage the parameters cannot be identified. However, it is likely that the segregation of the data sets into two groups described by equations (1) and (2) does reflect a real behavioural difference in movement. To determine what that behaviour might be will necessitate analysis of the parameters and this requires far more density–distance data than is available.

Received 12 December 1979; accepted 18 April 1980.

1. Taylor, R. A. J. *Ecol. Ent.* **3,** 63–70 (1978).
2. Taimr, L., Sedivy, J., Bergmannova, E. & Hanker, I. *Acta entomol. bohemovslav.* **64,** 325–332 (1967).
3. Morris, K. R. S. *Bull. ent. Res.* **37,** 201–250 (1946).
4. Many of the papers in *Population Control by Social Behaviour* (eds Ebling, F. J. & Stoddart, D. M.) (Institute of Biology, London 1978).
5. Pearson, K. & Blakeman, J. *Drap. Co. Res. Mem. Biomed. Ser.* **3,** 1–54 (1906).
6. Dobzhansky, T. & Wright, S. *Genetics* **28,** 304–340 (1943).
7. Taylor, R. A. J. & Taylor, L. R. *Population Dynamics* (eds Anderson, R. M., Turner, B. D. & Taylor, L. R.) 1–27 (Blackwells, Oxford, 1979).
8. Taylor, L. R., Woiwod, I. P. & Taylor, R. A. J. *J. Anim. Ecol.* **48,** 955–972 (1979).
9. Johnson, N. L. & Kotz, S. *Distributions in Statistics. Continuous Univariate Distributions* I 197 (Houghton Mifflin, Boston, 1970).
10. Waggoner, P. E. & Bingham, C. *Soil Science* **92,** 396–401 (1961).
11. Taylor, L. R. & Taylor, R. A. J. *Nature* **265,** 415–421 (1977).
12. Parker, R. R. *J. econ. Ent.* **9,** 325–354 (1916).
13. Yates, W. W., Lindquist, A. W. & Butts, J. S. *J. econ. Ent.* **45,** 547–548 (1952).
14. MacLeod, J. & Donnelly, J. *J. Anim. Ecol.* **32,** 1–32 (1963).
15. Hawks, C. *J. Appl. Ecol.* **9,** 617–632 (1972).
16. Wadley, F. M. & Wolfenbarger, D. O. *J. agric. Res.* **69,** 229–308 (1944).
17. Urquhart, F. A. *The Monarch Butterfly* (Toronto University Press, Toronto, 1960).
18. Parsons, J. & Duncan, N. *J. Anim. Ecol.* **47,** 993–1005 (1978).
19. Murry, M. D. & Carrick, R. *CSIRO Wild. Res.* **9,** 160–188 (1964).
20. Greenwood, P. J., Harvey, P. H. & Perrins, C. M. *J. Anim. Ecol.* **48,** 305–313 (1979).
21. Greenwood, P. J. & Harvey, P. H. *J. Anim. Ecol.* **45,** 887–898 (1976).
22. Hägerstrand, T. *Les Déplacements Humains* (ed. Sutter, J.) 61–83 (Union Européenne d'Éditions, Monaco, 1962).
23. Robinson, J. & Luff, M. L. *Ecol. Ent.* **4,** 289–296 (1979).
24. Wallace, B. *Am. Nat.* **100,** 551–561 (1966).

Cameral liquid transport and buoyancy control in chambered nautilus (*Nautilus macromphalus*)

Lewis Greenwald*, Peter D. Ward† & O. E. Greenwald*

*Department of Zoology, Ohio State University, Columbus, Ohio 43210
†Department of Geology, University of California, Davis, California 95616

Studies of cephalopod buoyancy[1] show that transport of cameral liquid by the shallow water cuttlefish (*Sepia*) can be explained by a reduction of the liquid's osmotic pressure, followed by osmosis out of the chamber. This mechanism seems insufficient to explain chamber emptying in the chambered nautilus (*Nautilus macromphalus*), which is frequently found below 240 m, the depth beneath which simple osmotic emptying cannot function[2,3]. At 240 m, the hydrostatic pressure forcing water into the chambers of the nautilus shell exceeds the maximum osmotic emtying pressure. Because deep water experiments were not feasible, it was our aim to determine whether nautilus could transport cameral liquid against osmotic pressure gradients, and to consider mechanisms that could account for transport against both osmotic and hydrostatic gradients. These possible mechanisms include enhanced siphuncular blood concentration (possibly caused by a countercurrent multiplier in the siphuncle[4]) which could 'draw' water from chambers below 240 m, and 'local osmosis'[6], resulting from enhanced solute concentrations in siphuncular intercellular spaces. Physiological and ultrastructural evidence for the latter is presented here.

To expose the siphuncle to osmotic pressure differences tending to draw water into a chamber, we drilled a hole into a 20-ml chamber and removed any liquid. Then we added 5 ml of NaCl-enriched seawater (either 1.3 or 1.9 osmolal). To give the animals an 'incentive' to empty their chambers, we drilled a hole in an adjacent chamber and filled it with seawater, causing the animal to sink to the bottom of the aquarium (1 m deep).

After 10–15 days we measured volumes and osmolalities of liquid remaining in the experimental chambers. Of 13 animals, 12 transported some liquid out (the animal that did not was omitted). For nine animals with 1.3-osmolal solutions in their chambers, the rate was 159 μl d^{-1} ± 80 (95% confidence interval), and for three animals whose chambers contained 1.9 osmolal solutions, 218 μl d^{-1}. The osmolality of heart blood of these and other animals was 1.062 (range 1.054–1.069, 17 animals); the osmolality of the seawater was 1.045. By the end of the experiment the osmotic pressure of the experimental cameral liquids had fallen to 1.262 and 1.770 osmolal, respectively, still well above the blood concentrations. Siphuncular blood samples were not obtained.

Thus the siphuncle transports liquid by some mechanism other than simple osmotic flow. This transport against osmotic gradients, as well as transport against hydrostatic gradients, such as would occur below 240 m, could be explained by local osmosis, which requires a cellular architecture of intercellular spaces or basolateral infoldings of the transporting cells[7]. According to Denton[5], siphuncular cells are "packed with mitochondria" and the basal and lateral membranes of these cells are "folded to form canaliculi". This description recalls other transporting cells thought to use local osmosis[8]. Our observations of siphuncular cells (Fig. 1) are consistent with this description. Our micrograph is from a siphuncle that was emptying cameral liquid (1.7 osmolal) against the osmotic gradient at a rate of 310 μl d^{-1}. The numerous mitochondria along the lateral infoldings (canaliculi) suggest that solute-coupled water transport occurs at these small infoldings rather than at the level of the large basal infoldings. Neither large basal infoldings nor canaliculi are present in siphuncles that

0028–0836/80/270055–02$01.00

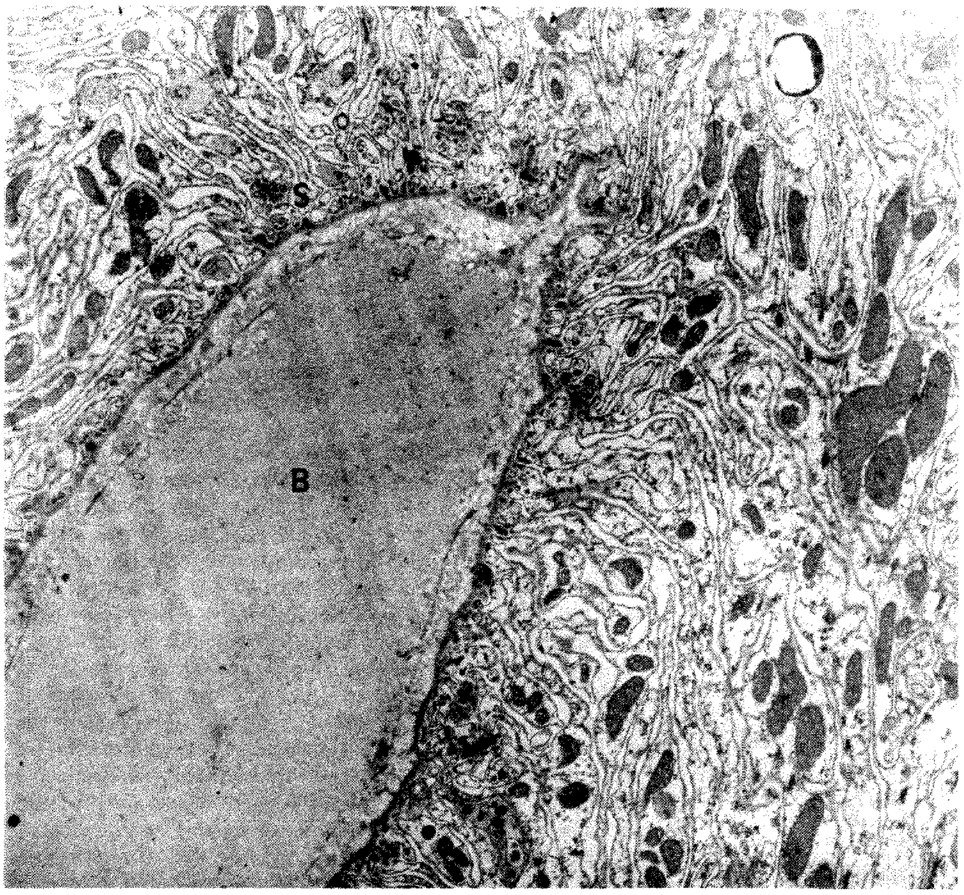

Fig. 1 Low power electron micrograph (×5,000) of a siphuncle cell. The large basal infolding (B) can be seen as well as the network of small channels (S) that lead into the large basal infolding. Numerous mitochondria (M) can be seen in the cytoplasm between the small channels.

have not yet begun to empty cameral liquid.

Nautilus adjusts its rate of emptying and consequent buoyancy development to meet its needs. When we did not flood incentive chambers and the animals were buoyant, as they become in the laboratory, emptying of hyperosmotic solutions was slow (Fig. 2). These animals increased their emptying rates when incentive chambers were flooded, to make the animals sink. Other animals that had been emptying rapidly (and had flooded incentive chambers) decreased their emptying rates when we emptied and plugged the incentive chambers to make the animals float.

This work was supported by NSF grant PCM 7823624 to L.G. and P.D.W. We thank Professor E. J. Denton for helpful criticism, Drs Yves Magnier, Director of the Aquarium of Nouméa, New Caledonia, and Paul de Boissezon, Director of the ORSTOM Laboratory in Nouméa where this work was done.

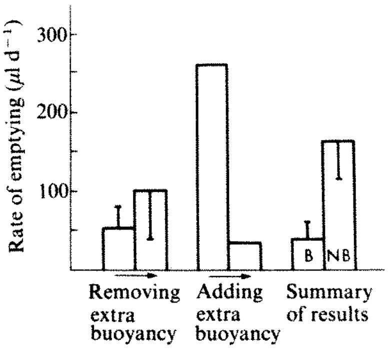

Fig. 2 Rates at which cameral liquid was emptied from experimental chambers of nautilus in different conditions. See text for explanation. The lines extending from the means are the 95% confidence intervals. The difference in emptying rates between all buoyant (B) and non-buoyant (NB) animals (last panel) is highly significant ($P < 0.01$, Student's t test).

Received 13 November 1979; accepted 25 April 1980.

1. Denton, E. J., Gilpin-Brown, J. B. & Howarth, J. V. *J. mar. biol. Ass. U.K.* **41,** 351–364 (1961).
2. Denton, E. J. & Gilpin-Brown, J. B. *J. mar. biol. Ass. U.K.* **46,** 723–759 (1966).
3. Denton, E. J. & Gilpin-Brown, J. B. *Adv. mar. Biol.* **11,** 197–268 (1973).
4. Alexander, R. McN. *The Invertebrates* (Cambridge University Press, Cambridge, 1979).
5. Denton, E. J. *Phil. Trans. R. Soc.* **B262,** 277–287 (1971).
6. Diamond, J. M. & Bossert, W. H. *J. gen. Physiol.* **50,** 2061–2083 (1967).
7. Tormey, J. McD. & Diamond, J. M. *J. gen. Physiol.* **50,** 2031–2060 (1967).
8. Diamond, J. M. in *Membrane Transport Processes* (ed. Hoffman, J. F.) (Raven Press, New York, 1978).

Ovipositing butterfly (*Pieris brassicae* L.) distinguishes between aqueous extracts of two strains of *Cannabis sativa* L. and THC and CBD

Miriam Rothschild

Ashton Wold, Peterborough PE8 5LZ, UK

J. W. Fairbairn

School of Pharmacy, University of London, Brunswick Square, London WC1, UK

The ovipositing female butterfly has proved a useful tool for separating closely related strains of various plant species. Using the large white (*Pieris brassicae*), we have been able to distinguish between the Turkish and Mexican strains of *Cannabis sativa*, and demonstrate that the butterfly is sufficiently sensitive to differentiate between purified THC (tetrahydrocannabinol) and CBD (cannabidiol) – two substances which taste and smell alike to the human observer.

Table 1 Oviposition on cabbage sprayed with aqueous extracts (soups) from leaves of *Cannabis sativa*

Cannabis strain and spray used on cabbage leaf	No. of trials	Egg batches (excluding singles)	No. of eggs laid	No. of times first choice of ovipositing females	Remarks
Cabbage extract	4	35	482*	1	No significant difference
v					
Tap water		47	462	3	
Boiled cabbage extract	2	ND	1,141	ND	The slight deterrent in extract seems to be dissipated by boiling away volatiles
v					
Cabbage extract			747		
Mexican extract	18	8	135*	All tap water	Powerful deterrent present in Mexican strain
v					
Tap water		181	1,418		
Mexican extract	10	3	132	1	Little if any difference between trials of treated or untreated leaves
v					
Untreated cabbage leaf		52	1,493	9	
Mexican extract, 2 leaves	3	0	0	All cabbage	Two leaves did not increase laying on *Cannabis* sprayed cabbage
v					
Untreated cabbage, 1 leaf		31	1,463		
Turkish extract	18†	29	773	4	Repellent quality of Turkish strain far less than that of Mexican strain
v					
Tap water		76	1,421	14	
Mexican extract	26‡	9	510	1	16 of the leaves treated with Mexican extract were not laid on, but all leaves treated with Turkish extract were
v					
Turkish extract		65	1,691	25	
Mexican extract	5	12§	13	ND	1978 trial
v					
Untreated cabbage		251§	537	ND	
Mexican extract	1	17§	37	ND	1979 trial
v					
Untreated cabbage		91§	669	ND	
Mexican extract (steamed)	2	38§	143	ND	1978 trial
v					
Untreated cabbage		36§	75	ND	
Mexican extract (steamed)	2	15§	40	ND	1979 trial
v					
Untreated cabbage		122§	546	ND	

*Eggs counted in only 2 and 5 of these trials, respectively. †Eggs counted in 10 trials; egg batches counted in 14 trials. ‡Egg batches counted in 23 trials. §No. of egg batches including singles. Results obtained from female ovipositing in dual choice chamber. Experiments performed by L. Lundgren. ND, not determined.

We sprayed cabbage leaves with aqueous extracts (soups) of plants which do not serve as normal hosts for *P. brassicae*. The ovipositing female will lay sparingly on most of these leaves, totally reject a few, and sometimes lay as freely as on controls sprayed with cabbage extract or tap water. Cabbage (*Brassica oleracea*, greyhound strain) and *Cannabis sativa* (Turkish strain containing predominantly CBD (UNC 354) and Mexican strain containing predominantly THC (UNC 347))[1] were grown under glass at Ashton from seed produced in the UK. Leaves for the experiments were cut from the same plant, matched for size and position on the stem. Butterflies from Brian Gardiner's Cambridge strain[2] of *P. brassicae* were reared at Ashton.

Aqueous extracts were prepared by macerating 5 g of *Cannabis* (or other) foliage in a domestic blender for 5 min, and adding 5 oz tap water. The blender was not allowed to warm up. The resulting opaque green fluid was filtered through Whatman No. 1 paper, and a measured amount was sprayed on to each cabbage leaf. Maceration probably liberates unusual volatiles from *Cannabis*, cabbage and any other plant, and such extracts from its own food plant may slightly alter the butterflies' reaction to a leaf (Table 1). In other experiments volatiles were removed by heating the extract slowly after filtration for 30 min until all the characteristic odour had evaporated, leaving only a generalized 'green' or 'vegetable' odour. Lost fluid was replaced by an equivalent amount of tap water, and refiltered to remove green matter that had precipitated during heating; the resulting fluid was a clear brownish yellow. Ethanolic solutions containing 1% CBD and 1% THC were also tested by spraying on to the surface of cabbage leaves.

Two leaves were offered simultaneously to free-flying ovipositing females in a large greenhouse (4.5 × 7.5 m). Placed on reversed flower pots (6–12 inches apart), they were left *in situ* from 1000 h to 1400 h. These pots, with leaves, were transposed at intervals to avoid position effects. In sunny weather the leaves were resprayed twice during the 4-h period. Females were used on the second day of egg laying which resulted in a high proportion of small egg batches.

Aqueous extracts of *Cannabis sativa* sprayed on to the normal host plant drastically reduced egg laying by *P. brassicae*, but the Mexican THC strain proved far more repellent than the Turkish CBD strain. Table 1 shows that, matched against a control sprayed with tap water, egg batches are outnumbered 22:1 on leaves sprayed with Mexican strain, but only 3:1 with Turkish strain.

If well steamed, extracts of both plants, but more especially the Turkish strain, lost their principal oviposition deterrent. In several trials (Table 2) leaves treated with steamed Turkish soup, and once or twice with Mexican soup, attracted more oviposition than the controls, confirming that the steam of volatiles of both plants contained the more active deterrents.

Since slight repellent qualities were usually retained by steamed extract, and some cannabinoids, although in reduced amounts, would occur in the aqueous residue, we tested THC and CBD (dissolved in ethanol) against various controls and each other (Tables 2, 3) and found that 2–3 times as many eggs were laid on leaves sprayed with CBD than THC.

The ovipositing large white is known to react to a variety of visual and sensory cues, including the presence of mustard oils in foliage, egg batches on both leaf surfaces, feeding larvae and injuries to the plants[3]. It is nevertheless surprising to find that

Table 2 Oviposition on cabbage sprayed with steamed aqueous extracts (soups) from leaves of *Cannabis sativa*

Strains of *Cannabis* and spray used	No. of trials	No. of egg batches (excluding singles)	No. of eggs laid	No. of times first choice of ovipositing female	Remarks
Steamed Mexican extract		1			1979 trials. Repellent quality of steamed extract was more marked than in 1978
v	11		ND	All cabbage	
Steamed cabbage extract		114			
Steamed Turkish extract			42		Less difference between Turkish steamed extract and cabbage
v	3	ND		ND	
Steamed cabbage extract			96		
Steamed Mexican extract			638	5	5 Trials counted. Markedly less deterrent quality in steamed than unsteamed extract
v	7	ND			
Unsteamed Mexican extract			72	0	
Steamed Turkish extract			405	3	4 Trials counted. This difference is less marked than between Mexican steamed and unsteamed
v	9	ND			
Unsteamed Turkish extract			319	1	
Steamed Mexican extract			11	1	All leaves with Turkish extract were laid on, but 4 leaves with Mexican extract had no eggs laid on them
v	6	ND			
Steamed Turkish extract			121	5	
Steamed Mexican extract		0	0	0	Turkish steamed extract preferred to Mexican steamed extract, but many more eggs laid when tap water used
v					
Steamed Turkish extract	2	2	11	0	
v					
Cabbage and tap water		2	70	4	
Steamed South African extract		3		0	A THC strain of *Cannabis*. A huge number of eggs on control leaf on both surfaces
v	7	(very small)	ND		
Steamed cabbage extract		87		7	

Table 3 Oviposition on cabbage sprayed with purified THC and CBD

Spray	No. of trials	No. of egg batches (excluding singles)	No. of eggs laid	Remarks
THC		21	1,301	Leaves sprayed with THC always carry fewer batches and fewer eggs than CBD sprayed leaves
v	24	11 trials	all trials	
CBD		52 counted	3,261 counted	
THC		46	1,119	A few trials were made in 1979, and showed a greater contrast than in previous trials
v	12		6 trials	
Tap water		145	2,211 counted	
CBD		100	3,859	Fewer egg batches were laid on CBD sprayed leaves. They were sometimes larger than on controls, suggesting an oviposition stimulant but not an attractant
v	19	16 trials	9 trials	
Tap water		227 counted	2,739 counted	
THC		3	83	Suggests THC less repellent than Mexican extract
v	2			
Mexican extract		0	0	
THC and Tween		6	176	The repellent character of THC compared with CBD is well illustrated in these trials
v				
CBD and Tween	8	16	506	
v				
Tween		8	202	
CBD+ethanol		36		Ethanol alone is less repellent than either CBD+ethanol or THC+ethanol
v				
Ethanol	4	37	ND	
v				
Tap water		133		

Table 4 Oviposition on cabbage sprayed with THC and CBD

	No. of egg batches laid			No. of eggs laid			
Spray	First trial	Second trial	Third trial	First trial	Second trial	Third trial	Remarks
THC	16		8	478	211	ND	In two out of three trials CBD sprayed leaves had more eggs than the control. In one case the THC-sprayed leaf had more eggs laid on it
v		9+3 singles					
CBD	16+		5	678	561	ND	
v	several singles	12+8 singles					
Cabbage+ tap water	17	12	8	404	383	ND	
CBD	9	4		437	111		In both trials CBD-sprayed leaves carried more egg batches and more eggs than the control
v							
Cabbage+ tap water	8	1		350	21		

ND, not determined.

this butterfly can distinguish between the aqueous extracts of two such similar strains of a plant species which does not, in nature, serve as a host. It seems that the major deterrent factors are in the volatiles emanating from these solutions; however, after steaming the extract, there remain non-volatile elements (which have not been identified) in the residue, which influence the ovipositing behaviour of the butterfly. It is therefore interesting to find that the large white can distinguish between two very similar cannabinoids (differing from each other only by a ring closure which changes a substituted terpinoid (CBD) into a dibenzopyran (THC). Although present in small quantities these probably constitute two of the non-volatile repellents in the plants, and the relative unattractive nature of the THC could contribute to the greater repulsive qualities of the Mexican strain.

It is difficult to determine whether the initial choice of a leaf is made after merely a close approach or a rapid or brief contact. It will be seen (Table 2) that out of 26 trials the Mexican extract leaf was only once selected for ovipositing before the Turkish extract leaf. Recognition of a leaf sprayed with CBD and THC occurred after, rather than before 'touch down'.

The tendency for females to lay larger batches (containing more eggs than the controls) on certain CBD-treated leaves (Table 4) suggests that there may be an ovipositing stimulant, but not an attractant, in this substance. There is no doubt that several different factors contribute to the production of large egg batches, quite apart from the age and past history of the females concerned.

The few results we obtained with Mexican steamed extract in 1979 (Table 2) differed from those of other years. Thus, after heating and steaming, the residue retained much of its original repellent quality. Possibly the THC concentration was higher. Moreover, the spring had been exceptionally cold, and in an unheated greenhouse all the plants suffered. Indeed it would be surprising if the secondary plant substances—always disconcertingly variable[1,4]—were similar in all respects to those found in the previous crops.

We thank Lennart Lundgren for help with the dual choice chamber, Brian Gardiner for butterflies and M. G. Rowan for material and advice.

Received 8 January; accepted 16 April 1980.

1. Fairbairn, J. W. & Liebmann, J. A. *J. Pharm. Pharmac.* **26,** 413–419 (1974).
2. David, W. A. L. & Gardiner, B. O. C. *Bull. ent. Res.* **56,** 581–593 (1966).
3. Rothschild, M. & Schoonhoven, L. M. *Nature* **266,** 352–355 (1977).
4. Turner, C. E., Elsohly, M. A., Cheng, P. C. & Lewis, G. *J. natural Prod.* **42,** 317–319 (1979).
5. Lundgren, L., Andersson, B. A. & Stenhagen, G. *Report from the Swedish Environment Protection Board SNV PM.* **1036,** 1–119 (1978).

A curiosity of light adaptation

J. D. Mollon & P. G. Polden

University of Cambridge, Department of Experimental Psychology, Downing Street, Cambridge CB2 3EB, UK

By standard psychophysical procedures[1] it is possible to arrange that visual discriminations depend only on signals originating in the violet-sensitive receptors of the eye. A person's vision then shows several characteristic properties: differential sensitivity is lower than when the green- and red-sensitive cones contribute to detection, spatial and temporal resolution is poorer, and a number of anomalies of adaptation reveal themselves[1–9], including the saturation that we have demonstrated when violet targets are presented on steady blue or violet adapting fields[10]. 'Saturation' refers to the empirical finding that as the intensity (I) of the short-wavelength field increases, the threshold intensity (ΔI) for detecting a violet target rises much more rapidly than is described by Weber's law ($\Delta I/I$ = constant). These earlier results (replicated here; see Fig. 2, right-hand data), were obtained in what would conventionally be regarded as equilibrium conditions, in that thresholds were measured after 4 min of adaptation to the steady field. Here we examine a very odd aspect of the phenomenon: the threshold reaches its saturated state only after passing through a much lower value[11,12].

Figure 1 shows (for 3 observers) the time course of the threshold for a 436-nm target during the first 3 min after the onset of a composite adapting field. The latter consisted of a 440-nm component of $10^{10.6}$ quanta s^{-1} deg^{-2} and a 575-nm component of $10^{11.7}$ quanta s^{-1} deg^{-2}. The second, yellow, component would traditionally be termed an 'auxiliary field' (ref. 1, p. 198); it serves to suppress the red- and green-sensitive cones. The left-most data points of Fig. 1 represent the threshold 1 s after the onset of the composite field; the threshold is elevated relative to its dark-adapted value (not shown). Thereafter the threshold falls (as would normally be the case during the first few seconds of light adaptation), passes through a minimum, and then rises with remarkable speed.

For observers J.D.M. and D.D. the function at its steepest has a slope of 1 dB s^{-1}. To record accurately these rapid changes in sensitivity we have revived a special psychophysical method described by Cornsweet and Teller[23]. An ordinary staircase procedure[12], such as is traditionally used to track a changing threshold, would require a very large step size if it were to track faithfully the extremely rapid changes seen in Fig. 1; but then the precision of the estimate at any given delay (Δt) would be low. The modified procedure (called here the 'method of a thousand staircases') is designed to obviate this difficulty. In the present example, the observer receives 13 exposures to the adapting fields, each exposure, or run, lasting 3 min and successive runs being separated by 15-min intervals to allow the visual system to recover. During each run, test flashes (and accompanying warning tones) are presented at 3-s intervals. On the first run of the series the test flashes are all presented at the same intensity and the observer indicates by pushbuttons whether he has seen each flash. The response corresponding to each value of Δt is stored by the computer that controls the experiment. On the next run the computer adjusts the intensity of the flash at a given Δt according to the response previously given at that Δt but independently of responses given earlier in the current run. The new response at each Δt is now stored and is used to determine the flash intensity at that Δt on the third run; and so on. The adjustments between runs are made according to the rules for a single staircase[13], but what is unusual is that a large number (here 60, but in principle unlimited) of staircases are being maintained concurrently, each staircase corresponding to a single Δt. The final thresholds plotted in Fig. 1 are based on the intensity levels visited at a given Δt in the last eight runs.

Figure 2 places the phenomenon of Fig. 1 in context. Consider first the data to the right. These constitute an increment–threshold function ('threshold-vs-intensity' (t.v.i.) curve) for 436-nm targets presented on a 440-nm field and were obtained in steady-state conditions, in that measurements at each intensity of the field were preceded by 4 min of adaptation to the field. A fixed yellow (575 nm) auxiliary field of $10^{11.2}$ quanta s^{-1} deg^{-2} was present throughout. The broken line has a slope of unity and corresponds to Weber's law. The thresholds deviate upwards from this line, showing the operational saturation described earlier. At the highest intensity of the 440-nm field, another class of cones becomes responsible for detection[10] and the function flattens. A conventional, random double-staircase procedure[13] was used to obtain these data.

In the central panel of Fig. 2, log threshold is plotted as a function of Δt, with the intensity of the 440-nm field as parameter. These data were obtained by the method of a thousand staircases and they show how the threshold reaches its final 'equilibrium' value. The broken lines project the

0028–0836/80/270059–04$01.00

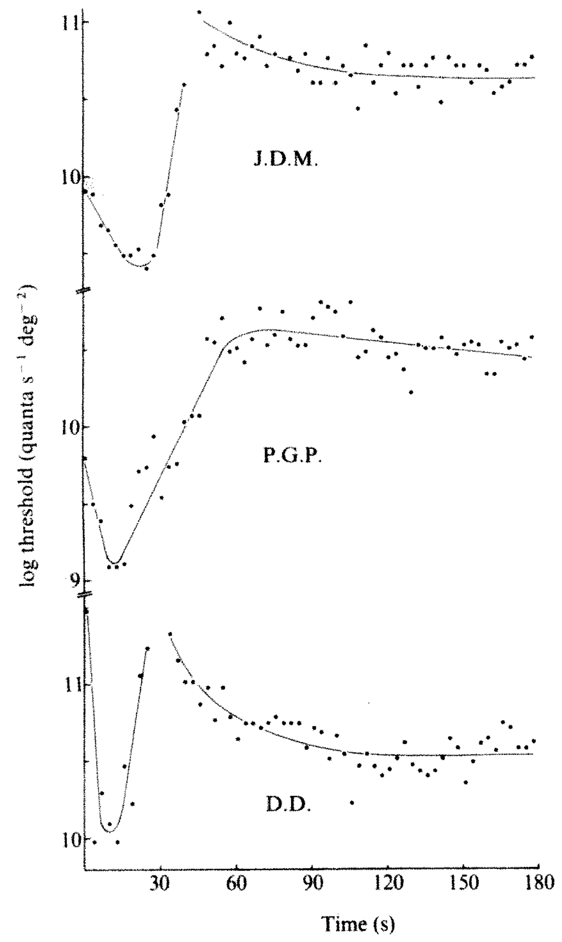

Fig. 1 Variation of log threshold intensity for detecting 436-nm flashes during the first 3 min of adaptation to a composite adapting field consisting of a 440-nm component at an intensity of $10^{10.6}$ quanta s^{-1} deg^{-2} and a 575-nm component at an intensity of $10^{11.7}$ quanta s^{-1} deg^{-2}. (The nominal chromaticity coordinates of this composite field are $x=0.45$, $y=0.47$.) The target flash subtended 1 deg of visual angle, was delivered to the centre of fovea and had a duration of 200 ms; the steady adapting fields were concentric with the target flash and subtended 6.5 deg. Target flashes were presented at 3-s intervals, each being preceded by a warning tone. A period of 2 min of dark adaptation preceded the onset of the fields. The solid lines are interrupted at values of Δt at which insufficient light was available to measure a threshold. Observers are denoted by initials.

asymptotic threshold levels to their rightful places on the t.v.i. curve. The 575-nm field remained the same intensity throughout and was combined in different sessions with different intensities of the 440-nm field.

The behaviour of the threshold changes systematically with small changes in the intensity of the 440-nm field. In all cases, the threshold passes through a minimum before rising again, but the more intense the field the earlier the minimum occurs and the steeper the slope of the rising part of the function. The latter trend can be seen in the data of Stromeyer *et al*[12]. Ancillary evidence suggests that for $\Delta t > 45$ s the upper limit to the family of functions in Fig. 2 depends on detection by a recovering long-wavelength mechanism (see also ref. 12, Fig. 14). At the lower field intensities, the functions resemble those given by Augenstein and Pugh[8] for light adaptation to long-wavelength fields alone. The left-most panel of Fig. 2 is discussed below.

Hitherto, we have treated the 575-nm field merely as an auxiliary field, serving to adapt the long- and middle-wavelength cones. If we assume that the spectral sensitivity of the short-wave receptors is approximately that of the psychological mechanism Π_3 (ref. 1, p. 18), then in our conditions the 575-nm field will contribute never more than 1% to the total number of photons absorbed in those receptors. Yet Fig. 3 demonstrates that this field (and thus probably a signal originating in the long- and middle-wavelength cones) is crucial to the temporal variation in sensitivity. In the control condition of this experiment (solid circles, Fig. 3) the onsets of the fields were simultaneous as before, but in the experimental condition (open circles) the onsets were uncoupled, the onset of the 575-nm field being delayed by 40 s relative to that of the 440-nm field. The delay chosen is equal to a Δt at which the threshold would have passed its minimum if the onsets of the fields had been simultaneous. Yet 40 s of pre-adaptation to the violet field has little effect on the function: the onset of the delayed yellow field finds the threshold close to the value for $\Delta t = 1$ s in the control condition and the threshold then passes through its curious oscillation as before; the rising part of the function is displaced along the abscissa by a delay (47 s) that is slightly greater than the imposed delay of the yellow field. Because it seems to matter only slightly whether or not the retina has been pre-exposed to the 440-nm component, the phenomenon must depend substantially on a signal originating outside the short-wavelength receptors. However, the 440-nm component (and thus, probably, the adaptive state of the violet-sensitive receptors) must be independently important, as variation in its intensity produces the family of functions seen in Fig. 2. The 7-s discrepancy noted in the present results may be attributable to the difference in the adaptive state of the short-wavelength receptors.

We relate the present phenomenon to a general model of the short-wave mechanism[14,15], in which it is supposed that signals originating in the short-wavelength receptors are transmitted only via chromatically opponent pathways[16-18] and that the sensitivity of the psychophysically defined short-wavelength mechanism depends on (1) the adaptive state of the short-wavelength receptors and (2) the balance of short- and long-wavelength signals reaching a chromatically opponent site. A crucial assumption is that a chromatically opponent channel is most sensitive to input perturbations when it is close to the centre of its operating range; as it is 'polarized' (that is, driven to one or other end of its operating range by, for example, a saturated blue or a saturated yellow field), incremental or decremental inputs are increasingly attenuated. In our experiments, yellow fields alter the measured sensitivity to short-wavelength targets primarily by altering the polarization of the opponent site, for they negligibly stimulate the short-wavelength receptors. The violet fields act both at short-wavelength receptors and at the opponent site, but, in the presence of the yellow field, contribute negligibly (<5%) to absorptions in the long- and middle-wavelength cones. Note that the most sensitive state of the opponent channel almost certainly does not correspond to the condition of equal rates of isomerization in the three classes of receptor; there is good evidence that the signal from the violet-sensitive receptors is disproportionately weighted in its contribution to this channel[19].

As a working hypothesis we suppose that the present phenomenon arises from a temporal variation in the signal delivered to the opponent site from the long- and middle-wavelength cones. A 575-nm field of $10^{11.2}$ quanta s^{-1} deg^{-2} has a troland value of $10^{5.0}$ and will bleach approximately 85% of the pigment in these cones[20]; most of the change in the proportion of unbleached pigment will occur in the first minute after onset of the field[21]. During this time the signal reaching the opponent site from these cones will presumably fall rapidly, owing both to bleaching and to other processes of receptor adaptation (see, for example, ref. 22). The photo-sensitivity of the short-wavelength cones is not known but our calculations suggest that they will not be substantially bleached by our 440-nm field. So we assume that during light adaptation to our composite field the signal from the long- and middle-wavelength cones is changing more rapidly than

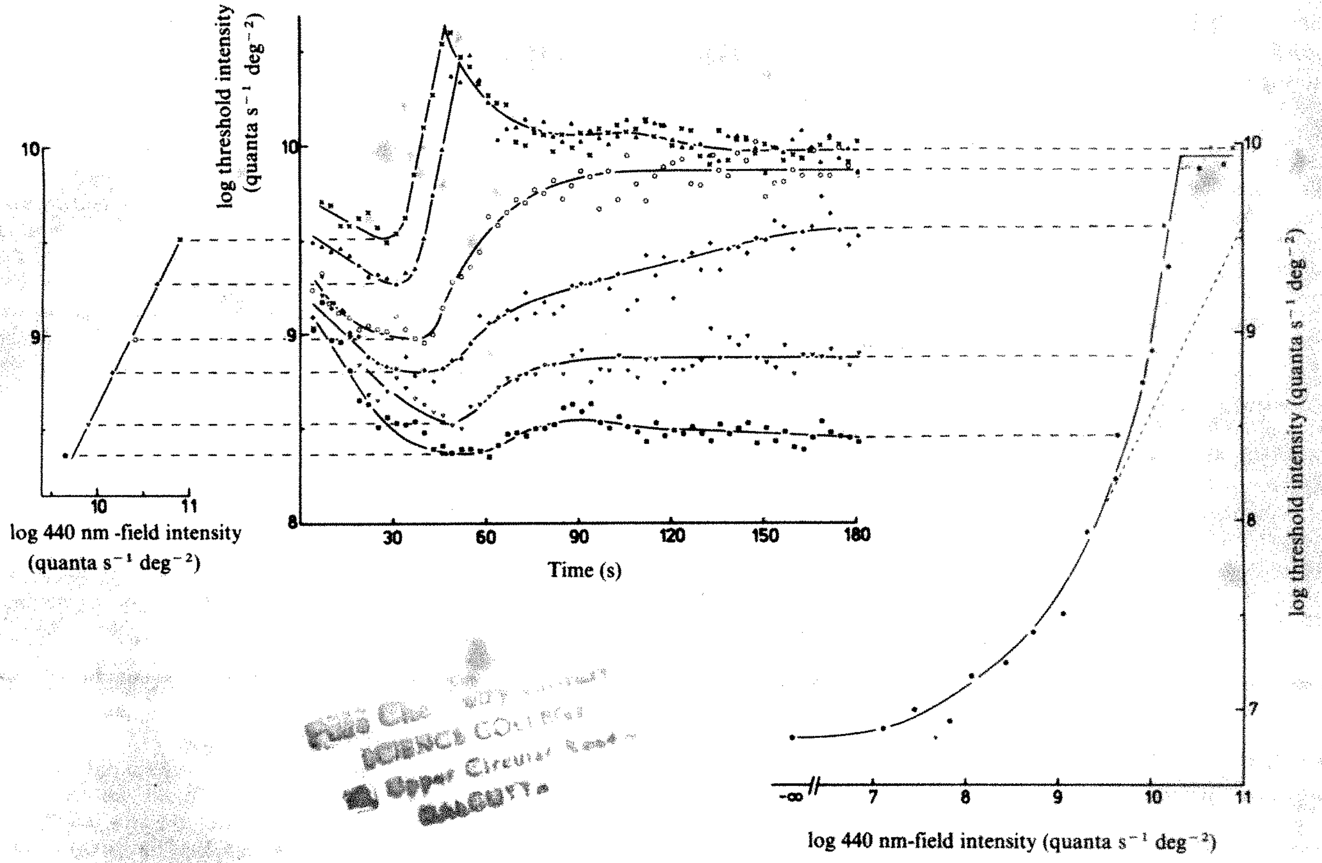

Fig. 2 Right-hand side: a conventionally obtained increment–threshold function for 436-nm test flashes presented on steady 440-nm fields of increasing intensity. A 575-nm auxiliary field of fixed intensity ($10^{11.2}$ quanta s^{-1} deg^{-2}) was present throughout. Thresholds were measured using a randomized double-staircase procedure and the plotted values are based on a sequence of 32 responses obtained between 3.5 and 5.5 min after onset of the composite adapting field, earlier responses being used to place the staircases close to the estimated threshold. Stimulus parameters were as for Fig. 1. Observer: J.D.M. Centre: temporal course of the threshold for detecting 436-nm test flashes during the first 3 min of adaptation to a series of composite fields consisting of a fixed 575-nm component of $10^{11.2}$ quanta s^{-1} deg^{-2} and 440-nm components of intensities: × $10^{10.88}$, ▲ $10^{10.63}$, ○ $10^{10.39}$, + $10^{10.14}$, ▽ $10^{9.88}$, ■ $10^{9.64}$ quanta s^{-1} deg^{-2}. Two experimental sessions were devoted to each of the latter values and the order of sessions was randomized. Left-hand side: minimal thresholds as a function of the log intensity of the 440-nm field. The solid line has a slope of unity.

that from the short-wavelength cones. The opponent site passes from being polarized in the yellow direction to being polarized in the other direction and the threshold, correspondingly, falls, passes through a minimum, and then rises again.

A further feature of the parametric results of Fig. 2 (central panel) is compatible with the hypothesis outlined above. The minima of the several functions should correspond to instants at which the opponent site is in the same (maximally sensitive) state. Differences between the minimal thresholds must then depend only on variations in sensitivity at more distal sites in the channel that carries the signal. In the left-most panel of Fig. 2 we plot the minima against the intensity of the 440-nm field: these values, unlike the asymptotes (right-most panel), obey Weber's law closely. As Weber's law (whatever its ultimate explanation) characterizes the threshold for large achromatic targets presented on bright steady fields, it is the behaviour that might be predicted when we hold constant the state of the opponent site. In other experiments we have held constant the 440-nm component of the field and varied the 575-nm component: in this case the minimum threshold, though reached at different values of Δt, varies little in its absolute value, as would indeed be predicted if (1) sensitivity at the distal site is predominantly set by the 440-nm component and (2) the minima represent equivalent states of the opponent site.

Is the hypothesis supported by the observer's

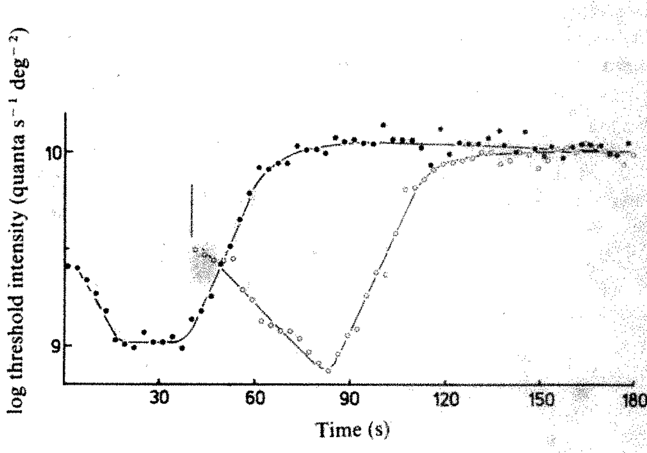

Fig. 3 Solid points: variation of log threshold intensity for detecting 436-nm test flashes during the first 3 min of adaptation to a composite adapting field consisting of a 440-nm component at an intensity of $10^{10.4}$ quanta s^{-1} deg^{-2} and a 575-nm component at an intensity of $10^{11.2}$ quanta s^{-1} deg^{-2}. Observer: J.D.M. Open points: results obtained when the onset of the 575-nm component of the field was delayed by 40 s. All points are plotted relative to the time of onset of the 440-nm component of the field. The onset of the delayed yellow field is indicated by a vertical bar.

phenomenological experience? Assuming that it is the central region of the field that is most relevant, the CIE chromaticity coordinates of the composite fields used for the measurements of Fig. 2 range from $x = 0.47$, $y = 0.50$ to $x = 0.36$, $y = 0.32$; but these chromaticities are not a good guide to the appearance of intense stimuli in transitional conditions. Formal phenomenological reports were obtained in separate runs in the conditions of Fig. 2. At onset, all fields were 'dazzlingly' bright and they varied in hue from 'yellow' to 'pale violet' according to the intensity of the 440-nm field. In all cases, after about 10 s, the field darkened strikingly and turned a grey or slate blue colour. After 60 s the colour was always pinkish, and, after 120 s, greyish. The sudden darkening always occurred a few seconds before the independently measured loss of sensitivity, and the value of Δt at which it occurred varied less with field intensity than did the point of minimum threshold. We therefore hesitate to relate the phenomenology to the processes, probably retinal, revealed by the sensitivity measurements; and the reader will have noticed that throughout this article we have avoided the term 'blue–yellow opponent channel'.

We thank C. R. Cavonius, D. MacLeod, A. Reeves, C. F. Stromeyer, and P. Whittle for comments and advice, and D. Diaper for help with the observations. This work was supported by MRC grant no. G976/139.

Received 16 January; accepted 16 April 1980.

1. Stiles, W. S. *Mechanisms of Colour Vision* (Academic, London, 1978).
2. Willmer, E. N. *J. theor. Biol.* **2,** 141–179 (1961).
3. Trezona, P. W. *Vision Res.* **10,** 317–332 (1970).
4. Brindley, G. S. *Physiology of the Retina and Visual Pathway* 2nd edn (Arnold, London, 1970).
5. Rodieck, R. W. *The Vertebrate Retina* (W. H. Freeman, San Francisco, 1973).
6. Mollon, J. D. & Polden, P. G. *Nature* **258,** 421–422 (1975).
7. Mollon, J. D. *Nature* **268,** 587–588 (1977).
8. Augenstein, E. J. & Pugh, E. N. Jr *J. Physiol., Lond.* **272,** 247–281 (1977).
9. Boynton, R. M. *Human Color Vision* (Holt, Rinehart and Winston, New York, 1979).
10. Mollon, J. D. & Polden, P. G. *Nature* **265,** 243–246 (1977).
11. Mollon, J. D. & Polden, P. G. *Invest. Ophthal. vis. Sci.* **17,** Supplement 177 (1978).
12. Stromeyer, C. F., Kronauer, R. E. & Madsen, J. C. *Vision Res.* **19,** 1025–1040 (1979).
13. Cornsweet, T. N. *Am. J. Psychol.* **75,** 485–491 (1962).
14. Pugh, E. N. & Mollon, J. D. *Vision Res.* **19,** 293–312 (1979).
15. Polden, P. G. & Mollon, J. D. *Proc. R. Soc.* B (in the press).
16. Guth, S. L., Alexander, J. V., Chumbly, J. I., Gillman, C. B. & Patterson, M. M. *Vision Res.* **8,** 913–928 (1968).
17. Boynton, R. M. in *Experimental Psychology* (eds Kling, J. W. & Riggs, L. A.) (Holt, Rinehart and Winston, New York, 1971).
18. Mollon, J. D. & Krauskopf, J. *Vision Res.* **13,** 27–40 (1973).
19. Pugh, E. N. Jr & Larimer, W. *Vision Res.* (in the press).
20. Rushton, W. A. H. & Henry, G. H. *Vision Res.* **8,** 617–631 (1968).
21. Cornsweet, T. N. *Visual Perception,* 153 (Academic, New York, 1970).
22. Baylor, D. A. & Hodgkin, A. L. *J. Physiol., Lond.* **242,** 729–758 (1974).
23. Cornsweet, J. N. & Teller, D. Y. *J. opt. Soc. Am.* **55,** 1303–1308 (1965).

Visual acuity is better for letters in rows than in columns

R. D. Freeman

School of Optometry, University of California, Berkeley,
California 94720

The spatial resolving capacity of the visual system is usually measured with charts containing letters of different sizes displayed in horizontal rows or, less often, in vertical columns. Although previous studies suggest that acuity may not be equal for these two arrangements[1–7] it is implicitly assumed in clinical tests that orientation of an array of letters is of no consequence to the measurement. The work reported here shows that this assumption is incorrect. While undergoing an examination in an eye clinic, I noticed that letters of a given size seemed more difficult to identify when they were arranged in vertical compared with horizontal arrays. Subsequently, I tested a group of subjects using letters presented pseudo-randomly with different inter-letter spacings, in rows or columns. Subjects were required to identify letters from left to right or from top to bottom in each isolated row or column. A significantly higher number of errors was made for letters in columns than for those in rows. The effect does not depend on order or direction of letter presentation, and it is not found when acuity determinations are made using a non-letter test symbol. To explore the conjecture that the effect could be associated with previous experience, two additional groups of subjects were tested. First, bilingual Chinese, whose first language is read in both horizontal and vertical arrays, were tested using Chinese characters and English letters. Second, acuity determinations were made with young children who could identify letters but did not read. In each case, acuity was not significantly different for horizontal or vertical presentations, a finding consistent with the notion that learning may influence the development of visual resolution.

The tests were carried out with slides containing pseudo-random combinations of eight letters—E, H, R, N, O, X, D and V—arranged in groups of columns or rows. Each letter appeared once at a given inter-letter separation (see below). The slides were mounted in frames for use in a standard vision chart projector. Before the tests, the refractive condition of each subject was carefully determined. Subjects were rejected if a visual anomaly or considerable refractive error was found. Using appropriate ophthalmic lenses if required, subjects monocularly viewed letters that each initially subtended an anticipated threshold level of 4 arc min at the eye. (A 7.1-mm letter viewed at 20 ft subtends 4 arc min and if correctly read, an acuity of 20/15 is indicated.) Letters were presented in a column or row and all eight letters were shown at each of five inter-letter separations (2, 4, 8, 16, and 32 arc min). For each subject, the zoom lens on the projector was adjusted so that letters were small enough to be near threshold, as estimated by approximately 75% correct identification. Letters of all separations were then systematically presented in columns or in rows and subjects were asked to identify them from top to bottom or from left to right, respectively. Half of the subjects were tested using columns followed by rows and the other half were tested in the reverse order. No differences were found related to order of presentation. Ten letters were used at each inter-letter spacing, but only the inside eight were scored to avoid possible complications of edge effects at the ends of each row or column.

Results for 11 subjects, given in Fig. 1*a*, show that for both columns and rows, the error rate increases with decreased separation between letters, as could be anticipated from previous work[8]. However, in addition, the mean error rate is clearly higher for columns than for rows of letters and the overall difference is highly significant ($\chi^2 = 26.12$, $P = 0.0062$).

What can account for this difference in acuity between horizontal and vertical arrays of letters? An optical explanation of the effect can be ruled out immediately. The subjects used did not have high amounts of ocular astigmatism, and the moderate or small astigmatic errors found were of both vertical and horizontal types. In either case, these errors were fully corrected with lenses. Furthermore, when grating test targets are used to determine acuity, no differences are found between vertical and horizontal orientations[9,10]. This applies also to laser-created interference-fringe gratings for which the effect of the eye's optics are essentially bypassed[10].

One must therefore propose an alternative explanation for the effect found here and an obvious possibility is that the development of visual acuity for arrays of letters is associated with learned patterns of reading. Specifically, because we learn to read rows of letters, finest acuity develops correspondingly for horizontal displays. Because we also learn to read from left to right, acuity may be superior for this direction compared

0028-0836/80/270062-03$01.00

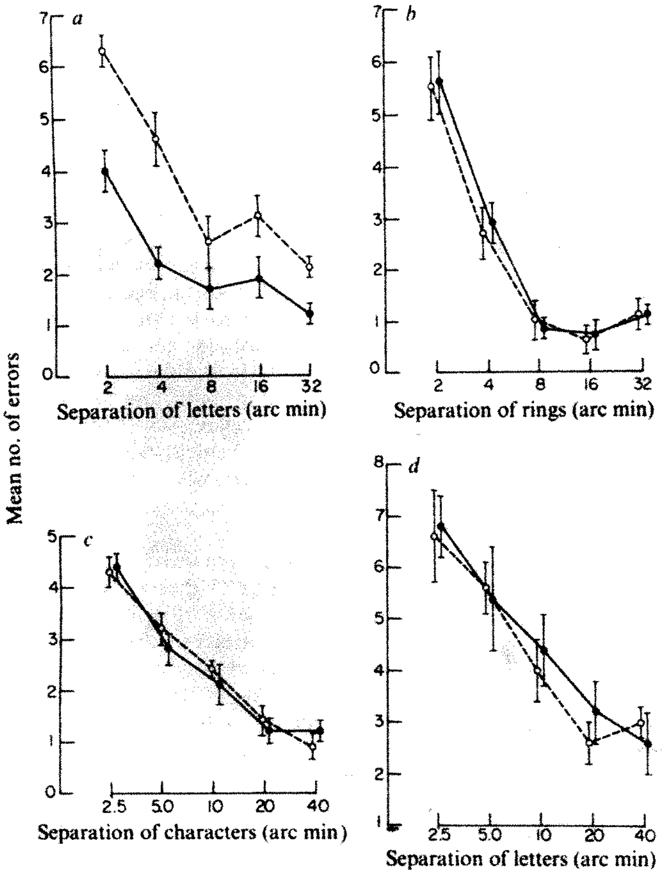

Fig. 1 Results are given for visual acuity tests using letters with adults (*a*) or children (*d*), Chinese characters with Chinese subjects (*c*), or Landolt rings (*b*), presented in vertical columns (open symbols, dashed lines) or horizontal rows (filled symbols, solid lines). Each point represents the mean number of errors for eight presentations at given inter-letter (or character or ring) separations. Vertical bars represent ±1 s.e.m. Abscissae are scaled logarithmically.

with the reverse. To examine this possibility, a second group of subjects, most of whom were included in the first group, was tested with the same letter chart used before. Only, in this case, letters were identified from right to left in rows or from bottom to top in columns. Results were very similar to those shown in Fig. 1*a*, with a significantly higher number of errors found for columns than for row arrays. The acuity effect is therefore selective for orientation but not for direction. If there is a direction-selective component, a more sensitive measure which might incorporate temporal factors is required for its study.

The hypothesis linking visual acuity development and experience applies to letters that must be recognized. For simpler acuity targets that require detection only, learned reading habits do not apply and therefore, differences between rows and columns would not be expected. To determine this, acuity was measured using Landolt rings, which contain a gap at the top, bottom, left or right whose subtense is 1 arc min at 20 ft. These were presented in rows or columns with inter-ring separations, just as in the previous case. The same group of subjects, whose letter acuities are shown in Fig. 1*a*, were tested using Landolt ring targets and the results are given in Fig. 1*b*. Clearly, there is no difference between acuities for rings in rows as compared with columns. In both cases, the data show a very high mean error rate for closely spaced rings, suggesting that this type of detection task may be more difficult than letter identification when test arrays are dense. It thus seems that acuity differences between rows and columns of test objects may apply specifically to letters; this is consistent with the idea that they are related to learned reading patterns.

It would be possible to test this notion more directly by measuring acuity of subjects whose language is read and written primarily in vertical rather than horizontal arrays. In this case, acuity would be expected to be reduced for rows instead of columns of letters. However, there are apparently no common languages that are arranged only in vertical columns. On the other hand, modern Chinese is read and written in both columns and rows so that no bias would be expected on the basis of learned reading patterns. Ideally, it would be best to test Chinese subjects who do not read or write English. This was not practical, but it was possible to measure acuities of bilingual Chinese subjects for whom English is a second language learned during teenage years. Following thorough refractions, acuities were determined using eight standard Chinese characters, chosen for simplicity, which each subtended 5 arc min initially. Inter-character separations were 2.5, 5, 10, 20 and 40 arc min. In addition, acuities were also determined with this group using the English letter chart. The results for characters, presented in Fig. 1*c*, clearly show that there are no acuity differences between rows and columns (confirmation is provided by the χ^2 statistic). Results with this same group using English letters showed a tendency for an increased number of errors for column arrays, but this trend is not significant (χ^2 statistic).

Although unlikely, it could be argued that there are inherent racial differences in visual resolving capacities between these Chinese subjects and the American group tested previously. The possibility is easy to rule out, however, by measuring acuity for English letters using Chinese–American subjects who have never learned to read or write characters. Five subjects in this category were tested with the same chart as used for the initial group of Americans. The results were virtually identical to those for the latter group and it may thus be concluded that inherent racial factors are not involved in the findings described here.

One additional group of subjects was tested. If an acuity bias for horizontally arranged letters develops as a result of learned reading patterns, subjects who know the alphabet but do not yet read should not demonstrate a difference between rows and columns of letters. Five children, aged 4–5 y, were refracted and then shown the eight letters used on the chart to insure that they could identify them. Acuities were then determined, the results for which are shown in Fig. 1*d*. As might be expected, variability is greater than that for the other groups, but there are no consistent differences between rows and columns.

Taken together, the results of this study suggest that visual acuity performance for letters is related to reading patterns learned in childhood. The finding which is not compatible with this idea is that the acuity difference between rows and columns holds for right to left identification as well as the reverse. It is possible, of course, that a directional effect could be found using different tests. In any case, the neural mechanism that underlies the relatively high acuity for horizontal arrays may be concerned primarily with fixation. For example, contours adjacent to a letter that interfere with its resolution[11,12] may be more effectively masked in row arrays. The advantage of horizontal letter displays, in terms of acuity, may be relevant to other work showing that reading speed is slower[3,4] and word or pseudo-word identification poorer[5–7] for vertical compared with horizontal arrangements of letters. Further study is required to determine the relative importance of factors such as spacing and numbers of letters in a given array. In addition, it would be interesting to know if eye movement patterns differ for reading in row as opposed to column arrangements.

I thank Dr G. Kaprielian for help with this study, Dr C. Chan for constructing Chinese characters and Dr Doris Lin for help with Chinese translations. This work was supported by Research Career Development Award EY00092 and grant EY01175 from the USPHS.

Received 13 February; accepted 10 April 1980.

1. Mishkin, M. & Forgays, D. G. *J. exp. Psychol.* **43,** 43–48 (1952).
2. Orbach, J. *Am. J. Psychol.* **65,** 555–562 (1952).
3. Aulhorn, O. *Pflügers Arch. ges. Physiol.* **250,** 12–18 (1948).
4. Tinker, M. A. *J. exp. Psychol.* **68,** 444–449 (1955).
5. Bryden, M. P. *J. exp. Psychol.* **84,** 120–122 (1970).
6. Mewhort, D. J. & Beal, A. L. *J. exp. Psychol.: Hum. Perception Performance* **3,** 629–640 (1977).
7. Krueger, L. E. *Cognitive Psychol.* **1,** 341–357 (1970).
8. Duke-Elder, S. & Abrams, D. *System of Ophthalmology* Vol. 5 (Klimpton, London, 1970).
9. Appelle, S. *Psychol. Bull.* **78,** 266–278 (1972).
10. Freeman, R. D. & Thibos, L. N. *J. Physiol., Lond.* **247,** 687–710 (1975).
11. Flom, M., Weymouth, F. & Kahneman, K. *J. opt. Soc. Am.* **53,** 1026–1032 (1963).
12. Loomis, J. M. *Vision Res.* **18,** 335–339 (1978).

Eye movement in strabismic cats

Max Cynader* & Laurence Harris

Department of Psychology, Dalhousie University, Halifax, Nova Scotia, Canada B3H 4JI

Strabismus is a common clinical condition in which the visual axes of the eyes do not intersect on the object being viewed[1]. As such, the ability to achieve single binocular vision by fusing the images of a single object in the two eyes is lost. In most cases of strabismus, one of the two eyes is clearly deviated and the other eye is used for fixation, although in some cases each eye is used alternately for fixation[2,3]. While much attention has been devoted to the motor capabilities of the deviating eye in strabismus[1–3], little attention has been given to the visuomotor competence of the other eye. We report here that, if one eye of a kitten is made to deviate by surgery, the visuomotor capacities of the other, 'normal', eye are affected. A reduction in the ability to follow the movement of a large striped drum is observed with binocular viewing, even when stimuli are viewed monocularly with the normal eye. This means that anomalous visual input from the deviated eye during stimulation is not the cause of the reduced oculomotor capacities.

Divergent strabismus was induced in three 10-day-old kittens by severing the medial rectus muscle of the right eye. The left eye was not touched. The kittens were then reared normally in a well-lit laboratory environment until they were 8–12 months old. At this time the normal undeviated eye of the cat was prepared for eye movement recording by implanting a magnetic search coil according to the technique of Robinson[4]. In addition, head restraining tubes were attached to the skull by means of dental acrylic[5]. Surgery was performed under Alfathesin anaesthesia and the animals were allowed at least 2 weeks to recover before recording began. The eye movements of the three strabismic cats were compared with those of three normal cats studied with the same techniques.

We primarily studied eye movements evoked in response to visual and vestibular stimuli in the horizontal plane. When a large striped drum is rotated about a cat, a characteristic pattern of eye movement called optokinetic nystagmus (OKN)[6] is evoked with a time course resembling a sawtooth. The slow phase of this response matches the velocity of the drum in normal cats and thus compensates for the motion of the drum and permits clear vision. Figure 1 compares the velocity of the slow corrective phase of optokinetic nystagmus (measured in the nondeviating eye) of strabismic cats with that of normal cats as a large striped drum is rotated about the animal at various velocities. The results show that the normal cat is able to match the velocity of his eyes to that of the drum rather well over most of the velocity range tested.

By contrast the velocity match of the apparently normal eye of the strabismic cat with that of the drum is much less accurate. For all drum velocities above 4° per s, the eye rotated more slowly than did the drum. This lessened response to visual stimulation is unlikely to be due to any generalized deficit in oculomotor capacity, due, for example, to mechanical impediments which might have resulted from implantation of the eye coil or from the early surgical procedures on the other eye. The eye movement responses to vestibular stimulation as assessed by rotating the cat sinusoidally in the dark were the same in normal and strabismic cats. In both normal and strabismic cats, the vestibulo-ocular reflex was able to compensate for the head and body movement induced by rotating the cat[5,7]. Thus, the deficit in oculomotor capabilities seems to be specifically related to the response to visual stimuli.

The results illustrated in Fig. 1 were obtained with both eyes open and did not permit assessment of the contribution of vision with each eye to the reduced oculomotor response of the nondeviating eye. Accordingly we measured optokinetic responses of the 'normal eye' to visual stimuli presented through either eye. The interpretation of the monocular stimulation findings (Fig. 2) is rendered more difficult by the finding that monocularly-viewed stimuli moving medially (that is, rightward viewed through the left eye) were more effective at eliciting OKN than lateral-directed stimuli even in normal cats[8]. This difference in the effectiveness of medial and lateral-directed stimuli was also observed with monocular stimulation of the nondeviating eye in the strabismic cats. It is clear, however, that the efficiency of OKN was decreased markedly for both medial and lateral stimulus motion, relative to that of the normal animals. This defect in monocularly-evoked OKN rules out anomalous visual input through the deviating eye during the stimulation period as a possible cause of the reduced OKN observed with binocular stimulation. Visuomotor performance mediated by stimuli presented through the deviating eye was also severely impaired. Figure 2*b* shows optokinetic responses of the nondeviating eye to visual stimuli viewed monocularly through the deviating eye. These data show that reduced OKN followed stimulation of the deviating eye when stripes moved in either direction. The

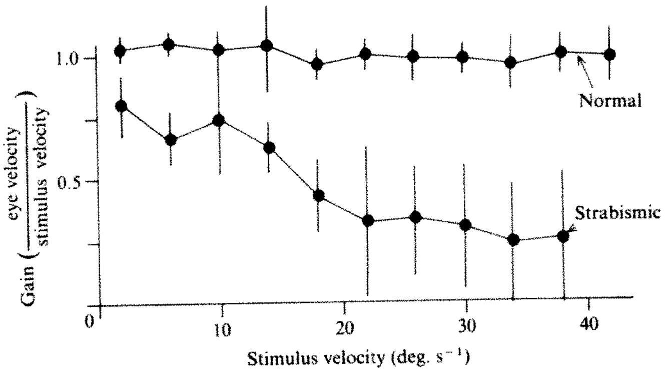

Fig. 1 The gain of optokinetic nystagmus as a function of drum speed for the normal and strabismic cats. The gain of the response is the velocity of the slow phase[6] of the optokinetic response divided by the velocity of the drum. A gain of 1 indicates perfect following of the drum by the eyes. The gain of the normal cats is close to 1 over most of the velocity range tested while that of the strabismic cats is markedly lower. The drum consisted of a large cardboard cylinder 90 cm in diameter on which high contrast black and white vertical stripes (period 20°) were painted. Background luminance was 0.1 cd m^{-2}.

---

*To whom correspondence should be addressed.

0028-0836/80/270064-02$01.00

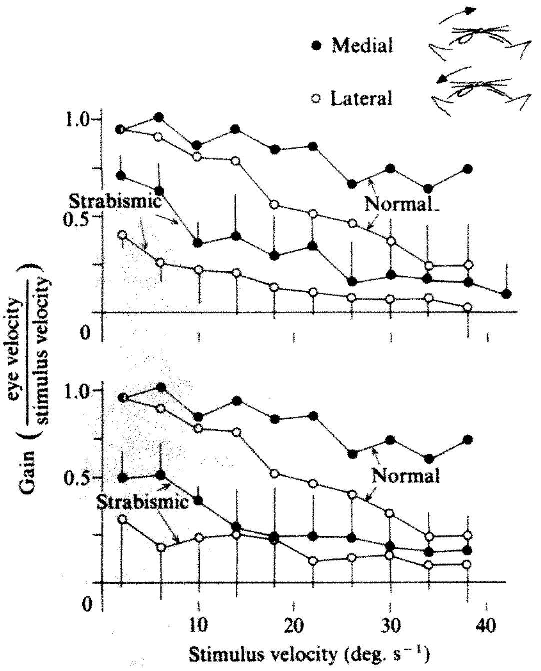

Fig. 2 *a*, The gain of the slow phase of optokinetic response in normal and strabismic cats when stimuli are viewed with the nondeviated eye only. The gain of the reflex is lower for laterally-directed high velocity drum movement than medially-directed movement in both the normal and strabismic cats. The gain in both directions is considerably lower for the strabismic cats than it is for normal cats even though the strabismic animals viewed the stimulus through the nondeviated eye. In normal cats, the gain of the reflex is the same regardless of whether the monitored eye or the other eye alone views the stimulus, as would be expected from Hering's Law[16]. *b*, Responses to drum motion when the strabismic animals view through the deviating eye alone are compared with those of normal cats viewing monocularly. The deficits observed in the visuomotor capacities of the strabismic cats are similar regardless of which eye views the moving stimulus. The standard deviations (s.d.) have been omitted from the curves representing responses of the normal cats for clarity. A typical value for the s.ds in this case is 0.15. Drum parameters are as in Fig. 1.

deficits of OKN were similar with stimulation of either the deviating eye or the nondeviating eye.

The present results show that the visually-evoked eye movements mediated through an apparently normal eye can be altered by surgical exodeviation of the other eye. The eye movement deficit seems to be specific to visual stimulation as vestibular stimulation evoked normal oculomotor responses. The mechanism underlying this reduced visuomotor competence remain unknown but several anomalies identified in various parts if the visual system in strabismic cats[9–11] help towards its understanding. We have recently recorded visual responses in the nucleus of the optic tract (NOT) of strabismic and normal cats[11]. Our findings in this structure, which has an essential role in optokinetic nystagmus[12,13], indicate marked changes in binocular connectivity among NOT neurones following surgically-induced strabismus. These neural changes may provide a basis for the visuomotor deficits found in the strabismic cats. It would be interesting to see if similar defects exist in the normal eye of human strabismics, particularly in view of the recent findings suggesting defects on OKN in the normal eye of amblyopic humans[14,15].

This research was supported by USPHS grant no. EY02248 and grants nos MT-5201 and A9939 from the MRC and NRC of Canada.

Received 12 March; accepted 3 April 1980.

1. Alpern, M. & Davson, H. eds *The Eye* Vol. 3, 1–127 (Academic, London, 1969).
2. Burian, H. M. & Von Noorden, G. K. *Binocular Vision and Ocular Motility* (C. V. Mosby, St Louis, 1974).
3. Duke, Elder, S. & Wybar, K. in *System of Ophthalmology* Vol. 6 (C. V. Mosby, St Louis, 1973).
4. Robinson, D. A. *IEEE*, Trans. Biomed. Electron. BME-10, 137–145 (1963).
5. Harris, L. R. & Cynader, M. *Invest. Ophthalm.* **18,** suppl. 263 (1979).
6. Ter Braak, J. W. G. *Arch neerl. Physiol.* **21,** 309–376 (1936).
7. Cohen, B. *Handbook of Sensory Physiology: Vestibular System* Vol. 6, Part 1 (ed. Kornhuber, H.) 477–540 (Springer Berlin, 1973).
8. Honrubia, V., Ward, P. H. & Scott, W. *Acta otolaryng* **64,** 388–402 (1967).
9. Hubel, D. H. & Wiesel, T. N. *J. Neurophysiol.* **28,** 1041–1059 (1965).
10. Cynader, M., Mustari, M. & Gardner, J. G. *Soc. Neurosci. Symp.* **4,** 99–120 (1979).
11. Cynader, M. & Hoffmann, K. P. (in preparation).
12. Collewijn, H. J. *J. Neurobiol.* **6,** 3–21 (1975).
13. Hoffmann, K. P. *Brain Res.* **99,** 359–366 (1975).
14. Schor, C. M. & Levi, D. *Invest. Ophthalm.* **18,** suppl. 201 (1979).
15. Crone, R. A. *Docum. Ophthalm.* **45,** 9–18 (1977).
16. Hering, E. *The Theory of Binocular Vision* (eds Bridgeman, B. & Stark, L.) 17–46 (Plenum, New York, 1977).

Genetic control of sensory connections in *Drosophila*

Philippe Vandervorst & Alain Ghysen

Laboratoire de Génétique, Université Libre de Bruxelles, 67 rue des Chevaux, 1640 Rhode-St-Genèse, Belgium

The function of the nervous system depends on the formation of a net of appropriate connections. This process must be at least partly under genetic control, yet the genetic analysis of the development of specific nerve connections has so far made little progress (reviewed in ref. 1). This is in part because of the immense complexity of the connective net. The problem is simpler in the case of insect secondary neurones which are derived from the epidermis and send their axons centripetally towards the central nervous system[2]. The arrangement of sense organs on the body surface is very reproducible in many cases, so that given neurones can be recognized unambiguously in different individuals. In *Drosophila*, the genetic analysis of development has so far concentrated on the epidermis. The genetic control of segmentation is relatively well understood[3,4] and it has been found that segments are progressively subdivided in smaller developmental units called compartments[5]. This led to the speculation that sensory neurones belonging to different compartments might have different properties[6]. Here we show that the stimulation of mechanoreceptor bristles at different positions on the notum and legs of *Drosophila* specifically evoke different behavioural responses. This specificity depends on the segmental and in some cases on the compartmental identity of the bristle, but not on the site of entry of the axon into the central nervous system.

Decapitated flies remain alive and standing for up to 20 h. They remain motionless if left undisturbed, although they are able to stand up if overturned, or to walk a few steps if pushed. The tickling of single bristles induces several reactions: wing scissoring, withdrawal of the stimulated body part, and vigorous cleaning by a leg. The latter reaction was analysed in more detail, for it provides a specific and easily scored response. The response evoked by the different macrochaetes on the humerus and notum is quantified in Fig. 1. The microchaetes on the notum were also examined, but their small size and high density makes it impossible to stimulate them individually. It appears from Fig. 1 that the notum is divided in two regions, one where all the bristles evoke a response of the first (and to some extent of the second) leg, and the other which stimulates the third leg. It should be noted that no bristle evoked specifically a response of the second leg, but that such a response was observed in many cases as an alternative to the response of the first leg, mostly after the latter had already responded repeatedly to

0028-0836/80/270065-03$01.00

continuing stimulation of a given bristle. In order to characterize the specificity of the response further, we have analysed two mutations which result in the development of a supernumerary notum at an ectopic location. The mutation *wingless* transforms the wing to a notum in mirror image symmetry to the normal notum[7]. In this case the axons from the ectopic bristles join those from the normal bristles and enter the thoracic ganglion at the normal place[8]. We have confirmed that the ectopic bristles induce the same response as their normal homologues[8]. The double mutation *bithorax*^{3} *postbithorax* transforms the bare, vestigial metanotum into a mesonotum bearing the whole complement of notal bristles[9]. Here the axons from the ectopic bristles enter the thoracic ganglion much posterior to the normal place[10]. The stimulation of these ectopic bristles gives a pattern of responses which is identical to the pattern of the normal mesonotum both in the specificity and in the frequency of the responses (Fig. 2).

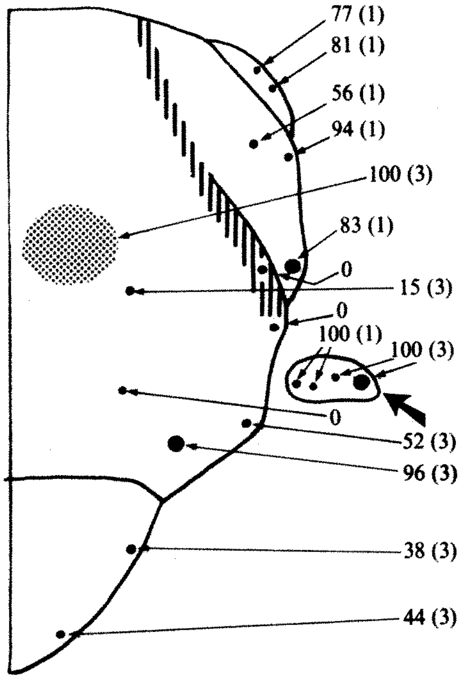

Fig. 1 Frequency and specificity of response to stimulation of the bristles on the notum and tegula. Flies of wild type Canton S strain were exposed to ether, decapitated and left to recover for 1–2 h in a moist environment. Stimulation was achieved by gently touching individual bristles with a hair. A micromanipulator was used in some cases. The numbers give the proportion of flies (out of 48) where a given bristle evoked a cleaning movement by a leg. The numbers in parentheses indicate which leg responded (1: prothoracic leg, 3: metathoracic leg). Bristles represented by large dots were selected for the analysis of the homoeotic situation in Fig. 2. The tegula is drawn at the side of the notum (arrow). The dotted area represents the region where groups of microchaetes were stimulated. The dashed stripe separates the zones which evoke responses of the first and third legs respectively.

The bristles on the legs were also characterized (Table 1). As for the microchaetes on the notum, most of the leg bristles are too small and dense to be stimulated individually. However it appeared that groups of microchaetes on the anterior and posterior regions of the first and third legs give different responses, and therefore the bristles of the two regions have been listed separately in Table 1. We have attempted to define more precisely the limit between the leg bristles which give an 'anterior' response and those which evoke a 'posterior' response in the case of the femur and tibia of the first and third legs. The results are shown in Fig. 3; the figure also shows the boundaries separating the anterior and posterior developmental compartments of these legs[11]. The coincidence between the sensory and the compartmental boundaries is obvious.

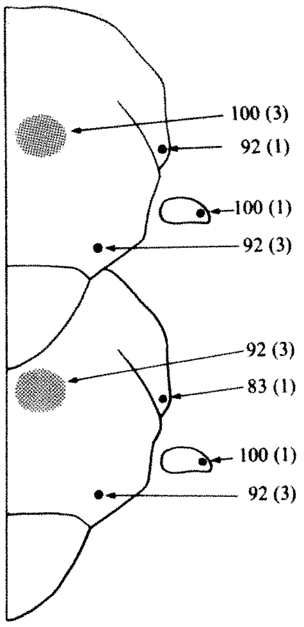

Fig. 2 Frequency and specificity of the responses in the mutant bx^3pbx/Ubx^{105}. The normal mesonotum is above, the transformed metanotum is below. The bristles marked by large dots on Fig. 1 have been selected because they give a high frequency of response. The numbers are as in Fig. 1, except that 12 flies were analysed.

There is a second situation where an apparently homogeneous population of bristles is divided by a compartmental boundary. The limit between the thorax and wing compartments runs through the tegula, a sclerite at the base of the wing. It is remarkable that within this small area, two of the bristles evoke an intense response of the first leg while two others induce a movement of the third leg (Fig. 1, arrow). However, in this case the identity between sensory and compartment boundaries cannot be assessed, since the exact position of the compartment boundary has been reported as variable within the tegula[12].

Table 1 Frequency and specificity of responses to stimulation of leg bristles in wild-type *Drosophila*

	wtd	2nd	contra
AFe 1	83		33
PFe 1	13	92	
ATi 1	63		46
PTi 1	71	21	4
AFe 2	100		
PFe 2	100		
ATi 2	100		
PTi 2	100		
AFe 3	33	88	4
PFe 3	71		15
ATi 3	79	21	
PTi 3	63		25

The left column indicates the stimulated area. AFe and PFe: anterior and posterior femur; ATi and PTi: anterior and posterior tibia; 1, 2 and 3: first, second and third legs. The next three columns represent the three responses which have been scored. wtd: withdrawal of the stimulated leg; 2nd: cleaning of the stimulated leg by the second (mesothoracic) leg; contra: cleaning of the stimulated leg by the contralateral leg. The numbers represent the per cent of flies (out of 48) where a given stimulation evoked a given response. The numbers add up to more than 100 because the stimulation of a given set of bristles may evoke different responses.

Our results on wild-type flies indicate that the connections established by a sensory neurone depend on its position in two different ways. In the case of the legs, the specificity of the response clearly depends on the segmental identity of the neurones. Furthermore, within each leg, groups of bristles with different specificities can be detected. In those cases where a detailed analysis could be done, the limit between groups of bristles which evoke different responses appeared to coincide with the position of the anterior–posterior compartment boundary. The same is probably true in the case of the tegula, although the position of the compartment boundary is not as precisely defined as it is in the legs. These results show that the choice of a given pattern of connections depends on the segmental and compartmental identity of the neurone. Recent experiments have shown that the establishment of a given projection in the central nervous system also depends on the developmental history of the sensory neurone in the locust[13], and on the segmental and compartmental identity of these neurones in *Drosophila*[14].

In the case of the notum, the different specificities of the anterolateral and dorsoposterior bristles must depend on something other than the compartmental identity since all these bristles belong to the same compartment. In this case, the decision to establish a given type of connection appears to depend on the position of the bristle along the anteroposterior (and possibly mediolateral) axis of the body. A similar dependence of the evoked behavioural response on the position of the sense organ along a body axis has been reported in the pupa of *Sphinx ligustri*[15]. Our results indicate that the neurones retain their specific pattern of connections even when they enter the central nervous system at an abnormal place. This may be related to the fact that ectopic or misrouted neurones which enter the central nervous system at an abnormal place can nevertheless establish a normal projection[10].

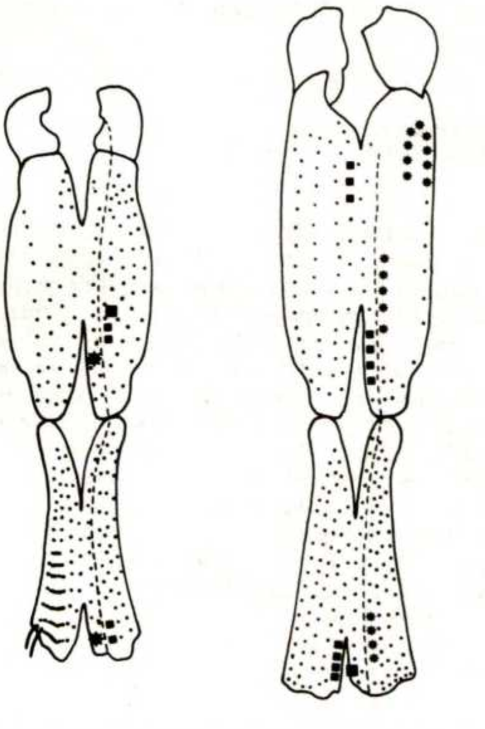

Fig. 3 Response of single bristles or rows of bristles on the prothoracic (left) and metathoracic (right) legs. All the leg bristles are represented by dots. Bristles which induce a withdrawal of the leg or a cleaning response of the contralateral leg are marked with asterisks, bristles which induce a cleaning movement of the mesothoracic leg are marked with solid squares. The broken line shows the position of the anterior–posterior compartment boundary. The chaetotaxy of the legs and position of the boundary are from ref. 11.

The behavioural approach used in this work was originally suggested by Don Ready. We thank R. Thomas for support and critical reading of the manuscript. This work was carried out under a contract between the Belgian government and the University of Brussels. P.V. is supported by the IRSIA; A.G. is chercheur qualifié of the FNRS.

Received 23 November 1979; accepted 11 April 1980.

1. Quinn, C. & Gould, J. L. *Nature* **278,** 19–23 (1979).
2. Wigglesworth, V. B. *Q. J. microsc. Sci.* **94,** 93–112 (1953).
3. Lewis, E. B. *Nature* **276,** 565–570 (1978).
4. Garcia-Bellido, A. & Capdevila, M. P. in *The Clonal Basis of Development* (eds Sobtenly, S. & Susex, I.) 3–21 (Academic, New York, 1979).
5. Garcia-Bellido, A., Ripoll, P. & Morata, G. *Nature new Biol.* **245,** 251–253 (1973).
6. Crick, F. H. C. & Lawrence, P. A. *Science* **189,** 340–347 (1975).
7. Sharma, R. P. & Chopra, V. L. *Devl Biol.* **48,** 461–465 (1976).
8. Deak, I. I. *Devl Biol.* **66,** 422–441 (1978).
9. Lewis, E. B. *Am. Zoologist* **3,** 33–56 (1963).
10. Ghysen, A. *Nature* **274,** 869–872 (1978).
11. Steiner, E. *Wilhem Roux' Archiv.* **180,** 9–30 (1976).
12. Morata, G. & Lawrence, P. A. in *The Clonal Basis of Development* (eds Sobtenly, S. & Susex, I.) 45–60 (Academic, New York, 1978).
13. Anderson, H. & Bacon, J. *Devl Biol.* **72,** 364–373 (1979).
14. Ghysen, A. *Devl Biol.* (in the press).
15. Bate, M. *J. exp. Biol.* **59,** 95–107 (1973).

Testosterone-sensitive neurones respond to oestradiol but not to dihydrotestosterone

K. M. Kendrick & R. F. Drewett

Department of Psychology, University of Durham,
Durham DH1 3LE, UK

Testosterone is aromatized to oestradiol in the brain, and it has been suggested that its effects on the brain are produced by this metabolite[1]. Oestradiol does indeed restore sexual behaviour in castrated rats[2,3], but it is much more effective if combined with a second metabolite, dihydrotestosterone[4,5]. This may be because the two hormones have a synergistic effect on the brain; or because the central effect of oestradiol synergises with the peripheral effects of dihydrotestosterone (which include stimulation of penile development). Evidence that the corticomedial amygdala (CMA) and the preoptic area of the rat brain are both involved in the control of sexual behaviour led us to examine the neurones of the stria terminalis that connect the two[6,7]. These neurones are hormone-sensitive; their absolute refractory period is lengthened by castration and reduced again by testosterone. So we have investigated the aromatization hypothesis further by examining the effect of oestradiol and dihydrotestosterone on these testosterone-sensitive neurones. Oestradiol has exactly the same effect as testosterone; dihydrotestosterone has no effect, whether it is given alone or in combination with oestradiol.

Thirty-two virgin, adult male Wistar rats (400–650 g) were divided at random into four groups of eight and castrated under ether anaesthesia. Eight weeks or more after castration, rats in each group were assigned to treatment with (1) 5 µg oestradiol benzoate (OB), or (2) 1 mg 5α-dihydrotestosterone propionate (DHTP), or (3) 1 mg DHTP + 5 µg OB, or (4) oil vehicle alone. These doses were chosen because they restore full sexual behaviour in the castrated male rat when OB and DHTP are given in combination[4,5], but not when each is administered alone[2–5]. Treatments were administered as two daily 0.1-ml subcutaneous injections, for 18–22 d. The hormones were provided for us in unlabelled, coded bottles, and we did not know which animal received which treatment until the experiment was finished and the code was broken.

For electrophysiological recording the animals were anaesthetized with urethane (1.3 g per kg, intraperitoneally)

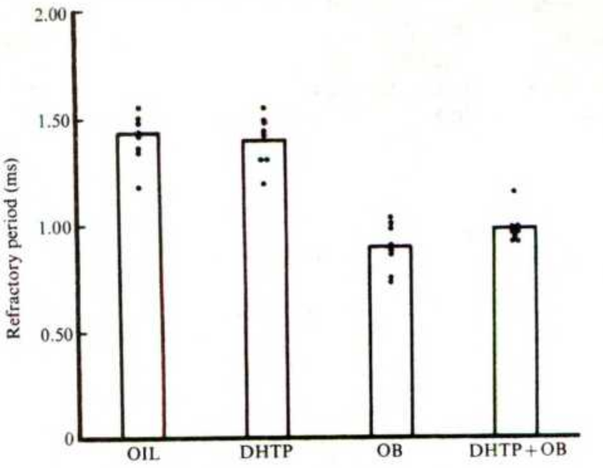

Fig. 1 Absolute refractory period of CMA neurones projecting to the MPH in castrated rats treated with oil (69 neurones from eight rats); DHTP (74 neurones from eight rats); OB (80 neurones from eight rats), or DHTP+OB (87 neurones from eight rats). Figure gives the overall mean and individual means (dots).

and mounted in a conventional stereotaxic frame (Kopf Instruments). Coordinates for electrode placement were the same as given in refs 6 and 7. A monopolar stainless steel electrode, insulated to within 0.5 mm of the tip, was used to stimulate the medial preoptic-anterior hypothalamic area (MPH) with cathodic monophasic pulses (current 50–500 μA; duration 0.5 ms). Glass micropipettes filled with 0.5 M sodium acetate plus 2% pontamine blue were used to make single-unit extracellular recordings from CMA neurones. No recording electrode was used in more than one animal. At the end of each experiment a small current was passed through the stimulating and recording electrodes to facilitate histological localization. The rats were perfused *in situ* with a 10% formol saline to which a small amount of potassium ferrocyanide had been added. Brains were mounted in paraffin wax, sectioned at 15 μm and stained in cresyl violet and luxol fast blue.

Absolute refractory periods were determined in a total of 310 CMA neurones stimulated antidromically from the MPH. The criteria for antidromic invasion and the method for estimating the absolute refractory period of CMA neurones were the same as in refs 6 and 7. The results were analysed as follows. The refractory periods for all neurones isolated in a given rat were reduced to a single mean. These means (eight for each of the four groups) were then analysed by analysis of variance, followed by the Scheffé test[8].

Results are shown in Fig. 1. Overall analysis of variance showed that the groups were significantly different ($F = 56.80$, with d.f., 3, 28; $P < 0.001$). The Scheffé test showed that oestradiol significantly reduced the refractory period (oil compared with OB, $P < 0.001$). Dihydrotestosterone (unlike testosterone[6,7]) had no effect when given alone (oil compared with DHTP was not significant) and no additional effect when given in combination with oestradiol (OB compared with DHTP+OB, not significant.)

The mean absolute refractory period for neurones in the group of gonadally intact rats in our earlier experiment was 1.01 ms, with 95% confidence limits of 0.89 and 1.13 ms; the mean for the group of castrated rats was 1.61 ms with 95% confidence limits of 1.37 and 1.85 ms. The mean absolute refractory periods for the OB and the DHTP+OB groups in this experiment (0.90 and 0.98 ms) are therefore within the 95% confidence limits of our earlier intact group and those for the group treated with DHTP (1.40 ms) are within the 95% confidence limits of our earlier castrated group. These comparisons demonstrate that the refractory periods for CMA–MPH neurones in animals that are castrated but treated with oestradiol are not significantly different from those in gonadally intact animals.

Thus, our results show that oestradiol has the same effect on a population of testosterone-sensitive forebrain neurones as testosterone itself, as would be predicted from much indirect evidence. Dihydrotestosterone, on the other hand, has no effect on these neurones, and does not enhance the effect that oestradiol has on them.

Although we have not excluded the possibility that higher doses of dihydrotestosterone might have such an action, these results suggest that in behavioural experiments with the two hormones in doses comparable to our own, the increased sexual behaviour that is induced by dihydrotestosterone is not attributable to an action of the hormone on forebrain neurones comparable with that of testosterone and oestradiol. There is independent evidence that dihydrotestosterone has a different site of action, for the stimulating effect of testosterone on spinal sexual reflexes is mimicked by dihydrotestosterone, but not by oestradiol[9].

This investigation was supported by SRC grant 76300492 and MRC grant G979/439/N. We thank D. Harper for help with histology.

Received 13 February; accepted 16 April 1980.

1. Naftolin, F., Ryan, K. J. & Davies, I. J. in *Subcellular Mechanisms in Reproductive Neuroendocrinology* (eds Naftolin, F., Ryan, K. J. & Davies, I. J.) 347–355 (Elsevier, Amsterdam, 1976).
2. Södersten, P. *Horm. Behav.* **4,** 247–256 (1973).
3. Paup, D. C., Mennin, S. P. & Gorski, R. A. *Horm. Behav.* **6,** 35–46 (1975).
4. Baum, J. J. & Vreeburg, J. T. M. *Science* **182,** 283–285 (1973).
5. Larsson, K., Södersten, P. & Beyer, C. *J. Endocr.* **57,** 563–564 (1973).
6. Kendrick, K. M. & Drewett, R. F. *Science* **204,** 877–879 (1979).
7. Kendrick, K. M. thesis, Univ. Durham (1979).
8. Keppel, G. *Design and Analysis* 144–145 (Prentice-Hall, New Jersey, 1973).
9. Hart, B. L. *Physiol. Behav.* **23,** 107–109 (1979).

Activity-dependent extracellular K^+ fluctuations in canine Purkinje fibres

Richard P. Kline*†‡, Ira Cohen*, Robin Falk* & Joel Kupersmith†

*Department of Physiology and Biophysics, SUNY, Stony Brook, New York 11794

†Departments of Pharmacology and Medicine, Mount Sinai School of Medicine, CUNY, New York, New York 10029

Cardiac Purkinje fibres are important in cardiac electrophysiology and pathology due to their specialized role in the ventricular conducting system, and their properties as a second cardiac pacemaker[1]. Changes in extracellular K^+ activity (K_0) affect the conduction velocity[2] and the natural automatic rate of the Purkinje fibre[3]. Both anatomical[4] and electrophysiological[5,6] studies of the Purkinje fibres have demonstrated the possibility of K_0 fluctuations in the narrow intercellular clefts. We investigated, using K^+ selective electrodes, the effect of the K_0 fluctuations observed during activity in canine Purkinje fibres. Summation of K_0 fluctuations during single action potentials leads to elevation of baseline K_0 during rapid trains. However, unlike in ventricular muscle where depolarization is seen[7,8], membrane potential in non-automatic Purkinje fibres hyperpolarizes in response to rapid beating. Prolonged depletions of extracellular K^+ following long periods of overdrive are associated with slowly changing membrane currents, which markedly influence automaticity, action potential duration, and membrane potential.

Free running canine Purkinje fibres were removed from left and right ventricles and perfused in well oxygenated Tyrode solutions containing the following, 4 mM KCl, 2 mM $CaCl_2$, 130 mM NaCl, 1 mM $MgCl_2$, 0.4 mM NaH_2PO_4, 12 mM $NaHCO_3$, and 6 mM glucose. *p*H was maintained at between

---

‡To whom correspondence should be addressed at: Department of Pharmacology, BSB-274, Mount Sinai School of Medicine, 10 East 101 Street, New York, New York 10029.

0028–0836/80/270068–04$01.00

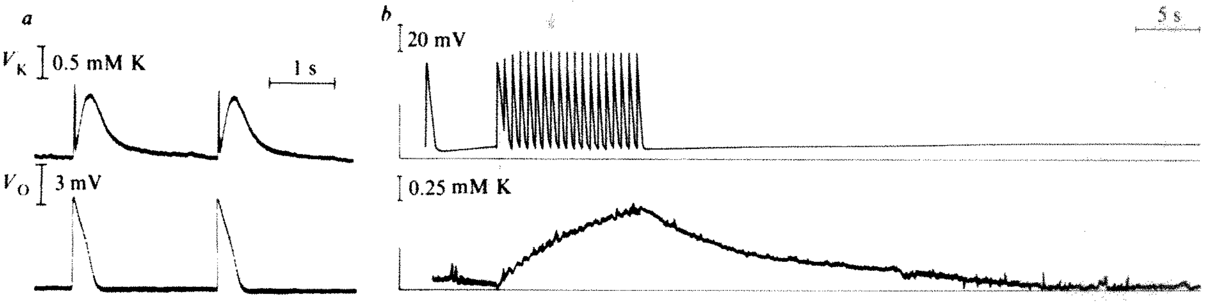

Fig. 1 (*a*), Top trace. (V_k) is the differential output of the two K^+ electrode barrels and represents the K_0 fluctuations during two single beats. The initial spike on this trace is an artefact due to the inability to reject stimulus voltage. Bottom trace: (V_0) is simultaneous output of the K^+ electrode reference barrel (37 °C). (*b*), Top trace. (V_m) is membrane potential measured with a conventional intracellular microelectrode. Bottom trace: (V_k) is differential output of K^+ electrode and represents K_0. No beat to beat accumulations are seen with this electrode tip position. K_0 accumulates slowly during 10 s of stimulation at 1 beat per 600 ms (37 °C).

'.2 and 7.4; the temperature was kept stable at the levels ndicated.

Double barrel K^+ sensitive electrodes (Corning liquid ion xchanger 477317) were constructed from theta glass double hannel tubing and calibrated for selectivity and response time sing methods previously described[7]. To measure K^+ activity evels, the output of the Tyrode-filled reference barrel (V_0) was ubtracted from the output of the K^+ selective barrel ($V_k + V_0$). The differential channel output (V_k) represents the K^+ activity evels, which for small changes vary approximately linearly with K^+ activity.[8]

Due to the somewhat slower response time of the K^+ elective barrel (20 ms), capacitive compensation was used to peed this barrel while a variable 'roll off' filter (Bloom) was sed to slow the reference barrel output before differential mplification. Common mode rejection of the two barrels was djusted to within 0.1% by a variable gain circuit.

K^+ electrode experiments were performed on the largest of he canine Purkinje fibres to facilitate manipulation of the lectrode and minimize the effect of tissue dimpling. Voltage lamp experiments were performed using the two-microelectrode voltage clamp method[6] on the short fibres of arrow radius (length, 1.5 mm; radius 0.15 mm). These fibres were dissected into short sections while being continually perfused with a high calcium (4 mM) Tyrode solution. In these mall fibres, clamp steps could be applied with acceptable evels of current magnitude and a good spatial homogeneity[9]. These fibres have K^+ currents similar to those described in ungulate[10].

To measure K_0 fluctuations, K^+ electrodes were slowly inserted through the sheath of the fibre bundle under constant observation through a dissecting microscope. To minimize tissue distortion, electrodes were made with fine tips (1–2 μm in total outer diameter). In fact, frequently cells were inadvertently punctured while the K^+ electrode was being advanced, such that normal action potentials were measured with the reference barrel, along with very high K^+ activity levels (but no beat to beat fluctuations) on the differential output. On withdrawal (or further advance) of the electrode tip, there was an abrupt fall in measured K^+ levels. At the same time, potential on the reference barrel returned to within several millivolts of ground level. One criterion for determining that the K^+ electrode was located extracellularly was that measured K^+ activity levels during quiescent equilibrium states were near bath levels, and were responsive to changes in bath K^+ levels[8].

Figure 1*a* shows K_0 accumulation measured during a single action potential. This beat to beat fluctuation occurs only when the electrode is near a cell membrane. The accumulation developed rapidly during the plateau of the action potential and then began to subside during fast repolarization. There is an initial rapid fall of K_0 which may have been influenced by the effect of active uptake processes on the narrow cleft spaces. During rapid beating, in addition to the K_0 fluctuations during single beats, there is an overall accumulation as beats occur progressively earlier during diastolic decay of K_0 (ref. 8). The post train decay of K_0 now exhibits a slow tail following the initial rapid decline, where the time constant of the slow

Fig. 2 K_0 fluctuations (V_k) during and after 1, 2 and 5 min periods of overdrive at 1 beat per 300 ms. K_0 undershoot of the baseline implies extracellular K^+ depletion. Solid arrow 'up' indicates start of stimulus drive; arrow 'down' indicates stimulus drive off (37 °C).

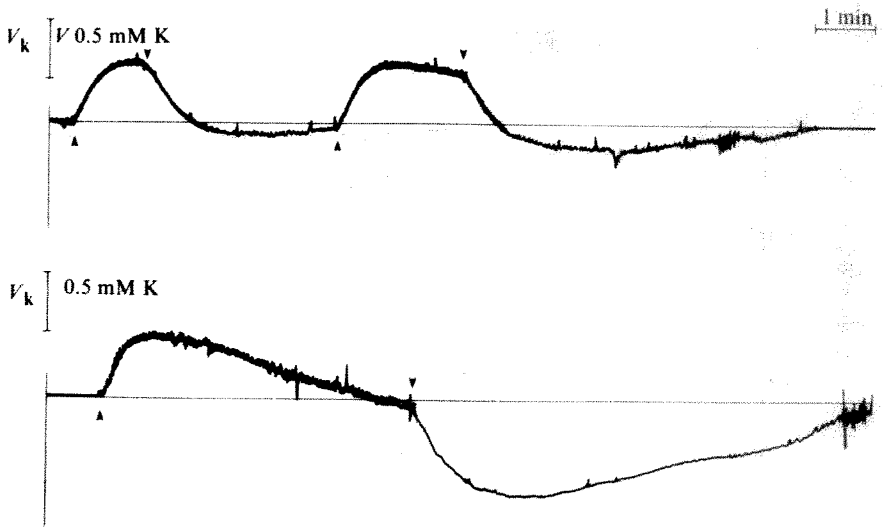

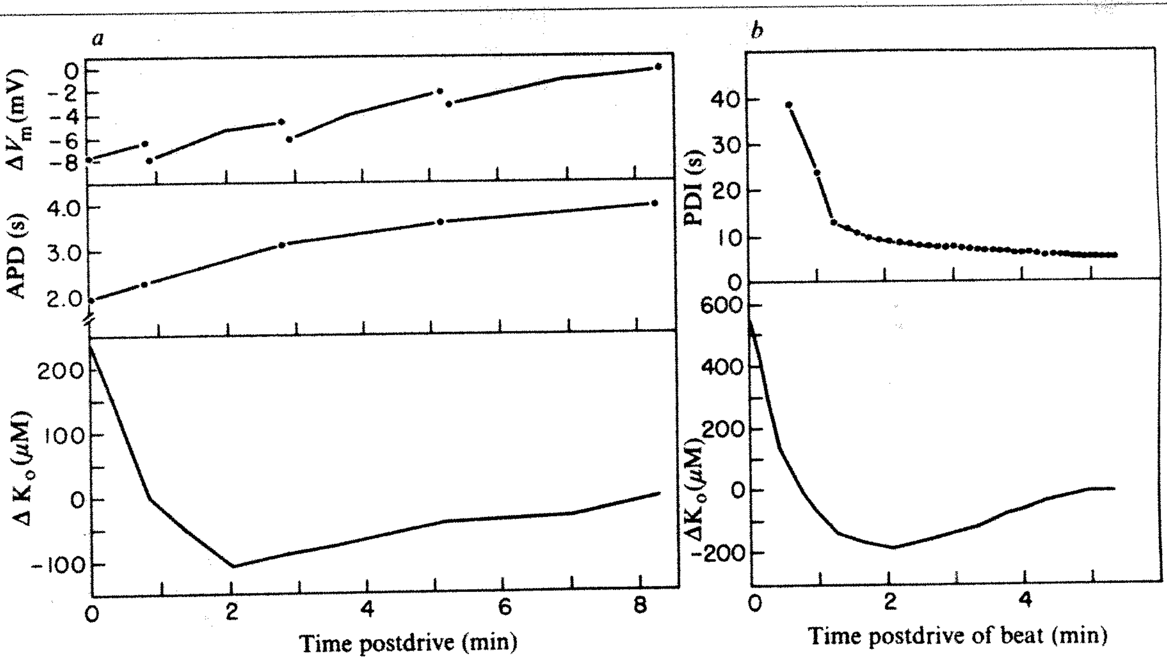

Fig. 3 (*a*), Return of V_m and action potential duration (APD) to control values following overdrive, plotted with simultaneously measured K$^+$ depletion. The '0' value on the K$_0$ axis corresponds to baseline levels of K$_0$(22 °C). (*b*), Comparison of return of automaticity with K$_0$ postdrive. Each point in the top panel represents a single action potential. Vertical axis is duration of previous diastolic interval (PDI) for each beat. (37 °C; difference in time course of undershoot in *a* and *b* is due to temperature difference.)

component reflects the diffusion relaxation time for the entire cylindrical preparation[7].

If the electrode tip is in a more superficial position in the fibre bundle, beat to beat accumulations are not seen. This is probably due to the longer diffusion pathway between the clefts and the electrode tip, and the resulting time average of observed K$_0$ levels[7]. As shown in Fig. 1*b*, K$_0$ accumulates progressively during 1 min of beating. We also measured intracellular potential (V_m) with a nearby conventional microelectrode, and found that the membrane hyperpolarizes during the K$_0$ accumulation.

With overdrive of more than 1 min, K$_0$ levels plateau and later slowly subside back to baseline. The most likely reasons for the decline in K$_0$ are stimulation of the Na$^+$-K$^+$ pump due to intracellular Na$^+$ accumulation[11,12] and decreased K$^+$ efflux per beat, due in part to action potential shortening (unpublished observation). When beating is terminated, K$_0$ levels fall rapidly and undershoot the baseline for a prolonged period. This prolonged postdrive undershoot is evidence of persistent Na$^+$-K$^+$ pump activity[11]. Figure 2 shows such K$_0$ accumulation and depletion associated with rapid stimulus trains of varying length (1, 2 and 5 min). The magnitude and duration of the K$_0$ undershoot increases with longer periods of overdrive[11]. Cooling the preparation to 22 °C also prolonged the undershoot.

With an intracellular microelectrode in a nearby cell, we monitored membrane potential (V_m) simultaneously with K$_0$ values. On cessation of stimulation following a period of overdrive, membrane potential is hyperpolarized and automaticity is suppressed. This phenomenon of overdrive suppression was originally described by Vassalle[13]. In addition, action potential duration is shortened following

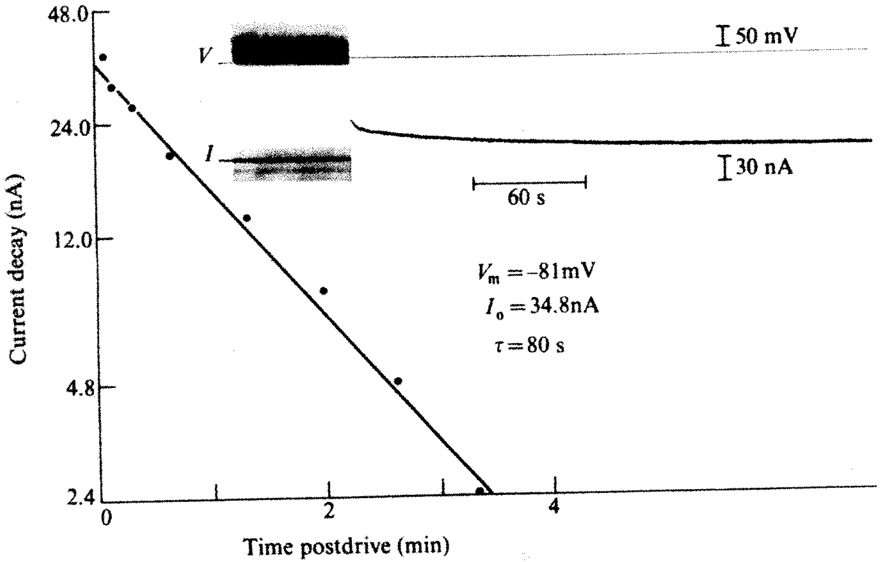

Fig. 4 Clamp current following overdrive (inset) is shown for 4 min voltage clamp to −81 mV (V, voltage trace; I, current trace).

drive. Figure 3*a* plots the postdrive return of action potential duration and membrane potential following a period of overdrive. Figure 3*b* plots the postdrive return of automatic activity versus K_0 for a spontaneously rhythmic fibre. The effect of overdrive on the membrane electrophysiological parameters gradually subsided during a period of minutes, and closely coincided with the duration of the K_0 undershoot.

As the post overdrive variations in these three parameters can be explained by a decaying outward current[13,14], we attempted to measure that current using the voltage clamp[15,16]. Following a similar period of rapid drive, we measured currents using sustained voltage clamp pulses at various holding potentials. Figure 4 (inset) shows the current recorded during a 4-min clamp pulse to −81 mV, following a period of overdrive. A decaying outward current is readily seen. The time constant of the current is 80 s, 1–2 orders of magnitude larger than the time constant of the pacemaker current (I_{K_2}) measured at this holding potential[10,17]. This slow current is dependent on there being a preceding period of overdrive, and is enhanced as the drive duration is lengthened.

However, the current does not seem to be independent of potential. As the postdrive clamp potential becomes more positive, the magnitude of the current decreases. Between −50 and −40 mV, the current becomes biphasic, and eventually at more positive potentials reverses polarity. The time constant of the decay of the slow current also seems to vary with potential. This may arise from :(1) contamination of an electrogenic pump current due to K_0 accumulation or depletion acting on other currents; (2) contamination of an electrogenic pump current by another time- and voltage-dependent current (I_x); (3) a direct effect on pump current of changing levels of K_0 in the clefts: (4) a dramatic dependence of passive ionic fluxes on post drive clamp potential, causing, for example, an increase in sodium loading at depolarized potentials; or, (5) a complicated dependence of pump current on membrane potential. Further experiments are needed to determine why slow current decay varies in this way with potential.

In summary, there is direct evidence for beat to beat changes in extracellular K^+ activity in canine Purkinje fibres. These fluctuations may provide some of the time dependence of the K^+ currents in both the plateau and diastolic potential ranges, by altering both the K^+ equilibrium potential and K^+ conductance [18]. It is also possible that transient changes in K_0 during extra-systoles and short periods of triggered automaticity may influence the following beats. Therefore, these activity-dependent fluctuations in K_0 and the associated membrane currents may be important factors affecting both the generation and maintenance of some ventricular arrhythmias.

These studies were supported by HL 20558, the Hearst Foundation, the Suffolk Heart Association, HL 25135, and an RCDA to I.C.

Received 10 December 1979; accepted 2 April 1980.

1. Hurst, J. W. *The Heart* (McGraw Hill, New York, 1974).
2. Fozzard, H. & Dominguez, G. *Circ. Res.* **26,** 565–574 (1970).
3. Vassalle, M. *Am. J. Physiol.* **208,** 770–775 (1965).
4. Hellam, D. C. & Studt, G. W. *J. Physiol., Lond.* **243,** 637–660 (1974).
5. Baumgarten, C. M. & Isenberg, G. *Pflügers Arch. ges. Physiol.* **386,** 19–31 (1977).
6. Cohen, I., Daut, J. & Noble, D. *J. Physiol., Lond.* **260,** 75–103 (1976).
7. Kline, R. P. & Morad, M. *J. Physiol., Lond.* **280,** 537–558 (1978).
8. Kline, R. P. & Morad, M. *Biophys. J.* **16,** 367–372 (1976).
9. Jack, J., Noble, D. & Tsien, R. W. *Electic Current Flow in Excitable Cells* (Clarendon, Oxford, 1975).
10. Cohen, I., Falk, R. & Kline, R. P. *J. Physiol., Lond.* **296,** 72P (1979).
11. Kunze, D. L. *Circ. Res.* **41,** 122–127 (1977).
12. Deitmer, J. W. & Ellis, D. *J. Physiol., Lond.* **284,** 241–259 (1978).
13. Vassalle, M. *Circ. Res.* **27,** 361–377 (1970).
14. Gadsby, D. & Cranefield, P. *J. gen. Physiol.* **73,** 819–837 (1979).
15. Gadsby, D. & Cranefield, P. *Proc. natn. Acad. Sci.* **76,** 1783–1788 (1979).
16. Eisener, D. A. & Lederer, W. J. *J. Physiol., Lond.* **296,** 75–76P (1979).
17. Noble, D. & Tsien, R. W. *J. Physiol., Lond.* **195,** 185–214 (1968).
18. Atwell, D., Eisner, D. & Cohen, I. *Q. Rev. Biophys.* (in the press).

0028–0836/80/270071–03$01.00

Single acetylcholine-activated channels show burst-kinetics in presence of desensitizing concentrations of agonist

B. Sakmann, J. Patlak & E. Neher

Max-Planck-Institut für biophysikalische Chemie, D-3400 Göttingen-Nikolausberg, Am Fassberg, FRG

High resolution measurements of the current through individual ion channels activated by acetylcholine (AChR-channels) in frog muscle have shown that these currents are discrete pulse-like events with durations of a few milliseconds[1,2]. Fluctuation and relaxation measurements of end-plate currents have led to the conclusion that the rate of channel opening increases with agonist concentration, and that the channel, once open, closes spontaneously[3–6]. Katz and Thesleff have shown, however, that in the continued presence of ACh, the initial end-plate current declines to an equilibrium value with a time constant of several seconds[7]. This reversible phenomenon is referred to as receptor desensitization. We report here that in the presence of ACh concentrations sufficient to cause desensitization, single channel current pulses appear in groups. From the temporal sequence of the pulses, we have derived estimates of the rates of activation and desensitization of the AChR-channel.

Experiments were performed on the extra-synaptic membrane of denervated fibres of frog (*Rana pipiens*) cutaneous pectoris muscle, using the extra-cellular patch clamp method for the application of agonist and to record membrane current[8]. AChR-channels in the extra-synaptic membrane are heterogeneous in their mean 'open times' (E.N. and B.S., in preparation). The predominant extra-synaptic AChR-channel has been described as having open times four to five times longer than the synaptic-type channel. However, about 10% of the channels we observed had properties comparable to subsynaptic AChR-channels. This report includes only measurements from channels of this latter type to facilitate comparison with previous measurements of end-plate currents.

Figure 1*a* shows the current recorded from a patch of membrane in the presence of 5 μM ACh starting less than 1 s after the agonist-containing pipette had been sealed on to the muscle fibre. The current switched randomly between the resting level and four equally spaced amplitudes, indicating that at least four channels were active. The progressive decrease in the number of amplitudes reached in the continued presence of ACh indicated a decrease in the number of open channels. This decrease characterizes the time course of receptor desensitization and results in complete inactivation of the current because of the low density of AChR-channels in the extrasynaptic membrane. However, after this initial desensitization, 'bursts' of single channel currents are observed at irregular intervals. Figure 1*b* shows a sequence of four such bursts recorded in the presence of 10 μM ACh about 30 s after the pipette had been sealed against the membrane. Initially the membrane is at the resting level. At time A, the current begins to fluctuate rapidly between the resting and another discrete level which in its amplitude corresponds to that flowing through a single open channel. At time B, about 800 ms later, the membrane current returns to the resting level. These rapid fluctuations define a current burst which is followed by an interburst interval during which the membrane is at the resting level. The sequence of bursts and interburst intervals becomes apparent in the presence of ACh concentrations >2 μM.

We interpret this pattern of current to reflect fluctuations of single AChR-channels between three states: closed, open and a desensitized, non-conducting state. At the beginning of the record shown in Fig. 1*b*, according to this model, all AChR-channels of the membrane patch under investigation are in a desensitized state. At time A, a single receptor-channel complex converts from the desensitized to the open/closed state. It then fluctuates rapidly between the open and the closed state and converts again to the desensitized state at B. However, the pattern of current shown in Fig. 1*b* is also reminiscent of the behaviour of single AChR-channels in the presence of channel-blocking substances[9]. Because some agonists themselves can block channels, the observed fluctuations of current during a burst could also reflect blocking of open channels by ACh molecules[10]. The two alternative mechanisms can be distinguished by their predictions for the agonist concentration dependence of the kinetics of fluctuations of current within a burst.

In the first interpretation, the rapid fluctuations are due to the changes of state: closed $\underset{\alpha}{\overset{\beta'}{\rightleftarrows}}$ open. In this two-state scheme β' and α are the rate constants of channel opening and closing respectively: α should be independent of the ACh concentration and can be measured as the reciprocal decay constant, τ_0^{-1}, of the distribution of the durations of current pulses (mean 'open time') during a burst. On the other hand, β', measured as the reciprocal decay constant, τ_C^{-1}, of the distribution of intervals between pulses, (mean 'closed time') should increase with the ACh concentration, because β' is an apparent rate constant, whose value is assumed to depend on agonist-binding steps preceding channel openings. In contrast, a channel-blocking mechanism would predict the opposite. The mean open time would shorten as the agonist concentration was raised, and the mean closed time would be independent.

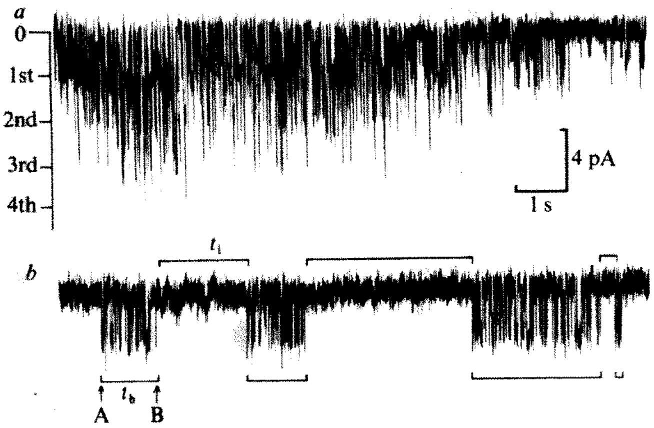

Fig. 1 Onset of desensitization and burst kinetics on small patches of extra-junctional membrane of chronically denervated frog muscle in the maintained presence of constant ACh concentrations. *a*, Record from a membrane patch starting when the agonist-containing patch pipette was sealed against the membrane. Four discrete levels of current can be resolved, as indicated roughly by the scale on the left. Individual step sizes are $\simeq 3$ pA, as expected for open ACh-activated channels at −130 mV membrane potential. The occurrence of currents reaching the fourth level indicates that at least four channels are active simultaneously. The maximum current amplitude reached decreases during this record until the membrane patch is at the resting level. ACh concentration was 5 μM; membrane potential, −130 mV; temperature, 11 °C. Inward current was downwards. The background noise, seen clearly on the resting level, caused some spread of the current amplitudes at each level. All records have been filtered at 500 Hz low pass. *b*, Bursts of current fluctuations follow the period of initial current inactivation. This record was started 34 s after the placement of the patch pipette and following a current pattern comparable to that shown in (*a*). The arrows marked A and B indicate the onset and cessation of fluctuations between the resting and the first current level and delineate that which is defined as a single channel current burst. Brackets indicate the measurement of t_b and t_i, burst duration and the inter-burst interval, respectively. Although occasionally bursts occur simultaneously, giving rise to currents reaching the second level (not illustrated), most bursts late in the record only reach the first level of current. This indicates that only a single channel is active. Conditions are the same as in (*a*), except that the pipette contained 10 μM ACh. The calibration scales apply to both traces.

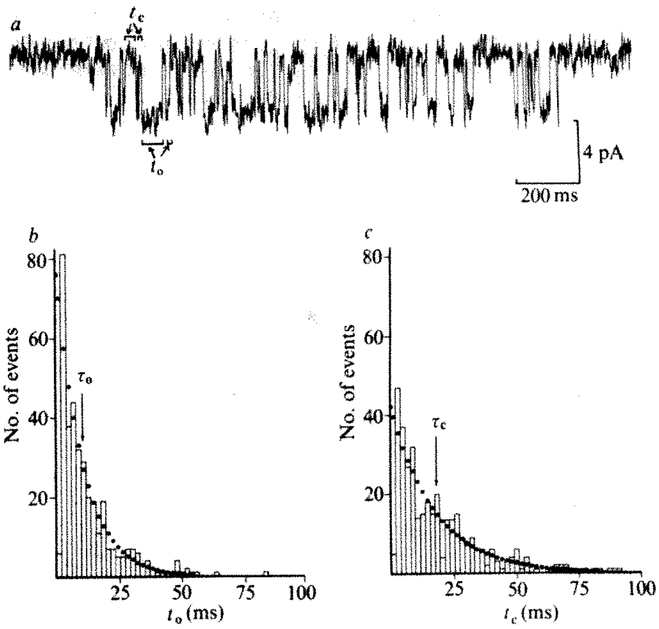

Fig. 2 Analysis of the rapid fluctuation of current during a burst. *a*, A single recorded burst in the presence of 10 μM ACh shown at higher time resolution than those in Fig. 1*b*. Brackets indicate the measurement of individual channel open times, t_0, and closed times, t_C. The membrane potential was −130 mV; temperature, 12 °C. *b* and *c*, Histograms of distributions of open and closed times measured during several sequential bursts at 10 μM ACh, −130 mV membrane potential and 12 °C. Records of currents were stored on an FM tape recorder, subsequently sampled and stored digitally on a PDP 11/34 computer. The sampling interval was 0.5 ms. Individual open and closed times were measured semi-automatically and stored to construct frequency-of-occurrence histograms. The histograms were fitted with single exponential curves, as indicated by the dotted line, using a least-squares fitting routine weighted for the statistical nature of the underlying events. The arrows indicate the best fit decay constants τ_0 and τ_C for the distribution of open and closed times, respectively. τ_0 was 10.6 ms and τ_C was 18 ms at 10 μM ACh.

We have, therefore, analysed quantitatively the distribution of open and closed times within bursts at various concentrations of ACh. Figure 2*a* shows a burst, illustrating the time course of the channel's conductance fluctuations. The distributions of open and closed times can be fitted by single exponentials (Fig. 2*b*, *c*), as expected for first-order kinetic processes. Figure 3*a* shows single bursts recorded in the presence of various concentrations of ACh and Fig. 3*b* summarizes our measurements as a plot of the values of τ_0^{-1} and τ_C^{-1} in double log scales as a function of ACh concentration. The mean open times are not measurably concentration dependent. Measurements at −90 mV and −130 mV show that mean open times increase with increasing membrane hyperpolarization. The e-fold increase per 65-mV change is close to the value reported for single channel measurements at low ACh concentration[1]. The rate constants of channel closing derived from these values are of the order of 100–250 s^{-1}, comparable to the values inferred from end-plate current fluctuation analysis[4]. Channel closed times decrease with agonist concentration. In the range of 5–50 μM ACh, the relation between τ_C^{-1} and ACh concentration is roughly described by a power law with an exponent of about 1.4. This suggests an increase of the apparent rate constant of channel opening from ~25 s^{-1} to ~500 s^{-1} in this concentration range. It is consistent with a reaction scheme that involves the binding of two ACh molecules preceding the opening of a single channel[5,6]. The intersections between the lines in Fig. 3*b* define the concentration of ACh for which the mean open time equals the mean closed time. These concentrations, 22 µM at −90 mV and 17 µM at −130 mV, are estimates of the apparent dissociation constants for channel activation by ACh in our conditions. These results support the hypothesis that the rapid current fluctuations during a burst reflect transitions of a single channel between the open and closed states. They rule out a channel-blocking mechanism.

The repeated appearance and disappearance of bursts of current, as illustrated in Fig. 1*b*, reflects fluctuations of AChR-channels between the open/closed and a desensitized state occurring on a much slower time scale than the open–closed transitions of the channel. At even lower time resolution, however, bursts seem to be an element of a pattern of current to which we refer as 'clusters' of several bursts (Fig. 4). Clusters are evident because the interburst intervals are much shorter than the mean intervals between the clusters.

Bursts and interburst intervals within a cluster vary stochastically in duration, and bursts become shorter at higher ACh concentrations. The separation of bursts is not always seen as clearly as in Fig. 1*b*, and in some cases it is difficult to define the beginning and end of individual bursts. However, at 20 µM ACh, bursts are clearly resolved (Fig. 4). The mean values of burst durations and interburst intervals at this concentration are 420 ± 12 ms and 180 ± 10 ms (± s.e.), respectively. Clusters of bursts have durations of several seconds and are separated by irregular intervals of several tens of seconds. For example, the cluster of eight bursts illustrated in Fig. 4 was recorded 18 s after the pipette had touched the muscle membrane; the next cluster occurred 23 s later. The duration of clusters is variable and decreases with increasing agonist concentrations. At 20 µM ACh, the average duration of clusters is 4.8 ± 2 s, whereas the average duration of the interval between clusters is 34 ± 4 s. A simple explanation for these observations is that the AChR-channel can exist in two different states of desensitization. Thus at 20 µM ACh, the sequence of bursts and burst intervals reflects the kinetics of a fast component of desensitization with apparent rate constants of $\simeq 2\,s^{-1}$ and $\simeq 5\,s^{-1}$ for the conversion to and from the desensitized state, respectively. The kinetics of a slow component are measured by the average duration of clusters and the average interval between clusters. At 20 µM ACh, the apparent rate constants are $\simeq 0.2\,s^{-1}$ and $\leqslant 0.03\,s^{-1}$ for the transitions between open/closed and this desensitized state.

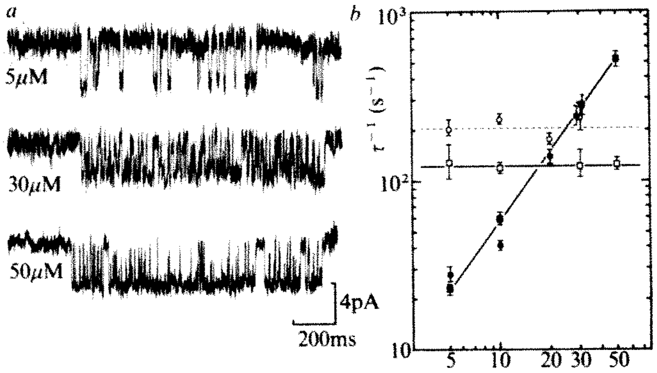

Fig. 3 Agonist concentration dependence of open and closed times during current bursts. *a*, Examples of bursts recorded in the presence of three different ACh concentrations as indicated on the left side of each record. All three records were taken at −130 mV membrane potential, 11 °C. As the ACh concentration increases, the duration of intervals between pulses of current decreases. At ACh concentrations $<20\,\mu M$ ACh, the channels are, during a burst, mostly in the closed state, whereas at $>20\,\mu M$ ACh, the channels are predominantly in the open state. *b*, Log log plot of the inverse of the best fit τ_0 and τ_C values, measured as shown in Fig. 2*b* and *c* against ACh concentration. Open symbols are values for the channel mean open times, τ_0, and closed symbols are for the channel mean closed times, τ_C. Circles were measurements at −90 mV, squares at −130 mV membrane potential. The solid lines were drawn through the −130 mV data, the dotted through the −90 mV. All lines were drawn by eye. Each point represents the best fit exponential to histograms made by summation of the histograms from many bursts in the same conditions. Standard error brackets refer to the calculated standard error of the best fit values of τ to their respective histograms. Channel open times are not measurably dependent on ACh concentration but increase with membrane hyperpolarization. The channel closed times are strongly dependent on ACh concentration: the slope of the line drawn was 1.4. No consistent change of mean closed times with changes in membrane potential was measureable.

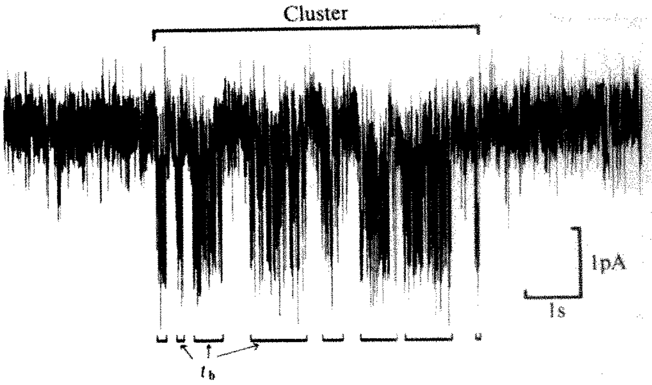

Fig. 4 Occurrence of single channel bursts in clusters as revealed at low time resolution. This record was obtained in the presence of 20 µM ACh 18 s after the establishment of the pipette-membrane seal. Membrane potential was −90 mV, 12 °C. At this slow sweep speed it is no longer possible to resolve individual pulses of current, but a clear grouping of bursts of pulses is apparent. The lower brackets indicate the durations of eight individual bursts, while the upper bracket illustrates the duration of a cluster. In frequency-of-occurrence histograms of the interval between current pulses, three widely separated exponential components are measureable. The fastest component respresents the distribution of channel closed times within bursts, the intermediate one the distribution of inter-burst intervals and the slowest component represents the time intervals between clusters. The wide separation of the means of the various interval distributions justifies the separation of groups of pulses into bursts and clusters.

The results demonstrate that at least three kinetic processes control the AChR-channel conductance state in the presence of desensitizing concentrations of ACh. The rapid fluctuations of current in the millisecond time range represent transitions of single AChR-channels between their open and closed states. The slow kinetic process, in the time range of several seconds, which is measured as the repeated occurrence of clusters, can tentatively be related to the onset of and recovery from desensitization as observed in measurements of end-plate current[11–13]. In addition, we have presented kinetic evidence for an agonist–receptor interaction that leads to a desensitized state of the receptor–channel complex in the intermediate time range of hundreds of milliseconds.

J.P. is supported by a postdoctoral fellowship from the Muscular Dystrophy Association of America.

Received 12 November 1979; accepted 8 April 1980.

1. Neher, E. & Sakmann, B. *Nature* **260**, 799–802 (1976).
2. Sakmann, B. & Heesemann, J. *Pflügers Arch. ges. Physiol.* **382**, R136 (1979).
3. Katz, B. & Miledi, R. *J. Physiol., Lond.* **224**, 665–699 (1972).
4. Anderson, C. R. & Stevens, C. F. *J. Physiol., Lond.* **235**, 665–691 (1973).
5. Sheridan, R. E. & Lester, H. A. *J. gen. Physiol.* **70**, 187–219 (1977).
6. Sakmann, B. & Adams, P. R. in *Advances in Pharmacology and Therapeutics* **1** (ed. Jacob, J.) 81–90 (Pergamon, Oxford, 1978).
7. Katz, B. & Thesleff, S. *J. Physiol., Lond.* **138**, 219–228 (1978).
8. Neher, E., Sakmann, B. & Steinbach, J. H. *Pflügers Arch. ges. Physiol.* **375**, 219–228 (1978).
9. Neher, E. & Steinbach, J. H. *J. Physiol., Lond.* **277**, 153–176 (1978).
10. Adams, P. R. & Sakmann, B. *Proc. natn. Acad. Sci. U.S.A.* **75**, 2994–2998 (1978).
11. Magazanik, L. G. & Vyskočil, F. *J. Physiol., Lond.* **249**, 285–300 (1975).
12. Adams, P. R. *Pflügers Arch. ges. Physiol.* **360**, 135–144 (1975).
13. Scubon-Mulieri, B. & Parsons, R. L. *J. gen. Physiol.* **69**, 431–447 (1977).

Effect of lesion of cortical dopamine terminals on subcortical dopamine receptors in rats

C. J. Pycock, R. W. Kerwin & C. J. Carter

Department of Pharmacology, Medical School, University of Bristol, Bristol BS8 1TD, UK

Since the demonstration of dopamine-containing nerve terminals within cortical regions[1,2], studies have confirmed the existence of a dopaminergic projection to the medial prefrontal cortex[3,4]. Cortical dopamine (DA) may be a functional neurotransmitter, as there are selective high-affinity receptor binding[5,6] and uptake sites[7,8] within this area, a DA-selective adenylate cyclase system[8,9], cells responsive to iontophoretically applied DA[10], and a pool of DA amenable to release *in vivo*[11] or *in vitro*[12,13]. Lesions of either midbrain cell bodies in the ventral tegmental area[14,15] or of frontal cortical areas directly[16], with subsequent loss of DA terminals from the medial prefrontal cortex, induce hyperactivity in rats[16], and enhanced behavioural responses to amphetamine[16,17]. Lesion of subcortical DA pathways results in the opposite effects, suggesting that frontal cortical DA systems may have an inhibitory role in motor behaviour[15,16]. Dopamine-dependent hyperactivity and stereotypy is believed to be mediated from extrapyramidal and mesolimbic DA-innervated sites[18]. We previously noted that loss of catecholamine terminals within the frontal cortex of the rat results in increased DA turnover and utilization in subcortical striatal and limbic regions after one week[19]. We now show evidence of both enhanced presynaptic and post-synaptic mechanisms in the terminal regions of the ascending nigrostriatal and mesolimbic DA pathways one month after destruction of DA terminals within the medial prefrontal cortex of the rat. The increased ^{3}H-ADTN and ^{3}H-spiperone binding, enhanced DA-induced stimulation of adenylate cyclase and potentiated uptake capacity for DA within striatum and nucleus accumbens may demonstrate a functional basis for the observed potentiated behavioural responses.

Destruction of catecholamine terminals within the area of the medial prefrontal cortex was performed by infusion of 6-hydroxydopamine (6-OHDA) into this site. Male Porton rats (220–250 g) were pretreated with the noradrenergic uptake blocker desmethylimipramine[20] (DMI, 25 mg per kg, intraperitoneally (i.p.), 30 min before lesion) to increase the relative toxic specificity of 6-OHDA for DA terminals. Animals were anaesthetized (chloral hydrate, 300 mg per kg), and immobilized in a Kopf stereotaxic frame. Two groups of rats received bilateral injections of either solvent (1.5 μl 0.1% nitrogen-bubbled sodium metabisulphite solution) or 6-OHDA (Sigma) (8 μg per 1.5 μl per 2 min) into the medial prefrontal cortex (coordinates A + 10.3; V + 1.0; L ± 0.8 mm)[21] (Fig. 1).

Four weeks after surgery, the spontaneous and (+)-amphetamine (1 mg per kg, i.p.)-induced locomotor activity of both sham and lesioned rats was tested in an open field. Remaining rats were killed for biochemical assessment of the effects of the 6-OHDA/DMI lesion. Paired corpus striatum, nucleus accumbens and the region of the medial prefrontal cortex were rapidly dissected out and regional concentrations of DA and noradrenaline (NA) were measured using a sensitive radiometric enzymatic assay with [^{3}H]-S-adenosylmethionine (15 Ci mmol^{-1}, Radiochemical Centre, Amersham) as the methyl donor[22]. The high-affinity benztropine-resistant[23] uptake of NA, and the DMI-resistant uptake of DA, within the lesion site and adjacent cortical areas were also compared (see Fig. 1). In addition, the DMI-resistant uptake of DA in the striatum and nucleus accumbens was measured in the two animal groups. Concentrations of the major DA metabolites homovanillic acid (HVA) and 3,4-dihydroxyphenylacetic acid (DOPAC) within striatum and nucleus accumbens were measured fluorimetrically[24], and the basal and dopamine (5–50 μM)-stimulated adenylate cyclase activity assayed in these regions according to the technique of Clement-Cormier and coworkers[25]. Further, (+)-butaclamol-sensitive ^{3}H-spiperone (20 Ci mmol^{-1}; Radiochemical Centre, Amersham) binding using a range of 100–2,000 pM radioactive ligand[27], and also the 2-amino-6,7-dihydroxy-1,2,3,4-tetrahydronaphthalene (ADTN)-sensitive binding of ^{3}H-ADTN (4.9 Ci mmol^{-1}; Radiochemical Centre, Amersham) using a range of 5–40 nM radioactive ligand[28] were studied in striatal

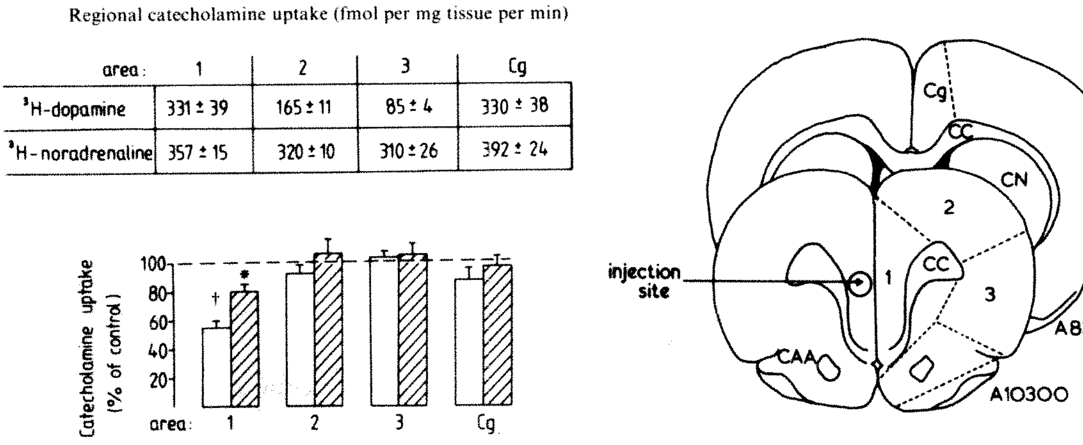

Regional catecholamine uptake (fmol per mg tissue per min)

area:	1	2	3	Cg
^{3}H-dopamine	331 ± 39	165 ± 11	85 ± 4	330 ± 38
^{3}H-noradrenaline	357 ± 15	320 ± 10	310 ± 26	392 ± 24

Fig. 1 The site and effect of 6-OHDA lesions of the medial prefrontal cortex on regional frontal cortical high-affinity catecholamine uptake. Transverse sections of the rat brain, levels A8380 and A10300[21], indicate site of injection (bilaterally, area 1) and adjacent areas taken for regional assay (areas 2, 3 and Cg). For regional high-affinity catecholamine uptake, areas were dissected from the appropriate plane and tissue from both sides of each animal pooled and chopped in two directions at 0.2 mm intervals using a McIlwain tissue chopper. Slices were weighed (5–10 mg per tube) incubated at 37 °C in 2 ml oxygen-bubbled Krebs–Ringer bicarbonate buffer, *p*H 7.4 for 10 min. ^{3}H-DA (specific activity 5 Ci mmol^{-1}, Radiochemical Centre, Amersham) or ^{3}H-NA (specific activity 10.7 Ci mmol^{-1}, Radiochemical Centre, Amersham) were added to each tube to give a final concentration of 0.1 μM. For DA uptake, 0.5 μM DMI was present in the buffer to restrict any uptake into NA terminals[20]; for NA uptake, 1 μM benztropine was present to restrict any uptake into DA terminals[23]. Uptake was terminated after 5 min by rapid filtration on to Whatman GF/B filters, and, following washing with 15 ml ice-cold buffer, radioactivity was determined by liquid scintillation counting. Tissue and filter blanks were assessed by measuring the uptake of radioactivity at 0 °C. The results of the regional high-affinity catecholamine uptake were calculated as fmoles per mg tissue per min (upper trace). Uptake in 6-OHDA lesioned animals was expressed as a percentage of that obtained in sham-operated rats (lower trace); open columns represent DA uptake, hatched columns for NA uptake. Each point is the mean of six values; vertical bars denote standard errors. Cg, cingulate cortex; CN, caudate nucleus; CC, corpus callosum; CAA, anterior commissure.
$*P < 0.05$; $\dagger P < 0.01$ (Student's *t* test).

0028-0836/80/270074-04$01.00

Table 1 Changes in regional concentrations of noradrenaline and dopamine and its metabolites in cortical and subcortical sites in rats following 6-OHDA lesions of the medial prefrontal cortex

Substance tested	Medial prefrontal cortex		Striatum		Nucleus accumbens	
	Sham	Lesion	Sham	Lesion	Sham	Lesion
NA	0.84 ± 0.03	0.58 ± 0.12* (68)	—	—	—	—
DA	0.11 ± 0.02	0.04 ± 0.01† (38)	11.94 ± 0.87	12.61 ± 0.84 (106)	7.97 ± 0.85	9.35 ± 0.40* (117)
HVA	—	—	0.63 ± 0.06	0.77 ± 0.04* (124)	0.93 ± 0.08	1.31 ± 0.10† (141)
DOPAC	—	—	1.21 ± 0.09	1.87 ± 0.40† (155)	1.33 ± 0.14	1.94 ± 0.27* (146)

Lesioned animals were pretreated with DMI (25 mg per kg, i.p.) and 6-OHDA (8 μg in 1.5 μl) injected bilaterally into the medial prefrontal cortex. Sham animals received bilateral injections of vehicle (1.5 μl 0.1 % sodium metabisulphite solution) into the same site. Biochemical assays were conducted 30 days after surgery. Results are the mean of seven observations and are expressed as μg per g wet weight tissue ±1 s.e.m. Figures in parentheses indicate the per cent value of sham-operated concentrations.

*$P < 0.05$.

†$P < 0.01$ (Student's t test).

and nucleus accumbens membrane preparations.

Total specific binding of ^{3}H-ADTN and ^{3}H-spiperone was significantly increased in the membrane fraction prepared from both striatum and nucleus accumbens examined from the 6-OHDA lesioned animals (Fig. 2). Scatchard analysis of the data indicated that this was due to an increase in receptor numbers in both regions for both ligands (ADTN: B-values for striatum, control 113 ± 10 fmol per mg protein compared to 146 ± 9 for lesioned group ($P < 0.05$); nucleus accumbens, control 78 ± 4 fmol per mg protein compared to 90 ± 5 for lesioned group ($P < 0.05$). Spiperone: B-values for striatum, control 0.81 ± 0.07 pmol per mg protein compared to 1.08 ± 0.09 for lesioned group ($P < 0.05$); nucleus accumbens, control 0.91 ± 0.05 pmol per mg protein compared to 1.33 ± 0.11 for lesioned group ($P < 0.05$)). Additionally, there appeared to be a small decrease in receptor affinity for ^{3}H-ADTN binding in the striatum (K_d values: control 0.87 nM, lesion 1.54 nM). There appeared to be no change in receptor affinity with dissociation constants ranging from 0.22 to 0.49 nM for ^{3}H-spiperone binding, or for ^{3}H-ADTN binding in the nucleus accumbens, the regression analysis showing that the slopes did not significantly deviate from parallelism between sham-operated and lesioned animals. All binding data represents mean ± s.e.m. of eight determinations.

Dopamine (5–50 μm) markedly stimulated adenylate cyclase activity in striatal and accumbens homogenates. This effect was significantly greater in 6-OHDA lesioned animals at all doses of DA giving maximal stimulation in the striatum ($P < 0.05$) and at the 20 μM dose of DA in the nucleus accumbens ($P < 0.05$, Fig. 3). Furthermore, the cortical lesions resulted in significant increase in the high affinity DMI-resistant uptake of DA in both extrapyramidal and mesolimbic sites. Accumulation of DA into striatal slices from 6-OHDA/DMI lesioned rats was $1{,}067 \pm 71$ fmol per mg tissue per min compared to 754 ± 70 fmol per mg tissue per min in vehicle-injected animals ($2P < 0.02$). Accumulation of DA into slices from nucleus accumbens was 649 ± 86 fmol per mg tissue per min in 6-OHDA/DMI lesioned rats: control animals accumulated 435 ± 32 fmol per mg tissue per min ($2P < 0.02$, $n = 10$).

We have previously reported the behavioural and biochemical sequelae of such lesions, 10 days after surgery[16,19]. Because the additional binding and uptake studies were performed 1 month after surgery, we repeated these experiments at this later time to verify the effects of the lesion. At 1 month these lesions enhanced spontaneous and amphetamine (1 mg per kg, i.p.)-induced locomotor activity in the perimeter squares of an open field compared to sham-lesioned animals (spontaneous, $P < 0.05$; amphetamine-induced, $P < 0.01$, $n = 8$). Similarly the biochemical parameters at 1 month paralleled those results reported at 10 days after surgery. Briefly 6-OHDA lesions of the medial prefrontal cortex reduced DA concentrations to 38 % ($P < 0.01$) and NA concentrations to 68 % ($P < 0.05$) within this site (Table 1). These results were supported by a 48 % decrease in high-affinity DMI-resistant DA uptake and a 21 % decrease in high-affinity benztropine-resistant NA uptake (Fig. 1). These significant changes in catecholamine uptake were only observed in the region of the medial prefrontal cortex (area 1), adjacent regions and the cingulate cortex showed no differences between 6-OHDA lesioned and sham-operated animals (Fig. 1). In addition to changes in cortical catecholamine content, significant increases (+17 %) in the DA content of the nucleus accumbens ($P < 0.05$), and HVA and DOPAC concentrations in both striatum and nucleus accumbens were recorded in 6-OHDA lesioned rats (Table 1).

Lesions of 6-OHDA of the medial prefrontal cortex produce significant loss of both DA and NA from this site, together with an apparent enhancement of subcortical DA systems as indicated by increases in concentrations of DA and its metabolites, in basal and dopamine-stimulated adenylate cyclase, in ^{3}H-ADTN and ^{3}H-spiperone receptor binding and enhanced high-affinity uptake of DA within the striatum and nucleus accumbens. The neurotoxic effects of the lesion seem to be confined to the medial prefrontal cortex as adjacent regions and the cingulate cortex showed no changes in high-affinity catecholamine uptake. The lesion was associated with an increase in both spontaneous and amphetamine-induced locomotor activity.

The biochemical data would suggest a facilitation of DA mechanisms within extrapyramidal and mesolimbic sites which would support the enhanced behavioural responses. This increase would seem to involve both pre- and postsynaptic mechanisms within the striatum and nucleus accumbens as indicated by the recorded increase in DA utilization (increased DA metabolite concentrations), DA uptake, and increase in adenylate cyclase and receptor number. The exact site of these receptor increases is not known as not all postsynaptic DA receptors seem to be linked to adenylate cyclase[29] and a recent report suggests only a poor correlation between ^{3}H-spiperone binding and DA-sensitive adenylate cyclase suggesting that two different populations of DA receptors may be involved[30]. Furthermore it has been suggested that the neuroleptic may also label central serotonin receptors which would obviously confuse interpretation of the results[31]. However, an identical binding pattern is observed in lesioned animals using ADTN, a rigid analogue of DA which is believed to bind specifically to DNA receptors[28].

Such an apparent increase in both presynaptic and postsynaptic neurotransmitter mechanisms seem paradoxical as a decreased presynaptic function is usually associated with an increased postsynaptic sensitivity[32] and vice versa[33]. Thus the appearance of increased activity at both pre- and postsynaptic sites is a novel situation which is very interesting because of its accordance with the post-mortem biochemical data seen in schizophrenia, where increases in DA concentrations in nucleus accumbens[34], and enhanced neuroleptic binding in both nucleus accumbens and striatum[35,36] have been a documented feature of this disease. On the basis of other reported data, such a unilateral increase in pre- and postsynaptic activity is not completely without precedent, as recent findings describe increased behavioural responses following chronic treatment with DA agonists[37,38].

The mechanism by which loss of catecholamine terminals within the prefrontal cortex induces supersensitivity within subcortical DA pathways is not known. It may reflect an increased number of active DA terminals in these sites, but whether such changes are purely a physiological consequence of reducing cortical DA function, or related to collateral sprouting[39] following damage to the mesocortical DA projection remains to be resolved. In a previous study we showed that such lesions will also bring about changes in other neurotransmitter functions within the basal ganglia[19]. It therefore seems that the frontal cortical catecholamine system may be intimately concerned with the regulation of subcortical DA pathways. The medial prefrontal cortex sends projections to the striatum[40], nucleus accumbens[41], ventral tegmental area[40], and to the substantia nigra[42], thus providing potential routes through which such control may be mediated. The development of supersensitive central receptor sites is of much interest to the clinician, and an increase in either affinity or number of subcortical DA receptors has been suggested in development of Parkinson's disease[43], schizophrenia[35,36] and the dyskinesias[44]. Indeed a recent report has presented evidence for the development of supersensitive striatal DA receptors in rats following chronic neuroleptic treatment[45], a situation that may explain tardive dyskinesias which often develop in this type of drug therapy. That an apparent supersensitive subcortical DA system can also develop after lesions of the prefrontal cortex may have far reaching implications as to the possible involvement of this site in the aetiology and management of neurological and psychiatric disorders hitherto attributed to dopaminergic function in subcortical areas.

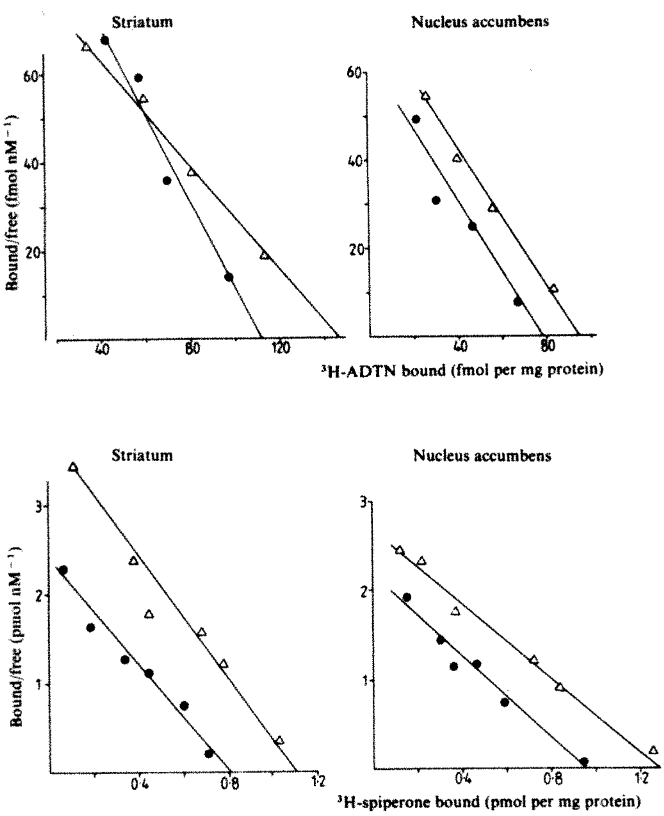

Fig. 2 Effect of 6-OHDA lesions of the medial prefrontal cortex on ^{3}H-ADTN (upper traces) and ^{3}H-spiperone (lower traces) binding to membrane fractions prepared from rat striatum and nucleus accumbens. Tissue pooled from nine sham-operated or nine 6-OHDA lesioned animals for each ligand, 30 days after surgery. Total specific ADTN binding was obtained by displacement with 1 μM ADTN[28] and total specific ^{3}H-spiperone binding was obtained by displacement with 1 μM (+)-butaclamol[27]. Data is shown as representative Scatchard plots of radiolabelled ligand receptor binding from sham-operated (●) and 6-OHDA lesioned animals (△), each point being the mean of quadruplicate determinations. At saturating concentrations of ^{3}H-spiperone specific binding typically represented 500 c.p.m.; nonspecific being typically 200 c.p.m. At saturating concentrations of ADTN specific binding was typically 900 c.p.m.; nonspecific being 400 c.p.m.

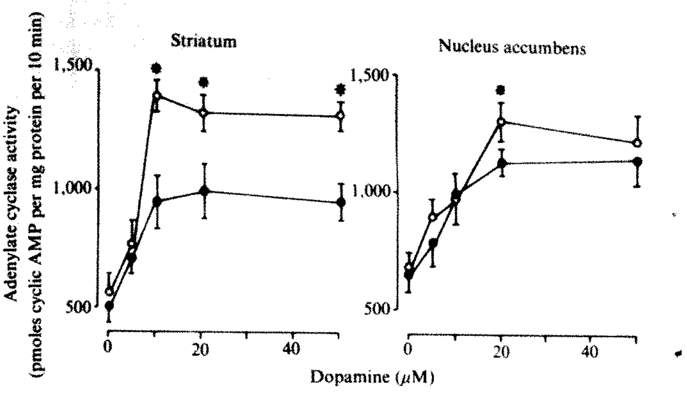

Fig. 3 Effect of 6-OHDA lesions of the medial prefrontal cortex on dopamine-sensitive adenylate cyclase activity in rat striatum and nucleus accumbens. Tissue pooled from six sham-operated or 6-OHDA lesioned rats, 30 days after surgery. DA-sensitive adenylate cyclase activity was determined according to the technique of Clement-Cormier *et al.*[25] and cAMP in the samples was assayed using the method of Brown *et al.*[26]. The results shown represent activity in tissue from sham-operated animals (●) and 6-OHDA lesioned rats (○) and represents the mean ± 1 s.e.m. of three determinations each assayed in triplicate. The data shown is obtained from a single assay and is one of several experiments carried out in identical conditions and giving similar results. Significant differences from sham-treated animals ($P<0.01$) are indicated by the asterisks and are determined non-parametrically from data pooled from two separate assays ($n=6$).

We thank Mrs Shirley Burns and Miss Sarah Pay for technical assistance, and Dr Tom Blackburn for supplies of ADTN. C.J.C. and R.W.K. are supported by the MRC.

Received 13 August 1979; accepted 16 April 1980.

1. Fuxe, K., Hökfelt, T., Johansson, O., Lidbrink, P & Ljungdahl, Å. *Brain Res.* **82**, 349-355 (1972).
2. Thierry, A. M., Blanc, G., Sobel, A., Stinus, L. & Glowinski, J. *Science* **182**, 499-501 (1973).
3. Lindvall, O., Björklund, A. & Divac, I. *Brain Res.* **142**, 1-24 (1978).
4. Emson, P. C. & Koob, G. F. *Brain Res.* **142**, 249-267 (1978).
5. Fields, J. Z., Reisine, T. D. & Yamamura, H. I. *Brain Res.* **136**, 578-584 (1977).
6. Laduron, P. M., Janssen, P. F. M. & Leysen, J. E. *Biochem. Pharmac.* **27**, 323-328 (1978).
7. Tassin, J. P., Thierry, A. M., Blanc, G. & Glowinski, J. *Naunyn-Schmiedeberg's Arch. Pharmac.* **282**, 239-323 (1974).
8. Tassin, J. P. *et al. Brain Res.* **154**, 241-251 (1978).
9. Von Hungen, K. & Roberts, S. *Eur. J. Biochem.* **36**, 391-401 (1973).
10. Bunney, B. S. & Aghajanian, G. K. *Life Sci.* **19**, 1783-1792 (1976).
11. Myers, R. D. & Mora, F. *Brain Res. Bull.* **2**, 105-112 (1977).
12. Saldate, M. C. & Orrego, F. *Brain Res.* **130**, 483-494 (1977).
13. Arnold, E. B., Molinoff, P. B. & Rutledge, C. O. *J. Pharmac. exp. Ther.* **202**, 544-557 (1977).
14. Le Moal, M., Cardo, B. & Stinus, L. *Physiol. Behav.* **4**, 567-574 (1969).
15. Tassin, J. P. *et al. Brain Res.* **141**, 267-281 (1978).
16. Carter, C. J. & Pycock, C. J. *Brain Res.* (in the press).
17. Le Moal, M., Stinus, L. & Simon, H. *Nature* **280**, 156-158 (1979).
18. Costall, B., Marsden, C. D., Naylor, R. J. & Pycock, C. J. *Brain Res.* **123**, 89-111 (1977).

19. Pycock, C. J., Carter, C. J. & Kerwin, R. W. *J. Neurochem.* **34,** 91–99 (1980).
20. Glowinski, J. & Axelrod, J. *Nature* **204,** 1318–1319 (1964).
21. König, J. F. R. & Klippel, R. A. *The Rat Brain: A Stereotaxic Atlas of the Forebrain and Lower Parts of the Brainstem* (Williams and Wilkins, Baltimore, 1963).
22. Cuello, A. C., Hiley, R. & Iversen, L. L. *J. Neurochem.* **21,** 1337–1340 (1973).
23. Coyle, J. T. & Snyder, S. H. *Science* **166,** 899–901 (1969).
24. Westerink, B. H. C. & Korf, J. *J. Neurochem.* **29,** 697–706 (1977).
25. Clement-Cormier, Y. C., Parrish, R. G., Petzold, G. L., Kebabian, J. W. & Greengard, P. *J. Neurochem.* **25,** 143–149 (1975).
26. Brown, B. L., Albano, J., Ekins, R. P. & Sgherzi, A. *Biochem. J.* **121,** 561–562 (1971).
27. Creese, I., Burt, D. R. & Snyder, S. H. *Life Sci.* **17,** 1715–1720 (1975).
28. Seeman, P., Woodruff, G. N. & Poat, J. A. *Eur. J. Pharmac.* **55,** 137–142 (1979).
29. Kebabian, J. W. & Calne, D. B. *Nature* **277,** 93–96 (1979).
30. Quik, M. & Iversen, L. L. *Eur. J. Pharmac.* **56,** 323–330 (1979).
31. Leysen, J. E., Niemegeers, C. J. E., Tollanaere, J. P. & Laduron, P. M. *Nature* **272,** 168–171 (1978).
32. Creese, I., Burt, D. R. & Snyder, S. H. *Science* **197,** 596–598 (1977).
33. Bartholini, G. *J. Pharm. Pharmac.* **28,** 429–433 (1976).
34. Bird, E. D., Spokes, E. G. S. & Iversen, L. L. *Brain* **102,** 347–360 (1979).
35. Owen, F. *et al. Lancet* **ii,** 223–225 (1978).
36. Lee, T., Seeman, P., Tourtellotte, W. W., Farley, I. J. & Hornykeiwicz, O. *Nature* **274,** 897–900 (1978).
37. Smith, R. C., Strong, J. R., Hicks, P. B. & Samorajski, T. *Psychopharmacology* **60,** 241–246 (1979).
38. Weiner, W. J., Goetz, C. G., Nausieda, P. A. & Klawans, H. L. *Neurology* **29,** 1054–1057 (1979).
39. Gilad, G. M. & Reis, D. J. *Brain Res.* **160,** 17–36 (1979).
40. Leonard, C. M. *Brain Res.* **12,** 321–343 (1969).
41. Beckstead, R. M. *J. comp. Neurol.* **184,** 43–62 (1979).
42. Knook, H. L. *The Fibre Connections of the Forebrain* (Van Gorcum, Amsterdam, 1965).
43. Lee, T., Seeman, P., Rajput, A., Farley, I. J. & Hornykiewicz, O. *Nature* **273,** 59–61 (1978).
44. Marsden, C. D., Tarsy, D. & Baldessarini, R. J. in *Psychiatric Aspects of Neurologic Disease* (eds Benson, D. F. & Blumer, D.) 219–265 (Grune and Stratton, New York, 1975).
45. Clow, A., Jenner, P., Theodorou, A. & Marsden, C. D. *Nature* **278,** 59–61 (1979).

Behavioural variants of rat neuroblastoma cells

Lloyd A. Culp

Department of Microbiology, Case Western Reserve University, School of Medicine, Cleveland, Ohio 44106

Study of the biological function of the cells of the nervous system has benefited from the isolation of cloned glial or neuronal tumour cell lines that can be induced to differentiate in culture[1–3]. Many of their differentiated properties reflect specific biochemical changes at the cell surface, and we have observed changes in cytoskeletal organization and glycosaminoglycan-containing proteoglycan content in the tissue culture substratum adhesion sites of neuroblastoma cells during neurite extension[4]. To assist in defining structure function relationships of cell surface components of rodent neuroblastoma cells, I have used two cell-surface-active agents to select for phenotypically-stable variants of these cells which display some unique properties and which will be useful for further biochemical and physiological analyses.

The first selection, based on sensitivity to detachment of these cells from the tissue culture substratum by the Ca^{2+}-specific chelator EGTA, is shown in Fig. 1 for cloned rat neuroblastoma B104 cells[3]. Variants were isolated that resist EGTA-mediated detachment from the tissue culture dish on conventional treatment [shaking at 37 °C for 30 min with 0.5 mM EGTA in phosphate-buffered saline (PBS)]. The selection was performed in two different ways. In the first approach (Fig. 1*a*), undifferentiated B104 cells were treated with EGTA, gently pipetted to detach loosely-adherent cells, and rinsed several times with PBS. Cells resisting this treatment (approximately 5×10^{-5} of the original cell number) were incubated for several hours in fresh medium and trypsin-subcultured into fresh dishes. After 2 weeks, several colonies developed at a final selection frequency of 1×10^{-5}; these colonies were subjected to the same selection protocol two more times before cloning. Most of the colonies from this selection were resistant to EGTA at 0.5 mM and displayed a highly elongated fibroblastic morphology. These cells are referred to as E_RA variants; higher EGTA concentrations or longer trypsinization are required to subculture them. Several clones were tested and showed properties similar to those of the E_RA 12 clone described here.

In an alternative procedure (Fig. 1*b*), cells in the original culture that resisted EGTA detachment were permitted to regrow into colonies in the original culture dish instead of being treated with trypsin and transferred to fresh dishes. The original dish was covered with cellular substrate-attached material (SAM), substratum adhesion sites which pinch off from the cell surface during EGTA-mediated detachment of the cells[6]; it has previously been shown that oncogenic virus-transformed fibroblasts respond differently to SAM-coated substrata compared to serum-coated substrata than do normal fibroblasts[7,8]. SAM-coated substratum permits selection of a different type of variant, termed E_RB, at a frequency of $\sim2\times10^{-5}$. Most clones displayed properties similar to the E_RB9 clone described here. Both variant types have been stable over 9 months of culture (25–30 passages).

A third selection method was based on the sensitivity of rat B104 cells to agglutination and killing by the lectin concanavalin A (Con A) using protocols similar to those found successful in generating Con A-resistant fibroblasts[5]. A confluent washed cell layer was treated with 20 μg ml^{-1} Con A for 16 h in serumless DMEM. The nonviable agglutinated cells were pipetted off the dish and the resistant cells (frequency of 5×10^{-6}) were permitted to regrow into colonies on the same

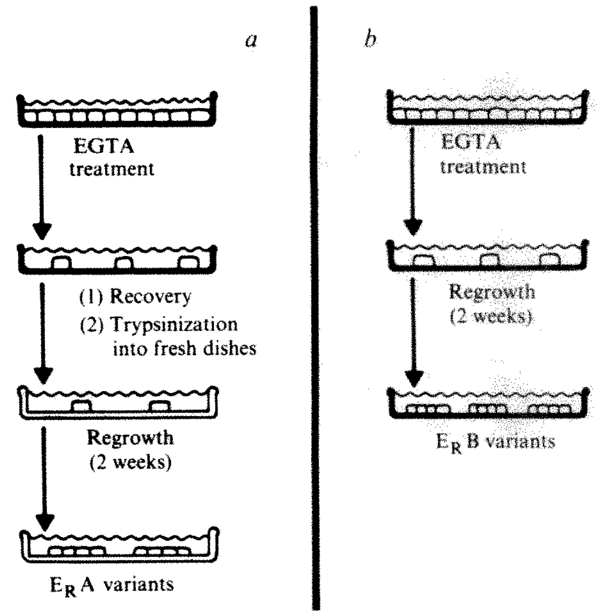

Fig. 1 Protocols for selection of EGTA detachment-resistant variants of rat neuroblastoma cells. Rat neuroblastoma cells (the B104 clone) were grown in 60 mm tissue culture dishes in DMEM (plus 7.5% fetal calf serum and penicillin and streptomycin) until they were just confluent ($\sim4\times10^6$ cells). In both selection protocols (*a* and *b*), the cell layer was rinsed twice with PBS and treated with 0.5 mM EGTA in PBS at 37 °C for 30 min by gentle shaking. Loosely-adherent cells were removed by gentle pipetting and the dish surface was rinsed twice with PBS. In protocol *b*, the dishes were refed with serum-containing medium to allow cell regrowth as a few sparse colonies on the SAM-coated substratum over a 2-week period. In protocol *a*, serum-containing medium was added back to the treated dishes for 4 h to permit recovery from EGTA-induced damage; the resistant cells were then trypsinized into fresh dishes to allow cell regrowth as a few sparse colonies over a 2-week period. Both of these protocols were repeated two more times before cloning of EGTA detachment-resistant cells.

0028-0836/80/270077-03$01.00

Table 1 Growth and differentiation of variants

Property	Cell type and response			
	B104	C_R4	E_RA12	E_RB9
(1) Density-dependent inhibition of growth*	−(>6)§	−(>5)§	−(>4)§	+(1.2)
(2) Form neurites in serum-containing medium	−	−	−	+
(3) Form neurites in serumless medium†	+	+	−‖	+
(4) Form neurites on SAM-coated substrata‡	−	−	−	+

The designation + indicates that more than 25% of the cells responded; − indicates that less than 1% respond.

*As determined by multilayering of cells and continued high DNA synthesis in cultures after confluence of the culture had been achieved. The numbers in parentheses are saturating densities (cells per cm^2 $\times 10^{-5}$).

†At 50% confluence of the culture, the cell layer was rinsed twice with PBS and refed with DMEM lacking serum. Twenty-four hours later, the culture was microscopically evaluated for neurite formation.

‡SAM-coated substrata (on 60 mm tissue culture dishes) were formed by growing rat C6 glioma or rat B104 neuroblastoma cells to confluence, detaching them by EGTA treatment, and rinsing the SAM layer with PBS before inoculating 5 ml of serum-containing medium containing 5×10^5 cells. The cells were grown for 48 h before evaluating whether they had formed neurites.

§Cells are multilayered at this density.

‖These cells elongated and fused with neighbouring cells to form multinucleated syncytia.

dish. This selection was performed three more times with the lectin showing much less of a cytotoxic effect on each subsequent treatment. This variant is referred to as C_R4.

The growth properties and morphology of all four cell types were determined. The doubling time during exponential growth was similar for 'wild-type' B104, E_RA 12, E_RB9, and C_R4 cells (18–20 h). B104, E_RA 12 and C_R4 cells grew to a very high density with multilayering of cells (Table 1). E_RB9 cells differed in that they became density-inhibited when they formed a criss-cross array of neurites at higher density (Fig. 2*d*) without the cell body alignment characteristic of the parental B104 cells (Fig. 2*a*). They differed from the other cells in containing neurites at any cell density in serum-containing medium (Fig. 2*c*, *d*), except for an initial 12–24 h recovery from subculturing damage. These cells are essentially constitutive for neurite formation and are less spread over the substratum than the E_RA 12 (Fig. 2*e*) or 'wild-type' B104 cells. C_R4 cells tend to be somewhat epithelioid in appearance (data not shown).

The ability of these cells to form neurites was then tested in various experimental conditions (Fig. 2 and Table 1). The B104 cells only formed neurites when they were starved of serum for 24 h (Fig. 2*b*). They did not form neurites when grown in serum-containing medium on substrata coated with rat C6 glioma or neurite-containing B104 neuroblastoma SAMs (generated by prior growth of these cells to confluence and EGTA-mediated detachment). The E_RB9 cells contained neurites in all experimental conditions tested. The E_RA12 variant did not form neurites in any condition and underwent massive fusion within 24 h in serumless medium to form highly elongated 'myotube-like' syncytia containing many nuclei. Also, at low density in serumless medium (Fig. 2*f*), the syncytia only contained 2–4 nuclei; with cells approaching confluence, the syncytia contained as many as 20 nuclei. These elongated cells frequently spanned the entire microscope field, and there was no evidence of growth cone formation in these cells. There was no appreciable syncytia formation when these cells were in serum-containing medium. C_R4 cells were similar to B104 cells in their ability to form neurites in serumless medium but not in serum-containing medium or during growth on SAM-coated substrata (Table 1). Thus, the selection protocol based on EGTA-mediated detachability and regrowth

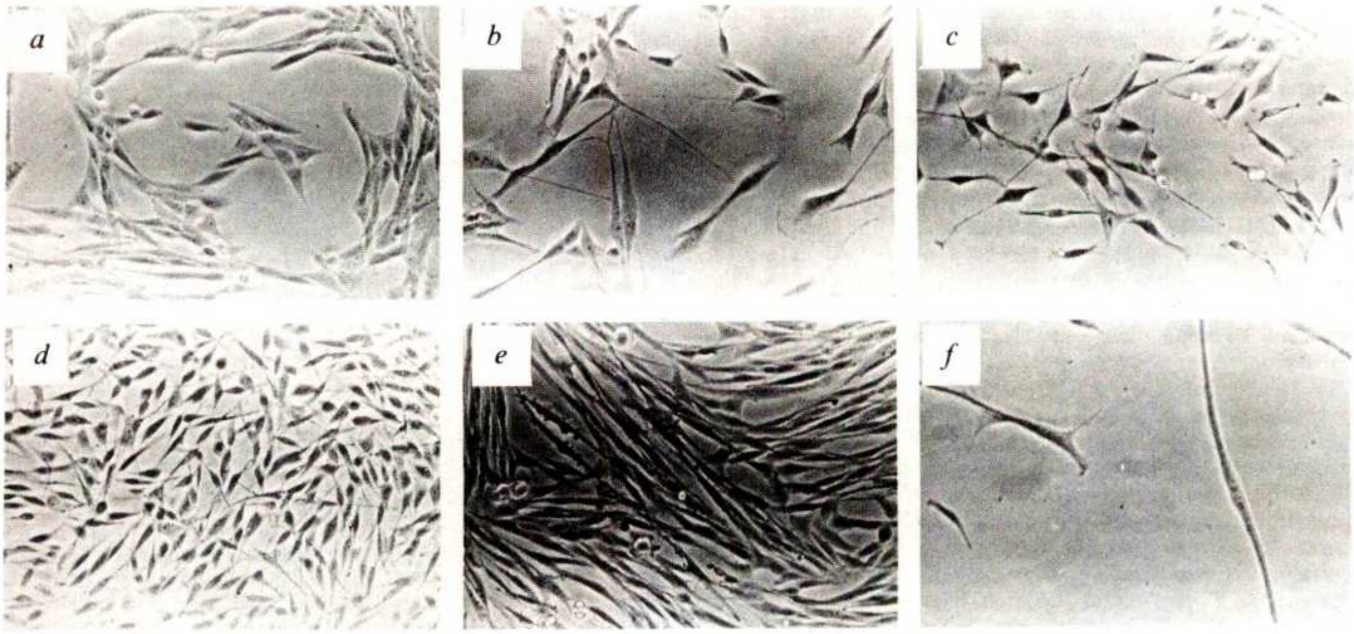

Fig. 2 Morphology and differentiation of EGTA detachment-resistant variant cells. Different cell types were plated into 60-mm tissue culture dishes at various densities and permitted to grow for at least 48 h before photographing the cultures under phase contrast optics (×90). For serumless cultures, the cell layer was rinsed twice with PBS and refed with serumless DMEM for 24 h before photography. The following are displayed: *a*, sparse B104 cells; *b*, neurite-containing B104 cells in serumless medium; *c*, sparse E_RB9 cells in serum-containing medium (note extensive neurite formation); *d*, density-inhibited E_RB9 cells in serum-containing medium (note the extensive array of criss-crossed neurites and the absence of alignment of cell bodies); *e*, E_RA12 cells as they approach confluence in serum-containing medium; and *f*, E_RA12 cells in serumless medium.

Table 2 Tumour formation in nude mice

Cell line	Tumour incidence		
	10^4 cells	10^6 cells	10^7 cells
B104	4/4 (3)	4/4 (1.5)	4/4 (1.5)
C_R4	4/4 (3.5)	4/4 (2)	4/4 (1.5)
E_RB9	0/4 (–)	4/4 (4)	4/4 (3)
E_RA12	0/4 (–)	0/4 (–)	0/4 (–)

Confluent cultures were rinsed twice with PBS and treated with 0.5 mM EGTA in PBS to detach cells. The cells were pelleted by centrifugation and washed once with serumless DMEM. The cells were suspended in serumless DMEM. 10^4, 10^6, or 10^7 cells were inoculated subcutaneously into each athymic nude mouse in 0.1 ml aliquots. Animals were palpitated twice a week to detect tumour formation. Tumour incidence is given as the number of tumour-bearing animals (always resulting in animal death)/number of animals inoculated. The numbers in parentheses indicate the number of weeks required to grow a 1 cm-diameter tumour.

on two different substrata generated variants strikingly different in their ability to generate neurites; both types of variant were distinct from respective parent cells.

The variant cells were also tested for their ability to form tumours in athymic nude mice (Table 2). Three different inocula of EGTA-detached cells were used, and mice were examined for tumour formation over a 3-month period. At all three inocula sizes, 'wild-type' B104 and C_R4 cells formed tumours in all mice with comparable speed. In these experiments, tumour formation always led to death of the animal. Even though E_RB9 cells are density-inhibited in culture, they formed tumours in these animals, although more slowly than B104 cells. E_RA12 cells, on the other hand, did not form tumours in any of the animals even at the highest inoculum size (10^7 cells); these cells are not density-inhibited in culture.

Thus the two EGTA selection protocols generated variants differing widely in tumorigenic potential and neurite differentiation. There is clearly no correlation between tumorigenesis and density sensitivity during *in vitro* growth. Regrowth of EGTA-treated cells on SAM-coated substrata selects for E_RB neurite-constitutive cells which apparently have lost the serum sensitivity for neurite formation as expressed in the parental cells; neurite extension and cell division are clearly not mutually exclusive events in these cells. The E_RA selection generates variants with an altered surface membrane that permits efficient cell fusion but not growth cone formation; the extensive elongation of these cells may also reflect some perturbation of cytoskeletal organization. Further study of these three variant classes should assist in establishing what cell surface properties are important in differentiation of these neural cells and in tumour formation in an appropriate host.

Many of these experiments were performed during a sabbatical leave in the laboratory of Dr Gordon Sato at the University of California, San Diego. Thanks are extended to Ms Bonnie Wolf for assistance in the tumorigenesis studies. L.A.C. was a Career Development Awardee of the NCI (1-K04-CA70709).

Received 29 January; accepted 2 April 1980.

1. Augusti-Tocco, G. & Sato, G. *Proc. natn. Acad. Sci. U.S.A.* **64,** 311 (1969).
2. Schubert, D., Humphreys, S., Baroni, C. & Cohn, M. *Proc. natn. Acad. Sci. U.S.A.* **64,** 316 (1969).
3. Schubert, D. *et al. Nature* **249,** 324 (1974).
4. Culp, L. A.,Ansbacher, R. & Domen, C. (in preparation).
5. Culp, L. A. & Black, P. H. *J. Virol.* **9,** 611 (1972).
6. Rosen, J. J. & Culp, L. A. *Exp Cell Res.* **107,** 139 (1977).
7. Culp, L. A. *J. Cell Biol.* **63,** 71 (1974).
8. Weiss, L., Poste, G., MacKearnin, A. & Willett, K. *J. Cell Biol.* **64,** 135 (1975).

0028-0836/80/270079-02$01.00

Ammonia inhibits phagosome–lysosome fusion in macrophages

A. H. Gordon*, P. D'Arcy Hart† & M. R. Young†

* Biophysics Division and †Laboratory for Leprosy & Mycobacterial Research, National Institute for Medical Research, Mill Hill, London NW7 1AA, UK

When foreign bodies, including many microorganisms, are ingested by cultured macrophages, they become enclosed in phagosomes, with which lysosomes usually fuse and then discharge their enzymes and other contents into the resulting phagolysosomes. Such fusion is, however, diminished or absent after the phagocytosis of some pathogens, notably *Mycobacterium tuberculosis*[1] and *Toxoplasma gondii*[2]. Assuming that the nonfusion is due to active inhibition by the intraphagosomal microbe, identification of an inhibitor should clarify the lysosomal control mechanism. It has been suggested that strongly acidic sulphatides present in virulent *tuberculosis*, which, like other substances with polyanionic structural features, can themselves block phagosome–lysosome fusion (P-LF)[3–5], may contribute to the negative lysosome response to ingested tubercle bacilli[4]. We report here another possibility, based on inhibition of fusion of yeast-containing phagosomes by filtrates from cultures of tubercle bacilli on traditional-type defined media; we show that the ammonia content of such filtrates is sufficient to account for their effect. This inhibition of fusion seems to be an hitherto unrecognized intracellular consequence of added ammonia, in striking contrast to the enhancement produced by some lipophilic amines[3].

Filtrates were obtained from surface-pellicle cultures of either *M. tuberculosis* virulent human strain H37Rv after 2–4 months on Ratledge–Hall 'normal' liquid medium[6], containing asparagine as sole nitrogen source, or *M. tuberculosis bovis* strain AN5 after 10 weeks on a modified Dorset–Henly liquid medium of similar composition. Lysosomes of mouse peritoneal macrophages in monolayer culture were prelabelled with acridine orange (AO) for darkfield vital fluorescence microscopy (VFM), or with ferritin for electron microscopy (EM)[3]. The cells were allowed to ingest fresh or 150-krad γ-ray-irradiated *Saccharomyces cerevisiae*, an organism which induces P-LF. Fusion was assessed by transfer of label into the yeast-containing phagosomes. With this test system (see ref. 3 for details), substantial inhibition of P-LF was obtained when the monolayers were exposed to either type of culture filtrate (diluted 1:5 or 1:10 in balanced salt solution (BSS)[7]) at 37 °C for 60 min immediately before the yeasts were offered for ingestion and then continuously until examination 45–60 min later (exposure to culture filtrate not being interrupted at any stage).

Experiments involving distillation, trapping in H_2SO_4 and gas chromatography suggested activity by a volatile base. Therefore, ammonia, a known constituent of *M. tuberculosis* cultures[8], was estimated in the culture filtrates, using glutamic transaminase and NADH (Sigma kit 170-UV), and was found to be as high as 20 mM. Replacement of culture filtrate by ammonia was tried and found to be effective in inhibiting P-LF, both by overall assessment using VFM and by quantitative assessment (based on screening surveys[1]) using EM (Table 1*a*, *b*). (Quantitative differences in estimating fusion between these two methods, and between fresh and irradiated yeasts, have been discussed elsewhere[3].) Corresponding to the formation of phagolysosomes by P-LF, degranulation (loss of lysosomes) takes place. Assessed by labelling the surviving lysosomes with AO, degranulation was much reduced by ammonia treatment of macrophages (Table 1*c*).

Ammonia rapidly enters lysosomes of macrophages and leaves rapidly after removal from the medium[9]. In the present

© 1980 Macmillan Nature Ltd

Table 1 Effect of ammonia on phagosome–lysosome fusion and degranulation in macrophages after ingestion of yeasts

Protocol	Optical system	Observation	Fusion or degranulation (%)	
			Untreated	Ammonia-treated
a	Fluorescence microscopy (AO label)	Phagosome–lysosome fusion	70	10
b	Electron microscopy (ferritin label)	Phagosome–lysosome fusion	92*(350)†	55*(390)†
c	Fluorescence microscopy (AO label)	Degranulation	90	25

a, Macrophage monolayers, after prelabelling with AO, were treated for 45 min with NH_4Cl (10 mM) in BSS at 37 °C and then exposed for a further 50 min to fresh yeasts at 10^6 cells per ml, the NH_4Cl still being present. (The results given are representative of 20 experiments, in 4 of which inhibition was evident using 1–2 mM NH_4Cl.) *b*, Macrophage monolayers, after prelabelling with ferritin, were treated for 45 min with NH_4Cl (5 mM) in BSS, then exposed for 30 min to irradiated yeasts (10^7 cells per ml). After washing to remove excess yeasts, incubation was continued for 45 min and the macrophages were then fixed. NH_4Cl (5 mM) was present throughout (including the yeast pulse and the washing). *c*, Similar to *a* but the yeasts, at 5×10^7 cells per ml, were applied for 30 min only, after which incubation was continued for 150 min, NH_4Cl (10 mM) being present throughout all stages; AO labelling was at the end of this period, immediately before examination. Figures denote percentage loss of AO-labelled lysosomes (results are representative of six experiments).

*Difference between results is significant ($P < 0.01$).

†Number of individual phagosome profiles counted.

work the lysosomes were seen to swell to a degree dependent on dose (evident by VFM and EM). At concentrations up to 10 mM for 2–3 h at 37 °C, the cells remained apparently healthy by light microscopy, with normal uptake of yeasts; by EM, autophagic vacuoles were few and mitochondria seemed normal in appearance. Moreover, when ammonia-treated macrophages that showed inhibition of P-LF were washed well with BSS and incubated for several hours, the lysosomal swelling declined and normal fusion pattern was restored.

Ethylamine and methylamine hydrochlorides were tested in the yeast system and showed some inhibitory activity. In view of this, and the behaviour of other amines tested by us previously, an interesting series with respect to effect on P-LF emerges. Lipophilic secondary or tertiary amines (for example, di- and tri-*n*-butylamine, dihexylamine, dibenzylamine, chloroquine and tetracaine) accelerated P-LF; lower tertiary and secondary amines (such as diethylamine and triethylamine) enhanced slightly; most primary amines tested (for example, *n*-butylamine and ethanolamine) also enhanced slightly[3]. Now we have the opposite effect, that is, some inhibition by the lower primary amines, ethylamine and methylamine, and much stronger inhibition by ammonia. The negative or weakly positive results of testing individual amines other than ammonia for inhibitory activity are in accord with further experiments with culture filtrate which indicate that the latter's ammonia content is sufficient to account for most, if not all, of its fusion-inhibitory activity in the yeast system. These experiments comprised comparison of activities of NH_4Cl and culture filtrate at equivalent ammonia concentrations, and repetition of the trapping experiment mentioned above, but after preliminary removal of the ammonia by treatment with glutamic dehydrogenase, NADH and α-ketoglutarate.

Ammonia raises intralysosomal *p*H (ref. 9) and inhibits degradation of lysosomal proteins[10–12]; so also do some other bases, including methylamine, tributylamine and chloroquine[9–11,13,14]. The present observation that ammonia has the opposite effect on P-LF to that of chloroquine and tributylamine makes it unlikely that its inhibitory activity operates through interference with *p*H and protein metabolism.

Thus, judged by fluorescence and electron microscopy, and by lysosomal degranulation, ammonia can inhibit P-LF in macrophages when *S. cerevisiae* is the target. Moreover, *M. tuberculosis* produces sufficient ammonia when grown *in vitro* to account for most or all of the fusion-inhibitory effect of its culture fluid in this yeast system. The possibility that *M. tuberculosis* achieves its fusion-inhibitory effect by the production of ammonia or relevant amines within phagosomes of macrophages is now being studied.

We thank Mr D. Andrews for a sample of culture filtrate, Mrs S. N. Payne and Mr N. L. Hemmings for analyses, and Miss K. H. Sullivan, Mr J. B. Gawor and Mr I. D. Parker for technical help.

Received 22 February; accepted 24 April 1980.

1. Armstrong, J. A. & D'Arcy Hart, P. *J. exp. Med.* **134,** 713–740 (1971).
2. Jones, T. C. & Hirsch, J. G. *J. exp. Med.* **136,** 1173–1194 (1972).
3. D'Arcy Hart, P. & Young, M. R. *Nature* **256,** 47–49 (1975); *Expl Cell Res.* **114,** 486–490 (1978); *Expl Cell Res.* **118,** 365–375 (1979); in *Mononuclear Phagocytes—Functional Aspects* (ed. van Furth, R.) (Martinius Nijhoff, The Hague, in the press).
4. Goren, M. B., D'Arcy Hart, P., Young, M. R. & Armstrong, J. A. *Proc. natn. Acad. Sci. U.S.A.* **73,** 2510–2514 (1976).
5. Geisow, M. J., Beaven, G. H., D'Arcy Hart, P. & Young, M. R. *Expl Cell Res* **126,** 159–165 (1980).
6. Ratledge, C. & Hall, M. J. *J. Bact.* **108,** 312–319 (1971).
7. Hanks, J. H. & Wallace, R. E. *Proc. Soc. exp. Biol. Med.* **71,** 196–200 (1949).
8. Long, E. R. *Chemistry and Chemotherapy of Tuberculosis* 3rd edn, 80–85 (Baillière Tindall & Cox, London, 1958).
9. Ohkuma, S. & Poole, B. *Proc. natn. Acad. Sci. U.S.A.* **75,** 3327–3331 (1978).
10. Seglen, O., Grinde, B. & Solheim, A. E. *Eur. J. Biochem.* **95,** 215–225 (1979).
11. Reijngoud, D-J., Oud, P. S., Káš, J. & Tager, J. M. *Biochim. biophys. Acta* **448,** 290–302 (1976).
12. Wibo, M. & Poole, B. *J. Cell Biol.* **63,** 430–440 (1974).
13. Reijngoud, D-J. & Tager, J. M. *FEBS Lett.* **64,** 231–235 (1976).
14. Goldstein, J. L., Brunschede, G. Y. & Brown, M. S. *J. biol. Chem.* **250,** 7854–7862 (1975).

Does the variability of the cell cycle result from one or many chance events?

Arthur L. Koch

Department of Biology, Indiana University,
Bloomington, Indiana 47405

Smith and Martin[1,2] proposed the transition probability (TP) model to explain the significance of the variability of the cell cycle length of individual cells within a clone or culture. This postulates that the cell cycle length consists of a fixed period of time, which is the same for all members of the population, plus a variable period which is distributed according to a negative exponential function among the individual cell cycles. This variable part is contained entirely within G1, may be controlled hormonally by the organism, and is assumed to result from a single first order random process that terminates the variable part of the cell cycle with constant probability. As originally proposed, the model failed to account for timing of the fastest third of the population[3]. Minor and Smith[4] assumed that there is biological variability in the previously presumed constant part of the cycle and that this variability accounts for the failure to see an abrupt discontinuity. They proposed that most of this kind of variation can be cancelled out by comparing sister cells. Thus, they proposed a second plot to test their model, the β-plot. This is a two-cycle semi-logarithmic plot of the percentage of sister-sister cells having a smaller difference in age at division than the time value corresponding to the abscissa of the graph. Their model predicts a straight line starting at 100% at time zero. Any model would require this value at time zero, but theirs requires that the plot be straight and parallel to the terminal slope of the α-plot. Shields and Smith[5] and Shields[6] have convincingly shown that for tissue culture cells of both mouse cell lines and *Staphylococcus albus*, the β-plots are linear for 97–98% of the cell populations and parallel to the α-plots. This has been taken as strong support for the TP model. Recently, in

developing computer simulation of a growth controlled (GC) model[7], I found that certain properties, such as the linearity of β-plots, are very sensitive to the presence of subpopulations of cells with longer doubling times. My major purpose here is to point out three statistical aspects of the cell cycle that are strongly influenced by growth rate heterogeneity for any model of the cell cycle.

The GC model as used here assumes that the sizes at successive divisions are uncorrelated and that the cell division produces daughter cells of equal size. I have assumed both a gaussian normal distribution and a negative exponential distribution and that growth of individual cells may follow exponential, linear or bi-linear growth laws. The negative exponential distribution was chosen because it is non-normal, moderately skewed in the positive direction and is the form assumed by the TP model. In addition, such a distribution would apply if the actual separation of the completed daughter cells proceeds by a process whereby the splitting into two separate cells has a constant probability with time[8] after the cells had physiologically divided.

Figure 1 shows computer-generated α- and β-plots for various combinations of distributions and growth laws. Calculation has been made for the case in which the coefficient of variation of the sizes of cells in the act of division (cv_d) is 0.1. It can be seen that the negative exponential–linear growth model gives linear β-plots; it is, in fact, equivalent to the TP model. However, the α-plot for this case has a quite different terminal slope. When exponential growth is assumed, both choices for the distributions of sizes at division give parallelism between the β-plot and the terminal part of the α-plot, but both are curved downwards. Table 1 gives the statistical parameters of these distributions and other statistics for these submodels.

For a single case, that of the prokaryote, *Escherichia coli*, there are reasons independent of the statistical data for choosing the GC model corresponding to the first line of Table 1. The distribution of sizes of cells showing constriction in electron micrographs is approximately gaussian and not exponential[9,10]. The coefficient of variation of sizes of cells engaged in cell division is small ($cv_d = 8$–14%)[11–13]; the rate of macromolecular synthesis is exponential[14]. Evidence for equality of cell division in producing equal-sized daughters is presented elsewhere[10,13], as are other types of evidence in favour of the model[12,13,15].

Some, but not all, of the statistical data for *E. coli* concerning cell cycle lengths agree with this GC submodel. The coefficient of variation of the distribution of ages at division ($cv_\tau = 20$–25%) is very nearly twice the coefficient of variation of the sizes of cells at division ($cv_d = 8$–14%)[13]. The model also predicts values of ρ_{ss}, the correlation coefficient of sister:sister ages at division of about 0.5 (see first line of Table 1). Values this high or higher have been observed in all studies except where cell division is very asymmetrical.

Certain experimental findings with *E. coli* and other prokaryotes are not predicted but are generally observed. They are: (1) that the measured correlation of ages at division of mother and daughters, ρ_{md}, is usually observed to be more positive as values near -0.5 predicted by the model (Table 1); (2) that the measured skewness of the distribution of ages at division, γ_1, is generally moderately positive instead of being nearly zero as predicted by the theory (Table 1); (3) that the β-plot is linear instead of exhibiting a downward curvature (see Fig. 1). Other choices of growth laws or distributions of division sizes do not give agreement (see Table 1 and Fig. 1). However, these three discrepancies can be fully resolved in a way which leaves the basic model intact by assuming that a small fraction of the cells in the population grow more slowly than do the majority. From Table 1 it can be seen that admixture with 2–3% more slowly growing cells decreases ρ_{md} and increases γ_1 towards values typically observed in the literature. Figure 2 shows α- and β-plots for the gaussian–exponential GC model with $cv_d = 0.1$ repeated from Fig. 1 together with the plots for hypothetical populations in which

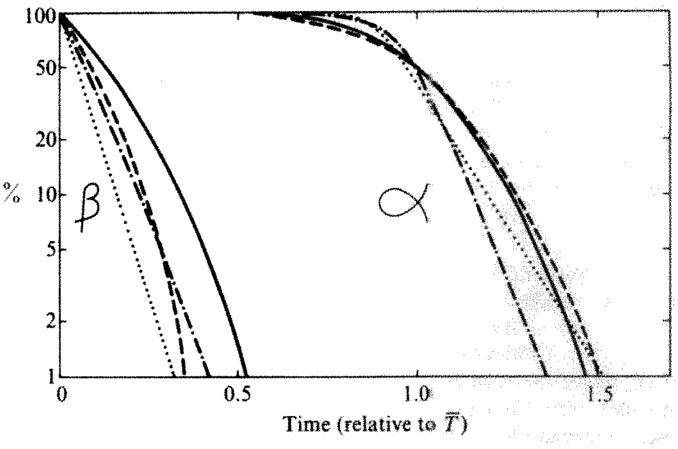

Fig. 1 α- and β-plots for four submodels of the growth controlled model of the cell division cycle. It was assumed that the coefficient of variation of the sizes of cells at division, cv_d, is 0.1 and that cell division partitions cell substances precisely. The submodels differ in the shape of the distribution of sizes at cell division and the mode of growth:

Distribution	*Growth law*	
Gaussian	Exponential	——
Gaussian	Linear	– – – –
Negative exponential	Exponential	– · – · –
Negative exponential	Linear	·····

Table 1 Statistical properties of growth controlled models of the cell cycle

Division distribution	Growth law	Coefficient of variation of the age distribution cv_τ	Skewness γ_1	Kurtosis† β_2	Sister : sister correlation ρ_{ss}	Mother : daughter correlation ρ_{md}
Gaussian	Exponential	0.204	-0.001	2.989	0.501	-0.501
Admixed with:						
2% delayed 0.57 Gen.		0.217	$+0.271$	3.758	0.775	-0.226
3% delayed 0.52 Gen.		0.219	$+0.305$	3.697	0.877	-0.125
Gaussian	Linear	0.221	0	2.886	0.200	-0.400
Gaussian	Bi-linear*					
$C = 1.3$		0.215	0	2.916	0.501	-0.501
$C = 1.6$		0.175	0	2.916	0.501	-0.501
Negative exponential	Exponential	0.136	0	4.651	0.502	-0.501
Negative exponential	Linear	0.157	$+1.196$	6.418	0.200	-0.399

All models are calculated for the assumption that the size of cells at division has a coefficient of variation (cv_d) of 0.1.

*C equals the size of the cell at which the rate of growth doubles relative to the mean birth size.

†For a normal distribution $\beta_2 = 3$.

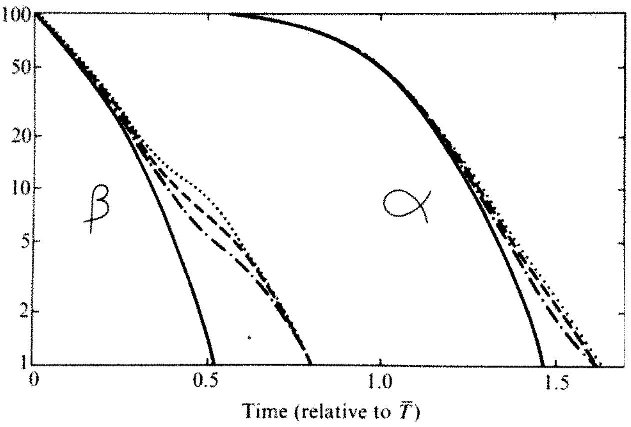

Fig. 2 The effect of straightening the β-plot by the admixture of a few per cent of more slowly growing cells. Calculations are for the gaussian distribution of sizes at division, exponential growth and $cv_d = 0.1$. ———, No admixture; –·–·–, 2% delayed 0.57 of $\bar{T}$; – – – –, 3% delayed 0.52 of $\bar{T}$; …., 4% delayed 0.49 of $\bar{T}$.

2, 3 or 4% are presumed to be delayed in division for about 0.5 of a mean generation compared with the majority population. In each percentage of admixture, I have fitted for the delay that gives the most linear β-plot.

The following conclusions follow from these considerations. (1) A small subfraction of slowly growing cells can greatly affect some but not others of the statistical properties of the life-lengths of cells in a growing culture. The coefficient of variation of the ages at division, and its relationship to the variation in size at division are not as responsive to the presence of a small proportion of more slowly growing cells. (2) The mother-daughter correlation, ρ_{md}, the skewness and kurtosis of the age distribution, γ_1 and β_2, and the curvature of the β-plots are very sensitive to admixture and therefore give little information about the events timing the cell cycle of the bulk of the cells of the population. (3) If there were a very few per cent of a population growing more slowly than the bulk of the cells, the transition probability model would fit the available data for a variety of cell lines very poorly. (4) In one case, that is, for *E. coli*, the gaussian–exponential submodel of the growth controlled model is known to apply because of the results of measurements not involving cell cycle length observations. These measurements involve electron microscopy, molecular biological measurements and autoradiography. In addition, the statistical properties not sensitive to admixture are consistent with the model. Consequently, for this case we believe that admixture of a small amount of a more slowly growing population accounts for the properties mentioned in (2). (5) Because it is virtually impossible to eliminate the possibility of a small, slowly growing subfraction experimentally, the measures mentioned in (2) are less useful and should not be used as a point of argument. (6) It is argued that instead, measurements of the distribution of cell properties at division and at other critical times in the cell cycle, and the growth kinetics of individual cells throughout the cell cycle be used as the basis for cell division models that apply to the majority class of cell populations as other cell types are studied. (7) Although the TP model may function for some cell lines, a single stochastic even cannot be adduced as timing the cell division cycle in any cell line based on the available types of data.

Received 4 December 1979; accepted 8 March 1980.

1. Smith, J. A. & Martin, L. *Proc. natn. Acad. Sci. U.S.A.* **70,** 1263–1267 (1973).
2. Smith, J. A. & Martin, L. in *Cell Cycle Controls* (eds Padilla, G. M., Cameron, I. L. & Zimmerman, A.) 43–60 (Academic, New York, 1974).
3. Pardee, A. B., Shilo, B.-Z. & Koch, A. L. *Cold Spring Harb. Conf. Cell Proliferation* **6,** 373–392 (1979).
4. Minor, P. S. & Smith, J. A. *Nature* **248,** 241–243 (1974).
5. Shields, R. & Smith, J. A. *J. cell. Physiol.* **91,** 345–356 (1977).
6. Shields, R. *Nature* **273,** 755–758 (1978).
7. Koch, A. L. & Schaechter, M. *J. gen. Microbiol.* **29,** 435–454 (1962).
8. Powell, E. O. *J. gen. Microbiol.* **18,** 382–417 (1958).
9. Woldringh, C. L. *J. Bact.* **125,** 248–257 (1976).
10. Woldringh, C. L., De Jong, M. A., Van en Berg, W. & Koppes, L. *J. Bact.* **131,** 270–299 (1977).
11. Koch, A. L. *J. gen. Microbiol.* **43,** 1–5 (1966).
12. Schaechter, M., Williamson, J. P., Hood, J. R. Jr & Koch, A. L. *J. gen. Microbiol.* **29,** 421–434 (1962).
13. Koch, A. L. *Adv. microbial Physiol.* **16,** 49–98 (1977).
14. Ecker, R. E. & Kokaisl, G. *J. Bact.* **98,** 1219–1226 (1969).
15. Newman, C. & Kubitschek, H. E. *J. molec. Biol.* **121,** 461–471 (1978).

The insulin gene is located on chromosome 11 in humans

David Owerbach*, Graeme I. Bell*, William J. Rutter* & Thomas B. Shows†

*Department of Biochemistry & Biophysics, University of California, San Francisco, California 94143
†Biochemical Genetics Section, Roswell Park Memorial Institute, New York State Department of Health, Buffalo, New York 14263

The polypeptide hormone insulin is required for normal glucose homeostasis. Insulin deprivation results in diabetes, a disease affecting up to 5% of the human population[1,2]. In some animals there are two insulin genes[3]; however, in most others, including humans, a single gene is present. The conclusion that there is a single insulin gene in humans is based on the finding of a single insulin species and on genetic studies involving mutant insulin alleles[4,5]. As the pattern of inheritance of insulin defects is not sex linked, the insulin gene must be located on an autosomal chromosome[5]. Recently, genomic DNA segments containing the human and rat insulin genes have been cloned and the DNA has been sequenced[6–8]. The fact that mouse and rat insulins are identical[3] suggests that the insulin gene sequences and organization are similar. A knowledge of the restriction endonuclease map for the human and mouse insulin genes enables human or mouse insulin DNA sequences to be distinguished in somatic cell hybrids between the two species. In the present study, somatic cell hybrid gene mapping methodologies[9] have been used to determine the chromosome localization[10] of the human insulin gene. Human–mouse cell hybrids with different numbers and combinations of human chromosomes were examined for the presence of specific human chromosomes and the human insulin gene using cloned human and rat cDNA probes. A 14-kilobase DNA fragment containing the human insulin gene was present in some cell hybrids and was easily distinguished from the DNA fragments containing the mouse insulin gene found in all cell hybrids. Co-existence of the 14-kilobase fragment and chromosome 11 indicate that the insulin gene resolves on chromosome 11 in humans.

Human and mouse parental cells were fused with β-propriolactone-inactivated Sendai virus or polyethylene glycol in monolayer culture and hybrid cells were cloned and propagated in hypoxanthine, aminopterin, thymidine (HAT) selection medium (see ref. 9). The cell hybrids were isolated and characterized by isozyme and karyotype analysis (Table 1)[9]. Genomic DNA was prepared from 15 cell hybrids, each containing a full complement of mouse but a reduced number of human chromosomes. This DNA was digested to completion with *Eco*RI restriction endonuclease. The fragments were separated by agarose gel electrophoresis, and then transferred to filters by the method of Southern[11]. Cloned cDNA fragments containing the coding sequences for rat[7] and human[12] preproinsulin mRNA were labelled by nick translation[13] and used as probes for insulin gene sequences in the DNA from human/mouse hybrid cells. Filters were hybridized and washed as described in Fig. 1 legend. Although the human probe cross-hybridizes with mouse DNA sequences, preliminary experiments showed that the best resolution of both human and mouse insulin sequences in cell hybrids was obtained by using a mixed ^{32}P-labelled probe to both rat and

0028-0836/80/270082-02$01.00

Table 1 The distribution of human insulin, LDH A and human chromosomes in human–mouse cell hybrids

			Chromosomes*																											
Hybrid	Insulin†	LDH A‡	1	2	3	4	5	6	7	8	9	10	11	12	13	14	15	16	17	18	19	20	21	22	X	Y	9/X	7/9	X/15	15/X	17/3
WIL-2	−	−	−	−	−	−	−	−	−	+	−	+	−	+	−	−	+	−	+	−	−	−	+	−	+	−					
WIL-8Y	+	+	−	−	−	−	−	+	+	−	−	+	+	−	−	+	−	−	+	+	−	+	+	−	+	−					
TSL-2	−	−	−	+	−	−	+	+	−	−	−	+	−	+	−	−	−	−	−	+	−	+	+	−	+	−					+
TSL-5	+	+	−	−	−	+	+	−	−	−	−	+	+	+	−	−	−	−	+	+	−	−	+	−	−	−					
TSL-6	−	−	−	−	−	−	+	−	−	−	−	+	−	−	−	−	−	−	−	−	+	−	−	−	−	−					+
TSL-8	−	−	−	−	−	−	−	−	−	−	−	−	−	−	−	−	−	−	+	+	−	+	−	−	−	−					
RAS-8	+	+	+	+	+	+	+	+	+	+	−	+	+	+	+	+	+	+	+	+	+	+	+	+	+	−					
RAS-9DT	+	+	+	+	+	+	−	−	+	+	+	+	+	+	−	+	+	+	+	+	+	+	+	+	+	−					
SIR-8	+	+	+	+	+	+	+	−	+	+	+	+	+	+	+	+	+	+	+	+	+	−	+	+	+	+					
XTR-3BSAgA	−	−	−	−	−	+	+	+	+	+	+	+	−	−	−	+	−	−	+	+	+	−	+	−	−	−					
DUA-5	+	+	−	−	+	−	+	−	−	−	−	−	+	−	−	+	+	−	+	+	−	−	+	−	−	−			+	+	
DUM-13	+	+	+	+	+	+	−	+	+	+	−	+	+	−	+	−	+	+	+	+	+	+	+	+	+	−			+		
ALR-2	+	+	+	−	+	+	+	+	+	−	+	+	+	+	+	+	+	+	+	−	+	+	+	−	−	−	+				
JSR-6C	−	−	−	+	+	−	+	−	−	−	−	+	−	−	−	+	+	+	−	+	−	−	−	−	+	−		+			
JSR-24D	+	+	+	−	+	−	+	+	−	+	−	+	+	−	+	+	+	+	+	+	+	+	+	−	+	−		+			

Chromosomally characterized human cell lines were used for parental cells. WIL hybrids (human WI-38 × mouse LM/TK$^-$), RAS hybrids (mouse RAG × human SH 421) and SIR hybrids (human GM 469 × mouse RAG) are derived from chromosomally normal human parental cell lines[22–24]. The remaining hybrid sets were derived using chromosomally characterized human translocation lines for regionally localizing human genes. TSL (GM 2808 × LM/TK$^-$) hybrids involve the [46,XX,t(3;17)(p21;p13)] translocation and segregate the 17qter→17p13::3p21→3pter translocation[25]. XTR (GM 2899 × RAG) hybrids involve the [46,X,t(X:3)(q26;q13)] translocation[26]. DUA (DUV × A9) and DUM (DUV × RAG) hybrids involve the [46,X,t(X;15)(p11;q11)] translocation and segregates the Xqter→Xp11::15q11→15qter and 15pter→15q11::Xp11→Xpter chromosomes[27]. The ALR (AnLY × RAG) hybrids involve the [46,X,t(X;9)(q12;p24)] translocation and segregates the Xqter→Xq12::9p24→9qter chromosome[28]. The JSR (JoSt × RAG) hybrids involve the [46,XX,t(7;9)(q22;p24)] translocation and segregates the 7pter→7q22::9p24→9pter chromosome[29].

*In each hybrid, chromosomes have been determined by Giemsa-trypsin staining[28] and follow the Paris system of human nomenclature[31]. In addition, enzyme markers whose genes have been assigned to each human chromosome, except the Y, have been tested on each hybrid and confirm the chromosome analysis (data not shown)[9,23,32].

†The insulin gene was measured as the 14-kilobase fragment.

‡The LDH A gene has been assigned to chromosome 11 by several laboratories (see ref. 30) and co-segregates with the insulin gene.

human insulin genes and washing the filters at high stringency.

In the control mouse cell line, three DNA fragments of 9, 1.8 and 1.4 kilobases hybridized with ^{32}P-labelled rat–human insulin probe (Fig. 1, channel 1). These results are similar to those obtained with rat DNA[7,8]. As both mouse and rat have two non-allelic insulin genes[3], and as one of the rat insulin genes contains an *Eco*RI site[7,8], the simplest interpretation of the data is that one of the mouse insulin genes also contains an *Eco*RI site. Thus, three DNA fragments containing insulin-specific sequences would be detected.

In the control human cell line (Fig. 1, channel 2), and in all human parental lines used in this study, a single *Eco*RI fragment of 14 kilobases hybridized with the rat–human ^{32}P-insulin probe. This agrees with the findings of Bell *et al.*[6], who showed that the human insulin gene is contained in a 14-kilobase *Eco*RI fragment. The presence of a single-size class of *Eco*RI fragments of human DNA containing insulin gene sequences also provides additional support for the existence of a single insulin gene in humans.

DNA from all 15 cell hybrids contained the mouse *Eco*RI fragments, whereas only some had the 14-kilobase human fragment (see Fig. 1 for representative data). The absence of the 14-kilobase *Eco*RI human fragment indicated the absence of the human chromosome on which the insulin gene is located. As the mouse sequences served as an internal hyridization control, the absence of the human 14-kilobase fragment was not due to other factors such as poor DNA transfer from the agarose gel or loss of DNA from the nitrocellulose filter. The segregation of the human insulin gene, human chromosomes and the chromosome 11 enzyme marker, lactate dehydrogenase A(LDH A) in the 15 human–mouse cell hybrids is shown in Table 1. All 22 autosomes and the X and Y chromosomes were scored both by karyotype and isozyme analysis (Table 1, see also ref. 9). For example, three hybrids (WIL-8Y, TSL-5, DUA-5) contained the human insulin gene but did not retain chromosome 1; it is thus obvious that the insulin gene is not on chromosome 1. The 14-kilobase human insulin fragment was invariably found when human chromosome 11 and LDH A were present in the cell hybrid (Table 1). None of the other chromosomes or enzyme markers co-existed with the 14-kilobase fragment (Table 1). The correlation of human chromosome 11 and the human insulin gene and the lack of correlation with any other human chromosome, conclusively demonstrate the localization of this gene on chromosome 11.

Restriction analysis of somatic cell hybrid DNA is a very useful addition to genome mapping technology. Any gene for which a molecular probe is available can be mapped. Several laboratories have mapped the β-globin genes to the short arm of chromosome 11 (refs 14–17). Our procedure for mapping the human insulin gene includes the use of 10% dextran sulphate in the hybridization mixture, which increases the rate and extent of hybridization with the probe[18]. With 10 µg of cell hybrid DNA and 3×10^4 c.p.m. of probe per cm^2 filter, it is possible to score the insulin-containing DNA fragment in less than 24 h exposure to X-ray film. These conditions permit the use of small numbers of cells (3–6×10^6) which can be obtained either from cell culture or from cells previously frozen for recovery in 10% glycerol, 20% fetal calf serum and tissue culture medium. These frozen cells, previously typed by chromosome and enzyme analyses, can be thawed, washed and used as a source of DNA without growing additional cells and rechecking the chromosome and enzyme complements. Finally, the use of probes and hybridization conditions that detect both mouse and human genes permit the use of mouse genes as an internal standard, thus eliminating external artefacts.

The causes of idiopathic diabetes mellitus are largely unknown. Some forms of the disease can be the consequence of the destruction of insulin-producing β cells of the pancreas after viral infection or by chemicals[1,2]. One example of diabetes, resulting from the production of a mutant insulin with altered biological properties, has also been reported[19]. In juvenile-onset or insulin-dependent diabetes a gene on chromosome 6 near the human lymphocyte antigen D locus (HLA-D) may influence the susceptibility of this form of the disease[2]. The present work demonstrates this locus is not in the vicinity of the insulin gene. There is also a hereditary disposition to the most common form of the disease, maturity-onset or insulin-independent diabetes[1,2]. If maturity-onset diabetes is a consequence of an altered insulin gene, the chromosome localization predicts that there should be a correlation among related diabetic individuals between diabetes and alleles of closely linked genes present on chromosome 11. Several genes have already been localized to specific regions of chromosome 11. The insulin gene may be precisely localized on chromosome 11 by examining hybrids

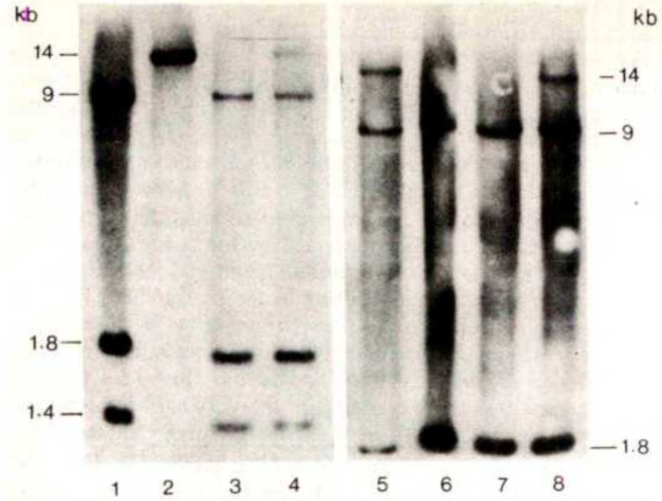

Fig. 1 Analysis of human and mouse insulin related DNA fragments present in restriction endonuclease digests of mouse, human and human–mouse cell hybrid DNA. DNA was prepared from a human T-cell lymphoblastoid cell line, RAG mouse cells and the 15 cell hybrids listed in Table 1. Approximately 4×10^6 cells of each hybrid clone were obtained from cells previously stored frozen in 10% glycerol, 20% fetal calf serum and tissue culture medium and were thawed, washed three times with Hank's balanced salt solution and DNA prepared as previously described[20]. Hybrid cells collected from monolayer culture were also used and prepared in the same way. 20–40 μg of high molecular weight DNA was obtained from 4×10^6 cells. The DNA was digested to completion with endonuclease *Eco*RI. Digested DNA (10–20 μg) was separated by electrophoresis through a 1% agarose slab gel and transferred by the method of Southern[15] to a nitrocellulose filter. pcRI-354 and pcHI-1 were labelled with ^{32}P *in vitro* by nick translation[17] with [α-^{32}P]dCTP and [α-^{32}P]dATP (NEN) to specific activities of $1\text{–}3\times10^8$ c.p.m. per μg. Before hybridization, nitrocellulose filters were treated for 2 days at 42 °C in 10 ml of a mixture of 50% deionized formamide, 5 × SSC (0.75 M NaCl, 75 mM trisodium citrate), 5 × Denhardt's reagent[21], 50 mM sodium phosphate buffer (*p*H 6.5) and 500 μg ml^{-1} sonicated denatured salmon sperm DNA (Sigma). Filters were then hybridized overnight at 42 °C in a 10 ml solution consisting of 50% deionized formamide, 5 × SSC, 1 × Denhardt's reagent, 20 mM sodium phosphate buffer (*p*H 6.5), 200 μg ml^{-1} sonicated denatured salmon sperm DNA, 10% sodium dextran sulphate 500 (Pharmacia)[18] and 2.5 ng ml^{-1} each of heat-denatured ^{32}P-labelled rat and human insulin cDNAs. Filters were then washed three times at room temperature with 2 × SSC, 0.1% SDS for 10 min each followed by three additional washes with 0.1 × SSC, 0.1% SDS at 50 °C for 15 min each. Labelled DNA bands were detected by exposing the filters to X-ray film for 1–5 days in the presence of an intensifying screen (Dupont). The insulin DNA patterns are shown for: (1), mouse RAG cells; 2, human T-cell lymphoblasts; 3, hybrid TSL-2; 4, hybrid SIR-8; 5, hybrid DUA-5; 6, hybrid JSR-6C; 7, hybrid TSL-8; 8, hybrid TSL-5. Fragments of *Hin*dIII-digested λ DNA were used as molecular weight markers. Channels 5–8 were run on a different slab gel and the 1.4-kilobase (kb) mouse insulin DNA fragment migrated off the gel. On long exposures, the autoradiographs of several hybrids (for example, channels 6, 7) showed high backgrounds. On shorter exposures, using the 9.0-kilobase mouse insulin fragment as a reference point, the 14-kilobase region could be accurately scored.

bearing translocations of this chromosome. Extensive information on the genetic loci of chromosome 11 may eventually allow the use of chromosome 11 markers to predict the probability of diabetes in individuals. Eventually, all or parts of chromosome 11 may be used in genetic engineering experiments for correcting diabetes in affected individuals.

We thank Dr R. Pictet for helpful discussions, L. Haley, M. Byers and R. Eddy for technical assistance, and L. Spector and C. Young for assistance in preparing the manuscript. This work was supported by NIH grant AM 21344 to W.J.R. and NIH grants GM 20454 and HD 05196 to T.B.S.

Received 31 December 1979; accepted 16 April 1980.

1. Notkins, A. L. *Scient. Am.* **241,** 62–73 (1979).
2. Craighead, J. E. *New Engl. J. Med.* **299,** 1439–1445 (1978).
3. Humbel, R. E., Bosshard, H. R. & Zahn, H. in *Handbook of Physiology* Section 7, Vol. 1 (eds Steiner, D. F. & Freinkel, N.) 111–132 (Williams & Wilkins, Baltimore, 1972).
4. Gabbay, K. H., DeLuca, K., Fisher, J. N., Mako, M. E. & Rubenstein, A. H. *New Engl. J. Med.* **294,** 911–915 (1976).
5. Gabbay, K. H., Bergenstal, R. M., Wolff, J., Mako, M. & Rubenstein, A. H. *Proc. natn. Acad. Sci. U.S.A.* **76,** 2881–2885 (1979).
6. Bell, G. I., Pictet, R., Rutter, W. J., Cordell, B., Tischer, E. & Goodman, H. M. *Nature* **284,** 26–32 (1980).
7. Cordell, B. *et al. Cell* **18,** 533–543 (1979).
8. Lomedico, P. *et al. Cell* **18,** 545–558 (1979).
9. Shows, T. B. *Isozymes: Current Topics in Biological and Medical Research* (eds Rattazzi, M. C., Scandalios, J. G. & Whitt, G. S.) (Liss, New York, 1977).
10. Shows, T. B. & McAlpine, P. J. *Cytogenet. Cell Genet.* (in the press).
11. Southern, E. M. *J. molec. Biol.* **98,** 503–517 (1975).
12. Bell, G. I. *et al. Nature* **282,** 525–527 (1979).
13. Rigby, P. W. J., Dieckmann, M., Rhodes, C. & Berg, P. *J. molec. Biol.* **113,** 237–251 (1977).
14. Desseroth, A. *et al. Proc. natn. Acad. Sci. U.S.A.* **75,** 1546–1460 (1978).
15. Scott, A. F., Phillips, J. A. & Migeon, B. R. *Proc. natn. Acad. Sci. U.S.A.* **76,** 4563–4565 (1979).
16. Gusella, J. *et al. Proc. natn. Acad. Sci. U.S.A.* **76,** 5239–5243 (1979).
17. Jeffreys, A. J., Craig, I. W. & Francke, U. *Nature* **281,** 606–608 (1979).
18. Wahl, G. M., Stern, M. & Stark, G. *Proc. natn. Acad. Sci. U.S.A.* **76,** 3683–3687 (1979).
19. Tager, H. *et al. Nature* **281,** 122–125 (1979).
20. Wigler, M. *et al. Cell* **16,** 777–785 (1979).
21. Denhardt, D. *Biochem. biophys. Res. Commun.* **23,** 641–646 (1966).
22. Shows, T. B. *Proc. natn. Acad. Sci. U.S.A.* **69,** 348–352 (1972).
23. Shows, T. B., Scrafford-Wolff, L., Brown, J. A. & Meisler, M. H. *Somatic Cell Genet.* **5,** 147–158 (1979).
24. Koch, G. A. & Shows, T. B. *Cytogenet. Cell Genet.* (in the press).
25. Naylor, S. L. *et al.*, in preparation.
26. Naylor, S. L. *et al. Cytogenet. Cell Genet.* (in the press).
27. Champion, M. J., Brown, J. A. & Shows, T. B. *Cytogenet. Cell Genet.* **22,** 498–502 (1978).
28. Shows, T. B. & Brown, J. A. *Proc. natn. Acad. Sci. U.S.A.* **72,** 2125–2129 (1975).
29. Shows, T. B. *et al. Cytogenet. Cell Genet.* **21,** 99–104 (1978).
30. Shows, T. B., Brown, J. A. & Lalley, P. A. *Cytogenet. Cell. Genet.* **16,** 231–234 (1976).
31. ISCN An International System for Human Cytogenetic Nomenclature *Cytogenet. Cell Genet.* **21,** 313–404 (1978).
32. Naylor, S. L., Klebe, R. J. & Shows, T. B. *Proc. natn. Acad. Sci. U.S.A.* **75,** 6159–6162 (1978).

Electrophoresis of proteins in intercellular bridges

Richard I. Woodruff & William H. Telfer

Department of Biology, University of Pennsylvania, Philadelphia, Pennsylvania 19104

Cytoplasmic polarity giving rise at mitosis to daughter cells with distinct but complementary morphogenetic functions has been proposed by Jaffe and co-workers to have transcellular ion currents as one of its essential physiological steps[1]. The clearest evidence is from fucoid eggs in which such currents have been shown to parallel the prospective axis of germination[2,3]. The currents are caused by stabilized accumulations of cation pumps on one side of the cell, and of permeability channels on the opposite side[4]; they are strong enough to suggest that the accompanying gradient in electrical potential could have an electrophoretic effect on the distribution of cytoplasmic constituents, including those that serve as morphogenetic determinants. Although ion currents correlated with axes of morphogenesis have thus been clearly established, their effects on intracellular localizations and morphogenetic activity have remained speculative[5]. We report here evidence that an endogenously generated gradient in electrical potential in the oocyte–nurse cell syncytium of *Hyalophora cecropia* can, in fact, influence the distribution of soluble proteins in a cytoplasmic continuum.

The system consists of seven nurse cells linked to each other and to a single oocyte by seven cytoplasmic bridges, which are clustered in a complex at the centre of the group (Fig. 1). The mitotic divisions giving rise to the eight cells entail incomplete cytokinesis, and the cells subsequently remain in cytoplasmic continuity throughout their 9-month life span[6]. By the time vitellogenesis begins in the oocyte, the bridges are 30-μm wide channels containing no membrane barriers to intercellular diffusion, and little evidence of orientated cytoskeletal elements in their core of cytoplasm[7]. Despite this structural simplicity, nurse cell products migrate into the oocyte in an apparently polarized fashion[8,9]. The bridges provided an opportunity to test for intracytoplasmic electrophoresis because, as we showed previously[7], the equilibrium potential of the nurse cells is several millivolts more negative than that of the ococyte. Furthermore, a negatively charged, fluorescein-labelled, rabbit serum globulin (FSG), when micro-injected into the oocyte, was unable to cross

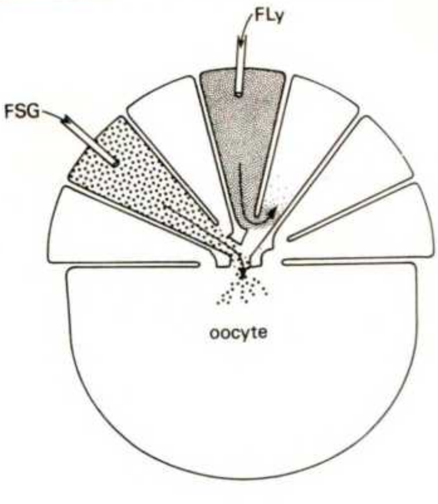

Fig. 1 Diagram of the oocyte and seven nurse cells and the distribution of the seven intercellular bridges that connect them. Also shown are examples of the behaviour of fluorescent serum globulin (FSG) and lysozyme (FLy) after injection into nurse cells.

the bridges into the nurse cells, although it readily moved in the opposite direction when injected into a nurse cell (Fig. 1).

These results showed definitively that the bridges are polarized both electrically and in their ability to transmit protein. Although they were thus consistent with the potential gradient being the polarizing force, satisfactory proof of this proposal needs evidence that basic proteins move through the bridges in the opposite direction from that of the acidic FSG. Our first efforts to test this possibility used fluorescein-conjugated histones, but were thwarted by the tendency of these proteins to adsorb onto cytoplasmic particles at the site of injection before they could diffuse to the intercellular bridges. We have now repeated the experiments with fluorescein-labelled lysozyme (FLy), a basic protein with an isoelectric point of 11.5, and obtained much clearer results. In 40 follicles the oocytes were injected with FLy and in every case fluorescence spread throughout the ooplasm, across the intercellular bridges and into the nurse cells (Fig. 2*a*, *c*). Fixation ranged from 1 to 2 h after micro-injection. In 25 additional follicles a nurse cell was injected and in no case did fluorescence spread to the oocyte (Fig. 2*b*, *d*), even after 2 h of incubation. FLy therefore crossed the bridges only in a direction opposite to that shown earlier for FSG.

An additional difference between FSG and FLy was seen in their capacities to move from nurse cell to nurse cell. In the earlier work FSG micro-injected into nurse cells moved directly to the oocyte, but was never seen to enter the other nurse cells,

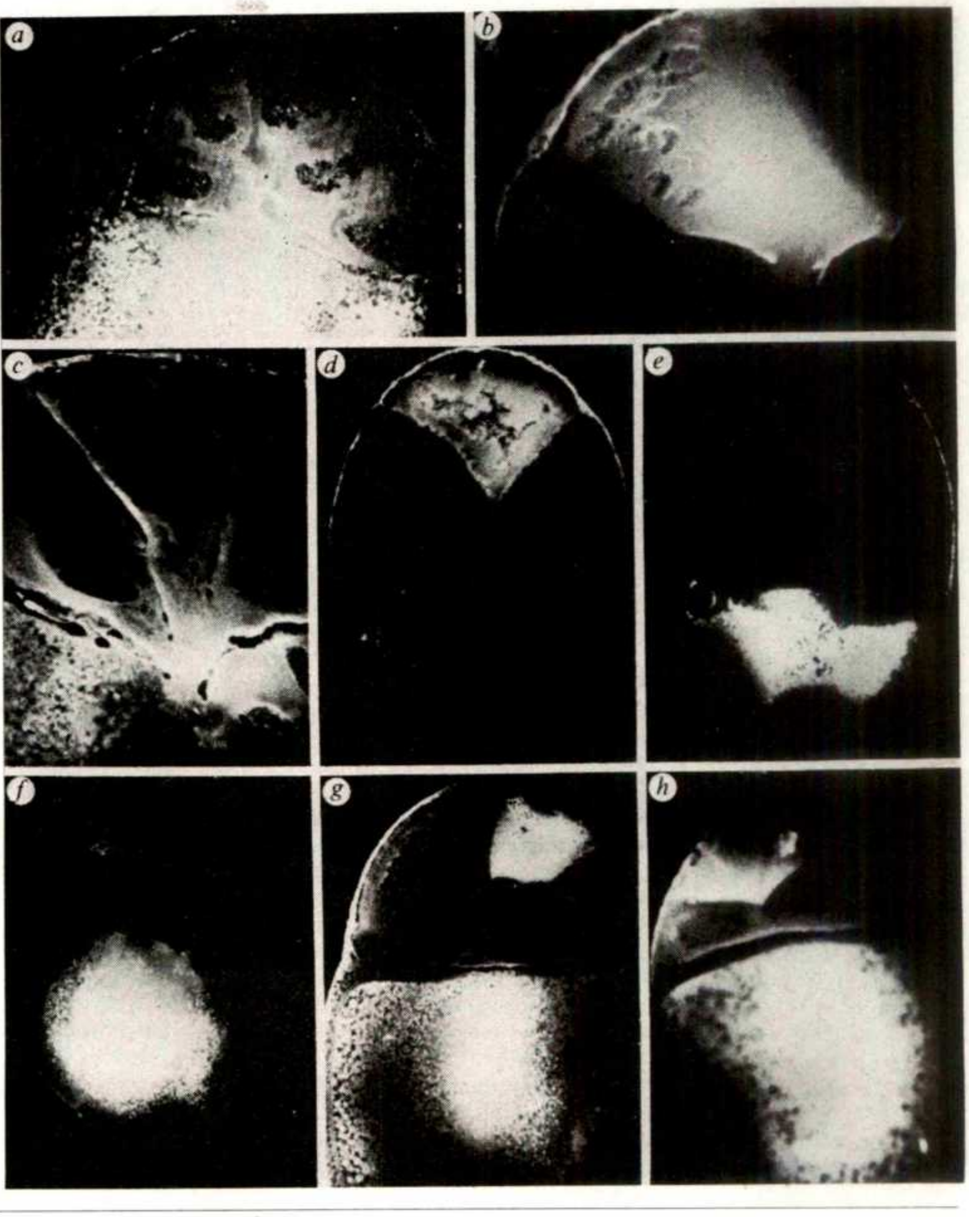

Fig. 2 Fluorescence photomicrographs of follicles injected with proteins labelled with fluorescein isothiocyanate FITC by the method of Nairn[15]. Micro-injection was carried out hydrostatically as described earlier[7]. The follicles were incubated in blood from the animal diluted 1:2 with dissecting solution[16]. In dilutions as great as 1:10, blood protein concentration is still sufficient to maintain membrane permeability and steady-state potentials identical to those which occur in whole blood. Following injection and 1–2 h incubation, follicles were fixed either by freeze substitution (*a*, *c*) or in Carnoy's acid-alcohol (*b*, *d*–*h*), embedded in paraffin, sectioned and examined with a fluorescence microscope. Photographs were taken with Kodak Tri-X pan film (ASA 400). *a*, *c* Fluorescent lysozyme (FLy) micro-injected into oocytes; *b*, *d*, FLy micro-injected into nurse cells. Note in *b* that protein has entered a co-bridged nurse cell (see Fig. 1), but failed to cross into the oocyte. *e*, *f*, Methylcarboxylated FLy (MCFLy) micro-injected into oocytes gave no detectable fluorescence in the nurse cells. *g*, *h*, MCFLy micro-injected into nurse cells. Magnification: in all cases shown, here and in Fig. 3, the width of the nurse cell cap adjacent to the oocyte was about 450 μm.

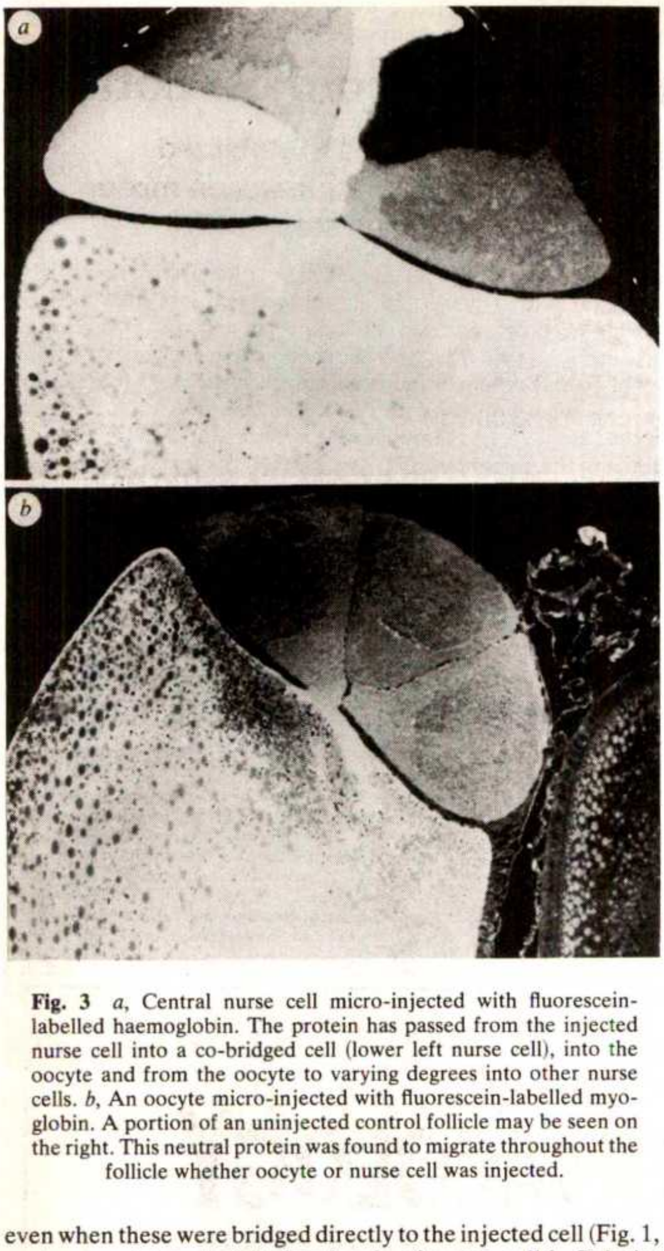

Fig. 3 *a*, Central nurse cell micro-injected with fluorescein-labelled haemoglobin. The protein has passed from the injected nurse cell into a co-bridged cell (lower left nurse cell), into the oocyte and from the oocyte to varying degrees into other nurse cells. *b*, An oocyte micro-injected with fluorescein-labelled myoglobin. A portion of an uninjected control follicle may be seen on the right. This neutral protein was found to migrate throughout the follicle whether oocyte or nurse cell was injected.

even when these were bridged directly to the injected cell (Fig. 1, centre quartet and right hand pair of nurse cells). Polarity apparently extends throughout the bridge complex, and whenever the negatively charged FSG entered this zone, it was unable to move in a direction away from the oocyte. By contrast, when nurse cells were injected with FLy, label entering the zone containing the bridge complex, although unable to proceed into the oocyte, was able to enter the nurse cells directly bridged to the injected cell (Fig. 2*b*). FLy thus seems to diffuse against the electrical potential gradient more readily than FSG.

To confirm that the differences in behaviour resulted entirely from the positive charge of lysozyme and not in part from its small size (molecular weight 14,600), the electrical properties of this protein were altered by methylcarboxylation of its ε-amino groups[10]. The polarity of lysozyme movement in the bridges was now completely reversed—it behaved exactly as FSG had behaved in the earlier work (Fig. 2*e*–*h*), passing from nurse cell to oocyte (48 injections), but not from nurse cell to nurse cell or from oocyte to nurse cell (40 injections). To extend the correlation between charge and mobility through the bridges, we also injected fluorescein-conjugated haemoglobin (21 injections) and myoglobin (28 injections), both of which have isoelectric points close to neutrality, and found that they were able to move in both directions across the bridges (Fig. 3*a*, *b*). When the fluorescein-labelled proteins were compared by electrophoresis in agarose plates at *p*H 7.0, they were found to exhibit the following sequence of mobilities towards the cathode: lysozyme > haemoglobin = myoglobin > methylcarboxylysozyme ⩾ serum globulin. The charge dependence of the mobility of these proteins decisively supports the idea that the potential gradient across the bridges is steep enough to polarize the movement of soluble proteins.

Is the intracytoplasmic electrophoresis observed here a unique adaptation to the transport requirements of the oocyte–nurse cell syncytium or an exceptionally clear example of a more ubiquitous mechanism of polarity? The widespread occurrence of transcellular ion fluxes in developing cells[1,11] suggests that intracytoplasmic potential differences are not unusual. The intercellular bridges, which are a special feature of our system, focus the potential gradient at the equator of the complex, and allow a qualitatively clear result in which fluorescent proteins either do or do not pass through to the uninjected cell. Although the diffusion of our fluorescent probes may prove not to be so dramatically restricted in polarized cells that lack an equatorial constriction, intercellular bridges occur more commonly than might be supposed. Many dividing cells generate transitory bridges of cytoplasm late in cytokinesis[12,13], and ionic communication through these channels attenuates gradually until division is complete[14]. Any dividing cell that is electrically polarized, therefore, should generate a transiently focused gradient in potential steep enough to restrict diffusion to the degree seen here for the oocyte–nurse cell syncytium.

This work was supported by US NSF grant PCM77-16455. R.I.W. is Professor of Biology at West Chester State College.

Received 18 March; accepted 8 May 1980.

1. Jaffe, L. F. *Membrane Transduction Mechanisms* (eds Cone, R. A. & Dowling, J. E.) (Raven, New York, 1979).
2. Jaffe, L. F. *Proc. natn. Acad. Sci. U.S.A.* **56,** 1102–1109 (1966).
3. Nuccitelli, R. *Devl Biol.* **62,** 13–33 (1978).
4. Robinson, K. R. & Jaffe, L. F. *Science* **187,** 70–72 (1975).
5. Quatrano, R. S., Brawley, S. H. & Hogsett, W. E. in *Determinants of Spatial Organization* (eds Subtelny, S. & Konigsberg, I. R.) (Academic, New York, 1979).
6. Mandelbaum, I. *J. Morph.* (in the press).
7. Woodruff, R. I. & Telfer, W. H. *J. Cell Biol.* **58,** 172–188 (1973).
8. Pollack, S. & Telfer, W. H. *J. exp. Zool.* **170,** 1–24 (1969).
9. Hughes, M. & Berry, S. *Devl Biol.* **23,** 651–664 (1970).
10. Grundlach, H. G., Stein, W. H. & Moore, S. *J. biol. Chem.* **234,** 1754–1761 (1959).
11. Jaffe, L. F. & Nuccitelli, R. *A. Rev. Biophys. Bioengng* **6,** 445–476 (1977).
12. Flemming, W. *Arch. microsk. Anat. Entw. Mech.* **37,** 685–751 (1891).
13. Byers, B. & Abramson, D. H. *Protoplasma* **66,** 413–435 (1968).
14. Ashman, R. F., Kanno, Y. & Loewenstein, W. R. *Science* **145,** 604–605 (1964).
15. Nairn, R. C. *Fluorescent Protein Tracing* (Churchill Livingston, New York, 1976).
16. Woodruff, R. I. *Devl Biol.* **69,** 281–295 (1979).

Corrigendum

In the *News and Views* item on 'Dendochronology' by Sara Champion, *Nature* **284,** 663 (1980), reference should have been included in paragraph four to the work of Hubert Polge and in particular to his paper, *Br. Arch. Rep.* S51, 77 (1978).

Erratum

In the letter 'Inhibin is absent from azoospermic semen of infertile men' by R. S. Scott and H. G. Burger, *Nature* **285,** 246–247 (1980), the following was omitted from line 13 on page 247 'relationship of inhibin concentrations to those of serum FSH in spontaneous disorders of the seminiferous epithelium has not been studied. It has been previously shown that a reciprocal'.

BOOK REVIEWS

What price conservation?

Kenneth Mellanby

The Common Ground: A Place for Nature in Britain's Future? By Richard Mabey. Pp.280. (Hutchinson: London, 1980.) £8.95.

WILDLIFE conservation is an important interest of a section of the British public — voluntary conservation organizations such as the Royal Society for the Protection of Birds, the Society for the Promotion of Nature Conservation and the many County Naturalists Trusts have several hundred thousand members. But the majority of the people of Britain are uninformed and indifferent. Is it therefore reasonable to expect wider support — and more money — from central government?

The British Nature Conservancy Council (NCC) is the official organization set up by Parliament "for the purpose of nature conservation and fostering the understanding thereof" and has the task of "maintaining the heritage of wildlife and natural features". Lack of funds and of popular support have always restricted the NCC in its work. During the financial year 1978–79 it received a grant from public funds of £9,535,000 of which £1,725,000 was earmarked for the purchase of the Ribble marshes, a wetland area of international importance for birdlife which would otherwise have been drained and used for intensive arable farming. Unfortunately this grant is unlikely to be increased or even maintained in value, particularly in the face of economic cutback. As one way of gaining support, and in an attempt "to widen the public debate in nature conservation", the NCC asked Richard Mabey to make a special study of the place of nature in Britain. He was helped by the NCC, but was given a free hand to write his own book.

For some centuries Britain has been fortunate in producing gifted amateur naturalists who have often done more than the professional scientists to observe and record our wildlife and the changes in the countryside. Richard Mabey is already well known as a worthy recruit to this body of men and women, and for his books which include *Food for Free* (Collins: London, 1975) which describes the fruits, fungi and other delicacies which the observant may gather in our fields, woods and hedges, and *The Unofficial Countryside* (Collins: London, 1973) which deals with the city and suburbia, and shows how nature adapts to human interference, which may stimulate the spread of many species of wild plants and animals. In *The Common Ground* he deals with human effects on what most people consider to be the natural countryside of Britain.

Of course Richard Mabey is well aware that almost all the landscape in Britain today has been affected by human activity, and that this situation, though changing year by year, has obtained for hundreds of years. Nevertheless, until recently, wild plants and animals were allowed to exist, often in greater numbers than were found in the dull and uniform forest which covered most of the country before agriculture changed the face of the land.

Here Richard Mabey deals at some length with old deciduous woods. Though they now only cover a fraction of the countryside, until relatively recently they continued, as a result of traditional management practice, to be beautiful, diverse and fascinating to the naturalist. They provided recreation for many and biological interest to the observant. Many such woods have now been felled and the land farmed, others have been transformed into uniform stands of exotic conifers.

In the same way farmland, with its hedges and shelterbelts, with old unimproved grassland and a multitude of ponds, allowed native species to flourish. In the past 30 years, farming has become much more productive, but the interest of the countryside and the abundance of wildlife in intensively farmed areas has greatly decreased. Hedges have been grubbed up, ponds filled and old grass with its wealth of wild flowers has been replaced with short-term leys of rye grass and clover.

The description of rural Britain in this book, based on its author's first-hand experience and his careful observation, is depressing to anyone with the slightest interest in natural history. Although only a few species of animals and plants have actually been exterminated, the numbers of many others have been drastically reduced. The whole pattern and diversity of the landscape has been altered and impoverished. However, Richard Mabey is no elitist. He has no time for those who think that conservationists should concentrate their efforts on safeguarding a few reserves rich in rare species, where the public is excluded, while the whole of the rest of the countryside is sterilized. He clearly loves wildlife, and wants to share it with as many people as possible. To him the common species may be as valuable as the scarce, and he wants wildlife to be readily visible in all parts of rural Britain.

Though the NCC has a statutory duty to set up and maintain nature reserves, it fully agrees with Mabey that these are only a part of its responsibilities. Experience has shown that isolated reserves may be of decreasing importance, for they may lose the very species that they were set up to preserve. Thus Monks Wood National Nature Reserve, one of the few areas of old woodland in eastern England, has been known as a site supporting rare and local butterflies for over 150 years. These butterflies appeared to flourish in the nineteenth century when the wood was used for coppice and timber, and in the first part of the twentieth century when its main importance was as a pheasant shoot. Clear felling of much of the wood did not harm the Lepidoptera. Since 1953, when it became an official reserve, and has been managed primarily for wildlife, no fewer than 10 of the 14 species of butterfly most sought by entomologists have disappeared. This may partly be because of inefficient management; as I had this responsibility for part of the time I know that we still do much in ignorance of the results. But I think that the main reason is that a woodland reserve of 150 hectares (and, by our standards, this is a large lowland wood) is too small to support many insect populations if it is an island in an area from which exchange and reinforcement does not take place.

How then can we encourage the return of our wildlife, and how can we convince the public that this is something they should support? Richard Mabey is too honest to pretend that he has any easy answers. He sees the point of view of the farmer, and does not pretend that conservation, or a return to the methods of previous centuries, will increase his income or his productivity. He makes a number of useful points about the way public and voluntary bodies can make minor contributions. His main suggestion is that "we need an imaginative land-use policy — a 'land ethic' — which recognizes that the fate of wildlife is inextricably connected with our own, and that nature conservation touches on the quality (and perhaps the continuance) of all our lives".

I agree strongly with his views on a land-use policy. Earlier this year, as the then chairman of the Environmental Division of the Institute of Biology, I organized a conference on this very subject. In it we discussed the various sectional demands for land — agriculture, forestry, water collection, recreation, waste disposal, nature conservation. Conservationists were agreed that we need to find some way of giving priority to wildlife even when economic forces work in the opposite direction. The difficulty is to find a reason for wildlife conservation which is convincing to those not already committed.

While I fully agree with Richard Mabey that wildlife may contribute greatly to the quality of life — at least of my own life, as one much involved in this field — I am doubtful whether I can support the idea that human continuance on the globe is in any way involved. I was equally worried by the recent *World Conservation Strategy*, produced by the International Union for Conservation of Nature and Natural Resources (see *Nature* **284**, 113; 1980), which relates wildlife conservation to sustainable development. I fear that conservationists may sometimes claim too much. On a world scale it may be wise to try to preserve all species, particularly plants which may have an unexpected potential or contain genetic material which may contribute to better cultivars of food species. I personally would be very upset if the large wild mammals of Africa and Asia were exterminated, but were I a peasant farmer whose crops were consumed by elephants and whose stock was killed by lions I would welcome the elimination of animals which, to me, were pests. British farmers have only gained from the extinction of the wolf, the bear and the beaver, however much some conservationists would welcome the reintroduction of these species.

The modern arable farm in Britain, which has done so much to harm wildlife, has not suffered in the process. The land is producing higher yields, and by any reasonable measure the fertility of the soil is being steadily improved. The disasters arising from monoculture, reduced rotations and increased fertilizer use which some ecologists foretold have not been apparent, though wildlife (including weeds and pests) has been devastated. I am unable to advance any purely economic reason when I try to persuade a farmer to take active steps to encourage wildlife. I have to rely on aesthetic, scientific or even spiritual values — in fact on the 'quality of life'.

Fortunately many farmers are willing to set aside small patches of land where cover may develop and wildlife survive. This is good conservation, but it makes no contribution to agricultural efficiency, in fact it probably reduces productivity slightly. This is the sort of compromise which the late Ivor Brown described as the British genius for making the second best of both worlds.

For, from the point of view of wildlife, it is only a second-best solution. If we are really serious, we must be prepared to establish far more and far larger nature reserves, even sacrificing good agricultural land for this purpose. We must also persuade farmers and foresters to make real sacrifices in productivity. Perhaps *The Common Ground* will help to produce a climate of opinion where such developments are possible. In any event it is an excellent book which will make its readers, even those within the conservation movement, better informed. By showing them how serious have been our losses, it should encourage them to redouble their efforts to protect our wildlife. Whether it will appeal to the non-caring majority is another question. ☐

Kenneth Mellanby was employed by the Nature Conservancy from 1961 to 1973, and was the first director of Monks Wood Experimental Station. He is President of the Bedfordshire and Huntingdonshire Naturalists Trust.

World of the stellar life-cycle

J. D. Barrow

White Dwarfs, Black Holes: An Introduction to Relativistic Astrophysics. By R. Sexl and H. Sexl. Pp. 198. (Academic: New York and London, 1979.) \$13.50, £7.60.

STARS often die very violent deaths and their mortal nature has caused modern astronomers to focus more and more attention upon the circumstances and consequences of their demise. In so doing, astronomers have become astrophysicists. Supernovae, pulsars, quasars, black holes and the entire body of high-energy cosmic phenomena require for their elucidation a delicate amalgam of knowledge concerning nuclear and quantum physics tempered by an understanding of the all-encompassing effects of gravity.

The more massive a star, the higher the temperature and rate of nuclear ignition in its central regions, the faster it evolves and the more dramatic its death throes. After their nuclear fuel is exhausted the most massive stars collapse; at first slowly but then catastrophically. A huge explosion can transform this unstable stellar state into a supernova explosion, expelling the outer layers of the star and scattering heavy elements and high-energy particles out into space in dramatically visible fashion.

Our Sun is not in the heavyweight stellar league. A member of the stellar bourgeois, it awaits a slower and quieter death. Although at present it burns only about 10^{16} of its 10^{30} kg of fuel every day, eventually, like all stars, it will suffer an irresolvable energy crisis. When the internal supply of fusible hydrogen is exhausted, exothermic fusion of other heavier elements must be employed to stave off the pressures of gravitational collapse. Gravitational potential energy can be tapped by adjusting to a more stable configuration with a contracted core and extended outer regions. The star inflates and appears superficially cooler and redder; it has become a 'red giant'. In such a bloated state our Sun would have expanded to encompass the orbit of Mars.

As the central temperature rises inexorably, heavier and heavier elements undergo exothermic nucleosynthesis until a turning point is reached: even if the temperature is high enough for the fusion of elements heavier than iron, these fusion processes are endothermic. The star has now lost its conventional means of pressure support.

The smallest stars, with mass less than ~ 1.5 that of the Sun, can form a stable, compact state termed a 'white dwarf'. To reach such a configuration the Sun would have to shrink one-million-fold to a size comparable with the Earth and, in so doing, increase its average density to about 10^3 kg per cubic centimetre. It would sit securely locked between the opposing forces of gravity and electron degeneracy pressure. The reason gravity can be countered is the exclusive nature of subatomic society. No two particles of a type that includes neutrons, protons and electrons can occupy the same energy state. In cool 'laboratory' gases pressure is determined by the kinetic energy of the constituent molecules and energy can be extracted by dropping an atomic electron into a lower energy orbit. In degenerate material the energy niches fill from the bottom upwards and no low-energy slots are left vacant. The density, rather than the temperature, determines the kinetic energy of the electrons. Once in the white dwarf state a dying star can only cool to a dark ember. Such are the non-linearities of gravity that, the larger a star in its youth, the smaller the dwarf it becomes in death.

If a star exhausts its nuclear fuel when a little larger than 1.5 Suns, its internal stresses can become so large that electrons are eventually torn from their atomic orbits and crushed into the nuclei. The result is a closely packed lattice of about 10^{57} neutrons, squashed to a nuclear density one-billion times higher than within a white dwarf. A strongly repulsive degeneracy pressure now arises between the neutrons and the squeezing is halted, eventually leaving a 'neutron star' in stable equilibrium, just a few kilometres in diameter. Free neutrons decay into protons and electrons in about ten minutes but the neutrons in a neutron star, like those comprising an atomic nucleus, do not undergo such decay. The resulting proton would have to occupy an extremely unfavourable energy state.

White dwarfs and neutron stars have been observed by radio, X- and gamma-ray astronomers and rapidly rotating neutron stars provide an explanation for the 'pulsar' phenomenon.

The fate of the heaviest stars is well known to the average reader: unstoppable collapse to a 'black hole' state of ever-increasing density. A point of no return, the 'event horizon', is encountered by infalling material and no known forces can support the star once it has been encompassed by this surface. The collapse proceeds inevitably to an unknown singular state.

This is the exotic life-cycle of stellar bodies and its documentation often requires a description of matter in gravitational fields too strong for Newton's classical theory to be accurate. And this is the world that the Sexls equip the student to explore. *White Dwarfs, Black Holes* is a translation of a new edition of their successful German text explaining the nature of general relativity, gravitational waves, relativistic astrophysics and elementary cosmology. It is clear and concise, didactic in style and eminently suitable for final-year undergraduates in physics or astronomy. General relativity is described in qualitative terms (no prior familiarity is assumed and no tensor analysis is developed in the text) with a good description of its experimental status although, unfortunately, the observations of the binary pulsar are not included. The authors maintain a good balance between theory and observation by concentrating upon hard, testable results rather than speculative possibilities. However, it is odd to see some of the theory of primordial nucleosynthesis developed without a glimpse at the observational data on cosmic abundances of very light elements. The authors use physical reasoning wherever possible and avoid the use of inessential mathematics. SI units are used throughout and illustrations are skilfully employed to augment, rather than merely re-state, the textual material. A series of exercises are scattered through the text and many have 'solutions' provided. Some of these questions are a little too open-ended to be useful for private study because specific background references are not provided.

Unfortunately referencing is often scanty and imprecise. There is a considerable amount of name-dropping in the text without reference to sources or follow-up articles, and the bibliography is categorized in a fashion that may be too general for students. A list of specific semi-popular articles would have been useful here. But these are second-order problems in a book that is clearly written, well produced and realistically priced. I recommend it to any student who is contemplating graduate work in astrophysics, to teachers seeking a well-ordered foundation course, or indeed to anyone curious to know what relativistic astrophysics is about. □

J.D. Barrow is a Research Lecturer in the Department of Astrophysics at the University of Oxford, UK.

Experts on vacua

John Yarwood

Methods of Experimental Physics. Volume 14, *Vacuum Physics and Technology.* Edited by G.L. Weissler and R.W. Carlson. Pp. 593. (Academic: New York and London, 1979.) $55, £13.80.

THIS BOOK contains a great deal of useful information, concisely and well-written by a number of American authors, all of whom are widely experienced in vacuum science and technology and have up-to-date knowledge gained in academic or industrial research.

The difficulty in judging the book is to assess at whom it is aimed. Despite the fact that the purpose (according to the title of this series) is experimental, a fairly sophisticated mathematical notation is almost always used by the authors so that a reader of that useful type of person — the technician — is, by and large, ruled out. The style is really more suited to the postgraduate student of science or technology.

Roughly the first half of the text is concerned with the production and measurement of vacuum (mostly high and ultrahigh). Although the authors frequently give ideas and explanations which are novel, the topics concerned have received much attention in textbooks and journals over the past 30 years or so. One wonders, therefore, whether it wouldn't have been preferable to omit most of the well-worn material and concentrate on the more novel second half, beginning with "Metal Vacuum Systems and Components". Here, modern information is provided about components and materials and their most effective use in the design of vacuum systems for specific applications.

The book contains no information about how the undergraduate student should go about undertaking practical work in vacuum science and technology. However, it will be most useful to the member of academic staff who is concerned with the development of such practical experiments and wishes to write them up satisfactorily for undergraduates, students beginning research and for special short courses. □

John Yarwood retired in 1978 as Head of Physics at the Polytechnic of Central London, UK, and is the editor of Vacuum.

First of a series on inflammation

G. P. Lewis

Handbook of Inflammation. Volume 1, *Chemical Messengers of the Inflammatory Process.* Edited by J. C. Houck. Pp.422. (Elsevier/North-Holland: Amsterdam and New York, 1979.) $75, Dfl. 154.

IN THE introduction to this first volume of the *Handbook of Inflammation*, the editor, John C. Houck, gives a splendid though brief account of the various steps in the inflammatory process. The book has then been arranged so that the mediators connected with each stage have been discussed.

Our old friend histamine comes first, but brought up to date in a very interesting way. In addition to the work of recent years on H_2 receptor-mediated actions, the author reviews current ideas on the possible regulatory function of histamine on activities of inflammatory cells. This theme of cell–cell interactions mediated by soluble mediators is taken up again later in the book in several chapters. Lymphokines, which were originally thought only to be the soluble products of activated T-lymphocytes, have now been shown to be not strictly restricted to immune activation pathways. The author of this particular chapter points out that release of soluble intracellular mediators might be a basic method of biological communication and describes lymphokines and cytokines as a plethora of inflammatory mediators which even includes viral and immune interferon.

The kinin system is described in some detail with the emphasis on biochemical aspects; only two of the 46 pages cover the role of kinins in inflammation. The review very adequately covers the relationships between the kinin and fibrinolytic systems and Hagemann factor, and the repetition of much of this in a later chapter on Hagemann factor seems to be unnecessary.

There have been so many reviews on prostaglandins in the past year or so that I was pleased to see only one modest chapter on this subject. But with the increasing knowledge of the importance of products of arachidonic acid metabolism other than prostaglandins, it seems unfortunate that this chapter did not include more information about thromboxane and the lipoxygenase products including SRS-A.

The book includes a very comprehensive chapter on complement and chemotaxis in which old and new methodologies in this complicated field are explained and compared.

In addition to discussions on mediators which might affect intracellular activities, there are two accounts of some cellular components which might be affected and which might play a role in the tissue damage which accompanies chronic inflammatory conditions. These are the lysosomal enzymes of which we are told there are more than 40 which are mostly hydrolytic and the acid cathepsins. They might well play a role not only in causing tissue damage but also in the formation of biologically active degradation products. But in spite of an enormous amount of research in this field, the extent of the involvement of these enzymes is not known. However, the discussions include an interesting description of the control mechanisms involved which might give a pointer to the direction that future work should take.

Volume 1 concludes with three fascinating chapters about factors controlling the growth of cells. Many of us who have become familiar with the mediators of the vascular changes and cell migration and activation in inflammation are not so familiar with growth factors and their inhibitors. The significance of macrophage growth factor in biology, for example, is just beginning to emerge. The future will reveal how important are the factors controlling differentiated cell populations at sites of inflammation and their role in inflammation and tissue repair.

Not only is the proliferation of inflammatory cells a significant aspect of inflammation but the proliferation of endothelial cells in growing blood vessels is also important, particularly in tissue repair. The editors decided to cover this aspect with a review on tumour angiogenesis which I personally found exciting and stimulating.

Finally we are treated to another fascinating account, this time about chalones, the tissue-specific inhibitors of cell proliferation. The chapter starts with the story of the early theoretical considerations and the early experimental evidence for the existence of chalones, and goes on to describe the arguments of mitotic stimulators versus mitotic inhibitors. A final glimpse into the future suggests the possibility of inhibiting the mast cell proliferation in *Urticaria pigmentosa* with a mast cell chalone.

There is no doubt that this first volume of the *Handbook* is a valuable addition to the literature on inflammation. It is a pity that the book, superficially well produced, has suffered from deplorable copy-editing and proof-reading — over 200 typographical and grammatical errors, and discrepancies in the references, have been noted in just two chapters. A list of these has been sent to the publishers, who will hopefully take greater care over subsequent volumes. □

G. P. Lewis is Professor of Pharmacology in the Institute of Basic Medical Sciences, Royal College of Surgeons, London, UK.

Science from the Serengeti

Hans Kruuk

Serengeti: Dynamics of an Ecosystem. Edited by A.R.E. Sinclair and M. Norton-Griffiths. Pp.389. (University of Chicago Press: Chicago and London, 1980.) $28.50, £17.10.

THE STREAM of papers emanating from the once so active Serengeti Research Institute has dwindled over the past decade, and the Institute is now only a shadow of its former self. The large concerted effort by scientists from many disciplines to provide an ecological basis to the management of this huge ecosystem in Tanzania has virtually stopped. What is the result of all this effort? *Serengeti* is a sample of the diversity of output of the Serengeti Research Institute, with contributions from a dozen of its former scientists; the book is an attempt to take stock, and to evaluate some of the research in terms of conservation and management. It is clearly focused on the phenomenon for which the Serengeti is justly famous, the vast population of migratory ungulates.

Of the 13 chapters, three by A.R.E. Sinclair describe the Serengeti background, the history and the migrations of its animal populations; the interactions between the most important migratory and resident ungulates and the vegetation are studied in detail in a further four chapters by S.J. MacNaughton, P.J. Jarman and Sinclair, L. Maddock, and M. Norton-Griffiths. C.J. Pennycuick analyses the cost of locomotion to the migrants, R. Hilborn and Sinclair describe simulation studies of the Serengeti populations, and P.J. and M.V. Jarman compare ungulate social organizations. Three chapters, one by B.C.R. Bertram, one by J.P. Hanby and J.D. Bygott, and one by D.C. Houston look at the large predators and scavengers, their social systems, population changes and adaptations to the herbivore migrations.

The book is more a collection of distinct individual contributions than a united evaluation. However some of these contributions are outstanding; I was particularly struck by MacNaughton's beautiful experimental approach to the grazing relationships. Norton-Griffiths' clear analysis of the relation between animal populations and movements, climate, fire and other factors in this huge ecosystem should be an example to many other studies in this field. The predator chapters give a summary of much of the work that has been done on the Serengeti carnivores, and they indicate once again the complicated consequences for the carnivores' social organization of a rapidly increasing prey population. At the end of the book there is a useful list of over 300 references to the scientific publications of the Research Institute.

In general, the quality of all the chapters is good, and the book is full of fascinating observations which more than overshadow its shortcomings. One feels the absence of a chapter on the botanical and soil studies carried out in the Serengeti — everything is seen through zoologists' eyes. The two introductory chapters with their categoric statements fall somewhere between reviews and new contributions, without doing full justice to either of these functions. Scientific modesty would be served if it were pointed out that present population levels of ungulates are well above anything that was predicted as 'equilibrium' only a few years ago, thus indicating some of the limitations of the work of ecologists in such an ecosystem, even when the most elegant predictive models are used. And clearly it is prudent not to attempt to explain these population increases only in terms of the eradication of rinderpest in the early 1960s, since non-vulnerable species also increased — a fact conveniently forgotten in some of the chapters.

These are relatively minor grumbles, however, as are the irritation of the printing errors and the unaccredited photographs in one batch in the middle of the book which are not related to the text. What I missed most of all was a final chapter by the editors in which they could have pulled the strings together instead of leaving the papers as separate entities.

Despite all this, the book stands as an important monument to the efforts of the Serengeti Research Institute, and I have no doubt that it will be a work of reference for many studies elsewhere. I hope that before long the Institute itself will again be in a position to make full use of it. □

Hans Kruuk is a Principal Scientific Officer at the Institute of Terrestrial Ecology, Banchory, UK.

Microwave spectroscopy

H.W. Kroto

Modern Aspects of Microwave Spectroscopy. Edited by G.W. Chantry. Pp. 513. (Academic: London and New York, 1979.) £38.80, $89.50.

YET another expensive volume containing articles by several authors! I have never been totally convinced that this is a satisfactory way to publish reviews. Such books often suffer from one or more of three main defects: the material tends to be three or four years out of date on publication, the various chapters may be uneven in quality and balance, and finally, more often than not, many chapters are intrinsically re-hashes of previously published reviews, often by the same authors. On the whole this book is better than average on these three scores and, indeed, microwave spectroscopy is one of the few areas for which there does not exist a surfeit of such books.

The first chapter, "Microwave Spectrometers" (G.W. Chantry and G. Roussy), gives rather brief general descriptions of various experimental techniques which are used to carry out microwave spectroscopy. Although it gives a useful overview I felt the chapter was too short to cover microwave hardware in sufficient depth. The technical aspects are important as microwave spectrometers are no longer commercially available. The chapter has a comprehensive compilation of references.

The second and third chapters are entitled "Microwave–Microwave Double Resonance" (J.G. Baker) and "Infra Red–Microwave Double Resonance Techniques" (H. Jones), respectively. Both are very useful, detailed reviews of the double-resonance method. They complement each other well and are presented at about the right level. The latter includes a section on optical-microwave experiments and so the two chapters, taken together, give a quite comprehensive survey of a technique which has revolutionized high-resolution molecular spectroscopy.

The fourth chapter on modern submillimetre microwave scanning spectroscopy, by A.F. Krupnov, highlights recent advances in the automation of the beautiful wide-band millimetre wave scanning spectroscopy technique pioneered by this author. The techniques described here would be useful were they available to the scientific community. However, the direct experimental value of this chapter is limited because the necessary high-power microwave sources appear only to be available in the military installation at Gorki in the USSR.

Chapter 5, by J.W. Fleming, deals with interferometric spectroscopy at millimetre and submillimetre wavelengths. Although this is a useful review of the technique, I find it a curious choice for this collection, though it does give a welcome change of pace. I suspect that the audience for the other articles is biased towards higher resolution techniques and that this review may not be readily found by those to whom it would be most valuable.

The last contribution is yet another review on interstellar molecules, entitled "Astrophysics of Interstellar Molecules" (G. Winnewisser, E. Churchwell and C.M. Walmsley), and it is valid to ask whether another review is justified. This one is. It presents a different perspective as it is more strongly biased than previous reviews towards spectroscopy — as is appropriate for this volume. It is well balanced and covers the appropriate material comprehensively from a microwave spectroscopists point of view. In addition it is up to date with numerous useful tables.

In all, this is a timely volume for the practising microwave spectroscopist. □

H.W. Kroto is a Reader in Chemistry in the School of Molecular Sciences, University of Sussex, Brighton, UK.

A weather controversy

M.W. Moncrieff

Weather Modification. By G. Breuer. Pp. 178. (Cambridge University Press: Cambridge, UK, and New York, 1980.) Hardback £10.50; paperback £3.75.

WEATHER modification is an emotive subject among meteorologists, and over the past few decades there has been a great deal of controversy. The physics and dynamics of atmospheric phenomena are more complex than most physical systems and, more often than not, incompletely understood. However, the potentially significant social, agricultural and economic rewards of successful weather modification have ensured that a considerable amount of financial backing has been available for experiments, often in the absence of sufficient scientific knowledge. The 'seeding' of clouds by silver iodide crystals to enhance rainfall is one example of how a laboratory technique was applied to real atmospheric clouds before a quantitative knowledge of the physics and dynamics of these systems was available. This book illustrates the basic gulf between the practical application of simple techniques to control complex dynamical systems, with a considerable number of commercial, political and economic consequences, and the background of insufficient theoretical understanding. It is no surprise that debate exists with such contrasting motivations surrounding the subject.

The book, in three chapters, is generally well written and is informative to the non-specialist, and the above-mentioned gulf between theory and application is well documented. It is not intended for the specialist, who might be irritated by the large amount of speculative science and continual reference to political and military application; this is especially true of the last chapter. However, the extensive bibliography is useful to both specialist and non-specialist. In general, a balanced viewpoint on a highly controversial topic is retained, and the layman should obtain much useful information.

The first chapter provides a background largely dealing with the philosophy and history of the topic, and brings out the controversies of the subject, particularly that related to cloud seeding. The introduction to the basic physics is unfortunately rudimentary and out of date. The reader may be left with the mistaken impression of cloud physics and dynamics being a very inexact science; recent advances in computational and mathematical techniques are not considered and the cloud models are typical of those seen in school textbooks. An important aspect stressed is the inadequate statistical significance tests in most cloud-seeding experiments, recognized as a major criticism of the subject in general.

The second chapter is undoubtedly the most quantitative and scientific; subjects such as fog dispersal, seeding of convective and orographic clouds, hail and lightning suppression, and the modification of hurricanes are discussed. The author covers experiments in many countries, mainly the USA, USSR and Australia. An interesting historical review of the basis of cloud-seeding, beginning with Langmuir's first laboratory experiments and the initial euphoric and extravagant claims made about weather control, is included. The seeding of cumulus clouds is reviewed in some detail, but the seeding of orographic clouds has probably been the most successful and has the best history of controlled scientific experiment, especially in the USA. It is no surprise that the modification of hurricanes has achieved little success since the basic dynamics, particularly in the growing stages, are not well understood. The most speculative discussion is centred on the modification of large-scale weather systems and climatic change. This has not yet been deliberately attempted, although man-made effects, such as carbon dioxide production due to industrialization, affect climate although their importance is debatable. The possible causes of climatic change are not reviewed in any detail, but these are also beyond the scope of the book. The economic and political interests in weather modification, particularly in cloud seeding, are described. The importance of the financial support by these interests is probably considerable; scientific support in the subject is, by contrast, largely a by-product of more fundamental research.

The last chapter is mainly speculative and qualitatively deals with social, economic and legal aspects; this chapter is more suitable for the non-scientist. I feel that it is somewhat laboured, could have been condensed considerably and is something of an anticlimax. The importance of military and political interests in research and experiment are again brought out, and perhaps this, above all, emphasizes the lack of proportion in the weather-modification picture. Indeed, it is not clear from this book that the present approach to weather modification is any more scientific than the original experiments in cloud seeding. □

M. W. Moncrieff is a Lecturer in Atmospheric Physics at Imperial College, University of London, UK.

Rats in the lab

Maurice Smith

The Laboratory Rat. Volume I, *Biology and Diseases.* Edited by H.J. Baker, J. Russell Lindsay and S.H. Weisbroth. Pp. 448. (Academic: New York and London, 1979.) $52.50, £29.40.

THIS IS the first of two volumes on the laboratory rat, following earlier publications on the laboratory rabbit and guinea pig which were also sponsored by the American College of Laboratory Animal Medicine.

Contributions from 24 authors have been brought together in 15 chapters and two appendices, forming a most comprehensive reference work. The success of the editors in consolidating the technical material available has been balanced by their equivalent success in producing a readable and yet authoritative work which should be available for reference by almost any worker using laboratory bred rats. This is best illustrated by the first chapter which describes in great detail and clarity the origin of the major outbred strains and the early development of inbred strains.

That this is a mainly American story is some reflection of the earlier recognition by the American research world of the need for defined laboratory animals. However it is significant that despite the understandable selection of authors mainly from the USA, those asked to write the chapters on taxonomy, genetics and inbred strains were British, which is due recognition for the work done in Britain on this aspect of laboratory animal science.

The biological chapters in the first half of the book cover genetics, anatomy, physiology, haematology, clinical biochemistry, nutrition, feeding and housing. They show a refreshing recognition of the relationship between biological and experimental variables, which is sometimes not adequately recognized by those using animals as experimental tools.

One of the best examples of this approach is Chapter 8, "Housing to Control Research Variables", which replaces what could have been a standard chapter on housing with a consideration of the effects of physical, chemical and microbial factors on biological responses.

The chapters on disease are without exception well done and each may be considered a definitive text in its own right, especially when supported by the very comprehensive references which are a characteristic of the book as a whole.

There are, however, occasional anomalies which could cause misunderstanding among British readers. Examples of this are the description of *Corynebacterium kutscheri* as the causative agent of pseudotuberculosis, which in the UK is usually attributed to *Yersinia pseudotuberculosis*. Also, at no point is the term chronic respiratory disease (which is generally recognized in the UK) used in reference to respiratory infection. There is a tendency to deal with respiratory infections as quite separate conditions, and the mixed nature of the outbreaks of respiratory disease so commonly found in conventional rat colonies is not sufficiently emphasized.

It is particularly gratifying that chapters on neoplasia and lesions associated with ageing have been included, while the chapter on human health hazards will prove very useful to those involved with safety problems in animal units.

The appendices on drug dosage and selected normative data are welcome and useful additions. It is to be hoped that some consideration may be given to the enlargement of these sections in future editions.

The book is profusely illustrated throughout with black and white photographs of excellent quality together with more-than-adequate tables, diagrams and figures. Understandably, colour has not been used, but despite this the quality of the publication with its strong hard-backed binding is of the high standard one has come to expect from ACLAM.

Volume I of *The Laboratory Rat* is without doubt a timely and very welcome addition to the literature. I await Volume II, *Research Applications*, with considerable interest and with the certain knowledge that *The Laboratory Rat* will become the standard work of reference on this subject. □

Maurice Smith is Director of Central Animal Services at the University of Cambridge, UK, and Laboratory Animal Consultant to the Open University, Milton Keynes, UK.

Reproduction in perspective

Barry Cross

Oxford Reviews of Reproductive Biology. Volume 1, 1979. Edited by C.A. Finn. Pp. 485. (Clarendon/Oxford University Press: Oxford and New York, 1979.) £30.

UNLIKE several biological disciplines of recent origin, the biology of reproduction has cast its spell on enquiring man for centuries, if not millenia. Even so the acceleration of activity in the last three decades has been remarkable, with research proliferating in the new universities and colleges as well as in long-established academic institutions. Whereas 40 years ago reproductive research was almost exclusively a male preserve, the recession of sex discrimination has brought a tide of female workers to reproduction laboratories, much to the advantage of the subject. Dr Anne McLaren FRS is the chairman of the editorial board of this annual review series and two of the chapters in the first volume are written by talented women scientists.

The book contains seven reviews of uniformly high quality, clearly written and appropriately comprehensive. The authors, who are all at the height of their investigative careers, do not skimp, plagiarize or patronize the reader. They dig deep into the foundation of their respective subjects often referring to much earlier work, and critically examine much present-day dogma.The mix is certainly not what one would expect to find in a textbook on the subject or in an introduction for the educated layman. It perhaps most obviously reflects the impact of refinements in chemical techniques on physiological problems. We have authoritative discussions on the current status of relaxin (D. G. Porter), uterine proteins (R. J. Aitken), molecular biology of spermatogenesis (A.R. Bellvé) and preservation of semen (P. F. Watson), as well as on the established favourites — sexual differentiation of the brain (J. E. Booth), control of gonadotrophins (C. A. Wilson) and milk secretion (R. C. Richards). All are treated in a refreshing way and make stimulating as well as informative reading.

The text is efficiently edited by Professor C.A. Finn and contains very few misprints. Some readers may feel that the scarcity of figures is a disadvantage and that the quality of some of the micrographs in the plates at the end of the book is not very impressive.

But these are small defects, and annual reviews in the series will be eagerly awaited.

Barry Cross is Director of the ARC Institute of Animal Physiology, Babraham, Cambridge, UK, and Head of its Neuroendocrine Group.

BOOKS RECEIVED

Computer science

CRONHJORT, B. (ed.) Real Time Programming 1978. Proceedings of the IFAC/IFIP Workshop Mariehamn/Aland, Finland. Pp. viii + 129. ISBN-0-08-024492-0. (Oxford, New York, Toronto, Sydney, Paris, Frankfurt: Pergamon Press, 1980.) $22.50 £10.50.

NOVAK, M. (ed.) Software for Computer Control. Proceedings of the Second IFAC/IFIP Symposium on Software for Computer Control, Prague, Czechoslakia. Pp. xii + 420. ISBN-0-08-024448-3. (Oxford, New York, Toronto, Sydney, Paris, Frankfurt: Pergamon Press, 1979.) $73.00.

SWARTZLANDER, E.E. jr. (ed.) Computer Arithmetic. Benchmark Papers in Electrical Engineering and Computer Science/21. Pp.xiii + 378. ISBN-0-87933-350-2. (Stroudsburg, Penn.: Dowden, Hutchinson & Ross, Inc. 1979.) Distributed world wide by Academic Press, $45.00.

THE ELECTRICAL RESEARCH ASSOCIATION LTD. The Engineering of Microprocessor Systems. Guidelines on System Development. Pp. xii + 175. ISBN-0-08-025435-7 Hardback ISBN-0-08-025434-9 flexi. (Oxford, New York, Toronto, Sydney, Paris, Frankfurt: Pergamon Press, 1979.) $15.00 £7.50 Hardback $6.00 £2.95 flexi.

Applied biology

AYRES, J.C., MUNDT, J.O. and SANDINE, E. Microbiology of Foods. Pp.708. ISBN 0-7167-1049-8 (Freeman: Oxford, 1980.) £10.80.

BRIGGS, M. H. and CORBIN, A. (eds) Advances in Steroid Biochemistry & Pharmacology Vol. 7. Pp. 125. ISBN 0-12-037507-9 (Academic: London and New York, 1980.) $23.00; £9.80.

BROWN, K. and COOPER, S. J. (eds) Chemical Influences on Behaviour. Pp. 670. ISBN 0-12-136780-0. (Academic: London and New York, 1979.) £39.20; $90.50.

BROWN, V.K. Acute Toxicity: In Theory and Practice. Pp.159. ISBN 0-471-27690-1. (John Wiley & Sons: Chichester, 1980.) £10.00.

CAMPBELL, P. N. and MARSHALL, R. D. (eds) Essays in Biochemistry. vol 15. Pp. 130. ISBN 0-12-158115-2. (Academic Press: Published for Biochemical Society, 1979.) $11.50; £4.80.

CROMPTON, C. R. Additive Migration from Plastics into Food. Pp. ix + 234. ISBN-0-08-022465-2. (Oxford, New York, Toronto, Sydney, Paris, Frankfurt: Pergamon Press, 1980.) $47.00 £21.00.

GALJAARD, H. Genetic Metabolic Diseases: Early Diagnosis and Prenatal Analysis. Pp. xvi + 880. ISBN 0-444-80143-X (Elsevier/North-Holland: Amsterdam, 1980.) Dfl. 285.00; US$ 139.25.

GIBSON, J. E. Thin Shells; Computing and Theory. Structures and Solid Body Mechanics series. Pp. ix + 289. ISBN-0-08-023275-2 hardback ISBN-0-08-034204 flexi. (Oxford, New York: Pergamon, 1979.) $30.00 £15.00 hardback $15.00 £7.50 flexi.

HARWOOD, R. F. and JAMES, M. T. Entomology in Human and Animal Health. Seventh edition. Pp. vi + 548. ISBN-0-02-451600-3. (New York: Macmillan Publishing Co., Inc.; Toronto: Collier Macmillan Canada, Ltd.; London: Baillière Tindall. 1980.) £18.00.

HECHT, S.M. (ed.) Bleomycin: Clinical, Biochemical, and Biological Aspects. Pp.351. ISBN 3-540-90395-X. (Springer: Berlin, Heidelberg and New York, 1979.) DM 79.00; $34.50.

JANTSCH, E. The Self-Organizing Universe. Scientific and Human Implications of the Emerging Paradigm of Evolution. Systems Science and World Order Library. Pp. xvii + 343. iSBN-0-08-024312-6 hardback ISBN-0-08-024311-8 flexi. (Oxford, New York, Toronto, Sydney, Paris, Frankfurt: Pergamon Press, 1979.) $44.00 £20.00 hardback $15.00 £6.65 flexi.

JORGENSEN, S. E. Lake Management. Water Development, Supply and Management. Pp. xii + 167. ISBN-0-08-022432-6. (Oxford, New York: Pergamon, 1980.) $36.00 £15.50.

NRIAGU, J. O. (ed.) The Biogeochemistry of Mercury in the Environment. Topics in Environmental Health, Volume 3. Pp. xv + 696. ISBN-0-444-80110-3. (Amsterdam, New York, Oxford: Elsevier/North-Holland Biomedical Press, 1979.) US $136.50 Dfl. 280.00.

OUCHTERLONY, O. and HOLMGREN, J. (eds) Cholera and Related Diarrheas Molecular Aspects of a Global Health Problem: 43rd Nobel Symposium co-sponsored by WHO Pp. 246. ISBN 0079-645X (S. Karger: Basel, 1980.) SFr. 115.; DM 138; $69.00.

PARRY, D.A.D. and CREAMER, L.K. (eds) Fibrous Proteins: Scientific, Industrial and Medical Aspects. Vol 1. Pp. 508. ISBN 0-12-545601-4. (Academic: London and New York, 1980.) £19.80; $46.00.

PARRY, D. A.D. and CREAMER, L. K. (eds) Fibrous Proteins: Scientific, Industrial and Medical Aspects. Vol. 2. Pp.257. ISBN 0-12-545602-2. (Academic: London and New York, 1980.) £13.00; $30.00.

PLIMPTON, P. A. (ed.) Jottings of a Harvard Botanist. Pp. 401. ISBN 76-52949 (Harvard University Press; Cambridge, Massachusetts and London, 1980). £7.80.

PLOMIN, DeFRIES and McCLEAN. Behavioural Genetics: A Primer Pp. 417. ISBN 0-7167-1128-1. (Freeman: San Francisco, 1980.) $15.00 Flexi; $25.00 Hardback.

POLLARA, B., PICKERING, R.J., MEUWISSEN H.J. and PORTER, I.H. (eds) Inborn Errors of Specific Immunity. Pp. 469. ISBN 0-12.559650-2 (Academic: New York and London, 1980.) $34.00.

POLLOCK, J. R. A. (ed.) Brewing Science Vol 1. Food Science and Technology: A Series of Monographs. Pp. 604. ISBN 0-12-561001-7. (Academic: London and New York, 1979.) £33.00; $76.00.

RICHARDS, V. (ed.) Current Cancer Immunology. Progress in Experimental Tumour Research. Volume 25. Pp.xii + 296. ISBN-3-8055-3033-1. (Basel, Munchen, Paris, London, New York, Sydney: S. Karger, 1980.) SFr. 145 DM 174 approx. US $87.00.

SMITH, G. (ed.) Proceedings of the Sixth International Congress on Hyperbaric Medicine. University of Aberdeen, Scotland. 1977. Pp. xii + 468. ISBN-0-08-024918-3. (Oxford, New York, Toronto, Sydney, Paris, Frankfurt: Pergamon Press, 1979.) $50.00 £25.00.

SUMMERFIELD, R. J. and A. H. BUNTING. Advances in Legume Science. Vol. 1 of the Proceedings of the International Legume Conference Kew, 31st July-4th August 1978. Pp. 667. ISBN 0-85521-223-3 (Royal Botanic Gardens: Richmond, 1980.) £15.00.

THYS, J.P., KLASTERSKY, J., and YOURASSOWSKY, E. (eds) Aerobic Gram-Negative Bronchopneumonias. Proceedings of the Symposium on Aerobic Gram-Negative Bronchopneumonias, Brussels, September, 1978. Pp. 183. ISBN-0-08-025533-7. (Oxford, New York, Toronto, Sydney, Paris, Frankfurt: Pergamon Press, 1980.) $25.00 £11.00.

UNITED NATIONS ECONOMIC COMMISSION FOR EUROPE. Problems of the Agricultural Development of Less-favoured Areas in Europe. Proceedings of a Symposium of the Committee on Agricultural Problems Economic Commission for Europe and Food and Agriculture Organisation on 22-26 May, 1978. Pp. xxi + 252. ISBN-0-08-024456-4. (Oxford, New York, Toronto, Sydney, Paris, Frankfurt: Pergamon Press, 1979.) $35.00 £17.50.

UNITED NATIONS ECONOMIC COMMISSION FOR EUROPE. Energy Aspects of the Forest Industries. Proceedings of a Seminar organized by the Timber Committee of the United Nations Economic Commission for Europe. Italy, 13-17 November 1978. Pp. xiii + 416. ISBN-008-025661-9. (Oxford, New York, Toronto, Sydney, Paris, Frankfurt: Pergamon Press, 1979.) $54.00 £25.00.

WEBB, M. (ed.) The Chemistry, Biochemistry and Biology of Cadmium. Topics in Environmental Health Volume 2. Pp. xiii + 465. ISBN-0-444-80109-X. (Amsterdam and New York: Elsevier/North-Holland Biomedical Press, 1979.) US $80.50 Dfl. 165.00.

WEISS, D. W. Tumour Antigenicity and Approaches to Tumour Immunotherapy: Current Topics in Microbiology and Immunology 89. Pp. 83. ISBN 3-540-09789-9. (Springer: Berlin, Heidelberg and New York, 1980.) DM 29.00; US $17.20.

WELCH, E. B. Ecological Effects of Waste Water: with hydrographic characteristics by T. Lindell. Pp. 337. ISBN 0-521-22495-0. (Cambridge University Press: Cambridge, 1980.) £15.00; Pbk £5.50.

WINEFIELD, H. R. and PEAY, M. Y. Behavioural Science in Medicine. Pp. xiii + 344. ISBN-0-04-610014-8 hardback ISBN-0-04-610015-6 flexi. (London and Sydney: George Allen & Unwin; Beaconsfield: Beaconsfield Publishers, 1980.) £10.50 hardback £5.95 flexi.

WALKER, B. H. (ed.) Management of Semi-Arid Ecosystems. Developments in Agricultural and Managed-Forest Ecology, 7. Pp. viii + 398. ISBN-0-444-41759-1. (Amsterdam and New York: Elsevier Scientific Publishing Company, 1979.) US $78.00 Dfl. 160.00.

ZUCKERMAN, A. J. A. Decade of Viral Hepatitis Abstracts 1969-79. Pp. 501. 0-444-80190-1. (Elsevier/North-Holland: Amsterdam, 1980.).

ZUCKERMAN, A. J. and HOWARD, C. R. Hepatitis Viruses of Man. Experimental Virology Series. Pp. xi + 269. ISBN-0-12-78150-3. (London, New York, Toronto, Sydney, San Francisco: Academic Press, 1979.) £16.80 $39.00.

Psychology

BERKOWITZ, L. (ed.) Advances in Experimental Social Psychology. Volume 12. Pp. ix + 358. ISBN-0-12-015212-6. (New York, San Francisco, London: Academic Press, 1979.) $24.00.

GRUNEBERG, M.M. and MORRIS, P.E. (eds) Applied Problems in Memory. Pp. xiii + 289. ISBN-0-12-305150-9. (London, New York, San Francisco: Academic Press, 1979.) £12.40 $29.00.

KEEHN, J. D. (ed.) Origins of Madness. Psychopathology in Animal Life. Pp. vii + 422. ISBN-0-08-023725-8. (Oxford, New York, Toronto, Sydney, Paris, Frankfurt: Pergamon Press, 1979.) $40.00 £20.00.

RIEBER, R. W. (ed.) Language Development and Aphasia in Children: New Essays and a translation of Kindersprache und Aphasie by Emil Fröschels. Pp.236. ISBN-0-12-588280-7. (Academic: New York and London, 1980.) $16.00.

RUSSELL, B. Education and the Social Order. Pp. 158. ISBN-0-04-370080-2. (London, Boston, Sydney: Unwin Paperbacks, 1980.) £1.75 flexi.

SCHARFETTER, C. General Psychopathology: An Introduction. Translated by H. Marshall. Pp. 239. ISBN 0-521-22812-3. (Cambridge University Press: Cambridge, 1980.) £20.00; Pbk £6.95.

SIMON, H. A. Models of Thought. Pp. xviii + 524. ISBN-0-300-02347-2. (New Haven and London: Yale University Press, 1980.) £28.35.

WILDEN, A. System and Structure: Essays in Communication and Exchange. 2nd Ed. Pp. 592. ISBN 0-422-76710-7. (Tavistock London, 1980.) £14.00 Hardback, £6.95 Pbk.

Sociology

BAYLEY, L. G. Local Government Is It Manageable? A Critical and Up-to-date Assessment of Local Government Operations with Examples and Explanations. vii + 125. ISBN-0-08-024279-0. (Oxford, New York, Toronto, Sydney, Paris, Frankfurt: Pergamon Press, 1980.) $13.00 £5.50.

BERTING, J., GEYER, F. and JURKOVICH, R. (eds) Problems in International Comparative Research in the Social Sciences. Papers from a Symposium on the Theory and Methods of International Comparative Research in the Social Sciences. Pp. xiii + 180. ISBN-0-08-0252247-8. (Oxford, New York, Toronto, Sydney, Paris, Frankfurt: Pergamon Press, 1980.) $22.00 £10.00.

CARTER, R.L. and HILL, K.Q. The Criminal's Image of the City. Pergamon Policy Studies on Crime and Justice. Pp.x + 97. ISBN-0-08-024633-8. (New York, Oxford, Toronto, Sydney, Frankfurt, Paris: Pergamon Press, 1979.) £6.25.

COOPER, C.L. and PAYNE, R. Current Concerns in Occupational Stress. Wiley series on studies in Occupational stress. Pp. x + 341. ISBN-0-471-27624-3. (Chichester, New York, Brisbane, Toronto: John Wiley & Sons, 1980.) £11.75.

DAMMANN, E. The Future in Our Hands. What we can all do towards the shaping of a better World. Pergamon International Library of Science, Technology, Engineering and Social Studies. Pp. xviii + 171. ISBN-0-08-024284-7 hardback ISBN-0-08-024283 flexi. (Oxford, New York, Toronto, Sydney, Paris, Frankfurt: Pergamon Press, 1979.) $20.00 £9.00 Hardback $10.00 £4.50 flexi.

GOLDSMITH, M. and KING, A. (eds) Issues of Development Towards a New Role for Science and Technology; Science, Technology and Global Problems. Proceedings of an International Symposium on Science and Technology for Development, Singapore, January, 1979. Science, Technology and Global Problems Series. Pp. xxiv + 277. ISBN-0-08-024691-5. (Oxford, New York, Toronto, Sydney, Paris, Frankfurt: Pergamon Press, 1979.) $35.00 £17.50.

GRIEVES, F. L. (ed.) Transnationalism in World Politics and Business. Pergamon Policy Studies on U.S. and International Business. Pp. xiii + 217. ISBN-0-08-023892-0. (New York, Oxford, Toronto, Sydney, Frankfurt, Paris: Pergamon Press, 1979.) £8.75.

HALE, N.C. Birth of a Family. The New Role of the Father in Childbirth. Pp.x + 196. ISBN-0-385-14162-9. (New York: Anchor Press/Doubleday, 1979.) np. Flexi.

HARRISON SHRYOCK, R. The Development of Modern Medicine: An Interpretation of the Social and Scientific Factors Involved. Pp. 473. ISBN 299-07534-6. (University of Wisconsin Press: London and Madison, 1980.) £4.50 Pbk; £10.50.

McAUSLAN, P. The Ideologies of Planning Law: Urban and Regional Planning Series Vol. 22. p.282. ISBN 0-08-025198-6 (Pergamon: Oxford, 1980.) Flexi $20.00; £8.50 Hardback $40.00; £17.00.

MORELL, J. A. Program Evaluation in Social Research. Pergamon International Library. Pp. xvi + 193. ISBN-0-08-023359-7. (New York, Oxford, Toronto, Sydney, Frankfurt, Paris: Pergamon Press, 1979.) £4.50 flexi.

O'BRIEN, J.T. and MARCUS, M. (eds) Crime and Justice in America. Critical issues for the Future. Pergamon Policy Studies on Crime and Justice. Pp. xx + 361. ISBN-0-08-025549-3 Flexi ISBN-0-08-023857-2 Hardback. (New York, Oxford, Toronto, Sydney, Frankfurt, Paris: Pergamon Press, 1979.) Flexi £13.75 Hardback.

PYKE, M. Long Life: Expectations for Old Age. Under the Auspices of the British Association for the Advancement of Science. Pp.166. ISBN 0-460-04481-8. (J.M. Dent: London, Toronto and Melbourne, 1980.) £6.95; Pbk £3.95.

SAVITCH, H.V. Urban Policy and the Exterior City. Federal State and Corporate Impacts upon Major Cities. Pergamon Policy Studies 41. Pp.xv + 359. ISBN-0-08-023390-2. (New York, Oxford, Toronto, Sydney, Frankfurt, Paris: Pergamon Press, 1979.) £15.00.

SHRADER-FRECHETTE., K. S. Nuclear Power and Public Policy: The Social and Ethical Problems of Fission Technology. Pp. 176 ISBN 90-277-1080-5. (D. Reidel: Dordrecht, Boston and London, 1980.) US $10.50; Dfl. 20.00 Pbk/Cloth Dfl. 38.00; US $19.95.

ANNOUNCEMENTS

Awards

The Harvey Prize in Science and Technology for 1980 has been awarded to **Professor Michael O. Rabin** (Hebrew University); the Harvey Prize in Human Health for 1979 is awarded to **Professor Ephraim Racker**, (Cornell University).

The Hamburg Foundation Jung-Stiftung für Wissenschaft und Forschung has awarded the Ernst-Jung-Prize for medicine 1980 to **Sir Alan Parks**, (St Mark's Hospital, London).

The 1st Margaret Grant Memorial Fellowship has been awarded to **E. Shyam Prasad Reddy** (Centre for Cellular and Molecular Biology, Regional Research Laboratory, Hyderabad, India).

The following Junior Beit Fellowships for Medical Research have been awarded: **David John Adams; Ian Brown; Elizabeth Gready Hill; Elinor Nancy Lupton; Alexandra Marie Thomson**.

The Geological Society of London has made the following awards for 1980: The Wollaston Medal to **Professor Augusto Gansser**; The Murchison Medal to **Professor J.V. Smith**; The Lyell Medal; to **Professor J.R.L. Allen**; The William Smith Medal to **Mr G. Armstrong**; The Wollaston Fund, Murchison Fund and equal moieties of the Lyell Fund to **Drs R.H. Sibson, M.P. Coward, G.S. Boulton** and **M.R. Leeder**, respectively; The President's Awards to **Drs A.P. Heward, J.K. Leggett** and **B.W.D. Yardley**.

The Institute of Physics has made the following awards for 1980: Charles Vernon Boys Prize to **Dr A.E. Costley** (National Physical Laboratory, Teddington); DuddellMedal and Prize to **Professor A.V. Crewe** (University of Chicago); Max Born Medal and Prize to **Professor Dr H. Faissner** (Rheinisch-Westfälische Technische Hochschule, Aachen); Glazebrook Medal and Prize to **Mr M.C. Crowley-Milling** (CERN, Geneva); Guthrie Medal and Prize to **Professor M.E. Fisher** (Cornell University); Maxwell Medal and Prize to **Professor D.J. Wallace** (University of Edinburgh); Rutherford Medal and Prize to **Professor P.G. Murphy** (University of Manchester) and **Dr J.J. Thresher** (Rutherford Laboratory, Didcot); Prize for the 1979 Graduateship Examination of the Institute to **Mr D.B.Mackay** (Napier College of Commerce and Technology, Edinburgh); Honorary Fellowship of the Institute to **Professor V.F. Weisskopf** (Massachusetts Institute of Technology).

Person to person

The Bioelectrochemical Society (BES) has been founded with the aim of stimulating cooperation among all scientists interested in the investigation, interpretation and practical utilization of biological phenomena by using electrochemical theories and methods. For information apply to Prof. Dr H.W. Nürnberg, Institute of Chemistry 4 Applied Physical Chemistry, Nuclear Research Center, PO Box 1913, D-5170 Jülich, FRG.

In 1967 a meeting of British research workers in the mucopolysaccharide field resulted in the formation of a Club. One of the first meetings, with the French Connective Tissue Club in Paris lead to the formation of the Federation of European Connective Tissue Societies FECTS which met for the first time in 1968. In September (1980) the Collagen Club and the Mucopolysaccharide Club come together to form the British Connective Tissue Society.

Information on intra-thecal overdoses of penicillin is required by J.L. Kay, 14 Ardayre Rd, Prestwick, Scotland. Any factual documented source would be helpful, perhaps reference to toxic effects, such as to the brain and central nervous system, clincial tests, possibly information on animal experiments in related fields and LD 50 tests.

Harvard professor seeks for January 1981 to June 1981 furnished house or flat, preferably in Central London, suitable for two persons plus guest room and study. No children or pets! If exchange is desired: Our 3-bedroomed house is in Lexington (Boston area), 15 min from Harvard, 20 min from MIT, MGH, on 1 acre among trees. Write to Mrs G. Holton, 14 Trotting Horse Drive, Lexington, Massachusetts 02173.

A scientist would like to exchange — for 1 year beginning September 1980 — 3-bedroomed house in an attractive Jerusalem suburb (4 miles from University campus, convenient to University and Medical centres, fully furnished for similar or smaller house or apartment in London. M. Goldberg, Bet Zeit 63, D.N. Harei Yehuda, Israel.

Appointments

Dr J.E. Eastoe is appointed to the Chair of Oral Physiology in the University of Newcastle upon Tyne from 1 October 1980.

Dr David Phillips has been appointed to the new Wolfson Chair of Natural Philosophy in the Royal Institution which was recently endowed by the Wolfson Foundation.

Professor M.H. Williams, currently Professor of Computer Science at Rhodes University, Grahamstown, South Africa, has been appointed to the Chair of Computer Science at Heriot-Watt University, Edinburgh.

Professor Harold W. Woolhouse has been appointed Director of the John Innes Institute, Norwich, and Professor of Biology in the School of Biological Sciences at the University of East Anglia from 1 October 1980.

Dr Paul Freeman has been appointed Director of the Department of Industry's National Engineering Laboratory at East Kilbride to succeed **Mr Denis Mallinson.**

Meetings

16-18 July, **Tropical Animal Production,** Merida (Centre for Tropical Animal Production, Escuela de Medicina Veterinaria, Universidad de Yucatan, Apartado 116D, Merida, Mexico).

21-15 July, **Soil Conservation,** Bedford (Dr R. Morgan, NCAE, Silsoe, Bedford, UK).

23-25 July, **590th Meeting of the Biochemical Society**, Sheffield (The Biochemical Society, 7 Warwick Court, High Holborn, London WC1, UK).

1-4 September, **Environment and Safety Exhibition and Conference,** London (International Environment and Safety Exhibition and Conference, London (International Environment and Safety, Labmate Ltd, Newgate, Sandpit Lane, St Albans, Herts, UK).

3-5 September, **Polymerization Mechanisms,** Liverpool, (Dr John Gibson, The Royal Society of Chemistry, Burlington House, London W1, UK).

9-11 September, **Industry and Environment,** Loughborough (Administrative Officer, I & E Conference, University of Technology, Loughborough, Leicestershire, UK).

15-18 September, **Oxygen and Life,** Birmingham (Dr J.F. Gibson, The Royal Society of Chemistry, Burlington House, London W1, UK).

15-19 September, **Management Studies for Chemists,** Slough (Miss L. Hart, The Royal Society of Chemistry, 30 Russell Square, London WC1, UK).

nature

10 July 1980

Progress on chemical weapons treaty

The decision of the United States House of Representatives to fall in with the Pentagon's request for funds to manufacture chemical weapons again is a serious, even a sombre, development. For the best part of a decade, both the Administration and Congress have been more concerned with the disposal of chemical weapons than their production. From time to time, the US Army has excited public interest and anger by its often clumsy arrangements for shipping unwanted chemical munitions about the place, with the consequence that the dumping of useless weapons at sea has been superseded by more rational techniques for the chemical decomposition of the active ingredients. Although the munitions disposed of by these means have usually been unserviceable or even unsafe, the mere act of disposal has chimed in well with the widespread belief that preparations for chemical warfare would serve no useful purpose, and might even damage the discussions between the Soviet Union and the United States about the form that might be taken by an international convention to prohibit chemical weapons. To be sure, the Pentagon has made no secret of its ambitions to get back into the production business, but Congress (the paymaster) has been stolidly unwilling to agree. Now, it appears, all this has changed (see page 100). Last week the House of Representatives agreed to provide the US Army with the funds needed to clear a site in Arkansas. In the next few weeks, it is almost certain that the appropriation for a pilot plant to manufacture binary chemical munitions will follow. Why has there been such a turnabout?

The influences on the US Congress are plain enough. Especially in an election year, few congressmen will wish to stand out against the Department of Defense. It would be different if detente had not collapsed, or been eroded, by the events in Asia in the past six months. Reports of the Soviet use of chemical weapons in Afghanistan, however insubstantial they may be, must tend also to undermine the resolve of Congress. Yet there must be a more intricate explanation of the sudden flurry of interest in chemical warfare, which is not confined to the United States. Last week, in Britain, a group of Conservative MPs gave it as their view that British cities are especially vulnerable to attack by chemical weapons. In doing so, they amplified some of the concern that members of the British government have expressed about Soviet intentions and the inconclusiveness of the Soviet-American discussions towards the draft of a treaty. What can be the explanation?

The erosion of detente has understandably set people's nerves on edge, but strategic developments in Europe have no doubt also helped to stimulate the current preoccupation with chemical weapons. The West German Chancellor, Mr Helmut Schmidt, makes no secret of his anxiety about the increasing numbers of medium-range missiles on the territory of the Warsaw Pact, not yet matched by the deployment of American cruise missiles within NATO. Yet there is no chance of an agreement to limit these developments while Salt II remains unratified. Until quite recently, European opinion would not have been excessively alarmed by this imbalance. While it has been customary (as it is prudent) to speculate on the ways in which short and medium-range weapons might be used in anger within the confines of Europe, people have usually been willing to accept that the strategic forces of NATO would be used if there were more than token trouble. The novel development is that this confidence has also been eroded, largely as a result of the hesitancy of American foreign policy in recent months. Are these also the circumstances which have led to the speculations that gas might be used in Europe without provoking a strategic response?

If so, it would be helpful that the strategic limitations of chemical weapons should be kept clearly in mind. Whatever the technical sophistication of modern chemical weapons, their strategic limitations remain what they have always been. It is unthinkable that the use or the threatened use of chemical weapons could be used to win a decisive advantage in some major conflict — or that an attempt to use them in this way by any state would fail to excite a nuclear response. The technical utility of chemical weapons, such as it may be, lies in the battlefield — and the Second World War shows that the fear of retaliation may be enough to engender restraint. The possibility that chemical weapons might be used in a nuclear war to win some larger advantage, perhaps that of making it safe to occupy some large tract of ground without first blowing it to pieces, is more real, yet still remote. It is hard to see even the most determined combatants trading the occupation of some other state's territory for the destruction of their own. In short, chemical weapons cannot by themselves substantially shift the balance of strategic strength in any major conflict, which is not to say that the military may not regard them as potentially useful in other kinds of conflicts.

So why not get rid of them? This question has been in the air for the past decade or so. Since 1974, the Soviet Union and the United States have been trying to work out the bare bones of an agreement on the subject. So far, there have been no fewer than eleven rounds of talks on the subject (and the twelfth is now going on at Geneva). A report on progress was presented to the Committee on Disarmament, and another is promised for later this year. While the past six months have seen a slackening of interest, some progress has been made. Yet the problems recognized as serious at the beginning persist.

Verification, as always, is a stumbling block, especially because plants for manufacturing the components of binary chemical munitions may be indistinguishable from ordinary chemical plants. Last year's report on the negotiations used the term "adequate verification" and suggested an international secretariat to supervise the way in which verification would be carried out. It is, however, hard to see the most significant potential signatories of a treaty to ban chemical weapons accepting the degree of detailed inspection that their potential adversaries could require. Any treaty that comes about will therefore demand of its participants a degree of trust in each other (as well as in their sources of intelligence) that has not been much in evidence in the past few years. Yet the closely analogous convention on biological weapons has survived even last year's outbreak of anthrax in the neighbourhood of Sverdlovsk. A convention on chemical weapons could be drafted along similar lines — for which reason it would be a great benefit if the Soviet Union were to provide a more detailed account of the anthrax outbreak than it has so far provided.

The scope of a treaty banning chemical weapons is another of the issues with which people have been wrestling for the past several years. Here again it is hard to see how a fully watertight treaty could ever be drafted. Some materials used in the manufacture of nerve gases have a legitimate place in the chemical industry (while phosgene is widely used as a chemical intermediate). The expressed intention of the Soviet Union and

0028-0836/80/280095-02$01.00

the United States of using incapacitating gases for domestic riot control is another serious snag. Here again, however, there is no reason why even the major powers should not accept a certain degree of fuzziness in what might be required of fellow signatories. It is not as if a violation of whatever treaty there might be would give the violator a decisive advantage.

So what are the prospects that a treaty will eventually be negotiated? And to what extent will the course of events be influenced by the willingness of the House of Representatives to let the Department of Defense have its pilot plant? Given that the Soviet Union (but also France) has the means of using chemical weapons tactically, and on the assumption that, even if the American pilot plant were followed by a full-scale production plant, the munitions produced would be similarly earmarked, there is no reason why the talks at Geneva should be interrupted. Indeed, the new development may persuade the Soviet Union that it would be prudent to make faster progress.

And there is little doubt that, if they chose to do so, the major powers could agree on the text of a treaty that would satisfy their own interests. They have learned, in the past several years, that it is possible to live with measures of arms control whose terms are not as specific as meticulous lawyers would ask. So the prospects for the treaty must depend on whether (and if so when) the major powers decide that the time has come to edge back towards detente. Many will hope that they take the plunge sooner rather than later. When that time comes, they will encounter one of the other longstanding problems of arms control — the unwillingness of other states to sign on somebody else's dotted line. On chemical weapons, France and China at least are likely to insist on their freedom to do what they do at present. Especially now that France has rejoined the enlarged Committee on Disarmament, has not the time come when the major powers should surrender the initiative to the committee? No harm, but only good, could come of such a step.

Two views on technological change

How will new technology affect the structure of society? Off and on, for the past few decades, people have been brooding on this kind of issue. This week, it became known that the British Labour Party is cautiously on the side of the pessimists. An unpublished report due to be considered by the party's National Executive later in the month correctly concludes that recent development in the technology of microprocessors will mean even more unemployment in the United Kingdom unless economic growth keeps pace with increases of productivity now foreseen; predictably, it goes on to argue that increased state intervention in the management of technical and social change is needed. This view neatly follows the publication by the OECD of a report called "Science and Technology in the new socio-economic context" prepared by what the OECD calls a "Group of Experts" for the longstanding Committee for Scientific and Technological Policy (see page 98). The OECD document comes to the same conclusion as the Labour Party, but if anything its prescription is more a charter for interference by social scientists than by governments.

During the past three years, there has been a more or less constant grumble that the applications of microprocessors now in prospect have serious consequences for people's jobs. Some will change in character. Some will disappear altogether. These calculations are correct, although the timing is as ever unsure. It does not follow, however, that microprocessors mean mass unemployment. With this as with any technological innovation, improved productivity in one important sector of industry will mean increased wealth, increased demand for goods and services and therefore more jobs in other sectors. The steam engine, whatever the Luddites said and did about it, was as dramatic a source of increased productivity as ever microprocessors will be — and the end result, at least in countries where steam engines were allowed to make a mark, was more jobs. The only reason not to welcome the coming of the microprocessors is that in some places the potential benefits of their increased productivity will not materialize, or will not be matched by comparable increases of productivity stemming from other new technologies.

The Labour Party document, to its credit, has the wit to recognize that this must be the case. The issue that will be disputed is whether more government intervention is the best way of safeguarding the future of jobs in Britain. The dispute is partly ideological. The Labour Party believes in government intervention. The present government does not. Since neither has a monopoly of wisdom, the need is to decide what governments can and cannot do. Providing every classroom or at least each school with a microcomputer might provide a sporting chance that people leaving school were familiar with one new technology, but is this the wisest course when the state school system is crying out for funds with which to buy books, mathematics text-books among them? Equally, the Department of Industry's scheme for helping industrialists become familiar with the new technology, useful though it may be to some of the participants, is no substitute for investors' sense that they can profitably invest in the British economy, and industrialists' sense that the taxation system will allow them to keep some of the profits. In short, what governments can do is to manage the climate for innovation. Governments themselves are less good at innovation. (This is no excuse for the continued delay in deciding whether in Britain the Department of Industry is to let the microprocessor company INMOS have its second £25 million; the government has a moral obligation that will not go away with the passage of time.)

Broadly speaking, these are the conclusions of the OECD report. The committee marshals impressive evidence which gives the lie to the cynical view that research and development is irrelevant to industrial innovation. The correlation between industrial (as distinct from government) spending on research and development and eventual prosperity is strong. But which is the chicken and which the egg? The OECD committee, while recognizing the difficulty, puts the issue beyond doubt. Governments wishing to foster innovation must foster research and development by industry, but without falling back on short-term fiscal incentives. It is a hard and self-denying recipe, that would entail in Britain some attenuation of the government's own research enterprise. Yet the case for doing more, not less, when times are hard is undeniable.

On the reasons for the hiatus in the affairs of the industrialized countries in the past seven years, the OECD is nothing if not robust. When money is being drained out of the economy, largely by OPEC, cannot be the best time for innovation or even mere change. All that is easier when things are going well. Yet this is a turning point in many people's affairs. More productivity is in the long run the only way out of the crisis. Although the report is short on references to the economists' gurus, Keynes and Friedman alike, it leaves the clear impression that the committee that prepared it considered that innovation is not so much a problem as an answer to an unstated problem. The committee's dissident voice, Professor Emma Rothschild, found this escalator uncomfortable because she had no clear idea where it is going. That is too much to ask.

That is the sensible part of the OECD report. It is less sensible that much of the document is taken up with the supposed need of what is fashionably called technological forecasting. This, after all, is a discipline which has yet to demonstrate itself as such. Many will suspect the phrase to be yet another licence for social scientists to make contradictory assertions about the consequences of technological innovations. The trouble, of course, is that the consequences are almost always unpredictable. All that can confidently be said is that some consequences are profound. What societies faced with rapid technological change thus need of their governments is flexibility — a capacity (and a willingness) to meet unforeseen social changes with compassion and imagination.

0028-0836/80/280096-01$01.00

Red faces (and hot tempers) on 2,4,5-T

The controversy over the use of the herbicide 2,4,5-T in the United Kingdom became even more heated last week with the revelation of a difference of opinion between government agencies over how to determine the safety of the herbicide. Thus Mr John Locke, the director-general of the Health and Safety Executive (HSE), pleaded for a more effective relationship between the executive and the Advisory Committee on Pesticides (PAC) of the Ministry of Agriculture, Fisheries and Food (MAFF).

Locke was speaking at the opening of a new HSE centre at the Royal Show (see page 100). His call for more "tying up" between HSE and PAC is, on the surface, a plea for more rationality in the review processes for toxic substances, but it underscores the strain both organizations are suffering in determining the safety or otherwise of 2,4,5-T.

The director-general's comments were voiced two days before a meeting of the HSE's Advisory Committee on Toxic Substances (ACTS), where 2,4,5-T was the main item on the agenda. Like all HSE advisory committees, ACTS has representatives from both the Trades Union Congress (TUC) and the Confederation of British Industries (CBI). With the TUC already on record as calling for a ban on 2,4,5-T, feelings were bound to run high. By all accounts it was a stormy meeting, with the TUC representatives expressing their dissatisfaction with PAC's review processes for herbicides and pesticides.

As a general rule, the TUC's representatives on ACTS believe that, where issues of health and safety are concerned, HSE should be responsible. The unions suspect the impartiality of MAFF in reviewing the toxicity of chemicals which can be of benefit to agriculture. At the meeting last week, they asked why PAC claimed in its eighth review of 2,4,5-T (published in March last year) that only three tonnes of the herbicide were used annually in Britain, when the real figure is now known to be about twenty times as much. They also want to know the names of all UK manufacturers importing, exporting or selling products containing 2,4,5-T.

Recent Customs and Excise figures confirm that some 116 tonnes of 2,4,5-T were imported into the UK in 1979. With the publication of these revised estimates, the unions are all the more sceptical of the review processes.

MAFF is seriously embarrassed by the error about the tonnage of 2,4,5-T used in Britain. PAC had assumed — wrongly — that the Forestry Commission was the largest user of the herbicide in the UK, and the three tonne figure was based on 2,4,5-T use in silviculture. It is now known that far more 2,4,5-T is used on grassland; on the basis of a recent survey, the use of 2,4,5-T in Britain last year is now put at 58 tonnes.

One especially serious aspect of the affair is that the PAC estimates were given to the Royal Commission on Environmental Pollution during its inquiry into agricultural pollution. In the report of this inquiry published last year, the royal commission gave 2,4,5-T a clean bill of health, partly on the grounds that British usage was relatively small. Members of the commission were wondering this week how the record should be set straight.

PAC is now reviewing the herbicide for the ninth time in the light of information about 2,4,5-T and its dioxin (2,3,7,8-tetrachlorodibenzo-*p*-dioxin) contaminant published in the past two years.

The subcommittee responsible, on the instructions of Mr Peter Walker, Minister of Agriculture, has now met a delegation from the National Union of Agricultural and Allied Workers (NUAAW) to hear the union's case against 2,4,5-T. In three and a half hours of often heated discussion, the union delegation insisted that 2,4,5-T should be banned. The delegation was told that the dioxin content of 2,4,5-T now set at a maximum of 0.01 parts per million in the UK is so low that it represents no threat. The herbicide itself is a teratogen in some rodent species at concentrations of 35 milligrams per kilogram of body weight, 10,000 times the concentrations at which dioxin is a teratogen. With the new 2,4,5-T formulation, 2,4,5-T will exert a teratogenic effect before dioxin.

The subcommittee also believes that there is a sufficient safety factor in the assessment of the carcinogenic risks from dioxin. The most reliable study suggests that dioxin is a carcinogen at dose levels of 0.1 microgram per kilogram of body weight per day in rodents. With the new formulation, to consume such a quantity of dioxin, rodents would need to take in 2,4,5-T at concentrations about one-tenth to a half of their body weight.

The subcommittee's recommendations on 2,4,5-T will be considered at a PAC meeting on 24 July. The same evidence will also be reviewed at a special meeting of ACTS at the end of August. Whatever the outcome of these meetings, it is clear that the trade union campaign against 2,4,5-T has had a considerable effect on HSE and MAFF.

The unions see the visit of the NUAAW deputation to the PAC scientific subcommittee as a precedent. But it is unlikely that the trades unions will be satisfied with this modest advance. The unions are openly campaigning for a change in the review process, and it was only natural that John Locke should appeal to MAFF for some help in devising a system which will satisfy all parties.

Alastair Hay

Supreme Court reprieves benzene

Washington

Strict regulation of toxic substances must be backed up by adequate scientific data on their potential danger. This was the message delivered by the US Supreme Court last week when it rejected a proposal by the Department of Labor's Occupational Safety and Health Administration (OSHA) to reduce permitted exposure levels to benzene to one part per million.

Following evidence which emerged in the early 1970s of a link between benzene exposure and various blood disorders — in particular, leukaemia — OSHA produced new regulations in 1977 which would have reduced permitted exposure levels from the current 10 parts per million.

The proposed regulation has been attacked by the chemical and petroleum industries, where more than a million workers are exposed to benzene in products from gasoline additives to paint solvents. The industries claimed that the regulations were unnecessarily restrictive; and that the cost of meeting them — measured in hundreds of millions of dollars — was incommensurate with the expected benefits.

Using such arguments, the American Petroleum Institute last year persuaded a judge in New Orleans to rule the proposed regulation invalid. Much attention had been focused on OSHA's decision to appeal to the Supreme Court, largely because the judge critized OSHA for not weighing the expected benefits of the regulations against the costs of meeting them.

In the event, the Supreme Court skirted around the cost-benefit issue. Only one member — Justice Lewis Powell — insisted that a full cost-benefit analysis should have been carried out; and the matter awaits resolution in two further cases which the court has agreed to hear next year.

No less significant, however, is the substance of the court's ruling in a case which Chief Justice Warren Burger described as raising "difficult unanswered questions on the frontiers of science and medicine". The court ruled that OSHA must demonstrate that a toxic chemical poses a "significant" risk before making a regulation.

This judgement directly undermines one of the fundamental principles on which OSHA's regulatory strategy is at present based. So far, the agency has argued that, where a chemical is suspected of having low-level toxic effects but the scientific and epidemiological evidence is insufficient to characterize these precisely, it must be

0028-0836/80/280097-02$01 00

assumed that there is no threshold below which the chemical can be considered "safe" — and industry is required to lower exposure to the limits of technological feasibility.

OSHA acted on benzene even though the evidence of increased leukaemia incidence among workers in Turkey and Ohio involved people who had been exposed to considerably more than 10 ppm over long periods of time.

The agency argued that only a technological feasibility strategy would suffice to guarantee the protection of workers, but the Supreme Court, in a 5-4 vote, agreed with industry critics that a more thorough scientific and technological justification must be produced. Admitting the existence of considerable uncertainties, the court accepted that the agency is not required to prove its point "with anything approaching scientific certainty".

Even so, in writing the majority opinion, Justice John Stevens said that OSHA had failed to produce "substantial evidence" that the new benzene rules were "reasonably necessary and appropriate" to remedy a "significant risk of material health impairment". OSHA, he said, had not produced empirical evidence or scientific opinion to show that exposure to benzene at or below the 10 ppm level had in fact caused cancer.

Predictably, the court's decision has been welcomed by industry, which has long protested at the expense of meeting the "lowest technologically feasible" criterion. Agency officials admitted that they were "disappointed" with the ruling, but vowed to press on with regulating benzene and other toxic substances.

The closeness of the Supreme Court's decision and the fact that different members gave different reasons for concurring are likely to cushion the impact. Indeed, if OSHA can produce more evidence on benzene, then the tough standard could still stand.

In a strongly worded dissenting opinion, four of the nine justices said they felt OSHA had already produced enough evidence to justify the low exposure limit. And a fifth said that, given additional evidence, he might be persuaded by OSHA's case.

David Dickson.

Soviet environment

Spending more

SOVIET capital investment in environmental protection and the conservation of endangered species will be trebled in the next Five Year Plan (1981-1985), according to what TASS has described as "preliminary data". Since the official figures for the present plan include 11,000 million rubles of direct state funding and 50,000 million from the budgets of industrial enterprises and institutions, this suggests an investment of at least 180,000 million rubles (£125,000 million) in the next five years.

The TASS announcement followed the passing of two major environmental bills, on clean air and the protection of fauna, by the Supreme Soviet. Enactment of the laws was preceded by unusually extensive reporting in *Pravda*, perhaps because of the undoubted pride which the members of the Supreme Soviet show in their progress to date. No other country, observed Deputy P.P. Vavilov, president of the All-Union Academy of Agricultural Sciences, has on its statute books laws of comparable scope, which even protect insects and soil fauna with a direct bearing on soil fertility.

Vavilov nevertheless emphasized that, even when the act becomes law in 1981, further research will be needed to ensure that its provisions are implemented in strict accordance with ecological principles.

What nobody mentioned in the debate, but what must surely have been in the minds of many of the deputies — especially those from central Russia, central Asia, Byelorussia and Estonia — was the present threat from wolves and wolf-dog crossbreeds which, according to some estimates, have doubled in numbers over the past ten years, following cutbacks in hunting and the disbanding of skilled hunting teams. The threat is particularly acute in Estonia.

No less complex are the management problems raised by the clean air bill. Air pollution has been a major problem in many Soviet cities for a considerable time, and one of the earliest preparations for the Moscow Olympic Games was the designing of electric runabout cars for the Olympic village, to reduce the effect of petrol fumes on the athletes.

Not only cities are at risk, however. In the Supreme Soviet debate, Deputy V.M. Kanun from Zhitomir spoke of the pollution threat to the Polessian forests — in spite of the expenditure, during the current Five Year Plan, of "tens of millions of rubles" on anti-pollution measures. Deputy Yu. A, Izrael', Chairman of the State Committee on Hydrometeorology and Environmental Monitoring, observed that the Union-wide anti-pollution monitoring service now has air-pollution monitoring projects in 450 cities; nevertheless, as Deputy Kipel' observed, "many plants and factories go on polluting the atmosphere and water in the same old way".

Water, in fact, is not specifically the subject of the new legislation, although, according to Deputy Izrael', progress in this field is one of the "major successes" of the environmental control programme. "Almost all the rivers of the European part of the USSR", he said, "have become cleaner".

Nevertheless, water may well soon be better regulated. A 200-person multidisciplinary research team, led by Vladimir Lazanskii, head of the All-Union Research Institute for Water Conservation, has completed a detailed computer analysis of the ecology of 26 of the largest rivers in the USSR and fifteen seas and lakes. On the basis of this study, the team has put forward several proposals ranging from the automated control of water conservation complexes and the introduction of closed-cycle processes for metallurgical works to the special processing of rain water and snow melt bearing particles of petroleum products.

Vera Rich

Industrially financed research, OECD countries

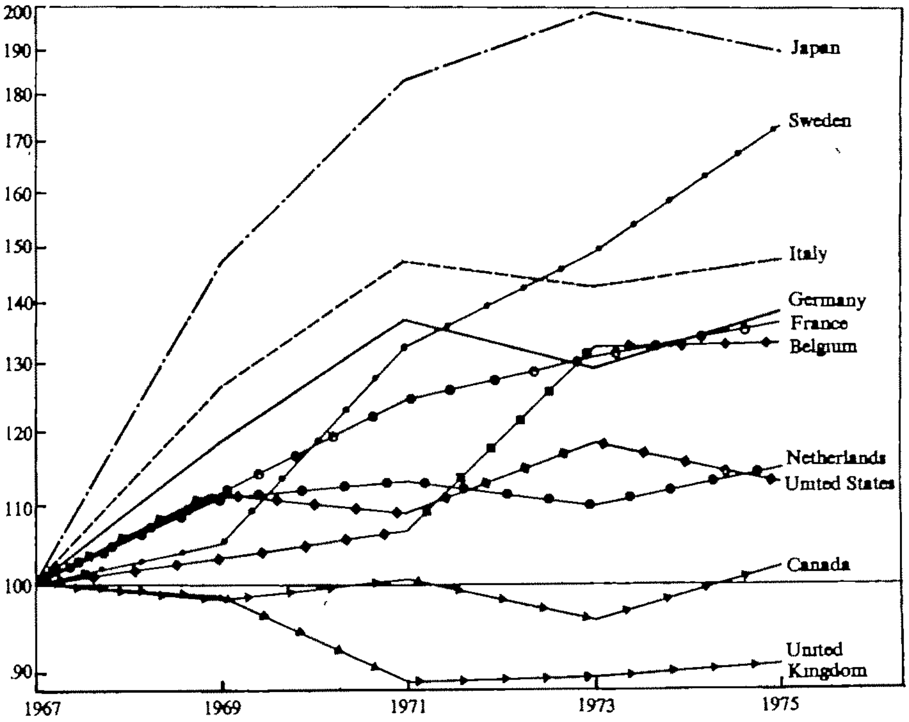

0028-0836/80/280098-01$01 00

Biotechnology

France now

A GROUP of French scientists has set up a commercial organization for the exploitation of genetic manipulation. Known as *Transgène*, the company has an initial capital of 40 million French francs. Although the capital has been provided by industrial companies, the sponsors of the new venture include the CNRS (Centre National de la Recherche Scientifique), L'Institut National de la Recherche Agronomique, L'Institut National de la Santé et de la Recherche Medicale and the Pasteur Institute.

The new organization will be based at its own laboratories near Strasbourg and its policy will be determined by a scientific committee including Professor Philippe Kourilsky from the Pasteur Institute and Professor Pierre Chambon from the Louis Pasteur University of Strasbourg. It is intended that the scientific committee will include some scientists from outside France. The scientific director of the enterprise has been recruited but not yet named.

It is understood, however, that the director is at present the head of research at a European pharmaceutical company and is not French.

The formation of *Transgène* has been talked of for several months. The capital for the enterprise has been provided by a consortium of companies organized by the Compagnie Financière de Paris et des Pays Bas (Paribas) and includes the oil company Elf, the French liquid air company Air Liquide and the champagne and brandy firm of Moet-Hennessy. The commercial head of the new enterprise will be the director of research at Parisbas, M. Robert Lattès. It appears that this French initiative has been prompted — some would say provoked — by the publicity given in the past few months to the doings of the Swiss-based company Biogen, but the organizers of *Transgène* also have in mind the steps taken in the United States during the past few years to put genetic manipulation on a commercial footing. Although nothing is known as yet of the work on which *Transgène* will be engaged, it is expected that the company will be recruiting a staff of between 50 and 80 people, most of whom will be based at the laboratories in Strasbourg.

Transgène appears to have hit on a novel way of reconciling the conflict of interest between university researchers and commercial interests that inevitably arises in such circumstances. Fifteen per cent of the shares are to be held by the sponsors of the enterprise, including the Pasteur Institute and the CNRS. A further eight per cent of the shares will be the property of a foundation yet to be established whose function will be to support basic research in the general field of molecular biology — a task that will become feasible if and when Transgène makes money.

The Strasbourg laboratory will not be completed for two years. In the meantime Transgène is hoping to make arrangements for research to begin on a contract basis in some other laboratory, possibly at the Louis Pasteur University. The scientific staff will be recruited in time to begin work at the turn of the year but the initial scientific objectives will not be defined until the scientific board is complete around October.

University industry

Surrey consults

SHORTAGES of funds are increasingly making British universities search for alternative sources of finance. The University of Surrey has in this way branched out beyond the usual pattern of university work. Last week it formally opened a new institute to tackle industrial health and safety problems.

Surrey's Institute of Industrial and Environmental Health and Safety has actually been operating for 18 months. So far, it has earned about £700,000, one-third from grants and donations and the rest from specific contracts. According to its director, Professor James Bridges, the institute is already almost entirely self-financing and hopes eventually to make a profit which can be ploughed back into the university. The members of the institute's staff are either tenured in an academic department, on short-term research council contracts or have been specifically employed by the institute on annual rolling contracts.

The institute is an amalgamation of several different academic units (the Wolfson Bionalytical Unit, the Materials Handling Research Unit, the Industrial Biomedical Unit and the Toxicology Unit). It also includes two new units, the Isolator (Gnotobiotics) Unit and the Occupational Health and Hygiene Service. The last of these is the most unexpected. It carries out no research as such, but aims to provide local industries too small to employ their own specialists with advice on health and safety problems.

The Occupational Health and Hygiene Service appears to be an effective way of making links with local industry. An investigation of sore throats and bronchitis at one local factory led to the Wolfson Bioanalytical Unit being called in to take air samples. It finally identified the source of irritation as chromium carried from one part of the plant to another when the wind was in a particular direction. The Wolfson Unit also solved a problem in the handling of glass fibre resins in a local factory after a similar introduction.

Most of the institute's work so far has been funded by larger organizations. The Materials Handling Unit, for example, has completed an ergonomic study for the EEC of the body stresses caused when men lift heavy objects, and is now doing a similar study of female workers for the UK Health and Safety Executive.

The Isolator Unit was created to build up on a previous collaboration with Vickers Medical Limited to design and make medical isolators out of flexible film. The unit is now designing film units for isolating experimental animals and protecting workers handling drugs and other potentially dangerous materials. The Toxicology Unit is engaged on fundamental work on biochemical pathways in man and animals, but most of its contract work consists of *in vitro* testing for mutagenesis and carcinogenesis.

The institute acts more as a research association than a university research department. According to its staff, the prospects for the next year or two are good, with plenty of work on hand. Thereafter, the institute will have to live on its wits, helped by whatever reputation it acquires in the meantime.

Judy Redfearn

Poles protest at academic censors

SCIENTIFIC publications should be totally exempt from state censorship, according to a report by the Polish "DiP" group *(Doswiadczenie i Przyslosc* — Experience and the Future). This unofficial body, which includes leading figures from the academic and literary professions, Party and church, was originally established in November 1978 as a discussion group to consider the economic crises facing Poland. Unable to hold the open discussions they had planned, the members of DiP have relied on questionnaires. The first such survey, "Report on the state of the country and ways of putting it right", was made in May 1979; the second, "How do we get out of this?" in December 1979 and January 1980. This second report is now in circulation.

Questionnaires were completed by 141 people. (Some of those approached declined to take part saying that they had no faith in the sense of the exercise.) The sample included 65 scientists, of whom 39 were university lecturers and professors — biologists, physicists, mathematicians and agronomists. The result is a penetrating study of the economic and social problems of the Polish People's Republics.

A necessary condition for any reforms to be successful, it says, is that confidence should be restored in the government. To this end, *inter alia*, a free flow of information is essential. A proper definition of material liable to censorship (military and industrial secrets) should be laid down, and academic publications exempted from the censors.

0028-0836/80/280099-01$01.00

Chemical weapons

Congress agrees

Washington

Citing circumstantial evidence of the use of poison gas by Soviet troops in Afghanistan, the US Congress has taken the first step towards ending an eleven-year moratorium on the production of chemical weapons.

By-passing the White House — which has nevertheless so far raised no objection — the House of Representatives last week approved the army's use of funds to renovate facilities at its Pine Bluff Arsenal in Arkansas to house the production of so-called binary chemical weapons.

The amount of money is relatively small — $3.1 million out of a total military construction budget of $4,800 million. A further $19 million will be needed to equip an intended pilot plant for the production of 155 mm binary shells. Given minimal opposition, either from within Congress or from the Administration, legislators pushing for the pilot plant are confident they can persuade the House to provide the extra cash, and that the Senate will go along. If so, the Pine Bluff plant could be in operation by 1983.

The Department of Defense has planned for two further extensions of the plant at a cost of $185 million — production plants for 8-inch artillery shells containing the British nerve agent VX and for so-called "big eye" bombs for the US Navy, like the 155 mm shells containing the nerve gas GB.

Binary weapons, the latest thing in the military gas-man's catalogue, offer safe storage and use; two relatively innocuous chemical components which react to produce a military gas only after the weapon has been primed. The US Army has been working on their developmnt since the mid-1960s.

In 1974, Congress turned down a proposal to manufacture them, on the grounds that the Soviet-American negotiation of a treaty covering chemical weapons, begun that year, would be jeopardized.

Officially, those talks still drag on. In each of the past two years, the Department of Defense has asked Congress for funds for binary weapons production, pleading Soviet superiority in both offence and defence. On each occasion, the request has been blocked by the White House.

Now the political climate has changed. Although Presidents Carter and Brezhnev agreed last year in Moscow to encourage the negotiations, the Soviet presence in Afghanistan has brought progress to a standstill. The future of the treaty, some US officials consider, will now depend on broad political considerations and not on the question whether or not the United States is producing chemical weapons.

Reports of the Soviet use of chemical agents in Afghanistan helped to change the mood of Congress and the Administration, although the details are still far from clear. US officials say there is now "strong" evidence of the use of riot-control agents, "middling" evidence of incapacitating agents, but that evidence of the use of lethal nerve agents is "weak". They support a proposal for an international fact-finding mission to gather more precise details of events in Afghanistan.

These reports, combined with accusations of Soviet development of biological weapons after the anthrax outbreak in Sverdlovsk, have created a climate in which support for a unilateral moratorium is waning. Some critics nevertheless remain vocal. Chemical weapons are of little real tactical value, "contributing nothing to fire power unless the other side chooses to use chemical first" says Professor Matthew Meselson of Harvard University.

In Congress, however, those who have previously resisted the chemical weapons programme have no plans to organize opposition to the new developments. Some argue that, since the army's existing stock of wet-eye nerve bombs is deteriorating and could become a serious health hazard, the production of binary weapons would be the lesser of two evils.

The White House occupies neutral ground. It has not supported the congressional amendments to its defence request, but neither has it opposed them. In the present climate, if Congress does give the green light to the chemical weapons facility, a presidental veto is unlikely.

David Dickson

British farming

Science on show

Agricultural shows still have the same appeal for the British public as they did in Thomas Hardy's day. The Royal Agricultural Society of England's annual show, however, is more than family entertainment. The theme of last week's show, like that of recent years, was the application of science in agriculture. Publicly supported research was much in evidence.

The Ministry of Agriculture, Fisheries and Food (MAFF) has always prided itself on the value of its research and development to the agricultural industry. In the wake of the Rothschild reorganization, almost half of the work done by the institutes of the Agricultural Research Council (ARC) is under contract from government departments. This year, for example, MAFF is spending about £34 million on basic research, matched by a similar contribution from the ARC. About £2 million will come from other sources. The Agricultural Development and Advisory Service (ADAS) will spend £54 million on getting the results of research to the farmer. The work of ADAS and ARC institutes was therefore prominent at the Royal Show. No doubt in an attempt to stave off the criticism that much of this research is too basic to bear on farmer's practical problems, the exhibits included examples of both pure and applied research.

The National Vegetable Research Station (NURS) displayed its basic research on the introduction of resistance to tobacco mosaic virus into tomato plants. It is also seeking to interest British food processors and growers in varieties of small outdoor tomato plants which yield fruit that is superior to (although more expensive than) Italian canned tomatoes.

Import substitution is a recurrent theme. The NVRS, proud of having helped to reduce the level of British onion imports since the early 1970s by the introduction of Japanese varieties which can be planted all the year round, is now working towards the home-grown baked bean.

On animal nutrition, the Rowett Research Institute is improving on the starch equivalent as a means of assessing the metabolic value of feeding stuffs. The Animal Diseases Research Association was last week offering advice on the prevention of hypothermia in lambs and the Meat Research Institute on the measurement of fat deposition in live animals. The long-term objective is to find better ways of controlling the proportion of fat to lean meat.

In these and other wys, the Royal Show has become an annual celebration of the notion that British agriculture is outstandingly efficient. The increase of agricultural productivity in the past 30 years is certainly impressive. The belief that British agriculture is the most efficient in the world has become almost a myth, difficult to challenge.

Such a challenge has come, however, from the Centre for Agricultural Strategy at the University of Reading. In a report published last week, the centre says that British agriculture is by no means streets ahead of European agriculture. Belgium, the Netherlands and Denmark may be doing better. The centre agrues that British farmers have invested too much capital in their businesses, especially in farm machinery. The Royal Show last week would have tempted them further down this primrose path.

Judy Redfearn

Fusion

Studied design

Planning time is running out for the INTOR project, the international design study of a thermonuclear reactor set up last year by the International Atomic Energy Agency. At the ten-day biennial conference on fusion and plasma physics just ended in Brussels, the members of the international design team (Euratom, Japan, the Soviet Union and the United States) confirmed that their final report will be with the IAEA next June. Then, it is acknowledged, will be the time for tackling

0028-0836/80/280100-02$01.00

the political problems.

INTOR stands for International Tokamak Reactor. The objective so far has been to define the design parameters of a 620 MW (thermal) tokamak which would test engineering systems required in a commercial fusion reactor. The objectives of INTOR are to produce a token amount of electricity and to demonstrate tritium breeding and 25-50 per cent availability. Decisions on the future of the project will be taken by members of the design team only when the final report is ready.

For the time being, the team is innocent of politics. The first difficult step will come when the design study is complete and it is necessary to set up a full-time design group.

If ever built, INTOR will be a net consumer of electricity and tritium. The reactor would use a charge of 3 kg of tritium which would have to be replaced every six months. Average electrical power consumption would be 200 MW. Capital costs would be of the order of the cost of the American Engineering Test Facility, about $1,000 million. **Robert Walgate**

US fusion

Middle course?

Washington

Magnetic fusion research in the United States will be further encouraged by a new report prepared for the Department of Energy. The report concludes that research is now sufficiently encouraging to justify a new stage of engineering experimentation.

Even so, the report falls short of endorsing the Engineering Test Facility being promoted by some members of the fusion research community. It says that the proposed high neutron flux and heavy usage, as well as the role of the ETF as a direct stepping-stone to commercial fusion, are "too ambitious" and "inappropriate at this stage".

The report recommends instead that the department should construct, at an estimated cost of less than $1,000 million over ten years, a more modest Fusion Engineering Device (FED) based on the tokamak design. This device, the report says, should be sited at a new Center for Fusion Engineering (CFE).

The proposals come from a subcommittee of the department's Energy Research Advisory Board, chaired by Dr Solomon Buchsbaum of Bell Laboratories. Officially they are still in draft form; but they are likely to form the backbone of the Administration's response to critics who claim it has been dragging its feet on the commercial application of fusion.

The Buchsbaum committee in passing attacks a previous report prepared two years ago by a similar committee chaired by Dr John Foster of TRW Industries. That argued that it would be unwise to pursue an ambitious programme based on the tokamak design, urging that research support should be spread more widely.

The Administration has responded by increasing support for alternative designs, in particular for the Elmo Bumpy Torus being developed at the Oak Ridge National Laboratories (*Nature*, 1 May), to the chagrin of the potential commercial sponsors of fusion techology, who have felt that the Foster committee was too cautious.

Leading the attack has been Mr Mike McCormack, chairman of the energy subcommittee of the House Science and Technology Committee. Mr McCormack has been pushing hard for an accelerated fusion research and development programme. Last year his subcommittee appointed a 12-member Fusion Advisory Panel which recommended that the ETF, being designed at Oak Ridge, should be built in 1987.

The Buchsbaum committee is the response to the McCormack initiative by Dr Edward Frieman, director of the Office of Energy Research. It justifies its shift of view by citing recent "rapid scientific progress" and says that the US is now ready to embark on the exploration of the engineering feasibility of fusion.

Among recent successes are:

- validation of empirical predictions of achievable electron energy confinement times;
- demonstration in experiments with neutral beam currents that the heating of plasma to ignition temperature is feasible;
- the absence of evidence that impurities will tend to accumulate in the centre of high density plasmas; and
- the existence of several promising schemes for steady-state current drive using radio-frequency or particle-injection techniques.

These and other developments, the committee says, make it appropriate to move on to the study of ignited plasmas — where fusion reactions proceed without external energy being supplied. This would be one of the principal goals of the FED, which would also be used to explore reactor technology and to study safety questions. But the new report, like that of the Foster committee, asks that attention should continue to be given to alternative designs in case the tokamak configuration disappoints.

The committee therefore supports the proposal for a large tandem mirror machine, if only to prove the principle that open-confinement systems may be feasible; this may be included in the 1982 budget request. The committee also asks that work on the Elmo Bumpy Torus should be strengthened to clarify some immediate physics issues, but adds that the proposed $75 million investment is "too large, given the existing uncertainties in the physics of the EBT configuration".

The appearance of the committee's draft report aptly coincided with a debate in the House of Representatives on the Department of Energy's proposed 1981 budget. As part of a general attempt to trim long-range energy research, the House Appropriations Committee had proposed that the magnetic fusion budget be reduced by $23 million from the Administration's request for $396 million (an 11.5 per cent increase over this year).

Waving copies of the Buchsbaum report, House members were able to restore the money by an amendment which also reduced some of the proposed cuts in high-energy and nuclear physics research programmes. But Mr McCormack is not satisfied. He is now talking of introducing a supplementary budget request later in the year to bring the fusion budget more into line with the Buchsbaum proposals, which recommend that the total budget be almost doubled over the next five to seven years.

Not unexpectedly, the Buchsbaum report is less bullish than Mr McCormack. It says that heavy spending on the engineering aspects of fusion will not be necessary until 1983-84. By then, results from the Tokamak Fusion Test Reactor at Princeton will be available, and should help to decide the design details of the proposed Fusion Engineering Device.

David Dickson

New NSF director

Dr John B. Slaughter (below) was nominated to take over from Richard C. Atkinson as director of the National Science Foundation last week. Slaughter, an engineer by training, has been persuaded to return to the NSF after leaving only a year ago to become academic vice-president and provost of Washington State University. He had previously been assistant director of NSF for astronomical, atmospheric, earth and ocean sciences. Atkinson, a psychologist, has already taken up an appointment at the University of California.

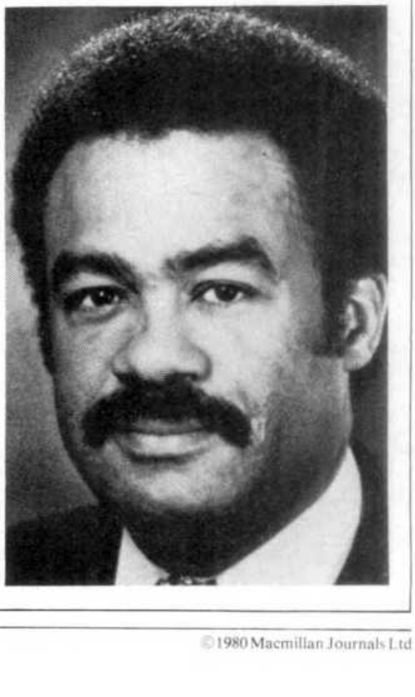

0028-0836/80/280101-01$01.00

Albanian science

Isolated still

Albania is embarking on its own characteristically isolated programme of science and technology. At the two-day plenary meeting of the Central Committee of the Albanian Workers' Party last month, the main theme was the need to increase the level of scientific research and to apply research and development more effectively for the development of the country.

The issue is timely. The five-year plan (1981-85) now being prepared includes increases of industrial and agricultural production of 40-42 per cent. But with the departure of the Chinese, "self-reliance" has become the order of the day. Addressing the plenum, Ramiz Alia of the Party's Political Bureau paid a glowing tribute to the Albanian "specialists, technicians and workers" who had had to take over the various technological projects left unfinished when the Chinese quit.

According to Alia, Albania is now able to design and set up "self-reliantly" every object the economy needs, whether "industrial, hydrotechnical, railway or cultural". Self-reliance is also to be the watchword for the future. In the natural sciences, he stressed the need for research in applied nuclear physics and the mastering of neutron and laser technology for both industrial and military use. Research projects in biophysics should also, he said, be started.

On the applied side, Alia emphasized the importance of water management; he said that 52 per cent of the arable land in Albania is now irrigated — the highest proportion in Europe. Alia also called for strains of wheat capable of producing 70 to 80 quintals per hectare, an increase of 10 to 15 per cent compared with existing hybrids. Alia said that fundamental work was needed to reach the target of 95 per cent extraction of useful minerals.

The first Secretary of the Central Committee of Albania, Enver Hoxha, in his closing address to the plenary session, put the Party's demand in more general terms. Albania, he said, has now reached an advanced stage of economic and social development, so that what is now required of science is "a generalization, improvement and an entire positive transformation in practice and theory — a qualitative break, a revolution in production technique, technology or organization". Technological advance, however, must not be accompanied by a drift from agriculture. Development of the agricultural sciences and the intensification of agricultural production is aimed at maintaining the current demographic distribution, in which some two-thirds of the Albanian population live in the countryside. **Vera Rich**

CORRESPONDENCE

Cruel Malthus

SIR, — Peter Laslett[1] does injustice, I believe, to British social science in stating that, except perhaps for John Maynard Keynes, "Thomas Robert Malthus may be quite justifiably called . . . the most important of all English-speaking social scientists". From the "population principle" which Malthus claimed[2] to have "established in the first six pages" of his 1798 *Essay*, Malthus concluded that poverty was caused primarily by the "vices" of the poor themselves.

Accordingly, "to assist the poor in such a manner as to enable them to marry as early as they please and rear up large families is a physical impossibility[3]". Ferociously consistent, this mild-mannered cleric and professor advocated abolition of the poor laws which sheltered, though inadequately, the helpless poor. He opposed repeal of the corn laws, universal suffrage, and a regularly meeting representative parliament.

Malthus's stature as a social scientist may be judged from his pronouncement[4] that "The structure of society in its great features will probably always remain unchanged. We have every reason to believe that it will always consist of a class of proprietors and a class of labourers." Yet his doctrine, which was born during the French Revolution, has surfaced repeatedly in various guises at times of social stress.

This recurrence is not particularly surprising. Malthus himself stated the political utility of his "principle" quite baldly in later editions of the *Essay*[5].

"Among the poor themselves, its effects would be still more important. That the principal and most permanent cause of poverty has little or no *direct* relation to forms of government or the unequal division of property; and that as the rich do not in reality possess the *power* of finding employment and maintenance for the poor, the poor cannot in the nature of things possess the *right* to demand them, are important truths flowing from the principle of population which when properly explained would by no means be above the most ordinary comprehension.

"And it is evident that every man in the lower classes of society who became acquainted with these truths would be disposed to bear the distresses in which he might be involved with more patience; would feel less discontent and irritation at the government and the higher classes of society on account of his poverty; would be on all occasions less disposed to insubordination and turbulence; and if he received assistance either from any public institution or from the hand of private charity, he would receive it with more thankfulness, and more justly appreciate its value.

"If these truths were by degrees more generally known . . . the lower classes of people as a body would become more peaceable and orderly, would be less inclined to tumultuous proceedings in seasons of scarcity, and would at all times be less influenced by inflammatory and seditious publications from knowing how little the price of labour and the means of supporting a family depend upon a revolution.

"The mere knowledge of these truths, even if they did not operate sufficiently to produce any marked change in the prudential habits of the poor with regard to marriage, would still have a most beneficial effect on their conduct in a political light; and undoubtedly one of the most valuable of these effects would be the power that would result to the higher and middle classes of society of gradually improving their governments without the apprehension of those revolutionary excesses, the fear of which at present threatens to deprive Europe even of that degree of liberty which she had before experienced to be practicable, and the salutary effects of which she had long enjoyed."

While Malthus's hopes for pacifying the "poorer classes" have not been conspicuously successful, the doctrine has found a new use in the post-war years, as the poor in the developing countries have raised demands on their erstwhile rulers. The Malthusian resurgence[6] assuages the conscience of the "class of proprietors" in the rich countries and facilitates inaction by their governments.

Yours faithfully,
HARRY GRUNDFEST

College of Physicians and Surgeons,
Columbia University,
New York, NY, USA.

---

1. *Nature,* **285,** 173 (1980).
2. 6th Ed., **2,** 453.
3. 7th Ed., 479 (1872).
4. *ibid.,* 480.
5. *ibid.,* 479.
6. Grundfest, H., *Monthly Review,* **3,** 247 (1951).

Nuclear protest

SIR, — Your leading article of 19 June concerning nuclear power exemplified many of the elitist opinions of the scientific "community". It appears you would like the public to reach an understanding of "the niceties of nuclear power" similar to its understanding of the relation between salary rises and inflation. The simplistic view of the economy (salary rises cause inflation) that many people have has been impressed on them by successive governments and the Tory press. Is this how you want the nuclear power debate to proceed?

Your arrogant suggestion that the willingness of people to demonstrate is sustained only by the division of "professional" opinion is insulting to the many demonstrators who have arrived at an anti-nuclear position after careful consideration of available information on all the aspects of nuclear power.

The "key to the future of nuclear power" does not belong with a small and self-interested clique of professionals; it belongs with society as a whole. The real trouble with the nuclear debate is not that it is too polite but that it centres on technical discussion while ignoring the political, for example, the proliferation of nuclear weapons that is already accompanying the proliferation of nuclear power, the setting up of an armed secret police force and the denial of trade union rights (which is one of the main political reasons for developing nuclear power, according to Thatcher). Hopefully, members of the public will continue to see through the "leave it to the experts" myth.

Yours faithfully,
BRIAN CUMMINS
ALAN BEARD
DAVE SMITH

Edinburgh Science for People,
Biochemistry Department,
University of Edinburgh, UK.

0028-0836/80/280102-01$01.00

NEWS AND VIEWS

How to use geothermal energy

from S.W. Richardson & A.A.L. White

WITHIN the next decade it will be possible to obtain large quantities of hot water from permeable geological formations buried deep in the sedimentary basins of the UK[1]. The temperature of the water is restricted by the terrestrial heat flow and the occurrence of suitable formations to a maximum of 110°C (ref. 2) but this limit could be extended if the technology is developed to extract heat from impermeable crystalline rocks[3].

There is a multitude of possible uses for this relatively low grade heat but here we consider the relative merits of just two such applications: the generation of electricity and the provision of district heating. These uses are very different in structure. District heating is, at first sight, the obvious application — and has dominated official thinking for several years[4] — but is capital intensive due to the cost of the network of pipes needed for distribution. The plant required to convert the heat into electricity is relatively cheap but provides a much less efficient use of the energy due to the low conversion efficiencies of heat engines operating at these low temperatures. To illustrate the differences between these schemes we investigate the case of two hypothetical entrepreneurs, one considering investing in boreholes and a distribution network hoping to make a profit by selling heat to householders; the other aiming to sell geothermally generated power to the electricity utility.

It is reasonable to assume that the scheme which offers the higher return on capital is more likely to be implemented. Costs and income for converting a small city to district heating are found using figures produced for the Combined Heat and Power reports[5-7]. Electrical generation is provided by 10 MWe plant based on the Rankine cycle with an organic working fluid and costs are taken from American generic studies[8,9]. The geothermal energy is assumed to be provided by pairs of production-reinjection boreholes or 'doublets' sunk into proven aquifers at 3 km depth containing water at 100°C. Aquifer transmissivity is taken to be 3.5×10^{-4} m^2 s^{-1} and flow rates of 50 kg s^{-1} are maintained by pumping. The cost of providing these holes[8] is £1.0M per doublet for a scheme involving a number of doublets.

District heating

Allowing for heat exchanger effectiveness and losses in the distribution system, we assume that each doublet will be able to provide water at 90°C to the householder. With a 60°C (ref. 5) return temperature this represents some 6.3 MWth, sufficient to provide for 1520 households (see p.85 of ref. 5). The cost of the distribution network varies with the housing density[5,7] and the capital costs of this scheme are as follows.

Household density per hectare	12	20	50	150
Heat load, MW km^{-2}	6	10	25	75
Distribution pipework cost per household £ (1980) (ref 5, p 80)	2600	1270	600	520
Total costs per doublet £M (1980)	4.95	2.93	1.91	1.79

It has been assumed that £1 (1976) = £1.6 (1980) and that all the boreholes are drilled within the city (extra significant figures are included allowing the argument to be followed in detail).

The energy papers found that each household will require 39 GJ per year[6] so the installation of the network will allow the entrepreneur to sell 5.9×10^{13} J per year.

The sale price of this heat will be determined by the price of alternative fuels since householders will not choose to convert their existing wet central heating system, or pay to have a number of radiators installed, unless the heat is considerably cheaper: indeed a major obstacle to district heating could be the need to coerce people to join the system[7]. However, in this work we have assumed 100% penetration of the heat market as this was the figure used to derive the costs in the energy papers. The current UK prices for heating alternatives, making due allowance for the inefficiency of domestic boilers, are shown below. Geothermal district heat sold at each of these prices produces the annual income shown.

Fuel	Price, £ per GJ	Income, £ per year
Gas	1.95	116,000
Coal	2.40	142,000
Oil	5.50	325,000

Against income must be set the pumping costs since the 'doublet' operation will require some 250 kWe. At 38% load factor[6] this represents £29,000 per yr. where the electricity is purchased from a utility at 3.5p per kWh. The net incomes are shown as percentages of the capital costs in the Figure and are seen to vary from 2% per yr. if the heat were supplied at gas prices to a sparse area of 12 households per hectare, to 16% if heat were supplied at oil prices to a densely populated area with heat demand from 150 households per hectare.

Obviously a geothermal district heat scheme will be relatively attractive in a fuel economy dominated at the present time by oil. This is the case in France and explains the energetic French exploitation of their geothermal resources in heating schemes. In Britain, where the heating market is dominated by gas, geothermal district heating schemes will be rather less attractive as an investment.

The income from each doublet may be increased if it is possible for the householders to accept a lower return water temperature of 50°C, allowing each borehole to supply 2,025 households. However, the network costs increase in proportion and the returns on capital are not significantly altered.

Similarly the load factor of the geothermal system could be increased by adding fossil fuel fired boilers to the network to provide for peak demands. However, the network extension required to accept the boreholes' output cause the improvements, if any, to be of second order.

Electricity generation

The efficiency of Rankine cycle generation from a hot water geothermal source is[10]

$$\eta = \alpha \left[1 - \frac{T_0}{T_2 - T_1} \ell n \left[\frac{T_2}{T_1} \right] \right]$$

where T_0 is the heat rejection temperature determined by the environment, T_2 is the

---

A.A.L. White is a Research Officer at the Central Electricity Generating Board's Marchwood Engineering Laboratories. S.W. Richardson, a Lecturer in Geology and Fellow of St. Edmund Hall Oxford, is currently on leave at Marchwood.

0028-0836/80/280103-02$01.00

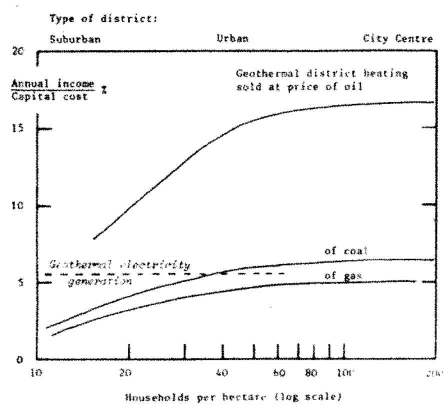

How return on capital for a geothermal district heating scheme varies according to the household density and the equivalent fuel price.

geothermal source temperature and T_1 is the temperature at which the geothermal fluid is reinjected into the aquifer. α is an empirical constant which is determined by the losses in the power cycle and we take the value $\alpha = 0.6$[8]. For $T_2 = 373$ K, $T_1 = 308$ K and $T_0 = 298$ K, $\eta = 0.073$ and the gross electrical output is 1 MW per doublet. The capital cost of the plant is £754,000[8] and the cost of the boreholes and connections to the central plant is £1.34M per doublet. Total capital is thus £2.09M for a net electrical output of 750 kWe. Operating at an 80% load factor this entrepreneur is able to sell some 5.3×10^6 kWh each year to the utility worth £116,000 at the current price of 2.2p per kWh paid by the Electricity Council's Area Boards. The return on capital is 5.5% per year.

Relative and absolute merits of the applications

Of the two schemes, electricity generation would have a higher return on capital if the price at which the other sold heat were determined by gas, for all dwelling densities. For a density of 40 households per hectare it would require an increase in the price of gas by 30% with the electricity price unchanged for district heating to hold the advantage. On the other hand, if the price of heat were fixed by oil, district heating would provide the better investment for densities greater than 12 households per hectare. The relative merit of the schemes is not sensitive to the assumed temperature of the aquifer.

It should be noted that we have stacked the odds in favour of district heating, in three respects particularly. First, the boreholes are assumed to be within the district they serve. Heat transmission would materially raise the capital cost of the scheme. Second, we have included no 'overheads' allowance for the district heating scheme. For the electricity scheme most of these costs are included in the difference between the Area Board's buying and selling price for electrical energy. Third, we have assumed (with refs 5 and 7) 100% market penetration. To achieve this, district heating would in fact have to set its price considerably below that of competing fuels.

Neither of the schemes is particularly attractive in absolute terms; but should energy prices as a whole increase relative to other costs this particular conclusion could well be reversed. In a regime under which a large proportion of electricity is generated from fossil fuels, major relative changes in electricity and fossil fuel prices seem unlikely.

We conclude that the generation of electricity from low grade heat is at least as likely to become an attractive proposition as the provision of geothermal district heating in countries which, like Britain, generate a large proportion of their electricity from fossil fuels. Paradoxically, the geothermal electricity option saves money but wastes fossil fuels: we suspect that none but the most high minded will be put off. □

---

1. Oxburgh, E.R. *Nature* **262**, 526 (1976).
2. Oxburgh, E.R. *et al.* in *Advances in European Geothermal Research EECXII/185/80EN* Brussels (1980).
3. Batchelor, A.S. in *Advances in European Geothermal Research EECXII/185/80EN* Brussels (1980).
4. Garnish, J.D. *Energy Paper* no. 9 HMSO (1976).
5. Wright, J.K. *et al. Energy Paper* no. 20 HMSO (1977).
6. Cassels, J.M. *et al. Energy Paper* no. 34 HMSO (1979).
7. Marshall, W. *et al. Energy Paper* no. 35 HMSO (1979).
8. Milora, S.L. & Tester, J.M. *Geothermal Energy as a Source of Electric Power* (MIT Press, 1976).
9. Cummings, R.G. & Morris, G.E. *Los Alamos Scientific Laboratory Report LA7888* (1979).
10. White, A.A.L. *Inst. Elect. Eng. Proc.* **A** (in the press).

Changes in length-of-day and atmospheric circulation

from Kurt Lambeck

OBSERVATIONS reported in this issue of *Nature* (Hide *et al.* p141) show that zonal components of atmospheric momentum contribute to high frequency changes in the length-of-day.

For many years astronomers have observed fluctuations in the Earth's rate of rotation — or changes in the length-of-day — that are attributable to various forces acting on the Earth's mantle and to a redistribution of mass within the Earth, oceans and atmosphere. Despite the smallness of these departures from uniform rotation — changes in length-of-day of about 10^{-3} s typically occur over time intervals of a few days to several years, and changes of about 10^{-2} s occur over several decades — they have intrigued geophysicists for many years and a complete discussion requires one to delve into atmospheric and oceanic circulation problems, into the Earth's elasticity and anelasticity and into magnetohydrodynamics of the core[1,2] (Fig. 1). Astronomers measure the integrated amount τ by which the Earth is slow or fast

Fig. 1 Schematic illustration of the forces that perturb the Earth's rotation. Topographic coupling of the mantle to the core has been referred to as 'Core Phrenology' by R.R. Hide while the beetles, following T. Gold, represent the effect of continental drift.

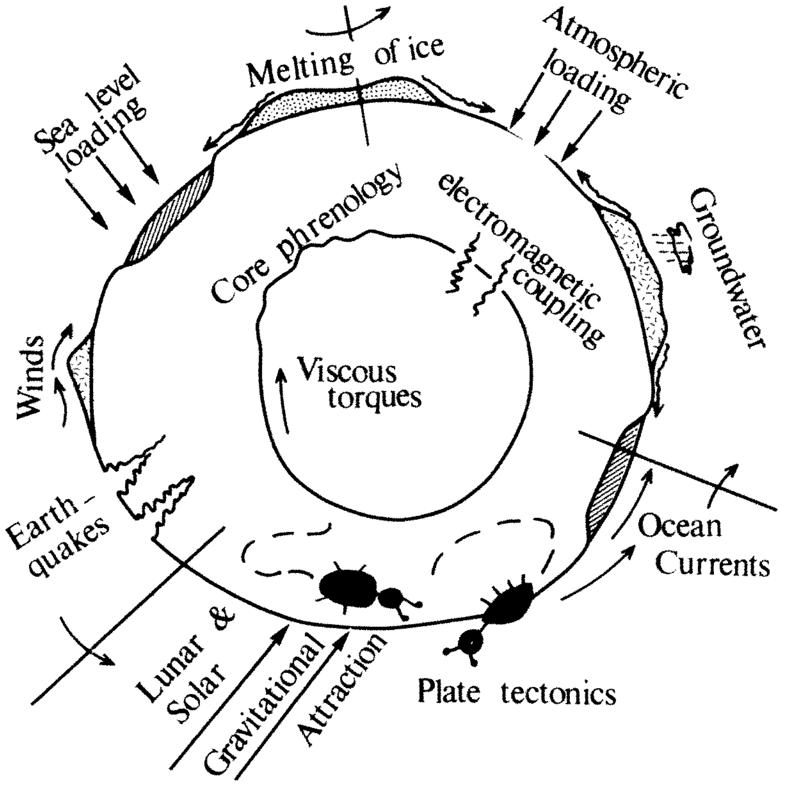

0028-0836/80/280104-02$01.00

after a certain time interval by comparison with a uniform time scale and the first derivative of this function gives a measure of the change in the length-of-day. Figure 2 illustrates the spectrum of the proportional changes in the length-of-day. Present techniques give accuracies for τ of about 1.5×10^{-3} s for an integration time of about 5 days[3] but new observational techniques based on laser range measurements to artificial satellites or to the Moon and long-baseline radio-interferometry have been developed. Preliminary results[4,5] indicate that improvements in resolution and precision are imminent.

We can anticipate that a new part of the length-of-day spectrum will rise above the measurement noise level (see Fig. 1). For example, rapid changes in length-of-day may occur in conjunction with very large earthquakes, similar to the Chandler wobble problem[6,7], in which the direction of the rotation axis is displaced relative to the Earth's crust when large earthquakes occur. Such changes will only be evident if there is no 'meteorological noise' in the length-of-day data or if the meteorological contribution to the length-of-day changes can be reliably evaluated from the meteorological data.

The contribution of the atmosphere to the broad spectrum of rotation perturbations has long been recognized as being important. A satisfactory quantitative comparison of the zonal angular momentum computed from wind data with astronomical observations was made only relatively recently[8] but it is now recognized[9] that variations in length-of-day with frequencies between about 0.2 cycles yr^{-1} and 4 cycles yr^{-1} are mainly a consequence of an exchange of angular momentum between the Earth and the atmosphere. This conclusion was substantiated by Lambeck and Hopgood in a recent compilation of ten years of zonal angular momentum[10]. At higher frequencies (i.e. $\gtrsim$ 4 cycles yr^{-1}) the atmosphere may contribute significantly to the length-of-day spectrum[1,9]. A quantitative comparison of the length-of-day observations with the zonal winds in this frequency range has now been attempted by Hide and co-workers, (this issue of *Nature* p141) based on data collected in 1979 during the first CARP Global Experiment.

Hide *et al.* have attempted to evaluate the zonal component of the angular momentum of the atmosphere at 12 hourly intervals using wind and pressure data collected during two 8 week periods in 1979. Where observations were incomplete they were supplemented by values deduced from numerical circulation models. A comparison with the astronomical length-of-day data, particularly for the second period, indicates a generally good agreement and confirms that the atmosphere makes a significant contribution to the high frequency changes in length-of-day. In particular, observed changes in length-of-day over five day periods can be attributed to rapid exchanges of angular momentum between the solid Earth and the atmosphere. From Hide *et al.*'s Fig. 3 it is also clear that shorter period, atmospherically induced, changes in rotation can be anticipated when the new methods of observing the rotation are fully exploited. What Hide *et al.*'s results show is that for precise and high-resolution length-of-day observations to be of geophysical use, the zonal wind field must be globally known with an accuracy and resolution that is at least as good as that collected during the first CARP Global Experiment. Such a major undertaking is justifiable for meteorological reasons. If future work substantiates Hide *et al.*'s conclusion then it may also become possible to use the high frequency and irregular length-of-day fluctuations as global contraints in numerical modelling of the circulation and, in particular, this may lead to a better understanding of how the atmospheric torques are distributed over the Earth's surface.

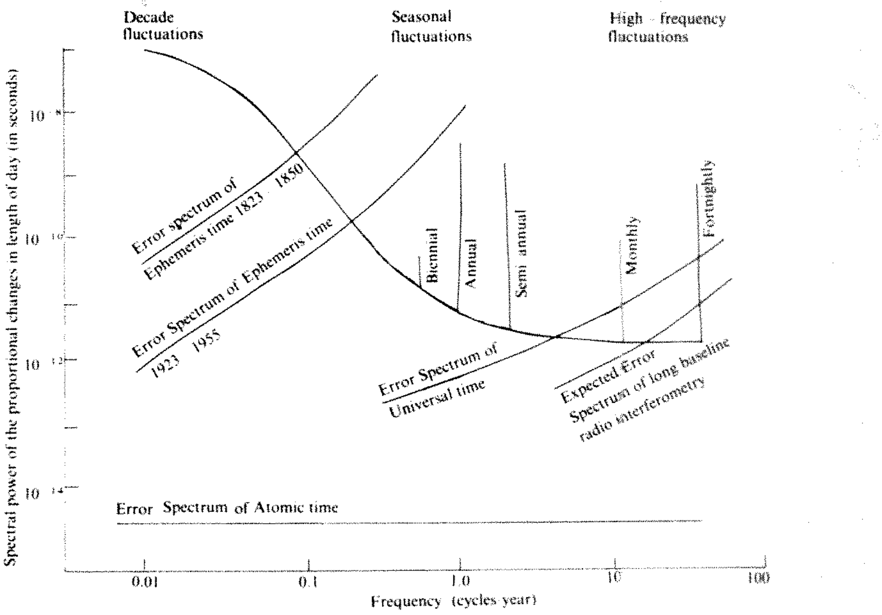

Fig. 2 Schematic spectrum of the proportional changes in length-of-day based on astronomical observations taken since the early nineteenth century. The error spectrum of Universal time is that which can be attained with astronomical observations since the introduction of atomic time. The error spectrum of ephemeris time is appropriate to the older data for the indicated time-intervals.

Towards the other end of the length-of-day spectrum, meteorological influences do not appear to be very important[1,10] although some contribution cannot be excluded. Recently it has been suggested by Currie[12] that there is an 11 year length-of-day fluctuation asociated with the solar cycle. Such a suggestion has been made previously[13] but this conclusion is hard to reconcile with the quality of the earlier astronomical data. For example, prior to 1850 the astronomical data becomes only barely significant when averages are taken over 10 years while from 1923–55 only 5 year averages are significant (Fig. 2). Only since the introduction of atomic time in 1955 can one be certain that fluctuations with about 10 year periods will reflect real changes in rotation. This being said, a relation between solar activity and the Earth's rotation cannot be dismissed if there is a solar influence on the zonal circulation as was suggested most recently by Nastrom and Belmont[14]. Attempts at evaluating the contribution of the atmosphere to long period length-of-day variations have not been wholly successful through lack of complete and reliable meteorological data but they do indicate that the winds can contribute at most about 10–20% to the decade length-of-day fluctuations[1,10].

Partly by an elimination process, core-mantle coupling processes[1,15] remain the most likely contenders for these decade fluctuations but here, as at the higher frequencies, the atmospheric contributions should be eliminated before other geophysical mechanisms can be reliably evaluated. Hide *et al.*'s results shows that this indeed can be done. ☐

Kurt Lambeck is Professor of Geophysics in the Research School of Earth Sciences, Australian National University, Canberra.

---

1. Lambeck, K. *The Earth's Variable Rotation; Geophysical Causes and Consequences* (Cambridge University Press, 1980).
2. Munk, W.H. & MacDonald, G.J.F. *The Rotation of the Earth* (Cambridge University Press, 1960).
3. *Annual reports of the Bureau International de l'Heure*, Paris.
4. King, R.W., Counselman, C.C. & Shapiro, I.I. *J. geophys. Res.* **83**, 3377 (1978).
5. McCarthy, D.D. & Pilkington, J.D.H. *Time and the Earth's Rotation* (Reidel, 1979).
6. O'Connell, R.J. & Dziewonski, A.M. *Nature* **262**, 259 (1976).
7. Mansinha, L., Smylie, D.E. & Chapman, C.H. *Geophys. J.R. astr. Soc.* **59**, 1 (1979).
8. Lambeck, K. & Cazenave, A. *Geophys. J.R. astr. Soc.* **32**, 79 (1973).
9. Lambeck, K. & Cazenave, A. *Phil. Trans. R. Soc. A***284**, 495 (1977).
10. Lambeck, K. & Hopgood, P. *Geophys. J.R. astr. Soc.* (in the press).
11. Hide, R., Birch, N.T., Morrison, L.V., Shea, D.J. & White, A.A. *Nature* **285**, 114 (1980).
12. Currie, R.G. *Geophys. J.R. astr. Soc.* **61**, 131 (1980).
13. Stoyko, A. & Stoyko, N. *Bull. Acad. R. Belg. Ser 5* **55**, 279 (1969).
14. Nastrom, G.D. & Belmont, A.D. *J. geophys. Res.* **85**, 443 (1980).
15. Hide, R. *Phil. Trans. R. Soc. A***284**, 547 (1977).

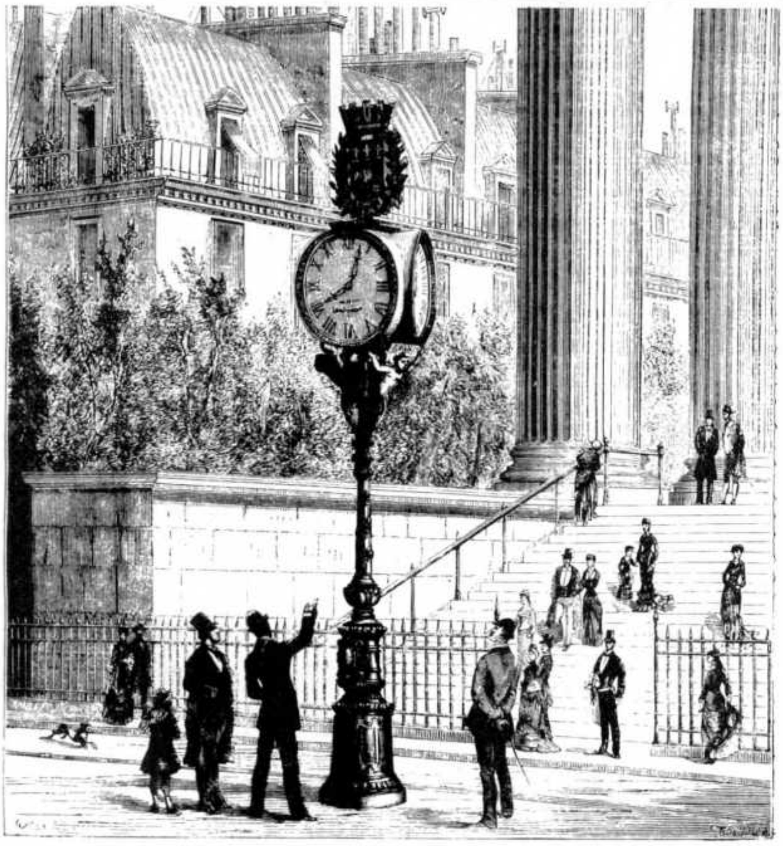

The Pneumatic Clock on the Place de la Madeleine.

100 years ago

To distribute the time with accuracy and uniformity in a large city is a problem of great utility and extreme importance. This problem has been all but completely solved by the pneumatic clocks erected since March last in the principal streets of Paris and among a considerable number of subscribers, who, for a halfpenny a day, receive dials with pneumatic receivers established in the public streets and in private buildings.
From *Nature* **22**, 8 July, 126, 1880.

Neurological mutants affecting myelination

from Richard P. Bunge

THEIR names (twitcher, quaking, jimpy, shiverer, trembler and dystrophic) suggest characters from a Dickens novel. They are, in fact, colloquial designations of the neurological abnormalities characterizing 6 strains of mutant mice, each with severe abnormalities of the myelin sheath within some part of their nervous system. These mutants provide important models of human disease and were the subject of a recent international meeting.*

The spiral membrane of the myelin sheath is formed by an intriguing feat of cellular acrobatics. The myelin forming cell extends a cellular process over a length of nerve fiber and deposits an expanding sheet of plasma membrane as a 'jelly roll' around the axon. As this cell process extends, the cytoplasm between the layers of plasmalemma is extruded and the spiralled membrane compacts into a multilayered sleeve; this provides the insulating properties that increases conduction velocity. The myelination process, which occurs during the fetal and neonatal period, requires a large metabolic investment in the synthesis of prodigious amounts of new cell membrane; about 1/3 of the weight of the mature mammalian central nervous system is myelin.

Each of the curiously named myelin deficient mutants appeared on stage at the Seillac meeting but for one it was a debut. Twitcher provides a direct example of the results of a degradative enzyme deficiency in myelin-forming cells. This autosomal recessive mutant, first observed in 1976 at the Jackson Laboratory, has been studied by Duchen and his colleagues at the Institute of Neurology in London. They have observed that both the central nervous system (CNS) and peripheral nervous system (PNS) contain excessive numbers of macrophages laden with peculiar crystalloid inclusions and multiangular bodies. These were found in areas of myelin loss and closely resembled cells that occur in the human degenerative disorder known as human globoid cell leukodystrophy, or Krabbe's disease. When Suzuki and Kobayashi at Albert Einstein in New York measured enzyme activities in this mutant they found a severe shortage of the enzyme that catalyzes the breakdown of one of the most prominent myelin glycolipids, cerebroside, to ceramide and galactose. Whereas myelination begins in a relatively normal manner in these mice, the amount of myelin present progressively declines as cerebroside accumulates. The twitcher mouse thus seems to provide a model of the fatal Krabbe's disease.

Such exact modelling of human disease is uncommon but two of the other mouse mutants present pathological pictures resembling rare hereditary human disease. In the X-linked mutant jimpy (*msd* seems to be an allele) there is little myelin and the few myelin forming cells present in the CNS appear immature. Because there is little evidence of myelin breakdown or lipid storage it is considered a primary failure of CNS myelination, a condition comparable to the Pelizaeus-Merzbacher disease in man. Infants often succumb during the first 3 or 4 years of life. The primary lesion in both the human and mouse disease is not known but work presented by Braun and co-workers of Montreal suggests that a membrane precursor to myelin accumulates in the jimpy mutant but is not converted into myelin.

The mutant trembler presents primarily PNS abnormalities including abnormal and sparse myelination with the concurrent deposition of connective tissue components which in time enlarge the peripheral nerve trunks. Aguayo and colleagures of Montreal (*Soc. Neurosci. Symp.* **4**, 362; 1979) note that conduction velocity is much slowed in these nerves, that axon diameter is reduced and that Schwann cell proliferation continues at abnormally high rates into adulthood. Drawing on their experience with nerve transplantation (including the transplantation of human nerve biopsy specimens into immunosuppressed mice), this group has shown that trembler Schwann cells express their characteristic abnormality with axons in normal mice, and that Schwann cells from patients with Charcot-Marie-Tooth disease (an hereditary human disease with marked peripheral nerve hypertrophy) express a very similar phenotype with normal mouse axons.

The dystrophic mouse was discovered in 1975 (Bradley & Jenkinson *J. Neurol. Sci.* **25**, 249; 1975) and was initially considered a model of muscle disease. It has been found to have a peculiar lesion in the nerve roots of its PNS, involving a more or less total failure of Schwann cell

---

*A meeting on Neurological Mutations affecting Myelination was held at Seillac, France, April 13-17, 1980. The organiser was Nicole Baumann and support provided by the French agency, INSERM. The proceedings will be published by Elsevier — North Holland.

Richard P. Bunge is Professor of Anatomy and Neurobiology, Washington University School of Medicine, St. Louis, Missouri.

0028-0836/80/280106-02$01.00

performance in these areas. Bunge and colleagues from St. Louis presented arguments at the meeting that this type of lesion could best be explained by an abnormality of extracellular matrix (ECM) within the nerve, i.e. a deficiency in the microenvironment of the Schwann cell. This contention derives from evidence that Schwann cell development is retarded if only axonal contact is available without simultaneous contact with appropriate ECM material (Bunge & Bunge *J. Cell Biol.* **78**, 943; 1978).

Centre stage was reserved for a relatively new mutant, shiverer (the mutant *mld* may be an allele). Interest in this mutant derives from the specific lack of one of the major myelin componets — basic protein (Dupouey *et al. Neurosci. Letters* **12**, 113; 1979). This constituent is of special interest for it causes a severe and sometimes fatal immune response when presented as an antigen with Freunds adjuvant. It previously had been assigned a quite specific role in normal myelin structure — that of stabilizing the compacted membranes of the myelin sheath. It was therefore not unexpected that CNS myelination was found to be severely deficient in this mutant (Privat *et al. Neurosci. Letters* **12**, 107; 1979) but it was surprising that myelin within the PNS, which also lacks basic protein, was quite normal in appearance, even at the level of the electron microscope (Kirschner & Ganser *Nature* **283**, 207; 1980). This mutant was much discussed at the Seillac meeting; several attendees suggested that available data indicate a different role for basic protein in CNS and PNS myelin. □

Timing in embryological development

from Michael H.L. Snow & Patrick P.L. Tam

NORMAL tables of embryonic development give the impression that the developmental processes are neatly co-ordinated, both spatially and temporally. The precision of timing of events is much stressed and frequently quoted in hours and minutes elapsed since the initiation of development. Certainly the synchrony observed between embryos of one species growing in a defined environment seems much more than mere coincidence. Evidence is accumulating that suggests a timing mechanism operates to control the emergence of developmental events. It is envisaged as a clock consisting of five components; the driving force (main-spring), operating an oscillatory mechanism (pendulum, balance wheel), which produces periodicity of emergent events (chimes on the hour), and all depending upon a linkage mechanism between oscillator and event (cog-wheels), and a capacity for adjustment in response to disturbance (correction for fast or slow running), (Brady *Biological Clocks*, Arnold, 1979).

In biological terms little is known about the driving force, the linkages or the homeostatic mechanisms but they can be presumed to exist. Studies have focussed on oscillators and the periodic events. More often than not the oscillatory mechanism has been ascribed to events in the cell cycle, DNA replication, cytokinesis. The premise that these reflect the operation of a clock has arisen from the characteristic regularity of the process in different tissues, and cell types. However the distinction made between proliferative cycles, which merely increase the number of identical cells, and quantal cell cycles, which generate daughters with developmental options different from the mother cell (Holtzer *et al. Q. Rev. Biophys.* **8**, 523; 1975) suggests that differentiative events may be gated by a periodicity not necessarily associated with cell cycles. Recent work throws some light on this subject.

The cell nucleus is generally regarded as the control tower for cellular functions and it has been implicated in the timing of various developmental events. In Ascidian embryos the specific expression of the enzyme acetylcholinesterase in presumptive muscle cells of the neurula (Whittaker *J. Embryol. exp. Morph.* **55**, 43; 1980) has been shown to be under a stringent control apparently directly related to the number of DNA replications undergone in the nucleus. The timing of its appearence is unaffected when cell or nuclear divisions are prevented by metabolic inhibitors (Satoh *J. Embryol. exp. Morph* **54**, 131; 1979). In the mouse embryo, cavitation of the morula to form a blastocyst seems more plausibly related to nuclear events since it is not governed by chronological time, nor interfered with by manipulation of cell number or supression of cytokinesis (Smith & McLaren *J. Embryol. exp. Morph.* **41**, 79; 1977).

Nevertheless, the nucleus can be excluded from other closely timed developmental events. In the mouse the time of compaction of the morula prior to blastocyst formation is not altered by changes in cell number, cell division, nuclear: cytoplasmic ratio or inhibition of DNA replication (Johnson, Pratt & Handyside in *Cellular and Molecular Aspects of Implantation*, Plenum, 1980). Similarly in *Xenopus* eggs periodic changes in contractile activity in the cortex of the cell are observed in perfect phase with cleavage divisions but persist in the absence of actual cell division and also continue when the cell is deprived of its nucleus (Hara, Tydeman & Kirschner *Proc. natn. Acad. Sci. U.S.A.* **77**, 462; 1980). Cytoplasmic or membrane associated mechanisms need to be considered for the control of these events. At the molecular level in the mouse the timing of synthesis of 'tissue-specific' polypeptides is the same in normal or experimentally disturbed embryos (Johnson, Handyside & Braude in *Development in Mammals* **2**, (ed. Von Blerkom & Brockway) North-Holland 1977; *Devel. Biol.* **44**, 148; 1975).

It is an attractive idea that the future development of the embryo is timed by a clock set in motion at the very beginning of development but is this feasible? The control of somitogenesis in Amphibian embryos is a later event that is precisely timed, regular and is currently explained in terms of a clock model (Cooke *3rd. Symp. Brit. Soc. Devl. Biol.* Cambridge University Press, 1977; Pearson & Elsdale *J. Embryol. exp. Morph.* **51**, 27; 1979; Elsdale & Pearson *J. Embryol. exp. Morph* **53**, 245; 1979). In mammals the later molecular events concerning the *in vitro* appearence of amylase activity in pancreatic primordia (Wessels & Cohen *Devel. Biol.* **15**, 237; 1977; Spooner, Cohen & Faubion *Devel. Biol.* **61**, 119; 1977) and the onset of responsiveness to androgen by mouse mammary tissue (Kratochwil *Devl Biol.* **61**, 358; 1977) seem to relate to chronological age rather than cell cycle parameters since the biochemical changes coincide with the timing expected *in vivo* despite the fact that tissue mass and cell number may be quite different from that in the embryo *in utero*.

It is unlikely however that the whole embryo is controlled by a single clock. Recent studies in the mouse in which embryos recover from a severe size reduction show that the neural ectoderm, the somatic tissues of somite and limb-bud, and the germ cell population recover according to different timetables and appear to be under separate intrinsic controls (Snow & Tam *Nature* **279**, 555; 1979). So, either the clocks can be changed independently at tissue or organ level by an exogenous insult or, during development when various cell populations are set aside each one becomes a mosaic of time zones. It is intriguing to speculate whether the obvious co-ordination of tissue interactions in normal embryogenesis arises as the result of the harmonics generated by signals of differing periodicity originating from the different time zones. Such a system is reminiscent of the phase-shift model for spatial and temporal organisation proposed by Goodwin and Cohen (*J. Theoret. Biol.* **25**, 49; 1979). □

Michael H. L. Snow & Patrick P. L. Tam are in the MRC Mammalian Development Unit, University College, London.

0028-0836/80/280107-01$01.00

Cree-Ojibwa hunting and the hare-lynx cycle

from Robert M May

MANY animal species exhibit well defined cyclic variations in abundance. Of particular fascination to ecologists are the dramatic cycles shown by many mammals in the boreal region of North America; these include the 3–4 year cycles of mice, voles and lemmings and the 10–11 year cycles of the snowshoe hare, lynx and other fur bearers. Indeed the hare-lynx cycle, which shows pronounced and regular oscillations extending back nearly 200 years, is presented in essentially all introductory ecology texts as the classic example of prey-predator oscillations (with discussion centering on whether the driving mechanism is the predation of lynx on hare, or predation of hare on their food supply with the lynx then entrained). A most readable review is by Hutchinson[1].

The cycles in populations of fur bearing animals are, in the main, deduced from records of pelt sales, kept by the Hudson's Bay Trading Company and administrative agencies of the Canadian North. From time to time, people have questioned the assumption that these records accurately reflect the abundance of the harvested species. Thus Elton and Nicholson[2] and Keith[3] have considered — and dismissed — the possibility that fluctuations in prices, caused either by business cycles in nineteenth century Europe or by factors intrinsic to the fur trade, have driven the cycle. Cyclic epidemics of disease affecting the trappers have also been suggested, but seem unlikely[4,5]. A more substantial suggestion, made independently by Gilpin[6] and Weinstein[7], is that pelt records may reflect changes in the foraging strategy of the trappers, rather than changes in the population densities of the fur bearing animals.

Winterhalder[8] has recently combined ecological studies with historical evidence about the foraging practices of Cree and Ojibwa Indians in northern Ontario, in an exploration of the extent to which apparent population cycles are artefacts of fur trapping practices.

Winterhalder first surveys studies showing that hare was a major component in the diets of boreal forest people. Particularly in the nineteenth and early twentieth centuries, when moose were scarce in, or absent from, northern Ontario (and possibly also from parts of Manitoba and Quebec), hare and fish were the main items in native diets. Winterhalder next examines the energy budgets for foraging for hare by Cree. In years of peak abundance there are around 1,200 hare per km^2, and he estimates a net acquisition rate of around 5,200 kcal per hr for time invested in snaring hares. At the trough of the hare cycle, the creatures are patchily distributed, but average around 13 hare per km^2 and their net yield to Cree hunters is about 1,200 kcal per hr. (These figures are based on trapping with stationary wire snares, which were not widely used before 1910; the older balance poles with snare loops made of string were probably not more than 10% less efficient). These figures suggest hare snaring would allow trappers to feed their families with relatively small investments of time and energy, when hare were abundant; the activity consumed significantly more time and energy when hare were relatively scarce. Finally, Winterhalder shows that[8] "until the twentieth century interior fur trappers could not exchange pelts for significant quantities of food. Dry goods, metal implements, tea, tobacco, and in some cases alcohol were available, but it was a recurrent problem for trading companies to transport or obtain sufficient food provisions even to maintain trading post personnel." Thus native trappers seldom had the option of exchanging pelts for food, and in times of shortage the pursuit of species highly ranked as food-producing resources necessarily had priority over those valuable mainly for their pelts.

These facts and inferences can be recast in the language of MacArthur and Pianka's[9] theory of optimal foraging. To this end, Winterhalder separates the species sought mainly for food from those sought mainly for pelts, making allowance for some intermediate types. The food species, ranked roughly in the order of their net value (food value less costs of pursuit and capture), include moose, hare, beaver, fish and muskrat. The fur bearers include lynx, otter, mink, marten, fisher, beaver, muskrat, and hare. When highly ranked food resources (moose and hare) were plentiful they provided ample food that could be easily obtained (often by women and adolescents), allowing male trappers to[8] "concentrate on the second economy represented by the fur trade". But when hare became scarce (and with moose rare or absent throughout much of the nineteenth century), more attention had to be devoted to lower ranking food resources, such as fish and muskrats, thus lowering the overall efficiency of the food quest. This in turn restricted the time available for participating in the fur trade; nor could furs be exchanged for staple foods. As a result, pelt-counts should be expected to cycle in parallel with the population abundance of hare.

Winterhalder also quotes from trader's reports, compiled by Bishop[10] from the Hudson's Bay Trading Company Archives. For instance, "the Indians say that they cannot hunt furs for want of Rabbits for they say that there is a few Martens on thir Lands but they cannot Make Traps for want of Provisions to live on."

Several interesting predictions follow from this analysis.

First, the above mechanism would have the peak abundance of pelts of most fur bearers, such as lynx, fisher and marten, occurring roughly contemporaneously with the peak of hare abundance (and therefore, presumably, the peak of hare pelt-counts). The dynamical properties of prey-predator associations, on the other hand, would have the predator populations lagging those of their hare prey, typically by about one quarter of the period of the cycle. This dichotomy is not discussed by Winterhalder, who observes that either explanation of the cyclic fluctuations in those animals sought mainly for fur (and not for food value) is roughly consistent with the data. Gilpin's[6] analysis, however, suggests the predator cycles do not lag significantly behind the hare cycles; this work could be taken to support the view that cycles in pelt records of fur bearers are artefacts of Cree-Ojibwa foraging strategies, rather than measures of the population dynamics of the animals themselves.

Second, Winterholder observes that pelt-count cycles are more pronounced in the nineteenth than in the eighteenth and twentieth centuries. This was also a time when moose and caribou were relatively absent from the hunting grounds of the Cree and Ojibwa; without this important food source to buffer fluctuations in the hare population[8], "the correlation between hare abundance and native attention to the fur trade should be strongest".

Third, muskrat is an interesting species in that it ranks relatively low both as a food source and in fur value. Winterhalder suggests that in times of hare-feast muskrat would have been spurned, but that in times of hare-famine the native hunters drew heavily on this less desirable food source, and sold the ensuing pelts. The resulting prediction is that peaks in muskrat pelt-counts should come in the troughs of hare abundance, and have nothing to do with the absolute abundance of muskrats as such. A somewhat irregular pattern of this kind is actually observed, particularly in the second half of the nineteenth century (when, as noted above, all patterns were more marked, by virtue of the absence of

Robert M. May is Class of 1877 Professor of Zoology at Princeton University.

1 Hutchinson, G E *Introduction to Population Ecology* (Yale Univ Press, New Haven, 1978)
2 Elton, C & Nicholson, M *J Anim Ecol* 11, 96 (1942)
3 Keith, L B *Wildlife's Ten Year Cycle* (Univ Wisconsin Press, Madison, 1963)
4 Elton, C & Nicholson, M *J Anim Ecol* 11, 215 (1942)
5 Moran, P A P *Aust J Zool* 1, 163 (1953)
6 Gilpin, M E *Am Nat* 107, 707 (1973)
7 Weinstein, M S *Am Nat* 111, 806 (1977)
8 Winterhalder, B P *Am Nat* 115, 870 (1980)
9. MacArthur, R H & Pianka, E R *Am Nat* 100, 603 (1966)
10 Bishop, C A *The Northern Ojibwa and the Fur Trade* (Holt, Rinehart and Winston, Toronto, 1974)
11 Pease, J L, Vowles, R H & Keith, L B *J Wildl Mgmt* 43, 43 (1979)
12. May, R M (ed) *Theoretical Ecology Principles and Applications* (Blackwell, Oxford, 1976)

0028-0836/80/280108-02$01.00

moose).

There are, of course, extensive field studies of the population dynamics of snowshoe hare, and, to a somewhat lesser extent, of lynx. These studies show the populations do in fact cycle, with periods of 10–11 years, Indeed, Bryant (of the University of Alaska) has shown that many of the deciduous plants browsed by snowshoe hare in Alaska manifest defensive responses to heavy browsing, by producing resins or other compounds that are repellent or toxic to hares[11]. The time lag in mounting this response is around 2–3 years; such a time lag in the regulatory mechanism will tend to produce population cycles of period $4 \times (2 \text{ to } 3) \simeq 10$ years in the overall prey (food)-predator (hare) system[12]. Species predatory upon the hare will then track this cycle.

In short, there is direct evidence to show that populations of hares and other boreal fur bearers do exhibit oscillations. But the nature of the foraging economy of the Cree-Ojibwa hunters must be kept in mind when we try to draw inferences about populations from records of pelts traded; peltcounts tend to amplify and sharpen the underlying population cycles of fur bearers (such as fisher and marten) and some cases (such as the out-of-phase muskrat cycles) may be pure artefacts. ☐

Primary productivity in the sea

from Richard W. Eppley

PEOPLE have been measuring primary production in the oceans using the ^{14}C method of E. Steemann Nielsen for nearly 30 years, yet they still argue about the accuracy and meaning of the measurements. Some of the debate concerns methodological details of little interest beyond the circle of measurers, but a larger part questions our understanding of photosynthetic mechanisms, the absorption of sunlight by plants in the sea, quantum efficiency of photosynthesis as a function of depth and submarine irradiance, metabolic adaptations of algae and other matters of broader interest. Oceanographers debated these issues 2-5 June at the 31st Brookhaven Symposium on Biology in the presence of experts in the laboratory study of photosynthesis and algal physiology. The productivity of coral reefs and seaweeds was also discussed along with the significance of global oceanic production for human affairs.

Measurement of ocean photosynthesis is no longer the exclusive territory of algal ecologists and physiologists as the experimental seawater samples contain minute animals that graze on the contained phytoplankton and bacteria — a microcosm exists within the productivity bottles. While this has long been known, we now realise that we must assess the flow of photosynthetic products among tiny animals and bacteria — the province of microbiologists and protozoologists — as well as among phytoplankton in order to estimate primary production. There is also concern that many oceanic species may not survive the mechanical and chemical insults of the measurement conditions and thus photosynthetic production may be underestimated by present methods. The size of the underestimate is unknown. There is agreement, however, that the problem is more extreme for the central oceanic gyres, such as the Sargasso Sea and comparable regions in the South Atlantic and North and South Pacific. Guesses of the magnitude of the underestimate seem to range from a factor of two to an order of magnitude for these areas. However most of a day's production in such regions is eaten, digested, defecated, decomposed and the organic-bound nutrients recycled during the day-night cycle of the 24-hour day. Thus, even those measurements suggesting higher values for production, such as daytime increases in oxygen in the water and in the concentration of organic particles, living and dead, involve daytime increases that disappear by the following dawn. Upward revision of the photosynthetic rates would not imply more food for fish although it would require some new thinking about the rates of elemental recycling in the surface waters and the ecological significance of microbial food webs. Our understanding and the validity of 30 years of historical measurements of production in the central oceans are more at stake than practical matters.

Z. Dubinsky (University of Bar Ilan, Israel) confirmed J. E. Tyler's earlier finding that the quantum yield of photosynthesis is very low at the sea surface and increases to near maximum expected values at the bottom of the photic zone. Jack Myers (University of Texas, Austin) explained why the theoretical maximum quantum yield (0.125 from the Z-scheme of photosynthesis with equimolar reaction centres for photosystems I and II) is rarely attained: the photochemical reaction centres are not always open to traffic. A. Ley (Rockefeller University, New York) found the reaction centres of unicellular red algae were not present in equimolar amounts; this would reduce the maximum quantum yield expected in dim light, depending on the proportion of reaction centers I and II. The practical problem of the quantum efficiency of photosynthesis arose in an argument over central ocean productivity. The arguments for order-of-magnitude greater production would require unrealistically high differences in quantum efficiencies between coastal and open-ocean regimes. Production would be 1-2 grams carbon m^{-2} day^{-1} in both yet the fraction of sunlight absorbed by phytoplankton is an order-of-magnitude greater in coastal than oceanic waters.

Many of those present were interested in photosynthesis light curves (T. Platt, Bedford Institute, Dartmouth, Canada) the regulation of chlorophyll, and other photosynthetic pigments in algal cells (P. Falkowski, Brookhaven National Laboratory; J. Marra, Lamont-Doherty Geological Observatory) and the vertical distribution of photosynthetic pigments in the ocean (S. W. Jeffrey, CSIRO, Australia). Falkowski presented the interesting hypothesis that regulation of cellular chlorophyll content by light may involve a competition for ATP between ammonium assimilation leading to protein synthesis on the one hand and the use of glutamate in the biochemical synthesis of chlorophyll on the other. Both Marra and Falkowski suspect that the rapid adjustment of cellular pigment content with changing irradiance and light quality (i.e. with depth) can serve as tools to study rates of vertical water motions in the photic zones. Here biology may provide information on the near surface circulation that is difficult to assess with physical observations.

Developing conceptually adequate mathematical models of ocean phtosynthesis and phytoplankton growth rate (realted to photosynthetic production by the phytoplankton standing stock) has been a difficult task. Nevertheless, T. Bannister (University of Rochester) has achieved a satisfying model which could be fitted to the old data of J. Myers and J. R. Graham on *Chlorella* and the new data of E. Laws (University of Hawaii) for the diatom *Thalassiosira fluviatilis*. The latter data set and modelling includes nitrogen, phosphorus and light-limited growth. Several generalizations from the work will be useful in the field assessments: both the dark respiration rate and the ratio of chlorophyll a to carbon in phytoplankton are linear functions of growth rate, and the photosynthesis light saturation term is not altered when growth rate is reduced by nutrient limitation.

Titbits of information were offered in profusion in the lecture hall and in the corridors. For example, R. Rivkin (Johns Hopkins University) has succeeded in measuring with ^{14}C the photosynthesis of individual cells of some large dinoflagellates. Cell division in diatoms seems to be less under the control of a biological clock than in dinoflagellates (S. W. Chisholm, MIT). It is still not clear whether photo-

Richard W. Eppley is a Research Biologist at the University of California, San Diego.

0028-0836/80/280109-02$01.00

Interferon nomenclature

AT a recent, specially-convened meeting an international group of scientists attempted to devise a system to define and classify the interferons*. The following is the unanimous report from the group.

The committee accepted the definition for interferon: "To qualify as an interferon a factor must be a protein which exerts virus non-specific, antiviral activity at least in homologous cells through cellular metabolic processes involving synthesis of both RNA and protein."

The preferred abbreviation for interferon is IFN, each interferon to be identified according to animal of origin: e.g. human (Hu IFN); murine (Mu IFN); bovine (Bov IFN); rat (Rat IFN); chicken, porcine, feline, equine interferon, etc. However, it may be necessary in some cases to apply generic nomenclature: e.g. monkey = *Rhesus* interferon, etc.; fish = *Salmo* interferon, etc.; bat = *Taderida* interferon etc.

Interferons will be classified into types on the basis of antigenic specificities, type designations to be alpha (α), beta (β) and gamma (γ), corresponding to previous designations of leukocyte (Le), fibroblast (F), and type II (immune) interferons, respectively. The old terminology of 'leukocyte', 'fibroblast' and 'immune' interferons were, by committee consensus, abolished, as they clearly were misnomers: both leukocyte and fibroblasts can produce each of these two types of interferon, and 'immune' interferons are often induced by mitogens rather than by immune recognition reactions. Also, the abbreviation 'F' has often been used to designate either fibroblast or fast migrating interferons. Alpha and beta interferons are usually acid-stable and correspond to what have been called type I IFNs; gamma interferons are usually acid-labile and correspond to what has been called type II IFNs. If there are discovered to be classes of IFN which are not presently recognized, they could be designated sequentially IFN-delta, epsilon, etc. The Table lists the new nomenclature for human and murine interferons and the corresponding designations which have been or are being employed. Interferon preparations may contain more than one type: for example, interferons derived from human lymphoblastoid cells and interferons from murine fibroblasts contain both IFN-α and IFN-β. These can be designated as to predominant type. Thus, the interferons presently employed in clinical trials are either HuIFN-α or HuIFN-β, or admixtures thereof.

The committee's recommendations apply at present only to human and murine IFNs, since there is insufficient information about IFNs from other animal species to allow differentiation into types. Workers using IFNs from other species are encouraged either to attempt preliminary classification based on antigenic homology with existing antisera specific for human or mouse alpha, beta or gamma IFNs, or to establish sequence homology with the known types of human and mouse interferons.

It is recognized that there may be size, charge, sequence and other heterogeneities within the designated IFN types. Currently, there is insufficient information available about the nature of these differences to allow designation of specific subtypes. Properly documented differences in molecular size appear to be useful parameters for differentiation until more stringent criteria (amino acid sequence, monoclonal antibodies) become available. Molecular weight designations may be indicated in parentheses, e.g. Hu IFN-α (18K) or Mu IFN-β (38K), or subtypes of IFNs based on specific amino acid sequence differences can be classified as Hu IFN-α_1, HuIFN-β_2, etc.

Indication of interferon origin for those that behave antigenically similarly may also be helpful. Thus, interferon from human lymphoblastoid cells and interferon from human leukocytes are both classified antigenically as HuIFN-α, yet these interferons differ in certain amino acids. Therefore, the nomenclature HuIFN-α (Ly) or HuIFN-α (Le) may be used until such time as specific differences in amino acid loci have been established and subtype designations can be assigned. Also, it is now recognized that there are a number of forms of HuIFN-α that differ in certain amino acids; eventually these may be designated according to specific amino acids and their locations. Schemes for such designation of subtypes of each of the major IFN types will be developed at subsequent meetings of the Nomenclature Committee. The next meeting of the committee will be held in April 1981. Suggestions and comments for consideration by the committee should be forwarded to the committee's Chairman.

The committee hopes that scientists and scientific journal editors will adopt the proposed nomenclature to avoid the proliferation of terms for the same substances and the indiscriminate naming of newly discovered factors. □

Old and new nomenclature for human and mouse interferons

New Nomenclature	**Old Nomenclature**	
	Human	**Mouse**
IFN-α	Le (leukocyte), type I, pH 2 stable, foreign cell-induced	F (fast), C, type I, pH 2 stable
IFN-β	F (fibroblast), Fi, type I, pH 2 stable	S (slow), A,B, type I, pH 2 stable
IFN-γ	IIF (immune), type II, T, pH 2 labile, antigen-induced, mitogen-induced	immune (IIF), type II, pH2 labile, T, antigen-induced, mitogen-induced

---

The meeting was sponsored by the National Institute of Allergy and Infectious Diseases and the World Health Organization — US National Centre on Interferon and was held at the National Institute of Health in Bethesda, Maryland on March 7, 1980. Those attending were: William E. Stewart II (Chairman; Interferon Laboratories, Memorial Sloan-Kettering Cancer Center, 1275 York Avenue, New York, New York 10021, US), J. Edwin Blalock (Galveston, TX), Derek C. Burke (Coventry), Charles Chany (Paris), June K. Dunnick (Bethesda), Ernesto Falcoff (Paris), Robert M. Friedman (Bethesda), George J. Galasso (Bethesda), Wolfgang K. Joklik (Durham, N.C.), Jan T. Vilcek (New York), Julius S. Youngner (Pittsburgh) and Kathryn C. Zoon (Bethesda).

---

respiration is significant for marine phytoplankton (J. Burris, Pennsylvania State University). On a global average the fate of about 80% of the primary production is to be recycled within the photic zone. The relative importance in nutrient recycling of bacteria, microzooplankton, larger zooplankton and nekton in the photic zone appears to vary between the continental shelf, the slope water and the open ocean (W. G. Harrison, Bedford Institute, Dartmouth, Canada).

Harrison's paper is indicative of the expanding interest of biological oceanographers in the fate of primary production. Globally, about 20% of it appears to sink out of the photic zone. J. Walsh (Brookhaven National Laboratory) postulated that a large fraction of this sinking flux on the continental shelf off New York is buried in the sediments of the upper continental slope, as shown by the relatively high sediment organic carbon content and a low (~ 6) ratio of carbon to nitrogen in the organic matter. Models of carbon flows in the circulation of the deep ocean (M. Fiadeiro, Yale University, New Haven) suggest what the magnitude of the sinking flux of organic carbon may be. Unhappily, the experimental measurements of the flux in the North Pacific using particle interceptor traps are inconsistent with the models. Further collaboration among the several oceanographic disciplines seems required to clarify such problems and especially to define the significance of sinking organic particles as sinks and transporters of atmospheric carbon dioxide from fossil fuel burning. □

0028-0836/80/280110-01$01.00

Zeolitic structures as revealed by high-resolution electron microscopy

L. A. Bursill*, Eliz. A. Lodge & J. M. Thomas†

Department of Physical Chemistry, Cambridge University, Lensfield Road, Cambridge CB2 1EP, UK

Interpretable images at 3–5 Å resolution of synthetic A-type zeolite suggest possible mechanisms of vitrification and introduction of dislocations into zeolitic structures. Techniques may be developed to extend the lifetime of these, and possibly other, beam-sensitive cage or tunnel structures. Evidence also exists for Si^{4+}/Al^{3+} ordering in the aluminosilicate framework.

ZEOLITE silicates are of considerable practical and academic interest in view of their role as catalysts, ion-exchangers, gas-purifiers, environmental cleaning agents and, following vitrification, as potentially useful matrices for the burial of radioactive waste[1]. For both channel and cage varieties synthetic adaptation has given rise, *inter alia*, to ultrastable zeolites possessing specific catalytic activity for either the cracking of petroleum or the production of gasoline from methanol, using highly silaceous hydrophobic molecular sieve solids such as ZSM-5 (ref. 1). The general chemical formula of a zeolite is $M_xD_y.Al_{x+2y}Si_{n-(x+2y)}O_{2n}.mH_2O$ where M and D may be mono- and divalent cations respectively, usually alkalis and alkaline earths in nature, but other ions in synthetic varieties. Dehydration of zeolites is usually complete at 350 °C (refs 1, 2) and is often reversible: dehydrated zeolites are strong desiccants, however, and molecules other than water may rapidly fill the channels[1].

Crystallographic studies and their implications for practical applications have been reviewed elsewhere[1,2] and an atlas of known zeolite structures is available[3], although most structural work has relied on X-ray methods[2]. Gard[4], however, used electron diffraction to obtain evidence for a pseudosymmetric cell doubling of a 'Union Carbide' zeolite A. Although his data led to a refinement of the structure when the weak reflections were measured by X-ray goniometry[5], the wide range of zeolitic structural variations remains to be fully appreciated[1]. Thus there may be marked differences between hydrated and dehydrated forms[2] and it is not always practicable to locate all of the M, D and H_2O sites or the sites of other ion-exchanged entities. Often crystals are too small (~0.1 μm) for X-ray studies. Moreover, there are apparently many possibilities for the occurrence of short-range order, antiphase domain structures, topological transformations, coherent intergrowth, polytypism and stacking disorder. These are particularly relevant in considering the synthesis of new phases having desirable catalytic, sieve, or other properties. In several areas of solid state chemistry, such as transition metal oxides and chalcogenides, alloys and silicates high resolution electron microscopy has proved invaluable in elucidating the local atomic arrangement which may, in many cases, be lost or not readily detected using X-ray diffraction alone[6,7].

There have been very few reports of high-resolution studies of zeolites. Although Menter[8] first observed images showing $d_{111} = 14.7$ Å spacings in a synthetic faujasite in 1958 it was not until 1978 that Sanders[9] obtained the first high-resolution (~3 Å) two-dimensional image of a (Linde L) zeolite. Sanders, however, used a zeolite as a resolution test object for a 1-MeV electron microscope and no new information about the structure was obtained. This sparsity of electron microscopic data stems principally from the electron beam sensitivity of zeolites, which vitrify within seconds, or at most minutes on examination in normal electron microscope illumination conditions. This beam sensitivity is probably linked with the water present in zeolites.

We report here the observation at high resolution (3–5 Å) of two-dimensional structure images of a synthetic Na-A zeolite. Interesting changes associated with the crystalline/glass transformation and the first observation of dislocations in zeolites are also described.

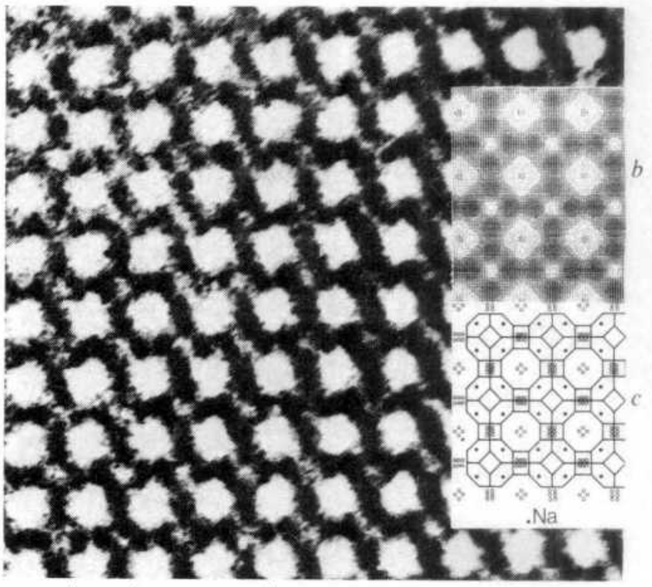

Fig. 1 *a* High-resolution image of zeolite A, [001] projection. *b*, Computer simulated image corresponding to $C_s = 2.5$ mm; crystal thickness = 50 Å; objective lens defocus, −1,040 Å; effective resolution, 3.1 Å. *c*, [001] projection of zeolite A aluminosilicate framework, Na atoms are indicated by ● and ○. Scale bar, 12.3 Å.

---

*Permanent address: School of Physics, The University of Melbourne, Parkville, 3052, Australia.

†To whom correspondence should be addressed.

0028-0836/80/280111-03$01.00

Stabilization of zeolites for electron microscopy

We hypothesize that the primary source of the crystalline/glass transformation induced by the electron beam is the production of ionized species, in particular hydroxyl ions, which lead to bond softening and bending in the aluminosilicate framework. This, when accompanied by elastic stresses associated with dehydration, will strongly favour collapse of the structure and consequent transformation to a grossly disordered (glassy) state. We, therefore, set out to dehydrate some well crystallized zeolites by heating in air, or *in vacuo*, before examination in the electron microscope, by ion-exchanging H_2O by inorganic salts, either during or after synthesis, and began a systematic study of a wide range of zeolites to discover which of these are least beam sensitive. However, in the case reported here, we were able to increase the longevity of the crystalline state significantly by simply pumping the specimens overnight *in situ* in the electron microscope (at $\sim 10^{-7}$ torr).

Experimental

The NaA zeolite samples used here were prepared by the Charnell method[10]. Their nominal stoichiometry is $Na_{12}(AlO_2)_{12}(SiO_2)_{12}.27H_2O$ when fully hydrated. Fine crystals, ~10–50 μm diameter, of this zeolite were placed in an agate mortar and crushed using a hard vertical thrust of the pestle, whereby a remarkably high incidence of ⟨100⟩ zone axis diffraction patterns were obtained. Such specimens were rapidly tilted into the symmetrical orientation using a JEOL-200 CX side-entry goniometer. Many such crystals showed good lattice images on the viewing screen and some of these persisted for a sufficiently long time (1–3 min) to enable objective lens astigmatism to be corrected and the optimum defocus established before photography. Exposure times were typically 4–11 s, using Kodak 4463 electron image film developed in D19 for 8 min.

Two sets of objective lens pole pieces were used having spherical aberration coefficients $C_s = 2.5$ mm and 10 mm respectively. Calculations of the corresponding lens transfer functions at 200 kV showed that at the Scherzer defocus[11] the 'interpretable image' resolution limits were ~3 and 4.1 Å respectively. Previously it had been shown that 3 Å limit could be achieved, for example with parawollastonite and cordierite, only if a suitably reduced gun bias setting was used, along with low beam divergence (semi-cone angle $\alpha \lesssim 1$ mrad) and if all sources of acoustical vibrations were eliminated.

Experimental results

Figure 1*a* shows a high-resolution image for the [001] orientation. Note the large white blobs and also much smaller white blobs linking the former along ⟨100⟩. The dark intensity surrounding the small tunnels can be just resolved into four dark blobs. Figure 2*a* shows a wider view of the crystal. A strip of essentially structureless contrast may be seen along the thin edge. This is presumably amorphous as it shows a characteristic lack of fringe contrast which extends progressively into the crystal with increasing exposure to the electron beam. At the same time the electron diffraction spots gradually fade giving way to a diffuse halo pattern. In many cases it was possible to record only two images before all structural detail was lost. The interface between glass and crystal is surprisingly sharp in Fig. 2*a*, showing unit cell steps (~12 Å high) along ⟨100⟩ directions. Note changes in contrast giving a patchy appearance. Some patches (~150–200 Å diameter) show a loss of fringe detail in one of the ⟨100⟩ directions (A), others show generally reduced (B) or virtually no (C) visible structure. Note especially that small islands of fringes (D) may be found, apparently completely surrounded by glass. These remnants of structure show fringes only along ⟨110⟩. Further inspection of Fig. 2*a*, by sighting along [100], reveals what seems to be an extended dislocation (circled). Further dislocations are more obvious in Fig. 2*b*, which shows nearly the same area, but was recorded using larger objective lens defocus. Patches are now more clearly outlined, by dark lines resembling Fresnel fringes, and terminating half-planes (dislocations) are seen to be associated with the interface between patches of fringes misoriented by ~5–10° with respect to the bulk.

Figure 3 shows a pincer-shaped intrusion of glassy material into a Na A crystal. The latter introduces a dislocation and extensive (~100–200 Å) strained regions around the intrusion tip.

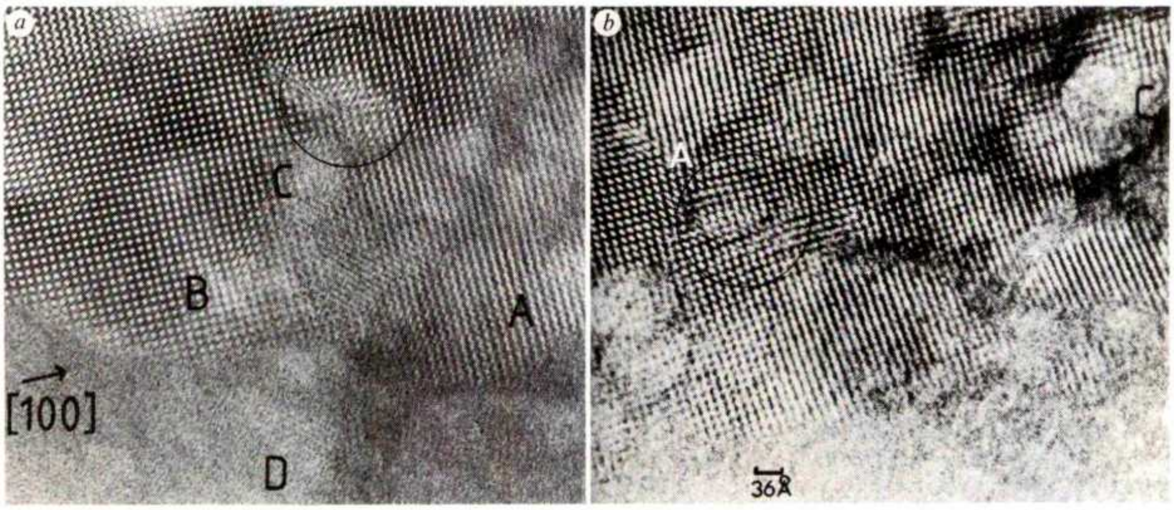

Fig. 2 *a*, *b*, Wider view of zeolite A crystal for two defects of focus showing development of glassy strip along thin edge of crystal and the appearance of patches ~150 Å diameter showing preferential loss of one set of {100} fringes (A), weak (B) or absent structural detail (C) and islands of weak {110} fringes (D) completely surrounded by glassy material. Note occurrence of extended dislocations (circled), sight along ⟨100⟩.

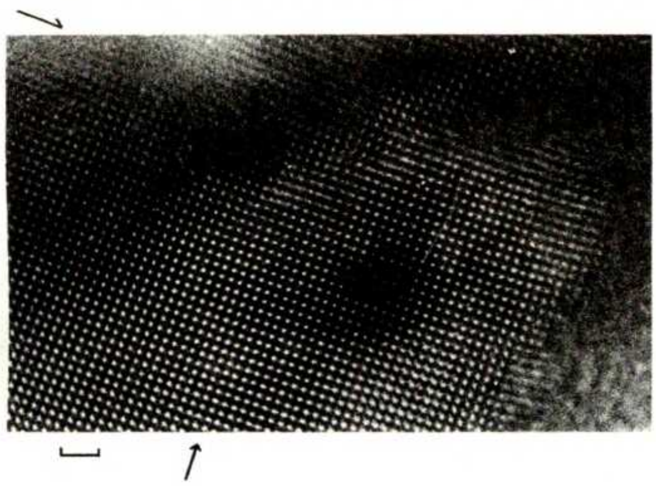

Fig. 3 Area of Na A showing pincer-shaped intrusion resembling a glass-filled Griffith crack. A dislocation may be seen by sighting along the rows of tunnels (indicated by arrows).

Discussion

The ideal chemical formula is $Na_{12}(AlO_2)_{12}(SiO_2)_{12}$. $27H_2O$ when fully hydrated, with cubic unit cell $a = 24.6$ Å, containing eight formula units[5]. The aluminosilicate framework contains two types of polyhedra: one a simple cubic arrangement of eight tetrahedra and the other a truncated octahedron of 24 tetrahedra (β cage). Their combination (Fig. 1*c*) produces a large cavity (α cage) with tetrahedral centres occupying the apices of a truncated cuboctahedron, free diameter 11 Å. We have used the 12.3 Å psudo-cell[12], space group Pm3m, for convenience here, as there are not observable effects in the [001] projection due to Si/Al ordering. However, we have obtained evidence, from electron diffraction patterns of [110], $[11\bar{2}]$ and $[21\bar{3}]$ zones that Si/Al ordering does take place in our zeolite preparation. Thus *hkl* (all odd) reflections satisfying $h + l = 2n$ were observed[13]. This confirms the recent criticism of space group Fm3c for Na A on the basis of high-resolution magic-angle spinning ^{29}Si NMR studies[13,14]. The proposed Si/Al ordering scheme contradicts Loewenstein's rule[15]. Zeolite A is thought to retain its structure on dehydration, which is reversible, after which the cell parameter decreases by only 0.02 Å (ref. 2).

Computer simulated images were obtained using multislice techniques[16] and programs previously developed by Jefferson *et al.*[17]. Computed images of zeolite Na A showed a faint grey blob in the centre of the α cage (large tunnels) if atomic coordinates for the Na atoms were included (Fig. 1*b*). These did not occur on the experimental images, suggesting that some Na atoms were either absent or had moved away from the centres of the tunnels on dehydration. In fact, the image match was improved by leaving out those Na^+ atoms having low partial site occupancy (indicated by open circles in Fig. 1*c*). Otherwise the image match was achieved assuming effective resolution of 3.1 Å. Further improvements in resolution (to 2.4 Å) are expected when ultra-high-resolution pole pieces ($C_s = 1.2$ mm) become available. However, we have clearly demonstrated that high-resolution images of zeolitic silicates may be obtained and that details of the contrast may be matched by computer simulation. Both large and small channels have been located. Further calculations and even higher resolution experimental images are necessary to determine whether specific cation-exchange sites may be located, but we expect that certain heavy ions may be found. We have already shown that the images are sensitive, in optimum defocus conditions and for sufficiently thin crystals, to the cation content of the larger tunnels.

Na A zeolite shows interesting contrast effects associated with transformation to the vitreous state. At least three processes seem to be operating. Thus, for Fig. 2*a* there is an extremely sharp interface, containing unit steps of 12 Å, which seems to advance into the crystal one unit cell at a time, starting at the thin edge. Second, there are patches or islands of structure, B and C in Fig. 2*a*, which are misoriented by several degrees with respect to the bulk of the crystal. These sometimes show a deterioration in image visibility suggesting loss of crystallinity (A, B) whereas other patches appear completely vitreous. Patches of types A and B imply a preferential breakdown of the structure on {100} planes whereas remnants of {110} planes may continue to exist even in areas completely surrounded by glass (D). Apparently, vitreous regions ~150-Å diameter form inside the bulk crystal, although we cannot rule out the possibility that regions having roughly circular cross-section are propagating into the crystal from upper or lower surfaces. Lattice rotation and the consequent production of dislocations may arise from the changes in cell parameter associated with the breakdown of {100} planes or with elastic strain due to changes in density of partially or completely transformed material. However, inspection of the structural drawing (Fig. 1*c*) immediately suggests that the origin of preferential breakdown on {100} planes is due to shear across the relatively weakly bonded structural units linking β-cages. This may be associated with the loss of Na and consequent rearrangement of the aluminosilicate framework, possibly by face-sharing of β-cages forming sodalite type structure units[2,3]. (Note that sodalite may be obtained from zeolite A by a three-dimensional crystallographic shear operation $\{100\}\langle\frac{1}{2}00\rangle$). The circled extended dislocations in Fig. 2*b*, *c* may well represent the initial stages of this process. More detailed analysis of the defects shown in Fig. 2, may lead to structural models for the dislocations and for transition structures.

A third transformation mechanism is suggested by the dislocation and strained region, surrounding the pincer-shaped glassy intrustion in Fig. 3. This resembles a glass-filled Griffith crack. Thus eventually relatively large areas (0.1–0.5 µm) will be split off from the bulk crystal. This mechanism also leads to islands of crystalline or paracrystalline regions surrounded by glass. (Similar intrusions were observed in a [011] zone axis image of zeolite A.)

This work was supported by the SRC, the University of Melbourne, and Unilever Limited. We thank Dr C. J. Adams for Na A specimen, and Drs D. A. Jefferson and G. R. Millward for their cooperation.

Received 24 March: accepted 23 April 1980.

1. Barrer, R. M. *Zeolites and Clay Minerals as Sorbents and Molecular Sieves* (Academic, London, 1978).
2. Breck, D. W. *Zeolite Molecular Sieves* (Wiley, New York, 1974).
3. Meier, W. M. & Olsen, D. H. *Atlas of Zeolite Structure Types* (Juris Druck, Zurich, 1978).
4. Gard, J. A. *Proc. 2nd Eur. Reg. Conf. Electron Microscopy*, Delft **1**, 203–206 (1961).
5. Gramlich, V. & Meier, W. M. *Z. Kristallogr.* **133**, S134–149 (1971).
6. Cowley, J. M. (ed.) *Modulated Structures, Kailua-Kona, 1979* (AIP Conf. Ser. No. 53 American Institute of Physics, New York, 1979).
7. Kihlborg, L. (ed.) *Chem. Scr.* **14** (1978/79).
8. Menter, J. W. *Adv. Phys.* **7**, 299 (1958).
9. Sanders, J. V. in *Physics of Materials* (eds Borland, D., Clareborough, L. & Moore, A. W.) 244–250 (University of Melbourne Press, 1978).
10. Charnell, J. F. *J. Cryst. Growth* **8**, 291–294 (1971).
11. Cowley, J. M. *Diffraction Physics* (North-Holland, Amsterdam, 1975).
12. Reed, T. B. & Breck, D. W. *J. Am. chem. Soc.* **78**, 5972–5977 (1957).
13. Bursill, L. A., Lodge, Eliz A. & Thomas, J. M. (in preparation).
14. Engelhardt, G., Zeigar, D., Lippmaa, E. & Mägi, M. *Z. anorg. allg. Chem.* (in the press).
15. Loewenstein, W. *Am. Miner.* **39**, 92 (1954).
16. Goodman, P. & Moodie, A. F. *Acta crystallogr.* **A30**, 280–289 (1974).
17. Jefferson, D. A., Millward, G. R. & Thomas, J. M. *Acta crystallogr.* **A32**, 823–835 (1976).
17. Mallinson, L. G., Jefferson, D. A., Thomas, J. M. & Hutchison, J. L. *Phil. Trans. R. Soc.* **A295**, 537–552 (1980).

Atmospheric angular momentum fluctuations and changes in the length of the day

R. Hide*, N. T. Birch*, L. V. Morrison†, D. J. Shea‡ & A. A. White*

*Meteorological Office, Bracknell, Berkshire RG12 2SZ, UK
†Royal Greenwich Observatory, Herstmonceux Castle, Hailsham, East Sussex BN27 1RP, UK
‡National Center for Atmospheric Research, Boulder, Colorado 80307

Fluctuations in the angular momentum of the Earth's atmosphere correspond fairly well with equal and opposite fluctuations in the angular momentum of the Earth's 'solid' mantle. A decrease of 20% of the relative angular momentum of the atmosphere during the second half of May 1979 was accompanied by a speeding up of the rotation of the mantle causing the length of the day (l.o.d.) to decrease by 0.6×10^{-3} s. Although motions in the Earth's liquid core produce the more pronounced 'decade' variations in the l.o.d. there is no evidence that core motions produce l.o.d. variations on much shorter time-scales.

FLUCTUATIONS in the angular momentum $\mathbf{M}_a$ of the Earth's atmosphere are of considerable interest to geophysicists and astronomers concerned with the dynamics of the 'solid' Earth as well as to meteorologists concerned with the general circulation of the atmosphere and numerical models[1-6]. All components of $\mathbf{M}_a$ exhibit fluctuations due to changes in the distribution of mass in the atmosphere and in the pattern of winds, and these will be associated with changes in the rate of rotation of the underlying planet and with movements of the poles. We are investigating these fluctuations as new wind and pressure observations become available from FGGE (First GARP global experiment where 'GARP' is Global Atmospheric Research Programme), which started at the beginning of December 1978 and lasted for 1 year. A detailed study of fluctuations in all components of angular momentum in the Earth–atmosphere system based on these new data will be reported elsewhere. Here we outline our determinations of the main contribution to fluctuations in the axial component of $\mathbf{M}_a$, namely that due to changes in the distribution and strength of zonal winds. (The main direct effect of redistribution of mass in the atmosphere is the alteration of the direction of $\mathbf{M}_a$ which is shown largely as the slight compensating movements of the pole of rotation of the solid Earth[1,2].) The results are a valuable check on established methods for measuring variations of the Earth's rotation on a time scale of several weeks, and should prove particularly useful in testing new methods for monitoring more rapid fluctuations of the Earth's rotation. These new methods[4], notably very long base-line interferometry and laser ranging to artificial satellites and the Moon will eventually provide useful data on the general atmospheric circulation.

The density of the atmosphere decreases rapidly with height and more than 95% of the mass of the atmosphere is contained within the troposphere, which extends from the ground to an altitude of ~10 km, and the lower stratosphere. These regions of the atmosphere rotate faster on average than the underlying solid Earth with a typical relative speed of about 10 m s^{-1}. Exactly how this super-rotation (a term used for the generally more rapid relative motions found in the very tenuous regions at heights around 300 km) is produced and maintained against the tendency for friction to oppose differential motions between the atmosphere and the underlying planet is a central problem in dynamical meteorology.

In the absence of energy sources such as solar heating, internal radioactivity, and tidal forces due to the Moon, Sun and planets, the solid parts of the Earth (crust, mantle and inner core) and fluid parts (atmosphere, oceans, liquid outer core) would rotate together as a rigid body with angular velocity $\mathbf{\Omega}$ equal to the angular momentum $\mathbf{M}+\mathbf{M}_a$ of the whole system (magnitude $5.85 \times 10^{33}\,\mathrm{kg\,m^2\,s^{-1}}$) divided by its principal moment of inertia $I + I_a = 8.04 \times 10^{37}\,\mathrm{kg\,m^2}$ where I_a is the principal moment of inertia of the atmosphere. During the development of the three-dimensional and non-axisymmetric global atmospheric circulation following the imaginary switching-on of the main source of energy for atmospheric motions, solar heating, $\mathbf{M}_a$ would increase by an amount $\delta\mathbf{M}_a$ (magnitude $\doteqdot 1.5 \times 10^{26}\,\mathrm{kg\,m^2\,s^{-1}}$), associated mainly with the average super-rotation of the troposphere and lower stratosphere at average angular speed $|\delta\mathbf{M}_a|/I_a$ relative to the underlying plant, about the main rotation axis. As $I_a = 1.42 \times 10^{32}\,\mathrm{kg\,m^2}$ then $|\delta\mathbf{M}_a|/I_a \doteqdot 10^{-6}\,\mathrm{rad\,s^{-1}} \doteqdot 1.5 \times 10^{-2}|\mathbf{\Omega}|$. To conserve the angular momentum of the whole system a change $\delta\mathbf{M} = -\delta\mathbf{M}_a$ in $\mathbf{M}$ would occur, largely manifested as a reduction in the magnitude of the angular velocity of the solid Earth by an amount $|\delta\mathbf{\Omega}| \doteqdot |\delta\mathbf{M}_a|/I \doteqdot 2 \times 10^{-12}\,\mathrm{rad\,s^{-1}} \doteqdot 3 \times 10^{-8}|\mathbf{\Omega}|$. Thus the l.o.d. $= 2\pi/|\mathbf{\Omega}|$ would increase by about 3×10^{-3} s which is small in absolute terms but comparable in magnitude with the largest changes in the l.o.d. revealed by astronomical transit observations. Fluctuations in the relative angular momentum $(\mathbf{M}_a - I_a\mathbf{\Omega})$ of the atmosphere of 20% in magnitude could therefore produce changes in the length of the day of 6×10^{-4} s and as there are observed changes of this magnitude on meteorological time scales of weeks and months it is reasonable to suppose that these changes might be produced by the fluctuations in the net couple $\mathbf{C}$ applied by the atmosphere to the underlying planet[1-3].

The couple $\mathbf{C}$ is a result of the instantaneous imbalance between the positive couple exerted by the atmosphere on the Earth in mid-latitudes, where the zonal component of surface winds is generally eastward (westerly) and the negative couple in tropical regions, where the surface (Trade) winds have a westward (easterly) zonal component, and to a much lesser extent in polar regions, where westward surface flow is found. Although comparatively large (and negative) during the setting-up process, this imbalance usually amounts to no more than a few per cent and fluctuates in sign, exhibiting persistent quasi-biennial, seasonal and irregular variations. Direct determinations of $\mathbf{C}$ cannot yet be made: even with a complete set of surface wind and pressure observations, an understanding of boundary layer processes and airflow over

0028-0836/80/280114-04$01.00

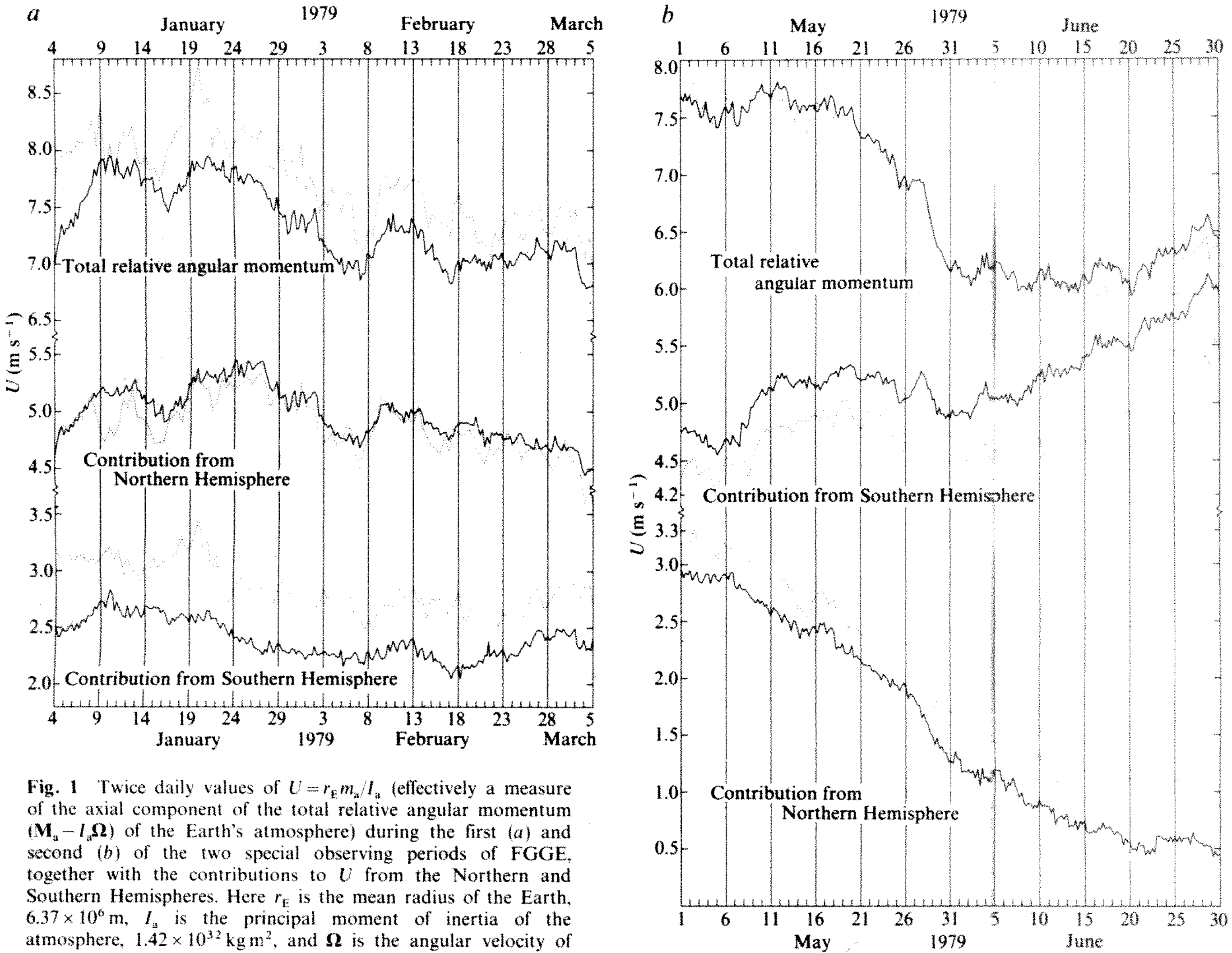

Fig. 1 Twice daily values of $U = r_E m_a / I_a$ (effectively a measure of the axial component of the total relative angular momentum $(\mathbf{M}_a - I_a\mathbf{\Omega})$ of the Earth's atmosphere) during the first (*a*) and second (*b*) of the two special observing periods of FGGE, together with the contributions to U from the Northern and Southern Hemispheres. Here r_E is the mean radius of the Earth, 6.37×10^6 m, I_a is the principal moment of inertia of the atmosphere, 1.42×10^{32} kg m^2, and $\mathbf{\Omega}$ is the angular velocity of the solid Earth relative to an inertial frame. Solid lines are based on the analysis scheme used by the British Meteorological Office and the broken lines on the US National Meteorological Center analysis scheme.

and around mountain ranges well beyond the present knowledge would be required. But values of **C** can be inferred indirectly from variations in the distribution and magnitude of zonal winds or from determinations of associated variations in the l.o.d.

Angular momentum budget

In examining the angular momentum budget of the solid and fluid parts of the Earth allowance should be made for the contributions from the oceans and fluid core as well as from the atmosphere. The relative angular momentum associated with ocean currents is very much less than $(\mathbf{M}_a - I_a\mathbf{\Omega})$ so that direct angular momentum transfer between the oceans and the solid Earth should produce negligibly small effects. On the other hand the relative angular momentum associated with motion in the liquid metallic outer core might be as much as $10 \times (\mathbf{M}_a - I_a\mathbf{\Omega})$ in magnitude, and indeed it is generally considered that angular momentum transfer between the core and solid mantle is responsible for the biggest fluctuations ($\doteqdot 5 \times 10^{-3}$ s) observed in the l.o.d., the so-called 'decade variations'[1,2,5,6]. It is unlikely (as the present study implies) but not yet certain that the core can produce significant l.o.d. changes on time scales less than a few years; this is a matter for more extensive future investigations of residual effects based on accurate determinations of l.o.d. changes and of the atmospheric contribution[5]. Conversely, the expected relationship between short-period l.o.d. fluctuations and changes in $\mathbf{M}_a$ is likely to involve the moment of inertia I_m ($= 7.1 \times 10^{37}$ kg m^2) of the crust and mantle, not the moment of inertia I of the whole Earth, which is $\sim 10\%$ greater than I_m.

The quantity

$$m_a \equiv \int_{-\frac{1}{2}\pi}^{\frac{1}{2}\pi} \int_0^{2\pi} \int_{r_s}^{\infty} \rho(r,\theta,\lambda,t)\, u(r,\theta,\lambda,t)\, r^3 \cos^2\theta \, dr\, d\lambda\, d\theta \tag{1}$$

is the axial (parallel to $\mathbf{\Omega}$) component of the relative angular momentum $(\mathbf{M}_a - I_a\mathbf{\Omega})$ of the whole atmosphere. Here ρ and u are the density and zonal (west–east) component of wind velocity at a time t at a point with spherical polar coordinates θ (latitude), λ (longitude) and r (distance from the centre of the Earth), the volume integration being taken over the whole atmosphere, from the surface $r = r_s$ of the Earth upwards. The density and pressure in the atmosphere satisfy the hydrostatic relationship $\partial p/\partial r = -\rho g$ where g is the acceleration due to gravity. Because the effective thickness of the atmosphere is very small compared with the mean radius r_E ($= 6.37 \times 10^6$ m) of the underlying planet, within the atmosphere g does not depart significantly from its mean surface value of 9.81 m s^{-2} and so both r and g can be treated as constants in equation (1). Thus, we have

$$m_a \doteqdot \frac{r_E^3}{g} \int_{-\frac{1}{2}\pi}^{\frac{1}{2}\pi} \int_0^{2\pi} \int_0^{p_s} u(p,\theta,\lambda,t) \cos^2\theta \, dp\, d\lambda\, d\theta \tag{2}$$

where p_s is the surface pressure.

It is convenient to introduce as a measure of m_a a quantity U with dimensions of speed (m s^{-1}):

$$U = r_E m_a / I_a \qquad (= 4.48 \times 10^{-26} m_a) \qquad (3)$$

U is thus equal to the relative zonal velocity at the equator of a solid body having the same mass distribution and total angular momentum as the atmosphere.

Relative zonal velocity

Determinations of U have been made from data obtained at 12-h intervals during the two periods 4 January (0GMT)–5 March (0GMT) and 1 May (0GMT)–30 June (0GMT) 1979. The procedure adopted is to evaluate U from finite interval approximations to the continuous integral (2) using values of the zonal wind defined at grid points on a global three-dimensional mesh. These grid-point values are obtained from the raw observations (which are, in general, not made at the grid-points) by an elaborate analysis method involving temporal as well as spatial interpolation and weighting based on forecast fields generated by a numerical circulation model[7]. These results are referred to as the Meteorological Office (MO) results. To give a preliminary estimate of the errors involved, the MO results were compared with what we call the NMC results. The latter were obtained by recalculating U from an analysed data set from the US National Meteorological Center: this data set had been produced using the analysis scheme in operation at the NMC[8]. Any discrepancies between the MO results and the NMC results can be mainly attributed to differences in analysis schemes, but also to the fact that the basic data sets were not quite identical. Figure 1*a* shows the variation of U for the first special observing period as well as the separate contributions from the Northern Hemisphere (NH) and Southern Hemisphere (SH). The difference between the two global variations is largely accounted for by the discrepancy in the SH values, the NH values being in much better agreement. Even in the SH the discrepancy seems to be more systematic than random, so that changes with time are quite well correlated between both records; however, this is not definite in view of the absence of marked trends in both SH records. The global angular momentum is dominated by the NH contribution. This is expected because of the large pole–Equator temperature gradient in the NH winter, which produces a large vertical variation of zonal winds, and the comparative weakness of mean surface winds. The NH makes a comparatively large contribution to changes in the global angular momentum. This is consistent with the hypothesis that interaction of the energetic winter hemisphere circulation with orography is the main mechanism responsible for fluctuations in U.

Figure 1*b* shows the variations of U and the contributions from the NH and SH during the second period. Fluctuations in the NH and SH contributions to U in the MO and NMC results are similar, but there are quasi-systematic differences. Thus the NMC results are systematically lower than the MO results for the SH contribution, whereas the reverse is the case for the NH contribution: nevertheless, the two global results are in good agreement. The SH contribution to U dominates during the second period, and the time variation reflects mainly the seasonal decline of the NH contribution. This is associated, of course, with the weakening of the NH zonal circulation as the temperature difference between low and high NH latitudes decreases. Changes on time scales of 1–2 weeks are generally less marked than in the first period, possibly because of the comparative scarcity of land masses and mountain ranges in the SH and the weakness of the NH circulation in summer. However, the most marked change of U found in these results did take place during the second period.

Discussion

A comprehensive error analysis is not yet available; this will form part of future studies. However, the appearance of the same major changes in U in both MO and NMC results presented here suggests that these features are real. A decline in U of ~1 m s^{-1} between 21 January and 7 February is conspicuous in both MO and NMC results (Fig. 1*a*) and an even more spectacular decline, ~1.5 m s^{-1}, appears between 18 May and 2 June in both records also (Fig. 1*b*).

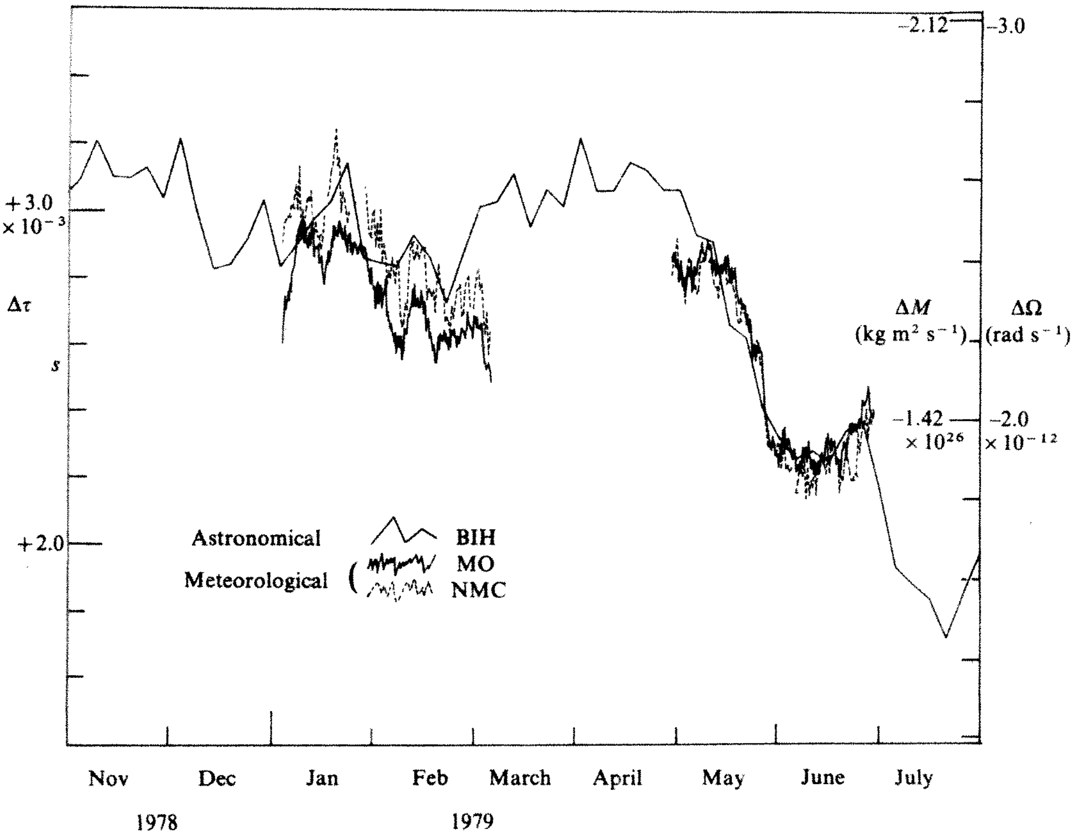

Fig. 2 Comparison of the expected changes in the length of the day (Δτ) derived from the meteorological results displayed in Fig. 1 alongside observed changes from astronomical measurements (see text).

We now compare the meteorological results with estimates of l.o.d. variations, as revealed by astronomical observations. These estimates can be made by comparing universal time (UT), defined by the Earth's rotation, with atomic time (TA). UT1 is based on the rate of rotation of the Earth as determined astronomically from transits of stars and Doppler tracking of artificial satellites; TAI is the international atomic time scale based on a certain resonance of the caesium atom and can be regarded as perfectly uniform for the present discussion. It is necessary to allow for all significant tidal effects[1,2,10]. This was achieved by taking values of the difference between TAI and UT1 at intervals of 5 days as published by the Bureau International de l'Heure (BIH) in Paris, which have already been corrected for annual and semi-annual tides and diurnal nutation, and removing effects due to fortnightly and monthly lunar tides (M_f and M_m (ref. 1)), thus obtaining a quantity $f(n)$, where n is an integer specifying the pentad to which f refers. (The amplitudes of these tides were taken from Table 14.3 of ref. 10.) The values of $f(n)$ were then smoothed to eliminate high-frequency scatter and the first derivative $\Delta\tau(n)$ at each pentad was calculated. This was done using the following 11-point convolute (which exploits the fact that the data were equally spaced in time):

$$\begin{aligned}\Delta\tau(n) \equiv (429\times 5)^{-1}\{89f(n)&+84(f(n-1)+f(n+1))\\ &+69(f(n-2)+f(n+2))\\ &+44(f(n-3)+f(n+3))\\ &+9(f(n-4)+f(n+4))\\ &-36(f(n-5)+f(n+5))\} \qquad (4)\end{aligned}$$

If TAI–UT1 is in seconds, $\Delta\tau(n)$ measures the change in the length of the day relative to the reference day of 86400 SI seconds, which by convection is the average length of the mean solar day during the nineteenth century and corresponds to an angular speed $\Omega_0 = 7.29211515\times 10^{-5}\,\mathrm{rad\,s^{-1}}$ (see ref. 6). The results are joined by a light continuous line in Fig. 2. The right ordinate gives the corresponding values of $\Delta\Omega(n)$ and $\Delta M(n)$ where

$$\Delta\Omega = (\Omega - \Omega_0) \equiv -\Omega_0^2\Delta\tau/2\pi \qquad (5)$$

and

$$\Delta M \equiv -\Omega_0^2 I_m \Delta\tau/2\pi \qquad (6)$$

which is the concomitant change $I_m\Delta\Omega$ in the angular momentum of the Earth's mantle.

If the fluctuations δm_a (as measured by δU, see equation (3) and Fig. 1) in the axial component of relative angular momentum $(\mathbf{M}_a - I_a\mathbf{\Omega})$ of the atmosphere manifest themselves largely as equal and opposite variations in the axial component of the angular momentum of the mantle of the Earth $I_m\Omega = I_m(\Omega_0 + \Delta\Omega)$ then the corresponding fluctuations $\delta\Omega$ in Ω (and in $\Delta\Omega$ since Ω_0 is constant by definition, see equation (5)) are such that $\delta\Omega$ satisfies

$$\delta\Omega \doteqdot -\delta m_a/I_m \qquad (7)$$

The corresponding fluctuations in the length of the day are given by

$$\delta(2\pi/\Omega) \doteqdot \delta m_a(2\pi/\Omega_0^2 I_m) \doteqdot \delta U(2\pi I_a/\Omega_0^2 r_E I_m) \qquad (8)$$

Values of the quantity

$$U(2\pi I_a/\Omega_0^2 r_E I_m) \qquad (9)$$

are plotted in Fig. 2, based on the MO and NMC results presented in Fig. 1. If the hypothesis expressed by equation (8) is correct and the values of $\Delta\tau$ evaluated by the 11-point smoothing procedure (see equation (4)) are dependable, then the curves representing the meteorological data in Fig. 2 should resemble the shape of the curve representing the astronomical data but be separated by a constant vertical distance $\Delta\tau_*$, to be determined from the data. Thus

$$\Delta\tau \doteqdot \Delta\tau_* + U(2\pi I_a/\Omega_0^2 r_E I_m) \qquad (10)$$

Comparison of these results shows that this is so, especially during the second special observing period. Indeed the curves are nearly coincident; that is to say $\Delta\tau_* \ll \Delta\tau$. This unexpected result implies that the net reduction of the angular momentum of the mantle due to the combined effects of tidal friction and other agencies (including any couples acting on the base of the mantle as a result of motions the liquid core of the Earth) since the nineteenth century is close in magnitude to the mean relative angular momentum of the atmosphere in 1979.

The likely connection between fluctuations in the zonal winds and in the l.o.d. has long been appreciated[1–3] but the earliest studies were handicapped by the incomplete wind data. Now, as a result of FGGE, it has become possible to make a close comparison between the changes in the angular momentum of the atmosphere and the mantle. The agreement overall shown in Fig. 2 between the expected changes in the l.o.d. according to the meteorological results and the changes observed astronomically is good, particularly during the second special observing period. The 11-point smoothing was chosen because it reduced the considerable scatter in the 'raw' astronomical results and yet preserved apparently real fluctuations greater than about 10^{-4} s. The agreement shown in Fig. 2 indicates that the meteorological results provide some control on the degree of smoothing that might safely be applied to the astronomical data. Previously this has only been possible from a consideration of the internal errors, which is an unreliable procedure.

Conclusions

By continuing the surveillance of the atmosphere it should be possible to subtract the changes in the angular momentum of the atmosphere from the astronomically determined changes in the angular momentum of the mantle and thus find the residual changes due to interaction between the mantle and the core. The magnitude and temporal behaviour of this interaction will be of particular interest. When the new methods for monitoring the Earth's rotation based on very long base-line interferometry and laser ranging to artificial satellites and the Moon are fully operational, it should also prove possible to carry out a more detailed comparison with the meteorological data. The results of such an investigation will be reported elsewhere.

It is impossible to acknowledge by name all the individuals to whom we are indebted for data, useful discussions and other help, but we should particularly like to mention Dr P. Bender, Mr P. Hart, Professor K. Lambeck, Dr A. Oort, Mr N. Saker, Dr D. Smith and Dr G. Wilkins. R.H. is grateful to Dr C. Leith and other members of the Atmospheric Analysis and Prediction Division for facilities generously made available during a visit to the National Center for Atmospheric Research, Boulder, Colorado.

Received 25 February; accepted 28 April 1980.

1. Munk, W. H. & MacDonald, G. J. F. *The Rotation of the Earth* (Cambridge University Press, 1960).
2. Lambeck, K. *The Earth's Variable Rotation* (Cambridge University Press, 1979).
3. Lambeck, K. & Cazenave, A. *Geophys. J. R. astr. Soc.* **38,** 49–61 (1974); *Phil. Trans R. Soc.* A**284,** 495–506 (1977).
4. McCarthy, D. D. & Pilkington, J. D. H. (eds) *Time and the Earth's Rotation* (Reidel, Dordrecht, 1978).
5. Hide, R. *Phil. Trans. R. Soc.* A**284,** 547–554 (1977).
6. Morrison, L. V. *Geophys. J. R. astr. Soc.* **58,** 349–360 (1979).
7. Lyne, W. H. & Birch, N. T. *Met 0 20 Tech Note No II/142* (Meteorological Office, Bracknell, 1979).
8. Bergman, K. H. *The NMC Operational Global Data Assimilation Scheme* (NMC, NWS, NOAA, Washington DC 1979).
9. *The Explanatory Supplement to the Astronomical Epmeneris and the American Empheris and Nautical Almanac* (HMSO, London, 1974).
10. Melchior, P. *The Tides of the Planet Earth* (Pergamon, Oxford, 1978).

Evidence for live ^{247}Cm in the early Solar System

Mitsunobu Tatsumoto
US Geological Survey, MS 963, Box 25046, Denver, Colorado 80225

Tadashi Shimamura*
Department of Chemistry and Geochemistry, Colorado School of Mines, Golden, Colorado 80401

Variations of the ^{238}U/^{235}U ratio in the Allende meteorite, ranging from −35‰ to +19‰, are interpreted as evidence of live ^{247}Cm in the early Solar System. The amounts of these and other r-products in the Solar System indicate values of (9,000 ± 3,000) Myr for the age of the Galaxy and ~8 Myr for the time between the end of nucleosynthesis and the formation of meteoritic grains. Three possible explanations are presented for the different values of the latter time period which are indicated by the decay products of ^{247}Cm, ^{26}Al, ^{244}Pu and ^{129}I.

THE nuclide ^{247}Cm decays to ^{235}U with a half life ($t_{1/2}$) of 15.6 Myr. As both parent and daughter are actinides, the existence of live ^{247}Cm at the time when solids formed in the primitive nebula would only cause variations in the present ^{238}U/^{235}U ratio if chemical fractionation separated Cm from U. Thus, uranium isotopes in primitive solids may provide important information on the time scale (T) for galactic nucleosynthesis and the time interval (Δ) between the termination of nucleosynthesis and the formation of solids in the early Solar System[1].

Earlier age estimates, based on the normal ^{238}U/^{235}U ratio, 137.88 (ref. 2), the ^{238}U/^{232}Th ratio, and/or these ratios in combination with the ^{187}Re/^{187}Os, ^{244}Pu/^{238}U and ^{129}I/^{127}I ratios[3-11], indicate that galactic nucleosynthesis occurred on a time scale T of $\sim 10^4$ Myr and that solids formed after an interval Δ of $\sim 10^2$ Myr. However, recent discoveries of the decay product of ^{26}Al ($t_{1/2} = 0.73$ Myr) in Allende[12,13] and the decay product of ^{107}Pd ($t_{1/2} = 6.5$ Myr) in the Santa Clara iron meteorite[14] imply that the interval Δ may instead be ~ 1 Myr.

In addition to isotopic anomalies from *in situ* decay of short-lived radionuclides which existed in the early Solar System, the discovery of isotopically anomalous oxygen in Allende was interpreted as evidence that meteorites trapped ^{16}O-enriched interstellar dust grains[15]. It has also been suggested that the oxygen anomaly indicates incomplete mixing of material injected from a nearby supernova (SN) which triggered the collapse of the presolar nebula[16], or isotopic differences between the various chemical components of the interstellar medium which were taken up differentially as solids formed[17]. The discovery of nucleogenetic anomalies, in addition to radiogenic ones, has overthrown the dogma of isotopic homogeneity in the pre-solar nebula, and raised doubts about the validity of classical nucleocosmochronology.

Recently, Arden[18] reported that the ^{238}U/^{235}U ratio is as low as 46 in an acid-etched residue of Allende, and additional analyses seemed appropriate to verify these findings. We report here the results of precise measurements of uranium isotopes in various phases of the Allende, C3V carbonaceous chondrite. Variations in the isotopic composition of uranium are attributed to the existence of ^{247}Cm and to chemical fractionation of ^{247}Cm/U in the early Solar System. The levels of ^{247}Cm indicated by our results are then used in the Cm–U–Th cosmochronometer to consider the SN trigger[16] and the presolar grain[15,17] hypotheses.

Experimental techniques and standards

The isotopic composition of uranium and concentrations of U and Th in inclusions and acid resistant residues of Allende were precisely determined by using a spike enriched in ^{233}U, ^{236}U and ^{230}Th and by pulse-counting on a two-stage, NBS-type mass spectrometer[19]. Details of the present study will be published elsewhere[20]. The ^{233}U–^{236}U double-spike was used to monitor mass fractionation of uranium isotopes.

By this technique, the ^{238}U/^{235}U ratio can be reproducibly determined in 1 ng of standard uranium, NBS-U-500, to within ±0.01% of the certified value. However, in 0.1–1.0 ng of a standard of natural uranium, NBS-950a, this ratio can be determined only to within ±0.5‰ (2σ). The reproducibility of ^{238}U/^{235}U ratio measurements on a standard solution of NBS-950a and on terrestrial basalts is shown in Fig. 1. The accuracy of the ratio measurement on small amounts of uranium depends solely on the count rate of ^{235}U, and 0.1 ng of natural uranium always provided a signal of more than 100 counts per second (c.p.s.). When the count rate of ^{235}U is less than 50 c.p.s., the apparent value of the ^{238}U/^{235}U ratio tends to become smaller because of background contribution to the ^{235}U signal.

Uranium anomalies in chondrules and inclusions

Inclusions of Allende were separated from a specimen coated with fusion crust using stainless steel tools under a laminar flow bench in an ultra-clean laboratory. Inclusions supplied from the National Museum of Natural History and several inclusions left from the previous U–Pb chronology study[21] were also analysed. Some of the inclusions were analysed by electron microprobe for mineralogy. The isotopic compositions which we measured for U in these inclusions are shown in Fig. 2.

Our results demonstrate that: (1) inclusions of Allende indeed display variations in the ^{238}U/^{235}U ratio, ranging from −4 to +3.5% of the terrestrial value, 137.88, whereas Arden[18] reports normal to lower values in all samples except one; (2) spinel-bearing pink aggregates show definite negative isotopic anomalies in the ^{238}U/^{235}U ratio ranging from −4 to −0.5%, but all white to grey aggregates show positive anomalies ranging from +0.5 to +3.5%; and (3) the Mg-rich chondrules show no definite anomaly pattern, with variations of +3 to −3% in the ^{238}U/^{235}U ratio, whereas this ratio ranges from normal to +2% in the Ca–Al-rich chondrules.

Such large variations in the ^{238}U/^{235}U ratio (up to 7%) cannot be the result of isotopic fractionation alone and will

---

*Present address: Department of Chemistry, University of California, San Diego, La Jolla, California 92093.

0028-0836/80/280118-05$01.00

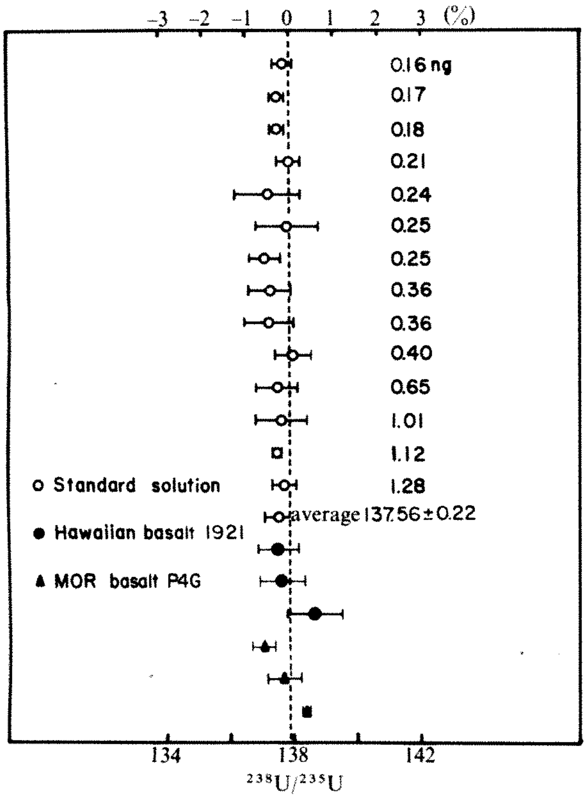

Fig. 1 Reproducibility of $^{238}U/^{235}U$ ratio measurements on the NBS-950a standard and on terrestrial basalts.

therefore be taken to indicate Cm/U fractionation. In view of the fact that ^{244}Pu ($t_{1/2} = 81$ Myr) and ^{129}I ($t_{1/2} = 16$ Myr) survived the interval Δ, it would be reasonable to assume that ^{247}Cm ($t_{1/2} = 16$ Myr) was also present in early Solar System condensates. If chemical fractionation of Cm/U occurred, then the grey to white aggregates trapped actinides with a lower Cm/U ratio than did the pink aggregates. Although the mineral components responsible for these fractionations are not known to us, it seems plausible that the orange-red V-rich spinel or Ti-bearing fassaite[22] may have lower $^{238}U/^{235}U$ ratios because $^{247}Cm^{3+}$ may have entered V^{3+} or Ti^{3+} crystal sites in preference to UO_2^{2+}.

Alternative explanations for the variations observed in the $^{238}U/^{235}U$ ratio include: (1) differences in recoil effects when the U isotopes were produced by α-decay; (2) contributions to the presolar nebula of transbismuth elements from two or more r-processes of nucleosynthesis with different $^{238}U/^{235}U$ production ratios; (3) contributions from two or more nucleosynthesis events which occurred at different times; (4) an 'early' cosmic-ray irradiation which preferentially destroyed ^{235}U (ref. 23); or (5) the presence of live ^{242}Pu ($t_{1/2} = 0.38$ Myr), the precursor of ^{238}U, in the early Solar System. The latter possibility is indicated if Lee *et al.*[24] are correct in concluding that ^{26}Al levels in Ca–Al-rich inclusions of Allende require a very short formation interval after nucelosynthesis, Δ <3 Myr. In any case, the early Solar System contained other r-products, ^{244}Pu and ^{129}I, with half lives comparable with that of ^{247}Cm. Thus, Cm/U fractionation is the most probable cause for the ^{235}U excess.

Uranium anomalies in acid etched residues

Because the mineral phases responsible for the negative and positive anomalies were not clearly identified in this early phase of our study, we prepared HCl–HF insoluble residues of Allende matrix to see if the anomalous uranium might reside in the minerals (carbon, chromite and spinel) which contain isotopically anomalous noble gases and tellurium[25–29]. The presence of anomalous noble gases and tellurium in such residues implies a signature of presolar grains which might be the source of isotopically anomalous uranium.

Our procedure for preparing these residues is that of Anders' group[25–27]. After removal of most visible inclusions, an insoluble residue of 154 mg was prepared from 31 g of the Allende matrix by treatment with HCl–HF at room temperature. The residue was then etched repeatedly, for periods of 24 h, in 6 M HCl. Etching was conducted in a Teflon container at 150 °C, with the dissolution of chromite, and probably spinel. After five HCl etchings, the solution was essentially colourless, indicating that the chromite ($FeCr_2O_4$), and probably the spinel ($MgAl_2O_4$), were dissolved. We denote this fraction as 'spinels'. The black residue which remained was then etched for 24 hours in concentrated HNO_3 (16 M) at 200 °C. In these conditions, the 'carbon' was dissolved leaving a yellowish-white residue. This residue was further treated with concentrated $HClO_4$ for one day at 150 °C.

The dissolution of 'spinels' in HCl at elevated temperatures was verified by a mock experiment on terrestrial chromite and spinel. The HCl dissolution was used instead of the H_3PO_4–H_2SO_4 mixture[27,29] to minimize analytical blanks. The dissolution of 'carbon' may be accompanied by the dissolution of an ill-defined mineral 'Q' (refs 25–27). We denote this fraction as 'carbon' because it was obviously the dominant phase which dissolved when the residue was treated with concentrated HNO_3 at 200 °C.

Measured concentrations of U and Th in each fraction and the isotopic compositions of U are presented in Table 1. Due to the low ^{235}U count-rate in fraction 2 the data for 'spinels' have large experimental uncertainties. In spite of this, the high $^{238}U/^{235}U$ ratio in 'spinels' is quite significant because, as noted above, measured $^{238}U/^{235}U$ ratios tend to become small when the ^{235}U signal is less than 50 c.p.s. The amounts of U in fractions 3, 4, 5 and 7 were too low for reliable isotopic analysis.

The $^{238}U/^{235}U$ ratio in carbon is low, and the intermediate value of $^{238}U/^{235}U$ in fraction 1 is probably due to physical flotation of some extremely fine, black particles which later dissolved when the decantate was converted in an HNO_3 medium for purification of U by anion exchange.

We estimate the $^{238}U/^{235}U$ ratio in the total acid residue to be ~116 from the values observed in fractions 1, 2 and 6. However, as our residue was prepared from matrix-rich portions, the results of this estimate do not necessarily provide support for the low values reported by Arden[18].

The extremely high value of the $^{238}U/^{235}U$ in fraction 2, when 'spinels' dissolved, seems to be inconsistent with Arden's report[18] of extremely low values of this ratio in residues which had been previously exposed to various oxidizing conditions. Regardless of whether HCl + HF or HNO_3 + HF were used in the first etching stage, Arden observed low values of the $^{238}U/^{235}U$ ratio, ~50, in the final stage of etching when the residues contained extremely small amounts of uranium, 10^{-11} g.

The most significant results of this etching experiment are: the high value of the $^{238}U/^{235}U$ ratio in fraction 2 when 'spinels' dissolved; and the extremely low value of this ratio in fraction 6 when 'carbon' dissolved. Enriched ^{235}U in 'carbon' and its depletion in 'spinels' parallel abundances of the heavy and light isotopes of Xe and Te in these[25–27,29]. If heavy isotopes of Xe and Te in carbon are from actinide fission, it implies that excess ^{235}U there may be due to an initial enrichment of live ^{247}Cm. These large anomalies are unlikely to be artefacts of the acid treatment, such as the selective extraction of radiogenic ^{235}U from 'spinels' because of α-recoil effects, and its adsorption on 'carbon', for the following reasons: (1) active sites for adsorption of uranium onto carbon would be swamped with uranium of normal composition which was released from the silicates during the earlier HCl–HF treatments; (2) the high $^{238}U/^{235}U$ ratio in the spinel-rich

Table 1 Data of Allende HCl–HF residue (154 mg)

Fractions	Amount (cm^3)	U* (p.p.b.)	Th* (p.p.b.)	% Blank U	% Blank Th	$\frac{Th}{U}$	$\frac{238†}{235} \pm 2\sigma_m$	^{235}U (c.p.s.)
1 6 M HCl	20	1.79	17.89	40	32	9.99	123.16 ± 0.66	242-33
2 6 M HCl	20	0.58	3.11	42	45	7.2	163.50 ± 1.26	67-16
3 6 M HCl	20	0.19	2.18	200	76	11.5	—	—
4 and 5 as above	20	—	—	—	—	—	—	—
6 16 M HNO_3	10	0.99	1.12	28	200	1.1	89.88 ± 2.79	244-88
7 11 M $HClO_4$	2	0.11	0.83	110	135	7.6	—	—

*Concentrations are for total residue; p.p.b., parts per 10^9. †Blank corrected ratios, errors are 2 × mean standard deviation.

fraction 2 is in accordance with the high values of this ratio in the spinel-rich, white inclusions which were mechanically separated from Allende; and (3) we are unaware of any chemical treatments which can separate the isotopes of such dissimilar elements as uranium, xenon and tellurium to produce the unusual isotopic compositions reported in acid-etched residues of Allende. We will, therefore, assume that variations in the $^{238}U/^{235}U$ ratio were produced be the decay of ^{247}Cm in the early Solar System.

The curium–uranium–thorium cosmochronometer

In the following calculations of the duration of galactic nucleosynthesis (T) and the interval Δ, we follow Fowler's[30] model of an exponentially decreasing rate of galactic nucleosynthesis with a last minute spike event. Local variations from a smooth exponential decline in the nucleosynthesis rate do not seriously detract from the general versatility of this model[31]. In fact, the last minute spike[7,8,30] is remarkably similar to recent models of a SN trigger which injected freshly synthesized material into a presolar nebula[16,32] of elements from earlier, collective nucleosynthesis processes.

If the transbismuth nuclides were produced by an r-process at a different site (core[33]?) from the explosive carbon-burning or hydrogen–helium-burning shells where ^{16}O and ^{26}Al were produced[34–36], then the high $^{238}U/^{235}U$ ratio and low concentration of ^{244}Pu in spinel might be explained by early condensation of spinels before mixing with the heavy r-process nuclides[37]. In this regard, note that the uranium which we extracted from 'spinels' represents a mixture of uranium from spinel, chromite and other spinels. Thus, the weakness of our experiment is its failure to set a firm upper limit on the value of the $^{238}U/^{235}U$ ratio which might be found by selective dissolution of the mineral components in our 'spinels'.

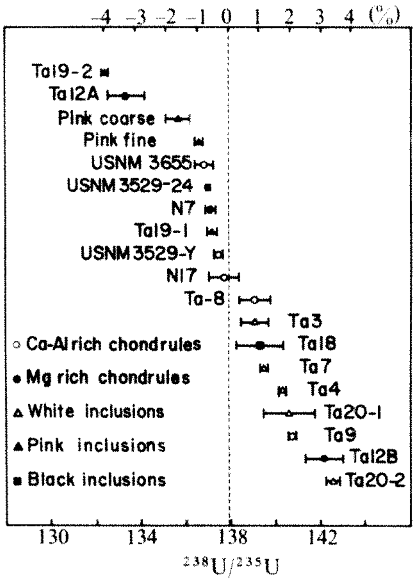

Fig. 2 Uranium isotopic compositions in the Allende inclusions. Pink aggregates, N7 and N17, were described earlier[21]. USNM samples are from the National Museum of Natural History.

Alternatively, if excess ^{16}O and ^{26}Mg are the result of material injected from a nearby SN[16,32], then classical nuclear cosmochronology may be affected[33,38,39]. However, the ^{16}O and ^{26}Al may alternatively have been produced locally, in the early Solar System[40,41]. Moreover, there have been many studies which suggest that isotopic homogeneity, rather than isotopic heterogeneity, was the dominant trait of the presolar nebula, for example, the negative results in attempts to find isotopically anomalous Ca, Sr, Ba and Sm in all Allende inclusions[24,42] analysed, except two Ca–Al-rich ones, and the finding of isotopically normal Sr and Nd in the HCl–HF etched residues of Allende[43]. These findings suggest that it would be premature to dismiss classical cosmochronology.

We will, therefore, use our results to compute values of T and Δ from the Cm–U–Th chronometer and compare these with values of T and Δ suggested by other radionuclides, such as, ^{244}Pu and ^{26}Al. For this calculation, we assume that the value of $^{238}U/^{235}U$ of 137.88 in bulk meteorites and terrestrial rocks is characteristic of solar uranium, although microscopic mineral constituents and inclusions of meteorites contain anomalous uranium.

According to Fowler's[30] model of exponentially declining nucleosynthesis, the production rate, P_A, of isotope A at time t is $P_A(t) = P_A(t=0)\exp(-\Lambda t)$. Thus, the primordial abundance ratio of isotopes A and B at the time of formation of planetary solids can be expressed as:

$$\frac{N_A(T+\Delta)}{N_B(T+\Delta)} = (P_A/P_B)\exp\{(\lambda_B - \lambda_A)\Delta\}$$

$$\times \frac{S\{1-\exp(\Lambda T)\} + (1-S)(\Lambda/\Omega_A)\{1-\exp(\Omega_A T)\}}{S\{1-\exp(\Lambda T)\} + (1-S)(\Lambda/\Omega_B)\{1-\exp(\Omega_B T)\}}. \quad (1)$$

In these equations, Λ is the decay constant of the assumed exponential form for nucelosynthesis, $\Omega_A = \Lambda - \lambda_A$ and $\Omega_B = \Lambda - \lambda_B$ where λ_A and λ_B are the decay constants of A and B, and S is the fraction of elements in the Solar System that was produced by a spike nucleosynthesis event which occurred at time T, at the termination of galactic nucleosynthesis of Solar System material.

To obtain the chronology of r-process nucleosynthesis from ^{247}Cm–U, the degree of fractionation of Cm/U in Solar System material must be known. However, the fractionation factor for ^{247}Cm at $T+\Delta$ is unknown. For simplicity, we therefore assume, in the first case, that the addition of freshly synthesized ^{247}Cm and U in the spike resulted in the present value of N_{235}/N_{238} is 1/137.88 in the Earth and in many bulk meteorites for unfractionated Cm/U abundances, and that the present value of N_{235}/N_{238} of 1/163 in 'spinels' represents the base value for the most extreme Cm/U fractionation, that is, this represents the value when there has been no ^{247}Cm contribution to 'spinels' uranium. Accordingly, the amounts of

^{247}Cm, ^{235}U and ^{238}U in the early Solar System were, assuming the meteorite age to be 4.55×10^3 Myr:

$$\frac{N^{G}_{235}(T+\Delta)+N^{S}_{235}(T+\Delta)+N^{G}_{247}(T+\Delta)+N^{S}_{247}(T+\Delta)}{N^{G}_{238}(T+\Delta)+N^{S}_{238}(T+\Delta)}= (1/137.88)\exp\{(\lambda_{235}-\lambda_{238})(4.55)\}=0.3163 \qquad (2)$$

and the ^{247}Cm-free ratio of ^{235}U/^{238}U was

$$\frac{N^{G}_{235}(T+\Delta)+N^{S}_{235}(T+\Delta)}{N^{G}_{238}(T+\Delta)+N^{S}_{238}(T+\Delta)}= \{1/163\}\exp\{(\lambda_{235}-\lambda_{238})(4.55)\}=0.2675. \qquad (3)$$

In these equations, the superscripts G and S designate contributions from galactic and spike nucleosynthesis, respectively. Then for this case, the ratio of ^{247}Cm to ^{238}U at time $T+\Delta$ is

$$\frac{N^{G+S}_{247}(T+\Delta)}{N^{G+S}_{238}(T+\Delta)}=0.3163-0.2675=0.0487. \qquad (4)$$

For the above model we have three input data which are associated with the r-process, ^{247}Cm/^{238}U, ^{235}U/^{238}U and ^{232}Th/^{238}U. These were used to determine the values of T, Δ, Λ and S, using the values of constants listed in Table 2. For values of $\Lambda=(0.1$ to $1.0)\times 10^{-9}\,\mathrm{yr}^{-1}$ and $S=0.01$ to 0.1, we found that the most internally consistent solution is obtained for $\Lambda=0.6\times 10^{-9}\,\mathrm{yr}^{-1}$ and $S=0.05$. Curves of Δ versus T for $\Lambda=0.6\times 10^{-9}\,\mathrm{yr}^{-1}$ are shown in Fig. 3. This solution yields a galactic age, $T_G=(T+\Delta+4{,}550\,\mathrm{Myr})=9{,}100\pm 2{,}800$ Myr, (assuming $\pm 10\%$ uncertainty in production rates and $\pm 5\%$ uncertainty on the Th/U ratio), and a decay interval $\Delta \sim 8$ Myr, with limits of 0–90 Myr for the above uncertainties.

Detailed calculations including the constraints imposed by the abundances of ^{244}Pu, ^{129}I and ^{26}Al will be presented elsewhere[20]. However, note that the ^{244}Pu/^{238}U curve intersects the ^{235}U/^{238}U (1/163) and ^{232}Th/^{238}U curves at $\Delta \simeq 100$ Myr, if the ^{244}Pu/^{238}U ratio at $t=T+\Delta$ is 0.016 (ref. 44) or 0.035 (ref. 45). However, the curve for ^{244}Pu/^{238}U $=0.087$, which Podosek and Lewis[46] observed in a Ca–Al-rich Allende inclusion crosses the curves of ^{235}U/^{238}U and ^{232}Th/^{238}U at $\Delta=8$ Myr. These calculations are based on values of $\Lambda=0.6\times 10^{-9}\,\mathrm{yr}^{-1}$ (see Fig. 3).

The assumption that the ^{238}U/^{235}U ratio in 'spinels' contains a negligible contribution from spike-produced ^{247}Cm but that 5% of other r-products in spinels came from this last nucleosynthesis spike, may not be correct if spinels formed before contamination with the spike r-products. However, note that the value which we calculated for the initial ^{247}Cm/^{238}U ratio, 0.049, is the same order of magnitude as values reported for the initial ^{244}Pu/^{238}U ratio, 0.016–0.087 (refs 44–46).

The value calculated above for the decay interval, $\Delta \sim 10$ Myr, is somewhat higher than the value of $\Delta < 3$ Myr which Lee *et al.*[24] obtained from data indicating that ^{26}Al/^{27}Al $\simeq 5\times 10^{-5}$ when Ca–Al-rich inclusions of Allende formed. Note, however, that Lorin and Christophe Michel-Lévy[47] found evidence of much higher initial ^{26}Al/^{27}Al ratios, up to 1×10^{-3}, in hibonites in inclusions of Leoville and Allende. Recently Lee *et al.*[48] reported a very low initial ^{26}Al/^{27}Al value of 2×10^{-7} in HAL inclusion of Allende. The difference between initial values of ^{26}Al/^{27}Al in hibonites of Leoville and in HAL inclusion of Allende corresponds to an interval of 9 Myr between the formation times of these objects[41], if the source of Al in these objects originally had the same ^{26}Al/^{27}Al ratio. This suggests that hibonite grains formed directly from freshly synthesized material, or very soon after this material was added to the presolar nebula, and that solidification of 1–10-mm size objects occurred ~10 Myr later.

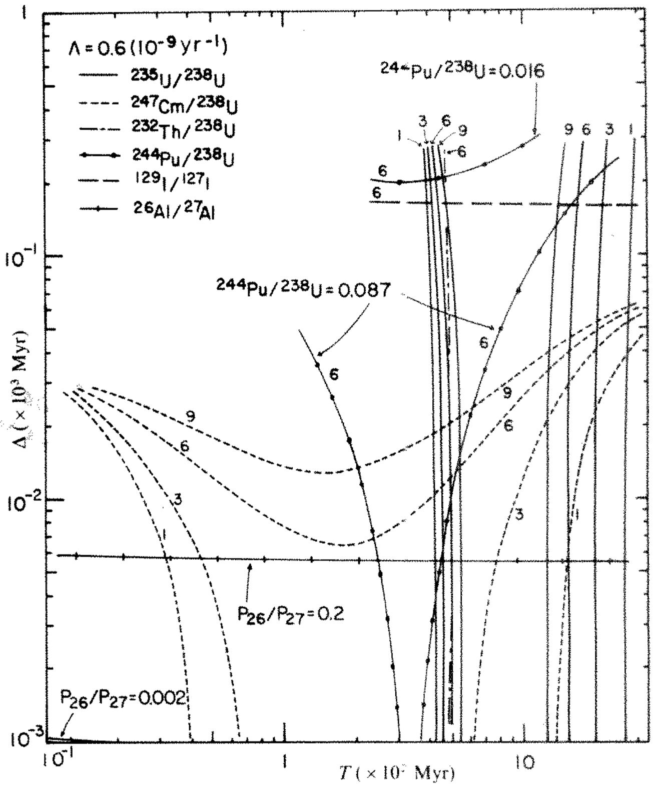

Fig. 3 Trajectories of Δ and T values of the ^{235}U/^{238}U, ^{232}Th/^{238}U, ^{247}Cm/^{238}U, ^{244}Pu/^{238}U and ^{26}Al/^{27}Al ratios for $\Lambda=0.6\times 10^{-9}\,\mathrm{yr}^{-1}$ of case 1. They are calculated following Fowler's model[30] of exponential galactic nucleosynthesis [exp $(-\Lambda T)$] and a last minute spike (S). Numbers on the trajectories are S (%). For the trajectories of ^{232}Th/^{238}U, ^{244}Pu/^{238}U, ^{129}I/^{127}I and ^{26}Al/^{27}Al, only values corresponding to $S=6\%$ are shown. Production ratios assumed for P_{26}/P_{27} are 0.002 and 0.2, and values assumed for the ^{244}Pu/^{238}U ratio at time $T+\Delta$ are 0.087 and 0.016

Conversely, these results may suggest that the production ratio of ^{26}Al/^{27}Al from some thermonuclear process in the SN was about two orders of magnitude higher[36] than that calculated for carbon burning[35,49].

For the second case, we assume that there was no contribution of any transbimuth r-products from the spike to 'spinels'. In this model, we assume that the 'spinels' represent grains which formed in the outer shell of the SN[37] and that these were injected into the presolar nebula, where the average mixture of all r-products is represented by the present value of $(^{238}\mathrm{U}/^{235}\mathrm{U})=137.88$ when no fractionation of Cm/U occurred.

This can be described by analogous forms of the equations used for case 1,

$$\frac{N^{G}_{235}(T+\Delta)+N^{G}_{247}(T+\Delta)}{N^{G}_{238}(T+\Delta)}=0.2675. \qquad (5)$$

If we assume that $N^{G}_{238}(T+\Delta)\simeq N^{G}_{238}(T+\Delta)+N^{S}_{238}(T+\Delta)$, then

$$\frac{N^{S}_{235}(T+\Delta)+N^{S}_{247}(T+\Delta)}{N^{G}_{238}(T+\Delta)}=0.0487. \qquad (6)$$

Because ^{247}Cm decays to ^{235}U, the numerator of equation (6) does not change during the period of free decay and cannot be used to calculate the value of Δ. However, if there is negligible

Table 2 Values of constants used in computations

	Decay constants (10^{-9} yr^{-1})		
λ_{247}	43.3	λ_{244}	8.41
λ_{235}	0.98485	λ_{129}	41.0
λ_{238}	0.155125	λ_{26}	950
λ_{232}	0.04948		
	Abundance ratios (at $T+\Delta$)		
^{247}Cm/^{238}U	0.0487 ± 0.0267	^{244}Pu/^{238}U	0.087‡, 0.016§
^{235}U/^{238}U	0.2675 ± 0.027	^{129}I/^{127}I	$(1.07 \pm 0.41) \times 10^{-4}$‖
^{232}Th/^{238}U	2.48 ± 0.12*	^{26}Al/^{27}Al	5×10^{-5}¶
	Production ratios		
P_{247}/P_{238}	0.837 ± 0.126†	P_{244}/P_{238}	0.90 ± 0.1#
P_{235}/P_{238}	1.64 ± 0.25†	P_{129}/P_{127}	1.52 ± 0.5#
P_{232}/P_{238}	1.80 ± 0.1#	P_{26}/P_{27}	2×10^{-3}**, 0.2††

*$(^{232}\mathrm{Th}/^{238}\mathrm{U})_{\mathrm{now}} = 4.0 \pm 0.2$. †ref. 3; ‡ref. 46; §ref. 44; ‖ref. 55; ¶ref. 24; #ref. 56; **ref. 49; ††ref. 36.

decay of ^{235}U, ^{238}U and ^{232}Th over the time period Δ, that is, $\lambda_{235}, \lambda_{238}, \lambda_{232} \ll 1/\Delta$, then $N^{G+S}_{235}(T+\Delta) = N^{G+S}_{235}(T)$, and so on, and if we assume that $N^{G+S}_{232}(T) \simeq N^{G}_{232}(T)$, then equation (1) yields $T_G = (9.4 \pm 2.7) \times 10^9$ yr, $\Lambda = 0.45 \times 10^{-9}$ yr^{-1} and $S = 0.02$ for case 2 (where $S = 0$ for all r-products in 'spinels').

If this model is correct, then the Cm/U ratio in 'carbon' has been increased by a fractionation factor of $\simeq 4$. Such a fractionation factor is quite reasonable from thermodynamic considerations[50]. We prefer case 2, where neither Cm nor U from the spike contributed to 'spinels', because case 1 requires a large fractionation of spike-produced Cm/U in 'spinels'. The duration of galactic r-process nucleosynthesis from our calculations, although model dependent, seems to be consistent with the revised age of the Universe which was recently reported from a new calculation of the Hubble constant[51].

For case 2, we assumed that grains of 'spinels' are fresh condensates from the triggering SN event and that this event also contributed transbismuth r-products to the presolar nebula. On the other hand, Lattimer *et al.*[32] note that the difference between values of the decay interval indicated by radiogenic Xe isotopes ($\Delta \sim 100$ Myr) and Mg isotopes ($\Delta \sim 1$ Myr) may imply that the last SN event was a source of ^{26}Al, but not a source of r-products. According to this hypothesis, the presolar nebula consists of interstellar type gas and dust which had been enriched in r-products when the nebula passed through a galactic spiral arm[52] ~100 Myr before this last SN event. If interstellar material had been cycled, by star formation and stellar ejections, with such a frequency[34] that the mean residence time of material in the interstellar medium is short, <100 Myr, then our calculations are compatible with the proposal of Lattimer *et al.*[32]. However, our calculations would not be warranted if the residence time of interstellar material is large, >1,000 Myr, as estimated by Clayton[17].

Conclusion

The Cm–U–Th chronometer yields values of $T = 9{,}000 \pm 3{,}000$ Myr and $\Delta \sim 8$ Myr. This value of Δ is larger than that implied from the decay product of ^{26}Al, $\Delta < 3$ Myr, but smaller than that suggested by the decay products of ^{244}Pu, $\Delta \sim 100$ Myr.

We suggest three possible explanations for the different values of Δ. (1) The short-lived r-products were produced on the last passage of the protosolar cloud through a galactic spiral arm[52], ~10 Myr before ^{26}Al was synthesized[32] in the explosion of a nearby SN which triggered the collapse of the presolar nebula[16]. (2) Both ^{26}Al and the short-lived r-products were produced in the nearby SN but Al condensed from material in outer shells of the SN ~10 Myr before the condensation of r-products, ^{247}Cm and ^{244}Pu, from the stellar interior[33]. Retention of Xe generally started ~100 Myr later, except in such cases as the Ca–Al-rich inclusion of Allende for which the ^{244}Pu–^{136}Xe chronometer indicates $\Delta \simeq 8$ Myr (ref. 46). (3) The ^{26}Al/^{27}Al production rates were different in different regions of the nearby SN, being higher by a factor of ~100 in H–He layers[36] than in that of carbon burning[35]. In this case, the observation of $^{26}\mathrm{Al}/^{27}\mathrm{Al} = 5 \times 10^{-5}$ would correspond to a value of $\Delta \sim 6$ Myr (see Fig. 3).

Alternatively, the primitive solar nebula may have contained large scale elemental and isotopic heterogeneities from the debris of a single SN which produced the bulk of the elements in the Solar System[53]. Note also that the ^{238}U/^{235}U ratio may have been altered by an early cosmic ray irradiation[23,54]. If so, then the calculations reported here, and previously calculated values of T and Δ, are unwarranted.

We thank O. K. Manuel, D. D. Clayton and D. M. Unruh for comments on this manuscript, A. K. Vuletich for assistance with mass spectrometry and Edward Anders for attracting our interest to the HCl–HF residues of Allende. USNM samples were provided by Brian Mason. This research was supported by NASA Interagency Transfer Order T-2407A.

Received 31 December 1979; accepted 21 April 1980.

1. Blake, J. B. & Schramm, D. N. *Nature* **243,** 138 (1973).
2. Barnes, I. L. *et al. Proc. 3rd Lunar Sci. Conf.* 1465 (Pergamon, Oxford, 1972).
3. Burbridge, E. M., Burbridge, G. R., Fowler, W. A. & Hoyle, F. *Rev. Mod. Phys.* **29,** 547 (1957).
4. Fowler, W. A. & Hoyle, F. *Ann. Phys.* **10,** 280 (1960).
5. Kohman, T. P. *J. chem. Educ.* **38,** 73 (1961).
6. Cameron, A. G. W. *Icarus* **1,** 13 (1962).
7. Wasserburg, G. J., Schramm, D. N. & Huneke, J. C. *Astrophys. J. Lett.* **157,** L91 (1969).
8. Hohenberg, C. M. *Science* **166,** 212 (1969).
9. Dicke, R. H. *Astrophys. J.* **155,** 123 (1969).
10. Schramm, D. N. & Wasserburg, G. J. *Astrophys. J.* **162,** 57 (1970).
11. Clayton, D. D. *Astrophys. J.* **139,** 637 (1964).
12. Gray, C. M. & Compston, W. *Nature* **251,** 495 (1974).
13. Lee, T., Papanastassiou, D. A. & Wasserburg, G. J. *Geophys. Res. Lett.* **3,** 41 (1976).
14. Kelly, W. R. & Wasserburg, G. J. *Geophys. Res. Lett.* **5,** 1079 (1978).
15. Clayton, R. N., Grossman, L. & Mayeda, T. K. *Science* **182,** 485 (1973).
16. Cameron, A. G. W. & Truran, J. W. *Icarus* **30,** 447 (1977).
17. Clayton, D. D. *Earth planet. Sci. Lett.* **36,** 381 (1977).
18. Arden, J. W. *Nature* **269,** 788 (1977).
19. Shield, W. R. (ed.) *NBS Technical Note* 456 (US Government Printing Office, Washington, DC, 1968).
20. Shimamura, T. & Tatsumoto, M. *Geochim. cosmochim. Acta* (submitted).
21. Tatsumoto, M., Unruh, D. M. & Desborough, G. A. *Geochim. cosmochim. Acta* **40,** 617 (1976).
22. Douty, E. & Clarke, J. R. *Am. Miner.* **58,** 230 (1973).
23. Fowler, W. A., Greenstein, J. L. & Hoyle, F. *Geophys. J. R. astr. Soc.* **6,** 148 (1962).
24. Lee, T., Papanastassiou, D. A. & Wasserburg, G. J. *Astrophys. J. Lett.* **211,** L107 (1977).
25. Lewis, R. S., Srinivasan, B. & Anders, E. *Science* **190,** 1251 (1975).
26. Srinivasan, B., Gros, J. & Anders, E. *J. geophys. Res.* **82,** 762 (1977).
27. Lewis, R. S., Gros, J. & Anders, E. *J. geophys. Res.* **82,** 779 (1977).
28. Frick, U. & Moniot, R. K. *Proc. 8th Lunar Sci. Conf.* 226 (Pergamon, Oxford, 1977).
29. Ballad, R. V., Oliver, L. L., Downing, R. G. & Manuel, O. K. *Nature* **277,** 615 (1979).
30. Fowler, W. A. in *Cosmology, Fusion and Other Matters,* 67 (Colorado Associated University Press, 1972).
31. Schramm, D. N. *A. Rev. Astr. Astrophys.* **12,** 383 (1974).
32. Lattimer, J. M., Schramm, D. N. & Grossman, L. *Astrophys. J.* **219,** 230 (1978).
33. Hillebrandt, W. *Space Sci. Rev.* **21,** 639 (1978).
34. Clayton, D. D. *Icarus* **32,** 255 (1972).
35. Truran, J. W. & Cameron, A. G. W. *Astrophys. J.* **219,** 226 (1978).
36. Arnould, M., Hillebrandt, W. & Thielemann, E. in *22nd int. Astrophys. Colloq.,* Liege (1978).
37. Clayton, D. D. *Astrophys. Space Sci.* **65,** 179 (1979).
38. Clayton, D. D. *Space Sci. Rev.* **24,** 147 (1979).
39. Lee, T. *Rev. Geophys. Space Phys.* **17,** 1591 (1979).
40. Heymann, D. & Dziczkaniec, M. *Science* **191,** 79 (1976).
41. Lee, T. *Astrophys. J.* **224,** 217 (1978).
42. Patchett, P. J. *Nature* **283,** 438 (1980).
43. Tatsumoto, M., Shimamura, T., Patchett, P. J. & White, W. M. *Lunar planet. Sci.* **11,** 1125 (1980).
44. Podosek, F. A. *Earth planet. Sci. Lett.* **8,** 183 (1970).
45. Wasserburg, G. J., Huneke, J. C. & Burnett, D. S. *Phys. Rev. Lett.* **22,** 1198 (1969).
46. Podosek, F. A. & Lewis, R. S. *Earth planet. Sci. Lett.* **15,** 101 (1972).
47. Lorin, J. C. & Christophe Michel-Lévy, M. *4th int. Conf. Geochron. Cosmochron. and Isotope Geol., USGS Open File Report* 78–701, Snowmass, CO 257 (1978).
48. Lee, T., Russell, W. A. & Wasserburg, G. J. *Lunar planet. Sci.* **10,** 713 (1979).
49. Arnett, W. D. & Wefel, J. P. *Astrophys. J. Lett.* **224,** L139 (1978).
50. Boynton, W. V. *Earth planet. Sci. Lett.* **40,** 63 (1978).
51. Aaronson, M. *et al. Astrophys. J.* (in the press).
52. Reeves, H. in *On the Origin of the Solar System* (ed. Reeves, H.) 376 (CNRS, Paris, 1972).
53. Manuel, O. K. & Sabu, D. D. *Trans. Mo. Acad. Sci.* **9,** 104 (1975).
54. Kuroda, P. K. *Geochem. J.* **13,** 83 (1979).
55. Hohenberg, C. M. *Earth planet. Sci. Lett.* **3,** 357 (1967).
56. Fowler, W. A. in *Proc. Robert A. Welch Foundation Conf. on Chemical Research* Vol. 21 (ed. Milligan, W. O.) 61 (Houston, 1978).

The influence of codon context on genetic code translation

Lionello Bossi* & John R. Roth

Department of Biology, University of Utah, Salt Lake City, Utah 84112

A class of mutations that increase the efficiency of a suppressor tRNA in translating a particular amber codon has been characterized. The increased efficiency is due to a mutation resulting in a change in the mRNA that affects the nucleotide adjacent to the 3′ side of the UAG triplet. Thus the interaction of tRNA with mRNA is influenced by mRNA sequences outside the triplet codon.

THE triplet words of the genetic code are known to be read by transfer RNA molecules which interact with the respective codons on the messenger RNA. The specificity and accuracy of reading are overwhelmingly due to standard base-pairing between three bases on the mRNA (the codon) and three bases in the tRNA (the anticodon). It is generally assumed that no additional nucleotides in the mRNA other than the three residues which make up a codon are involved in the interaction with a single tRNA species. In the past few years, however, several studies have suggested that reading of a given codon may be influenced by mRNA sequences external to this codon; this influence has been described as the effect of the reading context on translation[1–8]. We have closely investigated this aspect of the decoding process and present here direct evidence that mRNA sequence outside of the codon has a role in determining the efficiency of translation.

Mutant tRNAs, acting as informational suppressors, are tRNA species whose activity can be followed individually *in vivo*. In the appropriate genetic system, the measurement of suppression efficiency can be correlated directly with the activity of the suppressor tRNA. It is then possible to analyse various factors that can influence the activity of the tRNA, such as structural alterations of ribosome, tRNA or mRNA. This approach led us to study the effects of a mutation affecting tRNA structure (*hisT*) on the suppression properties of informational suppressors in *Salmonella typhimurium*.

The *hisT* mutation causes the lack of pseudouridine from the anticodon region of several tRNAs[9–12]. In spite of its pleiotropic effects on many tRNA species, the *hisT* mutation does not impair cell viability. The only detectable phenotypic change is the altered regulation (constitutive expression) of the histidine operon, consequent to the lack of two pseudouridine residues from the anticodon region of histidine tRNA[9]. During our study, it became evident that the activity of the glutamine-inserting amber suppressor *supE*[13] (which normally contains two pseudouridine residues in the anticodon region[12,14,15]) is reduced considerably by *hisT*[16] (unpublished results). The reduced efficiency of the suppressor offered the basis for the genetic selection of mutations increasing the efficiency of *supE*. Mutants were isolated in which the inhibitory effect of *hisT* on suppression is overcome by an increase in the efficiency of the translation step at the nonsense site. Interestingly, some of these mutations affect the reading context at the nonsense site by changing the mRNA sequence adjacent to the nonsense codon.

Effect of *hisT* on *supE* suppression efficiency

The ability of *supE* to suppress amber mutations in the *hisD* gene of the *his* operon was tested in both *hisT*$^+$ and *hisT*$^-$ genetic backgrounds. These tests show that at some mutant sites the *hisT* mutation causes a reduction in *supE* efficiency so severe that the mutants are not phenotypically corrected by *supE* in the presence of a *hisT* mutation. For some other mutations, however, suppression by *supE* still occurs in spite of the presence of a *hisT* mutation. Thus, the effect of *hisT* on *supE* efficiency seems to depend on the particular mutant site being read. A detailed description of these experiments will be published elsewhere.

We considered three possible explanations for the site-specificity of the effects of *hisT*. First, some mutant sites may yield a protein with poor activity when suppressed by *supE*. Such sites may require a fully active *supE* tRNA in order to show phenotypic correction. Second, some mutant sites may show strong polarity effects. These sites might require very efficient suppression in order to overcome the tendency to terminate mRNA production. Third, some amber codons may be poorly read by a suppressor tRNA due to the influence of the reading context. That is, the efficiency of the suppressor tRNA in reading a particular site may depend on the nature of the residues in the immediate neighbourhood of that site. UAG codons located in unfavourable reading contexts would require a strong suppressor to overcome these reading difficulties. Such context effects on suppression efficiency have been reported previously[1–7].

Each of these explanations is, in principle, consistent with the initial data presented above if the *hisT* mutation impairs the function of *supE* tRNA. However, there are compelling reasons, outlined below, for rejecting the first two hypotheses.

The first explanation seems untenable because some of the amber sites whose suppressibility is impaired by *hisT* affect the N-terminal portion of the *hisD* protein, which is dispensable for catalytic activity[17,18] (unpublished results of T. Kohno, I. Hoppe and J.R.). It seems unlikely that the nature of the amino acid insertion in this region could seriously affect protein function. This possibility is further contradicted by the behaviour of amber mutation *hisD6404*. As described below, this site has a glutamine residue in the wild-type sequence. The *hisT* mutation impairs the ability of *supE* (a glutamine-inserting suppressor) to suppress *hisD6404*. Thus the *hisT* effect is seen even though the suppressed protein is wild type in structure.

The second hypothesis implies that the *hisT* inhibition of suppression would have greater effects on the correction of strongly polar mutant sites. This seems unlikely in view of the genetic map distribution of sites whose suppression is strongly affected by *hisT*. In general, the polarity effect of nonsense mutations is a function of their position in the gene, with more polar mutations located nearer the promoter-proximal end of the gene[19]. The mutations we have studied show no correlation between map position and effect of *hisT* on their suppressibility by *supE* (data not shown).

Our initial observations are consistent with the idea that reading of a particular amber codon is influenced by the sequence of bases surrounding that codon in the mRNA

---

*Permanent address: I Istituto di Chimica Biologica, II Facolta' di Medicina e Chirurgia, University of Naples, Italy. Present address: European Molecular Biology Laboratory, Heidelberg, FRG.

0028-0836/80/280123-05$01.00

(context). The variable effects of *hisT* on suppressibility of different amber mutations might depend on differences in the context of the UAG codons at the various sites. Several possible mechanisms for these effects are discussed later.

If mRNA context influences the readability of a particular codon, then reading efficiency should be altered if the base sequence near that codon is changed. We did this by selecting mutations that improve the suppression efficiency of *supE* for a particular amber site. The dispensable (N-terminal) region of the *hisD* gene offered a convenient system, because the sequence changes in this region that could affect suppression efficiency were not expected to influence the catalytic activity of the suppressed protein.

Isolation of context mutants

In order to select context mutants, a strain was constructed which carries *hisT*, *supE* and a particular amber mutation in *hisD* whose suppression is abolished by *hisT*; such a strain is a histidine auxotroph in spite of the presence of the suppressor. His$^+$ revertants were isolated and screened for individuals that still contained all the parental genetic markers, but had acquired an additional mutational change within the *hisD* gene that restored suppressibility to the amber mutation (change in reading context).

The full genotype of the strain used (TT4242) and the results of the selection are shown in Table 1. The starting amber mutation is *hisD6404*, mapping in the operator-proximal, dispensable region of the *hisD* gene. Mutation *his01242* is a regulatory mutation that causes the *his* operon to be expressed constitutively at high levels[16,20]; the presence of this regulatory mutation eliminates any further effect of *hisT* on operon expression. Mutation *leu-414* is an amber mutation in the *leu* operon whose suppression by *supE* is also abolished by the presence of a *hisT* mutation. As Table 1 shows, the presence of *leu-414* considerably facilitated the search for context mutants in the initial screening. All the His$^+$ revertants arising due to other events (reversion of *hisT*, occurrence of other nonsense suppressor mutations, or any mutation relieving the negative effect of *hisT*) became simultaneously His$^+$ and Leu$^+$. Table 1 shows that this class included the majority of revertants.

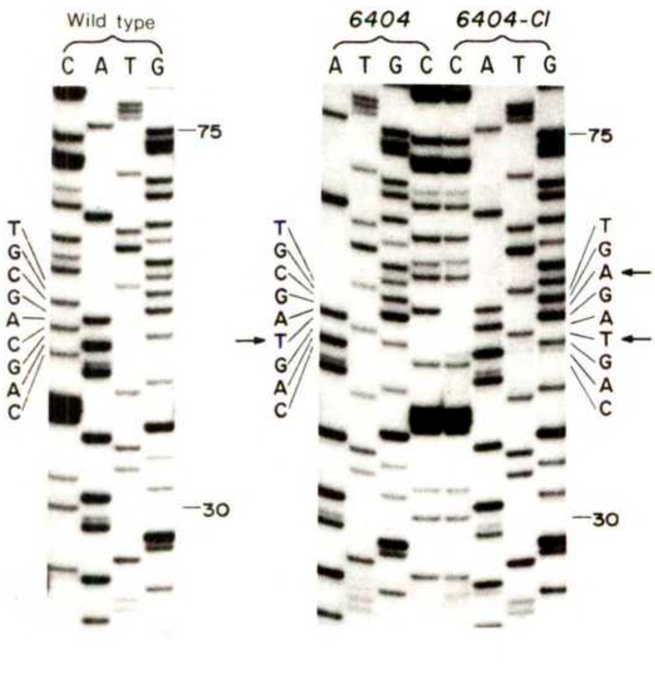

Fig. 1 DNA sequence of *hisD6404* and of its context change. The mutations *hisD6404* and *hisD6404-C1* were placed on M13H0176 (ref. 22) using a genetic procedure (our work in preparation; and unpublished results with H. M. Johnston and S. Lam) which involved the isolation of a Tn5-generated deletion in the *hisG* gene of the transducing phage and subsequent recombination between the phage and a chromosomal *his* region carrying the *hisD* mutations. Single-stranded phage DNA was prepared according to Barnes[22]. The DNA sequence was determined by the procedure described by Sanger *et al.*[23]. Because the orientation of the *his* region present on M13Ho176 is opposite to that on the phage genes, the sequencing gels directly give the *hisD* message sequence. The autoradiograms shown from left to right represent the sequences of wild type, *hisD6404* and *hisD6404-C1*. Two arrows indicate the amber and the context mutations, respectively.

The context mutants were sought among the His$^+$ Leu$^-$ revertants and had to be distinguished only from revertants of the *hisD6404* which had lost the nonsense mutation. This screening could be performed at an early stage of mutant isolation, due to a morphological property of colonies of *Salmonella* strains derepressed for the histidine operon. Such colonies show a wrinkled morphology when grown on 2% glucose, due to interference with cell division caused by high concentration of the *hisH* and *hisF* gene products[21]. When a derepressed operon contains a polar mutation located operator-proximal to *hisH* and *hisF*, the reduced expression of these genes prevents the wrinkled morphology. When this mutation reverts to prototrophy (His$^+$), the morphology of the revertant colonies can be either wrinkled (if the reversion event removes the polarity block), or smooth (if the reversion is due to the activity of a suppressor). (Suppression efficiency is usually insufficient to eliminate polarity completely.) In our case, because of the presence of the regulatory mutation *his01242*, the true revertants of *hisD6404* appeared as wrinkled colonies on the selection plates and could be distinguished from smooth-colony revertants whose His$^+$ character was due to the activity of *supE*. In Table 1 only the smooth His$^+$ Leu$^-$ revertant colonies are reported, all of which therefore are due to increased suppression and are potential context mutants.

A more direct genetic test was carried out on the putative context mutants to verify the continued presence of the *hisD6404* amber mutation. Phage lysates were prepared on the revertants using the generalized transducing bacteriophage P22. The lysates were used to transduce isogenic recipient strains carrying a *his* operon deletion, with and without suppressor *supE*. Because this deletion in the recipient strains completely removes the *hisD* gene, donors carrying the *hisD* mutation can give His$^+$ transductants only with a recipient strain carrying the amber suppressor, *supE*. Results are shown in Table 2. All the six potential context mutants (hereafter designated *hisD6404-C1,2* and so on) give transductants only with the *supE*-carrying recipient. Thus they still contain an amber mutation; DNA sequencing (see later) shows this to be the original *hisD6404* mutation. Furthermore, when the context variants of *hisD6404* were transduced into a recipient also carrying a *hisT* mutation, His$^+$ transductants were seen. This shows that the mutation which relieves *hisT* inhibition of suppression, is present on the same transducing fragment as mutation *hisD6404*.

Other genetic crosses were carried out to rescue *hisD6404* from the *hisD6404-C* (context) revertants. These experiments indicated that the mutations improving *supE* suppression map in the *hisD* gene, very close to *hisD6404* (data not shown).

DNA sequence of *hisD6404* and its context variants

The first structural genes of the histidine operon (*hisG* and *hisD*) have been cloned in both orientations on the single-stranded DNA phage M13 by Barnes[22]. The resulting M13Hol transducing phages make it possible to determine the DNA sequence using the method of Sanger *et al.*[23,24] (W. M. Barnes, manuscript in preparation). Therefore, to determine

Table 1 Isolation of mutants with improved suppressibility of *hisD6404*$_{\text{am}}$

Revertant phenotype	Revertants per 4×10^8 cells
His$^+$ Leu$^+$	105
His$^+$ Leu$^-$	6

The genotype of the parent strain TT4242 is:

his01242 hisD6404$_{\text{am}}$ *leu414*$_{\text{am}}$ *supE20 hisT1504 zej-636*::Tn5*

Cells of TT4242 were grown to stationary phase, and spread (2×10^8 cells per plate) on minimal medium supplemented with 0.3 mM leucine. Spontaneous His$^+$ revertants were isolated and scored for their leucine requirement. Of the His$^+$ Leu$^-$ class only the smooth colonies were saved (see text). The numbers given represent the combined revertants from two cultures.

**zej-636*::Tn5 designates a transposable kanamycin-resistance element (Tn5) co-transducible with the *hisT* locus.

Table 2 Context mutants retain the *hisD6404* mutation

Strain no.	Relevant genotype recipients	His$^+$ transductants with indicated donor strain *hisD* genotype of donor:	
		6404 (TT4242)	*6404-C1* (TT4265)
TT522	*his*Δ	−	−
TT3157	*his*Δ *supE*	+	+
TT3138	*his*Δ *supE hisT*	−	+

Transducing phage P22 was grown on strain TT4242 and on its six His$^+$ Leu$^-$ revertants. The phage lysates were used to transduce the three recipient strains:

TT522 (*his0-F644 zee-1*::Tn*10**)
TT3137 (*his0-F644 zee-1*::Tn*10** *leu-414*$_{\text{am}}$*supE20* *zej-636*::Tn5†)
TT3138 (*his0-F644 zee-1*::Tn*10** *leu-414*$_{\text{am}}$*supE20* *zej-636*::Tn5† *hisT1504*)

His$^+$ transductants were selected on minimal medium supplemented with 0.3 mM leucine (+ indicates that His$^+$ recombinants were observed). All the potential context mutants (isolates 1–6) showed the same behaviour as isolate *6404-C1* (shown above).

**zee-1*::Tn*10* designates a transposable tetracyclin-resistance element (Tn*10*) co-transducible with the histidine operon.

†*zej-636*::Tn5 designates a transposable kanamycin-resistance element (Tn5) co-transducible with the *hisT* locus.

the DNA sequence of *hisD6404* and of the *hisD6404-C* variants, these mutations were placed by recombination onto M13Hol 76 (one of the M13Hol phages[22]). The availability of a detailed restriction map of the *hisG-hisD* region of the *his* operon (Barnes, manuscript in preparation) and of a fine structure genetic map of the *hisD* gene (I. Hoppe and J.R., unpublished results) enabled us to choose a convenient restriction fragment as a primer in the sequencing procedure. Autoradiograms of the sequencing gels for the *hisD* region where the mutations are located are shown in Fig. 1. The inferred mRNA sequences between nucleotides 46 and 54 of the *hisD* gene are shown for wild type, for *hisD6404* and for *hisD6404-C1*, respectively, in Table 3. The result confirms the context hypothesis. The amber mutation *hisD6404* transforms a glutamine codon, CAG, into an amber codon, UAG. The context mutation which permits suppression by *supE* (*hisT*$^-$) generates a change in the residue following the UAG codon, a substitution of adenine for cytosine. All six context mutants (which included two independent groups of isolates) were sequenced. All have the same mutational change as *hisD6404-C1* (data not shown). Thus *hisT* inhibition of *supE* activity at this site can be reversed by changing the reading context of the suppressed nonsense codon.

Basis of the context effects

Initially, two general mechanisms were considered to explain the effect of the context mutation on suppression. First, the *hisD6404* UAG codon may be in a context which requires the presence of pseudouridine in *supE* tRNA (*hisT*$^+$) for the codon to be read efficiently. This suggests that pseudouridine residues in the anticodon region of *supE* tRNA are only essential for reading UAG in certain contexts. By altering context (as in mutant *hisD6404-C1*) one might generate a site which could be read by *supE* tRNA in the absence of the pseudouridine modification. Second, the *hisD6404* UAG codon may be poorly read even by a normal, fully modified suppressor tRNA (*hisT*$^+$). Lack of pseudouridine may impair the ability of *supE* tRNA to read all UAG sites regardless of context effects. This reduction in tRNA efficiency would be critical only at sites that were already poorly read by normally modified suppressor tRNA. The context change might improve readability of the amber codon sufficiently to overcome the *hisT* effect and to provide phenotypic correction.

The two possibilities can be distinguished by quantifying the effect of the context change on the efficiency of *supE* when the suppressor tRNA is fully modified (*hisT*$^+$). The first hypothesis predicts that the context mutation would only improve efficiency of a *supE* tRNA lacking pseudouridine in the anticodon region (*hisT*$^-$). The second hypothesis predicts that the context change would affect the efficiency of normally modified *supE* tRNA (*hisT*$^+$) as well. We have measured the effects of context on *supE* efficiency in both conditions (Table 4). It is clear that codon context strongly affects the activity of *supE* even when the suppressor tRNA is fully modified (*hisT*$^+$); the efficiency of *supE* in reading the same UAG codon varies over a 10-fold range depending on the nature of the base adjacent to the 3′ side of the codon. This suggests that the *hisT* mutation has no role in establishing the context effects (second hypothesis above); rather, the presence of *hisT* reduces (more than 10-fold) the activity of the suppressor at both sites. The *hisT* mutation prevents phenotypic suppression of *hisD6404* because *supE* is initially very inefficient at this site; the reduction in suppression caused by *hisT* reduces the amount of suppressed protein to a level below the threshold required for growth. The context change improves suppressor efficiency and, therefore, can be detected as a His$^+$ revertant in *hisT*$^-$ strains.

Context effects are tRNA specific

Context effects on tRNA efficiency involve aspects of tRNA structure other than simply the anticodon, because different tRNAs with the same anticodon are affected in different ways. Data on the effect of the *hisD6404* context change on the efficiency of various nonsense suppressors are presented in Table 5. A series of strains was constructed which carried *hisD6404* or *hisD6404-C1* and one of a series of amber suppressors. Each strain was assayed for its *hisD* enzyme level; enzymatic activity was taken as a measure of the translation efficiency at the amber site. As Table 5 shows, the context alteration of *hisD6404-C1* does not affect the efficiency of ochre suppressor *supG*; the change increases the efficiencies of amber suppressors *supE* and *supF*, but decreases the efficiency of amber suppressor *supD*.

For two reasons we conclude that the tRNA specificity of context effects is not due to qualitative differences in the suppressed proteins. First, the suppressed site is located in a non-essential part of the *hisD* protein. Second, the same effects of context on various suppressors are seen when polarity relief is used instead of *hisD* activity as a measure of suppressor efficiency. This was shown by assaying the level of *hisB* enzyme (Table 6). The *hisB* gene is located promoter-distal to *hisD* and is subject to polarity effects of the *hisD6404* mutation. While the magnitude of the context effect is reduced in these results, the general nature of the results agrees closely with the *hisD* assays in Table 5.

The results in Tables 5 and 6 provide further information on the nature of context effects. It has been proposed that the context effect on suppression can be explained by assuming

Table 3 mRNA sequence of the context mutant

Wild-type sequence	CAG	CAG	CGU
		↓	
hisD6404 (amber)	CAG	UAG	CGU
			↓
hisD6404-C1 (context mutant)	CAG	UAG	AGU

that the efficiency of peptide termination at a nonsense codon varies depending on the site of that codon[1,2]. Our results argue against this explanation. If the context mutation in *hisD6404-C1* generates a less efficient termination signal, then the change should cause an increase in the efficiency of all suppressors at that site. This is clearly not the case for suppressors *supG* and *supD*. The tRNA specificity of the context effects is important to the possible implications of these effects for coding in general.

Discussion

We have shown that the efficiency of the amber suppressor *supE* in translating the UAG codon can vary over one order of magnitude depending on the nucleotide adjacent to the 3′ side of the codon. The result demonstrates the role of codon context in determining suppression efficiency. In the mutant analysed, the suppressor inserts the same amino acid (glutamine) present in the wild-type sequence, and therefore measurements of enzyme activity directly reflect the actual efficiency of the *supE* tRNA in translation. Other authors have also shown that some site-specific differences in suppressor efficiencies are not due to protein differences[1-7]. Several models have been proposed to explain these effects; one proposes that context effects result from variation in efficiency of termination at the nonsense site[1,2]. The tRNA specificity data presented here argue strongly against that. Although the detailed explanation for context effects is unclear, two alternative hypotheses are consistent with our data.

According to the first, the nucleotide adjacent to the 3′ side of the codon may influence the rate of initial tRNA interaction with the codon. Basically, the increase in the affinity of the *supE* tRNA anticodon for the UAG codon caused by the presence of an adenine residue (instead of a cytosine residue) at the position adjacent to the 3′ side of the UAG, can be explained in two ways: (1) it may permit formation of a fourth base pair (A–U) involving the invariant U residue adjacent to the 5′ side of the tRNA anticodon; or (2) it may increase the stacking energy of the codon–anticodon interaction. A uracil residue is present in the position adjacent to the 5′ side of the anticodon in all the known tRNA species. The possibility that this nucleotide could base-pair with an A residue adjacent to the 3′ end of the codon has been proposed to explain data analogous to ours; Tanaguchi and Weissmann showed that the binding efficiency of fMet-tRNA for the initiation codon, AUG, of the $Q\beta$ coat cistron is increased more than threefold when the G residue adjacent to the 3′ side of the AUG in the wild-type sequence, is replaced by an A residue[8]. The hypothesis that such an additional base-pair is compatible with tRNA structure has been proposed also by Uhlenbeck *et al.*[27], after finding that the molar association constant (in absence of ribosomes) between fMet-tRNA and the tetranucleotide AUGA is more than 10-fold higher than that with AUGC, AUGG, AUGU, or that with the trinucleotide AUG. On the other hand, it is hard to explain the fact that other suppressor tRNAs (all carrying the U residue in the appropriate position) do not show an increase in efficiency at a codon followed by A (Table 5). Therefore, one should consider the alternative possibility that the nucleotide adjacent to the 3′ end of the codon has a role in contributing to the stacking energy of the codon–anticodon interaction. This possibility is suggested by Grosjean *et al.*[28], who have shown the influence of the nucleotide adjacent to the 3′ side of the anticodon on the stacking energy of anticodon–anticodon complexes. The behaviour of suppressors other than *supE* could be explained by assuming that the effect of the nucleotide adjacent to the 3′ end of the codon depends on particular features of the anticodon loop.

An alternative hypothesis to explain the context effects considers that the base change at the 3′ side of the UAG codon generates a new neighbouring codon; the arginine codon, CGU, is replaced by the serine codon AGU. The efficiency of each translation step could depend on optimal 'fitting' of tRNA pairs on the ribosome. This hypothesis implies that tRNA–tRNA interactions occur when these molecules are occupying the A and P sites of the ribosome during translocation. Such interactions could affect the efficiency of the peptide elongation step. According to this hypothesis, *supE* tRNA is able to transfer the growing peptide chain more efficiently to the Ser-tRNA$_{\text{AGU}}$ than to the Arg-tRNA$_{\text{CGU}}$.

Although the possibility of tRNA–tRNA interaction on the ribosome is speculative, several bits of genetic data support the notion. The best characterized frameshift suppressors are mutations which alter the structure of a tRNA such that a four-base code word is read, and the translational reading frame is shifted[29-31]. This indicates that a given tRNA can dictate the distance that the ribosome moves along the message in the translocation step of protein synthesis. This process is easily understood if an incoming tRNA interacts with the incumbent tRNA in order to determine the position of the next code word. The frameshift suppressor tRNA, by occupying a four-base codon forces a codon in the +1 frame to be read by tRNA in the next translation step. The ribosome slavishly translocates this new, improperly positioned tRNA to the peptidyl site in the translocation step.

A recently characterized frameshift suppressor, *sufJ*, further supports the idea that tRNA–tRNA interactions dictate reading frame. The *sufJ* suppressor reads any four-base code word whose first three bases are ACC (our work in preparation). The fact that any base can occupy the fourth position suggests that this fourth base is not actually read.

Table 4 Effect of context on suppression efficiency

Relevant genetic background	*HisD* activity resulting from suppression of indicated site (wild type) -$\underline{\text{CAG}}$C-	 (*hisD6404*) -$\underline{\text{UAG}}$C-	 (*hisD6404-C1*) -$\underline{\text{UAG}}$A-
Wild type	107.3 (TR5830)	<0.2 (TT4427)	<0.2 (TT4428)
supE	100.0 (TT4424)	2.1 (TT4241)	21.2 (TT4268)
supE hisT	93.3 (TT4425)	<0.2 (TT4242)	1.0 (TT4271)

A set of otherwise isogenic strains was built carrying either *hisD*$^+$, or *hisD6404*, or *hisD6404-C1* (context alteration) in addition to combinations of mutant and wild-type alleles of *supE* and *hisT*. The number and the full genotype of these strains is as follows:

TR5830 (*his01242 leu-414*$_{\text{am}}$)
TR4424 (*his01242 leu-414*$_{\text{am}}$*supE20 zej-636*::Tn5*)
TT4425 (*his01242 leu-414*$_{\text{am}}$*supE20 zej-636*::Tn5* *hisT1504*)
TT4427 (*his01242 hisD6404*$_{\text{am}}$*leu-414*$_{\text{am}}$*zej-636*::Tn5* *zeb-618*::Tn*10*†)
TT4241 (*his01242 hisD6404*$_{\text{am}}$*leu-414*$_{\text{am}}$*supE20 zej-636*::Tn5*)
TT4242 (*his01242 hisD6404*$_{\text{am}}$*leu-414*$_{\text{am}}$*supE20 zej-636*::Tn5* *hisT1504*)
TT4428 (*his01242 hisD6404*$_{\text{am}}$*-C1 leu-414*$_{\text{am}}$*zej-636*::Tn5* *zeb-618*::Tn*10*†)
TT4268 (*his01242 hisD6404*$_{\text{am}}$*-C1 leu-414*$_{\text{am}}$*supE20 zej-636*::Tn5*)
TT4271 (*his01242 hisD6404*$_{\text{am}}$*-C1 leu-414*$_{\text{am}}$*supE20 zej-636*::Tn5* *hisT1504*)

Radiological assays of the histidinol dehydrogenase enzymatic activity were carried out according to Ciesla' *et al.*[25]. The value of the activity in strain TT4424 (*hisD*$^+$ *supE*) was taken as 100; all other activities are expressed relative to this value. The results are the average of three determinations.

**zej-636*::Tn5 designates a transposable kanamycin-resistance element co-transducible with the *hisT* locus.

†*zeb-618*::Tn*10* designates a transposable tetracyclin-resistance element inserted at 41 min of the *Salmonella typhimurium* genetic map.

Table 5 Effect of codon context on several suppressors

Suppressor genotype	*HisD* enzyme activity resulting from suppression of indicated site (*hisD6404*) -UAGC-	 (*hisD6404-C1*) -UAGA-
sup^+	<0.2 (TT4427)	<0.2 (TT4428)
supG (*lys*)	0.8 (TT4286)	1.0 (TT4287)
supF (*tyr*)	3.4 (TT4278)	7.7 (TT4280)
supD (*ser*)	16.6 (TT4274)	6.7 (TT4276)
supE (*gln*)	2.0 (TT4241)	19.8 (TT4268)

Isogenic strains were built carrying either *hisD6404* or *hisD6404-C1* and the nonsense suppressors listed. The genotype of these strains is as follows:

TT4286:*his01242 hisD6404*$_{am}$*leu-414*$_{am}$*supG50 zej-636*::Tn5
TT4287:*his01242 hisD6404*$_{am}$*-C1 leu-414*$_{am}$*supG50 zej-636*::Tn5
TT4278:*his01242 hisD6404*$_{am}$*leu-414*$_{am}$*supF30 zej-636*::Tn5
TT4280:*his01242 hisD6404*$_{am}$*-C1 leu-414*$_{am}$*supF30 zej-636*::Tn5
TT4274:*his01242 hisD6404*$_{am}$*leu-414*$_{am}$*supD10 zej-636*::Tn5
TT4276:*his01242 hisD6404*$_{am}$*-C1 leu-414*$_{am}$*supD10 zej-636*::Tn5

The genotypes of sup^+ and *supE* containing strains are in the legend to Table 4. The enzymatic activity of the histidinol dehydrogenase was assayed as described in the legend to Table 4. Enzyme levels presented are relative to the level measured in strain TR5830 ($hisD^+ sup^+$). Results are the average of three determinations.

Table 6 Effect of codon context on the suppressor ability to relieve polarity

Suppressor genotype	*HisB* enzyme activity resulting from relief of polarity at the indicated *HisD* site (*hisD6404*) -UAGC-	 (*hisD6404-C1*) -UAGA-
supF (*tyr*)	5.6 (TT4278)	9.4 (TT4280)
supD (*ser*)	10.6 (TT4274)	5.9 (TT4276)
supE (*gln*)	0.9 (TT4241)	6.0 (TT4268)

HisB enzyme level was determined according to Martin *et al.*[26]. The activity measured in strain TR5830 ($hisD^+ sup^+$) is 17.1. All the values are corrected by subtraction of the *hisB* enzyme level in strains TT4427 (*hisD6404* sup^{WT}) or TT4428 (*hisD6404-C1* sup^{WT}). Strains carrying ochre suppressor *supG* gave *hisB* activity values below the detection level. Strain genotypes are in the legends to Tables 4 and 5.

Instead, the suppressor tRNA may read ACC and sterically prevent any tRNA from occupying the codon immediately adjacent to ACC. Thus the next tRNA must read the next unhindered triplet (out of phase).

If our observations on context effects for nonsense suppression apply to decoding in general, one is led to some interesting conjectures. If the efficiency of reading any particular codon can vary over a 10-fold range, depending on codon context, it is clear that these effects could have enormous influence on the rate of protein synthesis in particular regions. The phenomenon could be used by the cell as an additional regulatory device. According to translation modulation theories, translation rates can be set by the use of codons whose tRNAs are present at a low level in the cell[32–33]. As Stent pointed out[33], modulation of translation would more specifically be achieved by using modulating sequences longer than the codon. Invocation of context effects seems, therefore, especially appropriate. A particular rare codon may or may not have modulating function depending on the reading context in which it is located.

The possibility that context affects translation suggests a role for the minor isoaccepting tRNA species whose presence has been reported in many organisms. Changes in the abundance of these minor species have been observed during changes in growth conditions[34], development[35–37] and neoplasia[38]. It seems possible that these minor tRNA species might be able to read their particular codon when it occurs in a context which is poorly read by the isocoding major tRNA species. Shifts in these minor tRNAs could vary the overall rate of translation or could optimize production of proteins synthesized in large amounts in particular conditions.

Three examples may support these speculations. The first concerns the finding by Zilberstein *et al.*[39] that extracts of interferon-treated cells cannot completely translate haemoglobin mRNA unless a purified minor Leu-tRNA species is added. This minor Leu-tRNA could not be replaced by the major isocoding (CUG) tRNA species. The second case concerns tRNA genes carried by bacteriophage T4 (and other viruses). Guthrie and McClain have shown that one of the T4 tRNAs is essential for phage growth on a natural isolate of *Escherichia coli*[40]. The essential tRNA is a minor Ile-tRNA species recognizing the codon AUA. A tRNA species with the same codon specificity is, of course, already present in the infected host. It seems possible that the viral tRNAs permit translation of T4 messages in which the context of some codons permits only inefficient reading by the tRNA complement of some natural hosts. The third example is the *Bombix mori* posterior silk gland in which a novel Ala-tRNA species appears while huge amounts of silk protein are being produced[37,41]. One can speculate that to produce a large quantity of a particular protein, it may be necessary to eliminate even minor problems of context inherent in translation of message for that protein. The new silk gland Ala-tRNA may serve such a purpose. These three examples can all be interpreted as extreme cases in which there are restrictions of codon context that can be overcome by particular tRNA species. In summary, our data on the tRNA specificity of context effects suggest that any given codon may be read preferentially by one or another member of an isocoding tRNA family, depending on the context in which that codon appears.

We thank Wayne Barnes for facilities, for training L.B. in DNA sequence techniques, and for the communication of unpublished data. We also thank Bruce Ames and Stanley Artz for purified ^{14}C-labelled histidinol, and Fred Winston, Jeffrey Miller and David Botstein for the characterized suppressor mutants of *Salmonella typhimurium*.

Received 18 February; accepted 16 April 1980.

1. Salser, W. *Molec. gen. Genet.* **105,** 125–130 (1969).
2. Fluck, M. M., Salser, W. & Epstein, R. H. *Molec. gen. Genet.* **151,** 137–149 (1977).
3. Yahata, H., Ocada, Y. & Tsugita, A. *Molec. gen. Genet.* **106,** 208–212 (1970).
4. Akaboshi, E., Inouye, M. & Tsugita, A. *Molec. gen. Genet.* **149,** 1–4 (1976).
5. Colby, D. S., Schedl, P. & Guthrie, C. *Cell* **9,** 449–463 (1976).
6. Feinstein, S. I. & Altman, S. *J. molec. Biol.* **112,** 453–470 (1977).
7. Feinstein, S. I. & Altman, S. *Genetics* **88,** 201–219 (1979).
8. Taniguchi, T. & Weissmann, C. *J. molec. Biol.* **118,** 533–565 (1978).
9. Singer, C. E., Smith, G. R., Cortese, R. & Ames, B. N. *Nature new Biol.* **238,** 72–74 (1972).
10. Cortese, R., Kammen, H. O., Spengler, S. J. & Ames, B. N. *J. biol. Chem.* **249,** 1103–1108 (1974).
11. Ciampi, M. S., Arena, F., Cortese, R. & Daniel, V. *FEBS Lett.* **77,** 75–82 (1977).
12. Turnbough, C. L., Neill, R. J., Landsberg, R. & Ames, B. N. *J. biol. Chem.* **254,** 5111–5119 (1979).
13. Winston, F., Botstein, D. & Miller, J. H. *J. Bact.* **137,** 433–439 (1979).
14. Yaniv, M. & Folk, W. R. *J. biol. Chem.* **250,** 3243–3253 (1975).
15. Hachiro, I., Fumiaki, Y., Hitoshi, S. & Ozeki, H. *J. molec. Biol.* **132,** 649–662 (1979).
16. Johnston, H. M., Barnes, W. M., Chumley, F. G., Bossi, L. & Roth, J. R. *Proc. natn. Acad. Sci. U.S.A.* **77,** 508–512 (1980).
17. Ino, I., Hartman, P. E., Hartman, Z. & Yourno, J. *J. Bact.* **123,** 1254–1264 (1975).
18. Creeb, J., Atkins, J. F. & Loper, J. C. *J. Bact.* **106,** 421–431 (1971).
19. Newton, W. A., Beckwith, J. R., Zipser, D. & Brenner, S. *J. molec. Biol.* **14,** 290–301 (1965).
20. Roth, J. R., Anton, D. N. & Hartman, P. E. *J. molec. Biol.* **22,** 305–323 (1966).
21. Murray, M. L. & Hartman, P. E. *Canad. J. Microbiol.* **18,** 671–681 (1972).
22. Barnes, W. M. *Gene* **5,** 127–139 (1979).
23. Sanger, F., Nicklen, S. & Coulson, A. R. *Proc. natn. Acad. Sci. U.S.A.* **74,** 5463–5467 (1977).
24. Barnes, W. M. *Proc. natn. Acad. Sci. U.S.A.* **75,** 4281–4285 (1978).
25. Ciesla', Z., Salvatore, F., Broach, J. R., Artz, S. W. & Ames, B. N. *Analyt. Biochem.* **63,** 44–55 (1975).
26. Martin, R. G. *et al. Meth. Enzym.* **17,** 3–44 (1971).
27. Uhlenbeck, O. C., Baller, J. & Doty, P. *Nature* **225,** 508–510 (1970).
28. Grosjean, H., Söll, D. G. & Crothers, D. M. *J. molec. Biol.* **103,** 499–519 (1976).
29. Roth, J. R. *A. Rev. Genetics* **8,** 319–346 (1974).
30. Riddle, D. & Carbon, J. *Nature new Biol.* **242,** 230–234 (1973).
31. Kohno, T. & Roth, J. R. *J. molec. Biol.* **126,** 37–52 (1978).
32. Ames, B. N. & Hartman, P. E. *Cold Spring Harb. Symp. quant. Biol.* **28,** 349–356 (1963).
33. Stent, G. S. *Science* **144,** 816–820 (1964).
34. Chase, R., Tener, G. M. & Gillam, I. C. *Arch. Biochem. Biophys.* **163,** 306–317 (1974).
35. White, B. N., Tener, G. M., Holden, J. & Suzuki, D. T. *Devl Biol.* **33,** 185–195 (1973).
36. Delaney, P. & Siddiqui, M. A. Q. *Devl Biol.* **44,** 54–62 (1976).
37. Meza, L. *et al. FEBS Lett.* **77,** 255–260 (1977).
38. Kuchino, Y. & Borek, E. *Nature* **271,** 126–129 (1978).
39. Zilberstein, A., Dudock, B., Berissi, H. & Revel, M. *J. molec. Biol.* **108,** 43–54 (1976).
40. Guthrie, C. & McClain, W. H. *Biochemistry* **18,** 3786–3795 (1979).
41. Sprague, K. U., Hagenbüchle, O. & Zuniga, M. C. *Cell* **11,** 561–570 (1977).

Analysis of regulation of *Klebsiella pneumoniae* nitrogen fixation (*nif*) gene cluster with gene fusions

Ray Dixon, Robert R. Eady, Guadalupe Espin, Susan Hill, Maurizio Iaccarino*, Daniel Kahn & Mike Merrick

ARC Unit of Nitrogen Fixation, University of Sussex, Brighton BN1 9RQ, UK

*CNR Istituto Internazionale di Genetica et Biofisica, Via Gugliemo Marconi 10, 80125 Naples, Italy

Gene fusions in which the lac *genes are under the control of each promoter in the* Klebsiella pneumoniae *nitrogen fixation* (nif) *gene cluster have been constructed. These fusions have been used to examine positive control of the cluster and the response of individual genes to repression by ammonia and oxygen. De-repression of* nif *transcriptional units is coordinate and molybdate is required for maximal expression of the structural gene operon, which is autogenously regulated.*

THE process of biological nitrogen fixation, the conversion of nitrogen to ammonia, is rate-limiting in many agricultural areas. Nitrogenase, the enzyme complex which catalyses the reduction of dinitrogen, is comprised of two redox proteins both of which contain iron–sulphur centres and one of which also contains molybdenum[1]. These component proteins are irreversibly inactivated by oxygen. A cofactor (FeMo-co) containing Mo, Fe and S, presumed to carry the active site of nitrogenase, can be separated from the Mo–Fe protein[2]. Both a reductant and ATP are required for enzyme activity[3]; approximately 15 mol of ATP are consumed per mol dinitrogen reduced. In view of this high energy requirement and the extreme oxygen sensitivity of the component proteins it is not surprising that nitrogenase synthesis is tightly controlled.

The nitrogen fixation (*nif*) gene cluster of *Klebsiella pneumoniae* consists of at least 15 genes organized into 5 polycistronic and 3 monocistronic transcriptional units (Fig. 1)[4–7]. The structural genes *nifK* and *nifD* code for the β and α subunits, respectively, of nitrogenase Kp1 (Mo–Fe protein) and *nifH* codes for Kp2 (Fe protein) of nitrogenase. The *nifB*, *nifN* and *nifE* gene products are involved in the synthesis or processing of the iron–molybdenum cofactor, and the *nifM* gene product is required for Kp2 activity[8]. *NifF* and *nifJ* are involved in electron transport to nitrogenase[9]. The phenotype of *nifA* mutants suggests that *nifA* gene product is a positive activator of *nif* transcription[8,10]. The functions of the remaining five gene products are unknown.

Regulatory studies have so far indicated that the nitrogenase structural genes are subject to repression by ammonia and by oxygen[11] and there is some evidence that molybdate is involved in the regulation of nitrogenase[12]. In addition, glutamine synthetase, the product of the *glnA* gene, has been implicated as a general positive effector of enzyme systems which, including nitrogenase, are involved in the assimilation of 'poor' nitrogen sources[13]. There are, however, serious obstacles to studies on regulation of the individual transcriptional units in the *nif* gene cluster, because most of the gene products have not been conclusively identified and there is no simple assay for any of the individual gene products. To overcome these difficulties we have used the recently developed technique of Casadaban and Cohen[14] to construct gene fusions in which the *Escherichia coli lac* genes are fused to a promoter of interest. Such gene fusions have enabled us to monitor the response of each

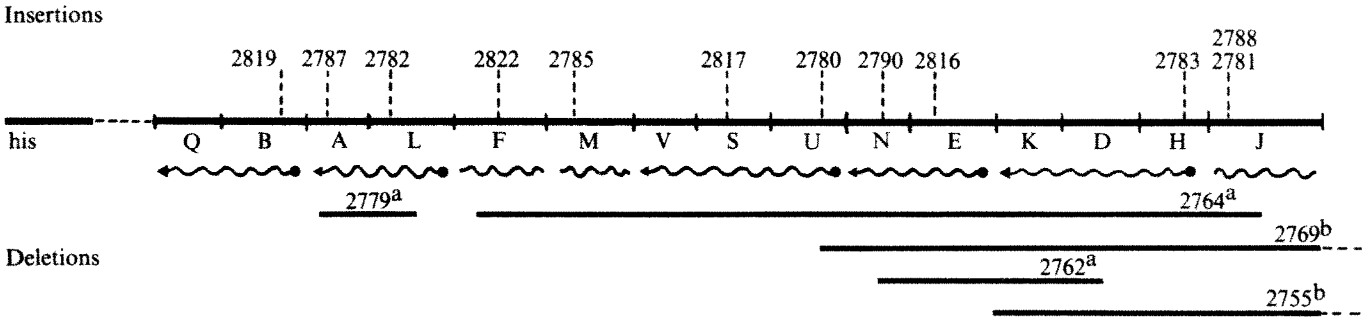

Fig. 1 Map of the *K. pneumoniae nif* gene cluster showing the location of insertions and deletions induced by phage Mud(Ap*lac*). The wavy lines indicate the eight transcriptional units and the arrows show the direction of transcription where known. The map is not drawn to scale. Transposition of Mud(Ap*lac*) into the conjugative plasmid pMF100, which carries the *his–nif* region of the *K. pneumoniae* genome was induced either by induction of an *E. coli* Mud(Ap*lac*) lysogen, UNF511 (*his trp lys lacΔ str*) carrying pMF100 at 37 °C or by infection of *E. coli* strain JC3272 carrying pMF149 (a Mu-sensitive derivative of pMF100) with a mixed lysate of Mu*cts* and Mud(Ap*lac*) at 30 °C. Insertion mutations in the plasmid were selected on the basis of co-transfer of *his* and ampicillin resistance in crosses carried out at 30 °C with an *E. coli* Mu*cts* lysogen, UNF514 (*his trp lacΔ recA56 spc*). In both cases the transposition frequency of Mud(Ap*lac*) was approximately 10^{-3} with respect to plasmid transfer. *nif–lac* fusions were obtained by screening for colonies which failed to grow anaerobically on nitrogen-free (NFDM[20]) agar, but could form blue colonies on NFDM plates containing serine (100 μg ml^{-1}) and the indicator dye 5-bromo-4-chloro-β-D-galactoside (40 μg ml^{-1}). Mud(Ap*lac*) insertions were mapped against a set of *K. pneumoniae nif* point and deletion mutations described in ref. 7. Allele numbers above the map are independent insertions in which β-galactosidase is under the control of a *nif* promoter. Black lines beneath the map represent Mud(Ap*lac*)-induced deletions in which (a) β-galactosidase is repressed by ammonia (under *nif* control) or (*b*) β-galactosidase is constitutive (under the control of a promoter outside *nif*).

0028–0836/80/280128–05$01.00

Table 1 β-Galactosidase activities of *nif–lac* fusion strains in various genetic backgrounds

							β-Galactosidase units in:		
		UNF619 *nif*$^+$			UNF686 Δ(*his–nif*)		UNF1716 Δ(*his–nif*) *glnA201*	UNF1721 Δ(*his–nif*) *gln-205*	UNF686 Δ(*his–nif*) *nifA2013*::Tn*10**
Fusion allele	$-NH_4^+$ +Mo	$-NH_4^+$ −Mo	$+NH_4^+$	$-NH_4^+$ +Mo	$-NH_4^+$ −Mo	$+NH_4^+$	$-NH_4^+$	$-NH_4^+$	$-NH_4^+$
nifB2819:: Mud(Ap*lac*)	400	250	9	440	250	6	24	9	—
nifA2787:: Mud(Ap*lac*)	790	—	24	940	—	14	13	8	—
*nif*Δ*2779*:: Mud(Ap*lac*)	710	600	20	1,040	600	17	16	7	—
nifL2782:: Mud(Ap*lac*)	730	600	25	890	700	23	13	9	—
nifF2822:: Mud(Ap*lac*)	700	400	16	700	400	15	56	35	—
nifM2785:: Mud(Ap*lac*)	900	900	22	520	500	24	13	8	25
nifS2817:: Mud(Ap*lac*)	220	—	18	120	—	11	11	19	10
nifU2780:: Mud(Ap*lac*)	900	550	15	680	800	14	11	7	—
nifN2790:: Mud(Ap*lac*)	950	500	23	580	500	14	9	9	19
nifE2816:: Mud(Ap*lac*)	610	—	10	660	—	7	19	9	—
nifH2783:: Mud(Ap*lac*)	3,500	500	7	500	500	11	9	8	9
nifJ2781:: Mud(Ap*lac*)	1,070	1,000	60	1,050	1,000	111	222	120	263

Derivatives of pMF100 carrying the Mud(Ap*lac*) insertions with or without a Tn*10* insertion in *nifA* were introduced into various *K. pneumoniae* strains. All strains are *lac*Δ MuhP1 lysogens derived from KP5022 (*nif*$^+$ *hisD2 hsdR1*) or UNF1522 (Δ(*his–nif*) *2633 hsdR1 str*). UNF619 and UNF686 are also *recA*. Cultures were grown anaerobically in bijoux bottles in nitrogen-free medium (NFDM)[20], containing 2 mg ml^{-1} $(NH_4)_2SO_4$ ($+NH_4^+$) or 100 µg ml^{-1} serine in the presence ($-NH_4^+$, +Mo) or absence ($-NH_4^+$, −Mo) of molybdate (100 µM). In the latter case, removal of traces of molybdenum was achieved by extracting both glucose and phosphate with 8-hydroxyquinoline and chloroform[21], and by washing the glassware in 50% nitric acid (v/v). Cells were collected, resuspended in ice-cold saline phosphate buffer containing 100 µg ml^{-1} chloramphenicol and assayed for β-galactosidase using the procedure and units of activity described by Miller[22]. Dashes indicate that the appropriate value was not determined.

*The *nifA2013*::Tn*10* (ref. 7) insertion was transduced onto the plasmids with phage PlCmclr100 by selecting for tetracycline resistance and screening for cotransfer of both tetracycline and ampicillin resistance.

transcriptional unit to various effectors and to determine the kinetics of de-repression of individual operons.

Construction of *nif–lac* fusions

We used phage Mud(Ap*lac*)[14], a defective derivative of Mu which retains Mu transposition functions, carries part of the transposon Tn*3* encoding ampicillin resistance (Ap) (which cannot itself transpose) and has the *lac* structural genes inserted in the phage such that when the phage inserts into a gene in the appropriate orientation, transcription proceeds through the S end of Mu into *lacZ*.

We have selected a large number of *nif–lac* fusions after transposition of Mud(Ap*lac*) into the Nif$^+$ conjugative plasmid pMF100. Around 20% of Mud(Ap*lac*) insertions resulted in a Nif$^-$ phenotype, although the majority of insertion events (261 out of 315 mutants obtained from several independent crosses) produced deletions which mapped to one side of the prophage. *lac* was expressed in some of these deletions and two classes were observed: (1) those with end points within *nif* in which *lac* was under the control of a *nif* promoter and was repressed by ammonia, and (2) those with more extensive deletions in which *lac* was fused to a promoter outside *nif*, resulting in the expression of β-galactosidase in the presence of ammonia (Fig. 1). All *nif–lac* fusions which did not carry adjacent deletions gave poor or no growth on lactose in the presence of ammonia. Precise mapping of these non-deleted strains has shown that the fusions are located in 11 out of 15 *nif* genes, with at least one fusion in each of the transcriptional units (Fig. 1).

Ammonium repression

Measurements of β-galactosidase activity in *K. pneumoniae* strains carrying various fusions suggest that all *nif* promoters respond to NH_4^+ repression, although the extent of repression varies among different fusions (Table 1). These observations confirm and extend previous data on ammonia repression of some of the *nif* transcriptional units as measured by RNA–DNA hybridization experiments[15] or by detection of *nif*-specific polypeptides[8].

Positive control

The *nifA* gene product has been suggested to act as a specific positive control factor for *nif* transcription[8–10]. We have therefore investigated the role of *nifA* in the regulation of the *nif* genes by constructing *nifA*, *nif*::*lac* double mutants. Transposon Tn*10* was inserted into the *nifA* gene, thus inactivating its function, and in all fusions tested, β-galactosidase activity was decreased considerably in the absence of an active *nifA* product (Table 1). Introduction of plasmids carrying a *nifA* mutation and a *nif–lac* fusion into a *nifA*$^+$ background restored β-galactosidase activity (data not shown). However, the *nifA* gene product is not apparently required for transcription from the *nifL* promoter, as significant levels of β-galactosidase were observed in the *nifL* and *nifA* fusions and in the fusion *nif2779*::Mud(Ap*lac*), which is deleted for most of *nifA* and *nifL*.

The properties of various mutations affecting the synthesis or activity of glutamine synthetase suggest that either the enzyme itself or a product of one or more regulatory genes, including *glnF* and *glnG* (*glnR*), acts as a general positive effector for various operons involved in nitrogen metabolism[16,17]. The response of *nif–lac* fusions to two *gln* mutations, *glnA201*, a mutation in the structural gene for glutamine synthetase, and *gln-205*, a *glnA*-linked regulatory mutation which prevents *nif* de-repression (G.E. and M.M. unpublished), is shown in Table 1. Transcription of all *nif* operons is affected by these mutations. This result does not allow us to distinguish whether the positive effector acts at only a single site within *nif* or whether all *nif* transcriptional units are subject to this control. Previous studies on *nif*-specific mutations which are independent of this regulation suggest that the effector may act at a single *nif* promoter and that the other transcripts are positively controlled by a *nif*-specific regulatory protein[18]. Our data are consistent with this model, as we have shown in Table 1 that transcription of the *nifLA* operon is dependent on a *gln* gene product.

The *nifJ* gene showed a unique response to various effectors. A high level of residual activity was observed in the *nifJ* fusion both in *glnA*, *gln-205* and *nifA*:: Tn*10* backgrounds as well as in ammonia-grown cultures (Table 1). Similar results were obtained with an independent *nifJ* fusion, *nifJ2788*::Mud(Ap*lac*). It is possible that there is a less stringent requirement for *nifA* product at the *nifJ* promoter.

Regulation of the *nifHDK* operon

In the majority of cases, no significant difference was observed in the steady-state levels of β-galactosidase when merodiploid strains of genotype *nif*$^+$/*nif*::*lac* were compared with haploid strains of genotype Δ*nif*/*nif*::*lac*. The exception was a *nifH*::*lac* fusion which showed a seven-fold increase in a *nif*$^+$ compared with a total *nif* deletion background (Table 1), suggesting that this operon is autogenously regulated.

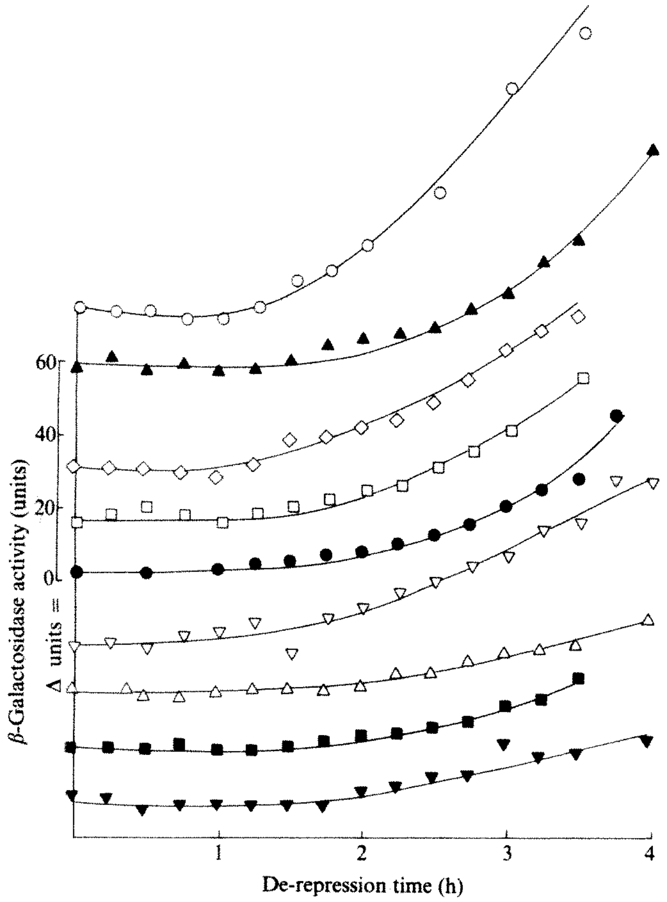

Fig. 2 Kinetics of de-repression of *nif–lac* fusions. Cultures were grown in NFDM plus $(NH_4)_2SO_4$ (1.5 mg ml^{-1}) overnight at 28 °C under N_2, collected by centrifugation and resuspended in NFDM at 25 °C. Cultures were bubbled with N_2 and samples (0.2 ml) removed at the times indicated for estimation of β-galactosidase activity. For clarity the curves are displaced and the data on the ordinate plotted as the change in β-galactosidase activity (units) observed during de-repression. All strains were derivatives of UNF619 (*nif*$^+$ *hisD2 hsdR1 lacΔ recA56 sr1300*::Tn*10* MuhP1) carrying *nif–lac* fusions in pMF100 (shown in Fig. 1). ○, *nifH2783*::Mud(Ap*lac*); ▲, *nifN2790*::Mud(Ap*lac*); ◇, *nifM2785*::Mud(Ap*lac*); □, *nifJ2781*::Mud(Ap*lac*); ●, *nifF2822*::Mud(Ap*lac*); ▽, *nifU2780*::Mud(Ap*lac*); △, *nifB2819*::Mud(Ap*lac*); ■, *nifL2782*::Mud(Ap*lac*); ▼, *nifA2787*::Mud(Ap*lac*).

Because the *nifH*::Mud(Ap*lac*) insertion exerts a strong polar effect on *nifD* and *nifK*, it is possible that any of the products of the operon could affect the level of *nifH* expression. Table 2 shows the β-galactosidase activities of merodiploid strains carrying various mutations in *trans* to a *nifH*::*lac* fusion on the *K. pneumoniae* chromosome. (Levels of activity were generally lower than those with *nifH*::*lac* located on the plasmid (Table 1), suggesting a possible effect of plasmid copy number, and in these experiments there was a threefold increase in the diploid (*nifH*::*lac*/*nif*$^+$) strain compared with the haploid (*nifH*::*lac*) level.) When the plasmid carried a Tn7 insertion in *nifK* or *nifD* or a deletion extending from *nifL* into *nifD*, β-galactosidase activities were 33–55% of the *nif*$^+$ level. However, not all Tn7 insertions in *nifH* gave a significant decrease in β-galactosidase activity (Table 2); this may reflect differences in polarity exhibited by Tn7 insertions in *nifH*. Only three out of seven Tn7 insertions in *nifH* had reduced levels of activity, whereas two *nifD* and three *nifK* insertions exhibited less than 55% of the *nif*$^+$ control (data not shown). These results suggest that the *nifK* and/or *nifD* gene products are involved in regulation of the operon. As none of the mutations tested can complement the *nifH*::*lac* insertion, nitrogenase activity *per se* is not required for stimulation of *nifH* transcription.

Involvement of molybdenum

Molybdenum is essential for nitrogenase activity, as it is a component of the iron–molybdenum cofactor of Kp1 protein. Hence, growth on molecular nitrogen is dependent on the presence of molybdate in the medium. As there is conflicting evidence concerning the involvement of molybdate in the regulation of nitrogenase synthesis in *K. pneumoniae*[12,19], we have re-examined this question using *nif–lac* fusion strains grown in the presence or absence of molybdate (100 μM). The absence of molybdate did not affect the β-galactosidase activity of ammonia-grown *nif–lac* fusion strains. None of the operons showed an absolute requirement for molybdate for de-repression and, in the haploid situation, β-galactosidase activities did not differ significantly in the presence or absence of molybdate (Table 1). Thus, molybdate has no regulatory function *per se*. In the diploid situation, only the *nif*$^+$/*nifH*::*lac* strain responded to molybdate addition and *lac* expression was increased sevenfold (Table 1). These results show that both the presence of molybdate and product(s) of the *nifHDK* operon are required for maximal expression from the *nifH* promoter. It is therefore most likely that a molybdoprotein, presumably Kp1 protein, is involved in autogenous regulation of the operon. We have been unable to distinguish whether the presence of molybdate influences the stability of this protein or whether insertion of molybdenum into Kp1 is necessary for the formation of a regulatory active species.

Oxygen repression

Oxygen represses nitrogenase synthesis as well as inactivating the nitrogenase component proteins[11]. Synthesis of β-galactosidase from all the *nif* promoters was inhibited in both *nif*$^+$ and *nif* deletion backgrounds when NH_4^+-grown cultures were resuspended in N-free medium and bubbled vigorously with air for 6 h. The degree of expression among different fusions varied from 3% (*nifH*) to 43% (*nifL*) of the activity obtained with control cultures sparged with nitrogen.

Additional experiments were carried out in an oxystat in which a defined and constant dissolved oxygen tension (D.O.T.) could be maintained. When a *nif*$^+$ strain was grown in ammonia, resuspended in N-free medium and maintained at a D.O.T. of 0.5%, de-repression was inhibited and synthesis of nitrogenase polypeptides could not be detected in pulse-labelling experiments (S. Hill and C. Kennedy, unpublished observations). Synthesis of β-galactosidase from the *nifH* promoter was also repressed as expected in these conditions, but synthesis from the *nifL* promoter in both *nif*$^+$ and *nif* deletion backgrounds was unaffected (Table 3). Thus, oxygen repression of the *nifHDK* operon is not mediated by inhibiting transcription at the *nifLA* promoter, at least at low oxygen tensions. At higher D.O.T.s (3% and 5%, Table 3) the *nifL*::*lac* fusion was apparently subject to oxygen repression as predicted from the bubbling experiments. The *nifHDK* operon is, therefore, far more sensitive to oxygen repression than the *nifLA* operon.

Table 2 Effect of mutations in *trans* on β-galactosidase synthesis from *nifH*::*lac*

Plasmid allele in *trans*	β-Galactosidase units	% *nif*$^+$
—	385 ± 35	30
nif$^+$	1,269 ± 107	100
nifK2185::Tn7	481 ± 90	38
nifD2197::Tn7	530 ± 20	42
nifD2210::Tn7	410 ± 3	32
nifΔ(L-D)8758	618 ± 68	49
nifH2191::Tn7	1,095 ± 25	87
nifH2212::Tn7	1,137 ± 67	90
nifH2213::Tn7	533 ± 37	42

Derivatives of plasmid pRD1 carrying *nifΔ(L-D)8758* or Tn7 insertions in *nifH*, *nifD* or *nifK* (ref. 7) were introduced into UNF725 (*nifH2783*::Mud(Ap*lac*) *hsdR1 lacΔ recA56 sr1300*::Tn*10* MuhPl). Cultures were grown and assayed for β-galactosidase activity as in Table 1.

Table 3 Effect of oxygen on β-galactosidase activity in *nifL* and *nifH* fusions

		Units of β-galactosidase activity under O_2 as % of that under N_2			
Fusion allele on plasmid	Strain background	Cultures bubbled with air	Cultures maintained at a D.O.T. (% saturation) of:		
			0.5	3.0	5.0
nifL2782	Δ(*his–nif*)	32 ± 9	123 ± 10	68	54 ± 6
	nif$^+$	43 ± 17	116 ± 3	64	—
nifH2783	Δ(*his–nif*)	10 ± 3	32 ± 3	—	—
	nif$^+$	3 ± 1	15 ± 3	—	—

Cultures were grown in NFDM[20] plus excess NH_4^+ overnight at 30 °C under N_2, collected by centrifugation and resuspended in NFDM at 30 °C. β-galactosidase activity was measured after vigorously bubbling 5 ml aliquots of culture with either air or N_2 for 6 h. Alternatively, β-galactosidase activity was determined after 4.5 h exposure either to the indicated D.O.T. in an oxystat supplied with air plus N_2, or to N_2. —, Not tested.

Kinetics of *nif* de-repression

Pulse-labelling experiments on cultures released from NH_4^+ repression have shown that the *nifK*, *nifD* and *nifH* polypeptides are synthesized approximately 1 h before nitrogenase activity can be detected, indicating either that de-repression of *nif* operons is not coordinate or that there is a rate-limiting step in establishing a functional nitrogenase system[11]. To examine this question more thoroughly, the onset and rate of de-repression for diploid (*nif*$^+$/*nif*::*lac*) fusion strains have been determined following transfer from NH_4^+ to N-free medium. The appearance of nitrogenase activity measured by acetylene reduction was reproducible in all strains tested, occurring 2–2.5 h after transfer to N-free medium. Control experiments in which rifampicin (100 µg ml^{-1}) was added before de-repression, indicated that there was no significant increase or decrease in the residual level of β-galactosidase activity in the absence of *nif* transcription. The onset of β-galactosidase de-repression occurred at 1–1.5 h in all cases, but the rates of enzyme synthesis varied among the different fusions (Fig. 2). Although the levels of β-galactosidase activity in fusion strains do not necessarily represent the efficiencies of the various *nif* promoters, the de-repression curve for *nifH* agrees well with pulse-labelling data on the rate of nitrogenase synthesis during de-repression[11], and the relative amounts of β-galactosidase synthesized from the other promoters generally correlate with the relative rates of synthesis of detectable *nif*-specific polypeptides observed on polyacrylamide gels. Note that synthesis of β-galactosidase from the *nifA*, *nifL* and *nifB* promoters occurred initially at a slower rate than with the other fusions. The slow de-repression of *nifB* may account for the late appearance of acetylene-reducing activity. Consistent with this hypothesis, nitrogenase activity of crude extracts prepared from cultures in the 'early' stages of de-repression is stimulated by addition of purified FeMo-co (R.R.E., unpublished results).

To examine regulation of the *nifHDK* operon in more detail, we also compared the de-repression kinetics of *nifH* diploid and haploid strains grown in the presence and absence of molybdate. Three typical curves are shown in Fig. 3: *a*, The *nif*$^+$/*nifH*::*lac* diploid fusion in the presence of molybdate showed a linear increase in β-galactosidase activity from the onset of de-repression for at least 7 h after transfer from NH_4^+ to N-free medium. *b*, The *nifH*::*lac* haploid strain, grown either with or without molybdate, initiated de-repression of β-galactosidase as in *a* but subsequently showed a cut-off in synthesis after 3.5–4 h in N-free medium. The *nif*$^+$/*nifH*::*lac* diploid strain in the absence of molybdate also showed a cut-off similar to that of the haploid strain. (For simplicity only the curve for the haploid *nifH*::*lac* fusion in the presence of molybdate is shown in Fig. 3.) *c*, A *nifH*::*lac*, *nifA*::Tn*10* double mutant showed no increase in β-galactosidase activity in the presence of molybdate, indicating that the *nifA* product is necessary for the onset of de-repression.

Thus, de-repression of the operon is clearly initiated in the absence of molybdate or in the haploid strain lacking the *nifH*, *nifD* and *nifK* products. The cut-off indicates there is an insufficient level of a regulatory molecule to maintain transcription from the *nifH* promoter in these conditions.

Discussion

Our data suggest that all the operons in the *nif* gene cluster are subject to positive control, which is ultimately mediated either by glutamine synthetase itself or by a gene product involved in glutamine synthetase regulation. We assume that this positive effector activates transcription at the *nifLA* promoter and that the *nifA* product specifically promotes transcription of other *nif* operons. Alternatively, it is conceivable that the positive effector involved in glutamine synthetase regulation is required in addition to the *nifA* product at these promoters. We have also shown that the *nifHDK* operon is subject to autogenous regulation and that the availability of molybdate and at least the *nifK* and *nifD* gene products are required for maximal expression from the operon promoter. This conclusion is also consistent with the finding that the level of Kp2 protein is low in strains carrying insertion mutations in *nifK* and *nifD*[4,8]. In wild-type nitrogen-fixing bacteria, autogenous regulation of the *nifHDK* operon might provide a useful mechanism for preventing synthesis of inactive nitrogenase.

All transcriptional units in the *nif* gene cluster are repressed by ammonia and as there is no evidence for a *nif*-specific repressor which responds to ammonia, it is possible that this repression is mediated through the level of a *gln* gene product. The latter control system is probably not involved in oxygen repression because mutants which produce nitrogenase in the

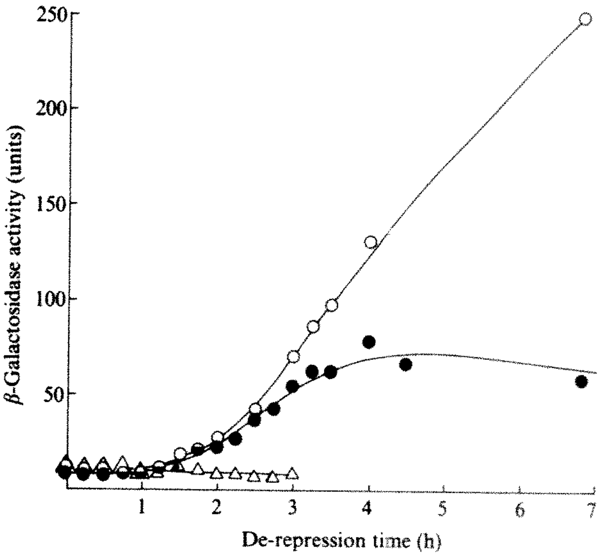

Fig. 3 Effect of strain background on de-repression kinetics of *nifH*::*lac*. Cultures were grown and assayed for β-galactosidase activity as in Fig. 2. Strains were derivatives of UNF619 and UNF686 described in Table 1 legend. *a*, *nif*$^+$/*nifH2783*::Mud(Ap*lac*) (○); *b*, Δ(*his–nif*)/*nifH2783*::Mud(Ap*lac*) (●); *c*, Δ(*his–nif*)/*nifH2783*::Mud(Ap*lac*), *nifA2013*::Tn*10* (△). When grown in the absence of molybdate both diploid (*nif*$^+$/*nifH*::*lac*) and haploid (*nifH*::*lac*) strains gave similar curves to ●. For description of curves *a–c*, see text.

presence of ammonia remain subject to oxygen regulation[11]. It is also unlikely that the products of the *nifHDK* operon are involved in oxygen repression because the level of β-galactosidase activity in a haploid polar *nifH::lac* fusion strain was lower under a D.O.T. of 0.5% than the control under nitrogen. It is possible that one of the other products of the *nif* gene cluster acts as an oxygen sensor and can mediate oxygen repression at a low D.O.T., whereas at higher oxygen concentrations there is a more general effect on the *nif* gene cluster which may also extend to other oxygen-repressible systems in the cell.

The isolation of regulatory mutations in each of the *nif* transcriptional units should considerably enhance our knowledge of the regulation of this complex gene cluster.

We thank Dawn Allitt, Marie Clark, Simon Harrison and Eugene Kavanagh for technical assistance, John Postgate for constructive criticism of the manuscript, and Malcolm Casadaban for supplying unpublished information and useful strains. M.I. and D.K. were supported by EMBO fellowships.

Received 4 March; accepted 23 April 1980.

1. Eady, R. R. & Smith, B. E. in *A Treatise on Dinitrogen Fixation*, Sections I, II (eds Hardy, R. W., Bottemly, F. & Burns, R. C.) 399–490 (Wiley, New York, 1979).
2. Shah, V. K. & Brill, W. J. *Proc. natn. Acad. Sci. U.S.A.* **74**, 3249–3253 (1977).
3. Eady, R. R. & Postgate, J. R. *Nature* **249**, 805–810 (1974).
4. Merrick, M., Filser, M., Kennedy, C. & Dixon, R. *Molec. gen. Genet.* **165**, 103–111 (1978).
5. Elmerich, C., Houmard, J., Sibold, L., Manheimer, I. & Charpin, N. *Molec. gen. Genet.* **165**, 181–189 (1978).
6. MacNeil, T., MacNeil, D., Roberts, G. P., Supiano, M. A. & Brill, W. J. *J. Bact.* **136**, 253–266 (1978).
7. Merrick, M. *et al. J. gen. Microbiol.* **117**, 509–520 (1980).
8. Roberts, G. P., MacNeil, T., MacNeil, D. & Brill, W. J. *J. Bact.* **136**, 267–279 (1978).
9. Hill, S. & Kavanagh, E. *J. Bact.* **141**, 470–475 (1980).
10. Dixon, R., Kennedy, C., Kondorosi, A., Krishnapillai, V. & Merrick, M. *Mol. gen. Genet.* **157**, 189–198 (1977).
11. Eady, R. R., Issack, R., Kennedy, C., Postgate, J. R. & Ratcliffe, H. D. *J. gen. Microbiol.* **104**, 277–285 (1978).
12. Brill, W. J., Steiner, A. L. & Shah, V. K. *J. Bact.* **118**, 986–989 (1974).
13. Tyler, B. *A. Rev. Biochem.* **47**, 1127–1162 (1978)
14. Casadaban, M. & Cohen, S. N. *Proc. natn. Acad. Sci. U.S.A.* **76**, 4530–4533 (1979).
15. Janssen, K. A., Riedel, G. E., Ausubel, F. M. & Cannon, F. C. in *Proc. 3rd int. Symp. Nitrogen Fixation*, Vol. I (eds Orme-Johnson, W. H. & Newton, W.) 85–93 (University Park Press, Baltimore, 1980).
16. Pahel, G. & Tyler, B. *Proc. natn. Acad. Sci.* U.S.A. **76**, 4544–4548 (1979).
17. Kustu, S., Burton, D., Garcia, E., McCarter, L. & McFarland, N. *Proc. natn. Acad. Sci. U.S.A.* **76**, 4576–4580 (1979).
18. Ausubel, F. M., Reidel, G., Cannon, F., Peskin, A. & Margolskee, R. in *Genetic Engineering for Nitrogen Fixation* (ed. Hollaender, A.) 111–126 (Plenum, New York, 1977).
19. Kennedy, C. & Postgate, J. R. *J. gen. Microbiol.* **98**, 551–557 (1977).
20. Cannon, F. C., Dixon, R. A., Postgate, J. R. & Primrose, S. B. *J. gen. Microbiol.* **80**, 227–239 (1974).
21. Kelly, M. & Lang, G. *Biochim. biophys. Acta* **223**, 86–104 (1970).
22. Miller, J. H. in *Experiments in Molecular Genetics*, 162–172 (Cold Spring Harbor Laboratory, New York, 1972).

LETTERS

IUE observations of the UV spectrum of comet Bradfield

P. D. Feldman*, H. A. Weaver*, M. C. Festou†, M. F. A'Hearn‡, W. M. Jackson§, B. Donn, J. Rahe||¶, A. M. Smith|| & P. Benvenuti||#

*Johns Hopkins University, Baltimore, Maryland 21218
†University of Michigan, Ann Arbor, Michigan 48109
‡University of Maryland, College Park, Maryland 20742
§Howard University, Washington, DC 20059
||Goddard Space Flight Center, Greenbelt, Maryland 20771
#ESA-VILSPA, Madrid, Spain

Comet Bradfield (1979l), discovered shortly after perihelion, on Christmas day 1979, is characterized by a retrograde orbit of period ≈250 yr. This orbit was very favourable for observation by the IUE satellite[1], and the first observations, the preliminary results of which are reported here, were made on 10 and 11 January 1980. Previously, comprehensive vacuum UV cometary spectra were available only for Comet West (1976VI) from rocket observations[2,3] and Comet Seargent (1978m) obtained with IUE[4], hence three comets have now been observed in the wavelength region where most of the major constituents are detectable spectroscopically. The UV spectra of these comets are remarkably similar, despite large differences between them in the gas-to-dust ratio and the different heliocentric distances at which the observations were made, and although the statistical basis is still very small, the implication for cosmogony is that nearly all comets have the same primary composition and origin.

At the time of these observations the comet was 0.71 AU from the Sun, 0.61 AU from Earth, and had a total visual magnitude ≈4. The visual appearance of the comet was diffuse with a weak central condensation and with only a slight trace of an ion tail. The comet could be tracked on its centre of brightness by the fine error sensor of the IUE. Drift was found to be no more than 1–2 arc s h^{-1}. All observations were made with the large (10 × 20 arc s) apertures of the spectrographs and the pointing accuracy was verified by the presence of the weak continuum near 2,900 Å in the centre of the slit.

The short wavelength spectrum is shown in a 2-h exposure in Fig. 1. The vertical scale has been reduced to average surface brightness per Å in the 10 × 20 arc s slit. As noted below, the use of the large slit permits a limited amount of spatial imaging on extended sources[5] to a resolution of ≈6 arc s, but the spectra presented here represent the average over the entire slit. The dominant features in the spectrum other than H I Lyα which is highly over-exposed are O I λ1,302, C I λλ1,561, 1,657 and 1,931 and S I λ1,813, as in the spectrum of Comet West[2,3]. The brightness in a given line or multiplet is obtained by integrating over the instrumental spectral band-pass which varies from ≈6 Å for a point source to ≈11 Å for a diffuse source uniformly filling the entire aperture. Table 1 gives the average brightness for these features. The C II λ1,335 multiplet and CO fourth positive bands observed by Feldman and Brune[2], are present in the smoothed spectrum of Fig. 1 slightly above the noise at about the same level relative to the C I lines as in the spectrum of Comet West. It is surprising that the spectrum of Comet

Table 1 Average brightness of spectral features at 0.71 AU

Species	Wavelength (Å)	Brightness (kR)
H I Lyα	1,216	160
O I	1,304	0.33
C I	1,561	0.12
	1,657	0.55
	1,931	0.05
S I	1,807–1,826	0.26
CS (0,0)	2,576	1.40
(0,1)	2,663	0.15
CO_2^+	2,890	0.60
OH (1,0)	2,820	7.6
(0,0)	3,085	370
(1,1)	3,142	12
CO^+ (0,1) + (1,2)	2,321	0.39
(0.2) + (1,3)	2,436	0.18

---

†Permanent address: Service d'Aéronomie du CNRS, Verrières-le-Buisson, France; ¶Permanent address: Astronomical Institute, Universität Erlangen, Nürnberg, FRG.

0028-0836/80/280132-04$01.00

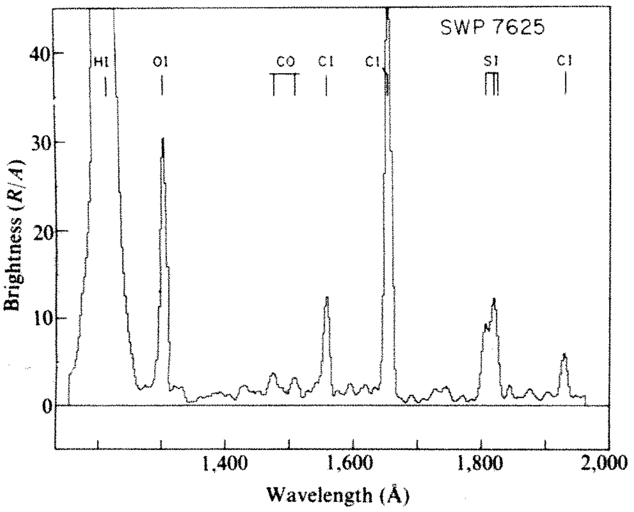

Fig. 1 Low dispersion, short wavelength spectrum of Comet Bradfield taken with the IUE spectrograph slit centred on the visible centre of brightness on 10 January 1980. The exposure time was 2 h.

Bradfield is so similar to that of Comet West considering the differences in appearance, heliocentric distance and gas production rate at the times of observation as well as the difference in projected slit area of the two instruments. This suggests that reactions among the neutral and ionized species in the inner coma may not play a significant part in altering the composition of the coma following photodestruction of the mother molecules evaporated from the cometary nucleus.

The average brightness of the H I Lyα emission, which is saturated in the spectrum of Fig. 1, is determined from a 60-s exposure and is found to be 160 kR which indicates an optically thick atomic hydrogen column along the line-of-sight to the centre of the coma. The O I multiplet at 1,302 A is nearly optically thick as it is excited by resonance scattering of the solar λ1,302 lines because the heliocentric velocity of the comet was 24 km s^{-1}. In previous observations of Comets Kohoutek and West[2] this velocity was ≈50 km s^{-1} which shifted the cometary oxygen absorption outside the solar line profile and it was assumed that fluorescent pumping by solar H I Lyβ radiation was the excitation source[6].

A 2-h exposure of the long wavelength spectrum is shown in Fig. 2. Once again the dominant features are the CO$^+$, CS, $CO_2{}^+$, and OH bands identified previously[3], but now the identification of CS is confirmed by the presence of the (0,1) band at 2,663 Å and the (1,0) band at 2,507 Å in addition to the saturated (0,0) band at 2,576 Å, all three of which are degraded towards the red. The three OH bands are also saturated but the average brightness of these bands can be found from shorter exposures. These are all listed in Table 1. The weak continuum observed near 2,750 and 2,950 Å suggests a very small dust-to-gas ratio for this comet, consistent with visual observations.

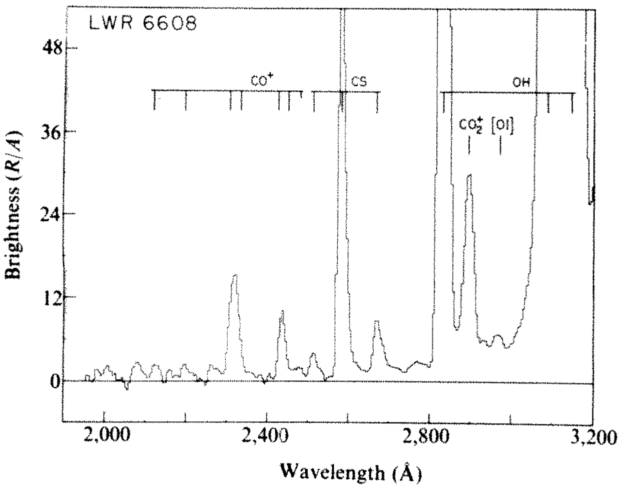

Fig. 2 Same as Fig. 1, but a 2-h exposure with the long wavelength spectrograph.

One peculiarity of this spectrum is the absence (or extreme weakness) of the (0,0) and (1,0) bands of the CO$^+$ first negative system near 2,190 and 2,112 Å, respectively. Both of these bands are also absent or very weak in the IUE spectrum of Comet Seargent[4]. In the rocket spectra of Comet West[2,3] the (0,0) band was the strongest CO$^+$ feature. It does not seem likely that fluorescent pumping by solar radiation can explain this difference as the observed strong bands near 2,300 (0,1 and 1,2) and 2,420 Å (0,2 and 1,3) originate on the same $v'=0$ and 1 levels of the upper $B^2\Sigma^+$ state of CO$^+$ and in an optically thin ion coma the band intensities would be proportional to the Franck–Condon factors for the transitions. One possibility is that the CO$^+$ in our field of view is optically thick along the line-of-sight in the $v''=0$ ground state and as a result (0,0) and (1,0) band photons are re-absorbed and pumped into transitions such as (0,1) and (1,2). The difference with the Comet West data can be explained by the difference in field of view, 5 × 35 arc min for the experiment of Feldman and Brune[2] compared with 10 × 20 arc s for IUE, a factor of ≈3,200 in solid angle. Thus, most of the radiation observed by Feldman and Brune is from CO$^+$ significantly further away from the nucleus where the CO$^+$ is not optically thick along the line-of-sight, and the relative band intensities are close to the theoretically expected values. A consequence of this explanation is the inference that CO$^+$ is produced in large abundance within 3,000 km of the nucleus. However, this hypothesis is not consistent with visual spectra obtained later in the month (January 30.0) which showed only very weak emission in the CO$^+$ comet tail bands near 4,000 Å (C. McCracken, personal communication) and only a faint visual ion tail.

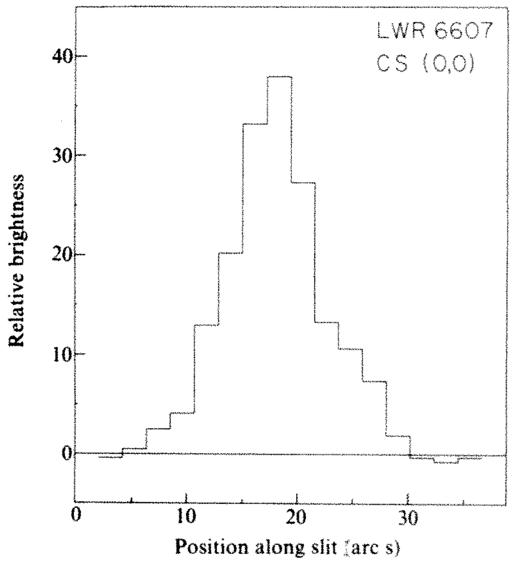

Fig. 3 Variation of the brightness of the CS (0,0) band at 2,576 Å across the spectrograph slit. At the instrumental resolution of 6 arc s, the CS seems to have a point-source origin.

Several very weak features were observed in both Fig. 1 and Fig. 2 and may, in fact, be real emission features such as additional CO fourth positive bands or the [O I] line at 2,972 Å. There is strong evidence that the [O I] 2,972 Å feature is real as it is also present above the dust continuum in the spectra of Comet West[2,3]. This transition (^1S–^3P), known to atmospheric spectroscopists as the 'trans-auroral' line of oxygen, is produced at 5% of the rate of the 'auroral green line' at 5,577 Å (^1S–^1D). The green line has been proposed[7] but not conclusively identified in cometary spectra due to the masking effect of the solar scattered continuum, the nearby (1,2) Swan band of C_2 and the presence of this line in the night airglow, but it is clear that oxygen in the ^1S state is produced in the coma. Preliminary calculations indicate that direct photodissociation of H_2O by solar H I Lyα radiation is sufficient to account for the observed surface brightness of the λ2,972 Å feature.

The spatial variations of the UV emissions can be studied in two ways. For those emissions with short scale lengths there is an appreciable variation in brightness within the 10 × 20 arc s aperture of the spectrographs and the variation can be mapped with a spatial resolution of ≈6 arc s. Otherwise it is necessary to take several different exposures with the spectrograph slit offset by a known amount from the centre of visual brightness of the coma. An example of the former is the CS (0,0) band at 2,576 Å, for which the spatial variation in the large slit from a 30-min exposure is shown in Fig. 3. The horizontal scale is the linear distance from the centre of the coma appropriate to the Earth–comet distance at the time of observation. The sharp decrease in brightness away from the centre of the comet suggests a ρ^{-1} brightness dependence characteristic of a parent molecule density distribution which varies as R^{-2} close to the nucleus, where R is the distance from the centre of the comet and ρ is the distance from the centre projected onto the sky. It is thus very probable that CS exists as a parent molecule in the cometary ice or is the dissociation product of an extremely short-lived parent molecule.

The second technique, several exposures centred at different distances from the visible centre of brightness, is shown for the OH (0,0) band at 3,090 Å in Fig. 4. The three data points are compared with the predictions of a Haser model[8] to give both the scale length (at 1 AU) and the OH production rate. However, the results are sensitive to the choice of the assumed H_2O outflow velocity and for our purpose we took extreme cases of 0.5 and 1.0 km s^{-1}. The other parameters needed[9] are the H_2O lifetime, 8.2×10^4 s, and the OH outflow velocity, 1.15 km s^{-1}. The two curves in Fig. 4, virtually indistinguishable from each other, correspond to values of $\tau_{OH} = 1.0 \times 10^5$ s and 5.0×10^4 s for the respective values of $v_{H_2O} = 0.5$ and 1.0 km s^{-1}. The corresponding values of the OH (and presumably H_2O) production rate at 0.71 AU are $Q_{OH} = 1 \times 10^{29}$ s^{-1} and 2×10^{29} s^{-1}, respectively. The range of deduced values of τ_{OH} (at 1 AU) is in accord with the theoretical value of 7.5×10^4 s given by Jackson[10] for a heliocentric velocity of 24 km s^{-1}. According to Festou[9], the lifetime derived by means of Haser's model is a lower limit to that obtained from a model which properly accounts for the spatial distribution of the OH radicals produced by photodissociation. The water production rate, reduced to 1 AU, of 0.5–1×10^{29} s^{-1}, is considerably lower than that of several 'new' comets as given by Keller and Lillie[11], consistent with the identification of this comet as a long-period comet which has made numerous passes through the inner Solar System.

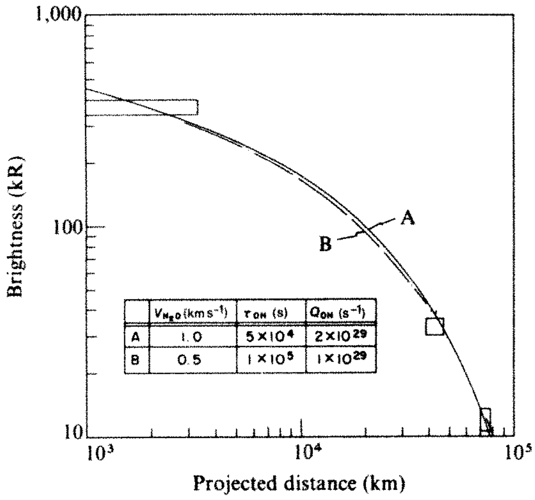

Fig. 4 Comparison of the OH (0,0) band brightness profile with a radial outflow model using the parameters defined in the insert. Data from three exposures are shown as rectangular boxes, the horizontal size being the projected length of the spectrograph slit on the comet and the vertical size the measurement uncertainty.

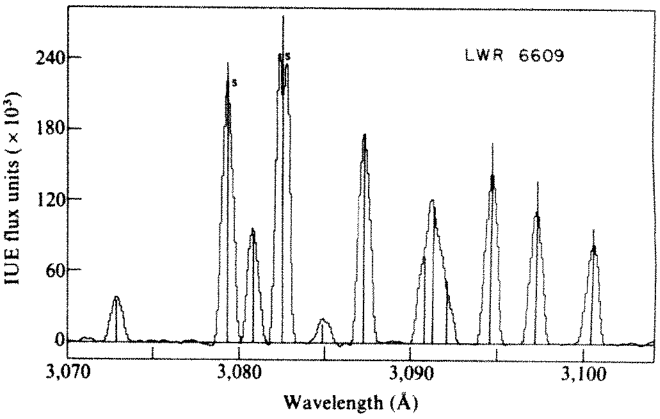

Fig. 5 High dispersion spectrum of the OH (0,0) band taken from a 15-min exposure. The wavelengths shown are vacuum wavelengths. The ordinate is in IUE flux units which are not corrected for the absolute spectral response of the instrument. The theoretical intensities have been multiplied by the approximate spectral response curve of the long-wavelength camera which varies steeply in this spectral region. The $P_1(1)$ line near 3,082 Å was saturated (S) in the observed spectrum and is off-scale in the theoretical calculation.

Assuming that CS is evaporated from the nucleus with the same outflow velocity as H_2O, it is possible to determine the relative production rate of these two molecules. A g-factor for the CS (0,0) band at 2,576 Å of 7×10^{-4} photons per s per molecule at 1 AU was adopted which leads to a value of the ratio $Q_{CS}/Q_{H_2O} \approx 5 \times 10^{-4}$. Thus, although CS is a prominent feature of the UV cometary spectrum it is clearly only a minor species in the comet.

The high resolution capability of the IUE spectrographs was used to study further the resonance fluorescence excitation of the OH (0,0) band, the strongest emission feature in the cometary spectrum. A 15-min, high-dispersion exposure is shown in Fig. 5, along with the predicted relative intensities as calculated for the heliocentric distance, r, and radial velocity, $\dot{r}$, at the time of observation[12]. The excellent agreement between theory and observation over the velocity range 24–28 km s^{-1} indicates that no process other than fluorescence is important in controlling the OH level populations. The dependence of the spectrum on $\dot{r}$ is strikingly illustrated by comparison of Fig. 5 with a similar, high-dispersion spectrum of this band from Comet Seargent (1,978m) (ref. 4), which differed in heliocentric radial velocity by ~10 km s^{-1}. The large changes in the spectrum with radial velocity indicate that the fluorescence efficiency (g-factor) is also a function of radial velocity. The velocity dependent g-factors, needed to convert low resolution fluxes to column densities as above, were obtained from this high resolution analysis.

These new results are only the preliminary analysis of the data obtained at the first opportunity for IUE observations of Comet Bradfield. Observations were continued, at the rate of one a week corresponding to increments in heliocentric distance of ~0.1 AU, through February, and should provide important information about the variation of the production rates of the UV active species with distance from the Sun. As the first comet to be so regularly observed in the vacuum UV, Comet Bradfield will greatly increase our understanding of the physics and chemistry of the cometary atmosphere.

We thank the IUE Observatory staff for acquisition and reduction of the data and for all their assistance. B. G. Marsden and M. P. Candy provided up-to-the-minute ephemerides. The work at Johns Hopkins University is supported by NASA grant NSG 5393.

Note added in proof: Further analysis has disclosed that the features at 2,321 and 2,436 Å are incorrectly identified as CO$^+$; rather they are a Mulliken band of C_2 and the second order HILyα image, respectively. The absence of CO$^+$ bands in the UV is thus consistent with the absence of this species in the visible spectrum.

Received 17 March; accepted 23 April 1980.

1. Boggess, A. *et al. Nature* **275,** 377–385 (1978).
2. Feldman, P. D. & Brune, W. H. *Astrophys. J. Lett.* **209,** L45–L48 (1976).
3. Smith, A. M. & Casswell, L. *Astrophys. J.* (submitted).
4. Jackson, W. M. *et al. Astr. Astrophys.* **73,** L7–L9 (1978).
5. Clarke, J. T., Moos, H. W., Atreya, S. K. & Lane, A. L. *Science* (submitted).
6. Feldman, P. D., Opal, C. B., Meier, R. R. & Nicolas, K. R. in *The Study of Comets* (eds Donn, B. *et al.*) 773–795 (NASA SP-393, 1976).
7. Swings, P. *Q. Jl R. astr. Soc.* **6,** 28–69 (1965).
8. Haser, L. *Bull. Acad. r. Belg.* **43,** 740–750 (1957).
9. Festou, M. thesis, Univ. Paris VI (1978).
10. Jackson, W. M. *Icarus* **41,** 147–152 (1980).
11. Keller, H. U. & Lillie, C. F. *Astr. Astrophys.* **62,** 143–147 (1978).
12. Schleicher, D. & A'Hearn, M. F. (in preparation).
13. Despois, D., Gerard, E., Crovisier, J. & Kazès, I. *Trans. IAU* (in the press).

Tidal effects on the mass profile of galactic haloes

Avishai Dekel*, Myron Lecar† & Jacob Shaham*

*Racah Institute of Physics, The Hebrew University of Jerusalem, Jerusalem, Israel
†Harvard-Smithsonian Center for Astrophysics, Cambridge, Massachusetts 02138

Most spiral galaxies are believed to be embedded in dark massive haloes[1,2]. The main observational evidence for their presence is the rotation curves of edge-on disks at large radii measured both by optical[3,23] and radio (21 cm)[4] techniques: rotation velocities remain constant to distances of several tens of kiloparsecs, far beyond the main visible bodies of the galaxies. This suggests the existence of a dark halo whose mass, if spherical, varies linearly with distance R from the galactic centre and hence has a density profile which falls off as R^{-2}. The extended 'flat' shape of the haloes poses a problem for most theoretical hypotheses of galaxy formation because simulations of collapse[5–8] and of violent mergers[9] predict a spherical density profile which is rather Hubble-like ($\rho \propto R^{-3}$) or even steeper. The time scale for two-body relaxation, which can lead to a flatter, isothermal, density profile, is much larger than the Hubble time. If, as Gunn[10] and Gott[6] have suggested, secondary cosmological infall produces the $\rho \propto R^{-2}$ haloes, special initial conditions are required: (1) the central perturbation, which is the progenitor of the galaxy, needs to be initially embedded in a bound homogeneous background—an assumption which might not be fully justified for relatively isolated galaxies; and, (2) the infall must be such that there is no dissipation so that most of the mass should already be in the form of compact objects before halo formation. We suggest, as an alternative mechanism, tidal interactions between haloes, or possibly between their smaller building blocks, while in the hierarchical gravitational clustering process. In this process typical tidal encounters are slow, such that relative orbital velocities of the interacting systems are comparable to the internal velocities of the stars in each system. The two systems are slightly unbound.

Our suggestion is based on N-body simulations which we performed to study the tidal effects of such encounters on the mass-profile of spherical systems[11]. On adopting the common view, that the dark material is not gaseous[12–14] but is rather composed of condensed bodies (such as unevolved low-mass stars, dead remnants of old stars, and primordial black holes[15]), a dissipationless N-body system was assumed to represent properly a galactic halo. The numerical experiments were based on the N-body code developed by Aarseth[7,16,17]. It integrates the equations of motion of N softened particles, which interact through a potential

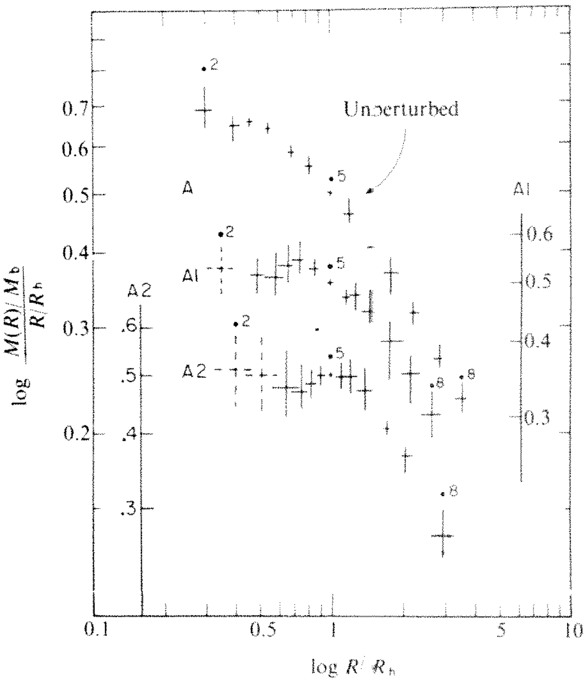

Fig. 1 Rotation curves of two tidally perturbed haloes, A1 and A2, are compared with the unperturbed one at the same final time. The mass and the radius are in fractional units relative to the mass, M_b, and the half-mass-radius, R_h, of the remnant bound system. The symbols correspond to given fractions of the bound mass, separated by 5%, and the error bars correspond to temporal deviations over three successive crossing-times. The curves are vertically shifted by a factor of 1/2 relative to each other. The parameters for the cases A1 and A2 are the following, perturber mass/halo mass = 2; relative velocity at closest approach = 1.05 the parabolic velocity; closest approach distance = 4.6 R_h, 2.8 R_h; fractional mass loss = 0.22, 0.33; final R_h/original R_h = 0.8, 0.74. Note that both the fractional and absolute flat regions become more extended.

$$\phi_{ij} = -Gm_i m_j/[(r_i - r_j)^2 + \varepsilon^2]^{\frac{1}{2}}. \qquad (1)$$

The softening parameter, ε, is chosen to suppress the two-body relaxation effects that arise due to the small number of particles in our experiment.

In our experiments, a 250-body system was tidally perturbed by a point perturber of comparable mass. The encounter velocities were slightly above parabolic and the closest approach distances, p, were between 2.5 R_h and 5 R_h, where R_h was the half-mass-radius. In such conditions, each 'shell' of stars expands, gradual stripping occurs outside ~R_h and up to one-third of the original mass may become unbound. As Fig. 1 shows, the effect on a system which initially has a decreasing $M(R)/R$ profile ($\rho \propto R^{-3}$) is to steepen the profile in the outer parts, and to produce, or extend, an inner region of constant $M(R)/R$, to encompass 50–70% of the bound mass. Hence, this mechanism, whose exact relaxation nature is not yet understood theoretically, produces systems which might show flat rotation curves over a large fraction of their mass (but not a relaxed flat outer envelope, as was discussed previously[18,19]). Tandem encounters of the same system tend to strip the outer parts and produce a smaller system, which retains a flat inner profile.

Most of the stripped stars in our simulations did not become bound to the perturber but rather escaped from the two-body system altogether. This indicates that stripped material from a realistic, N-body, perturber would not become bound to the perturbed system and, therefore, have no substantial effect on its mass profile. We therefore assume that

0028-0836/80/280135-02$01.00

our results for a point perturber are, for similar p values, also qualitatively representative for an N-body perturber. This assumption is supported by the consistency of our results for the energy-gain and mass-loss with those obtained by other simulations of encounters between identical systems[11]. The substantial amount of stripped material might remain bound to a larger group, forming a common background halo which might later infall and produce even more extended envelopes around the haloes.

If slow hyperbolic encounters are to be considered responsible for $M \propto R$ profiles, one should estimate how frequently they occur in a cosmological context. Tidal encounters are found to be effective whenever $p \leqslant 5\,R_h$, so that the geometrical cross-section for such an encounter is much larger than that for a merger, which occurs for $p \leqslant 2.5\,R_h$ (refs 9, 20, 21). The time scale for mergers in a small group is estimated analytically to be of the order of the dynamical time scale of the group[22], and N-body simulations show that about one-third of the galaxies have undergone mergers, mostly in the first generation of their clustering. One may, therefore, conclude that the proposed mechanism is quite relevant in small groups.

A weak lower limit on the rate of encounters can be estimated for 'field' galaxies. A straightforward *nσv* calculation shows that the number, N, of effective encounters since the epoch of halo formation, Z_{form}, is

$$N \sim 0.05\,\Omega_0\,(1+Z_{\text{form}})^2 \left(\frac{R_h}{60\,\text{kpc}\,h_{50}^{-1}}\right)\left(\frac{v}{300\,\text{km s}^{-1}}\right) \qquad (2)$$

where v is the typical peculiar velocity of galaxies. Each quantity in equation (2) has uncertainties but N does seem to be a number of the order of unity. There might be an additional contribution to N from dark haloes which do not have visible cores (galaxies)[13].

The suggested mechanism predicts a correlation between the degree of clustering of a galaxy (be it a field galaxy, a member of a small group or a member of a large one) and the fractional extension of its $M \propto R$ region. Note also that tidal encounters lead to haloes which are both less massive and have larger fractional $M \propto R$ regions, whereas cosmological infall should lead to larger $M \propto R$ regions in more massive haloes.

Tidal interactions might also be helpful in the merger picture for halo formation, as suggested by White and Rees[22]. There, each merger is preceded and followed by several tidal encounters which might reproduce inner $M \propto R$ regions even when the mergers themselves may steepen their profiles[9].

Another important indication from our results is the tendency for complete removal of haloes after many encounters. This is seen from the fact that, as a result of a tidal encounter, each 'shell' of stars expands, so that most parts of the system become less bound, an easy target for further stripping. It is expected, therefore, that galaxies now in rich clusters have lost most of their haloes due to successive encounters during their clustering process, and that galaxies observed to have haloes could not have undergone too many tidal encounters.

We thank Dr Sverre J. Aarseth for his code and help, Drs S. Michael Fall and Martin J. Rees for helpful comments.

Received 25 February; accepted 23 April 1980.

1. Ostriker, J. P., Peebles, P. J. E. & Yahil, A. *Astrophys. J. Lett.* **193,** L1 (1974).
2. Faber, S. M. & Gallagher, J. S. *A. Rev. Astr. Astrophys.* **17,** 135 (1979).
3. Rubin, V. C. *Comments Astrophys.* **8,** 79 (1978).
4. Krumm, N. & Salpeter, E. E. *Astr. Astrophys.* **56,** 465 (1977).
5. Peebles, P. J. E. *Astr. J.* **75,** 13 (1970).
6. Gott, J. R. *Astrophys. J.* **186,** 481 (1973); **201,** 296 (1975); *Ann. Rev. Astr. Astrophys.* **15,** 235 (1977).
7. Aarseth, S. J. & Lecar, M. *A. Rev. Astr. Astrophys.* **13,** 1 (1975).
8. Larson, R. B. *Mon. Not. R. astr. Soc.* **166,** 585; **169,** 229 (1974); **173,** 671 (1975).
9. White, S. D. M. *Mon. Not. R. astr. Soc.* **184,** 185 (1978).
10. Gunn, J. E. *Astrophys. J.* **218,** 592 (1977).
11. Dekel, A., Lecar, M. & Shaham, J. *Astrophys. J.* (in the press).
12. Bergeron, J. & Gunn, J. E. *Astrophys. J.* **217,** 892 (1977).
13. Rees, M. J. in *The Evolution of Galaxies and Stellar Populations* (eds Tinsley, B. M. & Larson, R. B.) 339 (Yale University Observatory, 1978).
14. Peebles, P. J. E. in *Physical Cosmology* (Gordon and Breach, Edinburgh, in the press).
15. Dekel, A. & Shaham, J. *Astr. Astrophys.* **74,** 186 (1979); Preprint, Hebrew Univ. of Jerusalem (1980).
16. Aarseth, S. J. *Gravitational N-body Problem* (ed. Lecar, M.) 373 (Reidel, Dordrecht, Holland, 1972).
17. Ahmad, A. & Cohen, L. *J. comp. Phys.* **12,** 389 (1973).
18. Layzer, D. *Gen. Rel. Gravit.* **8,** 3 (1977).
19. DaCosta, L. N. & Knobloch, E. *Astrophys. J.* **230,** 639 (1979).
20. Roos, N. & Norman, C. A. *Astr. Astrophys.* **76,** 75 (1979).
21. Aarseth, S. J. & Fall, S. M. *Astrophys. J.* **236,** 43 (1980).
22. White, S. D. M. & Rees, M. J. *Mon. Not. R. astr. Soc.* **183,** 341 (1978).
23. Rubin, V. C., Ford, W. K. Jr & Thonnard, N. Preprint, Carnegie Inst. of Washington (1980).

Interpretation of type I OH maser sources

W. H. Kegel

Institut für Theoretische Physik der Johann Wolfgang Goethe-Universität, Frankfurt am Main, FRG

D. A. Varshalovich

Ioffe Physical Technical Institute of the Academy of Sciences of the USSR, Leningrad, USSR

OH maser sources of type I, which are related to regions of star formation, have been known for more than a decade. However, despite great effort no satisfactory theoretical interpretation has yet been given. (For general reviews on cosmic masers see refs 1–5.) A model for the interpretation of type I OH maser sources is suggested here. This model combines the effect of velocity and magnetic field gradients with radiative pumping by means of the ($^2\Pi_{3/2}$, $J=5/2 \rightarrow {}^2\Pi_{1/2}$, $J=5/2$) transition. Due to an overlap of particular hyperfine components, inversion of the 1,665 MHz line is favoured.

Type I OH maser sources are characterized by an extreme intensity corresponding to a radiation temperature up to 10^{13} K in one or both of the main lines, the 1,665 MHz-line usually being the stronger, and by a high degree of circular polarization (up to 90%).

Schemes involving optical pumping[6–11], chemical pumping[12,13], and collisional pumping (refs 12, 15, 16, and C. H. Townes and W. D. Gwinn, unpublished data) have been used to explain the intensities. Although all these mechanisms may produce population inversions, difficulties arise when a more quantitative interpretation of the observations is attempted. For example, consider a radiative pumping scheme: on one hand it is not easy (though possible) to have enough pump photons to explain the observed high luminosities in the radio lines, on the other hand it is difficult to have an efficient pump mechanism and a large absolute value of the optical thickness in the maser line at the same time, because the absolute value of the optical thickness of the pump line along the same line of sight is in general larger than that of the maser line[4]. Note also that the upper and the lower levels of either of the main lines are distinguished only by their parity, while all other quantum numbers are identical. Thus to every spectral line connecting to the lower level there is a corresponding line connecting to the upper level. Inversion can, therefore, come about only by difference effects and not by selection rules.

To explain the high degree of polarization a model has been proposed which invokes gradients of the velocity and the magnetic field[17,18]. If the velocity and the magnetic field change along the line of sight, it can be hypothesized that in a certain region for a particular direction of propagation, the derivatives of the frequency shifts of the maser line due to the Doppler and the Zeeman effect just cancel each other out. This leads to a larger absolute value of the optical depth than one would have without Zeeman splitting.

If κ is the absorption coefficient

$$\kappa = \kappa_0 \exp\{-(\Delta v/\Delta v_{\text{th}})^2\} \qquad (1)$$

0028-0836/80/280136-03$01.00

we estimate the optical thickness in the line by

$$\tau = \kappa_0 \Delta l \qquad (2)$$

where Δl is the path length along the line of sight over which the frequency shift changes by an amount corresponding to the thermal width $\Delta\nu_{th}$ of the line. Using a Taylor expansion for the radial velocity (v_r) and the magnetic field (H); we obtain for the frequency shift along the line of sight:

$$\Delta\nu \simeq (\Delta\nu)_0 + \left[\frac{\nu_0}{c}\frac{\mathrm{d}v_r}{\mathrm{d}l} + \gamma\frac{\mathrm{d}H}{\mathrm{d}l}\right]\cdot\Delta l + \frac{1}{2}\left[\frac{\nu_0}{c}\cdot\frac{\mathrm{d}^2 v_r}{\mathrm{d}l^2} + \gamma\frac{\mathrm{d}^2 H}{\mathrm{d}l^2}\right]\cdot(\Delta l)^2 \qquad (3)$$

($\gamma = 3.31$ MHz Oe^{-1} for the 1,665 MHz-line and 1.99 MHz Oe^{-1} for the 1,667 MHz-line.)

For those lines for which the Zeeman effect is not important we can estimate Δl from the linear term in equation (3):

$$\Delta l_1 = \left|\frac{v_{th}}{\mathrm{d}v_r/\mathrm{d}l}\right|. \qquad (4)$$

If, however,

$$\frac{\nu_0}{c}\frac{\mathrm{d}v_r}{\mathrm{d}l} + \gamma\frac{\mathrm{d}H}{\mathrm{d}l} = 0 \qquad (5)$$

the linear term in equation (3) cancels and we have to determine Δl from the second-order term.

$$\Delta l_2 = \left|\frac{2v_{th}}{\dfrac{d^2 v_r}{\mathrm{d}l^2} + \dfrac{c\gamma}{\nu_0}\dfrac{\mathrm{d}^2 H}{\mathrm{d}l^2}}\right|^{1/2} \qquad (6)$$

As γ has a different sign for the different Zeeman components, this increase in the optical depth occurs only in one of the Zeeman components while in the other there is a decrease.

Thus, if this mechanism were operating, one would expect the maser radiation to consist mainly of only one of the Zeeman components. Observations show that in most cases the right hand and the left hand circularly polarized radiation come from different volume elements.

We suggest that type I OH masers may be due to a combination of the above effect with a particular scheme of optical pumping. For this we note that the relative Zeeman splitting ($\Delta\lambda/\lambda$) is much larger for the radio lines than for the IR lines. Thus, if condition (3) is satisfied for the maser line, the same cannot be true for the IR lines. Therefore we can apparently construct a model in which the absolute value of the optical depth in the maser line is large while that in a potential pump line stays at moderate values ($\tau \sim 1$).

To achieve the pumping we consider the effect of overlap of IR-lines; such pumping schemes have been suggested elsewhere[19,20]. Note that any IR-pumping scheme which is to invert the main lines has to use transitions with $\Delta J = 0$. Among these, the transitions connecting the states with $J = 5/2$ have the largest overlap and seem therefore to be the most important. According to the frequencies given by Destombes *et al.*[21], in the ($^2\Pi_{3/2}$, $J = 5/2$)→($^2\Pi_{1/2}$, $J = 5/2$) multiplet there is an almost complete overlap between two main lines, the ($F = 3^- \rightarrow F = 3^+$) and the ($F = 2^- \rightarrow F = 2^+$) transitions. The frequency difference is 0.5 MHz, corresponding to $\Delta\nu/\nu \simeq 8 \times 10^{-8}$, which is considerably less than the line width for any reasonable temperature. In contrast, the frequency difference between the ($F = 3^+ \rightarrow F = 3^-$) and the ($F = 2^+ \rightarrow F = 2^-$) transitions is 57.5 MHz corresponding to $\Delta\nu/\nu = 0.9 \times 10^{-5}$, which is much wider than typical line widths in OH-maser sources (see Fig. 1). Thus the optical depth in the first pair of lines is about twice that for the latter. If we now consider the radiation from an IR-source outside the OH-cloud, at a point within the cloud at which the optical thickness in the non-overlapping IR-lines is about unity, the intensity in the overlapping lines is about one-third of that in the non-overlapping ones. Thus the rate of absorption from the lower half of the ($^2\Pi_{3/2}$, $J = 5/2$) Λ-doublet is ~6 times larger than that from the upper half. (A factor or two comes from the fact that the non-overlapping lines cover a wider frequency range.) This effect produces a population inversion in the ($^2\Pi_{3/2}$, $J = 5/2$)-state as well as in the ($^2\Pi_{1/2}$, $J = 5/2$)-state. Both are transferred to the ground state by the other IR-transitions.

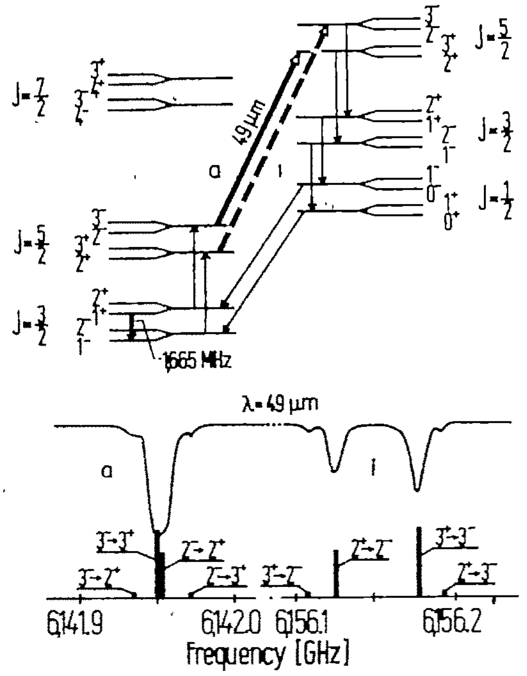

Fig. 1 Energy level diagram of the OH molecule (not to scale) and spectrum of the 49 μm multiplet.

The total number of absorbed pump photons is proportional to $L_{\nu,\mathrm{IR}} \cdot \Delta\nu_p$. The maser region is determined by Δl_2 (equation (6)). As the Zeeman effect is not important for the IR-lines, $\Delta\nu_p$ is much wider than the thermal line width and we can approximate

$$\Delta\nu_p = \frac{\nu_{p,0}}{c}\frac{\mathrm{d}v_r}{\mathrm{d}l}\Delta l_2 = \nu_{p,0}\frac{v_{th}}{c}\frac{\Delta l_2}{\Delta l_1}. \qquad (7)$$

$L_{\nu,\mathrm{IR}}$ may be estimated either from models for IR-sources or from measurements. For W3(OH) $L_{\nu,\mathrm{IR}}$ was determined[22] to be of the order of 4×10^{25} erg s^{-1} Hz^{-1} at $\lambda = 49$ μm.

We now make some quantitative estimates using an oversimplified model. As type I OH-masers occur in regions of star formation, it seems reasonable to consider a collapsing cloud with a central IR-source. If we assume that the kinetic energy density is larger than the magnetic energy density everywhere, the hydrodynamics of the collapse is essentially not altered by the magnetic field and we may assume radial symmetry (the magnetic field lines will also be essentially radial).

For free infall, we have

$$v(r) = v_0 (r_0/r)^{1/2} \qquad (8)$$

$$n(r) = n_0 (r_0/r)^{3/2} \qquad (9)$$

$$H(r) = H_0 (r_0/r)^2. \qquad (10)$$

In this model condition (3) is satisfied if

$$r^{1/2}(3p^2 - r^2) = \alpha(r^2 - p^2)^{1/2} \qquad (11)$$

where p is the impact parameter of the line of sight and

$$\alpha = \frac{4c\gamma H_0 r_0^{3/2}}{\nu_0 v_0}. \tag{12}$$

For simplicity we consider the central ray ($p=0$) only. Along this the maser region is around r_m which is determined from equation (11) to be

$$r_m = (-\alpha)^{2/3}. \tag{13}$$

With $p=0$ we find

$$\frac{\Delta l_2}{\Delta l_1} = \left[\frac{2v_0 r_0^{1/2}}{3v_{th}(-\alpha)^{1/3}}\right]^{1/2}. \tag{14}$$

This ratio, which is independent of r_0, gives the increase of the optical depth of the maser line over the value without Zeeman effect. It also corresponds to the ratio $\Delta\nu_p$ to the thermal width of the pump line. If we assume $v_0 = 5\,\mathrm{km\,s^{-1}}$, $H_0 = 10^{-3}$ Oe and $T_{kin} = 50\,\mathrm{K}$, which seem to be reasonable parameters, we have $\alpha = 0.48\, r_0^{3/2}$ and $\Delta l_1/\Delta l_2 \simeq 4.4$.

We estimate the number of available pump photons on one side by

$$W_{ph} \simeq 4\pi r_s^2 \cdot \pi B_\nu(T_s)\Delta\nu_p \tag{15}$$

where r_s and T_s are the radius and the temperature of the central IR-source. With $r_s \simeq 10^{15}\,\mathrm{cm}$ and $T_s \simeq 300\,\mathrm{K}$ we obtain $W_{ph} \simeq 10^{44}$ photons $\mathrm{s^{-1}}$ which seems to be about of the right order of magnitude. If, on the other side we estimate W_{ph} from the IR-luminosity measured[22] for W3(OH), we obtain about two orders of magnitude more photons. For these photons to be absorbed, the optical depth in the pump lines has to be about unity, that is we have to have $\Delta l_2 \kappa \simeq 1$. With the above assumed parameters this leads to the requirement that $n_{OH} \cdot r_0 \simeq 10^{17}\,\mathrm{cm^{-2}}$. With $r_0 \simeq 10^{16}\,\mathrm{cm}$ this requires an OH density of about $10\,\mathrm{cm^{-3}}$ or with $n_{OH}/n_{H_2} \simeq 10^{-5}$ a hydrogen density of $\sim 10^6\,\mathrm{cm^{-3}}$, which seem to be reasonable.

These estimates show that the proposed scheme may indeed explain the observed properties of type I OH-sources. In particular it explains: (1) the large differences in the relative intensities for the different subsources, these are because the intensity depends on the gradients of the radial velocity and the magnetic field along the line of sight, which vary much more than other physical parameters; (2) the high degree of polarization; (3) why in general the 1,665 MHz-line is more intense than the 1,667 MHz-line. This is expected if in the maser region the number of 49 μm-photons absorbed in the ($F = 2^+ \rightarrow F = 2^-$) transition is larger than that absorbed in the ($F = 3^+ \rightarrow F = 3^-$) transition. This is based on the lowest order consideration in which the satellite transitions ($\Delta F \neq \Delta J$) in the IR-lines are neglected. In this approximation the pump routes for the 1,665 MHz and the 1,667 MHz-line are decoupled and may be considered independently of each other. The number of photons absorbed in a line per cm³ per s is $\kappa I \Delta\nu$ with $I = I_0 e^{-\tau}$. If we further assume that the ratio of the occupation numbers of the different hyperfine components of the ($^2\Pi_{3/2}$, $J = 5/2$)-state corresponds to that of their statistical weights (7/5), the ratio of the absorption coefficients of the pump lines is also given by that number. It then follows, that the number of photons absorbed in the ($F = 2^+ \rightarrow F = 2^-$) transition of the 49 μm-line is larger than that of the ($F = 3^+ \rightarrow F = 3^-$) transition if the optical thickness τ of the latter is larger than 0.31. In more detailed investigations, however, one has to consider the complete multi-level system containing all levels and transitions possibly involved in the pumping scheme.

From the conservation of angular momentum, the IR-lines which provide the pumping would also be expected to be circularly polarized.

This work was performed while D.A.V. was a guest at the Institut für Theoretische Astrophysik, Heidelberg. His visit was supported by the Deutsche Forschungsgemeinschaft. This research is part of the Sonderforschungsbereich 132, which is also sponsored by the Deutsche Forschungsgemeinschaft.

Received 20 February; accepted 23 April 1980.

1. Litvak, M. M. *A. Rev. Astr. Astrophys.* **12,** 97 (1974).
2. ter Haar, D. & Pelling, M. A. *Rep. Prog. Phys.* **37,** 481 (1974).
3. Goldreich, P. in *Atomic and Molecular Physics and the Interstellar Matter* (eds Balian, R., Encrenanz, P. & Lequeux, J.) (North-Holland, Amsterdam, 1975).
4. Kegel, W. H. in *Problems in Stellar Atmospheres and Envelopes* (eds Baschek, B., Kegel, W. H. & Traving, G.) (Springer, Berlin, 1975); *Appl. Phys.* **9,** 1 (1976).
5. Cook, A. H. *Celestical Masers* (Cambridge University Press, 1977).
6. Perkins, F., Gold, T. & Salpeter, E. E. *Astrophys. J.* **145,** 361 (1966).
7. Litvak, M. M., McWhorter, A. L., Meeks, M. L. & Zeiger, H. J. *Phys. Rev. Lett.* **17,** 821 (1966).
8. Shklovsky, I. S. *Astr. Tsirk.* No. 372 (1966); No. 424 (1967).
9. Litvak, M. M. & Dickinson, M. M. *Astrophys. Lett.* **12,** 113 (1972).
10. Litvak, M. M. *Astrophys. J.* **156,** 471 (1969).
11. Burdyuzha, V. V. & Varshalovich, D. A. *Astr. Zh.* **50,** 481 (1973) [*Soviet Astr.* **17,** 308 (1974)].
12. Gwinn, W. D., Turner, B. E., Goss, W. M. & Blackman, G. L. *Astrophys. J.* **179,** 789 (1973).
13. Kegel, W. H. *Astr. Astrophys.* **32,** 227 (1974).
14. Johnston, I. D. *Astrophys. J.* **150,** 33 (1967).
15. Litvak, M. M. *Science* **165,** 855 (1969).
16. Kegel, W. H. *Astr. Astrophys. Suppl.* **38,** 131 (1979).
17. Cook, A. H. *Mon. Not. R. astr. Soc.* **171,** 605 (1975).
18. Varshalovich, D. A. & Burdyuzha, V. V. *Astr. Zh.* **52,** 1178 (1975) [*Soviet Astr.* **19,** 705 (1976)].
19. Litvak, M. M. *Astrophys. J.* **156,** 471 (1969).
20. Pelling, M. *Mon. Not. R. astr. Soc.* **178,** 441 (1977).
21. Destombes, J. L., Marliere, C., Baudry, A. & Brillet, J. *Astr. Astrophys.* **60,** 55 (1977).
22. Thronson, H. A. & Harper, D. A. *Astrophys. J.* **230,** 133 (1979).

Determination of ^{129}I using tandem accelerator mass spectrometry

D. Elmore*, H. E. Gove*, R. Ferraro*, L. R. Kilius†, H. W. Lee†, K. H. Chang†, R. P. Beukens†, A. E. Litherland†, C. J. Russo‡, K. H. Purser‡, M. T. Murrell§ & R. C. Finkel||

*Nuclear Structure Research Laboratory, University of Rochester, Rochester, New York 14627
†Department of Physics, University of Toronto, Toronto, Canada M5S 1A7
‡General Ionex Corporation, Newburyport, Massachusetts 01950
§Department of Chemistry, B-017, University of California at San Diego, La Jolla, California 92093
||Scripps Institution of Oceanography, University of California at San Diego, La Jolla, California 92093

Iodine-129, with a half life of 15.7 Myr (ref. 1), is one of the longest lived of the cosmogenic radionuclides. Although the primordial supply of ^{129}I is now extinct, ^{129}I is continuously being produced in the atmosphere primarily by cosmic ray reactions on xenon[2], in the Earth primarily by spontaneous fission of ^{238}U (ref. 3), and in meteorites and the Moon primarily by proton and neutron induced reactions on Te and Ba (ref. 4). The relatively large quantity of ^{129}I introduced into the environment from the nuclear age may be useful as a tracer in groundwater hydrology[5]. Fissiogenic ^{129}I in large granite formations (batholiths) could be used to establish the suitability of these sites for long term nuclear waste storage, because groundwater movement would carry away the more soluble iodides and disturb the equilibrium ^{129}I/^{238}U ratio. The concentration of ^{129}I in meteorites can be combined with results for shorter-lived radionuclides to provide information on the constancy of the galactic cosmic ray flux over longer time scales than previously possible and also on the preterrestrial history of meteorites. We have applied the new atom counting technique to ^{129}I analysis with a sensitivity (the minimum number of atoms in the sample required to obtain a quantitative result) of less than 10^7 atoms of ^{129}I in a 1-mg sample. An AgI standard with a known ^{129}I/^{127}I ratio of 10^{-11} was determined to ±10%, and the background contribution from a reagent grade AgI sample gave an upper limit to the ratio of about 3×10^{-13}. We used a time-of-flight measurement to distinguish ^{129}I from the stable ^{127}I ions that were not separated by the mass analysis system. Our results for the meteorites Bruderheim and Dhajala represent the first direct (that is, not inferred[6] from radiogenic Xe) determination of ^{129}I in meteorites. A Xe molecular negative ion was discovered but we show that it is not a problem for ^{129}I analysis.

0028-0836/80/280138-03$01.00

Because of its long half life, ^{129}I measurement by counting its β decay is not very sensitive and is useful only for samples with high activity[7]. Although our mass spectrometry measurements of ^{129}I are the first to use an accelerator, McHugh and Sheffield[8] used a three stage mass spectrometer with a negative ion sputter source to detect carrier free ^{129}I with a sensitivity near 10^9 atoms for samples with a ^{129}I/^{127}I ratio of about 10^{-7}. Their measurements were limited by interference from the ^{127}I tail and from molecular ions near mass 129 such as $^{97}MoO_2^-$ which could not be differentiated from $^{129}I^-$.

The neutron activation technique has been quite successful, with numerous reports[3,9] of ^{129}I measurements in natural samples with sensitivities typically in the range 10^{10}–10^{12} atoms. The neutron activation technique involves counting 12-h ^{130}I produced from the ^{129}I(n, γ) ^{130}I reaction in a high flux reactor. A careful chemical pre-separation is used to reduce interference from reactions such as ^{133}Cs(n, α)^{130}I and induced fission on uranium. Interference from 13-day ^{126}I produced by ^{127}I(n, 2n) often limits the sensitivity[2,3], and for this reason Rook *et al.*[10] followed neutron activation with isotope separation of mass 130 and then used β–γ coincidence counting of ^{130}I. The sensitivity was improved somewhat for samples with high ^{127}I content but this procedure still does not discriminate against ^{130}I produced from trace impurities and from the ^{127}I(3n, γ) ^{130}I multistep reaction[2]. By contrast, our method offers simplified sample preparation, a single analysis step taking $<$1h, no interference from impurities, background only from the ^{127}I tail, and a potential improvement in sensitivity by several orders of magnitude. This will allow ^{129}I measurements in considerably smaller samples, and will not require the use of natural iodine concentrators such as animal thyroids, seaweed, and brine.

The apparatus used in the present work is the same as that used for ^{36}Cl (ref. 11) and ^{26}Al (ref. 12) except that the final ionization detector was replaced with a 2.2-m time-of-flight (TOF) detector. The ^{129}I can be identified on the basis of mass alone as the only stable isobar of ^{129}I is ^{129}Xe, a noble gas that is not expected[13] to form negative ions (but see below). However, interference is expected from the stable ^{127}I, two mass units away. The I^- beam (1–5μA) produced from NaI or AgI samples in the Cs sputter source was accelerated to the 5 MV tandem terminal, stripped of several electrons, then accelerated again to ground potential. Charge state +5 ions with an energy of 30 MeV were selected by the 90° analysing magnet and 10° electrostatic deflector. These analysers eliminated all molecules and gave a combined resolution in M/q of ~0.5% FWHM. Although the ^{129}I is thus separated by 3 FWHM from the ^{127}I, a combination of charge exchange and scattering in the acceleration tubes and analysers allowed up to 200 counts per s (c.p.s.) of ^{127}I to pass into the detector. As the interfering $^{127}I^{5+}$ ions passed two magnetic analysers, most of them had the same magnetic rigidity (ME/q^2) as the $^{129}I^{5+}$ ions at the detector and therefore differed by 1.5% in energy (E) and in velocity ($\propto (E/M)^{\frac{1}{2}}$). Heavy-ion detectors are not available with an energy resolution adequate to resolve ions at this mass and energy, so we measured the velocity with TOF. The start signal was obtained[14,15] from the electrons produced by the iodine ions passing through a 5 μg cm^{-2} carbon foil; the stop signal was obtained from a 100-mm^2 area Si surface barrier detector. The Si detector also gave an energy signal adequate to resolve ions in lower charge states having nearly the same E/q and velocity.

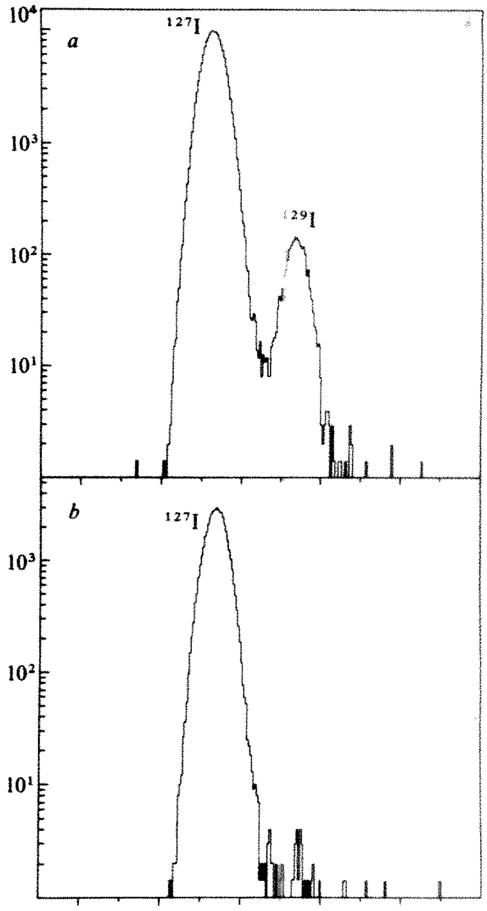

Fig. 1 Time-of-flight spectra for runs on: *a*, an AgI sample enriched to $^{129}I/^{127}I = 10^{-11}$; *b*, AgI made from reagent grade NaI. These events have been gated with a window on the total energy signal. The peaks are separated by 5.2 ns and the overall time resolution is 1.2 ns FWHM.

Table 1 Measured ^{129}I concentrations

Sample	AgI weight (mg)	Counting time (min)	Total ^{129}I (counts)	$^{129}I/^{127}I$ (10^{-12} g per g)	^{129} atoms in sample
NSRL-20003, enriched AgI	~10	89	3052	9.0 ± 0.6†	4.3×10^8
NSRL-20304, reagent blank AgI	~10	10	39	<0.3	$<1.4 \times 10^7$
NSRL-21601, chemistry standard*	1	27	203	8 ± 2†	4.7×10^7
NSRL-21701, Bruderheim*	1	48	160	6 ± 2‡	2.8×10^7
NSRL-21801, Dhajala*	1	33	88	7 ± 2‡	3.3×10^7

*The two meteorite samples were obtained from 6.74 g and 22.2 g of Bruderheim and Dhajala. For these and the chemistry blank ~1 mg of iodine carrier and 5 mg of AgCl were added.

†The two enriched samples (ICN Cat. no. 67325) had an expected $^{129}I/^{127}I$ ratio of $(9.8 \pm 0.5) \times 10^{-12}$.

‡The meteorite results for the $^{129}I/^{127}I$ ratio were normalized to the chemistry standard.

TOF spectra for runs on the standard and blank (Fig. 1) show that the ^{127}I peak is adequately resolved for samples having an $^{129}I/^{127}I$ ratio down to about 10^{-12}. We determined that the apparent levelling off of the ^{127}I tail at the ^{129}I location in the TOF spectrum for the blank was not due to ^{129}I or ^{129}Xe in the sample by moving the analysers off the mass 129 peak and noting that the intensity of the tail remained a factor of ~10^3 below the ^{127}I peak. The ^{127}I rejection factor for each of the analysis stages was approximately as follows: inflection magnet, 3; 90° magnet, 10^5; electrostatic analyser, 10^4; TOF, 10^3.

Although Xe^- is probably unstable, XeF^- has been accelerated in tandems (H. E. Wegner and P. Thieberger, personal communication) and xenon may form other stable or metastable molecular negative ions. As Xe is a likely contaminant in the samples and in the residual gas of the ion source, we felt that it was important to determine whether there is any ^{129}Xe contribution to the mass 129 peak. With the analysis system set for ^{129}I from the reagent AgI blank, pure Xe gas was introduced into the source until the pressure increased a factor of two to 5×10^{-5} torr. The mass 129 counting rate then increased from 1 c.p.m. (which corresponded to a background level of $^{129}I/^{127}I = 6\times10^{-13}$) to 5 c.p.m. Further optimization with a source geometry more appropriate for a gas sample led to a maximum counting rate of 3,500 c.p.m., and this dropped by more than a factor of 100 soon after the gas was turned off. A mass scan with the inflection magnet (which directly follows the ion source) revealed that the Xe was being injected into the tandem as a molecular negative ion with $M/q = -131$ (such as $^{129}XeH_2^-$) although the $^{129}Xe^-$ ion could not be completely ruled out because of the limited resolution of the inflection magnet. (The resolution of the post-acceleration analysis and TOF were adequate to positively identify mass 129, charge state 5 ions. This, together with the high counting rate that was correlated with Xe pressure, is strong evidence that we were counting only $^{129}Xe^{5+}$). The counting rate was low compared to what might be expected from the $\sim10^{10}$ Xe atoms being exposed to Cs in the sputter source. This can be explained if the probability of forming the (molecular) negative ion is low, if the cross-section for destruction in electric and magnetic fields is high, or if the ion is metastable with a life time short compared with the 15 μs trip to the terminal of the tandem. We estimate that if the residual gas in the source contains Xe in atmospheric concentrations (1.1 p.p.m.) and the Xe content of the samples is low (<1 p.p.m.) then the ^{129}Xe will not contribute to the ^{129}I background until a sensitivity for ^{129}I of one part in 10^{18} is reached.

The $^{129}I/^{127}I$ ratios (Table 1) were obtained by cycling the magnets between the two isotopes: the ^{129}I was counted for 3–5 min, then the $^{127}I^{5+}$ current was measured in a Faraday cup following the 90° analyser. The transmission efficiency of the TOF detector ($\sim$30%) was continuously monitored with the ^{127}I ions. The 1σ errors are estimated from the scatter in the individual cycles and reflect both statistics and random fluctuations in the ion source output and accelerator transmission. Systematic errors such as those due to mass fractionation and current calibration contributes an additional uncertainty of $\sim$20% to results for the standards, but most of these effects cancel out for the meteorite results because they are reported as ratios to the standard.

Preparation of the meteorite samples and an interpretation of their ^{129}I content will be subjects of another paper. The results given in Table 1 demonstrate that 10–20 g of meteorite are adequate for detailed ^{129}I analysis. The upper limit for the $^{129}I/^{127}I$ ratio of 0.3×10^{-12} for the reagent blank implies that the background level for a 1 mg AgI sample corresponds to less than 2×10^6 atoms of ^{129}I.

We are presently modifying the apparatus to reduce the ^{127}I tail and increase the sensitivity. A new inflection magnet with a resolution $M/\Delta M$ of better than 150 will reduce the number of $^{127}I^-$ ions that are injected into the accelerator by 2 or 3 orders of magnitude and will also reduce the contribution from a Xe molecular negative ion. This magnet, together with improved vacuum in the electrostatic analyser, should reduce the ^{127}I interference so that it no longer limits the sensitivity. At the same time the sensitivity will be further improved by increasing the $^{127}I^-$ beam current to over 10 μA with a new ion source and by obtaining better transmission in the TOF detector. We anticipate being able to measure $^{129}I/^{127}I$ ratios in 1-mg iodide samples below 10^{-15}, a level that has already been reached with ^{36}Cl detection[16].

We thank T. S. Lund and the rest of the NSRL staff for technical assistance. This work was supported by the NSF Grant 77-29843 and in part by the NSERC of Canada. R. P. B. is a Killam fellow.

Received 10 April; accepted 28 April 1980.

1. Emery, J. F. *et al. Nucl. Sci. Engng* **48,** 319–323 (1972).
2. Edwards, R. R. & Ray, P. *USAEC Rep.* NYO-3624-3 (1969).
3. Purkayastha, B. C. & Martin, G. R. *Can. J. Chem.* **34,** 293–300 (1956).
4. Kohman, T. P. *Carnegie-Mellon Univ. Rep-NYO-844-71,* 50–62 (1967).
5. Edwards, R. R. *Science* **137,** 851–853 (1962).
6. Podosek, F. A. & Lewis, R. S. *Earth planet. Sci. Lett.* **15,** 101–109 (1972).
7. Spernol, A. *et al. Int. J. appl. Radiat. Isot.* **28,** 615–624 (1977).
8. McHugh, J. A. & Sheffield, J. C. *Analyt. Chem.* **37,** 1099–1101 (1965).
9. Brauer, F. P. *Proc. 2nd Conf. Nuclear Methods in Environmental Research* CONF-740701, 328–343 (1974).
10. Rook, H. L., Suddueth, J. E. & Becker, D. A. *Analyst. Chem.* **47,** 1557–1561 (1975).
11. Elmore, D. *et al. Nature* **277,** 22–25, 246 (1979).
12. Kilius, L. R. *et al. Nature* **282,** 488–489 (1979).
13. Hird, B. & Ali, S. P. *Can. J. Phys.* **57,** 867–870 (1979).
14. Lang, W. & Clerc, H.-G. *Nucl. Instrum. Meth.* **126,** 535–539 (1975).
15. Kilius, L. R. thesis, Univ. Toronto (1978).
16. Nishiizumi, K. *et al. Earth planet. Sci. Lett.* **45,** 285–292 (1979).

Channel CO_2 in cordierites

Th. Armbruster & F. D. Bloss

Department of Geological Sciences, Virginia Polytechnic Institute and State University, Blacksburg, Virginia 24061

The formulae commonly cited for cordierite usually ignore the occupants of the structural channels that run parallel to the c-axis. Recently, however, it has been shown[1] that two of the more common channel occupants, Na^+ and molecular H_2O, significantly modify cordierite's refractive indices (α, β, γ), optic angle ($2V_x$), unit cell dimensions, and the distortion index (Δ) defined by Miyashiro[2]. Indeed, for 11 natural cordierites, excluding indialites, Δ correlates almost entirely with channel Na^+ and/or H_2O and with R_a, the average radius of the ions occupying the octahedral sites, but not (as long believed) with Al/Si ordering. After heating at 800 °C for 6 h, Δ increased for the four crystals remeasured, and $2V_x$ increased for the nine optically (−) crystals but decreased to below 90° for the two optically (+) crystals. Selkregg and Bloss[1] attributed these effects to loss of channel H_2O and/or Na^+ but did not explain why the two (+) crystals became (−) after heating. We report here that loss of molecular CO_2, a frequently reported channel occupant[3–5], was the reason. We observe that for Mg-cordierite, $2V_x$ is $\sim$87° if its channels are vacant, decreases to 45° or less as channel H_2O increases and increases to 114° with increasing channel CO_2 (but no H_2O). Channel CO_2 is apparently the long-sought-for cause of optically (+) cordierites.

The previously unexplained occurrences of (+) and (−) cordierites on opposite sides of a fault[6] probably represent control of CO_2 distribution by the fault. The seemingly capricious variation of $2V_x$, for cordierites with comparable Mg/Fe ratios, probably results from channel occupancy by varying proportions of H_2O and CO_2 and, perhaps, other channel occupants. In view of the importance of the channel occupants, the formula for cordierite should perhaps be

$$\mathrm{Na}_{x+2y}(\mathrm{Mg,Fe,Mn})^{\mathrm{vi}}_{2-y}(\mathrm{Al}_{4-x}\mathrm{Be}_x\mathrm{Si}_5)^{\mathrm{iv}}\mathrm{O}_{18}\cdot n[\mathrm{H_2O,CO_2}]$$

where y allows for vacancies in the octahedral sites[1,7] which, like substitution of Be^{2+} for Al^{3+}, seem to correlate with channel Na^+. The formula does not accommodate the tetrahedral vacancies reported by Wallace and Wenk[7], or additional channel occupants, but these might be relatively minor in amount and effect.

Cordierite occurs in a wide variety of metamorphic and igneous rocks and, by its presence or absence, conveys information regarding their conditions of formation. In the ceramic industry, its easy synthesis and high resistance to thermal shock favour its use in spark plugs, catalytic supports to treat automobile exhaust and, in the future, for fabrication of turbine engines. Consequently, solution of the long-standing

0028–0836/80/280140–02$01.00

mystery of why some cordierites are optically (+) but most are (−) seemed important because the factors involved, whether chemical or structural, might influence the stability and conditions of formation of cordierite.

Spindle stage studies[8] of 20 natural cordierites disclosed five to be optically (+) with $2V_x > 90°$. Microprobe analyses revealed no significant compositional differences that correlated with optic sign. However, IR spectra between 200 cm^{-1} and 4,000 cm^{-1} exhibited not only H_2O bands, but also CO_2 absorption bands near 2,350 cm^{-1}. These were intense for the (+) cordierites but weaker for the (−) cordierites. Refractive indices measured to 0.0005 by the double variation method disclosed that the (+) cordierites possessed higher refractive indices and birefringence (γ–α) compared with optically (−) crystals with the same iron content. When heated to 800–1,200 °C to expel the more volatile channel occupants, $2V_x$ increased for the (−) crystals but decreased for the (+) crystals.

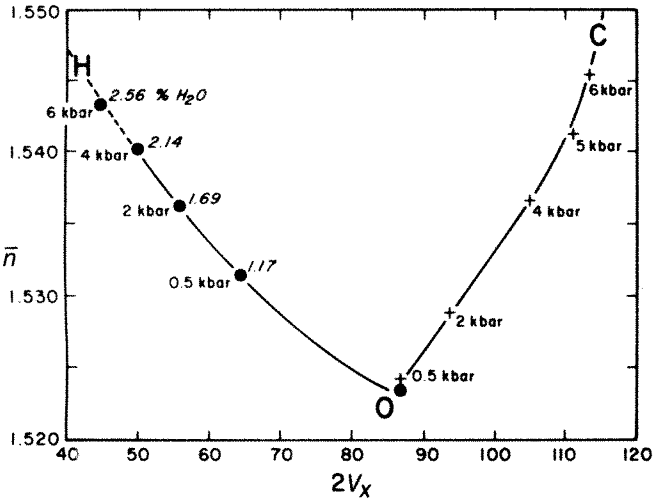

Fig. 1 Plot of the average index $\bar{n}$ [$\bar{n} = (\alpha + \beta + \gamma)/3$] versus $2V_x$ (averaged for wavelengths 400, 666 and 900 nm) for White Well cordierite after tempering at 1,300 °C for 30 h (point O), for this same material after CO_2 was forced into it at increasing CO_2 pressures (plus signs on line OC), and after H_2O was forced into it (● on line HO). The weight percentages of H_2O were estimated using the equations of Medenbach *et al.*[9]. Weight percentages of CO_2 are yet to be determined but the increase in $\bar{n}$ clearly shows that increasing quantities of CO_2 are being forced into the channels as CO_2 pressure increases.

The influence of channel CO_2 and H_2O on the optical properties of Mg-cordierite was more directly investigated using a (−) cordierite from White Well, Australia ($a = 17.065$Å, $b = 9.724$Å, $c = 9.346$Å; optic orientation, $a = Z$, $b = Y$, $c = X$). This specimen's optical properties were measured before and after tempering for 30 h at 1,300 °C in air to expel channel CO_2 and H_2O. Crystals thus tempered were also examined after being annealed for 30 days at 600 °C and at various pressures of H_2O and of CO_2 (from decomposition of $Ag_2C_2O_4$). The results (Fig. 1) clearly reveal the opposite effects on $2V_x$ of CO_2 and H_2O; however, both increase the average index $\bar{n}$ [$\bar{n} = (\alpha + \beta + \gamma)/3$]. Surprisingly, IR spectra of the tempered material taken before its rehydration or recarbonation revealed Si–OH groups and/or H_2O that either survived the 1,300 °C heating or re-entered after heating. Microprobe analyses showed that about half of the channel Na had also survived this heating.

Table 1 reveals that the birefringence (γ–α) increases significantly with CO_2 and that the distortion index Δ decreases significantly with channel H_2O and CO_2. Thus decarbonation of a CO_2-rich cordierite by heating will cause Δ to increase whereas $2V_x$ and (γ–α) will decrease. This inverse correlation between $2V_x$ and Δ as channel CO_2 increases thus opposes the statement of Miyashiro[2] that, in general, the larger Δ, the larger $2V_x$ will be.

Table 1 Optical properties, cell edges* and distortion index Δ for the White Well cordierite†

	Natural	Tempered	Carbonated at 4 kbar	Hydrated at 4 kbar
α	1.5345	1.5235	1.5326	1.5386
c (Å)	9.346	9.340	9.348	9.346
β	1.5392	1.5254	1.5381	1.5440
b (Å)	9.724	9.722	9.723	9.725
γ	1.5423	1.5275	1.5456	1.5450
a (Å)	17.065	17.076	17.059	17.060
(γ–α)	0.0078	0.0040	0.0130	0.0064
Δ	0.243°	0.260°	0.241°	0.237°
$2V_x$ ‡	76.4°	87.0°	105°	50.0°

*From back reflection Weissenberg photographs.
†Optic orientation, $c = X$, $b = Y$, $a = Z$.
‡Average of measurements at 400, 666, and 900 nm.

IR spectra for single cordierite crystals[3] were later interpreted[4] as showing that 80% of the channel CO_2 molecules were aligned perpendicular to c ($= X$) with the other 20% possibly aligned parallel to c. The increases in refractive indices produced by carbonation of the tempered White Well cordierite—$\Delta\alpha = 0.0091$, $\Delta\beta = 0.0127$, $\Delta\gamma = 0.0181$; average increase 0.0133—suggest a dominant alignment of CO_2 parallel to the a-axis ($= Z$) because $\Delta\gamma$ significantly exceeds the average index increase of 0.0133. Alignment of CO_2 molecules parallel to the c-axis is not supported by this present evidence because $\Delta\alpha$ ($= 0.0091$) is significantly below the average increase of 0.0133.

The marked increase in refractive indices with channel CO_2 for cordierite suggests that H_2O contents, if calculated using the measured refractive indices and Fe contents for cordierite[10], will be too high when significant CO_2 is also present. Work in progress indicates that the amounts and relative proportions of channel H_2O and CO_2 will be readily determinable for single crystals of cordierite if spindle-stage measurements of $2V_x$ and refractive indices are followed by microprobe analyses for Na, Fe, Mg, and Mn. We know of no other technique, so relatively simple and routine, that can determine the same data for a single grain. Knowledge of the relative proportions and amounts of the volatile species trapped in the channels of cordierite has potential use as an indicator of metamorphic and magmatic fluids.

We thank Professors G. V. Gibbs, D. A. Hewitt, P. H. Ribbe, and D. R. Wones for criticism of the manuscript and other aid. We also thank Professor Lucian Zelazny for use of the IR equipment in his laboratory. H. R. Wenk loaned us a preprint of the Wallace and Wenk paper.

Received 7 March; accepted 25 April 1980.

1. Selkregg, K. & Bloss, F. D. *Am. Miner.* (in the press).
2. Miyashiro, A. *Am. J. Sci.* **255,** 43–62 (1957).
3. Farrell, E. F. & Newnham, R. E. *Am. Miner.* **52,** 380–388 (1967).
4. Farmer, V. C. *The Infrared Spectra of Minerals* (Mineralogical Society, London, 1974).
5. Goldman, Don S., Rossman, G. R. & Dollase, W. A. *Am. Miner*, **62,** 1144–1157 (1977).
6. Kuznetsova, F. V., Bondareva, G. V. & Russakova, V. A. *Mineralogy of Cisbaikalia*, (ed. Shmakin, B. M.) 147–157 (11th Meet. int. Miner. Ass., 1978).
7. Wallace, J. H. & Wenk, H. R., *Am. Miner*, **65,** 96–111 (1980).
8. Bloss, F. D. *The Spindle Stage: Principles and Practice* (Cambridge University Press, in the press).
9. Medenbach, O., Maresch, W. V., Mirwald, P. W. & Schreyer, W. *Fortschr. Miner.* 1, 57, 99–101 (1979).
10. Lepezin, G. G., Kuznetsova, I. K., Lavrent'ev, Yu. G. & Chmel'nicova, O. S. *Contr. Miner. Petrol*, **58,** 319–329 (1976).

A fault plane solution for the Carlisle earthquake, 26 December 1979

Geoffrey King

Department of Geodesy and Geophysics, Madingley Rise, Madingley Road, Cambridge CB3 0EZ, UK

Deformation at plate boundaries is well determined from the fault parameters of large earthquakes but within plates relatively little is known. Although other methods of measuring *in situ* stress are available only intra-plate earthquakes provide information about stresses at depths of several kilometres[1]. Accurate location and the determination of fault parameters for intra-plate earthquakes is difficult because such earthquakes are rare and generally too small to be widely recorded. This problem has been overcome in parts of the eastern USA by installing permanent dense seismometer networks, and brief aftershock studies of the type described here. Our aftershock study has provided an accurate location of a significant UK earthquake, and a reliable measure of compression direction in a region of Europe distant from the influence of Alpine motion.

On the 26 December 1979 at 03h 57min an earthquake occurred north of Carlisle. The same day the Institute of Geological Sciences (IGS) in Edinburgh reported the shock to be $m_b = 5.0$ and probably located close to Longtown. Their assessment of epicentral position was based on the occurrence, earlier in 1979, of three smaller shocks (now taken to be foreshocks) which occurred in the area. The region has some history of activity with an earthquake occurring in 1786 which was felt at distances of 300 km (similar to the recent earthquake) and a sequence of four earthquakes in 1901 (ref. 2).

Damage from the earthquake was slight but created wide publicity and interest. A preliminary survey of intensity was determined by telephoning local police stations in the area and confirmed the IGS view that an epicentre near Longtown was probable. On the basis of the foregoing evidence, an aftershock study using Sprengnether MEQ800 smoked drum recorders was initiated. Eight instruments were taken by car to Carlisle, arriving in heavy rain and floods, and one instrument was installed at 1800 GMT on the same day as the earthquake. A small earthquake at 05.39 on 27 December confirmed, with a 1.1 s S–P time, that the aftershock sequence was likely to be close to Longtown. An array of instruments indicated in Fig. 1 was deployed. A maximum of seven stations were operated simultaneously. Station 1 was moved because of site noise. Other changes in instrument disposition were carried out in response to preliminary locations with a view to optimizing location accuracy and fault plane solution resolution.

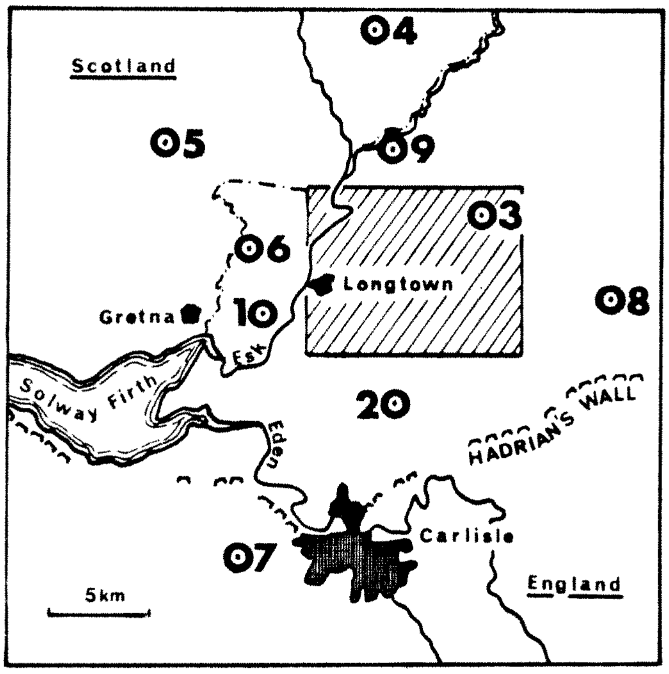

Fig. 1 The area of the survey showing station locations. The shaded area is enlarged in Fig. 2.

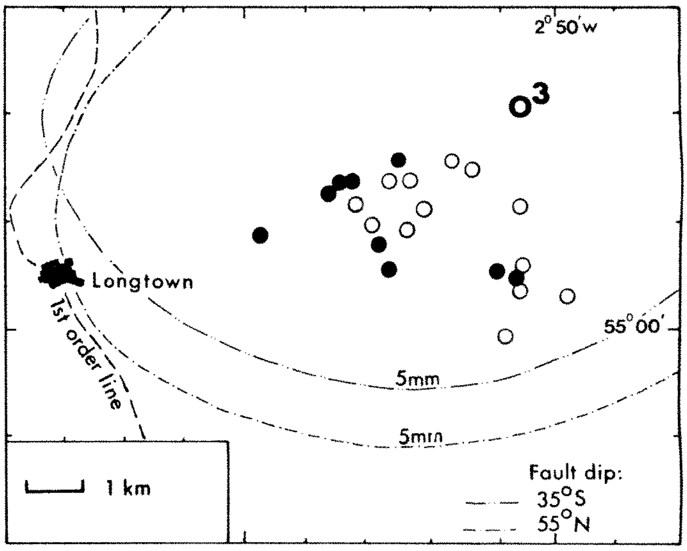

Fig. 2 Epicentral locations. ●, Shocks located with an error less than 1 km; ○, shocks located with an error less than 2 km. The 5-mm contour of predicted uplift is shown for both possible fault planes. The route of a first-order levelling line is also shown. The velocity model used for the locations and the fault plane solution was marginally the best of a set used to test the stability of the locations. It had a 3.3 km s^{-1} layer 1-km thick, a 5.0 km s^{-1} layer 4-km thick, a 5.7 km s^{-1} layer 15-km thick and the Moho velocity was taken to be 8.0 km s^{-1}. Because of the obvious lateral variation of the geology of the region on a scale comparable with the size of the seismograph array and the model insensitivity of the location procedure, the model adopted has no definite geological significance.

Selecting good sites proved impossible with many seismometers placed in the muddy middles of rain flooded fields. This reduced noise from rural roads and noise from the many trees and bushes. However, despite these difficulties, good low noise records were obtained. During the evening of 27 December temperatures dropped well below freezing and the ground remained frozen until after the stations were removed. The improvement of coupling was substantial and some seismometers were chipped out of the ice with difficulty. There was no wind during the recording period and cultural noise was generally low, only increasing on the 2 January 1980; 1 January, 1980 was particularly quiet. Low noise at this time was particularly fortunate as a major burst of seismic activity started in the early hours of the New Year with the major aftershock ($m_b = 3$) of the sequence occurring at 05.06 GMT.

Twenty-seven earthquakes were recorded on four or more stations. Of these 22 provided satisfactory hypocentral locations (with errors less than 2 km) and nine were located to

0028-0836/80/280142-02$01.00

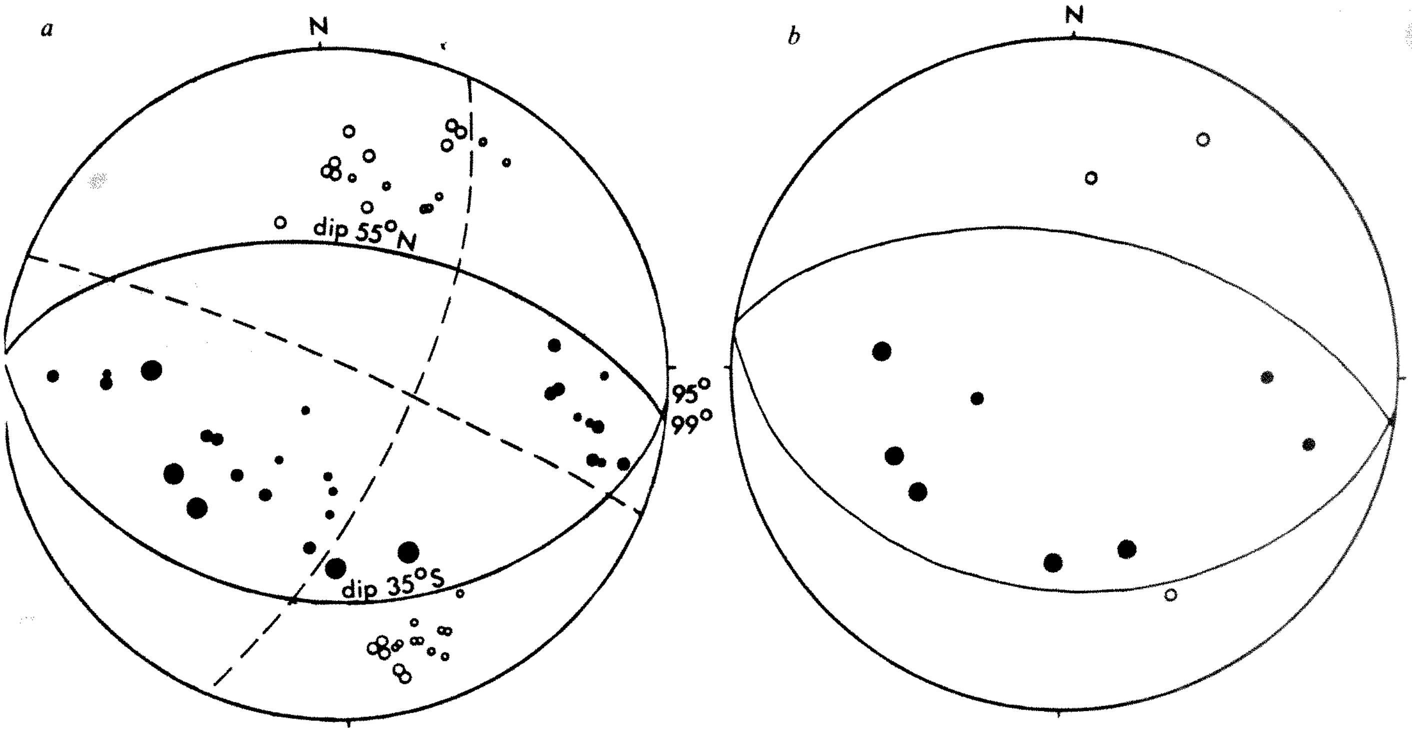

Fig. 3 *a*, Composite fault plane solution for the earthquakes shown in Fig. 2. Large circles, well located earthquakes; small circles, moderately located earthquakes: solid circles, compressions; open circles, dilatations. The very large circles are distant stations, and are all compressional. These latter data constrain the solution to be thrusting shown by solid lines and not strike-slip shown by dotted lines (the aftershock distribution also supports this conclusion). The nodal planes strike at 99° or 95° with dips of 35°S or 55°N respectively. *b*, The fault plane solution using only data for the aftershock at 05.06 GMT on 1 January 1980.

within 1 km. Location was carried out using the HYP071 location program[3] using a rough estimate of velocity structure. No reliable information is available to constrain the shallow velocity structure apart from a general knowledge of the geology and travel time residuals in the location process. However, even velocity structures that caused systematic station residuals to appear did not change most locations by more than 1 km.

Many first motions were clearly readable. These are shown as a composite fault plane solution in Fig. 3*a*. The data from the portable stations alone do not exclude the possibility of a strike-slip solution. However, first motion data from more distant permanent stations for the main shock and some aftershocks exclude the strike-slip possibility.

The consistency of the fault plane solution also indicates that the chosen velocity structure was satisfactory and that the hypocentral depths which range between 3 and 12 km (mostly clustered near 7 km) are reasonable. However, an examination of the depth distribution of aftershocks does not provide any guide to which of the nodal planes in the fault plane solution is the orientation of the fault plane. The scatter suggests that more than one fault plane was involved in the aftershock sequence.

Using the relations described by Kanamori and Anderson[4] the magnitude of the earthquake can be converted to an approximate moment of 8×10^{23} dyn cm. Using a rigidity modulus of 3×10^{11} dyn cm^{-2} and assuming a typical displacement to fault diameter ratio of 10^{-4} (a stress drop of 30 bar) the earthquake source could have been an average of 30 cm of slip on a plane 3.5 km in diameter. The aftershock distribution which has dimensions not much greater than 3.5 km independently supports this rough estimate.

Using a dislocation model[5] the surface displacements for the earthquake can be calculated from the foregoing results. An uplift of 2 cm is expected approximately above the epicentre and the area over which displacement greater than 0.5 cm is predicted is shown in Fig. 3. A first-order levelling line crosses the region[6] and displacements on this line should be observable.

No direct guide to the nature of the source is provided from the geology of the area. In the region of the aftershocks the surface is covered by alluvium generally not more than a few tens of metres thick. Beneath this is some 600 m of Triassic sandstone with shales (perhaps with conglomerates at the base) and this in turn overlies 800–1,600 m of Carboniferous limestones interbedded with sandstones. The Carboniferous rests unconformably on Upper Silurian sediments (greywakes) folded and probably tilted near to vertical. This sequence is thought to extend to a depth of around 12 km.

All hypocentral locations lie within the Upper Silurian which is extensively faulted where it is exposed. Recent work has drawn attention to a major suture in these formations (the Iapetus suture) thought to pass through the region of the earthquake[7,8]. It is possible that the Carlisle earthquake is a reactivation of planes of weakness broadly associated with this suture.

I thank Graham Nielson and Chris Browitt of the IGS Edinburgh for advice and information, and Jerry Leggett for describing the geology of the region. The NERC are thanked for providing equipment and rapidly funding the venture. Peter King and Moira Dunlop provided field assistance.

Received 26 February; accepted 25 April 1980.

1. Sykes, L. R. *Rev. Geophys. Space Phys.* **16,** 621–688 (1978).
2. Davidson, C. *History of British Earthquakes* (Cambridge University Press, 1924).
3. Lee, W. H. K. & Lahr, J. C. *U.S. Geol. Surv. Open-File Rep.* 75–311 (1975).
4. Kanamori, H. & Anderson, D. L. *Bull. seism. Soc. Am.* **65,** 1073–1095 (1975).
5. Mansinha, L. & Smylie, D. E. *Bull seism. Soc. Am.* 1433–1440 (1971).
6. Close, C. *Abstracts of the Primary Lines of the Second Levelling in England and Wales* (Ordnance Survey Office, Southampton, 1921).
7. Phillips, W. E. A., Stillman, C. J. & Murphy, T. *J. geol. Soc. Lond.* **132,** 579–609 (1976).
8. Leggett, J. K., McKerrow, W. A. & Eales, M. H. *J. geol. Soc. Lond.* **136,** 755–770 (1979).

Ocean bottom seismograph measurements in the Central Aleutians

Cliff Frohlich*, John G. Caldwell†, Alexander Malahoff‡, Gary V. Latham* & Jeff Lawton*

*Marine Science Institute, University of Texas, 700 The Strand, Galveston, Texas 77550
†4806 Grapevine, Houston, Texas 77045
‡National Ocean Survey, Cx4 NOAA Administration, Rockville, Maryland 20852

Bathymetric profiles of most oceanic trench regions show a well-defined outer rise seawards of the trench with numerous normal faults between the trench axis and the crest of the outer rise. Several investigators (see ref. 1 for review) have shown that the gross bathymetric features can be modelled quite well if they result from a simple mechanical bending of the subducting lithospheric plate. These results have encouraged searches for seismic evidence of the bending stresses predicted by the models. However, the available teleseismic studies[2] do not determine precisely the relative depths of events on the outer rise, or the precise locations of events relative to the trench. In 1979 we successfully deployed nine ocean-bottom seismometers[3] (OBS) which operated for 6 weeks on the outer trench slope in the Central Aleutians between the trench axis and the crest of the outer rise (Fig. 1). The locations, depths and focal mechanisms of the earthquakes located by this network all strongly support the bending hypothesis. In particular, we observed a band of seismicity on the outer trench slope extending ~60 km seaward of the trench axis (Fig. 1). The shallow events (Fig. 2) exhibit normal faulting (Fig. 3) and suggest tension in the upper part of the plate, while the deeper events (Fig. 2) exhibit thrusting mechanisms and suggest compression (Fig. 3). We suggest here that low magnitude seismic activity may be a common feature associated with the well-known normal faulting on the outer trench slope.

The 1979 OBS network located about 100 earthquakes (Fig. 1), including 30 events seaward of the trench axis. Eight of the OBS stations were deployed in an array (Fig. 1) of interlocking triangles with a station spacing of ~30 km. These eight stations covered a rectangular area ~40 km wide, extending from the trench axis to ~60 km seaward of the trench axis. A ninth station (Fig. 1) was deployed ~120 km seaward of the trench axis. No events were located more than 60 km seaward of the trench axis, and (S–P) times observed at the seawardmost station suggest that no such events occurred.

Nineteen of these events were located within about 20 km of the array, and 11 should have especially well determined depths, as they were observed at four or more stations with at least some observations of both P and S phases. Of these 11 events, the depths of seven were shallower than 13 km below sea level, or within about 6 km of the ocean floor, and the remaining four events were located with depths between 30 and 50 km below sea level. None of these earthquakes were located between depths of 13 and 30 km. The station spacing of 30 km allows the determination of relative depths with a precision of 10–15 km for events within or near the station network. Although location using alternate velocity models alters the depths determined for the events, the group of seven events shallower than 13 km remained distinctly shallower than the group of four events deeper than 30 km when these events were located using several different velocity models.

Previously, very little seismic activity has been reported seaward of the trench axis near the site of the present study. Near the trench only one teleseismic event with a tensional focal mechanism has been reported within ~400 km of our network[2,4], the event of 22 February 1958, with magnitude 6.75. No events were located seaward of the trench by a network of eight OBS stations that operated on the inner trench wall for 6 weeks in 1978 (Fig. 1). In addition, none of the events located seaward of the trench by the 1979 OBS network were located by the Adak network of seven land stations (Fig. 1) on the volcanic islands ~140 km north of the trench. In this region only 10 events, all with magnitude between 3.0 and 4.9, have been located by the Adak land network[5] since its installation in 1974. Apparently events seaward of the trench axis are seldom observed by stations landward of the trench either because phases from them are attenuated by structures in or near the trench, or else simply because most of the events are quite small. However, our data show that events with magnitudes of 2.0 and smaller do occur quite regularly in the zone seaward of the trench axis.

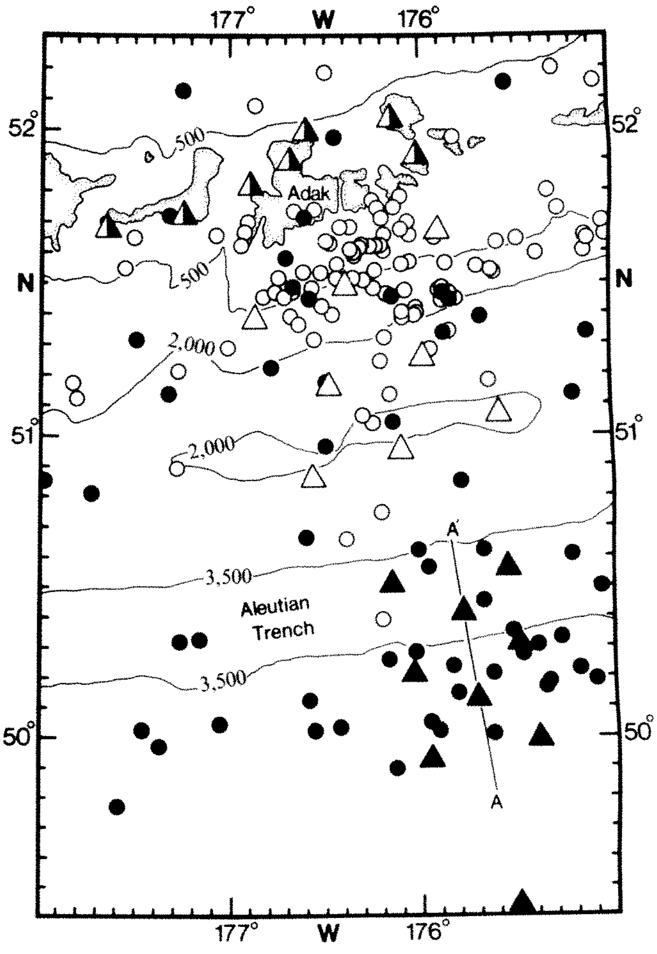

Fig. 1 Location of OBS and land stations in the Central Aleutians, and events located by the 1978 and 1979 OBS network; ▲, 1979 OBS station; △, 1978 OBS station; ◭, land station; ●, earthquake located by 1979 OBS stations; ○, earthquake located by 1978 OBS stations. Bathymetric contours are in fathoms. These events were located by using a program written by C.F. and a layered crustal structure similar to that used by Engdahl[5]. The line between A and A′ shows the location of the cross-section in Fig. 2.

With one exception, all the clear first motions of the events within our net were compressions (Fig. 3). For the shallow events, these compressional observations all lie near the edge of the projection of the focal sphere. This does not constrain the focal planes, but for a double couple mechanism, the observations are consistent only with normal faulting. For the deeper events, all the first motions lie in the centre of the projection of the focal sphere. As before, these observations do

0028–0836/80/280144–02$01.00

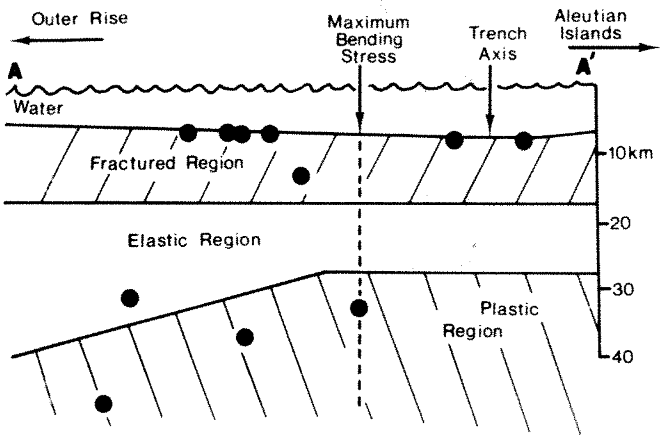

Fig. 2 Vertical cross-section perpendicular to strike of Aleutian Trench (Fig. 1) showing depths of 11 especially well-recorded earthquakes (●) that occurred within or close to the 1979 OBS network (no vertical exaggeration). Note that the Pacific plate extends to the left of the figure, and that it becomes subducted to the right of the figure beneath the Aleutian Islands. The depth chosen for each of these events is that of the minimum weighted r.m.s. residual on plots of r.m.s. residual versus depth. The location of the zone of maximum bending stress as well as the extent of the fractured, elastic and plastic regions were determined by Caldwell[7] from a study of the bathymetry in the Central Aleutians. For a model with a horizontal compressive stress of 5 kbar, he found that the effective elastic thickness of the lithosphere was ~55 km about 120 km seaward of the trench axis, but that the bending causes the elastic portion of the lithosphere to thin to ~10 km near where the maximum bending stress occurs 18 km seaward of the trench axis. Beneath the elastic zone, the compressional stresses exceed the elastic yield stress, producing earthquakes with compressional (thrusting) mechanisms below a depth of ~25 km. The upper 10–15 km of the lithosphere is a region of little strength[2,8], where extensional fractures produce normal faulting events.

not constrain the focal planes, but in this case are consistent only with a thrusting mechanism.

These observations are consistent with normal faulting mechanisms in a shallow zone of extension a few km deep, overlying a quiet zone extending to a depth of ~30 km, which in turn overlies a zone of compression between 30 and 50 km which produces thrusting events. These results are quantitatively consistent with an elastic–plastic model[6] of the lithosphere with parameters determined solely from the bathymetry in the Central Aleutians[7] (Fig. 2). The extremely shallow events with tensional mechanisms are produced by extensional failure in the weak upper portion of the bending plate, while the deeper events occur where the compressional bending stresses exceed the yield stresses in the lower portion of the plate. From our data, the presence of seismicity seaward of the trench axis (Fig. 1) suggests that the yield stress is exceeded to at least 60 km from the trench axis.

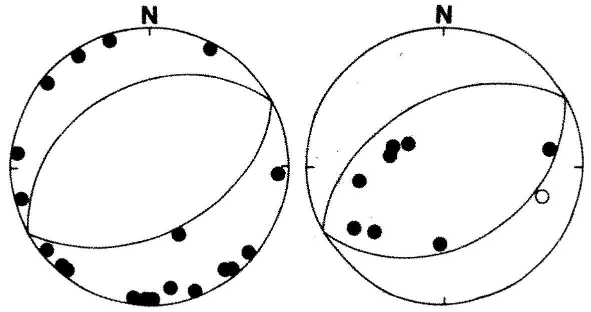

Shallower events Deeper events

Fig. 3 Composite first motions for the seven shallowest events and the four deeper events that appear in the cross-section (Fig. 2). Compressions (●) and dilatations (○) are plotted on an equal area lower hemisphere projection. The focal planes shown are not constrained by the available first motions, but show clearly that the shallow events are consistent with tensional stresses oriented normal to the trench axis, whereas the deeper events are consistent with compressional stresses oriented normal to the trench axis.

Although we have determined reliable depths for only a few events, the present study provides the strongest seismic evidence available suggesting that plate bending occurs on the outer trench slope. Previously, earthquakes whose (S–P) times indicated they occurred seaward of the trench have been detected by an isolated OBS station on the outer trench slope[9], but this station could not locate the events. The uncertainty in the locations of our located events (Fig. 2) is considerably smaller than is possible for teleseismically located events, although our results are generally consistent with teleseismic observations of events seaward of the trench in several island arcs[2,10].

We thank Selena Billington and Wayne Pennington for useful discussions, and Jim Dorman, A. K. Ibrahim and Don Forsyth for reviewing an earlier version of this manuscript. This work was funded by the National Ocean Survey under contract MO-A01-78-00-4120, and cooperative agreement NA79AA-H-0082. We also appreciate the hospitality and support of the captain and crew of the NOAA ship Discoverer, from which we deployed the OBS stations.

Received 10 March; accepted 11 April 1980.

1. Forsyth, D. W. *Rev. Geophys. Space. Phys.* **19**, 1109–1114 (1979).
2. Chapple, W. M. & Forsyth, D. W. *J. geophys. Res.* **84**, 6729–6749 (1979).
3. Latham, G. V. *et al. Offshore Tech. Conf.* 1467–1470 (1978).
4. Stauder, W. *J. geophys. Res.* **73**, 7693–7701 (1968).
5. Engdahl, E. R. *Am. geophys. Un. Monogr.: Ewing Ser* **1**, 259–271 (1977).
6. McAdoo, D. C., Caldwell, J. G. & Turcotte, D. L. *Geophys. J. R. astr. Soc.* **54**, 11–26 (1978).
7. Caldwell, J. G. thesis, Cornell Univ. (1978).
8. Caldwell, J. G. & Turcotte, D. L. *J. geophys. Res.* **84**, 7572–7576 (1979).
9. Nagumo, S. & Kasahara, J. *Am. geophys. Un. geophys. Monogr.* **19**, 155–167 (1976).
10. Hanks, T. C. *J. geophys. Res.* **84**, 2343–2347 (1979).

Northern Hemisphere sea-ice and glacial development in the late Cenozoic

Stanley V. Margolis

Department of Oceanography, University of Hawaii, Honolulu, Hawaii 96822

Yvonne Herman

Department of Geology, Washington State University, Pullman, Washington 99164

Evidence for the initiation of glacial ice-rafting, and for the development of sea-ice cover has been found in sediment cores from the central Arctic Ocean spanning early Pliocene (~4.5 Myr BP) to Recent time. The glacial evidence reported here includes ice-rafted quartz grains, exhibiting glacially formed surface features, and benthic foraminifera endemic to continental shelves in core sediments from the Alpha Rise. The oldest evidence of ice-rafting occurs in sediments palaeomagnetically dated at ~4.5 Myr BP. Variations in sediment facies indicate varying climatic regimes, and degrees of icecover in the Arctic Ocean since early Pliocene time.

Planktonic foraminiferal fauna compositions and surface features of quartz sand grain in sedimentary cores recovered from drifting ice platforms in the Arctic Ocean from the crest and upper flank provinces of the Alpha Cordillera (Table 1) have been analysed to determine the history of sea ice

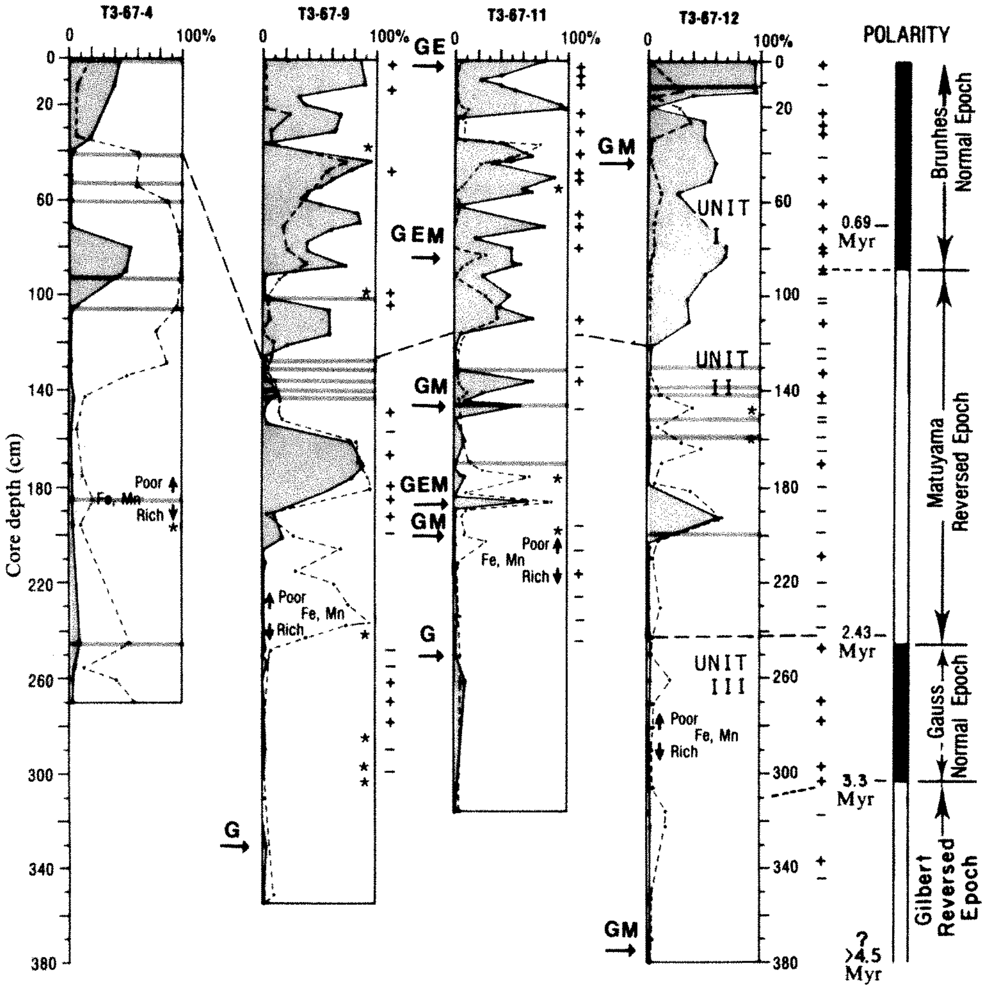

Fig. 1 Palaeomagnetic time scale[1] (right) and percentage of microfauna in coarse fraction (>62 µm) in cores T3-67-4, -9, -11, and -12. Shaded areas, microfauna; white areas, clastic particles. Dashed line and dots represents the percentage of the total planktonic foraminiferal population composed of *G. quinqueloba* and *G. egelida*. Dark horizontal bands are zones in which benthic foraminifers constitute 10% of the total fauna. *, low latitude planktonic foraminifera; +, −, magnetic polarity determinations[1, 11–18]. Dashed lines between cores show age and unit correlations based on palaeomagnetics and lithology. Arrows indicate levels from the cores where quartz sand grains were analysed, and the letters on top of arrows indicate environmental determinations: G, glacial surface features; M, marine (subaqueous abrasion) features; E, aeolian features[3,4]. Figure modified after ref. 2.

development, iceberg production and polar ice-cap growth of the surrounding continents. Magnetic stratigraphy of these cores[1] and radiometric dates, together with biostratigraphic and lithological correlations (Fig. 1), provide age control points since the early Pliocene[2]. N. D. Opdyke (personal communication) has suggested that core T3-67-12 contains the Gauss/Gilbert boundary at a depth of about 310 cm, and that the bottom of the core is between 4.5 and 5 Myr old. R. Z. Poore (personal communication) thinks that the bottom of this core is still in Gauss sediments with a maximum age of ~3.0 Myr. Opdyke's interpretation is shown in Fig. 1. Within this time interval, we have recognized three major oceanic sediment regimes in the Arctic, here represented as climatic units. The earliest, Unit III, contains sediments deposited between ~4.5 and 2.5 Myr (ref. 1) and consist of manganese–iron micronodule-bearing red clays. Rock fragments and mineral grains of ice-rafted origin were identified from three samples from this unit (Fig. 1). As this represents perhaps the oldest described evidence of Arctic Ocean ice-rafting, confirmation of the glacial (ice-rafted) origin of these sediments was sought by scanning electron microscopic examination of surface features on sand grains for environmental determinations[3,4]. Quartz sand grains from Unit III from sediments ~4.5 Myr BP (ref. 1) exhibit surface features (Fig. 2) consistent with a cycle of glacial abrasion before their transport to this region from the surrounding shelves and/or continents. Quartz sand grains were selected from the >62 µm washed fraction from representative sections of each climatic unit. The samples examined are indicated by arrows on Fig. 1. Two samples, not illustrated, from Drill Station A-4 (Table 1) which contains sediments of Brunhes age belonging to Unit I were also examined and found to contain glacial and glacial marine features. About 50 grains were selected randomly from each sample, to represent the range of sizes and shapes present. The grains were petrographically examined to ensure that they were unicrystalline quartz, and then examined by scanning electron microscopy to determine the occurrence and distribution of environmentally diagnostic surface features as described in refs 3, 4. A more thorough presentation of these data will be published elsewhere. Grains also show evidence of subaqueous abrasion (Fig. 2) indicative of either current or wave action after the glacial abrasion. The grains examined from these samples correspond to the 'glacial' and 'glacial marine' categories[3,4]. Sand grains such as these could be derived from glacial deposits from the continental regions surrounding the Arctic Ocean, as well as from shelves, and transported by icebergs, shelf ice, or sea ice hundreds of kilometres to their present site.

The funa in sediments from Unit III is sparse, constituting <1% of coarse fraction (>62 µm, Fig. 2). The planktonic foraminifera are dominated by the robust, polar, left-coiling *Neogloboquadrina pachyderma* complex, some of which are corroded. Shell fragments are abundant, and the solution susceptible tests of juvenile specimens are rare in this unit.

Scattered occurrences of low latitude planktonic foraminifers in this unit as well as in the 'foraminifera-poor' layers of Units II and I have been reported elsewhere[2,5] (Figs 1,3). Their presence was suggested to be due to transport by ocean currents from the Atlantic and Pacific during periods of more active water exchange between the Arctic and adjacent oceans[6] or to transport by shelf ice (Y. H. unpublished data). Barents Sea data indicate that shells of planktonic organisms carried from low latitudes by the warm Norway Current and deposited on the floor of the Barents Shelf may have been incorporated into grounded shelf ice. Subsequently, during periods of calving and drift over the Arctic, the incorporated debris was dropped to the sea floor. Benthic foraminifera are represented by deep-water (solution-resistant) agglutinated forms and robust, calcareous elements^{2,5}. Rare, shallow-water elements are also present, indicating transport by icebergs and/or islands from shelf areas^{2,5}.

The Unit III/II boundary is defined by simultaneous lithological and faunal changes, and coincides very roughly with the Gauss/Matuyama boundary (Fig. 1). The change is from the red clays in Unit III to tan silts in Unit II, which contain more abundant coarse ice-rafted sediments. Ice-rafted quartz sand grains from this unit differ from those of Unit III not only in abundance, but also in their surface features. Grains from Unit II show a greater percentage of subaqueous abrasion, overgrowths, and also aeolian features in comparison to features of glacial origin (Fig. 2). The aeolian/subaqueous/glacial combination are typical of periglacial environments presently found in Alaska^{3}.

Planktonic foraminifers in Unit II are dominated by the extant subpolar species *Globigerina egelida* and *Globigerina quinqueloba*. These two solution susceptible species constitute up to 99% of the fauna in cores raised from depths shallower than ~2,400 m; however, their relative abundance decreases considerably in deeper water sediments^{2,5} (Figs 1 and 3). The right-coiling subpolar *N. pachyderma* complex attains highest frequencies in this unit's sediments^{5} (Fig. 3).

The benthic foraminifers have both deep- and shallow-water representatives. Among the latter, species belonging to *Elphidium*, endemic to continental shelves, are abundantly represented, constituting up to 50% of the benthic elements (Fig. 3). Deep-water species are varied, both calcareous and arenaceous elements being common^{5}.

The Unit II/I boundary is again defined by both faunal and lithological changes, and occurs near the Brunhes/Matuyama magnetic boundary^{2} (Fig. 1). Brunhes sediments, representing the last major climatic regime, are composed of alternating foraminifera-rich and foraminifera-poor layers. The former represent conditions similar to those prevailing today (perennial sea–ice cover)^{5}; the latter perhaps short, milder, lower salinity intervals, comparable to those of the Matuyama epoch. The planktonic fauna is dominated by the polar left-coiling *N. pachyderma* complex; however, *G. quinqueloba*, capable of withstanding low salinities (Y.H. unpublished data), attains high frequencies near several of the foram-rich/foram-poor boundaries; benthic foraminifers are varied and ice-rafted debris is scattered throughout Brunhes sediments (Figs 1 and 3).

Two samples from the foram-rich zones of Unit I show surface features indicative of glacial marine and aeolian periglacial origin (Fig. 2), while grains from the foram-poor zones show typical glacial surface features similar to those from Unit II Matuyama sediments.

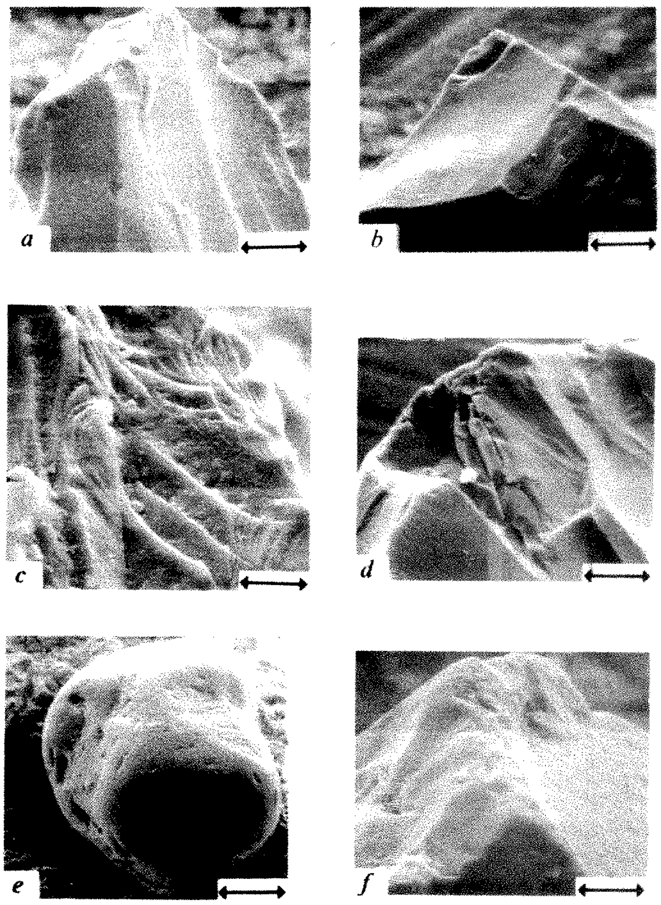

Fig. 2 Scanning electron micrographs of quartz sand grains from Arctic Ocean cores shown in Fig. 1. *a*, Sand grain from core T3-67-9, 330 cm depth (Unit III). Showing sharp angular outline, step shaped fractures and conchoidal fractures; typical of grains subject to glacial action, scale bar, 20 μm. *b*, Edge of quartz grain from core T3-67-12, 375 cm depth (Unit III), showing conchoidal fractures, semi-parallel steps, striations, and other features shown in *a*, scale bar, 20 μm. *c*, Sand grain from core T3-67-11, 85 cm depth (Unit I) showing high relief, large breakage blocks and conchoidal fractures typical of grains of glacial origin, scale bar, 10 μm. *d*, Grain from core T3-67-11, 188 cm depth (Unit II) showing typical glacial surface features over a larger area of the grain, scale bar, 20 μm. *e*, Grain from core T3-67-11, 188 cm depth (Unit II) showing abrasion features and rounded outline typical of grains with a history of marine-subaqueous transport, scale bar, 200 μm. *f*, Grain from core T3-67-9, 330 cm depth (Unit III) showing glacial features modified by aeolian features along right-hand margin, and on centre ridge, scale bar, 20 μm.

The differences between quartz grains from the three units can be summarized as follows: samples from Unit III contain fewer and smaller (<250 μm) grains and higher percentage of rounded aeolian and subaqueously abraded grains. Grains with glacial evidence also show superimposed features of subaqueous and aeolian origin. Samples from Unit II contain a greater number of large (>250 μm) and angular grains, exhibiting a mixture of aeolian and subaqueously abraded features. Unit I samples contain many large angular grains of glacial origin, with relatively few grains of mixed transport cycles.

Table 1 Locations, depths and lengths of cores

Core	Lat.	Long.	Depth (m)	Length (cm)
D.St.A.2	83°52′N	168°12′W	1,521	206
D.St.A.4	84°21′N	168°49′W	2,041	116
T3-67-3	79°11′N	175°09′W	2,285	380
T3-67-4	79°22.7′N	174°46′W	1,760	272
T3-67-9	79°37.9′N	172°07′W	2,237	356
T3-67-11	79°34.9′N	172°30′W	2,810	250
T3-67-12	80°21.9′N	173°33′W	2,867	374

The number of quartz grains of glacial increases in progressively younger sediments, while there is a decrease in the number of grains exhibiting features of mixed origins. In Brunhes sediments, however, there seems to be periods during which sediment transport conditions similar to those of the Matuyama prevailed.

There is relatively little information on pre-Pleistocene sediments from the Arctic Ocean. Ling *et al.*^{7} reported evidence for a warm, ice-free Arctic Ocean during Eocene and later times. A warm, temperate Arctic climate for the Palaeogene is discussed by Frakes and Kemp^{8}. The evidence of vigorous vertical mixing and relatively high biological production of the Arctic surface water preclude the existence of perennial ice cover between the late Miocene and the late Pliocene^{2,5,9}.

About 2.5 Myr ago a dramatic change in the structure of the Arctic Ocean water masses occurred, including the inception of density stratification. A stable, low-salinity, surface-water mass,

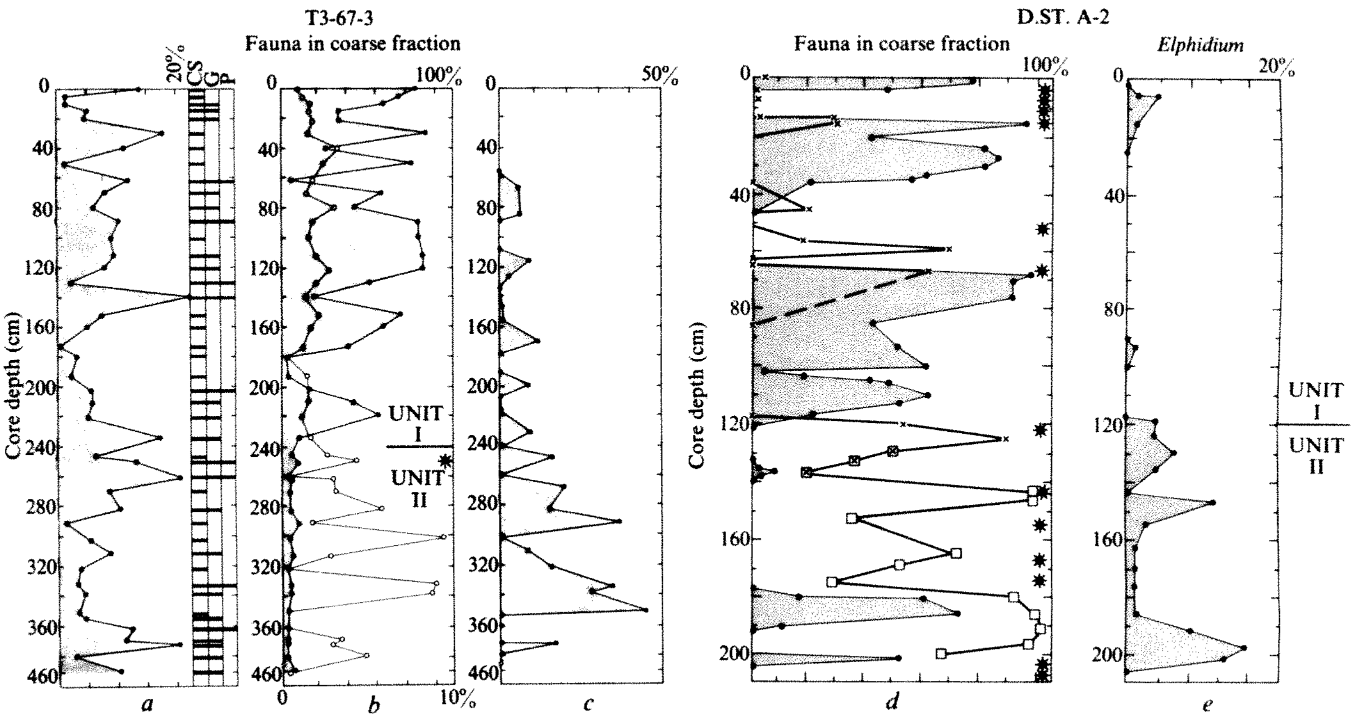

Fig. 3 Core T3-67-3. *a*, Percentage of coarse fraction (>62 μm). CS, coarse sand; G, granules; P, pebbles. *b*, Percentage of microfauna in the coarse fraction (>62 μm). Shaded areas represent the microfauna, white areas the clastics; values are indicated at the top of the diagram. ○, percentage of dextral *G. pachyderma* out of the total *G. pachyderma* population; values are indicated on the abcissa at the bottom of the diagram. *, low latitude planktonic foraminifera. *c*, Percentage of *Elphidium* spp. out of the total benthic foraminiferal fauna. (Modified after ref. 2.) *d*, Percentages of microfauna in the coarse fraction (>62 μm), D. Sta A2. Shaded areas represent the microfauna, white areas the clastic material. ×, percentages of *G. quinqueloba* out of the total planktonic foraminiferal fauna. □, percentages of *G. egelida* of the total planktonic foraminiferal fauna. *, low latitude planktonic Foraminifera. *e*, Percentages of *Elphidium* spp. a shallow-water genus out of the total benthic foraminiferal fauna. (Modified after ref. 2.) Drill Station A2.

essential for sea ice formation, was developed at this time[2,5]. Whether temperatures were sufficiently low for pack ice to form, even seasonally, cannot be ascertained for certain with the present data. While most data suggest that global Matuyama temperatures were higher than Brunhes temperatures (see refs 11–17), Kennett[18] interprets his results to indicate the opposite. It can be assumed, however, that given the stratification, sea-ice cover was present during the winter. A major climatic threshold was crossed ~0.7 Myr ago, when, as a result of continued global cooling, perennial sea-ice cover developed over the Arctic Ocean[2,5].

Clark, however, has stated that the Arctic Ocean has been covered continuously with perennial ice from the middle Cenozoic to the present and that the ice cover was much thicker during the deposition of the 'foraminifera-poor beds' than today[19]. At present, the ice attains thicknesses of 3–4 m at the end of winter, decreasing to ~2–3 m in summer[20]. Field observations and theoretical calculations indicate that sea ice reaches an equilibrium thickness at ~4 m (ref. 21). Furthermore, evidence exists for much drier climates, with reduced snowfall during glacial episodes in the north polar region. This is a direct consequence of increased continentality caused by broadening of coastal plains due to lowered sea level[9], and reduction of moisture available to the atmosphere when ice covered extensive land and ocean areas.

Recently discovered calcareous nannofossils in Unit III sediments as well as in 'foraminifera-poor zones' and in transition sediments between foraminifera-poor and foraminifera-rich zones also preclude the existence of perennial ice cover during the deposition of these sediments[22] and further supports the interpretation of Herman[2,5] concerning the evolution Arctic oceanic-climate during the past 5 Myr.

Glacial–marine (ice-rafted) sediment was previously reported from the North Pacific Ocean by Krinsley[23] who found glacial surface features on quartz grains of late Pliocene age from DSDP site 178 (Alaskan Abyssal Plain). Other investigators[24–26] found evidence of ice-rafting in the North Pacific, Bering Sea, and the Norwegian–Greenland Seas in sediments of middle Pliocene age (≃2.4–3 Myr old), which is consistent with the oxygen isotopic evidence for major development of Northern Hemisphere glaciers about this time[27]. One core raised at site 344 (76°08.98′N; 07°52.52′E) contains glacial marine sediments throughout the Pliocene. It is not certain whether the entire Pliocene was recovered nor what processes of sedimentation were responsible for the deposition of the glacial marine debris: "ice rafting, turbidity currents or sedimentary suspension in water" has been suggested.

Occurrence of ice-rafted quartz sand grains and shallow-water benthic foraminifers endemic to continental shelves on the crest and upper flank provinces of the Alpha Rise in sediments deposited ~4.5 Myr ago[2] firmly establishes that high latitude Northern Hemisphere mountain glaciers developed and perhaps extended to sea level at least as early as the early Pliocene. In addition, the variations in sediment types, microfaunal and floral compositions, and abundance of ice-rafted and glacially produced detritus, all indicate the history of development of ice cover in the Arctic Ocean. Corroboration by similar data from other Arctic Ocean sites would make this date highly significant with respect to our understanding of the chronology of Northern Hemisphere glaciations and the eventual onset of the Pleistocene glacial/interglacial climatic cycles. Oxygen isotope analysis of calcareous foraminifera and nannoplankton from these cores is planned to correlate these sediment sequences with isotopic stratigraphies established elsewhere in the world's oceans.

We thank Kenneth Hunkins and his colleagues for collecting the cores, R. R. Capo and Floyd W. McCoy for sampling and shipping the core samples, D. M. Hopkins, R. Poore and J. Kennet for reviews. Coring operations were supported by several ONR grants to K.H. Curatorial services were supported by Lament-Doherty Geological Observatory grants ONR N00014-75-C-0210 and NSF DES 72-01568 A03. S.V.M. was supported by NSF grants OCE76-81961 and OCE78-25283, and by RHREP grants to Y.H.

Received 18 October 1979; accepted 21 April 1980.

1. Hunkins, K., Be, A. W. H., Opdyke, N. D. & Mathieu, G. in *The Late Cenozoic Glacial Ages* (ed. Turekian, K.) 215 (Yale University Press, 1971).
2. Herman, Y. *Marine Geology and Oceanography of the Arctic Sea* 283 (Springer, Berlin, 1974).
3. Margolis, S. V. & Kennett, J. P. *Am. J. Sci.* **271,** 1 (1971).
4. Margolis, S. V. & Krinsley, D. H. *Am. J. Sci.* **274,** 449 (1974).
5. Herman, Y. *Science* **169,** 474 (1970).
6. Herman, Y. *Nature* **201,** 386 (1964).
7. Ling, H. Y., McPherson, L. M. & Clark, D. L. *Science* **18,** 1360 (1973).
8. Frakes, L. A. & Kemp, E. M. *Nature* **240,** 921 (1972).
9. Herman, Y. & Hopkins, D. M. *Science* (in the press).
10. Dawson, M. R., West, R. M., Langston, W. Jr & Hutchinson, J. H. *Science* **192,** 781 (1976).
11. Donahue in *Progr. Oceanogr.* (ed. Sears, M.) 133 (Pergamon, New York, 1967).
12. Hays, J. D. & Opdyke, N. D. *Science* **158,** 1001 (1967).
13. Olsson, R. K. *Init. Rep. DSDP* Leg **5,** 557 (1970).
14. Bandy, O. L., Casey, R. E. & Wright, R. C. *Antarctic Res. Ser.* 15, **4,** 1 (1971).
15. Casey, R. E. *Palaeogeogr. Palaeoclimat. Palaeoecol.* **12,** 115 (1972).
16. Ingle, J. C. Jr *Init. Rep. DSDP* Leg **18,** 949 (1973).
17. Poor, R. Z. & Berggren, W. A. *J. Foram. Res.* **4,** 91 (1974).
18. Kennett, J. P. *Deep Sea Res.* **17,** 125 (1970).
19. Clark, D. L. *Bull. geol. Soc. Am.* **82,** 3313 (1971). Clark, D. L. *Can. Soc. petrol. Geol. Mem.* **4,** 501 (1975).
20. Charlesworth, K. *The Quaternary Era* (Arnold, London, 1957).
21. Maykut, G. A. & Untersteiner, N. *J. geophys. Res.* **76,** 1550 (1971).
22. Worsley, T. & Herman, Y. *Science* (in the press).
23. Krinsley, D. H. *Init. Rep. DSPD* Leg 925 (1973).
24. Kent, D., Opdyke, N. D. & Ewing, M. *Bull. geol. Soc. Am.* **82,** 2741 (1971).
25. Schroll, D. W. & Creager, J. S. *Init. Rep. DSDP* Leg **19,** 897 (1973).
26. Schrader, H. J., Bjorklund, K., Manum, S., Martini, E. & van Hinte, J. *Init. Rep. DSDP* Leg **38,** 1197 (1976).
27. Shackleton, N. J. & Kennett, J. P. *Init. Rep. DSDP* Leg **29,** 801 (1975).
28. Talwani, M. *et al. Init. Rep. DSDP* Leg **38,** 389 (1976).

Why are distasteful prey not cryptic?

John L. Gittleman & Paul H. Harvey

School of Biological Sciences, University of Sussex, Falmer,
Brighton BN1 9QG, UK

Bright coloration among unpalatable prey is common[1]. Turner[2] has suggested that, as with Fisher's explanation for the evolution of distastefulness itself[3], such aposematic coloration has been favoured by kin selection. Distasteful aposematic prey tend to live in kin groups and predators sampling from such groups will learn to avoid conspicuous prey more readily than cryptic prey and, as a consequence, fewer members of conspicuous kin groups are preyed upon[2,4–6]. We know of no clear evidence that vertebrate predators take fewer trials when learning to avoid conspicuous rather than cryptic distasteful prey[6,7]. Here we report results from a series of experiments that provide such evidence.

For 3 days post-hatch, male Warren Sex-Link chicks were fed on dyed blue and green chick crumbs of equal size, hue and texture, that were presented on a grey background against which we could detect no selective predation[8]. On day 4, individual chicks were placed in a holding box for 1 min before being released through a sliding door into a testing arena (80 × 60 cm) with a hardboard painted floor. The floor was interchangeably blue or green and on it were scattered 1,000 chick crumbs which had been made distasteful (by including 4 g quinine sulphate and 2 g mustard powder per 100 ml of dye solution). At this density the crumbs do not act as background to each other and selective predation by the chicks is similar to that at lower densities[9]. The crumbs were all the same colour, either blue or green. Individual chicks were allowed to feed for 2 min and were retested every hour for 13 h, that being the number of trials after which each chick had refused food on at least one occasion. Details of housing, lighting conditions, food preparation, the testing arena and feeding before experimentation, are as described elsewhere[7]. There were four treatments—floor and food blue, floor and food green, floor blue and food green, floor green and food blue—with nine chicks assigned to each.

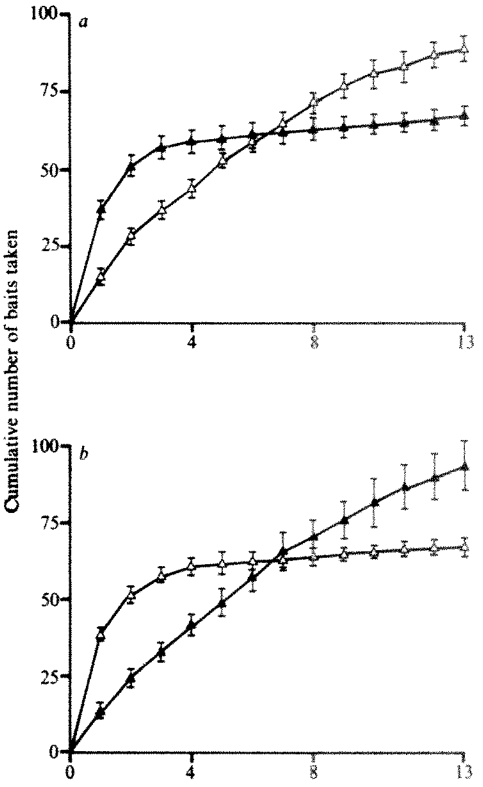

Fig. 1 Cumulative number of baits taken in successive trials. Experimental series: *a*, background green; *b*, background blue. Closed symbols represent experiments with blue food and open symbols green food. 95% confidence limits are shown.

The number of crumbs taken during the first (n_1) and subsequent trials (n_s), together with the number of trials before each chick refused food for the first time are shown in Table 1. In the first trial, more blue than green baits were taken when each was presented on a green background (Mann–Whitney $U = 0$, $P < 0.01$). Similarly, during the first trial more green were taken than blue when each was presented on a blue background ($U = 0$, $P < 0.01$). This we interpret as demonstrating crypticity of the crumbs against matching backgrounds. However, by the final trial the situation had changed: more green baits than blue had been taken ($n_1 + n_s$) against the green background ($U = 2$, $P < 0.01$), and more blue baits than green had been taken on the blue background ($U = 0$, $P < 0.01$). From the results shown in Fig. 1 it is apparent that the responses to the two treatments in each experiment were still diverging when testing was stopped.

These experiments indicate that chicks learn to avoid conspicuous more readily than cryptic distasteful prey. One or both of two mechanisms could be operating. First, the

Table 1 The number of crumbs taken during the first trial (n_1), the total number taken during the 12 subsequent trials (n_s), and the number of trials before each of the 36 chicks was tested and refused to feed for the first time (r)

Crumb colour	Blue			Green			Blue			Green		
Background colour	Blue			Blue			Green			Green		
	n_1	n_s	r	n_1	n_s	r	n_1	n_s	r	n_1	n_s	r
	15	67	9	41	29	6	45	30	4	10	60	9
	18	82	11	35	36	4	39	26	5	16	85	11
	11	68	10	33	25	4	40	20	3	9	96	10
	20	65	10	40	26	3	35	36	5	20	84	11
	17	72	9	29	33	4	36	28	4	14	73	7
	16	70	10	44	25	3	35	33	6	10	87	9
	13	72	10	38	26	5	38	29	5	15	89	11
	9	81	12	36	35	4	42	27	5	17	79	10
	19	77	10	39	31	3	37	28	6	13	66	9

0028–0836/80/280149—02$01.00

appearance of conspicuous prey *per se* is learned more readily than that of cryptic prey. Second, eating large numbers of prey in a short time is a more powerful reinforcer than eating even greater numbers of prey over a longer time period. Either mechanism provides a proximate explanation for the functional hypothesis. Note that in these trials the chicks were not offered a food choice and that, therefore, the experiments do not mimic the evolution of aposematic coloration[7]. Whether the effect described here is large enough to favour the evolution of conspicuous coloration among unpalatable prey depends on various behavioural parameters, such as prey group size and the availability of other foods to the predator, in addition to the degree of unpalatability or toxicity of the prey.

We thank Dr P. P. G. Bateson for suggesting the type of experimental design used here, Dr J. R. Krebs for introducing us to the problem, Drs J. J. D. Greenwood and P. J. Greenwood for helpful criticism, and Mr Martyn Stenning for technical assistance.

Received 22 January 1979; accepted 2 May 1980.

1. Edmunds, M. *Defence in Animals* (Longmans, Harlow, 1974).
2. Turner, J. R. G. *Nat. Hist.* **84,** 28–37 (1975).
3. Fisher, R. A. *The Genetical Theory of Natural Selection* (Clarendon, Oxford, 1930).
4. Rettenmeyer, C. W. *A. Rev. Ent.* **15,** 43–74 (1970).
5. Matthews, E. G. *Am. Nat.* **111,** 213–222 (1977).
6. Harvey, P. H. & Greenwood, P. J. in *Behavioural Ecology: an Evolutionary Approach* (eds Krebs, J. R. & Davies, N. B.) 129–154 (Blackwell, Oxford, 1978).
7. Gittleman, J. L., Harvey, P. H. & Greenwood, P. J. *Anim. Behav.* (in the press).
8. Gittleman, J. L. thesis, Univ. Sussex (in preparation).
9. Willis, A. J., McEwan, J. W. T., Greenwood, J. J. D. & Elton, R. A. *J. Anim. Ecol.* (in the press).

Dopaminergic A10 neurones are involved in cognitive functions

Hervé Simon*†, Bernard Scatton‡ & Michel Le Moal*

* Laboratoire de Neurobiologie des Comportements, Université de Bordeaux II, 146 Rue Léo Saignat, 33076 Bordeaux Cedex, France
‡ Synthélabo-LERS, 31 Avenue P. V. Couturier 92220 Bagneux, France

Delayed response tasks are widely considered to be particularly sensitive in demonstrating cognitive deficits after lesions of the prefrontal cortex in all species of mammals[1]. In rodents, these deficits are usually tested in a T-maze and are more pronounced after lesion of the anterior part of the striatum than after prefrontal cortex ablation[2]. In effect, the striatum is capable of assuming cortical functions either when the prefrontal cortex is poorly developed as in the lower mammals[3] or immature as in the early life of primates[4]. The prefrontal cortex and anterior striatum—the so-called prefrontal system[5]—are functionally and anatomically related. The prefrontal area specifically involved in delayed alternation[6] receives projections from the mediodorsal thalamic nucleus (MD)[7] and sends axons to the anterior striatum as well as to the MD[3,7]. Recently, a detailed anatomical study of the connections of the prefrontal system revealed the existence of important projections from the mesencephalic dopaminergic A10 neurones and the mediodorsal nucleus that converge on the prefrontal cortex[8]. Axons of the A10 system also project to the anterior part of the striatum[9,10]. The influence of dopaminergic A10 neurones on frontal lobe functions remains obscure, but some observations concerning the behavioural, pharmacological and biochemical effects of neuroleptics and psychostimulants have supported the idea that these dopaminergic neurones could have a role in the pathogenesis of schizophrenia[11–13]. Furthermore, the major symptoms observed in schizophrenic patients such as cognitive and attention disturbances have been attributed to a dysfunction of both prefrontal cortex and striatum[14–16]. Thus, in addition to their anatomical connections, the dopaminergic A10 neurones may be functionally related to the prefrontal cortex and striatum. These data encouraged us to investigate whether A10 neurones are functionally related to the prefrontal system and in particular if they are involved in cognitive processes measured in a delayed alternation task. We demonstrate here that selective lesions of dopaminergic A10 neurones in the rat produce a severe and specific impairment in retention of delayed alternation. On anatomical and behavioural grounds the dopaminergic A10 system could therefore be considered as a rather better indicator of frontal system function than the mediodorsal thalamic nucleus.

Fifteen male Sprague–Dawley rats (300–350 g) received, under ketamine anaesthesia (150 mg kg^{-1} intraperitoneally (i.p.)), bilateral stainless steel guide cannulae (0.65 mm) aimed 6.5 mm above the A10 cell bodies region. Stereotaxic coordinates were: 4 mm posterior to the bregma, 0.5 mm lateral to the midline and 2.2 mm below skull surface. Fifteen days after surgery, the delayed alternation experiment began according to the procedure of Wikmark *et al.*[2]. Briefly, animals deprived of food for 12 h were trained to enter alternately each arm of a T-maze for food with a fixed time between trials. Twenty-one trials were carried out daily until each rat made five errors or less in 3 consecutive days (91.66% of correct responses in 60 trials).

After the learning period, the animals were divided into control ($c = 6$) and experimental ($e = 9$) groups receiving vehicle or 6-hydroxydopamine (6-OHDA, 2 μg $\mu\mathrm{l}^{-1}$) injections respectively. The injections were made in unanaesthetized animals by lowering bilaterally an injection needle (0.30 mm) through the guide cannulae to the region of A10 cells (8.7 mm below the skull surface). A second injection was performed in similar conditions 3 d later. After another 10 d, the animals were tested for retention of delayed alternation according to the same paradigm as that used in the learning sessions. Training continued until the pre-injection criterion was reached.

Post-operative performances and gross behavioural analysis showed that experimental (6-OHDA–A10) animals presented a severe impairment in retention of delayed alternation. As indicated in Table 1, control rats showed no deterioration in performance between pre- and post-operative behavioural testing, as the number of errors was not statistically different. Moreover, the number of trials in retention was only slightly higher than the number of 60 trials imposed to reach the criterion. On the other hand, the 6-OHDA–A10 rats performed badly. In the first 60 post-injection trials, the 6-OHDA–A10 rats made many more errors than the control group ($t = 7.1$; $P < 0.001$). There was no difference in the errors made by the

Table 1 Learning and retention scores of delayed alternation responses

	Errors in the last 60 pre-operative and in the first 60 post-operative trials (mean ± s.e.m.)		No. of trials to reach criterion (mean ± s.e.m.)	
Group (*n*)	Pre-operative	Post-operative	Pre-operative	Post-operative
Control (6)	4.7 ± 0.3	5.1 ± 0.7	146.6 ± 12.3	70 ± 4.5
6-OHDA–A10 (9)	4.7 ± 0.2	19.6 ± 1.2*	148.9 ± 10	313.3 ± 33.9

There was a significant difference between control and experimental (6-OHDA–A10) groups in the number of errors in the first 60 post-operative trials and the number of post-operative trials needed to reach the criterion (Student's *t*-test, $P < 0.001$). As indicated by the number of errors in the first 60 post-operative trials compared with the last 60 pre-operative trials, the control animals did not show any deterioration of performance. On the contrary, many more post-operative than pre-operative trials were needed by the experimental (6-OHDA–A10) rats to reach the criterion (*paired test, $P < 0.01$).

---

† To whom correspondence should be addressed.

0028–0836/80/280150—02$01.00

Table 2 Learning and retention scores of visual discrimination

Group	(n)	Errors in the first 60 trials (mean ± s.e.m.) Post-operative	No. of trials to reach the criterion (mean ± s.e.m.) Pre-operative	Post-operative
Control	(5)	6.6 ± 0.5	116 ± 4	72 ± 5
6-OHDA–A10	(7)	6.3 ± 0.4	111.4 ± 6	71.4 ± 4

No statistical difference was observed between control and 6-OHDA–A10 lesioned rats. The number of trials for all rats in retention was only slightly greater than the 60 trials imposed to reach the criterion.

Table 3 Dopamine and serotonin contents after 6-OHDA injection (2 × 2 $\mu g\ \mu l^{-1}$) in the region of dopaminergic A10 cell bodies

		Dopamine (ng per g)			Serotonin (ng per g)	
Group	(n)	Frontal cortex	Nucleus accumbens	Anterior striatum	Frontal cortex	Hippocampus
Control	(6)	126 ± 10	8,290 ± 590	8,190 ± 1,310	539 ± 62	342 ± 33
6-OHDA–A10	(9)	39.7 ± 5.7	1,260 ± 150	2,230 ± 670	495 ± 26	241 ± 25

Note that 6-OHDA–A10 rats showed a big depletion of dopamine in forebrain projections, whereas serotonin levels were not significantly modified in the frontal cortex and decreased only slightly in the hippocampus. Values are mean ± s.e.m.

6-OHDA–A10 group between the first 60 post-operative trials (32.66%) and the first 60 initial trials in the learning period (32.40%). Post-operatively, the number of trials to reach the criterion was greater in 6-OHDA–A10 rats compared not only with the control group ($t = 5.6$; $P < 0.001$) but also with their own pre-injection level of performance ($t = 5$; $P < 0.001$). Gross behavioural analysis showed that, during the pre-operative learning of the delayed alternation response, the two groups of rats exhibited collateral behaviours such as rearing, stopping and returning before entering the chosen arm of the T-maze. These collateral behaviours were frequently observed at the beginning of acquisition and then disappeared progressively as the number of errors decreased. Post-operatively it was observed that the 6-OHDA–A10 rats demonstrated more collateral behaviours than the control rats. This difference was particularly evident during the 20 trials of the third post-operative session, that is when the control rats nearly reached the criterion (mean of rearings: $e = 2.10$, $c = 0.33$; stops: $e = 4.2$, $c = 2$; returns: $e = 2.20$, $c = 0.67$). According to these results the mean running time from the start box to the goal box of the T-maze was greater in 6-OHDA–A10 rats ($e = 4.5$ s, $c = 2.08$ s; Student's t-test: $t = 6.9$; $P < 0.001$). This running time did not shorten during the following trials, possibly indicating that post-operatively the experimental animals did not really relearn the task but rather developed a new strategy to reach the criterion. These behavioural observations might explain the nature of the deficit observed in the delayed task after lesion of A10 neurones. The experimental animals showed post-operatively more collateral or 'irrelevant' behaviours because they presented attentional deficits manifested by an enhanced distractibility or responsiveness to environmental stimuli. This renders the animals unable to select relevant information. In this respect, it is interesting that the frontal syndrome has also been interpreted in terms of attentional deficits[17].

Whatever the nature of the perturbation observed, the specificity of our results could be criticized. First, considering the fact that the experimental animals reached the food reward more slowly than control animals, the retention impairment could be explained by motivational deficits. To test this hypothesis, animals were trained in a straight alley divided into a start box, a runway and a goal box containing food reward. The running time for deprived animals to reach the goal box was considered as an index of their motivational state. Each animal was made to run daily in 10 consecutive trials over a period of 5 d. At the end of the experiment, it was found that the running time did not differ between the experimental (mean: 6.28 ± 1.31 s) and the control groups (mean: 5.93 ± 1.12 s). Second, it remained important to investigate if the perturbation observed in the delayed alternation task was not the result of more general learning disabilities. In this respect, it has been found that prefrontal lesioned animals have deficits in delayed alternation but not in discrimination tasks[1]. To test the specificity of a perturbation of delayed alternation after lesion of A10 neurones we carried out an additional experiment. Twelve naive rats maintained on 90% of *ad libitum* body weight, were trained in a Y-maze of the Lashley type for a visual discrimination task. Food reward signaled by light was randomly placed in the right or left arm of the maze. Twenty trials took place daily until the animals reached the criterion of 90% correct responses (6 errors or less in 3 consecutive sessions of 20 trials each). Then, the rats were divided into control ($n = 5$) and experimental ($n = 7$) groups. The control group rats received a saline injection and the experimental group 6-OHDA injections in the A10 cell bodies region, strictly according to the procedure previously used for the delayed alternation test. Fifteen days after the injections the rats were tested for retention of visual discrimination. As indicated in Table 2, the number of trials to reach the criterion and the mean of errors in the first 60 post-operative trials are similar for the two groups of rats.

At the end of the behavioural experiments, animals were decapitated and the brain quickly removed. The posterior part of the brain was kept out for histological examination of injection sites and the anterior part was used for biochemical assays as described previously[18]. Table 3 shows the biochemical results. Note that brain dopamine content of 6-OHDA rats was greatly depleted in the forebrain projections of A10 cell bodies such as the frontal cortex (−68.5%), the nucleus accumbens (−84.8%) and the anterior part of the striatum (−72.8%), whereas endogenous serotonin corresponding to raphe projections was not modified in the frontal cortex or only slightly decreased in the hippocampus (−29.5%).

In conclusion, our results suggest that the dopaminergic A10 neurones have a fundamental role in the processes required for the retention of the delayed alternation response. Supporting this view, it has recently been found that 6-OHDA injections in the frontal cortex of the monkey[19] and rat[20] or in the striatum of the rat[20,21] disrupted the delayed alternation response.

Moreover, we have demonstrated the critical influence of brainstem neurones on higher mental functions, such as cognitive processes, which have often been attributed exclusively to the prefrontal cortex. It could be considered that the sensory information reaching the A10 neurones[22] and conveyed to the prefrontal cortex and striatum are of particular importance for the normal functioning of the prefrontal system. Careful analysis of these A10–prefrontal system interrelations may be of special interest for future research dealing with cognitive representational functions and some pathophysiological states.

This work was supported by a grant from DGRST (78 7 2780) and INSERM (ATP 39.76.71).

Received 25 Februrary; accepted 2 May 1980.

1. Markowitsch, H. J. & Pritzel, M. *Psychol. Bull.* **84,** 817–837 (1977).
2. Wikmark, R. G. E., Divac, I. & Weiss, R. *Brain Behav. Evolut.* **8,** 329–339 (1973).
3. Öberg, R. G. E. & Divac I. *Acta neurobiol. exp.* **35,** 647–659 (1975).
4. Goldman, P. S. *Exp. Neurol.* **32,** 366–387 (1971).
5. Rosvold, H. E. & Szwarebart, M. K. in *The Frontal Granular Cortex and Behavior* (eds Warren, J. M. & Akert, K.) 1–15 (McGraw-Hill, New York, 1964).
6. Larsen, J. K. & Divac, I. *Physiol. Psychol.* **6,** 15–17 (1978).
7. Leonard, C. M. *Brain Res.* **12,** 321–343 (1969).
8. Divac, I., Björklund, A., Lindvall, O. & Passingham, R. E. *J. comp. Neurol.* **180,** 59–72 (1978).
9. Simon, H., Le Moal, M., Galey, D. & Cardo, B. *Brain Res.* **115,** 215–231 (1976).
10. Simon, H., Le Moal, M. & Calas, A. *Brain Res.* **178,** 17–40 (1979).
11. Hökfelt, T., Ljungdahl, A., Fuxe, K. & Johansson, O. *Science* **184,** 177–179 (1974).
12. Snyder, S. H., Banerjee, S. P., Yamamura, H. I. & Greenberg, D. *Science* **184,** 1243–1253 (1974).
13. Stevens, J. R. *Archs gen. Psychiat.* **29,** 177–189 (1973).
14. Hornykiewicz, O. *Neuroscience* **3,** 773–783 (1978).
15. Joseph, M. H., Frith, C. D. & Waddington, J. L. *Psychopharmacology* **63,** 273–280 (1979).
16. Lidsky, T. I., Weinhold, P. M. & Levine, F. M. *Biol. Psychiat.* **14,** 3–12 (1979).
17. Nauta, W. J. H. *J. Psychiat. Res.* **8,** 167–187 (1971).
18. Scatton, B. *Eur. J. Pharmac.* **46,** 363–369 (1977).
19. Brozoski, T. J., Brown, R. M., Rosvold, M. E. & Goldman, P. S. *Science* **205,** 929–931 (1979).
20. Simon, H. *J. Physiol., Paris* (in the press).
21. Dunnett, S. B. & Iversen, S. D. *Neurosci. Lett.* Suppl. **3,** 207 (1979).
22. Le Moal, M. & Olds, M. E. *Brain Res.* **167,** 1–18 (1979).

The role of ventral bundle noradrenergic neurones in sensory components of sexual behaviour and coitus-induced pseudopregnancy

S. Hansen, E. J. Stanfield & B. J. Everitt*

Department of Anatomy, University of Cambridge, Downing Street, Cambridge CB2 3DY, UK

Interaction of the female rat with the male in standardized laboratory conditions is characterized by two categories of behaviour. The first, known as proceptive behaviour, consists of a series of rapid movements by which she approaches and leaves the male, hopping and darting and wiggling her ears[1]. This behaviour, which is a response to visual, olfactory, and probably auditory cues from the male, serves to attract his sexual interest. As soon as the male mounts her, this behaviour is abruptly terminated and is replaced by a second (receptive) pattern[1]. The female becomes completely immobile and dorsiflexes her vertebral column to display a lordotic posture, which exposes her vagina and facilitates intromission by the male; this pattern results from tactile stimulation received by the female from the male as he mounts her[2,3]. Both these behaviours are under endocrine control since the female rat will only show them if she is exposed to the ovarian hormones oestradiol and progesterone[4]. However, proceptivity and receptivity clearly differ with regard to the neural mechanisms responsible for their activation, since different groups of afferent stimuli are required to set them in motion. We now show that a specific part of the ascending systems of noradrenergic neurones in the brain, that is carried in the ventral noradrenergic bundle[5], is critically involved in the mechanisms by which tactile stimuli elicit receptive, but not proceptive, behaviour in the female rat. The same system is also involved in the process by which genital stimuli activate another neuroendocrine phenomenon, the induction of pseudopregnancy.

The first experiment was carried out on ovariectomized animals injected daily with a low dose of oestradiol monobenzoate (0.2 μg) and with a single injection of progesterone (0.5 mg) between 4 and 6 hours before behavioural testing. Figure 1*a* shows that animals in which an electrolytic lesion of the ventral noradrenergic bundle had been made (Fig. 2) continued to display proceptive behaviours towards the male. However, in contrast to controls (who showed high levels of receptivity) ventral noradrenergic bundle-lesioned animals displayed greatly reduced levels of lordosis (receptive behaviour). The procedure was then repeated except that instead of an electrolytic lesion, 6-hydroxydopamine (6-OHDA) was injected at the same site. This neurotoxin induces selective degeneration of noradrenergic neurones when placed discretely in the small dose and volume (2 μg base in 0.5 μl Ringer's solution) used here[6]. Figure 1*a* shows that this resulted in similar behavioural consequences, females continuing to show proceptive behaviour, but only low levels of lordosis when they were mounted by the male. Table 1 shows that both electrolytic lesions (Fig. 2) and those produced by the neurotoxin 6-OHDA (Fig. 2) produced similar neurochemical changes, in that noradrenaline uptake in the hypothalamus was substantially decreased, whereas that in the cerebral cortex (which is supplied by the dorsal noradrenergic pathway) was unaffected. Very little or no nonspecific damage was seen around the site of injection of 6-OHDA and careful histological examination revealed that lemniscal and spinothalamic projections were undamaged. These experiments therefore suggest that the behavioural results that we observed were produced specifically by decreasing the noradrenaline content of the subcortical brain after a ventral noradrenergic bundle lesion.

The second experiment was carried out on intact animals showing regular oestrous cycles. The vagina of each rat was covered with tape to prevent intromissions during sexual interaction and so avoid episodes of pregnancy or pseudopregnancy. Such animals show recurrent periods of active sexual behaviour ('heat') every fourth day. Electrolytic lesions in the ventral noradrenergic bundle similar to those made in the first experiment did not prevent the postoperative occurrence of normal 4-day vaginal oestrous cycles, although these took longer to be re-established after operation than in the sham-operated

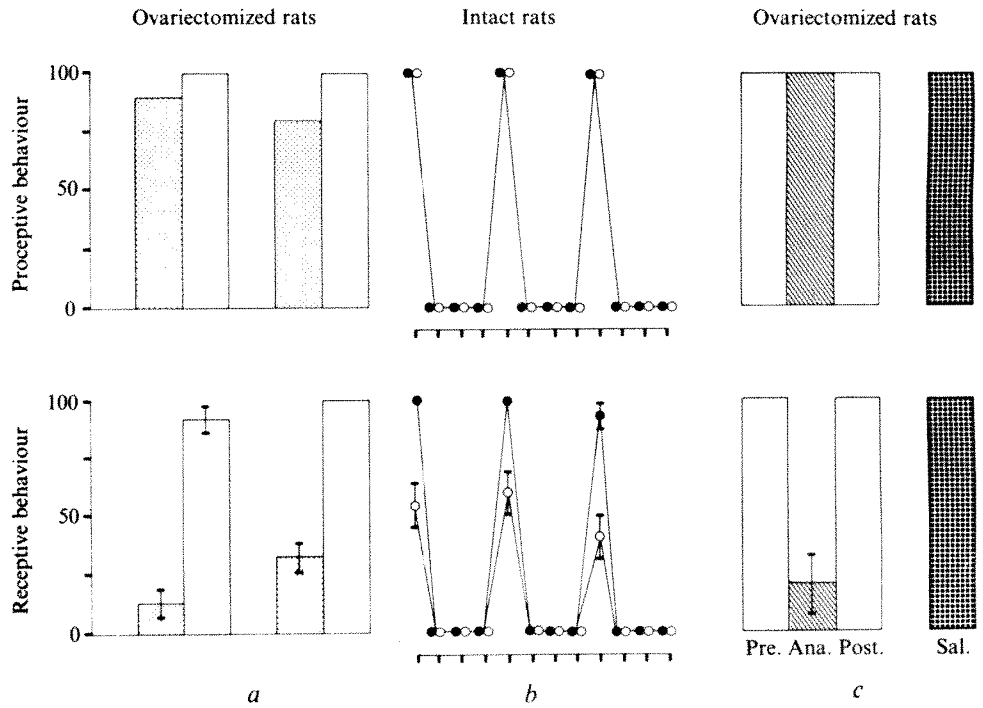

Fig. 1 The effects of ventral noradrenergic bundle (VNAB) lesions or procaine on the receptivity and proceptivity of female rats. *a*, Electrolytic lesions (1.5 mA, 10 s, insulated platinum electrode 0.4 mm o.d., columns 1 and 2) or 6-hydroxydopamine lesions (2 μg base in 0.5 μl 0.9% NaCl with 0.2% absorbic acid injected over 5 min through a cannula 0.3 mm o.d., columns 3 and 4) of the VNAB in ovariectomized rats treated with oestradiol and progesterone. Lesioned females are represented by cross-hatched columns, the receptive behaviour of lesioned females was significantly lower than controls ($P < 0.05$, Mann–Whitney *U*-test) in both cases. Coordinates for lesions were AP −0.5; L ±0.6; V −6.5 according to Konig and Klippel[15]. *b*, VNAB lesions in intact females, showing behavioural effects during three consecutive oestrous cycles (time scale on abcissa in days). Lesioned rats showed impaired lordosis responses (receptivity) during each period of oestrus ($P < 0.05$) while proceptivity was unaffected. Each female had her vagina covered to prevent intromissions. *c*, In ovariectomized oestrogen and progesterone treated rats, procaine-induced anaesthesia of the perineum (Ana.) significantly reduced ($P < 0.05$) receptivity when compared with pre- or post-anaesthesia scores or injection of normal saline (Sal.) at the same sites in the same volume as procaine. Proceptive behaviour was unaffected.

0028-0836/80/280152—03$01.00

controls (26.2 ± 2.4 days compared with 17.2 ± 1.3 days, $P<0.05$). However, Fig. 1*b* shows that the behavioural consequences which followed this procedure in intact animals were very similar to those seen in ovariectomized, oestrogen-treated ones described above. Both lesioned and control animals showed proceptive behaviours every fourth day on the night preceding the presumed time of ovulation. Only the controls showed high levels of receptivity while lesioned rats responded to attempted mounts by only infrequent lordosis. Thus, ventral noradrenergic bundle lesions produced the same behavioural syndrome in animals responding to their own hormones as was observed in ovariectomized animals given oestrogen and progesterone exogenously.

One interpretation of these results is that somatosensory information received from the male during mounting was not gaining access to the neural mechanism responsible for initiating lordosis (receptive) postures in the female rat. We therefore compared these results to those from a third experiment in which we studied behaviour after anaesthetizing the skin in the female's perineal region, to which the male applies tactile stimuli during mounting. Procaine was injected at four sites (0.25 ml per site as a 2% solution) around the perivaginal area as described previously[3]. Figure 1*c* shows that this procedure produced behavioural effects remarkably similar to those following ventral noradrenergic bundle lesions, rats showing marked deficiencies in receptivity but not in proceptivity.

Although these experiments showed, in a behavioural context, that the ventral noradrenergic bundle was clearly important in the transmission of tactile information generated during sexual interaction, we wanted to know whether this system of neurones could function similarly in any other neuroendocrine context. Tactile stimulation of the uterine cervix during copulation in the rat results in daily surges of prolactin which, by extending the lifespan of the corpus luteum, induces pseudopregnancy[7]. This stimulus can be mimicked by gently stimulating the cervix with a glass rod for 40 s during proestrus[8]. In a fourth experiment we found that 8 out of 11 unlesioned females so treated (73%) became pseudopregnant judging by the occurrence of persistent basal cells in their vaginal smears which were taken daily for about a week following stimulation. However, a similar procedure applied to 9 rats with lesions of the ventral noradrenergic bundle resulted in only 2 (22%) becoming pseudopregnant, the remainder continuing to show vaginal cycles after stimulation (Fisher's exact probability test $P=0.032$). This experiment suggests that the ventral noradrenergic pathway is concerned with somatosensory information important in neuroendocrine contexts other than those of regulating behaviour. But whether this only applies to stimuli derived from the genitalia, as explored in the present experiments, or can also extend to other parts of the body and other behavioural or physiological contexts, awaits further study.

It is known that tactile stimuli important in eliciting the receptive posture reach the brain via fibre systems running in the anterolateral columns of the spinal cord[9], and many of these fibres terminate in the vicinity of cell groups which contribute to the ventral noradrenergic bundle, particularly those lying in the ventro-lateral medulla and in the region medial to the superior olivary complex. It has also recently been shown that tritiated oestradiol is taken up into many noradrenergic cell bodies in the brain stem[11], which suggests a more direct relationship may exist between hormones which alter behaviour or pituitary secretion and this part of the noradrenergic pathway.

Table 1 Effects of electrolytic or neurotoxin lesion on the *in vitro* uptake of ^{3}H-noradrenaline by hypothalamic synaptosomes and slices or cerebral cortex slices

	% Decrease in active uptake of ^{3}H-noradrenaline *in vitro*	
Lesion	Hypothalamus	Cerebral cortex
Electrolytic	59.3%*	8%(NS)
6-Hydroxydopamine	65.8%*	13%(NS)

Incubations were performed in Krebs–Ringer bicarbonate buffer[16] with ^{3}H-noradrenaline at a concentration of 10^{-7} M. Data are expressed as % reductions compared with controls (sham lesions resulted in no significant depletions (<5%). The degree of reduction in active uptake is closely related to the degree of neuronal destruction[17]. NS, Not significant.

* $P<0.01$, comparison of original counts by *t*-test.

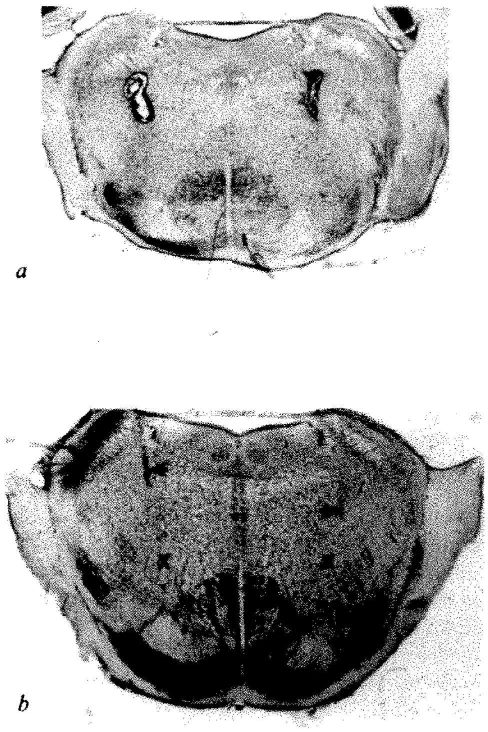

Fig. 2 Representative photomicrographs of electrolytic lesions of the VNAB (*a*) and the site of injection of 6–OHDA (*b*) which resulted in neurotoxic lesion of VNAB. In *a* the maximum dorsal–ventral extent of the lesion is shown, high power examination revealed necrosis and glial infiltration medial to the macroscopic lesion site. In *b* small glial scars can be seen (arrows) which indicate the site of descent of the micro-cannulae through which 6–OHDA was injected at depth *X*. No gross damage around the injection sites can be seen indicating that nonspecific effects of the injection were minimal. The neurochemical consequences of these lesions are shown in Table 1.

We suggest that ascending noradrenergic neurones carried in the ventral noradrenergic bundle and distributed to sub-cortical (hypothalamic and limbic) areas of the brain, may be an important pathway by which tactile information generated during sexual interaction modulates both behaviour and pituitary function. It becomes important to define, therefore, those sites in the brain where noradrenergic neurones exert these effects. Our preliminary evidence suggests that they may depend on the subsequent modulation of dopaminergic mechanisms: thus the switch from active to passive (proceptive to receptive) elements of the female's behaviour may be achieved by a corresponding, somatosensory-induced switch (decrease) in dopaminergic activity[12] mediated by the ventral noradrenergic pathway. Similar mechanisms may also underlie coitus (somatosensory)-induced prolactin secretion, particularly since this hormone (as well as lordosis) is under inhibitory dopaminergic control[13,14]. Furthermore, it is possible that these sub-cortically projecting noradrenaline-containing neurones may be involved in the transmission of somatosensory information in contexts wider than those reported here.

S.H. was in receipt of an award from the European Training Program in Brain and Behaviour Research. This work was supported in part by an MRC Programme grant to Joe Herbert who we also thank for constructive criticism of the manuscript. Address all correspondence to B.J.E.

Received 21 February; accepted 2 May 1980.

1. Beach, F. A. *Horm. Behav.* **7,** 105–138 (1976).
2. Pfaff, D. W. & Lewis, C. *Horm. Behav.* **5,** 317–335 (1974).
3. Kow, L. M. & Pfaff, D. W. *Brain Res.* **101,** 47–66 (1976).
4. Hansen, S. & Sodersten, P. *J. Endocr.* **77,** 373–379 (1978).
5. Ungerstedt, U. *Acta physiol. scand. Suppl.* **367,** 1–48 (1971).
6. Bloom, F. E. *J. neural Transmission* **37,** 183–187 (1975).
7. Smith, M. S., McLean, B. K. & Neill, J. D. *Endocrinology* **98,** 1370–1377 (1976)
8. Castro-Vasquez, A. & McCann, S. M. *Neuroendocrinology* **28,** 3–10 (1979).
9. Kow, L. M., Montgomery, M. O. & Pfaff, D. W. *Brain Res.* **123,** 75–88 (1977).
10. Zemlan, F. P., Leonard, C. M., Kow, L. M. & Pfaff, D. W. *Expl Neurol.* **62,** 298–334 (1978).
11. Heritage, A. S., Evant, L. D. & Stumpf, W. E. *J. comp. Neurol.* **176,** 607–630.
12. Caggiula, A. R., Antelman, S. M. Chiodo, L. A. & Lineberry, C. G. in *Catecholamines: Basic and Clinical Frontiers* Vol. II (eds Udsin, E., Kopin, I. J. & Barchas, J. (Pergamon, Oxford, 1979).
13. Yen, S. S. C. in *Reproductive Endocrinology* (eds Yen, S. S. C. & Jaffe, R. B.) 152–170 (Saunders, Baltimore, 1978).
14. Everitt, B. J., Fuxe, K., Hokfelt, T. & Jonsson, G. *J. comp. Physiol. Psychol.* **89,** 556–572 (1975).
15. Konig, J. F. R. & Klippel, R. A. *The Rat Brain: A Stereotaxic Atlas of the Forebrain and Lower Parts of the Brain Stem* (Williams and Wilkins, Baltimore, 1963).
16. Lidbrink, P., Jonsson, G. & Fuxe, K. *Neuropharmacology* **10,** 521–536 (1971).
17. Jonsson, G. & Sachs, Ch. *J. Pharm. exp. Ther.* **180,** 625–635 (1972).

Spontaneous and mechanically evoked activity due to central demyelinating lesion

K. J. Smith

Sobell Department of Neurophysiology, Institute of Neurology,
Queen Square, London WC1N 3BG, UK

W. I. McDonald

University Department of Clinical Neurology, Institute of Neurology,
Queen Square, London WC1N 3BG, UK

Patients with multiple sclerosis commonly complain of tingling and other sensory disturbances which may occur spontaneously or in response to movement. These symptoms are associated with plaques of demyelination in the corresponding sensory pathways but the physiological abnormalities underlying the symptoms are not understood. We have examined sensory fibres traversing a central demyelinated lesion resembling that of multiple sclerosis for evidence of activity which could account for the symptoms. We present here evidence for the existence of spontaneously and mechanically induced trains of action potentials propagating in both directions from the lesion.

Lesions were induced under anaesthesia (Saffan, Glaxo) in nine cats by the direct microinjection of lysophosphatidylcholine (LPC) into the dorsal column between L_1 and L_3 (ref. 1). The cats were reanaesthetized 7 to 14 days later, given atropine (300 µg) and rigidly held in a stereotactic frame. A laminectomy was performed from T_9 to L_7. Skin flaps were raised to form a recording paraffin pool, maintained at 37 ± 0.5 °C. Dorsal rootlets caudal and rostral to the lesion were isolated and raised on recording electrodes connected via unity gain cathode followers to differential preamplifiers. The data were processed using a small laboratory computer (Biomac 1000; Data Laboratories). The lesions were examined histologically.

Many of the rootlets caudal to the lesion in each of the cats contained spontaneously active units firing with fairly steady frequencies of between 15 and 45 impulses per second (Fig. 1*a*). Some spontaneously active units fired in bursts with, for example groups of about 5 impulses at 110 Hz separated by intervals of approximately 0.1 s (Fig. 1*b*). This pattern of firing bears a striking resemblance to that of the motor discharges associated with myokymia in multiple sclerosis[2].

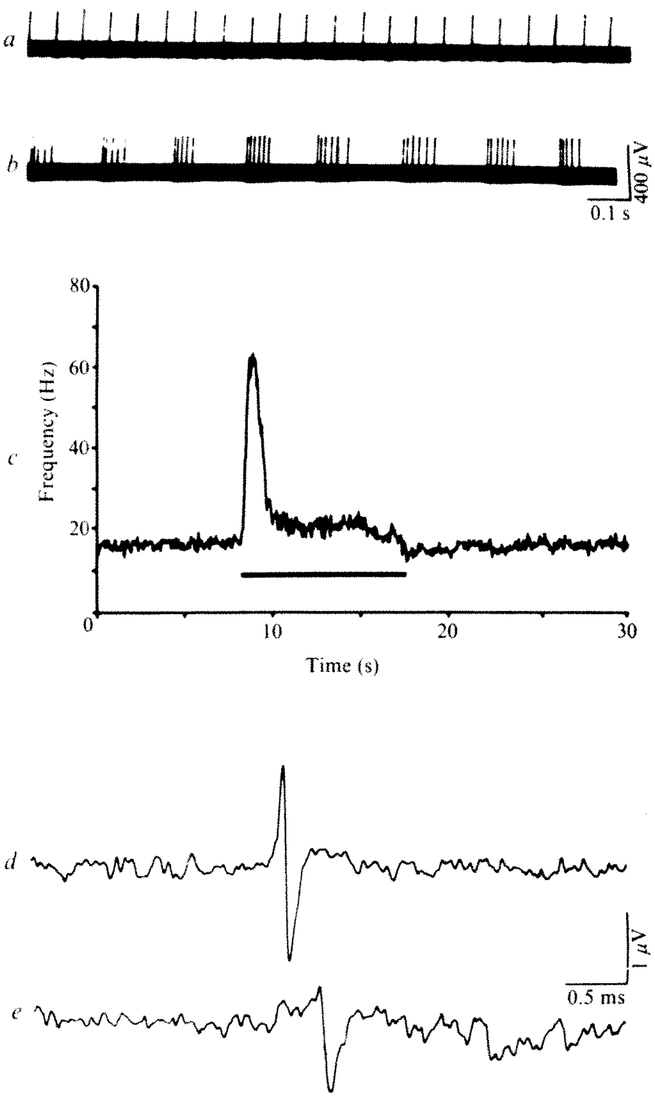

Fig. 1 *a* and *b*, Differential recordings of a steady (*a*) and a bursting (*b*) spontaneously active unit isolated in a teased dorsal root filament, caudal to the lesion, 14 days after LPC injection. *c*, Shows the firing rate of a steadily discharging, mechanosensitive unit recorded from a caudal dorsal root, 8 days after the injection of LPC. The bar marks the duration of a 0.75 mm compression of the lesion with a glass rod. *d* and *e*, Averaged records (n = 4,096) of the same spontaneously active unit, 14 days after LPC injection. Recordings were made 16 mm (*d*) and 6 mm (*e*) rostral to the lesion (conduction velocity = 30 m s^{-1}). The averager was triggered from the antidromic spikes of the unit in a teased dorsal root filament caudal to the lesion. The recordings were made with an imposed delay of 2 ms.

Small deformations (<1 mm) of the dorsal columns with a glass rod at the site of the lesion increased the firing rate of the spontaneously active units (Fig. 1*c*) and frequently recruited firing in units which were previously silent. The firing evoked by sustained deformations typically consisted of a phasic burst of activity followed by a slower, tonic discharge which subsided over about 30 s. Since the resting discharge pattern was not altered by comparable deformations of the dorsal column remote from the lesion, we conclude that the impulses were generated at the lesion in fibres which were unusually mechanosensitive. Tingling sensations, however, are likely to depend on impulses ascending the dorsal columns and it was therefore necessary to establish the existence of abnormal centripetal as well as centrifugal activity. The difficulty of distinguishing abnormal from normal ascending activity in the dorsal columns was overcome by the use of spike-triggered averaging[3] ($n = 128-16{,}284$) and the demonstration that, in some fibres, the descending impulses were time-locked to ascending impulses (see Fig. 1*d*, *e*). The averager was triggered from activity in a single nerve fibre isolated in the central end of a severed dorsal root caudal to the lesion. The input to the averager was connected to an uninsulated platinum wire which was inserted into the dorsal column rostral to the lesion using a micro-manipulator. A delay line (Mullard TDA 1022) was incorporated in the recording circuit when required. Of the 15 fibres examined with this recording arrangement we were able to find three in which there was clear evidence of synchronized trains of action potentials above and below the lesion. Two of the three fibres had quite steady firing frequencies for many hours and the other fibres fired in bursts. The relative latencies of the ascending and descending spontaneous action potentials established that they arose in the lesion. The fibres were also unusually mechanically sensitive at this site. In one fibre it was possible to determine the conduction velocity by recording the ascending action potential at two locations rostral to the lesion (Fig. 1*d*, *e*). From this measurement it was possible to determine the approximate site of origin of the impulses and this fell within the lesion.

The mechanism of origin of the time-locked ascending and descending impulses is uncertain. The simplest explanation is that they arose within the lesion in fibres with intact axons but abnormal myelin sheaths. Ectopic activity is known to occur in congenitally dysmyelinated axons[4]. It is, however, possible that the ascending impulses arose in surviving fibres by ephaptic excitation from spontaneous activity in adjacent severed fibres. Severed fibres exist in the LPC lesion at 14 d[1], as they do in the lesion of multiple sclerosis[5] and are known to generate spontaneous activity whether cut centrally (our unpublished observations) or peripherally[6]. Ephaptic cross-activation has been reported in congenitally dysmyelinated spinal roots of dystrophic mice[4]. Whether demyelinated, but previously normal nerve fibres can be similarly excited remains to be determined.

The present experiments provide clear evidence of spontaneous and mechanically induced trains of action potentials arising in a central demyelinating lesion and propagating in both directions from the lesion. We think it likely that such abnormal activity contributes to some of the sensory symptoms of human disease associated with comparable lesions. For example, many patients with multiple sclerosis or compressive lesions of the cervical spinal cord experience transient paraesthesiae on neck flexion. During this manoeuvre the cervical spine changes in length by several centimetres[7] and we have shown that much smaller deformations (<1 mm) can initiate transient abnormal discharges of a duration similar to that of the paraesthesiae. Length changes also occur in the optic nerve during eye movements and in patients with demyelinating optic neuritis such movements are sometimes associated with the perception of flashes of light[8]. The long-sustained, resting spontaneous discharges similarly provide a sufficient explanation for the continuous paraesthesiae often experienced during acute relapses of multiple sclerosis.

Received 5 March; accepted 29 April 1980.

1. Blakemore, W. F., Eames, R. A., Smith, K. J. & McDonald, W. I. *J. neurol. Sci.* **33,** 31 (1977).
2. Hjorth, R. J. & Willison, R. G. *J. neurol. Sci.* **20,** 117 (1973).
3. Kirkwood, P. A. & Sears, T. A. *J. Physiol., Lond.* **245,** 58P (1974).
4. Rasminsky, M. *Ann. Neurol.* **3,** 351 (1978).
5. Prineas, J. W. & Connell, F. *Ann. Neurol.* **5,** 22 (1979).
6. Wall, P. D. & Gutnick, M. *Expl Neurol.* **43,** 580 (1974).
7. Brieg, A. *Adverse Mechanical Tension in the Central Nervous System* (J. Wiley, London, 1978).
8. Davis, F. A., Bergen, D., Schauf, C. L., McDonald, W. I. & Deutsch, W. *Neurology (Mineap.)* **26,** 110 (1976).

0028-0836/80/280155—03$01.00

Intrathecal morphine inhibits substance P release from mammalian spinal cord *in vivo*

T. L. Yaksh*, T. M. Jessell†‡, R. Gamse§, A. W. Mudge§ & S. E. Leeman§

*Department of Neurologic Surgery, The Mayo Clinic, Rochester, Minnesota 55901
†Department of Pharmacology, Harvard Medical School, Boston, Massachusetts 02115
§Laboratory of Human Reproduction and Reproductive Biology and Department of Physiology, Harvard Medical School, Boston, Massachusetts 02115

The central terminals of small diameter primary sensory neurones associated with the transmission of noxious cutaneous stimuli are located predominantly in the superficial dorsal horn of the spinal cord[1-3]. Some of these neurones synthesize substance P (ref. 4) and transport this peptide to their central and peripheral terminals[5-7]. Substance P is released from the dorsal horn *in vitro* following potassium depolarization[8,9]; from spinal cord after electrical stimulation of dorsal roots[10] and from dissociated sensory neurones grown in culture[11]. The iontophoretic application of substance P produces a long-lasting excitation of dorsal horn neurones that are also excited by noxious cutaneous stimuli[12-14]. One population of opiate receptors in the dorsal horn seems to be located on primary afferent terminals[15,16]; the release of substance P from primary sensory neurones is inhibited by opiates *in vitro*[8,11]. At present, however, there is no direct evidence that substance P is released from sensory neurones, *in vivo*, following activation of nociceptive afferents. We report here that substance P-like immunoreactivity is released from the mammalian spinal cord, *in vivo*, following chemical stimulation of sensory neurones with capsaicin and by the activation of high threshold peripheral afferents. Furthermore, release of substance P evoked by high intensity stimuli is completely inhibited by intrathecal morphine.

Experiments were performed on rats and cats, anaesthetized with chloralose–urethane and placed in a stereotaxic frame. A length of PE-10 polyethylene tubing, serving as an inflow cannula, was inserted into the subarachnoid space, via the cisterna magna, to the caudal region of the lumbar enlargement[17]. The spinal cord was superfused at $100\ \mu l\ min^{-1}$ with artificial cerebrospinal fluid (CSF) containing bovine serum albumin ($120\ \mu g\ ml^{-1}$) and bacitracin ($30\ \mu g\ ml^{-1}$ in rats and $300\ \mu g\ ml^{-1}$ in cats). In rats, superfusate was withdrawn with a push-pull syringe pump through a second cannula, placed in the cisterna magna. Superfusate from cat spinal cord was removed with a PE-90 cannula, inserted concentrically over the PE-10 cannula to the rostral region of the lumbar enlargement. Samples were collected at 10-min intervals in rats and 30-min intervals in cats.

After superfusion of the rat spinal cord in the absence of any evoking stimulus, the levels of substance P released were too low for reliable measurement in most experiments (<5 fmol per 10 min). Superfusion of the spinal cord with potassium chloride (40 mM) resulted in the release of 78 ± 9 fmol (mean ± s.e.m.; $n = 4$) substance P during the 10-min collection period. In the fraction following potassium stimulation, release of substance P returned to basal levels. Addition of 2·0 mM cobalt to the superfusing medium prevented the evoked release of substance P.

---

‡To whom correspondence should be addressed at Department of Pharmacology, St George's Hospital Medical School, Cranmer Terrace, London SW17 0RE, UK.

In the cat it was possible to detect a significant release of substance P from the spinal cord in the absence of any evoking stimulus: 7–15 fmol were measured in each 30-min collection period with very little variation during the course of an experiment (Fig. 1). To examine whether substance P is released from the spinal cord following activation of specific afferent fibre populations, we stimulated the cat sciatic nerve bilaterally, while superfusing segments of the spinal cord receiving sensory input from the sciatic nerve. During stimulation, the compound action potential was monitored to determine the stimulus intensity required to activate Aαβ fibres alone, and that required to recruit Aδ and C fibres. At stimulus intensities sufficient to recruit only low threshold Aαβ afferents, there was no measurable increase in the release of substance P (Fig. 1). The collaterals of large myelinated fibres that are activated by low intensity stimuli terminate with deeper laminae of the dorsal horn. Thus, by superfusing the surface of the spinal cord, we cannot exclude that substance P is actually released from those terminals, but cannot diffuse into the spinal superfusate. Increasing the stimulus intensity to activate Aδ and C fibres produced a 4·9±0·6 fold (mean±s.e.m.; $n=4$) increase in substance P release (Fig. 1). In the fraction following stimulation, the release of substance P returned to pre-stimulation values.

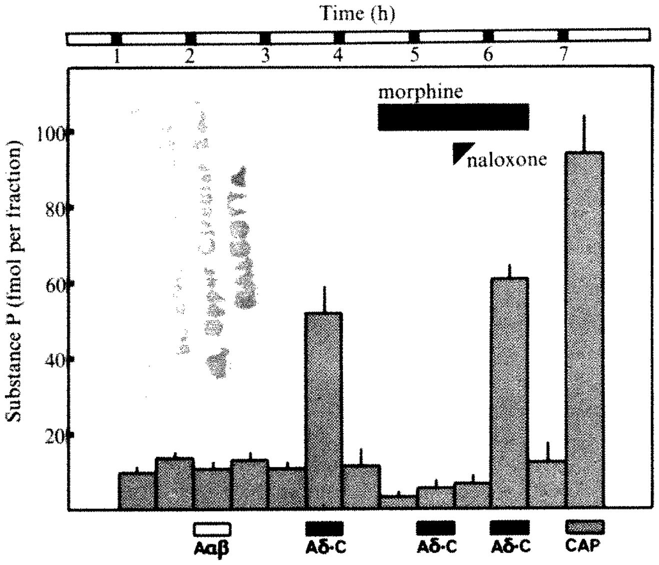

Fig. 1 Release of substance P from superfused cat spinal cord in response to sciatic nerve stimulation and capsaicin. Cats were anaesthetized with chloralose–urethane (100 mg per kg) and prepared with a tracheal tube and jugular and carotid catheters. An incision was made in the cisterna magna and the perfusion cannula was inserted after retraction of the arachnoid layer. The perfusion cannula consisted of a length of polyethylene PE-90 (1.0 mm outer diameter) tubing through which was passed a length of polyethylene PE-10 tubing. The PE-10 served as inflow cannula while the PE-90 was used as collection cannula. Both cannulae were inserted through the retracted incision in the cisterna membrane 37–40 cm down the spinal cord (upper sacral region) and the PE-90 cannula was then retracted 10 cm. Perfusion was therefore localized to the upper sacral and lumbar spinal cord. The position of the inflow and outflow cannulae was determined by X rays after infusion of radio-opaque dye. The sciatic nerve was exposed and prepared for stimulation and recording of the compound action potential. Stimulation of the nerve was performed with rectangular pulses (3–4 V, 0.05 ms, 50 Hz for activation of Aα and Aβ fibres and 40–50 V, 0.05 ms, 50 Hz for recruitment of Aδ and C fibres). Superfusate in all experiments consisted of NaCl, 151.1 mM; KCl, 2.6 mM; $MgSO_4$, 0.9 mM; $CaCl_2$, 1.3 mM; $NaHCO_3$, 21.0 mM; K_2HPO_4; 2.5 mM, gassed with 95% O_2 and 5% CO_2 before perfusion. Perfusion samples (3 ml) were collected into glacial acetic acid (final concentration of 2 N) and immediately frozen and lyophilized. Samples were reconstituted in 1.0 ml assay buffer, neutralized and aliquots of each fraction were used to determine the content of substance P, by radioimmunoassay, using antibody R6P with a sensitivity of 1.5 fmol per assay tube[33]. Serial dilutions of synthetic substance P and immunoreactivity in superfusate samples produced parallel dilution curves. Each value is the mean± s.e.m. from four separate experiments.

We have also examined whether the spinal application of morphine at concentrations known to elicit analgesia[18] can affect substance P release from cat spinal cord *in vivo*. Following superfusion with 5×10^{-4} M morphine sulphate (equivalent to 427.5 μg morphine base superfused over a 30-min period), the resting release of substance P was substantially decreased, in two animals to levels below the sensitivity of the assay (Fig. 1). Furthermore, bilateral stimulation of the sciatic nerve at intensities that clearly caused the release of substance P before the addition of morphine now failed to increase the release of substance P (Fig. 1). Following intraperitoneal injection of naloxone hydrochloride (1 mg per kg), stimulation of the sciatic nerve at the same intensity in the continued presence of intrathecal morphine, fully restored the evoked release of substance P (Fig. 1).

Peripheral application of the homovanillic acid derivative, capsaicin, produces a severe burning pain[19] that reflects the activation of C fibres in sensory nerves[20]. Subcutaneous administration of capsaicin to neonatal rats results in the degeneration of small sensory neurones[21], some of which contain substance P[22].

Capsaicin also depletes substance P from the dorsal horn of adult rats[23,24]. Administration of capsaicin directly onto the spinal cord, *in vitro*, causes a calcium-dependent release of substance P[9,25]. In the present experiments, superfusion of the cat spinal cord with 3×10^{-4} M capsaicin produced a greater than tenfold increase in the release of substance P (5 experiments, Fig. 1). The actions of capsaicin in the spinal cord seem to be restricted to nociceptive primary sensory neurones[23,26]. Thus, the demonstration of a capsaicin-evoked release of substance P from cat spinal cord, *in vivo*, provides further evidence that substance P may be involved in the transmission of noxious peripheral stimuli.

Our results with sciatic nerve stimulation provide direct evidence that substance P is released from mammalian spinal cord *in vivo* by activating nociceptive sensory afferents. The naloxone-reversible inhibition of substance P release by morphine applied directly to the spinal cord at concentrations known to elicit analgesia, may represent one substrate for the direct spinal analgesic actions of the opiates[18]. The opiate inhibition of substance P release reported by Mudge *et al.*[11] is a direct effect on sensory neurones. These authors also found that enkephalin could inhibit calcium influx into cultured sensory neurones by modulating voltage-sensitive channels and suggested that inhibition of substance P release from terminals could be mediated by the same mechanism.

The precise relationship between enkephalin and substance P-containing neuronal elements in the dorsal horn is still unclear. Substance P is highly concentrated within lamina I of the dorsal horn, where primary afferent terminals are rarely postsynaptic in axo-axonal contacts[3]. Furthermore, although there are a variety of enkephalin-containing elements within the superficial dorsal horn[27–29] few of these seem to contribute to axo-axonal contacts with primary afferents[30]. It remains to be seen if other neurotransmitters present in the dorsal horn that can elicit direct spinal analgesia[31,32] also inhibit the release of substance P *in vivo*.

We thank Robert Dailey and Gail Harty for technical assistance. Somatostatin antibody was a gift from J. Fernstrom and M. Arnold. T.M.J. was a Harkness Fellow of the Commonwealth Fund. A.W.M. was supported by training grant GM-00919. This work was supported by the Mayo Foundation and NS 14629 (to T.L.Y.) and NIH grant AM16510 (to S.E.L.).

Received 17 September 1979; accepted 7 May 1980.

1. Rethelyi, M. *J. comp. Neurol.* **172,** 511–528 (1977).
2. Light, A. R. & Perl, E. R. *J. comp. Neurol.* **186,** 117–132 (1979).
3. Ralston, H. J. & Ralston, D. D. *J. comp. Neurol.* **184,** 643–684 (1979).
4. Harmar, A., Schofield, J. & Keen, P. *Nature* **284,** 267–269 (1980).

5. Takahashi, T. & Otsuka, M. *Brain Res.* **87,** 1–11 (1975).
6 Hökfelt, T., Kellerth, J.-O., Nilsson, G. & Pernow, B. *Science* **190,** 889–890 (1975).
7. Hökfelt, T. *et al.* in *Substance P* (eds Von Euler, U. & Pernow, B.) 117–145 (Raven, New York, 1977).
8. Jessell, T. M. & Iversen, L. L. *Nature* **168,** 549–551 (1977).
9. Gamse, R., Molnar, A. & Lembeck, F. *Life Sci.* **25,** 629–636 (1979).
10. Otsuka, M. & Konishi, S. *Nature* **164,** 83–84 (1976).
11. Mudge, A. W., Leeman, S. E. & Fischbach, G. D. *Proc. natn. Acad. Sci. U.S.A.* **76,** 526–530 (1979).
12. Henry, J. L. *Brain Res.* **114,** 439–451 (1976).
13. Randic, M. & Miletic, V. *Brain Res.* **128,** 164–169 (1977).
14. Zieglgansberger, W. & Tulloch, I. *Brain Res.* **166,** 273–282 (1979).
15. Lamotte, C., Pert, C. B. & Snyder, S. H. *Brain Res.* **112,** 407–412 (1976).
16. Jessell, T. M., Tsunoo, A., Kanazawa, I. & Otsuka, M. *Brain Res.* **168,** 247–259 (1979).
17. Yaksh, T. L. & Rudy, T. A. *Physiol. Behav.* **17,** 1031–1036 (1976).
18. Yaksh, T. L. & Rudy, T. A. *J. Pharmac. exp. Ther.* **202,** 411–428 (1977).
19. Jancso, N. *Proc. 3rd Int. Pharmac. Meeting* 33–35 (Pergamon, London, 1966).
20. Szolcsanyi, J. *J. Physiol., Paris* **73,** 251–259 (1977).
21. Jancso, G. Kiraly, E. & Jancso-Gabor, A. *Nature* **270,** 741–743 (1977).
22. Gamse, R., Holzer, P. & Lembeck, F. *Br. J. Pharmac.* **68,** 207–213 (1980).
23. Jessell, T. M., Iversen, L. L. & Cuello, A. C. *Brain Res.* **152,** 183–188 (1978).
24. Yaksh, T. L., Farb, D. H., Leeman, S. E. & Jessell, T. M. *Science* **206,** 481–483 (1979).
25. Theriault, E., Otsuka, M. & Jessell, T. M. *Brain Res.* **170,** 209–213 (1979).
26. Nagy, J. *et al. Brain Res.* **186,** 435–444 (1980).
27. Hökfelt, T., Ljungdahl, A., Terenius, L., Elde, R. & Nilsson, G. *Proc. natn. Acad. Sci. U.S.A.*, **74,** 3081–3085 (1977).
28. Glazer, E. J. & Basbaum, A. I. *Soc. Neurosci. Abstr.* **5,** 723 (1979).
29. Hökfelt, T., Terenius, L., Kuypers, H. G. & Dann, O. *Neurosci. Letts* **14,** 55–60 (1979).
30. Hunt, S. P., Emson, P. C. & Kelly, J. S. *Neurosci. Letts.* Suppl. 3, **200** (1979).
31. Yaksh, T. L. & Wilson, P. R. *J. Pharmac. exp. Ther.* **208,** 446–453 (1979).
32. Reddy, S. V. & Yaksh, T. L. *Brain Res* **189,** 391–401 (1980).
33. Mroz, E. & Leeman, S. E. in *Methods of Hormone Radioimmunoassay* 121–137 (Academic, New York, 1979).

The role of D-1 and D-2 receptors

M. Schachter*, P. Bédard*, A. G. Debono*, P. Jenner*, C. D. Marsden*, P. Price*, J. D. Parkes*, J. Keenan†, B. Smith†, J. Rosenthaler‡, R. Horowski§ & R. Dorow§

*University Department of Neurology, King's College Hospital and Institute of Psychiatry, London SE5 9RS, UK. †Department of Chemical and Clinical Pathology, King's College Hospital, Royal Bethlem and Maudsley Hospitals, London SE5 8AZ. ‡Sandoz, Basle, Switzerland. §Schering, Berlin, FRG.

Dopamine receptors in intracerebral motor and endocrine systems[1,2] have been divided into two main types, D-1 and D-2, dependent on the presence or absence of adenylate cyclase linkage[3]. Here we have investigated a number of dopamine agonist and antagonist drugs in man that have different actions on D-1 and D-2 receptors in animals. Motor and endocrine effects in parkinsonian subjects seem to depend on drug interaction with D-2, but not D-1, receptors. These results may have important implications for the design of anti-parkinsonian and antipsychotic agents.

Many dopamine agonists and antagonists have selective actions on D-1 and D-2 systems, as determined by adenylate cyclase stimulation[4-6] and membrane binding studies[7-9], but examination of possible differences in motor, hormonal and other behavioural effects of these compounds in man has proved difficult because of individual variations in drug pharmacokinetics and the response[10]. Despite these problems, we have attempted to establish the magnitude of the motor, growth hormone and prolactin responses to known plasma levels of levodopa and the dopamine-like ergot derivatives, bromocriptine and lisuride[11,12]. Dopamine in low concentration is an agonist at D-2, and in higher concentration at D-1 receptor sites[13], but the ergot derivatives which act as agonists at D-2 receptors in micromolar concentrations have antagonist actions in nanomolar concentrations on striatal D-1 receptors[14,15]. We have also studied the effects of pimozide, a non-selective dopamine receptor antagonist[16], *cis*-flupenthixol, an effective antipsychotic with D-1 antagonist effects on the striatum[8,17], (blockade of adenyl cyclase activity shows a linear relationship with ^{3}H-*cis*-flupenthixol binding in striatal tissue), and the D-2 antagonists metoclopramide, sulpiride, oxiperomide and tiapride[18], on levodopa-stimulated motor and hormonal changes. These drugs were given to subjects with Parkinson's disease, in which dopamine sensitive adenylate cyclase activity is reduced by at least 50% (ref. 19), although the number of D-2 receptor sites in the striatum is increased, as determined by ^{3}H-haloperidol binding[20]. Following levodopa treatment, specific ^{3}H-spiperone binding approaches normal values[21]. Receptor changes and the loss of presynaptic neurones must influence the motor response to levodopa in parkinsonism: for instance, normal subjects do not readily develop levodopa dyskinesias[22]. Pituitary and hypothalamic dopamine receptor assays have not been reported in parkinsonian patients, but prolactin and growth hormone responses to levodopa are similar to those in age- and sex-matched normal controls[23].

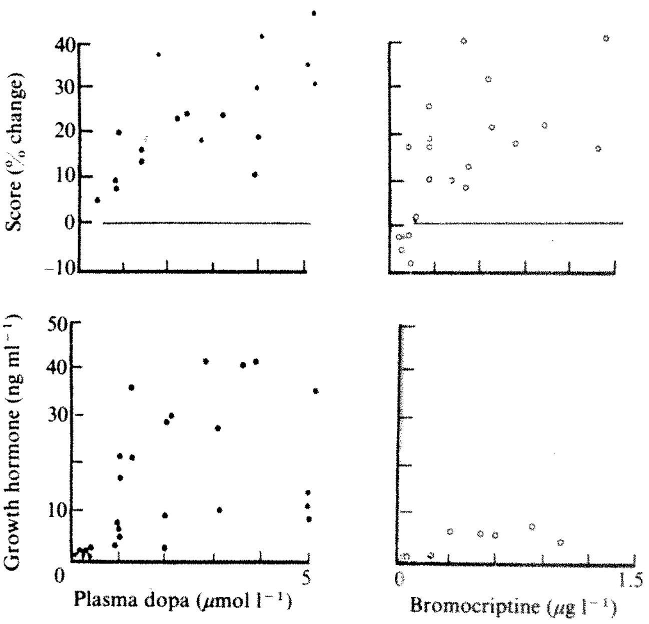

Fig. 1 Peak plasma dopa (μmol l^{-1}) or bromocriptine (μg l^{-1}) level, peak percentage reduction in parkinsonian disability score (score units), and peak elevation of plasma growth hormone level (ng m^{-1}) after single oral doses of levodopa (1 g) or bromocriptine (12.5–100 mg) in subjects with parkinsonism. With dopa, relationship between plasma drug level, motor and growth hormone effect; $r = 0.69$, $P < 0.01$, $n = 18$ and $r = 0{\cdot}50$, $P < 0{\cdot}05$, $n = 27$, respectively; and with bromocriptine, $r = 0.50$, $P < 0.05$, $n = 20$ and $r = 0.10$, not significant, $n = 7$.

Levodopa, bromocriptine and lisuride caused dose-dependent improvement in tremor, akinesia and rigidity, together with dyskinesias, a rise in growth hormone level and a fall in prolactin level in most subjects. Emesis, visual and auditory hallucinosis and delusions occurred with each drug. Bromocriptine and lisuride, but not levodopa, occasionally induced sleep. Systolic and diastolic erect and supine blood pressure fell by 10–20 mm Hg following levodopa, 1 g orally (p.o.), bromocriptine, 100 mg p.o., and lisuride, 0.01 mg intravenously (i.v.). Neither the

Table 1 Timing and duration of response to dopamine agonists

	Peak drug plasma level (min)	Peak therapeutic effect (min)	Peak plasma growth hormone elevation (min)	Peak plasma prolactin depression (min)
Levodopa, 1g p.o.	80	90 (180)	90 (120)	45 (150)
Bromocriptine, 100 mg p.o.	100	130 (480)	170 (120)	60 (480)
Lisuride, 0.15 mg i.v.	—	30 (120)	45 (120)	60 (240)

Values are means after single doses of levodopa, bromocriptine and lisuride in a subject with Parkinson's disease. The total duration of each response is shown in parentheses.

0028–0836/80/280157—03$01.00

Table 2 Effect of levodopa, bromocriptine and lisuride in Parkinson's disease, and of antipsychotic drugs on levodopa-mediated endocrine changes

	No. of patients	Mean peak plasma levodopa level (μmol l^{-1})	Parkinsonism reduction in disability score	Dyskinesia mean dyskinesia score	Growth hormone rise in plasma level (ng ml^{-1})	Prolactin fall in plasma level (%)
Levodopa, 1 g p.o.	(18)	4.5 ± 1	31 ± 4	4 ± 2	20 ± 3	41 ± 10
Bromocriptine 100 mg p.o.	(4)	—	37 ± 8	7 ± 2	6 ± 4*	41 ± 11
Lisuride, 0.15 mg i.v.	(4)	—	25 ± 5	1 ± 1	22 ± 8	43 ± 11
Levodopa, 1 g and pretreatment with antagonists at stated intervals:						
Metoclopramide, 60 mg p.o. 1 h	(14)	5.1 ± 1	21 ± 5	2 ± 1	6 ± 1†	48 ± 15
Pimozide, 6 mg p.o., 1 h	(11)	4.4 ± 1	13 ± 4†	1 ± 1	15 ± 5	
Tiapride, 200 mg p.o., 1 h	(2)	5.2 ± 1	26 ± 4	1 ± 1	16 ± 8	55
Oxiperomide, 10 mg p.o. 1 h	(5)	4.9 ± 2	27 ± 5	1 ± 1	24 ± 5	46 ± 12
cis-flupenthixol, 3 mg p.o. 4 h	(5)	—	17 ± 3	0	20 ± 3	76 ± 6
Sulpiride, 400 mg p.o. 2 h	(5)	—	14 ± 2†	0	2 ± 1‡	50 ± 7
Placebo (sulpiride), p.o. 2 h	(5)	—	31 ± 4	2	18 ± 3	62 ± 12

Mean (±s.e.m.) peak motor and hormonal changes after single doses of dopamine agonists, and after single doses of levodopa, 1 g p.o. preceded at the stated intervals by a range of antipsychotic drugs are shown. Motor responses: peak reduction in parkinsonian disability score and peak dyskinesia score (both King's College Hospital rating scales) are shown. Hormonal responses: peak increase in plasma growth hormone level (ng per ml) and peak reduction in plasma prolactin level (maximum percentage fall from basal level in case of agonists, and from peak stimulated level in case of antagonists) are shown. All observations are over a 4-h period.

* Rise after bromocriptine less than after levodopa or lisuride ($P < 0.05$ in each case, Student's *t*-test).

† Reduction in anti-parkinsonian effect after pimozide, and in growth hormone peak after metoclopramide, compared with levodopa alone ($P < 0.01$ in each case, Student's *t*-test).

‡ Reduction in anti-parkinsonian effect and growth hormone peak after sulpiride compared with levodopa and placebo ($P < 0.025$, Wilcoxon's signed rank test).

motor nor the hormonal responses were biphasic, that is, deterioration in parkinsonism did not precede improvement, and elevation of prolactin level or depression of growth hormone level did not precede the opposite effect. Peak motor and hormonal responses were simultaneous with peak plasma levels of each drug, although each compound had a different pharmacokinetic profile (Table 1). In equipotent anti-parkinsonian doses, the peak rise in plasma growth hormone level with levodopa (20 ± 3 ng ml^{-1}) and lisuride (22 ± 6 ng ml^{-1}) was greater than with bromocriptine (6 ± 3 mg ml^{-1}); $P < 0.05$ in each case.

The dopamine antagonist drugs had comparable motor and hormonal effects (Table 2). Sulpiride (400 mg) and pimozide (6 mg) were most active, and tiapride (200 mg) and oxiperomide (10 mg) were least active in producing antagonism of levodopa-induced motor and hormonal responses. All antagonists caused hyperprolactinaemia, and prolactin levels subsequently fell following levodopa (1 g). All antagonists reduced the severity of levodopa-induced dyskinesias, but also reduced the therapeutic effect of levodopa, with the exception of tiapride (200 mg) and oxiperomide (10 mg). No antagonist prevented the hypotensive action of levodopa.

The motor, endocrine and behavioural effects of levodopa, bromocriptine and lisuride in Parkinson's disease are thus very similar despite the different effects of these drugs on D-1 and D-2 receptors in animal models. The low peak plasma growth hormone response to bromocriptine compared to equipotent anti-parkinsonian doses of levodopa or lisuride may be due to the action of bromocriptine as a weak noradrenergic antagonist[23]. However, lisuride has similar adrenergic effects to bromocriptine[12].

In animal tissues, bromocriptine has dose-dependent antagonist or agonist effects on D-1 receptors, and in behavioural studies causes reduced exploratory activity before motor activation[24]. These changes have been attributed to separate pre- and post synaptic effects of bromocriptine[25], but a dual response with motor and hormonal inhibition at low plasma levels, and stimulation at high levels, is not evident in Parkinson's disease. However, bromocriptine may act as a partial rather than a complete agonist in the motor system, as clinical improvement with very high plasma bromocriptine levels is not always as great as that accompanying lower levels[10].

As with dopamine agonists, there are no distinctions between the actions of selective D-2 and non-selective D-1 and D-2 receptor antagonists in parkinsonism, apart from differences in potency. Metoclopramide and pimozide are both competitive antagonists to the anti-parkinsonian and growth hormone-elevating actions of levodopa, despite different effects on striatal D-1 and D-2 systems, and the other D-2 antagonists also block these responses. Oxiperomide and tiapride prevent levodopa-induced stereotypies but not motor hyperactivity in rodents[26], and in critical dosage have specific antidyskinetic effect in parkinsonism without impairing the therapeutic action of levodopa[27], although the apparent selectivity of these drugs has not been satisfactorily explained.

The motor and endocrine effects of levodopa, bromocriptine, lisuride and also of different dopamine antagonists in parkinsonism can be attributed to the effects of these drugs on D-2 non-adenylate cyclase linked receptors. The physiological significance of the dopamine-sensitive adenylate cyclase is obscure. Phosphodiesterase inhibitors—including caffeine and oxpentifylline—given to retard the breakdown of cyclic AMP have little or no therapeutic effect in parkinsonism[28]. Hormonal responses to dopamine in peripheral tissues, as shown for example by the release of parathormone from the parathyroid, are mediated by dopamine-stimulated increase in intracellular cyclic AMP[29] and cyclic AMP can mimic the hyperpolarizing effect of dopamine when applied directly to ganglionic neurones[30]. However, prolactin suppression by dopamine in pituitary cells does not involve adenylate cyclase mechanisms[15]. The presence of this enzyme in striatal neurones may be more important in determining the intracellular rather than the electrophysiologically significant membrane response to dopamine.

We thank Janssen, Sandoz, Schering and SESIF for gifts of drugs and Mrs P. Asselman for technical assistance.

Received 25 February; accepted 2 May 1980.

1. Ungerstedt, U. *Acta physiol. scand.* Suppl. **82,** 1–48 (1971).
2. Fuxe, K. *Acta physiol. scand.* **58,** 383–384 (1963).
3. Kebabian, J. W. & Calne, D. B. *Nature* **277,** 93–96 (1979).
4. Thorner, M. O. *Clin. Endocr. Metab.* **6,** 201–222 (1977).
5. Schorderet, M. *Neurosci. Lett.* **2,** 187–191 (1976).
6. Kebabian, J. W., Petzold, G. L. & Greengard, P. *Proc. natn. Acad. Sci. U.S.A.* **69,** 2145–2149 (1972).
7. Schwarcz, R., Creese, I., Coyle, J. T. & Snyder, S. H. *Nature* **271,** 766–768 (1978).
8. Hyttel, J. *Life Sci.* **23,** 551–556 (1978).

9. Seeman, P., Lee, T., Chau-Wong, M., Tedesco, J. & Wong, K. *Proc. natn. Acad. Sci. U.S.A.* **72**, 4376–4380 (1975).
10. Price, P., Debono, A., Parkes, J. D., Marsden, C. D. & Rosenthaler, J. *Br. J. clin. Pharmac.* **6**, 303–308 (1978).
11. Corrodi, H., Fuxe, K., Hokfelt, T., Lindbrink, P. & Ungerstedt, U. *J. Pharm. Pharmac.* **25**, 409–413 (1973).
12. Horowski, R. & Wachter, H. *Eur. J. Pharmac.* **36**, 373–378 (1976).
13. Kebabian, J. W. *Life Sci.* **23**, 479–484 (1978).
14. Schmidt, M. J. & Hill, L. E. *Life Sci.* **20**, 789–794 (1977).
15. Pieri, L., Keller, H. H., Burkard, W. & Daprada, M. *Nature* **272**, 278–280 (1978).
16. Anden, N-E., Butcher, S. G., Corrodi, H., Fuxe, K. & Ungerstedt, U. *Eur. J. Pharmac.* **11**, 303–314 (1970).
17. Miller, R. J., Horn, A. S. & Iversen, L. L. *Molec. Pharmac.* **10**, 759–766 (1974).
18. Jenner, P., Elliott, P. N. C., Clow, A., Reavill, C. & Marsden, C. D. *J. Pharm. Pharmac.* **30**, 46–48 (1978).
19. Shibuya, M. *J. neural Transmission* **44**, 287–295 (1979).
20. Lee, T., Seeman, P., Rajput, A., Farley, I. J. & Hornykiewicz, O. *Nature* **273**, 59–61 (1978).
21. Riesine, T. D. *et al. Life Sci.* **21**, 335–344 (1977).
22. Cotzias, G. C., van Woert, M. H. & Schiffer, L. M. *New Engl. J. Med.* **276**, 374–379 (1967).
23. Parkes, J. D. *Adv. Drug Res.* **13**, 247–343 (1977).
24. Dolphin, A. C., Jenner, P., Sawaya, M. C. B., Marsden, C. D. & Testa, B. *J. Pharm. Pharmac.* **29**, 727–736 (1977).
25. Marsden, C. D., Jenner, P., Parkes, J. D., Price, P. & Reavill, C. in *Dopaminergic Ergot Derivatives and Motor Function* (eds Fuxe, K. & Calne, D. B.) 313 (Pergamon, New York, 1979).
26. Costall, B. & Naylor, R. J. *Eur. J. Pharmac.* **33**, 301–312 (1975).
27. Bedard, P., Parkes, J. D. & Marsden, C. D. *Br. med. J.* **1**, 954–956 (1978).
28. Shoulson, I. & Chase, T. N. *Neurology, Minneap.* **25**, 722–724 (1975).
29. Brown, E. M., Carull, R. J. & Aurbach, G. D. *Proc. natn. Acad. Sci. U.S.A.* **74**, 4210–4213 (1977).
30. McAfee, D. A. & Greengard, P. *Science* **178**, 310–312 (1972).

α-Adrenergic receptors modulate β-receptor affinity in rat kidney membranes

Elizabeth A. Woodcock & Colin I. Johnston

Monash University, Department of Medicine, Prince Henry's Hospital,
Melbourne, Australia

Adrenergic receptors were first classified into two classes—α and β—on the basis of the relative pharmacological potencies of agonist compounds[1], and this classification has been supported by subsequent studies. In some tissues, such as the heart and liver[2,3], they exert similar physiological responses, and in other tissues, such as the uterus and vasculature, they have opposing roles[4,5]. The occurrence of both classes of receptor in the same tissue leads to the problem of what determines whether the overall response observed is α-type or β-type, as adrenaline and noradrenaline bind to both receptor classes. Furthermore, direct binding studies have demonstrated that the two receptor classes are distinct and separate entities[6]. We show here that stimulation of α-receptors in renal membranes causes a specific decrease in the affinity of the agonist compound isoprenaline for β-receptors in the same membranes. This demonstrates that interactions occur between renal α- and β-adrenergic receptors. Such interactions may modulate the response of the kidney to sympathetic stimulation.

Adult Sprague–Dawley rats were killed by cervical dislocation. Kidneys were removed immediately and homogenized in 0.25 M sucrose in buffer (50 mM Tris-HCl, *p*H 8.1, 10 mM $MgSO_4$). The homogenate was centrifuged twice at 2,000*g* for 5 min and the final supernatant was centrifuged at 30,000*g* for 15 min. The pellet was washed three times with buffer and finally resuspended in buffer at a protein concentration of 5–10 mg ml^{-1}. Binding studies were carried out as described in detail elsewhere[7]. Renal membranes (0.1 ml) were incubated with 5 nM ^3H-dihydroalprenolol (^3H-DHA, Searle Nucleonics) in a final volume of 0.5 ml in 50 mM Tris-HCl, *p*H 8.1, 10 mM $MgSO_4$, 10^{-4} M pyrocatechol and 0.1% ascorbic acid. Incubation was carried out at 37 °C for 10 min and was terminated by filtration through Whatman GF/C glass fibre filters. The filters were washed with 10 ml ice-cold buffer. Specific binding was defined as binding displaceable by 10^{-5} M isoprenaline and constituted 60–70% of the total binding at 5 nM ^3H-DHA. The characteristics of ^3H-DHA binding sites in these conditions were those expected of β-receptor binding and have been described in detail elsewhere[7]. The relative potencies of adrenergic agonists in competing for binding were isoprenaline > (−)adrenaline ≥ noradrenaline ≫ (+)adrenaline = dopamine. (−)Propranolol was 100 times more potent than (+)propranolol. The α-adrenergic agents phenylephrine and phentolamine competed for binding only at concentrations greater than 10^{-5} M. No competition for ^3H-DHA binding by clonidine was observed at concentrations up to 10^{-4} M. Renal membranes contained 33 ± 3 (s.e.m.) fmol per mg of β-receptors, measured by ^3H-DHA binding. The affinity of the receptors for ^3H-DHA was 1.5 ± 0.4 nM ($n = 6$). Receptor concentration and affinity were calculated by Scatchard analysis[8].

The affinity of the β-adrenergic agonist isoprenaline for renal β-receptors measured in competition experiments with ^3H-DHA was decreased in the presence of 10^{-6} M clonidine from 72 ± 4 nM to 185 ± 20 nM (average of 10 experiments; $P < 0.005$) (Fig. 1). This effect of clonidine was specific for agonists as clonidine had no effect on the affinity of the antagonist propranolol for the same membrane receptors (Fig. 1). Similarly, clonidine had no effect on ^3H-DHA binding in the absence of isoprenaline. ^3H-DHA bound in the presence of 10^{-6} M clonidine was 96% ± 4.4 of controls containing no clonidine. The addition of clonidine also caused a change in the Hill coefficient calculated from the isoprenaline displacement curves. In the presence of 10^{-6} M clonidine, the Hill coefficient increased from 0.75 ± 0.05 to 1.04 ± 0.05 (average of 10 experiments; $P < 0.005$). A Hill coefficient of less than one indicates either multiple classes of binding sites or negative cooperativity. K_I values measured in such conditions represent the average isoprenaline affinity at 50% of maximum isoprenaline binding.

The reduction of β-adrenergic agonist affinity was found to be a specific α-adrenergic receptor-mediated effect. The effect of clonidine was concentration dependent and was maximal at 10^{-8}–10^{-7} M. A decreased isoprenaline affinity was observed with clonidine concentrations as low as 10^{-9} M (Table 1). Moreover, the effect was due to the α-adrenergic agonist action of clonidine, as a similar reduction in isoprenaline affinity occurred with another α-agonist compound, phenylephrine. The α-adrenergic antagonist phentolamine antagonized the effect of clonidine (Table 1). Phentolamine alone had no effect on isoprenaline affinity.

In many different tissue preparations, the affinities of β-receptors for agonist compounds are decreased in the presence

Table 1 Modulation of isoprenaline affinity for renal β-adrenergic receptors

Additions	K_I isoprenaline (nM)	No. of experiments
None	72 ± 4	10
10^{-6}M Clonidine	185 ± 20*	10
10^{-7}M Clonidine	176 ± 31†	4
10^{-8}M Clonidine	172 ± 11‡	4
10^{-9}M Clonidine	112 ± 15†	4
10^{-5}M Phenylephrine	210 ± 42‡	4
10^{-6}M Clonidine plus 10^{-5}M phentolamine	105 ± 8§	4
10^{-4}M GTP	245 ± 12‡	4
10^{-4}M GTP plus 10^{-6}M clonidine	215 ± 31§	4

Values are mean ±s.e.m. *P* values were calculated using a paired *t*-test. K_I values were calculated using the formula: $K_I = I_{50}(I + L/K_L)$, where I_{50} is the concentration of the drug causing 50% inhibition of binding. L and K_L are, respectively, the concentration and the dissociation constant of the ^3H-DHA.

* $P < 0.005$ relative to controls; † $P < 0.025$ relative to controls; ‡ $P < 0.01$ relative to controls; § $P < 0.05$ relative to 10^{-6}M clonidine; § NS relative to 10^{-4}M GTP.

0028–0836/80/280159—02$01.00

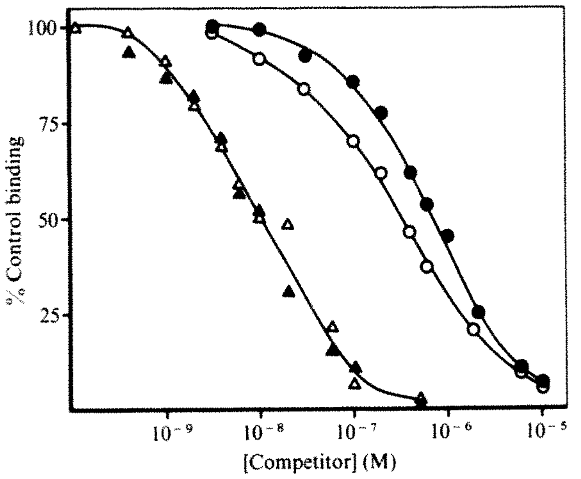

Fig. 1 Effect of clonidine on the affinities of isoprenaline and propranolol for rat kidney β-receptors. ^{3}H-Dihydroalprenolol (5 nM) was incubated with renal membranes in the presence of increasing concentrations of isoprenaline or propranolol and the percentage of control specific binding was determined. A typical experiment is shown. Average values of isoprenaline affinity (K_I) in the presence and absence of clonidine in 10 experiments are given in Table 1. ○, Isoprenaline; ●, isoprenaline and 10^{-6}M clonidine; △, propranolol; ▲, propranolol and 10^{-6}M clonidine.

of GTP and certain GTP analogues[9]. In rat kidney membranes isoprenaline affinity was reduced by 10^{-4} M GTP. The effects of clonidine and GTP were not additive, for in the presence of 10^{-4} GTP, clonidine (10^{-6} M) did not further reduce isoprenaline affinity (Table 1).

There are marked differences in the characteristics of agonist and antagonist binding[10,11]. Receptor affinity for antagonists remains remarkably constant and the Hill coefficient for antagonist binding is generally close to 1.0, indicating a single class of non-interacting binding sites. The Hill coefficient for agonist binding is generally less than 1.0. Also, agonist affinity can be modulated by a variety of agents including guanyl nucleotides[9], Mg^{2+}ion[12] and cholinergic agonists[13]. In general, these factors are thought to influence the apparent binding affinity of agonists through a primary effect on adenylate cyclase or the coupling mechanism between receptor and cyclase[14]; renal α-adrenergic receptors inhibit adenylate cyclase[15]. It is likely that the observed reduction of β-adrenergic agonist affinity in renal membranes by α-adrenergic agonists is also related to an effect on adenylate cyclase.

The kidney contains a functionally heterogeneous population of β-receptors. Although there is little direct evidence, both α- and β-receptors are thought to be present in the renal vasculature[16] on the juxtaglomerular cells[17,18] and β-receptors have been demonstrated on renal tubules[19]. The observed interaction between α- and β-receptors in renal membranes probably occurs in only one of these functional groups. This may explain why the observed shift in isoprenaline affinity is small compared with that caused by GTP in other tissues[9,12]. However, the lack of any additive effect of clonidine and GTP suggests that these two agents influence the same receptor population. This interaction between α- and β-receptors seems to be specific to the kidney, as we have been unable to demonstrate any effect of clonidine on isoprenaline affinity in cardiac membranes.

This work was supported by grants from the Life Insurance Medical Research Fund of Australia and the National Heart Foundation of Australia. We thank Ms C. Olssen for technical assistance.

Received 29 January; accepted 9 May 1980.

1. Ahlquist, R. P. *Am. J. Physiol.* **153**, 586–600 (1948).
2. Watanabe, A. M., Hathaway, D. R., Besch, H. R. Jr, Farmer, B. B. & Harris, R. A. *Circulation Res.* **40**, 596–604 (1977).
3. Exton, J. H. *Biochem. Pharmac.* **28**, 2237–2240 (1977).
4. Borda, E., Sauvage, J., Sterin-Forda, L., Gimino, M. F. & Gimeno, A. L. *Eur. J. Pharmac.* **56**, 61–67 (1979).
5. Fleisch, J. H. *Blood Vessels* **11**, 193–211 (1974).
6. Wood, C. L., Caron, M. G. & Lefkowitz, R. J. *Biochem. biophys. Res. Commun.* **88**, 1–8 (1979).
7. Woodcock, E. A. & Johnston, C. I. *Hypertension* **2**, 156–161 (1980).
8. Scatchard, G. *Ann. N.Y. Acad. Sci.* **51**, 662–672 (1949).
9. Hegstrand, L. R., Minneman, K. P. & Molinoff, P. B. *J. Pharmac. exp. Ther.* **210**, 215–221 (1979).
10. Limbird, L. E. & Lefkowitz, R. J. *Proc. natn. Acad. Sci. U.S.A.* **75**, 228–232 (1978).
11. Weiland, G. A., Minneman, K. P. & Molinoff, P. B. *Nature* **281**, 114–117 (1979).
12. Bird, S. J. & Maguire, M. R. *J. biol. Chem.* **253**, 8826–8834 (1978).
13. Watanabe, A. M. *et al. J. biol. Chem.* **253**, 4833–4836 (1978).
14. Maguire, M. E., Ross, E. M. & Gilman, A. G. *Adv. Cyclic Nucleotide Res.* **8**, 1–83 (1977).
15. Beck, N. P., Reid, S. W., Murdaugh, H. V. & Davis, B. B. *J. clin. Invest.* **51**, 939–944 (1972).
16. La Grange, R. G., Sloop, C. H. & Schmidt, H. E. *Circulation Res.* **33**, 704–712 (1973).
17. Johnson, J. A. *et al. Am. J. Physiol.* **230**, 410–418 (1978).
18. Pettinger, W. A., Keeton, T. K., Campbell, W. B. & Harper, D. C. *Circulation Res.* **38**, 338–346 (1976).
19. Morel, F., Chabardes, D. & Imburt-Teboul, M. *Proc. 7th int. Cong. Nephrology*, Montreal, 209–216 (Karger, Basle, 1978).

Cleavage of endorphins to des-Tyr endorphins by homogeneous bovine brain aminopeptidase

Louis B. Hersh*, Thomas E. Smith*
& Jeffrey F. McKelvy†

*Department of Biochemistry, The University of Texas Health Science Center at Dallas, Dallas, Texas 75235
†Departments of Psychiatry and Biochemistry, The University of Pittsburgh School of Medicine, Pittsburgh, Pennsylvania 15261

Attention has recently focused on the possible biological roles of peptides related to β-lipotropin (β-LPH)[1,2]. In particular, observations suggest that certain peptide fragments derivable from β-LPH, including γ-endorphin (β-LPH_{61-77}) and α-endorphin (β-LPH_{61-76}), may be involved in various modes of behavioural adaptation[2,3]. Structure–activity studies on behavioural actions of γ-endorphin, an opioid peptide, revealed that the omission of N-terminal tyrosine resulted in a non-opioid peptide, des-Tyr-γ-endorphin, which exhibited greater behavioural activity than γ-endorphin[3]. Subsequent biochemical studies provided evidence for the association with brain synaptic plasma membranes of peptidase activities which could produce γ- and α-endorphins and their des-Tyr derivatives from exogenous β-endorphin[4]. This and earlier observations[4–6] suggest that regulatory physiological events are focused on the N-terminal tyrosine residue; enzymatic reactions exerted at this residue are thus of great interest. We recently purified to homogeneity an aminopeptidase from bovine brain which catalyses the hydrolysis of Met[5]- or Leu[5]-enkephalin by sequential release of amino acids from the amino terminus of the enkephalin molecule[7]. The ability of this enzyme, purified from bovine[7], monkey[8] or rat[9] brain, to use endorphins as substrates has not been previously examined. We now present quantitative studies which show that homogeneous bovine brain enkephalin aminopeptidase catalyses the hydrolysis of the N-terminal tyrosine from γ-, α- and β-endorphins with substantial turnover numbers and yields only the des-Tyr derivatives. These results suggest that this enzyme may be involved in regulating the concentrations of opioid- and opioid-derived biologically active peptides in the brain.

We incubated homogeneous bovine brain aminopeptidase, previously shown to catalyse the hydrolysis of Met^5- and Leu^5-enkephalins[7] ($K_m = 22$ µM, $V_{max} = 20$ µmol per min per mg enzyme for the Tyr^1-Gly^2 bond), with synthetic α-, β- and γ-endorphins, and compared their hydrolysis with that of Met^5-enkephalin in the same experimental conditions by subjecting aliquots of the incubation mixtures to amino acid analysis at various times of incubation. All the commercial synthetic peptides were tested before use by HPLC and amino acid analysis and judged to be pure. The enzymatic digestions were carried out in incubation conditions in which linear rates of

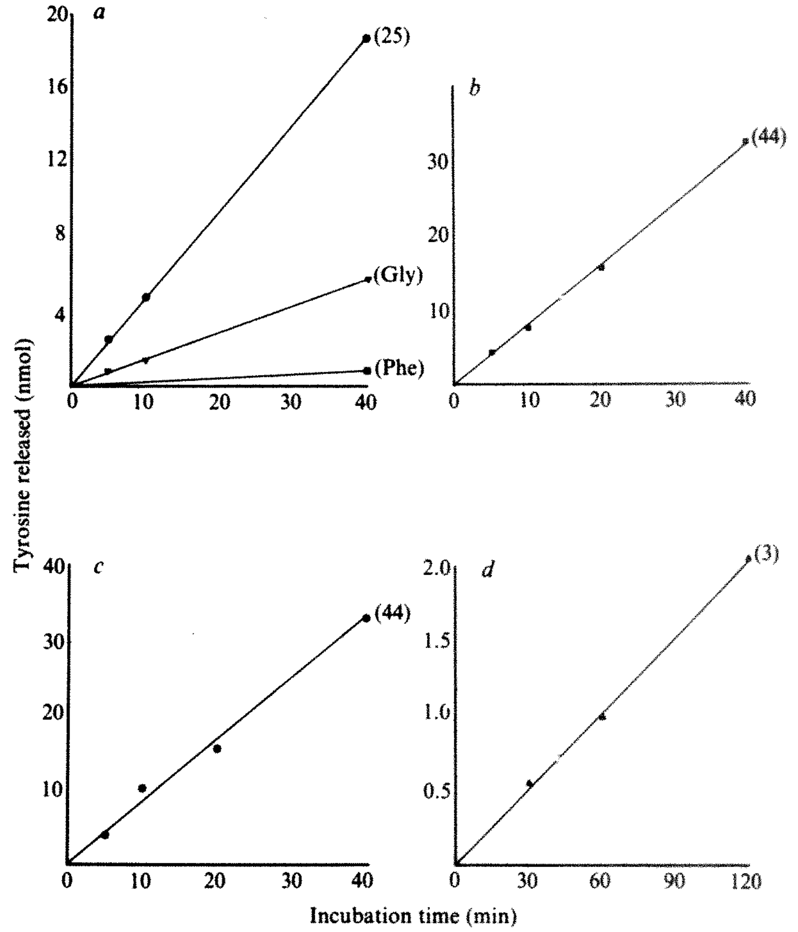

Fig. 1 Release of tyrosine from Met^5-enkephalin and α-, β-, and γ-endorphin catalysed by bovine brain aminopeptidase. Reaction mixtures containing 50 mM Tris-HCl buffer, *p*H 7.4, 0.5 mM substrate (Peninsula) and bovine brain aminopeptidase in a total volume of 150 μl were incubated at 37 °C. At the time points indicated, a 35-μl aliquot was withdrawn, diluted to 0.5 ml with water and boiled for 1 min. The boiled solution was filtered through a 0.45-μm Millipore filter, washed with 1.5 ml of water and the combined effluents lyophilized. The lyophilized samples were dissolved in 100 μl of sodium formate buffer (0.2 M in sodium ion) at *p*H 2.21 and applied directly to an amino acid analyser microbore single column system containing DC-4A cation exchange resin (Pierce). The amino acids were eluted using a three-buffer programme: 0.2 M sodium formate *p*H 3.28, 0.2 M sodium formate *p*H 4.38, and 0.2 M sodium borate *p*H 10.2. The amino acids were identified and quantified by comparison with standards run at various intervals between samples. Analyses were carried out on an Aminco Aminolyzer fluorometric liquid chromatography system equipped with a Shimadzu digital integrator. The fluorogenic reagent used was a *o*-phthalaldehyde. *a*, Tyrosine and glycine release from Met^5-enkephalin using 23 ng of enzyme; *b*, tyrosine release from α-endorphin using 115 ng of enzyme; *c*, tyrosine release from γ-endorphin using 115 ng of enzyme; *d*, tyrosine release from β-endorphin using 172 ng of enzyme. The values in parentheses represent the percentage of the substrate degraded.

hydrolysis were measured. Control incubations in which enzyme and substrate, respectively, were omitted, or in which boiled enzyme was used, revealed that no free amino acids were generated by non-enzymatic breakdown of substrate or by enzyme autolysis.

As shown in Fig. 1, homogeneous bovine brain aminopeptidase catalyses the release of the N-terminal tyrosine residue from Met^5-enkephalin and from α-, γ- and β-endorphins. As shown in Table 1, the rate of hydrolysis of α- and γ-endorphins was approximately 30% that of Met^5-enkephalin whereas β-endorphin was hydrolysed at a much lower rate—0.5% relative to Met^5-enkephalin. It is interesting that whereas glycine was also released from Met^5-enkephalin at about one-third the rate of tyrosine, no glycine was liberated from α- or γ-endorphin, even in conditions in which over 40% of the tyrosine was released. These results suggest that, unlike des-Tyr-Met^5-enkephalin, des-Tyr-α- and des-Tyr-γ-endorphins adopt a conformation resistant to further degradation by the aminopeptidase. This resistance could contribute to the metabolic stability of these peptides and thus to their biological activity. Note also that the homogeneous bovine brain aminopeptidase exhibited substantial turnover numbers for the hydrolysis of the N-terminal tyrosine of α- and γ-endorphins, 689 and 634 min^{-1} relative to 2,040 min^{-1} for Met^5-enkephalin (Table 1). This rapid rate of reaction with these endorphins raises the possibility of an *in vivo* role for the aminopeptidase in partitioning peptide fragments derived from β-endorphin between opioid and non-opioid pathways in response to functional demands. The rate of release of N-terminal tyrosine from β-endorphin was much lower than that for the other endorphins; although the extent of cleavage was relatively small in the conditions used, the enzyme seemed to produce only the des-Tyr fragment of β-endorphin. Whether this reaction, which would produce a non-opioid derivative of β-endorphin, is of physiological significance, for example, by being modulable by regulatory agents, is a subject for further study.

Our results provide new biochemical evidence in support of the hypothesis that des-Tyr α- and des-Tyr-γ-endorphins may have a role in brain function, as we have observed that a homogeneous brain aminopeptidase catalyses the cleavage of the N-terminal tyrosine residue from α- and γ-endorphins at a rapid rate to yield the des-Tyr derivatives with no further cleavage of the peptide. The relationship between this activity and the production of des-Tyr-α- and des-Tyr-γ-endorphins from β-endorphin by a rat brain "synaptic plasma membrane" (SPM) fraction observed by Burbach *et al.*[4], is not known. However, in the latter study, marker enzyme data were not presented to aid in understanding to what extent the vesiculation known to accompany the preparation of such membranes may have resulted in the inclusion of synaptoplasmic elements, possibly including the soluble aminopeptidase which we have described. It will be interesting to compare the properties of the SPM-associated production of des-Tyr α- and des-Tyr-γ-endorphins with those tabulated for our homogeneous enzyme preparation in terms of sensitivity to mercurials, puromycin and chelators. On the other hand, it may be that these are separate

Table 1 Rate of tyrosine release from Met^5-enkephalin and α-, β- and γ-endorphin by bovine brain aminopeptidase

Substrate	Rate of tyrosine release (μmol per min per mg enzyme)	Turnover number (min^{-1})
Met^5-enkephalin	20.4 (6.1)	2,040
α-Endorphin	6.5	634
γ-Endorphin	6.9	689
β-Endorphin	0.10	10

The data from Fig. 1 were used to calculate the rate of tyrosine release. The value in parentheses is the rate of glycine release.

*For hydrolysis of the Tyr^1–Gly^2 bond; molecular weight of the enzyme, 100,000 (ref. 7).

activities, and that the soluble aminopeptidase acts on a different metabolic pool of endorphins. *A priori*, based on our lack of knowledge of the modes of action of peptides in intercellular communication in the nervous system, there is no reason to assume that soluble enzymes metabolizing peptides could not be importantly involved in the use of peptides as primary output signals. In addition, many enzymes formerly considered to be soluble on the basis of extractability properties are now known to exhibit transient associations with subcellular organelles, such as hexokinase with mitochondria[10] and choline-acetyltransferase with synaptic vesicles[11], and are solubilized from such organelles by metabolites as part of regulatory intracellular processes. It will be of interest to investigate brain peptidase activities from this perspective.

This research was supported by grant DA-02243 from the National Institute of Drug Abuse (L.B.H. and J.F.M.), grant I-391 from the Robert A. Welch Foundation (L.B.H.), grant GM-21650 from the NIH (T.E.S.) and grant GB-4034 from the NSF (J.F.M.). J.F.M. is a recipient of Research Career Development Award AM-00331 from the NIH.

Received 7 March; accepted 2 May 1980.

1. Rossier, J. *et al. Nature* **270**, 618–620 (1977)
2. deWied, D in *Characteristics and Functions of Opioids* (eds VanRee, J M & Terenius, L.) 113–122 (Elsevier, Amsterdam, 1978).
3. deWied, D., Kovacs, G. L., Bohus, B., VanRee, J M & Greven, H. M *Eur J Pharmac* **49**, 427–436 (1978)
4. Burbach, J. P H *et al. Nature* **283**, 96–97 (1980)
5. Frederickson, R. C. A. *Life Sci* **21**, 23–42 (1977)
6. Smyth, D G, Massey, D. E., Zakarian, S. & Finnie, M D. *Nature* **279**, 252–254 (1979)
7. Hersh, L. B. & McKelvy, J F *J Neurochem* (in the press)
8. Hayashi, M *J Biochem.* **84**, 1363–1372 (1978).
9. Schnebli, H. P., Phillipps, M A. & Barclay, R. K. *Biochim biophys Acta* **569**, 89–98 (1979)
10. Felgner, P. L., Messer, J. L & Wilson, J E *J biol Chem* **254**, 4946–4951 (1979)
11. Fonnum, F. *Biochem J* **109**, 389–398 (1968).

Identification of a tetrodotoxin-sensitive Na^+ channel in a variety of fibroblast lines

J. Pouysségur, Y. Jacques & M. Lazdunski

Centre de Biochimie, Faculté des Sciences, Parc Valrose, 06034 Nice, France

The action potential Na^+ ionophore of excitable cells can be activated either by alkaloid compounds such as veratridine, or by small polypeptide toxins extracted from scorpion venom or sea anemone[1,2]. One of the main features of this Na^+ channel is that it is blocked by tetrodotoxin (TTX). However, we report here that during analysis of Na^+ influx in resting fibroblasts, we found that a variety of fibroblast lines also possess a TTX receptor. Veratridine and sea anemone toxin act synergistically to stimulate Na^+ influx 7 to 10-fold in hamster and rat fibroblasts. As in excitable cells, this toxin-stimulated Na^+ influx is blocked by TTX. Addition of serum to hamster fibroblasts arrested in G_0 stimulates Na^+ influx three-fold. Observations that TTX does not prevent serum-activated Na^+ influx, initiation of DNA synthesis and cell proliferation suggest that the fast Na^- channel which we have identified in fibroblasts is not involved in growth control.

The gating system of the Na^+ channel in excitable cell systems such as nerve, skeletal muscle, cardiac cell and neuroblastoma is altered by veratridine and sea anemone toxin II[3–5]. These toxins also reveal 'silent' channels[6]. Figure 1 shows that the well known action of these toxins on excitable membranes is also observed in fibroblasts. The kinetics of $^{22}Na^+$ uptake in the Chinese hamster lung fibroblast line CC139 (ATCC) are shown in Fig. 1*a*. Veratridine at 100 µM or sea anemone toxin at 10 µM have no effect on $^{22}Na^+$ influx. However, when added together, these toxins effect a 5–10-fold stimulation in the 5-min Na^+ uptake in these fibroblasts (Fig. 1, Table 1). The toxin-activated influx is completely inhibited by TTX. Half-maximal inhibition is observed at 20–40 nM TTX. The apparent affinity of TTX for the fibroblast Na^+ channel is identical to that found in similar studies with spiking neuroblastoma cells[5]. Also, the number of Na^+ channel receptors might be even higher in CC139 than in neuroblastoma cells, as suggested by comparison of the toxin-stimulated Na^+ fluxes of these two cell lines (Table 1).

When Na^+ efflux through the $(Na^+ + K^+)$ATPase system is inhibited with ouabain, the addition of veratridine (100 µM) and sea anemone toxin (10 µM) to CC139 cells leads to rapid lysis (Fig. 2), which is due to an increase in cell osmotic pressure caused by massive Na^+ entry. Cell lysis is prevented when TTX is added before the other toxins, when ouabain is omitted (Na^+ escapes from the cells) or when external Na^+ is replaced by choline$^+$.

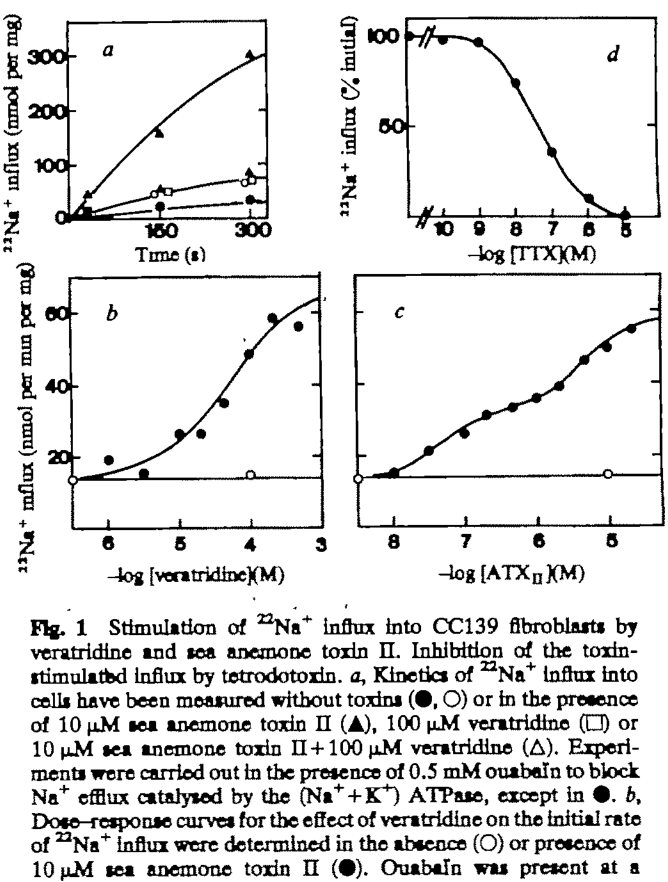

Fig. 1 Stimulation of $^{22}Na^+$ influx into CC139 fibroblasts by veratridine and sea anemone toxin II. Inhibition of the toxin-stimulated influx by tetrodotoxin. *a*, Kinetics of $^{22}Na^+$ influx into cells have been measured without toxins (●, ○) or in the presence of 10 µM sea anemone toxin II (▲), 100 µM veratridine (□) or 10 µM sea anemone toxin II + 100 µM veratridine (△). Experiments were carried out in the presence of 0.5 mM ouabain to block Na^+ efflux catalysed by the $(Na^+ + K^+)$ ATPase, except in ●. *b*, Dose–response curves for the effect of veratridine on the initial rate of $^{22}Na^+$ influx were determined in the absence (○) or presence of 10 µM sea anemone toxin II (●). Ouabain was present at a concentration of 0.5 mM. *c*, Dose–response curves for the effect of sea anemone toxin II (ATX$_{II}$) determined in the absence (○) or presence of veratridine (100 µM) (●). Ouabain was present at a concentration of 0.5 mM. *d*, Inhibition by TTX of the stimulating effect induced by the mixture of sea anemone toxin II (10 µM) and veratridine (100 µM) on the initial rate of $^{22}Na^+$ influx in the presence of 0.5 mM ouabain. $^{22}Na^+$ influx into confluent monolayers of CC139 cells was determined at 37 °C essentially as described previously for neuroblastoma cells[5]: culture medium of 35-mm dishes was first replaced by 1 ml of a saline solution buffered with 25 mM HEPES-Tris (*p*H 7.4) and containing 140 mM NaCl, 5.4 mM KCl, 1.8 mM $CaCl_2$, 0.8 mM Mg SO_4, 5 mM glucose and 0.1 mg ml^{-1} bovine serum albumin. After a 5-min preincubation of cells in this medium, $^{22}Na^+$ influx was then initiated by replacing the preincubation medium by 1 ml of the same saline solution isotopically labelled with $^{22}NaCl$ (2 µCi ml^{-1}). Ouabain (0.5 mM) and toxins were present in this uptake medium except when indicated. $^{22}Na^+$ influx was stopped 5 min later by removing the radioactive medium and washing the cells three times with 1 ml of a Na^+- and K^+-free saline solution at room temperature. In these conditions less than 5% of intracellular $^{22}Na^+$ is lost during the 15 s of the washing procedure. After solubilization of cells in 1 ml of NaOH (0.1 M), radioactivity was determined by scintillation counting and the initial rate of $^{22}Na^+$ influx calculated from the amount of $^{22}Na^+$ taken up in 5 min assuming linear kinetics. The time points of *a* were determined as described for the 5-min uptake points.

0028–0836/80/280162—03$01 00

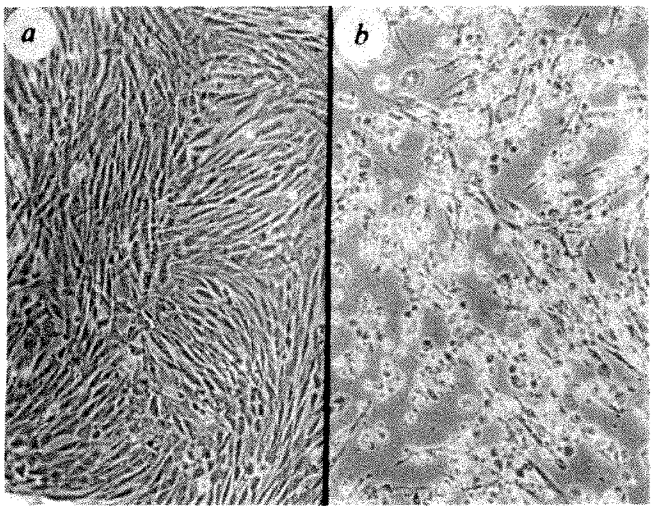

Fig. 2 Veratridine and sea anemone toxin-induced cell lysis in CC139 fibroblasts. Cells cultured in Dulbecco's modified Eagle's medium supplemented with 10% fetal calf serum were incubated with no drug (*a*) or with 100 μM veratridine + 10 μM sea anemone toxin and 0.5 mM ouabaïn (*b*). Phase contrast micrographs were taken 12 h after drug addition. Cell swelling is seen only after at least 30 min and 1 h before cell lysis (few cells) is detected. However, 2–3 h are required to see massive cell lysis. Incubation of the cells with ouabaïn alone or with the toxin mixture in the absence of ouabaïn over 24 h does not induce cell lysis (not shown).

Although CC139 cells have the morphology of fibroblasts, form fibrosarcoma tumours and do not generate action potentials, the origin of this established cell line cannot be known definitively. We therefore looked for fast Na^+ channels in two other fibroblast lines of Chinese hamster (CHO and CHL-V79), in a rat Fisher fibroblast line[7] and its polyoma virus-transformed derivative, and in chick embryo fibroblasts. Interestingly, all the cells possess a Na^+ channel stimulated by the mixture of veratridine and sea anemone toxins (Table 1). Although the stimulation effected by these toxins varied from 1.5- to 10-fold depending on the cell line, 30–50 nM TTX elicited half-maximal inhibition of Na^+ influx in all the cells tested. These results demonstrate the ubiquity of the fast Na^+ channel in fibroblasts from different origins.

It has been proposed that an increase in Na^+ influx might be the initial mitogenic signal in many cell systems[8]. Therefore, we have investigated whether the fast Na^+ channel of CC139 fibroblasts has any role in controlling their division. These cells can be arrested in G_0 by serum depletion. Figure 3 shows that reinitiation of DNA synthesis by 10% fetal calf serum is preceded by a very early threefold stimulation of Na^+ influx. The influx in these conditions is not blocked by TTX. This result, together with the observations that TTX does not affect the Na^+ uptake of growing fibroblasts, prevent reinitiation of DNA synthesis or alter cell division (not shown), strongly suggests that the TTX-sensitive Na^+ channel of fibroblasts is not involved in growth control.

Accordingly, these fibroblasts, like excitable cells, have receptors for veratridine, sea anemone toxin and TTX. The dose–response curves for the association of the different toxins with their respective receptors occur in a range of toxin concentrations which is similar for fibroblasts (Fig. 1*b*, *c*, *d*) and for excitable cells such as neuroblastoma[5]. Veratridine or sea anemone toxin alone significantly stimulate $^{22}Na^+$ entry through the TTX-sensitive Na^+ channel of neuroblastoma cells, and the two toxins act in synergy. In contrast, neither toxin alone stimulates $^{22}Na^+$ entry into fibroblasts (Fig. 1*a*); the mixture of the two toxins is essential for activation of the TTX-sensitive Na^+ channel. Electrophysiological studies are under way in an attempt to understand the differences between TTX-sensitive Na^+ channels in fibroblasts and those in excitable cells like neuroblastoma cells. Also, we hope to use the toxin-activable Na^+ channel of CC139 fibroblasts as a Na^+ microinjection device with which to

Table 1 Effect of veratridine and sea anemone toxin II on Na^+ influx in various fibroblast cell types

Cell type	Origin	5 min $^{22}Na^+$ uptake (nmol per mg protein) Basal	 Veratridine + sea anemone toxin	Stimulation (fold)
CC139	Chinese hamster lung fibroblast (ATCC)	72	570	7.9
CHL-V79	Chinese hamster lung fibroblast (ATCC)	88	95	1.1(2.1)
CHO	Chinese hamster ovary (Toronto's strain)	67	190	2.8(4.7)
FR-3T3	Rat Fisher fibroblasts[7]	16	154	9.6
3T3-PY	Rat Fisher-polyoma transformed	67	132	2
CEF	Secondary chick embryo fibroblast	67	93	1.4
NIE-115	Neuroblastoma	46	320	7

$^{22}Na^+$ uptake was measured as described in Fig. 1 legend, in the presence of 0.5 mM ouabaïn (basal) or 100 μM veratridine + 10 μM sea anemone toxin II for the toxin-stimulated influx. Values in parentheses represent the toxin-stimulation factor when cells were arrested by serum deprivation (serum deprivation reduces basal Na^+ influx, see Fig. 3). All values represent the average of duplicate experiments (less than 10% difference was observed in duplicate determinations).

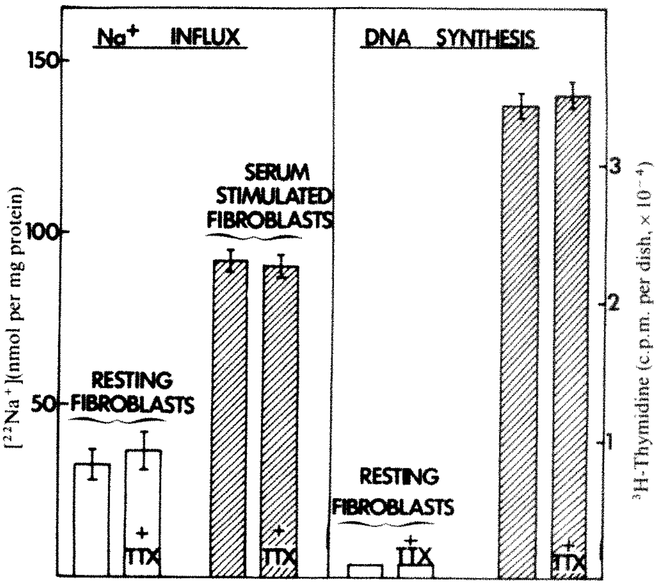

Fig. 3 Serum induced Na^+ influx and DNA synthesis in quiescent fibroblasts. Confluent CC139 fibroblasts were arrested in G_0/G_1 by incubating the cells in serum-free medium for 30 h. Na^+ influx was measured in the presence of 0.5 mM ouabaïn. Values represent 5 min $^{22}Na^+$ uptake in resting fibroblasts or in cells stimulated for 5 min with 10% fetal calf serum (hatched bar). For measurements of DNA synthesis, serum-deprived cells were incubated for 24 h in the presence of 0.5 μCi ^3H-thymidine without (empty bar) or with (hatched bar) 10% fetal calf serum. Where indicated +TTX, tetrodotoxin was added at 10^{-5} M during Na^+ uptake studies or during the 24 h of thymidine incorporation.

analyse the possible role of increased Na^+ influx in mitogenicity. These cells respond well to purified growth factors[9]. Finally, the toxin-effected cell lysis shown in Fig. 2 provides a powerful selection procedure for developing the genetics of Na^+ gating membrane components in a diploid and rapidly growing cell line.

We thank Mrs A. Franchi for technical assistance and Dr M. Murphy for reading the manuscript.

Received 18 February; accepted 7 May 1980.

1. Narahashi, T. *Physiol. Rev.* **54,** 813–889 (1974).
2. Lazdunski, M. *et al.* in *Function and Molecular Aspects of Biomembrane Transport* (eds Quagliariello, E., Palmieri, F., Papa, S. & Klinkenberg, M.) 25–42 (Elsevier, Amsterdam, 1979).
3. Catterall, W. A. & Nirenberg, M. *Proc. natn. Acad. Sci. U.S.A.* **70,** 3759–3763 (1973).
4. Fosset, M., De Barry, J., Lenoir, M. C. & Lazdunski, M. *J. biol. Chem.* **252,** 6112–6117 (1977).
5. Jacques, Y., Fosset, M. & Lazdunski, M. *J. biol. Chem.* **253,** 7383–7392 (1978).
6. Romey, G., Jacques, Y., Schweitz, H., Fosset, M. & Lazdunski, M. *Biochim. biophys. Acta* **556,** 344–353 (1979).
7. Seif, R. & Cuzin, F. *J. Virol.* **24,** 721–728 (1977).
8. Koch, K. & Leffert, H. *Nature* **279,** 104–105 (1979).
9. Pérez, R., Franchi, A. & Pouysségur, J. *2nd int. Cell Biol. Meet.*, Berlin (in the press).

Loss of immune competence with age may be due to auto-anti-idiotypic antibody regulation

Myron R. Szewczuk & Rita J. Campbell

The Host Resistance Program, Department of Pathology, McMaster University Medical Centre, Hamilton, Ontario, Canada L8N 3Z5

The decline in immune function with ageing involves both a loss of B-cell function[1,2] and a decline in T-cell function[3-5]. This picture has been complicated by the recent observation that normal old mice produce more B-cell mitogen-induced autoantibodies to syngeneic erythrocytes than do young animals[6]. They also produce elevated levels of IgM and IgA anti-IgG autoantibodies[7] and increased suppressor-cell activites[8-10]. It is therefore difficult to explain the relationships between autoantibody production, increased suppressor-cell activities and the loss of immune competence in old animals. Recently, auto-anti-idiotypic antibody regulation has been proposed to explain a rapid decline in the antibody-forming cell response to antigen during a normal immune response in young adult mice[11]. Schrater *et al.*[12] have suggested that this antibody, produced during the immune response, combines with B-cell-surface antigen receptors and thus inhibits antibody secretion. If the number of B cells is normal in old animals[13], but their function is impaired, it may be that the decline in immune competence with age is due to auto-anti-idiotypic antibody regulation, perhaps affecting the B-cell-surface antigen receptors and preventing the cell from responding normally to exogenous antigens. We have therefore investigated whether auto-anti-idiotypic antibody could be detected in immune splenic B cells from old and young mice of the same strain. We report here that auto-anti-idiotypic antibody regulation seems to have a role in the loss of B-cell function with age.

We first immunized various aged C57BL/6J male mice intraperitoneally (i.p.) with a highly thymic-dependent antigen, trinitrophenylated bovine γ-globulin (TNP-BGG) in complete Freund's adjuvant (CFA). Splenic anti-TNP plaque-forming cell (PFC) responses were assayed 2 weeks after immunization. As shown in Table 1, 4-month-old mice produced high numbers of IgM, IgG and IgA anti-TNP PFCs whereas the 1- and 2-month-old mice produced relatively low numbers. However, mice of 8 months or older showed a significant decline in the number of anti-TNP PFCs in the three isotypes studied as compared with the PFC responses of the 4-month-old group. Thus, aged ani-

Table 1 Effect of age on the number of splenic anti-TNP PFCs in C57BL/6J mice given TNP-BGG

		Splenic anti-TNP PFCs per 10^8 cells		
Age (months)	No. of mice	IgM PFCs	IgG PFCs	IgA PFCs
1	13	1,090 (±0.56)	1,594 (±0.83)	559(±0.65)
		$P<0.001$	NS	$P<0.001$
2	26	1,146(±0.91)	1,464(±0.58)	1,479(±0.62)
		$P<0.005$	$P<0.02$	$P<0.001$
4	19	2,325(±0.48)	2,323(±0.55)	3,153(±0.42)
8	25	1,978(±0.39)	1,266(±0.35)	1,288(±0.59)
		NS	$P<0.001$	$P<0.001$
11	3	1,807(±0.39)	1,024(±0.57)	1,499(±0.37)
		NS	$P<0.05$	$P<0.01$
15	5	707	987	833
24	2	351(±0.40)	337(±1.10)	456(±1.62)
		$P<0.001$	$P<0.001$	$P<0.001$

Male mice received 500 μg TNP-BGG in CFA i.p. Splenic anti-TNP PFCs per 10^8 nucleated cells were assayed 2 weeks after immunization. Data presented are the geometric means of pooled spleens from three to five animals from three to six independent experiments. The data from the 11- and 24-month groups are geometric means from individual spleens. The data from the 15-month group are from pooled spleens from five animals from one experiment. The value in parentheses is the natural logarithm of s.d. obtained from natural log-transformed data. The *t*-test was used to evaluate the statistical significance of differences on natural long-transformed data. NS, Not significantly different. Anti-TNP PFCs were determined by the method of Jerne *et al.*[21] as modified for a slide assay by Dresser and Greaves[22]. Rabbit anti-mouse IgG and rabbit anti-mouse IgA were used at predetermined optimal dilution (1:300), to develop indirect IgG and IgA plaques, respectively. The IgA-developing serum was prepared in rabbits by using pure mouse myeloma MOPC 315 (IgAλ2). The antiserum was depleted of anti-light-chain activity by passage through a pure mouse IgG-Sepharose 4-B immunoadsorbent column. The IgG-developing serum was prepared in rabbits by using purified mouse IgG (Miles, Lot 51). The antisera showed only a single line against normal mouse sera and pure IgG on Ouchterlony analysis. Pure mouse IgA or IgG when added to the PFC assay inhibited the development of only IgA or IgG PFCs, respectively, when the respective developing sera were added. Before developing indirect plaques, goat anti-μ was used to inhibit >95% IgM plaques during the first incubation period. The anti-μ antiserum was prepared in goats by using pure mouse MOPC 104E (IgMλ1) (Bionetics, Lot AJ110). It was passaged through a pure mouse IgG–Sepharose 4-B immunoadsorbent column to deplete anti-light-chain activity.

Table 2 Effect of age on the heterogeneity of affinity of splenic anti-TNP PFC responses in C57BL/6J mice

		Heterogeneity index		
Age (months)	No. of mice	For IgM PFCs	For IgG PFCs	For IgA PFCs
2	15	0.88±0.52	2.27±0.13	1.50±0.18
		($P<0.001$)	($P<0.02$)	($P<0.001$)
4	12	1.64±0.49	2.04±0.27	2.12±0.20
8	20	0.51±0.38	1.22±0.83	0.63±0.63
		($P<0.001$)	($P<0.001$)	($P<0.001$)
15	5	0.33	0.50	0.37
24	2	0	0	0.87±0.62
				($P<0.001$)

Male mice received 500 μg TNP-BGG in CFA i.p. Splenic anti-TNP PFCs were assayed 2 weeks after immunization. The Shannon heterogeneity index[15] was used to describe the degree of heterogeneity of affinity of the IgM, IgG and IgA anti-TNP PFC population of pooled spleens from three to five mice. The values presented are the means ± s.d. from three or four independent experiments. The values from the 15-month group were obtained from a single pool of five mice from one experiment. The values from the 24-month group were obtained from individual spleens and presented as means ± s.d. from two animals. The larger the index, the greater the heterogeneity. The *t*-test was used to evaluate the statistical significance in the heterogeneity indices as compared with the 4-month-old group.

0028-0836/80/280164—03$01.00

Table 3 Effect of age on the appearance of anti-idiotype-blocked hapten-augmentable, anti-TNP PFCs during the normal immune response to TNP-BGG in C57BL/6J mice

Age (months)	No. of mice	TNP-EACA	Splenic anti-TNP PFCs per 10^8 cells					
			IgM PFCs	(% aug PFCs)	IgG PFCs	(% aug PFCs)	IgA PFCs	(% aug PFCs)
2	15	–	2,154		2,035		1,838	
		+	2,283	6%	2,340	15%	2,022	10%
4	10	–	2,084		1,350		2,394	
		+	2,272	9% (NS)	1,755	30% ($P<0.005$)	2,729	14% (NS)
8	15	–	3,818		1,856		2,196	
		+	5,765	51% ($P<0.001$)	3,972	114% ($P<0.001$)	4,085	86% ($P<0.001$)
15	5	–	707		987		833	
		+	1,308	85%	2,240	127%	1,974	137%
24	2	–	351		337		456	
		+	1,127	221%	896	166%	880	43%

Male mice received 500 μg TNP-BGG in CFA i.p. Splenic anti-TNP PFCs per 10^8 nucleated cells were assayed 2 weeks after immunization. Data presented are the geometric means of 10–15 animals from two or three independent experiments. Spleen tissues were assayed as a single pool from five animals in each experiment. Spleen tissues from the 15-month-old group were assayed as a single pool from five mice in one experiment. Spleen tissues from the 24-month group were assayed as individual spleens and geometric means of two animals from one experiment are presented. Percentage augmentation of PFCs by optimal hapten concentration ($1\times10^{-9}-1\times10^{-7}$ M TNP-EACA) is calculated as: 100×(PFCs in presence of hapten – PFCs in absence of hapten)/PFC in absence of hapten. The *t*-test was used to evaluate the statistical significance of differences on natural log-transformed data as compared with the 2-month group.

mals exhibited a loss of IgM, IgG and IgA PFCs in their primary immune response to TNP-BGG. These results are consistent with other data reported for this strain, with a loss of IgM anti-sheep red blood cell (SRBC) PFCs *in vitro* in mice over 4 months of age[14].

We then investigated the heterogeneity of the PFC response during ageing. The distribution of PFCs with regard to avidity was determined by hapten inhibition of plaque formation in mice of different ages and can be quantitated using the Shannon function[15] as heterogeneity index, thereby permitting a simple statistical evaluation of the data. This index is expressed as a $\log_2$ term and increases with increasing heterogeneity of the PFC distribution. The heterogeneity indices calculated from these data (distributions not shown) show a significant decrease in heterogeneity of splenic PFCs with age (Table 2). Thus, IgM, IgG and IgA PFCs from 8-month-old animals are significantly ($P<0.001$) less heterogeneous than PFCs from 4-month-old animals. The affinities of IgM and IgG PFCs from the 24-month-old animals are completely restricted but the IgA PFCs still retain some heterogeneity, although this is significantly ($P<0.001$) less than that in the 4-month-old group. Thus, with ageing, there is a progressive decrease in heterogeneity, characterized by a loss of high-avidity PFC subpopulations in older animals.

Auto-anti-idiotypic antibodies have been shown to be responsible for a decline in the number of PFCs, a reduction in the heterogeneity of avidity of PFCs and the occurrence of hapten-augmentable PFCs (anti-idiotype blocked)[12]. We therefore investigated the effect of age on the appearance of anti-idiotype-blocked, hapten-augmentable anti-TNP PFCs. As shown in Table 3, 8-month-old mice, during the primary immune response to TNP-BGG, produced a significantly ($P<0.001$) high percentage of hapten-augmentable PFC responses in the IgM (51%), IgG (114%) and IgA (86%) isotypes studied as compared with the 2-month-old group, which did not show any appreciable (6–15%) hapten-augmentable PFCs. Older mice also produced a high percentage of hapten-augmentable PFC responses, ranging from 85% to 221% in the three isotypes. These data support the hypothesis that auto-anti-idiotypic antibody de-regulation of splenic anti-TNP PFC responses of old mice is responsible for the age-associated decline in the number and heterogeneity of avidity of the PFCs in the three isotypes studied.

Other studies[16] describe an assay for anti-idiotypic antibody that makes use of the ability of such antibody in the immune sera to inhibit plaque formation by idiotype-producing cells. This inhibition was reversible by the hapten, TNP-ε-amino-*n*-caproic acid (EACA). Results in Table 4 show that pools of immune sera from 8-month or older mice immunized 14 days previously with TNP-BGG in CFA caused a hapten-reversible block of plaque formation by spleen cells from TNP-BGG immune 2-month-old mice. In contrast, immune sera from 2-month-old mice failed to inhibit the PFC response.

Table 4 Anti-idiotypic antibody activity in immune sera from ageing C57BL/6J mice as assayed by hapten-reversible plaque inhibition

Serum source	Anti-TNP titre (reciprocal)	% Of control response					
		PFCs from spleen 1			PFCs from spleen 2		
		IgM PFCs	IgG PFCs	IgA PFCs	IgM PFCs	IgG PFCs	IgA PFCs
NMS	<2	100	100	100	100	100	100
Immune 2-month-old	80	100	110	99	78	83	95
Immune 4-month-old	80	78	52	96	72	75	96
Immune 8-month-old	160	42	23	73	31	57	71
Immune 11-month-old	80	62	33	88	53	39	50
Immune 15-month-old	160	47	40	88	52	37	60
Immune 24-month-old	160	42	23	45	ND	ND	ND

Immune spleen cells were obtained from individual 2-month-old C57BL/6J male mice that had been immunized i.p. with 500 μg TNP-BGG in CFA 14 days before assay. The control values (PFCs determined in the presence of normal mouse serum [NMS]) ranged for 1,667 IgM, 5,451 IgG and 3,608 IgA anti-TNP PFCs per 10^8 nucleated cells from spleen 1 and 2,073 IgM, 2,439 IgG and 10,829 IgA PFC's from spleen 2. Immune cells at $3\text{–}5\times10^7$ cells per ml were incubated with immune sera or NMS at a 1:10 final dilution for 5 min at 4°C. The cells were washed once, resuspended to the original volume, and plated. The inhibition of plaque formation was completely reversible by addition of hapten. The data illustrated are from one representative experiment out of six independent experiments. Anti-TNP titre was determined by passive hemagglutination. ND, Not determined.

The NMS pool was obtained from 10 C57BL/6J male mice at 10 weeks of age. Pools of immune sera were obtained from groups of 3–10 C57BL/6J male mice at various indicated ages, which had been immunized with 500 μg TNP-BGG in CFA i.p. 14 days before collection of sera.

The above findings suggest that the loss of immune competence in the splenic B-cell population may be due to auto-anti-idiotypic antibody regulation. The nature of the stimulus for the production of auto-anti-idiotypic antibody with age is unknown. However, the reported[13] increased appearance of new or altered antigenic determinants on the surface membrane of lymphoid cells from old mice or possibly alterations in I-region products with age[17], may serve as an attractive model to explain the increased appearance of auto-anti-idiotypic reactive B-cell clones. Also, auto-anti-idiotypic antibody may contribute to the increased suppressor cell activities in old animals. This is supported by the findings that anti-idiotypic antibody can induce the activation of suppressor T cells in normal young adult mice [18–20]. This type of observation has not been demonstrated in old animals. Furthermore, the relationship between auto-anti-idiotypic antibody regulation in old animals and auto-immune disease remains unclear.

This work was supported in part by grants-in-aid of research from the Banting Research Foundation and the Muscular Dystrophy Association of Canada. M.R.S. is a MRC of Canada Scholar.

Received 26 March; accepted 2 May 1980.

1. Callard, R. E. & Basten, A. *Eur. J. Immun.* **8,** 552 (1978).
2. Callard, R. E., Basten, A. & Waters, L. K. *Cell. Immun.* **31,** 26 (1977).
3. Goodman, S. A. & Makinodan, T. *Clin. exp. Immun.* **19,** 533 (1975).
4. Mathies, M., Lipps, L., Smith, G. S. & Walford, R. L. *J. Geront.* **28,** 425 (1973).
5. Krogsrud, R. L. & Perkins, E. H. *J. Immun.* **118,** 1607 (1977).
6. Meredith, P. J., Kristie, J. A. & Walford, R. L. *J. Immun.* **123,** 87 (1979).
7. Van Snick, J. L. & Masson, P. L. *J. exp. Med.* **151,** 45 (1980).
8. Goidl, E. A., Innes, J. B. & Weksler, M. E. *J. exp. Med.* **144,** 1037 (1976).
9. Callard, R. E., Fazekas de St. Groth, B., Basten, A. & McKenzie, I. F. C. *J. Immun.* **124,** 52 (1980).
10. Segre, D. & Segre, M. *J. Immun.* **116,** 735 (1976).
11. Rowley, D. A., Köhler, H., Schreiber, H., Kaye, S. T. & Lorback, I. *J. exp. Med.* **144,** 946 (1976).
12. Schrater, A. F., Goidl, E. A., Thorbecke, G. J. & Siskind, G. W. *J. exp. Med.* **150,** 138 (1979).
13. Callard, R. E., Basten, A. & Blanden, R. V. *Nature* **281,** 218 (1979).
14. Singhal, S. K., Roder, J. C. & Duwe, A. K. *Fedn Proc.* **37,** 1245 (1978).
15. Brillouin, L. in *Science and Information Theory* (Academic, New York, 1956).
16. Goidl, E. A., Schrater, A. F., Siskind, G. W. & Thorbecke, G. J. *J. exp. Med.* **150,** 154 (1979).
17. Gleichmann, E., Gleichmann, H. & Wilke, W. *Transplant. Rev.* **31,** 156 (1976).
18. Eichmann, K. *Eur. J. Immun.* **5,** 511 (1975).
19. Nisonoff, A., Ju, S. T. & Owens, F. L. *Immun. Rev.* **34,** 89 (1977).
20. Kim, B. S. *J. exp. Med.* **149,** 1371 (1979).
21. Jerne, N. K., Nordin, A. A. & Hendry, C. in *Cell Bound Antibody* (eds Amox, B. & Koprowski, H.) 109 (Wistar Institute Press, Philadelphia, 1963).
22. Dresser, D. W. & Greaves, M. R. in *Handbook of Experimental Immunology* (ed. Weir, D. M.) 271 (Blackwell, Oxford, 1973).

Phenotypic changes of phytohaemagglutinin-stimulated hairy cells

Paul Guglielmi, Jean-Louis Preud'homme & Georges Flandrin

Laboratory of Immunochemistry and Immunopathology (INSERM U 108 and Laboratory of Oncology and Immunopathology of CNRS) and Laboratory of Cytology, Research Institute on Blood Diseases, Hôpital Saint-Louis, Paris, France

Hairy cell leukaemia (leukaemic reticuloendotheliosis) appears to be a homogeneous and well defined disease on the basis of clinical presentation, light and electron microscopic features and cytochemical characteristics[1], but the study of immunological markers of hairy cells (HC) from many patients reveals apparent heterogeneity. The most common phenotype associates B-cell and monocytic properties: HC usually express monoclonal surface (and in certain cases cytoplasmic) immunoglobulins, receptors for IgM and IgG Fc, and mouse erythrocytes, and Ia-like antigens. Additionally, they are capable of phagocytosis, glass adherence, lysozyme and peroxidase synthesis[2–18]. However, most of these features are not constant and cases have been reported in which HC fail to express one or more of these properties. In certain cases HC even display a T-cell phenotype, while, in others, features of both T and B cells are expressed[16,19–22]. Moreover, in two recently studied patients, the phenotype of HC in the blood differed from that in the spleen (B+T in the blood and B in the spleen)[16]. These surprising discrepancies led us to hypothesize that HC from the same individual might be able to express different phenotypes following an appropriate stimulus. We therefore studied immunological parameters of HC stimulated by mitogens and the results indeed showed that after stimulation by phytohaemagglutinin (PHA) the cells switched from B to T or B+T phenotypes.

The three patients studied were affected with clinically and morphologically typical HC leukaemia. They had not previously received specific therapy. In patient Go., HC were obtained twice (3 months apart) from leukaemic blood. On both occasions, cell suspensions resulting from Ficoll centrifugation contained 10% lymphocytes and 90% HC as shown by cytological and cytochemical examination. Cells obtained from the spleen (splenectomy) were almost all HC in patient Cha. and 95% HC in patient Que. Cells from both blood and spleen were studied for lymphocyte markers and cultured with or without PHA; cultured cells were serially examined for cell number, tritiated thymidine incorporation, cytology and lymphocyte markers (see legend to Table 1).

Table 1 Immunological markers of fresh and cultured hairy cells (% positive cells)

Patients	Cells studied	SIg	cIg	γFcR	E rosettes	Anti-T serum
Go.	Fresh cells	77$\delta\lambda$	0	89	8	ND
	Day 4 cultured cells					
	Control	90$\delta\lambda$	56$\mu\lambda$	67	8	20*
	PHA	0	0	12	69	61*
Go. Expt 2	Fresh cells	71$\delta\lambda$	82$\mu\lambda$	73	37	25
	Day 3 cultured cells					
	Control	69$\delta\lambda$	82$\mu\lambda$	69	10	12
	PHA	0	0	2	80	82
Cha.	Fresh cells	38$\gamma\kappa(\mu\delta)$	0	1	1·5	1
	Day 14 cultured cells					
	Control	90$\gamma\kappa(\mu(\delta)$	0	51	4	5
	PHA	0·5	0	0	83	92
Que.	Fresh cells	95$\delta\lambda(\mu)$	67$\mu\lambda$	90	6	5
	Day 14 cultured cells					
	Control	83$\delta\lambda(\mu)$	57$\mu\lambda$	99	1	3
	PHA	2	50$\mu\lambda$	96	88	90

The cells obtained from blood or spleen were studied for cytological (Giemsa staining and tartrate-resistant acid phosphatase activity) and immunological parameters, then cultured at 1×10^6 cells ml^{-1} in RPMI 1640 medium containing 10% fetal calf serum (Gibco) either with or without PHA (PHA M, Gibco, final concentration 0.6%). Cultured cells were repeatedly studied for cytology, cytochemistry, cell numeration, thymidine incorporation and immunological features. Surface and cytoplasmic immunoglobulins (SIg and cIg) were assessed by direct immunofluorescence with rhodamine-conjugated rabbit F(ab')2 fragments prepared in our laboratory as previously described[23]. Conjugates polyvalent for human Ig and monospecific for μ, γ, σ, α, κ and λ chains were used. Ig Fc receptors (γ Fc R) were detected by immunofluorescence with immune complexes in conditions in which the positive cells are predominantly B cells[24]. E-rosette forming cells were enumerated according to a classical method[25]. Human T-lymphocyte specific antigens were studied by indirect immunofluorescence with a rabbit antiserum raised against peripheral T cells and a rhodamine-coupled sheep F(ab')2 fragment anti-rabbit IgG (ref. 26). ND, Not determined.

* Performed on day 7, when the control and PHA-stimulated cultures contained 26% and 81% E-rosetting cells respectively.

In the first study of cells from patient Go., the fresh HC displayed a B-lymphocyte phenotype with $\delta\lambda$ monotypic SIg (5–20% of the cells also stained for μ, γ and κ, which probably

0028–0836/80/280166—03$01.00

corresponded to exogenous Ig bound to Fc receptors since only δ and λ chains were subsequently found on cultured cells), γFcR and no T-cell markers (Table 1). PHA-stimulated cells were not examined before day 4 of culture. At this time, more than 90% of the cells in both PHA-stimulated and control cultures were typical HC on morphological grounds. In the control culture, the B phenotype remained stable except that monotypic cIg (IgM λ) became detectable. On the contrary, PHA-stimulated HC had lost SIg and γFcR, formed E rosettes and were strongly stained by anti-T serum, thus displaying a T-lymphocyte phenotype. The immunological phenotype in both control and PHA-stimulated cultures remained the same for the 5 following days, then most PHA-stimulated cells died. During this period, the appearance of PHA-stimulated cells changed: 50% of cells on day 5 and 60–70% the following days were large blast cells showing a strong acid phosphatase positivity which was tartrate-sensitive. Cell numbers were relatively stable and roughly similar in control and stimulated cultures. Relatively low levels of thymidine incorporation were found with stimulation indices of 18.6 and 3.0 on days 4 and 6 after PHA-stimulation (similar observations were made in patients Cha. and Que. with stimulation indices varying between 7.5 and 9.7 in PHA-stimulated cultures on days 4 and 6). These data and the rapidity (24 h) of morphological changes suggest that the T-blast cells may be derived from the PHA-stimulated HC.

When studied again 3 months later, fresh HC from patient Go.'s blood showed two features different from those found at first examination: most HC contained cytoplasmic μ and λ chains and a fair number had T-cell markers. Since 90% of the cells were HC, the obvious overlap of figures for T and B markers (Table 1) indicates that some HC had a mixed B+T phenotype. This mixed phenotype was lost in the control cultures (Table 1 and Fig. 1*a*) where HC retained B-cell characteristics only (the cells staining with the anti-T serum on days 3 and 6 were small lymphocytes by phase contrast microscopy). Daily study of PHA-stimulated cells showed a rapid loss of B-cell markers and the acquirement of T markers (Fig. 1*b* and Table 1). Morphological changes similar to those initially found were observed; the cells had a typical HC appearance till day 4 and were large blast cells on the following days.

Only 38% of fresh HC in patient Cha.'s spleen had monotypic SIg(γκ). Between 6 and 10% of the cells also stained for μ and δ, respectively. All these Ig chains were probably synthesized by the cells since they were found in control cultures at repeated examinations over 3 weeks. In non-stimulated cultures, we observed a progressive increase in the number of SIg-bearing cells (up to 90% on day 14) and the appearance of γFcR which was not detectable on fresh cells (Table 1). The changes occurring after PHA-stimulation had a slower kinetics than in patient Go. On day 5, the cells had lost SIg expression but only 10% formed E rosettes. These cells were virtually all HC by morphological criteria. Then, the percentage of E-rosetting cells increased. After day 12, most cells displayed T-cell features (Table 1). However, these cells were blast cells lacking cytological and cytochemical characteristics of HC. PHA-stimulated cells could not be studied after day 15 due to cell death.

Fig. 1 B and T cell markers of patient Go.'s blood cells cultured *a*, without or *b*, with PHA (second experiment). ●, E rosettes; ▲, SIg; ■, cIg; ○, γFcR. The number of cells staining with the anti-T serum paralleled that of E rosettes (not shown).

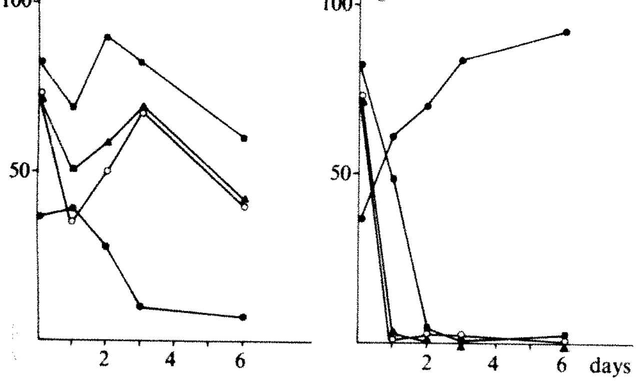

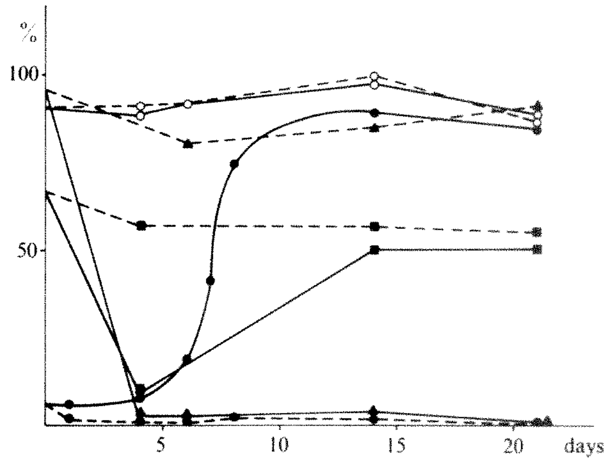

Fig. 2 B- and T-cell markers of patient Que.'s spleen cells in control (dotted lines) and PHA-stimulated (solid lines) cultures. ●, E rosettes; ▲, SIg; ■, cIg; ○, γFcR.

Study of patient Que.'s fresh spleen HC showed a B phenotype with SIg (δλ on most cells and also μ on some), cIg(μλ) and γFcR (Table 1). A faint surface staining and a globular cytoplasmic staining for γ, μ, κ and λ was additionally found and it was shown to be due to adsorption and pinocytosis of exogenous Ig. The B-cell phenotype remained stable in the control culture (Table 1 and Fig. 2, dotted lines). After PHA-stimulation, SIg rapidly disappeared whereas the number of cells with γFcR was constant. After an initial drop, the number of cells containing cytoplasmic μ and λ chains returned to pre-culture levels. The number of cells forming E rosettes and staining with anti-T serum sharply increased from day 4 to day 8 and then the phenotype of PHA-stimulated cells was unchanged until day 21 (Table 1 and Fig. 2, solid lines). Further study was not possible due to cell death. During these phenotypic changes and in contrast with the first cases, stimulated HC retained their typical morphological features. Therefore, the origin of these cells with a mixed T–B phenotype from the HC in this patient was supported by morphology and by the retention of some of the original B-cell markers (especially monoclonal cytoplasmic μ and λ chains).

This study provides three major findings: (1) when HC from the same patient were studied twice, their properties were not the same; (2) spontaneous variations were observed in control cultures: acquirement of cIg or of γFcR, switch from a B+T to a B phenotype. These data are in agreement with the finding of a different phenotype in the spleen and the blood from two patients[16]. Moreover, sequential studies of immunological markers in the same patients showed clear-cut fluctuations, as reported very recently[27]; (3) the most striking finding in our study is that PHA stimulation induced a switch from a B (patients Go. and Cha.) or a B+T (patient Go.) phenotype to a T phenotype, or from a B to a B+T phenotype (patient Que.). The two T-cell markers found on these cells were distinct since we were unable to inhibit E-rosette formation by preincubation with anti-T serum. Cells binding sheep erythrocytes were actual E rosettes and not immune rosettes which could have resulted from secretion or surface expression of Ig with anti-sheep red cell activity, as sometimes observed in CLL[28]. Indeed, rosetting was obtained only in the thermal and incubation conditions needed for T cells; it was not inhibited by incubation with anti-Ig sera and the cells did not form plaques with sheep erythrocytes. It must be stressed that these E rosettes were centered by lymphoid cells (as shown by phase contrast microscopy and

Giemsa staining of cytocentrifuge slides) and were not just clumps of red cells due to PHA in the medium (which was indeed a problem during the 2 or 3 first days of culture although HC were washed several times before rosette assay).

In two cases, there is no doubt that the cells which showed T-cell properties after PHA-stimulation did not result from the expansion of normal T cells and were derived from the original HC since: (1) These cells were still typical HC by morphological and cytochemical criteria. (2) In patient Que., they continued to express γFcR and the same intracytoplasmic Ig chains as the fresh cells. (3) In patient Go., the changes were too rapid (already clear-cut after 1 day of culture) to have been accountable by the growth of normal T cells. (4) Low levels of mitogenic stimulation and roughly stable or slightly decreased cell numbers similarly negate this hypothesis. In patient Cha., the cells with T-cell markers on day 12 of culture which could not be identified as HC upon morphological grounds were nevertheless probably derived from HC. Indeed, day 5 PHA-stimulated cultures from this patient's cells contain exclusively typical HC which had lost SIg while 10% of them had become E positive. The morphological changes subsequently observed are probably similar to those observed in patient Go., in whom typical HC with T-cell properties were replaced by blast cells probably derived from them (since this morphological change was observed within 24 h).

Since HC have peculiar surface properties, one could hypothesize that T-cell markers in PHA-stimulated cultures may not be endogenous but result from adsorption of membrane molecules released in the culture medium by PHA-stimulated normal T cells. This hypothesis may be ruled out for the following reasons: (1) cells from control cultures were incubated for 1 h, 3 h and overnight at 37 °C in supernatant media of PHA-stimulated cultures containing mostly cells with T markers. This incubation did not result in any change of the phenotype of these cells. (2) On several occasions, in patient Go., control and pokeweed-mitogen stimulated cultures contained a fair number of T cells (10–30%, with a similar percentage of large blast cells on Giemsa-stained smears) whereas HC in these cultures had no T-cell markers; (3) This hypothesis may hardly explain the loss of B cell features.

It is therefore clear that PHA actually induces major phenotypic changes of HC. This phenomenon is reversible since, when cultured cells with newly acquired T cell features were washed several times to remove the bulk of PHA and incubated in fresh medium without PHA, they lost T-cell characteristics and expressed the same B-cell properties as before culture within 2 days. Preliminary results of studies performed with other mitogens showed that concanavalin A induced changes similar to those observed with PHA, whereas we observed a plasmacytic differentiation after stimulation with the mitogen from nocardia opaca. If similar changes occur *in vivo*, our observation conciliates the published discrepancies in immunological phenotypes and HC may be considered as very remarkable cells capable of expressing different properties after an appropriate stimulation.

We thank Dr Larry B. Vogler for reviewing the English form of this manuscript, and A. Dimitriu for performing some of the tests. This work was supported by DGRST (grant no. 80.7.220).

Received 14 February; accepted 7 May 1980.

1. Bouroncle, B. A. *Blood* **53,** 412–436 (1979).
2. Preud'homme, J. L. & Seligmann, M. *Blood* **40,** 777–794 (1972).
3. Catovsky, D., Pettit, J. E., Galetto, J., Okos, A. & Galton, D. A. G. *Br. J. Haemat.* **26,** 29–37 (1974).
4. Haegert, D. G., Cawley, J. C., Collins, R. D., Flemans, R. J. & Smith, J. L. *J. clin. Path.* **27,** 967–972 (1974).
5. Fu, S. M., Winchester, R. J., Rai, K. R. & Kunkel, H. G. *Scand. J. Immun.* **3,** 847–851 (1974).
6. Jaffe, E. S., Shevach, E. M., Frank, M. M. & Green, I. *Am. J. Med.* **57,** 108–114 (1974).
7. King, G. W., Hurtubise, P. E., Sagone, A. L., Lo Buglio, A. F. & Metz, E. N. *Am. J. Med.* **59,** 411–416 (1975).
8. Scheinberg, M., Brenner, A. I., Sullivan, A. L., Cathcart, E. S. & Katayama, I. *Cancer* **37,** 1302–1307 (1976).
9. Burns, G. F. *et al. Blood* **52,** 1132–1147 (1977).
10. Burns, G. F., Cawley, J. C., Barker, C. R., Goldstone, A. H. & Hayhoe, F. G. J. *Br. J. Haemat.* **36,** 71–84 (1977).
11. Ütsinger, P. D., Yount, W. J., Fuller, C. R., Logue, M. J. & Orringer, E. P. *Blood* **49,** 19–27 (1977).
12. Gordon, J. & Smith, J. L. *Clin. exp. Immun.* **31,** 244–250 (1978).
13. Golomb, H. M., Vardiman, J., Sweet, D. L., Simon, D.& Variakojis, D. *Br. J. Haemat.* **38,** 161–170 (1978).
14. Reyes, F., Gourdin, M. F., Farcet, J. P., Dreyfus, B. & Breton-Gorius, J. *Blood* **52,** 537–550 (1978).
15. Rieber, E. P. *et al. Br. J. Haemat.* **42,** 175–188 (1979).
16. Jansen, J., Schuit, H. R. E., Schreuder, G. M. Th., Muller, H. P. & Meijer, C. J. L. M. *Blood* **54,** 459–467 (1979).
17. Cohen, H. J., George, E. R. & Kremer, W. B. *Blood* **53,** 764–775 (1979).
18. Yanovich, S., Marks, S. M., Rosenthal, D. S., Moloney, W. C. & Schlossman, S. F. *Cancer* **43,** 2348–2351 (1979).
19. Burns, G. F. *et al. Nature* **268,** 243–245 (1977).
20. Cawley, J. C. *et al. Blood* **51,** 61–69 (1978).
21. Saxon, A., Stevens, R. H. & Golde, D. W. *Ann. intern. Med.* **88,** 323–326 (1978).
22. Hernandez, D., Cruz, C., Carnot, J., Dorticos, E. & Espinosa, E. *Br. J. Haemat.* **40,** 504–506 (1978).
23. Preud'homme, J. L. & Labaume, S. in *In vitro Methods in Cell-Mediated and Tumor Immunity* (eds B. R. Bloom & J. R. David) 155–169 (Academic, New York, 1976).
24. Winchester, R. J., Hoffman, T., Ferrarini, M., Ross, G. D. & Kunkel, H. G. *Clin. exp. Immun.* **37,** 126–133 (1979).
25. Jondal, M., Holm, G. & Wigzell, H. *J. exp. Med.* **136,** 207–215 (1972).
26. Brouet, J. C., Preud'homme, J. L. & Seligmann, M. *Blood Cells* **1,** 81–90 (1975).
27. Burns, G. F., Worman, C. P. & Cawley, J. C. *Clin. exp. Immun.* **39,** 76–82 (1980).
28. Brouet, J. C. & Prieur, A. M. *Clin. immun. Immunopath.* **2,** 481–487 (1974).

The immunoglobulin μ constant region gene is expressed in mouse thymocytes

David J. Kemp, Anne Wilson, Alan W. Harris & Ken Shortman

The Walter and Eliza Hall Institute of Medical Research, Post Office, Royal Melbourne Hospital, Victoria 3050, Australia

It has been a matter of controversy whether the functional capacity of T cells to discriminate between antigens is mediated via immunoglobulin, an immunoglobulin-like molecule, or by the product(s) of unrelated genes. The progenitors of immunoglobulin-secreting cells, B cells, express membrane-bound immunoglobulin as the antigen-specific receptor on their surface[1]. For T cells, although products of immunoglobulin heavy chain variable region genes are implicated as receptor components[2–4], there has been no compelling immunochemical evidence for participation of either immunoglobulin light chains or heavy chain constant regions (see refs 2–6 for the disparate views). Recently, using cloned immunoglobulin DNA sequences as hybridization probes, we have demonstrated that the immunoglobulin C_μ gene, but not the C_κ gene, is expressed as polyadenylated RNA in some T cell tumour (T lymphoma) cell lines[7]. Individual T lymphoma lines yielded up to three discrete μ RNA species of different sizes (1.9, 2.2 and 3.0 kilobases), each species being different in size from the major μ RNA species present in B lymphoma cells (2.4 and 2.7 kilobases)[7,8]. We show here that cells from the normal mouse thymus contain μ RNA species, indistinguishable in size from those in T lymphoma cells, but contain little if any κ RNA.

To detect μ and κ RNAs in T- and B-cell RNA preparations, we used as probes DNA fragments[7] derived from plasmids bearing cDNA copies of a μ (ref. 9) and a κ (ref. 10) mRNA. Polyadenylated RNA from the cells was fractionated by agarose gel electrophoresis, blotted from the gel onto diazobenzyloxymethyl paper and hybridized with the ^{32}P-DNA probes[11]. RNA species which hybridized were detected by autoradiography. Thymocytes were prepared[12] from 5–6-week-old male CBA mice with care to exclude parathymic lymph nodes. They were found to be contaminated by 0.2–0.3% of surface immunoglobulin-positive cells, presumably B cells. The contaminating B cells were depleted at least threefold by treatment of the thymocytes with antiserum against Ia^k followed by rabbit complement[13]. To evaluate further whether contaminating B cells might contribute to immunoglobulin RNA in thymocyte RNA preparations, we characterized RNA obtained from three sources of B cells: normal spleen, spleen cells from

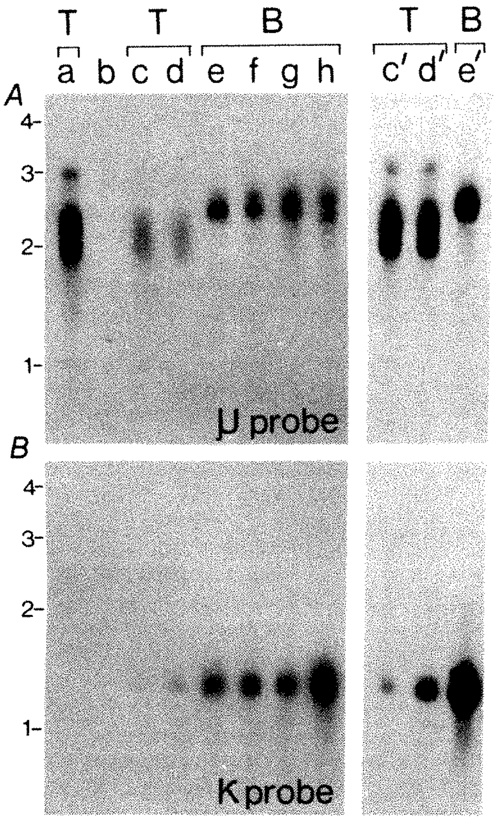

Fig. 1 Detection of *A*, μ RNA; and *B*, κ RNA in T and B cells. Polyadenylated RNA isolated from the cells indicated was denatured, fractionated by agarose gel electrophoresis, transferred to diazobenzyloxymethyl paper[11], hybridized with ^{32}P-DNA from cloned μ (ref. 9) and κ (ref. 10) cDNAs and autoradiographed for 3 days (tracks a–h) or 10 days (tracks c', d', e'), all as described previously[7]. Polyadenylated RNA (5 μg) was loaded onto tracks a–d and 0.5 μg onto tracks e–h. The sizes (in kilobases) are indicated on the left. The cells used for RNA preparation were: lane a, STRij-4-2.2 T lymphoma cells[7]; lane b, EMT6 sarcoma cells[7]; lanes c, d, c' and d', thymus cells prepared from 5–6 week old male CBA/CaHWehi mice. The cells used for the RNA preparation in lanes c and c' had been treated[13] with antiserum against Ia^k (prepared in the congeneic A.TH anti-A.TL combination) followed by rabbit complement treatment and removal of damaged cells[12]. Anti-Ia^k/complement treatment reduced the number of surface immunoglobulin-positive cells (determined by immunofluorescence) from 0.2% to <0.06% and lowered the level of functional B cells detected in a limit dilution assay[13] by at least 10-fold; lanes e, e', spleen cells, prepared from CBA.nu mice; lanes f and g, spleen cells, prepared from DBA/2 mice. The spleen cells used for lane f had been treated with anti-Thy-1 plus complement followed by damaged-cell removal, a procedure which removed 29% of the cells and all detectable T cells; lane h, W231.1 B lymphoma cells.

athymic nude mice and spleen cells treated with anti-Thy 1 plus complement to remove T cells.

Autoradiographs revealing species of RNA hybridizing with radioactive μ and κ probes are shown in Fig. 1. Relative contents of μ and κ RNA estimated from densitometric measurements on the autoradiographs are listed in Table 1.

In thymocyte RNA we detected μ RNA species of 1.9, 2.2 and 3.0 kilobases (Fig. 1*a*, tracks c, d, c' and d'). They were of the same size and relative abundance as μ RNA species from STRij-4 T lymphoma cells (track a). In contrast, each of the three different types of B cell preparations tested contained μ RNA species of 2.4 and 2.7 kilobases, analogous to the two species from WEHI-231 B lymphoma cells (tracks e–h and e'). As expected[7], the control RNA from the sarcoma cell line EMT6 (track b) contained no detectable μ RNA. In comparing the intensity of the μ RNA signals in the various tracks shown in Fig. 1, note that 10 times more RNA from thymocytes and STRij-4 T lymphoma cells than from splenic B cells and WEHI-231 B lymphoma cells was loaded on to the gel, as the μ RNA content of thymocytes was 10- to 20-fold lower than that of B cells.

It is crucial to know whether the μ RNA species are authentic products of the C_μ gene as, for example, hybridization of an RNA species distantly related to the C_κ gene has been observed in a T lymphoma[14]. The results shown in Fig. 1*A* were obtained using a probe representing only domains 1 and 2 of the C_μ gene[7]. When a cloned segment containing only C_μ domains 3 and 4 (ref. 7) was used as the probe, μ RNA species identical to those shown in Fig. 1*A* were detected in anti-Ia^k purified thymocytes (data not shown). Hence the thymocyte μ RNA species must each contain sequences from both the 5' and 3' halves of the C_μ gene, as is the case with T lymphoma μ RNAs[7]. We have also examined the thermal stability of hybrids formed with thymocyte RNA and the probe for domains 3 and 4. The hybrids formed with each thymocyte μ RNA species were stable to incubation at 65 °C in 0.036 M Na$^+$. In these conditions, this DNA probe forms stable hybrids only with the C_μ gene[15], not with any other sequence in the mouse genome. Thus the thymocyte μ RNAs are authentic products of the C_μ gene.

As κ chains comprise about 95% of the known immunoglobin light chains in the mouse, we expected that κ RNA would be readily detectable in B cells and this was borne out (Fig. 1*B*, tracks e–g). κ RNA was also detectable in RNA from crude thymocyte preparations (Fig. 1*B*, track d), but in lower amounts than in any of the B cell preparations (Table 1). We think most of the κ RNA comes from cells of the B lineage, because it was lowered by about threefold by depletion of B cells and plasma cells from the thymocyte population (Fig. 1*B*, track c); the resultant molar ratio of κ RNA to μ RNA was only one tenth of that found in purified B cells (Table 1). To delineate further the cellular origins of both μ and κ RNA in thymocyte preparations, we fractionated CBA mouse thymocytes on the basis of their buoyant density by centrifugation on continuous albumin gradients. The procedure used produces a marked separation of the minor, immunologically active, low Thy-1, cortisone-resistant, medullary subset (concentrated in fraction 2, Table 1) from the major subset (mostly found in fractions 3–4)[16]. The few contaminating activated B cells and immunoglobulin-secreting plasma cells are concentrated in the least dense fraction[17]. While μ RNA of the characteristic T lymphoma size classes was found

Table 1 Relative μ and κ RNA contents of T and B cells

Cells	Purification	κ RNA / μ RNA*
Expt 1		
STRij-4-2.2	Cloned cell line	<0.01
Thymus	None	0.25
Thymus	Anti-Ia^k	0.085
Spleen	None	0.90
Spleen	Anti-Thy-1	1.00
Spleen	From athymic nude mouse	0.72
WEHI-231.1	Cloned cell line	1.83
Expt 2		
Thymus	None	0.065
Thymus	Fraction 1 (ρ = 1.0630–1.0730)	0.28
Thymus	Fraction 2 (ρ = 1.0730–1.0752)	0.024
Thymus	Fraction 3 (ρ = 1.0752–1.0798)	0.014
Thymus	Fraction 4 (ρ = 1.0798–1.0824)	<0.02
Thymus	Fraction 5 (ρ = 1.0824–1.0910)	<0.02
Spleen	Anti-Thy-1	1.00

*The relative amounts of μ (or κ) RNA in each sample were determined by quantitative densitometry on autoradiographs prepared as described in Fig. 1 legend. These values were normalized to the values obtained for T cell-depleted spleen cells, assuming the latter value to be 1.0 mol κ RNA per mol μ RNA.

in all density fractions with little evidence for selective concentration in any fraction, the molar ratio of $\kappa : \mu$ RNA decreased to ≤ 0.024 in fractions 2–5 (Table 1). More than 90% of the total κ RNA was concentrated in the least dense fraction, which contained only 12% of the thymocytes. We conclude that the κ RNA originates from contaminating plasma cells or activated B cells. Since plasma cells (as evidenced by plasmacytomas) contain about 100–1,000 times more immunoglobulin mRNA than do B cells[7,8], they would contain at least 40,000 times as much κ RNA as our purified thymocytes (present data). Plasma cell contamination at a level of 1 in 40,000 could be present in thymocytes and might be the origin of immunoglobulin κ chains which others have found to be synthesized by thymocyte suspensions[18]. Our results certainly do not confirm earlier reports[19,20] suggesting the presence of similar amounts of κ RNA in spleen and thymus cells.

The average μ RNA content of about 5–10 molecules per thymocyte is similar to that found in some T lymphoma cell lines that we have studied[7]. We do not know, however, what proportion of thymocytes contain μ RNA. Expression of the μ but not the κ gene in thymocytes suggests a close parallel with pre-B cells[21] and this analogy is extended by the recently reported presence in an immature B cell lymphoma line[8] of μ RNA species with sizes (2.1 to 3.0 kilobases), similar to those in T lymphoma lines.

Our demonstration here of C_μ gene expression in normal thymocytes complements our results with cloned T lymphoid cell lines[7]. Together they constitute a strong case that the C_H locus functions in at least some cells of the T lineage, perhaps to encode a component of the T cell antigen receptor.

We thank Sue Kyne and Angela Apa for technical assistance, Jerry Adams and Suzanne Cory for helpful discussions and Judy Layton for determining immunofluorescence. This work was supported by grants from the National Health and Medical Research Council (Australia) and the National Cancer Institute (USA).

Received 18 March; accepted 13 May, 1980.

1. Warner, N. L. *Adv. Immun.* **19,** 67–216 (1974).
2. Biaz, H., Wigzell, H. & Bazin, H. *Nature* **264,** 639–642 (1976).
3. Hämmerling, G. J., Black, S. J., Berek, C., Eichmann, K. & Rajewsky, K. *J. exp. Med.* **143,** 861–869 (1976).
4. Rubin, B., Hertel-Wulff, B. & Kimura, A. A. *J. exp. Med.* **150,** 307–321 (1978).
5. Marchalonis, J. J. *Contemp. Topics molec. Immun.* **5,** 125–160 (1976).
6. Parkhouse, R. M. E. & Abney, E. R. in *B and T cells in Immune Recognition* (eds Loor, F. & Roelants, G. E.) 211–234 (Wiley, Chichester, 1977).
7. Kemp, D. J., Harris, A. W., Cory, S. & Adams, J. M. *Proc. natn. Acad. Sci. U.S.A.* (in the press).
8. Perry, R. P. & Kelley, D. E. *Cell* **18,** 1333–1339 (1979).
9. Adams, J. M., Gough, N. M., Webb, E. A. & Cory, S. *Biochemistry* (in the press).
10. Gough, N. M., Adams, J. M. & Webb, E. A. *Biochemistry* (in the press).
11. Alwine, J. C., Kemp, D. J. & Stark, G. R. *Proc. natn. Acad. Sci. U.S.A.* **74,** 5350–5354 (1977).
12. Shortman, K., Williams, N. & Adams, P. *J. immun. Meth.* **1,** 273–287 (1972).
13. Nossal, G. J. V. & Pike, B. L. *J. Immun.* **120,** 145–150 (1978).
14. Rabbitts, T. H., Forster, A., Smith, M. & Gillam, S. *Eur. J. Immun.* **7,** 43–48 (1977).
15. Cory, S. & Adams, J. M. *Cell* **19,** 37–51 (1980).
16. Shortman, K., von Boehmer, H., Lipp, J. & Hopper, K. *Transplantn Rev.* **25,** 163–210 (1975).
17. Williams, N., Kraft, N. & Shortman, K. *Immunology* **22,** 885–899 (1972).
18. Putnam, D., Clagett, J. & Storb, U. *J. Immun.* **124,** 902–912 (1980).
19. Storb, U *et al. Proc. natn. Acad. Sci. U.S.A.* **73,** 2467–2471 (1976).
20. Storb, U. (1978). *Proc. natn. Acad. Sci. U.S.A.* **75,** 2905–2908 (1978).
21. Siden, E. J., Baltimore, D., Clark, D. & Rosenberg, N. E. *Cell* **16,** 389–396 (1979).

An unusual translocation of immunoglobulin gene segments in variants of the mouse myeloma MPC11

Hannelore Schnell, Michael Steinmetz
& Hans G. Zachau

Institut für Physiologische Chemie, Physikalische Biochemie und
Zellbiologie der Universität München, Goethestrasse 33,
D-8000 München 2, FRG

Israel Schechter

Department of Chemical Immunology, The Weizmann Institute of
Science, Rehovot, Israel

Immunoglobulin light chain genes of the mouse are composed in germ-line DNA of four separate segments, the leader, V (variable), J (joining) and C (constant) segments. In immunocompetent cells a V and a J gene segment are joined by a site-specific recombination event[1,2]. In variants of the mouse myeloma MPC11 a so-called kappa (κ) light chain fragment is expressed[3] which consists of the MOPC321 leader peptide, joined to the κ constant region peptide[4,5]. Using the Southern blotting technique[6] we found that the gene coding for the light chain fragment has apparently been generated by an aberrant translocation of a V gene segment identical or very similar to the MOPC321 V gene segment into the large intervening sequence between the J and the C gene segments. The resulting deletion of the splice signals of the J segments could be the reason for the observed splicing between leader and C region sequences, a phenomenon which may be of general interest for the understanding of the splicing mechanism.

Two variants of myeloma MPC11 were investigated. In one only the κ light chain fragment is found; in the other one in addition an intact κ light chain with MPC11 leader and variable region peptides is expressed. The variants are called MPC11 (Lf) and MPC11 (L+Lf), respectively. High molecular weight DNA isolated from mouse liver and the two MPC11 variants was digested with various restriction nucleases and fractionated on agarose gels. Liver DNA has been shown to contain the C gene segment in an arrangement very similar if not identical to the one found in germ-line DNA[7]. After denaturation the DNA fragments were transferred to nitrocellulose filters[6] and hybridized with a nick-translated plasmid probe specific for the C gene segment plus about 2,000 base pairs of surrounding genomic DNA sequences. Figure 1 shows the autoradiograms obtained after digestion of the three DNAs with *Eco*RI, *Sst*I, *Bam*HI, and *Eco*RI plus *Hpa*I. The chain length of fragments observed in these and other digestion experiments are compiled in Table 1. In the *Eco*RI digests of both, MPC11 (L+Lf) and MPC11 (Lf) DNA a 19 kilobase band was identified while liver DNA (not shown) yielded the known[7,9,11] 15 kilobase fragment. The 19 kilobase band of MPC11 (L+Lf) is composed of two fragments of similar length as could be shown by digestion with for example *Bam*HI. Two fragments were formed, the smaller of which was also found in digests of MPC11 (Lf) DNA (Fig. 1). The *Bam*HI fragment of liver DNA differs from the two fragments of MPC11 DNA. A pattern of corresponding and non-corresponding fragments was also obtained in the analysis of the C region specific fragments with *Hpa*I (Fig. 2). The *Bam*HI and *Hpa*I fragment patterns already indicate the existence of two differently rearranged κ light chain genes in MPC11 (L+Lf) DNA. Only one of the rearranged κ genes is preserved in MPC11 (Lf) DNA which must be the one responsible for the synthesis of the L chain fragment.

According to the known amino acid sequence[10] of the MPC11 L chain and the nucleotide sequence of the five J gene segments[8,9] either J1 or J2 should be the target of the site-specific recombination process which leads to the formation of the complete MPC11 L chain gene. Restriction nucleases which cleave in the large intervening sequence between J2 and the C gene segment should then generate the same fragment from MPC11 (L+Lf) and liver DNA (compare Fig. 2). This was the case in *Bgl*II, *Xba*I, and *Sst*I digests (Figs 1, 2). The additional fragments in MPC11 (L+Lf) DNA digests correspond to the

0028-0836/80/280170—04$01.00

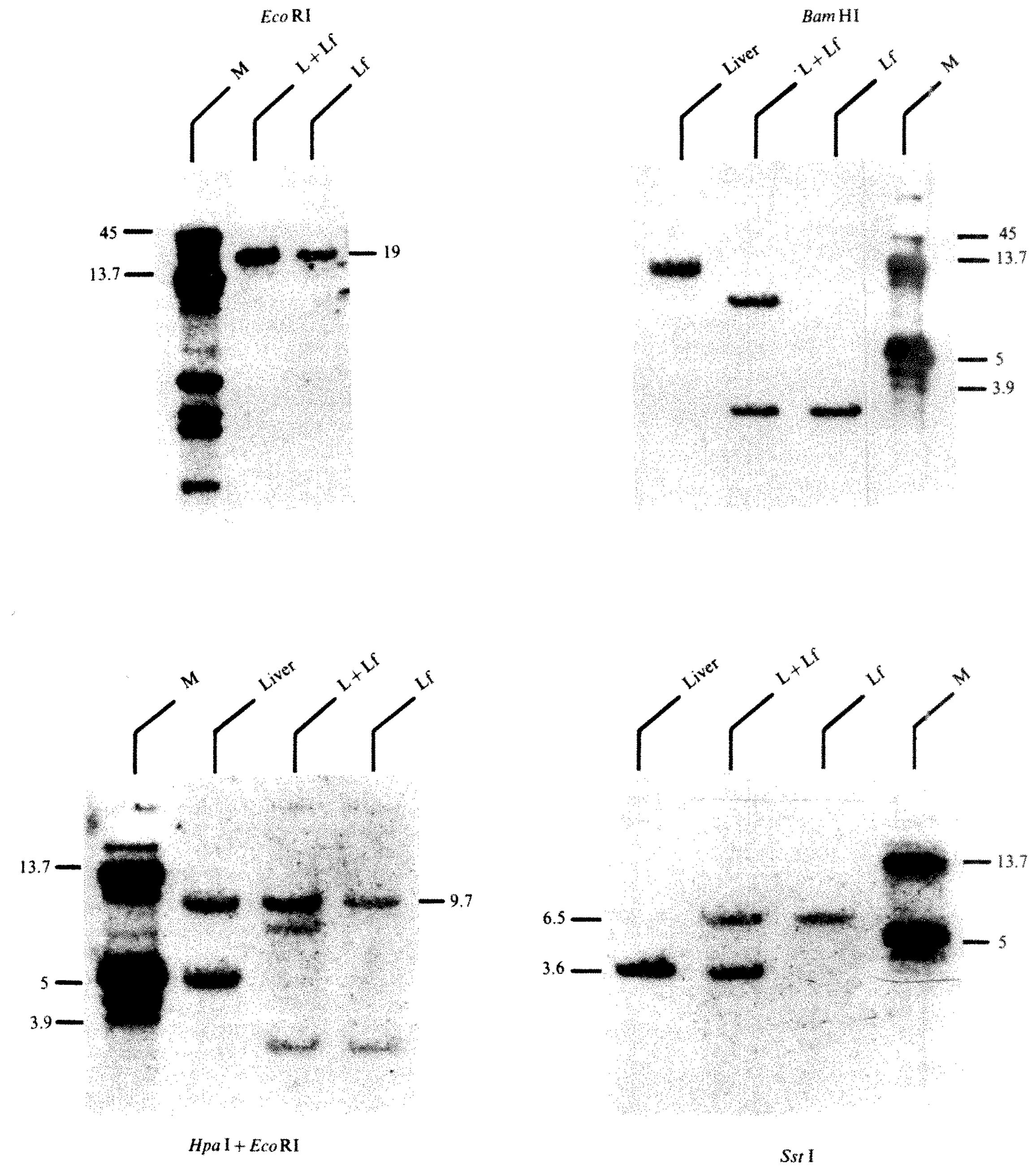

Fig. 1 Identification of DNA fragments containing the κ C gene segment in restriction endonuclease digests of mouse liver, MPC11 (L + Lf) and MPC11 (Lf) DNA. Clone 66.2 (ref. 3) designated MPC11 (L + Lf) and clone NP-2 (ref. 3) designated MPC11 (Lf), originally provided by R. Laskov (Hebrew University, Jerusalem), were maintained as solid tumours by subcutaneous transplantation in inbred BALB/c mice. DNAs were prepared according to ref. 13. Samples of 10 µg of DNA were digested with 10 units of *Eco*RI, *Bam*HI, *Sst*I (Bethesda) or *Hpa*I (Boehringer Mannheim) plus *Eco*RI for 3 h at 37 °C in volumes of 150–200 µl. Plasmid DNA when mixed with mouse DNA was completely digested. DNA digests were electrophoresed on a 0.7% or 0.5% (*Eco*RI digest) agarose gel in Tris-EDTA-phosphate buffer[14] containing 1 µg ml^{-1} ethidium bromide at 1.4 V cm^{-1} overnight. The gels were then exposed to 254 nm light for 5–10 min[15] and submitted to the transfer procedure[6]. The hybridization probe had been constructed by subcloning in pBR322 the 2.8 *Hin*dIII-*Bam*HI fragment containing the C gene segment of the 14 kilobase *Eco*Ri fragment from myeloma DNA[7]. The subcloned fragment is identical to the corresponding fragment from liver DNA (ref. 7, Fig. 2). Nick-translation[16,17] of the plasmid DNA with [α-^{32}P]dATP and [α-^{32}P]dCTP led to 2×10^{8} c.p.m. per µg DNA. Filters which had been baked for 2 h at 80 °C *in vacuo* were preincubated in 3 × SSC, 10 × Denhardt's solution[18] for 3 h at 68 °C and subsequently in 2 × SSC, 6.6× Denhardt's solution, 50 µg ml^{-1} sheared and heat-denatured salmon sperm DNA, 0.1% SDS for 1 h at 68 °C. The filters were then incubated in a graduate in a volume of 2.5 ml of the latter solution supplemented with 40 ng ml^{-1} heat-denatured nick-translated probe for 15 h at 68 °C under constant rotation. After this hybridization filters were washed six times for 5–10 min each in 2 × SSC, 6.6× Denhardt's solution, 0.1% SDS at 68 °C and twice in 1 × SSC, 0.1% SDS at 65 °C 15 min each. Some of the filters were further washed in 0.1 × SSC, 0.1% SDS at 65 °C, which did not alter the band pattern shown. Dry filters were exposed to Kodak X-Omat R film for 2 d at −80 °C with a SE6 intensifying screen from Cawo (Schrobenhausen, West Germany). The slots contain the following: liver, L + Lf, Lf, restriction fragments of mouse liver DNA, MPC11 (L + Lf) and MPC11 (Lf) DNA, respectively. The hybridization marker (M) consisted of 100 pg each of a *Pst*I, *Hin*dIII, *Bam*HI, and *Hpa*I digest of the genomic clone Ch4A 173/1 (ref. 7) and 100 pg of a *Hin*dIII plus *Pst*I digest of a pBR322 subclone[12] containing the 2.7 kilobase *Bgl*II fragment with the C gene segment from liver DNA (compare Fig. 2). Fragment sizes are given in kilobases.

fragments in MPC11 (Lf) DNA digests, indicating that the recombination in the MPC11 (Lf) genome has occurred to the right of the *Sst*I cleavage site in the large intervening sequence.

The previous conclusions are based on the assumption that the C gene segment itself and its 3′ flanking sequence has not been altered. This is made likely by the occurrence of identical fragments in the digests of the three DNAs (12 kilobases in the

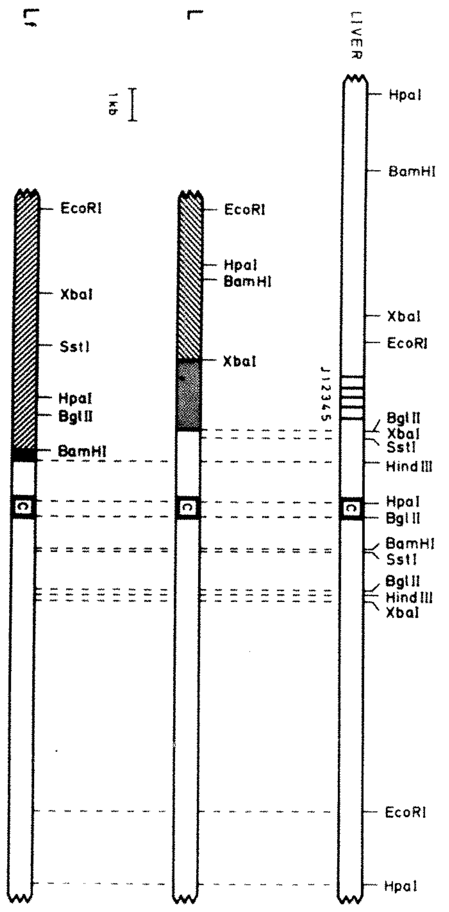

Fig. 2 Organization of the κ C gene segment in mouse liver, MPC11 (L+Lf) and MPC11 (Lf) DNA. Only those restriction endonuclease cleavage sites which were identified by Southern gel blotting experiments are shown. J (positions according to refs. 8, 9) and C gene segments are indicated by bars and boxes. Regions on the MPC11 DNA which differ from each other and from those on the liver DNA are shown as hatched boxes. DNA segments carrying the recombination site are indicated as stippled boxes.

*Hpa*I and 2.3 kilobases in *Bgl*II digests) and is further supported by double digestion experiments with pairs of restriction nucleases which cleave in the C gene segment and the 3′ flanking sequence and therefore should lead to the identification of the same DNA fragment in all three genomes. In *Hpa*I plus *Eco*RI digests of the three DNAs the expected 9.7 kilobase fragment was found (Fig. 1). Also, *Hpa*I plus *Xba*I, *Bgl*II plus *Sst*I, and *Bgl*II plus *Bam*HI digests yielded fragments which were common to the three DNAs (Table 1). The other fragments in the double digestion experiments are obviously derived from the 5′ flanking sequences of the C gene segment.

To show directly that the recombination process leading to the formation of the Lf genome gave rise to a deletion of the J gene segments *Eco*RI and *Xba*I digests of the MPC11 DNAs were hybridized with the *Eco*RI-*Bgl*II fragment from liver DNA containing the J gene segments (Fig. 2; compare also refs 8, 9) which had been subcloned[12] in pBR322. No hybridization band could be detected in digests of MPC11 (Lf) DNA whereas a 19 kilobase *Eco*RI resp. a 2.2 kilobase *Xba*I fragment (Table 1), obviously derived from the chromosome containing L chain gene, was identified in digests of MPC11 (L+Lf) DNA (not shown).

The mapping data on the MPC11 L and Lf genes are summarized in Fig. 2 and compared to the arrangement of the J and C gene segments in liver DNA. From our data the region where the recombination has occurred can be confined to the *Xba*I-*Bgl*II fragment for the MPC11 L chain gene (in agreement with the sequence data in refs 8–10) and to the *Bam*HI-*Hin*dIII fragment for the Lf gene (stippled boxes in Fig. 2). The *Hin*dIII sites to the left of the C gene segment have been found at the same positions on all three mouse DNAs. The localization of the recombination site involved in the formation of the Lf gene was supported by the results of *Hin*fI digestions of MPC11 (Lf) DNA (data not shown) although the interpretation of the blots was complicated, probably due to methylation of some of the restriction sites.

Since the Lf mRNA of MPC11 contains the MOPC321 light chain leader sequence it was of interest to search near the C gene segment of the MPC11 DNA for this sequence and also for MOPC321 V gene sequences. The hybridization probes we had available for these experiments were a *Pst*I subclone of MOPC321 cDNA comprising the leader sequence and a small part of the MOPC321 V gene segment as well as a *Bam*HI subclone containing only V region sequences (Fig. 3 legend). In *Eco*RI digested liver DNA we identified with either probe all DNA fragments which are known[11] to contain MOPC321 V region related sequences (in addition two small DNA fragments

Table 1 Length of some restriction nuclease fragments containing C or J gene segments

	LIVER			MPC11 (L+Lf)				MPC11 (Lf)	
	common	shared	unique	common	shared	unique L	unique Lf	common	unique Lf
*Eco*RI			15			19	19		19
*Bam*HI			12			8.5	3.1		3.1
*Hpa*I	12		13	12		7.5	3.3	12	3.3
*Bgl*II	2.3	2.7		2.3	2.7		3.2	2.3	3.2
*Sst*I		3.6			3.6		6.5		6.5
*Xba*I		5.4			5.4		9.7		9.7
*Hin*dIII	4.2			4.2				4.2	
*Hpa*I + *Eco*RI	9.7		5.1	9.7		7.5	3.3	9.7	3.3
*Hpa*I + *Xba*I	3.1	2.3		3.1	2.3		3.3	3.1	3.3
*Bgl*II + *Sst*I	1.1	2.6		1.1	2.6		3.2	1.1	3.2
*Bgl*II + *Bam*HI	1.0	2.7		1.0	2.7		2.0	1.0	2.0
*Eco*RI			15			19			None
*Xba*I			3.7			2.2			None

DNA fragments were identified by hybridization with a subclone containing the C gene segment (Fig. 1 legend), except for the last two digests where a subclone containing the J gene segments (see text) had been used. 'Common' fragments were found in all three digests and 'shared' ones only in the liver and the MPC11 (L+Lf) DNA digests; 'unique' fragments are derived exclusively from the liver, the L, or the Lf genome. Appropriate sizes are given for the fragments as they are obtained in Southern blot analysis while for the markers (Fig. 1) the more exact values are used which were determined by mapping of cloned fragments.

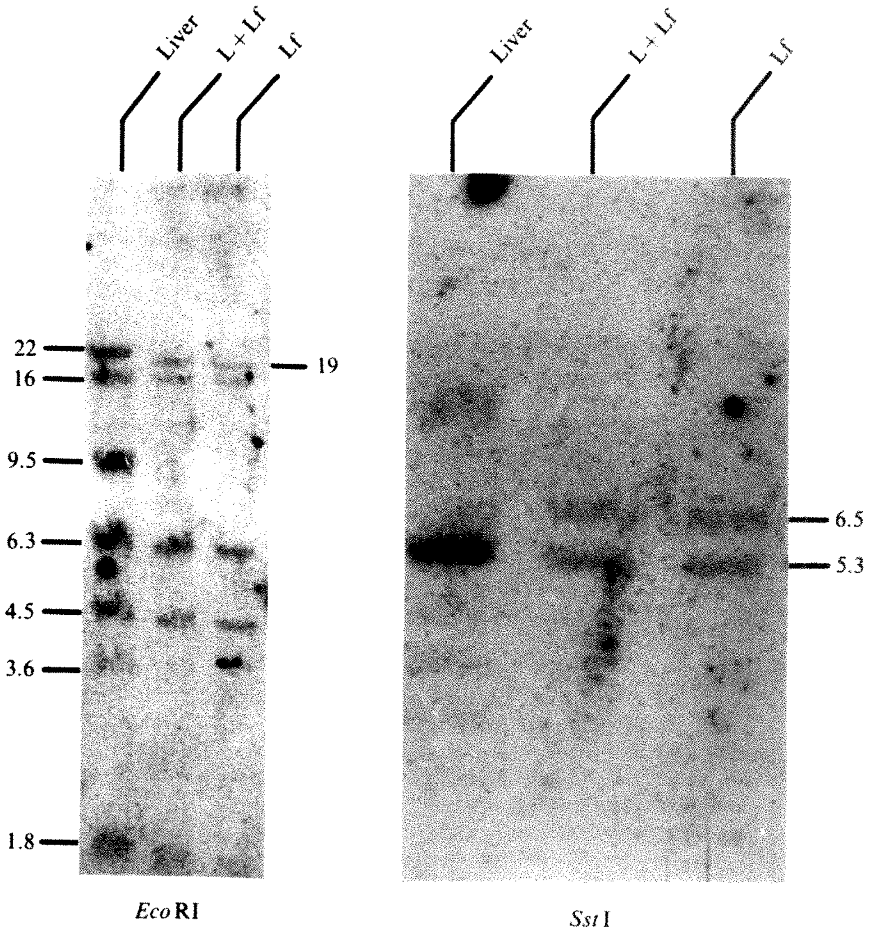

Fig. 3 Identification of restriction nuclease fragments in mouse liver, MPC11 (L+Lf) and MPC11 (Lf) DNA which hybridize to MOPC321 V region probe. Nuclease digestions, electrophoresis, markers, blotting, and hybridizations were as in Fig. 1, with the following exceptions: electrophoretic separation of the *Eco*RI digested DNA was for 3 d at 1 V cm^{-1} in the cold room; preincubation of the filters was in 6 × SSC and hybridization in 4 × SSC instead of 3 × SSC and 2 × SSC, respectively; after hybridization the filters were washed with 1 × SSC and autoradiographed for 9 d with a SE6 intensifying screen. As hybridization probes for the *Eco*RI and *Sst*I blots subcloned *Pst*I-*Pst*I and *Bam*HI-*Bam*HI fragments were used, respectively, which had been derived from a MOPC321 cDNA clone[20,21]. The *Pst*I fragment of ~160 base pairs contains a short GC-tail, 13 base pairs of the MOPC321 5′ untranslated region and the entire leader sequence plus the V region DNA sequence up to the codon for ^{23}Cys (I. Schechter and A. Bothwell, in preparation). The ~100 base pair *Bam*HI fragment contains part of the MOPC321 V region DNA sequence from a Gly codon at position 57, 64, or 66 to the ^{93}Gln codon[20,21]. Very similar or identical patterns were obtained when the *Bam*HI probe was used for the *Eco*RI digest and the *Pst*I probe for the *Sst*I digest.

could be identified which are not shown in Fig. 1 of ref. 11). In the *Eco*RI digests of both MPC11 DNAs three of these fragments (22, 9.5 and 3.6 kilobases) were absent while a 19 kilobase fragment not found in the liver DNA digest was seen (Fig. 3). The absence of germ-line V gene fragments and the appearance of a new fragment indicate that MOPC321 leader and V region segments have been arranged. In the *Eco*RI, *Sst*I, and the *Xba*I digests of both MPC11 DNAs the new fragments are identical in size to the fragments detected with the C region probe in the Lf genome (Table 1); this refers to the fragments of 19 kilobases (Fig. 3), 6.5 kilobases (Fig. 3), and 9.7 kilobases (not shown), respectively. It is of particular interest that very similar or identical hybridization patterns were found with the leader and the V gene probes (Fig. 3 legend). The results are best interpreted by assuming that in the MPC11 Lf genome the V gene segment of MOPC321 or a segment with a closely related V gene has been translocated into an aberrant position inside the large intervening sequence. It is not known yet whether the sequences at this recombination point bear similarity to the ones at or near the known J gene segments. Probably the whole region comprising the MOPC321 leader and V gene segments or a large part of this region has been translocated. Since apparently the J region with its splice points is deleted in the MPC11 (Lf) genome (see above; Fig. 2) the mRNA coding for the light chain fragment has to be formed by a splicing event (or events) in the pre-mRNA between the leader and C region. Further work is needed to establish whether the translocation of the MOPC321 gene segments into the large intervening sequence occurs directly or through a V–J joining and subsequent deletion of part of the intervening sequence including the splice signal.

We thank Ms F. Kantor for preparing the *Pst*I subclone of MOPC321 cDNA clone, E. Zeelon for preparing myeloma DNA, R. E. Streeck for samples of *Hin*dIII, *Bgl*II, *Xba*I, and T. Igo-Kemenes for *Bam*HI. The work was supported by Bundesministerium für Forschung und Technologie and Fonds der Chemischen Industrie.

Received 11 February; accepted 29 April 1980.

1. Bernard, O., Hozumi, N. & Tonegawa, S. *Cell* **15,** 1133–1144 (1978).
2. Seidman, J. G., Max, E. & Leder, P. *Nature* **280,** 370–375 (1979).
3. Kuehl, W. M. & Scharff, M. D. *J. molec. biol.* **89,** 409–421 (1974).
4. Rose, S. M., Kuehl, W. M. & Smith, G. P. *Cell* **12,** 453–462 (1977).
5. Burstein, Y. & Schechter, I. *Biochemistry* **17,** 2392–2400 (1978).
6. Southern, E. M. *J. molec. Biol.* **98,** 503–517 (1975).
7. Steinmetz, M., Zachau, H. G. & Mach, B. *Nucleic Acids Res.* **6,** 3213–3229 (1979).
8. Sakano, H., Hüppi, K., Heinrich, G. & Tonegawa, S. *Nature* **280,** 288–294 (1979).
9. Max, E., Seidman, J. G. & Leder, P. *Proc. natn. Acad. Sci. U.S.A.* **76,** 3450–3454 (1979).
10. Smith, G. P. *Biochem. J.* **171,** 337–347 (1978).
11. Lenhard-Schuller, R., Hohn, B., Brack, Ch., Hirama, M. & Tonegawa, S. *Proc. natn. Acad. Sci. U.S.A.* **75,** 4709–4713 (1978).
12. Steinmetz, M. & Zachau, H. G. *Nucleic Acids Res.* **8,** 1693–1707 (1980).
13. Blin, N. & Stafford, D. W. *Nucleic Acids Res.* **3,** 2303–2308 (1976).
14. Loening, U. E. *Biochem. J.* **113,** 131–138 (1969).
15. Lis, J. T., Prestidge, L. & Hogness, D. S. *Cell* **14,** 901–919 (1978).
16. Maniatis, T., Jeffrey, A. & Kleid, D. G. *Proc. natn. Acad. Sci. U.S.A.* **72,** 1184–1188 (1975).
17. Rigby, P. W. J., Dieckmann, M., Rhodes, C. & Berg, P. *J. molec. Biol.* **113,** 237–251 (1977).
18. Denhardt, D. T. *Biochem. biophys. Res. Commun.* **23,** 641–646 (1966).
19. Jeffreys, A. J. & Flavell, R. A. *Cell* **12,** 429–439 (1977)
20. Zeelon, E., Schechter, I., Moult, J., Sussman, J., Amster, O. & Zamir, A. *Isr. J. med. Sci.* (in the press).
21. Zeelon, E., Shinar, S., Kantor, F. & Schechter, I. *Isr. J. med. Sci.* (in the press).

Secretion requires a cytoplasmically disposed sulphydryl of the RER membrane

Robert C. Jackson*, Peter Walter & Günter Blobel

Laboratory of Cell Biology, The Rockefeller University,
New York, New York 10021

The capacity of the rough endoplasmic reticulum (RER) membrane of eukaryotic cells to translocate nascent presecretory proteins from the cytosol to the intracisternal space is preserved on cell fractionation and can be assayed *in vitro*[1]. Two attempts to characterize this translocation activity have been reported. Warren and Dobberstein[2] reported that microsomal membranes can be depleted of their translocation activity by extraction with a solution of high ionic strength (500 mM KCl) and that activity can be restored to the depleted membranes by re-addition of the salt extract. On the other hand, Walter *et al.*[3] reported that KCl extraction of the microsomal membrane does not result in complete depletion of its translocation activity. However, mild trypsinization of the microsomal membrane released a tryptic fragment(s) from the membrane which, when recombined with a tryptically inactivated membrane fraction, restored translocation activity[3]. We now show that both the trypsin and the KCl extracted factors, but not the membrane-integrated remainder of the translocation apparatus, contain at least one sulphydryl group that is essential for activity.

Our assay for the translocation activity of microsomal membranes takes advantage of the obligate coupling of translocation to proteolytic processing of nascent presecretory proteins[3-5]; hence, the ratio of 'processed' prolactin to 'unprocessed' preprolactin is a readily quantifiable measure of the translocation activity of the microsomal membrane.

It was previously noted[6] that *N*-ethylmaleimide, a sulphydryl-modifying reagent, inhibited translocation. Our data here confirm this observation. Preincubation of ribosome-stripped microsomal vesicles with 1.5 mM *N*-ethylmaleimide completely inhibited translocation, as virtually no processed prolactin was synthesized (Figs 1, 2, compare lanes 2 and 3).

A quantitative analysis of this inhibition by various concentrations of *N*-ethylmaleimide and other sulphydryl-modifying reagents (TLCK, a trypsin inhibitor, is mildly reactive with sulphydryl groups[7]) is shown in Fig. 3. We also analysed duplicate aliquots of these same modified samples by the signal peptidase-independent translocation assay described by Warren and Dobberstein[2]. In this, translocation activity is determined from the ability of the microsomal membrane to protect translocated polypeptides from proteolytic digestion, as quantitated by an increase in trichloracetic acid-precipitable radioactivity. Values comparable to those presented in Fig. 3 (data not shown) were obtained. *N*-Ethylmaleimide was the most effective inhibitor of translocation. At a concentration of less than 1.0 mM, *N*-ethylmaleimide completely inhibited translocation (Fig. 3*a*, *b*). Although the other sulphydryl-modifying reagents tested were also effective, concentrations in excess of 1.0 mM were required to achieve complete inhibition of translocation in the given conditions. Interestingly, the bound ribosomes of 'native' rough microsomes do not protect the sensitive sulphydryl group(s) from *N*-ethylmaleimide modification. As shown in Fig. 3*b*, *N*-ethylmaleimide-modified rough microsomes, when stripped of ribosomes by EDTA extraction and subsequently assayed for translocation activity, are inhibited to the same extent as an equivalent amount of microsomes which had been stripped of ribsomes before *N*-ethylmaleimide modification.

To rule out the possibility that the observed inhibition of the synthesis of processed prolactin could have resulted from an inactivation of signal peptidase rather than an impairment of translocation, *N*-ethylmaleimide-modified stripped microsomes were dissociated with sodium deoxycholate and assayed for signal peptidase activity in a post-translational assay[8,9]. The results (Fig. 4) demonstrate that signal peptidase is not inactivated by *N*-ethylmaleimide modification.

The fact that the translocation apparatus can be separated into soluble and membrane-associated fragments enabled us to localize the sensitive sulphydryl group(s) to either of these fragments. Soluble fragments were prepared as previously described[3], by subjecting EDTA-stripped and KCl-extracted microsomal vesicles to low concentrations of trypsin (7 μg ml^{-1}). Although such a mild treatment does not completely separate the membrane from the soluble portion of the translocation apparatus, it avoids the rapid inactivation of the solubilized fragments observed at higher concentrations of trypsin[3]. Centrifugation yielded a supernatant fraction that was further incubated in the absence or presence of *N*-ethylmaleimide. These fractions are referred to as t_7-sup or t_7n-sup, respectively.

Membrane-associated fragments, on the other hand, were prepared by digestion of EDTA-stripped, salt-extracted microsomal vesicles with a high concentration of trypsin (60 μg ml^{-1}). This harsher treatment generates a membrane fraction that is completely translocation inactive by itself (see Figs 1, 2, lane 7)

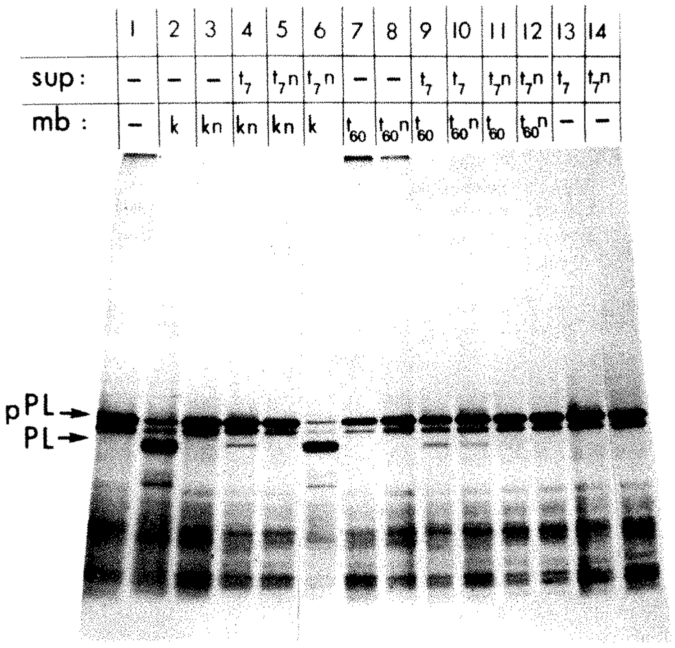
1 2 3 4 5 6 7 8 9 10 11 12 13 14
sup: – – – t7 t7n t7n – – t7 t7 t7n t7n t7 t7n
mb: – k kn kn kn k t60 t60n t60 t60n t60 t60n – –
pPL
PL

Fig. 1 The sulphydryl group required for translocation is located on a cytoplasmically disposed, trypsin-sensitive domain of the translocation apparatus. Supernatant (sup) and membrane (mb) fractions were prepared from mildly (7 μg ml^{-1}) and extensively (60 μg ml^{-1}) trypsin-digested samples of EDTA and KCl-stripped rough microsomes (k-mb) as previously described[3]. Aliquots of these fractions were reacted with 1.5 mM *N*-ethylmaleimide for 30 min at 25 °C, then quenched with a 10 fold molar excess of dithiothreitol (DTT). Both modified and unmodified fractions were assayed for their ability to support and/or reconstitute the translocation of preprolactin across the microsomal membrane. Samples of the indicated fractions were added to a wheat-germ *in vitro* translation system[10] programmed with bovine pituitary RNA and supplemented with human placental ribonuclease inhibitor[11] at a final concentration of $0.006A_{280}$ units ml^{-1}. In assaying for the reconstitution of translocation by the t-sup fractions, 3 μl of the indicated supernatant fraction were added to a typical 25-μl translation mixture. (3 μl of t-sup are derived from $0.126A_{280}$ units of stripped microsomes.) Where indicated, membranes were present at a final concentration of 2.3 A_{280} units ml^{-1}. Translation products were separated by polyacrylamide gel electrophoresis in SDS_4 and detected by autoradiography. Translocation capacity is assessed from the ability of the added fractions to process preprolactin (pPL) to prolactin (PL). The membrane fractions are: k-mb, KCl and EDTA-stripped rough microsomes; kn-mb, *N*-ethylmaleimide-modified k-mb; t_{60}-mb, extensively (60 μg ml^{-1}) trypsinized k-mb; t_{60}n-mb, *N*-ethylmaleimide-modified t_{60}-mb. The supernatant fractions are: t_7-sup, supernatant from mildly (7 μg ml^{-1}) trypsinized k-mb; t_7n-sup, *N*-ethylmaleimide-modified t_7-sup.

---

* Present address: Department of Biochemistry, Dartmouth Medical School, Hanover, New Hampshire 03755.

0028-0836/80/280174—03$01.00

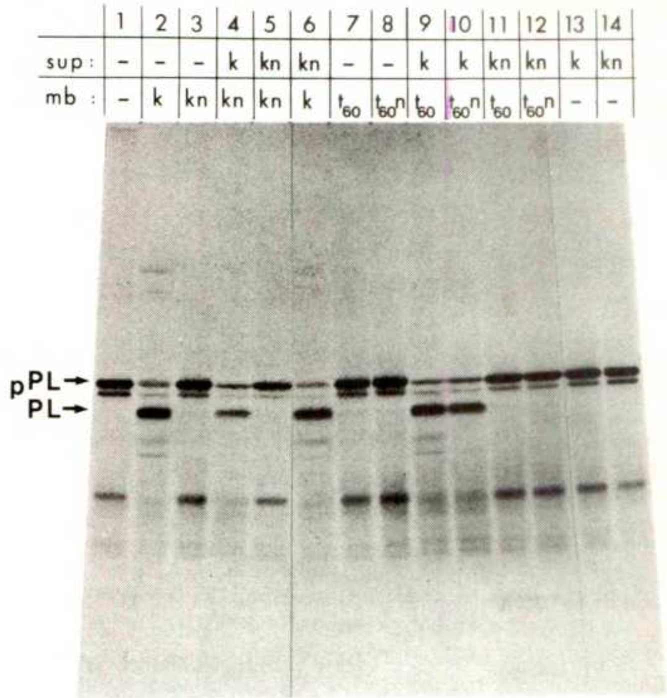
1
2
3
4
5
6
7
8
9
10
11
12
13
14
sup:
- - - k kn kn - - k k kn kn k kn
mb:
- k kn kn kn k t60 t60n t60 t60n t60 t60n - -
pPL→
PL→

Fig. 2 A factor removed from EDTA-stripped rough microsomes by extraction with 0.5 M KCl also contains an essential sulphydryl moiety. EDTA-stripped rough microsomes were extracted with 0.5 M KCl, as described by Warren and Dobberstein[2]. Aliquots of the KCl extract (k-sup) and membrane (k-mb) fractions were modified with 1.5 mM *N*-ethylmaleimide as described in Fig. 1 legend. Samples of the modified and unmodified supernatant and membrane fractions were assessed for their ability to support and/or reconstitute translocation activity as indicated by their ability to process preprolactin to prolactin. In assaying for the reconstitution of translocation by the t-sup and k-sup fractions, 3 μl of these supernatant fractions were added to a typical 25-μl translation mixture. (3 μl of k-sup are derived from 0.154A_{280} units of EDTA-stripped microsomes.) Where indicated, membranes were present at a final concentration of 2.3 A_{280} units ml^{-1}. The abbreviations used are: k-sup, 0.5 M KCl extract of EDTA-stripped rough microsomes; kn-sup, *N*-ethylmaleimide-modified k-sup; other abbreviations are as in Fig. 1.

but retains its competence to serve as acceptor for the solubilized fragment(s) and thereby to restore translocation activity (Fig. 1, lane 9). Before assaying for translocation activity, the trypsinized membrane fraction was further incubated in the absence or presence of *N*-ethylmaleimide. The resulting fractions are referred to as t_{60}-mb or t_{60}n-mb, respectively.

The effects of *N*-ethylmaleimide treatment of these various fractions as well as some essential controls are shown in Fig. 1. Two conclusions can be drawn from the data. First, *N*-ethylmaleimide inactivated only the trypsin-solubilized fragments, but not the membrane-integrated remainder of the translocation apparatus (compare lanes 11, 12 with 9, 10). Thus, the important sulphydryl group(s) is located in the cytosol-exposed, trypsin-sensitive domain of the translocation apparatus. Furthermore, as *N*-ethylmaleimide readily permeates membranes, and as reconstitution of translocation is not affected by *N*-ethylmaleimide modification of t_{60}-mb (Fig. 1, lane 10), the residual t_{60}-mb cannot contain any sulphydryl groups essential for translocation, that is, the essential sulphydryl is located exclusively on the cytosol-exposed domain of the translocation apparatus. Second, non-trypsinized control membranes (k-mb) must contain membrane-integrated fragments comparable to those that are experimentally generated by trypsinization (t_{60}-mb fraction). This was previously suggested by the finding that the translocation activity of trypsin-inactivated membranes could be increased to levels greater than those of untrypsinized membranes by the addition of saturating concentrations of the trypsin-solubilized supernatant factor[3]. Here it is indicated by the finding that a non-trypsinized, but *N*-ethylmaleimide-modified membrane fraction (kn-mb) which is translocation inactive (see Fig. 1, lane 3) can be partially reactivated by a t_7-sup fraction (lane 4). In other words, the control,

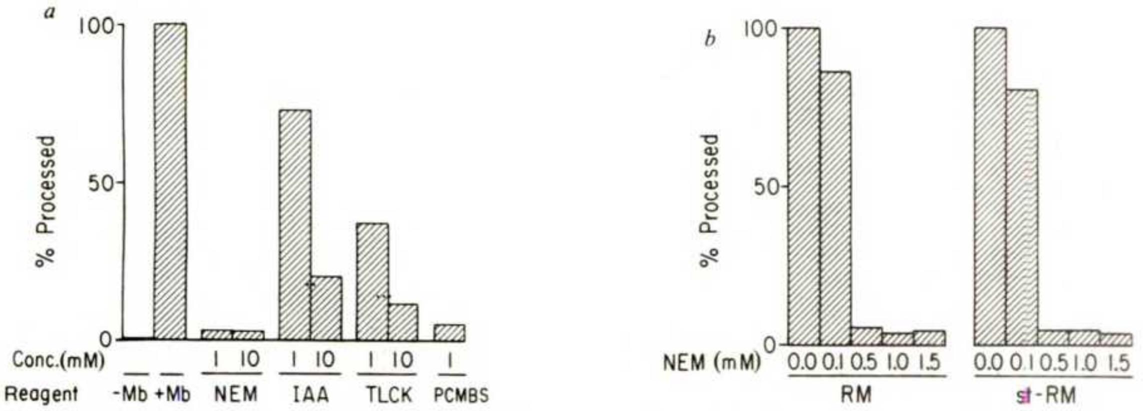

Fig. 3 *a*, Inhibition of precursor processing (and translocation) by sulphydryl-modifying reagents. Stripped rough microsomes (st-RM) were prepared as previously described[3,12] with the exception that DTT was excluded from all buffers. Modification reactions (50 μl) contained stripped microsomes at a final concentration of 46.5 A_{280} units (determined in 5% SDS), 1% Trasylol, 0.2 M sucrose, 100 mM triethanolamine-HCl (TEA-HCl), *p*H 7.5, 40 mM KCl, 0.8 mM $MgCl_2$ and the indicated concentration of freshly prepared sulphydryl-modifying reagent. Reactions were quenched after 30 min at 25 °C by the addition of at least a 10-fold molar excess of DTT. The DTT-inactivated sulphydryl-modifying reagents were removed from the modified stripped microsomes by centrifugation in a Beckman cellulose nitrate airfuge tube containing a sucrose step gradient comprised of 80 μl of 0.5 M sucrose, 10 mM TEA-HCl, *p*H 7.5, 1 mM DTT and 25 μl of 2.0 M sucrose in the same buffer. After centrifugation (5 min, at 30 lb per sq. inch, 100,000g_{av}) the microsomes were removed from the 2.0–0.5 M sucrose interface with a Hamilton syringe, brought to a total volume of 20 μl with 10 mM TEA-HCl, *p*H 7.5, and 1 mM DTT, and assayed for their ability to support translocation (see text) and processing of preprolactin to prolactin. Translocation assays were carried out in a final volume of 50 μl in a wheat-germ translation system[10] supplemented with human placental ribonuclease inhibitor[11] at a final concentration of 0.006 A_{280} units ml^{-1}. The wheat-germ system was programmed with pituitary RNA and supplemented with the appropriately modified membranes at a final concentration of 2.3 A_{280} units ml^{-1}. The ^{35}S-Met-labelled products were separated by gel electrophoresis in SDS, detected by autoradiography of the dried gel and quantitated by excising and counting the portion of the gel containing the ^{35}S-Met-labelled preprolactin and prolactin products[3,12]. Processing is expressed as per cent of control, unmodified membranes (+mb). In this particular experiment, the absolute amount of preprolactin processed by the unmodified membranes was 35.0% of the total preprolactin synthesized. The abbreviations used are: *N*-ethylmaleimide, NEM; iodoacetamide, IAA; *p*-chloromercuribenzene sulphonic acid, PCMBS; *N*-α-*p*-tosyl-L-lysine chloromethyl ketone, TLCK; sodium dodecyl sulphate, SDS. *b*, The processing (and translocation) activity of both rough and stripped rough microsomes is inhibited by *N*-ethylmaleimide modification. A rough microsomal fraction (RM), 107 A_{280} units ml^{-1}, was divided into two samples. Ribosomes were removed from the microsomes of one of these samples by mixing the sample with one volume of a ribosome-stripping solution containing 0.25 M sucrose, 40 mM EDTA and 50 mM TEA-HCl, *p*H 7.5. The stripped microsomes (st-RM) were separated from EDTA by centrifugation. Aliquots of both the stripped and the unstripped microsomes were modified with the indicated concentration of *N*-ethylmaleimide (NEM) as described in *a*. After inactivation of residual *N*-ethylmaleimide with DTT, ribosomes were removed from the rough microsomal fractions by EDTA extraction, as described above. The modified, stripped microsomes were separated from inactivated *N*-ethylmaleimide and EDTA by centrifugation and assayed for translocation activity (see *a*). In this particular experiment, the absolute amount of preprolactin processed by the unmodified stripped microsomes was 74.5% of the total preprolactin synthesized.

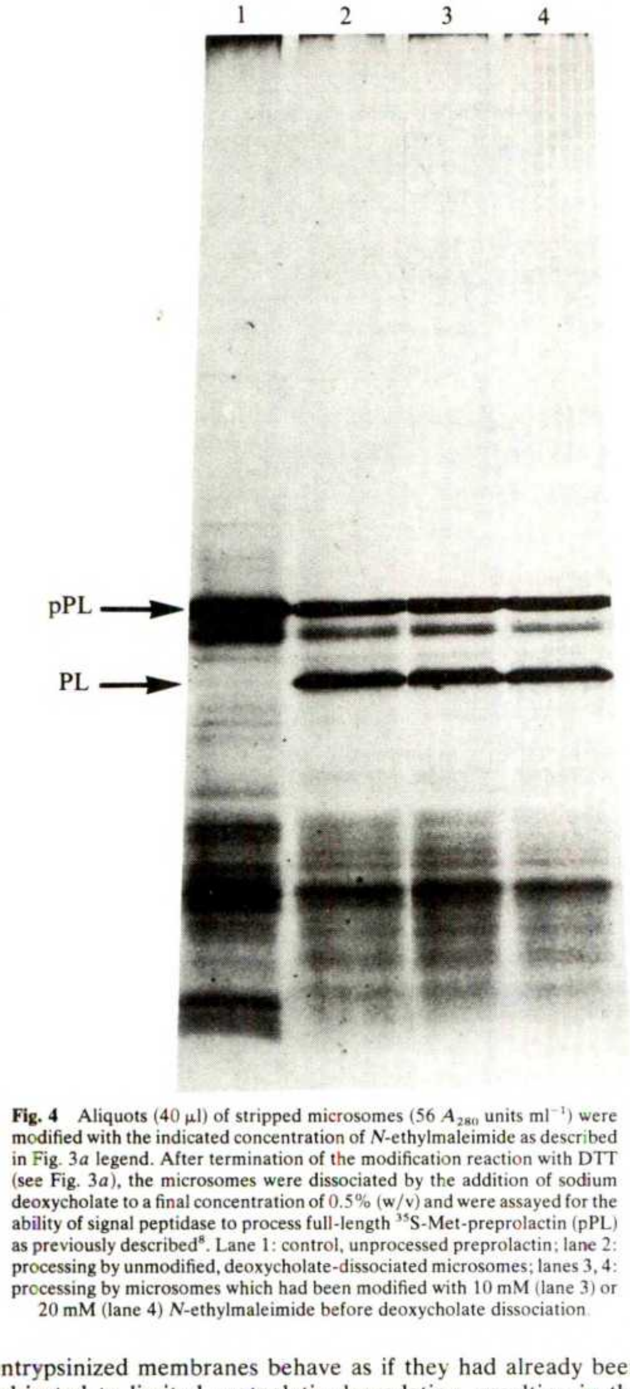

Fig. 4 Aliquots (40 μl) of stripped microsomes (56 A_{280} units ml^{-1}) were modified with the indicated concentration of *N*-ethylmaleimide as described in Fig. 3*a* legend. After termination of the modification reaction with DTT (see Fig. 3*a*), the microsomes were dissociated by the addition of sodium deoxycholate to a final concentration of 0.5% (w/v) and were assayed for the ability of signal peptidase to process full-length ^{35}S-Met-preprolactin (pPL) as previously described[8]. Lane 1: control, unprocessed preprolactin; lane 2: processing by unmodified, deoxycholate-dissociated microsomes; lanes 3, 4: processing by microsomes which had been modified with 10 mM (lane 3) or 20 mM (lane 4) *N*-ethylmaleimide before deoxycholate dissociation.

untrypsinized membranes behave as if they had already been subjected to limited proteolytic degradation, resulting in the production of some nonfunctional but reactivatable translocation sites. As expected, the observed reactivation of the kn-mb fraction is eliminated when a t_7n-sup fraction (Fig. 1, lane 5) is substituted for the t_7-sup fraction.

In the controls in Fig. 1, we show that neither the t_7-sup (lane 13) nor the t_7n-sup (lane 14) fractions are themselves capable of supporting translocation in the absence of added membrane. An additional control (lane 6) demonstrates that the t_7n-sup fraction does not inactivate translocation by added k-mb, indicating that our procedures (see Fig. 3*a*) for quenching *N*-ethylmaleimide are effective and that the observed effects of the *N*-ethylmaleimide-modified fractions are not due to a carryover of residual *N*-ethylmaleimide.

The presence of nonfunctional, but reactivatable translocation sites in untrypsinized k-mb suggested that the 'salt factor' of Warren and Dobberstein[2] is in reality a salt-extractable, proteolytic fragment of the translocation apparatus, comparable to that experimentally generated by trypsin. Therefore, one would expect that the salt factor, like the trypsin-generated soluble fragment(s), might also contain a sulphydryl group(s) that is essential for activity. These expectations were indeed borne out by data shown in Fig. 2. Although in our hands KCl extraction does not result in a complete loss of translocation activity, our KCl extract (k-sup) fraction does contain a salt factor which is able to restore translocation activity to trypsin-inactivated microsomes (Fig. 2, lane 9), to *N*-ethylmaleimide inactivated microsomes (Fig. 2, lane 10) and to microsomes inactivated by both trypsin and *N*-ethylmaleimide (Fig. 2, lane 4). In fact, the ability of the KCl extract to restore translocation is quantitatively superior to that of the tryptic extract (compare Figs 1 and 2, lanes 4, 9, 10). Although this difference in activity may reflect a genuine difference in the absolute reactivation capacity of the KCl and tryptic factors, other explanations (particularly tryptic inactivation of a substantial portion of the trypsin-solubilized factor) are also likely. Nevertheless, like its trypsin-generated counterpart, the salt factor is readily inactivated by *N*-ethylmaleimide (Fig. 2, compare lanes 5, 11, 12 with lanes 4, 9, 10). The control (Fig. 2, lane 6) demonstrates that the *N*-ethylmaleimide-inactivated salt factor does not affect translocation of EDTA-stripped, KCl-extracted membranes (Fig. 2, compare lane 6 with lane 3), indicating that the observed effects of the *N*-ethylmaleimide-modified fractions are not due to a carryover of residual *N*-ethylmaleimide.

From these experiments, we conclude that the translocation-reactivating factors present in k-sup and t_7-sup are functionally and structurally similar, in that both restore translocation activity to *N*-ethylmaleimide- or trypsin-inactivated test membranes, and both contain an essential sulphydryl group(s). Although both these factors are probably derived from the same parent molecule, differences in their extractability (the trypsin factor is released in the absence of salt) suggest that tryptic digestion removes a smaller fragment of the parent translocator protein than is generated by the endogenous tissue protease(s) which produces the salt factor. Presumably, it is this additional domain of the salt factor which is responsible for the differential salt extractability of the salt and tryptic factors. In any case, the observation that the cytoplasmically disposed domain of the translocation apparatus contains an essential sulphydryl which can be readily modified provides us with a tool which should be extremely useful in the purification and characterization of the polypeptides responsible for translocation of nascent secretory and membrane proteins across the membrane of the rough endoplasmic reticulum.

This work was supported by US Public Health Service grant CA12413. R.C.J. is the recipient of Postdoctoral Fellowship GM05829 from the National Institute of General Medical Science.

Received 29 October 1979; accepted 25 February 1980.

1. Blobel, G. & Dobberstein, B. *J. Cell Biol.* **67**, 852–862 (1975).
2. Warren, G. & Dobberstein, B. *Nature* **273**, 569–571 (1978).
3. Walter, P., Jackson, R. C., Marcus, M. M., Lingappa, V. R. & Blobel, G. *Proc. natn. Acad. Sci. U.S.A.* **76**, 1795–1799 (1979).
4. Lingappa, V. R., Devillers-Thiery, A. & Blobel, G. *Proc. natn. Acad. Sci. U.S.A.* **74**, 2432–2436 (1977).
5. Shields, D. & Blobel, G. *Proc. natn. Acad. Sci. U.S.A.* **74**, 2059–2063 (1977).
6. Katz, F. N., Rothman, J. E., Lingappa, V. R., Blobel, G. & Lodish, H. F. *Proc. natn. Acad. Sci. U.S.A.* **74**, 3278–3282 (1977).
7. Shaw, E. in *The Enzymes* 3rd edn, Vol. 1, 71–147 (Academic, New York, 1970).
8. Jackson, R. C. & Blobel, G. *Ann. N.Y. Acad. Sci.* (in the press).
9. Jackson, R. C. & Blobel, G. *Proc. natn. Acad. Sci. U.S.A.* **74**, 5598–5602 (1977).
10. Dobberstein, B. & Blobel, G. *Biochem. biophys. Res. Commun.* **74**, 1675–1682 (1977).
11. Blackburn, P., Wilson, G. & Moore, S. *J. biol. Chem.* **252**, 5904–5910 (1977).
12. Shields, D. & Blobel, G. *J. biol. Chem.* **253**, 3753–3756 (1978).

Efficiency of the adaptive response of *Escherichia coli* to alkylating agents

John Cairns

Imperial Cancer Research Fund, Burtonhole Lane,
London NW7 1AD, UK

When cultures of *Escherichia coli* are exposed to a low level of the alkylating agent *N*-methyl-*N*′-nitro-*N*-nitrosoguanidine (MNNG) they accumulate mutations for about 20 min and then

0028–0836/80/280176—03$01.00

become resistant to further mutagenesis by that level of MNNG[1]. This 'adaptive response,[2] has been shown to be due, at least in part, to induction of the rapid repair of O^6-alkylguanine[3–5] which appears to be the main mutagenic and carcinogenic lesion produced by simple alkylating agents[6,7]. A similar kind of repair has been demonstrated in the livers of rats exposed to nitrosamines[8], and this presumably helps to protect animals against carcinogenesis by the various alkylating agents that are widespread in our environment. It seemed important, therefore, to find out just how effectively such adaptive responses can control mutation rates.

The very efficiency of the response of *E. coli* to MNNG imposed certain constraints on the experiment to measure residual mutation rates. To prepare cultures of adapted bacteria which are free from the mutants that initially arose when adaptation was being induced, it is necessary to start each culture with only a few thousand adapted bacteria. But measurement of the subsequent very low mutation rate of bacteria growing in the presence of the level of MNNG to which they are adapted requires samples of at least 10^7 bacteria. It was therefore necessary to prepare a low *p*H, low phosphate[9] growth medium in which MNNG was sufficiently stable to survive for more than 12 bacterial generations (10–15 h). In practice, the stability of MNNG in such a medium is best checked by observing the distribution of mutant clone sizes in replicate cultures; for, if its concentration is effectively unchanged for the course of the experiment and the mutation rate (m) per cell per generation is therefore constant, the proportion of cultures of N bacteria that contain x or more mutants will follow the distribution of clone sizes, described by Luria[10] for mutations that arise at random in an exponentially increasing population: namely

$$x \sum_{i=x}^{i=N} P_i \rightarrow 2mN, \quad \text{as} \quad \frac{2mN}{x} \rightarrow 0 \qquad (1)$$

and the proportion of cultures that contain one or more mutants will be

$$\sum_{i=1}^{i=N} P_i = 1 - \exp(-2mN) \qquad (2)$$

[In the present instance, it is not necessary to consider the time of duplication of different genes in the cell cycle, because the experiments are solely concerned with comparisons between mutation rates at a single locus and furthermore do not deal with fractional generation times.]

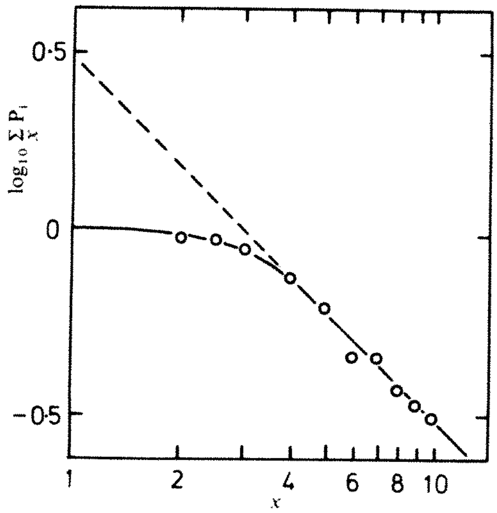

Fig. 1 The distribution of arg^+ revertant clone sizes in cultures of *E. coli* AB 1157 growing in the presence of 0.5 μg ml^{-1} MNNG. If the mutation rate is constant, the proportion of such cultures that contain x or more revertants will approach $2mN/x$ (equation (1)), and the best estimate of mN can be obtained by fitting a line of slope −1 to a plot of the logarithm of these proportions against log x and then measuring the intercept at $x = 1$. Here, the intercept gives log (2 mN) equal to 0.48, or 2 mN equal to 3. As N equalled 4×10^7, m equals 4×10^{-8}.

From either of these equations it is possible to measure the spontaneous mutation rate of unadapted bacteria growing in the absence of MNNG and the overall mutation rate (provoked plus spontaneous) of adapted bacteria growing in the presence of the concentration of MNNG to which they have been adapted. What the MNNG-provoked mutation rate would have been, in the absence of the adaptive response, can be determined simply by exposing a strain that cannot induce the response[11] to the medium in which the adapted bacteria had been growing; after a period of one generation these non-adapting bacteria will contain mN mutants.

The results of such an experiment are shown in Table 1 and Fig. 1. Most mutant clones in the adapted cultures are small (that is, of recent origin) and have the expected distribution (Fig. 1). The extra mutation rate in the MNNG-adapted cultures was 3.5×10^{-8} arg^+ per generation, but the medium in which these bacteria were growing produced $20{,}000 \times 10^{-8}$ arg^+ per generation in an adaptation-deficient strain. In these particular conditions, therefore, the adaptive response was lowering the mutation rate about 6,000-fold. This is a surprising result. Each DNA base in *E. coli* serves as template once every 2,500 s. For adaptation to lower 6,000-fold the probability that an altered base serves as a source of mutation, the adaptive response may have to render each premutational lesion such as O^6-methylguanine harmless within 0.5 s: (of course, the process would not have to be completed so quickly if the enzymes for post-replication mismatch repair can recognize and correct structures such as O^6-methylguanine·thymine base pairs). Conceivably, the reaction succeeds in being rapid because the catalytic reactant restores the normal base-pairing properties of the guanine

Table 1 Measurement of the mutation rate produced by 0.5 μg ml^{-1} MNNG in bacteria that are either adapted or unable to adapt

	Cells plated	arg^+ revertants	Mutation rate per generation $\times 10^8$
AB 1157	4×10^7	0, 0, 0, 0, 0, 0, 0, 0, 0, 0, 0, 0, 0, 0, 0, 0, 0, 0, 0, 0, 0, 0, 1, 1, 1, 1, 1, 1, 1, 2, 2, 5	0.5*
AB 1157 in 0.5 μg ml^{-1} MNNG	4×10^7	0, 2, 2, 3, 3, 3, 3, 3, 4, 4, 4, 4, 5, 5, 5, 5, 5, 7, 7, 7, 8, 9, 13, 19, 23, 42, 55, 89, 239, ~2,000	4.0†
AB 1157 *ada* 5	6×10^7	0, 0, 0, 0, 1, 1, 1, 1	~0.4*
AB 1157 *ada* 5 1 hr in supernates of MNNG cultures	1×10^6	174, 181, 192, 196, 204, 204, 211, 231	20,000

A culture of *E. coli* AB 1157 (*arg, his, leu, pro, thr, thi*) was grown in a low *p*H, low phosphate medium containing 0.1 M NaCl, 0.04 M KCl, 0.02 M NH_4Cl, 1 mM $MgCl_2$, 0.5 mM KH_2PO_4, 0.2 mM Na_2SO_4, 0.1 mM $CaCl_2$, 0.01 mM $FeCl_3$, 0.025 M Tricine (Sigma) *p*H 6.1, plus required amino acids (20 μg ml^{-1}) and vitamins (0.1 μg ml^{-1}) and 0.6% glucose. When the bacterial concentration had reached 10^7 per ml, MNNG was added to give a level of 0.1 μg ml^{-1} for one generation and 0.5 μg ml^{-1} for a further generation. At this point the culture was diluted to 2,000 bacteria per ml, and 32 3-ml aliquots were prepared in the absence of MNNG and 32 in the presence of 0.5 μg ml^{-1} MNNG. After 18 h incubation (when the cultures contained, by microscope count, 2×10^7 bacteria per ml), each aliquot was centrifuged, resuspended in 0.5 ml minimal medium and plated on minimal plates lacking arginine, to give the number of arg^+ revertants. These two sets of cultures therefore provided estimates of the spontaneous reversion rate and the sum of spontaneous and MNNG-provoked mutation rate to arg^+. At the same time, the supernatant medium from the MNNG-containing cultures was used to suspend similar cultures of the adaptation-defective strain AB 1157 *ada* 5 (ref. 11). After exposure for 1 h (roughly one generation) these cultures were centrifuged and similarly plated on arginine-deficient plates.

* Mutation rate determined by equation (2).

† Mutation rate determined by equation (1) (see Fig. 1).

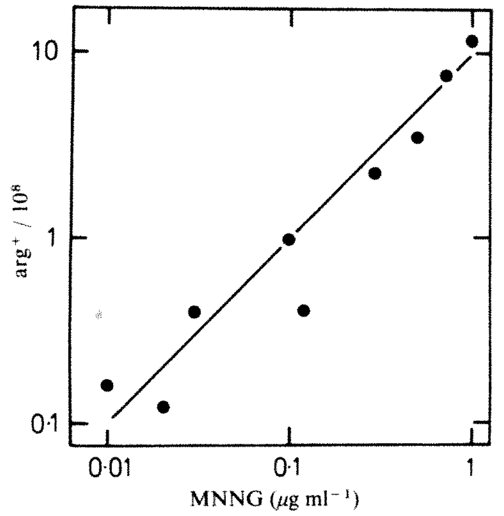

Fig. 2 The extra mutation rate of *E. coli* AB 1157 growing in the presence of various concentrations of MNNG. The mutation rate (*arg*$^+$ revertants per generation) was determined as described in Table 1 and Fig. 1; the spontaneous rate (1.2×10^{-9}) has been subtracted.

in one step by providing an alternate site of attachment for the alkyl group[5], and this is why each reactant molecule apparently can act only once[4]. Whatever the mechanism, it is interesting that the adaptive response succeeds in being at least as efficient as the 'error-free' repair of pyrimidine dimers produced by ultraviolet light[12,13] even though dimers are presumably much less of a threat because, unlike alkylated bases, they cannot be copied and so are not an immediate source of mutation.

The above calculation was based on the assumption that the low residual mutation rate in adapted bacteria is due to the very rare occasions when an O^6-methylguanine happens to be copied before it is repaired; and if that is correct, the mutation rate in adapted cultures should be directly proportional to the rate of production of alkylated bases (that is, proportional to mutagen concentration). However, more complex relationships between dose and response are imaginable. For example, the adaptive response could be 100% efficient once induced, but a small proportion of the cells might fail to undergo induction; in this case, very low levels of mutagen might be more mutagenic than higher levels. Such questions are of practical importance in assessing the likely risks from low levels of carcinogens, and so these experiments with bacteria were extended to cover a range of MNNG concentrations.

As Fig. 2 shows, adapted cultures of *E. coli* growing in the presence of MNNG have an increase in mutation rate that is approximately proportional to MNNG concentration. Interestingly, a similar result has been seen when rats are continuously exposed to dimethyl or diethyl nitrosamine in their drinking water (R. Peto, personal communication). Doses below 1 p.p.m. (that is, below about 0.1 mg per kg per day) produced an incidence of liver cancer that was roughly proportional to dose; but between 1 and 10 p.p.m. the age-specific incidence increased about 1,000-fold. For these alkylating agents it seems clear, therefore, that brief exposures are much more mutagenic for certain bacteria and high dose rates are much more carcinogenic for certain animals than might be expected from the response to continuous low dose rates.

Received 28 February; accepted 2 May 1980.

1. Samson, L. & Cairns, J. *Nature* **267**, 281–283 (1977).
2. Jeggo, P., Defais, M., Samson, L. & Schendel, P. *Molec. gen. Genet.* **157**, 1–9 (1977).
3. Schendel, P. F. & Robins, P. E. *Proc. natn. Acad. Sci. U.S.A.* **75**, 6017–6020 (1978).
4. Robins, P. & Cairns, J. *Nature* **280**, 74–76 (1979).
5. Karran, P., Lindahl, T. & Griffin, B. *Nature* **280**, 76–77 (1979).
6. Loveless, A. *Nature* **223**, 206–207 (1969).
7. Goth, R. & Rajewsky, M. F. *Proc. natn. Acad. Sci. U.S.A.* **71**, 639–643 (1974).
8. Montesano, R., Brésil, H. & Margison, G. P. *Cancer Res.* **39**, 1798–1802 (1979).
9. Lawley, P. D. & Thatcher, C. J. *Biochem. J.* **116**, 693–707 (1970).
10. Luria, S. E. *Cold Spring Harb. Symp. quant. Biol.* **16**, 463–470 (1951).
11. Jeggo, P. *J. Bact.* **139**, 783–791 (1979).
12. Miura, A. & Tomizawa, J. *Molec. gen. Genet.* **103**, 1–10 (1968).
13. Witkin, E. M. *Mutat. Res.* **8**, 9–14 (1969).

0028–0836/80/280178—03$01.00

Virus-specific effects of interferon in embryonal carcinoma cells

Timothy W. Nilsen, Debra L. Wood & Corrado Baglioni

Department of Biological Sciences, State University of New York
at Albany, Albany, New York 12222

Embryonal carcinoma (EC) cells are susceptible to infection by a variety of viruses[1], but do not become resistant to infection by Semliki Forest virus[2] or vesicular stomatitis virus[3] (VSV) on treatment with interferon. These observations have led to the conclusion that interferon does not induce an antiviral state in EC cells[2,3]. We report here, however, that EC cells treated with interferon become resistant to infection by two picornaviruses and two *ts* mutants of VSV, whereas they remain sensitive to wild-type VSV, Sindbis and influenza virus infection. These results suggest that a partial antiviral state is induced in EC cells by interferon and that the induced antiviral protein(s) interferes with the replication of specific viruses. A significant common feature of these viruses is their replication through structures containing double-stranded RNA (dsRNA)[4].

Interferon induces in human and mouse cells the synthesis of a few proteins that are detected by gel electrophoresis[5,6]. Among these are two enzymes, an oligonucleotide polymerase and a protein kinase (see ref. 7 for refs), which are activated by dsRNA in extracts of interferon-treated cells. The polymerase converts ATP into a series of oligonucleotides characterized by 2'5'-phosphodiester bonds and designated 2-5A (ref. 8). The 2-5A activates an endoribonuclease that degrades RNA[9,10]. The protein kinase (PK_{ds}) inhibits protein synthesis by phosphorylating the α subunit of initiation factor eIF-2 (ref. 7). Wood and Hovanessian[3] assayed these enzymatic activities in extracts of interferon-treated EC cells and observed an increase in 2-5A polymerase activity comparable to that in mouse L cells, whereas the PK_{ds} was not significantly increased in EC cells. As these cells did not become resistant to VSV infection[3], the induction of 2-5A polymerase could not be correlated with an antiviral state. In a different cell system, however, the induction of 2-5A polymerase is closely correlated with the inhibition of replication of a picornavirus, encephalomyocarditis virus

Table 1 Effect of interferon on virus yield and induction of 2'5'-oligo(A) polymerase and protein kinase

Cells	PCC4		L	
Interferon treatment	–	+	–	+
EMCV yield	8	3	8	4
VSV yield	8	8	8	4
2'5'-oligo(A) synthesis	10	680	10	2,440
Protein kinase	2	2	2	30

Cultures of control and interferon-treated cells (100 units ml^{-1} for 20 h) were infected for 48 h as described in Fig. 1 legend. The cultures were frozen and thawed three times and centrifuged for 10 min at 30,000*g*. The virus yield was measured by end-point dilution of the supernatant and quantification of the cytopathic effect on L-cell monolayers. Virus samples of known titre were assayed in parallel; virus yield is expressed as the $\log_{10}$ of the titre in plaque-forming units per ml. Cytoplasmic extracts were prepared from control and interferon-treated cells grown in 75-cm^2 flasks. The cells were washed with saline and homogenized as described elsewhere[16], with the addition of 0.5% Triton X-100 to the homogenization buffer. The S30 fraction obtained by centrifugation for 5 min at 30,000*g* was assayed for 2-5A synthesis with poly(I) · poly(C)-paper as described by Stark *et al.*[26]. The synthesis of 2-5A obtained with 100 µl of S30 in 16 h is expressed in pmol of ATP converted into oligonucleotides out of an input of 250 nmol of ATP per 50-µl reaction. The protein kinase activity was assayed by measuring the phosphorylation of a 67,000 molecular weight polypeptide as described elsewhere[27]. The S30 was centrifuged for 90 min at 150,000*g* and the pellet obtained resuspended and incubated with [^{32}P]ATP and 1 µg ml^{-1} of poly(I) · poly(C); the phosphorylated proteins were resolved by gel electrophoresis, detected by autoradiography and quantified by scanning the autoradiographs as described elsewhere[27]. The protein kinase activity is expressed in units of peak area, relative to a reference polypeptide present in both L and PCC4 cells.

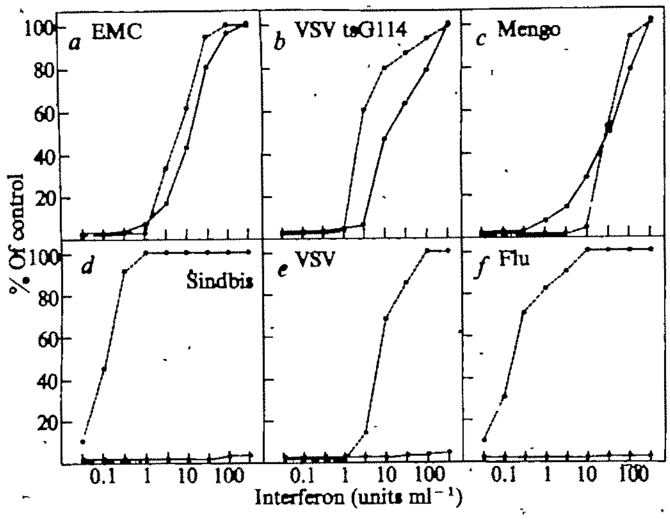

Fig. 1 Antiviral effects of interferon in embryonal carcinoma (●—●) and L cells (○– –○) infected with different viruses. The PCC4AzaR1 and L929 cell lines were maintained in monolayer cultures in Dulbecco modified Eagle's medium containing 10% heat-inactivated calf serum. Before infection the cells were seeded at about 3×10^5 cells per 16-mm well in 24-well cluster plates (Costar). The amount of virus required to produce a complete cytopathic effect in 48 h was determined for both cell types by end-point dilution of concentrated virus stocks. The cytopathic effect was quantified by the viral dye uptake method[15] The L cells were infected by adding 0.2 ml of virus stock diluted in medium minus serum to each well. After 1 h at 37 °C for all viruses except the *ts* mutants of VSV, which were kept at 30 °C, 0 8 ml of medium containing 1% fetal calf serum was added and the infection continued for 48 h. As the PCC4 cells were infected more effectively while the cells were not adhering to the plastic wells, these cells were resuspended by shaking, infected and allowed to re-attach Treatment with the concentration of interferon indicated in the abscissa (NIH reference units) was for 20 h before infection. At the start of the interferon treatment the PCC4 cells were suspended as described above for virus infection The cytopathic effect was quantified after 48 h of infection. In all experiments control infected and non-infected cells were examined in parallel cultures. The A_{540} of the dye taken up by the latter cells was taken as 100%; the A_{540} of the control infected cells represents the 0% value shown in the ordinate. Typical A_{540} values were 2.5 for uninfected cells and 0.15 for untreated infected cells. Mouse interferon was obtained from Ehrlich ascites tumour cells infected with Newcastle disease virus and partially purified to about 10^7 units per mg of protein[13]. The viruses used are indicated Vesicular stomatitis virus (VSV) was the Indiana serotype strain. Identical results were obtained with both VSV *ts* mutants G114 and G11 and therefore the results with tsG114 only are shown. Flu designates the WSN strain of influenza virus

(EMCV)[11]. Moreover, this inhibition is observed even when induction of PK_{ds} is prevented by actinomycin D (ref. 11). In view of these observations, it was of interest to investigate the response of interferon-treated EC cells to picornavirus infection.

The EC cell line PCC4, derived from the transplantable ascitic form of the OTT 50-60 teratocarcinoma[12], and L929 cells were grown in monolayer cultures. These cells were treated with increasing concentrations of mouse interferon prepared from Ehrlich ascites tumour cells[13] and infected with different viruses as described in Fig. 1 legend. The viruses were: EMCV and Mengo, two picornaviruses; VSV and its two mutants tsG11 and tsG114 (ref. 14); Sindbis and influenza virus. All the viruses infected both L and EC cells, as shown by quantification of the cytopathic effect by a viral dye uptake method[15]. Low concentrations of interferon protected L cells from all viruses tested. In contrast, concentrations up to 300 units ml⁻¹ of interferon did not protect EC cells from VSV, Sindbis or influenza virus. Interferon concentrations comparable to those effective for L cells, however, protected EC cells from infection by EMCV, Mengo and the VSV mutants.

To confirm that interferon has a protective effect on EC cells, we also measured virus yield in control and interferon-treated cells infected with EMCV and VSV (Table 1). Treatment with interferon reduced virus yield by four logs in both cells infected with EMCV, but had no effect on the yield of VSV in EC cells. The protective effect of interferon in EC cells, therefore, is clearly virus specific.

In subsequent experiments, we confirmed that only one of the two enzymatic activities induced by interferon is elevated in EC cells, whereas both are increased in L cells (Table 1). The 2-5A polymerase was induced in EC cells by interferon, but the kinase was not. The 2-5A synthesized by EC and L cell extracts was characterized by its elution from DEAE-cellulose with 0.35 M KCl[16] (Table 1) and by its biological activity in an endonuclease activation assay[9]. Oligonucleotides synthesized with extract of interferon-treated PCC4 and L cells activated a HeLa cell endonuclease, whereas corresponding fractions from incubations with extract of control cells did not (data not shown).

These observations suggest a possible correlation between the inhibition of replication of specific viruses in EC cells and the induction of the 'antiviral protein' 2-5A polymerase. Although the precise mechanism of action of this enzyme has not been determined, the following observations suggest that the 2-5A polymerase has some role in preventing replication of picornaviruses: (1) 2-5A is formed in interferon-treated cells infected with EMCV[17]; (2) 2-5A introduced into intact cells inhibits protein synthesis and causes RNA breakdown[18,19]; (3) preferential degradation of viral RNA is observed when the replicative intermediate (RI) of EMCV is incubated with extracts of interferon-treated cells (the RI is the RNA component of the replicative complex)[20]; (4) EMCV replicates by forming base-paired structures. This was shown by isolating cross-linked RI from infected cells treated with aminomethyltrioxalen[4]. This compound intercalates into duplexes and forms covalent bonds on irradiation[21]. Cross-linked RNA could not be detected in cells infected with wild-type VSV, but was detected in cells infected with two *ts* mutants that are sensitive to interferon protection in EC cells[4].

Interferons are glycoproteins that are operationally defined in terms of their antiviral activity against a wide range of viruses. With the recent advances in our understanding of the molecular basis of the antiviral state[7], it has become clear that several defence mechanisms are activated in interferon-treated cells; for example, an inhibitor of viral mRNA methylation[22] and a reduction in the amount of G protein incorporated into VSV[23] have been reported. The fact that interferon does not protect EC cells from VSV infection presumably means that these latter defence mechanisms are not operational in EC cells. In most cells interferon activates a spectrum of antiviral defence mechanisms, whereas in EC cells it elicits a restricted antiviral state, possibly limited to the induction of 2-5A polymerase.

A better understanding of the different antiviral mechanisms and of the replication of different viruses may ultimately provide a satisfactory explanation for the present and previous observations. A genetically determined virus-specific effect of interferon, for example, is due to the *Mx* allele in A2G mice[24]. Haller *et al.*[25] have reported that macrophages of *Mx* mice can be protected from influenza virus by much smaller interferon concentrations than are necessary to protect macrophages of other mice; no difference in protection is observed, however, on infection with EMCV or VSV. These authors speculate that the antiviral state is composed of a multitude of specific antiviral mechanisms and envisage the *Mx* gene as regulating the expression of a component of the antiviral state[25]. Each component may be both genetically and developmentally regulated, as shown by this report and by our observations on embryonal carcinoma cells.

This work was supported by NIH grant AI-16076. The VSV *ts* mutants were obtained from Drs Gail W. Wertz and Philip Marcus, Mengo was obtained from Dr Jean Lucas Lenard and other viruses from Dr James McSharry.

Received 11 March, accepted 15 May 1980.

1. Teich, N. M., Weiss, R. A., Martin, G. R. & Lowy, D. R. *Cell* **12**, 973–982 (1977)
2. Burke, D. C., Graham, C. F. & Lehman, J. M. *Cell* **13**, 243–248 (1978)
3. Wood, J. N. & Hovanessian, A. G. *Nature* **282**, 74–76 (1979)
4. Nilsen, T. W., Wood, D. L. & Baglioni, C. *Virology* (in the press)
5. Gupta, S. L., Rubin, B. Y. & Holmes, S. L. *Proc natn Acad Sci U S A* **76**, 4817–4821 (1979)
6. Knight, E. Jr & Korant, B. D. *Proc natn Acad Sci U S A* **76**, 1824–1827 (1979)
7. Baglioni, C. *Cell* **17**, 255–264 (1979)
8. Kerr, I. M. & Brown, R. E. *Proc natn Acad Sci U S A* **75**, 256–260 (1978)

9. Baglioni, C., Minks, M. A. & Maroney, P. A. *Nature* **273,** 684–687 (1978).
10. Clemens, M. J. & Williams, B. R. G. *Cell* **13,** 565–572 (1978).
11. Baglioni, C., Maroney, P. A. & West, D. K. *Biochemistry* **18,** 1765–1770 (1979).
12. Stevens, L. C. *Devl Biol.* **21,** 364–382 (1970).
13. Kawakita, M. *et al. J. biol. Chem.* **253,** 598–602 (1978).
14. Pringle, C. R. *J. Virol.* **5,** 559–567 (1970).
15. Borden, E. C. & Leonhardt, P. H. *J. Lab. clin. Med.* **89,** 1036–1042 (1977).
16. Minks, M. A., Benvin, S., Maroney, P. A. & Baglioni, C. *J. biol. Chem.* **254,** 5058–5064 (1979).
17. Williams, B. R. G., Golgher, R. R., Brown, R. E., Gilbert, C. S. & Kerr, I. M. *Nature* **282,** 582–586 (1979).
18. Williams, B. R. G. & Kerr, I. M. *Nature* **276,** 88–90 (1978).
19. Hovanessian, A. G., Wood, J., Meurs, E. & Montagnier, L. *Proc. natn. Acad. Sci. U.S.A.* **76,** 3261–3265 (1979).
20. Nilsen, T. W. & Baglioni, C. *Proc. natn. Acad. Sci. U.S.A.* **76,** 2600–2604 (1979).
21. Isaacs, S. T., Shen, C. I., Hearst, J. E. & Rapoport, H. *Biochemistry* **16,** 1058–1064 (1977).
22. Sen, G. C. *et al. J. Virol.* **21,** 69–83 (1977).
23. Maheshwari, R. K., Jay, F. T. & Friedman, R. M. *Science* **207,** 540–541 (1980).
24. Lindemann, J., Lane, C. A. & Hobson, D. *J. Immun.* **90,** 942–951 (1962).
25. Haller, O., Arnheiter, H., Lindemann, J. & Gresser, I. *Nature* **283,** 660–662 (1980).
26. Stark, G. R., Dower, W. J., Schimke, R. T., Brown, R. E. & Kerr, I. M. *Nature* **278,** 471–473 (1978).
27. West, D. K. & Baglioni, C. *Eur. J. Biochem.* **101,** 461–468 (1979).

A new papillomavirus associated with alimentary cancer in cattle

M. Saveria Campo[*], Martin H. Moar[*],
William F. H. Jarrett[†] & Helen M. Laird[†]

[*] Department of Zoology, University of Edinburgh, Edinburgh, UK
[†] Department of Veterinary Pathology, University of Glasgow, Glasgow, UK

A high incidence area of carcinoma of the alimentary tract of cattle has been reported[1–4]. The carcinomas are preceded by papillomas which may transform to malignancy. A papillomavirus was isolated from these warts and was shown to occur as a widespread infection of cattle in the UK[2]. In the high cancer area there is a marked increase in the overall incidence of this infection, an increase in the number of papillomas per animal and an increase in the number of specific sites of infection as compared with cattle from adjacent areas where cancers are not found. The papillomas are found in young animals but carcinomas do not develop until the cows are over 7 yr old. There is strong circumstantial evidence[1] that the factor associated with the increased multiplicity of papillomas and the subsequent malignant transformation is the ingestion of bracken fern. This plant is known to possess radiomimetic, mutagenic and carcinogenic activity. Preliminary experimental evidence supports the circumstantial data and we also have preliminary evidence of the presence of viral genome sequences, without production of virus, in the cells of carcinomas. In addition to the alimentary papillomas of the type described above, three more major patterns of bovine papillomatosis are found in the UK[5]—cutaneous fibropapillomatosis, papillomatosis of the skin of the udder and teats, and papilloma of the penis. We have extracted papillomaviruses from all the above tumours, and our results, published in a preliminary form elsewhere[5], indicate that the different lesions are caused by different papillomaviruses. Here we report the partial characterization of the virus involved in alimentary tract tumours and its differentiation from other bovine papillomaviruses. The system seems to present a dissectable model for investigating the mechanistic relationship between the viral infection and the ingestion of an environmental 'carcinogen'.

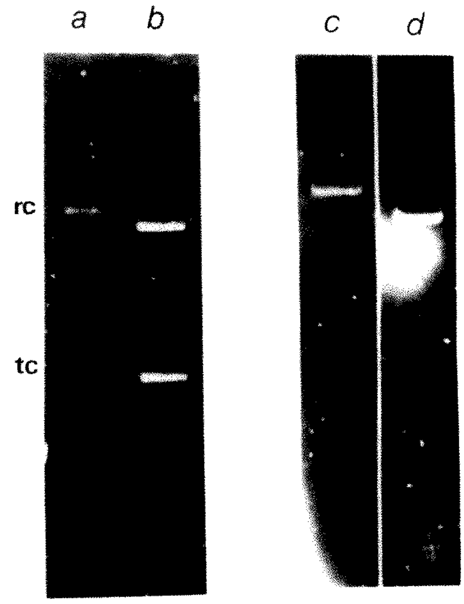

Fig. 1 Comparison between BCPV and BAPV DNA. *a*, Unrestricted BCPV DNA, and *b*, unrestricted BAPV DNA, electrophoresed in a 1% agarose gel. rc, relaxed circles; tc, twisted circles. *c*, *Hin*dIII-restricted BCPV DNA, and *d*, *Bam*HI-restricted BAPV DNA, electrophoresed in a 0.7% agarose gel. The MWs ($\times 10^{-6}$) are shown on the right. The MW of BAPV DNA was calculated by using the known MW of BCPV DNA as reference. Cutaneous and oesophageal papillomas were finely homogenized in TS buffer (10 mM NaCL, 1 mM Tris *p*H 8.0, 1 mM EDTA). The debris was pelleted at 2,000 r.p.m. for 5 min and the supernatant centrifuged at 10,000*g* for 15 min. Virions were pelleted from the 10,000*g* supernatant by centrifugation at 35,000 r.p.m. for 90 min. The virion pellet was resuspended in TS buffer and the virions were banded in a CsCl gradient at 1.36 g ml^{-1}. The band containing the virus was collected and, after dilution with TS buffer, the virions were pelleted at 35,000 r.p.m. for 2.5 h. The final pellet was resuspended in TS buffer and the virions were disrupted by adding SDS to 0.5%. The viral DNA was extracted with phenol, precipitated with alcohol and resuspended in 10 mM Tris, *p*H 7.8, and 1 mM EDTA. Unrestricted DNA was electrophoresed in a 1% agarose gel and restricted DNA in a 0.7% agarose gel in E buffer[16], at 5 V cm^{-1}. The DNA was visualized by staining the gel with ethidium bromide and by photography under UV light. Conditions of restriction are as in Fig. 2 legend.

Virus was isolated from a variety of papillomas by homogenization and density gradient centrifugation on CsCl. The papillomas were of four of the types recognized in cattle in the UK[5]. Alimentary papillomavirus (BAPV) was obtained from oesophageal warts; each isolate was made from a single abattoir animal which had several tumours but no concurrent carcinoma, and no other type of papillomas. DNA was purified from the virus and was present in two forms, twisted circles (form 1) and relaxed circles (form 2) (Fig. 1*b*). In agarose gel electrophoresis, both forms migrated ahead of the corresponding forms of DNA isolated from the virus (BCPV) of cutaneous fibropapillomas (Fig. 1*a*, *b*). This suggested that BAPV has a genome of lower molecular weight (MW) than BCPV. BAPV is cut at one site by *Bam*HI restriction endonuclease and this linear molecule shows a higher electrophoretic mobility than BCPV DNA linearized by *Hin*dIII (Fig. 1*c*, *d*). The MW of DNA of BAPV in the above experiments was calculated as approximately 4.5×10^6, or 10% smaller than the normally quoted MW for papillomavirus DNA[6,7].

We have analysed BAPV DNA with six restriction enzymes and compared it with physical maps generated in a similar fashion which we have made of BCPV DNA, and also with DNA from virus isolated from a group of tumours commonly found on the teats of cows and the penis of bulls that we have designated bovine paragenital papillomavirus (BPPV)[5].

Because of the limited amount of viral DNA obtainable from single alimentary tract papillomas, we found it inconvenient and wasteful to analyse restriction patterns by ethidium bromide fluorescence. We circumvented this problem by labelling some of the virus DNA by nick-translation[8] and by hybridizing the radioactive DNA to Southern blots[9] containing nanogramme amounts of restricted DNA. The results are presented in Fig. 2. *Bam*HI and *Hpa*I produce unit length linear DNA (Figs 1*d*, 2*a*, *h*); therefore, there is only one cleavage site for these enzymes in the DNA. *Eco*RI produces two fragments (Fig. 2*f*), *Hin*dIII three fragments (Fig. 2*d*) and *Hin*dII four fragments (Fig. 2*b*). The viral DNA is not restricted by *Bgl*II (not shown) and therefore has no cleavage site for this enzyme.

The MWs of the restriction fragments are listed in Table 1. The total MW of the viral genome obtained by adding the MWs of individual restriction fragments generated by any one enzyme ranges from 4.43×10^6 to 4.5×10^6, thus confirming our previous estimate.

0028-0836/80/280180—03$01.00

When the DNA is digested with *Eco*RI + *Bam*HI, the *Eco*RI fragment B disappears and two smaller fragments are produced (Fig. 2*g*). The *Bam*HI site therefore maps within *Eco*RI fragment B. Restriction with *Hin*dIII + *Bam*HI produces three detectable fragments (Fig. 2*e*). The first two correspond to *Hin*dIII fragment A and fragment B, respectively, and the third fragment corresponds to *Hin*dIII fragment C minus a low MW fragment that we could not detect in this particular gel. The *Bam*HI site is thus located within *Hin*dIII fragment C. When the DNA is restricted with *Hin*dII + *Bam*HI, five fragments are produced (Fig. 2*c*). Three fragments correspond, respectively, to *Hin*dII fragments, B, C and D. *Hin*dII fragment A is split into a major fragment and a very low MW fragment. This places the *Bam*HI site within *Hin*dII fragment A. Restriction with *Hpa*I + *Bam*HI produces two fragments (Fig. 2*i*). As the recognition sites of *Hpa*I are a subset of those of *Hin*dII[10], the double restriction shows that the single *Hpa*I site coincides with the *Hin*dII site at 0.278 map units (see below and Fig. 3). Restriction with *Eco*RI + *Hin*dIII, and *Eco*RI + *Hin*dII places the two *Eco*RI sites within fragments A and C of both *Hind* enzymes (Table 1). Of the three *Hin*dIII sites, two map within *Hin*dII fragment A and one within *Hin*dII fragment B (Table 1).

The MWs of the fragments obtained in all double digest experiments are listed in Table 1. Arbitrarily assigning the zero map unit to the single *Bam*HI site, and taking into account the fractional length of all the restriction fragments, these can be ordered in a circular map (Fig. 3).

This map differs considerably from the restriction maps of papillomavirus DNA from both the typical cutaneous warts and the paragenital (teat and penis) lesions[5] (M.S.C. *et al.*, in preparation). The differences between the viruses are not confined to the position of the restriction sites along their genomes: in liquid hybridization experiments, carried out in 2 × SSC at 70 °C, BAPV DNA failed to cross-hybridize to the DNA of the other two viruses, whereas the latter cross-reacted with each other to at least 55% as estimated from the S_1 nuclease resistance of the hybrids. Moreover, BAPV DNA did not hybridize to Southern blots of large amounts (up to 0.5 μg) of restricted BCPV DNA or restricted BPPV DNA, and conversely, neither of the latter hybridized to blots of *Hin*dII- and *Hin*dIII-restricted BAPV DNA. These results show that the alimentary tract papillomavirus is not a deletion mutant of the other two viruses, but belongs to a type of its own.

In contrast, the extensive cross-hybridization between the typical BCPV DNA and BPPV DNA and the respective restriction fragments immobilized on nitrocellulose showed that the sequence homology between these two types of virus is not confined to a particular region of the genome, but is spread throughout the whole of it[5]. Similar results have recently been obtained by Law and colleagues[11].

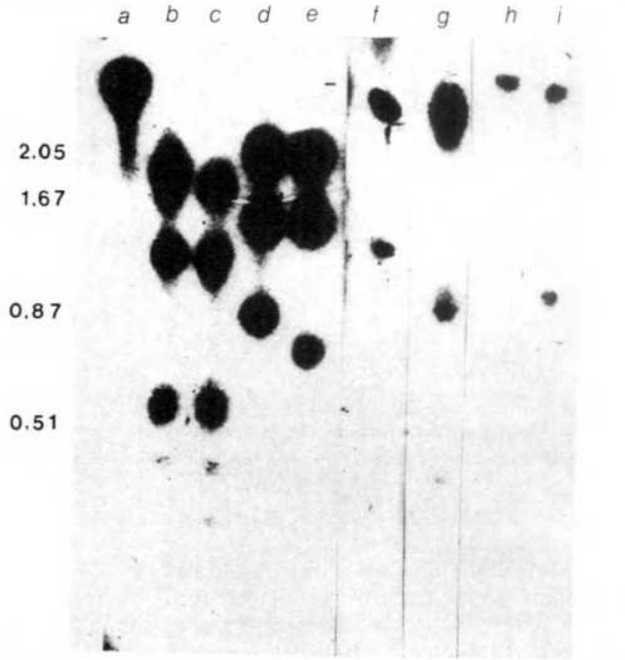

Fig. 2 Restriction fragments of BAPV DNA. *a*, *Bam*HI; *b*, *Hin*dII; *c*, *Hin*dII + *Bam*HI; *d*, *Hin*dIII; *e*, *Hin*dIII + *Bam*HI; *f*, *Eco*RI; *g*, *Eco*RI + *Bam*HI; *h*, *Hpa*I; *i*, *Hpa*I + *Bam*Hi (all Boehringer). The buffers used were as recommended by Boehringer laboratories. Nanogramme amounts of viral DNA were digested and the resulting fragments were electrophoresed in a 1.5% agarose gel as described in Fig. 1 legend. The DNA fragments were transferred to nitrocellulose[9] and hybridized overnight to nick-translated[8] ^{32}P-labelled viral DNA, in Denhart-2 × SSC at 70 °C (ref. 17). The nitrocellulose sheet was extensively washed in 1 × SSC at 70 °C, dried and exposed to a flash-activated X-ray film (Kodak X-Omat H) at −70 °C (ref. 18) for 3 weeks. The *Hin*dII fragments of BCPV DNA, visualized both by ethidium bromide fluorescence and by hybridization to ^{32}P-BCPV DNA, were used as MW markers. The sharpness of the stronger high MW bands has been lost so that the presence of the much fainter low MW bands can be seen.

Marked differences between BAPV on the one hand and BCPV and BPPV on the other were also found at the level of antigenic determinants. Whereas BCPV and BPPV have a major determinant in common, no serological cross-reaction was observed with BAPV[5] (W.F.H.J. *et al.*, in preparation). Thus, BCPV and BPPV seem to belong to the same group and, although distinguishable, are much more closely related to each other than they are to BAPV.

Two types of bovine papillomavirus, BPV 1 and BPV 2, have recently been described[12]. Although the precise body localization of the papillomas from which these viruses were purified is not specified in that work, BPV 1 corresponds to our BPPV and BPV 2 to our BCPV. Also, bovine papillomavirus with a genome of MW 4.5×10^6 has recently been found by Pfister *et*

Table 1 Molecular weights and fractional lengths of the restriction fragments of BAPV DNA

MW ($\times10^{-6}$)	Fractional length	MW ($\times10^{-6}$)	Fractional length	MW ($\times10^{-6}$)	Fractional length	MW ($\times10^{-6}$)	Fractional length	MW ($\times10^{-6}$)	Fractional length
*Eco*RI		*Hin*dIII		*Hin*dII		*Eco*RI + *Bam*HI		*Hin*dIII + *Bam*HI	
A 3.15	70.0	A 2.13	47.4	A 2.10	47.9	3.14	70.0	2.13	47.4
B 1.35	30.0	B 1.48	32.9	B 1.30	29.6	1.00	22.1	1.48	32.9
4.50		C 0.88	19.6	C 0.56	12.8	0.36	8.0	0.70	15.6
		4.49		D 0.42	9.5	4.50		4.31	
				4.38					
*Hin*dII + *Bam*HI		*Hin*dIII + *Eco*RI		*Hin*dII + *Eco*RI		*Hin*dII + *Hin*dIII		*Hpa*I + *Bam*HI	
1.82	41.5	1.48	33.2	1.52	34.7	1.32	29.8	3.3	73.3
1.30	29.6	1.30	29.2	1.30	29.6	1.22	27.3	1.2	26.6
0.56	12.8	0.79	17.7	0.60	13.7	0.88	19.9	4.5	
0.42	9.6	2 × 0.44	9.9	0.42	9.5	0.56	12.7		
0.26	5.9	4.45				0.43	9.7		
4.36									

The MWs were calculated as in Fig. 2 legend. In two different experiments, the measurement error ranged from 0.01×10^6 to 0.15×10^6 for individual fragments. The fractional lengths were calculated from the percentage of the MW of a single fragment over the total MW. In the case of *Hin*dII + *Eco*RI double digest and of *Hin*dII + *Hin*dIII double digest, where small fragments were missing, presumably because they failed to bind to the nitrocellulose, the fractional length was calculated on the total MW of the single digest.

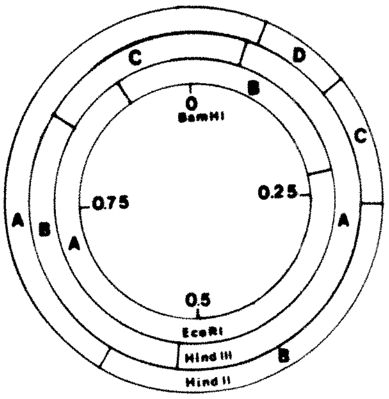

Fig. 3 Restriction map of BAPV DNA. The circular genome has been divided into tenths, and the restriction enzyme sites have been mapped according to the fractional length of the fragments produced by a given enzyme. Zero map unit has been arbitrarily assigned to the single *Bam*HI site. The approximate map positions of the other restriction sites are: *Hpa*I = 0.278; *Eco*RI = 0.220, 0.920; *Hin*dIII = 0.040, 0.514, 0.844; *Hin*dII = 0.057, 0.152, 0.278, 0.587

al.[13] in cutaneous papillomas from Australian cattle, but not in papillomas from German cattle where only the typical cutaneous type was found. Despite the similarity in MW, the DNA restriction map of the Australian virus found by those authors differs from the DNA restriction map of the small virus we have found in alimentary tract papillomas. Experiments in progress suggest that 'rice grain'-type lesions of the teat papillomatosis are caused by yet another type of papillomavirus. This would bring the number of different bovine papillomaviruses to five. We are now investigating the relationship between the several viruses at the molecular, immunological and pathological levels. We injected BAPV into the soft palate of 18 calves and into the skin of the neck of 6. After 2 months, all 18 calves injected in the palate showed marked papillomatosis, whereas no cutaneous papillomas have so far (8 months) been detected in the calves injected subcutaneously. Studies on the infectivity of BAPV are in progress. The viral DNA purified from the experimentally induced alimentary tract papillomas is indistinguishable in MW and restriction pattern from the one used to induce the tumours. In addition, the sera from the tumorous calves failed to cross-react with antisera raised against the other viruses, confirming the uniqueness of BAPV. The finding that BAPV does not induce cutaneous warts complements the finding of Olson and his colleagues[14], who, although able to induce cutaneous warts experimentally in cattle with BCPV, failed to infect the alimentary tract.

Thus, although our analysis of these viruses is incomplete, our initial studies of their epidemiological, pathological, immunological and molecular heterogeneity provide increasing evidence of a close relationship between the type of papillomavirus and the type and site of lesion caused by them. This is particularly interesting in view of the fact that, as far as we know, only BAPV is associated with the only benign papillomas that commonly undergo malignant transformation in cattle. A similar situation is found in humans: epidermodysplasia verruciformis, a papilloma with marked tendency to malignant transformation, is caused by HPV-5 (previously classified as HPV-4), a human papillomavirus differing from the other, more common, viruses associated with ordinary skin warts[15]. In addition, preliminary evidence indicates that bovine alimentary carcinoma cells contain BAPV DNA sequences, but not BCPV or BPPV DNA sequences, thus further suggesting that only the alimentary virus is involved in carcinogenesis.

This work was carried out with the aid of grants from the Agricultural Research Council (AG. 17/112), the NIH (N01 CP 81022), and the Cancer Research Campaign (916/800/2). We thank Mr Brian O'Neil, Mrs Ellen Leighton, Mrs C. Burke and Mrs C. McLay for technical assistance.

Received 30 January; accepted 8 May 1980.

1. Jarrett, W. F. H., McNeil, P. E., Grimshaw, T. R., Selman, I. E. & McIntrye, W. I. M. *Nature* **274,** 215–217 (1978).
2. Jarrett, W. F. H., Murphy, J., O'Neil, B. W. & Laird, H. M. *Int. J. Cancer* **22,** 323–328 (1978).
3. Jarrett, W. F. H. *Bull. Cancer* **65,** pt 2, 191–194 (1978).
4. Jarrett, W. F. H. in *Antiviral Mechanisms in the Control of neoplasia* (ed. Chandra, P.) 39–45 (Plenum, New York, 1979).
5. Jarrett, W. F. H. *et al. 7th Cold Spring Harb. Conf. Cell Proliferation* (1980).
6. Crawford, L. V. *Adv. Virus Res.* **14,** 89–125 (1969).
7. Favre, M., Orth, G., Croissaut, O. & Yanir, M. *Proc. natn. Acad. Sci. U.S.A.* **72,** 4810–4814 (1975).
8. Rigby, P. W. J., Dieckmann, M., Rhodes, C. & Berg, P. *J. molec. Biol.* **113,** 237–251 (1977).
9. Southern, E. M. *J. molec. Biol.* **98,** 503–517 (1975).
10. Garfin, D. E. & Goodman, H. M. *Biochem. biophys. Res. Commun.* **59,** 108–116 (1974).
11. Law, M., Lancaster, W. D. & Howley, P. M. *J. Virol.* **32,** 199–207 (1979).
12. Lancaster, W. D. *J. Virol.* **32,** 684–687 (1979).
13. Pfister, H. *et al. Virology* **96,** 1–8 (1979).
14. Olson, C., Gordon, D. E., Robl, M. G. & Lee, K. P. *Archs envir. Hlth* **19,** 827–837 (1969).
15. Orth, G. *et al. Proc. natn. Acad. Sci. U.S.A.* **75,** 1537–1541 (1978).
16. Loening, U. E. *Biochem. J.* **113,** 131–138 (1969).
17. Denhart, K. *Biochem. biophys. Res. Commun.* **23,** 641–646 (1966).
18. Laskey, R. A. & Mills, A. D. *FEBS Lett.* **82,** 314–316 (1977).

A pyrimidine dimer–DNA glycosylase activity associated with the *v* gene product of bacteriophage T4

Eric H. Radany & Errol C. Friedberg

Laboratory of Experimental Oncology, Department of Pathology,
Stanford University, Stanford, California 94305

Mutations in the *v* gene of bacteriophage T4 are associated with a marked increase in sensitivity to killing by UV radiation at 254 nm, but not to a variety of other forms of base damage to DNA[1–4]. Early studies from this laboratory provided evidence for a role of the *v* gene in the excision of pyrimidine dimers (PD) from DNA. Specifically, it was shown that extracts of T4v^+-infected *Esherichia coli* catalyse the formation of single-strand breaks (nicks) and/or alkali-labile sites in UV-irradiated duplex DNA[5]. Comparable hydrolysis of phosphodiester bonds is not observed with extracts of *E. coli* infected with the mutant T4v_1 (ref. 5). The product of the *v* gene has been extensively purified in a number of laboratories[6–9]; however, convincing evidence of purification to physical homogeneity has not yet been presented.

Characterization of the partially purified *v*-gene product yielded results that were consistent with the interpretation that this gene codes for an endonuclease activity (endonuclease V of T4 or T4 UV endonuclease) that directly catalyses the hydrolysis of phosphodiester bonds 5′ to PD in duplex DNA, creating nicks with 3′OH and 5′P termini[6,8,10,11]. The additional observations that the enzyme attacks single-stranded DNA containing PD[6,11] and that no other form of base damage in DNA thus far examined is recognized as substrate[1–4,12], support the notion that the activity coded by the *v* gene recognizes PD in DNA specifically.

Grossman *et al.*[13] and Haseltine *et al.*[14] have recently suggested an alternative mechanism for the incision of DNA containing PD. Their suggestion stems from the analysis by gel electrophoresis, of the length of DNA fragments generated by incubation of a sequenced region of the *E. coli lac* operon containing PD, with UV endonuclease activities from *Micrococcus luteus*. A knowledge of the exact nucleotide sequence of the substrate used allowed for a very precise prediction of the length of the oligonucleotide products generated following denaturation of the DNA, if the enzyme activity catalysed cleavage of phosphodiester bonds immediately 5′ to PD sites. Their experiments yielded unexpected results which have been interpreted in terms of an alternative molecular mechanism for the enzymatic incision of UV-irradiated DNA at PD sites, that is, a PD-specific DNA glycosylase catalyses cleavage of the 5′ *N*-glycosylic bonds of the dimerized pyrimidines and the resulting apyrimidinic sites are attacked by apurinic/apyrimidinic (AP) endonuclease, resulting in cleavage of phosphodiester bonds. This two-step mechanism is entirely consistent with the observation of nicks bearing 3′OH and 5′P termini located 5′

0028-0836/80/280182—04$01.00

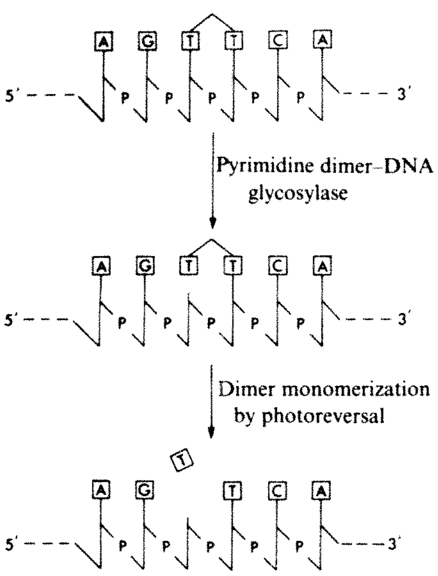
A
G
T
T
C
A
5'
3'
P
Pyrimidine dimer–DNA glycosylase
Dimer monomerization by photoreversal
T

Fig. 1 Diagrammatic representation of experimental protocol. Only one strand of a duplex DNA molecule is shown. The figure indicates postulated hydrolysis of the 5' glycosylic bond of a thymine–thymine dimer, yielding an apyrimidinic site. Subsequent monomerization of the dimer by direct photoreversal results in the release of the 5' thymine of the dimer as free thymine.

with respect to PD in duplex UV-irradiated DNA incubated with *M. luteus* correndonucleases I and II (ref. 15).

In view of the remarkable similarity in the properties of so-called T4 endonuclease V and *M. luteus* correndonucleases I and II, we have sought evidence for a PD-DNA glycosylase activity in preparations of T4 enzyme known to catalyse the nicking of UV-irradiated DNA. Enzyme-catalysed hydrolysis of the *N*-glycosylic bond linking either one of the dimerized pyrimidines to deoxyribose in DNA would leave the corresponding base in covalent linkage only with its partner in the dimerized structure (Fig. 1). Subsequent monomerization of the PD should result in the liberation of free thymine (Fig. 1) which can be readily detected by established chromatographic techniques. Our experimental approach has been to demonstrate that the formation of free thymine from UV-irradiated DNA is dependent both on incubation with T4 enzyme activity, and on the monomerization of PD by the technique of direct photoreversal.

Regarding the latter procedure, it has been clearly demonstrated by others that the formation of pyrimidine dimers in DNA by exposure to UV radiation at about 254 nm is a reversible process[16,17]. When *E. coli* DNA is irradiated at 254 nm under standard conditions, the rates of PD formation and reversal ultimately become equal and a state of dynamic equilibrium is attained in which ~7% of radioactively labelled thymine is in PD. Thus, further irradiation at 254 nm under these conditions does not result in measurable net dimer formation or dimer monomerization. However, when *E. coli* DNA is initially irradiated at 254 nm in the presence of $AgNO_3$, photosensitized dimer formation results in the conversion of as much as 20% of the thymine to thymine-containing PD[18]. Further irradiation of this DNA at 254 nm following removal of the photosensitizer results in measurable reversal of PD, until once again a steady state is reached at a level of ~7% thymine-containing PD. In the present experiments we have employed the technique of direct photoreversal to investigate the release of free thymine from *E. coli* DNA (containing about 17% of its thymine in PD) previously incubated with or without a T4 enzyme preparation.

Figure 2 shows the sedimentation profiles in alkaline sucrose gradients of UV-irradiated DNA incubated with the T4 enzyme. It is clear that the smallest amount of enzyme used in these experiments is saturating with respect to the number of DNA strand breaks and/or alkaline labile sites generated in the DNA. Unirradiated DNA incubated and sedimented under identical conditions showed no reduction in sedimentation velocity in alkaline sucrose gradients (data not shown). The incubation conditions described in Fig 2 also result in the release of free thymine. (Table 1 and Fig. 3). However this product is only observed when, following incubation of UV-irradiated DNA with the T4 enzyme preparation, the reaction mixture is subjected to direct photoreversal. Free thymine is not detected when unirradiated DNA incubated with enzyme is subjected to photoreversing light (Table 1), nor is this result obtained when UV-irradiated DNA not previously incubated with the enzyme is exposed to photoreversing light (Table 1).

These results strongly suggest that the T4 enzyme preparation contains a DNA glycosylase activity that catalyses the hydrolysis of one of the *N*-glycosylic bonds linking the dimerized pyrimidines to deoxyribose in DNA (Fig. 1). This suggestion is consistent with the fact that PD are quantitatively the major photoproduct in DNA irradiated at 254 nm, and to our knowledge are the only known photoproducts in DNA that can generate thymine as a product of their photolabilization. Our conclusions are also supported by the results of extensive previous studies with the T4 enzyme which have demonstrated that this activity recognizes pyrimidine dimers exclusively in UV-

Table 1 Release of free thymine from DNA containing thymine dimers

			Total free [^{3}H] thymine detected	
^{3}H-labelled thymine-labelled substrate	T4 enzyme	Incident photo-reversal fluence (kJ m^{-2})	(c.p.m. per ml of reaction mixture $\times 10^{-3}$)	(% of [^{3}H] radioactivity as thymine-containing PD)
Unirradiated *E. coli* DNA	Absent	0	<0.04	<0.001
	Absent	11.5	<0.04	<0.001
	Present	0	<0.04	<0.001
	Present	11.5	<0.04	<0.001
UV-irradiated *E. coli* DNA (17.5% thymine as thymine-containing PD)	Absent	0	<0.04	<0.001
	Absent	4.3	ND	—
	Absent	8.2	ND	—
	Absent	12.3	<0.04	<0.001
	Present	0	<0.04	<0.001
	Present	4.3	14.4	16.5
	Present	8.2	21.3	24.3
	Present	12.3	26.6	30.4

[^{3}H]thymine-labelled *E. coli* DNA (1.5×10^4 c.p.m. μg^{-1}) was prepared by standard methods. DNA containing 17.5% of ^{3}H-thymine in PD was produced by germicidal irradiation at 254 nm with an incident fluence of 2 kJ m^{-2} in the presence of Ag^+ photosensitizer according to the procedure of Rahn and Landry[18]. Tritiated UV-irradiated or unirradiated DNA (100 μg ml^{-1}) was incubated at 37 °C with or without 9.4×10^4 units ml^{-1} of the phosphocellulose fraction of T4 endonuclease[9] in 10 mM Tris–HCl *p*H 7.8, 10 mM Na_2 EDTA, 100 mM NaCl for 45 min in a total volume of 3.0 ml. Following incubation, each was deproteinized by incubation at 60 °C with 50 μg per ml Proteinase K for 1 h followed by extraction with an equal volume of $CHCl_3$. Irradiated or unirradiated ^{3}H-DNA (131 μg total) that had been incubated in the presence or absence of enzyme was diluted with 10 mM Tris–HCl *p*H 7.5, 1 mM Na_2EDTA to give a final activity of 5.0×10^5 ^{3}H c.p.m. ml^{-1}. Unlabelled DNA was added to these mixtures to bring the final A_{254} to 2.0. The mixtures were then subject to photoreversing irradiation and duplicate aliquots (0.2 ml) were withdrawn at the incident fluences stated. ^{14}C-thymine (9,530 c.p.m. NEN) was added to each aliquot as an internal marker for the chromatographic identification of free ^{3}H-thymine by TLC. The aliquots were evaporated to dryness and the residue extracted three times with 15 μl absolute ethanol. The extracts were spotted directly on thin layer plates and developed as described previously[22]. [^{3}H] and [^{14}C] radioactivity were measured in individual chromatogram fractions; total [^{3}H] free thymine was calculated by normalization to 100% recovery of the [^{14}C] standard. Separate ^{14}C-thymine samples were run with each chromatogram to allow for correction of channel spillover during radioactive counting of the two isotopes in a Beckman LS 250 liquid scintillation spectrometer. Replicate measurements agreed to within 5%. (ND = none detected.)

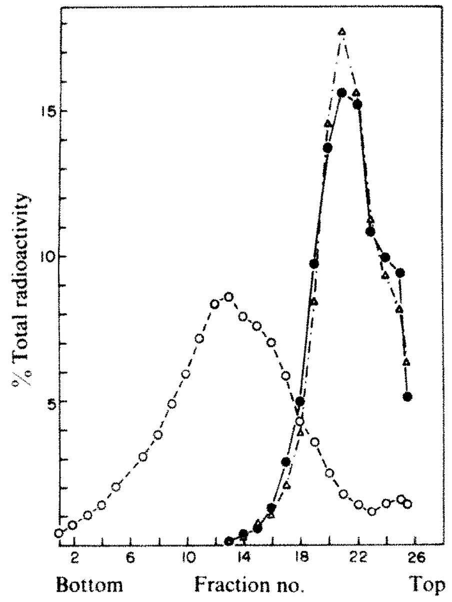

Fig. 2 ^{3}H-thymine DNA (0.5 μg, 21% thymine-containing PD) was prepared as described in the legend to Table 1 and incubated at 37 °C for 30 min with (●) or without (○) 9.4×10^4 units per ml of the phosphocellulose fraction of T4 endonuclease[9] in 50 μl reactions containing 10 mM Tris–HCl pH7.8, 10 mM, Na_2EDTA, 100 mM NaCl. The reactions were stopped by the addition of 50 μl 5% alkaline sucrose, and layered onto 4 ml 5–20% alkaline sucrose gradients. The DNA was sedimented at 30,000 r.p.m. in an SW56 rotor for 11 h at 20 °C. The gradients were fractionated and processed for measurement of radioactivity as described by Reynolds[23]. To demonstrate apparent completion of incision, a reaction containing enzyme was prepared and incubated as above, and then incubated with an additional aliquot (4.7×10^3 units) of enzyme for a further 30 min (△). Incubations with even higher amounts of enzyme yielded identical sedimentation profiles (data not shown).

irradiated DNA[2,7,11,19–21]. Thus, for example, removal of PD by enzymatic photoreactivation of UV-irradiated DNA in permeabilized *E. coli* results in the loss of all sites sensitive to the T4 enzyme[20]. In addition, in both duplex and single stranded UV-irradiated DNA incubated with the enzyme there is a stoichiometric relationship between the calculated number of PD in the DNA and the measured number of strand breaks[7,11,19,21]. Further evidence in support of PD-DNA glycosylase activity associated with the T4 enzyme preparation is provided by independent studies by Seawell *et al.* (manuscript submitted). Using the same preparation of T4 enzyme, these investigators have shown that under incubation conditions that are strictly limiting with respect to enzyme concentration, UV-irradiated DNA is subject to hydrolysis of phosphodiester bonds in strong alkali or following incubation with AP endonuclease at near-neutral pH. These are expected properties of DNA containing apyrimidinic sites generated by the action of a DNA glycosylase activity. Alkaline lability of T4 enzyme-treated UV-irradiated DNA and/or the presence of AP endonuclease activity associated with the T4 DNA glycosylase is also indicated in the present studies by the reduced sedimentation velocity of the DNA in akaline sucrose gradients shown in Fig. 2.

Table 2 Photoreversal-dependent release of free thymine from UV-irradiated DNA incubated with extracts of *E. coli* infected with phage T4v^+ or T4v_1

Extract of *E. coli* infected with	Free thymine (c.p.m./20 μl of reaction mixture) Photoreversal	No photoreversal
Phage T4v^+	380	<20
Phage T4v_1	<20	<20

Extracts of *E. coli* cells infected by wild type (v^+) and mutant (v_1) phage T4 were prepared by sonication in 50 mM Tris–HCl, pH 8.0 as described previously[7]. Extracts (0.87 mg total protein in each) were incubated at 37 °C for 30 min with 150 μg ^{3}H-thymine labelled *E. coli* DNA (3.0×10^4 c.p.m. per μg, 10% of [^{3}H] in thymine-containing PD) plus 35 mM Tris–HCl pH 8.0, 10 mM Na_2 EDTA, 100 mM NaCl. The final volume of each of the two incubation reactions was 1.6 ml. Following reaction, the mixtures were extensively deproteinized by incubation with 100 μg per ml Proteinase K at 60 °C for 2 h, followed by extraction with phenol and $CHCl_3$. The mixtures were made 0.5 M in NaCl and the DNA was precipitated overnight at −20 °C with two volumes of absolute ethanol. The DNA was collected by centrifugation and resuspended at a concentration of 150 μg ml^{-1} in 10 mM Tris–HCl pH 7.5, 1 mM EDTA. Half of each reaction mixture was subjected to 10 kJ m^{-2} photoreversal irradiation fluence; the other half was kept as a control. Aliquots (20 μl) of each reaction were spotted on thin layer chromatography plates. Free thymine was determined as described in the legend to Table 1. [^{14}C] thymine standard samples were run on adjacent lanes of the same thin-layer plate.

Note from Table 1 that the highest photoreversing fluence used in these experiments (12 kJ m^{-2}) is not yet saturating with respect to free thymine formation. Yet even at this fluence, the amount of radioactivity present in the free base is equivalent to that present in ~30% of the thymine-containing PD measured in the DNA. Since the DNA is uniformly labelled with ^{3}H-labelled thymine, each thymine-containing dimer attacked by the enzyme and subsequently reversed by irradiation, should release on the average one half of its radioactivity as free thymine (Fig. 1). Thus the radioactivity in free thymine equivalent to 30% of the thymine-containing PD in DNA represents the product of the reversal of 60% of such dimers. Clearly the PD-DNA glycosylase demonstrated in these experiments is not a minor contaminant of the T4 enzyme preparation used.

Finally, our studies indicate that the T4 PD–DNA glycosylase is a product of the v gene of phage T4, since extracts of T4-infected *E. coli* failed to catalyse the production of free thymine under the experimental conditions described (Table 2). A question of obvious interest is whether or not the v gene also codes for an AP endonuclease activity that is physically associated with the PD–DNA glycosylase activity. The release of free thymine dependent on the photoreversal of PD in DNA provides the basis for a specific and convenient assay of T4-induced PD–DNA glycosylase activity and we are currently purifying this enzyme to physical homogeneity from T4-infected

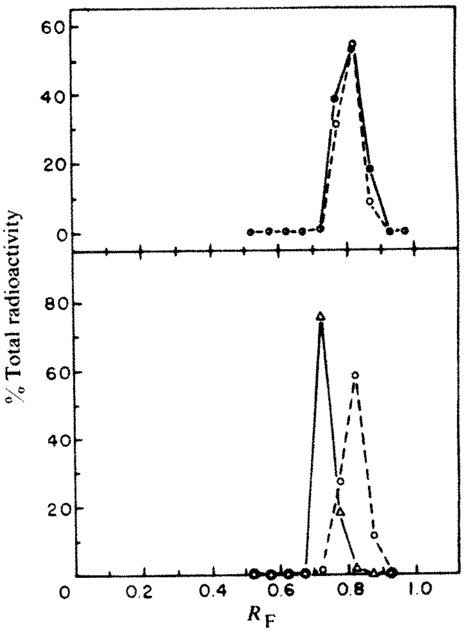

Fig. 3 Chromatographic identification of free ^{3}H-thymine in the ethanol-soluble phase generated by photoreversal irradiation of T4-enzyme treated irradiated DNA. Upper panel; portions of the ethanol-soluble phase of the photoreversal reaction containing added ^{14}C-thymine were applied to silica gel thin-layer chromatography plates and developed with water-saturated ethyl acetate/n-propanol (4 : 1)[17]. The plates were then fractionated at 0.05 R_f increments and the radioactivity in each fraction was determined after elution into water by liquid scintillation spectrometry[22]. Phosphorylated species migrate in this system with an $R_f = 0.1$ (ref. 17). Lower panel: ^{3}H-thymidine and ^{14}C-thymine were mixed and applied to an adjacent lane of the same plate depicted in the upper panel and analysed identically following development. No radioactivity migrated with an $R_f < 0.5$ in either chromatogram (data not shown). ●, [^{3}H] reaction product; △, [^{3}H]TdR standard; ○, [^{14}C]T standard.

E. coli. The availability of purified enzyme will hopefully facilitate a more detailed examination of the relationship of PD–DNA glycosylase to AP endonuclease activity, and of other questions concerning the detailed molecular mechanism of the incision of UV-irradiated DNA by this enzyme.

We thank Ms Pat Seawell for the preparation of T4 enzyme used, Ms Seawell and Drs Ann Ganesan, Thomas Bonura, Rick Reynolds and Jack Love for helpful discussions. These studies were supported by research grants from the USPHS and The Foundation—March of Dimes, and by contract with the US Department of Energy. E.H.R. is supported by an MSTP training grant from the USPHS and E.C.F. is the recipient of a research career development award from the USPHS.

Received 19 December 1979; accepted 7 May 1980.

1. Harm, W. *Virology* **19,** 66–71 (1963).
2. Friedberg, E. C. *Mutat. Res.* **15,** 113–123 (1972).
3. Ito, I & Sekiguichi, M. *Jap. J. Genet.* **51,** 29–33 (1976).
4. Nishida, Y., Yasuda, S. & Sekiguchi, M. *Biochim. biophys. Acta* **442,** 208–215 (1976).
5. Friedberg, E. C. & King, J. J. *Biochem. biophys. Res. Commun.* **37,** 646–651 (1969).
6. Yasuda, S. & Sekiguchi, M. *Proc. natn. Acad. Sci. U.S.A.* **67,** 1839–1845 (1970).
7. Friedberg, E. C. & King, J. J. *J. Bact.* **106,** 500–507 (1971).
8. Yasuda, S. & Sekiguchi, M. *Biochim. biophys. Acta* **442,** 197–207 (1976).
9. Friedberg, E. C., Ganesan, A. K. & Seawell, P. C. *Meth. Enzym.* (in the press).
10. Friedberg, E. C. & Lehman, I. R. *Biochem. biophys. Res. Commun.* **58,** 132–139 (1974).
11. Minton, K. Durphy, M., Taylor, R. & Friedberg, E. C. *J. biol. Chem.* **250,** 2823–2829 (1975).
12. Friedberg, E. C. *Photochem. Photobiol.* **21,** 277–289 (1975).
13. Grossman, L., Riazuddin, S., Haseltine, W. A. & Lindan, C. *Cold Spring Harb. Symp. Quant. Biol.* **43,** 947–955 (1979).
14. Haseltine, W. A. *et al. Nature* (in the press).
15. Riazuddin, S. & Grossman, L. *J. biol. Chem.* **252,** 6287–6293 (1977).
16. Setlow, R. B. *Science* **153,** 379–386 (1966).
17. Setlow, R. B. *Prog. nucleic Acid. Res. molec. Biol.* **8,** 257–295 (1968).
18. Rhan, R. O. & Landry, L. C. *Photochem. Photobiol.* **18,** 29–38 (1973).
19. Friedberg, E. C. & Clayton, D. A. *Nature* **237,** 99 (1972).
20. Ganesan, A. K. *J. molec. Biol.* **87,** 103–119 (1974).
21. Ganesan, A. K., Smith C. A. & Van Zeeland, A. A. in *DNA Repair: A Laboratory Manual of Research Procedures* (eds Friedberg, E. C. & Hanawalt, P. C.) (Dekker, New York, in the press).
22. Cook, K. H. & Friedberg, E. C. *Analyt. Biochem.* **73,** 411–418 (1976).
23. Reynolds, R. J. *Mutat. Res.* **50,** 43–56 (1978).

Calcium-induced decrease in membrane fluidity of sea urchin egg cortex after fertilization

Judith Campisi* & Carl J. Scandella

Department of Biochemistry, State University of New York,
Stony Brook, New York 11794

Fertilization of the sea urchin egg is a dramatic example of cell activation resulting from the interaction of an external stimulus, the spermatozoon, with the cell surface[1]. Growing and quiescent cells may have different membrane states[2]. Here we report membrane fluidity measurements on a surface membrane fraction, the cortex, isolated from unfertilized and fertilized eggs. The fluidity of the fertilized egg cortex, measured by electron spin resonance (ESR) spectroscopy using 5-doxylstearate as a probe, is less than that of the unfertilized cortex. In the intact egg the intracellular Ca^{2+} concentration increases after fertilization and this transient rise seems to be localized in the cortex[3]. The addition of Ca^{2+} to the cortex fraction isolated from unfertilized eggs triggers a fluidity decrease *in vitro*. The fluidity decrease seems to represent a Ca^{2+}-induced change in membrane structure rather than a direct interaction of Ca^{2+} with phospholipid headgroups.

Bulk membrane fluidity of sea urchin eggs increases after fertilization or partial activation by ammonia[4,5]. We could not determine the effect of fertilization on plasma membranes of intact eggs because 5-doxylstearate probably partitions throughout egg membranes[5] and plasma membrane accounts for only a smalll percentage of the membrane present. The egg cortex can be isolated in a functional form[6–9] (see Table 1 legend for details). The cortex fraction contains several components in addition to plasma membrane. The extracellular vitelline layer of the unfertilized egg becomes the fertilization envelope after fertilization[10]. The hyaline layer surrounding the fertilized egg cortex holds the blastomeres together[11]. Cortical granules, membrane-delimited vesicles ~ 1 μm in diameter, line the inner surface of the plasma membrane of unfertilized eggs and fuse with the plasma membrane within seconds of fertilization[10]. The addition of Ca^{2+} to the unfertilized egg cortex triggers the discharge of cortical granules *in vitro*[6,10], a process analogous to the cortical granule exocytosis which occurs as the intracellular Ca^{2+} level rises after fertilization[3]. When viewed by scanning electron microscopy or phase contrast microscopy, our cortex fraction consisted of nearly intact cortical hulls and smaller, morphologically unidentifiable membrane fragments. On addition of Ca^{2+} to the unfertilized egg cortex fraction the cortical granules disappeared and each cortical fragment twitched and became less opaque by phase contrast microscopy. By this visual assay our cortex preparation was apparently more than 90% pure. The purification of plasma membrane in this fraction was at least 10-fold, as judged by the specific activities of mitochondrial and endoplasmic reticulum enzyme markers, and nucleic

Table 1 Enzyme and nucleic acid content of cortex fractions

Sample	Cytochrome *c* oxidase specific activity U per mg protein per min	Relative	NADH oxidase specific activity U per mg protein per min	Relative	Nucleic acid protein (w/w)
Unfertilized egg homogenate	1.38	(100%)	0.48	(100%)	0.135
Unfertilized egg cortex	0.092	6.5	0.056	11.6	0.012
Fertilized egg homogenate	1.33	(100%)	0.65	(100%)	0.128
Fertilized egg cortex	0.11	8.3	0.083	12.7	0.013

Enzyme activities, protein and DNA content were measured for cortex fractions isolated from unfertilized and fertilized *Strongylocentrotus purpuratus* eggs. The procedures used were modifications of the methods described by Schatten and Mazia[7] and Grainger[9]. The samples were maintained at 15 °C throughout the isolation. The jelly coat was removed by incubating eggs for 2 min in seawater (Instant Ocean, Aquarium Systems) titrated to *p*H 5 with HCl. Dejellied, unfertilized eggs were washed in isolation medium containing (mM): glycine, 350; NaCl, 300; $MgCl_2$, 4; EGTA, 10; Tris base added to a final *p*H of 7.6. The eggs were hand-homogenized (8–20 strokes) in a Teflon–glass homogenizer in isolation medium containing 0.2 mg ml^{-1} soybean trypsin inhibitor. Cortices were collected by centrifugation at 700*g* for 10 s, washed once with isolation medium–soybean trypsin inhibitor, then washed twice with isolation medium. For cortex isolation from fertilized eggs, 3 volumes of 10 mM dithiothreitol in artificial seawater titrated to *p*H 9.1 with Tris base were added to dejellied, fertilized eggs 20 s after addition of sperm. This treatment dissolved the fertilization envelope[20]. After 4 min, 9 volumes of Ca^{2+}-free seawater were added with stirring. Ca^{2+}-free seawater contains (mM): NaCl, 460; $MgCl_2$, 55; KCl, 10; $NaHCO_3$, 2.5; EGTA, 10; titrated to *p*H 8.0 with Tris base. After 10 min stirring, the eggs were allowed to settle, then washed with isolation medium and homogenized as described above. Protein and nucleic acid were assayed spectrophotometrically[21]. Cytochrome *c* oxidase and NADH oxidase were assayed as described elsewhere[22,23].

---

* Present address: Laboratory of Tumor Biology, Sidney Farber Cancer Institute, 44 Binney Street, Boston, Massachusetts 02115.

0028-0836/80/280185—02$01.00

acid content (Table 1). From the data of Schroeder[12] we estimate that 50% of the membrane surface in the cortex fraction is plasma membrane and 50% cortical granule membrane. The purity of plasma membrane in the cortex fraction compares favourably with that of other purified plasma membrane fractions from animal cells despite the presence of cortical granules.

We measured membrane fluidity in the cortex fraction isolated from fertilized and unfertilized eggs. The order parameter, *S*, derived graphically from the ESR spectrum of 5-doxylstearate, decreases from 1 to 0 as the system becomes less ordered[13]. 5-Doxylstearate does not reside in neutral lipid droplets in these conditions[5], and the rapid, anisotropic motion revealed in the ESR spectrum means that 5-doxylstearate is probably not bound to protein[5]. Thus, an increase in order parameter may be interpreted as a decrease in membrane fluidity[5]. *S* measured for fertilized egg cortices isolated 30 min after fertilization is 3.2 ± 1.3% greater than when measured for unfertilized cortices from the same batch of eggs (Table 2). This change is about 50% greater than the change in *S* of bulk membranes[4,5], and is in the opposite direction. The response of this surface membrane fraction to fertilization seems to be distinct from the response of intracellular membranes.

An increase in *S* also accompanied the *in vitro* discharge of cortical granules of the unfertilized egg cortex (Table 3). In expts 1–5, cortical granules were discharged by adding a sufficient quantity of 0.1 M $CaCl_2$ just to titrate the 10 mM EGTA present in the isolation medium. The average ΔS observed for calcium addition *in vitro* was about the same as the average ΔS observed in the cortex fraction after fertilization. For example, the average $\%\Delta S$ measured at ambient temperature for unfertilized relative to fertilized egg cortices was 3.4 ± 1.8 compared with an average $\%\Delta S$ of 3.3 ± 0.6 for the change induced by addition of Ca^{2+}, measured at ambient temperature. The cortical granules of unfertilized egg cortices spontaneously discharge in isolation medium lacking EGTA. Spin labelled cortices allowed to undergo spontaneous discharge after removal of EGTA also exhibited an increase in *S* (expt 6). Mild heat treatment in the presence of EGTA discharges cortical granules. Cortices treated for 2 min at 40 °C in isolation medium containing 10 mM EGTA exhibited a similar increase in *S* (expt 7).

Table 2 Order parameter of cortices isolated from unfertilized and fertilized eggs

Expt	Temperature	*S* unfertilized cortex	*S* fertilized cortex	ΔS (%)
1	Ambient	0.669	0.683	2.1
2	Ambient	0.657	0.687	4.6
3	12 °C	0.756	0.777	2.8

Each experiment represents cortices isolated from the eggs of a different animal. 5-Doxylstearate in methanol was dried onto the wall of a test tube under a stream of nitrogen. A cortex suspension (1 ml) (Table 1) was added, the mixture was incubated for 10 min at 15 °C, then a cortex pellet was collected by centrifugation for 10 s at 700 *g*. The wet cortex pellet was washed with 0.5 ml isolation medium, then transferred to a Pasteur pipette sealed at one end. The molar ratio of spin label added to cortex phospholipid was approximately 1:30. ESR spectra were recorded from samples in sealed Pasteur pipettes on a Varian E-104A or E-4 ESR spectrometer equipped with a Varian temperature control accessory. Microwave power was 10 mW and modulation amplitude was 1 or 2 G. *S* was measured graphically from the spectra[13]. Multiple measurements of these samples indicated that the accuracy of the $\%\Delta S$ measurement is ±0.5%.

The exocytosis of cortical granules seems to be self-propagating in *vivo*[10] and *in vitro*[6] and a release of Ca^{2+} from the cortex may be involved[3]. Ca^{2+} interacts with the polar head group of phospholipids, rendering them less fluid[14], but that is an unlikely mechanism for the effects described here. The intrinsic association constant of Ca^{2+} for negatively charged phospholipids is of the order of $10\ M^{-1}$ (S. McLaughlin, unpublished results). We estimate that the Ca^{2+} concentration is less than 1 μM for all the samples studied here except those lacking EGTA or containing added Ca^{2+}. The intracellular Ca^{2+} concentration was estimated to reach 2.5–4.5 μM after fertilization[3]. At these concentrations less than 1% of the negatively charged lipids should carry bound Ca^{2+}, even considering that the surface concentration of Ca^{2+} may be 100-fold greater than the bulk concentration because of the effect of the membrane surface potential[15]. It seems clear that Ca^{2+} triggers the observed decrease in fluidity of the cortex but it apparently acts through membrane proteins rather than directly on the phospholipid bilayer.

Table 3 Effect of *in vitro* cortical granule discharge on order parameter of unfertilized egg cortex

Expt	Method of discharge	Temperature (°C)	*S* before discharge	*S* after discharge	ΔS (%)
1	Add $CaCl_2$	Ambient	0.595	0.617	3.7
2	Add $CaCl_2$	Ambient	0.591	0.608	2.9
3	Add $CaCl_2$	12	0.727	0.748	2.9
4	Add $CaCl_2$	12	0.771	0.818	6.1
5	Add $CaCl_2$	12	0.753	0.776	3.0
6	Remove EGTA	12	0.759	0.790	4.1
7	Heat	12	0.747	0.800	7.1

Each experiment represents cortices isolated from a different animal. Measurements were made as described in Table 2 legend. $CaCl_2$ was added to washed, labelled cortices as 0.5 M $CaCl_2$–0.5 M Tris base. The *p*H after Ca^{2+} addition was 7.6 ± 0.1. EGTA was removed by washing with isolation medium lacking EGTA. Heat discharge was effected by warming the sample to 40 °C for 2 min. Multiple measurements on these samples indicated that the accuracy of the $\Delta S\%$ measurement is ±0.5%.

Fluorescence photobleaching recovery measurements on mouse eggs revealed 10–100-fold slower rates of lateral diffusion on the cell surface after fertilization[16]. Studies on the rheological properties of the sea urchin egg surface showed that the cortex of the cell stiffens in response to fertilization[17]. These results seem consistent with the decrease in fluidity reported here.

These changes in fluidity are sufficient to alter the activity of membrane-bound enzymes such as adenyl cyclase and $(Na^+ + K^+)$ATPase by several fold (refs 18, 19 and M. Sinensky, unpublished results), assuming that the enzymes undergo the same change in fluidity as does the spin probe. The fluidity change could have an important role in the transition of the membrane from its quiescent to its proliferating state[2].

Part of this work was carried out in the laboratory of V. D. Vacquier. This work was supported by NIH grants HD-12986 (to V.D.V.) and GM-23218 (to C.J.S.), and by NIH training grants GM 07212 and CA 09176.

Received 19 November 1979; accepted 15 May 1980.

1. Epel, D. *Curr. Topics dev. Biol.* **12,** 186–292 (1978).
2. Pardee, A. B., de Asua, J. & Rosengurt, E. in *Control of Proliferation in Animal Cells* (eds Clarkson, B. & Baserga, R.) 547–561 (Cold Spring Harbor, New York, 1974).
3. Steinhardt, R., Zucker, R. & Schatten, G. *Devl Biol.* **58,** 185–196 (1977).
4. Campisi, J. & Scandella, C. J. *Science* **199,** 1336–1337 (1978).
5. Campisi, J. & Scandella, C. J. *J. biol. Chem.* (in the press).
6. Vacquier, V. D. *Devl Biol.* **43,** 62–74 (1975).
7. Schatten, G. & Mazia, D. *Expl Cell Res.* **98,** 325–337 (1976).
8. Detering, N. K., Decker, G. L., Schmell, E. D. & Lennarz, W. J. *J. Cell Biol.* **75,** 899–914 (1977).
9. Grainger, J. thesis, Univ. California (1978).
10. Schuel, H. *Gamete Res.* **1,** 299–382 (1978).
11. Citkowitz, E. *Devl Biol.* **24,** 348–362 (1971).
12. Schroeder, T. E. *J. Cell Biol.* **79,** 171a (1979).
13. Gaffney, B. J. *Meth. Enzym.* **32**B, 161–198 (1974).
14. Chapman, D. *Q. Rev. Biophys.* **8,** 185–235 (1975).
15. McLaughlin, S. *Curr. Topics Membrane Transport* **9,** 71–144 (1977).
16. Johnson, M. & Edidin, M. *Nature* **272,** 448–450 (1978).
17. Hiramoto, Y. *Expl Cell Res.* **89,** 320–326 (1974).
18. Sinensky, M., Pinkerton, F., Sutherland, E. & Simon, F. R. *Proc. natn. Acad. Sci. U.S.A.* **76,** 4893–4897 (1979).
19. Klein, I., Moore, L. & Pastan, I. *Biochim. biophys. Acta* **506,** 42–53 (1978).
20. Paul, M. & Epel, D. *Expl Cell Res.* **65,** 281–288 (1971).
21. Kalb, V. F. & Bernlohr, R. W. *Analyt. Biochem.* **82,** 362–371 (1977).
22. Wharton, D. C. & Tzagoloff, A. *Meth. Enzym.* **10,** 245–250 (1967).
23. Avruch, J. & Wallach, D. F. H. *Biochim. biophys. Acta* **233,** 334–347 (1971).

BOOK REVIEWS

The essential Lamarck

R.W. Burkhardt

Lamarck ou le Mythe du Précurseur. By M. Barthélemy-Madaule. Pp.185. (Editions du Seuil: Paris, 1979.) Approx. 55F, £7.

JUST as it was once common in natural history to view a wide array of species as existing primarily for the benefit of man, so too was it once common in the history of science to consider a large number of scientists as being adequately understood once they were identified as the 'precursors' of later thinkers. It is a mark of the growing maturity of the history of science that the 'precursoritis' that plagued the field as recently as a generation ago has now generally disappeared. French historians of science, most notably Alexandre Koyré and Georges Canguilhem, were prominent among those who argued that precursorship is a concept that is antithetical to the appreciation of scientific ideas in the past. Now Madeleine Barthélemy-Madaule, Professor of Philosophy at the Université de Picardie, has taken the insight of Koyré and Canguilhem and applied it to the case of Jean-Baptiste Lamarck (1744–1829), the French biologist who for about a century has been acclaimed, especially in France, as one of the great precursors of modern evolutionary thought.

Lamarck is a good choice for illustrating the problems of the notion of precursorship. His name is well known, but the ideas for which he is remembered fail to illuminate either the nature of his own work or the scientific problems of his day. Madaule's book is not the first study to make this point. The rethinking of Lamarck's place in the history of science began with papers written by Charles Gillispie in the 1950s and has continued up to the present. It is refreshing, nonetheless, to find that a book published in Lamarck's own country on the 150th anniversary of his death is directed more toward the issue of relocating Lamarck in his own historical context than toward the issues of who deserves the title of 'founder of evolution' or what Darwin owed to Lamarck.

Madaule has not attempted to provide an extensive treatment of Lamarck's life and work. She has sought instead to examine some of Lamarck's essential concepts in order to make clearer the interrelations of the ideological and the scientific elements of Lamarck's thought. At the same time she has sought to put to rest the "myth" of the precursor. As she explains, this is to be achieved through "the exploration of the possibilities of an epoch, the vigilant notation of the concepts that are utilized and of those that are not" (page 74). After an introductory chapter on Lamarck's life, she successively considers his ideas on nature, the relation between the animal "series" and environmental "circumstances", the inheritance of acquired characters, and adaptation. These are concepts in Lamarck's thought which have often been discussed, but Madaule manages to bring good sense and originality to her analysis of each of them. Her final chapter surveys how Lamarck came to be identified as a precursor of various later thinkers.

M. LE CHEVALIER DE LAMARCK.
Professor of Botany of the National Institute

Mary Evans Picture Library

The author's treatment of the role of "ideology" in Lamarck's thought is intriguing, but it is surprisingly narrow given her references to Canguilhem's and Althusser's thoughts on ideology in science. The ideological element she identifies in Lamarck's thinking is a theological one, manifesting itself in Lamarck's concepts of nature and the animal series and the relation of these concepts to Lamarck's thoughts on "the Supreme Author of all things". Madaule's observations on the ambiguities and tensions in Lamarck's presentation of these concepts are excellent and constitute an important contribution to Lamarckian scholarship. However, her reference to the ideological element in Lamarck's thinking as a "survival" (page 76), her view of the progressive elimination of this element along the route from Lamarck's evolutionary theory to Darwin's (page 139) and her phrase "ideological contamination" (page 141) suggest that she is operating with a restricted and generally negative view of the role of ideology in science. It is curious that Lamarck's commitment to a naturalistic explanation of mental as well as physical phenomena does not qualify in some measure as "ideological" and is not subjected to closer historical and philosophical scrutiny.

It is also curious that in a book devoted to placing Lamarck's thought in its own historical context considerable space is given to the issue of whether or not recent developments in molecular genetics have brought back the possibility that acquired characters may indeed be inherited. It would have been more appropriate to devote this space to examining how Lamarck's thinking developed over time, how the concepts selected for treatment here fit in with the rest of his scientific and philosophical thought, or how his views compared with those of his contemporaries. Madaule only scratches the surface of this part of the historical task. Generally speaking, her philosophical orientation makes her more sensitive to the apparent relation of elements within Lamarck's thinking at a given time than to the ways in which his thought was a dynamic, evolving entity. Her discussion of Lamarck's thoughts on species, for example, confuses the structural relations within one of Lamarck's general discourses for the historical situation in which the problem of species change came to be especially crucial for him.

Madaule acknowledges that history is reconstructed according to the concerns of the historian. What she has tried to offer the reader is "a Lamarck seen in his own epoch through the dimensions of a perspective produced by the contemporary world" (page 175), the perspective in question being that which concerns itself with the interrelations of science and ideology. She has succeeded in demonstrating the interest of Lamarck's case for the history of science, even though there is much more of interest in Lamarck's thinking than she mentions. Given the important kinds of questions she has posed, and allowing that new perspectives will provide additional questions to ask about Lamarck's case in the future, there is every likelihood that Lamarck will continue to be of considerable interest for the history of science when his next major anniversary comes around. □

R. W. Burkhardt is Associate Professor of History at the University of Illinois, Urbana, and author of The Spirit of System: Lamarck and Evolutionary Biology.

Reviews of bonding

S. R. Elliott

Electrons and Transitions. Vol. 39 of *Structure and Bonding.* Series editors J. D. Dunitz, J. B. Goodenough, P. Hemmerich *et al.* Pp.120. (Springer: Heidelberg and New York, 1980.) DM64,$35.90.

VARIOUS themes are common to the different branches of chemistry; one such, underlying inorganic and physical chemistry in particular, is bonding and its concomitant structure. This is the title of a continuing series published by Springer, each book comprising a collection of articles. The latest addition is Vol. 39, subtitled *Electrons and Transitions.*

This volume contains three articles. The first, by D. W. Clack and K. D. Warren, is entitled "Metal–Ligand Bonding in 3d Sandwich Complexes". The review concentrates on the bonding between the metal and the ligand rings for various series of first-row transition metal sandwich complexes containing from three- to eight-membered carbocyclic rings. Experimental data from electronic spectra, ESR and photo-electron spectroscopy are compared with the predictions obtained principally from the authors' INDO SCF molecular-orbital calculations. The article runs to 41 pages and 80 references are included.

The second article, "Ligand Polarization Model for the Spectra of Metal Complexes: The Dynamic Coupling Transition Probabilities", is by S. F. Mason. Crystal field theory, the principal independent-systems model in which metal–ligand overlap is neglected, has been extremely successful in accounting for the character of the structure and bonding of metal complexes. Nevertheless, its shortcomings are not confined to neglect of metal–ligand electron exchange. In a first-order independent-systems treatment, either the ligands perturb the metal ion (crystal field theory) or, in the other extreme, the metal ion perturbs the ligands (ligand polarization model). This article, of 39 pages and 82 references, considers applications of the latter approach to oscillator strengths of lanthanide and transition metal complexes, rotational strengths of chiral coordination compounds and the Faraday effect terms of achiral complexes.

The final article, by L. R. Balsenc, is "Sulfur Interaction with Metallic Surfaces and Interfaces studied by Auger Electron Spectroscopy (AES)". This sets out to review the contribution of AES to the studies of the behaviour of sulphur on and with metallic surfaces including, amongst others, gas adsorption and desorption kinetics, surface and grain boundary segregation, corrosion, passivation and catalyst poisoning. This technique has several advantages; it is very surface-sensitive and adsorption-site positions can be deduced from the angular-dependent Auger emission from single crystal substrates, and the method's high speed of data acquisition is of great use in kinetic studies. In contrast to another commonly used technique, X-ray photo-emission spectroscopy (XPS), AES is some 20 times more sensitive for sulphur detection, although XPS is far superior in the elucidation of the chemical state of the atoms by means of the 'chemical shift' since the shift is very small compared with the Auger peak width and hence easily obscured. The review is short, only 32 pages, but contains an extensive bibliography, and will be of interest in both the academic and industrial spheres.

In summary, this is a well presented book with only one niggling detail, the use of the American spelling, sulfur, although all other usage is English; the book's appeal should lie primarily with researchers in those fields represented by the articles included. □

S. R. Elliott is University Demonstrator in the Department of Physical Chemistry, University of Cambridge, UK.

Floras finished and in progress

Peter D. Moore

Flora Europaea, Vol.5. Edited by T. G. Tutin, B. H. Heywood, N. A. Burges *et al.* Pp. 452. (Cambridge University Press: Cambridge, UK, and New York, 1980.) £37.50, $85. *Flora Palaestina,* Part 3. Text pp. 481, plates 757. By N. Feinbrun-Dothan. (Israel Academy of Sciences and Humanities: Jerusalem, 1979.) IL500, $55.

"THE publication of this final volume of *Flora Europaea* represents a landmark in European floristics". So begins the preface to Vol. 5, and one can detect a flavour of relief coupled with the justifiable pride of this statement. The concept of a European flora was formed some 26 years ago and it was then hoped that it could be completed within 12 years; but the gestation period of this *magnum opus* proved far longer than was anticipated. This must make the final parturition a yet more satisfying occasion for the editorial committee.

The final volume is dedicated to the monocotyledons and it follows the same style adopted in previous volumes. The British botanist will find few surprises in the arrangement and nomenclature; we are already accustomed to such transmutations as *Endymion* to *Hyacinthoides* and we could have predicted movements within the genus of marsh orchids, *Datylorhiza. D. purpurella* and *D. praetermissa* are now regarded as subspecies of *D. majalis.* The subspecies *ericetorum* of *maculata* is absorbed into ssp. *maculata.*

These, however, are trivia. The importance of this work is the establishment of an authoritative description and definition of the flora of the whole of Europe. It is the first such account ever published and it is unlikely to be surpassed in our generation. The editors are to be admired for having devoted a large portion of their working lives to the project, and Cambridge University Press are to be congratulated on undertaking such a gargantuan publishing task and for the high standards of production. The complete set of five volumes now costs in excess of £150, but this is a wise investment for any serious botanist, amateur or professional, who wishes to be fully informed about the wealth of Europe's flora.

The development of the *Flora Europaea* project has not been an isolated process. Floras covering adjacent regions of south-west Asia are proceeding apace. Within the Soviet Union, *Flora Europaea* covers the entire area west of the Ural Mountains, to 60°E, and on the southern side of the Black Sea P.H. Davis' work *Flora of Turkey and* *the East Aegean Islands* is continuing to develop. Publication of this series of volumes from the University of Edinburgh Press began in 1965 and still proceeds. Similarly, to the south of the Caspian, K. H. Rechinger, based in Vienna, continues to work upon *Flora Iranica*, which commenced publication in the early 1960s.

A further, well advanced project is *Flora Palaestina* which is being published by the Israel Academy of Sciences and Humanities, Jerusalem. The recently published third part of this series covers the Ericaceae to Compositae, and the geographical range of the Flora encompasses Israel and the west and east banks of the Jordan rift valley, south to Elat and Aqaba. There are keys to genera and species of Palestinian plants plus detailed descriptions of each species. These descriptions include notes concerning the ecology and habitats of the plants, as well as their geographical range within the study area and their full world range. These are useful notes which are not generally found in *Flora Europaea* because of pressure on space.

Each part of *Flora Palaestina* is accompanied by a volume of plant drawings which are of very high artistic quality and botanical accuracy. Five artists have been employed in this task, but a commendable uniformity of style has been maintained. Since a fair proportion of the plants illustrated are widely distributed in the eastern Mediterranean, these drawings will prove useful and interesting to European botanists as well as to the Israelis. Which leads one to the question whether a similar set of illustrations could be prepared to accompany *Flora Europaea?* Herculean, perhaps, but nevertheless a profitable exercise. □

Peter D. Moore is Senior Lecturer in Plant Sciences at King's College, University of London, UK.

Pore structure and flow modelling

D. J. Gunn

Porous Media. By F. A. L. Dullien. Pp. 396. (Academic: New York and London, 1980.) $42, £23.60.

IN THE preface Professor Dullien gives the primary purpose of this book as "presenting in an organised manner the most pertinent information available on the role of pore structure and then putting it to use in the interpretation of experimental data and the results of model calculations". In pursuit of these aims the, book is divided into two principal parts, the first of which is devoted to the description of pore structure, the second to flow properties of porous media.

Work on pore structure is described in two 70-page chapters. In Chapter 2, "On Capillarity in Porous Media", the description of capillary pressure measurements in porous media is followed by a description of pore network models of capillary tubes and capillary pressure functions generated by network models. In Chapter 3 porosity and permeability are defined, the measurement of pore size and pore size distribution is considered, and the measurements of pore size distribution are described for a range of materials. Single-phase flow in porous media is considered in Chapter 4 and includes a survey of some of the available correlations between flow and pressure gradient, statistical permeability models and network models, with sections on gas flow and diffusion, and non-Newtonian flow. The description of multiphase flow of immiscible fluids, Chapter 6, is mainly directed to the flow of oil and water through both consolidated porous solids and unconsolidated solids, while the last major part of the book is Chapter 7 on miscible displacement and dispersion.

The emphasis of the book is on fundamental studies of interest in petroleum recovery and production, although topics such as the formation, flow and dispersion of micro-emulsions that are of interest in secondary recovery are not considered in detail. The book would have been more helpful if the description of models for flow and dispersion in porous media was more critical. The most important criteria for the success of a model description are that the model should be well founded, and that it should describe experimental phenomena without invoking significant further measurements to define the parameters of the model when applied to a particular situation. Some of the model descriptions of dispersion in porous media, although considered in some detail in the book, have not been shown to relate to experimental measurements of dispersion, while the use of a bivariate pore size distribution to estimate permeability requires more experimental work than a direct measurement!

However, for those who have already been introduced to the study, the publication of a research monograph on flow in porous media is timely because of the economic importance of techniques for secondary oil recovery. Further, it is very useful to have this comprehensive survey available as an aid in process development and in the mathematical modelling of field flows. □

D. J. Gunn is Reader in Chemical Engineering at the University College of Swansea, UK.

Macromolecules in 3D

Colin Blake

Teaching Aids for Macromolecular Structure. Compiled by Richard J. Feldmann and David H. Bing. Instructor manual pp.114 with 116 stereoslides; student kit 49 stereoslides with viewers. (Taylor-Merchant: New York, 1980.) Instructor kit $210, student kit $15.

THE APPLICATION of the X-ray diffraction technique to crystalline and paracrystalline biological materials has produced a solid body of information on the structure and function of many biological macromolecules. After an initial period of scepticism concerning the significance of the results, this material has now become reasonably well integrated into the broad field of biochemistry, and is now routinely taught at the undergraduate level, not only to biochemists, but also to those in other more biological or physical sciences. Teaching this material is however fraught with problems, most of which derive from the sheer complexity of biological macromolecules. Although the repetitive structures of DNA, the α-helix, β-sheet and even the collagen helix are fairly easy to visualize, the molecules of t-RNA, supercoiled DNA and most proteins and enzymes are much more difficult to illustrate. To overcome these difficulties a variety of short cuts are no doubt taken; the most extreme is to ignore all of an enzyme except its catalytic site, which at best does less than justice to enzymes and at worst gives a completely distorted view of the *raison d'être* of the subject, the attempt to understand the characteristic integration of structure and function exhibited by biological macromolecules. To say this does not necessarily imply criticism of the people who use the short cuts; it probably has much more to do with the sheer difficulty of producing teaching material that shows the extent of the structure – function integration. Even with a complete set of plastic and wire models, and mono and stereo slides there are problems: models are either too small or too complex to point out particular features to a class of students, and slides, even those in stereo, have of necessity to be simplified and cannot show all the features of a complete molecule. And, of course, many departments are not comprehensively equipped in this way.

With these problems as an overt background, a new aid for teaching macromolecular structure has just become available. Called TAMS, an acronym for Teaching Aids for Macromolecular Structure, it has been compiled by Richard Feldmann of NIH and David Bing of The Harvard Medical School. TAMS consists of a large ring-back folder containing a students' text, a teachers' text and a collection of 116 2″ x 2″ colour stereo slide pairs. A selection of the slides has been included on seven large cards which together with a simple but ingenious stereo viewer are packaged in a small plastic wallet for use by individual students. Although a small stereo viewer is included in the TAMS folder the stereo slides are intended for projection to the class using two normal slide-projectors (a stereo projector may not be suitable), an aluminized screen and polarized viewing glasses. Details of the simple modifications needed to be made to the projectors and an address where the screen and glasses can be obtained are included.

The text of TAMS is essentially a straightforward description of the contents of each slide, and need not be considered further. The slides are the heart of the system and it is on their technical quality and illustrative suitability that TAMS must be considered. One must say at once that the technical quality of the slides is quite superb. The vast majority of them are computer-drawn, coloured and shaded views of space-filling models of nucleic acids, proteins and their ligand complexes, that paradoxically do not, and at the level of accuracy shown, could not exist. Nevertheless the illusion of looking at three-dimensional, coloured space-filling models of a variety of biological macromolecules is totally convincing and one that students will readily accept, certainly with enjoyment and one hopes also with understanding and insight. Technically these slides are so good that one feels rather churlish in making criticisms: but there are two aspects on which I feel some dissatisfaction. First, although the muted colours are very agreeable to look at there are some difficulties in distinguishing the colours that are described as "light charcoal" and "pale blue" but which appear as very similar shades of light blue-grey. Also, the bluish shading of white spheres and the white highlights on pale blue or even pink spheres can lead to confusion. Secondly, and more importantly, the very success of the space-filling illusion appears to have seduced the compilers into using them almost exclusively, when many more line drawings would have been very valuable in providing aids to identifying particular features in the often complex space-filling picture.

Having established the technical excellence of the slides, one now has to consider how well they illustrate the seven "themes" of TAMS: Peptide Bond, Alpha Helix, Beta Sheet, Tertiary Structure, Quaternary Structure, Prosthetic Groups and Active Sites. Here I must confess to active disappointment, particularly in the case of the student cards, with both the overall organization of the material and the way in which it is illustrated in individual slides. The first student card on the Peptide Bond gets off to a very bad start. Four of its seven views illustrate a molecule called Synthetic Di-Alanine, with no more explicit description in either student or teacher text, but which is not the expected alanylalanine but an acetyl derivative whose additional methyl group perversely complicates the intended illustration of the spatial relationship of the methyl side chains and the peptide group. The final slide on this card shows a proline residue almost edge-on in the myoglobin molecule which thankfully illustrates rather ineffectually the text's repetition of that old misconception that prolines cannot be accommodated in helices. Why it was decided not to use this card to illustrate the Ramachandran dipeptide analysis, or why the card on Tertiary Structure does not consider the Levitt and Chothia classification of protein structure is not explained in the text, but what is shown in no way replaces these important insights into the principles of protein structure. The card on Active Sites brings out another problem — that of identifying particular residues in a complex, space-filling picture. Because no visual guide is given it is really very difficult, even when one knows what one is looking for, to identify the serine and histidine in the active sites of the serine proteinases. I can see many students giving up slides like this, and there are quite a number of them, simply because of the difficulties of identification. In contrast the other kind of slides in which specific features are picked out in particular colours can be immediately comprehended and represent the proper use of the system. One has to conclude that the primary requirement of teaching material, that it should be closely organized and absolutely clearly illustrated, has not been consistently borne in mind when TAMS was being planned. Finally, the choice of material in the cards and in the main body of the slides is not as comprehensive as it might be: there are no examples of fibrous proteins or carbohydrates, no illustrations of viruses apart from two slides of the filamentous type, there is insufficient consideration of intracellular proteins and too much emphasis on certain small proteins, most notably parvalbumin and cytochrome *c*. Of course one is aware that the authors are dependent on information being made available from recent research, which may account in part for the restricted choice of material, but certainly not all.

I have no wish to overemphasize the deficiencies in the choice and display of the material in TAMS. There are many slides which are both a joy to look at and which illustrate important aspects of protein and nucleic acid structure that could scarcely be demonstrated in any other way. The small set of views of nucleic acid structures is particularly striking, and especially that of supercoiled DNA, while in the enzyme collection the visualization of the deep cavities in which the active sites of carbonic anhydrase and carboxypeptidase are located is most successfully carried off. Once seen, many teachers will see slides of this kind as essential and irreplaceable visual aids to their courses in macromolecular structure. For this reason TAMS must be welcomed and Feldmann and Bing commended for overcoming the considerable technical and commercial difficulties they undoubtedly faced in making these slides generally available. Nevertheless a slight sense of disappointment of an opportunity missed persists. In the second edition of TAMS, one would ask the compilers to ignore McLuhan's notorious motto "The medium is the message" which they use to preface the text, and suggest that they keep the medium but think about improving the message. □

Colin Blake is in the Laboratory of Molecular Biophysics at the University of Oxford, UK.

Polymer science and scaling

M.A. Moore

Scaling Concepts in Polymer Physics. By Pierre-Gilles de Gennes. Pp.320. (Cornell University Press: Ithaca, New York, and London, 1979.) $38.50, £23.

OUR KNOWLEDGE of the physics of long, flexible polymer chains has been greatly extended in recent years by important developments in both experimental and theoretical techniques. On the experimental side the advent of high-flux neutron beams has made it possible to observe a labelled chain in a sea of chemically identical but unlabelled chains. This is done by replacing some of the protons of a polymer by deuterons which scatter neutrons more intensely than protons. Extensive data on long-range conformations and correlations have now become available. A traditional tool for studying polymers in solution has been that of light scattering, which has been improved almost beyond recognition by the development of the 'photon beat' method which now allows study of the dynamics of polymer chains in the frequency range 1^6–10^6 cycles.

Alongside this development in experimental technique there has been a sharpening in our theoretical understanding brought about by the discovery of the close connection between polymer statistics and phase transitions. This discovery has enabled concepts useful in the study of critical phenomena such as scaling and critical exponents to be transferred to the field of polymer science. De Gennes has been the foremost worker in this area and his book is essentially a collection of the results which he and his co-workers have obtained by the application of scaling ideas. These results have been largely confirmed by the new experimental methods and the general agreement between theory and experiment is most impressive. However, the scaling method only gives an understanding of 'universal' properties such as, for example, the molecular weight dependence of the dimensions of a flexible polymer molecule in solution. Numerical prefactors, which are specific to a given monomer, are not predicted by this approach.

In the book the scaling concept is applied to a great variety of topics. Polymers in dilute and semi-dilute solution, theta solvents and good solvents, gels, melts and the dynamics of single chains and networks are just some of the problems successfully treated. It is not easy to apply scaling ideas and much physical insight is needed to get correct results. De Gennes has such insight and he is also adept at explaining his reasoning. Further work is now needed to derive scaling results in a more systematic way, and in the last chapter de Gennes outlines the renormalization group which probably provides the best way of putting the scaling approach on a firmer theoretical foundation.

The book is written mainly for experimentalists in polymer sciences who wish to incorporate the recent theoretical advances into their mode of thinking and for polymer theorists who want to achieve a qualitative understanding of the scaling method. It is an excellent work and no worker in the field can afford to be without a copy. ☐

M.A. Moore is Professor of Theoretical Physics in the University of Manchester, UK.

Applied bifurcation theory

Michael Berry

Bifurcation Theory and Applications in Scientific Disciplines. Edited by O. Gurel and O.E. Rössler. Pp.708. (New York Academy of Sciences: New York, 1979.) $85.

THIS IS a collection of over 50 papers presented at a conference held in New York in 1977. Bifurcation is sudden qualitative change in the solutions of an equation or system of equations, produced by the smooth variation of one or more parameters. As might be expected on the basis of such a general definition the papers cover a vast range of subjects, well indicated by the titles of sections into which the book is divided: mathematics, biology, chemistry and chemical engineering, physics, ecology, economics, engineering, and experimentation and simulation. What all these subjects have in common is that they involve nonlinear equations, and the reason for the emergence of bifurcation theory as a separate discipline is that for some classes of nonlinear equations the bifurcation behaviour is beginning to be well understood.

In the simplest case of all, dynamics is ignored (i.e. the system's state is considered to change very rapidly) and bifurcation theory reduces to the classification of equilibria, accomplished by Thom's theory of catastrophes. In several papers here a refined version is applied to analyse the types of buckling that occur in elastic structures under increasing load in the presence of imperfection (of design or manufacture) described by several parameters.

When dynamics is taken into account, the variety of possible bifurcations is much greater, but the following sequence of events is quite common: as a parameter P increases, a stable equilibrium bifurcates into a stable closed orbit (Hopf bifurcation), which in turn bifurcates into one of twice the length, and so on, in a cascade of successive 'subharmonic bifurcations' accumulating at a finite value of P, beyond which the motion is aperiodic and chaotic. Such behaviour occurs, for example, in the ecological equations for the numbers of individuals in successive generations of a population reproducing in an environment with finite resources, or in the physiological control equations governing respiratory and haematological disorders, or in preturbulent fluid regimes with different Reynolds' numbers. In several papers the mathematical models give a very good description of experimental results, but when structurally stable behaviour is expected (and found) in a wide variety of contexts, it is important to be quite precise about what theory is being tested.

The general standard of exposition is high, but I cannot resist quoting one example of intolerable jargon:

> The bootstrap principle of adaptability theory is: The assumption of the hierarchical and compartmental structurability of the state description of biological systems is self-justifying within the framework of adaptability theory in the sense that such structurability is a necessary condition for efficient adaptability.

I strongly recommend this book to anybody wanting an introduction to this fertile new field of applied mathematics. ☐

Michael Berry is Professor of Physics at the University of Bristol, UK.

Source book on cadmium

M.H. Martin

The Chemistry, Biochemistry and Biology of Cadmium. Edited by M. Webb. Pp.476. (Elsevier/North-Holland: Amsterdam and New York, 1980.) Dfl. 165, $80.50.

THIS book is the second volume in a series on topics in environmental health, and consists of 11 chapters by different authors.

Most of the contributions are concerned with mammals including human beings, and indeed the editor states that the book attempts to integrate the toxicological aspects of cadmium in animals (*sensu* mammals) and human beings with the chemistry and biochemistry of the cadmium ion. The singling out of soils, plants and aquatic organisms as other environmental components to be considered serves to highlight the absence of contributions on air, terrestrial invertebrates and non-mammalian terrestrial vertebrates. In addition the preponderance of discussion on metallothioneins (cadmium, zinc, copper and mercury), some three chapters amounting to 22% of the book and also mentioned in the aquatic context, further unbalances the presentation.

In his remarkably brief preface, scarcely half a page, the editor states that he expects that the individual chapters of the book will be read as complete entities. To this end the various articles provide useful reviews on specific topics by authoritative contributors. The various chapters are relatively up to date, most including references to some 1979 literature, although some appear to have been completed before others. In fairness to the individual authors space could have been found in the preface to mention dates of completion of the reviews.

The presentation is relatively lavish and is consistent with the Elsevier/North Holland Biomedical Press standards, with matching price. Like many books of this multi-author type, its main use is likely to be as a source book of specific aspects of cadmium biochemistry rather than as a comprehensive treatment of the environmental biology, toxicology and biochemistry of cadmium. ☐

M.H. Martin is Senior Lecturer in Botany at the University of Bristol, UK.

Blackwell Scientific

In their advertisement (p.xxi) in the 12th June issue of *Nature*, titles and authors of two books were transposed. *Introduction to Modern Virology*, 2nd edn, is by S.B. Primrose and N.J. Dimmock; *Pharmaceutical Microbiology*, 2nd edn, is by W.B. Hugo and A.D. Russell.

BOOKS RECEIVED

Mathematics

KURATOWSKI, K A Half Century of Polish Mathematics Remembrances and Reflections International Series in Pure and Applied Mathematics volume 108 Pp viii + 204 ISBN-0-08-023046-6 (Oxford, New York, Toronto, Sydney, Paris, Frankfurt Pergamon Press, 1980.) $22 00 £10 00

PAN-TAI-LIU (ed) Dynamic Optimization and Mathematical Economics Mathematical Concepts and Methods in Science and Engineering-19 Pp x + 269 ISBN-0-306-40245-9 (New York and London Plenum Press, 1980) $29 50

WILSON, R J and BEINEKE, L W (eds) Applications of Mathematical Graph Theory Pp xii + 423 ISBN-0-12-757840-4 (London, New York, San Francisco Academic Press, 1979) £18 50 $39 00

Astronomy

ADAMS, D J Cosmic X-ray Astronomy Monographs on Astronomical Subjects 6. Pp 150 ISBN 0-85274-374-2 (Adam Hilger Bristol, 1980)

AKASOFU, S -I (ed) Dynamics of the Magnetosphere Proceedings of the A G U Chapman Conference held at Los Alamos Astronomy Scientific Laboratory Astrophysics and Space Science Library 78 Pp xi + 655 ISBN-09-277-1052-X (Dordrecht, Boston, London D Reidel Publishing Company, 1979) Dfl 130 US $68 50

AUDOUZE, J and VAUCLAIR, S An Introduction to Nuclear Astrophysics The Formation and the Evolution of Matter in the Universe Geophysics and Astrophysics Monographs 18 Pp xx + 164 ISBN-90-277-1012-0 Hardback ISBN-90-277-1053-8 flexi (Dordrecht, Boston, London, D Reidel Publishing Company 1979) Dfl 75 US$39 50 hardback

DAVIES, D R and HOPWOOD, D A (eds) The Plant Genome. Forth John Innes Symposium and Second International Haploid Conference Pp 273 ISBN 0-9506844-0-6 (John Innes Charity Norwich, 1980) £7 00

DAVIES, P Other Worlds Space, Superspace and the Quantum Universe Pp 207 ISBN 0-460-04400-1. (J M Dent London, Toronto and Melbourne, 1980) £7 50

FELDMAN, D H Beyond Universals in Cognitive Development PATH series Pp xx + 204 ISBN-0-89391-025-5 (New Jersey Ablex Publishing Corporation, 1980) $17 50.

SOLOMON, P M and EDMUNDS, M G (eds) Giant Molecular Clouds in the Galaxy Third Gregynog Astrophysics Workshop Pp xiii + 344 ISBN-0-08-023068-7 (Oxford, New York Pergamon, 1980) £18 00 $41 00

WHYTE, A J The Planet Pluto Pp 158 ISBN 0-08-024648-6 (Pergamon: Oxford, 1980) $17 50

Physics

BABIC, V M and KIRPICNIKOVA, N Y The Boundary-Layer Method in Diffraction Problems Springer Series in Electrophysics Volume 3 Pp vi + 140 ISBN-3-540-09605-1 (Berlin, Heidelberg, New York Springer-Verlag, 1979) DM 39 50 approx US $21 80

BRAUNLICH, P (ed) Thermally Stimulated Relaxation in Solids Topics in Applied Physics Volume 37 Pp xiii + 331 ISBN-3-540 09595-0 (Berlin, Heidelberg, New York Springer-Verlag, 1979) DM 98 approx US $54 90

BURSTEIN, E and KAWAMURA, H (eds) Inelastic Light Scattering Proceedings of the 1979 US-Japan Seminar held at Santa Monica, California, USA, January, 1979 Pp vii + 109 ISBN-0-08-025425-X (Oxford, New York Pergamon Press, 1979) $20 00 £9 00

GIANCOLI, Douglas C Physics Principles with Applications Pp 805 ISBN 0-13-672600-3 (Prentice/Hall International Hemel Hempstead, 1980) £12 95

GUNTHER, H NMR Spectroscopy An Introduction Pp 436 ISBN 0-471-27579-4. (John Wiley & Sons Chichester, 1980) Pbk £7 95

HARRISON, W A Electronic Structure and the Properties of Solids The Physics of the Chemical Bond Pp 582 ISBN 0-7167-1000-5 (Freeman Oxford, 1980) £16 30

IRIBARNE, J V and CHO, H R Atmosphere Physics Pp 212 ISBN 90-277-1033-3 (D Reidel Dordrecht, Boston and London, 1980) Dfl 40 00, $15 95

KITTEL, C and KROEMER, H Thermal Physics 2nd Ed ISBN 0-7167-1088-9 (Freeman, Reading, 1980) £10 80

KOLLMAN, W (ed) Computational Fluid Dynamics Pp 612 ISBN 0-89116-171-6 (Hemisphere. Washington, 1980) $55 00

KOLLMANN, N (ed) Prediction Methods for Turbulent Flows Pp 467 ISBN 0-89116-178-3 (Hemisphere Washington, New York, and London, 1980) $47 50

SINGER, T P , VON-KORFF, R W and MURPHY, D L (eds) Monoamine Oxidase Structure, Function, and Altered Functions Pp 557 ISBN 0-12-646880-X (Academic New York and London, 1980) $39 00

Chemistry

CADOGAN, J I G (ed) Organophosphorus Reagents in Organic Synthesis Pp 603 ISBN 0-12-154350-1 (Academic London and New York, 1980) £38 00 $89 50

CANTOR, C R and SCHIMMEL, P R Biophysical Chemistry Part I The Conformation of Biological Macromolecules Pp 503 ISBN 0-7167-1042-0 (Freeman, California, 1980) $35 00 Board, $19 50 Pbk

COOK, T M and CULLEN, D J Chemical Plant and its Operation (including Safety and Health Aspects) A Manual for Chemical Operators, Process Workers, Plant Technicians and Maintenance Staff in the Chemical and Allied Products Industries Second SI Edition Pp. ix + 173 ISBN-0-08-023813-0 ISBN-0-08-023812-2 hardback (Oxford, New York, Toronto, Sydney, Paris, Frankfurt Pergamon Press, 1980) £3 50 $7 95 flexi £6 50 $16 50 hardback

FLURRY, R L Jr Symmetry Groups: Theory and Chemical Applications Pp 356 ISBN 0-13-880013-8 (Prentice/Hall Hemel Hempstead, 1980) £17 25, £35 80

HOBZA, P and ZAHRADNIK, R Weak Intermolecular Interactions in Chemistry and Biology Studies in Physical and Theoretical Chemistry 3 Pp viii + 346 ISBN-0-444-99785-7 (Amsterdam, Oxford, New York Elsevier Scientific Publishing Company, 1980) $48 75 Dfl 100.00

SILCOCK, H L (ed) Solubilities of Inorganic and Organic Compounds Volume 3 Ternary and Multicomponent Systems of Inorganic Substances Part 1 Pp iv + 943 Part 2 Pp iv + 1170 Part 3 Pp iv + 1208 ISBN-023570-0 Vol 3 ISBN-0-08 023599-9 3 vol set (Oxford, New York, Toronto, Sydney, Paris, Frankfurt Pergamon Press, 1970) £275 00 $595 00, 3 vol set £475 00 $990 00

Technology

BISWAS, A K and DAVENPORT, W G Extractive Metallurgy of Copper 2nd Ed International Series on Materials Science and Technology Vol 32 Pp 438 (ISBN 0-08-0240735 (Pergamon Oxford, 1980) Flexi $20 00, £10 00 Hardback $50 00, £25 00

CAD'80 Proceedings of 4th International Conference on Computers in Design Engineering Pp xiv + 774 ISBN 0-86103-026-5 (IPC Science and Technology Press Guildford, Surrey, 1980) £22 50

CASH, J R Stable Recursions with Applications to the Numerical Solution of Stiff Systems Pp 223 ISBN 0-12-163050-1 (Academic London and New York, 1980) £15 00, $34.50

CHALMERS UNIVERSITY OF TECHNOLOGY First Symposium on Wave Energy Utilization 30th October-1st November Pp 556 (Chalmers University of Technology Gottenburg, 1979) ISBN 91-7032-002-0

CONNOR, F R Electronic Devices Introductory Topics in Electronics and Telecommunication Pp ix + 121 ISBN 0-7131-3413-5 (London Edward Arnold (Publishers) Ltd 1980) £3 95 flexi

DAVIDSON, F P , MEADOR, C L and SALKELD, R (eds) How Big and Still Beautiful? Macro-Engineering Revisited AAAS Selected Symposia Series Pp xxvii + 383 ISBN 0-89158-792-6 (Boulder, Colorado Westview Press, 1980) $28 50

DIXON, A E and LESLIE, J D (eds) Solar Energy Conversion An Introductory Course Selected Lectures from the 5th Course on Solar Energy Conversion, University of Waterloo, Ontario, Canada Pp xi + 1312 ISBN 0-08-024744-X (Toronto, Oxford Pergamon Press, 1979) $60 00 £30 00

FAZZOLARE, R A and SMITH, C B (eds) Changing Energy Use Futures Second International Conference on Energy Use Management October, 1979 Los Angeles Vol I Pp xliv + 441 + Appendix Vol II Pp xliv + 509 Volume III Pp xliv + 509 Vol IV Pp xliv + 636 + Appendix ISBN-0-08-025099-8 (New York, Oxford Pergamon Press, 1979) $400 00

GOODMAN, G T and ROWE, W D Energy Risk Management Pp 351 ISBN 0-12-289680-7 (Academic London and New York, 1979) £14 80, £34 50

HEYWOOD, R W Equilibrium Thermodynamics for Engineers and Scientists Pp 450 ISBN 0-471-27630-8 (John Wiley & Sons Chichester, 1980) £7 95 pbk, £20 00, $50 00 Cloth

MANDL, C Applied Network Optimization Pp 175 ISBN 0-12-468350-9 (Academic London and New York, 1980) £11 80, $27 50

MILLER, S E and CHYNOWETH, A G (eds) Optical Fiber Telecommunications Pp xv + 705 ISBN-0-12-497350-7 (New York, San Francisco, London: Academic Press, 1979) $48 50

MOO-YOUNG, M and FARQUHAR, G J (eds) Waste Treatment and Utilization Theory and Practice of Waste Management Proceedings of the International Symposium held at the University of Waterloo, Canada, July 5-7, 1978 Pp vii + 565 ISBN-08-023831-9 (Oxford, New York, Toronto, Sydney, Paris, Frankfurt Pergamon Press, 1979) £32 00 $70 00

PATANKAR-S V Numerical Heat Transfer and Fluid Flow Series in Computational methods in Mechanics and Thermal Sciences Pp 197 ISBN 0-07-048740-5. (Hemisphere London, Washington and New York, 1980)

PAVITT, K (ed) Technical Innovation and British Economic Performance, A Science Policy Research Unit Book Pp 353 ISBN 0-333-262255 (Macmillan London, 1980) £20 00

Earth sciences

ANDERSON, B W Gem Testing Pp xii + 434 ISBN-0-408-00440-1 (London, Boston, Sydney, Wellington, Durban, Toronto The Butterworth Group, 1980) £12 00

BERGER, R and SUESS, H E (eds) Radiocarbon Dating Proceedings of the Ninth International Conference Los Angeles and La Jolla 1976 Pp 787 ISBN 0-520-03680-8 (University of California Press Berkeley, Los Angeles and London, 1980) £33 00, $68 75

Biology

BARKER, K R and BRELAND, O P A Laboratory Manual of Comparative Anatomy McGraw-Hill Series in Organismic Biology Pp viii + 199 ISBN-0-07-003656-X (Hightstown, New Jersey McGraw-Hill Book Company, 1980) flexi

BARLOW, N D and DIXON, A F G Simulation of Lime Aphid Population Dynamics Simulation Monographs Pp 165 ISBN 90-220-0706-5 (Centre for Agriculture Publishing and Documentation Wageningen, The Netherlands, 1980) Dfl 35 00

BATT, R A L Influences on Animal Growth and Development Studies in Biology no 116 Pp 60 ISBN 0-7131 2769-4 (Edward Arnold. London, 1980) £2 40

BECK, J S Biomembranes Fundamentals in Relation to Human Biology Pp 172 ISBN0-07-004263-2 (Hemisphere Washington, 980) $19 95

BERNHARDT, D , FUKAREK, F , GUNTHER, E and KAMPFE, L Evolution und Stammesgeschichte der Organismen Pp 411 Bestellnummer-532-957-1 (Jena VEB Gustav Fischer Verlag, 1980) DDR 23,00M Flexi

BOTHWELL, T H , CHARLTON, R W , COOK, J D and FINCH, C A Iron Metabolism in Man Pp xi + 576 ISBN-0-632-00233-9 (Oxford, London, Edinburgh, Melbourne Blackwell Scientific Publications, 1979)

BOULLIN, D J Cerebral Vasospasm Neurosciences series Pp ix + 337 ISBN-0-471-27639-1 (Chichester, New York, Brisbane, Toronto John Wiley & Sons, 1980) £15 00

OGDEN, C G and HEDLEY, R H An Atlas of Freshwater Testate Amoeba Pp. 222 ISBN 0-19-858502-0 (Oxford University Press Oxford, 1980) £17 50

PEPE, F A , SANGER, J W and NACHMIAS, V T (eds) Motility in Cell Function Proceedings of the First John M Marshall Symposium in Cell Biology Pp xxvi + 479 ISBN-0-12-551750-5 (New York, London, Toronto, Sydney, San Francisco Academic Press, 1979) $28 50

PEPEU, G , KUHAR M J and ENNA, S J Receptors for Neurotransmitters and Peptide Hormones. Advances in Biochemical Psychopharmacology Vol 21 Pp 516. ISBN 0-89004-408-2 (Raven New York, 1980) $48 00

PHILLIPS, R D , GILLIS, M F KAÜNE, W T and MAHLUM, D D (eds) Biological Effects of Extremely Low Frequency Electromagnetic Fields Proceedings of the Eighteenth Annual Hanford Life Sciences Symposium at Richland, Washington, October, 1978. Pp. xiv + 577 (Tennessee Technical Information Center, U S Department of Energy, 1979) $10.50 pbk Available from National Technical Information Service, U S Department of Commerce, Springfield, Virginia

History of science

COHEN, R S and STACHEL, J J (eds) Selected Papers of Leon Rosenfeld. Boston Studies in the Philosophy of Science Vol XXI Pp 929 ISBN 90-277-0651-41 (D Reidel. Dordrecht, 1979) Dfl 185 00, US $75 00 Paperback Dfl 70 00, US $28 50

DIMSDALE, J E (ed) Survivors, Victims, and Perpetrators Essays on the Nazi Holocaust Pp 474 ISBN 0-89116-145-7 (Hemisphere Washington, 1980) $19 50

SIMPSON, G G Splendid Isolation The Curious History of South American Mammals Pp 266 ISBN 0-300-02434-7 (Yale University Press New Haven and London, 1980) £11 00

LAUGHLIN, W. S. and HARPER, A B The First Americans: Origins, Affinities and Adaptations. Pp 340 ISBN 437-30295 (Gustav Fischer New York and Stuttgart, 1980) £14.00

LINDZEY, G (ed) A History of Psychology in Autobiography Vol VII Pp 472 ISBN 0-7167-1120 (Freeman Oxford, 1980) £8 10 Pbk, £13 30 Board

PACT A Specialist Seminar on Thermoluminescence Dating Oxford Laboratory for Archaeology and the History of Art July 1978 Pp 509 ISBN 2-8017-0226-2 (Council of Europe Parliamentary Assembly Strasbourg 1980) Vols 2

RUSSELL, B Political Ideals Pp 80 ISBN 0-04-320120-2 (Unwin Paperbacks London, 1980) £1 50 Pbk

SCHREIBER, H G. The Philosophy of Life and the Universe Pp. xii + 169 ISBN-533-03232-6. (New York, Washington, Atlanta, Los Angeles, Chicago: Vantage Press, 1980.) $6 50.

nature

17 July 1980

What to do about new herbicides

THE British government has made a muddle for itself over the herbicide 2,4,5-T, rightly held by farmers to be one of the best ways of ridding fields of nettles, thistles and other weeds. Since the middle of the Vietnam War, it has been known that commercial preparations of the material are potentially dangerous because of the small quantities of dioxin which they contain. The Seveso accident dramatized the potential danger of the contaminant. Since then, the British government (like many others) has taken steps to limit the concentrations of dioxin permitted in manufactured lots of the herbicide, but by doing so has appeared merely to excite the morbid interest of trades unions and their members. In recent weeks, unions with as little naturally in common as the National Union of Agricultural and Allied Workers (NUAAW) and the Association of Scientific and Managerial Staffs (ASTMS) have taken up cudgels against this apparently beneficent chemical (*Nature*, 10 July), asking that its use should be stopped. The government's capacity to make a rational response, or even to decide what to do, has been entirely undermined by the belated and shamefaced confession by the Minister of Agriculture on 20 June that his department has misled not merely itself but other bodies to which it has proffered reassuring advice by its mistaken estimate of the amounts of 2,4,5-T used in Britain.

The toxicology of the dioxin and of 2,4,5-T are by no means precisely catalogued, but some of the bare bones of the story are simple. Dioxin, an exceedingly stable chemical, causes chloracne in largeish doses but is also teratogenic and is known also to be carcinogenic. So much is clear from laboratory studies but also, unhappily, from accidents in which human beings have been put at risk. Laboratory studies have also shown that 2,4,5-T itself may be a teratogen. Whether it is also carcinogenic at doses which are not also acutely toxic remains an open question. But it is beyond doubt that dioxin is a much more potent teratogen than the pure herbicide. Such laboratory evidence as exists is unfortunately incomplete. The Advisory Committee on Pesticides (PAC) of the Ministry of Agriculture, Fisheries and Food quoted in March 1979 data which suggest that mice and hamsters suffer teratological consequences only at doses which are also toxic. Doubt has however been cast on this conclusion, so that there are some who say that the effective teratological doses of the two materials are related by a factor of 10^{-4} or thereabouts. If this should be the case and because the permitted concentration of dioxin in otherwise pure chemical 2,4,5-T is one part in 100 million, the foetus of a pregnant woman eating commercial 2,4,5-T by the spoonful is more likely to be damaged by the principal ingredient than by the dioxin contaminant. The recognition of this possibility has come as a shock to many observers of the scene, and to the NUAAW in particular. It is of course ironical that the government, by taking steps to limit the damage that might be done by the contaminant in a commercial herbicide, should have served only to focus attention on the potential dangers of the herbicide itself.

None of this suggests that 2,4,5-T as used in Britain (or elsewhere that intensive agriculture is practised) should be considered an immediate danger. The total amount of the active ingredient used in Britain appears (whereby hangs a tale) to be of the order of 100 tonnes a year, something of the order of 100 grams a year for each of, say, a million agricultural workers. The current recommendation of the Food and Agriculture Organization and the World Health Organization is that 24 milligrams per day entails no risk of teratogenic damage. Even if British agricultural workers perversely chose not to spray all the herbicide on nettles but, rather, ate it or fed it to their pregnant wives, a substantial fraction of the total quantity now used would have to be diverted in this way before widespread damage was caused. Because most of the herbicide used does actually end on nettles and not in people's cups of tea, because 2,4,5-T is distinguished from dioxin by its relative instability and because the indirect consequences of the use of the material are likely as a consequence to be small, it is hard to think that harvested food can be seriously contaminated.

So why is there so much fuss? The most serious issue is that questions have been raised about the basis for the recommendations of PAC about the safe levels of 2,4,5-T. The question is by no means an easy one to settle. Such data as are to be found in the literature are not part of systematic and controlled studies, while many of them derive from the early 1970s when the need to distinguish between the effects of dioxin and 2,4,5-T was not fully appreciated (and the technical capacity to distinguish between them analytically was only meagre). Yet there is some reason to suspect that the recommendations of PAC are not as solid as they might have been. This, no doubt, is one of the issues that the several government committees concerned, PAC itself but also the committees of the Health and Safety Executive (HSE), will be trying to resolve before the summer is out. Nobody should be surprised if it turns out that the available data are insufficient for an informed conclusion to be possible.

Whatever the outcome, it is inevitable that the mere shadow of doubt cast on the recommendations of PAC will call into question the constitution of that body, which is one of those vaguely defined entities of which British bureaucracy is proud to boast. The committee is for practical purposes responsible for licensing the uses made of pesticides. Its positive recommendations have the force of legal licences. Negative recommendations are the equivalent of bans. To outsiders, the great anomaly in the constitution of PAC is that manufacturers are not required by law to submit new pesticides, or new formulations of old pesticides, to the committee. Compliance has always been, and remains, voluntary. Even so, to the surprise of many people, the system has worked well and imaginatively — the regulation of the organochlorine pesticides has, for example, been sensible. Equally surprising, there is no evidence that manufacturers deliberately keep new products from the eyes of the committee — the fear that there would in that case be a statutory scheme is enough to keep them all on the straight and narrow path. Such loopholes in the British arrangements for the regulations as there are centre on the import of materials manufactured overseas but not recommended by PAC, but again there is no evidence that this is substantially abused. The danger now, for the Advisory Committee on Pesticides, is that if it should turn out that it has erred on the side of what may seem to be complacency in such an important (or at least controversial) matter as 2,4,5-T, the pressures for converting from a voluntary to a statutory scheme will be almost irresistible. That would mean, for all concerned, more bumbledom.

The second issue that will keep the civil servants busy through the summer is that the Ministry of Agriculture has grossly underestimated the quantity of 2,4,5-T being used in Britain. For the past two years, the ministry has been saying that the quantity was something like three tonnes a year, largely on the basis of a survey by major users, the Forestry Commission in particular. Quite inexplicably the ministry, proud as it is of its connections

0028-0836/80/290193-02$01.00

with farmers through the Agricultural Advisory Service, failed to appreciate that the chief use of 2,4,5-T is for spraying crops and grassland to get rid of weeds. But even the revised estimate of 50 tonnes a year has had to be doubled to more than 100 tonnes in the light of figures supplied by Customs and Excise of the quantities of the herbicide imported. The broader issue here is that the ministry has for several years resisted complaints that its surveys of the use of pesticides on British farms are adequate.

What, while these questions are being resolved, are the unions (and their members) to do and think? By all accounts, PAC will make a detailed investigation of the specific allegations of damage done to people that have been mentioned by the agricultural workers, but that cannot be a quick job. What the union must do is what it should have been doing all along — to make sure that workers spraying pesticides wear adequate protective clothing. Mr Clive Jenkins of ASTMS is frying other fish. To his usual preoccupation with the recruitment of members, he appears to have added a wish to back the Health and Safety Executive rather than the Ministry of Agriculture as the arbiter of what pesticides are safe. His inclinations are understandable, for union representation on HSE is laid down by law. In reality, however, both executive and ministry have a finger in the protection of agricultural workers, while HSE is solely responsible for the occupational risks of chemical plants where 2,4,5-T may be manufactured. Even Mr Jenkins is on solid ground when he argues that the executive has dealt ineptly with recent problems. Whatever the strength of these complaints, however, it would be a great misfortune if the use of a herbicide whose value is unquestioned were to be needlessly and prematurely banned simply because the government has made a hash of this affair.

Nato, France and the neutron bomb

WHILE many parts of France enjoy the spectacle of protests against the building of civil nuclear power stations, there has been hardly a complaint at the French government's announcement that one of its recent nuclear tests was that of a neutron bomb. Just possibly the explanation is that French taxpayers accept the theory of strategic deterrence hook, line and sinker, and are persuaded that French neutron bombs are intended never to be used but that the civil nuclear power stations being built in France are meant to be used, and quickly. It is, however, more probable that the silence which has greeted the announcement of the neutron bomb betokens a general agreement by the French population with the national strategy which has been working out since the mid-1950s. Whatever the explanation of the domestic reaction, opinions appear to have been much changed by the new development. The *Suddeutcher Zeitung* was saying last week, for example, that the neutron bomb means that France is no longer a token nuclear power. What does it all mean?

For the best part of a quarter of a century, France has been the odd man out in European defence. The roots of the present policy appear to go back to Gaullist days, and to the theory advocated by General Jean Gallois that each nation should possess a nuclear striking force somehow commensurate with its own importance to a potential adversary. In reality, they probably have more ancient origins. It is too easily forgotten that the French have long memories, as long perhaps as those of the Irish. The French experience of two world wars is a sufficient justification of the conviction that nation states should in the last resort be masters of the means of their own defence. The painful withdrawal of France from NATO was as much a reflection of this belief as of overt distrust of the assurances in the NATO treaty or of disagreement with NATO strategy. Only this can properly explain how, even with the passage of two decades, France remains on the sidelines, now consulting closely with NATO and behaving as if a full-blown member, but stolidly opposed to rejoining the club.

From this point of view, the development of the neutron bomb is logical enough. So long as France holds to the view that the time may come when the defence of France by Frenchmen (without help from elsewhere) may be necessary, it plainly makes sense that France should be equipped with those nuclear weapons which, at least in theory, could be used tactically in European circumstances without inviting massive retaliation from the other side. Whether, of course, the financial cost of this new investment is worthwhile, only the government of France can judge. Apparently, however, the taxpayers most immediately concerned have no objection. Two years or so from now, which is the soonest the new weapons could be deployed, France may thus be the only nuclear power to risk deploying these new weapons in a theatre where their use makes sense.

The consequences for states on both sides of the German border are not easy to foresee. The most comforting calculation is that France will equip itself with only a modest force of neutron bombs, one so modest that it could have no decisive influence in a major European conflict. Certainly there has been no protest yet from the East at what the French are planning that compares with the trouble evoked when the United States announced its intention to deploy neutron weapons in Europe more than a year ago. Perhaps the President of France was able to stave off trouble when he met Mr Brezhnev in Warsaw last month, or perhaps the protest is yet to come. Whatever the future, however, it seems inevitable that the latest developments in France will change the regard of other European states for the non-NATO member among them. But this time, unlike the early 1960s, France will tend to be regarded not as the black sheep of Europe but as a symbol of the implicit belief now strengthening in Europe that European responsibility for its own defence is not merely prudent but necessary. The Gallois doctrine, after a long hiatus, is catching on.

So is there a chance that in the years ahead Western Europe as a whole will accept that it must, in the last resort, be responsible for its own defence? And what will be the consequences? The tendencies in this direction which have become apparent in the past few years differ markedly from those which carried France out of NATO twenty years ago. There are few in Western Europe who now doubt the commitment of the United States to European defence. Their anxiety, rather, is that this commitment has been one of the few reliable components of a foreign policy which has as often mystified as reassured. Escapades such as the abortive attempt to rescue the American hostages in Iran are worrying for Europeans not so much because of the direct risk of a conflagration, limited though it might well have been, but because they cast doubt on the machinery for consultation within NATO and on the process of policy formation in Washington. These doubts will not go away when the American election has been decided. There are also, however, other forces tending to strengthen European hankerings after a European defence policy. It becomes increasingly anomalous that the European Community has only the most slender means for formulating policy towards the rest of the world — the brief declarations tagged on to communiques such as that issued from Venice a few weeks ago are no substitute for a foreign policy. Moreover, it becomes ever more apparent that Western Europe is evolving its own sense of priorities as to how relationships with the East should be conducted. Chancellor Schmidt's visit to Moscow, sceptically regarded at the outset by the United States, has nevertheless opened the possibility of constructive discussions about medium-range missiles in Europe that could, if by some remote chance they succeeded, be a great boon to the industrialized West and East alike. On the face of things, the French neutron bomb (not yet a weapon) is a gesture of national independence, but it will curiously also help to strengthen Western Europe's growing tendency towards coherence and indendence.

0028-0836/80/290194-01$01.00

Congress supports technology centres

Washington

Plans are now being advanced to implement one of the key proposals made by the Carter Administration last year to help stimulate technological innovation — the setting up of a number of "generic technology" centres. The proposal has so far escaped budget cuts in Congress.

The purpose of each "generic technology" centre would be to carry out research and development in a particular area of technology underlying a range of industrial needs, rather than being related to any specific product. Typical examples given include welding, tribology, the study of new composite materials and the general area of automated manufacturing.

Officials at the Department of Commerce are now putting together detailed proposals from industry to establish three or four such centres. The hope is that, if Congress can be persuaded to allocate the $5 million requested for the programme, initial work on the centres would be under way by the beginning of the next fiscal year on 1 October.

The idea behind the centres is that the government should provide seed money to stimulate research of a type which no individual company may be prepared to support, but which is likely to benefit groups of companies or whole industries. Each centre would be jointly funded by industry, initially with the government picking up most of the bill, but with government support dropping to 20 per cent or less after five years.

Each centre, according to details published by the department last month, will have responsibilities in three main areas: first, to maintain a substantial in-house research and development effort; second, to provide a range of technical services, including consultants, information, training facilities and technology evaluation; and, finally strategic planning of technology development.

The idea has already found many sympathetic ears in the US Congress. The Senate, for example, recently passed an innovation bill, originally proposed by Senator Adlai Stevenson, Jr, chairman of the Science and Space Subcommittee, aimed specifically at encouraging research links between industry and universities by setting up a number of "centres for industrial technology". The Senate bill has already been accepted in principle by the Science and Technology Committee of the House of Representatives.

The private sector is also keen. Technology centres were one of the chief recommendations of the Research and Development Advisory Panel to last year's domestic policy review of innovation. The committee recommended that direct federal support of new technology generic to process or product innovation in wide spectra of industries "should be strengthened and recognized as federal policy". Its chairman, Dr Jack Goldman of the Xerox Corporation, remains enthusiastic about the Stevenson bill.

Some controversy remains, however. For example, should the universities be research contractors for groups of companies setting up a particular generic technology centre, as the Department of Commerce seems to recommending? Or should universities be given a more prominent role from the start as the point of contact between government and industry?

The second strategy has been advocated by the National Science Foundation, which has set up a number of university-based co-operative research centres under a programme initiated in 1973. The most successful of these has been the Polymer Research Center at the Massachusetts Institute of Technology, now self-financing from industry sources with an annual budget of $600,000.

NSF's own plans for expanded efforts in this direction had to be trimmed by $2 million when the Administration revised its budget request to Congress in April. But NSF officials are convinced that their approach, using universities as "surrogates" for federal contact with industry, has several advantages over what one refers to as the Commerce Department's "pie in the sky" efforts to forge ambitious links between government and industry virtually from scratch.

David Dickson

Carnesale for NRC chairman

Washington

Dr Albert Carnesale, professor of public policy at Harvard University and deputy director of the Center for Science and International Affairs there, was nominated last week by President Carter for the newly-upgraded chairmanship of the Nuclear Regulatory Commission (NRC). Dr Carnesale is a nuclear engineer by training, with experience of both arms limitation and non-proliferation negotiations. This, together with his reputation as a "moderate" on nuclear issues, has led both anti-nuclear and pro-nuclear groups to greet his appointment with a cautious welcome.

Carnesale's involvement in nuclear energy debates, for example as a participant in the Ford-Mitre study of 1976 and as head of the technical coordinating committee for the US delegation to the International Nuclear Fuel Cycle Evaluation (INFCE), nevertheless suggests that his views are closely aligned with the Administration's position on sensitive issues such as nuclear reprocessing and non-proliferation policy.

Dr Carnesale received a master's degree in engineering at the Drexel Institute in Philadelphia, and subsequently a PhD at North Carolina State University. After five years working as a nuclear engineer with the defence contractors Marietta Martin, he joined the Arms Control and Disarmament Agency, and was a senior adviser to the US delegation which negotiated the first Strategic Arms Limitation Treaty (Salt I) in 1972.

He returned to North Carolina State University as head of the division of environmental studies in 1972, subsequently moving to Harvard in 1974, where he now teaches a class at the Kennedy School on "Technology, War and Peace", while remaining a government adviser on various defence and nuclear issues.

Dr Carnesale refuses to be drawn on specific ideas about the current problems of the NRC, which has been under considerable strain following its handling of the Three Mile Island accident and its aftermath last year. But he said last week that he considers the safety of existing reactors to be "the first item of business for anyone".

On the reprocessing of spent fuel, whose deferral by President Carter is now under renewed attack in Congress, Dr Carnesale points out his agreement with the conclusion of the Ford-Mitre study (subsequently accepted by INFCE) that at present there is no economic case for recycling fuel from thermal reactors.

He considers the INFCE exercise to have been a "success" in generating an international dialogue on nuclear fuel cycle issues, even though it failed to endorse many aspects of US policy. "It has to be judged in a far wider perspective than the reports themselves", he says. But he refuses to be drawn on whether the United States, as some of the more ardent congressional supporters of its non-proliferation policy had argued, should have taken a bolder stance in registering areas in which it disagreed with the final consensus.

Waiting for approval . . .

0028-0836/80/290195-02$01.00

This is one area where Dr Carnesale's views are likely to be closely examined by Congress when it considers his nomination. The NRC's refusal to grant an export licence for nuclear fuel to India has already prompted moves to circumscribe its responsibilities for reviewing exports as detailed by the Non-Proliferation Act signed in 1978. Legislators are soon to consider whether to veto President Carter's decision to overrule the NRC and grant the licences. But they will want to know how sympathetic Dr Carnesale is to the proposals of Mr Gerard Smith, head of the INFCE delegation, that some of the more stringent provisions of the NNPA be amended.

Dr Carnesale's appointment is said to have been actively canvassed within the White House by the Office of Science and Technology Policy, keen to defuse what has recently been called "the most politicized agency in town" — as well as to see strong leadership given to a body which, prior to the Three Mile Island accident, relied more heavily on collegial decision-making by its five commissioners.

David Dickson

Policy analysis

UK adventure?

Can pure reason throw light on the relationship between technical innovation and social change, assisting the first and softening the consequences of the second? This is the inspiration of the brave gamble launched last week in London by the Leverhulme Trust, the Science Research Council (SSRL). Between them, the three organizations plan to spend £2.55 million setting up an organization known as the Technical Change Centre. Sir Michael Swann, the retiring chairman of the BBC, will run the governing body of the new centre, but a director has yet to be found.

The centre is intended as an instrument of policy analysis; it will seek, in other words, to influence events. Its sphere of operations was last week defined more confidently by example than by precept — it may look into public perceptions of the hazards of nuclear power, opportunities in but also the social consequences of microelectronics and the question whether academic training at the postgraduate level is good or bad for British industry. The sponsors' interest in the gamble is best explained by Sir Michael Swann's plaintive question why Britain, the leader in technological innovation for two centuries, should have failed so dismally since the Second World War.

Swann is the boss

The centre has venerable antecedents. Four years ago, the SSRC flirted with the notion of setting up in Britain an equivalent of the Washington-based Brookings Institution, but failed to find charitable partners for that venture. The new venture is in part a survivor of that plan, but with the difference that the SRC is an equal partner with the SSRC, that the Leverhulme Trust will contribute 60 per cent of the cost of the first five years and that the terms of reference, still broad, have been made more narrow.

Last week, the sponsors of the centre were frank in their estimate of their success. Much will depend on the director they can recruit; they also confess that they may be beaten by the intractability of the problems they tackle. They plan to make a cool appraisal of their venture (which may get under way by the beginning of 1881) in about four years. If things are going well, they would hope to give it at least a second lease of life.

Precisely how the centre's work will evolve plainly awaits the appointment of a director. For Sir Michael Swann emphasized last week that its policy will evolve independently of the interests of the sponsors. He explained, however, that the SSRC has a special interest in policy analysis of this kind more or less as an end in itself, while the SRC has a more specific interest in receiving advice on how its own budget should be disposed.

The core of the governing body has already been recruited, and includes the chairmen of the two sponsoring research councils (Sir Geoffrey Allen and Mr Michael Posner), Dr Duncan Davies (Chief Scientist at the Department of Industry), Sir Alastair Pilkington (soon to retire as chairman of Pilkington Brothers, the glassmakers) and Mr Philip Hughes (chairman of Logica Limited, a software house). It is intended that the board, when complete, should include representatives of trades unions.

Sir Michael Swann says that the absence of the Agricultural and Medical Research Councils from the list of sponsors has no significance, but plainly the new centre will be looking to them as well as to other organizations for funds with which to carry out sponsored research; the funds so far available amount to just over £500,000 a year, but the centre would hope to recruit a further £200,000 a year of soft money. While most of its work will be carried out in-house, it will also support work at other centres in the United Kingdom, thus no doubt helping to ensure that it is not regarded too much as a threat by existing academic centres.

Teaching companies

Victims of success

The British Science Research Council and the Department of Industry are in difficulties about the financing of their joint teaching company scheme. Paradoxically, their problems have arisen because the scheme is proving more successful than originally foreseen.

When the teaching company scheme was set up five years ago, the aim was to secure the participation of about 20 companies by 1980. Interest has been such, however, that 33 companies are now involved and many more are hoping to join. The SRC and DoI agreed to fund the scheme on a fifty-fifty basis but the rapid expansion has meant that this year the DoI may not be able to pay its share. The total cost of the scheme has risen from £0.5 million in 1979 to an estimated £1.5 million this year, of which the DoI can contribute only £600,000.

The SRC is confident that it will be able to take up the slack in 1980; the real problems will arise in future years, especially if expansionary pressures persist. The SRC's contribution could probably increase to about £1 million a year, but other sources of finance would then have to be found. A panel of industrialists, civil servants and academics is to be set up at the end of this month, with a remit to make recommendations by the end of the year.

The objective of the teaching company scheme is to introduce industry to the skills universities have to offer and at the same time to provide recent graduates with industrial experience. Typically, a company agrees to take on three recent graduates, called associates, in each of the first two years of membership.

The SRC and DoI between them pay the associates' basic salaries, incidental expenses, cost of any special equipment they need and the cost of any replacement staff needed in universities. The company's major expense is usually that of implementing recommendations for improvements.

The pressures to expand the scheme come not only from companies wishing to join but also from those already in the scheme who say they have found it so useful that they are reluctant to leave. So far, only two companies have actually left the scheme. Because of the pressure on funds, the SRC is now beginning to talk to several companies about ways of terminating formal membership.

Both industry and universities seem to be enthusiastic about the scheme. Industry effectively gets a free consultancy service and is able to tap otherwise inaccessible resources. Universities have the opportunity to put some of their academic work into practice.

Judy Redfearn

0028-0836/80/290196-01$01.00

Technological forecasting

Rush programme

The European Commission's FAST project, a five-year programme in science and technology forecasting set up in 1979, is up to its eyes in applications for funds. Invitations to tender for part of the £1.35 million budget were sent out early this year; and by the deadline of 10 April some 224 applications had been received from 176 institutions. Research projects relating to Europe 10, 20 and 30 years ahead must be completed by mid-1982, although the 30-40 successful applicants will be officially notified only in September.

FAST's director, Ricardo Petrella, says this compression of the timetable is inevitable, given that the programme was funded for only five years by a decision of the Council of Research Ministers on 25 July 1978. The FAST team of six scientists and four assistants spent most of 1979 defining the nature of the programme. The research phase of the programme now beginning must end during 1982 and early 1983 with the specification of research and development priorities for Europe the ultimate object of the exercise.

For the participating universities and research institutes, there will be little time to come to grips with what are complex issues — "microelectronics innovations in the context of the international division of labour", for example, and "social acceptability of biotechnology-based activities". This may account for what one observer outside the commission has called the unimaginative nature of most of the applications.

The applications are also biased to short-term issues. Petrella's team distinguished three broad sectors of problems — work and employment, the role of information technologies and the role of biotechnology — which Petrella identifies as of greatest importance over periods of 10, 20 and 30 years respectively. Some 100 applications were received for research in the first sector, 70 in the second but only 35 in the third. The final selection of projects will, however, be more uniformly divided.

The short perspective of the FAST applications might have mattered less if a parallel proposal within the European Science Foundation had come to fruition. The plan had been that the ESF, an independent body uniting national research councils throughout Europe, should have mounted an "additional activity" on "the socio-economic consequences of technical development", paid for by those among its members wishing to participate. This proposal, which would have been concerned with more basic and less policy-orientated objectives than is FAST, was thrown out by the ESF's social science committee last year.

One of the objectives of FAST, defined by the 1978 European Council decision, is "to establish an *ad hoc* system of collaboration between specialized research groups within the community and so create a series of community forecasting networks". All very well — but what can be done on a European scale that is not already being done nationally? ("Send me the answer on a postcard", one UK government science adviser asked one of the FAST team.) It is a question of scale and regionality, according to Mark Cantley, head of the FAST biotechnology programme. Investigation of the manpower and training implications of biotechnology-based industries, for example, requires consideration of international transfers and coordination. The distribution of benefits and risks associated with microelectronics and its applications is similarly a regional matter.

FAST itself is also under test, however. The earlier, small-scale "Europe plus 30" study recommended the establishment of a Community Forecasting Institute. The council rejected that in 1978 and instead set up FAST for a provisional five years. Petrella and his team naturally hope that the experiment will be continued.

Robert Walgate

Soviet energy

No shortage?

The Soviet Union and its socialist allies have no energy crisis ahead, according to Petr Neporozhnii, the Soviet Minister of Energy and Electrification. This confidence, he said, was based on estimates of the Soviet Union's fuel reserves — more than 50 per cent of the world reserves of coal and more than 33 per cent of the world reserves of oil and gas. Furthermore, the Soviet Union's hydroelectric capacity is potentially larger than that of the United States, Canada and Japan taken together.

The minister was speaking on the English-language service of Moscow Radio beamed to North America. Inevitably, he compared Soviet energy policy with that of the United States. The latter, he said, has in its oil shales "more than several Saudi Arabias" — but the "American monopolies" find it more profitable to import oil and raise retail prices of oil products than to develop new deposits. The minister glossed over the fact that one of the main barriers to the use of shale is environmental pollution. Estonia, which burns much shale in thermal power stations, is a major source of pollution in the Baltic area.

Neporozhnii's confidence is to a large extent supported by the latest figures from PetroStudies (Malmo). This independent team monitors Soviet oil and energy exports on the basis of trade figures with individual countries. According to the report for 1979, published last week, the Soviet Union is now the second largest oil exporter in the world (next to Saudi Arabia), exporting 164 million tonnes in 1979, and for the past six years has been the world's leading oil producer, with an annual target for 1980 of 606 million tonnes. The same confidence was shown by Dr Mikhail Tolkachev of the Soviet Academy of the National Economy, reporting to a meeting of the International Institute of Applied Systems Analysis earlier this month. This year, said Tolkachev, Soviet natural gas production is expected to reach 4.2 million m^3 per day, an increase of more than half a million m^3 since last year.

Soviet claims to energy sufficiency are not new. Neporozhnii's talk, however, is interesting in that it virtually ignored nuclear power, except for a passing mention of plans for integrating the Soviet grid with those of the various Comecon countries and the construction of the new ETL-750 transmission line to connect Rzeszow in Poland with the Khmelnitskaya atomic power station in the Ukrainian SSR. This is the more surprising since Neporozhnii put considerable stress on the Soviet planners' 'concern for the future" — as exemplified in the long-range energy plan launched 20 years ago with the construction of the Bratsk power station in Siberia. The same concern, said the minister, has led to long-term plans for the production of synthetic liquid fuel, the use of solar and geothermal energy and even "the heat of ordinary sea water".

To most Soviet energy planners, however, nuclear power is usually a key topic in any speech on energy prospects. In April 1979, Academician Anatolii Aleksandrov, president of the Soviet Academy of Sciences, and himself formerly a leading figure in the nuclear energy programme, stressed that it was atomic energy and coal which would help the Soviet Union to avoid what he called the "imminent energy crisis". The Soviet nuclear programme does not, however, appear to be keeping up with the demand.

Last month, at an All-Union conference on nuclear power held, appropriately, at Energodar, Sapozhnikov, one of Neporozhnii's deputy ministers, stated that the construction of nuclear power stations must be doubled and new commissioned capacity raised to 7,000-10,000 MW per year. The target is an overall nuclear generating capacity of 100,000 MW within the next 10-12 years.

According to Fedor Ovchinnikov, another deputy minister of energy, the short-term programme is for water-moderated water-cooled reactors of up to 1,500 MW capacity. Officially at least, there are no anxieties on environmental grounds. Yurii Markov, a spokesman for the Ministry of Energy and Electrification, wrote recently in *Sovetskaya Rossiya* that Soviet nuclear power stations are so safe that their surroundings "are used as recreation areas, where families come and picnic, gather mushrooms and berries and go fishing in the cooling ponds".

Vera Rich

0028-0836/80/290197-01$01.00

Technological change

Worry about jobs

Washington

The new report on science and technology policy (see *Nature,* 10 July, page 96) published by the Organization for Economic Cooperation and Development (OECD) is being cold-shouldered in Washington largely because of its warning that undirected technological change may be contributing to the rising level of unemployment. The report, prepared by a group of outside experts, sets out to identify the main elements of the social and economic environment for science and technology which are likely to affect OECD countries during the 1980s.

The report emphasizes the need to revitalize technological innovation in order to help remedy many of the afflictions of the 1970s, especially sluggish economic growth and escalating inflation. To this uncontroversial conclusion, however, it adds that technological innovation must be guided so as to ensure that its potential benefits are not overshadowed by the destruction of jobs.

The extent to which technical change, in both manufacturing and service industries, may be contributing to growing unemployment, expected to reach 8.5 per cent next year, is receiving more and more attention, particularly at state and local levels. Pennsylvania's legislature, for example, is considering a bill intended to reduce unemployment by banning automatic petrol stations and toll collection booths, among other measures.

In Washington, by contrast, the government resists the notion that it must act to soften the impact of technical change on employment. Last year's domestic policy review of industrial innovation, for example, concluded merely that "the key to successful adjustment is warning time"; and the national Labor Technology Forecasting System subsequently promised by President Carter has yet to materialize. The dominant argument is that once rapid economic growth has been re-established, jobs lost through technical change in one sector of industry will be replaced elsewhere. In any case, there is growing antagonism towards government intervention in the regulation of innovation, so that the lack of enthusiasm for the OECD report is no surprise.

The report started as an internal study within OECD to examine the relationship of technical change to the problems of inflation, unemployment and long-term economic growth. In part, it was intended as a counter-analysis to the official OECD report "Towards full employment and price stability", produced by a committee chaired by Professor Paul McCracken and published in 1977.

The new report challenges the McCracken thesis at two related levels. First, it argues that the economic problems faced by OECD countries in the early and mid-1970s were not, as McCracken suggested, merely a manifestation of cyclical economic changes that could be resolved through conventional policy instruments. Rather, the new report argues, they reflected deeper structural changes requiring a more radical approach.

More specifically, the report challenges the McCracken committee for underestimating the impact of technical change on social and economic policy, and for characterizing the declining rate of innovation as a problem that will resolve itself "naturally" with a revival in demand. Instead, the report argues that adequate policies for science and technology must be central to any attempt to tackle the joint problems of high inflation and unemployment. These problems, it argues, tend to depress the rate of innovation; but a slackening of innovation makes their solution more difficult.

Government action is therefore necessary, the report argues, to ensure both a faster and a "more balanced direction" for technical change. But in the United States, where most government economists accept the McCracken thesis, this has met with a certain scepticism. A particular source of irritation has been the report's warning that a general substitution of capital-intensive for labour-intensive techniques in manufacturing industry may be exacerbating unemployment.

Professor Richard Nelson of Yale University, a member of the OECD expert group, admits that the committee which prepared the report was "schizophrenic" on the employment issue. Thus it argues that "a significant acceleration of technical advance and productivity growth would make the unemployment problems easier to deal with" but also warns that more capital-intensive technology may further worsen the condition of the labour market.

The report adds that structural unemployment is now an "important feature of the economic landscape". The hypothesis is an increasingly familiar one in Europe, particularly in Britain where it has been argued forcefully by, among others, Professor Christopher Freeman of the Science Policy Research Unit at the University of Sussex, a member of the group which prepared the OECD report. Economists here prefer to point to similar concerns in the late 1950s and early 1960s that the automation of production might create serious unemployment; in the event, excess labour was absorbed into the rapidly-growing service sector.

Academic economists tend to be more agnostic than their government colleagues. Dr Robert Lund of the Massachusetts Institute of Technology, who has examined studies carried out at Sussex on the impact of microelectronics, says that "we did not find the kinds of employment impacts that seemed to be predicted". But he adds that "I do not know if we have enough data to say that we have the right answers".

Government policy-makers are less equivocal. The OECD report came in for substantial criticism when a draft was circulated last year. Strenuous, and ultimately successful, efforts were subsequently made within OECD to ensure that the report was published as the opinion of a group of experts rather than with the organization's official backing.

The net result, however, is that the report's potential impact on policy has been blunted, which Professor Nelson for one regrets. "On the employment question, it may not be quite right, but it is more correct than some of the discussions now taking place." **David Dickson**

Thermonuclear fusion

Soviets bid half

Brussels

The cost of the International Test Fusion Reactor (INTOR), estimated at $1,000 million, would be more than halved if the machine were built in the Soviet Union. This is the opinion of Dr L G Golubchikov, head of the fusion division of the Soviet State Committee on the Utilization of Atomic Energy who has been seeking to stimulate a greater commitment to the project from the West during his participation in the eighth international conference on plasma physics which ended last week.

The project, which so far consists largely of a design study, is being planned by the International Atomic Energy Agency (IAEA). American reaction at the conference, however, was cool. It might cost half as much, but it would take twice as long, was one opinion.

INTOR, whose study by the IAEA was proposed by the USSR in May 1978, is nevertheless agreed to be a constructive exercise in one respect: by concentrating attention on the severe engineering difficulties of the tokamak fusion reactor, it is helping to define the experimental questions which must be tackled in the next generation of large tokamaks (JET in Europe, T-15 in the USSR, TFTR in the United States and JT-60 in Japan). However, it is also generally agreed (except by the USSR) that the INTOR design is unlikely to see the light of day as a piece of hardware, at least in the medium term.

What appears most likely is that the recent proposal (*Nature,* 10 July) for a Fusion Engineering Device (FED) in the United States at a hardware cost of $1,000 million will capture (and double) the US fusion budget. FED, largely the work of the Princeton Plasma Physics Laboratory, is less ambitious than the Oak Ridge National Laboratory's proposal, the Engineering Test Facility (ETF), which in turn was less ambitious than INTOR. Moreover, it is felt in the US Department of Energy that collaboration with the USSR on a project of the scale of INTOR would be fraught with bureaucratic difficulties.

0028-0836/80/290198-02$01.00

Japan would also consider collaborating with the United States on FED although it is a little early for formal approaches to have been made. Professor Husini, a Japanese representative on the IAEA's International Fusion Research Council, said last week that Japan would be "very interested" in such a joint venture, on the basis of sharing costs.

This leaves the European Community in the cold beyond JET, unless it also joins in FED, which is by no means out of the question. The European Commission has been considering the next European Torus (NET) in a small committee headed by the Italian physicist Professor R Toschi of Frascati; but, said one Italian, "the FED recommendation means NET will have to be completely rethought. Perhaps we can build a device a step beyond FED and five years later."

The USSR would clearly be disappointed if INTOR goes little further than the project definition, which is to be presented to the IAEA next year. "The West has the bigger energy problem" said Golubchikov. The Soviet authorities are thus less bullish about fusion. It would thus assist the Soviet fusion community greatly if the next steps could be international. And Golubchikov believes the technical problems that will face FED or INTOR will be so great that Soviet participation will be necessary if there is to be rapid progress. After all, the USSR invented the tokamak — which appears to be the only viable ignition device at present — and built the only working superconducting tokamak (T7).

Robert Walgate

Laboratory merger

Harwell again

Several large research facilities in Britain will be completed late, and Britain's capacity to contribute to new international projects will be impaired, as a result of pressures on the budget of the Science Research Council. This is the view of Sir Geoffrey Allen, chairman of the SRC, speaking at an Open Day at the newly-merged Rutherford and Appleton Laboratories last week. Although the science budget has been let off relatively lightly in recent public expenditure cuts, he said, a 10–15 per cent increase of the budget would be needed to complete existing projects within the original timetables and to start new ventures.

One victim of these enforced delays is the Spallation Neutron Source, at present under construction at Chilton, across the fence from Harwell. It will now be completed in 1984, two years later than originally planned, largely because it has been necessary to spread out the funding of the £12 million project. Allen is also concerned that Britain may not be able to contribute fully to the building of a new European synchrotron radiation source (*Nature*, 20 May) or to the European Space Agency's plan to build an astrometry satellite, Hipparcos.

The proposed European synchrotron radiation project, devised by the European Science Foundation, would require a new international agreement among the partners; Allen plainly fears that the SRC budget may be too tight to allow Britain to contribute. Hipparcos presents a different problem. It will be paid for out of ESA's mandatory science budget to which all member states, including Britain, contribute annually on the basis of GNP. Allen's concern here is that British laboratories should recapture some of the cost by making viable bids for the ESA contracts.

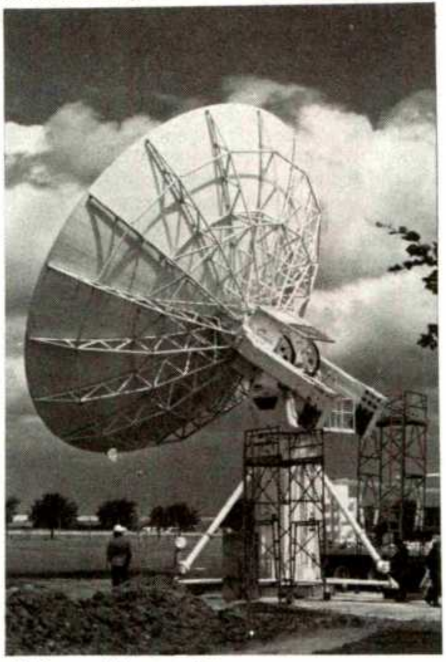

Dish awaiting satellite

The merging Appleton and Rutherford Laboratories are hoping to overcome this manpower problem by training and redeploying people as their projects come to an end, or as timetables are extended. The laboratories claim some success in these directions, but acknowledge that there must be limits to the extent to which staffs with different, highly specialised backgrounds, for example in radio and space physics (Appleton) and high-energy physics (Rutherford), can be fully redeployed.

A major reason for the merger is to save costs, including some staff. The SRC hopes to shed about 40 administrative jobs by not replacing those who choose not to move to the new site. Most of the scientific staff are expected to move, however, and those who do not will be replaced. So far about a third of the 300 Appleton staff have moved. The rest will do so before the end of 1981.

The plan to close the site of the Appleton laboratory at Ditton Park cannot be implemented precisely as originally hoped, however. Some of its instruments will not be compatible with the Chilton site; some millimetre wave and radio equipment, for example, will be sited 60 miles away to avoid interference from the spallation neutron source and 70 MeV linac.

Judy Redfearn

Siberian science

Marchuk on top

Last month's meeting of the Supreme Soviet confirmed the appointment of Academician Gurii I Marchuk as head of the State Committee for Science and Technology. The confirmation was a formality; Marchuk's appointment took effect last January, when the then head, Academician Vladimir A Kirillin, resigned (coincidentally on the day that Academician Andrei Sakharov was exiled to Gor'kii).

Marchuk came to the State Committee from the Siberian branch of the Academy of Sciences, of which he had been chairman since 1975. That branch, based on the science centre of Akademgorodok outside Novosibirsk, was originally set up, in 1957, as part of Khruschev's overall plan to decentralize the economy. Its activities have always, therefore, been closely related, at least formally, to the needs of Siberia.

The Siberian branch would therefore share the blame if science failed to play a full part in the opening up of the Siberian heartland. In the autumn of 1976, criticism of the Siberian branch did in fact break out. The State Monitoring Committee at the outset criticized the Academy of Science's Far Eastern Science Centre for failing to make a proper practical contribution to the national economy. The campaign turned to more and more prestigious institutions, finally attacking the Siberian branch itself. At that point, Marchuk fought back, and with an impressive battery of arguments demonstrated that, so far from slacking, the branch was alive and flourishing and more than pulling its weight.

In his new job as head of the State Committee, Marchuk is responsible for the whole of Soviet science planning, the coordination of research and development and the subsequent implementation of research. Marchuk's Siberian experience will be invaluable, for Siberia remains the major area of Soviet capital investment.

Last April, a special conference of the Central Committee of the CPSU advocated increased investment in the fossil-fuel-bearing regions of West Siberia, apparently because a lack of amenities is making it hard to attract scientists and engineers to the area. The new Baikal-Amur Mainline railway was planned from the beginning as a joint exercise in engineering, ecology, demography and economics.

Plans to divert the major Siberian rivers south were, however, delayed during the last five-year plan, although, in response to complaints at the possible global environmental consequences, the Soviet government announced that no such changes would occur. It has however mounted a major environmental study of the region, with the result that Siberian

0028-0836/80/290199-02$01.00

environmentalists have had unparalleled opportunity for field work in the past decade. This has involved the photography of the area from manned and unmanned spacecraft, ground-level geophysical surveys (which on one occasion discovered glaciers far to the south of where they were expected) and the drawing up of ecological guidelines for the engineers. There must be no tree-felling on slopes of more than 15 degrees and no insecticides — construction gangs plagued by the ubiquitous Siberian mosquitoes must use protective netting or swatters.

In spite of all this care, a recent report from the Chita Hydrometeorological Observatory suggests that the development of the BAM zone is running into environmental problems. In the north Transbaikal area, it appears, there is very little wind; the air masses remain static for a considerable time and industrial emissions become concentrated. Long before the BAM railway itself is officially opened, the pollution in the Chara valley is already, say the Chita scientists, some 50-100 per cent greater than that in the European part of the USSR — the centre, at present, of Soviet industry.

Vera Rich

CORRESPONDENCE

Biko's doctors

SIR, — The Faculty of Medicine of the University of the Witwatersrand has strongly attacked the decision of the South African Medical and Dental Council that there was no evidence of improper or disgraceful conduct on the part of the doctors who treated Mr Steve Biko before his death in detention. The Faculty Board has resolved unanimously to dissociate itself publicly from the council's decision, taken at a closed meeting on 17 June 1980.

At a meeting held on Friday, 27 June, the Board of the Witwatersrand University Medical Faculty unanimously adopted a resolution on the "Biko doctors". The resolution reads: "The Faculty of Medicine of the University of the Witwatersrand, Johannesburg, has considered the decision of the South African Medical and Dental Council, taken at a closed meeting on 17 June 1980, that there was no evidence of improper or disgraceful conduct on the part of the doctors who treated Mr Steve Biko before his death, and that there was thus no need for a disciplinary hearing.

"Bearing in mind the revelations under cross-examination at the inquest, and the fact that the magistrate presiding at Mr Biko's inquest had considered that the matter of the Biko doctors should be referred to the South African Medical and Dental Council, the Faculty expresses its deep concern and disquiet at the finding that there was no evidence of improper or disgraceful conduct and that the matter should be dropped. The faculty feels that there was *prima facie* evidence of improper or disgraceful conduct, which should have been subjected to the careful scrutiny of a Medical Council Disciplinary Committee hearing.

"The Faculty is of the opinion, furthermore, that this decision of the Medical Council may seriously affect the good standing of the South African medical profession both at home and abroad and, therefore, publicly dissociates itself from this decision.

Further, the Faculty endorses and supports the Guidelines for Medical Doctors concerning Detainees and Prisoners, adopted by the 29th World Medical Assembly of the World Medical Association in Tokyo in October, 1975, and known as the "Declaration of Tokyo". This states, *inter alia*, that a doctor must have complete clinical independence in deciding upon the care of a person for whom he or she is medically responsible (Article 5), and that a doctor shall in all circumstances be bound to alleviate the distress of his fellow men, and no motive — whether personal, collective or political — shall prevail against this higher purpose (Article 8).

"The Executive of the Board of the Faculty of Medicine is requested to ensure that the views of the Board are communicated widely to the public and to the medical community, both in South Africa and abroad."

In accepting this resolution, the Faculty stressed that "We are not saying that the doctors are guilty. We are saying that there is sufficient evidence for a Disciplinary Committee enquiry to be instituted and that a decision should be taken about the behaviour of the doctors on the basis of a full, fair, impartial and thorough Disciplinary Committee hearing. The South African Medical and Dental Council is supposed to be the watch-dog of the ethics of our profession and they have been zealous — and some would suggest over-zealous — in the severity of the punishment that they have meted out, not only for major infringements but for what many would regard as minor infringements of the ethics of medical practice. Yet, in the present case, it is difficult to accept that the Medical and Dental Council has applied its collective mind to the problem of the Biko doctors in a purely objective and dispassionate way."

In moving the resolution, Professor Clive Rosendorff, Head of the Department of Physiology at the Medical School, made this statement:

"This is all a source of great embarrassment and distress to many doctors in South Africa who are proud of the high ethical standing of their profession, both within this country and abroad. I believe that we have a responsibility to indicate to the world that we disapprove of the decision of the Medical Council to drop the matter. We should like it to be known that we dissociate ourselves, as an institution and as a body of concerned citizens and doctors, from their decision. We do this because we feel that it is morally indefensible for a matter as important and serious as this to be dropped before it has reached the Disciplinary Committee stage. We do this because we feel that the ethical standards of our profession have been compromised; because as doctors we have a humane concern for our patients and their welfare; because we are worried about the possible effects of the decision of the Medical Council on the future treatment of prisoners and detainees by the authorities; and because we are worried about the repercussions of the Medical Council's decision abroad. Already there are signs of a campaign to cut ties with doctors from South Africa, both at international congress level and in the recognition of our degrees abroad.

"Countries with which we have most dealing and reciprocity agreements, Great Britain, Australia, New Zealand, the Netherlands, Belgium, the United States of America, Canada, have always been happy to accept the *bona fides* of the S.A. Medical and Dental Council. However, there are already indications that rethinking on this point has started. The British Medical Association Ethics Committee is to examine the Biko doctors decision of the S.A. Medical and Dental Council. In Geneva, the World Health Assembly has called on member countries to review their medical ties with South African doctors."

My Faculty believes that it is vitally important that we distance ourselves from the decision of the Council. As a group of concerned doctors and Medical School teachers, we are worried that the South African Medical and Dental Council might, by its decision, have called in question its own credibility as an objective and unbiased guardian of the high standards of the medical profession in South Africa.

Yours faithfully,

PHILLIP V. TOBIAS

Dean, Medical School,
University of Witwatersrand,
Johannesburg, S A

Russian continues

SIR, — May I, as Head of the Department of Russian and Soviet Studies at the University of Lancaster, be allowed to comment briefly on Vera Rich's piece in the last issue of *Nature* (3 July). Her remarks concerning the diminishing provision for the study of Russian in Britain, in contrast to the proposed expansion in Finland, are entirely justified. Her statement, however, suggesting there has been an "overnight decision to close down the Russian Department of the University of Lancaster" is incorrect and seriously misleading.

As part of a broader policy document which purported to be a strategy for the 1980s, a small Vice-Chancellorial committee at Lancaster recently *recommended* the gradual phasing-out of five small academic departments, including Russian. The document was subjected to widespread and vociferous criticism throughout the University and was finally *withdrawn* at a meeting of the University Senate on 11 June.

The department, therefore, still exists and will continue to exist — with an increased undergraduate enrolment in 1980-81. Moreover, in addition to its full degree programme of Russian history, politics, language and literary studies, and in the context of your article, it plans to mount a new elementary Russian language course which will be available for scientists who wish to acquire a reading knowledge of Russian and hence gain access to a major "medium of scientific communication".

Yours faithfully,

ALAN WOOD

University of Lancaster, UK

Dioxin disclaimer

SIR, — I wonder if you would be kind enough to allow me to comment on Alastair Hay's article in *Nature* (6 March) which indirectly implies that I had some part in the non-publication of the two investigations of Coalite workers.

Firstly I was never involved in the treatment of Coalite cases. Secondly, not only did I never suggest suppression of the data, but I repeatedly urged its publication — unsuccessfully.

It should be mentioned that the second and more far-reaching study to which Hay has referred was suggested to Coalite by the HSE since the first study was considered inadequate. I have never been shown the results of this second study by the company but obtained them by unofficial means.

Yours faithfully,

K.D. CROW

Princess Margaret Hospital
Swindon, UK

0028-0836/80/290200-01$01 00

NEWS AND VIEWS

Tectonics of the Northwest European Continental shelf

from P.E. Kent

BOTH academic and industrial organisations are involved in exploration of continental shelves, but it is only intermittently that the large amount of data assembled by industry is made generally available. One of these occasions — five years from the previous major release[1] — took place at a conference held in London in February[2].

The conference in 1975 had been concerned mainly with the results of industrial exploration of the North Sea, at a time when drilling in the outer basins was just beginning. This year there was an increased input from other sources — notably regional compilations on the North Sea area by the Institute of Geological Sciences, and on the Norwegian offshore by the Norwegian Petroleum Directorate, while the oil companies added to North Sea data and described for the first time the structure and stratigraphy of the more westerly basins.

In the North Sea itself the nature of the crystalline floor was described from cores and radioactive dating at fifty sites. There is, as previously deduced, continuity of continental crust across the North Sea with a degree of attenuation indicated by gravity measurements and with Caledonian metamorphics with granite intrusions extending as far south as a line from Dundee to Stavanger. The area between this line and the Welsh-Brabant massif is occupied by lightly tectonised sediments, which have locally yielded Lower Palaeozoic faunas. It was again emphasised that development of the North Sea basin began in the Upper Palaeozoic, and that the Mesozoic fault pattern frequently relates to Caledonian progenitors.

Although the additions to North Sea data and detailed descriptions of additional fields are of considerable importance, the main access of new knowledge is of the basins nearer the edge of the continental shelf, from the Barents Sea to the Bay of Biscay, outlined in the following paragraphs.

The Norwegian Shelf, terminated seaward by the Faeroe-Shetland and Voring Plateau escarpments and extending to 68°N, is occupied by a series of basins partly separated by longitudinal and transverse faulted highs. In these basins sedimentary thicknesses exceed 12 kilometres, often in highly asymmetrical trap door-type half-graben basins which ended their fault-development with the 'Late Cimmerian' phase and which were essentially growth-fault controlled. Stratigraphic horizons have been partly dated in relation to those of the adjoining North Sea, and it is deduced that the greater part of the sedimentary sequence is Mesozoic, but that basinal development began in the Carboniferous.

In contrast to the northern North Sea, but in line with other fault controlled Mesozoic basins, inversion took place during the Cretaceous.

In the Barents Sea, more remote and also still undrilled, dating of horizons is less certain and depends on a combination of local dredgings, regional and stratigraphic trends (with Svalbard as a northerly control point) and deduction from world wide events.

The area shows two sub-basins, each with large salt diapirs which originated below the presumed Permian and hence believed to be Devonian/Carboniferous. The existence of salt of this date, if substantiated by drilling, could have an important influence on our understanding of Permo-Triassic salt deposition.

West of the Shetlands the notable feature has been discovery of a very large oilfield on the Rona Ridge. This has been credited with reserves in place of 3.5–4 billion barrels (around 500 million tons), but it is a heavy oil which will present major problems in extraction. The reservoir is mainly of Carboniferous and Devonian sandstones capping the scarp of a large down-to-the-ocean fault which bounds the main Rockall basin. The adjoining trap-door type basin on the eastern side of the Rona ridge is too shallow to have generated significant amounts of hydrocarbons, and it has to be concluded that the source rocks for this very large field lie in the deep Rockall trough itself, an area consequently considered increasingly attractive for future exploration.

The Northern Irish Sea, the site of discovery of a large gas field, is confirmed as essentially a Permo-Triassic basin analogous to the Cheshire Basin on land. An unexpected feature however is the discovery that it underwent inversion — a process of relatively rapid uplift at the end of the Mesozoic, partly counteracting the long period of Permo-Triassic subsidence, a feature now recognised widely on this continental shelf.

The Kish Bank Basin, a simple trapdoor subsidence lying off the Irish coast near Dublin, illustrates particularly well progressive basinal development from Upper Palaeozoic to Tertiary. The tectonised older Palaeozoic floor is followed by Carboniferous — possible Visean, then Westphalian B, C and D — Permian, Triassic and Jurassic (the latest formation surviving). The Carboniferous, Lower and Upper Triassic each thicken towards the 5,000m down-throw boundary fault system, which developed as deposition continued and moved also in the post-Jurassic, finally in the Oligocene.

In Cardigan Bay a very deep Mesozoic and Tertiary basin lies alongside the seaward continuation of the NE-SW Bala fault, which has a westerly downthrow of 4,000 metres. The oldest beds identified are Upper Carboniferous; these are overlain by Permo-Triassic and Jurassic sediments which total 7,000 metres in the centre of the basin. Contrary to earlier expectation the

---

P.E. Kent is a former chairman of the National Environment Research Council and the Petroleum Exploration Society of Great Britain.

*The conference was held jointly by the Institute of Petroleum, the Ecological Society and the Petroleum Exploration Society of Great Britain. The Proceedings will be published by the Institute of Petroleum in 1980.

0028-0836/80/290201-02$01.00

Cretaceous is absent, and the faulted earlier Mesozoic is directly overlain by Tertiary sediments. In line with the development of other Mesozoic basins on the continental shelf it could be presumed that movement of the bounding fault was syn-sedimentary, but the five deep boreholes drilled in the basin were not sufficiently close to the fault to encounter marginal fans, if these exist. The Cretaceous may have been present and been eroded, perhaps a case of inversion of subsidence as in analogous basins elsewhere around Britain.

The Celtic Sea Basin: The Celtic Sea conceals one of the larger basins of the continental shelf, extending 300 km southwards from the Irish coast. Like the other basins of the region, the Celtic Sea basin has a long history, with late Palaeozoic rocks (Lower Permian) proved at depth. Basin development until the late Mesozoic was controlled by rift development. Undifferentiated continental Permo Triassic rocks and a largely complete Jurassic sequence ending with the Purbeck was followed by a thick development of strata in the Wealden facies (indicated as some 1,200 metres thick in the Kinsale Head field); the Wealden apparently extending through the Neocomian to early Albian — appreciably longer than in southern England.

The Kinsale Head gas-bearing structure is an anticlinal feature produced by an inversion of the central part of the basin, a process which gently arched the later Wealden and overlying beds — a close analogy to the English Weald.

The Fastnet Basin: The Fastnet Basin, an appendage of the Celtic Sea Basin extending southwestwards almost to the continental margin in Irish waters, is a fault-bounded subsidence, measuring 110 km from NE to SW and 35–40 km across, which has been investigated by gravity, aeromagnetic and repeated seismic surveys followed by nine exploration wells, unfortunately without any economic discovery. The general structural style is analogous to that of most other basins on the continental shelf, with a thick packet of earlier Mesozoic rocks affected by strong faulting which died out before or during the Upper Cretaceous. An Upper Palaeozoic floor was reached in two wells which respectively identified Lower Carboniferous (Tournaisian) and Devonian, succeeded by a 'normal' continental Permo-Triassic development and a greatly expanded Lower Jurassic. Unconformable Cretaceous begins with a Wealden episode more limited in time than that of the Celtic Sea but similar in facies and age (Berriasian) to that of southern England. It is itself unconformably transgressed by 'Greensand', Chalk and Tertiary sediments.

The closely spaced faulting is dominantly extensional, down-to-basin, most faults being truncated by the Cretaceous unconformity, but others dying out in the Upper Cretaceous. The few which have large displacements in the Upper Cretaceous show evidence of throw reversal, this being associated with extensive basin inversion. The inversion process began in the Lower Cretaceous and resulted in attenuation of both that formation and the Chalk over the area where the Jurassic is thickest, the Chalk itself being absent over an area 20 × 10 km.

The listric faulting developed during the Jurassic can be seen as extension in relation to the incipient Atlantic continental parting, but the development of strong basin inversion (normally characteristic of internal basins) might be taken to indicate that the limit of the continental crust lies at least tens of miles oceanward of the shelf break.

The Bay of Biscay: The concept of the Cretaceous anti-clockwise rotation of the Iberian peninsula relative to the rest of Europe is widely accepted and the paper submitted to the 1980 Conference most usefully integrated this incident with the results of oil company exploration along the northern Spanish coast. The continental split took place centrally in a little-disturbed shelf covered by Triassic and Jurassic rocks. The preliminary stretching associated with the development of the oceanic wedge produced tension faulting and the consequent development of trapdoor subsidence, with greatly expanded Upper Jurassic and Lower Cretaceous sedimentation in the marginal 7 km deep Spanish Trough in the south and in the shallower Armorican Trough to the north of the incipient parting. On the new evidence the split radiates not from Biarritz but 120 km further north in the Parentis basin. The Spanish Trough suffered strong compression in association with the Pyrennean orogeny (Upper Eocene) and has by some been regarded as the foredeep of a subduction zone, but if the stratigraphical datings given in this paper are confirmed the sedimentary accumulation long predated this compressional phase.

In summary, the basins on the Northwest European Continental Shelf lying north of the Hercynian orogenic belt are known in the majority of cases to have a history extending back to Carboniferous or Devonian, with the main subsidence taking place during the Permo-Triassic and Jurassic. Throughout this period the stress system seems to have been consistent and to have been relieved by tensional, often listric, faulting which may well be symptomatic of thinning of the underlying crust by a process of plastic stretching. This long taphrogenic period ended with the inception of Upper Cretaceous and Tertiary simple miogeosynclinal subsidence — a process which was however interrupted in a majority of the basins by an episode of inversion of the former downwarp. In some cases this inversion may be related to a shortlived change in shear stresses but it was apparently not limited to subsidences produced by Mesozoic faulting and is not yet fully understood. □

---

1. Woodland, A.W. (ed.) *Petroleum and the Continental Shelf of North West Europe* Vol. 1 (Applied Science, Berking, UK, 1975).
2. Illing, L.V. (ed.) *Petroleum Geology of the Continental Shelf of North-west Europe* (Heyden, London, in the press).

Special sites in genetic recombination

from John Rosamond

At the end of the 1978 Cold Spring Harbor Symposium, Frank Stahl suggested that genetic recombination was ceasing to be simply a geneticists domain, and that the time was right for a more biochemical approach. A number of people seem to have taken notice of this since considerable effort is being expended on the *in vitro* formation and analysis of intermediates in recombination. Of particular interest is the work of Stahl himself, and his collaborators at the University of Oregon, on the nature of special sites for genetic recombination. Their recent work suggests that such sites may be structurally complex (*Cell,* **19,** 785; 1980) and of fundamental importance in recombination.

Generalised recombination involves the exchange of genetic information between homologous chromosomes, and it used to be thought that the frequency with which recombination occurred was equal throughout all regions of homology. That this expectation is not always met was first shown by genetic studies of recombination in fungi[1]. The frequency of exchange was higher in some regions of homology than others, implying the presence of special sites (hotspots) in the genome which influence the frequency of recombination in that region. More recently, Stahl and his collaborators have been examining similar sites which promote recombination in bacteriophage λ. Their studies on these sites, termed Chi, not only have provided interesting information on the mechanism of genetic recombination at the molecular level, but also suggest that the involvement of special sites, such as Chi, in genetic recombination may be more widespread than was originally envisaged.

Chi sites are not present in wild-type bacteriophage λ, but are found as mutations that arise in response to selective pressure on a specific part of the λ life cycle. After infecting *Escherichia coli,* the λ genome circularises and replicates, initially by a Cairns-type 'theta' mechanism, to produce a pool of monomeric circular molecules, before

---

John Rosamond is in the Microbiology Unit, Department of Biochemistry, University of Oxford.

0028-0836/80/290202-03$01.00

switching to the 'rolling circle' mode of replication. Most progeny chromosomes are derived from the concatamers produced in this way, since the monomeric circular molecules are not a substrate for encapsidation. Transition from 'theta' to 'rolling circle' replication is facilitated by two λ genes, *red*$^+$ and *gam*$^+$; the *red*$^+$ gene product promotes replication by creating replication forks, while the *gam*$^+$ gene product inhibits a host nuclease which would otherwise prevent rolling circle replication. (This nuclease, exonuclease V, is the product of the *recB* and *recC* genes and is involved in a bacterial recombination pathway).

Consequently, when phage that are defective in these genes (λ *red gam*) are grown on *recBC*$^+$ bacteria, rolling-circle replication is prevented, and in order to organise the DNA into a form that can serve as a substrate for encapsidation, the monomer genomes must be recombined to form dimeric molecules. λ *red*$^-$ *gam*$^-$ phage do this relatively inefficiently, thereby producing small numbers of progeny phage and therefore small plaques.

In these circumstances, there are obvious advantages to be gained by increasing the efficiency with which the host recombination system is being used. Consequently, when λ *red*$^-$ *gam*$^-$ phage are repeatedly grown on a *recBC*$^+$ host, the small-plaque forming phage are eventually overgrown by mutants with a large plaque phenotype[2]. This is the Chi$^+$ phenotype, which arises after mutation in one of at least four loci dispersed throughout the λ genome. It was suggested that these mutations (χ^+) increased the yield of progeny phage by accelerating the rate limiting step in the recombination pathway being used to form the dimeric precursors of mature phage DNA; it is the nature and properties of these χ^+ mutations that Stahl and co-workers have been investigating.

The presence of a χ^+ mutation in the λ genome increases the frequency of recombination near the mutation by about 10-fold. This stimulation decreases with distance, but can still be detected up to 2×10^4 base pairs away from Chi. There are four recombination pathways open to λ, and, in principle, Chi$^+$ might have enhanced recombination mediated by any or all of these. It transpired, though, that the action of Chi$^+$ is specific to the major bacterial recombination system, the so-called *recBC* pathway, which required the product of the *recA* gene as well as those of *recB* and *recC*[3]. This discovery led to the suggestion that Chi sites occurred in the *E. coli* genome as well as in λ, and functioned in bacterial recombination. Indeed it was found that λ *red*$^-$ *gam*$^-$ which include the *E. coli bio* operon behaved as though they carried a Chi$^+$ site, since they made large plaques on *recB*$^+$ hosts[4]. This property was not peculiar to the *bio* operon though, since by cleaving *E. coli* DNA with *EcoRI* and inserting random fragments into the λ genome, Malone *et al.*[5] estimated that Chi hotspots were present naturally in the *E. coli* chromosome at a density of 1-2 per 10^4 base pairs. Similar experiments, in which *EcoRI* fragments of DNA from *Saccharomyces cerevisiae* were inserted into λ, showed that yeast DNA also carries Chi sites[6].

Meanwhile, the phenotype of the χ^+ mutations in λ had been investigated in more detail and it was found that the enhancement of recombination due to Chi$^+$ was asymmetric (*Mol. Gen. Genet.* **140**, 29; 1975). Thus, χ^+C in the λ *cII* gene stimulated recombination to a greater extent in the *J-N* region to the left of χ^+C than it did in the *P-R* region to the right, although χ^+C was closer to the *P-R* interval. This leftward bias of Chi$^+$ activity was common not only to all the Chi$^+$ sites arising by mutation in λ, but also to all the naturally occurring Chi$^+$ sites found on the *EcoRI* fragments of *E. coli* DNA[6].

Of the several possibilities for this directional bias of Chi activity, two are most likely; either Chi could itself be an asymmetric sequence, in which case the directionality of Chi$^+$ activity will be dependent on the orientation of the sequence, or else the directionality could be imposed by some aspect of phage λ biology. If the directional bias were due solely to the orientation of the Chi elements, then artificially reversing the Chi sequence should lead to a reversal of the directional bias. Experiments to test this were done by excising *chi*$^+$-carrying *EcoRI* fragments of *E. coli* DNA from λ *red*$^-$ *gam*$^-$ phage and

---

NATURE

100 years ago

A sad balloon accident has taken place at Le Mans, and may be referred to as illustrating some useful facts relating to aëronautics. A man named Petit had ascended with two balloons connected by a long rope. The smaller, which was placed above, carried his son, almost a boy; Petit being in the larger with his wife. There was not much wind, and this foolish experiment would have ended without accident if Petit had not forgotten to loosen the neck of the balloon, so that no escape was left for the gas which was gradually expanding. When the balloon arrived at an altitude of 400 to 500 metres it burst in the vicinity of the "equator," and descended with great velocity, dragging the smaller balloon. Petit, who was devoid of any scientific knowledge, supposed his son was in danger, and with true heroism he cut the rope connecting the two balloons when at 250 to 300 metres from the ground. He placed his wife on the ring and remained himself in the car. The shock was so terrible that his spinal cord was broken, and he died on the following day. His wife was very badly hurt, and though in danger, is alive. If Petit had not cut the rope by an act of unintelligent devotion he would very likely have escaped, and his son would not even have touched the ground.

Through the kindness of General Myer we have received some further details concerning the extraordinary memory credited to the man in charge of the hat room at the Fifth Avenue Hotel, New York, referred to in Nature, vol. xxi. p. 562. He is an Irish-American about thirty years of age, Gilmartin by name, and has occupied his present position about a year. His sole duty consists in looking after hats during meal hours. The fact of his possessing a remarkable memory is indisputable, but still he is not looked upon as a prodigy by the hotel officials. They state that a Tommy Hart, now dead, who figured conspicuously in the "Stoke trial," was for a long time in charge of their hat-room, and was this man's superior as regards memory, and cited other instances of men now employed in different hotels throughout the country whom they consider his equals. It is very evident, however, that he possesses a wonderful talent for selecting the right hats, and mistakes are rare with him.

An occurrence, which may be partially or wholly attributable to the earthquake which Switzerland has recently undergone, is reported by the *Times* Geneva correspondent from Quarten, in the canton of St. Gall. A short time ago the people of the neighbourhood noticed signs of uneasiness about the Schnebelberg. The summit of the mountain appeared to be in a very precarious position, and it was feared that it might slip down and overwhelm the Schnebelwald, an extensive wood in the valley below. In anticipation of a possible catastrophe, great efforts were made to cut down and carry away as many trees as possible, though the men engaged in the work wrought at the peril of their lives. On Sunday fortnight, when fortunately there was nobody in the wood, a deafening report, like the firing of heavy artillery, resounded through the valley, and the mountain was hidden from view by a thick cloud of dust. When it dispersed, the Schnebelberg was seen to be shorter by a few metres, and the beatiful wood in the Murgthal has disappeared beneath a huge avalanche of stones and earth.

News from the Azores states that a disturbance of the earth has occurred in the island of St. George, resulting in the formation of another small island of about 18,000 square yards, and distant 600 yards from the shore.

It is stated that Col. Prjevalsky and his party are prisoners in the hands of the Chinese, who, it will be remembered, prevented him from proceeding to Lhassa.

From *Nature* **22**, 15 July, 252-254, 1880.

re-inserting them in the opposite orientation[7]. After inversion, some fragments that had been Chi^{+} become Chi^{-} and some Chi^{-} became Chi^{+}, while others showed no change in their phenotype. In all cases, though, the Chi^{+} phenotype showed the original leftward bias in stimulation of recombination. Clearly, reversing the Chi element does not lead to a reversal of the directional bias, which implies that some aspect of this bias is a property of λ and not of Chi. Nonetheless, the fact that the Chi^{+} phenotype is orientation dependent suggests that the Chi sites themselves are asymmetric nucleotide sequences.

Direct proof of this has come from the work of Gerry Smith and colleagues at Oregon[8,9]. They found the nucleotide sequence around the χ^{+} mutation in λ *cII* ($\chi^{+}C$) was strikingly devoid of any unusual structural features, such as obvious symmetrical regions, though they were unable, having determined the sequence of a single χ^{+} locus, to deduce the boundaries of the Chi site.

More recently, they have sequenced a second Chi site in λ (χ^{+} *B*, lying between *xis* and *redA*); comparison of this sequence with χ^{+}C sequence reveals a surprising extent of homology[10]. Within a region of 30 base pairs, there are 23 base pairs common to both sequences. The largest uninterrupted common sequence is 9 base pairs, with another common sequence of 6 base pairs to its left. Not only is the sequence asymmetric, but it may be that the nucleotide sequence of Chi sites is hyphenated, with regions of random base sequence separating specific nucleotide sequences. Such nucleotide sequences are found at the recognition sites of the Type I restriction endonucleases, and here too the asymmetry of the recognition site is reflected in the asymmetry of the restriction enzyme activity[11]. Again, though, the extent of the common sequence essential for the Chi^{+} phenotype cannot be identified; this will require the determination of the nucleotide sequence both of other Chi sites, particularly the *chi*$^{+}$ loci that occur naturally in *E. coli*, and of *chi*$^{-}$ revertants. Given the frequency with which Chi sites occur in the *E. coli* genome, if subsequent work shows them to have a complex, hyphenated sequence, this finding would argue both for a strong selective pressure for the maintenance of these sites and for their having a fundamentally important function. At present, although we know that Chi sites in *E. coli* DNA are capable of stimulating recombination when introduced into the λ genome, evidence that these sites perform a similar function *in situ* is circumstantial, at best.

Another major consideration is the mechanism by which Chi acts and the implications of that mechanism (be it confined to λ, or of more widespread application). Since, as noted above, we know that the stimulation of recombination by Chi^{+} is specific for the so-called *recBC* pathway, the underlying assumption is that Chi^{+} is recognised by a protein, so as to accelerate a rate-limiting step in the recombination process. The *recBC* pathway requires the activity of proteins coded by the *recA*, *recB* and *recC* genes (and possibly the *lexC* gene product as well); it remains possible that other, as yet unidentified, proteins are involved. We now think that the *recA* protein is involved in one or more of the early events in recombination, and probably promotes the formation of heteroduplex molecules[12]. We are less certain when (or how) *recBC* protein acts, although there is genetic evidence to suggest that it is involved late in recombination, perhaps in the resolution of heteroduplex DNA to form recombinant molecules[13]. Since it is thought that Chi also acts late in the *recBC* pathway[13] it seems more likely that the Chi nucleotide sequence is recognised by the *recBC* gene product than by the *recA* gene product. Disappointingly, efforts to show a specific interaction between Chi^{+} sequences and the *recBC* enzyme have been unsuccessful, although the problem is complicated by the diversity of the activities and mechanisms of the *recBC* enzyme[14,15].

Nonetheless, Stahl has offered a working hypothesis to describe the mechanism of Chi-stimulated recombination in phage λ, a component of which is that Chi is a specific site for the nucleolytic activity of the *recBC* enzyme[16]. Whether this idea is correct, and what its application might be to genetic recombination in other organisms, remains to be determined. □

1. Murray, N.E. *Genetics* **48**, 1163 (1963).
2. Henderson, D. & Weil, J. *Genetics* **79**, 143 (1975).
3. Stahl, F.W. & Stahl, M.M. *Genetics* **86**, 715 (1977).
4. Malone, R.E. & Chattoraj, D.K. *Mol. Gen. Genet.* **143**, 35 (1975).
5. Malone, R.E. *et al. J. Mol. Biol.* **121**, 473 (1978).
6. Chattoraj, D.K. *et al. Cold Spring Harbor Symp. Quant. Biol.* **43**, 1063 (1978).
7. Faulds, D. *et al. J. Mol. Biol.* **131**, 681 (1979).
8. Smith, G.R. Faulds, D.H. & Sprague, K.U. *Cold Spring Harbor Symp. Quant. Biol.* **43**, 1067 (1978).
9. Sprague, K.U., Faulds, D.H. & Smith G.R. *Proc. natn. Acad. Sci. U.S.A.* **75**, 6182 (1978).
10. Smith, G.R., Schultz, D.W. & Crasemann, J.M. *Cell* **19**, 785 (1980).
11. Rosamond, J., Endlich, B. & Linn, S. *J. Mol. Biol.* **129**, 619 (1979).
12. McEntee, K., Weinstock, G.M. & Lehman, I.R. *Proc. natn. Acad. Sci. U.S.A.* **76**, 2615 (1979).
13. Birge, E.A. & Low, K.B. *J. Mol. Biol.* **83**, 447 (1974).
14. Rosamond, J., Telander, K.M. & Linn, S. *J. Biol. Chem.* **254**, 8646 (1979).
15. Telander-Muskovitch, K.M. & Linn, S. *ICN-UCLA Symposia on Molecular and Cellular Biology* **xix** in the press.
16. Stahl. F.W. *Ann. Rev. Genet.* **13**, 7 (1979).

The structure of zeolites

from L. V. C. Rees

ZEOLITES are silicates of sodium, potassium or calcium. There are two varieties of zeolites, with three dimensional cage-like lattice or open channel structure that allow zeolites to be used as 'molecular sieves'. The high-resolution electron microscope pictures of zeolites described in the previous issue of *Nature* (**286**, 111; 1980) were first revealed when a few early results were shown at two recent meetings.* The excitement they caused there undoubtedly arose from the ability of zeolite chemists to actually see the windows in the aluminosilicate crystals and not to be entirely dependent on the subjective interpretations of X-ray crystallographers.

Some of the most heated discussions took place among the small group of X-ray crystallographers who argued about the existence or otherwise of zero-coordinated cations in some zeolite structures and about the quality of the data presented by the respective X-ray groups[2]. The lack of large single crystals of zeolites was also bemoaned. It is, therefore, somewhat refreshing to actually observe the unit cells in these high-resolution microscope photographs and to find that Thomas and colleagues had to grind the 10-50 μm crystals down to smaller dimensions before they could be studied in the microscope! Not only can one now observe the apertures in these structures but we should be able to see the cations sitting in these windows when the resolution of the microscope is improved to 2.4Å and when zeolites which are known to contain cations in the apertures after dehydration are studied (for example, potassium form zeolite A).

High-resolution electron microscopy should also be of great help to zeolite chemists. Zeolites, when used as catalysts by the petroleum industry for the cracking of hydrocarbons, require to be frequently decoked at high temperatures. Much effort has gone therefore, in producing zeolites which are more thermally stable. The rates of vitrification in the electron beam described in the *Nature* paper by Bursill *et al.* should, hopefully, provide information on some of the factors which affect the thermal stability of zeolites. A method of treating zeolite Y to produce thermally, ultra-stable zeolite Y has been developed[3]. In this treatment aluminium ions are removed from the framework and deposited in the zeolite channels as hydroxoaluminium cations. Much doubt still exists as to the exact nature of these aluminium products and on the effect of the loss of the framework aluminium on

---

L. V. C. Rees is in the Department of Chemistry, Imperial College of Science and Technology, London.

*The British Zeolite Association met in Thornaby-on-Tees, 12–13 April, 1980 and the Fifth International Zeolite Meeting was held in Naples, 2-6 June, 1980.

0028-0836/80/290304-02$01.00

the crystallinity of the zeolite. High-resolution electron microscopy could possibly observe these hydroxoaluminium cations and, along with electron diffraction, the structure of the resulting framework could be ascertained.

Bifunctional zeolite catalysts are widely used for hydrogenation-dehydrogenation reactions. These catalysts contain the usual Bronsted and Lewis acid sites necessary to produce carbonium ions but also contain atomic platinum or other metallic elements in the zeolitic cavities. These metal atoms often diffuse from the cavities and aggregate on the surface of the zeolite crystals and the catalyst loses much of its effectiveness. High-resolution electron microscopy would be a useful tool to ascertain the factors affecting this aggregation process, provided the specimens display sufficient beam stability for adequate imaging to be performed.

Natural mordenites and synthetic mordenites are found to give the same X-ray diffraction patterns. From these X-ray studies the structure of mordenite has been determined. This zeolite has a main elliptical channel, running parallel with the *c* axis of dimensions 0.67 × 0.70nm. Natural mordenite, referred to as small-port mordenite, has an effective diameter of channel of ~ 0.4 nm while synthetic mordenite, called large-port mordenite has channels consistent with the proposed structure.

The absorbate molecules which can enter the natural mordenite channels are much smaller than the molecular which can be adsorbed in the synthetic mordenites. It has been suggested that a few fault planes in the natural mordenites would produce these results in this zeolite with a one-directional channel system. However doubts still remain as to the exact reason for this difference and it would be interesting to look at these two different forms using high-resolution electron microscopy.

The paper of Bursill *et al.* presents evidence of Si^{4+}/Al^{3+} ordering. This is another fascinating result of their studies. In a recent "Workshop on the Adsorption of Hydrocarbons in Zeolites" held in Berlin, Aldershaft from 19-22 November, 1979 Engelhardt *et al.* presented exciting results obtained by high resolution, magic-angle ^{29}Si n.m.r. which suggested that in a zeolite A which had an exact 1:1 ratio of Si:Al the majority of the Si ions in the framework were bonded through oxygens to three Al and one Si ions. Thus some Al-O-Al bonding must exist in this zeolite and Loewenstein's rule is not obeyed. Other confirmation of these findings can be found in the literature, for example four of the X-ray reflections in the paper by Pluth and Smith[4] do not comply with the Fm3c space-group proposed by these authors but are consistent with the Fm3 space-group which would exist if Si/Al ordering occurred in their zeolite A sample[5].

In the past many chemical analyses of zeolite A have found excess Al to be present in the material. To abide by Loewenstein's rule Barrer and Meier proposed[6] that some $NaAlO_2$ was occluded in the sodalite cages. However these new results suggest that this conclusion may not be necessary and we await further studies with great anticipation. ☐

1 Bursill, L.A., Lodge, E.A. & Thomas, J.M. *Nature* 286, 111 (1980)
2 Smith, J V. *Proceedings of the Fifth International Conference on Zeolites* 194, (ed Rees, L V C, Heyden, London 1980)
3 McDaniel C V & Maher P.K *Molecular Sieves* 186, (Society of Chemical Industry, London 1968)
4 Pluth, J.L. & Smith, J.V. *J Phys Chem* 83, 741 (1979)
5 Lodge, E.A, Bursill, L A & Thomas J M. in preparation
6 Barrer, R M & Meier, W M *Trans. Faraday Soc* 54, 1074 (1958)

Epidermal growth factor and mitogenesis

from Colin R. Hopkins

FOR exploring the interactions of hormones with their target cells epidermal growth factor (EGF) is an extraordinarily versatile probe. It can be loaded with radioactive, fluorescent, photoaffinity and even particulate labels without loosing its ability to find and follow its receptor. Because, in addition, it provokes a mitogenic response in the most widely used fibroblast cell lines EGF is currently the favourite of all labelled ligands.

The receptors for labelled EGF on cells cultured in low serum are of one class and randomly distributed[1-6]. On binding the peptide, the receptors aggregate and are then taken into the cell by endocytosis. The number and size of the receptor aggregates and the pattern of redistribution varies considerably in different systems and it is not yet clear if this is due to differences in the various kinds of EGF probe or to real differences in cell surface behaviour. Certainly the relationship between the degree of receptor occupation, the rate of receptor internalization and the strength of mitogenic stimulus is very complex. Thus, although only one class of EGF receptors appears to exist on most cells[7] several studies have shown that only a small proportion of the total population needs to be occupied for the maximum mitogenic response to be generated[8,9]. At low concentrations of peptide the rate of receptor internalization correlates well with mitogenic potency, but at higher concentrations internalization continues to increase proportionally but mitogenicity is much reduced[10].

Clathrin-coated pits, which play such a prominent role in low density lipo-protein uptake[11], play an important[3] and even exclusive[12] role in internalization of EGF in some cells whereas in others[5] uncoated pits seem to predominate. If coat components are found to play a part in either receptor attachment[14], or intracellular routing[15], then the differences may be functionally very important, perhaps relating to the selection of alternative intracellular destinations.

Ferritin-tagged EGF allows the identification of receptor complexes by electron microscopy[16]. After uptake, the complexes remain associated with the limiting membrane of the endocytosed vesicle until it becomes transformed into a multivescular body (MVB). The MVB forms when receptor-rich vesicles are pinched off from the limiting membrane of the vesicle into its internum. Within about 30 minutes the receptor-bearing vesicles disappear and the MVB transforms into a secondary lysosome containing free ferritin particles. This scheme neatly accounts for the earlier work of Das and Fox[9] who showed that the complete membrane bound EGF-receptor complex, and not just the EGF peptide, is degraded in the lysosome.

As the path of the EGF-receptor complex has been followed as far as the point of degradation, the crucial question is which step gives rise to the second messenger(s) responsible for mitogenesis. Is there a membrane based receptor-transducer mechanism acting near the beginning of the pathway, or is there a lysosomal 'activation mechanism' generating active fragments (cf Diptheria toxin[17]) acting near the end? Chemical modulations of the EGF-induced mitogenic response may help to choose between these alternatives although the most intriguing effects are induced by agents like amine compounds and colchicine, which have ill defined sites of action.

Among the more specific effects of these early stage modulators of EGF mitogenicity are those induced by phorbol esters[18,19] and glucocorticoids[20], which have been shown to alter the affinity of EGF receptors, and retinoids, which selectively increase the number of EGF

Colin R. Hopkins is Professor of Cell Biology at the University of Liverpool.

0028-0836/80/290205-02$01.00

receptors available[21]. The importance of receptor aggregation has been indicated by the finding that cyanogen bromide-treated EGF which binds, but is poorly mitogenic, can be made considerably more potent when crosslinked with EGF antibody[22]. Here, the most straightforward interpretation — that potency is related to the number of occupied receptors able to aggregate and internalize — holds.

The effects of methylamine and colchicine, both of which enhance the potency of EGF without affecting the initial EGF-receptor interaction[23,24] are open to several interpretations. Methylamine seems capable of acting at two sites at least, since it has been shown to prevent the patching of rhodamine-labelled EGF (and prevent clustering into coated pits)[25] as well as reducing the rate at which EGF is degraded[26,27]. Studies using ferritin-labelled EGF show that concentrations of methylamine (10-30mM) which prevent visible patching of the fluorescent label allow some internalization of the EGF-receptor complex to occur[16]. It cannot be concluded, therefore, that the increase in EGF mitogenicity caused by methylamine is due solely to the prevention of internalization.

Ammonium compounds and amines have been shown to reduce EGF degradation so the potentiation of the mitogenic response seen with methylamine may be partly due to its action at the lysosomal level. The possibility that this is mediated by the inhibition of lysosomal hydrolase[28] has been removed by a study[29] in which leupeptin, the specific cathepsin B inhibitor, was used to inhibit EGF breakdown. While leupeptin retarded degradation so that EGF accumulated intracellularly the mitogenic response still correlated with the concentration of peptide in the medium. The effect of methylamine must, therefore, occur before the breakdown of the EGF-receptor complex. As an effect of amines is to reduce the formation of receptor-bearing vesicles within the MVB,[16] the vesiculation of receptor-rich membrane, either at the prelysosome stage, or at the plasma membrane seems a likely site for amine action.

A general mechanism, proposed by Maxfield[25] and Davies,[30] whereby receptor aggregation induced by monovalent ligands may be inhibited by agents interfering with transglutaminase, an enzyme capable of cross-linking adjacent glutamyl and lysyl residues, may explain the effects of methylamine. Methylamine is a strong inhibitor of transglutaminase at concentrations which inhibit patching of rhodamine labelled EGF[23] and as it readily penetrates cell membranes, it may act in a similar way at intracellular sites too.

These recent studies clearly show that the intact EGF-receptor complex is responsible for transmitting the mitogenic signal. The site of transduction is unclear, but the correlation between a reduction in the rate of degradation and enhanced potency suggests that the dismantling of the EGF-receptor complex and the termination of transduction are closely linked[24].

The role of endocytosis in the processing of the EGF-receptor complex remains unsolved. For the full mitogenic potency of EGF to be expressed, there is growing evidence that the target cell must be exposed to the peptide for periods of several hours[8,10,29,33] and thus the rapid rate at which receptor complexes are dispatched from the surface is particularly difficult to understand. All options must remain open, since at the present time there is no compelling reason why internalization should be regarded as an integral part of the transduction mechanism. Indeed, the possibility that signalling by the EGF receptor complex begins with aggregation on the cell surface and then continues throughout the lifetime of the complex is clearly worthy of serious consideration. □

1. Schlessinger, T., Schechter, Y., Willingham, M.C. & Pastan, I. *Proc. natn. Acad. Sci. U.S.A.* **75**, 2659 (1978).
2. Haigler, H., Ash, J.F., Singer, S.J. & Cohen, S. *Proc. natn. Acad. Sci. U.S.A.* **75**, 3317 (1978).
3. Gorden, P., Carpentier, J., Cohen, S. & Orci, L. *Proc. natn. Acad. Sci. U.S.A.* **75**, 5025 (1978).
4. Maxfield, F.R., Schlessinger, J., Schechter, J., Pastan, I. & Willingham, M.C. *Cell* **14**, 805 (1978).
5. Haigler, H.T., McKanna, J.A. & Cohen, S. *J. Cell Biol.* **81**, 382 (1979).
6. Hopkins, C.R., Boothroyd, B. & Gregory, H. *J. Cell Biol.* **83**, 233a (1979).
7. Carpenter, G. & Cohen, S. *A. Rev. Biochem.* **10**, 194 (1979).
8. Schechter, Y., Hernaez, L. & Cuatrecasas, P. *Proc. natn. Acad. Sci. U.S.A.* **75**, 5788 (1978).
9. Das, M. & Fox, C.F. *Proc. natn. Acad. Sci. U.S.A.* **75**, 2644 (1978).
10. Fox, C.F. & Das, M. *J. supramolec. Struct.* **10**, 595 (1979).
11. Anderson, R.G.W., Brown, M.S. & Goldstein, J.L. *Cell* **10**, 351 (1977).
12. Willingham, M.C., Maxfield, F.R. & Pastan, I.H. *J. Cell Biol.* **82** 614 (1979).
13. Heuser, J. *J. Cell Biol.* **84**, 560 (1980).
14. Goldstein, J.L., Anderson, R.G.W. & Brown, M.S. *Nature* **279**, 679 (1979).
15. Rothman, J.E. & Fine, R.E. *Proc. natn. Acad. Sci. U.S.A.* **77**, 780 (1980).
16. McKanna, J.A., Haigler, H.T. & Cohen, S. *Proc. natn. Acad. Sci. U.S.A.* **76**, 5689 (1979).
17. Pappenheimer, S. & Gill, J. *Science* **182**, 353 (1973).
18. Lee, F. & Weinstein, S. *Science* **202**, 213 (1979).
19. Brown, K.D. *Biochem. biophys. Res. Commun.* **86**, 1037, (1979).
20. Baker, J.B. & Cunningham, D.D. *J. supramolec. Struct.* **9**, 69, (1978).
21. Jenten, A.M. *Nature* **284**, 626 (1980).
22. Schechter, Y., Harnaez, L., Schlessinger, J. & Cuatrecasas, P. *Nature* **278**, 835 (1979).
23. Maxfield, F.R., Davies, P.J.A., Klempner, L., Willingham, M.C. & Pastan, I. *Proc. natn. Acad. Sci. U.S.A.* **76**, 5731 (1979).
24. Brown, K.D., Friedkin, M. & Rozengurt, E. *Proc. natn. Acad. Sci. U.S.A.* **77**, 480 (1980).
25. Maxfield, F.R., Willingham, M.C., Davies, P.J.A. & Pastan I. *Nature* **277**, 661 (1979).
26. Carpenter, G. & Cohen, S. *J. Cell Biol.* **71**, 159 (1976).
27. Brown, K.D. *Cell Biol. Int. Rep.* in the press.
28. Ohkuma, R. & Poole B. *Proc. natn. Acad. Sci. U.S.A.* **75**, 3327 (1978).
29. Savion, N., Vlodavsky, I. & Gospodarowicz, D. *Proc. natn. Acad. Sci. U.S.A.* **77**, 1466 (1980).
30. Davies, P.J.A., Davies, D.R., Levitzki, A., Maxfield, F.R., Milhaud, P., Willingham, M.C. & Pastan, I.H. *Nature* **283**, 162 (1980).
31. Ostlund, R.E., Pfleger B & Shonfeld, G., *J. clin. Invest.* **63**, 75 (1979).
32. Carpenter, G. & Cohen, S. *J. Cell Physiol.* **88**, 227 (1976).

The fenlands

from Peter Moore

THE fenlands of East Anglia have long provided a source of energy, in the form of peat, and a rich agricultural resource for the inhabitants of the area. Darby (*Medieval Fenland,* Cambridge University Press; 1940) collated much information concerning the exploitation of these lands and shows that as early as the 13th century peat was being cut for fuel in the fens. Drainage of the fens for agricultural development first became extensive in the 17th century, but it was not until the mid 19th century that the immense engineering problems involved in drainage were efficiently tackled. The installation of pumping machinery at that time led to permanent lowering of water tables and the full agricultural potential of the fens could be realized.

One consequence of drainage, which is evident even by casual observation, is the lowering of the land surface which has resulted from 'peat wastage'. Much of fenland now lies between -1.5 and -2.5m below Ordnance Datum, which means that the maintenance of low water tables in the soils requires the pumping of water into elevated drainage channels and rivers on its way to the sea. Despite the obvious nature of this development, however, there are no precise records of the rate of fall in the land surface, nor of the influence of various land use practices upon this rate.

The process of peat wastage has resulted from the gradual oxidation of surface layers as microbial activity has been stimulated by the lowering of soil water tables and the consequent removal of anoxic conditions. In addition, the peat has contracted in its structure as a result of drying and some has been lost by wind erosion, combustion and removal by man. Land use practices will have played an important part in influencing the rate of these processes.

Around 1848 (the precise date not certain) a cast iron post was sunk through the peat and embedded on wooden piles in the underlying clay at Holme Fen, 10 km south of Peterborough, and the history of this post has been the subject of research by Hutchinson (*J. Ecol.* **68**, 229; 1980), himself a civil engineer. When first established, the top of the post was flush with the peat surface and since that time many scattered observations and measurements have been conducted upon its progressive protrusion as the land surface fell. Hutchinson has collated these data and related them to records of the installation of new pumping machinery at various times and to variations in land use in the area.

The first drainage resulted from the

Peter Moore is in the Department of Botany, King's College, London.

0028-0836/80/290206-02$01.00

construction of a channel in 1850. Within eight years, this gravity drainage system had produced a fall in the peat surface of almost 2m. A suction pump was then added, resulting in a further 0.7m fall over the next 20 years. This pumping was accompanied by the development of arable agriculture, which may have accelerated the surface lowering. A second pump, introduced in 1877 resulted in another rapid fall of a further 0.5m over the next ten years.

Agricultural depression then led to the abandonment of cereal growing over the site and the area was left as rough grazing and scrub game cover. No further lowering appears to have taken place until a further pump was introduced in 1920, but by this time a birch woodland had developed and, despite yet another pump being added in 1962, the total surface fall over the past century has been only about 0.7m.

The overall conclusions, therefore, are that the greater part of the fall in surface level occurred immediately after the introduction of drainage and can be accounted for simply on the basis of peat contraction as it dried, rather than by any loss of organic material. In the later stages of drainage, however, lowering was more gradual and was less closely related to improved drainage; here oxidation may have begun to assume the major role.

Of particular interest is the relationship between land use and shrinkage under constant drainage processes. The replacement of arable by pastoral farming resulted in a considerable deceleration of wastage. On the basis of this observation, Hutchinson questions the wisdom of the current emphasis upon arable farming in the fenlands. The conservation of these organic soils could, he claims, be more effectively achieved by keeping water extraction to the minimum acceptable level and by changing the agricultural emphasis to pasture. □

Cometary science

from M.K. Wallis

OBSERVATIONS of comets in the ultraviolet spectral region show great promise because most major components of the cometary coma (atmosphere) can be covered, instead of only dust and minor radicals such as CN and C_2.

Early in 1970, the first UV observations revealed huge atomic hydrogen comas, 15×10^6 km diameter in comet Bennett, fluorescing in H Lyα (1,216 Å). During the same period, observations at 1,304 Å and 3,085 Å showed that comas of atomic oxygen and the hydroxyl radical, though less extensive, were of comparable density. The relative proportions suggested H_2O as the unobserved parent molecule — and was seen as confirming the Whipple hypothesis of comets being 'dirty' ice conglomerates.

Comet Bradfield discovered last Christmas day, just after perihelion at 0.7 AU, is favourably placed for observation from the International Ultraviolet Explorer (IUE) satellite: Feldman *et al.* (*Nature* **286**, 132; 1980) have reported the first of a very promising series of results. Optically the comet appears small and unexciting, containing little dust and hardly a trace of an ion tail. But in the UV, it is remarkably similar to the two others, Comets West and Seargent, observed in this range (1,200–3,200 A) where H, O, CO, C, S, CS, OH, CO^+, CO_2^+ are identified. A high resolution scan of the OH (O, O) band is shown, the relative intensities of the components implying that the excitation is simply resonant fluorescent. Doubtless, a future detailed study will reveal some departure from purely resonant equilibrium, due to collisional disturbances of the populations as discovered in pioneering Liège studies of CN and CH bands (reviewed by Arpigny in *The Study of Comets NASA SP*-**393**, 797; 1976). Such investigations are delicate, requiring allowance for doppler shifts across a solar spectrum of high resolution. But with appropriate modelling they can give parameters hardly accessible except by a cometary space-probe, namely, the OH expansion velocity and density temperature of the colliding agents (H and e).

For inferring the rate of sublimation of H_2O from Comet Bradfield, there are some uncertainties, particularly those due to the expansion velocities of different components. Past authors have assumed different values and generally normalized on H rather than OH (Keller & Lillie, *Astr. Astrophys.* **62**, 143, 1978). After adjustment, the result for the new comet comes surprisingly similar to previous comets — less H_2O by a factor of 2-4, and only three times less than Comet Tago-Sato-Kosaka, a much more active and typically impressive comet. Given that outgassing from a single icy nucleus should vary as the surface area, it's rather suspicious that now five comets, adjusted to the same heliocentric distance, should have such similar rates of loss of H_2O.

The velocity of expansion of the inferred H_2O is unknown but taken by Feldman *et al.* as 0.5 or 1.0 km s^{-1}. Though uncertain, it's clear the velocity is well above the 0.25 km s^{-1} corresponding to ice subliming into vacuum at about 200 K. Arpigny's spectroscopic studies of CH confirm enhanced velocities (0.7-1.3 km s^{-1}) and also show that the temperature of the colliding agent is several hundred K. Clearly, cometary comas do not expand adiabatically into space, but are heated probably by the kinetic energy of fragments from chemical dissociation, such as photo-dissociation of H_2O releasing 2 eV per molecule (Shul'man *Dinamika kometnikh atmosfer* § 3.3; Kiev, 1972; Wallis, *Mon. Not. R. astr. Soc.* **166**, 181; 1974). This heat source more than compensates for adiabatic cooling and energy loss through rotational excitations of H_2O and other molecules in the bulk of the coma (Shimizu *Astrophys. Space Sci.* **40**, 149; 1976). The chemical energy would go primarily to H-atoms, being the light dissociation fragment. Its transfer to the heavier molecules, such as OH and H_2O is effected through collisions. Larger comets with larger collisional zones would have higher expansion velocities — if allowed for, this effect would increase the surprisingly narrow spread in derived outgassing rates.

Because the apertures of the IUE spectrographs were relatively small ($4.5\times9\times10^3$ km at the comet), the variation in intensity of the intense (O, O) band of OH out through the coma could be followed. Assuming velocities and transformation rates for the parent H_2O and the OH then allows deduction of the absolute production rates. For simplicity Feldman *et al.* use the Haser-Mokhnach model describing the transformation under steady radial expansion, but take the OH to have the 1.15 km s^{-1} velocity from photo-dissociation which should of course be isotropic in the local expansion frame. At large radial distances this simplification is acceptable (Wallis in *Cometary Missions* Remeis-Sternwarte Bamberg **12** (132), 97; 1979) but its use in the region of OH production ($3\text{–}10\times10^4$ km) means the result is rather uncertain. Unfortunately, as the H Lyα coma is optically thick in the central region, no comparable rate from the H production is derived. The only comet for which simultaneous H and OH results are available over an extended period is Comet Tago-Sato-Kosaka (Keller and Lillie *Astr. Astrophys.* **62**, 143, 1978). The aperture used there was much larger (2×10^5 km at the comet) and the 26 observations show two notable characteristics: the deived OH production dropped twice as fast as H during the first three days (comet moving from 0.78–0.84 AU) and the ratio of OH:H production over most of the observation period was 0.3 rather than the 0.5 expected if H_2O was dominant. As the authors commented, the uncertainty of the ratio is large, so future comparative results from Comet Bradfield will be of great interest.

M. K. Wallis is in the Department of Applied Mathematics and Astronomy, University College, Cardiff.

0028-0836/80/290207-02$01.00

Delsemme and Combi (*Astrophys. J.* **228**, 330, 1979) also suggested recently on the basis of their comet Bennett optical observations of the 'forbidden' oxygen transition [O I] 6,300 Å, that most of it cannot arise from H_2O or OH — perhaps photodissociating CO_2 produces the excited atoms O(^{1}D), but dissociative recombination of CO^+ could be an alternative source. However, CO^+ is found to be very weak in comet Bradfield's UV and optical spectra. Comet Bradfield's 'trans-auroral' line [O I] 2,972 Å detected by IUE is tentatively attributed to photodissociation of H_2O, but CO_2 or OH are more plausible; alternatively dissociative recombinations of CO_2^+ or OH^+ are energetically capable of giving the O(^{1}S).

Some years ago Vanysek and Wickramasinghe (*Astrophys. Space Sci.* **33**, L19; 1975) proposed that cometary particulates could be H_2CO polymers, this being more plausible on abundance grounds than the commonly assumed silicate grains. For interstellar grains, it seems now to be clear from the $3\mu m$ absorption feature that there can only be a small proportion of H_2O-ice, while general abundance arguments imply an organic composition (Whittet *Nature* **281**, 708; 1979; Hoyle & Wickramasinghe *Astrophys. Space Sci.* **69**, 511; 1980). So cometary scientists need to consider more carefully whether H_2O-ice really does constitute a major fraction of comet nuclei — the continuing IUE observations of Comet Bradfield could lead to a resolution of this fundamental issue. □

Natural Killer cells

from Rod Langman

NATURAL KILLER cells *in vitro* and *in vivo* was the theme of an Armand Hammer Cancer Workshop held at The Salk Institute, April 7-11, 1980. The three key questions that emerged from the discussions were, 1) Do NK cells show target specificity in killing? 2) Do NK cells operate as a tumour surveillance mechanism *in vivo*? 3) Have NK cells any other *in vivo* function?

NK activity can be specified by its lack of MHC restriction (which distinguishes it from T-cell killing) and the failure of anti-immunoglobulin reagents to inhibit it (which distinguishes it from ADCC or K-cell activity). Although it was thought that NK activity was tumour cell specific, there are now many exceptions to this generalization. It is now clear that there is some degree of specificity for particular cell lines or cell types, but it is not clear whether this is due to a difference in the target cells' ability to respond to NK lytic signals, or to a failure of the NK cells' ability to recognize the target, there being evidence for both possibilities.

The most convincing case of NK recognition specificity came from the cloned lines of NK cells described by Harvey Cantor (Sidney Faber Cancer Centre, Boston) which specifically kill target cells bearing a gp70 dependent determinant. Target cells not lysed by one NK clone could be rendered susceptible to lysis by infection with Moloney virus and killing by this NK clone could be inhibited by partially purified Moloney virus proteins. NK clones, which carry the Thy 1 and Lyt 5 markers, were derived from normal spleen after removal of Lyt 1$^+$ and Lyt 2$^+$ cells, and cloned in 'T-cell growth factor' medium. There were reports by Ron Herberman (NIH, Bethesda), Rolf Kiessling (Karolinska Institute, Stockholm), Hans Wigzell (Upsalla), and Noel Warner (University of New Mexico, Albuquerque) all showing that NK cells from different sources gave unique patterns of NK lysis on panels of target cells.

The Lyt-5 marker has proved valuable in Cantor's hands for dissecting the regulatory activity of interferon on NK cells. A selected Lyt-5$^-$, NK$^-$ cell population upon incubation with interferon gains the Lyt-5$^+$, NK$^+$ phenotype, and at the same time itself begins to release interferon thus providing a positive feedback control loop. The rapid growth of interest in the anti-tumour effect of interferon means that this kind of control will attract increasing attention.

The question of specificity as a function of the ability of target cells to resist NK lytic signals was raised when John Collins (Salk Institute, La Jolla) reported that NK resistant fibroblast cell lines could be rendered NK sensitive by the addition of cycloheximide before or during the NK assay. There was some discussion whether cycloheximide inhibited a 'repair' process operating in target cells, or an interferon induced protection of NK lysis. While neither explanation was entirely satisfying, there is little doubt that target cells vary drastically in their sensitivity to NK lysis.

John Collins also reported that NK activity might be relevant to tumour surveillance *in vivo*. Starting with fibroblast cell lines that had been transformed *in vitro* and found to be tumourigenic only in immune-deprived (thymectomised, irradiated, foetal liver restored) mice, he found that these lines were also NK sensitive. However, after passage through the immune deprived mice, the cell lines were tumourigenic in normal mice, and these tumours were now NK resistant. The immune deprived mice are deficient in NK activity at the time of tumour inoculation, but by 2-3 months these mice have half-normal levels of NK. The inability of these *in vitro* derived cell lines to grow as tumours in normal mice is closely correlated with acquired NK resistance. Reconstitution experiments in this system are in progress and may provide the best evidence to date that NK activity is indeed relevant to early surveillance against incipient tumours *in vivo*.

There were indications that NK activity might be involved in normal lymphopoiesis. Ross Basch (New York) presented preliminary evidence that the subpopulation of thymocytes killed by NK includes the large subcapsular cells which can 'home' back to the thymus in cell-transfer experiments. Rolf Keissling then emphasized the remarkable similarity between NK cells and those that cause hybrid-histoincompatibility (in some F$_1$ hybrid combinations, there is a failure of haematopoietic stem cells from one of the parental strains to repopulate irradiated F$_1$ recipients). Not only were the H-2D linked genetic controls and inhibitors of NK activity and hybrid-histoincompatibility essentially the same, but up to 20% of normal bone marrow cells can be killed by NK, although no data were available as to which bone marrow cells were killed. Jonathan Sprent (Philadelphia University) noted that in similar F$_1$ hybrid combinations, mature parental T and B cells fail to recirculate or function. These results, taken together, suggest the NK activity may in normal *in vivo* conditions play some part in regulating lymphopoiesis.

Throughout the meeting, it was difficult to avoid the impression that NK and killer T-cells were in some way related. Since NK lysis can be a property of both the killer and the target, there is a resemblance between restricted T-cell killing and NK. Consider in the case of NK activity a cell-surface marker protein that is essentially constant from species to species and is subject to modifications due to viral infection, or even transformation, of the cell. If the NK system had a small repertoire of receptors capable of recognizing modifications of the marker protein, it might represent a surveillance system, albeit rather unspecific and inefficient. One therefore wonders if the NK system is a relic which recalls a stage in the evolution of contemporary killer T-cells. In an immunodeficient animal such as the athymic Nude, this relic could still provide valuable protection in the absence of a fully functional T-cell immune system. □

Rod Langman is Assistant Research Professor in the Developmental Biology Laboratory, The Salk Institute, La Jolla, California.

0028-0836/80/290208-01$01.00

Mid-Atlantic Ridge: zero-age geochemical variations between Azores and 22°N

H. Bougault*

Chief Scientist of the MAPCO Cruise, Centre Océanologique de Bretagne—BP 337, 29273 Brest, France

M. Treuil

Chief Scientist of the Project, Laboratoire de Géochimie Comparée et Systématique, 4, Place Jussieu, Tour 24/25 E3-75230 Paris, France

The MAPCO cruise of the RV J. Charcot sampled zero-age basalts along the Mid-Atlantic Ridge from the Azores Triple Junction to 24°N. Preliminary shipboard geochemical analyses together with earlier data show that some trace elements are not randomly distributed along the ridge. The latitude of the Hayes transform delineate two regions of rare earth element distribution: north from Hayes, is flat to light rare earth (or equivalent) enriched; south from Hayes, is light rare earth (or equivalent) depleted. These findings indicate large scale heterogeneity of the upper mantle.

THE IPOD program (International Phase for Ocean Drilling) has obtained many samples of igneous rocks from the ocean floor during the past five years. The studies related to this sampling and to samples collected by the more classical dredging method have provided many data which have been interpreted and discussed in terms of the fundamental processes of basalt genesis and the composition of the upper mantle. Some of these compositions are impossible to relate to one another by conventional magmatic processes of fractional crystallization, accumulation of crystalline phases and partial melting. In addition to these conventional processes, two main hypotheses have been proposed to account for the chemical heterogeneities in oceanic basalts that are observed at different scales. One of these hypotheses invokes magma mixing in one form or another; the second hypothesis assumes primitive heterogeneity of different source regions in the upper mantle. One interpretation does not preclude the other. Mixing, either of more or less fractionated liquids derived from the same source[1–3] or of liquids derived from different sources[4,5], is necessarily restricted to local areas. The mantle heterogeneity concept can also be considered as a large-scale (regional) property[6–9]. The research reported here is an attempt to examine regional heterogeneities along a portion of the Mid-Atlantic Ridge.

Area and techniques of analysis

The RV J. Charcot is equipped with a multi narrow-beam echo-sounding system (SEABEAM)[10] which produces a real-time bathymetric map of the sea floor. The system scans an area whose width, normal to the ship's track, is two-thirds of the depth. Because it allows the immediate observation of large scale structures and of fine scale features (20-m contour interval), the SEABEAM system permits relatively easy recognition of the rift valley and fracture zones (large-scale structures) and choice of a dredge site based on observation of fine scale features (such as, central high, volcano, steep slope). The objective of our analysis was to locate the inner floor of the central valley to dredge 'zero age' basalts. The rift valley area chosen for dredging was first surveyed by a track, approximately perpendicular to the ridge axis, roughly 30 miles long (15 miles to either side of the axis). This track was enhanced by a return profile located ~1.5–3 miles to the north or south of the initial crossing. In addition to providing information for dredging, each of these tracks constitutes data for structural interpretation. Dredge surveys and intermediate transits allowed us to obtain 54 transects of the ridge between 35°N and 24°N. Five profiles were made over each of three major transforms, Oceanographer, Hayes and Atlantis.

During this cruise, a new deredging system, 'active weight', was tried and used successfully. It is a percussion system: when the tension of the cable at the level of active weight, which is situated in front of the dredge, is approximately 3 tons, an impulse of 25 tons is communicated to the dredge. The system can act repeatedly at the bottom as it is reset by a return spring when no tension exists between the active weight and the dredge. Ten dredges along the ridge axis, with tracks of 0.5–1.5 miles, were attempted with this system and each dredge was half full to full of rocks. With this dredging method and with simultaneous use of SEABEAM, well positioned dredges can apparently be achieved with a minimum length of the dredge track, probably less than 0.5 miles.

Table 1 Different characteristics between the FAMOUS area (36°N) and sites 395, 396 (22°N). /Ch for Ta/La and Hf/La means normalized ratios*

	$\frac{\text{Ta/La}}{\text{ch}}$	$\frac{\text{Hf/La}}{\text{ch}}$	$^{206}Pb/^{204}Pb$	$^{87}Sr/^{86}Sr$	ΔNd
22°N					
(leg 45, 46)	0.56	2. – 2.6	18.0	0.7025	+13
FAMOUS	1.09	0.77 – 1.4	18.8	0.7028	+10

*Refs 20, 21.

---

*The members of the MAPCO (part 1 and 2) scientific team were: J. Y. Bervas, P. Beuzart, P. Cambon, M. El Azzouzi, G. Floch; J. Guichardot-Wirrmann, S. Monti, J. L. Olivet (Centre Océanologique de Bretagne), J. Durand, S. Savary (IPG St-Maur), C. Bassoulet, P. Tarits (IPG Paris), J. Argyriadis (Orsay), J. P. Eissen (Strasbourg), A. Y. Le Dain (Montpellier), A. Gourgaud (Clermont Ferrand), P. Fetter (Tunis), J. L. Joron, G. Meyer (Lab. P. Sue, CNRS), J. Stroup (Albany, US), A. Graham (British Museum (Natural History) London, UK) & D. Wood (Birmingham, UK).

0028-0836/80/290209-04$01.00

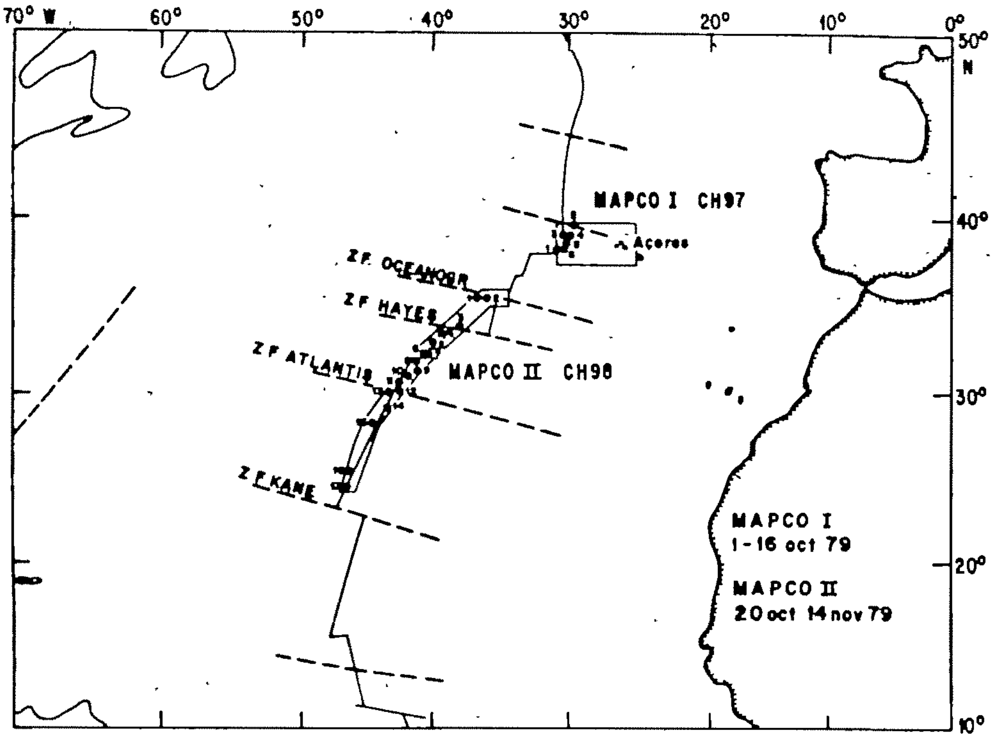

Fig. 1 Map of the studied area. Dots represent dredge sites

Thin sections were made on board and an X-ray fluorescence unit, similar to the unit used on board the Glomar Challenger[11,12], allowed us to obtain selected trace element and major element data. The precision of the data is comparable to that of an onland laboratory: ±1% (relative) for major elements and ±2 p.p.m. (absolute) for trace elements.

The primary objective of the first part of MAPCO (CH 97) was the structural analysis of the Azores Triple Junction between 39°N and 37°N (reported elsewhere); the primary objective of the second part of MAPCO (CH 98) and the secondary objective of MAPCO (CH 97) was to sample zero age basalts from the axis of the Mid-Atlantic Ridge The secondary objective of MAPCO (CH 98) was to collect bottom topographic profiles, with emphasis on examining the progressive increase in average depth of the rift valley floor from North to South along the ridge.

Results and discussion

Six dredges were attempted proximal to the Azores Triple Junction during MAPCO (CH 97) and four of these were successful, 17 dredges were conducted as close as possible to zero age during MAPCO (CH 98) and 16 were successful (Fig. 1). The morphologic nature of basalt samples recovered during both parts of the cruise is varied. Two-thirds of the total recovered material is comprised of pillow basalt; one-quarter is comprised of segments of glassy crust varying from 1 to 10 cm in thickness and up to 40 cm in length. The remainder of the material is comprised of small broken fragments. Most of the samples are remarkably fresh and have clean vitreous surfaces. The pillow basalts exhibit characteristic radial fracturing, glassy margins, and have very well preserved extrusive forms of lava fingers or tubes up to 15 cm long. The basalt crusts or sheets are glassy on both sides; the presumed upper portion of these crusts has a ropy appearance and the glass is occasionally oxidized and veneered by sediment, while the lower surface contains portions of thin vertical walls of large cavities (up to 20 cm diameter) and/or frozen droplets of basalt. In dredges CH 98 11 and 12 we recovered massive glass blocks up to 15 cm diameter, glass shards, and thin flat sheets (1 cm thick) of glass. The crusts or sheets are interpreted to be either fragments of large pillows or tubes that were rapidly emptied, or fragments of surfaces of lava lakes[13]. In addition to these basalt samples, scoriaceous basalts of probable subaerial origin were dredged at 900 m depth in the Azores Triple Junction area (CH 97 DR 05). One fragment of granitic metamorphic rock (garnet, cordierite) and a large number of blocks of sediment were recovered in dredge CH 98 DR 06 situated roughly 10 miles west of the rift valley axis.

Most of the basalt samples (two-thirds) are aphyric to subaphyric (phenocrysts <5%) Nearly all of these basalt fragments contain a few rounded plagioclase phenocrysts, possibly better referred to as xenocrysts, and one or two samples also contain rounded olivine phenocrysts. Microphenocrysts of euhedral olivine, quench olivine and plagioclase are all common. The remainder of the samples are porphyritic basalts (5–30% megacrysts, phenocrysts and/or microphenocrysts). Plagioclase is by far the dominant phenocryst phase; crystals are as large as 1 cm in length and are often rounded and partially reversely zoned. Some are better characterized as glomerocrysts. Most contain inclusions of glass or microcrystalline material. Olivine is a common, though usually minor, phenocryst phase. It is occasionally seen as rounded crystals up to 0.5 mm across but is generally subhedral to anhedral and fresh. Olivine contains rare small red-brown spinel. Clinopyroxene is observed infrequently as a phenocryst phase in these basalts, but is spectacularly present in dredge CH 97 DR 05 (in the Azores Triple Junction area) where it forms 15% of the rock

Extensive geochemical data from the northern region (Azores Triple Junction and FAMOUS area) and the southern

Table 2 Duplicate analyses of three samples of CH 97 DR 02—Sr, measured from the same pellet preparations as for Nb, Zr and Y determinations, has been used to improve the classification of rock types within one dredge, because of its relative higher precision, Ti was measured from a glass disk preparation

	Sr	Nb	Zr	Ti	Y
101 a	138.0	14.1	75	7,020	26
101 b	136.4	13.6	78		
202 B a	141.6	13.1	76	6,900	26
202 B b	141.1	13.7	74		26
304 a	150.0	15.1	71	6,720	24
304 b	149.3	13.1	74		24

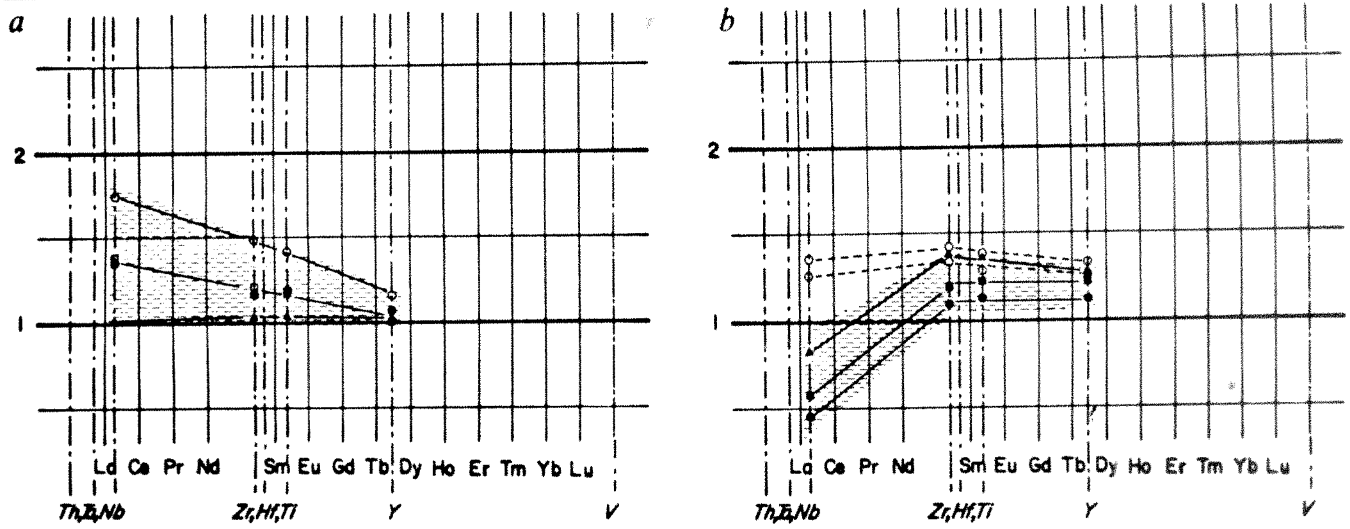

Fig. 2 Examples of extended rare earth diagrams including non rare earth hygromagmaphile elements. *a*, The spectrum observed in the Azores Triple Junction–FAMOUS area (data from refs 14, 16, 17, 23, 25); *b*, 22°N (data from refs 18, 19, 23). The preferred normalizing abundances corresponding to non rare earth elements are, in p.p.m.; Th, 0.028; Nb, 0.53; Ta, 0.031; Zr, 5.13; Hf, 0.128; Ti, 460; Y, 2.16; V, 22. In *a*, flat to light rare earth patterns, Nb, Ta and La plot at the same ordinate position (normalized Ta/La or Nb/La ratios are ≃1.09); *b*, light rare earth depleted patterns, Nb and Ta plot at a lower ordinate position than La (normalized Ta/La ratio is ≃0.5) see text.

region (22°N) have been interpreted as suggesting that there are significant differences in the isotopic compositions and trace element chemistry of the upper mantle sources between these two areas[14–20]. Table 1 summarizes these data for the FAMOUS area and 22°N (ref. 21). Clearly from our present knowledge only isotopic data obtained from basalts can be interpreted unambiguously in terms of mantle sources. Hygromagmaphile element ratios such as Hf/La (similar to Zr/La or Sm/La) in basalts depend on both mantle source and partial melting. The two different ranges of Hf/La in the FAMOUS area and at 22°N are interpretable in terms of different mantle sources (one for each region) in agreement with the isotopic data. The range of this ratio in each area is probably due to different extents or ways of melting[22,23]. As the main target of the MAPCO cruise is the examination of regional heterogeneities along a portion of the Mid-Atlantic Ridge, namely the transition between the Azores Triple Junction–FAMOUS area and 22°N, selected hygromagmaphile elements or their ratios can help, at least in part, to describe these heterogeneities or this transition.

It has been shown for some samples that elements whose ions present a rare gas electronic structure can be included in the rare earth Coryell–Masuda plot[24,25]; a comparative geochemical study of more than 300 oceanic basalts showing different rare earth patterns gave precise normalization values and relative behaviour of non rare earth hygromagmaphile elements compared with rare earth elements[26]. Figure 2 presents such a diagram for samples from the Azores Triple Junction–FAMOUS region and from 22°N (refs 14–19, 23, 25).

In the northern region the extended rare earth patterns are from flat to light rare earth enriched (Azores Triple Junction, FAMOUS, Sites 411, 412, 413 and 332, 334, 335 of DSDP);

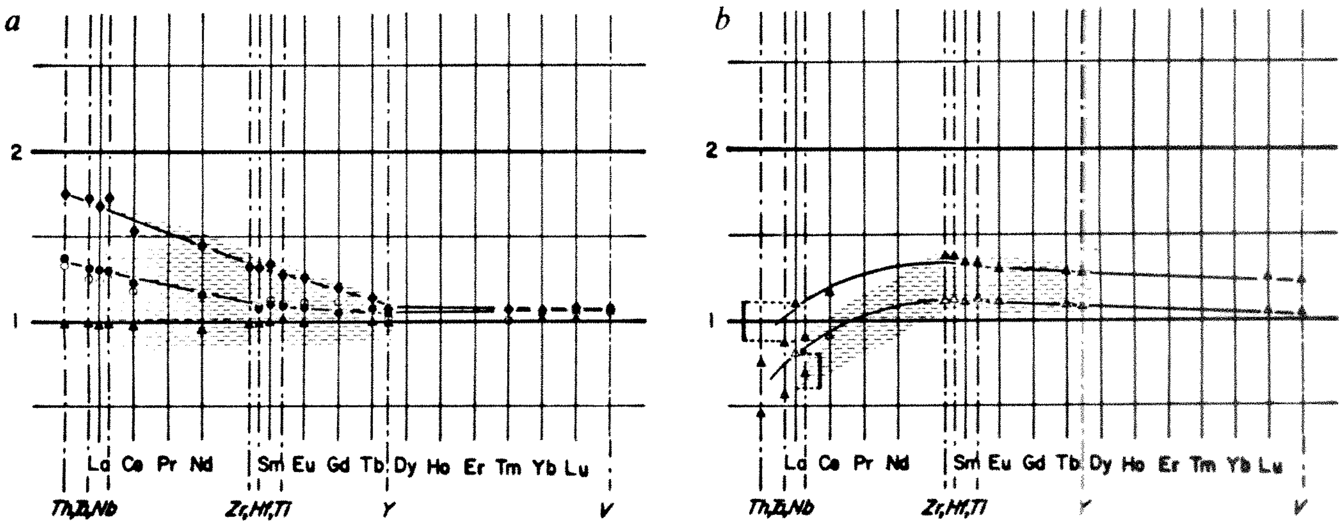

Fig. 3 *a*, Spectrum of non rare earth normalized patterns observed north from the Hayes transform. The end members of this spectrum are CH 97 DR 03 101, 39°N in the Triple Junction (○) and CH 98 DR 03 201, 33°N immediately north from Hayes fracture zone (FZ) (▲). The □, CH 97 DR 05 3.. at 38°N, ● CH 98 DR 02 1.. at 35°N (immediately south from Oceanographer FZ) have been chosen as examples showing similar distributions at different latitudes in this area. *b*, Spectrum of non rare earth normalized patterns observed south from Hayes transform. The plotted samples selected for examples are CH 98 DR 04, 33°N immediately south from Hayes FZ (●), CH 98 DR 07, 32°N (■) and CH 98 DR 17 301, 24°N (▲). The two exceptions (○) correspond to two groups in dredge CH 98 DR 08 at 31°N.

Table 3 Sr, Nb, Zr, Ti and Y data obtained on board; the figure in parentheses corresponds to the number of analysed samples

	Sr	Nb	Zr	Ti	Y
CH 97					
DR 02 See Table 1					
DR 03 39°06′N 29°54′W					
101 (1)	365	29	160	12,060	32
DR 05 38°42′N 29°57′W					
1.. (3)	397	28	155	11,460	27
2.. (4)	241	16	104	8,100	26
3.. (6)	192	13	86	6,840	21
DR 06 38°31′N 30°18′W					
1.. (6)	260	31	135	11,100	32
CH 98					
DR 02 35°11′N 36°14′W					
1.. (2)	155	12	75	7,400	26
201 (1)	110	8.5	74	8,220	33
DR 03 33°44′N 37°40′W					
1.. (2)	95	6	46	4,770	23
201 (1)	102	5	57	5,220	24
4.. (2)	92	6	61	5,850	25
DR 04 33°30′N 39°05′W					
1.. 2.. (4)	99	1.5	63	6,240	28
DR 05 33°02′N 39°20′W					
101 (1)	93	2	86	8,100	35
DR 06 32°17′N 40°21′W					
101 (1)	87	2	91	8,880	37
DR 07 32°17′N 40°11′W					
1.. (4)	93	2	80	8,000	34
DR 08 31°54′N 40°58′W					
1.. 501 (3)	133	12	134	10,260	45
102 (1)	111	9.5	111	8,580	38
2.. (2)	81	2	90	8,340	38
DR 09 31°28′N 40°57′W					
101, 301 (2)	91	2	87	8,460	36
201 (1)	89	1	69	6,780	30
DR 10 31°04′N 41°25′W					
101 (1)	110	3.5	113	10,080	42
2.. (2)	101	1.5	77	7,620	32
3.. (2)	75	1.5	71	6,960	31
DR 11 30°41′N 41°49′W					
1.., 3.., 4.. (7)	92	1.5	92	8,650	36
DR 12 30°10′N 41°55′W					
103, 204 (2)	92	2.5	103	9,600	41
DR 13 29°56′N 42°46′W					
204 et 301 (2)	122	3	105	8,940	36
DR 14 29°17′N 43°05′W					
101, 304 (2)	105	1.5	85	7,750	32
103, 201, 301 (3)	110	2.5	93	8,750	35
DR 15 27°46′N 44°05′W					
102, 301 (2)	113	1.5	95	8,190	32
2.. (2)	113	2.5	52	5,220	23
DR 16 25°16′N 45°20′W					
1.. (2)	128	3.0	100	8,300	33
201 (2)	119	3.5	112	9,360	39
202 (1)	124	5	92	7,320	30
DR 17 24°28′N 46°15′W					
101 (1)	148	3.8	121	9,300	35
201 (1)	167	2.6	99	7,260	31
301 (1)	136	3.5	125	10,260	38
401 (1)	138	3.0	110	9,000	34
Preferred chondrite abundance		0.53	5.13	460	2.16

the normalized Ta/La or Nb/La ratio ($\simeq 1$) is independant of the light rare earth enrichment (as well as for 45°N, site 410, and Reykjanes sites 407, 408 and 409). In the southern region (22°N) the extended rare earth patterns are systematically light rare earth depleted; the normalized Ta/La or Nb/La ratio is 0.5. Knowing this behaviour of hygromagmaphile elements, rare earths and non rare earths, it is possible to use Nb, Zr, Ti and Y concentrations measured through X-ray fluorescence on board to obtain chondrite normalized diagrams equivalent to a rare earth diagram. The data may be interpreted in terms of mantle heterogeneity if these diagrams show sufficiently large differences as we know that a range of Sm/La or Zr/Nb ratios can be observed within a restricted area (FAMOUS and site 411, 412, 413 of DSDP).

Table 2 shows duplicate analyses of samples CH 97 DR 02 used to test the accuracy of measurements on board. Table 3 shows from north to south the results obtained during the cruise. Examination of these data indicates that the distribution of these elements is not random along the axis of the Mid-Atlantic Ridge as mentioned for rare earths by White and Schilling[27]. Nb concentrations, the most hygromagmaphile element investigated, clearly show lower values in the southern region than in the northern region. The range of variation of (Nb, Zr, Ti, Y) chondrite normalized patterns are shown in Fig. 3. North from the Hayes transform these patterns are flat to Nb enriched (equivalent to light rare earth enriched); south from the Hayes transform they are Nb depleted (equivalent to light rare earth depleted); one exception in the southern region is observed in CH 98 DR 08 where two groups of samples show flat or only slightly Nb depleted patterns.

The large difference of the chondrite normalized plots of Nb, Zr, Ti and Y (equivalent to rare earth plots) between north and south from Hayes transform allow us to interpret these preliminary results in terms of regional mantle heterogeneity. The suggested limit (latitude of the Hayes transform) will have to be confirmed by isotopic data. It will be also interesting to study the Ta/La ratio between the Hayes transform and 22°N to confirm whether or not the single normalized Ta/La ratio found so far ($\simeq 0.5$) for light rare earth depleted material comparatively to the single value ($\simeq 1$) observed for flat to light rare earth enriched materials.

The MAPCO cruise was supported by the Groupe Croute Océanique du Comité IPOD—France, the CNRS and CNEXO. We thank J. Bonnin for help in formulating this program and D. Needham for assistance with the cruise plan. The active weight system used during the cruise was developed by J. P. Allenou with the support of J. Y. Bervas. We also thank the Captain, the officers and the crew of the RV J. Charcot. Contribution no. 685 from the Departement de Geophysique, Géologie et Géochimie marines du C.O.B.

Received 16 January; accepted 25 April 1980.

1. O'Hara, M. J. *Nature* **266,** 503–507 (1977).
2. Rhodes, J. M., Dungan, M. A., Blanchard, D. P. & Long, P. E. *Tectonophysics* **55,** 35–61 (1979).
3. Bryan, W. B., Thompson, G. & Michael, P. G. *Tectonophysics* **55,** 63–85 (1979).
4. Schilling, J. G. *Nature* **242,** 565–571 (1973).
5. Sun, S. S., Tatsumoto, M. & Schilling, J. G. *Science* **190,** 143–147 (1975).
6. O'Nions, R. K., Hamilton, P. J. & Evensen, N. M. *Earth planet Sci. Lett.* **34,** 13–22 (1977).
7. Tarney, J., Wood, D. A., Varet, J., Saunders, A. D. & Cann, J. R. *Deep Drilling Results in the Atlantic Ocean: Oceanic Crust, Maurice Ewing* Ser. **2,** 285–301 (1979).
8. Bougault, H., Joron, J. L. Treuil, M. *Deep Drilling Results in the Atlantic Ocean: Oceanic Crust, Maurice Ewing* Ser. **2,** 352–368 (1979).
9. *Proc. R. Soc.* (in the press).
10. Renard, V. & Allenou, J. P. *Int. Hydrogr. Rev.* **56,** 35–67 (1979).
11. Bougault, H. *Init. Rep. DSPP* Leg **37,** 643–657 (1977).
12. Melson, W. G., Rabinowitz, P. D., Natland, J. H., Bougault, H. & Johnson, H. P. *Init. Rep. DSDP* Leg **45,** 5–20 (1979).
13. Francheteau, J., Juteau, T. & Rangin, C. *Nature* **281,** 209–211 (1979).
14. O'Nions, R. K. & Pankhurst, R. J. *Init. Rep. DSDP* Leg **37,** 599–602 (1977).
15. Drach, V., Müller-Sohnins, D., Köhler, H. & Huckenholz, H. G. *Init. Rep. DSDP* Leg **45,** 535–590 (1977).
16. Puchelt, H., Emmermann, R. & Srivastava, R. K. *Init. Rep. DSDP* Leg **37,** 581–590 (1977).
17. Schilling, J. G., Kingsley, R. & Bergeron, M. *Init. Rep. DSDP* Leg **37,** 591–598 (1977).
18. Rhodes, J. M., Blanchard, D. P., Dungan, M. A., Rodgers, K. V. & Brannon, J. C. *Init. Rep. DSDP* Leg **45,** 447–460 (1979).
19. Bougault, H., Treuil, M. & Joron, J. L. *Init. Rep. DSDP* Leg **45,** 493–506 (1979).
20. Bougault, H., Joron, J. L. & Treuil, M. *Proc. R. Soc.* (in the press).
21. Allègre, C. J., Brèvart, O., Dupré, B. & Minster, J. F. *Proc. R. Soc.* (in the press).
22. Langmuir, C. H., Bender, J. F., Bence, A. E., Hanson, G. N. & Taylor, S. R. *Earth planet. Sci. Lett.* **36,** 133–156 (1977).
23. Bougault, H., Cambon, P., Corre, O., Joron, J. L. & Treuil, M. *Tectonophysics* **55,** 11–34 (1979).
24. Sun, S. S., Nesbitt, R. W. & Sharaskin, A. Ya. *Earth planet. Sci. Lett.* **44,** 119–138 (1979).
25. Wood, D. A. *et al. Earth planet. Sci. Lett.* **42,** 77–97 (1979).
26. Bougault, H., Joron, J. L. & Treuil, M. (in preparation).
27. White, W. H. & Schilling, J. G. *Geochim. cosmochim. Acta* **42,** 1501–1516 (1978).

Flow patterns in the central North American ice sheet

W. W. Shilts

Terrain Sciences Division, Geological Survey of Canada, 601 Booth Street, Ottawa, Canada K1A 0E8

Patterns of glacial dispersal of lithologically distinctive erratics around Hudson Bay show the central portion of the North American Laurentide ice sheet to have been made up of at least two land-based centres, one that grew and dissipated in Keewatin, and one that grew and dissipated in Nouveau Quebec–Labrador.

AN accurate model of the flow patterns of the central portion of the North American ice sheet is of fundamental importance in reconstructing the palaeogeography of northern North America for the past million or more years. The configurations of the margins of the Laurentide sector of the Wisconsinan ice sheet during the last 10,000 yr of its existence have been detailed satisfactorily, but inferences about the ice flow patterns during glacial maxima and locations and growth mechanisms of centres of glacial outflow have been hampered by a paucity of data from the Canadian Arctic and sub-Arctic. Most inferences on these earlier events have been drawn indirectly from geophysical data, from limited isostatic data on raised and tilted lacustrine or marine shorelines, and from broad, large-scale reconnaissance mapping of glacial features (largely by airphoto interpretation).

Over the past decade much relatively detailed information has been obtained on the lithological character of glacial sediments, the orientation of ice-inscribed or ice-moulded features, and on the general stratigraphic framework of glacial sediments around Hudson Bay. These data, by defining paths of glacial transport of distinctive bedrock lithologies, permit the postulation of several constraints on timing and configuration of glacial flow for the central parts of the Laurentide ice sheet (at least as it was constituted during the Wisconsinan). These constraints have lead to a preliminary model for glacial flow that conflicts with many aspects of recently published ice sheet reconstructions[1–3]. Furthermore, although the model is crude, its gross features are unequivocal and are sufficiently accurate to use as a basis for speculating on the configurations, palaeoclimatological conditions and dynamics of the last Laurentide ice sheet.

The data on which the maps and conclusions of this article are based are principally the petrological compositions of till and related sediments from: (1) the Hudson Bay Lowlands and adjacent areas of the Canadian Shield; (2) southern District of Keewatin; and (3) Coats and Mansel Islands (Fig. 1). The petrology of tills has been characterized by determining the percentages of several distinctive pebble lithologies in the 2–6-mm fractions of $\sim$1,200 samples of surface and older tills. Pebble lithologies and geochemical and mineralogical dispersal patterns were noted for a further 7,000+ samples of till collected in southern District of Keewatin[4–6]. Field observations of erratic types present at each of several hundred localities throughout these regions have been integrated with the quantitative data, as have pebble lithologies of glacial or related bottom sediments collected from Hudson Bay by C. F. M. Lewis and B. V. Sanford.

The petrological data are supported by observations of orientations of ice-inscribed or ice-moulded features compiled or generalized from the Glacial Map of Canada[7], from measurements of striation directions on boulders or boulder pavements in tills exposed in stratigraphic sections in the Hudson Bay Lowlands, and from measurements of orientation of striations on bedrock, of fluting, and of minor moraine or drumlins within a 200,000-km^2 area where detailed mapping of surficial geology has been carried out in southern Keewatin and on Coats and Mansel Islands.

Bedrock sources of erratics around Hudson Bay

Figure 1 shows the locations of the major geological domains within and around Hudson Bay. The older Precambrian terrane is largely underlain by non-calcareous, crystalline gneiss and igneous intrusive rocks. These 'crystalline' rocks include major belts of deformed, metamorphosed volcanogenic and associated sedimentary strata that generally retain some of their original lithological characteristics.

Superimposed on the 'crystalline' terrane are belts of Proterozoic sedimentary and volcanogenic rocks that are generally much less affected by metamorphism and which contain lithologically distinctive facies. One of these, the Dubawnt Group[8], comprises a sequence of generally red sedimentary and volcanogenic formations that underlie an area of several tens of thousands of square kilometres west and south-west of Baker Lake.

Another Proterozoic depositional basin, the Circum-Ungava geosyncline[9], forms an almost continuous belt of sediments, including locally significant occurrences of iron formation, basic volcanic rocks, and basic or ultrabasic igneous rocks. The sediments of that part of the basin in and adjacent to Hudson Bay are predominantly dark grey to black greywackes, slates, various facies of iron formation, and minor dolomitic units.

A thick sequence of gently dipping, unmetamorphosed Palaeozoic carbonate rocks with minor clastic facies underlies much of Hudson Bay and extends for several hundred kilometres on land south and south-west of the Bay[10].

Because of the distinctive lithological differences among the erratics derived from each of these major geological domains, pebble lithologies in the tills around Hudson Bay are grouped into four general and easily defined categories. For convenience, these four types of erratics will be referred to as crystalline erratics, red erratics, dark erratics, and carbonate erratics, in order of the above discussion of their source areas.

Outcrop patterns of these four lithological types are such that by mapping the areal distribution of the glacial erratics derived from each, one can place constraints on the glacial flow paths that must have prevailed during transport of the erratics from their source outcrops. In this way flow lines can be generalized for the central part of the Laurentide ice sheet. By establishing patterns of dispersal of erratics for the surface drift, and by comparing lithologies of older glacial deposits with the youngest, inferences bearing on the similarity or dissimilarity of flow patterns for older glacial events may be

0028–0836/80/290213–06$01.00

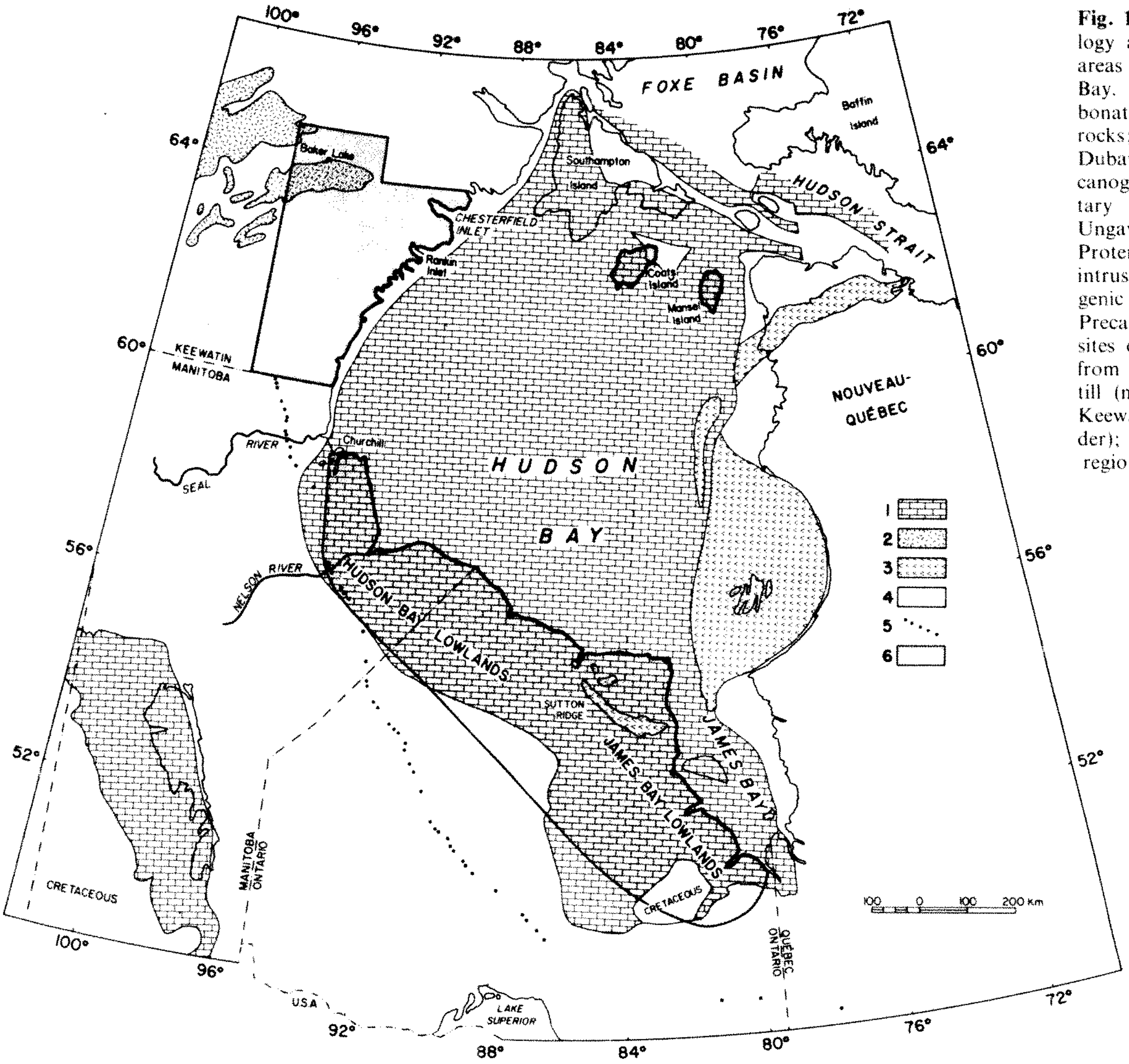

Fig. 1 Generalized geology and principal study areas around Hudson Bay. 1, Palaeozoic carbonate and minor clastic rocks; 2, Proterozoic Dubawnt Group, red volcanogenic and sedimentary rocks; 3, Circum-Ungava geosyncline, Proterozoic sedimentary, intrusive, and volcanogenic rocks; 4 crystalline Precambrian terrane; 5, sites of samples collected from boreholes through till (not shown north of Keewatin–Manitoba border); 6, principal study regions discussed in text.

Library SCIENCE COLLEGE

evaluated. Furthermore, by documenting the distance travelled by erratics during any one glacial event, one can make rough calculations of the time required for the distance of transport, as has already been done for the Dubawnt (red) erratics mapped on the mainland west of Hudson Bay[11].

Dispersal patterns around Hudson Bay

Dispersal of Carbonate erratics: south and south-west of Hudson Bay, carbonate erratics have been displaced hundreds of kilometres westward and southward onto crystalline Precambrian bedrock (Fig. 2). Carbonate erratics (20–30%) have been found in the fine gravel fraction of fine-grained, calcareous till 250 km from the nearest carbonate outcrops. The northern limit of westward carbonate dispersal is sharply defined in the vicinity of Seal River, just north of Churchill, Manitoba (L. A. Dredge, personal communication). Till from boreholes drilled north of Seal River bears no Palaeozoic carbonate erratics and has a non-calcareous matrix at least as far north as Chesterfield Inlet. South of James Bay, the Ontario–Quebec border (long. 79°30′) roughly divides the area of carbonate dispersal to the west from the area of non-calcareous drift to the east. Other than in the area of the late glacial Cochrane readvance, south-east of James Bay, no evidence has been found of eastward dispersal of Palaeozoic erratics east of James Bay or Hudson Bay (refs 12–14, and J. S. Vincent, personal communication). The rare Palaeozoic and Proterozoic erratics found east of the Bay and cited by Lee[15] as evidence of eastward dispersal are confined to zones of postglacial marine submergence and were undoubtedly emplaced by some form of ice rafting[13].

Although calcareous Palaeozoic debris could have been displaced eastward or westward from ice centred on Hudson Bay at some earlier time and could have been eroded and transported back into or across the Bay during later flow from Quebec or Keewatin centres, one would expect that at least some of the calcareous debris would have been left behind to be incorporated into the drift that now covers the areas adjacent to Hudson Bay. Certainly in other areas, where later ice flow has been at considerable angles to earlier flow, some components of the earlier flow have been left behind, although their frequencies are attenuated and their dispersal patterns modified. Such relict evidence of earlier dispersal has been observed in southern Keewatin[11] and in the Appalachian region of southern Quebec[16] where later major ice movements have not completely effaced earlier dispersal patterns.

Dispersal of dark erratics: dark grey to black sedimentary and volcanic rock fragments are widely distributed in drift throughout much the same area as that covered by till rich in carbonate erratics (Fig. 2). Isolated observations of dark erratics, iron formation and jasper have been interpreted[17,18] to indicate a source within the Circum-Ungava Proterozoic sequence that both underlies the eastern part of Hudson Bay and projects through the Palaeozoic cover in the Sutton Ridge[10]. V. K. Prest (personal communication, 1979) has noted widespread occurrence of dark erratics and oölitic jasper erratics in northwestern Ontario at least 1,000 km west of their nearest possible Proterozoic sources in association with fossiliferous Palaeozoic carbonate erratics over 600 km west of their nearest source. Dark erratics and associated iron formation commonly comprise 10–20% of the erratics (2–6 mm) in tills lying on Palaeozoic outcrops west and southwest of Hudson and James Bays. West of Hudson Bay, dark erratics are rare (generally ⩽5%) north of Seal River, and those that are found could reasonably be related to local sources within greenstone belts. Dark erratics make up at least 50% of the Precambrian erratics on Mansel Island and are found there in association with haematite–magnetite iron formation and other erratics which are common lithologies within the Circum-Ungava geosyncline[9]. Dark erratics are found on the east coast of Coats Island but are uncommon west of there.

Dark erratics are also found in older tills in numerous exposures throughout the Hudson Bay Lowlands and in a series of 6–20-m deep boreholes drilled in multiple tills overlying crystalline terrane west of the Lowlands. At given sites within the Lowlands, the concentrations of dark erratics (and also crystalline erratics) are generally similar among till sheets, including till sheets which predate the last interglacial stage[19,20].

Dispersal of red erratics: the pattern of dispersal of red erratics has been discussed in detail elsewhere[11] for that portion of the district of Keewatin east of the Keewatin ice divide. No red erratics occur north of a south-east-trending line from Baker Lake to the coast of Hudson Bay, just north of Rankin Inlet. In this region a well-developed southeastward-trending dispersal train of red erratics is superimposed on a poorly defined southerly train created during an earlier glacial flow event. Red erratics comprise 1–2% of the fine gravel in eskers and till on Coats Island. Distinctive cobble and boulder-size fragments of the red Pitz and Christopher Island Formations of the Dubawnt Group are numerous on Coats Island and can be ascribed confidently to outcrops that occur exclusively within a 100 km long belt that extends southwestward from the east end of Baker Lake (A. N. Lecheminant, personal communication).

No red erratics were found on Mansel Island, nor were they found in till-like bottom sediments from the floor of Hudson Bay between Coats and Southampton Islands. Red erratics comprise 1% of the gravel fractions of till samples near the Manitoba border, but no certain red erratics have been found as far south as Churchill. Although the true pattern of dispersal of red erratics between the Keewatin mainland and Coats Island is poorly known, the main part of the dispersal train seems to narrow northwards and to make at least a 90° bend, a configuration confirmed by the pattern of distribution of red erratics in till-like sediments from the bottom of Hudson Bay.

Dispersal of crystalline erratics: crystalline erratics are found virtually everywhere that it has been possible to make observations in the region covered by Figs 1 and 2. Crystalline erratics make up ~10% of the gravel fractions of all tills sampled in the southern Palaeozoic portion of the Hudson Bay Lowlands and make up 20% or more of the gravel-sized erratics occurring in tills from Hayes River–Nelson River northward. Crystalline erratics make up the bulk of the Precambrian erratics on both Coats and Mansel Islands. In the

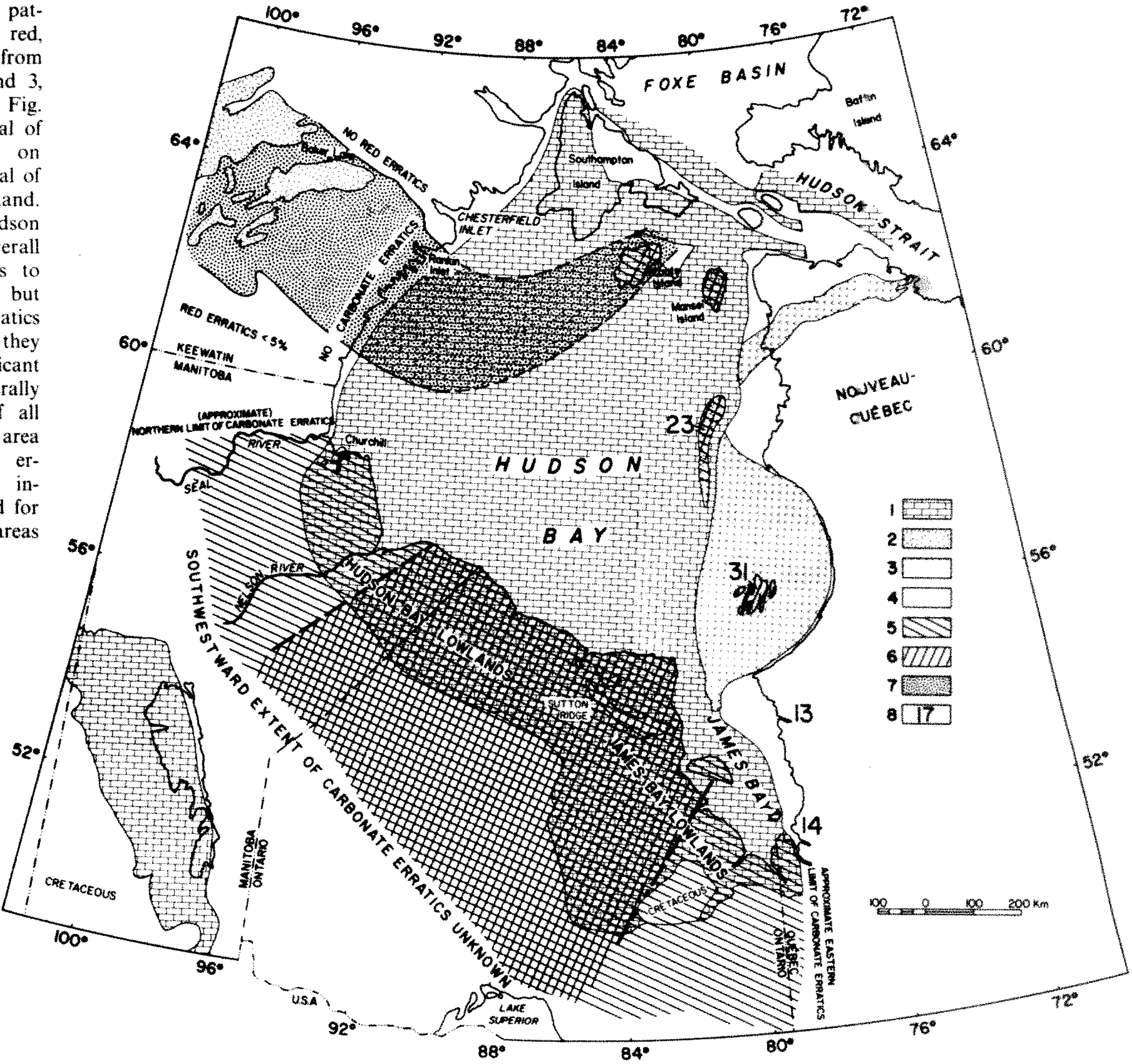

Fig. 2 Dispersal patterns of carbonate, red, and dark erratics from source areas 1, 2 and 3, respectively. 1–4, as Fig. 1; 5, area of dispersal of carbonate erratics on land; 6, main dispersal of dark erratics on land. South-west of Hudson and James Bays overall dispersal corresponds to carbonate pattern but dispersal of dark erratics is only shown where they make up a significant proportion, generally more than 15%, of all erratics; 7, principal area of dispersal of red erratics; 8, numbers indicate references used for data on erratics in areas indicated.

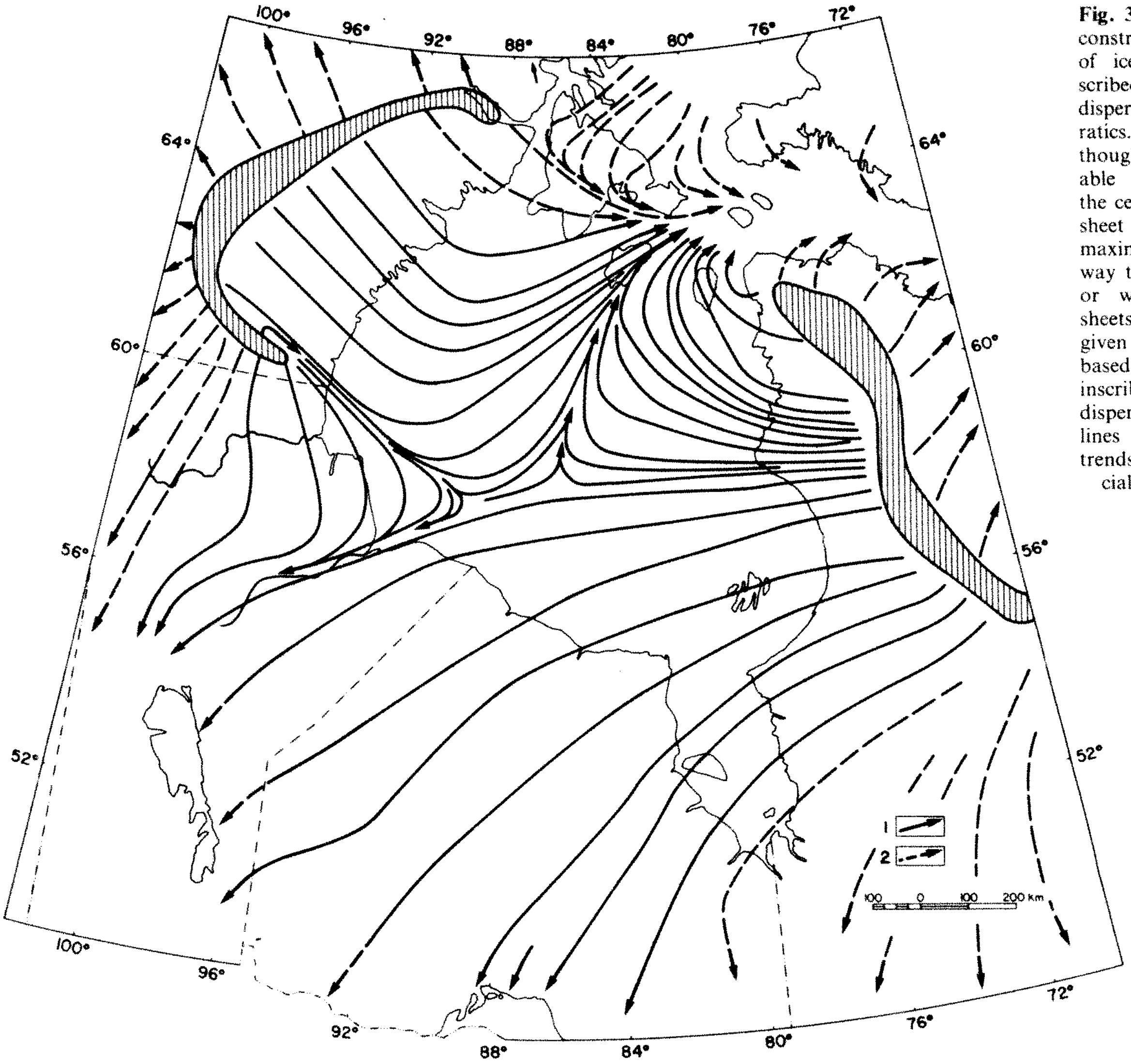

Fig. 3 Ice flow lines reconstructed from trends of ice moulded or inscribed features and from dispersal patterns of erratics. Although this is thought to be a reasonable reconstruction for the central part of the ice sheet at the last glacial maximum, there is no way to tell precisely how or where the two ice sheets interfaced at any given time. 1, Flow lines based on ice moulded or inscribed features and on dispersal patterns; 2 flow lines based on ice flow trends shown on the glacial map of Canada[7].

regions underlain by crystalline bedrock, crystalline erratics generally make up more than 95% of the gravel fraction, except down-ice from major dispersal areas of more erodable, less metamorphosed outcrops, such as the Palaeozoic carbonates or Dubawnt red beds.

In the district of Keewatin, geochemical and mineralogical dispersal patterns from several mineralized or mineralogically distinctive bedrock sources within the crystalline terrane east of the Keewatin ice divide invariably indicate eastward or southeastward glacial transport towards Hudson Bay.

Directions of flow from striation measurements

Numerous observations have been made (refs 19, 20 and B. G. Craig, unpublished data) of southwesterly oriented striations on boulder pavements within or between till sheets and on bedrock throughout the southwestern part of the James Bay and Hudson Bay Lowlands. Skinner's data clearly show that all tills preserved south-west of James Bay, including pre-Missinaibi (pre-Sangamon) tills, were deposited by glacier ice flowing from east-northeast. An exception to this general flow pattern is an area of clay-rich till associated with southeasterly oriented drumlins and striations that were probably formed during the Cochrane readvance[21], a southward and eastward late glacial surge. Observations[19,20,22] of southeasterly oriented striations on till stones and on Precambrian bedrock near the western edge of the Hudson Bay Lowlands from Churchill to the Ontario–Quebec border indicate that although southwesterly flow dominated all glaciations of this region, at some time during at least one glaciation, ice flow was southerly to southeasterly.

Hardy[14], among others, has shown that striations preserved in the eastern part of the Hudson Bay Lowlands invariably indicate ice flow westward or southwestward toward Hudson Bay. Andrews and Falconer[23] show that ice flow across the Ottawa Islands in the east-central part of Hudson Bay varied from northeastward to westward.

On Coats and Mansel Islands several directions of striae and fluting were noted, most being northward or northeastward, sub-parallel to the long axes of those islands. On Coats Island, however, the last direction of ice flow was eastward, presumably directly from Southampton Island or northern Keewatin.

In areas outside those discussed above striation directions are known or assumed to be similar to the main trends shown on the glacial map of Canada[7].

Discussion

Traditionally, the concepts regarding the configuration of the central part of the Laurentide ice sheet have been derived largely from observations of the amount of isostatic uplift of marine and lacustrine shorelines and from gravity data that seem to indicate that a significant amount of isostatic adjustment has yet to be made over Hudson Bay. These data have led to the belief that the locus of greatest ice loading, and hence the centre of glacial outflow at the maximum development of the last Laurentide ice sheet, was over Hudson Bay itself, notwithstanding the abundant glacial geomorphological evidence from regions adjacent to the Bay, all of which indicates ice flow radially away from centres of dispersal located in Keewatin and Nouveau Quebec. The terrestrial centres or ice divides have been explained as late glacial phenomena[24], formed when marine waters split a Hudson Bay ice dome into eastern and western segments with concomitant readjustment of ice flow patterns. Thus, the geomorphological features were thought to have been formed during the last 2,000–4,000 yr of the ice sheet's existence.

However, the time-transgressive nature of marine limit[11] combined with significant amounts of restrained rebound[11,25] in areas of marine inundation make interpretation of maximum uplift data difficult around Hudson Bay. In addition, recent measurements of marine limit on southeastern Southampton Island (124–157 m)[26], Coats Island (124 m) and the Ottawa Islands (156–163 m)[23] are lower than would be expected if the northern or north-central part of Hudson Bay had been loaded more heavily than adjacent areas on land. Vincent and Hardy[27] have shown convincingly that lacustrine strandlines which predate the marine incursion south-east of James Bay, are tilted upward towards a centre of uplift in Nouveau Quebec and not towards a centre over Hudson Bay as would be expected if an ice dome had existed there.

Although there is no firm evidence relating to the origin of the gravity anomalies that are found in parts of Hudson Bay, crustal blocks within the Bay seem to be in equilibrium with their adjacent terrestrial counterparts[28], suggesting that the anomalies may be in part a permanent feature of the crust under the basin.

From the above dispersal and geomorphological data, a map (Fig. 3) has been prepared showing probable flow directions in the central part of Laurentide ice sheet near a glacial maximum, but at an unspecified point in time.

The dispersal patterns of Fig. 2 show that an ice dome or domes could not have existed in the Hudson Bay basin unless some special conditions existed, such as the presence of a melt lake[3] or a frozen bed under the central portion of the ice sheet. Such conditions would have prevented erosion and transportation of the Palaeozoic carbonate rocks from beneath the Bay. Two facts that argue against special conditions are the consistent eastward dispersal patterns from distinctive sources in the crystalline terrain east of the Keewatin ice divide, well above and west of the central depression, and the abundant evidence of repeated episodes of intense erosion of the Palaeozoic and Proterozoic rocks that underlie the southern half of the Hudson Bay depression. The configuration of erratic dispersal patterns suggests, rather, that independent ice masses existed on either side of Hudson Bay.

The well defined northern limit of westwardly displaced carbonate lithologies along the Seal River in northern Manitoba indicates that ice from the Quebec centre never affected the western shore of Hudson Bay north of that river. The presence of red erratics on Coats Island and their absence on Mansel Island indicates that ice from a Keewatin centre was confined to the western portions of Hudson Bay, but the presence of dark erratics on Coats Island suggests that at some time ice from a Quebec centre flowed at least as far west as Coats Island. In any case, the dispersal patterns at the mouth of the Bay indicate that terrestrial ice flow centres were established well before marine waters divided the ice sheet. The lack of carbonate erratics east of Hudson Bay supports the interpretation that the pattern of westward dispersal of carbonate and dark erratics west and south-west of Hudson Bay was not related to a centre of dispersal within the Bay but to a centre on land to the east.

The general picture conveyed by the reconstruction depicted in Fig. 3 is one of independent Quebec and Keewatin ice masses in contact along discrete zones. The zone of contact in the northern part of the Bay was more or less between Coats and Mansel Islands. The contact zone depicted through the Hudson Bay Lowlands could have been as far north as Seal River and as far south as approximately the Quebec–Ontario border, based on the limits of carbonate dispersal. It is drawn at the Nelson River in this reconstruction because the amount of crystalline erratics in youngest tills north of Nelson River is considerably higher than in tills south of the river. The moderate concentrations of crystalline erratics in tills south of the river are assumed to have their origin principally in the crystalline terrain east of Hudson Bay. North of Nelson River the frequency of crystalline erratics doubles, and because there is no reason that a source area east of Hudson Bay would cause this enhancement, it is thought that much of the crystalline component was carried southward by Keewatin ice, from sources north-west of the lower reaches of Nelson River.

The shift through time of the contact of the Quebec and Keewatin ice masses in the southwestern Hudson Bay Lowlands explains the commonly observed presence of two sets of striae, one indicating flow from north or north-west, and one indicating flow from east or north-east. When the glacier from a Quebec–Labrador centre flowed over a given site, the latter sets of stria were formed; when Keewatin ice displaced the Quebec ice at the same site, the former directions prevailed. The strong evidence of westward to southwestward dispersal through the western Hudson Bay Lowlands suggests, however, that the Keewatin centre had a minor role in most of the Lowlands, either by virtue of its inability to erode and transport or because it did not flow long enough over most of the region to effect significant erosion and transportation.

That the position through the Hudson Bay Lowlands of this zone of contact between Quebec and Keewatin ice masses seems to have shifted considerable distances with time probably reflects the relative strengths and timing of ice build-up in the two centres of ice dispersal. It is tempting to speculate that within the central part of the Laurentide ice sheet the Labrador–Quebec centre of outflow predominated in the early and maximum stages of glaciation and that the Keewatin centre became relatively stronger during the later stages. Certainly in the last stages of glaciation there was a significant break in the vicinity of the Quebec–Ontario border between ice retreating towards a centre in Quebec and ice retreating generally northward or northwestward towards a Keewatin centre. The Cochrane readvance[14,30] seems to have been independent of the Quebec ice and may, therefore, have emanated from an ice mass shrinking toward a Keewatin centre.

The magnitude of the distances of transport of all erratics, more than 1,000 km in the case of the carbonate and dark erratics and at least 600 km in the case of the red erratics, demonstrates that ice flow was maintained from Keewatin and Quebec centres of outflow along discrete flow paths for significant periods of time, as already suggested elsewhere[11,30]. The duration of ice flow necessary to effect these distances of transport for erratics of any given till sheet must have been of the order of several tens of thousands of years if the reasoning used by Shilts *et al.*[11] or by Boulton *et al.*[29] is followed.

That erratic transport occurred along specific flow lines over such long periods of time seems to be incompatible with the concept that there could have been any prolonged period of glacial flow with a configuration other than that depicted on Fig. 3. Thus, it is concluded from the constraints of time and configuration of dispersal discussed above that ice flow was maintained from centres located east and west of Hudson Bay throughout one or more glacial stades of the Wisconsinan Stage. Lithological similarities between pre-Wisconsinan and Wisconsinan tills in the Hudson Bay Lowlands suggest that similar centres also existed during earlier glaciations.

Conclusions

In the region around Hudson Bay, the configuration of dispersal patterns for distinctive suites of glacial erratics indicates that a centre of ice flow or ice dome could not have existed over the Bay unless some special conditions existed that prevented erosion and transportation of debris from the Bay's limestone floor. Dispersal data agree with glacial geomorphological data in that they indicate ice flow from centres on land in Keewatin and in Nouveau Quebec–Labrador.

The distance of dispersal along clearly defined flow paths from the centres east and west of Hudson Bay is so great that the time required to form the major erratic trains of the Wisconsinan glaciation may have spanned most of that glacial stage, leaving little time for the development of a major ice dome over Hudson Bay.

Thus, I conclude that it is unlikely that an ice dome could have existed over Hudson Bay during the Wisconsinan nor is it likely, based on compositions and striated boulder pavements of pre-Wisconsinan tills of the Hudson Bay Lowlands, that an ice dome existed during the earlier glacial stages represented by these deposits. Centres of ice dispersal are thought, rather, to have developed and decayed on land east and west of Hudson Bay. Hudson Bay received ice flowing from Keewatin and Quebec throughout the last glacial stage. Reconstructions of the palaeoclimatology and dynamics of the Laurentide ice sheet might better be based on the multiple dome model presented here rather than on the less complex 'single dome' model.

Samples and unpublished data on which the discussions of glacial flow southwest of Hudson Bay are based were provided by Polar Gas Consortium through W. D. Roggensack and by B. C. McDonald, R. G. Skinner, B. G. Craig and C. F. M. Lewis. Canadian Coast Guard icebreaker CCGS Pierre Radisson provided helicopter support and a logistical base for study of Coats and Mansel Islands. Analyses of samples from Keewatin were partially funded by Atomic Energy of Canada Limited. Most of the analyses of pebble fractions were carried out by C. A. Kaszycki and P. Honarvar.

Received 26 November 1979; accepted 22 April 1980.

1. White, W. A. *Geol. Soc. Am.* **83,** 1037 (1972).
2. Hughes, T., Denton, G. H. & Grosswald, M. G. *Nature* **266,** 596 (1977).
3. Sugden, D. E. *J. Glaciol.* **21,** 367 (1978).
4. Shilts, W. W. *Boreas* **6,** 203 (1977).
5. Klassen, R. A. & Shilts, W. W. *Inst. Min. Metal. Prosp. Areas of Glac. Ter.* 80 (1977).
6. DiLabio, R. N. W. & Shilts, W. W. *Geol. Surv. Can.* Pap. 77-1A, 479 (1977).
7. Prest, V. K., Grant, D. R. & Rampton, V. N. *Geol. Surv. Con.* Map 1253A (1970).
8. Donaldson, J. A. *Geol. Surv. Can.* Pap. 64–20, 1 (1965).
9. Dimroth, E., Baragar, W. R. A., Bergeron, R. & Jackson, G. D. *Geol. Surv. Can.* Pap. 70-40, 45 (1970).
10. Sanford, B. V., Grant, A. C., Wade, J. A. & Barss, M. S. *Geol. Surv. Can.* Map 1401A (1979).
11. Shilts, W. W., Cunningham, C. M. & Kaszycki, C. A. *Geology* **7,** 537 (1979).
12. Hillaire-Marcel, C. *Cah. Géogr. Québ.* **20,** 185 (1976).
13. Dionne, J-C. *Rev. Geogr. Montreal* **28,** 453 (1974).
14. Hardy, L. thesis, McGill Univ. (1976).
15. Lee, H. A. *Geol. Soc. Am.* **70,** 219 (1959).
16. McDonald, B. C. & Shilts, W. W. *Geol. Soc. Am.* **76,** 683 (1971).
17. Bell, R. *Geol. Surv. Can. A. Rep. 1886* pt G. 1 (1887).
18. Prest, V. K. *Geol. Surv. Can.* Pap. 63–66, 1 (1963).
19. McDonald, B. C. *Geol. Surv. Can.* Pap. 68–53, 78 (1969).
20. Skinner, R. G. *Bull. geol. Surv. Can.* **225,** 1 (1973).
21. Hughes, O. L. *Geol. Soc. Am.* Spec. Pap. 84, 535 (1965).
22. Tyrrell, J. B. *Ont. Bur. Mines* **22** pt 1, 161 (1913).
23. Andrews, J. T. & Falconer, G. *Can. J. Earth Sci.* **6,** 1263 (1969).
24. Lee, H. A., Craig, B. G. & Fyles, J. G. *Geol. Soc. Am.* **68,** 1760 (1957).
25. Andrews, J. T. *Geol. Surv. Can.* Pap. 68–53, 49 (1969).
26. Bird, J. B. *Acta geogr. Univ. lodz.* **24,** 75 (1970).
27. Vincent, J-S. & Hardy, L. *Géogr. Phys. Quat.* **31,** 357 (1977).
28. Hall, D. H. *Geol. Surv. Can.* Pap. 68–53, 337 (1969).
29. Boulton, G. S., Jones, A. S., Clayton, K. M. & Kenning, M. J. *British Quaternary Studies, Recent Advances* 231 (Clarendon, Oxford, 1977).
30. Prest, V. K. *Geol. Surv. Can. Econ. Rep.* **1,** 676 (1970).
31. Jackson, G. D. *Geol. Surv. Can.* Pap. 60–20, 1 (1960).

Invertible DNA determines host specificity of bacteriophage Mu

Pieter van de Putte, Steve Cramer & Micheline Giphart-Gassler

Department of Molecular Genetics, State University of Leiden, Wassenaarseweg 64, 2333 Al Leiden, The Netherlands

The function of the invertible G region of bacteriophage Mu is apparently to confer different host specificities on Mu. Two products of genes S *and* U, *situated in the G region are not needed for the infectivity of Mu G(−) particles. In the Mu G(−) phage the* S *gene product and the 21-K polypeptide, presumably the product of gene* U, *are missing. Instead, two other polypeptides with different molecular weights are observed.*

THE invertible G region of bacteriophage Mu is 3,000 base pairs long and has short inverted repeats at its ends[1]. When Mu is propagated lytically in *Escherichia coli* K12 the G region is fixed in one particular orientation G(+), whereas when Mu stocks are prepared by induction of a Mu *cts* prophage the DNA consists of 50% G(+) and of 50% G(−) molecules[1,2].

A Mu gene *gin* situated in the β part of the Mu genome (Fig. 1) is essential for the inversion of the G area[3]. Only G(+) particles can infect *E. coli* K12 (refs 3, 4), but it has been speculated that the G(−) particles may be infectious for organisms other than *E. coli* K12 (ref. 5).

We now provide evidence that Mu G(−) particles are viable and have a different host specificity from G(+) particles.

Propagation in *Citrobacter freundii*

It has been reported that Mu can be propagated in cells of *C. freundii* but that the organism seemed to have, besides a restriction system directed against foreign DNA in general, a second restriction system specifically directed against phage Mu, because Mu plated with a low efficiency on *C. freundii* r$^-$ strains[6]. However, the presence of such a specific restriction system seems unlikely. Another explanation is that *C. freundii* cells are not sensitive to the Mu G(+) phages, which are the predominant product of lytic growth on *E. coli* K12, but to the G(−) form. To test this, the efficiencies of plating (e.o.p.) of different Mu phage preparations were determined on *E. coli* K12 and *Citrobacter* hosts. It seems that the lytically propagated Mu phage Mu*c*2000, a clear plaque mutant of Mu c^+, has an extremely low e.o.p. of 2.5×10^{-9} on the r$^-$ strain of *Citrobacter* (Table 1, line 1) whereas the e.o.p. of a Mu*cts* lysate obtained by induction is the same on *E. coli* K12 as on *C. freundii* (Table 1, line 2). This simple experiment strongly suggests that *C. freundii* is sensitive for Mu G(−) phages. (The nine log difference found between the e.o.p. of lytic Mu and induced Mu on *C. freundii* is much larger than could be expected from the e.o.p. data obtained by De Graaf *et al.*[6]. This difference is a result of the way the Mu phage was prepared by these authors: a spontaneous induction lysate of a Muc^+ lysogen with $\sim 10^5$ plaque-forming units (PFU) per ml^{-1} consisting of 50% G(+) and 50% G(−) particles was

0028-0836/80/290218-05$01.00

directly used to make confluent lysis plates on *E. coli* K12. The lysate of ~10^9 PFU ml^{-1} obtained in this way still contained 10^5 G(−) particles which led to an e.o.p. of nearly 10^{-4} on the *C. freundii* r^- strain.) That the orientation of the G area is involved in this phenomenon follows also from the behaviour of induced Mu*ctsgin*[3] phages. In this Mu mutant G is fixed in the + orientation and consequently the phages form no plaques on the *Citrobacter* host (Table 1, line 3).

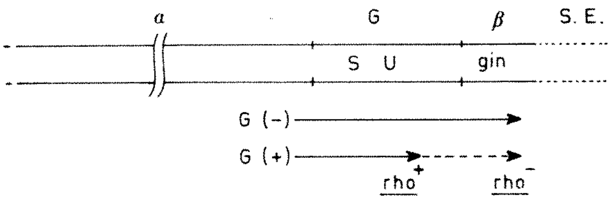

Fig. 1 A model for the expression of *gin* during lytic development of Mu G(+) and Mu (G−) phages.

G inversion during lytic development

When Mu*c*2000 was propagated lytically on *C. freundii* and titrated on different hosts it was found that the e.o.p. on an *E. coli* K12 r^- host was much higher (factor of 10^6) than when lytically propagated Mu on *E. coli* K12 was plated on *Citrobacter* (compare lines 1 and 5, Table 1). Apparently, G inversion is more frequent during lytic development of G(−) phages than of G(+) phages. A likely explanation for this is that the expression of *gin* is dependent on the orientation of the G area. In the + orientation the G area might act as a transcription barrier for *gin* expression, if the *gin* promoter is located in the α region of Mu (Fig. 1). This idea is supported by the following result: when Mu*c*2000 is propagated on an *E. coli* K12 *suA* strain, which is defective in the transcription termination factor ρ (ref. 7), the relative number of G(−) phages in a G(+) lysate is much enhanced (Table 1, line 4). In the prophage state expression of *gin* leads to a randomization of the orientation of the G region. However, our experiments show that Mu phages propagated lytically on *E. coli* K12 normally contain very few G(−) phages. This suggests that in the prophage state *gin* is expressed from a different promoter and that this promoter is shut off during lytic development.

Propagation on other hosts

Other *E. coli* strains and bacterial species were tested for sensitivity to Mu G(+) and G(−) phages. With induced Mu*cts*62 phage we found plaques on lawns of *E. coli* C and of *Shigella sonnei*. Two *Klebsiella* strains, *Salmonella typhimurium*, an *Aerobacter* strain, and *E. coli* B were found to be Mu resistant.

Mu*c*2000 G(−) phages propagated on *C. freundii* form plaques on lawns of *E. coli* C and *S. sonnei* with an efficiency approximately a factor 10^7 higher in comparison with Mu*c*2000 G(+) propagated on *E. coli* K12 (Table 1, lines 1 and 5). This suggests that *S. sonnei* and *E. coli* C are also sensitive to Mu G(−) phages.

However, there are some complications. As *E. coli* C is deficient in restriction functions the e.o.p. of induced Mu*cts* on *E. coli* C should be 1. In fact the e.o.p. on *E. coli* C and on *S. sonnei* is much lower than 1 and, moreover, is difficult to determine accurately. Besides the few normal plaques found, a large number of extremely faint plaques were seen. This is probably due to a poor adsorption of Mu*cts*62 to *E. coli* C and *S. sonnei* which is not related to G inversion. Phage Mu*c*2000, which compared to Mu*cts*62 adsorbs better to *E. coli* K12, also forms uniform clear plaques on *E. coli* C and *S. sonnei*. However, when these phages are propagated on *E. coli* C or *S. sonnei* and plated on *Citrobacter* or vice versa (Table 1, lines 5 and 7) still mutual differences in the e.o.p. of a factor 10–30 are observed. The reason for these differences is not yet known and was not further investigated.

Restriction enzyme analysis

The orientation of the G region is easily determined using restriction enzymes such as *Hpa*I, which cut asymmetrically in the G region[8]. Figure 2 shows the analysis of different DNAs treated with *Hpa*I. The *Hpa*I digest of Mu DNA derived from phage lysates prepared on *E. coli* K12 is shown in lane *b*. The *Hpa*I–E fragment of about 3,500 base pairs contains part of the G region. Mu*cts*62 DNA obtained from an induced phage lysate contains an additional *Hpa*I fragment of ~3,800 base pairs derived from the 50% G(−) molecules (Fig. 2, lane *c*). Of these two *Hpa*I fragments only the 3,800 base pair fragment is present in the DNA of Mu phage propagated in *C. freundii* (lane *d*). The G region must be almost exclusively in the G(−) orientation in this DNA because the fragment present in the Mu G(+) has disappeared. Mu DNA from phage propagated on *C. freundii*, *E. coli* C and *S. sonnei* (lanes *d–f*) gave the same restriction pattern.

Genes in the G region

Amber mutations in the genes *S* and *U* have been mapped inside the G region[9]. The G(−) phage cannot infect cells of *E. coli* K12 which might indicate that the *S* and *U* gene products are not made during lytic development of G(−) phages. A likely explanation for this is that *S* and *U* genes are expressed from a promoter located outside the G region in the α part of Mu (see Fig. 1). The expression of these genes from such a promoter will then be blocked after G inversion. To test whether the *S* and *U* gene products are essential for Mu G(−) phages we made induced lysates from an *E. coli* K12 strain lysogenic for Mu*ctsSam* and another which is lysogenic for Mu*ctsUam* and determined the titres on different strains lacking nonsense suppressors. Normal titres were found on the

Table 1 Plating efficiencies of Mu phage lysates on different hosts

	Phage	Mode of propagation	Host	Efficiencies of plating				
				E. coli K12 r^-	*E. coli* K12 r^+	*C. freundii* r^-	*S. sonnei* r^+	*E. coli* C (r^-)
1	Mu*c*2000	lytic	*E. coli* K12	1	1	2.5×10^{-9}	$<10^{-9}$	$<10^{-9}$
2	Mu*cts*62	induced	*E. coli* K12	1	1	1	(10^{-6})	(4.10^{-5})
3	Mu*cts*62*gin*	induced	*E. coli* K12	1	1	$<10^{-9}$	$<10^{-9}$	$<10^{-9}$
4	Mu*c*2000	lytic	*E. coli* K12*supA*	1	1	10^{-6}	—	—
5	Mu*c*2000	lytic	*C. freundii*	2.6×10^{-3}	2.0×10^{-6}	1	8.5×10^{-3}	7.5×10^{-2}
6	Mu*c*2000	lytic	*S sonnei*	3.1×10^{-4}	—	6.9×10^{-2}	1	2.5
7	Mu*c*2000	lytic	*E. coli* C	1.0×10^{-5}	—	2.7×10^{-2}	2.0×10^{-1}	1

All lytically propagated phage were made by the confluent lysis method. When the phage is propagated on a particular strain and titrated on the same strain, the efficiency of plating (e.o.p.) is arbitrarily set at 1. The e.o.p. values for induced Mu*cts*62 on *S. sonnei* and *E. coli* C (line 2) are given in parentheses as these values were extremely variable and dependent on plating conditions. All titrations were on 1.8% agar plates containing 1% Difco trypton broth; 0.8% NaCl and 0.5% Difco yeast extract.

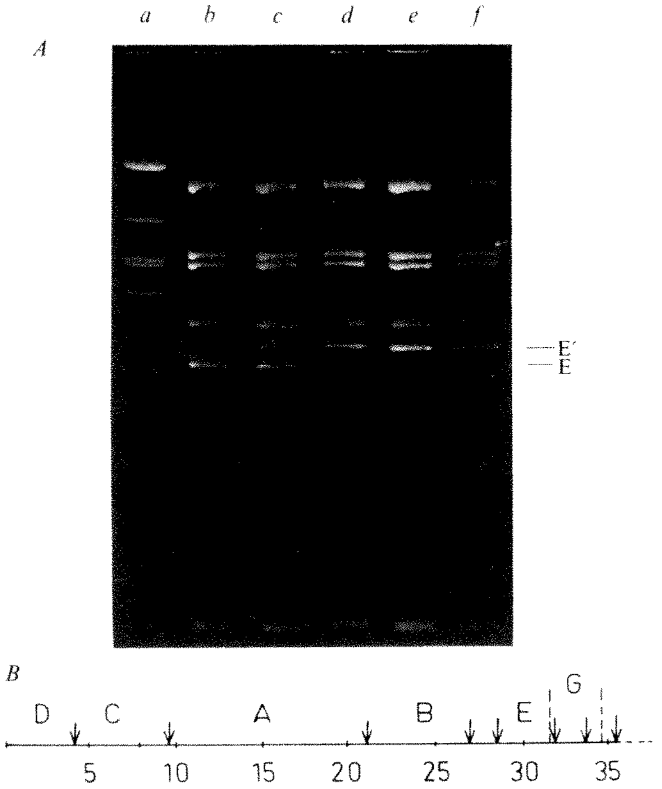

Fig. 2 *A*, DNA fragment patterns obtained from *Hpa*I digests of DNA derived from Mu lytically grown in *E. coli* K12 (*b*). Mu grown by induction of a Mu*cts*62 lysogen (*c*), Mu grown lytically in *C. freundii* (*d*), *S. sonnei* (*e*) and *E. coli* C (*f*). λDNA digested with *Eco*RI (*a*). Mu DNA was prepared by phenol extraction of phage, purified by equilibrium centrifugation in CsCl. *Hpa*I (a gift from Dr van Ormond) reactions were carried out in 20 mM Tris-HCl *p*H 7.4, 7 mM $MgCl_2$, 60 mM NaCl and 7 mM β-mercaptoethanol for 1 h at 37 °C. The digested DNA was subjected to electrophoresis on a 1% agarose slab gel. Electrophoresis buffer contained 89 mM Tris, 89 mM boric acid, 2.5 mM Na_2EDTA, *p*H 8.3 (TEB). After electrophoresis at room temperature at 1.5 V cm^{-1}, the gel was soaked in TEB containing 5 μg ml^{-1} ethidium bromide. The DNA bands were visualized under UV light and photographed with a polaroid camera. The *Hpa*I-E fragment of the G(+) and the E′ fragment of the G(−) orientation are indicated. *B*, the *Hpa*I restriction map of the Mu DNA is slightly different from the one described by Allet *et al.*[8].

C. freundii strain and no plaques were found on the *E. coli* K12 strain with the *Sam* lysate and very few with the *Uam* lysate (Table 2). These results indicate that the *S* and *U* gene products are not essential for Mu G(−) phages. (The non-permissiveness of *C. freundii* for nonsense mutations was tested with an induced *Bam* lysate (Table 2, line 1).)

The *S* protein has a molecular weight (MW) of 56,000 (ref. 10) for which a coding capacity of 1,500 base pairs is needed. We have looked at the structural proteins in Mu virions, propagated lytically in *E. coli* K12 and in *S. sonnei* (see Fig. 3). It seems that the 56,000-MW polypeptide, the product of gene *S*, is absent from phages propagated on *Shigella*. We see instead a polypeptide of MW 48,000. A gene coding for this size polypeptide would be about 1,300 base pairs long and would fit nicely into that part of the G region that can be deleted in Mu G(+) DNA. We propose that the 48,000-MW polypeptide is analogous to the *S* protein and shall refer to it as *S*′.

Table 2 Number of PFU per ml of Mu amber induction lysates on *C. freundii* and *E. coli* strains

Lysogen	Indicator strains *E. coli* K12, *supE*	 *E. coli* K12 su^-	 *C. freundii* r^-su^-
E. coli K12, *supE*::(Mu*cts*62*Bam*)	1.4×10^9	< 10	< 10
E. coli K12, su^-::(Mu*ctsSam*)*	1.1×10^5	< 10	2.4×10^8
E. coli K12, *supE*::(Mu*ctsUam*)*	5.2×10^7	2.1×10^2	4.5×10^8

For plating conditions see Table 1 legend. *The difference in the genetic background (su^- and *supE*, respectively) of the *Sam* and *Uam* lysogens was a coincidence and has no influence on the interpretation of the data.

A 21,000-MW structural protein present in phage propagated on *E. coli* K12 is absent from phage propagated on *S. sonnei*. Instead we see a 26,000-MW polypeptide (Fig. 3). The 21,000-MW polypeptide is a good candidate for the *U* product and 26,000-MW for the analogous *U*′. Support for the identification of the *U* gene product with a 21,000-MW protein comes from the work of Magazin *et al.*[11] who reported that the λ-pMu hybrid 82-573, that contains β and the G region, codes for a 41,500 and 20,500-MW protein.

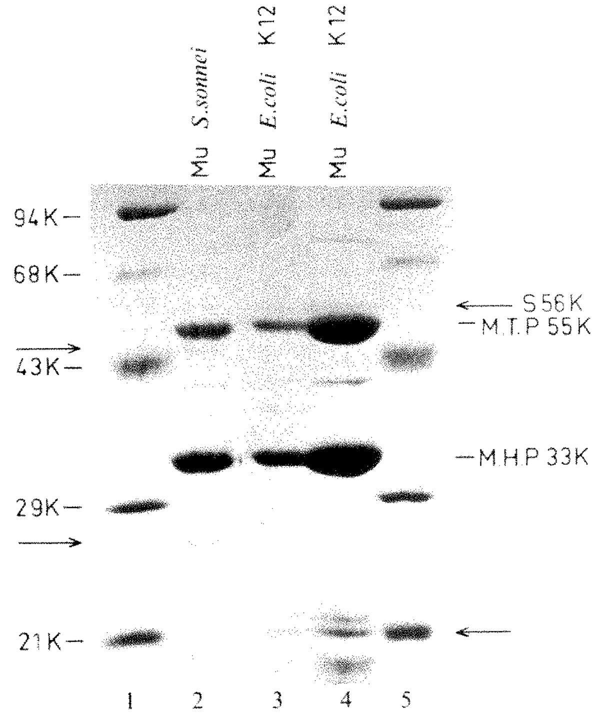

Fig. 3 Electrophoretic separation of the polypeptides of Mu G(+) (two different concentrations) and Mu G(−) phage particles. The molecular weight standards (Biorad; MW range 10,000 to 100,000) were electrophorised in lanes 1 and 5. Mu lysates were obtained by confluent lysis on *E. coli* K12 G(+) or *S. sonnei* G(−). Purified phages were obtained by banding in CsCl and dialysing against 0.01 M Tris-HCl *p*H 7.0; 0.01 M $MgCl_2$. The phages were precipitated in 5% trichloroacetic acid at 0 °C for 2 h and were centrifuged for 30 min at 45,000 r.p.m. in a SW 50.1 rotor. The pellets were solubilized in Laemmli sample buffer[19] and the *p*H adjusted to 6.8. The proteins were desaggregated by heating the samples at 100 °C for 3 min. Polypeptides were separated by electrophoresis through a 20-cm long linear 12.5–20% polyacrylamide gradient slab gel in the presence of SDS at 150 V for 18 h. Polypeptide bands were visualized by staining with Coomassie brilliant blue.

Aspects of regulation

These experiments provide evidence for a new type of regulation of gene expression. This is achieved by the inversion of a stretch of DNA which contains structural genes. We have shown that in bacteriophage Mu inversion of a 3,000 base-pair DNA region, the G region, results in a different host specificity of the phage. This inversion gives new adsorption properties and an extension of the host range of phage Mu. A second regulatory aspect of the inversion phenomenon is that the frequency of inversion during lytic development of the phage seems to be regulated by the invertible region itself. In one orientation the region acts as a ρ-dependent transcription

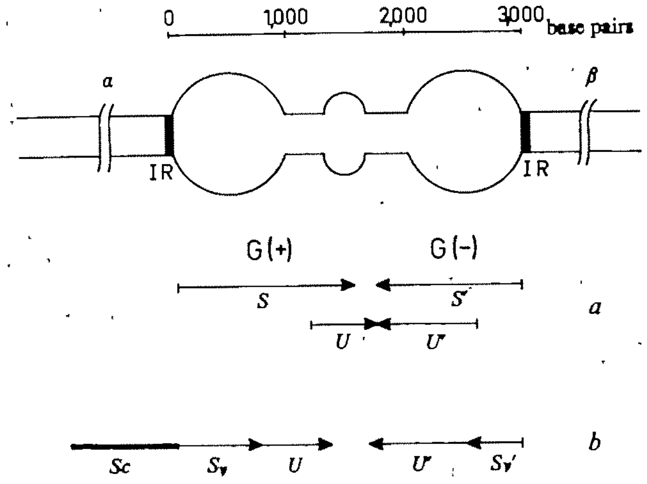

Fig. 4 Two models for the organization of the G region of bacteriophage Mu In model *a*, gene *S* is completely inside the G region based on the observation that no *S* ambers were found to map outside the G region[9] The position of gene *U* is drawn as far as possible to the right taking into account that the rightmost 1,300 base pairs of the G region are non-essential for Mu G(+) phages[3] Gene *U* could also be located completely inside gene *S* The presence of separate genes *S'* and *U'* for Mu G(−) phages is supposed because the *S* and *U* gene products are non-essential for Mu G(−) particles The sizes are based on the appearance of two new polypeptides in Mu G(−) virions instead of the *S* and *U* gene products which have disappeared (Fig 3). The drawing of the heteroduplex structure of G is according to the EM measurements of Chow *et al.*[13]. In model *b*, the *S* and *U* genes do not overlap and there is a common part of *S* and *S'* indicated with Sc outside the G region The genes *S* and *S'* differ from each other in the part located inside G, indicated with S_v and S'_v respectively.

barrier for the expression of a gene *gin*. The *gin* gene is situated outside the invertible region in the β part of Mu and is needed for the inversion of the G area[3]. It is also of interest that the gene *mom* is located adjacent to *gin* (A. Toussaint, personal communication) and might be coordinately expressed with *gin*. The *mom* gene codes for a modification function of a general nature[12]. If the function of G inversion is to prepare the phage for entering new hosts it will be extremely advantageous for the phage if a modification function is expressed simultaneously with *gin* to protect the phage DNA against foreign restriction enzymes.

Organization of the invertible region

All amber mutations in the genes *S* and *U* have been mapped inside the invertible region G. *S* codes for a 56,000-MW protein while *U* probably codes for a 21,000-MW polypeptide[10]. We have shown that these two gene products are only essential for Mu G(+) phages as *S* and *U* amber mutants plate on *C. freundii*, which is sensitive to Mu G(−) phages. Therefore, we postulate that two other genes which we indicate as *S'* and *U'* are also situated in the G region and are expressed in Mu G(−) phages instead of the *S* and *U* genes. We have some experimental evidence for the existence of *S'* and *U'*. The *S* and *U* gene products are present in Mu virions propagated in *E. coli* K12 which is sensitive to Mu G(+). However, these proteins are absent in Mu G(−) virions and are replaced by two new polypeptides with molecular weights of 48,000 (presumably S') and 26,000 (presumably U'). More recently, we have isolated amber mutants of Mu G(−) phages which are likely candidates for mutants in the genes *S'* and *U'*. Three of these amber mutants seem to behave as non-ambers in *E. coli* K12. They fall in two complementation groups and are rescued by λ-pMu hybrid phages containing the β and G regions of Mu.

As some 4,100 base pairs are needed to code for *S*, *S'*, *U* and *U'* their genes have to partially overlap if they are to be accommodated in the G region. Probably, *S* and *U* overlap each other as only 1,700 base pairs of DNA are available to code for *S* and *U*. This follows from the fact that 1,300 base pairs of the right part of G can be deleted in Mu G(+) phages without loss of viability[3]. We propose that *S'* and *U'* genes are situated in the 1,300 base pairs that can be deleted in the Mu G(+) phages. Such a model is presented in Fig. 4*a*. However, if *S* is situated partially outside the G region, it is not necessary to postulate overlapping genes (see Fig. 4*b*). The presence of G-like structures in P_1 and P_7 (refs 13, 14) supports model *a*. It is tempting to suggest that G is a unit involved in adsorption which has or had in the past the capacity to transpose itself to other DNA molecules. In fact the G region shows similarities with transposable elements as this region is bordered by inverted repeats and a *recA* independent recombination system (gin) acts on these repeats. If model *b* is correct then a striking analogy exists with immunoglobulins. The polypeptide chains in an immunoglobulin molecule have a constant region and a variable region coded for by separate genes which are fused, probably by a deletion, a transposition or an inversion[15,16]. According to Fig. 4*b*, *S* and *S'* would also consist of a constant common part coded for by a region outside the G area and a variable part located inside G. A more precise determination of the position of *S* and analysis of the four proteins will reveal whether model *a* or *b* is correct.

It is important to consider how a structure like the G region was created: it contains two pairs of genes, one pair being silent while the other is expressed. From electron microscopic studies it seems that the middle part of the G region, about 1,000 base pairs, shows an inverted homology except for a small part around the centre (see also Fig. 4). This suggests a rather extensive homology between *S* and *U* on one hand and *S'* and *U'* on the other hand. Such an extensive homology within G could be explained if G has evolved from a tandem duplication of *S* and *U* followed by an inversion of one duplicate. Subsequently one duplicate could have changed in such a way that adsorption to other hosts became possible. The nature of these changes is not yet known but apparently involves at least the sizes of the structural tail fibre proteins (S' <S and U'>U). It is of interest that we have found mutants of Mu that make slightly larger or smaller *S* proteins. These were found during the screening in minicells of amber mutants of Mu unrelated to *S*, indicating that changes in *S* might occur with a rather high frequency. In this way Mu might maintain a high degree of flexibility to adapt to changes in the environment in respect to the availability of host receptor sites.

Analogies with G inversion

Several other organisms exhibit regulatory mechanisms analogous to G inversion in Mu in that gene expression is controlled by genetic rearrangement. One example is the phase variation observed in *Salmonella typhimurium*[17]. This organism produces two types of flagella encoded by two different genes. The orientation of a promoter situated on an invertible region of 800 base pairs adjacent to one of the structural genes determines which of the two genes is expressed. Another analogy is with the regulation of the different mating type elements in yeast, a and α, which are expressed only after transposition from a silent position in the chromosome to the mating locus (cassette model[18]). In this type of mechanism, structural genes (genetic 'cassettes') are moved and thus activated. G inversion in Mu has aspects of both types of mechanism: like phase variation, host range switching in Mu involves inversion; like mating type inversion, the structural genes themselves move.

We thank Dr Jan van der Embden whose observations on G-like structures in *S. aureus* phages stimulated the initiation of our experiments, and Dr Ira Herskowitz for interesting discussions on cassette-type controls. This work was supported by Euratom grant 194-76 Bian to M.G.G.

Received 21 December 1979; accepted 16 April 1980.

1. Daniell, E., Abelson, J., Kim, J. S. & Davidson, N. *Virology* **51,** 237 (1973).
2. Hsu, M. T. & Davidson, N. *Proc. natn. Acad. Sci. U.S.A.* **69,** 2823 (1972).
3. Kamp, D., Kahmann, R., Zipser, D., Broker, T. R. & Chow, L. T. *Nature* **271,** 577 (1978).
4. Symonds, N. & Coello, A. *Nature* **271,** 573 (1978).
5. Howe, M. M. *Nature* **271,** 608 (1978).
6. De Graaf, J., Kreuningen, P. C. & Van de Putte, P. *Molec. gen. Genet.* **123,** 283 (1973).
7. Richardson, J. P., Grimley, C. & Lowery, C. *Proc. natn. Acad. Sci. U.S.A.* **72,** 1725 (1975).
8. Allet, B. *et al.* in *DNA Insertion Elements, Plasmids and Episomes* (eds Bukhari, A. I. *et al.*) 745 (Cold Spring Harbor Laboratories, New York, 1977).
9. Howe, M. M., Schumm, J. W. & Taylor, A. L. *Virology* **92,** 108 (1979).
10. Giphart-Gassler, M., Wijffelman, C. A. & Reeve, J. N. *J. molec. Biol.* (submitted).
11. Magazin, M., Reeve, J. N., Maynard-Smith, S. & Symonds, N. *FEMS Microbiol. Lett.* **4,** 5 (1978).
12. Toussaint, A. *Virology* **70,** 17 (1976).
13. Chow, L. T. and Bukhari, A. I. *Virology* **74,** 242 (1976).
14. Toussaint, A. *et al. Virology* **89,** 146 (1978).
15. Tonegawa, S., Hozumi, N., Matthussens, G. & Sculler, R. *Cold Spring Harb. Symp. quant. Biol.* **41,** 877 (1976).
16. Honjo, T. & Kataoka, T. *Proc. natn. Acad. Sci. U.S.A.* **75,** 2140 (1978).
17. Zeig, J., Hilmen, M. & Simon, M. *Cell* **15,** 237 (1978).
18. Hicks, J. B., Strathern, J. N. & Herskowitz, I. in *DNA Insertion Elements, Plasmids and Episomes* (eds Bukhari, A. I. *et al.*) 457 (Cold Spring Harbor Laboratories, New York, 1977).
19. Laemmli, U. K. *Nature* **227,** 680 (1970).

A mouse α-globin-related pseudogene lacking intervening sequences

Elio F. Vanin, Gregory I. Goldberg, Philip W. Tucker* & Oliver Smithies

Laboratory of Genetics, University of Wisconsin, Madison, Wisconsin 53706

A mouse α-globin-related pseudogene ($\psi\alpha30.5$) completely lacks intervening sequences, and could not code for a functional globin polypeptide because of frameshifts. The widespread occurrence of globin pseudogenes in other species suggests that they are not 'dead' genes but may be important in controlling globin expression.

INTERVENING SEQUENCES (introns) interrupt many eukaryotic genes[1–5]. In productive globin genes, that is, those producing functional globin polypeptides, these sequences are transcribed but are removed from the primary nuclear transcripts before the resulting mRNA is translated in the cytoplasm (reviewed in refs 6, 7). The functions of intervening sequences are not known.

The mouse genome has at least seven non-allelic globin genes: two adult β genes (β^{maj} and β^{min}), two β-type embryonic genes (y and z), two adult α genes and an α-type embryonic gene (x). An adult α and two adult β genes have been cloned and sequenced[8–13]. Each of the two β-globin genes has at the same position in the coding region a small 116-base pair intervening sequence[11,13] which has only three nucleotide differences between the two genes[13]. A second larger intervening sequence, 650 base pairs long in β^{maj} and 628 base pairs in β^{min}, differs considerably in sequence between these two genes[13], although it is in the same position in both. Intervening sequences have been found in the coding regions of all productive β-type globin genes described to date, including the adult β-type genes from rabbit[4,14], chicken[15] and man[16], and the human fetal β-type globin genes, $^{G}\gamma$ and $^{A}\gamma$ (ref. 17). An adult α-globin gene[9] from BALB/c mouse has also been shown to contain two intervening sequences, 122 and 134 base pairs long, which occur in positions analogous to those of the β-type globins. A human adult α-globin gene has comparable intervening sequences (ref. 18, and S. Liebhaber and Y. W. Kan, personal communication).

We describe here the nucleotide sequence of an α-globin 'pseudogene', which we call $\psi\alpha30.5$, previously isolated[19,20] from the DNA of outbred CD1 Swiss mice (Charles River Mouse Farms). $\psi\alpha30.5$ is clearly related to the productive mouse α-globin gene, but it lacks the two intervening sequences found in the productive gene; the intervening sequences are as cleanly missing as in fully processed mRNA. This unusual gene also has several additions and deletions, from 1 to 12 base pairs long, relative to the sequenced productive mouse α-globin gene[9]. These additions and deletions introduce frameshifts which would prevent $\psi\alpha30.5$ from producing a functional α-globin polypeptide; this is why we refer to it as an α-globin pseudogene.

Nishioka, Leder and Leder (personal communication) have recently isolated and sequenced the gene equivalent to $\psi\alpha30.5$ from BALB/c mice, and we have found that AKR/J and SWR/J mice have an *Eco*RI fragment of DNA in their genomes comparable in size and hybridization properties to the $\psi\alpha30.5$ fragment. Globin pseudogenes are also found in other species[18,21–23], and this widespread occurrence raises many questions about their evolution and function.

Restriction map of $\psi\alpha30.5$ and sequencing strategy

The α-globin pseudogene 30.5 was isolated, as clone Charon3AMm30.5 (refs 19, 20), from a random collection of recombinant bacteriophages containing *Eco*RI fragments of liver DNA from the Swiss mice. Figure 1*a* shows the restriction enzyme map of the 4.7-kilobase pair *Eco*RI

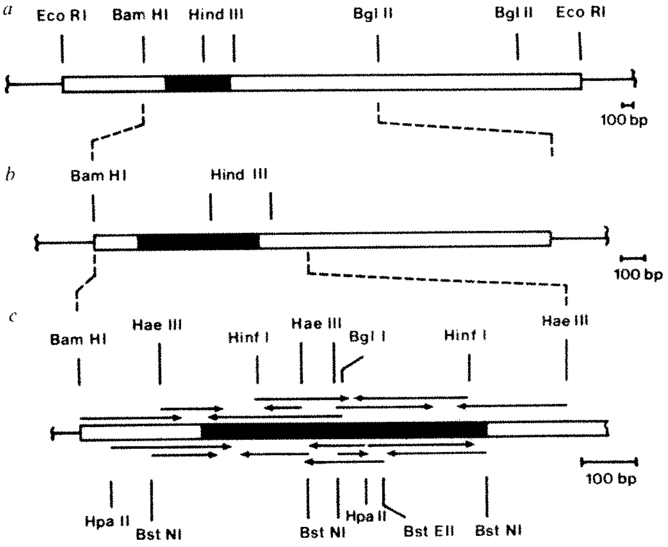

Fig. 1 Restriction maps and sequencing strategy for $\psi\alpha30.5$. *a*, Map of the 4.7-kilobase pair *Eco*RI fragment of mouse DNA in clone Charon3AMm30.5 (refs 19, 20). *b*, The *Bam*HI/*Bgl*II fragment subcloned into the *Bam*HI site of pBR322 before sequencing. *c*, The strategy used in sequencing $\psi\alpha30.5$. The black areas show the region of the cloned DNA which is homologous to mouse α-globin mRNA. The horizontal arrows show the directions of sequencing. ^{32}P-end-labelling and DNA sequencing were by the Maxam and Gilbert procedures[42] modified as described by Slightom *et al.*[17]. Other experimental procedures were essentially as described elsewhere[17]. bp, Base pairs.

---

*Present address: Department of Biochemistry, University of Mississippi Medical Center, Jackson, Mississippi 39216.

0028-0836/80/290222-05$01.00

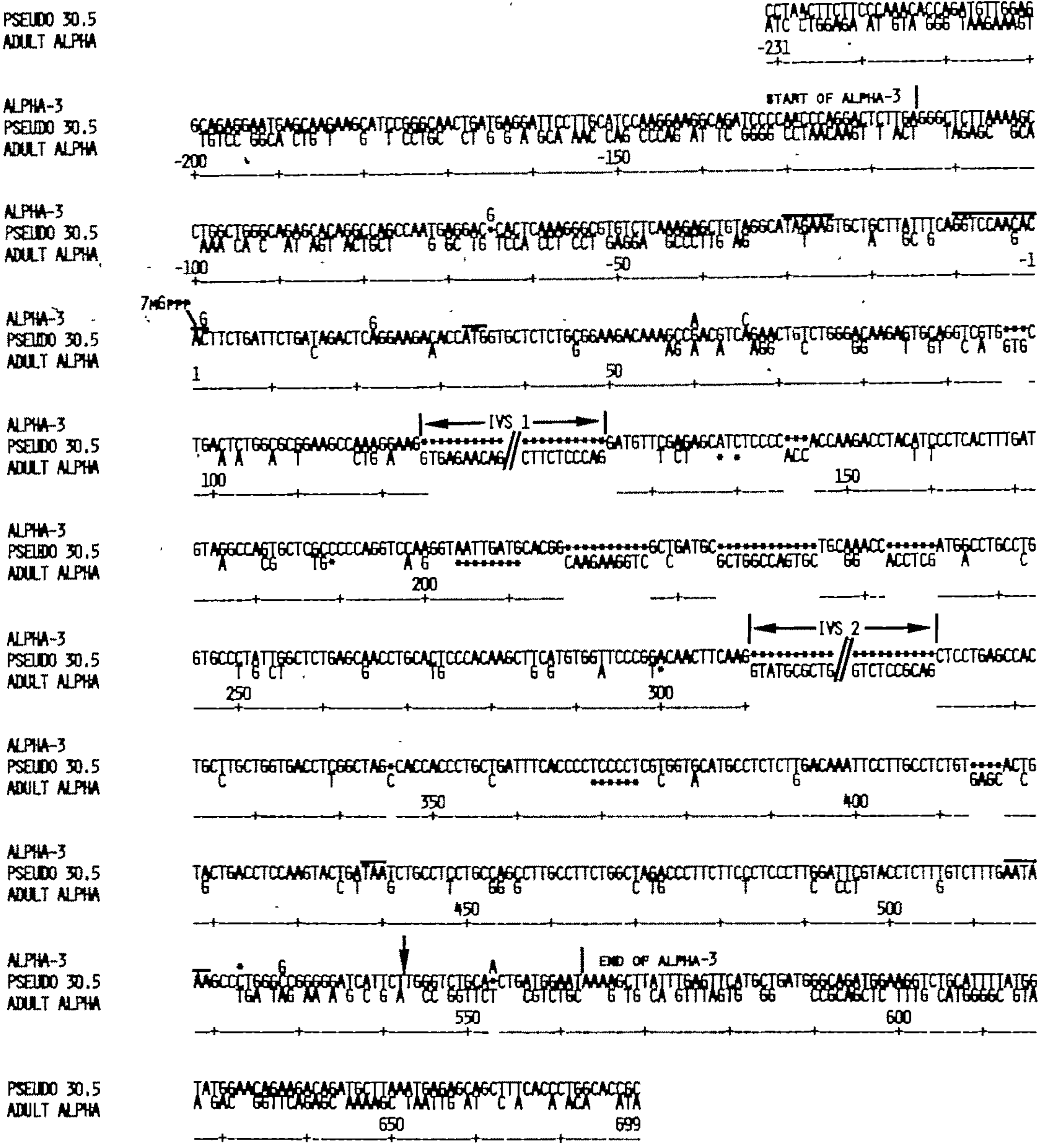

Fig. 2 The nucleotide sequence of the α-globin pseudogene, $\psi\alpha30.5$. The nucleotide sequence of $\psi\alpha30.5$ (pseudo 30.5, middle lines) is compared with the sequence of a productive adult α-globin gene[9] (adult alpha, lower lines), and to the sequence of an equivalent pseudogene (alpha-3, upper lines) isolated from BALB/c mice and sequenced by Nishioka, Leder and Leder (personal communication). The sequence of $\psi\alpha30.5$ is listed in full. Where either of the other sequences differs from $\psi\alpha30.5$ the differing bases are shown; where they are identical only the sequence of $\psi\alpha30.5$ is shown. Asterisks indicate that no bases are present at the indicated positions. The numbering system on the counting scale refers to $\psi\alpha30.5$, with number 1 corresponding to the nucleotide homologous to the first nucleotide of α-globin mRNA. The intervening sequences, IVS 1 and IVS 2, of the adult α-globin gene are shown. Potentially important signals are overlined (see text). 7mGppp shows the position of the cap of adult α-globin mRNA. The arrow after nucleotide position 541 indicates the probable 3′ end of α-globin mRNA (G. N. Pavlakis and J. N. Vournakis, personal communication). Note that the α3 sequence data do not cover nucleotide positions before −115 and after +561.

fragment in Charon3AMm30.5. Figure 1*b* shows the region subcloned into pBR322 before nucleotide sequencing, and Fig. 1*c* outlines the strategy used for nucleotide sequencing.

$\psi\alpha30.5$ is related to an adult α-globin gene

Figures 2 and 3 present the nucleotide sequence for $\psi\alpha30.5$ and compare it with the sequence of a productive α-globin gene from BALB/c mice[9]. The sequence of the equivalent pseudogene, α3, from BALB/c mice (Y. Nishioka, P. Leder and A. Leder, personal communication) is also given in Fig. 2. The nucleotide numbering system used refers to $\psi\alpha30.5$ and assigns number 1 to the nucleotide in $\psi\alpha30.5$ which is homologous to the first nucleotide of α-globin mRNA. The schematic comparison of the nucleotide sequences of $\psi\alpha30.5$ and of the productive α-globin gene presented in Fig. 3 indicates where the two sequences are identical (dark areas) and at the same time emphasizes where they differ in length (triangles above and below the horizontal lines). The points where α-globin mRNA begins and ends are indicated by vertical arrows.

The first feature revealed by the sequence data of Fig. 2 and the schematic comparison of Fig. 3 is that $\psi\alpha30.5$ is very closely related to the productive mouse α-globin gene. If we disregard additions and deletions, $\psi\alpha30.5$ is identical in sequence to the mouse α-globin gene in 84% of the region coding for mRNA. When $\psi\alpha30.5$ is compared with the nucleotide sequence of the mouse β^{maj} globin gene[11] there is only 54% identity, which is not significantly different from the 58% identity found when the sequences of mouse α- and β^{maj}-globin genes are compared with each other. These comparisons show that $\psi\alpha30.5$ is a member of the α-globin family rather than the β-globin family, which confirms our previous hybridization data[20]. Also, $\psi\alpha30.5$ seems more like the mouse adult α-globin gene than the mouse embryonic α-type globin gene, *x*; the nucelotide sequence of $\psi\alpha30.5$ has codons corresponding to an adult α-globin amino acid sequence rather than to the embryonic globin sequence[24] in nine discriminating positions which can be compared. Comparisons of the nucleotide sequence of $\psi\alpha30.5$ with the sequences of the coding regions of all the adult α-globin genes for which sequence data are available show that $\psi\alpha30.5$ is more closely related to the mouse adult α-globin gene[9] (84% identity) than to either the human adult α-globin gene (74%) (S. Liebhaber and Y. W. Kan, personal communication) or the rabbit adult α-globin gene[25] (72%).

$\psi\alpha30.5$ lacks both intervening sequences

The second feature revealed by the data presented in Figs 2 and 3 is that $\psi\alpha30.5$ completely lacks the two intervening sequences characteristic of productive globin genes. The absence of the intervening sequences in $\psi\alpha30.5$ is clean, in that the nucleotide sequence immediately 5′ and 3′ to the intervening sequences in the adult α-globin gene[9] are contiguous in ψα30.5; the nucleotide sequence in these regions of ψα30.5 is exactly the same as that seen in fully processed mouse α-globin mRNA (ref. 26, our unpublished observations, and G. N. Pavlakis and J. N. Vournakis, personal communication). It is as if the intervening sequences had never been there or had been perfectly excized.

ψα30.5 is an α-globin pseudogene

Inspection of the nucleotide sequence of ψα30.5 shows that it has several signals which might be expected in a productive α-globin gene. There is a sequence (TAGAAG) at nucleotide positions −30 to −25 comparable to the version of the Pribnow-like box[27] found in the productive α-globin gene (TATAAG) and thought to be important in the initiation of transcription[9]. There is a sequence (GGTCCAACACAC) at the nucleotide positions −10 to +2 comparable to the (GTTCGTCCTCAC) sequence postulated by Ziff and Evans[28] to be important in the 'capping' of mRNA. The expected translation initiation codon (ATG) and chain terminator codon (TAA) occur at the appropriate nucleotide positions (33–35 and 438–440). Finally, there is a sequence (AATAAA) at positions 514–519 which is identical to the so-called poly(A) addition signal (AATAAA) of Proudfoot and Brownlee[29]. We do not know whether these regions could provide adequate signals for all stages of normal transcription and translation, as the absolute requirements of these signals are not known. However, it is quite remarkable that, although the region of strong homology between ψα30.5 and the productive α-globin gene is extensive enough to include all these potential signals, beyond the outside signals the homology is virtually non-existent (see Figs 2, 3). Thus, on the 5′ (upstream) side of the two genes, the strong homology extends to nucleotide position −34, a few bases upstream from the Pribnow-like box[27]. On the 3′ (downstream) side of the two genes, the strong homology ends at nucleotide position 522, a few bases downstream from the Proudfoot–Brownlee sequence[29]. The strong homology does not extend to the 3′ end of α-globin mRNA, which is close to nucleotide position 541 (G. N. Pavlakis and J. W. Vournakis, personal communication).

Even if ψα30.5 could be transcribed into RNA which was then processed to yield a functional message, it could not code for a functional α-globin polypeptide. Figure 4 shows the amino acid sequence which corresponds to the nucleotide sequence of ψα30.5 on the assumption that it is translated in the same reading frame as the productive α-globin gene. The first 34 of these amino acid residues are very similar to those found in α globins[30], but a frameshift after amino acid residue 34, due to the addition in ψα30.5 of two bases, results in three chain terminator codons (one of each variety) shortly thereafter, and also causes the coded amino acid sequence to become unrelated (in italics) to α globin. Other frameshifts, due to the addition or deletion of non-integral triplets of nucleotides, occur elsewhere in the sequence of ψα30.5, and restore it to the α-globin reading frame briefly from residues 53 to 56 and again from residues 134 to 140.

Because ψα30.5 is clearly related in nucleotide sequence to an adult α-globin gene (Figs 2, 3), but could not code for a functional α-globin polypeptide (Fig. 4), we call it an α-globin pseudogene. This terminology does not exclude the possibility that ψα30.5 codes for a non-globin polypeptide. For example, it is conceivable (although unlikely) that ψα30.5 codes for a polypeptide homologous to α globin in its N-terminal and C-terminal regions but shorter because of the excision of a currently unrecognized intervening sequence covering the chain terminators caused by the frame shifts.

The α-globin pseudogenes in two mouse strains are almost identical

Comparison of the nucleotide sequences of ψα30.5 and the equivalent gene, α3, from BALB/c mice (Y. Nishioka, P. Leder and A. Leder, personal communication) shows (Fig. 2) that they are almost identical (>99% identity excluding deletions and additions). Both lack the two intervening sequences, and both are pseudogenes in the sense that frameshifts would prevent them from producing functional globin polypeptides. The number of differences between the α-globin pseudogenes from the two strains is close to the level attributable to errors in sequencing; thus, relative to ψα30.5, the BALB/c pseudogene has five base substitutions and three single base additions or deletions

How did the α-globin pseudogene ψα30.5 evolve?

Any evolutionary history of the α-globin pseudogene, ψα30.5, must take into account the following key observations: (1) all characterized productive globin genes of both α- and β-type have two intervening sequences at homologous places in their coding regions; (2) ψα30.5 lacks the intervening sequences cleanly; (3) ψα30.5 is much more closely related to an adult α-globin gene than to the β-type genes, and more to the mouse than to the human or rabbit adult α-globin genes; (4) ψα30.5 could not code for a functional globin polypeptide.

The first of these key observations has led to the suggestion by Leder *et al.*[8] that two intervening sequences became evolutionarily fixed in primitive globin genes before the α- and β-type genes diverged. If this is correct, three general types of evolutionary history can be suggested for ψα30.5. Each has problems, and we have no means of excluding any of them, although we favour the second.

First, ψα30.5 could be the present-day descendant of an old duplicate of a primitive globin gene which had never had intervening sequences. In this case, there are two important residual problems. Why did the pseudogene persist for so long, especially after it became unable to produce a functional globin chain? What mechanism or selective pressures caused it to co-evolve with the productive globins genes to the extent that it is recognizably related to an α-globin gene and particularly to a mouse adult α-globin gene? The simplest explanation for the evolutionary persistence of pseudogenes is

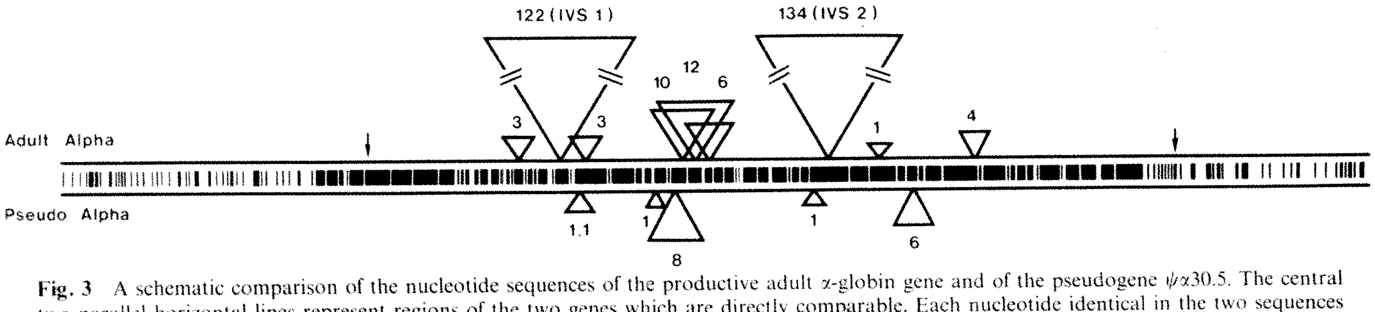

Fig. 3 A schematic comparison of the nucleotide sequences of the productive adult α-globin gene and of the pseudogene ψα30.5. The central two parallel horizontal lines represent regions of the two genes which are directly comparable. Each nucleotide identical in the two sequences is represented by a vertical stroke between these two horizontal lines; therefore, dark regions represent segments of extensive nucleotide homology. The triangles show places where the two genes differ in their lengths, and indicate the number of nucleotides in each length difference. (The triangle labelled 1,1 represents two single base additions separated by one base.) Triangles are drawn above the parallel lines when the adult α gene is longer, and below the lines when pseudogene ψα30.5 is longer. Two vertical arrows show where α-globin mRNA begins and ends.

1..........5.............10.............15................21/23........26
(Met)ValLeuSerAlaGluAspLysAlaAspValArgThr*Val*TrpAspLys*Ser*AlaGlyArgAlaAsp*Ser*GlyAla

27.....................35
GluAla*Lys*GlyArgMetPhe*Gly*Ser*IleSerProProArgProThrSerLeuThrLeuMet* * *AlaSerAlaArg*

54........57
ProGlnValGlnGly*Asn* * *CysThrGly* * *CysCysLysProTrpProAlaTrpCysProIleGlySerGluGln*

ProAlaLeuProGlnAlaSerCysGlySerArgThrThrSerSerSer * *AlaThrAlaCysTrp* * *ProArgLeu*

134...136
AlaProProCys * *PheTyrProSerProArgGlyAlaCysLeuSer* * *GlnIleProCysLeuCys*ThrValLeu

137......140
ThrSerLysTyr * *

Fig. 4 The amino acid sequence corresponding to the nucleotide sequence of $\psi\alpha30.5$ on the assumption that it is translated in the same reading frame and from the same initiator codon as the productive α-globin gene. The numbered scales show amino acid residue numbers in α globins. In frame α-globin amino acids are underlined. Amino acids in a different reading frame from α globin, or that have never been seen in an α globin, are italicized. Asterisks indicate chain terminator codons.

that they serve some important function, even though they are unable to code for globin polypeptides. The similarities between $\psi\alpha30.5$ and the adult α gene might then be a consequence of strong selective pressures keeping their sequences from diverging, or it might be due to the existence of mechanisms other than selection for maintaining similarities between related genes within a species. Recent nucleotide sequence data from our laboratory suggest that the human $^{G}\gamma$ and $^{A}\gamma$ fetal globin genes have remained very similar as a result of intergenic exchanges of DNA occurring during recombinational events comparable to gene conversion[17].

Second, $\psi\alpha30.5$ could be the descendant of a much more recent duplicate of a mouse adult α-type globin gene which had both intervening sequences. In this case, the important residual problem is explaining how they were then lost so exactly. The exact loss of both intervening sequences by random deletions at the DNA level would require an improbable series of events the selective advantages of which are individually difficult to imagine. It is easier to imagine that a molecular mechanism exists able to remove intervening sequences exactly from DNA in a fashion comparable to that used at the RNA level. Evidence in support of such a mechanism is provided by recent data on the preproinsulin genes of chicken[31], rat[9,32] and human[33]. All three species have a preproinsulin gene, with two intervening sequences in homologous positions. However, the rat, unlike the chicken and human, has an additional functional preproinsulin gene containing only the smaller first intervening sequence. Bell *et al.*[33] and Perler *et al.*[31] postulate that the two rat genes arose from a duplication, after which the larger intervening sequence was eliminated from one of the genes.

Third, a completely different type of evolutionary scheme can be imagined whereby $\psi\alpha30.5$ was recently derived from mouse adult α-globin mRNA. It is conceivable that a reverse transcript of a mouse α-globin mRNA was reintroduced into the genome, perhaps by recombination with a pre-existing α-globin gene. We know of no precedents for this type of mechanism except those related to the retroviruses, although the general concept was strongly advocated by Temin[34] in his protovirus hypothesis. This type of evolutionary scheme faces a major problem in accounting for the introduction of the reverse transcript into the germ line, because globin mRNA is normally produced in erythropoietic cells belonging to a cell lineage that is developmentally and temporally separated from the germ-cell lineage. Although the reverse transcript scheme is in general compatible with the sequence data for $\psi\alpha30.5$, special explanations would be required to account for the fact that the extent of the homology between the $\psi\alpha$ and α genes does not coincide exactly with the mRNA boundaries.

Have globin pseudogenes any function?

$\psi\alpha30.5$ is not unique in being a globin pseudogene. Maniatis and his collaborators have isolated several globin-related DNA sequences which cannot be identified with known globin polypeptides. In rabbits a gene, designated β_2, is found 5′ to the productive adult β gene[21]; it has limited sequence homology to adult and embryonic β-globin probes, it lacks a detectable mRNA transcript in the erythroid tissues examined (anaemic blood and bone marrow), and its larger intervening sequence does not hybridize to the larger intervening sequence of the productive adult β-globin gene[22]. Similar sequences ($\psi\beta_1$ and $\psi\beta_2$) which do not correspond to any of the β-type globin polypeptides have been identified in humans[23]. $\psi\beta_1$ is on the 5′ side of the productive adult β-type genes, and $\psi\beta_2$ is on the 5′ side of the embryonic ε gene. A gene, $\psi\alpha_1$, which does not code for any known globin polypeptide, has also been identified on the 5′ side of the two productive human adult genes[18]. Thus, each of these unusual genes is located in a comparable position on the 5′ side of productive globin genes. (Note, however, that the position of $\psi\alpha30.5$ in the mouse genome is not yet known.)

Although the human sequences $\psi\beta_1$ and $\psi\beta_2$ have not been studied in detail, the nucleotide sequences of both the rabbit gene β_2 (E. Lacy and T. Maniatis, personal communication) and the human gene $\psi\alpha_1$ (N. Proudfoot and T. Maniatis, personal communication) have been found to differ from the sequences of the corresponding productive globin genes in several ways which would make them incapable of coding for functional globin polypeptides. They are consequently also pseudogenes, although they differ from the pseudogene $\psi\alpha30.5$ in having intervening sequences. However, their intervening sequences are unusual in ways which would be expected to prevent them from being spliced out in the normal manner (E. Lacy, N. Proudfoot and T. Maniatis, personal communication). Thus, there are pseudogenes having unusual (or absent) intervening sequences associated with productive α- and β-type globin genes in all species for which detailed information is available. This leads us to conclude that they are probably important, and it is attractive to consider them as controlling, in some fashion, the productive globin genes. We think it unlikely that the globin pseudogenes are dead genes without function.

How might pseudogenes control productive genes?

We are investigating the possibility that pseudogenes might be 'diverting genes' able to modulate the expression of productive genes by diverting transcription into a degradative pathway. This possible mode of action of pseudogenes has two prerequisites: first, that each globin pseudogene and its related productive genes are members of the same transcriptional unit, although not necessarily of the same transcript; second, that a mechanism exists to select which portion of this unit is used. If the pseudogene portion is selected for transcription from the unit, the transcript would be degraded because the pseudogene lacks normal intervening sequences. If a productive gene portion is selected, processing of the transcript, transport out of the nucleus and translation could occur normally. Examples of processes similar to those envisaged here can be found in the literature: in adenovirus type 2, different portions of the late transcript are used in different mRNAs[35]; in a globin-SV40 system, transcripts not associated with normal intervening sequences do not yield globin polypeptides[36,37].

A second possibility is that $\psi\alpha30.5$ is an 'antigene', by which we mean that $\psi\alpha30.5$ is transcribed from the opposite (complementary) strand of DNA from that used in the productive gene. Such an anti-transcript would have the potential for forming an RNA–RNA heteroduplex with the productive gene transcript in a manner similar to that proposed by Davidson and Britten[38] for the transcripts of some repetitive DNAs. The resulting structure, with a form similar to that shown in Fig. 3, might function as a positive controlling element in erythroid tissues, or as a negative element in non-erythroid tissues. (This idea does not exclude the possibility that pseudogene anti-transcripts form ternary complexes with the transcripts of the corresponding productive genes and the small stable nuclear RNAs recently implicated in RNA processing by Lerner *et al.* and Rogers and Wall[39,40].)

Preliminary experiments aimed at exploring the transcriptional status of the $\psi\alpha30.5$ pseudogene have been done in erythroid tissue. We prepared ^{32}P-end-labelled fragments from $\psi\alpha30.5$ DNA which could be used as specific probes for the 'sense' and 'antisense' transcripts of the $\psi\alpha30.5$ pseudogene. We tested, by the Berk and Sharp procedure[41], the ability of total RNA from mouse fetal liver cells (an erythroid tissue) to form RNA–DNA hybrids capable of protecting these probes from S_1 nuclease. We have been unable in these preliminary experiments to find evidence for significant protection by the fetal liver RNA of either the sense or the antisense probes derived from $\psi\alpha30.5$, using conditions which allow easy detection of globin precursor RNA (A. J. Kinniburgh, personal commmunication). Thus, if the pseudogene is transcribed in erythroid tissues, its available transcript must be at a steady-state level lower than that of globin precursor RNA. This result agrees with that already cited for the rabbit pseudogene β_2 (ref. 22).

The general hypothesis that pseudogenes control the productive genes in some fashion, nevertheless, remains attractive and we are investigating the hypothesis further, including tests in non-erythroid tissues. Certainly, the widespread occurrence of globin pseudogenes argues strongly for their functional importance.

We thank Drs Y. Nishioka, A. Leder, P. Leder, N. Proudfoot and T. Maniatis for sequence data before publication, Natalie Borenstein and John Devereux for technical assistance, Dr J. L. Slightom for advice in the DNA sequencing, and Drs A. J. Kinniburgh and J. Ross for advice and help in the experiments testing for transcription of $\psi\alpha30.5$. This work was supported by NIH grants AM20120 and GM20069 to O.S., and GM21812 to Dr F. R. Blattner, whom we thank for the shared use of laboratory equipment. The recombinant DNA experiments were carried out in accordance with NIH guidelines.

Received 25 March; accepted 2 May 1980.

1. Breathnach, R., Mandel, J. L. & Chambon, P. *Nature* **270,** 314–319 (1977).
2. Braćk, C. & Tonegawa, S. *Proc. natn. Acad. Sci. U.S.A.* **74,** 5652–5656 (1977).
3. Leder, P. *et al. Cold Spring Harb. Symp. quant. Biol.* **42,** 915–920 (1977).
4. Jeffreys, A. J. & Flavell, R. A. *Cell* **12,** 1097–1108 (1977).
5. Lomedico, P. *et al. Cell* **18,** 545–558 (1979).
6. Crick, F. *Science* **204,** 264–271 (1979).
7. Abelson, J. *A. Rev. Biochem.* **48,** 1035–1069 (1979).
8. Leder, A. *et al. Proc. natn. Acad. Sci. U.S.A.* **75,** 6187–6191 (1978).
9. Nishioka, Y. & Leder, P. *Cell* **18,** 875–882 (1979).
10. Tilghman, S. M. *et al. Proc. natn. Acad. Sci. U.S.A.* **74,** 4406–4410 (1977).
11. Konkel, D. A., Tilghman, S. M. & Leder, P. *Cell* **15,** 1125–1132 (1978).
12. Tiemeier, D. C. *et al. Cell* **14,** 237–245 (1978).
13. Konkel, D. A., Maizel, J. V. Jr & Leder, P. *Cell* **18,** 865–873 (1979).
14. van den Berg, J. *et al. Nature* **276,** 37–44 (1978).
15. Dodgson, J. B., Strommer, J. & Engel, J. D. *Cell* **17,** 879–887 (1979).
16. Lawn, R. M., Fritsch, E. F., Parker, R. C., Blake, G & Maniatis, T. *Cell* **15,** 1157–1174 (1978).
17. Slightom, J. L., Blechl, A. E. & Smithies, O. *Cell* (in the press).
18. Lauer, J., Shen, C.-K. J. & Maniatis, T. *Cell* **20,** 119 (1980).
19. Blattner, F. R. *et al. Science* **202,** 1279–1284 (1978).
20. Smithies, O. *et al. Science* **202,** 1284–1289 (1978).
21. Lacy, E., Hardison, R. C., Quon, D. & Maniatis, T. *Cell* **18,** 1273–1283 (1979).
22. Hardison, R. C. *et al. Cell* **18,** 1285–1297 (1979).
23. Fritsch, E. F., Lawn, R. M. & Maniatis, T. *Cell* **19,** 959–972 (1980).
24. Melderis, H., Steinheider, G. & Ostertag, W. *Nature* **250,** 774–776 (1974).
25. Heindel, H. C., Liu, A., Paddock, G. V., Studnicka, G. M. & Salser, W. A. *Cell* **15,** 43–54 (1978).
26. Pavlakis, G. N. *et al. Cell* **19,** 91–102 (1980).
27. Pribnow, D. *Proc. natn. Acad. Sci. U.S.A.* **72,** 784–788 (1975).
28. Ziff, E. B. & Evans, R. M. *Cell* **15,** 1463–1475 (1978).
29. Proudfoot, N. J. & Brownlee, G. G. *Nature* **263,** 211–214 (1976).
30. Dayhoff, M. O. (ed.) in *Atlas of Protein Sequence and Structure* Vol. 5, Suppl. 2, 191–223 (National Biomedical Research Foundation, Washington, DC, 1976).
31. Perler, F. *et al. Cell* (in the press).
32. Cordell, B. *et al. Cell* **18,** 533–543 (1979).
33. Bell, G. I. *et al. Nature* **284,** 26–32 (1980).
34. Temin, H. M. *A. Rev. Genet.* **8,** 155–177 (1974).
35. Nevins, J. R. & Darnell, J. E. *Cell* **15,** 1477–1493 (1978).
36. Hamer, D. H., Smith, K. D., Boyer, S. H. & Leder, P. *Cell* **17,** 725–735 (1979).
37. Hamer, D. H. & Leder, P. *Cell* **17,** 737–747 (1979); **18,** 1299–1302 (1979).
38. Davidson, E. H. & Britten, R. J. *Science* **204,** 1052–1059 (1979).
39. Lerner, M. R., Boyle, J. A., Mount, S. M., Wolin, S. I. & Steitz, J. A. *Nature* **283,** 220–224 (1980).
40. Rogers, J. & Wall, R. *Proc. natn. Acad. Sci. U.S.A.* **77,** 1877 (1980).
41. Berk, A. J. & Sharp, P. A. *Cell* **12,** 721–732 (1977).
42. Maxam, A. M. & Gilbert, W. *Proc. natn. Acad. Sci. U.S.A.* **74,** 560–564 (1977).

Proximity of mRNA5′-region and 18S rRNA in eukaryotic initiation complexes

Kunio Nakashima*, Edward Darzynkiewicz† & Aaron J. Shatkin

Roche Institute of Molecular Biology, Nutley, New Jersey 07110

Messenger RNA was covalently linked to 18S ribosomal RNA in eukaryotic 40S and 80S initiation complexes by photoreaction with an RNA cross-linking agent, 4′-substituted psoralen. The sites of interaction of the mRNA capped 5′-region included some 3′-ends of 18S rRNA.

An early step in protein synthesis is the binding of mRNA to ribosomal small subunits. The resulting initiation complexes in prokaryotes apparently are stabilized by base pairing between the 3′-terminal sequence of 16S ribosomal RNA,...CCUCCUUA, and a purine-rich nucleotide stretch located in mRNA on the 5′-side of the AUG initiator codon[1-3]. The suggestion that mRNA–rRNA interactions are similarly involved in the initiation of eukaryotic translation[4] has been a topic of considerable speculation[5-9]. Comparative analyses have demonstrated a highly conserved 3′-terminal sequence in the small rRNAs of *Escherichia coli*[1], *Bacillus stearothermophilus*[10] and maize chloroplast[11] as well as in yeast[12], slime mould, wheat, silkworm, mouse[5], rat[13] and rabbit[14] but the CCUCC sequence implicated in prokaryotic initiation is absent from eukaryotic 18S rRNA. Thus, conservation of the 3′ sequence may be related to rRNA processing or events other than initiation of protein synthesis. However, some eukaryotic viral[15] and cellular[16] mRNAs contain within their noncoding 5′ region nucleotide sequences complementary to the 3′ end of 18S rRNA and consequently at least could contribute to stable initiation complex formation.

Psoralens are tricyclic photoreactive compounds that intercalate into nucleic acids. Irradiation of polynucleotide-bound psoralen with long wavelength UV light produces adducts with pyrimidine bases. Because psoralens are bifunctional agents, they can also form cross-links between interacting pyrimidine-containing nucleotide sequences[17]. 4′-Substituted derivatives of psoralen with improved

---

*Present address: Department of Biochemistry, Yamagata University School of Medicine, Zao-Iida, Yamagata, Japan 990–23.

†Permanent address: Department of Biophysics, Institute of Experimental Physics, University of Warsaw, Warsaw, Poland.

0028–0836/80/290226–05$01.00

photoreactivity have been synthesized recently and have already proved useful for investigating genome structure–function relationships in RNA viruses[18]. For example, photoreaction of reovirus with 4′-aminomethyl-4,5′,8-trimethylpsoralen (AMT) produced RNA–RNA cross-links between the two complementary strands comprising the viral genome and inactivated its template function for the virion-associated RNA polymerase[19]. These findings suggested that AMT photoreaction would be useful for probing other types of nucleoprotein complexes, such as those formed between mRNA and ribosomes during initiation of protein synthesis.

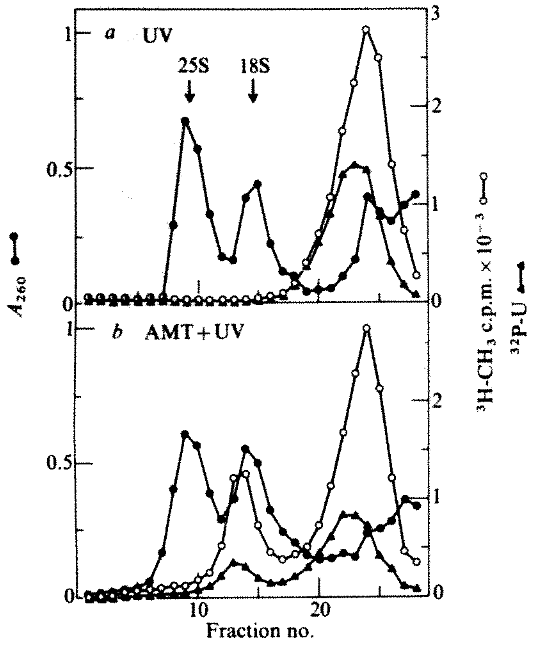

Fig. 1 Cross-linking of reovirus mRNA to 18S rRNA in wheat germ 40S initiation complexes. Reovirus mRNA radiolabelled with ^{3}H-methyl in the 5′-terminal cap, m^{7}GpppG^m and internally with ^{32}P-UMP was synthesized *in vitro* as described previously[43]. The viral mRNA was nicked to fragments sedimenting at 4–6S by incubation in 50 mM NH$_4$HCO$_3$, *p*H 10, at 98 °C for 3 min. The fragments were used to form 40S initiation complexes by incubation in wheat germ translating extracts in the presence of 0.2 mM sparsomycin to block elongation and 0.4 mM guanosine-5′-(β,γ-methylene)triphosphate to decrease 60S subunit joining to 40S–mRNA complexes[23]. Complexes were isolated by centrifugation for 4 h and 189,000*g* in the SW40 rotor in 10–30% glycerol gradients containing 10 mM Tris-HCl (*p*H 7.4), 0.75 mM Mg acetate and 70 mM KCl[20]. Fractions containing 40S initiation complexes (which also included free 60S subunits) were combined and irradiated with long wavelength UV light for 20 min at 0 °C in the absence (*a*) and presence (*b*) of 2.8 × 10^{-4} M 4′-aminomethyl-4,5′,8-trimethylpsoralen (AMT) as described previously[44]. The irradiated mixtures were incubated at 37 °C for 1 h with proteinase K (1 mg ml^{-1}) and 0.5% SDS, and the RNA was extracted with water-saturated phenol and analysed by centrifugation (SW-41, 131,000*g*, 16 h, 5 °C) in 10–30% glycerol gradients containing 50 mM Tris-HCl, *p*H 7.4, 150 mM NaCl and 1 mM EDTA. Fraction aliquots were counted in Aquasol (NEN) after determining the $A_{260\,\mathrm{nm}}$.

We have used this approach to look for RNA–RNA interactions between the ends of radiolabelled mRNA and rRNA in eukaryotic initiation complexes.

Cross-linking of reovirus mRNA and 18S rRNA in wheat germ 40S and 80S initiation complexes

Most eukaryotic mRNAs are monocistronic. During initiation of translation ribosomes bind to mRNA at or near the 5′ cap and re-position, perhaps by a scanning mechanism, at the 5′-proximal AUG codon to start polypeptide synthesis[6]. Previous studies with reovirus mRNA and mRNA fragments labelled with ^{3}H-methyl in the 5′ cap, m^{7}GpppG^m, and at internal sites with ^{32}P have demonstrated that capped molecules are selectively bound to ribosomes[20–22]. Thus when ^{3}H-methyl, ^{32}P-UMP labelled, alkali-fragmented reovirus mRNA (chain length ~200 nucleotides) was incubated in wheat germ cell-free translating extract in conditions of 40S initiation complex formation, 32% of the ^{3}H and 4% of the ^{32}P was bound to ribosomal small subunits and sedimented in a glycerol gradient in a position close to 40S subunits; similar results have been described previously[23,24]. To determine whether mRNA and rRNA were closely apposed in these complexes, pooled fractions from the 40–60S region of the gradient were irradiated at $\lambda_{352\,\mathrm{nm}}$ in the presence and absence of the RNA cross-linking agent, AMT, and the RNA was extracted from the initiation complexes and analysed by gradient sedimentation. As shown in Fig. 1*a*, initiation complexes irradiated in the absence of AMT yielded labelled mRNA

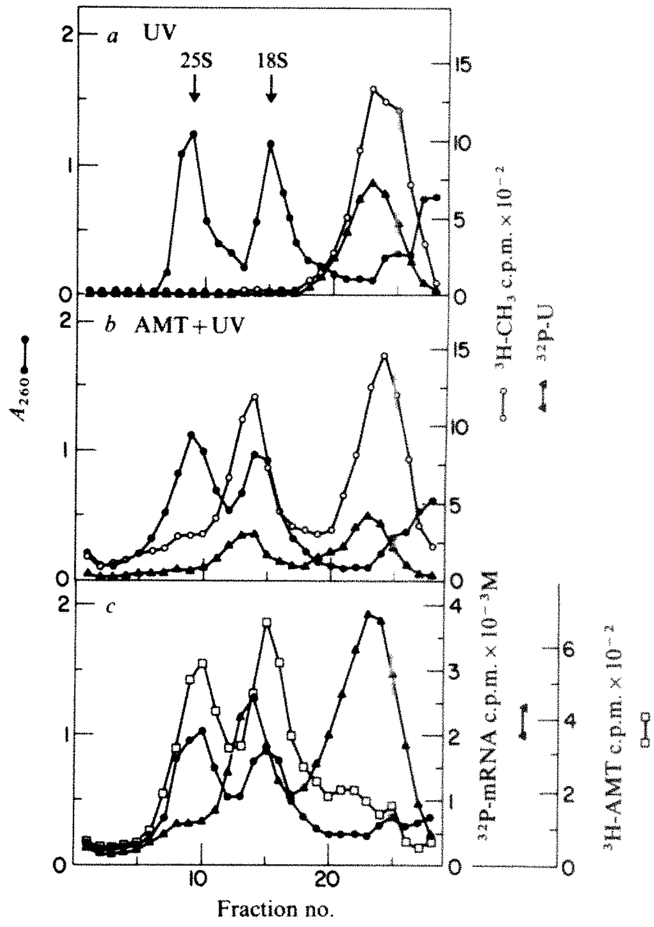

Fig. 2 Cross-linking of reovirus mRNA to 18S rRNA and covalent binding of ^{3}H-AMT to rRNAs in wheat germ 80S initiation complexes. Radiolabelled reovirus mRNA fragments were incubated as in Fig. 1 except that mixtures contained 0.2 mM GTP in place of guanosine-5′-(β,γ-methylene)triphosphate to obtain 80S complexes. Complexes containing double-labelled fragments were isolated by glycerol gradient centrifugation and UV-irradiated in the absence (*a*) or presence (*b*) of 2.8 × 10^{-4} M AMT. For *c*, fragments were prepared from mRNA synthesized in the presence of all four [α-^{32}P]labelled ribonucleoside triphosphates and unlabelled S-adenosylmethionine, and the incubation mixture, rather than isolated initiation complexes, was irradiated for 20 min in 1.4 × 10^{-4} M ^{3}H-labelled AMT (specific activity 1.4 × 10^5 c.p.m. μg^{-1}. RNA was extracted and analysed by glycerol gradient centrifugation as described in the legend to Fig. 1.

fragments that sedimented at the top of the gradient, well-separated from the rRNAs. By contrast, complexes that were irradiated in the presence of AMT yielded a significant portion of both the ^3H (28%) and ^{32}P (25%) sedimenting in a position slightly faster than the small ribosomal RNA (Fig. 1*b*).

Like 40S initiation complexes, 80S complexes irradiated with AMT also yielded a large fraction (38%) of the radioactive mRNA fragments cross-linked to 18S rRNA (Fig. 2*a*, *b*). Apparently there was little interaction of mRNA fragments with the large rRNA in initiation complexes. However, the rRNAs in both ribosomal subunits were accessible to psoralen photoreaction. As shown in Fig. 2*c*, in conditions which resulted in cross-linking of ^{32}P-labelled mRNA fragments to 18S rRNA, both rRNAs formed ^3H-labelled AMT adducts; psoralen average molar ratios were 0.8 and 1.5 for the small and large rRNAs, respectively.

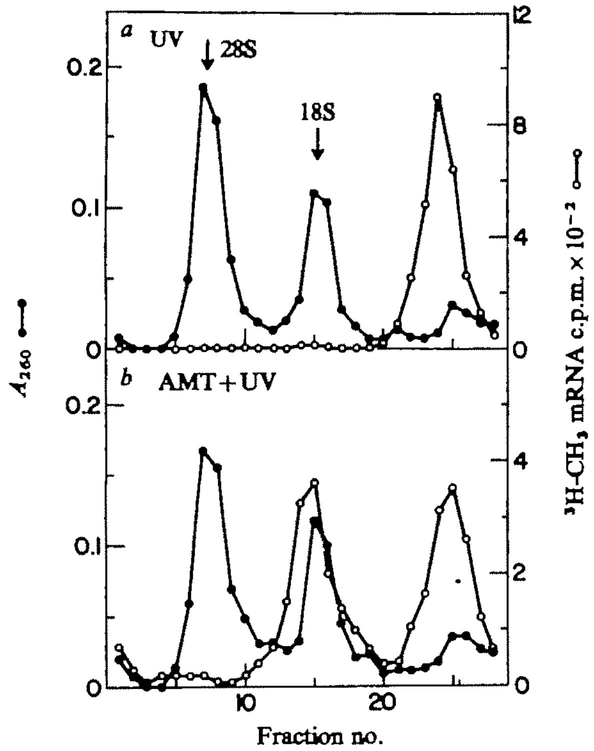

Fig. 3 Cross-linking of vesicular stomatitis virus mRNA to 18S rRNA in reticulocyte 80S initiation complexes. ^3H-methyl-labelled viral mRNA containing all radioactivity in the 5′-terminal cap, m^7GpppA^m was synthesized *in vitro* in the presence of 2 μM *S*-adenosyl-L-[Me-^3H]methionine (specific activity 70 Ci $mmol^{-1}$)[45]. Rabbit reticulocyte lysates (treated with haemin)[46] were used to form 80S initiation complexes as in Fig. 2. Gradient fractions containing complexes were combined, irradiated in the absence (*a*) or presence (*b*) of 2.8×10^{-4} M AMT, and the extracted RNA analysed as described for Fig. 1.

Results essentially the same as those in Figs 1 and 2 were obtained with intact mRNA and when sedimentation analyses were done in denaturing conditions in 99% Me_2SO-sucrose gradients, although the ribosomal and mRNAs were less well resolved. With either intact mRNA or fragments, interaction with 18S rRNA was dependent on initiation complex formation. Cross-linked hybrid molecules were not obtained by AMT photoreaction of a mixture of mRNA and purified rRNAs. Furthermore, cross-linking of ^3H-methyl, ^{32}P-AMP-labelled mRNA to rRNA was not observed following AMT photoreaction of incubation mixtures that were complete except for the absence of ATP which is required for mRNA binding to ribosomes[25,26].

Interaction of 18S rRNA with other mRNAs in rabbit reticulocyte and wheat germ initiation complexes

Various other 5′-terminally labelled viral mRNAs including *in vitro* transcripts synthesized by the virion-associated RNA polymerases of vesicular stomatitis (VSV), influenza and cytoplasmic polyhedrosis (CPV) viruses and genome RNAs of tobacco mosaic (TMV) and satellite tobacco necrosis (STNV) viruses were tested. Each of these RNAs interacted with the 18S rRNA in wheat germ initiation complexes as detected by AMT photoreaction (data not shown). In addition, 40S and 80S initiation complexes formed in rabbit reticulocyte lysates gave results similar to those obtained in the wheat germ system. For example, when initiation complexes of reticulocyte 80S ribosomes and fragmented VSV mRNA containing 5′-terminal ^3H-methyl-labelled m^7GpppA^m were photoreacted with AMT, 47% of the ribosome-bound radioactivity cross-linked to, and sedimented with the 18S rRNA (Fig. 3).

Capped ribopolymers, synthesized by incubating polynucleotide phosphorylase, ribonucleoside diphosphates and ^3H-methyl-m^7GpppG^m-C in primer-dependent conditions, have proved useful for studies of structural and compositional effects on mRNA binding to ribosomes[27]. Capped poly(U) forms only 40S initiation complexes with wheat germ ribosomes while capped poly(A, U) associates with 80S monosomes[27]. However, as observed with natural mRNA, AMT photoreaction of the 40S-capped poly(U) complexes or of the capped poly(A, U)–40S and 80S complexes resulted in polymer cross-linking to 18S rRNA only (data not shown).

Sites of cross-linking of 18S rRNA to 5′ end of mRNA

Initially we attempted to test whether the 3′ region of 18S rRNA interacts with mRNA during initiation by using prelabelled ribosomes but were unsuccessful in radiolabelling the 3′ terminus of rRNA *in situ* by incubating wheat germ extracts with ^{32}P-pCp and RNA ligase[28]. Instead we used the same technique to label purified, cross-linked hybrids of 18S rRNA and mRNA fragments isolated from AMT-photoreacted wheat germ 80S initiation complexes. They were formed with 5′ ^3H-methyl-labelled reovirus mRNA that had been treated at *p*H 10 before ribosome binding to produce mRNA fragments containing a 3′-terminal phosphate. As a consequence, ^{32}P-pCp-labelling of the cross-linked RNA–RNA complexes was apparently limited to free hydroxyl groups at the 3′ end of the rRNA strands. The radiolabelled sample, which included an excess of 18S rRNA from ribosomes that did not bind mRNA in addition to rRNA–mRNA complexes, was digested with RNase T_1. The resulting oligonucleotide fragments were loaded onto a column of acetylated dihydroxyboryl (DBAE)-cellulose in conditions that result in the selective binding of those oligonucleotides that contain 2′,3′-*cis*-diols[29]. Since the ^{32}P was present as ^{32}P-pCp at the 3′ end of rRNA (and T_1 RNase digestion results in oligonucleotides with a 3′-terminal phosphate), 99% of the ^{32}P-labelled fragments did not bind to the resin. The ^3H radioactivity, however, bound to the extent of 78% as expected for mRNA fragments containing 5′-terminal $m^7G^{5'}ppp^{5'}G^m$, that is, a 2′,3′-*cis*-diol in the 5′-linked m^7G (ref. 30). The bound oligonucleotides were eluted and rechromatographed on DBAE-cellulose. There was quantitative binding of the ^3H-labelled material, and more than 70% of the ^{32}P-labelled oligonucleotides were retained on the resin in the second pass (Fig. 4*a*), presumably due to cross-linking to capped mRNA fragments since in the absence of AMT photoreaction there was little ^{32}P rebinding.

The DBAE-bound sample was eluted and analysed by electrophoresis in a 20% polyacrylamide gel in denaturing conditions in 7 M urea. Although the capped oligonucleotides released from at least six of the reovirus mRNA species by RNase T_1 digestion are 8 to 10 nucleotides long[31], the ^3H-labelled cross-linked sample migrated as a broad peak of chain length ~15 to ~35 nucleotides as estimated from the position of marker dyes, bromophenol blue and xylene cyanol (Fig. 4*b*). The ^{32}P-labelled oligonucleotides were resolved into a fraction that co-migrated with the peak of ^{3}H and a larger, more heterogeneous component near the xylene cyanol dye. On the basis of the known 3′- and 5′-terminal sequences of rRNA and reovirus mRNAs, RNase T_1 treatment would release from 3′-^{32}P-pCp-labelled wheat germ 18S rRNA[5] the radioactive oligonucleotide, AUCAUUG-^{32}P and from a mixture of ^{3}H-methyl-labelled reovirus mRNAs, several 5′-capped A,U-rich oligonucleotides of chain length 8–10 nucleotides[31]. Cross-linking by AMT of the rRNA 3′ end to mRNA 5′ fragments would result in hybrids of minimum size ~15–17 nucleotides, a value corresponding reasonably well to the double-labelled peak at fractions 46–47 in Fig. 4*b*. The formation of cross-links involving pyrimidine residues distal to the 3′ end T_1 fragment of rRNA might have two related effects consistent with the higher ^{32}P/^{3}H ratio in the longer oligonucleotides: increased accessibility of the 3′ end for ^{32}P-pCp addition by RNA ligase and decreased susceptibility for complete cleavage by RNase T_1. Alternatively the radioactivity profiles may reflect cross-linking of some mRNA 5′ ends to other sites in the 18S rRNA. Results similar to those in Fig. 4 were obtained with reovirus mRNA–18S rRNA cross-linked fragments from wheat 40S and rabbit 80S initiation complexes.

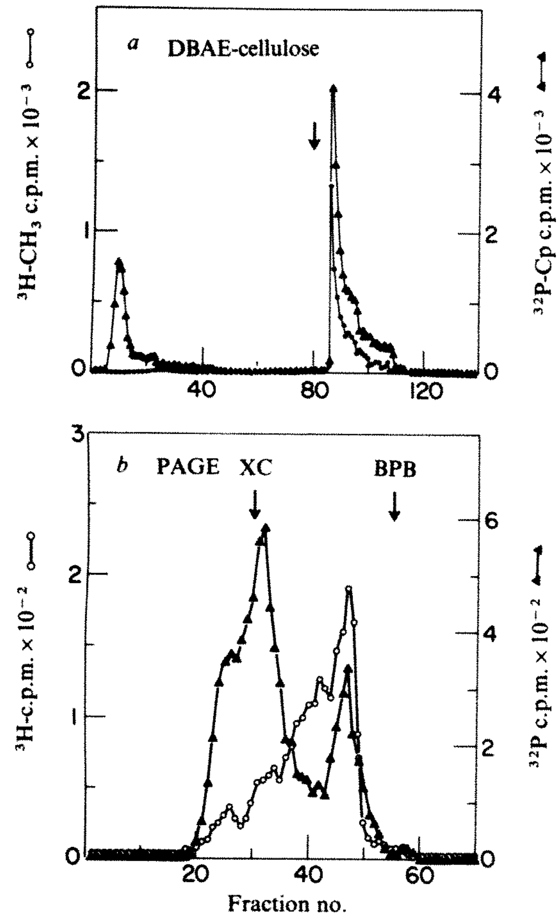

Fig. 4 Analysis of RNase T_1 digest of 5′ ^{3}H-methyl labelled reovirus mRNA cross-linked to 3′-^{32}P-labelled 18S rRNA. Wheat germ 80S initiation complexes were isolated, photoreacted with AMT and the cross-linked complexes of mRNA fragments with 18S rRNA were obtained as in Fig. 1. rRNA in the complexes was radiolabelled at the 3′ end by incubation with ^{32}P-pCp and T_4 RNA ligase[28]. After digestion with RNase T_1 (200 μg RNA, 100 units T_1 in 0.5 ml 20 mM Tris-HCl buffer *p*H 8 containing 0.1 mM EDTA) at 37 °C for 1 h, the digest was added to 2 ml of buffer A[30] and applied to a column (0.6 × 5 cm) of acetylated dihydroxyboryl-substituted cellulose (DBAE-cellulose). After extensive washing with buffer A, bound material was eluted with 1 M sorbitol in buffer A and precipitated by addition of 3 volumes of ethanol and standing overnight at −20 °C. The precipitated RNA was recovered by centrifugation and rechromatographed on DBAE-cellulose (*a*). Aliquots of fractions were counted in Aquasol. The RNA in fractions 85–115 (arrow indicates start of sorbitol elution) was recovered by ethanol precipitation and analysed by electrophoresis in a 20% polyacrylamide gel in the presence of 7 M urea. The 0.6 × 10 cm cylindrical gel was fractionated into 1 mm slices that were dissolved in 18% H_2O_2 before counting in Aquasol (*b*). XC, xylene cyanol dye; BPB, bromophenol blue dye.

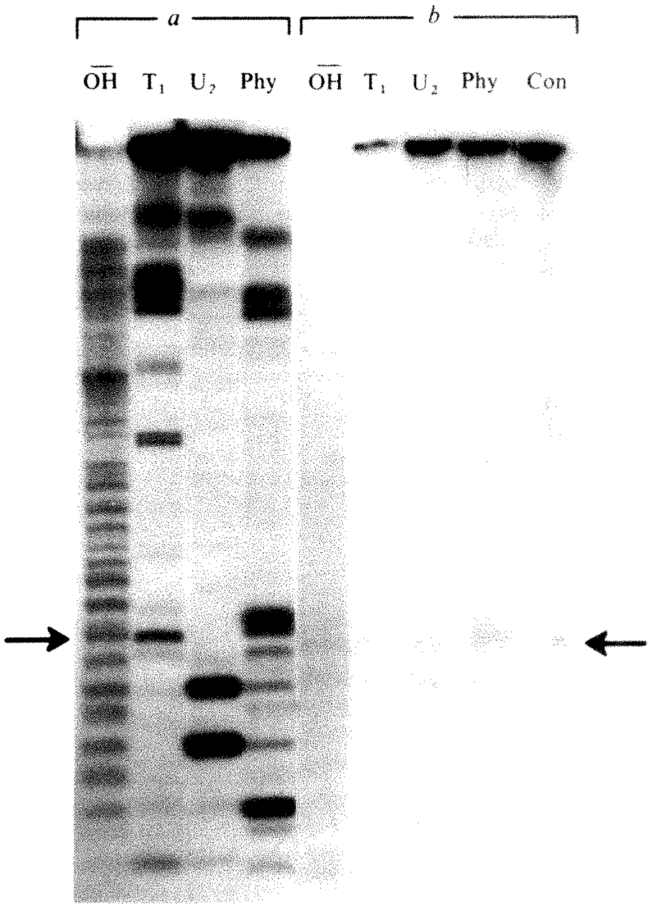

Fig. 5 Nucleotide sequence analyses of 18S rRNA and mRNA–rRNA complexes. AMT cross-linked complexes of mRNA and 18S rRNA that had been 3′-end labelled with ^{32}P-pCp, RNase T_1 digested and selectively bound to DBAE-cellulose two times (fractions 85–115 in Fig. 4*a*) were recovered by ethanol precipitation and irradiated with short wavelength UV light (254 nm) for 2 h at 0 °C in conditions that photoreverse AMT cross-links[32]. After photoreversal, the ^{32}P-labelled fragments were analysed by partial enzymatic digestion and polyacrylamide gel electrophoresis[33] in comparison with 3′-terminally ^{32}P-labelled 18S rRNA. *a*, Wheat germ 18S rRNA labelled at the 3′ end with ^{32}P-pCp; *b*, RNase T_1 fragment from photoreversed rRNA–mRNA complexes. Arrows indicate 18S rRNA 3′-terminal T_1 oligonucleotide. $\overline{\text{OH}}$, alkaline hydrolysate; T_1, U_2 and Phy, the respective RNase digests using conditions described previously[47]; Con, RNase T_1 fragments from photoreversed complexes not further digested.

To confirm that the DBAE-bound, ^{32}P-labelled oligonucleotides included 3′ ends of 18S rRNA, the cross-linked, double-labelled fragments eluted from the resin were irradiated at a wavelength of 254 nm to photoreverse the AMT cross-links[32]. The photoreversed sample was analysed in a polyacrylamide sequencing gel in comparison with 3′-^{32}P-labelled wheat germ 18S rRNA[33]. Partial enzymatic digests of the rRNA in non-denaturing conditions yielded patterns consistent with the published 3′ sequence[5] including a nuclease-resistant, presumptive hairpin structure extending from about residue 10 to 30 (Fig. 5*a*). Although some of the radioactivity in the irradiated oligonucleotide sample remained near the gel origin, the released ^{32}P-labelled material migrated in a position corresponding to the T_1 limit oligonucleotide of rRNA (Fig. 5*b*, Con, arrows). This oligonucleotide yielded a series of shorter products on digestion with alkali (OH). RNase T_1 treatment released some radioactivity which migrated near position 1 as in T_1 digests of rRNA, but most of the oligonucleotide remained undegraded (T_1). It was also relatively resistant to *Physarum* RNase I in these partial digestion conditions (Phy). RNase U_2 treatment yielded two additional bands that corresponded in position to oligonucleotides obtained from rRNA by U_2 digestion (U_2). These results indicate that the DBAE-selected, cross-linked fragments included some of the ^{32}P-pCp-labelled 3′-terminal T_1 oligonucleotide from 18S rRNA.

Role of base pairing

Several lines of evidence[2,3,34–36] support the early suggestion that initiation codon selection in prokaryotic mRNAs is influenced by base pairing between the 3′ sequence of 16S rRNA and a polypurine region about 10 nucleotides to the 5′ side of the initiator triplet. Similar kinds of experiment in eukaryotes have not been reported, but sequences complementary to the conserved 3′ end of 18S rRNA occur in the 5′ noncoding regions of many eukaryotic mRNAs. In some cases the complementarity is striking, with calculated stabilities for the potential mRNA–rRNA base-paired structures in the same range as prokaryotic initiator regions[15,37,38], and in polyoma virus mRNA the 5′ leader contains multiple copies of such a sequence[39]. In other functional eukaryotic mRNAs, including species of reovirus[31] and VSV mRNA[40], the potential for stable base pairing between 5′ ends and 18S rRNA 3′-termini is so low as to suggest that it could have at most a minor influence on initiation, indicating that this type of base pairing is not obligatory for eukaryotic protein synthesis. The observation that the translation of prokaryotic virus mRNAs in wheat germ extract is strongly enhanced after enzymatic addition of a 5′ cap supports this conclusion[41].

In an effort to test experimentally whether mRNAs interact with rRNAs during eukaryotic initiation, we have used photochemical reaction with the RNA–RNA cross-linking agent, AMT. By using ^{3}H-methyl-labelled capped mRNA and ^{32}P-pCp-labelling of rRNA, we detected cross-linking between mRNA 5′ fragments and 18S rRNA 3′ sequences in both 40S and 80S initiation complexes. It is not clear if cross-linking occurs at many sites in the 18S rRNA or is restricted to the 3′ end. Although the findings indicate that the opposite ends of mRNA and 18S rRNA are proximally located at least in some initiation complexes, the interaction clearly is not strictly homologous to 'Shine and Dalgarno' base-paired structures. One obvious difference noted previously[5] is the variation among eukaryotic mRNAs in the position of the rRNA complementary sequences relative to the initiator AUG, compared with the fixed position in prokaryotic mRNAs. However, since different 5′ leaders precede the initiator codon in eukaryotic mRNAs and ribosomes apparently re-position at the 5′-proximal AUG after attaching near the cap[6], 18S rRNA 3′-complementary sequences with functional effects on initiation could occur at different places within the 5′ noncoding region of various mRNAs. Another consideration is that some mRNAs, and particularly synthetic ribopolymers such as capped poly(U), contain too few 5′-proximal nucleotides complementary to the 3′ sequence of 18S rRNA to form a stable base-paired structure of the prokaryotic type. By the cross-linking method capped poly(U), as well as mRNAs like adenovirus hexon mRNA which can form a stable base-paired structure between 5′ leader sequences and 18S rRNA 3′ ends[15], would be fixed to 18S rRNA by the formation of AMT diadducts between pyrimidines that are even transiently juxtaposed. In some cases cross-linking presumably could also occur without base-pairing by the sequential reaction of AMT with two pyrimidines.

It is important to emphasize that although initiation-dependent interactions, perhaps base-pairing, between mRNA 5′-terminal regions and 18S rRNA can be detected by AMT cross-linking, their functional role if any in eukaryotic protein synthesis remains to be established. However, a stable interaction compatible with base-pairing has been demonstrated between 18S rRNA and globlin mRNA in 40S initiation complexes formed in a reconstituted mammalian cell-free protein synthesizing system (B. Erni and T. Staehelin, personal communication). It may be possible to test whether this interaction has a function in translation by using cloned rDNA including specific fragments complementary to the 3′ end of 18S rRNA[34,35,42].

We thank Alba LaFiandra and Maureen Morgan for assistance, Drs M. Kozak and Y. Furuichi for discussion, Dr J. Hearst for ^{3}H-AMT, and the following for gifts of virus or viral mRNA: Drs A. Marcus (TMV), J. Clark (STNV), Y. Furuichi (CPV), A. Banerjee (VSV) and R. Krug (influenza virus).

Note added in proof: Recent studies indicate that mRNA cross-linking is mainly within the ribosome-protected region.

Received 24 January; accepted 18 April 1980.

1. Shine, J. & Dalgarno, L. *Proc. natn. Acad. Sci. U.S.A.* **71,** 1342–1346 (1974).
2. Steitz, J. A. & Jakes, K. *Proc. natn. Acad. Sci. U.S.A.* **72,** 4734–4738 (1975).
3. Duan, J. J., Buzash-Pollert, E. & Studier, F. W. *Proc. natn. Acad. Sci. U.S.A.* **75,** 2741–2745 (1978).
4. Shine, J. & Dalgarno, L. *Nature* **254,** 34–38 (1975).
5. Hagenbüchle, O., Santer, M., Steitz, J. A. & Mans, R. J. *Cell* **13,** 551–563 (1978).
6. Kozak, M. *Cell* **15,** 1109–1123 (1978).
7. Barelle, F. E. & Brownlee, G. G. *Nature* **274,** 84–87 (1978).
8. Both, G. W. *FEBS Lett.* **101,** 220–224 (1979).
9. De Wachter, R. *Nucleic Acids Res.* **7,** 2045–2054 (1979).
10. Sprague, K. U., Steitz, J. A., Grenley, R. M. & Stocking, C. E. *Nature* **267,** 462–465 (1977).
11. Schwartz, Z. & Kössel, H. *Nature* **279,** 520–522 (1979).
12. de Jonge, P., Klootwijk, J. & Planta, R. J. *Nucleic Acids Res.* **4,** 3655–3663 (1977).
13. Alberty, H., Raba, M. & Gross, H. J. *Nucleic Acids Res.* **5,** 425–434 (1978).
14. Hunt, J. A. *Biochem. J.* **120,** 353–363 (1970).
15. Ziff, E. B. & Evans, R. M. *Cell* **15,** 1463–1475 (1978).
16. Schroeder, Jr, H. W., Liarakos, C. D., Gupta, R. C., Randerath, K. & O'Malley, B. W. *Biochemistry* **18,** 5798–5808 (1979).
17. Pathak, M. A., Krämer, D. M. & Fitzpatrick, T. B. in *Sunlight and Man—Normal and Abnormal Photobiologic Responses* (eds Pathak, M. A. *et al.*) 335–387 (University of Tokyo Press, 1974).
18. Isaacs, S. T., Shen, C. J., Hearst, J. E. & Rapoport, H. *Biochemistry* **16,** 1058–1064 (1977).
19. Nakashima, K., LaFiandra, A. J. & Shatkin, A. J. *J. biol. Chem.* **254,** 8007–8014 (1979).
20. Both, G. W., Furuichi, Y., Muthukrishnan, S. & Shatkin, A. J. *Cell* **6,** 185–195 (1975).
21. Muthukrishnan, S., Morgan, M., Banerjee, A. K. & Shatkin, A. J. *Biochemistry* **15,** 5761–5768 (1976).
22. Kozak, M. & Shatkin, A. J. *Meth. Enzym.* **60,** 360–375 (1979).
23. Kozak, M. & Shatkin, A. J. *J. biol. Chem.* **251,** 4259–4266 (1976).
24. Kozak, M. & Shatkin, A. J. *Cell* **13,** 201–212 (1978).
25. Marcus, A. *J. biol. Chem.* **245,** 962–966 (1970).
26. Trachsel, H., Erni, B., Schreier, M. H. & Staehelin, T. *J. molec. Biol.* **116,** 755–767 (1977).
27. Both, G. W., Furuichi, Y., Muthukrishnan, S. & Shatkin, A. J. *J. molec. Biol.* **104,** 637–658 (1976).
28. England, T. E. & Uhlenbeck, O. C. *Nature* **275,** 560–561 (1978).
29. Rosenberg, M. *Nucleic Acids Res.* **1,** 653–671 (1974).
30. Furuichi, Y., Shatkin, A. J., Stavnezer, E. & Bishop, J. M. *Nature* **257,** 618–620 (1975).
31. Kozak, M. *Nature* **269,** 390–394 (1977).
32. Rabin, D. & Crothers, D. M. *Nucleic Acids Res.* **7,** 689–703 (1979).
33. Donis-Keller, H., Maxam, A. M. & Gilbert, W. *Nucleic Acids Res.* **4,** 2527–2538 (1977).
34. Eckhardt, H. & Lührmann, R. *J. biol. Chem.* **254,** 11185–11188 (1979).
35. Taniguchi, T. & Weissmann, C. *Nature* **275,** 770–772 (1978).
36. Roberts, T. M., Bikel, I., Yocum, R. R., Livingston, D. M. & Ptashne, M. *Proc. natn. Acad. Sci. U.S.A.* **76,** 5596–5600 (1979).
37. Azad, A. A. & Deacon, N. J. *Biochem. biophys. Res. Commun.* **86,** 568–576 (1979).
38. Tsujimoto, Y. & Suzuki, Y. *Cell* **18,** 591–600 (1979).
39. Legon, S. *J. molec. Biol.* **134,** 219–240 (1979).
40. Rose, J. K. *Cell* **14,** 345–353 (1978).
41. Rosenberg, M. & Paterson, B. M. *Nature* **279,** 696–701 (1979).
42. Manning, R. F., Samols, D. R. & Gage, L. P. *Gene* **4,** 153–166 (1978).
43. Furuichi, Y. & Shatkin, A. J. *Proc. natn. Acad. Sci. U.S.A.* **73,** 3448–3452 (1976).
44. Nakashima, K. & Shatkin, A. J. *J. biol. Chem.* **253,** 8680–8682 (1978).
45. Nakashima, K., Chanda, P. K., Deutsch, V., Banerjee, A. K. & Shatkin, A. J. *J. Virol.* **32,** 838–844 (1979).
46. Pelham, H. R. B. & Jackson, R. J. *Eur. J. Biochem.* **67,** 247–256 (1976).
47. Darzynkiewicz, E. & Shatkin, A. J. *Nucleic Acids Res* **8,** 337–350 (1980).

Monoclonal antibodies which recognize different cell types in the rat retina

Colin J. Barnstable

Department of Neurobiology, Harvard Medical School, 25 Shattuck Street, Boston, Massachusetts 02115

Seven monoclonal antibodies have been produced against a membrane preparation from adult rat retina. Three antibodies reacted with particular regions of rat photoreceptor cell surfaces: RET-P1 labelled the cell bodies, outer and inner segments (rods but not cones), RET-P2 labelled only outer segments and RET-P3 labelled only the cell bodies. Three antibodies reacted with glial cells; RET-G2 and RET-G3 were specific for Müller cells, RET-G1 also labelled glia elsewhere in brain. The seventh antibody (RET-N1) reacted with many types of neuronal cells.

It is widely believed that differences between classes of neural cells are expressed in part by distinct patterns of cell-surface molecules[1-3]. Cell-surface molecules such as transmitter receptors and ion channels are basic to the function of the nervous system[4,5]. These and other surface molecules may be important in determining the exquisite specificity of synaptic connections.

Antibodies are almost uniquely suited for the detection of such cell-surface molecules since they can be used in histochemical assays to resolve single cells in mixed cell populations; they can be used in quantitative biochemical assays to determine the amount, molecular nature and tissue distribution of the antigens recognized; and perhaps most importantly, they can be raised against essentially any antigen or cell type of interest. Progress in producing antibodies against any but the broadest classes of neural cell types has, until recently, been hindered by the heterogeneity of the immune response generated against the available antigens[6-9]. The technique introduced by Milstein and co-workers[10,11], whereby antibodies are produced by cloned cell lines, has overcome many of these difficulties. Such monoclonal antibodies have already been of great value in biochemical, functional and genetic analyses of cell surface molecules[12-15].

We have chosen the visual system, and particularly the retina, as a model system in which to study the differences in cell-surface molecules of different subclasses of neural cells. This system has the advantage that many of the cells involved in the transmission of visual information from the photoreceptors to the primary visual cortex have been identified and reasonably well characterized with respect to their physiological responses and synaptic interactions[16-18]. The retina has the additional advantages that it is readily accessible, it has only seven basic neural cell types, its layered structure generally allows assignment of cell type from position alone[19], and it is a region of the vertebrate central nervous system (CNS) from which single dissociated cells have been isolated and successfully used in physiological[20] and biochemical studies[21,22].

This article describes initial observations on seven monoclonal antibodies that recognize cell-surface molecules of rat retina. Three of these antibodies react with photoreceptors, although each stains subregions of the cell surface in a distinct way. Three antibodies react with Müller cells, the main glial cell type of retina, and the seventh reacts with many classes of neuronal cells throughout the brain.

Production and immunological characterization of antibodies

Retinas were dissociated from adult CD rats (Charles River Breeding Laboratories) and a crude membrane pellet prepared as described by Barclay *et al.*[23]. Female BALB/c mice were given two intraperitoneal injections of 200 μg of membrane protein in Freund's adjuvant 3 weeks apart. Three weeks after the second injection mice were given an intravenous injection of 100 μg of membrane protein in saline. Four days later spleens were removed and used for fusions. Spleen cells were fused with either P3-NS1/1-Ag4-1 or 8653 myeloma cells (gifts of C. Milstein and P. Goodfellow, respectively), and hybrid cultures selected and cloned as described previously[15,24].

Hybrid- and clone-culture supernatants were tested for antibody activity using an indirect trace radioactive binding assay as described by Williams[25]. Target particles consisted of adult rat retina that had been lightly homogenized and fixed with 0.5% paraformaldehyde[26]. Bound mouse immunoglobulin was detected using a ^{125}I-labelled F(ab$'$)$_2$ fragment of an affinity-purified rabbit anti-mouse IgG antibody.

The seven antibodies described here have been selected from the products of four separate fusions. All seven antibodies were found to be of the IgG1 subclass when tested by Ouchterlony double diffusion against subclass-specific sera.

The antibodies were initially selected for study because the early culture supernatants did not react in a binding assay with rat thymocytes or by immunofluorescence with a fibroblast cell line grown out from newborn rat lung (data not shown). Thus they seemed to recognize antigens that were not expressed by all rat tissues. To study the antigen expression by different tissues in a more quantitative way, each antibody was absorbed with crude membrane preparations from retina, cerebral cortex and cerebellum, with liver as a control non-neural tissue. The amount of membrane needed to inhibit antibody-binding activity by 50% was determined (see Table 1 legend) and was used as a measure of the level of antigen expression of that particular tissue (Table 1). Because these

Table 1 Tissue distribution of antigens recognized by anti-retina antibodies

Antibody	Antigenic activity of membrane			
	Retina	Cortex	Cerebellum	Liver
RET-P1	50	<1	<1	<1
RET-P2	2,326	<1	<1	<1
RET-P3	15	<1	<1	<1
RET-G1	238	1,724	600	<1
RET-G2	87	<1	1.3	7
RET-G3	100	<1	5	8
RET-N1	312	91	161	<1

Crude membrane fractions[23] were prepared from each tissue. Aliquots of monoclonal antibody solution, at a dilution chosen so as to be limiting in the assay, were incubated with varying concentrations of membranes for 2 h at 4 °C. The residual antibody activity was then measured using a trace radioactive binding assay. At least 10 dilutions of each membrane preparation were used with each antibody. The antigenic activity is defined as the dilution of a 20 mg membrane protein per ml solution necessary to give 50% inhibition of the binding activity of an equal volume of antibody solution. The values given in the table are taken from inhibition curves, the points of which were each the mean of two separate inhibitions each assayed in duplicate.

0028-0836/80/290231-05$01.00

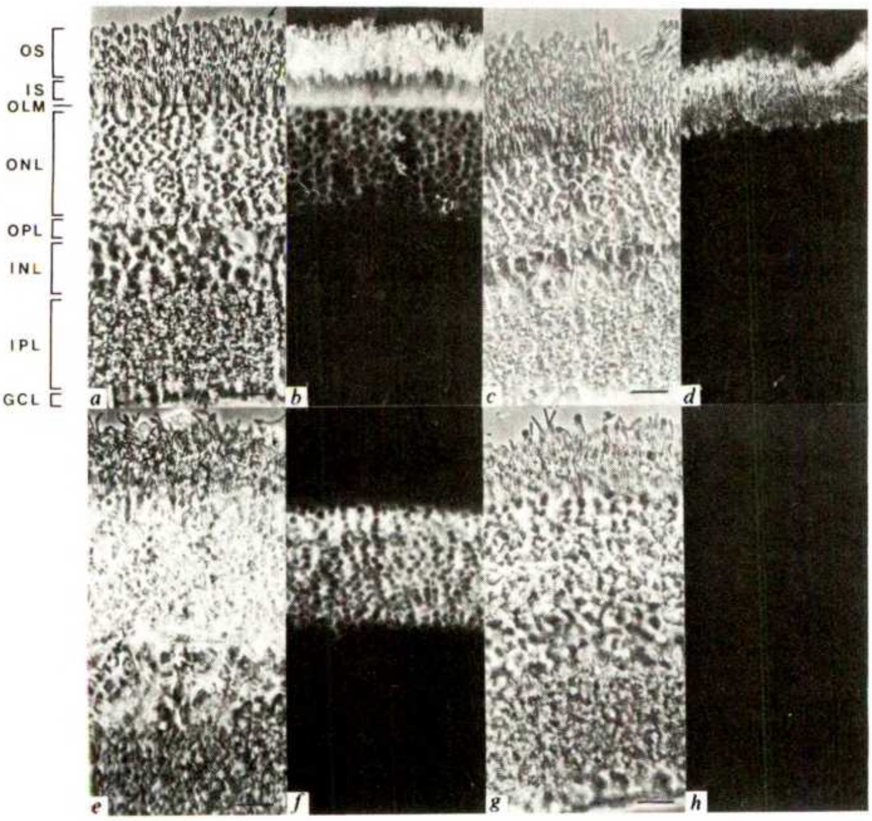

Fig. 1 Immunofluorescent labelling of sections of adult rat retina by antibodies RET-P1, RET-P2 and RET-P3. Rats were killed by cervical dislocation and the retinas rapidly dissected. They were fixed for 1 h at 4 °C in 1% parafomaldehyde, 0.1% glutaraldehyde in 0.1 M sodium phosphate buffer *p*H 7.6. After fixation the retinas were soaked in 30% (w/v) sucrose overnight. Sections (15 μ) were cut on a freezing microtome and dried onto subbed slides. Sections were preincubated with 5% (w/v) bovine serum albumin (BSA) in phosphate buffer for 1 h at 4 °C and then with the primary antibody for 18 h at 4 °C. The slides were washed in two changes of a large excess of phosphate buffer for 10 min each at 4 °C. Sections were then treated with a rhodamine-conjugated goat anti-mouse IgG preparation (Cappell) which was diluted in a solution of equal parts of 5% BSA in phosphate buffer and normal rabbit serum. Before use, the rabbit serum was passed over a column of mouse IgG coupled to Sepharose 4B to remove any heterophile anti-mouse IgG antibodies. After incubation for 45 min at room temperature the slides were again washed with two changes of phosphate buffer and then a coverslip applied using 50% glycerol in phosphate buffer as mounting medium. Slides were examined with a Zeiss ICM35 microscope. White light photographs were taken with phase contrast optics. Fluorescence photographs were taken using epi-illumination and excitation–barrier filter and reflector combination 48-77 15-9902. Photographs were taken on H & W Control film with 2 min exposures for fluorescence and an automatic light meter for phase contrast photographs. *a, b*, RET-P1 antibody; *c, d*, RET-P2 antibody; *e, f*, RET-P3 antibody; g, *h*, control using a monoclonal antibody against a human cell-surface glycoprotein. *a, c, e*, g, Phase contrast; *b, d, f, h*, fluorescence. The arrow at the top right corner of *a* indicates the only outer segment that can be detected as unlabelled in *b*. OS, outer segments; IS, inner segments; OLM, outer limiting membrane; ONL, outer nuclear layer; OPL, outer pelxiform layer; INL, inner nucelar layer; IPL, inner plexiform layer; GCL, ganglion cell layer. Scale bar represents 20 μ.

values are functions of both quantity of antigen and antibody affinity, only comparisons between different tissues for the same antibody are meaningful. From Table 1 it can be seen that RET-P1, RET-P2 and RET-P3 antigens were predominantly if not exclusively localized in retina because only retina membrane was able to give measurable inhibition of antibody binding activity. RET-G2 and RET-G3 antigens were expressed strongly by retina, weakly by cerebellum and liver and not detectably by cortex. Neither antigen was detectable by immunofluorescent staining of cerebellum or liver sections (data not shown) so that it is not yet possible to ascribe the absorption to the presence of a few cells with high levels of antigen expression, many cells with low levels of antigen expression or even some nonspecific absorption that affects these two antibodies but not the others. RET-G1 and RET-N1 antigens were strongly expressed by all three brain regions but were not detectable on liver. Although the absorption has the advantage of being quantitative, it cannot be used to determine which cell types in a tissue are expressing the antigen. For this, immunofluorescent staining of tissue sections was carried out.

Antibodies RET-P1, RET-P2 and RET-P3 specifically label photoreceptors

The immunofluorescent staining of sections of adult rat retina given by RET-P1 is shown in Fig. 1*a* and *b*. With the exception of the outer plexiform layer, the whole of the photoreceptor layer was labelled. Clear ring fluorescence was found around almost all of the photoreceptor cell bodies. The packing between the cell bodies appeared looser towards the outer limiting membrane and the intervening spaces often showed fluorescence. This was probably due to the fibres which connect the cell bodies with their inner segments[27]. The photoreceptor inner segments were labelled at about the same intensity as the cell bodies but the outer segments had a much brighter fluorescence. These differences presumably represented differences in antigen density which supports previous observations that the composition of the outer segment membrane is different from that of the rest of the cell[28,29]. This was much more decisively demonstrated by the staining pattern given by antibodies RET-P2 (Fig. 1*c*, *d*) and RET-P3 (Fig. 1*e*, *f*). Within the limitations of the fluorescence assay, RET-P2 antigen was located exclusively on the outer segments and RET-P3 antigen was located exclusively on the photoreceptor cell bodies. These differences in labelling patterns seen with these three antibodies suggest that some photoreceptor membrane molecules are common to all regions of the cell while others are restricted to discrete areas of the cell. It is not yet known whether this restriction is caused by some form of anchorage of particular molecules in a fluid membrane to submembranous or extracellular elements or by localized areas of insertion of newly synthesized molecules in a non-fluid membrane.

Experiments are now under way to determine the chemical nature of the RET-P1, RET-P2 and RET-P3 antigens to see whether both membrane proteins and lipids are restricted in their localization. In addition, production of other antibodies that label specific regions of photoreceptors will allow an estimate of the number of compartments into which the photoreceptor cell membrane is divided.

Although RET-P2 antibody was not absorbed by cerebellum membrane, immunofluorescent labelling of cerebellum sections showed that it reacted with structures at the level of the initial segment of the Purkinje cell (data not shown). The exact nature of the labelled structures and their relationship to the photoreceptor outer segments have yet to be determined. Neither RET-P1 nor RET-P3 stained any cerebellar structures.

The rat retina consists almost entirely of rods[30], so that judging whether or not the three antibodies reacted with both rods and cones was almost impossible. To investigate this, the three antibodies were tested on a number of different species to see whether or not any of them reacted with a retina containing a higher proportion of cones. RET-P2 and RET-P3 seem to be specific for rat but RET-P1 reacted with several species (including BALB/c mice from which the antibody-producing spleen cell was derived). A group of photoreceptors in a section of retina from the tiger salamander (*Ambystoma tigrinum*) is shown in Fig. 2. Cells 1, 3 and 5 are rods although the outer segment of cell 3 was removed during dissection. All three cells stain throughout their length with the most intense fluorescence being in the outer segment. The bright band at the junction of the inner and outer segments was probably due to labelling of the deep membrane invaginations at this region. These invaginations have been shown to represent the initial stage of pinching off of the disks of the outer segment[31]. Cells 2 and 4 have the morphology of cones, that is, narrower cell bodies, narrower but longer inner segments and slender outer segments. The outer segments of cells 2 and 4 are almost certainly damaged but there is no trace of fluorescence on any part of the cell. This would indicate that antigen RET-P1 is restricted to rods. As can also be seen in Fig. 2, the axons and synaptic pedicles of the rods were labelled. In several cases fine labelled processes were found to be given off from the thick pedicles. The lack of staining of the outer plexiform layer in the rat retina found with this antibody may simply be because such staining was below the threshold for visualization or alternatively may be real and may represent a difference in antigen compartmentalization between the two species.

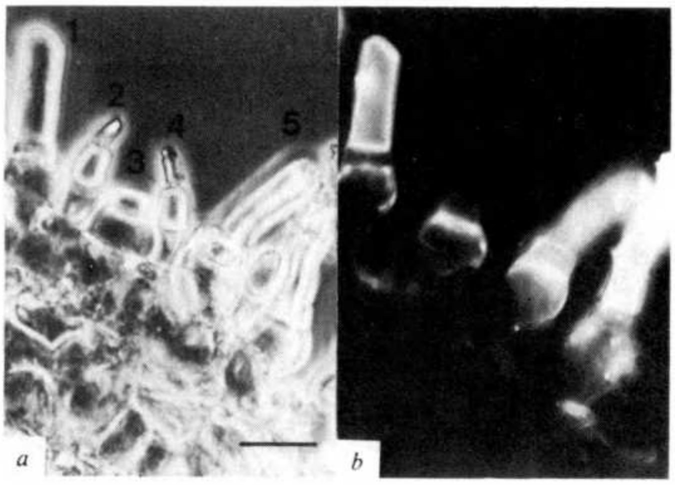

Fig. 2 Immunofluorescent labelling of tiger salamander photoreceptors by antibody RET-P1. Sections were prepared and treated as described in Fig. 1 legend except that the animals were dark-adapted for 4 h before being killed. *a*, Phase contrast; *b*, fluorescence. Scale bar represents 20 μ.

One obvious candidate for a photoreceptor-specific marker is the light-sensitive molecule rhodopsin. A rabbit antiserum raised against bovine rhodopsin stained both the outer and inner segments of frog photoreceptors[32]. This pattern was not given by any of the three antibodies described here. In addition, the anti-rhodopsin serum stained both rods and cones. None of these antibodies was inhibited by a partially purified preparation of bovine rhodopsin (a gift of Dr E. A. Schwartz) used at concentrations where whole retina membrane gave complete inhibition (data not shown). Thus, it is unlikely that any of these three antibodies recognize rhodopsin but final resolution of this must await a chemical analysis of the respective antigens.

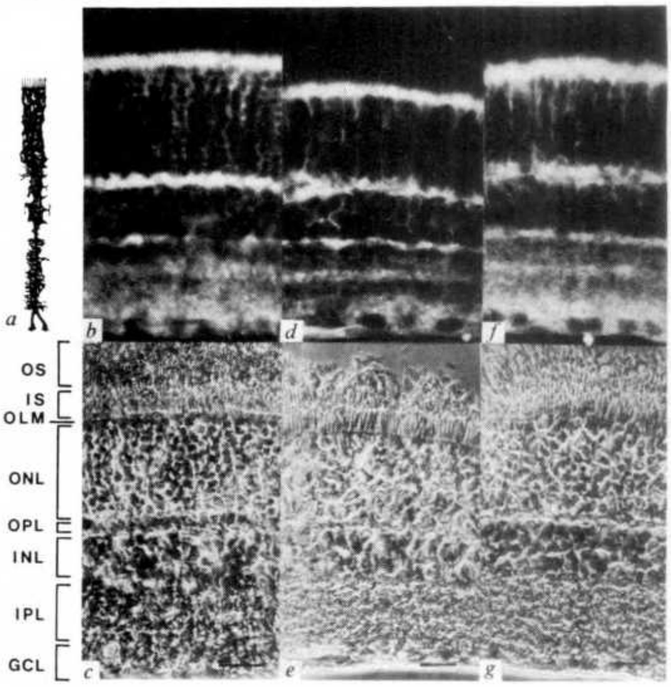

Fig. 3 Immunofluorescent labelling of sections of adult rat retina by antibodies RET-G1, RET-G2 and RET-G3. Sections were prepared and treated as described in Fig. 1 legend. *a*, A Müller cell taken from Golgi-stained retina as drawn by S. R. Cajal (ref. 35, p. 298); *b*, *c*, RET-G1 antibody; *d*, *e*, RET-G2 antibody; *f*, g, RET-G3 antibody. *b*, *d*, *f*, Fluorescence; *c*, *e*, g, phase contrast. Designation of retinal layers is described in Fig. 1 legend. Scale bar represents 20 μ.

Antibodies RET-G1, RET-G2 and RET-G3 specifically label Müller cells

Müller cells have a unique morphology in that they are the only cell type to extend radially across the retina from the outer limiting membrane to the inner limiting membrane[33,34]. The essential features of their structure, as shown in the Golgi-stained cell (Fig. 3*a*), were clearly picked out in the immunofluorescent labelling of sections of adult rat retina given by antibodies RET-G1 (Fig. 3*b*, *c*), RET-G2 (Fig. 3*d*, *e*) and RET-G3 (Fig. 3*f*, g). At the outer limiting membrane, each antibody labelled the fine finger-like Müller cell processes that extend up between the inner half of the photoreceptor inner segments. Thick radial processes passing through the outer nuclear layer were also labelled although the single focal plane shown in the photographs was not always adequate to show a single process traversing the whole width of that layer. Such fibres could frequently be followed visually. Virtually no tangential labelling was seen in the outer nuclear layer, indicating that the photoreceptor cell bodies had not reacted with the antibodies. The labelling in the inner nuclear layer was harder to interpret but probably represented Müller fibres following the contours of the cell bodies in this region on their way to the inner plexiform layer.

In very few cases was it possible to see a clear ring of fluorescence around a cell body as would have been expected if the neuronal cell bodies had been labelled. Those few cell bodies that were labelled had the position expected for Müller cell bodies. The radial Müller fibres give off fine tangential processes in the plexiform layers causing both plexiform layers to be labelled. The labelling of the inner plexiform layer showed three bands of higher intensity. One band was located at the junction of the inner nuclear and inner plexiform layers, one band was about half way through the inner plexiform layer and the other thick band was at the junction of the inner plexiform and ganglion cell layers and was continuous with the labelling of the bulbous feet that surround the ganglion cell bodies and optic fibres and end at the inner limiting membrane. This banded appearance of the inner plexiform layer, which probably reflects the density of tangential glial projections, was closely similar to the autoradiographic staining of Müller cells seen following uptake of radioactive GABA *in vitro* (refs 36, 37 and unpublished observations with R. W. Baughman).

As a further demonstration that antibody RET-G1 was reacting with Müller cells, immunofluorescent labelling of enzymatically dissociated adult rat retina cells[38] was carried out. The results (Fig. 4) clearly show that this antibody labelled cells with the morphology characteristic of Müller cells. Cells with the morphology of bipolar cells and a variety of amacrous cells were not labelled in these preparations.

Müller cells and astrocytes have a number of structural and functional features in common, such as close apposition to neuronal processes[39], potassium ion transport[40], and γ-aminobutyric acid transport[41]. Thus it was not surprising to find an antibody, RET-G1, that reacted with glial cells in all regions of brain. The results in Table 1 show that cerebral cortex and cerebellum express more RET-G1 per mg membrane protein than retina although the differences provide no information about the relative amounts expressed per cell.

In cerebellum, the cells expressing this antigen were found in all layers. The area illustrated in Fig. 5*c* shows labelled cell bodies in the granular layer and processes passing up through the unlabelled Purkinje cell layer to the molecular layer. Further studies will be necessary to determine whether this antigen is also on oligodendrocytes and glia of the peripheral nervous system. RET-G2 and RET-G3 antigens were expressed by Müller cells but not to a significant extent by other glia. The nature and function of these two 'Müller-cell specific' antigens are unknown. The two can be distinguished by their fluorescent labelling pattern on adult retina. RET-G2 antibody gave a relatively even labelling but RET-G3 antibody gave a highly punctate pattern of labelling in the inner plexiform layer. Studies at the electron microscope level will show whether these areas of increased labelling are related in any way to other structures in the inner plexiform layer, such as areas of glial processes close to synapses.

Antibody RET-N1 recognizes a neurone-specific antigen

Antibody RET-N1 labelled several cell types in sections of adult rat retina (Fig. 5*a*). It labelled the whole length of the photoreceptor inner segments but not the outer segments or cell bodies although some very faint labelling was found over the outer nuclear layer. Both plexiform layers were stained and many cell bodies in the outer half of the inner nuclear layer could be recognized. Axons of bipolar cells could be seen leaving some of these cells and passing through to the inner plexiform layer. There seemed to be fewer labelled cells in the inner half of the inner nuclear layer which may indicate that some amacrine cells were unlabelled. The ganglion cells were labelled. No traces of the characteristic glial labelling pattern—radial fibres in the outer nuclear layer and glial feet around the ganglion cells—were found. The absorption results (Table 1) indicated that RET-N1 antibody reacted with cortex and cerebellum. In agreement with this, the antibody was found to label cells at all levels in the cerebral cortex (data not shown). In cerebellum it also labelled several cell types. In the portion shown (Fig. 5*b*) it labelled Purkinje cells and brightly labelled pinceaux of basket cell terminals around the Purkinje cell initial segment. Many other cell bodies in the granular layer and processes in the molecular layer were also labelled, although in a pattern different from that given by antibody RET-G1. Thus antigen RET-N1 may be a marker for most if not all neurones of the CNS although further work will be necessary to show whether or not it cross-reacts with types of glial cells not found in the retina such as oligodendrocytes. It will also be of interest to determine whether antibodies RET-G1 and RET-N1 label glia and neurones, respectively, of the peripheral nervous system as these are of neural crest rather than neural tube embryonic origin. Experiments to investigate this are under way.

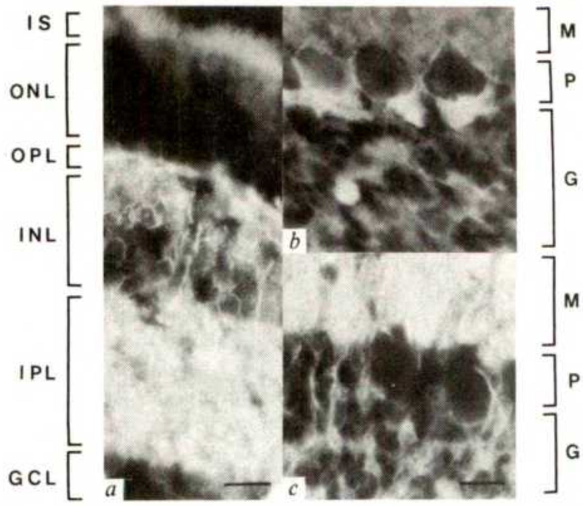

Fig. 5 *a*, Immunofluorescent labelling of adult rat retina by antibody RET-N1. The section preparation, labelling and the designation of retinal layers is as in the legend to Fig. 1. *b*, Immunofluorescent labelling of adult rat cerebellum by antibody RET-N1. *c*, Immunofluorescent labelling of adult rat cerebellum by antibody RET-G1. For *b* and *c* animals were anaesthetised with Nembutal and perfused through the ventricle with 2% paraformaldehyde in phosphate buffer. Cerebella were then dissected and treated as for retina. M, molecular layer; P, Purkinje cell layer; G, granular layer. Scale bar represents 20 μ.

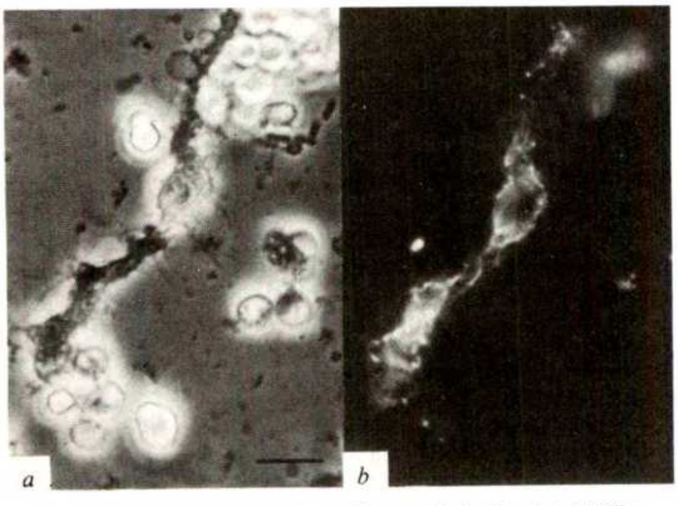

Fig. 4 Immunofluorescent labelling of enzymatically dissociated Müller cells by RET-G1 antibody. Retinas were dissected from adult rats and cells dissociated using published procedures[38]. The cell suspension was allowed to settle to the bottom of Petri dishes and the labelling carried out using 1-h incubations at room temperature for primary and fluorescent antibodies. Three rinses with HEPES-buffered Hank's salts solutions were carried out after each antibody incubation, care being taken not to disturb the cells. Scale bar represents 10 μ.

Discussion

The results presented above show clearly that monoclonal antibodies can be produced against subclasses of neural cells. It has yet to be shown formally that each antibody interacts with an integral cell-surface molecule rather than extracellular matrix or intracellular membrane material, but this seems likely. Fixation by itself is not an efficient way of allowing visualization of internal antigens in tissue sections. Addition of detergent to sections similar to those illustrated neither changed nor enhanced the labelling pattern, suggesting that external rather than internal antigens were recognized. Final demonstration of the cell-surface location of the antigens will be achieved by a combination of electron microscopic immunocytochemistry, biochemistry and studies in tissue culture on living cells.

The antibodies described here will be valuable for several studies. For example, they will be useful for studying the topography and development of particular cell types in the intact organism. Preliminary experiments have established that RET-P1, RET-P2 and RET-P3 are expressed at different stages of photoreceptor development and RET-G1, RET-G2 and RET-G3 are expressed at different stages of Müller cell development. Thus they are markers not only for adult cells but also for immature cells at discrete stages of development. Whether such stages are intrinsic to neural cells after the initial step of determination or whether they require distinct environmental triggers is not known. Experiments are in progress to test these alternatives by following cell maturation in defined *in vitro* culture systems.

Another use of antibodies such as those described above, and others now being characterized, will be for the separation of cells and subcellular fractions from adult and developing tissue for a variety of physiological and biochemical studies.

There is also the additional hope that production of antibodies that recognize particular neural cell subclasses may lead to the identification of cell-surface molecules that mediate functions specific to those subclasses and may, therefore, aid in an understanding of the molecular and genetic basis of neural cell development and function.

I thank Torsten Wiesel for his continuing encouragement and support of this work, Peter MacLeish for help with the salamander retina, Robert Baughman, Ed Furshpan, Peter Parham and Elio Raviola for their comments on the manuscript, Lynn Mangini, Karl Reich and Jane Soukup for technical assistance, and Cathy Cross for photography. This work was supported by grant EY006C6 from the National Eye Institute, NIH, and fellowship DRG-242 from the Damon Runyon–Walter Winchell Cancer Fund.

Received 12 February, accepted 17 April 1980

1. Sidman, R L *3rd Lepetit Colloquium on Cell Interactions* (ed Silvestri, L G), 1–13 (North-Holland, Amsterdam, 1972)
2. Moscona, A A (ed) *The Cell Surface in Development* (Wiley, New York, 1974)
3. Rutishauser, V, Brackenbury, R, Thiery, J P & Edelman, G M *Birth Defects Original Article Series* XIV, 305–316 (1978)
4. Krnjević, K. *Physiol Rev* 54, 418–540 (1974)
5. Hall, Z, Kelly, R & Fox, C F. (eds) *Cellular Neurobiology* (Liss, New York, 1977)
6. Fields, K. L, Gosling, C, Megson, M & Stern, P L *Proc natn Acad Sci U S A* 72, 1296–1300 (1975)
7. Schachner, M, Ruberg, M. Z & Carnow, T B *Brain Res Bull* 1, 367–377 (1976)
8. Stallcup, W. B & Cohn, M *Expl Cell Res* 98, 285–297 (1976)
9. Raff, M C *et al* *Brain Res* 174, 283–308 (1979)
10. Köhler, G. & Milstein, C. *Nature* 256, 495–497 (1975)
11. Galfre, G., Howe, S C, Milstein, C, Butcher, G. W & Howard, J C *Nature* 266, 550–552 (1977)
12. Standring, R, McMaster, W R, Sunderland, C A & Williams, A F *Eur J Immun* 8, 832–839 (1978)
13. White, R. A H *et al* *J exp Med* 14, 664–673 (1978)
14. Reinherz, E L, Kung, P C, Goldstein, G & Schlossman, S F *Proc natn Acad Sci U S A* 76, 4061–4065 (1979)
15. Barnstable, C J *et al* *Cell* 14, 9–20 (1978)
16. Werblin, F. S & Dowling, J E *J Neurophysiol* 32, 339–355 (1969)
17. Hubel, D H & Wiesel, T N *J Physiol, Lond* 155, 385–398 (1961)
18. Hubel, D H & Wiesel, T. N *Proc R Soc* B198, 1–59 (1977)
19. Dowling, J E & Boycott, B B *Proc R Soc* B166, 80–111 (1966)
20. Bader, C R, MacLeish, P R & Schwartz, E A *J Physiol, Lond* 296, 1–26 (1979)
21. Lam, D M K *Cold Spring Harb Symp quant Biol* 40, 571–579 (1975)
22. Sarthy, V P & Lam, D M K *J Neurochem* 32, 455–461 (1979)
23. Barclay, A N, Letarte-Muirhead, M & Williams, A F *Biochem J* 151, 699–706 (1975)
24. Brodsky, F M, Parham, P, Barnstable, C J, Crumpton, M J. & Bodmer, W F *Immun Rev* 47, 3–61 (1979)
25. Williams, A F *Contemporary Topics molec Immun* 6, 93–116 (1977)
26. Barclay, A N. *Brain Res* 133, 139–143 (1977)
27. Cajal, S R. *The Structure of the Retina* (Translators Thorpe, S A & Glickstein, M) (Thomas, Illinois, 1972)
28. Young, R W *J. Ultrastruct Res* 23, 462–473 (1968)
29. Papermaster, D S, Converse, C A & Zorn, M A *Expl Eye Res* 23, 105–116 (1978)
30. La Vail, M M *Invest Ophthal* 15, 64–70 (1976)
31. Cohen, A I *Vision Res* 10, 445–453 (1970)
32. Dewey, M. M, David, P K, Blasie, J K & Barr, L *J molec Biol* 39, 395–405 (1969)
33. Uga, S & Smelser, G K *Invest Ophthal* 12, 295–307 (1973)
34. Miller, R E & Dowling, J E *J Neurophysiol* 33, 323–341 (1970)
35. Cajal, S R *Histologie du Système Nerveux de l'Homme et des Vertébrés* Vol II (CSIC, Madrid, 1955)
36. Neal, M J & Iversen, L L *Nature new Biol* 235, 217–218 (1972)
37. Voaden, M J. in *Transmitters in the Visual Process* (ed Bonting, S L) 107–125 (Pergamon, Oxford, 1976)
38. Sarthy, P V. & Lam, D M K *Brain Res* 176, 208–212 (1980)
39. Peters, A, Palay, S L & Webster, H de F *The Fine Structure of the Nervous System* (Saunders, Philadelphia, 1976)
40. Kuffler, S W, Nicholls, J G & Orkand, R K *J Neurophysiol* 36, 855–868 (1966)
41. Iversen, L L & Kelly, J S. *Biochem. Pharmac* 24, 933–938 (1975)

LETTERS

Pressure balance and pressure distribution along the dayside ionopause of Venus

O. L. Vaisberg*, D. S. Intriligator† & V. N. Smirnov*

* Space Research Institute, USSR Academy of Sciences, Moscow, USSR
† University of Southern California, Los Angeles, California 90007

The pressure distribution within the magnetic barrier just outside the ionopause of Venus is shown here to be similar to expected solar wind pressure variation provided the more realistic shape of the ionopause is taken into account. The ionospheric pressure just below the magnetic barrier is about equal to the solar wind pressure while magnetic field pressure within the magnetic barrier amounts to about two-thirds of both ionospheric and solar wind pressures. So we can expect that one-third of magnetic barrier pressure is accounted for by the hot plasma contribution.

The existence of a bow shock near Venus was established during the Mariner 5 fly-by mission[1] and Venera 4 lander mission[2] in 1968. The close location of this shock to the planet demonstrated that Venus does not have a significant internal magnetic field and that the ionosphere of the planet is capable of deflecting a major part of the incoming solar wind plasma.

The Venera 9 and Venera 10 mission in 1975–76 made detailed studies of the shock and the wake region of Venus[3–5]. Recently the Pioneer Venus Orbiter (PVO) performed important measurements of the structure of the venusian ionosphere and its interaction with the solar wind[6,7]. Above 200 km the dayside ionosphere is in a state of diffusive equilibrium with the O^+ ions as the main constituent. The elevated electron and ion temperatures in the ionosphere together with the number density below the ionopause provide, in most cases, enough pressure to sustain the solar wind dynamic pressure. The height of the ionopause is strongly influenced by the solar wind pressure[8–12].

The magnetic field measurements from the PVO show that the magnetic pressure within the ionosphere is in most cases negligible, but that above the ionopause there is a region of increased magnetic field where the magnetic field pressure approximately equals the solar wind dynamic pressure. This region of increased magnetic field presumably transfers solar wind pressure to the ionosphere[10,13–16].

Joint data on the solar wind, magnetic field and ionosphere are available only for the first period of PVO observations in December 1978 when the region of solar zenith angle (SZA) $\geq 61.5°$ was studied. It is frequently assumed that external pressure exerted on the venusian ionopause changes as a simple newtonian law of specular reflection, $\cos^2 \psi$ (where ψ is the SZA). But the deviations of the ionopause shape from that of a spherical surface should give rise to significant deviations from the $\cos^2$ law for large SZA. Further improvement may be

0028-0836/80/290235—03$01 00

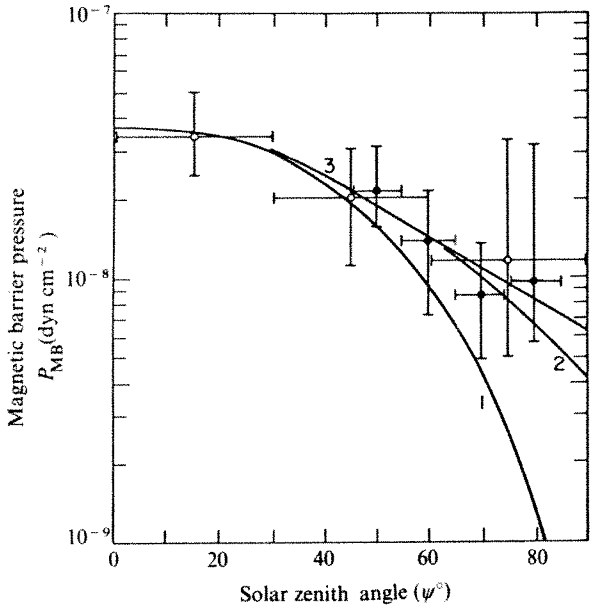

Fig. 1 Dependence of magnetic field pressure in the magnetic barrier on solar zenith angle. ●, From ref. 19; ○, from ref. 16. Curves are: 1, $\cos^2 \psi°$; 2, $\cos^2 \chi°$, with χ equal to expected angle between normal to ionopause and solar wind flow direction; and 3, hydrodynamic pressure variation along the boundary[17,18]. Curves are normalized to subsolar pressure value 3.7×10^{-8} dyn cm^{-2}.

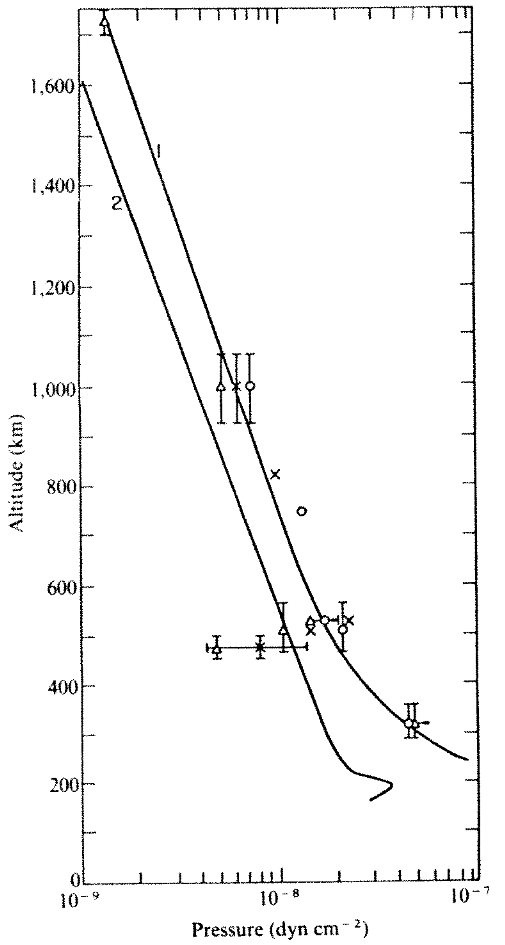

Fig. 2 Solar wind pressure (P_{SW}), magnetic barrier pressure (P_{MB}), increased by a factor of 1.5, and total (kinetic and magnetic) pressure of the ionosphere (P_I) below the ionopause plotted against observed ionopause altitudes on first orbits of PVO. Line 1 is drawn to show the change of pressure values at the ionopause with altitude for SZA range 65°–75°. Mean ionospheric pressure model, line 2, obtained from means of measured number densities and ion and electron temperatures for the same SZA range[6,7]. ○, P_{SW}; △, P_I; ×, $1.5 \times P_{MB}$.

obtained by taking into account a more realistic approximation of the external pressure. To obtain an estimate of the external pressure variation with SZA we assumed that the surface of the ionopause can be obtained from a simple ionospheric pressure balance[17,18]. The parameter H/r_0, ratio of the ionospheric scale height to planetocentric subsolar dimension of obstacle, defining the approximate shape of the ionopause, was taken equal to 0.07 (ref. 10). Figure 1 shows that the mean magnetic field pressure in the region just outside the ionopause, or in the 'magnetic barrier' closely follows the expected pressure variation along the boundary of the obstacle. The mean magnetic pressure within the magnetic barrier and its variations were taken from refs 16, 19. To fit the observations the pressure curves were normalized to 3.7×10^{-8} dyn cm^{-2} at $\psi = 0$ and this value is representative for mean subsolar magnetic barrier pressure for the PVO period of observations. Data of Fig. 1 confirm that pressure within the magnetic barrier is determined by the pressure of external flow and show that this condition holds up to SZA ~90°.

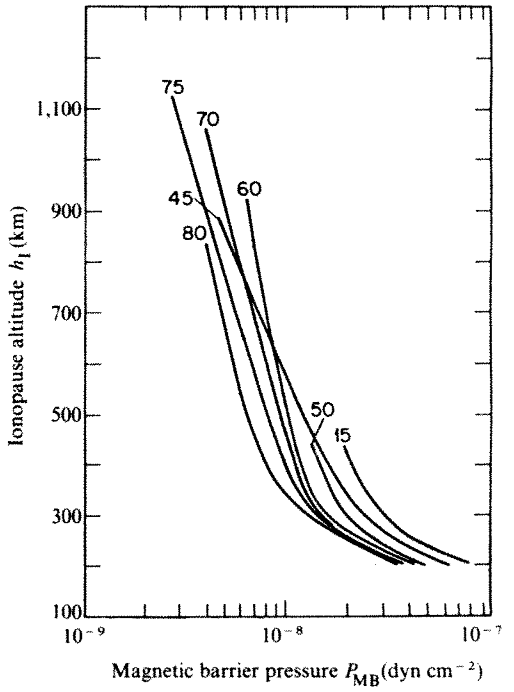

Fig. 3 Magnetic barrier pressure distribution versus height for different solar zenith angles (indicated) obtained according to data of refs 16, 19.

Distribution of measured values of ionospheric pressure just below the ionopause, magnetic pressure within the magnetic barrier, and solar wind pressure versus height of the ionopause for December 1978 are shown in Fig. 2. Data are limited to SZA between 63° and 90°. Solar wind pressure was estimated from the measured ρV^2 value corrected for pressure distribution along the boundary (curve 3, Fig. 1). Magnetic field pressure was multiplied by a factor of 1.5 to fit both the solar wind pressure and ionospheric pressure. Figure 2 shows good agreement between the measured ionospheric pressure below the ionopause and the solar wind pressure corrected for angle of incidence. It shows also that although the magnetic barrier has a major role in the transfer of solar wind pressure to the ionosphere, the plasma pressure within the magnetic barrier may provide up to one-third of the total pressure.

Comparison of the behaviour of the ionospheric pressure just below the ionopause with the mean ionospheric pressure distribution for the same SZA range apparently shows significant differences between these distributions suggesting modification of the subionopause layer due to changing solar wind conditions.

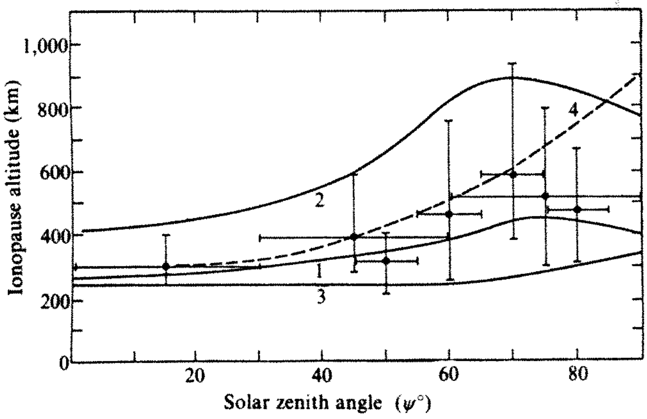

Fig. 4 Observed ionopause altitudes versus solar zenith angle. Expected 'instant' ionopause profiles are shown for close to the mean solar wind ram pressure value (curve 1); one half of it (curve 2); and doubled mean pressure value (curve 3). Dashed line, model ionopause profile for $H/r_0 = 0.07$ and $r_0 = 6{,}350$ km.

The magnetic pressure distribution within the magnetic barrier as a function of the ionopause altitude and as a function of SZA was obtained using data from (refs 16, 19). This distribution, shown in Fig. 3 enables the 'instant' profile of the ionopause to be found for a given solar wind pressure, provided that the hot plasma contribution to the magnetic barrier pressure is taken into account. Assuming that the plasma pressure within the magnetic barrier is one-third everywhere, the shapes of the ionopause for close to the mean solar wind condition, half and double this value were obtained. Figure 4 shows that the behaviour of the model profiles is in reasonable agreement with the observed mean ionopause altitude dependency on SZA and with the observed distribution of ionopause crossings. Also, it can be seen that both the observational data and the ionopause model show that at SZA ~70° the shape of the venusian ionopause differs significantly from the simple hydrostatic equilibrium model of the ionopause (curve 4 in Fig. 4). This implies the important role of solar wind heating of the subsolar ionosphere[15,20,21] and the significant influence of transport processes within the ionosphere at large SZA[12].

. The model of the subionopause pressure distribution with height and with the solar zenith angle seems to represent reasonably the observed behaviour of ionopause crossings at different SZA and allows one to obtain an 'instant' profile of the ionopause for given solar wind pressure.

Received 10 March; accepted 24 April 1980.

1. Smith, E. J., Davis, L. Jr, Coleman, P. J. Jr & Sonett, C. P. *J. geophys. Res.* **70,** 1571–1586 (1965).
2. Dolginov, Sh. Sh., Eroshenko, E. G. & Zhuzgov, L. N. *Kosm. Issled.* **6,** 562–567 (1968).
3. Dolginov, Sh. Sh., Eroshenko, E. G., Zhuzgov, L. N., Buzin, V. B. & Sharova, V. A. *Pisma Astr.* **2,** 88–90 (1976).
4. Gringauz, K. I. *et al* in *Physics of Solar Planetary Environments* (ed. Williams, D. J.) 918–932 (American Geophysical Union, Washington DC, 1976).
5. Vaisberg, O. L. *et al.* in *Physics of Solar Planetary Environments* (ed. Williams, D. J.) 904–917 (American Geophysical Union, Washington DC, 1976).
6. *Science* **203,** 743–808 (1979).
7. *Science* **205,** 41–121 (1979).
8. Bauer, S. J., Donahue, T. M., Hartle, R. E. & Taylor, H. A. Jr *Science* **205,** 109–111 (1979).
9. Kliore, A. J., Woo, R., Armstrong, J. W., Patel, I. R. & Croft, T. A. *Science* **203,** 765–768 (1979).
10. Knudsen, W. C. *et al. Science* **203,** 757–759 (1979).
11. Taylor, H. A. Jr *et al. Science* **203,** 752–754 (1979).
12. Taylor, H. A. Jr *et al. Science* **203,** 755–757 (1979).
13. Russell, C. T. *J. geophys. Res.* **82,** 625–631 (1977).
14. Russell, C. T., Elphic, R. C. & Slavin, J. A. *Science* **203,** 745–748 (1979).
15. Brace, L. H. *et al. Science* **203,** 763–765 (1979).
16. Elphic, R. C., Russell, C. T., Slavin, J. A., Brace, L. H. & Nagy, A. F. *Geophys. Res. Lett.* (submitted).
17. Spreiter, J. R., Alksne, A. Y. & Summers, A. L. in *Physics of the Magnetosphere* (eds. Carovillano, R. L., McClay, J. F. & Radoski, M. R.) 304–378 (Reidel, Dordrecht, 1968).
18. Spreiter, J. R., Summers, A. L. & Rizzi, A. W. *Planet. Space Sci.* **18,** 1281–1290 (1970).
19. Russell, C. T., Elphic, R. C. & Slavin, J. A. *Proc. Magnetospheric Boundary Layer conf.* 231–239 (ESA SP-148, 1979).
20. Scarf, F. L., Taylor, W. W. L. & Green, J. M. *Science* **203,** 748–750 (1979).
21. Knudsen, W. C. *et al. Science* **205,** 105–107 (1979).
22. Ivanov-Kholodny, G. S. *et al. Soviet Phys. Usp.* **20,** 1025–1027 (1977).
23. Ivanov-Kholodny, G. S. *et al.* 21*st COSPAR Meet.*, Innsbruck, (1978).

Hydromagnetic dynamo in the cores of Uranus and Neptune

M. Torbett & R. Smoluchowski

Department of Astronomy, University of Texas, Austin, Texas 78712

The explanation of the origin of a magnetic field of Uranus is difficult because the structure of the planet's interior is not well known and the strong thermal flux, which is associated with the operation of hydromagnetic dynamos in Jupiter and Saturn, seems to be absent or very low. We show here that the composition, physical state and electrical conductivity of the planet's core permits the generation of a magnetic field within the very low observational limits of its heat emission. We also suggest that the higher density and higher pressures in the core of Neptune could explain the suspected absence of a measurable field on that planet even though it is a relatively strong source of heat.

While there are no rigorous theories which would permit us to make quantitative predictions of the magnetic fields of various planets it is usually possible to explain the presence or absence of these fields and sometimes even give a semiempirical estimate of their strengths[1–3]. Observations[4] of 0.5-MHz pulses analogous to jovian emission suggested that Uranus has a magnetic field but the planet had resisted efforts to explain its field's origin in a satisfactory manner. It now seems that a detailed consideration of convection and electrical conductivity in the planet's core indicates the presence of a thermally driven hydromagnetic dynamo.

The generation of magnetic fields in planets, whether by a thermally or precessionally driven dynamo, is very sensitive to details of the models of their interiors. The development of a satisfactory model of Uranus has been hampered by the availability of only approximate values of some of the important parameters, by the lack of good equations of state and by the difficulty in fitting, within reasonable limits, what is known about the chemical composition and evolution of the outer planets. In particular there is still an uncertainty of about a factor of two in the rotational velocity of the planet[5,6]. This velocity strongly affects the structure of the outer parts of the planet and, to a much smaller degree, the size of the core. We have shown previously[7] that a two-layer model of Uranus could account for the presence of a magnetic field only if the planet had a layer of metallic hydrogen or of a metallically conducting molecular hydrogen and even then probably only if the dynamo were precessionally driven by Miranda. This conclusion was forced by the fact that in this model the core turned out to be solid while the layer containing liquid H_2O, NH_3 and so on had much too low an ionic electrical conductivity even though, as shown by experiment (W. J. Nellis, A. C. Mitchell, R. S. Hawke and R. K. Keeler, personal communication), the water would be pressure dissociated but not yet metallic. The above result was independent of the rate of rotation of the planet within the limits mentioned above.

The new three-layer model of Uranus of Hubbard and MacFarlane[8] led us to review the situation as the model uses new equations of state and, within a wide range of rotational velocities, it seems to fit better the observational parameters as well as the chemical constraints. First, the model excludes the presence of a metallic or of a suitably conducting molecular hydrogen layer. Second, just as in the two-layer model, the liquid 'ice' layer has too low an ionic conductivity to permit the operation of a magnetic dynamo although a thin layer of 'metallic' H_2O could appear right at the core boundary. It remains then to analyse the planet's core which has a radius of 7,700 km

0028–0836/80/290237—03$01.00

($r_c/R_u \sim 0.3$), and contains 38, 25, 25 and 12% of SiO_2, MgO, FeS and FeO respectively. The melting temperatures of these compounds as a function of radius in the core were calculated using the same method as in our previous paper (assuming the Grüneisen parameter to be the same for FeO and FeS) and the densities at which these compounds should become metallic were estimated using Herzfeld's molar refractivity criterion[9]. The results are shown in Figs 1 and 2. It seems that in an isothermal core FeS and FeO are always liquid, MgO is always solid while SiO_2 is solid in the inner part of the core. FeO and FeS are metallic throughout the core, the sulphide being known to change from a low gap semiconductor to a metal at pressures of the order of kilobars[10]. MgO and SiO_2 are metallic up to ~85% of the radius of the core.

It can be shown that initial gravitational condensation and radioactive heating led to a temperature of the interior of Uranus which was probably in excess of that required to keep the core metallic and entirely liquid. The outward flow of this heat produced convection which kept the core well mixed during this early high temperature phase. As the core cooled, however, large differences in the density of its constituents produced gravitational, diffusion controlled, separation between the heavy iron compounds and other lighter constituents which led to a significant evolution of additional heat. Further cooling of the core resulted in the formation of solid MgO which floated towards the surface of the core thereby releasing energy which in turn slowed down the cooling and the segregation. This self-regulating aspect of the process, reminiscent of that proposed[11] for the H–He system in the giant planets and necessary to explain the present magnetism and excess luminosity of Saturn[12], may be still active because the theory is certainly not rigorous enough to ensure that the melting temperature of MgO near the surface of the core is indeed 1,000 K higher than the calculated temperature at this radius. It seems reasonable, therefore, to conclude that even now the core of Uranus is not isothermal but adiabatic. Unfortunately, lack of knowledge of the phase diagram of the multicomponent alloy and especially of mutual solubilities of the components in the early stages of the evolution of the planet makes a quantitative prediction of the rate of heat generation in the core almost impossible. The total energy available from gravitational interchange in the core can be estimated, however, to be $\sim 10^{39}$ erg which distributed over a time scale of 10^{10} yr yields an average flux of the order of 40 erg cm^{-2} s^{-1} at the surface of the planet, a value compatible with the observational[13] upper limit for Uranus of about 10^2 erg cm^{-2} s^{-1}. The total original primordial energy of the planet was probably not less than 10^{40} erg. The range of possible compositions of cores of the giant planets introduces an uncertainty of about a factor of two into the above estimates.

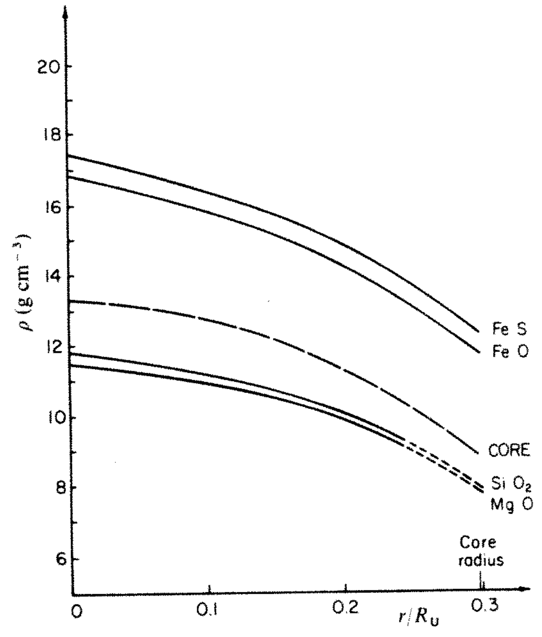

Fig. 1 Density profiles of the core and of its constituents: solid line, metallic; dashed line, non-metallic. R_U is the radius of the planet.

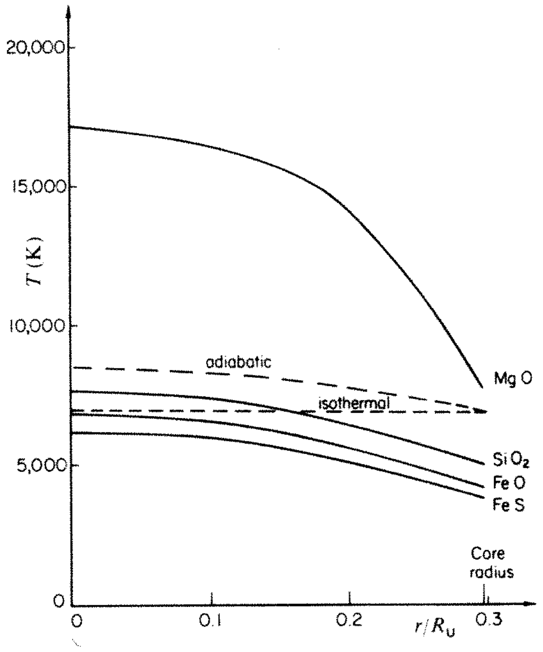

Fig. 2 Melting temperature profiles of the constituents of the core (solid line) and the temperature gradients in the core (dashed lines). R_U is the radius of the planet.

Assuming a superadiabaticity of $\nabla - \nabla_s = 10^{-6}$, a thermal expansion coefficient of the order of 10^{-6} and a mixing length $l \sim 10^{-3} r_c$ one obtains for the convective velocity in the core $v \sim 10^{-1}$ cm s^{-1}. In view of the highly heterogeneous chemistry of the core it seems reasonable to put electrical conductivity $\sigma = 10^{-5}$ e.m.u. which is typical of low conductivity metals. With these values for v and σ, the necessary condition for the operation of a thermally driven hydromagnetic dynamo—the magnetic Reynolds number, $R = \sigma \mu L v$ where μ is the permeability and L is the size of the core, has to be greater than 10—is amply satisfied. The heat flux carried by this convection, as estimated using the expression $\Phi = \rho C_p v l T\ (\nabla - \nabla_s)\ (2H_p)^{-1}$ (Scalo, personal communication) is about 10 erg cm^{-2} s^{-1} at the surface of the planet. Here H_p is the pressure scale height and C_p is the specific heat, about 5×10^6 erg g^{-1} deg^{-1}.

The presence of an internal heat source in the core implies, of course, that the central temperature of the planet is somewhat higher than in the original model[9], but this does not significantly affect the model's other features because the presence of a comparable flux is already taken into account and the thermal pressure is negligible. The approximate adiabatic gradient is also indicated in Fig. 2 showing that, except for MgO, all constituents of the core are liquid. One may add that Busse's semi-empirical rule[2] applied to Uranus' core leads to a surface field of the order of 10^{-1} G.

Applying the same kind of reasoning to the three-layer model of Neptune[8] one concludes that because of higher densities and pressure nearly half of the volume of its core is solid as compared to about one-third on Uranus. Thus one may expect the differentiation, the heat evolution, the rate of convection and the magnetic field of the core to be much lower than on Uranus. On Neptune, just as on Uranus, the ionic conductivity of the liquid 'ice' layer is too low and the probable layer of 'metallic' H_2O at the core boundary too thin to permit the operation of a hydromagnetic dynamo even in the presence[14] of the high heat flux.

It seems, therefore, that a slightly modified three-layer model of Uranus explains in a natural way the presence of a magnetic field on this planet and does not require making rather problematic assumptions which were necessary for the two-layer model. Application of a similar analysis to the three-layer model of Neptune explains its very low, if any, magnetic field in spite of the high thermal flux.

This work was supported by NASA grant NSG 7505 Sup. 1.

Received 11 February; accepted 23 May 1980.

1. Stevenson, D. J. *Icarus* **22,** 403 (1974).
2. Busse, F. H. *Phys. Earth planet. Inter.* **12,** 350 (1976).
3. Smoluchowski, R. *Phys. Earth planet. Inter.* **20,** 247 (1979).
4. Brown, W. L. *Astrophys. J.* **207,** L209 (1976).
5. Dunham, E. & Elliot, J. L. *Bull. Am. astr. Soc.* **11,** 568 (1979).
6. Smith, H. J. & Slavsky, D. B. *Bull. Am. astr. Soc.* **11,** 568 (1979).
7. Torbett, M. & Smoluchowski, R. *Geophys. Res. Lett.* **6,** 675 (1979); *Lunar planet. Sci.* (in the press).
8. Hubbard, W. B. & MacFarlane, J. J. *J. geophys. Res.* **85,** 225 (1980).
9. Ross, M. *J. chem. Phys.* **56,** 4651 (1972).
10. Stiller, H., Siepold, U. & Vollstaedt, H. *Fiz. Svoistva Gorn. Porod. Miner. Vys. Temp. Mater. Vses. Soveshch.* **4,** 198 (1974).
11. Salpeter, E. E. *Astrophys. J.* **181,** L183 (1973).
12. Stevenson, D. J. *Science* **208,** 746 (1980).
13. Hubbard, W. B. *Icarus* **35,** 177 (1978).

Solar cycle changes in the polar solar wind

W. A. Coles*, B. J. Rickett*, V. H. Rumsey*, J. J. Kaufman*, D. G. Turley*, S. Ananthakrishnan†, J. W. Armstrong‡, J. K. Harmons§, S. L. Scott|| & D. G. Sime¶

*Department of Electrical Engineering and Computer Sciences, University of California, San Diego, La Jolla, California 92093
† Radio Astronomy Centre, Tata Institute for Fundamental Research, Ootacamund 643001, India
‡ Jet Propulsion Laboratory, 4800 Oak Grove Drive, Pasadena, California 91103
§ Arecibo Observatory, Arecibo, Puerto Rico 00612
|| Owen's Valley Radio Observatory, Box 387, Big Pine, California 93513
¶ High Altitude Observatory, National Center for Atmospheric Research, PO Box 3000, Boulder, Colorado 80307

Although the 11-yr cycle of solar activity was first recognized in 1843 (ref. 1) and was subsequently traced back to the seventeenth century[2–4], it is still only poorly understood. The most obvious indicators of the activity cycle are sunspots, flares, plages, and so on. The corona as seen during an eclipse also reflects the cycle, appearing flattened at the poles near solar minimum and almost spherical near the solar maximum. All such phenomena are intimately linked to the solar magnetic fields, which exhibit complex but systematic variations. Whereas there are satisfactory qualitative models (see refs 5, 6) for the magnetic variations, the underlying physics is still obscure. The solar cycle also influences the Earth causing, for example, changes in geomagnetic activity, the magnetosphere and aurorae, the ionosphere, the flux of galactic cosmic rays and possibly the weather. These modulations are not well understood but must be transmitted by one or more of the following: electromagnetic radiation; solar wind thermal plasma and its magnetic field; energetic particles. We here present new observations on the changing three-dimensional form of the solar wind, which helps to relate some of the modulations.

The solar wind also shows the effects of the solar cycle, but changes observed by ecliptic spacecraft are minor compared with the dramatic changes observed in the corona for example. Two processes are apparent in the observations of 1962–74 (ref. 7). First, at sunspot maximum, there is an increase in flare-associated transient disturbances in the solar wind. Second the quasi-static structures of the solar wind such as magnetic sectors and high speed streams are much more evident and stable during the declining and minimum years of activity. In fact the dominance of the high speed streams during the declining phase of the cycle is the most obvious change in the ecliptic solar wind. We show that an understanding of the three-dimensional wind structure explains the occurrence of such streams.

Direct spacecraft observations have reached ±16° in latitude although most are confined to ±10°. These show very high latitude gradients of velocity during streams[8,9], and they have helped to clarify the magnetic sector structure[34] but they are obviously limited in defining the overall latitude structure. However, the indirect techniques of interplanetary scintillation (IPS) (refs 10–13) and comet-tail observations[14] can cover essentially all latitudes albeit with reduced precision. IPS observations from 1971 to 1979 show that the solar wind does respond dramatically to the solar activity cycle but the primary effects are in the polar regions.

The IPS method, pioneered by Dennison and Hewish[15] relies on three spaced antennas to record signals from a small diameter radio source. The scintillations in the strength of the signals at each antenna are caused by inhomogeneities in the solar wind; the signals are cross-correlated to yield time offsets, from which the speed of the scintillation pattern can be deduced.

The UCSD observatory, which operates at 74 MHz, and the methods of data analysis have been described elsewhere[16,17]. A careful comparison of ecliptic IPS observations with spacecraft observations[18] has 'calibrated' the IPS method. From this work we conclude that the IPS-observed speed is within ±50 km s^{-1} of the solar wind speed at the point where the radio-wave scattering is strongest. We thus adopt the simplified interpretation that the IPS speed gives an estimate of the solar wind speed at that single point in space. We make IPS observations of eight radio sources daily, from which we typically obtain useful solar wind speed estimates at 3–5 such effective locations. The heliographic latitude of these locations spans 60 °S to 70 °N. However, the coverage is not continuous; northern latitudes (>20°) are observed from March–July and October–November, while southern latitudes (>20°) are observed June–July, each year (see Fig. 1 of ref. 19).

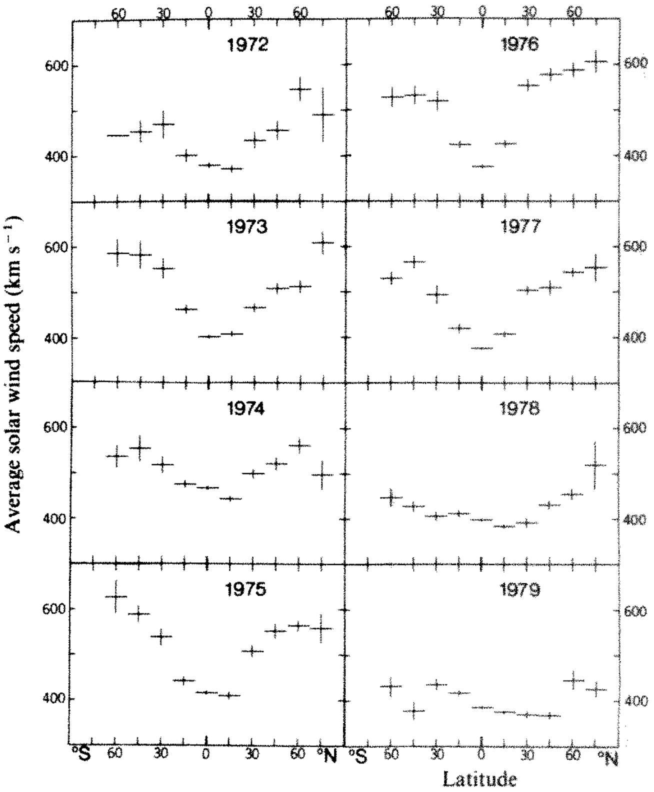

Fig. 1 Solar wind speed measured by IPS averaged into 15° intervals in heliographic latitude for the years 1972–79. The error bars are ± twice the standard deviation in the average.

0028–0836/80/290239—03$01.00

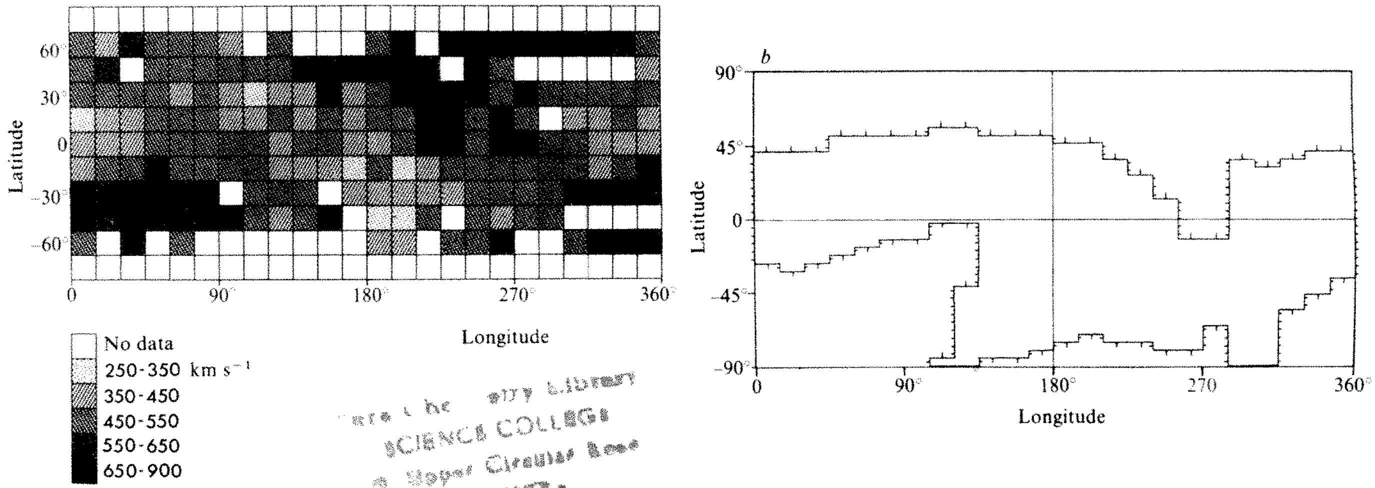

SCIENCE COLLEGE Upper Circular Road CALCUTTA

Fig. 2 *a*, The average solar wind speed in 15°×15° bins of heliographic latitude and longitude coded by the grey scale as indicated. The IPS data were averaged for Carrington rotations 1612–1617 (March–July 1974). *b*, Coronal holes indicated by a contour of low *K*-coronameter polarization brightness (1.5×10^{-8} pB); the tick marks point towards low brightness, that is towards the holes. Data, supplied by Drs R. and S. Hansen, are averaged for the same period as *a*.

The solar wind speed can be averaged over longitude to provide the speed versus latitude plots of Fig. 1. Their characteristic U-shape shows that the wind speed is on average considerably faster at high latitudes than at the solar equator[20]. This phenomenon is best described as evidence for persistent fast polar streams from the north and south poles. In studying the long-term changes in Fig. 1, we must be aware of the reduced number of observations at high latitudes, with a corresponding increase in the error bars with latitude. Nevertheless, we can identify three phases in the evolution of the polar streams.

First, during the years of declining activity 1973–75, equatorial speeds are somewhat elevated and there is a gradual increase of speed between 0° and ±60°. The distribution of mean wind speed with latitude and longitude averaged over six rotations is shown in Fig. 2*a*. Here it is apparent that the polar streams are tilted from the axis, remaining opposite each other but centred near latitudes of ±50°. These streams are wide enough to reach the ecliptic, where they are seen as two fast streams per rotation and also cause an increase in the mean speed[7]. Figure 2*b* shows that these fast streams come from coronal holes, where the polar holes are shown to be tilted in much the same way.

The second phase, 1976–77 (Fig. 1), shows slower equatorial speeds and a sharp transition from slow to fast between 15° and 30° in both the north and south. This corresponds to a better alignment of the polar streams with the rotation axis, as revealed in latitude–longitude plots[21]. Note that the gradient of the mean speed is greater than 10 km s^{-1} per degree between 15° and 30°. This is comparable with instantaneous measurements of the latitude gradient made with two spacecraft (see refs 8, 9). The polar holes were also wide and axially aligned during these years of solar minimum as shown by *K*-coronameter data[22] and by eclipse photographs which are elongated along the equator due to low densities over the poles[23].

The third phase, 1978–79, shows a flattening of the U-shape curve, that is a dramatic reduction in the wind speed at 30–60 °N and S, implying that the polar streams are much narrower. Note that this change probably occurred at the same phase of the previous cycle. Hewish and Symonds[10] observed higher speeds at north latitudes than at the equator in 1966, but not in 1967. Their restricted data coverage meant they could not draw any strong conclusions, but it is now clear that this is the same change which we see 11 yr later.

The polar holes also contracted during 1977, as the new sunspots emerged at mid-latitudes. This implies that bipolar magnetic regions are dominating the mid-latitudes restricting the extent of the open field regions (polar holes). Figure 3 compares average wind speed at 0, 30° and 60° with the area of the polar holes from 1971 to 1979. Hole area estimates from observations of He 10,830 Å made at Kitt Peak are plotted for 1974–78, together with earlier estimates by various techniques[24]. The areas are given as percentages of 4π sr at the photosphere. The slowing of the wind at 30° and 60° north and south in late 1977 to the present (a narrowing of the polar streams), is closely matched by the shrinking of the polar holes.

The latitude boundary of the polar holes and polar streams are compared in Fig. 4 (assuming axial symmetry). The stream boundary is chosen to be the latitude at which the velocity is 500 km s^{-1}. There are clearly large changes in the width of the polar streams. Between 1974 and early 1977, the polar stream boundaries were near ±30° showing that 50% of 4π sr were occupied by solar wind with an average wind speed > 500 km s^{-1}. By contrast, from late 1977 to the end of 1979, the polar stream boundaries moved up to ±65°, showing that the fast polar wind occupied only 9% of 4π sr.

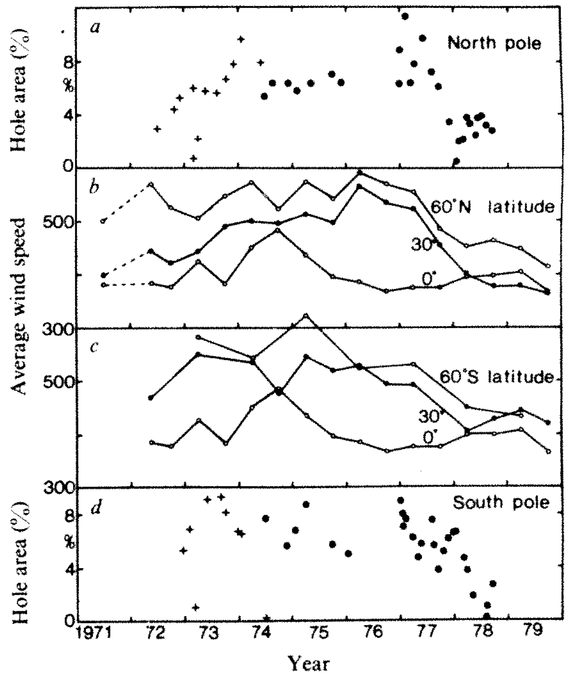

Fig. 3 The solar wind speeds averaged into 15° latitude intervals for six month periods are plotted against time in *b* and *c*. Single rotation estimates of polar coronal hole areas derived from photospheric observations are plotted for the north polar hole in *a* and for the south in *d*. Symbols indicate techniques from ref. 24. The slowing of the wind above ±30° latitude in 1978 is matched by a narrowing of the polar holes.

When these changes in the fast polar streams are compared with changes in the polar coronal holes, it is apparent that the polar hole boundaries do not change as much as the polar stream boundaries. Although there are real variations between rotations, the mean hole boundaries remain at ±60° (13% solid angle) through early 1977, shrinking to ±70° (6% solid angle) in 1978. Data are not yet available for 1979. The ratio of the solid angle for fast polar streams to that for coronal holes defines an expansion factor which characterizes the degree to which the coronal holes open out faster than radial as they become fast streams. This ratio decreased from 3.8 for 1974–77 to 1.5 for 1978. Whereas the numerical value of the ratio cannot be easily related to the areal expansion factor as defined and measured for a northern polar hole[25], the change in the ratio indicates that the areal expansion factor of the polar holes decreased substantially as the holes narrowed. A large expansion factor implies that the solar wind is accelerated to supersonic speeds closer to the base of the corona than for a smaller areal expansion[26].

The agreement with IPS observations in 1967 and 1968, and the agreement with the polar hole variations shows that the changes in the fast polar stream are part of the solar cycle. Studies of polar faculae over many solar cycles[27] suggest that the polar holes narrow for several years at the peak of activity. The polar magnetic field polarity also reverses near solar maximum. Clearly the polar holes; defined as unipolar open field regions, must undergo a major change and disappear altogether when the fields reverse. Eclipse photographs tell a similar story. The flattened images at solar minimum indicate the large low density holes over the polar regions; the circular images at solar maximum indicate no such polar holes. The changing three-dimensional solar wind structure reported here helps explain the solar cycle modulations of several phenomena.

The average level of geomagnetic activity varies with solar cycle but the pattern shows differences from one cycle to the next. Two mechanisms are thought to be responsible[28]: the increase in solar wind transients near the maximum phase of the cycle, and the increase of ecliptic fast streams in the declining phase. Both processes cause enhanced geomagnetic activity index. However, their relative importance change from cycle to cycle, so that the peak index sometimes occurs near the maximum phase, sometimes in the declining phase, or sometimes extends between the two. In particular, it has been suggested[29] that the previous solar cycle (number 20) was unusual in the dominance of ecliptic streams and associated geomagnetic activity during the declining phase. Such cycle-to-cycle variability is easier to understand in the context of the three-dimensional stream structure. The recurrent ecliptic streams are seen when the long-lived polar streams are tilted far enough from the axis to intersect the ecliptic. For obscure reasons, such tilting is greatest in declining solar activity. However, we suggest that the degree of tilt varies from one cycle to the next causing recurrent ecliptic streams and accompanying geomagnetic activity to be more pronounced in some 11-yr cycles than in others.

The average flux of galactic cosmic rays detected at the Earth is also modulated by the sunspot cycle, such that minimum cosmic ray flux occurs at sunspot maximum and vice-versa[30]. The spherically symmetrical diffusion models for this modulation predict an 11-yr variability in the strength of inhomogeneities in the magnetic field and also a radial gradient in the cosmic ray flux, both of which are now contradicted by observations[31]. The present results indicate a need for models where the magnetic geometry in three-dimensions is important (such as those of Jokipii *et al.*,[32]), especially when combined with the recent correlation of polar hole area and cosmic ray flux[33]. We suggest that at solar minimum wide polar holes connect to wide fast polar streams, which are presumably unipolar and may in turn be connected to the interstellar magnetic field, allowing easy access of cosmic rays. At solar maximum the polar holes are constricted by high latitude active regions, causing a narrowing of the polar streams, that is a smaller area of easy access which reduces the cosmic ray flux.

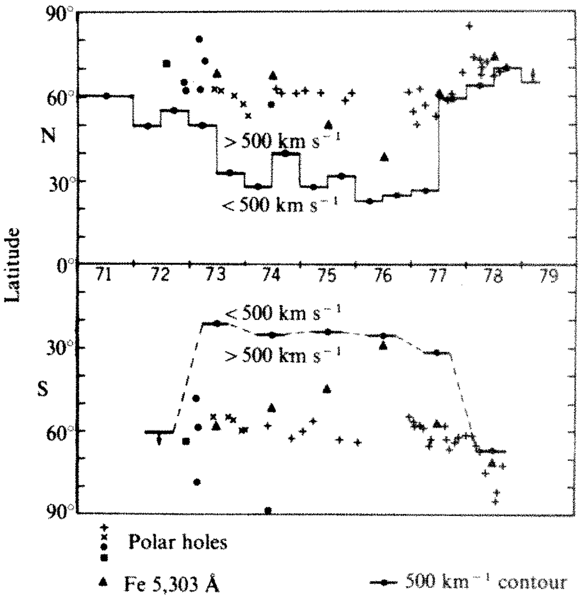

Fig. 4 Solid curve (in the north) and horizontal bars (in the south) indicate the contour of 500km s^{-1} average solar wind speed. The latitude boundaries of the polar holes are indicated by various symbols: +, He 10,830 Å; ×●■, different techniques (see ref. 24); ▲, Fe 5,303 Å (threshold at 1.5×10^{-6} of disk centre brightness, data from Sacramento Peak Observatory).

Fast solar wind streams from the polar coronal holes persist for at least 6 yr but contract as the solar activity cycle approaches maximum. The polar coronal holes are observed to narrow at the same time, presumably in response to the changing solar magnetic field. The link between coronal holes and fast wind streams is thus extended to polar latitudes and to a major fraction of the 11-yr cycle. This picture throws considerable light on the problem of solar cycle modulation of galactic cosmic rays, geomagnetic activity and the presence of fast ecliptic wind streams.

This research has been supported from the start by the Atmospheric Sciences Division of the NSF (ATM 78-6770), and since 1977 by the A. F. Geophysical Laboratories (F19628-77-C-0161).

Received 14 March; accepted 8 May 1980.

1. Schwabe, H. *Astr. Nachr.* **20,** (1843).
2. Wolf, R. *Astr. Mitt. Zürich* **1,** 8 (1856).
3. Maunder, E. W. *Mon. Not. R. astr. Soc.* **50,** 251–260 (1890).
4. Eddy, J. A. *Science* **192,** 1189–1192 (1976).
5. Babcock, H. W. *Astrophys. J.* **133,** 572–587 (1961).
6. Leighton, R. B. *Astrophys. J.* **156,** 1–41 (1969).
7. Gosling, J. T., Asbridge, J. R., Bame, S. J. & Feldman, W. C. *J. geophys. Res.* **81,** 5061 (1976).
8. Rhodes, E. J. & Smith, E. J. *J. geophys. Res.* **80,** 917–928 (1975).
9. Schwenn, R. *J. geophys. Res.* **83,** 1011 (1978).
10. Hewish, A. & Symonds, M. D. *Planet. Space Sci.* **17,** 313–320 (1969).
11. Vitkevich, V. V. & Vlasov, V. I. *Soviet Astr.* **13,** 669–676 (1970).
12. Coles, W. A. & Maagoe, S. *J. geophys. Res.* **77,** 5622–5624 (1972).
13. Watanabe, T., Shibasaki, K. & Kakinuma, T. *J. geophys. Res.* **79**, 3841–3843 (1974).
14. Brandt, J. C., Harrington, R. S. & Rosen, R. G. *Astrophys. J.* **196,** 877–878 (1975).
15. Dennison, P. A. & Hewish, A. *Nature* **213,** 343–346 (1967).
16. Armstrong, J. W. & Coles, W. A. *J. geophys. Res.* **77,** 4602–4609 (1972).
17. Coles, W. A. & Kaufman, J. J. *Radio Sci.* **13,** 591–597 (1978).
18. Coles, W. A., Harmon, J. K., Lazarus, A. J. & Sullivan, J. D. *J. geophys. Res.* **83,** 3337–3341 (1978).
19. Coles, W. A. & Rickett, B. J. *Solar Geophysical Data, Explanation of Data Reports,* No. 390, 13–15 (1977).
20. Coles, W. A. & Rickett, B. J. *J. geophys. Res.* **81,** 4797–4799 (1976).
21. Sime, D. G. & Rickett, B. J. *J. geophys. Res.* **83,** 5757–5762 (1978).
22. Hundhausen, A. J. in *Proc. Symp. on Solar Cycle from Space,* Wellesley (NASA, 1979).
23. Allen, C. W. *IAU Symp. on Solar Corona,* 241 (1961).
24. Sheeley, N. R. Jr in *Proc. Symp. on Solar Cycle from Space*, Wellesley (NASA, 1979).
25. Munro, R. H. & Jackson, B. V. *Astrophys. J.* **213,** 874–876 (1977).
26. Kopp, R. A. & Holzer, T. E. *Solar Phys.* **49**, 43–56 (1976).
27. Sheeley, N. R. Jr *J. geophys. Res.* **81,** 3462–3464 (1976).
28. Crooker, N. U., Feynman, J. & Gosling, J. T. *J. geophys. Res.* **82,** 1933–1937 (1977).
29. Gosling, J. T., Asbridge, J. R. & Bame, S. J. *J. geophys. Res.* **82,** 3311–3314 (1977).
30. Pomerantz, M. A. & Duggal, S. P. *Rev. Geophys. Space Sci.* **12,** 343–357 (1974).
31. Fisk, L. A. *Solar System Plasma Physics* (Reidel, Dordrecht 1979).
32. Jokipii, J. R. & Kopriva, D. A. *Astrophys. J.* **234,** 384–392 (1979).
33. Hundhausen, A. J., Sime, D. G., Hansen, R. T. & Hansen, S. F. *Science* **207**, 761–762 (1980).
34. Smith, E. J., Tsurutanik, B. T. & Rosenberg, R. L. *J. geophys. Res.* **83,** 717 (1978).

Peninsula method of ULF signal generation

A. C. Fraser-Smith & O. G. Villard Jr

Radioscience Laboratory, Stanford Electronics Laboratories,
Stanford University, Stanford, California 94305

Natural pulsations of the geomagnetic field in the ultra-low-frequency range (ULF; <5 Hz) have been studied for many years, but progress has been limited by the lack of controlled experiments on their generation and propagation. Clearly, a method for producing the pulsations artificially on a controlled basis would contribute greatly to our understanding of their properties. In 1975 we participated in a theoretical study[1] that described a method for generating artificial Pc 1 geomagnetic pulsations (0.2–5 Hz) by driving a large alternating electric current with frequency in the Pc 1 range around a relatively nonconducting peninsula in an enclosed sea or large saline lake. The study predicted that the alternating magnetic field of the current loop in the sea could disturb the lower ionosphere above the peninsula and that hydromagnetic (HM) waves at the Pc 1 frequency would propagate away from the disturbed region to large distances in the ionosphere and magnetosphere. Two important conditions for the generation to take place were that the amplitude of the ULF magnetic field fluctuations should be greater than $\sim$1 nT (refs 2, 3) and that suitable propagation conditions should exist for the HM waves. We report here the results of two experiments on the 'peninsula method' of Pc 1 pulsation generation conducted during 1975–76. Our results, when combined with those from a recent peninsula experiment by Soviet scientists[4,5], strongly support the proposed method of Pc 1 pulsation generation.

Our peninsula experiments used the North Neck Peninsula on Chappaquiddick Island, Massachusetts (Fig. 1), which is located in an enclosed body of seawater (enclosure of the peninsula provides well defined boundary conditions and protection from wave action; it is not a necessary condition for ULF signal generation). During the summer of 1975 we carried out a passive experiment using the seawater around the peninsula as a receiving loop. Two electrodes constructed of thin copper sheet $\sim$0.45 m square were inserted in the water on either side of the peninsula and connected by shielded cables (total length, 300 m; total resistance, $\sim 10\ \Omega$) to an electronics package consisting of a ULF differential amplifier, a timer, a calibrator and a low pass filter with an overall voltage gain of 200 at a frequency of 1 Hz. The resistance of the cable–seawater–cable circuit as seen by the electronics package was $\sim 12\ \Omega$, implying that the resistance between the two electrodes was roughly $2\ \Omega$. The output of this system, which had a flat frequency response over the Pc 1 frequency range, was recorded on a slow-speed analogue magnetic tape recorder.

Measurements of ULF geomagnetic pulsation activity were made each night between 26 August and 5 September, and several well defined Pc 1 events were recorded. A spectrogram of one particularly long-lasting and large-amplitude event is shown in Fig. 2, together with spectrograms of the same event as seen at Roberval, Quebec, and at Stanford, California (see Fig. 3 for locations of the stations). Although this was a preliminary experiment, and some desirable controls were necessarily lacking, it demonstrated that Pc 1 pulsations could be measured across the neck of a peninsula. Further, the high signal-to-noise ratio of the measurements, as shown by the data in Fig. 2, supported the peninsula current loop concept, as a large receiving area would be required to provide the high ratio.

An exploratory small-scale active experiment was conducted during the summer of 1976. Electrodes were installed at roughly the same locations on either side of North Neck Peninsula as during 1975, but this time they were larger and were constructed of galvanized iron pipe. They were spaced $\sim$180 m apart and connected to a ULF current source by heavy-gauge insulated aluminium wire (wire diameter 0.52 cm), and the resistance of the current path was $0.4\ \Omega$, as compared with $12\ \Omega$ the previous year. The ULF current source used four automobile starter relays in a bridge circuit to produce a pseudo sine wave alternating current; it could deliver a maximum current of 60 A into the $0.4\ \Omega$ load, and its frequency was adjustable in the range 0.5–12 Hz. Power was provided by two 12-V automobile batteries connected in series.

There were three parts to this active experiment: (1) a fluxgate magnetometer was used to measure the magnetic field produced on the peninsula and its vicinity; it had a flat frequency response from d.c. to 500 Hz, and its noise level was $\sim$1–2 nT in the 0.2–5 Hz band; (2) a three-axis electric field (or current) probe was constructed and used to measure the ULF currents flowing in the seawater around the peninsula. It had three orthogonal pairs of contacts spaced 0.5 m apart, and each pair fed a preamplifier with a voltage gain of 100 and a bandpass of 0.5–5 Hz. The calibrated outputs from the preamplifiers were separately monitored on a portable chart recorder, and the minimum electric field amplitude that could be measured was about $1\ \mathrm{mV\ m^{-1}}$. (3) Finally, measurements of the magnetic field produced above the peninsula were made with the total field magnetometer on a P-3C Orion aircraft.

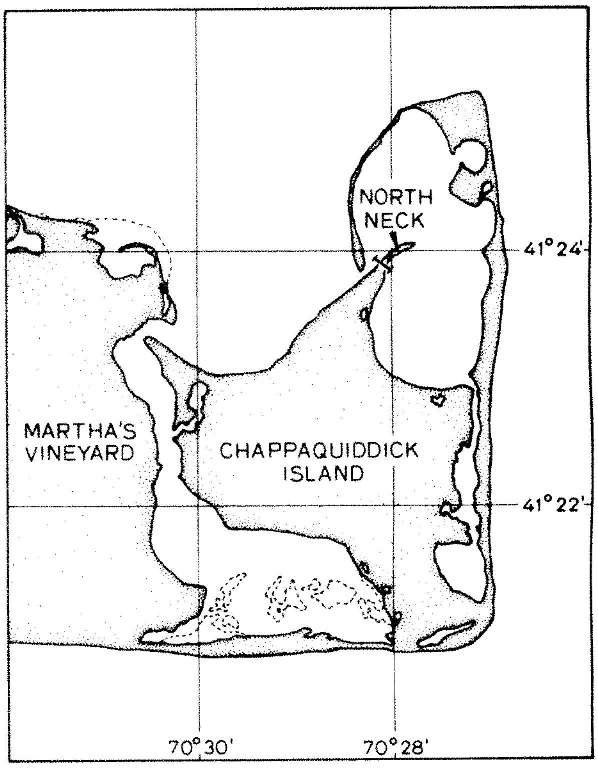

Fig. 1 Map of Chappaquiddick Island, Massachusetts. The experiment was conducted on North Neck, which projects into Cape Poge Bay (upper right), and the location of the electrodes on either side of the Neck is superimposed on the map. The longitude lines are 2.8 km apart.

0028-0836/80/290242—02$01.00

The magnetic field measurements on the peninsula were largely dominated, as expected, by the field of the electrode feed wires. This field was calculated, and it was found that the calculated values were ~20% greater than the measured values. The difference can be attributed to current flow directly through and under the peninsula. Noise caused by boat motion limited the probe measurements to points within ~300 m of the electrodes, and the principal result of these measurements was finding that the current flow was largely radial at all distances where measurements were possible. This finding indicated that some of the current paths would enclose a large area: a necessary condition for a large magnetic moment for the 'peninsula antenna'. Further evidence for this latter condition was provided by the aircraft measurements, which were made during eight passes over the peninsula at altitudes in the range 160–320 m. The sensitivity of the magnetometer was reduced after each pass, and even on the last pass, with minimum sensitivity (measurement range 0–40 nT), the peninsular current loop produced off-scale readings.

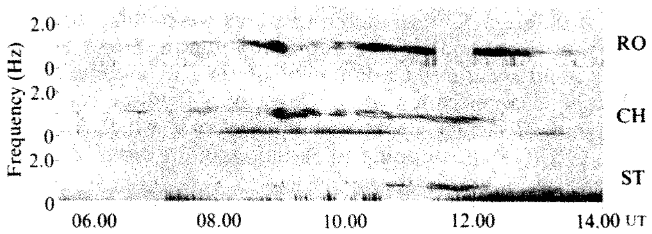

Fig. 2 Spectrograms of a long-lasting Pc 1 geomagnetic pulsation event, as recorded at Roberval, Quebec (RO), Chappaquiddick Island, Massachusetts (CH), and at Stanford, California (ST), on 2 September 1975. The recording at Chappaquiddick Island was made with a 'peninsula antenna'; the other recordings were made with conventional ULF solenoid antennas. A power failure caused the blank interval in the Roberval record.

Although these experiments supported the feasibility of the peninsular current loop concept, they only gave indirect information about the magnetic fields produced in the ionosphere. We therefore computed the amplitude of the magnetic field produced at an altitude of 100 km above the peninsula during our active experiment, using a standard finite difference relaxation method to obtain the electric potentials and current distribution in the seawater and then the Biot–Savart law for the magnetic field. The amplitude obtained was 0.017 ± 0.008 pT. This is about 49 times larger than the field that would be produced by the same total current flowing through a wire laid along the shoreline of the peninsula from one electrode to the other. Assuming a 20% loss of current through the peninsula (as suggested by our magnetic field measurements) the field produced by the peninsula–seawater combination is still ~35–40 times larger than the comparison value. Note that this comparison does not take into account the greater power that would be required to drive the current through the wire outlining the peninsula.

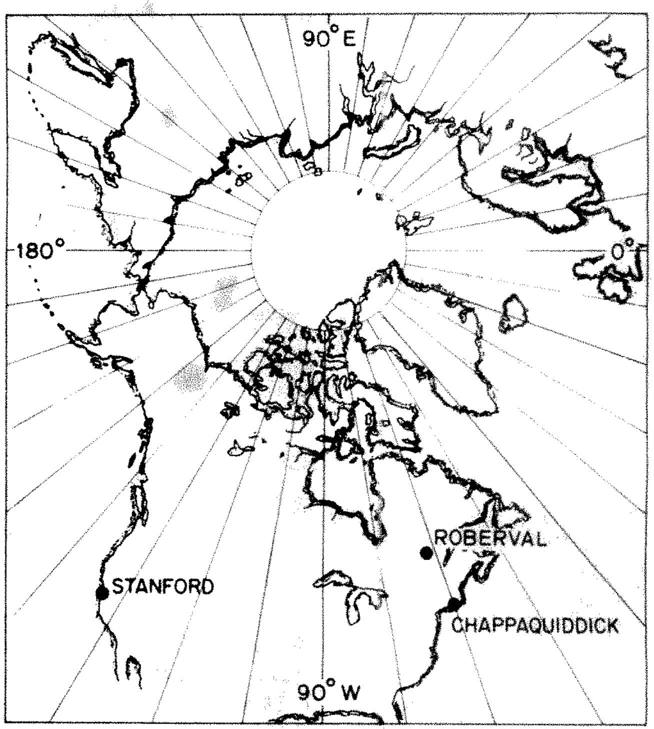

Fig. 3 Map of North America, showing the relative geographic locations of the ULF recording stations at Chappaquiddick, Massachusetts; Roberval, Quebec; and Stanford, California.

An experiment was recently reported by Soviet scientists in which a large current produced by a portable magnetohydrodynamic (MHD) pulse generator was driven through the sea surrounding the Rybachiy Peninsula (69°N, 32.5°E), and the resulting magnetic field was measured over the adjacent Kola Peninsula[4,5]. The maximum duration of the current pulses was ~6 s, and measurements showed that the equivalent magnetic moment of the current loop around the peninsula was 10^{14} A m^2. This loop was reported to take an equivalent area of about 5,000 km^2, implying that the amplitude of the current was 20 kA. As the resistance of the loop was 90 mΩ (this includes the resistance of the cables joining the MHD generator to the sea on either side of the peninsula; these cables weighed 160 tons), a power of about 36 MW was required. Measurements of the magnetic field were made at distances up to 750 km from the peninsula, and at 320 km the electric and magnetic fields had amplitudes of about 0.01 V m^{-1} and 1 nT, respectively.

These results are in good agreement with the predictions of Lipa *et al.*[1]. Note the very small resistance of the peninsula current loop and the resulting large current (and loop magnetic moment) for a moderate power. They imply that a substantial (⩾2 nT) ULF magnetic field can be produced in the lower ionosphere above the peninsula: one of the primary requirements for the artificial generation of Pc 1 pulsations. Unfortunately, the Soviet experiment seems to have been wholly devoted to the deep electromagnetic sounding of the Earth's crust, and no measurements to detect artificially generated Pc 1 pulsations were reported.

We conclude that the proposed 'peninsula method' for ULF signal generation in the ionosphere and magnetosphere[1] is not only feasible but that it is likely to have considerable economic advantages over the use of a large horizontal wire loop on the ground. These advantages include lower construction and running costs and the production of much greater ULF magnetic field amplitudes in the lower ionosphere per unit of input power.

We thank D. M. Bubenik, J. L. Buxton and H. Lewis for assistance, Mr and Mrs G. F. Hodder and the late Mr and Mrs E. Hartell on Chappaquiddick for their co-operation, and also the personnel at the US Naval Air Station at Brunswick, Maine, who made the airborne measurements. This work was supported by the US Defense Advanced Research Projects Agency through an Office of Naval Research Contract and by the Office of Naval Research.

Received 20 February; accepted 9 May 1980.

1. Lipa, B. J., Fraser-Smith, A. C., Villard, O. G. Jr & Storey, J. R. *Nature* **258,** 311–313 (1975).
2. Greifinger, C. *J. geophys. Res.* **77,** 6761–6773 (1972).
3. Harker, K. J. *J. geophys. Res.* **80,** 3100–3110 (1975).
4. Morokhov, I. D., Velikhov, Ye. P. & Volkhov, Yu. M. *Atomnaya Energiya* (in Russian) **44,** 213–219 (1978).
5. Gorbunov, G. I. *et al. Dokl. Akad. Nauk SSSR* **247,** 578–582 (1979).

$\Sigma^{\pm}$ lifetimes and longitudinal acceleration

C. E. Roos, J. Marraffino, S. Reucroft*, J. Waters, M. S. Webster* & E. G. H. Williams

Department of Physics and Astronomy,
Vanderbilt University, Nashville, Tennessee 37235

A. Manz, R. Settles* & G. Wolf

Max-Planck-Institut für Physik und Astrophysik, Föhringer Ring 6,
D-8000 München 40, FRG

The interactions of 420–500 MeV/c K$^-$ in the 11T hydrogen bubble chamber HYBUC have been used to produce a sample of 120,000 $\Sigma^{\pm}$ decays in flight[1,2]. We describe here how these decays were used to investigate the effects of longitudinal accelerations between 0.5 and $5.0\times10^{15}g$ on particle lifetimes. Any observed effect of acceleration on lifetime would indicate that the Lorentz transformation and/or the dynamics of particle decay is sensitive to acceleration. These data suggest that accelerations which change the Lorentz factor and which can return a relativistic elementary particle clock to rest do not cause any observable change in lifetime. This null result complements earlier measurements of the effects of transverse acceleration on muons[13]. Thus ensembles of elementary particles are ideal clocks which are invariant under intense accelerations.

The momentum range of the $\Sigma^{\pm}$ in the HYBUC sample (200–650 MeV/c) is particularly suited to the study of the effects of acceleration on lifetime, because the proper time for decay in the sigma rest frame is a significant fraction of the stopping time as measured in the laboratory. The mean decay length for a momentum of 200 MeV/c at production is 40% of the particle range for Σ^- and 21% for the Σ^+. The average value of this ratio over the momentum range of this experiment is 10% for the Σ^- sample and 5% for the Σ^+ sample.

The slowing down of the sigmas in hydrogen is an electromagnetic process with forces and accelerations that are large compared with gravity. The average accelerations are of the order of $10^{15}g$. The instantaneous accelerations are much greater than these average values and estimates are model dependent. Impact parameter calculations give instantaneous accelerations as high as $10^{22}g$.

The values of the lifetime $c\tau$ have been determined using the maximum likelihood method with a lifetime function normalized with a finite interval of proper time for each event. The lower limit of these intervals corresponds to cutoffs which eliminate scanning losses due to short sigma tracks (0.4 cm for Σ^+, and 0.6 cm for Σ^-). The upper cutoff is the minimum of: (1) the path length at which the sigma would have left the chamber; (2) the path length at which the sigma would stop; (3) a large proper time cutoff ($c\tau = 15$ cm for Σ^+, 20 cm for Σ^-). To take into account the energy loss in liquid hydrogen, the proper time τ is obtained by integrating the instantaneous momentum over the path length,

$$c\tau = m\int \mathrm{d}x/p(x)$$

where x is the distance travelled in the laboratory and the momentum $p(x)$ is obtained from the range–momentum tables and kinematic fits to the event. Note that this integral assumes the accuracy of special relativity applied to transformations from the laboratory system to the particle rest frame.

As the acceleration which a particle experiences depends on its momentum, we have examined $\Sigma^{\pm}$ lifetimes as a function of both the momentum at production and decay. Using the momentum at production is less subject to bias than at decay. However, if the history of acceleration has any observable effect on an elementary particle, then one could distinguish particles on the basis of this effect and, therefore, the momentum and rate of energy loss at the time of decay are of interest. Nuclear interactions are momentum dependent and could affect the lifetimes as a function of momentum. They, however, are <1% in our sample and the scanning requirement of a clear decay vertex would exclude small angle scattering events[2]. The $\Sigma^{\pm}$ samples were divided into five equal momentum bins as functions of the momentum at both production and at decay. The 20 different lifetime determinations were obtained by a maximum-likelihood method and are plotted in Figs 1 and 2. There is no measured variation of lifetime as a function of longitudinal acceleration at the level of a few per cent and ensembles of sigmas behave as ideal clocks, which are not changed by average stopping accelerations of the order of $10^{16}g$.

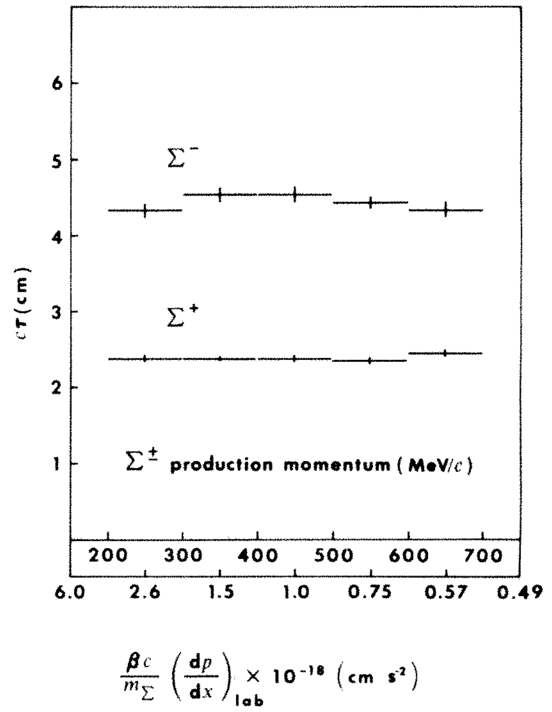

Fig. 1 The $\Sigma^{\pm}$ lifetimes $c\tau$ (cm) as a function of production momentum and rest frame longitudinal acceleration.

Broadening the discussion we note that our mean values of $c\tau$ for the $\Sigma^{\pm}$ are in close agreement with earlier experiments[3]. The particle data tables do not show any observed systematic difference in elementary particle lifetimes as a function of the stopping power of the detector. Sigma lifetimes have been measured in 'free flight'[4] and in nuclear emulsion[5–12] and these measurements are also plotted in Fig. 2. These lifetimes are constant to within a few per cent.

The effect of transverse acceleration on the muon lifetime has been investigated by the $g-2$ muon experiment at CERN[13]. Relativistic muons were held in an orbit by magnetic fields which produced accelerations of $10^{18}g$ perpendicular to the muon's

---

* Present address: EP Division, CERN, Geneva, Switzerland.

0028–0836/80/290244—02\$01.00

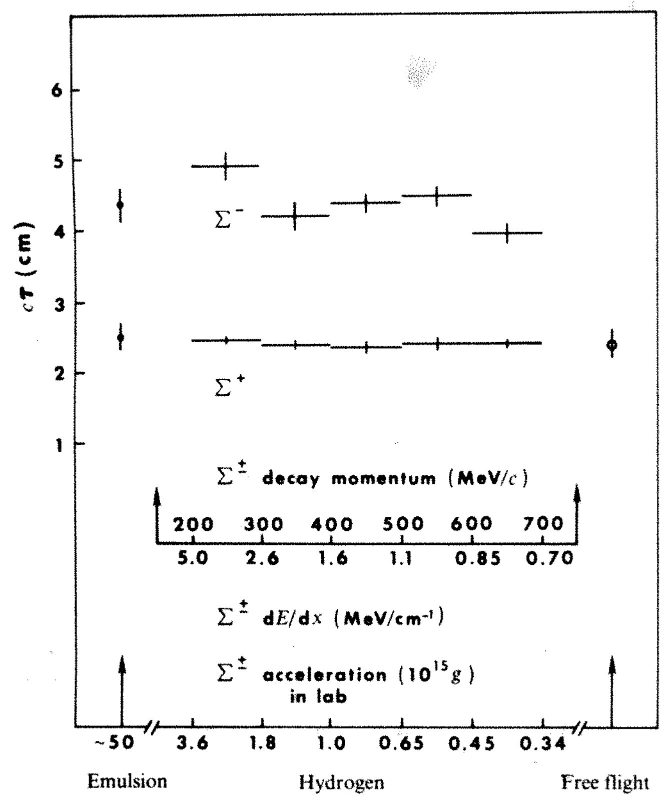

Fig. 2 The $\Sigma^{\pm}$ lifetimes $c\tau$ (cm) as a function of momentum at decay. The longitudinal acceleration depends on the stopping power of the detector. The lifetimes from HYBUC data (hydrogen) are compared with the lifetimes measured with emulsion[5–12] and free flight[4]. The rate of energy loss at minimum ionization is 22 times greater in emulsion than hydrogen.

velocity. The measured values of $c\tau$ for orbiting and free muons were the same to better than 1%. This remarkable result indicates that in the case of transverse acceleration, ensembles of muons can be considered as an ideal clock[13].

Longitudinal acceleration permits us to start two clocks in the laboratory, to accelerate one, return it to rest and then to compare it with the clock that has remained at rest. Transverse accelerations alone would not permit the same experiment. The data indicate that the behaviour of a clock is independent of both longitudinal and transverse accelerations. Arguments that accelerations change the clock are not correct.

We have shown that there is no observed dependence of lifetime on acceleration at the level of a few per cent over the range from 'free flight' to 10^{18}g, and we conclude that the Lorentz transformation gives the correct relationship between clocks subject to acceleration.

We thank Dr J Bell for enjoyable discussions and critical comments. This work was supported by the NSF grant 073-08392 and the Bundesministerium für Forschung und Technologie, FRG.

Received 4 February; accepted 2 May 1980.

1. Settles, R. *et al. Phys. Rev.* **D20,** 2154–2169 (1979).
2. Marraffino, J. *et al. Phys. Rev.* **D21,** 2501–2509 (1980).
3. Particle Data Group *Phys. Lett.* **75B,** 1–250 (1978).
4. Cook, V., Ewart, T., Masek, G., Orr, R & Platner, E. *Phys. Rev. Lett.* **17,** 223–228 (1966).
5. Puschel, W. *Nucl. Phys.* **20,** 254–274 (1960).
6. Evans, G. *et al. N. Cimento* **15,** 873–898 (1960).
7. Freden, S. *et al. N. Cimento* **16,** 611–624 (1960).
8. Kaplon, M. *et al. Ann. Phys.* **9,** 139–168 (1960).
9. Chiesa, A. *et al. N. Cimento* **19,** 1171–1182 (1961).
10. Barkas, M. *et al. Phys. Rev.* **124,** 1209–1223 (1961).
11. Bhowmik, B. *et al. Nucl. Phys.* **53,** 22–32 (1964).
12. Tovee, D. *et al. Nucl. Phys.* **B33,** 493–514 (1971).
13. Bailey, J. *et al. Nature* **268,** 301–304 (1977).

Time–temperature relations in the magnetization of assemblies of single domain grains

D. Walton*

Department of Physics, McMaster University, Hamilton, Ontario, Canada L8S 4M1

A theory for important magnetization processes such as magnetic viscosity and the production of a moment on cooling in a magnetic field is presented here. The results for viscous phenomena differ from those obtained by others in that the time dependence of the viscosity depends on the size distribution of the magnetic grains. The moment produced on cooling in a magnetic field is calculated for an arbitrary distribution of grains for the first time. The effect of the cooling rate on the moment produced is found not only to be independent of that distribution but also of the temperature dependence of the saturation magnetization.

The moment produced on cooling is affected by the rate of cooling. Cooling rate effects have been considered by York[1], Pullaiah *et al.*[2] and Dodson and McClelland-Brown[3] who all derive results for assemblies of identical grains. They show that the blocking temperature is higher, the higher the cooling rate, and the resultant moment is reduced. In determining palaeointensities, then, a difference in cooling rates will lead to differences in the field intensity deduced. When rocks which are cooled over millions of years are measured using cooling times of minutes the difference can be quite large, and a severe overestimate of the ancient field will result.

Previous authors have only calculated this effect for assemblies of identical grains. However, the magnetization which is observed is an integral over a distribution of grains of different sizes. This integral is found not to be sensitive to the grain size distribution, and the cooling rate effect to be sample dependent only if the magnetic constituents are different.

The calculation of magnetic viscosity presented here uses fewer approximations than generally used, and the time-temperature relation obtained differs from the expressions which can be found in the literature (see ref. 4 for detailed references).

All materials which display viscosity are in disequilibrium. The viscosity is the evolution of the system towards an equilibrium state. Consider an assembly of identical particles, of which n^+ are oriented so that their energy is higher than that of the remaining n^- which are in a ground state. The difference $n = n^+ - n^-$ will tend towards an equilibrium value n_{eq} at a rate given by

$$\frac{dn}{dt} = -\frac{(n - n_{\text{eq}})}{\tau} \tag{1}$$

where τ is a relaxation time.

This equation integrates easily to yield

$$n - n_{\text{eq}} = (n - n_{\text{eq}})_{t=0}\, e^{-t/\tau} \tag{2}$$

Note that although this calculation is for single domain grains, the results apply to all systems which obey equation (1).

If equation (2) is multiplied by the appropriate moment and integrated over all assemblies the change in total magnetization with time is obtained. The moment is JV where J is the saturation magnetization per unit volume.

The relaxation time is given by

$$\tau^{-1} = c\, e^{-KV/kT} \tag{3}$$

---

* Present address: Department of Geodesy and Geophysics, University of Cambridge, Madingley Road, Cambridge CB3 0EZ, UK.

0028–0836/80/290245—03$01.00

Where c is a rate assumed to be constant, K is the anisotropy constant, k is Boltzmann's constant and T the temperature. Only K and V will vary. Thus defining $W_V(K)$ as the probability that a grain of volume V will have a K lying between K and $K+\mathrm{d}K$, similarly that $N(V)$ is the probability that V lies between V and $V+\mathrm{d}V$, and N is the number of grains

$$M(t)=M_{\mathrm{eq}}+N\int\int W_V(K)\,JV(n-n_{\mathrm{eq}})_{t=0} \times\exp[-ct\,\mathrm{e}^{-KV/kT}]N(V)\,\mathrm{d}V\,\mathrm{d}K \qquad (4)$$

where

$$M_{\mathrm{eq}}=N\int\int n_{\mathrm{eq}}JVN(V)W_V(K)\,\mathrm{d}V\,\mathrm{d}K.$$

The first term in the integrand corresponds to viscous decay of the initial magnetization in zero field, the second to the acquisition of a moment from a demagnetized state.

Evaluating the time derivative of equation (4) and assuming that $W(K)$ is independent of V:

$$M'(t)=N\int W(K)\,\mathrm{d}K\int JV\Delta n_0(K,V)[-c\,\mathrm{e}^{-KV/kT}] \times\exp[-ct\,\mathrm{e}^{-KV/kT}]N(V)\,\mathrm{d}V \qquad (5)$$

where $\Delta n_0(K,V)=(n-n_{\mathrm{eq}})_{t=0}$.

As $c\simeq10^{10}\,\mathrm{s}^{-1}$ the integrand is small for small KV. It increases rapidly with KV as KV approaches about 30 kT, reaches a maximum, and decays exponentially as KV increases further due to the term $\mathrm{e}^{-KV/kT}$.

Thus the V integration can be performed using saddle point methods[5]. If V_{B} is the solution of $KV_{\mathrm{B}}=kT\ln ct$

$$tM'(t)=\int_{K_{\min}}^{K_{\max}}\frac{(2\pi)^{1/2}}{e}\Delta n_0(K,V_{\mathrm{B}})N(V_{\mathrm{B}}) \times\frac{kT}{K}JV_{\mathrm{B}}W(K)\,\mathrm{d}K \qquad (6)$$

A suitable average, $\bar{K}$, can always be found such that

$$tM'(t)=\frac{(2\pi)^{1/2}}{e}\Delta n_0\left(\bar{K},\frac{kT}{\bar{K}}\ln ct\right)N\left(\frac{kT}{\bar{K}}\ln ct\right) \times\left(\frac{kT}{\bar{K}}\right)^2(\ln ct)J \qquad (7)$$

$\bar{K}$, of course, is temperature dependent, and must lie between he maximum and minimum possible values of K.

This result leads to three conclusions: first, that the time and emperature dependence are connected through $T/\bar{K}$ and $\ln ct$. Second, that the form of this relationship depends on the previous history of the sample, and it is impossible to draw general conclusions from experimental results unless the initial state has been specified. Third, that it depends on the grain size distribution. This last result differs from Dunlop's[4] who concludes that this distribution is not critically important.

The simplest initial state is probably that in which the sample has been completely demagnetized. Consider then the acquisiton of a viscous moment by a completely demagnetized sample: In this case

$$\Delta n_0=-n_{\mathrm{eq}}=-JV_{\mathrm{B}}H/3kT \qquad (8)$$

and

$$tM'(t)=\frac{(2\pi)^{1/2}}{3\mathrm{e}}\frac{J^2H}{\bar{K}}\left(\frac{kT}{\bar{K}}\ln ct\right)^2N\left(\frac{kT}{\bar{K}}\ln ct\right) \qquad (9)$$

It should be possible to express the distribution as a power series

$$N(V)=\sum_r a_rV^r$$

In the following only one term in the series will be used, but the extension to the general case is obvious.

Thus, assuming $N(V)=AV^r$, and if the anisotropy is due to the shape of the grains, $\bar{K}=aJ^2$, and

$$tM'(t)=BH\left(\frac{kT\ln ct}{J^2}\right)^{2+r} \qquad (10)$$

where B is a constant.

A parameter which is frequently quoted is the viscosity coefficient.

$$S=\frac{\partial M(t)}{\partial\ln t}=tM'(t) \qquad (11)$$

S is often found to be proportional to the temperature[3,4,6]. This is true at low temperatures where J does not change very much, therefore r must be -1. (Note that a log normal distribution yields $r\sim-1$ for the larger grains.) However, equation (10) would suggest that the intervention of the temperature dependence of J would lead to a more complex temperature dependence in general.

Equation (10) is readily integrated to yield

$$M(t)=\frac{BH}{3+r}\left(\frac{kT}{J^2}\right)^{2+r}(\ln ct)^{3+r} \qquad (12)$$

A good way to determine $N(V)$ or r would be to plot $M(t)$ versus T (or T/J^2 if high temperature results are used) for equal values of t.

The expression obtained for the viscous moment differs from those obtained by others.

First, the moment depends on $(\ln ct)^m$ where m is determined by the grain size distribution. In general, however, it will be difficult to observe this experimentally because $(\ln ct)^m\simeq(\ln c)^m+(\ln c)^{m-1}(\ln t)$, and a $\ln t$ dependence will be observed except after very long times.

Second, the simple relationship $M(T_1\ln ct_1)=M(T_2\ln ct_2)$ which is frequently used[7] will not hold in general.

The time and temperature dependence of magnetic viscosity depends on the previous history of the sample. Therefore, unless $N(V)$ at $t=0$ is known an experiment on magnetic viscosity may yield bizarre, but meaningless, results. This is probably most important for experiments on viscous decay. On the other hand, if viscous acquisition is being measured it is probably safest to start with a completely demagnetized sample.

Finally, an interesting comparison of equation (12) with experiment is possible: Pullaiah *et al.*[3] remark that a magnetization acquired by heating a specimen of magnetite at 400 °C for 10 days is not removed before 550 °C if heating steps of 5 min are used. The samples were, in fact, expected to be completely demagnetized by 450 °C if the relationship between time and temperature is the one they derive, namely

$$\frac{T_1\ln ct_1}{[J(T_1)]^2}=\frac{T_2\ln ct_2}{[J(T_2)]^2}$$

However, equation (12) indicates that the relation should be

$$\left(\frac{T_1J^2(T_2)}{T_2J^2(T_1)}\right)^{2+r}=\left(\frac{\ln ct_1}{\ln ct_2}\right)^{3+r}$$

With this result if $r=-1$ (which roughly corresponds to a log normal distribution), the temperature for complete demagnetization becomes 500 °C, and for $r=-1.6$ it is 550 °C.

Similar arguments can be used to explain Pullaiah *et al.*'s observation that unblocking of NRM occurs at temperatures lower than they expected.

Next it is interesting to calculate the moment acquired during cooling.

The solution of equation (1) is complicated by the fact that n_{eq} and T are functions of time. Formally the solution is

$$n=\left\{\exp\left(-\int_0^{t_f}\frac{\mathrm{d}t}{\tau}\right)\right\}\int_0^{t_f}\frac{n_{\mathrm{eq}}(t)}{\tau}\exp\left[+\int_0^{t}\frac{\mathrm{d}t}{\tau}\right]\mathrm{d}t \qquad (13)$$

where t_f is the time at which the moment is measured after the material has cooled. Equation (13) may be rewritten

$$n=\int_0^{t_f}\tau^{-1}n_{\mathrm{eq}}(t)\left\{\exp\left[-\int_t^{t_f}\tau^{-1}\,\mathrm{d}t\right]\mathrm{d}t\right\}\tag{14}$$

For small t, that is initially, the argument of the exponential is large and therefore the integrand is small. It is small again as $t\rightarrow t_f$ because the relaxation time τ becomes very large. Thus, the method of steepest descents is again appropriate, and letting

$$g(t)=-\frac{KV}{kT}-\int_t^{t_f}c\,\mathrm{e}^{-KV/kT}\,\mathrm{d}t\tag{15}$$

the value of n is

$$n=(2\pi)^{1/2}\frac{n_{\mathrm{eq}}(t_c)c}{(|g''(t_c)|]^{1/2}}\exp\left[-\frac{KV}{kT(t_c)}-\int_{t_c}^{t_f}\frac{\mathrm{d}t}{\tau}\right]\tag{16}$$

t_c is obtained from $g'(t_c)=0$. In fact t_c will never be needed explicitly, but the condition $g'(t_c)=0$ gives, if $\mathrm{d}/\mathrm{d}t(K/T)=\alpha$

$$\frac{KV}{kT}=\ln\left(\frac{kc}{V\alpha}\right)\tag{17}$$

This equation may be solved for the temperature; this temperature would then be the blocking temperature. It will be convenient to modify the definition slightly so that the blocking temperature is

$$T_{\mathrm{B}}=\frac{(2\pi)^{1/2}}{e}\,\frac{K_{\mathrm{B}}V}{k\ln(kc/V\alpha)}\tag{18}$$

where K_{B} must be evaluated at the blocking temperature.

Now, returning to equation (16) we can evaluate n by introducing the expression for n_{eq}, equation (8)

and

$$g''(t_c)=-\frac{V}{k}\frac{\mathrm{d}\alpha}{\mathrm{d}t}-\left(\frac{V\alpha}{k}\right)^2\tag{19}$$

In equation (16) the values of J and α, which are temperature-dependent, are evaluated at T_{B}. For single domain grains, where shape anisotropy dominates, K is proportional to J^2 (ref. 8).

The parameter α depends on the particular way in which the material cools and is temperature and time dependent in general. The algebra becomes simpler if α is assumed to be constant. This is a relatively good approximation: it corresponds to a cooling law such that $\mathrm{d}/\mathrm{d}t(1/T)=$ constant. A similar approximation is made in ref. 3. If α is constant

$$\int_{t_c}^{t_b}\tau^{-1}\,\mathrm{d}t=-\frac{k}{\alpha V}\left[\left(\frac{1}{\tau}\right)_{t=t_b}-\left(\frac{1}{\tau}\right)_{t=t_c}\right]=1\tag{20}$$

as

$$(\tau)_{t=t_b}\gg(\tau)_{t=t_c}=\tau_b$$

combined with equations (20) and (21), (16) yields the eminently reasonable result that n is given by the equilibrium expression evaluated at the blocking temperature:

$$n=\frac{J_{\mathrm{B}}VH}{3kT_{\mathrm{B}}}$$

The magnetization is now

$$M=N\iint JV\left[\frac{J_{\mathrm{B}}VH}{3kT_{\mathrm{B}}}\right]N(V)W(K)\,\mathrm{d}V\,\mathrm{d}K\tag{21}$$

K may be replaced by its average as before, however, its temperature dependence must be retained.

Assuming that $N(V)$ obeys a power law $N(V)=AV^r$, equation (21) becomes

$$M=\frac{NJHA}{3k}\int_{V_0}^{V_m}\frac{J_{\mathrm{B}}}{T_{\mathrm{B}}}V^{2+r}\,\mathrm{d}V\tag{22}$$

It is convenient to integrate with respect to either J_{B} or T_{B}. Assuming that $\bar{K}=bJ^p$ and that $J=J_0(1-T/T_c)^{1/n}$, equation (22) yields a hypergeometric function which reduces to

$$M\cong\frac{NAJH}{3kT_c}\,\frac{p}{n}(V_m)^{3+r}\left[\left(\frac{kT_c}{V_m bJ_0^p}\right)\ln\frac{ke}{\alpha V_{\mathrm{eff}}}\right]^{1/p}\tag{23}$$

In obtaining this result $\ln kc/V\alpha$ which varies slowly with V has been assumed to be constant, and taken outside the integral. V_{eff} is an appropriate average V.

V_m is the blocking volume at the highest temperature of interest. Most of the moment is produced in the range from about 50 K below the Curie temperature to room temperature. Therefore V_m will be taken to be the volume of those grains whose blocking temperature is ~50 K below the Curie temperature. V_m is ~30 times V_0, the blocking volume at room temperature.

Note that the grain size distribution only influences the cooling rate effect by possibly affecting V_{eff}, and this is completely negligible. Note also that the cooling rate dependence does not depend on the temperature dependence of J, at least of the order of the approximation used here.

We can now estimate the effect of a change in cooling rate on the resultant moment: $\ln(kc/V_{\mathrm{eff}}\alpha)$ may be estimated as follows, $\alpha=[\Delta(\bar{K}/T)/\Delta t]$ so that in going from the Curie temperature to room temperature $\bar{K}/T$ increases from zero to K_0/T_0 where K_0 and T_0 refer to room temperature, thus

$$\frac{kc}{V_{\mathrm{eff}}\alpha}=\frac{kT_0}{V_{\mathrm{eff}}\mathrm{K}_0}c\Delta\mathrm{t}$$

now $V_{\mathrm{eff}}K_0/kT_0$ is of the order of 30 and if $c\sim3\times10^{10}$

$$\ln\left(\frac{kc}{V_{\mathrm{eff}}^{\alpha}}\right)\cong\ln(10^9\Delta t)$$

If Δt is changed by a factor of 10 the moment should change by about 6% for magnetite. For haematite[4], on the other hand, if $K=aJ^4$ the change should only be about 3%.

These results are in broad agreement with the calculations of Dodson and McClelland-Brown[3], in the sense that the integrated change in moment is in the low range of values obtained by them for an assembly of identical grains.

At present the only experimental results are those of Fox and Aitken[9]: for various samples of pottery they obtain an increase of between 3% and 9% in the moment for a decrease of an order of magnitude in the cooling rate. This agrees with the results obtained above as the carriers of the magnetization in pottery are believed to be monodomain grains of magnetite. It would be desirable, however, to have more precise experimental results.

An approximate expression for the moment produced during cooling from just below the Curie temperature has been obtained. We conclude that: the effect of cooling rate on the resulting moment is not sensitive to the grain size distribution or the temperature dependence of J. But is sensitive to the form of the temperature dependence of K on J; an order of magnitude increase in cooling rate leads to a 6% decrease in moment for magnetite, but only 3% for haematite.

I thank Dr D. J. Dunlop for comments, Dr M. J. Aitken for communicating experimental results before publication. This work was supported by a grant from the Natural Science and Engineering Council of Canada.

Received 5 February; accepted 23 May 1980.

1. York, D. *Earth planet. Sci. Lett.* **39,** 94–97 (1978).
2. Pullaiah, G., Irving, E., Buchan, K. L. & Dunlop, D. J. *Earth planet. Sci. Lett.* **28,** 133–145 (1975).
3. Dodson, M. H. & McClelland-Brown, E. *J. geophys. Res.* (in the press).
4. Dunlop, D. J. *Rev. Geophys. Space Phys.* **13,** 855–901 (1973).
5. Arfken, G. *Mathematical Methods for Physicists*, 2nd edn (Academic, New York, 1970).
6. Shimizu, Y. *J. Geomagn. Geoelectr.* **11,** 125–138 (1960).
7. McElhinny, M. W. *Paleomagnetism and Plate Tectonics* (Cambridge University Press, 1973).
8. Stacey, F. D. & Banerjee, S. K. *The Physical Principles of Rock Magnetism* (Elsevier, Amsterdam, 1974).
9. Fox, J. M. W. & Aitken, M. J. *Nature* **283,** 462 (1980).

Identification and estimation of carbonate minerals at low levels by evolved CO_2 analysis

A. E. Milodowski

Department of Geology, King's College, Strand,
London WC2R 2LS, UK

D. J. Morgan

Institute of Geological Sciences, 64/78 Gray's Inn Road,
London WC1X 8NG, UK

Recent differential thermal analysis (DTA) investigations of carbonate minerals using a flowing CO_2 furnace atmosphere[1,2] have shown that amounts as low as 0.25% (2,500 p.p.m.) may be detected in natural or synthetic mixtures, a significant improvement on that possible using static air DTA or conventional X-ray diffraction techniques. We show here that carbonate minerals can be routinely detected in the hundreds of p.p.m. concentration range using a non-dispersive IR CO_2 detector linked to a DTA furnace and describe modifications to the technique which permit the detection of certain carbonates below 100 p.p.m. The method described gives both an analytical determination of CO_2 and an identification of the mineral species responsible for CO_2 generation. It should be of use in the study of trace constituents in rocks, sediments, soils and ores and as a quality control technique in industrial processes.

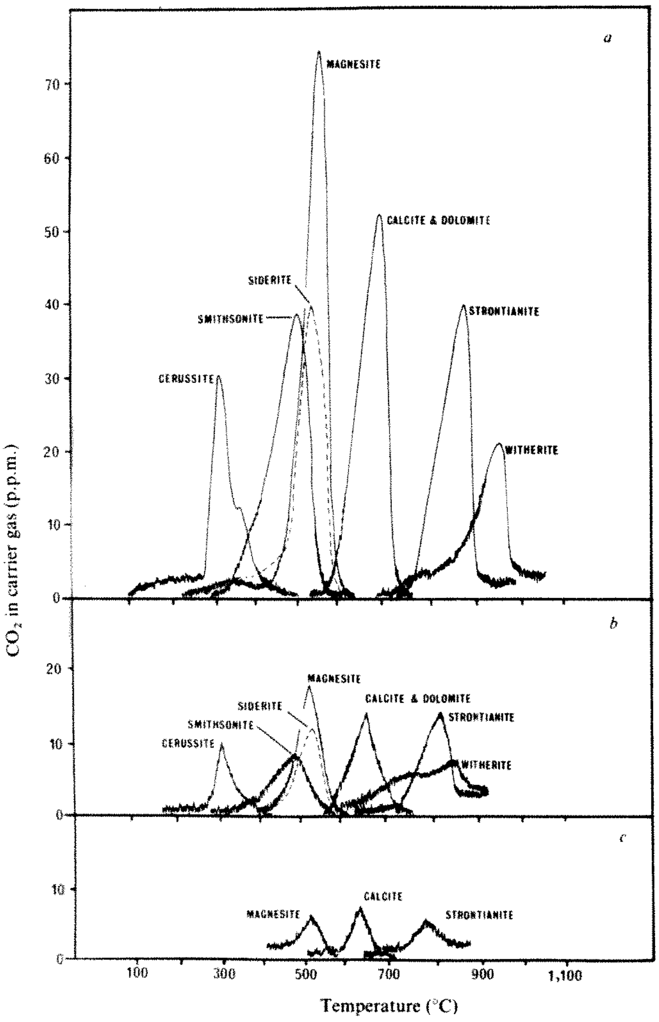

Fig. 1 CO_2 evolution profiles obtained from: *a*, 0.2%; *b*, 500 p.p.m.; and *c*, 50 p.p.m. nominal concentrations of carbonate minerals in alumina. Evolution profiles in *a* and *b* were obtained using a carrier gas flow rate of 300 ml min^{-1} and in *c* with a flow rate of 100 ml min^{-1}.

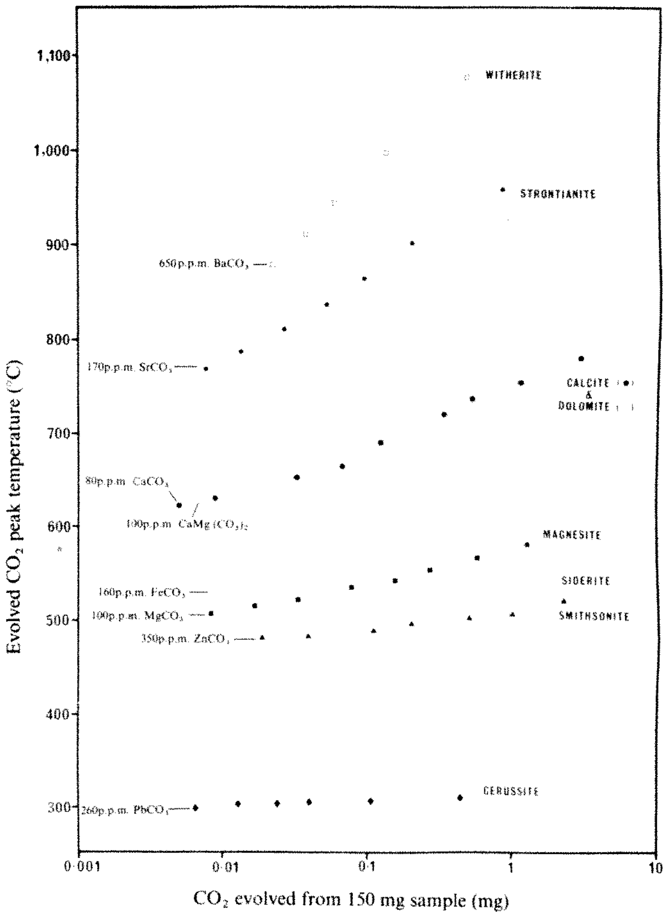

Fig. 2 Plot of evolved CO_2 peak temperature versus log mass of CO_2 evolved for the eight carbonates investigated.

Details of the DTA–EGA (CO_2) system have been given previously[3]. Briefly, this consists of a DTA furnace swept at 300 ml min^{-1} by a carrier gas stream consisting of a 2 : 1 mixture by volume of nitrogen and oxygen and linked by a stainless steel line to a non-dispersive IR CO_2 detector. This has two analysis cells capable of measuring up to 1,000 and 10,000 p.p.m. CO_2 in the carrier gas stream, although for the present study only the most sensitive cell was used. Output signals from the detector are fed into an external chart recorder which also monitors sample temperature. Additional, more sensitive ranges on the chart (0–500 and 0–100 p.p.m. fsd) are obtained through ×2 and ×10 signal amplification switches on the detector.

A standard mass of sample (150 mg) is lightly packed into a dimped Pt-crucible and this placed in the DTA head. A heating rate of 15 °C min^{-1} is used. Areas of the CO_2 evolution profiles on the chart are measured with a planimeter and the amount of CO_2 evolved obtained by calculation[3].

Eight X-ray pure natural anhydrous carbonates were examined: witherite, strontianite, calcite, dolomite, magnesite, siderite, smithsonite and cerussite. Each mineral was ground to pass a 200-mesh sieve and mixed with alumina to give a dilution sequence covering the range 2% to 50 p.p.m. The alumina/carbonate mixtures were placed in glass screw-top bottles and mechanically shaken for 20 min. No precautions were taken to obtain a statistically uniform 150 mg sample for analysis as the amount of carbonate mineral present was determined from the area of the CO_2 evolution profile.

Figure 1*a–c* shows CO_2 evolution profiles given by the eight carbonates at nominal concentrations ranging from 0.2% to 50 p.p.m. At 0.2% (Fig. 1*a*) all the carbonates give sharp peaks

0028–0836/80/290248—02$01.00

with virtually no baseline drift. Areas of the peaks vary in proportion to the CO_2 contents of the minerals which range from 52.2% for magnesite to 16.5% for cerussite. Detection limits are obviously influenced by this factor, although with decreasing concentrations other factors become increasingly important. In the concentration range examined, CO_2 release from witherite is governed more by solid-state reaction with alumina than by simple dissociation[4]. As a result, CO_2 evolution occurs over a relatively large temperature range and the mineral does not give recognizable peaks at concentrations <500 p.p.m. Kinetics of the dissociation are also relevant: cerussite, although containing less than half the CO_2 content of smithsonite, can be detected at lower levels because of its sharp CO_2 evolution profile (Fig. 1*a*, *b*).

Figure 2 summarizes the data obtained for the dilution sequences using a carrier gas flow rate of 300 ml min^{-1}. Values in p.p.m. to the left of the figure represent the lowest concentration at which each mineral gives a well-defined CO_2 peak. Reducing the carrier gas flow rate would be expected to improve detection limits due to the effective increase in CO_2 content of the carrier gas. However, at slower flow rates convection currents in the furnace assume a much greater importance. These are especially noticeable in the 150–450 °C range and cause irregular flushing of the evolved CO_2 and a consequent increase in background noise-to-signal ratio in the detector. Detection limits for cerussite and smithsonite, which dissociate within this temperature range, were not, therefore, significantly improved at slower carrier gas flow rates although satisfactory CO_2 peaks were obtained from magnesite, calcite and strontianite at nominal concentrations of 50 p.p.m. using a carrier gas flow rate of 100 ml min^{-1} (Fig. 1*c*).

Plots of evolved CO_2 peak temperature versus log mass of CO_2 evolved (Fig. 2) are straight lines which become shallow curves in the lower concentration ranges (this curvature is experimental and is a function of the rate of diffusion of CO_2 from the carbonate–alumina mixture). In general, the higher the dissociation temperature of the carbonate, the greater the slope of the line, a similar relationship to that existing between plots of DTA dissociation peak temperature and mass of the various carbonates at higher concentrations[5]. The exception is siderite which shows no variation in CO_2 peak temperature with dilution; note that Warne[6] found that the temperature of the endothermic DTA peak of this mineral was also relatively insensitive to dilution.

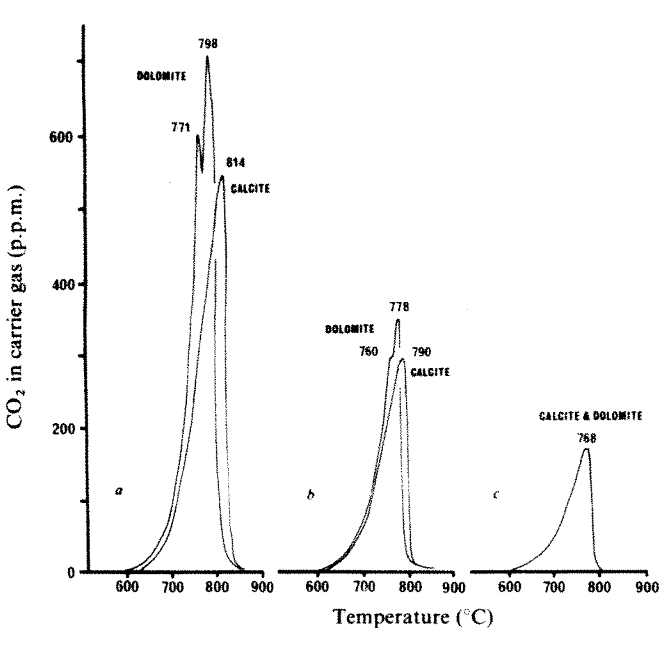

Fig. 3 CO_2 evolution profiles of calcite and dolomite obtained with a porous cap on top of sample crucible. *a*, 2%; *b*, 1%; and *c*, 0.5% nominal concentrations.

The CO_2 peak temperature–concentration relationships presented in Fig. 2 provide the basis for both identification and quantification of individual carbonates present at low levels in natural mixtures although it is apparent that distinction between calcite and dolomite is impossible in the experimental conditions used and some difficulty might be anticipated in differentiating between magnesite, siderite and smithsonite, especially when variations in thermal behaviour of the natural minerals are taken into account. This topic will be discussed in detail elsewhere but note here that placing a porous cap over the Pt-crucible resulted in a marked separation of dolomite and calcite peaks at concentrations of 1% and above (Fig. 3). Evolution of CO_2 from magnesite is also retarded to a much greater extent than from siderite or smithsonite by the porous cap and this mineral is readily distinguishable in 0.5% artificial mixtures with the other two carbonates.

This work was carried out while A.E.M. was in receipt of a Natural Environment Research Council CASE studentship. The paper is published by permission of the Director, Institute of Geological Sciences.

Received 10 March; accepted 6 May 1980.

1. Warne, S. St. J. *Nature* **269,** 678 (1977).
2. Warne, S. St. J. & Mitchell, B. D. *J. Soil Sci.* **30,** 111–116 (1979).
3. Morgan, D. J. *J. thermal Analysis* **12,** 245–263 (1977).
4. Wentworth, S. A., Sharp, J. H. & Bye, G. C. *Proc. Soc. analyt. Chem.* **5,** 245 (1968).
5. Smykatz-Kloss, W. *Differential Thermal Analysis* (Springer, Berlin 1974).
6. Warne, S. St. J. *Chemie Erde* **35,** 251–255 (1976).

Coral morphology, diversity and reef growth

John Chappell

Department of Biogeography and Geomorphology, Australian National University, Canberra, Australia

The shape of reef corals is affected by light level[1,2] and by wave stress[3,4], leading to the well-known zonation of coral form associations with exposure and depth[3–6]. Growth form also seems to be constrained by geometric factors[2,7,8]. Similarly, coral calcification rate, of importance both for coral form and for net reef growth, is light dependant[9,10], and may be affected by other factors such as wave stress and sediment flux. Here the growth structure of raised Pleistocene reefs in New Guinea, of both fringing and barrier types, is explained in terms of variations of coral framework growth rate across the reef profile. A model for growth rate in terms of wave stress, light level and other variables is outlined, first by examining the effects of these factors on coral form and diversity.

Growth form responses to several factors are outlined in Fig. 1, on the following basis. (1) Light response: Porter's general argument that surface-to-volume ratio should diminish as light increases[7] is contradicted by types which show globose to platy polymorphism[1,2]. A better index, consistent with Porter's argument, is the ratio of polyp-covered surface to the projected surface area seen from above. (2) Hydrodynamic stress response: adaptation will be to increase structural strength as wave/current stress increases[3,11,12]. (3) Sediment flux effect: advantageous forms, where sediment flux is high, would intercept the smallest proportion of settling sediment per unit surface area, for a given polyp size[13]. (4) Subaerial exposure: significant on many reef flats, the best adaptation is likely to be that which maximizes stored water capacity by minimizing surface-to-volume ratio as well as maximizing sideways spreading. Note that Fig. 1, outlining these responses, is not exhaustive and interpolations can be made in any row, for example, types 7 and 8 have similar or lower polyp surface/projected surface ratios than type 1, and can be placed at the left in row 1.

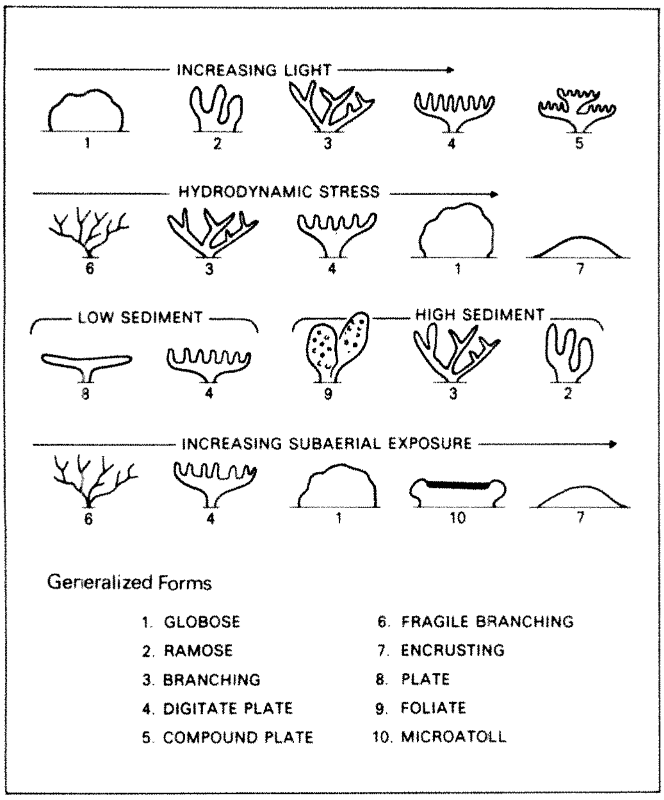

Fig. 1 Coral form responses to environmental stresses.

Net reef growth not only depends on coral calcification rate, but is also affected by the type of framework built by the local assemblage of forms. Figure 1 indicates that form assemblage will vary with the net balance of the four stress factors, which vary with position, as follows. Light diminishes with depth, although it seems not to be stressful until the depth where photo-adaptation (increasing zooxanthellae) ceases to change[1,14]. Wave stress increases with square of wave height and declines negative-exponentially with depth. The stress imposed by settling sediment should increase slowly down the windward forereef; it is significant on the reef flat, and also is high where sediment overspill to the backreef is high. Subaerial exposure on the reef flat increases with height above lowest spring tide level. These variations are shown in Fig. 2 for an idealized reef cross-section. Characteristic coral community forms, projected in Fig. 2 in the light of Fig. 1, are consistent with zonations described by others[3,6,15]. Note that when wave exposure is very high, the encrusting coral zone at the reef margin (shown at '7' in Fig. 2) often is replaced by algal bioherm[3,16].

Hypothetical diversity curves also are shown in Fig. 2, based on net stress (= sum at any point of stresses shown graphically in Fig. 2). Diversity ranges from maximum when environmental stress is small, down to zero when any factor is limiting[17]. Diversity curves in Fig. 2 are based on an assumed inverse-linear relationship between net stress and diversity. The curve for the forereef compares well with Porter's results from a Panama reef[18] when these are smoothed to eliminate variations related to local topographic effects. No account is taken, in compiling Fig. 2, of the 'intermediate disturbance' effect[19] on diversity of events such as cyclones.

Coral morphology and diversity zonation have been accounted for by others in terms of depth variation of wave stress and light[3,4,16,17]. In this regard, the semi-quantitative relationships underlying Fig. 2 are valuable. It is also suggested that growth of coral framework is constrained by the four stress factors in the same way as is diversity in Fig. 2, that is, that growth diminishes as net stress increases until any factor becomes limiting. This is tested by simulating reef growth and comparing the results with known reef growth structures.

A simple computer model to simulate reef development was arranged as follows. Each of the four stress factors was given a range 0–1 and net stress taken as the arithmetic mean at any point on the evolving profile. Growth ceases where any factor

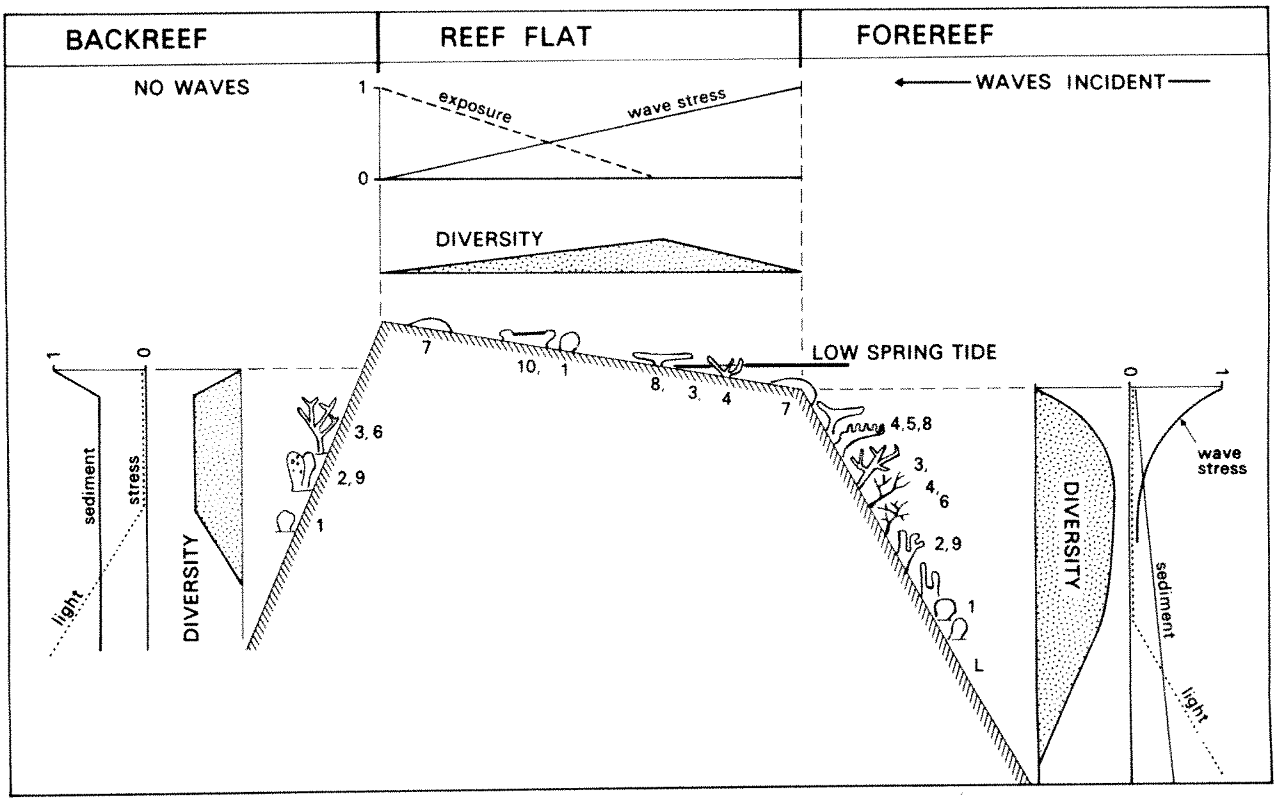

Fig. 2 Idealized variation of coral community forms and diversity from sums of stresses across simple reef section.

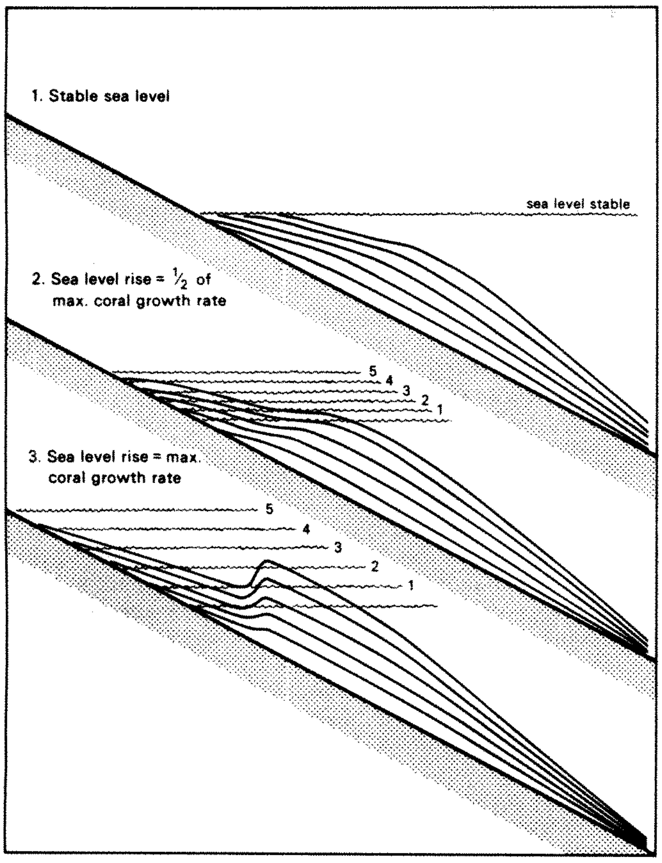
1. Stable sea level
sea level stable
2. Sea level rise = ½ of max. coral growth rate
5
4
3
2
1
3. Sea level rise = max. coral growth rate
5
4
3
2
1

Fig. 3 Reef growth: computer model results using stress factors as in Fig. 2, with different rates of sea-level rise.

reaches the limiting value of 1. Wave behaviour was modelled as Airy waves outside the breaker line, solitary waves inside it, with standard equations for bed shear, and so on.[20] Energy dissipation at wave break was assumed to be 75%. Maximum possible growth rate was 1 cm yr^{-1}. Light stress was assumed 0–15 m depth and to increase then to become limiting at 40 m. Waves of 2 m at 8 s (800 W m^{-1} of wave crest) were input (assumed not to be limiting). Sediment flux, taken as equivalent to the rate of wave energy loss from bed friction, was assumed limiting when wave power loss reached 100 W m^{-1} per m of wave advance. These values are taken in accordance with my observations of modern and Pleistocene reefs at Huon Peninsula, New Guinea[21], with which model results are compared, below. Variations from these values alters scaling dimensions but not the form of the results.

Reef development is affected by previous topography which developed sub-aerially during Pleistocene low sea levels[22,23]. This is simplified in the model by using a rectilinear initial substrate, which accords with the New Guinea case[21]. The rate of sea-level rise during deglaciation, relative to maximum potential growth rate of framework, is also important for reef growth structure[21], although the extent to which Darwin's hypothesis, that barrier and lagoon structure arises from rising relative sea level (submergence), is debated[22]. Accordingly, Fig. 3 shows three runs of the computer model, with sea-level rise rates of 0.0 cm yr^{-1}, 0.5 cm yr^{-1}, and 1.0 cm yr^{-1} respectively. The first two cases induce formation of a fringing reef; in the third case a barrier and lagoon develops.

The model is compared with late Pleistocene reefs for which the growth history is known, shown in Fig. 4. These developed during sea-level changes centred on the last interglacial period, 135–120 kyr ago, and are now exposed well above sea level through tectonic uplift, at Huon Peninsula, New Guinea[21] (examples 1, 2 in Fig. 4), and at Atauro Island, Timor[24] (example 3). Also shown is the pattern of 'absolute' sea-level change for the period[24,25]. Mean growth rates differ between the Huon and Atauro examples; Huon reef VIIa grew 50 m in <10,000 yr (>0.5 cm yr^{-1}), while the Atauro reef grew 40 m throughout the entire interval of 145–115 kyr (0.13 cm yr^{-1}). The rate difference is not due to uplift rate or substrate slope differences as these are matched in one or the other of the Huon cases (Fig. 4), and is probably caused by clastic sediment flux which is much greater at volcanic Atauro than at Huon Peninsula, where the hinterland is limestone. This is supported by the fact that Huon Peninsula coasts away from the limestone region have a volcanogenetic hinterland, high clastic flux, and only minor reefs. Coral zonation in the Huon reefs, described by Chappell[21], is consistent with Fig. 2 (no major algal bioherm occurs at reef crest on this moderate-energy coast); these zones are simplified to backreef (B), shallow forereef (S), and so on, in Fig. 4. Major facies boundaries trace the course of reef growth.

The structures in Fig. 4 compare well with computer model predictions in Fig. 3 when growth rate–sea-level rise rate relationships are considered. Maximum growth rates in Holocene reefs at Huon Peninsula, which are comparable to the raised Pleistocene reefs, are around 0.8 cm yr^{-1} (ref. 26). Sea-level rise for the NW Huon section slightly exceeded this, at ~1.0 cm yr^{-1} (uplift for this section being only 0.05 cm yr^{-1}), and a barrier–lagoon structure developed (see model case 3 in Fig. 3). Relative sea-level rise rate for the south-east Huon case is lower than maximum potential growth rate, at 0.6 cm yr^{-1}, due to rapid tectonic uplift (0.4 cm yr^{-1} at this section), and a fringing reef formed (see model case 2 in Fig. 3). In the Atauro case the potential reef growth rate seems to have been much lower than

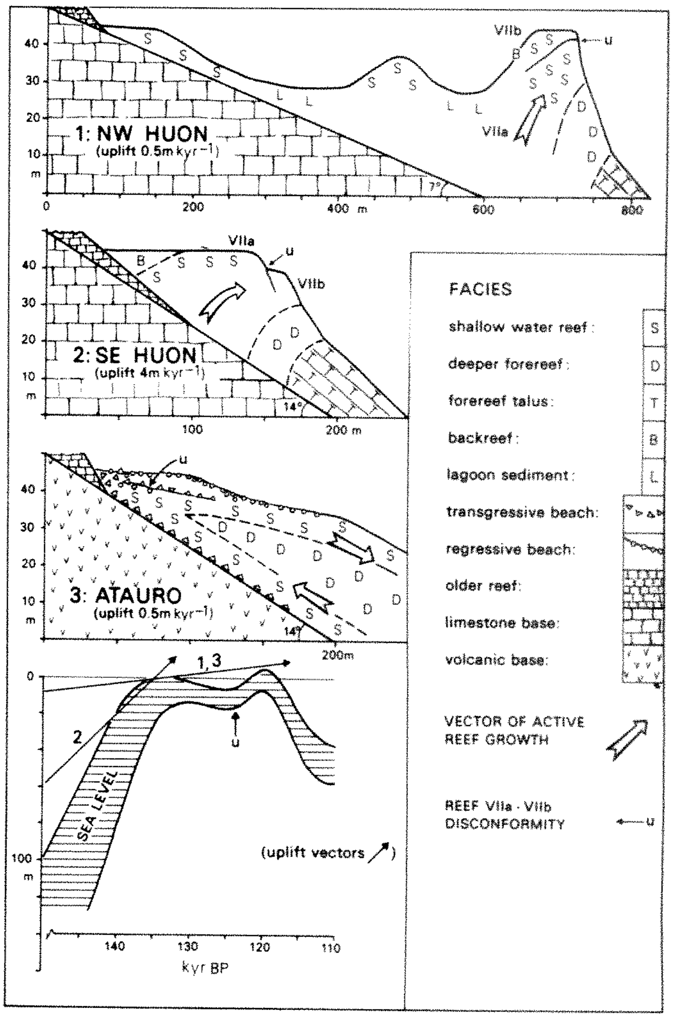

Fig. 4 Mapped cross-sections of late Pleistocene reefs at Huon Peninsula, New Guinea[21], and Atauro Island, Timor[24].

relative sea-level rise rate, resulting in formation of a transgressive shelving reef which continued to grow slowly through the interglacial and into the early phase of the subsequent falling sea level.

In conclusion, raised Pleistocene reefs at Huon Peninsula, where major variations of uplift rate along the coast provide the opportunity for examining reefs formed under different relative rates of sea-level rise, are compatible with a model for reef development which relates growth rate to net environmental stress. As the model is semi-quantitative, its predictions as to growth rates, coral forms and coral diversity, as functions of the four stress factors invoked, are readily testable through further observations.

Received 18 January; accepted 9 May 1980.

1. Jaubert, J. *Proc. 3rd int. Coral Reef Symp. Miami,* **2,** 483–488 (1977).
2. Graus, R. R. & MacIntyre, I. G. *Science* **193,** 895–897 (1976).
3. Geister, J. *Proc. 3rd int. Coral Reef Symp.* **1,** 23–29 (1977).
4. Morton, J. *Proc. 2nd int. Coral Reef Symp.* **2,** 55–69 (1974).
5. Vaughan, T. W. *U.S. natn. Mus. Bull.* **49,** 1–427 (1907).
6. Wells, J. W. *Mem. geol. Soc. Am.* **67,** 773–782 (1957).
7. Porter, J. W. *Ecology* **53,** 745–748 (1972).
8. Barnes, D. J., *Bull. mar. Sci.* **23,** 280–289 (1973).
9. Barnes, D. J. & Taylor, D. L. *Helgol. Wiss. Meeresunters* **24,** 284–291 (1975).
10. Chalker, B. E. & Taylor, D. L. *Proc. R. Soc.* **B190,** 323–331 (1975).
11. Vosburgh, F. *Proc. 3rd int. Coral Reef Symp.* **1,** 477–482 (1977).
12. Graus, R. R. *Proc. 3rd int. Coral Reef Symp.* **2,** 464–469 (1977).
13. Jackson, J. B. C., in Larwood, G. & Rosen, B. R. (eds) *Biology and Systematics of Colonial Organisms; Syst. Assoc. Spec.* Vol. 11, 499–555 (1979).
14. Porter, J. W. in *Growth, Maintenance, and Change of Coral Reefs* (ed. Barnes, D. J.) (in the press).
15. Pichon, M. *Proc. 2nd int. Coral Reef Symp.* **2,** 55–68 (1974).
16. Adey, W. H. & Burke, R. *Bull. geol. Soc. Am.* **87,** 95–109 (1976).
17. Rosen, B. R. *Underwater Ass. Rep. 1 (NS)* 1–16 (1975).
18. Porter, J. W. *Am. Nat.* **110,** 731–742 (1976).
19. Connell, J. *Science* **199,** 1302–1310 (1978).
20. Komar, P. D. *Beach Processes and Sedimentation,* 1–429 (Prentice-Hall, Englewood Cliffs, 1976).
21. Chappell, J. *Bull. geol. Soc. Am.* **85,** 553–570 (1974).
22. Purdy, E. in *Reefs in Time and Space,* 9–76 SEPM Spec. Publ. (1974).
23. Shinn, E. A. *et al. Proc. 3rd int. Coral Reef Symp.* **2,** 1–8 (1977).
24. Chappell, J. & Veeh, H. H. *Bull. geol. Soc. Am.* **89,** 356–368 (1978).
25. Chappell, J. & Thom, B. G. *Nature* **272,** 809–810 (1978).
26. Chappell, J. & Polach, H. *Bull. geol. Soc. Am.* **87,** 235–240 (1976).

A water depth model for the evolution of the planktonic Foraminiferida

Malcolm B. Hart

Department of Environmental Sciences, Plymouth Polytechnic,
Drake Circus, Plymouth PL4 8AA, UK

Recent papers on the evolution of the planktonic Foraminiferida have stressed the importance of repeated patterns[1,2] in the Neogene and Palaeogene, as well as in the Cretaceous[1–4]. Most authors have recognized the importance of gross morphological characters (the biocharacters of Steineck and Fleischer[2]) and used them to illustrate the evolution of the superfamily Globigerinacea, as well as a prime tool in classification. Cifelli[1] and Frerichs[4] relate such patterns of evolution to the available palaeotemperature data[5], and while temperature is clearly important I shall show that it is not the complete story. Here the evolution of the planktonic Foraminiferida is reconsidered in the light of recent advances in the understanding of distributional controls of the modern fauna. I suggest that well-known 'iterative' trends indicate successive attempts at colonizing deeper levels in the water column.

In the planktonic environment, and especially in the surface waters where the planktonic Foraminiferida are most abundant, faunas avoid competition by adjusting their regional distributions to the different surface water and temperature regimes and by sometimes seeking different levels in the water column in their adult growth form. Bé[6] has summarized his extensive knowledge of the modern fauna, and confirmed a threefold subdivision of the water column; shallow-water fauna (0–50 m), intermediate-water fauna (generally 50–100 m) and deeper-water fauna (with adults normally below 100 m). This distribution can be identified in the Cretaceous using oxygen isotope data[7] or, more conventional, stratigraphic information[8].

Using planktonic:benthonic ratios (counted on the 500–250 μm grain-size-fraction) a depth curve[8] has been produced for the Albian–Santonian interval of the Cretaceous succession in south-east England. A sample interval of 1 m (or less) was used throughout that study and the reliability of the graphs produced was tested by regional correlation[9,10]. That water depth curve has many major features in common with other postulated depth curves for the same area[11,12], although there are some minor differences[13]. Onto this depth curve Hart and Bailey[8] have reconstructed the evolutionary trends of the mid-Cretaceous planktonic Foraminiferida, placed at their predicted water depth (following the Bé[6] model) and confirmed by their distribution in the shelf seas prevailing over north-west Europe at that time. In all the examples cited, mid-Cretaceous evolution either proceeds horizontally within the same depth zone, or migrates downwards into a lower depth zone. I know of no examples of evolution following a trend up into a higher level in the water column. As indicated by Hart and Bailey[8], the distribution of an individual species and its appearance in time is, therefore, a function of the water depth available over the shelf during any particular interval. Differences in the known stratigraphic ranges of certain species are to be expected when one compares the UK succession with those recorded in the oceans by the Deep Sea Drilling Project[14], or even areas like the Tethyan/Alpine region of Southern Europe[15]. Using this experience of the mid-Cretaceous fauna the central part of Fig. 1 was constructed, and then extended to include both the late Cretaceous/Cenozoic and the Triassic/Jurassic/early Cretaceous, with the aid of data from the literature[1–6]. The depth preferences for each of the biocharacters is given where this is possible (following refs 6, 8), although this is clearly a great approximation the further one goes back through the geological record. There are also some characters that do not appear in all parts of the record, the most obvious being the lack of twin-keeled forms in the Palaeogene and Neogene, and the absence of biserial morphotypes at present.

Throughout the preparation of Fig. 1 the regional distributions of genera and species, together with their palaeoecological associations, have been considered. While the proposed model seems to cover most stratigraphic situations, there are clearly many cases where local palaeo-oceanographic conditions have created apparently anomalous occurences of deeper-water morphotypes in what are regarded as shallow-water sediments (for example, *Globotruncana* spp. in the Campanian/Maastrichtian marginal calcarenites of Scania, S. Sweden; *Rotalipora* spp. in the Lower Middle Cenomanian calcareous sands of south-east Devon[9]; the apparently contradictory distribution of certain spinose/smooth species in parts of the Palaeogene; and the occurrence of some species of *Acarinina* and *Morozovella* in Palaeogene shallow-water sediments). Interesting, and important, as these individual cases may be, they do not negate the longer-term, overall trends outlined here.

Following my experience of mid-Cretaceous planktonic foraminiferal evolution[8], it is possible to consider the complete Triassic to Recent time interval. Figure 1 shows the successive appearance of certain biocharacters exhibited by the whole superfamily Globigerinacea from its benthonic source (fully discussed by Masters[16]) in the Triassic(?). This original, primitive, shallow-water 'globigerinid' form remains virtually unchanged until the mid-Cretaceous (Aptian) when the first evolutionary explosion began. During, and following, the Aptian and Albian there was a very rapid appearance of new morphotypes of planktonic Foraminiferida, and their suggested depth stratification from this time onwards up the geological succession can be enclosed by the dotted line shown in Fig. 1, and contours the repeated conquest of deeper, surface, water habitats. This 'envelope' is also represented in Fig. 2, on which are also indicated the oceanic anoxic events of Schlanger and

0028-0836/80/290252—03$01.00

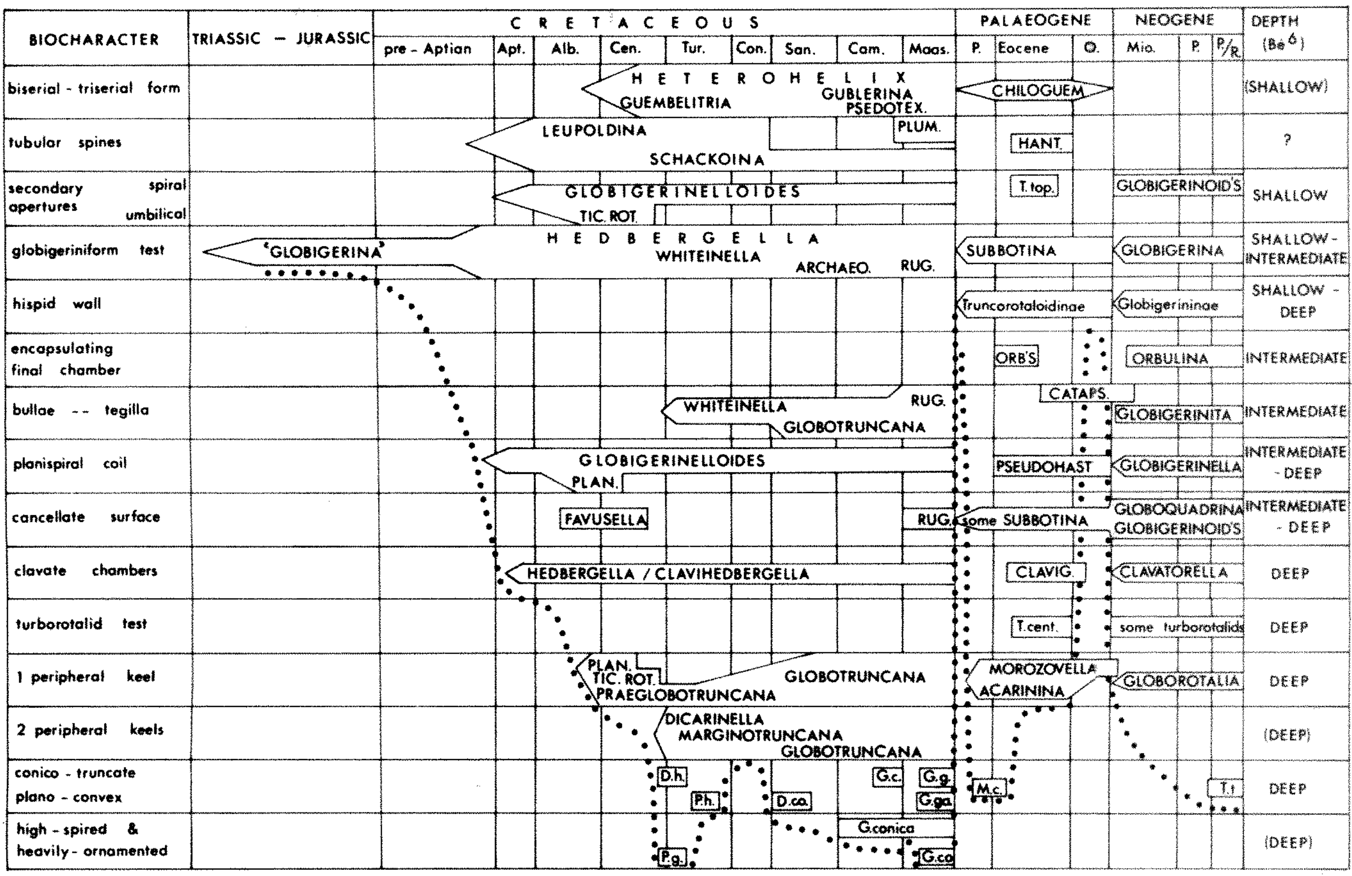

Fig. 1 Depth stratification model for the evolution of the planktonic Foraminiferida. *Pseudotex., Pseudotextularia*; *Chiloguem., Chiloguembelina*; *Plum., Plummerita*; *Hant., Hantkenina*; *Tic., Ticinella*; *Rot., Rotalipora*; *T. top., Truncorotaloides topilensis* (Cushman); *Globigerinoid's, Globigerinoides*; *Archaeo., Archaeoglobigerina*; *Rug., Rugoglobigerina*; *Orb's, Orbulinoides*; *Cataps., Catapsydrax*; *Plan., Planomalina*; *Pseudohast., Pseudohastigerina*; *Clavig., Clavigerinella*; *T. cent., Turborotalia centralis* (Cushman & Bermudez); *D.h., Dicarinella hagni* (Scheibnerova); *P.h., Praeglobotruncana helvetica* (Bolli); *G.c., Globotruncana calcarata* Cushman; *G.g., G. gagnebini* Tilev; *G.ga., G. gansseri* Bolli; *D.co., Dicarinella concavata* (Brotzen); *M.c., Morozovella caucasica* (Glaessner); *T.t., Truncorotalia truncatulinoides* (d'Orbigny); *P.g., Praeglobotruncana gibba* Klaus; and *G.co., Globotruncana contusa* (Cushman).

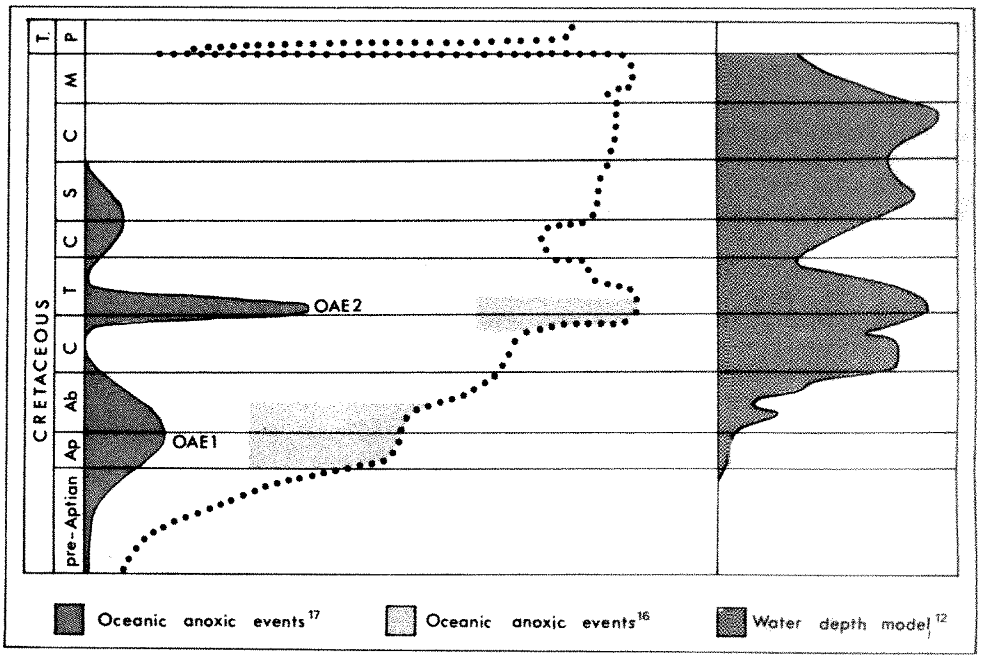

Fig. 2 Depth stratification model compared with the transgression/regression model of Hancock[12] and Cretaceous anoxic events[17,18].

Jenkyns[17] (together with the modifications proposed by Arthur and Schlanger[18] and Jenkyns[19]). These anoxic events coincide with the levels of maximum faunal change (for example, the late Cenomanian–early Turonian boundary, the Aptian–Albian interval, and the Coniacian–Santonian interval). The 'envelope' is also similar, in broad outline, to many published transgression/regression models[11,12], especially that figured by Schlanger and Jenkyns[17]; the present curve is produced simply by matching foraminiferal test morphology against a Recent water depth scale[6].

This close similarity suggests that the evolution of the planktonic Foraminiferida may be a function of increasing water depth on or near the shelf, which is, after all, where productivity is at its highest. This would be particularly true if a rising sea level was actively eroding its shorelines, thereby providing a vital nutrient source (Fig. 4 of ref. 19). This argument cannot, however, be applied to the Miocene–Pliocene interval where the same evolutionary patterns have been produced by a falling sea level. The same problem exists if one applies a temperature model; rising temperatures in the mid–late Cretaceous, and generally falling temperatures in the Miocene–Pliocene. Perhaps one should consider the stability of the stratification of the water column as the control. The oceanic anoxic events[17–19] imply a certain degree of stagnation of the water column, probably created by overproduction of phytoplankton in the surface waters, and a lack of O_2-rich waters being introduced into the ocean basins from cold polar sources. In such a situation the oceans probably become very sluggish and highly stratified. Such a stratification of the water column immediately implies a host of physical/chemical constraints[20] including temperature. If the plankton in the water column were stimulated into high productivity by a rising sea level over the extensive Cretaceous shelf seas, there is the possibility that the associated O_2-depletion of the water could have contributed to the localized (and in some cases quite widespread) stagnation of the ocean floor (and the expanded shelf areas at times of high sea level) in a highly stratified situation.

During three main intervals of time (mid-late Cretaceous, Palaeogene and Neogene) the planktonic Foraminiferida apparently adapted (or were forced to adapt) to the status quo, and when the stratification was disturbed (by the terminal Cretaceous Event[21], and the late Oligocene Event) they were then obliged to repeat their evolution as a direct response to the new situation.

This response has provided the successive appearance of the morphological features reported in Fig. 1 and the concomitant palaeotemperature values recorded by Douglas and Savin[7]. These various attempts to occupy the same levels in the water column have produced some remarkable examples of homeomorphy. Perhaps the best is the repeated evolution of the deeper-water plano-convex forms, with the successive appearance of the completely unrelated *Praeglobotruncana helvetica* (Bolli), *Dicarinella concavata* (Brotzen), *Globotruncana gansseri* Bolli, *G. gagnebini* Tilev, *Morozovella caucasica* (Glaessner), and *Truncorotalia truncatulinoides* (d'Orbigny). A not so extreme form of this morphotype (*Globotruncana stuartiformis* Dalbiez) was assigned to deeper levels in the water column on the basis of isotopic determinations by Douglas and Savin[7].

While the proposed model (Fig. 1) is clearly for further discussion and research it does highlight many problems of foraminiferal classification. Can Masters[16] be supported in his attempts to rejuvenate the use of *Globigerina* for Cretaceous species, when some workers in the Cenozoic feel unjustified in using that name back beyond the Neogene? It would also seem to indicate that in many places in the Cretaceous we are not using a phylogenetic classification, although the desirability/undesirability of such an approach is not being promoted by this account.

The recent work on isotopes/palaeotemperatures[7] has suggested a depth stratification model for planktonic Foraminiferida as far back as the Albian, and this is supported here. Also, if one could establish a direct relationship between eustatic changes (and their associated transgressions and regressions), phytoplankton productivity, evolution, and the production of anoxic sediments at selected levels in the geological record (particularly in the Cretaceous) then this would provide an interesting avenue of palaeo-oceanographic research.

The author acknowledges financial assistance from the School of Environmental Sciences Staff Research Fund, and the award of a research grant by the NERC. I also thank all my colleagues who have helped in the formulation of the above ideas.

Received 3 March; accepted 15 May 1980.

1. Cifelli, R. S. *Syst. Zool.* **18,** 154–168 (1969).
2. Steineck, P. L. & Fleischer, R. L. *J. Paleont.* **52,** 618–635 (1978).
3. McGowran, B. *Micropaleontology* **14,** 61–80 (1968).
4. Frerichs, W. E. *J. Paleont.* **45,** 963–968 (1971).
5. Emiliani, C. *Science* **154,** 851–857 (1966).
6. Bé, A. W. H. in *Oceanic Micropalaeontology* Vol. 1 (ed. Ramsay, A. T. S.) 1–100 (Academic, London, 1977).
7. Douglas, R. G. & Savin, S. M. *Mar. Micropaleont.* **3,** 175–196 (1978).
8. Hart, M. B. & Bailey, H. W. *Aspekte der Kreide Europas* (ed. Weidmann, J.) 527–542 (IUGS, Ser. A, No. 6, 1979).
9. Carter, D. J. & Hart, M. B. *Bull. Br. Mus. nat. Hist.* (*Geol.*) **29,** 1–135 (1977).
10. Hart, M. B. & Carter, D. J. *J. foramin. Res.* **5,** 114–126 (1975).
11. Cooper, M. R. *Palaeogeogr. Palaeoclimat. Palaeoecol.* **22,** 1–60, (1977).
12. Hancock, J. M. *Proc. geol. Ass.* **86,** 499–536 (1976).
13. Vail, P. R. *et al. Mem. Am. Ass. petrol. Geol.* No. 26 (1977).
14. Hart, M. B. *Cretaceous Research* Vol. 1 (in the press).
15. Robaszynski, F. & Caron, M. *Cahiers de Micropaleontologie* Part 1, 1–185; Part 2, 1–181 (1979).
16. Masters, B. A. *Oceanic Micropalaeontology* Vol. 1 (ed. Ramsey, A. T. S.) 301–731 (Academic, London, 1977).
17. Schlanger, S. O. & Jenkyns, H. C. *Geol. Mijnb.* **55,** 179–184 (1976).
18. Arthur, M. A. & Schlanger, S. O. *Bull. Am. Ass. petrol. Geol.* **63,** 870–885 (1979).
19. Jenkyns, H. C. *J. geol. Soc.* **137,** 171–188 (1980).
20. Degens, E. T. & Stoffers, P. *Nature* **263,** 22–27 (1976).
21. Thierstein, H. R. & Berger, W. H. *Nature* **276,** 461–466 (1978).

Intramolecular photochemical electron transfer in a linked porphyrin–quinone molecule as a model for the primary step of photosynthesis

Te-Fu Ho, Alan R. McIntosh & James R. Bolton

Photochemistry Unit, Department of Chemistry,
University of Western Ontario, London, Ontario, Canada N6A 5B7

The primary photochemical process in algal and green-plant photosynthesis is a one-electron transfer reaction from a chlorophyll donor species to an electron-acceptor molecule, with the electron transfer taking place across the thylakoid membrane probably within a special reaction-centre protein[1]. A similar process takes place in bacterial photosynthesis. We have mimicked this reaction through the synthesis described here using the method of Kong and Loach[2], of a single molecule (P–Q) (I) containing a porphyrin (P) linked to a quinone (Q) by a hydrocarbon chain. When illuminated with visible light an intramolecular electron transfer occurs from the porphyrin to the quinone creating the biradical $\mathrm{P}^{+\cdot}$–$\mathrm{Q}^{-\cdot}$ which can be detected by electron paramagnetic resonance (EPR) spectroscopy. In certain conditions the electron transfer is reversible.

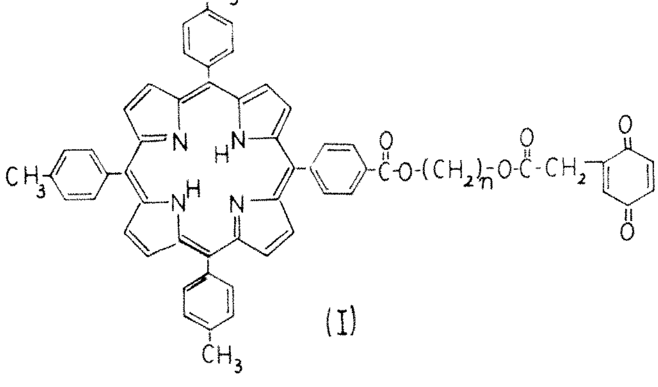

(I)

There has been considerable interest in constructing various models to mimic the *in vivo* photochemical system. These have ranged from models of the primary donor and intermediate electron-acceptor complexes[3-5], monolayer assemblies[7-10], vesicles[11,12], intramolecular exciplex complexes[13-18] to chlorophyl–quinone electron transfer in solution[19]. The P–Q compounds with $n = 2$ and 3 were previously synthesized by Kong and Loach[2]. They reported that the benzoquinone oxidation state quenches the fluorescence of the attached porphyrin in dioxane and petroleum ether with a very low fluorescence yield in the latter solvent. Tabushi *et al.*[20] reported that in (II) fluorescence was considerably quenched compared to that of the unlinked porphyrin. They have attributed the fluorescence quenching to electron transfer but presented no direct evidence for such a mechanism.

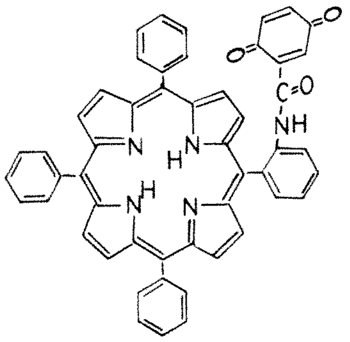

(II)

In the synthesis of P–Q (I with $n = 3$) we followed the method of Kong and Loach[2] except that we started with the more stable 2,5-dimethoxylphenylacetic acid. The purity of the final compound was assessed by NMR and mass spectra which were consistent with (I) and by obtaining a single spot on thin layer chromatography using two separate solvents on silica gel. We also found that the fluorescence of P–Q ($n = 3$) in methanol at room temperature is quenched to an extent of 90% compared with that of the free porphyrin; however, this observation alone does not prove that photochemical electron transfer has taken place. More direct evidence can be obtained from EPR measurements. Both steady-state and transient EPR measurements were carried out for concentrations of P–Q between 10^{-4} and 10^{-3} M in a frozen methanol plus 2% chloroform solution between 12 and 165K. The P–Q UV–visible optical spectrum obeys Beer's law for concentrations up to 5×10^{-4} M. Above that there are some changes in the spectrum which could be due to dimerization. However, all measurements were carried out down to 10^{-4} M with little or no change in behaviour. For $T < 150$K, photolysis with a 200 mW 647 nm Spectra Physics Krypton cw laser beam or with a Phase-R 620 nm pulsed dye laser generated an irreversible light-induced EPR signal. The spectrum (Fig. 1*a*) was found to be nearly invariant for temperatures below ~150K. The *g* factor and the lineshape are similar to those of the unlinked porphyrin $\mathrm{P}^{+\cdot}$ (Fig. 1*c*). However, on subtracting the $\mathrm{P}^{+\cdot}$ spectrum from that of Fig. 1*a* (to the extent of one-half of the latter's integrated intensity), the difference spectrum of Fig. 1*e* is obtained, which is neither that of $\mathrm{P}^{+\cdot}$ (Fig. 1*c*) nor the unlinked quinone $\mathrm{Q}^{-\cdot}$ (Fig. 1*d*). We have performed several control experiments in which the unlinked components P and Q were photolysed in methanol at low temperatures. When the concentration of Q is 1,000 times that of P, we observe irreversible intermolecular electron transfer, as shown in the EPR spectrum of Fig. 1*b*. When the spectrum of $\mathrm{P}^{+\cdot}$ is subtracted from Fig. 1*b* in the same manner as before, the difference spectrum of Fig. 1*f* is generated. This spectrum is similar to that of the unlinked $\mathrm{Q}^{-\cdot}$ (see Fig. 1*d*) allowing for some spin exchange broadening effects. However, when P and Q are mixed at the same low concentration, the quantum efficiency of production of the EPR photolysis spectrum is much less than that generated by photolysis of the same concentration (2×10^{-3} M) of the P–Q complex as shown in Fig. 2. Both meso-tetratolylporphyrin in chloroform/methanol and meso-tetra(4-carboxyphenyl)porphyrin in methanol were used, and nearly the same low yield of radicals was obtained.

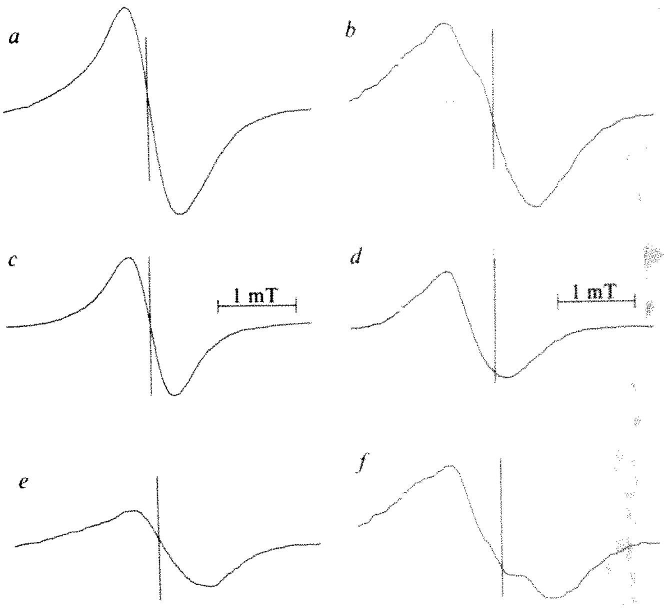

Fig. 1 Typical irreversible EPR spectra observed after the 200 mW 647 nm Krypton cw laser photolysis (except for *c* and *d*) of linked and non-linked P and Q compounds in methanol observed at 100K with EPR detection conditions of 0.2 mT modulation amplitude at 100 kHz and 1 mW microwave power at ~9.0 GHz. The vertical line in each case indicates the P^{+} *g* factor: *a*, photolysis spectrum observed from the linked compound P–Q at 2×10^{-3} M concentration; *b*, photolysis spectrum observed from 10^{-4} M meso-tetra(4-carboxyphenyl)porphyrin with 10^{-1} M benzoquinone; *c*, meso-tetratolylporphyrin radical cation (obtained by iodine oxidation) at half of the integrated amplitude or concentration of part *a*; *d*, spectrum of semireduced quinone (obtained by the air oxidation of 2,5-dihydroxyphenylacetic acid) at half of the integrated amplitude or concentration of part *a*; *e*, difference spectrum of *a* (P–Q) minus *c* (P^{+}) which removes the theoretical 50% contribution of P^{+} from the PQ photolysis spectrum; *f*, difference spectrum of *b* (P^{+} and Q^{-}) minus *c* (P^{+}) which removes the theoretical 50% contribution of P^{+} from the separated component spectrum.

On the basis of these steady-state EPR measurements, we conclude that the irradiation of P–Q results in an initial intramolecular electron transfer with high yield; however, there is also probably a low-yield contribution to the spectrum resulting from some electron transfer into the solvent or intermolecular transfer to the quinone moiety of another P–Q molecule.

As a further test of our intramolecular electron transfer hypothesis, we carried out flash-photolysis experiments with EPR detection[21] as the temperature was raised from 90 to ~160K (about 15° below the melting point of methanol). A large irreversible EPR signal was generated by photolysis at about 140K, as shown in Fig. 2. However, as the temperature approached 160K, the EPR kinetics became almost totally reversible, as shown in Fig. 3. The reversibility at 160K was very strong as the recorder pen of the Varian E-12 100 kHz EPR spectrometer jumped with each ~1 mJ flash of the red-filtered Photochemical Research Associates Model 610A Pulsed Light Source. The magnetic field profile of the EPR transients matched very well to the spectrum shown in Fig. 1*a*. Note that no reversible EPR signal could be observed by photolysis of solutions of the mixed unlinked components P and Q in conditions identical to those in Fig. 3 at 160K.

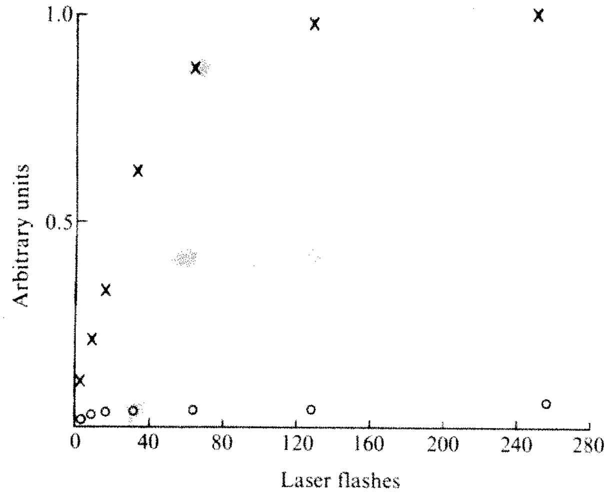

Fig. 2 Amplitude of the $g = 2.0$ EPR photolysis spectra induced by 620 nm photolysis at 140K in methanol followed by rapid cooling to 100K (where the spectra were measured as in Fig. 1) plotted as a function of the number of pulsed dye laser flashes with ~20 mJ per flash and a flashing rate of 1 Hz: for 2×10^{-3} M P–Q (×), and for meso-tetra(4-carboxyphenyl)porphyrin and benzoquinone each at 2×10^{-3} M (○).

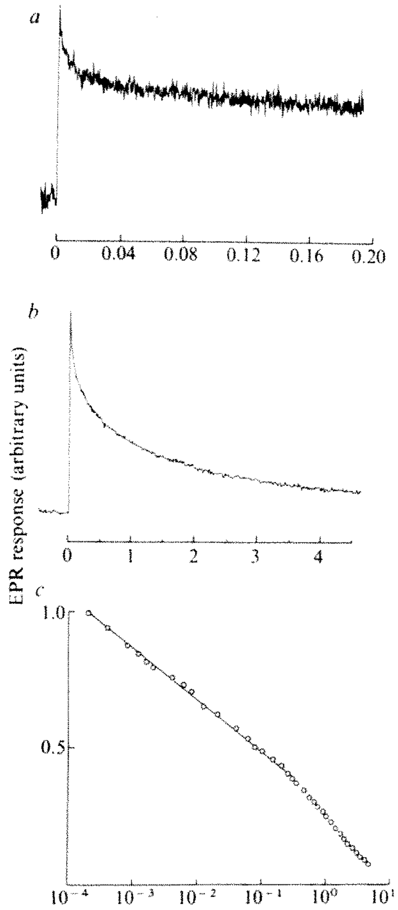

Fig. 3 Typical flash induced reversible EPR kinetics observed at 160K at the first derivative low field maximum of the spectrum of Fig. 1*a* for 2×10^{-3} M P–Q in methanol. The pulsed xenon light source was filtered by a Corning CS-262 filter with ~1 mJ per flash and the flashing rate was 0.1 Hz with 256 flashes accumulated in each kinetic trace and with EPR detection conditions of 0.5 mT modulation amplitude at 100 kHz and 5 mW microwave power at ~9.0 GHz: *a*, time domain of 200 ms; *b*, time domain of 5 s; *c*, logarithmic time domain up to 5 s.

Note that the observed electron-transfer kinetics (see Fig. 3) are approximately logarithmic in time over nearly four orders of magnitude, as shown in Fig. 3*c*. Ke *et al.*[22] have carried out a quantitative analysis of the charge recombination in photosystem I of green plants at low temperatures, and have shown that log *t* kinetics can be observed for an intramolecular electron-transfer process. They showed that the log *t* kinetics can be explained by assuming a rectangular distribution function for the distances separating the reacting species, or for some other parameter, such as the activation energy, for which the rate constant is an exponential function. On the basis of the restricted temperature domain for the observations of electron-transfer reversibility in the present work, we assume that we are observing a rectangular distribution in activation energies rather than a distribution of donor–acceptor distances leading to a temperature-independent electron tunnelling expression. Thus, at ~15° below the melting point of methanol, we assume that there is a range of activation energies for the electron to return to the primary donor arising from the relative motion of the donor and acceptor ends of P–Q at this temperature. This range of activation energies could arise from the various conformations of the hydrocarbon chain linking the quinone acceptor to the porphyrin donor.

We have used the route of Kong and Loach[2] to synthesize a donor–acceptor-molecule which, in certain conditions, exhibits reversible photochemical intramolecular electron transfer. Similar photochemical reactivity for P–Q has been observed at room temperature in acetronitrile (J.L.Y. Kong and P. A. Loach, personal communication). This system is an excellent model for the primary photochemical electron-transfer process in reaction centres of photosynthesis as both the confinement of donor and acceptor together and reversible photochemical electron transfer have been duplicated. This well-characterized model system should give us considerable insight into the mechanism of the *in vivo* reaction. We are continuing these studies with a view to stabilize the charge separation reaction and to study the effect of distance and molecular structure on the kinetics and mechanism of the intramolecular electron-transfer process.

This research was supported by a Strategic Grant in Energy from the Natural Sciences and Engineering Research Council of Canada. We thank Professor P. A. Loach for helpful discussions. This is publication no. 242 of the Photochemistry Unit.

Note added in proof: It has come to our attention that Dalton and Milgrom[23] have prepared porphyrins with attached quinones. However, they only report substantial fluorescence quenching.

Received 14 February; accepted 9 May 1980.

1. Sauer, K. in *Bioenergetics of Photosynthesis* Chap. 3, 115–180 (ed. Govindjee) (Academic, New York, 1975).
2. Kong, J. L. Y. & Loach, P. A. in *Frontiers of Biological Energetics—Electrons to Tissues*, Vol. 1 (eds Dutton, P. L., Leigh, J. S. & Scarpa, A.) 73–82 (Academic, New York, 1978). *Abstract No. THPMA12 of the 7th Annual Meeting of the American Society for Photobiology*, Asilomar (1979); *J. Het. Chem.* (in the press).
3. Katz, J. J. in *Light Induced Charge Separation in Biology and Chemistry* (eds Gerischer, H. & Katz, J. J.) 331–359 (Dahlenkonferenzen, Verlag Chemie, Berlin, 1979).
4. Wasielewski, M. R. in *Frontiers of Biological Energetics—Electrons to Tissues* Vol. 1 (eds Dutton, P. L., Leigh, J. S. & Scarpa, A.) 63–72 (Academic, New York, 1978).
5. Pellin, M. J., Kaufmann, K. J. & Wasielewski, M. R. *Nature* **278,** 54–55 (1979).
6. Boxer, S. G. & Bucks, R. R. *J. Am. chem. Soc.* **101,** 1883–1885 (1979).
7. Kelly, J. M. & Porter, G. *Proc. R. Soc.* **A319,** 319–329 (1979).
8. Kuhn, H. in *Light-Induced Charge Separation in Biology and Chemistry* (eds Gerischer, H. & Katz, J. J.) (Dahlenkonferzen, Verlag Chemie, Berlin 1979).
9. Janzen, A. F., Bolton, J. R. & Stillman, M. J. *J. Am. chem Soc.* **101,** 6337–6341 (1979).
10. Janzen, A. F. & Bolton, J. R. *J. Am. chem. Soc.* **101,** 6342–6348 (1979).
11. Ford, W. E., Otvos, J. W. & Calvin, M. *Proc. natn. Acad. Sci. U.S.A.* **76,** 3590–3593 (1979).
12. Kurihara, K., Sukigara, M. & Toyoshima, Y. *Biochim. biophys. Acta* **547,** 117–126 (1979).
13. Chandross, E. A. & Thomas, H. T. *Chem. phys. Lett.* **9,** 393–396 (1971).
14. Okada, T. *et al. Chem. phys. Lett.* **14,** 563–568 (1972).
15. Ide, R., Sakata, Y. & Misumi, S. *JCS Chem. Commun.* 1009 (1972).
16. Gnädig, K. & Eisenthal, K. B. *Chem. phys. Lett.* **46,** 339–342 (1977).
17. Mataga, N., Migita, M. & Nishimura, T. *J. molec. Struct.* **47,** 199–219 (1978).
18. Migita, M., Kawai, M., Mataga, N., Sakata, Y. & Misumi, S. *Chem. phys. Lett.* **53,** 67–70 (1978).
19. Tollin, G. *Bioenergetics* **6,** 69–87 (1974); *J. phys. Chem.* **80**, 2274–2277 (1976).
20. Tabushi, I., Koga, N. & Yanagita, M. *Tetrahedron. Lett.* No. 3, 257–260 (1979).
21. McIntosh, A. R., Manikowski, H. & Bolton, J. R. *J. phys. Chem.* **83,** 3309–3314 (1979).
22. Ke, B., Demeter, S., Zamarev, K. I. & Khairutdinov, R. F. *Biochim. biophys. Acta* **545,** 264–284 (1979).
23. Dalton, J. & Milgrom, L. R. *JCS Chem. Commun.* 609 (1979).

Inhibition of photosynthesis in *Arabidopsis* mutants lacking leaf glutamate synthase activity

C. R. Somerville & W. L. Ogren*

Department of Agronomy, University of Illinois, Urbana, Illinois 61801

The CO_2 released in photorespiration is believed to result from a complex mitochondrial reaction in which glycine is converted to equimolar amounts of CO_2, NH_3 and the C-1 group of N^5,N^{10}-methylene-tetrahydrofolate[1-3]. Because photorespiratory CO_2 production may amount to 80 μmol per h per g fresh weight[4,5] the stoichiometry of the decarboxylation reaction indicates that NH_3 release from glycine exceeds primary NO_3^- reduction[6,7]. Leaf cells must therefore be capable of rapid NH_3 re-assimilation in photorespiratory conditions. It has been suggested[8] that NH_3 could be refixed directly into glutamate by mitochondrial glutamate dehydrogenase (GDH), utilizing the NADH generated during glycine decarboxylation[1,9,10]. This seems unlikely[11,12] because of the high K_m for NH_3 exhibited by GDH *in vitro*. An alternative suggestion[11,12], that photorespiratory NH_3 could be re-assimilated into glutamate by the sequential action of cytoplasmic glutamine synthetase (GS) and the chloroplast enzyme glutamate synthase (GOGAT)[13,14], is supported by circumstantial evidence from *in vitro* studies[12,15]. Here we provide direct evidence for such a pathway, based on the results of experiments with mutants of *Arabidopsis thaliana* (L.) Heynh which are deficient in leaf GOGAT activity.

These mutants are inviable in atmospheric conditions that permit photorespiration, but are fully viable and phenotypically indistinguishable from the wild type when maintained in an atmosphere that suppresses photorespiration[5] (1% CO_2 in air). This conditional lethal phenotype, shared by several other mutants with defects in photorespiratory carbon metabolism[16,17], provided the basis for the isolation of the mutants[16].

Leaf extracts of wild-type *Arabidopsis* contained levels of ferredoxin-dependent GOGAT activity (Table 1) comparable to that observed in other species[11,18]. NADH or NADPH (0.2 mM) were relatively ineffective as electron donors, supporting about 4% of the activity obtained with ferredoxin in otherwise identical assay conditions (results not presented). Leaf extracts of the mutant lines CS30, CS103 and CS113 contained less than 5% of the wild-type level of ferredoxin-dependent GOGAT activity (Table 1). Mixing of mutant and wild-type extracts resulted in additive activity, suggesting that the low activity of mutant extracts was not due to the presence of an inhibitor. The presence of normal levels of ribulose bisphosphate (RuBP) carboxylase activity in all extracts indicates that recovery of chloroplast enzymes was similar in each case. Extracts of the mutants also contained normal levels of activity for GDH, GS and several enzymes related to photorespiration (results not presented). Thus, the mutants seem to be specifically defective in the synthesis of functional leaf GOGAT.

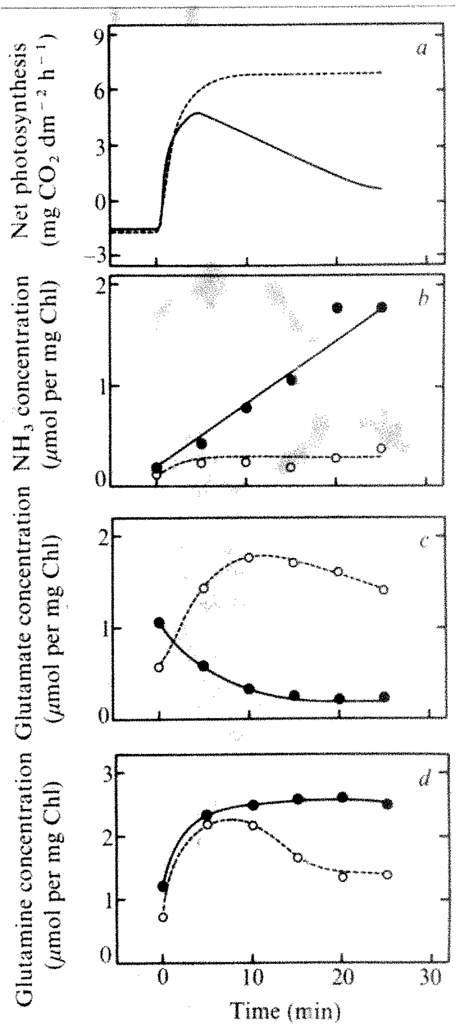

Fig. 1 Changes in *a*, photosynthesis rate and levels of *b*, NH_3; *c*, glutamate; and *d*, glutamine during illumination of wild-type and mutant *Arabidopsis* in photorespiratory conditions. Plants were grown in a 1% CO_2 atmosphere[16] on an artificial medium irrigated with a solution containing 2.5 mM KH_2PO_4 (pH 6.5), 5 mM KNO_3, 2 mM $Ca(NO_3)_2$, 2 mM $MgSO_4$ and micronutrients. The plants were placed in darkness in standard atmospheric conditions several hours before use to allow equilibration of metabolite pools. The plants were then placed in a photosynthesis chamber at 25 °C and continuously flushed with a gas stream (357 μl l^{-1} CO_2, 50% O_2, balance N_2) which exited through an infrared gas analyser. At time zero, the plants were illuminated at 300 μeinsteins m^{-2} s^{-1}. At the indicated intervals, plants were removed from the chamber and the leaf material ground in 2 ml chloroform/methanol/water (5:12:1). An additional 1.5 ml of chloroform and 1 ml of water was added, and the phases separated by centrifugation. Chlorophyll was determined on an aliquot of the organic phase. NH_3 was assayed in an aliquot of the aqueous phase by a colorimetric procedure[21]. Amino acid concentrations were determined with a Beckman (Model-119CL) amino acid analyser. Mutant and wild-type averaged 1.8 mg chlorophyll per g fresh weight. The response of the *gluS* mutant strain CS113 is indicated by the solid lines and symbols (●) and that of the wild type by broken lines and open symbols (○). Chl, chlorophyll.

A single nuclear mutation seems to be responsible for the enzyme deficiency and the conditional lethal phenotype. Reciprocal F_1 hybrids from crosses of wild-type and mutant lines showed the wild-type phenotype and had about 50% of wild-type GOGAT activity (Table 1). The mutant phenotype, scored as the onset of chlorosis after 4 days exposure to standard atmospheric conditions[15,16], segregated 3:1 (wild type:mutant) in the F_2 progeny resulting from crosses of wild-type × mutant. F_1 hybrids, obtained by crossing the mutants in all possible combinations, showed the mutant phenotype and were deficient in GOGAT activity (see for example CS103 × CS113, Table 1). The lack of complementation is evidence that the mutants carry defective alleles of the same gene, which we have designated *gluS*. Co-segregation of the mutant phenotype and enzyme deficiency was tested by first scoring the F_2 progeny from a wild-type × CS113 cross for the mutant phenotype at the rosette stage. The plants were revived by transfer to a CO_2-enriched environment for 2 weeks, then 64

---

* Also at US Department of Agriculture, Science and Education Administration-Agricultural Research, Urbana, Illinois 61801.

0028-0836/80/290257-03$01.00

randomly chosen plants were assayed individually for GOGAT. We observed an absolute correspondence between low enzyme activity and mutant phenotype.

The photosynthetic characteristics of the *gluS* mutants are similar to those of *Arabidopsis* mutants deficient in phosphoglycolate phosphatase[16] and serine–glyoxylate aminotransferase[17]. In atmospheric conditions that limit the oxygenation of RuBP[5] (1% CO_2 and 21% O_2 or 350 µl l^{-1} CO_2 and 2% O_2), photosynthesis (carbon dioxide fixation) continued indefinitely at wild-type rates (results not presented). However, in photorespiratory conditions (357 µl l^{-1} CO_2, 50% O_2, balance N_2), the photosynthesis rate of the mutants was initially similar to the wild type but rapidly declined to about 7% of that rate (Fig. 1*a*). The inhibition was reversible, for if the mutants were subsequently shifted to atmospheric conditions which suppressed photorespiration, photosynthesis was fully restored within about 30 min. Photosynthesis was also restored, irrespective of atmospheric conditions, by placing the plants in darkness for a similar period.

The inhibition of photosynthesis and reduced viability of the mutants in standard atmospheric conditions may be attributed to the accumulation of high levels of NH_3 during illumination in photorespiratory conditions (Fig. 2*b*). During 25 min of illumination in 357 µl l^{-1} CO_2, 50% O_2, balance N_2, free NH_3 in mutant CS113 increased 20-fold to a final intracellular concentration of about 3 mM. In the same conditions the concentration of NH_3 in the wild type remained below about 0.4 mM. The high concentration of NH_3 in the mutants would be expected to cause the observed inhibition of photosynthetic CO_2 fixation by uncoupling photophosphorylation[19]. In conditions of high CO_2 or low O_2, carbon flow through the photorespiratory pathway is negligible[5] so that little NH_3 is released from glycine. Photosynthesis and growth of the *gluS* mutants are therefore unimpaired in conditions which prevent photorespiration.

The accumulation of NH_3 in the *gluS* mutant in photorespiratory conditions is attributed to the virtual disappearance of free glutamate in leaf tissue (Fig. 1*c*), and thus the lack of an amino acceptor for re-assimilation of NH_3 by GS. The reduction in glutamate corresponds roughly to the increase in glutamine (Fig. 1*d*) as NH_3 is initially refixed by GS. The glutamine pool in the mutant then stabilizes because further synthesis is prevented by the lack of glutamate, and the GOGAT deficiency prevents conversion of glutamine to glutamate. The observation that NH_3 is not rapidly refixed into glutamate verifies the suggested[11] low *in vivo* activity of GDH in an assimilatory direction and confirms the importance of the GS/GOGAT pathway in the re-assimilation of photorespiratory NH_3[11,12].

Table 1 Glutamate synthase activity in extracts of wild-type and mutant lines of *Arabidopsis*

Strain	Glutamate synthase activity*	RuBP carboxylase activity*
Wild type	5.3	30.4
CS30	0.2	29.7
CS103	0.2	29.7
CS113	0.1	30.7
F_1 (W1 × CS113)	2.8	31.1
F_1 (CS103 × CS113)	0.3	31.5
Mixture†	2.8	30.0

Extracts were prepared by grinding leaf material in 50 mM KH_2PO_4 (*p*H 7.2), 12.5 mM *β*-mercaptoethanol, 0.5 mM EDTA and 0.5 mM EGTA. The extracts were centrifuged (30,000*g* for 15 min), passed through a column of Sephadex G-75, and dialysed against the same buffer for 12 h. Glutamate synthase activity was determined by measuring the formation of ^{14}C-glutamate from labelled 2-oxoglutarate. The complete 500 µl assay mixture[18] contained: 25 µmol KH_2PO_4 (*p*H 7.2), 6.2 µmol *β*-mercaptoethanol, 0.25 µmol EDTA, 0.25 µmol EGTA, 5 µmol aminooxyacetate, 1 µmol L-glutamine, 1 µmol ^{14}C-oxoglutarate (0.5 µCi µmol^{-1}), 50 µg spinach ferredoxin (Sigma), 0.8 mg $Na_2S_2O_4$, 0.8 mg $NaHCO_3$ and 60–70 µg of extract protein. The reaction was initiated by the addition of the dithionite and bicarbonate and terminated after 10 min at 24 °C by the addition of 60 µl of 3% H_2O_2. Product formation was measured by liquid scintillation counting following fractionation of the labelled compounds by ion exchange chromatography. Control reactions, lacking reductant, produced 1% of the d.p.m. obtained in the complete reaction mixture. RuBP carboxylase activity was measured as described previously[16]. Protein was determined by a dye binding assay[20].

*Enzyme activity is expressed as µmoles of product per h per mg protein.

†Equal volumes of wild-type and mutant (CS113) extract were mixed immediately before assay.

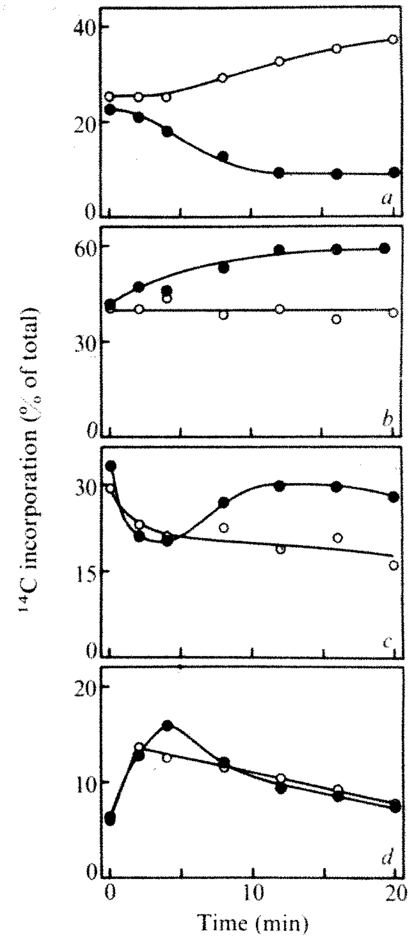

Fig. 2 Products of $^{14}CO_2$ assimilation by wild-type and mutant *Arabidopsis*. Intact plants were placed in a photosynthesis chamber and flushed with a humidified gas stream containing 350 µl l^{-1} CO_2, 21% O_2, balance N_2. At time zero the plants were illuminated (300 µeinsteins m^{-2} s^{-1}). At the indicated intervals the system was closed and $^{14}CO_2$ introduced. After 2 min the plants were quickly (3–5 s) removed to liquid nitrogen. The labelled products were extracted and separated as described previously[16]. The CO_2 concentration in the chamber remained between 300 and 350 µl l^{-1} during the period of incorporation. *a*, Basic fraction (amino acids); *b*, acid-1 fraction (organic acids and sugar monophosphates); *c*, combined acid-2 and acid-3 fractions (mostly sugar diphosphates); *d*, neutral fraction (sugars). The response of the mutant strain CS113 is indicated by solid symbols and that of the wild type by open symbols.

The low intracellular concentration of glutamate caused a plethora of secondary metabolic aberrations evident from the pattern of $^{14}CO_2$ incorporation into the products of photosynthesis (Fig. 2). In this experiment, plants were allowed to photosynthesize in standard atmospheric conditions for various periods, then given a short (2 min) pulse of $^{14}CO_2$ and the photosynthetic products were analysed. During the first few minutes, the labelling pattern of mutant and wild type were essentially indistinguishable. However, after several minutes of photosynthesis, the proportion of label in the amino acid fraction of the mutant dropped considerably (Fig. 2*a*). This is attributed to reduced availability of glutamate as an amino donor for the synthesis of glycine from glyoxylate. As a result, the intracellular concentration of serine declined to about one-fifth of the wild-type level (data not presented) as serine was utilized, by way of serine–glyoxylate aminotransferase, for glycine synthesis.

The central role of glutamate in cellular metabolism precludes a succinct description of the manifold effects resulting from glutamate depletion. In this respect it is not surprising that the mutants are inviable in normal atmospheric conditions. More surprising, perhaps, is the normal growth of the mutants in non-photorespiratory conditions. This implies that the plant does not require leaf GOGAT activity for NH_3 assimilation from primary nitrate reduction. Rather, the sole requisite function of leaf GOGAT seems to be the re-assimilation of photorespiratory NH_3.

We thank R. H. Hageman for growth chamber facilities, J. M. Widholm for amino acid analyses, and M. E. Hageman for technical assistance. This research was supported in part by grant No. 5901-0410-9-0341-0 from the USDA Competitive Research Grants Office.

Received 10 March; accepted 16 April 1980.

1. Bird, I. F., Cornelius, M. J., Keys, A. J. & Whittingham, C. P. *Phytochemistry* **11,** 1587–1594 (1972).
2. Kisaki, T., Yoshida, N. & Imai, N. *Pl. Cell Physiol.* **12,** 275–288 (1971).
3. Canvin, D. T., Lloyd, N. D. H., Fock, H. & Przybylla, K. in *CO_2 Metabolism and Plant Productivity* (eds Burris, R. H. & Black, C. C.) 161–176 (University Park Press, Baltimore, 1976).
4. Keys, A. J., Sampaio, E. V. S. B., Cornelius, M. J. & Bird, I. F. *J. exp. Bot.* **28,** 525–533 (1977).
5. Chollet, R. & Ogren, W. L. *Bot. Rev.* **41,** 137–179 (1975).
6. Brunetti, N. & Hageman, R. H. *Pl. Physiol.* **58,** 583–587 (1976).
7. Miflin, B. J. *Planta* **105,** 225–233 (1972).
8. Tolbert, N. E. *Encyclopedia Pl. Physiol.* (New Ser.) **6,** 338–352 (1979).
9. Douce, R., Moore, A. L. & Neuburger, M. *Pl. Physiol.* **60,** 625–628 (1977).
10. Woo, K. C. & Osmond, C. B. *Aust. J. Pl. Physiol.* **3,** 771–785 (1976).
11. Lea, P. J. & Miflin, B. J. *Encyclopedia Pl. Physiol.* (New Ser.) **6,** 445–456 (1979).
12. Keys, A. J. *et al. Nature* **275,** 741–743 (1978).
13. Lea, P. J. & Miflin, B. J. *Nature* **251,** 614–616 (1974).
14. Wallsgrove, R. M., Lea, P. J. & Miflin, B. J. *Pl. Physiol.* **63,** 232–236 (1979).
15. Anderson, J. W. & Done, J. *Pl. Physiol.* **60,** 354–359 (1977).
16. Somerville, C. R. & Ogren, W. L. *Nature* **280,** 833–836 (1979).
17. Somerville, C. R. & Ogren, W. L. *Proc. natn. Acad. Sci. U.S.A.* **77,** 2684–2687 (1980).
18. Wallsgrove, R. M., Harel, E., Lea, P. J. & Miflin, B. J. *J. exp. Bot.* **28,** 588–596 (1977).
19. Good, N. *Biochim. biophys. Acta* **40,** 502–517 (1960).
20. Spector, T. *Analyt. Biochem.* **86,** 142–146 (1978).
21. McCullough, H. *Clin. chim. Acta* **17,** 297–304 (1967).

Regulation of wound ethylene synthesis in plants

Thomas Boller* & Hans Kende†‡

*Botanisches Institut der Universität Basel, 4056 Basel, Switzerland
†Institut für Allgemeine Botanik, Eidgenössische Technische Hochschule, 8092 Zürich, Switzerland

Ethylene is produced by plants at specific stages of their life cycle and is involved in the regulation of many developmental processes, such as fruit ripening, flower fading, leaf abscission, growth in aquatic plants and initiation of flowering in bromeliads[1,2]. Ethylene is also formed when plants are subjected to stress by, for example, wounding, noxious chemicals, drought or waterlogging[1–3]. In both cases the biosynthetic pathway begins with methionine[1–5]. It proceeds to ethylene by way of *S*-adenosylmethionine (SAM) and 1-aminocyclopropane-1-carboxylic acid (ACC), a recently discovered intermediate[6,7], in ripening fruit[7,8] and auxin-treated pea stem sections[9,10]. We now report that wound-induced ethylene synthesis also proceeds by way of ACC and that it is regulated at the level of the ACC-forming enzyme (ACC synthase). Wounding of pericarp tissue of tomato fruit (*Lycopersicon esculentum* Mill.) results in rapid enhancement of the activity of ACC synthase and, consequently, in a greatly increased rate of ACC synthesis.

Cut tomato fruit evolves large amounts of wound ethylene[11–13]. We found that disks excised from the pericarp of green tomatoes produced relatively little ethylene in response to isolation (Table 1), but when each disk was further cut into 12 sectors (wounding), there was a substantial increase in ethylene production. In the same tissue, production of ACC increased even more rapidly as a result of wounding (Table 1). Aminoethoxyvinylglycine (AVG) is a potent inhibitor of ethylene biosynthesis[2] and of ACC synthase from tomato fruit[8]. When sectors of pericarp were incubated on 0.1 mM AVG after wounding, ethylene production was inhibited 89% after the first hour (2.07 nmol per g per h in control compared with 0.23 nmol per g per h in AVG-treated sectors).

In further experiments, we determined the activity of ACC synthase at short intervals after wounding of pericarp tissue and correlated the results with the time course of ACC accumulation and ethylene production. The activity of ACC synthase, as determined *in vitro*, was low in freshly cut sectors, tripled within 20 min and increased 10-fold within 40 min (Fig. 1), remaining fairly constant thereafter. The amount of ACC in the tissue increased approximately linearly after a lag of about 20 min; thus, the accumulation rate of ACC *in vivo* essentially paralleled the activity of ACC synthase *in vitro* (Fig. 1). The activity of ACC synthase was only about 20% of that expected from the rate of *in vivo* ACC synthesis, and we have been unable to discover where the loss occurred. Finally, the rate of ethylene formation, calculated from the total formed after wounding, increased after a lag of 30 min for at least 100 min and was proportional to the amount of ACC in the tissue.

Table 1 Effect of wounding on ethylene and ACC production

		Ethylene		ACC	
Incubation time (h)	Treatment	nmol per g	nmol per g per h	nmol per g	nmol per g per h
0		—	—	1.27	—
1	Intact	0.12	0.12	3.81	2.54
1	Wounded	0.72	0.72	8.73	7.46
2	Intact	0.25	0.13	3.77	—
2	Wounded	3.04	2.32	18.40	9.67

Disks of 11.5 mm diameter were cut from the pericarp of glasshouse-grown green tomato fruit (cv. Linda) and trimmed to 3 mm by removing extra tissue that formerly faced the inside of the fruit. They were incubated in pairs, epidermis facing upwards, on moist filter paper in 25-ml serum vials sealed with rubber stoppers at 28 °C. Disks were wounded by cutting each into 12 equal sectors. Ethylene was determined by gas chromatography[15]. ACC was extracted with ice-cold ethanol (4 ml for two disks), and insoluble residue was removed by centrifugation. The supernatant was taken to dryness and the residue was redissolved in 1 ml water. Of this, 0.1 ml was tested in the ACC assay of Lizada and Yang[16], based on the liberation of ethylene from ACC in alkaline solution containing Hg^{2+} and NaOCl. We had verified that all material in the crude ethanolic extract which released ethylene in the ACC assay of Lizada and Yang co-chromatographed with authentic ACC on cellulose thin-layer plates (solvent 2 of Boller *et al.*[8]).

The tissue already had the capacity to liberate ethylene from ACC during the lag phase, as reflected by the high rate of ethylene production in freshly cut sectors incubated on 10 mM ACC (Fig. 2). The rate of ethylene production during the first 10 min after cutting was 0.66 nmol per g per h and increased to a steady rate of about 2 nmol per g per h within 80 min. The maximum rate of ethylene formation was reached faster in tissue on 10 mM ACC than in that on 1 mM ACC. Attainment of the maximum rate of conversion of ACC to ethylene was probably delayed because of the time required to take up ACC into the pericarp sectors. The maximum rate of ACC-dependent ethylene formation might have been limited by

---

‡Permanent address: MSU-DOE Plant Research Laboratory, Michigan State University, East Lansing, Michigan 48824.

0028–0836/80/290259–02$01.00

saturation of an ACC uptake system and/or by saturation of the ethylene-forming system.

Ethylene synthesis after wounding, as in other situations, is inhibited by cycloheximide[5,14]. When sectors of pericarp were incubated on cycloheximide (25 µg ml^{-1}) for 2 h, the tissue produced 86% less ethylene and contained 84% less ACC and 96% less ACC synthase activity than untreated sectors.

These results indicate that ethylene is produced from ACC in tomato pericarp tissue in response to wounding. Such ethylene formation seems to be induced through rapid enhancement of ACC synthase activity. Because cycloheximide inhibits the development of this enzyme activity, it is likely, though not proven, that ACC synthase is newly formed rather than activated when the tissue is wounded. The last step in ethylene formation—conversion of ACC to ethylene—does not seem to be regulated in wounded tissue. This follows from two kinds of experiments. First, wounded pericarp disks already had the capacity to convert added ACC to ethylene during the lag phase of wound-induced ethylene synthesis. Second, when no ACC was added, the rate of ethylene formation was proportional to the level of endogenous ACC throughout the experiment. This also indicates that the system converting ACC to ethylene is not saturated at the concentrations of ACC reached in the wounded tissue.

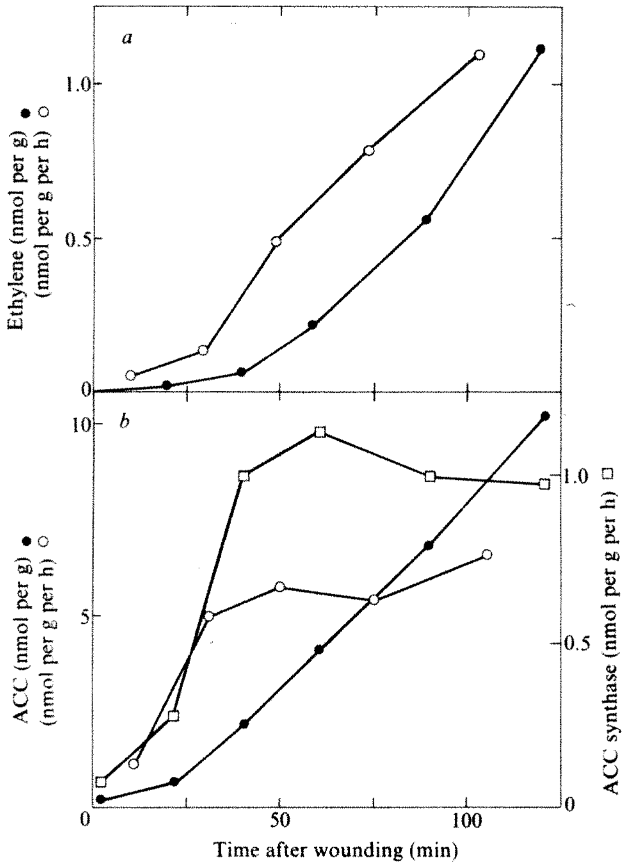

Fig. 1 Ethylene evolution, ACC content and ACC synthase activity in wounded pericarp disks from green tomato fruit. *a*, Ethylene production. From each of two freshly harvested tomato fruits (cv. Moneymaker), seven disks were cut. Each was wounded immediately by cutting into 12 equal sectors. Pairs of wounded disks, one from each fruit, were incubated for different times on moist filter paper in sealed 25-ml serum vials. After incubation, ethylene was determined[1,5], and the tissue was frozen in liquid N_2. Data are mean values from three identically incubated samples. The rate of ethylene production was calculated for each time interval of the experiment. *b*, ACC content and activity of ACC synthase. The frozen sectors from *a* (six disks, 1.8 g fresh weight total) were combined, pulverized in liquid N_2 with pestle and mortar and extracted in 3 ml 0.1 M K-HEPES buffer, *p*H 8, containing 4 mM dithiothreitol (DTT) and 0.4 µM pyridoxal phosphate. After centrifugation (10 min at 10,000*g*), two 0.1-ml samples of supernatant solution were used directly for ACC determination[16]. The rate of increase in ACC content was derived for each time interval of the experiment. The true rates of ACC formation were probably 10% higher if all ethylene formed was derived from ACC. Centrifuged extract (2 ml) was desalted on a column of Sephadex G-50 (2 × 6 cm) with 2 mM K-HEPES buffer, *p*H 8, containing 0.1 mM DTT and 0.2 µM pyridoxal phosphate as eluting buffer, and the eluted protein was used to determine ACC synthase activity with 50 µM SAM as substrate[8]. Enzymatically formed ACC was determined according to Lizada and Yang[16].

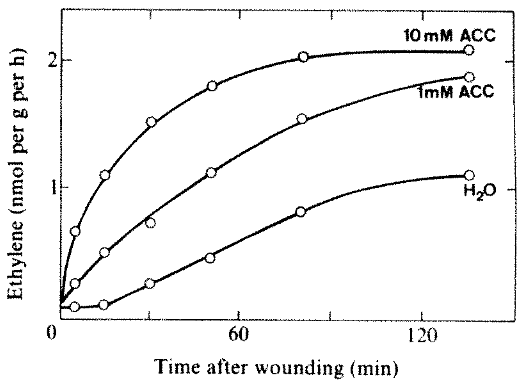

Fig. 2 Rate of ethylene formation in wounded pericarp incubated on ACC. Freshly cut disks of pericarp from a single tomato (cv. Linda) were cut into 12 sectors each, and the sectors from two disks were incubated in sealed 25-ml serum vials on filter paper wetted with water or 1 mM or 10 mM solutions of ACC. Ethylene was determined by gas chromatography[15] after 10, 20, 40, 60, 100 and 170 min. From these data, the mean rate of ethylene formation was calculated for each time interval. Control vials containing ACC solutions without tissue produced less than 2 pmol h^{-1} ethylene.

The regulation of wound ethylene synthesis in tomato pericarp resembles that of ethylene synthesis in senescing tomatoes. In the latter case, the activity of ACC synthase and the concentration of ACC increase during maturation of the fruit, when ethylene formation is initiated[8]. Similarly, auxin at high concentrations seems to induce ethylene synthesis in etiolated pea epicotyls by enhancing ACC synthase activity[9]. It remains to be seen whether developmental, stress and hormonal stimuli all regulate the activity of ACC synthase through the same mechanism or whether different modes of control are exerted to modulate the activity of this important enzyme in ethylene synthesis.

We thank Professor Ph. Matile, in whose laboratory this work was carried out, for his hospitality, Dr G. Défago for plant material and Mr P. Mötteli for technical assistance. The work was supported in part by NSF grant PCM 77-08522 to H.K.

Received 11 February; accepted 2 May 1980.

1. Abeles, F. B. *Ethylene in Plant Biology* (Academic, New York, 1973).
2. Lieberman, M. *A. Rev. Pl. Physiol.* **30**, 533–591 (1979).
3. Yang, S. F. & Pratt, H. K. in *Biochemistry of Wounded Plant Tissues* (ed. Kahl, G.) 595–622 (Walter de Gruyter, Berlin, 1978).
4. Hanson, A. D. & Kende, H. *Pl. Physiol.* **57**, 538–541 (1976).
5. Hyodo, H. *Pl. Physiol.* **59**, 111–113 (1977).
6. Lürssen, K., Naumann, K. & Schröder, R. *Z. Pflanzenphysiol.* **92**, 285–294 (1979).
7. Adams, D. O. & Yang, S. F. *Proc. natn. Acad. Sci. U.S.A.* **76**, 170–174 (1979).
8. Boller, T., Herner, R. C. & Kende, H. *Planta* **145**, 293–303 (1979).
9. Jones, J. F. & Kende, H. *Planta* **146**, 649–656 (1979).
10. Konze, J. R. & Kende, H. *Planta* **146**, 293–301 (1979).
11. Meigh, D. F., Norris, K. H., Craft, C. C. & Lieberman, M. *Nature* **186**, 902–903 (1960).
12. Lee, T. H., McGlasson, W. B. & Edwards, R. A. *Radiat. Bot.* **10**, 521–529 (1970).
13. Herner, R. C. & Sink, K. C. Jr *Pl. Physiol.* **52**, 38–42 (1973).
14. Saltveit, M. E. Jr & Dilley, D. R. *Pl. Physiol.* **64**, 417–420 (1979).
15. Kende, H. & Hanson, A. D. *Pl. Physiol.* **57**, 523–527 (1976).
16. Lizada, C. & Yang, S. F. *Analyt. Biochem.* **100**, 140–145 (1979).

Heterozygosity at enzyme loci and morphological variation

Paul Handford*

Rockefeller University, New York City 10021

*Present address: Zoology Department, University of Western Ontario, London, Canada N6A 5B7

Two recent reports[1,2] have concerned the relationship between genic heterozygosity, as indicated by electrophoretically detected enzyme loci, and an individual's tendency to depart from the mean on a variety of morphological traits. Using different methods to assess differences in morphological variances between homozygote and heterozygote classes, both conclude that homozygotes show a significantly higher level of morphological variation. These conclusions are important in that they seem to extend the phenomenon from studies on manipulated stocks of organisms[3] to variation in natural populations. As Eanes[2] points out, it is necessary to determine the generality of this result. Both these studies[1,2] consider poikilotherm animals (a fish and an insect), so it would be particularly interesting to look for the relationship in homoiotherms. As a contribution to this end, I present here the results (Table 1) of an analysis of variation in the Rufous-collared sparrow, *Zonotrichia capensis*[4]. I found no difference in levels of variation either between the homozygote and heterozygote classes or between classes of individuals heterozygous at different numbers of loci. My results thus suggest a difference between homoiotherms and poikilotherms in this phenomenon.

My data concern variation at four enzyme loci (mannose-6-phosphate dehydrogenase, M6PI; 6-phosphogluconate dehydrogenase, 6-PGD; glucose-6-phosphate dehydrogenase, G6PD and α-glycerophosphate dehydrogenase, α-GPD) and in 11 metrical characters (tarsus, tail length and three bill, four toe and two wing measures). As the sexes differ significantly on several variables they are considered separately.

There are some difficulties in comparing levels of variation among population samples or subsamples. These and some possible solutions are reviewed by Van Valen[5]. In the univariate case, one customarily compares sample variances. Additional variables may justifiably be considered independently, provided there is low correlation between them. This is the approach adopted by Eanes[2], considering variation in two wing characters in the butterfly *Danaus plexippus*. It is unwise, however, to test the null hypothesis, σ^2 homozygotes $= \sigma^2$ heterozygotes, by use of an F-test. The F-distribution is rather sensitive to deviations from normality of the measured distributions, which can give spuriously high values of F. The simplest way to test such a null hypothesis is that given by Levene[6]. One constructs a new variable $y_i = |x_i - \bar{x}|$ for each case i and tests the samples for differences in y by means of a t-test.

In most circumstances it is probably best to consider variation in several characters collectively, by some multivariate method, rather than separately, as even small degrees of correlation between variables introduce potential bias through, in effect, making the same test several times. This is particularly relevant when using the sign test[7] to assess a hypothesis. Mitton[1] has used two techniques for extracting a single measure of variability from his seven meristic characters: computing the mean coefficient of variation, c.v., and the determinant of the variance–covariance matrices, $|\Sigma|$. These are compared among the homozygote and heterozygote classes, and the results tested by the sign test. In fact, matrices may be tested for homogeneity of dispersion, and a probability ascribed[8], but one should note some undesirable properties of $|\Sigma|$ as a statistic of multivariate variability. If even one of the characters used in computing $|\Sigma|$ has a very low variance, then $|\Sigma|$ becomes very small regardless of variation in other characters. Small differences in such very small numbers will have large effects on the ratios between them, and so interpretation of these ratios becomes difficult and potentially misleading. Similarly, any degree of correlation between variables, which is almost inevitable when using more than three or four variables, reduces $|\Sigma|$ to very small values. Table 1 shows the results of applying a multivariate test for matrix homogeneity. Three of five tests among males are significant, but probably spurious given the very tiny values of $|\Sigma|$ (of the order of 10^{-20}). Van Valen[5] also discusses the use of principal components in this kind of analysis. This approach eliminates the problem of correlated variables, but exaggerates the problem of low variance in one or more variables, as the last principal components to be extracted

Table 1 Comparison of variability in morphological characters among genetic subgroups in samples of Rufous-collared sparrows, *Zonotrichia capensis*

	Loci									
	M6PI		6PDG		G6PD		α-GPD		Heterozygosity	
	Hom	Het	Hom	Het	Hom	Het	Hom	Het	Low	High
Males										
N	76	49	103	22	74	38	88	37	68	44
Σs^2	0.054	0.070	0.059	0.061	0.062	0.063	0.060	0.060	0.055	0.075
Hom/Het	0.782 NS		0.962 NS		0.983 NS		1.000 NS		0.739 NS	
Matrix homogeneity, P	0.041*		0.372 NS		0.037*		0.321 NS		0.008†	
Females										
N	37	10	36	11	37	9	41	6	21	25
Σs^2	0.059	0.043	0.059	0.042	0.058	0.055	0.058	0.039	0.063	0.52
Hom/Het	1.387 NS		1.398 NS		1.059 NS		1.502 NS		1.196 NS	
Matrix homogeneity, P	—		0.000†		—		—		0.585 NS	

Heterozygosity is the number of loci, of four, at which an individual is heterozygous. In males, Low = 0–1 loci; in females, Low = 0 loci. Different criteria were used to make sample sizes comparable. Σs^2 is the simple sum of all character variances within given subgroups. Hom/Het is the ratio $\Sigma s^2_{\text{hom}}/\Sigma s^2_{\text{het}}$; significance level tested by Levene's method (see text). Matrix homogeneity is the P level given by a multivariate test for the homogeneity of the two variance–covariance matrices. Where no value is given, as in the females, this is because the test could not be carried out due to matrix singularity caused by there being more morphological variables than cases in the heterozygote class. NS, Not significant. All analyses performed on ln-transformed measurements.

0028–0836/80/290261–02$01.00

usually account for a very small fraction of the total variance in the sample. There are no objective methods available appropriate to the present purpose, for setting a level for exclusion of these later components, and in any case this loses information.

By analogy with the univariate case, Van Valen recommends the use of total sample variance for j variables, $\Sigma_j s_j^2$. This eliminates problems of correlation and low variances by making them irrelevant. If the variables are log-transformed, scale effects are eliminated as is the need for some multivariate c.v. Differences in Σs^2 may again be tested for significance by an extension of Levene's test: $y_i = (\Sigma_j (x_{ij} - \bar{x}_j)^2)^{\frac{1}{2}}$, again using a t-test for differences in $\bar{y}$. The results of such an analysis of my data fail to show significantly different levels of variation either between the homozygote and heterozygote classes considered separately, or between classes of individuals heterozygous at different numbers of loci. Because the studies of Mitton[1] and Eanes[2] use other methods of analysis, it is not possible to make a close comparison between their results and mine. However, some points are worth mentioning. First, the absence of a significant result in this single sample from one species does not, of course, demonstrate the absence of the effect. What it does is raise the possibility of a difference between homoiotherms and poikilotherms in this regard, one which is consistent with other considerations about development and adaptation, as indicated below. It has been widely suggested that development of homoiotherms is more resilient to environmental insult than that of poikilotherms and invertebrates, and that their growth rates and final size are more determinate[9]. Again, genetic enzyme polymorphism among vertebrates as a whole is lower than among invertebrates, and homoiotherms are slightly, though non-significantly, less variable than are poikilotherm vertebrates[10]. This perhaps reflects different tactics of adaptation among very different kinds of organisms, and suggests the possibility that heterozygosity and polymorphism may have quite different significance in organisms with widely different organization and ecological situations[11]. This specifically suggests a relationship between levels of genic heterozygosity, body size and mobility which is consistent with predictions from Levins' theory of adaptive strategies in relation to environmental grain[12]. Thus, vertebrates which are typically larger and more mobile, so experiencing the environment in a more fine-grained fashion, exhibit lower levels of genic polymorphism. There are other studies considering variability and heterozygosity (at the population level), but these also consider variation in poikilotherms and invertebrates[13,14]. Clearly, there is a need for investigation of variation in a wider range of taxa, particularly the higher vertebrates, before we can make generalizations about the relationship between genic heterozygosity and morphological variability.

This work was supported by NSF grant GB38344 to Fernando Nottebohm. I thank Roger Green, Shiva Singh and the reviewers for their comments.

Received 20 November 1979; accepted 11 April 1980.

1. Mitton, J. B. *Nature* **273,** 661–662 (1978).
2. Eanes, W. F. *Nature* **276,** 263–264 (1978).
3. Lerner, I. M. *Genetic Homeostasis* (Oliver and Boyd, Edinburgh, 1954).
4. Handford, P. & Nottebohm, F. *Evolution* **30,** 802–817 (1976).
5. Van Valen, L. *J. theor. Biol.* **45,** 235–247 (1974); *Evolutionary Theory* **4,** 33–43 (1978).
6. Levene, H. in *Contributions to Probability and Statistics* (eds Olkin, I. *et al.*) 278–292 (Stanford University Press, 1960).
7. Sokal, R. R. & Rohlf, F. J. *Biometry* (Freeman, San Francisco, 1969).
8. Cohen, E. & Burns, P. *SPSS-MANOVA-Multivariate Analysis of Variance and Covariance* (Document No. 413, Rev. A, Northwestern University, Evanston, 1977).
9. Case, T. J. *Q. Rev. Biol.* **35,** 243–282 (1978).
10. Nevo, E. *Theor. Pop. Biol.* **13,** 121–177 (1978).
11. Selander, R. K. & Kaufman, D. W. *Proc. natn. Acad. Sci. U.S.A.* **70,** 1875–1977 (1973).
12. Levins, R. *Evolution in Changing Environments.* (Princeton University Press, 1968).
13. Soulé, M. E. *Taxon* **20,** 37–50 (1971); *Am. Nat.* **106,** 429–446 (1972); *Evolution* **33,** 396–401 (1979).
14. Soulé, M. E. & Baker, B. *Heredity* **23,** 611–614 (1968).

0028–0836/80/290262–03$01.00

Vitamin D_3 metabolites and PTH synergistically stimulate bone formation of chick embryonic femur *in vitro*

Hiroyoshi Endo*, Mamoru Kiyoki†,
Kohtaro Kawashima*,
Tatsuyuki Naruchi† & Yoshinobu Hashimoto†

*Department of Physiological Chemistry, Faculty of Pharmaceutical Sciences, Teikyo University, Sagamiko, Kanagawa 199-01, Japan
†Teijin Institute for Bio-Medical Research, 4-3-2 Asahigaoka, Hino-shi, Tokyo 191, Japan

Bone remodelling depends on a balance between formation and resorption. Little is known of the biological factors involved in bone formation, whereas there is much evidence that physiological factors, such as parathyroid hormone (PTH) and active metabolites of vitamin D_3, influence resorption. Cells responsible for osteogenesis and osteoclasis occur in close proximity, suggesting that both might be controlled by the same physiological factors in the micro-environment of the body fluid. To clarify the factors stimulating bone formation or accelerating osteogenic cell activity, we have examined the effects of vitamin D_3 metabolites and PTH on bone formation *in vitro*. We report here that combinations of those metabolites especially 1α,25-$(OH)_2D_3$ and 24R,25-$(OH)_2D_3$, directly stimulate calcification on bone synergistically with PTH.

We used the culture system described before[1,2]. Femora of 9-day-old chick embryos were obtained by removing adherent soft tissues under a dissecting microscope. Each femur was transferred to a roller tube containing 1.5 ml of medium. To allow for differences between embryos, the bones from one side of an embryo were cultivated in control medium and those from the opposite side of the same embryo in experimental medium. Basal medium was a mixture of BGJb-HW2 (ref. 3) and 11-day-old chick embryo extract (CEE), (9:1). PTH ($1\ \mathrm{U\,ml^{-1}}$), 1α,25-$(OH)_2D_3$ (0.02 and $2.0\ \mathrm{ng\,ml^{-1}}$), 24R,25-$(OH)_2D_3$ (0.5 and $50.0\ \mathrm{ng\,ml^{-1}}$) and 25-OH-$D_3$ ($2.5\ \mathrm{ng\,ml^{-1}}$) were added to the mixture, singly or in combination, to examine their effect on calcification. Roller tubes were incubated at 37 °C for 6 days, rotating 10 times per hour in a roller drum which held them at an angle of 5°. The medium was replaced every other day. At the end of cultivation, the calcium of most pair-mate bones was determined and

Table 1 Calcium level of 9-day-old chick embryonic femur after 6 days cultivation using PTH added to the basal medium as control

Treatment	Concentration ($\mathrm{ng\,ml^{-1}}$)	No. of pairs	Calcium level (μg per femur) Control bones	Calcium level (μg per femur) Treated bones	Calcification ratio*
1α,25-$(OH)_2D_3$ +24R,25-$(OH)_2D_3$ +25-OH-D_2	0.02 0.5 2.5	11	4.42 ± 0.74	7.54 ± 0.79	2.07 ± 0.16†
1α,25-$(OH)_2D_3$ +24R,25-$(OH)_2D_3$	0.02 0.5	13	4.40 ± 0.63	7.71 ± 0.60	2.04 ± 0.24†
1α,25-$(OH)_2D_3$ +25-OH-D_3	0.02 2.5	10	5.61 ± 0.56	5.71 ± 0.57	1.05 ± 0.09
24R,25-$(OH)_2D_3$ +25-OH-D_3	0.5 2.5	8	7.65 ± 0.69	8.93 ± 0.43	1.15 ± 0.11
1α,25-$(OH)_2D_3$	0.02	6	5.03 ± 0.79	5.55 ± 0.99	1.05 ± 0.06
1α,25-$(OH)_2D_3$	2.0	5	6.60 ± 1.12	6.96 ± 0.79	1.38 ± 0.25
24R,25-$(OH)_2D_3$	0.5	5	10.88 ± 1.21	11.13 ± 1.12	1.06 ± 0.05
24R,25-$(OH)_2D_3$	50.0	5	8.74 ± 1.21	8.14 ± 0.83	0.97 ± 0.08
25-OH-D_3	2.5	5	5.65 ± 1.74	5.80 ± 1.46	1.00 ± 0.13

Values represent mean ± s.e.m. The amount of calcium deposited in the femur was determined by OPCP method[15]. Control femur was cultivated in the basal medium plus PTH.

*The ratio of calcium levels in treated femora to pair-mate control bones.

†$P < 0.005$.

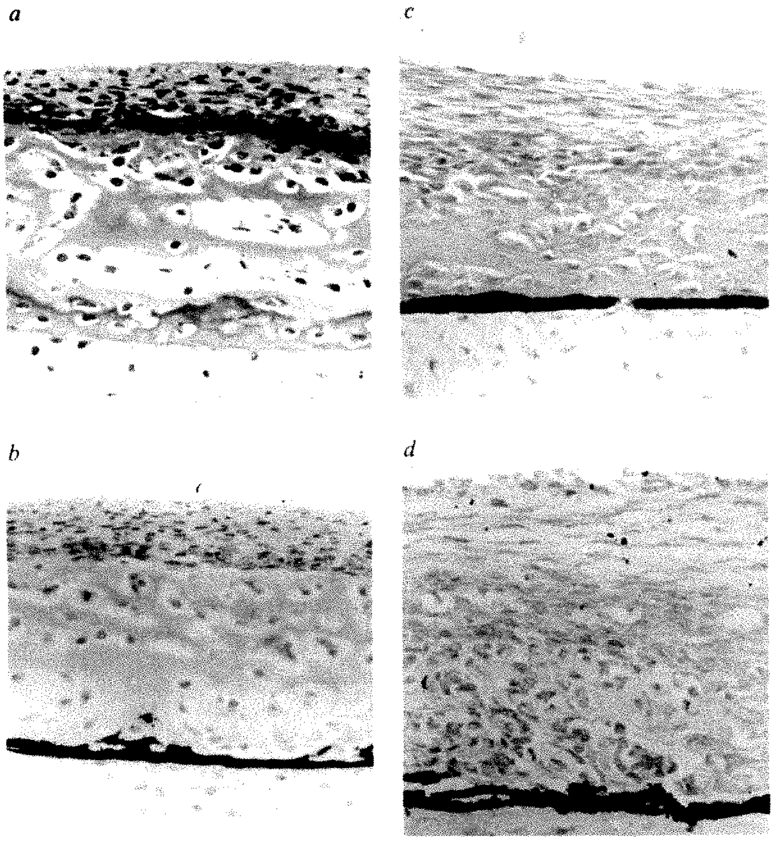

Fig. 1 Diaphyses of the femora from 9-day chick embryos after 6 days cultivation. *a*, Bone cultured in the medium CEE:BGJb-HW2 (1:9) (haematoxylin and eosin stain); *b*, the same specimen as in *a* (von Kossa's stain); *c*, bone cultured in medium containing the three metabolites of vitamin D_3 (von Kossa's stain); *d*, bone cultured in medium containing PTH (von Kossa's stain); *e*, bone cultured in medium containing PTH and the three metabolites of vitamin D_3 (haemotoxylin and eosin stain); *f*, the same specimen as in *e* (von Kossa's stain. All ×400.

histological development of residual pairs was examined microscopically with haematoxylin–eosin and von Kossa's stain.

Femora cultured in basal medium or in medium with vitamin D_3 metabolite(s) formed only osteoid tissue with no calcification (Fig. 1*a*–*c*). In medium containing PTH alone, mineralization scarcely occurred (Fig. 1*d*), although the bone elongated significantly[4]. In medium plus PTH and three kinds of vitamin D_3 metabolites, however, the diaphyseal cortex of the bone became heavily calcified (Fig. 1*e*, *f*).

The amount of calcium deposited in the femur treated with all three vitamin D_3 metabolites in the presence of PTH was 2.07 times greater than that in control bone treated with PTH alone. Similarly, combined treatment with 1α,25-$(OH)_2D_3$ and 24R,25-$(OH)_2D_3$ in the presence of PTH gave a value of 2.04 for that calcification ratio. When combined with 25-OH-D_3 in the presence of PTH, however, neither 1α-25-$(OH)_2D_3$ nor 24R,25-$(OH)_2D_3$ stimulated calcium deposition, the calcification ratio being 1.05 and 1.15 (Table 1). Moreover, no single treatment with 1α,25-$(OH)_2D_3$ or 24R,25-$(OH)_2D_3$ in the presence of PTH affected calcification, even at high concentrations (Table 1). 1α,25-$(OH)_2D_3$, when combined with 24R,25-$(OH)_2D_3$, could be replaced by the synthetic vitamin D_3 analogue 1α,24R-$(OH)_2D_3$ (ratio 1.93), although the synthetic vitamin alone with added PTH did not enhance calcification (ratio 1.03). Bone growth in medium plus PTH alone was 1.04 times that in medium alone, and in medium plus three kinds of vitamin D_3 metabolite the ratio was 1.17 (Table 2). Treatment with any one of these vitamin D_3 metabolites alone did not affect calcification.

Many observations made *in vivo* have suggested that vitamin D_3 metabolites could be involved in bone mineralization[5]. Our results show that these metabolites, especially the combination of 1α,25-$(OH)_2D_3$ and 24R,25-$(OH)_2D_3$, stimulate bone formation under the synergistic influence of PTH. These can activate bone resorption[6,7], and so our result suggested that bone could be remodelled successfully by simultaneous activation of both osteoclastic and osteogenic processes.

1α,25-$(OH)_2D_3$ is the most active metabolite of vitamin D_3 for many biological processes[8], and we have now demonstrated that 24R,25-$(OH)_2D_3$ is important for ossification, with mineralization proceeding only in the presence of both metabolites. This supports *in vivo* studies which suggested that 24R,25-$(OH)_2D_3$ may be active in bone

Table 2 Calcium level of 9-day-old chick embryonic femur after 6 days cultivation using basal medium as control

Treatment	Concentration (ng ml^{-1})†	No. of pairs	Calcium level (µg per femur) Control bones	 Treated bones	Calcification ratio*
PTH	1†	11	6.35±1.00	6.89±0.81	1.04±0.13
1α,25-$(OH)_2D_3$ +24R,25-$(OH)_2D_3$ +25-OH-D_3	0.02 0.5 2.5	7	9.60±1.15	10.27±0.58	1.17±0.15
1α,25-$(OH)_2D_3$ +24R,25-$(OH)_2D_3$	0.02 0.5	6	6.45±1.47	7.31±1.43	1.14±0.06
1α,25-$(OH)_2D_3$	0.02	5	10.06±0.30	10.12±0.85	1.01±0.07
1α,25-$(OH)_2D_3$	2.0	5	9.84±1.46	8.84±1.46	0.93±0.11
24R,25-$(OH)_2D_3$	0.5	5	10.40±0.39	9.52±0.76	0.91±0.05
24R,25-$(OH)_2D_3$	50.0	5	9.92±0.87	8.76±0.27	0.92±0.10

Values represent mean±s.e.m. The amount of calcium deposited in the femur was determined by OPCP method[15]. Control femur was cultivated in the basal medium.

*The ratio of calcium level in treated femora to pair-mate control bone.

†PTH concentration was 1 unit ml^{-1}.

formation[9,10], possibly in combination with 1α,25-$(OH)_2D_3$ (ref. 11).

The role of PTH in bone formation, however, has been controversial, with some studies suggesting that it inhibits bone collagen synthesis[12], and other evidence indicating that it increases bone formation[13,14]. Our results demonstrate that PTH is essential for the calcification of bone. We are now studying the role of CEE and the dose–response relationship of PTH and vitamin D_3 metabolites in stimulating bone formation *in vitro*.

Received 2 August 1979; accepted 16 April 1980.

1. Endo, H. *Expl. Cell Res.* **21**, 151–163 (1960).
2. Ito, Y., Endo, H., Enomoto, H., Wakabayashi, K. & Takamura, K. *Expl. Cell Res.* **31**, 119–127 (1963).
3. Endo, H. *Connective Tissue* **6**, 139–148 (1974).
4. Kawashima, K., Iwata, S. & Endo, H. *Bone Metabolism* **6**, 114–117 (1973).
5. De Luca, H. F. in *Vitamin D Metabolism and Function* (Springer, Berlin, 1979).
6. Margroab, A. & Sheppard, H. *Endocrinology* **100**, 629–634 (1977).
7. Robertson, W. F., Peacock, M., Atkins, D. & Webster, L. A. *Clin. Sci.* **43**, 715–718 (1972).
8. De Luca, H. F. & Schnoes, H. K. *A. Rev. Biochem.* **45**, 631–666 (1976).
9. Orony, A., Goodwin, D., Noff, D. & Edelstein, S. *Nature* **276**, 517–519 (1978).
10. Kanis, J. A. *et al. Br. med. J.* **1**, 1382–1386 (1978).
11. Malluche, H. H. *et al.* in *Vitamin D: Basic Research and its Clinical Application*, 425–427 (De Gruyter, Berlin, 1979).
12. Dirtrich, J. W., Canalis, E. M., Maina, D. M. & Raisz, L. G. *Endocrinology* **98**, 943–949 (1976).
13. Kalu, D. N., Pennock, J., Doyle, F. H. & Foster, G. V. *Lancet* **i**, 1363–1366 (1970).
14. Flanagan, B. & Nichols, G. *J. clin. Invest.* **44**, 1795–1801 (1964).
15. Connerty, H. V. & Briggs, A. R. *Am. J. clin. Path.* **45**, 290–296 (1966).

Leukotriene B, a potent chemokinetic and aggregating substance released from polymorphonuclear leukocytes

A. W. Ford-Hutchinson, M. A. Bray, M. V. Doig, M. E. Shipley & M. J. H. Smith

Biochemical Pharmacology Research Unit, Department of Chemical Pathology, King's College Hospital Medical School, Denmark Hill, London SE5 8RX, UK.

Arachidonic acid is metabolised either by cyclooxygenases to produce prostaglandins and thromboxanes or by lipoxygenases to produce mono-, di- and trihydroxyeicosatetraenoic acids (HETEs). Polymorphonuclear leukocytes (PMNs) release HETEs, including mono- and dihydroxy fatty acids, when exposed to stimuli such as the calcium ionophore A23187 (refs 1, 2). The mono-HETEs are assumed to be of particular importance with respect to effects on leukocyte function because they have been shown to possess both chemotactic and chemokinetic activities towards PMNs and eosinophils[3,4]. However, we have now shown that the chemokinetic and aggregating activities released from rat and human PMNs exposed to ionophore A23187 (ref. 5) are not due to the release of mono-HETEs but to that of 5,12-di-HETE (leukotriene B). This compound is active over the concentration range 10 pg ml^{-1} to 5 ng ml^{-1}.

Rat peritoneal or human peripheral PMNs, when exposed to ionophore A23187, release substances into the surrounding media which cause the aggregation and chemokinesis of other PMN suspensions[5]. The release of the activities was prevented by drugs known to inhibit lipoxygenase pathways of arachidonic acid (AA) metabolism.

The aggregating and chemokinetic activities released following exposure of human PMNs to ionophore A23187 were extracted into diethyl ether after acidification of the media. Both activities could be recovered from a silicic acid column following elution with ethyl acetate and >95% of the biological activity was recovered in a single UV absorbent peak following HPLC (see Fig. 1). Identical results were obtained with rat PMNs. This peak had a retention time identical to that previously reported for leukotriene B (5, 12-dihydroxy 6,8,10,14-eicosatetraenoic acid)[1]. Ultraviolet spectra were obtained for the methyl ester of the compound which showed three major bands ($\varepsilon_{\mathrm{mx}}^{\mathrm{MeOH}}$ 262±2, 271±2 and 282±2 nm), indicating the presence of three conjugated double bonds[6]. Gas–liquid chromatographic analysis of the active fraction showed a major peak with a C value of 23.6. The mass spectrum of this compound is shown in Fig. 2 and the substance was identified as leukotriene B by comparison with the spectra previously reported for this compound[7].

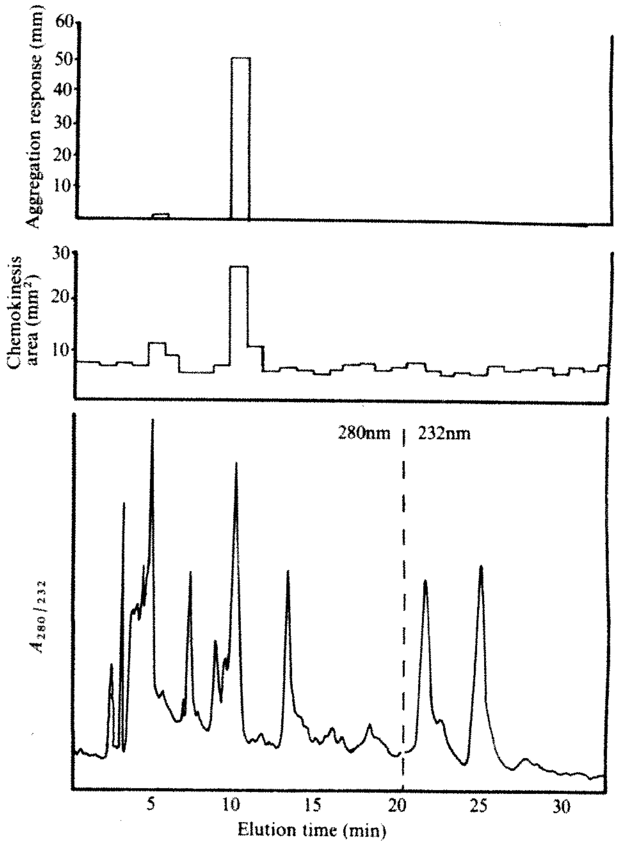

Fig. 1 Separation by HPLC of lipoxygenase products released by human PMNs exposed to 10 μM ionophore A23187 for 4 min as previously described[5]. The reaction was terminated by the addition of 1.5 vol. methanol, the cells were removed by centrifugation and the supernatant was acidified to *p*H 3.5 and extracted twice with diethyl ether. The ether extracts were washed once with water and dried under vacuum. The residue was dissolved in diethyl ether/hexane (20:80) and applied to a silicic acid column equilibrated with the same solvent[1]. The column was subsequently eluted with ethyl acetate, the ethyl acetate was removed under vacuum and the residue dissolved in 50 μl methanol for application to a reverse phase HPLC column (4.6 × 250 mm packed with Spherisorb 5ODS eluted at a flow rate of 1 ml min^{-1} with a mixture of methanol/water (75:25, v/v) plus acetic acid (0.01%)[1]. HPLC columns were calibrated with a mixture of dimethylphthalate, di-*n*-butylphthalate and pyrene using as a solvent methanol/water (85:15, v/v). The elution times for 15-, 12- and 5-HETE were 24, 26.5 and 31.5 min, respectively. HPLC fractions were dried under vacuum and resuspended in medium for assay as below. Chemokinetic activity towards human PMNs was assayed in an agarose microdroplet assay[11], the results being expressed as the increase in the area of migration when compared with that of cells in the presence of medium alone. Aggregation of rat PMNs was assessed by nephelometry in a Payton aggregometer, the results being expressed as the change in transmittance as measured (in mm) on the recorder[12].

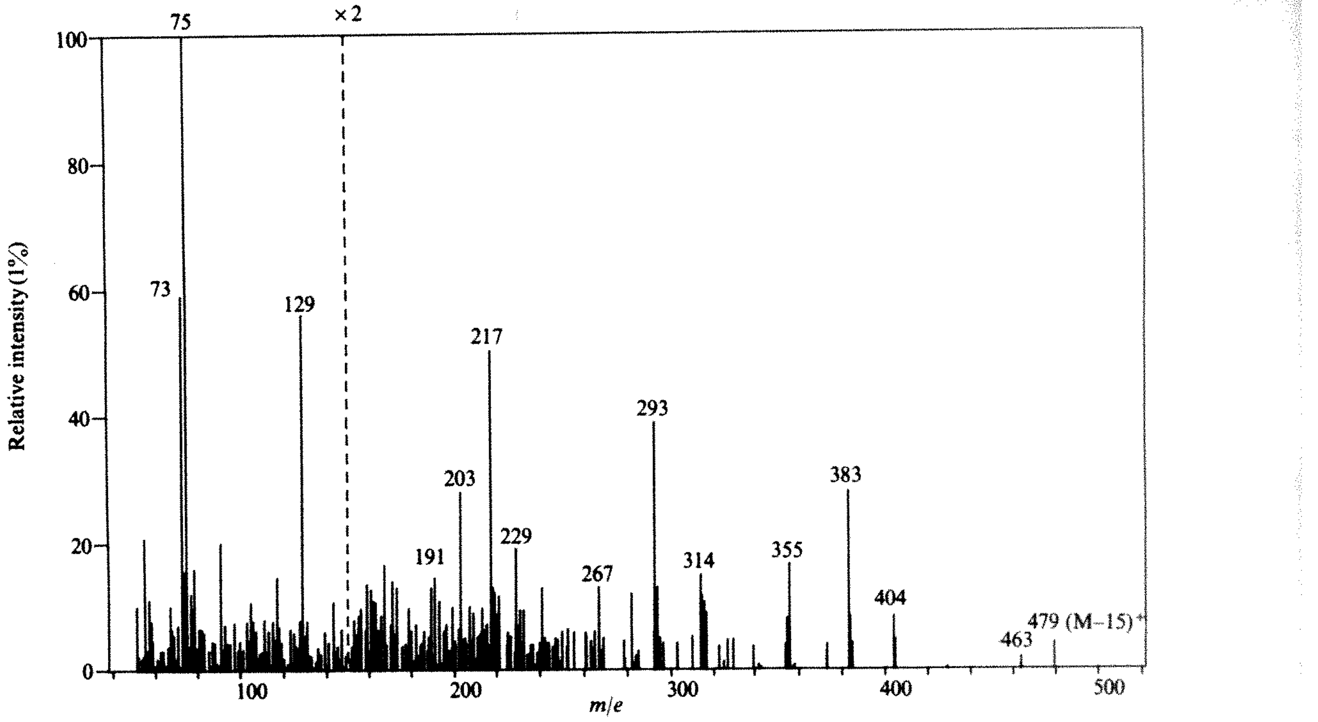

Fig. 2 Mass spectrum of the trimethylsilyl derivative of the methylester of leukotriene B obtained from rat peritoneal PMNs after incubation with A23187. The active fraction obtained from the HPLC column was methylated with diazomethane and further derivatized to the trimethylsilyl ether with bis (trimethylsilyl) trifluoroacetamide. The sample was chromatographed on a 20 m SE54 WCOT column coupled to a VG Micromass 16F mass spectrometer. Spectra were put on to a data system in the following conditions; electron energy 70 eV, trap current 180 μA and source temperature 240 °C. Peaks at *m/e* 281 and 355 represent bleed peaks from the column.

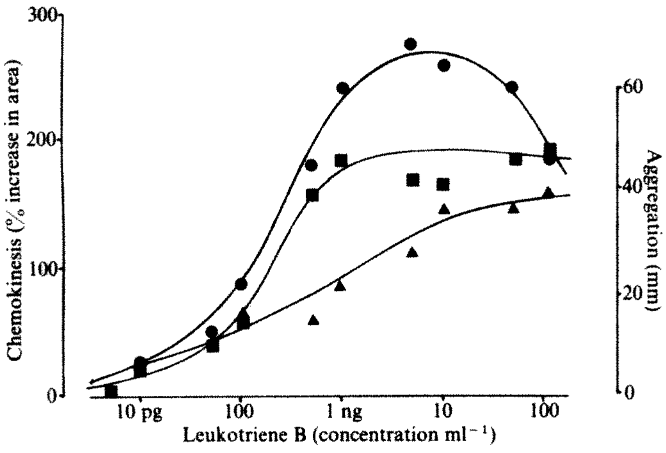

Fig. 3 The effects of leukotriene B on the chemokinesis of human PMNs (●) and the aggregation of rat (■) and human (▲) PMNs. Leukotriene B was prepared from 10^9 rat peritoneal PMNs incubated with calcium ionophore A23187 and was purified by ether extraction, silicic acid chromatography and HPLC and tested in aggregation and chemokinesis assays as described in Fig. 1 legend. The concentration of leukotriene B was determined using an $\varepsilon_{281}^{\mathrm{MeOH}}$ of 39,500 (ref. 6), 9 μg being recovered from 10^9 cells. Each point represents two separate experiments carried out on separate days ($n = 8$–16, standard errors were always $< 10\%$ of the mean).

Figure 3 shows the effects of leukotriene B on the chemokinesis of human PMNs and the aggregation of rat and human PMNs. Dose-related effects were seen over the range 10 pg ml^{-1} to 5 ng ml^{-1}, ED$_{50}$ values for human PMN chemokinesis, human PMN aggregation and rat PMN aggregation being 250, 560 and 170 pg ml^{-1}, respectively.

These results show that leukotriene B exhibits comparable activity on a molar basis to that observed for the complement peptide C5a and the synthetic peptide fMet-Leu-Phe. Furthermore, leukotriene B seems to be 100–1,000 times more active as a chemokinetic agent than the mono-HETEs[3,8] and in the present experiments no aggregating or chemokinetic activity was recovered in the fractions where the mono-HETEs would be expected to elute.

Release of lipoxygenase products, including leukotriene B, may be a common feature of exposure of PMNs to a variety of inflammatory stimuli[2,4]. Such release may be associated with the O_2 uptake, O_2^- production and stimulation of hexose monophosphate shunt activity that occur following exposure to such stimuli[9] and may also be involved in PMN degranulation[10]. The much greater potency of leukotriene B, compared with that reported for the mono-HETEs, suggests that the latter compounds are of less biological significance. It will be of some interest to study the role of leukotriene B *in vivo* with respect to the accumulation of inflammatory cells at sites of inflammatory and allergic reactions.

We thank the Arthritis and Rheumatism Council (M.A.B.), the Science Research Council (M.V.D.) and Lilly Research Ltd for financial support.

Received 29 February; accepted 29 April 1980.

1. Borgeat, P. & Samuelsson, B. *Proc. natn. Acad. Sci. U.S.A.* **76,** 2148–2152 (1979).
2. Stenson, W. I. & Parker, C. W. *J. clin. Invest.* **64,** 1457–1465 (1979).
3. Goetzl, E. J. & Sun, F. F. *J. exp. Med.* **150,** 406–411 (1979).
4. Goetzl, E. J., Weller, P. F. & Sun, F. F. *J. Immun.* **124**, 926–933 (1980).
5. Bray, M. A., Ford-Hutchinson, A. W., Shipley, M. E. & Smith, M. J. H. *Br. J. Pharmac.* (in the press).
6. Borgeat, P. & Samuelsson, B. *J. biol. Chem.* **254,** 7865–7869 (1979).
7. Borgeat, P. & Samuelsson, B. *J. biol. Chem.* **254,** 2643–2646 (1979).
8. Palmer, R. J., Stepney, R., Higgs, G. & Eakins, K. E. *Prostaglandins* (submitted).
9. Bokoch, G. M. & Reed, P. W. *Biochem. biophys. Res. Commun.* **90,** 481–487 (1979).
10. Smolen, J. & Weissman, G. *Advances in Prostaglandin and Thromboxane Research* (Raven, New York, in the press).
11. Smith, M. J. H. & Walker, J. R. *Br. J. Pharmac.* (in the press).
12. Cunningham, F. M., Shipley, M. E. & Smith, M. J. H. *J. Pharm. Pharmac.* **32,** 377 (1980).

Identification of an interferon in murine placentas

Arnold K. Fowler*, Carl D. Reed* & David J. Giron†

*Carcinogenesis Intramural Program, National Cancer Institute, Frederick Cancer Research Center, Frederick, Maryland 21701
†Department of Microbiology and Immunology, Wright State University, School of Medicine, Dayton, Ohio 45435

It is becoming increasingly apparent that interferon exerts a major role in cellular regulatory processes. Besides its well known antiviral properties[1], interferon has been shown to affect cell surface antigen expression[2,3], lymphoid cell function[4,5], as well as cellular protein synthesis[6,7] and growth[8-11]. To date, however, there is little information available on the mechanism of interferon production *in vivo* except in response to a variety of exogenously administered viral and nonviral systemic inducers. We report here the detection of a pregnancy-associated elevation of interferon, or an interferon-like component, in selected reproductive tissues of mice.

Ten-week-old virgin NIH Swiss mice, a random-bred strain, were killed at specific times after mating. Female mice were examined daily and mating was indicated by the appearance of a copulation plug and was referenced as day 1 of gestation. Mice were maintained on a 12 h light cycle at a temperature of 24 °C. Lab chow and water were available *ad libitum*. At autopsy the uteri were aseptically excised, carefully trimmed and the conceptuses removed. The conceptuses of individual mice were then pooled and after the 10-day stage dissected into placental and embryonic/fetal components. Earlier conceptuses (7-day stage) from individual mice were also pooled but were not dissected further. Immediately after removal, a 20% (w/v) homogenate of each specimen was prepared in phosphate-buffered saline (*p*H 7.2) and clarified for 30 min at 2,500*g*. Following storage at −76 °C the samples were defrosted and the level of antiviral activity was determined by the 50% plaque reduction (PR_{50}) method as described previously[12]; see legend to Fig. 1. The titre of antiviral activity is expressed as the reciprocal of the highest dilution that inhibited plaque formation by 50%. One unit of antiviral activity is equivalent to 0.5 NIH (G002-904-511) reference units.

Preliminary studies showed the presence of an antiviral activity in mouse placental extracts. Biological and biophysical characterization of this activity as an interferon was determined by its protection of L-cell cultures against the cytopathic effects (CPE) of MM virus and is summarized in Table 1. The antiviral activity was sensitive to treatment with trypsin, actinomycin D, and heat and was neutralized by anti-interferon γ globulin. Also, it was not inactivated by low *p*H treatment (at *p*H 2) and was not removed by high speed centrifugation. By these criteria, the placental component exhibits the properties of virally induced, Type 1, interferon[13,14]. It seems highly unlikely that the inhibition of CPE resulted from a nonspecific mechanism, such as an interference of virus attachment to the target L-cells by the tissue extracts, as the antiviral activity of the placental component requires a transcriptional event (sensitive to actinomycin D) and furthermore, is neutralized by specific anti-interferon γ globulin.

The interferon levels of uterine, placental and fetal tissues at various stages of gestation are shown in Fig. 1. As may be noted, interferon was detected in most uterine samples between 10–15 days of gestation; however, specimens taken before and after this interval of pregnancy, as well as from virgin mice ($n = 3$, data not shown), had no detectible titre (< 10 units ml^{-1}). This transient appearance of interferon in the gravid uterus developed abruptly and was highest at the 13-day stage (300 units ml^{-1}). By comparison, interferon was found in all placental samples examined, and its level increased significantly during pregnancy. This increase was most dramatic between 10- and 13-day stages (8-fold) but continued until the 17-day stage. Subsequently, the interferon level generally plateaued at approximately 2,000 units ml^{-1} until term. In other data not shown, the mean interferon level of 7-day old conceptuses from three individual mice was found to be essentially the same as 10-day placentas (110 as compared to 120 units ml^{-1}) and approximately 3-fold greater than 10-day fetuses (33 units ml^{-1}; right panel). Note that no fetal specimen had an interferon level greater than 80 units ml^{-1} and further, that interferon-positive fetal samples were clustered around the 10-day stage, a stage at which contamination by extra-embryonic tissues is difficult to avoid. After this stage only one out of 6 fetal samples had a detectable interferon level.

These results clearly demonstrate a progressive increase in the level of interferon in the mouse placenta during gestation. Significant levels were detected in this organ as early as 10 days after mating, and most likely, the interferon detected in the 7-day conceptus was largely of placental origin. In contrast, little if any interferon was found in embryonic/fetal tissues. This observation is consistent with earlier reports that the placenta forms an effective barrier limiting migration of interferon into fetal circulation[15,16]. Although a decrease in the efficacy of the placental barrier to interferon migration has been reported in the pregnant rat near term[17], we have found no evidence of transplacental transfer of interferon into mouse fetuses in late gestation. This discrepancy may be attributed either to species differences or to the stage of gestation as we have not examined fetuses beyond the 18-day stage. The presence of an interferon antagonist in mouse embryos[18] may also contribute to the apparently low levels of interferon in the embryo.

The significance of the transitory appearance of interferon in the uterus is more difficult to interpret. Although the level of interferon seems to be sufficiently elevated to indicate an active production or an accumulation process, we have not ruled out the possibility that uterine contamination by placental material

Table 1 Characterization of antiviral activity as interferon*

Treatment†	24 h CPE‡
None	0
*p*H 2.0	0
Ultracentrifugation	0
Trypsin	4†
Actinomycin D	4†
Heat	4†
Anti-IF γ globulin	4†
Virus control	4†
Cells controls§	0

*Placental extract containing 3,000 PR_{50} units of antiviral activity diluted 1:10 in Dulbecco's MEM was used. A 1:100 dilution of this sample completely protected L-cell cultures against the cytopathic effects (CPE) of MM virus.

†*p*H adjusted to 2.0 with 1 M HCl; after 24 h at 4 °C, *p*H adjusted to 7.0 with 1 M NaOH. Ultracentrifugation, Sample centrifuged at 100,000*g* for 2 h; supernatant fluid collected and assayed for antiviral activity. Trypsin, 0.25% trypsin for 30 min at 37 °C. Actinomycin D, L-cell monolayer cultures were treated with Actinomycin D (0.5 µg ml^{-1}) for 1 h before assay of the sample for antiviral activity. Heat, The sample was incubated at 56 °C for 4 h. Anti-interferon γ globulin: The sample was incubated with an equal volume of anti-IF γ globulin (30) for 30 min at 37 °C.

‡L-cell monolayer cultures were treated in duplicate for 4 h with each preparation. All the cultures, with the exception of cell controls, were then challenged with MM virus (about 10 p.f.u. per cell) and scored for CPE 24 h later. 0 = No CPE; 4+ = 100% CPE.

§Each preparation had its own cell control which was treated identically to the test sample but was not infected. Cell controls were all CPE negative.

0028-0836/80/290266-02$01.00

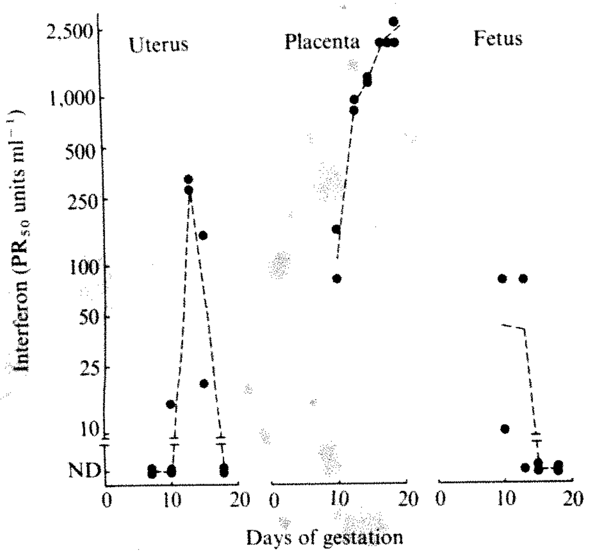

Fig. 1 Interferon levels of uterine, placental, and fetal tissues from NIH Swiss mice at various stages of gestation. For assay, twofold dilutions of each sample were made in Dulbecco's minimal essential medium supplemented with 10% fetal calf serum. Each dilution was added to duplicate monolayer cultures of L929 cells. After 18 h at 37 °C, the cultures were washed and challenged with approximately 100 plaque forming units (p.f.u.) of encephalomyocarditis virus (strain MM) and incubated for 48 h. The cultures were then stained and the plaques counted. Each point represents the antiviral activity of the tissue from an individual pregnant mouse.

is the source of the observed interferon. However, of the three explanations, the last seems least probable since a contamination of major proportion (>33%) would be necessary to account for uterine interferon level at the 13-day stage (300 units ml^{-1}). On the other hand, the production or accumulation of interferon in the gravid uterus, specifically between 10 and 15 days of gestation, would suggest stringent regulation.

The inductive event(s) of interferon production in the pregnant mouse and the mechanism of its concentration in the placenta are not known; however, studies in progress indicate that the maximum level of placental interferon in mice is under genetic control. We have not so far detected interferon in the serum (<10 units ml^{-1}) of either virgin or pregnant NIH Swiss mice. Whereas this may be interpreted as evidence favouring the *de novo* synthesis of interferon by the placenta, it does not preclude the possibility that this organ possesses an extraordinary capacity to concentrate interferon from maternal systemic pools. In the latter situation, induction by chronic parasitic infections in the mouse population could provide such a source of interferon. In our experiments, however, we have also examined tissues from specific pathogen-free NIH Swiss mice and in all cases, placental interferon levels of barrier-maintained mice were similar to mice housed in our conventional facility.

The demonstration that interferon accumulates in mouse placenta is interesting from several points of view. The placenta is an organ which occupies the intermediate zone between the maternal and fetal organisms. It is an organ of protective, endocrine, and immunological functions and is considered intricately involved in fetal acceptance[19]. Although a role for interferon in any of these events is conjectural, this class of glycoproteins exhibit numerous biological properties that are compatible with those of successful gestation. In addition to its viral prophylactic activity, interferon influences a variety of other physiological processes ranging from cell surface and growth control to immunoregulation. In this regard it is particularly noteworthy that prolongation of graft survival across H-2 barriers results with systemic interferon inducers[20,21], as well as with the direct administration of interferon[21–23]. Likewise, cell-mediated immunity in both graft-versus-host[24] and delayed-type hypersensitivity[25,26] reactions was reduced by interferon treatment. These results and the findings that interferon also inhibits DNA synthesis induced in mouse lymphocytes *in vitro* by mitogens and allogeneic cells[27–29] suggest a possible involvement of interferon in the immunoregulation of fetal acceptance. As we have also detected an antiviral activity in a human term placenta, the presence of interferon in this organ may not be unique to the murine species.

Received 26 November 1979; accepted 18 April 1980.

1. Isaacs, A. & Lindenmann, J. *Proc. R. Soc.* **B147,** 258–267 (1957).
2. Lindahl, P., Leary, P. & Gresser, I. *Proc. natn. Acad. Sci. U.S.A.* **70,** 2785–2788 (1973).
3. Lindahl, P., Gresser, I., Leary, P. & Tovey, M. *Proc natn. Acad. Sci. U.S.A.* **73,** 1284–1287 (1976).
4. Johnson, H. M. & Baron, S. *CRC Critical Reviews in Biochemistry* **4,** 203–227 (1976).
5. Johnson, H. M. & Baron, S. *Pharmac. Ther.* **A 1,** 349–367 (1977).
6. Brouty-Boye, D., Macieira-Coelho, A., Fiszman, M. & Gresser, I. *Int. J. Cancer* **12,** 250–258 (1973).
7. Fuse, A. & Kuwata, T. *J. gen. Virol.* **33,** 17–24 (1976).
8. Paucker, K., Cantell, K. & Henle, W. *Virology* **17,** 324–334, 1962.
9. Gresser, I. *et al. Proc. Soc. exp. Biol. Med.* **142,** 7–10 (1973).
10. Dahl, H. & Degré, M. *Acta path. microbiol. scand.* **84,** 285–292 (1976).
11. Stewart II, W. E., Gresser, I., Tovey, M. G., Bandu, M.-T. & LeGoff, S. *Nature* **262,** 300–302 (1976).
12. Giron, D. J., Allen, P. T., Pindak, F. F. & Schmidt, J. *Appl. Microbiol.* **21,** 387–393 (1971).
13. Giron, D. *Appl. Microbiol.* **18,** 584–588 (1969).
14. Youngner, J. S. & Salvin, S. B. *J. Immun.* **111,** 1914–1922 (1973).
15. Ho, M., Postic, B. & Yang, H. Ke. in *The Systemic Induction of IF*, in: *CIBA Foundation Symposium on IF* (eds Wolstenholme, G. E. W. *et al.*) 19–35 (Churchill, London, 1967).
16. Overall Jr., J. C. & Glasgoio, L. A. *Science* **167,** 1139–1141 (1970).
17. Mendelson, J., Kapusta, R. & Dick, V. *Am. J. Obstet. Gynec.* **107,** 902–907 (1970).
18. Cembrzynska-Nowak, M. *Archs Immun. Ther. Exp.* **25,** 663–668 (1977).
19. Jones, B. M. & Kemp, R. B. *Nature* **221,** 829–831 (1969).
20. Mobraaten, L. E., DeMaeyer, E. & DeMaeyer-Guignard, J. *Transplantation* **16,** 415–420 (1973).
21. Cerottini, J.-C., Brunner, K. T., Lindahl, P. & Gresser, I. *Nature new Biol.* **242,** 152–153 (1973).
22. DeMaeyer, E., Mobraaten, L. & DeMaeyer-Guignard, J. *C. r. hebd. Séanc. Acad. Sci., Paris* **277,** 2101–2103 (1973).
23. Hirsch, M. S., Ellis, D. A., Black, P. H., Monaco, A. P. & Wood, M. L. *Transplantation* **17,** 234–236 (1974).
24. Hirsch, M. S., Ellis, D. A., Proffitt, M. R. & Black, P. H. *Nature new Biol.* **244,** 102–103 (1973).
25. DeMaeyer-Guignard, J., Cachard, A. & DeMaeyer, E. *Science* **190,** 574–576 (1975).
26. DeMaeyer, E., DeMaeyer-Guignard, J. & Vandeputte, M. *Proc. natn. Acad. Sci. U.S.A.* **72,** 1753–1757 (1975).
27. Lindahl-Magnusson, P., Leary, P. & Gresser, I. *Nature new Biol.* **237,** 120–121 (1972).
28. Rozee, K. R., Lee, S. H. S. & Ngan, J. *Nature new Biol.* **245,** 16–18 (1973).
29. Heron, I., Berg, K. & Cantell, K. *J. Immun.* **117,** 1370–1373 (1976).
30. Giron, D. J., Liu, R. Y., Hemphill, F. E., Pindak, F. F. & Schmidt, J. P. *Proc. Soc. exp. Biol. Med.* **163,** 146–150 (1980).

Detection of a cell-surface antigen correlated with organ-specific metastasis

P. J. Shearman, W. M. Gallatin & B. M. Longenecker

Department of Immunology, University of Alberta, Edmonton, Alberta, Canada T6G 2H7

Despite the fact that tumour cells with the potential for metastasis may circulate randomly, many demonstrate a preference for specific organs. Recently, several investigators have selected variant tumour cell lines with enhanced capacity to metastasize to specific organs, mainly using the spontaneously originating B16 melanoma cell line of the mouse and tumour variants with enhanced capacity to metastasize to the lungs[1], brain[2] and liver[3]. We previously reported[4,5] the derivation of a liver-specific metastatic variant of a Marek's disease (MD) virus-transformed, non-producer[4,6] lymphoma cell line. MD is a naturally occurring, herpes virus-induced, T-cell lymphoma of chickens which bears pathological and aetiological similarities to Burkitt's lymphoma in man. This makes MD a useful model for study[7]. One similarity is the pattern of metastasis in which both lymphomas induce a high incidence of ovarian and liver lesions[8,9]. We now report the existence of a cell-surface antigen, detectable by a monoclonal antibody, correlated with organ-specific metastasis.

To quantify liver-specific metastasis in our system, we inject tumour cells intravenously into day 11 chick embryos and enumerate metastatic liver foci which form during 6 days of further incubation[4]. MDCC-AL2, a cell line which has been selected for liver-specific metastasis, forms many more embryonic liver foci than MDCC-RP1 or MDCC-AL1, lines not selected for organ-specific metastasis, or MDCC-AL3, selected for metastasis to the ovary[4]. Following the same *in ovo* procedure, cell lines which have been selected for increased virulence (RP1 < AL1 < AL2 < AL3) form increasingly more tumour foci on the chorioallantoic membrane (CAM) of the chick embryo. As these embryo assays are sensitive and convenient, we used them in inhibition assays to attempt to detect specific cell-surface antigens expressed on our liver-metastasizing, variant cell line, AL2.

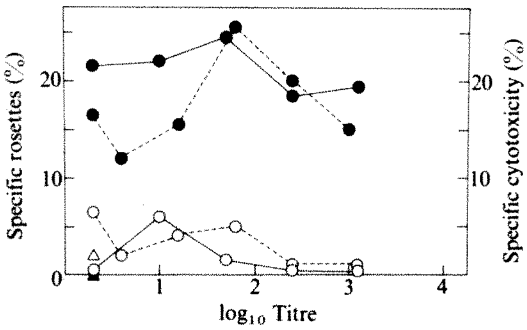

Fig. 1 Indirect rosettes (solid lines) were formed by incubating dilutions of hybridoma 1.20 culture supernatant with MDCC-AL2 cells (●) or MDCC-AL3 cells (○) for 60 min at 4 °C. After three washes in culture medium, chicken red blood cells with rabbit anti-mouse immunoglobulin antiserum (Cappel) coupled to their surfaces by a modified 1-ethyl-3-(3-dimethylaminopropyl) carbodiimide (Sigma) technique were added at a 10:1 red cell-to-target cell ratio and incubated for 180 min at 4 °C. Specific rosettes were calculated by subtracting background rosettes formed without culture supernatant. Complement-mediated cytotoxicity (broken lines) was accomplished by incubating RP1 (▲), AL1 (△), AL2 (●) or AL3 (○) cells with dilutions of hybridoma 1.20 culture supernatant and guinea pig complement for 45 min at 37 °C. The cells were washed once in culture medium and cytotoxicity determined by dye exclusion. Specific cytotoxicity (broken lines) was calculated by subtracting cytotoxicity due to complement alone. In both assays, each point represents the average of two determinations.

For the generation of anti-tumour cell hybridomas, five CBA/J mice were injected intravenously with 10^8 AL2 cells. Three days later the spleen cells from the mice were pooled and fused with 315.43 myeloma cells as described previously[10]. Hybrid clones exhibiting positive direct or indirect agglutination activity in their culture supernatants against AL2 cells were picked and grown for further analysis. Sixteen clones proved to be stable and antibody-producers. Of these, nine clones seemed to detect chicken major histocompatibility complex (MHC, B locus) antigens. Only one clone produced antibody which reacted with all types of chicken cells tested, normal and malignant, and was considered to be anti-chicken panspecific. One clone produced antibody reacting with all lymphocytes tested regardless of MHC type. Four clones produced antibody which reacted with RP1, AL1, AL2, AL3 and another MD-derived lymphoma cell line, MDCC-MSB1, but which did not react with normal lymphocytes or erythrocytes. One clone, 1.20, produced antibody which reacted specifically with AL2 cells (Fig. 1) and showed little or no reactivity against chicken red or white blood cells of various genotypes, or tumour cells of the other MD-tumour cell lines.

To test whether the 1.20 antigen might be associated with specific liver metastasis, we measured the capacity of 1.20 antibody to inhibit liver foci induced by AL2 cells in the *in ovo* assay[4]. It was found that preincubation of AL2 cells with 1.20 monoclonal antibodies (Table 1) specifically blocks the ability of AL2 cells to colonize the embryonic liver without affecting the ability of the same cells to produce CAM foci. In contrast, CH-4 monoclonal antibodies which detect a chicken MHC antigen[10] not found on AL2 cells, or 1.24 monoclonal antibodies which detect a public MHC antigen common to all MDCC-RP1-derived cell lines tested, inhibited neither CAM nor liver foci. To test another monoclonal antibody binding to AL2 cells, the capacity of 1.20 antibodies to inhibit liver foci was compared with that of 1.5 monoclonal antibodies, similar in specificity to 1.24 antibodies. This test (Table 2) was done with or without the prior complement-mediated killing of AL2 cells. Hybridoma 1.20 but not 1.5 monoclonal antibodies significantly inhibited the development of liver foci in the presence of complement. It is noteworthy that 1.5 monoclonal antibodies, which directly agglutinate the AL2 cells, caused a significant enhancement in the number of CAM foci induced by AL2 cells, suggesting that large emboli of tumour cells might be nonspecifically trapped in the CAM. In the same conditions, however, 1.5 monoclonal antibodies did not cause a significant enhancement in liver foci; this is consistent with our previous observations[4] which suggest that homing of AL2 cells to the embryonic liver is a specific process and not simply a nonspecific trapping of emboli of tumour cells. The fact that 1.5 monoclonal antibodies caused a slight, but not significant, reduction in the number of liver foci suggests that at least a few of the liver focus-forming cells may have been trapped within cell aggregates. As different classes of mouse antibody may affect the homing of metastatic tumour cells differentially, we have standardized the class of antibody used. All the monoclonal antibodies used in our studies are IgM (unpublished data). This is in keeping with our previous observations[10] which show that the mouse preferentially responds to chicken MHC antigens with antibodies of the IgM class in the same conditions with which the hybridomas were produced for the present study.

Two different *in vitro* assays, indirect rosette formation and complement-mediated cytotoxicity, were used to verify the specificity of 1.20-derived monoclonal antibodies. Both of these assays showed that approximately 20% of AL2 cells have detectable cell-surface antigen (Fig. 1). AL3 cells demonstrated a small but significant number of 1.20 antigen-positive cells.

To determine if the frequency of 1.20 antigen expression in a cell line correlates with the degree of liver metastasis exhibited by the cell line, we derived limiting dilution clones of metastatic variants AL2 and AL3. Six clones were isolated from AL2 and four from AL3. All 10 clones are non-producers for virus, tested as for the parent cell lines (data not

Table 1 Specific inhibition of liver metastasis by monoclonal antibody

Monoclonal antibody added	CAM foci	Liver foci
None	60 ± 17 (8)	63 ± 11 (8)
CH-4	59 ± 16 (8)	78 ± 21 (5)
1.20	61 ± 11 (7)	32 ± 10 (9)
1.24	68 ± 17 (10)	56 ± 6 (8)

Assays for chorioallantoic membrane (CAM) and embryonic liver foci were performed as described previously[4]. For CAM foci, 1×10^3 MDCC-AL2 cells were injected intravenously per embryo, and for liver foci, 3×10^4 AL2 cells were used. Before injection, cells were left untreated or preincubated for 30 min with ascites antibodies from hybridomas CH-4, 1.20 or 1.24 at a final dilution of 1:100. Results are expressed as means ± s.d. with number of embryos per group in parentheses. Statistically significant differences were obtained in comparing results in liver foci for 1.20 with controls ($P < 0.001$); 1.20 with CH-4 ($P < 0.01$) and 1.20 with 1.24 ($P < 0.001$).

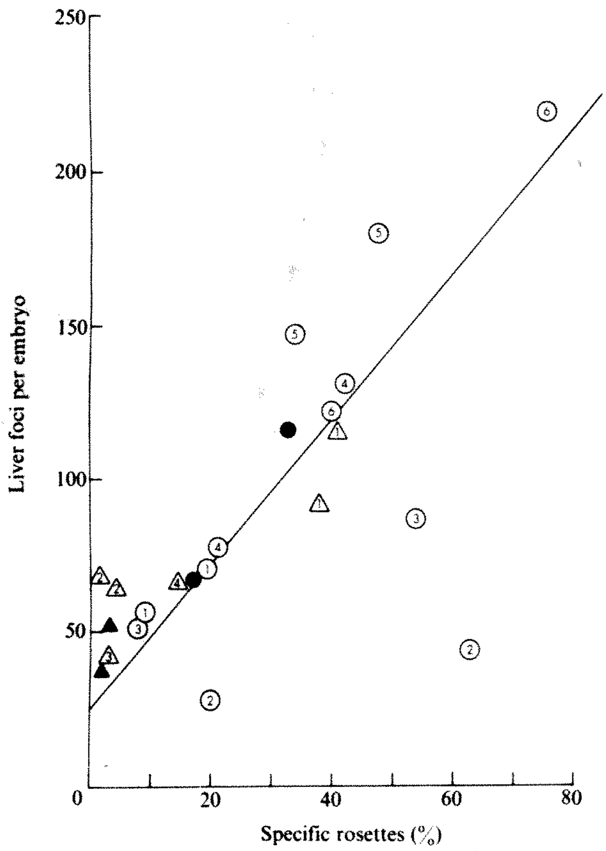

Fig. 2 The cell lines MDCC-AL2 (●) plus six limiting dilution clones (numbers in circle) and MDCC-AL3 (▲) plus four clones (numbers in triangles) were tested for 1.20 antigen frequency by the indirect rosette assay and for liver metastatic ability by the liver focus-forming assay[4] on two occasions. Indirect rosettes were formed as described in Fig. 1 using a 1.20 antibody dilution of 1:100. A cell dose of 3×10^5 cells per embryo was used in the liver focus-forming assay. Paired values of 1.20 antigen frequency and average number of liver foci per embryo are plotted for each cell line and clone. These values demonstrate a correlation coefficient of 0.70 ($P < 0.001$).

Table 2 Specific inhibition of liver metastasis by monoclonal antibody plus complement

Monoclonal antibody added	CAM foci	Liver foci
None	70 ± 51 (5)	88 ± 14 (6)
C′	60 ± 38 (7)	75 ± 11 (6)
1.20	115 ± 33 (7)	62 ± 23 (7)
1.20 + C′	93 ± 15 (7)	34 ± 12 (8)
1.5	184 ± 58 (7)	76 ± 11 (8)
1.5 + C′	86 ± 29 (6)	63 ± 9 (8)

Assays for CAM and embryonic liver foci were performed as described previously[4]. Before injection, AL2 cells were incubated for 45 min at 37 °C with the culture supernatants (full strength) from hybridomas 1.20 or 1.5 in the presence or absence of guinea pig complement (C′). The cells were washed and the cell concentrations were readjusted so that 1×10^3 viable AL2 cells were injected per embryo for CAM foci and 1×10^5 viable AL2 cells were injected per embryo for embryonic liver foci. 1.20 plus complement killed ~20% of AL2 cells and 1.5 plus complement killed ~40% of AL2 cells at the concentrations used. Results are expressed as means ± s.d. with number of embryos per group in parentheses. Statistically significant differences were obtained in comparing results in CAM foci for control or 1.5+C′ with 1.5 alone ($P < 0.01$); also for results in liver foci for C′ or 1.5+C′ with 1.20+C′ ($P < 0.001$); 1.20 and 1.20+C′ ($P < 0.02$); Control and 1.20 ($P < 0.03$).

shown)[4,6,11]. According to the work of Fidler and co-workers[12], these clones should vary in their metastatic ability and possibly their antigenic profile. We tested each clone as well as the parent cell lines on two occasions for both indirect rosette-forming cells and liver focus-forming ability. Cell line AL2 and its clones ranged from 8 to 75% in frequency of 1.20 antigen-positive cells. AL3 and its clones ranged from 1 to 41%. For the liver focus assay, we injected a relatively large number of cells to allow maximal precision of the assay. The paired observations are plotted in Fig. 2 and show that the number of liver foci formed by a clone is directly proportional to the number of 1.20 antigen-positive cells in that clone ($r = 0.70$, $P < 0.001$). Clone AL3.1 demonstrates a high frequency of 1.20 antigen-positive cells and showed high liver metastatic ability on both occasions. In contrast, all the other AL3-derived clones have a low value for each of these parameters as does the uncloned parental line AL3. Note that there is some day-to-day variation in 1.20 antigen expression and liver focus-forming ability, although successive assays correlate very highly. Thus, although correlated and possibly associated in a functional sense, the parameters of antigen expression and metastasis may vary in the strength of the correlation between them for a given clone. This is not unexpected as metastasis is a complex series of events only one of which involves specific organ recognition. Kerbel[13] has reported that random cloning produces unstable metastatic variants in contrast to the work of Fidler[12]. Stable metastatic variants were produced only after treatment with mutagens and lectins[13]. In our studies, we have found a strong and relatively stable correlation between 1.20 antigen expression and liver metastasis. This strengthens the argument in conjunction with the 1.20 antibody-mediated inhibition of liver metastases that the 1.20 antigen is involved in determining liver-specific metastasis.

Thus, we have described the existence of a cell-surface antigen, detectable by a monoclonal antibody which is correlated with specific liver metastasis of a lymphoma cell line. Cell populations with a low capacity to form liver foci have a low expression of the 1.20 antigen specificity and cell populations with a high capacity to form liver foci have a high level of 1.20 antigen expression. Monoclonal antibodies directed against the 1.20 antigen inhibit specific liver metastasis by AL2 cells but do not inhibit CAM lesions, which is a measure of the invasiveness of the cell line[4]. Our working hypothesis is that the 1.20 antigen has a functional role in the interaction of a blood-borne, metastasizing tumour cell with the target organ, the liver. The metastatic process is a complex series of events[12] and our results with clone AL3.1 have shown that 1.20 antigen expression is a necessary but not a sufficient condition in the determination of successful liver metastases.

This work was supported by the NCI and MRC of Canada. B.M.L. is a Research Associate and W.M.G. is a Research Student of the NCI of Canada.

Received 4 December 1979; accepted 21 April 1980.

1. Fidler, I. J. *Nature new Biol.* **242,** 148–149 (1973).
2. Nicolson, G. L. & Brunson, K. W. *Gann* **20,** 15–24 (1978).
3. Tao, T., Matler, A., Vogel, K. & Burger, MM. *Int. J. Cancer* **23,** 854–857 (1979).
4. Shearman, P. J. & Longenecker, B. M. *Int. J. Cancer* **25,** 363–369 (1980).
5. Report of the Ad hoc Committee on Avian Cell Line and Transplantable Tumour Nomenclature *Avian Path.* **8,** 487–498 (1979).
6. Nazerian, K. *et al. Avian Dis.* **21,** 69–76 (1976).
7. Klein, G. in *Oncogenesis and Herpesvirus* (eds Briggs, P. M., de Thé, G. & Payne, L. N.) 501–515 (IARC, Lyons, 1972).
8. Payne, L. N. in *Oncogenesis and Herpesvirus* (eds. Briggs, P. M., de Thé, G. & Payne, L. N.) 21–37 (IARC, Lyons, 1972).
9. Wright, D. H. in *Oncogenesis and Herpesvirus* (eds Briggs, P. M., de Thé, G. & Payne, L. N.) 217–229 (IARC, Lyons, 1972).
10. Longenecker, B. M., Mosmann, T. R. & Shiozawa, C. *Immunogenetics* **9,** 137–148 (1979).
11. Longenecker, B. M., Pazderka, F., Stone, H. S., Gavora, J. D. & Ruth, R. F. *Infect. Immun.* **11,** 922–931 (1975).
12. Fidler, I. J., Gerstein, D. M. & Hart, I. R. *Adv. Cancer Res.* **28,** 149–250 (1978).
13. Kerbel, R. S. *Am. J. Path.* **97,** 609–622 (1979).

T-cell hybridoma bearing heavy chain variable region determinants producing (T,G)-A--L-specific helper factor

Zelig Eshhar, Ron N. Apte, Ilana Löwy, Yinon Ben-Neriah, David Givol & Edna Mozes

Department of Chemical Immunology, The Weizmann Institute of Science, Rehovot, Israel

Thymus-derived lymphocytes (T cells) exert their regulatory effect (help or suppression) on the antibody production by B cells either by direct cell to cell interaction or by soluble mediators or factors[1,2]. The low frequency of specific T cells, the heterogeneity of their responses and their relatively short life span have hampered the molecular characterization of the antigen recognition unit of T cells, and its structure is largely unknown. The lymphocyte hybridization technique, which has been found very useful for the production of B-cell hybridomas secreting specific monoclonal antibodies[3], has also been used for the generation of homogeneous and stable T-cell hybridomas with unlimited growth potential[4,5]. So far the only specific effector function demonstrated in the established T hybridomas is the property to generate a factor(s) which suppresses antibody responses[6-8]. We now describe the establishment of hybrid lines which exhibit characteristic T-cell markers. One of the hybridomas (denoted R-9) releases into the culture supernatant factor(s) with helper activity specific to the synthetic polypeptide (T,G)-A--L and bears surface determinants of the immunoglobulin heavy chain variable region (V_H). Such hybrid cell lines are of great value for studies on the nature of the T-cell receptor.

Cell fusion was carried out essentially as described previously[9], using 41% polyethylene glycol 1500 (PEG) as fusing agent (Table 1). The AKR/J thymoma line BW5147, which lacks the enzyme hypoxanthine guanine phosphoribosyl transferase (derived by Dr R. Hyman), was fused with an enriched population of activated T cells. Activation of T cells to (T,G)-A--L was carried out by the transfer of thymocytes from C3H.SW ($H-2^b$) mice into irradiated (750 R) syngeneic recipients together with 10 μg of (T,G)-A--L (ref. 10). One week after transfer and 24 h before hybridization, 'educated' T cells from the spleens of the recipient mice were cultured on monolayers of (T,G)-A--L-bearing splenic adherent cells. This procedure augments the helper activity of (T,G)-A--L educated cells (R.N.A. and E.M., unpublished). After hybridization, cell suspensions were distributed into 24-well culture plates (Costar) and selected for 3 weeks in medium containing hypoxanthine, aminopterin and thymidine (HAT). Hybrid populations were grown in Dulbecco's modified Eagle's medium (DMEM) containing 15% horse serum (DMEM-HS). One month after fusion, 21 individual hybridoma cultures had been established.

The hybrids were screened for the presence of T-cell surface markers, immunoglobulin constant and variable (V_H and V_L) determinants[11] and (T,G)-A--L-specific biological activity. Most of the hybrid lines expressed the Thy 1.1 and Thy 1.2 alleles (originated from the parental BW5147 and C3H.SW lymphocytes, respectively). None of the hybridomas reacted with anti-V_L or anti-Ig antibodies, whereas 5 out of the 21 lines reacted with anti-V_H antibodies. Three of the V_H-positive hybrid lines—R-9, R-11 and R-17—affected the antibody response to (T,G)-A--L. R-11 demonstrated suppressive activity which will be described elsewhere. Here we present the characteristics of the R-9 hybrid line which exhibits antigen-specific helper activity.

Detailed analysis of the surface antigens (double immunofluorescence staining) and karyotype of R-9 hybridoma are shown in Table 1. The hybrid nature is indicated by the average chromosome number (65), which is higher than diploid (40), and by the expression of the H-2 and Thy-1 alloantigens of both parental strains on R-9 cells. Cytotoxicity assays using anti-Lyt reagents and rabbit complement resulted in 40% lysis of the R-9 cells with anti-Lyt-1.1, whereas no lysis was observed following treatment with anti-Lyt-2.1. Hybrids were not analysed for the Lyt-3.2 marker. The presence of immunoglobulin variable-region determinants was detected by using the $F(ab')_2$ of specifically purified rabbit antibodies against isolated V_H and V_L fragments derived from M-315 myeloma protein[11]. Most of the R-9 cells did express V_H determinants whereas neither BW5147 cells nor R-19 (another hybrid line derived from the same fusion) reacted with anti-V_H antibodies. The distribution of stained cells was further analysed by the fluorescence-activated cell sorter (FACS-II) as depicted in Fig. 1. Whereas R-9 cells were labelled with anti-V_H antibodies in a manner which suggests a homogeneous population of the stained cells, they failed to react with either anti-V_L or anti-Ig antibodies. Computer analysis of the relative cell number stained with anti-V_H indicated that 70–85% of R-9 cells were positively labelled. BW5147 cells were not stained by either anti-V_H or anti-V_L antibodies (Fig. 1).

The antigen-specific activity of the hybrid lines was evaluated by their ability to produce a factor(s) with helper activity in the (T,G)-A--L-specific antibody response. Supernatants from 48–72-h cultures (containing $1-2 \times 10^6$ hybrid cells per ml) were injected together with (T,G)-A--L and 2×10^7 primed B cells into irradiated syngeneic recipients. Mice were bled 10–14 days later and (T,G)-A--L-specific antibodies in their sera were determined as shown in Table 2. Supernatants from R-9 and R-17 hybridomas induced anti-(T,G)-A--L responses when transferred together with T-cell-depleted primed spleen cells and (T,G)-A--L. Such activity was not manifested by supernatants of BW5147 cells and 19 other hybridomas of which R-19 is a representative. The degree of help provided by the active supernatants was not as high as with the T cells in the unfractionated primed spleen cells, but it was comparable to that of 5×10^6 (T,G)-A--L-activated T

Table 1 Cell-surface markers and karyotype analysis of T hybridomas

Antisera or antibodies	BW5147	R-9	R-19
		% Stained cells	
Anti-Thy 1.1 (1:100)	>95	>95	>95
Anti-Thy 1.2 (1:100)	<5	>90	85
Anti-$H-2^k$ (1:20)	>95	>95	>95
Anti-$H-2^b$ (1:20)	<5	>95	>95
Anti-Ig (0.5 mg ml^{-1})	<5	<5	<5
Anti-V_H (0.3 mg ml^{-1})	<10	82	<10
Anti-$V_L(\lambda)$ (0.3 mg ml^{-1})	<5	<10	<5
Anti-$V_L(\kappa)$ (0.3 mg ml^{-1})	<5	<5	<5
Karyotype*	41(40–45)	65(60–72)	65(59–75)

Fusion was carried out by the addition of 41% PEG 1500 in serum-free DMEM to a cell pellet of 36×10^6 enriched activated T cells from C3H.SW mice ($H-2^b$, Thy 1.2, Lyt 1.1, Lyt 2.1, Lyt 3.2) and 10×10^6 AKR/J BW5147 thymoma. After 2 min at 37 °C, PEG was gradually diluted with serum-free DMEM and after centrifugation the cells were suspended in DMEM-HS to a concentration of 10^5 viable BW cells per ml. Aliquots (1 ml) were distributed into each well of 24-well culture plates. Medium containing HAT was added the next day and cultures were fed each third day with fresh HAT medium. The % of stained cells was analysed by indirect immunofluorescence using fluorescein-conjugated (FITC) rabbit antibodies against mouse IgG (Miles-Yeda) that were intensively absorbed with mouse T-cell lines and thymocytes for the detection of the murine alloantisera. FITC coupled to $F(ab')_2$ of goat anti-rabbit IgG was used for the detection of the rabbit antibodies against the murine variable region (V_H and V_L) and whole immunoglobulins (Ig). Anti-Thy 1.2 and anti-Thy 1.1 are monoclonal antibodies. Anti-$H-2^k$ antiserum was obtained by the immunization of C3H.SW mice with C3H/DiSn lymphocytes and for the production of anti-$H-2^b$ antiserum C3H/DiSn lymphocytes and for the production of anti-

*Chromosome number was detected 8 months after fusion. In each determination 10 mitotic cells were counted. The range of chromosome number is given in parentheses.

0028-0836/80/290270-03$01.00

Table 2 (T,G)-A--L-specific helper activity of culture supernatants of T hybridoma R-9

Cells and supernatants transferred into irradiated recipients	Expt 1	Expt 2	Expt 3
	Antibody response to (T,G)-A--L (c.p.m.)		
2×10^7 (T,G)-A--L-primed spleen cells	12,185	9,777	13,562
2×10^7 (T,G)-A--L-primed B cells*	1,880	2,029	754
2×10^7 (T,G)-A--L-primed B cells + 5×10^6 (T,G)-A--L 'educated' T cells†	4,947	4,370	5,163
2×10^7 (T,G)-A--L-primed B cells + supernatant of BW5147	2,671	1,659	NT
2×10^7 (T,G)-A--L-primed B cells + supernatant of line R-19‡	NT	NT	1,508
2×10^7 (T,G)-A--L-primed B cells + supernatant of line R-17‡	5,125	NT	NT
2×10^7 (T,G)-A--L-primed B cells + supernatant of line R-9‡	4,164	4,619	4,380
2×10^7 (T,G)-A--L-primed B cells + R-9 eluate from a (T,G)-A--L–Sepharose column§	15,393	NT	NT
	Antibody response to ovalbumin (c.p.m.)		
2×10^7 Ovalbumin-primed spleen cells	11,257	9,843	
2×10^7 Ovalbumin-primed B cells*	4,521	2,523	
2×10^7 Ovalbumin-primed B cells + supernatant of line R-9	4,346	1,820	
2×10^7 Ovalbumin-primed B cells + supernatant of BW5147	4,054	NT	
2×10^7 Ovalbumin-primed B cells + supernatant of line R-17	7,008	NT	

Cells and supernatants were transferred into 750-R irradiated C3H SW recipient mice together with 10 µg of (T,G)-A--L or 100 µg of ovalbumin. Antibody responses in antisera of mice bled 12–14 days after transfer were measured by plate radioimmunoassay; 0.05 mg ml^{-1} of either (T,G)-A--L or ovalbumin diluted in phosphate-buffered saline PBS were used to coat the wells of flexible plates. Antigen-coated plates were incubated with aliquots of 1:20 dilution of pooled sera (5–10 mice per group). The plates were then incubated with ^{125}I-labelled goat anti-mouse Fab. Results are expressed as mean c.p.m. of triplicate wells. NT, Not tested.

*Anti-Thy 1.2 and complement-treated primed spleen cells.

†Educated T cells obtained from spleens of irradiated recipients 1 week after transfer of 10^8 thymocytes and immunization with 10 µg (T,G)-A--L in complete Freund's adjuvant.

‡Supernatants (1 ml) of hybridoma cultures grown to a concentration of $1-2\times10^6$ cells per ml were injected into each recipient mouse together with B cells and antigen.

§R-9 supernatant was passed through a (T,G)-A--L–Sepharose column. Elution was with 0.1 M NH_4OH. The dialysed eluate was injected at a twofold concentration of the original supernatant.

cells (Table 2). The antigen specificity of the help provided by the factor was analysed in a parallel system using ovalbumin-primed splenic lymphocytes. As shown in the lower section of Table 2, R-9 supernatants which contain helper factor for (T,G)-A--L failed to reconstitute the anti-ovalbumin response in recipients of ovalbumin-primed B lymphocytes. However, R-17 supernatants functioned as non-antigen-specific mediators and provided help both to (T,G)-A--L and ovalbumin responses.

A further confirmation for the (T,G)-A--L specificity of R-9 supernatants is provided by the high efficiency of an eluate of a (T,G)-A--L–Sepharose column in replacing T cells in antibody production to (T,G)-A--L. As shown in Table 2 the antibody levels produced in recipients of (T,G)-A--L-primed B cells reconstituted with such an eluate (at a twofold concentration of the original supernatant) are comparable to those observed in recipients of primed spleen cells.

To determine whether the antigen-specific factor carries V_H determinants, as shown for R-9 hybrid cells, the above eluate of a (T,G)-A--L column was applied to immunoadsorbents made of anti-V_H and of anti-mouse immunoglobulin. The effluents and the 0.1 M NH_4OH eluates of these columns were analysed for their helper activity in an *in vitro* antibody production system[12] which enabled us to assay small doses of the factor. In this system nitro-iodophenyl (NIP)–ovalbumin primed spleen cells served as a source of hapten-specific B cells. The ability of the different R-9 fractions to provide help to these cells in the presence of NIP–(T,G)-A--L was determined by measuring the NIP-specific plaque forming cell (PFC) responses (Table 3). As shown in Table 3, the eluate of a (T,G)-A--L–Sepharose column provided (T,G)-A--L-specific helper activity; this was also shown *in vivo* in the transfer experiments (Table 2). In addition, as demonstrated in Table 3, the activity of the (T,G)-A--L–Sepharose eluate was removed by an anti-V_H–Sepharose column and could be eluted from this immunoadsorbent with 0.1 M NH_4OH. On the other hand, the helper activity could not be retained in an eluate of a guinea-pig anti-mouse immunoglobulin immunoadsorbent. Thus, the (T,G)-A--L-specific helper factor of R-9 hybridoma possesses the same V_H determinants as the cell line itself.

The R-9 hybrid line has expressed V_H determinants and produced active helper factors for 15 months since its establishment. This line could be cryopreserved and fully retained its properties. R-9 cells have been further cloned on soft agar. All 45 clones analysed reacted with the anti-V_H antibodies. Preliminary screening revealed helper activity in about 50% of the clones.

Antigen-specific helper and suppressor T cells and their products have been reported to possess determinants encoded by the I region of the major histocompatibility complex[13–18] and variable-region gene products[19–23]. We have previously described the generation and partial characterization of a helper T-cell factor specific for the synthetic polypeptide (T,G)-A--L[10,24]. The helper T-cell-replacing factor could be absorbed to immobilized antigen, anti-I-A antibodies and anti-idiotypes against (T,G)-A--L-specific antibodies[13,14,22]. Similarly, factors with suppressor activity have been shown to possess both I-J and idiotypic determinants[16,17,23]. More general reagents of potential reactivity against the T-cell receptor are the anti-V-region antibodies directed against the common framework-related determinants (V_H)[11]. Such anti-V_H antibodies effectively interfered with T-cell activities[25] and reacted with some T-cell products[26]. In accordance, we report here the establishment of an immunoglobulin-negative V_H-positive T-cell hybrid line producing a (T,G)-A--L-specific helper factor which bears V_H determinants.

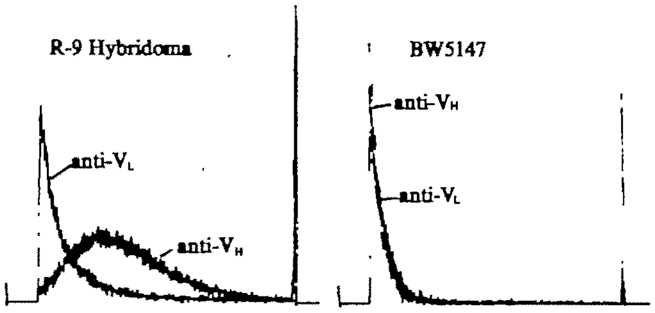

Fig. 1 Immunofluorescence profile of R-9 hybridoma and its parental BW5147 thymoma labelled with either anti-V_H or anti-$V_L(\lambda)$ purified rabbit $F(ab')_2$ antibody fragments. Fluorescein conjugated $F(ab')_2$ of goat anti-rabbit IgG was used for staining. Abscissa, fluorescence intensity; ordinate, relative cell number.

Table 3 (T,G)-A--L-specific helper factor of R-9 hybrid line possesses V_H determinants

NIP-OVA primed spleen cells cultured with:	NIP specific PFC per 10^6 viable cells*			
	NIP-(T,G)-A--L		NIP-FGG	
	Expt 1	Expt 2	Expt 1	Expt 2
—	279±43	81±23	175±24	66±28
(T,G)-A--L-primed spleen cells	1,333±76	500±33	375±25	47± 8
Eluate from (T,G)-A--L–Sepharose†	1,045±57	487±23	213±31	111±17
Effluent from anti-mouse Ig–Sepharose	416±36	388±71	196±33	103±38
Eluate from anti-mouse Ig–Sepharose‡	230±13	102±31	114±45	46±26
Effluent from anti-V_H–Sepharose	175±20	62±32	151±19	48±17
Eluate from anti-V_H–Sepharose‡	621±58	413±34	108±24	73±27

NIP–Ovalbumin primed spleen cells were cultured in microtitre plates (10^6 per well) together with either (T,G)-A--L-primed spleen cells (2.5×10^5 per well) or the different effluents and eluates (final concentration 25%). Either NIP-(T,G)-A--L or NIP-FGG (fowl γ-globulin) (1 μg) was added to each well. Culture conditions were as described elsewhere[12].

*Indirect plaque forming cells (PFC) were determined using NIP-sheep red blood cell indicator cells. Results are expressed as the mean number of quadruplicates tested ± s.e. NIP–Ovalbumin primed spleen cells cultured in the presence of homologous antigen gave 1,794 PFC and 678 PFC whereas the background without antigen was 68 PFC and 50 PFC in Expts 1 and 2 respectively.

†R-9 eluted from (T,G)-A--L–Sepharose column (as described in Table 2 legend). This affinity-purified fraction was further passed through the rabbit anti-V_H and guinea pig anti-mouse IgG–Sepharose columns.

‡Elution was with 0.1 M NH_4OH.

Experiments are under way to characterize the products of R-9, the first T-cell hybridoma which is a constitutive producer of (T,G)-A--L-specific helper factor and bears surface variable-region determinants. The information obtained may clarify the nature of the molecular association between MHC-coded determinants and immunoglobulin variable-region gene products in the T-cell recognition unit.

We thank Ms Heidy Zinger and Ms Tova Waks for technical assistance, Dr Patrick de Baetselier for analysing the hybridomas in the FACS, and Drs R. Hyman, A. Peled and A. Rothstein for BW5147 thymoma, anti-Lyt 2.1 antibodies, and anti-Thy 1.2 and 1.1 antibodies, respectively. This research was supported in part by a grant from the National Council for Research and Development, Israel, and the DKFZ, Heidelberg, FRG. Z.E. is an incumbent of the Recanati Career Development Chair in Cancer Research. R.N.A. is a recipient of the Wolf Michaels postdoctoral fellowship.

Received 23 January; accepted 29 April 1980.

1. Katz, D. H. & Benacerraf, B. *Adv. Immun.* **15,** 1–94 (1972).
2. Tada, T. & Okumura, K. *Adv. Immun.* **28,** 1–87 (1980).
3. Köhler, G. & Milstein, C. *Nature* **256,** 495–497 (1975).
4. Goldsby, R. A., Osborne, B. A., Simpson, E. & Herzenberg, L. A. *Nature* **267,** 707–708 (1977).
5. Hammerling, G. J. *Eur. J. Immun.* **7,** 743–746 (1977).
6. Kontianen, S. *et al. Nature* **274,** 477–480 (1978).
7. Taussig, M. J., Corvalan, J. R. F., Binns, R. M. & Holliman, A. *Nature* **277,** 305–308 (1979).
8. Taniguchi, M., Saito, T. & Tada, T. *Nature* **278,** 555–558 (1979).
9. Galfre, G., Howe, S. C., Milstein, C., Butcher, G. W. & Howard, J. C. *Nature* **266,** 550–552 (1977).
10. Taussig, M. J., Mozes, E. & Isac, R. *J. exp. Med.* **140,** 301–312 (1974).
11. Ben-Neriah, Y., Lonai, P., Gavish, M. & Givol, D. *Eur. J. Immun.* **8,** 792–796 (1978).
12. Mishell, R. I. & Dutton, R. W. *J. exp. Med.* **126,** 423–442 (1967).
13. Taussig, M. J., Munro, A. J., Campbell, R., David, C. S. & Staines, N. A. *J. exp. Med.* **142,** 694–700 (1975).
14. Isac, R., Dorf, M. E. & Mozes, E. *Immunogenetics* **5,** 467–475 (1977).
15. Feldmann, M. *et al.* in *Ir Genes and Ia Antigens* (ed. McDevitt, H. O.) 315–323 (Academic, New York, 1978).
16. Tada, T., Taniguchi, M. & David, C. S. *Cold Spring Harb. Symp. quant. Biol.* **41,** 119–127 (1977).
17. Thèze, J., Kapp, J. A. & Benacerraf, B. *J. exp. Med.* **195,** 839–856 (1977).
18. Okumura, K., Herzenberg, L. A., Murphy, D. B., McDevitt, H. O. & Herzenberg, L. A. *J. exp. Med.* **144,** 685–698 (1976).
19. Binz, H. & Wigzell, H. *J. exp. Med.* **142,** 197–211 (1975).
20. Eichmann, K. & Rajewsky, K. *Eur. J. Immun.* **5,** 661–666 (1975).
21. Krawinkel, U., Cramer, M., Melchers, I., Imanishi-Kari, T. & Rajewski, K. *J. exp. Med.* **147,** 1341–1347 (1978).
22. Mozes, E. & Haimovich, J. *Nature* **276,** 56–57 (1979).
23. Germain, R. N., Ju, S.-T., Kipps, T. J., Benacerraf, B. & Dorf, M. E. *J. exp. Med.* **149,** 613–622 (1979).
24. Isac, R. & Mozes, E. *J. Immun.* **118,** 584–588 (1977).
25. Eichmann, K., Ben-Neriah, Y., Givol, D. & Lonai, P. *Eur. J. Immun.* (in the press).
26. Cramer, M. *et al. Eur. J. Immun.* **9,** 332–338 (1979).

0028–0836/80/290272–03$01.00

Small subunit of I–A subregion antigens determines the allospecificity recognized by a monoclonal antibody

Jack Silver, Susan L. Swain* & Jeffrey J. Hubert

The Department of Cellular and Developmental Immunology, Scripps Clinic and Research Foundation, 10666 North Torrey Pines Road, La Jolla, California 92037

*Department of Biology, University of California San Diego, La Jolla, California 92037

The murine major histocompatibility complex (MHC) codes for three groups of identifiable cell-surface proteins, the K, D molecules, the I–A subregion antigens and the I–E subregion antigens. All three groups of molecules display a high degree of serologically detectable polymorphism[1] and consist of two noncovalently associated polypeptides[2–8]. Amino acid sequence and peptide comparisons among allotypes of K, D and I–E molecules reveals that one polypeptide is relatively constant, whereas the other is highly variable[9–13]. Thus, it is likely that only one of the two polypeptides, the variable component, determines the antigenic specificities recognized by alloantisera. In contrast to the K, D and I–E molecules, both subunits of I–A molecules display substantial structural differences when comparisons among allotypes are made[4,14–16]. Therefore, we have investigated whether one or both subunits of I–A molecules determine their alloantigenic specificities. Our results, presented here, indicate that only one of the two subunits determines a particular allospecificity recognized by a monoclonal antibody.

I–A molecules radiolabelled with ^{3}H-phenylalanine were isolated from B10.A(5R) mice by indirect immunoprecipitation with (B10.A × A)F_1 anti-B10.A(5R) antisera[14] (Fig. 1*b*). I–A molecules were isolated from B10.A(4R) and [B10.A(4R) × B10.A(5R)]F_1 mice with monoclonal antibody 10-2.16 (Fig. 1*a*,*c*), which is unreactive with B10.A(5R) mice and putatively directed against the public antigenic specificity Ia.17 based on its pattern of reactivity (Table 1 and ref. 17). The larger (A_α) and small (A_β) chains were purified by SDS-polyacrylamide gel

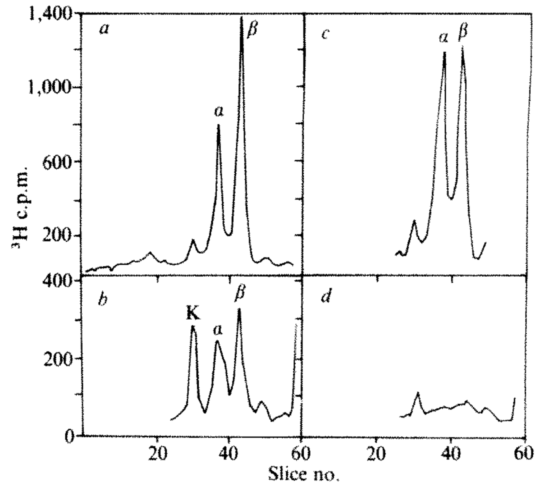

Fig. 1 SDS-PAGE profiles of I–A antigens immunoprecipitated from B10.A(4R) (*a*), B10.A(5R) (*b*) and [B10.A(4R) × B10.A(5R)]F_1 (*c*) mice. I–A antigens consist of two polypeptide chains designated α (molecular weight 37,000) and β (MW 28,000). The antiserum used to immunoprecipitate I–A antigens from B10.A(5R) mice is multispecific and also precipitates the H–2K molecule (MW 45,000). *d* Illustrates the inability of monoclonal antibody 10-2.16 to precipitate any I–A molecules from B10.A(5R) mice.

Table 1 Cytotoxic activity of reagent from 10-2.16

Spleen from:	I–A	I–E/C	Reciprocal titre
B10.BR	k	k	160
B10.D2	d	d	<10
B10.A	k	k/d	160
B10.A(4R)	k	b	160
B10	b	b	<10
B10.G	q	q	<10
B10.S	s	s	320
PL/J	u	u	160
B10.LPRIII	r	r	160
B10.M	f	f	160
B10.A(5R)	b	k/d	<10

Monoclonal antibody used to precipitate I–A subregion antigens from B10.A(4R) and [B10.A(4R) × B10.A(5R)]F_1 mice was produced by collecting and concentrating supernatants from cultures of hybridoma 10-2.16. This hybridoma was originally produced by fusing splenocytes from a CWB mouse immunized with C3H cells with the NS-1 myeloma. Cytotoxic activity was measured as described previously[32]. The resultant monoclonal antibody only lyses cells which possess the I–$A^{k,s,f,r,u}$ subregion, and is putatively directed against the antigenic specificity Ia.17 based on this pattern of reactivity[17].

electrophoresis (PAGE)[18] and tryptic peptide maps were obtained as described elsewhere[19–21]. A_α chains isolated from B10.A(4R) and B10.A(5R) mice (designated A_α^k and A_α^b, respectively) are distinguishable by their tryptic peptide maps (Fig. 2*a*), as are the A_β chains isolated from B10.A(4R) and B10.A(5R) mice (designated A_β^k and A_β^b, respectively) (Fig. 3*a*). Peptide mapping of the A_α and A_β chains immunoprecipitated from [B10.A(4R) × B10.A(5R)]F_1 mice with monoclonal antibody 10-2.16 directed against the I–A molecule of the B10.A(4R) parent (I-A^k) reveals that they consist solely of the A_β^k chain (Fig. 3*b*) and a mixture of A_α^k and A_α^b chains (Fig. 2*b*). The absence of an A_β^b chain in the immunoprecipitate is not due to the inability of these F_1 mice to express the A_β^b chain; antiserum directed against I–A^b antigens precipitates the A_β^b chain from F_1 mice.

We conclude from these results that the allospecificity Ia.17 recognized by monoclonal antibody 10-2.16 is determined by the β chain according to the following rationale: when a monoclonal reagent specific for I–A from parent 1 is used to precipitate I–A molecules from an F_1 offspring, several results are possible. If the specificity is determined only by the α chain, the α chain from parent 1 but not from parent 2 would be found in the F_1 precipitate. Conversely, if only the β chain determines the specificity, the β chain of parent 1 but not of parent 2 would be found. Finally, if both chains are responsible, both α and β chains from parent 1 and none from parent 2 would be found. Because the antibody displays specificity for the A_β^k chain and none for the α chains, we conclude that the β chain determines the antigenic specificity recognized by the monoclonal antibody. The observation that both α chains are found in the F_1 indicates that both α chains can freely associate with the A_β^k chain. Immunoprecipitation of both α chains cannot be due to their recognition by the monoclonal antibody, because then the monoclonal antibody would be expected to react with and precipitate I–A molecules from B10.A(5R) mice, which it does not (Table 1 and Fig. 1). However, we cannot rule out the possibility that the antigenic determinant recognized by monoclonal antibody 10-2.16 actually resides on the α chain and is generated when either A_α^k or A_α^b associate with the specific A_β^k chain.

Thus, only one of the two subunits of I–A subregion antigens, the β chain, has a crucial role in determining the antigenic determinant recognized by the monoclonal antibody. This, combined with studies that attribute the molecular polymorphism of the murine I–E subregion and K, D gene products, and their respective human analogues the HLA-DR[19–21] and HLA-A,B,C[22,23] antigens, to one of two subunits, makes it tempting to propose that only one chain, the β chain, is generally responsible for the alloantigenic specificities of I–A antigens. To substantiate this hypothesis, reagents against several other I–A specificities must be tested.

Assignment of the alloantigenic specificities of I–A molecules to one subunit has important functional implications. Genetic[24] and serological[25] studies suggest that T-cell recognition of allotype-specific I–A molecules on B cells and macrophages is a prerequisite for the development of optimal immune responses. If T cells perceive I–A antigens with a specificity similar to antibody, it is also possible that only the β chain determines allotype-specific recognition of I–A molecules by T cells. The free association of both α components with the A_β^k component may be interpreted to mean that both α components have a common effector function and may be substituted for one another.

In contrast to the proposal that the β subunit alone determines I–A antigenic specificities, the findings of Fatham *et al.*[26] may be construed to suggest that some antigenic specificities perceived by T cells are due to unique combinations of α and β chains. These authors found that some cell-surface antigenic determinants controlled by the MHC and recognized by T cells in mixed lymphocyte culture (MLC) reactions, are unique to F_1 animals and absent from both parental types. Although some of these specificities may be attributed to complementation of two MHC genes required for the expression of I–E molecules, as has been demonstrated by several investigators[27,28], others cannot be explained on this basis. The observation that α and β chains from an F_1 animal are capable of associating in a random manner introduces the possibility of generating antigenic specificities unique to the F_1 offspring and absent from both types, and may explain the findings of Fathman *et al.* If α and β chains can reassociate in a random fashion, F_1 animals should have four distinct sets of I–A complexes, two that are unique to the F_1 and not found on either parental types and one from each parental type. From a functional viewpoint, if I–A molecules are perceived by T cells in both MLC reactions and T–B or T–macrophage cell interactions in a similar fashion, an F_1

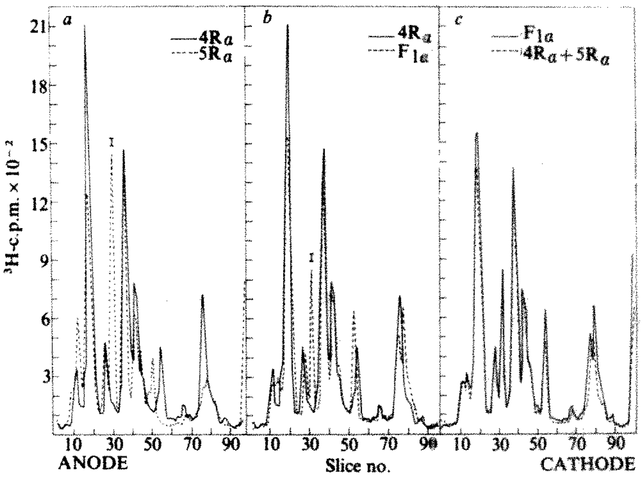

Fig. 2 Comparative tryptic peptide maps of the A_α chains immunoprecipitated from B10.A(4R), B10.A(5R) and [B10.A(4R) × B10.A(5R)]F_1 mice. The A_α chain isolated from B10.A(5R) mice (designated A_α^b) displays a peptide peak (I) that is absent from the A_α chain isolated from B10.A(4R) mice (designated A_α^k) (*a*). The peptide map of the A_α chain isolated from [B10.A(4R) × B10.A(5R)]F_1 mice displays peak I, which is unique to the A_α^b chain (*b*). Furthermore, this peptide map is virtually identical to that derived from a mixture of the A_α^b and A_α^k chains (*c*). Positional differences (1–2 gel slices) of peptides and the apparent 'splitting' of the peak near slice 80 (*c*) are due to minor variations in gel slicing.

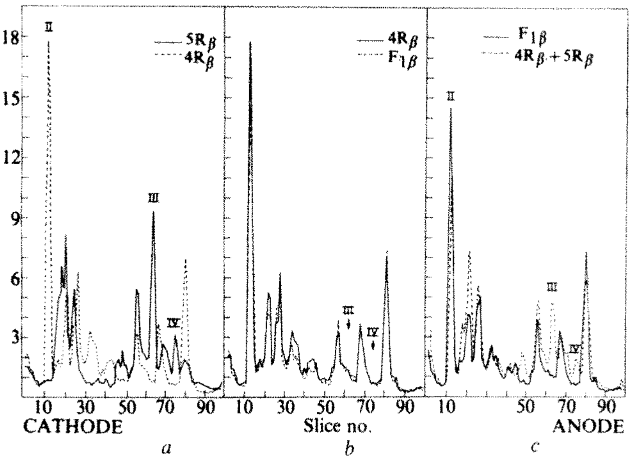

Fig. 3 Comparative tryptic peptide maps of the A_β chains immunoprecipitated from B10.A(4R), B10.A(5R) and [B10.A(4R) × B10.A(5R)]F_1 mice. The A_β chain isolated from B10.A(5R) mice (designated A_β^b) displays several unique peptides (III and IV); the A_β chain isolated from B10.A(4R) mice (designated A_β^k) also has one unique peptide (II) (*a*). The peptide maps of A_β chains isolated from [B10.A(4R) × B10.A(5R)]F_1 and B10.A(4R) mice are virtually identical (*b*). Clearly, the A_β chain isolated from [B10.A(4R) × B10.A(5R)]F_1 mice does not comprise a mixture of A_β^b and A_β^k chains, as its peptide map is different from that derived from the mixed A_β^b and A_β^k chains (*c*).

animal might be expected to possess some T cells that are capable of interacting with B cells and macrophages only from F_1 animals and not from either parental type. Although experiments by others clearly demonstrate that cells of F_1 animals can interact with cells of either parental type[29–31], functional studies designed specifically to determine the possibility of F_1 specific interactions have not been performed. It is important to discover whether such unique F_1 determinants frequently have an important role or are only found in rare cases.

The analytical method used in the present studies provides a general means of determining which chain confers the unique allospecificity on any complex consisting of multiple subunits, provided that both subunits from both parents are distinguishable and that monoclonal antibody or an operationally monospecific alloantiserum directed against the allospecificities is available. Furthermore, this method does not require retention of alloantigenicity after separation of noncovalently associated subunits to determine which subunit carries the allospecificities. Additional studies with several monoclonal antibodies directed against I-A^k and other allospecificities will enable us to assess definitively the relative contributions of the A_α and A_β polypeptides to the alloantigenicity of I-A subregion antigens.

This work was supported by NIH grant CA 23030. J.S. holds an established investigatorship from the American Heart Association. Hybridoma 10-2.16 was donated by Dr Len Herzenberg.

Received 12 December 1979; accepted 18 April 1980.

1. Shreffler, D. C. & David, C. S. *Adv. Immun.* **20**, 125–195 (1975).
2. Silver, J. & Hood, L. E. *Nature* **249**, 764–765 (1974).
3. Silver, J. & Hood, L. E. *Nature* **256**, 63–64 (1975).
4. Cullen, S. E., Freed, J. H. & Nathenson, S. G. *Transplantn Rev.* **30**, 236–270 (1976).
5. Silver, J., Cecka, J. M., McMillan, M. & Hood, L. E. *Cold Spring Harb. Symp. quant. Biol.* **41**, 369–377 (1976).
6. Silver, J., Russell, W. A., Reis, B. L. & Frelinger, J. A. *Proc. natn. Acad. Sci. U.S.A.* **74**, 5131–5134 (1977).
7. McMillan, M., Cecka, J. M., Murphy, D. B., MCDevitt, H. O. & Hood, L. E. *Proc. natn. Acad. Sci. U.S.A.* **74**, 5135 (1977).
8. Cook, R. G., Uhr, J. W., Capra, J. D. & Vitetta, E. S. *J. Immun.* **121**, 2205–2212 (1978).
9. Silver, J. & Hood, L. E. *Proc. natn. Acad. Sci. U.S.A.* **73**, 599–603 (1976).
10. Silver, J., Walker, L. E., Reisfeld, R. A., Pellegrino, M. A. & Ferrone, S. *Molec. Immun.* **16**, 37–42 (1979).
11. McMillan, M., Cecka, J. M., Murphy, D. B., McDevitt, H. O. & Hood, L. E. *Immunogenetics* **6**, 137–147 (1978).
12. Freed, J. H. & David, C. S. in *Current Trends in Histocompatibility* (eds Reisfeld, R. A. & Ferrone, S.) (Plenum, New York, in the press).
13. Cook, R. G., Vitetta, E. S., Uhr, J. W. & Capra, J. D. *Molec. Immun.* **16**, 29–35 (1979).
14. Silver, J. & Russell, W. A. *Immunogenetics* **8**, 339–346 (1979).
15. Cook, R. G., Capra, J. D., Bednarczyk, J. L., Uhr, J. W. & Vitetta, E. S. *J. Immun.* **123**, 2799–2803 (1979).
16. Silver, J. in *Current Trends in Histocompatibility* (eds Reisfield, R. A. & Ferrone, S.) (Plenum, New York, in the press).
17. Oi, V. T., Jones, P. P., Goding, J. W., Herzenberg, L. A. & Herzenberg, L. A. *Curr. Topics Microbiol. Immun.* **81**, 115–129 (1978).
18. Silver, J. *Transplantn Proc.* **9**, 661–665 (1977).
19. Silver, J. & Ferrone, S. *Nature* **279**, 436–437 (1979).
20. Silver, J. & Russell, W. A. *Nature* **279**, 437–438 (1979).
21. Silver, J. & Ferrone, S. *Immunogenetics* **10**, 295–298 (1980).
22. Grey, H. M. *et al. J. exp. Med.* **131**, 1608–1612 (1973).
23. Nakamuro, K. Tanigaki, M. & Pressman, D. *Proc. natn. Acad. Sci. U.S.A.* **70**, 2863–2865 (1973).
24. Katz, D. H., Graves, M., Dorf, M. E., Dimuzio, H. & Benacerraf, B. *J. exp. Med.* **141**, 263–268 (1975).
25. Frelinger, J. A., Niederhuber, J. E. & Shreffler, D. C. *Science* **188**, 268–270 (1975).
26. Fathman, C. G., Watanabe, T. & Augustin, A. *J. Immun.* **121**, 259–264 (1978).
27. Jones, P. P., Murphy, D. B. & McDevitt, H. O. *J. exp. Med.* **148**, 925–939 (1978).
28. Silver, J. *J. Immun.* **123**, 1423–1425 (1979).
29. Paul, W. E., Shevach, E. M., Pickeral, S., Thomas, D. W. & Rosenthal, A. S. *J. exp. Med.* **145**, 618–630 (1977).
30. Swierkosz, J. E., Rock, K., Marrack, P. & Kappler, J. W. *J. exp. Med.* **147**, 554–570 (1978).
31. Sprent, J. *J. exp. Med.* **147**, 1142–1158 (1978).
32. Feeney, A. J. & Hämmerling, U. *Immunogenetics* **3**, 369–379 (1976).

Increased proton conductance pathway in brown adipose tissue mitochondria of rats exhibiting diet-induced thermogenesis

Sarah L. Brooks*, Nancy J. Rothwell*,
Michael J. Stock*,
Anne E. Goodbody† & Paul Trayhurn†

*Department of Physiology, St. George's Hospital Medical School, London SW17 0RE, UK
†Dunn Nutrition Laboratory, University of Cambridge and MRC, Cambridge CB4 1XJ, UK

It has recently been demonstrated[1] that in rats induced to overeat by being fed a varied and palatable diet (the 'cafeteria diet') there is a marked increase in heat production which serves to reduce, or prevent, the development of obesity. This diet-induced thermogenesis is associated with increases in sympathetic activity, and with changes in brown adipose tissue. Following cafeteria feeding, brown adipose tissue hypertrophies and exhibits increased lipolysis and an apparently greater thermogenesis in response to noradrenaline. These metabolic changes resemble those seen during non-shivering thermogenesis in cold-adapted rats, and it was proposed[1] that non-shivering thermogenesis and diet-induced thermogenesis have a similar metabolic origin which depends on the unique capacity of brown adipose tissue for thermogenesis. During non-shivering thermogenesis heat is produced in brown adipose tissue through a proton conductance pathway across the inner mitochondrial membrane that dissipates the proton gradient generated by respiration[2]. The activity of the proton conductance pathway can be modulated by purine nucleotides, and changes in the pathway seem to be related to the level of purine nucleotide binding to brown adipose tissue mitochondria. We now report results which indicate that the proton conductance pathway is augmented in cafeteria-fed rats, and suggest that it operates to dissipate their excess energy intake through diet-induced thermogenesis.

In the first experiments, the activity of mitochondrial enzymes and the effect of purine nucleotides on mitochondrial respiration were determined with brown adipose tissue of normal and cafeteria-fed animals. Groups of adult, male Sprague–Dawley rats (Charles River) were maintained on either the conventional stock diet (PRD, Christopher Hill Group) or the cafeteria diet (see refs 1, 3 for details) for up to

0028–0836/80/290274–03$01.00

20 days in a room maintained at 24 °C. As in previous studies[1], the cafeteria-fed rats overate and exhibited increased metabolic rates and an increased thermogenic response to injected doses of noradrenaline. After 10–20 days the rats were killed and the interscapular brown adipose tissue was removed and homogenized, and the total protein content and cytochrome oxidase (EC 1.9.3.1.) activity were measured. Mitochondria prepared from homogenates were also assayed for protein, and for cytochrome oxidase and α-glycerophosphate dehydrogenase (EC 1.1.1.99.5.) activity. Details of the methods used and the results obtained are shown in Table 1.

Cafeteria feeding resulted in a near doubling of interscapular brown adipose tissue (BAT) mass and total protein content. There were also large increases in the total activity of the two mitochondrial respiratory enzymes, related to a twofold increase in mitochondrial protein content of the brown adipose tissue of cafeteria-fed rats. The enzyme changes were not due to increases in specific activity (that is, activity per mg mitochondrial protein) nor to differences in the recovery of mitochondria, and indicate that the oxidative capacity of this brown adipose tissue depot increases substantially during overfeeding.

These changes resemble those seen in cold-adapted animals[4–6] where high rates of mitochondrial respiration in brown adipose tissue result from a combination of increased oxidative capacity and reduced respiratory control[2]. Respiratory control can be partially restored by incubating mitochondria in the presence of albumin but significant improvements require the further addition of purine nucleotides[7]. In the present study, respiratory rates of brown adipose tissue mitochondria from cafeteria-fed rats were 30% greater than those from control animals, even when incubated with albumin to avoid differences due to any uncoupling effect of endogenous fatty acids (Table 2). However, the addition of GDP (Sigma) resulted in a marked 'tightening' of respiratory control such that respiratory rates were decreased in both groups and the differences between them were abolished. This effect of GDP could be overcome by adding the uncoupling agent carbonyl cyanide *p*-trifluoromethoxyphenylhydrazone (FCCP, Sigma). These results indicate that brown adipose tissue mitochondria from cafeteria rats are more 'loosely coupled' than those from control rats.

Table 1 Mitochondrial enzyme activities in interscapular brown adipose tissue from control and cafteria-fed rats

	Control	Cafeteria
Weight of animals (g)	196.5 ± 3.3	190.7 ± 2.5 NS
Interscapular brown adipose tissue mass (mg)	275 ± 10	538 ± 18*
Total brown adipose tissue protein (mg)	32.4 ± 2.4	58.7 ± 4.0*
Total cytochrome oxidase activity (μmol cytochrome *c* oxidized per min per mg tissue)	19.8 ± 3.3	44.2 ± 7.1†
Mitochondrial cytochrome oxidase activity (μmol cytochrome *c* oxidized per min per total mitochondrial preparation)	5.1 ± 0.7	11.8 ± 1.5†
α-Glycerophosphate dehydrogenase activity (μmol O_2 consumed per min per total mitochondrial preparation)	0.58 ± 0.03	1.62 ± 0.19*

The animals used were aged approximately 6 weeks. Protein content of tissue homogenates and mitochondrial preparations was determined using a protein dye reagent kit with a bovine serum albumin standard (Bio-Rad). Mitochondria were prepared using the isolation procedure described by Slinde *et al.*[16]. Cytochrome oxidase activity was determined spectrophotometrically using a modification of the assay described by Yonetani and Ray[17] and α-glycerophosphate dehydrogenase activity was assayed polarographically[18]. The specific activities of the two enzymes (that is, activity per mg mitochondrial protein) were not different in the two groups but the amount of mitochondrial protein isolated was different—3.5 ± 0.3 and 7.1 ± 0.4 mg in control and cafeteria-fed groups, respectively ($P < 0.001$). Comparison of cytochrome oxidase activities in whole tissue homogenates and mitochondrial preparations indicates that the fractional yield of mitochondria was identical in both groups. Results are mean values ± s.e.m., $n = 8$. NS, Not significant ($P > 0.05$).

*$P < 0.001$; †$P < 0.01$, compared with control values.

Table 2 Respiration of mitochondria from brown adipose tissue of control and cafeteria-fed rats

	Mitochondrial respiration (nmol O_2 per mg protein per min)	
	Control	Cafeteria
+ Albumin (5 mg ml^{-1})	32.3 ± 2.0	42.7 ± 2.6*
+ GDP (1 mM)	20.2 ± 1.2	18.7 ± 2.3 NS
+ FCCP (5 μM)	35.3 ± 2.6	38.3 ± 3.4 NS

The age and weight of the rats used were similar to those in Table 1. Mitochondria were prepared by the method of Slinde *et al.*[16], and oxygen consumption was measured at 25 °C in a Clark-type oxygen electrode (Rank Brothers) using the conditions described by Nicholls[7]. Mitochondrial protein was measured as in Table 1. Results are mean values ± s.e.m., $n = 8$. NS, Not significantly different ($P > 0.05$) from controls.

*$P < 0.01$.

The action of purine nucleotides on mitochondrial respiratory control in BAT is due to inhibition of the proton conductance pathway[2]. This inhibition is associated with the binding of the purine nucleotides to an inner membrane protein (molecular weight 32,000) unique to brown adipose tissue mitochondria. Changes in mitochondrial GDP binding have been used to study the capacity of the proton conductance pathway during cold-adaptation in rats[8,9], and during early development in both rats[9] and guinea pigs[10], as well as to investigate abnormalities in heat production in brown adipose tissue from genetically obese (*ob/ob*) mice[11]. In view of the similarities between non-shivering thermogenesis and diet-induced thermogenesis an experiment was carried out to compare the purine nucleotide binding capacity of brown adipose tissue mitochondria isolated from cafeteria- and stock-fed rats maintained in warm and cold environments.

Similar rats to those used in the first experiments were housed at either 24 °C (warm-adapted) or 4 °C (cold-adapted) and fed the stock diet for 15 days, after which time half the animals at each environmental temperature were allowed access to the cafeteria diet. We have previously shown[12] that

Table 3 Purine nucleotide (GDP) binding to interscapular brown adipose tissue mitochondria from cafeteria and control rats maintained at either 24 °C (warm) or 4 °C (cold)

	Warm control	Warm cafeteria	Cold control	Cold cafeteria
Animal weights (g)	326.3 ± 18.1	306.0 ± 25.5	296.6 ± 11.8	327.4 ± 21.2
Mitochondrial protein recovered (mg)	5.7 ± 0.9	8.7 ± 0.9*	17.2 ± 1.4‡	21.0 ± 1.3‡
GDP binding (pmol GDP per mg mitochondrial protein)	52.6 ± 7.4	135.3 ± 24.0†	249.8 ± 17.8‡	237.5 ± 14.6‡
n	7	5	5	5

The rats used in these experiments were aged approximately 10 weeks. Mitochondria were prepared by the method of Slinde *et al.*[16], and the protein content of each preparation was determined colorimetrically by a modified Lowry assay[19] using bovine serum albumin as a standard. Mitochondrial GDP-binding was measured essentially as described by Nicholls[20] with the modifications of Desautels *et al.*[6]; ^{3}H-GDP and ^{14}C-sucrose (both Radiochemical Centre) incubations were carried out for 7 min at room temperature. Results are mean values ± s.e.m.

*$P < 0.05$; †$P < 0.01$; ‡$P < 0.001$, compared with warm controls.

cafeteria feeding in the warm produces quantitatively similar increases in metabolic rate, noradrenaline sensitivity and brown adipose tissue mass, to those seen with cold-adapted stock-fed controls. In the present study, animals were killed after 10–20 days on the experimental diets and brown adipose tissue mitochondria prepared for determination of GDP-binding capacity. Details of the methods used and results obtained are shown in Table 3.

Cafeteria feeding in the warm environment resulted in a significant 2.5-fold increase in GDP-binding per mg mitochondrial protein compared with warm-adapted controls. Thus, the high diet-induced thermogenesis resulting from cafeteria feeding apparently leads to a marked increase in the proton conductance of brown adipose tissue mitochondria, similar to that observed with cold-adaptation. It is unlikely that the increased GDP binding of cafeteria-fed rats over that of the controls was due to the isolation of a different population of mitochondria or to differences in the purity of the preparations, because the specific activities of the two respiratory enzymes (cytochrome oxidase and α-glycerophosphate dehydrogenase) were almost identical for both groups.

Cold-adaptation produced a greater than fourfold increase in GDP binding per mg mitochondrial protein in both stock- and cafeteria-fed rats. The results for the cold-adapted control group are similar to those reported by Desautels *et al.*[8], and although an additive effect of cold and cafeteria feeding on metabolic rate and noradrenaline sensitivity has been seen in earlier experiments[12], this is not reflected in the GDP-binding results for the cold-adapted cafeteria group in the present study.

The present results are the first report of an effect of diet and energy intake on the capacity of brown adipose tissue mitochondria for thermogenesis. They support our earlier suggestion[1] that the mechanisms of diet-induced thermogenesis and non-shivering thermogenesis are similar, and are consistent with the improved cold tolerance of overfed rats[12].

Genetically obese animals (*ob/ob* and *db/db*) have impaired thermogenesis[13–15], which has been associated with a lowered purine nucleotide binding in their brown adipose tissue mitochondria[11]. This finding, together with the results of the present study, suggest that brown adipose tissue has an important regulatory role in energy balance, as well as in body temperature.

This work was supported by the MRC, the Rank Prize Funds and SW Thames Regional Health Authority.

Received 21 February; accepted 2 May 1980.

1. Rothwell, N. J. & Stock, M. J. *Nature* **281**, 31–35 (1979).
2. Nicholls, D. G. *Biochim. biophys. Acta* **549**, 1–29 (1979).
3. Rothwell, N. J. & Stock, M. J. *J. comp. Physiol. Psychol.* **93**, 1024–1034 (1979).
4. Jansky, L., Votapkova, Z. & Feiglova, E. *Physiologia bohemoslov.* **18**, 443–451 (1969).
5. Barnard, J., Skala, J. & Lindberg, O. *Comp. Biochem. Physiol.* **33**, 499–508 (1970).
6. Heick, H. M. C., Vachon, C., Kallai, M. A., Begin-Heick, N. & Leblanc, J. *Can. J. Physiol. Pharmac.* **51**, 751–758 (1973).
7. Nicholls, D. G. *Eur. J. Biochem.* **49**, 573–583 (1974).
8. Desautels, M., Zaror-Behrens, G. & Himms-Hagen, J. *Can. J. Biochem.* **56**, 378–383 (1978).
9. Sundin, U. & Cannon, B. *Comp. Biochem. Physiol.* **65B**, 463–471 (1980).
10. Rafael, J. & Heldt, H. W. *FEBS Lett.* **63**, 304–308 (1976).
11. Himms-Hagen, J. & Desautels, M. *Biochem. biophys. Res. Commun.* **83**, 628–634 (1978).
12. Rothwell, N. J., Schönbaum, E., Smith, I. C. H. & Stock, M. J. *J. Physiol., Lond.* **300**, 458 (1980).
13. Trayhurn, P., Thurlby, P. L. & James, W. P. T. *Nature* **266**, 60–62 (1977).
14. Trayhurn, P. & James, W. P. T. *Pflügers Arch. ges. Physiol.* **373**, 189–193 (1978).
15. Trayhurn, P. *Pflügers Arch. ges. Physiol.* **380**, 227–232 (1979).
16. Slinde, E., Pedersen, J. I. & Flatmark, T. *Analyt. Biochem.* **65**, 581–585 (1975).
17. Yonetani, T. & Ray, G. S. *J. biol. Chem.* **240**, 3392–3398 (1965).
18. Gurr, M. I., Mawson, R., Rothwell, N. J. & Stock, M. J. *J. Nutr.* **110**, 532–542 (1980).
19. Schacterle, G. R. & Pollack, R. L. *Analyt. Biochem.* **51**, 654–655 (1973).
20. Nicholls, D. G. *Eur. J. Biochem.* **62**, 223–228 (1976).

Insulin stimulates sugar transport in giant muscle fibres of the barnacle

P. F. Baker & A. Carruthers

Department of Physiology, University of London King's College,
Strand, London WC2R 2LS, UK

Insulin stimulates sugar transport in vertebrate skeletal muscle but the mechanism of insulin action is unknown[1]. It has been reported that Na transport in giant muscle fibres of the barnacle (*Balanus nubilis*) is sensitive to insulin[2] but no one has examined the sensitivity of sugar transport to insulin in this preparation. We show here that insulin does, indeed, stimulate sugar transport in barnacle muscle. The great advantage of barnacle muscle over all other muscles used so far for investigating the mechanism of insulin action is its large size, which facilitates measurements on single cells and permits the experimenter to control the intracellular environment of the muscle fibre by the technique of internal dialysis[3]. Using single muscle fibres it is possible to show that acceleration of sugar transport by insulin is associated with a fall in ionized Ca, a fall in cyclic AMP and a rise in cyclic GMP. Working with internally dialysed muscle fibres we find that insulin only increases sugar transport when the dialysis solution contains ATP. In the absence of insulin, sugar transport in dialysed muscle is increased by a rise in ionized Ca, a fall in cyclic AMP and, when the internal Ca is elevated, by a rise in cyclic GMP.

D-Glucose is taken up and metabolised by barnacle muscle fibres. For this reason, the non-metabolised sugar 3-*O*-methylglucose was used throughout the present study. In addition to their sensitivity to insulin, 3-*O*-methylglucose fluxes in barnacle muscle show several features in common with sugar transport in mammalian tissues. Sugar uptake and exit consist of two components: a saturable component (apparent $K_m = 5\,\mathrm{mM}$, $V_{max} = 17\,\mathrm{pmol\,cm^{-2}\,s^{-1}}$) which is reduced by both phloretin (apparent $K_i = 10^{-4}\,\mathrm{M}$) and cytochalasin B (apparent $K_i = 5 \times 10^{-6}\,\mathrm{M}$), and a component which increases linearly with sugar concentration and is insensitive to phloretin or cytochalasin B.

Porcine insulin stimulates reversibly the rate of sugar uptake and exit in isolated muscle fibres in a concentration-dependent manner (half-maximal stimulation seen at $1.2\,\mathrm{U\,ml^{-1}}$). Barnacle muscle fibres bind ^{125}I-insulin: this can be displaced by cold insulin, and in the presence of $1\,\mathrm{U\,ml^{-1}}$, the insulin space of single fibres is about five times greater than that of mannitol or sucrose. Both insulin binding and the activation of sugar transport become saturated at roughly the same concentration of insulin and on the assumption that all the radioactivity is bound to the surface of the muscle, the number of insulin binding sites is 600 per μm^2. These findings suggest that barnacle muscle fibres have receptors for insulin but we do not know whether barnacles possess endogenous insulin or an insulin-like peptide. The stimulatory action of insulin is confined to the phloretin- or cytochalasin B-sensitive component of sugar transport. In the presence of these inhibitors, insulin has no effect on sugar fluxes but in their absence it increases the rate of sugar uptake 2.4-fold and the rate of sugar exit approximately 2.5-fold. Denatured insulin, $ZnCl_2$ ($60\,\mu\mathrm{M}$) and albumin ($0.5\,\mathrm{mg\,ml^{-1}}$) are unable to mimic the effect of native insulin. Analysis of the kinetics of sugar uptake shows that insulin increases the V_{max} with little or no effect on the apparent K_m.

Insulin has been claimed to exert its action on sugar transport through changes in cyclic nucleotide levels or ionized Ca[1,2,4–6]. These possibilities can be examined directly using single barnacle muscle fibres. The effect of insulin on cyclic nucleotide levels is shown in Fig. 1. Insulin ($5\,\mathrm{U\,ml^{-1}}$) elicits a roughly simultaneous rise in cyclic GMP and fall in cyclic AMP levels which can be detected as early as 2 min after

0028-0836/80/290276-04$01.00

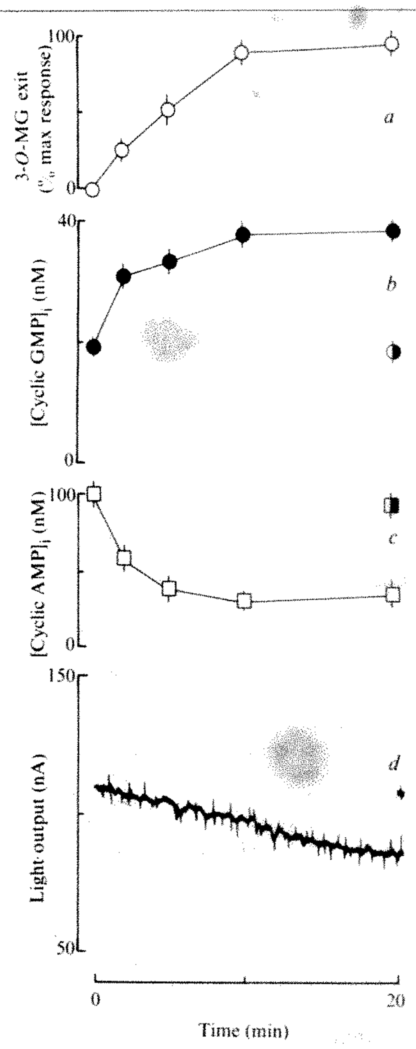

Fig. 1 *a–d* The effects of insulin ($5\,\mathrm{U\,ml^{-1}}$) on 3-*O*-methylglucose (3-*O*-MG) exit, cyclic nucleotide levels and aequorin light output in barnacle muscle. *a*, Time course of the stimulation of sugar exit in single muscle fibres by insulin Fibres were bathed in seawater, composition (mM): NaCl, 442; KCl, 10; $MgCl_2$, 53; $CaCl_2$, 11; Tris, 10, *p*H 7.6. Each point consists of four or more fibres. Mean fibre diameter, 1,326 µm; temperature, 11 ± 1 °C. *b*, Time course of the rise in cyclic GMP levels caused by insulin. Each point consists of six separate determinations. The concentration of cyclic GMP following 20 min incubation in insulin-free seawater (◑) is shown below the points. Temperature, 12 °C. Recovery of exogenous cyclic GMP added to barnacle muscle homogenate was 89.2%. *c*, Time course of the fall in cyclic AMP levels caused by insulin. Each point consists of five or six separate determinations. Cyclic AMP levels corresponding to 20 min incubation in seawater (◨) are shown above the points. Temperature, 12 °C. Recovery of exogenous cyclic AMP added to barnacle muscle homogenates was 93.4%. *d*, Time course of the change in intracellular free Ca as a result of exposure to insulin. The fibre was injected with aequorin and left in flowing seawater for 2 h to allow the aequorin to diffuse uniformly across the cell. The figure is a tracing of the photomultiplier output as displayed on a pen recorder. The light output was stable before application of insulin. Above the record at 20 min is shown the level to which light output recovered after 20 min in insulin-free seawater. Fibre diameter, 984 µm; temperature, 11 °C.

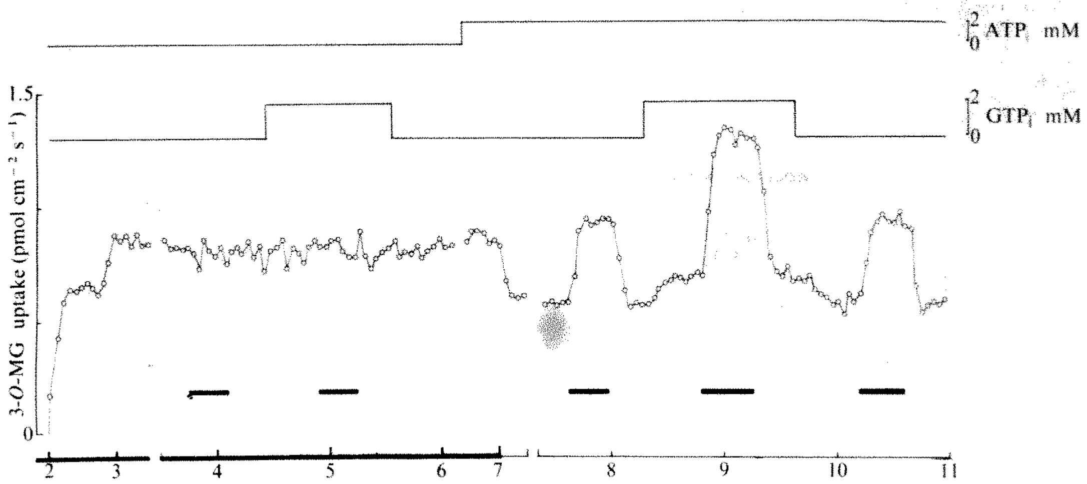

Fig. 2 The effect of insulin on 3-*O*-methylglucose uptake in an internally dialysed muscle fibre. The fibre was dialysed with a solution of the following composition (mM): K aspartate, 150; NaCl, 32; $MgCl_2$ (in excess of ATP), 10; $CaCl_2$, 1.5; EGTA, 5; HEPES, 5; PIPES, 5; NaCN, 2; ECCP, $2\,\mu\mathrm{g\,ml^{-1}}$; phenol red, 2, *p*H 7.0. The osmolarity was adjusted to 975 mosM with sucrose. ATP was added to the solution as MgATP. In calculating the concentration of ionized Ca, the log of the stability constant for Ca-EGTA at *p*H 7.0 was taken as −6.723. Internal ATP and GTP concentrations are shown above the points. External application of insulin ($5\,\mathrm{U\,ml^{-1}}$) is indicated by the solid bars. The external 3-*O*-methylglucose concentration was 2 mM in all dialysis experiments. The fibre was dialysed for 2 h with a solution containing 0 ATP before external application of isotope. Fibre diameter, 985 µm; temperature, 10 °C. As in Fig. 4, sugar uptake is expressed as $\mathrm{pmol\,cm^{-2}\,s^{-1}}$.

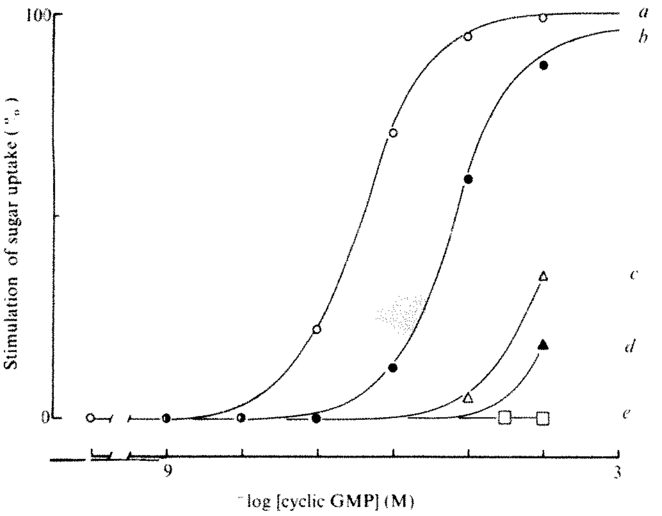

Fig. 3 The effect of raised internal free Ca on the activation of 3-*O*-methylglucose uptake by cyclic GMP. The data are pooled from six fibres. Each curve shows the cyclic GMP-dependent activation of sugar uptake at different Ca levels. The small activation caused by raising the internal ionized Ca concentration is subtracted from each point. The ionized Ca levels are 0.91, 0.5, 0.41, 0.27 and 0.12 μM for curves *a*–*e*, respectively. Curves *a*–*c* are calculated by Lineweaver–Burk analysis, on the assumption that the maximum stimulation in all cases is 100%. The apparent Michaelis constants for cyclic GMP are: curve *a*, 4.12×10^{-7} M; curve *b*, 6.92×10^{-6} M; curve *c*, 1.9×10^{-4} M. Curves *d* and *e* are drawn by eye. Mean fibre diameter 1,241 μm; temperature, 10 °C.

adding insulin to the medium. The changes in cyclic nucleotide levels seem to precede the change in the rate of sugar exit; this is not inconsistent with the possibility that insulin increases sarcolemmal sugar permeability through alterations in cyclic nucleotide levels.

The hypothesis that insulin acts in muscle by mobilizing intracellular Ca can be tested directly in the barnacle muscle fibre using the Ca-sensitive photoprotein aequorin. Fibres were injected axially with aequorin and the light emitted passed along a fibre optic system to a photomultiplier (EMI, 9635 B) the output of which was displayed on a pen recorder. Resting light output was calibrated by use of a variety of Ca-EGTA buffers[7] and, on the assumption of an internal ionized Mg of 4 mM (ref. 8) and *p*H of 7.2 (ref. 9), the light output was found to correspond to a free internal Ca of 70 nM. On exposing fibres loaded with aequorin and isotopic 3-*O*-methylglucose to insulin (5 U ml^{-1}), there was a simultaneous increase in the rate of sugar exit and a small, but reproducible, fall in the resting light output (Fig. 1). This effect on light output was not mimicked by $ZnCl_2$ (60 μM), denatured insulin or albumin (0.5 mg ml^{-1}). A fall in light output was rather unexpected in view of the claims that insulin may increase intracellular ionized Ca. It is well known that intracellular ionized Ca can be manipulated by altering external Ca or replacing external Na with Li, and the effects of these manoeuvres on sugar fluxes were examined. Removal of external Ca reduced light output by some 70% and replacement of Na by Li increased light output eight-fold; however, sugar exit in both conditions was unaffected. We conclude that although insulin seems to reduce internal free Ca in barnacle muscle, its effect on sugar transport in this preparation seems not to be related in any simple way to the myoplasmic ionized Ca concentration.

Another way to examine this problem is to use internally dialysed muscle fibres[3]. With this technique it is possible to clamp the ionized Ca to some predetermined level using Ca-EGTA buffers; if a change in ionized Ca is a prerequisite of insulin action, it should be impossible to elicit any response to insulin in conditions of dialysis with solutions containing EGTA buffers. This was certainly not the case. Figure 2 shows that, provided ATP was in the dialysis solution, insulin stimulated the rate of sugar uptake in the presence of a buffered Ca concentration of 120 nM and the stimulatory effect of insulin was enhanced when GTP (2 mM) was also included in the internal solution. This action of insulin was not seen in dialysed fibres exposed to cytochalasin B. These observations suggest that although intracellular ATP is essential for insulin action, alterations in internal ionized Ca are probably not necessary.

Figure 2 also shows that ATP *per se* has an effect on sugar fluxes. In the nominal absence of ATP the uptake of sugar increased. This is consistent with the well known effects of metabolism and anoxia on sugar fluxes in muscle cells[6]. The concentration of ATP which produced half-maximal inhibition of 3-*O*-methylglucose uptake was 0.4 mM.

Using the dialysed muscle fibre it is possible to examine whether any of the alterations in cyclic nucleotide levels or ionized Ca brought about by application of insulin are capable

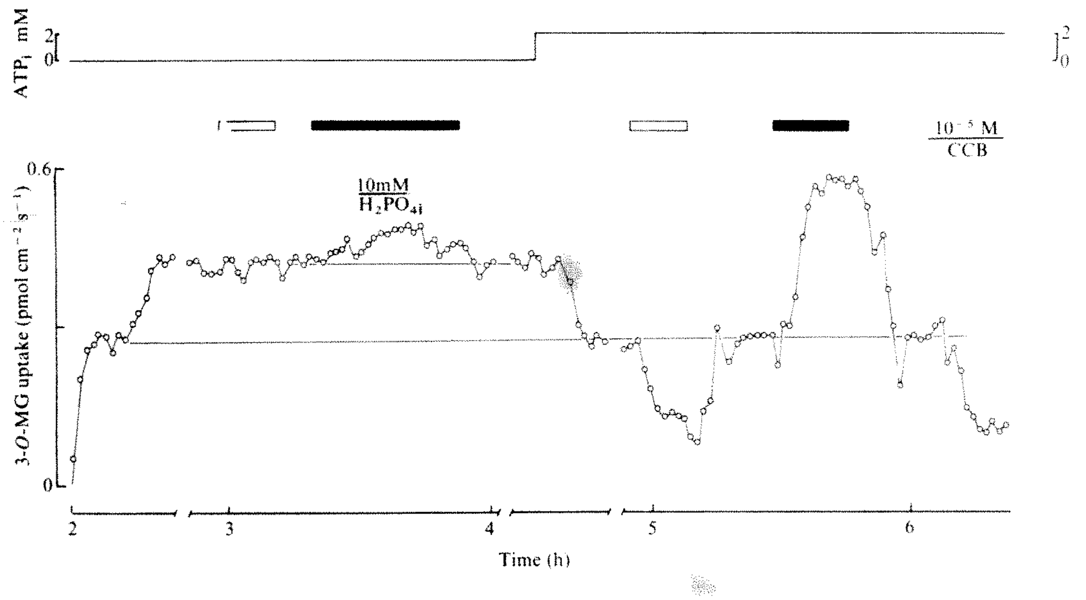

Fig. 4 Effect of cyclic nucleotides on sugar uptake in dialysed muscle. Internal solution as in Fig. 2. Internal ionized Ca = 0.91 μM. The internal ATP concentrations are shown above the points. Internal application of cyclic AMP (10^{-6} M) and cyclic GMP (10^{-4} M) are indicated by the open and closed bars, respectively. Cytochalasin B (CCB) was applied externally at the end of the experiment. Fibre diameter, 1,098 μm; temperature 10 °C.

themselves of mimicking the action of insulin on sugar fluxes. Raising internal Ca from 0.12 to 0.91 μM produced a small increase in the rate of sugar uptake averaging 1.27-fold. It follows that a fall in ionized Ca as seen after application of insulin should, if anything, reduce sugar uptake.

Internal application of cyclic AMP reduced the rate of sugar uptake in dialysed muscle. When cyclic AMP (100 μM) was added to an internal solution containing 2 mM ATP and a free Ca of 0.12 μM, 3-*O*-methylglucose uptake was reduced to 29.1 ±4.5% of control values ($n=5$). This inhibition of uptake was half maximal at 10^{-6} M cyclic AMP_i and was independent of the internal free Ca concentration.

When the internal free Ca was low (0.12 μM), internal application of cyclic GMP had no effect on the rate of sugar uptake. On raising the internal ionized Ca from 0.12 to 0.91 μM, however, cyclic GMP_i (100 μM) rapidly and reversibly stimulated the rate of 3-*O*-methylglucose uptake 2.13-fold ($n=4$). Raising internal free Ca seemed to increase the affinity of the system for cyclic GMP. Thus, increasing internal free Ca from 0.5 to 0.91 μM reduced the concentration at which cyclic GMP stimulated the rate of sugar uptake from 6.9×10^{-6} to 4.2×10^{-7} M (see Fig. 3). Figure 4 shows that ATP_i must be present for both cyclic AMP and cyclic GMP to influence the rate of sugar transport.

These results show that sugar uptake can be affected by changes in ionized Ca, cyclic AMP and cyclic GMP; however, can the measured changes in these parameters in intact muscles account quantitatively for the observed stimulation of sugar fluxes in dialysed muscles? Although the changes are somewhat smaller than those needed to alter sugar fluxes in dialysed fibres, it is unlikely that cyclic nucleotide levels are uniform across the fibre. Bearing in mind the peripheral location of adenylate cyclase in the plasma membrane, it is very possible that cyclic AMP is at appreciably higher concentrations in the myoplasm close to the sarcolemma. If this is the case, a fall in cyclic AMP could certainly play a part in mediating the increase in sugar transport brought about by insulin. The experiments on dialysed fibres suggest that alterations in cyclic GMP could be important when the background level of ionized Ca is raised, for instance during exercise; however, it is possible that dialysis removes some small molecular weight factor that is synergistic with cyclic GMP.

Received 12 January; accepted 15 April 1980.

1. Czech, M. P. *A. Rev. Biochem.* **46,** 359–384 (1977).
2. Bittar, E. E., Schultz, R. & Harkness, C. *J. Membrane Biol.* **34,** 203–227 (1977).
3. Brinley, F. J. Jr & Mullins, L. J. *J. gen. Physiol.* **50,** 2303–2331 (1967).
4. Fain, J. N. in *MTP Int. Rev. Sci., Biochem. Ser. 1* Vol. 8 (ed. Rickenberg, H. V.) 1–23 (University Park Press, Baltimore, 1974).
5. Illiano, G., Tell, G. P. E., Siegel, M. I. & Cuatrecasas, P. *Proc. natn. Acad. Sci. U.S.A.* **70,** 2443–2447 (1973).
6. Clausen, T. *FEBS Symp.* **42,** 481–499 (1977).
7. Baker, P. F., Hodgkin, A. L. & Ridgway, E. B. *J. Physiol., Lond.* **218, 709–755 (1971).**
8. Brinley, F. J. Jr, Scarpa, A. & Tiffert, T. *J. Physiol., Lond.* **266,** 545–565 (1977).
9. Boron, W. F. & Roos, A. *Am. J. Physiol.* **231,** 799–809 (1976).

Evidence for two insulin receptor populations on human erythrocytes

Victoria Herzberg, J. Mark Boughter, Sandra Carlisle & Donald E. Hill

Department of Pediatrics, University of Arkansas for Medical Sciences, Little Rock, Arkansas 72201

Human erythrocytes specifically bind ^{125}I-insulin in a manner similar to cells in which insulin exerts a physiological response[1]. In addition, erythrocytes are of practical value for correlating *in vitro* insulin binding with *in vivo* carbohydrate intolerance[2,3]. The competitive binding of labelled and unlabelled insulin to erythrocyte receptors is typically curvilinear when plotted according to Scatchard[4]. The curvilinear nature of the Scatchard plot describing insulin binding to membrane receptors, although originally attributed to heterogeneous sites[5], has been more recently interpreted as negative cooperativity between homogeneous sites[6]. Evidence reported here, however, suggests that there are two populations of insulin receptors on erythrocytes. Specific concentrations of concanavalin A (Con A), a lectin which mimics insulin activity[7], are shown here to inhibit one population of receptors leaving another population unaffected.

As Fig. 1 shows, Con A competes with labelled insulin for the erythrocyte receptors. After increasing the concentration of Con A to 5 μg ml^{-1}, a 50% reduction in ^{125}I-insulin binding was observed. Concentrations of Con A greater than 20 μg ml^{-1} presented problems with cell agglutination.

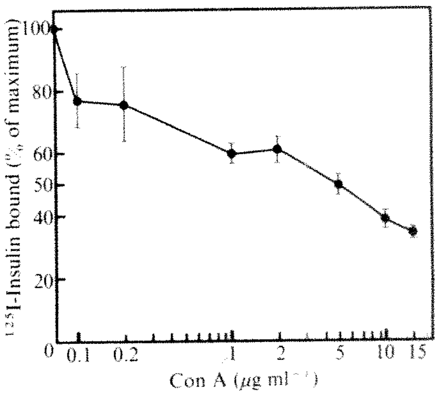

Fig. 1 Effect of Con A on the specific binding of ^{125}I-insulin to human erythrocytes. Data from five normal adult volunteers are expressed as mean ± 2s.d. Blood was collected in EDTA, and erythrocytes were purified on Isolymph (Gallard-Schlesinger) gradients[10], yielding a relatively homogeneous population of mature erythrocytes (0.01% granulocytes; ≃1% reticulocytes). Crystalline porcine insulin (Lilly) was labelled with ^{125}I to a specific activity of 125–150 μCi per μg (refs 16, 17). 1.5×10^{9} erythrocytes were added to a series of tubes in which ^{125}I-insulin (0.2 ng ml^{-1}) and increasing amounts of Con A (Sigma, grade IV) were mixed with Tris-HEPES buffer (*p*H 8.0, 284 mosmol per kg) to give a final volume of 0.5 ml. The erythrocyte receptor assay was as described before[1], with the following modifications: (1) ^{125}I-insulin was repurified on Sephadex G-50 immediately before use; (2) cells were incubated for 4 h (15 °C) to attain equilibrium binding, and (3) non-specific binding was determined in the presence of unlabelled insulin (10 μg ml^{-1}) and was subtracted from all data points before analysis.

In Fig. 2*a*, the individual curvilinear Scatchard plots obtained by the competitive binding of labelled and unlabelled insulin to erythrocyte receptors are illustrated with the 'best fit' line derived by 'Ligand' (ref. 8), a computer program designed to consider simultaneous analysis of n ligands binding to m classes of binding sites. In this instance, a single ligand (insulin) was investigated. The broken lines represent two heterogeneous, non-interacting binding sites mathematically derived from the 'best fit' line, illustrating each binding species as though the other were not present. The slope of each line represents the affinity (K_1, K_2) while the abscissa intercepts (R_1, R_2) approximate the maximum binding capacity of the two receptor populations. One receptor population (I) has a high affinity and low capacity for insulin, whereas the other (II) has a low affinity and high capacity for insulin. These lines may also be derived graphically as described by Rosenthal[9].

The experimentally determined insulin binding data obtained in the presence of Con A (Fig. 2*b*) approximate the mathematically derived site II. Variations in the concentration of Con A which proved optimal for linearization of the Scatchard plot were noted when erythrocytes from different

0028–0836/80/290279–03$01.00

individuals were tested; however, in all cases, a linear component whose correlation coefficient varied from −0.90 to −0.98 was observed. Insulin binding in the presence of Con A therefore demonstrates complete inhibition of binding site I and clearly delineates site II. The suppression of insulin binding at site I by Con A may result from steric hindrance by the larger Con A molecule binding to a contiguous site, direct competition for the same site, or indirect competition for a necessary binding component. The disclosure of site II indicates that this site may be physically removed and (or) biochemically distinct from site I.

Table 1 compares the values for the affinity and maximum binding capacity obtained by Ligand analysis of the individual Scatchard plots. Both the experimental (+Con A) and the theoretical (−Con A) binding values for site II mathematically approximate the same line. The affinity reported here cannot be directly compared with published values of average affinity constants which are based on receptor occupancy and the negative cooperativity model[6]. The maximum binding capacity, used to determine the number of sites per cell, varies considerably in the literature depending on the highest concentrations of ligand chosen by the investigator for extrapolation of the Scatchard plot to provide an abscissa intercept; for example, reported values for erythrocytes vary from 34 (ref. 10) to 2,000 (ref. 1) sites per cell. There are approximately 11 sites per cell calculated from the R2 value in Table 1, and R1 represents an average of approximately one site per cell; yielding a total of 12 insulin binding sites per erythrocyte when analysed by a two-site model. In view of these data, the difficulty in documenting a physiological response to insulin in erythrocytes is understandable.

Experimental parameters investigated in these experiments describe receptor characteristics well within the normal physiological range of circulating insulin concentrations (0.2–20 ng ml^{-1} = 5–475 μU ml^{-1}). As insulin concentrations are increased beyond this range, experimental data demonstrate that trace amounts of labelled insulin continue to be bound, accounting for the asymptotic nature of the Scatchard plot. This nonsaturable component can be treated mathematically by the Ligand program.

Erythrocytes demonstrate both enhanced dissociation[1] and, as shown here, heterogeneous populations of receptors. Enhanced dissociation of ^{125}I-insulin from receptors in the presence of excess unlabelled insulin has been explained by negative cooperativity between homogeneous receptors[6]. However, the phenomenon of enhanced dissociation cannot be explained by the presence of non-interacting, heterogeneous sites[11]. It is thus possible that there are site–site interactions among receptors of a single type, as suggested for adipocyte insulin receptors[12], or that one receptor population consists of an aggregated form of the other receptor population.

There are several interesting parallels between membrane receptors for Con A and insulin. Con A erythrocyte receptors are associated with physical particles on the membrane which influence glucose flux[13], and a specific minor membrane glycoprotein known to influence anion permeability[14]. Both of these transmembrane functions are stimulated by insulin in hormone-sensitive cell types. Insulin has also been shown to interfere with Con A binding sites on myoblasts, thus inhibiting the Con A-stimulated formation of myotubules[15]. Although these observations seem to favour a common or physically adjacent site for Con A and insulin membrane receptors, it is also possible that these molecules compete for the component(s) necessary for aggregation of receptor sites, a phenomenon observed for both Con A[14] and insulin[18] receptors. The data reported here augment these important similarities between Con A and insulin receptors and also provide evidence for heterogeneous populations of insulin receptors on human erythrocytes.

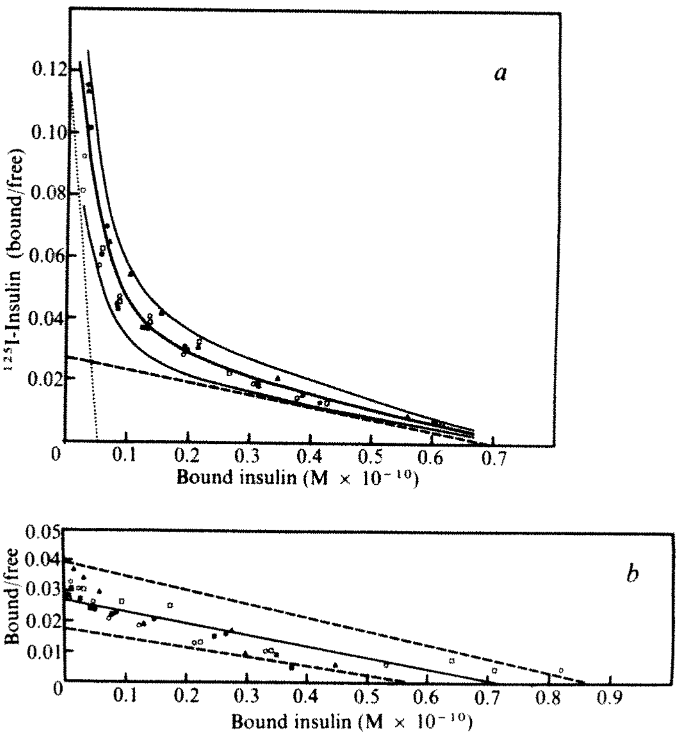

Fig. 2 Scatchard plots of insulin binding to erythrocytes from five individuals (as in Fig. 1) in the absence (*a*) and presence (*b*) of Con A. The ratio of bound to free insulin is plotted as a function of the molar quantity of bound insulin. Insulin concentrations varied from 0.2 to 100 ng ml^{-1} in the absence of Con A and from 0.2 to 20 ng ml^{-1} in the presence of Con A. *a*, Computer resolution of the curvilinear Scatchard plot, shown as the best fit line ± 2s.d. yields high affinity (......) and low affinity (– – – –) components. *b*, Data points obtained in the presence of Con A (5–10 μg ml^{-1}) are shown in comparison to receptor site II (——) ± 2s.d. (----) as determined by computer analysis of data in the absence of Con A.

Table 1 Comparison of binding parameters between Scatchard plots in the presence and absence of Con A

	Site I		Site II	
	K_1	R_1	K_2	R_2
	$\times 10^{10}$ M^{-1}	$\times 10^{-12}$ M	$\times 10^{8}$ M^{-1}	$\times 10^{-11}$ M
No Con A*	2.25 ± 1.07	5.39 ± 1.6	3.83 ± 0.81	7.11 ± 0.72
+Con A†	Undetectable		3.95 ± 0.56	7.03 ± 0.90

The values for affinity (*K*) and maximum binding (*R*) were determined from data illustrated in Fig. 2 and averaged to determine the mean ± s.e. (*n* = 5).

*From experimental data points shown in Fig. 2*a*.

†From experimental data points shown in Fig. 2*b*.

We thank Dr Dan Sheehan for verifying the original Rosenthal analyses, Drs David Rodbard and Peter Munson for helping us implement the 'Ligand' program; Drs David Straub and Jim Norris for reviewing the manuscript, and Dr Sanford Roth for initial suggestions. This work was supported by institutional grants from the University of Arkansas for Medical Sciences.

Received 31 January; accepted 16 April 1980.

1. Gambhir, K. K., Archer, J. A. & Bradley, C. J. *Diabetes* **27**, 701–708 (1978).
2. Wachslicht-Rodbard, H., Gross, H. A., Rodbard, D., Ebert, M. H. & Roth, J. *New Engl. J. Med.* **300**, 882–887 (1979).
3. Robinson, T. J. *et al. Science* **205**, 200–202 (1979).
4. Scatchard, G. *Ann. N.Y. Acad. Sci.* **51**, 660–672 (1949).
5. Gavin, J. R. III, Gorden, P., Roth, J., Archer, J. A. & Buell, D. N. *J. biol. Chem.* **248**, 2202–2207 (1973).
6. De Meyts, P., Bianco, A. R. & Roth, J. *J. biol. Chem.* **251**, 1877–1888 (1976).
7. Cuatrecasas, P. *J. biol. Chem.* **248**, 3528–3534 (1973).

8 Munson, P J & Rodbard, D *Analyt Biochem* (in the press)
9 Rosenthal, H E *Analyt Biochem* **20**, 525–532 (1967)
10 Herzberg, V L, Boughter, J M, Carlisle, S K, Ahmad, F & Hill, D E *Pediat Res* **14**, 4–7 (1980)
11 Rodbard, D *Am J Physiol* **237**, E203–E205 (1979)
12 Olefsky, J M & Chang, H *Diabetes* **27**, 946–958 (1978)
13 Pinto da Silva, P. & Nicolson, G L *Biochim biophys Acta* **363**, 311–319 (1974)
14 Gordon, J A, Staehelin, L A & Kuettner, C. A *Expl Cell Res* **110**, 439–448 (1977)
15 Kahn, C. R, Baird, K L, Jarrett, D B & Flier, J S *Proc natn Acad Sci U S A* **75**, 4209–4213 (1978)
16 Freychet, P, Roth, J & Neville, D M *Biochem biophys Res Commun* **43**, 400–408 (1971)
17 Schneider, B, Straus, E & Yalow, R *Diabetes* **25**, 260–267 (1976)
18 Sandra, A, Leon, M A & Przybylski, R J *Endocrinology* **105**, 391–401 (1979)

An effect of chloride on (Na+K) co-transport in human red blood cells

A. R. Chipperfield

Department of Physiology, University of Dundee,
Dundee DD1 4HN, UK

In certain conditions, internal K can stimulate active Na:K transport as well as Na:Na exchange through the ouabain-sensitive Na, K exchange pump[1]. When the exchange was examined during a study of the action of internal K, it emerged that the removal of K_o (the main requirement for Na:Na exchange[2,3]) reduced the ouabain-insensitive Na efflux. Thus, in eight experiments done variously with outdated cells or high and low $[K]_o$, PCMBS-treated cells, the K_o-dependent Na efflux ranged from 0.18 to 0.70 µEquiv per ml cells per h. This conflicts with the well established view that the K_o-dependent and ouabain-sensitive components of Na efflux are identical[3,4]. However, the K_o-dependent, ouabain-insensitive Na efflux was found to go through the (Na+K) co-transport system, which was further found to show a dependence on chloride ions.

In a further eight experiments, specifically designed to test the effect of K_o on the ouabain-insensitive Na efflux, the same pattern emerged. The K_o-dependent, ouabain-insensitive efflux varied from 0.16 to 0.96 µEquiv per ml cells per h (or from 8 to 41% of the total). But why did this happen in this study and not before? The reason seems to be because Ca, Mg and phosphate are absent in the external medium (this unusual feature derives from an earlier study of the kinetics of the pump[5] where any possible interference was to be avoided; this does not affect the sensitivity to ouabain). Thus, when any of the ions Ca, Mg or phosphate were present the effect of K_o was reduced and with all three present it was abolished. Moreover, it was not seen when Na_o was replaced by Li or by Mg. Thus, there may be several reasons why a K_o-dependent, ouabain-insensitive Na efflux has not been seen before.

Table 1 Tracer ^{24}Na efflux from human RBC in the presence of ouabain

External medium	Na efflux (µEquiv per ml cells per h) With 150 mM $[Cl]_o$	 With 30 mM $[Cl]_o$
Complete	2.19±0.31	1.73±0.12
K-free	1.74±0.14	1.78±0.14
Complete+ furosemide (1 mM)	1.48±0.12	1.59±0.14
K free+ furosemide (1 mM)	1.65±0.17	1.65±0.14

Tracer ^{24}Na efflux from outdated human RBC was measured as described elsewhere[1–5] in a medium containing 142 mM NaCl, 8 mM KCl, 8 mM Tris–Cl, *p*H 7.5, 10 mM inosine[16] and 0.1 mM ouabain. When K was omitted, KCl was replaced by NaCl external [Cl] was reduced by replacing NaCl, KCl and Tris–Cl by the corresponding nitrates. The results of this and the other four similar experiments show that the K_o-dependent, ouabain-insensitive flux in 150 mM external chloride is statistically significant (Student's *t* test, $P<0.003$); in contrast, this component of Na influx is not significant in media containing 30 mM $[Cl]_o$, furosemide or both. Results are the means of three determinations (±s.e.m.)

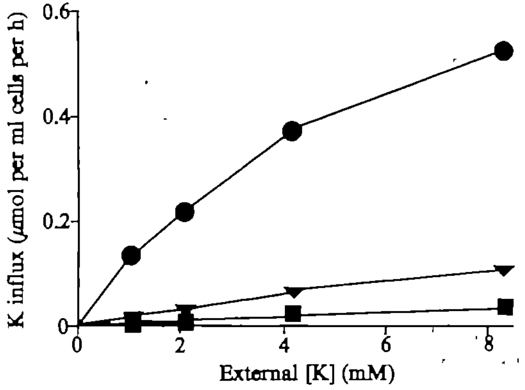

Fig. 1 External [K] dependence of ouabain-insensitive K influx into human RBC. K influx was measured as described in Table 2 (experiment 2): each point is the mean of two determinations (errors, which are not shown were comparable to those in Table 2). ●, Control: 150 mM $[Cl]_o$; ▼, 30 mM $[Cl]_o$; ■, 150 mM $[Cl]_o$ with 1 mM furosemide (the results for 30 mM $[Cl]_o$ with 1 mM furosemide (not shown) were the same as for 150 mM with furosemide).

If there is a ouabain-insensitive, K_o-dependent component of Na efflux, it is most likely to be related to the furosemide-sensitive (Na+K) co-transport system identified in RBC by Wiley and Cooper[6]. If so, is it related to the furosemide-sensitive, external Cl-dependent K:K exchange in ascites cells[7,8]? The results of one of five experiments designed to test these possibilities are shown in Table 1. Three features were noted: (1) furosemide inhibited the ouabain-insensitive, K_o-dependent efflux, (2) on replacing most of the Cl_o with nitrate, Na efflux was reduced and (3) the ouabain-insensitive, K_o-dependent efflux was smaller in nitrate-containing media.

These results, taken together with the studies mentioned before[6–8], are consistent with the idea that a large part of the Na efflux goes by a (Na+K+Cl) co-transport system. If this is so, then the furosemide-sensitive K influx should be reduced on lowering $[Cl]_o$. The results of the first experiment in Table 2 (leaving aside, for the moment, the tests with phloretin) bear out this prediction.

The results of the second experiment in Table 2 show that similar results were obtained when K influx was assessed using ^{86}Rb as tracer (this was also true for Rb influx). Accordingly, this technique was used in further comparisons with earlier work. Thus, the saturable, furosemide-sensitive passive K influx[2,3,6] was reduced on lowering $[Cl]_o$ (Fig. 1). There was a roughly linear dependence on $[Cl]_o$ (ref. 8) of K influx (Fig. 2). With anions other than nitrate, there was a substantial furosemide-sensitive K influx with bromide but not with

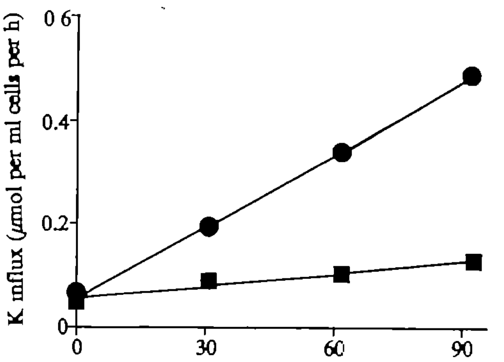

Fig. 2 External [Cl] dependence of ouabain-insensitive K influx into human RBC. K influx was measured as described in Table 2 (experiment 2): each point is the mean of three determinations (errors (not shown) were comparable to those in Table 2). ●, Control; ■, with 1 mM furosemide.

0028-0836/80/290281-02$01.00

Table 2 K influx into human RBC in the presence of ouabain

External medium	Experiment 1 K influx (tracer ^{42}K) (μEquiv per ml cells per h) Control	 With furosemide	Experiment 2 K influx (tracer ^{86}Rb) (μEquiv per ml cells per h) Control	 With furosemide
Complete	0.83 ± 0.04	0.26 ± 0.00	0.99 ± 0.00	0.25 ± 0.00
30 mM [Cl]	0.36 ± 0.01	0.25 ± 0.02	0.36 ± 0.05	0.29 ± 0.01
Complete + phloretin	0.46 ± 0.04	0.24 ± 0.03	0.64 ± 0.01	0.24 ± 0.00
30 mM [Cl] + phloretin	—	—	0.28 ± 0.01	0.24 ± 0.02

K influx into outdated human RBC was measured as described elsewhere[1–5] in the same conditions (and with the same changes) as those given in Table 1; the concentration of phloretin used was 0.1 mM. The results shown are the mean of three determinations (± s.d.).

sulphate or acetate: bicarbonate raised both the furosemide-sensitive and furosemide-insensitive components of K influx. These new observations on cation and anion affinities fit the previous findings[2,3,6,8]. It was also shown that passive K influx was half-maximally inhibited by 5×10^{-6} M furosemide.

Three other sets of results should be mentioned. First, experiments on fresh cells: here, the effects of furosemide and $[Cl]_0$ reduction on Na efflux were the same but K_0 had no effect (giving another reason why this flux has not been seen before). Second, experiments with phloretin: this drug reduced, but did not abolish, the K_0- and Cl_0-dependent Na efflux and likewise for K influx (Table 2). Moreover, furosemide and phloretin together inhibited no more than furosemide alone. Evidently, the co-transport system is the same as the phloretin- and furosemide-sensitive (Na-Li) counter-transport system identified in RBC by Tosteson and co-workers[9]. Third, there is the extensive work by Wieth on anion and cation effects on passive fluxes in RBC[10,11]; some of his results, for example, an increase in Na influx in 120 mM nitrate, seem to conflict with mine. The most likely explanation for these discrepancies is that his media contained Ca, Mg and phosphate, all of which may alter the results (see above) as well as bicarbonate, which alters passive permeability too[10].

(Na + K) co-transport[6] is clearly affected by chloride but direct evidence for Cl^- transport by the same system in RBC is lacking. On the other hand, furosemide-sensitive co-transport (or counter-transport) for each pair of ions has been found in several tissues and often these are invoked to explain ion distributions that do not seem to be in equilibrium[6–9,12–14]. Is it reasonable to speculate that some of these share the same pathway? Certainly, this view would be consistent with the idea that 'dissipative' fluxes may be coupled to uphill movements of another species[15].

I thank Mrs C. J. Hall for technical assistance, the Scottish Hospitals Endowments Research Trust for financial support and Hoechst UK Ltd for the gift of furosemide.

Note added in proof: A recent, independent study by Dunham *et al.*[17] also bears on the chloride dependence of furosemide-sensitive fluxes.

Received 13 September 1979; accepted 21 April 1980.

1. Garay, R. P. & Garrahan, P. J. *J. Physiol., Lond.* **231**, 297–325 (1973).
2. Garrahan, P. J. & Glynn, I. M. *J. Physiol., Lond.* **192**, 189–216 (1967).
3. Glynn, I. M. Lew, V. L. & Luthi, U. *J. Physiol., Lond.* **207**, 371–391 (1970).
4. Glynn, I. M. *J. Physiol., Lond.* **136**, 148–173 (1957).
5. Chipperfield, A. R. & Whittam, R. *J. Physiol., Lond.* **260**, 371–385 (1976).
6. Wiley, J. S. & Cooper, R. A. *J. clin. Invest.* **53**, 245–755 (1974).
7. Tupper, J. T. *Biochim. biophys. Acta* **394**, 586–596 (1975).
8. Bakker-Grunwald, T. *Biochim. biophys. Acta* **513**, 292–295 (1978).
9. Pandey, G. N. *et al. J. gen. Physiol.* **72**, 233–247 (1978).
10. Funder, J. & Weith, J. O. *Acta physiol. scand.* **71**, 168–185 (1967).
11. Weith, J. O. *Acta physiol. scand.* **79**, 76–87 (1970).
12. Heinz, E., Geck, P., Pietrzyk, C., Burckhardt, G. & Pfeffer, B. *J. supramolec. Struct.* **6**, 125–133 (1977).
13. Russell, J. M. *J. gen. Physiol.* **73**, 801–818 (1979).
14. Eveloff, J., Hildmann, B., Kinne, R. & Murer, H. *J. Physiol., Lond.* **285**, 9P–10P (1978).
15. Lew, V. L. & Beauge, L. in *Membrane Transport in Biology* Vol. 2 (eds Giebisch, G., Tosteson, D. C. & Ussing, H. H.) 81–115 (Springer, Berlin, 1979).
16. Whittam, R. & Wiley, J. S. *J. Physiol., Lond.* **199**, 485–494 (1968).
17. Dunham, P. B., Stewart, G. W. & Ellory, J. C. *Proc. natn. Acad. Sci. U.S.A.* **77**, 1711 (1980).

0028-0836/80/290282-04$01.00

High-affinity binding sites for juvenile hormone I in the larval integument of *Drosophila hydei*

Gerhard Klages & Hans Emmerich

Institut für Zoologie, Technische Hochschule Darmstadt,
Schnittspahnstrasse 10, D 6100 Darmstadt, FRG

Martin G. Peter

Institut für Organische Chemie und Biochemie, Rheinische Friedrich-Wilhelms-Universität Bonn, Gerhard-Domagk-Strasse 1, D 5300 Bonn, FRG

Insect juvenile hormones (JH) maintain larval characteristics of insects during growth and development. At high JH titres the larval hypodermis is programmed to secrete larval cuticle in the following moult[1]. Generally, the molecular events preceding the response of a target cell to a hormonal stimulus involve binding of the hormone to specific receptor molecules. There are little data available on the primary mechanism of action of JH at the molecular level. We have demonstrated the specific uptake and retention of JH-I in the cytosol of larval *Drosophila hydei* integument *in vitro* (G.K. and H.E., in preparation). We now report the discovery of high-affinity, high-specificity JH-binding principles that exhibit characteristic properties of hormone receptors, in the cytosol of early third instar *D. hydei* larval integument.

Because it has been established that receptors for steroid hormones in vertebrates[2] and invertebrates, especially the fruitfly *Drosophila*[3,4] and the crayfish *Orconectes*[5], exist in the cytosol of target cells in only very low concentrations, we started our search for receptors of the non-steroid JH using competition experiments with standard techniques. A large excess of nonradioactive racemic (2*E*,6*E*)-10,11-*cis*-JH-I was competed with either racemic or optically pure preparations of JH-I (ref. 6) labelled with tritium at high specific activity. The results are shown in Fig. 1: the presence of competible (specific) JH-I binding sites becomes apparent from the competition curves for both racemic and optically active preparations of radiolabelled JH-I. However, remarkably different results were obtained; first, the enantiomerically pure, naturally occurring (10*R*,11*S*)-JH-I is bound to cytosol

Table 1 Competitive displacement of [*methoxy*-^{3}H](10*R*,11*S*)-JH-I from partially purified high-affinity JH-binding sites by enantiomerically pure (10*R*,11*S*)-JH-I and racemic JH-I, respectively

Competitor (ng per test tube)	% Displacement of [*methoxy*-^{3}H](10*R*,11*S*)-JH-I by (10*R*,11*S*)-JH-I	 Racemic JH-I
0.4	24.7	1.7
1.3	48.8	10.0
9.1	54.8	20.9

High-affinity JH-binding sites were prepared by gel filtration of cytosol through Sepharose 6-B, equilibrated with TMG-buffer, *p*H 7.2, at 0 °C. The specific JH-binding sites were contaminated with nonspecific JH-binding sites. 8,600 c.p.m. [*methoxy*-^{3}H](10*R*,11*S*)-JH-I (0.32 ng per test tube = 1.1 nM) were incubated for 1 h at 4 °C with the indicated concentrations of (10*R*,11*S*)-JH-I or racemic JH-I. Bound radioactivity was measured in 100-μl aliquots by the charcoal adsorption technique. The enantiomerically pure (10*R*,11*S*)-JH-I was extracted from 3–4 day old *Hyalophora cecropia* accessory glands. The purification method of extracts includes low temperature precipitation of lipids, TLC on silica gel, chromatography on Sephadex LH-20, and HPLC on LiChrosorb Si 60 and Si 100. Purity was controlled by analytical HPLC on LiChrosorb Si 100.

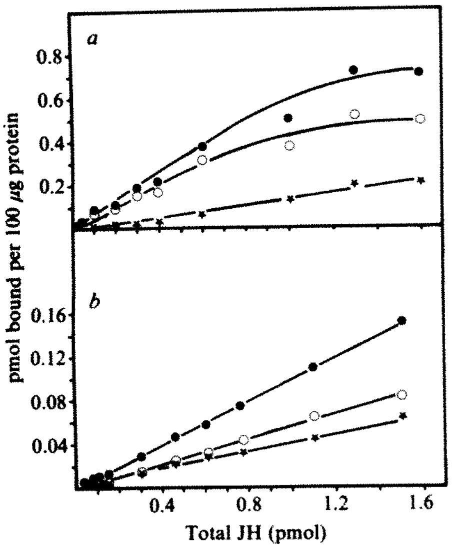

Fig. 1 Binding of *a*, enantiomerically pure [*methoxy*-^{3}H] (10*R*,11*S*)-JH-I (specific activity ~58 Ci mmol^{-1} (ref. 6)) and *b*, racemic [10-^{3}H]-JH-I (specific activity 11.5 Ci mmol^{-1}, NEN) to cytosol components. Larval integuments from early third instar larvae (120 h) were prepared and homogenized as described elsewhere[14]. Cytosol (120,000*g* supernatant) was prepared in TMG-buffer, *p*H 7.2, consisting of 10 mM Tris(hydroxy-methyl)-aminomethane, 15 mM β-mercaptoethanol, 20% glycerol, 1 mM EDTA, 50 mM KCl (all from Merck, Darmstadt), and 0.43 mM Trasylol (Bayer). JH metabolism was inhibited with 1 mM *p*-hydroxymercuribenzoate (Serva)[14]. Samples (100 μl) (containing 80–120 μg protein as determined in aliquots by the Lowry method[15]) of the cytosol were equilibrated for 30 min at 4 °C with increasing concentrations of [*methoxy*-^{3}H](10*R*,11*S*)-JH-I (0.02–1.6 pmol per 100 μl sample) or racemic [10-^{3}H]JH-I (0.04–1.5 pmol per 100 μl sample) in the absence (●) and presence (★) of a 100-fold excess of unlabelled racemic JH-I (Eco-Control), respectively. Bound and free radioactivity was separated by the charcoal adsorption technique with 0.42% dextran-coated charcoal (Serva)[8]. 100 μl of the supernatant (bound radioactivity) were measured by liquid scintillation counting using Aqualuma (Baker) as scintillation cocktail. The means of two duplicates, normalized on the basis of 100 μg cytosol protein are plotted. Specific binding (○) was considered as difference of total binding (●) and nonspecific binding (★).

constituents with a higher affinity than the racemic JH-I, even if the possibility is considered that 50% of the latter, represented by the (10*S*,11*R*) enantiomer, which does not occur naturally, is not bound at all. Second, in the concentration range tested, only the tritiated (10*R*,11*S*) enantiomer seems to be able to saturate the specific JH binding sites of the cytosol completely. It may be important to consider that with 1.6 pmol JH-I per test tube the limit of solubility is nearly reached in our buffer system on addition of the excess unlabelled JH-I. Third, the ratio of specific to nonspecific JH binding sites seems to depend on the optical purity of the hormone tested. Using tritiated (10*R*,11*S*)-JH-I it is 2.5, whereas it is only 1.5 using tritiated racemic JH-I.

Equilibrium dissociation constants (K_D) of JH binding sites were first determined in equilibrium conditions. Figure 2 shows the Scatchard[7] plots of binding data obtained with [*methoxy*-^{3}H](10*R*,11*S*)-JH-I and with racemic [10-^{3}H]JH-I. Increasing concentrations of the enantiomerically pure tritiated (10*R*,11*S*)-JH-I reveal the presence of two binding components with different affinities for the JH-I molecule. The apparent equilibrium dissociation constant (K_{De}) for the high-affinity JH-binding sites is 3.6×10^{-9} M. Similar equilibrium dissociation constants have been described for the macromolecular binding sites for ecdysteroids in *D. melanogaster* imaginal disks[3] and K_c cell lines[4]. The second JH-binding component exhibits a much lower affinity for JH-I ($K_{De}\approx10^{-7}$–10^{-6} M). Normalizing the data on the basis of protein content in the cytosol and correcting for low-affinity binding sites, a concentration of 7.7 pmol per mg cytosol protein is calculated for the free high-affinity JH-binding sites. With tritiated racemic JH-I (Fig. 2, inset), four JH-binding components are detectable. One of them shows a similar K_{De} value (4×10^{-9} M) to the high-affinity binding sites, detected with the enantiomerically pure JH-I. The additional binding components show apparent K_{De} values of 2×10^{-7} M, 8×10^{-7} M, and 10^{-5} M, with one of them ($K_{De}=2\times10^{-7}$ M) corresponding well to the haemolymph carrier protein ($K_{De}=1\times10^{-7}$ M)[8]. As it is essential to clarify whether this component results from contamination of the tissue preparation with haemolymph or whether it truly represents an intracellular constituent, we injected third instar larvae with ^{14}C-inulin solution. Following preparation of integuments 30 min after injection, the amount of label present was 0.65% of the total administered. Taking the concentration of the free JH-carrier protein into account[8], it is thus established that less than 4% of the 2×10^{-7} M JH-binding component found in the cytosol preparation results from contamination with haemolymph. It is therefore of interest first to isolate and characterize this JH-binding component for comparative studies with the haemolymph JH-carrier protein, and second, to investigate the possible role of the JH-carrier protein in the process of JH uptake into target tissues. An interesting analogy might be represented in this context by the mechanism of uptake of the diterpenoids retinol and retinoic acid in vertebrate target tissues[9].

An additional method was applied to obtain K_D values by measuring association and dissociation kinetics at 4 °C, using racemic [10-^{3}H]JH-I. The association of JH-I with cytosol constituents, shown in Fig. 3, follows second-order kinetics. Equilibrium between association and dissociation is reached after 30 min. Transformation of binding data into linear form (Fig. 3, inset) yields the association rate constant (k_{+1}) for total JH-binding sites. From the slope of the straight line, a k_{+1} of 2×10^6 M$^{-1}\times$min^{-1} is calculated. After reaching equilibrium the cytosol was chased with a 500-fold excess of non-labelled racemic JH-I. At appropriate times, bound radioactivity was measured in cytosol aliquots. From those data (not shown) a half-life time of approximatively 8 h at 4 °C for the hormone–macromolecule complex and a dissociation rate constant (k_{-1}) of 6.5×10^{-4} min^{-1} was calculated. The kinetic data are not impaired by a measurable loss of binding activity during the incubation period, due to the pronounced stability of the competible JH-binding sites at low temperatures; even after maintaining the cytosol for 2 days in

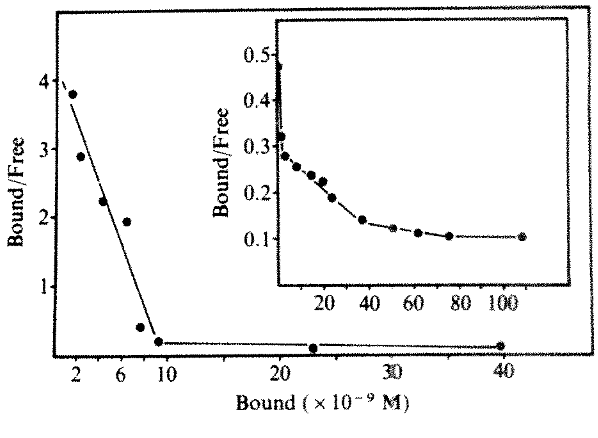

Fig. 2 Scatchard[7] analysis of ^{3}H-JH-I binding to cytosol components. Samples (100 μl) of larval integument cytosol, prepared as in Fig. 1, were equilibrated for 30 min at 4 °C with increasing concentrations of [*methoxy*-^{3}H](10*R*,11*S*)-JH-I (2–300 nM) or racemic [10-^{3}H]JH-I (1–1,100 nM) (inset), respectively. Bound radioactivity was measured as in Fig. 1. Each point represents the mean of duplicate experiments. Repeat experiments gave similar results.

ice, no change in binding behaviour was detectable. From the kinetic data an equilibrium dissociation constant (k_{-1}/k_{+1} $= K_D$) of 3.2×10^{-10} M results for the JH-binding sites, which is one order of magnitude lower than that obtained from the equilibrium binding data. Such differences are not uncommon in studies with protein–ligand complexes[10]. In any case, the K_D values obtained from both kinetic and equilibrium data clearly prove the presence of high-affinity JH-binding sites in the cytosol of *D. hydei* integument.

We do not know the biological significance of JH-binding sites showing different affinities for the JH molecule. We believe that the high-affinity binding sites might serve as JH receptors in the cytosol, comparable to those described for steroid hormones. Further support for this assumption is presented by experimental approaches towards this binding component. A molecule serving as JH receptor should meet the following requirements:

(1) receptors must be macromolecules. Gel filtration of crude cytosol preparations on Sephadex G-25 and on Sepharose 6-B, equilibrated with TMG-buffer, pH 7.2, without glycerol, revealed the macromolecular nature of specific JH-binding sites. Heating the macromolecular cytosol fractions for 10 min at 60 °C completely destroys the competible binding activity. (2) Receptors must show a high specificity for the natural hormone. The potential of some JH homologues and analogues to compete with [*methoxy*-^{3}H](10*R*,11*S*)-JH-I and racemic [10-^{3}H]JH-I for JH-binding sites was studied with crude cytosol. Among the compounds tested, racemic JH-I and JH-III were the most effective competitors of [*methoxy*-^{3}H]-(10*R*,11*S*)-JH-1 and racemic [10-^{3}H]JH-I bound to cytosol components (Fig. 4). The capacity to compete with the binding of [*methoxy*-^{3}H](10*R*,11*S*)-JH-I decreases in the following order: JH-I > JH-III > ethyl ester analogue of JH-III ≫ methyl farnesoate > ZR515. The sequence of competition efficiency with [10-^{3}H]JH-I is: JH-I ≈ JH-III > ethyl ester analogue of JH-III ≫ ZR515 > methyl farnesoate. Alterations in the structure of the JH-III molecule (the absence of the epoxy group as in methyl farnesoate or the presence of a ethyl ester group instead of a methyl ester group) markedly reduce the competing efficiency. It is of interest that the highly potent insect growth regulator ZR515, which has been used in pest control[11], indeed competes only very poorly with the JH-binding sites.

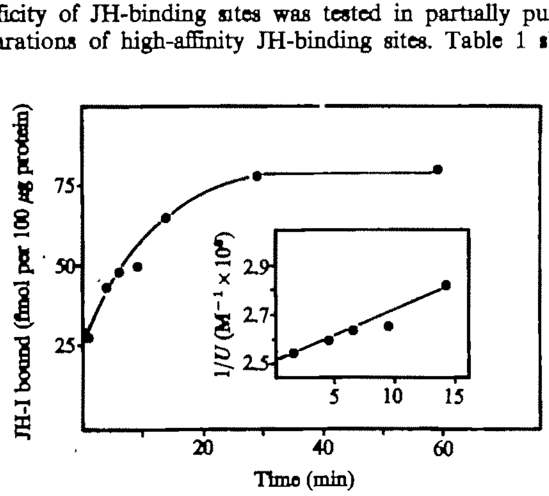

Fig. 3 Association kinetics of racemic [10-^{3}H]JH-I binding to cytosol components. Samples (100 µl) of larval integument cytosol, prepared as in Fig. 1, were incubated with 4 nM racemic [10-^{3}H]JH-I at 4 °C for the incubation periods indicated and bound radioactivity was measured as stated above. The means of two duplicates, normalized on the basis of 100 µg protein, are plotted. Inset, the inverse of unbound hormone concentration (1/*U*) is plotted as a function of time. The association rate constant (k_{+1}) for total JH-I binding is calculated from the slope of the straight line.

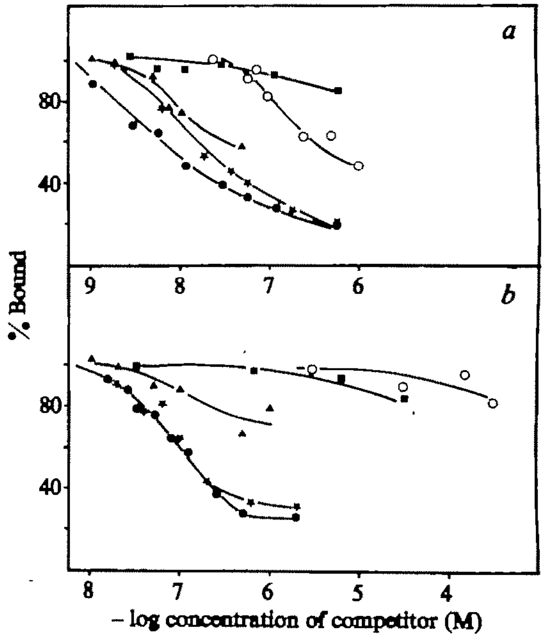

Fig. 4 Specificity of JH-binding sites in the cytosol of early third instar larvae integument. Samples (100 µl) of the cytosol, prepared as in Fig. 1, were equilibrated for 30 min at 4 °C with: *a*, 1.1 nM [*methoxy*-^{3}H](10*R*,11*S*)-JH-I (8,600 c.p.m. specific activity ~70 Ci mmol^{-1}) or *b*, 6.5 nM racemic [10-^{3}H]JH-I (8,600 c.p.m., specific activity 11.5 Ci mmol^{-1}) and increasing concentrations of competitors. Bound radioactivity was measured as stated above. Each point represents the mean of two to four duplicates. Tritiated JHs and unlabelled competitors were purified by HPLC on Porasil columns (Waters Associates) with *n*-hexane/8% ethyl acetate or 8% diethylether as solvent system and/or by TLC on silica gel plates with benzene/ethyl acetate (7:1). ZR515 (Zoecon) was 96.8% pure. ●, JH-I (methyl-2*E*,6*E*-*cis*-3,11-dimethyl-7-ethyl-10,11-epoxy-2,6-tridecadienoate) ★, JH-III (methyl-2*E*,6*E*-3,7,11-trimethyl-10,11-epoxy-2,6-dodecadienoate), ▲, (JH-III-E, ethyl-2*E*,6*E*-3,7,11-trimethyl-10,11-epoxy-2,6-dodecadienoate (a gift of H. Rembold, MPI f. Biochemie, Martinsried)); ○, FME (methyl-2*E*/*Z*,6*E*/*Z*-3,7,11-trimethyl-2,6,10-tridecadienoate), ■, ZR515, (isopropyl-2*E*,4*E*-11-methoxy-3,7,11-trimethyl-2,4-dodecadienoate).

Enantioselectivity as another means of determining the specificity of JH-binding sites was tested in partially purified preparations of high-affinity JH-binding sites. Table 1 shows that optically pure unlabelled (10*R*,11*S*)-JH-I competes with binding of [*methoxy*-^{3}H](10*R*,11*S*)-JH-I better than the racemic unlabelled JH-I, thus demonstrating enantioselective JH binding to the high-affinity JH-binding sites. Similar results have been reported previously for JH-specific haemolyph carrier proteins of *Manduca sexta*[12] and *Locusta migratoria*[13]. Surprisingly, especially at low competitor concentrations the unlabelled naturally occurring (10*R*,11*S*) enantiomer competes with the tritiated (10*R*,11*S*) enantiomer much better than the theoretically expected factor 2, when compared with the racemate. Considering only the data of Fig. 1, it may be suggested that the specific activity of the two radioactive JH-I preparations would have to be determined more carefully. This point, however, is of minor importance in the competitive binding studies depicted in Table 1. Clearly, there is a difference in binding behaviour of the racemate and the optically active preparation, the magnitude of which cannot be explained with our rationale on simple stereochemical arguments. A factor of 3 has been observed for the difference of binding of racemic and optically active JH-III preparations to the JH-carrier protein from larval *M. sexta* haemolymph[12]. Furthermore, in the *Galleria* bioassay, (10*R*)-JH-III is about three times more active than the racemate[12]. Due to the lack of more conclusive data, we have to consider the possibility that presently unknown effects govern the binding of radiolabelled JHs to their receptors.

The experiments performed so far present unequivocal evidence that high-affinity, high-specificity receptor-type JH-I binding sites are present in the cytosol of larval *D. hydei* integument. According to the general concept of hormone action, further work should analyse the interaction of these binding sites with other cellular components (nuclei) in order to investigate their physiological significance in more detail.

Received 20 December 1979; accepted 16 April 1980.

1. Riddiford, L. M. in *Invertebrate Tissue Culture, Applications in Medicine, Biology and Agriculture* (eds Kustak, E. & Maramorosch, K.) 213–222 (Publisher, town, 1976).
2. Jensen, E. V. & DeSombre, E. R. *A. Rev. Biochem.* **41,** 203–230 (1972).
3. Yund, M. A., King, D. S. & Fristrom, J. W. *Proc. natn. Acad. Sci. U.S.A.* **75,** 6039–6043 (1978).
4. Maróy, P., Dennis, R., Beckers, C., Sage, B. & O'Connor, J. D. *Proc. natn. Acad. Sci. U.S.A.* **75,** 6035–6038 (1978).
5. Kuppert, P., Wilhelm, S. & Spindler, K.-D. *J. comp. Physiol.* **128B**, 95–100 (1978).
6. Peter, M. G., Gunawan, S. & Emmerich, H. *Experientia* **35,** 1141–1142 (1979).
7. Scatchard, G. *Ann. N.Y. Acad. Sci.* **51,** 660–672 (1949).
8. Klages, G. & Emmerich, H. *Insect Biochem.* **9,** 23–30 (1979).
9. Chen, C.-C. & Heller, J. *J. biol. Chem.* **252,** 5216–5221 (1977).
10. Hansen, P. E., Johnson, A., Schrader, W. T. & O'Malley, B. W. *J. Steroid Biochem.* **7,** 723–732 (1976).
11. Henrick, C. A., Staal, G. B. & Siddall, J. B. *J. Agric. Fd Chem.* **21,** 352–359 (1973).
12. Schooley, D. A., Bergot, B. J., Goodman, W. & Gilbert, L. I. *Biochem. biophys. Res. Commun.* **81,** 743–749 (1978).
13. Peter, M. G., Gunawan, S., Gellissen, G. & Emmerich, H. *Z. Naturforsch.* **34c**, 588–598 (1979).
14. Klages, G. & Emmerich, H. *J. comp. Physiol.* **132,** 319–325 (1979).
15. Lowry, D. H., Rosenbrough, N. J., Farr, A. L. & Randall, R. J. *J. biol. Chem.* **193,** 265–275 (1951).

Molecular heterogeneity of benzodiazepine receptors

Werner Sieghart & Manfred Karobath

Department of Biochemical Psychiatry, University of Vienna,
Lazarettgasse 14, A-1090 Vienna, Austria

Benzodiazepines exhibit reversible, stereospecific high affinity binding to mammalian brain membranes, and the respective binding sites for ^{3}H-flunitrazepam represent pharmacologically and clinically relevant receptors for benzodiazepines[1–3]. Recently it has been demonstrated that reversibly bound ^{3}H-flunitrazepam becomes irreversibly attached to a specific membrane protein with apparent molecular weight of 50,000 when incubations were performed in the presence of UV light[4,5]. Irreversible binding of ^{3}H-flunitrazepam to this protein had pharmacological properties similar to reversible benzodiazepine receptor binding, indicating that ^{3}H-flunitrazepam is a photoaffinity label for the benzodiazepine receptor[5]. Using irreversible binding of ^{3}H-flunitrazepam and subsequent electrophoretic separation of the labelled proteins in SDS-gels followed by fluorography[6], we found that in hippocampus and several other brain regions at least two different types of benzodiazepine receptors exist. Each seems to be associated with a γ-aminobutyric acid (GABA) receptor.

Membranes from several rat brain regions were incubated with 10 nM ^{3}H-flunitrazepam at 0 °C for 90 min, and the samples were then irradiated with UV light for 10 min. Membranes were collected by centrifugation, dissolved in SDS and subjected to SDS-polyacrylamide gel electrophoresis and fluorography.

^{3}H-flunitrazepam irreversibly binds to a single protein band with an apparent molecular weight of 51,000 (P_{51}) in cerebellum (Fig. 1). Similarly, most of the ^{3}H-radioactivity bound to membranes from other brain regions is associated with a protein band with the same apparent molecular weight. The extremely weak labelling of this protein band in spinal cord agrees with the very low specific reversible binding (data not shown) of ^{3}H-flunitrazepam to membranes from this tissue. Thus, P_{51} seems to be identical to the labelled benzodiazepine receptor described previously[5]. However, in other brain regions in addition to P_{51} several other protein bands with apparent molecular weights of 53,000 (P_{53}), 55,000 (P_{55}) and 59,000 (P_{59}) are labelled with variable intensity. The most prominent of these additional bands is P_{55} which is most highly labelled in hippocampal membranes.

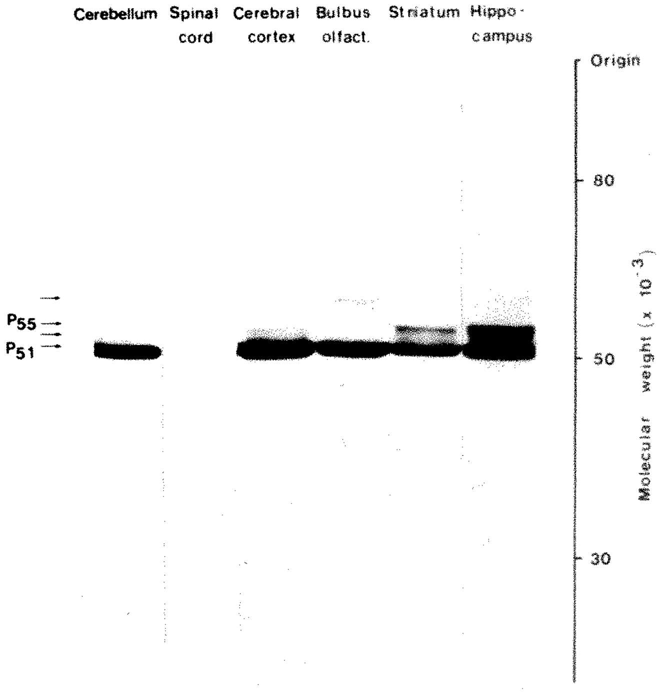

Fig. 1 Fluorography illustrating irreversible ^{3}H-flunitrazepam binding to membrane proteins from several rat brain regions. Tissues from several rat brain regions were homogenized with an Ultra Turrax for 30 s in 50 vol of 50 mM Tris–citrate buffer, *p*H 7.1, and centrifuged for 10 min at 48,000*g*. Pellets were washed four times by resuspension and recentrifugation in the same volume of buffer and stored at −20 °C for at least 18 h. After thawing, aliquots of membranes derived from 6 mg tissue wet weight were incubated with 10 nM ^{3}H-flunitrazepam (84.3 Ci mmol^{-1}, NEN) in a solution containing 50 mM Tris–citrate buffer, *p*H 7.1, and 150 mM NaCl (ref. 9). Incubations were performed at 0 °C for 90 min and the samples were then irradiated with UV light[5] for 10 min. Membranes were centrifuged at 48,000 g for 10 min, resuspended in 100 µl H_2O and 50 µl SDS stop solution (10% SDS (w/v), Tris–HCl 100 mM, *p*H 7.4, β-mercaptoethanol 5 mM, sucrose 0.1 g ml^{-1} and bromophenol blue tracking dye 0.02 mg ml^{-1}) and placed in a boiling water bath for 5 min. Electrophoresis on 10% SDS-polyacrylamide slab gels and protein staining of the gels was performed as described previously[10]. After treatment with PPO, gels were dried and subjected to fluorography at −70 °C on Kodak X-Omat R film[6] for 6 days. All radioactive bands disappeared after incubation of the samples with pronase but not after three extractions with chloroform–methanol (3:1), and thus represent proteins. The apparent molecular weights of the labelled protein bands, indicated by the arrows (59,000: P_{59}; 55,000: P_{55}; 53,000; P_{53} and 51,000: P_{51}) were determined by calibrating the gel with standard proteins of known molecular weight. The pattern of bound radioactivity was unchanged in cerebellar or hippocampal membranes isolated and labelled in the presence of the protease inhibitor phenylmethylsulphonyl-fluoride (PMSF, 100 µM). Furthermore, co-homogenization of cerebellum and hippocampus and irreversible binding of ^{3}H-flunitrazepam to the resulting mixed membranes revealed a pattern of labelled protein bands which was additive and did not show any enhanced degradation of the hippocampal bands. This indicates that the heterogeneity of ^{3}H-flunitrazepam binding proteins cannot be explained by regional differences in the degradation of a single protein with higher molecular weight. As the efficiency of labelling of the different protein bands is not necessarily identical, no attempt was made to estimate the quantitative contribution of the various bands to irreversible benzodiazepine receptor binding.

To characterize the pharmacological properties of irreversible ^{3}H-flunitrazepam binding to P_{51} and P_{55}, membranes from cerebellum and hippocampus were

Table 1 Influence of GABA and CL 218 872 on reversible and irreversible binding of ^{3}H-flunitrazepam to membranes or membrane proteins from rat cerebellum and hippocampus

	Specific ^{3}H-flunitrazepam binding (% of control)		
	Reversible	Irreversible	
		Membranes	Proteins
Cerebellum			
+ 10 μM GABA	200.7 ± 8.3	201.0 ± 0.2	251.7 ± 13.3
+ 1 μM CL 218 872	10.8 ± 1.5	16.9 ± 0.7	14.3 ± 0.4
Hippocampus			
+ 10 μM GABA	211.1 ± 2.9	198.8 ± 11.4	211.7 ± 11.1
+ 1 μM CL 218 872	45.9 ± 4.2	47.7 ± 0.2	49.9 ± 3.1

Cerebellar or hippocampal membranes were incubated with 0.4 nM ^{3}H-flunitrazepam either without additions (control) or in the presence of 10 μM GABA, 1 μM CL 218 872 or 2 μM diazepam as described in legend to Fig. 1. For the estimation of reversible binding, samples were then rapidly filtered as described previously[9]. For the estimation of irreversible binding to membranes samples were irradiated for 10 min with UV light after the 90 min equilibration period. In these conditions, irreversible binding of ^{3}H-flunitrazepam to membranes was about 30% of reversible binding. Exposure to UV light for a longer time period resulted in a higher percentage of irreversible binding but did not yield additional labelled protein bands. In this experiment the short irradiation time was selected because longer irradiation times change the kinetic properties of irreversible binding. After irradiation, 2 μM diazepam was added and samples were incubated at 30 °C for 60 min to remove non-irreversibly bound ^{3}H-flunitrazepam from membranes. Samples were then filtered and bound radioactivity was estimated as described previously[9]. For the estimation of irreversible binding to proteins, samples were treated as described in the legend to Fig. 2. As separation of the hippocampal proteins was not sufficient to allow for separate quantitation of the proteins in the gel system used, the region in the gel containing P_{51} to P_{55} was identified by fluorography, cut out and oxidized with a Packard Model 306 sample oxidizer to recover ^{3}H-radioactivity for liquid scintillation counting. Nonspecific binding (estimated in the presence of 2 μM diazepam) was subtracted from total binding to yield specific binding. Results are expressed as per cent of control binding (mean ± s.e.m.; $n = 3$). Control binding given in d.p.m. per mg wet weight was 1,643 and 3,170 (reversible binding), 579 and 1,046 (irreversible binding to membranes), 264 and 533 (irreversible binding to proteins) for cerebellum and hippocampus, respectively.

investigated. As can be seen in Fig. 2, irreversible binding of ^{3}H-flunitrazepam to P_{51} in cerebellum and to P_{51} and P_{55} in hippocampus is completely inhibited by diazepam, a centrally active benzodiazepine. In contrast, binding to these proteins is not inhibited by Ro 5-4864, which selectively inhibits binding to peripheral benzodiazepine binding sites[7] (data not shown). Furthermore, irreversible binding of ^{3}H-flunitrazepam to P_{51} in cerebellum and to P_{51} and P_{55} in hippocampus is stimulated by 10 μM GABA to a similar extent as is found with reversible binding to membranes from cerebellum or hippocampus (Fig. 2, Table 1). This stimulation by GABA is bicuculline sensitive (Fig. 2) indicating that GABA exerts its stimulatory effects on the labelling of the protein bands by way of a GABA receptor. These results indicate that irreversible binding of ^{3}H-flunitrazepam to P_{51} as well as that to P_{55} is similar to reversible benzodiazepine receptor binding. Thus, in different brain regions different types of benzodiazepine receptors may occur which are modulated by GABA receptors.

A heterogeneity of benzodiazepine receptors has been suggested previously when reversible benzodiazepine receptor binding was investigated in the presence of CL 218 872 (ref. 8). This substance, a triazolopyridazine, has anxiolytic but only weak sedative properties[8]. In contrast to benzodiazepines it inhibits reversible benzodiazepine binding with K_i values and Hill coefficients which differ in various brain regions[8]. We therefore investigated a possible differential effect of CL 218 872 on the irreversible binding of ^{3}H-flunitrazepam to the different binding proteins. Figure 2 shows that CL 218 872 inhibits irreversible binding of ^{3}H-flunitrazepam to P_{51} more strongly than binding to P_{55}. Such a selective effect can account for the different quantitative inhibition by CL 218 872 of reversible[8] and irreversible binding of ^{3}H-flunitrazepam in cerebellum and hippocampus (Table 1). These results seem to indicate that P_{55} is or is part of a pharmacologically different type of benzodiazepine receptor which is unrelated to that which contains the P_{51} protein. Both of these receptors seem to be associated with a GABA receptor. It should be emphasised, however, that additional types of benzodiazepine receptors could exist since the role of P_{53} and P_{59} in benzodiazepine receptor binding has not yet been investigated. In addition, each labelled band could consist of more than one labelled protein which differ in structure and properties but not in apparent molecular weight.

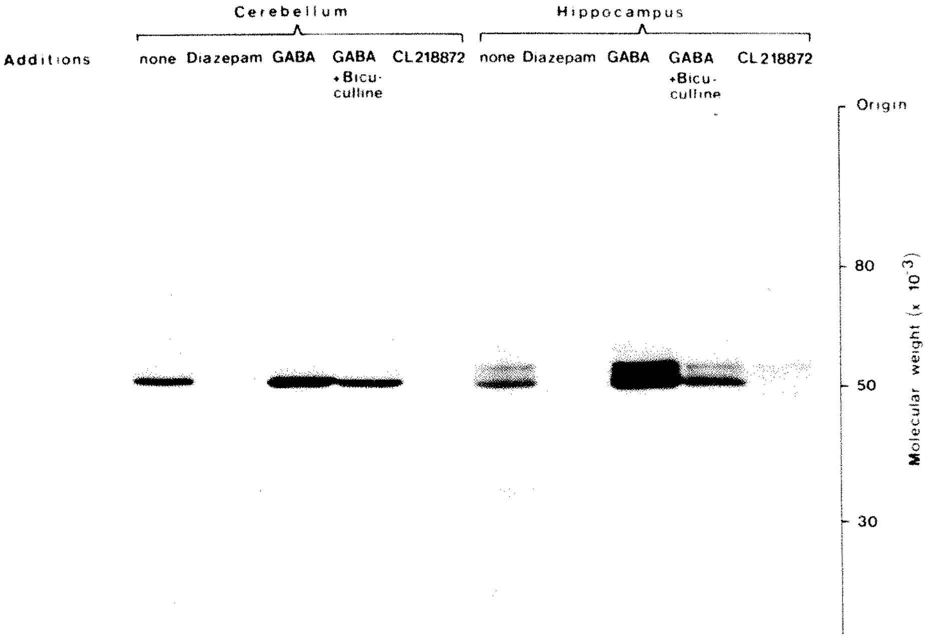

Fig. 2 Fluorography illustrating the influence of several drugs on irreversible ^{3}H-flunitrazepam binding to membrane proteins from cerebellum and hippocampus. Cerebellar or hippocampal membranes were incubated with 0.4 nM ^{3}H-flunitrazepam either without additions (lanes 1 and 6) or in the presence of 2 μM diazepam (lanes 2 and 7), 10 μM GABA (lanes 3 and 8), 10 μM GABA plus 10 μM bicuculline-methiodide (lanes 4 and 9), 1 μM CL 218 872 (lanes 5 and 10) or 1 μM Ro 5-4864 (experiment not shown). Incubation and irradiation of the samples as well as SDS-gel electrophoresis of the membrane proteins and fluorography of the gels was performed as described in the legend to Fig. 1.

Thus, this investigation indicates for the first time not only a pharmacological but also a molecular heterogeneity of benzodiazepine receptors. Using the present approach of irreversible labelling of benzodiazepine receptors followed by electrophoresis and fluorography, it seems possible to separate and isolate the different receptors. Furthermore, this technique can be used to develop new drugs which, in contrast to benzodiazepines, have selective effects on different types of benzodiazepine receptors.

We thank M. Forster for technical assistance. This work was supported by Fonds zur Förderung der wissenschaftlichen Forschung in Österreich.

Received 25 February; accepted 17 April 1980.

1. Möhler, H. & Okada, T. *Science* **198,** 849–851 (1977).
2. Squires, R. F. & Braestrup, C. *Nature* **266,** 732–734 (1977).
3. Speth, R. C., Wastek, G. J., Johnson, P. C. & Yamamura, H. I. *Life Sci.* **22,** 859–866 (1978).
4. Battersby, M. K., Richards, J. G. & Möhler, H. *Eur. J. Pharmac.* **57,** 277–278 (1979).
5. Möhler, H., Battersby, M. K. & Richards, J. G. *Proc. natn. Acad. Sci. U.S.A.* **77,** 1666–1670 (1980).
6. Laskey, R. A. & Mills, A. D. *Eur. J. Biochem.* **56,** 335–341 (1975).
7. Braestrup, C. & Squires, R. F. *Proc. natn. Acad. Sci. U.S.A.* **74,** 3805–3809 (1977).
8. Klepner, C. A., Lippa, A. S., Benson, D. I., Sano, M. C. & Beer, B. *Pharmac. biochem. Behav.* **11,** 457–462 (1979).
9. Karobath, M. & Sperk, G. *Proc. natn. Acad. Sci. U.S.A.* **76,** 1004–1006 (1979).
10. Krueger, B. K., Forn, J. & Greengard, P. *J. biol. Chem.* **252,** 2647–2773 (1977).

Axoplasmic transport of muscarinic receptors

Pierre Laduron

Department of Biochemical Pharmacology, Janssen Pharmaceutica, B-2340 Beerse, Belgium

The reality of axoplasmic transport is widely accepted; various neurotransmitters[1–3], enzymes[2–4], labelled proteins[5] and peptides[6] are known to move rapidly along the axons of different nerve fibres. In the terminals of sympathetic nerves, noradrenaline release is controlled by various regulatory mechanisms which imply the occurrence of presynaptic receptors[7]. In this regard, there is considerable indirect physiological evidence for the existence of muscarinic cholinergic receptors in the sympathetic nerve endings[7–9]; the stimulation by acetylcholine of such presynaptic receptors elicits an inhibitory effect on noradrenaline release[8,9]. We now provide direct biochemical evidence for the occurrence in dog splenic nerve of muscarinic receptors which seem to move along the axon as suggested by their rapid accumulation on either side of a ligature.

Ligature experiments were carried out in mongrel dogs anaesthetized with pentobarbital (30 mg per kg, intravenously). Splenic nerve fibres were dissected from the splenic artery near the bifurcation, and a silk thread ligature was tied round the splenic nerve[10]. At 18 and 48 h, and 11 days after the operation, 1-cm segments of the nerve were removed, two above (proximal to) and below (distal to) the ligature. Coeliac ganglia were also removed and control splenic nerves were taken from unoperated dogs. After clearing connective tissue from the nerve fibres, the segments were weighed and then homogenized in 50 volumes of ice-cold distilled water by means of an ultraturrax. The samples were further diluted to 1:200 with 0.05 M phosphate buffer, *p*H 7.4. Binding assays were carried out using 2 ml of tissue preparation with 2 nM ^{3}H-dexetimide (specific activity 17.5 Ci mmol^{-1}, IRE Fleurus, Belgium) or 2 nM ^{3}H-levetimide (specific activity 19 Ci mmol^{-1}, Janssen) as described previously[20]. After incubation for 20 min at 37 °C, 3 ml of cold buffer was added and the samples were then rapidly filtered on Whatman GF/B glass filters. Stereospecific binding was taken as the difference between binding measured in the presence of 2×10^{-7} M levetimide (inactive enantiomer) and 2×10^{-7} M dexetimide (blank value).

To characterize the ^{3}H-dexetimide binding sites in dog splenic nerves, various concentrations of dexetimide and levetimide were tested *in vitro* using a total homogenate. Figure 1 shows that dexetimide displaced the labelled ligand in the nanomolar range whereas levetimide was only effective in a micromolar concentration. This indicates the stereospecific nature of the binding which represents 50% of the total binding. Table 1 gives the IC_{50} values for different compounds; atropine, an antimuscarinic drug which belongs to a different chemical class from dexetimide, also competed with ^{3}H-dexetimide in the nanomolar range. Moreover, there was a good correlation between the IC_{50} values of muscarinic antagonists, oxotremorine and levetimide, in dog splenic nerves and rat brain. As nicotine is not active, but antimuscarinic drugs and oxotremorine are, ^{3}H-dexetimide binds in dog splenic nerves to receptors which have the characteristics of the muscarinic receptor. Further control experiments were carried out using ^{3}H-levetimide as ligand; here, there was no stereospecific displacement and the value of the total binding corresponded to the blank values in the ^{3}H-dexetimide binding. From these data, we conclude that the ^{3}H-dexetimide binding sites in dog splenic nerves are of muscarinic nature.

Stereospecific ^{3}H-dexetimide binding was measured in the proximal and distal part of dog splenic nerve at different times after ligature. Figure 1*a* shows that 18 h after constriction, the segments close to the ligature, P_1 and D_1, revealed more than a twofold increase in binding sites as compared with control nerves. In contrast, segments located 1 cm more proximally (P_2) or more distally (D_2) to the ligature and samples of the coeliac ganglion did not differ significantly from the control nerves. This accumulation in P_1 and D_1, so near the ligature, was still more pronounced 48 h after the operation (Fig. 2*b*). At that time the increase in binding sites was more than five times higher than control values in the proximal as well as in the distal part of the splenic nerves. This suggests a bidirectional transport of muscarinic receptors along the axon.

In contrast, the accumulation of noradrenaline was only detectable in the proximal segment, indicating a unidirectional transport for the biogenic amine, and confirming our earlier finding[10]. Interestingly, the increase of noradrenaline in the P_1 segment was of the same order of magnitude as the increase in muscarinic receptors measured in the binding assay. Here again, control experiments were carried out using ^{3}H-levetimide as ligand; there was no increase in binding in the P_1 and D_1 segments even 48 h after ligature and again the total binding corresponded to the blank value of ^{3}H-dexetimide binding.

To assess the origin of muscarinic receptors in the splenic nerves, ^{3}H-dexetimide binding was assayed in proximal and

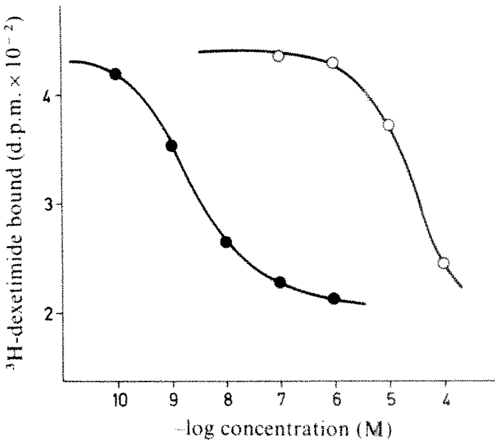

Fig. 1 Dose–response inhibition of dexetimide ((+)benzetimide) (●) and levetimide ((−)benzetimide) (○), expressed as −log concentration, in ^{3}H-dexetimide assay using a total homogenate from dog splenic nerves.

0028–0836/80/290287–02$01.00

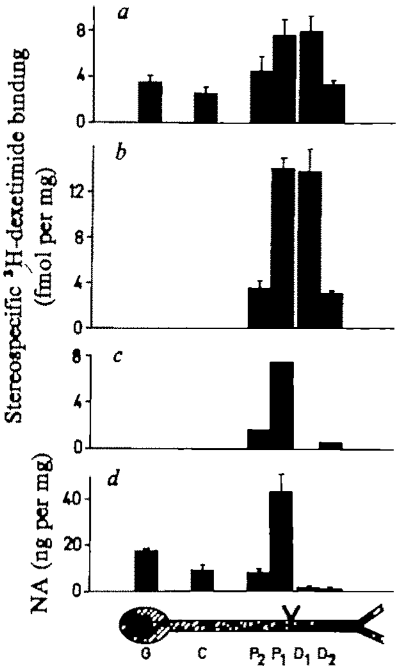

Fig. 2 Stereospecific ^{3}H-dexetimide binding and noradrenaline content in different segments of dog splenic nerves 18 h (*a*) 48 h (*b*, *d*) and 11 days (*c*) after ligature. Binding was assayed in duplicate; the results represent the mean (± s.e.m.) obtained from five or six animals except for *a* ($n=3$) and *d* ($n=1$). Noradrenaline was measured according to the method of Coyle and Henry[21] G = coeliac ganglion, C = control nerve from non-operated animals, P_1, P_2 and D_1, D_2 are, respectively, the proximal and distal part of ligated splenic nerves

distal segments 11 days after ligature Stereospecific binding sites were practically undetectable in the distal part, even in the segment closest to the constriction. In contrast, a clear-cut accumulation of binding sites remained detectable in the P_1 segment although to a lesser extent than that observed 48 h after the operation. This suggests that muscarinic receptors, like noradrenaline storage vesicles[1,10,11], originate from the perikarya of sympathetic neurones, in this case, in the coeliac ganglion

The above results provide biochemical evidence for the presence of muscarinic cholinergic receptors in sympathetic nerves, giving more support to the concept of presynaptic or prejunctional receptors. In the heart, a substantial fraction of muscarinic receptors have been identified biochemically at the presynaptic sites in the sympathetic nerve terminals[12].

The most interesting finding here is the rapid accumulation in dog splenic nerves of muscarinic receptors both above and below a ligature, suggesting a bidirectional axonal flow for such binding sites The fact that the rate of transport, about 1 mm h^{-1}, is practically the same as that previously found in similar conditions for noradrenaline storage vesicles, implies that muscarinic receptors are probably also associated with vesicle-like structures. Nevertheless, the rate of transport should be more precisely measured in smaller nerve pieces, this could provide a new approach to studying the turnover of receptors, as already reported for noradrenergic vesicles[13,14].

Table 1 Inhibition of stereospecific ^{3}H-dexetimide binding

	IC$_{50}$ (nM)	
	Dog splenic nerves	Rat striatum*
Dexetimide	2.2	1 4
Atropine	6 3	6.8
Oxotremorine	3,200	6,500
Levetimide	28,000	6,500
Nicotine	> 100,000	> 100,000

*The values were taken from refs 19 and 20

How these prejunctional receptors are transported along the axon remains unclear. However, the following sequence of events can be considered: synthesis of receptors like the proteins[15] and their association with subcellular organelles[11] in the perikarya; anterograde flow in the axon, at the terminals externalization of receptors by exocytosis, which makes the receptor available to ligand and thus functional, internalization by endocytosis (see ref 16), back to perikarya by retrograde axonal flow and recycling or degradation[17]. If this is the correct process, most of the binding sites in the perikarya, in the axon and partly in the nerve ending would be silent receptors. If such a view is transposed to the central nervous system, this could provide a plausible explanation for the very limited increase in binding sites in supersensitivity phenomena[18] when compared with the more pronounced pharmacological reactivity.

This work was partially supported by a grant of IWONL. I thank Dr J. Leysen for helpful discussions, D. Ashton for his help in preparing the manuscript, and J. D'Aubioul, W. Van Gerven, W. Gommeren and P. F M. Janssen for technical assistance.

Received 12 December 1979, accepted 28 April 1980

1 Dahlstrom, A *Phil Trans R Soc* B261, 325–358 (1971)
2 Banks, P & Mayor, D *Biochem Soc Symp* 36, 133–149 (1973)
3 Laduron, P in *Dynamics of Degeneration and Growth in Neurons* (eds Fuxe, K, Olson, L & Zotterman, Y) 245–256 (Pergamon, Oxford, 1974)
4 Lubinska, L & Niemierko, S *Brain Res* 27, 328–352 (1971)
5 Ochs, S *J Physiol, Lond* 277, 627–645 (1972)
6 Gmobetu, A & Said, S I *Nature* 281, 574–575 (1979)
7 Langer, S Z *Biochem Pharmac* 23, 1793–1800 (1974)
8 Loffelholz, K & Muscholl, E *Naunyn-Schmiedebergs Archs exp Path Pharmak* 265, 1–15 (1969)
9 Vanhoutte, P M *Fedn Proc* 36, 2444–2449 (1977)
10 Laduron, P & Belpaire, F *Life Sci* 7, 1–7 (1968)
11 Teichberg, S & Holtzman, E *J Cell Biol* 57, 88–108 (1973)
12 Sharma, V K & Banerjee, S P *Nature* 272, 276–278 (1978)
13 De Potter, W P & Chubb, I W *Biochem J* 125, 375–376 (1971)
14 Brimijoin, S *J Neurochem* 19, 2183–2193 (1972)
15 Droz, B *J Microsc* 6, 201–228 (1967)
16 Goldstein, J L, Anderson, R G W & Brown, M S *Nature* 279, 679–685 (1979)
17 Teichberg, S, Holtzman, E, Crain, S M & Peterson, E R *J Cell Biol* 67, 215–230 (1975)
18 Schwartz, J C, Costentin, J, Martres, M P, Protais, P & Baudry, M *Neuropharmacology* 17, 665–685 (1978)
19 Laduron, P M, Verwimp, M & Leysen, J E *J Neurochem* 32, 421–427 (1979)
20 Gorissen, H, Aerts, G & Laduron, P *FEBS Lett* 96, 64–68 (1978)
21 Coyle, J T & Henry, D *J. Neurochem* 21, 61–67 (1973)

Evidence against presynaptic α-adrenoreceptor modulation of cardiac sympathetic transmission

James A. Angus & Paul I. Korner

Baker Medical Research Institute, Commercial Road, Prahran, Victoria, Australia 3181

In addition to its well known actions on postsynaptic adrenoreceptors, noradrenaline released at the sympathetic nerve endings is now believed to modulate subsequent transmitter release through its actions on presynaptic receptors[1-7]. Much evidence in support of this hypothesis has been obtained from overflow studies in which labelled noradrenaline and metabolites released into the bathing solution are used as an assay of transmitter release. According to Langer[4] and Rand, McCulloch and Story[6], evidence to favour the existence of such a presynaptic mechanism includes the demonstration that α-adrenoreceptor antagonists produce enhanced transmitter overflow in steady-state conditions of sympathetic stimulation. They also suggest that α-adrenoreceptor-mediated potentiation of transmitter release would not be expected in response to a

0028–0836/80/290288–04$01 00

single pulse, as a threshold concentration of released noradrenaline is required to activate presynaptic inhibition of further release. In the myocardium both conditions have been obtained in the presence of phenoxybenzamine[5,6]. Surprisingly, although phentolamine is also a potent α-adrenoreceptor antagonist, the potentiation of transmitter release was less than the increase due to phenoxybenzamine[6]. Studies of transmitter overflow have generally been made with supraphysiological sympathetic stimulation of 5 Hz continuously for 30 s or 4 Hz for 60 s (refs 6, 7). We have used more closely physiological stimulation parameters delivered only during the atrial refractory period. We have now shown that phenoxybenzamine markedly potentiates the chronotropic response to a single pulse and also responses up to maximum stimuli. By contrast, phentolamine and yohimbine were totally without effect even at high concentration. The action of phenoxybenzamine was largely accounted for by its effect on uptake blockade. Taken together, our studies provide evidence against a physiological role of presynaptic α-adrenoreceptors in the heart

Guinea pig right atria were placed horizontally in Krebs' solution (composition in mM: Na^+ 144, K^+ 5.9, Ca^{2+} 2.5, Mg^{2+} 1.2, HCO_3^- 25, Cl^- 128.7, $H_2PO_4^-$ 1.2, SO_4^{2-} 1.2, EDTA 0.04, glucose 11) in a 50-ml organ bath at 37 °C with 1 µM atropine. Two Teflon-coated stainless steel wires, bared only at the tip, were placed on the surface of the atrium approximately 2 mm apart to record the surface electrogram. Following amplification, this signal was used to trigger a microprocessor-controlled period meter with an accuracy of better than 2 ms in the entire system. The cycle to cycle period (interval) was continuously displayed on a chart recorder. When required, intramural sympathetic nerve fibres were stimulated by applying square wave field pulses (2 ms duration, 100 mA) across the atrium from a pair of platinum electrodes. Field pulses were delivered from a Grass S88 stimulator following a 5-ms delay after the upstroke of the atrial electrogram signal (during the refractory period) to prevent arrhythmia[8]. Either a single field pulse or a train of four field pulses (one pulse following each of four consecutive atrial electrograms) were used as stimuli.

In control conditions, these low stimulation frequencies produced a marked tachycardia, that is, a decrease in the succeeding atrial period as measured from the P–P intervals of the atrial electrogram. After a single field pulse applied during the refractory period, atrial period fell by 30 ms, with the fall beginning at the next interval. The tachycardia then declined over the next 20 s. The mechanism underlying the time course of response is assumed to depend on the concentration of released noradrenaline in the synaptic cleft. The transmitter will activate postsynaptic β-adrenoreceptors to increase both rate and force of contraction until the concentration falls below the threshold level necessary to activate these receptors. The mechanisms responsible for the lowering of the biophase noradrenaline are a 'neuronal uptake mechanism' (or uptake$_1$) and an extraneuronal mechanism (uptake$_2$)[9,10]. After four pulses the fall in atrial period was approximately 150 ms. Maximum fall in atrial period was 200–250 ms observed with

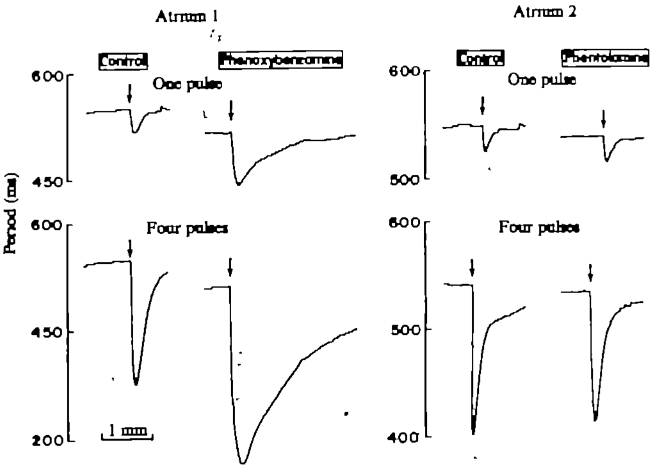

Fig. 1 Chart recordings of right atrial period from two tissues. Top: responses to sympathetic nerve stimulation effected by one square wave field pulse (2 ms duration, 100 mA) delivered during the refractory period in the presence of 1 µM atropine. Bottom: period responses to four field pulses delivered as a train of one pulse immediately after each of four spontaneous electrogram signals. Phenoxybenzamine (10 µM) was equilibrated with atrium 1 for 15 min followed by repeated washing for 30 min before restimulation. Phentolamine (10 µM) was left in contact with atrium 2 for 30 min before, and during, field stimulation. Both the peak fall in period and the duration of the tachycardia were significantly prolonged by phenoxybenzamine treatment but not by phentolamine.

Table 1 Effects of phenoxybenzamine, phentolamine, yohimbine and uptake block on the tachycardia response to sympathetic stimulation in guinea pig atria

	One pulse								Four pulses							
	Peak (ms)				Area (log units)				Peak (ms)				Area (log units)			
Treatment	Before	After	s.e.d.	P	Before	After	s.e.d.	P	Before	After	s.e.d.	P	Before	After	s.e.d.	P
Control ($n=8$)	31	31	1.5	NS	0.79	0.84	0.08	NS	134	149	7.8	NS	1.85	1.85	0.025	NS
Phenoxybenzamine																
3 µM ($n=5$)	18	39	9.4	NS*	0.78	1.15	0.11	<0.05	113	163	11.6	<0.02	1.70	2.03	0.09	<0.05
10 µM ($n=10$)	41	82	9.6	<0.001	0.83	1.52	0.04	<0.001	184	231	13.9	<0.01	1.76	2.3	0.08	<0.001
Phentolamine																
0.3 µM ($n=5$)	37	31	2.1	<0.05	0.70	0.62	0.04	NS	119	118	3.7	NS	1.70	1.59	0.07	NS
1 µM ($n=5$)	30	27	3.2	NS	0.88	0.77	0.07	NS	153	152	19.1	NS	1.78	1.65	0.03	<0.02
10 µM ($n=12$)	29	34	4.6	NS	0.79	0.88	0.06	NS	147	154	10.4	NS	1.78	1.88	0.05	NS
Yohimbine																
0.1 µM ($n=5$)	38	40	4.2	NS	0.85	0.91	0.09	NS	138	147	5.3	NS	1.79	1.88	0.08	NS
1 µM ($n=5$)	38	41	8.0	NS	0.85	0.83	0.08	NS	138	155	9.3	NS	1.79	1.83	0.09	NS
10 µM ($n=5$)	38	39	13.5	NS	0.85	0.87	0.23	NS	138	148	24.6	NS	1.79	1.99	0.17	NS
Uptake block																
($n=10$)	29	54	4.8	<0.001	0.86	1.51	0.07	<0.001	139	176	9.4	<0.005	1.76	2.36	0.07	<0.001

Peak responses are the maximum fall in period (ms) following either a single pulse or a train of four pulses of square wave field stimulation (2 ms duration, 100 mA) delivered across the atrium by two platinum electrodes during the refractory period of spontaneous sino-atrial rhythm. Area responses are the integrated change in atrial period over the whole response, that is, until the atrial period returns to resting values. The chart record of period was integrated by weighing. Logarithmic units of area were used to obtain homoscedastic observations. Mean values for peak and area responses before and after drug treatment are given together with s.e.d. within atria for each comparison. P values are the level of significance (n is the number of atria in each treatment). Phenoxybenzamine was left in contact with the atria for 15 min followed by repeated washing for 30 min before further field stimulation. Phentolamine, yohimbine and uptake block (combination of desipramine 0.1 µM and 17β-oestradiol 5 µM) were equilibrated with the atria for 30 min and left in the bath during stimulation.

*Considering log (peak) to avoid heteroscedasticity the difference was significant $P < 0.01$.

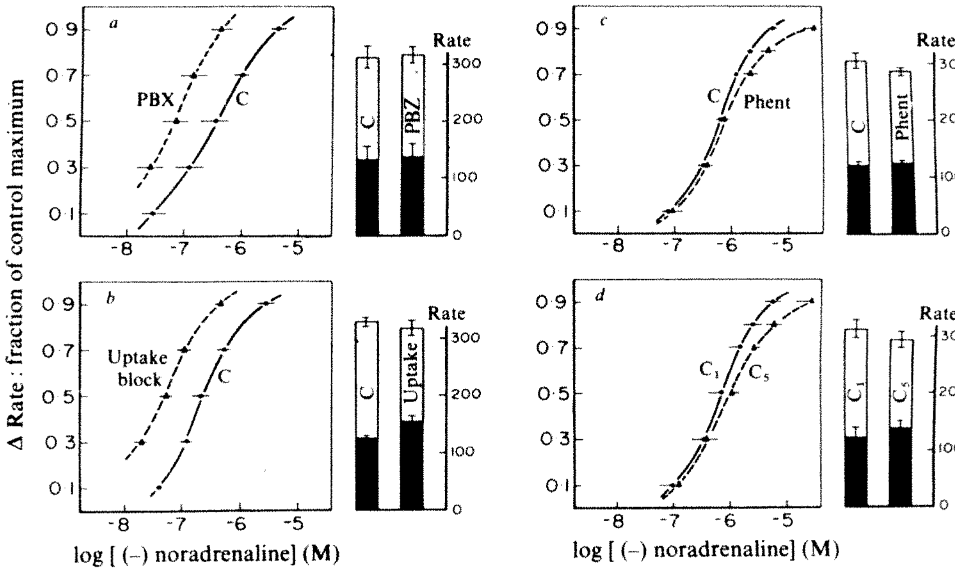

Fig. 2 Effect of phenoxybenzamine (PBX), phentolamine (Phent.) and uptake block to chronotropic response to exogenous (−)noradrenaline. Graphs: ●, first cumulative concentration–response curve to (−)noradrenaline; ▲, second curve after equilibration of test drug. For each atrium, curves were constructed by first expressing the change in atrial rate as a fraction of the maximum change obtained in the first curve. Mean ± s.e.m. values of log EC_{10}, EC_{30}, EC_{50}, EC_{70}, EC_{80} and EC_{90} values were determined from four atria. Histograms: black columns, resting atrial rate (beats min^{-1}) just before starting the noradrenaline curve; white columns, maximal atrial rate obtained with noradrenaline. Values are mean + 1 s.e.m. for four atria. *a*, Phenoxybenzamine (10 μM); 15 min equilibrium followed by 30 min washing before second curve. *b*, Uptake block; 30 min equilibration with 0.1 μM desipramine and 5 μM 17β-oestradiol before second curve. *c*, Phentolamine (10 μM), 30 min equilibration before curve. This curve was the fifth curve on each atrium; the previous curves were in the presence of 0, 0.3, 1 and 3 μM phentolamine and were similarly without significant effect on the noradrenaline responses. *d*, Control curves. C_1 refers to the first control curve and C_5 was the fifth curve to noradrenaline in each of four atria. Curves 2, 3 and 4 all lay between these two curves.

8–16 pulses. These findings indicate that the present method of atrial stimulation leads to immediate release of substantial amounts of sympathetic transmitter. Evidence that this transmitter was released from nerves was obtained by the observations that 0.1 μM tetrodotoxin completely blocked the response to one and two field pulses and almost abolished the response to four pulses without significantly altering resting atrial rate.

Pretreatment with phenoxybenzamine resulted in a marked potentiation in relation to the control response in both the peak and its duration after either one or four pulses (Table 1 and Fig. 1). If we assume that the tachycardia response is directly related to the synaptic cleft concentration of noradrenaline, the area under the atrial period response record will be a function of the concentration and duration of noradrenaline released by nerve stimulation. The peak responses to a single pulse doubled after phenoxybenzamine whereas the area increased by 2.4- and 4.9-fold after 3 and 10 μM, respectively (Table 1). In contrast, phentolamine, in concentrations that significantly antagonized α-adrenoreceptors in guinea pig aortic strips, did not increase the tachycardia response with respect to peak or duration to either one or four pulses, nor was there a significant depression of resting atrial period (Table 1 and Fig. 1). Yohimbine, which has been classified as being a more selective presynaptic α-adrenoreceptor antagonist than phentolamine[11], was also without significant effect on the response to sympathetic stimulation (Table 1).

Applying four field pulses within one refractory period (that is, four pulses over 40 ms equivalent to a frequency of sympethetic stimulation of ~100 Hz) decreased the atrial period by the same magnitude as four pulses delivered as one pulse following each atrial beat for four beats. However, phentolamine and yohimbine failed to potentiate the responses to either stimulation pattern. These findings contrast with some reports of an increase in the tachycardia response to sympathetic stimulation after phentolamine and yohimbine[12–15].

To explore the possibility that phenoxybenzamine potentiated the response to a single pulse by its well established property of uptake inhibition[9,16], we investigated the effect of a combination of desipramine and oestradiol, drugs classified as potent inhibitors of $uptake_1$ and $uptake_2$ (refs 17, 18). In the guinea pig heart the $uptake_2$ mechanism is of minor significance[19] and this was confirmed in the present study by the finding that desipramine alone potentiated the responses to field stimulation as much as did desipramine combined with oestradiol. The potentiation of response to a single pulse in the presence of the combination of the uptake blocking drugs was very similar to the potentiation observed following phenoxybenzamine (Table 1). Moreover, tachycardia responses to cumulative dose–response curves to exogenous noradrenaline were potentiated to a similar degree by phenoxybenzamine and uptake blockade (Fig. 2). By contrast, phentolamine at 0.3–10 μM had no significant effect on the resting atrial rate or the dose–response curves to noradrenaline (Fig. 2). Therefore, we conclude that uptake

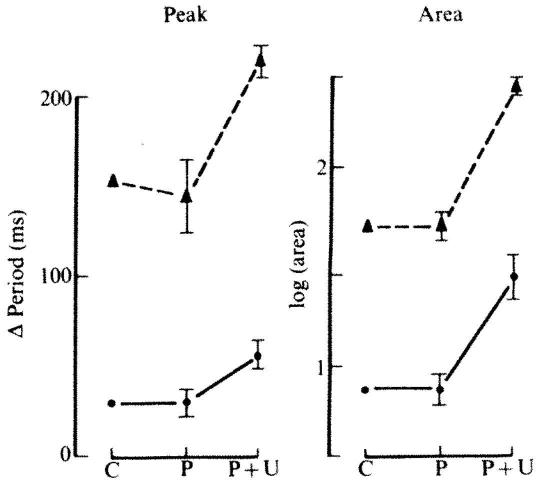

Fig. 3 Potentiation of right atrial period responses to sympathetic stimulation by uptake block in the presence of phentolamine. For each atrium responses were measured to one (●) and four (▲) field pulses in three conditions: (1) C, control, (2) P, in the presence of 10 μM phentolamine, and (3) P + U, in the presence of 10 μM phentolamine and uptake block (0.1 μM desipramine and 5 μM 17β-oestradiol). Points represent mean values from five atria; bars indicate ± 1 s.e.d. within atria between adjoining means. All values during P + U were significantly higher than either P or C ($P < 0.05$). Peak and area defined in Table 1 legend.

blockade is more likely to be the underlying mechanism of the phenoxybenzamine potentiation than α-adrenoreceptor antagonism.

The failure of phentolamine to enhance the chronotropic effect of sympathetic nerve stimulation despite a considerable increase in transmitter overflow has been previously observed[7,20]. However, Langer, Adler-Graschinsky and Giorgi[7] suggested that phentolamine had a veratramine-like direct depressant action on the sino-atrial node which (1) lowered the resting atrial rate, (2) attenuated the chronotropic response to exogenous noradrenaline and (3) prevented the tachycardia to sympathetic nerve stimulation. We can find no evidence for this depressant action of phentolamine on the resting atrial rate or on exogenous noradrenaline dose–response curves. Moreover, in the presence of a high phentolamine concentration (10 μM), uptake block treatment potentiated the response to one and four pulses of sympathetic stimulation to a similar degree to uptake block alone (Fig. 3). Similarly, pretreatment with 10 μM phenoxybenzamine in the presence of 10 μM phentolamine, still potentiated responses as before (area responses to one field pulse, log units: phentolamine 0.88, phenoxybenzamine 1.46, s.e.d. = 0.097, $t = 5.88$, $P < 0.01$, seven experiments).

In conclusion, our results indicate that phenoxybenzamine potentiates not only the response to a train of sympathetic nerve pulses but also markedly accentuates the effects of a single pulse. By contrast, the α-adrenoreceptor antagonists phentolamine and yohimbine did not potentiate the effects of either stimulus trains or single pulses. It seems likely that the potentiation produced by phenoxybenzamine was not due to its α-adrenoreceptor antagonist action but to its property of uptake block. This suggests that presynaptic α-adrenoreceptor modulation by synaptically released noradrenaline plays no part in cardiac sympathetic transmission, at any rate, at the physiological stimulus levels of the present experiments which were generally lower than those used in overflow studies.

We thank Mrs E. Anderson and Mr M. Lew for technical assistance and Mr M. Percy for the period meter. J.A.A. is a holder of an NH and MRC of Australia C.J. Martin Fellowship.

Received 30 November 1979, accepted 16 April 1980.

1 Farnebo, L O & Hamberger, B *Br J Pharmac* 43, 97–106 (1971)
2 Enero, M A, Langer, S Z, Rothlin, R P & Stefano, F J E *Br J Pharmac* 44, 672–688 (1972)
3 Starke, K *Naunyn-Schmiedebergs Arch Pharmak* 275, 11–23 (1972)
4 Langer, S Z *Br J Pharmac* 60, 481–497 (1977)
5 Rand, M J, Story, D F, Allen, G S, Glover, B & McCulloch, M W in *Frontiers in Catecholamine Research* (eds Usdin, E & Snyder, S H) 579–581 (Pergamon, Oxford, 1973)
6 Rand, M J, McCulloch, M W & Story, D F in *Central Action of Drugs in Blood Pressure Regulation* (eds Davies, D S & Reid, J L) 94–132 (Pitman, Tunbridge Wells, 1975)
7 Langer, S Z, Adler-Graschinsky, E & Giorgi, O *Nature* 265, 648–650 (1977)
8 Blinks, J R *J. Pharmac exp Ther* 151, 221–235 (1966)
9 Paton, D M in *The Mechanism of Neuronal and Extraneuronal Transport of Catecholamines* (ed Paton, D M) 49–66 (Raven, New York, 1976)
10 Iversen, L L *The Uptake and Storage of Noradrenaline in Sympathetic Nerves* (Cambridge University Press, 1967)
11 Starke, K, Borowski, E & Endo, T *Eur. J. Pharmac* 34, 385–388 (1975).
12 Lokhandwala, M F & Buckley, J P *Eur. J Pharmac* 40, 183–186 (1976)
13 Cavero, I *et al Br. J Pharmac* 67, 283–292 (1979)
14 Mouillé, P, Huchet, A-M, Lucet, B, Chelly, J. & Schmitt, H *J cardiovascular Pharmac* 1, 515–528 (1979)
15 Docherty, J P & McGrath, J C *Br J Pharmac* 66, 55–63 (1979)
16 Iversen, L L *Adv Drug Res* 2, 5–23 (1965)
17. Story, D F, Story, M. E, McCulloch, M W, Hope, W & Rand, M J *Clin exp Physiol Pharmac* 1, 429–439 (1974)
18 Salt, P J *Eur J Pharmac* 20, 329–340 (1972)
19 Trendelenburg, U *Trends pharmac Sci* 1, 4–6 (1979)
20 Adler-Graschinsky, E & Langer, S Z *Br J Pharmac* 53, 43–50 (1975)

Open time of channels activated by binding of two distinct agonists

Alain Trautmann & Anne Feltz*

Laboratoire de Neurobiologie, Ecole Normale Supérieure 75230 Paris Cedex 05, France

At the frog endplate, acetylcholine (ACh) causes depolarization by opening synaptic channels, and it is generally assumed that more than one molecule must bind to open one channel. This interpretation, proposed to explain the sigmoidicity of the dose–response curve[1,2], also accounts for the potentiating effect of pipette-released ACh on the response to nerve-released ACh[3]. We have described a similar cross-potentiation between ACh and carbachol (CCh)[4,5]. The response to simultaneous application of these two agonists is larger than the sum of the responses to separate application, and we have assumed that this reflects the binding of both ACh and carbachol to individual receptor molecules. One approach to an understanding of the molecular basis of transmitter action is to study the mean time a channel remains open in its presence. Because this mean 'open time' depends on the nature of the agonist used to activate a given receptor, we have measured this parameter in order to understand better the mechanism underlying the cross-potentiation. We compared the 'open times' observed when the two agonists were applied separately with those obtained when both were applied together. In each case, when a 'faster' agonist (one inducing 'short' open times) and a 'slower' agonist (one inducing 'long' open times) are applied together, the channels opened by combined activation have a short mean open time, as if these were only controlled by the faster agonist.

The open time of a channel at the frog endplate (τ) can be measured directly (by single-channel recording[8]), or it can be estimated indirectly from the relaxation of the endplate current when displaced from equilibrium. Displacement can be spontaneous, appearing in the form of fluctuations of thermal origin around a mean, and in that case noise analysis is used[6]; it can be caused by a concentration jump, in which case the decay of the endplate current is measured[7]; or, as τ is voltage-dependent, it can be caused by voltage jumps[9–11]. The estimation of τ is effectively independent of the method used, at least at a low concentration of agonist. We used the last method, where τ is given by the time constant of relaxation of the agonist-induced current after an instantaneous voltage jump.

Experiments were carried out on the frog endplate at a low temperature (3–5 °C) to reduce the rate of desensitization[5,12]. Membrane potential was controlled by a conventional two-electrode voltage clamp on an endplate region located under Nomarski optics. Identical voltage jumps were performed before (control) and after application of various agonists. Pure agonist-induced current was obtained by subtracting from the current measured in the presence of the agonist (before, during and after the voltage step) the 'nonsynaptic' current measured during a control jump[9–11]. Figure 1*a* (top trace) shows the CCh-induced current obtained by such a subtraction. Before the jump, at −90 mV, the agonist induced a current of 20 nA. After hyperpolarization to −140 mV, the CCh-induced current first increased as expected from the change in driving force on the channels that were open before the jump. The current then relaxed towards a new steady level. When the membrane potential was returned to the initial holding potential, the CCh-induced current first decreased rapidly, then more slowly, eventually returning to the value measured before the voltage step.

A semilogarithmic plot of current against time (Fig. 1*b*) shows that after reaching the new voltage (−140 mV), the

---

*Present address: Laboratoire de Physiologie Respiratoire, CNRS, 23 rue Becquerel, 67087 Strasbourg, France

0028-0836/80/290291-03$01.00

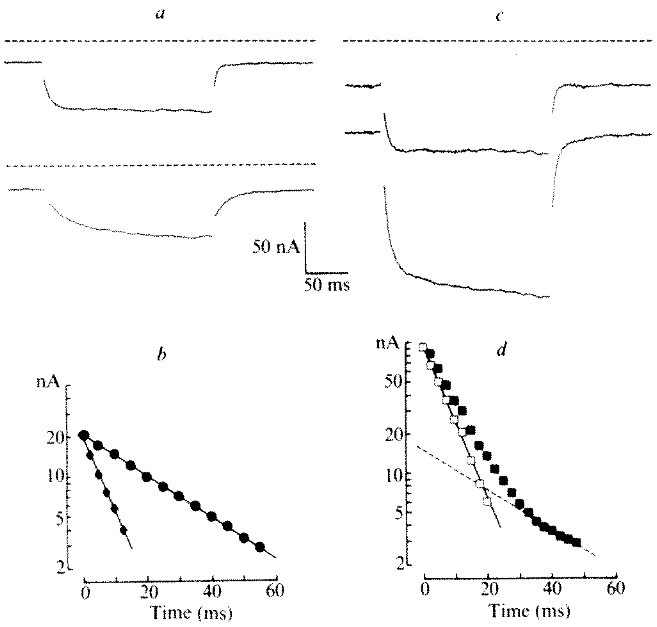

Fig. 1 Agonist-induced currents during a voltage jump lasting 205 ms from a −90-mV to a −140-mV holding potential. The voltage jump was performed before, then during agonist application. After subtraction of the control jump, the nonsynaptic contribution disappears, leaving the current flowing through the synaptic channels opened by the agonist. Each trace is an averaged signal on eight jumps. Dotted lines give the zero synaptic current. *a*, Current induced by the application of 10 μM CCh (top trace) and 37 nM SubCh (bottom trace). *b*, Semilog plot of the CCh-induced current (rhombs) and SubCh-induced current (circles) against time, after a jump at −140 mV. Both currents decay exponentially, with time constants of 7.6 ms and 27 ms respectively. *c*, The bottom trace shows the 'total current' resulting from the simultaneous application of 37 nM SubCh and 10 μM CCh, and the top trace shows the difference between the total current and the sum of the two currents given in *a*. *d*, Semilog plot of the total current (black squares) against time after a jump at −140 mV; the foot of the curve is fitted with an exponential (dotted line) of time constant 27 ms as in *b*. The difference between the total current and this slow component is given by the open squares, which can be fitted by an exponential with time constant 7.5 ms. The time constant of the 'difference' shown in *b*, top (semilog plot is not shown) is 5.7 ms. This figure is somehow shorter than the fast component, but this difference was not systematic in the various experiments (see text). The base line slopes slightly on all records; its time constants of several hundreds of ms are easily separable from the values we are studying. The perfusing medium was cooled at 3 °C to reduce desensitization. In the same line, a Ca-free Ringer was used, with the following composition (mM): NaCl, 115; KCl, 2; $MgCl_2$, 5; HEPES 2 mM and *p*H adjusted to 7.2. All data were recorded on a tape recorder Racal M4 and later analysed on a Hewlett Packard 9825A desk computer. Note the increase in noise level in *c* (compared with *a*): the phenomenon was recorded at a low gain (to avoid saturation on the tape), and reamplified later, with a resulting increase of the background noise from the tape.

current relaxed exponentially to a steady level, enabling us to estimate, at this potential, the mean open time of the channels controlled by CCh ($\tau_{\rm CCh}$).

Similar records obtained during the application of suberyldicholine (SubCh) show slower relaxations (Fig. 1*a*, bottom trace). In the voltage range studied, $\tau_{\rm CCh}$ and $\tau_{\rm SubCh}$ differ by a factor of 3–4, in good agreement with previous data[6,11]. Both values increase with hyperpolarization, and both double over a 50-mV range.

At the holding potential of −90 mV, separate applications of 10 μM CCh• and 37 nM SubCh resulted in an inward current of 20 nA and 25 nA, respectively. During simultaneous application of both agonists (10 μM CCh + 37 nM SubCh) cross-potentiation was observed: instead of the 45-nA current expected from purely additive effects, a total current of 87 nA developed. Moreover, when SubCh and CCh were applied together, the relaxation following a voltage jump was no longer exponential, but biphasic. The extra current produced by cross-potentiation was calculated by subtracting both the CCh-induced current and the SubCh-induced current shown in Fig. 1*a* from the agonist-induced current which developed during simultaneous application. Figure 1*c* (top trace) shows that this extra current relaxed along a single exponential with a time constant almost identical to that observed with CCh alone.

The subtraction of the two single-agonist relaxations from the double-agonist relaxation is justifiable only if the number of receptors bound by two molecules of a given agonist is the same when that agonist is applied alone and when it is applied in combination with the second agonist of the pair—a criterion that can be assumed to be met if the fraction of receptors activated by the agonist is small. In our experimental conditions, clearly only a small proportion of the receptors were activated, because the doses used induced a current of only 20 nA (10 μM CCh), whereas the current expected from activation of all the receptors (assuming a total of more than 10^7 receptors per endplate[13] and an elementary conductance of 25 pS[14]) is 1,000 times greater. Furthermore, because low concentrations of agonist and low temperatures were used, desensitization developed very slowly.

Given our experimental conditions, it thus seems possible to conclude that the receptor population was far from saturated and that desensitization was avoided, so that we could assume that the additional current seen with combined agonist application was due to the recruitment of a new group of receptors, each bound by one CCh and one SubCh molecule. Even if receptor saturation and desensitization were not completely avoided, neither of these factors would be expected to alter our principal finding—that the extra channels controlled by combined agonist application are opened for a short time.

The same conclusion as that drawn from subtracting the two relaxations can be reached directly from a semilog plot of the relaxation of the combined agonist-induced current against time (Fig. 1*d*). Two exponentials appear, with time constants the same as those obtained by separate application of the two agonists. Whereas the amplitude of the slow component remained equal to that obtained with SubCh alone, that of the fast component was four times larger than in the relaxation seen with CCh alone. This again suggests that the channels opened by combined application of SubCh and CCh behave as CCh-activated channels.

To investigate whether our observations were generally applicable, we looked at the characteristics of the channels during cross-potentiation between ACh and acetylthiocholine, SubCh, or CCh. These experiments were all performed after irreversible inactivation of acetylcholinesterase by *O*-ethyl-S_2-diisopropyl-amino-ethyl-methyl-phosphonothionate (MTP)[5]. In all cases, the agonist, which alone would have led to the shorter open time, $\tau_{\rm short}$ (so called faster agonist), seemed to determine the open time of the channels controlled by two agonists ($\tau_{\rm pot}$). In 12 experiments $\tau_{\rm pot}/\tau_{\rm short}$ was 1.08 ± 0.31 (± s.d.).

Our data thus suggest that the binding of a receptor molecule by two different agonists leads to channel opening for a time determined in most cases, if not always, by the faster of the two agonists. These results have to be taken into account in schemes describing normal channel activation. It has often been suggested that sequential binding of two agonist molecules is followed by isomerization of the receptor–channel complex and subsequent channel opening (see ref. 14 for a review). Our data are not easily interpreted with respect to such a model: if isomerization is the rate limiting step, it has to be assumed that for a mixed activation, isomerization depends only on the faster agonist, and that is not very satisfying. On the other hand, if binding is the rate limiting step, one can predict that the open time of the channels controlled by receptors bound by two agonists will be intermediate between the values characteristic of each agonist, which we did not find. A more general discussion would have to take into account other possibilities—if the two binding sites on one receptor are not identical, then models compatible with our results are possible.

This work was supported by grants from CNRS, INSERM (ATP 58-78-90) and DGRST. We thank P. Ascher and J. Kehoe for comments on the manuscript. Suberyldicholine was given by J. Heisemann and B. Sakmann.

Received 14 February; accepted 28 April 1980.

1. Katz, B. & Thesleff, S. *J. Physiol., Lond.* **138,** 63–80 (1957).
2. Jenkinson, D. H. *J. Physiol., Lond.* **152,** 309–324 (1960).
3. Hartzell, H. C., Kuffler, S. W. & Yoshikami, D. *J. Physiol., Lond.* **251,** 427–463 (1975).
4. Feltz, A. & Trautmann, A. *J. Physiol., Lond.* **293,** 64–65P (1979).
5. Feltz, A. & Trautmann, A. *J. Physiol., Lond.* **299,** 533–552 (1980).
6. Katz, B. & Miledi, R. *J. Physiol., Lond.* **230,** 707–717 (1973).
7. Magleby, K. L. & Stevens, C. F. *J. Physiol., Lond.* **223,** 151–171 (1972).
8. Neher, E. & Sakman, B. *Nature* **260,** 799–801 (1976).
9. Adams, P. R. *Br. J. Pharmac.* **53,** 308–310 (1975).
10. Sheridan, R. E. & Lester, H. A. *Proc. natn. Acad. Sci. U.S.A.* **72,** 3496–3500 (1975).
11. Neher, E. & Sakmann, B. *Proc. natn. Acad. Sci. U.S.A.* **72,** 2140–2142 (1975).
12. Magazanik, L. G. & Vyskocil, F. *J. Physiol., Lond.* **249,** 285–300 (1975).
13. Matthews-Bellinger, J. & Salpeter, M. M. *J. Physiol., Lond.* **279,** 197–213 (1978).
14. Colquhoun, D. in *The Receptors* **1** (ed. O'Brien, R. D.) 93–142 (Plenum, New York, 1979).

Proton NMR detection of acetylcholine status in synaptic vesicles

H. Stadler & H. H. Füldner

Max-Planck-Institut für biophysikalische Chemie, Postfach 968, D 3400 Göttingen 1, FRG

The storage granules of cholinergic nerve terminals, the synaptic vesicles, have a central role in the mechanism of cholinergic transmission, and direct evidence as to whether acetylcholine is stored in them in a free or partially immobilized form is therefore of interest. In some secretory systems it has become evident that low molecular weight secretion products are stored within the granules as complexes with proteins or proteoglycans[1]. The application of high resolution NMR spectroscopy to isolated granules[2–4] has recently elucidated the internal structure of secretory granules. We report here that proton NMR analysis of isolated cholinergic synaptic vesicles from *Torpedo marmorata* allows the identification of acetylcholine within the organelle. The spectrum shows that all the acetylcholine is dissolved in an essentially fluid phase within the core. Vesicular and uncompartmentalized acetylcholine can be distinguished from each other and in addition, any hydrolysis to choline and acetate can be monitored. The results open the possibility of studying dynamics of acetylcholine pools and their breakdown in cholinergic tissue by a direct and non-perturbing method.

After isolation[5], vesicles were pelleted, resuspended in a small volume, dialysed against isosmolar D_2O buffer and spectra recorded in a Bruker WH 270 FT spectrometer interfaced to a Nicolet B-NC 12 computer. Chemical shifts are given relative to the internal standard 3-(trimethylsilyl)-d_4-propionic acid, whose pH dependence has been observed where necessary[6]. Complete recording of integrals was assured by proper choice of the acquisition parameters. The temperature was kept at 5 °C.

Basically, three experiments were carried out. In the first experiment, the spectrum of intact vesicles was recorded (Fig. 1*a*). In the second, the acetylcholinesterase present as a contaminant[5] in the sample was blocked by diethyl-*p*-nitrophenyl phosphate (paraoxon). The vesicles were then lysed by several freeze–thaw cycles and the spectrum was taken (Fig. 1*b*). In the third experiment the esterase was left active, the vesicles were lysed and a spectrum with the resulting choline and acetate resonances was obtained (Fig. 1*c*).

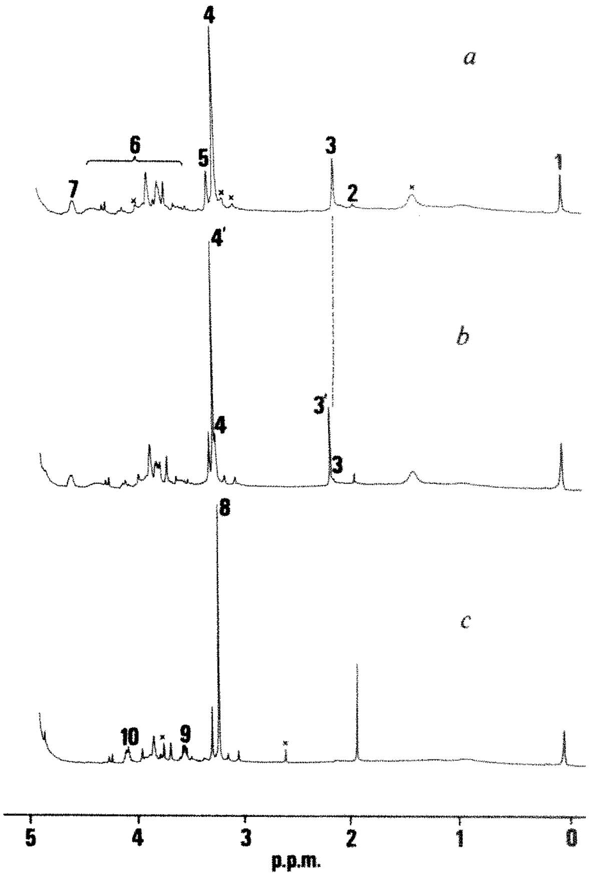

Fig. 1 Proton NMR spectra of isolated cholinergic synaptic vesicles from *Torpedo marmorata*. Vesicles were pelleted from the corresponding fraction from a sucrose density step gradient and suspended and dialysed against 0.4 M NaCl and 20 mM phosphate pD 7.4 made in D_2O and the spectrum recorded at 5 °C. *a*, Intact vesicles in the presence of 50 µM paraoxon (acetylcholine esterase blocker). *b*, The same preparation as *a*, but after lysis of vesicles and release of acetylcholine by repeated freezing and thawing. The dashed line indicates the chemical shift between resonances 3 and 3', the shift is present on all acetylcholine resonances (see text). *c*, Another vesicle preparation that has been lysed by freezing and thawing in the absence of an acetylcholine esterase blocker. The acetylcholine has been hydrolysed by the esterase present in the sample. Identified resonances: (1) 3-(trimethylsilyl)-propionic acid (internal standard, 1 mM); (2) free acetate; (3) and (3') $-CH_3$ protons of the acetyl residue of intact acetylcholine; (4) and (4') $-N-(CH_3)_3$ protons of acetylcholine; (5) trimethyloxamine; (6) resonances from residual sucrose and $-CH_2-$ protons from acetylcholine; (7) $-CH_2-$ protons of acetylcholine adjacent to the acetyl group; (8) $-N-(CH_3)_3$ protons of choline; (9) and (10) $-CH_2-$ protons of choline superimposed on sugar resonances; (×) unidentified resonances.

The simple spectrum of intact vesicles (Fig. 1*a*) contains the resonances of acetylcholine, trimethyloxamine (present in high concentrations in the body fluids of elasmobranchs[7]) and residual sucrose, together with a few minor unidentified resonances. Although ATP is present in vesicles in a 1:7 ratio relative to acetylcholine[5], its resonances could not be identified unambiguously. The membrane lipids gave only a very broad background.

Figure 2 shows the changes in the spectral region containing the $N(CH_3)_3$ and acetyl-CH_3 resonances when the vesicle preparation was subjected to several freeze–thaw cycles in the presence of the anticholinesterase. The progressive release of the intact acetylcholine as vesicles are broken is apparent.

0028–0836/80/290293–02$01.00

Three observations were noted: (1) The acetylcholine resonances of intact vesicles are shifted upfield relative to free acetylcholine as obtained after lysis or from a simple acetylcholine solution in our buffer (spectrum not shown). The shift ranges from about 0.02 p.p.m. to 0.04 p.p.m. for the various acetylcholine resonances (compare Fig. 1*a*, *b*). Although small, it is reproducibly above the resolution limit of 0.01 p.p.m. Possible explanations for this shift include susceptibility differences between the vesicle core and the external medium, differences in *p*H or ionic strength, and a weak interaction of acetylcholine with the negatively charged groups of a glycosaminoglycan found to be associated with the vesicles[8]. The effect of *p*H and ionic strength was insufficient to explain the observed shifts. (2) The integrals of corresponding resonances are identical before and after lysis. This means that all the vesicular acetylcholine is detected in the intact vesicles. (3) The stored form of acetylcholine shows only slightly bigger linewidths than the released one. Therefore, there is no doubt that the stored acetylcholine is dissolved; the differences in linewidths are presumably due to viscosity differences.

The result of the third experiment (several freeze–thaw cycles in the presence of active cholinesterase) is presented in Fig. 3. Here, vesicle breakdown and the immediate hydrolysis of the released acetylcholine are indicated by the disappearance of the acetyl-CH_3-resonance of intact acetylcholine and the concomitant appearance of the CH_3-resonance of free acetate. Correspondingly, all other acetylcholine resonances change over to those of choline (see Fig. 1*c*). This observation supports our deduction from the chemical shifts in the spectrum of acetylcholine that these were due to the difference between intra- and extravesicular acetylcholine. Another experiment of type 3 (omitting the freeze–thaw cycles) established that the half life of acetylcholine (~36 h) is long compared with the time of the experiments.

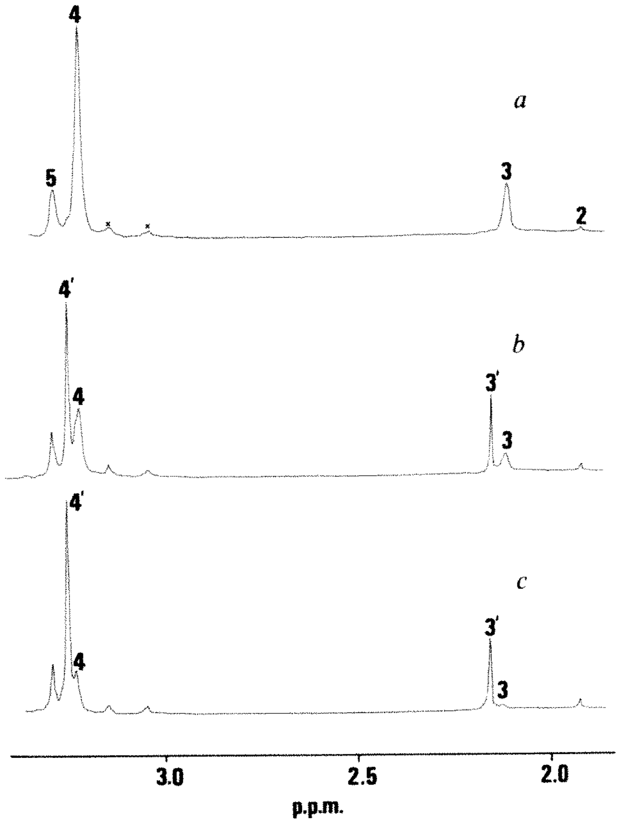

Fig. 2 Proton NMR spectra of cholinergic synaptic vesicles as a function of progressive release of acetylcholine from the vesicles by repeating freezing and thawing. Conditions and labelling as in Fig. 1*a*, *b*; a window of the resonances (2) to (5) is presented on an expanded scale. *a*, Intact vesicles before freezing and thawing; *b*, after 4 freeze–thaw cycles; *c*, after 12 freeze–thaw cycles.

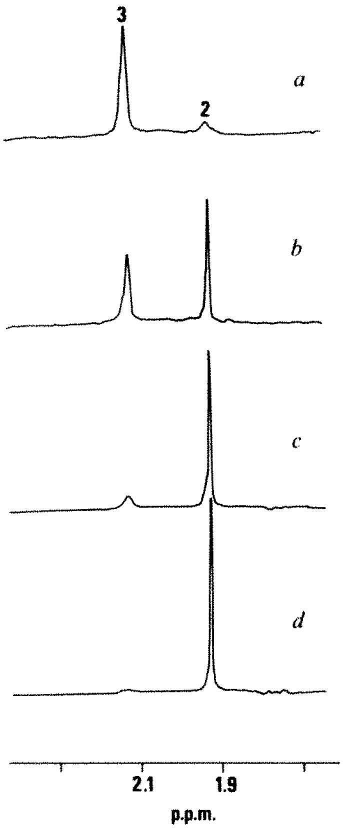

Fig. 3 Hydrolysis of acetylcholine progressively released from synaptic vesicles in the presence of unblocked acetylcholine esterase. Conditions as described in Fig. 1*c*, labelling as in Fig. 1. Part of the spectrum shown in Fig. 1*c* is presented. *a*–*d* Are spectra after 0, 2, 8 and 16 freeze–thaw cycles, respectively. Freezing and thawing of an acetylcholine solution in the same condition has no effect.

Pure Chem. Library
SCIENCE COLLEGE
Upper Circular Road
CALCUTTA

We accordingly conclude that the internal organization of acetylcholine in synaptic vesicles, in agreement with our recent findings that no soluble or easily releasable high molecular weight material is present in the core [5,13], constitutes a specialized version of a secretory organelle with fully dissolved storage product, thus fulfilling the need for quick acetylcholine release, which presumably occurs via exocytosis of vesicles during synaptic transmission. The result is consistent with density measurements suggesting that the vesicular acetylcholine is in an 'osmotically active' state [9,10].

As there is evidence that the dynamic structure of the internal content of an isolated secretory granule is identical with that of the granule in the intact organ[11], the shift differences mentioned might provide the basis for future NMR experiments using synaptosomes or intact (perfused) tissue to study the turnover and breakdown of acetylcholine pools, a matter of current interest[12].

We thank Dr V. P. Whittaker for support and Frl. U. Welscher for technical assistance. The work was supported by the SFB 33 project C6.

Received 6 February; accepted 23 April 1980.

1. Giannattasio, G., Zanini, A. & Meldolesi, J. in *Complex Carbohydrates of Nervous Tissue* (eds Margolis, R. U. & Margolis, R. K.) 338 (Plenum, New York, 1979).
2. Daniels, A., Korda, A., Tanswell, P., Williams, A. & Williams, R. J. P. *Proc. R. Soc.* **B187**, 353 (1974).
3. Casey, R. P., Njus, D., Radda, G. K. & Sehr, P. A. *Biochemistry* **16**, 972 (1977).
4. Ugurbil, K., Holmsen, H. & Shulman, R. G. *Proc. natn. Acad. Sci. U.S.A.* **76**, 2227 (1979).
5. Tashiro, T. & Stadler, H. *Eur. J. Biochem.* **90**, 479 (1978).
6. De Marco, A. *J. magn. Resonance* **20**, 527 (1977).
7. Cohen, J. J., Krupp, M. A. & Chidsey, C. A. *Am. J. Physiol.* **194**, 229 (1958).
8. Stadler, H. & Whittaker, V. P. *Brain Res.* **153**, 408 (1978).
9. Breer, H., Morris, S. J. & Whittaker, V. P. *Eur. J. Biochem.* **81**, 453 (1978).
10. Ohsawa, K., Dowe, G. H., Morris, S. J. & Whittaker, V. P. *Brain Res.* **161**, 447 (1979).
11. Daniels, A., Williams, R. J. P. & Wright, P. E. *Nature* **261**, 321 (1976).
12. Zimmermann, H. *Neuroscience* **5**, 1773 (1979).
13. Stadler, H. *Hoppe-Seylers Z. Physiol. Chem.* **359**, 326 (1978).

Metallothionein mRNA induction in HeLa cells in response to zinc or dexamethasone is a primary induction response

Michael Karin, Robert D. Andersen, Emily Slater, Karen Smith & Harvey R. Herschman

Molecular Biology Institute, Department of Biological Chemistry, and
Laboratory of Nuclear Medicine and Radiation Biology,
UCLA School of Medicine, Los Angeles, California 90024

Metallothioneins (MTs) are low molecular weight, heavy metal binding proteins unique in their high cysteine content and high affinity for Zn^{2+}, Cd^{2+}, Hg^{2+}, Ag^{2+} and Cu^{2+} (refs 1–3). The synthesis of MTs is induced by zinc or cadmium in the liver and kidney[4–8] and in cultured cells[9–12]. More recently MT induction by the steroid hormone dexamethasone (Dex) has been demonstrated in HeLa cells[13] and adrenalectomized rats[14]. Because glucocorticoid hormones lead to an intracellular accumulation of zinc[15–17], the question arises of whether the induction of MT gene expression by steroids is a 'primary induction response' (ref. 18), or due to elevated intracellular Zn^{2+}. The glucocorticoid-induced transport of Zn^{2+} is dependent on concurrent protein synthesis[10,19]. We now show that, in contrast to glucocorticoid-stimulated Zn^{2+} transport, the Zn^{2+} and Dex induction of translatable MT-mRNA is independent of concomitant protein synthesis but not RNA synthesis; that is, MT induction by either agent is a primary induction response[18].

We first compared the effects of Dex and Zn^{2+} on (1) the patterns of protein synthesis directed by total HeLa cytoplasmic RNA in a cell-free system, and (2) the patterns of soluble protein synthesis in the cells (Fig. 1). HeLa cells were grown as previously described[13]. To demonstrate an elevated MT-mRNA level in response to Zn^{2+} or Dex, confluent plates of HeLa cells were incubated for 6 h in control medium, 10^{-7} M Dex, or 3.7×10^{-5} M Zn^{2+}. At the end of this induction period the cells were collected by scraping, with a rubber policeman, into ice-cold phosphate-buffered saline. The cells were collected by centrifugation in a Beckman Microfuge B for 45 s. Total cytoplasmic RNA was extracted from the cells by the phenol–chloroform method of Anderson *et al.*[20]. Total cytoplasmic RNA extracted from HeLa cells was translated in the wheat-germ cell-free translation system described by Andersen and Weser[21] for translation of rat liver MT-mRNA. The incorporation of radioactivity into MT is a linear function of the amount of HeLa cell total cytoplasmic RNA added to the translation system up to 15 µg of total RNA per reaction mixture (data not shown). To examine the effects of Zn^{2+} and Dex on MT synthesis in the cells, additional plates were exposed to inducers for 6 h, shifted to cysteine-free medium and exposed for an additional hour to ^{35}S-cysteine (see Fig. 1 legend).

At the end of either the *in vitro* translation reaction or the radioactive labelling of the cultured cells, the fractions to be analysed were reduced and alkylated (ref. 21 and Fig. 1 legend) and subjected to electrophoresis on polyacrylamide gels. Due to its high cysteine content, reduced and carboxymethylated MT has a large net negative charge (carboxymethyl cysteine is negatively charged in the conditions used for electrophoresis). As a consequence, the carboxymethylated MT migrates abnormally rapidly on 20% polyacrylamide SDS gels (see ref. 21). In this gel system MTs migrate as a single band with an R_F of 0.72 relative to bromphenol blue, and are completely separated from all other proteins[21].

Lanes *a*, *c* and *e* of Fig. 1 are the reduced and carboxymethylated proteins synthesized in the cell-free system. The reduced and carboxymethylated soluble proteins extracted from ^{35}S-cysteine-labelled cells are in lanes *b*, *d* and *f*. The MT band (indicated by the arrows) is markedly increased by Dex (lanes *c*, *d*) and by Zn^{2+} (lanes *e*, *f*) in comparison with control cells (lanes *a*, *b*). Dex and Zn^{2+} clearly stimulate MT synthesis both in the cells and in the RNA-dependent *in vitro* translation system. Characterization, by both DEAE-Sephadex chromatography and electrophoresis on native polyacrylamide gels, of the Zn^{2+}- and Dex-induced MT from HeLa cells

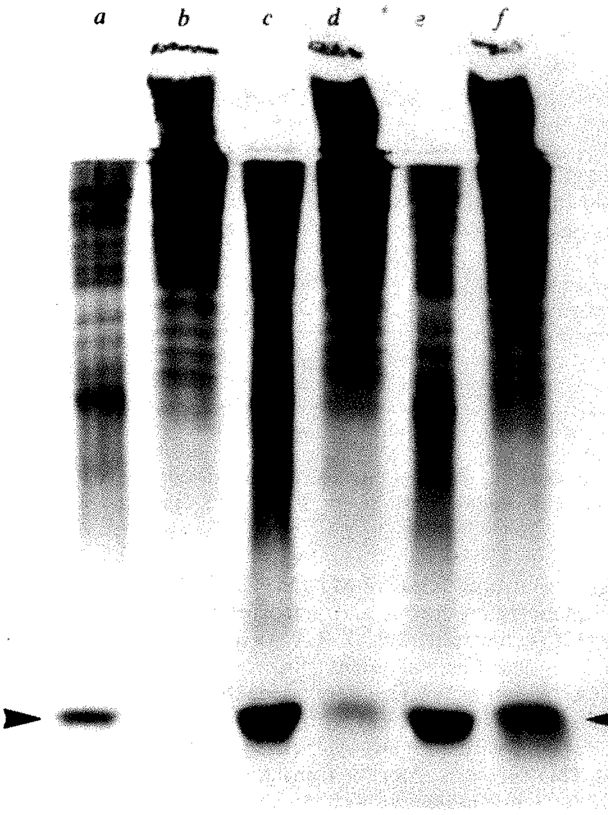

Fig. 1 Dexamethasone- and Zn^{2+}-induced stimulation of MT synthesis and MT-mRNA accumulation in HeLa cells cultured in serum-free medium. HeLa cells were incubated for 6 h with control medium (*a*, *b*), medium $+10^{-7}$ M Dex (*c*, *d*), or medium $+3.7 \times 10^{-5}$ M Zn^{2+} (*d*, *e*). At the end of the incubation period three culture plates for each point were collected and total cytoplasmic RNA was extracted. The cell-free translation was carried out as described by Andersen and Weser[21] in a total volume of 25 µl, optimal salt concentrations were 4.5 mM $MgCl_2$ and 65 nM KCl. Unlabelled cysteine was omitted from the amino acid mixture and replaced with 0.8 µM of ^{35}S-cysteine (translation grade, NEN 608 Ci mmol^{-1}). The reaction was initiated by adding exogenous RNA. All samples were assayed with both 10 µg (a subsaturating amount) and 15 µg (the peak of the concentration curve) of cellular RNA. At the end of the 2-h incubation at 25 °C the samples were carboxymethylated as previously described[21]. The remaining culture dishes were labelled from the 6th to the 7th hour with 30 µCi of ^{35}S-cysteine (NEN, 300–500 Ci mmol^{-1}). Radioactive labelling was carried out in cysteine-free medium containing the appropriate inducers. At the end of the 1-h pulse, the cells were collected and the soluble proteins extracted as described before[13]. Reduction and alkylation of proteins synthesized in the cells were done as follows. To 200 µl of the cell extract were added 20 µl of 1 M HCl and 20 µl of 0.25 M EDTA. After 20 min at room temperature, 300 µl of 8 M guanidine, 0.5 M Tris-Cl, 0.05 M EDTA, pH 8.5, containing 20 mM dithiothreitol were added. After 3 h incubation at 37 °C, 50 µl of 2 M neutralized iodoacetic acid were added and the mixture was incubated for another 90 min at 37 °C. The reaction was terminated by dialysing against H_2O for 24 h. All the samples were subjected to electrophoresis on 20% polyacrylamide, 0.1% SDS slab gels. Lane *a*, 76,000 c.p.m. of translation product from the cell-free protein synthesis reaction, synthesis directed by RNA from control cultures. Lane *b*, 151,000 c.p.m. of intracellular ^{35}S-cysteine-labelled soluble proteins from control cultures. Lane *c*, 81,000 c.p.m. of *in vitro* synthesized translation product directed by RNA from Dex-induced cultures. Lane *d*, 161,000 c.p.m. of intracellular labelled soluble proteins from Dex-induced cultures. Lane *e*, 77,000 c.p.m. of *in vitro* synthesized translation products directed by RNA from Zn^{2+} induced cultures. Lane *f*, 162,000 c.p.m. of intracellular labelled soluble proteins from Zn^{2+}-induced cultures. Electrophoresis and fluorography have been described previously[21–25]. The position of the MT band is indicated by the arrows.

0028–0836/80/290295–03$01.00

Table 1 Dexamethasone stimulation of zinc uptake by HeLa cells

	Expt 1 (confluent cells)	Expt 2 (confluent cells)	Expt 3 (exponential cells)
Control (6 h)	37,734 ± 953	37,543 ± 3016	21,474 ± 3772
Dex (6 h)	43,899 ± 220	43,140 ± 1689	26,200 ± 2848
Cycloheximide (6 h)	—	31,144 ± 1288	19,040 ± 2206
Dex + cycloheximide (6 h)	—	26,729 ± 3858	18,938 ± 891
Control (24 h)	57,903 ± 2780	—	—
Dex (24 h)	97,647 ± 2475	—	—

HeLa cells were incubated for the times indicated in our serum-free medium[13] with 0.5 μCi of $^{65}Zn^{2+}$ per plate. Dexamethasone, where indicated, was 10^{-7} M; cycloheximide was 10^{-4} M. At the end of the incubation period the cells were washed twice with 5 ml of cold phosphate-buffered saline. Cells were dissolved in 1 M NaOH. $^{65}Zn^{2+}$ content was measured in a Beckman Biogamma counter. Expts 1 and 2 were with confluent cells; expt 3 was with cells at half-maximal density.

suggests that both forms of MT (MT_I and MT_{II}, refs 2, 12) are induced by heavy metals and glucocorticoid hormones (M.K. and H.R.H., in preparation). R.A. *et al.*[20] have demonstrated that the wheat-germ system preferentially translates small mRNAs *in vitro*. We also see a reduction in high molecular weight proteins synthesized in the cell-free system (lanes *a*, *c*, *e*) compared with proteins synthesized in intact cells (lanes *b*, *d*, *f*). This does not affect the translation of MT-mRNA, which codes for a low molecular weight (6,000) protein.

To determine whether or not the elevation of MT-mRNA in response to the two different inducers is dependent on *de novo* synthesis of RNA and protein, we used inhibitors of RNA and protein synthesis (actinomycin D and cycloheximide). HeLa cells were exposed for 6 h to 10^{-7} M Dex or 3.7×10^{-5} M Zn^{2+}, either in the absence or presence of inhibitors. At the end of the 6-h exposure period total cytoplasmic RNA was extracted and translated in the cell-free system, using ^{35}S-cysteine to label the proteins synthesized. The reduced and carboxymethylated proteins were subjected to electrophoresis and fluorograms were prepared (Fig. 2). Lanes *a*, *b* and *c* are, respectively, proteins from control, Dex-induced and Zn^{2+}-induced cells in the absence of inhibitors. Lanes *d*, *e* and *f* are, respectively, proteins from control, Dex-induced and Zn^{2+}-induced cells in the presence of 1 μg ml^{-1} of actinomycin D during the 6-h induction period. Lanes *g*, *h* and *i* are, respectively, control Dex-induced and Zn^{2+}-induced cells in the presence of 10^{-4} M cycloheximide during the induction period. Once again, Dex and Zn^{2+} exposure leads to an elevation in translatable MT-mRNA (lanes *a*–*c*). Both the hormone- and metal-elicited elevations in MT-mRNA are inhibited by 1 μg ml^{-1} of actinomycin D (lanes *d*–*f*) but not by 10^{-4} M cycloheximide (lanes *g*, *h*, *i*). This concentration of cycloheximide blocks more than 90% of protein synthesis in HeLa cells (results not shown).

To quantitate the amounts of MT synthesized, a fluorogram prepared from the experiment shown in Fig. 2 was scanned with a densitometer. The optical density (a direct function of radioactivity, data not shown) in the MT band was summed and normalized to the amount of total radioactivity applied to the gel. Figure 3 shows the quantitative results from a densitometric analysis of a fluorogram from the same experiment shown in Fig. 2. In this particular experiment MT-mRNA was elevated about five-fold by 10^{-7} M Dex and six-fold by 3.7×10^{-5} M Zn^{2+}. Inclusion of 1 μg ml^{-1} actinomycin D in the culture medium during the induction period not only prevented the elevation of MT-mRNA, but also lowered its level relative to control cultures by 50–60%. In contrast, inclusion of 10^{-4} M cycloheximide did not inhibit the induction of MT-mRNA; in fact, cycloheximide caused an elevation in the level of MT-mRNA in both control and treated cultures.

We considered it essential to examine the role of RNA and protein synthesis in MT induction by Zn^{2+} and Dex at similar levels of induction. The Dex concentration used (10^{-7} M) causes maximal MT synthesis in response to this inducer. In contrast, we used a concentration of Zn^{2+} (3.7×10^{-5} M) which, although it causes approximately the same level of induction as maximal dexamethasone, results in only 20% of the maximal MT response to the optimal Zn^{2+} concentration (10^{-4} M). Variable cycloheximide enhancement of MT synthesis (40–100%) in Zn^{2+}-treated cultures and control cultures was observed in two *in vitro* translation experiments and four *in vivo* experiments of the type described in Fig. 1 legend. In contrast, we observed only 0–30% cycloheximide enhancement with Dex-treated cells. The stimulatory effect of cycloheximide observed in control- and Zn^{2+}-induced, but not Dex-induced expression of MT-mRNA may be due to the fact that in one condition (with Dex) the system is operating at maximal potential for that physiological condition, whereas in the other cases (control, Zn^{2+}) the system is operating in sub-optimal conditions of expression. Alternatively, the glucocorticoid receptor may have a short half life: its decay in the presence of cycloheximide may counterbalance a true stimulating effect of the drug. Recently, Enger *et al.*[22] have also used *in vitro* translation of mRNA in a wheat-germ system to demonstrate that induction of MT in cultured CHO cells in response to cadmium occurs as a consequence of an elevation in translatable message.

Cox[19] reported that exposure of HeLa cells to Dex leads to an increased uptake of Zn^{2+}. We find that Dex exposure of HeLa cells grown in serum-free medium also leads to a twofold elevation in the uptake of $^{65}Zn^{2+}$ after 24 h (Table 1, expt 1). Cox also reported the Dex-induced Zn^{2+} uptake was,

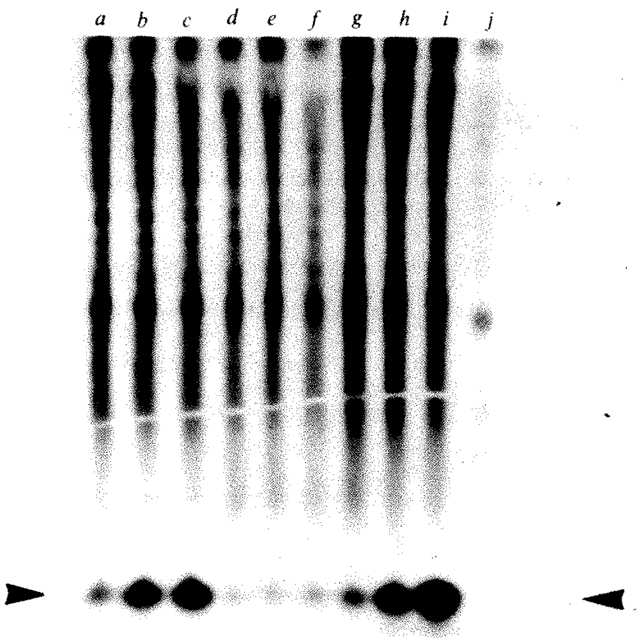

Fig. 2 *In vitro* translation of RNA preparations from control, Dex-treated and Zn^{2+}-treated HeLa cells and the effect of actinomycin D and cycloheximide on MT-mRNA accumulation. Confluent cultures of HeLa cells were incubated for 6 h in: *a*, control medium; *b*, medium containing 10^{-7} M Dex; (*c*, medium containing 3.7×10^{-5} M Zn^{2+}; *d*, control medium plus 1 μg/ml^{-1} actinomycin D; *e*, 10^{-7} M Dex plus 1 μg ml^{-1} actinomycin D; *f*, 3.7×10^{-5} M Zn^{2+} plus 1 μg ml^{-1} actinomycin D; *g*, control medium plus 10^{-4} M cycloheximide; *h*, 10^{-7} M Dex plus 10^{-4} M cycloheximide; *i*, 3.7×10^{-5} M Zn^{2+} plus 10^{-4} M cycloheximide; *j*, no exogenous RNA added to the translation system. At the end of the 6-h incubation period, total cytoplasmic RNA was extracted and translated in the cell-free system. The translation products were reduced and alkylated, dried down under vacuum in a desiccator and resolubilized in 50 μl of electrophoresis sample buffer. A 10-μl aliquot containing 40,000–60,000 c.p.m. was subjected to electrophoresis on 20% polyacrylamide, 0.1% SDS gels. The position of the MT band on the resulting fluorogram is indicated by the arrows.

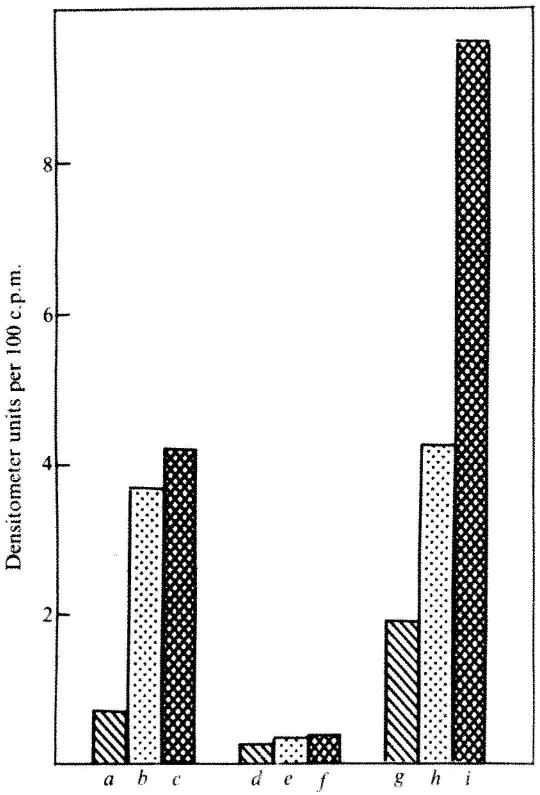

Fig. 3 Quantitation of the effects of RNA and protein synthesis inhibitors on elevation of MT-mRNA in response to Dex and Zn^{2+}. A fluorogram similar to that shown in Fig. 2, but in the linear response range, was scanned with an Optronics Photoscan model P-1000 digitalized densitometer, using a photometer window with a 200-μm raster. RNA at 10 μg per translation (a subsaturating concentration) was used. The density in the MT band was summed and normalized to the amount of radioactivity applied to each slot.

however, dependent on *de novo* RNA and protein synthesis[19]. We find that after 6 h of exposure to Dex there may already be a slight increase in $^{65}Zn^{2+}$ uptake. More importantly, in the presence of cycloheximide there is no Dex stimulation of $^{65}Zn^{2+}$ uptake over the 6-h induction period (Table 1, expts 2, 3). In contrast to Dex stimulation of Zn^{2+} transport, the induction of MT-mRNA is not blocked by cycloheximide (Figs 2, 3). In the HeLa system, glucocorticoid induction of MT is thus not a consequence of protein synthesis-dependent Zn^{2+} uptake into the cells, as suggested by Failla and Cousins[17] for primary rat hepatocytes.

Several of the currently studied steroid hormone induction systems are not primary induction responses. Hepatic induction of $\alpha 2\mu$-globulin mRNA by glucocorticoid hormones is inhibited by cycloheximide[23], in contrast to our results for glucocorticoid hormone induction of MT-mRNA. McKnight[24] has also reported that the induction in explants of chick oviduct of mRNA for both ovalbumin and conalbumin by oestrogen (or progesterone) is blocked by inhibition of protein synthesis. A primary induction system such as the Dex induction of MT synthesis in HeLa cells, in which no intervening protein synthesis need occur, should be much more amenable to cell-free analysis of transcription control by steroid hormones.

We conclude that (1) Dex and Zn^{2+} both lead to an elevation of the mRNA for MT in HeLa cells, (2) the elevation is dependent on *de novo* RNA synthesis (inhibition by actinomycin D), (3) the elevation is independent of *de novo* protein synthesis (insensitivity to cycloheximide), and (4) the elevation is not dependent on increased Zn^{2+} transport (Table 1). MT induction by both Dex and Zn^{2+} is a primary induction response[18], that is, it is not dependent on the induced synthesis of any protein intermediates. The MT induction system should provide an excellent experimental model both for the study of the physiological regulation by glucocorticoid hormones of Zn^{2+} metabolism and for the elucidation of the control mechanisms responsible for regulation of gene expression in eukaryotes by heavy metals and glucocorticoids.

This work was supported by DOE Contract DE AM03 76 SF00012 and EPA Contract IAG-D5-E-68 -A0. Film scanning was performed on equipment purchased with NIH research funds (GM16925) and supported by the Parvin Cancer Research Laboratories core grant. Scanning and integration software was prepared by Richard G. Fisher.

Received 16 July 1979; accepted 16 April 1980.

1. Margoshes, M. & Vallee, B. L. *J. Am. chem. Soc.* **79,** 4813–4814 (1957).
2. Kagi, J. H. R. & Vallee, B. L. *J. biol. Chem.* **236,** 2435–2442 (1961).
3. Sabbioni, E. & Marafante, E. *Envir. Physiol. Biochem.* **5,** 132–141 (1975).
4. Wisniewska, J. M., Trojanowska, B., Piotrowski, J. K. & Jakubowski, M. *Tox. appl. Pharmac.* **16,** 754–763 (1970).
5. Shaikh, Z. A. & Lucis, O. J. *Fedn Proc.* **29,** 298 (1970).
6. Winge, D. R., Premakumar, R. & Rajagopalan, K. V. *Archs Biochem. Biophys.* **170,** 242–252 (1975).
7. Squibb, K. S. & Cousins, R. J. *Envir. Physiol. Biochem.* **4,** 24–30 (1974).
8. Squibb, K. S. & Cousins, R. J. *Biochem. biophys. Res. Commun.* **75,** 806–812 (1977).
9. Webb, M. & Daniel, M. *Chem. biol. Interact.* **10,** 269–276 (1975).
10. Failla, M. L. & Cousins, R. J. *Biochim. biophys. Acta* **543,** 293–304 (1978).
11. Rudd, C. J. & Herschman, H. R. *Tox. appl. Pharmac.* **44,** 511–521 (1978).
12. Rudd, C. J. & Herschman, H. R. *Tox. appl. Pharmac.* **47,** 271–276 (1979).
13. Karin, M. & Herschman, H. R. *Science* **204,** 176–177 (1979).
14. Etzel, R. R., Shapiro, S. G. & Cousins, R. J. *Biochem. biophys. Res. Commun.* **89,** 1120–1126 (1979).
15. Cox, R. P. *Molec. Pharmac.* **4,** 510–521 (1968).
16. Cox, R. P. & Ruckenstein, A. *J. cell. Physiol.* **77,** 71–82 (1971).
17. Failla, M. L. & Cousins, R. J. *Biochim. biophys. Acta* **538,** 435–444 (1978).
18. Yamamoto, K. R. & Alberts, B. *A. Rev. Biochem.* **45,** 721–746 (1976).
19. Cox, R. P. *Science* **165,** 196–199 (1969).
20. Anderson, C. W., Lewis, J. B., Atkins, J. F. & Gesteland, R. F. *Proc. natn. Acad. Sci. U.S.A.* **71,** 2756–2760 (1974).
21. Andersen, R. D. & Weser, U. *Biochem. J.* **175,** 841–852 (1978).
22. Enger, M. D., Rall, L. B. & Hildebrand, C. E. *Nucleic Acids Res.* **7,** 271–288 (1979).
23. Chen, C. C. & Feigelson, P. *Proc. natn. Acad. Sci. U.S.A.* **76,** 2669–2673 (1979).
24. McKnight, G. S. *Cell* **14,** 403–413 (1978).
25. Laskey, R. A. & Mills, A. D. *Eur. J. Biochem.* **56,** 335–341 (1975).

Independent replication and expression of B-component RNA of cowpea mosaic virus

Rob Goldbach, Geertje Rezelman & Albert van Kammen

Department of Molecular Biology, Agricultural University, De Dreijen 11, 6703 BC Wageningen, The Netherlands

Cowpea mosaic virus (CPMV) is a plant virus with a split genome, composed of two single-stranded plus-type RNA molecules which are separately encapsidated in two (bottom and middle) nucleoprotein particles[1–3]. The protein capsids of the bottom (B) and middle (M) component are similar and consist of two proteins in equimolar amounts[4,5]. Both B and M components are necessary for virus multiplication, indicating that the genetic information is distributed between both (B and M) RNAs[6]. However, little is known about the location of genes on either RNA and the reason for a divided genome is unknown. Inoculation of cowpea protoplasts with complete virus (M + B components) results in the synthesis of at least seven virus-specific polypeptides, including the capsid proteins[7,8]. We show here that on inoculation of protoplasts with the separated components, the B component RNA is replicated and expressed independently, whereas the M component RNA is not. The results presented suit a model in which B RNA codes for early functions and M RNA for late functions during viral infection, supplying a possible explanation for the divided genome of CPMV.

The molecular weights (MWs) of M and B RNAs are 1.37×10^6 and 2.02×10^6, respectively[9]. Both RNAs possess a 3′-terminal poly(A) tail[10] and a protein covalently linked to their

0028-0836/80/290297-04$01.00

5′ termini[11,12]. Translation in a wheat-germ cell-free system and in extracts from rabbit reticulocytes results in the synthesis of large proteins which readily account for more than 80% of the coding capacity of both M and B RNA[13–15]. Pelham[15] has shown that in the reticulocyte system some processing of the large proteins occurs. However, no polypeptides corresponding to the viral coat proteins were observed. Mesophyll protoplasts can be isolated from the primary leaves of cowpea plants (*Vigna unguiculata* (L.)) and infected with CPMV[16]. We have analysed the proteins synthesized in this *in vivo* system after inoculation with separated B and M components.

Figure 1 shows the electrophoretic patterns of the proteins from mock-infected protoplasts and protoplasts inoculated with M, B or the mixture of M+B components. In agreement with earlier results[7,8], protoplasts infected with M+B components produce seven virus-specific polypeptides of MWs 170,000, 110,000, 87,000, 84,000, 37,000, 30,000 and 23,000. The polypeptide pattern obtained from protoplasts infected with M component alone is similar to that of the uninfected protoplasts. No virus-specific proteins were detected. In contrast, protoplasts infected with B component alone produce all virus-specific polypeptides with the exception of the (37,000 and 23,000 MW) capsid proteins. No immunoprecipitate with antiserum against virions was obtained from protoplasts infected with either M or B components, confirming the absence of coat proteins. The total of the MWs of the five B RNA-coded polypeptides greatly exceeds the coding capacity of the RNA. Peptide fingerprint experiments, using *Staphylococcus aureus* V8 protease, have shown, however, that the polypeptides of MWs 110,000, 87,000 and 84,000 are derived from the 170,000 MW polypeptide by post-translational cleavage (data not shown). The results shown in Fig. 1 raise the question of why B RNA alone can be expressed whereas M RNA cannot. Two possible explanations can be given. First, M RNA can only be translated when B RNA or B RNA-coded proteins are present in the cell. This explanation seems improbable as M RNA is readily translated *in vitro*. Second, B RNA codes for the viral replicase[17,18] and on infection of protoplasts with B component, B RNA is replicated to give a large quantity of RNA subsequently directing detectable translation. Translation of M RNA in protoplasts remains undetectable because multiplication of M RNA does not occur.

Table 1 Replicase activity in cowpea protoplasts inoculated with CPMV components

Protoplasts inoculated with	^{3}H-UTP incorporation per 13×10^6 protoplasts (c.p.m.)
	5,492
M	5,688
B	17,876
M+B	17,332

Portions of 13×10^6 protoplasts were inoculated with 3.5 μg M, 3.5 μg B or 7 μg (1:1 mixture) M+B components and incubated as described elsewhere[7]. The cells were collected 42 h after inoculation, resuspended in 1 ml of 50 mM Tris-HAc (*p*H 7.4), 10 mM KAc, 1 mM EDTA, 10 mM dithioerythritol (DTE) and 0.5 mM phenylmethylsulphonylfluoride (PMSF) and disrupted at 0 °C in a Thomas homogenizer with a Teflon pestle. Cell homogenates were centrifuged at 1,000*g* for 15 min. The supernatants were adjusted to 20% (v/v) glycerol and centrifuged at 31,000*g* for 30 min. The 31,000*g* pellets were resuspended in 0.4 ml 50 mM Tris-HAc (*p*H 8.2), 25% (v/v) glycerol, 50 mM KAc, 1 mM EDTA, 10 mM DTE and 0.5 mM PMSF. ^{3}H-UTP incorporation in the resuspended 31,000*g* pellets was measured in standard replicase assay conditions[18]. Although the ratio between the activities of uninfected and M+B-infected cells is only slightly more than 3, it was reproducible in other experiments. Moreover, in time course experiments (not shown) it was found that the extra activity in M+B-inoculated cells was induced at 15–30 h post-infection, that is, the period of maximal virus production[16].

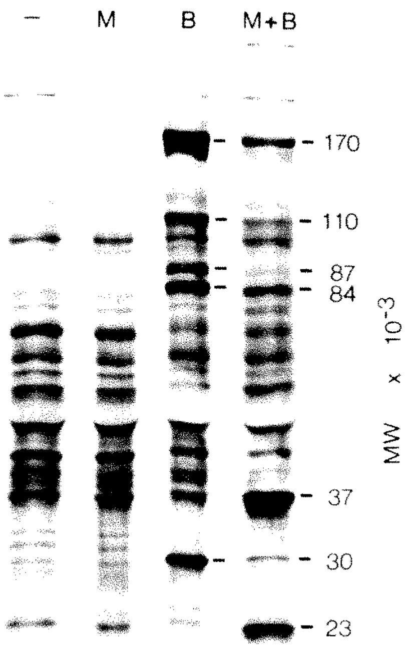

Fig. 1 Analysis on a 7–15% linear SDS-polyacrylamide gradient gel of ^{35}S-labelled proteins from uninfected protoplasts (–), protoplasts inoculated with purified M components (M), purified B component (B), and complete virus (M+B). CPMV was grown in *Vigna unguiculata* L. 'blackeye early ramshorn' and purified as previously described[27]. M and B components were separated by three cycles of centrifugation in a linear 15–30% zonal sucrose gradient (Beckman Ti 15 rotor, 16 h, 23,000 r.p.m. at 10 °C). By means of the local lesion infectivity assay[16] it was determined that M components were free of B and that B components contained less than 0.2% M. Portions of protoplasts (5 ml, 5×10^5 ml^{-1}) were mock-infected or inoculated with 7 μg M, 7 μg B or 14 μg (1:1 mixture) M+B virus components and labelled with 150 μCi ^{35}S-methionine 20–25 h after infection as described in detail elsewhere[7]. Neither actinomycin D nor any other inhibitor of host protein synthesis was added in this experiment. Soluble protein fractions (31,000*g* supernatants) were prepared and electrophoresed (using equal amounts of radioactivity) as previously described[7]. In the M+B slot the large (170,000–84,000 MW) virus-specific polypeptides are not as clearly visible as in the B slot, as most radioactivity is found in the capsid proteins (37,000 and 23,000 MW). MW markers used were: *Escherichia coli* RNA polymerase subunits (MWs 165,000 and 155,000), *E. coli* β-galactosidase (116,200), phosphorylase *a* (92,500), human transferrin (80,000), bovine serum albumin (68,000), catalase (57,500), γ-globulin (54,000 and 23,500), ovalbumin (46,000), lactate dehydrogenase (35,000) and tobacco mosaic virus coat protein (17,500).

To test the latter hypothesis, the RNA replicase activity was examined in infected and uninfected protoplasts using the assay conditions for CPMV replicase as described by Zabel *et al.*[17,18]. The results presented in Table 1 show that in protoplasts infected with a mixture of M+B the ^{3}H-UTP-incorporating activity increases three times over the activity measured in uninfected protoplasts. A similar increase in activity occurs in protoplasts infected with B component but not in those infected with M component. This finding strengthens the suggestion that B RNA contains information essential for viral RNA replication. This suggestion was substantiated by analysing the RNAs produced. Protoplasts inoculated with M, B or M+B components, or uninfected, were labelled by incubation with $^{32}PO_4$ 20–25 h after inoculation and then analysed for RNA. As shown in Fig. 2, protoplasts infected with a mixture of M+B components produce two RNAs which co-migrate with standard CPMV B RNA and M RNA. These RNAs are absent in uninfected protoplasts as well as in protoplasts infected with M component. However, protoplasts inoculated with B component efficiently produce ^{32}P-labelled B RNA. This finding verifies that B RNA replicates independently whereas M RNA does not.

The absence of M RNA (or fragments of M RNA) in protoplasts infected independently with M or B components was checked using cDNA made from B and M RNA. The results of the hybridization experiments presented in Table 2 show that M RNA is not synthesized in protoplasts inoculated with M component alone, whereas in protoplasts inoculated with the M+B mixture this RNA is readily detected. The results confirm that B RNA is made in protoplasts infected with B component alone. The amount of B RNA produced in these cells is comparable with the amount of this RNA in protoplasts infected with M+B, consistent with the independent expression of B as shown in Fig. 1. To a certain degree CPMV resembles another two-component virus, tobacco rattle virus (TRV). The large RNA of TRV is also able to replicate independently, whereas no coat protein is produced[19]. CPMV differs from TRV, however, in that inoculation of plants with B component does not result in infection detectable by local lesions.

The data obtained from the present experiments provide evidence that B RNA can be independently replicated, implying that this RNA codes for a protein involved in replication. Although in theory B RNA (but not M RNA) may code for a protein inducing the expression of a host gene, this possibility is very unlikely. A host gene must be proposed, which is 'sleeping' in normal (uninfected) conditions and acting harmfully during infection. It is plausible that B RNA codes for the viral replicase or a subunit of this enzyme. Zabel *et al.*[17,18] have isolated CPMV RNA replicase from virus-infected cowpea leaves and have shown that such replicase preparations contain a protein which binds CPMV RNA specifically and is absent in control preparations from healthy leaves. Together, these findings favour the hypothesis that CPMV RNA carries information for a protein required for viral RNA replication. They do not support the idea that plant viral RNA is replicated by a host enzyme, as has been suggested[20–22].

The results shown here suggest that M RNA codes for both capsid proteins, these being the only viral proteins absent in protoplasts infected with B component. A similar conclusion is reached from complementation studies using particles from different CPMV isolates[23,24]. The results are consistent with a model for the distribution of genes among the components of CPMV in which B RNA exclusively codes for early proteins (for example, the replicase or replicase subunit(s)) and M RNA for late proteins (for example, both capsid proteins). The usefulness of the split genome would therefore lie in its ability to regulate separately the expression of early and late genes.

Table 2 Hybridization of ^{32}P-labelled RNA from infected and uninfected protoplasts with cDNA made from B and M RNA

^{32}P-RNA from protoplasts inoculated with	Hybridization (c.p.m.) to M cDNA	B cDNA	Calf thymus DNA
—	165	122	93
M	173	147	130
B	290	2,966	161
M + B	1,665	2,342	152

Protoplasts were incubated with ^{32}P-orthophosphate 20–25 h after inoculation. For details see Fig. 2 legend. Portions of 100,000 c.p.m. ^{32}P-RNA were hybridized to 1 μg of filter-bound DNA for 18 h in 0.45 M NaCl and 0.045 M Na-citrate (*p*H 7.0) at 65 °C, essentially as described by R.G. *et al.*[25]. Complementary DNA from purified M and B RNA (M cDNA and B cDNA, respectively) was made as previously described[26].

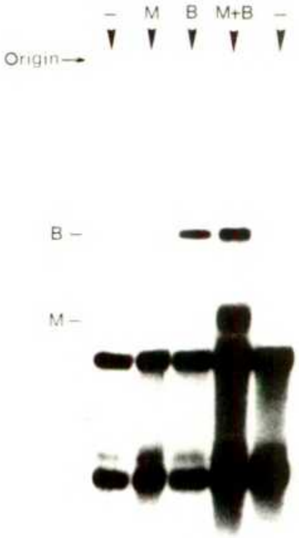

Fig. 2 Agarose gel electrophoresis of glyoxal-denatured RNAs from protoplasts infected with CPMV components. Portions of protoplasts (5 ml, 5×10^5 ml^{-1}) were inoculated with virus components as described in Fig. 1 legend. The cells were collected 20 h after inoculation, resuspended in phosphate-deficient medium[7] (10^6 cells ml^{-1}) and labelled for 5 h with ^{32}P-orthophosphate (1 mCi ml^{-1}) in the presence of actinomycin D (15 μg ml^{-1}). Total cell RNA was isolated by heating the cells for 5 min at 60 °C in a detergent mix (2% *p*-aminosalicylate, 1% Na-deoxycholate, 0.5% tri-isopropylnaphthalene sulphonate and 2% Sarkosyl in 50 mM Tris-HCl (*p*H 8.2) and 0.1 M NaCl) and centrifugation of the lysate on a 5.7 M CsCl cushion according to Glišin *et al.*[28]. Yields were: uninfected cells, 840 μg (7,900 c.p.m. per μg); M-inoculated cells, 780 μg (8,200 c.p.m. per μg); B-inoculated cells, 860 μg (10,200 c.p.m. per μg); M + B inoculated cells, 790 μg (9,400 c.p.m. per μg); c.p.m. were measured by scintillation counting. RNA samples (comprising 20,000 c.p.m.) from uninfected (–) protoplasts and those inoculated with M, B and M + B components were denatured with glyoxal and electrophoresed in a 1.5% agarose gel according to McMaster and Carmichael[29]. After the run the gel was dried and autoradiographed. B and M below the origin indicate the position of standard (unlabelled) virion B and M RNA in the gel. Recently, it has been reported[30] that the poly(A) tail of M RNA is heterogeneous in length (50–400 residues), whereas the length distribution of the poly(A) tail in B RNA shows a narrow distribution (50–150 residues). This heterogeneity is visible in the gel, where the band of B RNA is sharp but the band of M RNA rather diffuse.

We thank Drs J. Stanley and P. Zabel for helpful comments and Mr J. Verver for carrying out the RNA electrophoresis experiments. This work was supported by the Netherlands Foundation for Chemical Research (SON) with financial aid from the Netherlands Organization for the Advancement of Pure Research (ZWO).

Received 15 February; accepted 29 April 1980.

1. Van Kammen, A. *A. Rev. Phytopath.* **10,** 125–150 (1972).
2. Jaspars, E. M. J. *Adv. Virus Res.* **19,** 37–149 (1974).
3. Bruening, G. in *Comprehensive Virology* Vol. 11 (eds Fraenkel-Conrat, H. & Wagner, R. R.) 55–141 (Plenum, New York, 1977).
4. Wu, G.-J. & Bruening, G. *Virology* **46,** 596–612 (1971).
5. Geelen, J. L. M. C., Van Kammen, A. & Verduin, B. J. M. *Virology* **49,** 205–213 (1972).
6. Van Kammen, A. *Virology* **34,** 312–318 (1968).
7. Rottier, P. J. M., Rezelman, G. & Van Kammen, A. *Virology* **92,** 299–309 (1979).
8. Rottier, P. J. M. thesis, Wageningen Agricultural Univ. (1980).
9. Reijnders, L., Aalbers, A. M. J., Van Kammen, A. & Thuring, R. W. J. *Virology* **60,** 515–521 (1974).
10. El Manna, M. M. & Bruening, G. *Virology* **56,** 198–206 (1973).
11. Stanley, J., Rottier, P., Davies, J. W., Zabel, P. & Van Kammen, A. *Nucleic Acids Res.* **5,** 4505–4522 (1978).
12. Daubert, S. D., Bruening, G. & Najarian, R. C. *Eur. J. Biochem.* **92,** 45–51 (1978).
13. Davies, J. W., Aalbers, A. M. J., Stuik, E. J. & Van Kammen, A. *FEBS Lett.* **77,** 265–269 (1977).
14. Pelham, H. R. B. & Stuik, E. J. *Proc. Coll. Nucleic Acids and Protein Synthesis in Plants, CNRS,* 691–695 (1977).
15. Pelham, H. R. B. *Virology* **96,** 463–477 (1979).
16. Hibi, T., Rezelman, G. & Van Kammen, A. *Virology* **64,** 308–318 (1975).
17. Zabel, P., Weenen-Swaans, H. & Van Kammen, A. *J. Virol.* **14,** 1049–1055 (1974).

18. Zabel, P., Jongen-Neven, I. & Van Kammen, A. *J. Virol.* **29,** 21–33 (1979).
19. Lister, R. M. *Proc. Fedn Am. Soc. exp. Biol.* **28,** 1875–1889 (1969).
20. Ikegami, M. & Fraenkel-Conrat, H. *Proc. natn. Acad. Sci. U.S.A.* **75,** 2122–2124 (1978).
21. Ikegami, M. & Fraenkel-Conrat, H. *FEBS Lett.* **96,** 197–200 (1978).
22. Chifflot, S., Sommer, P., Hartmann, D., Stussi-Garaud, C. & Hirth, L. *Virology* **100,** 91–100 (1980).
23. Gopo, J. M. & Frist, R. H. *Virology* **79,** 259–266 (1977).
24. Thongmeearkom, P. & Goodman, R. M. *Virology* **85,** 75–83 (1978).
25. Goldbach, R. W., Bollen-de Boer, J. E., Van Bruggen, E. F. J. & Borst, P. *Biochim. biophys. Acta* **521,** 187–197 (1978).
26. Davies, J. W., Verver, J. W. G., Goldbach, R. W. & Van Kammen, A. *Nucleic Acids Res.* **5,** 4643–4661 (1978).
27. Klootwijk, J., Klein, I., Zabel, P. & Van Kammen, A. *Cell* **11,** 73–82 (1977).
28. Glišin, V., Crkvenjakov, R. & Byus, C. *Biochemistry* **13,** 2633–2637 (1974).
29. McMaster, G. K. & Carmichael, G. G. *Proc. natn. Acad. Sci. U.S.A.* **74,** 4835–4838 (1977).
30. Ahlquist, P. & Kaesberg, P. *Nucleic Acids Res.* **7,** 1195–1203 (1979).

Compressed microfibril models of the native collagen fibril

Benes L. Trus & Karl A. Piez

Laboratory of Biochemistry, National Institute of Dental Research, National Institutes of Health, Bethesda, Maryland 20205

A three-dimensional crystal model for packing of collagen molecules (type I) in the native fibril has recently been proposed by Hulmes and Miller[1]. It provides a straightforward explanation of the major features of the X-ray diffraction pattern, and is consistent with measurements of fibril density. However, there is independent evidence for a well defined microfibrillar substructure, which is absent from their model. This evidence, which is derived from electron microscopy[2-5] and studies of *in vitro* assembly[6,7], the pattern of covalent cross-links[8] and sequence analysis[9,10], is convincing. Therefore, we have searched for a means to reconcile this conflict. We now propose two models which contain five-stranded microfibrils compressed to place molecules (in cross-section) on a pseudo-hexagonal lattice. The unit cells are equivalent or related to the cell proposed by Hulmes and Miller[1]. In the simplest case, molecules, and thus microfibrils, are straight-tilted. However, it is not ruled out that molecules are supercoiled and microfibrils are straight. Noncrystallographic considerations[6,7,9,10] favour supercoiling.

The five-stranded microfibril in which D-staggered collagen molecules ($D = 67$ nm) form a 5_1 or 5_4 helix (Fig. 1*A*), originally proposed by Smith[11], has been the most widely accepted model for packing of collagen molecules. In the original interpretation by Miller and colleagues[12-14] of the X-ray diffraction pattern, the unit cell contained four 5-fold microfibrils in a tetragonal unit cell. A more recent study[15] suggests a sheared tetragonal cell. In the present study we retain the microfibril but compress it to place molecules on a pseudo-hexagonal lattice as illustrated in Fig. 1*B*. As proposed by Hulmes and Miller[1], we assume that the three strong X-ray diffraction reflections in the equatorial region with row-line spacings of 1/1.369, 1/1.328 and 1/1.264 nm^{-1} are the reciprocal distances between planes of molecules in the three sets that define the pseudo-hexagonal lattice. We suggest that a microfibril in isolation or in small bundles may have a symmetrical or loosely symmetrical 5-fold cross-section but that in large bundles (fibrils) the internal crystal energy is sufficient to distort the helix and force molecules onto a hexagonal lattice. Molecules may be straight or supercoiled, as discussed below. We envisage supercoiling as being accommodated by tilts of molecular segments, the angle varying about some average value. As a molecule coils about the microfibril axis it would appear at successive lattice points within the compressed microfibril cross-section. The trapezoidal cross-section, in general, would not rotate. The distortion required is consistent with NMR studies[16-18] which have shown that since collagen molecules in the native fibril are in rapid segmental motion in directions perpendicular to the fibril axis, intermolecular interactions must be fluid. In addition, systematic as well as random deviations from the lattice are possible as long as a large portion of the protein density is near the lattice planes. That is, the actual structure of the microfibril may be between the two extremes illustrated in Fig. 1*B*.

Table 1 Observed and calculated equatorial row-line spacings

Observed	Model 1	Model 2 Smaller cell	Model 2 Larger cell
3.800	3.777 (1, 0)	3.777 (1, 0)	3.777 (1, 1)
		3.837 (1, −1)	3.837 (2, 0)
2.651	2.582 (1, −1)	2.582 (1, −2)	2.621 (1, −2)
2.461	2.436 (0, 1)	2.436(0, 2)	2.436 (2, −2)
1.890	1.889 (2, 0)	1.889 (2, 0)	1.889 (2, 2)
1.748	1.748 (1, 1)	1.748 (1, 2)	1.748 (1, −3)
1.57	—	1.560 (2, 1)	1.560 (1, 3)
1.503	—	—	1.505 (5, −2)
1.369	1.369 (3, −1)	1.369 (3, −2)	1.369 (5, 1)
1.328	1.328 (1, −2)	1.328 (1, −4)	1.328 (6, −1)
1.264	1.264 (2, 1)	1.264 (2, 2)	1.264 (0, 4)

For convenience real spacings are given. Units are nanometres. Indices are shown in parentheses. Observed row-line spacings are from rat tail tendon[12-14]. For descriptions of models 1 and 2, see Figs 2 and 3, respectively.

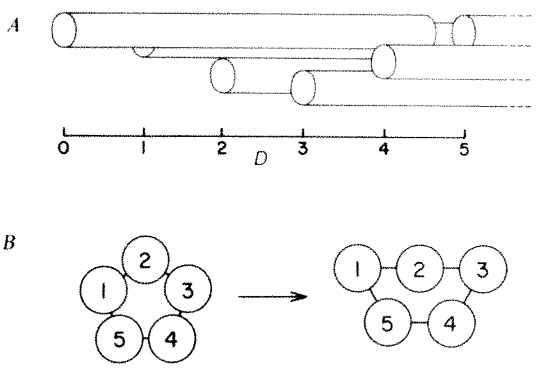

Fig. 1 Schematic representations of one end of a 5-fold microfibril of collagen molecules (*A*) and its conversion to a compressed microfibril where molecules in cross-section lie on a pseudo-hexagonal lattice (*B*). $D = 67$ nm. The numbers designate the D segment cut in the cross-section. Molecules may be straight as shown or supercoiled.

In model 1 the compressed microfibrils are arranged in a hexagonal pattern as shown in Fig. 2. Every point on the lattice of molecules is occupied and the unit cell contains a D segment of one microfibril. The unit cell is equivalent to that proposed by Hulmes and Miller[1], but the arrangement of molecules within the cell is different. Table 1 shows the agreement between observed and calculated row-line spacings. As can be seen in Fig. 2, the unit cell can be drawn in two equivalent ways, one of which was selected by Hulmes and Miller[1]. We have used the other because it is directly related to the unit cell of model 2.

The simplest way to explain the equatorial position of the 1/1.264-nm^{-1} reflection and the off-equatorial positions of the 1/1.328- and 1/1.369-nm^{-1} reflections is to straight-tilt molecules in the direction of the 1.264-nm plane so the tilting vector is 0° normal to that plane but about 4° normal to the other two planes. Here also, the unit cell of our model 1 is equivalent to the Hulmes and Miller[1] cell and thus provides as satisfactory an explanation of the X-ray diffraction pattern insofar as the analysis has been developed. However, we do not rule out the possibility that molecules are supercoiled about the microfibril axis rather than straight-tilted. The strong reflections near 1/1.3 nm^{-1} would then be explained by sampling of the transform of the supercoiled molecules. Because distorted helices are involved, this more complex

0028-0836/80/290300-02$01.00

situation requires a more complex analysis, which we have not attempted.

The advantage of supercoiled molecules is that the microfibrils are better defined and thus provide a better explanation of evidence for a microfibrillar substructure, already quoted. For example, *in vitro* studies[6,7] have shown that assembly of native fibrils from collagen monomer is a stepwise process involving thin filaments as intermediates. Lateral association of supercoiled microfibrils is consistent with these data whereas assembly of straight-tilted molecules implies a three-dimensional crystallization. Also, regularities in the amino acid sequence can be explained by supercoiling of molecules in a microfibril[9,10].

In model 2 we assume that the asymmetric unit contains *D* segments of two compressed microfibrils related by a noncrystallographic 2-fold axis. We have examined all possible arrangements and find one (Fig. 3*A*) in which the unit cell (Fig. 3*B*, smaller cell) accurately predicts the observed reflections in the near-equatorial region of the X-ray diffraction pattern (Table 1). The unit cell contains one asymmetric unit and its dimensions, not surprisingly in retrospect, are the same as those of the unit cell in model 1 except that one dimension is doubled. The advantage of model 2 is that it predicts one of two observed weak reflections not predicted by model 1, and it predicts a second reflection near the critical reflection at 1/3.8 nm^{-1} (Table 1). Both predicted reflections near 1/3.8 nm^{-1} arise from important structural features of the model (Fig. 3*B*) and thus both could be present but unresolved.

If the unit cell in model 2 is doubled (Fig. 3*B*), the second of the two reflections not predicted by model 1 is present and the fit to the observed reflection at 1/2.651 nm^{-1} is markedly improved (Table 1, larger cell). That is, the true unit cell may contain four compressed microfibrils. If so, they must in some sense be non-equivalent. The situation may be analogous to the earlier interpretation[12–14] of the X-ray diffraction data in which the unit cell contained four 5-fold microfibrils related by a 4-fold screw axis. Therefore, some of the arguments based on that model may still be valid. For example, the larger unit cell is consistent with recent electron microscopic evidence[5] for an 8-nm unit in collagen fibrils. Regularities in the amino acid sequence have also been interpreted in terms of a 4-fold screw axis[9,10], results which are not inconsistent with the distortion required for hexagonal packing of supercoiled molecules.

As in model 1, molecules in model 2 may be straight-tilted or supercoiled. The same arguments hold. A somewhat stronger case may be made for supercoiling in model 2 as the tilting vectors arising from the supercoil will be largely parallel to the long axes of the compressed microfibril cross-sections, which lie in the 1.264-nm planes. As already noted, this spacing gives rise to an equatorial reflection whereas the 1.369- and 1.328-nm planes give rise to reflections that are off-equatorial. However, a detailed analysis has not been done.

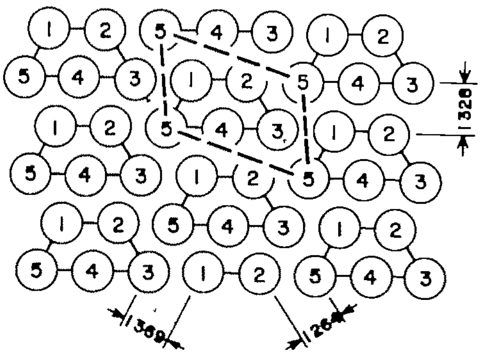

Fig. 2 Model 1. One possible arrangement of molecules in a native collagen fibril. The lines join sets of five molecules constituting a microfibril (Fig. 1). The lattice spacings are given in nanometres. The unit cell (dashed lines) has dimensions *a* = 2.668 nm, *b* = 4.136 nm and γ = 114.04° and contains one microfibril.

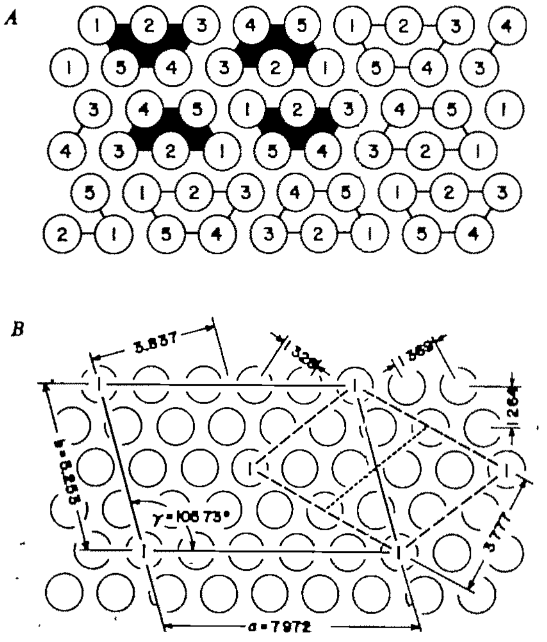

Fig. 3 Model 2. *A*, A second possible arrangement of molecules in a native collagen fibril. The lines join sets of five molecules constituting a microfibril (Fig. 1). The shading designates a group of four microfibrils which in the larger unit cell constitute the true repeating unit. *B*, The same arrangement showing the larger (solid lines) and smaller (dashed lines) unit cells, some of the major spacings and the dimensions of the larger unit cell. Distances are given in nanometres. The dimensions of the smaller unit cell are *a* = 5.335 nm, *b* = 4.136 nm and γ = 114.04°. The dotted line halves the smaller cell and defines a pseudo-cell identical to the unit cell of model 1.

Of course, the unit cell in model 1 can be doubled or quadrupled and microfibrils made non-equivalent; the unit cells of models 1 and 2 become identical. Therefore, evidence for a large unit cell does not favour one model over the other. It is also possible that different arrangements of microfibrils with varying degrees of order exist within a group of fibrils.

Further analysis and perhaps independent evidence will be needed to provide a definitive answer. What we have shown is that hexagonal packing of molecules is not inconsistent with some type of ordered microfibrillar substructure.

We thank Drs Hulmes and Miller for a copy of their manuscript[1] before its publication.

Note added in proof: We have recently learned that Katz and Li[19] in 1973 proposed the general idea that microfibrillar structures (5- and 7-stranded) could be contained within a hexagonal lattice of collagen molecules.

Received 24 January, accepted 2 May 1980

1 Hulmes, D J & Miller, A *Nature* 282, 878–880 (1979)
2 Piez, K A & Miller, A *J supramolec Struct* 2, 121–137 (1974)
3 Doyle, B B *et al* *Proc R Soc* B186, 67–74 (1974)
4 Ruggeri, A, Benazzo, F & Reale, E *J ultrastruct Res* 68, 101–108 (1979)
5 Parry, D A D & Craig, A A *Nature* 282, 213–215 (1979)
6 Gelman, R A, Williams, B R & Piez, K A *J biol Chem* 254, 180–186 (1979)
7 Gelman, R A & Piez, K A *J biol Chem* (in the press)
8 Light, N D & Bailey, A J *Biochem J* 185, 373–381 (1980)
9 Piez, K A & Trus, B L *J molec. Biol* 122, 419–432 (1978)
10 Traub, W *FEBS Lett* 92, 114–120 (1978)
11 Smith, J W *Nature*, 219, 157–158 (1968)
12 Miller, A & Wray, J S *Nature* 230, 437–439 (1979)
13 Miller, A & Parry, D A D *J molec Biol* 75, 441–447 (1973)
14 Fraser, R D B, Miller, A & Parry, D A D *J molec Biol* 83, 281–283 (1974)
15 Fraser, R D B & MacRae, T P *J molec Biol* 127, 127–133 (1979)
16 Torchia, D A & VanderHart, D L *J molec Biol* 104, 315–321 (1976)
17 Jelinski, L W & Torchia, D A *J molec. Biol* 133, 45–65 (1979), *J molec Biol* 138, 255–272 (1980)
18 Jelinski, L W, Sullivan, C E & Torchia, D A *Nature* 284, 531–534 (1980)
19 Katz, E P & Li, S H *J molec. Biol* 73, 351–369 (1973)

Structure of cytochrome c': a dimeric, high-spin haem protein

Patricia C. Weber*§, R. G. Bartsch†, M. A. Cusanovich*, R. C. Hamlin‡, A. Howard‡, S. R. Jordan*, M. D. Kamen†, T. E. Meyer†, D. W. Weatherford*, Nguyen huu Xuong‡ & F. R. Salemme*

*Departments of Biochemistry and Chemistry, New Chemistry Building, University of Arizona, Tucson, Arizona 85721
†Department of Chemistry A-002, University of California at San Diego, La Jolla, California 92093
‡Departments of Physics, Chemistry and Biology, University of California at San Diego, La Jolla, California 92093
§To whom correspondence should be addressed

The bacterial cytochromes c' (ref. 1) occur in various photosynthetic and denitrifying bacteria, where they are presumed to function in electron transport[2]. Most cytochromes c' are isolated as dimeric molecules composed of two identical subunits of ~14,000 molecular weight (MW), with each polypeptide chain incorporating a protohaem IX prosthetic group covalently bound through thioether linkages formed by condensation of two cysteine side chains with the haem vinyl groups[3]. Although a similar mode of covalent haem attachment is found in members of the well studied mitochondrial cytochrome c family[4], the cytochromes c' are, in contrast, high-spin haem proteins (hence the prime designation) which bind neutral ligands[5], characteristic properties generally associated with members of the oxygen-binding globin family[6]. Here we present a preliminary structural description of the cytochrome c' derived from the photosynthetic, purple non-sulphur bacterium *Rhodospirillum molischianum*, and show that it bears little structural resemblance to members of either the cytochrome c or globin structural families. The cytochrome c' monomer structure is, instead, principally organized as a left-twisted, 4-α-helical bundle, a structural motif previously observed in several other sequentially and functionally unrelated proteins[7-13].

R. molischianum cytochrome c' crystallizes in the orthorhombic space group $P2_12_12_1$ ($a=56.5$ Å, $b=71.8$ Å, $c=75.6$ Å) with a dimeric molecule (MW ~ 29,000) in the crystallographic asymmetric unit[14]. Native and heavy atom (K_2PtCl_6 and K_2HgI_4) intensity data were collected from three crystals on the multiwire area detector developed by Xuong and co-workers at the University of California at San Diego[15,16]. Heavy atom sites for the singly substituted platinum and doubly substituted mercury derivatives were determined by deconvolution of the respective heavy atom difference Patterson maps and referred to a common origin by calculating a difference Fourier map for each derivative based on phases derived from the other. Anomalous dispersion effects arising from the platinum and mercury derivatives were incorporated into the final phase refinement cycles (Table 1) as described by Matthews[17], giving an overall figure of merit of 0.72 for the 10,667 independent reflections phased to 2.5 Å resolution. The resulting map was contoured to allow construction of a 2 cm Å^{-1} Kendrew model of the dimer, which was built according to the established amino acid sequence of the molecule[18]. Preliminary atomic coordinates were measured from the model using an electro-mechanical optical superpositioning device[19]. Figure 1 shows a representative view of the electron density of the 2.5 Å resolution map, whose overall quality was sufficient to trace unambiguously the backbone chain and establish the majority of the side-chain conformations.

Table 1 Data collection and phase refinement for *R. molischianum* cytochrome c'

Crystal	Native	K_2PtCl_6*	K_2HgI_4†
No. of intensities measured (observations/unique reflections)	81,380/18,513	71,072/10,881	67,994/14,082
Scaling R	0.062	0.074	0.068
No. of reflections used in phase refinement	10,667	10,372	10,540
R_C	—	0.55	0.54
R_K	—	0.084	0.095
E/F_H	—	0.37	0.48
E''/E	—	0.23	0.25

The overall figure of merit, m, to 2.5 Å resolution is 0.72. E, E'' = r.m.s. differences between observed and calculated heavy atom and anomalous dispersion contributions, respectively. F_H = mean heavy atom contribution.

*Platinum site at $x/a=0.402$, $y/b=0.236$, $z/c=0.144$, $B=16.6$ Å^2.

†Mercury site 1 at $x/a=0.082$, $y/b=0.073$, $z/c=0.061$, $B=32.0$ Å^2, and mercury site 2 at $x/a=0.253$, $y/b=0.321$, $z/c=0.386$, $B=40.1$ Å^2.

$$R_C=\frac{\Sigma\left|\left|F_{PH}\pm F_P\right|-F_H(\mathrm{calc})\right|}{\Sigma\left|F_{PH}\pm F_P\right|}\text{ for centric reflections.}$$

$$R_K=\frac{\Sigma\left|F_{PH}(\mathrm{obs})-F_{PH}(\mathrm{calc})\right|}{F_{PH}(\mathrm{obs})}$$

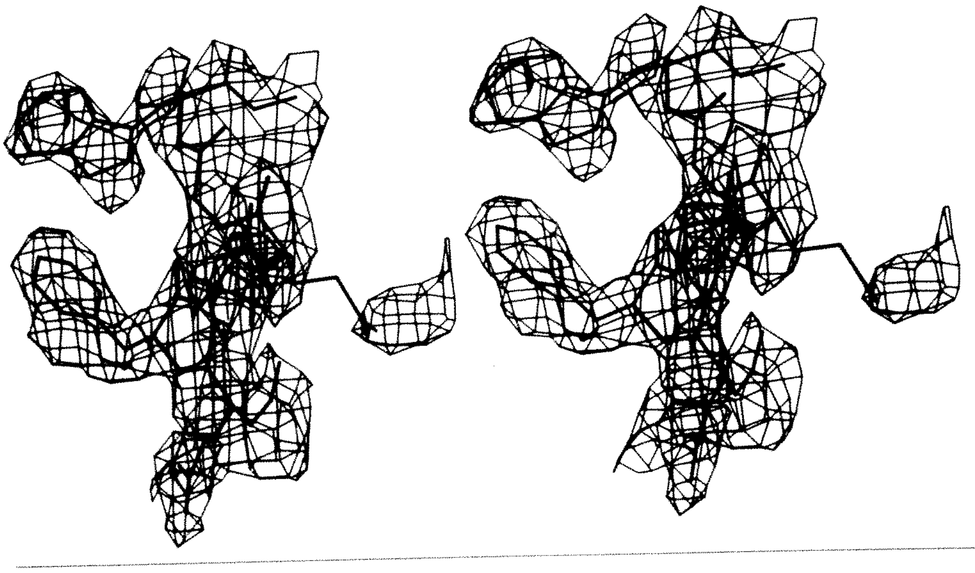

Fig. 1 Stereoscopic view of a segment of the C helix (residues Glu 81, Phe, Leu, Glu, Gly, Trp 86) superimposed on the 2.5 Å resolution MIR phased electron density map, showing a representative fit of the measured model coordinates. Prominent in the density are two aromatic residues situated in the protein interior and an external, solvent-exposed glutamate whose side chain is only partially defined at the present contour level which includes 15% of the unit cell volume.

0028-0836/80/290302-03$01.00

Fig. 2 Schematic representation of the *R. molischianum* cytochrome *c′* dimer viewed down the molecular diad axis. The cytochrome *c′* monomers are principally composed of four, roughly parallel α-helices shown here as sequentially labelled cylinders. The left-twisted 4-α-helical arrangement of the monomers is qualitatively repeated at the subunit interface, due to the pairwise interaction of two helices from each subunit. The haem groups, situated at one end of the helical bundle, are orientated roughly parallel to each other and to the subunit interface, with their propionate side chains pointed towards the molecular surface. Regions of essentially extended polypeptide chain (shaded) connect and terminate the helices in each monomer. Approximately one-half of the residues in the molecule exist in an α-helical conformation.

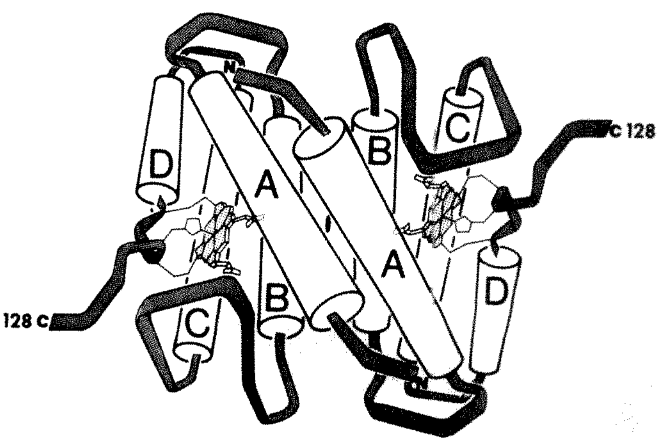

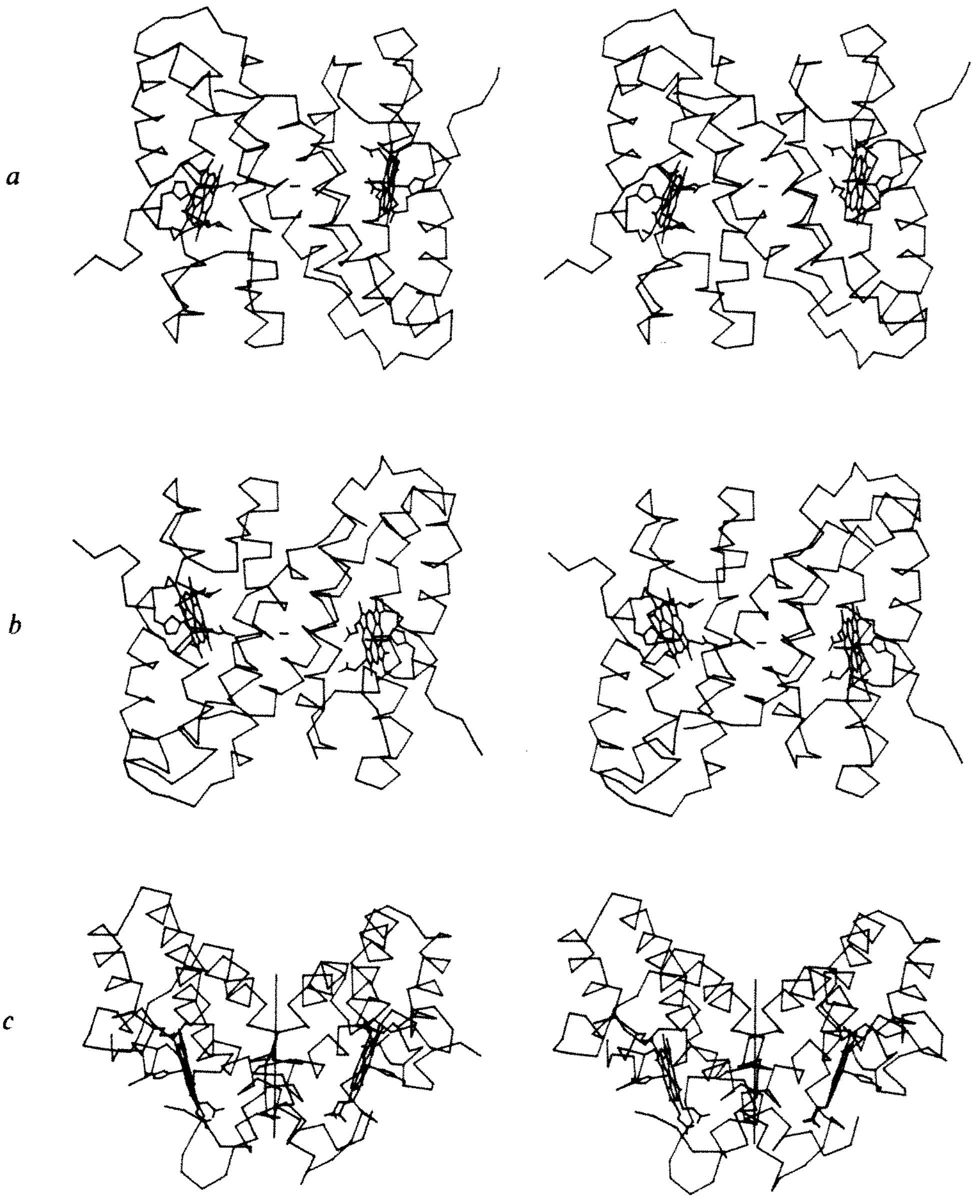

Fig. 3 Stereoscopic α-carbon drawings of *R. molischianum* cytochrome *c′*. *a* Shows the structure from the same aspect as Fig. 2, looking down the molecular diad axis at the molecular surface which has greatest haem exposure. The haem prosthetic groups, covalently bound near the carboxy termini, are separated in space by the two A helices, one from each subunit, which form the closest inter-helical interaction in the entire structure. The regions of extended polypeptide between helices are orientated towards this 'haem side' of the dimer. In contrast, the opposite side shown in *b* is primarily composed of α-helices. The ~110° crossing angle between subunits gives the dimer a V-shaded appearance when viewed normal to the diad axis as in *c*.

Figures 2 and 3 show schematic and α-carbon stereo representations of the cytochrome *c′* dimer. Each subunit is composed of a 128-amino acid polypeptide chain incorporating a covalently bound protohaem IX prosthetic group. Structurally, each monomer is composed of four, roughly parallel α-helices (sequentially labelled A–D) connected by more or less extended loops which join adjacent helix ends. Additional regions of essentially extended polypeptide chain occur at both the amino and carboxy termini of the molecule, the latter providing the covalent attachment points for the haem prosthetic group. The α-helices of the monomer pack with an overall left-handed twist along the direction of the helix axes. However, the helices of the bundle distinctly diverge at one end to accommodate the haem prosthetic group.

The cytochrome *c′* monomers pack about a non-crystallographic diad axis at an angle between bundle axes of approximately 110°, giving the dimer a V-shaped appearance when viewed normal to the diad symmetry axis (Fig. 3*c*). The subunit interaction is mediated by the pairwise interaction of the A and B helices of each monomer, to give a 4-α-helical, left-twisted AA′–BB′ bundle at the dimer interface whose geometry is qualitatively similar to the arrangement of the helices within each monomer. The fact that the subunit interface interactions are similar to those within each monomer, both with respect to the hydrophobic nature of the amino acid residues involved and the overall similarity in extent and geometry of the α-helical interactions, provides an explanation for the observation that some homologous species of cytochrome *c′* can only be dissociated in conditions which lead to protein denaturation[20].

The protohaem IX prosthetic group in cytochrome *c′* forms three covalent attachments with the polypeptide chain, all of which are derived from the pentapeptide sequence Cys-X-X-Cys-His at residues 118–122. Two of these are the haem thioether linkages which serve to orientate the haem so that its propionate-substituted edge lies roughly parallel to each monomer bundle axis, and roughly perpendicular to the dimer diad axis. The third haem–polypeptide interaction is formed by the fifth position axial ligation of the ferric haem iron with $N^{\varepsilon 2}$ of His 122. The sixth ligand ferric iron coordination site is either unoccupied or ligated by a solvent molecule, consistent with the high-spin character of the haem iron[21,22]. Space-filling representations of the molecular structure show the haem environment to be highly asymmetric, with the imidazole side chain of the fifth haem iron ligand and two-thirds of the corresponding haem surface being exposed to the solvent. In contrast, the distal haem surface, which faces towards the dimer interface, is surrounded by aromatic or otherwise hydrophobic amino acid residues. Many of these packing interactions are provided by residues of the A helix, which are orientated so as to restrict access of exogenous ligands to the sixth haem iron coordination site through the most direct route to the molecular surface.

Because of the geometry of the monomer–monomer packing interaction, both haem groups of the molecule are situated on the same face of the dimer in nearly parallel orientation. Although this structural arrangement suggests that the haems of cytochrome *c′* may be situated so as to allow their simultaneous interaction with some physiological oxidoreductase, it is equally possible that this arrangement provides the basis for inter-haem communication in the molecule. Of relevance to the latter possibility is the fact that the 24 Å iron–iron vector is nearly coincident with the A–A′ inter-helix contact normal vector, which at 6.0 Å is the shortest inter-helical interaction in the entire molecule. As described above, it is residues of the A helix which principally provide the packing interactions about the unliganded, distal haem surface. Thus, it seems possible that any local structural alterations accompanying haem ligation or oxidoreduction could be communicated between the haems due to the intimacy of the A–A′ helix packing interaction.

The principal similarity between the cytochromes *c′* and the mitochondrial cytochromes *c* is the common presence of a Cys-X-X-Cys-His sequence which provides the covalent attachment points and fifth axial ligand for the haem prosthetic group. Otherwise, the molecules are distinctly different with respect to overall chain folding, sequential location of the haem-binding peptide, spin state and extent of haem exposure to the solvent. Similarly, almost the only major feature shared by the cytochromes *c′* and the globins is their high-spin haem character, the general nature of the haem environments being otherwise quite different in the two molecules. Nevertheless, the fact that the cytochromes *c′* and globins are both high-spin haem proteins which can bind exogenous ligands and occur in both monomeric and higher aggregate forms[2,6], suggests interesting parallels between these molecules which require further investigation.

This work and facilities were supported by NIH grants GM18528-11 to M.D.K., RCDAK04EY0013 to M.A.C., GM20102, RR00757, to N.H.X., and GM21534, GM25664 to F.R.S. and NSF grants GB36019X to M.D.K., PCM7804349 to M.A.C. and PCM7722495 to N.H.X. Structure determination was done in partial fulfilment of the requirements for a PhD at the University of Arizona by P.C.W. who was a Carl S. Marvel Fellow. F.R.S. received a Dreyfus Teacher-Scholar Award and the University of Arizona Computer Center also provided support.

Received 6 February; accepted 25 April 1980.

1. Vernon, L. P. & Kamen, M. D. *J. biol. Chem.* **211,** 643–675 (1954).
2. Bartsch, R. G. in *The Photosynthetic Bacteria* (eds Clayton, R. K. & Sistrom, W. R.) 249–279 (Plenum, New York, 1978).
3. Barrett, J. & Kamen, M. D. *Biochim. biophys. Acta* **50,** 573–575 (1961).
4. Salemme, F. R. *A. Rev. Biochem.* **46,** 299–329 (1977).
5. Taniguchi, S. & Kamen, M. D. *Biochim. biophys. Acta* **74,** 438–455 (1963).
6. Perutz, M. F. *A. Rev. Biochem.* **48,** 327–386 (1979).
7. Bloomer, A. C., Champness, J. N., Bricogne, G., Staden, R. & Klug, A. *Nature* **276,** 362–368 (1978).
8. Stubbs, G., Warren, S. & Holmes, K. *Nature* **267,** 216–221 (1977).
9. Stenkamp, R. E., Sieker, L. C., Jensen, L. H. & McQueen, J. E. Jr *Biochemistry* **17,** 2499–2504 (1978).
10. Ward, K. B., Hendrickson, W. A. & Klippenstein, G. L. *Nature* **257,** 818–821 (1975).
11. Hendrickson, W. A., Klippenstein, G. L. & Ward, K. B. *Proc. natn. Acad. Sci. U.S.A.* **72,** 2160–2164 (1975).
12. Banyard, S. H., Stammers, D. K. & Harrison, P. M. *Nature* **271,** 282–284 (1978).
13. Mathews, F. S., Bethge, P. H. & Czerwinski, E. W. *J. biol. Chem.* **254,** 1699–1706 (1979).
14. Weber, P. & Salemme, F. R. *J. molec. Biol.* **117,** 815–820 (1977).
15. Cork, C., Hamlin, R. C., Vernon, W., Xuong, Ng. H. & Perez-Mendez, V. *Acta crystallogr.* **A31,** 702–703 (1975).
16. Xuong, Ng. H., Freer, S. T., Hamlin, R., Neilson, C. & Vernon, W. *Acta crystallogr.* **A34,** 289–296 (1978).
17. Matthews, B. W. *Acta crystallogr.* **20,** 82–86 (1966).
18. Ambler, R. P. in *Abstr. 3rd int. Symp. Photosynthetic Prokaryotes* (ed. J. M. Nichols) E17 (Oxford, 1979).
19. Salemme, F. R. & Fehr, D. G. *J. molec. Biol.* **70,** 697–700 (1972).
20. Cusanovich, M. A. *Biochim. biophys. Acta* **236,** 238–241 (1971).
21. Ehrenberg, A. & Kamen, M. D. *Biochim. biophys. Acta* **102,** 333–340 (1965).
22. Maltempo, M. M., Moss, T. H. & Cusanovich, M. A. *Biochim. biophys. Acta* **342,** 290–305 (1974).

Molecular dynamics of ferrocytochrome *c*

Scott H. Northrup, Michael R. Pear & J. Andrew McCammon*

Department of Chemistry, University of Houston, Houston, Texas 77004

Martin Karplus

Department of Chemistry, Harvard University, Cambridge, Massachusetts 02138

The cytochromes *c* function as single-electron carriers in the mitochondrial electron transport chain[1,2]. The native structures of the proteins from different species are quite similar[1,2], as are the structures of the reduced and oxidized forms[3,4]. The 103-residue polypeptide chain of tuna cytochrome *c* contains 5 α-helical segments (residues 2–13, 50–54, 61–69, 71–74, 89–100); the haem group is almost completely buried in a hydrophobic pocket and is covalently bonded to the polypeptide chain by thioether linkages involving Cys 14 and Cys 17 and by linkages to the iron involving His 18 and Met 80 (refs 1–3). NMR[5,6] and hydrogen exchange[7,8] studies indicate significant internal mobility in cytochrome *c*. In spite of the apparent similarity of the time-average structures of the reduced and oxidized proteins, the structural fluctuations are significantly larger in the latter form[2,7,8]. It has been suggested that the internal motions have a role in the electron transfer mechanism[2,9]. A 16-ps computer simulation[10–14] of the atomic motions in reduced tuna cytochrome *c* has now been completed; this reveals various correlations between the magnitudes of the atomic position fluctuations and the structural features of the protein.

The dynamical simulation method used here is similar to that used in earlier studies of the pancreatic trypsin inhibitor[10]. The protein potential energy function consists of a sum of terms associated with bonds, bond angles, dihedral angles, hydrogen bonds and nonbonded (van der Waals and electrostatic) interactions. The partial charges of the atoms have been reduced according to the distances of the atoms from the protein centre to approximate dielectric screening effects due to surrounding water[15]. To begin the simulation, the protein was dynamically equilibrated as follows. The X-ray structure[16,17] was first subjected to 100 cycles of steepest descent energy minimization[18] to relax any sizeable local stresses. The atoms were then assigned random maxwellian velocities corresponding to a temperature of 50 K and the classical equations of motion were solved for a 2-ps period using the fifth order Gear algorithm[10]. Repeated velocity assignments corresponding to increasing temperatures followed by 2-ps periods of dynamical relaxation were used to bring the protein to a final average temperature of 297 K; the total period of temperature adjustment was 12 ps. To equilibrate the protein further, the dynamics was continued for 20 ps; the average temperature remained at 297 K. The actual simulation was obtained by continuing the run for an additional 16 ps.

---

*To whom reprint requests should be addressed.

The time-average structure from the simulation is quite similar to the 2.0-Å resolution X-ray structure[16], except that several exposed, flexible sidechains have folded down on to the protein surface. The average r.m.s. deviation of C^α positions is 1.58 Å, while that for all heavy atoms is 1.90 Å. There is some correlation between the residues with the largest deviations and those which have somewhat different positions in different crystal structures[3]. The largest deviations occur at the protein surface, particularly in the exposed sidechains of Lys 25, 27, 39, 72, 73 and 87 and Arg 38, where some atoms moved nearly 9 Å. Concomitant with these sidechain shifts, the accessible contact surface area of the protein as determined by Richards' method[19] with a probe of 1.4-Å radius decreased from 1,751 Å^2 for the X-ray structure to 1,440 Å^2 for the dynamical average structure.

The fluctuations of the atoms about their average positions are sizeable and show interesting correlations with the time-average structure. The average r.m.s. fluctuation of the C^α positions is 0.70 Å and that of all heavy atoms is 0.85 Å. To compare interior and exterior fluctuations, averages were calculated for atoms in spherical shells of 3-Å thickness centred at the protein centre of mass. Shells with outer radii greater than 12 Å contain exterior atoms, because the average atomic density decreases rapidly with increasing radius for such shells. In the interior, the fluctuations are relatively small and increase slowly with shell size; the average r.m.s. fluctuations are 0.66, 0.70 and 0.73 Å for shells with outer radii of 6, 9 and 12 Å, respectively. In the exterior, the corresponding results are 0.98, 1.05 and 1.64 Å for shells with outer radii of 15, 18 and 21 Å, respectively. The average r.m.s. fluctuations for individual residues are correlated with their relative surface exposures in the time-average structure, with more exposed residues exhibiting larger fluctuations (Fig. 1*a*,*c*).

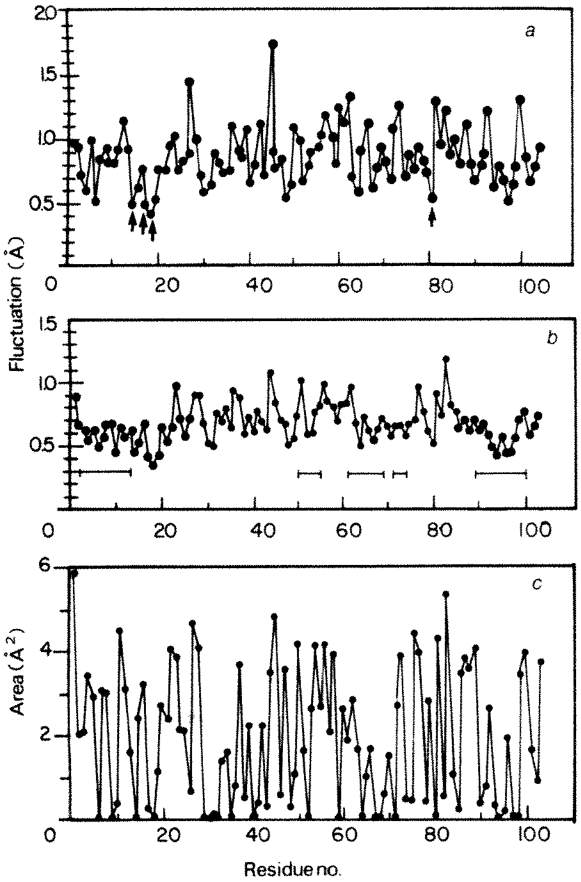

Fig. 1 *a*, Average r.m.s. atomic position fluctuation for each residue. Arrows indicate the residues (14, 17, 18 and 80) that are covalently bonded to the haem group. *b*, r.m.s. position fluctuations of the C^α atoms. Bars are drawn to indicate the α-helical segments. *c*, Exposed surface area of each residue in the dynamical average structure, divided by the number of heavy atoms in the residue. The exposed surface area is the accessible contact surface area as calculated by Richards's method[19] using a probe of 1.4-Å radius.

The haem group is expected to be relatively rigid due to the extensive pi electron delocalization in its ring system. The average r.m.s. fluctuation of the haem atom positions is 0.51 Å, which is significantly smaller than that of the other atoms in the protein interior. To assess the effect of the haem group on the mobility of nearby polypeptide atoms, a haem neighbourhood was defined by two cylindrical disks of 6-Å radius and 6-Å thickness lying on either side of the haem and coaxial with the iron. The average r.m.s. fluctuation of the 56 heavy atoms in this neighbourhood is 0.64 Å, compared with 0.72 Å for the other 411 heavy atoms of the protein interior. The average r.m.s. fluctuations are larger in the disk on the Met 80 side (0.71 Å) than in the disk on the His 18 side (0.56 Å).

The position fluctuations of the backbone atoms show a correlation with secondary structure (Fig. 1*b*). The average r.m.s. fluctuation of C^α positions in the α helices is 0.65 Å, while that of the other C^α atoms is 0.72 Å. Within the α helices, residues which have the smallest surface exposures tend to have the smallest fluctuations (for example, residues 6, 9, 10, 52, 64, 67, 71 and 74 in Fig. 1*a*,*c*).

The correlations of atomic mobility with structural features in cytochrome c are in general accord with the results of theoretical[10–14] and experimental[20,21] studies of other proteins. Relatively small fluctuations of interior atoms and of backbone atoms in regions of secondary structure were found in simulation studies of the pancreatic trypsin inhibitor[11–14] and in analyses of the X-ray temperature factors for myoglobin[20] and lysozyme[21]. The myoglobin study[20] also revealed an asymmetrical reduction in the fluctuations of protein atoms on the two sides of the haem group.

The dynamical simulation described here is being repeated with more rigorous equilibration. The magnitudes of the fluctuations will apparently be somewhat smaller, but the structural correlations will be unchanged. Detailed accounts of this simulation and of a planned simulation of the oxidized form will be presented in the future.

This work was supported in part by the NSF and by the Petroleum Research Fund, administered by the American Chemical Society. S.H.N. is a Robert A. Welch Foundation Postdoctoral Fellow.

Received 4 February; accepted 16 April 1980.

1. Dickerson, R. E. & Timkovich, R. in *The Enzymes*, **11**, 3rd edn, Ch. 7 (Academic, New York, 1975).
2. Salemme, F. R. *A. Rev. Biochem.* **46**, 299–329 (1977).
3. Mandel, N. *et al. J. biol. Chem.* **252**, 4619–4636 (1977).
4. Labhardt, A. & Yuen, C. *Nature* **277**, 150–151 (1979).
5. Campbell, I. D. *et al. FEBS Lett.* **70**, 96–100 (1976).
6. Cookson, D. J. *et al. Eur. J. Biochem.* **83**, 261–275 (1978).
7. Ulmer, D. D. & Kägi, J. H. R. *Biochemistry* **7**, 2710–2717 (1968).
8. Patel, D. J. & Canuel, L. L. *Proc. natn. Acad. Sci. U.S.A.* **73**, 1398–1402 (1976).
9. Hopfield, J.J. *Proc. natn. Acad. Sci. U.S.A.* **71**, 3640–3644 (1974).
10. McCammon, J. A., Wolynes, P. G. & Karplus, M. *Biochemistry* **18**, 927–942 (1979).
11. Karplus, M. & McCammon, J. A. *CRC Cr. Rev. Biochem.* (in the press).
12. McCammon, J. A. & Karplus, M. *A. Rev. phys. Chem.* (in the press).
13. McCammon, J. A., Gelin, B. R. & Karplus, M. *Nature* **267**, 585–590 (1977).
14. Karplus, M. & McCammon, J. A. *Nature* **277**, 578 (1979).
15. Linder, B. *Adv. chem. Phys.* **12**, 225–282 (1967).
16. Takano, T. *et al. J. biol. Chem.* **252**, 776–785 (1977).
17. Bernstein, F. C. *et al. J. molec. Biol.* **112**, 535–542 (1977).
18. Levitt, M. *J. molec. Biol.* **82**, 393–420 (1974).
19. Richards, F. M. *A. Rev. Biophys. Bioengng* **6**, 151–176 (1977).
20. Frauenfelder, H., Petsko, G. A. & Tsernoglou, D. *Nature* **280**, 558–563 (1979).
21. Artymiuk, P. J. *et al. Nature* **280**, 563–568 (1979).

MATTERS ARISING

Cometary evidence against the solar companion

WILKINS[1] has concluded, from his computation of the perturbation of cometary orbits, that the Sun cannot have a fast moving neutron star as a companion. His results exclude all objects other than a massive black hole ($350 M_\odot$) with velocity $\gtrsim 10^2\,\mathrm{km\,s^{-1}}$ as candidates for the solar companion whose existence was proposed by Harrison[2]. In a previous paper[3] I performed a closely similar calculation and concluded that an object of solar mass cannot be ruled out as a solar companion on the basis of cometary evidence, provided that its speed exceeds $20\,\mathrm{km\,s^{-1}}$. Our results are thus in conflict by several orders of magnitude.

In equation (8) of Wilkins' paper, the perturbation of a comet's energy is given, to an order of magnitude, by the difference in the potential exerted by the companion at the end points of the comet's orbit, that is

$$\Delta E \sim \frac{Gm_c}{D} \cdot \frac{r_{\odot i} \cos\theta}{D}.$$

If m_c and D are now increased, such that the ratio m_c/D^2 remains constant, the resulting perturbation is unchanged. This means that the perturbation as calculated by Wilkins would still exist if the Sun and comet were freely falling in a uniform gravitational field; the calculation must therefore be in error.

A correct evluation of the perturbation of the cometary orbit uses the gradient of the disturbing function due to the companion[4], as in equation (9) of ref. 3. In this case the perturbation

$$\Delta\left(\frac{1}{a}\right) \propto Gm_c/D^2 v$$

goes to zero as D becomes large, since the velocity v scales with D.

J. G. KIRK

Max-Planck-Institut für Physik & Astrophysik,
Institut für Astrophysik,
Karl-Schwarzschild-Strasse 1, 8046
Garching bei München, FRG

1. Wilkins, D. *Nature* **282**, 696–697 (1979).
2. Harrison, E. R. *Nature* **270**, 324–326 (1977).
3. Kirk, J. G. *Nature* **274**, 667–669 (1978).
4. Smart, W. M. *Celestial Mechanics*, 9 (Longmans, London, 1953).

WILKINS REPLIES—The black hole was mentioned as only one example satisfying the luminosity criteria of Pineault[1]. But its supposed distance (15,000 AU) and mass may need to be increased severalfold.

Note that Kirk uses a different reference frame to calculate ε, the specific energy (per unit mass) of the comet (K). Kirk finds ε_I relative to the instantaneous rest frame of the Sun (S), which is accelerated by the companion (C). I, however, determine ε_F relative to a fixed inertial frame, that of the Sun at apparition. These energies increase (Δ) as follows:

$$\Delta\varepsilon_I = \int (\mathbf{f}_{CK} - \mathbf{f}_{CS}) \cdot (\mathbf{v}_K - \mathbf{v}_S)\,dt \qquad (1)$$

$$\Delta\varepsilon_F = \int \mathbf{f}_{CK} \cdot \mathbf{v}_K\,dt - \int \mathbf{f}_{KS} \cdot \mathbf{v}_S\,dt \qquad (2)$$

(In general ε_I is the total energy of the binary system K–S referred to its centre of mass, divided by its reduced mass.) Here $\mathbf{f}_{ij}$ is the force (per unit comet mass) of body i on j. Equation (1) is the integral form of Kirk's equation (9), divested of esoteric notation. Integration by parts of equation (2) yields $\Delta\varepsilon_F = \Delta[\varepsilon_I + \mathbf{v}_S \cdot (\mathbf{v}_K - \mathbf{v}_S) + \mathbf{v}_S^2/\mathbf{2}]$, which also follows from the definitions of $\varepsilon_{F,I}$. Because the cross-term vanishes for a parabolic comet and because the last term $\simeq (Gm_c/Rv_C)^2$, where $R = r_{CS}$ at apparition, is small, $\Delta\varepsilon_F \simeq \Delta\varepsilon_I$.

The discrepancy between my results and those of Kirk arose from my too-crude approximation for the first integral of equation (2), and the second integral should have been three times larger than in my equation (6). Thus I did not realize that the two integrals would cancel almost completely, leaving a difference smaller than either by about r_i/R (defined after equation (3)).

A head-on approach of C towards S, at high speed v_C = constant, can be calculated analytically. Introducing the semi-major axis a through $1/a = -2\varepsilon_I/Gm_S$, one finds

$$(1/a) = -0.22(3\cos^2\psi - 1) \times (m_C/m_S)[(r_i/R)^2 + 0(r_i^3/R^3)]R^{-1} \qquad (3)$$

ψ is the polar angle from axis CS about S, of the comet's zero-energy radial infall to the Sun; the comet's distance from the Sun at a time $2R/v_C$ before apparition is denoted by $r_i = (9Gm_S/2)^{\frac{1}{3}}(2R/v_C)^{\frac{2}{3}}$. Averaging over the isotropic flux of comets, one finds that the mean value of $1/a$ is unchanged, but its r.m.s. spread due to C, equals $\sigma_C = 0.2 \times (m_C/m_S)(r_i/R)^2 R^{-1}$. Demanding that $\sigma_C < 2 \times 10^{-5}\,\mathrm{AU}^{-1}$ (as for comets without non-gravitational forces[2]) and setting $g_C = Gm_C/R^2$ yields the constraint

$$(g_C/10^{-6}\,\mathrm{cm}^{-2})^{\frac{3}{2}}(R/10^3\,\mathrm{AU})^{\frac{1}{2}} \times (30\,\mathrm{km\,s^{-1}}/v_C)^2 < 0.86 \qquad (4)$$

If, for example, the first two factors are each unity, this gives $v_C > 32\,\mathrm{km\,s^{-1}}$, exceeding Kirk's estimate. Actually, the lower limit should be still larger because an off-side collision prolongs the epoch of closest approach and unless v_C were augmented, σ_C would increase.

The smallness of Neptune's perturbations, however, forbids a close encounter unless the companion has speeds well above $10^2\,\mathrm{km\,s^{-1}}$. Let $T = 2R/v_C$ be the effective transit time (10^2 yr for $R = 10^3$ AU, $v_C = 10^2\,\mathrm{km\,s^{-1}}$). Neptune's known perturbations roughly limit

$$(Gm_C/R^3) \times \begin{cases} & ,\ T > 170\,\mathrm{yr} \quad (a) \\ (T/170\,\mathrm{yr})^2, & T < 170\,\mathrm{yr} \quad (b) \end{cases} \qquad (5)$$

to less[3] than $1.2 \times 10^{-24}\,\mathrm{s}^{-2}$. Case (a) yields

$$R > 5.3 \times 10^4\,\mathrm{AU}\,(g_C/10^{-6}\,\mathrm{cm\,s^{-2}}) \qquad (6)$$

This excludes a close approach lasting more than 170 yr. Only a briefer encounter, case (b), permits $R \sim 10^3$ AU, if the speed is high enough:

$$v_C > 440\,\mathrm{km\,s^{-1}}(R/10^3\,\mathrm{AU}) \times (g_C/10^{-6}\,\mathrm{cm\,s^{-2}})^{\frac{1}{2}} \qquad (7)$$

This easily predominates over the cometary limit above.

My article gave a limit on R three times smaller than in equation (6) because I had adopted the allowed tidal gradient[4] for a companion in circular orbit at $r_{CS} \leqq 75$ AU, which turns out unexpectedly to be three times larger than the value[3] for $r_{CS} = 150-600$ AU. Equations (5), (6) use the latter value, assuming that it has already stabilized at its large-distance limit.

Note added in proof: In work to be published I confirm that the right side of equation (4) never exceeds 0.86 for any fast encounter.

DANIEL WILKINS

Instituto di Astrofisica Spaziale del CNR,
CP 67, I-00044, Frascati, Italy

1. Pineault, S. *Nature* **275**, 727–730 (1978).
2. Marsden, B. G., Sekanina, Z. & Everhart, E. *Astr. J.* **83**, 64–71 (1978).
3. Rawlins, D. & Hammerton, M. *Mon. Not. R. astr. Soc.* **162**, 261–270 (1973).
4. Rawlins, D. & Hammerton, M. *Nature* **240**, 457 (1972).

0028–0836/80/290306–01$01.00

Redshifts and distances

In the recent review by Burbidge[1] I had expected to find a wide ranging discussion of all the important evidence both for and against cosmological origin of quasar redshifts. However, no mention is made of how the continuity of properties between galaxies and QSOs and amongst QSOs themselves supports the cosmological interpretation of all QSO redshifts, or how the number/redshift distribution of bright QSOs is found to be incompatible with non-cosmological redshifts[2]. Even within his rather restricted brief (dealing only with QSO/galaxy associations) Burbidge has failed to include results which do not favour his conclusions. He cites the existence of five 3C QSOs near bright galaxies as evidence for non-cosmological redshifts[3]. However, he does not mention several subsequent investigations[4–6] of much larger samples of QSOs which failed to detect a statistically significant excess of close pairs compared with that expected by chance for a random distribution of quasars and galaxies.

Burbidge ignores published criticism of at least one of the arguments he uses. His Fig. 1 shows a correlation between galaxy redshift and separation of the galaxy from the associated QSO, and this is taken as good evidence for the galaxies and the QSOs being physically associated. Nevertheless, it has been pointed out by Noerdlinger[7] and Browne and Cohen[5] that when pairs selected from heterogeneous samples are used, strong selection effects inevitably give rise to a redshift–separation correlation roughly of the form presented by Burbidge. Note that not only is the legend to Fig. 1 confusing because it refers to a symbol not present in the diagram, but also the line shown is certainly not the best fit to all the points.

Finally, to establish the reality of non-cosmological redshifts systematic investigations of well defined samples must be undertaken. Then, at least, it will be unnecessary to resort to estimating Arp's allocation of telescope time as a way of assessing the statistical significance of the results.

IAN W. A. BROWNE

Moss Cottage, Strawberry Lane,
Wilmslow, Cheshire SK9 6AH, UK

1. Burbidge, G. R. *Nature* **282**, 451 (1979).
2. Green, R. F. & Schmidt, M. *Astrophys. J. Lett.* **220**, L1 (1978).
3. *Burbidge, E. M., Burbidge, G. R., Solomon, P. M. &* Strittmatter, P. A. *Astrophys. J.* **170**, 233 (1971).
4. Hazard, C. & Sanitt, N. *Astrophys. Lett.* **11**, 77 (1972).
5. Browne, I. W. A. & Cohen, A. M. *Mon. Not. R. astr. Soc.* **182**, 181 (1978).
6. Nieto, J.-L. *Astr. Astrophys.* **70**, 219 (1978).
7. Noerdlinger, P. D. *Astrophys. Space Sci.* **38**, 457 (1975).

BURBIDGE REPLIES—Browne is clearly strongly biased in favour of the cosmological redshift hypothesis, because none of his criticisms considers that I omitted discussion of the many problems associated with that hypothesis. His remarks imply that I have omitted only work critical of the evidence for non-cosmological redshifts. In fact I attempted to demonstrate that there is good evidence for the existence of both cosmological and non-cosmological redshifts. I spent more time discussing the Arp evidence to attempt to redress the balance as the normal practice is to quote Stockton and ignore Arp.

In a previous review article[1], which was far more wide-ranging, I did discuss all of the earlier evidence for association between galaxies and QSOs. In my later article I only quoted the 3C survey evidence for historical reasons, as I was concerned with an account of the more recent work. I had overlooked the paper of Browne and Cohen[2] which should certainly be taken into account in evaluating my Fig. 1.

The results of Green and Schmidt[3] lay outside my restricted brief. Had I discussed their results I would also have had to discuss other evidence, such as the existence of peaks and periodicities in the redshift distribution, the Compton problem, the Hubble diagram for QSOs, and the existence of so-called superlight velocities, all of which have to be discussed and evaluated before a balanced picture can be obtained.

GEOFFREY BURBIDGE

Kitt Peak National Observatory,
950 North Cherry Avenue,
PO Box 26732,
Tucson, Arizona 85726

1. Burbidge, G. *Nature phys. Sci.* **246**, 17 (1973).
2. Browne, I. W. A. & Cohen, A. M. *Mon. Not. R. astr. Soc.* **182**, 181 (1978).
3. Green, R. F. & Schmidt, M. *Astrophys. J. Lett.* **220**, L1 (1978).

The Lizard complex as an ophiolite

KIRBY[1] has stated "Of prime importance to the proposed ophiolitic nature of the complex is the relationship between peridotite and gabbro... Green's lithological map and the author's field observations show that the gabbro is further restricted to the primary-type peridotite and does not occur in the recrystallized varieties except as isolated and deformed scraps".

This is an oversimplification: Green[2] refers to the mineralogical assemblage within the primary peridotite and not to a completely unrecrystallized condition. He wrote that the "coarse anhedral texture with curving grain boundaries" was igneous but concluded that "the primary peridotite assemblage has a...texture compatible with deep seated igneous crystallization or at least of crystallization in a hydrostatic or near hydrostatic stress environment. Although the banding and incipient augen foliation are ascribed to crystalline flow of the body at a very early stage, this flow has occurred at a rate accommodated in the rock without cataclasis or creation of granulitic or schistose fabrics".

All the evidence of Flett[3], Green[4] and Rothstein[5,6] taken together suggests that the rocks within the mass of primary peridotite south of Coverack have undergone a near solid-state deformation, although within this primary assemblage peridotite, in the lherzolites and harzburgites containing little or no troctolite, there are relics of primary textures and structures resembling crescumulates rather than settled gravity stratified cumulates. The deformation of the primary assemblage structures in this area is part of the continuity which exists between the two major areas of peridotite with respect to the trends of the near vertical foliation and banding, the primary mineralogy (to be reported elsewhere), and the rare earth content[7]. It would seem reasonable, therefore, to regard the peridotite as originally one body (albeit the eastern part not quite so heavily deformed as the western part). This being so the continuity extends between the two parts of the peridotite and the hornblende schists, and is broken, one way or the other, by the cross-cutting field relationships of the gabbro. This implies a contrary view to that expressed by Kirby[1] "that the association of peridotite and gabbro existed before their juxtapositioning with the surrounding hornblende schists (the event in which some of the peridotite was recrystallized)". This does not preclude the possibility of a deformed and recrystallized eastern part of the peridotite undergoing some partial melting.

A. T. V. ROTHSTEIN

Department of Geology,
Porstmouth Polytechnic,
Portsmouth, Hampshire PO1 3QL, UK

1. Kirby, G. A. *Nature* **282**, 58–61 (1979).
2. Green, D. H. *J. Petrol.* **5**, 134–188 (1964).
3. Flett, J. S. & Hill, J. B. *Mem. geol. Surv. U.K.* (1912, 1946).
4. Green, D. H. *J. Geol.* **72**, 543–563 (1964).
5. Rothstein, A. T. V. *Geol. Mag.* **108**, 393–398 (1971).
6. Rothstein, A. T. V. *Proc. geol. Ass.* **88**, 93–105 (1977).
7. Frey, F. A. *Geochim. cosmochim. Acta* **33**, 1429–1447 (1969).

KIRBY REPLIES—The interrelationships between the foliations in the primary peridotite and those in the secondary peridotites and schists are not well

0028–0836/80/290307–02$01.00

exposed anywhere. However, on the south-east coast of the Lizard peninsular the foliation and banding in the primary peridotite, although mostly poorly defined, dips at moderate angles. The foliation in the underlying hornblende schists is subhorizontal. Green[1] described an increase in the metamorphic grade of the schists in approaching the overlying peridotite, demonstrating that the peridotite was the local heat source. The non-parallelism of the foliations implies that there is not a continuum in deformations as proposed by Rothstein. It shows that the development of foliations in the schists is a later event. In the absence of a continuum of deformation, the cross-cutting relationships of gabbro in primary peridotite do not imply that the gabbro was intruded after the development of the hornblende schists and secondary peridotites. Gabbro is very rare in the secondary peridotites and where it does occur it is invariably highly deformed. I have seen no gabbro intrusive into hornblende schists. These admittedly simplified observations suggest that the gabbro was intruded into the primary peridotite before the deformational event which led to the formation of the hornblende schists and secondary peridotites, and further that it was preferentially intruded into parts of the primary peridotite that generally escaped later deformation. These relationships are typical of ophiolite complexes in which gabbro intrudes peridotite with mantle-tectonite fabrics towards the top of the complex whereas at the base, this peridotite contains little or no gabbro and is overprinted by a later deformation associated with the formation of hornblende schists, as summarized recently by Nicholas *et al.*[3].

G. A. KIRBY

Deep Geology Unit,
Institute of Geological Sciences,
Keyworth, Nottingham NG12 5GG, UK

1. Green, D. H. *J. Geol.* **72,** 543–563 (1964).
2. Nicholas, A., Boudier, F. & Boudier, J. L. *Am. J. Sci.* (in the press).

Evolution of bacterial cytochromes c_2

IN an attempt to uncover the phylogeny of cytochromes c_2, Ambler *et al.*[1] recently compared 13 cytochrome c_2 primary structures. The molecules they compared were from purple photosynthetic bacteria and could be classified on the basis of the length of their interhelical loops as belonging to three different cytochrome c_2 subclasses[2] (so-called short, medium and long cytochromes c_2). The molecular phylogeny reported by Ambler *et al.* is at apparent variance with a morphological one[3] and we should like to comment on this challenging fact.

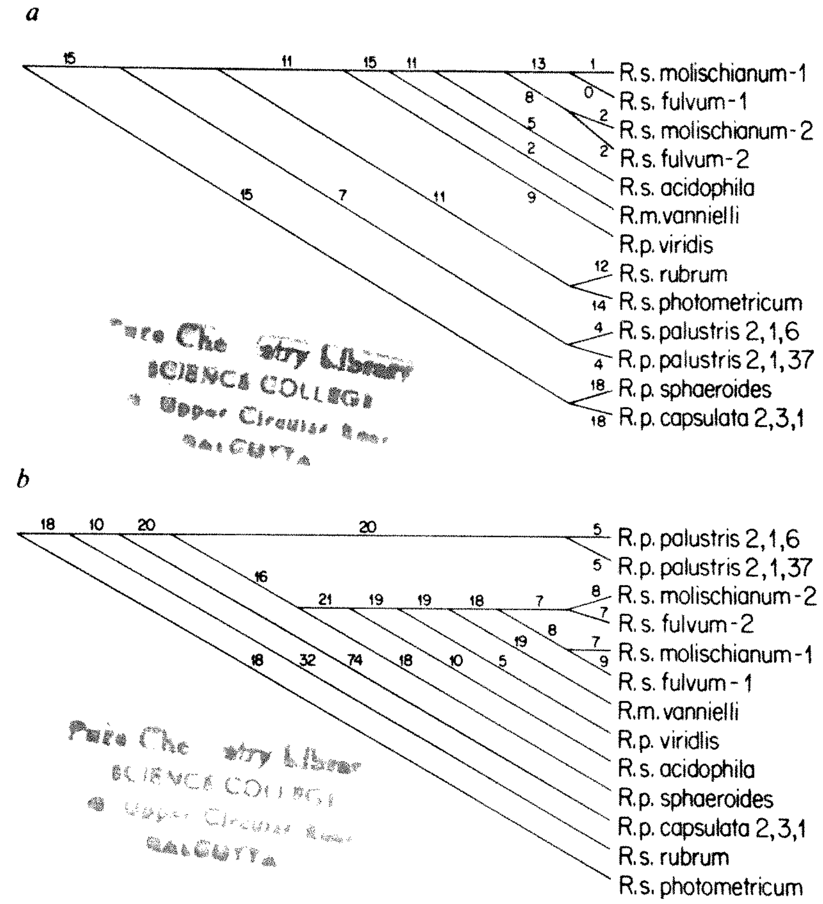

Pure Chemistry Library
SCIENCE COLLEGE
Upper Circular Road,
CALCUTTA

Pure Chemistry Library
SCIENCE COLLEGE
Upper Circular Road,
CALCUTTA

Fig. 1 Phylogenetic trees[7] of bacterial cytochromes c_2. For abbreviations see Table 1. *a*, Tree constructed using the similarity matrix of the unstructured segments. *b*, Tree constructed using the similarity matrix of the secondary structure segments. Numbers give branch lengths in arbitrary units.

The phylogeny of Ambler *et al.* is based on a per cent similarity matrix of the whole primary structures (a matrix element represents % of identical amino acid residues found in a pair of primary structures aligned to maximize homology). It has been shown previously[4,5] that different segments of the primary structure which correspond to individual secondary structure elements (helices, pleated sheets, turns) evolve at a different rate (that is, they display different percentages of similarity) according to the different functional constraints imposed on them. We have therefore constructed two similarity matrices of the 13 cytochrome c_2 structures: the first contains per cent similarities of those primary structure segments which are involved in the secondary structures, the second consists of per cent similarities displayed by unstructured segments. (Assignment of the segments to the secondary structure

Table 1 Similarity matrix of bacterial cytochromes c_2

	1	2	3	4	5	6	7	8	9	10	11	12	13
1. *Rm. vannielli*	100	59	57	51	46	52	55	38	38	42	41	35	28
2. *Rp. viridis*	65	100	52	43	43	43	45	33	32	42	41	32	28
3. *Rs. acidophila*	74	79	100	38	33	38	41	35	35	32	35	45	28
4. *Rs. molischianum-1*	68	60	69	100	84	70	75	30	36	35	35	29	26
5. *Rs. fulvum-1*	69	62	71	99	100	72	70	30	33	32	33	28	28
6. *Rs. molischianum-2*	76	69	75	78	79	100	86	30	36	35	35	25	26
7. *Rs. fulvum-2*	76	68	74	76	78	96	100	29	38	32	32	29	26
8. *Rs. rubrum*	54	51	54	56	57	62	60	100	54	41	39	41	38
9. *Rs. photometricum*	51	53	51	57	56	60	60	74	100	39	33	33	32
10. *Rp. palustris 2.1.6*	51	47	51	49	49	59	59	53	51	100	90	39	45
11. *Rp. palustris 2.1.37*	51	47	51	49	49	59	59	53	51	91	100	42	41
12. *Rp. sphaeroides*	35	35	37	34	35	41	43	49	47	32	32	100	43
13. *Rp. capsulata 2.3.1*	40	43	40	46	47	50	49	59	53	41	41	63	100

Numbers represent per cent identical amino acid residues in a pair of the primary structure segments compared. Above the diagonal (upper right): numbers obtained for segments with secondary structure; below the diagonal (lower left): numbers obtained for unstructured segments. Abbreviations *Rs.*, *Rhodospirillum*; *Rp.*, *Rhodopseudomonas*; *Rm.*, *Rhodomicrobium*.

0028-0836/80/290308-02$01.00

elements—four α-helices, two 3_{10} helices and three turns—is based on the three-dimensional structure of *Rhodospirillum rubrum* cytochrome c_2 (ref. 6) deposited with the Brookhaven Protein Data Bank.) The two matrices computed in this way clearly differ from one another (see Table 1). When phylogenetic trees[7] are constructed of them (Fig. 1), these also differ.

There are 135 amino acid positions in the cytochromes c_2, half of which (69) form helices and turns, the other half (66) being involved in unstructured loops. There is therefore no bias in favour of any of the two groups considered. They do differ evolutionarily, however, in that the secondary structure segments predominantly evolved by amino acid replacements whereas the unstructured loops harbour two-thirds of the deletions responsible for a distinction of the short, medium and long cytochromes c_2.

Thus, the following important points emerge as far as evolution of cytochromes c_2 is concerned. (1) Different phylogenies can be proposed for different segments of homologous primary structures, the phylogeny of the whole structure being a weighted average of the partial ones. (2) Because the differences can be correlated with typical features of the secondary structure, they seem to result from structural, rather then genetic causes.

Bacterial phylogeny is a notoriously difficult subject. Dickerson[8] and Woese *et al*[9]. have already tried to reconcile the cytochrome c_2 dilemma; this note, far from attempting to solve all the existing questions, aims at delineating a new approach to them.

We thank Dr Edgar Haber for discussions and for facilities used in the preparation of this manuscript.

JIŘÍ NOVOTNÝ

Molecular and Cellular
Research Laboratory,
Massachusetts General Hospital,
Harvard Medical School
Boston, Massachusetts 02114

ANTONÍN VÍTEK

Institute of Organic Chemistry
and Biochemistry,
Czechoslovak Academy of Sciences,
166 10 Prague 6,
Czechoslovakia

---

1. Ambler, R. P., Meyer, T. E. & Kamen, M. D. *Nature* **278,** 661–662 (1979).
2. Salemme, F. R. *A. Rev. Biochem.* **46,** 299–329 (1977).
3. Buchanan, R. E. & Gibbons, N. E. (eds.). *Bergey's Manual of Determinative Bacteriology* 8th edn (Williams & Wilkins, Baltimore, 1974)
4. Novotný, J. & Franěk, F. *Nature* **258,** 641–643 (1975).
5. Novotný, J., Vitek, A. & Franěk, F. *J. molec. Biol.* **113,** 711–718 (1977).
6. Salemme, F. R., Freer, S. T., Xuong, N. H., Alden, R. A. & Kraut, J. *J. biol. Chem.* **248,** 3910–3921 (1973).
7. Fitch, F. W. & Margoliash, E. *Science* **155,** 279–284 (1967).
8. Dickerson, R. E. *Nature* **283,** 210–212 (1980).
9. Woese, C. R., Gibson, J. & Fox, G. E. *Nature* **283,** 212–214 (1980).

Methotrexate binding to dihydrofolate reductase

RECENTLY, in discussing dihydrofolate reductase, Gready[1] described, with the emphasis on our paper[2], the finding that the inhibitor, methotrexate, binds to the enzyme with its pteridine ring 'upside down' with respect to the substrates dihydrofolate and folate. It is essential to point out that the most important observations leading to this conclusion were made by others.

In their report of the crystal structure of the enzyme–methotrexate–NADPH complex, Matthews *et al.*[3] discussed the implications for the stereochemistry of the reaction and specifically recognized the possibility that the substrates might bind the other way up. Shortly thereafter, Fontecilla-Camps *et al.*[4] determined the absolute configuration of 5,10-methenyl-tetrahydrofolate (which can be related to that of tetrahydrofolate itself; see ref. 2). This revealed the stereochemistry of reduction of dihydrofolate at C6, and by comparison with the results of Matthews *et al.*, showed that dihydrofolate does bind the other way up from methotrexate. This was pointed out by Hitchings[5]. Our NMR experiments extended this to folate, showing that both substrates have the same orientation on the enzyme, which, from the crystallographic work, differs from that adopted by methotrexate.

The interesting finding that substrates and structurally analogous inhibitors bind to dihydrofolate reductase in quite different orientations thus arises from a comparison of a number of separate observations.

G. C. K. ROBERTS
J. FEENEY
B. BIRDSALL

National Institute for Medical Research,
The Ridgeway, Mill Hill,
London NW7 1AA, UK

P. CHARLTON
D. YOUNG

University of Sussex,
Falmer, Brighton,
Sussex BN1 9RH, UK

---

1. Gready, J. E. *Nature* **282,** 674 (1979).
2. Charlton, P. *et al. Chem. Common.* 922 (1979).
3. Matthews, D. *et al. J. biol. Chem.* **253,** 6946 (1978).
4. Fontecilla-Camps, J. *et al.* in *Chemistry and Biology of Pteridines* (eds Kisliuk, R. L. & Brown, G. M.) 235 (Elsevier, Amsterdam, 1979).
5. Hitchings, G. H. *Enzyme Inhibitors as Drugs* (ed. Sandler, M.) (Macmillan, Basingstoke, 1980).

Effects of the Earth's rotation rate on climate

HUNT'S[1] investigation of the meteorological effects of a faster rotating Earth has application to palaeoclimatology, but his findings cannot explain the occurrence or character of the several late Precambrian glaciations.

Hunt's[1] article does not distinguish between middle and late Precambrian. Late Precambrian glaciation occurred $0.95–0.60\times10^9$ yr ago[3–5], whereas glaciation is unknown during the middle Precambrian $\sim1.5\times10^9$ yr ago[3]. Pannella's[2] curve of length of year suggests a 19–20-h day during the late Precambrian. Using Hunt's[1] Fig. 4, an Equator-to-Pole temperature difference of ~41 K and poles ~4 K colder than at present accordingly are indicated for late Precambrian glacial time; these estimations assume an obliquity of the ecliptic near that of today, which geological[3–7] and geophysical[3,5,8] data suggest may be invalid.

In the Precambrian conditions predicted by Hunt's[1] model—an increased Equator-to-Pole temperature gradient, with equatorial regions warmer and polar regions colder than those of today—glaciation would be confined to high palaeolatitudes, while low palaeolatitudes remained ice-free. Available palaeomagnetic data[3,5,8] reveal, however, a dominant picture of low palaeolatitude (~0–40°) glaciation in late Precambrian time; although some of the daata are difficult to interpret[9], circumpolar models of glaciation can be ruled out. Furthermore, Hunt's[1] findings cannot explain the marked episodicity of the seven or more glaciations since the middle Precambrian[3,4].

The major application of Hunt's[1] model lies in testing explanations of low-palaeolatitude glaciation in the late Precambrian. The concept of global glaciation[3,8] as a cause of preferred low-palaeolatitude glaciation is difficult to reconcile with an Earth possessing a warmer Equator and an Equator-to-Pole temperature gradient greater than at present. The alternative hypothesis of an increased obliquity of the ecliptic ($\gtrsim 54°$) in late Precambrian time[3–8] to reduce equatorial insolation and thereby confine glaciation to relatively low palaeolatitudes explains the data better.

G. E. WILLIAMS

BHP Melbourne Research Laboratories,
Clayton, Victoria 3168,
Australia

---

1. Hunt, B. G. *Nature* **281,** 188–191 (1979).
2. Pannella, G. *Astrophys. Space Sci.* **16,** 212–237 (1972).

0028-0836/80/290309-02$01.00

3. Frakes, L. A. *Climates Throughout Geologic Time* (Elsevier, Amsterdam, 1979).
4. Williams, G. E. *Megacycles: Long-Term Episodicity in Earth and Planetary History* (Dowden, Hutchinson & Ross, Stroudsburg, in the press).
5. Williams, G. E. *Geol. Mag.* **112,** 441–465 (1975).
6. Young, G. M. *Am. J. Sci.* **276,** 366–370 (1976); *Precambrian Res.* **3,** 137–158 (1976).
7. Kröner, A. *J. Geol.* **85,** 289–300 (1977).
8. McWilliams, M. O. (thesis, Australian National Univ. (1977); *Trans. Am. geophys. Un.* **59,** 1061 (1978).
9. Morris, W. A. *Geology* **5,** 85–88 (1977).

HUNT REPLIES—Current knowledge regarding climatic conditions during the Precambrian is fragmentary and subject to differing interpretations. However, there is considerably more information available than I was aware of, mainly in the geological literature, and I thank Dr Williams for providing very interesting data. Frakes[1] suggests that glacial conditions prevailed 2,300 Myr ago, followed by a warm period extending to 950 Myr when an interval of episodic ice ages commenced, terminating at about 600 Myr (ref. 2). If, as I suggested[3], 1,500 Myr ago the Earth was rotating 2–2.5 times faster than now with a somewhat smaller obliquity, climatic conditions should have been most conducive to an ice age. Thus the warm period which apparently then existed implies some very marked difference between the model and the actual atmosphere. What this difference was remains a mystery! With regard to the late Precambrian (600–1,000 Myr ago) when the Earth's rotation was closer to its present rate, Williams[2] suggests that glaciation was confined to low and middle latitudes, attributable to the Earth's obliquity then exceeding 54°. Clearly any such obliquity variations would create climatic conditions completely different from those of my model regardless of rotation rate effects.

The concept of climatic changes induced by obliquity variations has considerable attractions, but also unresolved problems. Williams[2] has suggested an obliquity cycle with a period of over 1,000 Myr and a total amplitude exceeding 54°. Wolfe[4], from Tertiary palaeobotanical data, has deduced obliquity variations of up to 25° in ~25 Myr. No mechanism is advanced to account for these obliquity changes. The absence of an identifiable mechanism, however, should not preclude them from consideration; rather it should stimulate a search for the cause. If such obliquity changes did occur this implies that current understanding of the Earth–Moon dynamical interaction over the ages as presented by MacDonald[5], for example, is deficient. The rotational period and obliquity variations with time shown in my Fig. 1 (ref. 3) were taken from MacDonald's[5] calculations, and had the great attraction of being dynamically based and mutually consistent.

One positive way to investigate the hypothesis of obliquity-induced climatic variations is to resort to numerical modelling; as noted by Williams this approach has considerable potential. In 1980 I intend to run the same model as used in my study[3], with an obliquity of 0° and a value near 60° as an initial contribution to this fascinating area of science. It is hoped this will throw light on the combined climatic effects of an increased rotation rate and extreme values of obliquity.

B. G. HUNT

Australian Numerical Meteorology Research Centre, PO Box 5089AA, Melbourne, Australia 3001

1. Frakes, L. A. *Climates Throughout Geologic Time* (Elsevier, Amsterdam, 1979).
2. Williams, G. E. *Geol. Mag.* **112,** 441–465 (1975).
3. Hunt, B. G. *Nature* **281,** 188–191 (1979).
4. Wolfe, J. A. *Am. Scient.* **66,** 694–703 (1978).
5. MacDonald, G. J. F. *Rev. Geophys.* **2,** 467–540 (1964).

Analysis of host specificity of temperate and tropical animals

IN the contingency-table analysis of the host specificity of temperate and tropical ambrosia beetles, Beaver[1] erred in using the percentages of species showing various grades of host specificity rather than the actual frequencies[2]. Depending on the sample size and the distribution of frequencies among cells, this procedure may either inflate or deflate the values of χ^2 and thus invalidate a test of independence of rows and columns. Also, Beaver[1] implied that a test of host specificity for xylomycetophagous beetles was carried out with a 2×4 table but no xylomycetophagous species was restricted to a single species of host plant. Thus, the data for this group should have been tested in a 2×3 design.

Corrected values of χ^2 for Beaver's[1] data are given in Table 1. Considering all species of both families of beetle, the evidence for increasing specialization with increasing latitude is considerably stronger than Beaver's analysis indicated. For phloeophagous species, the evidence is weaker than Beaver suggested but, for the most part, his hypothesis is strongly supported by data from this group of species. However, the data for the xylomycetophagous species are equivocal (4/6 country pairs show independence of rows and columns) and thus provide no evidence in support of Beaver's hypothesis. It is not clear whether this failure results from the small sample sizes for this group or from a fundamentally different pattern of resource utilization.

Table 1 Comparison* of the degree of specialization of feeding habits of Scolytidae and Platypodidae

	Countries compared					
Species group	Fr/Ca	Fr/Ma	Fr/Fi	Ca/Ma	Ca/Fi	Ma/Fi
All	15.085	165.121	70.169	245.781	100.747	20.505
Phloeophagous	13.058	37.753	40.718	55.899	40.905	12.110
Xylomycetophagous	1.640	19.339	2.148	9.583	4.161	5.126

*The null hypothesis states that there is no relationship between the degree of specialization and latitude. Data were tested in 2×4 (all species and phloeophagous species) or 2×3 (xylomycetophagous species) contingency tables. For 2×4 tables, critical values are 7.815, 11.345 and 16.266 for $\alpha = 0.05$, 0.01 and 0.001, respectively; corresponding critical values for 2×3 tables are 5.991, 9.210 and 13.816. The values of χ^2 comparisons among all pairs of countries are given. Ca, California; Fi, Fiji; Fr, France; Ma, West Malaysia.

STEPHEN SMITH

Faculty of Science,
Department of Biology,
University of Waterloo,
Waterloo, Ontario, Canada N2L 3G1

1. Beaver, R. A. *Nature* **281,** 139–141 (1979).
2. Zar, J. H. *Biostatistical Analysis* (Prentice-Hall, Englewood Cliffs, 1974).

BEAVER REPLIES—The point concerning the use of percentages in χ^2 tables is accepted. I had not intended to suggest that the xylomycetophagous species followed the pattern of the phloeophagous species and were less host specific in the tropics. As I noted[1], they show "a similar low specificity in both temperate and tropical regions". I think it probable that this difference from the phloeophagous species is related to the different methods of resource utilization. If the ambrosia fungi can grow in the dying or dead wood of a high proportion of the tree species present in a tropical forest, this forest may not appear more heterogeneous to an ambrosia beetle than a temperate forest.

R. A. BEAVER

Department of Biology,
The University of Zambia,
PO Box 2379,
Lusaka, Zambia

1. Beaver, R. A. *Nature* **281,** 139–141 (1979).

0028-0836/80/290310-01$01.00

BOOK REVIEWS

Peripatetic physicist

C.A. Russell

The Papers of Joseph Henry. Vol. 3: *January 1836–December 1837, The Princeton Years*. Edited by N. Reingold. Pp. 585. (Smithsonian Institution Press: Washington D.C., 1979.) $30.

THE PHYSICIST Joseph Henry (1797–1878) achieved lasting fame for his work on electromagnetism and, in particular, his anticipation (1830) of Faraday's discovery of electromagnetic induction. He became, in 1832, Professor of Natural Philosophy at Princeton, and in 1846 the first Director of the Smithsonian Institution in Washington. In his later years he was active in establishing the American Association for the Advancement of Science and the National Academy of Sciences. Today, his name is perpetuated in two main ways: by the unit of electrical inductance, the henry, and by the splendid collection of his personal papers in the archives of the Smithsonian Institution. It is this deposit which forms the nucleus of *The Papers of Joseph Henry*, currently in course of publication. Two volumes have already appeared dealing with, respectively, his years at Albany, New York, until 1832, and the first part of his Princeton period. The present book covers the years 1836–1837, subsequent volumes being planned for the remainder of his life.

For a book of this size merely to span two years may seem an excessively generous use of space, but as the editor rightly observes "the period covered was extraordinarily eventful". In the study of electricity the outlines of a coherent view of electromagnetism were beginning to emerge. Developments in optics, metallurgy and engineering were bearing fruit in lighthouse construction, instrumentation, shipbuilding and the new steam railways. Thanks partly to geological progress, searching questions were being asked about the nature of science and its relation to revealed religion. And Henry's own university was struggling to equip its laboratories in a manner fitting for the new challenges, even though its efforts coincided with the great economic depression of 1837. For Henry himself an even more significant event took place at this time: a scientific tour of Europe. In his own extensive reporting of this unforgettable experience lies the greatest interest of this remarkable collection of documents.

In the first part of the book we see Henry writing to his brother James on family matters, to his wife while away on a visit to Albany and to Benjamin Silliman on popular demonstrations in electromagnetism. He confides to his notebook a "record of experiments", chiefly on the lateral discharge of static electricity. Other correspondence fills out many intriguing details of the American scientific scene, and introduces us to a host of scientific figures both famous and obscure. The idea of a Continental trip was mooted in mid-1836 as a means of procuring the required scientific equipment. It was but one of many such journeys undertaken by Americans to post-Napoleonic Europe. Thereafter, foreign travel figures frequently in the correspondence until February 22 when he set sail for Europe. An increasing apprehension about the potential hazards of his voyage is evident in his letters. It would hardly have been dispelled by the request of a scientific colleague that he convey to Europe for distribution numerous copies of his latest paper, "On the gales and hurricanes of the Western Atlantic".

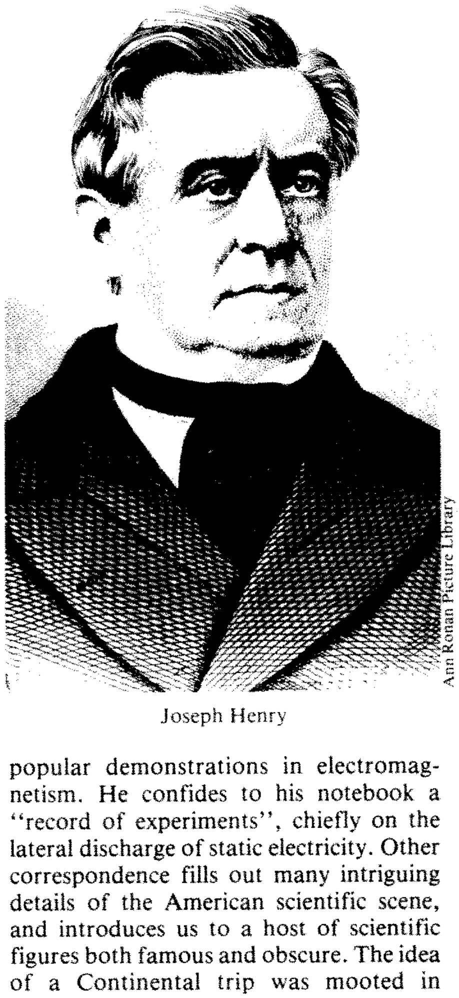
Ann Ronan Picture Library

Joseph Henry

The account of Henry's European tour is supplemented by one from his friend and counterpart in Philadelphia, A. D. Bache, who left for Europe a few months before Henry. Their two diaries illuminate the great sensitivity of Americans at that time to their reputation overseas. Nowhere is this more evident than in Henry's experiment in King's College, London, when he tried to obtain a spark from thermoelectricity; the successful outcome, which had eluded Faraday, gained in significance with each retelling of the tale and Henry became a folk-hero in his own country. During his London stay he frequently enjoyed the hospitality of Daniell's laboratory at King's College, and quickly became acquainted with most of the leading metropolitan scientists. His lodgings were chosen so as to be a few steps from the Royal Institution. Visits to Greenwich, Woolwich and an unnamed gasworks still further enlarged his circle of acquaintances, and he did not hesitate to characterize many of those he met. Sturgeon was reckoned to be "a very good experimenter but an indifferent lecturer"; Wheatstone was the most "talented" person he had encountered; but Faraday (who welcomed him into his own family circle and home) was "the greatest man".

From England Henry went to France where his diaries and letters reveal interesting details of transport, social life and an American's impressions of Paris. But scientifically it was less successful. Equipment ordered in France failed to be delivered, and he found considerable difficulty in meeting the great figures of French science. Partly this was due to a language problem, but also, as the editor admits, "many of Henry's opinions of France would provide ammunition for recent historiography arguing the decline of French science in the nineteenth century". Several times Henry wished he had spent less time in France and more in Britain.

The final part of his tour took him to Scotland where he gives graphic accounts of life in Edinburgh, trips to Scottish lighthouses and (especially) the Edinburgh

Observatory. Then, after attending the British Association meeting in Liverpool, and a brief visit to Cambridge, he set sail from Portsmouth on 22 October 1837 for his homeward journey.

It is impossible to do justice to the richness of material in these papers. A great number of Henry's contemporaries flit in and out of his pages: obscure instrument-makers, technicians, engineers and others on the periphery of science; relations, students, friends and casual acquaintances; politicians and royalty (though not much, for Henry was a staunch republican); poets and philosophers; and above all men and women active in science. We are treated to his views on race and slavery, on the status of women, on the cost of war, on the politics of science — and even on the philosophy of tea-making.

Popperfoto

Charles Wheatstone — the most "talented" person . . .

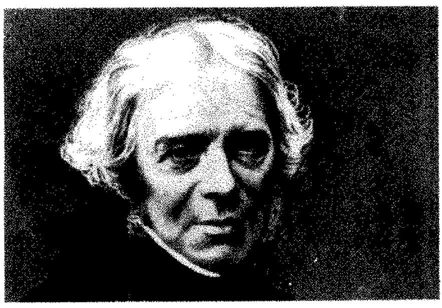
Popperfoto

Michael Faraday — "the greatest man".

The task of the editor and his assistants has included the provision of very full notes with (where possible) full identifications of individuals, places and incidents referred to in the papers. The massive index is a testimony to their thoroughness and care. Naturally, a few blemishes have been detected; there is now some doubt about the authenticity of "Newton's" telescope at the Royal Society (p. 189); the spectrum studied by Brewster was most certainly not that of "nitrous acid" (p. 482); the Brunel referred to on p. 225 as the engineer of the Great Western Railway was not Marc but his more famous son Isambard; and there are a few uncorrected colloquialisms in the notes and a small number of misprints. But these cannot detract from the great merits of a work that will be invaluable to social historians as well as historians of science working on that period. There are eight pages of portraits (though, curiously, not one of Henry himself) and several other illustrations in the text and endpapers. For a work of this size and complexity it is excellent value for money. Subsequent volumes will be awaited with keen interest.

C. A. Russell is Reader in History of Science at The Open University, Milton Keynes, UK.

Anecdotal astrophysics

G. T. Bath

Introduction to Advanced Astrophysics. By V. Kourganoff. Pp. 479. (Reidel: Dordrecht, The Netherlands, Boston and London, 1979.) Hardback Dfl. 135, $71.05; paperback Dfl. 55, $28.45.

WHEN Martin Schwarzchild wrote *Structure and Evolution of the Stars* (Princeton University Press) in 1958 (rightly referred to as "a remarkable treatise" in this book), the revolution in astrophysics which we have witnessed in recent years had already begun. For the first time computers provided a tool which led, using considerable intellectual ingenuity, to the solution of previously intractable equations describing the structure of stars and other cosmic objects. Radioastronomy had broken down barriers that restricted our view of the Universe to the optical region of the electromagnetic spectrum. New optical instrumental techniques were continuously developing and were a continuing source of unpredictable discovery.

Since then astronomy and its associated research fields have matured into a fully fledged science — one which in the UK currently receives 20% of the Science Research Council budget. The bulk of the electromagnetic spectrum is now visible through satellite or ground-based telescopes.

The new astronomies based on γ-ray, X-ray, ultraviolet and microwave observations have added a vast body of data ranging from the galactic binary X-ray sources to the cosmic microwave background. Nonetheless optical and radio wavelengths have retained their central position. In 1964 quasars were discovered, and the subject of active galaxies and galactic evolution was opened up by the mysterious optical spectra of the Cambridge 3C radio survey sources, 3C48 and 3C273. Even more startling was the way in which the persistent detective work of Bell-Burnell, Hewish and colleagues tracked down the neutron star using techniques developed to study interstellar scintillation. The Cambridge group quickly convinced the world of the reality of pulsars in 1968 (in a piece of teamwork which it does service to no one today to break down into isolated individual contributions as attempted in this book).

All this is well known. Less widely appreciated are the developments in optical instrumentation that have produced a rich source of surprises — solar oscillations, polarization and pulsations in white dwarfs, confirmation of accretion disks in stellar binary systems, complex quasar spectra reflecting structure around the quasar powerhouse and within the intergalactic medium, velocity dispersion studies providing a wealth of information on the morphology and evolution of galaxies — to mention but a few.

There is clearly a place, though competitors already exist, for a lucid, approachable and up-to-date introduction to the subject at postgraduate level: a book which reflects the past excitement, together with the logic and physics underlying models which account for these cosmic discoveries; something akin to *Structure and Evolution of the Stars.* Unfortunately, *Introduction to Advanced Astrophysics* does not provide this, at least in the way I would have hoped for.

The *Concise Oxford Dictionary of Current English* gives one definition of the word 'idiosyncrasy' as "mode of expression peculiar to an author". This book is a rich source of idiosyncrasy — of content, style, science and even English usage. In my view the author and publisher have not been successful in producing a well-balanced introduction to the study of astrophysics at the postgraduate level, which is their stated aim.

The book covers radiative transfer, stellar structure, white dwarfs, neutron stars and pulsars, binary systems and galactic X-ray sources, simple cosmological models, and, very briefly, extragalactic astronomy. The style is the lecture-note format elaborated to contain a multitude of *caveats* to simple introductory statements. These confuse the intelligent, inquiring reader, and distract from the main thrust of the subject. Most of the topics treated can hardly be described as advanced, and the treatment is muddled with anecdotes and asides.

Kepler's laws occupy 40 pages, the physics of X-ray binaries two, in a section totalling 70 pages, and the two pages on the physics are confused and misleading. Perhaps there is a place for an exhaustive discussion of the solution of binary orbital elements in a section devoted to X-ray sources, but not at the expense of a thorough discussion of the basic physical processes that power them, and make them what they are — amongst the powerful stellar energy sources in the Universe. It is a Sunday magazine supplement howler to state that in mass exchanging binaries "the very strong *gravitational field in the neighbourhood* of the compact object obliges the surrounding gas to flow over to the object" from the companion (my italics).

The English is eccentric and frequently grammatically incorrect. I am full of sympathy for the problems facing scientists whose mother tongue is not English. In the preface Professor Kourganoff, in his defence, quotes Zel'dovich: "Specific broken English (not Shakespearian or slang) plays the role played by Latin in the time of Copernicus". Broken English presents no difficulty, and can even have unsuspected advantages, when reporting original research. But textbooks are a different matter. The author has a responsibility to capture the reader's attention, to further his appreciation of the excitement of the subject, to have faith in the content and to help him use his intelligence. And that demands as much attention to style as to content. In this case I feel the author is not wholly at fault. The editor and publisher must also take some responsibility. ☐

G. T. Bath is a Research Fellow at Wolfson College and a Research Officer at the Department of Astrophysics, University of Oxford, UK.

Hormones from start to . . .

George Fink

Hormones and Evolution. Edited by E.J.W. Barrington. 2 vols, pp.989. (Academic: London and New York, 1979.) Each volume £30, $69.

Hormones and Evolution is an important treatise which tests the hypotheses that underlie the oft-quoted aphorisms of Peter Medawar — "Endocrine evolution is not an evolution of hormones but an evolution of the uses to which they are put" — and J.B.S. Haldane — "The evolution of vertebrate hormones was nearly complete in Silurian times". Medawar's hypothesis is proved correct for the steroids which, as shown in the interesting first chapter by Sandor and Mehdi, have been found in most species of animal and many species of plant (including prokaryotes). Sandor and Mehdi argue that the steroid nucleus (cyclopentanoperhydrophenanthrene) could have been synthesized abiotically, and because steroids interact with DNA (including the DNA of bacteriophages) they could be considered to be universal biomolecules which were among the first transmitters of chemical information. Medawar's hypothesis may also hold for the monoamines and the thyroid hormones the structure, but not function, of which remains unchanged among the vertebrates.

Common to the vertebrates and many invertebrates is the fact that the nervous and endocrine systems are linked by neuroendocrine cells, the transmitter most often being a peptide. Peptide hormones have recently attracted much interest, but even so the information obtained thus far, especially about their structure in lower vertebrates and invertebrates, is too meagre to enable us to determine for most compounds whether there has been a significant evolution of peptide structure as well as function. However, in agreement with Medawar's hypothesis, the mammalian thyrotropin releasing hormone (TRH), a tripeptide, is present in the brains of amphibians, reptiles and fish, but does not appear to release thyrotropin in these animals. Jackson suggests that TRH is a central neurotransmitter which, during evolution, acquires a role in the hypothalamic-pituitary system, first as a releasing factor for prolactin and then for thyrotropin. By contrast, the peptides of the neurohypophysis and the gut do appear to have undergone an evolution of structure as well as function. Thus, in mammals, gastrin and cholecystokinin are distinct, whereas in amphibians, fish and cyclostomes there appears to be only one gastrin/cholecystokinin molecule. In their review of the evolution of responses to the neurohypophysial principles, Sawyer and Pang point out the need in mammals for separate regulation of urine flow and milk ejection. This might explain why arginine vasopressin is the predominant pressor-antidiuretic peptide in the mammal, while arginine vasotocin predominates in non-mammalian vertebrates. Arginine vasotocin is about half as potent as oxytocin (the milk-ejection principle in mammals) in stimulating milk ejection and only half as potent as arginine vasopressin (which has little milk-ejection activity) in blocking diuresis. Thus, the switch from vasotocin to vasopressin, which only involves the substitution of phenylalanine for isoleucine (one base change in the codon), would confer a considerable advantage to the mammal. Further studies will be required to determine whether there are any common precursors for the invertebrate and vertebrate peptide hormones. Is there, for example, any relationship between the hyperglycemic hormone of the crustaceans and the gut and pancreatic hormones of the vertebrates?

As a treatise on comparative endocrinology, biologists will find this a most valuable handbook which they will wish to keep close to hand in the laboratory. Professor Barrington has chosen the topics and the authors carefully. Most vertebrate hormones and endocrine

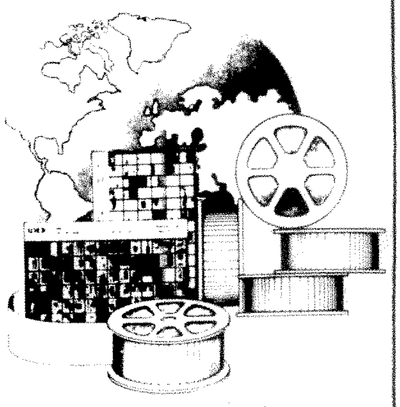

nature

is Available in
MICROFORM

For Complete Information
customers should write

University Microfilms
International

Dept F A
300 North Zeeb Road
Ann Arbor, MI 48106
U S A

Dept F A
18 Bedford Row
London WC1R 4EJ
England

Bring Your Library Up-To-Date With This ANS Edition...

O. J. Wick
HANDBOOK

Plutonium Handbook
A Guide to the Technology

992 pages — 8½" × 11"
Hardbound $98.00

American Nuclear Society
555 North Kensington Avenue
La Grange Park, IL 60525 USA

Please take my order for ____ book(s).
☐ Payment in full enclosed.
☐ Bill me and I accept postage and handling charges.

Name ____
Organization ____
Street ____
City ____
State ____ **Zip** ____

Circle No. 01 on Reader Enquiry Card.

systems are reviewed in detail, and one chapter each is devoted to the annelids, molluscs, crustaceans, insects and echinoderms. The chapters are mostly well written and illustrated, and reflect excellent scholarship. The authors, however, show a disappointing readiness to fit their data to prevailing views on evolution and the origin of life rather than looking for clues that might spark revolutionary ideas. There is one surprising omission — no chapter on the pineal gland which continues to tantalize the endocrinologist and evolutionist. Perhaps in man the pineal is *only* the seat of the soul (although recent studies suggest that it may also moderate gonadal function); but what an elevation in function from a mere phototransducer! □

George Fink is Director of the MRC Brain Metabolism Unit, University Department of Pharmacology, Edinburgh, UK.

Cookery book for immunologists

A.J. Munro

Selected Methods in Cellular Immunology. Edited by Barbara B. Mishell and Stanley M. Shiigi. Pp. 486. (W.H. Freeman: San Francisco and Oxford, 1980.) $29.95, £17.70.

THIS BOOK contains most of the principal methods used by cellular immunologists working with cells from mice. It started as a manual for teaching students and research workers in the Department of Microbiology and Immunology at the University of California, Berkeley, but has been expanded to include chapters from workers in other laboratories, although the majority of the 40 or more contributors are from the same department. The editing and the production of the book has ensured that the style of each contribution is very similar. Each chapter starts with a brief introduction, explaining the principle behind the method to be discussed. For example, there is a clear and precise description of limiting dilution analysis before details of how to measure the frequency of precursors of B-cells, helper T-cells and cytolytic T-cells.

About half of the procedures considered are only applicable to experiments using murine cells, but the rest are of general value and make the book of interest to all immunologists. The purification of immunoglobulins and their fragments and different assay procedures for detecting the reactions of immunoglobulins are described in useful detail. There is a section devoted to the method developed by Köhler and Milstein for the production of monoclonal antibodies from hybrid cell lines which will be particularly valuable to researchers trying this procedure for the first time.

Although most of the contributions contain a list of comments, often describing particular snags in the procedure or why particular reagents have been used, this is not always the case. One feels that, as with recipes, descriptions of methods should include some indication of which steps are essential, or which reagents were used because they happened to be conveniently at hand at that moment. A further criticism concerns the expense of some of the approaches suggested — by simple modification some of the procedures could be carried out at one-tenth of the cost.

The editors have not tried to make this collection of methods comprehensive, but nevertheless they have brought together most of the important techniques for studying cellular immunology and all immunologists will find valuable procedures clearly laid out. I have had considerable difficulty in reviewing this book, since whenever I brought it into the laboratory it vanished. And, like all good cookery books, it is rapidly accumulating stains on the more used pages. □

A.J. Munro works in the Division of Immunology, Department of Pathology, University of Cambridge, UK.

SCIENTIFIC BOOKSHOP

H. K. LEWIS can supply works in all branches of Pure and Applied Science. Catalogues on request. Please state interests.

SCIENTIFIC LENDING LIBRARY

Annual Subscription from £7.50.
(Available in U.K. only)

Reduced rates for multiple subscriptions.

Prospectus post free on request.

Quarterly List of New Books and new editions added to the Library sent post free to subscribers regularly.

H. K. LEWIS & Co. Ltd.

**136 GOWER STREET,
LONDON, WC1E 6BS**

Telephone: 01-387 4282
Telegrams: "Publicavit, London, WC1E 6BS."

Circle No. 11 on Reader Enquiry Card.

Mammals through the mists of time

Barry Cox

Mesozoic Mammals: The First Two-Thirds of Mammalian History. Edited by J.A. Lillegraven, Z. Kielan-Jaworowska and W.A. Clemens. Pp.321. (University of California Press: Berkeley and London, 1980.) Hardback $30, £18; paperback $8.75, £5.25.

THE EARLY days of mammalian evolution were perhaps the Dark Ages in more than one sense — because not only were the little early mammals probably nocturnal, but also their tiny remains are fragmentary and uncommon. It is not so long ago that it was said that all their known remains could have been put in a shoe-box and, though the volume of their known fossils has considerably increased, it is still true that the overwhelming majority are isolated teeth or tooth-bearing fragments of skull. Study of their evolution is therefore still largely a matter of comparative odontology, as is reflected by the names of their orders: Triconodonta, Symmetrodonta, Multituberculata etc. These Dark Ages are particularly frustrating, for they separate the period of reasonably well-known Permo-Triassic mammal-like reptile evolution, which culminated in the very mammal-like cynodonts, from the Cenozoic period of well-documented, diverse, fully-evolved marsupials and eutherians ('placentals').

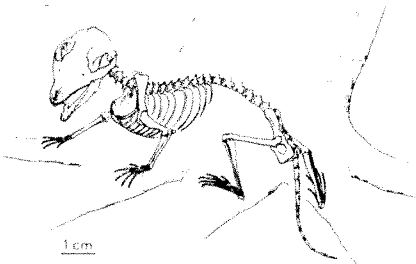

Jenkins and Parrington

Skeletal reconstruction of a Triassic triconodont

This book is therefore an extremely valuable synthesis of our current knowledge of Mesozoic mammals. It includes an introduction and 14 other chapters, by a total of 12 authors — mostly from the USA, but also including Dr Zofia Kielan-Jaworowska from Poland. After the Introduction, Chapter 2 provides a summary, on a world-wide basis, of the state of the record of Mesozoic mammals, giving faunal lists for each locality or group of localities, brief discussions (where necessary) of geological age assignments and information as to what parts of the mammals are actually known from those localities. Seven of the chapters are devoted to the morphology and systematics of the different orders of Mesozoic mammal. For each of these, one table

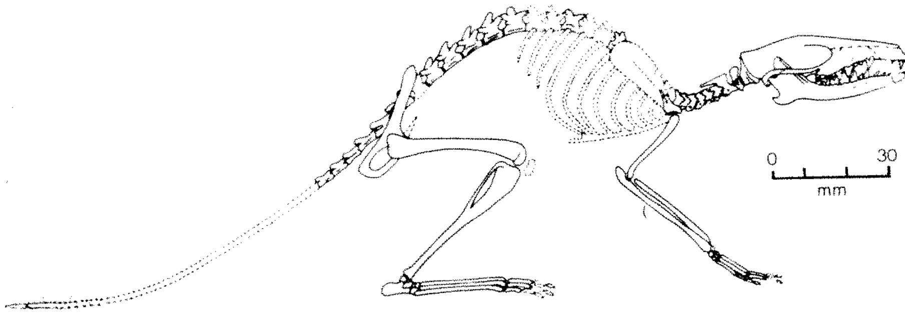

Z. Kielan-Jaworowska

Skeletal reconstruction of *Zalambdalestes lechei*

provides a complete listing of the taxonomic hierarchy from order to species, giving their authors, and another table shows the known distribution of the genera in space and time. The tables are followed by sections devoted to the anatomy, systematics, phylogeny and ecology of the order. There is also a brief chapter evaluating current opinion on the relationship between the monotremes and the Mesozoic groups.

The taxonomy of Mesozoic mammals used in the book is based on that of Simpson and Romer, and the editors have wisely decided that this was neither the place nor the time to embark on novel ventures in this field. Indeed, they have been extremely cautious, to the extent of refraining from formal use of the terms Prototheria and Theria in view of increasing scepticism about the theory that there was a corresponding fundamental dichotomy in early mammalian evolution. The book can therefore be used without needing to translate one's memory of well-established usage into some new-fangled (and perhaps transient) system of taxonomic/phyletic interpretation, which is a considerable relief.

Three evolutionary topics have been selected for treatment in particular detail. Crompton and Jenkins discuss the origin of mammals from mammal-like reptiles. The gap between the two groups has been gradually reduced, and little change would be needed in the braincase, jaw-joint and dentition of the small chiniquodont cynodonts known from the Middle Triassic to turn them into the tiny, insectivorous morganucodont mammals of the late Triassic. Crompton and Jenkins believe that, although there are some differences between the structure of the braincase in the therian and non-therian mammals, these are not great, and certainly not so great as to suggest that these two groups originated from the mammal-like reptiles separately.

Bown and Kraus give a clear, well-illustrated account of the origin of the tribosphenic molar, describing how it evolved from the three surfaces of the late Triassic symmetrodonts to the six surfaces of the early eutherians by the gradual proliferation of shearing surfaces. The proliferation was one aspect of the change in tooth shape that exploited the new masticatory process based on transverse shear rather than on simple puncture-crushing.

In the last of these three chapters, Lillegraven discusses reproduction in Mesozoic mammals. He provides a strong case for believing that it was the evolution of a trophoblast that could suppress maternal immunological rejection of the fetus that provided the eutherians with a decisive advantage over the marsupials. He also suggests that the pair-bonding or social structure, that in eutherians may have facilitated rapid genetic change and evolution, was impossible in marsupials because of the greater likelihood of maternal rejection of subsequent inseminations by the same, or a closely related, male.

At the end of the book Lillegraven, Kraus and Bown summarize the palaeogeographical changes that took place in the Mesozoic world. As they point out, it is in the late Cretaceous that the mammalian fossil record becomes most complete, and therefore the possibility of accurate biogeographical interpretation becomes greatest. But, even here, a good record is known from only two land areas, and only a few fragments are known from three others; in the remaining nine areas the fossil record is silent. Their concluding phrase — "We have much to learn" — may be taken as a suitable keynote, not only for this chapter, but for the book as a whole.

The book has an attractive format, most of the figures are clear and the editors are to be congratulated on an almost fault-free text. Though it would have been improved by the addition of an index, the organization of the book makes it easy to find topics and make cross-references. *Mesozoic Mammals* is an extremely valuable statement and synthesis of this field, both for those whose research lies in or near to it and also for those who have to try to explain it in the course of their teaching. ☐

Barry Cox is Professor of Zoology at King's College, University of London, UK.

Direct methods and the phase problem

C. J. Gilmore

Theory and Practice of Direct Methods in Crystallography. Edited by M. F. C. Ladd and R. A. Palmer. Pp.421. (Plenum: New York and London, 1980.) $35, £22.05.

DURING THE past 20 years, three developments have revolutionized X-ray crystallography. Two of them are well known even to the non-specialist. The automatic diffractometer has removed the drudgery of measuring the complicated diffraction pattern that results from the interaction of X-rays and crystals while, at the same time, increasing the speed and accuracy of the process. Similarly, processing this raw data to produce a crystal structure at an atomic level was also once an even more laborious business that has now been almost completely taken over by computers. As a result of these two advances over 2000 new crystal structures are reported each year; 20 years ago the figure was nearer 200.

One stumbling block still remains. The step between the diffraction experiment and obtaining the crystal structure is not trivial, since the relative phases of the diffracted X-ray beams need to be determined and they cannot be measured experimentally. This is the crystallographic phase problem and it is here that there has been a third major development that is less well known.

It is called 'direct methods' and is a technique by which phase angle information is obtained directly from the diffraction pattern by mathematical means. The subject started modestly enough 30 years ago as a mathematical curiosity and has grown to become the principal method by which the phase problem is now solved. It has allowed crystallographers to study a whole range of molecules that were previously inaccessible, and it has revolutionized our knowledge of structural chemistry.

It is by no means a static field and there has been a large influx of new ideas in the last decade, but strangely there have been very few books on the subject. Pioneering monographs by Hauptman and Karle (American Crystallographic Association: New York, 1953) and later Woolfson (Oxford University Press: Oxford, 1961) are now outdated or unavailable, and more recent books have either been conference proceedings or have restricted themselves to specialized aspects of the technique. Consequently, there is a need among crystallographers for a book that covers both theoretical and practical features of direct methods in an integrated and up-to-date way.

This book does not quite achieve this. It contains ten chapters that discuss various aspects of direct methods, each chapter having a separate author. The editorial hand could have been firmer. Apart from the inevitable problems of duplication and overlap, each contributor has been allowed to use his own nomenclature which is consequently different in every section. This will confuse the non-expert and so limit the overall usefulness of the book. The index, too, is rather poor.

There are, however, some excellent individual contributions. Rogers has written a thorough chapter on origin and enantiomorph definition, looking at what can be a difficult subject in a fresh and interesting way. Hauptman, who was one of the pioneers of direct methods, has contributed a clear and elegant summary of some recent theoretical developments including potentially important work on seminvariant theory. Another pioneer, Sayre, gives an account of phase expansion and refinement methods in his typically concise and illuminating style. There is also an interesting chapter by Argos and Rossmann on the molecular replacement method although its inclusion somewhat extends the customary boundaries of direct methods.

Whether these chapters justify buying the whole volume is of course a personal decision. In any case, the price is not unreasonable for a book of this length. However, the field is still open for a definitive book on direct methods in X-ray crystallography.

C. J. Gilmore is a Lecturer in Chemistry at the University of Glasgow, UK.

A wealth of virus lore

D.H. Watson

Introduction to Virology. By K. M. Smith and D. A. Ritchie. Pp.212. (Chapman and Hall: London and New York, 1980.) Hardback £12, $29.95; paperback £5.95, $14.95.

THE STRENGTH of this book lies in its wide-ranging selection of examples from the world of plant and invertebrate as well as of vertebrate and bacterial viruses. Fungal, protozoal, mycoplasma and spiroplasma viruses are also mentioned. The reader will also benefit from K. M. Smith's wide knowledge of the natural history of plant and insect viruses in particular, as well as from the beautiful electron micrographs (more profuse than is usual in a book of this size) which reach the excellent standard one would expect from this author. Many of these micrographs are of viruses not often represented in illustrations of more comprehensive texts.

The order of presentation is a little unconventional and in some respects illogical; an elementary introduction to the general characteristics of viruses and a survey of the morphology of some representative viruses are followed by chapters on purification, classification and nomenclature, virus diseases of a wide-ranging selection of organisms, spread of viruses and latency, satellite viruses and viroids.

At this stage are interpolated two basic chapters by Professor D.A. Ritchie on virus replication and virus genetics. The chapter on replication in particular is a masterly summary of replication of the various groups of viruses. However, many teachers of virology would, I think, agree that this core topic should have been brought forward since an understanding of the basic principles of replication is a necessary preliminary to the study of many of the topics discussed in earlier chapters, for example latency.

There follows a rather dated discussion of tumour viruses which only mentions virus isolation and electron microscopy as methods for establishing virus aetiology. Late in the book come tissue and cell culture of viruses and virus assay which are surely basic to much of the earlier chapters.

The book concludes with a chapter on control of virus disease. This is sketchy in the extreme and also somewhat dated. The student reading the paragraphs on interferon will surely contrast the low-key treatment of interferon with what he picks up from the media. The selection of thiosemicarbazone as the only chemotherapeutic agent discussed for animal viruses is also likely to give a somewhat distorted view.

The student requiring an introduction to the subject, either from the standpoint of another discipline or as background reading for an elementary course, would perhaps be better served by one of the other paperback volumes — say Primrose's *Introduction to Modern Virology* (Blackwell Scientific: Oxford) now appearing in a second edition, although Ritchie's chapter on replication would be very usefully read by him. Paradoxically, the book should perhaps be read by more advanced students because of the wealth of lore on viruses often perfunctorily treated in the more standard texts, and also for the wide selection of micrographs.

D. H. Watson is Professor of General Microbiology and Head of the Department of Microbiology in the University of Leeds, UK.

Mathematical plasma physics

R.J. Bickerton

Plasma Physics for Nuclear Fusion. By K. Miyamoto. Pp.610. (MIT Press: Cambridge, Massachusetts, 1979.) $50, £31.

PROFESSOR Miyamoto's book is aimed at postgraduate or advanced undergraduate students but it will be equally useful as a reference volume for research physicists in the field. The book was first published in Japanese in 1976 and has now just appeared in English. It appears to date effectively from about 1974 and is consequently dated in the more rapidly moving parts of the subject.

The book opens with arguments in favour of nuclear fusion based on apparently unsubstantiated figures for future energy requirements and for reserves of fossil fuels and uranium. There are then four sections in the book covering fundamentals, magnetohydrodynamics, kinetic description and finally heating diagnostics and confinement. Under fundamentals we have particle orbits, field configurations, Coulomb collisions and the Vlasov equation. The magnetohydrodynamic section includes toroidal equilibria of various kinds, plasma diffusion and a full range of instabilities. Topics considered under kinetic description are waves in cold and hot plasma, Landau damping and microinstabilities due to inhomogeneities in real or velocity space. The final section covers heating by a variety of methods, plasma diagnostic techniques and a survey of confinement experiments.

Professor Miyamoto's view of the world is clearly mathematical rather than physical. The treatment is comprehensive but monochrome with no attempt made to highlight important concepts and no concessions are made or detail sacrified in the interests of clarity. In many cases the mathematical working is fully displayed so that derivations can be followed step by step. One result is that the book is a heavy read and less than gripping. The main body of the book is very weak and largely silent on the extent to which the theory being presented has been tested by experiment. Although it can be justified by the title it is nevertheless sad that that reader is given no impression of the relevance of the main body of plasma physics to non-fusion fields, in particular to astrophysics.

The chief merit of the book is its completeness and in the detail of the presentation. As such it will be a useful reference book, although somewhat marred by a crop of misprints.

R.J. Bickerton is Associate Director (Science) at the JET Joint Undertaking, Abingdon, UK.

BOOKS RECEIVED

Mathematics

GROSS J. F. and POPEL, A. (eds) Mathematics of Microcirculation Phenomena. Pp. xi + 174. ISBN-0-89004-449-X. (Raven Press, New York, 1980.) $22.00.

LEITHOLD, L. College Algebra. Second edition. Pp. xi + 496. ISBN-0-02-369580-3. (Macmillan Publishing Co., Inc. New York; Collier Macmillan Publishers, London, 1980.) £10.95.

Astronomy

GEHRELS, T. Asteroids. Pp. xi + 1181. ISBN-0-8165-0695-7. (The University of Arizona Press, Tucson, Arizona. 1979.) $19.95.

MOORE, P. The Pocket Guide to Astronomy. Pp. 144. ISBN-0-671-25309-3. (Simon & Schuster, New York, 1980.) $5.95 limp.

Physics

BARDOS, C. and BESSIS, D. (eds) Bifurcation Phenomena in Mathematical Physics and Related Topics. Proceedings of the NATO Advanced Study Institute held at Cargèse, Corsica, June, 1979. NATO Advanced Study Institutes Series. Pp. ix + 596. ISBN-90-277-1086-4. (D. Reidel Publishing Company, Dordrecht, Boston, London, 1980.) Dfl. 115 US $59.50.

CHILD, M. S. (ed.) Semiclassical Methods in Molecular Scattering and Spectroscopy. Proceedings of the NATO ASI held in Cambridge, England, September, 1979. NATO Advanced Study Institutes Series. Pp. xi + 332. ISBN-90-277-1082-1. (D. Reidel Publishing Company. Dordrecht, Boston, London, 1980.) Dfl.75, US$39.50.

CONSTANTINSCU, F. Distributions and their Applications in Physics. International Series in Natural Philosophy Volume 100. Pp. x + 148. ISBN-0-08-018297-6. (Pergamon Press, Oxford and New York, 1980.) £13.50 $30.00.

DUMMER, G. W. A. (Editor-in-Chief) Semiconductor and Microprocessor Technology 1979. Selected papers presented at the 1979 annual SEMINEX Technical Seminar and Exhibition, London. Microelectronics and reliability. Volume 19, No. 5/6. Pp. 407-644. ISBN-0-08-026134-5. (Pergamon Press, Oxford and New York, 1980.) £23.00 flexi.

MARLOW, A. R. Quantum Theory and Gravitation. Pp. x + 267. ISBN-0-12-473260-7. (Academic Press, New York and London, 1980.)

PAMPLIN, B. R. (ed.) Molecular Beam Epitaxy. Pp. v + 174. ISBN-0-08-025050-5. (Pergamon Press, Oxford and New York, 1980.) US $35.00 £15.75.

Chemistry

BARD, A. J. and LUND, H. (eds) Encyclopaedia of the Elements: Organic Section, volume xiv. Pp. xii + 308. ISBN-0-8247-2514-X. (Marcel Dekker, Inc. New York and Basel, 1980.) SFr. 240.

BLYTHE, A. R. Electrical properties of polymers. Pp. x + 191. ISBN-0-521-21902-7 hardback ISBN-0-521-29825-3 paperback. (Cambridge University Press, Cambridge, 1980.) £4.50 pbk.

CALLEWAERT, D. M. and GENYEA, J. Basic Chemistry; General, Organic, Biological. Pp. xxii + 837. ISBN-0-87901-130-0. (Worth Publishers, Inc. New York, 1980.)

EYRING, H., LIN, S. H. and LIN, S. M. Basic Chemical Kinetics. A Wiley-Interscience Publication. Pp. vii + 439. ISBN-0-471-05496-8. (John Wiley & Sons, New York and Chichester, UK, 1980.) £20.00.

GOFFER, Z. Archaeological Chemistry. A Sourcebook on the Applications of Chemistry to Archaeology. Chemical Analysis: Vol. 55. A Series of Monographs on Analytical Chemistry and its Applications. A Wiley-Interscience Publication. Pp. xvi + 376. ISBN-0-471-05156-X. (John Wiley & Sons, New York and Chichester, UK 1980.) £15.80.

MURPHY, D. B. and ROUSSEAU, V. Foundations of College Chemistry. Third Edition. Pp. xvi + 767. ISBN-0-471-04621-3. (John Wiley & Sons, New York and Chichester, UK, 1980.) £13.00.

SHRINER, R. L., FUSON, R. C. The late, CURTIN, D. Y. and MORRILL, T. C. The Systematic Identification of Organic Compounds. A Laboratory Manual. 6th edition. Pp. xviii + 604. ISBN-0-471-78874-0. (John Wiley & Sons, New York and Chichester, UK, 1980.) £13.75.

Technology

BANKS, R. C., MATJEKA, E. R. and MERCER, G. Introductory Problems in Spectroscopy. Pp.326. ISBN-0-8053-0572-6. (Addison-Wesley: 1980.) flexi £9.

GUENOD, M. A. (ed.) Computer Aided Design of Control Systems. Preceedings of the IFAC Symposium, Zürich, Switzerland, August, 1979. Pp.688. ISBN-0-08-024488-2. (Pergamon: 1980.) $125,£55.

KIDD, C. V. Manpower Policies for the Use of Science and Technology in Development. Pergamon Policy Studies on Socio-Economic Development. Pp.183. ISBN-0-08-02124-2. (Pergamon: 1980.) £10, $20.

Earth Sciences

BOOTH, B. and FITCH, F. La Terre en Colère. Les Cataclysmes Naturels. Pp. 328. ISBN-2-02-005578-3. (Editions du Seuil, Paris, 1980.) np. flexi.

MACKENZIE, W. S. and GUILFORD, C. Atlas of rock-forming minerals in thin section. Pp.v + 98.ISBN-0-582-45591-X. (Longman Group Ltd., Harlow, Essex, 1980)

CADIOT, B. et al. Les tremblements de terre en France. Memoire du Bureau de recherches geologiques et minières No.96-1976. Pp.ii + 220. (Orleans: Bureau de Recherches Gèologiques et Minières, 1979.) F80,00 app. US$20. flrxi.

GOULD, S.J. Ever Since Darwin: Reflections in Natural History. Pp.285. ISBN 0-14-02. 2222-7. (Penguin: London, 1980.) £1.50.

GUTIERREZ, L.T. and FEY, W.R. Ecosystem Succession: General Hypothesis and a Test Model of a Grassland. Pp.231. ISBN 0-262-07075-8. (MIT; Cambridge, Massachusetts, 1980.) $25.00.

HARRIS, A.L., HOLLAND, C.H. and LEAKE, B.E. The Caledonides of the British Isles Reviewed. Pp.768. ISBN 0-7073-0257-9. (Scottish Academic Press: Edinburgh, 1980.) £40.00; $100.00.

JEANS, C. V. and RAWSON, P. J. Andros Island, Chalk and Oceanic Oozes: Unpublished work of Maurice Black. Pp.100. ISBN 0143-6635. (Yorkshire Geological Society: Leeds, 1980.)

KILDOW, J.D. Deepsea Mining. Pp. 251. ISBN 0-262-11-075-X. (MIT Press: Cambridge, Massachusetts, and London, 1980.)

KUNKEL, G. Taxonomic aspects of African economic Botany. Proceedings of the IX Plenary Meeting of A.E.T.F.A.T. Las Palmas de Gran Canaria, March, 1978. Pp.250. ISBN-84-500-3340-3. 6kew: The Secretary, Bentham-Moxon Trust, Royal Botanic Gardens, 1980. £11.00.

LONG, C. E. Discovering The Universe. Pp.511 ISBN 0-06044034-1 (Harper and Row: London and New York, 1980.) $14.95 Flexi.

MORAN, J.M., MORGAN, D. and WIERSMA, J.H. Introduction to Environmental Science. Pp.658. ISBN 0-7167-1020-X (Freeman: Reading, 1980.) £9.20.

MORNER, N. A. (ed.) Earth Rheology Isostasy and Eustasy. Pp.599. ISBN 0-471-27593-X. (John Wiley & Sons: Chichester, 1980.)

POINTINGS, G and THOMPSON, F. Hebridean Naturalist: Magazine of the Western Isles Natural History Society: Pp.72. ISBN. (Western Isles Natural History Society: Isle of Lewis, 1980.)

OWEN, D.F. What is Ecology? 2nd Ed. Pp. 234. ISBN 0-19-219155-1 (Oxford University Press: Oxford, 1980.) £6.50 hardback; £3.50 paperback.

REED, G. M. Surveys in General Topology. Pp.555. ISBN 0-12-584960-5. (Academic: New York and London, 1980.) $35.00.

RORISON, I.H. and HUNT, R. (eds) Amenity Grassland. An Ecological Perspective. Pp. xi + 261. ISBN-0-471-27666-9. (Chichester, New York, Brisbane, Toronto: John Wiley & Sons, 1980.) £19.00.

ROSE, A. W., HAWKES, H. E. and WEBB, J. S. Geochemistry in Mineral Exploration. Second ed. Pp.xvii + 657. ISBN-0-12-596250-9 cased ISBN-0-12-596252-5 paperback. (London, New York Toronto, Sydney, San Francisco: Academic Press, 1979.) $64.50 £28.00 Clothbound $29.00 £12.40 paperback.

SCHOPF, T. J. M. Paleoceanography. Pp.341. 0-764-65215-0 (Harvard University Press: London and Massachusetts, 1980.) £15.00.

TROMP, S.W. Biometeorology; The Impact of the Weather and Climate on Humans and Environment (Animals and Plants). Pp.xiv + 346. ISBN-0-85501-453-9. Heyden International Topics in Science. (London, Philadelphia, Rheine: Heyden, 1980.) £9.00 $18.00 DM41.50.

WRATTEN, S. D. and FRY, G. L. A. Field and Laboratory Exercises in Ecology. Pp.x + 227. ISBN-0-7131-2735-2. (London: Edward Arnold (Publishers) Ltd., 1980.) £7.50 pbk.

Biological Sciences

ALTMANN, J. Baboon Mothers and Infants. Pp. 242. ISBN 0-674-015856-9 (Harvard University Press: Cambridge, Massachusetts and London, England, 1980.) $17.50.

BRASIER, M.D. Microfossils. Pp. 193. ISBN 0-04-56200[illegible]-6 (George Allen & Unwin: Hemel Hempstead, 1980.) £12.00 Hbk; £6.50 pbk.

CLOUDSLEY-THOMPSON, J.L. Biological Clocks: Their Functions in Nature. Pp.138. ISBN 0-297-77685-1 (Weidenfeld & Nicolson: London, 1980.) £8.95.

DIXON, F.J. and KUNKEL, H.G. (eds) Advances in Immunology. Vol. 28. Pp. 532. ISBN 0-12-022428-3 (Academic: London and New York, 1980.) $57.50.

FOLEY, C.W., LASLEY J. F. and OSWEILER, G.D. Abnormalities of Companion Animals: Analysis of Heritability. Pp. viii + 270. ISBN-0-8138-0940-1 (London: Bailliere Tindall, 1980.) £10.00.

FRANKLIN, E.C. (Editor-in-Chief) Clinical Immunology Updated: Reviews for Physicians. Pp. 351. ISBN 0-444-00312-6. (Elsevier/North-Holland: New York, 1980.) $24.95.

GILULA, N.B. (ed.) Membrane-Membrane Interactions. Society of General Physiologists series Volume 34. Pp. xii + 218. ISBN-0-89004-377-9. (New York: Raven Press, 1980.) $27.00.

GOLDSTEIN, M., CALNE, D.B., LIEBERMAN, A. and THORNER, M.O. (eds) Ergot Compounds and Brain Function: Neuroendocrine and Neuropsychiatric Aspects. Advances in Biochemical Psychology Vol. 23. (Raven: New York, 1980.) $39.00.

GREGORIADIS, G. and ALLISON, A.C. (eds) Liposomes in Biological Systems. Pp. 412. ISBN 0-471-27608-1. (John Wiley & Sons: Chichester, 1980.) £20.00.

GRIFFITHS, B., HENNESSEN, W., HORODNICEANU, F. and SPIER, R. Proceedings of the General Meeting of European Society of Animal Cell Technology. Vol.46. Pp. xii + 316. ISBN 3-8055-0764-X. (Karger: Basel and New York, 1980.) SFr. 70.00; DM 84.00 US $42.00.

HOCHACHKA, P.W. Living without Oxygen. Closed and Open Systems in Hypoxia Tolerance. Pp. xi + 181. ISBN-0-674-53670-3. (Cambridge, Mass, London: Harvard University Press, 1980.) $17.50.

HORN, A.S., KORF, J. and WESTERINK, B.H.C. (eds) The Neurobiology of Dopamine. Pp. xvii + 723. ISBN-0-12-354150-6. (London, New York, San Francisco: Academic Press, 1979.) $83.00.

HORTON, J.D. (ed.) Development and Differentiation of Vertebrate Lymphocytes: Developments in Immunology Vol. 8. Pp. 280. ISBN 0-444-80195 (Elsevier/North-Holland, 1980.)

HUBINONT, P.O. (series editor) Progress in Reproductive Biology: Seasonal Reproduction in Higher Vertebrates Vol. 5. R.J. Reiter, San Antonio, Tex. B.K. Follett, Bristol. Pp. xii + 222. ISBN 3-8055-0246-X (Karger: Basel, New York and Paris, 1980.) SFR. 155.00; DM 186; US $93.00.

JEANNEROD, M. and HECKEN, H. Adaptation et restauration des fonctions nerveuses. Pp. 392. ISBN 2-85334-178-X. (Simep: Villeurbanne, France, 1980.)

KEENLEYSIDE, M.H.A. Diversity and Adaptation in Fish Behaviour: Pp. xiii + 208. ISBN 3-540-09587-X. (Springer: Berlin, Heidelberg and New York, 1979.) DM 69.00; US $38.00.

KEETON, W.T. Biological Science: 3rd Edition. Pp. 1079. ISBN 0-393-95021-2. (W.W. Norton: New York and London, 1980.) $19.95.

KERR, F.W.L. et al (Work Session Reports.) Neurosciences Research Program Bulletin. Volume Sixteen. Pp. iii + 661. ISBN-0-262-14033-0. (MIT Press:Cambridge, Massachusetts, and London, 1980.) $30.

LEWIS, W.H. (ed.) Polyploidy; Biological Relevance. Basic Life Sciences volume 13. Pp. xii + 583. ISBN-0-306-40358-7. (New York and London: Plenum Press, 1980.) $55.00.

McFADDEN, C.H. Study Guide: for the Third Edition of Keeton's Biological Science. Pp. 232. ISBN 0-393-95208-X. (W.W. Norton: New York and London, 1980.) $4.95.

MEISAMI, E. and BRAZIER, M.A.B. (eds) Neural Growth and Differentiation. International Brain Research Organization Monograph Series Volume 5. Pp. xvii + 528. ISBN-0-89004-378-7. (New York: Raven Press, 1979.) $48.00.

MISHELL, B.B. and SHIIGI, S.M. (eds.) Selected Methods in Cellular Immunology. Pp. xxix + 486. ISBN-0-7167-1106-0. (San Francisco: W.H. Freeman and Company, 1980.) $29.95.

MOORE, T.C. Biochemistry and Physiology of Plant Hormones. Pp. xii + 274. ISBN-3-540-90401-8. (Berlin, Heidelberg, New York: Springer-Verlag, 1979.) DM 49 approx. US $27.00.

OGDEN, C.G. and Hedley. R. H. An Atlas of Freshwater Testate Amoebae. Pp. 222. ISBN 0-19-858502-0. (Oxford University Press: Oxford, 1980.) £17.50.

PEPE, F.A., SANGER, J.W. and NACHMIAS, V.T. (eds) Motility in Cell Function. Proceedings of the First John M. Marshall Symposium in Cell Biology. Pp. xxvi + 479. ISBN-0-12-551750-5. (New York, London, Toronto, Sydney, San Francisco: Academic Press, 1979.) $28.50.

PEPEU, G., KUHAR, M.J. and ENNA, S.J. Receptors for Neurotransmitters and Peptide Hormones: Advances in Biochemical Psychopharmacology. Vol. 21. Pp.516. ISBN 0-89004-408-2. (Raven: New York, 1980.) $48.00.

PITT, J. I. The Genus Penicillium and its Teleomorphic States Eupenicillium and Talaromyces. viii + 634. ISBN 0-12-557750-8. (Academic: London and New York, 1980.) $92.00; £40.00.

PONTING, K. Sheep of the World. Pp. 155. ISBN-0-7137-0941-3. (Poole: Blandford Press, 1980.) £5.95.

PRASAD, K. N. Regulation of Differentiation in Mammalian Nerve Cells. Pp. xiii + 245. ISBN-0-306-40365-X. (New York and London: Plenum Press, 1980.) $24.50.

PROCTOR, J. and PROCTOR, S. Color in Plants and Flowers. Pp. 116. ISBN-0-89696-017-X. (New York: Everest House, 1978.) $9.95.

RIDDLE, P. N. Time-Lapse Cinemicroscopy. Biological Techniques Series. ISBN 0-12-588060-X (Academic: London and New York, 1979.)

ROBINSON, J. P. The Effects of Weapons on Ecosystems. UNEP Studies Series. Pp. ix + 70. ISBN-008-025656-2. (Oxford, New York, Toronto, Sydney, Paris, Frankfurt: Pergamon Press, 1979.) $10.00 £4.55.

RONALD, K. and DUGUY, R. (eds) The Mediterranean Monk Seal. UNEP Technical Series Volume 1. Pp. viii + 178. ISBN-0-08-025654-6. (Oxford, New York, Toronto, Sydney, Paris, Frankfurt: Pergamon Press, 1979.) $20.00 £9.00.

SCHMALZL, F. and HELLRIEGEL, K. P. (eds) Preleukemia. Pp. 194. ISBN 3-540-09798-1. (Springer: Berlin, Heidelberg and New York, 1979.) DM 48.00; US $26.90 Pbk.

SCHULSTER, D. and LEVITZKI, A. (eds) Cellular Receptors for Hormones and Neurotransmitters. Pp. 412. ISBN 0-471-27682-0 (John Wiley & Sons: Chichester, 1980.) £25.00.

SHANKS, R. G. (ed.) Methods in Clinical Pharmacology-Cardiovascular System. Pp. 106. ISBN-0333-28282-5. (Basingstoke: Macmillan Publishers Ltd. Scientific & Medical Division, 1980.) Hardback £10.00.

SPAWLS, S. Sun, Sand and Snakes. Pp. 254. ISBN-0-00-262760-4. (London: Collins and Harvil Press, 1980.) £6.95.

VOGEL, de E. F. Seedlings of Dicotyledons. Pp. 465. ISBN 90-220-0696-4 (Centre for Agricultural Publishing and Documentation: The Netherlands, 1980.) Dfl. 150.00.

WELLS, N. Medicines: 50 years of Progress 1930-1980. Pp. 60. (Office of Health Economics, Free of Charge at the Economics of Health Office, 1980.)

WOOLEY, D. E. and EVANSON, J. M. (eds) Collagenase in Normal and Pathological Connective Tissues. Pp. 292. ISBN 0-471-27668-5 (Wiley Interscience: Chichester, 1980.) £16.00.

WUTTKE, W., WEINDLE, A., VOIGT, K. H. AND DRIES, R. R. Brain and Pituitary Peptides: Ferring Symposium on Brain and Pituitary Peptides Munich 1979. Pp. vii + 240. ISBN 3-8055-0165-X. (S. Karger: Basel, New York and Munchen, 1980.)

Applied Biological Sciences

ALFIN-SLATER, R. B. and KRICHEVSKY, D. (eds) Human Nutrition: Nutrition and the Adult Macronutrients 3A. Pp. 290, ISBN 0-306-40287-4 (Plenum: New York and London, 1980.)

ARIENS, E. J. (ed.) Drug Design. Vol IX. Pp. 355. ISBN 0-12-060309-8. (Academic: New York and London, 1980.) $39.50.

BACH-y-RITA, P. (ed.) Recovery of function: Theoretical considerations for brain injury rehabilitation. Pp. 278. ISBN 3-456-890836-4. (Hans Hurer Publisher: Berne, Stuttgart and Vienna, 1980.) Fr. 34.00; DM 37.00 pbk.

BLOOR, C. M. and LIEBOW, A. A. The Pulmonary and Bronchial Circulations in Congenital Heart Disease. Topics in Cardiovascular Disease. Pp. 279. ISBN 0-306-40383-8. (Plenum: New York, 1980.) $32.50.

COHEN, E.N. Anaesthetic Exposure in the Workplace. Pp. 197. ISBN 0-85200-348-X. (MTP: Lancaster, UK, 1980.) £11.75.

COMMONWEALTH BUREAU OF NUTRITION. Anorexia nervosa. Annoted Biolography (1973-79) Pp. i + 179 ISBN 0-141-5441 (CNS, Bucksburn, Aberdeen, 1980.) £7.50.

COMMONWEALTH BUREAU OF NUTRITION: Aquaculture. Annotated Bibliography (1973-79) Pp. i + 179 ISBN 0-141-5441 (CNS, Bucksburn, Aberdeen, 1980.) £7.50.

DALTON, C. D. An Introduction to Practical Animal Breeding. Pp. 162. ISBN 0-246-11351-0. (Granda Publishing: St. Albans, 1980.) £4.95 Pbk.

EDDY, D.M. Screening for Cancer; Theory, Analysis, and Design. Pp. 308. ISBN 0-13-796789-6. (Prentice-Hall: 1980.) £19.45.

GETZ, M. E. Getz, Paper & Thin Layer Chromatographic Analysis of Environmental Toxicants. Pp. 164. ISBN 0-85501-451-2. (Heyden: London, Philadelphia and Rheine, 1980.) £7.30; $16.50; DM 34.50.

GNANAM, A., KRISHNASWAMY, S. and KAHN, J. S. Biological Applications of Solar Energy: Proceedings of the International Symposium on. Pp. 214. (Macmillan India: Madras, 1980.) Rs. 75.00.

KLEIN, G. (ed.) Viral Oncology. Pp. 860. ISBN 0-89004-390-6. (Raven: New York, 1980.) $85.00.

MANCINI, M. et al. Medical Complications of Obesity; Proceedings of the Serona Symposia, Vol. 26. Pp. 406. ISBN 0-12467150-0. (Academic: New York and London, 1980.) $43.50; £18.80.

NEEDHAM, J. R. Handbook of Microbiological Investigations for Laboratory Animal Health. Pp. xviii + 174. ISBN 0-12-515950-1. (Academic: New York and London, 1980.) £9.80 $21.00.

OLIVER, J. S. Forensic Toxicology: Proceedings of the European Meeting of the International Association of Forensic Toxicologists. Pp. 320. ISBN 0-7099-0362-6 (Croom Helm Ltd: London, 1980.) £14.50.

OPENSHAW, K. Cost and Financial Accounting in Forestry: Practical Manual Pp. 188. ISBN 0-08-021455-X. (Pergamon: Oxford and New York, 1980.) $13.75; £6.25 Pbk $27.50; £12.50 Board.

PLAATS, G. F. van der. Medical X-Ray Techniques in Diagnostic Radiology. Fourth Edition. Pp. 463. ISBN 0-333-26415-0 (Macmillan: London, 1980.) £35.00.

READ, S. E. and ZABRISKIE, J. B. Streptococal Diseases and the Immune Response. Pp. 830. ISBN 0-12-583880-8. (Academic: New York and London, 1980.) $45.00.

SHALHEVET, J. et al. (ed.) Irrigation of Field and Orchard Crops under simi-arid conditions. Revised edition. Pp. 110 ISBN 0-08-025511-6. (International Irrigation Information Center: Pergamon Press: Oxford and New York, 1980.) $9.00; £4.50.

SOPPER, W.E. and KERR, S.N. (eds) Utilization of Municipal Sewage Effluent and Sludge on Forest and Disturbed Land. Pp. 537. ISBN 271-00205-0. (Pennsylvania State University Press; 1980.) £12.

TURUSOV, V. S. (Editor-in-Chief) Pathology of Tumours in Laboratory Animals. Vol II. Tumours in the Mouse. Pp. 661. ISBN 92-832-1123-5. (World Health Organisation: International Agency for Research on Cancer, 1980.) Sw.Fr 100.00 US $60.00.

WAYNFORTH, H. B. Experiment and Surgical Technique in the Rat. Pp. 265. ISBN 0-12-738850-8. (Academic: London, 1980.) £11.80; £27.50.

WERTELECKI, W. and PLATO, C. C. (eds) Dermatoglyphics — Fifty Years Later. Pp. 800. ISBN 0-8451-1031-4. (Alan R. Liss: New York, 1980.) $76.00.

Psychology

BUTTERWORTH, B. (ed.) Language Production. Vol. 1. Speech and Talk. Pp. x + 478. (Academic: London and New York, 1980.) $64.50; £28.00.

General

ALLEN, M. Falconry in Arabia. Pp. 143. ISBN-0-85613-013-3. (London: Orbis Publishing, 1980.) £15.00.

BOOTH, D., RODIN, J. and MOGENSON, G. Appetite: The Journal for Research on Intake, its Control and its Consequences. Vol. 1. No. 1. March 1980. Pp.102. ISBN 0195-6663 (Academic: London and New York, 980.) £27.00 Pbk.

CAFFERTY, B. and HOOPER, D. A complete Defence to 1P-K4. A Study of Petroff's Defence, Second edition. Pergamon Chess Series. Pp. xiv + 149. ISBN-0-08-024089-5 hardback ISBN-0-08-024088-7 flexi. (Oxford, New York, Toronto, Sydney, Paris, Frankfurt: Pergamon Press, 1979.) $14.00 £6.50 hardback $8.00 £3.50. flexi.

COHEN, M. L., RONEN, N. and STEPAN, J. Law and Science: Selected Bibliography. Pp. 155. ISBN 0-262-03073-X. (MIT: Cambridge, Massachusetts, 1980.) $15.00.

COLINVAUX, P. Why Big Fierce Animals Are Rare. How the Natural World Works. Pp. x + 224. ISBN-0-04-574015-1. (London, Boston, Sydney: George Allen & Unwin Ltd., 1980.) £7.95.

DAVIDGE, R. W. Mechanical behaviour of ceramics. Pp. viii + 165. ISBN-0-521-21915-9 hardback IBSN-0-521-29309-X pbk. (Cambridge, London, New York, New Rochelle, Melbourne, Sydney: Cambridge University Press, 1980.) £3.95 pbk.

deRIVERO, O. B. New Economic Order and International Development Law. Pp. xvi + 141. ISBN-0-08-024706-7. (Oxford, New York, Toronto, Sydney, Paris, Frankfurt: Pergamon Press, 1980.)

DUNN, E.K. and BLACK, D. (eds) The Twelve Months of the Year. Pb. 120. ISBN-0-7153-7918-6 hardback ISBN-0-7153-7919-4 paperback. (Newton Abbot: David & Charles, 1980.) £3.95 paperback £5.95, hardback.

PRENEY, J. R. and NICOLSON, A. J. (eds) Sulfur in Australia. Pp. 268. ISBN-085847-059-4. (Australian Academy of Science: Canberra, 1980.) £26.50.

GOSSELIN, C. and WILSON, G. Sexual Variations: Fetishism, Transvestism and Sadomasochism. Pp. 169. ISBN-0-571-11538-1. (Faber & Faber: London, 1980.) £7.50.

GRANT, J. (ed.) The Book of TIme. Pp. 320. ISBN-0-7153-7764-7. (Newton Abbot: David & Charles, 1980. £10.50.

GRIFFITHS, F. and POLANYX, J. C. (eds) A Pugwash Symposium. Pp. xiii + 193. ISBN-0-8020-2356-8 hardback. ISBN-0-8020-6389-6 hardback.

GRIFFITHS, F. and POLANYI, J. C. (eds) The Dangers of Nuclear War. A Pugwash Symposium. Pp. xiii + 193. ISBN-0-8020-2356-7 hardback. ISBN-0-8020-6389-6 paperback. (Toronto, Buffalo, London: University of Toronto Press, 1980.) $15.00 hardback $5.95 paperback.

HAKEN, H. (ed.) Pattern Formation by Dynamic Systems and Pattern Recognition. Proceedings of the International Symposium on Synergetics at Schlob Elmau, Bavaria, Springer Series in Synergetics Volume 5. Pp. viii + 305. ISBN-3-540-09770-8. (Berlin, Heidelberg, New York: Springer-Verlag, 1979.) DM68 approx. US $37.40.

HAYNES, R. D. H. G. Wells: Discoverer of the Future. The Influence of Science on his Thought. Pp. xi + 283. ISBN-0-333-27186-6. (London and Basingstoke: The Macmillan Press, Ltd., 1980.) £12.00.

HEIM, A. Barking up the right Tree or Intelligence and Personality in Dogs. Pp. 208. ISBN-0-1214-9. (London: Pelham Books, 1980.) £6.50.

KRASNEGOR, N. A. (ed.) Behavioural Analysis and Treatment of Substance Abuse. Pp. 256. Stock No. 017-024-00939-3. (Department of Health, Education, and Welfare: National Institute on Drug Abuse Research 25 Monograph Series, Washington, 1980.) £4.50.

KRASNEGOR, N. A. (ed.) The Behavioural Aspects of Smoking. NIDA Research Mongraph Series 26. Pp. 192. Stock No. 017-024-009474. (Department of Health, Education and Welfare: Government Printing Office, Washington, 1980.) $12.00.

LUEPKE, N.-P. (ed.) Monitoring Environmental Materials and Specimen Banking. Proceedings of the International Workshop, Berlin (West) October, 1978. Pp. xiii + 391. ISBN-90-247-2303-5. (The Hague: Martinus Nijhoff, 1980.) Guilders 150.

MANUEL, F. E. A Portrait of Isaac Newton. Pp. 478. ISBN-0-584-95357-7. (Frederick Muller: London, 1980.) £11.75.

NARNHAM, P. Fantastic Invasion: Dispatches from Contemporary Africa. Pp. 271. ISBN-01-636-5764. (Jonathan Cape: London, 1980.) £6.50.

NUKI, G. (ed.) The Aetiopathogenesis of Osteoarthrosis. Pp. x + 212. ISBN-0-272-79434-1. (Tunbridge Wells: Pitman Medical Limited, 1980.) £15.00.

PAARLBERG, D. Farm and Food Policy: Issues of the 80s. Pp. 338. ISBN-0-8032-3656-5. (University of Nebraska Press: Lincoln, Nebraska, 1980.) £9.90.

SANDBANK, C. P. (ed.) Optical Fibre: Communication Systems. Pp. 347. ISBN-0-471-27667-7. (John Wiley & Sons: Chichester and New York, 1980.) £17.50.

SCHUTTE, H. R. Wirkungsmechanismen von Herbiziden und synthetischen Wachstumsregulatoren. Pp. 381. ISBN-533-286-9. (VEB Gustav Fischer Verlag, Jena E. Germany, 1980.)

SCHWARZBACH, M. Alfred Wegener und die Drift der Kontinente. Pp. 160. ISBN-3-8047-0582-0. (Stuttgart: Wissenschaftliche Verlagsgesellschaft mbH, 1980.) DM29.

SHAW, T. L. (ed.) An Environmental Appraisal of Tidal Power Stations: with particular reference to the Severn barrage. Pp. 220. ISBN-0-273-08463-1. (Pitman: London, 1980.) £9.75.

SIPRI: Stockholm International Peace Research Institute. Pp. 201. ISBN-0-85066-199-4. (Taylor & Francis: London, 1980.) £6.50; US $19.50 pbk.

STEVENSON, J. P. Trout Farming Manual. Pp. 183. ISBN-0-85238-102-6. (Fishing News Books: Farnham, Surrey, 1980.) £9.75 + 95p p&p.

STOCKHOLM INTERNATIONAL PEACE RESEARCH INSTITUTE. Nuclear Energy and Nuclear Weapon Proliferation. Pp. xxv + 462. ISBN-0-85066-184-6. (London: Taylor & Francis Ltd., 1979.) £14.00.

SZERI, A.Z. (ed.) Tribology: Friction, Lubrication, and Wear. Pp. 584. ISBN0-07-, 062663-4. (Hemisphere Publishing Corp: New York, 1980.) $32.00.

TURNER, E. M. (ed.) Kapchigai Defile: The Journal of Paul Nazaroff. Pp. 127. ISBN-0-584-10463-4. (Frederick Muller: London, 1980.) £7.95.

UNITED NATIONS ECONOMIC COMMISSION FOR EUROPE. The Gas Situation in the ECE Region Around the Year 1990. Proceedings of an International Symposium of the Committee on Gas of the Economic Commission for Europe, France, 1978. Pp. xviii + 373. ISBN-0-08-024465-3. (Pergamon: Oxford and New York, 1979.) $60.00, £27.00.

UNITED NATIONS ENVIRONMENT PROGRAMME. Directory of Institutions and Individuals Active in Environmentally-Sound and Appropriate Technologies. UNEP Reference Series. Pp. xviii + 152. ISBN-0-08-025658-9. $20.00, £9.00.

FREIMAN, G. It Seems I Am a Jew. A Samizdat Essay. Pp. 96. ISBN 0-8093-0962-9. (Southern Illinois University Press. Feffer and Simons: 1980.) Np.

KATSENELINBOIGEN, A. Soviet Economic Thought and Political Power in the USSR. Pergamon Policy Studies on the Soviet Union and Eastern Europe. Pp. 213. ISBN 0-08-022467-9. (Pergamon: 1980.) £12.50.

SLAPPEY, S.G. (ed.) The Future of Business—Annual Review 1980/81. Pergamon Policy Studies on U.S. and International Business. Pp. 113. Hbk ISBN 0-08-025585-X; Flexi ISBN 0-08-025584-1. (Pergamon: 1980.) Hbk £7.50; flexi £2.70.

STOCKHOLM INTERNATIONAL PEACE RESEARCH INSTITUTE. World Armaments and Disarmament. SIPRI Yearbook 1980. Pp. 514. ISBN 0-85066-201-X. (Taylor & Francis, 1980.) £19.

TASCA, D. (ed.) U.S.–Japanese Economic Relations; Cooperation, Competition, and Confrontation. Pergamon Policy Studies on U.S. and International Business. Pp. 135. ISBN 0-08-025129-3. (Pergamon: 1980.) £8.25.

nature

24 July 1980

Should academics make money outside?

When, and under what circumstances, is it proper that academics should be involved with commercial enterprises? This question — always teasing — has been made more urgent by developments in the past few months which have involved academic scientists in attempts commercially to exploit the new techniques of genetic manipulation. Those concerned are likely to be by this stage keenly aware that many of their academic colleagues are deeply resentful of some of the most publicized developments. Harsh things are said over normally genteel coffee tables. There is a danger that the atmosphere of academic research will be soured, the reputations of academic institutions damaged and, perhaps worse still, the progress of research in this important field impeded. What is to be done?

The events which have made this question an important issue are memorable enough. It is now more than a year since a group of molecular biologists at the University of California, linked both by their common scientific interests and by their membership of a company called Genetech, announced that they were in a position to develop the manufacture of insulin (and some other peptide hormones) by means of genetically manipulated strains of *E. coli*. The announcement, widely acclaimed as an important development, also prompted complaints that those concerned had fallen into unacademic habits of not talking as freely to their academic colleagues as would normally have been the case. Since then, the number of prominent academic molecular biologists caught up in extramural commercial activities has increased substantially, as has the volume of somewhat embittered complaint at what is going on. The activities of the company known as Biogen, based in Switzerland and organized principally by Professor Charles Weissmann of the University of Zurich, usually excite most comment, partly because of the distinction of the academic scientists linked with it, partly because of the company's willingness to talk about itself and partly because of the somewhat breathless press conference on the prospects of manufacturing interferon with genetically altered *E. coli* held improbably at the Waldorf–Astoria Hotel in Manhattan earlier this year. Colleagues of those involved have now taken to complaining that such events are likely to undermine the integrity of academic life, to cloud the supposed single-mindedness of academic researchers in the pursuit of what might be called the truth and to create restraints on the normally free flow of information within the academic community.

Everybody will agree that the issues raised by these developments are complicated and are unlikely to be resolved quickly. Several sets of conflicting considerations intereact. Perhaps the most serious impediment to a proper resolution of these difficulties is that, so far at least, too little has been done, by commercially inclined academics or by their critics, to define the issues which perplex them. No list of these could at this stage be complete, although a few bones of contention prominently stand out. It goes without saying that the issues, whatever they are, are most difficult when academics rather than, say, public employees are concerned, but this is not to say that important conflicts of interest do not arise when, for example, employees of the National Institutes of Health in the United States, or of the research councils in the United Kingdom, find themselves inclined to cash in on their expertise.

Universities are the chief testing grounds for the underlying principles because universities are proud to call themselves self-governing communities of scholars. Even if, in practice, many universities fall short of this ideal, seeming to be uneasy alliances of warring factions (departments) or grudgingly subject to the inclinations of their administrators, it is a mark of grace that the ideal is so often held to be desirable. Does it necessarily follow that extramural commercial interests by some members of such a community are incompatible with the ideals they and their colleagues hold? The answer is complicated by the way in which, especially in recent years, many governments have urged that universities should contribute more directly to the economies which ultimately support them, and by the way in which universities themselves, for the best of educational reasons, have sought to attract teachers with practical and even continuing experience of industry. It is also important that the problem is by no means a creation of the past few years. In what sense, if any, does a molecular biologist with an interest in the success of some commercial genetic manipulation enterprise differ from, say, an academic who happens to be a successful novelist or textbook author, or from one who spends a substantial part of his time consulting for an engineering company or a drug house?

The simplest conclusion, a necessary but not sufficient condition of propriety, is that an academic should carry out the duties required of him by his contract of employment. The difficulty here is that while it is relatively easy for heads of departments to assess a person's diligence (though not his flair) in teaching, the standard requirement that he or she should also be active in research is much harder to evaluate. This, no doubt, is why many universities now require that academics should spend no more than one day a week on outside work. It is a rule of thumb which does at least ensure that an academic with outside interests has some time in which to pursue research. (In the United States, the growing zeal of those responsible for the public audit of research grant expenditure may turn out to be a tighter restriction.) Such requirements, of course, cannot ensure either the quality or the single-mindedness of a person's research, but it is a fair guess that those most able to contribute to the success of commercial enterprises outside their universities are likely also to be among the most valuable teachers and the most creative researchers. In the present wave of grumbling about the activities of molecular biologists, allegations of the neglect of simple academic duties are conspicuous by their absence.

A much more serious charge is that external commercial interests create intolerable conflicts of interest within academic laboratories. For how, if academic A is linked with some company, can academic B talk freely, over coffee or at some departmental seminar, of his own work in a related field? The difficulty is real, and those who have complained at recent developments are entirely right to say that too much of this could easily endanger not merely the social climate but the creativity of university laboratories. It is partly for this reason that many universities (but, shamefully, not all) require that academics should declare their outside interests to the heads of their departments. That is the very least that they should ask. For one thing, even though the head of a department may be apprised of his colleagues' outside interests, other researchers appear often to be unaware of what their colleagues are about. In these democratic days, is there not at least a case for asking that the disclosure of people's outside interests should be common knowledge within each closely-knit group of colleagues? And would it not be seemly and also important that heads of departments should themselves be required to spill the beans to those who work for them? That disclosure on this limited scale might be embarrassing to the academics concerned, or that

0028-0836/80/300319-02$01.00

students might make trouble if they knew what their teachers were up to on the side, is unfortunate but unavoidable. Yet this, too, is merely a necessary but not a sufficient condition of seemliness.

The third and perhaps the most intractable cause of present discontent is, bluntly, that many academics are resentful of the money their colleagues stand to make from outside involvement. Even if, as seems probable, biotechnology turns out to be less like a gold mine than some people have been supposing, great disparities of income have arisen in the past and will no doubt arise in the years ahead. The problem is to decide what is seemly. If an academic should write a successful novel, his colleagues may envy him but they have no more right to complain than if he were to win a fortune in some lottery. If, on the other hand, his extramural rewards are dependent on some special knowledge derived from his position within the group of academics to which he belongs, his colleagues are rightly resentful. If his profit should in part derive from the use of university facilities, laboratories or computers for example, wider issues arise. In such circumstances, indeed, it is only equitable that a person's profit should be shared with the institution to which he belongs. A neat way of doing this emerges from the constitution of the French company *Transgène* (see *Nature*, 10 July) where the University of Strasbourg and the Pasteur Institute will each hold a small percentage of the shares.

There are many, no doubt, who will argue that even these three conditions — diligence, open disclosure and profit-sharing where special knowledge is involved — are insufficient. Others will be attracted by more ambitious if more cumbersome ways of enabling academics to contribute to industrial development — companies or corporations set up by universities, for example. Universities differ sufficiently among themselves for the outcome of full-blooded debate on these issues to vary from place to place. There would be no harm in that. The danger lies in the virtual absence of debate. Academics grumble among themselves, but have done very little to ensure that their grumbles are openly discussed. While that reticence persists, the capacity of universities to contribute to industrial development will be impaired, while their reputation as self-governing communities of scholars will be tarnished.

Reviving (in the US) an old British recipe

The United States Congress seems bent on an exercise that resembles the re-invention of the wheel. Last week (see *Nature*, 17 July) it became known that the Department of Commerce is working on plans for the setting up of a number of "generic technology" centres and that both the Senate and the House of Representatives are ready to approve whatever scheme comes forward. Generic technology is the ugly name for what appears to be basic research related to some branch of industrial technology. Both the Department of Commerce and the Congress have it in mind that public funds should be used to launch a number of these centres, but that the industries most likely to benefit should provide an increasing proportion of the budgets of the centres, allowing the federal budget to be used for other purposes after the five years or so. Opinions, it is reported, are divided on the question whether universities should be given an important role in the management of the new centres. The antecedents of this proposal are as respectable as anybody could — the report of the level-headed Advisory Panel on Research and Development that contributed to last year's grand review of federal policy.

In reality, the new proposal in the United States is a neat amalgam of two kinds of institutions already tried in Britain. Is it too much to ask that Congress might profit from a study of the mixed success of the British experiments? The two kinds of enterprises concerned are the industrial research associations, originally recommended in the United Kingdom while the First World War was under way, and which have been over a switchback of ups and downs since their creation, and the ecology centres set up by Mr Anthony Wedgwood Benn (nor Mr Tony Benn) during his spell in the then Ministry of Technology in the late 1960s. The research associations resemble the American centres now proposed in that they were originally financed in partnership between central government and the group of industrial companies most likely to benefit. The more recently created technology centres were intended to be concerned with rather more specific problems than those which provided bread and butter for the research associations, but it was intended from the start that they would be based in universities. Again (for this is the way that governments think) the intention was that industry should take over financial responsibility for these centres in the course of time.

How well have these parallel devices worked? Most probably it is unfair to judge their success from successive British governments' opinions of them, but the research associations have lived through a succession of unpleasant ups and downs. When the wind was blowing in their direction, in the late 1950s and early 1960s, public policy stemmed from the conviction that some of the ills of British industry might be cured if only there were a mechanism for making sure that basic research germane to important sectors of manufacturing industry was effectively undertaken. During this period, public funds were used on a modest but impressive scale and new research associations were from time to time created. They fell from favour for a variety of reasons. Some of them turned out to be second-rate. Some of them turned out to be more interested in the provision of market research than basic research. Others were undermined by the unwillingness of successful industrial subscribers with their own programmes of research and development to allow research associations more than a peripheral role. Central government, having agreed in the 1950s that the research associations should be a continuing charge on public funds, eventually changed its mind — and then found the process of making the research associations stand on their own feet more painful than it had imagined. The end result, however, is that some thirty substantial and apparently valuable research associations have survived from this half-century of initiative.

The British government's attempts to set up technology centres in universities have, by comparison, left hardly any trace. To be fair, the plan was hardly given a fair trial. Mr Anthony Wedgwood Benn (as he then was) swept into the Ministry of Technology in 1966 with a sheaf of plans for stimulating industrial research. To begin with, half a dozen centres of tribology (lubrication etc.) were set up, but plans to create a number of more broadly based centres were frustrated by the defeat of the Labour government in 1970. For what it is worth, some of these centres survive, making their way in the world with the help of funds from the University Grants Committee, the Department of Industry and fees for contract research. As such, they do not greatly differ from the industrially orientated centres for research and development that universities and polytechniques have set up on their own initiative.

What lessons should the United States Congress and the Department of Commerce draw from this experience? The first need is that they should know that it exists. Most probably, they should also reconcile themselves to providing support of some kind for the centres they plan to set up for rather longer than is now apparently foreseen. Industrial companies will pay up only when they know from experience that a new centre is doing a useful job. The successful research associations in Britain are those which have served industries (such as the water industry) where the potential members have little tradition of basic research. British experience throws little light on the usefulness of links with universities, but Congress might push in that direction.

0028-0836/80/300320-01$01.00

British biotechnology boat comes home

The plan to set up a British biotechnology company, much talked of recently (*Nature*, 5 June) came into the open this week. A company has been set up with an initial capital of £12 million, between 40 and 50 per cent of which will be provided by the National Enterprise Board. It is hoped that it can be registered as Celltech, but the formalities had not been completed on Monday.

The managing director will be Mr Gerard Fairtlough, until two years ago joint managing director of Shell UK Limited with responsibility for the £300 million turnover of the petrochemical part of the enterprise, and who has since then been a division head at the NEB.

Mr Fairtlough said this week that the NEB had been looking at the opportunities in biotechnology since the early autumn of last year, when it commissioned a study of the opportunities, apparently from Professor J D Watson, director of the Cold Spring Harbor Laboratory in the United States. At that stage the NEB had not known that Sir Alf Spinks was working on a report on biotechnology for the Advisory Council on Applied Research and Development (ACARD).

The new company will be jointly owned by the NEB (the largest shareholder) and four commercial partners — the Prudential Assurance Company Limited, the Midland Bank Limited, Finance for Industry and British and Commonwealth Shipping Limited. It is intended that roughly a third of the board of the company should be molecular biologists.

The new company plans to recruit between 50 and 75 people over the next two years. It will not build a laboratory of its own but will use existing premises. The location has not been finally decided, but may well be in Cambridge.

The company has taken trouble to come to good terms with the Medical Research Council, and claims that it has a "framework for collaboration" that will allow it to place contracts with MRC laboratories and to have access to MRC "ideas". The embryo company has also been talking to two other institutions, not openly identified but probably including the Imperial Cancer Research Fund.

Mr Fairtlough says that particular trouble has been taken to study the ways in which molecular biologists might be involved with the new company. Appreciating that some may wish to make money out of their skill, and that others are offended by the notion, it is planned that the company will make commercial arrangements only with the institutions to which people belong, leaving them to decide how individuals should be paid.

At the outset, the new company will make and sell monoclonal antibodies, but will also explore longer-term projects. It is laid down that the company should make money out of something within two or three years. The phrase "lean and hungry" is much used. The first opportunities will, it is said, be in the field of diagnostic tests.

At the same time, the NEB is anxious that the company should be financially strong enough to tackle "big things". The company will not always seek to market its own products to their ultimate users, but will be content with selling licences for manufacture by others where that seems the best course to follow.

The board of the NEB itself is said to be pleased at having launched its first "constructive project" — since the previous board resigned *en bloc* last November, the board has been primarily concerned with housekeeping. The fact that the NEB rather than the National Research Development Corporation has become the chief public sponsor of the new biotechnology company is not only a sign of its skill but a mark of the disfavour in which the NRDC finds itself with academic scientists in general and those working for the Medical Research Council in particular.

On the question why the present British government may have sanctioned this modest investment, Mr Fairtlough said that the involvement of private capital had been a necessary condition, given "the way our guidelines have been evolving". He said that the new company would succeed if it could show that it had a "distinctive competence" and if it combined a hard-headed appraisal of the market with a capacity to make better use of people's talents. He considers that Celltech will be able to establish better relations with academic scientists than companies such as Genetech and Biogen.

Supreme Court stirs up more fear

Washington

Recombinant DNA research is moving from the frying pan to the fire. Last month's decision by the US Supreme Court to permit the patenting of live micro-organisms has started a new round of public debate about the conditions under which recombinant DNA research should be carried out.

When the National Institutes of Health formulated safety guidelines in 1976, the main concern was the potential health hazard. Attention is now concentrated on the rights of ownership and control over natural processes.

The Supreme Court ruling has crystallized various areas of concern. Several scientists, for example, have expressed their fears that the decision to allow a patent on a strain of *Pseudomonas* bacterium, developed by research workers with the General Electric Company by inserting foreign plasmids, could create barriers to the free flow of research ideas. Others disagree, claiming that the requirement to publish details of a patent ensures that the information will be publicly available. And the American Society for Microbiology is sponsoring a meeting in Washington this week to explore such areas of disagreement.

The ASM meeting will debate "the proper role of the patent laws in genetic research and development". Questions to be discussed include that of whether the law should be modified to preclude exclusivity or monopoly over a microorganism; and,more generally, whether the decision is consistent with the objectives of the microbiological and biomedical scientific communities.

Professor Emilio Schaechter, chairman of the committee organizing the ASM meeting, highlights one particular area needing attention, that of how research using recombinant DNA techniques should be regulated in the private sector. Although NIH operate a system of voluntary compliance with their safety guidelines, they have no desire to act as a full-blown regulatory agency. NIH are considering delegating most safety decisions to local biohazard committees, and there is concern that the regulatory apparatus may be inadequate.

The Department of Labor's Occupational Safety and Health Administration is already taking steps to define its own role, including setting up a committee to outline voluntary control of the exposure of workers to processes involving recombinant DNA techniques.

Both the closeness of the Supreme Court decision — a five to four majority — and the justices' opinions on both sides provide an open invitation to Congress to look more closely at the patenting question. The four minority justices wrote "it is the role of Congress, not of the court, to broaden or narrow the reach of the patent laws". For the majority, Chief Justice Warren Burger admitted that the court's decision had been reached on a narrow interpretation of present patent law and added that Congress was free to amend the law to exclude from patent protection organisms produced by genetic engineering, or to "craft a statute specifically designed for such living things".

Pope John Paul II warned in an address to Unesco that genetic manipulation might be applied to "ends contradictory to those of humanity". Four days after the Supreme Court's decision was announced, religious groups representing Protestant, Catholic and Jewish viewpoints issued a statement which said that the questions raised by genetic engineering — who should control it, who would benefit and

0028-0836/80/300321-02$01.00

who might bear adverse consequences — dealt with "the fundamental nature of human life".

Finally, the whole issue may come under review by the newly established President's Commission for the Study of Ethical Problems in Medicine and Biomedical and Behavioural Research. Following an approach from the National Council of Churches, the commission is exploring whether any major reviews of the ethical implications of genetic manipulation are already in progress. If not, the subject might be selected for study by the commission when it meets in September.

David Dickson

Biotechnology

European setback

Brussels

THE European Commission's programme of research in biotechnology was seriously set back last week, when a meeting of CREST failed to endorse the programme or even to agree on a compromise. Over the past four years, the commission has developed a plan for spending £28 million over the next five years (half of it to be supplied by national governments) on a number of projects.

France was the chief stumbling block at last week's meeting of CREST, the committee which advises the European Community on research and development policy. French representatives argued for an alternative programme of fellowships to help train potential genetic engineers. The meeting of CREST was the last at which the biotechnology programme will be considered — a decision on what to do now rests with the Council of Ministers of the European Community, on which France will be able to exercise its veto.

According to reliable national sources, the council will have to choose between the commission's original plan, the French proposal and a compromise between the two supported by the United Kingdom. That would entail spending a total of £18 million over only four years and the elimination of some of the research projects proposed by the commission.

The CREST decision has caused much ill-feeling among European states. West German delegates at the meeting last week supported the French position, but more flexibly. One angry Dutch observer said last week that the smaller European states would feel misled by the larger states. An Italian offical said that France had opposed the commission's plan because it wished to keep all projects with "pace" to itself.

The difficulty now is that the Council of Ministers, when considering the biotechnology programme, will be advised by an *ad hoc* scientific subcommittee of COREPER — the committee of community ambassadors in Brussels, which is well used to taking political considerations into account. It could, for example, think of trading an agreement on the biotechnology programme for an agreement on sheepmeat.

There is nevertheless a chance that a compromise proposal may be adopted, if Germany can be persuaded to agree. The compromise would involve restricting the research projects to:

- the development of new reactors involving immobilized multi-enzyme systems;
- the transfer of genes to *Escherichia coli, Saccharomyces cerevisiae,* and other organisms;
- gene transfer in microorganisms and plants important important to agriculture;
- safety studies.

The compromise also emphasizes mobility of manpower, in line with the French proposals, by devoting 30 per cent of the budget to training of foreign nationals in national laboratories, training of industrial scientists in university laboratories, and short courses in biohazards and safety measures. However, the French proposal does not mention safety questions, which must be satisfactorily answered if public confidence in the emerging technology is to be maintained.

In Britain, the possible demise of the European initiative is seen more as a danger signal than as an unmitigated disaster. Dr Duncan Davies, Chief Scientist at the Department of Industry, and chairman of the Cabinet Official Committee on Biotechnology which has just produced a draft White Paper on biotechnology in Britain, told the House of Lords recently that the commission programme — as it would affect the UK — would amount to only 10 per cent of the probable British effort over the next five years.

At Imperial Chemical Industries Limited, which probably has the most advanced industrial biotechnical team in Britain, the loss of the European programme is seen as less sad for ICI than for "UK Limited". Things could be done on the European scale, said Dr Bernard Langley of ICI's Policy Group last week, "which would help everyone". Coordinating safety standards and experimentation and developing new host-vector systems were examples.

In academic circles, where the UK Spinks report on biotechnology recommended an immediate injection of 20 new posts, and cash, the loss of commission money is taken more seriously. "Unless we have more posts soon, we are in deep trouble" said one leading biotechnologist last week. "And I see no sign at all of the Department of Education and Science taking an intelligent interest in the issue." The loss of the European programme could be the end.

The draft version of the White Paper currently in circulation also may be little consolation to Britain's biotechnologists. According to one comment, "it offers everything short of real help".

Robert Walgate

Yugoslav academics

No liberalization

At least for academics and scientists in Yugoslavia, there seems to be little sign of the liberalization expected to follow Tito's death.

Ivan Supek, a leading Yugoslav nuclear physicist and an active participant in the Pugwash movement, has just published in Britain a defence of his view that scientific research must be based on ethical principals, and of his resolute opposition to nuclear weapons. His views, he claims, have been consistently misrepresented by the official Communist press, which treats him, at best, as some kind of Don Quixote.

Supek, who is now head of the Institute of the History and Philosophy of Science in Zagreb, was formerly in charge of the Rudjer Boscovic Institute of Theoretical Physics in Zagreb. While working there, he watched with increasing alarm the development of a nuclear institute on the outskirts of Belgrade where, he suspected, preparations were being made for the development of nuclear weapons.

His own anti-nuclear campaign of the 1960s was, he says, only one aspect of a growing discontent among intellectuals and scientists, who felt their status had been devalued by the Party in the name of the working class. The University of Zagreb's 300th anniversary in 1969 was seized on by the academics as a unique opportunity to redress the balance.

The appearance of Supek's apologia coincides with an appeal to the world academic community by seven professors from the University of Belgrade for support in their campaign against the latest revision of the Serbian law on universities.

These lecturers were closely associated with the philosophical journal *Praxis*, founded in the mid-1960s as the organ of the Croatian Society for Philosophy. Originally in the hands of Zagreb academics who took a generally social democratic line, it gradually became associated with the more liberal-marxist Belgrade philosophers. Finally, it was closed in 1975, and eight lecturers were suspended. They were not allowed to teach, lecture or publish; they did, however, draw a reduced salary and could benefit from the free health service.

Their status will however be radically changed by the revision of Serbian law on universities, passed on 5 June. Under the previous law, (introduced in 1974) lecturers could be suspended if they "damaged social interests". Under the new law, they can be sacked after two years' suspension. Persons already suspended for more than two years will be sacked in six months' time. The seven lecturers still under suspension (one has since found another post) maintain that this law has been brought in specifically to deal with their case. They further state that it is unconstitutional, being against the

Yugoslav Federal Labour code in which the specified grounds for dismissal do not include the nebulous charge of "damaging social interests", and because it specifically excludes any right of appeal. Most seriously, they see it as a violation of the Universal Declaration of Human Rights and the Helsinki Final Act, both of which have been ratified by Yugoslavia. They conclude that such "arbitrary interference and discrimination constitutes not only an act of harassment but an act of imperilling the very conditions of existence of a scholar".

Vera Rich

Scientists' pay

UK rumpus

A decade of discontent among scientists in the British Civil Service will come to a head on 5 August, when the dispute about salaries for 1980 will go to arbitration. The most immediate issue to be settled is whether the Civil Service will accept the latest pay offer by the Civil Service Department (CSD). Underlying the dispute, in which the Institution of Professional Civil Servants has taken most of the weight, is whether existing methods for settling Civil Service pay should apply to scientists.

The chief humiliation in this year's pay offer is that some grades of the scientific Civil Service are to be offered no increase of salary. After a period in which the general level of salary increases in the United Kingdom has been running at something like 20 per cent, it is not surprising that passions have been roused.

Thus the salaries of those at the top of the Senior Principal Scientific Officer grade will, if the CSD proposal is unchanged by the arbitration award, remain unchanged between 1979 and 1980.

Mr William McCall, general secretary of the IPCS, has said in a circular to his members that the offer of 1980 salaries is "disgraceful". The offer, if it is upheld by arbitration, may have repercussions outside the Civil Service, and among the staffs of research councils in particular.

The pay of scientists in the British Civil Service has been a contentious issue since the early 1970s, but the professionals within the service appear to be divided in how they would like to see the present arrangements changed. The ICPS bases its complaints chiefly on the use of what is called "pay research" to determine public servants' salaries.

This procedure entails the search for groups of scientists carrying out comparable work in the private sector of British industry. Quite independently, the use of pay research for determining civil servants' pay has recently been criticized in the United Kingdom on the grounds that the comparisons are flattering to the Civil Service and in any case take no account of the value of index-linked pensions to which retired public servants are entitled.

The IPCS objects to pay research because of the element of circularity which, it says, is likely to be introduced into the comparison because the Civil Service is the largest employer of scientists on research and development in the United Kingdom. But it also says that for some categories of senior people, suitable comparisons with private industry do not exist.

Other members of the scientific Civil Service are, on the other hand, anxious that there should be a more radical revision of the arrangements for regulating both pay and career prospects for scientists in the Civil Service. One body of opinion holds that the pay of scientists in the Civil Service compares well with that of scientists in,

Long-standing pay dispute continues

The dispute between the Civil Service Department of the British government and the Institution of Professional Civil Servants, the principal union representative of government scientists, has been rumbling on for two years. Since the early 1970s, the institution has reluctantly agreed that the pay of some categories of scientists should be determined on the recommendations of the Pay Research Unit Board, which is responsible for comparing civil servants' salaries with those of comparable groups outside.

The institution's misgivings about "pay research" for fixing the salaries of scientists stems from its belief that the Civil Service, which is the "largest single employer" of scientists working in research and development, is also a major influence on outside salaries. It also holds that pay research does not provide for the practice within the Civil Service of allowing for the promotion of individuals on the grounds of merit and says that career patterns outside are, in any case, quite different from those within the service.

The notion that civil servants should be fairly treated compared with people doing comparable civil work has been a cornerstone of Civil Service salary determinations since the Priestley Commission reported in 1956. More recently, however, the Fulton Commission on the organization of the Civil Service in 1968 advocated two further principles — the barriers between the scientific and the administrative branches of the Civil Service should be broken down and salaries in the two branches should be linked. From 1968 until recently, the salary scales of Principal Scientific Officers and of Principals (in the administrative branch) have thus been identical.

The first breach in this principle came last year, when Principal Professional and Technical Officers (including engineers) in the Civil Service were awarded a salary increase which, although three per cent above the general increase, gave them salaries which were £729 less than those of Administrative Principals.

This year, scientists within the Civil Service come off even worse. The offer from the Civil Service Department on 26 June, based on the work of the Pay Research Unit, would have increased the salaries of all but the more senior scientists in the Civil Service by between 14.0 per cent and 25.3 per cent. Senior Principal Scientific Officers, of whom there are more than 700, were however offered no increase of salary, while it was proposed that four points should be added at the bottom of the salary scale to be occupied by future entrants.

Senior Scientific Officers and Principal Scientific Officers also fare badly, with increases at the top of the pay scales concerned of 9.1 per cent and 6.2 per cent respectively. More significantly, to many civil servants, the link with the salaries of Administrative Principals has been broken — under the terms of the new offer from the Civil Service Department, the salaries of Principal Scientific Officers would in future be nearly £2,000 less than those of Administrative Principals.

The basis for the offer apparently rests, at least where the PSO grade is concerned, on the observation by the Pay Research Unit that in many industrial companies scientists are paid less than engineers. This has been held to justify the differential between the salaries of the Principal grades for scientists and engineers.

One of the issues in dispute between the Institution of Professional Civil Servants and the Civil Service Department is that of whether pay research can apply to the salaries of the small numbers of people in the grades of Senior Principal Scientific Officer and above. The CSD is insisting that comparisons with outside industry are possible at least for the SPSO grade.

There is also a dispute about the applicability of the agreed arbitration procedure.

Maximum salaries offered for 1980

Grade	No. in service (1979)	Salary offer	Percentage increase
Senior Principal SO*	728	£15,748	Nil
Principal SO	2,458	£12,050	6.2
Senior SO	3,830	£9,500	9.1
Higher SO	4,194	£7,900	17.3
SO	2,982	£6,400	16.7
Assistant SO	3,120*	£4,925	22.2

*SO = Scientific Officer.

0028-0836/80/300323-02$01.00

say, academic life, but that it would be in the long-term interest of those working as professional people within the Civil Service that something should be done to remove the barriers between the professional and administrative career tracks.

Although the Fulton Commission in 1968, in the course of its attack on the generalist as senior Civil Servant, advocated more administrative responsibility for professional civil servants, many scientists in the service are bitterly disappointed that so little has been done to implement these recommendations.

US science budget

Stability ahead?

Washington

Locked once again into the annual congressional switchback over research funds, science policy administrators in Washington have eagerly endorsed plans to place key aspects of the congressional budget review process on a multi-year basis. On 21 July, the House of Representatives passed a bill submitted by its Science and Technology Committee that would require the Administration to provide two-year (or longer) estimates of major research and development expenditures as part of its annual budget request to Congress.

The objective is that any authorization committee should then be able, if it so chose, to approve research programmes for two or more years. At present, most research spending has to be authorized annually (except for the National Institutes of Health, for which new authorizing legislation is now under consideration (*Nature*, 22 May)).

Multi-year authorizations would affect only part of the budget process. Decisions on appropriations (authority to spend) are usually more significant and these would continue to be decided annually. Even so, supporters of the new legislation hope that, if a companion bill can be coaxed from the Senate, the result will be a first step towards greater stability and continuity for research finding. Some even see it as a "pilot endeavour" for multi-year funding of federal programmes in general.

The idea appeals equally to Congress, to the Administration and to leaders of the research community. In the first place, it would cut down considerably on the amount of time and effort now required of all parties.

But as Dr Frank Press, director of the Office of Science and Technology Policy (OSTP), told a recent hearing on the bill, "by its nature, most research and development has to be carried out over a lengthy time-frame".

Some hope that the reduced commitment would provide more time for more detailed examination of specific policy proposals, and that multi-year authorization would help to improve the climate for long-range planning of research, a goal that frequently conflicts with the need to respond to fluctuating political demands. The result should be, according to the bill's supporters, that research and development expenditure is less vulnerable to short-term changes in the fiscal climate. As things are, research and development suffers because, although it is a relatively small proportion of the overall federal budget, it represents almost a quarter of that which is not predetermined by specific laws, those concerned with social security for example. Extending the timescale of federal planning for research happens also to accord with "the budgetary philosophy of this Administration", according to Mr Bowman Cutter, executive associate director of the Office of Management and Budget (OMB).

In practice, however, multi-year planning will be difficult; the Office of Technology Assessment has told the committee that simple and flexible methods will be needed for treating inflation for example. Inflation affects research and development differently from other part of the federal budget; Dr Press has told the committee that many areas of science suffer from the "natural" built-in inflation that comes about because research becomes more sophisticated and the equipment and technical support required correspondingly more costly.

The House committee has taken Press's point. The legislation now passed by the House would require OSTP to assist and advise OMB on the evaluation of the effects of inflation factors on research and development and to suggest how they should be allowed for.

Most of this is relatively uncontroversial. Less so are proposed changes in the reporting requirements which existing legislation imposes on the OSTP and the National Science Foundation (NSF) to keep Congress up to date with the direction and intentions of official research and development policy. In particular, the new bill would dispense with OSTP's annual report to Congress on the nation's research and development. Instead, the NSF would be required to produce a broad outlook every four years with revisions every two years. OSTP officials make little secret of their scepticism about the usefulness of such reports, hitherto required by the Presidential Science and Technology Advisory Organization Act of 1976, and the House Science Committee now appears to agree.

US unemployment

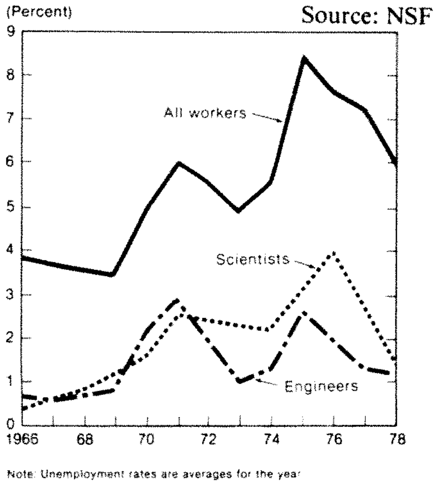

Note: Unemployment rates are averages for the year
SOURCES: Bureau of Labor Statistics and National Science Foundation

Some members of Congress, however, feel strongly that OSTP should be making public policy statements about the general health of research and development and the directions that it should be taking. They are thus unhappy about OSTP's apparent abdication of responsibility for long-range planning which, they claim, is explicitly required by its legislative mandate. Mr George Brown, a member of the House committee, in a minority report on the new bill, says OSTP has brought upon itself the difficulties it has encountered in preparing the reports required by law. There is reason to believe that the General Accounting Office is about to issue a report that is severely critical of OSTP on the same grounds.

David Dickson

India in space

One up so far

India has taken another step into the space age. Last week, the second test flight of the 17-tonne SLV-3 launcher successfully placed a small satellite into near-Earth orbit, making India one of a select group of countries with independent satellite launch facilities. SLV-3's first test flight last year ended in disaster when the rocket fell into the Indian Ocean 15 minutes after lift-off from the Sriharikota launch pad off India's east coast.

Mrs Gandhi's announcement that the second test flight was a success came during a debate in the Indian lower house (Lok Sabha) on defence ministry grants, leading some observers to speculate that the main impetus behind the rocket's development is military. India has never denied that its expertise in space technology could be used to launch reconnaissance satellites or develop intercontinental ballistic missiles, but it has always stressed that its space programme is intended to be peaceful and geared towards national development.

Space applications, such as remote sensing and telecommunications, form the major part of India's space programme. India has cooperated for several years with other countries such as the Soviet Union, France and the United States on remote sensing and telecommunications, one notable example being the SITE experiment with the US to bring educational television programmes to rural areas.

Rohini 1, the 40-kg satellite launched last week to record the flight characteristics of SLV-3 is the third Indian satellite to go into orbit. The Soviet Union launched the two others: Arybhata, a scientific satellite, in 1975 and Bhaskara, for Earth observation,

0028-0836/80/300324-02$01.00

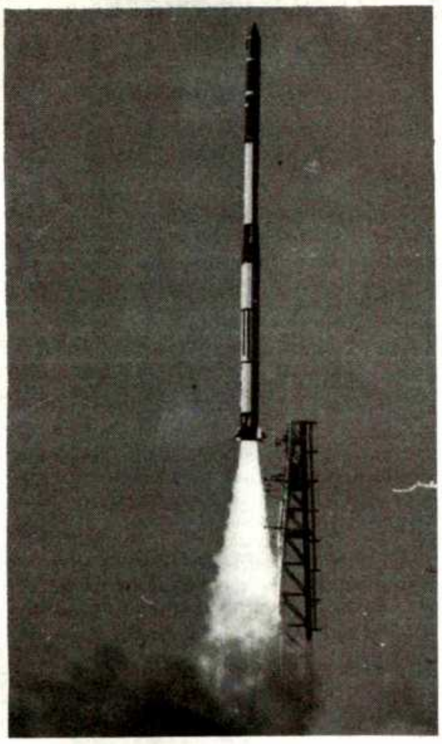

India: where next?

in 1979. Plans for further satellites include two more in the Rohini series. These will be larger than Rohini 1 and geared to specific scientific or applications tasks. India is also planning to launch an experimental telecommunications satellite, APPLE, on the third test flight of Ariane, the European launcher, next year.

The present SLV-3 rocket, based on NASA's Scout launcher, is too small, however, to launch some of the large satellites planned. Large liquid rocket motors are already being developed at the Vikram Sarabhai Space Centre on India's west coast for incorporation into future rockets capable of putting up to 800 kg into geosynchronous orbit.

The current launcher programme, which began in 1973, grew out of earlier experience gained in building sounding rockets at the Thumba equatorial rocket launching station.

Judy Redfearn

Nuclear explosions

No alarm

Washington

When can a cloud of dust particles resemble a nuclear explosion? When it is detected by a nuclear monitoring satellite, according to a report published last week by the US Office of Science and Technology Policy.

Spurred by speculation over the nature of a mysterious explosion apparently observed by a military Vela satellite over the lower Atlantic ocean last September, OSTP set up a panel of inquiry chaired by Dr Jack Ruina of the Massachusetts Institute of Technology.

The panel was at first inclined to agree with defence officials who claimed that the satellite had detected a clandestine nuclear explosion carried out by the South African Navy either on its own initiative or in collaboration with Israel.

After intense scrutiny of the data from the satellite, however, the panel now says that the flash of light seen by the satellite was "probably not" a nuclear explosion. Its alternative hypothesis is that the satellite was hit by a small meteroid, possibly as small as a speck of dust, and that this dislodged paint chips or other particles from the satellite's surface, which subsequently reflected sunlight into its detectors.

In support of this hypothesis, the scientists cite discrepancies in the data from the satellite's two sensors, indicating that the source may have been considerably closer to one sensor than the other.

In addition, there was a lack of any other evidence detected by stations on the ground — such as increased radiation or seismic activity — which would have corroborated the explosion hypothesis. Nor were there intelligence reports that a nuclear test had been carried out by either country. The Defense Intelligence Agency is not convinced. Before the OSTP report was released, the DIA leaked to the press its own conviction that a nuclear explosion had indeed been detected by the satellite, and that it had been carried out under weather conditions chosen to make detection difficult.

The White House, however, has adopted as its official position the OSTP panel's conclusion that there is insufficient evidence to prove a clandestine weapons test. According to State Department officials, this is the view that will prevail when a report on the incident is made to the Nuclear Non-Proliferation Treaty review meeting in Geneva next month.

David Dickson

Nuclear power

Ore running out?

The year just past was "another year of lost opportunities" according to the Nuclear Energy Agency (NEA), the OECD's own organization for the promotion of civil nuclear power. In its most recent annual report (the Eighth Activity Report covering 1979), the agency says that the growth of nuclear energy production in 1979 was a disappointing 2.2 per cent, compared with the average growth rate of 27.5 per cent a year during the period 1968-78. The pace of growth has paradoxically declined since the oil price rises of 1973.

On the face of things, however, the figures are not too bad. According to the report, there were 232 civil nuclear plants in operation at the end of 1979, and a further 229 under construction or on order, only seven more than in the previous year. New orders were almost offset by cancellation in West Germany, Spain and the United States.

Whatever happens to new orders, the output of nuclear electricity in the OECD area in 1990 is now almost certain to be between 33 per cent and 40 per cent of the energy equivalent of oil imports in that year, according to figures quoted in the report. The hiatus in the projected growth of the nuclear industry in 1979 is attributed to the international concern with nuclear proliferation, the Three Mile Island accident, uncertainty about waste disposal and "the related problems of public understanding".

On the consequences of the Three Mile Island accident, the NEA follows a judicious line. Its report says that the accident showed that nuclear power is not accident-free, that defence in depth can work in practice but also that the accident "has revealed a number of deficiencies in the way that reactor safety has been approached up to now". It urges that more attention should be paid to the malfunctioning of other than major items of equipment, and promises to do what it can to help.

One consequence of last year's hesitation about nuclear power is, according to NEA, that the uranium mining industry has become overcautious, thus threatening future growth.

World uranium reserves at costs up to $80/kg of uranium metal (the present economic limit on production) have increased by some 200,000 tonnes in the past two years, and now total 1.85 million tonnes. The increase came mainly from discoveries in Brazil and Canada and "improved knowledge" of deposits in Namibia, South Africa, Spain and the United States. NEA estimates that these reserves match the needs of Western nuclear power programmes between now and 2000-2005 but also considers that a significant portion of ore now identified will not be recovered "for technical or political reasons". So, the argument goes, there is an "urgent need" for the discovery of additional resources, reinforced by the wide range of the projections for nuclear power in 2025. The cumulative uranium requirements by that date range from 3.4 to 12 million tonnes, depending on nuclear power growth, the extent of reprocessing and the degree of development of fast breeders.

The NEA also looks forward to the exploitation of leaner ores, capable of yielding uranium at a cost of $\$130/\mathrm{kg}^{-1}$. Its upper estimate of the quantity of uranium in reserves now identified, not all of them explored, is put at 5.04 million tonnes, a quantity comparable with the estimated need of the nuclear industry by the second decade of the next century unless breeder technology is applied rapidly. Thus, the report concludes, the viability of the industry at the turn of the century will depend on the success of exploration in the coming ten years.

Robert Walgate

0028-0836/80/300325-01$01.00

CORRESPONDENCE

Geothermal electricity

SIR,— Richardson and White[1] have raised the interesting possibility that electricity generation from geothermal aquifers in the UK might be an economic proposition. It is unfortunate, however, that they have supported their proposal with spurious comparisons; for example, comparing the performance of purpose-built (and as yet undeveloped) organic Rankine cycle generating plant with conventional unadapted district heating systems.

They state that district heating "... has dominated official thinking for several years. . ." and cite[2] Energy Paper No 9. I would not in general wish to defend that development, which is now outdated, but it actually says (p.51): ". . .it seems that district heating would be economic only if higher temperatures or higher housing density were to become available".

Current thinking is that the major market for heat from geothermal aquifers in the UK (as in France) will indeed be for space heating, but at the group rather than district level. Heating of only a few large buildings from each pair of wells (doublet) is envisaged, which would be located as close to the buildings as possible. Few aquifers in the UK seem likely to yield temperatures in excess of 80°C, so it will be necessary to instal heating equipment capable of (1) operating at temperatures lower than those used in conventional systems and (2) extracting as much heat as possible from the geothermal fluid. These conditions have already been met in France, and suitable equipment is available. In particular, rejection temperatures can be nearer 25°C than the 60°C envisaged in ref. 1.

In the operation of a resource with a high capital cost and a low running cost resource such as geothermal energy, there is a powerful incentive to maximize the load factor. In the French installation a conventional boiler plant is used in parallel with the primary geothermal circuit, allowing geothermal to meet the "base" heating load while peak demands are met by fossil fuel. In this way, a geothermal doublet designed to meet 40% of the peak demand can typically supply 70% of the buildings' annual energy needs while achieving a load factor of 60% or more[3]. The relative capacities of geothermal and conventional plant will be determined by local conditions — including cost of conventional fuel at the site; analysis of the heat demand curve for similar buildings in the UK[4] suggests that comparable figures for a UK geothermal scheme would be about 50%, 89%, and 74% respectively.

In comparing the two modes of use, we recognize that in the UK, calculations must be based on estimates and will be of value only in assessing relative rather than absolute performance. For consistency, the approach adopted by Richardson and White[1] has been used to calculate the relative performance of electricity generation and group heating for a range of probable UK aquifer temperatures and attainable flow rates. The capital cost of the doublet (£1m) and the pumping power required (250 kWe) have been assumed constant for all cases. For group heating, the geothermal system is assumed to meet 50% of the buildings' needs with the remainder supplied by conventional boilers. The size of the heat load ("equivalent dwellings" at a density in excess of 100/hectare for a mixture of commercial and residential property) is allowed to vary according to the output of the geothermal well. Capital costs for distribution mains, building internals and boiler plant are calculated according to refs 1 and 5. The rejection temperature is taken as 30°C, distribution and heat exchange losses as 10°C, the load factor as 70%, and the heat is assumed to be sold at £2.0 per GJ. For electricity generation, the conditions given in ref. 1 have been used, while the capital cost of turbogenerator plant is assumed to be proportional to (gross output)$^{1/2}$ with the £748,000 for a 1 MWe plant of ref. 1 used as a baseline.

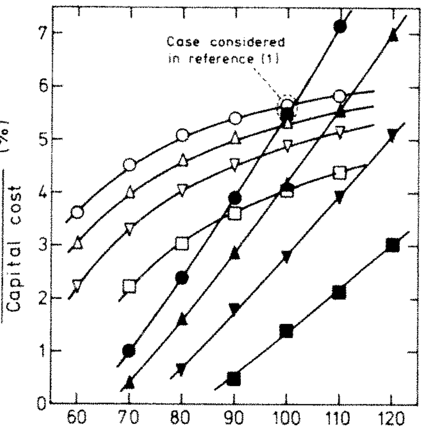

Fig.1 The effect of temperature and flow rate on the relative merits of group heating and electricity generation from geothermal aquifer sources in the UK.

Solid symbols, electricity generation; open symbols, group heating. Flow rates: ■ □, 20; ▼ ▽, 10; ▲ △, 40; ● ○, 50 kg s^{-1}.

The results are given in the figure. As might be expected, electricity generation becomes more attractive as temperature and flow rate increases but the return on capital is very sensitive to both parameters. Group heating is apparently less sensitive but this may be due to the method used for calculating capital costs. Comparing the data with those from French installations, capital costs derived from ref.5 seem very high, particularly for the larger schemes. Note also that the selling price of gas, in practice, varies from £2.03 per GJ (domestic user) to £2.47 per GJ (large industrial user). The cost of useful heat, even from gas, is thus nearer £2.90 per GJ than the £1.95 per GJ quoted in ref. 1, and the cost of heat from oil would be almost double. By contrast, the selling price of electricity is fixed (at 2.2 p/kWh); this calculation might then underestimate the relative advantage of direct heat uses over power generation.

Hence the advantages of electricity generation from low-enthalpy geothermal sources are not as clear-cut as Richardson and White[1] suggest. Until a borehole is drilled at any particular site, uncertainties will exist — particularly as regards flow rate.

However, such demand for heat will occur only in the larger towns, while many of the deep aquifers in the UK underlie rural areas where group heating would not be an option. If electricity production can be shown to be an economic proposition, then the contribution of geothermal sources to UK energy supply would be greatly increased.

J.D. GARNISH

AERE Harwell
Oxon, UK

References

1. Richardson, S.W. & White, A.A.L. *Nature* **286**, 103 (1980).
2. Garnish, J.D. *Energy Paper No.9* (HMSO, London 1976).
3. Garnish, J.D. *Pap. District Heating Association 3rd National Conf.* (1979).
4. W.S. Atkins & Partners (to be published)
5. Wright, J.K. *et al. Energy Paper No.20* (HMSO, London, 1977).
6. Milora, S.L. & Tester, J.W. *Geothermal Energy as a Source of Electric Power*, (MIT Press, 1976).

Banking DNA sequences

SIR, — We were glad to see your article "Banking DNA Sequences" (8 May) 1980, in which you make a persuasive case that there should be such a computerized data bank. We fully agree. In fact, we already have compiled such a computerized DNA sequence bank, which now considerably exceeds the 100-kilobase figure mentioned in your article. Our DNA data bank is a natural adjunct to our Protein Sequence Reference Data Collection[1] that has been supported for the past 15 years mainly by the Institute for General Medical Sciences of the US National Institutes of Health and by the National Aeronautics and Space Administration.

Many people are aware of our facilities and we do various searches and computer studies each week for people all over the world. Our computer system includes a large number of programs especially designed for analysing such collections of data. The most frequently used capability is a search of the amino acid and nucleotide sequences for segments that match a given segment. Sequences can be retrieved quickly and compared, and statistical assessments of similarity can also be made.

Our DNA Reference Data Bank is growing continually, despite the fact that the collection of these data is aggravated by the nonavailability of material in computer-readable form (as are, for instance, the protein crystallography data). The sequences are not even in clearly readable form in some journals. We would be happy to receive sequence data in computer-readable form to add to the collection when this information is published in journals. The sequence in this additional format would then be available to others.

You also entertain the notion that it matters little by whom or where a bank is started and that a successful operation could be a depository run by a keyboard operator who sent out tapes. Based on our years of experience, we must emphatically disagree. There have been many attempts to start data collections but few have continued in operation, mainly due to greatly underestimating the amount of effort and training required for such an undertaking. Will the users be satisfied to say, in their papers, "I looked over a few sequences and reached the conclusion that . . ." or would they prefer to say, with confidence, "I looked over all of the sequences so far elucidated . . ."? Who will find corrections that have been made to the old data? Will the users want the corrected sequence in the collection? Will they want other information, such as which portions of the nucleic acid sequence code for proteins? Also, who will solicit the new material? It doesn't just drift into a depository. If the users have questions about the collection, do they want to be able to communicate with someone and expect answers? Do the users want the data center to be delicately attuned to their needs?

We feel that making the data base intellectually accessible requires a considerable amount of effort and that such an effort is warranted by the central importance of nucleic acid sequence data to many fields, including medicine, genetics, and biochemistry.

M.O. DAYHOFF,
R.M. SCHWARTZ,
H.R. CHEN, L.T. HUNT,
B.C. ORCUTT, W.C. BARKER
National Biomedical Research Foundation
Georgetown University Medical Center
3900 Reservoir Road,
Washington, DC 20007

References

1. Dayhoff, M.O. (ed.) *Atlas of Protein Sequence and Structure* Vol.5 and Suppls 1–3 (National Biomedical Research Foundation, Washington, DC, 1972, 1973, 1976, 1979).

0028-0836/80/300326-01$01.00

NEWS AND VIEWS

Just so stories and cautionary tales

from Robert M. May and Miranda Robertson

SPECULATION about the evolution of social behaviour had its historical beginning in Darwin's perplexity about (and tentative explanation for) sterile castes among the social insects. The recent upsurge of interest in such questions derives largely from Hamilton's papers in 1964 (*J. theor. Biol.* **7**, 1 & 17), and their popularization in Wilson's *Sociobiology: The Modern Synthesis* (Harvard University Press, 1975). A fascinating glimpse into the sociology of science is provided by Paul Harvey's and Jon Seger's recent analysis of the citation of Hamilton's seminal papers; in the span 1964–1975, *Science Citation Index* records no more than 2-3 citations in any one year; after the appearance of Wilson's book in 1975, the citation rate explodes faster than exponentially. But Wilson's citation contains an error ("the genetical theory of social behaviour", replacing the original "the genetical evolution of social behaviour"), and this mutant form had risen to constitute 80% of all citations by 1978. Possibly as a result of the Harvey and Seger study, the mutation has not gone to fixation, and has decreased to 60% of all citations in the most recent SCI.

For a quantitative discussion of the general phenomenon of altruism, Hamilton introduced the notion of an individual's "inclusive fitness" (see *Nature* **260**, 390; 1976; **260**, 9; 1976). Suppose the performance of an altruistic act (such as uttering an alarm call upon noticing a predator, or, in the extreme, remaining sterile and helping raise relative's offspring) diminishes the fitness of the altruist by a factor $(1-c)$ relative to a non-altruist, but increases the fitness of the beneficiary by a factor $(1+b)$. Such altruism will be favoured by natural selection provided the cost c accrueing to the performer is less than the fitness benefit b conferred upon the recipient, discounted by the degree of relatedness, r, between them;

$$r > c/b \qquad (1)$$

In a diploid population with no inbreeding, sisters have $r=1/2$, and the altruistic extreme of sterile castes ($c=1$) will evolve only if $b > 2$. But in a simple haplo-diploid system, sisters have $r=3/4$, and the critical degree of benefit is the weaker $b > 4/3$. This observation is one of the crucial points of Hamilton's paper.

But these ideas about inclusive fitness are based on the phenotype (altruist and non-altruist), and do not deal with the underlying genotypes and genetic mechanisms. So when ethologists, geneticists and theoreticians met recently in Berlin to talk about the evolution of social behaviour*, much discussion centred on the extent to which quick and dirty conclusions obtained from inclusive fitness arguments can be trusted. Several authors (Cavalli-Sforza & Feldman *Theor. Pop. Biol.* **14**, 268; 1978; Charlesworth, Uyenoyama & Feldman, this Conference) have recently analyzed the population genetics of altruistic traits governed by one locus with two alleles. These formal, genetic studies reveal at least three shortcomings in the phenotypic inclusive fitness approach. First, the assumption that relatedness-discounted benefits and costs can be added in a simple linear fashion does not always hold; often, it will be more appropriate to compound the effects in multiplicative fashion. However, as long as both costs and benefits are relatively small, so that only weak selection operates, the difference between additive and multiplicative models is unimportant. Second, the structure of the coefficient of relatedness deduced from a genetic treatment can be different from that deduced by simple inclusive fitness arguments for the asymmetric cases of sister-brother and brother-sister in haplo-diploid species. For example, the haplo-diploid sister-brother coefficient is modified from $1/4$ to $(1/4)/(1+bh/4)$, where h measures the probability that the heterozygous genotypes Aa are altruists (the homozygotes AA being altruists, and aa being non-altruists). Although these complications simply are not taken into account in the inclusive fitness analysis of phenotypes, the structural differences between the two approaches are again negligible in the limit of weak selection (small b and c). Third, nonlinear dynamical behaviour in the genetic models can lead to stable polymorphism, with both altruistic A and non-altruistic a alleles persisting together; in linear or additive models, be they phenotypic or genetic, if an altrusitic trait can invade a population it will necessarily go to fixation.

All these differences between formally exact genetic analyses of relatedness and approximate inclusive fitness analyses are small if selection is weak. Moreover, the inclusive fitness approach provides intuitive biological understanding that is quite absent from the mathematical edifices of population gentics. Although far from unanimous, people at the conference took the view on balance that rough inclusive fitness arguments are likely to remain our main guide in thinking about the evolution of social behaviour.

More important, practical difficulties in assessing the costs c and benefits b in equation (1) will usually outweigh considerations of formal rigour. Among such difficulties identified in the conference discussions are how to combine different components (such as survival and reproductive success) into an aggregate measure of inclusive fitness, and how to determine paternity.

False assumptions about paternity, in particular, are now recognized as an important hazard in empirical tests of inclusive fitness. Clearly, the accuracy of quantitative measurements of inclusive fitness made on the basis of field observations will depend heavily on the confidence with which paternity can be assigned; and it has turned out to be a very wise ethologist indeed who knows his fathers. The important attempt by Trivers and Hare (*Science* **191**, 249; 1976; see also *Nature* **260**, 9; 1976) to explain the altruism of the hymenopteran worker castes by a quantitative study of data bearing on their inclusive fitness gains has been seriously

---

*The Dahlem Conference on the 'Evolution of Social Behaviour' was held in Berlin on February 18–22. The proceedings will be published as a book available from Dahlem Konferenzen, Delbrückstrasse 4c, D-1000, Berlin 33.

Robert M. May is the Class of 1877 Professor of Zoology at Princeton University, Miranda Robertson is an associate editor of Nature.

0028-0836/80/300327-03$01.00

eroded by, *inter alia,* the discovery that multiple matings are common in the ant species on which they based their calculations. (Alexander & Sherman *Science,* **196,** 494; 1977), and that coefficients of relationship are therefore not what they might seem.

Nor are the multiple matings of insects the only hazard to inclusive fitness analysis. Students of vertebrate behaviour have only recently begun to recognize the full extent of the gene dispersal going on behind their backs in what they fondly believed to be monogamous species. P. Marler (Rockefeller University) and M. Baker (Colorado State University) pointed out, for example, that reports of healthy clutches of young hatched by the 'monogamous' mates of vasectomized birds have been in the literature for at least five years (e.g. Bray, Kennelly & Guarino, *Wilson Bull.* **87,** 187; 1975). For the reproductive strategy of the fathers of such clutches, sociobiologists have coined the term kleptogamy (or, in conversation, sneaking). These studies on bird paternity, incidentally, also testify to the complications that so often beset field experiments of this kind: for many bird species (including the redwing blackbirds studied studied by Bray *et al.*) infertile eggs are distinguishable by their colour from fertile ones, and it could conceivably be that the unfaithful wives chose to stray only after discovering their spouses to be infertile.

In general, field workers are becoming increasingly wary of assumptions about paternity, and wherever possible checking the degree of relationship between altruists and beneficiaries by isoenzyme analysis. This policy was adopted by R. Metcalf (University of California) in his cost-benefit analysis of the alpha and beta castes of paper wasps (*Polistes*). Female paper wasps may found nests and rear young as solitary individuals, or they may cooperate with a sister. In the case of cooperating sisters, one wasp, the alpha female, lays all or nearly all of the eggs so that the beta female is rearing nieces and nephews. However, the co-ops are so much more productive than the nests of solitaries that the inclusive fitness of the beta female is greater than that of a solitary one. Since this conclusion is based on calculations of the average number of genes a beta wasp will share with her nephews and nieces, by comparison with the average number shared with her own young, it is clearly essential to know for certain that she is the full sister of the alpha. The precaution taken by Metcalf, who analyzed the polymorphic enzymes of the wasps to check their relationships, is increasingly adopted by sociobiologists and has certainly helped to reveal unsuspected heterogeneity in presumed inbred colonies.

It has been generally assumed that the altruistic wasp, bird or beast itself does not have access to accurate information about its relationship to its conspecifics, and simply directs its altruistic acts towards the individuals it grew up with. But strict kin selection could still work in the face of rampant polygyny, kleptogamy and general promiscuity provided that there were in fact an innate mechanism for distinguishing degrees of kinship. Greenberg's report (*Science* **206,** 1095; 1979) that such a mechanism exists in the primitively eusocial bee *Lasioglossum zephyrum* was therefore generally agreed to be one of the most important recent contributions to the literature. There is overwhelming evidence that social insects recognize colony mates, but until recently no-one had managed to distinguish between innate and environmental factors in determining such recognition. Greenberg reared laboratory-bred bees of 14 different degrees of kinship in isolation and was able to show that when they were allowed to form colonies they preferentially admitted close kin to the nest, the probability of admission being roughly proportional to the degree of kinship. An exactly analogous mechanism was reported by K. E. Linsenmair (University of Würzburg) in a desert-dwelling social isopod. It is not yet known whether vertebrates have similar innate abilities. Waldman's and Adler's evidence for kin recognition in frogs (*Nature* **282,** 611; 1979) does not distinguish between innate and environmental mechanisms; but if innate mechanisms turn out to be widespread, this will limit the applicability of J. Maynard Smith's (Sussex University) ingenious adaptations of game theory to define evolutionarily stable strategies (ESSs) for behaviour, one of whose underlying assumptions is usually that kin recognition is based on simple proximity. The whole question of 'hidden' assumptions in evolutionary theories of behaviour is clearly a sore point with empiricists, who expressed the view that theoreticians should make them more explicit. For example, the majority of empiricists are probably not aware that most (though not all) of the ESS calculations in the current literature assume haploidy, and therefore strictly apply to nothing higher that some insects. Most of the conclusions can, however, be shown to apply to sexual diploids; and given the inevitability of simplifying assumptions, probably the most useful thing a theoretician can do is try to give some indication of how sensitive his theory is to violation of its assumptions.

On the other hand, it is incumbent on the empiricists to produce data good enough to provide a serious test of the theory. It is the shallowness of some of the earlier ethological investigations that has led to their being castigated by some as evolutionary Just-So stories. Lively discussion centred on several interesting but unfinished studies in which individual males seem to adopt one of two or more alternative reproductive strategies (for an example, fighting to maintain a territory and/or a harem *versus* kleptogamy). Such studies have so far left open many questions. Are the different phenotypes associated with different genotypes, or are they dictated by environmental constraints? Do the different strategies correspond to different categories of animal, or can, for example, a male start his adult life as a 'sneak' and later progress to ownership of a harem?

A fundamental question that has been raised regularly by the principal detractors of what has become known as sociobiology, and often ignored by its practitioners, is: what evidence is there that a particular phenotype is, in fact, adaptive? Feldman quoted the example of meiotic drive as a mechanism for preserving maladaptive genes in a population. Other extreme examples of this sort are known or suspected, and there is every reason to

100 years ago

NATURE WELCOMES *SCIENCE*

We take the following from the New York *Nation*:— "For the English-speaking race, wherever planted, we should have supposed NATURE to be a sufficient scientific medium, and entitled to universal support. We are partly confirmed in this view by the quotations from NATURE in the first number of *Science*, a quarto weekly journal, edited by Mr John Michels, and published at 229 Broadway, in this city. Nevertheless, the editor's statement that the enterprise has been begun 'after consultation with many of the leading scientists in this country,' and his list of co-labourers seem to point to a real want, and to entitle this new 'record of scientific progress' to a friendly welcome. Its present size is sixteen pages, including the advertising sheet. The opening article, on the United States Naval Observatory, is from the pen of Prof. E.S. Holden." We wish our new contemporary every success, and trust that it may be the means of spreading a wide interest in science on the other side of the water.

A violent shock of earthquake occurred at Manila and throughout the Island of Luzon on July 18, which did immense damage, totally destroying several government buildings and other houses. Some of the native inhabitants were killed, but no Europeans suffered any injury. A slight shock was felt also on the 17th inst.

from *Nature* **22**, 24 July, 276 & 276, 1880.

suppose that selectively neutral behaviour can become fixed in a population by historical or evolutionary accident.

To paraphrase one of the more vociferous participants, the Romantic Age of sociobiology, with its excitement and imaginative speculations about the explanatory power of inclusive fitness notions, is giving way to a more sober appreciation of the experimental difficulties that must be overcome before contending theories can be sorted out. For many, the meeting helped to crystallize thoughts about assembling data of sufficient resolution to distinguish between theories, and to draw up a tentative agenda of theoretical and empirical problems that deserve attention. In this context, the generic format of the Dahlem Conferences (of which there have been some 20-odd, on a diversity of topics) deserves mention: canonically teutonic, with groups and subgroups forming and reforming in intricate, pre-ordained patterns, their most obvious function is to produce a book, whatever betide. But the groups at the sociobiology meeting were skillfully chosen, blending theorists and empiricists, optimists and pessimists, romantics and realists; most important, the four rapporteurs (Feldman, Harvey, Krebs, Oster) managed to extract from the discussions reports that seem to be useful signposts. □

Malignant transformation and protein phosphorylation

from Thomas Langan

DURING the past decade protein phosphorylation reactions have been found to function in the regulation of a large number of cellular processes. In addition to extensively studied systems such as cyclic AMP-dependent phosphorylation, many other less well-characterized protein kinases and protein phosphorylation reactions occur, suggesting that regulation by protein phosphorylation is more wide-spread than currently appreciated. Recent work, stemming from the original observations of Collett and Erickson[1], has indicated that certain proteins responsible for transformation of virally infected cells to the malignant state are protein kinases, or are closely associated with protein kinases. These kinases have now been shown to have the novel property of catalyzing the phosphorylation of tyrosine residues in their substrate proteins, rather than the usual serine or threonine residues[2-5]. The findings indicate that a unique class of protein kinases may catalyze a key reaction in the production of certain types of malignancy, and there are hints that similar kinases may participate in normal regulation of cell proliferation.

The best studied system is that of the Rous or avian sarcoma virus, an RNA virus in which a single viral gene, *src*, has been shown to be responsible for transformation of cells to the malignant state[6]. A 60,000 MW protein present in transformed cells has been identified as the product of this gene by the use of deletion and temperature-sensitive mutants and, more convincingly, by direct translation *in vitro* from fragments of viral RNA containing the *src* gene[7,8]. The protein (pp60^{src}) is phosphorylated in two distinct regions of the molecule[9] and as with certain other phosphoproteins, pp60^{src} seems to be itself a protein kinase. This activity is of the cyclic AMP-independent type and was originally revealed by the ability of pp60^{src} to catalyze transfer of phosphate from ATP to the heavy chain of IgG in immunoprecipitates of viral protein, prepared using antisera from tumour bearing animals[1,10]. The reaction is clearly not of functional significance, but the ability to phosphorylate a non-physiological substrate is very advantageous for assay purposes. Extensive studies with deletion and temperature sensitive mutants[1,10-12] and the demonstration of protein kinase activity in highly purified preparations of pp60^{src} [13,14] as well as in pp60^{src} made by *in vitro* translation of viral RNA[15,16] show that the protein kinase activity is a property of the *src* gene product and that the activity is essential for transformation of cells to the malignant state. While tight association of traces of a cellular kinase with the native form of pp60^{src} cannot be completely ruled out, they support the conclusion that the *src* gene product is either a protein kinase itself, or functions in close association with a cellular protein kinase.

As well as avian sarcoma virus, protein kinase activity has been found associated with several other transforming gene products, including those from the DNA-containing adenovirus, SV40, and polyoma viruses [17-21,2], and from the RNA-containing Abeleson murine leukaemia and Fujinama viruses[3,22]. In each case protein kinase activity is detected in immunoprecipitates of viral proteins using the assay developed by Collett and Erickson. However, phosphorylation in most cases occurs not on the immunoglobulin chain, but on the viral protein itself. Whether this represents an intermediate in the normal enzymatic reaction which is stable in the absence of a suitable substrate, or an autophosphorylation which may affect function is not clear. pp60^{src} also undergoes an apparent autophosphorylation reaction when in soluble form both *in vitro* and *in vivo*, and in addition is phosphorylated by the normal cellular cyclic AMP-dependent protein kinase at a separate site in the molecule[14,9]. Whether these phosphorylation reactions modulate function is again not clear. There is less evidence that the protein kinase activity is due to viral protein for viruses other than avian sarcoma and there are some reports that activity may not be present in purified forms of SV40 and hybrid SV40 large T antigen[18,23]. However, large T antigen is different in many ways from the other viral products which show kinase activity. Kinase activity is absent from immunoprecipitates when transformation-defective mutants of adenovirus, SV40 and polyoma are used, consistent with the conclusion that the transforming activity is a kinase although the possibility of an association between the viral protein and a cellular kinase remains.

That transformation-related protein kinases catalyze the phosphorylation of tyrosine residues in their substrates was first shown by Hunter and co-workers[2] in the polyoma system, where kinase activity is mainly associated with a tumour antigen of intermediate size (middle T). Phosphorylation occurs on the phenolic hydroxyl group of tyrosine. Protein kinases associated with other viral transforming gene products also phosphorylate tyrosine residues[3-5]. Previously, phosphorylated tyrosine residues were not known to occur in proteins, although modifications such as nucleotidyl derivatives of tyrosine are found in bacterial enzymes (for example, ref. 24). As each of these kinases associated with viral transforming gene products catalyzes the phosphorylation of tyrosine residues it seems probable that a unique class of protein kinases may be involved in the transformation of cells to the malignant state. This feature may be extremely useful in locating other kinases with similar or related functions, and in locating and measuring the phosphorylation of potential substrates.

By itself, the fact that phosphorylation occurs on tyrosine rather than on serine or threonine residues gives no clue to the molecular mechanism of transformation. One possibility is that the phosphorylation of cellular substrate proteins by the viral kinase (or by a cellular kinase which is activated by association with the viral protein) leads to functional alterations which initiate the transformation process. Since this is a highly pleiotropic response, many substrates could be involved. Kinase action *in vivo* is indicated by an approximately 10-fold increase in the phospho-

---

Thomas Langan is Associate Professor of Pharmacology at the University of Colorado School of Medicine.

0028-0836/80/300329-02$01.00

tyrosine content of total cell protein during transformation by avian sarcoma virus. When the *src* gene contains a temperature sensitive mutation, phosphotyrosine content rapidly declines to normal values and rises again as cells are shifted from permissive to restrictive temperatures and back[25]. Not all of the increase in phosphotyrosine can be accounted for by the apparent autophosphorylation of $pp60^{src}$ which occurs in transformed cells, indicating that tyrosine residues in cellular proteins are phosphorylated. Two specific proteins that appear to be substrates of cellular origin are under study. One is a 50,000 MW protein found in immunoprecipitates of $pp60^{src}$ because of its affinity for the kinase protein[4] and the second is a 34,000 MW protein that is clearly identifiable in normal cells, and which undergoes a transformation dependent and temperature-sensitive phosphorylation in virally infected cells[26,27]. The 34,000 MW protein, extensively purified from normal chicken cells, is phosphorylated by purified $pp60^{src}$ kinase, and tryptic digests phosphorylated *in vitro* and *in vivo* show the same patterns of tyrosine-containing phosphopeptides in two-dimensional maps[28]. Determination of the functions of the substrate proteins may not be a simple task and it is possible that $pp60^{src}$ has additional functions which are important for the transformation process.

Tyrosine phosphorylation may not be a universal feature of transformation mechanisms as although transformation by the related Abelson virus is associated with elevated phosphotyrosine in proteins (Hunter, pers. comm.) in several other viruses including, surprisingly, polyoma and SV40, there is no elevation[25]. However, the kinases in these cases may be more specific in catalyzing the tyrosine phosphorylation reactions required for transformation, so that no increase in total content is detectable. Two chemically transformed cell lines examined also did not have elevated phosphotyrosine levels.

DNA sequences closely related to the sequences in the avian sarcoma *src* gene are present in normal cells of vertebrates ranging from birds to man[29], and transcripts of these sequences are found in polyribosomes[30], indicating that the sequences code for a protein with a highly conserved general cellular function. In keeping with this, normal cells also contain a 60,000 MW protein which is structurally related to $pp60^{src}$, as indicated by immune cross-reaction and by peptide mapping, and which is also associated with protein kinase activity acting on tyrosine residues[31,32] (Erikson, pers. comm.). The amount of the normal cell protein is some 30-50-fold lower than that of $pp60^{src}$ in transformed cells. These findings suggest that the viral protein may be related to a normal cell protein involved in some universal cellular function such as maintenance of control over cell division. Malignant transformation might result from a qualitative change in the substrates phosphorylated, or from an uncontrolled increase in a normal cell phosphorylation reaction. In either case, investigation of the substrates phosphorylated by the normal cell protein and by any similar kinases seems worthwhile. One interesting candidate has already been identified. When cell membranes from human epidermoid cells bind epidermal growth factor the binding is associated with the phosphorylation of a membrane protein (possibly the receptor for the growth factor) and this phosphorylation occurs predominantly on tyrosine residues[34] (S. Cohen, pers. comm.). Future study of this as well as other protein phosphorylation reactions involving tyrosine residues may shed light on important control mechanisms in both normal and malignant cells. □

---

1. Collett & Erikson *Proc. natn. Acad. Sci. U.S.A.* **75**, 2021 (1978).
2. Eckhart *et al. Cell* **18**, 925 (1979).
3. Witte *et al. Nature* **283**, 826 (1980).
4. Hunter & Sefton *Proc. natn. Acad. Sci. U.S.A.* 77, 1311 (1980).
5. Collett *et al. Nature* in the press.
6. Hanafsa in *Comprehensive Virology* **10**, 401. (ed. Fraenkel-Conrat & Wagner.) (Plenum Press, New York 1977).
7. Purchio *et al. Proc. natn. Acad. Sci. U.S.A.* **74**, 4661 (1977).
8. Purchio *et al. Proc. natn. Acad. Sci. U.S.A.* **75**, 1567 (1978).
9. Collett *et al. J. Virol.* **29**, 770 (1979).
10. Levinson *et al. Cell* **15**, 561 (1978).
11. Rubsamen *et al. Proc. natn. Acad. Sci. U.S.A.* **76**, 967 (1979).
12. Sefton *et al. J. Virol.* **33**, 220 (1980).
13. Maness *et al. Proc. natn. Acad. Sci. U.S.A.* **76**, 5028 (1979).
14. Erikson *et al. Proc. natn. Acad. Sci. U.S.A.* **76**, 6260 (1979).
15. Erikson *et al. Nature* **274**, 919 (1978).
16. Sefton *et al. J. Virol.* **30**, 311 (1979).
17. Lassam *et al. Nature* **277**, 241 (1979).
18. Tjian & Robbins *Proc. natn. Acad. Sci. U.S.A.* **76**, 610 (1979).
19. Griffin *et al. Proc. natn. Acad. Sci. U.S.A.* **76**, 2610 (1979).
20. Smith *et al. Cell* **18**, 915 (1979).
21. Schaffhausen & Benjamin *Cell* **18**, 935 (1979).
22. Lee *et al. Proc. natn. Acad. Sci. U.S.A.* **77**, 2018 (1980).
23. Giacherio & Hager *J. biol. Chem.* **254**, 8113 (1979).
24. Adler *et al. J. biol. Chem.* **250**, 6264 (1975).
25. Sefton *et al. Cell* (in the press).
26. Erikson *et al. Cold Spring Harb. Symp. quant. Biol* **44**, (in the press).
27. Radke & Martin *Proc. natn. Acad. Sci. U.S.A.* **76**, 5212 (1979).
28. Erikson *et al. Phil. Trans. R. Soc.* (in the press).
29. Spector *et al. Proc. natn. Acad. Sci. U.S.A.* **75**, 4102 (1978).
30. Spector *et al. Cell* **13**, 381 (1978).
31. Collett *et al. Cell.* **15**, 1363 (1978).
32. Oppermann *et al. Proc. natn. Acad. Sci. U.S.A.* **76**, 1804 (1979).
33. Collett *et al. Proc. natn. Acad. Sci. U.S.A.* **76**, 3159, (1979).
34. Carpenter *et al. J. biol. Chem.* **254**, 4884 (1979).

Repressor represses cro represses repressor represses cro . . .

from Mark E. Furth

THE discovery of regulatory genes in bacteria and maize quickly invited speculation on how simple control elements such as repressors and operators might determine cell differentiation[1]. Are these elements connected in circuits to produce states of gene expression which can be propagated through many cell generations[2]? Stable regulatory circuits are easy to construct on paper, but more difficult to unravel in the laboratory. The choice between the lysogenic and lytic lifestyles of bacteriophage λ has served as one experimental model of a 'developmental switch' between alternative stable states. A regulatory circuit central to this switch has now been explained in exquisite molecular detail[3].

The circuit involves two proteins, encoded by genes *cI* and *cro*. Each protein represses the other's synthesis. The *cI* protein (often called the λ repressor) maintains the lysogenic state in which λ replicates passively, its DNA integrated into the chromosome of its bacterial host. In this state the repressor shuts off viral genes, including *cro*, which are required for active growth. The *cro* protein (called cro), in contrast, promotes lytic growth by shutting off the repressor gene *cI*. Either of the two stable states of gene expression, *cI* turned on and *cro* turned off, or *cro* turned on and *cI* off, can be maintained for many generations in cells carrying particular λ mutants[4]. These states are regulated by binding of the repressor and cro to an operator called O_R which lies between the *cI* and *cro* genes. The bound proteins control the initiation of messenger RNA synthesis at two distinct sites: the promoter P_{RM} for transcription of *cI*, and the promoter P_R for transcription of *cro* (see figure)[5,8,12]. How do the repressor and cro differentially affect the activity of these two promoters?

One key to the control of *cI* and *cro* expression lies in the fine structure of the operator. M. Ptashne and colleagues discovered several years ago that O_R contains three separate binding sites for repressor (O_R1, O_R2, O_R3; see figure)[7,17]. These sites are closely related, but the nucleotide sequence of each is unique. When cro was purified[9], its target sequences could be compared with those for repressor. Remarkably, although the two proteins show no obvious structural homology[10,11,18], they bind to the same three sites in O_R (ref. 12). However, the proteins differ in the order in which each occupies these sites. Repressor first binds coordinately to O_R1 and O_R2, and binds to O_R3 only at much higher protein concentration[13]. cro first binds to O_R3, and then to O_R1 and O_R2.[12]. This difference in the relative affinity for binding sites in the operator is critical to gene regulation, because occupation of each site by a repressor or cro molecule affects promoter activity in a specific way.

0028-0836/80/300330-02$01.00

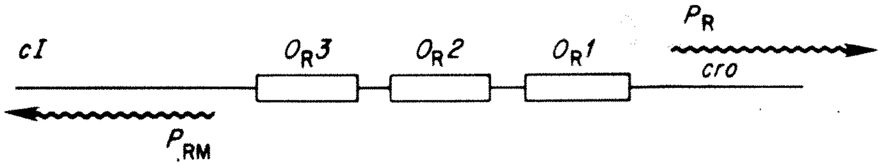

Fig. O_R region of λ DNA. Promoters P_{RM} and P_R direct transcription (wavy arrows) of genes *cI* (encoding repressor) and *cro* respectively. Repressor and cro proteins bind to sites O_R1, and O_R3. The distance between mRNA startpoints is 82 base pairs. Each binding site is 17 base pairs long.

B. Meyer, R. Maurer and M. Ptashne have identified the function of protein molecules bound to each site in the operator[14–16]. They devised a strategy to measure P_R and P_{PM} activity over a wide range of repressor and cro concentrations in intact cells, and to determine the effects of mutations in the three binding sites. The trick was to place the expression of an easily assayed enzyme, β-galactosidase, under the control of each phage promoter, and to introduce O_R mutations into the fused operons. Levels of the λ regulatory proteins were manipulated by similar genetic sleight-of-hand; the expression of *cro* or *cI* was placed under control of an inducible bacterial operon and the rate of synthesis was set by varying the concentration of the inducer. The special elegance of the approach is that it uncouples the synthesis of the regulatory proteins from the promoters which normally control their expression, so that measurements of promoter activity can be made under many steady-state conditions.

The results of studies with the fused operons show that each of the outer operator sites, O_R3 and O_R1, regulates transcription from the start-point adjacent to it, while the central site, O_R2, regulates both promoters. Either a repressor molecule or a cro molecule bound to O_R3 turns off transcription from P_{RM}, but does not turn off transcription from P_R. Conversely, either protein bound to $O_R{}^1$ or $O_R{}^2$ turns off transcription from P_R but not from P_{RM}[14,15]. Repressor, but not cro, bound to O_R2 has a second effect: it strongly stimulates transcription from P_{RM}[5,6,16].

The different order of binding of cro and repressor to the three sites in O_R, and the particular role of each site in determining promoter activity largely explain the stable states of *cI* and *cro* expression. Because cro binds preferentially to O_R3, it represses transcription of *cI* more readily than it represses transcription of its own gene. By contrast, because repressor binds preferentially to O_R1 and O_R2, it turns off transcription of *cro* more readily than it turns off transcription of *cI*. Thus, there are concentrations of cro which prevent synthesis of repressor but permit expression of *cro*, and there are concentrations of repressor which prevent synthesis of cro but permit, and actively maintain expression of *cI*.

What determines the order of occupation of the binding sites by the regulatory proteins, and how do bound protein molecules control the initiation of RNA synthesis? Ultimately, it should be possible to answer these questions at the atomic level of resolution. The present studies of molecular mechanisms focus attention on some of the protein-DNA and protein-protein interactions that contribute to gene regulation. A striking and unexpected finding is that cooperative interactions between bound repressor molecules help to govern the pattern of binding to sites in the operator.

Cro binds to the three sites in O_R independently, in the order set by the protein's intrinsic affinity for each site[12,13]. Repressor presents a more complex picture. Its intrinsic affinity for the isolated O_R1 sequence is about 15-fold greater than that for O_R2 or O_R3. Nevertheless, on an intact operator it binds O_R1 and O_R2 to about the same extent at concentrations at which O_R3 remains free. Johnson, Meyer and Ptashne attribute the coordinate binding at O_R1 and O_R2 to positive cooperative interactions between repressor molecules[13]. They argue that a molecule bound at O_R1 facilitates the binding of a second molecule at O_R2 by direct protein contact. When O_R1 is free, repressor molecules also can cooperate to fill O_R2 and O_R3. However, a molecule bound at the central site does not interact simultaneously with neighbours on both flanks, and at equilibrium the interaction between molecules at O_R1 and O_R2 is strongly favoured. A major consequence of this cooperative binding is to stabilize the state (O_R1, O_R2 bound by repressor, O_R3 free) in which cro synthesis from P_R is turned off while repressor synthesis from P_{RM} is stimulated. This is the predominant situation in a cell lysogenic for λ.

Table 1 Properties of repressor and cro

	Repressor	Cro
Gene	*cI*	*cro*
Size of monomer	236	66 amino acids
Active form	Dimer	Dimer
Order of binding to operator sites (wild-type O_R)	$O_R1 \simeq O_R2 > O_R3$	$O_R3 > O_R2 \simeq O_R1$
Cooperativity in binding to DNA	Yes	No

Table 2 Comparison of promoters P_R and P_{RM}

	P_R	P_{RM}
Intrinsic activity	High	Low
Positive control (stimulation)	No*	Yes, by repressor
Primary site for negative control by repressor or cro	O_R1, O_R2	O_R3

(*or weakly by cro: see ref. 8)

Table 3 Action at O_R2: Protein bound at O_R2

	Repressor	cro
Transcription from		
P_R:	Off	Off
P_{RM}:	High (stimulated)	Low (unaltered)

The capacity of bound repressor to prevent transcription from one promoter while enhancing transcription from another is one of the most striking features of the repressor/cro regulatory circuit. Both repressor and cro protein appear to shut off transcription simply by blocking access of RNA polymerase to a promoter[3,6,9,13,15]. However, the mechanism by which repressor boosts transcription from P_{RM} is not obvious. Meyer and Ptashne[16] have shown that repressor must directly effect this stimulation; it is not merely a consequence of turning off transcription from the nearby promoter P_R. They suggest that repressor at O_R2 interacts with RNA polymerase at P_{RM} to stabilize polymerase binding or to facilitate a subsequent step in the initiation of RNA synthesis[3,15,16]. The startpoint for transcription from P_{RM} lies only one base pair further from O_R2 than does the startpoint for transcription from P_R. Yet repressor bound to O_R2 helps RNA polymerase to initiate at one promoter, but excludes it from the other[15]. Whether repressor acts positively or negatively on transcription must therefore critically depend on the precise orientation of bound repressor with respect to the binding site for RNA polymerase. A remaining challenge is to find an exact molecular explanation for the Janus-like behavior of this regulatory protein.

Perhaps a more imposing challenge is to identify genetic regulatory circuits that control development of multicellular organisms, and which can be dissected as neatly as those of λ. One outstanding lesson from the phage model is that the action of each element of such a circuit can be finely tuned and very flexible, so that a single regulator or target sequence may affect gene expression in very different ways. ☐

Mark E. Furth is in the MRC Laboratory of Molecular Biology, Cambridge.

1. McClintock, B. *Cold Spring Harb. Symp. quant. Biol.* **21**, 197 (1956). Monod, J. Jacob, F. *Cold Spring Harb. Symp. quant. Biol.* **26**, 3[illegible]9 (1961).
2. Kauffman, S. *J. Theor. Biol.* **44**, 167 (1974).
3. Ptashne, M., Jeffrey, A., Johnson, A.D., Maurer, R., Meyer, B.J., Pabo, C.O., Roberts T.M. & Sauer R.T. *Cell* **19**, (1980).
4. Eisen, H. & Ptashne, M. in *The Bacteriophage Lambda* (et. Hershey, A.D.) (Cold Spring Harbor Laboratory, New York, 1971).
5. Reichardt, L.F. *J. mol. Biol.* **93**, 267 (1975).
6. Meyer, B.J., Klein, D.G. & Ptashne, M. *Proc. natn. Acad. Sci. U.S.A.* **72**, 4785 (1975). Walz, A., Pirrotta, V. & Ineichen, K. *Nature* **262**, 665 (1976).
7. Ptashne, M., Backman, K., Humayun, M.Z., Jeffrey, A., Maurer, R., Meyer, B.J. & Sauer, R.T. *Science* **194**, 156 (1976).
8. Takeda, Y. *J. mol. Biol.* **127**, 177 (1979).
9. Takeda, Y., Folkmanis, A. & Echols, H. *J. biol. Chem.* **252**, 6177 (1977).
10. Roberts, T.M., Shimatake, H., Brady C. & Rosenberg, M. *Nature* **270**, 274 (1977).
11. Hsiang, M.W., Cole, R.D., Takeda Y. & Echols, H. *Nature* **270**, 275 (1977).
12. Johnson, A., Meyer B.J. & Ptashne, M. *Proc. natn. Acad. Sci. U.S.A.* **75**, 1[illegible]8 (1978).
13. Johnson, A., Meyer B.J. & Ptashne, M. *Proc natn. Acad. Sci. U.S.A.* **76**, 5[illegible]6 (1979).
14. Maurer, R., Meyer, B.J. & Ptashne, M. *J. mol Biol.* **139**, 147 (1980).
15. Meyer, B.J., Maurer, R. & Ptashne, M. *J. mol. Biol.* **139**, (1980).
16. Meyer, B.J. & Ptashne, M. *J. mol. Biol.* **139**, (1980).
17. Maniatis, T. *et al.* *Cell* **5**, 109 (1975).
18. Saver, R.T. & Anderegg, R. *Biochem.* **17**,1092 (1978).

The problem of defining a substorm

from S. W. H. Cowley

ALTHOUGH the correlation between periods of geomagnetic disturbance and the occurrence of auroras had been known since the time of Celcius (1741), the first scientific reference to magnetospheric substorms seems to be found in the accounts of Herrick (1838) and Olmstead (1856) who noted that auroras often display 'fits of maximum intensity' at intervals of several hours. Interest in these 'auroral fits' and their associated short-lived polar magnetic disturbances waned towards the end of the nineteenth century, and for the next sixty years interest focussed instead on world-wide magnetic storms which develop and decay on time scales of a day or two. It was not until the exploitation of ground networks of all-sky auroral cameras and magnetometers during the International Geophysical Year (IGY, 1957-8) that it was finally realized that the polar 'fits' constituted the building-blocks of world-wide storms. Magnetic storms build up when intense 'fits', now fortunately renamed 'substorms', occur very frequently.

The phenomenology of the auroral substorm described by Akasofu (1964) on the basis of the IGY data is sketched in the accompanying figure, and this was followed by a monograph (1968) in which the evolution of high-latitude phenomena (for example, magnetic disturbance, ionospheric cosmic radio noise absorption, VLF radio emissions) was linked to a common time frame defined by the auroras. Auroral light emission is produced at $\sim$100-150 km altitudes by 1-10 keV electron bombardment of the upper atmosphere, the electrons originating in the Earth's magnetosphere (the region extending $\sim$10 Earth radii on the day side and at least $\sim$1000 on the night side containing the Earth's magnetic field and excluding, at least in part, the solar wind plasma). During the early sixties detailed satellite observations in the magnetosphere out to large distances, but linked to the polar regions by the Earth's magnetic field lines, were only just becoming available, but it was already clear that large changes in the field and charged particle populations occurred, and that the substorm concept provided an organizing framework.

Akasofu's (1964) auroral substorm consisted of two phases, 'expansion' and 'recovery', both lasting 30 min — 1 hour. Onset of expansion is signalled by a sudden brightening (in $\sim$1 min), usually near midnight local time, of one of a series of quiet auroral arcs which may have existed for several hours previously (Fig. a). Brightening is followed by rapid poleward motion, forming a bulge which expands also to the east and west (Fig. b). The western end develops a large scale fold or 'surge', and the quiet arcs along which it propagates can brighten just before the surge reaches and engulfs them. In the morning the arcs break up into patches, drifting eastward at speeds $\sim 300\,\mathrm{ms}^{-1}$. Recovery starts when the bulge reaches its highest latitude, begins to contract and the auroras gradually resume their quiet-time appearance (Fig c). The occurrence of such displays is very variable, but several during one day is not unusual.

The principal magnetic signature is a decrease in horizontal field strength under the auroral bulge due to an ionospheric westward 'electrojet' current of $\sim 10^6$ amps flowing within it, although smaller perturbations are observed down to low latitudes. In addition, a spatially widespread magnetic signal usually appearing as a damped, $\sim$1 min period sinusoid is initiated at the onset of expansion. This characteristic signal is known as a Pi-2 and is thought to be excited by rapid changes in plasma flow in the magnetosphere.

In principle the substorm onset time can be obtained to within a minute or two using either auroral or magnetic data, and such accuracy is often required, for example, to establish the relative timing of rapidly changing conditions at widely separated locations (for example, ionosphere and night side magnetosphere). In practice, however, timing substorms turns out not to be at all easy, as has become increasingly evident over the past decade, due both to the incomplete coverage provided by ground-based networks and to the increasing realization of their complexity. These problems have encouraged research groups to champion differing signatures as definitions of the substorm time-frame, resulting in a great deal of both scientific and etymological confusion, and providing the basis of much heated argument.

A resolution of these problems was attempted in August 1978, when a three-day workshop was held at Victoria, British Columbia, Canada, attended by nine prominent substorm researchers. Their brief was to attempt to reach consensus on a workable substorm definition, backed by a set of useable signatures. The results of their deliberations have been published very recently (Rostoker *et al. J. geophys. Res.* **85**, 1663; 1980).

The substorm picture discussed above is extended in the new descriptive definition offered by these authors in the recognition of 'multiple onsets', arising from observations of several discrete increases of activity during the expansion phase. Each of these increases is associated with a Pi-2 burst, the formation of a new westward-travelling surge in the auroras, and, as the surge crosses the local meridian, a discrete poleward expansion of the westward electrojet. The first increase in activity is termed the 'onset', and all subsequent increases prior to the start of recovery (defined as before), 'intensifications'. It is noteworthy that their definition includes the necessary appearance of at least one Pi-2 burst, the pulsations being taken to signify that the observed event is of an impulsive nature.

Fig. Sketches of auroras during substorms viewed looking down on the north pole showing (a) thin quiet arcs lying in an oval around the pole with a brightened arc at the equatorward border signalling substorm onset, (b) bulge formation by rapid poleward motion with a westward-travelling surge at its westernmost edge and eastward moving patches in the morning hours, and (c) auroras returning to quiet conditions during recovery. The coordinates are local time hours (longitude) and magnetic latitude.

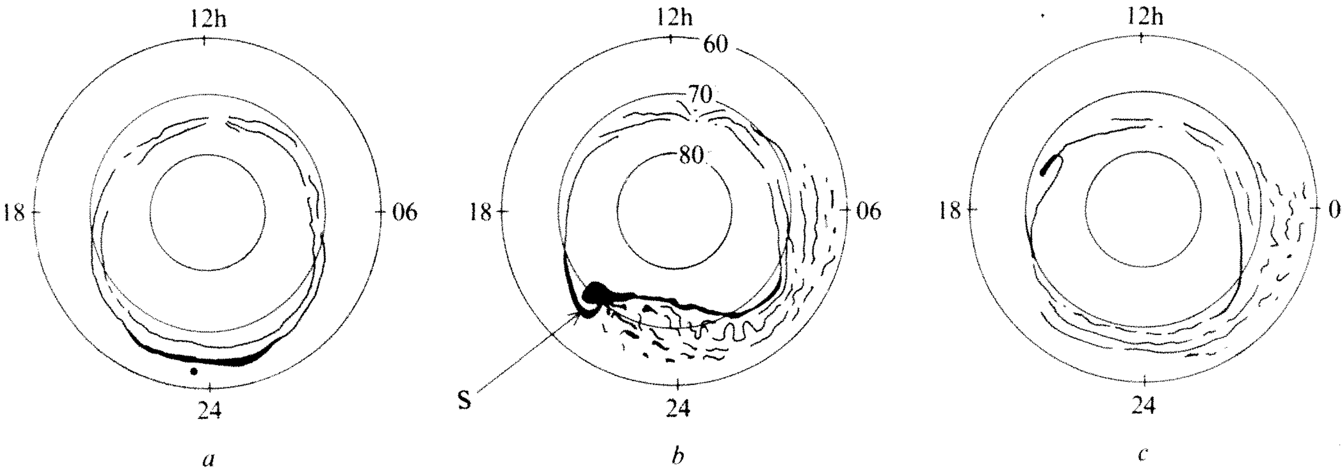

0028-0836/80/300332-02$01.00

The second and more important feature of their discussion, however, is concerned directly with the difficulties and ambiguities inherent in currently available ground-based data, and the circumstances required for the drawing of valid conclusions regarding the start of the expansion and recovery phases. It is pointed out, for example, that a single all-sky camera sees only a small part of the whole auroral display at any one time, and as a result the brightening of arcs just to the west of a surge followed by passage of the surge across the local meridian can easily be mistaken for a local onset. In the future any substorm onset time proposed on the basis of local auroral brightening should therefore, the authors say, be substantiated by showing that at the least no brightening occurred a few minutes earlier to the east of the station. Similar treatment is given to the magnetic signature, and it is finally uncompromizingly recommended that researchers use original magnetograms from "as many relevant observatories as possible" to determine individual substorm development. Standard magnetic indices, in common use at present, which are synthesized from a few auroral zone stations are to be eschewed.

Even if the above laborious practices are followed, however, not all onset and recovery times can be determined with confidence due to gaps in ground coverage. Indeed some substorms, particularly those of small amplitude which tend to occur at higher than normal latitudes, may not be detected at all. These inadequacies were particularly exposed in the last decade when the first whole auroral oval pictures became available via the imagers flown by the US Air Force Geophysical Laboratory on DMSP satellites and by Canadian experimenters on ISIS-2. In these systems the picture is built up on a line-by-line basis as the satellite traverses the polar regions at ~ 1,000 km altitudes, so that only one 'snapshot' (of the northern auroral zone) is obtained per orbit (~90 min). These images allowed a great step forward in understanding auroral morphology, but were, of course, unable to follow the changes during substorms. A radical solution to the problems emphasized by Rostoker *et al.* is therefore clear, although technically difficult and rather expensive. What is needed, as the authors point out, is a satellite auroral TV system with a resolution better than 10 km spatially and 1 minute in time, which can return images continuously for a period of several hours. Only with such data will the full story of the dynamic auroras be finally revealed. □

S. W. H. Cowley is an SRC Advanced Fellow in the Blackett Laboratory, Imperial College, London.

Radar measurements of estuarine currents and tides

from E.D.R. Shearman

An important step in the development of a new remote sensing system is reached when the research moves from comparisons with ground truth to the provision of area surveillance data in a form directly comparable with theoretical models. This point has now been reached for surface current measurement by High Frequency (HF) radar in the dekametric band as described by A.S. Frisch and B.L. Weber[1].

The discovery from which HF radar oceanography has grown was made in 1969 by D.D. Crombie[2]. In observations with a vertically-polarized 13.5 MHz radar, directed seawards from a coastal site, he detected Doppler-shifted echoes with a strong spectral line component at a shift of 0.376 Hz. This shift corresponds to a radial velocity which is that of gravity waves on the sea surface of wavelength 11 m, just half the radio wavelength. There is a selective scattering process, now known as Bragg scattering by analogy with the diffraction of X rays from the regular rows of atoms in a crystal lattice. This process sifts out from the chaotic superposition of waves of different lengths and different directions on the sea-surface those waves travelling radially towards or away from the radar and of wavelength half the radar wavelength.

By using a number of radar frequencies and by directing the radar beam in different directions it thus becomes possible to measure the wavelength spectrum and the directional spectrum of sea waves, whether wind-driven waves or swell. This has led to

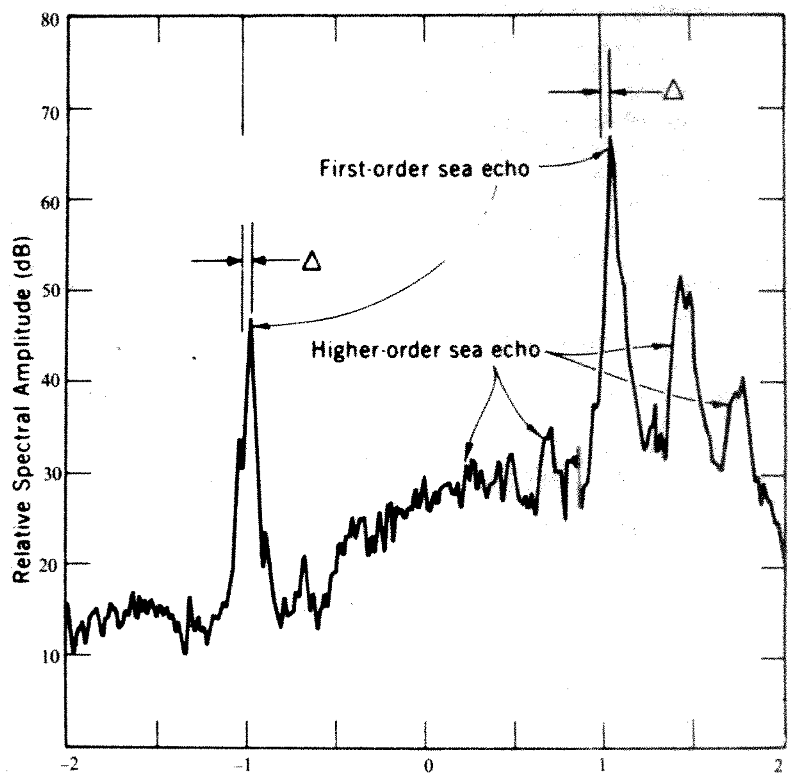

Fig. 1 Example of 9-sample average of 200 second HF ground-wave sea-echo power spectra at 9.4 MHz. Doppler frequency (horizontal axis) is normalised with respect to the expected position of the first order Bragg resonant peaks (here 0.313 Hz). Δ is the normalized shift of the record due to a surface current, as utilized in the NOAA current-measuring radar. Note the narrow Bragg peaks as seen with a narrow-beam radar. (After Barrick *et al*[7]).

E.D.R. Shearman is in the Department of Electronic and Electrical Engineering, University of Birmingham.

0028-0836/80/300333-02$01.00

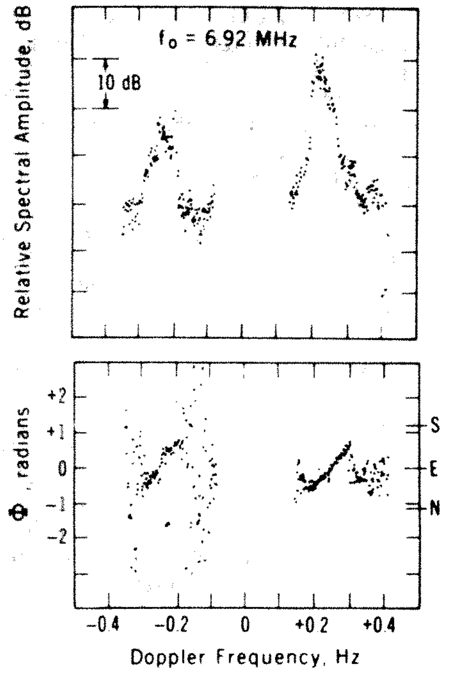

Fig. 2 Upper: Doppler spectrum of current-smeared sea echo from the Gulf Stream received on a wide-beam antenna.
Lower: Phase difference between two spaced antennas versus Doppler-shift, demonstrating that echoes from different directions are sorted by current-produced Doppler and can then be identified. (After Crombie *et al*[11]).

the remote measurement not only of wave spectra, but also, by inference, of sea-surface wind direction[3] and wind speed[4].

Theoretical investigations by Hasselmann[5] and by Barrick[6] make it possible to deduce the wavelength and the directional spectra of sea waves by inversion of second order features in the radar echo spectra from a single patch of ocean at a single radio frequency. The spectrum of Fig. 1, obtained at San Clemente Island, California[7], illustrates these first and second order features. These techniques already promise a capability for characterising sea-state over a large area of ocean. Crombie's coastal-sited 'ground-wave radar' technique can give coverage up to some 300 km with suitable power and frequency; 'sky-wave radar' using ionospheric refraction covers the area between 1,000 km and 3,000 km from the radar[8,9]. A useful review of the basic concepts of HF radar oceanography has been given by Barrick[10].

The paper by Frisch and Weber makes use of a different phenomenon from those employed in the above wave and wind measurements. In Fig. 1 it will be seen that the approach and recede first-order Bragg resonant frequencies, nominally at ±1 on the normalized Doppler frequency scale, are displaced from symmetry about zero, as if the approaching waves were travelling faster towards the radar than the receding waves away from the radar. This is what would be expected if the water surface were being carried towards the radar by the radial component of a tidal stream or current. (In the case of sky-wave propagation, such shifts can also be introduced by ionospheric motion, but this is not so for ground-wave radar).

If we consider a ground-wave radar located on the sea coast with an omnidirectional antenna, so that sea areas in all directions contribute to the received echo, a 'current-smearing' will occur. Returns from different directions will be Doppler-shifted by the current to different extents. Fig. 2 shows the results of an experiment done under conditions[11] in which reception took place on two spaced antennas. At the top is seen the current-smeared spectrum for the approach and recede Bragg resonant waves, while at the bottom is the phase difference between the two antenna signals plotted as a function of Doppler shift. This phase difference, Φ, would be expected to be given by $k_0 d \sin \alpha$ where d is the (known) spacing between the two receiving antennas, α the azimuthal angle relative to the normal to d, and k_0 is the (known) radar wave number. We see that by Doppler analysing the echoes, returns from each direction have been sorted by frequency and that it is then possible to measure their direction of arrival by simple relative phase measurement, at separated antennas. This is the principle of the NOAA current measuring radar[12].

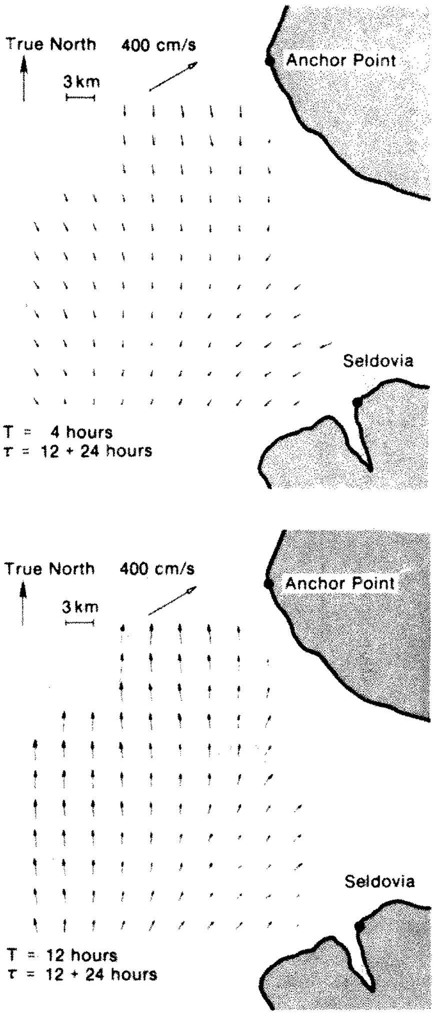

Fig. 3. Two maps depicting the tidal currents in the vicinity of Kachemak Bay at times 8 hrs apart. The current vectors are plotted at 3 km intervals relative to the southern radar site near Seldovia.

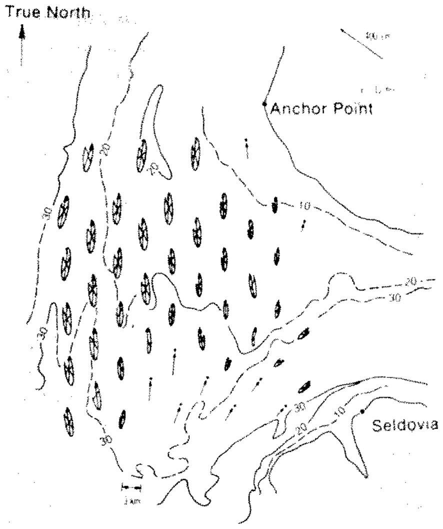

Fig. 4. Tidal ellipses for the 12 hour tidal velocity component in the vicinity of Kachemak Bay, starting at 00 hours on July 13, 1977. The arrow points to the current direction at 00 hours.

Frisch and Weber describe the deployment of two such radars in the Cook Inlet, Alaska. Fig. 3 shows a snapshot of current vectors obtained by putting together the radial current components measured from the two sites, Seldovia and Anchor Point. The data was analysed by extracting from the radar results at grid locations spaced 3 km apart, the North-South and East-West components of the current. The values of these components were available from observations taken every fifteen minutes throughout twenty-four hours. A least square fit was then carried out to estimate the nominal twelve and twenty-four hour tidal components for the surface currents as a function of position. The current velocity at the grid locations showed a considerable but orderly amplitude and phase variation over the radar coverage area.

A compact summary of the kind of results that can be obtained by this method is given in Fig. 4, here showing the tidal ellipses for the 12 hr component of tidal velocity. □

---

1. Frisch, A.S. & Weber, B.L. *J. geophys. Res.* **85**, 485(1980).
2. Crombie, D.D. *Nature* **223**, 1325 (1969).
3. Long, A.E. & Trizna, D.B. *IEEE., Trans. Ant. Prop.*, **AP-21**, 680 (1975).
4. Barnum, J.R., Maresca, J.W. & Serebeny, S.M. *IEEE., Trans. Ant. Prop.* **AP-25**, 128 (1977).
5. Hasselmann, K. *Nature Phys. Sci.* **229**, 16 (1971).
6. Barrick, D.E. *Remote Sensing of Environment*, **6**, No. 2, 201 (1977).
7. Barrick, D.E., Headrick, J.M., Bogle, R.W. & Crombie, D.D., *Proc. IEEE.*, **62**, No. 6, 673 (1974).
8. *Proc. IEEE. Special issue on modern radar technology and applications. Proc. IEEE* **62**, No. 6 (1974).
9. Shearman, E.D.R., Sandham, W.A., Bradley, E.N. & Bradley, P., *AGARD Conf. Proc.* **263**, 30 (1979).
10. Barrick, D.E. *Remote Sensing of the Troposphere* (ed. Derr, V.E.) Chap. 12 (US Govt. Printing Office, Washington 1972).
11. Crombie, D.D., *et al.* 1970. Reproduced in NOAA Technical Report ERL 373, WPL 47, (U.S. Dept. of Commerce 1976).
12. Barrick, D.E., Evans, M.W. & Weber, B.L. *Science* **198**, 138 (1977).

ARTICLES

Nd–Sr isotopic relationship in granitoid rocks and continental crust development: a chemical approach to orogenesis

Claude J. Allègre & Dalila Ben Othman

Laboratoire de Géochimie et Cosmochimie, Institut de Physique du Globe, Département des Sciences de la Terre, Universités de Paris VI et VII,
2 Place Jussieu, 75230 Paris Cedex 05, France

Nd and Sr isotopic compositions of young granitoid rocks from diverse locations show that none of them is derived from an oceanic mantle. Instead a large amount of recycled older continental crust must be involved in their genesis. In contrast old granitoids (older than 2,000 Myr) seem to have initial isotopic ratios of Nd and Sr quite close to the planetary mantle evolution line. These observations are interpreted as evidence of a quasi-continuous continental growth through geological time. We propose a mixing model to explain quantitatively the generation of granitoids from mantle and recycled continental materials.

THE process of orogeny incorporates a variety of stages such as folding, metamorphism and granitization, and its main chemical result is the formation of a piece of continental crust. As granitoids are the main components of continental crust, the problem of their genesis is linked to that of the origin and evolution of continents. Two extreme theories have been proposed:

(1) continental crust is created from the mantle by a continuous differentiation process throughout geological time;

(2) continental crust has been differentiated once from the mantle, early in the Earth's history, since then this material has been continuously recycled into the new crust.

The formation of granites can also be described by two models: either as the ultimate product of magmatic differentiation, or as a product of crustal anatexis[1,2]. Although using Sr or Pb isotopes as petrogenetic tracers has clarified some problems[2–7] no widely accepted model has been proposed so far.

Following the work by Richard *et al.*[8] Nd isotopes were used for extremely powerful tracer studies[9–13]. Their usefulness is due to two geochemical properties of rare-earth elements (REEs): they are not very mobile and large geochemical fractionation of the parent/daughter Sm/Nd ratio is difficult.

This article considers the application of the coupled Nd–Sr isotopic systems to the genesis of continental crust: old and young granitoids are compared.

Petrogenesis of recent granitoids

We have investigated the Nd systematics in granitoids younger than ~350 Myr (the age correction for ^{147}Sm *in situ* decay is, therefore, rather small) representative of the various geodynamic environments: (1) island-arcs (Japan); (2) continental subduction zones (Andes); (3) complex subduction areas (southern California Batholith, Sierra Nevada); (4) continental collision zones (Himalayan and European hercynian granites). Results for the major petrographic types of granitoids are given in Table 1 and illustrated in Figs 1 and 2.

Subduction zones

Japan. We have studied two typical Japanese granitoids from Okue and Owe in the centre of Honshu Islands, which are 21- and 12-Myr old respectively. Like the whole calc-alkaline suite, these granitoids are associated with the general subduction process. $\varepsilon^{i}_{Nd} = -3.3$ and -3.1 (see Table 1 for a definition of ε_{Nd}). Because these values are significantly lower than those for mid-oceanic[8–11] and island-arc basalts[12,13], direct derivation from a downgoing plate is ruled out. These granitoids are at least partly composed of crustal material, which may have been incorporated into the subducted plate as detritial sediments, or it might result from remelting of the overlying continental crust induced by the presence of hot basic or calc-alkaline magmas.

California. Two typical batholiths occur in California: in southern California and in the Sierra Nevada. Although the tectonic situation at the time of their formation is not clear, it is considered to be related to subduction processes[14].

The southern California batholith is a complex which includes many different types of granitoids with ages ranging from 80 to 103 Myr on the east and 105 to 130 Myr on the west[14]. Detailed studies by Silver *et al.*[14–17] using Sr and Pb isotopes and trace elements, and by Taylor and Silver[18] using ^{18}O/^{16}O and ^{87}Sr/^{86}Sr ratios, have shown that the batholith can be divided into a western and an eastern part, the former being older and emplaced at a shallower depth than the latter.

The variation of ^{18}O/^{16}O and ^{87}Sr/^{86}Sr seems to confirm that several sources are involved in the genesis of this batholith. The value $\varepsilon^{i}_{Nd} = +3.6$ for the San Marcos gabbro is consistent with that of mid-oceanic ridge basalts (MORB) contaminated by some crustal material. The Rubidoux granite, a 'charnockitic granite' has $\varepsilon^{0}_{Nd} = -1.4$. which is close to the present chondritic value, while for the Lakeview Tonalite $\varepsilon^{0}_{Nd} = -9.9$ which is very different from any mantle material value and implies a large crustal component.

In the study of the Sierra Nevada batholith by Hurley *et al.*[19] using the ^{87}Rb/^{87}Sr method, some isotopic heterogeneities were pointed out within the batholith. More recent studies[20] gave a better definition of this heterogeneity: this batholith is composed of many plutons almost continuously emplaced from 134 to 85 Myr and with some older ones around 160 Myr. In the southern California batholith there is a systematic variation from west to east for both Sr and Pb isotopes. Note that the four rocks studied here clearly do not constitute a comprehensive survey of the two massives. As the ε^{i}_{Nd} vary between -7 and -3.3 and is clearly outside any mantle trend, this implies the participation of crustal material in the genesis of these batholiths. Again, none of these granitoids can be considered as the direct product of mantle type material—remelting of old continental crust is needed. This agrees with the studies of Magaritz and Taylor and Armstrong *et al.*[21,22]. Both batholiths are heterogeneous and seem to contain oceanic material mixed with previous continental crust.

Peru. The tectonic environment in the Andes is important because it has been considered as the archetypal continental growth mechanism. Although we have studied only one granitoid, more extensive research has been carried out on the different types of lavas which are widely held to be the extrusive

0028–0836/80/300335—08$01.00

equivalent of true granitoids. We have studied two andesites, three rhyolites and one dacite, from the Barrosso and Arequipa volcanic fields in southern Peru. Sr and Pb isotope studies have shown that these rocks have been contaminated by continental crust[23,24]. This contamination seems to be differential and more extensive than for other samples. The values of ε^{i}_{Nd} are all negative between −1.4 and −5.1; none of these values are thus consistent with a pure derivation from oceanic mantle. These results agree with those of De Paolo and Wasserburg[9] which are based on the analysis of one andesite and imply a crustal contamination.

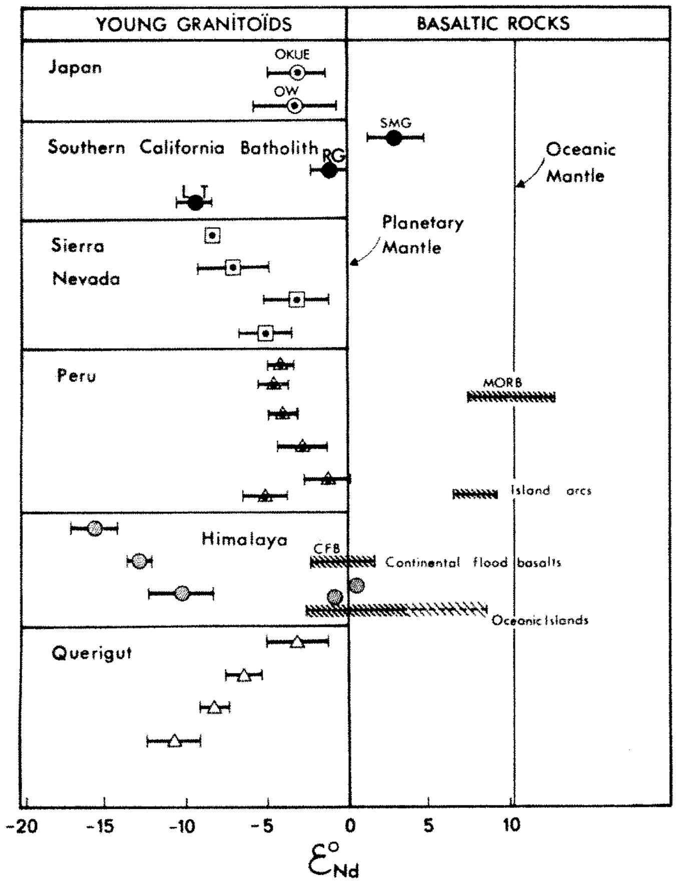

Fig. 1 Raw values of young granitoids expressed in ε^{o}_{Nd}. The reference values for MORB, oceanic islands, continental flood basalts and islands arcs are from refs 8, 9–11, 37: ⊙, Japan; ●, Southern California Batholith; ⊡, Sierra Nevada; ▲, Peru; ◉, Himalaya; △, Pyrenees, Quérigut; ◎, Costabonne; ◆, Aix les Thermes; ▲, In'zize. We adapted the technique of Richard *et al.*[8] to the granite problem. To dissolve all the accessory minerals (such as sphenes and zircons) often rich in REE, they were attacked in a Teflon bomb under pressure (see ref. 73), HNO_3 and $HClO_4$ were added, reevaporation took place and they were then dissolved in 6 M HCl. Measurements were made using the triple filament technic. The total blank is about 40 pg and is, therefore, negligible in our study. Notations are defined by:

$$\varepsilon^{o}_{Nd} = \frac{(^{143}Nd/^{144}Nd)_{sample,Today} - (^{143}Nd/^{144}Nd)_{Pla,Today}}{(^{143}Nd/^{144}Nd)_{Pla,Today}} \times 10^4$$

$$(^{143}Nd/^{144}Nd)_{Pla,Today} = 0.51264 \text{ (ref. 74)}.$$

$(^{143}Nd/^{144}Nd)_{sample,Today}$: measured value of the sample. $\varepsilon^{initial}_{Nd}$ for a sample of age T_1 is defined in the same way:

$$\varepsilon^{i}_{Nd} = \frac{(^{143}Nd/^{144}Nd)^{sample}_{I,T_1} - (^{143}Nd/^{144}Nd)_{Pla,T_1}}{(^{143}Nd/^{144}Nd)_{Pla,T_1}} \times 10^4$$

$$(^{143}Nd/^{144}Nd)_{Pla,T_1} = (^{143}Nd/^{144}Nd)_{Pla,Today} - (^{147}Sm/^{144}Nd)_{Pla}(e^{\lambda T_1 - 1});$$

$$(^{143}Nd/^{144}Nd)^{sample}_{I,T_1} \bullet (^{143}Nd/^{144}Nd)_{sample,Today} - (^{147}Sm/^{144}Nd)_{sample} \cdot (e^{\lambda T_1 - 1}).$$

The Sr isotopic composition has been measured in most samples following the technique described elsewhere[75]. For Sr, ε^{i}_{Sr} can also be defined in the same way[36].

The continental collision situation

The continental collision environment must exist in Himalayan granites and has also been proposed to account for the French hercynian segment[25].

The Himalayan granitoids can be divided into two categories: those which are situated along the Main Central thrust (MCT), a gigantic intracontinental thrust inside the Indian shield[25,26] and those which are on the edge of the Tsanpo suture, composing the Laddakh batholith.

The MCT granites are all leucogranites (aluminous, two mica alkaline granites). An age determination of 29 Myr for the Manaslu massif has been questioned[27], and the other Palung Daman and Makalu-Kakani granitoids seem to be slightly different and not well dated either[28]. However, for general stratigraphic reasons, the ages of these granites are taken as between 50 and 15 Myr (ref. 26) which gives initial $^{87}Sr/^{86}Sr$ ratios of around 0.780. Such high ratios clearly represent the remelting of old continental material, which agrees well with the petrological study by Lefort[26]. As expected, ε^{i}_{Nd} values are strongly negative, from −10.3 to −15.8 and are the lowest values ever reported for young granitoids. There is little doubt that these values, like those for Sr, indicate the almost pure remelting of old continental crust.

The Laddakh complex is a large granodiorite complex which represents the granitoids associated with the major collision between India and Eurasia. Two samples have been analysed with ε_{Nd} values of +1.8 and −1.4. Both values may be interpreted as a record of material derived from an oceanic crust contaminated by crustal material (as for California or Japan).

The 'pyrenean' granitoids have been extensively studied from the chronological, isotopic, and petrological points of view[29–34]. They were deposited during the hercynian orogeny and can be divided into two groups. The first is represented by early granites emplaced 320 Myr ago with a high initial $^{87}Sr/^{86}Sr$ ratio (0.712) characteristic of many gneissic xenoliths; a typical example is the Aix-les-Thermes 2-mica granite. The second group is younger (280 Myr) and has a lower initial $^{87}Sr/^{86}Sr$ ratio[29]. These granitoids are characterized by xenoliths of quartz dioritic composition and a complex set of different facies[32]. The Querigut granite[33] and the Costabonne granite belong to this second group.

According to Mattauer's interpretation of the hercynian orogeny in western Europe[34], these granites were generated during a continental collision very similar to the Himalayan one. All of the granites have negative ε^{i}_{Nd} values between −0.7 and −8.9 which again cannot be explained by direct derivation from the oceanic mantle. This conclusion is supported by trace element results[35].

Nd–Sr relationship on modern granitoids

The relationship between the Sr and Nd isotopic ratios of modern basalts suggested by Richard *et al.*[8] and demonstrated by others[10,11] is a very important and distinctive signature of mantle evolution[36]. It seems that the initial ratios of Sr and Nd of any material directly derived from the mantle would probably plot on this general trend. On the other hand, as we have already emphasized, the studies of Carter *et al.*[37] have shown that the Sr–Nd isotope diagram can clearly discriminate a mantle type origin from a lower or upper crustal origin. Therefore, the Nd–Sr diagram should give a clear distinction between different hypotheses of granitoid genesis. Let us consider the general trends in ε^{o} notations. The present terrestrial mean corresponds to $\varepsilon^{o}_{Nd} = 0$ ($^{143}Nd/^{144}Nd = 0.51264$) (see above) and by definition $\varepsilon^{o}_{Sr} = 0$ ($^{87}Sr/^{86}Sr = 0.70478$) (ref. 36). The oceanic mantle, and probably some of the subcontinental mantle plot in the upper left quadrant ($\varepsilon^{o}_{Nd} > 0$ and $\varepsilon^{o}_{Sr} < 0$). In this quadrant there is a negative correlation between ε^{o}_{Nd} and ε^{o}_{Sr}. Carter *et al.*[37] have shown that Lewisian granulites normally plot in the lower left quadrant ($\varepsilon^{o}_{Nd} < 0$ and $\varepsilon^{o}_{Sr} < 0$) although a few granulites do have positive ε^{o}_{Sr}. The old granitoids or gneisses in amphibolite facies

Table 1 Major petrographic types of the granitoids

Samples	^{147}Sm/^{144}Nd	^{143}Nd/^{144}Nd*	$\varepsilon^{0}_{\mathrm{Nd}}$†	ε^{i} Nd†	^{87}Sr/^{86}Sr	^{87}Sr/^{86}Sr‡ initial	^{87}Rb/^{86}Sr‡	Model Sr age (Myr)	Model Nd age (Myr)	Real Age (Myr)	$\varepsilon^{\mathrm{i}}_{\mathrm{Nd}}$	$\varepsilon^{\mathrm{i}}_{\mathrm{Sr}}$
Young granitoids												
Japan Okue 2		0.51247±9	−3.3	−3.3	0.7062±1	0.70610	2.15	49		21	−3.3	+11.3
Owe 2		0.51248±13	−3.1	−3.1	0.7077±1	0.70713	3.00	72		12	−3.1	+34.4
Himalaya												
Nepal 22 D. Manaslu	0.141	0.51183±7	−15.8	−16.3	0.74332±40§	0.7408§	5.98§	471	2,340	28	−16.3	+513.6
Palung A 404		0.51197±4	−13.1	−13.1	0.82131±50§	0.8000§	37.8§	223			−13.1	+1,456.0
Makalu 132	0.121	0.51211±10	−10.3	−10.10					1,110	26	−10.10	
Laddakh												
granodiorite HB68	0.108	0.51256±3	−1.4	−1.4	0.7050±1§	0.7045	0.170	190	65	51	+2.0	2.66
diorite HB74	0.617	0.51273±3	+1.8	+1.8	0.7048±1§	0.7045	0.352				−1.1	2.28
Southern Batholith of California												
San Marcos G. 60-5	0.153††	0.51279±5	+2.9	+3.6	0.7040	0.7032	0.38	−190	−565	120	+3.6	−18.2
Rubidoux G. EL 38		0.51257±5	−1.4		0.7121	0.7045	4.42	121		120		−1.0
Lakeview Tonalite 60-2		0.51213±4	−9.9		0.7058	0.7045	0.73	114		120		−1.1
Sierra Nevada												
R 5075		0.51228±11	−7.0	−7.0	0.7072±2	0.7063	0.68	293		90	−7.0	+23.6
R 5084		0.51247±10	−3.3	−3.3	0.7106±1	0.70937	1.13	404		90	−3.3	+64.4
R 5079		0.51237±8	−5.3	−5.3	0.7106±1	0.70950	0.97	474		90	−5.3	+66.6
R 4602	0.107	0.51220±2	−8.6	−6.6	0.7083±2	0.7063	0.79	361	775	180	−6.6	+24.4
Peru												
Granite P 293		0.51238±10	−5.1		0.7235±1	0.7105	4.02	342		230		83.4
Rhyolites												
P 255	0.094§§	0.51248±8	−3.1	−3.1	0.70705±5#	0.7070±3#	1.95#	87	246	1.74	−3.1	32.2
P 293	0.116§§	0.51257±4	−1.4	−1.4	0.73928±7#	0.7174±3#	909.0#	2.8	138	1.74	−1.4	171
P 292	0.138§§	0.51238±6	−5.1	−5.1	0.7484±6#	0.7174±3#	1172.4#	2.6	715	1.74	−5.1	206.1
Dacite												
P 254	0.086§§	0.51243±3	−4.1	−4.1	0.70619±6#	0.70618±6#	0.57#	209	298	1.74	−4.1	20
Andésites												
P 290	0.104§§	0.51242±4	−4.3	−4.3	0.70551±5#	0.70551±6#	0.54#	108	375	1.74	−4.3	10.3
P 289	0.085§§	0.51239±1	−4.9	−4.9	0.70574±4#	0.70574±6#	0.54#	151	352	1.74	−4.9	13.6
French Hercynian granites												
From Querigut												
Quartz diorite QT 08	0.137‡‡	0.51250±9	−2.7	−0.7	0.7085±9	0.70633	0.55	578	378	280	−0.7	26.7
Monozonitic granite QT 12	0.097‡‡	0.51230±6	−6.6	−3.2	0.7214±2	0.7101	2.89	426	540	280	−3.2	77.7
Granodiorite QT 52	0.112‡‡	0.51221±3	−8.4	−5.5	0.7136±7	0.7099	1.09	632	806	280	−5.5	68.6
Calcalkaline granite with bitotites QT 15	0.138‡‡	0.51208±9	−10.9	−8.9	0.7458±10	0.7153	7.78	383	1,540	280	−8.9	156.1
Granite Costabonne	0.142	0.51239±45‖‖	−4.9	−3.1	0.7230¶¶	0.711	3.03	445	741	265	−3.1	104.4
Aix les Thermes AX4	0.110	0.51204±60‖‖	−11.7	−8.2	0.7829¶¶	0.711	15.9	355	1,100	325	−8.2	92.6
Sahara												
Inzize	0.1197	0.51170±5	−18.3	−12.7					1,930	600	−12.7	
Precambrian granitoids												
Grenville												
5208 Wesport Granite	0.0920	0.51209±3	−10.7	+2.5	0.753**	0.704**	3.25	1,090	835	1,020	+2.5	+43.4
5210 Blue Mountain	0.1325	0.51210±9	−10.4	−0.37	0.727	0.7041±4	1.30	1,290	1,339	1,285	−0.37	+5.1
Rapakivi Parguasa (Venezuela)	0.092	0.51160±2	−20.3	−0.35	0.8405	0.7004±1	6.53	1,500	1,510	1,530	−0.35	−39.4
Tassendjanet												
L 418	0.085	0.51125±3	−27.1	+2.0	0.713±1	0.7018	0.39	1,950	1,930	2,090	+2.0	−10.3
M 697	0.086	0.51123±1	−27.5	+1.0					1,980	2,090	+1.0	
Ivory Coast Granite CI_2	0.107	0.51150±6	−22.3	+0.1	0.7141±6	0.7010±5	0.416	2,010	2,000	2,010	+0.1	−0.0
Swaziland												
S_1, S_A	0.115	0.51098±2	−32.3	+2.1					3,200	3,400	+2.1	
S_1, S_8	0.106	0.51066±2	−38.6	−0.2					3,400	3,400	−0.2	
China granites												
CHID	0.119	0.51150±3	−22.3	+0.8	0.7033±8##	0.7025±5##	0.023##	1,590	2,320	2,400	0.8	+18.9
CHIB	0.068	0.51073±5	−37.3	+0.9	0.7165±7##	0.7025±5##	0.417##	2,550	2,340	2,400	0.9	+8.6

* Normalized to ^{146}Nd/^{144}Nd = 0.7219; errors are 2σ mean.

† $\varepsilon^{0}_{\mathrm{Nd}}$ and $\varepsilon^{\mathrm{initial}}_{\mathrm{Nd}}$ relative to Juvinas; ^{143}Nd/^{144}Nd today = 0.51264; ^{147}Sm/^{144}Nd today = 0.1936; $\lambda\,^{147}\mathrm{Sm} = 6.54 \times 10^{-12}\ \mathrm{yr}^{-1}$.

‡ $\lambda\,^{87}\mathrm{Rb} = 1.39 \times 10^{-11}\ \mathrm{yr}^{-1}$; ^{87}Sr/^{86}Sr today = 0.70478; ^{87}Rb/^{86}Sr today = 0.087.

§ Ref. 27. ‖ Unpublished data. ¶ Ref. 28. # Ref. 23. ** Ref. 55. †† Ref. 12. ‡‡ Ref. 34. §§ Dupuy, unpublished data. ‖‖ Ref. 8. ¶¶ Ref. 76. ## Feldspar from CH1D and CH1B.

A number of ratios of ^{87}Sr/^{86}Sr, taken from the literature (for example, Aix les Thermes, and Costabonne) are given here with smaller number of digits (3 or 4) and without error bar, due to their ancient determination.

(^{87}Sr/^{86}Sr) initial ratios for Japan, Sierra Nevada, Querigut and part of Peru samples have been calculated from ages determined with other radiochronometers and with the $\lambda_{\mathrm{Rb}} = 1.39 \times 10^{-11}\ \mathrm{yr}^{-1}$. Ages for all the other samples have been determined from corresponding isochrons.

and old schists, which might be attributed to the upper or medium continental crust, plot in the lower right quadrant ($\varepsilon^{0}_{\mathrm{Nd}} < 0$, $\varepsilon^{0}_{\mathrm{Sr}} > 0$).

To compare the position of modern granites with that of other rock types more quantitatively, we have to remember that $\varepsilon^{0}_{\mathrm{Nd}}$ and $\varepsilon^{0}_{\mathrm{Sr}}$ values for the old granitoids and gneisses which form the basement in most continental areas strongly depend on their ages. Statistically the older they are, the lower their $\varepsilon^{0}_{\mathrm{Nd}}$ and the higher their $\varepsilon^{0}_{\mathrm{Sr}}$. This precludes the possibility of getting a simple field in a $\varepsilon^{0}_{\mathrm{Nd}}$–$\varepsilon^{0}_{\mathrm{Sr}}$ diagram for all types of continental crust and, therefore, we must consider each case individually.

In the ($\varepsilon^{\mathrm{i}}_{\mathrm{Nd}}$, $\varepsilon^{\mathrm{i}}_{\mathrm{Sr}}$) correlation diagram we shall consider the mantle correlation band and the quadrant defined by Carter *et al.*[37]. Plotting our results for young granitoids, we see that (Fig. 3) most modern granitoids plot in the lower right quadrant, roughly indicating that they show isotopic affinities with the upper or medium crust rather than with the granulite facies. Only the two granitoids of the southern California batholith plot in the lower left quadrant. These massifs may be derived from lower granulite crust (see ref. 37). Thus the correlation diagram qualitatively suggests that no young granitoid is an uncontaminated product of the mantle, and that they all contain some crustal recycled component. We can now study the mixing of a mantle component and a recycled crustal component more quantitatively. Such a theory was first proposed in 1965 (ref. 38) using isotopic evidence, but it can now be modelled.

The equations show (see Fig. 4*b*) that the mixing depends on three groups of parameters: (1) the isotopic compositions of the

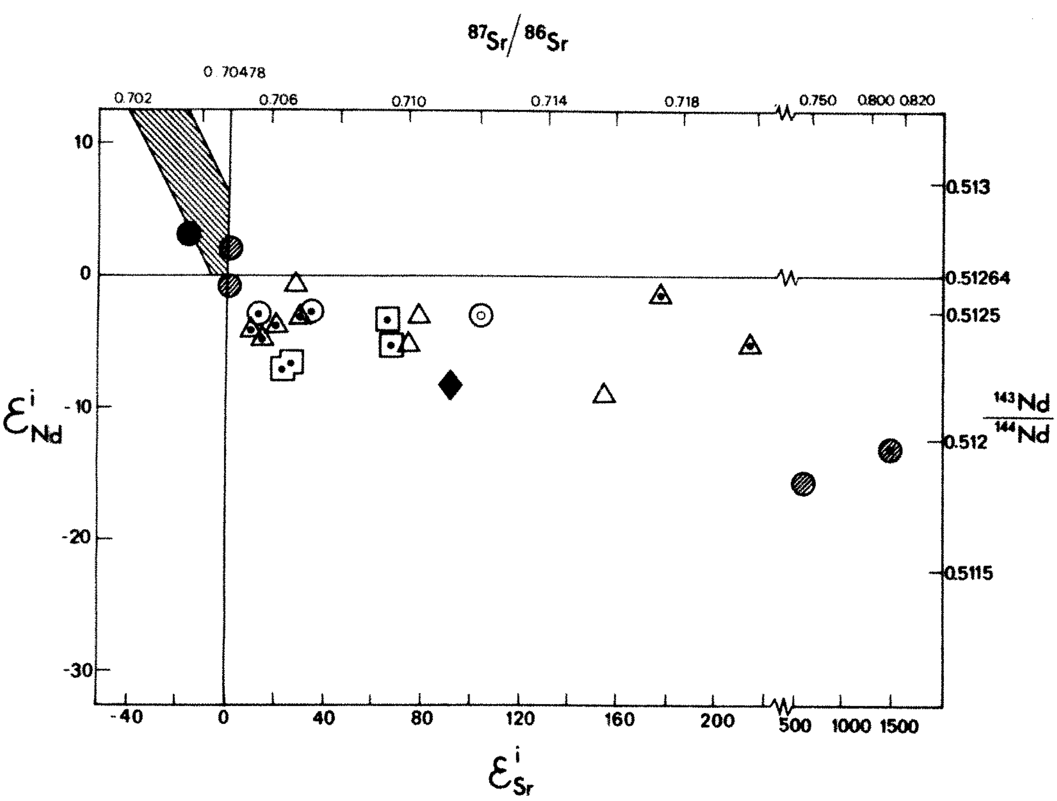

Fig. 2 Comparison of ε^i_{Nd} with ε^i_{Sr} for young granitoids. Symbols are as in Fig. 1.

two end-members, the mantle and the crustal component; (2) the ratios of Nd and Sr concentrations in crust and mantle, C^c_{Nd}/C^m_{Nd} and C^c_{Sr}/C^m_{Sr}; (3) the mass ratio of the two components, m^c/m^m.

We will select two different points for the isotopic composition of each component. We assume that the mantle component has the composition of a typical oceanic MORB mantle or that it has a planetary composition. For the crustal component we will fix the Sr isotopic ratio as $^{87}Sr/^{86}Sr = 0.720$, and take a 'young' crustal component with $^{143}Nd/^{144}Nd = 0.5125$ and an 'old' crustal component with $^{143}Nd/^{144}Nd = 0.5108$. These limits allow the observed results to be discussed in a general framework.

The mixing equations also involve the Nd and Sr crust/mantle concentration ratios. The values for both the upper and lower crustal component concentrations fall in a fairly narrow range[37,39,40]. The mantle component concentrations are more difficult to ascertain; this component may be a highly differentiated rock such as rhyolite, or a moderately differentiated one such as diorite[29]. It cannot be of typical basaltic nature because if it were the mixture with the crustal component would change the isotopic ratios so that the mixture would inherit a 'granitic' isotopic signature although it could be close to a basalt from the point of view of major element chemistry. For neodymium a crust/mantle concentration ratio of about 1 or 2 is reasonable. For strontium we can assume a crust/mantle concentration ratio of 0.3 which corresponds to the granite/diorite concentration ratio.

Most of our data plot in the field between the young and old crust mixing lines. For every young granite in Fig. 3, we can read in Fig. 4 its specific mixing ratio m^c/m^m. For a given ordinate in Fig. 4, a conservative estimate of the crust/mantle mixing ratio is provided by the interval between the ε_{Nd} values for the young and old crust mixing curves. A qualitative description in terms of young or old crust recycling can be obtained, rather than a precise young/old crust ratio or crust age. However, when the crust/mantle mixing ratio is found to be close to unity, a good approximation of crustal age is given by the Sm/Nd model age.

Most orogenic granitoids have been mixed with relatively young continental crust (Sm/Nd model ages: 600–1,200 Myr); this includes the Japan, Sierra Nevada, European Hercynian granitoids and Andean granitoids or andesites. For these areas the basement is not expected to be very old and, therefore, the results agree with the regional geology. The continental/mantle component mass ratio values are probably between 1 and 4. The highest ratio is that for the Himalayan anatectic granites which represent almost pure remelting of 1,100–2,300 Myr old basement. The hercynian granites from the Pyrenees have also a high m^c/m^m ratio.

The southern California batholith, on the other hand, plots outside the upper crust mixing curve field and would be accounted for by a mixture of mantle material and a lower crustal

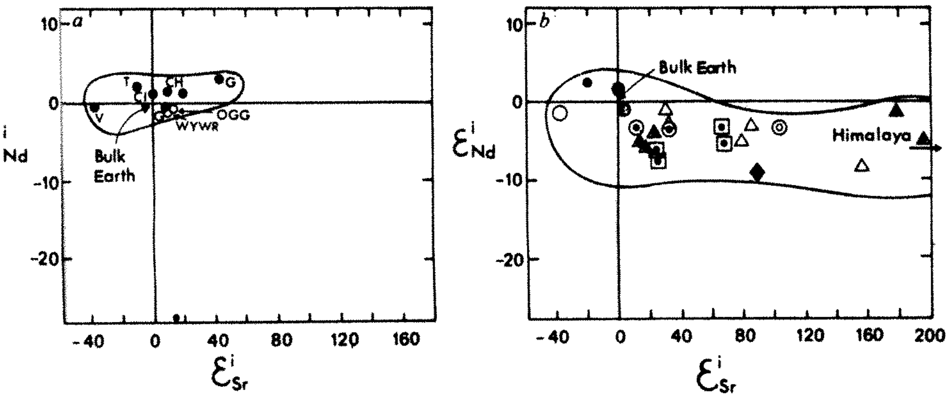

Fig. 3 *a*, *b* Comparison of ε^i_{Nd} with ε^i_{Sr} showing the contrast in the distribution of experimental points between granitoids older than 1,000 Myr (*a*) and those younger than 400 Myr (*b*).

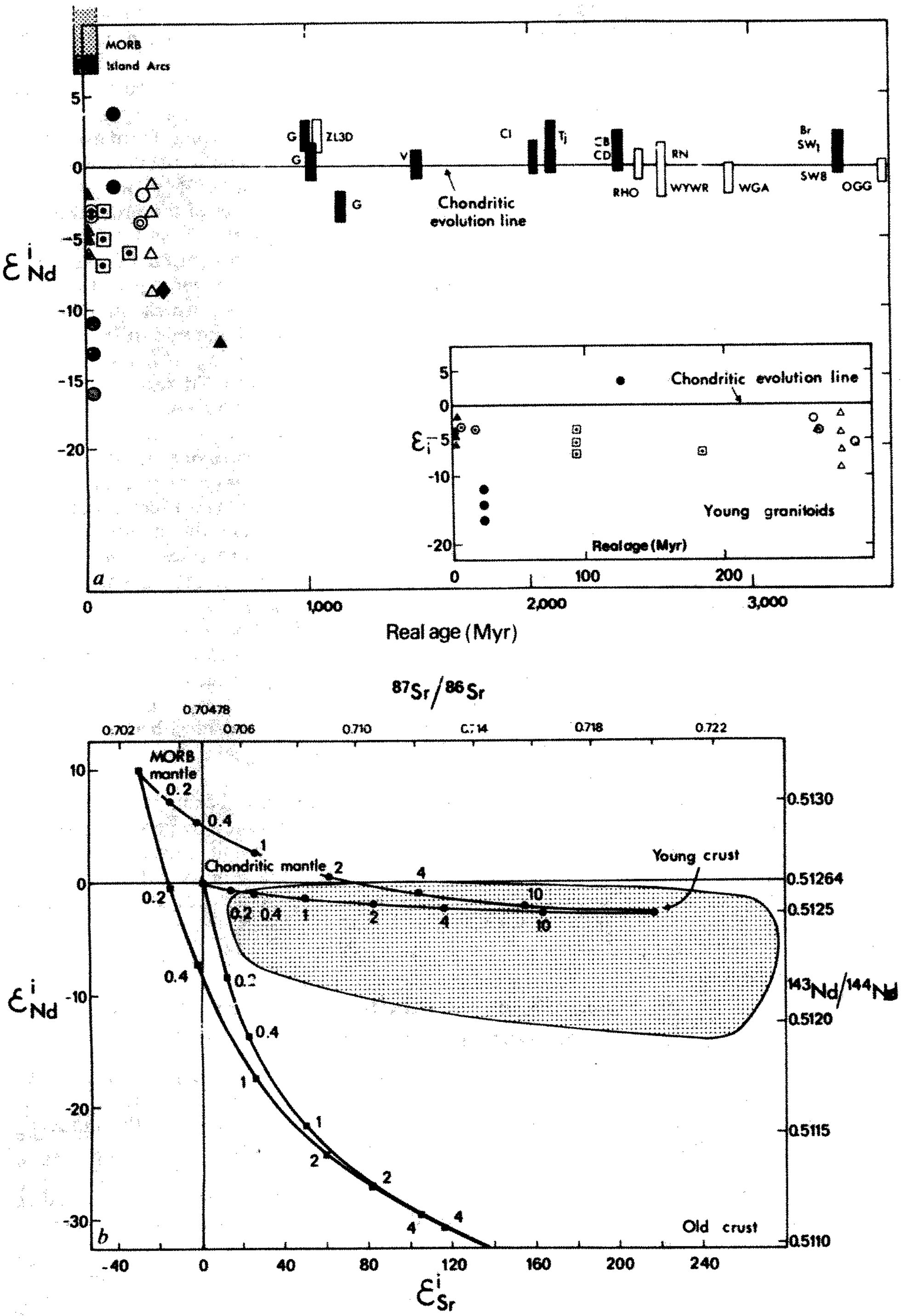

Fig. 4 *a*, Plot of ε^i_{Nd} with time (data from refs 9–12 and from the present study). As in Fig. 3 we can see the increase in deviation from the chondritic line with time. Young granites symbols are as in Fig. 1. Precambrian granites: this work: CI, Ivory Coast; Tj, Tassendjanet; C_B, C_D, North East China; SW_1, SW_8, Swaziland; V, Venezuela; G, Grenville. Other results: ZL 3D, Llano uplift; RHO, Great Dyke; RN_3, Preissac Lacorne B; WYWR, Louis Lake Gr_1 Wyoming; WGA, Anorthosite West Greenland; OGG, Amitsoq gneisses. *b*, Comparison of ε^i_{Nd} with ε^i_{Sr} illustrating the mixing model. The mixing is between two possible mantle materials (one MORB, one chondritic) and two possible continental crusts (old and young). Mixing equations:

$$R^m_{Nd}x + R^c_{Nd}(1-x) = R^\Sigma_{Nd}$$

$$R^m_{Sr}y + R^c_{Sr}(1-y) = R^\Sigma_{Sr}$$

where R_{Nd} is $^{143}Nd/^{144}Nd$ and R_{Sr} is $^{87}Sr/^{86}Sr$; R^m corresponds to the mantle input, R^c to the crustal input and R^Σ to the mixture.

$$x = \frac{C^m_{Nd}m^m}{C^m_{Nd}m^m + C^c_{Nd}m^c} = \frac{1}{1+(C^c_{Nd}/C^m_{Nd})(m^c/m^m)}$$

$$y = \frac{1}{1+(C^c_{Sr}/C^m_{Sr})(m^c/m^m)}$$

C^c_{Nd} (C^c_{Sr}) is the concentration of Nd(Sr) in the crustal component; C^m_{Nd} (C^m_{Sr}) the concentration of Nd(Sr) in the mantle component; m^c the mass of the crustal component; m^m the mass of the mantle component. The two curves indicate:

$$\frac{[\mathrm{Sr}]\text{ in mantle material}}{[\mathrm{Sr}]\text{ in continental material}} = 3.3$$

$$\frac{[\mathrm{Nd}]\text{ in mantle material}}{[\mathrm{Nd}]\text{ in continental material}} = 0.75$$

$$\frac{m_c}{m_m} = \frac{\text{mass of continental material}}{\text{mass of mantle material}}$$

The hatched area corresponds to the observed data.

component; such a conclusion does not contradict that of Taylor and Silver[18], but a more comprehensive study is needed to really understand the data. The position of the Skye anorogenic granite in the (ε^i_{Nd}, ε^i_{Sr}) diagram is close to the field of the Lewisian gneissic basement[37]. Its genesis has therefore involved remelting of an old basement.

The Nd and Sr isotopic results for most young granitoids leads to the main conclusion that there has been extensive involvement of previous continental crust. This effect is particularly important for continental collision orogenesis (almost pure crust remelting in the MCT from Himalayas). Subduction type orogeny involves more mantle material but with m^c/m^m values of 0.5–2. We can stress three points concerning the mixing process.

(1) Where the mixing[38] occurs has not been determined. It may take place in the geosyncline between volcanic rocks and detrital sediments, or during the intrusion of mantle diorite by assimilation, or even by sediments dragged down by the downgoing slab.

(2) Except for continental collision areas, the basement involved is not extremely old, which agrees with the border type models of continental growth (see below).

(3) Because Nd is extremely insoluble and not very mobile during water transport or metamorphism[41] the mixing process cannot be interpreted as selective contamination as it was for Sr or Pb. We had then to consider a volume-to-volume mixture. This is a characteristic of Nd isotopes and reinforces their usefulness.

Genesis of Precambrian granites

The Sm–Nd isotopic relationship of several Precambrian granitoid rocks have been investigated. They include:

Isua gneisses, 3,720-Myr old[42–44].

Amitsoq gneisses from Greenland, 3,650-Myr old[41–45].

Preissac Lacorne batholith from Quebec[46] and Lake Louis batholith from Wyoming, ~2,650-Myr old[47].

Lewisian gneisses, 2,920-Myr old[48].
Mountain Pass, California, with proposed[49] ages of between 1,400 and 1,700 Myr.
Llano uplift, 1 Myr old[50].

We have added several new examples:
The Swaziland (South Africa) granites, 3,400-Myr old[51].
The Tsien-Si metagranite (Republic of China), 2,400-Myr old.
The Tassendjanet granite (Sahara), 2,100-Myr old[52].
The Baoulé granite from Ivory Coast, 2,000-Myr old[53].
The Grenville granites from Ontario, 1,000–1,300-Myr old[54].
The Rapakivi granite from Venezuela, 1,500-Myr old[55].
The Pan African granodiorites from Morocco and Ahaggar, 600-Myr old[52].

For each granite, it is possible to measure the $^{143}Nd/^{144}Nd$ and $^{147}Sm/^{144}Nd$ ratios. If the geological age T_1 is known independently, the initial ratio can be calculated:

$$(^{143}\mathrm{Nd}/^{144}\mathrm{Nd})_{\mathrm{I},T_1} = (^{143}\mathrm{Nd}/^{144}\mathrm{Nd})_{\mathrm{meas}} - (^{147}\mathrm{Sm}/^{144}\mathrm{Nd})(e^{\lambda T_1} - 1)$$

De Paolo and Wasserburg[10] have shown that this calculation is reasonably reliable for Sm–Nd because this chronometer is practically insensitive to weathering and to weak metamorphism. Therefore, only a simple *in situ* age correction is needed to calculate all initial ratios $(^{143}\mathrm{Nd}/^{144}\mathrm{Nd})_{\mathrm{I},T_1}$. A convenient way of comparing the deviations from the planetary evolution curve is to use the initial $\varepsilon^{\mathrm{I}}_{\mathrm{Nd}}$ notation[10].

All of these granitoids have initial $^{143}Nd/^{144}Nd$ values which plot very close to the closed system planetary evolution line defined by De Paolo and Wasserburg[10].

Contrary to what is observed for recent granitoids, Nd isotopes favour a mantle origin for the Precambrian granitic rocks. Our present statistics on these initial ratios are poor and need to be improved. However, the general result is impressive compared with the results for modern granites, especially as our sampling covers different petrographic types in the Precambrian. The first interpretation would be that these granites were directly derived from the mantle through magmatic differentiation or segregation processes. However, we could also imagine a derivation from the mantle via a sedimentary cycle. In such processes, the sediments are volcanogenic greywackes which are melted a short time after their deposition. If this is the common process for granitoid formation, then our results indicate the participation of a large proportion of mantle material in the sedimentation during the Precambrian period. In some way these granites were freshly derived from the mantle and, therefore, the continental crust corresponding to these granites can be considered to be young.

As for modern granites, one important way of examining the Precambrian origin is to use the coupled Sr–Nd isotopes. As the initial ratio is more difficult to obtain for Sr because of the mobility of Rb and Sr, a complete study including whole rock isochrons is necessary to obtain such values.

The data for Precambrian granitoids plot around the origin of the diagram (Fig. 5*a*), even if the resulting Sr errors are larger than the Nd ones. Such a plot seems to indicate a tendency for departure from the planetary (bulk Earth) values with time, more clearly for Sr than for Nd. Comparing these diagrams with our mixing model reveals large differences in the isotopic geochemistry of Sr and Nd, and clarifies the scatter around the origin through geological time. The lower crust (granulite facies) has positive $\varepsilon^0_{\mathrm{Sr}}$ but quite negative $\varepsilon^0_{\mathrm{Nd}}$ (ref. 37). The fact that all experimental points plot around the origin of the Nd diagram eliminates the possibility of Precambrian granitoid originating from recycling of the lower crust[57].

The Nd and Sr evolution curves for the oceanic mantle have been determined by Zindler *et al.*[58] and C.J.A. *et al.*[59]. It is very interesting to plot on the same diagram the oceanic mantle evolution curve and the evolution curve for the initial ratio of granitoids (continental crust, see Fig. 4*a*). For the past 2,000 Myr, the younger the age, the more the oceanic mantle and continental crust curves diverge; this means that granitoids are not the result of pure oceanic mantle differentiation, thus recycling has been involved. This strongly suggests that the oceanic mantle isotopic evolution is due to the extraction of some material which is stored in the continental crust. A second observation is that the scatter of values for granitoids increases with time, so that the process is a statistical one. Third, we do not observe a sharp transition between old and young granitoids, but rather a continuous one. Thus, 1,000 or 500-Myr old granitoids are very important for studying the onset of the present divergence of continental crust and mantle evolution.

Various models[3,4,57,60], in which old continental crust was differentiated and then recycled through geological time, are ruled out by Nd data. Other models[2], which suggest that continental crust is derived from the mantle by a differentiation process, are not appropriate either (see Fig. 4*b*). The model of Moorbath[7] is difficult to reconcile with Nd results on young granitoids. Nd contamination is not selective or accidental, as it can be for Sr, and large masses of crustal component are involved in the genesis of young andesites or granodiorites.

One interpretation of our observations is by postulating two types of granite production processes: (1) a Precambrian type for which granitoids are derived from the mantle through complex magmatic fractionation processes (calc-alkaline differentiation); (2) a post 1,000 Myr type during which crustal anatexis became the major process.

Such a sharp transition is difficult to reconcile with petrographic observations since Moorbath *et al.* (ref. 61 and unpublished results) have clearly demonstrated the existence of crustal anatexis in the Archean, and others[62–64] have clearly demonstrated, for various types of granitoids linked with a calc-alkaline suite, that many Precambrian granites have close equivalents in modern ones.

In addition, such a sharp transition will bring back the 'catastrophy' problem usually poorly supported by geological observations. We will, therefore, assume a uniform set of processes for the genesis of granitoids through geological times, with an evolution in the characteristics of these processes. We suppose that the variation applies to the composition of the materials from which the granitoids derive.

Mantle–crust mixing model for granitoid formation and continental growth

We have seen that isotopic data for young granitoids can be understood through a mixing model involving a mantle component and a recycled crust component. Can this model be extended to the Precambrian granitoids?

Adopting the (*I*–*S*) classification of White and Chappell[65] which agrees with Didier and Lameyre's classification based on xenoliths[66], we examine the genesis of these two types of granitoids.

The (*S*) granitoids are derived from sediments or metasedimentary rocks. All sediments are composed of a recycled detrital component and a mantle component. For sediments which are abundant in metasedimentary piles such as greywackes or schists this type of dual origin is clear. In the Archean, the continental crust was not as developed as it is today: the mantle component was dominant in such sediments. With time, however, the isotopic signature shifted from a mantle value to a continental crust one. In recent times the continental component has dominated. Such a model explains quite well the observations by S. R. Taylor on shales. These authors claim that these are pure continental crust sediments while we believe that they are mixtures with a mantle component[67].

We admit that the (*I*) granitoids result from a mixture between an intrusive component of mantle origin (diorite) and its surroundings. These surroundings are composed of sediments or metasediments or granitoids.

The above reasoning may then be applied, but with a larger mantle contribution. Thus, both (*I*) and (*S*) granitoids can be explained through a mixing model, but does our model fit the data quantitatively?

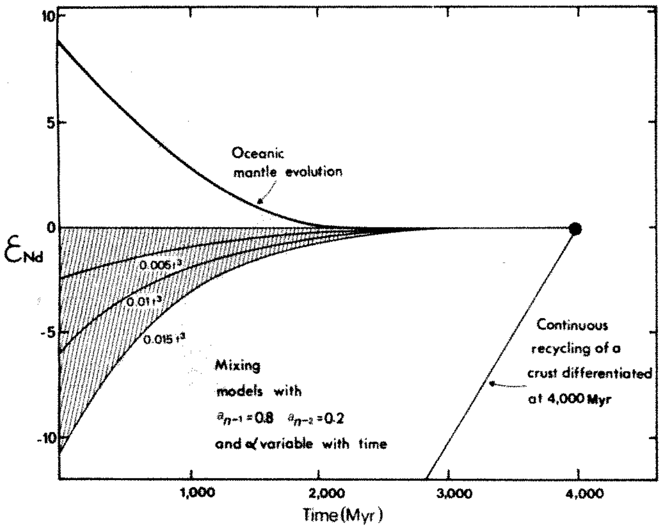

Fig. 5 Mixing model curves. Computed model with two last orogeneses entering the continental crust (last orogeny contribution is four times that of the one before). The degree of mixing between mantle and preexisting crust is assumed to be increasing with time as t^3, with more and more crust entering the orogenesis. The curves for oceanic mantle and continuously recycled crust differentiated at 4,000 Myr are also plotted as references.

Our hypothesis is based on the fact that continents have grown through geological time, although not always with the same rate. This growth takes place during orogeneses. These orogeneses are discontinuous events, at least locally. Therefore, we will use a finite difference method. Let $R_n(t)$ be the isotopic ratio (Nd or Sr) (at time t) of the granitoid formed during the nth orogenesis which occurred at time t_n (or age t_n). Let $R_{c,n}(t)$ be the isotopic ratio at time t (or age t) of the mantle. If α is the mass fraction of Nd (or Sr) from the preexisting crust involved in the mixing, then

$$R_n(t_n) = \alpha R_{c,n}(t_n) + (1-\alpha) R_m(t_n)$$

Because geological observations[68,69] and observations made on California and Laddakh granitoids suggest that the oceanic mantle is involved in continental growth, we will take the oceanic mantle isotopic ratio for $R_m(t)$. The crustal composition will be written as a polynomial:

$$R_{c,n}(t_n) = \sum_{i=0}^{i=n-1} a_i (R_i(t_i) + \mu_c \lambda (t_n - t_i))$$

with

$$a_i > 0 \quad \text{and} \quad \sum_{i}^{n-1} a_i = 1$$

and

$$\mu_c = \frac{^{147}\text{Sm}}{^{144}\text{Nd}}$$

in the continental crust. $a_i(R_{c,i}(t_i) + \mu_c \lambda (t_n - t_i))$ is the crustal contribution of the ith orogenesis to crustal composition. This approach uses the fact that μ_c is almost constant in granitoids of different ages.

The parameters a_i can be chosen in different ways: if we take $a_{n-1} = 0.8$, $a_{n-2} = 0.19$, $\sum_{i=1}^{n-3} a_i = 0.01$, recycling is restricted to the last two orogeneses. This hypothesis is supported by the erosion being proportional to the height of mountains, and is therefore only important for young mountains. It also agrees with the theory of continental growth by successive belts. We can choose a smoother law:

$$a_{n-1} = 0.4, \quad a_{n-2} = 0.3, \quad a_{n-3} = 0.2, \quad a_{n-2} = 0.08 \ldots$$

This assumption is supported by the fact that sediments are created by large rivers such as the Mississippi, the Yang Tse, the Mekong, and the Amazon, which flow through terrains of various ages.

Another hypothesis about the mixing parameter must be made. Although we assume that α is constant through geological time (this is the steady state approximation), it is more likely to have increased because during the Precambrian the mantle was more active[70–72] amd the continental crust not so developed and thus there were more volcanogenic sediments than at present. Observations of Archean sediments support this point of view[70].

As we have no evidence that continental differentiation started before 4,000 Myr, our calculations start from that date. Orogeneses are supposed to occur with a regular time interval of 500 Myr. In fact, each parameter is susceptible to variations and our model should be stochastic. However, the model is given here in its mean value form. Numerical calculations of these equations and comparison with observed data have shown that: (1) a mixing ratio α, which is constant through geological times does not fit the data; (2) the function α must depend on time as t^3 or t^4, but we cannot be more specific with the available data. (3) With the present data we cannot tell whether the last two or four orogeneses are involved in crust formation. The involvement of the four last crustal segments in the orogeneses would imply that the mixing coefficient is lower than if only two are involved. (4) The polynomial coefficient of an old orogeny may possibly become more important with time. This could occur if the Precambrian orogeny were to follow the centrifugal growing and then in modern time the plate tectonics focate the orogeny in random way relative to the age of crustal segments.

Figure 5 shows ε_{Nd} variations with time for $a_{n-1} = 0.8$ and $a_{n-2} = 0.2$ and different functions α. Hence with certain conditions the mixing model is seen to apply and now requires a more refined study, especially in the Precambrian.

Conclusion

Our model quantitatively fits the isotopic variation with geological age and explains the fact that Pb isotopes are a record of continental recycling whereas Sr is more appropriate for mantle derivation, Nd being an intermediate tracer.

We thank H. P. Taylor, P. M. Hurley, R. Kistler and Z. Peterman, J. R. Lancelot, P. Lefort, P. Brunel and S. Moorbath for samples, also P. M. Hurley, S. R. Hart, S. Moorbath, J. F. Minster, F. Albarede, and S. Fourcade for helpful discussions. D. Rousseau made some of the Sr isotope measurements. We thank P. Richard for his help in applying the Nd technique and O. Brevart for programming. S. Fourcade, O. Brevart and J. F. Minster reviewed the manuscript. This is contribution IPG 414.

Received 2 February; accepted 23 May 1980.

1. Engel, A. E. J. *Science* **140,** 143–152 (1963).
2. Hurley, P. M., Hugues, H., Faure, G., Fairbain, H. W. & Pinson, W. H. *J. geophys. Res.* **67,** 5315–5334 (1962).
3. Faure, G. & Powell, J. L. in *Strontium Isotope Geology*, 188 (Springer, Berlin, 1972).
4. Patterson, C. C. in *Isotopic and Cosmic Chemistry* (ed. Wasserburg, C. M.) 244 (North-Holland, Amsterdam, 1964).
5. Allègre, C. J. in *Structure et Dynamique de la Lithosphère* (eds Allègre, C. J. & Mattauer, M.) 372–433 Hermann, Paris, 1972.
6. Armstrong, R. L. *Rev. Geophys.* **6,** 175–199 (1968).
7. Moorbath, S. *Chem. Geol.* **20,** 151–187 (1977).
8. Richard, P., Shimizu, N. & Allègre, C. J. *Earth planet. Sci. Lett.* **31,** 269–278 (1976).
9. De Paolo, D. J. & Wasserburg, G. J. *Geophys. Res. Lett.* **3,** 743–746 (1976).
10. De Paolo, D. J. & Wasserburg, G. J. *Geophys. Res. Lett.* **3,** 249–252 (1976).
11. O'Nions, R. K., Hamilton, P. J. & Evensen, N. H. *Earth planet. Sci. Lett.* **34,** 13–22 (1977).
12. De Paolo, D. J. & Wasserburg, G. J. *Geol. Res. Lett.* **4,** 465–468 (1977).
13. Hawkesworth, C. J. *et al. Earth planet. Sci. Lett.* **36,** 253–262 (1977).
14. Silver, L. T. *Geol. Soc. Am. Abstr.* **13,** 193–194 (1977).
15. Silver, L. T., Allen, C. R. & Stehle, F. G. *Geol. Soc. Am. A. Meet.* 179–280 (1968).
16. Silver, L. T. & Early, T. O. *EOS* **58,** 532 (1977).
17. Silver, L. T., Early, T. O. & Anderson, T. H. *Geol. Soc. Am. Abstr.* **7,** 375–376 (1975).
18. Taylor, H. P. & Silver, L. T. *Int. Conf. Geochron. Cosmochron. Isotope Geol.* Aspen, 423–426 (1978).
19. Hurley, P. M., Bateman, P. C., Fairbain, H. W. & Pinson, W. H. Jr *Bull. geol. Soc. Am.* **76,** 165–174 (1965).
20. Kistler, R. W., Peterman, Z. E., Ross, D. C. & Gothfried, D. *Geological Science* **XIII** (School of Earth Science, Stanford University, 1973).
21. Magaritz, M. & Taylor, H. P. Jr *Can. J. Earth. Sci.* 1514–1536 (1976).
22. Armstrong, R. D., Taubeneck, W. H. & Hales, P. Q. *Bull. geol. Soc. Am.* **88,** 397–411 (1977).
23 Lancelot, J. R., Briqueu, L., Westphal, B. & Tatsumoto, M. *Int. Conf. Geochron. Cosmochron. Isotope Geol.*, Aspen, 240–241 (1978).
24. Briqueu, L. & Lancelot, J. R. *Earth planet. Sci. Lett.* **43,** 385–396 (1979).
25. Mattauer, M. *Earth planet. Sci. Lett.* **28,** 144–154 (1975).
26. Lefort, P. *Rev. Geogr. Phys. Geo. Dyn.* **13,** 5–12 (1971).
27. Hamet, J. & Allègre, C. J. *Bull. geol. Soc. Am.* **84,** 1429–1442 (1976).

28. Andrieux, J., Brunel, M. & Hamet, J. *Colloq. int. Cent. natn. Rech. Scient.* **268,** 31–40 (1976).
29. Vitrac-Michard, A. & Allègre, C. J. *Conr. Miner. Petrol.* **50,** 257–285 (1975).
30. Vitrac-Michard, A. & Allègre, C. J. *C. r. hebd. Séanc. Acad. Sci., Paris* **269,** 2174–2177 (1969).
31. Autran, A., Fonteules, M. & Guitard, G. *Bull. Soc. fr. Géol.* XII, 4, 673–731 (1970).
32. Le Terrier, J. thesis, Univ. Nancy (1972).
33. Lacroix, A. *Bull. Serv. Cart. Géol. Fr.* II, 71, 501–550 LXVII (1900).
34. Mattauer, M. *2ème Réun. Ann. Sci. Terre*, Nancy, 279 (1974.)
35. Fourcade, S. & Allègre, C. J. (in preparation).
36. Allègre, C. J., Ben Othman, D., Polvé, M. & Richard, P. in *Phys. Earth planet. Inter.* **19,** 293–306 (1979).
37. Carter, S. R., Evensen, N. M., Hamilton, R. K. & O'Nions. R. K. *Science* **202,** 743–747 (1978).
38. Allégre, C. J. & Dars, R. *Geol. Rdsch.* **55,** 226–237 (1965).
39. Heier K. S. *Fortsch. Miner.* **50,** 174–187 (1974).
40. Dupuy, C., Leyreloup, A. & Vernières, J. *2eme Symp. Origin and Distribution of Trace Elements* (Unesco, Paris, 1977).
41. Haskin, L. A. *et al. J. geophys. Res.* **71,** 6091–6105 (1966).
42. Moorbath, S., O'Nions, R. K. & Pankhurst, R. J. *Earth Planet. Sci. Lett.* **27,** 229–239 (1975).
43. Hamilton, P. J., O'Nions, R. K. & Evensen, N. H. *Nature* **272,** 41 (1978).
44. Vitrac-Michard, A., Lancelot, J. R., Allègre, C. J. & Moorbath, S. *Earth planet. Sci. Lett.* **35,** 449–453 (1977).
45. Moorbath, S. & Pankhurst, R. J. *Nature* **262,** 124–126 (1976).
46. Steiger, R. H. & Wasserburg, G. J. *Geochim. cosmochim. Acta* **33,** 1212–1232 (1969).
47. Naylor, N. S., Steiger, R. H. & Wasserburg, G. J. *Geochim. cosmochim. Acta* **34,** 1133–1154 (1970).
48. Hamilton, P. J., Evensen, N. H., O'Nions, R. K. & Tarney, K. *Nature* **277,** 25–28 (1979).
49. Lamphere, M. A. *J. Geol.* **72,** 381–399 (1964).
50. Zartmann, R. E. *J. Petrol.* **5,** 359–408 (1968).
51. Allsopp, H. L., Ulrych, T. J. & Nicolaysen, L. O. *Can. J. Earth Sci.* **5,** 605 (1968).
52. Allègre, C. J. & Caby, C. R. *C. r. hebd. Séanc. Acad. Sci. Paris* **275,** 2095–2098 (1972).
53. Bonhomme, thesis, Univ. Clermont Ferrand (1961).
54. Krogh, T. E. & Hurley, P. M. *J. geophys. Res.* **73,** 7107–7118 (1968).
55. Gaudette, H. E., Mendoza, V., Hurley, P. M. & Fairbarn, H. W. *Bull. geol. Soc. Am.* **89,** 1335–1340 (1978).
56. Hargraves, R. B. *Science* **143,** W 4251 363 (1976).
57. O'Nions, R. K. & Pankhurst, R. J. *Earth planet. Sci. Lett.* **38,** 211–236 (1978).
58. Zindler, A., Brooks, C., Arndt, T. N. & Hart, S. *Int. Conf. Geochron. Cosmochron. Isotope Geol.* Aspen, 469–471 (1979).
59. Allègre, C. J., Brevard, O., Dupré, B. & Minster, J. F. *Phil. Trans. R. Soc.* (in the press).
60. Fyfe, W. S. *Geol. Sci. Can.* **3,** 82–83 (1976).
61. Moorbath, S., Wilson, J. F. & Cotteril, P. *Nature* **264,** 536–538 (1976).
62. O'Nions, R. K. & Pankhurst, R. J. *Earth planet. Sci. Lett.* **22,** 328–338 (1974).
63. Tarney, J., Dalziel, I. W. & De Wit, M. J. *The Early History of the Earth* (ed. Windley, B. F.) 131–146 (London, 1976).
64. Barker, F., Wones, D. R., Sharp, W. N. & Desborough, G. A. *Precamb. Res.* **2,** 97–160 (1975).
65. White, A. J. R. & Chappell, R. W. *Tectonophysics* **43,** 7–22 (1977).
66. Didier, J. & Lameyre, J. *Contr. Miner. Petrol.* **24,** 219–238 (1969).
67. Taylor, S. R. *Chemical Composition and Evolution of the Continental Crust in The Earth: its Origin, Structure and Evolution* (ed. McElhinny, M. W.), 353–376 (Academic, New York, 1979).
68. Michot, P. *Revue univlle Mines* **9,** 249–261 (1968).
69. Goodwin, A. *Can. J. Earth Sci.* **12,** 2737–2759 (1977).
70. Veizer, J. & Jansen, S. *J. Geol.* **87,** 341–510 (1979).
71. Taylor, S. R. *Tectonophysics* **4,** 17–34 (1967).
72. Brevard, O. & Allègre, C. J. *Geol. Soc. Fr.* 16 (1979).
73. Krogh, T. E. *Yb. Carnegie Instn Wash.* **69,** 342–344 (1971).
74. Lugmair, G. W., Scheimin, N. B. & Marti, K. *Earth planet. Sci. Lett.* **27,** 79–84 (1975); *Proc. 6th Conf. Lunar Sci.* 1419–1429 (1975); *Proc. 7th Conf. Lunar Sci.* 2009–2033 (1976).
75. Birck, J. L. & Allègre, C. J. *Earth planet. Sci. Lett.* **39,** 37–51 (1978).
76. Vitrac-Michard, A. thesis, Univ. Paris (1975).

Continental crust composition and nature of the lower crust: constraints from mantle Nd–Sr isotope correlation

Barry L. Weaver & John Tarney

Department of Geology, The University of Leicester, Leicester LE1 7RH, UK

Calculations suggest that if the widespread upper mantle depletion in lithophile elements, as represented by the negative correlation between Nd and Sr isotopes in basalts, has resulted from continental crustal extraction, then extraction of observed Archaean crustal compositions best explains the Nd–Sr isotope relationship. Much of the lower continental crust must, therefore, have the high Nd/Sm and low Rb/Sr ratios typical of Archaean granulites.

RECENT developments in neodymium isotope geochemistry[1–3], and the combined use of both neodymium and strontium isotope data[4–9] on mantle-derived igneous rocks, have produced information on the Rb/Sr and Sm/Nd history of their mantle source regions[6–9]. Clearly much of the present upper mantle has suffered a time-integrated depletion of Rb relative to Sr and of Nd relative to Sm. Corresponding evidence on Archaean igneous rocks[2,4,10–12] suggests, however, that the Archaean mantle had broadly chondritic Sm/Nd ratios. Because the continental crust represents a reservoir which is enriched in Rb relative to Sr and in Nd relative to Sm and, overall, has higher ^{87}Sr/^{86}Sr and lower ^{143}Nd/^{144}Nd ratios than the mantle, and because there is strong isotopic evidence that the crust has grown with time since ~4,000 Myr ago[13–15], it is a reasonable assumption that extraction of continental crust may have caused the observed Rb/Sr and Nd/Sm depletion relative to primordial ratios in the present mantle. There is no unambiguous evidence that another major high Rb/Sr and high Nd/Sm reservoir exists which might complement the generally depleted nature of present upper mantle sources. Preliminary attempts have therefore been made to assess the effects of crustal extraction[16] (and crustal contamination[17]) on the Sr and Nd isotope systematics of the upper mantle reservoir.

Here we examine the crust–mantle isotopic relationship in more detail, but with respect to specific Precambrian crustal materials rather than quoted 'average' crustal compositions. This approach is more relevant because (1) the time scale on which mantle can be completely recycled is probably of the order of several hundred million years, (2) considerable crustal growth occurred during the early Precambrian[14,15], (3) the long half lives of ^{87}Rb and ^{147}Sm necessitate a long time lapse before changes in ^{87}Sr/^{86}Sr and ^{143}Nd/^{144}Nd ratios of the magnitude observed in the present-day mantle can develop[18], and (4) there are significant differences between Archaean and Phanerozoic crustal compositions[19].

The crustal data used in the calculations are based on the Archaean Lewisian complex of north-west Scotland, a region which contains juxtaposed segments of presumed upper and lower crustal orthogneisses[20], the geochemical[20–24] and isotopic (Sr, Nd and Pb)[12,25–30] characteristics of which are relatively well known.

Sr–Nd isotope correlation and crustal extraction

Measured Sr and Nd isotopic ratios in many young basalts exhibit a strong negative correlation[5,6] shown by the 'main trend' (defined by $\varepsilon_{\mathrm{Nd}} = -2.7\ \varepsilon_{\mathrm{Sr}}$) (ref. 16; see also Fig. 3) where $\varepsilon_{\mathrm{Nd}}$ expresses the deviation (in parts per 10^4) of ^{143}Nd/^{144}Nd ratios observed in igneous rocks at present from the ^{143}Nd/^{144}Nd ratio expected in a reservoir which has always had chondritic Sm/Nd (ref. 16). $\varepsilon_{\mathrm{Sr}}$ is defined similarly for ^{87}Sr/^{86}Sr ratios relative to a reservoir with bulk Earth Rb/Sr ratios[16]. Thus rocks derived from a mantle source which has suffered a time-integrated depletion of Rb relative to Sr and Nd relative to Sm will plot in the $+\varepsilon_{\mathrm{Nd}}$, $-\varepsilon_{\mathrm{Sr}}$ quadrant on the $\varepsilon_{\mathrm{Nd}}$–$\varepsilon_{\mathrm{Sr}}$ diagram. Mid-ocean ridge basalts invariably plot in this quadrant, as do many ocean island and continental basalts, although these latter tend to plot nearer to the bulk Earth composition. Basalts derived from mantle sources which seem to have been altered by

0028-0836/80/300342—05$01.00

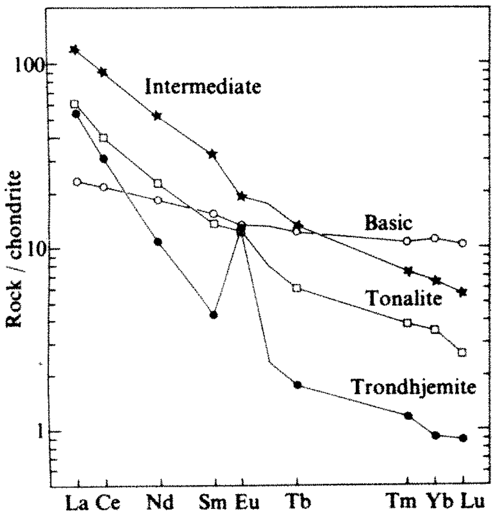

Fig. 1 Average rare-earth element patterns of the main rock types comprising the Lewisian lower crustal granulite complex, north-west Scotland (data from refs 12, 20–24, 37).

more radiogenic seawater Sr (ref. 31), or by continental material[17,32] are displaced from the 'main trend'.

The widespread upper mantle depletion in incompatible elements represented by the 'main trend' must be accommodated in models of mantle evolution. DePaolo and Wasserburg[17] consider the slope of the 'main trend' to be incompatible with upper crustal contamination of a uniform mantle reservoir, while Allègre *et al.*[18] have demonstrated that the mantle main trend correlation reflects melt extraction from the mantle rather than, for instance, mixing processes involving separate mantle reservoirs. In this case the slope of the Sr–Nd isotope correlation constrains the Rb/Sr and Sm/Nd ratios of the material extracted provided an assessment can be made of the Sr/Nd ratios of the extract and of the initial mantle source[16]. By assuming that the continental crust is the complement to the 'main trend' mantle depletion, and by noting that there was only very limited variation in the Sm/Nd and Sr/Nd ratios of the various published estimates of 'average' upper crust and total crust composition, DePaolo[16] was able to use the Sr–Nd isotope correlation to calculate the mean Rb/Sr ratio of the continental crust as lying within the range 0.044–0.10. As upper crustal compositions are quite well defined[33], it is the composition of the lower crust which is crucial in constraining models for the generation of the continental crust.

Crustal compositions

The Lewisian granulite facies gneiss complex is a prime candidate for Archaean lower crust, having the appropriate seismic characteristics[34,35] and having equilibrated in temperature–pressure conditions as high as 1,000 °C and 15 kbar (ref. 36), corresponding to depths of the order of 45 km. Nd isotope studies[12] have demonstrated that the immediate igneous precursors of these gneisses were generated from a mantle source with chondritic Sm/Nd ratios 2,920 Myr ago.

The complex is a heterogeneous mixture of ultramafic, mafic, intermediate, tonalitic and trondhjemitic gneisses, but tonalitic–trondhjemitic compositions dominate. Average rare-earth element (REE) patterns[37] for the main rock types are shown in Fig. 1. The tonalitic and trondhjemite patterns in particular are highly fractionated, with high Ce_N/Yb_N ratios (and Nd/Sm ratios) owing to the strong depletion in the heavy REE caused by residual garnet in the source during the partial melting event which produced the gneiss precursors[24,37]. Using these REE data plus previously published results for La, Ce, and Y (determined by X-ray fluorescence) on several hundred granulite samples[20], it is possible to calculate a weighted mean REE pattern for Lewisian lower crustal granulites (Fig. 2). Because of their very high Nd/Sm ratios and age, the Lewisian granulites are markedly unradiogenic with respect to Nd isotope ratios[12] in comparison with the bulk Earth. The granulites are also high in Sr, but are unusually low in Rb and other radioactive heat producing elements (K, U, Th) largely as a result of the removal of these elements by an active fluid phase during the granulite facies event[12,38]. Thus their Rb/Sr ratios are unusually low, and indeed the present day $^{87}Sr/^{86}Sr$ ratios of many granulites are below typical mantle values[39].

The amphibolite-facies gneiss sections of the Lewisian complex have a much smaller component of ultramafic, mafic and intermediate gneisses, and their mean major- and trace-element compositions are essentially identical to the tonalitic–trondhjemitic components of the granulite facies complex except that they have much higher Rb contents and Rb/Sr ratios. Although full representative REE data are not yet available for these gneisses, comprehensive X-ray fluorescence data for La, Ce and Y (refs 20–24), and limited data for Sm and Nd (ref. 12), allow a fairly accurate estimation of their Sm/Nd ratios, which must be close to the values for the tonalitic–trondhjemitic granulites. From their tectonic and metamorphic state we would regard these gneisses as being more representative of an intermediate crustal level rather than upper crust.

For comparison with these compositions we have also used the mean 'upper crust' composition and the corresponding 'lower crust' composition derived by Taylor[33] on the basis of the

Table 1 Continental crust compositions*

	Andesite model			Archaean	
	UC	TC	LC	LGr	LAm
SiO_2	66·0	58·0	54·0	61·2	67·3
TiO_2	0·6	0·8	0·9	0·5	0·3
Al_2O_3	16·0	18·0	19·0	15·6	15·9
FeO*	4·5	7·5	9·0	5·3	3·4
MgO	2·3	3·5	4·1	3·4	1·2
CaO	3·5	7·5	9·5	5·6	3·4
Na_2O	3·8	3·5	3·4	4·4	4·6
K_2O	3·3	1·5	0·6	1·0	2·2
Cr	35	55	65	88	27
Ni	15	20	23	58	16
Zr	240	100	30	202	199
Rb	110	50	20	12	62
Sr	350	400	425	569	541
Ba	700	350	175	757	838
Pb	15	7	3	13	18
Th	10·5	2·5	—	0·42	9
U	2·5	1	0·25	0·05	—
La	38	19	9·5	22	29
Ce	80	38	17	44	64
Pr	8·9	4·3	2·0	—	—
Nd	32	16	8	18·5	(25)
Sm	5·6	3·7	2·75	3·3	(4·3)
Eu	1·1	1·1	1·1	1·18	—
Gd	4·7	4·2	3·95	—	—
Tb	0·77	0·64	0·58	0·43	—
Dy	4·4	3·7	3·35	—	—
Ho	1·0	0·82	0·73	—	—
Er	2·9	2·3	2·0	—	—
Tm	0·5	0·4	0·35	0·19	—
Yb	2·8	2·2	1·9	1·2	—
Lu	0·4	0·3	0·25	0·17	—
Y	27	22	20	9	9
Ce_N/Yb_N	7·3	4·4	2·3	9·3	—

UC, TC, and LC are upper crust, total crust and (calculated) lower crust compositions respectively, based on andesite model for crustal growth[33]. LGr is mean composition of Lewisian granulites (= Archaean lower crust); LAm is mean composition of amphibolite-facies gneisses from Scotland and Greenland (= Archaean intermediate crustal level). Figures in brackets are interpolated values.

* Oxides in wt%, trace elements in p.p.m.

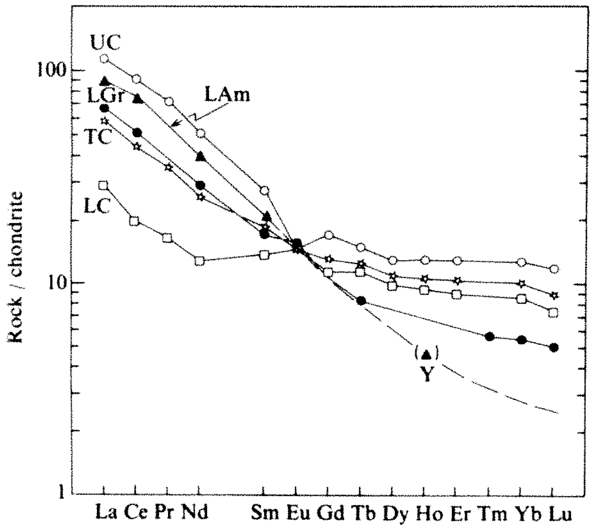

Fig. 2 Mean rare-earth element patterns of crustal components. UC, TC and LC are average upper crust, total crust and (calculated) lower crust compositions based on the andesite model for crustal growth[33]. LGr is mean rare-earth pattern for Lewisian lower crustal granulites (based on Fig. 1 plus data in refs 12, 20–24, 37). LAm, mean rare-earth pattern for Lewisian amphibolite-facies gneisses (based on data in refs 12, 20, 22, 38).

andesite model for crustal growth. Relevant data for these compositions and for the Lewisian granulite and amphibolite facies gneisses are given in Table 1, and the corresponding REE patterns are plotted on Fig. 2.

Results

The modelling of ε_{Nd}–ε_{Sr} (Fig. 3) follows the method used by DePaolo[16], except that the data in Table 1 are used to derive vectors on the ε_{Nd}–ε_{Sr} diagram for residual mantle compositions after extracting the various crustal components. Clearly a valid model should yield mantle vectors for the extraction of upper crust and lower crust which embrace the mantle 'main trend'. The vectors calculated are very dependent on the Sr/Nd ratio of mantle + crust, and less dependent on the parameter X_c (the fraction of Nd atoms in the crust + depleted-mantle system residing in the crust[16]). The values used here for the Sr/Nd ratio of mantle + crust and X_c are those of DePaolo[16]. Where upper crust and lower crust compositions have been treated separately the X_c factor has been adjusted accordingly. The method for calculating the vectors is given in Table 2 (see also ref. 16).

The slopes of the vectors for crust and mantle compositions plotted on Fig. 3 are directly proportional to the factors R_f in Table 2. The vectors for depleted mantle compositions in Fig. 3, derived respectively from the given crustal compositions, illustrate several interesting features. That resulting from the extraction of Lewisian granulites has a very steep trend. This arises because the mean Rb/Sr ratio of Lewisian granulites (0.021) is actually slightly lower than that estimated for the uniform mantle reservoir (0.029, ref. 16), hence resulting in little fractionation of ε_{Sr} in the residual mantle. Lewisian amphibolite facies gneisses, although having a rather higher mean Nd/Sm ratio than the granulites, have a much higher mean Rb/Sr ratio (0.13, Table 1) resulting in a much shallower slope of the residual vector.

The average upper crust composition of Taylor[33] has a similar Nd/Sm ratio to that of Lewisian gneisses, but has a high Rb/Sr ratio (0.31, Table 1), thus the corresponding residual mantle vector has a shallower slope than the mantle 'main trend' on Fig. 3. The calculated lower crust composition based on the andesite model actually plots in the $+\varepsilon_{Nd}$, $+\varepsilon_{Sr}$ quadrant, and the corresponding residual mantle vector has an even shallower slope than that produced by extraction of average upper crust. The andesitic lower crust, in fact, has a calculated Nd/Sm ratio less than chondritic, although the calculated full rare-earth pattern is slightly light-REE enriched (Fig. 2). However, if the upper crust was taken to be 30% of the total crust (rather than 33%), the calculated lower crust would then have a chondritic Sm/Nd ratio.

Figure 3 shows that extraction of an andesite bulk crust[33] from a mantle with chondritic Sr/Nd ratios could not produce the mantle 'main trend'. Because the vectors for the average upper crust of Taylor[33] and for the amphibolite facies Lewisian are similar, the determining factor in whether crustal extraction can reproduce the mantle Sr–Nd isotope trend is the nature of the lower crustal component. Apparently, the lower crust component in any crustal model is required to have a moderately high Nd/Sm ratio together with a very low Rb/Sr ratio—a chemical characteristic typical of Lewisian granulites. Extraction of continental crust with this composition as a component is compatible with a simple model for the generation of the mantle isotope correlation.

An independent test of mean crustal compositions can be made using the composition of the source of mid-ocean ridge basalts (MORB), assuming this to be the mantle residue complementary to the crustal extract. Thus if the Sr/Nd ratio of the MORB source can be defined it is possible to estimate the slope, on the ε_{Nd}–ε_{Sr} diagram, of the required crystal extract. Using the data of Sun and Nesbitt[41] for average MORB, together with reasonable assumptions of the residual mantle mineralogy, the degree of melting necessary to generate MORB

Table 2 Compositions of crustal components and calculated parameters used in ε_{Nd}–ε_{Sr} modelling

	Rb	Sr	Nd	Sm	Rb/Sr	Nd_N/Sm_N	Sr/Nd	$f_{Rb/Sr}$*	$f_{Sm/Nd}$*	$(R_f)_c$*	$(R_f)_{dm}$†
Upper crust[33]	110	350	32	5.6	0.31	1.82	10.9	9.8	−0.45	−0.046	−0.093
Total crust[33]	50	400	16	3.7	0.13	1.37	25.0	3.3	−0.28	−0.082	−0.038
Lower crust‡	20	425	8	2.75	0.047	0.92	53.1	0.62	−0.086	0.14	0.029
Lewisian amphibolite-facies gneiss§	74	580	25	4.1	0.13	1.92	23.2	3.4	−0.48	−0.14	−0.102
Lewisian granulite-facies gneiss§	12	570	19	3.3	0.021	1.82	30.0	−0.27	−0.45	1.67	0.78
Chondrite values	2.5	11	0.60	0.19	0.23	1.00	18.3	6.8	0.0	—	—

* $f_{Rb/Sr} = \frac{(Rb/Sr)}{0.029} - 1$ and $f_{Sm/Nd} = \frac{(Sm/Nd)}{0.317} - 1$; $(R_f)_c = \frac{f_{Sm/Nd}}{f_{Rb/Sr}}$

† $(R_f)_{dm}$ (dm, depleted mantle) calculated from (see ref. 16):

$$\frac{(R_f)_c}{(R_f)_{dm}} = \frac{(Sr/Nd)_c}{(Sr/Nd)_{dm}} \quad \text{where } (Sr/Nd)_{dm} \text{ derived from} \quad X_c \frac{(Sr/Nd)_c}{(Sr/Nd)_{Eth}} + (1 - X_c)\frac{(Sr/Nd)_{dm}}{(Sr/Nd)_{Eth}} = 1$$

$$X_c = 0.5 \quad \text{and} \quad (Sr/Nd)_{Eth} = 18.3$$

‡ Lower crust calculated from data in ref. 33 assuming upper crust and lower crust respectively one-third and two-thirds of total crust.

§ Mean Sm and Nd values calculated from data in refs 20 and 37, weighted by rock type. Note, amplibolite facies average is different to that of Table 1.

and utilizing published partition coefficient data for Rb, Sr, Nd and Sm (ref. 42), the composition of the MORB source can be calculated (Table 3). The R_t value for this source (Table 3), defining the slope on the ε_{Nd}–ε_{Sr} diagram, is in excellent agreement with the value of −0.25 obtained for the mantle 'main trend'. Altering the degree of partial melting required to generate MORB has little effect on the relevant element ratios (Table 3). Having obtained a value of $f_{Sm/Nd}$ for the MORB source it is also possible to calculate the present-day isotopic composition of this source, assuming the present Sm/Nd ratio has been maintained since time t. For an age of 2,500 Myr the present day MORB source would have $\varepsilon_{Nd} = 10.7$ and $\varepsilon_{Sr} = -30$, values similar to those observed in recent basalts[2,4,6]. This is at least consistent with the argument that Archaean crustal extraction may have been responsible for the widespread depletion of upper mantle sources.

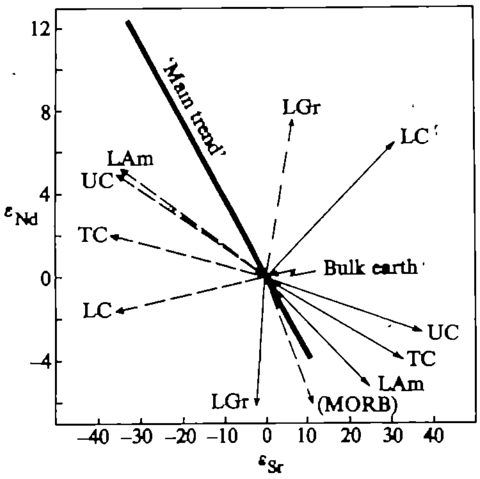

Fig. 3 Vectors showing the effect that extraction of different crustal components (Table 1, Fig 2) would have on the Sr and Nd isotope composition of residual mantle which initially had bulk Earth Rb/Sr and Sm/Nd ratios and chondritic Sr/Nd ratios. ———, Vectors for the crustal components themselves; – – –, corresponding residual mantle vectors shown as dashed lines; —–, the calculated crustal vector corresponding to the mantle source for typical mid-ocean ridge basalt.

The calculated complementary crustal component to this MORB mantle reservoir is detailed in Table 3 and defines a high (negative) slope vector on the ε_{Nd}–ε_{Sr} diagram (Fig. 3), which lies between the crustal vectors corresponding to Lewisian granulite and amphibolite facies gneisses. The trend of this vector reinforces the conclusion that a lower crust component with a composition similar to that of Lewisian granulites is necessary for reasonable models of crustal growth. Note that the present Rb/Sr ratios of Lewisian granulites are not primary values, but have been lowered by Rb removal during the granulite-facies event, while the Lewisian amphibolite-facies gneisses may have suffered some corresponding Rb-addition (as is also implied by the Sr isotope data, ref. 12). Correcting for these effects would move both Lewisian crustal vectors closer to that corresponding to the MORB source.

Nevertheless, even accepting a higher bulk crustal Nd/Sm ratio than that of average andesite, it does seem that the bulk crust must have a fairly low mean Rb/Sr ratio, as concluded by DePaolo[16], Using the R_t value for the bulk crust complement to the MORB source (Table 3) and a likely value of $f_{Sm/Nd}$ for the bulk crust (about −0.45, Table 2) yields an $f_{Rb/Sr}$ value of ~1 for the bulk crust, corresponding to a mean Rb/Sr ratio of 0.07. This value is low in relation to typical upper crustal values and must imply that a substantial proportion of the deeper continental crust has very low Rb/Sr ratios similar to those in Lewisian granulites.

Table 3 Calculated composition of MORB source and corresponding modelling parameters

	Average* MORB	MORB source†		
		$F = 0.10$	$F = 0.15$	$F = 0.20$
Rb	1.0	0.10	0 15	0.20
Sr	124	13 0	19.2	25.3
Nd	7.7	0.86	1.24	1.62
Sm	2.8	0.32	0.46	0.60
Sr/Nd	16.1	15.1	15.5	15.5
$f_{Rb/Sr}$	—	−0.74‡	−0.73	−0.73
$f_{Sm/Nd}$	—	0.17	0.17	0.17
R_t	—	−0.24	−0.23	−0 23
ε_{Nd} (2,500 Myr)	—	10.7§	10.7	10.7
ε_{Sr} (2,500 Myr)	—	−30.5	−30.1	−30.1

* Average MORB from ref. 41.

† MORB mantle source compositions calculated assuming residual mineralogy: O1 70, Opx 25, Cpx 5 and using partition coefficient data from ref. 42 and the equation:

$$C_{source} = C_{MORB}[D(1-F)+F]$$

where D = bulk distribution coefficient and F = fraction melted.

‡ R_t, $f_{Rb/Sr}$ and $f_{Sm/Nd}$ calculated as in Table 2.

§ ε_{Nd} and ε_{Sr} calculated from the relationship[16]:

$$\varepsilon_{Nd}(0) \approx 24.7\, f_{Sm/Nd} \cdot T \quad \text{and} \quad \varepsilon_{Sr}(0) \approx 16.5\, f_{Rb/Sr} \cdot T$$

Conclusions

The present modelling suggests that the Sr–Nd isotope correlation in the present upper mantle reservoir can be explained by extracting observed crustal compositions. However, crustal estimates based on Lewisian type crustal components seem to be more compatible with the isotopic constraints than crustal compositions based on the andesite model for crustal growth. Thus Archaean crust may, to a first approximation, complement the lithophile element depletion observed in modern MORB mantle sources. There are other interesting implications:

(1) Quoted 'average' upper crustal compositions are unlikely to be representative of the whole crust.

(2) The Precambrian crust, and particularly the lower crust, must have significantly higher Nd/Sm (and hence higher Ce_N/Yb_N) ratios than suggested by the andesite model for crustal growth.

(3) The higher Ce_N/Yb_N ratios implied for (and the heavy REE depletion observed in) many Archaean crustal rocks suggest a role for eclogite in Archaean crustal generation processes. Because the residues of crustal extraction need to be recycled into the mantle to generate the Sr–Nd isotope correlation, this suggests that some form of subduction may have operated in the Archaean.

(4) The requirement for high Ce_N/Yb_N ratios in the lower crust is not compatible with a lower crust dominated by the residues of partial melting or the cumulates from fractional crystallization.

(5) Even allowing for higher Ce_N/Yb_N ratios in the bulk Archaean crust, it is apparent that a substantial proportion of the deeper continental crust must have a very low Rb/Sr ratio. This may have arisen through transfer of Rb and other radioactive heat-producing elements (U, Th, K) from the deeper crust to the upper crust during the Precambrian. A consequence is that the Precambrian lower crust may constitute a substantial reservoir which is unradiogenic with respect to Pb Isotope ratios as well as to Sr and Nd isotope ratios[43,44].

B.L.W. acknowledges receipt of an NERC studentship. We thank Drs C. J. Hawkesworth, M. J. Norry, R. K. O'Nions, A. D. Saunders and R. S. Thorpe for helpful comments.

Received 28 December 1979, accepted 15 May 1980

1 Richard, P , Shimizu, N & Allègre, C J *Earth planet Sci Lett* 31, 269 (1976)
2 DePaolo, D J & Wasserburg, G J *Geophys Res Lett* 3, 249 (1976)
3. O'Nions, R K., Carter, S R , Evensen, N M & Hamilton, P J *A Rev Earth planet Sci* 7, 11 (1979)
4 De Paolo, D J & Wasserburg, G J *Geophys Res Lett* 3, 743 (1976)

5. DePaolo, D. J. & Wasserburg, G. J. *Geophys. Res. Lett.* **4,** 465 (1977).
6. O'Nions, R. K., Hamilton, P. J. & Evensen, N. M. *Earth planet. Sci. Lett.* **34,** 13 (1977).
7. Carter, S. R., Evensen, N. M., Hamilton, P. J. & O'Nions, R. K. *Earth planet. Sci. lett.* **37,** 401 (1978).
8. Hawkesworth, C. J., Norry, M. J., Roddick, J. C. & Vollmer, E. *Nature* **280,** 28 (1979).
9. O'Nions, R. K., Evensen, N. M., Carter, S. R. & Hamilton, P. J. in *Results of Deep Sea Drilling in the Atlantic: Ocean Crust* (eds Talwani, M., Harrison, G. C. & Hayes, D. E.) Maurice Ewing Ser. **2,** 342 (American Geophysical Union, Washington, 1979).
10. Hamilton, P. J., Evensen, N. M., O'Nions, R. K., Smith, H. S. & Erlank, A. J. *Nature* **279,** 298 (1979).
11. Hamilton, P. J., O'Nions, R. K. & Evensen, N. M. *Earth planet. Sci. Lett.* **36,** 263 (1977).
12. Hamilton, P. J., Evensen, N. M., O'Nions, R. K. & Tarney, J. *Nature* **277,** 25 (1979).
13. McCulloch, M. T. & Wasserburg, G. J. *Science* **200,** 1003 (1978).
14. Moorbath, S. *Nature* **254,** 395 (1975).
15. Moorbath, S. *Phil. Trans. R. Soc.* A**278,** 401 (1978).
16. DePaolo, D. J. *Earth planet. Sci. Lett.* **43,** 201 (1979).
17. DePaolo, D. J. & Wasserburg, G. J. *Geochim. cosmochim. Acta* **43,** 615 (1979).
18. Allègre, C. J., Ben Othman, D., Polve, M. & Richard, P. *Phys. Earth planet. Inter.* **19,** 293 (1979).
19. Nance, W. B. & Taylor, S. R. *Geochim. cosmochim. Acta* **41,** 225 (1977).
20. Sheraton, J. W., Skinner, A. C. & Tarney, J. in *The Early Precambrian of Scotland and Related Rocks of Greenland* 13 (eds Park, R. G. & Tarney, J.) (University of Keele, 1973).
21. Sheraton, J. W. *Earth planet. Sci. Lett.* **8,** 301 (1970).
22. Tarney, J., Skinner, A. C. & Sheraton, J. W. *24th Int. geol. Cong. Montreal* **1,** 162 (1972).
23. Tarney, J. in *The Early History of the Earth* 405 (ed. Windley, B. F.) (Wiley, London, 1976).
24. Tarney, J., Weaver, B. L. & Drury, S. A. in *Trondhjemites, dacites and related rocks* (ed. Barker, F.) 275 (Elsevier, Amsterdam, 1979).
25. Moorbath, S., Powell, J. L. & Taylor, P. N. *J. geol. Soc.* **131,** 213 (1975).
26. Moorbath, S., Welke, H. & Gale, N. H. *Earth planet. Sci. Lett.* **6,** 245 (1969).
27. Chapman, H. J. & Moorbath, S. *Nature* **268,** 41 (1977).
28. Pidgeon, R. T. & Aftalion, M. *Earth planet, Sci. Lett.* **17,** 269 (1972).
29. Pidgeon, R. T. & Bowes, D. R. *Geol. Mag.* **109,** 247 (1972).
30. Lyon, T. D. B. & Bowes, D. R. *Krystalinikum* **13,** 53 (1977).
31. Hawkesworth, C. J., O'Nions, R. K., Pankhurst, R. J., Hamilton, P. J. & Evensen, N. M. *Earth planet. Sci. Lett.* **36,** 253 (1977).
32. Carter, S. R., Evensen, N. M., Hamilton, P. J. & O'Nions, R. K. *Science* **202,** 743 (1978).
33. Taylor, S. R. in *Island Arcs, Deep Sea Trenches and Back-Arc Basins* (eds Talwani, M. & Pitman, W. C.) Maurice Ewing Ser. **1,** 325 (American Geophysical Union, Washington, 1977).
34. Hall, J. & Al-Haddad, F. M. *Scott. J. Geol.* **12,** 305 (1976).
35. Hall, J. & Simmons, G. *Geophys. J. R. astr. Soc.* **58,** 337 (1979).
36. O'Hara, M. J. *J. geol. Soc.* **134,** 185 (1977).
37. Weaver, B. L. & Tarney, J. (in preparation).
38. Tarney, J. & Windley, B. F. *J. geol. Soc.* **134,** 153 (1977).
39. Holland, J. G. & Lambert, R. St. J. *Precambrian Res.* **2,** 161 (1975).
40. O'Nions, R. K., Evensen, N. M., Hamilton, P. J. & Carter, S. R. *Phil. Trans. R. Soc.* A**258,** 547 (1978).
41. Sun, S.-S. & Nesbitt, R. W. *Earth planet. Sci. Lett.* **35,** 429 (1977).
42. Hanson, G. N. *J. geol. Soc.* **134,** 235 (1977).
43. Evensen, N. M., Hamilton, P. J. & O'Nions, R. K. *EOS* **60,** 406 (1979).
44. Tarney, J., Wood, D. A., Saunders, A. D., Cann, J. R. & Varet, J. *Phil. Trans. R. Soc.* (in the press).

Three-dimensional structure of *Escherichia coli* initiator tRNA$_f^{Met}$

Nancy H. Woo*, Bruce A. Roe† & Alexander Rich*‡

* Department of Biology, Massachusetts Institute of Technology, Cambridge, MA 02139
† Department of Chemistry, Kent State University, Kent, Ohio 44240

The crystal structure of Escherichia coli *tRNA$_f^{Met}$ an initiator transfer RNA, has been determined. While grossly similar to that of the chain-elongating yeast tRNA^{Phe}, there are three major differences. One involves the folding of the anticodon loop; in particular, the position of the constant uridine, U33. This difference was unexpected and may be of functional significance.*

ALL organisms use a specialized transfer RNA molecule, tRNA$_f^{Met}$, to initiate protein synthesis. These tRNAs are distinguished from chain-elongating tRNAs in several ways, perhaps the most important of which is that the aminoacylated initiator tRNA goes directly into the ribosomal P site while all other aminoacylated tRNAs go initially to the ribosomal A site and only later in protein synthesis translocate to the P site[1,2]. Despite significant differences in their nucleotide sequences, prokaryotic and eukaryotic initiator tRNAs are readily interchangeable in *in vitro* protein synthetic systems and thus form a single functional class. To understand the nature of the distinction between initiator and chain-elongating tRNAs, it is of value to compare the three-dimensional structure of an initiator tRNA with the known structure of the chain-elongating tRNA, yeast tRNA^{Phe} (refs 1–3). Here we report an X-ray diffraction analysis of the *Eschericia coli* tRNA$_f^{Met}$. We have crystallized this molecule in a form which diffracts to a resolution of 2.8 Å. The current analysis is based on data to 3.5 Å. The general shape of the molecule is similar to that of yeast tRNA^{Phe}, which has also been reported for yeast tRNA$_f^{Met}$ (ref. 4). One of the differences from yeast tRNA^{Phe} is in the anticodon loop and that may be functionally significant in view of recent solution studies[5].

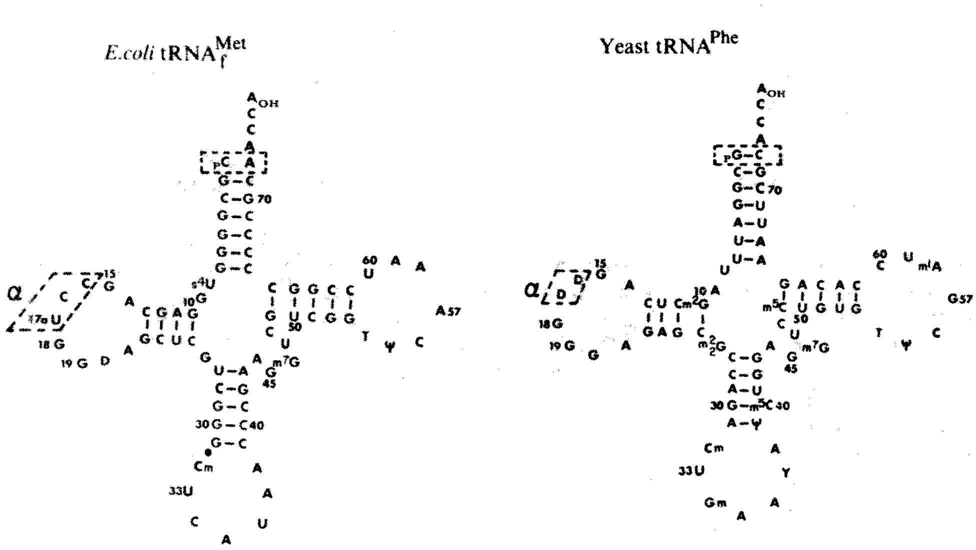

Fig. 1 The nucleotide sequence of the *E. coli* initiator tRNA, tRNA$_f^{Met}$, and the chain-elongating yeast RNA^{Phe}. The significant differences in the two sequences are indicated by the dashed boxes. The initiator tRNA contains unpaired bases at the end of its acceptor stem. The α region of the initiator tRNA contains one residue more than the corresponding region in yeast tRNA^{Phe}. The numbering system adopted here and in the text is that of Gauss *et al.*[23]

---

‡ To whom correspondence should be addressed.

0028-0836/80/300346—06$01.00

Crystallization and structure solution

E. coli tRNA$_f^{\rm Met}$ was prepared as described by Roe *et al.*[6], and Anandaraj and Roe[7]. The tRNA is crystallized in an orthorhombic lattice by vapour diffusion of 1–2% isopropanol into a solution containing 10 mM $MgCl_2$, 50 mM $(NH_4)_2SO_4$, 8 mM spermine and 2 mM $BaCl_2$ (ref. 8). Data to 3.5 Å (4,400 reflections) have been collected. Over 65% of the data in the shell 3.50–3.55 Å (217 reflections) diffract with an intensity significantly above background. Oligonucleotide binding, chemical modification, and NMR studies[2,9] all suggest that no major conformational differences exist between yeast tRNA$^{\rm Phe}$ and *E. coli* tRNA$_f^{\rm Met}$. In particular, no differences are found in the accessibility of nucleotides in E. coli tRNA$_f^{\rm Met}$, corresponding to those involved in tertiary interactions in yeast tRNA$^{\rm Phe}$, implying that the gross conformation of the two molecules is very similar. Consequently, the method of rotation and translation function searches was used to locate the initiator tRNA in its unit cell[11]. The search model was the known crystal structure of the yeast tRNA$^{\rm Phe}$.

The result of the searches was a unique position of the yeast tRNA$^{\rm Phe}$ search model in the *E. coli* tRNA$_f^{\rm Met}$ unit cell which formed a lattice without interpenetration of adjacent molecules. The initial model was formed by substituting the *E. coli* tRNA$_f^{\rm Met}$ base sequence into the yeast tRNA$^{\rm Phe}$ search model in such a way as to leave the conformation of the ribose–phosphate backbone intact. *E. coli* tRNA$_f^{\rm Met}$ contains one residue more in the variable α region of the D loop than yeast tRNA$^{\rm Phe}$ (see Fig. 1). The extra residue, C17, was not included in the initial model, nor was the 3′ terminal adenosine 76. The agreement between a molecular model and the observed diffraction data is measured by the residual function R, defined as $R=\sum\|F_0|-|F_c\|/\sum|F_0|$ where F_0 and F_c are the observed and calculated structure factors[12] which varies inversely with the agreement between model and data. The R value for the initial model was 0.44 at 6 Å, which compares favourably with residuals for protein models obtained using rotation–translation function search methods[10,13], as well as those obtained using multiple isomorphous replacement methods[14]. A complete description of the search procedure used is given in ref. 11.

Although the R for the initial model was encouraging and indicated that the hypothesis of gross similarity in conformation of *E. coli* tRNA$_f^{\rm Met}$ and yeast tRNA$^{\rm Phe}$ was correct, it also indicated that the model was far from perfect. This was further reflected by the R at 3.5 Å, which was 0.52. To determine if the disagreement was localized to some specific parts of the model, Fourier maps based on the initial model were calculated. At 3.5 Å resolution, both the difference Fourier, F_0-F_c, and the sum function Fourier, $2F_0-F_c$, showed that in most regions there was good agreement between the observed data and model but in some, the model was clearly wrong. These latter regions included the acceptor terminus, the D loop, and the anticodon loop. Fourier maps were also calculated from partial models in which those regions most at variance with the observed data were omitted; these included the entire anticodon loop, the entire D loop, the acceptor end. In both the F_0-F_c and $2F_0-F_c$ maps calculated using the partial models, chains of continuous electron density were seen which could account for the omitted portion of the model. Thus the phasing from the remainder of the model was sufficiently accurate to fix the positions of the omitted portions.

The initial model was rebuilt using the University of North Carolina molecular graphics facility. Electron density maps (F_0-F_c and $2F_0-F_c$) based on the complete model as well as those based on partial models were used to guide the fitting. The entire molecule was fitted to density and residue C17 inserted. The refit model was idealized using a restrained least-squares procedure[15]. The idealization involved both local geometry (bond angles and lengths) and hydrogen-bonding geometry of residues in the four stem regions. No attempt was made to preserve interactions between residues corresponding to those involved in tertiary bonding in yeast tRNA$^{\rm Phe}$ (refs 1–9). Limited refinement of the idealized model has been refined together (for example, the anticodon loop and stem, the D and T loops). No refinement of the complete molecule at one time has been done. An isotropic temperature factor of 40 Å has been assigned to the molecule and has not been refined. The current residual at 3.5 Å is 0.35. A fuller description will be given elsewhere (manuscript in preparation).

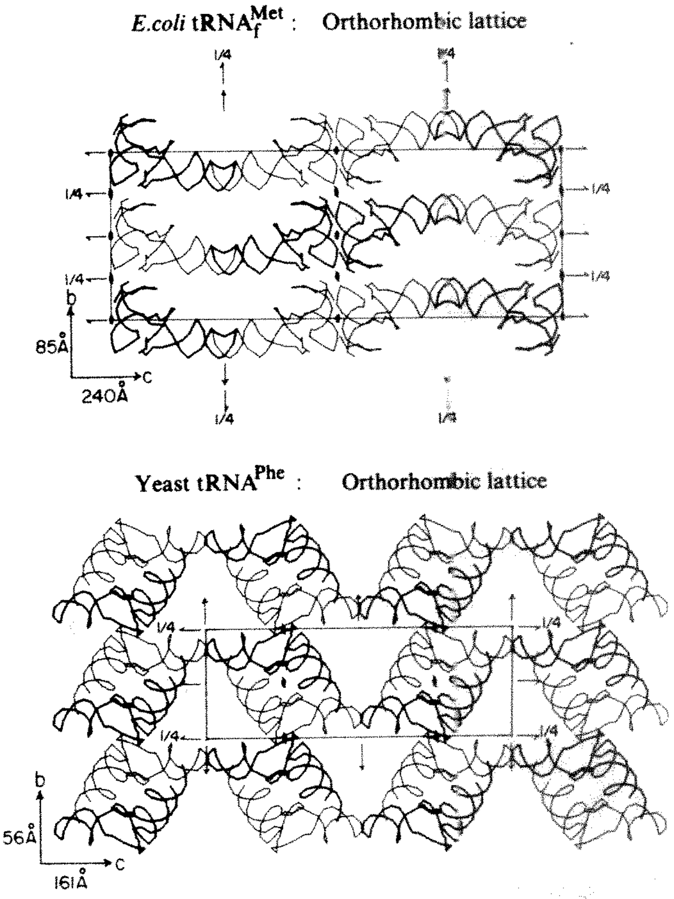

E.coli tRNA$_f^{\rm Met}$: Orthorhombic lattice
1/4
1/4
1/4
1/4
1/4
1/4
b
85Å
c
240Å
1/4
1/4
Yeast tRNA$^{\rm Phe}$: Orthorhombic lattice
1/4
1/4
1/4
1/4
b
56Å
c
161Å

Fig. 2 Crystal packing diagrams of the *E. coli* tRNA$_f^{\rm Met}$ and yeast tRNA$^{\rm Phe}$. The two packing diagrams are shown for comparative purposes. The diagrams show the projection of the molecular packing in the *bc* place. Molecules which lie above are drawn in heavier lines than those below. Crystal symmetry elements are indicated. The empty regions are solvent channels which in both crystals extend through the crystal along the *a* axis direction. The intermolecular contacts in the two crystals can be seen to be totally distinct. The *E. coli* tRNA$_f^{\rm Met}$ crystals belong to the orthorhombic space group $C222_1$, with cell dimensions $a=32$, $b=85$, and $c=240$ Å.

The lattice of *E. coli* tRNA$_f^{\rm Met}$ is shown in Fig. 2 with, for comparison, the orthorhombic lattice of yeast tRNA$^{\rm Phe}$. Long solvent channels extend through the crystal along the a axis direction in both lattices. The lattice contacts in the initiator tRNA crystal include interactions between the T stems of twofold related molecules, between the acceptor terminus of one molecule with the T and D loops of a C-centred related one, and between the anticodon loops of twofold related molecules. These interactions are all distinct from those seen in either the orthorhombic or monoclinic lattices of the yeast tRNA$^{\rm Phe}$ (refs 16, 17). Hence, any similarity in the overall shape of the *E. coli* initiator tRNA and the yeast tRNA$^{\rm Phe}$ cannot be attributed to crystal lattice forces.

The form of the molecule

Figure 3 shows side views of both *E. coli* tRNA$_f^{\rm Met}$ and yeast tRNA$^{\rm Phe}$. The two molecules are broadly similar in shape, the most striking difference being found in the acceptor ends. In the

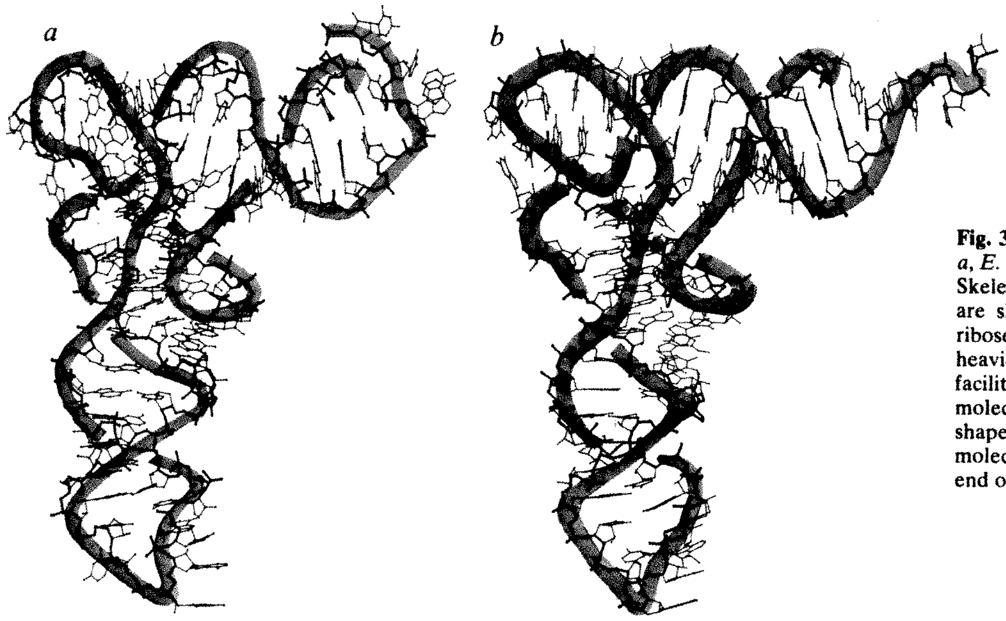

Fig. 3 A comparison of the structure of *a*, *E. coli* tRNA$_f^{Met}$ and *b*, yeast tRNA^{Phe}. Skeletal diagrams of the two molecules are shown. The continuous phosphate–ribose backbone has been drawn in heavier lines and shading has been used to facilitate tracing of the chain. The two molecules are seen in the fully extended L shape. The acceptor termini of both molecules are located at the upper right end of the L's and the anticodon loops at the bottom.

initiator tRNA, the last five nucleotides at the 3′ terminus curl back toward the acceptor end, rather than continuing the helical organization of the acceptor stem, as in yeast tRNA^{Phe}. This difference in the acceptor ends of the two molecules may arise from the fact that the *E. coli* initiator tRNA, as most other prokaryotic initiator tRNAs, has an unpaired set of bases at the end of its acceptor stem (Fig. 1).

Several sections of the 3.5 Å electron density map based on the current model are presented in Fig. 4. The sum function Fourier map, $2F_0 - F_c$, is shown to allow assessment of both the quality of the fit and the noise level of the map. The phosphate–ribose backbone is found in strong electron density, as are virtually all of the bases. A few bases do not lie entirely in density, which indicates that their position will probably shift slightly with further refinement. The low density peaks found in solvent regions indicate the noise level of the maps. No solvent has been included in the current model. Figure 4*a* shows a portion of the map including the 5′ side of the anticodon loop (see Fig. 4*e*). The position of uracil 33 differs in the initiator tRNA from that in yeast tRNA^{Phe} and will be discussed below. All of residue 33: phosphate, ribose, and base, lies in strong density. Figure 4*b* shows portions of the D stem and loop and the T loop. The D loop of the initiator tRNA was fitted using maps based on partial models to insert the extra residue in the α region. The base of residue 16 in the α region can be seen to lie in strong density, as do the bases of the D stem seen between phosphate 15 and ribose 23. The acceptor stem density is shown in Fig. 4*c*. The present model includes P76, the terminal phosphate, but not adenosine 76. The strong peak of density to the upper right of P76 is probably occupied by the ribose and the elongated extension may be the position of adenine 76. The strong density to the left of P76 is occupied by phosphates 73–75, which are part of the curled portion of the acceptor terminus (see Fig. 3). Figure 4*d* shows the anticodon arm at the point where the anticodon stem and D stem join to form one helix. At the left is a large region with a number of small peaks, which corresponds to the long solvent channel seen in Fig. 2. Figure 4*f* shows the D loop, T stem and acceptor stem. The generally good fit of the helix can be seen. Note the density corresponding to phosphate 73 which begins the curl seen in the acceptor terminus.

Figure 5 has stereo side and end views of *E. coli* tRNA$_f^{Met}$, and for comparison, yeast tRNA^{Phe}. In the side view of the initiator tRNA (Fig. 5*a*), one can see four of the five unpaired residues at the 3′ end (A76 is not yet in the model). Residue 72 is base-paired to residue 1 in chain-elongating tRNAs and eukaryotic initiators[1,2]; here it is rotated away from the base-pairing plane. The plane of adenine 72 is almost perpendicular to that of C1, and is in a curved stacking array with bases 73, 74, and 75. The 3′ terminus in this tRNA curves over the minor groove of the acceptor helix, bringing phosphate 76 close to phosphates 3 and 4 of the opposite strand. The significance of this conformation is not clear. Schulman *et al.*[18] have shown that modification of C1 to U1, with the resulting formation of a normal Watson–Crick base pair with A72, does not interfere with initiator function, but does enhance the ability of the initiator tRNA to bind to *E. coli* elongation factor, Ef-Tu. The curved stacking array of bases 72 through 75 appears to be stable in the crystal. It would be of interest to determine its stability in solution.

Although eukaryotic initiators differ from other tRNAs in the T loop, prokaryotic initiators differ in this loop only in the presence of A57 rather than the more common G57[1,2]. The major difference seen here in the initiator tRNA structure compared to yeast tRNA^{Phe} is the position of residue 57. A57 in the initiator tRNA is intercalated between G18 and G19 of the D loop, as is G57 in yeast tRNA^{Phe}, but is not drawn in as far as the backbone of the D loop (compare Fig. 5*a* and *c*). The position of G57 in yeast tRNA^{Phe} may be stabilized by the hydrogen bonds formed between N2 of G57 and riboses 18 and 19 (refs 19, 20). Such stabilizing forces are not possible when adenine is substituted for guanine, which may account for the differences. The current model of the initiator tRNA has not been constrained to include any tertiary interactions. The only constraints imposed have been on residues involved in the hydrogen-bonded stem regions. Most of the base positions in the current initiator tRNA model have been shifted from their original positions in the initial model by the refitting process. Tertiary interactionscannot be identified with certainty at the resolution of this report. However, they can be tentatively identified by the relative geometry and proximity of the bases. For example, O6 of G9 appears to be within hydrogen-bonding distance of the amino group of C12, an interaction which may be similar to that in yeast tRNA^{Phe} between A9 and A23. Most of the tertiary interactions seen in yeast tRNA^{Phe} appear also to exist in *E. coli* initiator tRNA. The precise identification of these interactions as well as the identification of the interactions of magnesium ions and spermine must, however, await the higher resolution analysis.

The major differences between the two structures are found outside the core region of the molecule. There are two significant sequence differences between *E. coli* tRNA$_f^{Met}$ and yeast tRNA^{Phe} (Fig. 1). The first is found at the end of the acceptor stem and may give rise to the difference in conformation of the 3′ OH end of the two molecules described earlier. The second is the size of the α region of the D loop. This region of the initiator structure was fit using Fourier maps based on a model in which the entire D loop was omitted. The α region residues are shown shaded in Fig. 5*a*, *c*. In the initiator tRNAs these residues are associated with strong density (see Fig. 4*c*) and appear to be more rigidly fixed than the two α residues in yeast tRNA^{Phe}. D16 and D17 in yeast tRNA^{Phe} point away from each other, while the three α bases in the initiator tRNA are close together, with C17 and U17a stacked upon each other (Fig. 5*b*). Although the α region in this initiator tRNA is one residue larger than that of yeast tRNA^{Phe}, it does not project further from the body of the molecule than the α region of yeast tRNA^{Phe} (Fig. 5*b*, *d*). Instead, the D loop accommmodates the extra residue by folding toward the body of the molecule, giving rise to a more tightly organized loop than in yeast tRNA^{Phe}. This may explain why tRNAs have a maximum of three nucleotides in the α region[1,2,8]: there is simply not enough room for an internally directed segment to accommodate a fourth nucleotide without encroaching on the body of the molecule.

The anticodon loops of *E. coli* $\text{tRNA}_\text{f}^{\text{Met}}$ and yeast tRNA^{Phe} are superficially similar in that the anticodon bases have roughly similar stacking (Figs 3 and 5*a*, *b*). However, an important difference lies in the orientation of the conserved residue U33 which is 5′ to the anticodon. In yeast tRNA^{Phe}, U33 folds into the anticodon loop and forms a hydrogen bond between N3 of U33 and phosphate 36 (refs 19, 20). U33 in *E. coli* $\text{tRNA}_\text{f}^{\text{Met}}$ has an almost opposite orientation; it is thrust away from the anticodon loop into the solvent region. An intermolecular lattice interaction involving uracil 33 may help stabilize its orientation; however, its identification is still tentative. The effect of this difference in U33 orientation on the anticodon loop folding in the two molecules can be seen in Fig. 5*b*, *d*. The loop in yeast tRNA^{Phe} is symmetrical while the loop of *E. coli* $\text{tRNA}_\text{f}^{\text{Met}}$ is skewed, so that the anticodon bases are in different positions relative to the anticodon stem in the two molecules. The orientation of residue 33 in the initiator tRNA involves a position of the ribose so that the 2′ hydroxyl of ribose 33 could perhaps form a hydrogen bond with phosphate 36. Phosphate 36 is also in a slightly different position than in yeast tRNA^{Phe}, being closer to the backbone of the 5′ side of the anticodon loop. Residues 34 and 35 are forced off to one side, producing the skewed shape of the loop. The shape of the anticodon loop may thus be determined by the group hydrogen bonding to phosphate 36: one conformation of the loop is found if the hydrogen-bonding group is ribose 33 and another if it is uracil 33. The two conformations show a marked difference in the position of phosphate 35 which in the initiator tRNA extends away from the anticodon loop in contrast to its more proximal position in the yeast tRNA^{Phe}.

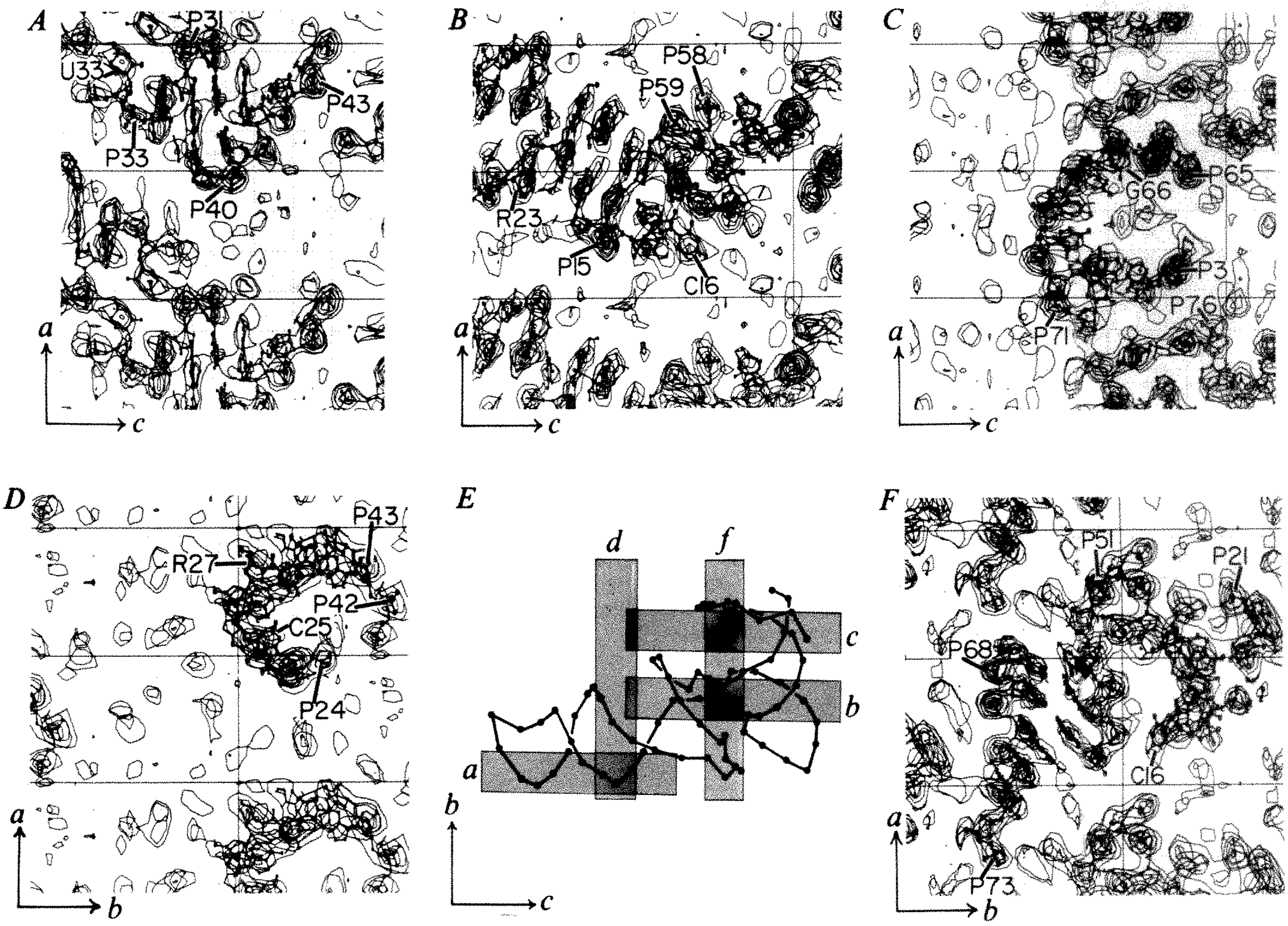

Fig. 4 Five different sections of the sum function Fourier map, $2F_0 - F_c$, are shown. Each section is the superposition of seven sections with a total thickness of 8 Å. In *e*, a schematic diagram is given which includes a plot of the phosphorous atoms in the backbone. The molecule is shown in the orientation of Fig. 2. The shaded bars indicate the regions of the molecule seen in the correspondingly labelled density section. The bars are all 8 Å wide and extend over 50 Å in the direction perpendicular to the page. The scale of this schematic is not the same as that of the density sections. In *a*–*d* and *f*, one-and-a-half unit cells are shown in the *a* direction. The horizontal lines are drawn at $x = 0$, $\frac{1}{2}$, and 1. The distance between each pair of lines is therefore 16 Å. In *b* and *c*, the vertical line is drawn at $z = 1/2$, and in *d* and *f*, at $y = 1/2$. In all sections the model has been drawn in addition to the contours of electron density. The principal molecule is drawn in heavy lines, symmetry-related molecules in light lines. The contouring begins at $0.275\ \text{e}\ \text{Å}^{-3}$ with intervals of $0.300\ \text{e}\ \text{Å}^{-3}$. In indicating various parts of the molecule, we have used P for phosphate, R for ribose, and A, G, C, U for bases.

Fig. 5

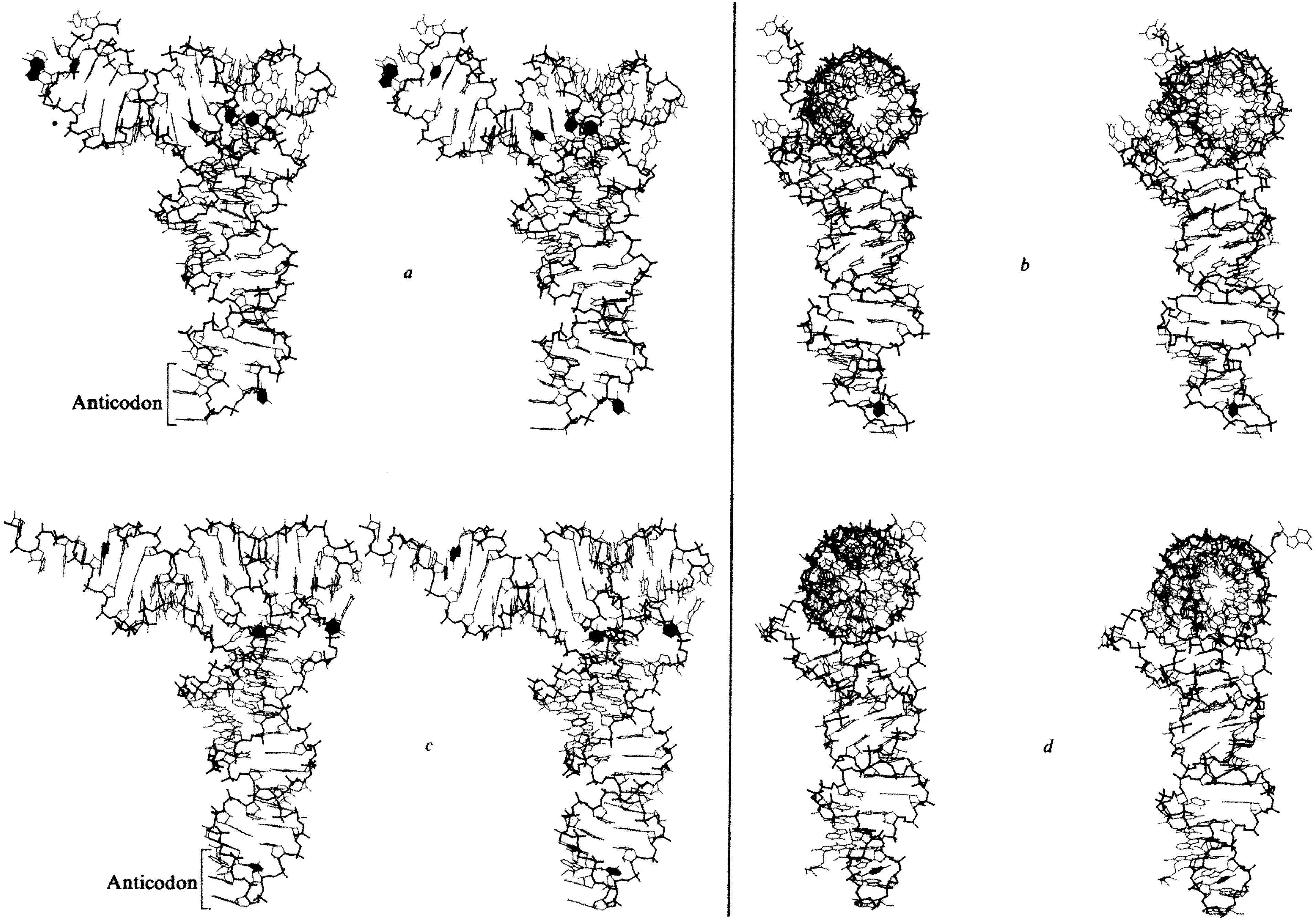

Fig. 5 Stereo diagrams of *E. coli* $\text{tRNA}_f^{\text{Met}}$(*a*, *b*) and yeast tRNA^{Phe} (*c*, *d*). *a* and *c* show side views of the two molecules and *b* and *d* views looking down the acceptor helix. In *a*, residues C1, A72, C16, C17, U17a, and U33 are shaded. Only residue U33 is shaded in *b* and *d*. In *c*, residues G1, C72, D16, D17, and U33 are shaded. The backbone of each molecule is emphasized with heavy lines.

Two different kinds of molecules

The structure presented here is based on data to 3.5 Å resolution and has been partially refined to a residual of 0.35. We have been able to interpret the structure at this resolution in more detail than might be expected because we have interpreted it comparatively with the refined 2.5 Å structure of the yeast tRNA^{Phe}. There are three regions in which the structure of the *E. coli* $\text{tRNA}_f^{\text{Met}}$ differs substantially from that of yeast tRNA^{Phe}. The first is the 3′ end of the molecule. The conformation observed in the initiator tRNA demonstrates the flexibility of this end of tRNA molecules which is consistent with its biological role: the transfer of the nascent polypeptide chain from one tRNA to the next[1,2,9]. The second difference is found in the α region of the D loop. The initiator tRNA accomodates its larger α region not by extending it further into solvent, but by drawing it closer to the body of the molecule, giving a more compact structure than seen in yeast tRNA^{Phe}. The third difference concerns the conformation of the anticodon arm. In their 4.5 Å analysis of yeast $\text{tRNA}_f^{\text{Met}}$, Shevitz *et al.* found an overall similarity in the shape of the yeast initiator tRNA to that of yeast tRNA^{Phe}, with a difference existing in the anticodon arm[4]. It will be of interest to compare the structures of the *E. coli* and yeast initiator tRNAs once the details of the latter are available. A recent biochemical study has implicated the anticodon loop conformation in distinguishing initiator tRNAs from chain elongation tRNAs by their endonuclease cleavage patterns[5]. In the present study, the major difference in the anticodon region concerns itself with the orientation of uridine 33. In *E. coli* $\text{tRNA}_f^{\text{Met}}$, the base projects away from the loop while in yeast tRNA^{Phe}, it points into the loop[19,20]. The effect of the different orientation is a position of ribose 33 which appears to allow the formation of a hydrogen bond between O2′ of the ribose with phosphate 36. It is important to emphasize, however, that the identity of this hydrogen bond, as of all the tertiary hydrogen bonds discussed above, is tentative until the higher resolution analysis is complete. Phosphate 36 is drawn toward the centre of the loop while phosphate 35 is forced away from the centre, giving rise to the skewed appearance of the loop (Fig. 5*b*) in contrast to that of yeast tRNA^{Phe} (Fig. 5*d*). The two loop conformations lead to a slightly different stacking arrangement of the anticodon bases. Although the position of uracil 33 in *E. coli* $\text{tRNA}_f^{\text{Met}}$ may be stabilized by a lattice interaction, it is not likely that the loop conformation is entirely determined by this interaction.

The difference in the anticodon loop conformation was not anticipated from either the nucleotide sequence or the results of earlier solution studies. The implication from the recent nuclease digestion study[5], however, is that the conformation detected there for the *E. coli* initiator tRNA is the same as that found in both lower and higher eukaryotic initiators. The generality of an initiator tRNA anticodon loop conformation may be the determining factor which permits initiators to enter the bind at the P site of the ribosome while chain-elongating tRNAs bind initially at the A site. The external position of uracil 33 and its concomitant failure to participate in hydrogen bonding within the anticodon loop offers an explanation for the cytosine in position 33 in higher eukaryotic initiators. In cytosine, N3 is not protonated so that a hydrogen bond between the base of residue 33 and phosphate 36 of the type seen in yeast tRNA cannot exist. However, even with cytosine in position 33, the hydrogen bond between ribose 33 and phosphate 36 suggested in the *E. coli* initiator tRNA could exist. One should recall here that higher eukaryotic initiators can be used in *in vitro E. coli* protein synthetic systems and vice versa[21].

The uridine swivel hypothesis

tRNAs move from the A site to the P site in the ribosome. The conformational difference in the anticodon loop which we observe between the chain-elongating yeast tRNA^{Phe} and the initiator *E. coli* $\text{tRNA}_f^{\text{Met}}$ may be a conformational shift which occurs when tRNA moves from one site to the other. A chain-elongating tRNA moving from the A site to the P site may interact with an element of the ribosomal machinery which flips the anticodon loop from one conformation to the other with a swivel motion of U33. If so, does the externally oriented uracil 33 play a structural role when the tRNA occupies the P site? Perhaps a ternary complex forms involving messenger RNA and tRNAs in the A and P sites, such that uracil 33 of tRNA hydrogen bonds to the anticodon arm of the A-site tRNA. This hydrogen bond could involve a 2′ hydroxyl of the A-site tRNA and O2 of uracil 33. In such an hypothesis, cytosine in position 33 would not modify the stability of the system. Furthermore, the hypothesis allows a plausible positioning of the tRNAs in the A and P sites in which the anticodon bases hydrogen bond to adjacent nucleotide triplets on the messenger RNA, and the CCA ends of the two molecules are close enough to effect a transfer of the nascent polypeptide chain. In this arrangement, the two codons of the message must be unstacked as suggested a few years ago[22]. A further description of this proposed ternary complex will be published elsewhere. The observed difference in the anticodon loop conformation of the *E. coli* initiator tRNA and the yeast tRNA^{Phe} may thus provide clues as to the manner in which tRNAs associate with each other in the ribosome.

This research was supported by grants from the NIH, NSF, NASA, and the American Cancer Society. We thank Dr F. P. Brooks and his colleagues at the Department of Computer Science, University of North Carolina at Chapel Hill, for their assistance with the GRIP-75 molecular graphics facility. We also thank Dr Gary Quigley for use of the program to plot Figs 2–5 and the coordinates in Figs 2 and 5, and both him and Andrew H.-J. Wang for their encouragement, advice, and assistance.

Received 8 October 1979; accepted 3 April 1980.

1. Sigler, P. B. *A. Rev. Biophys. Bioengng* **4,** 477–527 (1975).
2. Rich, A. & RajBhandary, U. L. *A. Rev. Biochem.* **45,** 805–860 (1976).
3. Quigley, G. J., Teeter, M. M. & Rich, A. *Proc. natn. Acad. Sci. U.S.A.* **75,** 64–68 (1978).
4. Schevitz, R. W. *et al. Nature* **278,** 188–190 (1979).
5. Wrede, Woo, N. H. & Rich, A. *Proc. natn. Acad. Sci. U.S.A.* **76,** 3289–3293 (1979).
6. Roe, B. A., Marcu, K. & Dudock, B. *Biochim. biophys. Acta* **319,** 25–36 (1973).
7. Anandaraj, M. P. J. S. & Roe, B. A. *Biochemistry* **14,** 5068–5073 (1975).
8. McPherson, A. Jr in *Methods of Biochemical Analysis* (ed. Glick, D.) 249–345 (Wiley, New York, 1976).
9. Goddard, J. P. *Prog. Biophys. molec. Biol.* **32,** 233–308 (1977).
10. Rossman, M. G. (ed.) *The Molecular Replacement Method* (Gordon and Breach, New York, 1972).
11. Woo, N. H. thesis, MIT (1978).
12. Stout, G. H. & Jensen, L. H. in *X-ray Structure Determination*, 245 (Macmillan, New York, 1968).
13. Ward, K. B., Wishner, B. C., Lattman, E. E. & Love, W. E. *J. molec. Biol.* **98,** 161–179 (1975).
14. Blundell, T. L. & Johnson, L. N. in *Protein Crystallography*, 428–429 (Academic, London, 1976).
15. Hedrickson, W. A. & Konnert, J. in *Biomolecular Structure, Conformation, Function, and Evolution* Vol. I (ed. Strinivasan, R.) 43–57 (Pergamon, Oxford, 1979).
16. Kim, S. H. *et al. Science* **185,** 435–440 (1974).
17. Robertus, J. D. *et al. Nature* **250,** 546–550 (1974).
18. Schulman, L. H., Pelka, H. & Sundari, R. M. *J. biol. Chem.* **249,** 7102–7110 (1974).
19. Quigley, G. J. & Rich, A. *Science* **194,** 796–806 (1976).
20. Jack, A., Ladner, J. E. & Klug, A. *J. mol. Biol.* **108,** 619–649 (1976).
21. Elson, N. A., Adams, S. L., Merrick, W. C., Safer, B. & Anderson, W. F. *J. biol. Chem.* **250,** 3074–3079 (1975).
22. Rich, A. in *Ribosomes*, 871–884 (Cold Spring Harbor Laboratory, New York, 1974).
23. Gauss, D. G., Gruter, F. & Sprinzl, M. *Nucleic Acids Res.* **6,** r1–r19 (1979).

Insertion of the eukaryotic transposable element Ty*1* creates a 5-base pair duplication

Philip J. Farabaugh & Gerald R. Fink

Section of Biochemistry, Molecular and Cell Biology, Cornell University, Ithaca, New York 14853

The his4–912 *mutation results from insertion of a transposable element into the 5′-non-coding region of the* his4 *gene of yeast. A duplication of 5 base pairs of wild-type* his4 *DNA flanks the inserted element. The major class of His$^+$ revertants result from excision of most of the transposable element, leaving an inserted segment of 334 base pairs flanked by the 5-base pair repeats.*

TRANSPOSABLE genetic elements in bacteria are capable of transposition to new sites and promoting chromosomal rearrangements including deletions, inversions and fusions[1,2]. The existence of eukaryotic transposable elements has been suggested on genetic and biochemical grounds. In maize, the genetic 'controlling elements' are capable of transposition to new sites and of catalysing gross rearrangements of the genome[3]. Reiterated DNA elements which have the same structure as a bacterial transposon have been isolated from *Drosophila*[4] and the yeast *Saccharomyces cerevisiae*[5]. The location of these elements varies between strains. The genetic properties of maize controlling elements and the biochemical properties of the *Drosophila* and yeast elements suggest that transposable elements similar to those found in prokaryotes exist in eukaryotes. In no case has an unstable mutation been shown biochemically to be the result of the insertion of a transposable element.

The *his4-912* mutation is due to the insertion of a transposable element (Ty*1*) into the *his4* locus of yeast[6]. The mutation is unstable and has given rise to translocations, deletions, a transposition and an inversion[7]. DNA sequence analysis of the wild-type *his4* gene and the *his4-912* mutant indicates that transposition of Ty*1* creates a 5-base pair duplication of DNA previously at the site. Excision of the element by recombination between the terminal 334-base pair repeats results in reversion to a His$^+$ phenotype. In *his4-912*, Ty*1* inserted into the 5′-non-coding region of the *his4* gene. The phenotype of the His$^+$ revertants of *his4-912* suggests that Ty*1* does not disrupt the *his4* promoter but that it interferes with *his4* expression by transcriptional competition.

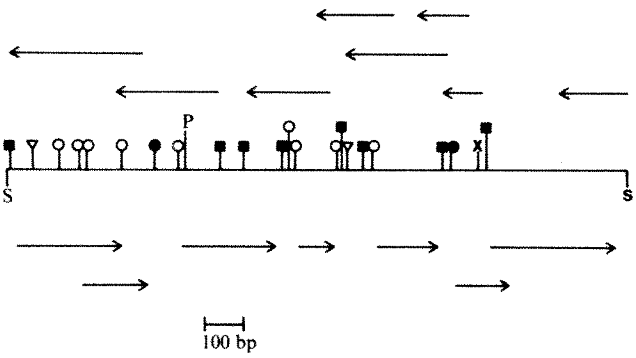

Fig. 1 The sequencing strategy for the 1,577-base pair (bp) *His4$^+$ Sal*I fragment. Those restriction sites used to determine the sequence are indicated: *Sal*I(S), *Hinf*I (■), *Taq*I(○), *Msp*I(▽), *Xho*I(×), *Sau*3A (●) and *Pvu*II(P). Each arrow above and below the map indicates the extent of the 3′ to 5′ sequence determined from a single experiment; the head of the arrow indicates the position of the nucleotide identified farthest from the end label. The restriction fragments for sequence analysis were generated by cleavage of either the *Sal*I plasmid (YIP302) or the *Sal*I fragment and labelled at their 3′ ends with either [α-^{32}P]dATP or dCTP using reverse transcriptase[29]. The labelled fragments were isolated and subjected to the Maxam–Gilbert chemical sequencing procedure and the reaction products separated by electrophoresis as described[30] except that 80-cm gels were used to enable us to read sequences very far from the label (±350 base pairs). The products were visualized by autoradiography and the sequence read from the film.

Analysis of *His4$^+$* and *his 4-912*

The *his4* locus was cloned as a 20×10^3-base pair *Bam*HI fragment on pBR313 (YIP300)[8]. Existing deletions of portions of *his4* localize the beginning of the gene to 500 base pairs from the end of an approximately 1,500-base pair *Sal*I fragment[9]. The Southern blot of labelled *his4* DNA to DNA from a *912* yeast strain and the restriction map of the *912* clone demonstrated that the *912*-insert was a Ty*1* element transposed to the same *Sal*I fragment[6].

We present here the DNA sequence from this *Sal*I fragment in *His4$^+$* and compare it with the DNA sequence from the *Sal*I fragment in *his4-912*. We analysed fragments of the *His4$^+$* segment which end at *Sal*I, *Hinf*I, *Taq*I, *Msp*I, *Xho*I and *Pvu*II sites to determine the complete nucleotide sequence of the wild-type 1,577-base pair fragment (Fig. 1). The *his4* coding frame extends through the last 474 base pairs of the top strand of the fragment. Many nonsense codons are dispersed throughout the region in the other two coding frames. Two early *his4$^-$* mutations differ from the wild-type sequence within this segment (T. Donahue, personal communication). The protein specified by the *his4* coding frame begins Met-Val-Leu-Pro-Ile; the amino terminus of the *his4* protein is the tetrapeptide Val-Leu-X-Ile (X was unidentified, ref. 10 and R. Bigelis, personal communication). These data show that the coding region for the amino-terminal portion of the *his4* protein begins at position +1 shown in Fig. 2.

The plasmid containing the *his4-912* mutation (YIP312) includes 19×10^3 base pairs of yeast DNA (the restriction map, as previously determined[6], is shown in Fig. 3). To analyse more easily the DNA sequence in the region of the two junctions between *his4* and the insert, we cloned the two *Sal*I fragments which span these junctions in pBR322 (YIP312-1 and YIP312-2; Fig. 3). The junction closest to *his4* was sequenced from fragments produced by cleavage of YIP312-1 with *Sal*I, *Hinf*I, *Sau*3A, *Taq*I and *Bgl*II. The junction distal to *his4* was sequenced using the restriction sites for the enzymes *Hinf*I, *Msp*I and *Sau*3A, which lie within a 900-base pair *Pvu*II fragment of YIP312-2 (Fig. 4*b*). The sequence of the *his4*-proximal junction extends 715 base pairs into the insertion element and the *his4*-distal sequence extends 369 base pairs in from the other junction (Fig. 2).

Ty*1* is a transposable element

The Ty*1* element is a 5,600-base pair region flanked by direct repeats of approximately 250 base pairs ('δ regions')[5]. The element is present in about 35 copies dispersed throughout the

0028-0836/80/300352—05$01.00

```
                                      -161
GTGACTCACGTTTTTTTATCAGTCATTCGATATAGAAGGTAAGA
CACTGAGTGCAAAAAAATAGTCAGTAAGCTATATCTTCCATTCT
                    TaqI

GTGACTCACGTTTTTTTATCAGTCATTCGATATAGAAGGTAAGATGTTGGAATAGAAATCAACTATCATCTACTAACTAGTATTTACATTACTAGTATATTATCATATACGGTGTTAGAA
CACTGAGTGCAAAAAAATAGTCAGTAAGCTATATCTTCCATTCTACAACCTTATCTTTAGTTGATAGTAGATGATTGATCAGAAATGTAATGATCATATAATAGTATATGCCACAATCTT
                    TaqI

GATGACGCAAATGATGAGAAATAGTCATCTAAATTAGTGGAAGCTGAAACGCAAGGATTGATAATGTAATAGGATCAATGATATAAACATATAAAATGATGATAATAATATTTATAGAAT
CTACTGCGTTTACTACTCTTTATCAGTAGATTTAATCACCTTCGACTTTGCGTTCCTAACTATTACATTATCCTAGTTACTATATTTGTATATTTTACTACTATTATTATAAATATCTTA
                                                                              Sau3A

TGTGTAGAATTGCAGATTCCCTTTTATGGATTCCTAAATCCTTGAGGAGAACTTCTAGTATATTCTGTATACCTAATATTATAGCCTTTATCAACAATGGAATCCCAACAATTATCTCAA
ACACATCTTAACGTCTAAGGGAAAATACCTAAGGATTTAGGAACTCCTCTTGAAGATCATATAAGACATATGGATTATAATATCGGAAATAGTTGTTACCTTAGGGTTGTTAATAGAGTT
             HinfI          HinfI                                                                         HinfI

CATTCACCCATTTCTCATGGTAGCGCCTGTGCTTCGGTTACTTCAAAAGGAAG ...   ~5100 bp   ... GTCGACACAAAGGCTTCGTTAACATGCACTTCAACTA
GTAAGTGGGTAAAGAGTACCATCGCGGACACGAAGCCAATGAAGTTTTCCTTC         of Ty1       CAGCTGTGTTTCCGAAGCAATTGTACGTGAAGTTGAT
                                                                           SalI

CAGAAGCAGAAATACACGCAGTCAGTGAAGCTATACCGCTATTGAATAACCTCAGTCACCTTGTGCAAGAACTTAACAAGAAACCAATTATTAAAGGCTTACTTACTGATAGTAGATCAA
GACTTCGTCTTTATGTGCGTCAGTCACTTCGATATGGCGATAACTTATTGGAGTCAGTGGAACACGTTCTTGAATTGTTCTTTGGTTAATAATTTCCGAATGAATGACTATCATCTAGTT
                                                                                                                    Sau3A

CGATCAGTATAATTAAGTCTACAAATGAAGAGAAATTTAGAAACAGATTTTTTGGCACAAAGGCAATGAGACTTAGAGATGAAGTATCAGGTAATAATTTATACGTATACTACATCGAGA
GCTAGTCATATTAATTCAGATGTTTACTTCTCTTTAAATCTTTGTCTAAAAAACCGTGTTTCCGTTACTCTGAATCTCTACTTCATAGTCCATTATTAAATATGGATATGATGTAGCTCT
Sau3A                                                                                                                  TaqI

CCAAGAAGAACATTGCTGATGTGATGACAAAACCTCTTCCGATAAAAAGATTTAAACTATTAACTAACAAATGGATTCATTAGATCTATTACATTATGGGTGGTATGTTGGAATAGAAAT
GGTTCTTCTTGTAACGACTACACTACTGTTTTGGAGAAGGCTATTTTTCTAAATTTGATAATTGATTGTTTACCTAAGTAATCTAGATAATGTAATACCCACCATACAACCTTATCTTTA
                                                                              HinfI   BglII

CAACTATCATCTACTAACTAGTATTTACATTACTAGTATATTATCATATACGGTGTTAGAAGATGACGCAAATGATGAGAAATAGTCATCTAAATTAGTGGAAGCTGAAACGCAAGGATT
GTTGATAGTAGATGATTGATCATAAATGTAATGATCATATAATAGTATATGCCACATACTTCTACTCGGTTTACTACTCTTTATCAGTAGATTTAATCACCTTCGACTTTGCGTTCCTAA

GATAATGTAATAGGATCAATGAATATAAACATATAAAATGATGATAATAATATTTATAGAATTGTGTAGAATTGCAGATTCCCTTTTATGGATTCCTAAATCCTTGAGGAGAACTTCTAG
CTATTACATTATCCTAGTTACTTATATTTGTATATTTTACTACTATTATTATAAATATCTTAACACATCTTAACGTCTAAGGGAAAATACCTAAGGATTTAGGAACTCCTCTTGAAGATC
        Sau3A                                                                 HinfI      HinfI

TATATTCTGTATACCTAATATTATAGCCTTTATCAACAATGGAATCCCAACAATTATCTCAACATTCACCCATTTCTCATAAGAAAAGGATATGACTATGAACAGTAGTATACTGTGTAT
ATATAAGACATATGGATTATAATATCGGAAATAGTTGTTACCTTAGGGTTGTTAATAGAGTTGTAAGTGGGTAAAGAGTATTCTAAACCTATACTGATACTTGTCATCATATGACACATA
                                       HinfI                                                                          -121
                                                                                 TAAGAAAAGGATATGACTATGAACAGTAGTATACTGTGTAT
                                                                                 ATTCTTTTCCTATACTGATACTTGTCATCATATGACACATA

ATAATAGATATGGAACGTTATATTCACCTCCGATGTGTGTTGTACATACATAAAAATATCATAGCACAACTGCGCTGTGTAATAGTAATACAATAGTTTACAAAATTTTTTTTCTGAATA
TATTATCTATACCTTGCAATATAAGTGGAGGCTACACACAACATGTATGTATTTTTATAGTATCGTGTTGACGCGACACATTATCATTATGTTATCAAATGTTTTAAAAAAAAGACTTAT
                                                                                                                         -1
ATAATAGATATGGAACGTTATATTCACCTCCGATGTGTGTTGTACATACATAAAAATATCATAGCACAACTGCGCTGTGTAATAGTAATACAATAGTTTACAAAATTTTTTTTCTGAATA
TATTATCTATACCTTGCAATATAAGTGGAGGCTACACACAACATGTATGTATTTTTATAGTATCGTGTTGACGCGACACATTATCATTATGTTATCAAATGTTTTAAAAAAAAGACTTAT

MetValLeuProIleLeuProLeuIleAspAspLeuAlaSerTrpAsnSerLysLysGlu
                                                         +60
ATGGTTTTGCCGATTCTACCGTTAATTGATGATCTGGCCTCATGGAATAGTAAGAAGGAA
TACCAAAACGGCTAAGATGGCAATTAACTACTAGACCGGAGTACCTTATCATTCTTCCTT

ATGGTTTTGCCGATTCTACCGTTAATTGATGATCTGGCCTCATGGAATAGTAAGAAGGAA
TACCAAAACGGCTAAGATGGCAATTAACTACTAGACCGGACTACCTTATCATTCTTCCTT
           HinfI              Sau3A
```

Fig. 2 Comparison of the *His4*⁺ and *his4–912* sequences indicates the location of Ty*1*. The *his4-912* sequence (roman letters) is homologous with the *His4*⁺ sequence (italic letters) up to position −161 from the right (the direction to *his4*) and −157 from the left. The sequence of 5 base pairs from positions −157 to −161 (large letters) is duplicated at either end of the element. The 334-base pair region into the element from either junction is a direct repeat of the δ element (indicated by bars above and below the Ty*1* sequence). The 5,600-base pair internal region of Ty*1* lies between the two δ elements. The sequence of 36 base pairs in from the right hand and 382 base pairs in from the other have been determined. At the junctions between the δ elements and the 5,600-base pair region there is a second 5-base pair duplication 5′-TGGTA-3′ (underlined). The non-coding region of *His4*⁺ (italics) includes two possible Hogness boxes (underlined) that could be associated with mRNAs beginning on the *his4*-side of the first ATG in the *his4* non-coding region (underlined).

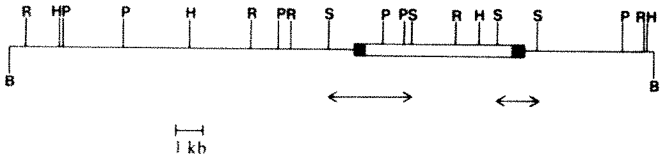

Fig. 3 The restriction map of the *his4-912* plasmid (YIP312) as described by Roeder and G.R.F.[5]. The sites for the enzymes *Bam*HI(B), *Eco*RI(E), *Hin*dIII (H), *Pst*I(P) and *Sal*I(S) are indicated. The boxed region represents the Ty*1* insert, and the δ repeats are indicated by the solid regions. The portions of this plasmid cloned in YIP312-1 and YIP312-2 are indicated by double-headed arrows below the map.

yeast genome and the δ regions are present in over 100 copies both as part of Ty*1* elements and as independent units. The Ty*1* element was inferred to transpose because it appeared in different locations in several strains of yeast. However, in no case was transposition directly observed.

The sequence of *his4-912* demonstrates that Ty*1* transposed into *his4*, as only the element itself has moved into the new site. The element which has inserted into *his4* is approximately 5,600 base pairs flanked by a perfect 334-base pair direct repeat. The *his4* wild-type sequence begins precisely at the ends of the terminal repeats, so no DNA other than Ty*1* has been inserted. Because insertion includes only Ty*1*, it could not have been caused by homologous recombination involving sequences flanking its original site. The DNA sequence of the *his4-912* mutation is consistent only with transposition of an intact Ty*1* into the 5′-non-coding region of *his4*.

The Ty*1* element in *his4-912* is flanked by a duplication of 5′-TAAGA-3′ (Fig. 5). This duplication was created during transposition, because the sequence appears only once in *His4*$^+$ DNA (nucleotides −161 to −157). The creation of flanking duplications is a characteristic of all prokaryotic transposable elements; both 5-base pair (IS*2*, Tn*3*, Mu and γ–δ) and 9-base pair duplications (IS*1*, Tn*5*, Tn*9*, Tn*10*) have been observed (summarized in ref. 11). Our finding that Ty*1* insertion creates a duplicated sequence in the target suggests that the mechanism of transposition is similar between a eukaryote and the prokaryotes.

A feature of the Ty*1* sequence which we cannot explain is the existence of a 5-base pair duplication of 5′-TGGTA-3′ at the internal δ junctions of Ty*1* (Fig. 2). The existence of a duplication of the sort created by Ty*1* transposition suggests that these junctions have also been created by transposition. There is no simple transposition process known or postulated that could account for this structure. It is also possible that this is either a random occurrence of a 5-base pair duplication or that the duplication is required for Ty*1* function.

The insertion of Ty*1* creates a 24-base pair inverted repeat

Although in *Escherichia coli* the insertion of transposable elements is not a site-specific event, the sites of insertion cluster in specific regions ('regional specificity') and many insertion mutations are found in these regions at a few specific sites ('hotspots'). Many transposons demonstrate regional specificity [Tn*3* (ref. 12), Tn*7* (ref. 13), Tn*9* (ref. 14), Tn*10* (refs 15, 16), Tn*501* and Tn*802* (ref. 17)]. DNA sequencing of Tn*10* (ref. 18) and Tn*3* (ref. 19) insertions shows directly that these elements have insertion hotspots. The hotspots for insertion of Tn*3* occur near a sequence in the target DNA which is homologous to the termini of the element. The insertion of Tn*3* at the hotspots creates an inverted repeat between the homologous sequences in the element and the site. Thus, some sequence homology is responsible for the specificity of insertion, although homologous recombination is not involved.

A sequence created by the insertion of Ty*1* into *his4* suggests that transposition is directed by limited sequence homology. The sequences 12 base pairs in either direction from one mutation junction form an inverted repeat with its centre of symmetry precisely at the junction (Fig. 5). The sequence, 5′-ACCCATTTCTCA/TAAGAAAAGGAT-3′ (the slash is the centre of symmetry and the junction), includes nine matches and two purine–purine matches. The sequence at the end of δ could be required for recognition of the preferred insertion site. The recognition does not involve homologous recombination, as that process would create a flanking direct repeat.

Excision of Ty*1*

The major class of His$^+$ revertants is caused by a sequence alteration at the *912* site. These revertants are His$^+$ at 37 °C and His$^-$ at 23 °C (ref. 7). The *his4* region from these revertants has suffered a large deletion of Ty*1* DNA, but still retains approximately 300 base pairs of the element[6]. The fact that the δ element is the same size as the remaining insert suggested that reversion resulted from recombination between the direct terminal repeats of δ, leaving a single δ. This process is called excision. The Tn*9* element, which is flanked by a direct repeat of IS*1*, also undergoes an excision of this sort[20].

We cloned the *his4* region of one cold-sensitive revertant, *his4-912R1*, using a modification of a previously described procedure[6]. Sequence analysis of the *his4* region from *his4-912R1* shows that the mutation results from the presence of a single δ element which is identical to those at the end of Ty*1* in *his4-912*. The δ element is flanked by the identical 5-base pair duplication flanking *his4-912*. We have sequenced 250 base pairs towards and into the *his4* gene and found no additional differences from *His4*$^+$. The sequence is entirely consistent with the recombination model for excision. Excision of Ty*1* by this specialized recombination could be responsible for the distribution of δ sequences in the yeast genome. As many as 50 δ sequences independent of Ty*1* are dispersed throughout the genome. These δ elements could mark the sites of previous Ty*1* excisions.

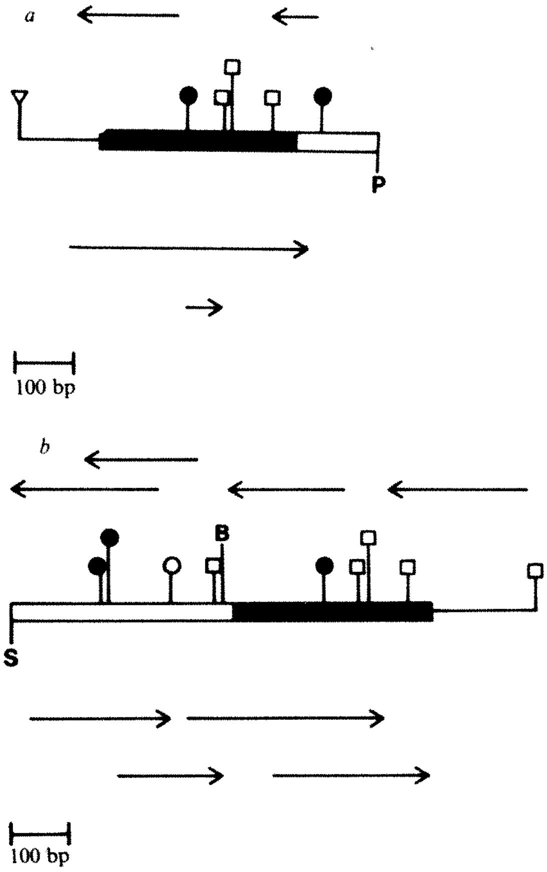

Fig. 4 The sequencing strategy for the two junctions of Ty*1* in *his4-912* is shown as described in Fig. 1 legend; the site for the enzyme *Bgl*II is indicated (B). The Ty*1* element is represented as in Fig. 3. *a*, The strategy for the *his4*-distal (left) region from plasmid YIP312-1. *b*, The strategy for the *his4*-proximal (right) region (YIP312-2).

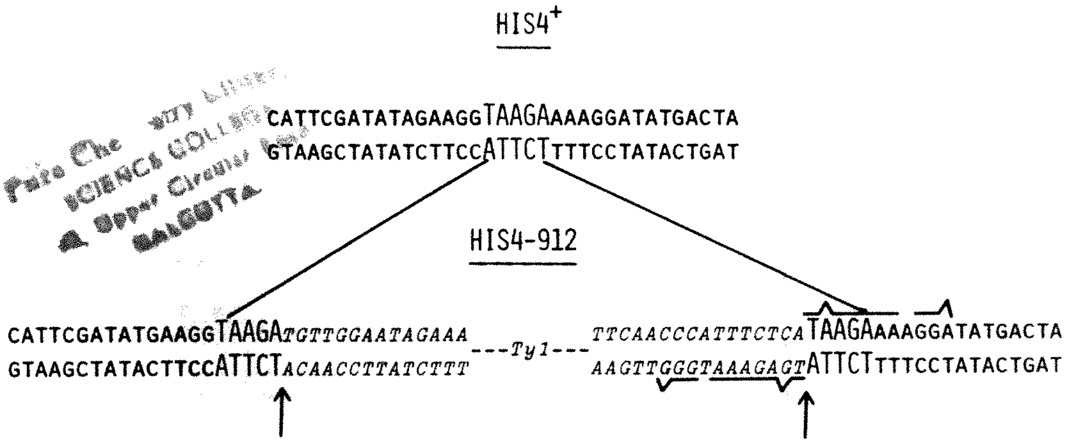
HIS4$^+$
CATTCGATATAGAAGGTAAGAAAAGGATATGACTA
GTAAGCTATATCTTCCATTCTTTTCCTATACTGAT
HIS4-912
CATTCGATATGAAGGTAAGATGTTGGAATAGAAA
GTAAGCTATACTTCCATTCTACAACCTTATCTTT
---Ty1---
TTCAACCCATTTCTCATAAGAAAAGGATATGACTA
AAGTTGGGTAAAGAGTATTCTTTTCCTATACTGAT

Pure Che... Science College, Upper Circular Road, CALCUTTA

Fig. 5 The sequences of *His4*$^+$ and *his4-912* junctions. The arrows are at the junction points. The regions homologous to *His4*$^+$ in the sequences of the two junctions are shown in roman lettering, the Ty*1* element in italics; the 5-base pair duplication is indicated by large letters. The lines in either direction from the right junction demonstrates the inverted repeat; a (–) indicates identity and a (Λ) indicates purine–purine partial identity.

Ty*1* is inserted into the region of the *his4* promoter

A comparison of the sequences of *His4*$^+$ and *his4-912* demonstrates that in the *his4-912* mutation Ty*1* lies in the 5′-non-coding region, 161 base pairs from the ATG responsible for initiation of *his4* translation (Fig. 2). Because the sequence encoding the *his4* polypeptide is unaffected and the mutation is distant from the structural gene, the His$^-$ phenotype of *his4-912* is likely to result from a block in the expression of the gene at the level of transcription.

Unfortunately, we do not know exactly where *his4* transcription begins. Comparison of the *his4* sequence with that of known eukaryotic promoters limits the position possible for *his4* transcriptional initiation. Regions where eukaryotic RNA polymerase II initiates have two common features. Translation begins at the first AUG following the site of transcriptional initiation[21]. As shown by studies on the *cycl* gene of *S. cerevisiae*, the only signal required for initiation of translation is the AUG[22]. This observation is supported by comparisons of 5′-non-coding regions of many eukaryotic mRNAs[23]. Based on these considerations the *his4* message must initiate downstream from the first ATG in the non-coding region (−88) between −87 and +1.

The second common feature of eukaryotic promoters is a sequence which is thought to be a recognition site for RNA polymerase II. Nearly all promoters have a sequence similar to 5′-TATAAATA-3′ (the 'Hogness box') which is centred approximately 28 base pairs on the 5′ side of the initial nucleotide of the message[24]. The promoter regions of the yeast genes *his3*[25], *cycl*[26], and the gene encoding glyceraldehyde-3-phosphate dehydrogenase[27] all include a sequence related to the Hogness box. If *his4* mRNA begins between −87 and +1, any Hogness box must lie between nucleotides −120 and −25. Two sequences similar to the Hogness box occur in this region: 5′-TATATAATA-3′, centred on −119, and 5′-CATAAAAA-3′, centred on −67. The His$^-$ phenotype of *his4-912* does not result from disruption of the DNA sequence in the region of either Hogness box.

Preliminary RNA blotting experiments indicate that the normal *his4* message is not produced in *his4-912* (C. Ilgen, personal communication). One possible explanation for the His4$^-$ phenotype of the *his4-912* mutation is that transcription initiated within the Ty*1* element disrupts the initiation of transcription at the normal *his4* promoter. The other possibility is that Ty*1* inserted into a site required for polymerase recognition. This would mean that the promoter includes sites in the region of −161 as well as the Hogness box.

The *his4-912R1* revertant created by excision of most of the Ty*1* element can distinguish between these two possibilities. In *his4-912R1* there is no new promoter either at the *his4*-proximal junction of the insertion or in the insertion itself, as this region is identical to that of *his4-912*. A promoter created at the *his4*-distal junction would result in transcription of the element itself. The element includes nine ATG codons each followed by several in-frame nonsense codons before the beginning of *his4*. Such a transcript would fail to express *His4*$^+$ because translation would initiate and terminate before the *his4* gene. The simplest hypothesis is that the *his4* promoter is located between the *his4-912* site (−161) and the beginning of the gene. The His$^-$ phenotype of *his4-912* could be attributed to transcriptional competition. Deletion of most of the element by excision eliminates the Ty*1* transcript so that initiation at the *his4* promoter occurs normally. The residual cold sensitivity of *his4-912* is not explained by this model. This phenotype could be due to some other pleiotropic effect of the δ element (such as that due to a minor transcript), or the presence of a δ element could alter the *his4* promoter. Many predictions of this model are being tested by RNA blotting experiments.

Sequence analysis of the Ty*1* element from *his4-912* demonstrates that Ty*1* is a transposon and is capable of transposition by a mechanism similar to that of bacterial transposons. Southern blotting analysis of His$^+$ revertants of *his4-912*[5] suggest that the element is also capable of promoting chromosomal aberrations similar to those catalysed by bacterial transposons. One mutant may be the result of a transposition-mediated inversion, similar to those seen with bacteriophage Mu[28]. The Ty*1* element also promotes events which differ from any observed in bacteria. These include deletions ending at apparently random locations in the element, chromosomal aberrations with breakpoints outside the element, and 'concerted' events[6,7], and suggest that the mechanism of action of Ty*1* is significantly different from that of prokaryotic transposons.

We thank Deborah Chaleff, Thomas Donahue, John Lis and Shirleen Roeder for their critical reading of this manuscript and for helpful discussions. This work was supported by NIH grant GM15408. P.J.F. was an American Cancer Society Postdoctoral Fellow. Experiments involving recombinant DNA techniques were carried out according to the NIH guidelines.

Received 25 February; accepted 16 May 1980.

1. Kleckner, N. *Cell* **11,** 11–23 (1977).
2. Bukhari, A. I., Shapiro, J. A. & Adhya, S. L. (eds) in *DNA Insertion Elements, Plasmids and Episomes*, 3–11 (Cold Spring Harbor Laboratory, New York, 1977).
3. McClintock, B. *Cold Spring Harb. Symp. quant. Biol.* **21,** 197–216 (1956).
4. Potter, S. S., Brorein, W. J., Dunsmuir, P. & Rubin, G. M. *Cell* **17,** 415–427 (1979).
5. Cameron, J. R., Loh, E. Y. & Davis, R. W. *Cell* **16,** 739–751 (1979).
6. Roeder, G. S. & Fink, G. R. *Cell* (in the press).
7. Chaleff, D. T. & Fink, G. R. *Cell* (in the press).
8. Hinnen, A., Farabaugh, P., Ilgen, C. & Fink, G. R. in *Eukaryotic Gene Regulation* (eds Axel, R., Maniatis, T. & Fox, C. F.) 43–50 (Academic, New York, 1979).
9. Farabaugh, P. & Fink, G. R. *Gene* (in the press).
10. Keesey, J. K., Bigelis, R. & Fink, G. R. *J. biol. Chem.* **254,** 7427–7433 (1979).
11. Grindley, N. D. F. & Sherrat, D. *Cold Spring Harb. Symp. quant. Biol.* **43,** 1257–1261 (1978).
12. Kopecko, D. J., Brevet, J. & Cohen, S. N. *J. molec. Biol.* **108,** 333–360 (1976).
13. Barth, P. T. & Grintner, N. J. *J. molec. Biol.* **113,** 455–474 (1977).
14. Johnsrud, L., Calos, M. & Miller, J. H. *Cell* **13,** 411–418 (1978).
15. Botstein, D. & Kleckner, N. in *DNA Insertion Elements, Plasmids and Episomes* (eds Bukhari, A. I., Shapiro, J. A. & Adhya, S. L.) 185–203 (Cold Spring Harbor Laboratory, New York, 1977).
16. Foster, T. J. *Molec. gen. Genet.* **154,** 305–309 (1977).
17. Grinsted, J., Bennett, P. M., Higginson, S. & Richmond, M. H. *Molec. gen. Genet.* **166,** 313–320 (1978).
18. Kleckner, N. *Cell* **16,** 711–720 (1979).

19. Tu, C.-P. D. & Cohen, S. N. *Cell* **19,** 151–160 (1980).
20. MacHattie, L. A. & Jackowski, J. B. in *DNA Insertion Elements, Plasmids and Episomes* (eds Bukhari, A. I., Shapiro, J. A. & Adhya, S. L.) 219–228 (Cold Spring Harbor Laboratory, New York, 1977).
21. Kozak, M. *Cell* **15,** 1109–1123 (1979).
22. Sherman, F., Stewart, J. W. & Schweingruber, A. M. *Cell* (in the press).
23. Baralle, F. E. & Brownlee, G. G. *Nature* **274,** 84–87 (1978).
24. Gannon, F. *et al. Nature* **278,** 428–433 (1979).
25. Struhl, K. & Davis, R. W. *Cell* (in the press).
26. Smith, M. *et al. Cell* **16,** 753–761 (1979).
27. Holland, J. P. & Holland, M. J. *J. biol. Chem.* **254,** 9839–9845 (1979).
28. Faelen, M. & Toussaint, A. *J. Bact.* **136,** 477–483 (1978).
29. Smith, D. & Calvo, J. *Nucleic Acid Res.* (in the press).
30. Maxam, A. & Gilbert, W. *Proc. natn. Acad. Sci. U.S.A.* **74,** 560–564 (1977); *Meth. Enzym.* **65** (in the press).

A signal sequence is not sufficient to lead β-galactosidase out of the cytoplasm

Felipe Moreno[*,§], **Audree V. Fowler**[†], **Michael Hall**[‡], **Thomas J. Silhavy**[‡], **Irving Zabin**[†] **& Maxime Schwartz**[*]

[*] Unité de Génétique Moléculaire, Institut Pasteur 25 rue du Dr Roux, 75724 Paris Cedex 15, France
[†] Department of Biological Chemistry, UCLA School of Medicine and Molecular Biology Institute, University of California, Los Angeles, California 90024
[‡] Frederick Cancer Research Center, Cancer Biology Program, Frederick, Maryland 21701

Escherichia coli *strains have been constructed in which* lacZ, *the gene for the cytoplasmic enzyme β-galactosidase, is fused to* lamB, *the gene for an outer membrane protein. One such strain produces a β-galactosidase which remains cytoplasmic even though it possesses the complete signal sequence of the* lamB *protein precursor at the amino-terminal end.*

ACCORDING to the signal hypothesis, proteins secreted from eukaryotic cells are synthesized as precursors with an extra NH_2-terminal sequence of predominantly hydrophobic amino acids[1,2]. That 'signal sequence' initiates binding of the translation complex to the endoplasmic reticulum, facilitating transfer of the protein across the membrane concomitant with translation. In most cases the signal sequence is removed by a 'signal peptidase' from the growing polypeptide during transfer, giving rise to the final protein product, which is localized on the luminal side of the endoplasmic reticulum. Evidence for this scheme in animal cells has come from the isolation, *in vitro*, of numerous precursors of secreted proteins, the discovery that they have extra amino acid sequences (15–30 residues) at their NH_2-terminus and the demonstration that secreted proteins are synthesized on polysomes bound to the endoplasmic reticulum whereas cytoplasmic proteins are synthesized on free polysomes[3–7]. On the basis of similar evidence, the hypothesis was extended to include the localization of non-cytoplasmic proteins in bacteria, with the cytoplasmic membrane having a role analogous to that of the eukaryotic endoplasmic reticulum[8–13]. (By non-cytoplasmic we mean proteins of the cytoplasmic or outer membranes, of the periplasmic space, or truly secreted proteins.)

We are using a genetic approach to evaluate the importance of the signal sequence in the export process[14–18]. One non-cytoplasmic protein which we have been studying is the product of gene *lamB* in *Escherichia coli.* Located in the outer membrane, it is involved in the transport of maltose and maltodextrins, and also serves as a receptor for several bacteriophages, including λ (refs 19–22). Comparison of the NH_2-terminal sequence of the mature protein[23] with that of the primary gene product[24,25] showed that *lamB* protein is synthesized as a precursor containing 24 extra amino acids at the NH_2 terminus. Mutations affecting this extra sequence prevent the export of the protein, which remains in the cytoplasm as an uncleaved precursor[26]. From this we conclude, as predicted by the signal hypothesis, that the extra sequence in the precursor of non-cytoplasmic proteins is essential for their export.

The question then is whether such an extra sequence possesses all the information required to lead any polypeptide out of the cytoplasm.

By means of gene fusion we have already shown that a polypeptide coded by a *lamB–lacZ* hybrid gene was exported, to some extent, to the outer membrane, although β-galactosidase, the product of *lacZ*, is normally cytoplasmic[15]. The amount of *lamB* DNA present in this hybrid gene (called 42-1) was 200–300 codons (out of a total of about 500 for the entire gene). We now describe two other fusion strains, in which there is much less *lamB* DNA in the hybrid gene. Our results demonstrate that the presence of a signal sequence at the NH_2 terminus of β-galactosidase does not suffice to lead this polypeptide out of the cytoplasm.

Construction and characterization of fusion strains

The application of gene fusion *in vivo*[27] to the selection of strains with *lamB–lacZ* hybrid genes has been described previously[15] (Fig. 1). It involves the insertion of phage Mu DNA into the *lamB* gene, the integration of a λ*plac* prophage into the Mu prophage, and a deletion of the Mu prophage. Two fusions will be described here, 61-4 and 52-4, derived from Mu insertions 61

Table 1 Purification of the hybrid proteins

	61-4		52-4	
	Total activity (units)	Specific activity (units per mg protein)	Total activity (units)	Specific activity (units per mg protein)
French press extract	9.9×10^8	2.5×10^4	3.3×10^9	5.1×10^4
38% Ammonium sulphate precipitate	4.3×10^8	7.6×10^4	1.8×10^9	2.2×10^5
DEAE-Sephadex A50 eluate	3.0×10^8	5.5×10^5	1.2×10^9	4.4×10^5

The 61-4 and 52-4 hybrid proteins were purified from 700 g and 1,000 g, respectively, of cells grown to late exponential phase at 30° C in M63 minimal medium[34] supplemented with 0.8% maltose. The purification was essentially as described by Miller[34] except that: (1) the extraction was carried out in the presence of 30 $\mu g\ ml^{-1}$ *p*-toluylsulphonyl fluoride to inhibit proteases present in the extract, (2) a precipitation step with 3% streptomycin sulphate was carried out before the ammonium sulphate precipitation, (3) DEAE Sephadex A50 was used instead of DEAE cellulose, (4) the sucrose gradient step was omitted and (5) 10^{-4} M Na-EDTA and 10^{-1} M β-mercaptoethanol were present in all buffers. The purified proteins were kept in the form of a 50% ammonium sulphate precipitate.

---

§ Present address: Servicio de Microbiologia, Centro Especial Ramon y Cajal, Madrid-34, Spain.

0028–0836/80/300356—04$01.00

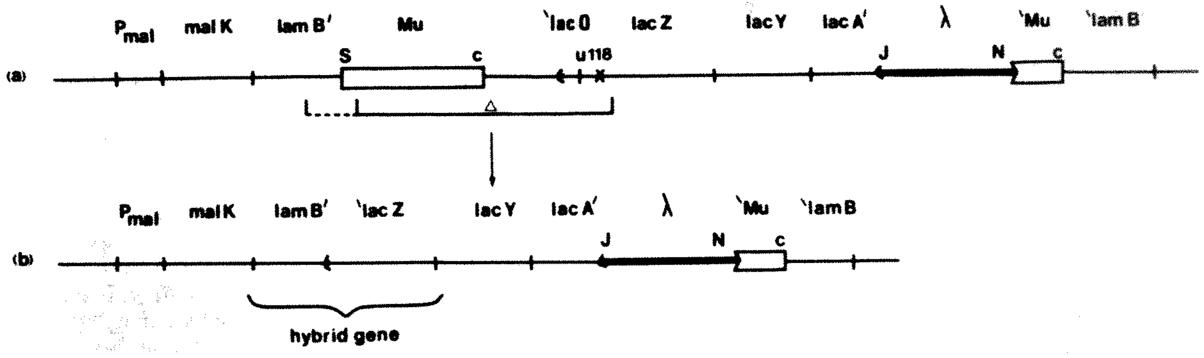

Fig. 1 Scheme for isolating *lamB–lacZ* fusion strains. Because the whole procedure has been previously described[15], only the last step is shown here. A thermoinducible Mu(cts) prophage was first inserted into *lamB* and a λ*plac Mu* prophage was then inserted into the *Mu* prophage, by recombination between homologous Mu DNA sequences. The structure of the resulting strain is shown in *a*. Pmal is the promoter of the *malK-lamB* operon. The S- and c-ends of the Mu prophage[44] are indicated. Primes, as in *lamB'* or *'lacO*, indicate that the genetic region referred to is deleted on the side the prime is written. U118 is an ochre mutation located in codon 17 of gene *lacZ* (ref. 45). Deletion events (Δ) removing all or most of the Mu(cts) prophage and extending past the U118 mutation yield strains whose genetic structure are shown in *b*. Such strains can be selected as thermoresistant (loss of the thermoinducible Mu(cts) prophage) and Lac$^+$ (elimination of U118 and production of a hybrid protein which has β-galactosidase activity).

and 52, respectively (Fig. 2). The presence of *lamB* DNA within the 52-4 hybrid gene was demonstrated by deletion mapping[15,28,29]. Because fusion 61-4 was derived from a Mu insertion located at the very beginning of *lamB*, the presence of *lamB* DNA in this hybrid gene could not be ascertained by this technique. Accordingly, we had to insure that *lacZ* was not fused to the promoter proximal gene *malK*. This was accomplished by demonstrating (as described in ref. 30) that the introduction of a non-polar amber mutation in *malK* (*malK*3 or *malK*4), in the *cis* position with respect to these fusions, had no effect on the synthesis of β-galactosidase. The introduction of such a mutation into known *malK–lacZ* fusions leads to the disappearance of β-galactosidase activity.

To locate the hybrid proteins in the cell, we prepared extracts and separated the cytoplasmic and envelope fractions as described elsewhere[14–16]. The hybrid proteins can be detected either by their enzymatic activity or by their migration on polyacrylamide gels in the presence of SDS. About 10% of the β-galactosidase activity sediments with the envelope in the case of 61-4, and 15% with 52-4. However, these figures, which result from assays carried out on unwashed envelope pellets, certainly represent overestimations of the amount of hybrid protein which is truly membrane bound. Indeed, when extracts of wild-type strains are centrifuged in the same conditions, about 10% of authentic β-galactosidase also sediments with the envelopes. The gel pattern in Fig. 3 confirms that the hybrid proteins are mostly cytoplasmic: the amount of envelope-bound protein is undetectable with 61-4 and is less than 3% with 52-4. Figure 3 also shows that the 61-4 polypeptide is slightly shorter than 52-4.

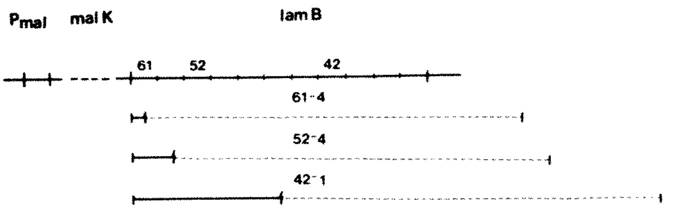

Fig. 2 Genetic structure of the *lamB–lacZ* fusions. Previous work[28] allowed us to divide gene *lamB* into 11 deletion intervals. The position of Mu insertions 61, 52 and 42 is shown on the first line. The structure of fusions derived from these Mu insertions is indicated below the map, with the *lamB* part of the hybrid gene shown as a heavy line and the *lacZ* part as an interrupted line. Only fusions 61-4 and 52-4 are described in this article, fusion 42-1 is described elsewhere[15]; it produces a hybrid protein which is partly exported to the outer membrane (see Fig. 3).

When 61-4 or 52-4 cells are submitted to cold osmotic shock[31], less than 2% of β-galactosidase activity, but about 90% of maltose binding protein[32], are released into the medium. Thus, the two hybrid proteins are not in the periplasmic space.

According to our fractionation data, therefore, the 61-4 and 52-4 hybrid proteins are chiefly in the cytoplasm, perhaps a very small fraction of the latter being bound to the membrane. That location accords with the growth properties of these two strains, which grow normally in the presence of maltose, an inducer of the *malK–lamB* operon, whereas other *lamB–lacZ* strains (such as 42-1, Figs 2, 3), which export some of the hybrid protein to the outer membrane, are sensitive to maltose[15,16].

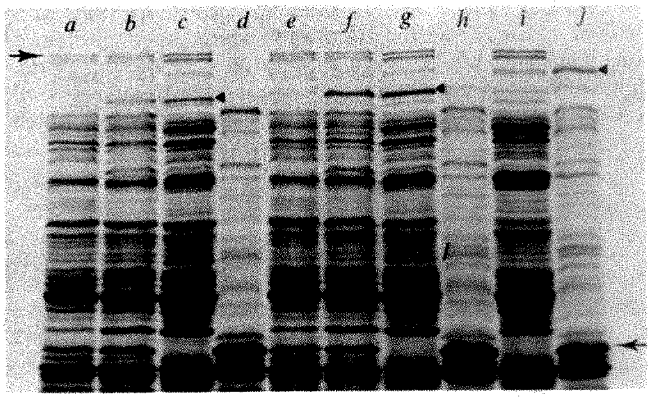

Fig. 3 SDS-polyacrylamide gel electrophoresis of whole cell extracts and cellular fractions of *lamB–lacZ* fusion strains. Whole cell extracts were prepared by growing the cells in the indicated media to mid-logarithmic phase, resuspending in 0.1 volume SDS sample buffer[46] and boiling for 2 min. Cytoplasmic and membrane fractions were prepared as previously described[14] by centrifuging at 100,000*g* for 1 h extracts obtained by sonication. All 'induced' samples correspond to cells grown at 30 °C for 4 h in maltose-glycerol M63 minimal medium supplemented with 5% complete medium (LB). 'Uninduced' samples correspond to cells grown in glucose M63 medium. The acrylamide concentration was 9%. Channels *a–d* are various preparations from the 61-4 fusion strain, channels *e–h* correspond to the 52-4 strain and channels *i* and *j* to the 42-1 strain. *a* And *e* are uninduced whole cell extracts; *b* and *f* are induced whole cell extracts; *c*, *g* and *i* are induced cytoplasmic fractions; *d*, *h* and *j* are induced membrane fractions. The membrane fractions displayed here correspond to 7.5 times more cells than the cytoplasmic fractions. The solid arrowheads indicate the *lamB–lacZ* hybrid proteins. The complete arrows indicate cytoplasmic and membrane markers: at the upper left the β and β' subunits of RNA polymerase and, at the lower right, major outer membrane protein Ia.

	1	2	3	4	5	6	7	8	9	10	11	12	13	14	15	16	17	18	19
	MET	ILE	GLU	ALA	ALA	HIS	GLU	LYS	ARG	GLU	SER	LEU	ALA	ALA	HIS	PRO	PRO	PHE	ALA
	1	2										27	28	29	30	31	32	33	34
	lamB	lamB										lacZ	lacZ	lacZ	lacZ	lacZ	lacZ	lacZ	lacZ
Intact Protein	●	●		●	●		●												
CNBr2*		●	●	●	●	●	●	●	●	●	●	●	●	●		●	●	●	●

Fig. 4 Amino-terminal sequence of the 61-4 *lamB–lacZ* hybrid protein. All sequencing was done using 0.1 M Quadrol in a Beckman 890C sequencer. The CNBr2* fragment was sequenced using a dual wash program[47]. The intact carboxymethylated protein was sequenced with a program similar to that of Hunkapiller and Hood[48]. All other procedures were as described previously[36] except that, recently, identification has also used HPLC. ● Indicates residue identified. The numbers above the sequence correspond to the position of the residue in the 61-4 protein, the numbers below correspond to the position of the residues in the *lamB* and *lacZ* gene products. According to the DNA sequencing data the *lamB* gene starts on the mRNA with two successive AUG codons. Therefore, the *lamB* protein precursor might be expected to start with two successive methionine residues. However the two hybrid proteins described here start with a single methionine residue, and there is some evidence that this is also true of the *lamB* protein precursor synthesized *in vitro* (ref. 25). We do not know whether this is due to an initiation of translation at the second, rather than the first AUG, or to a proteolytic cleavage of the first methionine. This introduces an ambiguity in the numbering of residues in the *lamB* gene product. We decided to call residue number 1 the single methionine which could be detected at the NH_2-terminal end of the hybrid proteins.

The 61-4 and 52-4 hybrid genes were transduced into other strains of *E. coli* K12 (see below). The transductants grew normally in the presence of maltose and synthesized a cytoplasmic β-galactosidase. Thus, the original fusion strains carried no unlinked mutation which might have prevented the export of hybrid protein.

Purification of the hybrid proteins

To facilitate purification we used genetic techniques to increase the amount of hybrid protein synthesized by fusion strains. Any hybrid gene obtained by our technique of gene fusion is located close to a λ prophage (Fig. 1). Induction of fusion strains with UV light yields λ transducing phages which carry the hybrid gene. When such phages are used to lysogenize another strain, multiple lysogens are obtained at a very high frequency, and these can be recognized by the amount of β-galactosidase which they synthesize[33]. After infecting MC4100 cells (deleted for the *lac* operon[27]) with a λ61-4 or a λ52-4 transducing phage, we selected presumed triple lysogens, which synthesized approximately three times as much β-galactosidase as the original fusion strain. Although they were of limited stability, these polylysogens could be used for protein purification, provided the number of transfers after their isolation was minimized.

Hybrid proteins were purified essentially according to the scheme used for authentic β-galactosidase[34] (Table 1). The 52-4 protein had a stability comparable to that of authentic β-galactosidase. The 61-4 protein, on the other hand, was rather unstable. For instance, it lost 90% of its activity after 10 days at 4 °C when kept in solution after elution from the DEAE Sephadex column.

Determination of NH_2 terminus of hybrid proteins

Hybrid protein sequences were analysed by techniques developed for use on a hybrid protein containing β-galactosidase and *lac* repressor sequences[35]. In wild-type β-galactosidase, the first two methionine residues are at positions 2 and 92 (ref. 36), and residues 3–92 yield a cyanogen bromide fragment called CNBr2. Hybrid proteins obtained as described in Fig. 1 legend always lack at least the first 17 amino acids of wild-type β-galactosidase, eliminating the first methionine. If the amino acid sequence which replaces the normal β-galactosidase NH_2 terminus contains no internal methionine, only one new fragment (CNBr2*) should result from treatment of the hybrid protein with cyanogen bromide. Indeed, with the 61-4 hybrid protein a single additional cyanogen bromide fragment was found that reacted with antibodies directed against wild-type CNBr2. The NH_2-terminal sequence of this peptide is the same as that of the intact hybrid protein (Fig. 4). The 52-4 hybrid protein, on the other hand, yielded three new peptides, due to the presence of methionine residues at positions 18 and 23 in the *lamB* portion of the hybrid protein[25]. To establish the sequence of the 52-4 hybrid protein up to the β-galactosidase sequence, it was therefore necessary to analyse the NH_2-terminal sequence on the intact protein, to purify the CNBr2* fragment and sequence its NH_2-terminal region, and to purify and sequence the smallest of the additional cyanogen bromide fragments.

As Figs 4 and 5 show, the 61-4 and 52-4 proteins contain *lacZ*

	1	2	3	4	5	6	7	8	9	10	11	12	13	14	15	16	17	18	19	20	21	22	23	24	↓ 25
	MET	ILE	THR	LEU	ARG	LYS	LEU	PRO	LEU	ALA	VAL	ALA	VAL	ALA	ALA	GLY	VAL	MET	SER	ALA	GLN	ALA	MET	ALA	VAL
	1	2	3	4	5	6	7	8	9	10	11	12	13	14	15	16	17	18	19	20	21	22	23	24	25
	lamB	lamB	lamB	lamB	lamB	lamB	lamB	lamB	lamB	lamB	lamB	lamB	lamB	lamB	lamB	lamB	lamB	lamB	lamB	lamB	lamB	lamB	lamB	lamB	lamB
Intact Protein	●	●	●	●	●	●	●	●	●	●	●	●	●	●	●	●	●	●		●		●	●	●	●
lamB 52-4 CNBrB																			●	●	●	●			
CNBr2*																								●	●

	26	27	28	29	30	31	32	33	34	35	36	37	38	39	40	41	42	43	44	45	46	47	48	49	50
	ASP	PHE	HIS	GLY	TYR	ALA	(ARG)	SER	GLY	ILE	GLY	TRP	THR	GLY	ARG	GLY	VAL	THR	GLN	LEU	ASN	ARG	LEU	ALA	ALA
	26	27	28	29	30	31	32	33	34	35	36	37	38	39		20	21	22	23	24	25	26	27	28	29
	lamB	lamB	lamB	lamB	lamB	lamB	lamB	lamB	lamB	lamB	lamB	lamB	lamB	lamB		lacZ	lacZ	lacZ	lacZ	lacZ	lacZ	lacZ	lacZ	lacZ	lacZ
Intact Protein	●																								
CNBr2*	●	●	●	●	●	●		●	●	●	●	●	●	●	●	●	●	●	●	●	●		●	●	●

Fig. 5 Amino-terminal sequence of the 52-4 *lamB–lacZ* hybrid protein. See Fig. 3 legend. The arrow indicates the site of cleavage by the signal peptidase. *lamB* 52-4 CNBrB is one of the three cyanogen bromide fragments obtained from the 52-4 protein but not from authentic β-galactosidase.

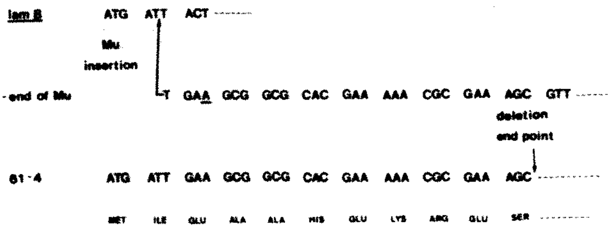
lam B
ATG ATT ACT
Mu
insertion
S-end of Mu
T GAA GCG GCG CAC GAA AAA CGC GAA AGC GTT
deletion
end point
61-4
ATG ATT GAA GCG GCG CAC GAA AAA CGC GAA AGC
MET ILE GLU ALA ALA HIS GLU LYS ARG GLU SER

Fig. 6 A reconstruction of the events which yielded the 61-4 fusion. The fragment of *lamB* sequence on the first line is from ref. 25. The Mu sequence on the second line is from Kahman and Kamp[39] and Allet[40]. (The sequence published by Allet[41] differs in two respects from that presented here: (1) the "A" underlined here is missing and (2) the prophage sequence would start at the "G" immediately following this "A".) Only the 'sense' strand of the DNA is shown here. The NH_2-terminal sequence of the 61-4 protein (shown on the last line) can be explained if we assume that the original Mu insertion and the final deletion (see Fig. 1) occurred as shown here by the two arrows.

polypeptides in which the first 26 or 19 amino acids, respectively, have been replaced by 11 or 40 other amino acids. The 61-4 polypeptide is therefore 15 amino acids shorter than the authentic *lacZ* polypeptide, whereas the 52-4 polypeptide is 21 amino acids longer. The fact that these sequences could be determined unambiguously shows that there was no extensive site-specific cleavage in the NH_2-terminal region of the hybrid polypeptides (see also Fig. 3).

Discussion

Because the NH_2-terminal sequence of the 61-4 hybrid protein contains only the first two amino acids of the precursor of the *lamB* protein (Fig. 4), it is not surprising that the hybrid protein remains in the cytoplasm. Indeed, other experiments have shown that most or all of the 24-amino acid signal sequence is essential for export of *lamB* protein from the cytoplasm[16,26,29]. This is also consistent with the observations that *phoA-lacZ* and *malE-lacZ* hybrid proteins containing truncated signal sequences remain in the cytoplasm, whereas wild-type *phoA* and *malE* products are exported to the periplasm[37,38]. The amino acid sequence also revealed that the deletion generating the fusion removed the first 26 codons of the *lacZ* gene. This is the largest amount found missing in any fusion strain synthesizing a hybrid protein still endowed with β-galactosidase activity[35,37].

One unexpected feature of the 61-4 protein is that its amino acid sequence in residues 3–11 is found neither at the NH_2-terminal end of the *lamB* protein precursor nor at that of β-galactosidase. This sequence is actually that which would be coded by the DNA sequence located at the S-end of prophage Mu[39,40]. Therefore, we believe that, in the case of the 61-4 strain, the deletion which constituted the final event in the creation of the fusion (Fig. 1) failed to remove a small portion of prophage Mu (Fig. 6). (There is some controversy regarding the nucleotide sequence in Mu DNA; our results could not be explained using the sequence originally reported by Allet[41]).

As might have been predicted from genetic data (Figs 1, 2), the 52-4 protein does not contain Mu-coded amino acids (Fig. 5). From residue 1 to 39 its sequence corresponds to the NH_2 terminus of the *lamB* protein precursor. Except for residue 40, which corresponds to the fusion joint, the rest of the sequence is from β-galactosidase. Therefore, this protein contains the entire signal sequence of the *lamB* protein precursor and is, nevertheless, chiefly located in the cytoplasm (Fig. 3). One interpretation of this result would be that the signal sequence is not sufficient information to initiate the transfer of a polypeptide through the cytoplasmic membrane. If the additional information required were encoded over a large fraction of the polypeptide, alternatives[42] to the signal hypothesis would have to be considered. Another possibility is that the signal sequence does suffice to initiate the transfer but that severe restrictions exist as to which amino acid sequences can be extruded through a membrane[43]. The enzyme β-galactosidase, which is normally cytoplasmic, may contain unfavourable sequences[17]. These sequences might block the transfer of the 52-4 protein at an early stage, so that this protein, weakly bound to the membrane by its NH_2-terminus, may fall back into the cytoplasm as synthesis proceeds. Whatever the interpretation, the fact remains that adding a signal sequence to at least one cytoplasmic protein—β-galactosidase—is not a sufficient condition to alter to any significant extent the cellular location of this protein.

We thank M. Hours for growing the cells necessary for protein purification. This work was supported by grants from the Délégation Générale à la Recherche Scientifique et Technique (77.7.1294) and the Centre National de la Recherche Scientifique (LA 270) to M.S., from the NSF (78-1-9974) and USPHS (AI 04181) to I.Z., and from the National Institute of General Medical Science (GM25524) to T.S.

Received 23 November 1979; accepted 23 April 1980.

1. Milstein, C., Brownlee, G. G., Harrison, T. M. & Mathews, M. B. *Nature new Biol.* **239,** 117–120 (1972).
2. Blobel, G. & Dobberstein, B. *J. Cell Biol.* **67,** 835–851 (1975).
3. Palade, G. *Science* **189,** 347–358 (1975).
4. Rothman, J. E. & Lodish, H. F. *Nature* **269,** 775–780 (1977).
5. Kreibich, G., Ulrich, B. L. & Sabatini, D. D. *J. Cell Biol.* **77,** 464–487 (1978).
6. Austen, B. M. *FEBS Lett.* **103,** 308–313 (1979).
7. Blobel, G. *et al. Symp. Soc. exp. Biol.* **33,** 9–36 (1979).
8. Randall, L. & Hardy, S. *Eur. J. Biochem.* **75,** 43–53 (1977).
9. Smith, W. P., Tai, P. C., Thompson, R. C. & Davis, B. D. *Proc. natn. Acad. Sci. U.S.A.* **74,** 2830–2834 (1977).
10. Inouye, H. & Beckwith, J. *Proc. natn. Acad. Sci. U.S.A.* **74,** 1440–1444 (1977).
11. Di Rienzo, J. M., Nakamura, K. & Inouye, M. *A. Rev. Biochem.* **47,** 481–532 (1978).
12. Lin, J. J. C., Kanazawa, H., Ozols, J. & Wu, H. C. *Proc. natn. Acad. Sci. U.S.A.* **75,** 4891–4895 (1978).
13. Chang, C. N., Model, P. & Blobel, G. *Proc. natn. Acad. Sci. U.S.A.* **76,** 1251–1255 (1979).
14. Silhavy, T. J., Casadaban, M. J., Shuman, H. A. & Beckwith, J. *Proc. natn. Acad. Sci. U.S.A.* **73,** 3423–3427 (1976).
15. Silhavy, T. J., Shuman, H. A., Beckwith, J. & Schwartz, M. *Proc. natn. Acad. Sci. U.S.A.* **74,** 5411–5415 (1977).
16. Emr, S. D., Schwartz, M. & Silhavy, T. J. *Proc. natn. Acad. Sci. U.S.A.* **75,** 5802–5806 (1978).
17. Bassford, P. J. Jr, Silhavy, T. J. & Beckwith, J. R. *J. Bact.* **139,** 19–31 (1979).
18. Silhavy, T. J., Bassford, P. J. Jr & Beckwith, J. R. in *Bacterial Outer Membranes* (ed. Inouye, M.) 203–254 (Wiley, New York, 1979).
19. Randall-Hazelbauer, L. & Schwartz, M. *J. Bact.* **116,** 1436–1446 (1973).
20. Wandersman, C. & Schwartz, M. *Proc. natn. Acad. Sci. U.S.A.* **75,** 5636–5639 (1978).
21. Wandersman, C., Schwartz, M. & Ferenci, T. *J. Bact.* **140,** 1–13 (1979).
22. Roa, M. *J. Bact.* **140,** 680–686 (1979).
23. Endermann, R., Hindennach, I. & Henning, U. *FEBS Lett.* **88,** 71–74 (1978).
24. Randall, L. L., Hardy, S. J. S. & Josefsson, L. G. *Proc. natn. Acad. Sci. U.S.A.* **75,** 1209–1212 (1978).
25. Hedgpeth, J., Clément, J. M., Marchal, C., Perrin, D. & Hofnung, M. *Proc. natn. Acad. Sci. U.S.A.* **77,** 2621–2625 (1980).
26. Emr, S., Hedgpeth, J., Clément, J. M., Silhavy, T. J. & Hofnung, M. *Nature* **285,** 82–85 (1980).
27. Casadaban, M. *J. molec. Biol.* **104,** 541–555 (1976).
28. Raibaud, O., Roa, M., Braun-Breton, C. & Schwartz, M. *Molec. gen. Genet.* **174,** 241–248 (1979).
29. Emr, S. & Silhavy, T. J. *J. molec. Biol.* (in the press).
30. Débarbouillé, M. & Schwartz, M. *J. molec. Biol.* **132,** 521–534 (1979).
31. Neu, H. C. & Heppel, L. A. *J. biol. Chem.* **240,** 3685–3692 (1965).
32. Kellermann, O. & Szmelcman, S. *Eur. J. Biochem.* **47,** 139–149 (1974).
33. Sanzey, B. *J. Bact.* **138,** 40–47 (1979).
34. Miller, J. H. in *Experiments in Molecular Genetics* (Cold Spring Harbor Laboratory, New York, 1972).
35. Brake, A. J., Fowler, A. V., Zabin, I., Kania, J. & Muller-Hill, B. *Proc. natn. Acad. Sci. U.S.A.* **75,** 4824–4827 (1978).
36. Fowler, A. V. & Zabin, I. *J. biol. Chem.* **253,** 5521–5525 (1978).
37. Sarthy, A., Fowler, A., Zabin, I. & Beckwith, J. *J. Bact.* **139,** 932–939 (1979).
38. Bedouelle, H. *et al. Nature* **285,** 78–81 (1980).
39. Kahman, R. & Kamp, D. *Nature* **280,** 247–250 (1979).
40. Allet, B. *Cell* **16,** 123–129 (1979).
41. Allet, B. *Nature* **274,** 553–558 (1978).
42. Wickner, W. *A. Rev. Biochem.* **48,** 23–45 (1979).
43. Van Heijne, G. & Blomberg, C. *Eur. J. Biochem.* **97,** 175–181 (1979).
44. Bukhari, A. I. *A. Rev. Genet.* **10,** 389–412 (1976).
45. Zabin, I., Fowler, A. V. & Beckwith, J. R. *J. Bact.* **133,** 437–438 (1977).
46. Laemmli, U. K. *Nature* **227,** 680–685 (1970).
47. Brauer, A. W., Margolis, M. N. & Haber, E. *Biochemistry* **14,** 3029–3035 (1975).
48. Hunkapiller, M. W. & Hood, L. E. *Biochemistry* **17,** 2124–2144 (1978).

LETTERS

Spontaneous production of cosmological fluctuations

Craig J. Hogan
Institute of Astronomy, Madingley Road, Cambridge CB3 0HA, UK

In the 'standard' hot big bang, fluctuations which give rise to galaxies and galaxy clusters must be present in the initial conditions; that is, they are already present at the earliest epoch when general relativity is valid. In a structureless big bang there seems to be only one way that the necessary fluctuations can be explained within the scope of conventional physics: a uniform universe with low specific entropy ($S \lesssim 1$) can spontaneously generate fluctuations by shattering into macroscopic fragments. Such a critical point probably occurs at nuclear density during the transition from pion condensate to nucleon gas; shattering at this epoch would create fragments of the order of a Chandrasekhar mass, providing both the lumpiness necessary to produce galaxy clusters and a potential energy source for the microwave background radiation.

The universe seems to be uniform on the very largest scales, and we know that it is fundamentally non-uniform on the smallest scales. Furthermore, we know that small irregularities introduced into a homogeneous Friedmann universe can grow with time. The obvious temptation is to try to show that all inhomogeneity, even on astronomical scales, ultimately originates from quantum effects operating in a universe which is initially as uniform as possible. Proposals along these lines have been made using, for example, Heisenberg uncertainty in the metric[1] and thermal fluctuations in particle positions[2]. Several authors have also invoked various types of phase transitions, including vacuum phase transitions at very early times[3,4], a nucleated quark–nucleon phase transition[5], and the conventional solid- or liquid–gas transitions[6,7]. Critical-point transitions are particularly good for generating fluctuations spontaneously because they afford an enormous amplification of quantum discreteness which is in principle limited only by conditions of causality: if such a transition occurs, matter is unstable and must shatter into macroscopic fragments[6,7]. A uniform expansion can 'tear apart' a uniform medium to leave a highly non-uniform expanding 'gas' of macroscopic lumps. Some fundamental constraints on such schemes are described here and a model proposed which does not rely on a speculative departure[1–3] from classical general relativity.

Although some quantum inhomogeneity always exists, it is possible to show that in the standard hot big bang no classical process can create the actual observed scale of inhomogeneity. Let us assume that quantum effects operating at epoch t_1 introduce density fluctuations with amplitude $\delta\rho/\rho \equiv \delta_M$ on a comoving scale labelled by its baryon charge M. At the present time t_0, ignoring dissipation effects and assuming $\Omega = 1$, linear Lifshitz gravitational growth gives

$$\delta_M(t_0) = (a_1/a_0)^2 (t_0/t_1)^2 \delta_M(t_1) \tag{1}$$

independent of the equation of state, where a is the scale factor. If gravitating energy and momentum are locally conserved in the sense required by classical general relativity[9] (which is generally true even during vacuum phase transitions[3,4]), then the spectrum of growing fluctuations introduced by any irreversible process on scales larger than the horizon must be[8,10–12,32]

$$\delta_M(t_1) \propto M^{-7/6} \tag{2}$$

This spectrum has been shown[10,12,32] to arise in a perfect fluid with an arbitrarily variable equation of state; any conservative matter is gravitationally identical to such a fluid on scales sufficiently large that the off-diagonal components of $T^{\mu\nu}$ are uncorrelated. Moreover, causal processes cannot move matter further than ct_1, so the density contrast on the horizon scale must be less than unity:

$$(\delta\rho/\rho)_{ct_1} \equiv \delta_H(t_1) < 1 \tag{3}$$

Using equation (2), causality limits the amplitude of $(\delta\rho/\rho)$ on any mass scale:

$$\delta_M(t_1) < (M/M_H(t_1))^{-7/6} \tag{4}$$

where M_H is the baryon charge within the horizon at t:

$$M_H(t_1) = M_H(t_0)(a_1/a_0)^{-3}(t_1/t_0)^3 \tag{5}$$

Thus in an initially uniform universe

$$\delta_M(t_0) < (a_1/a_0)^{-3/2}(t_1/t_0)^{3/2}(M/M_H(t_0))^{-7/6} \tag{6}$$

The actual universe is observed[8] to have $\delta_M \simeq 1$ on a length-scale $r_* \approx 3h^{-1}$ Mpc (where $h \equiv H_0/100$); since $ct_0 = 3{,}000\ h^{-1}$ Mpc, we need $\delta_{M_*} = 1$ for

$$M_*/M_H = 10^{-9} \tag{7}$$

This requirement, the Friedmann relations between a and t, and equation (6) put a lower limit on (a_1/a_0), that is an upper limit $z_{\max}$ on the redshift at which fluctuations can be created by a causal process. The reason for this limit is that with an initial spectrum of the form of equation (2) the amplitude $(\delta\rho/\rho)_H$ on the horizon scale (or any constant fraction thereof) decreases with time; although the amplitude of fluctuations increases, the universe actually grows 'smoother' with time. No classical process at a redshift greater than $z_{\max}$ can generate fluctuations which give rise to the observed structure.

Now in a hot universe[13]

$$(a_1/a_0) \cong (t_1/t_{eq})^{1/2}(t_{eq}/t_0)^{2/3} \tag{8}$$

where the epoch of equal matter and radiation densities is

$$(t_{eq}/t_0) = 10^{-7}\ (S/10^8)^2 \tag{9}$$

where S denotes the specific entropy in the fireball phase (again assuming $\Omega h^2 = 1$). The maximum redshift at which fluctuations can form if $\Omega h^2 \leqslant 1$ is

$$z_{\max} < 10^9\ (S/10^8)^{-2/3} \tag{10}$$

corresponding to a total (radiation + matter) density

$$\rho_1 \lesssim 2 \times 10^3\ (S/10^8)^{-4/3} \quad \text{g cm}^{-3} \tag{11}$$

But a high-entropy plasma with $S \gg 1$ is known[6] to be stable against any instability of the type required up to $\rho \simeq 10^{14}$ g cm^{-3}, so there is never any opportunity for fluctuations to form however matter behaves[15] at higher densities. The conclusion is that in a hot universe the macroscopic structure of the universe cannot be explained by any conventional physics—it must originate at an epoch when either classical causality or mass–energy conservation breaks down, and therefore lies in the domain of some theory of 'quantum gravity'. This conclusion (which has been assumed by most authors) remains valid even for 'tepid' universes[16] with a primordial S as low as 10.

Let us consider a cold degenerate universe[6,7,10,17] with $S \lesssim 1$. Particle interactions which might cause phase instabilities can be important even at relatively modest densities ~ 1 g cm^{-3}, as in the models of Zel'dovich and Layzer where the cosmic medium shatters due to solid-body or Van der Waals forces. The maximum redshift for forming fluctuations in a pressureless ($p \ll \rho c^2$) universe is

$$z_{\max} = (M_*/M_H(t_0))^{-14/9} \cong 10^{14} \tag{12}$$

corresponding to a density of

$$\rho_1 \lesssim 2 \times 10^{13}\ \text{g cm}^{-3} \tag{13}$$

so the limits imposed purely by causality present no problem for

0028-0836/80/300360—03$01.00

this type of model—there is a wide range of z in which fluctuations could be generated. Equation (13) shows that for any primordial S and any assumptions about supernuclear matter, a phase transition at strongly supernuclear density cannot by itself explain cosmic inhomogeneity unless correlated domains form on scales much larger than the horizon—again, requiring either special (non-uniform) initial conditions or a modification of general relativity[3,28]. We also know, from equation (11), that if a phase transition at nuclear density generates too much entropy (that is $S \gg 10$) it cannot be responsible for cosmic structure, so our model is constrained to remain cool.

One can place more stringent limits on t_1 by considering the process in more detail. In a shattering- or cracking-type phase transition, the size of the lumps created, and hence the distance over which matter is moved, is determined not by the velocity of light, but by the velocity of sound. Thus in equation (4) we should replace M_H by M_S:

$$\delta_M(t_1) \lesssim (M/M_S)^{-7/6} \tag{14}$$

where

$$(M_S/M_H)_{t_1} = (c_S/c)^3 = (p/\rho)^{3/2} \tag{15}$$

Because pressure forces balance cohesive forces in the solid phase, this condition is equivalent to Layzer's: the characteristic size arises because if the expansion energy of a 'fragment' exceeds its cohesion energy, it shatters into still smaller fragments until the two are about equal. Let us assume that the cosmic medium consists of e^-, p^+, and ν in equal abundance[10], so that the pressure is due mainly to degenerate relativistic electrons and neutrinos. Now $p \simeq \rho/3$ when the Fermi energy of the electrons $E_f \gtrsim m_p c^2$, thereafter, p/ρ decreases as a^{-1} until $E_f \sim m_e c^2$, and then like a^{-2}. Thus

$$(M_S/M_H)_{t_1} \lesssim (3a_1/a_2)^{-3/2} \tag{16}$$

where a_2 is the scale factor when $E_f \simeq m_p c^2$ (ref. 14):

$$z_2 = (a_0/a_2) = m_p c n_0^{-1/3}/\hbar(3\pi^2)^{1/3} \simeq 8 \times 10^{14} \tag{17}$$

But then equations (14), (7), and (1) say that the sound speed decreases so fast with z that the final fluctuations are maximized if $z \sim z_{max}$; that is, instabilities at lower or higher redshifts are always fundamentally insufficient to produce the observed clustering, but if a cold universe is unstable at nuclear density the amplitude is about right. (In fact, Zel'dovich and Layzer find that the amplitude of fluctuations from planet-sized lumps resulting from shattering at $\rho \sim 1$ is insufficient and needs to be supplemented with subsequent growth far in excess of the linear growth rate (equation (1)).

Thus, if a phase transition occurs in cold matter at $\rho \sim 10^{13-14}$ g cm^{-3} it would yield lumps of order the horizon size at that epoch, the Chandrasekhar mass:

$$M_H \simeq (\hbar c/G m_p^2)^{3/2} m_p \simeq 2 M_\odot$$

and would produce $(\delta\rho/\rho) \simeq 1$ on present day mass-scales of the order of 10^{12}–$10^{15} M_\odot$, possibly enough to explain the observed astronomical inhomogeneity. The surprising thing is that such a phase transition probably exists[18,31].

Recent theoretical work on the composition of cold matter in neutron stars indicates that the favoured phase at $\rho \approx 10^{15}$ g cm^{-3} is probably a solid Bose lattice of pions held in place by strong nuclear forces[18]. At lower densities the Fermi energy of pion decay products decreases, and at some point the equilibrium state becomes a Fermi gas of baryons and leptons. An additional uncertainty is introduced in cosmological cold matter because the relative chemical potentials of fermion species depend on the cosmological lepton–baryon ratio n_L/n_B (in neutron stars lepton number is not conserved because neutrinos can escape). Although more calculations are necessary to include this effect, it seems likely that a phase transition from pion condensate to Fermi gas occurs for at least some values of n_L/n_B. This phase transition is of the right type, and occurs at about the unique right time as calculated above, to produce the observed astronomical inhomogeneity.

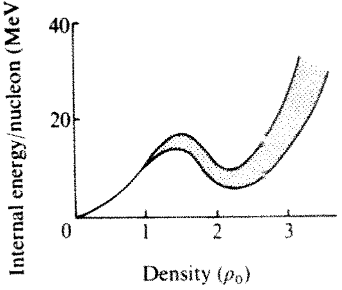

Fig. 1 Equation of state of cold matter around nuclear density.

Figure 1, after Irvine[18], shows the specific internal energy of cold matter $E(\rho)$ near nuclear density $\rho_0 \equiv 3 \times 10^{14}$ g cm^{-3}. There are theoretical uncertainties (shaded region), but it is clear that at zero temperature the conditions for thermodynamic instability[29] exist:

$$\begin{aligned}(\partial E/\partial \rho) &< 0\\ (\partial^2 E/\partial \rho^2) &< 0\end{aligned} \tag{18}$$

which require the solid Bose condensate to shatter at $\sim 2\rho_0$ into macroscopic fragments. (Note that matter with $S \gtrsim 1$ would not have this property: the internal energy then varies monotonically with ρ because it is dominated by thermal photons and neutrinos.) Chaotic conditions and large-scale motions persist for about a Hubble time, leaving lumpy single-phase matter with $\delta\rho/\rho \gtrsim 1$ at a mean cosmic density of the order of $\rho_1 \sim 10^{13-14}$ g cm^{-3}.

As the Jeans mass in a cold universe decreases with time after t_2, it is probable that fragments would collapse and survive as compact bound objects, providing a natural source of 'missing mass'. We also know that the fragments are initially of the order of a Chandrasekhar mass—they might end up as black holes, neutron stars, main-sequence hydrogen-burning stars or supermassive stars ($\gtrsim 100\ M_\odot$), depending on the exact details of the fragmentation and subsequent coalescence. Such objects are natural candidates for the energy sources necessary to explain the microwave background in a cold model[19–21].

There are some weak points in the above hypothesis which also provide crucial observational tests. Some potential problems are: (1) a fluctuation spectrum as steep as equation (2) cannot explain both galaxies and galaxy clusters if only gravitational forces are at work[8], it forms galaxies too early and hence with too high a density; (2) it is not certain that enough inhomogeneity on galaxy clustering scales $\gtrsim 10^{15} M_\odot$ can be generated with only the linear growth rate (equation (1)); and (3) the cosmic helium abundance cannot be calculated—even if n_L/n_B were known, the chaotic conditions caused by the phase transition would invalidate previous cold-universe calculations[10,22] by increasing the entropy and upsetting the equilibrium abundance of various particle species (for example, collapsing fragments would squeeze neutrinos into the confining Fermi gas). The first two of these problems can be solved by invoking hydrodynamic effects, for example, primordial fragments may form into super-massive exploding stars[21,30] which could unbind dense systems on scales $\lesssim 10^{12} M_\odot$ and/or amplify fluctuations on scales $10^{12} \lesssim M \lesssim 10^{15} M_\odot$. Such objects would certainly leave an imprint on the anisotropy[23] and spectrum[24–26] of the microwave background; they might also create helium and/or deuterium[27]. A fairly rigorous prediction of any shattering model is that present-day fluctuations on scales $\gg 10$ Mpc should be unaffected by such events and should still show the original $(\delta\rho/\rho) \propto M^{-7/6}$ spectrum.

Although there are complications with a cold big bang, it is clear from the preceding discussion that any other model attempting to produce structure in an initially uniform universe is likely to encounter difficulties of a much more fundamental nature unless it tampers with classical general relativity. If the structure we see today is not the shattered remnant of a cold universe, then it must be a relic of the preclassical era.

I thank Bernard Carr, David Layzer, P. James E. Peebles and Martin Rees for helpful comments, and the University of Cambridge for an Isaac Newton Studentship.

Received 25 February; accepted 3 June 1980.

1. Harrison, E. R. *Phys. Rev. D.* **1,** 2726 (1970); *Nature* **215,** 151 (1967).
2. Peebles, P. J. E. *Nature* **220,** 227 (1968).
3. Press, W. H. *Phys. Scr.* **21** (1980).
4. Sato, K. Preprint (Nordita, Copenhagen, 1980).
5. Lasher, G. *Phys. Rev. Lett.* **42,** 1646 (1979).
6. Layzer, D. in *Galaxies and the Universe* (eds Sandage, A., Sandage, M. & Kristian, J.) (University of Chicago Press, 1976).
7. Zel'dovich, Ya.B. *Soviet Phys. JETP* **16,** 1395 (1963); *JETP* **43,** 1982 (1962).
8. Peebles, P. J. E. *Cosmology: Physics of Large-Scale Structure* (Princeton University Press, 1980).
9. Hawking, S. W. & Ellis, G. F. R. *The Large Scale Structure of Space-Time* (Cambridge University Press, 1973).
10. Zel-dovich, Ya. B. *Adv. Astr. Astrophys.* **3,** 241 (1965).
11. Peebles, P. J. E. *Astr. Astrophys.* **32,** 391 (1974).
12. Press, W. H. & Vishniac, E. T. *Astrophys. J.* (submitted).
13. Weinberg, S. *Gravitation and Cosmology* (Wiley, New York, 1972).
14. Zel'dovich, Ya. B. & Novikov, I. D. *Relativistic Astrophysics*, Vol. 1 (eds Thorne, K. S. & Arnett, W. D.) (Midway, University of Chicago Press, 1978).
15. Weinberg, S. *Phys. Scr.* **21,** 773 (1980).
16. Carr, B. J. & Rees, M. J. *Astr. Astrophys.* **16,** 705 (1977).
17. Carr, B. J. *Mon. Not. R. astr. Soc.* **181,** 293 (1977).
18. Irvine, M. *Neutron Stars* (Clarendon, Oxford, 1978).
19. Layzer, D. & Hively, R. M. *Astrophys. J.* **179,** 361 (1973).
20. Rees, M. J. *Nature* **275,** 35 (1978).
21. Carr, B. J. Preprint (University of Cambridge, 1980).
22. Kaufman, M. *Astrophys. J.* **160,** 459 (1970).
23. Hogan, C. *Mon. Not. R. astr. Soc.* (in the press).
24. Woody, D. P. & Richards, P. L. *Phys. Rev. Lett.* **42,** 925 (1979).
25. Rowan-Robinson, M., Negroponte, J. & Silk, J. *Nature* **281,** 635 (1979).
26. Puget, J. L. & Heyvaerts, J. *Astr. Astrophys.* **83,** L10 (1980).
27. Epstein, R. I. *Astrophys. J.* **212,** 595 (1977).
28. Zee, A. *Phys. Rev. Lett.* **44,** 703 (1980).
29. Landau, L. D. & Lifshitz, E. M. *Statistical Physics* (Pergamon, Oxford, 1969).
30. Doroshkevich, A. G., Zel'dovich, Ya. B. & Novikov, I. D. *Soviet Astr.* **11,** 233 (1967); *Astr. Zh.* **44,** 295 (1967).
31. Shuryak, E. V. *Phys. Rep.* **61,** 71–158 (1980).
32. Bardeen, J. M. Preprint (Institute for Advanced Study, Princeton, 1980).

Some diurnal properties of clouds over the martian volcanoes

Garry E. Hunt*, Adrian O. Pickersgill*, Philip B. James† & Gordon Johnson‡

*Laboratory for Planetary Atmospheres, Department of Physics and Astronomy, University College London, Gower Street, London WC1E 6BT, UK

†Department of Physics, University of Missouri, St Louis, Missouri 63121

‡Jet Propulsion Laboratory, 4800 Oak Grove Drive, Pasadena, California 91103

Discrete white cloud systems have long been recognized as a martian atmospheric phenomenon. However, it was not until the Mariner 9 mission in 1971–72 that the cloud systems were found to be closely related to topographic features, in particular, the giant volcanoes on the Tharsis Ridge. Using the available Earth based observations, Smith and Smith[1] investigated the seasonal and diurnal behaviour of the clouds the Olympus Mons and Elysium regions. They found that the cloud activity was generally confined to late spring and early summer seasons in the northern hemisphere. This corresponds to $L_s = 60$–$150°$, where L_s is the aerocentric solar longitude and $L_s = 0$ for spring equinox in the northern hemisphere. The Viking Orbiters have observed martian atmospheric phenomena for eight seasons. During this period, the volcanoes have been frequently, but often irregularly, monitored. Unfortunately, the changes in the spacecraft orbit have meant corresponding variations in the surface resolution,.viewing geometry and local times of the observations. However, the available observations do provide important new insights into the diurnal properties of the volcanic cloud systems, which we describe here.

Cloud systems appear over the volcanoes in certain seasons of the martian year, and these spacecraft observations are in general agreement with the times of meteorological activity suggested by the ground based studies of Smith and Smith[1]. In the Elysium region, clouds were observed during the period $L_s = 46$–$141°$, while during $L_s = 230$–$17°$ there was no apparent atmospheric activity. Except for a period between $L_s = 2100$ and $L_s = 300°$, some form of cloud activity was observed throughout the year in the Tharsis region. However, this period of apparent inactivity corresponds to the time of two major dust storm events observed by the the Viking spacecraft (see, for example, ref. 2). This area of the planet was noticeably dusty, and frequently only the summits of these volcanoes were visible through the dust clouds. During these dust storms, the atmospheric water vapour abundance was greatly reduced[3] as the particles absorbed the atmospheric moisture. Furthermore, the thermal properties of the atmosphere were also affected by the presence of the dust, suppressing the diurnal variation and reducing the vertical structure[4,5]. These substantial changes to the thermodynamic state of the atmosphere account for the absence of clouds due to the dust storm period.

The cloud systems observed from the Earth cover areas of 10^5–10^6 km^2 and are first seen at periods around local noon. From Viking studies, we have found many much smaller clouds in the Tharsis region, occupying regions of only $\sim 5 \times 10^3$ km^2, which often develop in the early morning. Figure 1 shows such a localized cloud system for the Ascraeus region at $L_s = 225°$. Here we concentrate on a study of the diurnal properties of orographic cloud systems, monitored near Elysium, Olympus Mons, and the two northern peaks of the Tharsis system.

Figure 2 shows the development of a cloud system associated with Elysium from 07.00 to 12.51 LT at $L_s = 92.7°$, shortly after summer solstice. All of the clouds seen here are smaller than the classic afternoon clouds seen from the Earth. Each of the views in Fig. 2 were imaged in four filters. By comparing these images condensate clouds can be separated from surface details produced by slopes which appear as bright areas through all filters. In the first three pictures, the sunward facing slopes are brightly highlighted in a manner frequently observed at Elysium. The clouded western flanks show greatly reduced contrast as the wavelength is increased, unlike the sunward slopes which appear equally bright at all wavelengths. At 07.00 LT, the entire region is lightly clouded and surface features may be seen

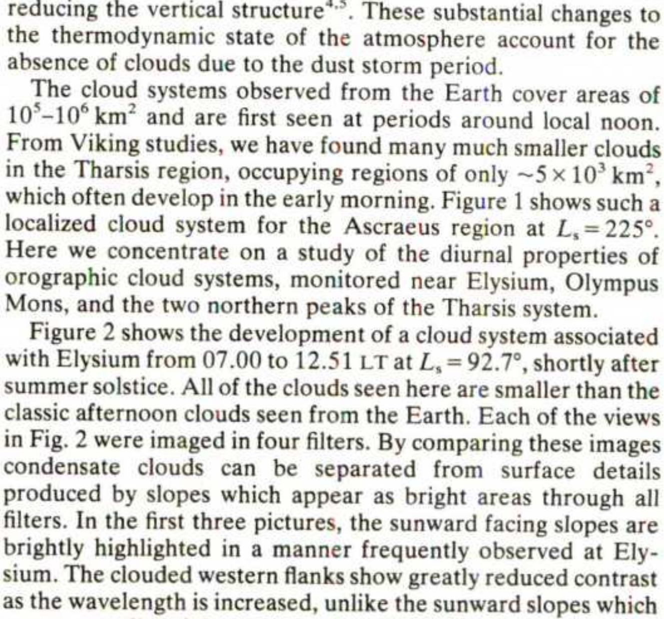

Fig. 1 Viking Orbiter 1, revolution 225, frame 5. A turbulent region of cloud is observed on the western flanks of Ascraeus Mons for 14.03 LT through a violet filter for $L_s = 210°$.

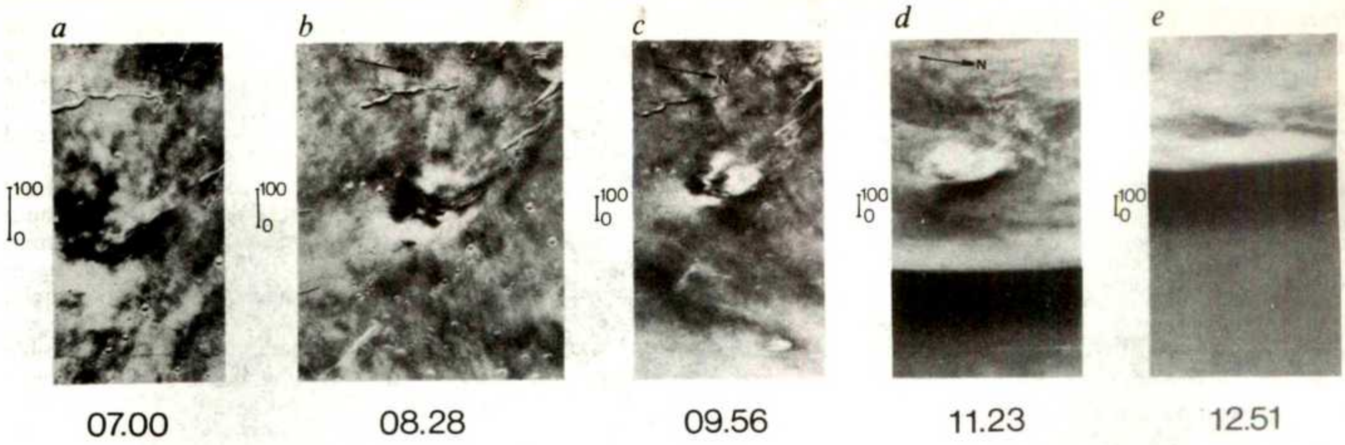

Fig. 2 The daily cycle of a cloud in the lee of Elysium Mons is shown as five time-sequence photographs taken between 07.00 and 12.51 LT. The LT of the frames are 07.00 (*a*), 08.28 (*b*), 09.56 (*c*), 11.23 (*d*) and 12.51 (*e*). The arrow-shaped lee wave cloud on the extreme left photograph is replaced by an almost circular region of cloud on the extreme right photograph. These photographs were taken by Viking Orbiter 1, orbit 710, through a violet filter for $L_s = 92.7°$.

through the denser patches, although with reduced contrast. The most prominent cloud is seen to the WNW of Elysium in the vague shape of an arrow whose head points towards the summit of the volcano. This cloud is more opaque than the mist in the surrounding region. The region has apparently not changed appreciably in the second view, obtained at 08.28 LT. The cloud to the WNW is still quite apparent although it is more concentrated than in the earlier view. By 09.56 LT (Fig. 2*c*), this cloud has clearly split into two pieces, with the main portion displaced substantially towards the north, while a plume, reminiscent of those seen in the Tharsis region[6] appears to the west. The larger component of the cloud is roughly 100 km in diameter.

The cloud's rapid growth seems to be starting in the 11.23 view shown in Fig. 2*d*. The dimensions of this cloud are roughly 200 km, so that the effective area has roughly quadrupled in the hour and a half since the previous picture. The region is somewhat hazy, and a field of scattered clouds seems to be developing to the north-west of the main cloud. The approximately 70° emission angles roughly double the effective optical depth from the earlier view and, therefore, enhance the haziness of the region. In the final view 12.51 LT, the cloud has grown to dimensions of ~350 km.

Figure 3 summarizes a diurnal sequence in the vicinity of Ascraeus Mons for $L_s = 121.5°$. The first images, corresponding to 05.50 and 07.30 LT show a pervasive fog which nearly obscures surface features on the flanks of Ascraeus. Comparison with the USGS topographic map of Mars suggests that the top of the cloud bank is ~15 km below the summit so that this is a very low lying cloud layer.

The cirrus-like clouds to the south-west of the summit in Fig. 3*a* seem to be of the variety catalogued by Briggs *et al.*[6] one (martian) year earlier. They are well over the terminator and, on the basis of their illumination, would have to be at least as high as the summit, which is 27 km. Two discrete clouds are seen to the west of the volcano in Fig. 3*b*. Ascraeus frequently exhibits clouds in this location and they sometimes take the form of extensive plumes such as those reported by Briggs *et al.*[6]. Apparent shadows suggest that these may be quite high, perhaps 10–15 km above the volcano summit. This feature is confined to the early morning hours at all seasons, and is a lee wave cloud system formed on the leewardside of the volcano. These features imply the existence of easterly winds at high altitudes in agreement with the predictions of circulation models[7,8].

The general cloudiness at low levels is still seen in Fig. 3*c*, obtained when the local time is 09.26 at the summit of Ascraeus. However, a variety of waves are present with wavelengths around 10 km. The orientation of the waves suggests streamlined flow around the volcano, but the presence of waves at opposed angles may imply a more complicated situation. There are no obvious surface features that could affect the flow and be identified as the source of the waves. However, in view of the wide variety of undulations on the planet, it is still possible that these waves are topographically induced. The time localization of these phenomena suggests that they may be the result of a change in the characteristics of the boundary layer which is strongly influenced by the thermal properties and opacity of the atmosphere. Bright areas to the east of the volcanoes are probably incidence angle effects since they have disappeared in the later view. It is not possible to make a more positive statement because the images are available only in the violet filter (450 nm).

By 11.23 LT (Fig. 3*d*) large clouds are seen developing to the west and south of Ascraeus and to the west of Pavonis, which suggests that these are the nuclei of two components of the w cloud monitored by the Earth based observers (see, for example, ref. 11). Cloudiness is also seen to the east of Ascraeus towards the canyons and the clouds in these peripheral areas appear distinctively convective. Estimates of heights from other pictures using presumed shadows suggest that these clouds are relatively low with altitudes of 4.5–6.5 km above the surface.

The present visible observations are supported from the Orbiter measurements of the thermal characteristics and water vapour distribution of the atmosphere. This then allows the composition of the clouds to be determined by the procedures developed by G.E.H.[9]. We find that the low lying fogs and the convective afternoon clouds (see also ref. 10) are water ice clouds. In this season, the atmospheric temperatures are far above the CO_2 condensation temperatures. The cirrus-type clouds are more difficult to characterize owing to their very diffuse nature. Certainly, as Hunt[11] has shown, we cannot yet exclude the possibility of CO_2 clouds at these high altitudes.

The diurnal development of clouds, shown in Figs 2 and 3, is related to the local stability and circulation of the atmosphere as influenced by the topography and local thermal properties of the surface. The volcanic areas have low surface inertias and this permits unusually large diurnal temperature variations in these areas[10]. Night-time cooling produces denser cold air at low elevations favouring the formation of the observed radiation fogs in the early hours of the morning. The water vapour content of the martian atmosphere seems to be limited by the amount which can be contained in a saturated, night-time atmosphere[12]. Regions of locally large cooling are, therefore, favoured sights for fogs. The atmospheric stability associated with these conditions, together with the downslope winds, favour early morning gravitational wave effects such as are seen particularly in the Tharsis region.

The rapid warming of the surface as noon approaches will lead to increased lapse rates and, perhaps, to eventual instability.

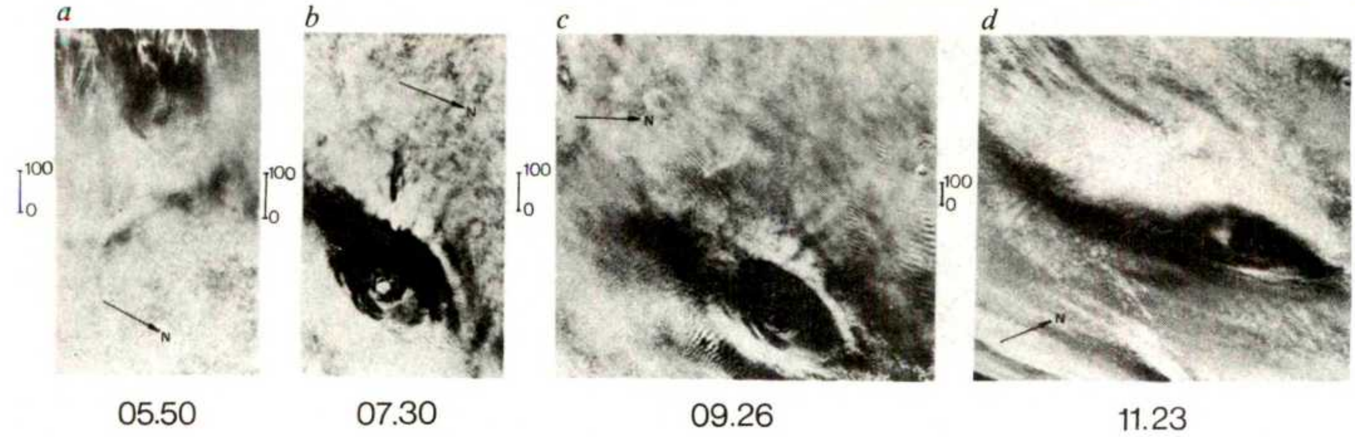

Fig. 3 The morning cycle of cloud in the vicinity of Ascraeus Mons shown as four time-sequenced photographs, taken between 05.50 and 11.23. The LT of the frames are 05.50 (*a*), 07.30 (*b*), 09.26 (*c*) and 11.23 (*d*). The scale and direction of north are shown. These photographs were taken by Viking Orbiter 1, orbit 774, through violet filter for $L_s = 121.5^\circ$.

Lindal *et al.*[14] have noted that lapse rates approach adiabatic only in these latitudes and seasons. The resulting convection will produce cumulus-like clouds by adiabatic cooling; this is supported by observations of such clouds in the region. Upward circulation in the atmosphere has been predicted to the west of the large volcanoes due to thermal forcing effects[13]. Cloud formation will also be enhanced by this convergence due to the positive vertical velocities; winds from the west due to this low level convergence may also contribute to adiabatic cooling of the parcels of air as they are carried up the slope of the Tharsis Ridge. The combination of these three effects seems plausible as an explanation for the diurnal cycle observed.

The reason for the pronounced seasonal variation is less easily seen, however, The spring and summer seasons in the northern hemisphere correspond generally to higher insolation and larger water vapour content in the atmosphere than does the rest of the year. As both factors should influence cloud formation, the general correlation is not surprising. However, in detail these factors fail to explain the abrupt boundaries of activity at $L_s = 60^\circ$ and $L_s = 150^\circ$ for Ascraeus and Elysium. The water at 25°N peaks at L_s between 140° and 150°, when the cloud activity is ending, and only gradually drops to equinox[15]. The large martian orbital eccentricity causes the insolation at noon at 25° latitude to be actually greater at the equinoxes than at solstice. Possibly, circulation changes when the south cap becomes stationary at $L_s \sim 150^\circ$ may effect the change; such circulation changes, from easterly to westerly winds, are predicted at that time by GCM[7]. If this change from easterly to westerly winds occurs the formation of convective clouds to the west of the volcanoes may be inhibited.

The Tharsis volcanoes are cloudy for a more extensive period and this is consistent with all these factors as the circulation and insolation at the equator do not vary as they do to the north. The cessation of activity from $L_s = 210^\circ$ to $L_s = 300^\circ$ is clearly associated with the major dust storms. These not only reduce the water content of the atmosphere drastically, but also tend to make the vertical profiles more isothermal than would normally be expected.

G.E.H. and A.O.P. were supported by the SRC. P.B.J. and G.J. were supported by NASA.

Received 30 April; accepted 26 June 1980.

1. Smith, S. A. & Smith B. A. *Icarus* **16**, 509–521 (1972).
2. Briggs, G. A., Baum, W. A. & Barnes, J. *J. geophys. Res.* **84**, 2795–2820 (1979).
3. Farmer, C. B. & Doms, P. E. *J. geophys. Res.* **84**, 2881–2898 (1979).
4. Martin, T. Z., Peterfreund, A. R., Miner, E. D., Kieffer, H. H. & Hunt, G. E. *J. geophys. Res.* **84**, 2830–2842 (1979).
5. Martin, T. Z. & Kieffer, H. H. *J. geophys. Res.* **84**, 2843–2852 (1979).
6. Briggs, G. A., Klaasen, K., Thorpe, T., Wellman, J. & Baum, W. *J. geophys. Res.* **82**, 4121–4150 (1977).
7. Leovy, C. B. & Mintz, Y. *J. atmos. Sci.* **26**, 1167–1190 (1969).
8. Pollack, J. B., Leovy, C. B., Mintz, Y. H. & Van Camp, W. *Geophys. Res. Lett.* **3**, 479–482 (1979).
9. Hunt, G. E. *J. geophys. Res.* **84**, 2865–2874 (1979).
10. Kieffer, H. H. *et al. J. geophys. Res.* **82**, 4249–4291 (1977).
11. Hunt, G. E. *Geophys. Res. Lett.* (in the press).
12. Davis, D. W. *J. geophys. Res.* **84**, 2875–2879 (1979).
13. Webster, P. J. *Icarus* **30**, 626–649 (1977).
14. Lindal, G. *et al. J. geophys. Res.* **84**, 8442–8457 (1979).
15. Farmer, C. B., Davies, D. W., Holland, A. L., La Porte, D. D. & Doms, P. E. *J. geophys. Res.* **82**, 4225–4248 (1977).

Black-body radiation as an inertial confinement fusion driver

F. Winterberg

Desert Research Institute, University of Nevada System, Reno, Nevada 89507

To ignite a thermonuclear microexplosion a power source of $\gtrsim 10^{14}$ W is required with an energy of $\gtrsim 10^6$ J focused down to $\lesssim 0.1$ cm. To meet these driver requirements, charged particle beams[1] and even hypervelocity projectiles[2] have been proposed as an alternative to lasers for which an energy $\gtrsim 10^6$ J is considered very large. Although charged particle beams and hypervelocity projectiles promise much larger energies the problem of the large driver power of $\gtrsim 10^{14}$ W remains. We propose here a two-stage driver concept which eliminates this problem. In it the initial energy is drawn from any of these drivers but is used here to generate an intense black-body radiation source. This black-body radiation is then used to drive the thermonuclear microexplosion target. This concept not only permits the initial driver power to be reduced by about two orders of magnitude from $\gtrsim 10^{14}$ W down to a few 10^{12} W, but also greatly relaxes the beam-focusing requirements as compared with direct pellet fusion.

The idea is depicted in Fig. 1. The thermonuclear target T is placed inside the centre of a small cavity filled with a tenuous high atomic number gas, for example, krypton or uranium hexafluoride. The inside of the wall is lined with a dense material P, for example gold or uranium. P is surrounded by an ablative layer A of low atomic number material. Beams B hitting the ablator from all sides ablatively implode the cavity. The implosion makes the wall P implode with the velocity v into the tenuous gas inside the cavity. This results in a shock

0028-0836/80/300364—03$01.00

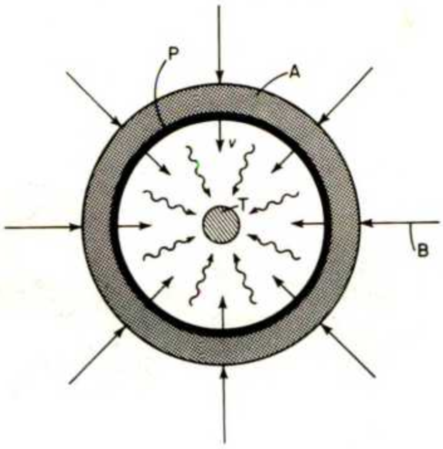

Fig. 1 The two-stage driver equipment: T, thermonuclear target; P, lining of dense material surrounded by an ablative layer A. Beams B, hit the ablator from all sides.

wave moving into this gas. The temperature T behind this shock wave is related to the implosion velocity[3] and one finds

$$T=\frac{A}{3R(Z+1)}v^2 \tag{1}$$

where A is the atomic weight, R the gas constant and Z the degree of ionization. Z depends on T and a useful approximation is

$$Z \simeq 6.6\times 10^{-3}T^{0.41} \tag{2}$$

The shock-heated high temperature gas, by bound–free, bound–bound and free–bound transitions, will then become an intense source of photons, and as a result the kinetic energy in the shock wave will be rapidly converted into black-body radiation. This happens on an atomic time scale of $\lesssim 10^{-8}$ s. The resulting black-body radiation is further compressed and greatly amplified by the cavity implosion, and is finally delivered to the target surface, assumed to be spherical of radius r_p at the rate

$$P(t)=4\pi r_p^2\sigma T^4 \tag{3}$$

where σ is the Stefan–Boltzmann constant. A power of 10^{14} W for a pellet surface of $\sim 10^{-1}$ cm^2 is reached at a temperature of $\simeq 3.6\times 10^6$ K. To store energy of $\simeq 10^7$ J at this temperature in the form of black-body radiation would require a volume of 75 cm^3; this suggests we use higher temperatures, as for a given energy the volume decreases as T^{-4}. For $T=10^7$ K the cavity volume would be only $\simeq 1.3$ cm^3. In the absence of photon losses through the cavity wall the black-body radiation changes with the cavity volume V as $VT^3=$constant, or with the cavity radius r as $rT=$constant. Therefore, if the initial cavity temperature is $T=5\times 10^6$ K, a twofold reduction in the cavity radius would raise the temperature to 10^7 K with a 2^4 fold increase in the radiative power delivered to the thermonuclear target. The initial and final radiative power would thus be $\simeq 3.6\times 10^{14}$ W and 5.75×10^{15} W. From equations (1) and (2) to reach the initial temperature would require $A=200$, $v=46$ km s^{-1} and krypton with $A=83$, $v \simeq 71$ km s^{-1}.

To make a shock wave in the tenuous gas the collision mean free path must be small compared with the cavity radius and one finds that the atomic number density must be $\gtrsim 10^{18}$ cm^{-3}. On the other hand, to store most of the incident energy into black-body radiation, the gas density cannot exceed $\sim 10^{21}$ cm^{-3}. Finally, if the thermonuclear target were to be bombarded with the full power derived from the Stefan–Boltzmann law, the cavity would have to be optically transparent, because otherwise the photons would diffuse through the gas at a much lower average velocity. Whether or not the gas is optically transparent is determined by the opacity coefficient[4]

$$\kappa \simeq 4.34\times 10^{25}\rho T^{-3.5} \tag{4}$$

from which the photon path length $\lambda_p=(\kappa\rho)^{-1}$ is derived. To make $\lambda_p > r \sim 1$ cm requires $\rho \lesssim 0.3$ g cm^{-3}, which for $A=200$ is an atomic number density of $\lesssim 10^{21}$ cm^{-3}. Therefore, an atomic number density of $\simeq 10^{19}$ cm^{-3} would satisfy all the conditions.

The concept depends on the black-body radiation photons being sufficiently confined during the cavity implosion. The diffusion of the photons through the cavity wall is given by the energy flux

$$j=\frac{\lambda_p c}{3}\frac{\partial}{\partial x}(aT^4) \tag{5}$$

where $a \equiv 4\sigma/c$. λ_p is the photon path length in the wall, which like the path length in the cavity must be computed using equation (4). Putting $j=aT^4v_d$ and $\partial(aT^4/\partial x) \simeq aT^4/x$ where x is the distance the photons have travelled into the wall with the diffusion velocity v_d, one finds

$$v_d/c \simeq (1/3)(\lambda_p/x) \tag{6}$$

For $T=10^7$ K, $\rho=18$ g cm^{-3} (uranium) one finds $\lambda_p \simeq 2\times 10^{-4}$ cm, and requiring $x \lesssim r \sim 1$ cm, that $v_d > 20$ km s^{-1}. Therefore, a cavity implosion velocity of $v \gtrsim 50$ km s^{-1} should be sufficient to confine the photons effectively.

Because the radiation flux absorbed by the thermonuclear target is inversely proportional to the opacity of the target and which according to equation (4) is proportional to $T^{-3.5}$, the power absorbed will rise in proportion to $T^{7.5}$ or $r^{-7.5}$. If, for example, the cavity radius decreases twofold, the power absorbed increases by the factor $2^{7.5} \simeq 180$. Most of the energy is, therefore, delivered to the pellet at peak power towards the end of the implosion process. This power amplification is due to the initial driver energy intermediately stored here in the form of black-body radiation which is only delivered at the end of the implosion process. Because of this the initial driver power can be reduced by a factor of about 100.

The short wavelength of the black-body radiation, given by $h\nu=kT$, and which is in the soft X-ray domain, is much better

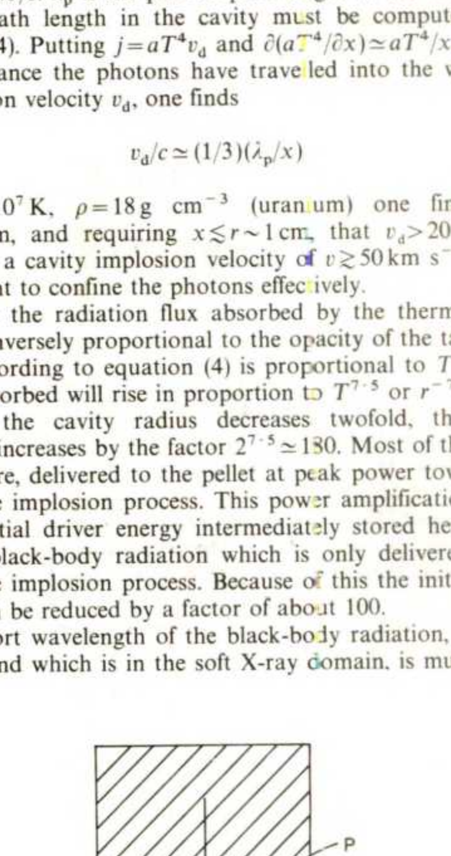

Fig. 2 A combination of the two-driver process with impact fusion. P, a hypervelocity projectile; C, conical cavity carved out of the anvil, AN; T, thermonuclear target.

suited than laser light to reach high density target compression, as it is matched to a plasma frequency of $\sim 10^4$ times compressed hydrogen. Furthermore, because of the isotropy of the radiation, there is no stimulated Brillouin backscattering as in laser fusion. A likely candidate to drive the cavity implosion seems to be an intense light ion beam (which can already be produced at the required power level) which is sufficiently well focused because the target area of the cavity is much larger than that of the pellet.

The rather low implosion velocity of $\sim 50\,\mathrm{km\,s^{-1}}$ suggests combining this concept with impact fusion where a hypervelocity projectile P accelerated to $v \sim 50\,\mathrm{km\,s^{-1}}$ implodes and amplifies black-body radiation in a conical cavity C carved out the anvil AN with the thermonuclear target T inside this same cavity. This concept is shown in Fig. 2.

Received 5 March; accepted 23 April 1980.

1. Yonas, G. *Scient. Am.* **239**, 50 (1978).
2. *Proc. Impact Fusion Workshop*, Los Alamos (1979).
3. Landau, L. D. & Lifshitz, E. M. *Fluid Mechanics*, 331, 358 (Pergamon, London, 1959).
4. Schwarzschild, M. *Structure and Evolution of Stars*, 67 ff (Princeton University Press, 1958).

Overlap of intense charged particle beams for intertial confinement fusion

J. A. Halbleib, P. A. Miller, L. P. Mix & T. P. Wright

Sandia National Laboratories, Albuquerque, New Mexico 87185

One approach to controlled thermonuclear fusion for power production requires the irradiation of centimetre-size targets containing heavy hydrogen (D–T) fuel by intense charged particle beams (CPB). Beam energy and pulse length requirements are ~1 MJ and 10 ns. In certain studies[1] the CPBs are beams of light ions, such as helium, with kinetic energies per nucleon in the range 1–5 MeV. These beams can be transported by preformed, current-carrying, plasma discharge channels. The fields from the channel currents (supplied by capacitor banks) confine the CPBs. These channels can be laser-initiated in a background gas that has a pressure between 10 and 100 torr. This gas blanket enables first wall loading, by X rays, shocks and thermal radiation to be mitigated. Although intense relativistic electron beams (REBs), which were developed before intense light ion beams, have achieved higher intensities[2], ion beams have more favourable deposition characteristics in targets[3]. Proton beams have driven exploding pusher targets[4] to implosion velocities of 20 cm μs^{-1} and have attained power of ~1 TW cm^{-2}, which is a factor of 40 below that estimated (G. Allshouse, personal communication) to be necessary for target ignition and for net system energy gain. To close the gap between present capabilities and future requirements, beam bunching and beam overlap are being studied. The current density gain *G* is important to the CPB overlap process and is the ratio of beam current density at the target surface to that of the individual beams in the transport channels; it depends on particle species, transverse energy, geometry of the channel-target interface, and so on. Detailed calculations[5–7] indicate that for electron beams, $G < 3$, while for practical cases of light ions, *G* can exceed 10. This is due to the difference in masses and effective temperatures of the two types of beams. Sources providing multiple ion beams are not available to test this overlap theory experimentally, hence it has been tested using a multiple electron beam system. Here we outline the experiment and describe the apparatus, and then summarize the theoretical treatment of beam overlap, describe diagnostic procedures, and compare the experimental results with calculations.

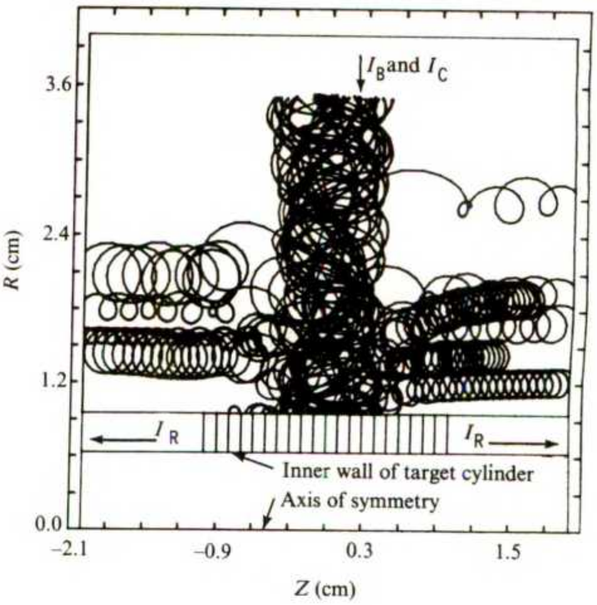

Fig. 1 *R–Z* trajectory plot for beam electrons incident on a 1.9 cm o.d. target cylinder. Target zoning for deposition analysis is indicated but trajectories inside the target are suppressed. I_B, I_C, and I_R are magnitudes of the beam currents, channel conduction currents and return currents ($3I_C$), respectively; directions of the electron flows are indicated by the arrows.

Several electron beams were generated simultaneously and transported through plasma channels[8,9] to a common cylindrical target. Targets with different diameters were used, and the total energy delivered to the targets was measured. As the diameter of the target decreases, progressively less of the energy reaches the target. The experiment aimed to measure the dependence of delivered energy on target diameter and to compare this with theoretical predictions. Agreement would imply that the physical models are correct in the present energy density regime, however, further work would still be required to investigate collective effects which may be important with higher-energy density systems[1,10–12].

The electron beam source was the Proto II accelerator[13] at Sandia National Laboratories. The front end of the accelerator could drive 12 separate electron beam diodes in parallel. These diodes were arranged in coplanar fashion in a 1-m diameter circle. On each accelerator shot, 12 pinched electron beams were generated, with six of these being stopped by 0.64 cm-thick solid aluminium or copper anodes. The other six were extracted from the diodes through thin compound diaphragms in the centres of the anodes. The six extracted beams were transported by preformed plasma channels of which the target was the common terminus. The channels were formed in parallel by the discharge of a 20 μF capacitor bank system charged to 65 kV. System inductance was 330 nH. The six plasma channels used for beam transport were formed in the ambient laboratory atmosphere and were guided by 25 μm diameter tungsten wires.

The phenomonology and limitations of plasma channel transport have been discussed in more detail elsewhere[1]. Basically, the channels start with initial diameters <1 mm and expand with radial velocities of ~1.5 mm μs^{-1}. The central part of each channel consists of singly ionized air at a few electron volts temperature, with a mass density reduced below ambient by a factor near four. There is much evidence that the tungsten wire plays a role only in initiating the discharge, and that it does not 'explode' nor affect subsequent channel dynamics. Thus the channels' features should be the same as if they had been laser-initiated. As the channels expand, the current rises to a peak in 4 μs; at this time the accelerator is fired. The conductivity of the channels is high enough to provide space-charge and current neutralization of the beam fields. Thus, ideally there are

0028–0836/80/300366—03$01.00

no collective effects, and the beam is guided only by the channel fields from the channel current. Consequently the peak current in each channel must be the Alfvèn current, which is ~65 kA for the 1.5 MeV electrons.

For this experiment, Proto II was operated in a mode that provides a pulse with nominal parameters of 1.5 MV, 3.5 MA, 20 ns FWHM, 5 TW, and 100 kJ. Thus the energy and power of each individual beam were ~8 kJ and 0.4 TW, and were transported 0.46 m. The aluminium targets had diameters ranging from 6 to 32 mm.

The time independent theoretical model for channel transport is based on an earlier technique[14] which combines coupled electron/photon collisional transport with electron transport in static, externally applied electric and magnetic fields of arbitrary spatial dependence. As the relatively short pulse REBs are not injected until the highly conducting plasma channels have been well established, the electrons of the charge and current neutralized beam are assumed to follow single particle trajectories in the quasi-static externally applied field of the channel conduction current. While the material geometry in the numerical model is constrained to be two-dimensional, cylindrical, and invariant with respect to rotation about an axis of symmetry, particle trajectory descriptions are fully three-dimensional. This three-dimensional capability is essential in the present application because of the azimuthal dependence of the multibeam source and because of the preferential orientation of the X-ray pinhole camera whose exposure environment is to be predicted by the model.

Figure 1 shows an *R–Z* plot of a random sample of trajectories for a 1.91-cm o.d., 1.27-cm i.d. cylindrical target. Only that portion of the electron trajectories outside the target is plotted. Experiments have confirmed efficient transmission along the plasma channels[6]. Consequently, trajectories are initiated in the model calculations at a distance of one betatron wavelength (~2.3 cm) beyond the geometrical beam 'overlap radius' (~1.2 cm) to ensure spatial phase mixing[15]. The overlap radius is defined as the radius at which the edges of the individual beams and channels start to merge. The magnetic field is a superposition of the fields due to the six-channel conduction currents and the axial return currents in the target cylinder. Field effects are ignored inside the solid target because of the high collision frequency. On the other hand, collisional effects are ignored outside the target.

Because the target radius is about three-quarters of the geometrical overlap radius in this calculation, ~100% of the beam strikes the target[5]. The beam/target coupling efficiency (per cent of the beam energy deposited in the target) is about 80%. Fig. 1 shows most of this energy is deposited within the beam radius. A few of the reflected electrons reenter the target. However, the majority of the reflected electrons (~20% of the beam energy) is lost through axial drift in the field of the return currents.

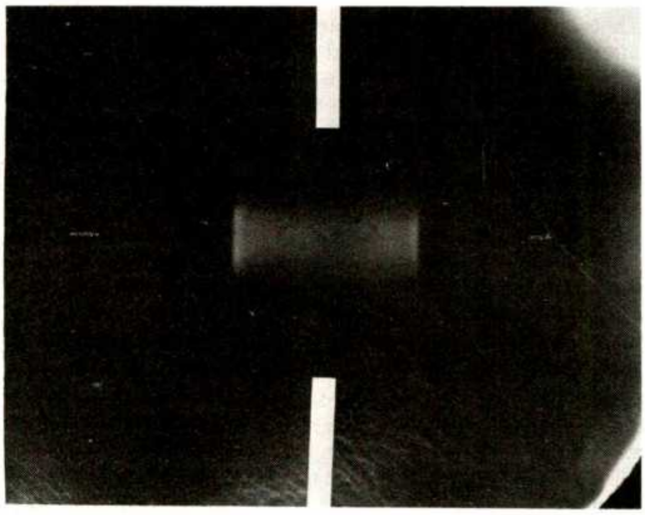

Fig. 2 X-ray pinhole photograph of six beams incident on a 1.9-cm o.d. target. The vertical axis of the cylinder is indicated.

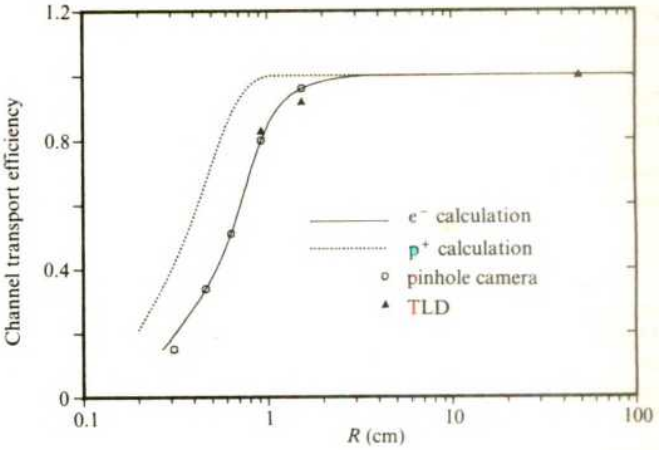

Fig. 3 Beam-target coupling efficiency as a function of target radius. For the 2-MeV proton reference calculation, the maximum angle of injection of protons into the channels was taken to be 8°.

The numerical model was also used to predict the coupling efficiencies and three-dimensional energy deposition profiles as a function of the target o.d. In addition, spatially and spectrally resolved predictions of the X radiation emitted within a small solid angle about a direction corresponding to the orientation of an experimental pinhole camera were obtained. According to the calculated results, the total X-ray emission in the direction of the pinhole should be proportional to the coupling efficiency.

The fraction of the beam energy transported to the central target cylinder was determined from measurements of the bremsstrahlung produced by the electron beams. An X-ray pinhole camera in the plane of the transport channels viewed the cylinder transverse to its axis. Thermoluminescent dosimeters (TLDs) were positioned at one end of the central target cylinder. Additional TLDs were placed behind the solid aluminium anodes of those beams which were not transported to provide a reference measurement of the dose expected when 100% of the electrons were stopped in aluminium.

Both diagnostics relied on the theoretical calculations presented above for interpretation of the results. The absolute TLD measurements were calculated to depend strongly on the kinetic energy of the electrons striking the aluminium (roughly as the square of the energy). The uncertainties in the absolute voltage monitor calibrations would have made this technique inaccurate if only one TLD reading had been made. However, the ratio of the TLD doses from the cylindrical targets to those from the solid anodes was calculated to be independent of voltage, to within the accuracy of the Monte Carlo calculation, over the range 0.5–1.6 MeV. This ratio was used to determine the transport efficiency for the 3.2-and 1.9-cm diameter cylinders.

The presence of electron drift losses near the ends of the cylinders would have complicated interpretation of TLD data for the smaller diameter cylinders. However, the X-ray pinhole camera was able to resolve this loss spatially and thus was used to infer the transport efficiencies to smaller cylinders. A typical X-ray photograph is shown in Fig. 2. Previous work[16] has shown that the image on the developed film is proportional to the energy absorbed in the film emulsion in this regime, and absolute calibrations were not required. The spatial distributions in the X-ray images were in good agreement with the theoretical predictions. The observed X-ray intensities were compared with the predicted intensities calculated using the techniques described above. By normalizing the experimental photographic intensities to the theory for the 3.2-cm diameter cylinder, the absolute transport efficiencies could be inferred for smaller diameter cylinders.

Figure 3 compares the transport efficiencies predicted using the numerical model and the experimental data. Surprisingly, the agreement between theory and experiment is much better than possible inaccuracies predict. The only significant disagreement occurs for the smallest cylinder for which the measurement is ~5% below the calculated transport efficiency of 19%. This result is strong support for the models used to calculate plasma channel formation, channel overlap geometry, electron and photon transport, and for the experimental procedures used. Figure 3 also shows a calculated prediction of transport efficiency for protons injected into the same channel system used here for the electron beams. The ions would reach a smaller radius with higher efficiency than do the electrons, and thus would irradiate a target with higher power. This result, along with their more favourable energy deposition properties[3] and the recent rapid advances in ion diode research[1,4], makes light ions more attractive than electrons for ICF use.

We thank P. Davis, D. Noack, R. Noack, W. Simpson and D. Zagar for technical assistance, and the data acquisition and Proto II operations crews for their perseverence and help. This work was supported by the US Department of Energy under Contract DE-AC04-76-DP000789.

Received 24 March; accepted 9 May 1980.

1. Miller, P. A., Johnson, D. J., Wright, T. P. & Kuswa, G. W. *Comments Plasma Phys. and Controlled Thermonucl. Fus.* **5,** 95–103 (1979).
2. Widner, M. M. *et al. Phys. Rev. Lett.* **43,** 357–360 (1979).
3. Clauser, M. J. *Phys. Rev. Lett.* **35,** 848–851 (1976).
4. Johnson, D. J. *et al. Phys. Rev. Lett.* **42,** 610–613 (1979).
5. Wright, T. P. *J. appl. Phys.* **49,** 3842–3850 (1978)
6. Wright, T. P. & Halbleib, J. A. Sr, *Sandia Rep.* SAND79-2064J; *Phys. Fluids* (in the press).
7. Halbleib, J. A. Sr & Wright, T. P. *Sandia Rep.* SAND79-2063J; *Phys. Fluids* (in the press).
8. Miller, P. A. *et al. Phys. Rev. Lett.* **39,** 92–95 (1977).
9. Benford, J. *J. appl. Phys.* **48,** 2320–2323 (1977).
10. Ottinger, P. F., Mosher, D. & Goldstein, S. A. *Phys. Fluids* **22,** 332–337 (1979).
11. Mosher, D., Colombant, D. G., Goldstein, S. A. & Lee, R. *IEEE Conf. Record-Abstr. 1978 IEEE int. Conf. Plasma Sci.* 113 (IEEE, New York, 1978).
12. Freeman, J. R. *et al. IEEE Conf. Record-Abstr. 1978 IEEE int. Conf. Plasma Sci.* 177 (IEEE, New York, 1978).
13. Martin, T. H., Johnson, D. L. & McDaniel, D. H. *Proc. 2nd int. Topical Conf. High Power Electron and Ion Beam Research and Technology* Vol. 2, 807–818 (Cornell University, New York, 1977).
14. Halbleib, J. A. Sr & VanDevender, W. H. *J. appl. Phys.* **48,** 2312–2319 (1977).
15. Wright, T. P. & Halbleib, J. A. Sr *Bull. Am. phys. Soc.* **24,** 949 (1979).
16. Dozier, C. M., Brown, D. B., Birks, L. S., Lyons, P. B. & Benjamin, R. F. *J. appl. Phys.* **47,** 3732–3739 (1976).

Opto–acoustic study of weak optical absorption of liquid methane

C. K. N. Patel, E. T. Nelson & R. J. Kerl

Bell Laboratories, Murray Hill, New Jersey 07974

The first opto-acoustic absorption spectra of liquid methane at 94 K in the region of 5,500–7,500 Å is reported here. The observed absorption bands are very weak with peak absorption coefficients of 16×10^{-3} to 1×10^{-4} cm^{-1} and are of importance in the study of spectra of outer planets (such as Jupiter and Neptune) for detecting the existence of liquid methane on these planets.

Methane is a minor constituent of the atmospheres of the outer major planets[1], Uranus, Neptune, Jupiter and Saturn, as well as of Titan, the largest satellite of Saturn. This is deduced from the absorption bands of CH_4 which dominate the visible and near IR spectra of these planets[2]. The long effective optical path lengths in the atmosphere of these planetary bodies enables the absorption bands to be readily observed using ground based telescopes. Further, the temperatures on some of these planetary bodies are such that CH_4 could exist as liquid droplets[3] or even as an ocean[4] on Titan. To provide correlations with laboratory data, and to deduce the CH_4 concentration of the atmospheres of the above planets from the optical astronomy data, an accurate determination of the positions of these weak absorption bands, their band strengths, and temperature dependences is needed. Because CH_4 at pressures of tens of atmospheres or even at liquid densities (~590 amagats) is very transparent in the visible region the laboratory data are difficult to obtain. Conventional optical absorption spectroscopy in the ~4,000–11,000 Å region has recently been carried out using a multipass cell to obtain absorption pathlengths of ~1 km for room temperature CH_4 at pressures up to 20 atm (ref. 5) resulting in density–pathlength products of up to 20 km amagat. Longer path lengths of up to 3.86 km at lower pressures were used in earlier studies[16,17]. These data show several absorption bands of generally decreasing strength towards shorter wavelengths. Conventional optical spectroscopy of liquid CH_4 has been recently reported[6] in the region of 6,190–19,000 Å using a cell length of ~3 cm. The sensitivity of these studies, however, is such that the shortest wavelength absorption feature reported is at $\lambda\sim6{,}190$ Å with a peak absorption coefficient of $\sim4\times10^{-3}$ cm^{-1}. The signal-to-noise ratio reported for this peak is only about 5 : 1, that is, the 6,190 Å peak height is ~5 times the system noise. If we extrapolate from Giver's high temperature gas data[5], liquid CH_4 should exhibit weaker absorption bands all throughout the visible region (4,000–7,000 Å). Measurements of these absorption bands are clearly beyond the capabilities of the conventional spectroscopy studies of Ramaprasad *et al.*[6] who used a density path length product ~19 m amagat although some improvement is possible by using longer (but perhaps experimentally difficult) path lengths. Note that the multipass long cell technique used by Giver[5] is not applicable to liquid CH_4 studies because of obvious practical problems.

We report here optical absorption spectrum of liquid CH_4 at ~94 K in the 5,500–7,500 Å region. Several absorption bands are observed, the strongest one being at 13,700 cm^{-1} with an absorption coefficient of $(1.6\pm0.2)\times10^{-2}$ cm^{-1} and the weakest one at 15,515 cm^{-1} with an absorption coefficient of $\sim(1\pm0.3)\times10^{-4}$ cm^{-1}. The signal-to-noise ratio for the weakest peak reported is such that we should be able to observe absorption features as small as $\sim10^{-6}$ cm^{-1}. Our measurements were carried out using an opto–acoustic (OA) detection technique[7] which has been shown to be ideally suited for measuring absorption coefficients of room temperature liquids at levels as low as $\sim10^{-7}$ cm^{-1} and which we have adapted for the study of cryogenic liquids. The OA cell used in the present liquid CH_4 measurements had an effective density path length product of ~6.33 m amagat. In addition to the position and the strengths of the absorption bands, we report their bandwidths, asymmetries and identifications. In general, the absorption peaks arise from combinations of harmonics of the various vibrational fundamentals of CH_4. Further, the absorption bands for liquid CH_4 show asymmetries and frequency shifts (from the gas phase data) which are reminiscent of the liquid benzene results[8].

The measurements were carried out using a pulsed laser immersed transducer OA gated detection technique[7], modified for low temperature studies. The all stainless steel OA cell[9] was attached to a liquid N_2 cryostat such that any desired temperature between 80 and 200 K can be obtained. Methane (Matheson, Ultra-High Purity grade) was directly condensed into the low temperature cell and its pressure was monitored using a capacitance manometer. Tunable pulsed laser radiation was obtained from either a flashlamp pumped dye laser (pulse energy ~1–3 mJ, pulse duration $\tau_p\sim1$ μs, and repetition rate ~10 pulses per s (p.p.s.)), or a doubled Nd : YAG pumped dye laser (pulse energy ~1–5 mJ, $\tau_p\sim10$ ns, and pulse repetition rate ~20 p.p.s.). The laser pulse energy was measured using a Laser Energetics pulsed joule-meter. The OA signal as well as the reference laser level signal sampled by box-car integrators were averaged and ratioed by a NOVA 800 minicomputer. We thus obtained spectra of normalized OA signal $S_\nu=V/E_{inc}$, where V is the OA signal from the PZT transducer and E_{inc} is the incident laser pulse energy, as a function of the dye laser frequency.

The transient acoustical output signal from the transducer (in form of ringing due to the 200 kHz resonant frequency of the

0028–0836/80/300368—03$01.00

Table 1 Observed data on optical absorption spectrum of liquid methane

	Liquid*					Gas†
Feature‡	Bandcentre§ (cm^{-1})	Peak absorption‖ (cm^{-1})	Width (cm^{-1})	Asymmetry¶	Identification	Bandcentre (cm^{-1})
1	13,700	1.6×10^{-2}	180	1.69	$4\nu_1+\nu_3$	13,755
2	14,170	1×10^{-3}	—	—	$3\nu_1+2\nu_3$	14,225
3	14,585	3×10^{-4}	—	—	$2\nu_1+3\nu_3$	14,652
4	14,935	7×10^{-4}	250	2.4	$4\nu_1+\nu_3+(\nu_2, \nu_4)$	14,992
5	15,170	—	—	—	—	—
6	15,300	—	—	—	—	—
7	15,410	—	—	—	$3\nu_1+2\nu_3+(\nu_2, \nu_4)$	—
8	15,515	1.2×10^{-4}	—	—	—	15,576
9	16,090	3×10^{-3}	224	1.67	$5\nu_1+\nu_3$	16,155
10	16,714	2.3×10^{-4}	240	—	$4\nu_1+2\nu_3$	16,750
11	17,320	2.5×10^{-4}	310	1.38	$5\nu_1+\nu_3+(\nu_2, \nu_4)$	17,361

* $T\approx94$ K, density length product 6.3 M amagat.
† $T\approx300$ K, data from ref. 5.
‡ See Fig. 1.
§ Bandcentres generally accurate to ±5 cm^{-1} for strong bands.
‖ Accuracy ±30%.
¶ See text for definition.

PZT transducer, and the reflections of acoustic waves generated from the condensed liquid) is delayed from the incident laser pulse by a delay, $\tau_D=d/v_a$, where d is the distance between the laser illuminated volume and the OA transducer, and v_a is the acoustic velocity in the condensed liquid. From a measurement of τ_D versus d we have determined the sound velocity in liquid CH_4 ($T=94$ K) to be $v_a=(1{,}455\pm18)$ m s^{-1}. This value is consistent with the currently accepted value[10].

Figure 1 shows the measured spectrum of normalized OA signal from liquid CH_4 at 94 K from 13,300 to 17,800 cm^{-1}. Several clearly recognizable absorption peaks are indicated. Spectral resolution which is typically ~1.5–2 cm^{-1} is much smaller than the observed widths of the absorption features. Note that the only previous measurements of liquid CH_4 in the visible reported[6] the strong peak at ~16,090 cm^{-1} with a signal-to-noise ratio of $\leqslant5$. We see many more absorption features with peak absorptions which are ~30 smaller than that for the 16,090 cm^{-1} band. And even for the weak features the signal-to-noise ratio exceeds 100 for an integration time of ~1.5 s per resolution element of 1.5–2 cm^{-1}. Note also that there are no regions of spectrum where liquid CH_4 absorption drops below ~10^{-4} cm^{-1}. All the observed absorption features show a pronounced asymmetry, the absorption tails being longer on the high frequency side of the peaks.

As reported earlier[7,9], the normalized OA signal, S_ν, can be related to the intrinsic absorption coefficient of the condensed material through the relationship

$$S_\nu=\frac{V}{E_{\rm inc}}=K\beta\frac{v_a}{C_p}\alpha_\nu \qquad (1)$$

where β is the thermal volumetric expansion coefficient, C_p the specific heat at constant pressure, α_ν the absorption coefficient ($\alpha_\nu l\ll l$ where l is the sample path length), and K is a constant that describes the OA conversion efficiency and includes such parameters as the geometry of the OA cell, the acoustic impedance mismatch between the liquid and the transducer, and the sensitivity of the PZT transducer. Thus a knowledge of all the relevant parameters in equation (1) is sufficient to extract the absorption coefficient from the observed normalized OA signal. Procedures such as this have provided an excellent estimate of the absorption coefficient of media at room temperature where a sensitivity $\Sigma=S_\nu/\alpha_\nu$, calibrated for one liquid can be approximated for another of known β, C_p, and ρ. An accurate determination of the sensitivity Σ for a given liquid requires that a suitable dye be incorporated into the liquid medium such that a very small concentration of the dye (small enough so that none of the parameters of the right-hand side of equation (1) other than α_ν are perturbed) produces an absorption which can be measured accurately by conventional optical techniques (and by the OA technique). Unfortunately no data are available for the low temperature condensed gases. For the present study, we have extrapolated our sensitivity measurements from benzene studies[7,8] to obtain absorption coefficient from the measured S_ν for liquid CH_4. For the strong absorption peak at 16,090 cm^{-1}, we thus obtain α $(16{,}090)\approx(3\pm1)\times10^{-3}$ cm^{-1}. This value is in a reasonable agreement with the one which can be deduced from ref. 6.

Table 1 shows the data on observed absorption bands including: (1) the band peak frequencies; (2) bandwidths of peaks which are sufficiently separated to make such a measurement meaningful; (3) band asymmetry parameter defined as the ratio of the half-width at half-height on the high frequency side of peak to that on the low frequency side of the peak; (4) the peak absorption coefficient (subtracting out the broad background absorption in case of weak absorption features); and (5) identifications of the peaks, using Giver's[5] scheme for gaseous methane. We also show in Table 1 relevant data from the gas phase studies of Giver[5].

(1) There is a systematic shift of ~35–50 cm^{-1} of the liquid CH_4 absorption peak positions towards low frequency side when compared with gaseous CH_4 data. This shift is thought to arise from the effect of local environment in liquid CH_4 and is qualitatively in agreement with the data on liquid[8] and gaseous benzene (ref. 11 and R. G. Bray, personal communication). Note that our liquid CH_4 data show well-defined subsidiary peaks/shoulders on the absorption features which are not visible in the gas data of Giver[5].

(2) The observed liquid CH_4 bandwidths vary from ~250 to 350 cm^{-1} and are much wider than those for gaseous CH_4, again in qualitative agreement with liquid/gaseous benzene studies. The higher harmonics in a given series have larger bandwidths.

(3) All the observed liquid CH_4 absorption features in the 5,500–7,500 Å region show pronounced asymmetries with the asymmetry parameter varying from ~1.4 to 2.4. The gaseous CH_4 (ref. 5) data on the other hand show no such asymmetry

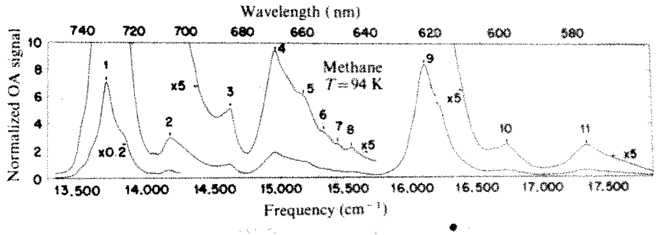

Fig. 1 Normalized OA signal as a function of dye laser frequency. Data including the absolute absorption coefficients for the indicated peaks are summarized in Table 1.

which is again thought to arise from local environment interactions in qualitative agreement with liquid/gaseous benzene studies (refs 8, 11 and R. G. Bray, personal communication) of its harmonic absorption in the visible region. We observe that the asymmetry of the absorption is a general characteristic feature of the absorption profiles of liquids.

(4) From the measured bandshapes one can derive integrated band strength (not done here). The absorption coefficients of the measured peaks vary from $\sim 1\times10^{-4}$ to $\sim 1.6\times10^{-2}$ cm^{-1}. From the signal-to-noise ratio for the smallest peaks (obtained using an integration time of 1.5 s per resolution element of 1.5 cm^{-1}), we conclude that we have the ability to measure absorption features as small as $\sim 10^{-6}$ cm^{-1} for liquids at low temperatures. The trend of the measured absorption coefficient for liquid CH_4 is similar to that for gaseous CH_4, that is the higher the harmonics the smaller the absorption coefficients.

(5) While major peaks have been reasonably well identified as arising from the combinations of harmonics of the four fundamental vibrational frequencies of CH_4, the minor peaks are not yet assigned.

The detailed knowledge about liquid CH_4 absorption spectrum provided here should now allow us to look carefully at the spectra of the outer planets to search for existence of liquid CH_4. (As pointed out by Ramaprasad *et al.*[6], detection of liquid CH_4, in form of an ocean on the planetary surface, is likely to be very difficult because only surface reflection is involved. However, for liquid CH_4 droplets in the planetary atmosphere, the sunlight penetrates and is reflected back from a surface or a cloud layer. Thus detection or setting an upper limit of the droplet fraction of CH_4 is feasible if high resolution high quality astronomical spectroscopic data are available.) Important information is to be gained from the position of the absorption bands as well as from their widths and shapes. As is seen above, these three features are characteristically different for liquid CH_4 from those for gaseous CH_4. For example, the existence of liquid CH_4 (in the form of droplets in the planetary atmosphere) can be deduced from the planetary astronomical absorption data if measurable differences are found in the peaks (positions, shapes, and widths) of the absorption bands (compared to the absorption peaks of gaseous CH_4).

Finally, our demonstration of the usefulness of liquid OA absorption measurement technique to low temperature liquids opens up an entirely new field of study. The ability to measure absorption coefficients as small as 10^{-6} cm^{-1} (an ability which we feel can be improved considerably) at cryogenic temperatures will undoubtedly provide exciting new data on liquids and solids. We have already begun to look at other liquified gases such as ethylene, and ammonia which are also important[12–14] in the atmospheres of the outer planets. We are modifying our OA measurement techniques to go to yet lower temperatures ~4 K to investigate H_2 and HD which are the major constituents[15] of these planets.

We thank Drs L. J. Lanzerotti and J. A. Tyson for helpful comments.

Received 21 March; accepted 20 May 1980.

1. Kuiper, G. P. (ed.), *The Atmospheres of Earth and Planets* (University of Chicago Press, 1952).
2. Lutz, B. L., Owen, T. & Cess, R. D. *Astrophys. J.* **203**, 541 (1976).
3. Danielson, R. E. *Icarus* **30**, 462 (1977).
4. Caldwell, J. in *Planetary Satellites* (ed. Burns, J. A.) 438–450 (University of Arizona Press, Tucson, 1977).
5. Giver, L. P. *J. quant. Spectrosc. Radiat. Transfer* **19**, 311 (1978).
6. Ramaprasad, K. R., Caldwell, J. & McClure, D. S. *Icarus* **35**, 400 (1978).
7. Patel, C. K. N. & Tam, A. C. *Appl. phys. Lett.* **34**, 467 (1979).
8. Patel, C. K. N., Tam, A. C. & Kerl, R. J. *J. chem. Phys.* **71**, 1470 (1979).
9. Patel, C. K. N. & Tam, A. C. *Nature* **280**, 302 (1979); *Appl. Opt.* **18**, 3348 (1979).
10. *International Thermodynamic Tables of Fluid State* Vol. 5 (Pergamon, Oxford, 1976).
11. Reddy, K. V., Bray, R. G. & Berry, M. J. in *Advances in Laser Chemistry* (ed. Zewail, A.) 48 (Springer, Berlin, 1978).
12. Ridgeway, S. T. *Astrophys. J. Lett.* **187**, L41 (1974).
13. Combes, M., Encrenaz, T., Vapillon, L., Zeau, Y. & Lesqueren, C. *Astr. Astrophys.* **34**, 33 (1974).
14. Encrenaz, T., Owen, T. & Woodman, J. H. *Astr. Astrophys.* **37**, 49 (1974).
15. McKellar, A. R. W. & Welsh, H. L. *Proc. R. Soc.* **A322**, 421 (1971).
16. Dick, K. A. & Fink, U. *J. quant. Spectrosc. Radiat. Transfer* **18**, 433 (1977).
17. Fink, U., Benner, D. C. & Dick, K. A. *J. quant. Spectrosc. Radiat. Transfer* **18**, 447 (1977).

Contact angles associated with thin liquid films in emulsions

M. P. Aronson & H. M. Princen

Lever Brothers Company, Research Division, 45 River Road,
Edgewater, New Jersey 07020

As a result of interaction forces, the tension of a thin liquid film can be lower than the sum of the interfacial tensions of the bulk surfaces bounding the film[1]. To satisfy conditions of mechanical equilibrium, this reduced film tension leads to a macroscopic contact angle between the film and its associated Plateau border[2]. We have observed and report here very high contact angles, in some cases approaching 90°, for aqueous films between oil droplets, stabilized by anionic surfactants in the presence of various electrolytes. The contact angle is found to depend on the nature of the surfactant head group, type and concentration of counter-ion, and temperature. These contact angles have a pronounced effect on the stability, structure and rheology of emulsions.

Consider the thin metastable liquid film and its Plateau border that form when a vertical rectangular glass frame is withdrawn from a surfactant solution (Fig. 1). The tension of the film, γ_f, is related to the normal bulk interfacial tension, γ by[3]

$$\gamma_f = 2\gamma + \Delta F = 2\gamma + \int_{\infty}^{h_e} \pi(h)\,\mathrm{d}h \qquad (1)$$

h is the film thickness, h_e is the equilibrium thickness, π is the 'disjoining pressure', and ΔF is the free energy of interaction per unit area of the film, that is, the reversible work of thinning the film from infinite thickness, where the surfaces do not interact, down to the equilibrium thickness, where attractive and repulsive interaction forces are in balance. [Strictly speaking[3], equation (1) should include a term πh_e. For the extremely thin films (so-called Newton black films) to be discussed in this study, this term is expected to be negligible.]

A mechanical analysis[4] of the region where the film and the Plateau border join indicates that, whenever $\Delta F < 0$, the two bulk surfaces will, on a macroscopic scale, intersect at a sharp angle, 2θ, such that

$$\gamma_f = 2\gamma \cos\theta \qquad (2)$$

It follows from equations (1) and (2) that

$$-\Delta F = 2\gamma(1 - \cos\theta) \qquad (3)$$

One of the many manifestations of a finite contact angle is the spontaneous clumping that occurs when two or more oil drops approach each other in an aqueous surfactant solution (Fig. 2).

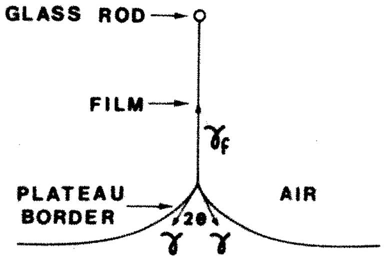

Fig. 1 Film and associated plateau border that are formed when a vertical glass frame is pulled out of a surfactant solution.

0028–0836/80/300370—03$01.00

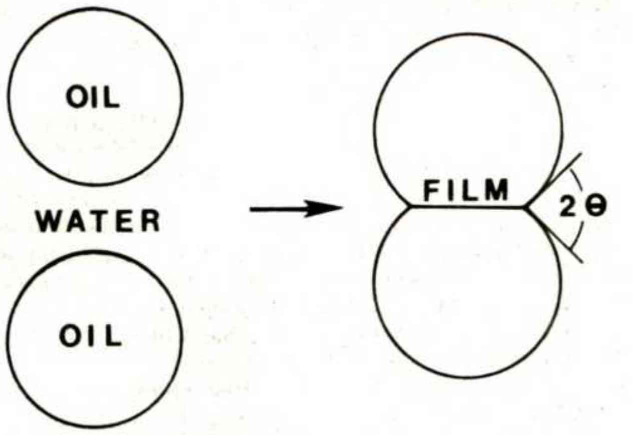

Fig. 2 The spontaneous flocculation of oil droplets when the contact angle, θ, is greater than zero.

When the contact angle is large, the droplets comprising the cluster are highly deformed, while remaining separated by an extremely thin film of intervening liquid of reduced tension.

Appreciable contact angles, as high as 15°, have been observed in aqueous films in air[5–8]. For lipid films in water, contact angles up to 8° have been reported[9,10]. If one assumes that interaction free energies for aqueous films in oil are of about the same magnitude as for aqueous films in air, one would, on the basis of equation (3), expect much larger angles for the former on account of their generally much lower interfacial tension.

Indeed, while studying[11] concentrated oil-in-water emulsions, we have observed very large contact angles, in some cases approaching 90° which would seem to be the theoretical limit. The emulsions were stabilized with anionic surfactants and contained added electrolyte. The contact angle was found to depend strongly on the composition of the aqueous phase (type of surfactant, and concentration and kind of counter-ion), while the nature of the oil phase had a relatively minor influence. We have used two classes of anionic surfactant: sodium alkyl sulphates and sodium alkyl carboxylates (soaps) in the presence of added LiCl, NaCl or KCl. With alkyl sulphates, the contact angle reached at a given electrolyte concentration increases in the order $Li^+ \ll Na^+ < K^+$. With alkyl carboxylates, the order seems to be reversed, although there is some doubt about the position of Li^+ because of the very low solubility of lithium soaps. Similar reversals in the relative effect of the alkali metal ions on properties of alkyl carboxylates and alkyl sulphates have been reported in other areas of colloid and surface chemistry[12]. With Na^+ as the counter-ion, the alkyl carboxylates give rise to much higher contact angles than do the alkyl sulphates. For example, with 0.3 m NaCl and 0.2% surfactant at 25 °C, the contact angles with dodecane are $\simeq 0°$ for SDS and $\simeq 57°$ for sodium oleate. Contact angles were also observed with other *n*-alkanes, as well as with paraffin oil and carbon tetrachloride. The results of this study, still in progress, will be presented elsewhere.

More recently, we have observed that the contact angle varies strongly with temperature. This is not unexpected, as this effect has been reported also for aqueous films in air[8]. Because of the much greater range of contact angles that can be obtained with aqueous films between oil, however, the phenomenon is much more dramatic. An example is given in Fig. 3 that shows dodecane droplets in an aqueous phase containing 0.25% sodium oleate, 0.25% sodium laurate and 0.6 m NaCl. At 25 °C, this system has a contact angle of about 70° which leads to the formation of flocs composed of highly deformed oil droplets. The floc is quite rigid and the individual droplets do not easily roll past each other. Very little water is seen to remain in the Plateau borders in the interior of each floc. Just as in polyhedral foams, these borders are of two types: 'linear' channels where three films meet at angles of 120°, and 'tetrahedral' corner pockets where four linear borders meet at angles of 109.47°. It can be shown[11] that the linear Plateau borders empty out when $\theta \geqslant 30°$ while the tetrahedral pockets do so when $\theta \geqslant 35.26°$.

When the dispersion is heated, the contact angle decreases and the cluster gradually decomposes into increasingly spherical droplets that begin to shift and rearrange (45 °C). Finally, at 60 °C, the contact angle is near 0°, and the floc now appears as a collection of discrete spherical droplets that are mobile. If, at this stage, the dispersion is cooled back to 25 °C, rigid flocs of deformed droplets again appear. They do not, of course, revert to the original configuration because of shifts that have taken place in the first cycle.

The presence of large contact angles can have a pronounced effect on several properties of an emulsion. For example, there is a dramatic increase in the rate and extent of sedimentation or creaming of an emulsion when $\theta > 10°$.

The structure of a concentrated emulsion, such as the cream layer formed on top of an initially dilute emulsion, is also very sensitive to the contact angle[11,13]. When the cream is formed by

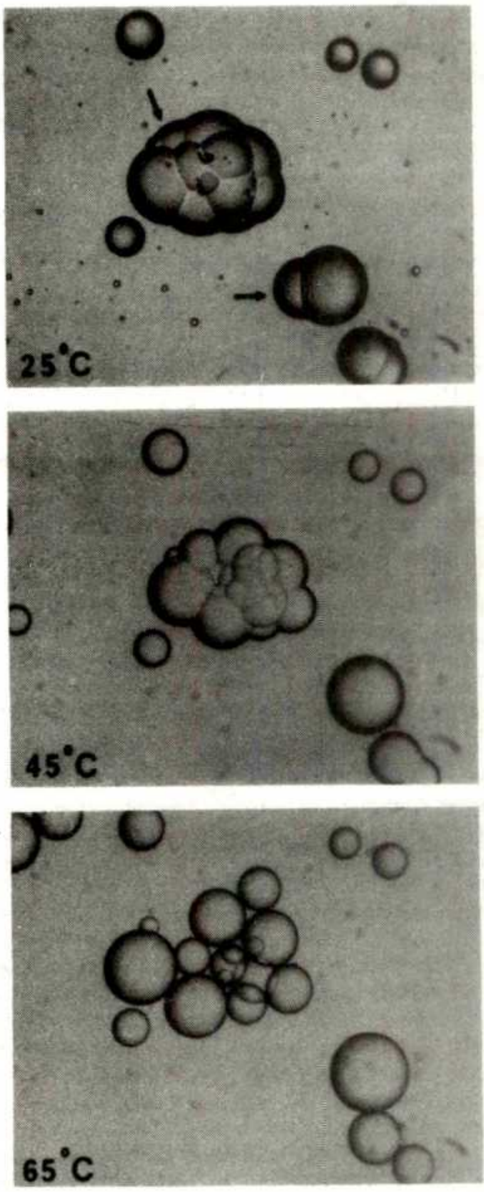

Fig. 3 The effect of temperature on the contact angle in flocs formed when dodecane droplets are dispersed in an aqueous solution of 0.25% sodium oleate, 0.25% sodium laurate and 0.6 M NaCl. The arrows indicate droplets that disappear during the experiment because of coalescence. Magnification, ~×90. An Olympus MG inverted microscope was used and heating was accomplished with a Mettler FP2 programmable hot stage. Contact angle equilibrium was generally achieved in less than 10 min.

sedimentation under gravity, an open network of flocs can form when $\theta \gg 0$. Appreciable amounts of water can be trapped in this network, leading to an expanded cream whose volume fraction of oil is <0.74 (the volume fraction corresponding to closest packing of monodisperse spheres). In this regard, this type of emulsion cream is analogous to the voluminous sediment encountered with a highly unstable colloidal dispersion of solid particles[14]. When such an expanded emulsion cream is compacted by mild centrifugation and then allowed to relax and equilibrate under normal gravity, much of the occluded water can be squeezed out, so that the resulting cream tends to have a final volume fraction of oil significantly greater than 0.74, as predicted by theory for the state of minimum free energy[11,13]. Indeed, using this method, we have prepared stable creams whose volume fraction is as high as 0.94 (ref. 11).

Note that some aspects of this work may have their parallel in biological systems. The cluster shown in Fig. 3 has a close morphological resemblance to a blastula, that is, the aggregate of living cells at the early stage of embryonic development. Of course, in biological systems the liquid phases would be reversed, that is, aqueous drops (cells) would be separated by lipid films (membranes).

We thank Lever Brothers Company for permission to publish this work.

Received 8 April; accepted 23 May 1980.

1. Derjaguin, B. V. *Acta phisicochim. URSS* **12,** 181–200 (1940).
2. Princen, H. M. & Mason, S. G. *J. Colloid Interface Sci.* **29,** 156–172 (1965).
3. De Feijter, J. A., Rijnbout, J. B. & Vrij, A. *J. Colloid Interface Sci.* **64,** 258–268 (1978).
4. De Feijter, J. A. & Vrij, A. *J. electroanalyt. Chem.* **37,** 9–22 (1972).
5. Princen, H. M. *J. phys. Chem.* **72,** 3342–3345 (1968).
6. Huisman, F. & Mysels, K. J. *J. phys. Chem.* **73,** 489–497 (1969).
7. Kolarov, T., Scheludko, A. & Exerowa, D. *Trans. Faraday Soc.* **64,** 2864–2873 (1968).
8. De Feijter, J. A. & Vrij, A. *J. Colloid Interface Sci.* **64,** 269–277 (1978).
9. Haydon, D. A. & Taylor, J. L. *Nature* **217,** 739–740 (1968).
10. Requena, J., Billett, D. F. & Haydon, D. A. *Proc. R. Soc.* **A347,** 141–159 (1975).
11. Princen, H. M., Aronson, M. P. & Moser, J. C. *J. Colloid Interface Sci.* **75,** 246–270 (1980).
12. Goddard, E. D. *Croatica chem. Acta* **42,** 143–150 (1970).
13. Princen, H. M. *J. Colloid Interface Sci.* **71,** 55–66 (1979).
14. Vold, M. J. *J. Colloid Interface Sci.* **18,** 684–695 (1963).

Hydrostatic pressure and long-chain organic molecule diffusion through a polymer matrix

A. R. Rennie & D. Tabor

Department of Physics, University of Cambridge, Madingley Road, Cambridge CB3 OHE, UK

Earlier papers from our laboratory[1–3] have described a sensitive but relatively simple technique using IR spectroscopy to study the diffusion of labelled organic molecules through a polymer matrix. The method showed that the behaviour agreed well with de Gennes[4] model of reptation which assumes that long organic molecules diffuse by the motion of segments consisting of 20 to 30 units in the backbone. We describe here an extension of this work and deal with the effect of hydrostatic pressure on the diffusion of two hydrocarbons (suitably labelled) with backbone units $N = 18$ and 45 through molten low density branched polyethylene at pressures ranging from atmospheric to 1,300 atmospheres. The results show that the diffusion coefficient D decreases as the pressure P is increased. To a close approximation $\log D$ decreases linearly with P implying an apparent activation volume, V. Typical values for $N = 18$, are $V = 55$ Å^3 at 150 °C and 70 Å^3 at 120 °C implying a thermal expansion of the free volume of order 0.5 Å^3 K^{-1}. For $N = 45$, $V = 80$ Å^3 at 120 °C.

The experiments were carried our using ICI Alkathene 11/01 branched polyethylene as the matrix. The diffusants were stearamide ($CH_3(CH_2)_{16}CONH_2$) with 18 backbone atoms and behenyl behenate ($CH_3(CH_2)_{20}COOCH(CH_2)_{20}CH_3$) with 45 units counting the oxygen in the ester linkage. Cylindrical specimens were prepared in the manner described earlier[1] one half containing about 1% diffusant and the other consisting of matrix polymer only. A thin slice cut from the cylinder perpendicular to the join is scanned in an IR microdensitometer tuned to the adsorption frequency of the carbonyl group in the diffusant. Initially the concentration is a step function. As a result of diffusion the profile changes and from the new shape the diffusion coefficient can be calculated.

The diffusion experiments are all carried out above the melting point of the polymer. First, this avoids problems involving different degrees of crystallinity as the molten material at any specified temperature has a reproducible 'morphology'. Second, the diffusion rates are far more rapid than with the solid polymer, an important practical consideration in view of the decrease in D as the pressure is increased. Third, the specimen may be contained in a metal clyinder and compressed by a piston—because it is liquid the pressure is entirely hydrostatic. The force on the piston is applied with dead weights using a converted lever-arm tensile-testing machine and in this way the pressure is maintained constant without the need for elaborate servo-mechanisms. The seals, which slide in the cylinder, are of the Bridgman unsupported area type[5]. The metal cylinder is heated by electrical resistances and thermocouples are inserted at various points near the specimen. Temperature control is reproducible to ±1 °C. After the specimen has been subjected to the required pressure and temperature for a specified time it is solidified rapidly, removed from the containing cylinder and then sliced for examination in the IR microdensitometer.

Figure 1 shows that $\log D$ decreases linearly with P. Assuming a simple Arrhenius relation of the form $D = D_0 \exp(-PV/kT)$ where V is the activation volume for diffusion, k the Boltzmann constant and T the absolute temperature, we obtained the values quoted in Table1.

From Table 1 we first note that the activation volumes are very much smaller than the molecular volumes of the diffusants themselves (400 Å^3 for stearamide, 1,000 Å^3 for behenyl behenate). It is not possible to provide a specific model to explain this. It could be associated with a crankshaft motion involving some 3–4 CH_2 units; or it could relate to a small overall dilation of the matrix to allow passage of the diffusant. However, we also note that the activation volume for the behenyl behenate is only a little larger than for the stearamide although the molecular volume is more than twice as large. This is consistent with the earlier work of Klein and Briscoe[2,3] which

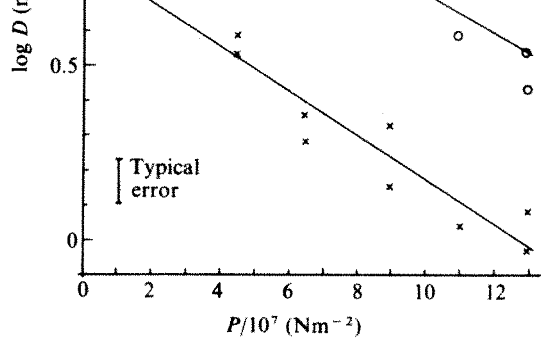

Fig. 1 Plot of $\log D$ against applied hydrostatic pressure, P, for stearamide at 150 °C (+) and 120 °C (○) and behenyl behenate at 120 °C (×).

0028–0836/80/300372—02$01.00

Table 1 Activation volumes, V, for diffusants in molten branched polyethylene

Diffusant	N	Temperature (°C)	V (Å^3)
Stearamide	18	150	55 ± 7
Stearamide	18	120	70 ± 8
Behenyl behenate	45	120	80 ± 8

indicated that however long the diffusant, motion occurs by the movement within individual segments each of which is about 20 carbons in length. Whatever the detailed mechanism it is clear that the diffusant is constrained by the surrounding matrix so that the activation process is easier the larger the available free volume. This accounts for the observation that the activation volume for stearamide decreases from 70 Å^3 at 120 °C to 55 Å^3 at 150 °C. Indeed, we may attribute this decrease to a thermal expansion of the free volume of the order 0.5 Å^3 K^{-1}.

It is interesting to compare these values for V with those deduced from the shear properties of polyethylene in the solid state. Ward[6] and Wilding and Ward[7] quote a value of ~50 Å^3 for bulk shear of linear polyethylene. Although the polymer was largely crystalline and highly oriented the deformation process involves radical disorganization of both the crystalline and the amorphous material in the specimen. Consequently, the mechanisms of motion may not be greatly different from those occurring in the melt. Similarly B. J. Briscoe (personal communication) quotes a value between 100 and 200 Å^3 for the shear of thin films of branched polyethylene. In these experiments the molecular length (and hence N) was many hundreds of times greater than the molecular length of the diffusants used in the present work. This again suggests that the unit involved in shear is a short segment, independent of the overall length of the polymer molecule. We hope to explore this aspect further by carrying out diffusion experiments with diffusants of increasing molecular length. If these data are to be used in the construction of molecular models of diffusion it should be noted once again that the activation volumes are very much smaller than the molecular volume of the segment itself.

A.R.R. thanks the SRC and ICI for a CASE studentship.

Received 31 March; accepted 30 May 1980.

1. Klein, J. & Briscoe, B. J. *Nature* **257**, 386 (1975); *Polymer* **17**, 481 (1976).
2. Klein, J. *Nature* **271**, 143 (1978).
3. Klein, J. & Briscoe, B. J. *Proc. R. Soc.* A**365** (1979).
4. de Gennes, P. G. *J. Chem. Phys.* **55**, 572 (1971).
5. Bridgman, P. W. *The Physics of High Pressure* 39 (Bell, London, 1949).
6. Ward, I. M. *Phil. Trans. R. Soc.* A**294**, 473 (1980).
7. Wilding, M. A. & Ward, I. M. *Polymer* **19**, 969 (1978).

Possible ozone reductions and UV changes at the Earth's surface

J. A. Pyle

Department of Atmospheric Physics, Clarendon Laboratory, University of Oxford, Oxford OX1 3BD, UK

R. G. Derwent

Environmental and Medical Sciences Division, AERE Harwell, Oxfordshire OX11 0RA, UK

During recent years there have been suggestions[1-3] that man's activities might reduce the thickness of the atmospheric ozone layer. Reductions in ozone could then give rise to an increase in potentially harmful solar UV radiation at the Earth's surface. Concern has been expressed particularly about the possibility of subsequent increases in skin cancer. Most calculations of ozone reduction have employed one-dimensional (height-only) models and few have calculated the solar radiation reaching the ground. Rather, it has been assumed that, for example, a 1% depletion in ozone is equivalent to a 2% increase in UV-B (the biologically important radiation in the wavelength range 280–320 nm) (refs 4, 5). However, studies using two-dimensional models[6,7] indicate that any change in ozone will not be uniform, but will show significant variations with latitude and season. We show here first, that the commonly accepted idea that a depletion of ozone of a particular figure is equivalent to an UV increase of twice that figure does not hold generally; second, we point out the importance of seasonal and latitudinal variations in ozone changes on the UV radiation reaching the Earth's surface.

Figure 1 shows the latitude–time cross-section of the depletion in total ozone calculated by one of us (J.A.P.) using a two-dimensional model of the atmosphere including detailed photochemistry and simulating a source of chlorofluorocarbons (CFCs). The features of the depletion are similar to a calculation in the model using a much simplified photochemical scheme[6]. Namely, maximum depletions are found in high latitudes where the total ozone is largest; smallest depletions occur in equatorial latitudes where ozone is a minimum throughout the year. Figure 2 shows two calculations, using the depletions found in Fig. 1, of the increase in solar UV radiation at 310 nm at the Earth's surface consequent on the reductions in ozone. The dashed line was obtained using the simple direct beam absorption scheme employed in the two-dimensional model, while the solid line uses the radiation scheme of Green *et al.*[8], which includes the effects of scattering by air molecules and aerosols. It can be concluded immediately from Figs 1 and 2 that the ratio of ozone reduction to UV increase is not constant; the ratio varies with latitude and time. A value of two is perhaps appropriate to mid-latitudes during winter but it is clear that this value cannot be used generally.

It is desirable to know the possible increase in radiation at all wavelengths in the UV-B and ideally these increases should be weighted by the action spectrum for skin cancer. However, as this spectrum is not available we have used that of mild sunburn or erythema[9]. Ideally, we would wish to examine the

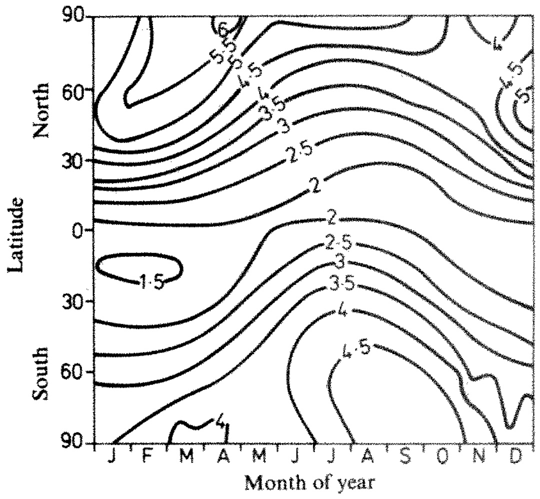

Fig. 1 Latitude–time cross-section of the percentage depletion in the total ozone amount in 1992 using the mean 1973–76 CFC production rates and the Oxford University two-dimensional model.

0028–0836/80/300373—03$01.00

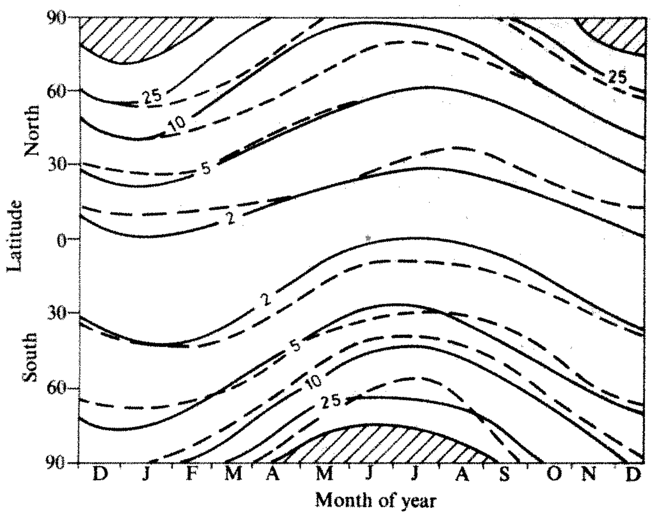

Fig. 2 Percentage change in UV radiation intensity in a narrow wavelength range centred at 310 nm resulting from CFC usage at 1992. Dashed line, calculations using a two-dimensional model; solid line, calculations using a simple UV radiation scheme.

perturbation in erythemally-weighted UV–B dose when the ozone depletion from CFC release reaches its steady state. Because of the many tens to hundreds of years that would be required and because of the detailed horizontal and vertical coverage in the two-dimensional calculations, the cost of running the model to steady state was considered prohibitive. However, the extrapolation of such predictions can be readily achieved by simple scaling up Fig. 1. A steady-state global ozone depletion of 13 ± 3% was selected on the basis of several UK modelling studies[10]. The slight annual increase in ozone depletion apparent in Fig. 1 during 1992, amounts to about a factor of 1.1–1.2. This slight upward drift when extrapolated into steady state introduces errors in the ozone depletion which are small in comparison with the errors in the chosen value itself.

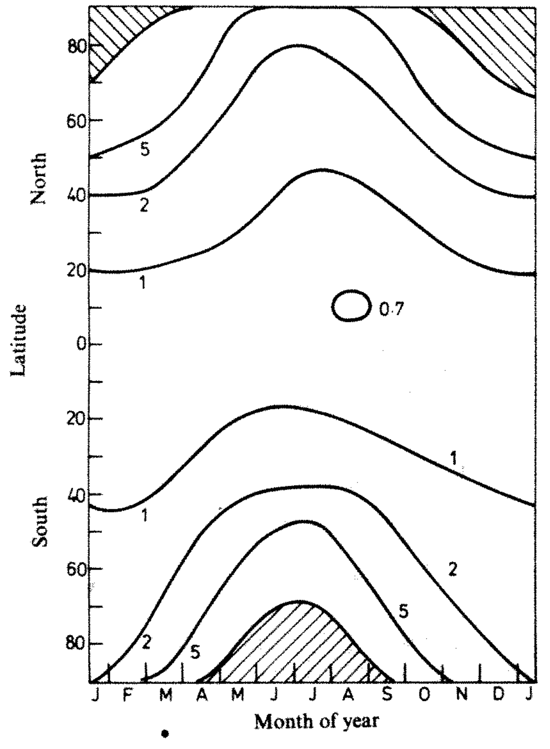

Fig. 3 Ratio of increase in erythemally-weighted UV–B dose to decrease in total ozone amount resulting from CFC usage.

The results shown in Fig. 1 were extrapolated to steady state with respect to CFC release, giving a global ozone depletion of ~13%. The radiation calculations including scattering were then used to compute the increase in the erythemally-weighted UV–B dose at steady state. A global increase of about 12% was found. Figure 3 shows the latitude–time section of the ratio of the percentage increase in UV–B dose to ozone depletion. Only in middle latitudes during winter does the ratio approach a value of 2 and for much of the globe the value is < 1, such that the global ratio, as implied above, is about unity.

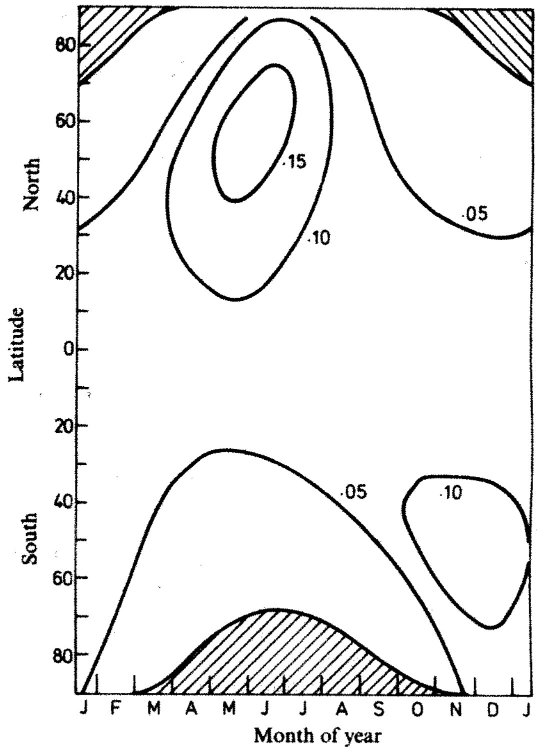

Fig. 4 Ratio of increase in erythemally-weighted UV-B dose from CFC usage to the dose at the Equator.

In high latitudes, the ratio does become larger and the significance of this is interesting. In Fig. 4 the increase in erythemally-weighted UV–B dose at the extrapolated steady state is compared with the dose at the Equator. The larger percentage increases in high latitudes seem to be of little significance when compared with the radiation reaching equatorial latitudes. However, plant and animal life in these high latitude regions coexist with small radiation doses so that we cannot necessarily infer that these changes will have only a small effect.

We conclude that no simple relationship exists between decreased stratospheric ozone and increased surface UV–B dose. The results of radiation calculations in steady-state one-dimensional models for a particular latitude should be treated with caution. Significant variations in the increased dose as a function of latitude and season have been demonstrated here. Inclusions of latitudinal and temporal effects will evidently be important in assessing the biological and botanical effects of possible future ozone depletions.

This work was sponsored by the Department of Environment.

Received 22 February; accepted 25 April 1980.

1. Johnston, H. S. *Science* **173**, 517 (1971).
2. Molina, M. J. & Rowland, F. S. *Nature* **249**, 810–812 (1974).
3. Crutzen, P. J. *Ambio* **3**, 201–210 (1974).
4. Council on Environmental Quality, Fluorocarbons and the Environment (USGPO, Washington DC, 1975).
5. Hammon, A. L. & Maugh, T. H. *Science* **186**, 335–338 (1974).
6. Pyle, J. A. *Nature* **271**, 42–43 (1978).
7. Pyle, J. A. *WMO Publ.* No. 511, 239–246 (1978).
8. Green, A. E. S., Sawada, T. & Shettle, E. P. *Photochem. Photobiol.* **19**, 251–259 (1974).
9. Komhyr, W. D. & Machta, L. *The Perturbed Troposphere of 1990 and 2020* (Department of Transportation, Washington DC, 1973).
10. Department of Environment, *Chlorofluorocarbons and their Effect on Stratospheric Ozone* (HMSO, London, 1979).

ELF radio signals in the auroral ionosphere generated by non-linear demodulation of LF and/or MF transmissions

T. Turunen

Geophysical Observatory, Sodankyla, Finland

P. S. Cannon[*] & M. J. Rycroft[†]

Department of Physics, The University, Southampton, UK

We have conducted experiments measuring ELF and VLF radio signals in the afternoon to early morning (local time) between 24 March and 4 April 1979 in Northern Scandinavia. Apart from those of a natural origin (atmospherics, chorus, and so on), we received timing signals, six pips which occurred on the hour UT; the duration of each pip, of frequency 1 kHz ± 0.5 Hz, was 105 ± 8 ms. A spectrogram of these is shown in Fig. 1. We have established that these are not due to non-linear demodulation of strong higher frequency radio signals in any part of the equipment. We consider that they are produced by non-linear demodulation of signals from two or more amplitude modulated transmitters in the USSR operating at 173, 200, 236, 263 and 657 kHz. The demodulation occurs only during enhanced auroral electrojet activity.

The equipment primarily used in this study involved three goniometer ELF/VLF receivers, one located at Sodankyla (Finland), one at Tromsø (Norway) and one at Arjeplog (Sweden). All stations are within the auroral zone. The goniometer system, described in detail by Bullough and Sagredo[1] and Jarvis[2], uses loop antennas, of area 58m^2; the goniometer modulation frequency was 27.5 Hz. Some measurements were made in parallel at Sodankyla using a VLF receiver designed at the Sodankyla Geophysical Observatory. This receiver was fed from a long (500 m) wire antenna. Additionally an ELF receiver (bandwidth 1 Hz–1 kHz), fed by a multiturn loop antenna, was operated during certain periods at Tromsø. Pips were detected by all these independent measuring systems. The ELF/VLF goniometer at Arjeplog was unfortunately disturbed by local interference at 1 kHz; thus recordings made there could not be used for detailed study.

As well as the timing pips, distorted music, distorted speech and station identifiers were occasionally heard. Broadcast band monitoring and subsequent reference to the World Radio and TV Handbook[3] identified the Russian First and Second Programmes on 173, 200, 236, 263 and 657 kHz as being the cause of these signals and, presumably, of the pips; timing signals were being transmitted on at least some of the above mentioned frequencies every time the 1-kHz pips were detected. Some of the stations transmitting these programmes are within 1,500 km of Sodankyla; these are Kaliningrad (173 kHz, 1 MW), Moscow (173 kHz, 500 kW), Syktyvkar (173 kHz, 300 kW), Leningrad (200 kHz, 150 kW), Moscow (200 kHz, 100 kW), Leningrad (236 kHz, 1 MW), Arkhangelsk (236 kHz, 150 kW), Moscow (263 kHz, 2 MW) and Murmansk (657 kHz, 150 kW) (Fig. 2). The field strength of the 173-kHz transmissions was measured by J. Sivusaami (personal communication) at Sodankyla during the daytime on 3 April 1979, and found to be $112\ \mu\text{V m}^{-1}$.

After completing the field experiments, 1 kHz amplitude modulated signals were injected into the goniometer receiving system, using a dummy aerial. Even with signals 52 dB stronger than those measured at 173 kHz, no demodulated output at 1 kHz was noted. Thus we conclude that the receiving system was linear and that the demodulation observed did not take place in the equipment.

The period of the experiment was characterized by two different levels of local geomagnetic activity. From 14 to 21 March, when no pips were recorded, the daily sum of K_{HDZ} indices, measured at the Sodankyla Geophysical Observatory, varied between 2 and 20. From 22 March to 4 April the corresponding values varied between 20 and 45 and, with the exception of 1 April, pips were recorded at least once each day. We conclude that pips were recorded only when the daily magnetic activity was moderately high. The probability of pips occurring is greatest in the local evening sector, at 19 and 20 UT. Only one measurement was available at 18 UT. Inspection of STARE (Scandinavian Twin Auroral Radar Experiment[4]) data and magnetograms from Sodankyla and Kiruna shows that an active auroral zone current system was always nearby during the times of pip occurrence. Additionally, in cases when the source location was possible, this location probably fell within the eastward electrojet.

On six occasions the signal-to-noise ratio was high enough to allow the determination of the azimuthal bearings of the 1-kHz signals both from Sodankyla and Tromsø, enabling the source to be located by goniometer triangulation. On five occasions the sources were approximately the same. Figure 3 shows this location with the worst case envelope of standard errors. The sixth location is also shown with its error diamond. On three more occasions a bearing angle, with 180° ambiguity, was obtained from Sodankyla. These directions are also shown in Fig. 3. They do not coincide with the direction of the five cases having roughly the same source location. The group of five events from the same location occurred at 19 or 20 UT; the sixth location was determined at 22 UT. Two of the directions determined from Sodankyla only are at 19 UT and the other at 21 UT. Two of the measurements belonging to the group of five events of the same source location were measured on the same day.

We summarize the results obtained as follows. During times of active auroral zone currents, and providing that the daily magnetic activity has been relatively high, there is a high probability of the occurrence of pips in Northern Scandinavia. These signals are considered to be due to a demodulation (self-detection) effect (in the lower ionosphere) of certain LF (and MF) AM broadcasting stations transmitting hourly time marks at 1 kHz within the programme schedule of the Russian Internal Service First and/or Second Programmes. The probability of their occurrence is highest around 19 and 20 UT, but a high probability at 18 UT is not ruled out, because of a data gap. At these times the signal-to-noise ratio is sometimes good enough to indicate that the signal source has a favoured location in the ionosphere (shown in Fig. 3) and that this location does not change with time; there are also other possible locations of the source.

Experimental evidence for the demodulation of HF radio signals in the presence of auroral electrojets has been reported by Kapustin *et al.*[5]. Theoretical treatments for the generation of ELF/VLF waves in the auroral ionosphere have been published

---

Present address: [*]Marconi Space and Defence Systems, Portsmouth, UK; [†]NERC British Antarctic Survey, Cambridge, UK.

0028–0836/80/300375—03$01.00

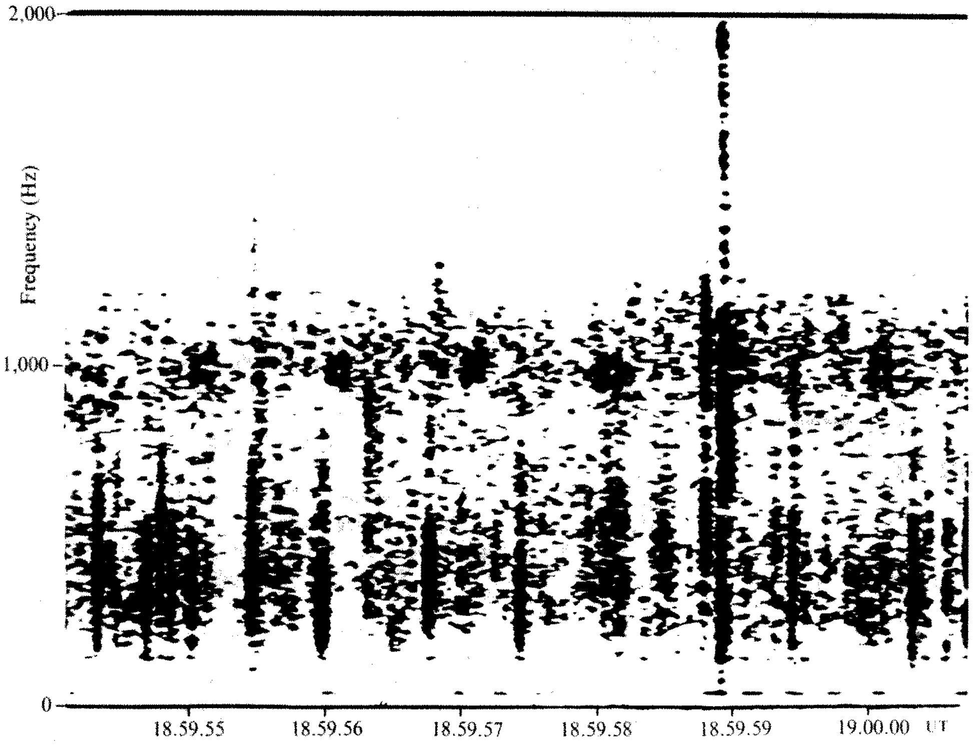

Fig. 1 Spectrogram showing atmospherics and six 1-kHz pips; frequency splitting of the signal, into upper and lower sidebands 55 Hz apart, is due to the goniometer modulation.

by Stubbe and Kopka[6,7] and by Kapustin *et al.*[5], and in the references cited therein. It is proposed there that ELF/VLF radio waves can be generated after heating the lower ionosphere with a strong HF wave having amplitude modulation at ELF/VLF. The modulation causes periodic changes in electron temperature which cause corresponding changes in the Hall and Pedersen conductivities. As a consequence, an a.c. component, at the frequency of the periodic heating, is formed in the auroral electrojet, which radiates a wave at the heating frequency. Stubbe and Kopka[6,7] consider the case when a limited area of auroral ionosphere is heated by a vertical narrow beam radio transmission at HF which can penetrate both the D and E layers in most conditions. This also applies to the experimental arrangements of Kapustin *et al.*[5].

We believe that we have found a basically similar phenomenon, but caused by obliquely propagating amplitude modulated LF and/or MF transmissions acting in the lower portion of the auroral D-layer. In the case of one transmitting station, maxima of the heating effect are located at any instant at positions where the maxima of the modulation of the direct wave and waves after experiencing several sky and ground reflections are essentially in phase with each other. When the same programme is transmitted from two stations an interference pattern is formed, with maxima in the heating power moving along roughly hyperbolic trajectories in space. The positions of these trajectories depend on the modulation frequency. Non-linear demodulation occurs only in regions where the appropriate ionospheric conditions are satisfied.

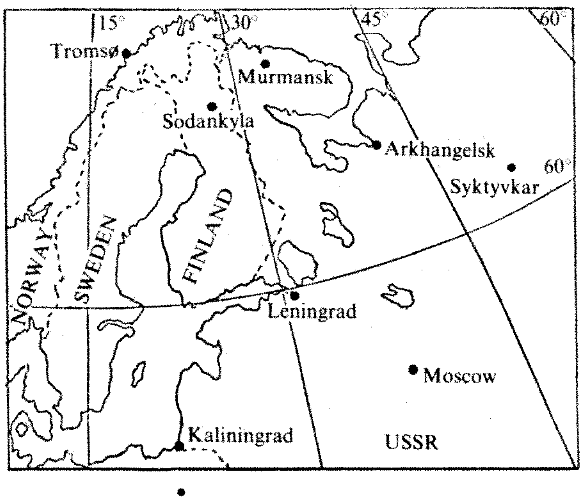

Fig. 2 Mercator projection of Scandinavia and North Western USSR, showing Soviet high power LF and MF broadcast stations within 1,500 km of Sodankyla, on 173, 200, 236, 263 and 657 kHz.

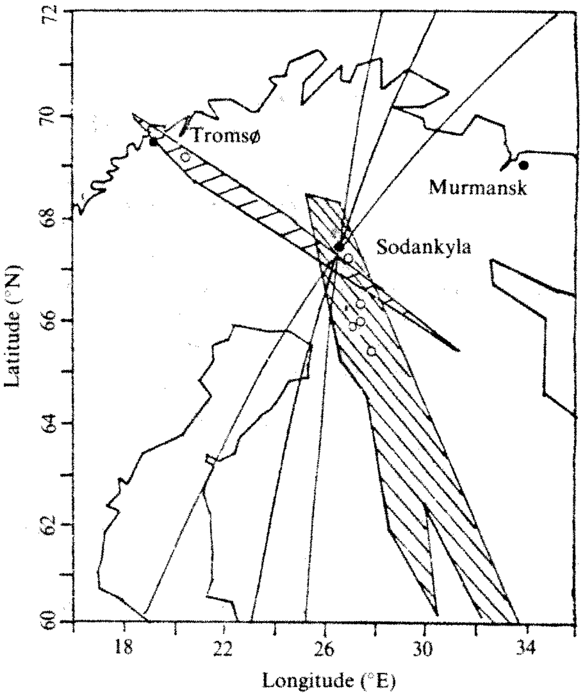

Fig. 3 Cartesian projection of Northern Scandinavia showing the positions (○) of the sources in the ionosphere of the 1-kHz pips, with the worst case error envelopes (hatched area). Additionally, three bearings with 180° ambiguity and a typical error of ±6°, are shown from Sodankyla.

In the case of three stations there are a few particular areas, which remain fixed, where the crests of the modulated waveforms occur and where the periodic heating maximizes. For four or more stations, the extra stations may, depending on their locations and the phases of modulation of their transmitted signals, contribute to the phenomenon.

We consider that at 1 kHz a proper phasing of the signals from at least three stations is obtained in the area in which we have located five sources. We then explain our discovery that pips occur only when the daily magnetic activity is above a certain threshold by this preferred area lying in the electrojet. On quiet days the main current system lies at higher latitudes beyond the particular area mentioned. The distortion of music or speech occurs because sources at different modulating frequencies have different fixed locations; not all of these may lie in areas suitable for ELF/VLF wave generation. This gives rise to a complicated and spectrally varying weighting of the signal. Other such areas may also be invoked to explain the sixth location shown in Fig. 3 and the three signals, observed only at Sodankyla, which had quite different propagation directions.

We thank our colleagues who took part in the present observational programme, and also members of the Measuring Station of the Finnish Broadcasting Company for measurements of various LF and MF transmitter field strengths.

Received 28 January; accepted 5 June 1980.

1. Bullough, K. & Sagredo, J. L. *Planet. Space Sci.* **21,** 899 (1973).
2. Jarvis, M. J. thesis, Univ. Southampton (1976).
3. *World Radio and TV Handbook* (Billboard, London, 1979).
4. Greenwald, R. A., Weiss, N., Nielsen, E. *Radio Sci.* **13,** 1021 (1978).
5. Kapustin, I. N. *et al. JETP Lett.* **25,** 228 (1977).
6. Stubbe, P. & Kopka, H. *J. geophys. Res.* **82,** 2319 (1977).
7. Stubbe, P. & Kopka, H. *Ionospheric Modification Experiments in Northern Scandinavia—a Description of the Heating Project* (Max Planck Institute für Aeronomie, MPAE-W-02-79-04, 1979).

The pear-shaped section of the Earth

D. G. King-Hele*, C. J. Brookes† & G. E. Cook*

* Royal Aircraft Establishment, Farnborough, Hants GU14 6TD, UK
† University of Aston, Gosta Green, Birmingham B4 7ET, UK

The Earth's gravitational field, and hence the shape of the Earth's sea-level surface, the geoid, can be determined from analysis of the motion of artificial satellites in orbit about the Earth. The method is particularly powerful in revealing the longitude-averaged meridional profile of the geoid, that is, an average slice through the poles, which from its north–south asymmetry is often called 'pear-shaped'. We now report an improved determination of this profile, which should be accurate to about 50 cm at latitudes up to 86°, and replaces our previous evaluation[1,2].

The Earth's gravitational potential may be expressed as the sum of (1) an infinite series of zonal harmonics independent of longitude, and (2) a double infinite series of tesseral harmonics, dependent on both latitude and longitude. Here we are only concerned with (1), and we express the longitude-averaged potential at an exterior point distant r from the Earth's centre at geocentric latitude ϕ in the standard form[3]

$$\bar{U} = \frac{\mu}{r}\left\{1 - \sum_{l=2}^{\infty} J_l \left(\frac{R}{r}\right)^l P_l(\sin\phi)\right\} \qquad (1)$$

where μ is the gravitational constant for the Earth, 398,600 km^3 s^{-2}, R is the equatorial radius, 6,378.14 km, and $P_l(\sin\phi)$ is the Legendre polynomial of degree l and argument $\sin\phi$. The J_l are constant coefficients: $J_2, J_4, J_6, \ldots$ express the effects of harmonics symmetrical about the Equator; J_3, J_5, $J_7, \ldots$ express the effects of north–south asymmetry, and it is these odd zonal harmonics that determine the pear-shape tendency of the Earth.

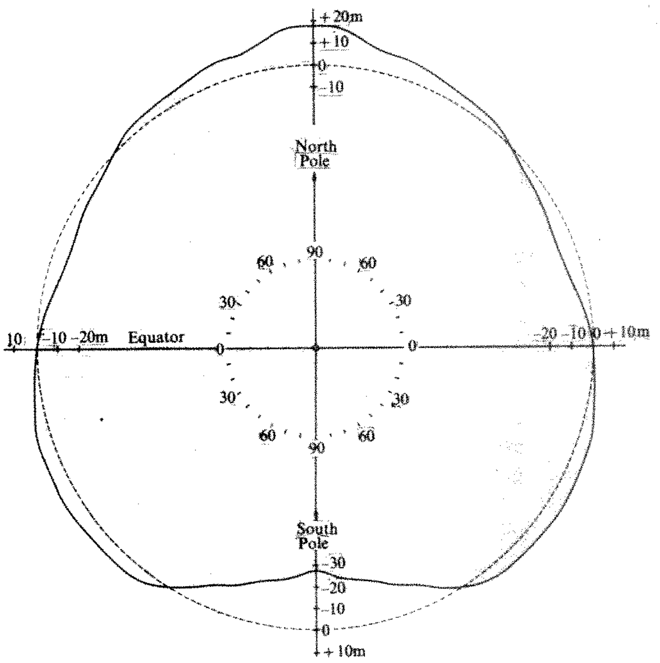

Fig. 1 Height of the meridional geoid section (solid line) relative to a spheroid of flattening 1/298.25 (dashed line) as given by our nine-coefficient set of odd harmonics and GEM 10B even harmonics.

A major effect of the odd zonal harmonics on satellite orbits is to alter the distance of perigee from the Earth's centre: although the north–south asymmetry of the Earth only amounts to about 40 m, it produces an oscillation several kilometres in amplitude. We have evaluated sets of odd zonal harmonics by analysing such oscillations in 28 satellite orbits, from near-equatorial to polar. Previously there was a lack of accurate orbits at inclinations near 63.4°, where the oscillation becomes very large. So two suitable satellites, Cosmos 248 and Cosmos 373 at inclinations 62.2° and 62.9°, have been specially observed optically for more than five years by the Hewitt camera at Malvern, the kinetheodolite at the South African Astronomical Observatory, and visual observers in Britain and elsewhere. The orbits of these satellites were determined from about 5,000 observations[4,5], and were used to evaluate the amplitudes of the oscillations in perigee distance, which amounted to 58.7 ± 0.2 km for Cosmos 373.

The methods for evaluating J_3, J_5, $J_7, \ldots$ were basically similar to those previously used, but with significant improvements in the theory. More than 500 solutions were computed, and the following nine-coefficient set is selected as the best[6]:

$$\begin{array}{lll}
10^9 J_3 = -2{,}530 \pm 4 & 10^9 J_9 = -90 \pm 7 & 10^9 J_{15} = -20 \pm 15 \\
J_5 = -245 \pm 5 & J_{11} = 159 \pm 9 & J_{17} = -236 \pm 14 \\
J_7 = -336 \pm 6 & J_{13} = -158 \pm 15 & J_{19} = -27 \pm 19
\end{array}$$

This set of values has standard deviations about 40% smaller than in the previous eight-coefficient set[2], and differs from the previous values by less than the sums of their standard deviations.

Figure 1 shows the profile of the longitude-averaged meridional section as given by this set of odd zonal harmonics and the even harmonics of the Goddard Earth Model 10B (ref. 7). The heights shown in the diagram are relative to a spheroid of flattening 1/298.25, which is drawn as a broken line. With the new profile, sea level at the north pole is 17.84 m above the spheroid, and sea level at the south pole is 27.23 m below the spheroid. So the 'pear-shape asymmetry', the north polar minus the south polar radius, is 45.1 m, compared with 44.7 m from the previous solution.

We have also derived 8- and 14-coefficient solutions as alternatives, but they give almost identical results, with differences of less than 30 cm in geoid height up to 86° latitude.

Comparison with the corresponding geoid profile from the most recent comprehensive gravity field[7], GEM 10B, which has a completely independent set of odd zonal harmonics, shows differences of less than 80 cm up to latitudes of 85°, the average difference being about 25 cm. The effect of changing the even harmonics from those of GEM 10B to the most recent set derived at the Smithsonian Astrophysical Observatory shows an average difference of only 20 cm. For these and other reasons, we suggest that the profile of Fig. 1 should be accurate to 50 cm up to latitudes of 86°. Over the remaining 0.2% of the Earth's surface very near the poles, the errors may be larger, possibly up to 1.5 m: basically, this increased error arises because there is so little of the Earth's mass at these latitudes.

Although the longitude-averaged geoid profiles agree well, the predicted amplitudes of the oscillations in perigee distance do not: at certain inclinations, the amplitudes given by our zonal harmonics differ from those given by GEM 10B by up to 350 m, even if the singularity near 63.4° inclination is excluded. So further improvements in the values of the zonal harmonics, utilizing satellites in chosen orbits specially observed, will be needed if orbital models capable of centimetric accuracy, to match centimetric laser observations, are ever to be developed.

Received 28 April; accepted 3 June 1980.

1. King-Hele, D. G. & Cook, G. E. *Nature* **246,** 86 (1973).
2. King-Hele, D. G. & Cook, G. E. *Planet. Space Sci.* **22,** 645 (1974).
3. Merson, R. H. & King-Hele, D. G. *Nature* **182,** 640 (1958).
4. Brookes, C. J. & Holland, D. *Planet. Space. Space Sci.* **26,** 611 (1978).
5. Brookes, C. J. *Planet. Space Sci.* **24,** 711 (1976).
6. King-Hele, D. G., Brookes, C. J. & Cook, G. E. *Geophys. J.R. astr. Soc.* (in the press).
7. Lerch, F. J. *et al. Paper Spring A. Meet. Am. Geophys. Un.* Florida (1978).

West Antarctic ice sheet fluctuations in the Antarctic Peninsula area

D. E. Sugden & C. M. Clapperton

Department of Geography, University of Aberdeen,
Aberdeen AB9 2UF, UK

The West Antarctic ice sheet is believed to be inherently unstable because much of it is grounded below sea level[1–4]. It has been suggested that the ice sheet has withdrawn from its late Wisconsin maximum position, grounded at the edge of the continental shelf, and is now undergoing collapse as a delayed response to the warming and sea-level rise of the Holocene[5], and that the ice sheet is likely to collapse shortly in response to rising CO$_2$ levels in the atmosphere[6]. We present here some geomorphological evidence from Alexander Island and the Antarctic Peninsula which does not agree with either hypothesis. Rather, following deglaciation from the Wisconsin maximum, there was less ice than at present around 8,000 yr ago. The ice shelf in George VI Sound has built up subsequently.

Alexander Island is a mountainous block of country approximately 450 km from north to south and 300 km from east to west. Jagged mountains rise to altitudes exceeding 3,000 m in the north of the island but more subdued tracts of dissected plateau 250–800 m altitude are more characteristic of the south and east. These topographical contrasts partly reflect the island's geology for, whereas the spectacular Elgar Mountains of the north are composed of plutonic rocks, the bulk of the island's plateau scenery in the south and east coincides with extensive areas of sedimentary strata, particularly shales, sandstones, volcanoclastics and conglomerates[7–9]. The adjacent part of the Antarctic Peninsula, similarly aligned from north to south, is 200 km across and includes mountains rising to 3,000 m. As on Alexander Island, the land is more extensively buried by ice fields towards the south. The Peninsula is geologically distinct from Alexander Island in that the bulk of it is composed of plutonic and volcanic rocks and a variety of gneisses, granites and lavas predominate[10]. It is believed that block faulting has separated the two land areas resulting in the trench of George VI Sound which is over 20 km wide, and 500 km long.

The Peninsula is covered by a northward extension of one of the three main ice domes comprising the West Antarctic ice sheet and from its axis the ice drains westwards and eastwards into ice shelves. The western ice shelf, 100–500 m thick, flows westwards across George VI Sound and abuts the east coast of Alexander Island where it is depositing a conspicuous moraine. This ice shelf terminates at either end of the Sound in environmental conditions where summer temperatures rise to within a few degrees of 0 °C. As such the ice shelf in George VI Sound is in a marginal environment for its survival[11]. Alexander Island itself supports an ice cap and ice fields which discharge outwards to each coast. Outlet glaciers flowing into George VI Sound ice shelf are quickly dominated by the more powerful ice flow from the Peninsula and are almost immediately deflected northwards and southwards.

Evidence of past glacial maximum conditions points to increased ice thicknesses on both Alexander Island and the Antarctic Peninsula, with both areas acting as independent centres of outflow. On eastern Alexander Island the evidence is in the form of glacial trough alignment, the direction and position of striations on plateau surfaces and interfluves, and erratic fans which can be traced from distinctive bedrock outcrops. Examples of these features in the Ablation Point area show how flow was consistently eastwards towards George VI Sound (Fig. 2). Compatible with this reconstruction is the absence of Peninsula erratics on the eastern plateaux of Alexander Island; although Peninsula-derived granites and gneisses are clearly identifiable in the moraine flanking the present ice shelf in George VI Sound, none were found above an altitude of 85 m. On Plateau surfaces in the Batterbee Mountains of the Peninsula across from Alexander Island the flow of a former ice cover was westwards into the Sound and then northwards parallel with the Sound. Clear evidence for this comes from roches moutonnées, striations, sub-glacial meltwater channels and the slope of high-level lateral moraines which cross the plateau at 400–670 m altitude (Fig. 3).

Previous reconstructions of maximum ice conditions in the late Wisconsin for this part of Antarctica show the ice flowing from the Peninsula axis across Alexander Island to the edge of the continental shelf on its west side[5,12]. The field evidence from eastern Alexander Island indicates ice-flow directions directly opposite to those implied by these previous reconstructions and implies that the ice masses were thinner, consisting of separate domes that were based on Alexander Island and on the Peninsula and becoming confluent in George VI Sound.

Some indication of the age of the last maximum glaciation was obtained from a shelly till deposit found on a spur 3 km north of Two Step Cliffs and lying between 94 and 114 m above the present ice shelf. The shells consist of fragments of *Hiatella solida*. They lie in a till with striated clasts and a typical glacial matrix (mean ϕ 0.21, sorting 4.05, skewness 0.39, kurtosis 0.82). Analysis of the lithology of the clasts and of the magnetic susceptibility of the matrix suggests the till is derived from sedimentary rocks characteristic of Alexander Island and is quite different to the Peninsula-derived ice shelf moraines in the vicinity originating on igneous rocks. The outer fraction of the shells gave a radiocarbon age of 32,160 ± 360 yr and the inner fraction 30,600 ± 660 yr (SSR 1499). That such an old radiocarbon age is likely to be a minimum was confirmed by the results of amino acid analysis on three separate shells which yielded total D/L ratios of 0.169, 0.113 and 0.147 (AAL 1297).

0028–0836/80/300378—04$01.00

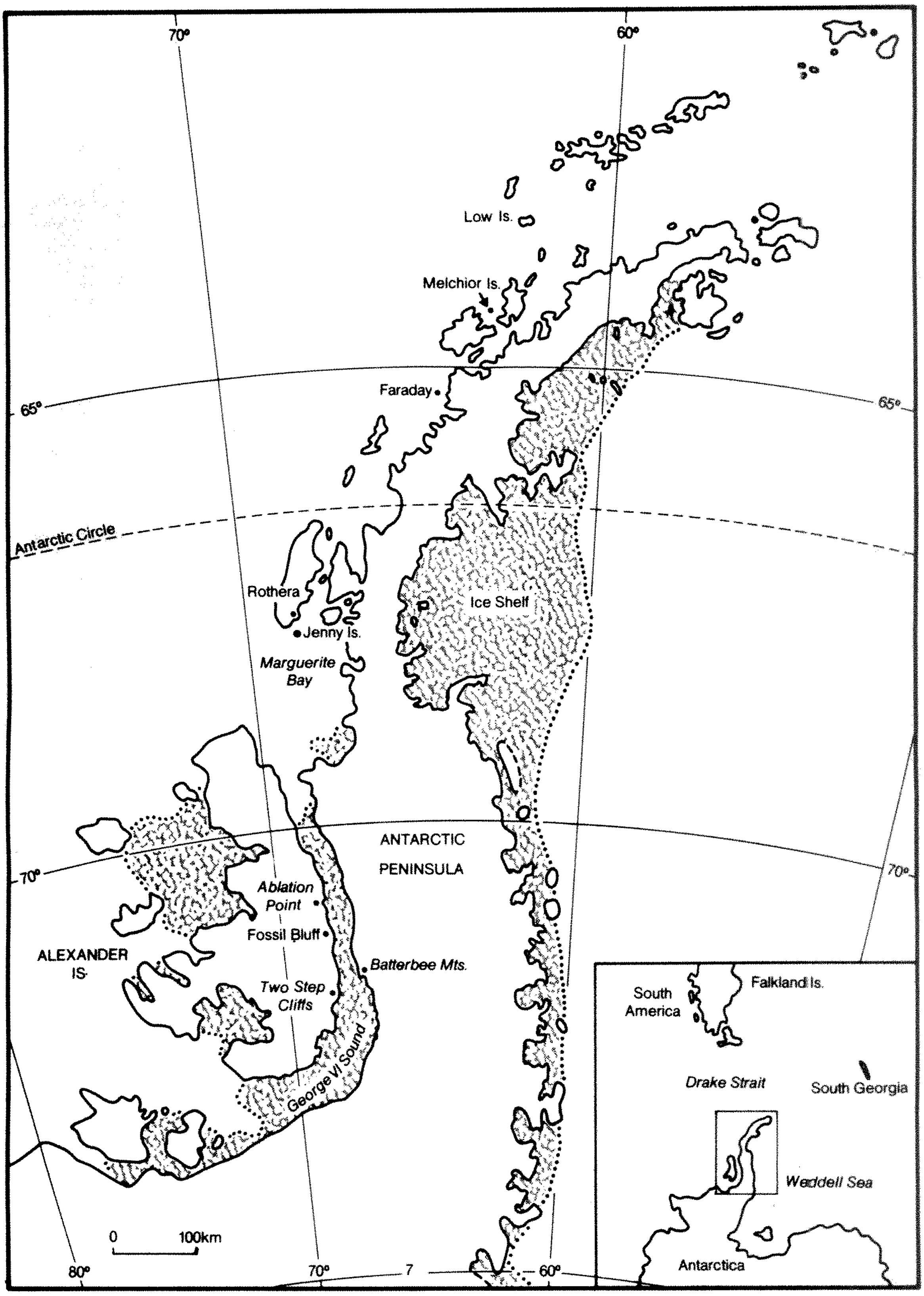

Fig. 1 The Alexander Island–Antarctic Peninsula area of West Antarctica.

We cannot place accurate absolute dates on these values without knowing the precise thermal history of the shells since their death. Nevertheless, a reconstruction of the most likely thermal history (in seawater or beneath a warm-based glacier) produces an age which is compatible with that of the last interglacial (G. H. Miller, personal communication). We can go even further and suggest that at the time of their growth the Sound was free of an ice shelf. The basis of this suggestion is the discovery from the J9 drill hole through 420 m of the Ross Ice Shelf, 430 km from the open sea, that no living infauna existed and that the sediments contained no animal traces or bioturbations[13]. As George VI Sound Ice Shelf is 300 m thick over 200 km distant from the open sea in the vicinity of Two Step Cliffs, it is reasonable to suggest that shells may be unable to thrive beneath its canopy and must, therefore, reflect open conditions in the Sound.

The most likely explanation of the shelly till is that it was formed by an enlarged ice sheet grounded in George VI Sound and just impinging on Alexander Island on the promontory north of Two Step Cliffs. In such a case the dates imply that the ice cover was substantially thicker in the Wisconsin than at present. In the absence of any alternative moraine limits it seems reasonable to attribute the maximum reconstruction described earlier to this Wisconsin advance.

Evidence of the Holocene history of the ice shelf comes from the moraine which flanks the ice shelf where it abuts onto Alexander Island. The moraine has two components. One is a landward ridge 5–30 m high which apparently contains no ice. The other is immediately adjacent and forms one to three ice-cored ridges. The crests of all the ridges are lower than the overall surface of the ice shelf. At Two Step Cliffs barnacles *Bathylasma corolliforme* (Hoek) were found in the landward of the two ridges. The presence of striated clasts and mechanical analysis of the matrix confirm that the deposit is till but with signs of water activity (mean ϕ 2.09, sorting 4.19, skewness −0.02, kurtosis 0.96). Radiocarbon dating of the outer fraction of the barnacles produced an age of 6,930±60 and the inner fraction 7,200±50 (SRR-1500). If one allows for a correction factor of ~750 yr for the ^{14}C deficiency in Antarctic waters based on radiocarbon dates on modern shells in the Antarctic Peninsula area[14,15] then the adjusted dates come out as 7,700 and 7,950 radiocarbon yr BP. This Holocene age is fully consistent with the results of amino acid analysis which revealed total D/L ratios of 0.028 and 0.01 (AAL 1298). The position and age of the barnacles implies that they were growing in George VI Sound around 8,000 yr ago and that subsequently they have been incorporated in the ice shelf moraine. There are two possible implications pertinent to the Holocene history of the ice shelf. The most likely is that the barnacles were growing in an ice-free Sound ~8,000 yr ago and the ice shelf has built up subsequently. The other less likely possibility is that the

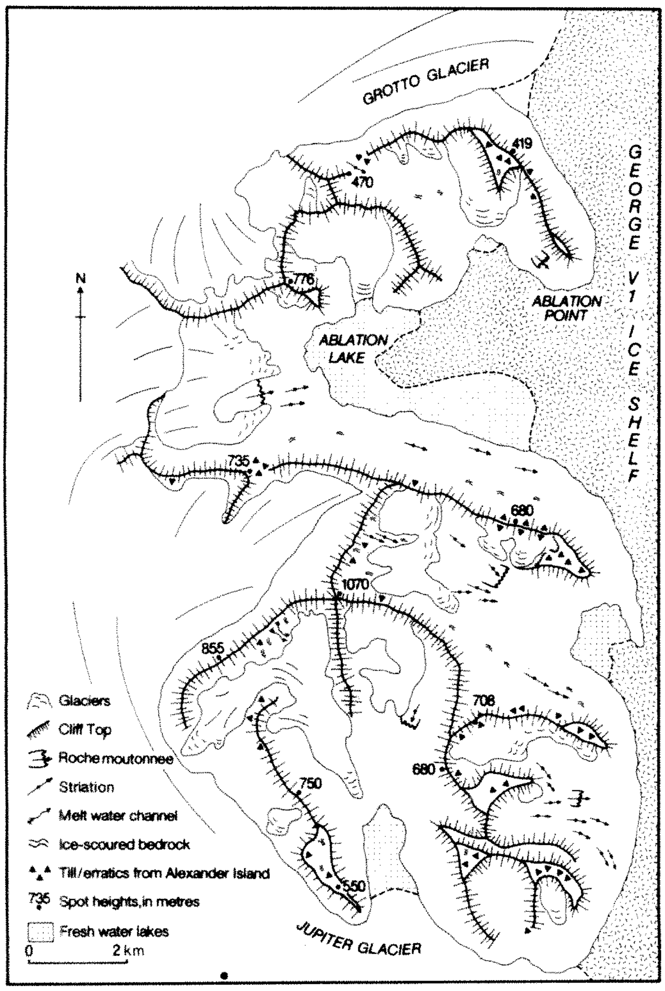

Fig. 2 Evidence of former ice movement from west to east across the Ablation Point area.

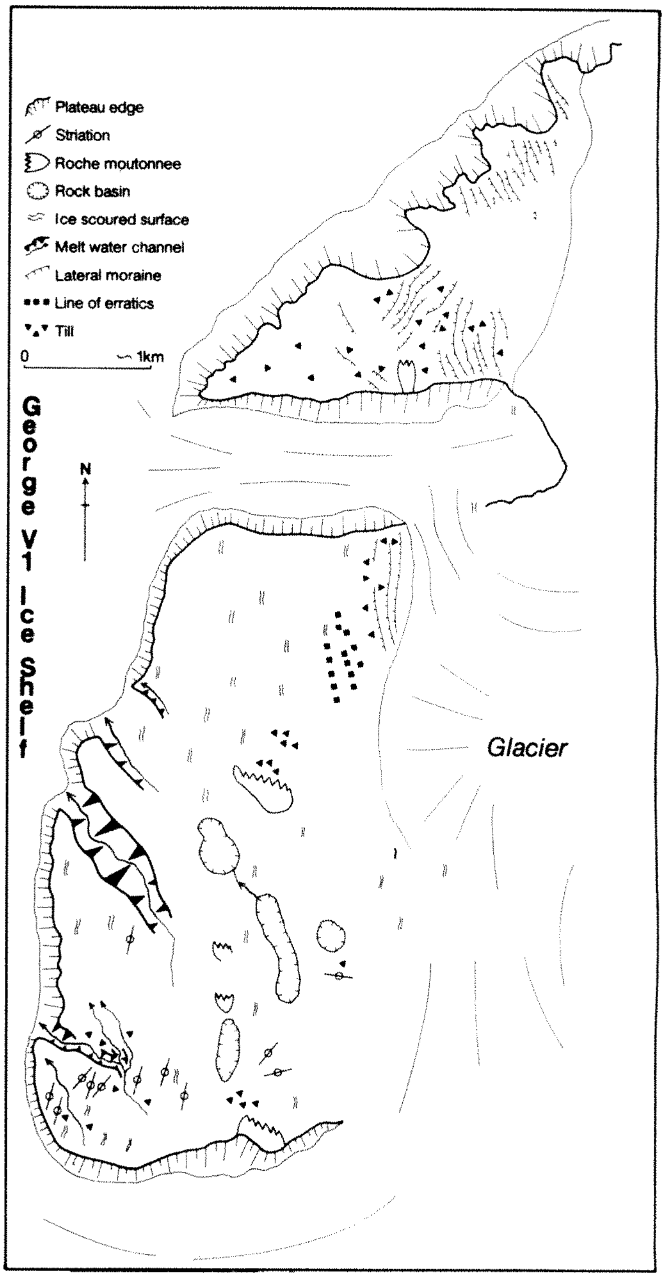

Fig. 3 Evidence of former ice movements sub-parallel to George VI Sound in the Batterbee Mountains area.

barnacles were growing beneath the ice shelf; in this case the implication is that the ice shelf has not been materially thicker than at present for ~8,000 yr (although it is possible that it has been thinner and less extensive).

These results of investigations in the Alexander Island and Antarctic Peninsula area yield five conclusions relevant to the history of the West Antarctic ice sheet.

(1) During the last maximum glaciation separate ice domes were centred over both Alexander Island and the Peninsula. This represents an ice thickness less than that predicted on theoretical grounds in the CLIMAP reconstructions[12].

(2) Amino acid analyses on shells suggest that the last maximum was achieved in the Wisconsin and followed an interval when the Sound may have been free of ice, perhaps during the last interglacial.

(3) George VI Ice Shelf, one of the most sensitive to environmental change in West Antarctica, has apparently reformed in the last 8,000 radiocarbon yr following a period of warmer conditions when the Sound was ice-free.

(4) Ice sheet fluctuations in this part of West Antarctica, especially the signs of a warmer period ~8,000 yr ago, seem to be in phase with world environmental changes as reflected for example by deep sea cores[16] and recent ice cores[17].

(5) With regard to the hypotheses concerning the possible instability of the West Antarctic ice sheet, one can conclude that in this sector: the ice in the last maximum was thinner than previously supposed and that there is no sign of progressive ice sheet collapse; rather there seems to have been an expansion in the last 8,000 yr as George VI ice shelf reformed; the West Antarctic ice sheet is able to survive without the presence of George VI ice shelf; so long as the ice shelf survives, then there is no need to fear imminent West Antarctic ice sheet collapse due to climatic warming as proposed by Mercer.

We thank NERC for financial support, the British Antarctic Survey for logistic support, Drs G. Oliver and W. Newman for identifying the shells, Dr D. Harkness for radiocarbon dating, Dr J. T. Andrews for amino acid analysis and Professor F. Oldfield for magnetic susceptibility measurements.

Received 29 February; accepted 23 May 1980.

1. Hughes, T. *J. geophys. Res.* **78,** 7884–7910 (1973).
2. Weertman, J. *Nature* **260,** 284–286 (1976).
3. Hughes, T. *Rev. Geophys. Space Phys.* **15,** 1–46 (1977).
4. Thomas, R. H., Saunderson, T. J. O. & Rose, K. E. *Nature* **277,** 355–358 (1979).
5. Hughes, T. *Rev. Geophys. Space Phys.* **13,** 502–526 (1975).
6. Mercer, J. H. *Nature* **271,** 321–325 (1978).
7. Horne, R. R. *Br. Antarct. Surv. Bull.* **22,** 61–76 (1969).
8. Bell, C. M. *Br. Antarct. Surv. Bull.* **33 & 34,** 1–16 (1973).
9. Bell, C. M. *Br. Antarct. Surv. Bull.* **39,** 35–44 (1974).
10. Adie, R. J. *Antarctic Research* (eds Priestley, R., Adie, R. J. & Robin, G. de Q.) 118–162 (Butterworths, London, 1964).
11. Mercer, J. H. *Int. Ass. Sci. Hydr.* **79,** 217–225 (1968).
12. Denton, G. H. & Hughes, T. J. (eds) *The Last Great Ice Sheets* (Wiley-Interscience, in the press).
13. Lipps, J. H., Ronan, T. E. & DeLaca, T. E. *Science* **203,** 447–449 (1979).
14. Sugden, D. E. & John, B. S. *Palaeoecology of Africa and of the Surrounding Islands and Antarctica*, Vol. 8 (ed. van Zinderen Bakker, E. M.) 139–159 (Balkema, Cape Town, 1973).
15. Harkness, D. D. *Br. Antarct. Surv. Bull.* **47,** 43–59 (1979).
16. Hays, J. D., Imbrie, J. & Shackleton, N. J. *Science* **194,** 1121–1132 (1976).
17. Lorius, C., Merlivat, L., Jouzel, J. & Pourchet, M. *Nature* **280,** 644–648 (1979).

Shelly microfossils near the Precambrian–Cambrian boundary, Mackenzie Mountains, northwestern Canada

S. Conway Morris

Department of Earth Sciences, Open University, Milton Keynes
MK7 6AA, UK

W. H. Fritz

Geological Survey of Canada, 601 Booth Street, Ottawa, Ontario
K1A 0E8, Canada

Our understanding of early metazoan evolution is being revolutionized by recent discoveries of pre-trilobite faunas. A fascinating aspect of this evolution is the appearance and development of metazoan skeletal parts near the Precambrian–Cambrian boundary. Fossils of these parts are best known from the lowermost stage (Tommotian) of the Cambrian in Siberia which contain archaeocyathids and small shelly fossils, the latter commonly of phosphatic composition[1–3]. Although the sudden, in terms of geological time, appearance of metazoan hard parts near the boundary is recognized as an outstanding evolutionary event, none of the proposals given to explain the 'Cambrian explosion' (see refs 4–6) has been widely accepted. Additional information from areas outside Siberia is now needed to broaden our knowledge on early Metazoa, and to assist a geological team, the Precambrian–Cambrian Boundary Working Group of the International Union of the Geological Sciences, that is locating, defining and correlating the Precambrian–Cambrian boundary on a world-wide basis. Here we report the discovery of a small fauna of microfossils near the boundary in the Mackenzie Mountains. New forms are present and a known species is used for correlation with the classic Precambrian–Cambrian sections in Siberia and successions elsewhere.

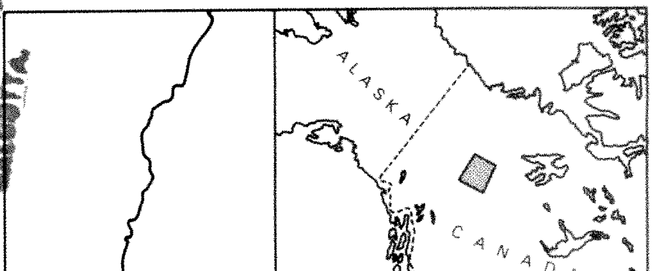

Fig. 1 Map locating sections 35, that contains shelly microfossils at GSC locality 94597, and 33. Section 35 is located between lat. 63°22·5′, long. 128°38.75′ (base of section) and lat. 63°22′, long. 128°35.75′ (top of section).

A sample from the Mackenzie Mountains (Geological Survey of Canada (GSC) locality 94597) collected by one of us (W.H.F.) yielded shelly microfossils after 660 g of limestone was digested in dilute acetic acid ~10%). The sample is from stratigraphic section 35 (ref. 7), located between the Keele and Natla Rivers, Northwest Territories (Fig. 1). Note that the sample came from a horizon 3,065 feet (934 m) stratigraphically below the next youngest fossil locality (GSC locality 94599) (Fig. 2) which is located in the Sekwi Formation[7,8] and yields cf. *Parafallotaspis grata* Fritz, the oldest described trilobite species from North America. GSC locality 95497 is in the middle of a 135 foot (41.4 m) thick limestone unit that has been correlated with map Unit 11 (ref. 7), an informal stratigraphic unit recognized by Blusson[9] a short distance to the east. In addition to the microfossils documented here, stromatolites and burrows were noted[7] at GSC locality 94597. These latter fossils, together with the light colour of the limestone, suggest the sampled limestone was deposited in shallow water.

The following microfossils were obtained: (1) A single specimen of *Protohertzina* cf. *P. anabarica* Missarzhevsky[10] (Fig. 3*a*–*c*). Both ends are broken, but the specimen is otherwise well preserved. *P. anabarica* is the genotype and four other species have been described[10–12]. The genus belongs to a group of phosphatic fossils known as protoconodonts that may form one

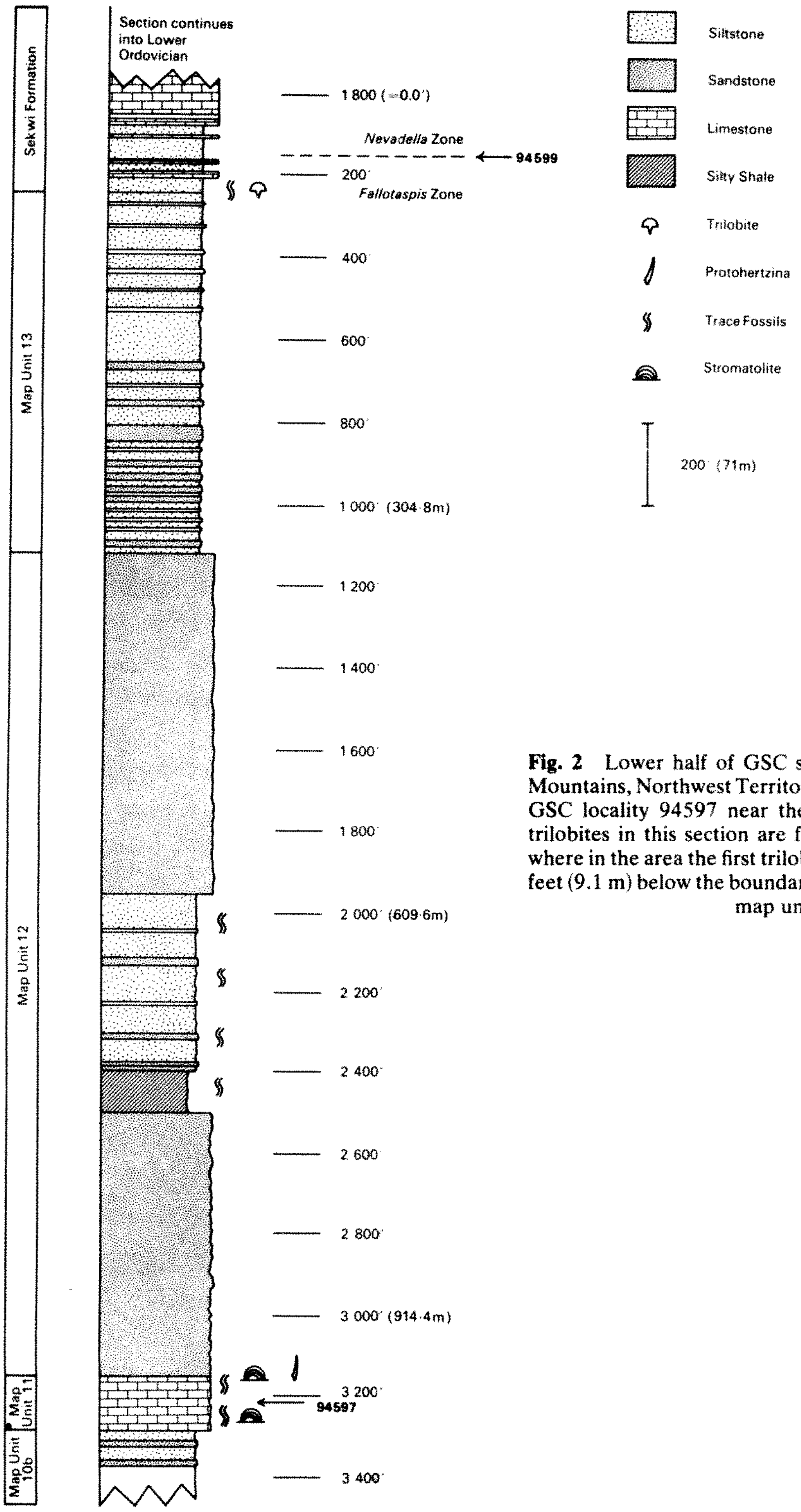

Fig. 2 Lower half of GSC stratigraphic section 35, Mackenzie Mountains, Northwest Territories. The shelly microfossils are from GSC locality 94597 near the base of the section. The earliest trilobites in this section are from GSC locality 94599, but elsewhere in the area the first trilobites occur slightly lower at about 30 feet (9.1 m) below the boundary between the Sekwi Formation and map unit 13 (ref. 8).

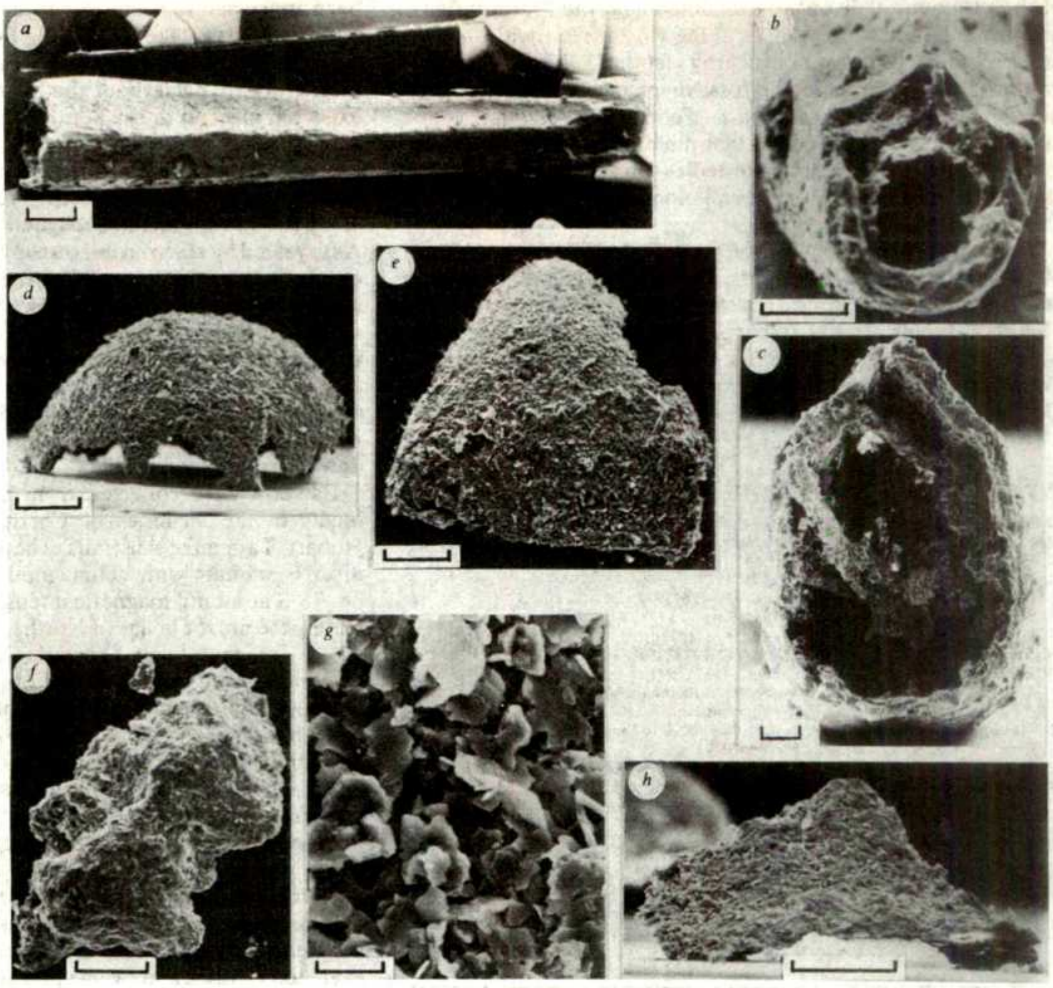

Fig. 3 Scanning electron micrographs of gold–palladium coated microfossils from GSC locality 94597. Each specimen is given a type number for storage in the National Type Fossil Collection, Geological Survey of Canada, Ottawa. *a–c*, *Protohertzina* cf. *anabarica* (GSC 45338). *a*, Posterior view; *b*, transverse section of distal end; *c*, transverse section of proximal end. *d–e*, Silicified concavo–convex microfossils of uncertain systematic position. *d*, Side view of GSC 45339; *e*, top view of GSC 45340. *f–h*, Microfossils, composed of agglutinated clay plates, possibly of foraminifer affinities; *f*, top view of GSC 45341; *g*, detail of exterior surface of GSC 45342 showing clay plates; *h*, side view of GSC 45343. Scale bars, 20 μm (*g*); 100 μm (*b*, *c*); 200 μm (*a*, *d*, *e*, *f*, *h*).

end of an evolutionary series leading to the true or eucondonts[4]. (2) Approximately 12 fossils composed of agglutinated platy grains, apparently of a clay mineral (Fig. 3*g*). The fossils are roughly orthoconical and in basal outline are irregularly oval (Fig. 3*f*, *h*). Several phyla have representatives with agglutinated tests, but the small size of these fossils prompts comparison with protistans and in particular the Foraminifera. The Lower Cambrian *Platysolenites* and *Spirosolenites*, regarded as the earliest agglutinated foraminifers, have a tubular form that is elongate in *Platysolenites* and coiled in *Spirosolenites*[13,14]. The agglutinated foraminifer *Iridia*, which belongs to the primitive suborder Allogromiina[15] has an irregularly hemispherical test, although with pseudochitinous base. As such a base is most unlikely to be fossilized, a comparison between the extant *Iridia* and these fossil forms may be valid (no intimate systematic relationship is at present claimed), and individuals of the latter may have lived adpressed to the substrate with pseudopodia extending from the margins. (3) About 200 silicified fossils with a pronounced concavo–convex shape (Fig. 3*d*, *e*). The degree of convexity varies, but hemispherical types predominate. In basal outline the specimens are usually slightly oval, but more elongate configurations are not uncommon. The lack of diagnostic shape or surface ornamentation precludes any useful speculation on their zoological affinites. This assemblage may well contain several different taxa. Use of very dilute acid (~1%) during rock digestion may produce more complete specimens.

Protohertzina anabarica has been recorded from the Siberian Platform (Anabar Shield) and Kazakhstan (Malij Karatau Ridge)[10]. In the north-west region of the Anabar Shield *P. anabarica* ranges through the latest Precambrian (?) Nemakit-Daldyn (= Manykay) Horizon[10], and in Kazakhstan it occurs in equivalent strata[16]. The Nemakit–Daldyn Horizon, which has been correlated with the upper beds of the Yudoma Suite in the classic Aldan River sections (refs 1, 2 and Rozanov in ref. 17), has a sparse shelly fauna which in addition to protoconodonts includes the worm tubes *Paleolina* and *Anabarites trisulcatus* (ref. 1 and Savitsky in ref. 17). A richer shelly fauna of Tommotian aspect has, however, been discovered close to the top of the Horizon near the type locality for *P. anabarica*[10] on the Kotujkan River in the Anabar Shield[18]. Current Soviet usage[1,2] generally places the Precambrian–Cambrian boundary at or very close to the first appearance of this richer fauna. Microfossils identified as *P. anabarica* have also been reported from the upper part (Huangshandong, Zhongyicun and Siaowaitoushan members; the latter two formerly comprised the Meischucun Formation) of the Tongying Formation[12,19] which is regarded as equivalent to the Tommotian of Siberia.

The presence of *P.* cf. *anabarica* in map unit 11 suggests that it is probably equivalent to part of the Nemakit–Daldyn Horizon or the lowermost Tommotian. Thus, according to current Soviet definition, the unit is close to the Precambrian–Cambrian boundary. If this correlation is correct the equivalents of the Tommotian Stage probably lie within map unit 12 and perhaps 13 (Fig. 2). The possibility remains that *P.* cf. *anabarica* has a higher stratigraphic range in the Mackenzie Mountains, but the great stratigraphic sequence (3,065 feet, 934 m) between *P.* cf. *anabarica* and the lowest Cambrian trilobites indicates otherwise.

Additional samples from the Mackenzie Mountains and elsewhere in the North American Cordillera are being processed, but the paucity of carbonate beds near the Precambrian–Cambrian boundary means that recovery of further microfossils may be limited. Recovery of other microfossils, such as acritarchs, through the use of stronger acids on clastic rocks has only begun and has so far met with limited success. Trace fossils in section 35 and nearby sections[7] should be studied for evidence of the pronounced diversification noted near the Precambrian–Cambrian boundary elsewhere in the world (see review in ref. 20). Preliminary field work at nearby section 33 (Fig. 1) provides grounds for optimism that this fossil diversification also exists in the Mackenzie Mountains (M. Fedonkin, personal communication). It is to be hoped that the diversification events in trace and shelly fossils can be tested against each other thereby improving intercontinental correlation of the Precambrian–Cambrian boundary.

We thank S. Bengtson, J. W. Cowie, G. S. Nowland and S. C. Matthews for helpful comments, J. Taylor, J. Hill, D. Newling and R. Carlton for technical assistance and P. Hammond and A. Mahoney typing. Initial research by S.C.M. was undertaken whilst a Research Fellow of St John's College, Cambridge. W.H.F. publishes with the permission of the Director of the Geological Survey of Canada.

Received 22 April; accepted 3 June 1980.

1. Matthews, S. C. & Missarzhevsky, V. V. *Q. Jl geol. Soc. Lond.* **131,** 289–304 (1975).
2. Rozanov, A. Yu *et al. Trudy̆ Inst. geol. Nauk, Mosk.* **206,** 1–380 (1969).
3. Zhuravleva, I. T. *Am. J. Sci.* **269,** 417–445 (1970).
4. Bengtson, S. *Acta Univ. Upsal.* **415,** 1–71 (1977).
5. Rhoads, D. C. & Morse, J. W. *Lethaia* **4,** 413–428 (1971).
6. Stanley, S. M. *Paleobiology* **2,** 209–219 (1976).
7. Fritz, W. H. *Geol. Surv. Pap. Can.* 78–23, 1–19 (1979).
8. Handfield, R. C. *Geol. Surv. Pap. Can.* 68–47, 1–23 (1968).
9. Blusson, J. L. *Geol. Surv. Pap. Can.* 71–22, 1–17 (1971).
10. Missarzhevsky, V. V. in *Palaeontological and Biostratigraphical Problems in the Lower Cambrian of Siberia and the Far East* (in Russian) 53–57 (1973).
11. Missarzhevsky, V. V. *Trans. Soviet–Mongolian palaeont. Expedn* 10–19 (1977).
12. Qian, Yi. *Acta palaeont sin.* **16,** 255–278 (1977).
13. Føyn, S. & Glaessner, M. F. *Norsk geol. Tidsskr.* **59,** 25–46 (1979).
14. Glaessner, M. F. *Bull. Bur. Miner. Resour. Geol. Geophys. Aust.* **192,** 61–65 (1978).
15. Loeblich, A. R. & Tappan, H. in *Treatise on Invertebrate Paleontology* Part C (Protista 2) (1964).
16. Mambetov, A. M. & Repina, L. N. in *Biostratigraphy and Palaeontology of the Lower Cambrian of Siberia* (in Russian), 98–138 (1979).
17. Cowie, J. W. & Glaessner, M. F. *Earth Sci. Rev.* **11,** 209–251 (1975).
18. Shishkin, B. B. *Geol. Geofiz. Novosibirsk* **4,** 111–114 (1974), (English translation in *Soviet geol. Geophys.* **15,** 97–99).
19. Qian, Yi, Chen, Menge & Chen, Yi-yuan *Acta paleont. sin.* **18,** 207–230 (1979).
20. Alpert, S. P. *Geol. Jl Spec. Issue* **9,** 1–8 (1977).

South-seeking magnetotactic bacteria in the Southern Hemisphere

R. P. Blakemore*, R. B. Frankel† & Ad. J. Kalmijn‡

* Department of Microbiology, University of New Hampshire, Durham, New Hampshire 03824
† Francis Bitter National Magnet Laboratory, Massachusetts Institute of Technology, Cambridge, Massachusetts 02139
‡ Department of Biology, Woods Hole Oceanographic Institution, Woods Hole, Massachusetts 02543

Several species of aquatic bacteria which orient in the Earth's magnetic field and swim along magnetic field lines in a preferred direction (magnetotaxis) have been observed in marine and freshwater sediments of the Northern Hemisphere[1,2]. Their orientation is due to one or more intracytoplasmic chains of single-domain magnetite particles[3]. These linearly arranged particles impart a net magnetic dipole moment to the bacterium, parallel to the axis of motility. Northern Hemisphere magnetotactic bacteria with unidirectional motility swim consistently in the direction of the magnetic field, that is, to the geomagnetic North[1,2,4]. This implies that their magnetic dipole is systematically orientated with the North-seeking pole forward. The magnetic polarity can be reversed by single, magnetic pulses of high field strength (1–2 μs, 300–600 G), and these bacteria then swim along magnetic field lines to the South[5]. Due to the inclination of the Earth's magnetic field, magnetotactic bacteria which swim to the North in the Northern Hemisphere are directed downward at an angle increasing with latitude. It has been suggested that this downward-directed motion confers a biological advantage by guiding the bacteria, when dislodged, back to the sediments[1]. On the basis of this hypothesis, magnetotactic bacteria of the Southern Hemisphere would be expected to swim to the South to reach the bottom. We report here several morphological types of magnetotactic bacteria present in sediments of the Southern Hemisphere. These bacteria indeed swim consistently to the South, hence downward along the Earth's inclined magnetic field lines, as hypothesized. As revealed by electron microscopy, they contain internal chains of electron-opaque particles similar to those observed in magnetotactic bacteria from the Northern Hemisphere. Like their Northern Hemisphere counterparts, their magnetic polarity can be permanently reversed and they cannot be demagnetized. We also report on Northern Hemisphere magnetotactic bacteria incubated in Southern Hemisphere magnetic conditions, confirming the biological relevance of downward directed motility.

Bacteria were collected from marine and freshwater sediments in the vicinities of Christchurch, New Zealand, and Hobart, Tasmania, Australia. These locales offered ecologically diverse habitats with geomagnetic characteristics (inclination 68–73°S at a total magnetic intensity of 0.59–0.63 G) approximately the mirror image of Northern Hemisphere environments where magnetotactic bacteria are found. Magnetotactic responses were recorded by optically monitoring bacterial motion in uniform magnetic fields of 0.2–2 G, provided by a pair of Helmholtz coils mounted to either side of a Zeiss OPMI 1 operation microscope (magnification ×83.2; working distance, 10 cm). The Helmholtz-coil axis was aligned with the horizontal component of the Earth's magnetic field; the polarity of the imposed field was selected by a toggle switch. The coils and the dark-field illuminator were battery operated. In the coil system, both freshwater and marine bacteria migrated along magnetic field lines in the direction opposite to that indicated by a magnetic compass needle. On reversal of the field, the organisms executed U-turns and swam opposite to the initial direction. The rates of migration were comparable to those observed in Northern Hemisphere bacteria. Thus, the magnetotactic responses of Southern Hemisphere bacteria are similar to those of the Northern Hemisphere species, except for their magnetically opposite direction of migration (South-seeking magnetotactic bacteria have also been observed in Victoria, Australia[6]).

Transmission electron microscopy of bacteria magnetotactically separated from sediments was carried out at the University of Canterbury, Christchurch, New Zealand, using a Hitachi HS-7S electron microscope operating at 50 kV. Samples were placed on parlodion-coated, carbon-reinforced, 300-mesh copper grids, and were lightly stained with uranyl acetate. Magnetic cells of various morphological types were observed to contain one or two chains of intracytoplasmic electron-opaque particles which vary in size and shape with cell type (Fig. 1). Thus, Southern Hemisphere magnetotactic bacteria also possess magnetosomes[7], the characteristic morphological feature of all magnetotactic bacteria examined thus far.

To establish the ferromagnetic nature of their orientation mechanism, bacteria were subjected to alternating 50-Hz magnetic fields over 1,000 G, produced by a small hand-held magnetic tape degausser (Tandy Corporation). Northern Hemisphere and Southern Hemisphere magnetotactic bacteria were examined in separate water drops on a microscope slide before and after exposure to the alternating magnetic field. On exposure, the degausser was slowly moved away from the water drops to obtain the field decay required for demagnetization. Whereas before exposure all the cells in these samples swam exclusively either to the North or to the South, after exposure each sample contained approximately equal numbers of North- and South-seeking cells. Magnetic reversals were also effected by approaching individual bacteria at the water–air interface with a sharp, magnetized needle. These observations indicate that bacteria from both hemispheres physically function as single-domain magnetic dipoles, in agreement with previous

0028–0836/80/300384—02$01.00

remagnetization studies using strong magnetic pulses of short duration[5].

In experiments carried out in Massachusetts, sediment samples containing North-seeking bacteria from New England were placed in an experimental chamber in which the vertical component of the local Earth's magnetic field was inverted, reproducing conditions in the Southern Hemisphere. Control samples were placed in a similar chamber with a field of normal inclination. The polarities of cells from the samples were determined periodically for several weeks, that is, over many generations. Whereas all samples contained almost exclusively North-seeking cells at the beginning of the experiment, with time the number of North-seeking cells in the experimental chamber decreased dramatically, and South-seeking bacteria gradually predominated. In the control samples no such changes occurred. Thus, downward-inclined fields select for North-seeking bacteria whereas upward-inclined fields select for South-seeking cells. This demonstrates that the vertical component of the Earth's magnetic field is the relevant parameter determining the predominant cell polarity.

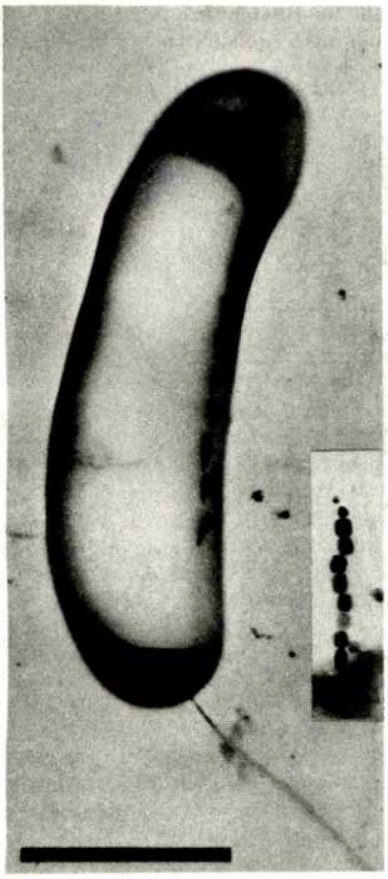

Fig. 1 Electron micrograph of a magnetotactic bacterium separated magnetically from freshwater sediments of New Zealand and stained with uranyl acetate. Inset shows one of two chains of particles found in a freshwater magnetotactic coccus of New Zealand. Both photographs are presented at the same magnification (scale bar = $1\ \mu m$). Whereas the particles shown in the inset are similar to those found in Northern Hemisphere magnetotactic bacteria, those in the rod-shaped species have a novel shape.

In conclusion, the prevalence of South-seeking magnetotactic bacteria in Southern Hemisphere sediments and in samples held in similar magnetic conditions in the Northern Hemisphere verifies the hypothesis that downward-directed motion is advantageous for and upward-directed motion detrimental to the survival of these magnetotactic bacteria with unidirectional motility. Magnetotaxis is a reliable means of keeping these microorganisms in or near the bottom sediments. As particles in the micrometre size range with densities close to 1.0 tend to remain suspended in water, gravity is virtually inconsequential in determining the vertical distribution of the bacteria.

The Earth's magnetic field provides a global orientation cue to which various organisms are known to respond. Only recently have detection mechanisms based on electromagnetic induction[8] and ferromagnetic alignment[5,9] been explained. In the bacteria, nature has shown the biological feasibility of synthesizing a highly organized ferromagnetic structure equivalent to a magnetic compass needle.

We thank Nancy Blakemore for her participation in the expedition to New Zealand and Tasmania, Australia, Drs T. Cole, L. Greenfield and W. D. Parkinson for hospitality and co-operation, M. Ingerfeld for assistance with electron microscopy, and H. Stram, D. Lobel, J. Perc, V. Kalmijn and T. Dourdeville for valuable contributions to this work. This work was supported by a research grant from the National Geographic Society, and the Office of Naval Research. The Francis Bitter National Magnet Laboratory is supported by the NSF and R.P.B. is supported, in part, by NSF grant PCM77-12175.

Received 14 February; accepted 9 May 1980.

1. Blakemore, R. P. *Science* **190,** 377 (1975).
2. Kalmijn, Ad. J. & Blakemore, R. P. *Proc. int. Un. physiol. Sci.* **13,** 364 (1977).
3. Frankel, R. B., Blakemore, R. P. & Wolfe, R. S. *Science* **203,** 355 (1979).
4. Moench, T. T. & Konetzka, W. A. *Archs Microbiol.* **119,** 203 (1978).
5. Kalmijn, Ad. J. & Blakemore, R. P. in *Animal Migration. Navigation and Homing* (eds Schmidt-Koenig, K. & Keeton, W. T.) 344 (Springer, New York, 1978).
6. Kirschvink, J. L. *J. exp. Biol.* (in the press).
7. Balkwill, D. L., Maratea, D. & Blakemore, R. P. *J. Bact* **141,** 1399 (1980).
8. Kalmijn, Ad. J. *Handbook of Sensory Physiology* Vol. III (ed. Fessard, A.) 147–200 (Springer, Berlin, 1974).
9. Frankel, R. B. & Blakemore, R. P. *J. Magn. magn. Mater.* **15–18,** 1562 (1980).

Laetoli Pliocene hominid footprints and bipedalism

M. H. Day

Department of Anatomy, St Thomas's Hospital Medical School,
London SE1 7EH, UK

E. H. Wickens

Department of Photogrammetry and Surveying, University College
London, Gower Street, London WC1 EGBT, UK

The ability to stand upright and walk on two legs is widely recognized as a crucial hominid adaptation that had profound effects on the course of human evolution. The relief of the upper limb from the task of supporting the trunk in locomotion would have permitted the efficient carriage of food, infants and later tools and weapons. Any or all of these activities could, it is believed, have improved the differential survival of early hominids. Precisely when upright stance and bipedal gait were first acquired within the hominid evolutionary line is not known, and so the discovery of apparently bipedal footprints of Pliocene age at site G, Laetoli, Tanzania is important in itself[1,2]. A study of the footprints, reported here, has shown that when these hominids walked, they transmitted their body weight and the forces of propulsion to the ground in a manner very similar to that of modern man.

Most of the evidence for early hominid upright posture and bipedal gait has been deduced from the anatomy of fossil hominid lower limb and pelvic bones from several African sites, including Sterkfontein and Swartkrans in the Republic of South Africa, Olduvai Gorge in Tanzania, Koobi Fora (formerly East Rudolf) in Kenya and the Afar site in Ethiopia[3–11]. Opinions have varied as to the degree of adaptation to bipedalism that the

0028–0836/80/300385—03$01.00

study of these fossil remains has disclosed[12-17]. The dates recorded for the sites where fossil hominid lower limb and pelvic bones have been found span from about 1.5 to 3.0 Myr BP, so that the discovery of what are believed to be bipedal footprints in 1978 and 1979 in a tuff dated at 3.6–3.75 Myr BP has added nearly 0.75 Myr to the known antiquity of bipedalism.

The fossil footprints of three individuals were made in a fine grained volcanic ash that subsequently became damp, perhaps after rain, and consolidated into a tuff retaining the imprints, often in considerable detail.

Because footprints made during walking reflect the way in which weight and propulsive forces are transmitted to the ground, we have compared the fossil footprints with those of modern man made experimentally on ground of similar consistency. Modern human footprints were made by walking over wet sand (grade 25/52, that is 0.30–0.6-mm grain size) in the laboratory so that clear impressions were made and retained for stereophotography. The instrument used was an Officene-Galileo stereometric camera on a 560-mm base, and the stereo images produced were contoured at 2-mm intervals on a Thompson–Watts Mk 2 plotting instrument. This technique—photogrammetry—is widely used by surveyors and map-makers as a precision method of determining surface form. The experimental footprint contour diagrams (Fig. 1) show the various depths that resulted from the differing pressures exerted on the ground in walking; the darker the colour, the deeper the impression. Similar diagrams were prepared from stereophotographs of replicas of three fossil footprints from two individuals (Figs 2, 3).

The remarkable similarities between the modern human footprint contour patterns and those of the fossil hominids can be seen at a glance. In more detail, heel and ball impressions are clear and transfer of weight and force progresses from heel to ball on the outer side of the foot outlining a medial arch. The heel and ball impressions are deep and surrounded by an irregular figure-of-eight pattern in each case. The ball impressions have oblique principal axes that run anteromedially towards the base of the great toe, where the impressions are especially deep, and lead on to the great toe impression itself as it digs into the soft ground during walking.

The similarity of the contour patterns of the three fossil footprints to the modern human examples is striking confirmation of the bipedal nature of the gait of the Laetoli Site G hominids already claimed from the footfall sequence[1,2]. The pattern of weight and force transference through the foot, well known in modern man[18], also seems to be very similar in the

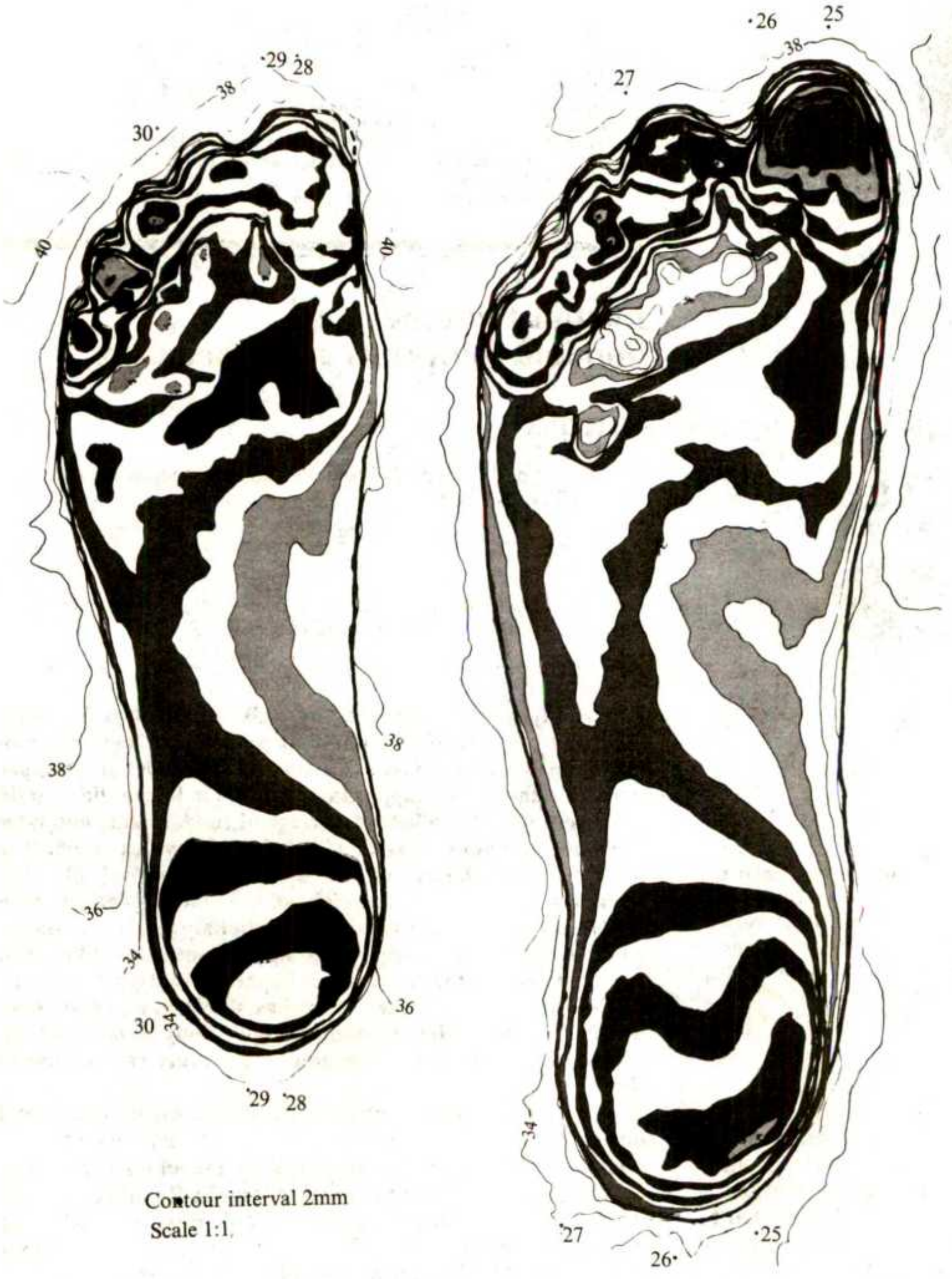

Fig. 1 Modern human female (*a*) and male (*b*) soft ground walking footprints. Contoured at 2-mm intervals.

fossil footprints and indicates that even at this early stage of hominid evolution bipedalism had reached an advanced and specialized stage. Ironically these fossil hominid footprints from Laetoli provide locomotor evidence without a single adult fossil hominid limb bone being known from the site. Nonetheless Pliocene hominid footprints, and their comparison with experimental modern human equivalents, may well prove to be more convincing evidence of early hominid bipedalism than osteological or morphometric analysis of fossil bones.

We thank Dr Mary Leakey for the opportunity to examine the Laetoli footprints; Mr A. A. Mturi, Director of Antiquities, Tanzania, Mr A. J. N. Mgina, Ngorongoro Conservation Authority, for help and cooperation; the Research Endowments Committee at St Thomas's Hospital for support, and colleagues in the Department of Photogrammetry and Surveying, University College London.

Received 10 December 1979; accepted 3 June 1980.

1. Leakey, M. D. *Antiquity* **52,** 133 (1978).
2. Leakey, M. D. & Hay, R. L. *Nature* **278,** 317 (1979).
3. Broom, R., Robinson, J. T. & Schepers, G. W. H. *Trans. Mus. Mem.* 4 (1950).
4. Napier, J. R. *Arch. Biol. Liège* **75,** Suppl. 673 (1964).
5. Davis, P. R. *Nature* **201,** 967 (1964).
6. Day, M. H. & Napier, J. R. *Nature* **201,** 967 (1964).
7. Day, M. H. & Napier, J. R. *Nature* **211,** 929 (1966).
8. Day, M. H. *Nature* **215,** 323 (1967).
9. Day, M. H. *Nature* **221,** 230 (1969).
10. Day, M. H. in *Earliest man and the Environment of the Lake Rudolf Basin* (eds Coppens, Y., Howell, F. Clark, Isaac, Glynn L1. & Leakey, R. E. F.) (Chicago University Press, 1976).
11. Johanson, D. C. & Taieb, M. *Nature* **260,** 293 (1976).
12. Dart, R. A. *Am. J. Phys. Anthrop.* **7,** 301 (1949).
13. Clark, W. E. Le Gros *The Fossil Evidence for Human Evolution* (The University of Chicago Press, 1955).
14. Robinson, J. T. *Early Hominid Posture and Locomotion* (Chicago University Press, 1972).
15. Day, M. H. *Symp. zool. Soc.* **33,** 29 (1972).
16. Zuckerman, S. *et al. Symp. zool. Soc* **33,** 71 (1972).
17. Lovejoy, C. O. & Heiple, K. G. *Nature* **235,** 175 (1972).
18. Barnett, C. H. *Lancet* **i,** 617 (1956).

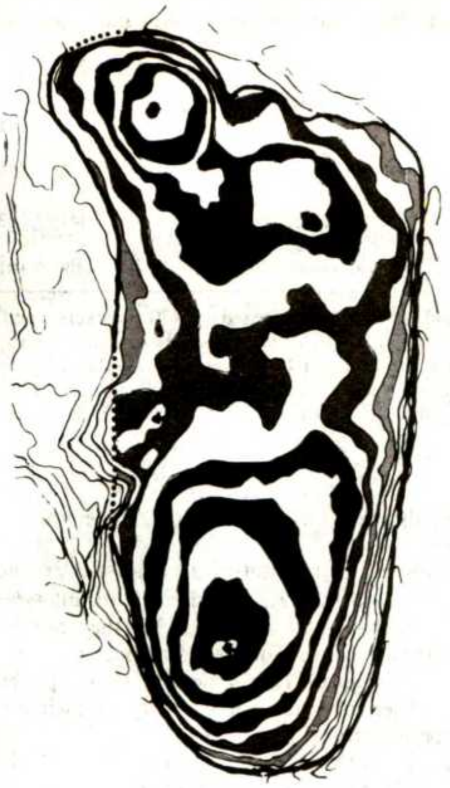

Fig. 2 A right fossil hominid footprint from site G, Laetoli. The footprint shows many points of similarity with those of modern man. Contoured at 2-mm intervals.

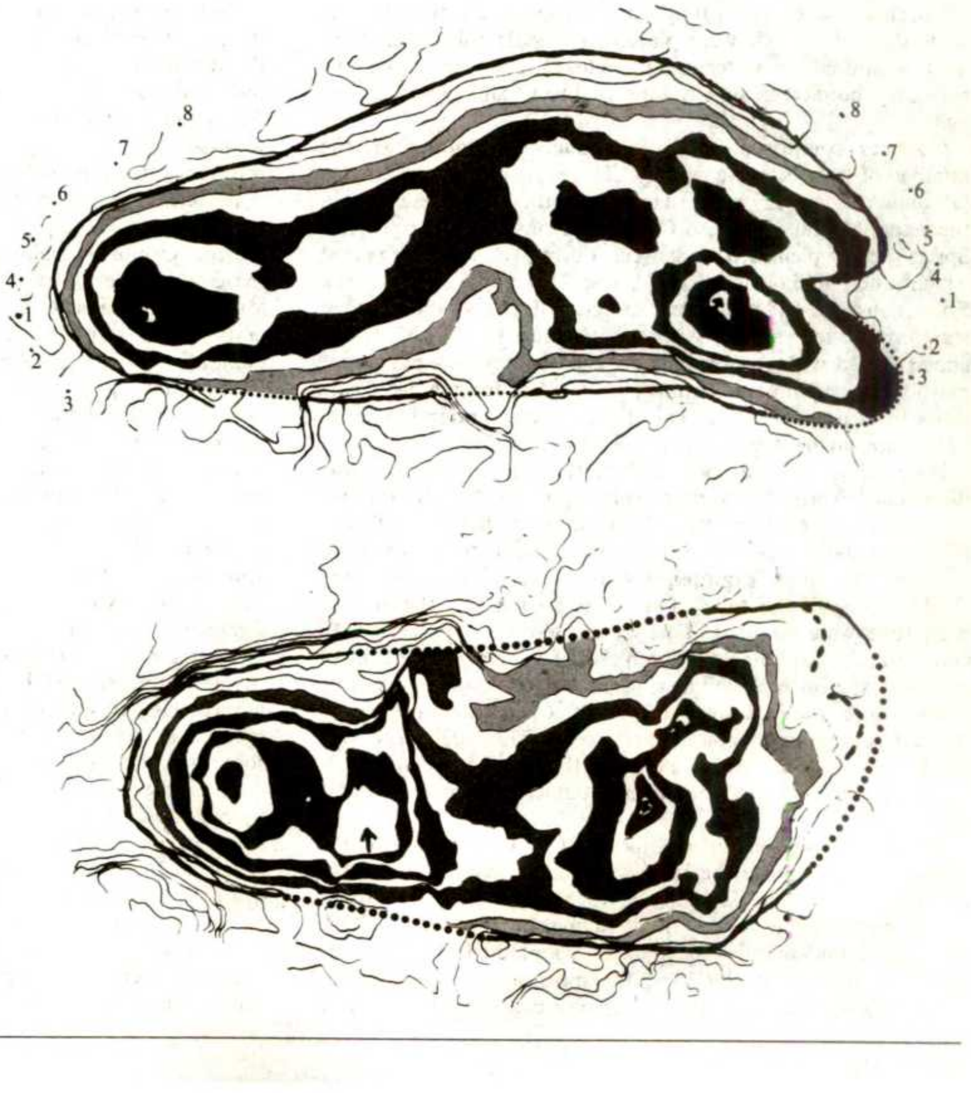

Fig. 3 Left (*a*) and right (*b*) fossil hominid footprints from a larger individual that also show striking similarities to those of modern man. Contoured at 2-mm intervals.

Environmental preference induced experimentally in ants (Hymenoptera: Formicidae)

Pierre Jaisson

Equipe de Recherche Associée au CNRS no. 885, Laboratoire d'Ethologie et Sociobiologie, Université Paris-Nord, Avenue J.B. Clément, 93430 Villetaneuse, France

In ants, early experience seems to influence the development of aggression[1,2] and the recognition of cocoons[3–6], but there has been no investigation of such influences on the ants' relationship with their habitat. There are, however, many descriptions of the use of plants as nests (*Azteca*[7], *Colobopsis*[8], *Oecophylla*[9] and *Pseudomyrmex*[10], for example), while habitat selection based on early experience is known among some vertebrates, principally amphibians[11–13], birds[14] and mammals[15]. In this context, my hypothesis is that the preference of an ant for a plant can be induced on the basis of previous entrainment to a plant stimulus. Using ants of the sub-family Formicidae, *Camponotus vagus* Scop. and *Formica polyctena* Först., I have demonstrated that early experience can induce an environmental preference and may explain specific associations that can be found in the wild between ants and plants.

C. vagus and *F. polyctena* seem to have close affinities with plants. The former lives inside wood, while the latter builds nests of twigs or pine needles. The two species are common in France, and colonies were collected either in Provence (near Vaison-la-Romaine, Vaucluse) in the case of *C. vagus*, or the Rambouillet forest (Yvelines). Laboratory colonies were established using very young ants which all emerged on the same day and which were placed in a glass tube (22 × 2 cm) with a source of water at the closed end, providing the necessary humidity; an envelope of black card obscured the light.

Colonies comprised 25–45 individuals, depending on the number of ants eclosing weekly. Three 5-cm sprigs of thyme (*Thymus vulgaris* L.) were placed near the water reservoir in the experimental colonies. Control colonies had no thyme. Sprigs were replenished each week during the training period which lasted 30 days for *C. vagus* and 21 days for *F. polyctena*. Food consisted of honey and water. All colonies were then transferred to tubes without thyme for 24 h; then, anaesthetized with carbon dioxide, each colony was put into a plastic box equidistant from two lateral horizontal plastic tubes fixed into the sides, one of which was randomly chosen to contain thyme (to avoid any effect of laterality).

Each tube was a potential nest. The apparatus was illuminated isotropically, with white light, so that the interior of each tube (covered by an envelope of black card) was relatively dark. On recovery from anaesthesia, the ants, avoiding the light, explored the box and finally chose the shade in one of the tubes. On the following day the ants in each tube were counted. This choice test was applied to 15 control and 9 experimental colonies of *C. vagus*, and 9 control and 13 experimental colonies of *F. polyctena*. The few ants remaining in the box were also counted but not included in the determination of colony preference. This preference was evaluated as the difference between the number of ants that chose the nest with thyme and the number that chose the nest without thyme.

Table 1 shows that all colonies of *C. vagus* trained to the thyme stimulus chose the tube containing thyme. Conversely, all but one of those familiarized to an environment without thyme preferred the tube without thyme. But even this colony, although found in the tube that had contained thyme at the beginning of the test, moved all the sprigs into the plastic box. Nevertheless, I decided that this colony had chosen the thyme side. In fact, the two tubes were empty when the count was made.

Table 1 Behaviour of young *C. vagus* and *F. polyctena*

		N	*T*+	*T*−	*d*
C. vagus	Experimental colonies	9	171	41	9
	Control colonies	15	72	330	1
F. polyctena	Experimental colonies	13	348	33	11
	Control colonies	9	89	181	2

Experimental colonies comprised 25–30 workers, and control colonies 30 workers for *C. vagus*; experimental and control colonies comprised 25–45 workers for *F. polyctena*. *N*, number of colonies; *T*+, ants that preferred the tube with thyme for all colonies; *T*−, ants that preferred the tube without thyme; *d*, colonies in which *T*+ > *T*−.

I used non-parametric statistical analysis: at the colony level, the χ^2 total correlation is highly significant ($\chi^2 = 16.5$; $P < 0.01$). This analysis was applied to all the colonies to test the nul hypothesis of a randomized distribution of the colonies between two possibilities (preference for thyme/preference for empty tube). The same test applied only to each group as a whole (experimental or control) confirms my first observations: in both cases the probability that the results represent a randomized distribution of the colonies during the choice test is less than 0.01. Thus the preference of the experimental group for the nest containing thyme is significant ($\chi^2 = 8.8$), as is that of the control group for the empty nest ($\chi^2 = 11.3$).

Wilcoxon's test gave the same results, but more precisely than χ^2. It enabled me to classify the colonies on the basis of the difference between the number of ants in the colony that preferred the tube with thyme and the number in the colony that preferred the empty tube. In other words, it enabled me to associate the qualitative and quantitative aspects of the preference (the tables show only the total group values).

In terms of the number of ants involved (namely their individual preference), χ^2, either total or calculated for each of the two groups, is highly significant, regardless of the fact that the colonies were artificially set up. However, there is a need for caution because each ant's choice between the two artificial nests is not standard: each new entry into a tube may be qualitatively different from the preceding entry.

The same applies to *F. polyctena*, as Table 1 shows, although after choosing the tube containing thyme, the two control colonies did not expel the sprigs. The same statistical treatment shows again that the behaviour of the colonies as a whole was heterogeneous ($\chi^2 = 6.19$; $P < 0.02$) and the experimental colonies had a significant preference for the tube containing thyme ($\chi^2 = 6.23$; $P < 0.02$). But the same test applied to control colonies gives a non-significant value ($\chi^2 = 1.77$). Wilcoxon's test does not improve the precision (only significant for the experimental group). However, the comparison of individual ant preference for the tube without thyme in the controls becomes significant ($\chi^2 = 31.3$; $P < 0.01$); nevertheless, it should be remembered that treatment of the individual results increases the information but modifies somewhat the significance of the choice test.

Thus, the behaviour of these two species differed according to previous experience: the experimental colonies, trained to thyme, chose the tube containing it, while the control colonies preferred the tube without thyme. However, these results were more clear-cut for *C. vagus*.

To test the possible importance of age, I examined environmental preference in older ants, collected from nests in the same localities as before. These experiments were carried out at the end of the season, when I could form only seven

0028-0836/80/300388—02$01.00

colonies of *C. vagus* and five of *F. polyctena*, to which the same training period and bioassay was applied. Table 2 shows, first, that adult ants reared in the presence of thyme suffered heavy mortality: 48.6% for *C. vagus* and 56.6% for *F. polyctena* (compared with 9.8% and 5.8% for the young ants). It seems to be deleterious for naive adult ants to be exposed to this plant, for which they have a spontaneous aversion (as known already in insects[16]). The aversion was revealed by the distribution of the workers, especially at the beginning of the training period: most of them remained close to the sprigs, rather than within the thyme as the young workers had done.

In the choice test, statistical analysis revealed responses much less clear than for the young ants. Preference for the empty tube seemed to be clear-cut for *C. vagus* ($\chi^2 = 5.14$; $0.05 > P > 0.01$), but not significant for *F. polyctena* ($\chi^2 = 5.26$; $0.05 > P > 0.01$).

Adult ants trained to the thyme always seemed to prefer a tube without thyme, even if this preference (in particular for *F. polyctena*) appeared less pronounced than for control colonies. Although the high mortality of the adults exposed to thyme affected the number of individuals, the sensitivity of the young workers seemed to be greater and their age more favourable for the establishment of an environmental preference.

The behaviour of workers in the presence of thyme varied according to age. Mature ants avoided contact with the plant more often than not, while the young ants entered the sprigs. This difference may enable the latter to develop an active preference for thyme on the basis of its presence during the neonatal period.

Table 2 Behaviour of mature *C. vagus* and *F. polyctena*

	N	*T+*	*T−*	*d*
C. vagus	7	11	115	0
F. polyctena	5	28	48	2

In each case there were 35 worker ants.

There have been reports of avoidance conditioning in mature ants for the odour of peppermint (used as a conditional stimulus)[17,18]. But the preference reported here could resemble more the olfactory conditioning discovered by Thorpe and Jones[19], as in two species of *Drosophila*[20,21], which if reared in a culture medium scented with peppermint oil, later showed a positive response to that odour. However, that phenomenon, which is difficult to interpret[22], develops only when peppermint is presented simultaneously with food during training[23]. Conversely, in my experiments food was presented very briefly at the nest entrance, away from the thyme.

I suggest that the induction of the preference for thyme in young ants is due to either passive familiarization or an association between favourable environmental factors (for example darkness and/or humidity in my experiments) and the odour of the plant. The repulsive nature of plant odour for young ants has not been established, and their sensory receptors might increase progressively in sensitivity as the ants develop, as shown for the phytophagous larva of *Manduca sexta* reared on a plant that it normally finds unacceptable[24]. A mechanism of this type, but independent of feeding, may contribute to the development of relationships of the sort involving the ants *Azteca* or *Pseudomyrmex*, which live exclusively on the plants *Cecropia* or *Acacia*, respectively.

Received 20 August 1979; accepted 25 April 1980.

1. Fielde, A. M. *Biol. Bull.* **10,** 1 (1902).
2. Fielde, A. M. *Indep. Aug.* **17,** 375 (1905).
3. Jaisson, P. *C.r. hebd. Séanc. Acad. Sci. Paris* **275,** 2721 (1972).
4. Jaisson, P. *Behaviour* **52,** 1 (1975).
5. Le Moli, F. & Passetti, M. *Att. Soc. Ital. Sci. Nat., Milano* **118,** 49 (1977).
6. Jaisson, P. & Fresneau, D. *Anim. Behav.* **26,** 1064 (1978).
7. Janzen, D. H. *Ecology* **50,** 147 (1969).
8. Wheeler, W. M. *Ants: Their Structure, Development and Behavior* (Columbia University Press, New York, 1910).
9. Way, M. J. *Bull. ent. Res.* **45,** 93 (1954).
10. Janzen, D. H. *Kans. Univ. Sci. Bull.* **47,** 315 (1967).
11. Wiens, J. A. *Copeia* **1970,** 543 (1970).
12. Wiens, J. A. *Anim. Behav.* **20,** 218 (1972).
13. Mushinsky, H. R. *Copeia* **1976,** 755 (1976).
14. Hildén, O. *Ann. zool. Fenn*, **2,** 53 (1965).
15. Wecker, S. C. *Ecol. Monogr.* **33,** 307 (1963).
16. Soliman, M. H. & Hay, D. A. *Experientia* **34,** 329 (1978).
17. Hoagland, H. *J. gen. Psychol.* **5,** 21 (1931).
18. Vowles, D. M. *J. comp. Physiol. Psychol.* **58,** 105 (1964).
19. Thorpe, W. H. & Jones, F. G. W. *Proc. R. Soc.* **B124,** 56 (1937).
20. Thorpe, W. H. *Proc. R. Soc.* **B127,** 424 (1939).
21. Cushing, J. E. *Proc. natn. Acad. Sci. U.S.A.* **50,** 163 (194[illegible]).
22. Alloway, T. M. *A. Rev. Ent.* **17,** 43 (1972).
23. Hershberger, W. A. & Smith, M. P. *Anim. Behav.* **15,** 259 (1967).
24. Schoonhoven, L. M. *Proc. Koninkl. Ned. Akad. Wetens., Amsterdam* **72,** 491 (1969).

Orientation bias of cat retinal ganglion cells

W. R. Levick & L. N. Thibos

Department of Physiology, John Curtin School of Medical Research, Canberra, Australia 2601

Kuffler[1] described the receptive fields of cat retinal ganglion cells as having a concentric arrangement. This has usually been taken to mean that they are approximately circular in form (see, for example, ref. 2). Hammond[3] tested the circularity of the centre component of receptive fields by plotting a contour of isosensitivity to a small flashed spot. He concluded that centres were often elliptical (average ratio of major to minor axis 1.23) and that more than 50% of the recorded cells had the major axis oriented within ±20° of the horizontal. Such data are important for discussions[4] of the neurophysiological basis of the 'oblique effect' (reduced visibility for periodic grating patterns when oriented away from the vertical or horizontal) observed in psychophysical experiments on humans because subcortical units are often assumed to be orientationally unbiased. Orientation selectivity is a prominent attribute of visual cortical neurones[5] so analysis has usually emphasized the distribution of orientation selectivity at that level[6–8]. The results presented here redirect attention to the retinal level since they reveal a previously unsuspected systematic relation between orientation bias of ganglion cells and their location relative to the area centralis.

Experiments were conducted on adult cats anaesthetized for surgical procedures with 1–2% Fluothane and maintained during data collection on a 70:28·5:1·5 mixture of nitrous oxide, oxygen and carbon dioxide, usually supplemented by intermittently administered urethane (about 0.6 g per day). Eye movements were controlled by continuous infusion of gallamine (5 mg per kg per h) and tubocurarine (0.7 mg per kg per h). The paralysis necessitated artificial ventilation. Extracellular recordings were made from ganglion cells with a tungsten-in-glass electrode[9] passed through a cannula penetrating the globe so as to leave the natural optical system undisturbed. Because optical quality of the retinal image may influence results special precautions were taken as follows. Corneal refraction was modified with a plastic contact lens of spherical form and zero power. The resulting ocular refraction was measured with a Hartinger refractionometer. The point of passage of the axis of the instrument through the dilated natural pupil (1% atropine drops) was adjusted so as to minimize astigmatism. An artificial pupil (3 mm diameter) was centred on this axis and close (about 1 mm) to the contact lens. The combination of spherical and cylindrical lenses indicated by the refractionometer was placed next to the pupil and further measurements were made to confirm the emmetropic state.

The stimulus was a sine wave grating (contrast 0.5, mean luminance 82 cd m^{-2}) drifting slowly (2 bars per s passing a given point) across the receptive field. The pattern was generated as a raster on the face of a cathode ray tube (Tektronix 608) which

0028–0836/80/300389—02$01.00

was centred on each receptive field in turn by means of a gimbal mounting. The orientation of the bars of the grating was controlled by a Dove prism also carried on the gimbal. The visual subtense of the pattern through the prism was about 20°. The screen was focussed at optical infinity with a +4 dioptre lens placed close to the prism between screen and prism. A computer (Hewlett Packard 2100) controlled both the production of the raster and the measurement of trains of impulses constituting the responses of a ganglion cell. The instant when a particular phase of each cycle of the grating passed the centre of the screen provided the synchronization for accumulating usually 100 cycles of response as a 'peri-stimulus time histogram' (PSTH).

As the spatial frequency of a grating was increased over the range 0.03–8 cycles per degree, modulation of a ganglion cell's discharge first increased to a maximum, then decreased. By working near the high-frequency limit for a modulated reponse from each ganglion cell it was easy to find instances where response modulation was strongly influenced by grating orientation. The orientations yielding maximum and minimum modulation were generally 90° apart. Two obvious examples are shown in Fig. 1. A convenient measure of response is the amplitude of the first harmonic component obtained by Fourier analysis of the PSTH. In the examples of Fig. 1 the ratio of maximum to minimum response was 3.2 for unit 1 and 10.7 for unit 2. In a sample of 250 units from five cats the distribution of the ratio ranged from 1.0 to 18.7 with the median at 1.86. By extrapolating the relations between response and spatial frequency to determine the spatial frequency at zero response ('cutoff frequency') for best and worst orientations, the behaviour may also be expressed as a ratio of cutoff spatial frequencies. Ratios of up to 1.6 have been encountered. Clearly the orientation dependence is a definite effect. However, the dependence was insignificant in 30% of the cells tested and this may explain why it was not reported previously[2].

In several animals where data were collected from many ganglion cells in a local patch of retina, it became evident that there was a clustering of best orientations. Patches from various locations had different best orientations. The central tendency of best orientations seemed to be consistently parallel to the line joining the patch to the area centralis. The uncertainties of combining diverse data from various animals influenced us to examine a substantial number of ganglion cells in a single preparation. A sequence of recordings was made along an approximately circular trajectory completely encircling the area centralis. Each unit was assessed as in Fig. 1 and the best orientation recorded as that yielding the maximum modulated response. The position of the centre of each receptive field was transferred to a fundus photograph with the aid of three independent assessments: (1) direct ophthalmoscopic visualization of the electrode tip relative to the pattern of retinal blood vessels; (2) hand mapping of receptive field centres on a frontal tangent screen; (3) noting azimuth and elevation readings on the gimbal carrying the centred cathode ray tube. The photograph was also marked with the centre of the area centralis estimated from the peak of ganglion cell density in the cresyl violet stained whole-mount of the retina and correlation of the blood vessel pattern in whole-mount and photograph.

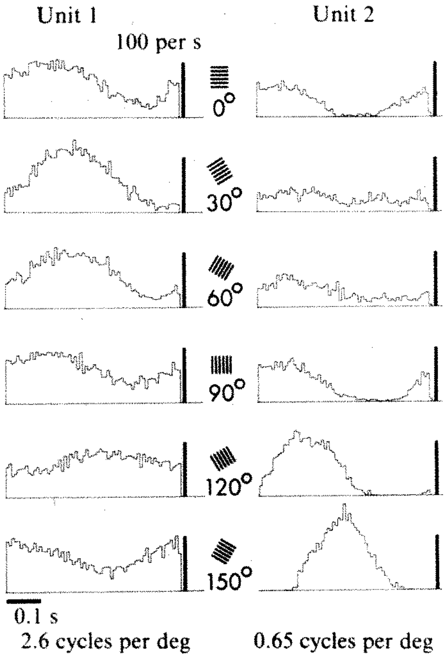

Fig. 1 Peristimulus time histograms (8 ms bin width) of responses to a sinusoidal grating (contrast 0.5) at various orientations (indicated schematically down centre column) drifting at a constant rate (2 c.p.s.) across the receptive field of two ganglion cells: left, on-centre brisk-sustained type; right, on-centre brisk-transient. Same vertical scale (solid bar at right of each, 100 impulses per s) for all PSTHs. Spatial frequencies indicated at bottom are just below the highest resolvable by each unit. The preferred orientations were judged to be 30°, 150° respectively. The positions of the cells relative to the area centralis are indicated (1, 2) in Fig. 2.

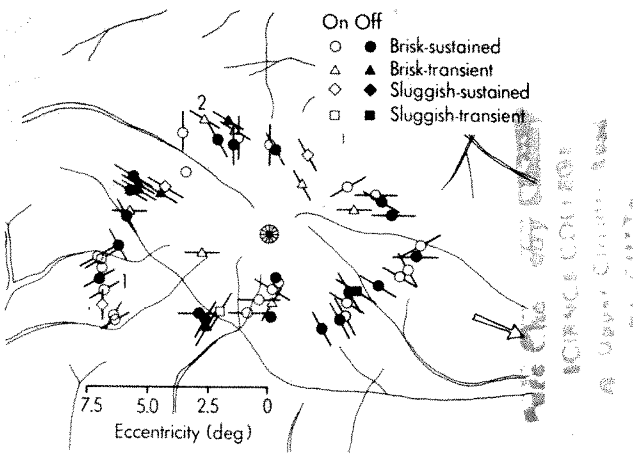

Fig. 2 Preferred grating orientation in relation to retinal location. Positions of receptive fields are indicated by symbols (keyed to unit class, top right) on a tracing of a fundus photograph showing pattern of blood vessels and centre of area centralis (spoked wheel symbol). A line through a symbol indicates the preferred orientation of that unit (no line–no orientation bias). The two units of Fig. 1 are distinguished: 1, 2. The arrow points along the line from area centralis to optic disk.

The result is displayed in Fig. 2 which is a tracing of the fundus photograph. Out of 57 units examined, 52 showed definite orientation bias. Their positions and best orientations are indicated. It is evident in a statistical sense that orientation bias was systematically related to retinal locus. A similar result was obtained in another experiment of the same design. The effect was observed in all classes of concentrically organized ganglion cells[10].

A particular point of interest in these results is that they indicate retinal regions where the information sent to the brain is biased in favour of obliquely oriented gratings. As far as we are aware, eccentric regions along oblique meridians have not been systematically explored in human psychophysical experiments.

Received 4 February; accepted 2 May 1980.

1. Kuffler, S. W. *Cold Spring Harb. Symp. quant. Biol.* **17,** 281–292 (1952); *J. Neurophysiol.* **16,** 37–68 (1953).
2. Enroth-Cugell, C. & Robson, J. G. *J. Physiol., Lond.* **187,** 517–552 (1966).
3. Hammond, P. W. *J. Physiol., Lond.* **234,** 64P–66P (1973); **242,** 99–118 (1974).
4. Appelle, S. *Psychol. Bull.* **78,** 266–278 (1972).
5. Hubel, D. W. & Wiesel, T. N. *J. Physiol., Lond.* **160,** 106–154 (1962).
6. Mansfield, R. J. W. *Science* **186,** 1133–1135 (1974); *Brain Res.* **149,** 229–234 (1978).
7. Rose, D. & Blakemore, C. *Expl Brain Res.* **20,** 1–17 (1974).
8. Finlay, B. L., Schiller, P. H. & Volman, S. F. *Brain Res.* **105,** 350–352 (1976).
9. Levick, W. R. *Med. Electron biol. Engng* **10,** 510–515 (1972).
10. Cleland, B. G. & Levick, W. R. *J. Physiol., Lond.* **240,** 421–456 (1974).

Voltage clamp discloses slow inward current in hippocampal burst-firing neurones

Daniel Johnston & John J. Hablitz

Program in Neuroscience and Section of Neurophysiology, Department of Neurology, Baylor College of Medicine, Houston, Texas 77030

Wilkie A. Wilson

Epilepsy Center, Veterans Administration Hospital, and Department of Pharmacology, Duke University Medical Center, Durham, North Carolina 27705

Hippocampal pyramidal cells, among the most-studied cortical neurones, display several interesting properties. In particular, intracellular recordings in both *in vivo*[1] and *in vitro*[2] preparations have shown that the pyramidal neurones of the CA3 region of the hippocampus have, in addition to the more conventional single spike, the capacity to generate spontaneous bursts of action potentials (APs). The burst-firing patterns have been well documented, but their underlying electrophysiological mechanisms are not completely understood. The bursts seem to be an intrinsic response of individual neurones and can be triggered by weak orthodromic stimulation or by direct depolarization of the somatic membrane. In molluscan and spinal systems, voltage-clamp techniques have revealed slow, voltage-sensitive, inward currents underlying this type of firing behaviour[3–7]. The use of these voltage-clamp techniques to study this phenomenon in hippocampal neurones has previously been precluded by the small size of the neurones and by the difficulty of recording from them in intact preparations. However, the development of methodology for voltage-clamping with a single microelectrode (SEC)[8] and for the maintenance of hippocampal slices *in vitro*[9] has made it possible for us to examine the membrane currents in these CA3 neurones. We report here a slow inward current in CA3 neurones and suggest that it is carried by calcium ions.

Experiments were carried out on hippocampal slices from guinea pigs weighing 300–700 g. Slices 400–600 μm thick were cut transverse to the longitudinal axis of the hippocampus and maintained *in vitro*, using standard techniques[9,10]. Intracellular recordings were obtained from CA3 neurones, using 3 M KCl- or 2 M CsCl-filled micropipettes (30–50 MΩ). Electrodes were selected carefully for current-passing capability and for rapid decay of tip potentials following cessation of current.

The circuit used for voltage clamping is based on that of Wilson and Goldner[8,11]. The technique uses a single microelectrode and rapid switching (3,000 Hz) between voltage-recording and current-passing modes. The membrane potential is sampled after the potential across the microelectrode has decayed and just before return to the current-passing mode. The sampled potential is fed into a standard voltage-clamp circuit and determines the amplitude of the next current pulse. For excursions of approximately ±30 mV from rest, a steady potential could be reached within 2 ms.

A standard voltage-clamp protocol was used, whereby step depolarizing commands were given to the cell while the current response was monitored. Figure 1*a* shows the response of a CA3 neurone, bathed in saline containing 1 μg ml^{-1} tetrodotoxin (TTX), to 300-ms commands. At small depolarizations, only the leakage current is seen; at larger depolarizations, a slow, inward-going current develops and peaks in about 50–100 ms. Either the inward-going current decays during the command, or an outward current develops and reverses the inward-going trend. The total current–voltage (I–V) relationship of this cell in

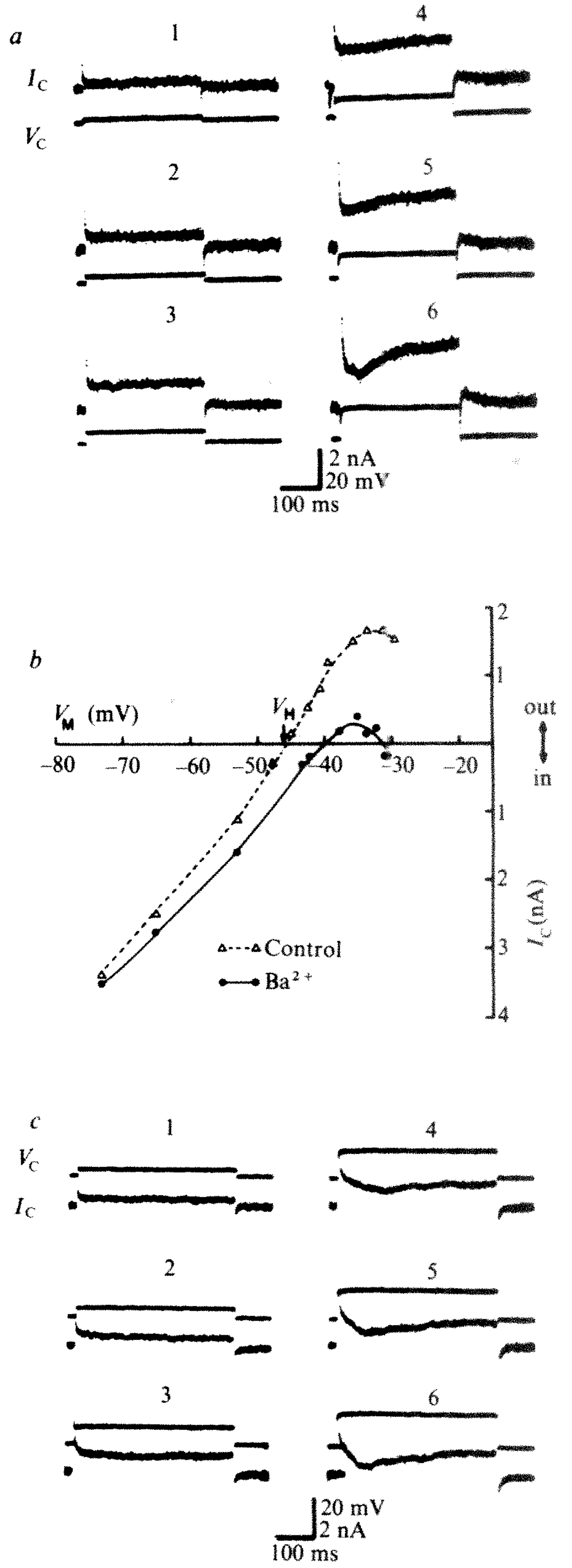

Fig. 1 Voltage-clamp data from a CA3 neurone in the presence of 1 μg ml^{-1} TTX. *a*, A series of depolarizing commands is given to the cell. Frames 1–3 show primarily leakage current. In frames 4–6, an inward-going current develops that peaks in 50–100 ms. I_c, clamp current; V_c, command potential. (See 1*b* for value of holding current.) *b*, I–V curve from same cell before and after applying a drop of 15 mM Ba^{2+}. Current is measured as the peak of the inward-going phase. V_M, membrane potential under voltage clamp; V_H, holding potential. After application of Ba^{2+}, the I–V curve becomes net inward at about −30 mV. *c*, Depolarizing clamp commands after applying Ba^{2+}.

0028-0836/80/300391—03$01.00

normal saline plus TTX is shown in Fig. 1*b*; the current is measured with respect to zero at the peak of the inward-going phase. A similar inward-going current has been observed in well over 50 CA3 neurones. In Fig. 1*c*, current from depolarizing commands is shown from the same cell after applying a drop of 15 mM Ba^{2+} from a coarse extracellular micropipette. It is clear that after the application of Ba^{2+} the total membrane current is less outward at all potentials, membrane current becomes net inward at about −40 mV (Fig. 1*b*), and the inward-going current is more prominent during the depolarizing commands (Fig. 1*c*). Since it is likely that the depolarizing commands activate both an outward K^+ current and a TTX-insensitive inward current simultaneously, and as Ba^{2+} has been shown, in several preparations, to block K^+ currents[12,13] as well as to substitute for Ca^{2+} as the charge carrier through Ca^{2+} channels[14,15], further manipulations were necessary to separate the inward and outward currents.

Internally applied caesium (Cs^+) has been shown to block outward K^+ currents in a variety of systems[16], and we used Cs^+ loading to reduce the K^+ contamination of the inward current in CA3 neurones. Neurones were impaled with micropipettes containing 2 M CsCl, and Cs^+ was iontophoresed for 1–10 min using 200–400-ms pulses at 2 Hz. Cs^+ injection typically increased the passive input resistance two- or threefold and seemed to block K^+ currents, as judged by: (1) the increased duration of the APs; (2) the decreased leakage conductance; and (3) the decreased outward current observed in voltage clamp. Moreover, the passive input resistance, as measured under current clamp, showed little decrease with depolarization up to about −40 mV, suggesting a substantial reduction in delayed rectification. Figure 2 shows an *I–V* relationship from a Cs^+-injected neurone in which Na^+ currents had previously been blocked by TTX. In this cell, the total membrane current was inward over the entire voltage range up to −10 mV, the limit to which we could clamp the cell reliably; a clear region of negative slope conductance in the range of −45 to −20 mV is demonstrated.

To test for the ionic sensitivity of this slow inward current, Co^{2+}, a potent inhibitor of Ca^{2+} inward currents in a variety of preparations[14,15], was applied to CA3 neurones. Figure 3*a* shows data from another Cs^+-injected CA3 neurone in a TTX-treated slice. Although in this cell the holding current is outward at the holding potential of −40 mV (Fig. 3*b*), the depolarizing commands activate a persistent inward-going current (see Fig. 3*a*, 3 and 4) that becomes net inward at about −25 mV. Hyperpolarizing commands from −40 mV show little leakage current (Fig. 3*a*, 1 and 2). A drop of 10 mM Co^{2+} was applied to this cell via a coarse extracellular micropipette. Figure 3*c* shows that following this application, the current response to step commands is quite different. No inward-going current is activated by

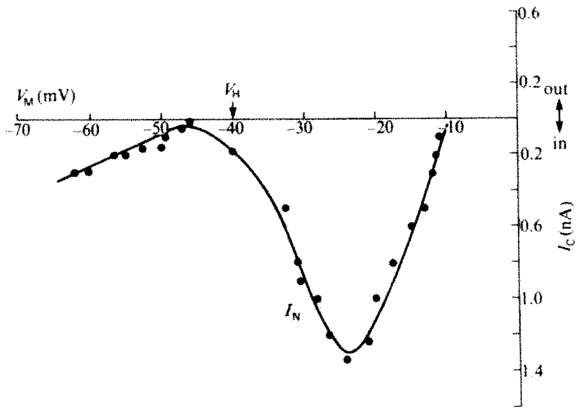

Fig. 2 *I–V* curve of a CA3 neurone, injected with Cs^+. The cell was treated with 1 μg ml^{-1} TTX, and Cs^+ was injected via the intracellular microelectrode. Total current is inward at all potentials. A prominent region of negative slope conductance is seen after Cs^+ loading.

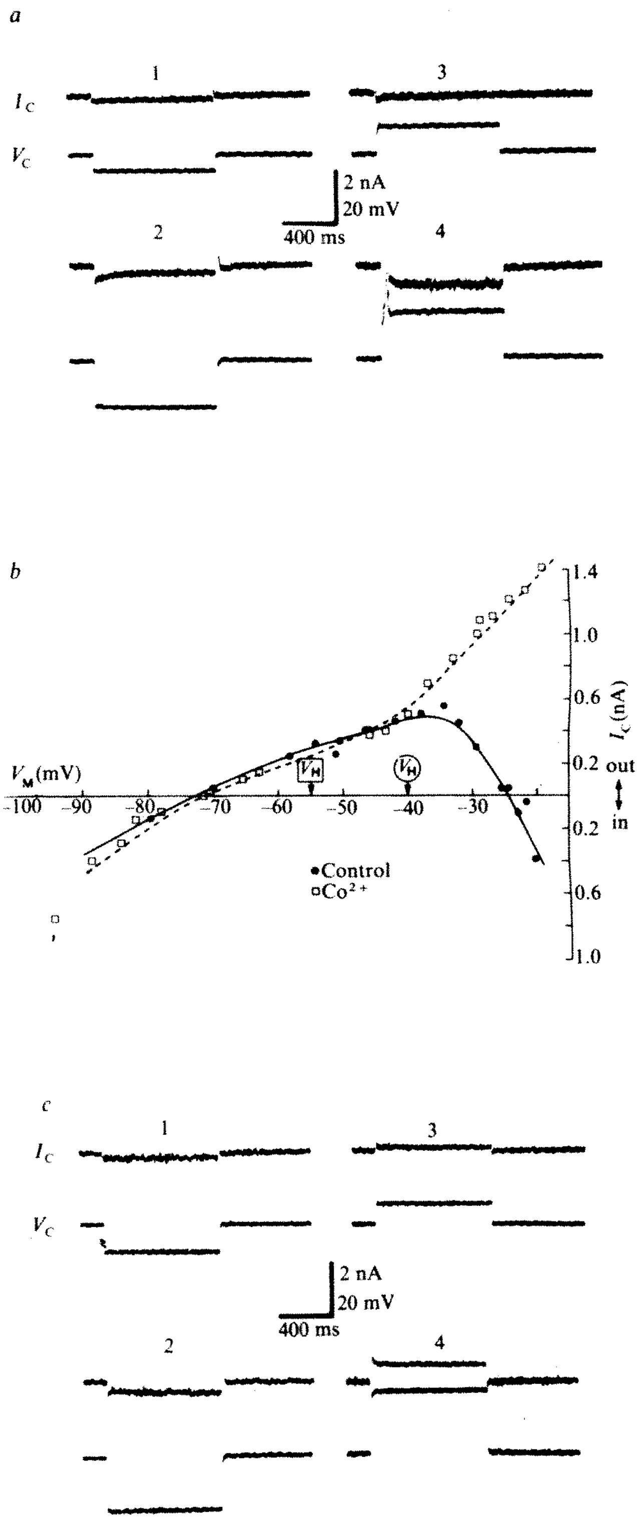

Fig. 3 Effects of Co^{2+} on a CA3 neurone. *a*, Voltage-clamp commands to another Cs^+-loaded cell exposed to 1 μg ml^{-1} TTX. Frames 1 and 2 show hyperpolarizing commands and the small leakage current. Frames 3 and 4 show depolarizing commands that activate an inward-going current that shows little or no decay during the command. (See *b* for value of holding current.) *b*, *I–V* curve before and after applying a drop of 10 mM Co^{2+}. The region of negative slope conductance is absent after Co^{2+}. Although a more negative holding potential was used after Co^{2+}, the depolarizing commands used reach well into the previous region of negative slope conductance, and no inward-going current is observed. This impalement was lost before measurements at the previous holding potential could be made. *c*, Voltage-clamp commands after application of Co^{2+}. The inward-going current is no longer present during the depolarizing commands.

depolarization, and the *I–V* curve shown in Fig. 3*b* displays no region of negative slope conductance. These data suggest that a slow, voltage-dependent, inward current is present in these cells, probably carried by Ca^{2+} ions. However, a TTX-resistant Na^+ current, which is affected by Ba^{2+} and Co^{2+} in the above manner, cannot be excluded. Although Cs^+ injection substantially reduced the outward-current contribution to the total membrane current, it did not block it completely. During large depolarizing commands (for example >20 mV from the holding potential), an outward current, possibly a Ca^{2+}-dependent K^+ current, developed. This latter current apparently was less sensitive to Cs^+ injection and contaminated our inward current measurements.

We appreciate the difficulties associated with attempting to voltage clamp neurones whose geometry is as complex as that of the hippocampal pyramids. However, an analysis of the cable properties of CA3 neurones suggests that their total electrotonic length is less than one space constant[11]. A twofold increase in input resistance as a result of Cs^+ injection theoretically would reduce the electrotonic length by a factor of $1/(2^{1/2})$, improving spatial control of voltage. Given such an electronic structure and twice the average membrane time constant of 23.6 ms (ref. 11), equation (32) of Rall[17] predicts a time constant of decay of about 7 ms for the passive current transient following a step change in potential at the soma. Empirically, we have found that this decay is complete in less than 7 ms.

After Cs^+ injection, the persistent inward current exerts almost complete control over the membrane potential in unclamped conditions. Small applied currents move the membrane potential rapidly into and out of the region of negative slope resistance (approximately −50 to −10 mV). This sensitivity to small potential changes suggests that the slow inward current is generated electrically near the recording site and is therefore amenable to voltage-clamp study.

When not voltage clamped, all of the neurones illustrated displayed spontaneous bursting behaviour after Ba^{2+} application or Cs^+ injection, even in the presence of TTX. The bursts consisted of one or more regenerative events, presumably Ca^{2+} spikes, triggered by slow depolarizations of the membrane potential. The voltage-clamp data and the behaviour of the unclamped cell are therefore in agreement.

Although the SEC is not capable of resolving currents underlying the action potential, we believe that it is more than adequate for resolution of the currents described here. This slow inward current in CA3 neurones is similar to the slowly inactivating inward current shown to be responsible for endogenous bursting in molluscan and spinal neurones[3–6], which suggests that the burst tendencies of CA3 neurones may arise from similar mechanisms. The results of the experiments with Cs^+ injection indicate that K^+ currents may be important in modifying the effect of an inward Ca^{2+} current. As in molluscan neurones[18], several K^+ currents undoubtedly exist and may control different aspects of bursting.

This work was supported by grants NS11535 and NS15772 from the National Institute of Neurological and Communicative Disorders and Stroke, NIH, USPHS.

Received 18 February; accepted 2 April 1980.

1. Kandel, E. R. & Spencer, W. A. *J. Neurophysiol.* **24,** 243–259 (1961).
2. Wong, R. K. S. & Prince, D. A. *Brain Res.* **159,** 385–390 (1978).
3. Wilson, W. A. & Wachtel, H. *Science* **186,** 932–934 (1974).
4. Eckert, R. & Lux, H. D. *J. Physiol., Lond.* **254,** 129–152 (1976).
5. Johnston, D. *Brain Res.* **107,** 418–423 (1976).
6. Partridge, L. D., Thompson, S. H., Smith, S. J. & Connor, J. A. *Brain Res.* **164,** 69–79 (1979).
7. Schwindt, P. C. & Crill, W. E. *Brain Res.* **120,** 173–178 (1977).
8. Wilson, W. A. & Goldner, M. M. *J. Neurobiol.* **6,** 411–422 (1975).
9. Schwartzkroin, P. A. *Brain Res.* **85,** 423–436 (1975).
10. Schwartzkroin, P. A. *Brain Res.* **128,** 53–68 (1977).
11. Johnston, D. *Biophys. J.* **25,** 304a (1979).
12. Sperelakis, N., Schneider, M. F. & Harris, E. J. *J. gen. Physiol.* **50,** 1565–1583 (1967).
13. Magura, I. S. *J. Membrane Biol.* **35,** 239–256 (1977).
14. Hagiwara, S. in *Membranes—A Series of Advances* Vol. 3 (ed. Eisenman, G.) 359–381 (Dekker, New York, 1975).
15. Akaike, N., Lee, K. S. & Brown, A. M. *J. gen. Physiol.* **71,** 509–531 (1978).
16. Tillotson, D. *Proc. natn. Acad. Sci. U.S.A.* **76,** 1497–1500 (1979).
17. Rall, W. *Biophys. J.* **9,** 1483–1508 (1969).
18. Thompson, S. H. *J. Physiol., Lond.* **265,** 465–488 (1977).

Circadian clock in *Limulus* brain increases response and decreases noise of retinal photoreceptors

E. Kaplan* & R. B. Barlow Jr†

Marine Biological Laboratory, Woods Hole,
Massachusetts 02543

The sensitivity and structure of ommatidia in the *Limulus* lateral eye exhibit circadian rhythms[1–3]. The cyclic changes are mediated by the activity of efferent optic nerve fibres[1] that originate in the brain and terminate in the retina[4,5]. We report here that the effects of the efferent input to the retina are detectable in single photoreceptor cells. At night the efferent input decreases photoreceptor noise (discrete waves of the membrane potential in darkness) and increases the photoreceptor response to light (amplitude of the receptor potential).

The receptor potential is a fundamental component in the process of visual excitation. It is believed to be formed in *Limulus* photoreceptors by the summation of discrete waves of membrane potential[6]. The statistical behaviour of the waves in light is consistent with the notion that they are triggered by single photon absorptions[7,8]. Discrete waves occurring in the dark are thought to result from thermal events in the excitatory process[9,10]. We found that the efferent input to the retina at night reduces the frequency of discrete waves occurring in the dark without reducing the efficacy of light to initiate them. Apparently the circadian clock can affect early steps in the process of visual excitation. The action of the clock suggests the existence of separate pathways for the spontaneous and light-evoked excitation of photoreceptor cells.

Figure 1 shows records of the membrane potential of a single, dark-adapted photoreceptor (retinular cell) *in situ*. On the day of this experiment an animal was taken from a natural light–dark environment in the early afternoon and fastened to a rigid platform in a seawater aquarium located in a light-proof cage. We removed a small section of cornea from one lateral eye and inserted a glass microelectrode into the exposed patch of retina. We impaled a single retinular cell in the late afternoon and optically isolated the ommatidium containing the cell with a light pipe aligned in contact with the cornea[11]. The cage was then closed to dark adapt the animal. Details of the technique have been described elsewhere[12]. The membrane potential of the retinular cell was recorded continuously from 6 to 10 p.m. We chose this particular period because the results of previous experiments indicated that efferent fibres in the optic nerve trunk become active about the time of sunset (~7 p.m.) and exert their maximal effects on the retina in the late evening hours (~10 p.m.)[1]. Each trace in Fig. 1 shows the membrane potential recorded from the cell in darkness for 20 s and in response to a 5-s flash of constant light intensity.

At 6 p.m. numerous discrete waves of membrane potential occurred in the dark, and the response to the test flash was small. As the evening progressed, the discrete waves occurring in the dark decreased in frequency and those in the light increased. At 10 p.m. no waves occurred in the dark, whereas numerous ones summated to produce the light response. It seems that at night the photoreceptor 'noise' decreased and response increased.

Figure 2 shows that pulses of current delivered to the optic nerve during the day mimic the effects recorded from photoreceptor cells at night. The intracellular data in Fig. 2 were recorded from a single dark-adapted retinular cell. For an additional measure of photoreceptor sensitivity we also recorded the electroretinogram (ERG) from the eye using a surface

---

Permanent addresses: *Rockefeller University, New York, New York 10021. †Institute for Sensory Research, Syracuse University, Syracuse, New York 13210.

0028–0836/80/300393—03$01.00

corneal electrode[1]. The intracellular recording at 2.30 p.m. is characteristic of the day-time state of the retina, that is, it contains many discrete waves in the dark and a relatively small response to light. Note that these features are also contained in the 6 p.m. record of Fig. 1. At 2.32 p.m. periodic episodes of current pulses were delivered to the distal end of the cut optic nerve to simulate endogenous efferent activity[1]. The effect of the nerve shock was to reduce the frequency of discrete waves in the dark and elevate the amplitude of both the receptor potential and ERG. Maximal response amplitudes were recorded after about 2 h of nerve shock (4.30 p.m.) at which time the current pulses were turned off. Subsequently, the receptor potential and ERG decreased in amplitude and discrete waves reappeared in the dark.

In Fig. 2 simulation of efferent optic nerve activity during the day produced night-time characteristics in the photoreceptor recordings; compare the 4.30 p.m. record with the 10 p.m. record in Fig. 1. Cessation of current pulses to the cut optic nerve at night led to the return of the day-time characteristics; compare the 8.30 p.m. record with the 6 p.m. record in Fig. 1.

The results reported here for single photoreceptor cells parallel those recorded from single optic nerve fibres *in situ*[1]. In both cases the time of day when the light-evoked response is elevated and spontaneous activity is depressed corresponds to the period of endogenous efferent activity. Also, in both cases, cutting the optic nerve abolished the circadian changes. Finally, shocking the cut optic nerve during the day produced the physiological effects characteristic of the night-time state of the retina. We therefore conclude that the reduction in noise and increase in response of the photoreceptor in Fig. 1 were mediated by the endogenous activity of efferent optic nerve fibres.

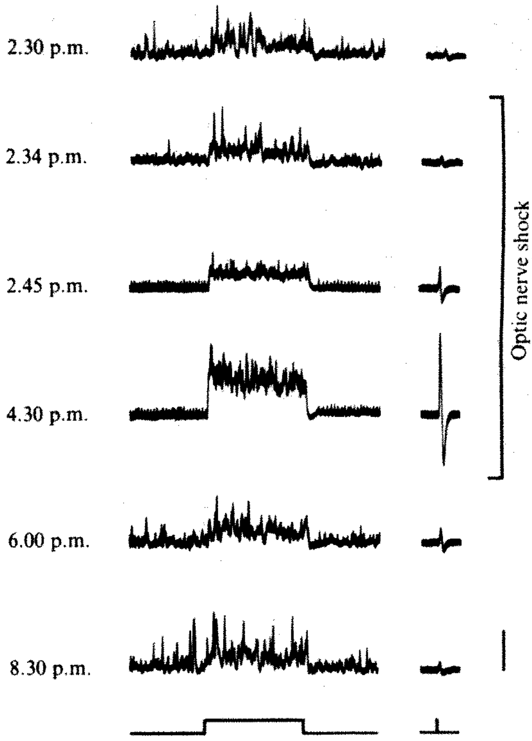

Fig. 2 Effect of optic nerve shock on visual responses of the *Limulus* lateral eye. On the left are intracellular records of a dark-adapted photoreceptor cell recorded with a glass microelectrode in response to 4-s flashes of constant intensity. On the right are electroretinograms (ERGs) recorded with a corneal electrode in response to 100-ms flashes. Before impaling the retinular cell, the optic nerve was exposed, sectioned and its distal end placed in a suction electrode. The 2.30 p.m. records are characteristic of the dark-adapted day-time state of the retina: small responses to light and frequent occurrence of discrete waves in the dark. At 2.32 p.m., current pulses were delivered to the cut nerve at the rate of 4 s^{-1} for 30 s every minute. This shock regime was chosen to simulate the maximum level of endogenous efferent activity recorded at night from the proximal end of cut optic nerves in other preparations. The effect of nerve shock was to elevate the responses to light and reduce the 'noise' in the dark. The increased response amplitudes correspond to about a 20-fold increase in visual sensitivity. The small spikes occurring in the dark are believed to originate in the second-order eccentric cells. They are often observed in experiments in which efferent activity is simulated by nerve shock but not when it is generated by the circadian clock as in Fig. 1. After the optic nerve shock was turned off at 4.30 p.m., the characteristics of the recorded responses returned to the day-time state and remained there until the cell was lost at 8.45 p.m. Cutting the optic nerve blocked the transmission of endogenous efferent activity to the retina at night and thus eliminated circadian changes of the type shown in Fig. 1. Duration of each intracellular record is 10 s. Scale bar, 10 mV for the intracellular data and 50 μV for the ERG records.

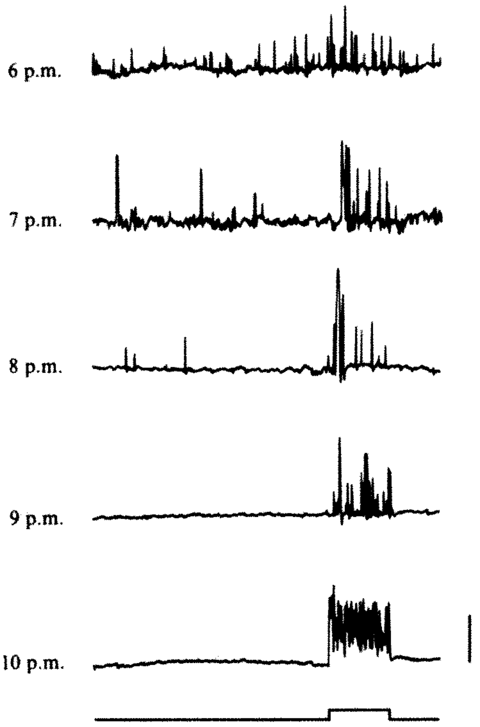

Fig. 1 Intracellular records from a retinular cell of the *Limulus* lateral eye *in situ*. The cell was impaled in the late afternoon with a glass microelectrode without disrupting the blood supply to the eye. At 5 p.m. the cage was closed to dark adapt the animal. The only light stimuli reaching the animal during the next 5 h (5 to 10 p.m.) were the 5-s test flashes (bottom trace) delivered by a light pipe isolated on the ommatidium containing the recorded retinular cell. In each trace a 20-s recording of the cell membrane potential in the dark precedes the response to the test flash. Based on the results of previous experiments, we estimate that the transmission of efferent optic nerve impulses to the retina from the circadian clock in the brain began between 6 and 7 p.m. By 9 p.m. efferent input seems to have abolished the occurrence of discrete waves in the dark and increased the response to the test flash. The recording was lost shortly after the 10 p.m. test. Cell resting potential was 50 mV. Scale bar, 10 mV. The intracellular recordings for this study were carried out with freshly collected crabs at the Marine Biological Laboratory, Woods Hole, Massachusetts.

The night-time increase in the amplitude of the photoreceptor response in Fig. 1 can be largely attributed to an increase in the number of photons caught by the retinular cells. Circadian changes in the morphology of the retinular cells and surrounding pigment cells maximally expose the photosensitive rhabdom to incident light collected by the corneal lenses[3].

The night-time reduction in photoreceptor noise cannot be attributed to any known cellular mechanism. The spontaneously occurring discrete waves in retinal cells seem to result from the thermal isomerization of single rhodopsin molecules, whereas the light-evoked waves result from the photo-isomerization of rhodopsin[9,10]. This seems to be a general property of photoreceptors[13,14]. If the spontaneous fluctuations in membrane potential are in fact initiated by thermal events, by what mechanism does the circadian input to the retina abolish the effects of thermal energy without influencing those initiated by light? Perhaps part of the chain of events triggered by light is separate from that initiated by thermal energy, and only the latter part is influenced by the efferent input to the retina. Whatever the answer, neural signals from the circadian clock seem to act at a stage preceding the excitatory conductance change in the photoreceptor membrane.

Our intracellular recordings did not reveal any additional information on the nature of the mechanisms that mediate the effects of the circadian clock. For example, no consistent changes in either the potential or the resistance of the photoreceptor membrane were detected. Long-term recordings of the type shown in Figs 1 and 2 are generally associated with a slight but steady increase in resistance as monitored by current pulses passed through the recording electrode. Such drifts in resistance are independent of the time of day and probably result from a gradual clogging of the microelectrode. Neither membrane potential nor resistance reflect the activity of efferent optic nerve fibres.

The elevated night-time sensitivity of the retina may partially compensate for diurnal changes in ambient illumination. The circadian rhythm of sensitivity corresponds reasonably well to that of the animal's locomotor behaviour[15]. Interestingly, the period of elevated sensitivity also corresponds to the time the animals congregate in shallow water to mate (C. M. Cavanaugh, unpublished observations).

In sum, the efferent input from a circadian clock enhances retinal sensitivity at night by increasing the quantum catch and decreasing the spontaneous activity of the retinular cells. The efferent input thereby increases the signal-to-noise ratio of the photoreceptor response. The efferent input seems to act at an early stage in the process of visual excitation.

This research was supported by NIH grants EY-00667, EY-00108 and EY-00188 and NSF grant BNS77-19436.

Received 17 January; accepted 7 May 1980.

1. Barlow, R. B. Jr, Bolanowski, S. J. Jr & Brachman, M. L. *Science* **197**, 86–89 (1977).
2. Chamberlain, S. C. & Barlow, R. B. Jr *Biol. Bull.* **153**, 418–419 (1977).
3. Barlow, R. B. Jr & Chamberlain, S. C. in *Effects of Constant Light* (eds Williams, T. P. & Baker, B. N.) (Raven, New York, 1980).
4. Chamberlain, S. C. thesis and Spec. Rep. ISR-S-17 (Institute for Sensory Research, Syracuse University, 1978).
5. Fahrenbach, W. H. *Z. Zellforsch.* **144**, 153–166 (1973).
6. Dodge, F. A. Jr, Knight, B. W. & Toyoda, J. *Science* **160**, 88–90 (1968).
7. Yeandle, S. *Am. J. Opthal.* **46**, pt 2, 82–87 (1958).
8. Adolph, A. R. *J. gen. Physiol.* **48**, 297–322 (1964).
9. Adolph, A. R. *J. gen. Physiol.* **52**, 584–599 (1968).
10. Srebro, R. & Behbehani, M. *J. Physiol., Lond.* **224**, 349–361 (1972).
11. Barlow, R. B. Jr *J. gen. Physiol.* **54**, 383–396 (1969).
12. Barlow, R. B. Jr & Kaplan, E. *J. gen. Physiol.* **69**, 203–220 (1977).
13. Yau, K. W., Lamb, T. D. & Baylor, D. A. *Nature* **269**, 78–80 (1977).
14. Yau, K. W., Matthews, G. & Baylor, D. A. *Nature* **279**, 785–786 (1979).
15. Barlow, R. B. Jr & Palfai, T. in *Research Report LSC*-14 4 (Institute for Sensory Research, Syracuse University 1971).

Light-induced calcium fluxes from outer segment layer of vertebrate retinas

S. Yoshikami, J. S. George & W. A. Hagins

Laboratory of Chemical Physics, NIAMDD, National Institutes of Health, Bethesda, Maryland 20205

Light affects the membrane potential of a vertebrate retinal rod or cone cell by transiently reducing its 'dark current', an inward flow of Na^+ through the plasma membrane covering the light-absorbing outer segment[1,2]. In rods most photons are absorbed by photopigment molecules in intracellular disk membranes that are physically separate from the plasma membrane[2–5]. Photochemical events in the disks probably control the Na^+ conductance of the plasma membrane through a chain of events that ultimately change the level of a diffusable substance in the cytoplasm of the outer segment. By combining reversibly with Na^+ carriers or channels in the plasma membrane, this 'internal transmitter' substance would modulate the dark current and thus the rod's membrane potential[6]. There is evidence that the internal transmitter is free Ca^{2+} (refs 7–10). Ca^{2+} buffer EGTA has a desensitizing effect on rods, consistent with a free cytoplasmic Ca^{2+} concentration of about 1 μM in darkness and release of 500–1,000 additional calcium ions for each absorbed photon[10]. However, there is insufficient proof that Ca^{2+} is released into the cytoplasm of rod outer segments by light and removed again in darkness. Reports that light reduces the total Ca^{2+} in outer segments have varied widely in their details[11–15]. Small amounts of Ca^{2+}, ~1 mol per mol of photoisomerized rhodopsin, are released by strongly illuminated isolated rod disks[16], but this is not enough to explain the large size of single photon responses[10,17]. We have studied net movements of Ca^{2+} in the receptor layer of albino rat retinas during the responses of the rods to light with the aim of detecting release of internal Ca^{2+} by a rise in its extrusion into the interstitial space.

Microelectrodes sensitive to free Ca^{2+} were made as described previously[18]. The siliconed tips were 2–3 μm in diameter and were filled for a length of 250 μm with *O*-nitrophenyl octyl ether containing 10% Na tetraphenylborate and 10% of the Ca^{2+} selective synthetic ionophore, ETH 1001 (Orion)[19]. The remainder of the electrode contained 0.1 M $CaCl_2$. Electrode resistances were 1–3,000 MΩ. the microelectrodes responded to step changes in Ca^{2+} activity from 0.5 to 5 mM with potential changes having an exponential rise of 130 ± 10 ms. Over the range of free $[Ca^{2+}]$, a_{Ca}, from 10^{-7} to 10^{-2} M, the Ca electrode potential V_{Ca} followed the equation

$$V_{Ca} = V_o + M \log_{10}(a_{Ca} + a_o) \qquad (1)$$

where V_o is a constant dependent on the solutions in the Ca and reference electrodes and M is 31 ± 1 mV per decade change in a_{Ca} at 37 °C. The apparent basal Ca activity due to electrode permeability to other ions, $a_o < 5 \times 10^{-8}$ M. Changes in *p*H of 1.5 unit on a background of 70 μM Ca^{2+} produced electrode potential changes of <20 μV. The electrodes were insensitive to changes in Mg^{2+}, Na^+, and K^+ (ref. 19).

The Ca electrode potential was referred to one of a pair of Ringer-filled micropipettes mounted in a cluster with it (shown in Fig. 1*a*). The entire assembly could be thrust under direct vision by IR microscopy[1] into the upturned receptor surface of an isolated retina so that the external voltage gradient V_d due to the dark current could be monitored with the change in potential of the Ca^{2+} electrode. As shown in Fig. 1*a*, electrode B and the Ca electrode were placed at the same depth in the retina so that the Ca signal was not mixed with light-induced changes in V_d.

Isolated rat retinas were prepared as previously described[1,2]. They were mounted in a chamber in a stream of physiological solution that passed parallel to the outer segment layer in laminar flow. The fluid velocity 50 μm above the rod tips was ~100 μm s^{-1}. An arrangement of valves allowed the fluid composition to be changed in 5 s. When more rapid changes in fluid composition were needed, a continuous jet of the desired fluid from a pipette in the bath was quickly lowered so as to sweep over the retina near the electrodes.

0028–0836/80/300395—04$01.00

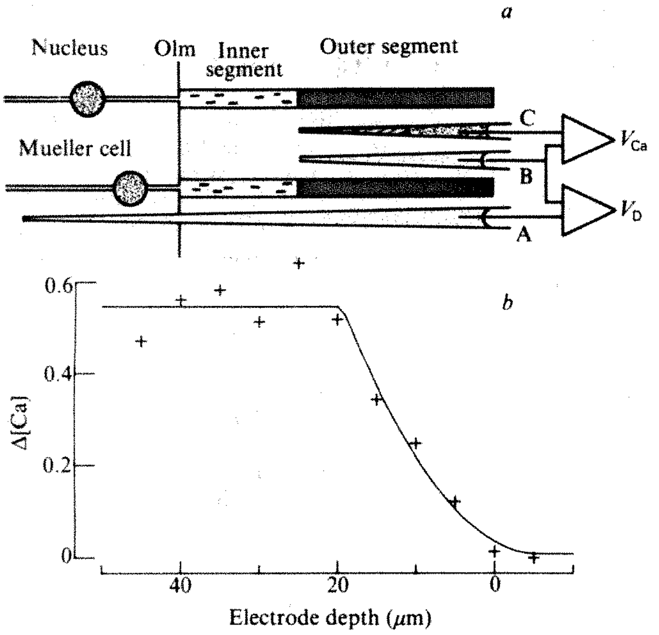

Fig. 1 Spatial distribution of the light-induced transient increase in interstitial [Ca^{2+}] with depth of the Ca-sensing electrode in the receptor layer. *a*, Diagram of the structure of the receptor layer to scale indicated at the bottom of *b*. Electrodes placed as shown in the interstitial spaces between the rods. *b*, Amplitude of the Ca^{2+} against depth. Each point is the mean area under the first 800 ms of the Ca transient obtained by averaging 16 flash responses. Curve: amplitude distribution to be expected from a source of Ca^{2+} limited to the outer segment layer of the retina. The assembly of three electrodes was moved in steps through the receptor layer. Stimuli: 2 μs, 560 nm, 110 photons absorbed per rod per flash. Ambient free [Ca^{2+}] 10 μM in a Ringers of composition similar to that of Fig. 2*a*.

Light causes a transient increase in the Ca^{2+} activity in the interstitial space of the outer segment layer. Figure 2*a* shows the effect of a 560-nm flash yielding 110 photons absorbed per rod on V_d recorded between electrodes A and B at depths of 75 and 25 μm from the rod tips and changes in the Ca^{2+} activity seen by the Ca electrode at 25 μm. The flash immediately shut down the dark current for about 1 s after which V_d returned to its initial level with a small overshoot. This waveform is characteristic of rat rods in the 70 μM unbuffered Ca^{2+} of the Ringer used. The Ca electrode showed a transient increase in a_{Ca} followed by a longer lasting decrease to slightly below the level before the flash. Although V_{Ca} was logarithmic in Ca^{2+} activity (equation (1)), the changes seen were so small relative to the background a_{Ca} that the relationship between ΔV_{Ca} and Δa_{Ca} was nearly linear. The time integral of the Ca^{2+} transient (smooth line) was nearly zero over the duration of the record. The rise in Ca^{2+} was ~1.2 μM at its peak just after the minimum in V_d.

If the Ringer was augmented with 10 mM Ca^{2+} buffer, nitrilotriacetic acid (NTA), and the Ca^{2+} and Mg^{2+} activities carefully adjusted to those of the control, the light-induced change in V_d was unaffected, but the Ca^{2+} transient was greatly reduced (Fig. 2*b*). This effect of NTA could not be attributed to its action as a buffer for H^+ or Mg^{2+}: there was 10 mM of the *p*H buffer HEPES present in both cases, and NTA is a weak Mg^{2+} buffer at the concentration used (500 μM Mg^{2+}). Thus the responses of the Ca electrode were probably due to changes in interstitial a_{Ca}.

With a fixed 10-μM free Ca^{2+} concentration in the Ringer and a stimulus of 80 photons absorbed per rod per flash, the size and shape of the Ca transient varied with electrode depth in the retina. Figure 1*b* shows data from Ca transients recorded at 5-μm intervals beginning 5 μm above the tips of the outer segments and extending inward to a depth of 45 μm. The points were computed from the time integrals of the responses 800 ms after the flashes. This time was near the peaks of the transients themselves. Small Ca transients could usually be seen even when the electrode was 25 μm above the retinal surface. These were much slower than the intraretinal ones and were caused by clouds of Ca^{2+}, released from distant retinal areas, drifting past the Ca electrode. In the space between the rods, the transients grew rapidly in size with increasing electrode depth in the region between the rod tips and the inner–outer segment junction at 25 μm depth. As the Ca electrode was advanced further, the transients remained at constant size or decreased slightly. In the dark, there was no detectable gradient of a_{Ca} in the extracellular space. Thus the Ca transients must indicate increased efflux and not a light-induced fall in a steady dark influx.

Viewed as a problem in one-dimensional diffusion of Ca^{2+} from sources in the receptor layer to sinks there and in the flowing Ringer stream, the concentration *c* of Ca^{2+} should follow the differential equation

$$\frac{\partial c}{\partial t} - D\frac{\partial^2 c}{\partial x^2} = F(x, t) \qquad (2)$$

where *D* is the diffusion coefficient of Ca^{2+} in the interstitial space perpendicular to the retinal surface and *F*(*x*, *t*) is the distribution of Ca^{2+} sources and sinks on the receptor cells. In

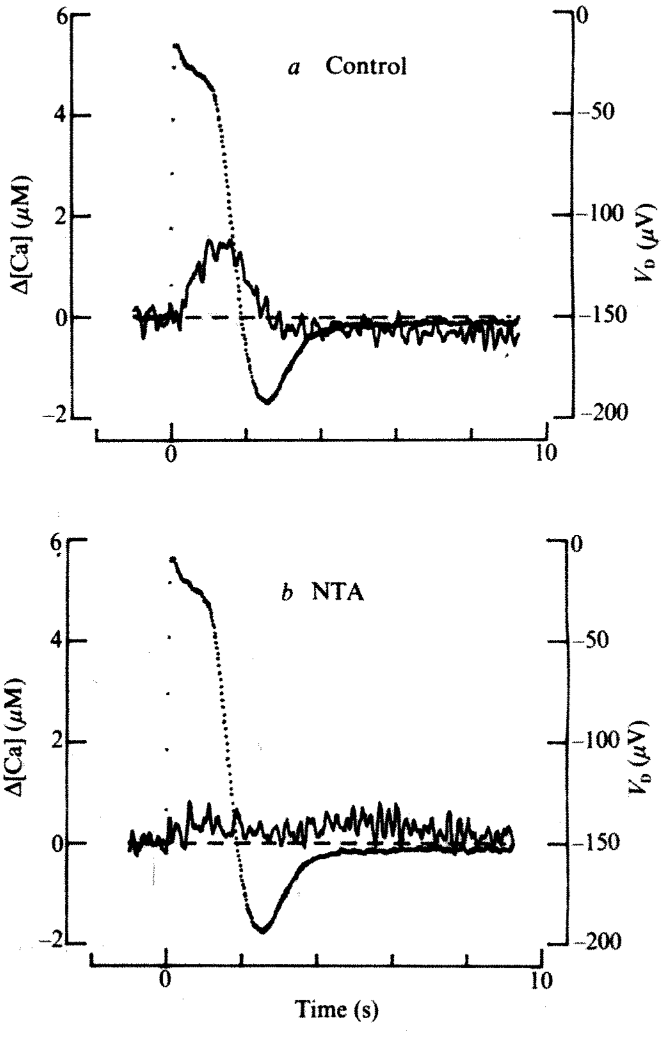

Fig. 2 Changes in interstitial dark voltage gradient V_d and free [Ca^{2+}] in the rod layer of an albino rat retina. Voltage-recording and Ca-recording electrodes placed as shown in Fig. 1*a*. Stimuli: 2 μs flashes of wavelength 540–580 nm that resulted in 110 photons absorbed per rod per flash. Dotted curves: changes in V_d. Continuous noisy curves: interstitial free [Ca^{2+}]. Dashes: drawn at signal levels seen just before flashes. Each curve is the mean of 16 responses. *a*, Control Ringer containing 136 mM NaCl, 0.5 mM $MgCl_2$, 2.7 mM KCl, 0.5 mM NaH_2PO_4, 11 mM glucose, 10 mM HEPES, and $CaCl_2$ added until the Ca electrode indicated a free [Ca^{2+}] of 70 μM. *p*H 7.14. *b*, Bathing Ringers same as control except that 10 mM nitrilotriacetic acid (NTA) was added and excess Ca^{2+} and Mg^{2+} were added by titration to achieve the same free metal concentrations as in *a*. The buffering effect of the NTA was negligible for H^+ and Mg^{2+} but reduced the concentration elevating effect of added Ca^{2+} to <10% of that of the control Ringers.

principle the two partial derivatives could be measured directly with electrode arrays and F computed as Ca^{2+} current sources and sinks[1], but the noise in the present data makes this procedure inaccurate. However, if the Ca transients are sampled at their peaks as in Fig. 1*b*, $\partial c/\partial t$ is negligible and equation (2) becomes an ordinary differential equation linking $c(x)$ with the Ca^{2+} source distribution $F(x)$. In Fig. 1 $c(x)$ is computed from equation (2) for a hypothetical distribution $F(x)$ (solid line) where the source is a uniform zone covering the entire length of the outer segments. No flow of Ca^{2+} is assumed to occur at the outer limiting membrane at $x = 45$ μm.

The data fit the hypothetical source distribution closely when its amplitude is properly scaled. In the outer segment layer, the transients grow in size roughly as the square of the electrode depth and not linearly as would be expected for Ca sources concentrated at the inner segments or more deeply. Unlike the computed curve, however, the data suggest some loss of Ca^{2+} towards the deeper retinal layers. The slight shift of the measured Ca source distribution (Fig. 1*b*) relative to the retinal elements of Fig. 1*a* is due to the 5-μm uncertainty in electrode position. Most of the Ca^{2+} arises in the region of the rod outer segments.

The internal a_{Ca} of rat rod outer segments is ~1 μM (ref. 10), and that of the external medium is much higher. Thus rods, like other eukaryotic cells, must regulate their internal Ca^{2+} with membrane pumps that exchange Ca^{2+} for Na^+ (refs 20, 21) or extrude Ca^{2+} via nucleotide phosphatases in the plasma membrane[22,23]. Is the light-induced Ca^{2+} efflux caused by a rise in the cytoplasmic a_{Ca} or by a light-stimulated increase in the activity of some Ca^{2+} extrusion mechanism? The results shown in Fig. 3 suggest the first mechanism perhaps augmented by the second through light-induced rod hyperpolarization.

If the NaCl in the bath is replaced with the depolarizing salt, potassium isethionate, the large V_d response shown in Fig. 3*a* (right) is completely abolished, but the interstitial increase in a_{Ca}, while slower and four times smaller, persists (Fig. 3*b*). Replacing the Na^+ in the medium with choline ions produces a similar result even though the rod membrane potentials should be hyperpolarized to near K^+ equilibrium potential in this solution. Since the residual Na^+ in both choline and K isethionate Ringers was less than 10 μM, it is unlikely that Na : K exchange causes the Ca^{2+} efflux in these solutions.

Can light still produce a Ca^{2+} efflux when plasma membrane calcium pumps are partly shunted by a divalent metal ionophore? If the rods are exposed to X-537A, the dark current and the V_d responses are greatly reduced at external $a_{Ca} > 10^{-5}$ M (ref. 8), but the light-induced rise in interstitial a_{Ca} remains large (Fig. 3*d*). Reducing the ambient a_{Ca} to 10 μM increases the dark current and V_d, but the Ca signal decreases slightly. Since X-537A increases the permeability of the plasma membrane to Ca^{2+}, it is likely that the increased Ca^{2+} efflux follows mainly from an increase in cytoplasmic a_{Ca}. Because the external $[Ca^{2+}]$ is greater than that in the cytoplasm even in the presence of X-537A, however, the Ca extrusion machinery must link the presumed light-induced rise in internal Ca^{2+} to that seen extracellularly, making it larger and faster.

If intracellular Ca^{2+} release causes the dark current shutdown, the kinetics of Ca^{2+} efflux should closely track the V_d waveform. To compare the kinetics of the two processes, the observed waveform of the transient increase in interstitial a_{Ca} must be transformed mathematically to allow for the finite volume v of the interstitial space (l cm^{-2}) and for the loss of Ca^{2+} by diffusion into the flowing Ringers. Neglecting the small unstirred layer at the retinal surface and solving equation (2) for the condition of no flow at the outer limiting membrane (OLM) (Fig. 1*a*) and for a uniform Ca^{2+} source distributed along the outer segments that instantaneously dumps Q mol cm^{-2} into the interstitial space yields a transient increase in a_{Ca} at 25 μm depth in the receptor layer that is close to a truncated exponential of the form

$$c(25, t) = 0.5\, c(25, 0) \exp(-t/\tau) \qquad (3)$$

where $c(25, 0) = Q/v$ and $\tau = 4l^2/\pi^2 D$ (ref. 24, equation 3.4.5, p. 101). Here l is the distance from the rod tips to the OLM. For this special position of the Ca electrode, the total outflux $J(t)$ from the entire length of outer segments thus is represented approximately by

$$2v\left(\frac{dc}{dt} + \frac{c}{\tau}\right) = J(t) \qquad (4)$$

For the receptor layer of the rat retina, measurements from electron micrographs yield $v = 650$ nl cm^{-2}. τ, Computed from a measured D for Ca^{2+} of 1.1×10^{-5} cm^2 s^{-1} in the rod interstices (W. A. H. and S. Y., unpublished) is 650 ms. Using these two experimental parameters and forming the sum on the left-hand

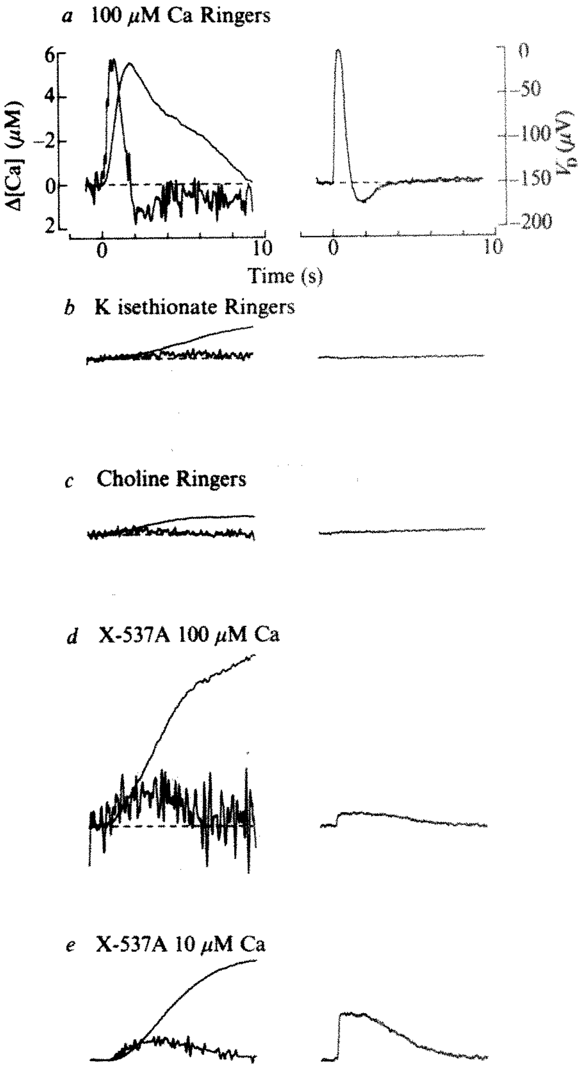

Fig. 3 Changes in dark voltage gradient V_d (right column) and extracellular free $[Ca^{2+}]$ (left column) in the rod layer of the rat retina in solutions of various compositions. Stimuli as in Fig. 2, electrode positions as in Fig. 1*a*. Temperature, 37 °C. *a*, Control. As in Fig. 2 but Ca^{2+} added to give *p*Ca 4.0. Mean of four responses. *b*, NaCl and KCl replaced with 140 mM K isethionate, *p*Ca 4.0. Mean of 96 responses at 15-s intervals. V_d response suppressed by the depolarizing solution, but there was a distinct light-induced increase in interstitial $[Ca^{2+}]$ as shown by its time integral (smooth line in left column). The total Ca^{2+} appearing was 25% of that in the control solution. *c*, NaCl replaced with 140 mM choline chloride. This solution should hyperpolarize the rod membrane potentials but suppress the dark current. As in *b*, the V_d response disappeared but there was a measurable Ca^{2+} release from the rod layer. *p*Ca 4.0. Mean of 96 responses. *d*, 10 μM of the divalent cation ionophore, X-537A was added to control Ringers at *p*Ca 4.0. The dark current and V_d were greatly reduced, but there was a large light-induced release of Ca^{2+} from the rod layer. Mean of eight responses. The large spikes in the Ca responses were electrical interference from the bath heater. 200 photons per rod . *e*, Same retina as in *d* but ambient free $[Ca^{2+}]$ reduced to 10 μM. Dark current and V_d response immediately increased, but Ca release was slightly reduced. Mean of eight responses. 200 photons per rod.

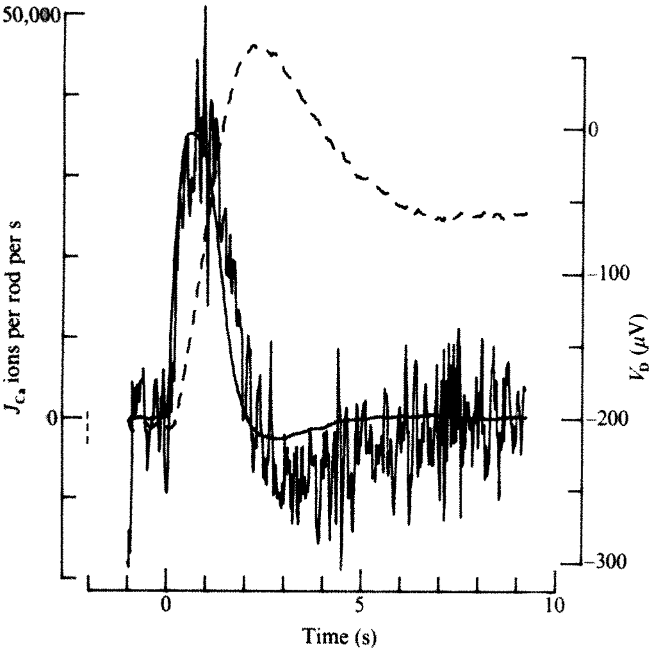

Fig. 4 Time courses of the light-induced Ca^{2+} flux from the rod layer compared with the light-induced reduction in V_d. Stimuli as in Fig. 2. Smooth line: V_d response convolved with an exponential response function of time-constant 130 ms to simulate the time-lag of the Ca electrode. Noisy curve: Ca^{2+} flux from the rods computed from equation 4. Dashes: time integral of Ca^{2+} flux in units of ions per rod on the left-hand scale. Mean of four responses to flashes of energy 110 photons absorbed per rod. The time course of the Ca efflux and the change in V_d are similar. Apparently about half of the Ca^{2+} released within 2 s of the flash is reaccumulated by the rod layer.

side of equation (4) by numerical differentiation of the experimental Ca transient yields the noisy curve in Fig. 4.

The Ca flux can now be directly compared with the waveform of the V_d response if the latter is first convolved with a truncated exponential with a 130-ms time constant to simulate the response lag of the Ca electrode. The result is a smooth line, shown in Fig. 4. The two waveforms are nearly identical, the duration of the Ca efflux being slightly longer and its peak not more than 100 ms later than the transformed V_d response.

The Ca^{2+} flux is large and biphasic. As much as half of the 45,000 ions leaving the outer segments in the first 2 s after the flash are apparently reabsorbed in the next 7 s (Fig. 4, dashed line). Since each rod absorbed 110 photons per flash, about 400 Ca^{2+} ions must have been extruded per photon response. If Ca^{2+} is the internal excitatory transmitter, the total Ca release must have been at least twice as large, because only cytoplasmic Ca^{2+} should reduce the Na^+ permeability of the plasma membrane. The observed release would only increase the cytoplasmic $[Ca^{2+}]$ by about 3 μM, a small fraction of the total Ca^{2+} in rod outer segments[14,25]. But if a steady 25-s light stimulus of intensity 9,500 photons per rod per s is used instead of a flash, the Ca^{2+} outflux is sustained for the entire period of illumination and amounts to about 100 $\mu mol\,l^{-1}$ of rod water. The light-sensitive Ca store is therefore large.

The light-induced Ca^{2+} effluxes seen here are fast enough, large enough, and of the spatial distribution to be expected from the Ca hypothesis. Moreover, the observed fast exchange of Ca^{2+} across the plasma membrane of rod outer segments explains the great sensitivity of the dark current to the $[Ca^{2+}]$ in the external medium. It remains to link the Ca^{2+} fluxes to enzymatic events in the disk membranes, such as the hydrolysis of GTP[26–29] and of cyclic GMP[30], and the binding of GDP[29]. *Note added in proof*: Since this paper was submitted, a preliminary account has appeared in *Fedn Proc.* **39,** 2066 (1980) and similar conclusions are reached by use of surface calcium electrodes by G. H. Gold and J. Korenbrot, *Fedn Proc.* **39,** 1814 (1980).

Received 12 December 1979; accepted 12 May 1980.

1. Hagins, W. A., Penn, R. D. & Yoshikami, S. *Biophys. J.* **10,** 380–412 (1970).
2. Penn, R. D. & Hagins, W. A. *Biophys. J.* **12,** 1073–1094 (1972).
3. Cohen, A. I. *Vision Res.* **10,** 445–453 (1970).
4. Rüppel, H. & Hagins, W. A. in *Biochemistry and Physiology of Visual Pigments* (ed. Langer, H.) 257 (1973).
5. Yoshikami, S., Robinson, W. E. & Hagins, W. A. *Science* **185,** 1176–1179 (1974).
6. Baylor, D. A. & Fuortes, M. G. F. *J. Physiol., Lond.* **207,** 77–92 (1970).
7. Yoshikami, S. & Hagins, W. A. in *Biochemistry and Physiology of Visual Pigments* (ed. Langer, H.) 245 (1973).
8. Hagins, W. A. & Yoshikami, S. *Expl Eye Res.* **18,** 229–305 (1974).
9. Pinto, L. H., Brown, J. E. & Coles, J. A. in *Vertebrate Photoreception* (eds Fatt, P. & Barlow, H.) 159 (1977).
10. Hagins, W. A. & Yoshikami, S. in *Vertebrate Photoreceptor* (eds Fatt, P. & Barlow, H.) 97 (1977).
11. Liebman, P. A. *Invest. Ophthal.* **13,** 700–702 (1974).
12. Hendricks, T., Daeman, F. J. M. & Bonting, S. L. *Biochim. biophys. Acta* **345,** 468–473 (1974).
13. Szuts, E. & Cone, R. A. *Fedn Proc.* **33,** 1471 (1974).
14. Szuts, E. & Cone, R. A. *Biochim. biophys. Acta* **468,** 194–208 (1977).
15. Hendricks, T., van Haard, P. M. M., Daeman, F. J. M. & Bonting, S. L. *Biochim. biophys. Acta* **467,** 175–184 (1977).
16. Kaupp, U. B. & Junge, W. *FEBS Lett.* **81,** 229–232 (1977).
17. Baylor, D. A., Lamb, T. D. & Yau, K.-W. *J. Physiol., Lond.* **288,** 589–611 (1979).
18. Heinemann, U., Lux, H. D. & Gutnick, M. J. *Expl Brain Res.* **27,** 237–243 (1977).
19. Simon, W., Ammann, D., Oehme, M. & Morf, W. E. *Ann. N. Y. Acad. Sci.* **307,** 52–70 (1978).
20. Reuter, H. & Seitz, N. *J. Physiol., Lond.* **195,** 451–470 (1968).
21. Mullins, L. J. *J. gen. Physiol.* **70,** 681–695 (1977).
22. Blaustein, M. P., Ratzlaff, R. W. & Kendrick, N. K. *Ann. N. Y. Acad. Sci.* **307,** 195–212 (1978).
23. Baker, P. F. *Ann. N. Y. Acad. Sci.* **307,** 250–268 (1978).
24. Carslaw, H. S. & Jaeger, J. C. *Conduction of Heat in Solids* 2nd edn (Oxford University Press, London, 1959).
25. Hagins, W. A. & Yoshikami, S. *Ann. N.Y. Acad. Sci.* **264,** 314–325 (1975).
26. Robinson, W. E. & Hagins, W. A. *Biophys. J.* **16a** (1977).
27. Robinson, W. E. & Hagins, W. A. *Photochem. Photobiol.* **29,** 693 (1979).
28. Wheeler, G., Matsuo, Y. & Bitensky, M. W. *Nature* **269,** 822–824 (1977).
29. Robinson, W. E. & Hagins, W. A. *Nature* **280,** 398–400 (1979).
30. Yee, R. & Liebman, P. A. *J. biol. Chem.* **253,** 7902–7909 (1978).

Co-infection by lactic dehydrogenase virus and C-type retrovirus elicits neurological disease

Larry R. Pease & William H. Murphy

Department of Microbiology and Immunology, The University of Michigan Medical School, Ann Arbor, Michigan 48109

Intraperitoneal injection of neuropathogenic strains of lactic dehydrogenase virus (LDV)[1–3] causes a histologically distinctive[4] fatal paralytic disease characterized by an inflammatory destruction of motor neurones in the brain stem and cord in C58 mice aged over 9 months. To elicit the disease in the naturally susceptible C58 strain requires an age-associated[5] or X-ray induced[6] loss of immunological competence[5], LDV infection[1–3] and genetic susceptibility[1,6]. Genetic studies[1,7] of the common inbred mouse strains showed that susceptibility to the disease was not linked to the major histocompatibility complex but correlated with the FV-1^n allele, susceptibility to spontaneous leukaemia, and infection by neuropathogenic strains of LDV[1–3]. These observations suggested that neuropathogenic strains of LDV elicit the disease only in those strains of mice that carry multiple copies of N-tropic C-type retroviruses in their genomes[8,9] and that are permissive for retrovirus replication. Presumably the expression of these viral genomes (high titres of virus in tissues correlating with age[9]) is the important factor. Here we present genetic evidence to support this hypothesis and briefly discuss the possible implications.

In Table 1 the mice in group 1 were selected to test whether there was a correlation between susceptibility to the disease, the number of copies of N-tropic C-type retroviruses in their genomes[8,9], their haplotype and their FV-1 genotype. The FV-1^b allele[10] dominantly restricts N-tropic C-type retrovirus replication. All of the strains (*a–e*) that were FV-1^n and are known to contain multiple copies of N-tropic C-type retroviruses in their genomes[8,9] were susceptible. The data for the congeneic AKR strains are of interest because they show that

0028-0836/80/300398—03$01.00

Tab! 1 Susceptibility of inbred mice to paralytic disease

Group		Inbred strains*		FV-1 type	Genomic copies of C-type retroviruses	Incidence of paralysis† age (months) 6	9	12
	a		k	n	Many		10/10	15/15
			k	n	Many		13/20	
			b	n	Many	0/17		5/6
			k	n	Many			16/16
			u	n	Many			6/11
			k	b	Many		0/24	
			k	n	Few	0/8		0/12
			d	n	Few	0/13		0/14
			b	b	Few		0/13	
			b	b	Few	0/19		0/10
		/Boy	b	n	Few		0/12	
			k	b	Few	0/18		
	a	/wm × C3H/HeJ	k/k	n/n		2/8	7/12	
	b	C58/wm × DBA/2J	k/d	n/n		2/8	5/8	
2	*c*	C58/wm × B10	k/b	n/b		0/26		0/10
	d	C58/wm × B10.BR	k/k	n/b		0/20		0/14
	e	C58/wm × BALB/cWm	k/d	n/b		0/11		0/19
Backcross progeny								
	a	(C58 × B10) × B10	k/b or b/b	n/b or b/b		0/43		
3	*b*	C58 × (C58 × B10)	k/k or k/b	n/n or n/b		18/53		6/12
	c	(C58 × B10) × C58	k/k or k/b	n/n or n/b		1/93		1/20

* In group 1, strains *a–c* are considered to have a 'high' incidence of leukaemia ranging from 40 to 90% depending on the colony. Strains *d* and *e* have a 'moderate' incidence of leukaemia ranging from 20 to 40%. The remaining mice listed have a 'low' incidence of spontaneous leukaemia (usually < 5%)[16]. AKR-H-2^b/Boy is congeneic to AKR/Boy and is H–2^b rather than H–2^k. AKR-FV-1^b/Boy is congeneic to AKR/Boy but is FV-1^b rather than FV-1^n. B6/Boy is a subline of C57BL/6 and is FV-1^b. The congeneic line B6-FV-1^n/Boy is FV-1^n. The C58/wm and BALB/cWm mice are our stock inbred lines. The following abbreviations were used: C58 for C58/wm, B10 for C57BL/10Sn, and B10.BR for B10.BR/SgSn. In Groups 2 and 3 the female is listed first for each breeding set; mice were 2–5 months old when mated.

† Mice received 550R of whole body X-ray irradiation 24 h before the intraperitoneal injection of LDV (10^7–10^8 infectious doses) derived from either line I*b* cells or from a stock prepared from the plasma of infected BALB/cWm mice[2]. The plasma stocks of LDV cause the same clinical and histopathological effects as line I*b* derived virus[2]. After infection, mice were held for 30 days and scored for the incidence of paralysis. Paralysed and disease-free mice (3–6 per group) were killed and the diagnosis of paralysis or its absence confirmed histologically as described previously[4]. The sex of mice did not affect their susceptibility in any of the test groups.

when H–2^b was substituted for H–2^k, mice were still susceptible (compare *c* with *b*). When FV-1^b was substituted for FV-1^n, mice were resistant (compare *f* with *b*). The mice in groups *g* and *h* were representative of strains that carry few copies of retroviruses in their genomes but are permissive (FV-1^n) for retrovirus replication. None contracted the disease. The strains in groups *i* and *j* contain few copies of retroviruses in their genomes, are not permissive (FV-1$^{b/b}$) for N-tropic C-type retrovirus replication, and were not susceptible. Introduction of the FV-1^n allele in place of FV-1^b (compare *k* with *i*) or H–2^k in place of H–2^b (compare *l* with *j*), did not confer susceptibility. These results confirmed our findings[1,7] that susceptibility or resistance was not H–2 linked and indicated that mice had to carry multiple copies of N-tropic C-type retroviruses in their genomes and be permissive for retrovirus replication to be susceptible.

The mice in group 2 were used to test whether mice presumed to be genetically susceptible, but containing too few copies of N-tropic C-type retroviruses in their genomes (mice in *g* and *h*, Group 1), would manifest paralytic LDV infection if they became infected by the appropriate C-type retrovirus. Thus, 'genetically susceptible' male mice 'deficient' in virus (C3H/HeJ and DBA/2J) were bred to C58 females. The assumption was that the C58 mothers would transmit virus to the newborn F$_1$ progeny either chromosomally or by the milk. Table 1 shows that the F$_1$ hybrids derived from the 'potentially susceptible strains' (groups *a* and *b*) were susceptible. The corresponding genetically resistant (FV-1$^{n/b}$) hybrids were not (groups *c–e*) even when the H–2^k haplotype (group *d*) was substituted for H–2^b (group *c*).

In group 3, test-cross progeny were tested to determine whether resistance segregated in accordance with the hypothesis that the FV-1^b allele determined resistance. The data show that all of the backcross progeny in control group *a*, which in principle inherited an FV-1^b allele, were resistant. In theory, 50% of the test-cross progeny in group *b* should have been FV-1$^{n/n}$ and susceptible if they were infected by an N-tropic C-type retrovirus by their mothers. The results confirmed this expectation with a somewhat lower incidence of disease (34%) in the incompletely susceptible 6-month-old indicator C58 mice[1,6,7]. Moreover, when backcross progeny were nursed on resistant (C58 × B10) mothers (group *c*) there was a strong maternal effect. Such an effect would be consistent with the failure to transmit virus to the progeny by the milk[11], or the transmission of antibody to the progeny by the milk, thereby protecting them from C-type retrovirus infection. Other mechanisms of conferring maternal resistance are not ruled out by the data[11].

If one accepts the genetic data at their face value they support the hypothesis that dual infection by LDV and N-tropic C-type retrovirus(es) was required to elicit a specific paralytic motor neurone disease in genetically susceptible mice. Expression of N-tropic C-type retrovirus genomes in FV-1$^{n/n}$ mice seemed to be an important factor in the susceptible strains. The paradox is that neither LDV[12] or the common C-type retroviruses are frankly cytopathic to cells either *in vitro* or *in vivo*. Although Gardner *et al.*[13] and McCarter *et al.*[14] have reported the occurrence of neuropathogenic C-type viruses in mice, LDV has not been evaluated as an essential contributory factor in such virus stocks. However, these investigators also have not claimed tha neurone destruction is a direct cytopathic response to vira infection. The striking feature of the model we describe is tha two viruses that are ubiquitous in mice, and that ordinarily d not cause overt disease, seem to act together to elicit a specif disease syndrome in a genetically susceptible host. The findings are of interest because they direct attention to ho unrelated viruses may interact together at the cellular lev provide an additional way to characterize phenotypically LD and mouse leukaemia virus strains, and may provide an additional insight to the complex interactions between viruses and their hosts in the slow viral infections of the nervous system[15].

This work was supported by funds from the Institute of Gerontology of the University of Michigan and by USPHS grant S07-RR-05383. All the 'Boy' mouse strains were from Dr Edward Boyse. The mice with a J designation and B10 and B10.BR lines were from Jackson Memorial Laboratory.

Received 18 February; accepted 27 May 1980.

1. Murphy, W. H., Nawrocki, J. F. & Pease, L. R. in *Animal Models of Neurologic Disease* (eds Behan, P. O. & Rose, C. F.) (Pitman, London, in the press).
2. Nawrocki, J. F., Pease, L. R. & Murphy, W. H. *Virology* **103,** 259–264 (1980).
3. Martinez, D., Brinton, M. A., Tachovsky, T. G. & Phelps, A. H. *Infect. Immun.* **27,** 979–987 (1980).
4. Lawton, J. W. M. & Murphy, W. H. *Archs Neurol.* **28,** 367–370 (1973).
5. Murphy, W. H., Tam, M. R., Lanzi, R. L., Abell, M. R. & Kauffman, C. *Cancer Res.* **30,** 1612–1622 (1970).
6. Duffey, P. S., Martinez, D., Abrams, G. D. & Murphy, W. H. *J. Immun.* **116,** 475–481 (1976).
7. Pease, L. R., Abrams, G. D. & Murphy, W. H. *J. Immun.* (submitted).
8. Lowy, D. R., Chattopadhyay, S. K., Teich, N. M., Rowe, W. P. & Levine, A. S. *Proc. natn. Acad. Sci. U.S.A.* **71,** 3555–3559 (1974).
9. Chattopadhyay, S. K., Lowy, D. R., Teich, N. M., Levine, A. S. & Rowe, W. P. *Cold. Spring Harb. Symp. quant. Biol.* **39,** 1085–1101 (1974).
10. Lilly, F., Duran-Reynals, M. L. & Rowe, W. P. *J. exp. Med.* **141,** 882–889 (1975).
11. Melief, C. J. M., Louie, S. & Schwartz, R. S. *J. natn. Cancer Inst.* **55,** 691–698 (1975).
12. Rowson, K. E. K. & Mahy, B. W. J. *Virol. Monogr.* **13,** 57–87 (1975).
13. Gardner, M. R. *et al.* in *Amotrophic Lateral Sclerosis* (eds Adams, J. M., Johnson, R. T. & Brazier, M. A. B.) 217–234 (1976).
14. McCarter, J. A., Ball, J. K. & Frei, J. V. *J. natn. Cancer Inst.* **59,** 179–183 (1977).
15. TerMeulen, V. & Hall, W. W. *J. gen. Virol.* **41,** 1–25 (1978).
16. Staats, J. *Cancer Res.* **36,** 4333–4377 (1976).

S100 protein is present in cultured human malignant melanomas

Richard Gaynor, Reiko Irie, Donald Morton & Harvey R. Herschman

Division of Hematology-Oncology, Department of Medicine; Division of Oncology, Department of Surgery; Department of Biological Chemistry and Laboratory of Nuclear Medicine and Radiation Biology, Center for the Health Sciences; University of California, Los Angeles 90024

S100 protein, so called because of its solubility in 100% saturated ammonium sulphate[1], is an acidic cytoplasmic protein specific for the nervous system[2,3]. It is localized primarily to glial elements of the brain, Schwann cells in the peripheral nervous system and satellite cells in sympathetic ganglia[4,5]. This brain-specific protein shows a close immunological relationship among a wide variety of vertebrates, as measured by a quantitative complement fixation technique[6]. Although strict serological conservation and tissue localization have been maintained among different species, no function for S100 protein has been determined. However, the appearance of S100 protein in brain is correlated with maturation of the nervous system in both rat and man[7,8]. Previous *in vitro* studies on the production and regulation of S100 protein in the C6 cell line derived from a rat astrocytoma indicated that cell contact and cessation of division induced S100 protein[9]. Neuroblastoma cell lines lack this protein[10,11] although it is found in other astrocyte cell lines. We are unaware of any reports of cell lines, other than those of glial origin, which produce S100 protein. Melanocytes are derived from neuroectodermal elements, and this common origin of glial cells and melanocytes prompted us to study whether S100 protein might be present in cell lines from human malignant melanomas. We now report the presence of S100 protein in five f seven continuous cell lines of human malignant melanoma.

All lines used in our studies were derived from metastatic elanomas, and were maintained in culture for 12–20 passages. Most lines have been characterized previously[12,13]. After the elanoma cells in tissue culture flasks were confluent, the cells ere collected and homogenized. The soluble protein was assayed by quantitative complement fixation for S100 protein, using rabbit antisera to bovine S100. Complement fixation curves for extracts of human brain and one of the melanoma cell lines are shown in Fig. 1. Five of seven cell lines from human melanomas were found to have S100 protein (Table 1). In two of the lines (lines 19 and 12) the amount of S100 protein exceeded that present in human brain medulla. Lymphocyte cell lines of the two patients from which M14 and M29 were derived were negative for S100, as were HeLa cells and a human sarcoma cell line. Cells from line M14 were injected into a nude mouse; the tumour resulting after 30 days had 2.2 μg of S100 per g of tumour. Of the lines studied, only M12 and M19 were melano-

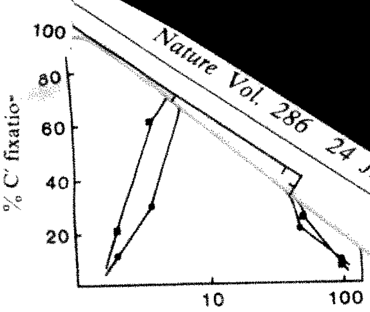

Fig. 1 Complement (C') fixation curves of S100 for human brain medulla (●) and M29 cell line (■). M29 cell line extract was prepared as described in Table 1 legend. The brain sample was homogenized with Tris buffer, 2 ml per g tissue, and spun at 40,000*g* for 10 min before S100 determination. Quantitative complement fixation using an 8,000-fold dilution of antiserum was carried out on extracts of M29 and human brain medulla.

Table 1 S100 protein values for melanoma cell lines and other tissues

Specimen	μg S100 per mg soluble protein
Melanoma cell lines	
M12	6.2
M14	1.0
M15	1.9
M19	30.0
M21	ND
M24	ND
M29	3.5
Other cells and tissues	
C6 rat glial cells	2.6
Brain cerebrum (human)	2.3
Brain medulla (human)	5.6
HeLa cells	ND
Sarcoma cell line (human)	ND
Lymphocyte cell lines	
L14	ND
L29	ND

Cell lines were cultured in 75-cm^2 culture flasks using RPMI 1640 medium with 20% fetal calf serum and maintained in 5% CO_2. Confluent cells were washed twice with phosphate-buffered saline (NaCl, 8 g l^{-1}; KCl, 0.2 g l^{-1}; $MgCl_2 \cdot 6H_2O$, 0.1 g l^{-1}; $Na_2HPO_4 \cdot 7H_2O$, 2.16 g l^{-1}) and once with complement fixation buffer (0.0 M trisma base, 0.14 M NaCl, 0.5 mM $MgSO_4$, 0.15 mM $CaCl_2$, 0.1% bovine serum albumin). Cells were collected by scraping into complement fixation buffer, homogenized and spun at 40,000*g* for 10 min. Quantitative complement fixation was carried out using a 6,000-fold dilution of antiserum as described by Levine[17]. S100 was quantified as described by Zuckerman *et al.*[18]. The serological specificity of our antiserum has previously been demonstrated by double diffusion in agar and by quantitative complement fixation analysis using soluble protein extracts of a variety of tissues as antigens[17,18]. Purified bovine S100 was used as a standard to quantify the amount of S100 present in the soluble portion of each specimen. ND, Not detectable.

8–0836/80/300400—02$01.00

tic. Line M19 cells are the source with the greatest specific activity of S100 protein so far reported.

The serological cross-reactivity of S100 protein is strongly conserved in different species[6]. To show that the S100 protein present in human brain was immunologically identical to that present in human melanoma, we examined the serological cross-reactivity, as measured by complement fixation. The ratio of antisera required to give the same percentage of complement fixation at equivalence for heterologous compared with homologous antigens provides a quantitative measure of cross-reactivity defined as the 'index of dissimilarity' (refs 14, 15). The maximal complement fixation values for brain extracts and extracts from melanoma cell lines at three dilutions of antiserum were plotted against the log of the antiserum concentration (Fig. 2). The superimposable lines for the brain and melanoma samples indicate immunological identity for the S100 protein from these two sources (that is, an 'index of dissimilarity' of 1.0).

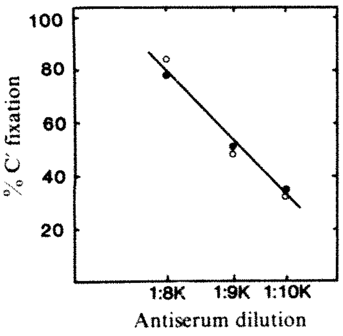

Fig. 2 Cross-reactivity of brain and melanoma cell line S100 protein. Maximal complement (C′) fixation values for brain extract (●) and melanoma (○) line M29 extract at these dilutions of antisera [1/8,000 (1 : 8 K), 1/9,000 (1 : 9 K), 1/10,000 (1 : 10 K)] are plotted against the log of the antiserum concentration. The superimposable lines for both samples indicate immunological identity for the S100 protein from these two sources.

We do not know whether S100 protein accumulation is a function only of malignant melanocytes or of all melanocytes. S100 protein does not accumulate in human skin (our unpublished observations); however, this may reflect the low density of melanocytes normally present. Malignant melanoma cell lines have previously been shown to possess receptors for nerve growth factor[16]. Either nerve growth factor receptors or S100 protein may serve as a tumour-associated marker for malignant melanoma.

R.G. is a Hematology–Oncology fellow (training grant CA-09247); R.I. holds a US-PHS RCDA (CA-00543). These studies were supported by grants CA 12582 (D.M.) and DOE DE AM03 76 SF00012 (H.R.H.).

Received 28 January; accepted 14 May 1980.

1. Moore, B. W. *Biochem. biophys. Res. Commun.* **6,** 739–744 (1976).
2. Moore, B. W. & MacGregor, D. *J. biol. Chem* **240,** 1647–1659 (1965).
3. Moore, B. W., Perez, V. J. & Gehring, M. *J. Neurochem.* **15,** 265–272 (1968).
4. Ludwin, S. K., Kosek, J. C. & Eng, L. F. *J. comp. Neurol.* **165,** 197–208 (1976).
5. Eng. L. F., Kosek, J. C., Forno, L, Deck, J. & Bigbee, J. *Trans. Am. Soc. Neurochem.* **7,** 211 (1976).
6. Kessler, D., Levine, L. & Fassman, G. *Biochemistry* **7,** 758–764 (1968).
7. Zuckerman, J., Herschman, H. R. & Levine, L. *J. Neurochem.* **17,** 251–256 (1970).
8. Herschman, H. R., Levine, L. & deVellis, J. *J. Neurochem.* **18,** 629–633 (1971).
9. Pfeiffer, S. E., Herschman, H. R., Lightbody, J. & Sato, G. *J. cell. Physiol.* **75,** 329–340 (1970).
10. Benda, P., Lightbody, J., Sato, G., Levine, L. & Sweet, W. *Science* **161,** 370–371 (1968).
11. Moore, B. *Proteins of the Nervous System* (Raven, New York, 1973).
12. Irie, R., Irie, K. & Morton, D. *Cancer Res.* **36,** 3510–3517 (1976).
13. Irie, R., Giuliano, A. E. & Morton, D. *J. natn. Cancer Inst.* **63,** 367–373 (1979).
14. Sarich, U. M. & Wilson, A. C. *Science* **154,** 1563–1564 (1966).
15. Nonno, L., Herschman, H. R. & Levine, L. *Archs Biochem. Biophys.* **136,** 361–367 (1969).
16. Fabricant, R., DeLarco, J. & Todaro, G. *Proc. natn. Acad. Sci. U.S.A.* **74,** 565–569 (1977).
17. Levine, L. in *Handbook of Experimental Immunology* (ed. Weir, D. M.) (Blackwell, Oxford, 1967).
18. Zuckerman, J., Herschman, H. R. & Levine, L. *J. Neurochem.* **17,** 251–256 (1970).

Polar redistribution of ^{125}I-labelled insulin on the plasma membrane of cultured human lymphocytes

Philippe Barazzone*, Jean-Louis Carpentier*, Phillip Gorden†, Emmanuel Van Obberghen† & Lelio Orci*

* Institute of Histology and Embryology, School of Medicine, University of Geneva, Geneva, Switzerland
† Diabetes Branch, National Institutes of Arthritis, Metabolism and Digestive Diseases, National Institutes of Health, Bethesda, Maryland 20014

Cultured human lymphocytes of the IM-9 line have specific binding sites for ^{125}I-insulin that have been characterized in detail[1,2]. When the hormone–cell interaction was studied by quantitative electron microscopic (EM) autoradiography, it was shown that initial binding was to the plasma membrane and that at 37 °C a small fraction of the ligand was internalized by the cell[3,4]. The internalized ligand was found preferentially localized in lysosomes in the Golgi region of the cell[5]. It is well known that di- or multivalent ligands redistribute in the plane of the membrane before internalization[6]. We now report that following initial binding the univalent ligand insulin also undergoes a polar redistribution ('capping') before internalization.

Cultured human lymphocytes have a polarity that can be distinguished in appropriately taken photomicrographs of thin sections of these cells (Fig. 1). The Golgi pole was arbitrarily assigned to half the cell and the opposite pole was assigned to the other half as indicated in Fig. 1.

In this study we have assumed that initial receptor binding is most accurately reflected at low temperature and at early times of incubation. When 0.2 nM ^{125}I-insulin was incubated at 15 °C for 2 min and the hormone–cell interaction examined by EM autoradiography, grains became distributed on the plasma membrane of the cell in a statistically indistinguishable fashion (Table 1). We interpret this to mean that insulin receptors or groups of receptors are initially distributed at each pole of the cell with equal frequency.

Table 1 Distribution of autoradiographic grains on the surface of IM-9 lymphocytes during incubation with 0.2 nM ^{125}I-insulin

	2 min, 15 °C	90 min, 15 °C	2 min, 37 °C	60 min, 37 °C
Golgi pole	53%	58%	72%	73%
Opposite pole	47%	42%	28%*	27%*

Number of grains analysed = 2 min, 15 °C: 148; 90 min, 15 °C: 154; 2 min, 37 °C: 140; 60 min, 37 °C: 164.

* As determined by the χ^2 test these grain distributions are significantly different ($P < 0.005$) from the grain distribution found after 2 min of incubation at 15 °C.

We next investigated whether this was true for insulin at physiological concentrations. Labelled insulin was, therefore, incubated with cultured lymphocytes for a longer period of time at 15 °C and 37 °C. By 90 min at 15 °C there was no statistically significant difference between the percentage of grains associated with each pole of the cell (Table 1). By contrast, by 2 min of incubation at 37 °C there was a preferential association of the ligand with the Golgi pole of the cell and the same distribution of the labelled material was apparent after 60 min of incubation (Table 1, Fig. 2). We have found that although the affinity of insulin for its receptor is decreased with increasing temperature, there is no change in the total number of receptors when the incubation temperature is raised from 15 to 37 °C (unpublished observations). We interpret the present data to mean that, although insulin initially binds with equal frequency to either

0028-0836/80/300401—03$01.00

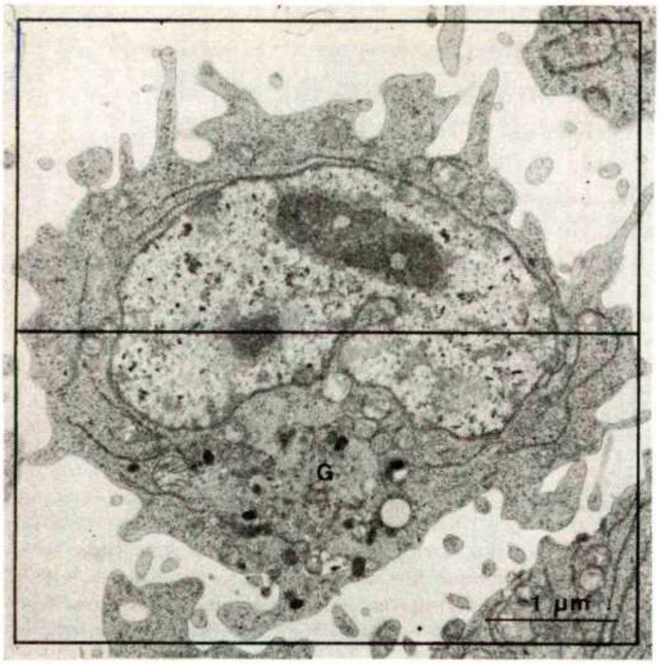

Fig. 1 The method used to determine the two plasma membrane segments of the lymphocytes for evaluation of ^{125}I-insulin redistribution (examples of lymphocytes with autoradiographic grains are shown in refs 3, 5, Figs 2, 6, respectively). Typically, the lymphocyte has an eccentric, indentated nucleus. The Golgi area (G) lies close to the indentation of the nucleus. A square divided in two equal rectangles by an horizontal line was superimposed on each cell so that the Golgi area fitted approximately the centre of one of the rectangles. The plasma membrane segment contained within that rectangle was considered as the 'Golgi pole' of the membrane; the number of autoradiographic grains present within ±250 nm of the plasma membrane in each rectangle was then recorded separately. Approximately 100 cells showing the typical morphology illustrated were evaluated in each experimental condition. Lymphocytes were incubated with 0.2 nM ^{125}I-insulin at 15 and 37 °C as described elsewhere[3,5]. At each time point selected cells were fixed with 4% phosphate-buffered (*p*H 7.4) glutaraldehyde, dehydrated, embedded in Epon and thinly sectioned. High-resolution autoradiography of the thin sections was carried out using Ilford L4 emulsion and Microdol-X developer after 3–5 weeks' exposure time[3,5].

pole of the cell, at 37 °C there is a rapid redistribution of the ligand in the plane of the membrane.

It has previously been shown in human fibroblasts that some ligands initially bind preferentially to specialized regions of the membrane known as coated pits[7–11]. The lymphocyte differs from the fibroblast in that the coated regions of the plasma membrane are much less marked with respect to the size of the coated segment and coat development. Although this factor must be taken into account in the analysis of our data, we find no initial preferential localization of labelled insulin to coated segments of the membrane after 2 min of incubation at either 15 or 37 °C. These data are similar to our findings of insulin binding in isolated hepatocytes, to those of Billheimer *et al.* for low-density lipoprotein (LDL) binding in circulating monocytes and to those of Haigler *et al.* studying epidermal growth factor (EGF) binding in A-431 epithelioid carcinoma cells[12–14], but may not rule out a participation of coated segments of the membrane in internalization of the labelled material.

Table 2 Relationship of autoradiographic grains to coated regions of the plasma membrane

	2 min, 15 °C	2 min, 37 °C
Total no. of grains examined	252	292
No. of grains associated with coated invaginations	5 (2%)	6 (2.1%)

The criteria for selection were: (1) the grain centre was ±250 nm from the plasma membrane, and (2) the plane of the section was appropriate for a clear identification of the plasma membrane. A grain was considered associated with a coated invagination if its centre was closer than 250 nm from a coated invagination. These methods are identical to those previously used for analysis of binding of ^{125}I-EGF and ^{125}I-LDL to cultured fibroblasts[9,10].

Schlessinger *et al.*[15] have shown in cultured mouse fibroblasts that, at high concentration, insulin conjugated to lactalbumin–fluorescein undergoes patching before internalization. Whether a similar process occurs in our cultured lymphocytes cannot be determined from these studies. The redistribution of insulin in the plane of the membrane to the Golgi pole of the cultured human lymphocytes seems more closely analogous to the phenomenon of capping. Taken with the data of Schlessinger *et al.*[15], the present results suggest that insulin binding to the cell surface induces a patch–cap formation similar to that described for di- or multivalent ligands[6]. In this respect, it is interesting that the capping of ^{125}I-insulin on the cell surface is qualitatively and, most importantly, quantitatively identical to that observed for a unique immunoglobulin (anti-insulin receptor antibody) which binds specifically to the insulin receptor[16], and which was isolated from a patient with a severe insulin resistance.

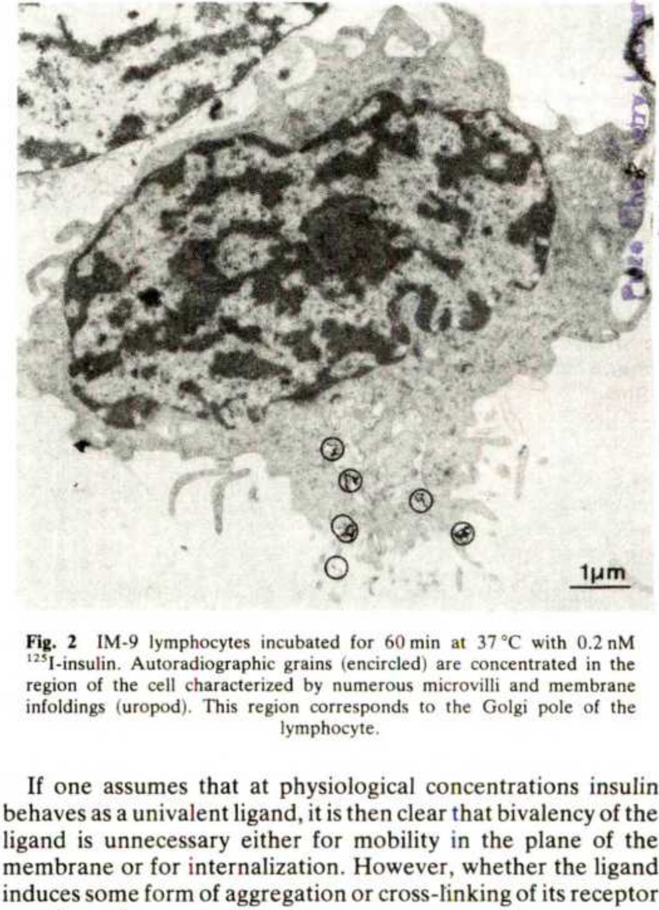

Pure Chemistry Library
SCIENCE COLLEGE
Upper Circular Road

Fig. 2 IM-9 lymphocytes incubated for 60 min at 37 °C with 0.2 nM ^{125}I-insulin. Autoradiographic grains (encircled) are concentrated in the region of the cell characterized by numerous microvilli and membrane infoldings (uropod). This region corresponds to the Golgi pole of the lymphocyte.

If one assumes that at physiological concentrations insulin behaves as a univalent ligand, it is then clear that bivalency of the ligand is unnecessary either for mobility in the plane of the membrane or for internalization. However, whether the ligand induces some form of aggregation or cross-linking of its receptor remains unknown.

Finally, we have proposed that endocytosis may be the major mechanism by which polypeptide hormone receptors are lost from the cell surface[5]. Micro-aggregation, lateral mobility and internalization of the hormone and its specific receptor in the plane of the membrane could provide a mechanism for selective loss of a single class of receptors analogous to the removal of specific immunoglobulins from the surface of lymphocytes[17].

This work was supported by grant 3.120.77 from the Swiss NSF. During this work P. Gorden was a visiting professor at the Institute of Histology and Embryology in Geneva.

Received 4 March; accepted 14 May 1980.

1. Gavin, J. R. III, Gorden, P., Roth, J., Archer, J. A. & Buell, D. N. *J. biol. Chem.* **248,** 2202 (1973).
2. De Meyts, P. in *Methods in Receptor Research* (ed. Blecher, M.) 301 (Dekker, New York, 1976).
3. Carpentier, J.-L. *et al. J. clin. Invest.* **61,** 1057 (1978).
4. Goldfine, I. D., Jones, A. L., Hradek, G. T., Wong, K. Y. & Mooney, J. S. *Science* **202,** 760 (1978).
5. Gorden, P. *et al. J. Cell Sci.* **39,** 77 (1979).

6. de Petris, S. in *Dynamic Aspects of Cell Surface Organization* Vol. 3 (eds Poste, G. & Nicholson, G. L.) 643 (North-Holland, Amsterdam, 1977).
7. Anderson, R. G. W., Brown, M. S. & Goldstein, J. L. *Cell* **10,** 351 (1977).
8. Orci, L. *et al. Expl Cell Res.* **113,** 1 (1978).
9. Carpentier, J.-L. *et al.. Expl Cell Res.* **121,** 135 (1979).
10. Gorden, P., Carpentier, J.-L., Cohen, S. & Orci, L. *Proc. natn. Acad. Sci. U.S.A.* **75,** 5025 (1978).
11. Willingham, M. C., Maxfield, F. R. & Pastan, I. M. *J. Cell Biol.* **82,** 614 (1979).
12. Carpentier, J.-L., Gorden, P., Freychet, P., Le Cam, A. & Orci, L. *J. clin. Invest.* **63,** 1249 (1979).
13. Billheimer, D. N., Ho, Y. V., Brown, M. S., Anderson, R. G. W. & Goldstein, J. L. *J. clin. Invest.* **61,** 678 (1978).
14. Haigler, M. T., McKanna, J. A. & Cohen, S. *J. Cell Biol.* **81,** 382 (1979).
15. Schlessinger, J., Schechter, T., Willingham, M. C. & Pastan, I. *Proc. natn. Acad. Sci. U.S.A.* **75,** 2659 (1978).
16. Carpentier, J.-L., Van Obberghen, E., Gorden, P. & Orci, L., in preparation.
17. Taylor, R. B., Duffus, M. R. M., Raff, M. C. & De Petris, S. *Nature new biol.* **233,** 225 (1971).

Increased human red cell cation passive permeability below 12 °C

G. W. Stewart, J. C. Ellory & R. A. Klein*

Physiological Laboratory, Downing Street, Cambridge CB2 3EG, UK

* Medical Research Council, Molteno Institute, University of Cambridge, Cambridge CB2 3EE, UK

The rate of most biological reactions declines as the temperature is reduced; indeed, cooling is often used to limit or terminate reactions. We report here a paradoxical temperature response of red cell K and Na permeability below 12 °C. This may be interpreted thermodynamically in terms of a membrane-ordering phenomenon, an observation supported by a variety of other physical measurements on red cell membranes reported in the literature.

Surprisingly few data are available on the effects of temperature on Na and K transport in human erythrocytes. This may be due in part to the presence of at least three components of Na and K movement in human red cells. These can be resolved as the ouabain-sensitive Na–K pump[1,2], the furosemide-sensitive Na–K co-transport system[3] and a residual process showing linear concentration dependence[1]. For normal human red cells, at 5 mM external K, K influx is roughly divided between these three processes in the proportion 60%, 35% and 5%, respectively, at 37 °C. We have measured the temperature dependence of the three components of K uptake over the temperature range 4–37 °C (Fig. 1). The two K transport systems which show saturable kinetics and which can be identified using known inhibitors (ouabain for the Na–K pump and furosemide, or other loop diuretics such as bumetanide, for the Na–K co-transport system), fell off sharply with decreasing temperature, no significant fluxes being measurable below about 4 °C (Fig. 1). In marked contrast, however, the residual K influx, which shows a linear K concentration dependence and is ouabain- and furosemide-resistant, reached a minimum at about 12 °C, below which temperature the flux began to increase again. In three experiments in which this flux was measured at 0 °C and 10 °C, the ratio K influx 0 °C : 10 °C was 2.1 ± 0.5 (s.e.m.). Ouabain- and furosemide-resistant Na efflux (Fig. 2), K efflux and Na influx (data not shown) all showed a similar paradoxical pattern of temperature dependence with a minimum at about 12 °C. In a second series of experiments, net Na accumulation was measured following long-term (22 h) incubation in media containing ouabain and bumetanide (used as an alternative to furosemide because of its greater potency). The results (Table 1) demonstrate that Na accumulation was significantly lower following incubation at 10 °C than with either 20 °C or 0 °C. This experiment, therefore, confirms the observations from tracer fluxes that there was a minimum around 10 °C for Na permeability, as also shown by Dalmark & Wieth[17].

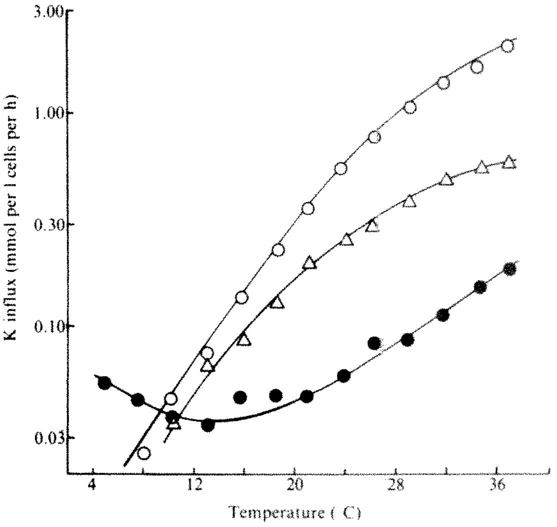

Fig. 1 The three components of K influx as a function of temperature. K influx was measured by previously described methods[15] using ^{42}K or tracer ^{86}Rb (ref. 16) in a 142 mM NaCl, 7.5 mM KCl, 15 mM MOPS (Sigma) and 5 mM glucose solution, *p*H 7.4, at 20 °C, 7.3 at 0 °C, 7.48 at 37 °C. Inhibitors (ouabain and furosemide, Hoechst) were added to final concentrations of 0.1 mM and 1 mM, respectively. Cells were preincubated at 37 °C for 15 min before cooling to allow binding. The cells were exposed to isotope for up to 3 h before rapid washing four times in ice-cold $MgCl_2$ 106 mM and Tris 10 mM. ○, Ouabain-sensitive; △, furosemide-sensitive; ●, ouabain/furosemide-insensitive.

Table 1 Changes in internal erythrocyte [Na] after storage as a function of temperature

	$[Na]_i$ µmol per gHb	Difference
Before storage	31.9 ± 0.1	
After storage		
20 °C	51.8 ± 0.3	19.9 ± 0.4
10 °C	46.7 ± 0.2	14.8 ± 0.2*
0 °C	52.0 ± 0.3	20.1 ± 0.4*

After washing 4× in (mM) NaCl 145, KCl 5, MOPS 15 and glucose 5, *p*H 7.4, at 20 °C, followed by 15-min incubation with inhibitors at 37 °C, cells were incubated for 22 h at 4% haematocrit at the temperatures shown with ouabain and bumetanide 10^{-4} M each, with continuous gentle mixing. After storage, the cells were washed 4× in 106 mM $MgCl_2$ and 10 mM Tris, packed and lysed in water. [Na] was measured by flame photometry and haemoglobin (Hb) was measured with Drabkin's reagent at 540 nm. The results are expressed per g Hb (± s.e.m., *n* = 6) to exclude any effects of temperature on cell volume.

*Significantly different at $P < 0.001$, Student's *t*-test.

Although ouabain binding shows a very low reversibility at 0 °C (ref. 4), it was important to rule out the possibility of reversal of bumetanide (or furosemide) binding at low temperatures. Cells were always pretreated with maximal concentrations of inhibitors for 15 min at 37 °C before flux measurements, and as the K concentration dependence of K influx, measured at 0, 4, 11 and 37 °C, was found always to be linear, reversal of inhibition at low temperatures, which would restore a saturable component of K influx, can be discounted. Possible participation of the anion transport protein in this effect (through, for example $NaCO_3^-$ or KCO_3^- transport)[5] is unlikely because the anion exchange flux rate is markedly inhibited by temperature between 10 and 0 °C (ref. 6). In any case 0.1 mM SITS (4-acetamido-4′-isothiocyanatostilbene-2,2′-disulphonic acid, sodium salt, BDH), a potent inhibitor of the anion transport system[7], had no effect. Membrane potential effects can be ruled out because both influx and efflux tracer cations were increased at low temperatures, and there was no significant temperature-dependent change in membrane potential (measured by the dis-C_3-(5) dye method[8]) in ouabain- and furosemide-treated cells.

In the present work, we have shown that the linear components of Na and K fluxes have minimum values at around

0028-0836/80/300403—02$01.00

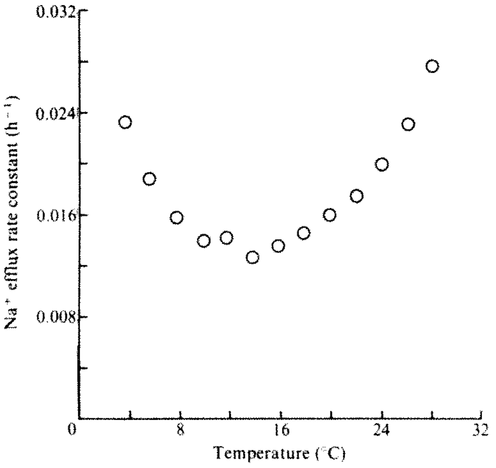

Fig. 2 Na efflux as a function of temperature. Fresh human cells were loaded with ^{24}Na as previously described[15]. Ouabain (10^{-4} M) and bumetanide (10^{-4} M) were added towards the end of the loading incubation to allow binding before rapid washing in cold 145 mM NaCl, 5 mM KCl, 15 mM MOPS and 5 mM glucose solution, containing the inhibitors.

12 °C. Wieth[9] has reported a temperature-dependent stimulation of the ouabain-insensitive Na and K fluxes in human erythrocytes by the anions SCN$^-$ and salicylate (used at 100 mM concentration) which gave rise to a flux minimum at about 18 °C. In thermodynamic terms such paradoxical behaviour could be the result of two mechanisms: the summation of two processes with enthalpies of activation of opposite sign (for example, Wieth[9] suggested that the ions SCN$^-$ and salicylate titrated fixed membrane charges exothermically at low temperatures) or the result of a single process whose entropy change is a function of temperature. According to Eyring's theory[10], the temperature dependence of diffusion (D) is given by

$$D = cTe^{-\Delta G^*/RT}$$

where c is a constant, T the absolute temperature, R the gas constant and ΔG^* the Gibbs free energy change for activation of the transition state. From the Gibbs equation $\Delta G^* = \Delta H^* - T\Delta S^*$ where ΔH^* and ΔS^* are, respectively, the enthalpy and entropy changes for activation. In the first case, ΔS^* is invariant with temperature. If ln D is differentiated with respect to $1/T$, one obtains

$$\frac{\mathrm{d}\ln D}{\mathrm{d}(1/T)} = -T - \frac{\Delta H^*}{R}$$

If $T \ll \Delta H^*/R$, this reduces to

$$\frac{\mathrm{d}\ln D}{\mathrm{d}(1/T)} = -\frac{\Delta H^*}{R}$$

the Arrhenius equation. If, in the second case, ΔS^* is a function of temperature denoted by $\Delta S^*(1/T)$, the expression becomes

$$\frac{\mathrm{d}\ln D}{\mathrm{d}(1/T)} = \frac{\mathrm{d}}{\mathrm{d}(1/T)}\left\{\frac{\Delta S^*(1/T)}{R}\right\} - \frac{\Delta H^*}{R} - T$$

The function ln D (and therefore D) can show a minimum if at some temperature

$$\frac{\mathrm{d}}{\mathrm{d}(1/T)}\Delta S^*(1/T) = \Delta H^* + RT$$

This equation expresses the thermodynamic condition necessary for a minimum to be observed in the relationship between ion flux and temperature, consistent with the present data. A temperature-dependent change in the entropy of activation for the transition complex could result from a change in membrane ordering. In this context workers using physical techniques to study membrane ordering have reported relevant observations: (1) Raman spectroscopy (Verma and Wallach[11]) showed discontinuities in lipid CH-stretching and membrane-bound β-carotene intensities in the temperature range −4 °C to 20 °C; (2) Tanaka and Ohnishi[12] demonstrated an inflection point at 18 °C in the phosphatidylcholine spin label line splitting for erythrocyte ghosts; (3) in ether-extracted erythrocyte ghosts, Cullis[13] found a change in ^{32}P nuclear magnetic resonance linewidth at about 20 °C; (4) using a fluorescence probe to assess membrane fluidity, Kapitza and Sackmann[14] observed a marked increase in this parameter between 12 and 17 °C. All these methods reflect membrane ordering and therefore entropy. However, as the temperature of the flux minimum is a function not only of $\mathrm{d}/\mathrm{d}(1/T)\Delta S^*(1/T)$ but also of ΔH^* and RT, points of inflection identified from these data cannot be simply related to the flux minimum described here.

Our flux measurements may therefore represent a functional correlate of the temperature-dependent changes in membrane ordering evidenced by other physical methods.

We thank Dr T. J. Rink for measuring membrane potential, Dr V. L. Lew for helpful discussions, and the Wellcome Trust for supporting G.W.S.

Received 13 February; accepted 16 May 1980.

1. Glynn, I. M. *J. Physiol., Lond.* **134,** 278–310 (1956).
2. Post, R. L. & Jolly, P. C. *Biochim. biophys. Acta* **25,** 118–128 (1957).
3. Wiley, J. S. & Cooper, R. A. *J. clin. Invest.* **53,** 745–755 (1974).
4. Joiner, C. H. & Lauf, P. K. *J. Membrane Biol.* **21,** 99–112 (1975).
5. Funder, J. & Wieth, J. O. *Alfred Benzon Symp.* **14,** 520–530 (eds Lassen, U., Ussing, H. H. & Wieth, J. O.) (Munksgaard, Copenhagen, 1980).
6. Dalmark, M. & Wieth, J. O. *J. Physiol., Lond.* **224,** 583–610 (1972).
7. Knauf, P. & Rothstein, A. *J. gen. Physiol.* **58,** 190–210 (1971).
8. Hladky, S. B. & Rink, T. J. *J. Physiol., Lond.* **263,** 287–319 (1976).
9. Wieth, J. O. *J. Physiol. Lond.* **207,** 563–580 (1970).
10. Stein, W. D. *The Movement of Molecules across Cell Membranes* (Academic, London, 1967).
11. Verma, S. P. & Wallach, D. F. H. *Biochim. biophys. Acta* **436,** 307–318 (1975).
12. Tanaka, K. & Ohnishi, S. *Biochim. biophys. Acta* **426,** 218–231 (1975).
13. Cullis, P. R. *FEBS Lett.* **68,** 173–176 (1976).
14. Kapitza, H. G. & Sackman, E. *Biochim. biophys. Acta* **595,** 56–64 (1980).
15. Ellory, J. C. & Dunham, P. B. *Alfred Benzon Symp.* **14,** 409–423 (eds Lassen, U., Ussing, H. H. & Wieth, J. O.) (Munksgaard, Copenhagen, 1980).
16. Fortes, P. A. G., Ellory, J. C. & Lew, V. L. *Biochim. biophys. Acta* **318,** 262–272 (1973).
17. Dalmark, M. & Wieth, J. O. *Biochim. biophys. Acta* **219,** 525–527 (1970).

Plateau potentials in pancreatic islet cells are voltage-dependent action potentials

Daniel L. Cook, Wayne E. Crill & Daniel Porte Jr

Veterans Administration Hospital, 4435 Beacon Avenue So., Seattle, Washington 98108

Islet cells stimulated by a steady glucose concentration above a certain threshold (usually 5–7 mM) display cyclic membrane potential changes[1]. This islet electrical activity consists of action potentials (spikes) superimposed on a depolarized plateau (see Fig. 1). Higher levels of glucose prolong the plateau phase and shorten the silent phase until the plateau potentials merge to produce continuous spiking at 20–25 mM. The fraction of each cycle spent in the plateau phase correlates with glucose concentration and insulin release rate[2], suggesting that control of the onset and offset of the plateau is important in the regulation of insulin release. The abrupt transitions between silent and plateau phases suggest that the plateau is a persistent, voltage-dependent action potential as in cardiac muscle. This idea is supported by evidence[3] that $\mathbf{Ca^{2+}}$ influx is stimulated by $\mathbf{K^+}$ depolarization of islets. However, this voltage dependency can be explained by electrical evidence[4,5] that the spikes are generated by voltage-dependent $\mathbf{Ca^{2+}}$ currents. Furthermore, there is evidence against the voltage dependency of the plateau because it seemed to be unaffected by intracellular current injection and $\mathbf{K^+}$ depolarization, which clearly affected spik-

ing[5,6]. As there are alternative explanations (see below) for these last negative findings, we have re-examined this important question using a new technique of direct electrical stimulation of entire, isolated islets using a suction electrode. Contrary to the previous negative findings, our present results clearly show that the plateau potential is a voltage-dependent, persistent action potential.

Pieces of pancreas from Swiss–Webster mice fed *ad libitum* were perfused in a Krebs–Ringer bicarbonate buffer gassed with O_2/CO_2 (95:5) and maintained at 37 °C. Individual islets (100–300 μm diameter) were microdissected free of exocrine tissue and held by the hollow glass electrode (90–200 μm inside tip diameter) with gentle suction (5–10 mm H_2O). A stimulus isolation unit provided constant current stimuli through this suction electrode. Standard electrophysiological techniques with glass microelectrodes (tip resistance 300–400 MΩ) were used to record islet cell membrane potentials. Because the suction electrode current passes through the entire islet, extracellular potentials within the islet cannot be assumed equal to the bath ground potential. Therefore, potentials measured during stimulation are not a true measure of transmembrane potential. Glucose-responsive islet cells were identified by their typical pattern of electrical activity and were used only if recordings were stable for at least 10 min. These records typically had silent phase potentials between −50 and −60 mV, and at the time of recording the islets had been exposed to 11.1 or 13.7 mM glucose for at least 30 min.

Figure 1, line 1, shows the rhythmic electrical response to 11.1 mM glucose. In line 2, this regular endogenous rhythm was interrupted by an 8-μA, 2-s-long depolarizing current (from the suction electrode) which evoked an all-or-none plateau potential indistinguishable from endogenous plateaus. The ensuing electrical rhythm is identical to that observed before the stimulus but is shifted as if a pacemaker had been reset. Line 3 of Fig. 1 demonstrates that this all-or-none response has a definite electrical threshold, as a slightly weaker stimulus (6 μA) did not initiate a plateau and had no effect on the plateau rhythm.

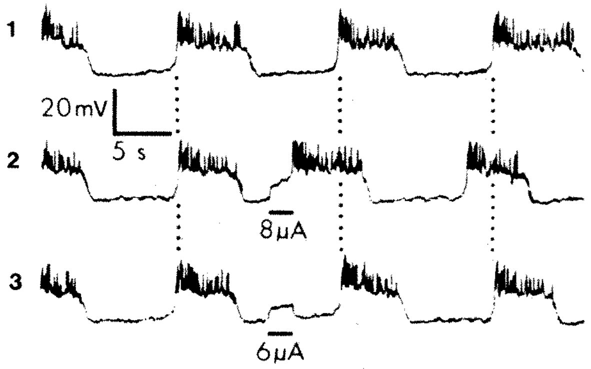

Fig. 1 Responses to depolarizing currents. Three excerpts from a membrane potential recording from a single islet cell in the presence of glucose (11.1 mM). Line 1, control activity; line 2, a premature plateau potential initiated by an 8-μA, 2-s-long depolarizing current presented 2 s into the silent phase; line 3, failure of a similar 6-μA stimulus to initiate a plateau.

Plateau termination is also voltage dependent because an endogenous plateau can be aborted by a brief (100 ms) hyperpolarizing stimulus current of −18 μA (Fig. 2, line 2). This all-or-none response has the same slow time course of repolarization and length of silent phase as seen in the endogenous activity. There is also a sharp stimulus threshold, as a slightly weaker current (−15 μA) does not interrupt the plateau (Fig. 2, line 3). Although not clearly shown in Fig. 2, artificial termination of plateaus interrupted and reset the endogenous rhythm as effectively as artificial plateau initiation (Fig. 1).

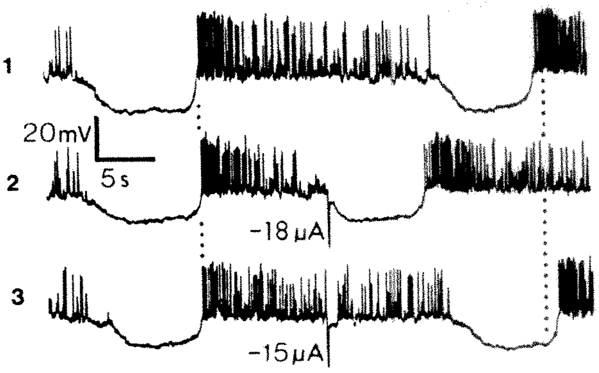

Fig. 2 Responses to hyperpolarizing currents. Membrane potential records from a second cell in the presence of glucose (13.7 mM). Line 1, control electrical activity; line 2, endogenous plateau prematurely terminated by a −18-μA, 100-ms-long hyperpolarizing current presented 10 s after the beginning of the plateau; line 3, failure of a similar −15-μA current to terminate a plateau.

For both the initiation and termination of plateaus in all cells tested, we have consistently observed a reciprocal relationship between stimulus current strength and stimulus duration (data not shown), as is characteristic of excitability phenomena in other systems. For example, in one cell, a 10-μA current required 2 s to trigger a premature plateau whereas a 20-μA current required only 1 s. Similar relationships were found for termination of plateaus, although typically, plateau initiation has required longer stimuli that plateau termination (1–2 s compared with 50–100 ms).

Previous studies[5,6] found that neither plateau length nor frequency was affected by stimulus currents passed through the recording electrode or by elevation of bath K^+ concentration. These results probably reflect the difficulty of driving a coupled[7] population of cells by stimulating a single cell, as well as accommodation to slow changes in K^+. More rapid (1–2 s) bath K^+ changes elicit premature plateaus (unpublished results) as readily as electrical stimulation through the suction electrode.

It is possible that our electrical stimuli affect plateau potentials indirectly by releasing endogenous islet neurotransmitters. However, this is unlikely because it seems to require that depolarizing stimuli selectively release acetylcholine (known to depolarize islet cells)[8] whereas hyperpolarizing stimuli selectively release catecholamines (known to hyperpolarize islet cells)[9]. A more likely explanation is that the electrical stimuli are directly activating and deactivating a voltage-dependent membrane conductance. This conductance change underlies the prolonged plateau depolarization which drives the more rapid spiking activity. Thus, the islet cell plateau potential resembles voltage-dependent, persistent action potentials seen in myocardial cells[10] and the slow potentials of molluscan pacemaker neurones[11]. The underlying ionic mechanism in islet cells is unclear but may be due to increased conductance to Na^+ or Ca^{2+} as in these other systems or to a decreased conductance to K^+, as proposed for islet cells[5].

The second key observation in the present work is that electrical stimuli interrupt and completely reset the rhythm of islet cell electrical activity. This seems to rule out electrically insensitive pacemaker mechanisms such as autonomous biochemical oscillators which merely drive membrane events. Furthermore, the pacemaker mechanism must depend on either the membrane potential directly or the fluxes of ions underlying the voltage changes. For instance, as in heart cells and molluscan neurones, one or more slow, voltage-dependent K^+ conductances may serve as the pacemaker. Alternatively, islet cells are known to possess an electrogenic Na^+–K^+ pump[12] and a Ca^{2+}-dependent, K^+ conductance[13]. Thus, intracellular accumulation of Na^+ or Ca^{2+} during the active plateau phase could, by either mechanism, activate a hyperpolarizing current which would eventually trigger plateau repolarization. Depletion of the cation pool during the silent phase would lead to slow depolarization and the next plateau.

Although the specific ionic mechanisms of the plateau conductance change and the pacemaker mechanism remain unclear, these data conclusively show the islet cell plateau potential to be a persistent, voltage-dependent action potential whose pacing must involve membrane potential or ion fluxes.

We thank H. P. Meissner and I. Atwater for technical advice. This work was supported by the US Veterans Administration and NIH research grants AM 12829 and 21185. D.L.C. was supported by a Juvenile Diabetes Foundation post-doctoral fellowship.

Received 24 March; accepted 13 May 1980.

1. Dean, P. M. & Matthews, E. K. *Nature* **219**, 389–390 (1968).
2. Meissner, H. P. & Schmelz, H. *Pflügers Arch. Ges. Physiol.* **357**, 195–206 (1974).
3. Henquin, J. C. & Lambert, A. E. *J. Physiol., Paris* **72**, 747–756 (1976).
4. Matthews, E. K. & Sakamoto, Y. *J. Physiol., Lond.* **246**, 421–437 (1975).
5. Atwater, I., Ribalet, B. & Rojas, E. *J. Physiol., Lond.* **278**, 117–139 (1978).
6. Cook, D. L., Porte, D. Jr & Crill, W. E. (abstr) *10th Cong. int. Diabetes Fedn*, 46 (Int. Cong. Ser. 481, Excerpta Medica, Amsterdam, 1979).
7. Meissner, H. P. *Nature* **262**, 502–504 (1976).
8. Gagerman, E., Idahl, L.-A., Meissner, H. P. & Taljedal, I.-B. *Am. J. Physiol.* **235**, E493–E500 (1978).
9. Dean, P. M. & Matthews, E. K. *J. Physiol., Lond.* **210**, 255–264 (1970).
10. Reuter, H. *A. Rev. Physiol.* **41**, 413–424 (1979).
11. Gola, M. in *Abnormal Neuronal Discharges* (eds Chalazonitis, N. & Boisson, M.) 243–261 (Raven, New York, 1978).
12. Meissner, H. P. *J. Physiol., Paris* **72**, 757–767 (1976).
13. Atwater, I., Dawson, C. M., Ribalet, B. & Rojas, E. *J. Physiol., Lond.* **288**, 575–588 (1979).

Linkage relationship between variable and constant region allotypic determinants of human immunoglobulin heavy chains

J. P. Pandey*, E. Tung*, S. Mathur*, K. K. Namboodiri†, A. C. Wang*, H. H. Fudenberg*, W. A. Blattner‡, R. C. Elston† & C. G. Hames§

*Department of Basic and Clinical Immunology and Microbiology, Medical University of South Carolina, Charleston, South Carolina 29403; †Department of Biostatistics, The University of North Carolina, Chapel Hill, North Carolina 27514; ‡National Institutes of Health, Bethesda, Maryland 20014; §Evans County Health Department, 2 North Newton Street, Claxton, Georgia 30417

Allotypic (genetic) variations in the variable (V) region of immunoglobulin chains have been extensively studied in the domestic rabbit[1-3]. The first allotypic determinant identified in the V region of human immunoglobulins, described in our laboratory, is designated Hv(1). Its detection, using protein McE and a rabbit antiserum to McE, and its mode of inheritance based on family and population studies, have been reported previously[4]. Briefly, Hv(1) is located in the V region of human immunoglobulin heavy (H) chains of G, M and A classes. It is inherited as an autosomal dominant trait, with a gene frequency in white people of 0.189 ± 0.023. The polymorphic nature of Hv(1) has also been confirmed in black people, studies on a large black kindred ($n = 80$) having confirmed its autosomal dominant mode of inheritance. The gene frequency (determined by the Elston–Stewart method using maximum likelihood[5]) in blacks is 0.278 ± 0.067. Hv(1) seems analogous to murine idiotypes of the so-called *Idx* category[6] and to rabbit V_H-region allotypes in that it is not restricted to any particular immunoglobulin class. This observation is consistent with our previous finding that the same V-region amino acid sequence is able to associate with constant (C) regions of different H-chain classes[7]. However, an important difference between Hv(1) and the idiotypic markers in mice and rabbits is that the former is presumably associated with the framework residues whereas the latter are associated primarily with the hypervariable regions. We now report results obtained from family studies which indicate absence of linkage between Hv(1) and the human C-region markers Gm (human IgG H chains) and Km (κ-type light chains). These results provide new information about the genetic control of immunoglobulin synthesis in man.

Serum samples from one large black kindred ($n = 80$) and one large white kindred ($n = 220$) and from three smaller white families ($n = 84$) were typed for Hv(1), Km(1) and nine Gm markers (1, 2, 3, 5, 6, 13, 14, 17, 21) by our standard haemagglutination inhibition method[4,8]. All sera were diluted 1:16 for detection of Gm and Km markers. The Hv(1) marker was detected by the use of serial dilutions, with inhibiting titres of 1:16 or greater considered as positive. The lod score method of Morton[9] was used to test for linkage between Hv(1) and the C-region markers, basing the likelihood on the complete pedigree structures[5,10]. This method takes advantage of available data from every sort of informative test cross, that is, from double intercrosses and single backcrosses as well as double backcrosses. It determines the relative odds that a sequence of genotypes among siblings resulted from linked loci with a certain percentage of meiotic crossing over, as compared with the possibility that the sequence occurred by chance from unlinked loci. For convenience, the ratio of these two probabilities—recombination fraction $\theta < 1/2$ (linkage) compared with $\theta = 1/2$ (no linkage)—is expressed as its logarithm. The $\log_{10}$ of this relative probability is called the log of the odds or 'lod score', and the value of θ which corresponds to the maximum value of the lod score is taken as the estimate of the recombination fraction θ. Computer program LIPED[10] was used to calculate lod scores. The lod scores for linkage between Hv(1) and Gm and Km markers were negative (Table 1). (A negative value argues against linkage, a lod score greater than 2 is suggestive of linkage, and a value greater than 3 is accepted as proof of linkage.) On the basis of the data presented here, close linkage between Hv(1) and Gm and Km is excluded.

Investigations in humans, as well as mice and rabbits, suggest that unlinked genes code for H chains, κ-type light (L) chains and λ-type L chains[11-14]. Absence of linkage between Hv(1) and Km is compatible with these observations. However, the absence of linkage between Hv(1) and Gm does not concur with findings in the rabbit and the mouse.

Most models of immunoglobulin genes predict close linkage between V- and C-region genes. V_H-region markers have been analysed in considerable detail with regard to linkage to C_H loci. Rabbit a-group allotypes, located on the V_H region, are linked to the d- and e-group allotypes located on the γ-chain of C_H (refs 15, 16), and in mice some idiotypic (V-region) markers are linked to C_H allotypes[6,17,18]. However, the results reported here are not entirely unprecedented. For example, one study of b-group allotypes and the LId idiotype in rabbits gave no evidence of linkage between V_L and C_L genes[19].

The simplest interpretation of the present finding is that Hv(1) is not a V-region allotype. However, extensive inhibition

Table 1 Lod scores for linkage between Hv(1) and Gm and Km markers

Recombination fraction (θ)*	Gm	Km
0.05	−9.93	−3.47
0.1	−6.33	−2.18
0.2	−2.72	−0.86
0.3	−0.99	−0.29
0.4	−0.19	−0.04

*Assuming that the recombination fractions (θ) in males and females are equal.

0028–0836/80/300406—02$01.00

experiments involving Fab and Fc fragments and isolated H and L chains, reported previously[4] demonstrated that the antigenic determinant for Hv(1) is located on the V region of human immunoglobulin heavy(1) chain. Another interpretation of our results is that [illegible] phenotypes are controlled by two [illegible] structural genes coding for the antigenic [illegible] genes controlling the [illegible] regulatory genes need not be [illegible] and the genes they regulate[20]. A [illegible] several species suggest that the [illegible], in which allotypes are encoded by [illegible] structural genes, may be an oversimplification. [illegible] humans, discrepancy between the genotype [illegible] expressed phenotype, and in rabbits, allotype [illegible] latent allotypes and the 'pecking order' in the [illegible] of allotypes, all suggest the existence of regulatory [illegible] which control the expression of structural genes coding immunoglobulin allotypes[21–27]. Indeed, it has been suggested that expression of other genetic polymorphisms (for example, HLA and ABO) may also be under the control of regulatory genes[28].

Alternatively, the loci for Hv(1) and Gm may be on the same chromosome, but very far apart. In murine H and L chains, the V-region structural genes are located at some distance from the C-region structural genes in the germ-line DNA[29–33]. When two loci are very far apart, their genetic behaviour in family studies is often indistinguishable from that of independently segregating loci (that is, those on different chromosomes). One approach to this problem is genetic mapping by the somatic cell hybridization technique[34]. Such studies are in progress in our laboratory.

We thank Vennie Moore for technical assistance, Charles Smith for editorial assistance, and Mary Marazita, John Thompson and Drs S. Hsia and T. Fogle for collection of some of the samples used in this study. This research was supported in part by USPHS grants HD-09938, CA-25746, RR-05767, MH-26721, HL-03341 and GM-16697 and NSF grant PCM-24809.

Received 20 December 1979; accepted 29 April 1980.

1. Dray, S., Young, G. O. & Gerald, L. *J. Immun.* **91,** 403–415 (1963).
2. Todd, C. W., *Biochem. biophys. Res. Commun.* **11,** 170–175 (1963).
3. Nisonoff, A., Hopper, J. E. & Spring, S. B. *The Antibody Molecule*, 346–370 (Academic, New York, 1975).
4. Wang, A. C. *et al. Science* **200,** 327–329 (1978).
5. Elston, R. C. & Stewart, J. *Hum. Hered.* **21,** 523–542 (1971).
6. Weigert, M. & Potter, M. *Immunogenetics* **4,** 401–435 (1977).
7. Wang, A. C., Wang, I. Y. & Fudenberg, H. H. *J. biol. Chem.* **252,** 7192–7199 (1977).
8. Vyas, G. N., Fudenberg, H. H., Pretty, H. M. & Gold, E. R. *J. Immun.* **100,** 274–279 (1968).
9. Morton, N. E. *Am. J. hum. Genet.* **7,** 277–318 (1955).
10. Ott, J. *Am. J. hum. Genet.* **26,** 588–597 (1974).
11. Steinberg, A. G. & Matsumoto, H. *Hum. Biol.* **36,** 77–85 (1964).
12. Mage, R., Lieberman, R., Potter, M. & Terry, W. D. in *The Antigens* V.1 (ed. Sela, M.) 299–376 (Academic, New York, 1973).
13. Natvig, J. B. & Kunkel, H. G. *Adv. Immun.* **16,** 1–60 (1973).
14. Kindt, T. J. *Adv. Immun.* **21,** 35–86 (1975).
15. Hamers-Casterman, C. & Hamers, R. *Immunogenetics* **2,** 597–603 (1975).
16. Mage, R. G. *Annls Immun. Inst. Pasteur, Paris* **130C,** 105–114 (1979).
17. Eichmann, K., Tung, A. S. & Nisonoff, A. *Nature* **250,** 509–511 (1974).
18. Mäkelä, O. & Weigert, M. in *Immune System: Genetics and Regulation* (eds Sercarz, E. E., Herzenberg, L. A. & Fox, C. F.) 123–125 (ICN-UCLA Symp., Academic, New York, 1977).
19. Sogn, J. A., Yarmush, M. L. & Kindt, T. J. in *Immune System: Genetics and Regulation* (eds Sercarz, E. E., Herzenberg, L. A. & Fox, C. F.) 91–97 (ICN-UCLA Symp., Academic, New York, 1977).
20. McClintock, B. *Proc. natn. Acad. Sci. U.S.A.* **36,** 344–355 (1950).
21. Lobb, N., Curtain, C. C. & Kidson, C. *Nature* **214,** 783–785 (1967).
22. Rivat, L., Gilbert, D. & Ropartz, C. *Immunology* **24,** 1041–1049 (1973).
23. Gutman, G. A., Loh, E. & Hood, L. *Proc. natn. Acad. Sci. U.S.A.* **72,** 5046–5050 (1975).
24. Wang, A. C. *Fedn Eur. biochem. Soc. Symp.* **36,** 19–31 (1975).
25. Strosberg, A. D. *Immunogenetics* **4,** 499–513 (1977).
26. Strosberg, A. D. in *Immune System: Genetics and Regulation* (eds Sercarz, E. E., Herzenberg, L. A. & Fox, C. F.) 115–122 (ICN-UCLA Symp., Academic, New York, 1977).
27. Yarmush, M. L., Sogn, J. A. & Kindt, T. J. *Annls Immun. Inst. Pasteur, Paris* **130C,** 143–156 (1979).
28. Bodmer, W. F. *Transplantn Proc.* **5,** 1471–1475 (1973).
29. Brack, C., Hirowa, M., Lenhard-Schuller, R. & Tonegawa, S. *Cell* **15,** 1–14 (1978).
30. Seidman, J. G., Max, E. E. & Leder, P. *Nature* **280,** 370–375 (1979).
31. Early, P. W., Davis, M. M., Kaback, D. B., Davidson, N. & Hood, L. *Proc. natn. Acad. Sci. U.S.A.* **76,** 857–861 (1979).
32. Davis, M., Early, P., Calame, K., Livant, D. & Hood, L. in *Eukaryotic Gene Regulation* (eds Axel, R., Maniatis, T. & Fox, C. F.) 393–406 (ICN-UCLA Symp., Academic, New York, 1979).
33. Davis, M. M. *et al. Nature* **283,** 733–739 (1980).
34. Croce, C. M. *et al. Proc. natn. Acad. Sci. U.S.A.* **76,** 3416–3419 (1979).

0028–0836/80/300407—02$01.00

A test for the selective origin of environmentally correlated allozyme patterns

J. M. Malpica & J. M. Vassallo

Departamento de Genética, INIA, Carretera de La Coruña Km.7,
Madrid-35, Spain

Differences in the kinetic and/or endurance properties of enzymes encoded by alternative alleles have been suggested as the basic level at which selection could act on allozyme polymorphisms[1,2]. The correlation between spatial differences in gene frequencies and an environmental variable (hereafter designated cline, in its widest sense), when not spurious, has been proposed to show the working of selection[3]. Let us suppose that a given cline has originated through an environmentally imposed selection on enzyme activity. Because differences in enzymatic activities among individuals can be split into structural-gene and 'genetic-background' components[4–6], selection should act on both components in the same direction. That is, a correlation should exist between the environmental variable and the background component and it should be of the same sign as that between the environmental variable and the frequency of the most active allele. It should be less likely for clines conforming to these expectations to be spurious. Here we have investigated the relationship between the alcohol dehydrogenase locus (*Adh*) polymorphism and temperature in Spanish populations of *Drosophila melanogaster* and have found that it meets the above criterion.

It has been shown that the specific activity is higher for the Adh^F than for the Adh^S allelic variant of the enzyme[7–9], and that loci other than *Adh* affect ADH activity[4,5], although the extent of the two effects has been questioned[10]. A temperature cline has been reported for this locus[8], but a widespread association of the Adh^S allele with an inversion in the same chromosome arm (II left; refs 11, 12 and our unpublished results) makes interpretation of the cline difficult.

We have chosen the average temperature of the coldest month of the year (t_{min}) as the environmental variable. (Average temperature of the year ($\bar{t}$) and average temperature of the hottest month (t_{max}) are correlated with it over locations; $r_{t_{min},\bar{t}} = 0.961$, d.f. $= 22$, $P < 0.001$; $r_{t_{min},t_{max}} = 0.712$; d.f. $= 22$,

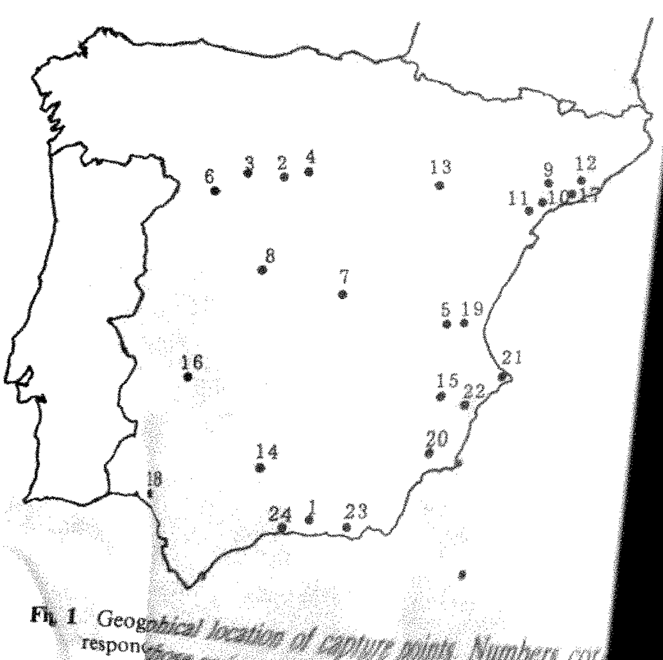

Fig. 1 Geographical location of capture points. Numbers correspond to those assigned to the samples in Table 1.

Table 1 Temperature clines of *Adh* and ADH activity measured in $Adh^{F/F}$ females

Sample	Minimum temperature	Adh^F frequency*		Enzyme activity, $Adh^{F/F}$ individuals		Arrangements Adh^F chromosome‡	
		n	Frequency	No. of groups of 10 ♀♀	per fly		LAI
1 Alpujarra	−0.31	119	0.962				
2. Peñafiel§	1.29	96	0.948				
3 I Cigales	2.10	94	0.957	9			
II§	2.10	95	0.947				
4 Fuentespina	2.35	104	0.899	16	3.084	4	
5 Utiel	2.35	129	0.950	11	2.937		
6 I Toro	2.86	121	0.992	12	2.843	47	
II§	2.86	96	0.995				
7 Fuente P.N.	3.34	124	0.952	2	2.250		
8 Cebreros§	4.07	95	0.984				
9 Montblanch	4.08	126	0.917	15	2.928		
10 Marsá	4.93	121	0.934	15	3.201		2
11 Gandesa	5.62	121	0.955				
12 S. Quintín	5.79	124	0.948	16	2.579		
13 Cariñena	5.95	73	0.932	15	2.073		
14 I Baena	6.51	76	0.882				
II§	6.51	118	0.915			43	6
15 Jumilla	7.27	123	0.866	11	2.885		
16 Castuera	7.36	122	0.906	3	2.420		
17 Vendrell	8.41	108	0.944	15	1.989		
18 Almonte	8.78	121	0.756				
19 Cheste	9.32	126	0.849	7	2.276		
20 Alhama§	9.40	95	0.653			49	0
21 Jalón	9.47	148	0.730	7	1.814		
22 I Aspe	10.07	127	0.728	15	1.780		
II§	10.07	95	0.742			82	3
23 Egido§	11.81	96	0.745			42	1
24 Torre de Mar	13.63	53	0.877				
Correlation with t_{min}			−0.749‖		−0.764¶		

* Results from captured wild flies; no significant differences were observed between sexes.

† ADH activity was assayed in descendents of the captured individuals, kept in population cages for no more than 3 months. The heads were electrophoresed and the b of $Adh^{F/F}$ individuals pooled in groups of 10. Reaction mixture: 0.5 ml of 6 mM NAD, 1 M isopropanol + 0.1 ml of homogenate (10 flies per ml), all in 0.05 M Tris-HCl b pH = 9.0 Assay temperature 25°C. Results in ΔE per m per fly, at 340 nm.

‡ Chromosomes extracted from wild captured males and assayed for cross-over suppression against an *all* chromosome[15]. LAI, Left arm inversion.

§ Samples captured in the same month, but a year later than the rest.

‖ Angular transformation has been applied to the frequencies (d.f. = 26, $P < 0.001$).

¶ d.f. = 13, $P < 0.001$.

$P < 0.001$.) There is a close correlation between the angular transform of Adh^F frequency and t_{min} (Table 1). The cline is not strictly latitudinal, in contrast with that observed on the US East Coast[8] (see Fig. 1 and Table 1).

We have assumed the among-populations differences in ADH activity, measured in $Adh^{F/F}$ individuals, to be due to the genetic background. This is a valid approach as the available evidence shows that there is little structural variability segregating within *Adh* electromorphs[13]. ADH activity was measured in $Adh^{F/F}$ individuals from 15 locations ($r_{\text{ang.transf.}Adh^F\text{freq.},t_{min}} = -0.747$) and a negative correlation with t_{min} was found (Table 1). Activities were expressed on a per fly basis as no significant over-locations correlations were found between body weight (x_1) and t_{min} or between body weight and activity per fly (x_2) ($r_{x_1,t_{min}} = -0.2814$, d.f. = 10, $0.4 > P > 0.3$; $r_{x_1,x_2} = 0.1339$, d.f. = 11, $0.7 > P > 0.6$).

In general, this type of result should reduce the probability of a non-selective origin for an observed environmentally correlated allozyme pattern. In our particular case, we note that the environmental variable is an *a priori* one, in the sense that a imilar cline has been described already[8]. The other potential ource of spuriousness, non-random association, can be easonably excluded, as the non-random associated gene (or lock of them) would have to fulfill the following conditions:) to be selected, (2) to have a relevant role in determining the zymatic activity, and (3) to be associated by chance with the ectrophoretic allele that modifies the activity in the same irection. In the present case, as the above statd association between Adh^S and the inversion is not absolu (our unpublished results), we have checked the frequen of left arm inversions within Adh^F chromosomes for so the samples in the cline (Table 1). They were always small significant differences were found between samples loc he first and the second half of the temperature range ($\chi_1^2 = 0.335, 0.6 > P$ 0.5).

We regard these results as strong support for the hypothesis a selective origin of the *Adh* cline in Spanish populations *D. melanogaster*. We do not imply that temperature is the age of the probable selection in the cline; any other temperature correlated variable (such as average concentration of alcohol i the food available to the flies) or a combination of them could b the actual agent.

The present study provides a new approach for investigatin the selective origin of clines. We believe it could be applied to fair proportion of enzymatic polymorphisms as, in most case there are differences in the specific activities between allel forms[1], and, at least in some species, spatial patterns of ge frequencies are not uncommon[11,14].

L. Silió carried out the activity assays. We thank F. Garcí Olmedo, G. N. Somero and C. Wills for their help in th preparation of this manuscript.

Received 25 February; accepted 15 May 1980.

1. Harris, H. *Can. J. Genet. Cytol.* **13**, 381–396 (1971).
2. Clarke, B. *Genetics* **79**, 101–113 (1975).
3. Lewontin, R. C. *The Genetic Basis of Evolutionary Change* (Columbia University Pr New York, 1974).
4. Ward, R. D. *Genet. Res.* **26**, 81–93 (1975).
5. McDonald, J. F. & Ayala, F. *Genetics* **89**, 371–388 (1978).
6. Bulfield, G., Moore, E. A. & Kacser, H. *Genetics* **89**, 551–561 (1978).
7. Gibson, J. *Nature* **227**, 959–960 (1970).
8. Vigue, C. L. & Johnson, F. M. *Biochem. Genet.* **9**, 213–227 (1973).
9. Day, T. H., Hillier, P. C. & Clarke, B. *Biochem. Genet.* **11**, 155–165 (1974).
10. Clarke, B., Camfield, R. G., Galvin, A. M. & Pitts, C. R. *Nature* **280**, 517–518 (1979
11. Voelker, R. A. *et al. Genetics* **88**, 515–527 (1978).
12. Briscoe, D. A., Robertson, A. & Malpica, J. M. *Nature* **255**, 148–149 (1975).
13. Sampsell, B. *Biochem. Genet.* **15**, 971–988 (1977).
14. Powers, D. A. & Place, A. R. *Biochem. Genet.* **16**, 593–607 (1978).
15. Lindsley, D. L. & Grell, E. H. *Genetic Variations of Drosophila melanogaster* (Carnegie Wash. Publ. 627, 1968).

Feline sarcoma virus polyprotein P115 binds a host phosphoprotein in transformed cells

Fred H. Reynolds Jr & Wim J. M. Van de Ven

Carcinogenesis Intramural Research Program, Frederick Cancer Research Center, Frederick, Maryland 21701

John R. Stephenson

Laboratory of Cellular and Molecular Biology, National Cancer Institute, Frederick, Maryland 21701

Several independent isolates of feline sarcoma virus (FeSV) have been described[1–3]. Such viruses are apparently derived by genetic recombination between feline leukaemia virus (FeLV) genomic RNA and host cellular genetic sequences with transforming potential[4]. Two FeSV isolates, one originally described by Gardner and the second by Snyder-Theilen, have been shown to encode polyproteins of around 115,000 molecular weight[5–8,18,19]. Both polyproteins contain FeLV structural components (p15, p12) at their amino terminus in addition to nonstructural carboxyl terminal components encoded by acquired sequences within the FeSV genome. We have previously shown that Gardner FeSV P115 contains multiple sites of phosphorylation within its nonstructural component and possesses an associated protein kinase activity[9]. In the present study we describe the expression in cells derived from a number of mammalian species, of a highly conserved cellular phosphoprotein with binding affinity for Gardner FeSV P115. This protein, designated P150, exhibits an associated protein kinase activity and is immunologically and structurally distinct from polyproteins encoded by the Gardner or Snyder-Theilen strains of FeSV.

In view of accumulating evidence implicating the non-structural components of Gardner and Snyder-Theilen FeSV encoded polyproteins in transformation (see ref. 10 for review), we analysed uninfected and FeSV transformed mammalian cells for the presence of proteins which exhibit specific binding affinity, and thus possible functional interaction with FeSV P115. Initially, ^{14}C-amino acid labelled control and Gardner FeSV transformed mink cells were analysed by immunoprecipitation and SDS-polyacrylamide gel electrophoresis (SDS-PAGE) using goat antisera directed against detergent-disrupted FeLV. In addition, a high-titred antiserum prepared by immunization of a goat with FeSV P115 partially-purified from Gardner FeSV(4070-A) pseudotype virions by gel filtration was used. As shown in Fig. 1, immunoprecipitation of FeSV P115 and its major cleavage product, P72, from Gardner FeSV transformed mink cells was obtained with either anti-FeSV P115 (lane *b*), or anti-FeLV (lane *a*), but not by normal goat serum (lane *c*). The viral specificity of these proteins is indicated by their absence from control mink cells (lanes *d-f*). Precipitation of Gardner FeSV P115 by anti-FeLV has previously been shown to be due to immunological recognition of FeLV p15 and p12 structural components[6,8,18,19]. An additional protein, of around 150,000 molecular weight (P150), was precipitated from both FeSV transformed and control mink cells by anti-FeSV P115 and from FeSV transformed but not control mink cells by anti-FeLV. These findings demonstrate recognition of P150 by our anti-Gardner FeSV P115 serum and raise the possibility that FeSV P115 may have binding affinity for P150. Such affinity could account for immunoprecipitation by anti-FeLV of P150 from FeSV transformed but not control mink cells.

To explain the above results it is necessary to account for precipitation of P150 from control mink cells by anti-FeSV P115. One possibility is that P150 might have been incorporated into FeSV pseudotype virions as a consequence of an affinity for FeSV P115. Antisera prepared by immunization with partially-purified FeSV P115 might thus recognize mink cellular P150 due to low level P150 contamination of the original immunogen. Alternatively, immunoprecipitation of P150 by anti-FeSV could reflect immunological cross-reactivity between the two proteins. A high-titred antiserum was prepared by repeated immunization of a Fisher rat with FeSV nonproductively-transformed syngeneic tumour cells. If P150 and FeSV P115 shared immunological determinants, sera prepared by this means should also recognize mink cellular P150. As shown in Fig. 1, immunoprecipitation of FeSV P115 and P72 from FeSV

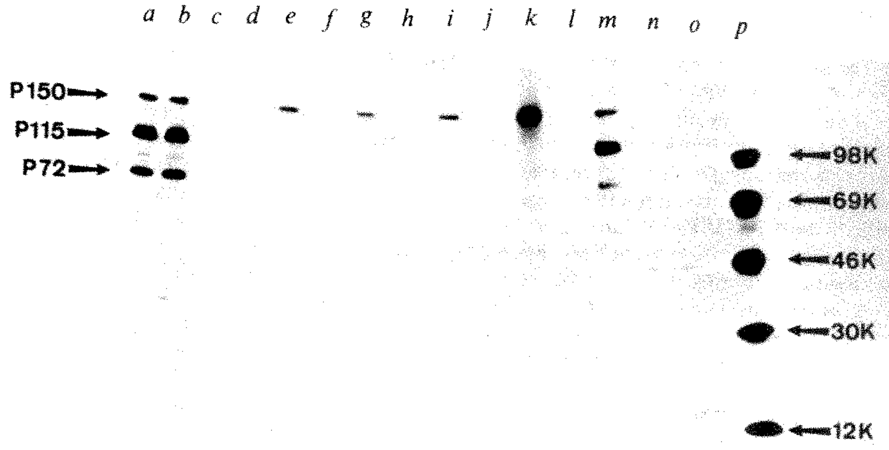

Fig. 1 Analysis by SDS-PAGE of polyproteins encoded by the Gardner strain of FeSV and 150,000 molecular weight cellular phosphoproteins. Cell lines have been previously described[6,8] and include a fetal mink cell line, CCL64 (*d–f, k, l, n*); a Gardner FeSV transformed subclone of CCL64, designated 64F3 (*a–c, m*), a kitten embryonic lung cell line, KeLu (*g, h,* 0) and a canine embryo thymus line, FCf2Th (*i, j*). Metabolic labelling of exponentially-growing cells for 2 h at 37 °C with either ^{14}C-amino acids (10 µCi per ml) (57 µCi/m Atom, Amersham) (*a–j*; *m*–0) or ^{32}P-orthophosphate (100 µCi per ml) (carrier-free), NEN) (*k, l*) was performed as reported previously[9]. Following labelling, cell monolayers were washed twice in serum-free Dulbecco's modified Eagles medium and disrupted at 4 °C in 10 mM sodium phosphate *p*H 7.2, 0.9% NaCl, 1% Triton X-100, 0.5% sodium deoxycholate and 0.1% SDS (PBSTDS) lysis buffer. Extracts (5 ml) were incubated at 4 °C for 18 h following addition of RNase A (200 µg ml^{-1}), RNase T$_2$ (0.1 µg ml^{-1}), DNase I (4.0 µg ml^{-1}), normal goat serum (25 µl), protein-A Sepharose Cl-4B (1.0 ml of 10% v/v suspension) (Pharmacia), and clarified by centrifugation at 100,000 *g* for 1 h. Specific proteins were immunoprecipitated by addition of 5 µl of specific antisera to 1 ml lysate, incubation for 18 h at 4 °C, addition of 50 µl of a 10% (v/v) protein-A Sepharose Cl-4B suspension and incubation for a further 2 h at 4 °C. Immunocomplexes were collected by centrifugation at 2,000*g* for 10 min, washed three times in PBSTDS, resuspended in 20 µl 0.65 M Tris-HCl *p*H 6.7, 1% SDS, 10% glycerol, 2.5% 2-mercaptoethanol and 0.1% bromophenol blue and heated for 2 min at 90 °C. Finally, samples were electrophoresed through a 5% acrylamide stacking gel and a 9 cm 5–20% linear polyacrylamide (30:0.8 acrylamide: bis-acrylamide) gradient separation gel in a Tris-glycine-SDS-buffer system at 20–30 mA (ref. 17). Radioactivity was visualized by autoradiography using Kodak X-0mat XR2 film. Sera used included goat anti-FeLV (*a, d*); goat anti-FeSV P115 (*b, e, g, i, k*), normal goat serum (*c, f, h, j, l*) and serum from a Fisher rat repeatedly immunized with syngeneic FeSV transformed tumour cells (*m–o*). Molecular weight standards include ^{14}C-labelled phosphorylase B (98,000), bovine serum albumin (69,000), ovalbumin (46,000), carbonic anhydrase (30,000) and cytochrome *c* 12,000 (P).

8-0836/80/300409—04$01.00

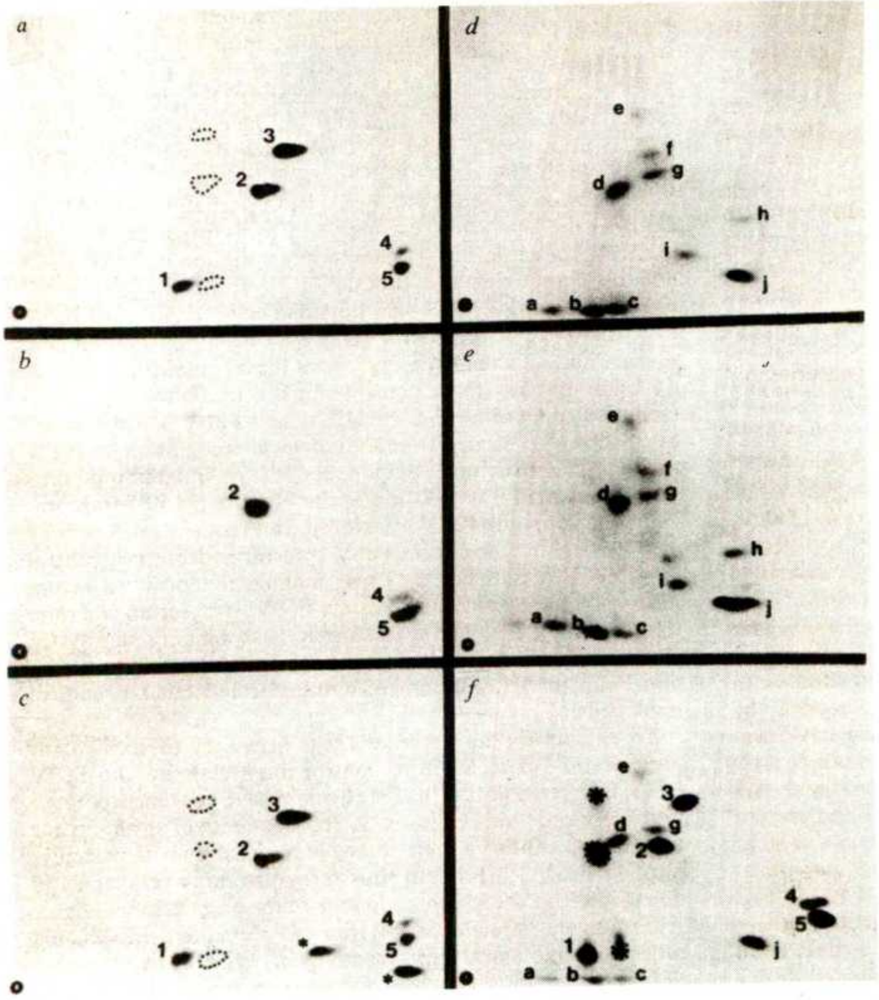

Fig. 2 Comparison by two dimensional tryptic peptide analysis of Gardner and Snyder-Theilen FeSV P115s to the 150,000 molecular weight phosphoproteins expressed in mink and cat cells. Proteins were labelled for 2 h at 37 °C with ^{35}S-methionine (200 μCi per ml) (1075 Ci mmol^{-1}, Amersham) and purified by immunoprecipitation and SDS-PAGE as described in the legend to Fig. 1. Following electrophoresis, gels were washed extensively with 10% trichloroacetic acid, and subsequently with a 10% solution of acetic acid and methanol in water and dried under vacuum. Labelled proteins were localized by autoradiography, and selected gel slices further washed in methanol (10%) and lyophilized. Proteins were digested by incubation of gel slices in tolylsulphonyl phenylalanyl chloromethyl ketone (TPCK)-trypsin (Worthington Biochemicals) (50 μg ml^{-1} in 0.05 M ammonium bicarbonate *p*H 8.0) for 6 h at 37 °C. Following filtration through a 0.45 μm Millex filter (Millipore) and removal of ammonium bicarbonate by repeated lyophilization, tryptic digests were incubated for 2 h at 0 °C in 0.1 ml of chilled performic acid (30% H_2O_2 and 90% formic acid (1:9) preincubated for 2 h at room temperature). Samples were diluted with 2 ml H_2O, lyophilized, resuspended in electrophoresis buffer comprised of acetic acid : formic acid : water (15:5:80) and spotted on 10 × 10 cm cellulose coated TLC glass plates (EM Laboratories). Electrophoresis was performed for 30 min at 500 V and chromatography was conducted in the second dimension in buffer containing butanol, pyridine, acetic acid and water (32:25:5:20). Radiolabelled tryptic peptides were visualized by autoradiography using Kodak X-Omat XT 2 film. Detection of peptides was enhanced by spraying TLC plates with a solution of 7% diphenyloxazole in diethyl ether. Proteins analysed included: Gardner FeSV P115, (*a*); Snyder-Theilen FeSV P115 (*b*); a mixture of FeLV Pr65^{gag}(*) and Gardner FeSV P115 (1–5) (*c*); CCL64 P150 (*d*); KeLU P150 (*e*); and a mixture of KeLu P150 (*a–j*) and Gardner FeSV P115 (*f*).

transformed (lane *m*), but not control mink (lane *n*) or cat (lane *o*) cells was obtained. The absence of detectable precipitation of P150 from uninfected control cells (lane *n*) argues against the possibility that P150 and FeSV P115 possess common immunological determinants.

The availability of a high-titred goat antiserum with specificity not only for FeSV P115 but also for mink cellular P150 provided a means for examining cells of additional species for immunologically cross-reactive proteins. As shown in Fig. 1, proteins similar in molecular weight to mink cellular P150 were precipitable from uninfected feline embryo and canine thymus cells by anti-FeSV P115 (lanes *g*, *i*) but not control (lanes *h*, *j*) goat serum. In other studies we have observed expression of analogous proteins in each of several established human tumour cell lines (data not shown). Thus, mink cellular P150 seems to be representative of a class of proteins of around 150,000 M_r expressed in cell lines of many different mammalian species.

To explore further the relatedness of the 150,000 molecular weight proteins in uninfected mink and cat cells both to each other and to the 115,000M_r Gardner and Snyder-Theilen FeSV encoded polyproteins, ^{35}S-methionine tryptic peptide mapping studies were performed. As shown in Fig. 2*a*, Gardner FeSV P115 contains five ^{35}S-methionine labelled peptides, none of which correspond to the two ^{35}S-methionine labelled peptides specific to the p30 component of FeLV Pr65^{gag} (Fig. 2*c*). Three of the five Gardner FeSV P115 peptides are also represented in Snyder-Theilen FeSV P115 (Fig. 2*b*) consistent with the contention that these independently-derived FeSV isolates possess common or overlapping acquired genetic sequences[4,8,19]. Additional minor peptides within the Gardner FeSV P115 peptide map, indicated by dotted circles, are probably nonspecific in that their presence is variable, and in contrast to the five major ^{35}S-methionine labelled peptides, is dependent on the species of origin of cells analysed. Analysis of mink and cat cellular P150s revealed 10 major ^{35}S-methionine labelled peptides which seemed very similar by two dimensional analysis (Fig. 2*d*, *e*). When analysed in a mixing experiment, none of the 10 ^{35}S-methionine labelled peptides specific to P150 corresponded to the five major ^{35}S-methionine labelled peptides present in Gardner FeSV P115 (Fig. 2*f*). This latter observation is consistent with the above described lack of immunological cross-reactivity between these two proteins and further argues against the possibility that P150 is encoded by cellular sequences homologous to those encoding the non-structural component of FeSV P115.

The non-structural components of Gardner and Snyder-Theilen FeSV 150,000 M_r polyproteins are known to contain multiple sites of phosphorylation[9]. It was thus of interest to establish whether the above described 150,000 M_r cellular proteins are also phosphorylated. To examine this possibility, we analysed extracts of cells metabolically labelled with ^{32}P-orthophosphate by immunoprecipitation and SDS-PAGE. As shown in Fig. 1, mink cellular P150 was efficiently labelled and was immunoprecipitated from mink cells by anti-FeSV P115 (lane *k*) but not normal goat serum (lane *l*), establishing its phosphorylated nature. Tryptic peptide analysis of ^{32}P-labelled P150s from mink and cat cells revealed each to possess 10 to 1 major well-resolved phosphopeptides. The high degree o relatedness of the tryptic peptide patterns of the two protein further indicates that these proteins are relatively conserve (data not shown).

We have previously reported[9] the presence of readily detect able levels of protein kinase activity in immunoprecipitates of

Gardner FeSV P115. The polyprotein itself has been shown to represent a major substrate for this enzymatic activity. Because of the above findings indicating the invariable presence of P150 in such immunoprecipitates, it was of interest to find whether cellular P150s exhibited similar reactivities in the absence of FeSV P115. Extracts of FeSV transformed and control mink cells were prepared, immune precipitated by anti-FeLV, anti-FeSV P115 and normal goat serum and analysed for protein kinase activity. Enzymatic reactivities and substrates involved were identified by SDS-PAGE. As shown in Fig. 3, both Gardner FeSV P115 and mink cellular P150 were efficiently labelled by this means. Incorporation of phosphate into both P150 and FeSV P115 was in the range of 10–20 fmol per min. Even in the absence of FeSV P115, efficient labelling of P150 was observed (lane *e*) establishing that *in vitro* [γ-^{32}P]ATP labelling of P150 is not dependent on an FeSV P115 associated protein kinase. Additional substrates for the P150 associated protein kinase included proteins of around 45,000–50,000 molecular weight in control and FeSV transformed mink cells and a 40,000 molecular weight protein detectable only in control mink cells. The significance of these proteins and their relationship to P150 remain to be determined.

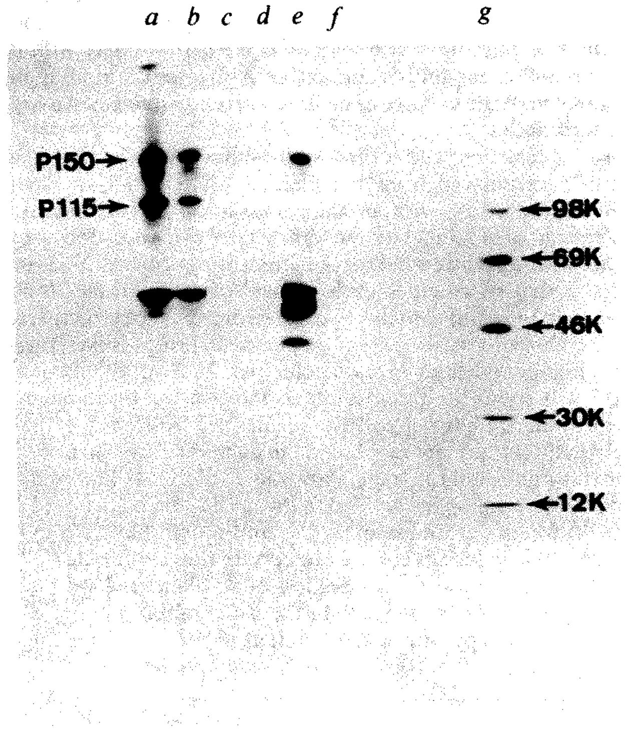

Fig. 3 Analysis of Gardner FeSV P115 and mink cellular P150 containing immunoprecipitates for protein kinase activity. FeSV transformed (*a–c*) and control (*d–f*) CCL64 mink cells were disrupted by repeated aspiration of 1.0×10^7 cells in 5 ml 10 mM Tris-HCl *p*H 7.2, 100 mM NaCl, 1 mM EDTA and 0.1% Triton X-100 through a 25-gauge needle. Disrupted cells were clarified by centrifugation at 2,000 r.p.m. for 10 min, preabsorbed by addition of 50 μl normal goat serum and 0.5 ml of a 10% (v/v) suspension of protein-A Sepharose Cl-4B (Pharmacia), incubated overnight at 4 °C and reclarified by centrifugation at 100,000*g* for 2 h. Following addition of 5 μl specific antiserum, lysates (1 ml) were incubated at 4 °C for 18 h, 50 μl of a 10% (v/v) protein-A Sepharose suspension was added and incubation continued for a further 2 h at 4 °C. Immunocomplexes were collected by centrifugation for 10 min at 2,000*g* and washed in PBSTDS. Protein kinase activity was assayed by resuspension of immunoprecipitates in 20 mM Tris-HCl, *p*H 7.2, 5 mM $MgCl_2$ buffer containing 1 μCi [γ-^{32}P]ATP (2000 Ci mMol^{-1}, NEN) and incubation for 10 min at 30 °C. Reactions were terminated by addition of 3 ml ice cold PBSTDS and nonprotein-bound [^{32}P] label removed by repeated centrifugation in excess PBSTDS. After the final wash, immunoprecipitates were analysed by SDS-PAGE as described in the legend to Fig. 1. Sera used included goat anti-FeLV (*a*, *d*); goat anti-FeSV P115 (*b*, *e*) and normal goat (*c*, *f*). Molecular weight standards are as described in the legend to Fig. 1.

Immunoprecipitation of P150 from both normal and FeSV transformed cells of various species by the anti-FeSV P115 serum used in the present study suggests that P150 is incorporated into pseudotype virions in association with FeSV P115 and represents a probable minor contaminant of the purified FeSV P115 used as the original immunogen. To test this possibility directly, immune precipitates of density-gradient purified FeSV(4070-A) and control 4070-A virions were analysed for protein kinase activity. As shown in Fig. 4, both P150 and FeSV P115 were precipitated from FeSV (4070-A) pseudotype virions by anti-FeLV but not by normal goat serum.

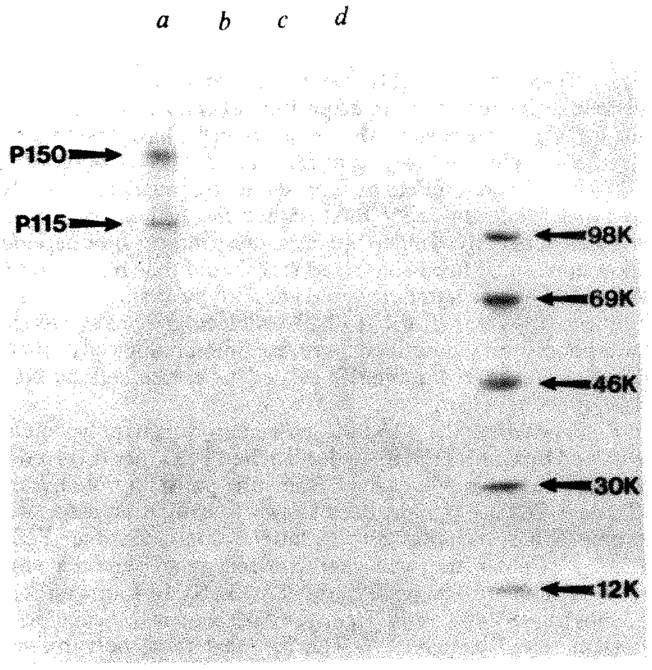

Fig. 4 Association of P150 and FeSV P115 in FeSV(4070-A) pseudotype virions. FeSV(4070-A) (*a*, *b*) and 4070-A (*c*, *d*) virions were purified by sucrose density gradient centrifugation, disrupted and analysed for protein kinase activity as described in Fig. 3. Sera used included goat anti-FeLV p12 (*a*, *c*) and normal goat (*b*, *d*). Molecular weight standards are as described in the legend to Fig. 1.

Both proteins represented efficiently labelled substrates for protein kinase activities present in these immune precipitates. Proteins of around 40,000–50,000 M_r seen in immunoprecipitates of FeSV transformed and control mink cells were not present in immunoprecipitates prepared from FeSV pseudotype virus, arguing against the possibility that their presence is necessary for the protein kinase activities associated with FeSV P115 and P150.

The present findings establish the expression in mink cells of a highly conserved 150,000 molecular weight cellular phosphoprotein with binding affinity for Gardner FeSV P115. Although the biological role of this cellular phosphoprotein is unknown, its affinity for FeSV P115 may have functional significance. P150 and FeSV P115 both represent efficient substrates for protein kinase activity present in immunoprecipitates of FeSV P115. While *in vitro* [γ-^{32}P]ATP labelling of mink cellular P150 is shown to proceed in the absence of FeSV P115, the converse is not necessarily true. Thus, the possibility that P150 possesses intrinsic protein kinase activity and is responsible for phosphorylation of FeSV P115 must be considered. Such a model would be consistent with the affinity that these proteins exhibit for each other. The possibility that both P150 and FeSV P115 possess intrinsic protein kinase activity or alternatively, that an as yet undetected cellular protein kinase is responsible for phosphorylation of one or more of these proteins cannot, however, be excluded.

It is of interest to compare the 150,000 molecular weight cellular phosphoproteins described above to a protein of similar molecular weight recently shown to be expressed in mouse thymus and to a lesser extent, spleen and bone marrow cells[11]. This latter protein, designated NCP 150, has not as yet been characterized with respect to phosphorylation and protein kinase activity. However, NCP 150 has been shown to share immunological determinants with the non-structural component of a 120,000 molecular weight polyprotein encoded by Abelson murine leukaemia virus and is apparently encoded by normal cellular sequences analogous to acquired cellular sequences represented within the AbLV genome. In contrast, on the basis of immunological and structural criteria, the 150,000 molecular weight cellular protein described in the present study is immunologically and structurally unrelated to FeSV P115. The possibility that this lack of relatedness is due to genetic drift subsequent to acquisition of cellular sequences by the FeSV genome seems to be excluded on the basis that three of five ^{35}S-methionine labelled tryptic peptides of Gardner FeSV P115 have been found to be represented by analogous peptides in Snyder-Theilen FeSV P115. Since the two sarcoma virus isolates were derived independently, these three tryptic peptides have apparently been conserved and should thus be present in feline P150 if the latter protein is encoded by analogous genetic sequences. Whether the 150,000 molecular weight cellular phosphoproteins described here are immunologically, structurally or even evolutionarily related to mouse cellular NCP 150, is not yet clear.

Evidence that the 115,000 molecular weight polyproteins encoded by Gardner and Snyder-Theilen FeSV are involved in transformation is increasing. Both are phosphoproteins and Gardner FeSV P115 has been shown to exhibit an associated protein kinase activity[9]. In this latter respect, Gardner FeSV P115 resembles the well characterized avian sarcoma virus transforming protein, pp60^{src} (refs 12, 13), SV40 T antigen[14], an adenovirus–SV40 hybrid T antigen (D2 protein)[15,16] and polyoma middle T antigen[20–22]. The fact that these polyproteins, encoded by independently-acquired cellular sequences, share tryptic peptides, argues for the existence within the normal cellular genome of a limited number of genetic sequences which, on insertion into the type C viral genome, can lead to malignant transformation. The identification of a highly conserved cellular phosphoprotein with associated protein kinase activity and binding affinity for FeSV P115 may have significance with respect to the elucidation of cellular regulation mechanisms involved in transformation of eukaryotic cells.

We thank S. E. VanLaningham-Miller and R. P. Nalewaik for technical assistance. This work was supported under NCI contract NOI-CO-75380, and by a fellowship awarded to W. J. M. Van de Ven by The Netherlands Organization for the Advancement of Pure Research (ZWO).

Note added in proof: Gardner FeSV P115-associated protein kinase specifically phosphorylates tyrosine acceptor sites represented both within P115 itself and in cellular P150.

Received 2 April; accepted 2 May 1980.

1. Snyder, S. P. & Theilen, G. H. *Nature* **221,** 1074–1075 (1969).
2. Gardner, M. B. *et al. Nature* **226,** 807–809 (1970).
3. McDonough, S. K., Larsen, S., Brodey, R. S., Stock, N. D. & Hardy, W. D. Jr *Cancer Res.* **31,** 953–956 (1971).
4. Frankel, A. E., Gilbert, J. H., Porzig, K. J., Scolnick, E. M. & Aaronson, S. A. *J. Virol.* **30,** 821–827 (1979).
5. Khan, A. S. & Stephenson, J. R. *J. Virol.* **23,** 599–607 (1977).
6. Stephenson, J. R., Khan, A. S., Sliski, A. H. & Essex, M. *Proc. natn. Acad. Sci. U.S.A.* **74,** 5608–5612 (1977).
7. Sherr, C. J., Sen, A., Todaro, G. J., Sliski, A. & Essex, M. *Proc. natn. Acad. Sci. U.S.A.* **75,** 1505–1509 (1978).
8. Van de Ven, W. J. M., Khan, A. S., Reynolds, F. H. Jr, Mason, K. & Stephenson, J. R. *J. Virol.* **33,** 1034–1045 (1980).
9. Van de Ven, W. J. M., Reynolds, F. H. Jr & Stephenson, J. R. *Virology* **101,** 185–197 (1980).
10. Stephenson, J. R., Khan, A. S., Van de Ven, W. J. M. & Reynolds, F. H. Jr *J. natn. Cancer Inst.* **63,** 1111–1119 (1979).
11. Witte, O. N., Rosenberg, N. E. & Baltimore, D. *Nature* **281,** 396–398 (1979).
12. Collett, M. S. & Erikson, R. L. *Proc. natn. Acad. Sci. U.S.A.* **75,** 2021–2024 (1978).
13. Levinson, A. D., Oppermann, H., Levintow, L., Varmus, H. E. & Bishop, J. M. *Cell* **15,** 561–572 (1978).
14. Griffin, J. D., Spangler, G. & Livingston, D. M. *Proc. natn. Acad. Sci. U.S.A.* **76,** 2610–2614 (1979).
15. Baumann, E. A. & Hand, R. *Proc. natn. Acad. Sci. U.S.A.* **76,** 3688–3692 (
16. Tjian, R. & Robbins, A. *Proc. natn. Acad. Sci. U.S.A.* **76,** 610–614 (1979).
17. Laemmli, U.K. *Nature* **227,** 680–685 (1970).
18. Khan, A. S., Deobagkar, D. N. & Stephenson, J. R. *J. biol. Chem.* **253,** 8894–
19. Barbacid, M., Lauver, A. V. & Devare, S. G. *J. Virol.* **33,** 196–207 (1980).
20. Griffin, J. D., Spangler, G. & Livingston, D. M. *Proc. natn. Acad. Sci. U.S.A.* 7 (1979).
21. Schaffhausen, B. S. & Benjamin, T. L. *Cell* **18,** 925–933 (1979).
22. Smith, A. E., Smith, R., Griffin, B. & Fried, M. *Cell* **18,** 915–924 (1979).

0028-0836/80/300412—03$01.00

Fraying of A-filaments into three subfilaments

Maria C. Maw & Arthur J. Rowe

Department of Biochemistry, School of Biological Sciences,
University of Leicester, Leicester LE1 7RH, UK

Since Huxley[1] established their bipolar structure, direct ele microscopy of A-filaments isolated from vertebrate sk muscle has yielded little further interpretable information the mode of packing of the myosin molecules within filament. Using A-filaments prepared from rat psoas muscle have now found it possible to induce clear fraying of these filaments into subfilaments, by exposure of the preparation to very low ionic strength before contrasting with uranyl acetate. The number of such filaments observed is generally (and never in excess of) three. Considerations of symmetry suggest that the formation of these frayed filaments is compatible only with a 'three-stranded' model for the native A-filament, a finding in agreement with the balance of evidence recently published using other techniques[2–5].

X-ray diffraction and other studies have shown that the cross-bridges emerge from the filament shaft in an approximately helical array, with an axial translation of 14.3 nm and axial repeat of 43 nm, but the diffraction evidence does not indicate with certainty whether the cross-bridge helix is 2-, 3- or 4-start[6,7]: that is, whether each 'crown' of cross-bridges (one 'crown' per 14.3 nm) contains two, three or four such structures. If the number of myosin molecules per cross-bridge is one, then *n* (the number of myosin molecules per 14.3 nm of filament length) will equal the number of 'strands' in the three helical models. If there are two myosin molecules per cross-bridge then it is virtually certain that $n = 4$, and the filament is two-stranded. Estimates published for *n* are shown in Table 1. As Squire has pointed out[2], opinion has tended to favour $n = 3$, and two recent studies[3,4] which determine mass per unit length have strongly supported this value, in contrast to certain other estimates[5].

While studying the reconstruction of A-filaments[8] we have used rat psoas muscle rather than the usual rabbit muscle, and electron microscopy of relaxed filament preparations revealed that a significant proportion of the A-filaments were 'frayed' at

Table 1 Estimates by various workers for *n*, the number of myosin molecules per 14.3-nm repeat in the A-filament of vertebrate skeletal muscle

Method	Estimated value for *n*	Ref.
Inference from observed symmetry (*E/M*)	3	This work
Quantitative SDS-PAGE of myofibrils	3.8 ± 0.5	5
	2.5	20
	2.7	21
	3.9	22
Mass per unit length determined by hydrodynamics	3.1 ± 0.2	4
Mass per unit length determined by quantitative electron scattering	2.7 ± 0.7	3
Particle counting (*E/M*)	4.3	22
Nucleotide binding to myofibrillar protein	3.5 ± 0.2	23
Calculation from myosin content and density of A-filaments per unit volume of muscle	4	24

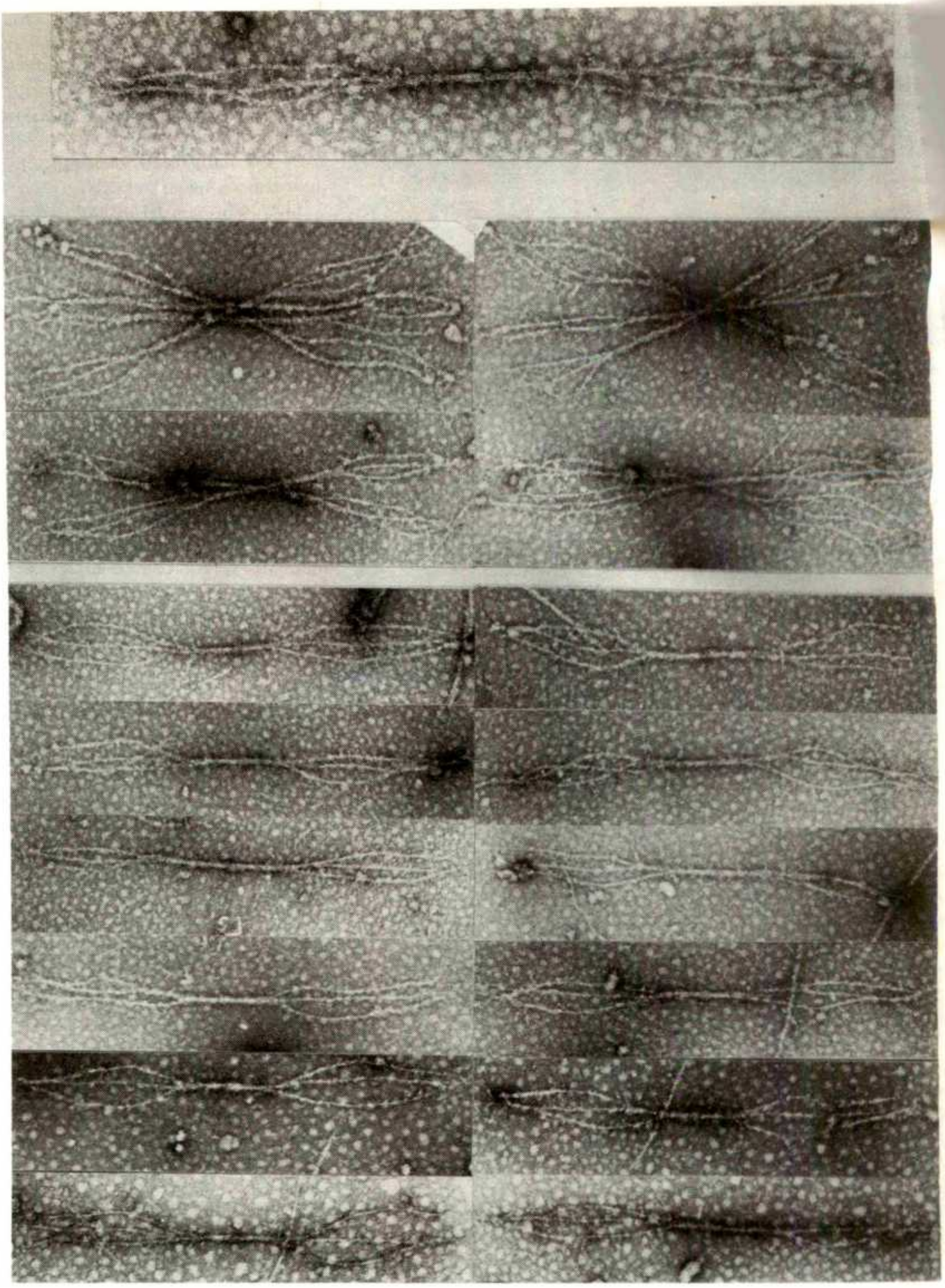

Fig. 1 Electron micrographs of A-filaments and small a-segments (second and third rows) in relaxed filament preparations prepared from rat psoas muscle by the method of Emes and Rowe[4]. The preparations were rinsed on the support grids first with 0.12 M KCl and then with several drops of distilled water before contrasting with unbuffered 2% uranyl acetate. 'Frayed' filaments of the type shown here are routinely seen when this procedure is followed, both in areas where the filaments are negatively contrasted (as shown) and were positive contrasting has occurred. top, ×114,500; Others, ×45,000.

the ends into subfilaments (Fig. 1). We have occasionally observed this effect with rabbit A-filaments prepared in identical conditions. Filaments that 'fray' are indistinguishable in length or width (of the 'non-frayed' region) from intact filaments (Fig. 2); as the proportion that fray varies from preparation to preparation, and even from area to area within the same specimen grid, it is unlikely to constitute a genuine subpopulation of filaments. The variation presumably arises from exact drying-down conditions which are not yet fully controlled.

More than 800 frayed filaments were photographed, measured and examined. In every case only two or three subfilaments were present. Where two subfilaments were counted one was usually significantly thicker than the other (Fig. 1); the thicker one is presumed to comprise two unfrayed subfilaments. We never observed an A-filament that frayed into more than three subfilaments. Fraying, which commences at the distal region, can proceed to any point along the filament axis (Fig. 2) up to a central region ~0.3 μm wide. Within experimental error this corresponds to the innermost stripe of the A-segment which stains with impure anti-C-protein (that is, stripe 9, following the terminology of Craig and Offer[9]). Although the subfilaments are not smooth and show evidence of projections which may be cross-bridges, a clear repeating structure has not as yet been demonstrated.

Subfilaments formed only when the preparation on the microscope grid was washed with several drops of distilled water before contrasting with uranyl acetate. In control experiments, preparations made by this technique showed from 32 to 79% of frayed filaments in randomly selected areas; however a further wash with 0.12 M KCl before contrasting produces almost complete reversal of the effect. No significant proportion of frayed filaments is found if washing with ammonium formate solution (pH 7, $I = 0.12$) is substituted for the distilled water wash. The simplest explanation for this phenomenon is that at

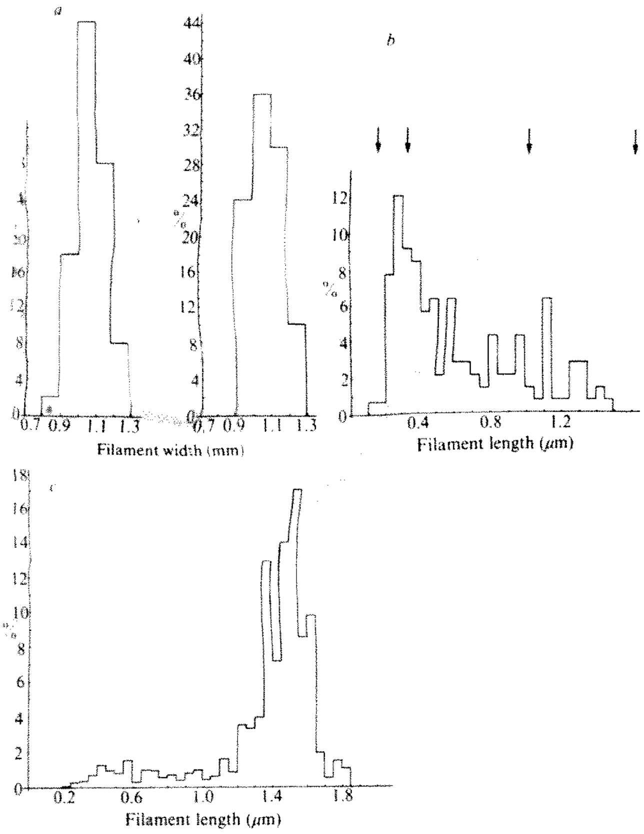

Fig. 2 Statistical analysis of the dimensions of frayed A-filaments showing: *a*, the measured width (×68,700) of the unfrayed central region, avoiding the presumed M-line region, as compared with the similarly measured width of normal, unfrayed filaments (R) from adjacent fields: *b*, the distribution of the length (from one side of the filament to the other) of the unfrayed central region of the frayed filaments, with vertical arrows showing (from L to R) the distances corresponding respectively to the M-line, stripe 9, stripe 1 (terminology of Craig and Offer[9]) and the filament tip: *c*, the length distribution (weight-averaged) of the frayed filaments, this being completely comparable to that obtained with normal, unfrayed filaments[4]. Approximately 800 filaments measured.

low ionic strength the expansion of the electrical double layer around the myosin molecules leads to greatly increased repulsive forces[10]. An increase in net negative charge on the filaments might be expected to have a similar effect, and with synthetic filaments made from rat myosin, Pinset-Härström and Truffy[11] show that high concentration of ATP induces a rather poorly defined tendency to fray. The whole phenomenon may be related to one of the first observations made on myosin, by Szent-Györgyi[12], who showed that prolonged dialysis of myosin solutions at low ionic strength (that is, synthetic filament preparations) against distilled water yielded clear but viscous solutions.

We therefore conclude that the A-filaments from rat psoas muscle contain three asymmetric units which appear as subfilaments after fraying. Our micrographs give no clear evidence to suggest that these subfilaments are packed in the intact A-filament into other than a simple linear array: certainly any large degree of coiling of the subfilaments seems implausible in the light of their ability to fray apart and then re-associate whilst loosely adsorbed on to a carbon film. Our evidence does not, of course, yield a direct estimate for *n*, but it is entirely compatible with 3-start helical models supported by recent measurements of mass per unit length of A-filaments[3,4].

This finding provides an important constraint on the type of molecular model which can be postulated for the A-filament. An obvious conclusion is that if the tails of the myosin molecules are organized into three subfilaments along the shaft, then all the myosin molecules cannot be equivalent at the level of near-neighbour contacts in the main cross-bridge region, and may not even be helically packed. This is not, however, a necessary conclusion. If the subfilaments arise as a result of fraying, initiated (as it seems) from the tip region, then detailed model-building (A.J.R., in preparation) shows that a model which will fray into three subfilaments can be devised, which conserves the conventionally made assumptions regarding equivalence and helical packing.

The finding of 3-fold physical symmetry in the A-filament is consistent with data such as the near-triangular appearance of the shaft in cross-sections[13]; however, no currently published model immediately suggests the fraying into three subfilaments now observed. The model of Pepe[14,15] packs the myosin tails into linear array, but it is two-stranded with respect to the cross-bridge lattice and hence unlikely to fray into three subfilaments. Moreover, recent evidence[16] casts doubt on the existence of the myosin dimer as a kinetic unit, almost certainly an essential feature of a two-stranded, two myosin/cross-bridge model. Squire's model[7,17], like that of Wray[18] for crustacean thick filaments, could only fray into subfilaments with pronounced coiling. The finding of Davey and Graafhuis[19] of three highly coiled subfilaments after tryptic digestion has been shown (A.J.R. and M.C.M., in preparation) to be an artefact of trypsin incubation. We conclude that a thorough re-examination of possible models for A-filament structure is now necessary, in which long-held but never fully proved assumptions as to the equivalence and helical packing of the molecular packing units may be called into question.

This work was supported by an MRC grant.

Received 3 March; accepted 30 May 1980.

1. Huxley, H. E. *J. molec. Biol.* **7,** 281–308 (1963).
2. Squire, J. M. *Nature* **281,** 99–100 (1979).
3. Lamvik, M. K. *J. molec. Biol.* **122,** 55–68 (1978).
4. Emes, C. H. & Rowe, A. J. *Biochim. biophys. Acta* **537,** 125–144 (1978).
5. Pepe, F. A. & Drucker, B. *J. molec. Biol.* **130,** 379–393 (1979).
6. Huxley, H. E. & Brown, W. J. *J. molec. Biol.* **124,** 383–434 (1967).
7. Squire, J. M. *J. molec. Biol.* **77,** 279–323 (1973).
8. Maw, M. C. & Rowe, A. J. *J. ultrastruct. Res.* **69,** 142–143 (1979).
9. Craig, R. & Offer, G. *Proc. R. Soc.* B**192,** 451–461 (1976).
10. Verwey, E. J. W. & Overbeek, J. Th. G. *The Theory of the Stability of Lyophobic Colloids* (Elsevier, Amsterdam, 1948).
11. Pinset-Härström & Truffy, J. *J. molec. Biol.* **134,** 173–188 (1979).
12. Szent-Györgyi, A. *The Chemistry of Muscular Contraction* (Academic, New York, 1951).
13. Luther, P. K. & Squire, J. M. *J. molec. Biol.* **125,** 313–324 (1978).
14. Pepe, F. A. in *Electron Microscopy* Vol. 2 (ed. Uyeda, R.) 53 (Maruzen, Tokyo, 1966).
15. Pepe, F. A. *J. molec. Biol.* **27,** 203–225 (1967).
16. Emes, C. H. & Rowe, A. J. *Biochim. biophys. Acta* **537,** 110–124 (1978).
17. Squire, J. M. *A. Rev. Biophys. Bioengng* **4,** 137–163 (1975).
18. Wray, J. S. *Nature* **277,** 37–40 (1979).
19. Davey, C. L. & Graafhuis, A. E. *Experientia* **32,** 32–34 (1976).
20. Potter, J. D. *Archs Biochim. Biophys.* **162,** 436–441 (1974).
21. Tregear, R. T. & Squire, J. M. *J. molec. Biol.* **77,** 279–290 (1973).
22. Morimoto, K. & Harrington, W. F. *J. molec. Biol.* **83,** 83–97 (1974).
23. Maruyama, K. & Weber, A. *Biochemistry* **11,** 2990–2998 (1972).
24. Huxley, H. E. in *The Cell* Vol. 4 (eds Brachet, J. & Mirsky, A. E.) (Academic, New York, 1960).

The yeast transposon Ty*1* generates duplications of target DNA on insertion

Jürg Gafner & Peter Philippsen

Microbiology Department, Biozentrum, University of Basel,
Klingelbergstrasse 70, CH-4056 Basel, Switzerland

Genetic elements which can transpose into different chromosomal sites causing modulation of gene expression have been found in maize[1] and several other organisms[2]. Most intensively characterized are those in enterobacteria: the insertion sequences, short DNA segments with probably no coding information, the transposable drug-resistance genes and the phage Mu (refs 2–4). The molecular details of transpositions in bacteria are under investigation; important results are the duplication of short target sequences at the integration site[5–15] and the identification of a transposase protein[16,17]. The yeast transposable element Ty*1* is present in about 35 copies per genome; it is 5,600 nucleotide pairs long with terminal direct

0028-0836/80/300414—05$01.00

repeats of 300 nucleotide pairs and is able to integrate into new chromosomal sites[18]. The resemblance of this yeast element to mobile elements in *Drosophila melanogaster*[19,20] is striking. The best characterized element, called copia, is present in about 30 copies in the *Drosophila* genome[19,21] and can integrate into many sites[22], in some cases as part of a large transposable segment[23]. Another remarkable structural resemblance exists with the proviral DNA of retrovirus, which can insert into different chromosomal sites, as found in avian sarcoma virus transformed rat cells[24]. We focus here on the DNA sequence at the termini of element Ty*1* (ref. 18). Our sequence data show that transposition in yeast and bacteria have several features in common, such as integration into different sites without any apparent sequence specificity and duplication of five nucleotide pairs of target DNA at the integration site. In addition, we find that the terminal repeats in two Ty*1* elements consist of identical 338 nucleotide pairs.

The upper part of Fig. 1 shows the basic structure of Ty*1* as deduced from heteroduplex experiments with cloned yeast DNA[18]; the 300 nucleotide pair repeats, called δ, flank a 5,000-nucleotide transcribed sequence which we call ε. Short sequences with homologies to the δ sequences at the Ty*1* termini were also found frequently alone in the chromosomal DNA[18]. These so-called solo δ sequences show up to 15% sequence divergence as determined by DNA sequence analyses in our early experiments (J. G., unpublished). Determination of whether the δ sequences at the Ty*1* termini also show some divergence or whether they are identical should clarify the problem of whether the synthesis of both termini is guided by one template or not. The integrated DNA of retroviruses, for example, probably has identical termini of several hundred nucleotides, as concluded from the known sequence arrangement of the template, the retrovirus RNA[33]. On the other hand, the direct or inverted terminal repeats of bacterial transposons need not be identical according to plausible transposition mechanisms[25,26]. In other words, the two termini need not originate from the same template in the transposition event.

Two separate Ty*1* elements were investigated: Ty*1*-B10, located to the left of the Sup4 locus on chromosome X in strain B596, and Ty*1*-D15 of unknown but different location in strain D585-11C (ref. 18). Cloned restriction fragments containing the Ty*1* termini were sequenced according to the Maxam and Gilbert protocol[27] and the strategy for this analysis is outlined in Fig. 1. The reading of the sequence gels reveals identical δ sequences of 338 nucleotide pairs at the four termini. Figure 2 shows part of the autoradiograms for the left terminus of Ty*1*-D15 and Fig. 3 gives the actual sequences with the identical parts written only once.

A single δ sequence does not show any immediately obvious coding or structural information. It contains 15 start codons and several octanucleotides similar to the sequence 5'-TATAAATA, which are common to eukaryotic promoter regions[28]; but the δ sequence also contains 53 stop codons i reading frames and the longest possible translation prod coded by a δ sequence would consist of 42 amino ac However, there is an open reading frame running out of th sequence starting at nucleotides 41–39 in the lower strand (3). A search for structural features revealed some short inver repeats up to 13 nucleotides long (Fig. 3), but these were located at the ends. Terminal short inverted repeats have be found in bacterial transposable elements and are probably functional importance[9,10].

Work on several other Ty*1* elements is in progress. We ha seen some divergence from the δ sequence in Fig. 3, but t alterations appear in both ends. It is possible that, despi variations among different Ty*1* elements, both termini a always identical.

Transposition events in bacteria create duplications of sho sequences of target DNA at the integration sites which are the flanking the transposed DNA. DNA sequence analysis show clearly that the number of the duplicated nucleotides, but no the sequence itself, is specific for a given transposable element: nucleotides for IS2, Tn*3* and Mu[11–14], 9 nucleotides for IS*1*, Tn*9*, Tn*10* and Tn*903* (refs 5–10) and 11 or 12 nucleotides for IS4 (ref. 15). Analysis of the sequences surrounding the yeast transposable element shows direct repeats of 5 nucleotides flanking the Ty*1*: 5'-GAAAC in the case of Ty*1*-B10 and 5'-ATTTT for Ty*1*-D15 (Fig. 4). For the first case it was demonstrated that these repeats originate from a duplication. As mentioned above, the Ty*1*-B10 is located to the left of the Sup4 locus on chromosome X. Cloned DNA from this locus of strain S288C, which lacks the Ty*1* at this position[18], was analysed. The sequences surrounding the Ty*1*-B10 were found with the 5'-GAAAC present only once (Fig. 4).

It is unlikely that the pentanucleotide which becomes duplicated is a recognition sequence for Ty*1* integration, because this pentanucleotide is different for Ty*1*-B10 and Ty*1*-D15. (A third case shows a 5'-GAGAA adjacent to Ty*1*; P.P., unpublished.) Looking for possible recognition characteristics or preferable sites of Ty*1* insertions, we only note that the 30 nucleotides on either side of each Ty*1* examined consist of 70% or more A + T pairs (Fig. 4). A preference for A + T-rich regions is also found for the bacterial IS*1* transposition[29].

Both Ty*1* elements analysed here also have direct 5-nucleotide repeats (5'-TACCA) at the junctions between the δ and ε segment (Fig. 4). These internal repeats might have functional significance although such internal duplications at comparable locations have not been observed in bacterial transposons.

The solo δ sequences mentioned above probably mark former sites of Ty*1* elements which were deleted by homologous recombination between the termini, leaving one δ sequence behind. Such deletion processes are known in bacteria for λ phages carrying the chloramphenicol transposon Tn*9*, which has direct repeated IS*1* termini; the deletion generates λ phage with

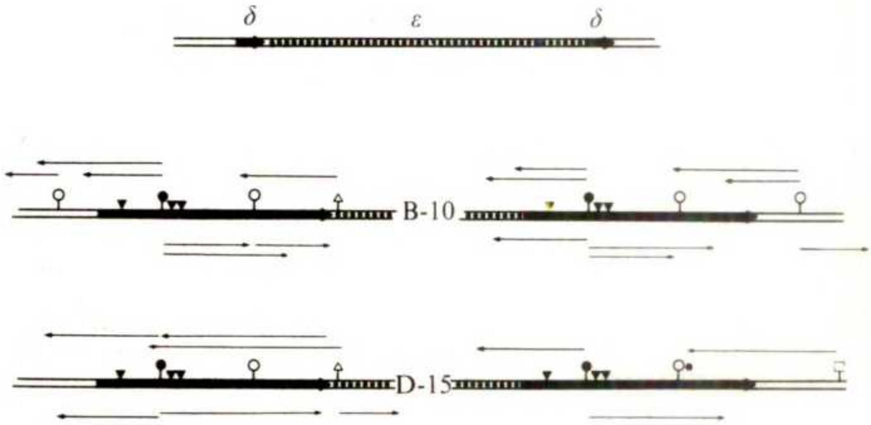

Fig. 1 Structure of Ty*1* and strategy of DNA sequence analysis. The general structure of an integrated Ty*1* is shown in the upper part (chromosomal DNA, double line; δ sequences, thick black arrows; ε sequence, dotted line). The δ sequences of Ty*1*-B10 and Ty*1*-D15 and of some adjoining DNA were sequenced according to Maxam and Gilbert[27]. The arrows mark the length and direction of sequences determined in restriction fragments which were labelled at their 3' ends and also sometimes at their 5' ends. *Xho*I (●), *Taq*I (○), *Hin*fI (▼), *Bgl*II (△) and *Hpa*II (□) restriction sites are indicated. Because of the sequence identity of the four δ sequences we did not determine in all four cases the sequence of both DNA strands.

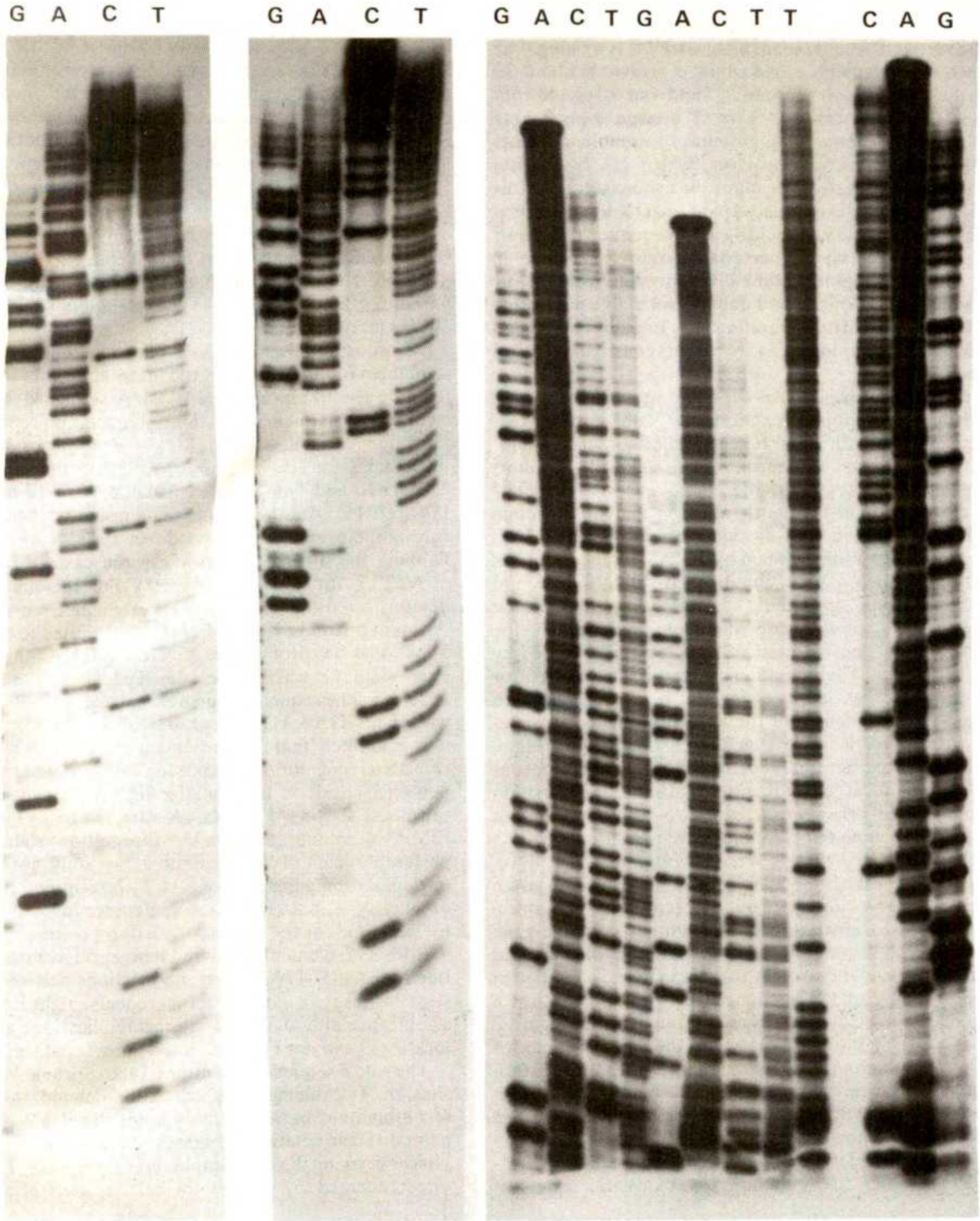

g. 2 Autoradiograms of sequence gels (left part of Ty*1*-D15, Fig. 1). Left, two 18% gels showing the sequence from the *Xho*I site towards the chromosomal DNA d towards the centre of the δ sequence, respectively. Right, 8% gel showing the sequence from the end of the δ sequence towards the *Xho*I site. Electrophoresis of the DNA in the left, middle and right tracks in the 8% gel continued for 8, 12 and 4 h, respectively.

ngle IS*1* sequence[30]. The observed sequence divergence
ng solo δ sequences (base differences and small deletions)
probably reflects either random mutations after the Ty*1*
tion, the terminal heterogeneity among different Ty*1*, or
ı. Clearly, the solo δ sequences are potential targets for a
Ty*1* integration if homologous recombination is involved.
omparable process in bacteria is the homologous recom-
ition between two IS*1* sequences from different replicons
ch creates transposable sequences flanked by two direct
eated IS*1*[31]. An interesting result concerning the question of
nilar mechanism for Ty*1* insertion comes from the analysis
he target sequence for Ty*1*-B10.

As presented above, the sequences to left and right of Ty*1*-B10 are identical to the continuous sequence of the same chromosomal site in strain S288C, which lacks the Ty*1*-B10, except for the duplicated pentanucleotide. By reading the S288C sequence (upper line, Fig. 4) in the inverse orientation, one recognizes the central part of a δ sequence (nucleotides 237–119 of Fig. 3 with point mutations and a deletion of nucleotides 175–179). By sequencing several hundred additional nucleotides on both sides of the S288C sequence and the Ty*1*-B10, we confirmed the Ty*1*-B10 transposition into the middle of a solo δ sequence but one inverted relative to the δ sequence termini of Ty*1*-B10. This rules out the necessity of a

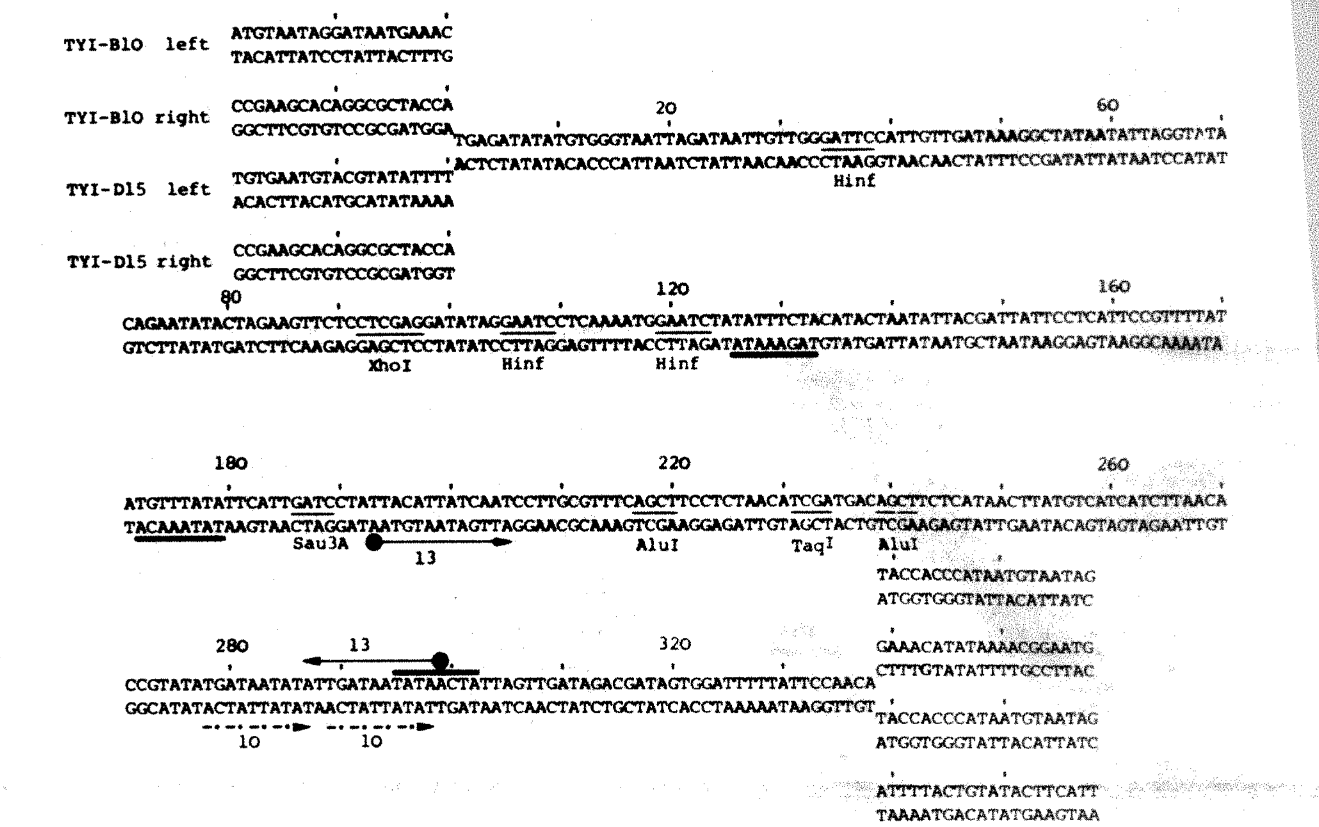

Fig. 3 Nucleotide sequences at the left and right termini of Ty*1*-B10 and Ty*1*-D15. The δ sequence of the four termini is written only once. The left termini start with a stretch of 20 nucleotides of the adjoining chromosomal DNA and continue at the end of the δ sequence with 20 nucleotides of ε DNA. The right termini start with 20 nucleotides of ε DNA and continue at the δ sequence end with 20 nucleotides of the adjoining chromosomal DNA. The three octanucleotides in the δ sequence which are very similar to the 'Hogness box' (5'-TATAAATA), common to eukaryotic promoter regions[28], are marked with a thick bar. Five other similar octanucleotides start at nucleotides 67 and 199 in the upper strand and at nucleotides 70, 143 and 171 in the lower strand. The longest open reading frame in the δ sequence consists of 42 codons (nucleotides 171–296 in the upper strand). One tandem repeat of 10 nucleotides and one inverted repeat of 13 nucleotides are indicated. The terminal sequence 5'-CCAACA appears inverted close to the beginning of the δ sequence (nucleotides 33–28). The adenosine phosphate at position 188 was difficult to read because of a very weak A signal at this position. The sequence of the opposite strand clearly showed a T at position 188. This was confirmed by cleavage with *Sau*3A restriction endonuclease. A poly-adenylation sequence is present at nucleotides 332–327.

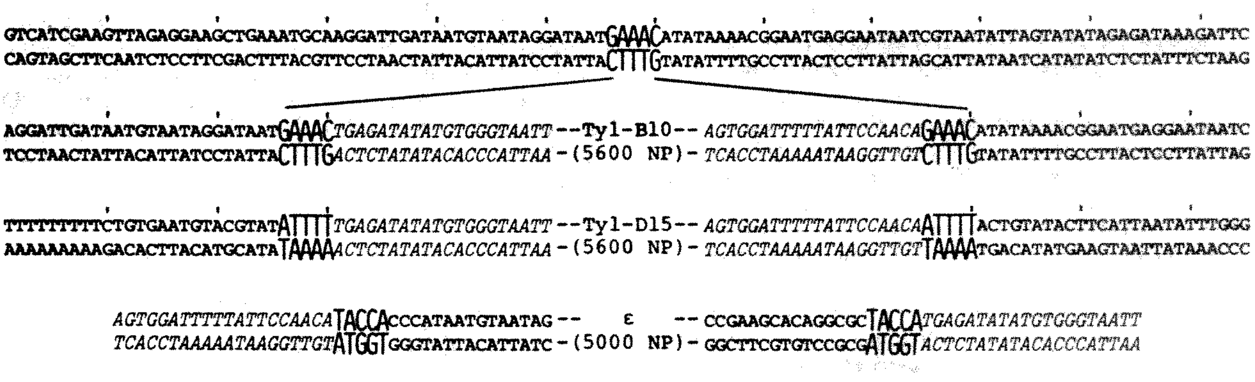

Fig. 4 Five nucleotide pairs duplication at δ sequence junctions. The first and second DNA sequences represent the same region left of the Sup4 locus in strain S288C (no Ty*1* inserted) and B596 (Ty*1*-B10 inserted), respectively. The relationship between the S288C and the B596 strain is unknown. The S288C sequence was obtained from both strands of a 130 nucleotide *Taq*I sequence. The third sequence shows the junction between the δ termini of Ty*1*-D15 and chromosomal DNA. The fourth sequence describes the internal Ty*1* junctions between δ and ε DNA.

sequence homology between the Ty*1* termini and the target DNA for Ty*1* transposition. This is consistent with most of the sequence data from the insertion sites of bacterial transposons, although sequence homology might be involved in Tn*3* transposition in the site selection but not the insertion process[32].

It is unclear whether the 5-nucleotide deletion in the S288C sequence as compared with the inverted δ sequence of Fig. 3 is of any importance for the transposition. This deletion creates the 5'-GAAAC, the actual site of integration for Ty*1*-B10 (Fig. 4). The sequence without the deletion reads 5'-*GAA*TA-TAA*AC* (nucleotides 182–173 of Fig. 3). Possibly, this sequence alteration made the A+T-rich region in the solo δ sequence more receptive for a Ty*1* transposition.

Our sequence data allow a comparison between an eukaryotic transposable element and the bacterial transposons on a molecular level. Shared features are the terminal repetition within the element, the duplication of target sequences at the sites of insertion and the lack of homologous recombination in the transposition process. We also noted some dissimilarities; the δ sequences at the Ty*1* termini lack inverted repeats at their ends the 5-nucleotide internal duplication at the δ–ε juncture Ty*1* is not found at comparable positions in bacterial sposons. When compared with higher eukaryotes, Ty*1* shows certain similarities with the proviral DNA of roviruses, such as the direct repetition of probably identical quences of several hundred nucleotides at the two ends the insertion into different chromosomal sites. As learn more about eukaryotic transposable elements we y find universal features for DNA transposition processes nature, although the various elements will surely have dividual characteristics.

ceived 14 March; accepted 16 May 1980.

1. McClintock, B. *Cold Spring Harb. Symp. quant. Biol.* **21,** 197-216 (1956).
2. Bukhari, A. I., Shapiro, J. A. & Adhya, S. L. (eds) *DNA Insertion Elements, Plasmids and Episomes* (Cold Spring Harbor Laboratory, New York, 1977).
3. Kleckner, N. *Cell* **11,** 11–23 (1977).
4. Starlinger, P. *Plasmid* (in the press).
5. Calos, M., Johnsrud, L. & Miller, J. H. *Cell* **13,** 411–418 (1978).
6. Grindley, N. D. F. *Cell* **13,** 419–426 (1978).
7. Kühn, S., Fritz, H. J. & Starlinger, P. *Molec. gen. Genet.* **167,** 235–241 (1979).
8. Johnsrud, L., Calos, M. P. & Miller, J. H. *Cell* **15,** 1209–1219 (1978).
9. Oka, A., Nomura, N., Sugimoto, K., Sugisaki, H. & Takanami, M. *Nature* **276,** 845–847 (1978).
10. Kleckner, N. *Cell* **16,** 711–720 (1979).
11. Rosenberg, M., Court, D., Shimatake, H., Brady, C. & Wulff, D. L. *Nature* **272,** 414 (1978).
12. Ghosal, D., Sommer, H. & Saedler, H. *Nucleic Acids Res.* **6,** 1111–1122 (1979).
13. Ohtsubo, H., Ohmori, H. & Ohtsubo, E. *Cold Spring Harb. Symp. quant. Biol.* **43,** 1269–1278 (1979).
14. Kamp, D. & Kahmann, R. *Nature* **280,** 247–250 (1979).
15. Habermann, P., Klaer, R., Kühn, S. & Starlinger, P. *Molec, gen. Genet.* **175,** 369–373 (1979).

We thank Ron Davis, John Cameron, Elwyn Loh and Peter Shalit for helpful discussions and for recombinant λ phage, Werner Arber, Tom Bickle and Tom Fox for their comments on this manuscript. The work was supported by grant no. 3.330.78 from the Swiss National Foundation for Scientific Research.

Note added in proof: Sequence analysis of the *Drosophila* mobile element copia show that the integration of copia also generates a 5-nucleotide paired duplication and that the first three and the last ten nucleotides of the terminal repeats in copia and Ty*1* are identical (B. Levis, P. Dunsmuir, W. Brorein & G. Rubin, personal communication).

16. Gill, R. E., Heffron, F. & Falkow, S. *Nature* **282,** 797–801 (1979).
17. Chou, J., Lemaux, P. G., Casadaban, M. J. & Cohen, S. N. *Nature* **282,** 801–806 (1979).
18. Cameron, J. R., Loh, E. Y. & Davis, R. W. *Cell* **16,** 739–751 (1979).
19. Finnegan, D. J., Rubin, G. M., Young, M. W. & Hogness, D. S. *Cold Spring Harb. Symp. quant. Biol.* **42,** 1053–1063 (1978).
20. Tchurikov, N. A., Ilyin, Yu. V., Ananiev, E. V. & Georgiev, G. P. *Nucleic Acids Res.* **5,** 2169–2187 (1978).
21. Strobel, E., Dunsmuir, P. & Rubin, G. M. *Cell* **17,** 429–439 (1979).
22. Potter, S. S., Brorein, W. J. Jr, Dunsmuir, P. & Rubin, G. M. *Cell* **17,** 415–427 (1979).
23. Gehring, W. & Paro, R. *Cell* (in the press).
24. Hughes, S. H. *et al. Cell* **15,** 1397–1410 (1978).
25. Shapiro, J. A. *Proc. natn. Acad. Sci. U.S.A.* **76,** 1933–1397 (1979).
26. Arthur, A. & Sherratt, D. *Molec. gen. Genet.* **175,** 267–274 (1979).
27. Maxam, A. & Gilbert, W. *Proc. natn. Acad. Sci. U.S.A.* **74,** 560–564 (1977).
28. Gannon, F. *et al. Nature* **278,** 428–433 (1979).
29. Meyer, J., Iida, S. & Arber, W. *Molec. gen. Genet.* (in the press).
30. MacHattie, L. A. & Jackowski, J. B. in *DNA Insertion Elements, Plasmids and Episomes* (eds Bukhari, A. I., Shapiro, J. A. & Adhya, S. L.) 219–228 (Cold Spring Harbor Laboratory, New York, 1977).
31. Iida, S. & Arber, W. *Molec. gen. Genet.* **177,** 261–270 (1980).
32. Tu, C. P. D. & Cohen, S. N. *Cell* **19,** 151–160 (1980).
33. Taylor, J. M. *Curr. Top. Microbiol. Immun.* **87,** 23–41 (1979).

Transcriptional control of two gene subclusters in the tRNA operon of bacteriophage T4

Alexander Goldfarb[*] & Violet Daniel

Biochemistry Department, Weizmann Institute of Science, Rehovot, Israel

In bacteriophage T4 DNA, transcription units recognized *in vitro* by host RNA polymerase consist of promotor-proximal 'immediate early' (IE) genes and promotor-distal 'delayed early' (DE) genes separated from each other by ρ-dependent transcription terminators[1]. *In vivo*, the transition from IE to DE transcription requires phage-specific protein synthesis and can be prevented by chloramphenicol (CAM)[2]. Most of the information about IE/DE transition has been obtained by hybridization analyses of mixtures of RNA species synthesized simultaneously on several T4 transcription units (for review see ref. 3). A useful model for the study of T4 gene expression at the level of primary transcripts and individual gene products is provided by the T4 tRNA operon, a cluster of genes coding for eight T4-specific transfer RNAs and two stable RNAs (species 1 and 2) of unknown function (Fig. 1). The 10 genes of the tRNA operon are arranged in two subclusters (I and II) with a promotor located about 1 kilobase pair upstream[4,5]. The primary transcripts and the final gene products of this region have been identified and isolated[6,7]. Moreover, this genetic region was recently cloned and a part of it sequenced[5,8]. We describe here the expression of T4 tRNA genes *in vivo* and *in vitro* in terms of the IE/DE concept and demonstrate that the two subclusters of the tRNA operon are subject to different modes of control.

The transcription of individual tRNA genes *in vitro* can be monitored by digesting the total synthesized RNA with nucleases present in the 100,000*g* supernatant (S-100) of *Escherichia coli* and analysing the stable products by gel electrophoresis[7,9]. Figure 2 shows the S-100 digestion products of RNA synthesized in the presence and in the absence of ρ-factor. As templates for transcription in this experiment we used wild-type T4 DNA (lanes 1, 2) or DNA with deletions in the tRNA operon (lanes 3–6), the map locations of which are shown in Fig. 1. The digestion products migrating in the 4S region of lanes 1 and 2 (Fig. 2*a*) were analysed by a second-dimension electrophoresis (Fig. 2*b*). One can see that factor ρ prevents the transcription of genes coding for tRNA^{Arg} and RNA species 1 and 2 from the wild-type DNA. However, in the presence of ρ, these genes are expressed from DNA containing deletion Δ119, and species 1 RNA is synthesized in the case of deletion Δ27. The addition of ρ does not block the expression of genes of subcluster I. These results can only be explained by assuming the existence of a ρ-dependent transcription terminator in DNA between subclusters I and II of the tRNA operon. The absence of ρ-effect in the case of deletions Δ119 and Δ27 seems to be due to the removal of this site from DNA by the deletions.

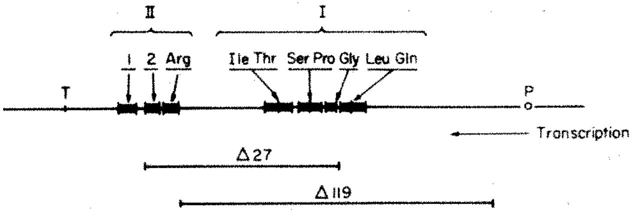

Fig. 1 T4 tRNA operon (modified from refs 4, 5, 7, 13). I and II, the two subclusters of stable RNA genes. The distance between promotor (P) and terminator (T) is about 3,000 base pairs. Lower bars represent deletions used in the present work.

The effect of ρ on the transcription of tRNA genes was further analysed at the level of primary transcripts. Elsewhere[7] we have studied the *in vitro* transcription of this region at high ionic strength when ρ-factor is not active and demonstrated that the major transcript of the wild-type tRNA operon is a 3.0-kilobase long RNA molecule (RNA species A_{wt}) which contains all 10

---

[*] Present address: Max-Planck-Institute for Biochemistry, Martinsreid bei Munchen, FRG.

0028–0836/80/300418—03$01.00

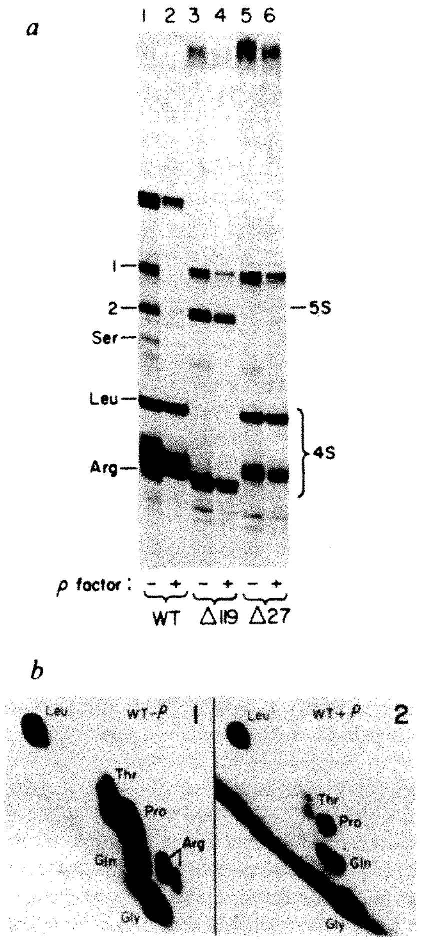

Fig. 2 Autoradiograms showing stable RNAs synthesized *in vitro* in the presence and absence of ρ-factor. DNA (10 μg) from wild-type (WT) T4 or psu_b^- deletion mutants Δ119 and Δ27 were transcribed by 4 μg RNA polymerase in 100-μl reaction mixtures containing 40 mM Tris-HCl *p*H 7.9, 10 mM $MgCl_2$, 7 mM 2-mercaptoethanol, 50 mM KCl, 0.25 mM each of ATP, GTP and UTP and 0.08 mM [α-^{32}P]CTP (1 Ci mmol^{-1}, Amersham); 4 μg of ρ-factor were added where indicated. After 15 min incubation at 37 °C, 5 μg ml^{-1} rifampicin was added and incubation continued for 10 min followed by addition of 10 μg DNase 1 (RNase-free, Worthington). After 10 min incubation the samples were deproteinized with phenol, RNA precipitated with ethanol, dried, dissolved and digested with 5 mg ml^{-1} 100,000*g* supernatant fraction of *E. coli* (S-100) for 2 h at 37 °C. The digestion products, after phenol deproteinization and ethanol precipitation, were separated by electrophoresis in acrylamide gels containing 6.6 M urea. The isolation of RNA polymerase and DNA, preparation of S-100, conditions of S-100 digestion and gel electrophoresis and identification of digestion products were as described elsewhere[7]. Factor ρ was purified according to ref. 14. *a*, Separation of S-100 digestion products in 10% acrylamide gel. *b*, Two-dimensional separation of 4S wild-type products. The 4S regions of lanes 1 and 2 of gel *a* were cut out and applied to 20% acrylamide gel slabs for the second-dimension electrophoresis.

genes of the operon and is terminated about 0.3 kilobases downstream from subcluster II. It was also shown that deletions Δ27 and Δ119 result in the synthesis of new deletion-specific transcripts A_{27} and A_{119} which are initiated and terminated at the same sites as the wild-type transcript A_{wt} (ref. 7). We now find (Fig. 3) that at low salt concentrations, transcripts A_{wt}, A_{27} and A_{119} are still synthesized on their respective DNA templates. The addition of ρ-factor results in the disappearance of the wild-type transcript A_{wt} whereas the two deletion-specific transcripts are still synthesized. This confirms the above conclusion about ρ-dependent termination of transcription between the two subclusters of tRNA operon.

On the basis of these observations one can expect that genes of subcluster II would not be transcribed *in vivo* in t absence of phage-specific protein synthesis. Accordingly, analysed the formation of phage-specific stable RNA in ce infected in the presence of CAM (Fig. 4). In this experiment v compared RNAs induced by wild-type phage (lanes 2, 4) a deletion mutant psu_b^- Δ119 (lanes 3, 5) in the presence (lanes 5) and absence (lanes 2, 3) of CAM. Note that in the presence CAM host transcription is not completely shut off by bacteri phage and the continued synthesis of bacterial tRNA gives high background. Nevertheless, the products of subcluster I tRNA^{Arg} and species 1 and 2, can be detected. It is clear tha CAM strongly inhibits the formation of these three products in the cells infected with wild-type phage. In the case of deletio Δ119, however, the formation of RNA species 1 and tRNA^{Arg} i CAM resistant. The CAM sensitivity of RNA species 2 can be attributed to its degradation in the absence of the product o bacteriophage gene *mb*: the product of this early gene has been shown to be required for the appearance of tRNA^{Pro}, tRNA^{Ser},

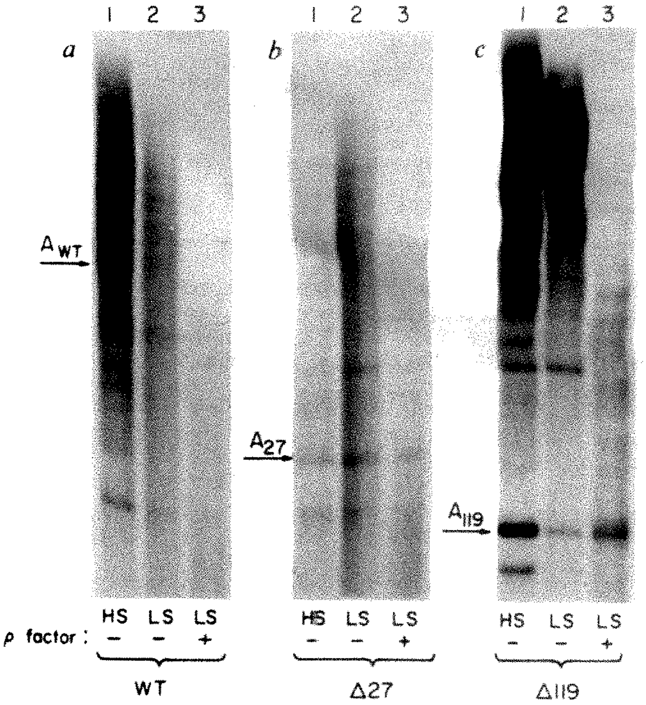

Fig. 3 Autoradiogram showing primary transcripts of T4 DNA made in the presence and absence of ρ-factor. DNA of wild-type T4 (WT) and deletion mutants psu_b^- Δ27 and Δ119 was transcribed at low (LS, 50 mM KCl) and high (HS, 250 mM KCl) salt concentrations. Otherwise, the conditions of transcription were as in Fig. 2. After the first phenol deproteinization, RNA transcripts were precipitated with ethanol, dissolved and separated in composite acrylamide–Agarose SDS gels as described elsewhere[7]. The lengths of RNA species A_{wt}, A_{27} and A_{119} are about 3,000, 1,500 and 750 nucleotides, respectively, *a*, *b*, 2.2% acrylamide–0.5% Agarose gels. *c*, 2.5% acrylamide–0.5% Agarose gel.

tRNA^{Ile} and RNA species 2 in the infected cell[10,11]. Although, in the absence of *mb* function these RNAs are transcribed and probably processed, they cannot be detected *in vivo*, apparently due to their fast degradation. As for tRNA^{Arg} and RNA species 1, we conclude that phage-specific protein synthesis is required for their transcription from the wild-type template but not from DNA with deletion Δ119. This, as well as the above *in vitro* experiments, demonstrate that the genes of subcluster II are expressed as DE functions in the wild-type phage and as IE functions in psu_b^-Δ119 (and Δ27) mutant.

he CAM inhibition of subcluster II transcription can hardly explained by the polar effect of nonspecific inhibition of slation[3] because tRNA genes are not likely to be translated ll. Rather, one can assume that a phage-specific protein se target sequence is situated between the two subclusters of A genes is responsible for the transcription of subcluster II.

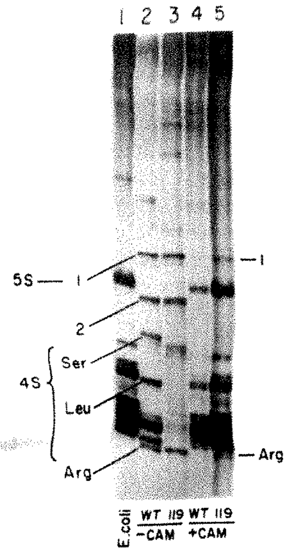

Fig. 4 Autoradiogram showing T4-specific stable RNAs induced in *E. coli* in the presence and absence of CAM. The cells of *E. coli* were infected with wild-type T4 (WT) or deletion mutant psu$_b^-$ Δ119 at MOI = 10 and labelled with ^{32}P as described elsewhere[7]. Where indicated, 100 μg ml^{-1} CAM was added to the culture 1 min before phage infection. RNA was extracted and separated in 10% acrylamide urea gel. Lane 1 shows stable *E. coli* RNAs.

The existence of a phage-specific product responsible for IE/DE transition has been postulated in T4 (ref. 3). Its action may be similar to the anti-termination effect of *N* gene product of bacteriophage λ (ref. 12). The study of such proteins has hitherto been hampered by the absence of suitable assay systems. Our results provide a convenient *in vitro* system for the search and analysis of the factors responsible for IE/DE transition.

We thank Drs K. Fukada and J. Abelson for psu$_b^-$ Δ mutants and for communicating their results before publication, and Mr Y. Tichauer for isolating ρ-factor. This research was supported in part by a grant from the US-Israel Binational Science Foundation (BSF), Jerusalem, Israel.

Received 4 January; accepted 29 April 1980.

1. O'Farrell, P. Z. & Gold, L. M. *J. biol. Chem.* **248,** 5512–5519 (1973).
2. Salzer, W., Bolle, A. & Epstein, R. *J. molec. Biol.* **49,** 271–296 (1970).
3. Rabussay, D. & Geiduschek, E. P. in *Comprehensive Virology* Vol. 8 (eds Fraenkel-Conrat, H. & Wagner, R.) (Plenum, New York, 1976).
4. Fukada, K., Ostuka, A. & Abelson, J. *J. molec. Biol.* **137,** 191–211 (1980).
5. Fukada, K., Gossens, L. & Abelson, J. *J. molec. Biol.* **137,** 213–234 (1980).
6. Goldfarb, A., Seaman, E. & Daniel, V. *Nature* **273,** 562–564 (1978).
7. Goldfarb, A. & Daniel, V. in preparation.
8. Fukada, K. & Abelson, J. *J. molec. Biol.* (in the press).
9. Nierlich, D. P., Lamfrom, H., Sarabhai, A. & Abelson, J. *Proc. natn. Acad. Sci. U.S.A.* **70,** 179–182 (1973).
10. Wilson, J. H. & Abelson, J. *J. molec. Biol.* **69,** 57–73 (1972).
11. McClain, W. H., Guthrie, C. & Barrell, B. G. *J. molec. Biol.* **81,** 157–171 (1973).
12. Adhya, A. & Gottesman, M. *A. Rev. Biochem.* **47,** 967–996 (1978).
13. Wilson, J. M., Kim, J. S. & Abelson, J. *J. molec. Biol.* **71,** 547–556 (1972).
14. Roberts, J. W. *Nature* **244,** 1168–1174 (1969).

Evolution of DNA sequences has been retarded in Malagasy primates

Tom I. Bonner*, Robert Heinemann† & George J. Todaro*

*Laboratory of Viral Carcinogenesis, National Cancer Institute, National Institutes of Health, Bethesda, Maryland 20205
†Program on Genetics, George Washington University, Washington, DC 20052

It is generally accepted[1] that there are six major groups of living primates: (1) lemurs (including all the primates of Madagascar), (2) lorises (including galago and potto), (3) tarsiers, (4) New World monkeys, (5) Old World monkeys and (6) apes (including man). Tree shrews, once considered to be primates, are now generally recognized[2] as not significantly more closely related to the six groups than other mammals. The first surviving primate lines to diverge from the common primate ancestor are believed to have given rise to one or more of the first three groups. However, the fossil record is insufficient to determine their relative branching order[3]. Furthermore, neither morphological considerations[2,4–7] nor studies of protein evolution[8,9] produce unanimity as to whether tarsiers are more closely related to the prosimians (the lemurs plus lorises) or the simians (the monkeys and apes). In an attempt to resolve these discrepancies, we have measured the DNA sequence *difference* between several primates. We report here that the evolution of DNA of primates from Madagascar is significantly less than that of all other groups of living primates. This is not expected in the simplest form of the theory of neutral selection and may be important for our understanding of evolution at the molecular level.

To measure genetic differences between the various primates as directly as possible, we followed Kohne *et al.*[10] in using the sequences which are present in a frequency of one copy per haploid genome, commonly referred to as single copy DNA. As the single copy fraction amounts to approximately half the DNA in the genome, the evolutionary fluctuations which can occur within a single gene are thoroughly averaged out. To determine the branching order in the early evolutionary history of the primates, we divide the living primates into four groups: lemurs, lorises, tarsiers and simians—New World plus Old World monkeys and apes. Our experiment consists of preparing ^{125}I-labelled single copy DNA from a representative species of each of the four groups, hybridizing each labelled DNA to the unlabelled total DNA of two to four members of each group in conditions such that each labelled DNA molecule hybridizes to an unlabelled molecule, and measuring the sequence divergence between the two species of DNA by measuring the melting temperature of the hybrid molecules. From experiments with various model systems, we can expect a 1 °C decrease in melting temperature for each ~1% nucleotide difference[11]. Thus, what we measure is the accumulation of single base mutations in the two lineages since their divergence. We expect that these accumulated mutations account for the bulk of the evolutionary difference between the species. We will not, however, measure any additions to, deletions from or rearrangements of the DNA. Thus, we may not detect some of the changes in gene regulation which would be expected to be relatively rare but evolutionarily quite significant[12,13].

Our results are shown in the form of melting curves (Fig. 1). From these it is clear that with labelled DNA from the simian, loris or tarsier groups, the most closely related DNAs are always from the lemur group. The only explanations for this are that either the data are defective or the lemurs have diverged substantially more slowly than the other groups. As the melting curves for all the DNAs within a single group are nearly identical when hybridized with ^{125}I-DNA from another group, the only

0028-0836/80/300420—04$01.00

possible defect would be one which simultaneously affects all the DNAs of a single group. This would require either the degradation of all the DNAs within one group or the presence of an impurity in some of the groups of DNAs that affects the stability of hybrids with some but not all of the other groups. The fact that all the homologous melting curves are nearly identical demonstrates that the DNAs of all four groups are comparable. When, as a further test, separate extractions (obtained from B. Hoyer) of DNAs from *Lemur catta* and tarsier were compared with those used for Fig. 1, identical results were obtained. Thus, we believe that the data can only be accounted for by the hypothesis that the lemur DNA has evolved more slowly than the other primate DNAs.

To construct a phylogenetic tree consistent with the data we must consider Fig. 1 quantitatively. If we define the hybridizable fraction of a given labelled DNA as the fraction which hybridizes to the homologous DNA, the data of Fig. 1 show that only 50–70% of the hybridizable DNA actually hybridizes to DNAs from other groups. The most reasonable explanation of this reduced hybridization is that a portion of the hybridizable sequences have diverged so much between the two groups that they are not able to form stable hybrids at the hybridization temperature. We can take these sequences into account if we use the melting temperature of the potentially hybridizable sequences rather than those which actually hybridize[10]. We therefore characterize each melting curve with the temperature (T_{50}H) at which 50% of the hybridizable sequences are bound to hydroxyapatite. These values are presented in Table 1. We then convert the measured T_{50}H values to the actual number of nucleotide substitutions which have occurred since the divergence of the two species. There is some uncertainty in this conversion as results from different model systems vary over 1.5–0.7 °C in melting temperature reduction per per cent nucleotide difference. We will assume the intermediate value of 1.0 °C in our calculations. However, choice of any conversion factor within the above range does not significantly affect the relative amounts of change along the different branches. An additional correction must be made because the degree of sequence divergence in our measurements is sufficiently great for the probability of multiple changes at the same site to be appreciable. Assuming only that a given base can mutate to any other base with equal probability, statistical corrections[14] can be made (see Table 2) and, as we are comparing about 10^9 nucleotides, the corrected values should reflect the actual number of base substitutions quite accurately. Once this correction is

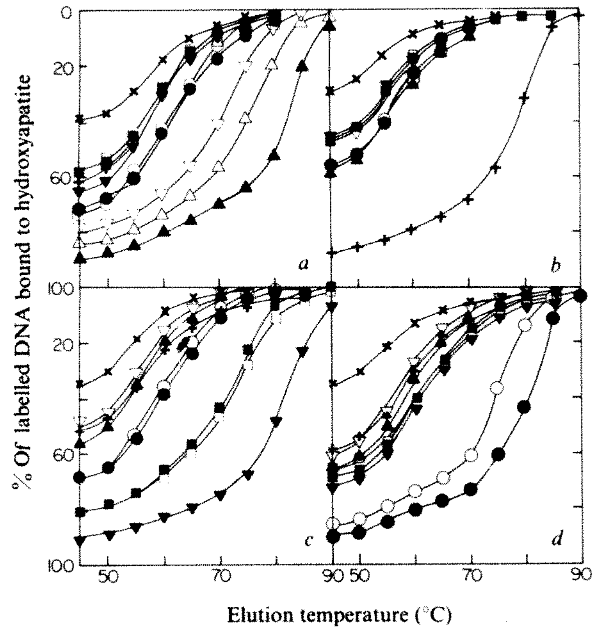

Fig. 1 Melting curves of hybrid DNA molecules formed between ^{125}I-labelled single copy DNAs and unlabelled cellular DNAs. DNAs were iodinated to a specific activity of 3×10^7 c.p.m. per μg by a modification of the procedure of Chan *et al.*[20], hybridized to a C_0t of 200 and fractionated on hydroxyapatite at 45 °C in 0.14 M phosphate buffer (PB, sodium phosphate, *p*H 6.8). The single copy fraction, that is, the fraction which did not bind, was then fractionated by electrophoresis on an alkaline 2% agarose gel and the portion between 200 and 1,200 nucleotides was used for the hybridizations. 100 μg of cellular DNA was hybridized with about 2,000 c.p.m. of labelled DNA in 1.0 M PB at 60 °C to a C_0t of 22,000, the hybrid was bound to hydroxyapatite in 0.14 M PB plus 0.02% SLS at 45 °C and eluted in 5 °C steps as described elsewhere[21]. The cellular DNAs are: ▲, human; △, baboon; ▽, spider monkey; +, tarsier; ▼, galago; □, slow loris; ■, slender loris; ○, *L. catta*; ●, *L. mongoz*; ×, pig or mouse. The labelled DNAs are: *a*, human; *b*, tarsier; *c*, galago; *d*, *L. mongoz*.

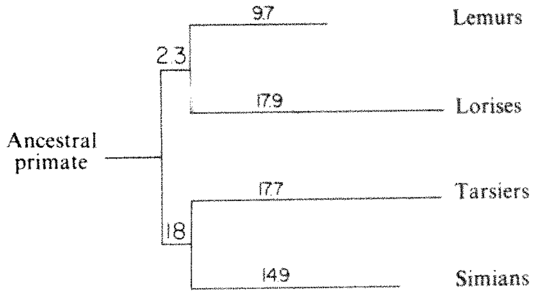

Fig. 2 Phylogenetic tree for the primates derived from the single copy DNA sequence divergences. The number of actual nucleotide substitutions since the divergence of the lineages as obtained from Table 2 were used to construct the tree as follows. The sum of the lemur and loris branches is given by the average of their reciprocal hybridizations. The difference between the lemur and loris branch lengths is obtained from the experiments in which labelled tarsier or simian DNA is hybridized to both lemur and loris DNAs (the differences within columns of Table 2). These values would be expected to be more accurate than the differences obtained by hybridizing labelled lemur and labelled loris DNAs to either simian or tarsier DNAs (the differences within rows of Table 2). Combining these values, we can solve for the length of the two branches. Similarly, we can solve for the length of the tarsier and simian branches. Using these four branch lengths we can then determine the length of the branch interconnecting the lemur–loris branch point and the tarsier–simian branch point necessary to fit the eight measurements which include this branch. Finally, these branch lengths are combined with the estimated distances measured with tree shrew DNA to determine the branch point with the common primate ancestor. The numbers on the branches represent the percentage of nucleotide substitutions along that branch.

Table 1 Sequence divergence as measured by reduction of hybrid melting temperature

Unlabelled DNA	Labelled single copy DNA			
	Human	Tarsier	Galago	*L. mongoz*
Human	0	24.6	29.3	23.4
Baboon	6.9	—	27.8	25.1
Spider monkey	11.2	26.4	30.7	24.5
Tarsier	26.2	0	30.2	26.9
Galago	26.7	30.1	0	22.1
Slow loris	27.6	—	11.5	23.0
Slender loris	28.6	28.6	11.3	23.1
L. catta	22.6	24.6	22.4	6.0
L. mongoz	21.2	24.6	22.0	0

The T_{50}H for each melting curve in Fig. 1 and for other melting curves which are not shown was determined as described in the text. The reduction in T_{50}H compared with the homologous DNA was averaged and this average is tabulated. The homologous T_{50}H values are 78.8–81.3, 78.1, 78.8–80.7 and 79.5–81.1 °C for human, tarsier, galago and lemur DNAs, respectively. The values for comparable pairs of DNAs are very close to those reported by Kohne, Chiscon and Hoyer[10]. The reciprocal values (for example, the divergence between human and tarsier as measured with either labelled tarsier or labelled human DNAs) are in general but not precise agreement. This difference probably results from the various labelled single copy DNAs not being precisely equivalent in sequence composition.

ble 2 Difference matrix in terms of per cent actual nucleotide substitutions

Unlabelled DNAs averaged within groups	Labelled single copy DNA Simian	Tarsier	Loris	Lemur
mian	0	32.0	38.2	30.1
arsier	33.0	0	39.7	34.3
oris	35.2	38.2	0	28.1
emur	26.6	30.6	27.1	0

The values of ΔT_{50}H from Table 1 were averaged over the various unlabelled DNAs within a taxonomic group and were converted to per cent actual nucleotide substitutions. The conversion assumes that 1 °C in ΔT_{50}H equals 1% sequence difference and that any given base can mutate to any other base with equal probability. The use of Holmquist's[14] equation (20) then corrects for multiple changes at a particular site in one lineage and for changes at the same site in both lineages.

made, it is clear that the total number of base substitutions along individual lineages should be additive. We can then use the six pairwise differences between the four primate groups to determine distances along each branch of the tree.

The only tree consistent with the data but without substantially negative branch lengths places the loris and lemur groups at one branch point separated by about 4% base substitution from the branch point between tarsiers and simians. It is not, however, possible to determine the location of the branch point for the divergence from the common primate ancestor without data which include a more distant DNA. We have therefore used single copy tree shrew (*Tupaia glis*) DNA which is so distant that we cannot directly measure ΔT_{50}H. We can, however, measure ΔT_{25}H values of 24.8, 26.8 and 28.0 °C for lemur, simian and loris groups, respectively. As Fig. 1 indicates that $\Delta T_{50}\mathrm{H} = 1.18 \times \Delta T_{25}\mathrm{H}$, we can extrapolate to obtain approximate ΔT_{50}H values of 29.3, 31.6 and 33.0 °C. When combined with the branch lengths derived in Fig. 2, these values indicate that the common ancestor branch point is located between the lemur-loris branch point and the simian–tarsier branch point. This position is consistent with both protein phylogenetic trees[8,9]. The full branching diagram can then be drawn as shown in Fig. 2. With the exception of the length of the lemur and simian branches, the tree is qualitatively quite similar to that of Dene *et al.*[8]. In particular, the first branching is that of the lemur–loris ancestor from the tarsier–simian ancestor, followed shortly after by further splitting in both these branches to give rise to the four separate groups. The slight shortening of the simian branch relative to the loris and tarsier branches may reflect the fact that simian generation times are two to four times greater than those of prosimians. Whether the extent of molecular evolution depends strictly on time or on the number of generations remains unclear[10,15]. The present data seem to support the latter hypothesis. However, the observation that lorises and tarsiers are approximately equidistant from the common primate ancestor whereas lemurs are nearly twice as close must have a different explanation because all three groups have comparable generation times. We believe that this result constitutes the first case in which a phylogenetic tree constructed using single copy DNA has branches of substantially unequal lengths.

As the *Lemur mongoz* and *L. catta* DNAs represent only one genus within the broader lemur group, the question arises as to how widespread the reduced divergence is within the lemur group as a whole. We have therefore tested the DNA from three additional genera of Malagasy primates, *Microcebus*, *Cheirogaleus* and *Propithecus*. Except for *Daubentonia*, the protein phylogenies[3,9] place *Microcebus* and *Cheirogaleus* as the most distant Malagasy relatives of the genus *Lemur* and place *Propithecus* approximately half as distant from *Lemur*. Hybridization with various labelled single copy DNAs indicates that the *Propithecus* branch length is the same as for the genus *Lemur* and that the *Microcebus* and *Cheirogaleus* branches are only slightly longer (that is, 12.5% actual substitution). Thus, reduced divergence rates occur throughout the lemur group. Similar evidence can be derived from the protein data of Sarich and Cronin[9]. Of 10 genera of Malagasy primates tested, 7 have branch lengths which are 61–83% of the loris group branch length. Considering all the evidence it is clear that essentially all the primates from Madagascar have had a reduced evolutionary rate since their divergence from the lorises.

Our results demonstrate that lemurs are genetically the most primitive of the modern primates in the sense that their DNAs most closely resemble that of the common primate ancestor. Although lemurs are considered quite primitive morphologically[1], this is unexpected on a molecular basis. Kimura[16] has argued that the genetic load imposed by the observed rate of DNA divergence is so great that only a few per cent of the DNA could be subject to natural selection and that most mutations must therefore be of neutral selective value. In this case the rate of fixation of base substitutions should be proportional to the mutation rate[16] and all the branch lengths would be expected to be equal, whereas in fact the average rate of DNA divergence for lemurs during the 50–70 Myr since their divergence from the lorises is approximately half that of the other prosimians. The reason for this discrepancy may be either that the bulk of the DNA is subject to selection or that the mutation rate is reduced for lemurs. The fact that this effect occurs for all Malagasy primates and not for their closest relatives, the lorises, implies that it is either an environmental effect or the result of a major genetic change which occurred after the divergence of the lemurs from the lorises and before the divergence of the various lemurs from each other.

There are three possible solutions. First, the basic premise of the theory of neutral selection could be wrong and most of the DNA could be subject to selection at the nucleotide level. If this is true, it follows that the Malagasy environment has required less adaptation than the environments experienced by other primates. Alternatively, the Malagasy primates could have a reduced mutation rate due to a change in the genes which affect the spontaneous mutation rate. This could happen in a somewhat trivial but strictly neutralist fashion as the result of a founder effect. If the lemurs are descended from a small number of ancestors which populated Madagascar[17–19], these individuals could have fortuitously represented a rare low mutation rate variant which was then perpetuated on Madagascar. In the absence of a founder effect, a reduced mutation rate in lemurs could also result from selection for an optimum spontaneous mutation rate without direct selection on the genome as a whole. As in the case of selection on the whole genome, this hypothesis would require that there has been a reduced selective pressure for change on Madagascar.

The selection and founder effect hypotheses could be evaluated by looking for the same effect in other orders of mammals present on Madagascar, such as carnivores or rodents. Assuming that such experiments do not establish the founder effect hypothesis, an understanding of the basis for the reduced evolutionary rate of the primates of Madagascar could resolve the question of whether darwinian selection or selective neutrality is the major force in molecular evolution.

We thank Dr Morris Goodman for suggesting these measurements, for his continuing help and for some of the prosimian tissues, especially the tarsier tissue which was made available to him by the Chicago Zoological Society. We also thank Dr Bill Hoyer for helpful discussions and for tarsier and *L. catta* DNAs, and the Duke University Center for the Study of Primate Biology and History for *Propithecus*, *Cheirogaleus* and *Microcebus* tissues. This work is in partial fulfilment of the requirements for the Ph.D degree to be submitted to the George Washington University by R.H.

Received 9 January; accepted 1 May 1980.

1. Charles-Dominique, P. & Martin, R. D. *Nature* **227**, 257–260 (1970).
2. Martin, R. D. in *Recent Advances in Primatology* Vol. 3 (eds Chivers, D. S. & Josey, K. A.) 3–26 (Academic, London, 1978).
3. Simons, E. L. in *Molecular Anthropology, Genes and Proteins in the Evolutionary Ascent of the Primates* (eds Goodman, M. & Tashian, R. E.) 35–62 (Plenum, New York, 1976).

4. Luckett, W. P. in *Phylogeny of the Primates* (eds Luckett, W. P. & Szalay, F. S.) 157–182 (Plenum, New York, 1975).
5. Schwartz, J. H. in *Recent Advances in Primatology* Vol. 3 (eds Chivers, D. S. & Josey, K. A.) 195–202 (Academic, London, 1978).
6. Noback, C. R. in *Phylogeny of the Primates* (eds Luckett, W. P. & Szalay, F. S.) 199–218 (Plenum, New York, 1975).
7. Martin, R. D. *Symp. zool. Soc. Lond.* **33,** 301–337 (1973).
8. Dene, H. T., Goodman, M. & Pyrchodko, W. in *Molecular Anthropology, Genes and Proteins in the Evolutionary Ascent of the Primates* (eds Goodman, M. & Tashian, R. E.) 171–195 (Plenum, New York, 1976).
9. Sarich, V. M. & Cronin, J. E. in *Molecular Anthropology, Genes and Proteins in the Evolutionary Ascent of the Primates* (eds Goodman, M. & Tashian, R. E.) 141–170 (Plenum, New York, 1976).
10. Kohne, D. E., Chiscon, J. A. & Hoyer, B. H. *J. hum. Evol.* **1,** 627–644 (1972).
11. Bonner, T. I., Brenner, D. S., Neufeld, B. R. & Britten, R. J. *J. molec. Biol.* **81,** 123–135 (1973).
12. King, M.-C. & Wilson, A. C. *Science* **188,** 107–116 (1975).
13. Britten, R. J. & Davidson, E. H. *Q. Rev. Biol.* **46,** 111–138 (1971).
14. Holmquist, R. *J. molec. Evol.* **1,** 115–133 (1972).
15. Sarich, V. M. & Cronin, J. E. *Nature* **269,** 354 (1977).
16. Kimura, M. *Nature* **217,** 624–626 (1968).
17. Walker, A. in *Calibration of Hominoid Evolution* (eds Bishop, W. W. & Miller, J. A.) 247–272 (Scottish Academic, Edinburgh, 1972).
18. Martin, R. D. *Phil. Trans. R. Soc.* **B264,** 295–352 (1972).
19. Tattersall, I. *Trans. N.Y. Acad. Sci.* **35,** 314–324 (1973).
20. Chan, H. C., Ruyechan, W. T. & Wetmur, J. G. *Biochemistry* **15,** 5487–5490 (1976).
21. Bonner, T. I. & Todaro, G. J. *Virology* **103,** 217–227 (1980).

Neutron scattering studies of *lac* repressor

M. Charlier*, J. C. Maurizot* & G. Zaccai†

* Centre de Biophysique Moléculaire, 1A, Avenue de la Recherche Scientifique, 45045 Orleans Cedex, France
† Institut Max von Laue-Paul Langevin, Avenue des Martyrs, BP, 156 Centre de Tri, 38042 Grenoble Cedex, France

The *lac* repressor, a tetrameric protein of identical subunits [molecular weight (MW) 4×38,500], interacts specifically with the *lac* operator, preventing the expression of the structural genes of the *lac* operon[1,2]. The presence of an inducer (such as isopropyl-β-D-thiogalactoside; IPTG) which binds to the repressor, prevents operator binding by lowering the association constant by a factor of 10^3 (ref. 3). Genetic and biochemical analysis have shown that the major part—if not all—of the binding site for the *lac* operator is located in the 60 N-terminal residues of the protein[1,4,5]. In certain conditions, limited trypsinolysis of the protein yields four N-terminal 'headpieces' each containing 51 or 59 residues, and a tetrameric core with full inducer binding activity[4,5]. It was shown recently that this headpiece is able to bind nucleic acids, and interacts with the *lac* operator[6], giving the same pattern of sensitivity with respect to the methylation of the bases as does the intact repressor[7]. We are studying the interaction of *lac* repressor with DNA by neutron scattering using contrast variation and discuss here measurements on the protein, its tryptic core and their complexes with IPTG. Our results demonstrate that the headpieces are located far (67 ± 10 Å) from the centre of mass of a somewhat elongated core, and that the inducer does not significantly change the radius of gyration of the protein.

Guinier plots[8] of *lac* repressor and its tryptic core are shown in Fig. 1. Two parameters were obtained from the Guinier plots—a radius of gyration of excess scattering length density, R_G, and the scattered intensity extrapolated to zero angle $(I/C)_0$, which is related to the MW and concentration C of the particle[9]. In this case, the MWs of the particles are well known[10] and the concentrations were measured by absorption spectrophotometry. These values provided a criterion for each measurement of $(I/C)_0$, as aggregation or interparticle effects would lead to misleading observations of both $(I/C)_0$ and R_G. Aggregation was not negligible above concentrations of about 5 mg ml^{-1} and appeared more readily in D_2O solvents, an observation which has also been made in other systems (B. Jacrot and G. Zaccaï, personal communication). Values of R_G and $(I/C)_0$ measured in different conditions are shown in Table 1. The difference between R_G in H_2O and D_2O is expected because of the hydrophilic amino acid residues lying predominantly on the protein surface[9]. There seems to be no change in R_G on binding of IPTG.

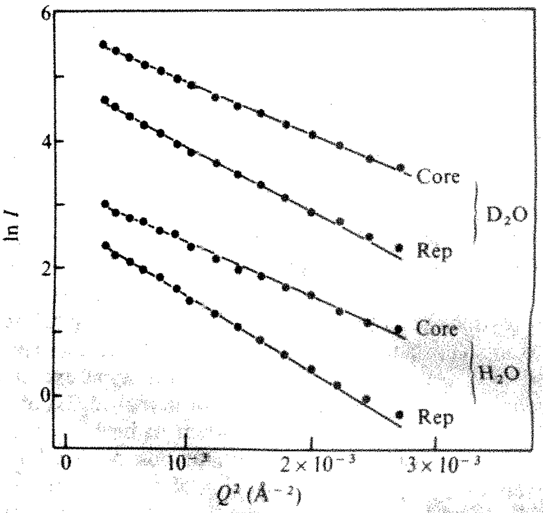

Fig. 1 Guinier plots of the scattering data for the *lac* repressor and its tryptic core. The logarithm of the scattered intensity is plotted against Q^2; $Q = (4\pi \sin \theta)/\lambda$, where θ is the half of the scattering angle and λ is the wavelength of the incident neutrons (10 Å in these measurements). Data were obtained with the protein concentrations 2.0 mg ml^{-1} (rep) and 2.5 mg ml^{-1} (core) in D_2O, and 5.0 mg ml^{-1} (rep) and 6.6 mg ml^{-1} (core) in H_2O. Buffers are described in Table 1 legend. The *lac* repressor was isolated by the method of Müller-Hill *et al.*[24]. The tryptic core was prepared according to Files and Weber[5]. For clarity, the curves are shifted arbitrarily along the ordinate axis.

The radius of gyration of a compact protein such as lysozyme or haemoglobin, for example, is proportional, to a good approximation, to the cube root of its molecular weight[11]. By extrapolating, we find the radii of gyration of compact multi-subunit proteins of MWs 128,000 and 154,000 to be about 30 Å and 32 Å, respectively. A higher value is observed for the tryptic core, and the experimental R_G of *lac* repressor is considerably larger. A larger R_G could indicate a less compact distribution of

Table 1 Neutron scattering data for *lac* repressor and its tryptic core

	Repressor	Core
MW	154,000	128,000
Volume (Å^3)	196,700	163,800
R_G HKPD (Å)	42.5 ± 1.5	35.0 ± 1.5
R_G DKPD (Å)	39.0 ± 0.2	34.2 ± 0.2
R_G DKPD + IPTG (Å)	39.2 ± 0.3	34.2 ± 0.2
$(I/C)_0$ obs. HKPD	0.0750 ± 0.0050	0.0620 ± 0.0010
$(I/C)_0$ calc.	0.0733	0.0608
D_{max} (Å)	115 ± 15	100 ± 15

MW and volumes are calculated from the sequence of the protein[10] using data given in ref. 9. R_G and $(I/C)_0$ are, respectively, the radius of gyration and the scattered intensity at 0 angle per mg per ml of protein normalized by the incoherent scattering of H_2O. The values are obtained from Guinier plots. $(I/C)_0$ calculated (calc.) is obtained from the formula

$$(I/C)_0 = 4\pi 10^{-3} \times (T/1 - T) \times t \times N_A \times [\sum b/\mathrm{MW} - \rho_S \times \bar{V} \times 10^{-24}/N_A]^2 \times \mathrm{MW}$$

where T is the neutron transmission of the sample in H_2O buffer, t the path length in cm, N_A the Avogadro's number, $\sum b$ the sum, in cm, of the scattering length of the amino acid residues (given in ref. 9), $\bar{V}$ the partial specific volume, ρ_S the neutron scattering density of water in cm Å^3 and MW the molecular weight[12]. HKPD buffer is 0.2 M potassium phosphate and 10^{-4} M dithiothreitol, *p*H 7.25, in H_2O; DKPD buffer is 0.2 M potassium phosphate, 0.5 M potassium chloride, 10^{-4} M dithiothreitol, *p*D = 7.25 in D_2O. The concentration of inducer IPTG (10^{-3} M) is large enough to complex all repressor or core molecules ($K_a \approx 10^6$ M^{-1}). D_{max} is the maximum dimension of the particle, calculated from Fourier transform of the scattering curves.

0028–0836/80/300423—03$01.00

cattering mass within a similar shape, or a more elongated hape.

By examining the scattering curves at large angles, a 'scatterng equivalent' to the shape of a particle can be deduced. It is a imple shape (an ellipsoid or a cylinder of given axial ratios, for xample) whose calculated scattering curve best approximates he observed curve. Scattering curves of *lac* repressor and its ryptic core are shown in Fig. 2. Up to $R_G \times Q \simeq 3$, the observed points fit very well to the curve calculated for a 2:1:1 prolate ellipsoid. The shape of compact proteins usually lies between that of a sphere and a 2:1:1 prolate ellipsoid. It is likely, therefore, that the large observed radius of gyration arises from a less compact packing of the subunits. The headpieces must be located so as not to change significantly the apparent shape of the particle. Although the data are poor in that region of Q, the shoulders in the scattering curves seem to be higher in D_2O buffers than in H_2O buffers. A similar observation has been discussed with respect to the packing of subunits in bacterial F_1-ATPase[12]. These shoulders must arise from a pronounced inhomogeneity in the scattering density distribution in the particle, probably associated with the packing of the subunits. The shoulders cannot be fitted by the scattering curves of homogeneous ellipsoids. Their heights as well as the angle at which they occur are approximately correct for hollow ellipsoids. Because the shoulder is higher in D_2O, we can say that the inhomogeneity is more pronounced in that solvent, as would be the case if there were solvent regions lined with hydrophilic amino acid residues 'within' the general ellipsoidal shape of the particle.

The maximum dimensions of the particles were deduced from the scattering curves in D_2O (the data from D_2O are better than those from H_2O solvents because of increased signal-to-background ratio) using the characteristic function given in ref. 8:

$$\gamma_0(r) = C' \times \int_0^\infty Q^2 I(Q) \frac{\sin Qr}{Qr} \, dQ$$

They are 115 ± 15 Å for *lac* repressor and 100 ± 15 Å for its tryptic core.

Assuming no major rearrangement on trypsin digestion, as supported by several experiments[13-15], the large R_G of *lac* repressor shows that the headpieces extend outwards from the core particle. The distance d between the centre of mass of each headpiece and the centre of mass of the protein can be calculated using the relationship (parallel axes theorem)

$$MR_G^2 = M'R_G'^2 + 4\,mr_G^2 + 4\,md^2$$

where M, M' and m are the masses of the repressor, the tryptic core and the headpiece, respectively, and R_G, R'_G and r_G are their respective radii of gyration. The calculation can be made for two extreme hypotheses concerning the conformation of the headpiece: either a spherical compact headpiece whose MW (6,400) leads to a radius of gyration of 10 Å, or an elongated ellipsoid with a long axis of 35 Å so as to cover half the operator, for example[16], leading to $r_G = 16$ Å. From these values, the calculated distances between the centre of mass of the protein and that of the headpieces are 67.5 ± 10 Å and 66.5 ± 10 Å, respectively. This calculation seems to be very insensitive to the assumed value of the radius of gyration of the headpiece. Combining these results with data on the structure of the headpieces[17] and its mobility[18,19], a model emerges with the headpieces as partly compact bodies at the end of flexible sequences attaching them to the core.

Two models have been proposed for the structure of *lac* repressor, based on packing considerations in microcrystals[20] and electron micrographs[21]. Our results do not allow us to confirm or reject either of these models. The size given by the authors is too uncertain to calculate valid radii of gyration and scattering curves (for example, the radii of gyration calculated from the extreme values given by Ohshima *et al.* are 38.4 and 45.5 Å)[21]. The situation of the headpieces at about 68 Å from the centre of mass implies an outward localization of these parts of the protein. Because at least two subunits are necessary to bind the operator[22,23] and because chemical cross-links between two headpieces have been observed[23], the headpieces must be arranged in pairs. In the elongated model proposed by Steitz *et al.*[20] the headpieces should be located in pairs near the extremities of the molecule. In this case, it is probable that the operator interacts with one pair of adjacent headpieces located at the same extremity of the repressor. In the model proposed by Ohshima *et al.*[21] more possibilities of localization exist; however, in any case, the headpieces must be located on the outside of the proposed volume. In this latter case the headpieces probably do not appear clearly in the electron micrographs after negative staining. Repressor could bind to the operator with the two adjacent interacting headpieces fitting perfectly the sequence of bases and the conformational state of the DNA. When the inducer is present the relative positions of the headpieces might vary in such a way that the positions of the interacting residues no longer fit the operator sequence exactly, to result in a decrease of three orders of magnitude in the association constant with DNA. This movement of the headpieces on IPTG binding might be small as it must not change the radius of gyration significantly. On the other hand, it could be quite large provided the distance between the headpieces and the centre of mass of the particle did not change; such a displacement would not change the radius of gyration at all. Experiments are in progress to test this model.

We thank C. Hélène and B. Jacrot for encouragement and useful discussions, and W. Gilbert for communication of unpublished results. Part of this work was supported by the Délégation Générale à la Recherche Scientifique et Technique (contract 79-7-0150 to J.C.M., ACC Mécanisme de Reconnaissance Moléculaire).

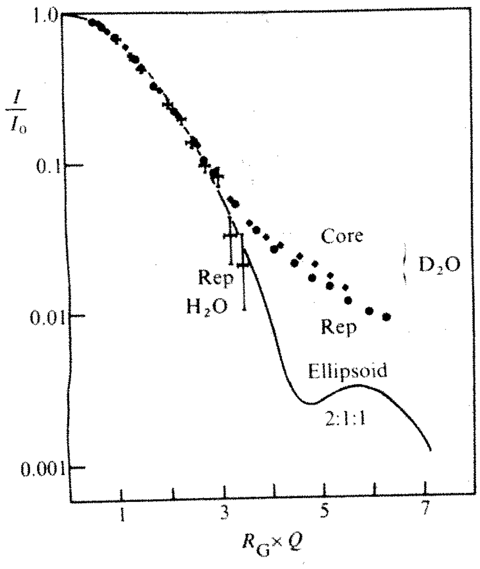

Fig. 2 Scattered intensity for large values of Q. Data are plotted against $R_G \times Q$, to compare directly the shape of normalized curves. Circles, diamonds and crosses are experimental values obtained for the indicated samples. The continuous line is the calculated curve for a prolate ellipsoid 2:1:1, according to ref. 8. Buffers are described in Table 1 legend. Protein concentrations are 5 mg ml^{-1} (rep) and 3.5 mg ml^{-1} (core) (neutron wavelengths 5 Å).

Received 17 December 1979; accepted 14 May 1980.

1. Müller-Hill, B. *Prog. Biophys. molec. Biol.* **30**, 227–252 (1975).
2. Bourgeois, S. & Pfahl, M. *Adv. Protein Chem.* **30**, 1–99 (1976).
3. Barkley, M. D., Riggs, A. D., Jobe, A. & Bourgeois, S. *Biochemistry* **14**, 1700–1712 (1975).
4. Platt, T., Files, J. G. & Weber, K. *J. biol. Chem.* **248**, 110–121 (1973).
5. Files, J. G. & Weber, K. *J. biol. Chem.* **251**, 3386–3391 (1976).
6. Geisler, N. & Weber, K. *Biochemistry* **16**, 938–943 (1977).
7. Ogata, R. T. & Gilbert, W. *Proc. natn. Acad. Sci. U.S.A.* **75**, 5851–5854 (1978).
8. Guinier, A. & Fournet, G. in *Small-angle Scattering of X Rays* (Wiley, New York, 1955).
9. Jacrot, B. *Rep. Prog. Phys.* **39**, 911–953 (1976).
10. Farabaugh, P. L. *Nature* **274**, 765–769 (1978).

11. Serdyuk, I. N., Zaccaï, G. & Spirin, A. S. *FEBS Lett.* **94,** 349–352 (1978).
12. Satre, M. & Zaccaï, G. *FEBS Lett.* **102,** 244–248 (1979).
13. Ramstein, J., Charlier, M., Maurizot, J. C., Szabo, A. G. & Hélène, C. *Bioch* [illegible] *iophys. Res. Commun.* **88,** 124–129 (1979).
14. Platt, T., Files, J. G. & Weber, K *J. biol. Chem.* **248,** 110–121 (1973).
15. Alexander, M. E., Burgum, H. A., Noall, R. A., Shaw, M. D. & Matthews, K. S *iochem. biophys. Acta* **493,** 367–379 (1977).
16. Ogata, R. T. & Gilbert, W. *J. molec. Biol.* (in the press).
17. Chandrasekaran, R., Jardetzky, T. S. & Jardetzky, O. *FEBS Lett,* **101,** 11–14 (1979).
18. Buck, F., Rüterjans, H. & Beyreuther, K. *FEBS Lett.* **96,** 335–338 (1978).
19. Wade-Jardetzky, N. *et al. J. molec. Biol.* **128**, 259–264 (1979).
20. Steitz, T. A., Richmond, T. J., Wise, D. & Engelman, D. *Proc. natn. Acad. Sci. U.S.A.* **71,** 593–597 (1974).
21. Ohshima, Y., Horiuchi, T. & Yanagida, M. *J. molec. Biol.* **91,** 515–519 (1975).
22. Geisler, N. & Weber, K. *Proc. natn. Acad. Sci. U.S.A.* **73,** 3103–3106 (1976).
23. Kania, J. & Brown T. *Proc. natn. Acad. Sci. U.S.A.* **73,** 3529–3533 (1976).
24. Müller-Hill, B., Beyreuther, K. T. & Gilbert, W. *Meth. Enzym.* **21** part D, 483–487 (1974).

The caries resistance of human teeth is determined by the spatial arrangement of hydroxyapatite microcrystals in the enamel

Gregor Cevc*†, Pavle Cevc†, Milan Schara† & Uroš Skalerič‡

* Institute for Biophysics, University E. Kardelj, Ljubljana, Lipičeva 2, 61000 Ljubljana, Yugoslavia
† Institute J. Stefan, University E. Kardelj, Ljubljana, Jamova 39, 61000 Ljubljana, Yugoslavia
‡ Dental Clinic, Medical School, University E. Kardelj, Hrvatski trg 6, 61000 Ljubljana, Yugoslavia

Teeth from different people differ in their susceptibility to caries. The beginning and the development of tooth decay depend on the presence of bacterial plaque[1] and on the structure of the tooth enamel[2]. But it has not been established whether the organic or the inorganic component of the enamel (which is comprised principally of hydroxyapatite microcrystals organized in a firm matrix), is responsible for most of the resistance of teeth to caries. We report here that the electron spin resonance (ESR) lines of the CO_3^{3-} defect of samples of enamel prepared from caries-resistant teeth differ significantly from the corresponding spectra of the caries-sensitive samples. We have traced these differences to the hydroxyapatite microcrystalline alignment in the tooth enamel, and found that this alignment is specific to indivduals and is therefore probably nutritionally or genetically determined.

We used samples of enamel 2 × 2 × 1 mm, cut from the human maxillary incisors of adults of different sex and age. The outer, square face was taken from the buccal tooth surface (insert in Fig. 1*a*). To facilitate comparison, several deciduous teeth were also measured and analysed. We had two groups of adult teeth: those removed (because of periodontal disease) from people with above average resistance to caries (25 samples) and those considered to be caries-sensitive because they were grossly decayed (26 samples). In the latter case, care was taken to prepare ESR samples from areas which were completely unaffected by caries.

All samples were γ-ray irradiated at room temperature to a final dose of 0.5 Mrad to introduce defects into the enamel. The CO_3^{3-} centre was predominant; this arises from electron capture by the CO_3^{2-} radical[3], but a weak signal of O^- was also observed. The lines were assigned by comparison of the irradiated enamel ESR spectra with those of synthetic hydroxyapatite. Irradiated samples were placed in sealed quartz–glass tubes for measurement on a Varian E-9 ESR spectrometer. Spectra were recorded with the magnetic field perpendicular to the square face of the sample and thus also perpendicular to the long axis of the tooth. Representative spectra were also recorded from enamel samples powdered in a mortar. The spectrometer was operated in the X-band range and only the central part of the spectra[4], corresponding to the CO_3^{3-} centre, was analysed.

The carbonate in the enamel may be contained within the hydroxyapatite lattice or present as a separate phase with counterions[5,6]. ESR studies of natural carbon-containing apatites have, however, shown that the CO_3^{3-} ESR lines originate from the carbonate radicals CO_3^{2-} which replace PO_4^{3-} in the apatite lattice and are therefore firmly bound to it[3]. For tooth samples, we compared the angular dependence of the ESR lines of the CO_3^{3-} and O^- defects (the orientation of the latter with respect to the crystal axes being well established from other studies of synthetic hydroxyapatites[5–7] and thereby obtained further evidence that the ESR-observable CO_3^{3-} indeed reflect the *order* within the hydroxyapatite matrix[4].

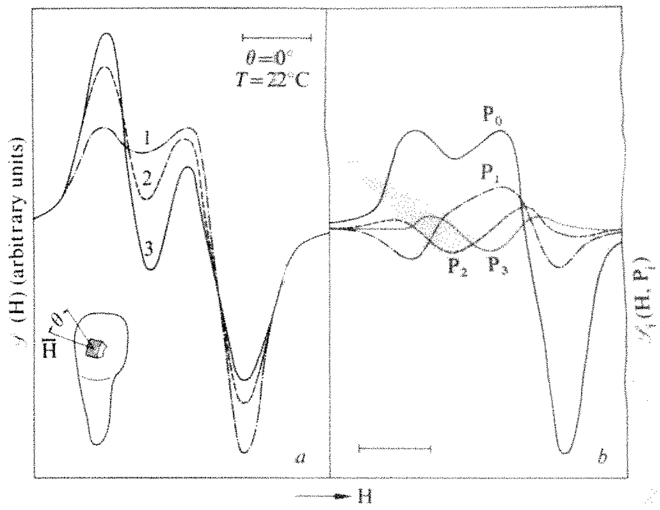

Fig. 1 Measured and simulated CO_3^{3-} centre ESR lines of γ-ray irradiated adult human incisor enamel. *a*, The experimental spectra of representative powdered (1), caries-sensitive (2) and caries-resistant (3) teeth; *b*, the first four calculated ESR spectra $\mathscr{S}_i(H)$, $i = 1,2,3,4$, which correspond to the angular distribution function of the CO_3^{3-} centre preferential axes given by the lowest four Legendre polynomials. Insert shows the site on the tooth buccal surface from where the samples were cut and their orientation in the magnetic field. Scale bars represent 10 G. $\vartheta = 0°$; temperature = 22 °C.

The ESR spectra of oriented, cut samples differ from spectra of powdered samples (Fig. 1*a*). As the ESR lines, which arise from the paramagnetic centres, mirror internal order within the sample, it is possible to deduce the orientational distribution function of these centres in the tissue studied. This function is correlated with the probability that the molecular axes of the observed centres are aligned preferentially in a certain direction with respect to the external magnetic field, corresponding to the state of the internal order of the system.

To understand and simulate the ESR spectrum, the energy states of the observed spin, which can be calculated from the values of the anisotropic hyperfine coupling tensor, as well as the lineshape parameters, must be known. In the procedure that we have developed[8] the ESR spectra of powdered enamel have first been simulated. A linear combination of the gaussian and lorentzian convolution functions[9] has been used. The optimal parameters have been determined in the standard way by minimizing the squared differences between the measured and the calculated spectra. Then, the ESR spectra of the corresponding partially ordered specimen have been simulated: the ESR line-determining parameters used were those obtained from the simulation of the powdered enamel spectra, and the Legendre polynomials[10] $P_i(\vartheta)$, $i = 1, 2, \ldots, 12$ have been

0028–0836/80/300425—02$01.00

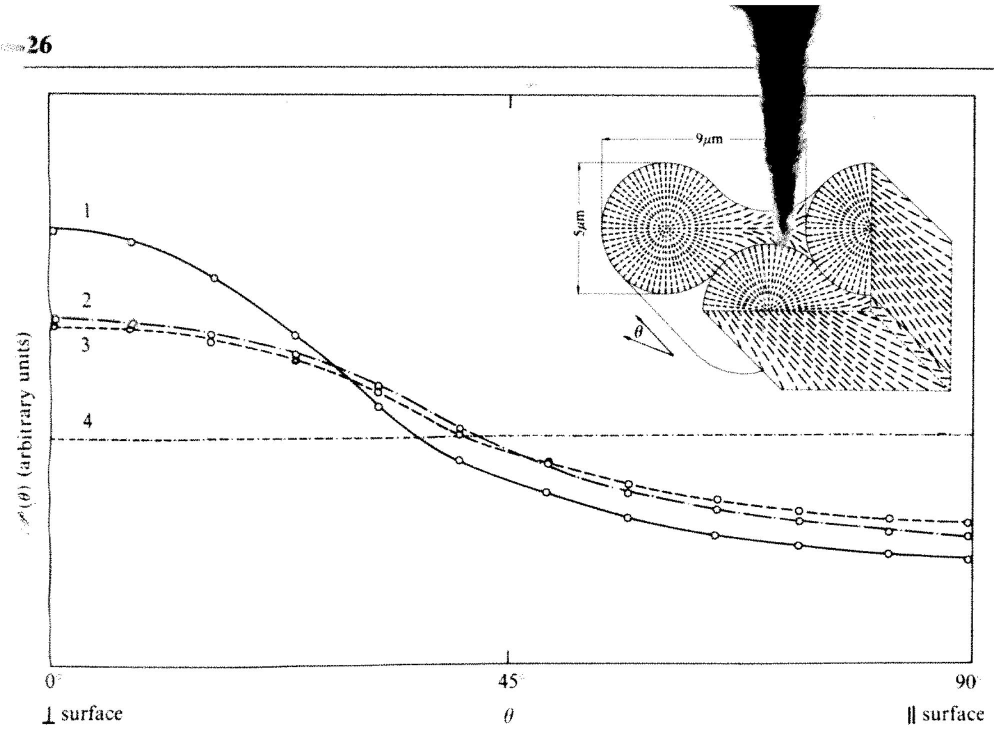

Fig. 2 The angular distribution function of the hydroxyapatite microcrystals within human incisor enamel. Their alignment is defined with respect to the normal to the tooth surface. The points have been obtained by summing the values of Legendre polynomials at respective angles and weighted by the factors α_i, defined in equation (1), and determined from the simulation of the tooth enamel ESR spectra. The curves correspond to the caries-resistent (1), caries-sensitive (2), milk (3) and powdered (4) human teeth. The insert presents schematically the arrangement of the hydroxyapatite microcrystals in lockhole-shaped tooth enamel prisms which are the basic units of the enamel[13].

assumed to represent the angular distribution function of the CO_3^{3-} centres — and therefore of the hydroxyapatite microcrystals — in the sample. The angle ϑ was defined with respect to the external magnetic field, that is, normal to the enamel surface (insert in Fig. 1*a*). We have calculated a set of the spectra $\mathcal{S}_i(\mathrm{H}) = \mathcal{S}_i\,(\mathrm{H}, \mathrm{P}_i(\vartheta))$, $i = 1, 2, .., 12$, (Fig. 1*b*), which have been normalized properly[11] as a basis for the expansion of the experimental spectrum of the tooth enamel $\vartheta(\mathrm{H})$ into the series

$$\mathcal{S}(\mathrm{H}) = \sum_{i=1}^{12} \alpha_i \mathcal{S}_i(\mathrm{H}) \qquad (1)$$

The factors α_i in the above sum therefore define the relative contributions of the hypothetical samples of known microcrystalline alignment, given by $\mathrm{P}_i(\vartheta)$, in the experimental ESR spectrum. This macroscopic sample spectrum is actually a result of the overlap of the particular ESR lines corresponding to the single hydroxyapatite microcrystals. The factors α_i therefore also reveal the relative amounts of the Legendre polynomials $\mathrm{P}_i(\vartheta)$ used for obtaining $\mathcal{S}_i(\mathrm{H})$ in the actual distribution function of these hydroxyapatite microcrystals in the bulk sample $\mathcal{P}(\vartheta)$

$$\mathcal{P}(\vartheta) = \sum_{i=1}^{12} \alpha_i \mathrm{P}_i(\vartheta) \qquad (2)$$

We conclude that the differences in the CO_3^{3-} centre ESR lines of the teeth studied (Fig. 1*a*), which correlate significantly to their resistance to tooth decay[4], are a consequence of a higher degree of alignment of the hydroxyapatite microcrystals in the enamel of the caries-resistant teeth as compared to caries-sensitive teeth.

The electron microscope studies of etched enamel have shown that the hydroxyapatite in the human enamel is ordered in well defined patterns[12,13]. Around the areas of well aligned microcrystals there are zones of lesser microcrystalline order. As yet, such studies have only yielded localized information about the tooth surface whereas our approach permits conclusions to be drawn about the order averaged over the whole sample, and can thus be compared with the neutron diffraction studies of apatite orientation in bones[14]. In this study we have found that the hydroxyapatite order, as revealed by the angular distribution function of microcrystals, extends throughout the outer layer of the enamel (Fig. 2). In this layer, which acts as the main tooth-protecting barrier, the enamel seems to be organized in such a way that the long axes of microcrystals are on average perpendicular to the tooth surface, an arrangement which confers optimal resistance to the detrimental influences of the oral environment (insert in Fig. 2). The more randomly oriented microcrystals (which contribute to the flat portion of the distribution function, $\vartheta = 45°–90°$) would imply little resistance of the corresponding regions to caries. However, these areas constitute the inner enamel parts and are therefore less significant for the overall sensitivity of the tooth to caries: the ESR spectra of the consecutive layers of tooth enamel show a decrease in alignment of microcrystals with distance from the tooth surface[4]. It may also be significant that milk teeth have a poorly organized hydroxyapatite matrix and in this respect resemble caries-sensitive teeth. The limited lifetime of milk teeth suggests that they need not be very resistant to caries (Fig. 2). In caries-resistant teeth, however, a larger proportion of the microcrystals is well oriented. In the angular distribution function this better alignment of hydroxyapatite in the outer enamel region is partially screened by the large background of more randomly oriented inner parts of bulky samples.

The alignment of the microcrystals in the hydroxyapatite matrix of human tooth enamel of different incisors of the same subject are alike[4]. We therefore conclude that the degree of hydroxyapatite microcrystal alignment is an individual property which may, for each individual, determine resistance to tooth decay. However, it remains to be seen whether nutritional or genetic factors, or both, are responsible.

Received 22 January; accepted 21 May 1980.

1. Kleinberg, J. in *Oral Microbiology* 3rd ed. (ed. Nolte, W. A.) 515–534 (Mosby, St Louis, 1977).
2. Frank, R. M. in *Caries Resistant Teeth* (eds Wolstenholme, G. E. & O'Connor, M.) 169–184 (Churchill, London, 1965).
3. Gilinskaya, L. G., Shcherbakova, M. Ya. & Zanin, Yu. N. *Kristallografiya* **15,** 1016–1019 (1971).
4. Cevc, P., Schara, M., Ravnik, Č. & Skalerič, U. *J. dent. Res.* **55,** 691–695 (1976); *Radiat. Res.* **51,** 581–589 (1972).
5. Elliot, J. C. *Calcium Tissue Res.* **3,** 293–307 (1969).
6. Elliot, J. C., Mackie, P. E. & Young, R. A. *Science* **180,** 1055–1057 (1973).
7. Mengeot, M., Bartram, R. H. & Gilliam, O. R. *Phys. Rev.* **B11,** 4110–4124 (1975).
8. Cevc, G., Cevc, P., Schara, M., Ravnik, Č. & Skalerič, U. *Period. Biol.* **78,** 178–179 (1976).
9. Abragam, A. & Bleaney, B. in *Electron Paramagnetic Resonance of Transition Ions*, 54–59 (Clarendon, Oxford, 1970).
10. Abramovitz, M. & Stegun, J. A. in *Handbook of Mathematical Functions*, 473 (Dover, New York, 1971).
11. Hentschel, R., Schlitter, J., Sillescu, H. & Spiess, H. W. *J. chem. Phys.* **68,** 56–66 (1978).
12. Hamilton, W. J. Jr, Judd, G. & Ansell, G. S. *J. dent. Res.* **51,** 1407–1420 (1972).
13. Scott, D. D., Simmelink, J. W. & Nygaard, V. *J. dent. Res.* **53,** 165–178 (1974).
14. Bacon, P. J. & Griffith, R. K. *J. appl. Crystallogr.* **12,** 99–103 (1979).

BOOK REVIEWS

Trials of Jewry

Vera Rich

It Seems I Am a Jew. By Grigori Freiman. Pp.98. (Southern Illinois University Press: Carbondale, Illinois/Feffer and Simons: London, 1980.) $9.95, £5.45.

OVER the past ten years, the problems facing Soviet Jews in general and Soviet Jewish scientists in particular have frequently been raised in both the general and the scientific press. To a large extent, however, this has been a matter of Jews wishing to emigrate to Israel: Jews, it may be argued, who have chosen to opt out of the Soviet system. What is less often realized is that in one branch of Soviet life there appears to be active discrimination against Jews, however little they themselves feel aware of their Jewish identity — namely in mathematics.

It Seems I Am a Jew, originally a *samizdat* (privately circulated) essay and now published in English translation, is basically a record of one man's experiences in trying to make for himself a career in mathematics while handicapped by the implications of the word 'Jew' in his internal passport, under Point 5, 'Nationality'. For, from the point of view of the Soviet administration, Jewishness relates not to religion, not to self-identification with an ancestral cultural tradition, but simply to ethnic descent. Thus in the case of some anti-Jewish prejudice or campaign, as with the notorious 'Doctors' plot' in the last days of Stalin, any person of Jewish descent, no matter how *déraciné*, is liable to fall victim.

Such prejudices or campaigns are, of course, totally contrary to the Soviet constitution. The Soviet press constantly reiterates that there is no 'anti-Semitism' in the Soviet Union and that Soviet policy is opposed only to 'Zionism'. Nevertheless, as Freiman's essay indicates, there is growing evidence that discrimination against Jews, particularly in the academic professions, and especially in mathematics, does exist. Promotions over one's head, unreasonable delays in the acceptance of a doctoral thesis, refusal (or at least non-provision) of a passport for foreign travel — these are phenomena all too common in the life of the Soviet Jewish intellectual. (Ironically, such incidents have sometimes driven a hitherto uncommitted Jew right into the arms of the emigration lobby. Aleksandr Ioffe, whose mathematical work recently formed the basis of a two-day seminar in London, had shown no signs of wanting to emigrate to Israel — until he was refused a passport to take a temporary post as 'visiting lecturer' in Paris.)

To such a situation, which could so easily become fraught and over-emotional, Freiman brings a rare, if black, humour. The 'documentary poem' of his attempts in the early 1950s to enrol as an external graduate student of mathematics, while working at the Kazan Institute of Aviation, is a masterly analysis of 'Catch-22' bureaucracy. Yet since that time, he says, the situation has significantly deteriorated, with admission of Jews to the more prestigious mathematical departments and institutes being phased out almost completely since 1970. The universities of Moscow, Leningrad and Novosibirsk, the main stepping-stones to a career in creative mathematics, have, says Freiman, virtually ceased to admit Jews. He describes a special selection process by which Jews and cerain other 'undesirables', such as Armenians, are concentrated for the entrance examination into special groups, which are then set far more difficult problems than the racially more acceptable candidates. Examples of these 'Jewish problems' are given in the text; further examples, from the examination of 1978 for the Moscow University Faculty of Mechanics and Mathematics, are cited in an appendix. Although there has been previous mention of such 'Jewis problems' in print, this is the first time tha a sufficient number have been cited t make it possible to assess them.

Grigori Freiman

Since this review was written, Professor Freiman has been dismissed from his post at *Kalinin State University*.

Judging from these, for 'speci selection' the examiners seem to favou number theory and classical geometry subjects in which intuition plays particularly significant role. One or two o the questions, incidentally, notably th solution in integers of the equation $x^y = y^x$ can be solved intuitively and virtuall instantaneously — in the context o pseudo-mathematical party-games. *If* however, a rigorous mathematical proo must be produced — orally, within 15 minutes, under the pressure of examination conditions, by a nervous 19 year old — the situation takes on a rather differen aspect. The standard Soviet explanation o such questions, as Freiman points out, is that the examiners cannot admit everyone but are on the look out for excellence. In that case, he asks, why do Jewish students who have come out in the top bracket of the All-Union Mathematical 'Olympiads' do so badly in the entrance examinations? (And why, one may add, are such supplementary tests of excellence not administered to all of the candidates?)

Yet the entrance examination is only the first of the problems to be faced in the academic careers of Soviet Jews. Not only are they refused admission to the best universities, but at every step their advancement is blocked. The thesis is turned down, not because *the aspirant* is called Goldberg *or Finkelstein*, but because it was not *quite* up to standard. The promotion bypassed Lazar Izaakovich *in* favour of Ivan Petrovich *not on grounds of* nationality, but simply because *the* ethnically Russian candidate happens to be the better, more qualified and more capable applicant. Such 'explanations' are notoriously difficult to refute — all the more so since, according to Freiman, the examiners, expert committees and appointments' boards all have to play a double game; knowing that they must reject a Jewish candidate, they *have to* produce an academic *alibi*. "The mathematics is mechanical . . ."; "He is a brilliant mathematician but superficial"; "He has about a hundred works to his name. He must be chasing after recognition". Such gems, taken, says Freiman, from the official stenographic reports of the various assessing bodies, show only too clearly the *cynical nature of their verdicts.*

Freiman's essay is *essentially* a personal statement, founded on his own *experience* and on data which he has been able to garner from acquaintances. He does not attempt to explain or find psychological or political motivation behind the drive to render Soviet mathematics *judenfrei*. He is content simply to state the facts as he sees them, and to cite, in an impassioned *J'accuse* addressed to the President of the Soviet Academy of Sciences, the names of half-a-dozen leading Soviet mathematicians, the Expert Committee for Mathematics and Mechanics of the Higher Attestation Committee (the body responsible for higher degrees) and the Steklov Institute of Mathematics of the Soviet Academy of Sciences. These few put prestigious persons and bodies, he says, have made Soviet mathematics "a cesspool of scientific unprincipledness".

Granted the conditions described in Freiman's essay, and the resolute official denials that anything in the nature of anti-Semitism can exist in the Soviet Union, it would seem virtually impossible for any impartial third party to assess the validity of Freiman's claims. A certain weight should undoubtedly be given to the fact that at the time of writing the essay Freiman himself was neither a refusnik nor an *émigré*. (Since then, he has filed an application to emigrate to Israel.) Weight, too, should be given to the style of the essay, remarkably free from the introspective self-pity that mars so many *samizdat* biographies of repression. One piece of evidence mentioned by Freiman is, however, open to checking by the Western reader — the virtual disappearance over the past few years of Jewish surnames from the contributors to the *Matematicheskii Sbornik* and other leading Soviet mathematical journals. Thanks to the various cover-to-cover translation bureaux, most of these journals are available, in their entirety, in English translations. Those readers who find Freiman's revelations difficult to accept can count for themselves. ☐

Vera Rich is a journalist who specializes in East European science affairs.

Publicity for exotic atoms

C.J. Batty

Exotic Atoms '79: Fundamental Interactions and Structure of Matter. Edited by Kenneth Crowe, Jean Duclos, Giovanni Fiorentini and Gabriele Torelli. Pp.403. (Plenum: New York and London, 1980.) $45, £28.35.

AN EXOTIC atom is an atom in which one of the electrons has been replaced by a negatively charged heavy particle such as a muon (μ), π or K-meson, antiproton ($\bar{p}$) or by a Σ-hyperon. It can be formed by stopping a beam of the appropriate particles in a suitable nuclear target. Once the heavy particle has been slowed down to an energy of order 1 keV it can be captured into a Bohr orbit about the nucleus of high principal quantum number *n*. It will then cascade down through its own sequence of atomic levels, first by Auger transitions with the emission of an electron and later by the emission of X-rays. Following each of these transitions it comes closer to the nucleus until at some stage nuclear capture takes place.

Studies of exotic atoms cover a whole range of disciplines from physical chemistry through atomic and solid-state physics to nuclear and elementary particle physics. This diversity of interests and applications is reflected in the 22 articles, of varying length, which appear in *Exotic Atoms '79*.

The exact mechanism by which the heavy particle is captured to form the exotic atom is not fully understood but the present volume contains an interesting review of this topic by Schneuwly under the heading of "Mesic Chemistry". Four other shorter articles deal with more specific aspects of capture by hydrogen and the properties of muonic-hydrogen atoms. A particularly fascinating review by J. Rafelski from CERN deals with the properties of mesomolecules of hydrogen in which the electron in the hydrogen molecule H_2^+ has been replaced by a muon. In the case of the heavier hydrogen isotopes spontaneous fusion can occur, a process first observed for the system μ^-pd at Berkeley in 1956, and there is now considerable interest in the properties of dd and dt mesomolecules.

Rather special examples of exotic atoms are muonium, the system μ^+e^-, and positronium, the system e^-e^+. The properties of muonium and positronium are reviewed by V. Hughes of Yale University, who has worked for many years in this field, and here one is particularly impressed by the elegance of the experiments and the precision of the results. Extensions of the exotic atom picture to consider bound states of quarks to form hadrons are discussed in three theoretical articles. Other topics reviewed include muon capture rates and parity non-conservation in atoms and molecules.

The whole field of muon spin rotation (μSR), so named because of its close analogy with nuclear magnetic resonance (NMR) and electron spin resonance (ESR), has expanded dramatically over the last few years and is now a valuable tool in the study of condensed matter as well as being a topic of study in its own right. It is therefore not surprising that almost half of the book is devoted to this subject. Topics covered include muon diffusion and trapping in solids, aspects of positive muons as impurities in metals, studies of μSR in semiconductors and in ferromagnetic metals, and some features of muonium chemistry.

The book is certainly a valuable contribution to publicizing the existence of a fascinating area of cross-disciplinary research, and will provide an excellent introduction to those meeting the subject for the first time and a valuable reference work for the more expert. ☐

C.J. Batty is on the staff of the Rutherford and Appleton Laboratories at Chilton, Oxfordshire, UK.

Neurophysiological methods in entomology

Melody Siegler

Insect Neurophysiological Techniques. By T.A. Miller. Pp.308. (Springer: Heidelberg and New York, 1979.) DM54, $29.70.

IN *Insect Neurophysiological Techniques*, T.A. Miller has compiled details of techniques taken from the published works of many authors, and from his own visits to and correspondence with several laboratories. The text is divided into four parts. I, "Materials", describes electrophysiological apparatus and accessories; II, "Actographs", reports the methods used over the past 25 years to measure insect activity; III, "Free-Moving and Tethered Preparations", describes the procedures selected researchers have used to record from nerve and muscle in cockroaches, locusts, crickets and flies; IV, "Organ and Tissue Preparations", emphasizes heart, gut and salivary gland preparations, methods of recording from cockroach ventral nerve cord, and nerve–muscle preparations of locust and cockroach leg. There is a reference section, containing selected literature prior to 1977, an appendix listing suppliers and an index. The book is the first in a series to be concerned with problems of experimental entomology.

Ideally, a book that emphasizes methodology should be accurate, clear, concise and well-organized, and be designed to make its contents readily accessible to the reader. *Insect Neurophysiological Techniques* falls far short of these ideals. The text is wordy, and almost awash with minutiae. Often it strays from the topic at hand, and large sections are misplaced or mistitled. There is a wealth of detail, but it is often repetitive or with no clear objective. I wish the author had exerted more of an organizing hand, carefully and firmly integrating the information from his diverse sources. Throughout, the level of presentation is uneven. For some topics, the writing is addressed to those readers with little or no laboratory experience; for others there is little introduction and much jargon. Too often minor points are given misleading emphasis, whilst crucial details are incorrect or omitted altogether. The dedicated and cautious reader will doubtless be able to extract some useful information but, in general, the book is not a particularly helpful introduction to the considerable advantages of insects for basic or applied research. □

Melody Siegler is a Research Fellow in the Department of Zoology, University of Cambridge, UK.

Insight into microbial development

Ian Dawes

Developmental Biology of Prokaryotes. Edited by J.H. Parish. Pp.297. (Blackwell Scientific: Oxford, 1980.) £19, $48.50.

THERE are few texts available that cover the many aspects of microbial development and those that are have been around for rather too many years to be of much use to students or teachers. There is, therefore, a need for a suitable text at a fairly advanced level and this book is an attempt to fill the gap.

It tries to do this by way of a brief introduction by the editor to prokaryotic diversity and unity, and to gene expression and its regulation. This is followed by ten chapters covering nine groups of organisms, each chapter written by an expert in his particular area. These include the cell cycle in *Escherichia coli*; bacterial sporulation (with two chapters in deference to the volume of research that has been carried out in this area); sphere-rod transitions in *Arthrobacter*; streptomycete differentiation; *Bdellovibrio* growth; prosthecate bacteria; cyanobacterial differentiation (filamentous and pleurocapsalean); and myxobacteria. A brief concluding chapter rounds off the book.

Foremost among the difficulties in trying to provide a text by this type of approach is the tendency to produce a collection of individual review articles, each a catalogue of the hopes, successes and failures of research in one particular area, at the expense of formulating a fundamental analysis of the subject. Is this not integrating differentiation? This book is no exception in that the two chapters that could provide an overview of the subject are too condensed to be of much value; much of the introduction is best dispensed with and the reader should consult, where necessary, the appropriate biochemistry bible of choice. The majority of material has, however, been chosen judiciously with a balanced coverage of the main bacterial development systems, although in future editions several chapters on bacteriophage development could be added to illustrate relevant control and assembly systems that have been worked out in considerable detail.

Several of the chapters are excellent. That on the cell cycle is stimulating, both for its breadth of coverage and for the critical discussion of possible models to account for the mechanisms controlling DNA replication and cell division. The two chapters on bacterial spores and sporulation also provide interesting reading despite the plethora of reviews already available on the subject. Inevitably, that concerned with the molecular biology of sporulation is beginning to date, as gene cloning techniques are rapidly exploited. Nonetheless, the chapter provides a useful summary of the main work that has been done on the control of spore formation. The authors of the remaining chapters have faced the difficulty (recognized by Parish) that "there is a lot of work to do on other groups of 'differentiating prokaryotes' to bring the state of knowledge up to the level of *B. subtilis*". In most cases, they have succeeded in avoiding the temptation to compare progress with that in *B. subtilis* by stressing the aspects of development that are unique to their system. There are occasional lapses, none more revealing than the several discussions of the lack of evidence for RNA polymerase changes during differentiation in *Caulobacter* and *Streptomyces*. One or two chapters lack freshness since the authors have little to add to recent reviews on the same subjects. Also noticeable in places is the inverse correlation between the number of pictures and the number of facts available for presentation. Also, at times, and to the greatest extent in the chapter on *Arthrobacter*, there is a tendency to catalogue biochemical studies, without regard to their relevance or completeness; this makes for less interesting reading.

These are, however, minor criticisms of a book that is valuable for the insight it gives into microbial development processes. Whilst not a text in the sense that it tries to unify the field of prokaryotic development, it provides excellent coverage of the main bacterial systems and should prove very useful to those who study, or teach, microbial development. □

Ian Dawes is a Lecturer in the Department of Microbiology, University of Edinburgh, UK.

A holistic approach to vision

Talbot H. Waterman

The Ecology of Vision. By J.N. Lythgc Pp.244. (Clarendon/Oxford Universi Press: Oxford, 1979.) £22, $49.

IN THE ecology of vision John Lythgoe h chosen a fascinating topic for a boo Obviously radiant energy mainly from t Sun has had far reaching effects on t nature of the Earth and its fitness for li More directly, sunlight supplies practica all of the energy needed by organisms survive, grow and evolve. In the compl mentary field of biological informatic and control natural light also functio everywhere in daily and seasonal pr gramming as well as in the spatial orie tation of both plants and animals.

Limiting one's attention to the phot biology of animals with well-develope functional eyes as implied by 'vision' st leaves an enormously challenging area be dealt with. Lying as it does at the inte section of comparative visual physiolog and ecology it has long been the major are of my own research and teaching. Indeed would have liked to write a book about th subject myself. Hence this appraisal c Lythgoe's work, while it may betray a trac of sour grapes, cannot fairly be attribute to disinterest.

However, coping well with the taxin demands of so broad and varied a subject a formidable goal. Starting with sola irradiation, the path leads insistentl through meteorological as well as sub marine optics to the biophysics and bio chemistry of visual pigments, the func tional organization of eyes, thence t visually mediated perception, orientation navigation, migration and behaviour.

Obviously most of these componen topics have often been reviewed in thei own right, sometimes with a high degree o competence. Even in the holistic sens there are several symposium volumes tha have essayed to survey the substantial are where natural radiation, ecology and sen sory physiology come together.

Thus the author of a book on this subjec not only has a big topic to deal with but h also has to encompass the previous contributions of numerous other scientists. Hence the questions: "What should be said that hasn't already been well said?" "What is the real point d'appui of the present approach?" and finally, "To whom is the work addressed?", are not trivial ones easily answered.

An unusually versatile author working resolutely with consummate skill might solve most of these problems if overall strong matching support was provided by his publisher. Yet weakness or failure in fulfilling one or more of the book's numerous desiderata will at b 'nice try' rather th pinion the present volume, while certainly timulating, is not unflawed and has roved to be rather disappointing.

On the positive side *The Ecology of ision* has, in addition to its subject, other rong points in its favour. Thus, the verall organization is fine. In outline there e two introductory chapters (80 pp.) on e photic environment and vision spectively. A middle section (89 pp.), in our chapters, details the visual con- equences of (1) low ambient light inten- ities (night, deep water, caves), (2) high urbidity of the medium (which often estricts aerial vision and always puts a evere limit on underwater visibility), (3) e interaction of directional illumination nd *preferred* lines of sight, and (4) spectral ias of non-white illumination (e.g. sky ght, mesopelagic irradiance and reflected ght from vegetation). The final chapter 35 pp.) surveys the organism–nvironment interaction as it relates to amouflage, conspicuousness and ecognition.

Thus the text overall is brief, and therefore appropriate to a broad readership which might not persist through a multi-authored encyclopaedic treatise. Yet Lythgoe has managed to include so varied a coverage that even the specialist is bound to find some fascinating correlations previously unappreciated. These fresh insights, however, may seem to lie around the periphery rather than near the centre of a given reader's area of expertise. For instance two topics of primary interest to me, compound eyes and polarization sensitivity, seemed among the less effective aspects of the book.

A further and notable positive feature of *The Ecology of Vision* is its wealth of illustrative material. This eye-catching potpourri of line drawings and colour as well as black-and-white half-tones is attractive both to the general reader and to the specialist, ranging from portrait sketches of many of the different animals cited in the text to excellent illustrations chosen from relevant research publications including Lythgoe's own. While the idea of illustrating many of the organisms referred to in this comparative study is welcome, its impact is blunted if adequate biological and aesthetic standards are not maintained. Rather rudimentary drawings of a six-legged spider, a crayfish with eight legs and a bifurcate rostrum, as well as a gecko apparently fitted with dentures, are extreme examples in point.

The bibliography, of 340 items, is reasonably up to date; however one disturbing aspect of the references is an almost total failure of the author to guide the reader to the most important sources of further original information. Thus few primary publications of innovative research workers are presented in any sort of historical or evaluative perspective. Lythgoe is surely not alone in this tendency to become lax or even irresponsible in identifying the seminal contributions to a field of science. Further, a number of experimental biologists whose contributions would loom large in some readers' view of the ecology of vision are not even mentioned: Karl von Frisch, Erich von Holst, H.K. Hartline and Werner Reichardt, for example.

This brings up another feature of the book which is particularly evident in the bibliography, namely its marked skewness towards the vertebrates. Sixty percent of the citations refer to this group and of these 57% in turn are references to fishes. This bias reflects the author's own research interest which has mainly been concerned with underwater visibility and fish vision.

Even with regard to fishes, major seemingly relevant topics are ignored. For instance the dorsal light reflex, sun compass behaviour, diurnal vertical migration, light-cued rhythms and photoperiodic influences, as well as the whole field of chromatophores and their control, are all omitted. Obviously the coverage of insects, spiders, crustaceans and cephalopods, all of which have highly developed vision, is even less representative of the great amount of research which has been done on their visual ecology.

One pervasive feature of the text suggests that the author may have surrendered his manuscript to the publisher before its due term. This is a certain lack of polish and style in the writing. In some sections repetitive and awkwardly coordinated passages are common, while the style at its least elegant may be epitomized by the disappointing introduction to Chapter 1 and the rather limp coda at the very end.

How can such a good idea for a book have materialized as unevenly as this? John Lythgoe provided an important and interesting topic generally well organized, well illustrated and well documented. But in spite of this the book fails to live up to its promise. The flaws are too many for it to be regarded as a prospective classic, though it is certainly a 'nice try'. □

Talbot H. Waterman is Professor of Biology at Yale University, New Haven, Connecticut.

Brain structures and behaviour

Richard Lynn

rain and Personality. By Graham E. owell. Pp. 113. (Saxon House: arnborough, UK, 1979.) £10.50.

N THIS *volume* Dr Powell reviews the urrent state of theory and knowledge of he relation between brain structures and ersonality. The methodology in this field onsists primarily of making lesions in ifferent parts of the brain and observing ubsequent changes in the personality of he subject. The first substantial advance vas the documentation in the nineteenth entury of the case of Phineas Gage, a onstruction worker whose frontal lobes ere severely damaged in an accident and vho subsequently became more happy-go-ucky and less socially responsible. In later ears this type of effect has frequently been eported following frontal lobe injury.

Dr Powell argues that to make progress in the field it is necessary to have a model of the major personality traits or dimensions. We assume that different brain structures serve particular personality traits. The brain can then be mapped by observing the effects of lesions in different parts of the brain on various personality traits. Dr Powell begins with Professor Eysenck's traits of neuroticism and extraversion and his theory that these are mediated by the amic and brain stem reticular This formulation has in difficulties. An made by J. Stress: 1971) who has proposed that introverts are more sensitive to punishment and that this sensitivity is mediated by the orbital frontal cortex, the medial septal area and the hippocampus. Here again, however, the new theory has met difficulties. In particular, it is still not clear whether damage to this system really does make people less introverted.

The author turns next to the more empirical studies. These consist of attempts to relate lesions of various brain structures to personality change, without any model of brain function. The chief results here are the reduction of aggressiveness following damage to the amygdala, the reduction of anxiety following damage to the cingulate gyrus and the reduction of sexual drive following damage to the hypothalamus. These findings have been used in the USA to reduce criminal aggressive and sexual behaviour. This is a useful source of knowledge of the brain mechanisms underlying these behaviours, although not one of which the author approves.

Looking at work on these problems in the century or so that has elapsed since the Phineas Gage case, one is left with a certain feeling of disappointment about the slowness of the progress that has been made. Perhaps the use of questionnaires such as Cattell's (*Personality and Learning Theory:* 1979), which measure narrower personality traits, would yield more decisive results. In the meantime, Dr Powell's book will be a useful starting point for those attempting to come to grips with the still largely unsolved problems in this field. □

Richard Lynn is Professor of Psychology at the University of Ulster, UK.

nature

31 July 1980

5\2\82

Public monopoly and private enterprise

The British government, no longer (one forgets) new, appears to have had a rush of blood to the head in the past few weeks in its reorganization of the public monopolies. With the British parliament well on the way to agreeing that the government should sell to the public a still undefined proportion of the shares in British Airways, it was flooded with a stream of proposals for the reorganization of other public monopolies. The British Post Office is to lose its monopoly on the carriage of letters. Three years from now, the telecommunications arm of the Post Office will no longer be the sole supplier of terminal equipment. To many people's surprise, the Central Electricity Generating Board is to lose its monopoly on the manufacture and sale of electricity, while British Rail is to divest itself of some of the largely peripheral activities which it has accumulated over the decades — the operation of docks and ferry services but also of hotels and golf courses. With such a flood of announcements, many British taxpayers must have been fearing that their government was about to break up the monopoly of the Inland Revenue by reverting to the ancient practice of putting-out to open tender the right to collect taxes.

In reality, of course, the explanation of this fever of activity is more mundane. It has taken the British government a year or so to put flesh on the bones of its declared intention of exposing the public monopolies to more effective competition. With the summer parliamentary recess about to begin, ministers are trying to clear their desks and also to stake a claim on parliamentary time for legislation in the next session, beginning in November. The hope that it would be possible to deal with the public monopolies more quickly, and in such a way as to reduce the government's need to borrow from the money markets in the current financial year, much cherished a year ago, has now faded — with some exceptions, assets cannot be sold in a hurry except at a loss. The danger now is not so much that the British government will give potential purchasers of public assets too good a bargain at the taxpayers' expense but that by dealing piecemeal with the problem of public monopoly will arrive at a patchwork of decisions which are self-contradictory, even mutually nugatory.

But why not do away with the public monopolies altogether? This is what some intemperate souls are inclined to ask. A little reflection will show that such a radical solution, however attractive it may seem, is entirely impractical. Public monopolies of one kind or another will persist for as long as modern states persist. The clinching example is that of sewage disposal in built-up areas such as cities. Nobody in his senses would suggest that the provision of such a service should be left to private enterprise (as it used to be in the eighteenth century and is still in some rural areas). The essence of the case for local monopolies in sewage disposal is that the cost of providing the service is to a very large extent a capital cost, that the cost of two competing systems would be approximately twice the cost of one and that, if both were to remain viable, the users of the service would be required collectively to pay twice as much as would otherwise be necessary. (Ironically, in Britain, local monopolies for sewage disposal were uncontentious until recently, when the service was administered by elected local authorities; their transfer to the newly constituted water authorities has raised all kinds of doubts about the basis on which the service should be charged for.)

The difficulties in which the independent railway systems of the United Kingdom found themselves at the height of the nineteenth century railway boom is still a memorable illustration of how competition may not always be beneficial. It is, however, important that the case for a public monopoly is not always strictly economic. Most national post offices have been given a monopoly to deliver mail on the grounds that same-cost delivery of a piece of mail to any address serves a valuable purpose in holding the community together.

At least in modern times, monopoly rights imply monopoly obligations. Because a monopoly can in principle make its customers pay through the nose for whatever service it provides, steps must be taken to prevent abuse. Even where public monopolies are financed by private, not public, capital, control of some kind is necessary, whence the great bureaucracies such as the Federal Communications Commission with which Washington is littered. Where monopolies are financed with public money, as in Britain, the agency of control is usually a nationalized industry and, paradoxically, consumers often have much less explicit evidence that their interests are well cared for. Governments are all too ready to issue directives which further short-term political interests against the long-term interests of consumers. (The way in which successive British governments have forced British Airways to buy British equipment against its wishes are only the most easily remembered scandal of this kind.) The objective of the recent wave of change in Britain is allegedly to make the public monopolies more efficient. The difficulty, by no means confined to Britain, is how to measure efficiency.

The crop of decisions that assailed the British parliament last week is from this point of view a mixed bag. The British government's decision that a proportion of the shares in British Airways should be sold to private investors is partly a money-making operation, although the government has also promised that it will "get the Treasury off the airline's back". For the rest, it is relying on the fond belief that once private investors are represented on the board of the airline, everybody will be more vigilant in looking for a healthy economic return on capital, so that the operation of the airline as a whole will be by definition optimally efficient. That expectation is, of course, naive. The best that can be hoped for is that the airline will be as efficient as it can be with one hand tied behind its back. For in the international jungle of air transport, the monopoly rights that matter are not those of being allowed to run an airline but of being allowed to land so many times a week at this or that airport, and these rights are controlled by governments, either bilaterally or through the International Air Transport Association (IATA). If nothing is done to make this system less restrictive than at present, there is no prospect that the reorganized airline will be better able to make efficient use of the technology of air transport than the airline that now exists.

The continued neglect of technology by the other public monopolies is indeed the most serious cause of discontent with the new arrangements now in prospect. In the delivery of mails, for example, private operators are to be allowed to compete with the British Post Office only in those circumstances in which it is feasible for them to charge at least £1 for each letter handled. Unless Sir Keith Joseph, the minister responsible, has cynically calculated that the Post Office will soon be charging much the same for its ordinary mail, this change will not markedly increase the pressure on the rump of the service to use automatic sorting devices more efficiently, to wonder about electronic mail or to devise other ways of making sure that people receive their mail. Similarly, although it is high time that the iniquitous monopoly of the telecommunications part of the British Post Office on the supply of terminal equipment was ended, that will not by itself

0028-0836/80/310431-02$01.00

ensure that the rump of the monopoly will not repeat the appalling errors of the past three decades — blowing hot and cold about electronic switching equipment and so on. Sir Keith Joseph, the minister responsible, has gone no further than the decision of the United States Supreme Court in 1968 (the "Carterfone decision") that the American public (but privately financed) monopoly should accept other people's equipment at the ends of its telephone lines. What is to happen, in Britain, when quite new kinds of organisations ask permission to set up special-purpose communications networks (say, for data transmission) which the public monopoly does not wish for the time being to provide? Again, on past form at least, people will have to do without the benefits of a technology that they wish to use.

The decision that the monopoly of the Central Electricity Board on the generation of electricity should be modified is, from this standpoint, the oddest of those now announced. In the old days, the publicly owned electricity utility used to prevent people generating electricity from windmills sited in their back yards, but has recently been more accommodating. The British Government has not yet explained just what advantages its new dispensation will provide. Presumably, however, it will be possible for large manufacturing plants to be equipped with their own electrical generating plants and even to sell some of the electricity surplus to their needs to consumers nearby. (Some, no doubt, will also think of building nuclear power stations.) On the face of things, however, it is hard to conceive of circumstances in which the independent generation of electricity in bulk offers advantages over the service the national grid can provide.

The scale on which electricity users opt out of the public monopoly will therefore be a crude measure of the monopoly's failure. But again, the right to opt out will not by itself ensure that the service as a whole is technically efficient.

These issues are important because the public monopolies are often closely involved with novel or advanced technology. Not only in Britain, they are also conspicuously less innovative than they might be. The modest relaxations of the monopoly rights now announced in Britain are welcome, but their consequences will be marginal. Yet some at least of the public monopolies are here to stay. The long-term interests of their customers require more radical ways than those now devised of ensuring that they are technically adventurous, neither dogs in the manger nor stick-in-the-muds.

Subject in search of discipline?

How should the education of scientists be broadened? And how should intending scientists be helped to understand the wider implications of their professions? These are questions with which teachers have been much concerned in recent years. Increasing numbers of them have taken to devising curricula that include elements labelled "social relations of science" and the like. In recent years, science courses in higher education have been the chief beneficiaries (if that is the word) of this enrichment, but now there are signs that the habit is also catching on in the schools. It is therefore worthwhile that the Nuffield Foundation should have commissioned Sir Alec Cairncross (a wily economist once the British Treasury's chief adviser) to take a cool look at schemes for broadening the curriculum in this way which have been introduced in recent years in British higher education. His report, now published (and to be had from the Nuffield Foundation, Nuffield Lodge, Regent's Park, London NW1), should give pause to all those who think that their students will be better scientists if they can be persuaded to attend courses on the ethics of radioactive waste disposal, the social responsibility of scientists and the moral implications of genetic manipulation.

It is now more than twenty years since British universities began flirting with this means of broadening the science curriculum. One of the first courses to be established (at the University of Manchester) remains both the most ambitious and the most interesting. It constitutes a serious attempt to provide an undergraduate course with roughly equal amounts of science (physics, chemistry, physiology, etc.) and other subjects (history of science, economic history and so on). The original hope was that it would yield graduates with a capacity to work either as scientists or more generally. There are some thirty graduates a year, but the course appears not to be at the centre of school-leavers' attention, while the people who emerge from it, cultivated though they are, rarely choose to practise as scientists. They contribute, rather to the pitifully small pool of people who work in business, industry or administration who also know what science is about. At other British universities, the experience of the past few years has been more disappointing. Some of the more ambitious attempts to set up genuinely amalgamating courses have had to be abandoned. Where science courses are supplemented with a small amount of more general chat about the social relations of science, the students appear enthusiastic but the value of their marginal activities cannot be evaluated.

It is easy enough to make fun of these extra components in the science curriculum. Sometimes they are superficial. Sometimes they are downright wrong-headed. University science teachers in British universities are, however, far too quick to make these and other scornful points. Cairncross says laconically in his report that "it is a great misfortune of English education that it leads to so early and final a decision between those who study science and those who do not. This is a huge understatement. Outside the United Kingdom, it may not be fully appreciated that students entering science courses are almost always people who have been for the preceding two years rehearsing at school the studies they will follow later, and that many of them have been preparing for this curious exercise for a further three years. (Cairncross's use of the word "English" is deliberate, for the Scottish universities are more liberal in what they require of new entrants.) The result is that the majority of those who enter science degree courses have long since ceased to bother with language (their own as well as other people's), with history and economics. Is it any wonder that complaints abound that new British graduates are tongue-tied or illiterate or just plainly ignorant of the social setting in which they will have to work? And in such circumstances, can it be right to demean the attempts that university teachers make, however inadequate they may be, to compensate for the deficiencies of the educational system of which they are only a part?

The only long-term remedy must be a reorganization of the educational system as a whole, but especially at the transition between secondary schools and universities. More immediately, there is a need for ways of enriching science courses in higher education that will be more substantial and more valuable than those now in vogue. Much of what is now provided for students under this heading centres around the much talked of Promethean dilemma. Nuclear fission means nuclear reactors but also nuclear proliferation. Molecular genetics means cheaper ways of making interferon (perhaps) but also (possibly) ways of undermining the natural course of evolution. The list of topics that make grist for this mill is endless. As ingredients of serious teaching, however, they are topics replete with pedagogical problems. The information available is incomplete. Books do not exist. The capacity of students maimed by their school education to grapple with the formless issues raised by such questions is quite inadequate. Their teachers are all too often bent on grinding other axes — political, ideological or religious. The Cairncross report has drawn attention to the need for some enrichment of science courses but has also spelled out the limitations of what is at present being taught. Has not the time now come for more serious attempts to make good the deficiencies of the British educational system? Science students might usefully be helped to keep up with a foreign language, to learn more serious economics or to discover in reorganized teaching laboratories that science is not cut and dried, as the textbooks have it, but as full of intellectual conundrums as any study of the humanities.

0028-0836/80/310432-01$01.00

Proliferation a test of nerve in Congress

Washington

United States non-proliferation policy is facing its toughest domestic test for almost a decade, as Congress decides whether or not to veto President Carter's decision to allow the further export of nuclear fuel to the Tarapur nuclear power plant in India. The Nuclear Regulatory Commission (NRC) has already ruled that the export of 38 tons of enriched uranium requested by India would violate the Nuclear Non-Proliferation Act of 1978 (NNPA). The act forbids the export of fuel or technology to countries which have not adopted international safeguards on all their nuclear facilities.

President Carter has since overruled the NRC on the grounds that denying India the fuel would seriously prejudice political and economic relationships with India.

The dispute has brought to a head not only strategic differences between Congress and the State Department but also tensions between the United States and India rampant ever since India exploded a nuclear device in 1974.

Mrs Gandhi's return to power last year, and her subsequent firm refusal to eschew the possibility of India developing its own nuclear weapons, put an end to hopes that agreement could be reached. Now the Administration is trying to persuade Congress that political tensions in South Asia, and the consequent advantage of remaining on good terms with India, should override more narrowly focused policies.

The Administration and its critics find themselves on opposite sides of a narrow dividing line. The NRC, for example, taking a strict interpretation of the NNPA, refused to grant an export licence partly on the grounds that the shipment of the fuel would take place more than two years after the NNPA had been signed, the grace period for compliance. But the Administration points out that the request had been received in 1977; that the delays were the result of US indecision for which India should not be penalized; and that subsequent licence requests will be treated differently.

Then there is the question of whether, if the export licence is granted, it will be used as a precedent by other countries — for example Argentina, Brazil, South Africa and Iraq — to claim exemption from the act. Administration critics are standing firm on this point. The Administration however disagrees.

Another question is whether denying the fuel to India would violate the 1963 agreement, under which the United States guaranteed to provide fuel supplies to Tarapur for 30 years and, if so, whether India would then feel free to ignore other restrictions in the agreement.

"If the US breaks the agreement, then India can do what it wants, including using plutonium from the fuel rods to make nuclear weapons", Dr Betty Lall of the US State Department said at a meeting organized by the Arms Control Association in Washington last week. Others, however, argue that India has long been aware that the obligation of the United States to supply fuel is contingent on India's compliance with US licensing requirements, however these may change.

Strict non-proliferationists favour the big stick. "Congress should draw a clear line and say 'no' to further nuclear commerce with India until the Indian government accepts international safeguards on all its nuclear activities", said a statement issued last week by several public interest groups, including the Natural Resources Defense Council and the Union of Concerned Scientists. The Administration still prefers to use softer methods, arguing that in the long run non-proliferation objectives have a better chance of success through dialogue rather than confrontation.

In Congress, which can overturn the President's decision if both houses agree by a simple majority before 12 September, the issue is in the balance. In the House of Representatives, feelings against the export licence are running high; a majority of members of the Foreign Affairs Committee, for example, have signed a statement calling the decision to grant the licence "a dangerous mistake".

In the Senate, there is also some strong opposition, headed by Senator John Glenn, chairman of the Government Affairs Committee's Energy and Nuclear Proliferation Subcommittee.

In an election year, however, political dynamics could prove crucial. A certain amount of the opposition seems to have been stimulated by a desire to embarrass the Administration. The House committee's statement opposing the licences, for example, was supported by two-thirds of the committee's Democrats, but three-quarters of its Republicans.

The Administration is at present trying to convince a sufficient number of Senate Democrats of the value of treating the licence as a special case, with a promise of further negotiation towards a definite outcome one way or the other. Given that both houses have to concur in any disapproval, the Senate's refusal to do so would be sufficient to allow the export to proceed.

David Dickson

Plagiarism strikes again

The spate of publications with which Dr E.A. Alsabti has scattered the scientific literature in the past few years now seems destined to be followed by a similar spate of retractions. The accompanying letter (see page 437) from Dr Akiro Shishido, Managing Editor of the *Japanese Journal of Medical Science and Biology (JJMSB)*, says that a notice will appear in the August issue of the journal explaining that the editorial board now considers that Alsabti's contribution to that journal describes research originally carried out by Dr Daniel Wierda and Dr T L Pazdernick, first published in the *European Journal of Cancer*.

It is not yet known how many of the 23 papers listed in *Index Medicus* under Dr Alsabti's name are likely also to fall under a cloud. It is, however, known that Alsabti's paper "Lymphocyte transformation in patients with breast cancer", published in the *Japanese Journal of Experimental Medicine* (49, 101; 1979) is virtually identical with "The effects of surgery on lymphocyte transformation in patients with breast cancer", published by Dr Sylvia M. Watkins in *Clinical and Experimental Immunology* (14, 69; 1973).

As in other papers published under his name, Dr Alsabti acknowledges his gratitude to His Royal Highness Crown Prince Hassan for "financial support and encouragement". To Dr Watkins's original list of references is added in the pirated version the reference "Alsabti, E.A., Lymphocyte transformation in bladder carcinoma, *J. Clin. Hematol. Oncol.* (1978), in press".

Meanwhile, an apparently unrelated case of plagiarism involving another Jordanian scientist, has come to light. Dr K.O. Kutschke, of the Canadian National Research Council, who is Editor of the *Canadian Journal of Chemistry*, says that in February 1978 his journal received for publication a manuscript called "Influence of electric charges on the corrosion of metals" a paper previously published by a group of Swedish authors — J.A. Hedvall, Nils-Gosta Vannerberg and P.O. Blomqvist — in *Acta chemica scandinavica* (22, 363; 1968).

In that case, Dr Kutschke explained this week, the plagiarized manuscript was not accepted for publication because the list of references included one to the Swedish group whose work had otherwise been pirated. Only curiosity, Dr Kutschke explained, prompted him to look up the original publication, whereupon he recognized the identity of the two papers.

On that occasion, it appears, the Jordanian author (whose name is being withheld) gave an address at a university in the eastern United States, but had given the University of Amman as the location of his research. On complaint from Dr Kutschke, the visiting appointment of the scientist was terminated.

0028-0836/80/310433 01$01.00

US budgets

End in sight?

Washington

"The best we can hope for is to try to salvage a disaster and just make it a very bad year," This is how one Washington lobbyist last week summed up the prospects for next year's research budget as Congress continued, at the President's request, to chip away at the budget.

Since the beginning of the year, the prospects for science have changed substantially. When President Carter delivered his original request to Congress in January, he proposed a 13 per cent growth for basic research, about 3 per cent above the anticipated rate of inflation.

In March, after what the President's Science Advisor Dr Frank Press has described as the "traumatic experience" of a review designed to cut public expenditure and balance the overall budget, the increase was reduced to 8 per cent, barely enough to keep pace with inflation. Now even this figure is looking optimistic.

As far as congressional authorization committees (which approve programmes for funding) are concerned, there have been relatively few problems in meeting the President's requests for cuts and in some cases even greater cuts have been made.

Both houses of Congress have agreed on an authorization bill for the National Aeronautics and Space Administration (NASA) which, at a total of $5,600 million, is $70 million above the revised request for the agency. The two houses agreed in particular to restore funding for some of the long-range support programmes that had been cut earlier.

Similarly the National Science Foundation has so far done relatively well. The House of Representatives and the Senate have passed very different authorization bills, with the latter incorporating provisions for a major "women in science" programme, and this could involve some redistribution of funds within the agency. But the total in each case is at or above the Administration's $1,074 million request.

But in the appropriations committees — which decide how the federal budget is to be allocated — it is a different story. Most appropriations bills have still to be acted on; but in their determination to pare the federal budget wherever possible, several appropriations committees have taken basic research as one of their targets.

The worst affected so far has been the Department of Energy, which supports a large proportion of the physics programme. The department's request for energy research activities, trimmed slightly by authorization committees, was recommended for a 12 per cent cut.

This proposal stimulated intense lobbying by universities and research laboratories, as well as the Office of Science and Technology Policy, and when the budget was debated on the floor of the House, an amendment proposed by Mr Don Fuqua, chairman of the House Science and Technology Committee, to restore most of this cut was agreed by a wide margin.

Furthermore the intense effort involved in protecting the energy research budget is being taken as an indicator of the strength with which scientists will increasingly have to fight to retain their share of the budget pie in other areas as well.

As far as other agencies are concerned, no action has yet been taken by Congress on the National Institutes of Health budget, which for the most part does not require separate authorization. Congress is unlikely to cut back on the Administration's request for a 5.2 per cent increase to $3,350 million; but neither is it likely to award the generous increase of previous years.

Some concern is being expressed about the Administration's decision to cut back heavily on the number of training grants. These may be traded in committee against the proposal to maintain at 5,000 the number of new and competing investigator-initiated research grants.

The House has authorized a total of $627 million for basic research in the Department of Defense, and the Senate has authorized a comparable figure. This is lower than the $644 million in the Administration's revised budget request, but still represents a real growth of 8 per cent over 1980 funding, far higher than for any other research agency. Also, for the third year in a row, the House appropriations committee has proposed cutting $30 million allocated to a competitive grants programme to the Department of Agriculture, in favour of support for programmed research support through designated land-grant colleges. As in previous years, this is likely to be partially restored in the Senate.

Despite protests that reducing the Environmental Protection Agency's research activities will restrict its effectiveness, the House has authorized a budget 3 per cent lower than the Administration had requested for research, from $413 million to $396 million.

David Dickson

International laboratory

Danes turn soft

Danish biologists are preparing to make a strong recommendation to their Minister of Education next month that Denmark should continue to belong to the European Molecular Biology Laboratory in Heidelberg. Their previous report on the question of continued membership of EMBL was lukewarm, and persuaded a government advisory committee to decide that Denmark should rescind the EMBL treaty from mid-1981 (*Nature*, 26 June).

That report, now in circulation, recommended that EMBL should increase the number of permanent scientific posts (there is at present only one) and have fewer short-term contracts (now about 50); there should be more detailed research plans than hitherto; and EMBL should submit its plans for the next five-year period (1985–90) to Denmark in time for a "well-founded" decision on membership.

Before then, says the report, the research councils should "consider whether it is desirable in principle that Denmark should participate in building up European laboratories in fields where the proportions of the problems and investment prevent attempts to establish national solutions or international collaboration in utilizing national laboratories" — thus implying that in fact EMBL was un-necessary.

EMBL's recruitment policy appears to be based in part on the assumption that the best molecular biologists are young, but the report concludes that these younger scientists require "a well-established environment with firm scientific traditions and with older experienced scientists" before they can achieve important results. Hence, the working party concluded, it is not possible to build up a good laboratory if nearly all the scientific staff are young postdoctoral fellows on short-term contracts.

Moreover "it must be expected that small working groups of scientists whose contracts are reviewed every three years will chiefly choose problems ensuring results within a short period, but on the other hand not offering great possibilities of all-important results".

The report also questioned the research management of EMBL, saying that "it does not appear very satisfactory that the individual working groups are not asked to submit fairly specific plans for their work and that the decision-making bodies, including among others the EMBL council, are given such a vague basis for making decisions". The research groups are also too small, the report considered, being no larger than those at national laboratories.

On the positive side, the report made special mention of the groups on data processing and the utilization of computers; this part of EMBL's activities was "very promising".

Nevertheless, it is felt strongly at EMBL that it is too soon to make a proper assessment of the laboratory's achievement. The laboratory was established in its present permanent headquarters in Heidelberg in 1978, and many of the staff were recruited then. The constitution of EMBL, modelled on that of the European sub-nuclear physics organization CERN, says that no person may apply for tenure until he or she has worked at EMBL for three years. Few have reached that position. The laboratory's director, Sir John Kendrew, says that there should be a marked increase in the number of tenured posts in a few years.

0028-0836/80/310434-02$01.00

EMBL acts as a service centre, with P3 and P4 laboratories, outstations using synchrotron light at Hamburg and neutrons at Grenoble, and instrumentation and computer groups at Heidelberg. So it is necessary, EMBL thinking goes, for the staff scientists concerned to pursue the most up to date lines of research, to keep them in touch with the immediate needs of the scientific community. Thus flexibility is a prime goal, and short-term contracts and small groups provide it.

The Danish meeting on EMBL towards the end of next month will consist not only of biologists. There will be representatives of the research councils for natural science, agriculture and medicine, just as there were on the original working party that produced the original report, so it is difficult to predict the outcome. However, whereas that report recommended that the government should foot the £120,000 EMBL bill, the new report may suggest that a single research council takes the subscription into its own budget. An obstacle may be that at present no Danish biologist works at EMBL, although a computer scientist and some ancillary staff do so.

Robert Walgate

Scientific instruments

Nature spin-off

The colour filters supplied with the 3 April issue of *Nature* have turned out to have an unexpected use. In some laboratories, it seems that the filters are superior to others on the market in the contrast they provide.

Dr R. Zeki of University College London, whose article on colour vision prompted the distribution of the set of three colour filters (*Nature* **284**, 412–421; 1980), said last week that he had received a number of comments on the value of the filters, which he had passed on to Polaroid, the manufacturers.

One of those who have found the red filter of particular value is Mr David Owen, a graduate student in the laboratory of Dr C. Harwood, of the University of Newcastle upon Tyne. One series of experiments is to identify extrachromosomal genetic elements in bacteria. The procedure is to separate DNA molecules by gel electrophoresis and to make molecules of different classes apparent by treating the gel with a fluorescent dye that binds to DNA.

Mr Owen explained last week that he had had some trouble finding a suitable filter for photographing the pattern of visible light stimulated by ultraviolet radiation, so he had tried "Dr Zeki's red filter".

"To our surprise", he said, "the resulting photographs were far superior . . . in that the DNA bands were clearly visible against a black background". The accompanying illustration is an example of such a photograph, in which the bright central band represents chromosomal DNA and the sidebands DNA from plasmids.

No agreed explanation of this result is available, although it seems likely that the narrowness of the transmission band of the red filter may account for the sharp contrast.

The Polarioid Corporation has apparently developed these filters largely for research purposes. A spokesman for the company said last week that filters with narrow transmission bands should be available from more conventional sources, but that the company might reconsider its decision that its filters would not be put on the market if the demand for them turned out to be sufficient.

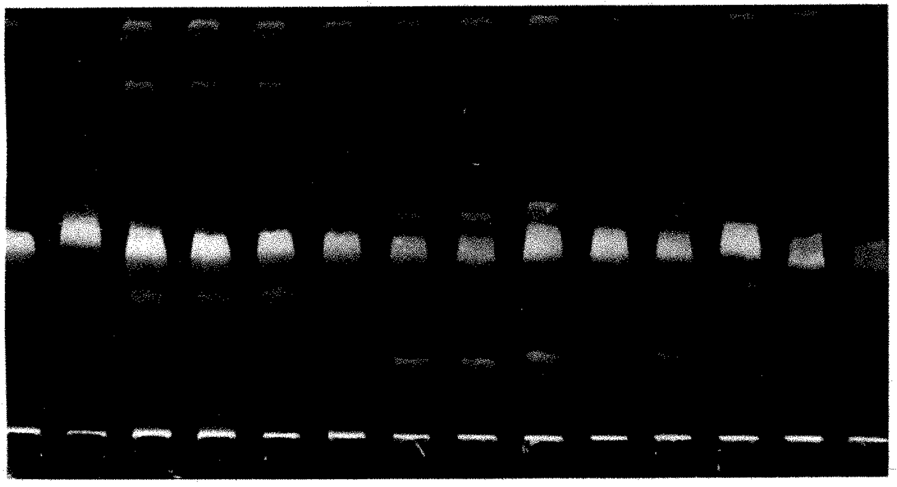

High-energy physics

Trouble ahead

Washington

As if bleak budget prospects were not enough, high-energy physicists in the United States are facing another delicate question — what to do about continued difficulties in the development of superconducting magnets for the 400 × 400 GeV accelerator (ISABELLE) now under construction at the Brookhaven National Laboratory on Long Island.

The official line is that a substantial effort must be maintained to resolve the difficulties, even if this means cutting further into the laboratory's operating funds for experiments and bringing in help from across the physics community.

But attention is now also being paid to what have been called "graceful failure modes". At best this could mean lowering the maximum energy of each of the two intersecting beams of protons from 400 to, say, 300 GeV; at worst, it could mean cutting losses and scrapping the whole project.

Given the continued risk of failure in the ambitious superconducting magnet programmes at Brookhaven and at Fermilab some physicists are suggesting that there is a need to broaden the base of the whole nuclear physics programme — in particular, by diverting resources to electron–positron machines directly competitive with Europe's proposed LEP in Geneva.

ISABELLE is scheduled for completion in 1986, when it will be able to explore the physics of proton–proton interactions at energies an order of magnitude higher than those which can be reached on comparable existing machines.

It had always been anticipated that developing superconducting magnets to deliver the required high fields would be difficult. But given the success of early prototype magnets, nobody realized how great the difficulties were likely to be.

ISABELLE will use 1.7-m quadrupole and 5-m dipole magnets, the former operating with a gradient of 6 kG cm^{-1}, the latter at a field strength of 50 kG. So far the quadrupoles have operated with no difficulty. But major problems have arisen with the dipoles, which have not reached either the planned maximum fields or field quality — and of which more than 700 will eventually be required.

Brookhaven has mounted an intense research and development programme to pinpoint the difficulty. The number of people working on the magnets has been increased almost four-fold over the past two years. And outside help has also been sought from the Massachusetts Institute of Technology's magnet laboratory and the Lawrence Berkeley Laboratory.

The problem is one of engineering rather than theory — that of keeping the magnets in a superconducting mode while building up the required field. Although Brookhaven scientists are optimistic that an answer will eventually be found, they admit that they are still uncertain about precisely what is going wrong.

ISABELLE's difficulties were a major focus of attention when a sub-panel of the Department of Energy's High-Energy Physics Advisory Panel met in Woods Hole, Massachusetts, last month to report on the current status and prospects of US high- energy physics.

Considerable discussion took place about whether, in the light of the "serious and unexpected setbacks" to ISABELLE's construction programmes, the specifications for its performance should be revised downwards. If each beam only

0028-0836/80/310435-02$01.00

operated in the 60 to 300 GeV range, it was argued, this would still be sufficient to produce a large amount of important physics, even without the possibility of investigating collision energies between 600 and 800 GeV.

In the end, the panel refrained from making any such formal proposal. But it did state that current information from Brookhaven was insufficient to assess whether the pilot production of the dipoles was likely to begin in mid-1981 as planned. "If it is not, the ISABELLE project will encounter significant delays", the sub-panel reported.

Brookhaven scientists have been heartened by the report's recommendation that the successful completion of ISABELLE — including any necessary R and D funding — should remain a top priority of the Department of Energy, as well as becoming "the responsibility of the entire national community".

At the same time, however, others are warning of the dangers of failure in what has become recognized, both at Brookhaven and to a lesser extent at Fermilab, as a high-risk/high-benefit programme still facing large engineering uncertainties.

"The US high-energy programme is now highly dependent on the successful solution of such engineering problems and I would recommend greater diversification to reduce that dependence", Dr Wolfgang Panofsky, director of the Stanford Linear Accelerator Centre (SLAC), told a meeting held in Washington last week to celebrate 50 years of particle accelerator construction.

SLAC is promoting its own proposal, developed by Dr Burton Richter, to construct a machine which would collide bunches of electrons and positrons, passed in tandem down the linear accelerator and then in separate directions around a ring at the end.

Dr Richter is pushing for early funding of the so-called Stanford Linear Collier (SLC), attempting to finesse experiments on CERN's LEP and claim discovery of the intermediate vector boson. The Woods Hole sub-panel examined the proposal closely, describing it as a "fascinating and challenging new departure in accelerator technology". However, the sub-panel refused to endorse SLC for immediate funding. In particular, questions were raised about whether SLC's predicted luminosity would be sufficient to make it truly competitive with LEP, which will also have a larger energy range.

David Dickson

Dead Sea

Coming to life

Theodore Herzl's dream of a canal from the Mediterranean to the Dead Sea is at last a cost-effective proposal, the Israeli government was informed last week. Use of the 400 m drop between the two seas to generate hydroelectricity could now match the cheapest generation from fossil fuel stations, according to a government-appointed working party chaired by Professor Yuval Neeman of Tel Aviv University.

Assuming an initial investment of $800 million, the canal with a cascade of hydroelectric installations would, said Dr Neeman, pay for itself in 30 years, simply from the 100–150 MW of hydroelectricity produced. In addition, the canal could provide the sites for nuclear power stations which cannot be accommodated along the crowded Mediterranean coast. (That between Ashquelon and Ashdod has been found to be earthquake-prone.) A thermal power station using the water from the canal but fired by local oil shale deposits could also be built at Ein Bokek.

Ecologically, the main benefit of the canal would be to replenish the waters of the Dead Sea. The only natural feeder of the Dead Sea is the lower Jordan, which draws its water from the Sea of Galilee and from its east bank tributary, the Yarmuk. The Sea of Galilee is however the source of water for virtually the whole country, while the Jordanians have almost completed a major irrigation project involving the diversion of the Yarmuk into the East Ghor Canal. When this is complete, the lower Jordan will shrink even further to a mere 200 million m^3 annually, mostly return flow from irrigation.

Evaporation loss from the Dead Sea is 1,200 m^3 a year, so that the sea has shrunk considerably — the S'dom potash works have become stranded and a special channel has been built to pump brine to the evaporation pans. By November 1978, in a Knesset debate on the proposed canal, both government and opposition were agreed that any further shrinkage could bring irreversible ecological damage.

Then came the drought of 1979. By September, the Dead Sea had split in two at the narrowest point (some 3 km across) and, according to Shlomo Drori of the Dead Sea Development Company, there was a dry plain some 12 km long between the northern part of the Sea and the sourthern fragment, then split into a number of pools. Meanwhile, plans were going ahead to use the Dead Sea for generating electricity on the "solar pond" principle, based on the temperature difference developed in brines exposed to sunlight where the density gradient is too great to allow convection mixing. The first solar pond power station was opened at Ein Bokek in December 1979.

The ecological advantages of the proposed canal are admitted by all concerned. Until now, they have been the paramount concern, with hydroelectricity considered rather as a valuable spin-off. As late as the Knesset debate of 1978 on the canal, Energy Minister Yitzak Moda'i stressed that electricity could still be generated more cheaply from fossil fuels. Professor Neeman's estimates, for the first time, reverse this situation. However, with the Israeli economy in a state of crisis — inflation is now running at 130 per cent per annum — it is by no means clear whether the government could raise the necessary $800 million.

Vera Rich

Biogenetic hormones

Insulin trial

Eli Lilley, the US pharmaceutical company, has taken another step along the road to producing human insulin on a commercial scale. Last week, it announced a $40 million programme to build two plants at its factories at Speke in the United Kingdom and Indianapolis in the United States for the commercial production of human insulin from genetically engineered bacteria. Ultimately, human insulin produced in this way should be much cheaper than the insulin currently extracted from pig and beef pancreas.

Full-scale production, however, is still a few years off. First, any problems cropping up with manufacture on a large scale will have to be resolved and extensive clinical trials have to be done. The first trials with insulin from the company's US laboratories began on healthy people earlier this month at Guy's Hospital in London. Initially at least, the trials are being conducted in the United Kingdom to avoid delay in getting permission from the Food and Drug Administration for trials in the United States.

The tests at Guy's Hospital mark the first time that any recombinant DNA hormone has been injected into humans. Preliminary tests to measure the effectiveness of the new insulin in reducing the blood glucose level of healthy people and their immune response to it should be complete in a few weeks. By the autumn, tests should begin on diabetics. It is expected that human insulin will be tolerated without the production of antibodies. Some diabetics do produce antibodies to insulin derived from pigs and cattle. One possible advantage of human insulin is that it will minimize or eliminate the risk to middle-aged diabetics of eye and liver damage.

The techniques Eli Lilly are using are those developed by Genentech (which will get a cut of the profits) whereby synthetic genes for the A and B insulin chains are put into an *Escherichia coli* plasmid. The bacteria expressing the two genes are fermented separately, killed and broken up to extract the A and B chains. The chains are then chemically combined to produce human insulin. So far, no method of getting genetically engineered bacteria to excrete their products has been found, but Eli Lilly claims that its method of extraction has produced pure insulin free from bacterial fragments.

The production of human insulin from recombinant DNA is more complicated

0028-0836/80/310436-02$01.00

than the production of antibiotics, where bacteria excrete the product. Nevertheless, it should prove far less costly than the current methods of extracting porcine and beef insulin. The cost of human insulin to the consumer, however, will depend on its penetration into the market and competition from other companies. When costs will come down is still uncertain, especially since Lilly cannot even say yet when it will be in a position to start commercial production.

Judy Redfearn

Environmental protection

Bulgaria ahead

Bulgaria is to spend more than 1,000 million lev (£500 million) on environmental protection during the next five years, President Todor Zhivkov announced recently. He was addressing a meeting held to celebrate the 80th anniversary of the Bulgarian National Agricultural Union.

In Bulgaria, President Zhivkov said, the Constitution makes environmental protection a nationwide matter, dealt with by specially created bodies at all levels of state management. Ecological problems are a compulsory subject in higher educational establishments and throughout the educational system. Special organizations have been set up to deal with erosion and bring reclaimed or neglected soil back into use. Bulgaria, he said, is a world leader in reafforestation, planting 400–500 decares per year.

Zhivkov unequivocally rejected the view of "bourgeois ideologists" who maintain that the violation of the established ecological balance is the result of the modern scientific–technological revolution. On the contrary, he said, this revolution is essentially "our greatest ally in harmonizing relations between society and nature". Although the published data on natural resources are so "very alarming", Zhivkov reiterated that "being aware of the danger is a signal for action, not a cause for pessimism".

Bulgaria is not rich in natural resources, and before the Second World War it was the most backward but one of the European countries (Albania ranked last). Now, however, Zhivkov claimed his country is a "developed industrial agrarian country", with an agriculture capable of feeding "one and a half Bulgarias" and a target of "two Bulgarias" in 1985. Referring to his African tour of two years ago, Zhivkov suggested that if Nigeria, Angola, Ethiopia and Mozambique could apply Bulgarian-type organization and technology to their agriculture, they too would be producing surpluses. Ethiopia, in particular, he said, has especially good soil which could not only support the present population but also "feed a neighbouring state".

Vera Rich

One journal disowns plagiarism

Sir — Your recent article "An Outbreak of Piracy in the Literature" makes it apparent that the *Japanese Journal of Medical Science and Biology* (*JJMSB*) was a victim of an outbreak of paper piracy by a person called Dr A. Alsabti. I am writing this letter on behalf of the Editorial Board of *JJMSB* to make our position clear. Our unfortunate experience shows how difficult it is to be aware of dastardly and minutely planned piracy of papers.

We first received this manuscript entitled "Effect of Platinum Compounds on Murine Lymphocyte Mitogenesis" on 20 November 1978 from the stated address — Department of Developmental Therapeutics, M.D. Anderson Hospital and Tumor Institute, University of Texas System Cancer Center. After careful reviewing, the manuscript was sent back on 25 December 1978 with referees' comments to Dr Alsabti at his changed address (7520 Brompton Blvd, No. 736, Houston, Texas 77025). The revised manuscript was received in our editorial office on 16 January 1979, but it was still not satisfactory for publication and it was again sent back to him on 12 February. The final revision was received on 2 March, and the editorial board accepted it for publication on 12 April 1979. On 11 May 1979, a galley proof was sent to him and he asked us to send any further correspondence to his new address — 7511 Teal Run, Houston, Texas 77071. On 11 June 1979 the paper was finally published in the April issue of our journal (*Japan. J. med. Sci. Biol.* 32, 53–65, 1979).

The editing of Dr Alsabti's paper therefore followed quite a normal course. However, it may be important to add here that we received three other manuscripts from him at around the same time. These were:

(1) Effects of tumor cell culture supernatants from various tumor cell line and normal tissues on macrophages.

(2) Tumor dormancy established in DBA/2 mice with P815Y mastocytoma cell lines.

(3) Tumor dormant state established in DBA/2 mice by sinecomitant immunization and challenge with lymphoma cells: Role of endogenous viruses in its mechanism.

All these papers were rejected.

Almost one year later we received a shocking letter from Dr D. Wierda of the Chemical Industry Institute of Toxicology, North Carolina, USA. His letter told us an almost unbelievable fact, that the paper entitled "Suppression of Spleen Lymphocyte Mitogenesis in Mice Injected with Platinum Compounds" contributed by himself and Dr T.L. Pazdernik to the *European Journal of Cancer* (15, 1013-1023; 1979) is identical to Dr Alsabti's "Effect of Platinum Compounds on Murine Lymphocyte Mitogenesis" published in our journal. Dr Wierda enclosed copies of proofs demonstrating the authenticity of his work and suspected that their manuscript was probably pirated during the process of review for the *European Journal of Cancer*. He added that their manuscript was received on 10 October 1978, accepted for publication on 5 January 1979 and published in the August 1979 issue of *European Journal of Cancer*.

In urgent response to Dr Wierda's letter I wrote to Dr Alsabti on 9 June 1980 to ask for an explanation of this unusual situation, specifying a time limit of 15 July, 1980. This letter was sent to his last corresponding address. I also asked Dr Freireich, head of the Department of Developmental Therapeutics, M.D. Anderson Hospital and Tumor Institute, to forward my letter to Dr Alsabti.

On 30 June 1980 Dr Freireich wrote to tell me that he could not forward my letter to Dr Alsabti as his address was unknown. However, he proved that Dr Alsabti had never conducted any scientific research worthy of publication, either in the laboratory or clinic, during his 7 months' stay in his department, and suggested further that his large number of publications are all either outright plagiarisms or were totally imaginary.

We have so far received no reply from Dr Alsabti, although the deadline we gave him has already expired. Furthermore, Dr Wierda notified me on 21 July of the article "Jordanian Denies He Pirated Papers" (in the 11 July issue of *Science*) in which Dr Alsabti claimed that he had not published the paper in *JJMSB*. We therefore decided to retract Dr Alsabti's paper to protect the characters of Drs D. Wierda and T.L. Pazdernik. *Japanese Journal of Medical Science and Biology* hereby announces retraction of his paper from our journal. Our "Retraction Notice" will appear in the coming August issue of *Japan. J. med. Sci. Biol.* 33 (4), 1980 as follows:

> **The Editorial Board of the** ***Japanese Journal of Medical Sciences and Biology*** here announces retraction of the following paper from the Journal:
>
> "Effect of Platinum Compounds on Murine Lymphocyte Mitogenesis" by E.A.K. Alsabti, O.N. Ghalib, and M.H. Salem. *Japan. J. med. Sci. Biol.* 32(2), 53-65, 1979.
>
> Judging from several lines of evidence (1–5), this work must have been authentically carried out by Drs D. Wierda, and T.L. Pazdernik, whose paper was almost simultaneously published in the *Eur. J. Cancer* (15 (8), 1013-1023, 1979) under the title of "Suppression of Spleen Lymphocyte Mitogenesis in Mice Injected with Platinum Compounds".
>
> 1. Letters from Drs D. Wierda & T L. Pazdernik
> 2. Correspondence to the Head of Department of Developmental Therapeutics, M D. Anderson Hospital and Tumor Institute, the University of Texas System Cancer Center, with which Dr Alsabti was affiliated.
> 3. *Nature* 285, 429-430 (1980)
> 4. *Science* 208, 1438-1440 (1980)
> 5. *Science* 209, 249 (1980).

Akira Shishido

National Institute of Health, Tokyo, Japan.

0028-0836/80/310437-01$01.00

CORRESPONDENCE

Biologists mis-cite

SIR,—The importance of checking original sources is well recognized, but doing so becomes harder as the literature grows. I describe here an attempt at quantification of the reliability of citations.

Since familiarity with the cited literature is essential, I selected 28 of my own, not faultless, publications and 136 related publications by other authors. These deal mostly with snail physiology and with ionic and acid–base regulation in animals.

Errors found include misquotation of quantitative data, confusion of hypothesis with fact, of crustaceans with molluscs, of one species with another and of experimental variations with natural variations; also invention, simplification and statements contrary to what was demonstrated. Along with 33 such errors occurring in 29 citing publications are 11 instances of correct information being used with a wrong reference, or with none. Some of the correct citations were almost too simple to be capable of being wrong (such as "Recent investigations include that of. . ."). Such citations can be useful, but at least 12 citing publications include apparently pointless references to the cited publications or, more important, omit others known to the authors that are clearly of greater relevance.

There are 3 instances of references being given in the text, but not in the bibliography, and 4 mistakes of the opposite kind. Of the 205 entries in the 136 bibliographies, 14 contain mistakes that could hinder, though not prevent, the location of articles (wrong page number, year or publisher). Other, mostly trivial slips, including altered punctuation and omission of words or letters, occur in a further 55 references, sometimes several in each. 58 of the bibliographies contain at least one error. Most errors are in titles, which, in accordance with editorial policies, many of the other references do not include.

Fifty-six per cent of the citing publications contained at least one of the above faults. Especially in bibliographies, slips must often be due to hasty note-taking before citation is specifically envisaged; the original lack of care may then be forgotten during preparation of the manuscript. Blanchard[1], in a letter since misrepresented in print, has described (I think) how he found that, of 6 references to a particular paper in chemistry, 4 contained errors in volume or page number. The assessment concerning the appropriateness of some of the citations is subjective, but is a reminder that other factors may influence an author's choice of citations than the interests of the reader[2,3].

R.F. BURTON

Institute of Physiology
University of Glasgow
Glasgow G12 8QQ, UK

References
1. Blanchard, D.C. *Science* **185**, 1003 (1974).
2. May, K.O. *Science* **156**, 890-892 (1967).
3. Garfield, E. *Current Contents, Life Sci.* **23**, 5-9 (1980).

Chemical warfare

SIR, — Your leading article of 10 July makes the point that verification of an agreement to ban chemical weapons, which was never easy, becomes even more difficult in relation to production of the components of binary chemical munitions. An alternative approach, assuming that an agreement had been reached, might be to monitor the stockpiling and/or issue of protective clothing (especially gas masks) for military or civilian use, and any military exercises in such clothing. If the major powers had entered into the agreement in good faith there would be no need for clothing capable of protecting against nerve agents, and certainly not of military exercises by troops wearing it. It is very unlikely that a country intending to use chemical weapons could do so without making preparations to protect its own personnel on a scale which would escape detection by the intelligence organizations of the other countries which were party to the agreement. From an agreed date, after sufficient countries had ratified the agreement, all clothing for protection against nerve gases would go into bonded stores, and any military exercises involving such clothing would be forbidden.

If the argument is valid, such an indirect monitoring should suffice to detect any intention to infringe the agreement — even though the most important factor remains confidence that in no country do chemical weapons serve its people's real interests.

J.H. HUMPHREY

17 Mortimer Crescent
London NW6 5NP, UK

Budapest disclaimer

SIR,—Your article by Vera Rich (5 June) refers to an interview with me at the Budapest International Fair. Having studied the contents of the article, I must state with the utmost regret that it lacks the desired accuracy. I therefore feel it appropriate to correct the article at some points.

At the beginning of our talk I conveyed to Miss Rich that as the Hungarian Academy of Sciences was not a participant at the 1980 Budapest International Fair, academic research was not being presented at this event. I explained that at the exhibition, in accordance with Hungarian science policy, attention was drawn to scientific results serving practical benefits and achieved at universities and other institutes of higher education within the sphere of the Ministry of Education. Furthermore, I emphasized that great effort has been and is still exercised by the Ministry of Education towards putting research results into practice as soon as possible, thus promoting progress in our country. Universities agree with us in setting these goals, as was confirmed by the fair. I continued by emphasizing the importance of the demand made by users in connection with practical research, but I did not say "We make what foreigners want to buy".

In the course of the ensuing discussion, Miss Rich raised the question of how our scientists react to research being directed towards practical purposes. In answer, I said that the great majority seems to exercise the necessary goodwill in this respect but that not everybody is fit to fulfill the demands required by practical research.

In this sense, the statement attributed to me in the article that I do not agree with the pragmatic orientation of our research policy is incorrect; what I said was that the intention of the authorities of giving a pragmatic orientation to research policy causes some of our scientists anxiety. Accordingly I cannot accept, being myself also an advocate of emphasizing the need for practical research, the statement attributed to me that "It is a pragmatic solution to direct more scientists to industry and not good for research".

I do not know which facts led Miss Rich to the conclusion that we place less emphasis on the socialist virtue of the development of scientific research in Hungary. I am convinced that this could only be a misunderstanding.

GYÖRGY PÁRIS

23 Szerb Street
H-1056 Budapest
Hungary

VERA RICH writes: I should feel most distressed if misunderstandings cloud Mr Paris's recollections of what I remember as a most friendly and open conversation. Although the Academy of Sciences was not, however, exhibiting this year, the pavilion was clearly marked on the official plan as housing, *inter alia*, the Academy. If, because of interpretation difficulties, I have inadvertently confused views that Mr Paris put forward on his own behalf with views he quoted from scientists who disagree with him, I would wish to point out, in tendering him my apologies, that it is by no means common to meet an official spokesman who is ready both to put his own view and to quote his opponents.

Adjectival concerns

SIR, — I suggest that we generalize the convention implicit in the naming of the Earth's year. We suffer from a surfeit of planetary adjectives — should one speak of the mercuric or mercurial year, the saturnian, saturnine or saturnalian? Can one, in a reputable journal, mention the venereal or uranal year? How much simpler to name the planetary years *ymer*, *yven*, *year*, *ymar*, *yjup*, *ysat*, *yura*, *ynep* and *yplu*! How fortunate that y is both vowel and consonant!

PETER RASTALL

Department of Physics
University of British Columbia
Vancouver, British Columbia
Canada V6T 1W5

Unsplit infinitives

Dr Glascock from Reading's an erudite man,
Full of wit and grammatical zeal;
In *Nature*[1] this May, he asked for a ban
On the customary scientists' spiel.

Speak active, not passive, Dr Glascock
  advised;
Attach participles where they belong.
Above all be sure that you are apprised
Of how syntax matters in song.

Alas (and alack), as they say in some places,
The verses we liked but we shortened the
  missive.
One way and another, the result was red faces;
Nature had split one of Glascock's infinitives!

Much worse was to come, to readers' chagrin.
Good Garton noticed the error[2]
And promptly blamed Glascock, not *Nature*,
  for sin.
What anger, what shock and what horror!

Nature now tenders both Garston and
  Glascock
Regrets for its error and shame;
What verbs should be split is for authors to
  say
It is we who shoulder the blame.

The moral's quite clear, as we know too well.
The jargon leaves much to desire.
But do not rely upon rhymed doggerel
And to Belloc do not aspire.

Editor, *Nature*

1. *Nature* 8 May p.66.
2. *Nature* 12 June p.434.

0028-0836/80/310438-01$01.00

NEWS AND VIEWS

Solar size variation

from David W. Hughes

Is the sun getting bigger, getting smaller or staying about the same size? Astronomers are divided as to the answer, some say it is shrinking, some say it remains constant.

John A. Eddy, of the High Altitude Observatory, Boulder, Colorado and Aram A. Boornazian, a mathematician with S. Ross and Co., Boston favour the shrinking Sun, and talk in terms of a contraction of about 0.1% per century. Their results were published in *The American Astronomical Society Bulletin* **11**, 437; 1979. A recent paper by Irwin Shapiro of the Massachusetts Institute of Technology contains results which disagree with those of Eddy and Boornazian. Shapiro concludes that the change is less than 0.03% per century.

Eddy and Boornazian used data obtained at the Royal Greenwich Observatory. At Greenwich the precise position of the centre of the Sun, with respect to the stars, was measured on every clear day at noon. The times at which the limbs of the Sun crossed a fixed meridian wire were recorded. Knowing the Earth's rotation rate and the Earth's orbit enables the time difference between the two crossings to be converted into a solar horizontal diameter. Values for this quantity are shown in Fig. 1.

The vertical solar diameter has also been measured since 1836 using a micrometer screw at the eyepiece. However inaccuracies in the mechanical screw and problems of atmospheric refraction make the vertical readings less accurate than the horizontal ones. The decrease in apparent Sun size as a function of time can be easily seen in the Greenwich data.

Sun transit measurements from the Naval Observatory, Washington, DC, were also analysed and the same decreasing trend was noticed. There was, though, a consistent difference between the two data sets, the Sun's horizontal diameter appearing to be 1 arc s larger from Washington, and the vertical diameter about 0.5 arc s smaller. (The Sun's diameter is about 1,917 arc s). This introduces one of the problems of the measuring technique. The results depend to an extent on the atmospheric transmission, a quantity that varies from place to place on the globe. The judgement of the time when the limb crosses a meridian wire is effected by irradiation, a physiological effect produced by the contrast between a bright object (the Sun in this case) and a dim one (the sky background). The Greenwich data shows for example a consistent difference between the apparent diameter of the Sun in winter and summer.

The Greenwich results indicate that the horizontal diameter is diminishing by 2.25 arc s per century and the vertical one by 0.75 arc s per century. The fact that the latter result suffers from atmospheric refraction makes the authors cautious about claiming that the Sun is changing its shape.

Now a constant shrinkage rate of 2.25 arc s per century for an object that is about 1,917 arc s in diameter means that the Sun shrinks to a point in 90,000 years time and was twice its present size 90,000 years ago. Both these are clearly ridiculous conclusions, the latter being completely unsupported by geological evidence, and Eddy and Boornazian are convinced that they are dealing with an oscillating Sun. The responsible agent could be thermal cycling in the convective zone or periodic variations in the convective efficiency, the period being hundreds of years, similar to the period between Maunder minima. The Kelvin-Helmholtz time scale of the convective envelope, the time it takes a photon to escape assuming that the photons movement is not assisted by convective motion, is also of the order of hundreds of years.

Before theoretical speculation gets out of hand let us consider the results of a more recent analysis that indicates that the Sun has been the same size for the last 250 years. The solar diameter can be easily obtained from an analysis of the observations of the transits of the planet Mercury in front of the Sun. These transits occur about 13 times per century, in May and November, when Earth and Mercury are nearly aligned, and have been carefully observed since 1677. The observations consist simply of the times of external and internal contact. Mercury has an apparent diameter of 10 arc seconds (1/200 that of the Sun) and takes about 5 hours to cross the Sun. The observed times of contact are affected by seeing conditions and the 'boiling' of the Sun's limb and are often uncertain by more than ten seconds.

Irwin I. Shapiro has published his analysis of the transit data in a recent edition of *Science* **208**, 51; 1980. His results are also shown in Fig. 1. The values obtained by the transit technique are free from any significant dependence on the variation in the rotation rate of the Earth and on our knowledge of the orbits of Earth and Mercury. The line through the

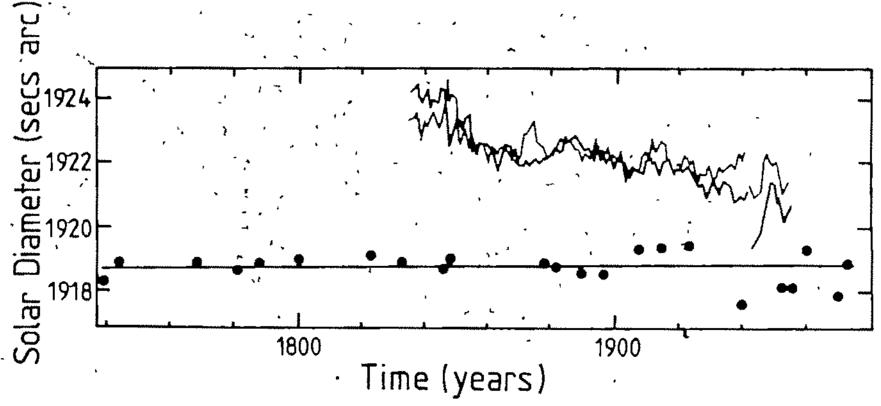

Fig. 1 The apparent diameters of the Sun as a function of time Upper graphs show the annual averages obtained by Eddy and Boornazian from the Royal Greenwich Observatory data (Thin line — vertical diameter, thick line — horizontal diameter). The dots represent the solar diameter as obtained from observations of the transit of Mercury by Shapiro

David W. Hughes is in the Department of Physics, University of Sheffield.

0028-0836/80/310439-02$01.00

data in Fig. 1 has a gradient of 0.05±0.10 arc s per century indicating that the Sun is possibly expanding but also that a conclusion that the Sun is of a constant size is entirely in keeping with the quoted uncertainties.

This result supports the findings of Sofia, O'Keefe, Lesh and Endal (*Science* **204**, 1306, 1979) who imply that changes in the solar constant (a measure of the energy output of the Sun) are directly related to the solar size. From the constancy of the solar constant Sofia *et al* conclude that the rate of change of solar diameter must be less than 0.6 arc s per century.

How do we explain Eddy's result? Firstly the difference shown in Fig. 1 between the solar diameter measured by Mercury transits and the diameter measured by meridianal transits is due to the irradiation effect caused by the solar disk — sky contrast. This can easily amount to the two s or so difference shown in Fig. 1. This irradiation is a function of atmospheric transparency and decreases as the transparency decreases. Greenwich being a suburb of London is obviously affected by the growth of London's population and the atmospheric effects of the increasing coal consumption between 1836 and 1950. Eddy and Boornazian find, however, that an unrealistic transmission decrease of at least 20% is required to explain their results. Irradiation effects also depend on the instrument, and the observing technique and the observer. The latter can be ruled out as over 100 different observers were responsible for the Greenwich data. In 1850 the instrument used was changed from the 5 inch transit to the 8 inch Airy transit circle. Also the means of recording the transit has varied. These changes complicate the interpretation.

So the mystery remains. Eddy and Boornazian are convinced that the sun is shrinking and claim that the fact that the 9 April 1567 solar eclipse was annular and not total indicates that the sun was bigger in the past. The situation is complicated by cyclic variations. Secchi and Rosa suggested in 1872 that the solar diameter varied with the 11 year sunspot cycle. Cimino (1945) and Giannuzzi (1955) found a 22 year period.

Looking to the future the SCLERA (Santa Catalina Laboratory for Experimental Relativity by Astrometry) f/100 photoelectric telescope could be used to measure the diameter to an accuracy of 0.01 arc s, a twenty-fold improvement in sensitivity, so the problem of size variation should be placed on a much sounder footing. The weather and sky transparency are better in Tucson, Arizona than in Greenwich or Washington and this should help too. □

Structure of bacteriophage Pf1

from R.A. Crowther

A NEW structural model for bacteriophage Pf1, differing in potentially important ways from that previously accepted, has just been proposed by Makowski, Caspar and Marvin (*J. molec. Biol.* **138**, 149; 1980).

Bacteriophage Pf1 is representative of a class of filamentous virus particles which infect gram-negative bacteria. The particles, which are about 1 μm long and 60 Å in diameter, contain a closed circular single-stranded DNA molecule of about 7,000 bases. The DNA is coated by many copies of a small protein of known sequence with a predominantly α-helical conformation. There is about 1 base of DNA per coat protein in Pf1, though the ratio is different in other phage, suggesting that interactions between DNA and coat may not be very specific. The ability to package single-stranded DNA molecules of arbitrary size makes filamentous phage, particularly M13, attractive as vectors for DNA cloning and sequencing.

An elongated structure built from a repeated unit would be expected to have helical symmetry and the X-ray diffraction patterns obtained from Pf1 confirm this. The detailed interpretation of the X-ray pattern has however been more controversial. Marvin and Wachtel (*Nature* **253**, 19; 1975) proposed a model for Pf1 assuming a helical repeat containing 22 coat protein molecules in 5 turns of a 15Å pitch helix. The model represented the coat subunit as a single α-helix coiled into a segment of a left handed concho-spiral. This interpretation was questioned by Makowski and Caspar (In *The single stranded DNA phages* eds. Denhardt, Dressler & Ray, p.627; 1978), who presented evidence favouring a subunit repeat of 27 units in 5 turns of a 15 Å pitch helix. The new model proposed jointly by the two groups is based on the latter assignment of helical symmetry, although the local structure is not much affected.

The X-ray diffraction pattern provides only part of the information needed to compute a map of the structure. Although the intensity of the various parts of the pattern is recorded the relative phase

Fig: The arrangement of α-helical segments in the virus particle. Two axial repeats of the inner layer of rod segments are shown in (a), two repeats of the outer layer in (c) and 2.5 repeats of both layers in (b). The α-helical segments in the virus protein subunit are represented as cylinders around the central core, occupied by DNA in the virus particle.

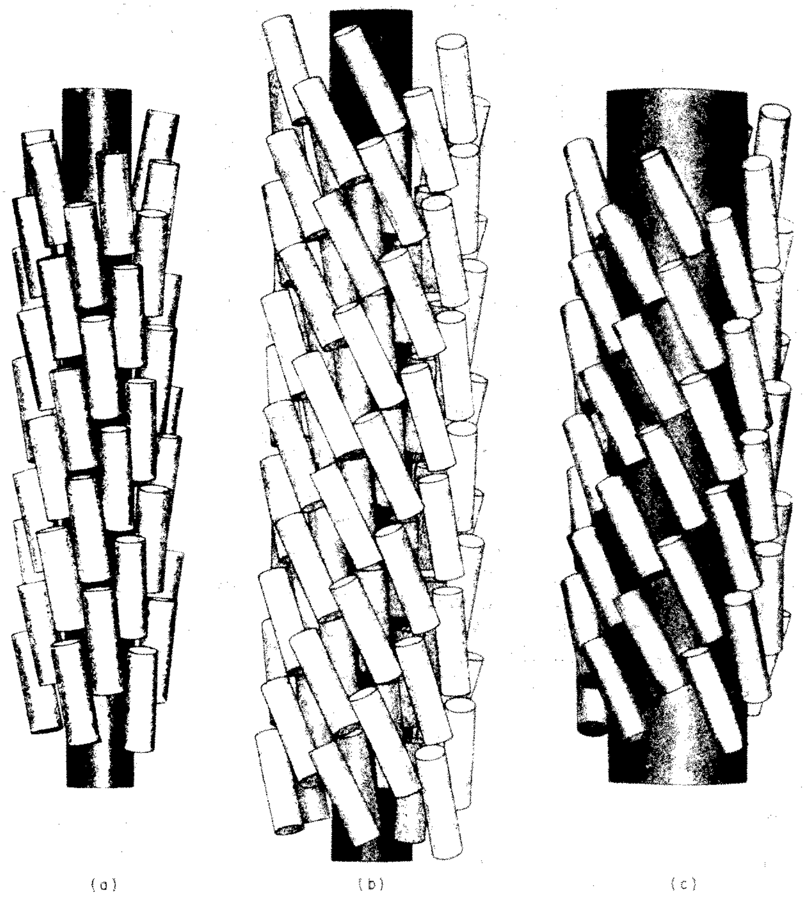

R.A. Crowther is in the MRC Laboratory of Molecular Biology, Cambridge.

0028-0836/80/310440-02$01.00

information is lost and must be regenerated by indirect means, such as introducing heavy atoms into the structure. This has not yet been possible for Pf1, so a more circuitous approach has been adopted by Makowski *et al.*, involving cycles of model building and iterative phase refinement. The stereochemical constraint of α-helical structure and the geometrical 'box' constraint of a particle of limited radius, within which all the scattering material must be confined, combine to produce what the authors claim is a unique structural solution consistent with the X-ray intensities to spacings of about 7 Å.

The picture that emerges of the coat protein (see figure) is of a segmented structure. One set of α-helical segments lies almost parallel to the particle axis at a radius of about 15 Å, while the other set of α-helical segments lies at about 25 Å radius and is tilted by about 25° to the particle axis. The resulting tightly packed and intricately interlocked structure conforms with accepted models for packing of α-helices and provides a stable 20 Å thick protein coat around the viral DNA. Unfortunately the model is not yet sufficiently detailed for the connectivity of the segments to be established. An inner segment might connect to an outer segment lying further along the virus giving an elongated though kinked subunit, reminiscent of the single α-helix of Marvin & Wachtel. More intriguingly the connectivity might be such that an inner segment joins to the outer segment overlying it at larger radius, giving a hair-pin fold to the molecule. The latter would produce a very compact coat protein, resembling the double α-helical hair-pin proposed as the primitive ancestor of the present day tobacco mosaic virus coat protein (McLachlan *et al. J. molec. Biol.* **136**, 203; 1980). More detailed studies are needed to choose between these possibilities but the outcome will clearly provide an important constraint on the molecular mechanisms proposed for viral morphogenesis. □

Plant opportunists

from Peter D. Moore

ADAPTABILITY is a valuable asset for an opportunist. The maxim applies as well to the struggling weed as to the business entrepreneur, as an increasing number of studies of the genetics and population biology of plant pest species is showing. Much of the interest in this area of botany stemmed from Bradshaw's work on variation within grasses such as *Argrostis tenuis* (see for example, *New Phytol.* **59**, 92; 1960) in response to intense selective pressures operating over limited spatial distances. In particular, it was the study of heavy metal pollution in areas disturbed by mining and dumping which led him and his students to an awareness of the genetical mosaic found in the plant cover as a response to such soil stresses (Jain & Bradshaw *Heredity* **21**, 407; 1966). In some cases it was possible to pinpoint the precise physiological adaptation involved in the provision of selective advantages, as in the case of Snaydon and Bradshaw's work (*New Phytol.* **60**, 219; 1961) on ecotypic variation in the grass *Festuca ovina* on alkaline and acid soils. Here, membrane selectivity (between sodium and potasium) was shown to be closely correlated with the environmental pH.

Complex variations and patterns in the micro-environment are frequently associated with human activity, as in the case of mine spoil, and consequently one might reasonably expect to find genetic diversification and intense local selection within those plant species which are especially dependent on man's activity, namely the weeds. This has indeed proved to be the case, for example, the work of Gadgil and Solbrig (*Am. Nat.* **106**, 14; 1972) on dandelions in North America, showed that these plants form a patchwork of genetically uniform populations, each of which has characters of growth, reproductive rate and seed size which could be regarded as adaptive responses to their varying local environment, such as degree of disturbance and frequency of mowing. (see *Nature* **252**, 191; 1974, **269**, 375; 1977).

But dandelions are somewhat peculiar in that they are apomictic and also can regenerate very effectively by vegetative means. Both of these characteristics lead to the conservation of a uniform genetic make-up within populations. Much interest has therefore been generated in the degree of variation and adaptation in other common weed species. An interesting series of papers concerning the genecology of a number of weeds has been published by Warwick and Briggs, who have been particularly interested in lawn plants. In the annual meadow grass, *Poa annua*, they found that some plants were prostrate and others erect, and that this growth habit was genetically determined (*New Phytol.* **81**, 711; 1978). The prostrate types were better able to withstand defoliation and were well adapted to lawn conditions, which is where they were generally located. The erect forms were associated with habitats in which catastrophes were common, such as disturbed soils, and devoted a greater proportion of their energy to reproduction. The erect types can therefore be regarded as r-selected with respect to the prostrate types.

A subsequent analysis of populations of the broad-leaved plantain, *Plantago major*, has demonstrated some similarities to and some differences from the meadow grass (*New Phytol.* **85**, 289; 1980). Populations were examined from regularly mowed lawns and from waste ground beside roads and canals. Again, there was a differentiation into populations with flattened, prostrate rosettes of leaves (found on lawns) and those with erect, tall shoots and leaves (found on roadsides). Naturally, when exposed to a régime of regular clipping at a height of 2 cm above ground level, the erect form suffered far more severe damage than the prostrate form. In this respect the plantains resembled the meadow grass. A consideration of Warwick and Briggs' data concerning the accumulation of vegetative and reproductive dry weight over the 14 weeks of the experiment, reveals some interesting contrasts to the meadow grass observations. Under control (unclipped) conditions, the reproductive structures (flower and fruiting spikes plus their scapes) of the lawn plantains account for between 62% and 65% of the total plant dry weight. The roadside populations, however, have a generally lower and more variable reproductive component, between 28% and 47% (based on population means). Thus, under control conditions, the prostrate form exhibits a greater degree of energy diversion to reproduction than the erect population, and this character is normally an indication of r-selection. Under clipped conditions, as one might reasonably predict, this difference is further exaggerated, for the shorter, less erect spikes of the lawn type are far more successful. After 14 weeks growth under a weekly mowing regime, the lawn population had a 52% to 54% investment in reproductive structures and the roadside plants were reduced to 13% to 17%.

Such clear indications of ecotypic variations have not, however, been found in all the lawn weeds examined by Warwick and Briggs. In the daisy, *Bellis perennis* (*New Phytol* **85**, 289; 1980), there was a great deal of variation within populations from grasslands of differing mowing and grazing histories. Transplantation into a regularly cut lawn did not necessarily diminish the reproductive vigour of some individuals from grazed habitats, but, in the case of the daisy, the importance of vegetative reproduction in the overall success of the plant is much greater than for either the plantain or the meadow grass. One cannot measure the full potential of a weed simply by its commitment to sexual reproduction. □

Peter D. Moore is in the Department of Plant Sciences, University of London King's College.

0028-0836/80/310441-01$01.00

New developments in iron-sulphur proteins

from R. Cammack

A NOVEL kind of iron-sulphur cluster has been found in a ferredoxin from the nitrogen-fixing bacterium *Azobacter vinelandii*. The cluster is unusual in that it contains a ring of three iron atoms linked by labile sulphide atoms. The iron-sulphur proteins are a class of proteins that contain clusters of iron atoms bound to cysteine and sulphide sulphur. They are an important group of biological electron transfer agents. For example, more than a dozen different types of iron-sulphur clusters have been detected in mitochondria where they are concerned with energy metabolism. Two years ago, the possibility that iron-sulphur clusters can have other functions was raised when F. J. Ruzicka and H. Beinert (*J. Biol. Chem* **253**, 2514; 1978) found that aconitase is an iron-sulphur protein. This enzyme of the Krebs tricarboxylic acid cycle of mitochondria has no known electron transfer function. It now seems likely that the iron-sulphur cluster in this enzyme is unusual in another respect, in that it may be a new type of three-iron cluster, similar to those recently proposed in certain bacterial proteins.

In the early 1970's it became established, by a combination of X-ray crystallography, spectroscopy and synthesis of chemical analogues, that all the iron-sulphur proteins contained either 1-iron, (Rd), 2-iron [2Fe-2S] or 4-iron [4Fe-4S] clusters (see figure). The 1-iron centres are found only in the rubredoxins of certain bacteria but the [2Fe-2S] and [4Fe-4S] clusters, in which iron is attached to sulphide sulphur and cysteine sulphur from the protein, has been found in many electron-transferring systems and enzymes. The iron-sulphur proteins are often described by the low-temperature electron-paramagnetic-resonance (EPR) spectra, since this is a good way of detecting them in biological systems. The [2Fe-2S] clusters and some of the [4Fe-4S] clusters give EPR signals in the reduced state at $g = 1.94$. Other [4Fe-4S] clusters give EPR signals around $g = 2.01$. However recent results suggest that a novel type of cluster may also give a $g = 2.01$ signal.

The centre of attention is a ferredoxin from *Azotobacter vinelandii*. This protein contains two iron-sulphur clusters with widely different redox potentials, +320mV and −424mV. Both give EPR signals at $g = 2.01$. The first cluster seems to be a conventional [4Fe-4S] type. The second one, however, seems to be different. Chemical analysis (which is, admittedly, notoriously difficult with these proteins) indicates that it contains fewer than four iron atoms. Preliminary X-ray crystallography of the ferredoxin at 4 Å resolution by C. D. Stout of the University of Pittsburgh showed that this cluster was smaller than the other and last year it was proposed (Stout *Nature* **279**, 83; 1979) that it might be a two-iron cluster. A clearer picture of the cluster has now emerged from an electron density map at 2.5 Å resolution (Stout, Ghosh, Pattabni & Robbins *J. Biol. Chem.* **255**; 19797; 1980).

A model (see figure) has now been fitted to the X-ray data and can be considered as a two-iron cluster which has opened at one side to introduce a third iron atom (numbered 3) and sulphide atom. Unlike all other iron atoms in iron-sulphur clusters, atom 3 does not have tetrahedral symmetry but appears to be almost square planar. Also, the ligands from the protein could not all be cysteine sulphurs as there are insufficient residues of this amino acid available.

The results of the X-ray analysis are still preliminary. Refinement of the full structure of the protein is not expected before the end of this year. However support for the existence of a three-iron cluster is provided by a totally different technique, ^{57}Fe Mössbauer spectroscopy. A paper from groups in Wisconsin and Minnesota (Emptage, Kent, Huynh, Rawlings, Orme-Johnson & Münck *J. Biol. Chem.* **255**, 17973; 1980) looks at the iron atoms in *A. vinelandii* ferredoxin. After subtracting the spectrum of the [4Fe-4S] cluster, the second cluster appears to contain two types of iron atom, in the ratio 2 : 1. As in other iron-sulphur clusters, the iron atoms are antiferromagnetically coupled together. The observation that the cluster gives the EPR signal at $g = 2.01$ in the oxidized form, but is non-magnetic in the reduced state, can readily be explained by a three-iron cluster. (This was a difficulty with the previously proposed two-iron cluster). The valence states of the iron atoms would correspond to $3Fe^{3+}$ in the oxidized state, and $2Fe^{3+}$ and Fe^{2+} in the reduced state, giving net charges for the cluster of +3 and +2, respectively.

If the existence of three-iron clusters is confirmed, there are already a number of proteins known that may also contain them. All of these given the EPR signal at $g = 2.01$. Mossbauer spectra of ferredoxin II from *Desulfovibrio gigas* indicate that it contains a [3Fe-3S] cluster on each polypeptide chain. Since the protein is a tetramer it appears to contain four such clusters (Interestingly ferredoxin I from the same organism contains [4Fe-4S] clusters in a trimeric unit of exactly the same polypeptide). Other, more complex proteins, may also contain the cluster. Emptage *et. al.* report that they have observed similar Mossbauer spectra from the enzyme glutamate synthase of *A. vinelandii* and from aconitase of beef heart mitochondria.

The presence of this iron-sulphur cluster in aconitase is intriguing. The cluster does not appear to participate in the enzyme reaction directly, but the enzyme is inactive unless the cluster is first reduced. It has therefore been suggested that the cluster somehow regulates the activity of the enzyme. If this idea becomes accepted, there are other examples known. Glutamine amidoribosyl transferase is an enzyme concerned with nucleic acid synthesis. The enzyme, both from human tissue and from *Bacillus subtilis* has been found to contain an iron-sulphur cluster (possibly of the [4Fe-4S] type). Again this has no obvious role in catalysis, but the enzyme is only active when the cluster is reduced.

It seems, as more types of iron-sulphur proteins continue to be discovered, that we have much to learn about the versatility of iron-sulphur clusters. □

R. Cammack is a Lecturer in the Department of Plant Sciences, University of London King's College

Atomic arrangements in the one-iron (rubredoxin, Rd) two-iron and four-iron clusters, and the proposed three-iron cluster.

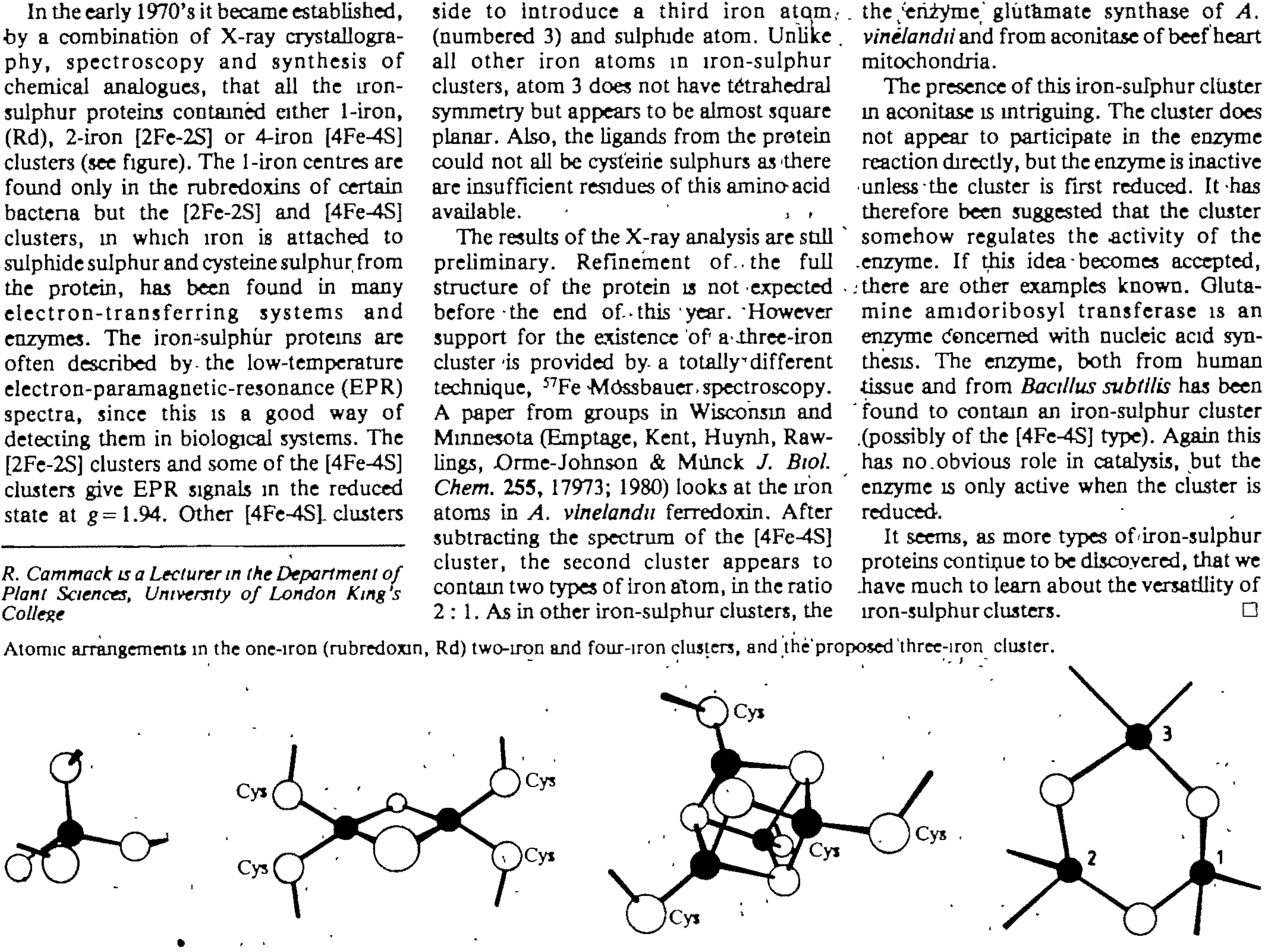

[Rd] [2Fe-2S] [4Fe-4S] [3Fe-3S]

0028-0836/80/310442-01$01.00

100 years ago

NEW SCHEME FOR DIRECTING BALLOONS

M. Gabriel Yon, one of the directors of the great Giffard captive balloon, and Mr. E.A. Pearse of Bristol, have each published a pamphlet on the direction of aërostats. The balloon of each inventor is to be elongated according to the principles of the experiments tried by Giffard in 1852 and by Dupuy de Lome in 1871. The propeller is to be moved by a gas-engine in the Pearse balloon, and by a steam-engine in the Yon balloon. M. Yon proposes to use the gas of the balloon as fuel, but only in proportion to loss of weight produced either by uncondensed steam or by consumption of petroleum.

Nothing can be said to be really impracticable in the Pearse scheme, although Mr. Pearse lacks the aëronautical training which distinguishes M. Yon, an aëronaut who ascended with M. Giffard in 1854, and has witnessed all his experiments. The only essential difference between M. Giffard's scheme and the new system is the place given to the fan, which M. Giffard attaches to the car. Practice will only decide whether the alteration projected is an improvement or otherwise. The reason alleged for the change is the bringing of the fan nearer to the centre of resistance. But it obliges the aëronaut to give to his fans a very small diameter, which requires an immense number of rotations in a second, and consequently represents a loss of power.

The calculations appear to have been made with care by M. Yon and Mr. Pearse. A trial would be greatly desirable, although it is impossible to suppose that the aërial carriage of Mr. Pearse or the directing balloon of M. Yon can possibly bring aëronauts to the North Pole for their inaugural trip, they may be instrumental in eliciting useful facts. We may add to the peculiarities of M. Yon's scheme that he uses a small globe inclosed in the lower part of the aërostat called a compensation sphere, and connected by a pipe with a ventilator, for keeping intact the form of his aërial machine. Mr. Pearse does not appear to be convinced of the urgent necessity of abstaining in any aërial construction from every complication which can be avoided at any cost, and he suggests the adoption of some accessory organs which, although designed to help aëronauts, would tax too much the lifting power or the attention of the aërial sailor. Mr. Pearse supposes that he will be able to navigate the air with an excess of weight, and does not pay attention to the intensity of motive power required to counteract gravitation even in a partial manner. He should certainly take advantage of the pamphlet written by his French competitor, who deals mostly with facts belonging to the public, and on which nobody can, in the present state of science, raise any claim as being his own property.

Both these pamphlets are greatly in advance of similar productions, and are creditable to their writers. Mr. Pearse's pamphlet has been only published for private publication. M. Yon's is printed with a number of plates representing many details; but a directing balloon is so complex a matter that this part of the publication can hardly be said to be complete.

Having been the builder of M. Depuy de Lome's balloon and one of his crew, M. Yon may be said to have witnessed all the great aeronautical constructions of the age. Next to M. Henry Giffard, of whom he claims to be the pupil, he is the most completely qualified aëronaut to work out the solution of the great problem to which a recent success in photography has given unexpectedly in some respects a practical result.

From *Nature* **22**, 29 July, 303, 1880.

The mechanism of two-nucleon transfer reactions

from P.E. Hodgson

SOME recent calculations made by Da Hsuan Feng *et al.* (*Phys. Rev. Lett.* **44**, 1037; 1980) greatly clarify the interpretation of two-nucleon transfer reactions. These reactions, particularly the (*p*,*t*) and the inverse (*t*,*p*) reactions, are extensively used to study nuclear structure but the interpretation of the experimental results has been hindered by lack of knowledge of the reaction mechanism. The distorted wave calculations of the reaction cross-sections tend to give the shapes of the angular distributions rather well, but the absolute magnitudes are very often much smaller than the experimental values. The situation compares unfavourably with that for the corresponding one-nucleon transfer reactions, which can usually be accounted for both in angular distribution and in absolute magnitude using the distorted wave theory.

Attempts to improve the calculations of the cross-section of the two-nucleon transfer reactions fall into two categories, those that concentrate on the nuclear reaction and those that concentrate on the nuclear structure. It has been found that the inclusion of additional reaction mechanisms — for example a two-stage process through an intermediate nucleus — gives additional contributions to the cross-section that brings it into closer accord with the experimental values. Another line of research is to include more detailed wavefunctions for the initial and final nuclear states, and these also tend to increase the calculated cross-section. There still remains, however, much uncertainty about the reaction mechanisms that have to be included, and the importance of higher-order nuclear configurations.

Da Hsuan Feng *et al.* use realistic triton and nuclear wave functions and succeed in fitting the experimental cross-sections both in magnitude and in angular distribution. The reaction was assumed to take place by the direct pickup of the two nucleons from the target nucleus by the incident proton to give the outgoing triton. The wavefunction of the proton and the triton are generated by the appropriate optical potentials, and the reaction matrix element is evaluated without making the assumption that the interaction potential has zero range, an assumption that is known to give good results for one-nucleon transfer reactions but not for two-nucleon transfer reactions.

The improved form of the triton wave function is an important feature of the new calculations. Most of the previous calculations included only the predominant spatially symmetric *S* state. But now the mixed-symmetry *S*′ and *D* states are included as well. This alters the selection rules and allows transitions to unnatural parity states to take place by a one-step process. The overlap integral between the wavefunctions of the initial and final nuclei satisfies a Schroedinger equation for two interacting particles in an external potential, and this was solved by an extended-basis shell model method. Overall, these new calculations are the first that use realistic transfer potentials, triton wavefunction and nuclear overlap functions and are thus the first detailed test of the validity of the distorted wave method as applied to two-nucleon transfer reactions.

To evaluate the success of this formulation, it was applied to the ^{18}O(p,t)^{16}O reaction at 20 MeV., the ^{48}Ca(t,p)^{50}Ca reaction at 12.08 MeV. and the ^{90}Zr(t,p)^{92}Zr reaction at 11.89 and 20 MeV., and the results for the first two of these reactions are compared with the experimental data in the figure. In both cases, and also for the third reaction, the

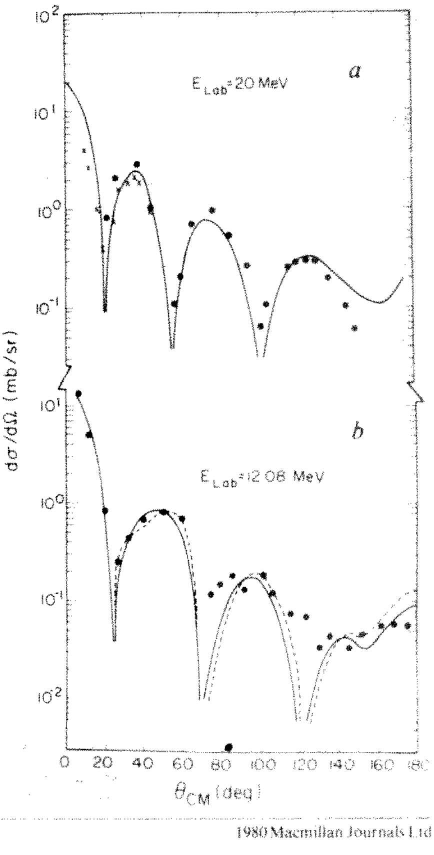

Figure: (a) Differential cross-section for the ^{18}O(p,t)^{16}O reaction compared with distorted wave calculations. (b) A similar comparison for the ^{48}Ca(t,p)^{50}Ca reaction. The dashed curve shows the result of using a different way of calculating the wavefunctions of the transferred nucleons.

P.E. Hodgson is in the Department of Nuclear Physics, University of Oxford.

0028-0836/80/310443-02$01.00

agreement is good both for the absolute magnitude of the cross-section and also for its angular variation. Since the optical potentials are obtained from the analysis of elastic scattering cross-sections, and the parameters of the nuclear structure part of the calculation are fixed in advance, there are no adjustable parameters in the calculations. The excellent fit to the data for different reactions at two energies for different nuclei shows that the essential features of the reaction have been included in the calculation. In particular, the results provide no evidence in favour of the suggestion that two-stage processes contribute appreciably to the cross-section.

Further work remains to be done to test these calculations against a wider range of data, and also to improve the method still further. In particular, the validity of the distorted wave method needs to be examined in more detail, and account needs to be taken of the possibility of exchanges between the ingoing proton and the target nucleus. However even in its present form the calculation is a significant advance on previous work, and should provide a powerful tool for nuclear structure studies.

Evolution and gaps in the fossil record

from Mark Ridley

CHARLES Darwin's theory of evolution differed from most of its alternatives in postulating that new parts evolved in many tiny stages from previously existing parts. Unfortunately, the intermediate stages hardly ever seemed to exist in the fossil record (Huxley's later trumpeting about *Archaeopteryx* notwithstanding). Darwin himself followed Lyell in blaming the fossil record — it was incomplete, unhistorical and misleading, so it did not count against this theory. If taken to an extreme the two ideas (that the fossil record is incomplete and that evolution proceeds at a fairly constant rate) can form an irrefutable system in which gradual temporal change in fossils is interpreted literally, but sudden jumps between species are attributed to gaps in the record. All the evidence is then consistent with a constant tempo of evolution.

A few years ago Eldredge (*Evolution* **25**, 156; 1971) and then Eldredge and Gould (*Models in Paleobiology* ed. J. W. Schopf; Freeman, San Francisco, 1972; *Paleobiology* **3**, 115; 1977), following on suggestions by Mayr, Simpson and others, argued that the gaps in the fossil record might be more real than apparent. They put forward a version of the theory of allopatric speciation that would automatically generate gaps in the fossil record. According to their theory: (1) the intermediates between species existed in small populations, and small populations are less likely to leave a record than large ones (2) evolution is rapid in the small isolated population, and (3) the intermediates did not exist in the same place as (and so are unlikely to be preserved with) their ancestor. Evolution, therefore, is not gradual and of constant tempo. There are short periods of rapid change at speciation, separated by longer periods in which there is no change. Eldredge and Gould christened this the 'punctuated equilibrium' model of evolution, and its alternative 'phyletic gradualism'.

Eldredge and Gould's forceful essay has inspired two controversies. One is over whether the fossil record does, in fact, show one pattern or the other, and the second concerns the validity of Eldredge and Gould's explanation of punctuated equilibria. Even if it is established that evolution is punctuated, Eldredge and Gould's theory of speciation is only one of a variety of possible explanations.

Biometrical studies, in which the range of variation is described for each interval within a continuous sedimentary unit, are essential for a test between phyletic gradualism and punctuated equilibria. Incompleteness of the record and typological taxonomy (in which each specimen is named by its similarity to a type specimen) will otherwise be confounding factors. A study of geographical variation is also desirable. If the samples contain specimens from the ancestral species pooled with increasing (as time passes) numbers from the allopatrically derived species, then gradual evolution can appear as an artefact even if the actual evolution was punctuated. Such pooling is less likely to occur if geographic variation is studied separately.

Gingerich has published several biometrical studies of mammal evolution, though his studies lack information about geographical variation (*Am. J. Sci.* **276**, 1; 1976; *Pap. Paleont. Mus, Paleont. Univ. Mich.* **15**, 1; 1976; *J. Paleont.* **53**, 153; 1979; Gingerich & Symons *Contr. Mus. Paleont. Univ. Mich.* **24**, 245; 1977). His most abundant data are for the condylarth *Hyopsodus* in the early Eocene (*Am. J. Sci.* **276**, 1; 1976), which looks as if it evoved gradually. Gould and Eldredge (*Paleobiology* **3**, 115; 1977) said that the rate of evolution in *Hyopsodus* was too slow to be important. However, the rate of change within a *Hyopsodus* species is similar to that at speciation. This is manifest phyletic gradualism even if only on small scale. More recently, West (*Paleobiology* **5**, 252; 1979) followed the descendants of Gingerich's *Hyopsodus* through a middle Eocene formation of at least one million years, and found no evidence of evolutionary change. So even if *Hyopsodus* did evolve gradually in Gingerich's study site, they showed prolonged stasis soon afterwards. Gingerich's other papers document phyletic gradualism in other condylarths and in primates, and there is now a steady trickle of papers (see recent issues of *Paleobiology*) variously substantiating either gradual or punctuated change.

Eldredge and Gould's microevolutionary theory has also been criticized. The first problem is whether speciation occurs in small populations. Anderson and Evensen (*Syst. Zool.* **27**, 421; 1978) have compared the sizes of the geographic ranges of recently diverged pairs of species of North American terrestrial vertebrates and found that "more than half of the recently divergent species pairs have the range of the smaller species greater than 30 percent of that of the larger species". Although uncertainty exists about just how recently the pairs of species diverged and about the relation between range and population sizes, Anderson and Evensen's data does not support Eldredge and Gould's claim that speciating populations are very small. It can also be asked whether evolution is rapid in small populations. Smaller populations have lower total rates of mutation which can cause lower rates of evolution (e.g. Maynard Smith *Am. Nat.* **110**, 331; 1976).

The second problem is to reconcile punctuated evolution with natural selection and genetics. The rate of evolution might either be controlled by the extent of genetical variation, or by the intensity of selection. On the latter possibility, the pattern of evolution is directly controlled by rates of change of the environment. The *Gryphaea* studied by Hallam (*Paleobiology* **4**, 16; 1978), for example, speciate rapidly when their ranges are fragmented by a fall in sea level. When the sea rises *Gryphaea* gradually evolve increased size. The other hypothesis is that rapid evolution results from rare, large mutations; chromosomal changes are possible examples. Chromosomal differences between species are well-known in a variety of taxa, and several authors have broached chromosomal mechanisms for rapid speciation in small populations (reviewed by M.J.D. White *Modes of Speciation* W.H. Freeman, San Francisco; 1978), which would cause a 'punctuated' pattern of evolution. One suggested mechanism is a change in a chromosome (such as a translocation or an inversion) within one local population. Heterozygotes for the mutation would probably be selected against, so that if members of this population interbred with the ancestral species there would be intense selection for reproductive isolation. However, even given a correlation between chromosome

---

Mark Ridley is in the Animal Behaviour Research Group, Oxford University.

0028-0836/80/310444-02$01.00

differences and speciation, it is not obvious which is cause and which effect, and nor can we be sure that chromosomal speciation would necessarily produce punctuated evolution. In his latest essay on the subject, Gould (*Paleobiology* **6**, 119; 1980) argues that large mutations are the main cause of punctuated evolution.

A third and interesting possibility is that gradual environmental change could cause punctuated evolution. In their original paper, Eldredge and Gould mooted that a species' gene pool is so intricately co-adapted that change is only possible by a thorough revolution. By co-adapted it is meant that a change in one part of the system will not be favoured without simultaneous changes in other parts. Thus when evolution occurs it will be by a sudden leap, with changes in many parts; natural selection does not favour piecemeal tinkering.

Ironically, an objection to any model in which punctuated evolution occurs with gradual environmental change comes from the very facts that led to the formation of the theory to begin with: geographical variation. Stepped clines (discontinuous variation in space) are known that do not coincide with obvious environmental discontinuities, such as the enigmatic spotting pattern of the butterfly *Maniola jurtina*, and these have been interpreted as quantum jumps between different co-adapted genetic systems (E.B. Ford *Ecological Genetics* Chapman & Hall, London; 4th edn, 1975, J.A. Endler *Geographic variation, speciation, and clines* Princeton University Press, 1977). However, continuous variation in space is commonly observed in many species and is difficult to reconcile with the theory that says that natural selection causes abrupt changes between different co-adapted states. Earlier this century gradual geographical variation was important in confuting the de Vriesian 'mutationist' theories of evolution. Gradual geographic variation probably evolves much too rapidly to be represented in the fossil record as gradual evolution, so the existence of gradual geographic variation is perfectly compatible with punctuated evolution over geological time. Gradual geographic variation, however, does not fit in well with the 'co-adaptation' theory of how natural selection brings this punctuated evolution about. □

Earthquake prediction

from David W. Simpson

In the early 1970s, principally because of observations of premonitory changes in velocity ratio and groundwater geochemistry in the USSR and crustal deformation studies in Japan, there was considerable optimism that earthquake prediction would soon become a reality. The intervening years have seen a greatly expanded program in earthquake prediction in the United States, but negative and conflicting results have dampened some of the initial enthusiasm, if not led to outright pessimism on the part of many US seismologists regarding the practical reality and imminence of reliable methods for predicting earthquakes. At a recent meeting* on a wide variety of topics related to earthquake prediction much of the original enthusiasm appeared to be re-emerging as it became clear that at least some earthquakes can be, and in fact have been, successfully predicted. It was also clear, however, that no universal panacea can be expected. Premonitory effects appear to vary widely with tectonic environment and earthquake magnitude. The premonitory signatures of large earthquakes in thrust regions of Soviet Central Asia, China and Japan appear to be clearer and to extend over a wider area than any such effects observed so far in strike-slip environments such as the San Andreas Fault of California.

On a time scale of tens of years, gaps in the occurrence of large earthquakes along major plate boundaries have proved to be one of the most successful methods for predicting the sites of future great shocks. Nishenko, McCann and Sykes (Lamont-Doherty Geological Observatory, Columbia) presented a map of the current 'seismic potential' of the circum-Pacific belt, in which they refined the idea of seismic 'gaps' by ascribing a high seismic potential to a gap only if historical or tectonic data indicate that it is a region capable of producing a large shock. Sykes *et al.* (Lamont-Doherty) used historical reports to extend the record of great earthquakes in the Alaska-Aleutian arc back to 1784 and showed repeat times of 50 to 100 years for great earthquakes in some regions. Large segments of this part of the plate boundary seem to rupture in temporally clustered sequences of large earthquakes (e.g., 1898-1907 and 1938-1965), separated by long periods of relative quiescence. Variations in seismicity in western Japan, and especially a south to north migration in the area to the west of the 1946 Nankaido earthquake were reported by Mogi (Tokyo University). He also showed how a recent model by Shimazaki and Nakata, in which rupture occurs at a constant ultimate stress (as opposed to a model of constant stress drop during an earthquake), can be used to explain the observation that the time interval between large earthquakes in western Japan is proportional to the stress drop in the preceding large earthquake. Takagi (Tōhoku University, Japan), in a detailed study of activity before and after the 1978 magnitude 7.4 Miyagi-oki earthquake, showed a migration of foreshocks towards the boundary between the oceanic slab and overriding plate, with aftershocks clustering along the boundary. Seismicity patterns in the Mexico-Central America segment of the circum-Pacific belt were described by McNally (California Institute of Technology), Ohtake *et al.* (National Research Center for Disaster Prevention, Japan) and Singh *et al.* (Instituto Geofisica, Mexico), who reviewed data which led to the successful prediction of the 1978 Oaxaca earthquake and showed repeat times of 30-40 years for this region. For at least 50 years following the 1906 San Francisco earthquake the level of seismicity in northern California was considerably lower than it had been in the preceding 50 years. Ellsworth *et al.* (US Geological Survey) suggested that a pair of magnitude 5.5 earthquakes in the San Francisco area in August 1979 and January 1980 show the activity to be returning to a more normal level. Pairs of earthquakes with similar temporal clustering have occurred a number of times in the area since 1836.

In continental areas, where the repeat times for large earthquakes are longer than for oceanic subduction zones and are usually beyond the range of instrumental or historical catalogues, geological data are being used to extend the record of occurrence of major earthquakes. Sieh (California Institute of Technology), Wallace (US Geological Survey) and Schwartz *et al.* (Woodward-Clyde consultants, San Francisco) showed how detailed mapping of displacement on major fault zones in the western US can be used to date past earthquakes to determine recurrence intervals and maximum magnitudes of prehistoric events. They showed a general increase in the recurrence interval from west to east: from tens to hundreds of years for large earthquakes along the San Andreas system to hundreds to thousands of years in Nevada and Utah.

Whereas most methods for long-term prediction are based on regularities and changes in the seismic cycle itself as revealed

---

David W. Simpson is in the Lamont-Doherty Geological Observatory of Columbia University, New York.

* The Third Maurice Ewing Symposium was held at Mohonk Mountain House, New Paltz, New York. Eighty-eight scientists from eleven countries attended under the sponsorship of the Lamont-Doherty Geological Observatory of Columbia University, with Lynn R. Sykes as Chairman of the Organizing Committee. Support was provided by the G. Unger Vetlesen Foundation, the National Science Foundation and the U.S. Geological Survey. The Proceedings will be published in 1981 by the American Geophysical Union.

0028-0836/80/310445-02$01.00

Insect diapause — stability and change

from A.D. Lees

GEOGRAPHICAL strains of insects often differ substantially in their diapause characteristics. The critical photoperiod required for diapause induction, the interactions between day length and temperature and the intensity (duration) of dormancy are particularly variable. When the area of distribution extends continuously over a wide range of latitudes these characters form a north-south cline with critical photoperiod and intensity diminishing towards lower latitudes and diapause sometimes fading out entirely in the sub-tropics. Following the classical work of Danilevsky (*Ent. Obozr.* **36**, 6; 1957), this has been accepted as evidence that geographical strains are closely adapted in their phenology (date of entry into diapause, voltinism etc.) to their own part of the geographical range of the species. Since photoperiod and temperature, as the main agents controlling diapause, vary systematically with latitude, the insect would receive a false indication of season in other parts of the range. This is expected to limit spread along a north-south axis and might have severe initial effects on introduced species, although some later readjustment by natural selection might well be looked for. In this connection, crosses between different strains have shown that quantitative differences in diapause-related characters such as critical photoperiod and diapause intensity depend on polygenic inheritance. Nevertheless, as emphasised by Tauber and Tauber (*Evolution of Insect Migration and Diapause* p.53-71, Springer-Verlag, 1978), these features can sometimes be modified quite rapidly by directional selection in the laboratory.

Introduced pests that fail to gain a foothold usually escape notice. For this reason the diapause status of the more successful invaders is especially worthy of scrutiny. In this issue of *Nature* (p.489) Goldson and Emberson show that the Argentine grass stem weevil *Hyperodes bonariensis*, introduced into New Zealand more than 50 years ago, has a remarkably stable photoperiodically controlled adult diapause, populations collected in areas extending over 8° of latitude having much the same critical photoperiod. It seems that the beetle might have achieved multivoltinism (and even greater destructiveness?) if diapause had been eliminated by selection. The absence of diapause in most indigenous New Zealand insects suggests that this condition is not required for winter survival.

In contrast, the photoperiodically controlled winter diapause of the Colorado potato beetle is well suited to its new environment in continental Europe. Introduced into France in 1922, *Leptinotarsa* has since spread eastwards as far as the USSR, occupying only slightly wider latitudinal limits than in N. America. It seems likely that the dispause control mechanisms and the voltinism have again remained relatively stable (de Wilde, *Soc. exp. Biol. Symp.* **23**, 263; 1969). The pink bollworm *Pectinophora gossypiella*, originating in India, is a pest which has been transported by commerce to virtually every cotton growing area in the world, mainly during the present century. The geographical strains tested by Ankersmit and Adkisson (*J. Insect Physiol.* **13**, 553; 1967) were found to have very similar critical photoperiods for diapause induction even though the populations came from widely separated latitudes (for example, El Paso 32°N and Colombia 3°N). However, many fewer insects from lower latitudes entered diapause at all, even in short days. In this species adaptive changes are already far advanced. In the cornborer *Pyrausta nubilalis* the evidence suggests that changes in the diapause status are progressing rapidly. Introduced into N. America from Europe before 1920, there has been a strong tendency for the univoltinism of populations in the north to give way to a bi- or multivoltine life cycle in the warmer states of Kansas and Missouri. According to the analysis of Beck and Apple (*J. econ. Ent.* **54**, 550; 1961), these changes involve both photoperiod and temperature control of the inductive daylength as well as more indirect effects of temperature on the rate of larval development. From these few examples it is clear that the adaptive changes shown by different insects are liable to be varied and complex. ☐

A.D. Lees is Professor of Insect Physiology, Imperial College, London.

---

by seismicity data, many intermediate- and short-term predictions rely strongly on indirect indicators of the earthquake preparation process. Aki (Massachusetts Institute of Technology) presented a method by which information from various independent precursors can be combined to improve estimates of the probability of the occurrence of a large earthquake. Thatcher (US Geological Survey) showed how geodetic measurements have been useful, especially in Japan and California, in identifying areas of increased stress as the possible sites for future earthquakes. The importance of inhomogeneities in the stress distribution on fault zones and the role of asperities in controlling the release of stress were discussed by Kanamori and Lay (California Institute of Technology) and Wyss (Institute für Geophysik, Zurich). A model of time dependent failure due to stress corrosion, in which the growth of cracks is controlled by a 'stress intensity factor' and the presence of asperities, was presented by Scholz *et al.* (Lamont-Doherty).

In short-term predictions, water-related effects are especially common. A number of papers described the observation of changes in radon content in groundwater and deep wells. Fu (State Seismological Bureau, Peking) and Wakita (Tokyo University) reported a variety of short-term precursors preceding recent earthquakes greater than magnitude 7 in China and Japan, many of which may be closely related to groundwater (e.g., water level, geochemical and temperature changes in wells, resistivity variations). Sobolev (Institute of Physics of the Earth, Moscow), in a summary of studies in Soviet Central Asia, showed premonitory changes of water levels in wells as far as 650 km from earthquakes of magnitude 7.

Reviews were presented of the national programs in earthquake prediction in the US, USSR, China and Japan. As described by Mogi (Tokyo University) and Rikitake (Tokyo Institute of Technology) the Japanese program, which began in 1965, involves a closely integrated organization of universities and government agencies monitoring a wide spectrum of geophysical, geological, geodetic and geochemical parameters, with special emphasis on the Izu Peninsula and Tokai district. In addition to the high level of data gathering and research, the Japanese have also made significant advances in raising public awareness of earthquake hazards and in preparing the public for earthquake emergencies. Participants at the meeting were vividly reminded of the sociological and economic importance of earthquake prediction by a series of Japanese films on the disastrous effects of major earthquakes and a Chinese video-tape showing the destruction caused by the 1976 Tangshan earthquake.

Large earthquakes occur in cycles which are long compared to the instrumental records available of seismicity and related geophysical parameters. The seismic cycle appears even longer when viewed in terms of the relatively short time during which data have been gathered specifically for earthquake prediction purposes. Even within the limitations of existing data, however, the meeting clearly showed that consistent patterns are emerging. As data gathering and interpretation improve, the challenges of the next few years will be to identify the techniques which are the most reliable; to test the significance of predictions based on those methods; and to integrate various techniques into an increasingly reliable procedure for earthquake prediction. ☐

0028-0836/80/310446-02$01.00

Nature Vol. 286 31 July 1980

REVIEW ARTICLE

Biomolecular structure determination by mass spectrometry

Howard R. Morris

Department of Biochemistry, Imperial College of Science and Technology, London SW7 2AZ, UK

Mass spectrometry, conventionally used with smallish molecules (less than 1,000 daltons), has surprisingly emerged as a powerful technique for the determination of the amino acid sequences of proteins and the structure of glycopeptides as well as for the characterization of biologically active materials of unusual structure such as the peptidolipids. Further applications to biomedical problems are foreseen.

THE past decade has seen a considerable advancement both in the technical capabilities of mass spectrometry and in its application to problems in biochemistry and medicine. Perhaps most surprising, given that most conventional mass spectrometers perform optimally on volatile samples of mass less than 1,000 daltons, has been the successful extension of mass spectrometry to the elucidation of the structures of complex and polar substances such as proteins and carbohydrates. The great power of modern mass spectrometry stems from several fundamental principles peculiar to the technique, not all of which have yet been properly or completely exploited. These are all illustrated in the text that follows but a summary of the concepts will be useful at this stage: (1) sensitivity: mass spectrometry is the most sensitive of all general methods of structure elucidation or quantitation, being routinely applicable to sample sizes of microgrammes or less. In favourable cases picogramme sensitivity has been achieved[1], and progress in the physics of ion generation, mass analysis and detection may eventually lead to the ultimate in sensitivity-generation, analysis and detection of a single ion (detection is already a reality). (2) Specificity: because the method provides an exact physicochemical measurement (mass with an accuracy of five decimal places for example), its specificity is unequalled by other widely used 'structure probes' such as radioimmunoassay. (3) Sample purity: mass spectrometry has a unique advantage over classical chemical methods or true spectroscopic methods of structure elucidation in that it does not require a pure sample of the compound whose structure is to be determined. It is the intention of this review to illustrate the power and potential of mass spectrometry by examples of its recent role in the determination of protein, peptide, glycopeptide and peptidolipid structure.

Protein sequence analysis

The demand for protein sequence analysis is greater than ever despite recombinant DNA technology, not least because the positive identification of initiator, termination and intron coding sequences demands comparison with amino acid sequence data. The underlying trend in protein sequence analysis is towards the rapid generation of sequence data, not necessarily complete, but sufficient, for example, to combine with crystallographic data to

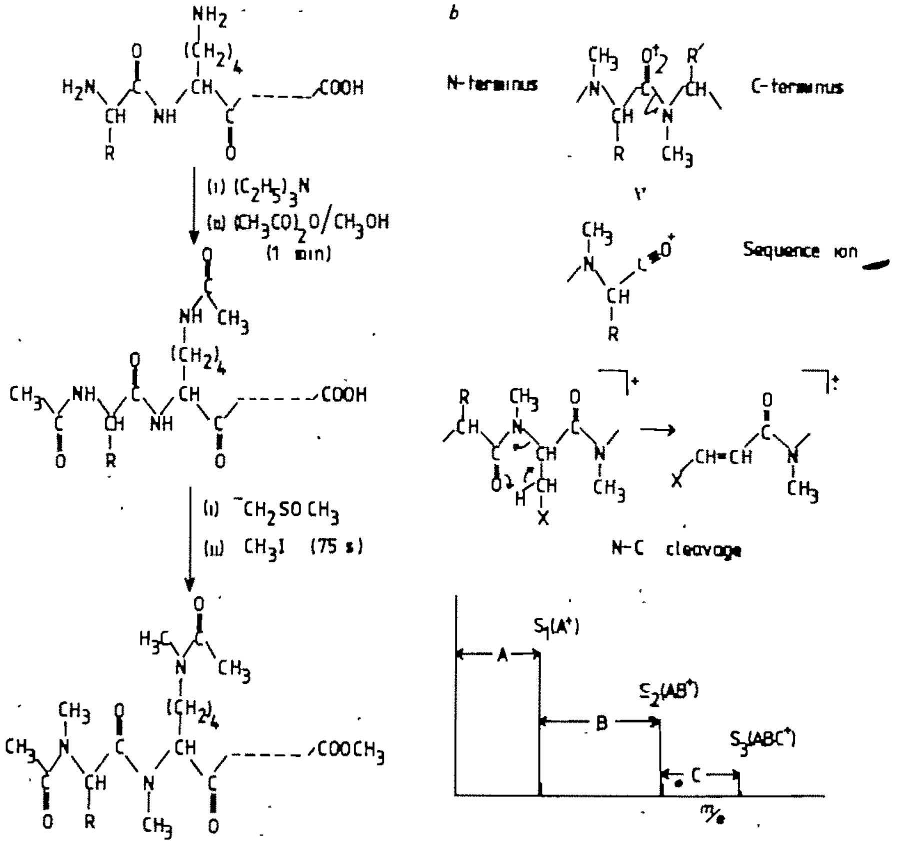

Fig. 1 *a*, General derivative-forming reactions applicable to 1–50 nmol of protein-derived peptides[10,11]. To be applicable to all common amino acids, the permethylation step must be restricted with respect to alkylation reaction time to prevent 'salt' formation[10]. Arginine-containing peptides require an additional mild hydrazinolysis step before acetylation. This reaction is carried out only on those peptides showing a positive stain test for arginine on the electrophoretogram[11] (see 'Strategy'). *b*, The formation of 'sequence ions' and N–C cleavage fragment ions from which the interpretation of the spectrum is made. N–C cleavage is only observed where 'X' corresponds to Phe, Tyr, His, Trp, Asn or Asp[13]. The schematic representation of a mass spectrum shows how the sequence is built up simply by counting mass differences (corresponding to the amino acids A, B and C) between sequence ions S_1, S_2 and S_3 (ref. 14).

0028-0836/80/310447—06$01.00

determine tertiary structure, to locate the protein coding in a DNA sequence, or to answer questions on the evolutionary divergence of enzymes. Partial sequence data, following chemical modification of the protein, can also be sufficient to reveal catalytic or binding sites.

It is now 20 years since studies on small synthetic peptides first indicated the possibility of sequence analysis by mass spectrometry[2,3], and 10 years since the mass spectrometric analysis of protein-derived peptides and peptide mixtures was first demonstrated[4]. Since then, considerable progress has been made, resulting in combined classical–mass spectrometric attack on total protein sequences, for example on ribitol dehydrogenase[5] and chloramphenicol transacetylase[6,7]. Only recently, however, was the first total protein sequence assignment made by mass spectrometry, independent of classical methodology, in work on dihydrofolate reductase[8,9]. Why has it been so difficult and taken so long to reach this stage? The short answer is that, as already mentioned, the mass spectrometer is not an obvious method of choice for the study of high molecular mass, complex polar molecules. The successful reconciliation of these apparently irreconcilable differences, to produce a methodology that has clear advantages over classical ones (whether manual or automated) has hinged upon the following developments in the areas of derivatization, fragmentation and strategy.

Derivatization and fragmentation

Several types of derivatives are currently in use, the choice depending very much upon the subsequent strategy, for example whether gas chromatography or direct probe insertion is to be used. In most of the protein studies reported to date, samples have been introduced directly via the probe, for which technique the *N*-acetyl, *N,O,S*-permethyl derivative[10] is preferred. Figure 1*a* summarises the method for obtaining volatile methylated derivatives.

The one feature of the early work that suggested that mass spectrometry might be useful for peptide sequencing was the observation of fragmentation at the peptide bond[2,3]. This 'sequence ion' formation, first observed for acyl peptide esters, is an even more pronounced fragmentation pathway when the amide bond is methylated, as in the permethylation reaction. Recognition of this important fragmentation pathway is not, however, sufficient for the successful interpretation of the mass spectrum; often the true molecular ion is not present, and other fragmentation pathways including radical or neutral losses from the molecular ion or other fragment ions[12] (Fig. 1*b*) must be recognized. The exact nuances of interpretation are too detailed for discussion here, but suffice it to say that current ideas on peptide sequence assignment go well beyond simple recognition of 'sequence ions', often to an understanding and recognition of every signal in the spectrum. This degree of sophistication has been generated by the study of hundreds of peptides in protein sequence analyses so that valuable sequence information can now be obtained from spectra, the interpretation of which might well have been abandoned 10 years ago because of 'ambiguous' assignments.

Strategy

Strategy is crucial to the ultimate success of mass spectrometric determination of biological structures. For example, should one use 'classical' enzymes, like trypsin, for an initial digestion of the protein followed by purification of all the peptides and redigestion of the larger ones? What purification methods will be compatible with mass spectrometry? Is it better to purify the peptides or their derivatives? And what derivatives should be made? Is it best to use high resolution, low resolution, electron impact or chemical ionization? Some of these questions are interrelated; for example, the initial choice of a dipeptidyl aminopeptidase (cathepsin) digest would exclude the production of derivatives by permethylation and would probably lead to gas chromatography–mass spectrometry (GC–MS) separation and identification of dipeptides. Such procedures have been developed[15] but have not yet been applied to proteins of unknown structure. Other GC–MS methods which have been developed include the examination of mixtures of small peptides as trifluoracetyl permethyl derivatives[16] or as polyamino alcohols[17,18].

The most widely applied mass spectrometric method used to date has been low resolution direct probe analysis of peptide mixtures[4,9]. The great advantage of this approach is that it can deal effectively with mixtures of all sizes of peptide from 2 to 15 residues and above. The ability to sequence unambiguously a mixture of peptides is unique to mass spectrometry[13], but the significance of this statement is only grasped when one realizes that the isolation and preparation of individual purified peptides is the rate determining step in any classical protein sequencing method; even when using an automated spinning cup sequencer, rarely more than 50–100 amino acids can be placed in sequence

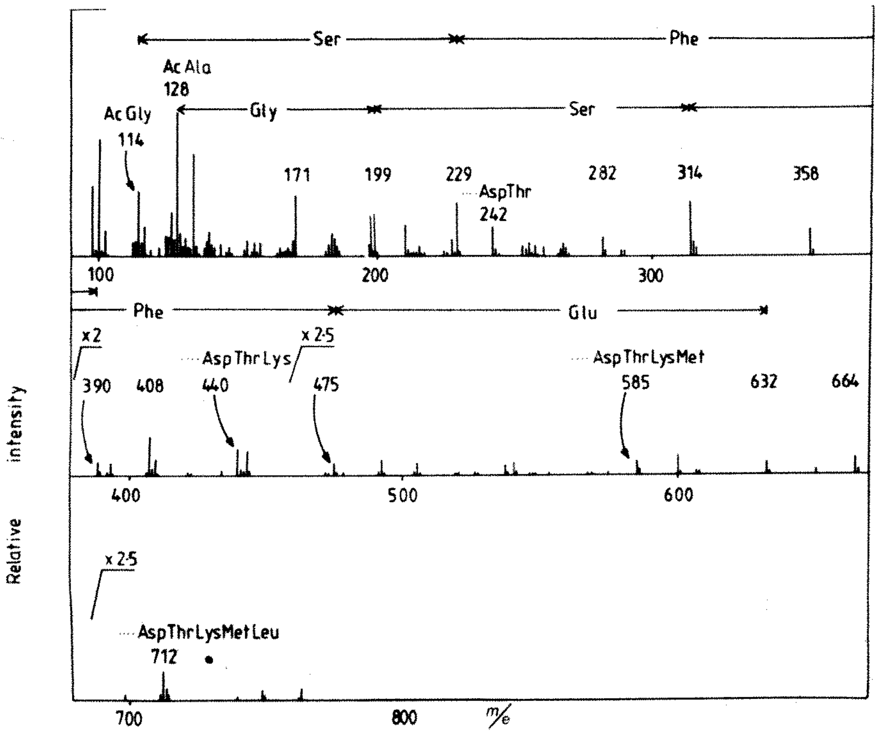

Fig. 2 A typical mass spectrum from the partially purified elastase digest of DHFR, at a source temperature of 240 °C. The assignment of major sequence ions is given, together with a sequence derived from N–C cleavage at aspartic acid. The latter assignment was made by working from high to low mass in the spectrum, looking for amino acid mass differences and expected losses (for example, methanol from Ser or Thr) until *m/e* 242. Since *m/e* 242 loses methanol to *m/e* 210, it must contain either a Ser or Thr. 242 minus serine (115 mass units) is 127—a meaningless N-terminal signal; however, 242 minus threonine (129 m.u.) is 113, which although not an abundant fragment (not well stabilized), is assigned to N–C cleavage at Asp, thus generating the sequence Asp-Thr-Lyr-Met-Leu. This, and the other sequences shown, were extended to higher mass at higher source temperatures[9].

by studying the intact protein. Mixture analysis provides a much needed way of bypassing this rate limiting step in the overall strategy. The principle is one of fractional distillation of the individual peptides from the mixture on the probe tip within the mass spectrometer, using either the probe or ion source heater[13,19]; the signals associated with any one peptide in the mass spectrum will rise and fall together at different rates to other components in the mixture, depending upon the separation achieved. The result is that each component can normally be sequenced unambiguously, the method being best suited to mixtures of two to five peptides.

To complete the strategy one needs a method of producing peptides of less than about 1,500 molecular mass. Cathepsins can be used[15], but they generate dipeptides, thus destroying the valuable 'overlap' information present in larger peptides. In contrast, trypsin or chymotrypsin may produce fragments too large for the mass spectrometer, and acid hydrolysis leads to loss of amides and other possible complications. It is best, therefore, to use nonspecific proteases, such as thermolysin[5], elastase[19] or subtilisin[20], which produce small peptides (2–15 residues) of ideal size for mass spectrometry.

The overall strategy developed is well illustrated by the study of the sequence of dihydrofolate reductase from methotrexate-resistant *Lactobacillus casei*. Here several digests were utilized, including elastase and subtilisin, and the large cyanogen bromide fragments isolated, to overlap and place the many peptides produced into a final sequence[8,9].

Peptide digests are separated by only one cation exchange column step, the effluent being screened analytically by high voltage paper electrophoresis before pooling of peptide mixture fractions, and derivatization. A typical spectrum from the elastase digest, together with its interpretation, is seen in Fig. 2.

Dihydrofolate reductase is the first protein of unknown structure to be fully sequenced by mass spectrometry without the aid of classical methods. Interestingly, with a molecular mass of 18,000 this must be the largest molecule ever to have had its structure determined by mass spectrometry[9].

New developments in computer automation of the interpretation of mass spectra—at present a skilled task—promise to reduce the time required to sequence a 20,000 dalton protein to about two man months. That, combined with the fact that in experienced hands one needs only 5–30 nmol of a peptide to sequence it, makes mass spectrometry both a complementary approach and a highly competitive alternative to classical techniques of protein sequencing, regardless of whether one chooses the GC–MS method[16–18] or the direct probe analysis method[4,5].

Glycopeptide analysis

Although glycopeptides are increasingly being recognized as an important group of substances, the determination of their structures has proven to be an especially difficult problem. It is difficult in that the structures are complex, demanding information on (1) protein sequence, (2) carbohydrate sequence, (3) nature of protein–carbohydrate linkage, for example O-glycosidic to serine, (4) nature of saccharide–saccharide linkage, for example 1–4, 1–3, and (5) configuration of linkage(s). In seeking such information, mass spectrometry offers the great advantage that it does not suffer from restrictions of compound class as do chemical approaches to the structure; given the normal difficulties encountered with any polar molecule, mass spectrometry can provide information on both the carbohydrate and protein structure from the same experiment. For example, it was necessary to study only two derivatives of AF8, an 'antifreeze' glycopeptide isolated from Antarctic fish blood plasma[21], to obtain information on each of the first four points above.

The peptide sequence of AF8 was established by studying the electron impact (N-terminal) and chemical ionization (C-terminal) spectra of an acetyl permethyl derivative of the glycopeptide. The spectra showed evidence of heterogeneity in several positions of the 14-residue peptide sequence (Fig. 3*a*), and the points of attachment of carbohydrate were clearly visible by the assignment of dehydrothreonine, formed by β-

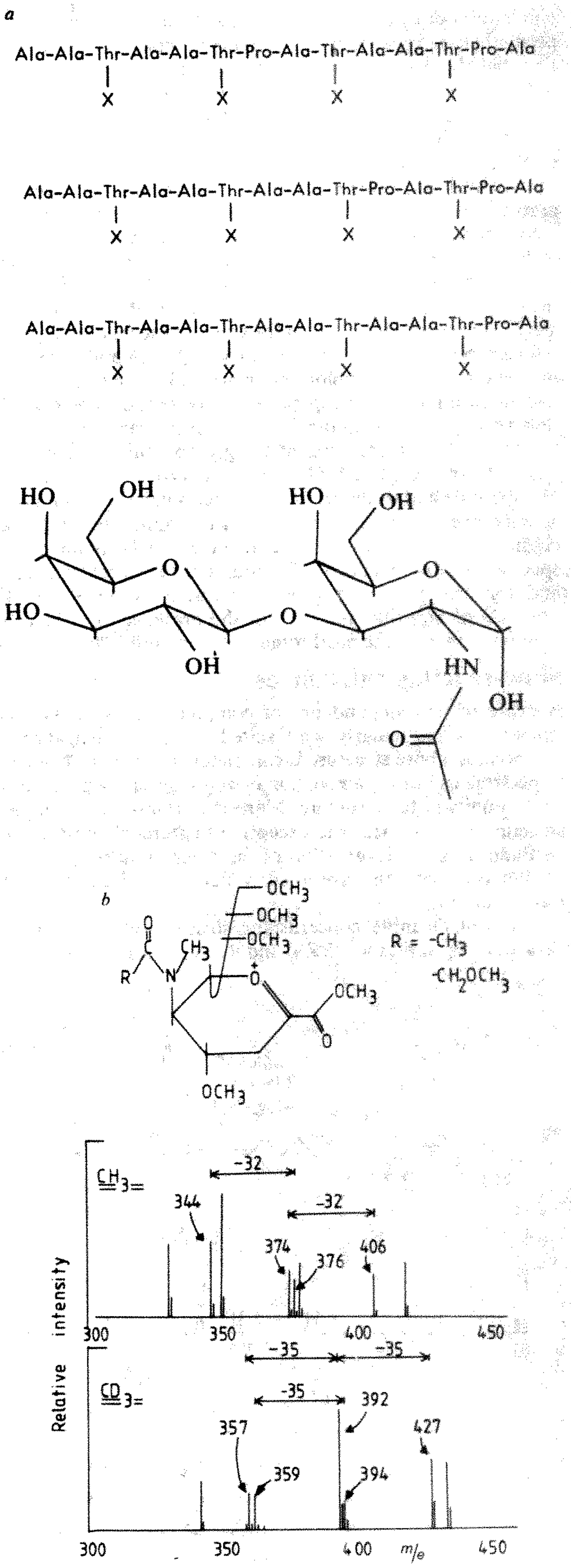

Fig. 3 *a*, The structure of the glycopeptide AF8 as deduced by electron impact, chemical ionization and field desorption mass spectrometry. *b*, The partial mass spectrum of a fragment of the glycoprotein prothrombin showing the presence of *N*-acetyl and *N*-glycolyl neuraminic acids. Sequence ions were confirmed by the stable isotope experiment shown.

elimination of carbohydrate during addition of the base in the permethylation reaction. Without any necessity for pre-separation, the eliminated permethyl carbohydrate was observed at a different source temperature (fractional distillation) and the sequence assigned as hexosyl-acetamidohexosamine. Interpretation of linkage between saccharides is normally based upon relative abundances of fragment ions which are much more pronounced in pertrimethylsilyl[22] rather than permethyl derivatives. In a separate experiment, the carbohydrate was eliminated from the peptide using sodium hydroxide, and again without any purification or separation, a trimethylsilyl derivative was prepared. Comparison of the spectra produced with those of standard 1–4 and 1–3 linked carbohydrates allowed an assignment of a 1–3 linkage in the amino disaccharide (Fig. 3*a*).

The potential of mass spectrometry in glycopeptide analysis is further illustrated by exploratory work on known structures[23,24] and on the unknown glycopeptide portion of the blood coagulation zymogen prothrombin[25]. Here, considerable information has been derived from one of the glycopeptides of molecular weight 4,500 (ref. 25). *N,O*-permethyl derivatives of the intact glycopeptide and its degradation products have been studied to characterize a number of sequences containing up to 10 saccharide units. Interestingly, several of the signals obtained in the spectra are very diagnostic of certain unusual saccharide units, and for example, have given conclusive evidence (via the presence of *m*/*e* 406 and 374) of the presence of *N*-glycolylneuraminic acid in the prothrombin glycopeptide[25] (see Fig. 3*b*).

Slow-reacting substances

Because of its independence of compound class, mass spectrometry is particularly well suited to the investigation of compounds whose structure is completely unknown. As long as a spectrum can be obtained, it may well suggest the presence of certain units in the structure. More importantly, the complete structure (usually with the exception of stereochemistry) may be deduced by interpretation of the fragmentation pattern in conjunction with the observed molecular weight (from the molecular ion).

A recent example concerns the structure elucidation of a slow-reacting substance (SRS) and its close relative, slow reacting substance of anaphylaxis, SRS-A[26], which is a mediator released from lung on antigen challenge, and believed to give rise to allergic bronchospasm (asthma) in man.

The structures of these pharmacologically similar substances have remained unknown since their discovery some 40 years ago[27]. Chemical clues have been uncovered (for example the probable incorporation of arachidonic acid and cysteine by radio-labelling experiments[28]), but these have been unconvincing because of the lack of purity of the preparations, and attempts to define the structures of SRSs have relied upon degradative experiments which are inevitably open to question[29]. Recently, following the earlier development of an HPLC purification procedure for SRS-A and the demonstration of its UV spectrum[30], the structures of SRS and SRS-A have been determined, based on the first mass spectra of derivatives of the intact molecules[31,32]. The SRS spectrum is shown in Fig. 4*a*. Definitive statements about the structure can now be made because of the exact physicochemical measurements available from the mass spectrum. For example, the molecular weight greatly reduces the number of structural possibilities, particularly since we can define this to five decimal places thus giving the atomic composition of this SRS. We can, however, go much further and use the fragmentation pattern of the molecule to define unambiguously the respective positions of certain structural features in the molecule. A detailed interpretation would not be appropriate here but some guidance is given in Fig. 4. In this way, we can show that SRSs form a novel class of 'peptidolipid'[31,32] and, in particular, SRS from rat basophil leukaemia cells and SRS-A from guinea pig lung are assigned the structure shown in Fig. 4*b*, and do not correspond to the recently revised structure of another SRS, termed leukotriene C[33]. Human lung SRS-A has previously been shown to co-chromatograph with guinea pig lung SRS-A[34], strongly suggesting that this also is the dipeptidyl structure shown in Fig. 4*b*.

Thus the mass spectrum can give a confidence of structural assignment on very small quantities of material (the above work was accomplished using less than 10 μg total material) in a manner unparalleled by any other physical or chemical technique. Importantly, the mass spectrum also shows what is *not* present in the structure; for example, we can say that neither the

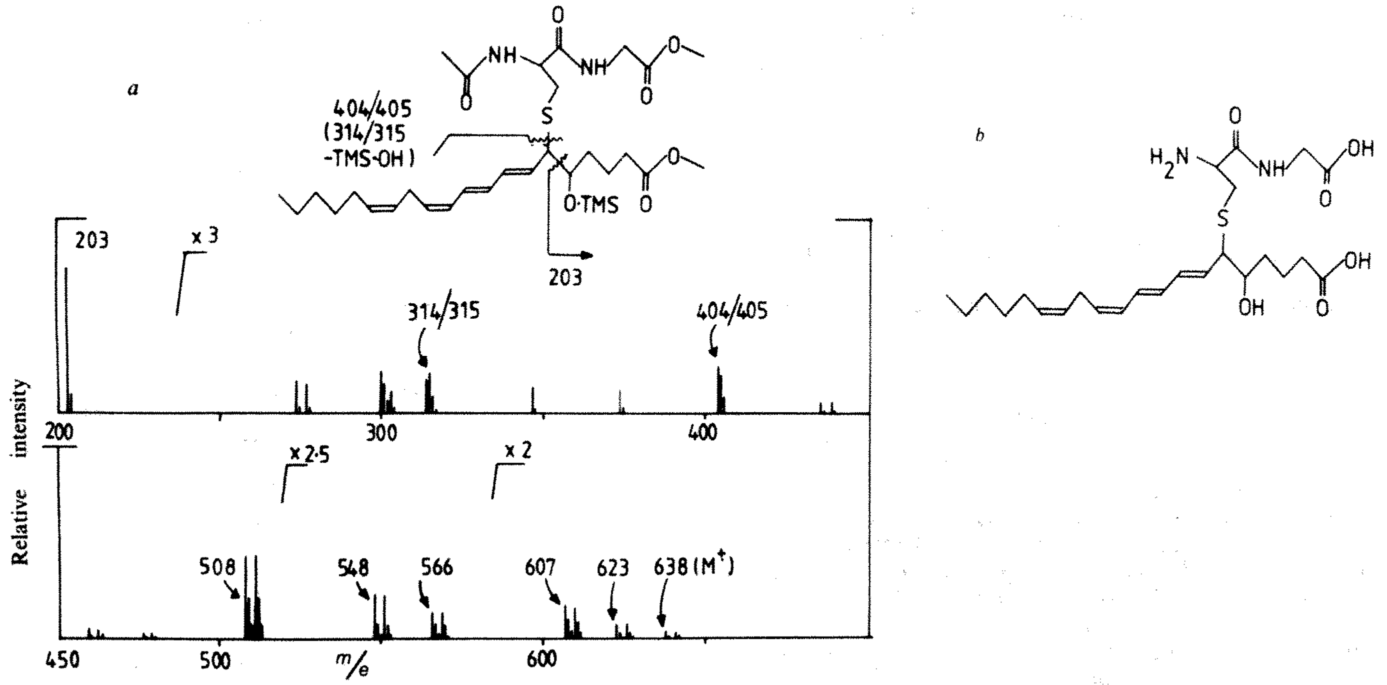

Fig. 4 *a*, The first mass spectrum of a slow reacting substance (SRS), as the trimethylsilyl ether of the *N*-acetyl, methyl ester derivative[31]. Analytical protein chemical data together with experiments on the destruction of biological activity had indicated the presence of a primary α-amino group in SRS and SRS-A[35]. The molecule was therefore located and differentiated from background by preparing the I:I ($^2H_3$:H_3) acetyl derivative of the unknown. The doublet signals found in the spectrum allowed unambiguous location of those ions corresponding to the unknown SRS, showing a molecular ion at *m*/*e* 638 and associated losses of CH_3 and OCH_3 at *m*/*e* 623 and 607 respectively. Signals at *m*/*e* 404, 405 and 314, 315 (loss of TMSOH) are diagnostic for the peptide attachment (C_6-S bond) and the arachidonate-derived portion of the molecule. *b*, The structure of the major SRS[31] from rat basophil leukaemia cells (RBL-1) and of SRS-A[32] from guinea pig lung, deduced from the above spectrum and associated data to be 5-hydroxy-6-cysteinyl-glycinyl-7,9,11,14-eicosatetraenoic acid. The mass spectrum does not define stereochemistry.

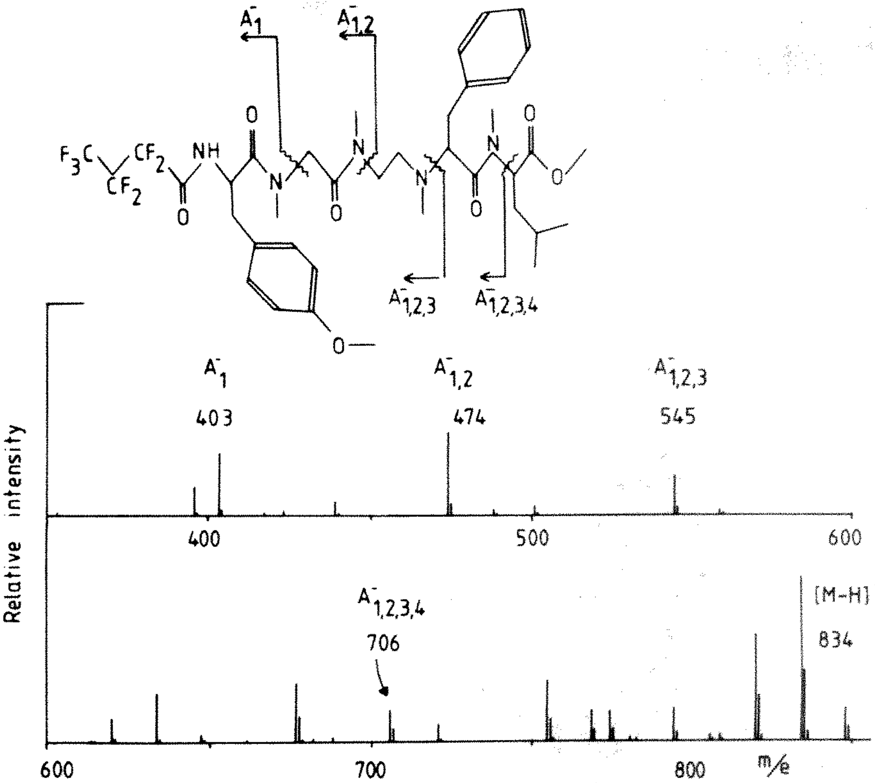

Fig. 5 The negative chemical ionization (NCI) spectrum of 1 nmol of leucine enkephalin as the *N*-heptafluorobutyryl permethyl derivative (A. Buko, D. F. Hunt, M. Judkins and H.R.M., unpublished work). The spectrum shows the increased relative abundance of high mass signals compared with typical EI or CI spectra (no amplification factors in drawing), together with retention of sequence ion information leading to structure (A_1, $A_{1,2}$ etc.) NCI spectra can be obtained routinely using this type of derivative at the 1 nmol level or less.

Pure Chemistry Library
SCIENCE COLLEGE
92 Upper Circular Road
CALCUTTA

RBL-SRS nor the lung SRS-A contain a glycineamide or sulphoxide which would be difficult to discount by chemical or enzymatic methods. Similarly we can say that they do not contain a sulphate moiety, widely expected from the results of destruction of biological activity by aryl sulphatase, reported in the literature.

New and novel amino acids, and 'blocked' proteins

Another important area of biochemistry in which mass spectrometry is playing a significant role is in the study of enzymatic regulation and control in the blood coagulation system.

As with the SRS study above, perhaps the most obvious strength of the mass spectrometric method is in the area of new structures, where no reference compounds exist with which to make a classical interpretation. Just such a situation arose quite surprisingly in 1974 from a sequence study of one of the blood coagulation zymogens, prothrombin. The outcome of this work was the discovery of a new amino acid, γ-carboxyglutamic acid (Gla), and its sequence location in 10 positions in the N-terminal region of prothrombin[36–38]. This amino acid was missed in classical sequencing procedures (in fact it was assigned as ordinary glutamic acid) due to a ready decarboxylation during Edman degradation or hydrolysis in the dansyl procedure.

Since this discovery, there has been considerable interest in the function and occurrence of Gla. In the original work on the identification of Gla, two unique mass spectrometric signals and two unique mass differences were established. These are diagnostic for the new amino acid and the observation of these signals in a mass spectrum allows a definitive assignment not just of the presence of Gla in a peptide but also of its exact location in the sequence[38]. Thus a recent study of the N-terminal portions of factors X_1 and X_2 (derived by activation of the zymogen factor X) has shown each to contain 12 Gla residues and the two sequences to be identical[39].

It should be clear from an understanding of the methods discussed earlier, that the assignment of novel amino acids, such as *N*-methyl lysine, in a peptide sequence reduces to an almost trivial problem. The use of perdeutero-methyl iodide in the permethylation reaction will allow assignment of natural methyl groups simply by counting the mass spectrum (normal lysine would have a mass of 204 mass units, whereas *N*-Me lysine would have a mass of 201 mass units).

Deuterated reagents may also be used to define the presence (or absence) of blocking groups on proteins or peptides. There are now a number of examples in the literature[40–43], including a method for use on proteins[44], which obviates the necessity for isolation of the blocked N-terminal peptide.

Neurochemistry

Mass spectrometry is playing an increasingly important part in studies on neuropeptides isolated, inevitably in very small quantities, from the central nervous system. Not only the quantity but also the purity may be inadequate for classical structural determination and, furthermore, the confidence in sequence assignment normally associated with protein sequence studies is not available when the sample is not necessarily of protein origin, and, therefore, may have unusual amino acids, unusual linkages or even may not be a peptide at all.

Such a situation occurred in the study of enkephalin, where amino acid analysis, gel column and electrophoretic data did not correlate well with the partial sequence data obtained by the dansyl–Edman method, and an ultraviolet fluorescence measurement raised the further possibility of a 'modified' tryptophan in the molecule[45]. Using the mass spectrometric methods developed for protein sequence analysis, it proved possible to identify two enkephalin pentapeptides, Tyr-Gly-Gly-Phe-Met and Tyr-Gly-Gly-Phe-Leu[46]; once the mass spectrometric sequence assignment had been made, and the tryptophan analogue discounted, then the classical data were found to correlate reasonably well with this interpretation.

A number of biologically active neuropeptides have been shown to possess blocked structures, and these pose considerable problems for classical methodology, but fewer problems for mass spectrometry since free peptides would be 'blocked' before study by making derivatives. The difference in 'degree of difficulty' is really quite remarkable here when we consider that the pioneering work on the structure elucidation of thyrotropin releasing hormone (TRH)[47,48] took some 10 years, and even today the structure of this simple blocked tripeptide would pose very considerable problems for the protein chemist to define, as an unknown. By contrast, the presence of blocking groups actually assists in the mass spectrometric investigation since the formation of a derivative for such a small peptide is no longer necessary. Of course, larger blocked structures still require derivative formation to remove hydrogen bonding and a recent example of this type of problem is the study of adipokinetic hormone[49], isolated from locust and responsible for lipid mobilization during flight. The mass spectrum of a permethyl derivative of adipokinetic hormone showed a pyrrolidone carboxylate group (*m/e* 98 and 126) blocking the N-terminus, and a signal at *m/e* 428 was interpreted as arising from a C-terminal amide: ... Trp-Gly-Thr-NH_2. The total structure was assigned as a fully blocked decapeptide, PCA-Leu-Asn-Phe-Thr-Pro-Asn-Trp-Gly-Thr-NH_2, and was the first peptide hormone of insect neuroendocrine origin to be completely characterized.

New developments

Several new technical developments promise to improve the analytical value of mass spectrometry still more. Space does not permit a detailed discussion, but briefly the areas covered include ionization techniques giving molecular weight information on underivatized peptides and glycopeptide antibiotics[50,51] (field desorption), new approaches to improve sensitivity of detection based upon negative chemical ionization[1,52], and developments in magnet technology which have already led to a tripling of the effective mass range of the mass spectrometer at full sensitivity, to over *m/e* 3,000. The potential of negative chemical ionization in the neurochemical area is illustrated in Fig. 5 showing the spectrum of a Leu-enkephalin derivative, illustrating the derivation of full sequence information at the 1 nmol level.

Thus mass spectrometry is of growing value in the determination of the structure of compounds of biological interest. It is already the method of choice in some cases and is likely to become so in others as the technique develops. In combination with procedures such as high pressure liquid chromatography which can separate picomolar quantities of peptides[53,54], mass spectrometry promises to allow the solution of further important chemical and biochemical problems, only just beyond the scope of present technology.

1. Lewy, A. J. & Markey, S. P. *Science* **201**, 741–743 (1978).
2. Anderson, C. O. *Acta chim. scand.* **12**, 1353–1355 (1958).
3. Biemann, K., Gapp, F. & Seibl, J. *J. Am. chem. Soc.* **81**, 2274–2276 (1959).
4. Geddes, A. J. *et al. Biochem. J.* **114**, 695–702 (1969).
5. Morris, H. R., Williams, D. H., Midwinter, G. G. & Hartley, B. S. *Biochem. J.* **141**, 701–713 (1974).
6. Dell, A. & Morris, H. R. *Advances in Mass Spectrometry in Biochemistry and Medicine* Vol. 1 (eds Frigerio, A. & Castagnoli, N.) 263–266 (Spectrum, New York, 1976).
7. Shaw, W. V. *et al. Nature* **282**, 870–872 (1979).
8. Batley, K. E. & Morris, H. R. *Biochem. Soc. Trans.* **5**, 1097–1098 (1977).
9. Morris, H. R. *Phil. Trans. R. Soc.* A **293**, 39–51 (1979).
10. Morris, H. R. *FEBS Lett.* **22**, 257–261 (1972).
11. Morris, H. R., Dickinson, R. J. & Williams, D. H. *Biochem. biophys. Res. Commun.* **51**, 247–255 (1973).
12. Dell, A. & Morris, H. E. *Biochem. biophys. Res. Commun.* **61**, 1125–1132 (1974).
13. Morris, H. R., Williams, D. H. & Ambler, R. P. *Biochem. J.* **125**, 189–201 (1971).
14. Morris, H. R. & Dell, A. *Instrumentation in Amino Acid Sequence Analysis* (ed. Perham, R. N.) 147–191 (1975).
15. Krutzsch, H. *Meth. Enzym.* **67E**, 391–404 (1978).
16. Priddle, J. D., Rose, K. & Offord, R. E. *Biochem. J.* **157**, 777–780 (1976).
17. Hudson, G. & Biemann, K. *Biochem. biophys. Res. Commun.* **71**, 212–220 (1976).
18. Khorana, H. G. *et al. Proc. natn. Acad. Sci. U.S.A.* **76**, 5046–5050 (1979).
19. Morris, H. R. *et al.*, *Biochem. J.* **137**, 409–411 (1974).
20. Dell, A. & Morris, H. R. *Biochem. biophys. Res. Commun.* **78**, 874–880 (1977).
21. Morris, H. R. *et al. J. biol. chem.* **253**, 5155–5162 (1978).
22. Kamerling, J. P., Vliegenthart, J. F. G., Vink, J. & de Ridder, J. J. *Tetrahedron* **27**, 4749–4757 (1971).
23. Karlsson, K.-A. *et al. FEBS Lett.* **94**, 413–417 (1978).
24. Nebelin, E. & Das, B. C. *FEBS Lett.* **107**, 254–258 (1979).
25. Taylor, G. W., Morris, H. R., Petersen, T. E. & Magnusson, S. *Adv. Mass Spectrometry* **8**, 672–681 (1980).
26. Kellaway, C. H. & Trethewie, E. R. *Q. Jl exp. Physiol.* **30**, 121–145 (1940).
27. Feldberg, W. & Kellaway, C. H. *J. Physiol., Lond.* **94**, 187–226 (1938).
28. Parker, C. W., Jakschik, B. A., Huber, M. G. & Falkenhei, S. F. *Biochem. biophys. Res. Commun.* **89**, 1186–1192 (1979).
29. Murphy, R. C., Hammarstrom, S. & Samuelsson, B. *Proc. natn. Acad. Sci. U.S.A.* **76**, 4275–4279 (1979).
30. Morris, H. R., Taylor, G. W., Piper, P. J., Sirois, P. & Tippins, J. R. *FEBS Lett.* **87**, 203–206 (1978).
31. Morris, H. R., Taylor, G. W., Piper, P. J., Samhoun, M. N. & Tippins, J. R. *Prostaglandins* **19**, 185–201 (1980).
32. Morris, H. R., Taylor, G. W., Piper, P. J. & Tippins, J. R. *Nature* **285**, 104–106 (1980).
33. Hammarstrom, S. *et al.*, *Biochem. biophys. Res. Commun.* **91**, 1266–1272 (1979).
34. Morris, H. R., Piper, P. J., Taylor, G. W. & Tippins, J. R. *Br. J. Pharmac.* **67**, 179–184 (1979).
35. Morris, H. R., Taylor, G. W., Piper, P. J. & Tippins, J. R. *Ag. Actions Suppl.* **6**, 27–36 (1979).
36. Magnusson, S., Sottrup-Jensen, L., Peterson, T. E., Morris, H. R. & Dell, A. *FEBS Lett.* **44**, 189–193 (1974).
37. Stenflo, J., Fernlund, P., Egan, W. & Roepstorff, P. *Proc. natn. Acad. Sci. U.S.A.* **71**, 2730–2733 (1974).
38. Morris, H. R., Dell, A., Peterson, T. E., Sottrup-Jensen, L. & Magnusson, S. *Biochem. J.* **153**, 663–679 (1976).
39. Thogersen, H. C. *et al. Biochem. J.* **173**, 613–627 (1978).
40. Frank, G. & Weeds, A. G. *Eur. J. Biochem.* **44**, 317–334 (1974).
41. Morris, H. R. & Dell, A. *Biochem. J.* **149**, 754 (1975).
42. Nystrom, L.-E., Linberg, U., Kendrick-Jones, J. & Jakes, R. *FEBS Lett.* **101**, 161–165 (1979).
43. Hofmann, T., Kawakami, M., Hitchman, A. J. W., Harrison, J. E. & Dorrington, K. J. *Can. J. Biochem.* **57**, 737–740 (1979).
44. Batley, K. E. thesis, Univ. Cambridge (1977).
45. Hughes, J., Smith, T., Morgan, B. & Fothergill, L. *Life Sci.* **16**, 1753–1758 (1975).
46. Hughes, J. *et al. Nature* **258**, 577–579 (1975).
47. Nair, R. M. G., Barrett, J. F., Bowers, C. Y. & Schally A. V. *Biochemistry* **9**, 1103–1106 (1970).
48. Burgus R. *et al. Nature* **226**, 321–325 (1970).
49. Stone, J. V., Mordue, W., Batley, K. E. & Morris, H. R. *Nature* **263**, 207–211 (1976).
50. Dell, A., Williams, D. H., Morris, H. R., Smith, G. A., Geeney, J. & Roberts, A. C. K. *J. Am. chem. Soc.* **97**, 2497 (1975).
51. Rinehart, K. L., Cook, C. J., Maurer, K. H. & Rapp, V. *J. Antibiot.* **27**, 1–6 (1974).
52. Hunt, D. F., Stafford, G. C., Crow, F. W. & Russell, J. W. *Analyt. Chem.* **48**, 2098–2105 (1976).
53. Rubinstein, M., Chem-Kiang, S., Stein, S. & Udenfriend, S. *Analyt. Biochem.* **95**, 117–121 (1979).
54. Morris, H. R., Etienne, A. T., Dell, A. & Albuquerque, R. *J. Neurochem.* **34**, 574–582 (1980).

ARTICLES

Evidence for differential intracellular localization of the *Acanthamoeba* myosin isoenzymes

Hana Gadasi & Edward D. Korn

Laboratory of Cell Biology, National Heart, Lung, and Blood Institute, Building 3, Room B1-20, National Institutes of Health, Bethesda, Maryland 20205

The three myosin isoenzymes of Acanthamoeba castellanii *coexist within a single cell and the native molecules probably have the same unusual polypeptide composition as the isolated enzymes. The two myosin I isoenzymes seem to be preferentially localized near the plasma membrane while myosin II seems to be much less concentrated near the plasma membrane than elsewhere in the cytoplasm.*

ACTIN and myosin provide the molecular basis for the diverse motility activities of eukaryotic cells[1]. Actins from muscle and non-muscle cells are very similar in structure and properties and almost all of the myosins are also structurally similar, containing a pair of heavy chains of molecular weight (MW) ~200,000 and two pairs of light chains with MWs of about 20,000 and 16,000. Because these non-muscle myosins can also self-assemble into bipolar filaments, it is widely, and not unreasonably, assumed

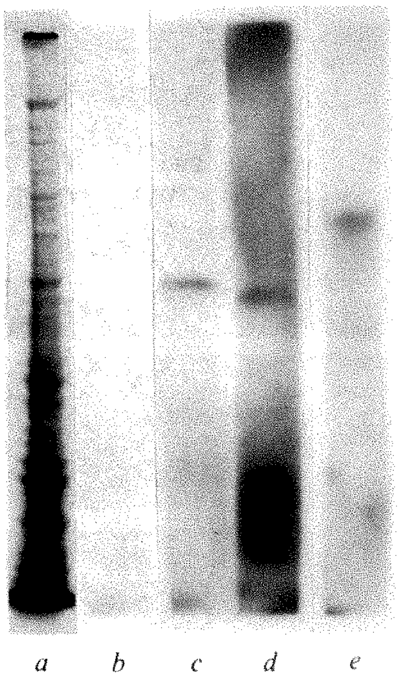

Fig. 1 Specificity of the reactions of the *Acanthamoeba* myosin heavy chain antibodies with polypeptides of whole amoebae. A centrifugal pellet of intact *Acanthamoeba castellanii* (0.1 ml) was boiled for 20 min in 3 ml sample buffer[8] containing 1% SDS, 5 mM EGTA, 5 mM EDTA, 0.5 mM phenylmethylsulphonyl fluoride and 0.1 mM pepstatin. Aliquots of 75 μl each were applied to multiple lanes of 5.6% polyacrylamide slab gels and electrophoresed according to Laemmli[8]. The polypeptides in one lane were stained with Coomassie blue and the polypeptides in the other lanes were transferred to diazobenzyloxymethyl paper as described in the text. The paper was cut into strips corresponding to individual lanes which were then exposed to one of four rabbit IgG fractions (1 : 50 dilution) and ^{125}I-labelled protein A (1×10^6 c.p.m. per lane) as described in the text. Autoradiographs were exposed for 18 h using Kodak no screen X-ray film NS 2T. Lane *a*, Coomassie blue stained polypeptides; lane *b*, non-immune IgG; lane *c*, anti-myosin IA heavy chain IgG; lane *d*, anti-myosin IB heavy chain IgG; lane *e*, anti-myosin II heavy chain IgG. The MWs of the radioactive bands in lanes *c*, *d* and *e* are 130,000, 125,000 and 170,000, respectively, relative to standards applied to the same gels, and their electrophoretic mobilities were identical to those of the heavy chains of the corresponding purified myosins on the same gels. Broad smears of apparent labelling (as in lane *d*) are common but irreproducible occurrences[9,11]. Occasionally, minor degradation products of the heavy chains were detected.

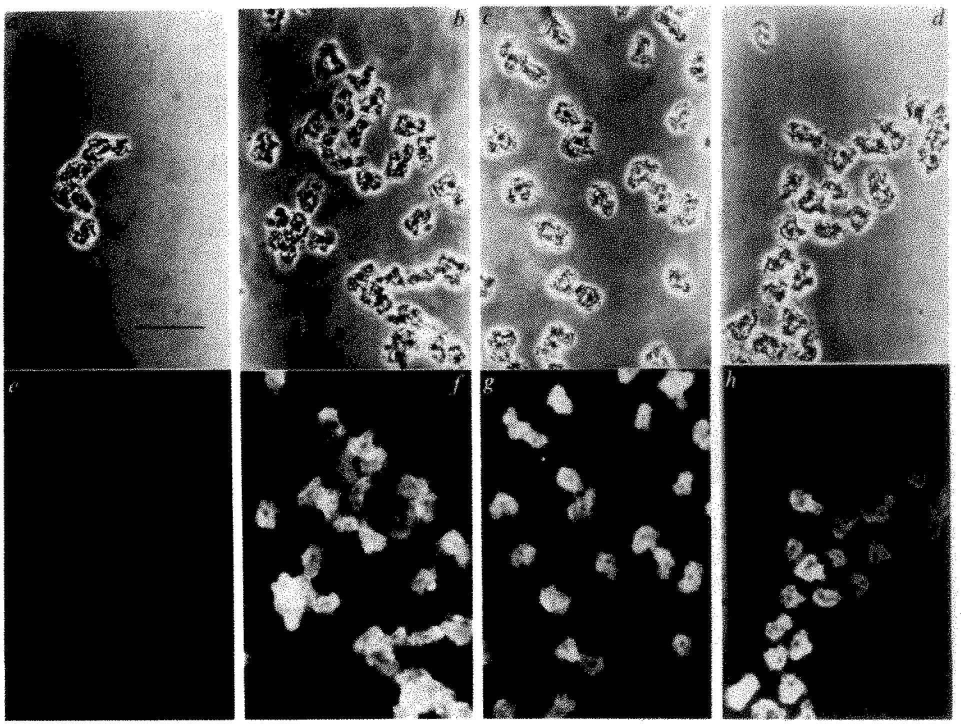

Fig. 2 Indirect immunofluorescence assay of the reaction of *Acanthamoeba castellanii* (Neff strain) with myosin heavy chain antibodies. Cells were allowed to adhere to clean glass slides and were fixed with 5% formaldehyde in phosphate-buffered saline (PBS) for 30 min and then treated with cold (−20 °C) acetone for 5 min. They were then sequentially treated with non-immune IgG in PBS, one of the specific antisera (1:200 dilution in PBS containing 1% bovine serum albumin (BSA)) and rhodamine-labelled goat anti-rabbit IgG (1:200 dilution in PBS containing 1% BSA). The cells were washed in 1% BSA in PBS between each treatment. Cells were photographed under phase contrast and fluorescent microscopy at the same magnification. All fluorescent microscopy photographs were made with 30 s exposure and were printed identically. Frames *a–d* are phase contrast and *e–h* are fluorescent micrographs of cells reacted with: *a*, *e*, non-immune IgG; *b*, *f*, antimyosin IA heavy chain IgG; *c*, *g*, anti-myosin IB heavy chain IgG; *d*, *h*, anti-myosin II heavy chain IgG. Scale bar, 40 μm.

that a sliding filament mechanism analogous to that responsible for contraction of skeletal muscle is responsible for activities such as amoeboid movement, cell division and phagocytosis in non-muscle cells.

The three myosin isoenzymes isolated from *Acanthamoeba castellanii* (Neff strain) are the only known apparent exceptions. As isolated, *Acanthamoeba* myosins IA and IB[2–5] are both single-headed enzymes of MW about 150,000–180,000. Myosin IA contains a heavy chain of ~130,000 MW and light chains with MWs of about 17,000 and 14,000, while myosin IB contains a heavy chain of ~125,000 MW and light chains with MWs of ~27,000 and 14,000. Both enzymes seem unable to form bipolar filaments[2]. A third myosin isoenzyme, *Acanthamoeba* myosin II, is structurally more conventional[6,7] and can form bipolar filaments *in vitro*[7]. It is a double-headed molecule with a pair of heavy chains of about 170,000 MW and two pairs of light chains of about 17,500 and 16,000 MWs, for a native MW of about 400,000. We have shown by peptide mapping[4] and immunochemical analysis[5] that the three *Acanthamoeba* myosin isoenzymes are products of different genes.

Because of the unusual structure of two of the *Acanthamoeba* myosin isoenzymes and because no other non-muscle cell has yet been shown to contain more than one species of myosin, we thought it important to establish: (1) if the isolated enzymes are in their native forms; (2) if the isoenzymes coexist in a single cell; and (3) whether the myosin isoenzymes are differentially localized within the cell. We have now obtained affirmative answers to all three questions through the use of specific antibodies raised against the isolated heavy chains of the three myosin isoenzymes. The differential localizations of the isoenzymes raise the interesting possibility that the different myosin species serve specific and different motility functions, and the unusual

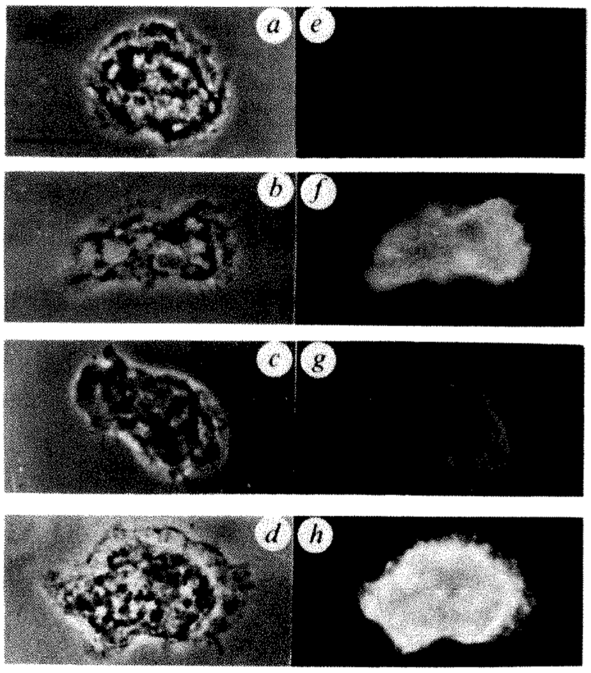

Fig. 3 Differential localization of myosin isoenzymes by indirect immunofluorescence. This experiment was identical to that described in Fig. 2. Frames *a–d*, phase contrast; *e–h*, fluorescence; *a, e*, non-immune IgG; *b, f*, anti-myosin IA heavy chain IgG; *c, g*, anti-myosin IB heavy chain IgG; *d, h*, anti-myosin II heavy chain IgG. Scale bar, 10 μm.

physical properties of the myosin I isoenzymes suggest that some of these functions might not involve the classical sliding filament mechanism.

Preparation of heavy chain antibodies

Previously[5], we had raised antibodies against the isolated myosins. Although the enzymes were highly purified, they were contaminated by small amounts of other amoeba proteins, which might also have elicited sufficient antibodies to make those antisera inappropriate for cytochemistry. Therefore, monospecific myosin heavy chain antibodies were prepared as follows. Highly enriched preparations of *Acanthamoeba* myosins IA, IB and II were obtained by direct immunoprecipitation with the appropriate antibodies previously raised against the isolated enzymes. The immunoprecipitates were separated by electrophoresis[8] on SDS-5.6% polyacrylamide slab gels and the gels were stained lightly with Coomassie blue. In each case[5], only a single major band, corresponding in mobility to the 130,000, 125,000 and 170,000-MW heavy chains of myosin IA, IB and II, respectively, was present above the dye front. These bands were cut out, washed, sonicated and injected into rabbits to elicit specific antibodies against each of the three heavy chains. Prepared in this way, the only possible contaminating antigens from the amoebae would be molecules which were precipitated from the amoeba extract by the antibody raised against the whole myosin and which also co-migrated electrophoretically with the myosin heavy chain. Such coincidence is unlikely. Immune and non-immune sera were precipitated with 45% ammonium sulphate and the IgG fractions were dissolved in phosphate buffered saline.

Specificity of heavy chain antibodies

We tested, in the same experiment, both the specificity of the three myosin heavy chain antisera and the possibility that higher molecular weight forms of the heavy chains might exist in the amoebae. Whole amoebae were boiled in 1% SDS containing several inhibitors of proteolytic enzymes and multiple identical samples were separated by SDS-polyacrylamide slab gel electrophoresis. One lane was excised and stained for polypeptides with Coomassie blue while the polypeptides in the duplicate lanes were transferred to diazobenzyloxymethyl paper[9]. The paper was cut into individual lanes which were incubated with a large excess of either non-immune sera or one of the specific myosin heavy chain antibodies followed by ^{125}I-protein A (ref. 10) and the positions of the bound antibodies were located by autoradiography.

The antibodies raised against the isolated heavy chains of myosin IA, IB and II reacted exclusively (Fig. 1) with polypeptides of molecular weights corresponding exactly to those of the heavy chains of the purified enzymes: 130,000, 125,000 and 170,000, respectively. Similar results have been obtained in 15 to 20 experiments including some in which the polypeptides were reacted with the antisera on the polyacrylamide gel without transfer to the paper. Occasionally, minor degradation products of the myosin heavy chains were detected but never a polypeptide of higher molecular weight than that of the heavy chains of the purified myosins. Degradation products were never detected when extracts of amoeba, rather than whole cells, were analysed, probably because the lysosomal proteases were removed before addition of SDS. To demonstrate that, if it were present in the amoebae, a polypeptide of the size typical of the heavy chains of other myosins would have been detected, we mixed pure chicken pectoralis muscle myosin with a sample of the amoebae just before they were added to the SDS solution. The undegraded 200,000-MW heavy chain of the chicken myosin was readily detected using its specific antibody. These experiments, therefore, provide strong evidence that the cells do not contain immunologically cross-reactive higher molecular weight forms of the heavy chains of *Acanthamoeba* myosins IA, IB and II.

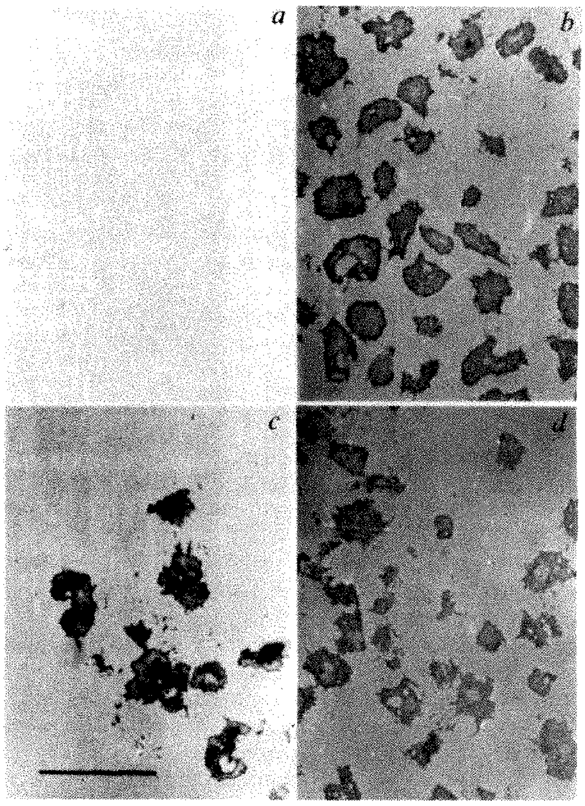

Fig. 4 Immunocytochemical localization of myosin isoenzymes. Sections (1 μm) were reacted with specific antisera (1 : 250 dilution) and subsequently with the peroxidase–anti-peroxidase system as described in the text. All micrographs were photographed and printed under identical exposures. Frame *a*, non-immune IgG; *b*, anti-myosin IA heavy chain IgG; *c*, anti-myosin IB heavy chain IgG; *d*, anti-myosin II heavy chain IgG. Scale bar, 40 μm.

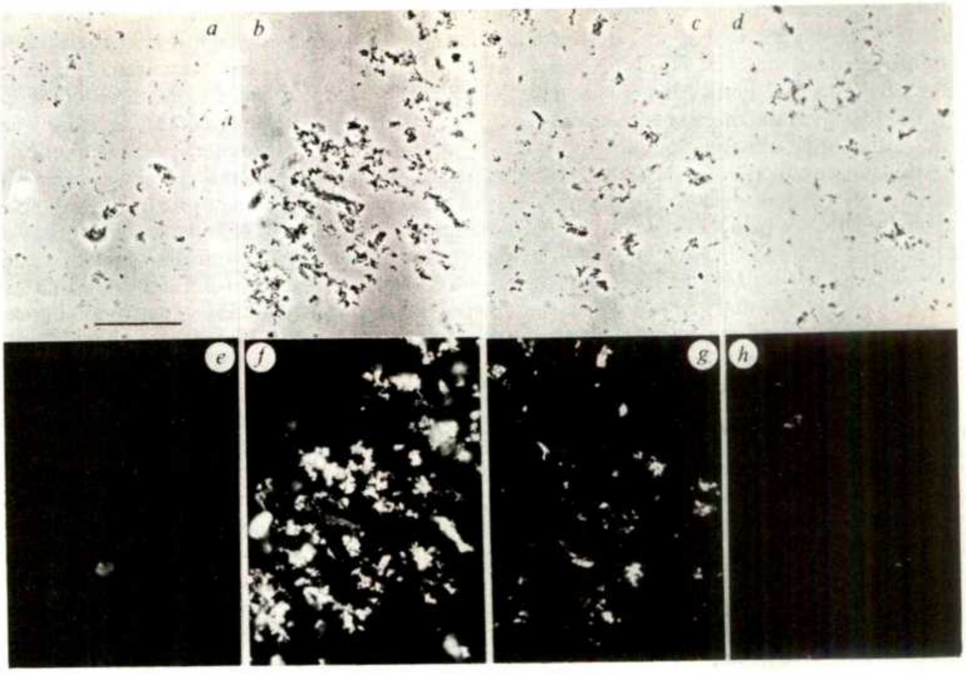

Fig. 5 Indirect immunofluorescence assay of isolated plasma membranes. Suspensions of purified plasma membranes[16] were fixed for 30 min with 3.7% formaldehyde and then reacted with specific antisera (1:50 dilution) followed by rhodamine-labelled goat anti-rabbit IgG (1:200 dilution). The membranes were then applied to slides and the same fields were photographed under phase contrast (*a*–*d*) and fluorescence (*e*–*h*). Exposure time was 20 s and all the fluorescent micrographs were printed under identical exposures. Non-immune IgG (*a*, *e*); anti-myosin IA heavy chain IgG (*b*, *f*) anti-myosin IB heavy chain IgG (*c*, *g*); anti-myosin II heavy chain IgG (*d*, *h*). Scale bar, 40 μm.

Myosin isoenzymes occur in the same cells

The data shown in Fig. 1 demonstrate that the antibodies to the myosin heavy chains could be used in cytochemical experiments to detect myosin II and the two myosin I isoenzymes in the presence of each other and without interference by other amoeba proteins. Although the antibodies to myosin IA and IB heavy chains also did not seem to cross-react (Fig. 1, lanes *c*, *d*), we were not certain that we could selectively detect myosin IA or IB in the presence of the other because previous antisera to the purified intact myosins IA and IB did cross-react[5] and because direct inspection of some of the autoradiograms obtained with antibody to myosin IA heavy chain indicated slight reaction with the 125,000-MW heavy chain of myosin IB.

We used the indirect immunofluorescence method to determine if each of the *Acanthamoeba* myosin isoenzymes occurs in every cell. Amoebae were allowed to crawl on clean glass slides[12]. The cells that adhered were fixed with formaldehyde and made permeable to antibodies by treatment with cold acetone. Cells were then exposed to antibodies to either myosin IA heavy chain, myosin IB heavy chain or myosin II heavy chain followed by rhodamine-labelled goat anti-rabbit immunoglobulin[13]. The same fields of cells were photographed at low magnification (×160) under phase contrast (Fig. 2*a*–*d*) or fluorescence (Fig. 2*e*–*h*) microscopy. As every cell on all of the slides was fluorescent irrespective of which of the three specific antisera was used, all the cells must have contained myosin II and at least one, but probably both, of the myosin I isoenzymes.

Intracellular localization of myosin isoenzymes

In Fig. 2, the fluorescent image of every cell exposed to the antibodies to myosin IA and myosin IB heavy chains is the same size as the corresponding phase contrast image (Fig. 2, *f* compared with *b* and *g* compared with *c*), whereas the fluorescent image of every cell exposed to the antibodies to myosin II heavy chain is smaller than the corresponding phase contrast image (Fig. 2, *h* compared with *d*). The reason for this difference can be seen at higher magnification, as in Fig. 3. Antibodies to myosin IA and IB heavy chains were bound more intensely at, or near, the plasma membrane than elsewhere in the cell (Fig. 3*f*, *g*) and, therefore, the fluorescent images of the cells have the same overall dimensions as the phase contrast images (Fig. 3*b*, *c*). On the other hand, the periphery of the cell and the cytoplasmic region adjacent to the plasma membrane reacted much less well with antibodies to myosin II heavy chain than did the rest of the cytoplasm (Fig. 3*h*). As a result, the fluorescent image of the cell is smaller than the corresponding phase contrast image (Fig. 3*d*). Therefore, the myosin I isoenzymes seem to be more concentrated at or near the plasma membrane, from where myosin II is mostly excluded. No reaction was detected with any antisera unless the cells were made permeable; none of the antigenic sites, therefore, is on the external surface of the amoeba.

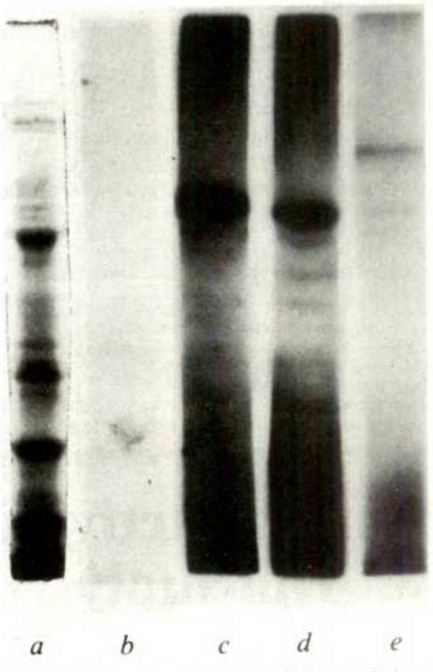

Fig. 6 Reaction of *Acanthamoeba* myosin heavy chain antibodies with plasma membrane polypeptides. Isolated plasma membranes of *Acanthamoeba castellanii* (Neff) were analysed identically as described for whole cells except that 7.5% polyacrylamide gels were used. Lane *a*, Coomassie blue stained polypeptides; lane *b*, non-immune IgG; lane *c*, anti-myosin IA heavy chain IgG; lane *d*, anti-myosin IB heavy chain. The autoradiograms (lanes *b* and *d*) were overexposed to detect the very low reaction with myosin II heavy chain and, therefore, minor degradation products of some of the heavy chains and nonspecific smears, may be detected in addition to the major bands. The major bands in lanes *c*, *d* and *e* are at the exact positions of the heavy chains of the respective purified myosins which were applied as standards to the same slab gel.

Additional evidence for the differential localization of *Acanthamoeba* myosins I and II was obtained by an independent immunochemical method. Transverse sections of cells fixed in glutaraldehyde and embedded in polyethylene glycol[14] were exposed to one of the three specific antisera and incubated with goat anti-rabbit immunoglobulin followed by rabbit anti-peroxidase immunoglobulin coupled to horseradish peroxidase[15]. The position of the bound peroxidase was determined cytochemically by incubation for 30 min with the peroxidase substrates, diaminobenzidine and hydrogen peroxide. When antibodies to myosin IA and IB heavy chains were used (Fig. 4*b*, *c*), the cell boundary was intensely stained with brown reaction product, and the cytoplasm was diffusely stained, the antibodies to myosin II heavy chain resulting in only diffuse staining of the cytoplasm (Fig. 4*d*).

Myosins of isolated plasma membranes

By indirect immunofluorescence, isolated plasma membranes[16] were found to react with antibodies to myosin IA and IB heavy chains (Fig. 5*f*, *g*) but not with antibodies to myosin II heavy chain (Fig. 5*h*). Myosin IA and myosin IB were also concentrated in the isolated plasma membranes as determined by specific staining of SDS-polyacrylamide electrophoretic gels. The intensity of the radioactive labelling of the 130,000- and 125,000-MW polypeptides of myosin IA and IB was very much greater than the barely detectable labelling of the 170,000-MW myosin II heavy chain (Fig. 6), in contrast to the essentially equivalent labelling of the three polypeptides in electrophoretic gels of the whole amoebae (Fig. 1). Also, the absolute intensity of labelling of the 130,000- and 125,000-MW peptides was very much greater for the plasma membranes (Fig. 6) than for whole amoebae (Fig. 1), although the same amounts of protein were applied. Both myosin I isoenzymes, therefore, were enriched in the isolated plasma membranes in comparison with myosin II and also relative to their own concentrations in the whole amoebae.

Conclusions

From the data in this and previous papers from our laboratory, we conclude that *Acanthamoeba castellanii* (Neff) contains three myosin isoenzymes: single-headed myosins IA and IB and double-headed myosin II having heavy chains of the unusually low MWs of 130,000, 125,000 and 170,000, respectively. The myosin I isoenzymes seem to be preferentially localized at or near the plasma membrane while myosin II seems to occur mainly, if not exlusively, deeper in the cytoplasm. We do not know if the myosin I isoenzymes are bound directly to the isolated plasma membrane or are associated with the actin filaments that lie immediately under the plasma membrane[17] and co-purify with the plasma membranes[18,19].

We must consider, of course, the possibility that the experimental data do not accurately reflect the distributions of the myosin isoenzymes in the living amoebae. When cells are fixed, soluble myosins might precipitate, or attach to actin filaments, in places where they do not normally occur, or myosins might be lost from cells during the subsequent steps of the cytochemical procedures. Similarly, myosin isoenzymes might differentially redistribute during the isolation of plasma membranes.

However, although none of these possible sources of errors has been unequivocally eliminated, we think it unlikely that three entirely independent methods, fixation by formaldehyde, fixation by glutaraldehyde and isolation of plasma membranes, would have given the same misleading result. Moreover, myosin II is larger and less soluble than myosin IA and IB and all three purified myosins bind tightly to F-actin, which greatly stimulates their Mg^{2+}-ATPase activities. There is no reason to suppose, therefore, that myosin II would be preferentially extracted from, or that myosins IA and IB would selectively and artefactually bind to, just that region of the cell which is particularly enriched in actin filaments. Nonetheless, it is important that the observations in this paper be confirmed by independent methods.

Finally, if the myosin I and II isoenzymes are, as we suggest, differentially localized, it is likely that they function in different cellular activities with the myosin I isoenzymes being involved in processes, possibly such as endocytosis, that occur at or near the cell surface. Because of the unusual physical properties of myosin IA and IB, their functions may involve actomyosin interactions of a type not previously proposed.

We thank Dr Susan Lowey for chicken pectoralis muscle myosin and its antibody, Dr Blair Bowers for guidance in the immunocytochemical procedures, Dr Michael Bustin for help with the immunofluorescence studies, and Mr Thomas Olszewski and Mrs Margaret Clark for technical assistance.

Received 19 February; accepted 9 May 1980.

1. Korn, E. D. *Proc. natn. Acad. Aci. U.S.A.* **75,** 588–599 (1978).
2. Pollard, T. D. & Korn, E. D. *J. biol. Chem.* **248,** 4682–4690 (1973).
3. Maruta, H., Gadasi, H., Collins, J. H. & Korn, E. D. *J. biol. Chem.* **254,** 3624–3630 (1979).
4. Gadasi, H., Maruta, H., Collins, H. J. & Korn, E. D. *J. biol. Chem.* **254,** 3631–3636 (1979).
5. Gadasi, H. & Korn, E. D. *J. biol. Chem.* **254,** 8095–8098 (1979).
6. Maruta, H. & Korn, E. D. *J. biol. Chem.* **252,** 6501–6509 (1977).
7. Pollard, T. D., Stafford, W. F. & Porter, M. E. *J. biol. Chem.* **253,** 4798–4808 (1978).
8. Laemmli, U. K. *Nature* **229,** 680–685 (1970).
9. Renart, J., Reiser, J. & Stark, G. R. *Proc. natn. Acad. Sci. U.S.A.* **76,** 3116–3120 (1979).
10. Adair, W. S., Jurivich, D. & Goodenough, U. *J. Cell Biol.* **79,** 281–285 (1978).
11. Ehrlich, H. B., Levinson, J. R., Cohen, S. N. & McDevitt, H. D. *J. biol. Chem.* **254,** 12240–12247 (1979).
12. Parker, R. C. *Methods of Tissue Culture* 3rd edn, 31 (P. Hueber, New York, 1961).
13. Lazarides, E. & Weber, K. *Proc. natn. Acad. Sci. U.S.A.* **71,** 2268–2272 (1974).
14. Mazurkiewicz, J. E. & Nakane, P. K. *J. Histochem. Cytochem.* **20,** 969–974 (1972).
15. Sternberger, L. A. *Immunocytochemistry* (Prentice-Hall, Englewood Cliffs, 1974).
16. Ulsamer, A. G., Wright, P. L., Wetzel, M. G. & Korn, E. D. *J. Cell Biol.* **51,** 193–215 (1971).
17. Bowers, B. & Korn, E. D. *J. Cell Biol.* **41,** 786–805 (1969).
18. Korn, E. D. & Wright, P. L. *J. biol. Chem.* **248,** 439–447 (1973).
19. Pollard, T. D. & Korn, E. D. *J. biol. Chem.* **248,** 448–450 (1973).

Surface activation of blood coagulation, fibrinolysis and kinin formation

Ronald L. Heimark, Kotoku Kurachi, Kazuo Fujikawa & Earl W. Davie
Department of Biochemistry, University of Washington, Seattle, Washington 98195

The activation of plasma prekallikrein by single-chain factor XII has been studied in the presence of high molecular weight kininogen and kaolin. The data indicate that factor XII can initiate blood coagulation, fibrinolysis or kinin generation in the presence of kaolin and does so by converting prekallikrein to kallikrein. An enzyme cascade is then generated leading to the formation of fibrin, plasmin or bradykinin in three closely related physiological events.

THE initiation of the contact phase of blood coagulation by a surface, such as glass or kaolin, leads to an enzyme cascade resulting in fibrin formation[1–3]. A similar enzyme cascade occurs during the formation of plasmin in the surface-activated fibrinolytic system and the generation of kinin in the presence of a surface.

0028–0836/80/310456—05$01.00

The molecular basis for the initiation of these three closely related processes has been difficult to explain as two of the proteins involved in the surface activation reaction, factor XII (Hageman factor, ref. 4) and prekallikrein[5,6] (Fletcher factor), are present in plasma as zymogens to serine proteases. Furthermore, these two proteins have an unusual relationship to each other in that factor XII$_a$ converts prekallikrein to kallikrein[6–10], and kallikrein converts factor XII to factor XII$_a$ (refs 9, 11–16). Thus, it has been difficult to determine whether factor XII$_a$, kallikrein or some other protein is responsible for initiating these cascade reactions. A third plasma protein, high molecular weight kininogen[17–20] (HMW kininogen), stimulates the activation of prekallikrein by factor XII$_a$ and the activation of factor XII by kallikrein[21–26]. HMW kininogen seems to function as a cofactor in these reactions.

The role of factor XII and factor XII$_a$

Considerable attention has been directed towards factor XII as the principal protein involved in the surface activation of blood coagulation, fibrinolysis and kinin formation. Bovine and human factor XII are single-chain glycoproteins with molecular weights of about 74,000 (refs 27–29). The bovine preparation has no detectable esterase or amidase activity in the absence or presence of a surface, such as kaolin, dextran sulphate, or sulphatide[26,30]. Furthermore, it shows very little reactivity towards serine protease inhibitors, such as diisopropyl fluorophosphate or antithrombin III and heparin, in the absence or presence of a surface. Bovine factor XII$_a$ is composed of a heavy chain (MW 46,000) and a light chain (MW 28,000), and these two chains are held together by a disulphide bond(s)[30]. The two-chain protein has substantial esterase and amidase activity and readily activates prekallikrein[31] and factor XI$_a$ (ref. 32) by the cleavage of a specific internal peptide bond(s) in each of these proteins. Bovine factor XII$_a$ is also readily inhibited by diisopropyl fluorophosphate or antithrombin III and heparin[30]. In contrast, single-chain human factor XII possesses amidase activity when previously exposed to ellagic acid–Sepharose[33]. Human factor XII, however, reacts about 600 times more slowly with diisopropyl fluorophosphate than factor XII$_a$ in the presence or absence of kaolin[34]. Accordingly, it has been suggested that factor XII may participate in the initiation of blood coagulation as a weakly active zymogen[34]. In whole plasma, radiolabelled human factor XII was shown to be converted to factor XII$_a$ during the coagulation process[35]. It was not established, however, whether the activation of factor XII was an initial or a secondary event in the contact activation reaction. Furthermore, it has not been clear from the various studies on human and bovine factor XII whether the single-chain molecule or the two-chain factor XII$_a$ participates as a catalyst in the initial reactions involving prekallikrein and HMW kininogen.

Involvement of factor XII in factor XI activation

Recently, Saito[24] reported the activation of human factor XI (plasma thromboplastin antecedent) by factor XII in the presence of HMW kininogen and ellagic acid. No evidence was obtained to indicate that human factor XII was converted into lower molecular weight fragments during the reaction. We have studied the activation of bovine factor XI by single-chain bovine factor XII in the presence of sulphatide, dextran sulphate or kaolin plus HMW kininogen[32]. In the latter experiments, factor XI (MW 124,000) was converted to factor XI$_a$ (MW 124,000) by the cleavage of an internal peptide bond in each of the two nearly identical chains of the precursor molecule. The bovine factor XII was converted to factor XII$_a$ in the latter portion of this reaction, however, by the newly generated factor XI$_a$ (ref. 32). Homogeneous preparations of bovine factor XI (ref. 36), factor XII (ref. 27) and HMW kininogen[26] were used in these studies. The activation of factor XI by factor XII provided direct evidence to support the concept that single-chain factor XII can act as a catalyst, but only in the presence of a highly specific substrate and a negatively charged surface.

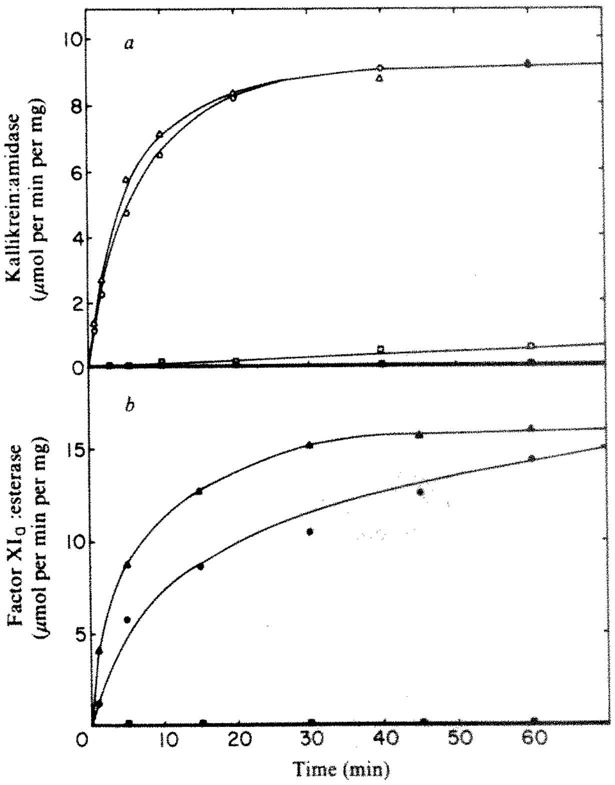

Fig. 1 Time course for the activation of *a*, plasma prekallikrein and *b*, factor XI by factor XII or factor XII$_a$ in the presence of HMW kininogen and kaolin. Factor XII or factor XII$_a$ (0.14 μg) was preincubated with HMW kininogen (0.4 μg) and kaolin (20 μg) for 5 min at 37 °C in 0.05 M Tris–HCl, *p*H 7.5, containing 0.1 M NaCl. Reactions were initiated by the addition of prekallikrein (9 μg) or factor XI (9 μg). Incubations were carried out in siliconized glass tubes in a final volume of 0.1 ml. Aliquots (10 μl) were removed at various times and assayed for kallikrein or factor XI$_a$. In the assay for kallikrein: amidase activity, the samples were added to 0.99 ml of 0.05 M Tris–HCl, *p*H 8.0, containing 0.15 M NaCl, 10 mg per ml polybrene, 50 μg lima bean trypsin inhibitor, and 0.1 ml of 1.5 mM benzoyl-Pro-Phe-Arg-*p*-nitroanilide. The initial rate of amide hydrolysis was followed at 37 °C by the change in absorbance at 405 nm using a Gilford recording spectrophotometer. For the factor XI$_a$: esterase activity, aliquots were added to a solution of factor XII antibody to stop the reaction and hydrolysis of tosyl-L-arginine- [^{3}H]-methyl ester was followed in a Beckman scintillation counter (SL-100C) as previously described[32]. The coagulation proteins were prepared from bovine plasma and all were homogeneous by SDS-polyacrylamide gel electrophoresis. Protein concentrations were determined by absorption at 280 nm using an $E_{280}^{1\%}$ of 10.9 for prekallikrein[37], 12.6 for factor XI (ref. 36), 14.2 for factor XII (ref. 27) and the same value for factor XII$_a$. Their specific activities in a clotting assay with their respective deficient plasmas were as follows: factor XII (180 u per mg), factor XII$_a$ (280 u per mg), HMW kininogen (11 u per mg), plasma prekallikrein (60 u per mg), and factor XI (280 u per mg). Factor XII was treated with diisopropyl fluorophosphate (1 mM) at 37 °C for 60 min to remove any traces of factor XII$_a$, and the diisopropyl fluorophosphate was removed by dialysis against the reaction buffer. *a*: ○, prekallikrein plus factor XII, HMW kininogen and kaolin; △, prekallikrein plus factor XII$_a$, HMW kininogen and kaolin; ■, prekallikrein plus HMW kininogen and kaolin; □, prekallikrein plus factor XII. *b*: ●, factor XI plus factor XII, HMW kininogen and kaolin; ▲, factor XI plus factor XII$_a$, HMW kininogen and kaolin; ■, factor XI plus HMW kininogen and kaolin.

Activation of prekallikrein by factor XII and/or factor XII$_a$

In the present report, we describe the activation of bovine plasma prekallikrein by single-chain factor XII as well as factor XII$_a$ in the presence of HMW kininogen and kaolin. In these experiments, a homogeneous preparation of single-chain plasma prekallikrein (MW 82,000)[37] was used as substrate. This preparation of prekallikrein contained no detectable kallikrein or factor XII activity. Bovine factor XII or factor XII$_a$ was added to optimum amounts of HMW kininogen and kaolin, and the activation reaction was initiated by the addition of prekallikrein. The factor XII or factor XII$_a$-to-prekallikrein weight ratio was 1:65. In these conditions, prekallikrein was rapidly converted to kallikrein (Fig. 1*a*). The generation of kallikrein was measured by its amidase activity towards benzoyl-L-prolyl-L-phenylalanyl-L-arginine-*p*-nitroanilide. The initial rate of kallikrein generation was almost the same with either factor XII (open circles) or factor XII$_a$ (open triangles). No lag phase or sigmoidal curve was observed for the activation of prekallikrein by factor XII. A lag phase would be expected, however, if the conversion of factor XII to factor XII$_a$ were essential in this reaction. No activation of prekallikrein occurred in the absence of factor XII or factor XII$_a$ (solid squares). A small amount of activation occurred in the absence of kaolin (open squares). When prekallikrein was omitted from the reaction, no amidase activity was generated.

To test for the possibility of an extremely rapid conversion of factor XII to factor XII$_a$ by kallikrein early in the activation reaction, the conversion of prekallikrein to kallikrein was studied using ^{3}H-labelled factor XII as the enzyme. These experiments are important because kallikrein readily converts factor XII to factor XII$_a$, and this reaction could greatly reduce any lag phase in the reaction if the activation of prekallikrein were catalysed only by factor XII$_a$. The ^{3}H-factor XII was prepared by reductive alkylation by the procedure of Means and Feeney[38] using ^{3}H-NaBH$_4$ and formaldehyde. The ^{3}H-factor XII had the same clotting activity as the unlabelled protein and contained approximately 143,000 c.p.m. per µg. Furthermore, when a catalytic amount of kallikrein was used to activate ^{3}H-factor XII in the presence of kaolin, the generation of factor XII$_a$ esterase activity occurred in parallel with the disappearance of single-chain factor XII and the appearance of two-chain factor XII$_a$. This was shown by SDS polyacrylamide gel electrophoresis of the reaction products in reducing conditions (data not shown).

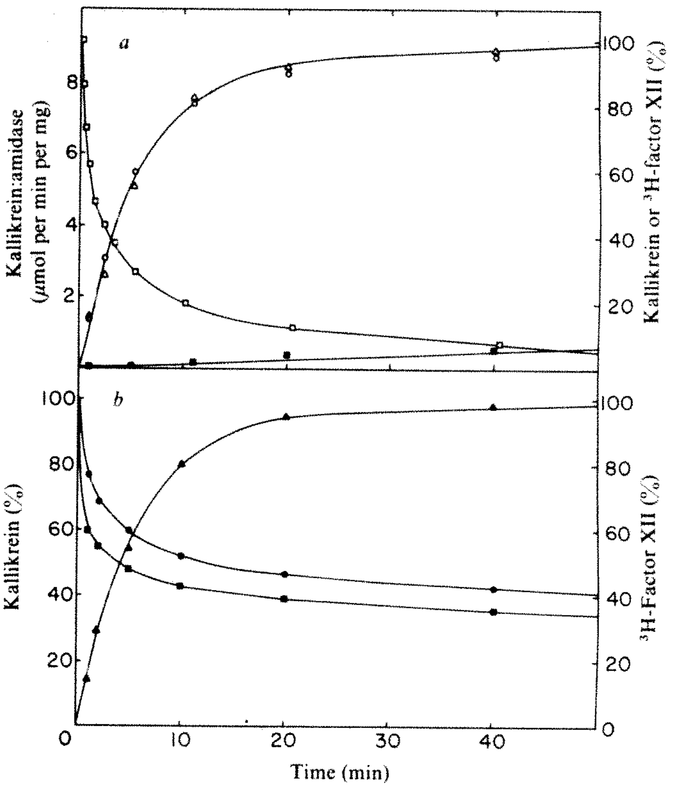

Fig. 2 *a*, Time course for the activation of plasma prekallikrein by ^{3}H-factor XII in the presence of HMW kininogen and kaolin. *b*, The reaction in the presence of RVV inhibitor II, a serine protease inhibitor from Russell's viper venom. ^{3}H-factor XII (0.84 µg) was preincubated with HMW kininogen (2.4 µg) and kaolin (120 µg) for 5 min at 37 °C in 0.05 M Tris-HCl, *p*H 7.5, containing 0.1 M NaCl. Reactions were then initiated by the addition of prekallikrein (55 µg) to give a final volume of 0.6 ml. Aliquots (10 µl) were removed at various times and assayed for kallikrein: amidase activity for the experiments shown in *a*. Samples (50 µl) were also subjected to SDS-polyacrylamide gel electrophoresis[39] in the presence of 5% 2-mercaptoethanol. The samples for electrophoresis were immediately added to sample buffer, boiled for 1 min, and then analysed on a 10% polyacrylamide slab gel. After staining (Coomassie brilliant blue R) and destaining, the gel was scanned with a Joyce-Loebl densitometer and the amount of kallikrein was determined from the tracings. To determine the amount of ^{3}H-factor XII, the gel was prepared for fluorography[40]. After developing the fluorogram, the band of ^{3}H-factor XII was sliced from the dried gel and the amount of radioactivity was determined by dissolving the gel slices in 30% H_2O_2 (99 vol:1 vol NH_4OH) followed by counting in Aquasol (NEN). The counting efficiency was 30%. *a*: ○, generation of kallikrein: amidase activity in the complete reaction mixture; ■, kallikrein: amidase activity in the absence of kaolin; △, generation of kallikrein as determined by densitometry of the stained gels; □, per cent ^{3}H-factor XII. *b*: ▲, generation of kallikrein in the complete reaction mixture plus RVV inhibitor II (114 µg), determined by densitometry of the stained gels; ■, per cent ^{3}H-factor XII in the reaction mixture containing 23 µg of RVV inhibition II; ●, per cent ^{3}H-factor XII in the reaction mixture containing 114 µg of RVV inhibitor II.

Activation of prekallikrein by factor XII

A time course for the activation of prekallikrein by ^{3}H-factor XII in the presence of HMW kininogen and kaolin is shown in Fig. 2*a*. The rate of formation of kallikrein (open circles) was very similar to that shown in Fig. 1*a*, and no lag phase was observed. The activation of prekallikrein was also followed by SDS-polyacrylamide gel electrophoresis on a slab gel using the method of Laemmli[39]. In these experiments, samples were removed at various times during the activation reaction by factor XII and examined in the presence and absence of 2-mercaptoethanol. In the absence of reducing agent, prekallikrein appeared as a band of MW 82,000. This indicated that little, if any, change in the molecular weight of prekallikrein occurred during its conversion to kallikrein. A difference in the SDS-polyacrylamide gel electrophoresis pattern of the prekallikrein was observed, however, after reduction of the samples with 2-mercaptoethanol. At zero time, prekallikrein appeared as a 82,000-MW band. During the first few minutes of the activation reaction, three new, faster-moving bands appeared, including a heavy chain (apparent MW 52,000) and a light chain (apparent MW 38,000 or 33,000). The appearance of these bands as measured by densitometry (Fig. 2*a*, open triangles) occurred in parallel with the formation of kallikrein as measured by its amidase activity (Fig. 2*a*, open circles). These data indicate that bovine prekallikrein was converted to kallikrein by the hydrolysis of an internal peptide bond in the single-chain precursor molecule in the presence of HMW kininogen and kaolin. The cleavage of bovine prekallikrein by factor XII is very similar to that reported earlier for human prekallikrein activated by human factor XII$_a$ fragments (ref. 10). The SDS-polyacrylamide slab gel was then prepared for fluorography[40] and the amount of radioactivity present in ^{3}H-factor XII was determined. At zero time, the radiolabelled protein migrated as a single band (approximate MW 74,000) on SDS-polyacrylamide gel electrophoresis in the presence of 2-mercaptoethanol. As the ^{3}H-factor XII was converted to ^{3}H-factor XII$_a$ by the newly generated kallikrein, the ^{3}H-factor XII$_a$ appeared as a heavy chain (MW 46,000) and a light chain (MW 28,000) in the presence of 2-mercaptoethanol. After 2.5 min, 35% of the prekallikrein was converted to kallikrein (Fig. 2*a*, open circles), while 40% of the factor XII was still present as a single-chain molecule (Fig. 2*a*, open squares). After 5 min, 60% of the prekallikrein was converted to kallikrein, while only 30% of the factor XII was still in the single-chain form. After 5 min, the weight ratio of kallikrein-to-factor XII was nearly 40 : 1, and the conversion of factor XII to factor XII$_a$ was occurring very rapidly. These data indicate that single-chain factor XII converts prekallikrein to kallikrein in the initial phase of the activation reaction in the presence of HMW kininogen and kaolin. This conclusion is further supported by the fact that the initial rate of prekallikrein activation by either factor XII or factor XII$_a$ was nearly identical (Fig. 1*a*), and this would not be the case if the prior conversion of factor XII to factor XII$_a$ were required. These experiments also demonstrate that the latter part of the prekallikrein activation reaction is catalysed primarily by factor XII$_a$ which is rapidly generated after the formation of kallikrein.

The activation of prekallikrein by single-chain ^{3}H-factor XII was further examined in the presence of an excess of RVV inhibitor II, a low molecular weight serine protease inhibitor from Russell's viper venom. This protein inhibits bovine plasma kallikrein with a K_i of 0.29 nM (ref. 41) but has no effect on factor XII or factor XII$_a$. Thus, it is useful to restrict the effect of kallikrein on the activation of factor XII. The conversion of prekallikrein to kallikrein in the presence of a 5-M and a 25-M excess of the RVV inhibitor II relative to prekallikrein is shown in Fig. 2*b*. The weight ratio of ^{3}H-factor XII-to-prekallikrein was 1:65. The formation of kallikrein was measured by SDS-polyacrylamide gel electrophoresis in the presence of 2-mercaptoethanol as described for Fig. 2*a*. In these experiments, the rate of generation of kallikrein (Fig. 2*b*, solid triangles) in the presence of either a 5-M or a 25-M excess of kallikrein inhibitor was the same as that in the absence of the kallikrein inhibitor (Fig. 2*a*, open triangles). As before, no lag phase was observed. The conversion of factor XII to factor XII$_a$, however, was substantially reduced in the presence of the kallikrein inhibitor. With a 5-M excess of RVV inhibitor II, 35% of the prekallikrein was converted to kallikrein in 2.5 min, while 55% of the factor XII was in the single-chain form (Fig. 2*b*, solid squares). With a 25-M excess of RVV inhibitor II, 35% of the prekallikrein was converted to kallikrein in 2.5 min, while 70% of the factor XII was still in the single-chain form (Fig. 2*b*, solid circles). If the conversion of factor XII to factor XII$_a$ were an absolute requirement for this reaction, then a lag phase would have been readily detected in these experiments and the inital rate would have been much slower than that found for an equivalent amount of factor XII$_a$. These data strongly suggest that single-chain factor XII converts prekallikrein to kallikrein in the presence of HMW kininogen and kaolin and does so at a very rapid rate.

Activation of factor XI by factors XII or XII$_a$

Similar experiments were then carried out for the activation of bovine factor XI by factor XII or factor XII$_a$ in the same reaction conditions used in Fig. 1*a*, except that factor XI was substituted for prekallikrein. Factor XII readily activated factor XI in the presence of HMW kininogen and kaolin (Fig. 1*b*, solid circles). In these experiments, factor XI$_a$ was measured by its esterase activity towards tosyl-L-arginine methyl ester. The initial rate of activation of factor XI by factor XII was 2–4 times slower than that of factor XII$_a$ (Fig. 1*b*, solid triangles). The rate of activation of factor XI by factor XII$_a$, however, was almost the same as the activation of prekallikrein by factor XII$_a$ or factor XII (Fig. 1*a*). As factor XII$_a$ is a more effective catalyst than factor XII in the activation of factor XI, the generation of factor XII$_a$ by kallikrein is required for the rapid activation of factor XI and the eventual formation of fibrin in whole plasma.

The cascade mechanism is initiated by factor XII

These data strongly suggest that the initial event in the activation of the intrinsic pathway of blood coagulation involves a substrate-induced catalysis by single-chain factor XII (Fig. 3). In this reaction, factor XII, bound to the kaolin surface, converts prekallikrein to kallikrein. The kallikrein thus generated converts the kaolin-bound factor XII to factor XII$_a$, which in turn converts factor XI to factor XI$_a$. Each of these three reactions is stimulated by HMW kininogen or kinin-free HMW kininogen. Human kinin-free HMW kininogen and bradykinin are formed after the generation of the kallikrein in the initial reaction. In the presence of calcium, factor XI$_a$ then converts factor IX to factor IX$_a$. Eventually, thrombin is formed and this leads to the conversion of fibrinogen to fibrin[1]. Although the present experiments were carried out with clotting factors from bovine plasma, similar data have been obtained in preliminary experiments with purified clotting factors from human plasma. Thus, the mechanism shown in Fig. 3 seems applicable to other mammalian plasmas.

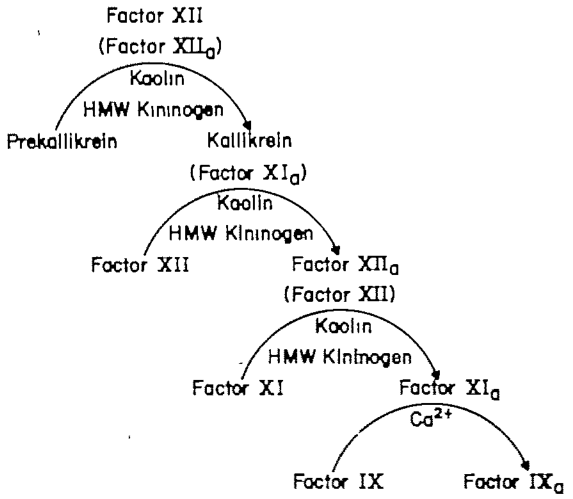

Fig. 3 A tentative mechanism for the surface activation of blood coagulation in the presence of kaolin.

Factor XII$_a$ will also activate prekallikrein after it is generated in the initial reactions. The activation of prekallikrein is not catalysed by kallikrein, factor XI$_a$ or prekallikrein. Factor XI$_a$ will activate factor XII when it is generated by factor XII$_a$ (Fig. 3). We have not observed, however, an activation of human or bovine factor XII by factor XI$_a$. Recently, Wiggins and Cochrane[42] have reported the cleavage of rabbit factor XII by factor XI$_a$. In whole plasma, the activation of factor XII is probably catalysed primarily by kallikrein rather than factor XI$_a$, as kallikrein is generated first and it is about four times more active in the activation reaction than factor XI$_a$ (ref. 26). Thus, factor XI$_a$ probably has only a minor role in the activation of factor XII. Factor XII will also activate factor XI in the presence of kaolin and HMW kininogen, although the rate is slower than that catalysed by factor XII$_a$. Thus, the initiation of blood coagulation by kaolin occurs at a faster rate in the presence of prekallikrein which is converted to kallikrein, and this in turn leads to the formation of factor XII$_a$. When plasma deficient in prekallikrein is preincubated with kaolin for approximately 10 min before the addition of calcium, it has a normal clotting time[22]. In these conditions, optimal levels of factor XI$_a$ are probably generated by single-chain factor XII and the formation of factor XII$_a$ via kallikrein is not required[32]. The correction of the kaolin clotting time of prekallikrein-deficient plasma by factor XII (refs 17, 27) can also be explained by the fact that elevation of the level of this protein will lead to the direct activation of factor XI and bypass the requirement for prekallikrein in these conditions.

Consequences of our studies

The present data provide a mechanism for the initiation of blood coagulation, as well as fibrinolysis, and kinin generation by single-chain factor XII in the presence of a surface, such as kaolin. By this mechanism, a trace of factor XII$_a$, kallikrein or some other plasma or cellular protease as previously suggested[3,21], is not required to initiate the reactions. Also, it is not necessary to postulate the participation of factor XII or prekallikrein as weakly active zymogens as suggested by Griffin and Cochrane[34], as factor XII is as active as factor XII$_a$ in the activation of prekallikrein in the presence of kaolin and HMW kininogen. Whether or not this mechanism will be applicable for other negatively charged surfaces is not clear. The physiological importance of the surface activation reaction is evident when blood comes in contact with a foreign surface *in vivo*. This occurs following the implantation of artificial heart valves where the incidence of thrombosis on the valve is 20–25% (ref. 43). Similar problems are encountered when patients with kidney failure are subjected to haemodialysis, when fibrin formation often occurs in the shunt.

This work was supported in part by grant HL 16919 from the NIH. K.K. is a recipient of a Research Career Development Award HL 00404 from the NIH. The nomenclature for the various coagulation factors is that recommended by an International Nomenclature Committee[44]. We thank Dr W. Kisiel for supplying the highly purified RVV inhibitor II.

Received 17 December 1979; accepted 7 May 1980.

1. Davie, E. W., Fujikawa, K., Kurachi, K. & Kisiel, W. *Adv. Enzy.* **48,** 277–318 (1979).
2. Ratnoff, O. D. & Saito, H. *Curr. Topics Hemat.* **2,** 1–57 (1979).
3. Kaplan, A. P. *Prog. Hemostasis Thromb.* **4,** 127–175 (1978).
4. Ratnoff, O. D. & Colopy, J. E. *J. clin. Invest.* **34,** 602–613 (1955).
5. Hathaway, W. E., Belhasen, L. P. & Hathaway, H. S. *Blood* **26,** 521–532 (1965).
6. Wuepper, K. D. *J. exp. Med.* **138,** 1345–1355 (1973).
7. Nagasawa, S., Takahashi, H., Koida, M., Suzuki, T. & Schoenmakers, J. G. G. *Biochem. biophys. Res. Commun.* **32,** 644–649 (1968).
8. Kaplan, A. P. & Austen, K. F. *J. Immun.* **105,** 802–811 (1970).
9. Cochrane, C. G., Revak, S. D. & Wuepper, K. D. *J. exp. Med.* **138,** 1564–1583 (1973).
10. Mandle, R. & Kaplan, A. P. *J. biol. Chem.* **252,** 6097–6104 (1977).
11. Kaplan, A. P. & Austen, K. F. *J. exp. Med.* **133,** 696–712 (1971).
12. Komiya, M., Nagasawa, S. & Suzuki, T. *J. Biochem.* **72,** 1205–1218 (1972).
13. Cochrane, C. G., Revak, S. D., Aikin, B. S. & Wuepper, K. D. in *Inflammation: Mechanisms and Control* (eds Lepow, I. H. & Ward, P. A.) 119–138 (Academic, New York, 1972).
14. Bagdasarian, A., Lahiri, B. & Colman, R. W. *J. biol. Chem.* **248,** 7742–7747 (1973).
15. Revak, S. D., Cochrane, C. G., Johnston, A. & Hugli, T. *J. clin. Invest.* **54,** 619–627 (1974).
16. Griffin, J. H. *Proc. natn. Acad. Sci. U.S.A.* **75,** 1998–2002 (1978).
17. Saito, H., Ratnoff, O. D., Waldmann, R. & Abraham, J. P. *J. clin. Invest.* **55,** 1082–1089 (1975).
18. Wuepper, K. D., Miller, D. R. & Lacombe, M. J. *J. clin. Invest.* **56,** 1663–1672 (1975).
19. Donaldson, V. H., Glueck, H. I., Miller, M. A., Movat, H. Z. & Habal, F. *J. lab. clin. Med.* **87,** 327–337 (1976).
20 Colman, R. W. *et al. J. clin. Invest.* **56,** 1650–1662 (1975).
21. Griffin, J. H. & Cochrane, C. G. *Proc. natn. Acad. Sci. U.S.A.* **73,** 2554–2558 (1976).
22. Meier, H. K., Webster, M. E., Mandle, R., Colman, R. W. & Kaplan, A. P. *J. clin. Invest.* **60,** 18–31 (1977).
23. Schiffman, S., Lee, P. & Waldmann, R. *Thromb. Res.* **6,** 451–454 (1975).
24. Saito, H. *J. clin. Invest.* **60,** 584–594 (1977).
25. Chan, J. Y. C., Habal, F. M., Burrowes, C. E. & Movat, H. Z. *Thromb. Res.* **9,** 423–433 (1977).
26. Fujikawa, K., Heimark, R. L., Kurachi, K. & Davie, E. W. *Biochemistry* **19,** 1322–1329 (1980).
27. Fujikawa, K., Walsh, K. A. & Davie, E. W. *Biochemistry* **16,** 2270–2278 (1977).
28. Claeys, H. & Collen, D. *Eur. J. Biochem.* **87,** 69–74 (1978).
29. Griffin, J. H. & Cochrane, C. G. *Meth. Enzym.* **45,** 56–65 (1976).
30. Fujikawa, K., Kurachi, K. & Davie, E. W. *Biochemistry* **16,** 4182–4188 (1977).
31. Heimark, R. L., Fujikawa, K. & Davie, E. W. *Fedn Proc.* **37,** 1587 (1978).
32. Kurachi, K., Fujikawa, K. & Davie, E. W. *Biochemistry* **19,** 1330–1338 (1980).
33. Ratnoff, O. D. & Saito, H. *Proc. natn. Acad. Sci. U.S.A.* **76,** 1461–1463 (1979).
34. Griffin, J. H. & Cochrane, C. G. *Semin. Thromb. Hemostasis* **5,** 254–273 (1979).
35. Revak, S. D., Cochrane, C. G. & Griffin, J. H. *J. clin. Invest.* **59,** 1167–1175 (1977).
36. Koide, T., Kato, H. & Davie, E. W. *Biochemistry* **16,** 2279–2286 (1977).
37. Heimark, R. L. & Davie, E. W. *Biochemistry* **18,** 5743–5750 (1979).
38. Means, G. E. & Feeney, R. E. *Biochemistry* **7,** 2192–2201 (1968).
39. Laemmli, U. K. *Nature* **227,** 680–685 (1970).
40. Bonner, W. M. & Laskey, R. A. *Eur. J. Biochem.* **46,** 83–88 (1974).
41. Iwanaga, S., Takahashi, H. & Suzuki, T. *Meth. Enzym.* **45,** 874–881 (1976).
42. Wiggins, R. C. & Cochrane, C. G. *J. exp. Med.* **150,** 1122–1132 (1979).
43. Spencer, F. D. in *Principles of Surgery* (ed. Schwartz, S. I.) 627–690 (McGraw-Hill, New York, 1969).
44. Wright, I. S. *J. Am. med. Ass.* **170,** 325–328 (1959).

Distinctive sequence of human mitochondrial ribosomal RNA genes

I. C. Eperon, S. Anderson & D. P. Nierlich*
MRC Laboratory of Molecular Biology, Hills Road, Cambridge CB2 2QH, UK

The nucleotide sequence spanning the ribosomal RNA (rRNA) genes of cloned human mitochondrial DNA reveals an extremely compact genome organization wherein the putative tRNA genes are probably 'butt-jointed' around the two rRNA genes. The sequences of the rRNA genes are significantly homologous in some regions to eukaryotic and prokaryotic sequences, but distinctive; the tRNA genes also have unusual nucleotide sequences. It seems that human mitochondria did not originate from recognizable relatives of present day organisms.

HUMAN mitochondrial DNA comprises a duplex closed circle of molecular weight 10×10^6, which has been shown to code for several proteins[1] and RNA species[2]. Two RNAs (12S and 16S) are conspicuous by their stability, methylation and equimolar synthesis[3,4], being the RNA components in 60S mitochondrial ribosomes[5,6]. These unique genes[7] are adjacent[8], and were mapped relative to the 4S RNA genes[9] and the *Hpa*II cleavage points in mitochondrial (mt) DNA[2,10].

It has been suggested that mitochondria are derived by endosymbiosis from prokaryotes, based on the sensitivity of ribosomes to antibiotics[11] and initiation of polypeptides with formylmethionine[12]. However, mammalian mitochondrial ribosomes and rRNAs are unusually small, and all but plant mitochondria also lack a 5S rRNA [13]. The rRNA sequences, being the only identified large genes with nuclear and prokaryotic counterparts, should clarify phylogenetic relatedness (for example, in chloroplasts the 16S rRNA gene[14] has shown near identity to that from *Escherichia coli*). This comparison should also clarify the sequences necessary for the function of these small rRNAs.

Most of the *Mbo*I fragments from human placental mt DNA have been mapped and cloned in the *Bam*HI site of the plasmid pBR322 (ref. 15); these have been used to determine the rRNA gene sequences presented here.

DNA sequence analysis

Figure 1 shows the map established for the restriction enzymes *Mbo*I (ref. 11) and *Hpa*II (ref. 10). The cloned *Mbo*I fragments 7, 14, 12, 3a, 18, 19 and 9 were sequenced using the dideoxy chain-termination method[16]. Single-stranded template was prepared by cleavage of the pBR322 moiety of the recombinant plasmid at the single sites for the enzymes *Hin*dIII or *Sal*I, followed by exonclease III digestion[17] which results in degradation of each strand from the 3′ end, exposing different strands in each case. An example is given in Fig. 2, which shows the sequence of the tRNA$^{\mathrm{Val}}$ gene and the 3′ end of the 12S rRNA gene.

Small inserts were sequenced using adjacent pBR322 restriction fragments as primers; larger inserts required the use of restriction fragments purified from the insert, which were often pretreated with exonuclease III to give sequence information within the region complementary to the restriction fragment[18]. Where the internal fragments were large, ribosubstitution of the 3′ end of the fragment was used to generate a new 5′ end for the extended chains on cleavage with alkali or ribonuclease. The published technique[19] was modified to allow direct ribosubstitution of the fragments before addition of the template:

---

* Permanent address: Department of Microbiology, College of Letters and Science, University of California, Los Angeles, California 90024.

0028–0836/80/310460—08$01.00

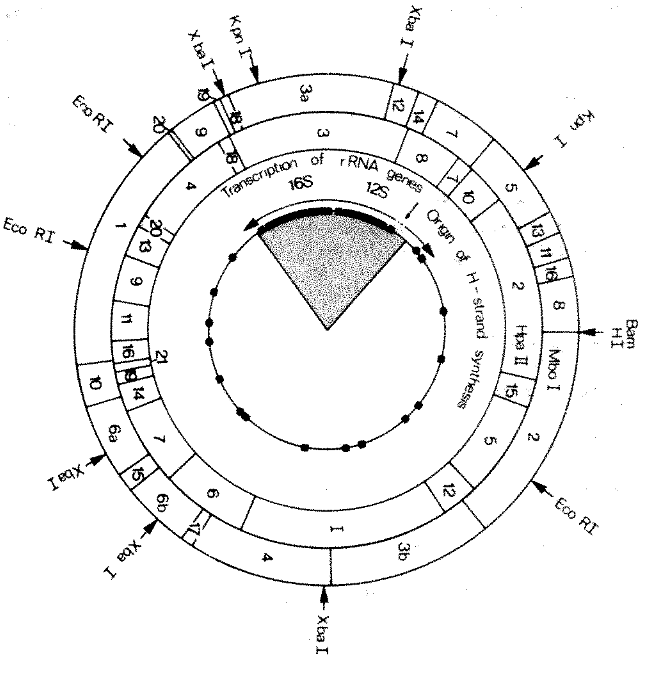

Fig. 1 The *Mbo*I restriction enzyme map of human mt DNA[11] is correlated with that of *Hpa*II[10], based on their alignments with some of the other enzyme cleavage sites marked and corrected according to the sequence in the region published here, which is shaded. The rRNAs are marked, as are the L-strand (■) and H-strand (●) sequence 4S RNAs[10]. The origin and direction of H-strand synthesis are shown.

incubation of the fragment with a ribonucleotide triphosphate and the Klenow fragment of DNA polymerase I at 37 °C allowed exchange of the 3′-terminal deoxyribonucleotide or 'filling-in' of the restriction fragment with the ribonucleotide. This eliminated the possibility that the overlapping ends of the exonuclease-degraded template could be substituted. EDTA was used to chelate Mn^{2+} during the reaction to prevent ribonucleotide incorporation during extension with deoxy- and dideoxynucleotides without recourse to column separation steps (I.C.E., unpublished).

Single-stranded template DNA prepared by exonuclease digestion can give a relatively high background and two other techniques were also used. One involved the separation of complete plasmid strands on alkaline RPC-5 columns (ref. 20 and B.A. Roe, manuscript in preparation) after cleavage of the closed circular duplex at a unique restriction enzyme site. This was most satisfactory where the pBR322 vector contained large inserts that were asymmetric with respect to the base compositions of the two strands, although recovery was variable. The second technique involved recloning of the isolated insert into the *Bam*HI site of the double-stranded form (RFI) of a derivative of the single-stranded bacteriophage M13 mp2 (refs 21–23).

To establish the orientation of the *Mbo*I fragments, and to ascertain whether very small fragments might have been missed in the mapping experiments, fragments prepared from the pBR322 clones were used for priming on HeLa mt DNA that had been digested by exonuclease III from the *Bam*HI, *Eco*RI or *Xba*I sites. The sequences obtained thus overlapped the *Mbo*I sites. Further confirmation was provided by sequence analysis of *Alu*I fragments (A. R. Coulson and F. Sanger, personal communication). The sequence obtained is shown in Fig. 3, with the *Mbo*I sites and extent of the probable genes indicated.

Organization of the genome

The tRNA genes have been assigned to the sequences shown (Figs 3, 4) by detection of likely clover-leaf structures (using the computer program TRNASU: R. Staden, unpublished) and features of the sequence that are common to all previously identified tRNAs[24,25]. The assignments correlate well with the map positions identified by electron microscopy of HeLa 4S RNA–mt DNA hybrids. No further likely tRNA genes were found when the possibility of insertions in the anticodon loop, analogous to those found elsewhere[26–28], was allowed.

The rRNAs were exactly located by the accurate homology with short sequences from the 5′ ends of the HeLa rRNAs[2], and found to abut tRNA genes at these termini (Fig. 3). The 3′ ends cannot be identified at present, although the extensive sequence homology to known small subunit rRNA sequences to within approximately 12 nucleotides from their 3′ termini (Figs 5, 6*a*) suggests that the 12S 3′ terminus is very close to the $tRNA^{Val}$ gene. This proximity agrees with mapping by electron microscopy, which has shown that the gap between the two rRNA genes is less than 500 base pairs[8] and that a 4S RNA maps between the two[9]. This closeness may involve a conjunction of the 12S rRNA and $tRNA^{Val}$ genes as at the 5′ end of both rRNA genes.

The lack of an intergenic sequence at some junctions suggests that a large initial transcript will be produced: this would agree with the large sizes of the HeLa mitochondrial transcripts hybridizing to the heavy (H) strand, the largest of which (9.0×10^5 MW, equal to the sum of the rRNAs) is found polyadenylated and unpolyadenylated[2,29]. The polyadenylated species has a short halflife compared with some other discrete mitochondrial 'poly(A)-containing' RNAs and is notable among these for being present in the polysomal fraction to a very small extent, as expected for a rRNA precursor. Resistance of restriction fragment–rRNA hybrids to exo- and endonucleolytic enzymes demonstrated that neither of the rRNA genes is 'split' by an intervening sequence in HeLa mitochondria[2].

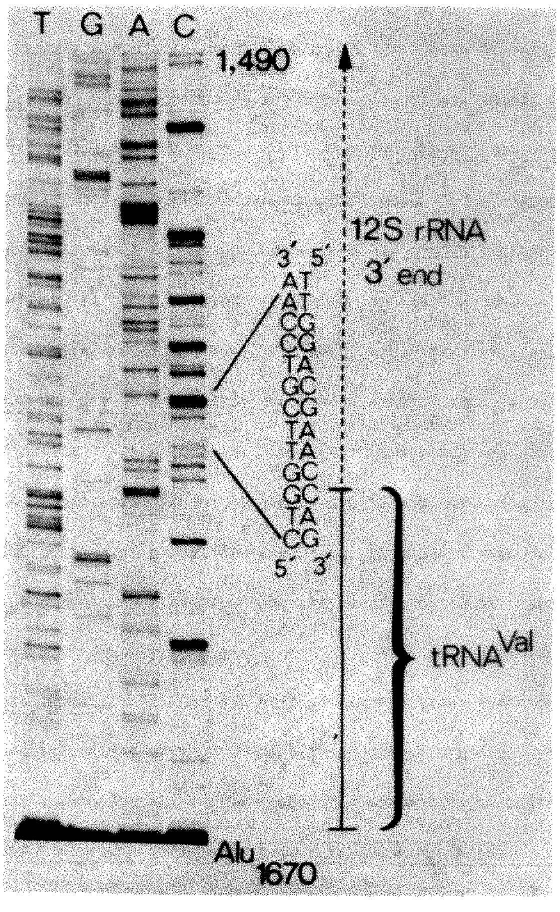

Fig. 2 A chain-termination sequencing gel showing the sequence through the $tRNA^{Val}$ gene and the 3′ end of the 12S rRNA, in the complementary sense. The primer is 223 bases long (the *Alu*I fragment from 1,671–1,894 of Fig. 3), and the resultant sequence from priming on exonuclease-treated template (*Ava*I digest of *Mbo*I fragment 3a cloned in pBR322) can be read from this 6% thin gel[86], run for 4 h, to a total polynucleotide length of 400 bases, that is, to 1,490 on Fig. 3. The sequence through the junction of the two genes is shown.

In *E. coli*, processing of the 16S rRNA probably involves initial cleavage by RNase III of a large inverted repeat that flanks the 16S gene[30], followed by at least RNase M16 cleavage to generate the mature 5′ terminus[31]. Eukaryotic nuclear rRNA transcripts also include large flanking sequences that are later removed[32,33], although the available sequence data do not suggest that these are inverted repeats (ref. 34 and K. G. Skryabin, personal communication). The 'butt-jointing' of mt tRNA genes at one or both end of the rRNAs implies a totally different processing mechanism, involving recognition of the structure or sequence of regions within mature transcripts and simple cleavages around the rRNA genes if both mature from the same transcript.

This mechanism implies a novel method for the production of the 3′ terminus of mature tRNAs, which in *E. coli* and *Bombyx mori* probably involves 3′,5′ exonuclease activity[35], as mitochondrial tRNA^{Phe} and tRNA^{Val} abut rRNA genes at their 3′ termini. However, single cleavage at the 5′ terminus of the tRNA genes would not be unusual: such a cleavage is catalysed in *E. coli* by RNase P, the rate being dependent on the secondary

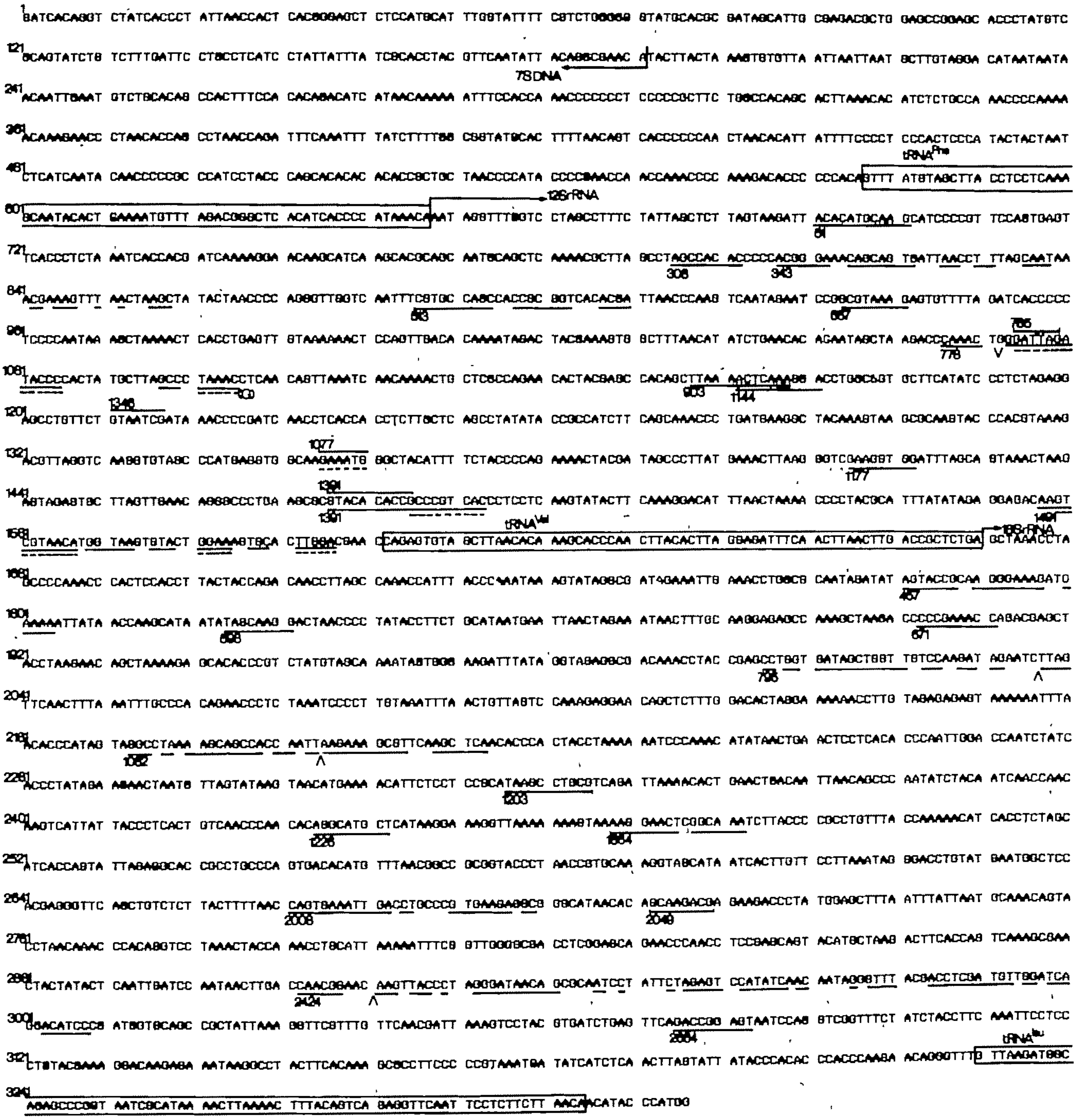

Fig. 3 The sequence of the region shaded in Fig. 1 is shown, with the tRNA genes boxed and the 5′ termini of the 12S and 16S rRNA genes shown; this is L-strand sequence, which corresponds to the RNA sequence. Numbers down the left-hand edge are those of this mt sequence, and those adjacent to underlining are those of the *E. coli* rRNAs. The 5′ terminus of 7S DNA, which is complementary to the strand shown, is also marked. Underlining shows regions of homology with the *E. coli* rRNAs ≥ 8 nucleotides, with surrounding smaller blocks in the same phase. Λ and V indicate that the *E. coli* rRNAs have one nucleotide more or less, respectively, in the areas of parallel sequence. Overlined regions are homologous to sequences (≥pentamers) identified by Woese *et al*[72] as universal among prokaryotes and kethoxal modifiable in 30S ribosomal subunits of *E. coli*. Broken underlining emphasizes those sequences that are identifiably homologous (assuming that sites would be in the same 5′–3′ order along the two rRNA sequences) to sites identified by Herr *et al.*[73] as those in 16S rRNA of *E. coli* that must be unmodified by kethoxal for 30S–50S subunit association.

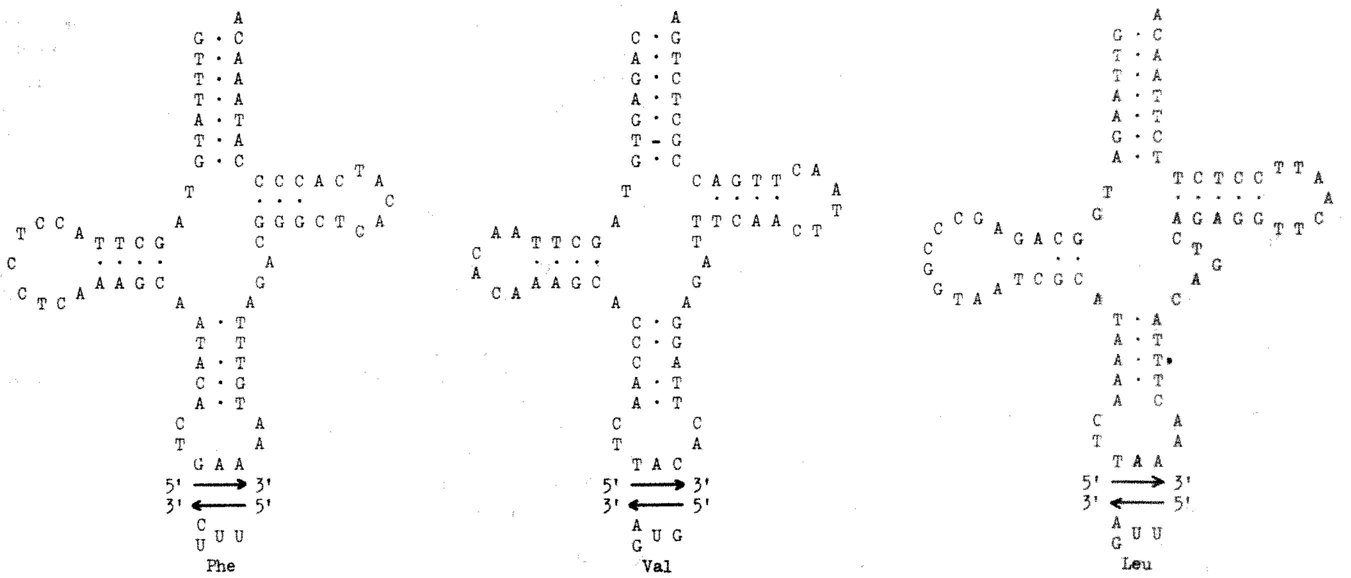

Fig. 4 A clover-leaf arrangement of the tRNA genes. The 3′ CCA sequence common to all other tRNAs is not encoded. G–U wobble is assumed in the codons recognized[46]. Loop I is the left-hand loop of this arrangement and often contains dihydrouridine, and loop IV is the right-hand loop which is usually characterized by the sequence G-T-pseudouridine-C.

or tertiary structure of the tRNA moiety of the substrate[36], and a similar *in vitro* activity has been isolated from the eukaryote, *B. mori*[35]. Cleavage around both termini of mt tRNA sequences in the primary transcripts by an analogous activity to RNase P is a possible general processing mechanism in human mitochondria, agreeing with the approximate correlation found between the length of mapped inter-tRNA sequences and the sizes of encoded proteins[2] and with the generally larger sizes of the polyadenylated RNA species.

The origin of H-strand replication of HeLa mt DNA was initially mapped by locating the D-loop within large restriction fragments by electron microscopy[37], and later by hybridization of the D-loop-forming 7S single-stranded DNA fragment to small restriction fragments with subsequent primed synthesis[38]. A sequence of the HeLa 7S DNA at its 5′ end and adjacent restriction fragment sequences have been published[39]. The placental sequence differs slightly from the HeLa sequence in that nucleotides 263–264 are A–C rather than just G, and there are three fewer Cs in the block 303–315.

The function of the region between the 5′ end of the 7S DNA (H-strand sequence) and the 5′ end of the first tRNA^{Phe} (light-strand sequence) seems likely to include that of initiating transcription of L-strand sense RNA, but there are no sequences resembling the initiation sequences found in *E. coli*[40] or those before the 5′ end of transcripts in eukaryotes. Further, there are no obvious repeated sequences analogous to the two or more promoters[41,42] or RNA polymerase binding sites[43] found before rRNA genes in *E. coli* and *Xenopus*[44] that have been postulated to play a part in the high level of transcription of these genes. The rRNAs in mitochondria are comparatively stable[4] and this, rather than a high frequency of transcription, may account for their predominance *in vivo*.

Sequences of tRNA genes

With the exception of those flanking the cytochrome oxidase subunit II gene in human mitochondria[45], previously published mt tRNA sequences have come from *Neurospora* or *Saccharomyces* and have shown most of the features common to prokaryotic and eukaryotic tRNAs. Only the initiator tRNA from *Neurospora crassa*[46], for example, seems to have radically altered those nucleotides identified [from X-ray crystallographic studies on yeast cytoplasmic tRNA^{Phe} (ref. 47)] as being involved in the loop I–loop IV tertiary interactions.

In contrast, the sequences presented here (Fig. 4, drawn on the assumption that stem lengths are conserved) differ considerably from other tRNA sequences. This is most noticeable in the lengths and sequences of loops I and IV, where many 'invariant' features are lacking, and in the poor base pairing in the stem to loop IV of tRNA^{Phe}. These changes may reflect altered possibilities of interaction between the two loops. The significance of the retained 'invariant' and common features cannot be assessed from so few sequences and will be discussed elsewhere.

Sequence analyses of the genes coding for the yeast ATPase subunit 9 (refs 48, 49) and cytochrome oxidase subunit II[45,50] (in human and yeast mitochondria) have recently shown, by comparison with the yeast and beef protein sequences respectively, that threonine (in yeast only) and tryptophan (and perhaps methionine in human mitochondria) are coded for by triplets which otherwise have different specificities in the 'universal' genetic code. The codons corresponding to the tRNAs published here, UUC(U), GUA(G) and UUA(G), do not seem to be anomalous in protein–DNA sequence comparison, and so probably do code for the amino acids shown (Fig. 4).

Like the sequences of yeast and *Neurospora* mt tRNAs[51], the human mt tRNA sequences published here show no greater homology to prokaryotes than to eukaryotes, seeming to form a rather distinct class. At some positions in tRNA sequences that are apparently characteristic of prokaryotes or eukaryotes, these genes frequently differ from both. The lack of agreement with a recent prokaryotic origin is emphasized by the inability of *E. coli* aminoacyl tRNA synthetases to charge mt tRNAs[52,53]. The HeLa cytoplasmic enzymes were partially successful in some cases[53] with HeLa mt tRNAs, one of which involved valine incorporation despite the fact that the human placental mt tRNA^{Val} has lost the conserved positions found in prokaryotic, eukaryotic and yeast mt tRNAs.

The 16S ribosomal RNA gene

Because relatively little is known about mitochondrial ribosomes, the significance of the sequence shown in Fig. 3 must be brought out by comparison with known sequences.

The homology of *E. coli* 23S rRNA[54] to this 16S rRNA does not extend to the 3′ end of the former sequence, resulting in some uncertainty about the length of the latter gene. Despite this and the considerable difference in probable lengths (2,904 to 1,559 nucleotides), there are regions of homology between the two. Regions with eight common nucleotides, with surrounding smaller blocks of homology in the same phase, have been shown in Fig. 3 where these regions occur in the same order in both sequences. The largest region of homology is found between nucleotides 2,910 and 3,010 of Fig. 3, corresponding to nucleotides 2,422–2,522 of the 23S rRNA. This is within the region that has been identified as involved in the interface between *E. coli* ribosomal subunits, the RNA being protected against kethoxal modification on 30S–50S association[55], although the exact sites of modification are not conserved. More extensive homology to this region of the 23S rRNA has been reported in a partial sequence of the yeast mt 21S rRNA gene[54]. Nucleotides 2,934 and 2,990 of Fig. 3 correspond to 21S rRNA nucleotides altered in chloramphenicol-resistant mutants of yeast and are therefore probably involved in binding the 3′ terminus of aminoacyl tRNAs. Only 2 of the 16 kethoxal-modifiable sites found in *E. coli* 50S subunits[54] occur within the underlined regions, suggesting a low level of conservation of exposed sequences in general.

The 12S ribosomal RNA gene

By contrast with the absence of sequences from cytoplasmic large rRNAs, some of the yeast small (18S) cytoplasmic rRNA sequence[6,7] is known, as is that of the *E. coli* 16S rRNA[56,57]. The involvement of the 3′ end of 16S rRNA in initiation of protein synthesis has led to the determination of short sequences at the 3′ ends of many small subunit rRNAs (Fig. 5).

The degree of complementarity[58] and binding[59] of the 3′-terminal sequence of *E. coli* 16S rRNA to a polypurine stretch before the initiation codons in bacteriophage RNA has been correlated with the level of translation of these RNAs. Complementarity alone, however, does not fully explain the level of binding, or the translational preferences of ribosomes from various bacterial species[60,61]. In contrast, eukaryotic ribosomes show comparatively little messenger discrimination; the 3′-terminal sequences of eukaryotic 18S rRNAs are highly conserved[62], and no region of complementarity has been identified in eukaryotic mRNAs that has any constant relationship to the initiation codon. The eukaryotic ribosome–Met tRNA$^{\mathrm{Met}}$ complex[63] may therefore not recognize internal regions of mRNA, but could 'scan' the mRNA for the first initiation codon[64], after binding near the 5′ end[65,66]; complex binding[65] and the monocistronic translation of prokaryotic mRNA are enhanced by a 'cap' (refs 67, 68).

The comparison shown in Fig. 6*a* clearly illustrates that the small subunit rRNA from human mitochondria lacks the polypurine-complementary sequence (CCUCC) found in prokaryotes. Although the exact 3′ end of the 12S rRNA has not been established, it is apparent (Fig. 6*b*) that any extended stem would be less stable than that of the analogous structure in *E. coli* if the rRNA gene does not overlap the tRNA$^{\mathrm{Val}}$ gene. This stability may be necessary for dissociation (after initiation) of the prokaryotic CCUCC sequence from the mRNA[59], and hence may be diagnostic of such a mode of initiation. No region of complementarity to the 3′ end of 12S rRNA has been found appropriately near the initiation codon for the cytochrome oxidase subunit II[46] or other structural genes (B.G. Barrell, personal communication).

The absence of these prokaryotic characteristics suggests that there is no sequence-specific binding of ribosomes and internal initiation, but rather that the long mitochondrial transcripts are processed to monocistronic units as in eukaryotes. If so, initiation seems likely to be dependent on the 5′ terminus *per se* or the first AUG codon for transcripts are not capped and in at least one case there would be no leader sequence (the AUG codon abuts a tRNA gene) unless translation preceded processing[46]. No eukaryotic transcripts are known where there is no leader sequence, although the cap structure does not seem to be invariably necessary for efficient translation, and the single prokaryotic example (λprm transcript[69]) is translated inefficiently. It is interesting, however, that the λprm transcript is translated; this suggests that initiation will occur at the AUG nearest to the 5′ end of mRNA, or that the 5′ end of mRNA is bound by the 30S–initiation factor complex. Mitochondria may represent a situation where there is no 12S–mRNA complementarity to favour internal initiation, nor a cap to enhance 5′-terminal binding, but a simpler mechanism underlying those developed elsewhere. If this is the case, the persistent failure of non-mitochondrial *in vitro* or *in vivo* systems to produce other than at best fragmentary translation products from mt RNA or DNA[70,71] may be ascribed to the use of the codon TGA (normally a terminator) to code for tryptophan[46,51], rather than a lack of initiation. One would, however, expect discrete products representing N-terminal peptides of proteins.

The 12S rRNA shows several other regions of homology to both *E. coli* and yeast small subunit rRNAs (Figs 3, 5, 6). The homology around the stem-loop structure near the 3′ end is

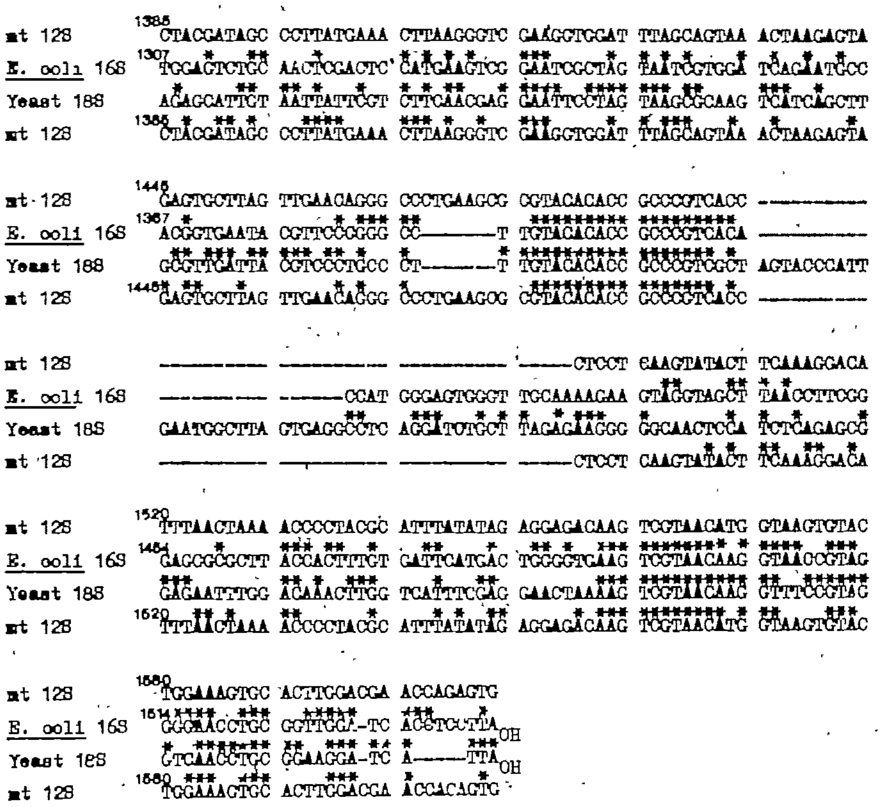
mt 12S 1385 CTACGATAGC CCTTATGAAA CTTAAGGGTC GAAGGTGGAT TTAGCAGTAA ACTAAGAGTA
E. coli 16S 1307 TGGAGTCTGC AACTCGACTC CATGAAGTCG GAATCGCTAG TAATCGTGGA TCAGAATGCC
Yeast 18S AGAGCATTGT AATTATTCGT CTTCAACGAG GAATTCCTAG TAAGCGCAAG TCATCAGCTT
mt 12S 1385 CTACGATAGC CCTTATGAAA CTTAAGGGTC GAAGGTGGAT TTAGCAGTAA ACTAAGAGTA
mt 12S 1445 GAGTGCTTAG TTGAACAGGG CCCTGAAGCG CGTACACACC GCCCGTCACC
E. coli 16S 1367 ACGGTGAATA CGTTCCCGGG CC—T TGTACACACC GCCCGTCACA
Yeast 18S GCGTTGATTA CGTCCCTGCC CT—T TGTACACACC GCCCGTCGCT AGTACCGATT
mt 12S 1445 GAGTGCTTAG TTGAACAGGG CCCTGAAGCG CGTACACACC GCCCGTCACC
mt 12S —CTCCT CAAGTATACT TCAAAGGACA
E. coli 16S —CCAT GGGAGTGGGT TGCAAAAGAA GTAGGTAGCT TAACCTTCGG
Yeast 18S GAATGGCTTA GTGAGGCCTC AGGATCTGCT TAGAGAAGGG GGCAACTCCA TCTCAGAGCG
mt 12S —CTCCT CAAGTATACT TCAAAGGACA
mt 12S 1520 TTTAACTAAA ACCCCTACGC ATTTATATAG AGGAGACAAG TCGTAACATG GTAAGTGTAC
E. coli 16S 1464 GAGCGCGCTT ACCACTTTGT GATTCATGAC TGGGGTGAAG TCGTAACAAG GTAACCGTAG
Yeast 18S GAGAATTTGG ACAAACTTGG TCATTTCGAG GAACTAAAAG TCGTAACAAG GTTTCCGTAG
mt 12S 1520 TTTAACTAAA ACCCCTACGC ATTTATATAG AGGAGACAAG TCGTAACATG GTAAGTGTAC
mt 12S 1580 TGGAAAGTGC ACTTGGACGA ACCAGAGTG
E. coli 16S 1514 GGGAACCTGC GGTTGGA-TC ACCTCCTTA OH
Yeast 18S GTCAACCTGC GGAAGGA-TC A—TTA OH
mt 12S 1580 TGGAAAGTGC ACTTGGACGA ACCAGAGTG

Fig. 5 The 3′ termini of mitochondrial *E. coli*[56,57] and yeast[34] small subunit rRNAs have been aligned to show the major blocks of homology, introducing gaps where appropriate. The scores for homologous nucleotides out of the total possible in this alignment are 45%, 57% and 45% for the pairs mitochondria·*E. coli*, *E. coli*·yeast and yeast·mitochondria, respectively. The mt DNA sequence has been extended for seven nucleotides into the tRNA$^{\mathrm{Val}}$ gene, illustrating the lack of homology there.

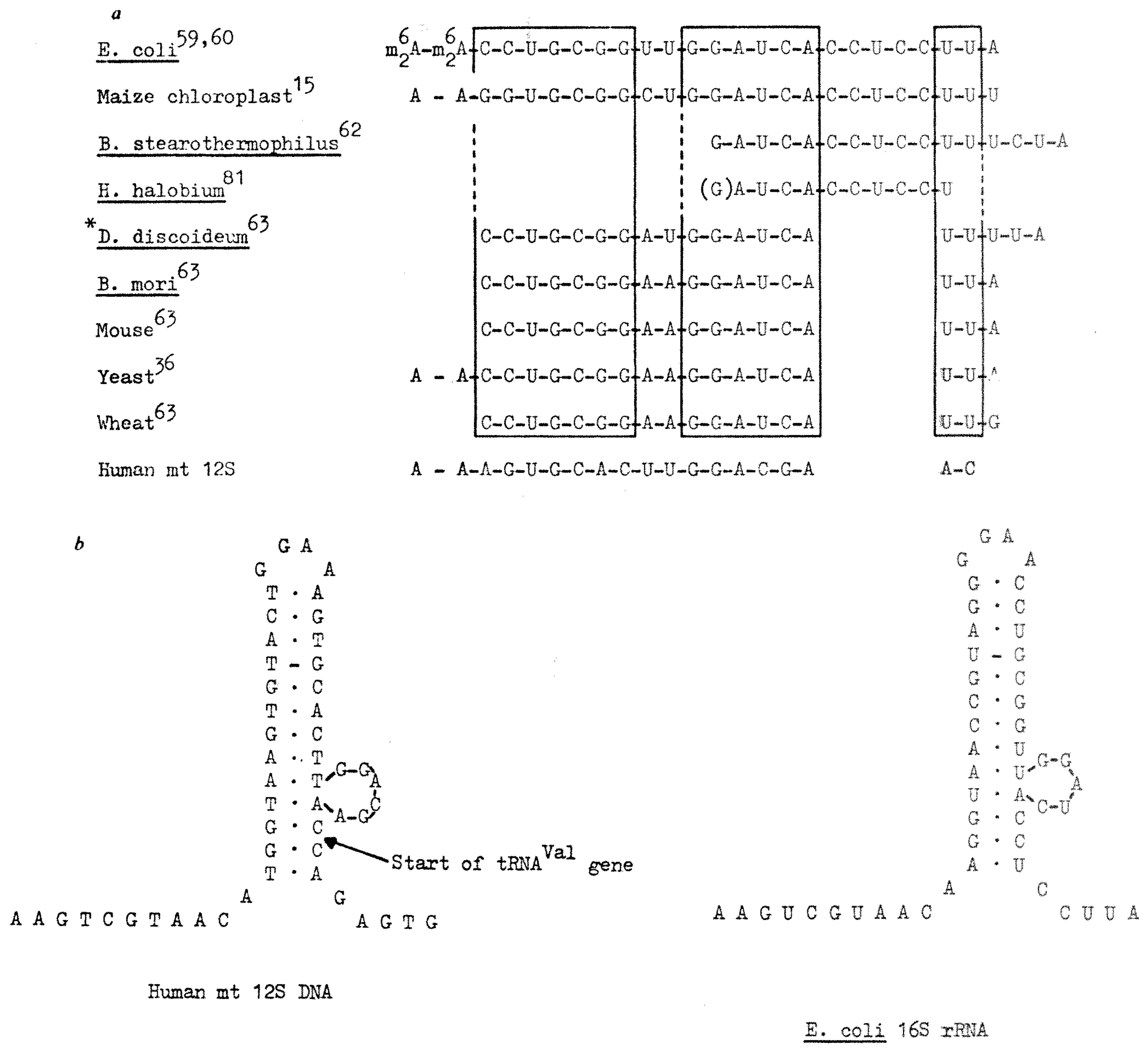
a
E. coli59,60 m62A-m62A-C-C-U-G-C-G-G-U-U-G-G-A-U-C-A-C-C-U-C-C-U-U-A
Maize chloroplast15 A - A-G-G-U-G-C-G-G-C-U-G-G-A-U-C-A-C-C-U-C-C-U-U-U
B. stearothermophilus62 G-A-U-C-A-C-C-U-C-C-U-U-U-C-U-A
H. halobium81 (G)A-U-C-A-C-C-U-C-C-U
*D. discoideum63 C-C-U-G-C-G-G-A-U-G-G-A-U-C-A U-U-U-U-A
B. mori63 C-C-U-G-C-G-G-A-A-G-G-A-U-C-A U-U-A
Mouse63 C-C-U-G-C-G-G-A-A-G-G-A-U-C-A U-U-A
Yeast36 A - A-C-C-U-G-C-G-G-A-A-G-G-A-U-C-A U-U-A
Wheat63 C-C-U-G-C-G-G-A-A-G-G-A-U-C-A U-U-G
Human mt 12S A - A-A-G-U-G-C-A-C-U-U-G-G-A-C-G-A A-C
b
Start of tRNAVal gene
A A G T C G T A A C
A G T G
Human mt 12S DNA
A A G U C G U A A C
C U U A
E. coli 16S rRNA

Fig. 6 *a*, The 3'-terminal sequences of small subunit rRNAs. The solid lines enclose regions of absolute homology in all previously determined sequences, including some prokaryotes not included here. Broken lines indicate incomplete sequences or a short 3' terminus. **Dictyostelium discoideum*. *b*, The small subsidiary loop proposed for *E. coli*[59] and the extended stem (of sequence GGAUCACCU) are unlikely to form in mitochondria unless the 12S gene overlaps the tRNA^{Val} gene.

broken, but differences from the other sequences are such as to retain the possibility of base pairing. The TG base pair and its flanking pairs are found in all the sequences known. The large block of homology in the region of nucleotides 1,476–1,495 (1,391–1,408 in the *E. coli* sequence, Fig. 5) is strongly conserved in mitochondria, eukaryotes and prokaryotes. Like the region just before the 3' stem-loop, there are important functional aspects to this sequence in *E. coli*, for part is a sequence that is universal among prokaryotes and accessible to modification by kethoxal in 30S subunits[72], and the remainder has been identified as crucial for 30S–50S subunit association[73]. Several other sequences are homologous to those found to be universal and accessible to modification in prokaryotes (Fig. 3), and 7 of the 14 kethoxal-modifiable sequences in *E. coli* 16S rRNA that are implicated in subunit association are recognizable in the 12S sequence. One of these is very similar to one of two sequences that might be involved in base pairing to 23S rRNA in *E. coli*[55,73], but there are no complementary sequences (>6 base pairs) in the mt 16S rRNA. The latter indeed has no regions absolutely homologous to the few association-protected oligonucleotides identified in *E. coli* 23S rRNA[55].

Evolution of human mt DNA

Although only one other small rRNA gene (16S rRNA of *E. coli*) has been sequenced, the sequences of the many small oligonucleotides produced by exhaustive ribonuclease T1 digestion of 16S rRNA have been used to deduce relatedness and highly conserved sequences among prokaryotes. Apart from obvious blocks of homology, comparisons of extensive rRNA sequences and judgements of similarity are hampered by the fact that the functional importance of the structure is not known in most regions. Unlike some proteins, it is not possible to draw conclusions as to similar chemical nature, structural role or frequency of substitution by the comparison of non-identical sequences. The use of 'catalogues' of oligonucleotides, each of which represents a phylogenetic character and is scored as absent or present, is therefore attractive, and does not require attempts at alignment of different sequences.

Previous evidence for an endosymbiotic origin of mitochondria has sought to demonstrate recent common ancestry with contemporary prokaryotic forms. However, these arguments have generally relied on features that are not due to mitochondrially coded components[74–76], and often the similarities are

Table 1 Degree of homology in small subunit rRNAs

Sequence	Oligonucleotide catalogue				
	E. coli	*R. spheroides*	*B. stearo-thermophilus*	*H. halobium*	Wheat mt 18S*
Human mt 12S rRNA gene	15(9.5)	34(11)	22–28‡(9)	30(12)	20(17)
E. coli 16S rRNA	†	167(17)	151(13)	53(19)	87(28)

Values given are the total number of nucleotides in ribonuclease T_1-generated oligonucleotides (⩾hexamers) that exactly match the two sequences, assuming a requirement for a G nucleotide before the oligonucleotide sequence. This stringency, together with the size requirements, reduces the number of *E. coli* oligonucleotides that match the 12S rRNA from 38 (see text) to 2 (a hexamer and a nonamer). The values in parentheses are the results expected when these catalogues are tested in this manner against randomly chosen sequences of the same length as the 12S or 16S rRNA (≏954 and 1,541 nucleotides, respectively). Oligonucleotides of unknown sequence were omitted.

* Wheat mt 18S and wheat cytosol 18S score 31, approximately the expected random level, when matched.

† As a test of the method, virtually all the oligonucleotides listed in ref. 72 matched the DNA sequence.

‡ Of the oligonucleotides which were shown with ambiguous sequences, one matched only when one of the two possible sequences was assumed.

more likely to have arisen by chance or convergence than are extensive sequence homologies.

The tRNA structures, unique genetic code and 3′-terminal sequence of the 12S rRNA suggest that mitochondria are less close to prokaryotes than the latter are to eukaryotes. This was further explored using oligonucleotide sequences from the published catalogues of small subunit rRNAs, which were fitted to the 12S rRNA gene sequence using the computer program SEQFIT[77]. Of the 114 oligonucleotides produced from *E. coli* 16S rRNA[72], only 38 matched the 12S rRNA, including 9 of the 29 'conserved' sequences but 14 of the 32 universal prokaryotic sequences[72]. With just 500 nucleotides known from the 5′ and 3′ termini of yeast cytoplasmic 18S rRNA (ref. 34 and K. G. Skryabin, personal communication), 29 *E. coli* oligonucleotides matched, 8 being conserved and 12 being universal sequences, suggesting (because the oligonucleotides do not all map at the ends of 16S rRNA) a far higher level of shared oligonucleotides (see Fig. 5) between prokaryotic and cytoplasmic rRNAs than either shares with mt rRNA.

To test evolutionary relatedness more stringently, hexanucleotides or larger from several catalogues were matched against the 12S mt rRNA and *E. coli* 16S sequences, and the total number of nucleotides in those oligonucleotides that matched was calculated (Table 1). These values are higher than those expected from matching unrelated sequences of the same lengths as those of the two rRNA genes to the individual catalogues. Table 1 shows that the Gram-negative bacterium *Rhodopseudomonas spheroides*[78] and the Gram-positive *Bacillus stearothermophilus*[79] are far more closely related to *E. coli* than either is to human mitochondria, contrary to conclusions from comparisons of respiratory chains[75] and from matrix-of-differences trees based on cytochrome *c* and 5S RNA homologies[76]. The close homology among all tested eubacterial rRNAs[79,80] confirms the distinctiveness of the mt 12S rRNA. Despite the molecular peculiarities of the 'archaebacterium' *Halobacter halobium*[81], it seems to be more closely related to eubacteria than to human mitochondria. The approximately equal homology of eukaryotes and eubacteria with Archaebacteria[80], together with the higher homology between the *E. coli* 16S rRNA and yeast cytoplasmic 18S rRNA (discussed above and shown in Fig. 5) than the homology of either with mt rRNA, suggests that the representatives tested from the major groups of organisms are more closely related to each other than to human mitochondria.

A catalogue from wheat mt rRNA has shown that, although not closely akin to prokaryotic sequences, it is nonetheless further removed from the wheat cytoplasmic rRNA[82]; it can be added from Table 1 that human mt rRNA is at least as distant. 5S rRNAs have only been found in plant mitochondria; if they are absent in other mitochondria the sequences of the larger rRNAs may differ for this reason. A difference between mt rRNAs from different organisms was expected, yeast mitochondria differing in rRNA methylation[83,84], arrangement of the genome[85] and genetic code from mammalian mitochondria, but the implied distance from wheat is surprising. Further work on the difference between cytoplasmic and mitochondrial rRNA from different organisms will be required to show the relative extents of divergence of these sequences and thus the patterns of selection and drift in mitochondria.

From the results presented here human mitochondria seem to represent a radical departure from previously examined organisms. The compact genome organization is probably linked to a requirement for processing so as to free the tRNAs and rRNAs, and perhaps to allow 5′-end recognition of mRNAs. Although there are conserved features, and perhaps functions, of these rRNA sequences, the extent of the differences from other rRNA genes has consequences for the mechanism of initiation of protein synthesis and argues, at least, for a more ancient origin of any endosymbiosis than 'recent common ancestry' (ref. 76) with prokaryotes or eukaryotes.

We thank Dr F. Sanger for encouragement and criticism, Dr B. G. Barrell and Mr R. Staden for advice on the computer techniques used, Dr B. A. Roe for strand separation on RPC-5, and Dr G. Attardi for the gift of HeLa mt DNA and for communicating results before publication. S.A. is a Research Fellow of the Cystic Fibrosis Foundation of America and D.P.N. was supported by a grant from the USPHS.

Note added in proof: The sequence of the region between nucleotides 324 and 933 of Fig. 3 has been determined in HeLa mt DNA; the 5′ sequence of the 12S rRNA differs only in being A at nucleotide 750 (ref. 87).

Received 21 January; accepted 19 May 1980.

1. Attardi, G. & Ching, E. *Meth. Enzym.* **56,** 66–79 (1979).
2. Attardi, G. *et al.* in *Proc. ICN–UCLA Symp. on Extrachromosomal DNA* (in the press).
3. Vesco, C. & Penman, S. *Proc. natn. Acad. Sci. U.S.A.* **62,** 218–225 (1969).
4. Attardi, B. & Attardi, G. *J. molec. Biol.* **55,** 231–249 (1971).
5. Attardi, G. & Ojala, D. *Nature new Biol.* **229,** 133–136 (1971).
6. Brega, A. & Vesco, C. *Nature new Biol.* **229,** 136–139 (1971).
7. Aloni, Y. & Attardi, G. *J. molec. Biol.* **55,** 271–276 (1971).
8. Robberson, D., Aloni, Y., Attardi, G. & Davidson, N. *J. molec. Biol.* **64,** 313–317 (1972).
9. Angerer, K., Davidson, N., Murphy, W., Lynch, D. & Attardi, G. *Cell,* **9,** 81–90 (1976).
10. Ojala, D. & Attardi, G. *Plasmid* **1,** 78–105 (1977).
11. Schatz, G. & Mason, T. L. *A. Rev. Biochem.* **43,** 51–87 (1974).
12. Buse, G. & Steffens, G. J. *Hoppe-Seyler's Z. physiol. Chem.* **359,** 1005–1009 (1978).
13. Cunningham, R. S., Bonen, L., Doolittle, W. F. & Gray, M. W. *FEBS Lett.* **69,** 116–122 (1976).
14. Schwarz, Z. & Kössel, H. *Nature* **283,** 739–742 (1980).
15. Drouin, J. *J. molec. Biol.* (in the press).
16. Sanger, F., Nicklen, S. & Coulson, A. R. *Proc. natn. Acad. Sci. U.S.A.* **74,** 5463–5467 (1977).
17. Smith, A. J. H. *Nucleic Acids Res.* **6,** 831–848 (1979).
18. Zain, B. S. & Roberts, R. J. *J. molec. Biol.* **131,** 341–352 (1979).
19. Brown, N. L. *FEBS Lett.* **93,** 10–15 (1978).
20. Eshaghpour, H. & Crothers, D. M. *Nucleic Acids Res.* **5,** 13–21 (1978).
21. Messing, J., Gronenborn, B., Müller-Hill, B. & Hofschneider, P. H. *Proc. natn. Acad. Sci. U.S.A.* **74,** 3642–3646 (1977).
22. Schreier, P. H. & Cortese, R. *J. molec. Biol.* **129,** 169–172 (1979).
23. Rothstein, R. J., Lall, L. F., Bahl, C. P., Narang, S. A. & Wu, R. *Meth. Enzym.* (in the press).
24. Clark, B. F. C. & Klug, A. in *Proc. 10th FEBS Meet.* 183–206 (1975).
25. Gaun, D. H., Grüter, F. & Springl, M. *Nucleic Acids Res.* **6r,** r1–r19 (1979).
26. Goodman, H. M., Olson, M. V. & Hall, B. D. *Proc. natn. Acad. Sci. U.S.A.* **74,** 5453–5457 (1977).
27. Valenzuela, P., Venegas, A., Weinberg, F., Bishop, R. & Rutter, W. J. *Proc. natn. Acad. Sci. U.S.A.* **75,** 190–194 (1978).
28. Knapp, G. Beckmann, J. G., Johnson, P. F., Furhonan, S. A. & Abelson, J. *Cell* **14,** 221–236 (1978).
29. Amalric, F., Merkel, C., Gelfand, R. & Attardi, G. *J. molec. Biol.* **118,** 1–25 (1978).
30. Young, R. A. & Steitz, J. A. *Proc. natn. Acad. Sci. U.S.A.* **75,** 3593–3597 (1978).
31. Dahlberg, A. E. *et al. Proc. natn. Acad. Sci. U.S.A.* **75,** 3598–3602 (1978).
32. Boseley, P., Moss, T., Mächler, M., Portmann, R. & Birnstiel, M. *Cell* **17,** 19–31 (1979).
33. Frankel, G., Cockburn, A. F., Kindle, K. L. & Firtel, R. M. *J. molec. Biol.* **109,** 539–558 (1977).
34. Skryabin, K. G., Karyev, A. S., Rubtsov, P. M. & Bayev, A. A. *Dokl. (Proc.) Acad. Sci. U.S.S.R.* **247,** 761–765 (1979).
35. Garber, R. L. & Altman, S. *Cell* **17,** 389–397 (1979).
36. Stark, B. C., Kole, R., Bowman, E. J. & Altman, S. *Proc. natn. Acad. Sci. U.S.A.* **75,** 3717–3721 (1978).
37. Brown, W. M. & Vinograd, J. *Proc. natn. Acad. Sci. U.S.A.* **71,** 4617–4621 (1974).
38. Ojala, D. & Attardi, G. *J. molec. Biol.* **122,** 301–319 (1978).
39. Crews, S., Ojala, D., Posakony, J., Nishiguchi, J. & Attardi, G. *Nature* **277,** 192–198 (1979).
40. Rosenberg, M. & Court, D. *A. Rev. Genet.* (in the press).
41. Young, R. A. & Steitz, J. A. *Cell* **17,** 225–234 (1979).
42. Gilbert, S. F., de Boer, H. A. & Nomura, M. *Cell* **17,** 211–224 (1979).
43. Mueller, K., Oebbecke, C. & Förster, G. *Cell* **10,** 121–130 (1977).

44. Moss, T. & Birnstiel, M. *Nucleic Acids Res.* **6,** 3733–3743 (1979).
45. Barrell, B. G., Bankier, A. T. & Drouin, J. *Nature* **282,** 189–194 (1979).
46. Heckman, J. E. *et al. Cell* **13,** 83–95 (1978).
47. Jack, A., Ladner, J. E. & Klug, A. *J. molec. Biol.* **108,** 619–649 (1976).
48. Macino, G. & Tzagoloff, A. *Proc. natn. Acad. Sci. U.S.A.* **76,** 131–135 (1979).
49. Hensgens, L. A. M., Grivell, L. A., Borst, P. & Bos, T. L. *Proc. natn. Acad. Sci. U.S.A.* **76,** 1663–1667 (1979).
50. Macino, G., Couzzi, G., Nobrega, F. G., Li, M. & Tzagoloff, A. *Proc. natn. Acad. Sci. U.S.A.* **76,** 3784–3785 (1979).
51. Larue, B., Cedergren, R. J., Sankoff, D. & Grosjean, H. *J. molec. Evol.* **14,** 287–300 (1979).
52. Martin, R. P. *et al. Nucleic Acids Res.* **5,** 4579–4592 (1978).
53. Lynch, D. C. & Attardi, G. *J. molec. Biol.* **102,** 125–141 (1976).
54. Brosius, J., Dull, T. J. & Noller, H. F. *Proc. natn. Acad. Sci. U.S.A.* (in the press).
55. Herr, W. & Noller, H. F. *J. molec. Biol.* **130,** 421–432 (1979).
56. Ehresmann, C., Stiegler, P., Carbon, P. & Ebel, J.-P. *FEBS Lett.* **84,** 337–341 (1977).
57. Brosius, J., Palmer, M. L., Kennedy, P. J. & Noller, H. F. *Proc. natn. Acad. Sci. U.S.A.* **75,** 4801–4805 (1978).
58. Shine, J. & Dalgarno, L. *Proc. natn. Acad. Sci. U.S.A.* **71,** 1342–1346 (1974).
59. Steitz, J. A. & Jakes, K. *Proc. natn. Acad. Sci. U.S.A.* **72,** 4734–4738 (1975).
60. Shine, J. & Dalgarno, L. *Nature* **254,** 34–38 (1975).
61. Sprague, K. U., Steitz, J. A., Grenley, R. M. & Stocking, C. E. *Nature* **267,** 462–465 (1977).
62. Hagenbüchle, O., Santer, M., Steitz, J. A. & Mans, R. J. *Cell* **13,** 551–563 (1978).
63. Hunter, A. R., Jackson, R. J. & Hunt, T. *Eur. J. Biochem.* **75,** 159–170 (1977).
64. Kozak, M. *Cell* **15,** 1109–1123 (1978).
65. Filipowicz, W. & Haenni, A.-L. *Proc. natn. Acad. Sci. U.S.A.* **76,** 3111–3115 (1979).
66. Ahlquist, P., Dasgupta, R., Shih, D. S., Zimmern, D. & Kaesberg, P. *Nature* **281,** 277–282 (1979).
67. Paterson, B. M. & Rosenberg, M. *Nature* **279,** 692–696 (1979).
68. Rosenberg, M. & Paterson, B. M. *Nature* **279,** 696–701 (1979).
69. Walz, A., Pirrotta, V. & Ineichen, K. *Nature* **262,** 665–669 (1976).
70. Moorman, A. F. M., Verkley, F. N., Asselbergs, F. A. M. & Grivell, L. A. in *Mitochondria 1977: Genetics and Biogenesis of Mitochondria* (eds Bandlow, W. *et al.*) 385–400 (De Gruyter, Berlin, 1977).
71. Chang, A. C. Y., Lansman, R. A., Clayton, D. A. & Cohen, S. N. *Cell* **6,** 231–244 (1975).
72. Woese, C. R. *Nature* **254,** 83–86 (1975).
73. Herr, W., Chapman, N. M. & Noller, H. F. *J. molec. Biol.* **130,** 433–449 (1979).
74. Henderson, C. E., Perham, R. N. & Finch, J. T. *Cell* **17,** 85–93 (1979).
75. Whatley, J. M., John, P. & Whatley, F. R. *Proc. R. Soc.* **B204,** 165–187 (1979).
76. Schwartz, R. M. & Dayhoff, M. O. *Science* **199,** 39 –403 (1978).
77. Staden, R. *Nucleic Acids Res.* **4,** 4037–4051 (1977).
78. Zablen, L. B. & Woese, C. R. *J. molec. Evol.* **5,** 25–34 (1975).
79. Fox, G. E., Pechman, K. R. & Woese, C. R. *Int. J. systemic Bact.* **27,** 44–57 (1977).
80. Magrum, L. J., Luehosen, K. R. & Woese, C. R. *J. molec. Evol.* **11,** 1–8 (1978).
81. Woese, C. R., Magrum, L. J. & Fox, G. E. *J. molec. Evol.* **11,** 245–252 (1978).
82. Bonen, L., Cunningham, R. S., Gray, M. W. & Doolittle, W. F. *Nucleic Acids Res.* **4,** 663–671 (1977).
83. Klootwijk, J., Klein, I. & Grivell, L. A. *J. molec. Biol.* **97,** 337–350 (1975).
84. Dubin, D. T., Taylor, R. H. & Daveport, L. W. *Nucleic Acids Res.* **5,** 4385–4397 (1978).
85. Borst, P. & Grivell, L. A. *Cell* **15,** 705–725 (1978)
86. Sanger, F. & Coulson, A. R. *FEBS Lett.* **87,** 107–1 0 (1978).
87. Crews, F. & Attardi, G. *Cell* **19,** 775–784 (1980).

LETTERS

Discovery of a very distant supernova

M. R. S. Hawkins

Royal Observatory, Blackford Hill, Edinburgh EH9 3HJ, UK

The luminosity and rapid time variation of supernovae suggest that they could be powerful cosmological probes. The main obstacle to such use has been the difficulty of finding sufficient high-redshift examples in time to make the necessary observations of the light curve. Here a very distant ($z \simeq 0.5$) supernova is reported together with photometric observations of its light curve.

On a given night a deep UK 1.2-m Schmidt plate would be expected to show between one and ten supernovae depending on the supernova rate and the usable limiting magnitude. In the present observing programme one sky-limited plate was taken per night, clear of Moon, for 3 weeks between two lunations. The plates could then be compared and a light curve measured for any supernova discovered with maximum near the beginning of the series. This could then be compared with a measured or estimated redshift. The main run of observations was made during August 1978 with the UK 1.2-m Schmidt in Australia. The field was centred on 21 h 28 min, −45° (1950) at a galactic latitude of −47° chosen as a compromise between time available on the telescope and minimum distance from the South Galactic Pole; the plate material is described in Table 1.

A Zeiss blink comparator was used to search for supernovae. Initially two plates were selected; the early epoch J3653, and J4410, a plate of similar quality near the beginning of the run. This produced 36 candidates which were appreciably brighter on the later plate. These images were then blinked with J4458, taken a month after J4410. Six of the candidates were found to have dimmed to their original magnitudes, and three of these were too faint to measure photometrically. The remaining prime candidates—SN1, SN4 and SN6—were all ~2 mag above the plate limit at their brightest. SN4 and SN6 appeared to be stellar with no obviously associated galaxy, but SN1 was clearly resolved.

Table 1 UK 1.2-m Schmidt plates measured

Plate no.	Date UT	Exposure (min)	Seeing (arc s)
J3653	8.10.77	70	DL-1
J4381	25.7.78	45	2–3
J4394	27.7.78	70	DL
J4401	30.7.78	70	DL
J4410	31.7.78	70	1
J4416	3.8.78	65	4
J4425	4.8.78	75	4
J4436	9.8.78	70	3
J4458	23.8.78	70	1

Field centre 21 h 28 min–45° 00′ (1950); emulsion IIIaJ; filter GG395. DL, diffraction limited.

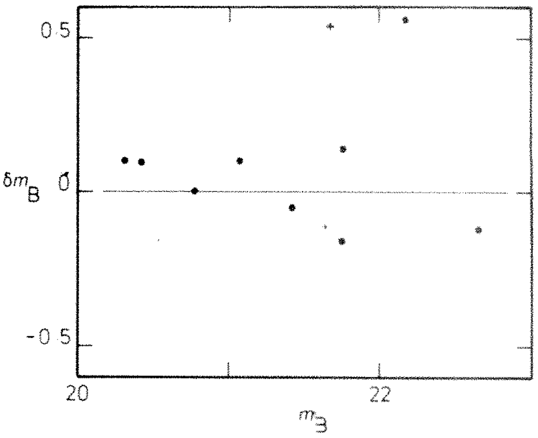

Fig. 1 Plot of residuals between mean magnitudes and magnitudes for plate J4394 against magnitude. +, The supernova image.

To obtain magnitudes three separate measurement procedures were used. A 'first look' was obtained by scanning in one dimension across the candidate image and four nearby comparison images spanning the full range of variation, using a Joyce-Loebl microdensitometer. The readings were converted to intensity using the step wedge calibration, and the area under the curves integrated to give relative magnitudes.

The magnitude scale was checked against photoelectric and electronographic standard magnitudes and no significant deviation from a slope of unity was found, even for brighter stars where saturation effects might be expected. Zero points were obtained by averaging the readings of each star and then plotting the measures for each plate against these mean magnitudes. A plot of relative magnitude of the candidate images against epoch revealed that SN4 and SN6 were not supernovae. They were both of more or less constant brightness on all plates except J4410, where they flared up by about one magnitude. Concentrating on SN1 an electronographic sequence was obtained of the field to fix the zero point of the mean magnitudes, which showed that at its brightest, the candidate image had $B = 21.4$ mag. The SN1 field was now remeasured on the Perkin–Elmer Data System (PDS) at the Royal Greenwich Observatory, including about eight comparison images comprising stars and galaxies, measured in square rasters. The images were analysed in two ways; first the volume under the images was integrated,

0028–0836/80/310467—03$01.00

and second a gaussian of variable height and radius was fitted to the image. These and the Joyce-Loebl measurements all gave substantially the same light curve, although they differed slightly over the measurement of individual images. The PDS integration method gave the smallest scatter and we use those measurements here.

Figure 1 shows residuals between plate J4394 and mean magnitude plotted against magnitude; the r.m.s. scatter of the residuals is 0.11 mag. The supernova candidate is shown by a cross, and the mean magnitude is taken from the early and late epoch plates; the cross is a 5σ point. Figure 2 shows magnitude plotted against epoch for SN1, the scatter being as expected, similar to that in Fig. 1. It is not usually possible to see the supernova as a distinct stellar image superimposed on an underlying galaxy on even the best plates. It looks more like a faint galaxy which suddenly becomes brighter and more star-like and then fades to its original form. The best early epoch plate (J3376) for SN1 shows a faint roughly circular galaxy with a rather compact centre. A positive classification of the galaxy type is not feasible for such a faint image but the general morphology is suggestive of an elliptical. J4381 is the first plate of the main series and here the image has become more point-like and distinctly brighter. On the next plate J4394, taken in very good seeing, the image is just resolved into a faint star-like object about 1 arc s west of the galaxy centroid. This is confirmed by positional measures from the PDS. For the other plates the image steadily fades as shown in Fig. 2, until it regains its early epoch magnitude. This object has all the properties expected of a distant supernova, and apart from some unlikely coincidences is hard to classify in any other way. Distinguishing a type I from a type II supernova is always difficult, even for nearby objects where spectroscopic information is available. Type II objects are, however, observed relatively infrequently, and if, as seems likely, the underlying galaxy is not a late-type spiral, a type II can be ruled out. To measure the decay time, the magnitudes in Fig. 2 must be modified by subtracting the flux from the underlying galaxy. The resulting light curve from the early and late epoch plates is shown in Fig. 3. A straight line was fitted to the readings to give the decay time, the best fit being

$$5.8 \pm 0.5 \text{ days mag}^{-1}$$

Repeating the fit after removing individual readings, and changing the value for the underlying galaxy by the standard error, still gave the best fit slope within the above error limits. Note that the last two observations, which after galaxy subtraction were the most uncertain, were not used. The resulting least-squares slope was 6.16 ± 0.67 days mag^{-1} which is not significantly different from the value given above. The r.m.s. difference of the stars about the best fit line was 0.19 mag, larger than the error in Figs 1 and 2. This is to be expected due to the effect of subtracting the underlying galaxy.

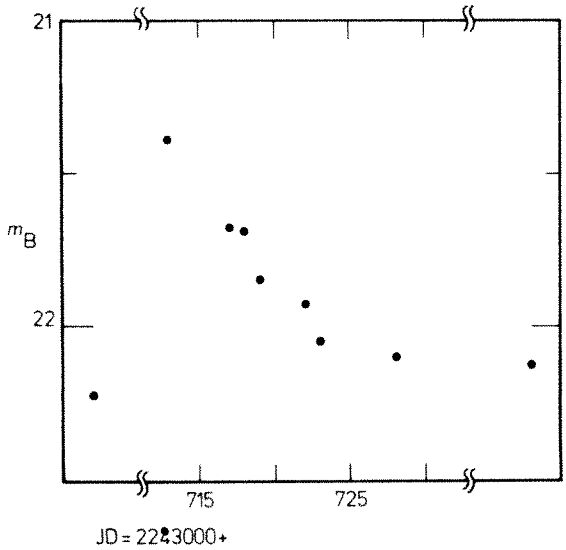

Fig. 2 Plot of magnitude against epoch for the supernova image.

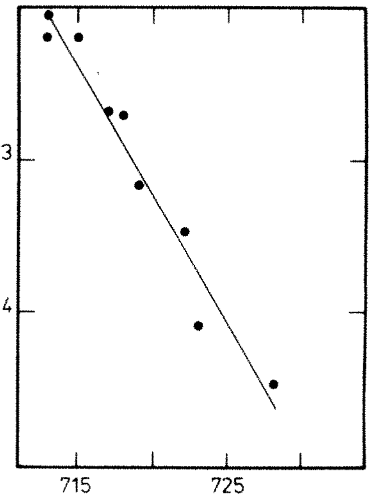

Fig. 3 Plot of magnitude against epoch for the supernova image after subtracting background galaxy flux. Also shown is the least-squares best fit straight line.

Rust[1] has found that the local value for the decay rate of a type I nearby supernova is 8.32 ± 1.95 days mag^{-1} which is compatible with the result found above, although SN1 is clearly not a local object. Unfortunately, we cannot yet obtain a redshift for the underlying galaxy due to its faint magnitude of $B = 22.23$. However, the brightest magnitude in Fig. 3 is $B = 22.06$ which sets a lower limit to the supernova brightness at maximum. Rust[1] found a mean absolute magnitude at maximum of $m_B = -19.53$ with a dispersion of 0.94 mag. The mean value gives a redshift of $z \simeq 0.6$ which in a Friedman cosmology would imply an increase of the decay time given by

$$T_0 = T_i(1+z) \qquad (1)$$

where T_i and T_0 are the intrinsic and observed decay rates respectively. Thus the expected decay rate at the redshift of 0.6 would be 13.3 ± 3.1 days mag^{-1}, which puts the observed value of 5.8 days mag^{-1} at 2.5σ, and in fact the slowest supernova known would have a decay rate of 7.2 days mag^{-1} at this redshift. Even if the absolute magnitude of the supernova were 2σ fainter than the mean value at $m_B = 17.6$, a redshift $z \simeq 0.3$ would be implied giving an expected decay rate of 10.8 ± 2.5 days mag^{-1}; this is still 2σ above the observed value. The most natural interpretation of these observations is that light from the supernova has not undergone a Doppler shift.

Another important effect must be taken into consideration. De Vaucouleurs and Pence[2] have pointed out that the change in the supernova spectral energy distribution as a function of time alters the observed decay rate in a particular bandpass with redshift—the observed magnitudes must be modified by a time-dependent k-correction. This makes supernovae appear to decay more quickly at high redshifts, and de Vaucouleurs and Pence give as the correction factor

$$T_0 = T(1+1.08z) \qquad (2)$$

where T is the observed decay time and T_0 is the decay time which would be observed were the passband redshifted to the rest frame of the supernova. The relation (2) is only claimed by de Vaucouleurs and Pence up to a redshift of $z = 0.15$; however, if this holds at the redshift of SN1 comparison of relations (1) and (2) shows that there will be essentially no observed change in the decay rate as a function of redshift in a Friedman cosmology, and that for a non-expanding universe the decay rate would actually become smaller. Applying the correction to the present observations puts the observed decay time within the bracket represented by the Friedman cosmology, and is evidence that the Universe is expanding; rejection of the correction implies a non-expanding Doppler cosmological redshift.

I thank the UK 1.2-m Schmidt Unit, Miss Faroos Saedi, Dr B. D. Kelly and Dr R. S. Stobie for assistance.

Received 18 April; accepted 10 June 1980.

1. Rust, B. W. thesis, Univ. Illinois (1974).
2. de Vaucouleurs, G. & Pence, W. D. *Astrophys. J.* **209,** 687 (1976).

A 2.2-Hz modulation of auroral electrons imposed at the geomagnetic equator

D. R. Lepine, D. A. Bryant & D. S. Hall

SRC Rutherford and Appleton Laboratories, Ditton Park,
Slough SL3 9JX, UK

The direct observation of high frequency ~3 Hz modulation of electron intensities during pulsating aurora is comparatively recent although, from TV and photometric studies, modulation of the visual aurora at these frequencies has been recognized for over a decade. We report here 2.2 ± 0.5 Hz oscillations in the intensities of 4–25 keV electrons producing a pulsating aurora. The electrons were measured from a Petrel sounding rocket launched from Kiruna, Sweden on 25 January 1979. The oscillations like the slower 1–20 s pulsations, exhibit a marked velocity dispersion implying an equatorial origin for both forms of modulation. VLF—hiss observed at about the same time at the Satellite GEOS 2, operating in the same equatorial region, shows remarkable similarities to the modulation in the particle fluxes. A connection between VLF emissions and auroral pulsations has been suggested by Coriniti and Kennel who argue that low frequency, 5–300 s period, micropulsations modulate whistler-mode wave amplitudes leading to variations in the rate of pitch-angle scattering of electrons from the magnetosphere. The isotropic angular distributions reported here suggest that this mechanism acting alone cannot explain the modulation in the present case.

A Petrel rocket, designated P216 in the UK National Programme, was flown from Kiruna, Sweden, to compare electron intensities seen in pulsating aurora with related parameters at the magnetically-conjugate geostationary satellite GEOS 2. The rocket was launched at 21.07.33 UT on 25 January 1979 during the recovery phase of a magnetic substorm. A low-light television, operating down range, showed that for part of its flight the rocket was in the vicinity of patches of aurora that pulsed irregularly with durations of maximum brightness of between 1 and 20 s. Electron intensities at the rocket, measured with channel multipliers and electrostatic analysers, exhibited similar pulsations. We are concerned here with shorter-period (0.46 ± 0.05 s) oscillations that occur in 4–25 keV electron intensities, at several intervals during the rocket flight superimposed on the maxima of the slower pulsations[1]. Particle modulation in the 3 ± 1 Hz frequency range has been observed previously[2] at low energies (< 70 eV), and more recently at high energies[3] (> 25 keV). The present observations are significant in that particles within the 4–25 keV range carry sufficient energy to account for the observed light emission and, therefore, may cause a 2–3 Hz modulation in light intensity frequently observed during pulsating aurora[4,5]. During these particular oscillations, however, due to the combined effects of velocity dispersion and the narrow range of spectrum energies involved, the precipitated energy-flux variations amount to only ± 3% of the ~25 mW m^{-2} energy-flux at pulsation maximum. Because of the low auroral intensity (~2 kR at 427.8 nm), this level of modulation equals the noise level of the optical instrumentation and we cannot confirm that the particle modulation reported here leads to a modulation in the optical brightness.

Examples of the oscillations are contained in Fig. 1, an energy-time spectrogram of electron intensities for the flight-time interval 217–250 s. These intensities were measured at pitch-angles 20 ± 3.5° with a detector whose electrostatic analyser swept through the energy range 1.2–25 keV every 143 ms. In the interval shown the rocket altitude ranged from 170 to 180 km. Oscillations at 2.2 ± 0.2 Hz are strongest during intervals A and B in which it is very noticeable that intensity changes at higher energies precede the corresponding changes at lower energies. This effect can be readily explained as velocity dispersion due to a distant source of modulation. A dispersion in the times of occurrence of 1–20 s pulsations at different particle energies was discovered by Bryant *et al.*[6], confirmed on subsequent occasions[7,8], and indeed found to be the case in this event[1]. The present results are, we believe, the first indication of dispersion in shorter-period oscillations.

To test more closely the hypothesis of a distant source of modulation, we have examined the intensity changes recorded by other detectors operating continuously at energies 3.9, 7.7 and 11.5 keV. These constant-energy detectors were sampled every 0.5 ms as they scanned through the pitch-angle range 15–55° every 57 ms, all sampling the same pitch angle at the

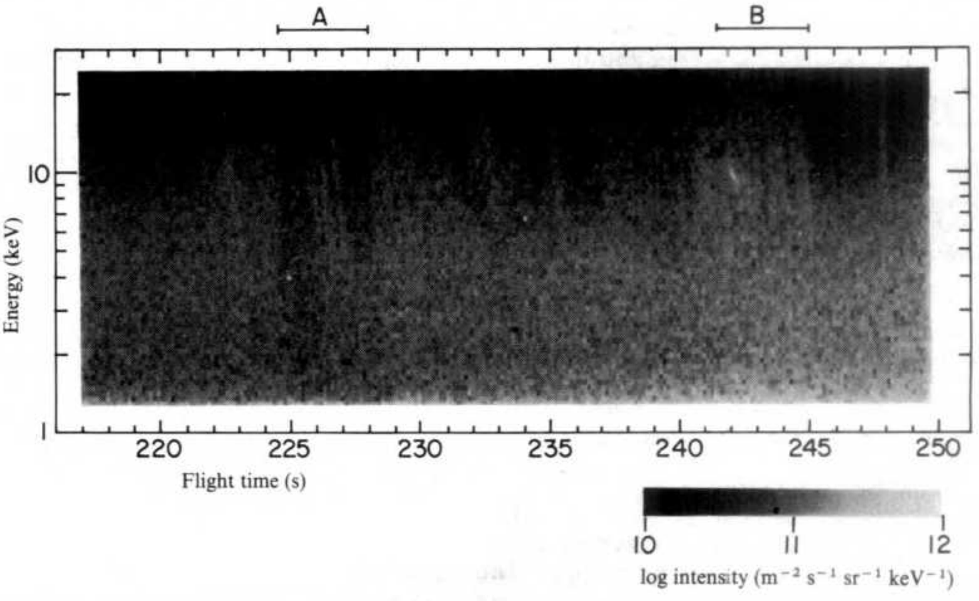

Fig. 1 Electron intensities measured at P216 during an interval of temporal changes. The intensities were measured at pitch angles 20 ± 3.5°. 2.2 Hz oscillations occurring during the intervals A and B are discussed in the text.

same time. In the intervals A and B intensities were found to be isotropic over the observed pitch-angle range at all three energies. Figure 2 shows intensity variations at the three energies in terms of fluctuations about a mean intensity at that energy. It is immediately apparent that the oscillations are quasi-periodic with a mean frequency of 2.2 Hz, and that the amplitude and phase are energy dependent. The oscillations are, when the time shift is taken into account, well correlated.

Because the vertical separation in Fig. 2 is proportional to reciprocal of velocity, sloping lines linking the oscillations provide clear evidence of velocity dispersion, if we assume that modulation is simultaneous at all energies and that particles travel with constant speed after modulation. The data clearly support the dispersion hypothesis, and point to a source distance of $42 \pm 5 \times 10^6$ m. The length of a particle trajectory from a rocket altitude to the geomagnetic equator ranges from, in the dipole approximation, 41 to 43×10^6 m for the pitch angles (15–55°) sampled here, so the analysis performed in Fig. 2 therefore suggests that the source of modulation is located in the equatorial region at a radial distance of about 5.4 R_E. The use of the dipole approximation requires justification, particularly when there is evidence for, on some occasions, a considerable stretching of field lines in the midnight sector of the magnetosphere. Using a comparison of plasma measurements made by the Vela satellites at 18 R_E, with satellite photographs of the auroral oval, Hones *et al.*[9] have deduced that the degree of stretching is variable, and that on some occasions field lines from approximately the latitude of Kiruna reach out to at least 18 R_E. Their result is consistent with the degree of stretching deduced from observations of variable dispersion[8], and therefore our present results indicate that, at the time of the rocket flight, the magnetic field was not severely stretched from its dipole-like configuration.

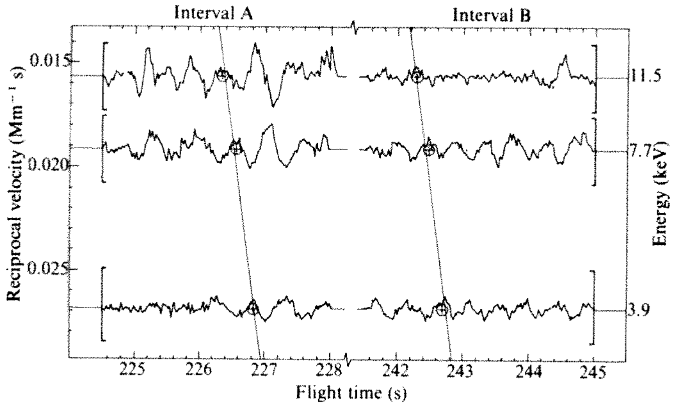

Fig. 2 Velocity dispersion of 2.2 Hz oscillations in the intervals A and B. Each trace shows electron intensity at a constant energy in terms of variations about a mean intensity at that energy. The encircled crosses indicate zero variation and an average time for the cycle on which they are drawn. The vertical separation of the traces is proportional to reciprocal velocity. The straight lines linking the oscillations provide clear evidence of dispersion, and correspond to a source distance of 42 Mm. [ ], Indicate ±25% variations. Random statistical errors are typically ±4%.

In view of the location of GEOS 2, close to the equatorial crossing point of magnetic field lines which at times connect with the area of Kiruna, measurements made at the satellite are well suited for comparison with those made at the rocket. An examination of particles of similar energy at GEOS 2, indicates that there are no changes, either inside or outside the loss-cone, corresponding to the longer-period pulsations. It is not yet clear whether 2.2 Hz oscillations in particle flux are detectable by the instruments on GEOS 2. However, VLF emissions measured at GEOS 2 during the rocket flight are noticeably modulated at a frequency close to that of the oscillations in electron intensities at the rocket. These emissions are strongest in a band centred on 500 Hz, and are of a type usually referred to as hiss. Figure 3 shows the amplitude of 500 Hz magnetic field fluctuations, measured by experiment S300 on GEOS 2, for the rocket flight interval 220–250 s. Oscillations at 2.8±0.6 Hz are very apparent between 221 and 225 s, and at 3.1±0.6 Hz between 241 and 243 s. Although these do not correspond exactly with events at the rocket they have a similar frequency and occur, like those at the rocket, in irregular bursts. A possible connection between the electron intensity oscillations and VLF activity is not entirely unexpected. Coroniti and Kennel[10] have argued that auroral pulsations are caused by a modulation of the rate of pitch-angle scattering in a diffusion region near the equator. In their model, electrons are scattered by resonance with whistler-mode electromagnetic waves whose growth rates depend on, among other parameters, the amplitude of magnetic micropulsations within the diffusion region. Although this is in many ways a promising explanation of auroral pulsations[11], there are

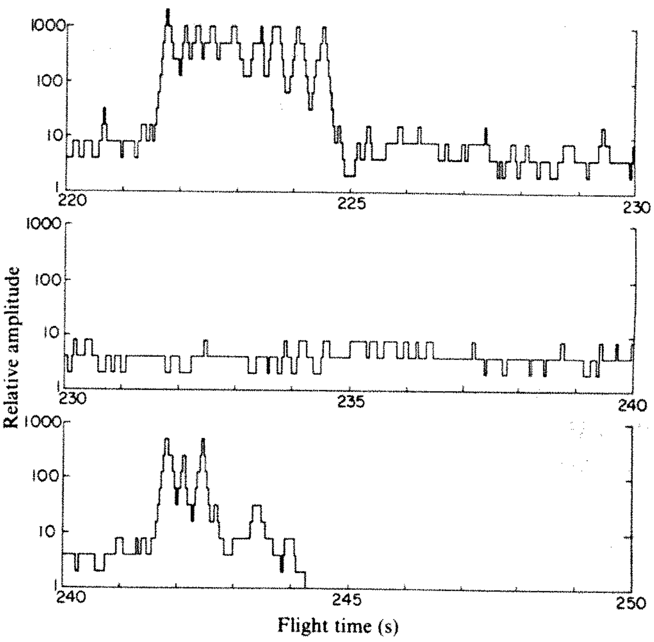

Fig. 3 Intensity of 500 Hz magnetic field fluctuations measured at GEOS 2 by the S300 wave experiment during the rocket flight interval 220–250 s. Oscillations at about 2.8 Hz can be seen between 221 and 225 s, and at about 3.2 Hz between 241 and 243 s.

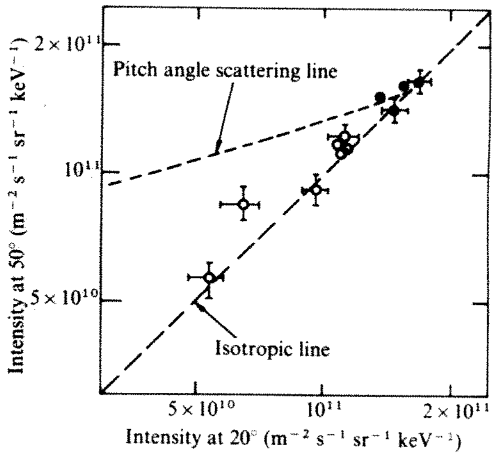

Fig. 4 Relation between intensities at pitch-angles of 50° and 20° for 11.5 keV electrons during interval A: ●, maxima; ○, minima intensities. The pitch-angle scattering line is calculated using a dipole approximation with $L = 5.4$ and a loss-cone of half-angle of 3.44° at the equator.

observations, as on earlier occasions[12], which create difficulties for this theory. Figure 4 shows the relationship between intensities at pitch-angles of 50° and 20° for 11.5 keV electrons during interval A. The broken line, marked pitch-angle scattering, indicates the expected degree of anisotropy for oscillations that are driven by changes in the rate of diffusion of trapped electrons from a reservoir of constant intensity of $1.6\times10^{11}\ \mathrm{m^{-2}\,s^{-1}\,sr^{-1}\,keV^{-1}}$ into a loss-cone created by atmospheric absorption. Although there is a suspicion that intensities at large pitch-angles exceed those at small pitch-angles, the observations follow more closely the isotropic line than the pitch-angle scattering one, indicating that variations in pitch-angle scattering are not the dominant feature controlling the oscillations. Intensities at other energies during intervals A and B follow closely the behaviour of the 11.5 keV electrons shown in Fig. 4, therefore pitch-angle scattering acting alone cannot explain their modulation. As the nature of the mechanism is unclear at this stage, the extent to which the similarity between the modulation seen at GEOS 2 and the modulation seen at the rocket indicates a real coupling between magnetospheric and ionospheric events remains to be evaluated.

We thank Drs H. Borg, P. Christiansen, P. Gough, A. D. Johnstone, A. Korth and G. Martelli for information and helpful discussions on GEOS 2 particle and wave measurements.

Received 10 March; accepted 23 May 1980.

1. Bryant, D. A. Rep. *3rd Workshop on IMS observations in Northern Europe*, Skokloster (1979).
2. Basto, R. A. & Raitt, W. J. *Planet Space Sci.* **26,** 21 (1978).
3. Sandahl, I., Ellasson, L. & Lundin, R. *Geophys. Res. Lett.* (in the press).
4. Royrvik, O. & Davis, T. N. *J. Geophys. Res.*, **82,** 4720 (1977).
5. Pemberton, E. V. & Shepherd, G. G. *Can. J. Phys.* **53,** 504 (1975).
6. Bryant, D. A., Collin, H. L., Courtier, G. M. & Johnstone, A. D. *Nature* **215,** 45 (1967).
7. Bryant, D. A., Courtier, G. M. & Bennett G. *J. atmos. terr. Phys.*, **33,** 859 (1971).
8. Bryant, D. A., Smith, M. J. & Courtier, G. M. *Planet. Space Sci.*, **23,** 867 (1975).
9. Hones, E. W., Ashbridge, J. R. & Bame, S. J. *Rep. 2nd General Scientific Assembly of the Int. Ass. Geomagnetism and Aeronomy*, Kyoto (1973).
10. Coroniti, F. V. & Kennel, C. F. *J. geophys. Res.* **75,** 1279 (1970).
11. Johnstone, A. D. *Nature* **274,** 119 (1978).
12. Smith, M. J., Bryant, D. A. & Edwards, T. E. *J. atmos. terr. Phys.* **42,** 167 (1980).

Observation of flaws in anodic films on aluminium

G. E. Thompson, K. Shimizu & G. C. Wood

Corrosion and Protection Centre, University of Manchester Institute of Science and Technology, PO Box 88, Manchester, M60 1QD UK

A thin compact oxide film forms naturally on aluminium in air and can be thickened by anodizing, to give widely used materials. However, highly localized processes can occur at flaws, which are always present in the films and they can lead to pit development[1] and influence the electrical properties[2] (dielectric breakdown and rectification). As awareness of the different behaviour at flaws increases, other interesting phenomena, such as electroluminescence[3], response to UV radiation[4] and electrolytic colouring[5], may be influenced by the activation of pre-existing flaws, or the generation of new flaws. Clearly, further knowledge of this kind is of fundamental and practical importance. Some of the more significant findings relating to the nature, shape and geometry of flaws observed after anodizing in ammonium pentaborate solution are outlined here.

Flaws or lighter regions ~73–200 nm in size, can be observed readily in the barrier films formed to various voltages at constant current density on as-received superpure aluminium (99.99 Al; 0.003 Cu; 0.002 Fe; 0.002 Si wt%) (Fig. 1). Stripped anodic films show that the pre-existing flaws are now 'decorated' by differently textured film, which spreads into the neighbouring featureless film in an approximately circular front (Fig. 1*a*, *b*) This texture changes further with increase in forming voltage and, at 200 V, the local islands have been identified as γ' alumina[3] (Fig. 1*c*). A change in the extent of crystallinity has also been suggested[6,7]. The corresponding ultramicrotomed sections show that the film formed to 50 V is relatively uniform, although occasional metal ridges protruding into the film from the metal–film interface are evident (Fig. 1*d*). Further thickening of the film has occurred at 100 V and distinct local regions of differently textured film are evident in approximately the outer half of the film (Fig. 1*e*). These apparently convex lens-shaped regions are sharply defined and are located above metal ridges at the metal/film interface. A more marked change in appearance is observed at 200 V, where the metal ridges are more clearly defined and the differently textured film is more extensive (Fig. 1*f*). The locally textured regions of film have spread laterally from their original position centred above the tip of the metal ridge. The islands of crystalline γ' alumina have become damaged during sectioning, but the micrograph suggests that they are thicker at their centres, and the thickness decreases progressively into the neighbouring barrier film. In addition, a narrow channel appears to be present in the barrier film above the crystalline island.

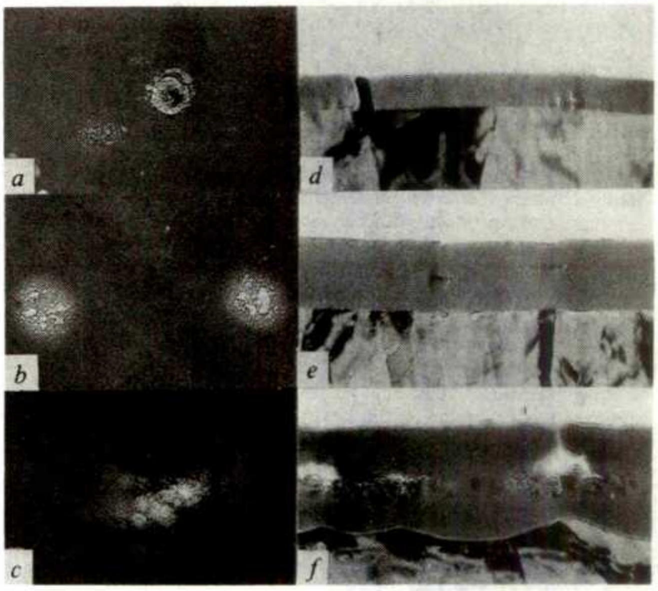

Fig. 1 Transmission electron micrographs of the films formed on as-received aluminium at $50\ \mathrm{A\,m^{-2}}$ in 0.1 M ammonium pentaborate solution at 298 K to various voltages. *a*, Stripped anodic film formed to 50 V, showing the decorated flaws. *b*, Stripped anodic film formed to 100 V showing the different textured appearance of the flaws. *c*, Stripped anodic film formed to 200 V, showing the island of crystalline γ' alumina. *d*, Ultramicrotomed section of the aluminium substrate and the film formed to 50 V. Occasional metal ridges can be seen at the metal–film interface. *e*, Ultramicrotomed section of the aluminium substrate and the film formed to 100 V, showing the sharply defined regions of differently textured film above metal ridges. *f*, Ultramicrotomed section of the aluminium substrate and the film formed to 200 V, showing the marked scalloping at the metal–film interface and the developing regions which have been identified as γ' alumina by electron diffraction[3]. Magnification ×78,000.

The number of the resultant islands of crystalline film is dependent on substrate preparation and cleaning or electropolishing markedly reduces their population density (from $2\times10^{12}\ \mathrm{m^{-2}}$ on as received specimens to about $10^9\ \mathrm{m^{-2}}$ after

0028–0836/80/310471—02$01.00

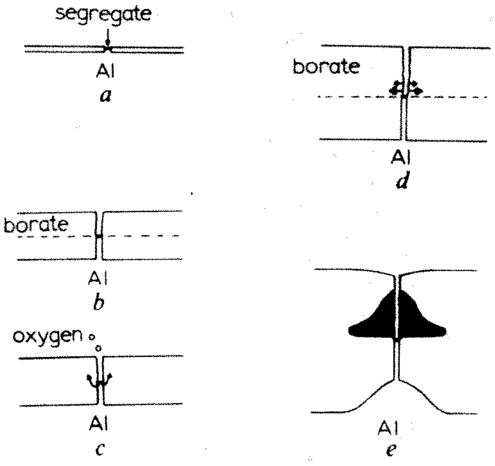

Fig. 2 The development of islands of crystalline film. *a*, An impurity segregate situated at the tip of a metal ridge protruding into the air-formed film. *b*, After anodizing, the segregate is located in the vicinity of the boundary between the borate-containing film material and the relatively pure alumina film. *c*, Gas evolution from the segregates proceeds during anodizing and high local field strengths may cause the aluminium ridge to be removed preferentially, thereby occluding the segregate in the film. *d*, Joule heating allows the development of local temperature rises in the solution-filled channel. The hotter region is situated just above the segregate, and direct heating of the film in this region causes the change in texture. *e*, Crystalline film develops as a result of direct heating and the original flaw passes through the centre of this material. Its development produces shielded regions, which hinder the development of the amorphous barrier film.

electropolishing). This suggests that they develop in the vicinity of surface impurity segregates rather than from effects in the depths of the metal, that is, second phase material, which may be revealed as the metal–film interface recedes during anodizing. Favoured sites for segregation of impurities, such as iron and copper, exist on rolled surfaces, that is, in the vicinity of metal ridges and troughs associated with rolling lines. Growth of the air-formed film, which is more voluminous than the aluminium consumed, then creates a distribution of flaws, comprised of metal segregates situated at the bottoms of channels in the film, which are located at the tips of metal ridges protruding into the film from the metal–film interface (Fig. 2*a*). A characteristic air-formed film is also likely to form over the segregates.

During anodizing, thickening of the air-formed film occurs by the usual growth processes involving ionic migration of Al^{3+} outwards and OH^- or O^{2-} ions inwards[8]. SIMS data (G.E.T. and G.C.W., unpublished work) suggest similar anion and cation transport numbers, leading to an inner relatively pure alumina film and deposition of an outer borate-containing film. However, film formation does not proceed directly above the segregates where an alternative anodic process, oxygen evolution occurs or in the shielded regions directly below the segregates. This manner of film growth results in the segregates being located at the tips of metal ridges protruding into about one-half of the total film thickness (Fig. 2*b*). Gas evolution from the segregates tends to maintain the channels above them open by mechanically disrupting the outer film, which attempts to bridge over them. Unless the shielding of the aluminium ridges is effective, high local field strengths may result in the consumption of this metal in lateral film growth, and the possible inclusion of some of the segregate into the film (Fig. 2*c*).

The areas of the bases of the segregates are extremely small compared with the macroscopic aluminium substrate and large effective current densities can be directed to these relatively low resistance pathways, with resultant large temperature rises due to local Joule heating effects. This is unlike the situation suggested to occur during pitting, at localized sites, where salt film formation proceeds rapidly and the temperature at the pit surface remains essentially unchanged[9]. As the film thickens further, more current is focused into these preferred regions, which is confirmed by the more ready observation of gas evolution at high cell voltages, with greater local heating effects. Heat is dissipated into the aluminium substrate and bulk solution, but because the segregates are located above the tips of relatively narrow metal ridges, it is likely that the rate of heat flow into the substrate is limited and the hottest zone in the solution-filled channel is situated just above the segregate (Fig. 2*d*).

Direct heating[10], or hydrothermal treatment[11], increases the extent of crystallinity of anodic films, at a rate dependent on their composition. Similar texture changes to those evident here initially have been observed during electron beam heating of anodic films[12], suggesting that they may be promoted by direct heating. However, there is presently little direct information about the magnitude of the local temperature rises. Figure 2*d* shows that the hot zone is adjacent to the borate-containing film material, which implies that this film material undergoes the more rapid change in texture and ultimate increase in crystallinity.

In the present situation the local heating is thought to develop continuously rather than in discrete bursts, which are more commonly associated with electron avalanching and dielectric breakdown. Direct heating promotes the increase in the extent of crystallinity of the material adjacent to the hotter regions of the channel and, as the barrier film thickens, the hot regions spreads up the channel resulting in an increase in the volume of the resultant crystalline island. The shape of the crystalline region is explained by the hotter region remaining just above the segregate, but with further barrier film thickening temperature rises adjacent to regions further up the channel promote local crystallization. The actual stage at which crystallinity appears is a compromise between the size and population density of the flaws and the film thickness, which govern the effective current density and local temperature rises generated. Anodizing in borate solution favours development of the islands[3], which suggests that the eventual crystallization process may be dependent on electrolyte conductivity and buffering capacity and/or film composition. Furthermore, it is not clear whether borate species incorporated in the film aid this process directly by reducing the crystallization temperature or migrate from the hotter regions during crystallization and whether borate species act as glass network formers or modifiers. However, the eventual development of these islands, which hinders the growth of the normal amorphous barrier film results in the development of scalloped metal regions at the metal–film interface (Fig. 2*e*).

Note also that electroluminescence is observed during the growth of these films in borate solutions. The significance of flaws, film composition and the development of crystalline film is in the stages of elucidation and will be reported elsewhere.

In conclusion, it is suggested that iron and/or copper impurities are responsible for the behaviour observed during anodizing in borate solution. They remain at the tips of metal ridges located at the bases of channels within the films and local temperature rises associated with Joule heating effects give rise to the development of crystalline film.

Received 31 March; accepted 22 May 1980.

1. Wood, G. C., Sutton, W. H., Richardson, J. A., Riley, T. N. K. & Malherbe, A. G. *Localized Corrosion*, NACE-3, 526–546 (1974).
2. Vermilyea, D. A. *J. electrochem. Soc.* **110,** 250–262 (1963).
3. Shimizu, K., Tajima, S., Thompson, G. E., & Wood, G. C. *Electrochim. Acta* (in the press).
4. Young, L. *Anodic Oxide Films*, 130–131 (Academic, New York, 1961).
5. Doughty, A. S., Thompson, G. E., Richardson, J. A. & Wood, G. C. *Trans. Inst. Metal Finishing*, **53,** 33–39 (1975).
6. Franklin, R. W. *Conf. Anodizing Aluminium*, Nottingham 96–100 (Aluminium Development Association, 1961).
7. Stirland, D. J. & Bicknell, R. W. *J. Electrochem. Soc.* **106,** 481–485 (1969).
8. Thompson, G. E., Furneaux, R. C., Wood, G. C., Richardson, J. A. & Goode, J. S. *Nature* **272,** 433–435 (1978).
9. Beck, T. R. & Alkire, R. C. *J. electrochem. Soc.* **126,** 1662–1666 (1979).
10. Aladjem, A., Brandon, D. G., Yahalom, J. & Zahavi, J. *Electrochim. Acta* **15,** 663–671 (1970).
11. Thompson, G. E., Furneaux, R. C. & Wood, G. C. *Trans. Inst. Metal Finishing* **55,** 117–128 (1977).
12. Thompson, G. E., Furneaux, R. C. & Wood, G. C. *Corros. Sci.* **18,** 481–498 (1978).

The structure and energetics of the conduction plane in Naβ Al$_2$O$_3$

J. R. Walker & C. R. A. Catlow

Department of Chemistry, University College London,
20 Gordon Street, London WC1H 0AJ, UK

An atomistic computer simulation study of the superionic conductor NaβAl$_2$O$_3$ is described here. This material is a layer structured compound in which highly mobile sodium ions are located in 'conduction planes' between spinel structured Al$_2$O$_3$ blocks[1]. Although we have investigated structural properties of the conduction plane, which have been widely studied by diffraction techniques, our results are also important to transport properties of the compound. We demonstrate that a very flat potential surface governs the distribution of Na$^+$ ions in the conduction plane. This finding is clearly compatible with superionic properties of the compound but also has consequences for analysis of structural data. Our calculations confirm that O^{2-} interstitials are stabilized by large relaxations of neighbouring lattice ions to give the cluster proposed earlier[2]. Defects in the conduction plane of β-Al$_2$O$_3$ are shown to be generally stabilized by large relaxations of surrounding ions, which favour defect formation in the compound, and which, therefore, cause the gross deviations from stoichiometry observed in β-Al$_2$O$_3$. Our results suggest a 'fluid' conduction plane structure (a fluidity which extends to the neighbouring spinel block ions) with only weak localization of the conduction ions into specific sites and strong stabilizing relaxations of conduction and spinel block ions around any defect species.

Two types of calculation are discussed. In the first, lattice energy calculations on stoichiometric NaβAl$_2$O$_3$ for a variety of sodium ion distributions, use the general lattice energy code, PLUTO[3], previously applied successfully to complex problems in the field of non-stoichiometry[4,5]. In the second, calculations of the energies of formation of defects within the conduction plane of stoichiometric NaβAl$_2$O$_3$ use another general computer code, the HADES III[4,6], which can be applied to all crystal symmetries. The HADES code is an improvement on earlier theoretical studies of Wong *et al.*, which omitted relaxation effects.

Both types of calculation require specification of the relevant interionic potentials. Shell model potentials (see refs 3, 6) are used. Thus to model NaβAl$_2$O$_3$ we take parameters from the lattice potential of Al$_2$O$_3$ (refs 4, 6) which are supplemented by a Na$^+$–O^{2-} potential obtained from a study of the crystal properties of Na$_2$O; for the shell parameters of the Na$^+$ ion we use the values reported in ref. 7. The present calculations were prompted by their successful application in other systems[5,6,8].

Three important cation sites in the conduction plane of NaβAl$_2$O$_3$, have been identified. Figure 1 shows the positions known as the Beevers–Ross, anti-Beevers–Ross and mid-oxygen sites. We have, therefore, performed three lattice energy calculations; in each case all the Na$^+$ ions were situated at one of the three sites. The Beevers–Ross configuration is found to have the lowest lattice energy. The other results are summarized in Table 1.

Table 1 Energies of Na$^+$ ion configurations

Configuration	Energy* (eV)
Mid oxygen	0.39
Anti-Beevers–Ross	0.15

* Energies are given per Na$^+$ ion and with respect to the Beevers–Ross configuration.

Several important consequences follow from these calculations. First, the Beevers–Ross sites are the most energetically favourable for the incorporation of Na$^+$ ions—a result in line with experimental observation[9]. But the differences between the energies of the Na$^+$ at this site and other configurations are very small—of the same order of magnitude as kT for elevated temperatures (500–1,000 K). The existence of such an exceptionally flat potential surface provides a qualitative explanation of the superionic nature of NaβAl$_2$O$_3$. Little resistance to Na$^+$ motion can be provided by the alumina framework, and the conduction mechanism and activation energy will be largely controlled by the interactions between the Na$^+$ ions. Second, the flatness of the potential surface will result in very large and anharmonic thermal parameters in any refinement of diffraction data on the material—a conclusion of obvious importance in structural studies of NaβAl$_2$O$_3$. Third, our present theoretical methods contain limitations. If the potential energy of the Na$^+$ ion between different sites in the conduction plane varies only by $\sim kT$, then transport properties of the solid cannot be adequately modelled by 'static' calculations of the type discussed here because the correlation between the motions of several species cannot be modelled by our technique which concentrates on isolated defect species. Dynamical simulations as reported by

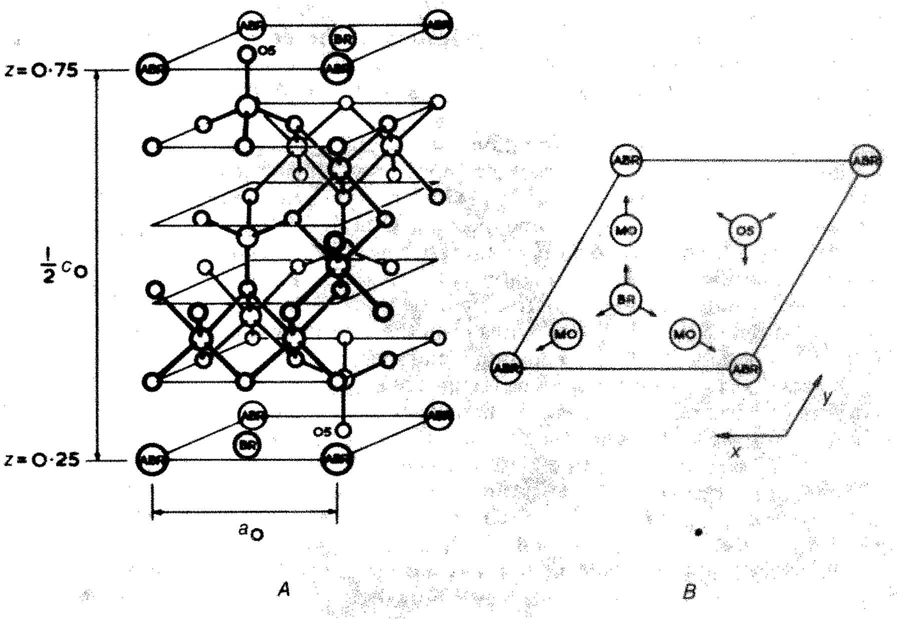

Fig. 1 The structure of β-Al$_2$O$_3$ with Beevers–Ross (BR), anti-Beevers–Ross (ABR) and mid-oxygen (MO) sites marked. *A*, 3D Structure. ∘, Al^{3+}; O, O^{2-}. *B*, Section of structure through conduction-plane.

0028–0836/80/310473—02$01.00

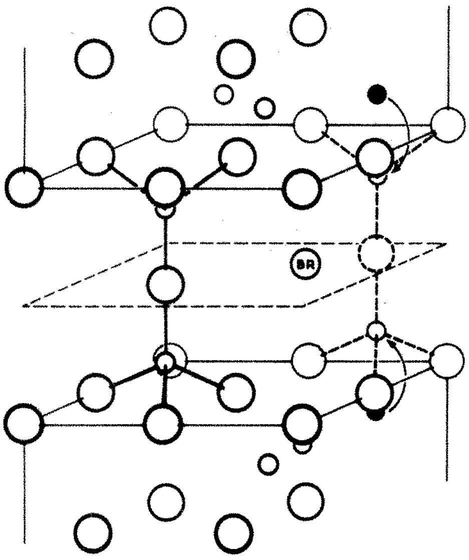

Fig. 2 Oxygen interstitial in conduction plane. The interstitial (◌) is stabilized by the movement of the Al^{3+} ions (●) as shown. A bridging oxygen ion is also shown.

Dixon and Gillan[10] for the superionic fluorite materials will be required.

Excess oxide ions in non-stoichiometric β-Al_2O_3 are incorporated in the conduction plane. Recent diffraction studies have suggested that these O^{2-} ions are stabilized by the displacement of two neighbouring aluminium ions from their lattice positions into 'interstitial' sites above and below the conduction plane; Fig. 2 illustrates the resulting complex. To test the feasibility of these proposals, we performed calculations using the HADES III program first on the conduction-plane O^{2-} interstitial, and second on the interstitial with both neighbouring displaced Al^{3+} ions. We found that displacement of both ions resulted in a stabilization energy of 1.0 eV. Our results confirm the Roth model. They also indicate a tendency for exceptionally large displacement of lattice ions around 'defects' in β-Al_2O_3.

We have performed calculations using the HADES III program of vacancy and interstitial energetics in β-Al_2O_3, and found, remarkably, that the formation of all defect species is energetically favourable. The result is not attributable to inadequacies in our lattice model, as the calculations converged successfully, without excessive ion dipoles developing. Rather, the favourable defect energies are due to the ability of the conduction plane and neighbouring spinel block ions to relax extensively around charged defects—a feature of the defect chemistry of β-Al_2O_3 already shown by the structure of the oxide interstitial, but which our work suggests is general to this material.

It is also clear that if defect formation is a favourable process in $Na\beta Al_2O_3$, then the stoichiometric compound would not be expected to be stable; the compound will disproportionate into a defective non-stoichiometric compound and Al_2O_3. Although our discussion cannot yet be more quantitative, we believe that we have identified the essential feature of $Na\beta Al_2O_3$ responsible for its unusual stoichiometry, namely the exceptional stability of defects which in turn arises from the very large ion relaxations possible around conduction plane species.

Our results suggest that the unique features of β-Al_2O_3 can be attributed to two related factors: the flatness of the sodium ion potential surface in the conduction plane; and the tendency for large ion relaxations around defect species in the plane. This 'fluidity' of the conduction plane is obviously the basic cause of the superionic properties of β-Al_2O_3. However, it raises serious problems for the detailed modelling of the material. Static simulations cannot yield information beyond the general guidance which the present results have provided. Molecular dynamic simulations are necessary. Preliminary results have been reported by de Leeuw[11], but detailed simulations would be of great interest.

We are grateful for financial support from AERE Harwell, and the Commission of the European Communities. We thank the SRC for permission to use the CRAY-1 computer at the Daresbury Laboratory.

Received 21 April; accepted 6 June 1980.

1. Kummer, J. T. in *Progress in Solid State Chemistry* Vol 1 (eds Reiss, H. & McCalden, J. O.) 141 (1972).
2. Rertn, W. L., Reichinger, F. & La Placa, S. U. in *Superionic Conductors* (eds Mahan, G. D. & Roth, W. L.) (Plenum, New York, 1977).
3. Catlow, C. R. A. & Norgett, M. J. *UKAEA Rep.*, AERE-M.
4. James, R. *UKAEA Rep.* AERE, Tp 814.
5. Catlow, C. R. A. & James, R. *Nature* **272,** 602 (1978).
6. Catlow, C. R. A., James, R., Mackrodt, W. C. & Stewart, R. *Phys. Rev. B* (in the press).
7. Catlow, C. R. A., Diller, K. M. & Norgett, M. J. *J. Phys.* C**10,** 1395 (1977).
8. Catlow, C. R. A. & Fender, B. E. F. *J. Phys.* C**8,** 3267 (1975).
9. Roth, W. L., Hamilton, W. C. & La Placa, S. J. *Am. Crystallogr. Ass. Abstr. Ser. 2* **1,** 169 (1973).
10. Dixon, M. & Gillan, M. J. *J. Phys.* C**11,** L165 (1978).
11. de Leeuw, S. W. & Peram, J. W. in *Fast Ion Transport in Solids* (eds Vashishta, P., Mundy, J. N. & Shenoy, G. K.) 345 (North-Holland, Amsterdam, 1979).

Conversion of carbohydrate into hydrogen fuel by a photocatalytic process

Tomoji Kawai & Tadayoshi Sakata

Institute for Molecular Science, Myodaiji, Okazaki 444, Japan

Attempts have been made to find green plants which produce low-molecular weight hydrocarbons[1,2] and to find seaweeds which produce hydrogen from water utilizing solar energy[3,4]. These attempts are aimed at finding methods of making use of the photosynthetic process in plants for direct production. Most green plants, however, synthesize carbohydrates, such as sugar, starch and/or cellulose, from water and carbon dioxide. The C_4 plants[5], such as corns and sugar cane, grow rapidly, utilizing solar energy with ~1% efficiency for the fixation of CO_2. This value is 10 times larger than that of the average efficiency of photosynthesis of plants, 0.1%. However, the carbohydrates produced by these plants cannot be used directly as fuel. Here we show a new route for the conversion of carbohydrates into hydrogen (a clean fuel in the hydrogen energy system), taking advantage of the photocatalytic process. We found that the irradiation of the carbohydrates, not only sugar or starch but also cellulose, in the presence of water and a $RuO_2/TiO_2/Pt$ photocatalyst powder leads to the efficient production of hydrogen gas.

This new process is expressed as equation (1) together with the photosynthesis of carbohydrates by green plants (equation (2)), as follows:

$$(C_6H_{12}O_6)_n + 6n\ H_2O \xrightarrow{h\nu,\ RuO_2/TiO_2/Pt} 6n\ CO_2 + 12n\ H_2 \qquad (1)$$

$$6n\ H_2O + 6n\ CO_2 \xrightarrow{h\nu,\ \text{green plant}} (C_6H_{12}O_6)_n + 6n\ O_2 \qquad (2)$$

$$12n\ H_2O \longrightarrow 6n\ O_2 + 12n\ H_2 \qquad (3)$$

Here, $(C_6H_{12}O_6)_n$ represents sugar (saccharose) ($n = 2$), starch ($n \simeq 100$) or cellulose ($n \simeq 1{,}000$–$5{,}000$) after hydrolysis.

Accordingly, the overall reaction results in the decomposition of water to produce hydrogen (equation (3)), the CO_2 being recycled. The reaction (1) proceeds almost without loss of energy (heat of combustion: 688 kcal mol^{-1} for $(C_6H_{12}O_6)_{n=1}$ and 680 kcal mol^{-1} for 12 H_2).

The typical experimental conditions are as follows: the powders of RuO_2 (Rare Metallic), TiO_2 (Katayama Kagaku) and Pt (Engelhardt) (weight ratio = 10:100:5) were mixed and ground in an agate mortar, and this powder was suspended in

0028-0836/80/310474—03$01.00

neutral water (40 ml) in a Pyrex glass bulb (280 ml). Then a sugar (600 mg, Nissin Seito pure white sugar) or a soluble starch (120 mg, Katayama Kagaku) was dissolved in the solution and the bulb was deaerated and illuminated by a 500 W Xe lamp. For the reaction of cellulose, a filter paper (Toyo Filter) was cut into pieces and put into neutral water or a 6 M NaOH water solution with the photocatalyst forming alkali-cellulose. The gases evolved were collected and analysed by a mass spectrometer, and the amounts of the gases were determined with a manometer with traps at −197, −78 and −10 °C, as described previously[6].

When the photocatalyst suspension in water with the substrate was illuminated, gas bubbles were vigorously generated out of the depth of the solution near the illuminated area. The bubbling stopped when the light was turned off. The evolved gases were mainly H_2 and CO_2, with very small amounts of CH_3OH and C_2H_5OH (less than 0.2% of the total amount). Table 1 summarizes the amounts of hydrogen evolved from sugar, starch or cellulose with water, and Fig. 1*a* shows the evolution of H_2 and CO_2 from sugar plotted against irradiation time. The ratio of the formation rate of H_2 to CO_2 was 3 : 1 to 4 : 1 at the initial stage, becoming about 2 : 1 in the stationary state. No CO, CH_4 and O_2 were evolved. When NaOH was put into the solution to form 6M NaOH solution during the reaction, only H_2 was evolved (Fig. 1*a*), and the CO_2 produced was absorbed in the solution presumably as Na_2CO_3 or $NaHCO_3$. Also with the cellulose in 6M NaOH aqueous solution, pure hydrogen was evolved (Table 1). The quantum yields of the H_2 production determined by monochromatic irradiation at λ = 380 nm for sugar, starch and cellulose were 1.2, 0.8 and 0.3% respectively in neutral water and 1.5, 1.3 and 1.0% respectively in 6M NaOH. These quantum yields, using the $RuO_2/TiO_2/Pt$ photocatalyst, were 100 times larger than those obtained with TiO_2 alone (Table 1). To confirm that no detectable amounts of other products were formed in the solution at the end of the reaction, an experiment was carried out with a small amount of sugar (13 mg, corresponding to 1 mmol of H_2 gas), using a Hg-ultra-high pressure lamp (500 W, Philips) which emits intense UV light ($\lambda < 320$ nm was cut by a Pyrex glass filter), instead of the Xe lamp. The sugar was then completely decomposed within 18 h producing only the corresponding H_2 and CO_2 gases (Fig. 1*b*). These results show that the reaction (1) occurs successfully in this experimental condition at room temperature, simply producing gaseous H_2 and CO_2. Surprisingly, the hydrogen was evolved not only from water and sugar, a relatively large molecule, but also from water and starch or cellulose, the stable macromolecule which consists of about a hundred to thousands of molecules of glucose.

Table 1 H_2 and CO_2 evolution from water and sugar, starch or cellulose on the $RuO_2/TiO_2/Pt$ photocatalyst suspended in neutral water and 6M NaOH solution, irradiated by 500 W Xe lamp

Reactant	H_2 (μmol/20 h)	CO_2 (μmol/20 h)	Quantum yield at λ = 380 nm (%)
Sugar + H_2O	280	133	1.2
Starch + H_2O	204	96	0.8
Cellulose + H_2O	70	42	0.3
H_2O	4	*	0.02
Sugar + 6M NaOH	341	—	1.5
Starch + 6M NaOH	320	—	1.3
Cellulose + 6M NaOH	244	—	1.0
Sugar + H_2O with TiO_2 catalyst	2	1.2	—

Experimental conditions: sugar (600 mg), starch (120 mg), cellulose (120 mg), $RuO_2/TiO_2/Pt$ photocatalyst (300 mg), H_2O (40 ml), 6M NaOH aqueous solution (40 ml). All the values fluctuated within at most ±10%. The rates of gas evolution represent the values at 50 h after the beginning of the irradiation. The quantum yield means the number of electrons used for the H_2 evolution divided by the number of incident photons, taking into consideration that two electrons produce one H_2 molecule.

* Oxygen (1.6 μmol per 20 h) was simultaneously evolved.

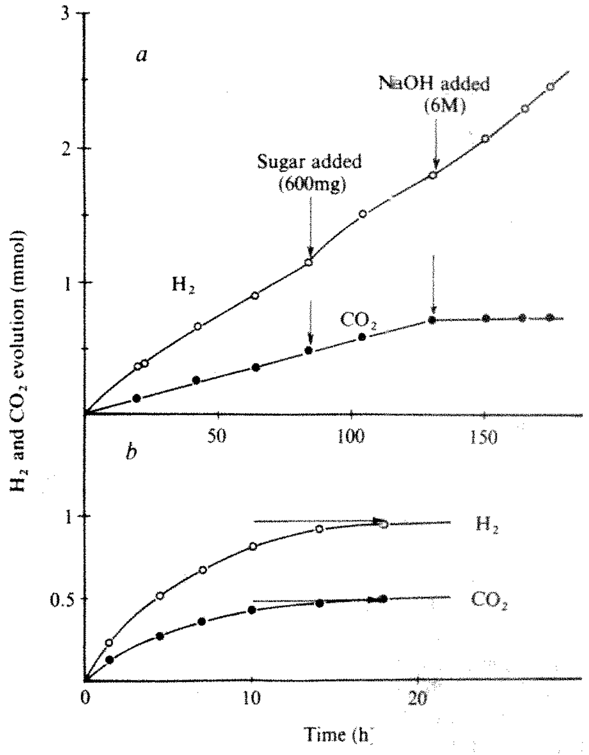

Fig. 1 *a*, H_2 and CO_2 evolution from sugar in water versus the irradiation time. Experimental conditions: sugar (600 mg), H_2O (40 ml), $RuO_2/TiO_2/Pt$ (300 mg), 500 W Xe irradiation. Additional sugar (600 mg) and NaOH (9.6 g) were put into the solution at 85 and 130 h after the start of the reaction, respectively. *b*, H_2 and CO_2 production with the irradiation time from a small amount of sugar. Experimental conditions: 500 W Hg-ultrahigh-pressure lamp, sugar (13 mg), H_2O (40 ml), $RuO_2/TiO_2/Pt$ (150 mg). Arrows (→) indicate the estimated amounts of H_2 and CO_2 which are produced from 13 mg of sugar according to equation (1).

The mechanism of the reaction could be explained by regarding the $RuO_2/TiO_2/Pt$ powder as an electrochemical microcell, as follows: the light of energy larger than the band gap of TiO_2 (3 eV) produces electron–hole pairs; then the separated electron and holes can make redox reactions at the surface of the particle with the molecules in the solution (Fig. 2). This particular $RuO_2/TiO_2/Pt$ photocatalyst is very active in reaction (1) (100 times more active than TiO_2 alone), presumably because RuO_2 is one of the best electrode materials for the oxidation of water[7] and Pt for hydrogen evolution[8]. As carbohydrate is expressed as $(CH_2O)_n$ and is an assembly of $(\mathrm{H{-}\overset{|}{\underset{|}{C}}{-}OH})_n$ which has alcoholic —OH groups, we chose CH_3OH and HCHO as the model C_1 compounds, and examined their photocatalytic reactions with water on the $RuO_2/TiO_2/Pt$ photocatalyst. It is already known that CH_3OH is photooxidized to form HCHO on a single crystal TiO_2 photoanode[9] ($CH_3OH + 2p \rightarrow HCHO + 2H^+$). In our experiment using $RuO_2/TiO_2/Pt$ powder, the CH_3OH was oxidized into HCHO, and simultaneously, H^+ was reduced to form H_2 (Quantum yield ≃44%). It was also observed that HCHO with water was finally converted into H_2 and CO_2 ($H_2 : CO_2 = 2 : 1$) on this photocatalyst ($HCHO + H_2O \rightarrow 2H_2 + CO_2$). Consequently, the carbon chains of carbohydrates in water would be successively oxidized by the hole at the oxidizing site of the catalyst to form H^+ and CO_2, while the electrons would reduce H^+ at the reducing site to form H_2, similar to the case of CH_3OH and HCHO. The larger amount of H_2 production at the beginning of the reaction would be due to the dehydrogenation of the carbohydrate to form >C=O, —CH=O or —COOH functional groups at the initial stage.

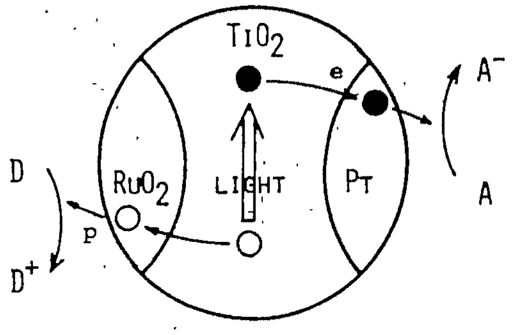

Semiconductor particle

Fig. 2 A schematic figure of the $RuO_2/TiO_2/Pt$ particle. O, Hole (p) in the valence band of TiO_2; ●, electron (e) in the conduction band. A and D represent acceptor and donor, respectively, of electrons in the solution. In reaction (1), carbohydrate and proton in the solution play the roles of D and A, respectively.

Note also that this $RuO_2/TiO_2/Pt$ photocatalyst can decompose water directly into H_2 and O_2 with a quantum yield of 0.02% at $\lambda = 380$ nm (Table 1).

As solar energy conversion into chemical energy by a man-made device with efficiency of >1% is not cheap or easy at this stage, the use of the photosynthetic power of green plants for making fuels is still effective[1]. In Brazil, a project is under way in which sugar taken from rapidly growing sugar cane is fermented into ethanol for use as a fuel, using bacteria[1,10]. The fermentation, however, is a delicate procedure, and occasionally an acid is formed instead of alcohol. In our method, the capture and the fixation of dilute CO_2 is left to the plants, and the produced carbohydrates are artificially converted into H_2 and CO_2 using the photocatalytic reactions on the stable inorganic semiconductor powder. This process may be called 'photoinduced fermentation'. The CO_2 evolved can be collected and may be fed back to the plants as concentrated CO_2 gas. In the concentrated NaOH solution, we can get pure hydrogen gas (Fig. 1*a*) and simultaneously Na_2CO_3 or $NaHCO_3$, important substances for the chemical industry. Furthermore, the rates of H_2 production from carbohydrates were greatly enhanced in 6M NaOH solution compared with that in neutral aqueous solution (Table 1). Another method for the production of pure hydrogen, utilizing reaction (1) in a photoelectrochemical cell is now under investigation: the carbohydrate with water is oxidized at a semiconductor photoanode to form CO_2 in one cell, with H_2 production from water at the cathode in the other cell.

Using the strong oxidizing power of the RuO_2/TiO_2 photocatalyst powder, we have demonstrated the photoinduced water–gas reaction with formation of H_2 from water and solid carbon[6], the direct decomposition of water into H_2 and O_2 (refs 11, 12) and, in this study, the decomposition of carbohydrate by $RuO_2/TiO_2/Pt$ to produce H_2. This method may also be applied to the decomposition of excrements containing cellulose, protein and fat, accompanied by the production of H_2 as a fuel. We are also interested in the possibility of the decomposition and scavenging of abandoned carbon compounds in nature (such as corpses of animals) using a semiconductor photocatalyst (Fe_2O_3, WO_3 and so on) instead of bacteria.

Received 4 March; accepted 15 May 1980

1. Calvin, M. *Photochem. Photobiol.* **23**, 425 (1976).
2. Nielson, P. B., Nishimura, H., Otvos, J. W. & Calvin, M. *Science* **198**, 942 (1977).
3. Benemann, J. R. & Weare, N. M. *Science* **184**, 174 (1974).
4. Miyamoto, K., Hallenbeck, P. C. & Benemann, J. R. *J. Ferment. Technol.* **57**, 287 (1979).
5. Hatch, M. D. & Osmond, C. B. *Encyclopedia of Plant Physiology* Vol. 3 (eds Stocking, C. R. & Heber, U.) 144 (Springer, Berlin, 1976).
6. Kawai, T. & Sakata, T. *Nature* **282**, 283 (1979).
7. Morita, M., Iwakura, C. & Tamura, H. *Electrochim. Acta* **23**, 331 (1978).
8. Bockris, J. O'M. & Reddy, A. K. N. *Modern Electrochemistry*, 35 (Plenum, New York, 1970).
9. Miyake, M., Yoneyama, H. & Tamura, H. *Chem. Lett.* 635 (1976).
10. Baum, M. *Nature* **282**, 550 (1979).
11. Kawai, T. & Sakata, T. *Proc. 7th int. Cong. Catal.*, Tokyo B38 (1980).
12. Kawai, T. & Sakata, T. *Chem. Phys. Lett.* **72**, 87 (1980).

Trace element abundances in basalts of Nauru Basin

R. Batiza*, R. L. Larson†, S. O. Schlanger‡, S. A. Shcheka§ & H. Tokuyama‖

*Department of Earth and Planetary Sciences, Washington University, St Louis, Missouri 63130
†Lamont-Doherty Geological Observatory of Columbia University, Palisades, New York 10964
‡Hawaii Institute of Geophysics, University of Hawaii at Manoa, Honolulu, Hawaii 96822
§Far East Institute of Geology, USSR Academy of Sciences, Vladivostok USSR
‖Ocean Research Institute, University of Tokyo, Nakano, Tokyo 164, Japan

Leg 61 of the Deep Sea Drilling Project (DSDP) was concerned with drilling a single continuously cored multiple re-entry hole at site 462 in the Central Nauru Basin (Fig. 1). Preliminary results of this drilling, which penetrated more than 1 km beneath the sea floor, were presented earlier[1,2]. One major result was the discovery of a late Cretaceous off-ridge volcanic/intrusive complex of basaltic composition and great thickness (>500 m). We now present trace element abundance data for these basalts. Results of the drilling provide further support for a relatively long-lived thermal and magmatic event in the late Cretaceous resulting in voluminous and widespread magmatism in the central and western Pacific consistent with earlier suggestions[3–5]. The trace element data show that most of the rocks produced during this event have trace element characteristics intermediate between those of normal and transitional mid-ocean ridge basalts (N- and T-type MORB)[6] and different from Hawaiian basalts[7]. These results indicate that basalts which are depleted in light rare earth elements (LREE) relative to the heavy REE may, in certain conditions, be erupted as voluminous intra-plate eruptions far from active ridge crests.

DSDP site 462 is located in the Central Nauru Basin in a region of low topographic relief and bottom depths of ~5,100 m (ref. 1) and lies on magnetic anomaly M-26 (~155 Myr BP)[8–10]. The Nauru Basin is bounded on the west and south by the Ontong–Java plateau[11–13], on the east and north by the Gilbert and Marshall ridges[3,5,10,14,15] and on the north-west by the Caroline Ridge[15–18] (Fig. 1). It is a region of well developed Mesozoic magnetic anomalies and since the mid-Cretaceous has been the site of turbidite deposition from the surrounding elevated regions[1]. Palaeomagnetic data show that the Nauru Basin basalts are all normally magnetized, indicating that they were largely emplaced during the Cretaceous long normal event which lasted from 109 to 80 Myr BP. As the age of the Pacific crust at this site is about 155 Myr BP, this magmatic event occurred off-ridge on oceanic crust at least 46 Myr old[1,8,19].

Based on on-board petrographic and X-ray fluorescence analyses for several major elements[1] and later shore-based chemical analyses of several hundred samples, it is clear that the basalts produced during the off-ridge magmatic episode in the Nauru Basin are mineralogically and chemically similar to MORB[1,6]. They are quartz and olivine-hypersthene normative and have mineralogy and major trace element characteristics which are very similar to many types of oceanic ridge basalt (see Table 1). However, they differ significantly and systematically in the following respects: (1) Nauru Basin basalts have higher FeO^*/MgO ratios for a given TiO_2 content than N-type MORB. For example, at TiO_2 contents of 1.0 wt %, FeO^*/MgO is 1.3–1.5 compared with 0.8–1.0 for N-type MORB[6,20]. Trends of FeO^*/MgO and TiO_2 wt % for Nauru Basin basalts are parallel to trends for N-type MORB but displaced to higher FeO^*/MgO ratios. (2) Spinels in Nauru Basin basalts have lower Mg/Mg +

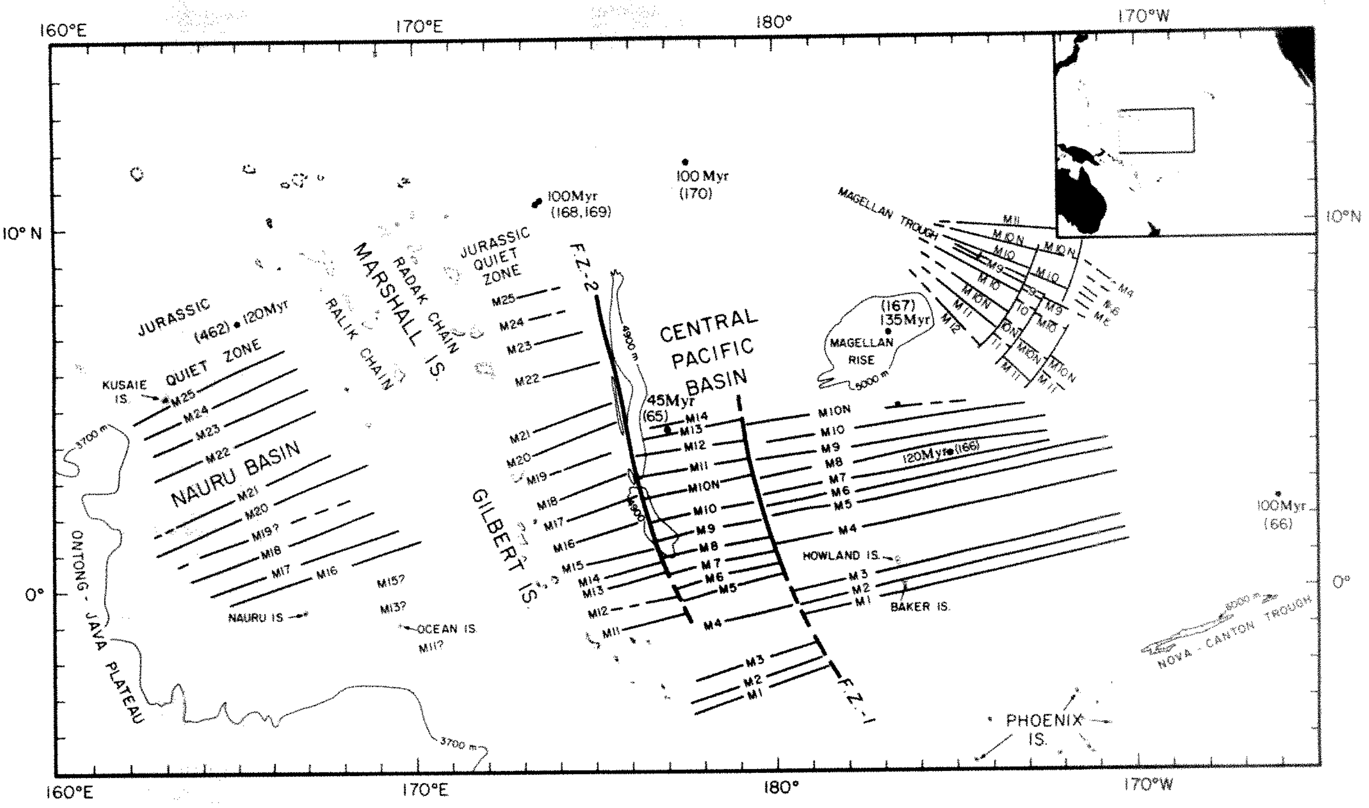

Fig. 1 Bathymetry of the western and central Pacific[23] showing the location of DSDP sites 462 and 169.

Fe^{2+} ratios (0.49–0.54) and higher Cr/Cr + Al ratios (0.54–0.73) than N-type MORB (0.6–0.8 and 0.4–0.6, respectively)[21] and these co-exist with olivine of generally lower Mg number (100 Mg/(Mg + Fe^{2+}) of olivines is 0.83–0.84) than found in N-type MORB. (3) Nauru Basin basalts have higher La/Sm ratios at given Sm contents than N-type MORB, but lower La/Sm ratios than transitional MORB[6] and Hawaiian tholeiitic basalts[7] (see Figs 2, 3). Abundances of Sc, Cr, Co, Ni, Sr, Hf and Zr fall within the range of abundances for MORB (Table 1). Thus, Nauru Basin basalts are depleted in LREE as are N-type MORB, but the level of depletion of LREE is significantly and systematically less than that of N-type MORB.

The geological evolution of the central and western Pacific during the Mesozoic is apparently quite complicated and may involve very rapid spreading rates from several relatively short-lived ridge crest segments, numerous ridge jumps and creation of thick volcanic piles[3,5,22,23]. The formation of abundant seamount and island chains[15,24], guyots[25] and high standing plateaus[5,13] is thought to have occurred in late Mesozoic time but the relationship between this widespread volcanism, vertical movements and plate geometrics and evolution remains problematic[3–5,10,26].

A possible clue to the nature of volcanic/tectonic evolution of the western and central Pacific is provided by the widespread occurrence of off-ridge basalts with trace-element abundances like those of the Nauru Basin elsewhere in the region. Basalts which are depleted in LREE but which have unusually high La/Sm ratios (relative to the N-type MORB) have been encountered in DSDP holes 169 (ref. 27), 289 (ref. 28) and 317 (ref. 29) drilled during Legs 17, 30 and 33. These basalts occur either as sills or as lava flows on plateau regions and contrast chemically with volcanic rocks of broadly similar age which form the seamounts and seamount chains of the western and central Pacific[24,29], all of which are alkalic and more enriched in LREE. It is possible that much of the crust in the area of the Darwin Rise[3], within which the Nauru Basin and other DSDP sites that encountered off-ridge basalt with MORB trace element abundances all lie, is pervasively intruded.

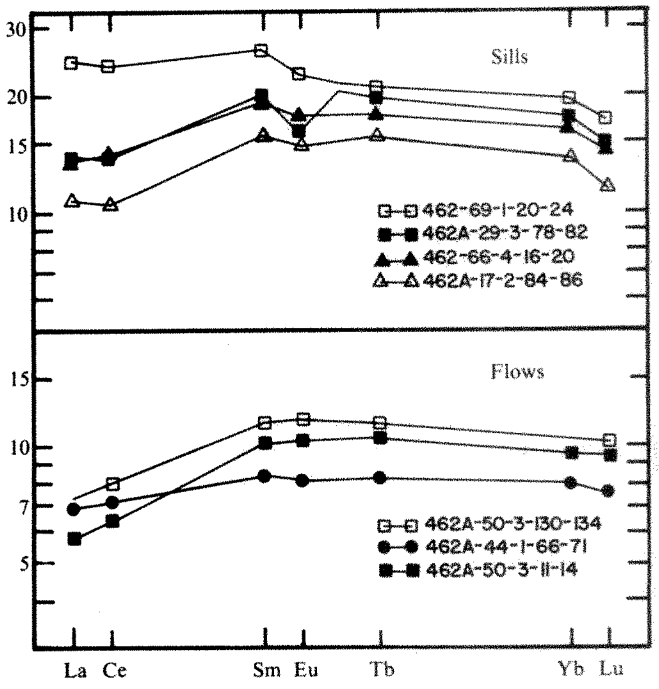

Fig. 2 Representative chondrite-normalized REE abundance patterns for several samples drilled during DSDP Leg 61. The sills (with interlayered sediment) comprise the upper portions of the Nauru Basin igneous complex and the flows occupy the lower portions of the section. Analyses were carried out by instrumental neutron activation analyses[32]. Rare earth and other trace element data will be reported elsewhere[33] but are available before then from R.B.

Table 1 Representative chemical analyses

Oxide (wt %) or element (p.p.m.)	Nauru Basin			Ontong–Java Plateau
	462-64-1-8-11	462A-20-1-115-121	462A-72-3-21-23	289-132-4-6-10
SiO_2	49.78	47.50	49.24	49.4
TiO_2	1.52	1.62	1.02	1.6
Al_2O_3	14.76	14.69	15.33	14.9
Fe_2O_3	3.62	2.88	3.52	4.1
FeO	9.07	10.15	7.30	7.5
MnO	0.21	0.26	0.19	0.14
MgO	7.01	7.09	7.70	6.6
CaO	9.44	11.14	12.29	10.6
Na_2O	2.19	2.26	1.95	2.3
K_2O	0.12	0.05	0.05	0.34
P_2O_5	0.17	0.18	0.13	0.14
H_2O^+	1.08	0.82	0.99	2.2
H_2O^-	0.67	1.08	0.81	
Total	99.64	99.72	100.52	99.82
La	4.29	4.13	2.59	4.45
Ce	13.1	11.53	7.41	11.77
Sm	3.33	3.18	2.19	3.59
Eu	1.29	1.11	0.81	1.12
Tb	0.95	0.82	0.61	0.85
Yb	3.78	2.98	2.28	3.09
Lu	0.55	0.45	0.35	0.48
Sc	51	41	45	46
Cr	228	179	313	298
Co	51	44	46	38
Hf	2.96	2.51	1.54	2.40

Analyses of two sills from hole 462, core 64 and hole 462A, core 20 and 1 flow from hole 462A, core 72. Analysis of a basalt from DSDP Leg 30 is given for comparison with the DSDS Leg 61 sills. Major element chemistry of the Leg 30 sample is from Stoeser[26] (sample 289-132-4-27). Major element analyses of Leg 61 samples were done by wet chemical techniques and trace elements by instrumental neutron activation analysis[32].

If this speculation is correct, very large portions of the Pacific may have been constructed by a combination of normal oceanic crustal creation processes (at ridges) together with voluminous off-ridge additions of basaltic material of broadly similar chemical composition. Perhaps coincidentally, the Caribbean flood basalts encountered during Leg 15 of DSDP have nearly identical trace element chemistry to the Nauru Basin and other basalts described previously[30] and the crustal ages and structures inferred from geophysical studies are also similar[9,31]. This may indicate that conditions leading to the generation of large volumes of intra-plate basalt chemically similar to MORB were not unique to the Pacific.

The major conclusions from the trace element data of Nauru Basin basalts and interpretation of these data in the light of volcanic and tectonic evolution of the central and western Pacific are as follows: (1) The Nauru Basin volcanic complex is composed of basalt which has trace element characteristics that are intermediate between N- and T-types of MORB. (2) Basalt of this compositon is widely distributed throughout the western and central Pacific in sills and aseismic plateaus, but it is not known if this distribution is continuous. Basalt of similar chemistry is also present in the Caribbean crust. (3) More tentatively, it may be concluded that the wide distribution of off-ridge basalt chemically similar to MORB in the crust of the western and central Pacific is an indication of unusual processes of crustal origin and evolution in this region. Clearly, though, much more information is required before the nature of such processes is determined.

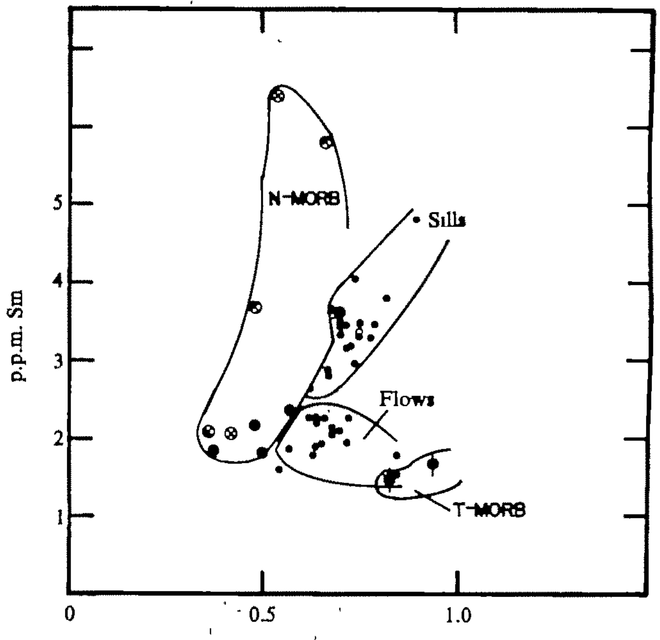

Fig. 3 (La/Sm) chondrite normalized enrichment factor as a function of Sm abundance for Leg 61 lavas (small dots). Also shown, for comparison, are normal mid-ocean ridge basalts (MORB) from the Siqueiros Fracture Zone[34] (circled crosses), analyses from Sun *et al.*[6] (large dots) and analyses from the Ontong–Java plateau (small circles). Note the clear separation of Leg 61 sills from flows and the intermediate La/Sm ratios of Leg 61 basalts. They occupy a field between normal and transitional types of MORB.

We thank Larry Haskin for allowing use of facilities for trace element determinations. This work was partly supported by NSF grant OCE7727001 and the Deep Sea Drilling Project.

Received 22 February, accepted 23 May 1980

1. Scientific Staff, DSDP Leg 61 *Geotimes* **23**, No. 12, 21–24 (1978).
2 Larson, R. L., Schlanger, S. O. & Scientific Staff Leg 61 in *Hawaii Symp. Intraplate Volcanism and Submarine Volcanism Abstr.*, 20 (1979).
3. Menard, H. W. *Marine Geology of the Pacific* (McGraw-Hill, New York 1964).
4 Hsu, K. J. & Schlanger, S. O. *Proc. 23rd int. Geol. Congr.*, Prague, Vol 1, 91–105 (1968).
5. Winterer, E. L. *Geophys. Monogr.* **19**, 269–278 (1976).
6. Sun, S.-S., Nesbitt, R. W. & Sharaskin, A. Ya. *Earth planet. Sci. Lett.* **44**, 119–138 (1979)
7. Schilling, J.-G. & Winchester, J. W. *Contr. Miner. Petrol.* **31**, 251–266 (1969).
8. Larson, R. L. & Hilde, T. W. C. *J. geophys. Res.* **80**, 2586–2594 (1975) Cande, S. C., Larson, R. L. & LaBrecque, J. L. *Earth planet. Sci. Lett.* **41**, 434–440 (1978)
9. Houtz, R. E. *J. geophys. Res.* **81**, 6321–6331 (1976)
10. Larson, R. L. *J. Geomagn. Geoelect. Kyoto* **28**, 219–236 (1976)
11 Winterer, E. L. & Riedel, W. R. *Init. Rep. DSDP* **7**, 3–8 (1971)
12. Packham, G. H. & Andrews, J. E. *Init. Rep. DSDP* **30**, 3–12 (1975)
13 Hussong, D. M., Wipperman, L. K. & Kroenke, L. W. *J. geophys. Res.* **84**, 6003–6010 (1979).
14 Emery, K. O., Tracy, J. I. & Ladd, H. S. *U.S. geol. Surv. Prof. Pap.* **260A**, 1–265 (1954)
15. Clague, D. A. & Jarrard, R. D. *Geol. Soc. Am. Bull.* **84**, 1135–1154 (1973)
16 Bracey, D. J. & Andrews, J. E. *Mar. geophys. Res.* **2**, 111–118 (1974).
17 Stark, J. T. & Hay, R. L. in *Military Geology of Truk Islands, Caroline Is* (eds Stark, J. T. *et al.*) 1–205 (U.S. Army, Chief of Engineers, Int Div, Hdqtrs U.S. Army Pacific, 1958)
18 Weissel, J. K. & Anderson, R. N. *Earth planet. Sci. Lett.* **41**, 143–158 (1978)
19 Larson, R. L. & Pitman, W. C. *Geol. Soc. Am. Bull.* **83**, 3645–3662 (1972)
20 Batiza, R., Rosendahl, B. R. & Fisher, R. L. *J. geophys. Res.* **82**, 265–276 (1977)
21 Sigurdsson, H. & Schilling, J.-G. *Earth planet. Sci. Lett.* **29**, 7–20 (1976)
22 Larson, R. L. & Chase, C. G. *Geol. Soc. Am. Bull.* **83**, 3627–3644 (1972).
23 Tamaki, K., Joshima, M. & Larson, R. L. *J. geophys. Res.* **84**, 4501–4510 (1979)
24 Natland, J. H. *Init. Rep. DSDP* **33**, 749–777 (1976)
25. Matthews, J. L. *et al. Science* **184**, 462–464 (1974)
26 Watts, A. B., Bodine, J. H. & Ribe, N. M. *Nature* **283**, 532–537 (1980)
27 Bass, M. N., Moberly, R., Rhodes, J. M. & Shih, C.-Y. *Init. Rep. DSDP* **17**, 429–503 (1973)
28 Stoeser, D. B. *Init. Rep. DSDP* **30**, 401–414 (1975)
29. Jackson, E. D., Bargar, K. E., Fabbi, B. P. & Heropoulos, C. *Init. Rep. DSDP* **33**, 571–630 (1976)
30 Bence, A. E., Papike, J. J. & Ayuso, R. A. *J. geophys. Res.* **80**, 4775–4804 (1975)
31. Burke, K., Fox, P. J. & Sengor, A. M. C. *J. geophys. Res.* **83**, 3949–3954 (1978).
32 Jacobs, J. W., Korotev, R. L., Blanchard, D. P. & Haskin, L. A. *J. radioanalyt. Chem.* **40**, 93–114 (1977).
33 Batiza, R. *Init. Rep. DSDP* **61** (in the press)
34. Johnson, J. R. *J. geophys. Res.* **84**, 1635–1651 (1979)

Deep water formation in the North Atlantic Ocean during the last ice age

Jean-Claude Duplessy

Centre des Faibles Radioactivités, Laboratoire Mixte CNRS-CEA, 91190-Gif-sur-Yvette, France

J. Moyes & C. Pujol

Institut de Géologie du Bassin d'Aquitaine, Université de Bordeaux I, 33405-Talence, France

Oxygen-18 records of benthic foraminifera from northeastern Atlantic and Southern Ocean cores are significantly different. This difference indicates that the deep water in the northeastern Atlantic Ocean during the last Ice Age was at least 1.3 °C cooler than in modern times. We show here that the occurrence of such a cold deep water mass implies that the North Atlantic was a sink for dense surface waters, replacing the Norwegian Sea where ice cover and stratification prevented the formation of deep water.

Over the last few million years, the Earth's climate has alternated between ice ages and warmer intervals. Although there have been many quantitative studies of the response of the ocean–atmosphere–ice system to climatic changes, most of these have been concerned with the history of ocean surface waters, based on faunal analysis of fossil plankton from deep sea sediments[1]. However, the formation and circulation of deep water are also affected by climatic changes. The present major source of North Atlantic Deep Water (NADW) is the Norwegian Sea, in which an inflow of warm saline surface water is progressively cooled during its transfer towards high latitudes. This loss of heat to the atmosphere within the Norwegian basin increases the density of the surface water so that it sinks to the bottom, where it overflows the sills in the Denmark strait and the Faeroe channel and moves southward into the Atlantic Ocean[2]. During the last ice age, however, the Norwegian Sea bottom water has been shown to be warmer than at present[3], so that the Norwegian Sea was not a sink for surface water, which followed from the disappearance of the Norwegian current[4] and stratification due to a permanent ice cover[5]. This implies a major change in the origin and circulation of the deep water of the Atlantic Ocean. Additional evidence for these changes is found in the benthic foraminiferal fauna changes of the North Atlantic Ocean during the last climatic cycle[6–8]; however, it has not been possible to interpret these faunal changes in terms of temperature variations of the NADW.

During the cruise FAEGAS 1 of the French RV Jean Charcot in the northeastern Atlantic, piston core CH 73139C was collected at 54°38′ N, 16°21′ W from a water depth of 2,209 m (Fig. 1). A sedimentological description of this core has been given elsewhere[9]. Radiocarbon dates have been obtained on the coarse fraction (>44 μm) which consists of a foraminiferal ooze with non-calcareous detrital material below 1 m. The mean sedimentation rate during the past 17,000 yr was calculated to be ~11.9 cm kyr^{-1} (Table 1).

Table 1 ^{14}C dates of cores CH 73139C and MD 73025

Core CH 73139C		Core MD 73025	
Depth (cm)	Age (yr)	Depth (cm)	Age (yr)
7–13	2,020 ± 200	35–39	6,880 ± 330
46–50	5,300 ± 260	76–80	8,230 ± 370
77–83	8,520 ± 350	152–159	8,950 ± 400
112–120	12,020 ± 480	182–186	9,930 ± 440
140–144	11,800 ± 480	226–230	10,400 ± 460
157–165	15,230 ± 770	276–280	12,620 ± 550
180–184	16,900 ± 900	324–329	17,700 ± 1,000
220–224	23,300 ± 2,100	355–359	19,000 ± 1,200
		416–420	24,700 ± 2,400

A ^{14}C half life of 5,730 yr has been used. No correction has been made to take into account isotopic fractionation in samples or apparent age of seawater carbon

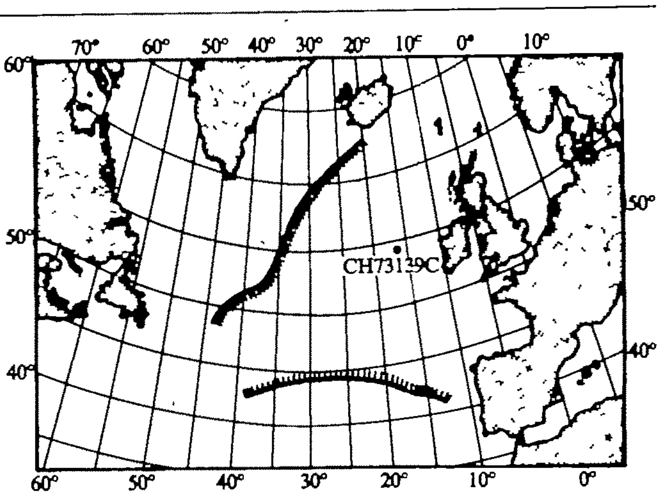

Fig. 1 Location of core CH 73139C. Lines with hachures indicate the extreme poleward and equatorward position of the polar front during isotopic stages 2, 3, 4. Core CH 73139C was north of the polar front during about half of this period[18].

We have measured the $^{18}O/^{16}O$ ratio of the benthic foraminiferal species *Cibicides wuellestorfi* and a mixture of *C. kullenbergi*, *C. gr.lo* and *C.*sp. (ref. 10). Analyses were performed using a Micromass 602 C mass spectrometer with experimental procedures described elsewhere[11]. Replicate analyses of the same carbonate gave a standard deviation of 0.07 ‰ for a single measurement. Results are expressed as $\delta^{18}O$ defined by the relationship:

$$\delta^{18}O = \left[\frac{(^{18}O/^{16}O)\ \text{sample}}{(^{18}O/^{16}O)\text{PDB}} - 1\right] \times 10^3$$

where PDB (Pee Dee Belemnite) is the Chicago PDB 1 standard.

Although most benthic foraminifera yield different oxygen isotopic values[12], all the *Cibicides* species from the same level in the sediment have identical oxygen isotopic ratios within experimental errors. Mean values for each level are reported in Table 2.

The isotopic record of benthic foraminifera in core CH 73139C is reported in Fig. 2*a* with a constant correction factor of 0.64 ‰ to take account of *Cibicides* departure from isotopic equilibrium[8,13]. This record is readily correlated with the standard sequence of stages to stage 6 as defined by Emiliani[14]. The absolute $\delta^{18}O$ values obtained and their variations with core depth closely match those from other cores from the North Atlantic Ocean[8,15], in agreement with the hypothesis that the major signal in these records reflects isotopic changes in the world's ocean water resulting from the variation of continental ice sheets.

The isotopic record shows that the sedimentation rate has varied during the last climatic cycle: assuming an age of 127,000 yr for the boundary between isotopic stage 5 and stage 6 (ref. 13), a mean sedimentation rate of 5 cm kyr^{-1} is obtained below 1.8 m, which is about half of that determined for the upper part of the core. However, the sedimentation rate did not remain constant during that time. From the late glacial maximum to the boundary between isotopic stage 4 and stage 5, a mean sedimentation rate of 5.9 cm kyr^{-1} can be calculated according to the time scale developed by Broecker and Van Donk[16]. Within stage 5, the fine structure of the isotopic record

0028–0836/80/310479—04$01.00

recognized first by Emiliani[17] is not in evidence in core CH 73139C. However, the $\delta^{18}O$ peak between 720 and 620 cm can be unambiguously correlated with isotopic substage 5e on the basis of $\delta^{18}O$ values similar to the modern ones and of the occurrence in the planktonic foraminiferal fauna of warm species like *G. crassaformis* which has been reported only during that substage in the north-east Atlantic ocean[18]. Assuming an age of 115,000 yr for the boundary between isotopic substage 5e and substage 5d, a mean sedimentation rate of 8.3 cm kyr^{-1} is calculated during substage 5e. In contrast, the sedimentation rate has dropped sharply between 115,000 and 75,000 yr BP (isotopic substages 5a to 5d) because only 1 m of sediment was deposited during that time. This low sedimentation rate (2.5 cm kyr^{-1}) is probably responsible for the blurring of the fine structure of the isotopic record[14]. Therefore, this part of the record will not be discussed in terms of palaeooceanographic change and we shall limit our discussion to the last 75,000 yr.

The present bottom water at the location of core CH 73139C is the North Atlantic Deep Water ($T = 3.3°$ C; $S = 34.96$); its $\delta^{18}O$ is +0.12 versus SMOW[19]. The measured $\delta^{18}O$ value for *Cibicides* in the upper 10 cm of core CH 73139C is +2.58 versus PDB. Using a correction factor of 0.64 to take account of *Cibicides* departure from isotopic equilibrium[8,13], we calculated an isotopic temperature of $+3.5 \pm 0.4°$ C, again in good agreement with the modern conditions. The upper part of the benthic record contains $\delta^{18}O$ variations of high amplitude, up to 1.9 ‰ between the Holocene and the last glacial maximum. Such large $\delta^{18}O$ changes have also been reported for two other deep sea cores from the North Atlantic Ocean[8,15]. These large variations reflect the fact that deep water in this area experienced large changes in physical parameters during the last climatic cycle.

In contrast, benthic records from the Pacific and Indian Oceans contain $\delta^{18}O$ variations of much smaller amplitude. One of the most detailed benthic records from this area is that of core MD 73025, collected in the diatom ooze belt at 43°49′ S, 51°19′ E in a water depth of 3,284 m during the cruise OSIRIS I of the French MS Marion Dufresne in the Indian Ocean. Radiocarbon dates (Table 1) have been obtained on the total carbon content of the sediment and indicate that the most recent sediment has been lost during the coring process. However, the first 2.5 m of the core are Holocene in age and the sedimentation rate is as high as 54.5 cm kyr^{-1}. Between 11,000 and 24,000 yr BP, the sedimentation rate was only 11.7 cm kyr^{-1} indicating a sharp decrease of the diatom production during the last Ice Age.

Digital $\delta^{18}O$ values for *Nonion* were reported by Duplessy[11]. The isotopic record of core MD 73025 extends to Emiliani's isotopic stage 6, and, due to the high sedimentation rate, provides one of the most detailed isotopic sequence covering the last climatic cycle. The present bottom water at the coring site is the circumpolar water ($T = +0.6$ °C; $S = 34.69$). Using the measured $\delta^{18}O$ values for *Nonion* in the upper 10 cm of core MD 73025, using a constant correction factor of +0.4 ‰ to compensate for *Nonion* departure from isotopic equilibrium[15], and using Shackleton's palaeotemperature scale which is valid for low temperature[20] when a $\delta^{18}O$ value of −0.3 versus SMOW is assumed for the Circumpolar Water[19], we calculated an

Table 2 Oxygen isotopic analyses ($\delta^{18}O$/PDB) of *Cibicides wuellestorfi* and *Cibides* sp.*

Levels	$\delta^{18}O$ (*Cibicides*) *wuellestorfi*	Levels	$\delta^{18}O$ (*Cibicides*) sp.
TOP	+2.59	340	+4.21
		350	+4.19
		360	+4.22
15	+2.58	370	
20	+2.57	375	+4.37
30	+2.60	380	
40	+2.64	390	+4.25
50	+2.67	400	+4.25
60	+2.66	410	+3.95
70	+2.75	420	+4.11
85	+2.82	435	+4.24
90	+2.83		
100	+2.89	450	+4.03
110	+2.93	460	+4.03
120	+3.40	470	+4.15
130	+3.41	480	+4.03
135	+3.46	490	+3.97
145	+3.42	500	+4.22
150	+4.06	510	+4.06
155	+3.88	520	+3.84
160	+4.34	530	+3.80
170	+4.73	540	+3.59
175	+4.51	550	+3.52
185	+4.46	560	+3.59
190	+4.53	570	+3.66
200	+4.48	580	+3.58
210	+4.22	590	+3.59
		600	+3.87
225	+4.62	610	+3.83
		620	+3.53
235	+4.61	630	+3.30
		645	+3.11
245	+4.50	665	+3.00
		680	+2.82
255	+4.14	690	+2.65
		700	+2.85
265	+4.10	710	+2.85
		720	+3.57
275	+4.22	730	+4.28
		740	+5.00
285	+4.49	750	+4.67
		760	+4.75
300	+4.68	770	+4.64
310	+4.39	780	+4.90
320	+4.41	790	+4.58
330	+4.25	795	+4.75

* Mean values are reported for each level.

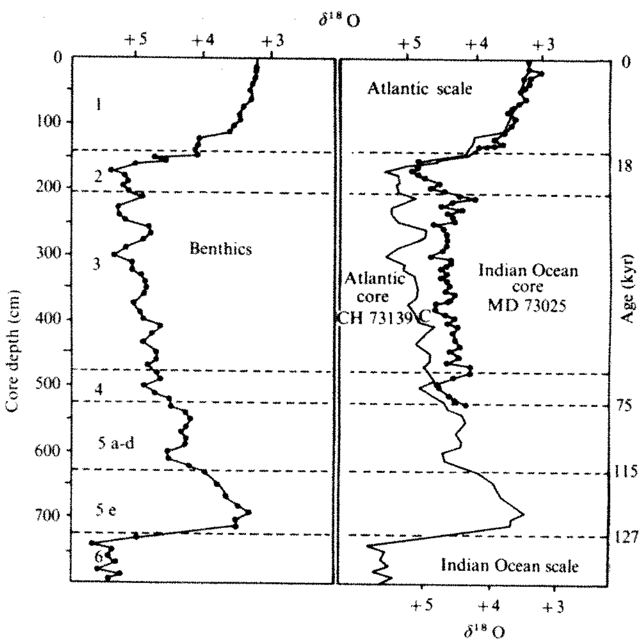

Fig. 2 *a*, Variations of $\delta^{18}O$ of *Cibicides wuellestorfi* and of a mixture of *C. kullenbergi*, *C.gr.io*, and *C.*sp. *b*, Variations of $\delta^{18}O$ of benthic foraminifera in North Atlantic core CH 73139C and southern Indian core MD 73025 with time during the past 75,000 yr. A constant correction factor of 0.64 ‰ for *Cibicides* in core CH 73139C and of 0.40 ‰ for *Nonion* in core MD 73025 have been applied to take account of departure from isotopic equilibrium[11,13,15]. Major isotopic stage boundaries[14] are correlated with dashed lines.

isotopic temperature of 0.8 ± 0.4 °C, in good agreement with the modern temperature at the site. In this record in which both modern and last glacial maximum conditions are well documented, the amplitude of the isotopic shift between isotopic stages 2 and 1 is only 1.6 ‰.

The isotopic record of core MD 73025 is readily correlated with that of the high sedimentation rate core V19 29 from the equatorial Pacific Ocean, analysed by Shackleton[21]. We therefore conclude that the benthic records from the Pacific and Indian Oceans show highly correlated variations with an amplitude of 1.6 ‰ which is 0.3 ‰ smaller than that of the northeastern Atlantic cores.

Figure 2*b* compares the $\delta^{18}O$ records of the southern Indian Ocean core MD 73025 (ref. 11) and the northeastern Atlantic core CH 73139C during the past 75,000 yr. Both cores are plotted with the same time scale, but the $\delta^{18}O$ of the Indian Ocean record has been shifted by 0.25 ‰ to compensate for the present-day difference between the two sites. As the same species has been continuously analysed along each core, this shift, which brings into coincidence the two Holocene mean $\delta^{18}O$ values, allows us to compare the isotopic records at the two sites independently of the correction factors introduced to take into account the departure from isotopic equilibrium in benthic foraminiferal species. The two records are clearly significantly different and cannot both simultaneously reflect only continental ice volume variations. This amplitude difference cannot be explained through a smoothing of the Indian Ocean record due to benthic mixing as this core has a very high sedimentation rate: using the mixing model of Peng *et al.*[22], ^{14}C data from core CH 73139C indicate an upper limit for the mixing layer thickness of 15 cm. This thickness, which is similar to that measured in most cores, is equivalent to a time interval of 1.400–3.000 yr, which is smaller than the duration of the full glacial conditions or any other climatic extreme. In fact, for both cores, the $\delta^{18}O$ values of glacial and interglacial extremes are well defined and practically unbiased by bioturbation. As North Atlantic Deep Water originates in the high latitudes of the North Atlantic Ocean whereas the circumpolar water originates mainly in the Weddel Sea[25] the differences between these two kinds of isotopic records indicate that the northern and southern sources of oceanic deep water have had different histories during global climatic variations.

The only explanation for such a difference between the isotopic records is a cooling of the northeastern Atlantic deep water: at present, Antarctic Bottom Water is formed during the winter when sea water freezes. As the ice forms, it rejects most of the salt from the water, so that the salinity and density of the water increase. As a result, this denser water sinks[23]. As increasing bottom water formation during glacial periods has been inferred from particle size analysis of sediments of the Vema Channel[24], this enhanced formation process which occurs at the freezing point cannot produce bottom water warmer than that produced at present. Thus, as a conservative estimate, we shall assume that the deep water from the southern Indian Ocean experienced no temperature change in the past and that the $\delta^{18}O$ record of core MD 73025 reflects the normal glacial effect, which is continental ice volume variations. Many hypotheses can be advanced to explain the higher amplitude of the benthic record of core CH 73139C. For instance, one might argue that benthic foraminifera were heavy because the glacial NADW became isotopically heavier than expected from the normal glacial effect, without any temperature change. This hypothesis, however, is in conflict with all the reconstructions of the glacial North Atlantic[1,25,26]. The surface salinity map for 18,000 yr BP clearly shows the occurrence of a well defined polar front at 42°N latitude, north of which the salinity decreased[26]. The $\delta^{18}O$ of the surface water should also decrease in the same way. Palaeooceanographic reconstructions clearly demonstrate that there are ways (Labrador current, glacial flow) to get high latitude melt water to intermediate latitudes, north of the polar front. Thus there would be no way that deep water forming in this area could become enriched in ^{18}O, and the 0.3 ‰ amplitude difference between the Atlantic and south Indian benthic records indicates that the glacial NADW was at least 1.3 °C cooler than at present.

A second hypothesis, agreeing with the occurrence of cold deep water, is that there was a complete absence of deep water formation in the North Atlantic during most of the last Ice Age, as suggested by the abundance of *U. peregrina*, a species living today in water with an oxygen content falling to below 5 ml per l (ref. 8). In such a case, the Southern Ocean would be the only source of the world ocean deep water. However, we can rule out this possibility as the benthic foraminifera from the North Atlantic Ocean were isotopically heavier than those of the southern Indian Ocean and Pacific Ocean[21] during isotopic stages 2 to 4. If the only deep water source were located in the southern Indian Ocean, all the deep waters should have the same oxygen isotopic composition and our data would indicate that the glacial NADW was cooler than the deep water source itself, which is impossible.

We thus conclude that the North Atlantic Ocean has been a source of deep water during the past 75,000 yr, even during the coolest periods. The benthic foraminiferal data of Streeter and Shackleton[8] clearly indicate that the dissolved oxygen content of this glacial NADW was sometimes low, reflecting large changes in the production rate of the NADW. During the period 15,000–75,000 yr BP, the glacial NADW was cooler than today. Our evidence is in direct conflict with the theories of Weyl[27] and Newell[28], who in their models of glacial ocean hypothesize warmer deep waters. In contrast, our results suggest that winter freezing in near shore areas, producing cold waters, is the most likely explanation of the isotopic composition of the benthic foraminifera in the North Atlantic Ocean during the last Ice Age. More cores will be necessary to determine the coolest deep water areas in the North Atlantic Ocean during the last climatic cycle, and thus the sources of the Glacial NADW.

As far as isotope stratigraphy is concerned, our data show that the major signal in the isotopic curves is an ice volume record but that minor fluctuations reflecting deep water temperature changes are superimposed on it. Until these temperature changes are more accurately known, worldwide correlations between isotopic records must be restricted only to the major trends which define Emiliani's stages.

We thank M. Kritz, H. M. Sachs, N. J. Shackleton and S. Streeter for reviews, J. Labeyrie for useful discussions B. Le Coat and J. Antignac for help in the isotopic analyses and A. Pujos-Lamy for the determination of the benthic foraminifera. The computer treatment of the data was made by D. Nordemann. Carbon-14 measurements were made by G. Delibrias. We acknowledge the support of our study by CEA, CNRS and DGRST, the support of cruise FAEGAS of the French RV Jean Charcot by CNEXO and the support of cruise OSIRIS I by TAAF.

Received 13 March, accepted 16 May 1980

1 Climap Project Members *Science* **191**, 1131 (1976).
2 Worthington, L. V in *On the North Atlantic Circulation*, 77–110 (John Hopkins University Press, London, 1976)
3 Duplessy, J. C , Chenouard, L. & Vila, F *Science* **188**, 1208 (1975).
4. Kellogg, T B *Geol Soc. Am Mem* **145**, 77–110 (1976)
5. Kellogg, T. B , Duplessy, J C & Shackleton, N J. *Boreas* **7**, 61 (1978)
6. Streeter, S. S *Quat Res* **3**, 131 (1973).
7. Schnitker, D *Nature* **248**, 385 (1974).
8. Streeter, S S & Shackleton, N. J. *Science* **203**, 168 (1979)
9. Pujol, C , Duprat, J., Gonthier, E , Peypouquet, J P & Pujos-Lamy, A *Bull. I G.B.A.* **16**, 65 (1974)
10 Pujos-Lamy, A. *Revta esp Micropaleontol.* **5**, 213 (1973)
11 Duplessy, J C in *Climatic Change* (ed Gribbin, J.) 46–47 (Cambridge University Press, 1978)
12 Duplessy, J C , Lalou, C & Vinot, A C. *Science* **168**, 250 (1970)
13 Shackleton, N J & Opdyke, N. *Quat Res.* **3**, 39 (1973)
14. Emiliani, C *J. geol* **63**, 538 (1955)
15 Shackleton, N J in *The Fate of Fossil Fuel CO_2 in the Oceans* (eds Andersen, N R. & Malahoff, A) 401–427 (Plenum, New York, 1977).
16. Broecker, W S & Van Donk, J *Rev Geophys Space Phys.* **8**, 169 (1970)
17 Emiliani, C *Ann. N Y Acad Sci* **95**, 521 (1961)
18 Ruddiman, W. F & McIntyre, A *Geol Soc. Am Mem* **145**, 111–146 (1976).
19 Craig, H & Gordon, L I in *Stable Isotopes in Oceanographic Studies and Paleotemperatures* 9–131 (Consiglio Nazionale delle Richerche, Pisa, 1965).

20. Shackleton, N. J. in *Les Méthodes Quantitatives d'Études des Variations du Climat au cours du Pléistocène* (ed. Labeyrie, J.) 203–209 (CNRS, Paris, 1974).
21. Ninkovich, D. & Shackleton, N. J. *Earth planet. Sci. Lett.* **27,** 20 (1975).
22. Peng, T. H., Broecker, W. S., Kipphut, G. & Shackleton, N. J. in *The Fate of Fossil Fuel CO_2 in the Oceans* (eds Andersen, N. R. & Malahoff, A.) 355–374 (Plenum, New York, 1977).
23. Sachs, H. M. *J. geophys. Res.* **81,** 3141 (1976).
24. Ledbetter, M. T. & Johnson, D. A. *Science* **194,** 837 (1976).
25. Alvinerie, J., Caralp, M., Latouche, C., Moyes, J. & Vigneaux, M. *Oceanologica Acta* **1,** 87 (1978).
26. McIntyre, A. *et al. Geol. Soc. Am. Mem.* **145,** 43–76 (1976).
27. Weyl, P. K. *Met. Monogr.* **8,** 37 (1968).
28. Newell, R. E. *Quat. Res.* **4,** 117 (1974).

Enrichment of dissolved phenolic material in the surface microlayer of coastal waters

David J. Carlson & Lawrence M. Mayer

Department of Oceanography, University of Maine at Orono, Walpole, Maine 04573

The sea surface microlayer often has greater concentrations of dissolved organic material (DOM) than subsurface water[1–5], but the chemical nature of this material remains unresolved. Most studies of microlayer organic chemistry have focused on lipid[6–9] and hydrocarbon components[10,11]. Carbohydrate material can account for a significant fraction of the microlayer DOM[4] supporting IR spectroscopic evidence which suggests that the microlayer material is predominantly carbohydrate-proteinaceous complexes[12]. Some similarity of the microlayer DOM to marine humic material has been noted[12–14]. We report here preferential enrichment of dissolved phenolic material in the surface microlayer of coastal waters.

Two major sources of phenolic substances in coastal marine waters are known. Terrestrial drainage delivers dissolved fulvic and humic material containing aromatic structures, partially phenolic, as important components[15,16]. Marine macroalgae, especially the Phaeophyta, have been shown to exude significant quantities of dissolved polyphenols[17].

The UV absorbance of seawater has been used to examine the distribution of DOM in marine waters[18]. Coastal waters exhibit UV absorbance in an inverse relationship to salinity, indicating a terrestrial origin for the substances causing absorption[18–21]. Brown[22] and Mrkva[23] have suggested that this riverine UV absorbance is due to aromatic compounds. The UV absorbance of macroalgal exudates has been ascribed to their polyphenol content[17]. Although UV absorbance has been shown to be inappropriate as an estimate of total DOM in coastal waters[24,25], it may be a useful parameter by which to monitor phenolic substances.

We have examined UV absorbance, dissolved organic carbon (DOC), and phenolic material in the bulk and surface microlayer waters of the Damariscotta and Saco River estuaries. The Damariscotta River estuary is a 30-km long, narrow embayment in central Maine with limited freshwater input, predominantly overflow from Damariscotta Lake. The Saco River is a major drainage in southern Maine with an 8-km long estuary. Microlayer samples were collected by immersing a 30 × 30 cm glass plate and withdrawing it vertically through the water surface[25]. The glass plate collects a surface layer of water 51 ± 2 μm ($\bar{x} \pm 95\%$ C.I.) thick. All samples were filtered through precombusted, rinsed glass fibre filters, and the absorbance at 280 nm measured in 10 cm quartz cells. DOC was measured by persulphate oxidation and FR detection[27] using an Oceanography International carbon analyser. Dissolved phenolic material was analysed by a modification of the Folin–Ciocalteu (F–C) test[28].

The UV absorption of the estuarine waters varies almost linearly with their phenolic reactivity (Fig. 1), supporting earlier suggestions that the UV absorbance of seawater reflects aromatic components. It is not possible definitively to identify the source of the phenolic material. Experiments with natural exudates from *in situ* macroalgae (*Ascophyllum nodosum* and *Fucus vesiculosis*) show that exudates have higher ratios of F–C reactivity to UV absorbance than do the lake, riverine and estuarine samples. However, the F–C reactivity, the UV absorbance, and the resultant reactivity to absorbance ratios of the exudates change with time (range indicated in Fig. 1), as does the UV absorbance of ethanol extracts of the same species[25], and this variation therefore causes some uncertainty as to the source of the estuarine phenolic materials. Bulk water and microlayer samples collected within the Damariscotta estuary show the same ratio of phenolic reactivity to ultraviolet absorbance as samples from Damariscotta Lake. Data from the Saco estuary, which has very little macroalgal input, show exactly the same trend as the Damariscotta estuary, demonstrating similarity between estaurine and lake- or river-derived phenolic material. Based on these data it seems that the surface microlayers of this estuary contain terrestrially derived phenolic material.

Data from the Damariscotta and Saco estuaries (Fig. 2) demonstrate consistent microlayer enrichment of UV absorbance, and hence phenolic material. The DOC levels, however, do not exhibit consistent enrichment. In addition, most samples plot above the line of equal microlayer partitioning of UV absorbance and DOC. Preferential enrichment of phenolic material relative to other DOC is therefore indicated.

Enrichment factors for UV absorbing material are plotted against salinity in Fig. 3. Enrichments of phenolic material occur at all salinities, but are demonstrably greater at higher salinities.

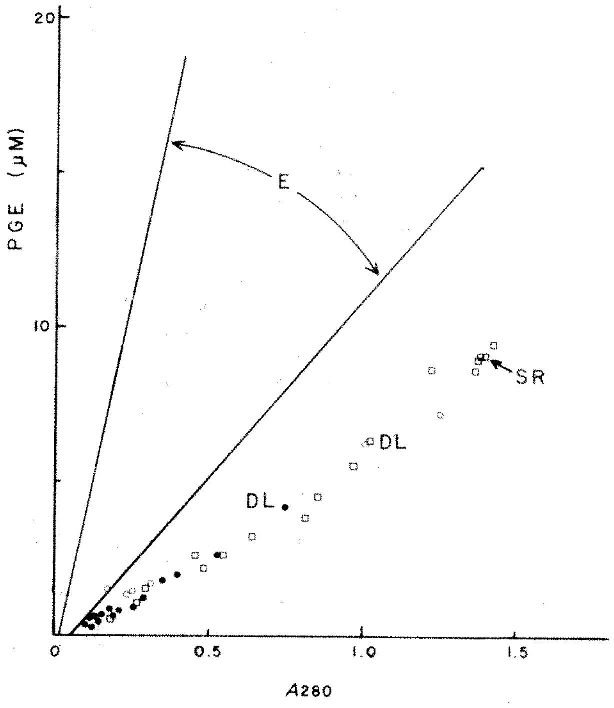

Fig. 1 Absorbance at 280 nm plotted against phenolic reactivity expressed as micromoles of phloroglucinol equivalent (PGE). Lower trend contains samples from Damariscotta transect of October 23, 24 and bulk water samples from the Saco R. estuary on 22 August, 1979. Macroalgal exudates (upper range) obtained by placing emersed fronds of *Fucus vesiculosis* and *Ascophyllum nodosum* in flasks of seawater before immersion by a rising tide. Data represent the difference between pre- and post-exudation values of PGE and A_{280} of the seawater in the flasks. Aliquots of the exudates were analysed after various time intervals. ●, Damariscotta bulk water; □, Saco bulk water; ○, Damariscotta surface microlayer; DL, Damariscotta Lake; SR, Saco River; E, algal exudates.

0028–0836/80/310482—02$01.00

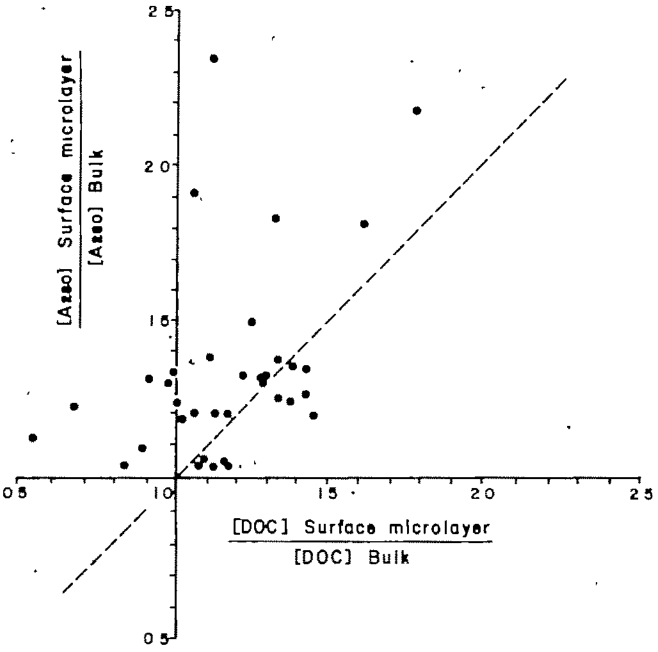

Fig. 2 Surface microlayer to bulk water ratios of DOC and UV absorbing material (A_{280}) in summer and fall 1979 samples from the Damariscotta River estuary and spring 1980 samples from the Saco River estuary. Only data without significant salinity differences between bulk and microlayer water are included. Dashed line indicates equal microlayer partitioning of DOC and UV absorbance. DOC values were 2.5–9.8 mg l^{-1} in bulk water and 2.6–11.9 mg l^{-1} in the surface microlayer.

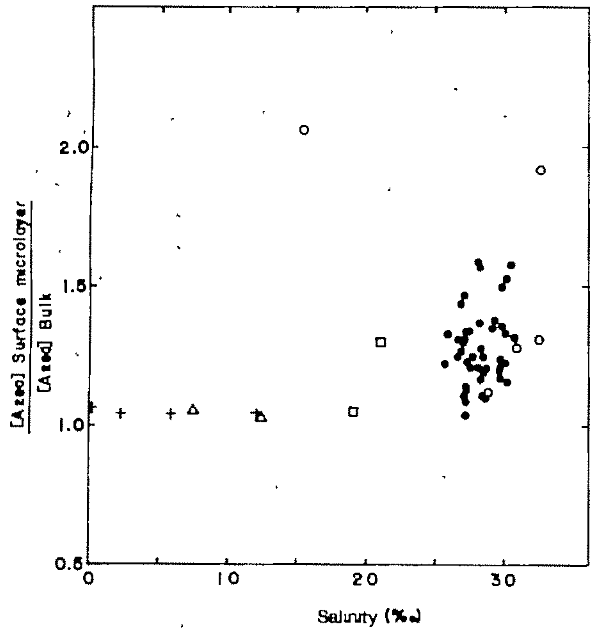

Fig. 3 Microlayer enrichments of UV-absorbance plotted against salinity in samples from the Damariscotta and Saco estuarine systems. Data in which salinity differences between microlayer and bulk water exist have been included by correcting the bulk water absorbance to the absorbance appropriate at the microlayer salinity. ●, Damariscotta summer, 1979; △, ○, Damariscotta autumn, 1979; □, Damariscotta spring 1980; +, Saco spring 1980.

We suggest three alternative explanations for this trend. First, Sholkovitz[29] has shown that terrigenous humic DOC becomes less soluble at high salinities. Higher partition coefficients at higher salinities can be explained if the dissolved phenolic material has similar chemical properties or if the enriched phenolic compounds are humates. Second, the rate of partitioning into the microlayer is unknown at this time; if these enrichments form slowly relative to the flushing time of terrigenous phenols through an estuary, then the higher enrichments at high salinities may simply reflect an ageing phenomenon. Third, if the UV absorbance at high salinities represents macroalgal rather than terrigenous phenolic material, we may be observing different partition coefficients for the two sources of phenols.

These strongly UV-absorbing molecules will be very susceptible to photo-oxidative transformations in the surface microlayer. This zone may therefore be a temporary sink and a reaction site leading to their resolubilization in bulk water as small degradation products[30] or to oxidation[31] and removal to the atmosphere. These aromatic compounds will also serve as important sources of hydrated electrons[32] or free radicals[31] in the microlayer.

Sea surface microlayers often contain greater numbers of bacteria than subsurface water[4,33–35], and have been suggested to be heterotrophically active environments[4,36]. However, apparent inhibition of bacterial activity in the microlayer has been reported[4,37], most notably in coastal waters[35,38]. The presence of phenolic material, potentially inhibitory to bacteria[36,39] and phytoplankton[40], in the surface microlayers of coastal waters may account for this reduction in microbial activity.

Funding for this study was provided by a National Wildlife Federation fellowship to D.J.C., the Faculty Research Fund of the University of Maine at Orono, and NSF grant OCE 79 20244. We thank the graduate students in the Department of Oceanography who assisted in the field work, and P. Rossi for her assistance with the graphics. The comments of W.B. Lyons and B. J. McAlice are gratefully acknowledged.

Received 22 January, accepted 29 May 1980

1 Goering, J J & Menzel, D W *Deep Sea Res* **12,** 839–843 (1965)
2 Williams, P M *Deep Sea Res* **14,** 791–800 (1967)
3 Nishizawa, J *Bull Plankton Soc Jap* **18,** 42–44 (1971)
4 Sieburth, J McN *et al Science* **194,** 1415–1418 (1976)
5 Hunter, K A & Liss, P S *Mar Chem* **5,** 361–379 (1977)
6 Garrett, W D *Deep Sea Res* **14,** 221–227 (1967)
7 Larsson, K, Odham, G & Sodergren, A. *Mar. Chem* **2,** 49–57 (1974)
8 Daumas, R A, Laborde, P L, Marty, J C & Saliot, A *Limnol Oceanogr* **21,** 319–326 (1976)
9 Kattner, G G. & Brockmann, U H *Mar Chem* **6,** 233–241 (1978)
10 Wade, T L & Quinn, J G *Mar Pollut Bull.* **6,** 54–57 (1975)
11 Marty, J C. & Saliot, A *Deep Sea Res* **23,** 863–873 (1976)
12 Baier, R E, Goupil, D W, Perlmutter, S & King, R *J Rech Atmos* **8,** 571–600 (1974)
13 MacIntyre, F *J Rech Atmos* **8,** 515–527 (1974)
14 Pellenbarg, R E *Estuarine Coastal Mar Sci* **6,** 187–195 (1978)
15 Ruggiero, P., Interesse, F S & Sciacovelli, O *Geochim cosmochim Acta* **43,** 1771–1775 (1979)
16 Weber, J H & Wilson, S A *Wat Res* **9,** 1079–1084 (1975)
17 Craigie, J S & McLachlan, J *Can J Bot* **42,** 23–33 (1964)
18 Ogura, N & Hanya, T. *Int J Oceanol Limnol* **1,** 91–102 (1967), *J Water Pollut Control Fed* **40,** 464–467 (1968)
19 Foster, P & Morris, A W *Wat Res* **8,** 137–142 (1974)
20 Sheppard, C R C *Wat Res* **11,** 979–982 (1977)
21. Butler, E I & Tibbetts, J *J mar Biol Ass U K* **52,** 681–699 (1972)
22 Brown M *Estuarine Coastal mar Sci* **5,** 309–317 (1977)
23 Mrkva, M. *J Water Pollut Control Fed* **41,** 1923–1931 (1969)
24 Wheeler, J R *Limnol Oceanogr* **22,** 573–575 (1977)
25 Ragan, M A & Craigie, J S *J exp mar Biol Ecol* (in the press)
26. Harvey, G W & Burzell, L A *Limnol Oceanogr* **17,** 156–157 (1972)
27. Menzel, D. W. & Vaccaro, R F *Limnol. Oceanogr* **9,** 138–142 (1964)
28 Singleton, V. L *Adv Chem* **137,** 184–211 (1974)
29 Sholkovitz, E R *Geochim cosmochim Acta* **40,** 831–845 (1976)
30 Hansen, H P *Mar Chem* **3,** 183–195 (1975)
31 Zafiriou, O C *Mar Chem* **5,** 497–522 (1977), *J geophys Res* **79,** 4491–4497 (1974)
32 Swallow, A. J *Nature* **222,** 369–370 (1969)
33 Crow, S A, Ahearn, D. G, Cook, W L. & Bourquin, A W *Limnol Oceanogr* **20,** 644–646 (1975)
34 Marumo, R, Taga, N & Nakai, T *Bull plankton Soc Jap* **18,** 36–41 (1971)
35 Kjelleberg, S & Håkansson, N *Mar Biol* **39,** 103–109 (1977)
36. Ahearn, D G, Crow, S A, Cook, W L & Bourquin, A W *Environmental Protection Agency Ecological Research Series* EPA-600/3-77-050, 1–22 (1977)
37 Sieburth, J McN *Mar Biol* 11, 98–100 (1971)
38 Dietz, A S, Albright, L J & Tuominen, T. *Can J Microbiol* **22,** 1699–1709 (1976)
39. Sieburth, J McN. in *Advances in Microbiology of the Sea* (eds Droop, M R & Wood, E J F.) **1,** 63–94 (1968)
40 McLachlan, J. & Craigie, J S *Can. J Bot* **42,** 287–292 (1964), *J. Phycol* **2,** 133–135 (1966)

Late Jurassic lizards from Como Bluff, Wyoming and their palaeobiogeographic significance

Donald R. Prothero

Department of Vertebrate Paleontology, American Museum of Natural History, New York, New York 10024

Richard Estes

Department of Zoology, San Diego State University, San Diego, California 92182

Fossils from the late Jurassic Morrison Formation, Como Bluff, Wyoming (Tithonian, ~140 Myr ago) show that three genera of European lizards from the later Jurassic of England and Portugal (*Cteniogenys, Paramacellodus, Dorsetisaurus*) also inhabited North America. These specimens corroborate evidence from mammal and other terrestrial vertebrate faunal similarities that western Europe and western North America had a continuous land connection in the late Jurassic. Some of this similarity, however, is pre-Tithonian, indicating that widespread mid-Jurassic transgressive seas in Europe were no barrier to vertebrate dispersal.

Between 1968 and 1970, a joint American Museum of Natural History–Yale University expedition made new collections at Quarry Nine, the famous 'mammal quarry', in the Upper Jurassic Morrison Formation at Como Bluff, Wyoming. The expedition collected many mammalian specimens described elsewhere[1], as well as dinosaur material, glyptopsid turtles[2], crocodiles, sphenodontids, frogs, lungfish, amioid fish and lizards. A review of this and previously known lizard material from the Morrison Formation has resulted in the identification of at least three genera of lizards. Only one, *Cteniogenys antiquus* Gilmore 1928, was known previously from North America; it has been shown to be an eolacertilian[3].

Hecht and Estes[4] reported an ilium of what they believed to be a true lacertilian from previous Quarry Nine collections, but did not name it. Lacertilian ('true') lizards are known from the late Jurassic of Europe and China[3,5]. A presumed lacertilian was described from the late Triassic of China[6], but one of us (R.E.) believes it to be an eolacertilian. The new material from the Morrison Formation not only verifies the occurrence of both eolacertilians and lacertilians in the late Jurassic of North America, but also shows for the latter group a well-established, derived, 'autarchoglossan' organization at this early time, which is in agreement with previous identifications of some Jurassic European forms as scincomorphs. The three lizard species identified in the Morrison Formation are classified as follows:

Order Squamata
Suborder Lacertilia
Infraorder Eolacertilia
Cteniogenys antiquus Gilmore 1928

The new collection includes two jaws referable to this species. (Other jaws, including the type specimen, were found in the original Marsh collections made at Como Bluff in 1879 and 1880.) *Cteniogenys* was later identified by Seiffert[3] from the late Jurassic (Kimmeridgian) fauna from Guimarota, Portugal. We agree with Seiffert's identification of *Cteniogenys* as an eolacertilian, closely related to the 'flying lizards', or kuehneosaurs, known from the late Triassic of Europe[7] and North America[8]. *Cteniogenys* is known from jaws, maxillae and parietals. The other species are true lacertilians, of which the first is:

Infraorder Lacertilia
Paramacellodus sp.

Paramacellodus oweni was first described from the late Jurassic Purbeck Formation of England, and allied with the cordyloid scincomorphs[5]. Several jaws referable to *Paramacellodus* (including two from the new collection) occur at Quarry Nine (Fig. 1*a,b*); they may represent the same species but the material is insufficient to determine this. Some postcranial material possibly referable to *Paramacellodus* also occurs in the new collection. The specimen (AMNH 11523) consists of a left prefrontal, a left scapulocoracoid, one trunk vertebra, a partial pelvis, seven caudal vertebrae, and a nearly complete left hind limb. The hind limb, pelvis and sacral vertebrae are articulated. All other elements are disarticulated, but closely associated on the block of matrix.

A detailed description of this material is in preparation, but the important features of AMNH 11523 can be summarized as follows. The prefrontal has a sculpture pattern like that of an unidentified Jurassic specimen from Portugal (Fig. 1*c,d*)[3] and may possibly represent the prefrontal of *Paramacellodus*. The scapulocoracoid (Fig. 1*e,f*) is fully lacertilian, with expanded coracoid region that resembles the derived condition in cordyloid lizards. In the pubis, the iliac blade differs in shape from the ilium described by Hecht and Estes[4], but both are generally similar in morphology to the ilia of some cordyloid lizards (Fig. 1*g–j*). In the tail (Fig. 1*k*), the transverse process of the sixth vertebra may show an autotomic septum, implying fragility of the tail. If so, the septum would split the vertebra into two parts as in many lizards. Comparison of AMNH 11523 with recent lizard skeletons showed that this autotomic configuration is very similar to that of comparably sized lizards belonging to several families, particularly some scincids; cordyloids have the autotomic plane anterior to the transverse process. The third species is:

Family Dorsetisauridae
Dorsetisaurus sp.

There are two dentaries of *Dorsetisaurus* sp.[5]. Neither specimen is well preserved (Fig. 1*l–n*), and both are visible only in lateral view. The elongated, flattened, blade-like teeth, some of which are antero-posteriorly expanded, make this identification clear. Hoffstetter, who originally described *Dorsetisaurus*, placed it in its own family Dorsetisauridae, with which we agree. He also included the family in the Anguimorpha; if so, dorsetisaurs would be very primitive members of that group.

The presence of three genera of small lizards in both North America and Europe in the late Jurassic is an indication of the close faunal affinities of the two regions at that time. Continental reconstructions show that the North American plate was still in contact with Europe at the end of the late Jurassic[11,12]. Como Bluff, Wyoming, and southern England were approximately 2,500 km apart, equivalent to the present distance between San Francisco, California and St Louis, Missouri. Some recent lizards have ranges larger than this. In addition, several other small animals apparently ranged from England to the present western United States. These include four genera of shrew-sized mammals[1,13,14] (*Docodon, Amblotherium, Ctenacodon, Trioracodon*), the crocodile *Goniopholis*[15], the dinosaur *Camptosaurus*[16], and the amioid fish *Ophiopsis*[17]. Also, most of the Morrison mammal taxa have their closest sister-groups in Europe, and a cladogram of therian mammals shows no separation of the taxa into European and American clusters, as might be expected if long-term endemism had taken place[1].

Direct comparisons have not been made in other groups, but most other elements in the Morrison fauna have their closest relatives in the European later Jurassic. Turtles from the early Cretaceous of England[18] and sphenodontids from the Kimmeridgian of Portugal[19] have been examined recently, and are most closely related to Morrison taxa. Complete faunal lists of the Kimmeridgian Guimarota fauna of Portugal have not yet been published, but the partial one given by Kühne[13] is very similar to that from the Purbeck and Morrison Formations. To date, the mammals[13,14], dinosaurs[20], crocodilians[21], turtles[22] and lizards[3] have been described, and most forms show their closest

0028–0836/80/310484—03$01.00

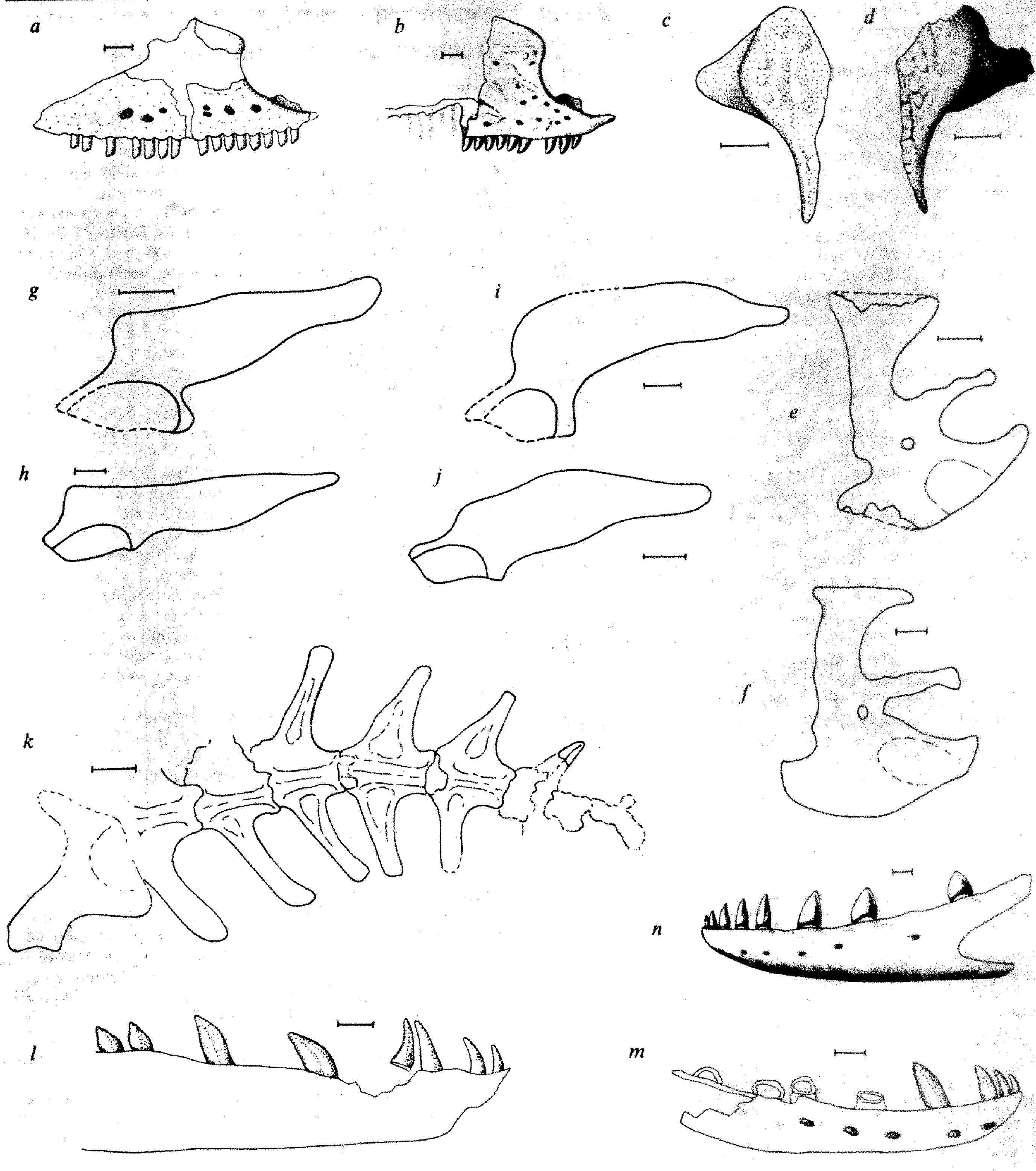

Fig. 1 *a*, *Paramacellodus* sp., right maxilla, Morrison Fm. *b*, *Paramacellodus oweni*, right maxilla, Purbeck Fm[5]. *c*, AMNH 11523, left prefrontal, Morrison Fm. *d*, GUI. 157, right prefrontal, Guimarota Beds[3]. *e*, AMNH 11523, left scapulocoracoid, Morrison Fm. *f*, Left scapulocoracoid of recent *Cordylus polyzonus* for comparison. *g*, AMNH 11523, left ilium, Morrison Fm, comparable with *h*, recent *Platysaurus guttatus*. *i*, YPM 1568, left ilium, Morrison Fm, comparable with *j*, recent *Cordylus warreni*. The fossil iliac blades show some differences, but are within the range of variation of modern cordyloid lizards. *k*, AMNH 11523, caudal vertebrae. *l–m*, *Dorsetisaurus* sp., dentary, Morrison Fm. Both specimens are badly broken. *n*, *Dorsetisaurus purbeckensis*, dentary, Purbeck Fm[5]. All scale bars, 1 mm.

affinities with forms from the Morrison and Purbeck Formations. Kimmeridgian sauropods from Portugal (*Apatosaurus*, *Brachiosaurus*) are congeneric with Morrison taxa[23]. Pre-Kimmeridgian Jurassic dinosaur faunas in both North America and Europe are highly similar[24–26]. Bathonian (middle Jurassic) mammals from England[27] and Scotland[28] show close affinities with Morrison mammals[1].

These strong faunal resemblances between western Europe and western North America seem to indicate a continuous land connection between these regions throughout the Jurassic. Yet reconstructions by Ager[29], Hallam[30], and Hallam and Sellwood[31] show both southern England and Portugal submerged or surrounded by seaways during most of the Jurassic. The maximum extent of Jurassic epicontinental seas was during the Oxfordian and Kimmeridgian (early late Jurassic)[30]. During the Tithonian, widespread tectonism uplifted large areas of land, reconnecting Europe and North America[30,31]. The amount of exposed land in the late Tithonian reached a maximum level matched only by the earliest Jurassic (Sinemurian–Pliensbachian) regression[30].

If the similarity of land faunas were restricted to the late Tithonian, then rapid migration during the maximum phase of regression would be sufficient to explain the lack of endemism. But the similarity persists throughout the Jurassic, indicating that the submergence was not continuous or effective enough to be a barrier to vertebrate migration. Hallam (personal communication) has suggested that the epicontinental seas were so shallow that the numerous short-term regressions occurring throughout the Jurassic[30] would create transient land corridors. Migration then reached a peak during the Tithonian when dry land connection extended across Europe and North America.

We thank M. C. McKenna, E. S. Gaffney, R. J. Emry and J. H. Ostrom for permission to study specimens in their care. The new Como Bluff specimens were collected by T. H. Rich, prepared by C. S. Schaff and curated by E. Manning. We thank H. Green, A. Hallam, J. Gauthier and E. Manning for helpful comments. D.R.P. was supported by a Columbia Faculty Fellowship and an NSF graduate fellowship and R.E. was supported by NSF grant DEB-77-14995.

Received 22 February, accepted 9 May 1980

1 Prothero, D R *Bull Am Mus nat Hist* (in the press)
2. Gaffney, E. S. *Bull Am Mus nat Hist* **162,** 91–136 (1979)
3. Seiffert, J *Mem Servs geol Port* **22,** 8–85 (1973).
4 Hecht, M K & Estes, R D *Postilla* **46,** 1–19 (1960)
5 Hoffstetter, R. *C r natn Rech Sci* **163,** 349–371 (1967)
6 Carroll, R L & Galton, P M *Nature* **266,** 252–255 (1977)
7 Robinson, P L *Proc geol Soc* **1601,** 137–146 (1962), *C r natn. Rech. Sci* **163,** 395–407 (1967)
8 Colbert, E H *Am Mus Novit* **2246** (1966), *Bull Am Mus nat Hist* **143,** 89–142 (1970)
9 Estes, R D & Prothero, D R (in preparation)
10 Etheridge, R *Copeia* **4,** 699–721 (1967)
11 Dietz, R S & Holden, J C *J. geophys Res* **75,** 4939–4956 (1970)
12 Smith, A. J & Briden, J C *Mesozoic and Cenozoic Palaeocontinental Maps* (Cambridge University Press, Cambridge, 1977).
13 Kuhne, W G. *Mem Servs geol Port* **14,** 1–20 (1968); in *Evolution and Environment* (ed Drake, E T) 109–123 (Yale University Press, New Haven, 1968)
14 Hahn, G *Palaeontographica Abt* A **133,** 1–100 (1969)
15 Owen, R. *Rep Br Ass Advmt Sci* **11,** 60–204 (1841)
16. Galton, P M *Publs biol Geol Milwaukee publ Mus* **2,** 41–54 (1977)
17 Bartram, A *J Linn. Soc* **56,** 183–205 (1975)
18. Evans, J. & Kemp, T S *Palaeontology* **19,** 317–324 (1976).
19 Cocude-Michel, M *Nouv Archs Mus Hist nat. Lyon* **7,** 1–187 (1963)
20 Thulborn, R A. *Mem Servs geol Port* **22,** 89–134 (1973)
21 Krebs, B *Mem Servs geol Port* **14,** 1–53 (1968)
22. Braun, H *Mem Servs geol. Port* **22,** 135–141 (1973).
23 de Lapparent, A. F & Zbyszewski, G *Mem Servs geol Port* 1–63 (1957)
24 Chang, A. J. in *Atlas of Palaeobiogeography* (ed Hallam, A) 359–362 (Elsevier, London, 1973)
25 Colbert, E H *Wandering Lands and Animals* (Dutton, New York, 1973), in *Implications of Continental Drift to the Earth Sciences* Vol. 1 (eds Tarling, D H & Runcorn, S. K) 395–412 (Academic, London, 1973)
26 Cox, C B *J Biogeogr* **1,** 75–94 (1974).
27 Freeman, E F *Proc. geol Ass* **87,** 231–235 (1976), *Science* **194,** 1053–1055 (1976), *Palaeontology* **22,** 135–166 (1979)
28 Waldman, M. & Savage, R. J G *J geol Soc Lond* **128,** 119–125 (1972).
29 Ager, D V in *Jurassic Northern North Sea Symposium* 1–43 (Stavanger, 1975)
30 Hallam, A. *Jurassic Environments* (Cambridge University Press, 1975), *Publs biol Geol Milwaukee publ Mus* **2,** 23–34 (1977), *Earth Sci Rev* **5,** 45–68 (1969); *Palaeogeogr Palaeoclim Palaeoecol* **23,** 1–32 (1978)
31 Hallam, A & Sellwood, B W *J. Geol* **84,** 301–322 (1976)

Green anole in Dominican amber

Olivier Rieppel*

Department of Zoology, Natural History Museum, Basel, Switzerland

A lizard of the iguanid genus *Anolis* enclosed in amber of Oligocene or Miocene age from the Dominican Republic represents the first complete vertebrate fossil in amber as well as the oldest and only complete fossil of its genus. The fossil *Anolis* is very closely related to a recent form and will shed some light on the evolution of its genus which otherwise has a poor fossil record.

The evolution of the iguanid genus *Anolis* on the Caribbean islands serves as a model for the ecology of colonization and speciation on small islands[1,2]. The evolution of the Caribbean *Anolis* has been reconstructed by Etheridge on the basis of osteology and by Gorman *et al.* on the basis of cytology. Their findings have been summarized by Williams[1]. Etheridge was able to divide the genus into an α and a β section. α *Anolis* lacks transverse processes on the caudal vertebrae whereas they are present on β *Anolis*. A striking result of Etheridge's analysis is that the α *Anolis carolinensis* from the south-eastern United States is not related to the β anoles from Mexico, but it has Caribbean affinities, being related to the species of the *carolinensis* complex of the western Caribbean. *Anolis carolinensis* invaded the continent from a tropical island. The geographic centre of the *carolinensis* complex today is Cuba. Some slightly more primitive α anoles occur on Hispaniola. Of these, members of the 'green anole species group' as defined by Williams[3], such as *A. chlorocyanus* or *A. coelestinus*, were found by Etheridge to be most closely related to and possibly ancestral to the *carolinensis* complex.

This phylogenetic scenario is usually assumed to have taken place during the Pleistocene. The genus *Anolis* is thought to have colonized the Caribbean islands after the Early Miocene inundation[1], but no fossil remains of these lizards older than the latest Pleistocene age have been reported, either from the Caribbean islands or from the southeastern United States. The oldest fossil *Anolis* remains are skin fragments enclosed in amber of Oligocene or Miocene age from Mexico[4].

In 1979, Dr C. Baroni-Urbani from the Natural History Museum in Basel obtained a more or less completely preserved specimen of *Anolis* in amber from the Mina 'La Toca', Cordillera Septentrional, Dominican Republic (Fig. 1). Dominican amber is thought to be of middle Oligocene or early Miocene age[5]. The generic affinities of the fossil lizard are indicated by the structure of the toes, which bear scansorial pads on the lower surface of their expanded distal parts (Fig. 1). X-ray analysis revealed an incompletely preserved skeleton. Important characters such as the structure of the pectoral girdle or the number of presacral vertebrae cannot be determined. However, caudal vertebrae can be shown to lack transverse processes, a feature characteristic of α anoles (Fig. 2).

In view of its uniqueness I propose to name the fossil anole:

Anolis dominicanus n. sp.

Holotype: Natural History Museum Basel, Department of Entomology collection no. P 52. Mina 'La Toca', Cordillera Septentrional, Dominican Republic.

Diagnosis: A member of the α section of the genus *Anolis*: ventral scales hexagonal, subimbricate, smooth; scales on tail imbricate, keeled, arranged in verticils comprising 4–5 middorsal scales; 22–24 lamellae under fourth toe.

Description: The fossil *Anolis* has a total length of approximately 71 mm; the head is 9.2 mm long; snout–vent length is 26.5 mm; the tail is complete and not regenerated. The left front limb is difficult to measure because of three-dimensional

---

*Present address: Paläontologisches Institut und Museum der Universität, Künstlergasse 16, 8006 Zürich, Switzerland

0028-0836/80/310486—02$01.00

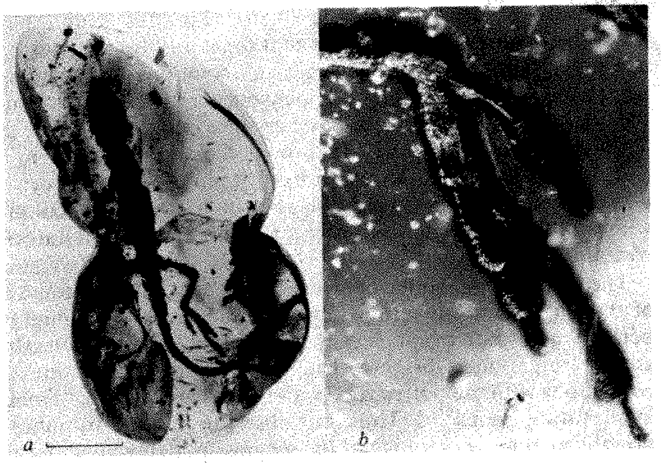

Fig. 1 *a*, *Anolis dominicanus* n. sp., holotype, as preserved in dorsal view. Scale bar, 10 mm. *b*, Lower surface of enlarged right pes, showing the lamellae on fourth digit.

distortion; it is approximately 12 mm long. The right hind limb can be measured accurately: its length up to the tip of the fourth toe is 17.3 mm. The total length of the specimen indicates either a juvenile or a small species.

The colour of the lizard has not been preserved. The squamation of the dorsum lies immediately below the surface of the amber and cannot be made out in detail. The scales on the ventrum are partially preserved. They are hexagonal, sometimes with a rounded posterior edge, subimbricate and smooth. The scales covering the gular region are only partially preserved. They are smaller than the ventral scales, granular, juxtaposed and smooth. Gular scales smaller than ventrals probably imply that the specimen is a female. A weakly expressed longitudinal gular fold is observed. The dewlap appears to have been small or vestigial, which might be correlated with the juvenility or with the sex of the specimen, or it might represent a primitive characteristic.

The tail is trigonal in cross-section. The scales of the tail are imbricate, keeled and arranged in verticils. The verticils are sometimes not distinctly set off from one another. They can well be made out in a middle section of the tail where I counted 5-4-5-4-4-4 middorsal scales in 6 verticils.

The lower surface of the expanded distal part of the fourth toe certainly bears more than 20 lamellae: the exact number is difficult to establish because of a break in the amber obscuring the view (Fig. 1). There could be 22–24 lamellae, 23 being a probable number.

As described above, all the visible characteristics of *A. dominicanus* match Williams's[3] definition of the Hispaniolan 'green anole species group', a group of four rather generalized species of moderate to small size and green colour, which live in the crowns of trees. Within the 'green anole species group', the first subgroup (*A. chlorocyanus*–*A. coelestinus*) is characterized by somewhat longer hind limbs (190% of head length) than the second subgroup (*A. aliniger*–*A. singularis*, hind limbs 162–172% of head length). *A. dominicanus* shows a relative length of the hind limb as it is observed in the *A. chlorocyanus*–*A. coelestinus* subgroup (Table 1). Among the green anoles of Hispaniola, *A. coelestinus* is the species with the relatively longest head. The proportions of the head are the same in *A. dominicanus* (Table 1).

Fig. 2 X-ray picture of a well preserved vertebra from the posterior part of the tail, showing the absence of transverse processes. The length of the vertebra equals ~1 mm.

Table 1 Body measurements of Hispaniolan green anole species

Species	*n*	SVL (mm)	HDL = % SVL	HLB = % HDL
A. chlorocyanus	9	34.5–70	31 (32.7) 34.8	178.4 (190.6) 206.6
A. coelestinus	11	26–77	29.8 (34) 38.4	180 (190.9) 200
A. aliniger	10	41.8–60.5	29.5 (31.7) 35	151.6 (162.3) 186.2
A. singularis	17	37–73	29.8 (32.5) 35.4	157.1 (172.3) 187
A. dominicanus	1	26.5	34.7	188

n, Number of specimens examined; SVL, snout–vent length, the maxima and minima values of all specimens examined are indicated; HDL, head length, expressed as % of snout–vent length; HLB, hind limb, expressed as % of head length. The figures indicate maxima and minima, and the arithmetic mean of all specimens examined is given in parentheses. Measurements are based on the following specimens: *A. chlorocyanus cyagnosticus*, MBS 19778, 20100, 20268, 20344–45; *A. c. chlorocyanus*, MBS 19834, 19975, 20302–03; *A. coelestinus*, MBS 3056–58, 19841–43, 19853–54, 20402–03, 20405; *A. aliniger*, MCZ 143367–76; *A. singularis*, MCZ 124629–45. MBS, Natural History Museum Basel; MCZ, Museum of Comparative Zoology, Harvard University.

In conclusion, the fossil *A. dominicanus* from Dominican amber is evidence of the presence of *α* anoles closely related to recent forms (especially *A. coelestinus*) since the Oligocene or early Miocene. This is a much earlier date than that which has usually been assumed to account for the evolution and dispersal of *α* anoles on the Greater Antilles.

I thank Drs E. E. Williams and R. Etheridge for loaning specimens, critically examining X-ray pictures and reading a draft of this report. X-ray analysis was done by Professor W. Stürmer.

Note added in proof: New dating of amber matrix from the Dominican Republic by Dr J. B. Saunders, Basel, indicates an age range of between 20 and 23 million years BP (lower part of early Miocene).

Received 25 April; accepted 20 May 1980.

1. Williams, E. E. *Q. Rev. Biol.* **44,** 345–389 (1969).
2. Williams, E. E. in *Evolutionary Biology* **6** (eds Dobzahnsky, T., Hecht, M. K. & Steere, W. 6, 47–89 (Appleton-Century-Crofts, New York, 1972)).
3. Williams, E. E. *Breviora* **227,** 1–16 (1965).
4. Lazell, jr, J. D. *J. Palaeont.* **39,** 379–382 (1965).
5. Sanderson, M. W. & Farr, T. H. *Science* **131,** 1313 (1960).

Unique adaptations for submarine pollination in seagrasses

J. M. Pettitt*, C. A. McConchie†, S. C. Ducker† & R. B. Knox†

* Department of Botany, British Museum (Natural History),
Cromwell Road, London SW7 5BD, UK
† School of Botany, University of Melbourne, Parkville, Victoria,
Australia 3052

Seagrasses are flowering plants that are adapted for pollination submerged in the sea. Many species, including the Australian sea nymph, *Amphibolis antarctica*, have filiform pollen grains. These grains have no exine[1–4]—the resistant pollen wall layer characteristic of terrestrial plants—and each may be up to 5 mm in length. The pollen has a similar density to seawater so that it remains suspended or floats after release from the anther. The stigma of the sea nymph and related seagrasses is a simple branched structure which protrudes between the leaves when receptive and has a surface secretion with cytochemically detectable enzymatic activity[1–3,5]. This stigma coating is not

0028-0836/80/310487—03$01.00

dispersed in seawater. However, submarine pollen–stigma interactions have never been observed in any species of seagrass. We demonstrate here that pollination in the sea nymph has several unusual features when compared with the events in terrestrial flowering plants. These features include the waterproof nature of the adhesive binding the pollen to the stigma surface, the unique mechanism for pollen germination in the inaperturate filiform grains, and the mode of pollen germination in the inaperturate filiform grains, and the mode of pollen tube penetration into the stigma. Taken together these characteristics suggest a considerably more refined level of adaptation to the marine environment than hitherto supposed.

Mature flowering plants of *Amphibolis antarctica* were collected from natural populations growing on the coast of Victoria, Australia, and held in aerated seawater aquaria at 14 or 22 °C. Ripe pollen from dehiscing anthers was taken up in a Pasteur pipette and applied to the stigmas in a stream of seawater. Grains adhered immediately on contact, and were allowed to remain for up to 48 h before fixation in buffered 2.5% glutaraldehyde and processing for light and electron microscopy[5].

The pollen grains are held tenaciously on the stigma by a meniscus of adhesive material which is formed on contact from the surface coating of both interacting surfaces (Fig. 1*a*). This adhesive is waterproof, a quality which contrasts with the adhesive of terrestrial plants. In *Gladiolus*, for example, water-soluble arabinoglactan proteins have been implicated in pollen–stigma adhesion[6,7]. Germinated pollen produced numerous tubes in the vicinity of the contact zone with the stigma (Fig. 1*b*). We have observed that the grains failed to germinate until they came into contact with the submerged stigma, suggesting that molecular transfer may be important for promoting pollen tube growth, as in the seagrass *Zostera marina*[8].

The filiform grains of seagrasses do not have preformed apertures—special sites for pollen tube emergence. Instead, the position of the aperture is first detectable cytologically by a marked loss of staining affinity in the wholly fibrillar wall[4] after attachment of the grain to the stigma (Fig. 1*c*). Our interpretation of this phenomenon is that focal autolysis forms the aperture. Reorganization of cytoplasmic components, including starch grains, is seen beneath the incipient aperture (Fig. 1*c*), but the first indication of pollen tube emergence is the appearance of a mucilaginous cap protruding through the aperture to form a bubble-like structure. This overlies the emerging tube cytoplasm (Fig. 1*d*) and the cap mucilage stains a light purple colour with toluidine blue, indicative of low molecular weight carbohydrates[9].

The formation of pollen apertures by means of focal autolysis of the wall is not known for any other flowering plant, and is perhaps a further adaptation to the aquatic environment. In germinating pollen of terrestrial angiosperms the intine is contiguous with the pollen tube wall in both aperturate[10,11] and inaperturate grains[12,13]. Thus, our observations call into question the assumed homology of the seagrass pollen wall with the intine of their land-based relatives, notwithstanding the structural and cytochemical similarities[2–5].

Hydration is an essential prelude to germination of the pollen of terrestrial angiosperms[6,11,12,14,15]. In seagrass pollen, however, the hydrodynamic principles must be different, although our observations show that submarine germination is triggered by stigma contact. The differences extend also to subsequent reproductive events. In *Amphibolis*, the germinating tubes grow within a water-resistant mucilaginous sheath towards the stigma surface where they make contact with the cuticle. Using light microscopy, we have observed digestion of the cuticle by the pollen tubes and entry of the tubes into the polysaccharide matrix of the receptive cell wall (Fig. 1*b*) as well as initial growth through the transmitting tissue to the ovary. This sequence first necessitates penetration of the cuticle, a process which accommodates one level of control in those terrestrial angiosperms with dry stigma types, where cutinase activation is implicated[6,12,14,16,17]. Precisely how these cutinases are produced and deployed in the seagrasses remains to be determined.

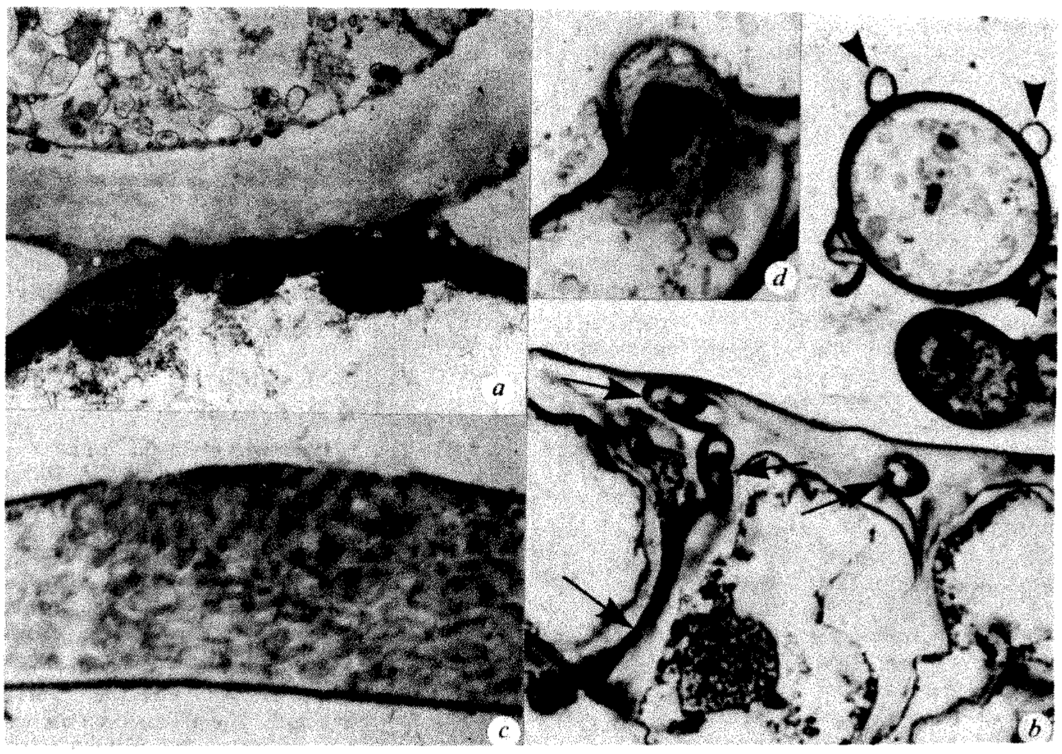

Fig. 1 *a*, A meniscus of insoluble adhesive forms at the point of contact between the pollen grain (upper half) and the stigma in *Amphibolis antarctica* and binds the two together. Electron micrograph of a section stained with silver proteinate after periodate oxidation[21] ×14,400. *b*, Pollen at the surface of the stigma. The filamentous grains have been sectioned transversely and the circular profiles of several pollen tubes passing towards the stigma are indicated by arrow heads. Pollen tubes are also present beneath the stigma cuticle in the walls of the receptive cells (arrows). Thick section of resin-embedded specimen stained with toluidine blue, ×1,200. *c*, The aperture for pollen tube emergence is formed by autolysis of the pollen grain wall. The site of the future aperture is first detectable by the loss of staining affinity in the wall and reorganization of the cytoplasmic components beneath the site. Staining as for *b*, ×800. *d*, After formation of the aperture tube emergence begins. The first structure to appear is a mucilaginous cap and immediately behind this is a zone of densely staining cytoplasm. The pollen grain wall forming the border of the aperture flanks the emerging pollen tube. Staining as for *b*, ×960.

The special adaptations to submarine pollination are important for an understanding of the mechanisms associated with discrimination of self (compatible) from foreign seagrass pollen in interspecific and intergenic matings. Two species of *Amphibolis* are sympatric in southern Australian waters and other seagrass genera occupy adjacent habitats. Although the flowering periods are often coincidental, authenticated hybrids are unknown. In terrestrial pollination systems, barriers to discriminate against foreign pollen operate at initial contact, before adhesion, when many foreign grains simply fail to hydrate, while others are blocked at later steps leading to fertilization[6,11,12,14,15]. Our observations of the seagrasses suggest that barriers to foreign pollination may operate at the moment of adhesion, or even at the time of stigma penetration within the waterproof coating. Experiments are now in progress to test the validity of these predictions.

It is generally believed that seagrasses are angiosperms which have adapted successfully to their marine environment by the loss or modification of terrestrial features[18,19]. In view of both the present discoveries and the distinctive structural and physiological features—such as filiform and flexible pollen grains up to 5 mm in length; precocious microspore mitosis following soon after tetrad period in pollen development[3,20]; the wholly fibrillar nature of the pollen wall in many species[1-5]; water-resistant surface-coating of the receptive stigma[1] which also possesses acid phosphatase activity[5] as well as esterase activity characteristic of terrestrial stigmas; and coincidence of flowering in some species with tide cycles[5]—the explicit phylogenies of the groups need to be determined.

We thank the Australian Research Grants Committee for financial support (to S.C.D. and R.B.K.) and the Royal Society for the award of a Royal Society and Nuffield Foundation Bursary to enable J.M.P. to work at the University of Melbourne.

Received 31 March; accepted 21 May 1980.

1. Ducker, S. C. & Knox, R. B. *Nature* **263,** 705–706 (1976).
2. Pettitt, J. M. & Jermy, A. C. *Micron* **5,** 377–405 (1975).
3. Pettitt, J. M. *Micron* **7,** 21–32 (1976).
4. Ducker, S. C., Pettitt, J. M. & Knox, R. B. *Aust. J. Bot.* **26,** 265–285 (1978).
5. Pettitt, J. M. *Ann. Bot.* **45,** 257–271 (1980).
6. Gleeson, P. A. & Clarke, A. E. *Biochem. J.* **181,** 607–621 (1979).
7. Clarke, A. E., Gleeson, P. A., Harrison, S. & Knox, R. B. *Proc. natn. Acad. Sci. U.S.A.* **76,** 3358–3362 (1979).
8. de Cock, A. W. A. M. *Bull. Soc. bot. Fr.* Suppl. 1–2, 145–148 (1978).
9. Pearse, A. G. E. *Histochemistry* Vol. 1, 3rd edn (Churchill, London, 1968).
10. Heslop-Harrison, J. *Ann. Bot.* **44,** Suppl. 1, 1–47 (1979).
11. Rowley, J. R. & Dahl, A. O. *Pollen Spores* **19,** 169–284 (1977).
12. Heslop-Harrison, Y. *Ann. Bot.* **41,** 913–922 (1977).
13. Ashford, A. E. & Knox, R. B. *J. Cell Sci.* (in the press).
14. Knox, R. B. & Clarke, A. E. *Contemp. Topics Immunobiol.* **9,** 1–36 (1980).
15. Heslop-Harrison, J. *Am. J. Bot.* **66,** 737–743 (1979).
16. Shayk, M. & Kollatukudy, P. E. *Pl. Physiol.* **60,** 907–915 (1977).
17. Heslop-Harrison, J. *A. Rev. Pl. Physiol.* **26,** 403–425 (1975).
18. Arber, A. *Water Plants* (Cambridge University Press, 1920).
19. Sculthorpe, C. D. *The Biology of Aquatic Vascular Plants* (Arnold, London, 1967).
20. Yamashita, T. *Beitr. Biol. Pfl.* **52,** 217–226 (1976).
21. Thiéry, J. P. *J. Microsc.* **6,** 987–1018 (1967).

Relict diapause in an introduced weevil in New Zealand

S. L. Goldson

Ministry of Agriculture and Fisheries, PO Box 24, Lincoln,
New Zealand

R. M. Emberson

Department of Entomology, Lincoln College, Canterbury,
New Zealand

The Argentine stem weevil *Hyperodes bonariensis* Kuschel, a stem boring weevil native to the southern part of South America, was first reported in New Zealand in 1927[1] where it has become a widespread and serious pest of Graminae. Recent investigations[2] have demonstrated the existence of reproductive hibernatory diapause induced by a critical photoperiod in the population in Canterbury, New Zealand (latitude 43°39′ S). Coincidentally, it was noted that similar ovarian diapause occurs in *H. bonariensis* found at a corresponding latitude (41° S) in the Bariloche region of Argentina[3]. Owing to the imminence of the autumnal equinox at diapause induction (early March in both localities), identical daylengths are experienced successively over a wide latitudinal range within a week. In the present report, examination of the New Zealand population at this time, sampled over at 8° range of latitude, revealed a corresponding synchronous induction of diapause without the usual latitudinal and therefore temperature-related shift in critical photoperiod[4]. This lack of temperature-related shift and the relatively mild winters suggest that the diapause behaviour of *H. bonariensis* throughout New Zealand is an adaptively inappropriate relict response resulting from the recently arrived weevils cueing into the same photoperiodic seasonality as their South American counterparts, which in regions such as Bariloche, must have evolved diapause behaviour to survive.

During a 3-day period, samples of weevils were collected from localities near sea level in the North Island of New Zealand between 35°39′ S and 40°23′ S and examined by dissection for diapause status. This allowed comparison with comprehensive data collected from Canterbury on *H. bonariensis* diapause induction during 1977–79.

The results, summarized in Table 1, show the similarity of diapause condition found in the populations sampled from four widely separated locations at the end of the second week of March. Surprisingly, the diapause-related physiological reorganization seemed somewhat further advanced in the populations collected from the warmer northern areas. This is indicated in Table 1 by the percentage of the population with clearly defined oocyte resorption bodies[5]. When a population is fully reproductive, oocyte resorption bodies are very rare and 80–90% of the reproductively competent weevils have eggs. Table 2 shows that during diapause induction (28 February–14 March) daylengths of increasing shortness were experienced in Whangarei (35°39′ S) about a week before identical daylengths were experienced at Lincoln (43°39′ S). This implies that the populations of weevils in the northern areas would have experienced the presumed common critical photoperiod shortly before their Lincoln counterparts and hence accounts for the slightly more advanced diapause condition of these northern populations.

Table 1 indicates that the time of diapause induction of Argentine stem weevil was completely unaffected by variation in mean daily temperature over a considerable latitudinal range. Such a response to photoperiod irrespective of ambient temperature is frequently observed in other species within a local region, as there is a stable correlation between the seasonal course of daylength and temperature. However, this correlation varies sharply with latitude. Daylength provides a reliable means of anticipating winter conditions independent of the vagaries of weather. In general, with an increase in latitude, the cooler conditions necessitate earlier onset of hibernatory diapause which is often regulated by longer critical photoperiods[4]. Thus, intraspecific latitude (and therefore temperature) related variation in critical photoperiod is to be expected in widely dispersed hibernating insect populations. In spite of this

0028–0836/80/310489—02$01.00

Table 1 Reproductive status of female *H. bonariensis* at four localities in New Zealand

Locality	Date sampled	% With eggs	% With oocyte resorption bodies	% Fertilized	% Fertilized with eggs	No.
Whangarei	13.3.80	6.5	48.3	67.7	9.5	31
Auckland	14.3.80	6.5	36.7	51.6	12.5	31
Palmerston North	11.3.80	0	30.4	34.8	0	23
Lincoln	13.3.79	10	15	30	33.3	20
	12.3.78	5	25	45	11.1	20
	13.3.77	14.3	—	71.4	20	20

Table 2 Environmental factors at the sampling localities[8]

Climatological station	Latitude	Daylength (hours and minutes)			Mean daily screen temperature (°C)					
		28 Feb.	7 March	14 March	March	April	May	June	July	August
A 54631 Glenbervie Forest Whangarei	35°39'S	12.52	12.38	12.21	16.5	14.7	12.3	10.2	9.0	9.7
C 64971 Mangere Auckland	36°58'S	12.57	12.42	12.25	17.8	15.8	13.2	11.0	10.2	10.8
E 05363 Palmerston North DSIR	40°23'S	13.04	12.46	12.27	16.1	13.7	10.7	8.4	7.8	8.9
H 32641 Lincoln	43°39'S	13.14	12.52	12.29	14.1	11.4	8.1	5.6	4.8	6.4

Daylength from nearest airport through NZ Civil Aviation Administration. Expressed as time from sunrise to sunset.

there was no evidence of a temperature-compensated shift in critical photoperiod among any of the *H. bonariensis* populations sampled (Table 2).

The results of this experiment confirm the exotic origin of the *H. bonariensis* population in New Zealand. With an estimated overall threshold temperature of development of ~10°C (ref. 6) there seems to be little adaptive reason for diapause during the comparatively mild New Zealand winters, particularly in the north. The seasonal behaviour of *H. bonariensis* in New Zealand is undoubtedly a relict response resulting from the insect cueing into a photoperiodic seasonality identical to that of its native habitat. In some South American localities the evolution of hibernatory diapause must have been necessary to allow the weevil to survive the relatively severe winter conditions, such as those of Bariloche (a ski resort) in Argentina. Here, at 41° S, *H. bonariensis* has been observed in diapause between March and July, as occurs in New Zealand.

The relict diapause behaviour of *H. bonariensis* in New Zealand therefore elegantly demonstrates the overriding effect of photoperiod on the adult stage resulting in diapause induction irrespective of other abiotic factors and the associated adaptive implications. In effect, the New Zealand weevils demonstrate a local diapause response over a wide geographical area (35°39′ S to 43°39′ S), suggesting their introduction from a localized source in Argentine. Furthermore, the complete absence of any latitudinal effect on the critical photoperiod indicates no evolutionary change in diapause behaviour since their establishment. This lack of adaptive evolution, and perhaps the very existence of diapause itself, confirms that *H. bonariensis* is a recent addition to New Zealand's insect fauna, which has very few native diapausing species[7].

The synchronous induction of reproductive diapause of this pest species has important practical implications. It means that any phenological management approach should be applicable throughout New Zealand without the need to establish and adjust for regional variation in biological responses.

Received 23 April; accepted 13 May 1980.

1. Marshall, G. A. K. *Trans. N. Z. Inst.* **67**, 316–340 (1937).
2. Goldson, S. L. *Proc. 2nd Australasian Conf. Grassland Invert. Ecol.* Preprint, 1–7 (1978).
3. Ahmad, R. *Entomophaga* **23**, 161–162 (1978).
4. Danilevsky, A. S., Goryshin, N. I. & Tyshchenko, V. P. *A. Rev. Ent.* **15**, 201–244 (1970).
5. Phipps, J. *Proc. R. ent. Soc.* **A31**, 78–86 (1966).
6. Goldson, S. L. thesis, Univ. Canterbury, New Zealand (1979).
7. Roberts, R. M. *N. Z. Ent.* **6**, 350–356 (1978).
8. *N. Z. met. Serv. Misc. Publ.* **143**, 1–77 (1973).

Gametocytogenesis by malaria parasites in continuous culture

D. C. Kaushal*, R. Carter*, L. H. Miller* & G. Krishna†

*Laboratory of Parasitic Diseases, National Institute of Allergy and Infectious Diseases, National Institutes of Health, Bethesda, Maryland 20205

†Laboratory of Chemical Pharmacology, National Heart, Lung and Blood Institute, National Institutes of Health, Bethesda, Maryland 20205

Asexual proliferation of malaria parasites proceeds by multiplication of the parasites within red cells. Following rupture of the host cells the released merozoites re-invade other red cells. On re-invasion, a proportion of merozoites become, not asexual parasites but gametocytes, the sexual stages infective to the mosquito vectors. Conversion of asexual parasites to gametocytes occurs not only during natural infections but also in continuous *in vitro* culture as reported first by Trager and Jensen[1–4] and by others[5,6]. We showed previously that the proportion of early intra-erythrocytic stages (ring stages) of *Plasmodium falciparum* which developed into gametocytes in culture was influenced by culture conditions[7]. Gametocyte formation was rare in conditions supporting rapid proliferation but frequent when parasite densities were static. We now show that nearly 100% of ring stages develop into gametocytes in response to 1 mM cyclic AMP in static cultures whereas in rapidly growing cultures few rings become gametocytes in response to cyclic AMP.

We have used the Z isolate of *P. falciparum* grown in continuous culture in human red cells as previously described[1] (see Table 1 legend). Complete development of *P. falciparum* gametocytes, either in culture or in man, takes approximately 10 days. During this time the gametocytes develop from ring forms into mature crescent-shaped parasites capable of undergoing gamete formation. One of the developmental stages of gametocyte maturation, the stage II gametocyte, is easily identified and occurs 48 h after ring formation. In our previous study[7] we devised a method for the daily measurement of the rate of production of gametocytes based on the percentage of rings that develop into stage II gametocytes 48 h later. Using this method,

0028-0836/80/310490—03$01.00

Table 1 Asexual parasitaemia and gametocyte production by *P. falciparum* in culture in the presence or absence of added cyclic AMP

Days after subculture		4	5	6	7	8	9
Rings*	No cyclic AMP	1.9±0.2	2.1±0.3	2.0±0.31	1.5±0.2	1.4±0.2	1.5±0.6
	With cyclic AMP	2.0±0.3	0.9±0.1	0.5±0.1	0.4±0.1	0.16±0.04	0.11±0.04
Stage II gametocytes*	No cyclic AMP	0.9±0.3	2.0±0.7	4.1±1.1	5.4±1.1	8.5±2.2	9.0±1.7
	With cyclic AMP	1.1±0.3	5.1±2.9	24.1±3.7	56.7±6.0	36.7±6.7	17.0±7.2
Stage III gametocytes*	No cyclic AMP	0.7±0.3	1.0±0.4	1.8±0.7	3.2±1.1	4.5±2.3	2.5±0.6
	With cyclic AMP	0.8±0.3	1.5±0.5	4.4±1.8	22.9±4.7	50.8±7.0	50.4±9.2
% Rings to gametocytes†	No cyclic AMP	2.5±0.7	3.3±0.6	4.4±0.6	6.1±1.1	—	—
	With cyclic AMP	11.4±2.9	58.1±8.2	70.8±5.7	37.7±18.4	—	—

Parasites were grown in human red cells in continuous culture using a method we have described previously[1] and based on the methods developed by Trager and Jensen[1] and by Haynes *et al.*[9] Cultures were grown in tissue culture flasks (Corning, 25 cm², polystyrene, 25100) in type A, Rh+ human red cells at a 5% haematocrit in culture medium. The culture medium was made up in double distilled water from RPMI 1640 powdered medium with glutamine and without bicarbonate (Gibco) to which was added HEPES buffer (Sigma) to 25 mM. Immediately before use sodium bicarbonate was added to 24 mM and the medium was supplemented to 10% with inactivated human serum, blood type A, Rh+. The complete medium was filtered through a 0.45 µm Nalgen filter. No antibiotics were used. Culture flasks contained 10 ml of the parasitized blood cell suspension and were laid on their broad sides (25 cm²) to give a medium depth of 4 mm and a cell depth of 0.2 mm. Medium was replaced daily and the flasks gassed with a mixture of 3% CO_2, 6% O_2, 91% N_2, hermetically sealed and maintained at 37°C. Fresh cultures were established by diluting a growing culture with uninfected red cells at a 5% haematocrit in culture medium to give an initial parasitaemia of 0.1–0.5%. The diluted cultures were thereafter dispensed into flasks and maintained as described above. Four days after setting up a *P. falciparum* culture in fresh red cells and medium, each flask was divided and 3 ml of the culture suspension was placed into each of two new flasks. The flasks were placed on their smallest end to give a medium depth of 3.3 mm and a cell depth of 0.17 mm. One flask was cultured as before with normal medium; in the other the medium was supplemented with 1 mM cyclic AMP. Ring stages and gametocyte densities were estimated daily from blood smears stained with Giemsa's stain. Stage II and stage III gametocytes are defined by morphological criteria and are estimated to be 2–3 and 3–5 days old, respectively (see refs 4, 7, 10). Results are given as the mean ± 1 s.e. of 9 separate experiments.

*Parasite counts are expressed as the number of parasites (gametocytes or rings) per 100 red cells

†The per cent of rings developing into stage II gametocytes 2 days later (see ref. 7 for full explanation)

we have studied the effect of cyclic AMP on the production of gametocytes in culture.

The mean densities of ring stages and gametocytes (stages II and III) during culture in the presence or absence of 1 mM cyclic AMP are shown in Table 1. Cyclic AMP was added and measurement of gametocyte production was begun after the parasites had been growing for 4 days in fresh red cells and medium. The percentage of rings which developed into gametocytes was 5–10 times greater in the presence of cyclic AMP. The data show that 24 h after their appearance as stage II gametocytes, they progressed quantitatively into stage III gametocytes. Measurement of the high proportion of rings developing into gametocytes in the presence of cyclic AMP is not, therefore, an artefact due to the accumulation of stage II gametocytes in culture.

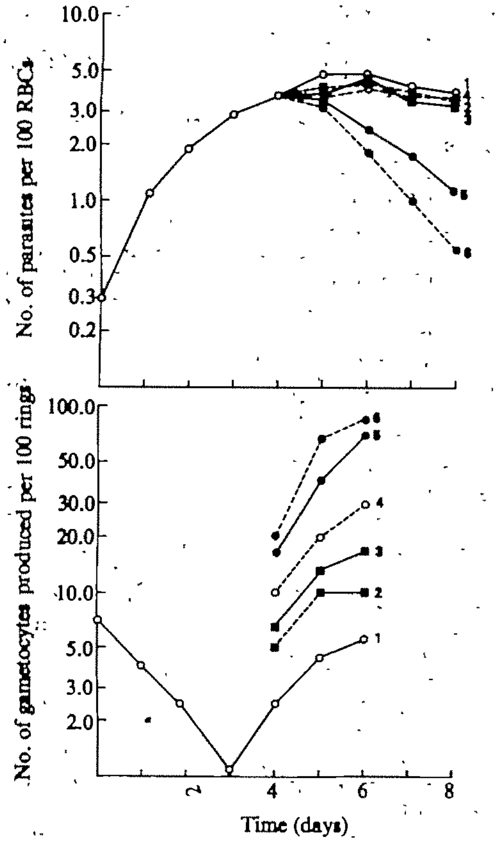

Fig. 1 The effects of different concentrations of cyclic AMP added from the fourth day of culture onward on the asexual parasitaemia and rate of gametocyte formation during *in vitro* culture of *Plasmodium falciparum*. in human red blood cells RBCs. (1) No cyclic AMP added; (2) 0.01 mM cyclic AMP; (3) 0.05 mM cyclic AMP; (4) 0.1 mM cyclic AMP; (5) 0.5 mM cyclic AMP; (6) 1.0 mM cyclic AMP.

When cultures were exposed to various concentrations of cyclic AMP (Fig. 1), 1 mM cyclic AMP mediated the greatest increase in the proportion of rings forming gametocytes. Higher concentrations (above 1 mM, data not shown) were lethal to all stages of the parasite. At concentrations as low as 0.01 mM the proportion of rings forming gametocytes was still more than twice that of cultures without added cyclic AMP.

Dibutyryl cyclic AMP, an analogue of cyclic AMP, was equally effective at equivalent concentrations in inducing gametocyte formation. Administration of 0.1 mM and 1 mM cyclic GMP and dibutyryl cyclic GMP had no effect on gametocyte formation. To test the effects of degradation products of cyclic AMP, we administered 5′-AMP, 3′-AMP, ADP and ATP, adenine and adenosine at concentrations of 0.1 mM and 1 mM. None of these compounds influenced gametocyte formation.

The following experiment was carried out to test the effect of cyclic AMP on the proportion of rings which develop into gametocytes at different times during culture. A parasite culture was diluted with fresh red cells and medium to achieve a parasite density of 0.5% and the culture divided equally into seven flasks. To each flask 1 mM cyclic AMP was added starting on a different day. The proportion of rings which were developing into gametocytes was measured 24 h after the addition of cyclic AMP. During the first 3 days after subculture, when there was rapid growth of the asexual parasites (Fig. 2), the proportion of rings which formed gametocytes following addition of cyclic AMP remained low (<10%) and even fell slightly (Fig. 2). Prolonged exposure of the parasites to 1 mM cyclic AMP during this period of rapid asexual growth was uniformly lethal to the asexual parasites (data not shown). In cultures without added cyclic AMP the proportion of rings forming gametocytes typically fell to very low levels (Fig. 2). From the fourth day onward the rate of asexual proliferation was very low and degenerate asexual parasites began to appear in culture. During this time the proportion of rings which spontaneously developed into gametocytes began to increase again. Moreover, during this phase of the culture, addition of 1 mM cyclic AMP elevated the proportion of rings which developed into gametocytes to about 10 times the spontaneous rate (Fig. 2). By the sixth day in culture, when 10–15% of rings spontaneously developed into gametocytes, almost 100% of rings were stimulated to become gametocytes 24 h after the addition of 1 mM cyclic AMP.

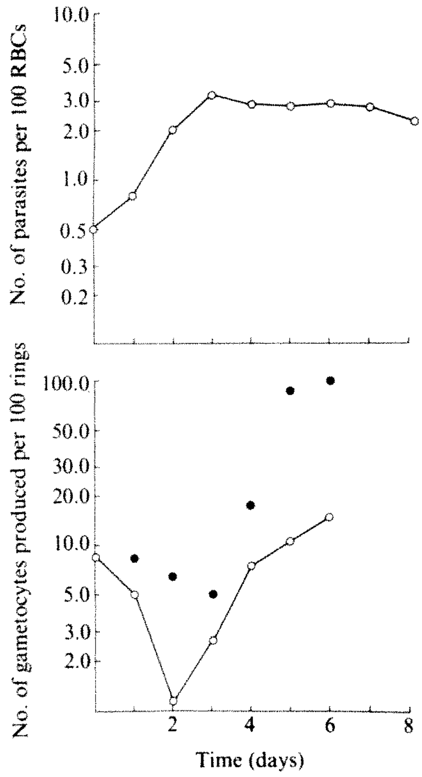

Fig. 2 The changing rate of formation of gametocytes from rings in response to cyclic AMP added on different days during the growth of *P. falciparum* in culture. A subculture of *P. falciparum*, set up by addition of fresh red cells and medium to a growing culture as described in Table 1 legend, was divided into 3-ml aliquots among seven flasks; the starting parasitaemia was 0.5%. One culture flask had no cyclic AMP added and showed the asexual growth and the daily rate of spontaneous formation of gametocytes from rings (○–○). To each of the other six flasks 1 mM cyclic AMP was added beginning on day 0 for flask 2, on day 1 for flask 3 to day 5 for flask 7. For each flask the rate of formation of gametocytes from rings was determined after the parasites had been exposed to cyclic AMP for 24 h (●). The rate of formation of gametocytes for flask 2 is shown on day 1, for flask 3 on day 2 and so on.

Our results demonstrate that the response to cyclic AMP by rings of *P. falciparum* in continuous culture changes according to the state of the culture. During rapid asexual proliferation, few rings develop into gametocytes in response to 1 mM cyclic AMP. Indeed, prolonged exposure to 1 mM cyclic AMP is lethal to the parasites. After rapid proliferation has ceased and the density of asexual parasites is constant, almost 100% of ring forms develop into gametocytes in response to 1 mM cyclic AMP. This change in responsiveness to cyclic AMP parallels the change in the rate of spontaneous gametocyte formation. Thus, during rapid asexual proliferation, spontaneous gametocyte formation falls to low levels or is absent; after asexual densities have become more or less constant, up to 10% of rings develop into gametocytes.

A similar change in responsiveness to a cyclic AMP stimulus was found in the amoeba *Dictyostelium discoideum. In* the presence of an adequate food source the free-living amoebae proliferated exponentially and did not respond to 0.001 mM cyclic AMP[8]. When the food supply became exhausted and exponential growth ceased, the amoebae became highly sensitive to cyclic AMP and formed aggregates in the early stages of spore formation. An analogous situation may apply to *P. falciparum* in culture. Parasites in cultures in which densities are not increasing are also in a state of near starvation; glucose levels become almost totally depleted before each addition of fresh culture medium. The state of starvation may, therefore, be associated with the development in the ring stages of a state of responsiveness to stimuli which induce gametocyte formation.

Received 28 November 1979; accepted 23 May 1980.

1. Trager, W. & Jensen, J. B. *Science* **193,** 673–675 (1976).
2. Trager, W. & Jensen, J. B. *Nature* **273,** 621–622 (1978).
3. Trager, W. *J. Protozool.* **26,** 125–129 (1979).
4. Jensen, J. B. *J. Protozool.* **26,** 129–132 (1979).
5. Carter, R. & Beach, R. F. *Nature* **270,** 240–241 (1977).
6. Phillips, R. S., Wilson, R. J. M. & Pasvol, G. *J. Protozool.* **25,** 394–398 (1978).
7. Carter, R. & Miller, L. H. *Bull. Wld Hlth Org.* **57,** Suppl. 1, 37–52 (1979).
8. Bonner, J. T. *et al. Devl Biol.* **20,** 72–87 (1969).
9. Haynes, J. D., Diggs, C. L., Hines, F. A. & Desjardins, R. E. *Nature* **265,** 767–769 (1976).
10. Smalley, M. E. *Nature* **264,** 271–272 (1976).

Determination and cellular commitment in the embryonic amphibian mesoderm

D. Forman & J. M. W. Slack

Imperial Cancer Research Fund, Mill Hill Laboratories,
Burtonhole Lane, London NW7 1AD, UK

In classical embryology, the term 'determination' was used to describe the process by which a region of the embryo became committed to form a particular part of the body and it was understood that there was a particular stage of development at which determination occurred with respect to each decision[1–3]. Some authors[4,5] insisted that only an irreversible commitment should be described as determination, but this leaves undefined the nature of the preceding events involved in its establishment. We show here that there may be several stages of commitment for an organ rudiment that can be distinguished from one another by the use of different methods for altering the pathway of development. We have investigated the region of the amphibian mesoderm that is destined to become somitic muscle in the course of normal development and applied to it a variety of isolation and grafting techniques. The results, which show an extensive period of lability within this region, can be used to explain how pattern formation might occur within the dorsoventral axis of the mesoderm.

In the experiments described here, the prospective somite region of the axolotl (*Ambystoma mexicanum*) was treated in one of four different ways as shown in Fig. 1. (1) The region was dissected out, wrapped in an ectodermal jacket obtained from the anteroventral region of a stage 13 embryo, and cultured in a buffered salt solution for 10 days. (2) After dissection, the explant was dissociated into single cells and allowed to reaggregate into clumps for 48 h. The clumps were then wrapped in ectoderm and cultured as in treatment (1). (3) After dissection, the explant was grafted into another embryo of the same stage to replace a piece of ventral mesoderm and the host embryo was allowed to develop for 12 days. (4) The region was dissected out, dissociated and reassociated, and then grafted ventrally to a host embryo of the same stage as the donor had been at the time of explantation. The host was allowed to develop for 12 days.

The results of treatment (1) show that at both neurula and head process stages the isolated tissue behaves in a similar way to normal development in that it differentiates predominantly into muscle (Table 1*a*, Fig. 2*a*). According to this criterion, one could therefore describe the prospective somite region of the mesoderm as being determined by the neurula stage and, indeed, the result is consistent with classical work using both urodele and anuran embryos, which indicated that the determination of this region had occurred by the time of gastrulation[6,7]. Some of the isolates also formed small amounts of pronephric tubules and/or mesenchyme. The formation of more than one tissue type is common in these experiments and we think that it may be the result of single cells or small groups of cells becoming detached from the main mass of tissue and behaving differently as a result. Because unwrapped controls remained undifferentiated, we believe that the ectodermal

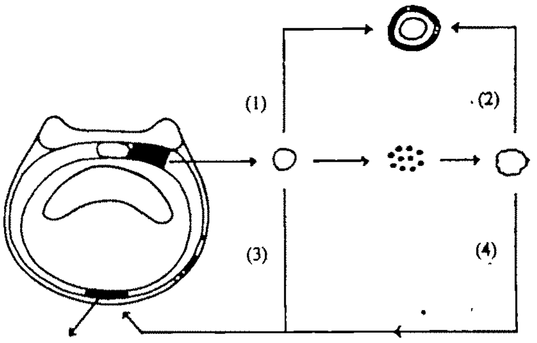

Fig. 1 The four experimental procedures. The diagram represents a transverse section through the trunk region of an axolotl neurula and shows the location of the prospective somite region (dorsal, shaded). This region was dissected out of the embryo on both sides with tungsten needles in ½ strength 'normal amphibian medium' (NAM)[11] containing 0.05% trypsin. The explants were washed, fused and allowed to round up in full-strength NAM for 30 min. Operations were carried out on neurulae (stages 15–18)[14], head process stages (21–24)[14] and tail bud stages (26–28)[14]. By the head process stage the somite region had begun segmentation at the anterior end (1) Explants were wrapped in ectoderm and cultured in NAM for 10 days. (2) Explants were dissociated by washing in Ca^{2+}/Mg^{2+}-free NAM and then treated for 5 min with Ca^{2+}/Mg^{2+}-free NAM containing 1 mM EDTA. The single cells were micropipetted into the centres of agar-coated 0.4-ml multiwell plates containing NAM. After 48 h of reaggregation, the resulting cell clumps were wrapped in ectoderm and cultured in NAM for 10 days (3) A piece of tissue, about one-quarter of the size of the prospective somite file, was grafted into the ventral region of host embryos of the same stage The embryos were allowed to develop in ½ strength and later $\frac{1}{10}$ strength NAM for 12 days. (4) A piece of dissociated–reaggregated tissue was grafted ventrally as in (3) All cultures were kept at 18 °C and after the appropriate period, the isolates or host embryos were fixed and processed for histological examination. Details of the methods used for obtaining embryos, operational procedures and tissue identification have been given previously[11]

jackets are essential for the successful differentiation of these isolates.

Treatment (2) gave significantly different results (Table 1*b*). At both neurula and head process stage there was now a much reduced tendency for the isolates to differentiate into muscle. Instead, the main tissue found was pronephric tubules together with substantial amounts of mesenchyme (Fig. 2*b*). We feel that the most likely interpretation of this result is that undifferentiated cells which would have turned into muscle turn into pronephros instead. The difference cannot be due to the selective overgrowth of one committed cell population by another because the culture medium used in these experiments is not nutritive and although the cells undergo several cleavage divisions there is no net growth of the tissue. Such selection would therefore have to be accompanied by massive cell death, which we do not observe. Because some undifferentiated cells persist in the isolates after the culture period, the only possible explanation based on selection is that the differentiation of committed pre-kidney cells is inhibited in treatment (1) and the differentiation of committed pre-muscle cells is inhibited in treatment (2). We cannot exclude this explanation but we believe it to be unlikely. By the tailbud stage of development the lability of the tissue seems to be lost because muscle is then the dominant cell type formed by the reaggregated isolates (Table 1*b*).

Table 1 Tissue types identified in isolated explants of prospective somite region of axolotl mesoderm

Stage from which tissue isolated	Cases	Muscle	Pronephros	Blood	Mesenchyme
a, Undissociated					
Neurula	8	7 (87%)	2 (25%)	0	6
Head process	13	13 (100%)	7 (54%)	0	9
b, Dissociated-reaggregated					
Neurula	15	6 (40%)	14 (93%)	0	15
Head process	12	2 (17%)	12 (100%)	0	10
Tailbud	8	7 (87%)	6 (75%)	0	7

Prospective somite regions which were grafted to the ventral position while donor and host embryos were at the neurula stage (treatment (3)) differentiated predominantly into erythrocytes (Fig. 2*c*,*d*). Small amounts of muscle and pronephric tubules were also found in some of the grafts (Table 2*a*). At later stages of development the grafts gave rise to more muscle and fewer erythrocytes (stages 19/20 in Table 2*a*) and by the head process stage the grafts differentiated mainly into muscle (Fig. 2*e*) and the few erythrocytes which were formed were dispersed around the outside of the graft tissue. This type of switch from position-dependent to source-dependent development has been reported by Yamada[8], although in his work on the newt *Cynops pyrrhogaster* the switch occurred rather earlier, at about stage 15.

If the prospective somite region is dissociated and reaggregated before being grafted to a ventral position (treatment (4)), the period of lability is even longer (Table 2*b*). As with the reaggregated isolates there was a much reduced differentiation into muscle and a much increased formation of pronephric tubules. There was also a significant formation of erythrocytes which was more extensive at the neurula than at the head process stage. Results with the undissociated controls confirm that these effects were not due to the fact that the reaggregated isolates were cultured for 48 h before grafting. Indeed, the 48-h culture period for the controls actually reduced the lability of the neurula stage ventral grafts; cultured grafts always maintained their capacity for muscle differentiation whereas non-cultured grafts did not (compare Table 2*a* neurula with Table 2*b* neurula control).

For all the operations reported in Table 2*a*, *b* we are confident that the tissues we identify are genuinely derived from the graft and not from the host. This is because grafts to the ventral position persist as readily visible clumps of tissue for many days, as shown in Fig. 2*c*. Also, 21 of these grafts, including cases from each experimental class, were carried out using triploid donor embryos and these triploid cells were later identified in the graft (Fig. 2*f*). In axolotls the number of nucleoli per nucleus corresponds to the ploidy[9] and so the identification of trinucleolar cells is proof of their donor origin. Nucleoli are readily visible in muscle and kidney cells and although they cannot be seen in mature erythrocytes they can be prominent in the erythrocyte precursor cells which are an intimate part of the graft tissue.

The results are summarized in Table 3.

It seems, therefore, that the prospective somite region is determined with respect to self-differentiation in isolation throughout the developmental period considered. However, the determination of the tissue can be modified by grafting to a ventral position up to the head process stage and can be modified by dissociation and reaggregation up to the early tailbud stage. This latter stage is the time at which muscle specific differentiation products can first be detected in the region (T. J. Mohun,

Table 2 Tissue types identified in grafted material following a graft of prospective somite region axolotl mesoderm to replace ventral mesoderm in a donor of equivalent stage

Stage at which graft performed	Cases	Muscle	Pronephros	Blood	Mesenchyme
a, Undissociated					
Neurula	16	4 (25%)	5 (31%)	15 (93)%	6
19/20	11	6 (55%)	1 (9%)	7 (63%)	3
Head process	10	9 (90%)	2 (20%)	7 (70%)	5
b, Dissociated–reaggregated					
Neurula	11	3 (27%)	7 (64%)	10 (91%)	4
Neurula control*	10	10 (100%)	1 (10%)	10 (100%)	2
Head process	10	2 (20%)	10 (100%)	4 (40%)	8
Head process control*	8	8 (100%)	3 (37%)	5 (62%)	1

* Controls were undissociated isolates cultured in salt solution for the time period during which dissociated cases were allowed to reaggregate.

R. Tilly, R. Mohun and J.M.W.S., unpublished data) and which we therefore consider to be the onset of cytodifferentiation. Thus, in this case there is no state of truly irreversible determination before cytodifferentiation.

Yamada[10] suggested that the dorsoventral pattern of structures in the mesoderm was specified by a graded signal emanating from the dorsal end of the tissue, which is the prospective notochord. Mesoderm closest to the notochord would be programmed to form the somites, the next layer would be programmed to form the kidney and the most ventral layer to form the blood islands. Our own previous work[11] supports the idea of a dorsal signal for the specification of the somite region and the experiments reported here suggest that the maintenance of this determined state may require the preservation of intercellular contacts. The fact that erythrocytes can be formed by grafts to the ventral position but not in isolates suggests the existence of a second 'blood inducing' signal which is present in the ventral region of the neurula. This would imply that in the absence of all signals the mesoderm would develop into kidney which is what we find in the isolated tissue after disaggregation and reaggregation.

Although this scheme of pattern formation is largely speculative, it is consistent with all our results and does bear some formal similarity to 'double gradient' models which have been advanced to explain other embryonic phenomena[12,13]. Further experiments to test its validity are in progress.

Table 3 Summary of results

a, Neurula	*Isolate*	*Ventral graft*
No dissociation	Muscle	Erythrocytes
Dissoc./reagg.	Pronephros	Erythrocytes (pronephros)
b, Head process		
No dissociation	Muscle (pronephros)	Muscle (erythrocytes)
Dissoc./reagg.	Pronephros	Pronephros

The predominant tissue was found in >85% of cases and the minor tissue in >50% of cases.

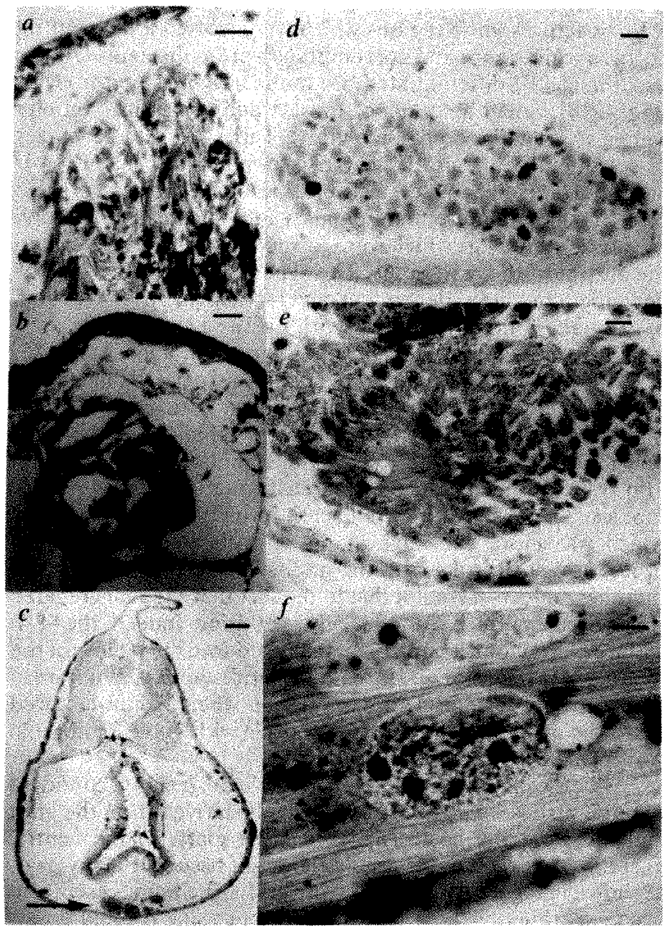

Fig. 2 *a*, Section through prospective somite region which was isolated from a neurula, wrapped in ectoderm and cultured for 10 days (treatment (1)). The tissue, although still containing yolk granules, has largely differentiated into muscle (scale bar, 50 µm). *b*, Section through prospective somite region which was isolated from a head process stage embryo, dissociated and reaggregated, wrapped in ectoderm and cultured (treatment (2)). The tissue has formed pronephric tubules (scale bar, 50 µm). *c*, Transverse section through the trunk region of an early larval stage axolotl which received a graft of prospective somite region into the ventral position (treatment (3)). The graft was carried out at the neurula stage, 12 days previously. The graft tissue is shown by an arrow (scale bar, 200 µm). *d*, High power view of the graft indicated in *c*, showing erythrocytes (scale bar, 20 µm). *e*, High power view of ventral graft of prospective somite region carried out at head process stage, showing muscle (scale bar, 20 µm). *f*, Donor muscle cell in graft region autonomously marked by possession of three nucleoli in the nucleus. Triploid donor embryos were obtained by a 10-min heat shock of 36 °C given 30–45 min after fertilization. The nucleoli are differentially stained by the Unna-Pappenheim stain (scale bar, 5 µm).

Received 25 March; accepted 5 June 1980.

1. Spemann, H. *Embryonic Development and Induction* (Hafner, New York, 1967).
2. Weiss, P. *Principles of Development* (Hafner, New York, 1969).
3. *CIBA Symp.* **40,** 103–110 (1976).
4. Waddington, C. H. *Principles of Embryology* (Allen and Unwin, London, 1956).
5. Needham, J. *Biochemistry and Morphogenesis* (Cambridge University Press, 1942).
6. Holtfreter, J. *Wilhelm Roux Arch. Entw Mech. Org.* **138,** 522–656; 675–738 (1938).
7. Holtfreter, J. & Hamburger, V. in *Analysis of Development* (eds Willier, B. H., Weiss, P. A. & Hamburger, V.) 230–296 (Saunders, Baltimore 1955).
8. Yamada, T. *Wilhelm Roux Arch. Entw Mech. Org.* **137,** 151–270 (1937).
9. Fankhauser, G. & Humphrey, R. R. *Proc. natn. Acad. Sci. U.S.A.* **29,** 344–350 (1943).
10. Yamada, T. *Biol. Bull. mar. biol. Lab., Woods Hole* **98,** 98–121 (1950).
11. Slack, J. M. W. & Forman, D. *J. Embryol. exp. Morph.* **56,** 283–299 (1980).
12. Hörstadius, J. *Experimental Embryology of Echinoderms* (Clarendon, Oxford, 1973).
13. Sander, K. *Adv. Insect Physiol.* **12,** 125–238 (1976).
14. Bordzilovskaya, N. P. & Detlaff, T. A. *Axolotl Newslett.* **7** (1979).

A hypolipaemic factor from the corpus cardiacum of locusts

I. Orchard & B. G. Loughton

Department of Biology, York University, Downsview,
Ontario M3J IP3, Canada

The glandular cells in the glandular lobe of the corpus cardiacum (CC) of locusts are the source of adipokinetic hormone (AKH), a hyperlipaemic hormone which has been characterized, sequenced and synthesized[1–4]. The release of AKH is under the synaptic control of axons within the nervi corporis cardiaca II (NCC II)[5]. We show here that a second factor with hypolipaemic activity is also under the control of axons within the NCCII. However, its release sites lie within the storage lobe. Insulin, at physiological doses equivalent to those found in vertebrates, mimics the action of the hypolipaemic factor, and axons which show immunoreactive staining with anti-insulin have been located within the storage lobe. The locust hypolipaemic factor and insulin seem to have some common molecular features.

The CC of locusts has proved an attractive resource for insect endocrinologists because of its anatomical division into storage (which is composed largely of the axon terminals of the median neurosecretory cells) and glandular (composed almost entirely of intrinsic neurosecretory cells) lobes. This has allowed the localization of the source of locust AKH[1–4] in the glandular lobe. The CC is supplied by two nerves, the paired nervi corporis cardiaca I (NCC I) which enter the anterior aspect of the storage lobe and expand to constitute the bulk of the storage lobe, and

0028-0836/80/310494—03$01.00

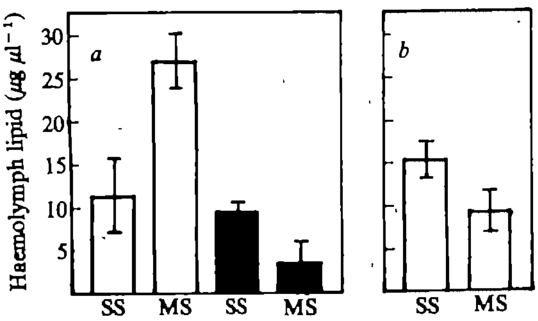

Fig. 1 *a*, Haemolymph lipid levels after injection of perfusate of the glandular lobe of the CC following its stimulation through the NCC II in the presence (solid bars) and absence (clear bars) of phenoxybenzamine. Note that the perfusate following maximal stimulation (MS, open bars) caused elevation of haemolymph lipid (hyperlipaemia) but that the perfusate following maximal stimulation in the presence of 10^{-6} M phenoxybenzamine caused a reduction in haemolymph lipid compared with controls (SS, open and closed bars). Release of hyperlipaemic hormone is obviously blocked in the presence of phenoxybenzamine but the release of hypolipaemic hormone is not. Mean ± s.e. of four assayed locusts. *b*, Haemolymph lipid levels after injection of perfusate of isolated storage lobe following stimulation of the NCC II. Note that the perfusate following maximal stimulation (MS) caused a reduction in haemolymph lipid (hypolipaemia). Mean ± s.e. of 12 assayed locusts. SS, Sub-threshold stimulation; MS, maximal stimulation.

the two nervi corporis cardiaca II(NCC II) which enter the storage lobe dorsally, close to the junction of storage and glandular lobes. We have recently demonstrated[5] that stimulation of the NCC II causes the release of hyperlipaemic factors from the glandular lobe (see Fig. 1*a*, MS open bars).

During experiments on the pharmacology of the neurotransmitters mediating the release of hyperlipaemic factors, we observed preparations which, when stimulated through the NCC II in the presence of the α-adrenergic blocking agent phenoxybenzamine, caused a reduction in the haemolymph lipid of the insects studied (Fig. 1*a*, MS, closed bars). We interpreted this finding as indicating the continued release of a hypolipaemic factor, evident only when the release of the hyperlipaemic hormone(s)[1–4] was inhibited by blocking the synapse between NCC II axons and the intrinsic cells of the glandular lobe to the CC. To substantiate this hypothesis we examined the hypolipaemic activity in greater detail.

AKH activity has been associated primarily with the glandular lobe[6]; therefore, it was expected that the source of the hypolipaemic factor should lie elsewhere. Because incubation of the CC in phenoxybenzamine without nervous stimulation did not bring about release of hypolipaemic activity, it was assumed that its release was controlled by axons of the NCC II. Mason[7] has shown that NCC II sends axons into both the storage and glandular lobes of the CC of *Schistocerca*. This was confirmed for *Locusta* by recording a propagated response from both storage and glandular lobes following stimulation of NCC II. Two approaches were adopted to confirm the presence of a hypolipaemic factor in the storage lobe of the CC. CCs were carefully dissected from mature adult female locusts so as to retain as much of the NCC I and NCC II as possible. Next, the glandular lobe was dissected away leaving the NCC II attached to the storage lobe. As several workers have pointed out[8] that the boundary between storage and glandular regions is not discrete, we could not always be certain that all the glandular lobe had been removed. The storage lobe was placed in 100 μl of physiological saline[9]. The cut end of the NCC II was then drawn into a suction electrode and stimulated with impulses of subthreshold current intensities at 5 Hz for 10 min. The bathing solution was collected and the preparation replaced with 100 μl of fresh saline. The procedure was repeated but the level of stimulation was increased to bring about a maximally propagated response in the form of a compound action potential recorded from the internal face of the ventral lobe of the storage lobe of the CC. The control saline (collected after sub-threshold stimulation) and the experimental saline (following recording of compound action potentials) were assayed for hypolipaemic activity. Groups of four adult male locusts (10–14 days old) were each injected with 20 μl of the test saline. After 45 min the insects were bled through the cervical membrane. The lipid in the haemolymph was estimated gravimetrically[5]. In two out of three storage lobes stimulated in this way, the 'experimental saline' caused a 38% diminution of haemolymph lipid when compared with controls (Fig. 1*b*). Stimulation of NCC I failed to cause release of a hypolipaemic factor. We believe that in the third experiment the storage lobe might have retained some glandular lobe contaminants as lipid levels increased on injection of this preparation.

In a second series of experiments the ventral lobe of the storage lobe was dissected out of mature female locusts and homogenized in 100 μl of saline. Aliquots of the saline extract were injected into adult male locusts. Control insects received injections of saline or extracts of fat body. The lipid levels in the haemolymph of the test insects were determined 45 min later. Figure 2 shows the effects of injections of storage lobe extracts on the lipid levels in the haemolymph of test insects. It can be seen that as little as 0.0025 equivalents of the storage lobe

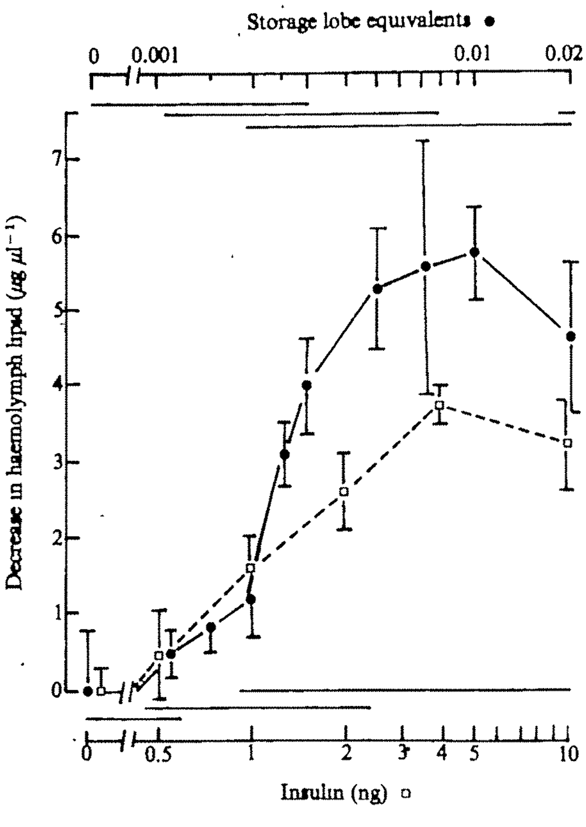

Fig. 2 Decrease in haemolymph lipid following injection of extracts of ventral lobe of the storage lobe of the CC or solutions of insulin (porcine). The resting level of lipid in the control insects for the storage lobe experiment was $10.1 \pm 0.8\ \mathrm{g\,l^{-1}}$, giving a maximum hypolipaemic effect of 57% reduction in haemolymph lipid. Resting level in the insulin experiment was $6.6 \pm 0.3\ \mathrm{g\,l^{-1}}$, giving a maximum hypolipaemic effect of 56% reduction in haemolymph lipid. The resting levels of lipid in the two sets of experiments reflect differences in the age and diet of the 'assay locusts'. The horizontal lines at the top and bottom of the figure denote homogeneous subsets formed by Student–Newman–Keul multiple range test ($\alpha = 0.05$) for storage lobe and insulin, respectively (results of one-way analyses of variance: for storage lobe, $F = 6.23$; d.f. = 9, 127; $P < 0.001$; for insulin: $F = 8.35$; d.f. = 5, 79; $P < 0.001$). The points are mean ± s.e.

caused a significant diminution of haemolymph lipid and that the hypolipaemic effect increased as higher concentrations of storage lobe were used.

In vertebrates, insulin decreases glucose levels in the blood and promotes lipid synthesis in the tissues. Several authors[10-12] have reported the presence of insulin-like molecules in insects. Furthermore, insulin has been shown to decrease the release of lipid from *Hyalophora* fat body *in vitro*[13]. Antibodies against porcine insulin (Sigma) were generated in rabbits and used to localize insulin immunoreactive substances in sections of brains and CC of locusts using the peroxidase–anti-peroxidase method[14]. Positive staining was detected in the ventral lobe region of the storage lobe and in median neurosecretory cells of the brain. The presence of insulin-like molecules in the CC prompted us to investigate the effect of insulin on the lipid levels in locust haemolymph. It can be seen from Fig. 2 that injection of insulin caused a marked decrease in haemolymph lipid. The similarity in the effect of extracts of storage lobe of the CC and insulin together with the presence of anti-insulin immunoreactive molecules in this part of the CC suggest the locust hypolipaemic factor and insulin have some common molecular features.

Although the hypolipaemic factor has not been demonstrated in the haemolymph, the manner of its release from the CC suggests that the hypolipaemic factor in the storage lobe of the locust CC is indeed a newly discovered hormone. A slight hypolipaemia has been reported in cockroaches following injection of extracts of whole CC or corpora allata[15] and Goldsworthy and Cheeseman[16] suggested the possibility of such a hormone following the observation of slight hyperlipaemia in starved locusts in the absence of changes in AKH titre in the haemolymph. The physiological significance of the hypolipaemic factor could be to overcome the inhibition of glycolysis in flight muscle brought about by increased levels of diglyceride in the haemolymph[16] or to restore haemolymph lipid levels to 'normal' following its dramatic increase during flight.

This work was supported by the National Research Council of Canada in the form of a Negotiated Development Grant to York University and NSERC grant A3645 to B. G. L. We thank Dr E. H. Miller for statistical analysis of the data.

Received 21 February; accepted 21 May 1980.

1. Stone, J. V., Mordue, W., Batley, K. E. & Morris, H. R. *Nature* **263,** 207–211 (1976).
2. Goldsworthy, G. J., Mordue, W. & Guthkelch, J. *Gen. comp. Endocr.* **18,** 545–551 (1972).
3. Mayer, R. J. & Candy, D. J. *J. Insect Physiol.* **15,** 611–620 (1969).
4. Carlsen, J., Herman, W. S., Christensen, M. & Josefsson, L. *Insect Biochem.* **9,** 497–501 (1979).
5. Orchard, I. & Loughton, B. G. (in preparation).
6. Rademakers, L. H. P. M. & Beenakkers, A. M. Th. *Cell Tissue Res.* **180,** 155–171 (1977).
7. Mason, C. A. *Z. Zellforsch.* **141,** 19–32 (1973).
8. Krogh, I. M. & Normann, T. C. *Acta zool., Stockh.* **58,** 69–78 (1977).
9. Hoyle, G. *J. Physiol., Lond.* **127,** 90–103 (1955).
10. Seecof, R. L. & Dewhurst, S. *Cell Differentiation* **3,** 63–70 (1974).
11. Tager, H. S., Markese, J., Kramer, K. J., Speirs, R. D. & Childs, C. N. *Biochem. J.* **156,** 515–520 (1976).
12. Duve, H. & Thorpe, A. *Cell Tissue Res.* **200,** 187–191 (1979).
13. Bhakthan, N. M. G. & Gilbert, L. I. *Gen. comp. Endocr.* **11,** 186–197 (1968).
14. Sternberger, L. A., Hardy, P. H. Jr, Cuculis, J. J. & Meyer, H. G. *J. Histochem. Cytochem.* **18,** 315–333 (1970).
15. Downer, R. G. H. & Steele, J. E. *Gen. comp. Endocr.* **19,** 259–265 (1972).
16. Goldsworthy, G. J. & Cheeseman, P. in *Comparative Endocrinology* (eds Gaillard, P. J. & Boer, H. H.) 423–436 (1978).

Influence of voluntary intent on the human long-latency stretch reflex

J. C. Rothwell, M. M. Traub & C. D. Marsden

University Department of Neurology, Institute of Psychiatry and King's College Hospital Medical School, De Crespigny Park, Denmark Hill, London SE5 8AF, UK

In man, sudden stretch of an actively contracting muscle evokes a classical monosynaptic spinal reflex followed by an automatic 'long-latency' response, both evident as bursts of activity in the electromyogram (EMG)[1]. This long-latency response, extensively investigated in the human long thumb flexor, but present in many other muscles[2], occurs too early to be voluntary and much indirect evidence suggests it represents the operation of a 'long-loop', perhaps transcortical, stretch reflex mechanism[3,4]. Some investigators have found that the long-latency responses may be modified substantially by the subject's intent, possibly by pre-setting of excitability levels within the central nervous system thereby influencing the 'long-loop' mechanism[5-9]. However, others have observed little effect of voluntary set on the automatic long-latency stretch response[10,11]. It is notable that these studies, which have yielded conflicting results, have involved different muscles in a variety of experimental conditions. In some studies a warning signal preceded muscular stretch, while in others control trials were interspersed with stretches. To resolve the dilemma we have examined the influence of these variables, and found that the automatic long-latency response can be modified most strongly in conditions when the voluntary reaction time is shortest, for example, when the timing of the stimulus can be predicted accurately. We suggest that modification of a long-loop stretch response is not due to some central pre-setting process, but merely represents interaction between a reflex of long latency and a subsequent very rapid voluntary event, occurring early because of predictability of the stimulus.

We have investigated the effect of voluntary intent on the long-latency stretch response in flexor pollicis longus (FPL) and biceps brachii of 10 normal volunteers. The experimental apparatus has been described previously[1,2]. In the experiments on FPL, the thumb was clamped at the proximal phalanx and the subject maintained a constant position of the distal phalanx of the thumb against a background force (2.5 N) offered by a low inertia motor. For biceps, the subject rested his upper arm on a table top at chest height and maintained his semi-pronated forearm vertical against a constant force (8 N) exerted by means of a light chain attached to the motor and pulling on the wrist to extend the elbow. Surface EMGs were recorded by a PDP 12 computer after being rectified and integrated. In each subject muscle stretch was produced every 10–20 s by sudden increases in motor force lasting 1s (to 5 N for FPL; 24 N for biceps). These disturbances were administered in three separate ways (*a*, *b* and *c* given in random order); (*a*) 500–650 ms after a warning bleep, the time being set by a pseudo-random generator; (*b*) a constant 8 s after the bleep; and (*c*) as in condition *a* but with 50% of randomly selected controls (unrecorded) in which the bleep was not followed by a change in motor force. Before each warning signal the subject was instructed in random sequence either to 'let go' by relaxing completely, or to 'resist' by flexing as hard as possible on perceiving the disturbance. It was stressed that he was to react to the stretch and not to the earlier bleep signal. The computer recorded each trial over a period of 250 ms before the disturbance. Sixteen 'let go' and sixteen 'resist' trials were averaged separately in each group. The duration of the long-latency response was measured from the rectified EMG records of the 'let go' trials in condition *c*. The size of the response was measured from the integrated EMG records as the percentage increase in activity over control levels extrapolated from the first 50 ms of the sweep.

It has been shown previously that when a stimulus is preceded by a warning signal, the simple reaction time increases with the length and variability of the fore-period[12]. Thus we expected the reaction time to be shortest in condition *a* in which the subject could predict the timing of the stretch stimulus most accurately. It was in this condition that the subject could voluntarily influence the size of the long-latency stretch response most effectively (Figs 1, 2). The addition of control trials (condition *c*)

0028–0836/80/310496—03$01.00

or increasing the length of the fore-period to 8 s (condition *b*), both of which made the exact timing of the disturbance less certain, reduced the influence of voluntary intent on the stretch response by a similar amount.

Interestingly, there was a considerably greater effect of voluntary set on the stretch response in biceps than in FPL. This was unlikely to be due to a difference in voluntary reaction time because the latency of the EMG response to an auditory stimulus was longer in biceps than in FPL (biceps 151 ms ±7.3 s.e.m. ($n = 8$); FPL 133±7.7 ($n = 8$); paired Student's t-test, $P < 0.005$). It is possible that because of the low inertia of the distal phalanx of the thumb, the stretch stimulus caused a relatively large and rapid change in length in FPL thus saturating the reflex output (see Fig. 1). However, when a smaller thumb disturbance was given (increase in force from 2.5 to 3.0 N) in condition *a*, the influence of voluntary set was reduced, presumably because of the increase in voluntary reaction time to the smaller stimulus.

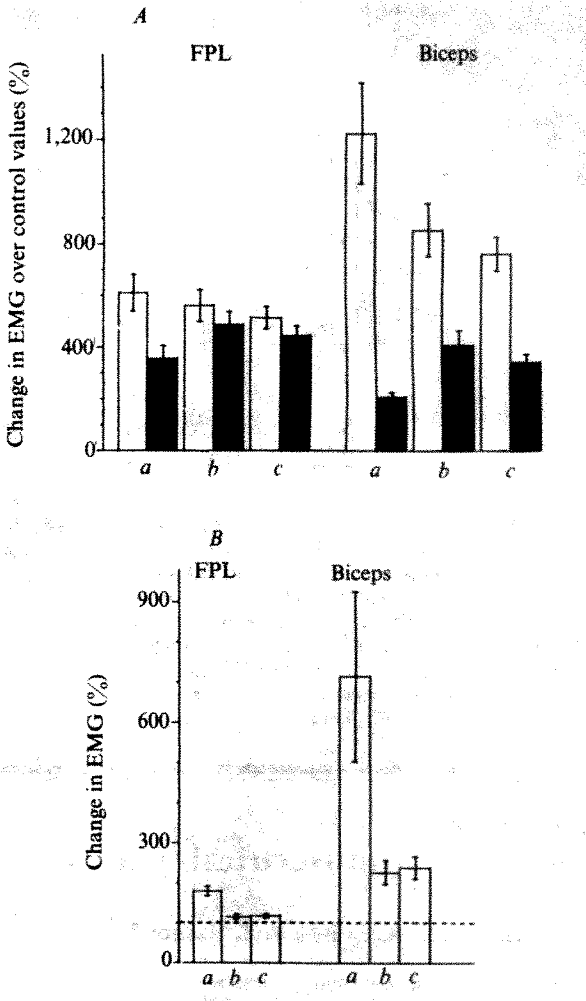

Fig. 2 *A*, Average size of the long latency stretch reflex (±1 s.e.m.) in FPL and in biceps of 10 subjects in the three different experimental conditions *a*, *b* and *c* (see text). Open bars indicate the size in the 'resist' (p) trials; hatched bars the 'let go' (l) trials. Size of reflex EMG was measured from integrated records and is expressed as a percentage of basal levels of activity calculated for the same duration as the reflex, but extrapolated from the control period immediately before the stretch stimulus. *B*, Mean percentage change (±1 s.e.m.) in the size of the stretch reflex during the 'resist' trials compared with the size in the 'let go' trials for each experimental condition (see text). The horizontal dotted line at 100% indicates that the reflex size was the same in both conditions.

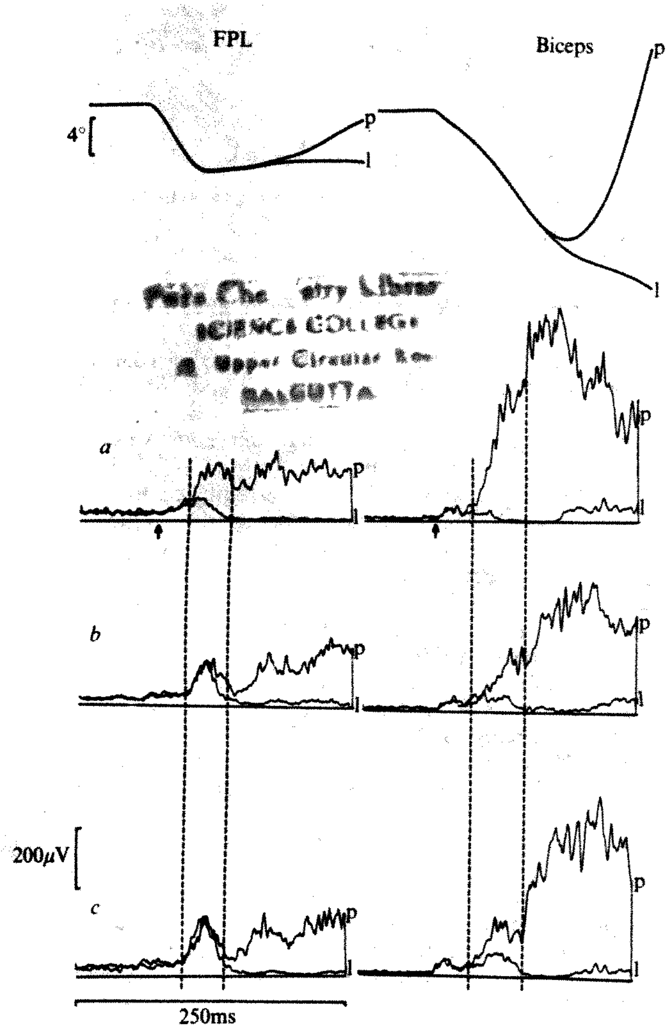

Pata Chemistry Library
SCIENCE COLLEGE
8 Upper Circular Ro
CALCUTTA

Fig. 1 The effect of prior instruction on the automatic long-latency response to muscle stretch in flexor pollicis longus (left-hand traces) and in biceps (right-hand traces) in a single subject. The top records illustrate the angular position of interphalangeal joint of the thumb and the elbow, the initial positions of the joints being 10° and 90° flexion respectively. The lower three traces show rectified EMG. The motor torque was increased 50 ms after the start of each sweep and the subject was instructed before each trial to 'resist' (p) or 'let go' (l) on perceiving the disturbance. Each trace shows the average of 16 p trials superimposed on the average of 16 l trials. The three experimental designs, *a*, *b* and *c*, performed as described in the text, in the sequence *b*, *c*, *a*. Position traces (top) are from trial *a*. The duration of the long-latency stretch response (vertical dotted lines) was estimated from the 'let go' (l) trials in trace *c*. A vertical arrow marks the onset of a small spinal latency component of the response with a latency of about 25 ms in FPL and about 15 ms in biceps.

In a subsidiary experiment the smaller stretch was administered together with a simultaneous electric shock (60 V; 50 μs) to the contralateral median nerve at the wrist (voluntary reaction to the electrical stimulus alone was 100 ms ±2.8 s.e.m.) so as to shorten the reaction time to a small non-saturating stretch stimulus. Now the influence of voluntary intent was enhanced to levels greater than observed in the conditions described previously for larger stretches (Figs 2, 3). In contrast, a simultaneous electric shock had no apparent effect on reflex size when given with a larger stretch when reaction time was already short (Fig. 3).

In conclusion, the degree of voluntary modification of the size of the long-latency automatic stretch response depends on factors which affect reaction time. The relatively small effects of

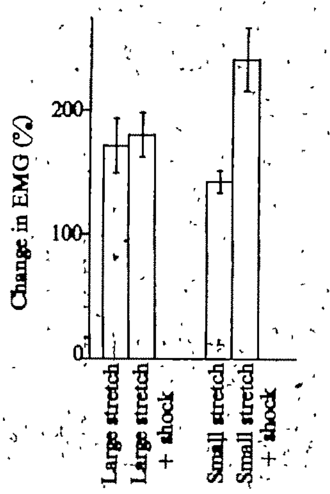

Fig. 3 Average percentage change (±1 s.e.m.) in the size of the long-latency stretch reflex in FPL of ten subjects during the 'resist' and 'let go' conditions when the stretch stimulus was given alone or paired with a simultaneous electric shock to the contralateral median nerve at the wrist. All trials performed under condition *a*, with a warning signal given 500–650 ms prior to the muscle stretch. Left bars, large stretch (from 2.5 to 5 N); right bars, small stretch (from 2.5 to 3 N). The electric shock was arranged to be above threshold for thenar muscle contraction.

voluntary intervention seen in FPL may be because it is impossible to administer a stretch stimulus which is both easily and therefore rapidly perceived, and yet which does not saturate the stretch reflex mechanism. In contrast, the stretch response in biceps does not saturate so easily (because the inertia of the arm precludes very rapid stretches with the apparatus used), so that the influence of rapid voluntary intervention is seen more easily than in FPL. Prior instruction, rather than pre-setting excitability levels in the long-loop pathways, seems to influence the automatic long-latency response to stretch by superimposing fast descending voluntary activity on the earlier automatic event.

Received 11 March, accepted 6 June 1980

1 Marsden, C. D., Merton, P. A. & Morton, H. B. *Nature* **238**, 140–143 (1972), *J. Physiol., Lond.* **257**, 1–44 (1976).
2 Marsden, C. D., Merton, P. A. & Morton, H. B. *J. Physiol., Lond.* **259**, 531–560 (1976)
3 Marsden, C. D., Merton, P. A. & Morton, H. B. *Lancet* **i**, 759–761 (1973)
4 Marsden, C. D., Merton, P. A., Morton, H. B. & Adam, J. *Brain* **100**, 185–200, 503–526 (1977)
5. Hammond, P. H. *J. Physiol., Lond.* **132**, 17–18P (1956)
6 Lee, R. G. & Tatton, W. G. *Can. J. neurol. Sci.* **2**, 285–293 (1975)
7. Evarts, E. V. & Granit, R. *Prog. Brain Res.* **44**, 1–14 (1976)
8 Iles, J. F. *Expl Brain Res.* **30**, 451–470 (1972).
9 Colebatch, J. G., Gandevia, S. C., McCloskey, D. I. & Porter, E. K. *J. Physiol., Lond.* **292**, 527–534 (1979)
10 Marsden, C. D., Merton, P. A., Morton, H. B., Adam, J. & Hallett, M. *Prog. clin. Neurophysiol.* **4**, 167–177 (1978).
11 Evarts, E. V. & Vaughn, W. J. *Prog. clin. Neurophysiol.* **4**, 178–192 (1978).
12 Klemmer, E. T. *J. exp. Psychol.* **51**, 179–184 (1956), **54**, 195–200 (1957)

Interaction of anaesthetics with electrical synapses

M. F. Johnston, S. A. Simon & F. Ramón*

Departments of Physiology and Anaesthesiology, Duke University Medical Center, Durham, North Carolina 27710

Studies of the interaction of anaesthetics with various preparations, from whole animals to organic solvents, have been continuing since Overton and Meyer found a correlation between anaesthetic potency and solubility in olive oil[1]. Although the physiological basis of anaesthesia is far from clear, one popular hypothesis is that anaesthetics act primarily by interfering with the normal functioning of chemical synapses[2–4]. This hypothesis is supported by experiments showing that these synapses are more sensitive to both local and general anaesthetics than are axons. The effects of anaesthetics on electrical synapses (gap-junctions or nexus) have not previously been studied. These ubiquitous structures, presumably responsible for cell-to-cell communication[5], are found in most vertebrate and invertebrate tissues. We report here the effects of several anaesthetics on electronic coupling between nerve cells, and show that electrical synapses are less sensitive to most anaesthetics than are chemical synapses and axonal membranes.

Experiments were performed on segmented giant axons of the nerve cord of crayfish (*Procambarus clarkii*). Each axonal segment is coupled to its neighbours by bidirectional electrical synapses near each segmental ganglion[6,7]. Measurements were made at the second or third abdominal ganglion. Intercellular coupling was determined by injecting hyperpolarizing square pulses of current and measuring the voltage responses at both sides of the intersegmental septum with intracellular microelectrodes. Septal resistance (R_s) and axon membrane resistance (R_m) were calculated from these measurements[7–9]. Propagated action potentials (p.a.ps) were also recorded as they travelled through the septal region. Control values for resting membrane potential and action potential amplitude are 88.9±2.0 mV and 123.8±3.8 mV (mean±s.d.), respectively. Septal resistance and membrane resistance averaged 40±17 KΩ and 188±18 KΩ, respectively.

Axons were bathed in a modified van Harreveld solution containing 205 mM NaCl, 13.5 mM $CaCl_2$, 5.4 mM KCl, 2.6 mM $MgCl_2$, and 5 mM HEPES, adjusted to *p*H 7.5. Anaesthetics, with the exception of ketamine which was obtained from Parke–Davis, were purchased from Sigma. All drugs were added extracellularly unless otherwise stated. The standard internal solution (SIS) contained 15 mM NaCl, 109 mM KF, 37 mM K citrate, 96 mM mannitol and 1 mM HEPES, adjusted to *p*H 7.5. The more water-soluble anaesthetics were added directly to the external solution. Octanol and nonanol were added to the external solution from 1M stock solutions in dimethylsulphoxide (DMSO). The final concentration of DMSO was always less than 0.5% (v/v), which by itself had no effect on electrical behaviour. Drug concentrations were increased until the axon would no longer maintain a propagated action potential. Experiments were performed at 15 °C.

Figure 1 summarizes data obtained when heptanol (3 mM) was applied externally. This figure shows propagated action potentials and the voltage–current relationships of the septal region during control (*a*, *d*), heptanol (*b*, *e*) and recovery (*c*, *f*). Data for other anaesthetics at various concentrations were obtained similarly.

Figure 1*b* shows that 3 mM heptanol blocks propagation of action potentials across the septum. These effects of heptanol are reversible (Fig. 1*c*). Blockade of action potentials can be explained, from septal *V–I* relationships, by an increase in resistance from 50 KΩ (Fig. 1*d*) to 600 KΩ (Fig. 1*e*). In these data only the *V–I* curves in the third quadrant (hyperpolarization) are relevant. The nonlinearity of the *V–I* relationships seen in the first quadrant is due to changes in membrane resistance during axon depolarization. Under voltage-clamp conditions the *V–I* relationships are linear over a voltage range of ±100 mV[8,9]. In Fig. 1*g*, the septal resistance obtained from the slope of the *V–I* relationships is plotted against time. Arrows at 30 and 80 minutes indicate the beginning and end of heptanol perfusion, respectively.

Table 1 summarizes the results obtained with local and general anaesthetics with regard to their effect on p.a.ps (column

---

* To whom correspondence should be addressed.

0028–0836/80/310498—03$01 00

Table 1 Effect of anaesthetics at the crayfish septal synapse

Anaesthetic	Concentration (mM)	Effect on p.a.ps	Coupling at synapse	Reversibility
Local				
Procaine	5.0	blocked	normal	++++
Benzocaine	3.0	blocked	normal	++++
Propranolol	1.0	blocked	normal	++
General				
Ketamine	2.0	delayed	normal	++++
n-Hexan-1-ol	10.0	blocked	slightly decreased	++++
n-Heptan-1-ol	3.0	blocked	uncoupled	++++
n-Octan-1-ol	1.0	blocked	uncoupled	+++
n-Nonan-1-ol	0.3	blocked	slightly decreased	+++

Scale: ++++, completely reversible; +, irreversible.

3), ability to electrically uncouple the axons (column 4), and reversibility (column 5). Table 1 shows that ketamine, procaine, propranolol (all of which exist in both the charged and neutral form at *p*H 7.5), and benzocaine (which is uncharged at *p*H 7.5), produced no significant changes in septal resistance despite their profound effects on p.a.ps. For the homologous series of *n*-alcohols, from hexanol to nonanol (C6–C9), the bulk concentrations correspond to approximately equal membrane concentrations[1]. Alcohols from C6 to C9, all of which block action potentials at the concentrations used, affect septal resistance with a marked dependence on alcohol chain length. Specifically, heptanol and octanol dramatically increased septal resistance whereas hexanol and nonanol produced only minimal changes (Fig. 2). For example, octanol applied externally increased junctional resistance from 40 KΩ to 1.3 MΩ. All the anaesthetics reduced the resting membrane potential by 2–10 mV.

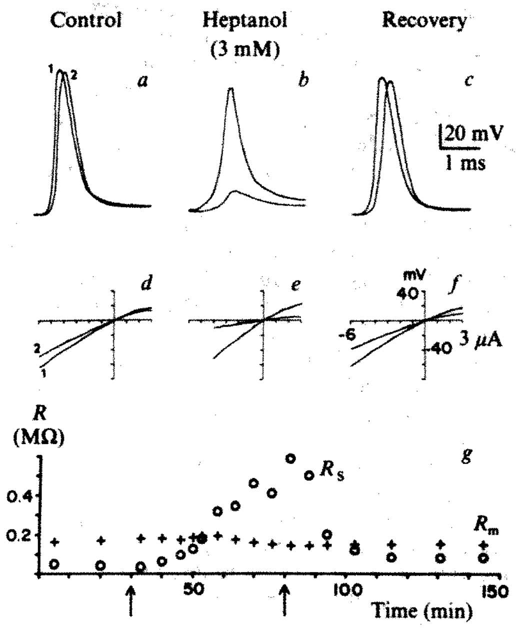

Fig. 1 Propagated action potentials (*a–c*) and voltage–current relationships (*d–f*) in the septal regions of an axon externally perfused with heptanol (3 mM). Data were obtained using three microelectrodes, one for current injection and the others for voltage measurements across the septum. Calibrations at *c* apply also to *a* and *b*, and those on *f* also to *d* and *e*. The small numbers beside the action potentials in *a* and the *V–I* relationships in *d* indicate (1) pre- and (2) postsynaptic recordings respectively. *g* shows septal (R_s, circles) and membrane (R_m, crosses) resistances calculated from the *V–I* relationships in the hyperpolarizing direction. Arrows at 30 and 80 min indicate the beginning and end of heptanol perfusion.

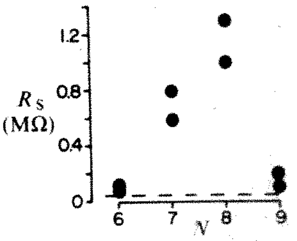

Fig. 2 Maximum septal resistance reached during external perfusion with hexanol (10 mM), heptanol (3 mM), octanol (1 mM) and nonanol (0.3 mM). Abscissa is alkyl chain length (*N*) of the alcohol. Results from two separate experiments are shown for each alcohol. The horizontal dashed line depicts the control value for septal resistance.

As octanol produced the greatest increase in R_s, additional experiments were performed to determine its 'site' of action. These experiments were performed using a technique previously developed to perfuse the interior of segmented axons[8,9]. When one of the axons was perfused with SIS and 1 mM octanol was added to the external solution, uncoupling was similar to that described above. When 10 mM octanol was perfused internally the action potential was blocked as expected[10]; however, the septal resistance remained unchanged.

The above results have implications for mechanisms of anaesthesia. In addition they provide information regarding modulation at electrical synapses: (1) from Table 1 it is clear that electrical synapses are less sensitive to representative anaesthetics than either chemical synapses or axonal membranes, virtually eliminating them from the scope of structures that might be involved in anaesthesia. (2) The lack of effect of certain anaesthetics on electrical synapses and the chain length effect exhibited by alcohols serve to exclude several possibilities regarding mechanisms responsible for uncoupling. Positively charged molecules propranolol, ketamine and procaine (at *p*H 7.5) and the neutral molecule benzocaine had no effect on septal resistance. Thus, generalized membrane changes due to surface charges[11,12], dipole potentials[13,14], thickness[14], tension[28] and membrane fluidity[15,16] produced by these molecules apparently do not affect the operation of electrical synapses. For many preparations the homologous series of alcohols behave in a manner consistent with their solubility in membranes. This is the case for axons[10,17], phospholipid bilayers[18–21], monolayers[22], red blood cells[1] and synapses in the abdominal ganglia of *Aplysia*[23]. Such is not the case for the electrical synapse we investigated. A different alcohol chain length behaviour was described by Gage *et al.*[25,26] on chemical synapses. These authors measured the time constants of decay of miniature end plate currents and found that the normal alcohols from C1 to C6 increased the time constant to decay, whereas octanol decreased it. Similarly, Richards *et al.*[18] showed that no simple correlation exists between an alcohol's ability to block nerve conduction and to perturb bilayer structure.

The striking differences in potency of these alcohols in uncoupling the crayfish synapse implies an interaction which is strongly dependent on the alkyl chain length. Furthermore, the persistence of coupling when octanol is applied internally suggests that this 'site' is accessible only from the external medium. This chain length effect does not exclude a possible role for the hydroxyl group (or other polar groups) in the uncoupling mechanism. It would be of general interest to know, in light of current models of electrical synapses[27], how heptanol and octanol act to uncouple these synapses.

We thank Professors P. B. Bennett, M. Harmel and J. W. Moore for their support. This project was supported by grants HL-22767 and HL-12157.

Received 14 April; accepted 28 May 1980.

1. Seeman, P. *Pharmac. Rev.* **24**, 583–655 (1972).
2. Richards, C. D. & White, A. F. *J. Physiol., Lond.* **252**, 241–257 (1975).
3. Richter, J., Landau, E. M. & Cohen, S. *Molec. Pharmac.* **13**, 548–559 (1977).
4. Katz, Y. & Simon, S. A. *Biochim. biophys. Acta* **471**, 1–15 (1977).
5. Loewenstein, W. R. *Biochim. biophys. Acta* **560**, 1–65 (1979).

6. Johnson, G. E. *J. comp. Neurol.* **36**, 323–373 (1924)
7. Watanabe, A. & Grundfest, H. *J. gen. Physiol.* **45**, 267–308 (1961).
8. Johnston, M. F. & Ramón, F. *J. Physiol., Lond.* (in the press).
9. Johnston, M. F. thesis, Duke Univ., Durham, North Carolina (1979)
10. Oxford, G. & Swenson, R. *Biophys. J.* **26**, 585–590 (1979)
11. Lee, A. G. *Molec. Pharmac.* **13**, 474–487 (1977).
12. Strichartz, G. *Anesthesiology* **45**, 421–441 (1969)
13. Simon, S. A. & Bennett, P. B. in *Molecular Mechanisms of Anaesthesia* Vol. II (ed. Fink, B. R.) (Raven, New York, in the press).
14. Reyes, J. & Latorre, R. *Biophys. J.* **28**, 185–196 (1979).
15. Trudell, J. R., Hubbell, W. L. & Cohen, E. N. *Biochim. biophys. Acta* **291**, 321–327 (1973)
16. Hille, B. *J. gen. Physiol.* **69**, 475–496 (1977).
17. Armstrong, C. M. & Binstock, L. *J. gen. Physiol.* **48**, 265–277 (1964)
18. Richards, C. D., *et al.* *Nature* **276**, 775–779 (1978)
19. Hill, M. W. *Biochim. biophys. Acta* **356**, 117–124 (1974)
20. Kondo, M. & Kasai, M. *Biochim. biophys. Acta* **311**, 391–395 (1973)
21. Jain, M. K., Wu, N. M. & Wray, L. V. *Nature* **255**, 494–496 (1975)
22. Nakagaki, M. & Ichonoseki, H. *Yakugaku Zasshi* **98**, 577–584 (1978)
23. Woodson, P. B. J., Traynor, M. E., Schlapfer, W. T. & Barondes, S. H. *Nature* **260**, 797–799 (1976).
24. Elliott, J. R. & Haydon, D. A. *Biochim. biophys. Acta* **557**, 259–263 (1979).
25. Gage, P. W., McBurney, R. N. & van Helden, D. *J. Physiol., Lond.* **274**, 279–298 (1978)
26. Gage, P. W., McBurney, R. N. & Schneider, G. T. *J. Physiol., Lond.* **244**, 409–429 (1975)
27. Unwin, P. N. T. & Zampighi, G. *Nature* **283**, 545–549 (1980).
28. Elliott, J. R. & Haydon, D. A. *Biochim. biophys. Acta* **557**, 259–263 (1979)

Diffusion of acetylcholine in the synaptic cleft of normal and myasthenia gravis human endplates

S. G. Cull-Candy, R. Miledi & O. D. Uchitel

Department of Biophysics, University College London,
Gower Street, London WC1E 6BT, UK

When acetylcholinesterase (AChE) is inactivated the time constant of decay of the miniature endplate current ($\tau_{m.e.p.c.}$) depends on the lifetime of the endplate channel and on the speed of clearance of acetylcholine (ACh) from the synaptic cleft[1–3]. The latter will be influenced by the binding of ACh to receptors, hence by their density and by the proportion of the ACh packet which attaches to them. By comparing $\tau_{m.e.p.c.}$ at various levels of receptor density, for example, following curare treatment, it is possible to estimate the proportion, *p*, of the ACh packet which normally attaches to the receptors[1]. We have estimated *p* at the normal human endplate and compared this with myasthenia gravis (MG) affected human endplates where, as a result of reduced receptor density, there is a reduction in miniature endplate potential (m.e.p.p.)[4] and m.e.p.c. amplitudes[5,6], α-bungarotoxin (α-Btx) binding[7,8] and ACh-sensitivity[9]. The properties of the ACh-induced channels are similar at normal and MG endplates[4,10] and it is unlikely that normal or MG channel properties are markedly altered by the various drug treatments used here[11,12]. Therefore, at treated normal and at MG endplates any reduction in the time constant of decay of m.e.p.cs indicates that the speed of clearance of the ACh from the cleft is increased. In the experiments reported here the proportion of the ACh packet which binds is estimated to be about 0.5 at normal human endplates. At MG endplates in the absence of cholinesterase activity m.e.p.cs decay more rapidly than normal and the proportion of the ACh packet attaching is reduced.

Human intercostal nerve muscle was obtained from myasthenia gravis and control patients. The preparation of muscle bundles and electrophysiological techniques for intracellular recording and voltage clamping were as previously described[5,6].

Application of neostigmine to human endplates increases the amplitude of the spontaneously occurring m.e.p.ps by inhibiting cholinesterase activity. The amplitude of m.e.p.ps and the time constant of decay of the miniature currents have been studied over a range of neostigmine concentrations to determine the optimum level required to inhibit cholinesterase. This was found to be 10^{-7} to 5×10^{-7} g ml^{-1} neostigmine; higher concentrations reduce the m.e.p.p. and m.e.p.c. amplitude. The amplitude and time course of m.e.p.cs were obtained at normal human endplates equilibrated in neostigmine (5×10^{-7} g ml^{-1}). Tubocurarine (TC) was then applied either iontophoretically or in the bathing medium (10^{-6} g ml^{-1}). At this concentration TC has no appreciable effect on endplate channel properties in frog muscle[11]. In addition, in some experiments α-Btx (5×10^{-7} g ml^{-1}) was used to block receptors partially, because even at doses higher than those used here it does not appreciably alter the characteristics of the remaining endplate channels[1]. M.e.p.cs were sampled during progressive block or during the recovery stage.

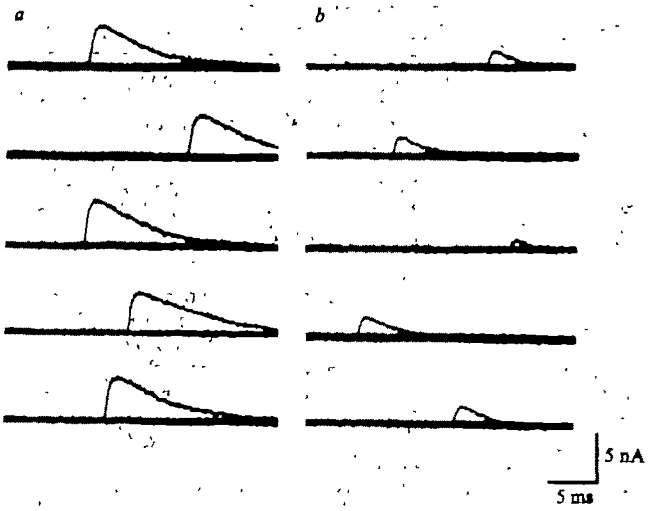

Fig. 1 M.e.p.cs recorded from a single normal human endplate in normal medium in the presence of neostigmine (5×10^{-7} g ml^{-1}) (*a*) and after application of tubocurarine and neostigmine (5×10^{-7} g ml^{-1}) (*b*). In the presence of TC the m.e.p.c. amplitude is reduced and the time constant of decay of the m.e.p.cs becomes briefer. M.e.p.cs are recorded under voltage clamp ($V_m = -80$ mV, $T = 22$°C) through a 500-Hz low pass filter which prolongs the rising phase and slightly attenuates the amplitude. The rising phase of m.e.p.cs is also prolonged by the presence of neostigmine. Tubocurarine is applied iontophoretically. Tetrodotoxin (5×10^{-7} g ml^{-1}) was present throughout.

Figure 1 shows examples of normal m.e.p.cs in neostigmine and m.e.p.cs at the same endplate following iontophoretic application of TC ($V_m = -80$ mV). The reduction in m.e.p.c. amplitude, to less than one-third the normal size in this example, is accompanied by a decrease in $\tau_{m.e.p.c.}$ as previously reported for partially blocked endplates in other species[1,13,14].

The ratio of control to curarized $\tau_{m.e.p.c.}$, which in anti-esterase-treated endplates reflects the relative rates of clearance of ACh from the synaptic cleft, was obtained either from a semilogarithmic plot of the m.e.p.c. decay phase or from power density spectra of m.e.p.cs. Figure 2 illustrates power spectra of m.e.p.cs obtained from a single voltage-clamped human endplate in normal medium (neostigmine 5×10^{-7} g ml^{-1}) and after bath application of TC. $\tau_{m.e.p.c.}$ is obtained from the half-power frequency, f_c, at which the spectral density is reduced to one-half of the zero-frequency asymptote, according to $\tau_{m.e.p.c.} = 1/(2\pi f_c)$. In the examples in Fig. 2 the frequency shift from 27 Hz in normal medium to 35 Hz in TC indicates a decrease in $\tau_{m.e.p.c.}$ from 5.89 ms to 4.54 ms on partial curarization.

It has been suggested[1] that if a fraction, *p*, of the ACh molecules in the cleft binds to receptors, diffusion will be slowed down by the factor $1/(1-p)$. Then from the ratio of the time constants of the control and curarized m.e.p.cs, τ/τ_{TC}, and the ratio of their amplitudes, α, it is possible to obtain an estimate of p: $\tau/\tau_{TC} = (1-\alpha p)/(1-p)$.

$$p = (\tau - \tau_{TC})/(\tau - \alpha\tau_{TC})$$

0028-0836/80/310500—03$01.00

Several kinetic assumptions involved in this relationship have previously been considered[1,14]. The fraction of the packet which attaches is reduced to αp by reducing the number of available receptors, for example, during curarization or at the human MG endplate, where the density of receptors is reduced by an anti-receptor antibody (reviewed in refs 15, 16). Thus, when p is known at untreated endplates it should vary as αp for different levels of receptor block. In the experiment in Fig. 2 the fraction, p, of the ACh packet attaching to receptors is 0.41. The range of values for p, obtained by treating with TC or α-Btx, was 0.4–0.6 at normal human endplates; the mean value for p was 0.56 ± 0.05 (±s.e., five endplates from three muscles).

We have found no significant difference between $\tau_{\text{m.e.p.c.}}$ at normal and MG endplates in normal bathing medium (that is, in the absence of esterase inhibitors) examined in four normal and four MG muscles (Table 1, see also ref. 10). On addition of neostigmine the decay time of both normal and MG m.e.p.cs increased markedly. For normal endplates $\tau_{\text{m.e.p.c.}}$ increased about three times whereas for MG endplates it was approximately doubled. Therefore, in the presence of neostigmine MG m.e.p.cs decay more rapidly than normal m.e.p.cs: $\tau_{\text{m.e.p.c.}}$ (normal) = 5.56 ms and $\tau_{\text{m.e.p.c.}}$ (MG) = 3.65 ms ($V_m = -80$ mV, $T = 22$°C). These values are significantly different, $P < 0.001$ (see Table 1). The simplest explanation for such a difference between normal and MG m.e.p.cs is that the rate of diffusion from the cleft is faster at MG endplates as a result of the reduced ACh-receptor density.

If we compare the mean value of $\tau_{\text{m.e.p.c.}}$ for myasthenia gravis and normal m.e.p.cs in neostigmine (Table 1), where the ratio of the mean m.e.p.c. amplitudes, $\alpha = 0.35$ (range of values for α at 20 endplates, 0.17–0.46), the fraction of the packet attaching at the normal endplate is estimated to be $p = 0.45$ (range of values at 20 endplates, 0.38–0.60). This is assuming that the reduced amplitude and rapid time course of MG m.e.p.cs results mainly from a decreased receptor density at MG endplates. Furthermore, the fraction of the packet, αp, expected to attach at MG endplates is about 0.16 (range of values, 0.08–0.20). We have recorded MG m.e.p.cs before and after treatment with TC or α-Btx. In these conditions m.e.p.cs become so small that accurate estimates of $\tau_{\text{m.e.p.c.}}$ are difficult to obtain. However, it was possible to obtain values at five MG endplates at a clamp potential of −120 mV. This increased the amplitude of the m.e.p.cs and because of the voltage sensitivity of the channel lifetime[10] caused a slight prolongation of $\tau_{\text{m.e.p.c.}}$. Although there has been no detailed study on the dependence of p on membrane potential, from the information available no marked change is expected. Table 1 shows typical values from a myasthenic endplate treated with α-Btx in which $p = 0.17$. The range of values of p obtained was 0.1–0.2; the mean value for p was 0.16 ± 0.03 (±s.e., five endplates in two muscles).

Table 1 Proportion of the ACh packet (p) attaching to receptors: *a*, for normal endplates by comparison of normal with myasthenic m.e.p.cs; *b*, for a normal endplate by curarizing normal m.e.p.cs; *c*, for a myasthenia gravis endplate by α-bungarotoxin treating MG m.e.p.cs

		$\tau_{\text{m.e.p.c.}}$ (ms)	$\tau_{\text{m.e.p.c.}}$ (ms) (neostigmine)	V_m (mV)	α*	p
a	Normal	1.77 ± 0.07 ($n = 15$)	5.56 ± 0.25 ($n = 16$)	−80	0.35	0.45
	Myasthenia gravis	1.80 ± 0.05 ($n = 18$)	3.65 ± 0.12 ($n = 20$)	−80		
		$\tau_{\text{m.e.p.c.}}$ (ms) (neostigmine)	$\tau_{\text{m.e.p.c.}}$ (ms) (neostigmine + TC or α-Btx)	V_m (mV)	α†	p
b	Normal	5.3	4.0 (TC)	−80	0.78	0.59
c	Myasthenia gravis	6.12	5.40 (α-Btx)	−120	0.36	0.17

Values in *a* are mean ±s.e., where n = no. of endplates examined. All measurements were made at 22°C.

* α = MG m.e.p.c. amplitude/normal m.e.p.c. amplitude.

† α = treated m.e.p.c. amplitude/untreated m.e.p.c. amplitude.

Therefore, the similarity in estimates of p (in the absence of esterase activity) obtained by curarizing normal endplates or by comparing normal with MG miniature currents, indicates that the curarized normal endplate resembles the MG endplate in certain respects. The fact that MG miniature currents decay faster than normal miniature currents may be explained by a loss of 'ACh binding sites' which results in a more rapid escape of ACh from the synaptic cleft. This renders unattractive the possibility that at MG endplates there is a decrease in the number of functional channels without a concomitant decrease in ACh binding sites. The reduced fraction of the ACh packet attaching at MG endplates falls within the range expected from the reduction in receptor density estimated from measurements of m.e.p.c. amplitudes. This suggests that the affinity of the receptors for ACh is similar at normal and MG endplates. It therefore seems that the presence of anti-receptor antibody on the postsynaptic membrane[17,18] or changes in the endplate geometry associated with myasthenia[9,19] do not have a predominant role in determining the time course of ACh diffusion out of the synaptic cleft.

We conclude that the fraction of the ACh packet attaching at anti-esterase-treated human endplates is similar to that previously reported for frog[1,20] and rat[12] endplates. In addition, the fraction of the ACh packet attaching at MG endplates seems to be about one-third of that at the normal human endplate, due to a reduction in available ACh receptors. This results in a faster than normal clearance of ACh at the MG endplate.

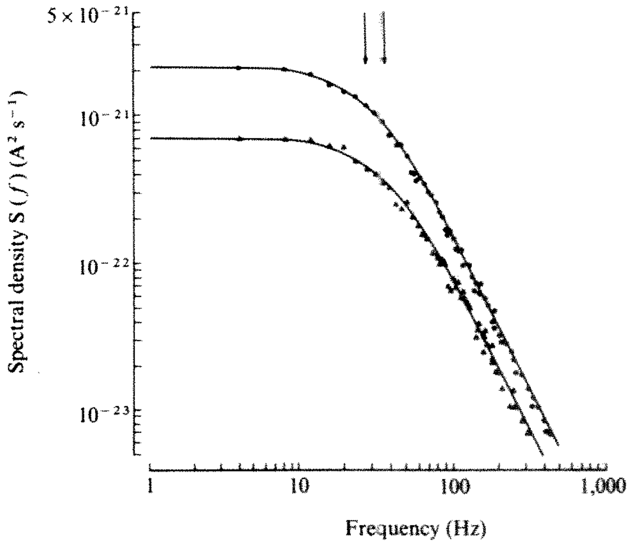

Fig. 2 Effect of tubocurarine on power density spectra of normal human m.e.p.cs from a single voltage-clamped endplate. ●, m.e.p.cs in normal medium, in the presence of neostigmine (2×10^{-7} g ml^{-1}) at a clamp potential $V_m = -80$ mV, $T = 22$°C. Averaged spectrum of 12 individual m.e.p.c. spectra. Cut-off frequency indicated by arrow is $f_c = 27$ Hz, hence $\tau_{\text{m.e.p.c.}} = 5.89$ ms. ▲, m.e.p.cs treated with tubocurarine (10^{-6} g ml^{-1} applied in the bathing medium) in the presence of neostigmine (2×10^{-7} g ml^{-1}), $V_m = -80$ mV, $T = 22$°C. Averaged spectrum of 13 m.e.p.c. spectra. Cut-off frequency indicated by arrow is $f_c = 35$ Hz, hence $\tau_{\text{m.e.p.c.}} = 4.54$ ms. The zero frequency asymptote is three times smaller for the spectrum of m.e.p.cs treated with TC indicating that the ratio: curarized m.e.p.c. amplitude/normal m.e.p.c. amplitude, $\alpha = 0.58$, where the ratio of the amplitudes, α, before and after TC is obtained from the ratio of the square roots of the respective spectral densities. Hence, from the relationship, $p = (\tau - \tau_{TC})/(\tau - \alpha\tau_{TC})$, $p = 0.41$ for this particular case.

We thank Professor B. Katz for helpful discussions, Mr J. R. Belcher and Dr J. Newsom Davis for help in obtaining biopsies, the patients for their collaboration and the MRC and the Muscular Dystrophy Association of the UK for support.

Received 27 March; accepted 2 June 1980.

1. Katz, B. & Miledi, R. *J. Physiol., Lond.* **231,** 549–574 (1973).
2. Kordaš, M. *J. Physiol., Lond.* **270,** 133–150 (1977).
3. Anderson, C. R. & Stevens, C. F. *J. Physiol., Lond.* **235,** 655–691 (1973).
4. Elmqvist, D., Hofmann, W. W., Kugleberg, J. & Quastel, D. M. J. *J. Physiol., Lond.* **174,** 417–434 (1964).
5. Cull-Candy, S. G., Miledi, R. & Trautmann, A. *Nature* **271,** 74–75 (1978).
6. Cull-Candy, S. G., Miledi, R. & Uchitel, O. D. *Nature* **277,** 236–238 (1979).
7. Fambrough, D. M., Drachman, D. B. & Satyamurti, S. *Science* **182,** 293–295 (1973).
8. Green, D. P. L., Miledi, R., Perez de la Mora, M. & Vincent, A. *Phil. Trans. R. Soc.* **B270,** 551–552 (1975).
9. Albuquerque, E. X., Rash, J. E., Mayer, R. F. & Satterfield, J. R. *Expl Neurol.* **51,** 536–563 (1976).
10. Cull-Candy, S. G., Miledi, R. & Trautmann, A. *J. Physiol., Lond.* **287,** 247–265 (1979).
11. Katz, B. & Miledi, R. *Proc. R. Soc.* **B203,** 119–133 (1978).
12. Colquhoun, D., Dreyer, F. & Sheridan, R. E. *J. Physiol., Lond.* **293,** 247–284 (1979).
13. Kordaš, M. *Int. J. Neuropharmac.* **7,** 523–530 (1968).
14. Colquhoun, D., Large, W. A. & Rang, H. P. *J. Physiol., Lond.* **266,** 361–395 (1977).
15. Grob, D. (ed.) *Ann. N.Y. Acad. Sci.* **274** (1976).
16. Vincent, A. *Physiol. Rev.* (in the press).
17. Engel, A. G., Lambert, E. H. & Howard, F. M. *Mayo Clin. Proc.* **52,** 267–280 (1977).
18. Lindstrom, J. M. & Lambert, E. M. *Neurology* **28,** 130–138 (1978).
19. Engel, A. G. & Santa, T. *Ann. N.Y. Acad. Sci.* **183,** 46–63 (1971).
20. Magleby, K. L. & Terrar, D. A. *J. Physiol., Lond.* **244,** 467–495 (1975).

Erythroid developmental agglutinin is a protein lectin mediating specific cell–cell adhesion between differentiating rabbit erythroblasts

F. Lynne Harrison & C. James Chesterton

Department of Biochemistry, King's College London, Strand,
London WC2R 2LS, UK

In many developmental systems β-galactoside-specific protein lectins have been identified as components which appear at the cell surface in concert with an initial requirement for cell–cell adhesion during tissue formation[1–8]. Although some of these lectins have been purified, there has been little direct evidence concerning their role in establishing specific cell–cell contact. A mammalian system where selective cell–cell adhesion is evident and which is amenable to study is that of erythroid differentiation in the adult bone marrow[9]. Here, the differentiation of erythroblasts takes place with the participants clustered together in the vicinity of a macrophage 'nurse' cell until the enucleation stage, when the immature reticulocyte is released and passes through the sinusoidal wall into the circulation. We show here that a small, β-galactoside-specific, protein lectin can be extracted from erythroblast-enriched marrow and purified to homogeneity. This factor, termed erythroid developmental agglutinin (EDA), exhibits properties which strongly suggest that it is responsible for inter-erythroblast recognition and adhesion *in vivo*.

EDA, purified from lactose washes of erythroblast-enriched rabbit bone marrow (see Fig. 1 legend), shows 95–100% Coomassie blue staining in a single component after electrophoresis on native, urea or SDS-containing polyacrylamide gels, where it exhibits a molecular weight of 13,000. No staining is observed with Schiff-periodic acid reagent, and GLC analysis for sugars in EDA hydrolysates detected less than 1 molar equivalent carbohydrate. Completely pure EDA can be obtained by repeating the affinity chromatography step once or twice more. The lectin electrofocuses as a single component at pH 5–6.

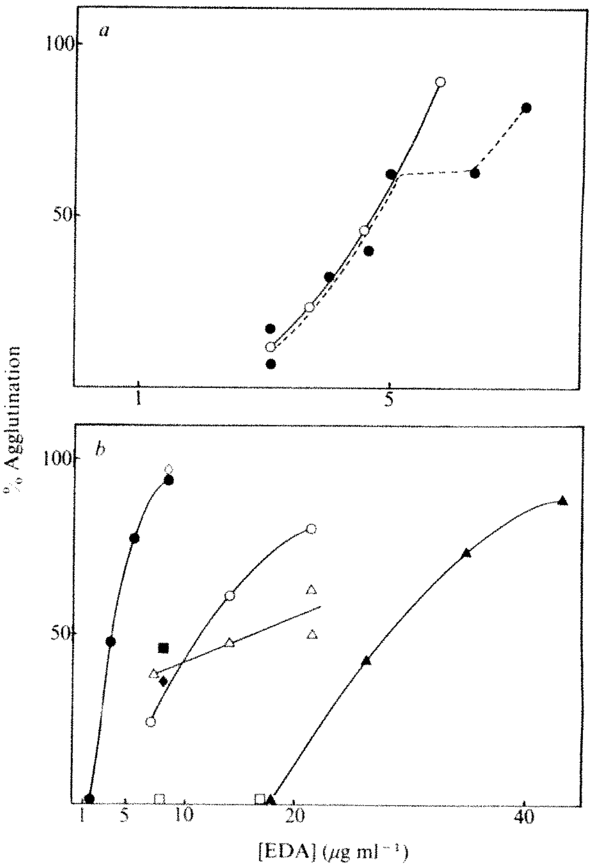

Fig. 1 *In vitro* agglutination studies. The ability of EDA to mediate intercellular cross-linking was tested using cells which were washed twice in MESL and resuspended in buffered medium. In addition, fractions enriched for erythroblasts, immature myeloid cells and marrow reticulocytes were prepared by sedimentation through a Percoll gradient (experimental details will be published elsewhere). The cellular composition of the fractions used was determined by cytocentrifugation and histological staining to be: 90% erythroblast, 5% myeloid, 5% reticulocyte; 69% myeloid, 26% reticulocyte, 5% erythroblast; and 87% reticulocyte, 4% erythroblast, 9% myeloid, respectively. Cell suspensions (0.25 ml, 10^7 cells per ml buffered medium) were mixed at room temperature by end-over-end rotation (4 r.p.m.) in small plastic vials at various EDA concentrations. Aliquots were taken throughout the incubation, diluted fivefold with 0.2% trypan blue in buffered medium (to check viability) and aggregation was assessed by counting the number of single cells present in a haemocytometer. The points plotted represent single cells lost after 10 min incubation with EDA. In the absence of EDA no agglutination was seen. *a*, Agglutination of a mixed cell population: ●, anaemic rabbit bone marrow; ○, erythroblasts for comparison. *b*, Agglutination of cell fractions: ●, erythroblasts; ○, myeloid cells; △, marrow reticulocytes; □, erythrocytes; ▲, Chinese hamster ovary cells. Erythroblasts in the presence of : ◇, 24 mM sucrose; ■, 0.66 mM lactose; ◆, 0.32 mM thiodigalactoside. EDA was purified from the bone marrow of 20 rabbits made anaemic by phenylhydrazine injection[11]. The tissue was gently disaggregated and the cells washed 3 × in a total of 30 ml MESL. After centrifugation at 27,000g for 15 min followed by 120,000g for 2 h, the washes were treated with 100% saturated $(NH_4)_2SO_4$ and centrifuged at 30,000g for 20 min. Pelleted protein was dissolved in MES (14 mM 2-mercaptoethanol, 2 mM EDTA, pH 8, 150 mM NaCl) and fractionated by gel filtration through Sephadex G-100. Fractions with haemagglutination activity[10] were concentrated by ultrafiltration, applied to a column of Sepharose 4B (4.4 × 28 cm) and eluted with MES. EDA was eluted after the main protein peak. Active fractions were concentrated by ultrafiltration.

The specific location of EDA *in vivo* was demonstrated by immunolabelling. The IgG fraction from anti-EDA antiserum raised in a sheep was absorbed out with that protein from an EDA preparation which did not bind to the affinity column and yielded a single precipitin line in a double-diffusion test against EDA or crude lactose extract. This was used to locate the agglutinin by standard indirect immunofluorescence techniques in whole marrow freshly obtained from healthy or anaemic rabbits. Fluorescence was detected only on the surface of erythroblasts and reticulocytes and this could be completely eliminated by preincubation of the cells and antibody with purified EDA (Fig. 2). Washing the marrow with 0.3 M lactose removes all the cell-surface agglutinin detectable in the same batch of unwashed marrow. Developing myeloid cells and the macrophage 'nurse' cell were not labelled unless in contact with an erythroblast (Fig. 2).

The agglutinin is capable of linking inert cells together by a mechanism blocked by β-galactosides. The assay used to monitor the lectin during preparation is a simple haemagglutination test with trypsinized rabbit erythrocytes[10]. EDA also gives a positive haemagglutination reaction when such cells are fixed in glutaraldehyde, a procedure which chemically cross-links and inactivates surface protein. This activity was inhibited by 0.6 mM lactose and 0.5 mM thiodigalactoside but was not affected by 230 mM sucrose, confirming previous observations on the behaviour of unfixed cells.

The *in vitro* specificity of EDA was first tested on lactose-washed cells from anaemic marrow, a mixed cell population. With increasing concentrations of the lectin, two phases of aggregation were seen. Approximately 60% of the cells agglutinated at 5 μg ml^{-1} EDA, and the remainder required a higher concentration (Fig. 1*a*). Phase contrast microscopy showed that the initial aggregates contained almost exclusively erythroblasts which stained preparations revealed constituted 67% of the marrow. The erythroid specificity suggested by these results and previously shown by immunofluorescent labelling was confirmed by the behaviour of different cell fractions in this assay. Lactose-washed erythroblasts from either healthy or anaemic rabbits were agglutinated by 2–8 μg ml^{-1} EDA, whereas immature myeloid cells required three or four times more lectin to achieve 50% aggregation, and a Chinese hamster ovary cell line needed a level over fivefold higher (Fig. 1*b*). Erythroblast agglutination was inhibited by low concentrations of β-galactosides (Fig. 1*b*). The intra-marrow concentration of EDA is not known, but an estimate can be made from the yield of agglutinin protein after purification. This is approximately 0.2 mg per rabbit or 40 μg ml^{-1} marrow from anaemic animals and 0.05 mg or 10 μg ml^{-1} from healthy rabbits; thus, the affinity of

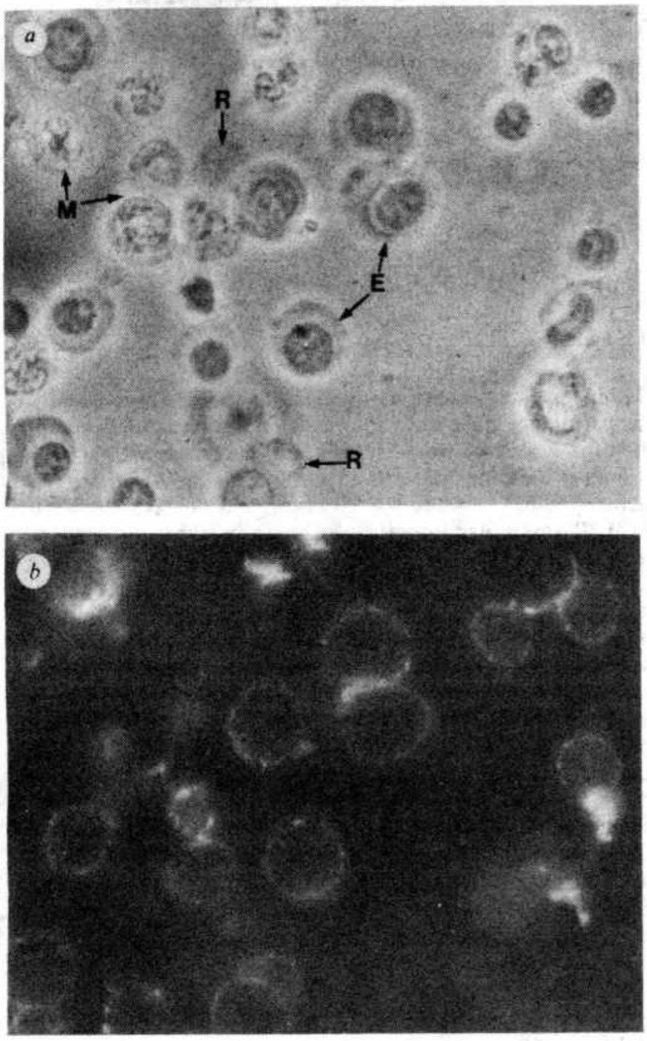

Fig. 2 Detection of EDA in fresh bone marrow by indirect immunofluorescent labelling. The marrow was gently disaggregated in Gibco 109 medium buffered with 25 mM HEPES and the suspension of cells allowed to settle on to microscope slides precoated with polylysine or concanavalin A. The immobilized cells were incubated with preimmune or anti-EDA IgG (3.4 mg ml^{-1}) followed, after washing, by fluorescein-conjugated rabbit anti-sheep IgG. After washing again, the cells were mounted in 80% glycerol in phosphate-buffered saline and viewed with a Vickers M17 microscope using visible light under phase contrast (*a*) or incident fluorescent illumination (*b*). Fluorescent labelling was detected strongly on the surface of erythroblasts (E) and weakly on marrow reticulocytes (R). No labelling was detected on the surface of myeloid cells (M). Furthermore, no labelling was seen in the following conditions: when IgG from a preimmune serum was substituted for anti-EDA IgG; if the cells and IgG were preincubated with 0.5 and 1.7 μg ml^{-1} EDA, respectively; or when the cells were prewashed with MESL (28 mM 2-mercaptoethanol, 2 mM EDTA, *p*H 8, 150 mM NaCl and 0.3 M lactose). ×1,155.

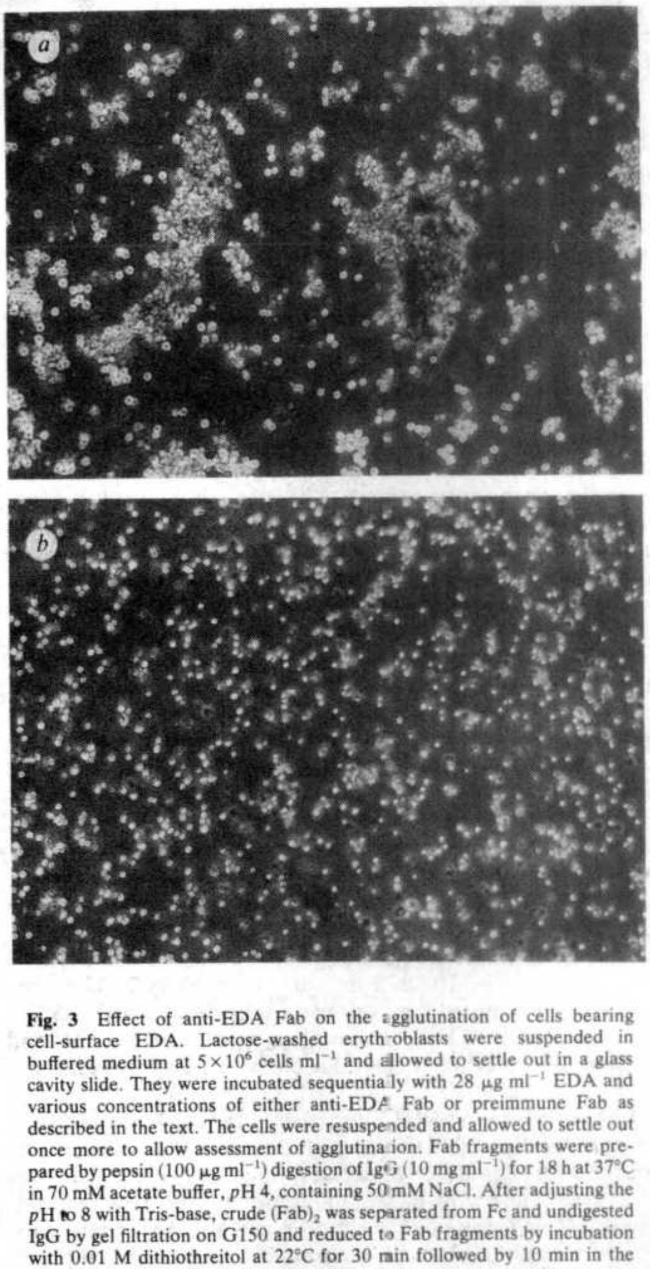

Fig. 3 Effect of anti-EDA Fab on the agglutination of cells bearing cell-surface EDA. Lactose-washed erythroblasts were suspended in buffered medium at 5×10^6 cells ml^{-1} and allowed to settle out in a glass cavity slide. They were incubated sequentially with 28 μg ml^{-1} EDA and various concentrations of either anti-EDA Fab or preimmune Fab as described in the text. The cells were resuspended and allowed to settle out once more to allow assessment of agglutination. Fab fragments were prepared by pepsin (100 μg ml^{-1}) digestion of IgG (10 mg ml^{-1}) for 18 h at 37°C in 70 mM acetate buffer, *p*H 4, containing 50 mM NaCl. After adjusting the *p*H to 8 with Tris-base, crude $(\mathrm{Fab})_2$ was separated from Fc and undigested IgG by gel filtration on G150 and reduced to Fab fragments by incubation with 0.01 M dithiothreitol at 22°C for 30 min followed by 10 min in the presence of 0.022 M iodoacetamide. The product was separated by repeating the gel filtration step and its purity was checked by SDS-polyacrylamide gel electrophoresis. (The method was communicated to us by M. Virji.) The photographs show erythroblasts after incubation with preimmune Fab (*a*) or anti-EDA Fab (*b*), both at 5 mg ml^{-1}. ×115.

EDA for the erythroblast surface which can be demonstrated *in vitro* seems to be adequate to account for the clustering seen *in vivo*.

The presence of EDA is coincident with the requirement for adhesion *in vivo*. Erythroblasts at all stages of differentiation discernible in the marrow were strongly labelled by anti-EDA IgG but marrow reticulocytes showed a weaker surface fluorescence (Fig. 2). Only faint fluorescence was observed on early circulating reticulocytes and none could be detected on late cells or erythrocytes. Erythroblasts, separated into fractions enriched for the various developmental classes by unit gravity sedimentation[11], all showed a similar degree of agglutination by EDA *in vitro*. However, aggregation of bone marrow reticulocytes required higher levels of agglutinin and erythrocytes were not visibly affected apart from a transient clustering at high EDA concentrations (Fig. 1*b*).

The immunofluorescence studies described above demonstrate that anti-EDA antibody binding does not displace EDA from the erythroblast surface. Therefore, it is possible that if EDA mediated cell aggregation by triggering a secondary mechanism at the cell surface, cell–cell adhesion would not be affected by the binding of an antibody molecule. On the other hand, if an EDA bridging mechanism induces agglutination, the presence of bound anti-EDA IgG, rendered monovalent by conversion to Fab fragments, would almost certainly stearically hinder the process. The experiment was carried out using lactose-washed erythroblasts which had been allowed to settle out into a monolayer on the surface of a cavity slide. The cells adhere to the glass strongly enough for the surrounding medium to be changed without significant disturbance. *In situ*, the erythroblasts were loaded with agglutinin and subsequently incubated with either control preimmune Fab or anti-EDA Fab. After subsequent resuspension, the cells were allowed to settle once more to enable assessment of their state of aggregation (Fig. 3). In the presence of up to 14 mg ml^{-1} control Fab protein, normal EDA-induced agglutination was observed whereas anti-EDA Fab at 14, 10 or 5 mg ml^{-1} completely blocked cell clustering; 2.5 mg ml^{-1} produced an inhibition of about 50%. A second batch of both preparations gave similar results and we find the experiment reproducible with cells from different animals.

Using the experimental advantages of the erythroid system, it has thus been possible to demonstrate that many of the criteria required for identifying molecules which link cells together *in vivo* are fulfilled by EDA. In particular, the fact that this agglutinin will cross-link inert cells and that its action when bound to erythroblasts is blocked by monovalent antibody strongly suggests that a bridging mechanism is involved. EDA is a typical small, acidic, β-galactoside-specific, protein lectin. It may be, therefore, that all such animal lectins act as cell–cell bridging molecules.

Perhaps the temporal role of the β-galactoside-specific lectins in development is now clearer. The inter-erythroblast adhesion mediated by EDA occurs at an early stage of tissue formation and is reversible, the erythroblastic island being a transient structure. Examination of the relationship of other such factors extracted from embryonic tissue to the developmental pattern of the embryo reveals that in all cases activity is only observed at an early stage[12-15]. It is possible that these have a similar role to that of the erythroid lectin. However, in most non-haemopoietic tissue, such links would be overridden by more powerful binding mechanisms. In the marrow, the cohesion is reversed and the maturing cell is lost irretrievably from its tissue of origin.

We thank Tessa Beswick for technical assistance, Susan Godsave, David Wraith and Nicholas Parsons for help with the agglutination experiments and EDA preparation, Dr Elizabeth Hounsell for GLC analysis, Neill Spencer and Karen Wells for analysis of EDA by electrofocusing, Dr N. Totty for Chinese hamster ovary cells, and all in the laboratory for aid in preparing the manuscript. L.H. is a Cancer Research Campaign-supported research fellow and the work was additionally funded from the SRC and MRC.

Received 14 March; accepted 3 June 1980.

1. Frazier, W. & Glaser, L. *A. Rev. Biochem.* **48,** 491–523 (1979).
2. Simpson, D. L., Rosen, S. D. & Barondes, S. H. *Biochemistry* **13,** 3487–3493 (1974).
3. Rosen, S. D., Kaur, J., Clark, D. L., Pardos, B. T. & Frazier, W. A. *J. biol. Chem.* **254,** 9408–9415 (1979).
4. Vacquier, V. D. & Moy, G. W. *Proc. natn. Acad. Sci. U.S.A.* **74,** 2456–2460 (1977).
5. Kobiler, D., Beyer, E. C. & Barondes, S. H. *Devl Biol.* **64,** 265–272 (1978).
6. Briles, E. B., Gregory, W., Fletcher, P. & Kornfeld, S. *J. Cell Biol.* **81,** 528–537 (1979).
7. Podleski, T. R., Greenberg, I. & Nichols, S. C. *Expl Cell Res.* **122,** 305–316 (1979).
8. Kobiler, D. & Barondes, S. H. *Devl Biol.* **60,** 326–330 (1977).
9. Weiss, L. in *Regulation of Haematopoiesis* Vol. 1 (ed. Gordon, A. S) 79–92 (Appleton-Century-Croft, New York, 1970).
10. Harrison, F. L. & Chesterton, C. J. *Biochem. Soc. Trans.* **6,** 662–664 (1978).
11. Clissold, P. M., Arnstein, H. R. V. & Chesterton, C. J. *Cell* **11,** 353–361 (1977).
12. Den, H., Malinzak, D. A. & Rosenberg, A. *Biochem. biophys. Res. Commun.* **69,** 621–627 (1976).
13. Mir-Lechaire, F. J. & Barondes, S. H. *Nature* **272,** 256–258 (1978).
14. Kobiler, D. & Barondes, S. H. *Devl Biol.* **60,** 326–330 (1977).
15. Simpson, D. L., Thorne, D. R. & Loh, H. H. *Nature* **266,** 367–369 (1977).

Abelson murine leukaemia virus transformation involves loss of epidermal growth factor-binding sites

Jonas Blomberg*, Fred H. Reynolds Jr†, Wim J. M. Van de Ven† & John R. Stephenson*

* Laboratory of Cellular and Molecular Biology, National Cancer Institute, Frederick, Maryland 21701
† Carcinogenesis Intramural Program, Frederick Cancer Research Center, Frederick, Maryland 21701

Malignant transformation by mammalian RNA sarcoma viruses has previously been shown to involve a reduction in receptor sites for a well characterized 6,000-molecular weight (MW) growth-promoting substance, designated epidermal growth factor (EGF)[1-3]. Although Abelson murine leukaemia virus (AbLV) resembles sarcoma viruses in its ability to transform embryo fibroblasts in cell culture[4], AbLV induces a rapid B-cell lymphoid leukaemia rather than fibrosarcomas *in vivo*[5,6]. The major translational product of AbLV is a highly phosphorylated polyprotein[7,8] of MW 120,000 which exhibits an associated tyrosine-specific protein kinase activity[9,10] and probable transforming function[11-14]. We show here that AbLV transformation resembles transformation by RNA sarcoma viruses with respect to the abolition of EGF-binding sites. EGF binding is restored to control levels following loss of polyprotein expression in morphological revertants of AbLV-transformed clones and remains uninfluenced in cell lines infected with transformation-defective (td) AbLV mutants encoding polyproteins deficient in protein kinase activity. These findings indicate that AbLV transformation involves a polyprotein-associated, tyrosine-specific protein kinase activity which mediates its effect through a mechanism resulting directly or indirectly in the abolition of EGF-binding sites.

The wild-type (wt) and td mutant AbLV FRE Fisher rat and CCL64 mink cell clones analysed in the present study are described in Table 1. In contrast to the wt AbLV-transformed clones, each of the td AbLV mutant clones is highly contact inhibted (data not shown) and lacks the capacity for colony formation in soft agar. Moreover, none of five td AbLV mutant clones were found to be tumorigenic on inoculation into a syngeneic Fisher rat host. Each of the td AbLV non-productively-infected clones express a 120,000-MW polyprotein, P120, at levels comparable with wt AbLV-transformed clones, but in contrast to the latter clones, the polyprotein expressed lacks detectable protein kinase activity. Two morphological revertants of one wt AbLV-transformed mink clone, 64Ab2-2, lack detectable AbLV P120 expression, protein kinase and ability to grow in soft agar. This defect in expression of transformation is cellular rather than viral in nature as demonstrated

0028-0836/80/310504—04$01.00

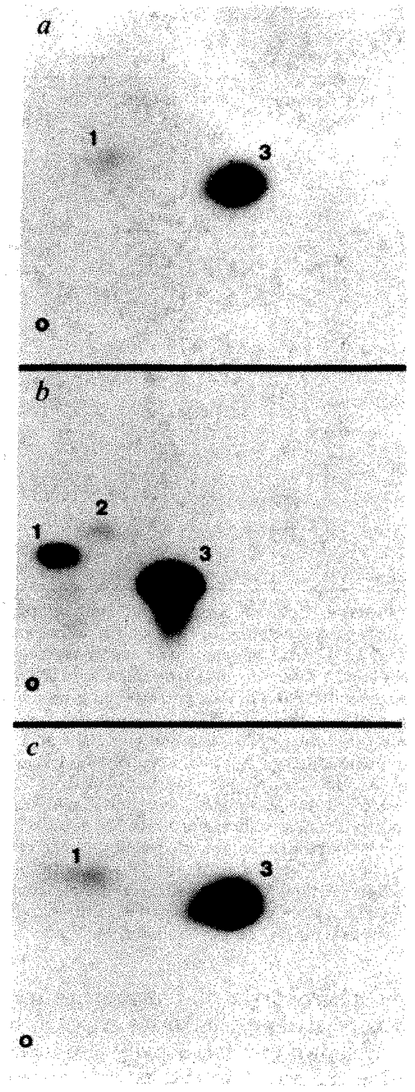

Fig. 1 Identification of amino acid acceptor residues phosphorylated *in vitro* by phosphotransferase activity. *In vitro* ^{32}P-labelled extracts of control FRE cells (*a*) or FRE cells infected with either wt AbLV (Cl 4-4) (*b*) or td AbLV (2-112-F2) (*c*) were hydrolysed in 6 M HCl at 100 °C for 1 h. Two-dimensional separation was carried out by electrophoresis at 500 V for 3 h in acetic acid/formic acid/water (15:5:80; *p*H 1.9) (horizontal dimension) and chromatography in 0.5 M ammonium hydroxide/isobutyric acid (3:5) (vertical dimension). *In vitro* phosphorylated amino acid residues were identified by comparing their position relative to phosphoamino acid standards stained with ninhydrin[19]. These included phosphothreonine, phosphotyrosine and phosphoserine and co-chromatographed with spots 1, 2 and 3, respectively.

by the presence of AbLV genomic sequences measured by molecular hybridization (data not shown) and the rescuability of wt AbLV by appropriate type C helper viruses[15,16].

The above findings do not indicate whether the lack of [γ-^{32}P]ATP-mediated *in vitro* phosphorylation of AbLV P120 is a defect in the AbLV P120-associated protein kinase activity, or whether it reflects an inability of P120 expressed in td AbLV-infected cells to act as substrate. To resolve these possibilities, we examined the levels of phosphotyrosine in representative wt and td AbLV-infected cell clones. As shown in Fig. 1, phosphotyrosine was not observed to a significant extent in control FRE rat cells but was readily detectable in a representative wt AbLV-transformed cell line. In contrast, appreciable levels of phosphotyrosine were not observed in td AbLV-infected cell lines. These findings suggest that the lack of phosphorylation of AbLV P120 in td mutant-infected clones does not simply reflect a lack of substrate activity.

In view of the previously reported loss of EGF-binding sites following transformation by avian and mammalian RNA sarcoma viruses[1-3], we examined the possibility that AbLV transformation might also result in abolition of EGF-binding sites. For this purpose, each of the above-described wt and td AbLV-transformed cell clones was analysed for the ability to bind ^{125}I-labelled EGF. As summarized in Table 1, EGF-binding by AbLV non-productively-transformed rat and mink cells was ~20-fold lower than that by uninfected control cell lines. Scatchard plot analysis shows this difference to be primarily due to a decrease in receptor site number rather than an altered binding affinity (Fig. 2). Although the absolute number of cellular binding sites on CCL64 mink cells was about sevenfold greater than exhibited by the FRE rat cell line, the binding affinities were similar. Mink or rat cells non-productively

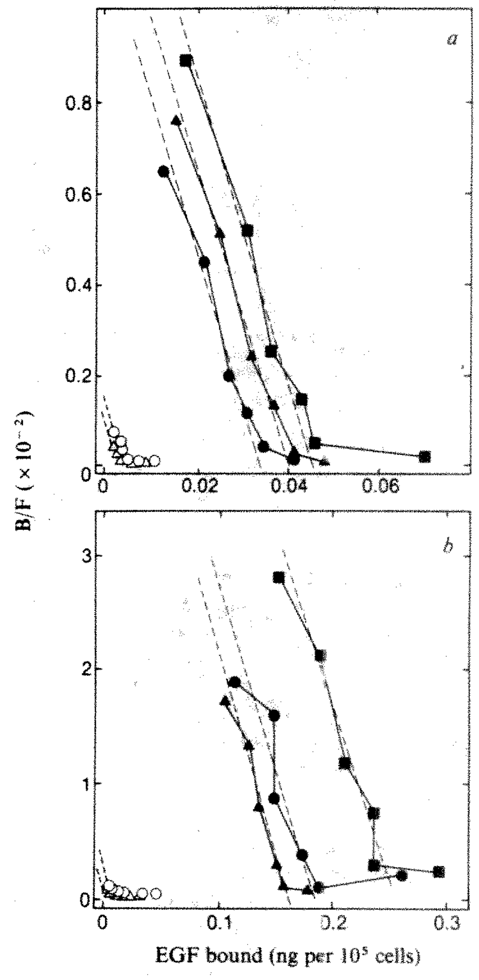

Fig. 2 Analysis of EGF-binding characteristics according to the method of Scatchard[25]. Mouse EGF (Collaborative Research) was labelled with ^{125}I at high specific activity (10–40 μCi per μg) according to previously published methods[17,18]. Cell lines were cultured at around 10^5 cells per well in 24-well cluster plates (Costar). After 48 h, individual wells were washed once with complete DMEM, incubated for 3 h at 37 °C in serum-free DMEM, and for an additional 4 h at 4 °C in 0.2 ml of HEPES buffered (*p*H 7.4) DMEM containing 0.1% ovalbumin and concentrations of ^{125}I-labelled EGF ranging from 5,000 to 500,000 c.p.m. Cells were then washed three times in serum-free medium, dissolved in 1% SDS (1 ml) and their radioactivity measured in a γ-scintillation counter. For cell number determinations, duplicate wells were stained with Sedi-stain (Becton-Dickinson). Results are based on triplicate determinations and are expressed as ng EGF bound per 10^5 cells and as the ratio of bound to unbound EGF (B/F). Cell lines tested are described in detail in Table 1 legend and include *a*, FRE (●), Cl 4-4 (○), 2-112-F2 (▲), 2-109-F5 (■), 2-112-RT2 (△), and *b*, CCL64 (●), 20-1-F6 (○), 64Ab2 (△), 9-104-7 (▲), 64 Ab2-2 (■).

Table 1 Correlation between AbLV P120 associated protein kinase activity, EGF binding and malignant transformation

Cell clone		Growth in soft agar (%)	AbLV P120 (μg per mg cell protein)	Protein kinase pmol ^{32}P incorporated	Phosphotyrosine (% of total cellular phosphoamino acids)	EGF receptor sites	
						No. per cell ($\times 10^{-4}$)	Affinity ($\text{l mol}^{-1} \times 10^{-8}$)
Rat							
Control:	FRE	<0.01	<0.02	<0.01	<0.3	2±0.5	3±1
wt AbLV transformed:	C14-4	16	0.9	0.7	2.8	0.1±0.1	3±2
	2-9-T2	14	1.1	0.5	3.1	0.1±0.1	2±2
td AbLV infected:	34-F2	<0.01	0.8	<0.1	<0.3	8±2	3±1
	2-109-F5	<0.01	1.3	0.03	NT	2±1	3±1
	2-612-F3	<0.01	1.1	<0.01	NT	6±2	3±1
	2-622-F5	<0.01	0.7	<0.01	<0.3	1±1	4±1
	2-112-F2	<0.01	0.8	0.02	NT	4±1	3±1
Retransformed td AbLV mutant:	2-112-RT2	20	1.1	0.5	1.5	0.1±0.1	3±1
Mink							
Control:	CCL64	<0.01	<0.02	<0.01	<0.3	15±3	3±1
wt AbLV transformed:	64Ab2	17	1.2	0.3	2.6	0.1±0.1	2±2
	20-1-F6	19	1.8	0.8	2.1	0.2±0.1	2±2
td AbLV infected:	9-104-7	<0.01	0.7	0.02	NT	12±2	4±1
	9-124-2	<0.01	1.3	<0.01	<0.3	8±2	3±1
	9-70-1	<0.01	0.6	<0.01	NT	22±3	3±1
Revertant:	64-Ab2-2	<0.01	<0.02	<0.01	<0.3	27±4	2±1
	64Ab2-56	<0.01	<0.02	0.01	NT	13±2	2±1

Cells were propagated in Dulbecco's modification of Eagle's medium (DMEM) supplemented with 10% calf serum (Colorado Serum Co.). Details of the isolation and preliminary characterization of each of these cell lines have been previously reported[16,17]. Plating efficiency in soft agar was determined as previously described[16,17]. Results represent mean values from three separate determinations. Levels of AbLV P120 expression were estimated on the basis of competitive immunoassays for their p12 structural components[16,17]. *In vitro* phosphotransferase assays were carried out as described previously[9]. Cells (1×10^7) were disrupted in 5 ml of 10 mM Tris-HCl buffer (*p*H 7.2) containing 100 mM NaCl, 5 mM $MgCl_2$, 0.1% Triton X-100, by repeated aspiration through a 19-gauge needle. Extracts were preabsorbed overnight with normal goat serum (50 μl) and 0.5 ml of a 10% v/v suspension of protein-A–Sepharose (Pharmacia), and clarified by centrifugation of 40,000*g* for 90 min. Immunoprecipitation was by addition of 5 μl goat anti-Moloney-MuLV and 50 μl protein-A–Sepharose (10% v/v suspension) to 1 ml extract, agitation overnight and collection of immunocomplexes by centrifugation at 2,000*g*. Protein kinase reactions were carried out by resuspension of immunoprecipitates or aliquots of total lysates in Tris-HCl buffer (*p*H 7.2) containing 5 mM $MgCl_2$, 1 μCi [γ-^{32}P]ATP 100 Ci mmol^{-1} (NEN) and incubation for 10 min at 30 °C. Samples were washed in ice-cold 10 mM sodium phosphate buffer (*p*H 7.2), 0.9% NaCl, 1% Triton X-100, 0.5% sodium deoxycholate and 0.1% SDS, collected by centrifugation at 2,000*g* for 10 min, transferred and collected on glass fibre filters (GF/C, Whatman) with 10% trichloroacetic acid containing 1 mM AMP. Incorporated radioactivity was quantified by liquid scintillation and results expressed as pmol ^{32}P incorporated into trichloroacetic acid-insoluble precipitates and corrected for nonspecific radioactivity at zero reaction time. Determination of phosphotyrosine as a percentage of total cellular phosphoamino acids was determined by scraping individual ^{32}P labelled phosphoamino acids from TLC plates; radioactivity was quantified by liquid scintillation. Results are expressed as the ratio of ^{32}P-labelled phosphotyrosine to total ^{32}P label in all three phosphoamino acids. NT, Not tested. The number of EGF-binding sites per cell and binding affinities are estimated on the basis of Scatchard binding plots prepared according to the method of Scatchard[25] and illustrated in Fig. 2. Results represent average values of two to four separate determinations±s.e.m. As recently discussed by Norby *et al.*[26], values obtained by this means may represent slight overestimations of the actual binding site numbers.

infected with each of eight td AbLV mutants examined, exhibited similar numbers of EGF-binding sites and binding affinities to the uninfected control cell lines from which they were derived. Moreover, as shown in Table 1, restoration of AbLV P120-associated protein kinase activity following retransformation of a representative td AbLV mutant clone by wt AbLV was associated with a reduction in the number of EGF receptors. Thus, the defect in transforming potential by td AbLV mutants is associated with simultaneous loss of protein kinase activity and an impairment in the process resulting in EGF-receptor site abolition.

As described above, morphological reversion of AbLV transformation is associated with loss of detectable levels of AbLV P120 expression. Thus, if AbLV P120-associated protein kinase activity is necessary for the abolition of EGF-receptor binding sites in AbLV-transformed cells, we would predict that such sites would reappear and that cellular phosphotyrosine levels would be reduced to those characteristic of nontransformed cells in revertant clones. To test this possibility, several morphological revertants of AbLV-transformed mink clones were analysed with respect to EGF-binding properties and levels of cellular phosphotyrosine. These clones are of particular interest because the transformation defect seems to be cellular in nature and to occur at high frequency[15,16]. As shown in Table 1, in both of the revertant cell clones examined, phosphotyrosine levels were reduced to control levels. Moreover, in both cell lines, EGF binding was restored to levels comparable to that exhibited by uninfected control cells.

To test the generality of restoration of EGF binding after morphological reversion of transformation, levels of EGF binding by uninfected control, Gardner feline sarcoma virus (FeSV)-transformed cells and morphological revertants of FeSV-transformed mink cells were examined. The Gardner FeSV transformation system was chosen because of its resemblance to AbLV in that FeSV has also been shown to encode a high molecular weight phosphorylated polyprotein translational product[17,18] with associated protein kinase activity[9]. In fact, we have more recently shown that this activity also has specificity for phosphotyrosine acceptor sites and have demonstrated elevated levels of phosphotyrosine in mink and rat cells following FeSV transformation[19]. As shown in Table 2, EGF binding was over 10-fold lower in FeSV-transformed than uninfected control mink cells. Following reversion of one such clone to a nontransformed phenotype, EGF binding was restored to control levels. Thus, an undefined mechanism resulting in simultaneous loss of expression of viral polyprotein expression and phenotypic transformation also leads to restoration of EGF-binding capacity.

The present findings establish an association between AbLV-induced transformation and reduction of EGF-binding sites and suggest that both depend on the presence of tyrosine-specific protein kinase, either intrinsic to, or associated with, AbLV P120. The fact that EGF binding by td AbLV mutant-infected

Table 2 EGF binding by uninfected control, FeSV-transformed and morphological revertant cell clones

Cell clone		EGF receptor sites	
		No. per cell ($\times 10^{-4}$)	Affinity $\text{l mol}^{-1} \times 10^{-8}$
Rat			
Control:	FRE	2±0.5	3±1
FeSV transformed:	FeSV-NPC14	0.1±0.1	2±1
Mink			
Control:	CCL64	15±3	3±1
FeSV transformed:	64-FeSV-14	0.3±1	2±1
Revertant:	64-FeSV-14-1	12±4	3±1

The isolation and preliminary characterization of these cell lines have been previously reported[14,16]. EGF receptor site numbers and binding affinities were determined as described in Table 1 legend.

cell lines is equal to that exhibited by uninfected control cells, despite levels of AbLV P120 expression comparable to those in wt AbLV transformants, suggests that if AbLV does directly interact with EGF-binding sites, its expression in the absence of protein kinase activity is not sufficient for transformation. For instance, phosphorylation of one or more tyrosine acceptor sites within the EGF receptor, AbLV P120 itself, or in some undefined cellular regulatory protein may be involved in the process. Alternatively, reduction of EGF binding associated with AbLV P120 protein kinase activity may be due to activation of one or more cellular growth-promoting factor(s) analogous to sarcoma growth factor (SGF) described by Todaro and colleagues[20].

Our results do not resolve the problem of whether the reduced EGF-binding activity associated with AbLV transformation is directly attributable to AbLV P120 protein kinase activity or whether loss of EGF binding represents a secondary phenomenon resulting from expression of the transformed phenotype. The previous demonstration, however, that EGF binding is reduced only partially in avian sarcoma virus-transformed cells and remains essentially unaltered in cells morphologically transformed by DNA viruses such as SV40 and polyoma, argues against the latter possibility. This difference in effect on EGF receptors by RNA and DNA tumour viruses of mammalian origin is somewhat surprising in view of results indicating that transformation by SV40 and polyoma may also involve protein kinase activities[21–24].

Activation of growth factor regulatory systems may represent one of several mechanisms for spontaneous and chemically and virally induced malignant transformation. In particular, the transforming function associated with acquired cellular sequences represented within recombinant genomes of certain RNA tumour viruses, such as AbLV, may be mediated by this pathway. A major advantage of the AbLV system for studies of the role of the growth-promoting factors in transformation relates to the fact that an AbLV-encoded protein with tyrosine-specific protein kinase activity and probable transforming function has been identified. In addition, many td AbLV mutants and morphological revertants have been isolated and characterized in some detail. AbLV transformation thus provides an excellent model system for further elucidation of the molecular events involved in malignant transformation.

We thank K. A. Seese and G. T. Blennerhassett for technical assistance. This work was supported by NCI contract NOI-CO-75380.

Received 14 February; accepted 5 June 1980.

1. Todaro, G. J., DeLarco, J. E. & Cohen, S. *Nature* **264,** 26–30 (1976).
2. Todaro, G. J. & DeLarco, J. E. *Cancer Res.* **38,** 4147–4154 (1978).
3. Carpenter, G. & Cohen, S. *A. Rev. Biochem.* **48,** 193–216 (1979).
4. Scher, C. D. & Siegler, R. *Nature* **253,** 729–731 (1975).
5. Abelson, H. T. & Rabstein, L. S. *Cancer Res.* **30,** 2213–2222 (1970).
6. Rosenberg, N. & Baltimore, D. *J. exp. Med.* **143,** 1453–1463 (1976).
7. Witte, O. N., Rosenberg, N., Paskind, M., Shields, A. & Baltimore, D. *Proc. natn. Acad. Sci. U.S.A.* **75,** 2488–2492 (1978).
8. Reynolds, F. H. Jr, Sacks, T. L., Deobagkar, D. N. & Stephenson, J. R. *Proc. natn. Acad. Sci. U.S.A.* **75,** 3974–3978 (1978).
9. Van de Ven, W. J. M., Reynolds, F. H. Jr & Stephenson, J. R. *Virology* **101,** 185–197 (1980).
10. Witte, O. N., Dasgupta, A. & Baltimore, D. *Nature* **283,** 826–831 (1980).
11. Stephenson, J. R., Kahn, A. S., Van de Ven, W. J. M. & Reynolds, F. H. Jr *J. natn. Cancer Inst.* **63,** 1111–1119 (1979).
12. Shields, A., Goff, S., Paskind, M., Otto, G. & Baltimore, D. *Cell* **18,** 955–962 (1979).
13. Van de Ven, W. J. M., Reynolds, F. H. Jr, Nalewaik, R. P. & Stephenson, J. R. *J. Virol.* **32,** 1041–1045 (1979).
14. Stephenson, J. R., Van de Ven, W. J. M., Khan, A. S. & Reynolds, F. H. Jr *Cold Spring Harb. Symp. quant. Biol.* **44** (in the press).
15. Reynolds, F. H. Jr, Van de Ven, W. J. M. & Stephenson, J. R. *J. Virol.* (in the press).
16. Sacks, T. L., Hershey, E. J. & Stephenson, J. R. *Virology* **97,** 231–240 (1979).
17. Stephenson, J. R., Khan, A. S., Sliski, A. H. & Essex, M. *Proc. natn. Acad. Sci. U.S.A.* **74,** 5608–5612 (1977).
18. Sherr, C. J., Sen, A., Todaro, G. J., Sliski, A. & Essex, M. *Proc. natn. Acad. Sci. U.S.A.* **75,** 1505–1509 (1978).
19. Reynolds, F. H. Jr, Van de Ven, W. J. M. & Stephenson, J. R. *J. biol. Chem.* (in the press).
20. DeLarco, J. E. & Todaro, G. J. *Proc. natn. Acad. Sci. U.S.A.* **75,** 4001–4005 (1978).
21. Tjian, R. & Robbins, A. *Proc. natn. Acad. Sci. U.S.A.* **76,** 610–614 (1979).
22. Griffin, J. D., Spangler, G. & Livingston, D. M. *Proc. natn. Acad. Sci. U.S.A.* **76,** 2610–2614 (1979).
23. Schaffhausen, B. S. & Benjamin, T. L. *Cell* **18,** 925–933 (1979).
24. Smith, A. E., Smith, R., Griffin, B. & Fried, M. *Cell* **18,** 915–924 (1979).
25. Scatchard, G. *Ann. N.Y. Acad. Sci.* **51,** 660–672 (1949).
26. Norby, J. G., Ottolenghi, P. & Jensen, J. *Analyt. Biochem.* **102,** 318–320 (1980).

'Activation-labile' glucocorticoid–receptor complexes of a steroid-resistant variant of CEM-C7 human lymphoid cells

Thomas J. Schmidt*, Jeffrey M. Harmon† & E. Brad Thompson

Laboratory of Biochemistry, DCBD National Cancer Institute,
NIH Bethesda, Maryland 20205

For cytoplasmic glucocorticoid–receptor complexes to enter and accumulate in the nucleus a temperature-dependent event, 'activation' is required[1–4]. Activation can be achieved *in vitro* by increased ionic strength[3–6], dilution or gel filtration[7] and is manifested by an increased affinity of steroid–receptor complex for DNA[3,5,7,8] and an altered elution profile from ion-exchange resins[9–11]. Munck and Foley have shown[12] that activated complexes isolated from thymocytes elute from DEAE-cellulose in a manner identical to complexes activated *in vitro*. We report here that DEAE-cellulose chromatography of steroid–receptor complexes from CEM-C7, a cloned human leukaemic T-cell line sensitive to the cytolytic action of glucocorticoids[13–15], and its steroid-resistant subclone 4R4 demonstrated that steroid receptors of clone 4R4 cannot form stable activated complexes. This defines a new defect in receptor action, activation lability (r^+act^l), which is unlike either the r^-, r^+nt^-, or r^+nt^i phenotypes previously described for mouse lymphoid variants[16–19].

Both the glucocorticoid-sensitive clone (C7) and the steroid-resistant subclone (4R4) contain specific, high-affinity binding sites for ^{3}H-dexamethasone, although the 4R4 sites display a somewhat lower affinity for dexamethasone than do those of its sensitive parent (Table 1). The source of this difference, which in itself cannot account for the total resistance of 4R4 to 10^{-6} M dexamethasone, may be clonal variation, or it may actually reflect subtle differences in the receptors. Since subsequent experiments indicate that glucocorticoid–receptor complexes of 4R4 are labile in the conditions of the whole cell binding assay (37 °C), the higher K_d obtained may result from non-equilibrium conditions. In fact, binding data obtained using cytosol assays performed at 0–4 °C suggest that both C7 and 4R4 receptors have the same high affinity (3×10^{-8} M) for dexamethasone (data not shown). A more striking difference in the properties of the receptor complexes of the two clones is their relative ability to translocate to the nucleus in physiological conditions (Table 1). No glucocorticoid–receptor complex was detected in the nucleus of 4R4 after incubation for 1 h at 37 °C in the presence of 5×10^{-8} M ^{3}H-dexamethasone, although 40% of the receptor complexes of clone C7 were detected in the nucleus in identical conditions. In contrast to the r^+nt^- mouse variants which generally display decreased but detectable nuclear accumulation of receptor complex (40% of the sensitive S49 wild type)[16,19], clone 4R4 exhibits no nuclear transfer.

Since glucocorticoid–receptor complexes of clone 4R4 could not be detected in the nucleus we examined the possibility that these receptor complexes were either unable to be activated (r^+act^-) or were labile (r^+act^l) in 'activating' conditions. DEAE-cellulose chromatography of glucocorticoid–receptor complexes from several cell types resolves these complexes into two forms: a high salt-eluting form which does not bind to DNA, nuclei or chromatin and probably represents the 'unactivated' form of the complex, and a low salt-eluting form which does bind to DNA, nuclei and chromatin, and which has been suggested to represent the 'activated' form of the glucocorticoid–receptor complex[11,12]. Figure 1*a* depicts the time course of activation of C7 cytoplasmic receptors which were pre-incubated for 2 h at 0–4 °C with 5×10^{-8} M [1,2,4(*n*)-^{3}H]triamcinolone acetonide (^{3}H-TA) and then activated at 20 °C in the presence of 0.2 M KCl for 0–30 min. Immediately after the 2 h incubation and removal of unbound ^{3}H-TA by gel filtration, most receptor complexes were eluted from DEAE-cellulose by 0.22 M potassium phosphate, that is in the 'unactivated' form (peak II). After activation for 15 min or 30 min there was a progressive shift of specifically bound ^{3}H-TA to a form which was eluted at 0.05 M potassium phosphate (peak I), so that after 30 min 50% of the total bound radioactivity was found in peak I with a proportional loss from peak II. The salt concentrations at which peak II and peak I were eluted are essentially the same as those for cytoplasmic receptor complexes detected in rat liver, HTC cells, LA9 cells, rat brain and adrenalectomized rat thymus (Y. Sakaue and E.B.T., unpublished data), and only activated receptor complexes from CEM cells bind to DNA-cellulose[23].

---

* Present address: Fels Research Institute, Temple University School of Medicine, Philadelphia, Pennsylvania 19140.

† To whom all correspondence should be addressed.

Figure 1*b* depicts the time course of attempted activation of 4R4 cytoplasmic receptors. Again the glucocorticoid–receptor complexes in the unactivated cytosol were eluted predominantly in peak II (0.21 M potassium phosphate). After activation for

Table 1 Characteristics of binding of ^{3}H-dexamethasone by sensitive (C7) and resistant (4R4) CEM cells

Clone	Binding (sites per cell)*	K_d*	% Nuclear translocation*
C7	20,000	1.2×10^{-8} M	40
4R4	5,900	7.3×10^{-8} M	0

Cells were grown in suspension in RPMI 1640 (NIH Media Unit) containing 10% heat-inactivated fetal calf serum (North American Biologicals) at 37 °C in a humidified atmosphere of 95% air, 5% CO_2. Clone 4R4 is one of 54 spontaneously derived steroid-resistant subclones of CEM-C7 selected in 10^{-6} M dexamethasone[15]. For the whole-cell binding assay cells were collected in mid-logarithmic phase and resuspended in Tricine-buffered RPMI 1640 at approximately 10^7 cells per ml. Aliquots (980 µl) of the cell suspensions were added to a series of borosilicate culture tubes (Fisher Scientific) which contained 10 µl of various concentrations of [1,2(*n*)^{3}H]dexamethasone (38 Ci mmol^{-1}; Amersham/Searle) in 95% ethanol plus either 10 µl of ethanol (uncompeted) or 10 µl of 5×10^{-3} M nonradioactive dexamethasone in ethanol (competed). Cell suspensions were incubated at 37 °C for 1 h. Following the incubation, 3 ml Hanks' balanced salt solution (BSS) at 22 °C were added to each tube, and the tubes were then centrifuged for 1 min at 1,200*g* in a clinical centrifuge. The cell pellets were then washed three times in 3 ml of BSS at 22 °C. Final cell pellets were resuspended in 1.6 ml BSS and 1.0 ml was added to 10 ml Aquasol liquid scintillation cocktail (NEN) and radioactivity was determined in a Beckman LS 9000 counter. A 0.2-ml aliquot of the cell suspension was counted (Coulter Model ZB) to determine final cell recovery. The difference between the total d.p.m. and the noncompeting d.p.m. represents specifically bound ^{3}H-dexamethasone and was expressed as sites per cell. K_d values and sites per cell were determined by analysing the data by the method of Scatchard[20]. For determination of nuclear translocation a minor modification of the procedure of Munck and Wira[21] was utilized.

* Values represent means of at least two determinations.

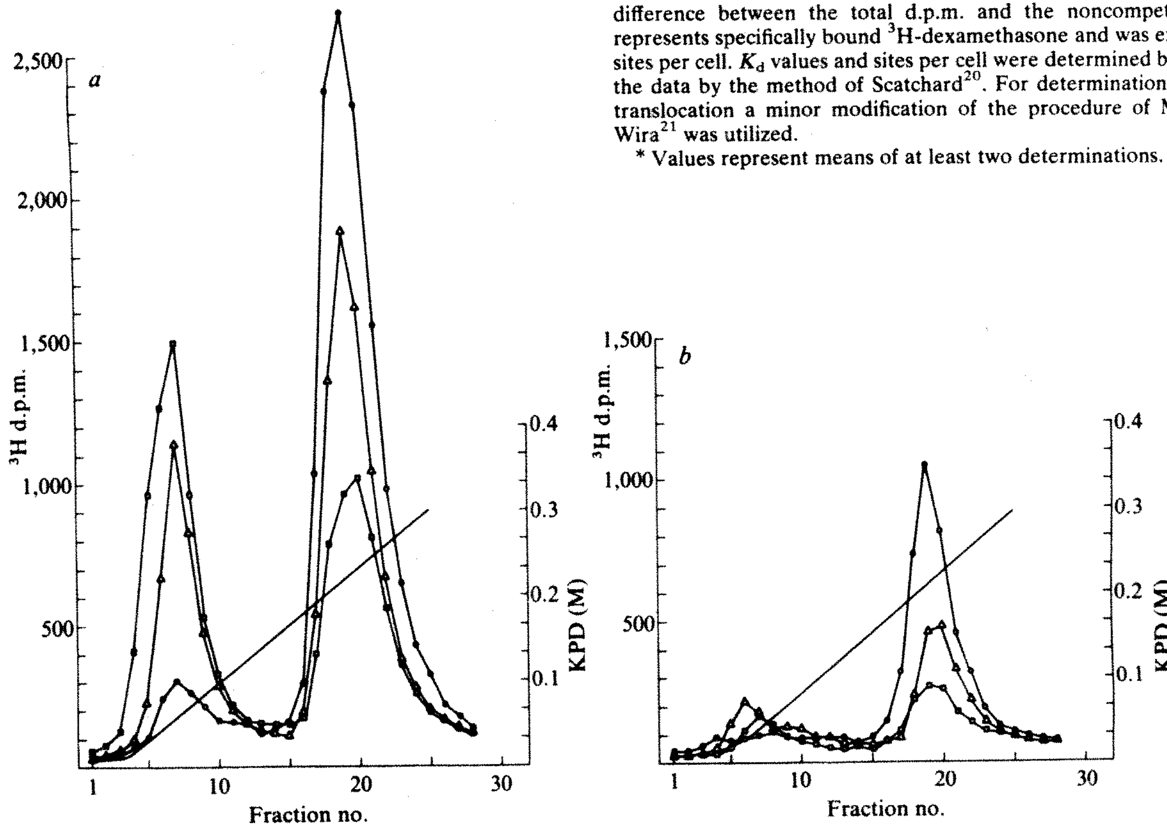

Fig. 1 Time course of activation (20 °C, 0.2 M KCl) of cytoplasmic [1,2,4*n*-^{3}H]triamcinolone acetonide–receptor complexes of CEM-C7 (*a*) and 4R4 (*b*) (○, unactivated control; △, 15 min activation; □, 30 min activation). Cells (1×10^6 cells per ml) were collected, washed once in an excess of ice-cold Hanks' BSS, and homogenized in 5 mM potassium phosphate buffer containing 0.5 mM dithiothreitol, *p*H 7.3 (KPD) at 4 °C with a Ten Broeck ground glass homogenizer. Cytosols were isolated after centrifugation for 1 h at 100,000*g* in a Spinco Model L refrigerated centrifuge. Cytosolic protein concentrations were determined by the method of Lowry *et al.*[22] and were 6 to 9 mg ml^{-1}. Cytosols were incubated for 2 h at 0–4 °C with approximately 5×10^{-8} M [1,2,4(*n*)-^{3}H]triamcinolone acetonide (29 Ci mmol^{-1}; Amersham/Searle) before activation. Following activation (20 °C, 0.2 M KCl) free steroid and salt were removed by passage over G25 columns (PD 10; Pharmacia) pre-equilibrated with 5 mM KPD buffer. 700 µl of the post-G25 cytosol were then loaded on to a DEAE-cellulose (DE52; Whatman) column (3 ml bed volume) which had been pre-equilibrated with 5 mM KPD. Bound radioactivity was then eluted by a linear 5 mM to 400 mM KPD gradient and 1.0-ml fractions collected. All chromatographic procedures were performed at 4 °C. Aliquots (400 µl) of each fraction were added to 10 ml of Aquasol and assayed for radioactivity. Salt concentrations were measured with a Radiometer electroconductivity meter. In similar experiments cytosols incubated with a 1,000-fold excess of nonradioactive TA failed to reveal any ^{3}H-TA bound to DEAE-cellulose columns. Since these lymphoid cells are devoid of progesterone receptors (J.M.H. and T.J.S., unpublished data) the binding of ^{3}H-TA can be assumed to be to glucocorticoid receptors.

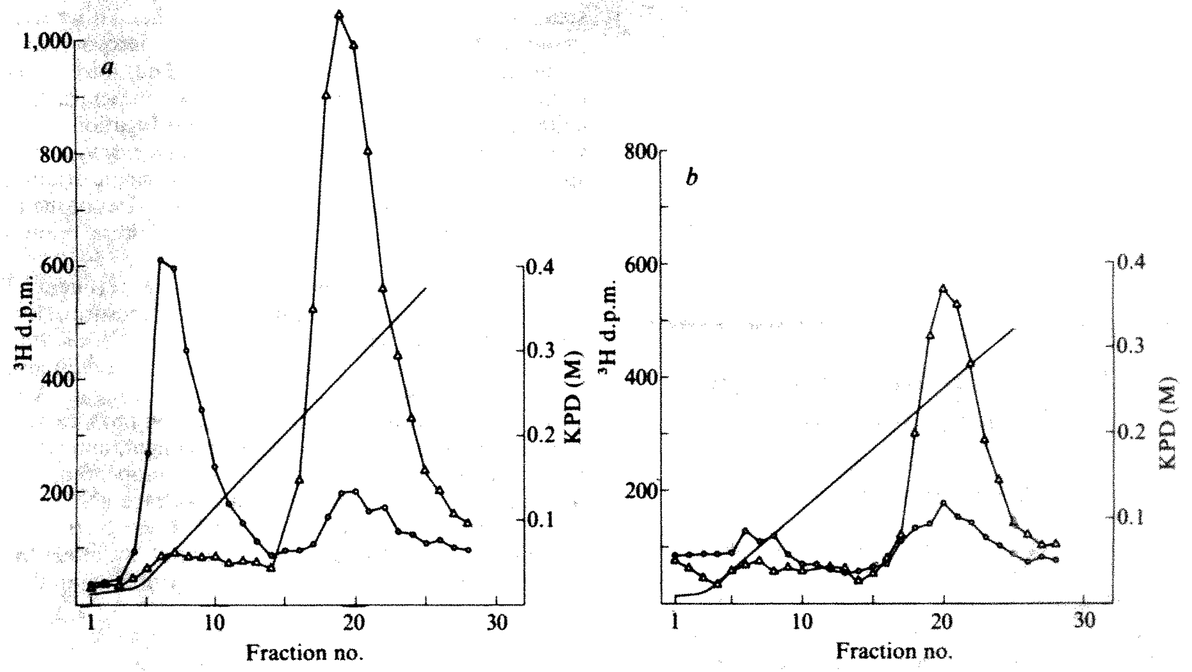

Fig. 2 DEAE-cellulose chromatograms depicting activation (30 min at 20 °C, 0.2 M KCl) of cytoplasmic [1,2,4(n)-^{3}H]triamcinolone acetonide–receptor complexes of CEM-C7 (a) and 4R4 (b) in the absence (○) and presence (△) of molybdate. Cell cytosols were prepared, incubated with ^{3}H-TA, and activated as in Fig. 1 with the exception that half of each cytosol was activated in the presence of 50 mM molybdate.

15 min there was a significant depletion in the radioactivity associated with peak II as seen for the wild type, but only a very small increase in the radioactivity associated with peak I (0.05 M potassium phosphate). Continued exposure to activation conditions for 30 min resulted in a further reduction of peak II with no further increase in the small amount of bound radioactivity eluted in peak I so that the total bound radioactivity was reduced by approximately 50%. These data clearly suggest that glucocorticoid–receptor complexes from 4R4 are labile in activation conditions. The small increase in peak I seen in the time course of activation of 4R4 receptor complexes after 15 min (Fig. 1b) suggests that at least some activation is possible. The subsequent disappearance of this peak after prolonged (30 min) activation suggests that it may be the activated form of the receptor complex which is labile. This instability could result from actual denaturation of the receptor protein or from dissociation of the steroid from receptor.

Sodium molybdate (Na_2MoO_4) inhibits the activation of glucocorticoid receptors from rat liver, rat thymus, mouse L cells and human leukaemic cells (T.J.S., unpublished data)[24,25]. It also inhibits the activation of avian oviduct progesterone receptors[26,27]. When 50 mM molybdate was incubated with C7 cytosol receptors during activation, the characteristic shift of steroid–receptor complex from peak II to peak I was not observed (Fig. 2a), demonstrating the ability of this compound to inhibit the activation of human lymphoid receptors. Attempted activation of 4R4 steroid–receptor complexes in the presence of 50 mM molybdate produced the result shown in Fig. 2b. In contrast to the loss of binding in the absence of molybdate, all of the binding was retained and eluted in peak II. This retention of binding most probably reflects the failure to generate a labile activated form of the 4R4 steroid–receptor complex in the presence of the inhibitor of activation, molybdate. Alternatively molybdate may have another, as yet undefined effect, whereby it is capable of stabilizing an otherwise unstable 'unactivated' form of the steroid–receptor complex.

Mouse lymphoid variants of S49 and W7, resistant to the cytolytic action of glucocorticoids, either lack receptor (r^-) or have receptor with diminished ability to enter the nucleus with reduced affinity for DNA-cellulose (r^+nt^-) or receptors which paradoxically bind more avidly to DNA cellulose (r^+nt^i)[16–19]. In the case of the r^+nt^- and r^+nt^i phenotypes it is presumed that activation is normal since it is the affinity of steroid–receptor complexes for DNA and not their ability to bind which is altered. We have identified a new phenotype, r^+act^l, in a steroid-resistant variant of a human leukaemic cell line. DEAE-cellulose chromatography of the glucocorticoid–receptor complexes of this resistant variant failed to demonstrate the formation of stable activated complexes. This result explains our failure to detect ^{3}H-dexamethasone–receptor complexes in 4R4 nuclei in physiological conditions and indicates an additional mechanism for the acquisition of steroid resistance. These results suggest that the predominant mechanism(s) of steroid resistance in human and mouse lymphoid cell lines may differ and the steroid-resistant variants of CEM-C7 may provide a more useful model system for the study of glucocorticoid resistance in human T-cell leukaemia.

This research was supported in part by an NIH Postdoctoral Fellowship (1F32 CA05447-02) awarded by the NCI to T.J.S. We thank Mrs Jean Regan for editorial assistance.

Received 16 November 1979; accepted 9 May 1980.

1. Munck, A. *et al. J. Steroid Biochem.* **3,** 567–578 (1972).
2. Rousseau, G. G., Baxter, J. D., Higgins, S. J. & Tomkins, G. M. *J. molec. Biol.* **79,** 539–554 (1973).
3. Baxter, J. D. *Proc. natn. Acad. Sci. U.S.A.* **69,** 1892–1896 (1972).
4. Higgins, S. J., Rousseau, G. G., Baxter, J. D. & Tomkins, G. M. *J. biol. Chem.* **248,** 5866–5872 (1973).
5. Milgrom, E., Atger, M. & Baulieu, E.-E. *Biochemistry* **12,** 5198–5205 (1973).
6. Kalimi, M., Beato, M. & Feigelson, P. *Biochemistry* **12,** 3365–3371 (1973).
7. Goidl, J. A., Cake, M. H., Dolan, K. P., Parchman, G. L. & Litwack, G. *Biochemistry* **16,** 2125–2130 (1977).
8. Cidlowski, J. A. & Munck, A. *Biochim. biophys. Acta* **543,** 545–555 (1978).
9. Atger, M. & Milgrom, E. *Biochemistry* **15,** 4298–4304 (1976).
10. Parchman, L. G. & Litwack, G. *Archs Biochem. Biophys.* **183,** 374–382 (1977).
11. Sakaue, Y. & Thompson, E. B. *Biochem. biophys. Res. Commun.* **77,** 533–541 (1977).
12. Munck, A. & Foley, R. *Nature* **278,** 752–754 (1979).
13. Norman, M. R. & Thompson, E. B. *Cancer Res.* **37,** 3785–3791 (1977).
14. Harmon, J. M., Norman, M. R., Fowlkes, B. J. & Thompson, E. B. *J. cell. Physiol.* **98,** 267–278 (1979).
15. Harmon, J. M., Norman, M. R. & Thompson, E. B. in *Steroid Receptors and the Management of Cancer* (eds Thompson, E. B. & Lippman, M.) 113–130 (CRC Press, Boca Raton, Florida, 1979).
16. Sibley, C. H. & Tomkins, G. M. *Cell* **2,** 213–220 (1974); Sibley, C. H. & Tomkins, G. M. *Cell* **2,** 221–227 (1974).

17. Yamamoto, K. R., Stampfer, M. R. & Tomkins, G. M. *Proc. natn. Acad. Sci. U.S.A.* **71,** 3901–3905 (1974).
18. Bourgeois, S., Newby, R. F. & Huet, M. *Cancer Res.* **38,** 4279–4284 (1978).
19. Pfahl, M., Kelleher, R. J. & Bourgeois, S. *Molec. cell Endocr.* **10,** 193–207 (1978).
20. Scatchard, G. *Ann. N. Y. Acad. Sci.* **51,** 660–672 (1949).
21. Munck, A. & Wira, C. *Meth. Enzym.* **36,** 255–264 (1975).
22. Lowry, O. H., Rosebrough, N. J., Farr, A. L. & Randall, R. J. *J. biol. Chem.* **193,** 265–275 (1951).
23. Harmon, J. M. *et al.* (in preparation).
24. Sando, J., Hammond, N. D., Stratford, C. A. & Pratt, W. B. *J. biol. Chem.* **254,** 4779–4789 (1979).
25. Leach, K. L., Dahmer, M. K., Hammond, N. D., Sando, J. J. & Pratt, W. B. *J. biol. Chem.* **254,** 11884–11890 (1979).
26. Toft, D. & Nishigori, H. *J. Steroid Biochem.* **11,** 413–416 (1979).
27. Moudgil, V. K., Nishigori, H., Essalu, T. E. & Toft, D. D. in *Molecular Mechanisms of Steroid Hormone Action* (eds Clark, J. H. & Roy, A.) (Springer, Berlin, in the press).

Insertion of *E. coli* photoreactivating enzyme into V79 hamster cells

Betsy M. Sutherland & S. G. Hausrath

Biology Department, Brookhaven National Laboratory, Upton, New York 11973

Photoreactivating enzyme mediates the specific repair of UV light [220–300 nm, (UV)]-induced cyclobutyl pyrimidine dimers in DNA[1]. It binds to dimer-containing DNA, and on absorption of light in the wavelength range 300–500 nm monomerizes the dimer, restoring biological activity to DNA[2]. The specificity of the enzyme for pyrimidine dimers in DNA allows its use as an analytical tool. If UV-induced biological damage is photoreactivable, dimers are probably a major cause of that damage. Thus dimers have been implicated in producing death and mutation in prokaryotes and in simple eukaryotes[3]. Although this photoreactivation test has great potential value in assessing the role of dimers in UV-induced damage in mammalian cells, its use in cultured mammalian cells has been limited by the dependence of photoreactivating enzyme levels on the cell species[4], genotype[5] and culture medium[6,7]. We have developed a method for insertion of *Escherichia coli* photoreactivating enzyme into mammalian cells, and show here that the inserted bacterial enzyme can mediate photoreactivation of pyrimidine dimers in V79 rodent cells.

We selected V79 Chinese hamster cells as a mammalian cell line with minimal endogenous photoreactivating enzyme (rodent cells contain no more than about 10% as much photoreactivating enzyme as do human cells[4]; also, V79 cells undergo excision repair very slowly[8–10]). Cells were grown in a minimal essential medium known to be unfavourable for photoreactivating enzyme production[6]. We also required an effective insertion agent which did not inactivate the *E. coli* enzyme. Polyethylene glycol (PEG) 6000 proved satisfactory in all these respects.

We first examined dimer monomerization in V79 cells treated with PEG, *E. coli* photoreactivating enzyme and visible light. Cells were grown in 60-mm plastic culture dishes overnight; the medium was removed, the cells were washed twice with 2 ml phosphate-buffered saline (PBS; 0.171 M NaCl, 3.4 mM KCl, 10.1 mM Na_2HPO_4, 1.9 mM KH_2PO_4), and 1 ml PBS was layered over the cells. They were exposed to UV light from a low pressure mercury bulb; UV exposures were measured with a Jagger meter[11] calibrated against a Yellow Springs Instrument Company radiometer. All procedures were carried out under Sylvania F40G0 safe lights. After exposure to UV light, the PBS was removed, and the cells treated for 2 min with 3 ml of insertion mixture[12] [prepared by mixing 30 g of PEG 6000, Biological Laboratories (which had been autoclaved for 30 min) with 60 ml of medium without serum at 45 °C. The mixture was then cooled to 37 °C]. The insertion mixture was removed, the cells drained briefly, rinsed with 1 ml PBS and 0.1 ml (1.1 mg) of partially purified photoreactivating enzyme from *E. coli* W 3350 λ *phr* (ref. 13) [fraction III (ref. 14), specific activity ~600 units mg^{-1}] was layered over the cells. The cells were allowed to stand at room temperature for 15 min, then either exposed to photoreactivating light from a 60-W incandescent bulb, or kept in the dark. Small amounts of PBS (~0.2 ml) were added to the dishes as required to prevent drying of the cells. Cells were collected by scraping into PBS, and centrifugation; their DNAs were extracted, then treated with the *Micrococcus luteus* dimer-specific UV-endonuclease (which makes a single-strand scission adjacent to each dimer)[15], and the relative sizes of the resulting DNAs determined from their electrophoretic mobilities in alkaline agarose[16,17].

Figure 1 shows the result of such an experiment. Trace *a* represents DNA from unirradiated cells. Exposure of the cells to $10\ J\ m^{-2}$ of UV radiation (trace *b*) produces UV endonuclease-sensitive sites (dimers) in the DNA, and thus a reduction in the size of the DNA after endonuclease treatment. After UV-irradiated cells were treated with insertion mixture and *E. coli* enzyme, followed by photoreactivating light, almost all of the UV endonuclease-sensitive sites disappeared, implying substantial monomerization of dimers (trace *c*). Treatment of the cells with insertion mixture plus photoreactivating enzyme in the absence of photoreactivating light did not affect the dimer content of the DNA (trace *d*), nor did incubation in the light of

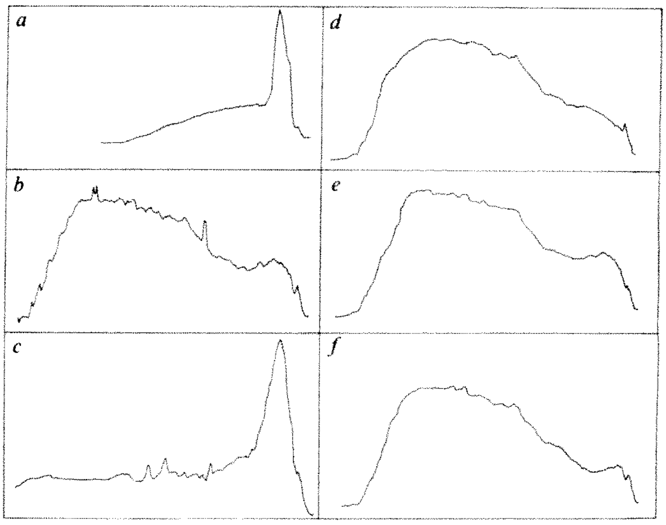

Fig. 1 Alkaline agarose gels of DNA from V79 cells which were: *a*, unirradiated; *b*, exposed to $20\ J\ m^{-2}$ of 254 nm radiation after treatment with PEG and photoreactivating enzyme and killed immediately; *c*, UV irradiated and treated with PEG, photoreactivating enzyme, then 60 min of photoreactivating light; *d*, UV irradiated, treated with PEG, photoreactivating enzyme and kept in the dark for 60 min; *e*, UV irradiated, treated with PEG (but no photoreactivating enzyme) and then 60 min photoreactivating light; *f*, UV irradiated and treated with photoreactivating enzyme (but no PEG) and 60 min photoreactivating light. Cells were collected by scraping into PBS, centrifuging at 5,000 r.p.m. in the SE12 rotor of the Sorvall RC2B for 5 min, resuspension in 0.25 ml buffer A-1 (50 mM Tris, *p*H 8, 10 mM EDTA, 0.4 M NaCl) and addition of 6 μl of freshly prepared 5% sodium lauryl sulphate, followed by 0.25 ml of redistilled phenol equilibrated with buffer A-1. The samples were rotated gently for 30 min, centrifuged, the upper layer removed and ethanol-precipitated. The precipitated DNA was centrifuged for 2 min in a Brinkman Microcentrifuge, drained briefly and resuspended in 20 μl of reaction buffer (30 mM Tris *p*H 8, 40 mM NaCl, 1 mM EDTA). To samples (10 μl) of the mixture was added 15 μg of a *M. luteus* dimer-specific endonuclease preparation[15]. The mixture was incubated at 37 °C for 20 min. A stop mixture (2 μl of 0.5N NaOH, 25% glycerol containing 0.125% bromocresol green) was added, and the mixture applied to a 12 × 14 cm agarose gel containing 0.29 g agarose, 59 mM NaOH and 4 mM Na_3EDTA. The gels were electrophoresed at 16V for 22 h, neutralized in 500 ml 0.1 M Tris, *p*H 8, stained in 0.1 M Tris *p*H 8 containing $0.5\ \mu g\ ml^{-1}$ ethidium bromide. The gels were photographed using Polaroid type 55 positive/negative film, and the negatives scanned using a Joyce–Loebl densitometer.

0028–0836/80/310510—02$01.00

Table 1 Fate of dimers in UV irradiated V79 cells

	Treatment	% Radioactivity in dimers $[(TT+UT)\times 10^2/\text{total}]$
1	No UV	0.009, 0.005
2	+UV, kill immediately	0.740
3	+UV, 90 min incubation in dark	0.722, 0.682, 0.702, 0.621
4	+UV, 40 min illumination	0.670, 0.650
5	+UV, 90 min illumination	0.562, 0.713
6	No UV, 90 min illumination	0.02

V79 cells were labelled for 24 h in a minimal essential medium containing 10% dialysed fetal calf serum (inactivated at 55 °C for 30 min), and 2 μCi ml^{-1} ^{3}H-thymidine (specific activity 60 mCi mmol^{-1}). Cells were washed with PBS, exposed to 500 J m^{-2} from a germicidal lamp with most of its emission at 254 nm, then killed immediately, kept in the dark or exposed to photoreactivating light from a 100-W incandescent bulb at 20 cm. Cells were collected by scraping into PBS and centrifuging at 15,000 r.p.m. in the Sorvall SE-12 rotor. The DNA was hydrolysed with 88% formic acid, chromatographed on silica gel thin-layer plates in ethyl acetate/H_2O/n-propanol (4 : 2 : 1)[24], sliced and counted in a LKB scintillation counter. Similar determinations for cells exposed to 50 J m^{-2} gave no indication of substantial excision or photoreactivation in the times used in the PEG insertion experiments.

cells treated with insertion mixture (but without photoreactivating enzyme) (trace *e*) or incubation in the light of cells treated with enzyme and photoreactivating light (but no PEG) (trace *f*).

As these experiments showed the apparent monomerization of cellular dimers by exogenous *E. coli* photoreactivating enzyme, it was important to show that the cells did not contain endogenous enzyme which might be mediating the reaction. We thus examined cellular photoreactivation and photoreactivating enzyme in three series of experiments. We first labelled the cells with ^{3}H-thymidine, and collected them without irradiation (Table 1, line 1), exposed them to UV (Table 1, line 2), kept them in the dark (line 3) or exposed them to photoreactivating light (lines 4, 5). Dimer photoreactivation in V79 cells grown in minimal essential medium was not detectable after either high (500 J m^{-2}) or low (50 J m^{-2}) UV exposures. We also examined the loss of UV-endonuclease sensitive sites in V79 cells untreated with insertion mixture or photoreactivating enzyme in experiments similar to those in Fig. 1. Exposure of UV light-irradiated cells to photoreactivating light did not affect the number of endonuclease sensitive sites in the DNA, thus indicating an absence of detectable endogenous photoreactivation. We also tested cell extracts directly for the presence of photoreactivating enzyme activity. No enzyme activity could be detected in standard photoreactivating enzyme assays[18]. We thus conclude that it is likely that the disappearance of dimers seen in Fig. 1 is mediated by *E. coli* photoreactivating enzyme inserted into the cells rather than by endogenous V79 enzyme.

This method for inserting *E. coli* photoreactivating enzyme into mammalian cells extends the range of cells in which photoreactivation of pyrimidine dimers can be examined. Several types of cells are especially suited for these studies. For example, rodent cells, in which excision and post-replication repair have been studied extensively[19], contain low levels of endogenous photoreactivating enzyme and have thus not been amenable to photoreactivation studies. In addition many cell strains derived from patients with xeroderma pigmentosum are deficient in photoreactivating enzyme and cellular photoreactivation[5,20]. Finally, even those mammalian cells which are capable of producing photoreactivating enzyme (presumably *Phr*$^+$) must be grown on suitable medium for expression of the *Phr* gene. The development of this method lifts this restriction and should allow examination of photoreactivation in a variety of media. Insertion of an enzyme which can specifically reverse pyrimidine dimers will allow a determination of the role of dimers and of other photoproducts in the induction of cellular damage.

Two other systems have been developed for insertion of exogenous repair enzymes. Smith and Hanawalt studied the action of the phage T4 endonuclease V in isolated nuclei of human cells[21]. Tanaka *et al.* used Sendai virus to insert the T4 endonuclease into intact human cells[22,23]. They both increased unscheduled DNA synthesis and survival (about a fivefold increase) on addition of Sendai virus plus the endonuclease.

Our attempts to insert *E. coli* photoreactivating enzyme into V79 cells with UV light inactivated Sendai virus were unsuccessful; we thus developed the PEG insertion method [Yarosh (personal communication) has used a similar method for insertion of *M. luteus* UV endonuclease into V79 cells], which has several advantages: (1) PEG is available commercially, and is stable, (2) it is not a potential biohazard and does not yield productive or latent infection of treated cells, and (3) it is gentle to the photoreactivating enzyme, which is inactivated by many reagents. Finally, because the *E. coli* photoreactivating enzyme is larger (monomer molecular weight 35,000; the enzyme also aggregates to form higher multiples) than enzymes inserted by the Sendai method (the molecular weight of the T4 endonuclease is 20,000), it may offer a general method of insertion of enzymes into mammalian cells.

This work was supported by grants and a Research Career Development Award to B.M.S. from the National Cancer Institute of the NIH, and the Department of Energy.

Received 6 March; accepted 27 May 1980.

1. Setlow, J. K. & Setlow, R. B. *Nature* **197,** 560–562 (1963).
2. Rupert, C. S. *J. gen. Physiol.* **45,** 725–741 (1962).
3. Setlow, R. B. *J. cell comp. Physiol.* **64,** Suppl. 1, 51–68 (1967).
4. Sutherland, B. M., Runge, P. & Sutherland, J. C. *Biochemistry* **13,** 4710–4715 (1974).
5. Sutherland, B. M., Rice, M. & Wagner, E. K. *Proc. natn. Acad. Sci U.S.A.* **72,** 103–107 (1975).
6. Sutherland, B. M. & Oliver, R. *Biochim. biophys. Acta* **442,** 358–367 (1976).
7. Mortelmans, K. *et al. Mutat. Res.* **44,** 433–446 (1977).
8. Cleaver, J. E. & Trosko, J. E. *Int. J. Radiat. Biol.* **15,** 411–424 (1969).
9. Trosko, J. E., Chu, E. H. & Carrier, W. L. *Radiat. Res.* **24,** 667–672 (1965).
10. Trosko, J. E. & Kasschau, M. R. *Photochem. Photobiol.* **6,** 215–219 (1967).
11. Jagger, J. *Radiat. Res.* **14,** 394–403 (1961).
12. Clark, M., Crenshaw, A. H. Jr & Shaw, J. W. *T. C. A. Man.* **4,** 801–804 (1978).
13. Sutherland, B. M., Court, D. & Chamberlin, M. J. *Virology* **48,** 87–93 (1972).
14. Sutherland, B. M., Chamberlin, M. J. & Sutherland, J. C. *J. biol. Chem.* **12,** 4200–4205 (1973).
15. Ahmed, F. E. & Setlow, R. B. *Cancer Res.* **39,** 471–479 (1979).
16. McDonell, M., Simon, M. N. & Studier, F. W. *J. molec. Biol.* **110,** 119–143 (1977).
17. Achey, P. M., Woodhead, A. D. & Setlow, R. B. *Photochem. Photobiol.* **29,** 305–310 (1979).
18. Sutherland, B. M. & Chamberlin, M. J. *Analyt. Biochem.* **53,** 168–176 (1973).
19. Lehmann, A. R. *Life Sci.* **15,** 2005–2016 (1975).
20. Sutherland, B. M. & Oliver, R. O. *Nature* **257,** 132–134 (1975).
21. Smith, C. A. & Hanawalt, P. C. *Proc. natn. Acad. Sci. U.S.A.* **75,** 2598–2602 (1978).
22. Tanaka, K., Sekiguchi, M. & Okada, Y. *Proc. natn. Acad. Sci. U.S.A.* **72,** 4071–4075 (1975).
23. Tanaka, K., Hayakawa, H., Sekiguchi, M. & Okada, Y. *Proc. natn. Acad. Sci. U.S.A.* **74,** 2958–2962 (1977).
24. Cook, K. H. & Friedberg, E. C. *Analyt. Biochem.* **74,** 411–418 (1976).

Innocuous biological freezing during warming

W. F. Rall*‡, D. S. Reid† & J. Farrant*

* Clinical Research Centre, Watford Road, Harrow HA1 3UJ, UK
† Unilever Research, Colworth House, Sharnbrook, Bedford
MK44 1LQ, UK

Intracellular freezing during the cooling of living cells is reported to reduce or abolish their recovery on thawing[1]. In microscopical and microprobe studies, low-temperature techniques may induce intracellular ice artefacts[2]. The amount of intracellular ice can be reduced either by selecting a slow cooling procedure that allows extracellular crystallization and cellular dehydration before the intracellular ice forms or by the ultrarapid cooling of very small samples to minimize the nucleation and growth of ice[3]. However, a few reports suggest that in some

---

‡ Present address: ARC Institute of Animal Physiology, Animal Research Station, 307 Huntingdon Road, Cambridge CB3 0JQ, UK.

0028–0836/80/310511—04$01.00

conditions intracellular ice may be either innocuous[4] or even sometimes beneficial[5] for the survival of function. We have therefore used here the technique of low-temperature light microscopy to examine the relationship between intracellular freezing and cell injury. We followed the morphological appearance of eight-cell mouse embryos during cooling and warming in medium containing dimethyl sulphoxide (DMSO; 1.5 M) and correlated it with their functional survival after thawing. Unexpectedly, we found that ice formed in the cytoplasm of embryos during slow warming in conditions when it did not form during cooling. Death of embryos, however, did not correlate with the temperature during slow warming at which intracellular ice appeared (−85 °C). The occurrence in some conditions of freezing at these low temperatures during warming has important implications both for the preservation of function of cells and for the preservation of morphology in electron microscopy.

The mouse embryo system was chosen because of the availability of a stringent *in vitro* survival assay (development to expanded blastocyst)[6] and the ease of observing the large blastomeres during cooling and warming on the low-temperature stage of a light microscope[7]. The embryos were cooled slowly (~0.5 °C min^{-1}) to −40 °C and then rapidly to < −150 °C. In these conditions, they exhibit high survival after rapid warming (~500 °C min^{-1}) but are dead after slow warming (<20 °C min^{-1})[5]. Injury following slow warming is believed to be associated with the migratory recrystallization of intracellular ice that formed during rapid cooling[8].

Figure 1 shows the typical microscopical appearance of two eight-cell embryos in DMSO (1.5 M) during cooling and warming. The formation of intracellular ice is usually characterized by the sudden blackening or 'flashing' of the cytoplasm when viewed using phase contrast optics[9]. This blackening is believed to result from the scattering of light by the surfaces of ice crystals and possibly gas bubbles[10]. During the slow cooling of the embryos to −40 °C (Fig. 1*a*–1*f*), extracellular freezing occurred and the blastomeres shrank as reported for other cells[11–13]. During the subsequent rapid cooling to ~ −150 °C (Fig. 1*g*), the appearance of the embryos did not change, indicating the absence of visible intracellular ice. However, when the embryos were then warmed slowly, they 'flashed' (Fig. 1*j*), suggesting the formation of intracellular ice when the temperature reached −85 °C. On continued slow warming, a complex series of phenomena was observed. Changes included: the gradual appearance (−85 to −70 °C; Fig. 1*j*–*l*) and disappearance (−70 to −40 °C; Fig. 1*l*–*q*) of a dark crystalline material outside the zona pellucida and perhaps within the perivitelline space, an abrupt increase in the mobility of this material at −70 °C (not visible in Fig. 1, but discernible in videotape recordings), the sudden appearance of the zona pellucida at −65 °C (Fig. 1*m*), a second darkening of the cytoplasm at −55 °C (Fig. 1*o*) and finally, the disappearance of the dark intracellular material at −40 °C. After thawing, the embryos appeared morphologically abnormal (Fig. 1*r*). When similarly cooled embryos were warmed rapidly (~250 °C min^{-1}) from −120 °C or below, both videotape and visual observations revealed none of these changes in appearance during warming. Furthermore, if slow warming was converted to rapid warming at ~ −75 °C, the second darkening of the embryos was not observed. In both these instances, the embryos were morphologically normal after thawing.

The critical temperature range associated with injury during slow warming was found from parallel survival studies. The embryos were cooled slowly to −40 °C and then rapidly to −196 °C. They were first warmed slowly (~2 °C min^{-1}) to various temperatures and then rapidly (~500 °C min^{-1}) to 20 °C (Fig. 2). The data demonstrate that the embryos survived slow warming providing conversion to rapid warming was done before the temperature reached −70 °C. Slow warming to −60 °C or above resulted in the death of the embryos. Functional injury therefore only occurred if slow warming was continued some 15–20 °C above the temperature (−85 °C) at

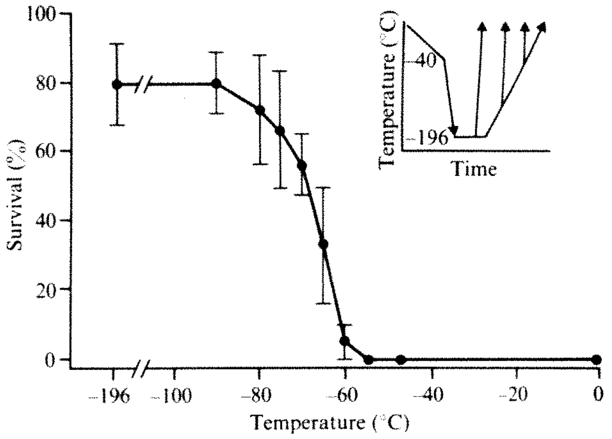

Fig. 1 Microscopical appearance of two eight-cell mouse embryos during cooling and warming. Embryos were flushed from the oviducts of superovulated TO (Crc: TO) or MF1 (Ola: MF1) female mice that had been mated ~64 h earlier with TO males. Embryos were collected and handled as described previously[18]. The embryos were placed into phosphate-buffered saline (PB1)[19] containing DMSO (1.5 M) for at least 20 min at ~20 °C to allow complete permeation of the DMSO[20]. Approximately 10 embryos were then placed into a small drop of the PB1–DMSO solution on a 13-mm diameter coverglass and immediately covered with another coverglass. A hole reinforcer for loose-leaf paper (WEB self-adhesive reinforcements, Westwood Stationery) on one of the coverglasses prevented the embryos from being crushed. The coverglass sandwich was then placed onto the temperature-controlled slide of a low-temperature microscope stage[7]. The appearance of the embryos was recorded on time-lapse videotape and photographed onto Ilford Pan-X film using phase-contrast optics on a Leitz Ortholux II microscope. The embryos were cooled slowly (~0.5 °C min^{-1}) from +4 to −40 °C and photographs *b*–*f* were taken at the indicated temperatures. Photograph *b* shows the extracellular ice front as it passes the embryos. The embryos were then cooled rapidly (~250 °C min^{-1}; photograph *g*). Subsequently, the embryos were warmed rapidly to −120 °C and then slowly (~2 °C min^{-1}) to ambient temperature (photographs *h*–*r*). Scale bar, ~50 μm.

Fig. 2 Survival of eight-cell mouse embryos cooled slowly to −40 °C and then rapidly to −196 °C as a function of the temperature at which slow warming was converted to rapid warming (see insert diagram). Embryos were collected as noted in Fig. 1 legend, and 10–15 embryos were transferred into glass test tubes (10 × 75 mm) which contained 0.1 ml PB1. The embryos were held at ~20 °C and an equal volume of PB1 containing DMSO (3.0 M) was added and mixed (final DMSO concentration 1.5 M). The embryos were held at ~20 °C for 20 min to allow complete permeation of the DMSO[20]. The samples were then placed into a −7 °C bath and 2 min later were nucleated with an ice crystal. After ~5 min, the samples were transferred into an alcohol bath at −7 °C that was cooling at ~0.5 °C min^{-1} (ref. 18). When the temperature of the bath reached −40 °C, the samples were quickly transferred into liquid nitrogen (−196 °C) and held for 15 min to 48 h. The samples were warmed either by direct transfer into a +37 °C water bath (~500 °C min^{-1}) or by transfer into stirred alcohol (300 ml in a 1-l beaker) initially at ~ −110 °C and allowed to warm in air (~2 °C min^{-1}). At different temperatures, samples were removed and warmed rapidly in a +37 °C water bath until the ice disappeared. After thawing the samples were diluted rapidly[5] and the embryos were washed in PB1 and cultured in Brinster's BMOC-3 medium[6]. Survival was measured as a percentage of cultured embryos developing to the expanded blastocyst stage in 48 h. Approximately 90% of the embryos frozen were recovered and cultured. Temperature was measured using copper–constantan thermocouples and a potentiometric recorder. Each data point represents five replicate tubes.

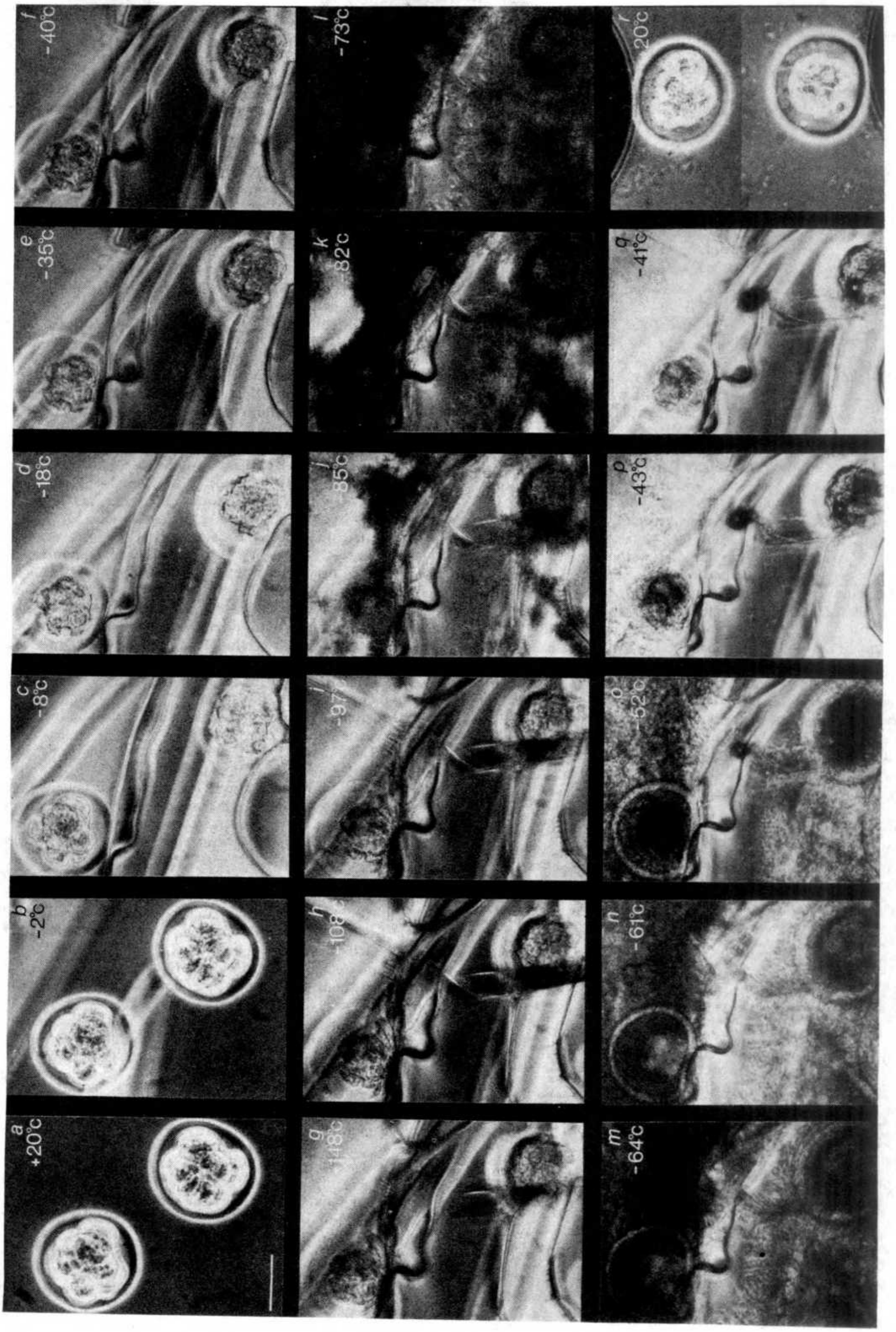
a
+20°C
b
-2°C
c
-8°C
d
-18°C
e
-35°C
f
-40°C
g
148°C
h
-108°
i
-97
j
85°C
k
82°C
l
-73°C
m
-64°C
n
-61°C
o
-52°C
p
-43°C
q
-41°C
r
20°C

which intracellular ice was first observed to form. We also examined whether the functional injury was reversible, by repeating the experiments described in Fig. 2 legend, except that instead of warming the embryos rapidly from various temperatures during slow warming, they were recooled rapidly from those temperatures into liquid nitrogen and then rewarmed rapidly in a +37 °C water bath. The survival was not significantly different from that in Fig. 2. This suggests that the injury resulting from some event that occurs during slow warming could not be reversed by a return to a lower temperature before rapid warming.

These results indicate that the absence of intracellular freezing during cooling is no guarantee that freezing will not occur within the cells during warming. This finding has important implications for those using low-temperature techniques for preservation of either structure or function. The initial formation of intracellular ice at −85 °C during slow warming clearly did not result in cellular injury, as injury occurred only when slow warming was continued for a further 20 °C (to about −65 °C). Furthermore, the embryos were injured before the second darkening of the cytoplasm at −55 °C and the melting of the intracellular ice at −40 °C. If the three events of flashing at −85 °C, darkening at −55 °C and disappearance of the dark crystalline material in the cytoplasm at −40 °C correspond, respectively, to devitrification (crystallization)[14,15], migratory recrystallization[15] and melting of ice in the cytoplasm, then our data showing injury at ~ −65 °C do not support a correlation of injury with these phase transitions of intracellular ice. This conclusion contradicts previous suggestions of the mechanism by which intracellular ice injures. Mazur has suggested that injury from intracellular ice and its migratory recrystallization is a direct physical consequence of the ice and the effect is on intracellular membranes[8,16]. If this were so, the injury should occur at the same temperature as, or soon after, migratory recrystallization. Farrant has suggested instead that injury results from osmotic forces mediated by the imbalance between the melting of intra- and extracellular ice[17]; with this idea most injury should occur after the intracellular ice melts. Three alternatives may account for the discrepancy between our survival data and the phase changes of intracellular ice. First, an invisible event may occur at −65 °C (for example, recrystallization of ice) that leads to injury. Second, one of the visible changes of intracellular ice (recrystallization at −55 °C) may be the damaging event and become inevitable once slow warming reaches −65 °C. Finally, the presence of intracellular ice may be innocuous and functional injury result from a change in another component of the system.

We thank Dr C. R. Coid for providing research facilities and Miss C. Evans for the photographic processing.

Received 13 March; accepted 21 May 1980.

1. Mazur, P. *Science* **168,** 939–949 (1970).
2. Dempsey, G. P. & Bullivant, S. *J. Microsc.* **106,** 261–271 (1976).
3. Farrant, J., Walter, C. A., Lee, H., Morris, G. J. & Clarke, K. J. *J. Microsc.* **111,** 17–34 (1977).
4. Sherman, J. K. *Anat. Rec.* **144,** 171–189 (1962).
5. Whittingham, D. G., Wood, M., Farrant, J., Lee, H. & Haley, J. A. *J. Reprod. Fert.* **56,** 11–21 (1979).
6. Brinster, R. L. in *Growth, Nutrition, and Metabolism of Cells in Culture* Vol. 2 (eds. Rothblat, G. H. & Cristofalo, V. J.), 251–286 (Academic, New York, 1972).
7. Reid, D. S. *J. Microsc.* **114,** 241–248 (1978).
8. Mazur, P. *Cryobiology* **14,** 251–272 (1977).
9. Smith, A. U. & Smiles, J. *Jl R. microsc. Soc.* **73,** 134–139 (1953).
10. Hobbs, P. V. *Ice Physics*, 619–621 (Clarendon, Oxford, 1974).
11. Diller, K. R. & Cravalho, E. G. *Cryobiology* **7,** 191–199 (1970).
12. McGrath, J. J., Cravalho, E. G. & Huggins, C. E. *Cryobiology* **12,** 540–550 (1975).
13. Leibo, S. P. *CIBA Fdn Symp.* **52,** 69–92 (1977).
14. Hildebrandt, W. H., Cocks, F. H. & Shepard, M. L. *J. mater. Sci.* **13,** 1099–1104 (1978).
15. MacKenzie, A. P. *Phil. Trans. R. Soc.* **B278,** 167–189 (1977).
16. Mazur, P. *Ann. N.Y. Acad. Sci.* **125,** 658–676 (1965).
17. Farrant, J. *Phil. Trans. R. Soc.* **B278,** 191–205 (1977).
18. Leibo, S. P. & Mazur, P. in *Methods in Mammalian Reproduction* (ed. Daniels, J.) 179–201 (Academic, New York, 1978).
19. Whittingham, D. G. *Nature* **233,** 125–126 (1971).
20. Rall, W. F., Mazur, P., McGrath, J. J. & Leibo, S. P., (in preparation).

0028–0836/80/310514—03$01.00

Precursor complement protein (pro-C4) is converted *in vitro* to native C4 by plasmin

Gabriel Goldberger & Harvey R. Colten

Division Cell Biology, Department of Medicine, the Ina Sue Perlmutter Cystic Fibrosis Research Center, Children's Hospital Medical Center and the Department of Pediatrics, Harvard Medical School, Boston, Massachusetts 02115

The fourth component of complement (C4) is a constituent of the classical serum complement pathway, one of the principle effectors of inflammatory reactions. A single chain protein (molecular weight (MW) 200,000), presumed to be the precursor of C4 (pro-C4), was first identified as a product of cell-free translation on polysomes from guinea pig liver homogenate[1]. Pro-C4 has since been detected in human[2,3] and guinea pig[4] plasma and intracellularly in macrophage[5] and liver cultures[1]. Native C4 is composed of three polypeptide chains of unequal size and linked by disulphide bridges—the α, β, and γ chains which have MWs of approximately 95,000, 75,000 and 31,000 respectively (ref. 6). Kinetic studies of C4 biosynthesis in tissue culture, a comparison of peptide maps from tryptic digests[7] and identity of the amino-terminal segments of guinea pig pro-C4 with β chain of guinea pig and human C4 (ref. 8) suggested that pro-C4 was a precursor of C4. However, conversion of pro-C4 to native C4 has not been demonstrated directly. We now report that the addition of plasmin to radiolabelled pro-C4 (in cell lysates of guinea pig macrophages) generated a protein with the characteristic size and subunit structure of native C4, establishing the precursor–product relationship between these proteins. These data also suggest that a plasmin-like enzyme is responsible for post-translational conversion of this procomplement (pro-C4) protein to C4 *in vivo*. Another enzyme, the C1s subunit of the first component of complement, cleaved pro-C4 at a single site, distinct from the plasmin cleavage sites, to generate fragments of approximate MWs 112,000 and 91,000. This experiment indicated that β-α-γ is the sequence of subunits in pro-C4.

A previous study[8], using a microradiosequencing method, showed that the β chain is the amino-terminal segment of pro-C4; the carboxy-terminal segment had not been ascertained. Hence, a preliminary study of pro-C4 structure was required to interpret results of experiments designed to convert the procomplement protein to native C4. Guinea pig macrophage cultures from starch-induced peritoneal exudates were incubated for 5 h in medium containing ^{35}S-methionine. The cell monolayers were then washed extensively and the intracellular radiolabelled protein containing pro-C4 was recovered in the supernatant following 100,000g centrifugation of a 0.5% Triton X-100 lysate of the cells. Culture medium served as the source of radiolabelled native C4.

The C1s subcomponent of the first component of complement is an enzyme that cleaves the amino terminus of α-chain of native C4 at a single site, liberating a fragment of MW 9,000 (C4a). To test whether this enzyme would be of use in deducing the sequence of subunits in the precursor protein, purified C1s was mixed in excess with radiolabelled pro-C4 in cell lysate or with ^{35}S-methionine-labelled native C4 secreted by macrophages in culture. After incubation for 60 min at 37°C the products were subjected to SDS-polyacrylamide gel electrophoresis (Fig. 1). In confirmation of published data[6], C1s treatment of native C4 resulted in alteration of the mobility of α chain (generation of α') due to loss of a 9,000-MW fragment. There was no apparent change in mobility of either β or γ chain. C1s also cleaved pro-C4 at a single site to generate two polypeptides of approximate MWs 112,000 (α'-γ) and 91,000 (β chain + 9,000-MW (9 K) fragment of α chain); no free α' chain

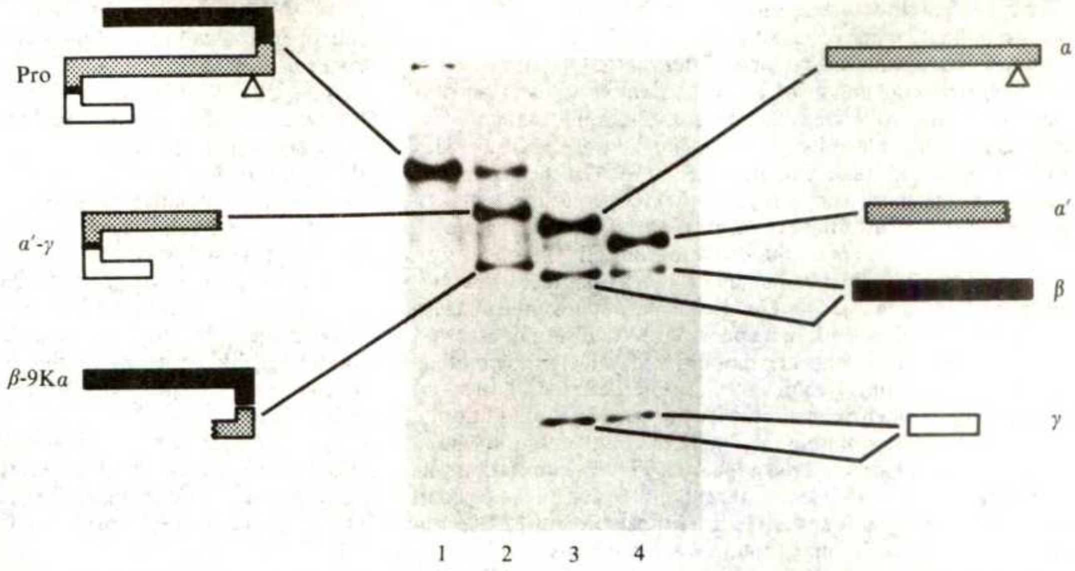

Fig. 1 Cleavage of pro-C4 and native C4 by C1s. Cell lysate (as a source of ^{35}S-methionine-labelled pro-C4) prepared as described in Fig. 3 legend and medium from the same cultures (as a source of radiolabelled native C4) were each mixed with purified C1s (140 μg ml^{-1} final concentration)[12] and the mixtures were incubated at 37 °C for 60 min. Controls consisted of lysate or medium incubated in identical conditions except that C1s was omitted. C4 antigen was isolated by precipitation[9] and the products of C1s action on pro-C4 and C4 were analysed by 1% SDS/9% polyacrylamide gel electrophoresis[13]. Lane 1, pro-C4; lane 2, pro-C4 treated with C1s; lane 3, native C4; lane 4, native C4 treated with C1s. The two fragments generated from pro-C4 by C1 cleavage were stable on prolonged incubation with the C1s enzyme. Their sizes (MWs 112,000 and 91,000) were estimated in a parallel experiment on cylindrical 1% SDS/5.6% polyacrylamide gels as described by Fairbanks *et al.*[14]. Δ, C1s cleavage site.

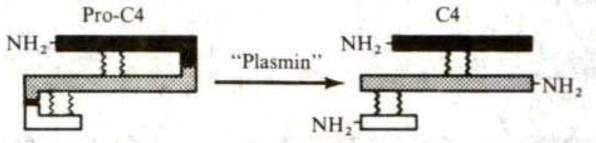

Fig. 2 Model of Pro-C4 with β chain (■) as the amino-terminal segment linked to α chain (▨) followed by γ chain (□) at the carboxy terminus. Conversion of pro-C4 to C4 mediated by plasmin or a plasmin-like enzyme according to data in Fig. 3 legend. The position and number of disulphide bridges are not known.

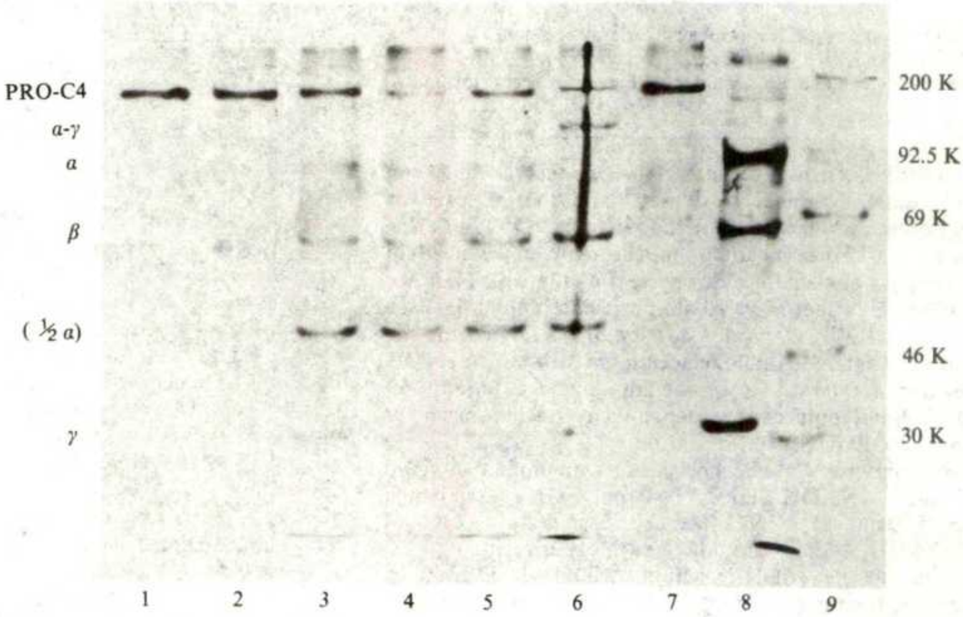

Fig. 3 Kinetics of pro-C4 cleavage by plasmin. Confluent cultures of macrophages from starch-induced peritoneal exudates in Hartley guinea pigs were established by plating 3 × 10^7 cells in 100-mm plastic Petri dishes (Falcon Plastics) with 10 ml Medium 199 containing 10% heated fetal bovine serum (FBS), 50 U ml^{-1} penicillin and 50 μg ml^{-1} streptomycin (P/S). After 2 h incubation at 37 °C in humidified 5% CO_2/95% air atmosphere, the monolayers were washed thrice with Hank's balanced salt solution (HBSS) then fed with 6 ml of supplemented (10% dialysed heated FBS, P/S and glutamine 2 mM) Dulbecco's modified Eagle's medium in which ^{35}S-methionine (>500 Ci mmol^{-1}) 85 μCi ml^{-1} was substituted for the corresponding unlabelled amino acid. Culture medium was removed after 5 h and the cells were washed extensively with HBSS then lysed in 6 ml KCl 100 mM, Tris 50 mM, *p*H 7.5 buffer with 0.5% Triton X − 100. Following one freeze–thaw cycle, the lysate was centrifuged at 100,000 *g* for 2 h at 4 °C and the supernatant stored at −90 °C. The cell lysate (1.7 ml) was mixed with 34 μl plasmin stock solution prepared as described below. An aliquot (300 μl) was immediately removed, mixed with benzamidine (20 mM final concentration) and stored at 0°C. The remainder was incubated at 37 °C and at timed intervals 300-μl aliquots were removed, benzamidine added and the samples stored at 0 °C. Controls consisted of lysate alone stored at 0 °C, and lysate alone incubated at 37 °C for 55 minutes. Sodium EDTA (2 mM final concentration) and a pseudoglobulin fraction of guinea pig serum[9] were added to each sample, then the mixture was centrifuged 10,000 *g* for 5 min at 4 °C. C4 antigen was precipitated from 250 μl of the supernatant according to the method in ref. 9. The precipitates were washed, dried and dissolved in 50 μl of a solution containing 10 mM Tris, 1 mM Na_2EDTA, 1% SDS, 10% glyerol, 60 μg pyronine-y, 4% 2-mercaptoethanol, boiled for 4 min then applied to a 1% SDS/9% polyacrylamide gel and electrophoresed[14]. The gel was stained, fixed and dried and an autoradiograph developed after 2 weeks at −70 °C. Lane 1, lysate untreated; lanes 2–6, lysate treated with plasmin at 37 °C for 0, 5, 10, 20, 55 min, respectively; lane 7, lysate incubated at 37 °C for 55 min in the absence of plasmin; radiolabelled native C4 from medium (see Fig. 1 legend) in lane 8 and MW markers in lane 9. Note the disappearance of pro-C4 following plasmin treatment and appearance of α, β and γ chains of native C4. Note also the 130,000- and 50,000-MW fragments. Plasminogen (2 mg ml^{-1}) purified on lysine Sepharose[15] was activated by incubation with urokinase (Abbot) 10% w/v for 30 min at room temperature. Plasmin activity was measured spectrophotometrically by hydrolysis of chromogenic substrate S-2251 (Ortho Diagnostics); 5 μl of the stock solution liberated 4.7 mM s^{-1}. MWs (K = × 10^3) are given on the right-hand side.

was seen. These data are consistent with the model of pro-C4 shown in Fig. 2 with β chain, the amino-terminal segment, then α chain and γ chain at the carboxy-terminus.

Enzymatic conversion of pro-C4 to native C4 was accomplished in the following experiment. Plasmin (human plasminogen and plasminogen activator) was mixed with radiolabelled cell lysate and incubated at 37 °C. At timed intervals, aliquots were removed and the reaction stopped with benzamidine (20 mM final concentration). C4 antigen was precipitated[9], and the precipitates were washed, dissolved and subjected to SDS-polyacrylamide gel electrophoresis in reducing conditions (Fig. 3). Treatment with plasmin resulted in a loss of pro-C4 protein and the appearance of disulphide-linked peptides with electrophoretic mobilities identical to the mobilities of the α, β and γ chains of unlabelled carrier C4 protein, mixed and co-electrophoresed with the samples. In addition, a protein of approximately 50,000 MW, interpreted to be a fragment of α chain ($1/2\ \alpha$), appeared. This interpretation was supported by the observation that the intensity of the α-band decreased, whereas β and γ chains were stable during plasmin treatment. An additional protein fragment consistent in size (MW 130,000) with an α–γ segment was also generated. The rate of cleavage of pro-C4 by plasmin was a function of enzyme concentration and temperature, and was inhibited by benzamidine (20 mM). Cleavage of pro-C4 was not observed in cell lysates alone, that is, those lacking plasmin, nor in the presence of plasminogen activator (human urokinase) alone. Moreover, the C1r subcomponent of C1, properdin factor D and urinary kallikrein each failed to generate C4 protein from pro-C4. Trypsin extensively degraded pro-C4 to a mixture of small molecular weight peptides.

The possibility that a plasmin-like enzyme converts pro-C4 to C4 *in vivo* is of interest in view of evidence that levels of plasminogen activator in monocytes[10] and macrophages[11] are modulated by a variety of stimuli, thus providing a potential mechanism for post-translational control of complement production.

We thank Drs Brian Tack for supplying plasminogen, Judy Andrews for purified C1s and C1r, Jocelyn Spragg for purified human urinary kallikrein, and A. E. Davis III for purified factor D. This work was supported by USPHS grants AI15033 and HL22487.

Received 24 March; accepted 28 May 1980.

1. Hall, R. E. & Colten, H. R. *Proc. natn. Acad. Sci. U.S.A.* **74,** 1707–1710 (1977).
2. Gigli, I. *Nature* **278,** 836–837 (1978).
3. Gorski, J. P. & Muller-Eberhard, H. J. *J. Immun.* **120,** abstr., 1775–1776 (1978).
4. Burge, J., Nicholson-Weller, A. & Austen, K. J. *Fedn Proc.* **38,** abstr., 1200 (1980).
5. Roos, M. H., Atkinson, J. P. & Shreffler, D. C. *J. Immun.* **121,** 1106–1115 (1978).
6. Schriber, R. D. & Muller-Eberhard, H. J. *J. exp. Med.* **140,** 1324–1335 (1974).
7. Parker, K. L., Roos, M. H. & Shreffler, D. C. *Proc. natn. Acad. Sci. U.S.A.* **76,** 5853–5857 (1979).
8. Abraham, G. N., Goldberger, G., Colten, H. R. & Williams, J. *Fedn Proc.* **38,** abstr., 1201 (1980).
9. Hall, R. E. & Colten, H. R. *J. Immun.* **118,** 1903–1905 (1977).
10. Greindder, D. K., Connorton, K. J. & David, J. R. *J. Immun.* **123,** 2808–2813 (1979).
11. Gordon, S., Unkeless, J. & Cohn, Z. A. *J. exp. Med.* **140,** 995–1010 (1974).
12. Bing, D. H., Andrews, J. M., Morris, K. M., Cole, E. & Irish, V. *Prep. Biochem.* (in the press).
13. Laemmli, U.K. *Nature* **227,** 680–685 (1970).
14. Fairbanks, G., Steck, T. L. & Wallach, D. F. H. *Biochemistry* **10,** 2606–2617 (1971).
15. Deutsch, D. G. & Mertz, E. T. *Science* **170,** 1095–1096 (1970).

A specific enzyme is not necessary for vanadate-induced oxidation of NADH

F. Vyskočil*, J. Teisinger† & Hana Dlouhá*

* Institute of Physiology, Czechoslovak Academy of Sciences,
142 20 Prague 4-Krč, Vídeňská 1083, Czechoslovakia
† Institute of Hygiene and Epidemiology, Prague 2, Czechoslovakia

It has recently been found that ortho- or metavanadate can effectively block $(Na^+ + K^+)$ATPase[1–4] and that it loses its blocking potency when reduced to the vanadyl (VO^{2+}) ion[5]. The question arose whether vanadate could be involved (reduced) in an NAD-linked enzymatic redox system of the cell. Here we have studied the effect of vanadate on malate dehydrogenase (MDH, EC1.1.1.37) catalysed oxidation of NADH during the formation of malate from oxalacetate *in vitro*. The MDH reaction was accelerated by vanadate, but we found that vanadate does not require the presence of any specific enzyme or substrate to mediate NADH oxidation.

Unless otherwise stated, the reaction medium contained 1×10^{-4} mol l^{-1} NADH and 8×10^{-4} mol l^{-1} Na_3VO_4 [stock solution: 500 mg of $NaVO_3$(Merck) dissolved in 1 ml of 1 mol l^{-1} NaOH] at the beginning of each experiment.

The rate of the MDH reaction (MDH 0.033 U ml^{-1}), measured continuously on an Eppendorf photometer at A_{366} as the amount of NADH lost in 0.1 mol l^{-1} Tris-HCl buffer (*p*H 7.2) at 37 °C, was accelerated in the presence of vanadate. The loss of NADH was, however, observed even without MDH, if only vanadate and NADH (and oxalacetate 0.5 mmol l^{-1}) were present in the reaction medium. The vanadate-accelerated MDH reaction (loss of 4.14 μmol of NADH per min) is thus the result of the sum of the MDH reaction (loss of 1.75 μmol of NADH per min) plus the vanadate–NADH (loss of 2.29 μmol of NADH per min). Vanadate can thus induce the oxidation of NADH (probably by accepting electrons itself), and this process does not require any further enzymatic support. According to our preliminary observations in the UV spectrophotometer, vanadate immediately forms a complex with NADH, within which the NADH reduction subsequently proceeds. This redox system might be masked in biochemical experiments in which buffers with EDTA (or biological samples containing this

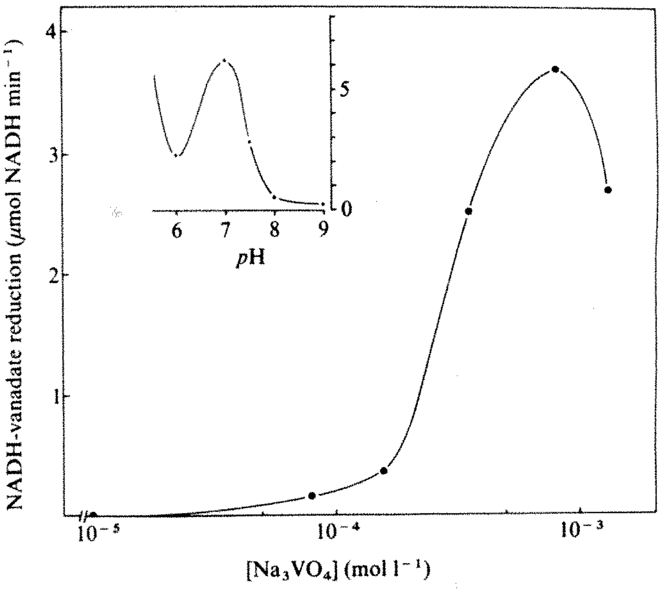

Fig. 1 Effect of vanadate on NADH oxidation in 0.1 mol l^{-1} phosphate buffer (*p*H 7.3) at 37 °C. Abscissa, concentration of vanadate [Na_3VO_4] in mol l^{-1}. Ordinate, the rate of NADH–vanadate reduction expressed as loss of NADH in μmol min^{-1} (see Erdmann *et al.*[7], Fig. 1). Inset, *p*H dependence of NADH loss (in μmol NADH per min, ordinate) in 0.1 mol l^{-1} phosphate buffer at 37 °C. Concentrations of vanadate and NADH at the beginning of experiments were 8×10^{-4} and 1×10^{4} mol l^{-1}, respectively. All results presented here are the means of 5–10 experiments. The s.e.m. values were always smaller than 5% of the mean and are therefore not indicated.

0028-0836/80/310516—02$01.00

Table 1 The rate of NADH oxidation in the presence of 8×10^{-4} mol l^{-1} vanadate in different reaction media

	mol l^{-1}	T(°C)	pH	−ΔNADH
Na-phosphate	0.1	17	7.3	2.18
Na-phosphate	0.1	27	7.3	2.41
Na-phosphate	0.1	37	7.3	3.84
Na-phosphate	0.1	37	7.0	6.15
Tris-HCl	0.1	37	7.2	5.20
HEPES-NaOH	0.01	37	7.0	1.70
Liley's solution	*	37	7.3	0.92
Histidine–NaOH	0.01	37	7.1	0.09
Imidazole-HCl	0.01	37	7.0	0.00

The rate of NADH oxidation is expressed as the loss of NADH in μmol min^{-1}, −ΔNADH. The concentration of NADH at the beginning of experiments was 10^{-4} mol l^{-1}.

The composition of Liley's solution[9] was (mol l^{-1}): Na^+ 149.8; K^+ 5.0; Ca^{2+} 2.0; Mg^{2+} 1.0; Cl^- 148.0; HCO_3^- 12.0; $H_2PO_4^-$ 1.0; glucose 11.0.

chelating compound) are used; in the presence of 1×10^{-3} mol l^{-1} EDTA no oxidation of NADH was observed, probably because inactive complexes are formed with vanadate[6].

A recent report[7] described the vanadate–NADH reductase activity of cardiac cell membranes. Because these authors claimed that there was no vanadate-induced NADH oxidation unless membrane proteins were present, we looked for the probable sources of this discrepancy. The only difference between our experiments and those of Erdmann *et al.*[7] was the buffer used in the reaction medium. When we started the vanadate–NADH reaction in a 0.01 mol l^{-1} imidazole-HCl buffer[7], we also found no oxidation of NADH. Contrary to the findings of Erdmann *et al.*[7], we observed no vanadate-dependent oxidation of NADH in the presence of membrane fractions isolated from rat and golden hamster heart[8] and other tissues (skeletal muscle, brain and liver). Subsequently, we checked several other buffers used for biochemical experiments (Table 1) and Liley's extracellular medium[9]. With the exception of the imidazole and histidine buffer, the vanadate–NADH reaction proceeded in all media.

The vanadate–NADH reaction in Tris-HCl medium was slowed to 50% by either 2.5 mmol l^{-1} Ca^{2+} or 20 mmol l^{-1} Mg^{2+}. The presence of Ca^{2+} and Mg^{2+} might therefore explain the rather slow rate of NADH oxidation in Liley's medium. The reaction is dependent on the concentration, pH (Fig. 1) and temperature (Table 1).

Similar results were obtained in the NADPH–vanadate reaction medium. Thus, 2.95 μmol NADPH was oxidized within 1 min in the presence of 8×10^{-4} mol l^{-1} vanadate and 7×10^{-5} mol l^{-1} NADPH at 37 °C in the Tris-HCl buffer.

Further examples can be presented concerning the more generalized role of vanadate in living redox systems. Vanadate–NADPH reduction was accelerated by 80% after the addition of 1 μmol l^{-1} β-hydroxy-β-methyl-glutaryl-CoA (HMGCoA). However, it is not clear whether the reduction of HMGCoA to mevalonate is triggered in this particular case by vanadate in the absence of hydroxylmethylglutaryl CoA reductase or whether HMGCoA only accelerates the transfer of electrons from NADH to vanadate within the complex. Whatever the explanation, this effect of vanadate might be of particular interest because the HMGCoA reductase is generally considered to be the rate determining enzyme for the conversion of acetate to cholesterol[10].

Received 31 January; accepted 27 May 1980.

1. Cantley, L. C. *et al. J. biol. Chem.* **252,** 7421–7423 (1977).
2. Beaugé, L. A. & Glynn, I. M. *Nature* **272,** 551–552 (1978).
3. Cantley, L. C., Resh, M. D. & Guidotti, G. *Nature* **272,** 552–554 (1978).
4. Karlish, S. J. D., Beaugé, L. A. & Glynn, I. M. *Nature* **282,** 333–335 (1979).
5. Cantley, L. C. & Aisen, P. J. *J. biol. Chem.* **254,** 1781–1784 (1979).
6. Ringbom, A., Siitonen, S. & Skrifvars, B. *Acta chem. scand.* **11,** 551–556 (1957).
7. Erdmann, E. *et al. Nature* **282,** 335–336 (1979).
8. Matsui, A. & Schwartz, A. *Biochim. biophys. Acta* **128,** 380–390 (1966).
9. Liley, A. W. *J. Physiol., Lond.* **132,** 650–666 (1956).
10. Rodwell, K. W., McNamara, D. J. & Shapiro, D. J. *Adv. Enzym.* **38,** 373–412 (1973).

Visualization of the structural polarity of microtubules

Steven R. Heidemann* & **J. Richard McIntosh†**

* Department of Physiology, Michigan State University, East Lansing, Michigan 48824
† Department of Molecular, Cellular and Developmental Biology, University of Colorado, Boulder, Colorado 80309

Microtubules (MTs) are intrinsically polar fibres[1–8]. Many models for the mechanism of MT-mediated transport and mitosis postulate an important role for MT polarity[7,9–12] because a symmetric fibre could not generate force in one direction along its surface. The lack of a convenient method to determine the polar orientation of cellular MTs has hindered experimental testing of these ideas. We report here a convenient technique for visualizing MT polarity based on conditions for tubulin assembly *in vitro* whereby MT elongation occurs with the associated formation of hooked, protofilament appendages on the MT wall (see Fig. 1). There is polarity information in such junctions between MT walls[13–15]; our method reveals the polarity of the cellular MT by the handedness of the hooked appendage as seen in cross-section (Fig. 1).

Microtubule protein (MTP) was prepared from porcine brain by the method of Shelanski *et al.*[16] After three cycles of polymerization, the protein was resuspended in 0.5 M PIPES pH 6.9, 2.5% dimethyl sulphoxide, 1 mM EDTA, 1 mM $MgCl_2$, and 1 mM GTP (hereafter called polymerization buffer (PB)) at 0 °C and spun at 250,000g for 3 h. The polymerization of MTP in PB is similar in its magnesium and GTP requirement and in its cold, calcium and colchicine lability to that which occurs in other polymerization buffers[17]. MTP will assemble to the same extent in PB in the presence of a strong detergent mixture, 1% Triton X-165, 0.5% deoxycholate, 0.2% SDS. MTP assembly in PB also shows the biased polar growth characteristic of other *in vitro* assembly conditions[5,7,18]. One end of isolated *Tetrahymena* ciliary axonemes elongated about twice as fast as the other at the protein concentrations tested. Elongation at each end of the axoneme was about three times as fast as growth at the comparable end in 0.1 M PIPES buffer.

The polymer initiated *de novo* in PB consists primarily of ribbons of laterally associated protofilaments, as previously reported for similar conditions[14,15], not true MTs. However, when true MTs nucleate the polymerization, the elongated polymer usually has an evident lumen, and ribbons of protofilaments join the MT wall, forming hooked appendages (Fig. 1). We have examined such polymers to see if one handedness of hook predominates by nucleating MT growth from basal bodies. The MTs of the basal body are known to be oriented with the fast growing end of their MTs pointing away from the cell[6]. When lysed and deciliated *Tetrahymena* were used to nucleate the assembly of MTP in PB, polymerization occurred largely as elongation from the basal bodies (Fig. 2a). Pellicles in MTP fixed before polymerization was initiated showed no MT growth (Fig. 2b). After polymerization, the organized geometry of basal bodies in the pellicle allowed us to observe the elongated polymers in known orientations with respect to the basal bodies that initiated them (Fig. 2c). We found that about 95% of the newly grown MTs had the hook-shaped appendages. Figure 2d is a composite of several such images as seen looking toward the basal body from outside the pellicle. Figure 2e shows MTs growing inward as seen from the basal body. We confirmed both in longitudinal sections and by negative staining that the hooks are protofilament sheets which make a junction with the MT wall. The cross-section images demonstrate that when the elongated MT is viewed from its fast growing end or '+end' towards its slow growing end or '−end'(ref. 8) the hooks are commonly right handed. On polymers growing outward from the basal body (those initiated at a fast end) we counted 562 MTs with right-handed hooks and 62 with left-handed hooks when viewed from +end to −end. On

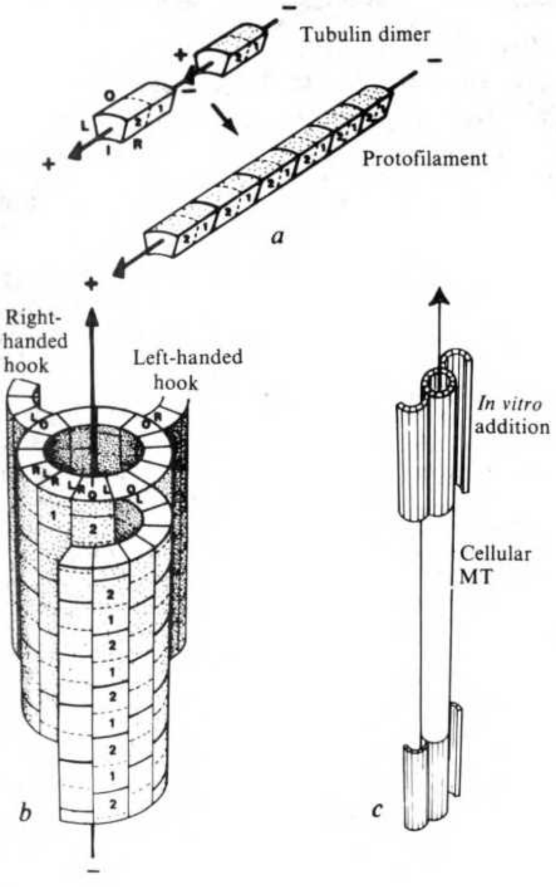

Fig. 1 Different associations of MTP. The tubulin dimer is pictured as having six dissimilar surfaces. + and − correspond to the distal and proximal ends, respectively, of a flagellar MT[22]. I and O are the surfaces which would be on the inside and outside of a normal MT, L and R are the two surfaces which associate laterally in the wall of a normal MT. The numbers 1 and 2 denote the different subunits of the tubulin dimer. The intradimer bonds are suggested by dashed line, interdimer bonds by solid ones. *a*, The head-to-tail association of dimers to form protofilaments. *b*, Protofilaments have associated laterally to form MT wall (L–R interactions) or in two alternative geometries to form junctions between MT walls, which also occur naturally[23,24]. Wall junctions and concomitant hooks of two possible hands are made by associating either the R or L surface of a protofilament with the O surface. A tacit assumption is made that the protofilament polarity of the hook wall is the same as that of the tubule itself. *c*, In our conditions neurotubulin adds *in vitro* to a cellular MT to form predominantly right-handed hooked MTs. The polarity orientation of a MT end can be determined from the observed hook-handedness of newly grown MTs.

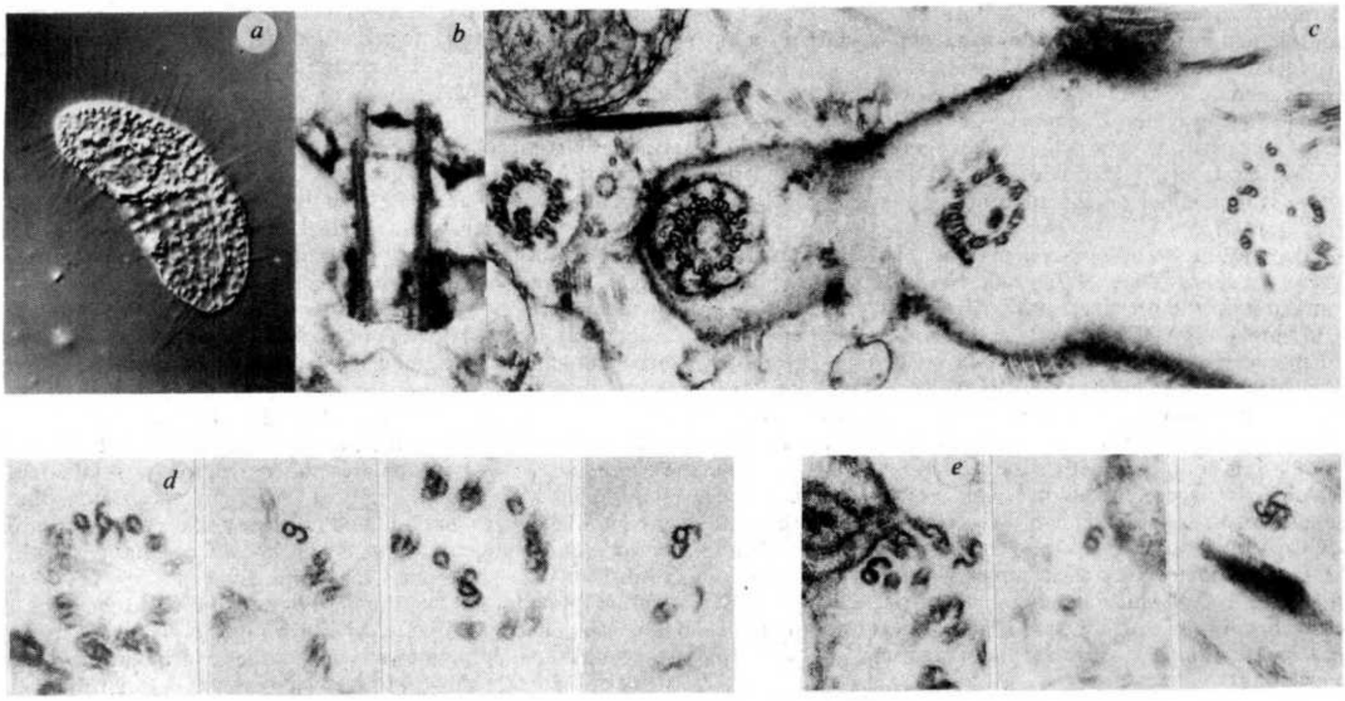

Fig. 2 *Tetrahymena* pellicles were used to nucleate growth of 1 mg ml^{-1} microtubule protein in PB at 37 °C for 6 min, then fixed by addition of an equal volume of 2% glutaraldehyde in 0.1 M PIPES. Fixed pellicles were allowed to settle onto polylysine-coated slides and were then treated with 0.2% tannic acid, rinsed in phosphate-buffered saline, post-fixed in $\frac{1}{2}$% OsO_4 for 2 min, dehydrated in 2-methoxyethanol and flat embedded in Epon. Individual pellicles were excised, serially sectioned and stained with uranyl acetate and lead citrate. Microscopy was performed on a Phillips 300 equipped with a goniometer stage to facilitate orientation of the tubules. *a* Is a Nomarski image of MT polymerization from such a pellicle after 6 min at 37 °C, ×600. *b* Was fixed at 0 °C (no growth), ×55,000. *c* Is 6 min of growth. The orientation of the growing MTs may be deduced from pellicle geometry, ×55,000. *d* Is a composite of MT images seen looking from the outside of the pellicle towards the basal body. *e* Shows MTs growing inward from the basal body; *d* and *e*, ×92,000.

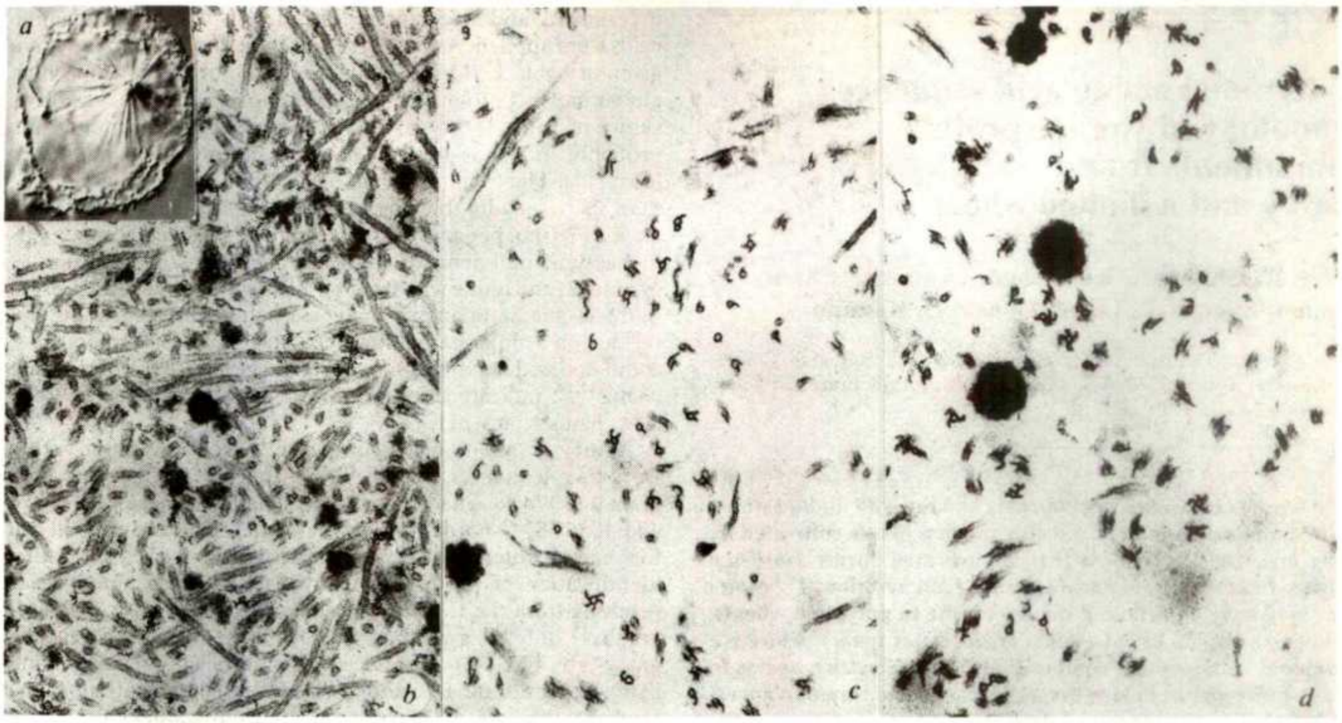

Fig. 3 Microtubule polarity in the mitotic aster of the HeLa cell. *a*, Nomarski image of a metaphase-arrested HeLa cell lysed in detergent-containing PB with 2 mg ml^{-1} MTP, ×750. *b*, An electron micrograph from a section approximately at the centre of an aster. Note that MTs are generally of normal morphology. *c*, The periphery of an aster in a section 'before' the aster centre. Note that most MTs have right-handed hook appendages. *d*, The periphery of an aster in a section 'beyond' the aster centre. The hooks are now left handed; however, the apparent observation point for these hooks is now proximal to the centre, in contrast to the distal vantage point of *c*; *b*, *c* and *d*, ×40,000.

MTs growing inward from the basal bodies, viewed from the same direction, we found 135 MTs with right-handed hooks and 25 MTs with left-handed hooks. Eight MTs displayed hooks of both handedness.

We next studied the polarity of mitotic MTs by using a remnant of the mitotic apparatus from HeLa cells. Hela cells stably blocked in metaphase with 0.04 μg ml $^{-1}$ of the microtubule poison nocodazole[19] contained large numbers of MTs with typical mitotic organization[20]. Lysis of nocodazole-poisoned cells in PB containing the detergent mixture described above preserved metaphase aster structures approximately 5 μm in diameter surrounded by a thin, fibrous cell remnant. These asters consisted of normal MTs, presumably those which existed in the drug-poisoned cell. Inclusion of 2 mg ml^{-1} MTP in the PB lysis buffer produced asters up to 20 μm in diameter (Fig. 3*a*). In these large asters, 85% of the MTs were normal within a 5 μm radius of the aster centre (Fig. 3*b*). In the area beyond a 5 μm radius, 80% of the MTs displayed the hooked appendages (Fig. 3*c*,*d*). Our interpretation is that exogenous brain tubulin added to the distal ends of pre-existing HeLa MTs to form hooked MTs. Serial sections from four such asters reveal predominately right-handed hooks when viewed looking toward the aster centre: 1752 MTs showed only right-handed hooks, 121 MTs bore only left-handed hooks and 66 MTs displayed hooks of both handedness.

Close to 90% of all hooks on neurotubules elongated from both basal body and astral MTs displayed a consistent handedness relative to the MT on which they formed. As the same predominant handedness of hook was seen on MTs growing in both directions from the basal body, we conclude that our method reveals the molecular polarity of a MT, not its direction of growth. For the same reason, we infer that the MTs which grew from the basal body have the same polarity as the A subfibre in the basal body itself. Hook handedness on the elongated MT therefore reflects the polarity of the MT which nucleated elongation. The preponderance of right-handed hooks on MTs extending from both asters and basal bodies indicates that the astral MTs have the same polarity relative to the mitotic centre as do the outer nine flagellar MTs relative to the basal body. That is, the fast or +end of the HeLa MT is distal to the mitotic centre. This is the same polarity as that of neurotubules initiated from the mitotic centres of lysed CHO cells[21,22]. This agreement supports our assertion that hook handedness is a valid marker of MT polarity. The observed bias toward right-handed hooks on MTs grown from both basal bodies and asters was strong (about 9:1) but not complete. Further, MTs with hooks of both hands were occasionally observed, so we conclude that left-handed wall junctions are not excluded. Our method reveals and uses a biased formation of right-handed wall junctions to visualize the molecular polarity of the MT.

This investigation was supported by Biomedical Research Support funds from the Colleges of Osteopathic Medicine and Natural Science, Michigan State University, and grants CD 8D from the American Cancer Society and PCM-77-14796 from the NSF to J.R.M. S.R.H. would like to thank the Department of Microbiology, M.S.U. for the use of their electron microscope.

Received 17 March; accepted 13 May 1980.

1. Amos, L. A. & Klug, A. *J. Cell Sci.* **14,** 523–549 (1974).
2. Crepeau, R. H., McEwen, B., Dykes, G. & Edelstein, S. J. *J. molec. Biol.* **116,** 301–315 (1977).
3. Baker, T. S. & Amos, L. A. *J. molec. Biol.* **123,** 89–106 (1978).
4. Dentler, W. L., Granett, S., Witman, G. B. & Rosenbaum, J. L. *Proc. natn. Acad. Sci. U.S.A.* **71,** 1710–1714 (1974).
5. Allen, C. & Borisy, G. G. *J. molec. Biol.* **90,** 381–402 (1974).
6. Rosenbaum, J. L. *et al. Ann. N.Y. Acad. Sci.* **253,** 147–177 (1975).
7. Margolis, R. L. & Wilson, L. *Cell* **13,** 1–8 (1978).
8. Bergan, L. G. & Borisy, G. G. *J. Cell Biol.* **84,** 141–150 (1980).
9. Subirana, J. A. *J. theor. Biol.* **20,** 117–123 (1968).
10. McIntosh, J. R., Hepler, P. K. & Van Wie, D. G. *Nature* **224,** 659–663 (1969).
11. Nicklas, R. B. *Adv. Cell Biol.* **2,** 225–297 (1971).
12. Margolis, R. L., Wilson, L & Kiefer, B. J. *Nature* **272,** 450–452 (1978).
13. Mandelkow, E-M. & Mandelkow, E. *J. molec. Biol.* **129,** 135–148 (1979).
14. Burton, P. R. & Himes, R. H. *J. Cell Biol.* **77,** 120–133 (1978).
15. Himes, R. H., Newhouse, C. S., Haskins, K. M. & Burton, P. R. *Biochem. biophys. Res. Commun.* **87,** 1031–1038 (1979).
16. Shelanski, M. L., Gaskin F. & Cantor, C. R. *Proc. natn. Acad. Sci. U.S.A.* **70,** 765–768 (1973).
17. Weisenberg, R. C. *Science* **177,** 1104–1106 (1973).
18. Summers, K. & Kirschner, M. W. *J. Cell Biol.* **83,** 205–217 (1979).
19. Zieve, G. W., Turnbull, D., Mullins, J. M. & McIntosh, J. R. *Expl Cell Res.* (in the press).
20. Heidemann, S. R., Zieve, G. W. & McIntosh, J. R. *J. Cell Biol.* (submitted).
21. Borisy, G. G. *J. molec. Biol.* **124,** 565–570 (1978).
22. Bergan, L. G., Kuriyama, R. & Borisy, G. G. *J. Cell Biol.* **84,** 151–159 (1980).
23. Turner, F. R. *J. Cell Biol.* **53,** 263–270 (1972).
24. Tilney, L. G. *et al. J. Cell Biol.* **59,** 267–275 (1973).

N-terminal amino acid sequence homology of storage protein components from barley and a diploid wheat

Peter R. Shewry*, Jean-Claude Autran†, Charles C. Nimmo, Ellen J.-L. Lew & Donald D. Kasarda

Food Proteins Research Unit, Western Regional Research Center, Agricultural Research, SEA, US Department of Agriculture, Berkeley, California 94710

Wild barley (*Hordeum spontaneum*) and the wild diploid wheat *Triticum boeoticum* were possibly the first plants cultivated by early man[1], giving rise to the domesticated forms *Hordeum vulgare L.* and *Triticum monococcum L.* In addition, *T. boeoticum* may have contributed the A genome to polyploid wheats, including common bread wheat (*Triticum aestivum*)[2] which is a hexaploid with genome composition ABD. *Hordeum* seems to be the older genus, having diverged from some common ancestor before the divergence of *Triticum* and other genera of the subtribe Triticinae[3]. Prolamins constitute the major storage protein fraction of both barley and wheat; they are located in the endosperm of the caryopsis and are soluble in alcohol–water solutions[4]. Barley and wheat prolamins (hordeins and gliadins, respectively) contain large amounts of glutamine and proline, which together make up 50–75 mol per cent of total amino acids[4,5]. The hordeins and gliadins are complex mixtures of components[6–8] that seem to be encoded by clusters of duplicated genes that have diverged to produce many distinguishable protein components. Despite the complexity of the gliadin mixture, the components retain considerable homology in their N-terminal region[9,10] and this has been reported for zeins, the prolamins of maize (*Zea mays*)[11], as well. Here, we report that a purified C-hordein component from barley is homologous in amino acid sequence with a purified ω-gliadin component from *T. monococcum* at 23 of 27 residues at the N-terminus. This result is in accord with the close relationship between the two species and indicates that, despite the propensity of prolamin genes to tolerate mutations, a significant portion of their sequences can be conserved over a period of time, which, although not accurately known, probably amounts to millions of years.

Prolamins were extracted from barley (*H. vulgare* Julia) and *T. monococcum* (from the University of Manitoba) as described previously[10,12]. The C-hordein component was obtained by ion exchange chromatography of the hordein mixture on CM-cellulose followed by gel filtration on Sephacryl S–300 (ref. 12). The ω-gliadin component from *T. monococcum* was obtained by ion exchange chromatography of the gliadin mixture on CM-cellulose according to the procedure of Booth and Ewart[13] except that the gradient ranged linearly from 5 to 43 mM in sodium acetate; this component was not purified further. Electrophoretic patterns of the purified components in aluminium lactate buffer, pH 3.2, where separation is based on net charge, are compared with those of the prolamin mixtures in Fig. 1. We estimated molecular weights of 57,000 for the C-hordein and 44,000 for the ω-gliadin by SDS polyacrylamide gel electrophoresis[6].

Amino acid analyses were carried out on a Durrum analyser, model D–500. Hydrolyses were for 24 h, tryptophan was not determined, and no corrections for destruction of labile amino acids were applied. Averaged results from duplicate analyses are given in Table 1. Both components were notable for their high glutamine and proline content (although glutamic acid only is shown in Table 1, this amino acid is present in C-hordein[12] and probably in the ω-gliadin[14] almost entirely in its amidated form[12,14]). The C-hordein had more proline and less glutamine than the ω-gliadin, but the sum of these two amino acids was close to 70 mol per cent for both components. Both components had about 9 mol per cent phenylalanine, only trace amounts of cystine/2, and lysine was absent from the C-hordein and present in the ω-gliadin in an amount corresponding to only about 0.5 residue on a molar basis. Low percentages of basic amino acids, combined with equivalent low percentages of free carboxyl side chains[12,14], indicate that these proteins will have few charged side chains at any pH.

Automatic amino acid sequencing[15] was carried out with a Beckman sequencer, model 890B, and DMAA peptide program 111374 (ω-gliadin) or 0.1 M Quadrol programs 011576 and 121178 (C-hordein). Duplicate analyses were carried out for each protein. In the first analysis of the ω-gliadin, identification of the phenylthiohydantoin (PTH) amino acids resulting from the Edman degradation[15] was by gas chromatography[16] only; this method was supplemented in the second analysis by TLC on polyamide sheets[17] and silica gel plates[18] and by hydrolysis to the free amino acid followed by analysis on the Durrum analyser. PTH amino acids from sequencing of the C-hordein were identified by HPLC[19], which clearly resolved and quantified all the PTH amino acids found in the first 28 cycles. The N-terminal sequences obtained are compared in Fig. 2. Initial yields in sequencing ranged from 50 to 76% of molar

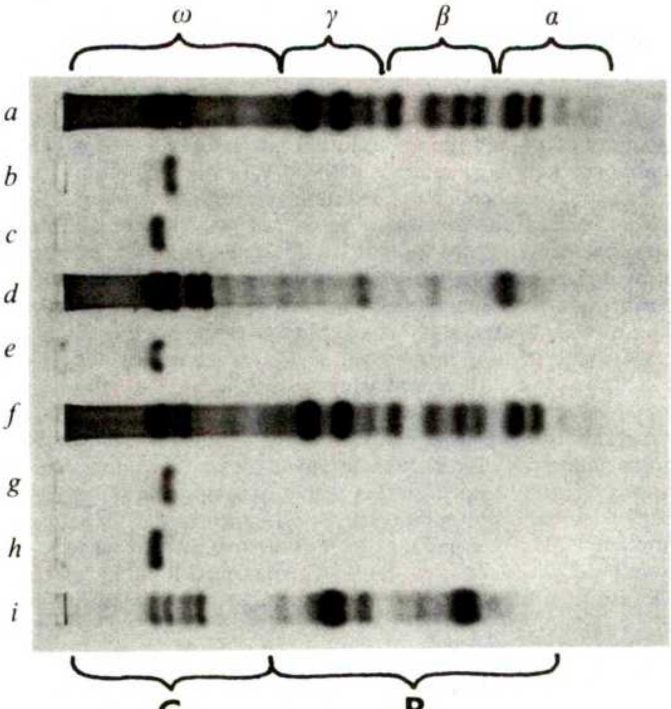

Fig. 1 Polyacrylamide gel electrophoresis[27] of purified protein components and the whole prolamin mixtures from which they were prepared, aluminium lactate buffer, pH 3.2, 3 M urea, migration from left (+) to right (−): *a*, prolamin mixture from *T. monococcum*; *b*, purified ω-gliadin from *T. monococcum*; *c*, purified C-hordein; *d*, prolamin mixture from barley (var. Julia); *e*, same as *c*; *f*, same as *a*; *g*, same as *b*; *h*, same as *c*; *i*, prolamin mixture from barley (Julia), but treated with 2% 2-mercaptoethanol to dissociate B-hordeins. The α-, β-, γ- and ω-regions (top) correspond to the usual assignments of electrophoretic mobilities for gliadin patterns of common wheats[5] and the B- and C-regions (bottom) correspond to the hordein patterns.

---

* Permanent address: Biochemistry Department, Rothamsted Experimental Station, Harpenden, Herts AL5 2JQ, UK.

† Permanent address: Institut National de la Recherche Agronomique, Laboratoire de Technologie des Cereales, 9 Place Viala, 34060 Montpellier, France.

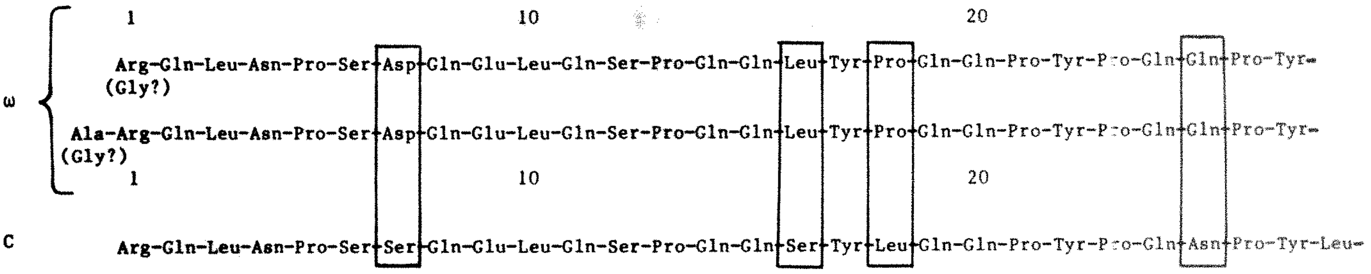
1
10
20
ω
Arg-Gln-Leu-Asn-Pro-Ser-Asp-Gln-Glu-Leu-Gln-Ser-Pro-Gln-Gln-Leu-Tyr-Pro-Gln-Gln-Pro-Tyr-Pro-Gln-Gln-Pro-Tyr-
(Gly?)
Ala-Arg-Gln-Leu-Asn-Pro-Ser-Asp-Gln-Glu-Leu-Gln-Ser-Pro-Gln-Gln-Leu-Tyr-Pro-Gln-Gln-Pro-Tyr-Pro-Gln-Gln-Pro-Tyr-
(Gly?)
1
10
20
C
Arg-Gln-Leu-Asn-Pro-Ser-Ser-Gln-Glu-Leu-Gln-Ser-Pro-Gln-Gln-Ser-Tyr-Leu-Gln-Gln-Pro-Tyr-Pro-Gln-Asn-Pro-Tyr-Leu-

Fig. 2 N-terminal amino acid sequences of the ω-gliadin component from *T. monococcum* (ω) and the C-hordein component from barley (C). Sequences are ordered from the first arginine residue to emphasize homology. Glycine was a minor residue at cycle 1 in the sequence of the ω-gliadin. Positions where the ω-gliadin and C-hordein sequences differ are marked.

amounts applied. The highest yield of 76% for one of the C-hordein analyses indicates there was no significant N-terminal blocking.

No important minor residues were noted in sequencing the C-hordein, but three amino acids were identified in the first cycle of the ω-gliadin sequence and two amino acids at each subsequent cycle. Alanine was the major residue at cycle 1 in the ω-gliadin, but glycine and arginine were clearly identified; in subsequent cycles it became clear that the second sequence appearing at about half the level of the major sequence was the same as that of the major sequence displaced by one cycle. It evidently resulted from a protein component without the terminal alanine (or glycine) residue. Electrophoresis of the purified ω-gliadin did not show any minor components in sufficient amount to account for the second sequence; however, it is unlikely that a component differing by only one neutral amino acid would be resolved. The extra residue could mean that at least two genes code for the proteins in our preparation, but post-translational modifications might modify a single component in such a way as to produce the 2:1 ratio of components we observed.

Comparison of the amino acid sequences of our two components (Fig. 2) shows that they differ only at four positions if we do not consider the N-terminal alanine residue that is present in part of the ω–gliadin preparation. This demonstrates a close relationship between *H. vulgare* and *T. monococcum*. No fossil evidence provides a measure of the time since divergence of *Hordeum* and *Triticum*. If we assume for purposes of speculation, however, that the rate of evolution of the N-terminal regions of our proteins is equivalent to that of one of the fastest evolving peptide systems characterized so far, the fibrinopeptides (9.0 amino acid substitutions per site per 10^9 yr)[20], then the time since divergence of our two species would be 16 Myr.

Table 1 Amino acid compositions (mol%) of the ω-gliadin protein from *T. monococcum* and the C-hordein protein from barley (var. Julia)

	ω-Gliadin	*C*-hordein
Asp	1.18	0.83
Thr	1.08	0.99
Ser	4.89	2.61
Glu	45.2	41.1
Pro	26.2	31.9
Gly	0.89	0.41
Ala	1.57	0.69
Val	0.80	1.11
Met	0.13	0.22
Ile	2.22	3.02
Leu	4.70	4.31
Tyr	1.17	2.29
Phe	8.09	9.03
His	0.56	0.60
Lys	0.13	0.0
Arg	1.04	0.84
Cys/2	Trace	Trace

The similar sequences we obtained for our C-hordein and our ω-gliadin from *T. monococcum* show little homology with any other N-terminal sequences reported for α-, β- or γ-gliadins of common wheat[9,10,21,22], rye prolamins[13] or maize prolamins[11]. Our sequence is the first reported, however, for any ω-gliadin component. Autran *et al.*[10] did not note evidence of our ω-gliadin sequence in sequencing of the whole prolamin mixture from the same accession of *T. monococcum*, but this is not surprising as ω-gliadins probably constitute less than 10% of the total mixture. Our C-hordein sequence is closely similar to sequences recently obtained for the total hordein mixture[23], the C-hordein mixture[24] and a partially purified C-hordein component[25].

In common bread wheat, which is hexaploid (genomes A, B and D), gliadin proteins are encoded by genes located on homoeologous (partially homologous, but non-pairing in the polyploid) chromosomes 1 and 6 of each genome[7,26–28]. Shepherd[29] has suggested that all gliadin genes were located originally on one chromosome and that translocation of part of this chromosome to another gave rise to the common ancestor that, in turn, differentiated into the progenitors of the common wheat genomes A, B and D. This common ancestor must have already differentiated from the line that gave rise to *Hordeum* as all the prolamin genes of barley are located on chromosome 5 with the B-hordeins and C-hordeins being coded by two separate, but linked, loci[30]. Our results suggest that the C-hordein locus of barley and the ω-gliadin loci located on homoeologous chromosomes of group 1 in common wheat are homologous. It is also possible that the B-hordein locus is homologous with the gliadin loci coding for α-, β- and γ-gliadins that are located on homoeologous chromosomes of group 6 in common wheat but this is more difficult to establish as B-hordein is blocked at the N-terminus[12,25].

We thank A. Noma for amino acid analyses, B. J. Miflin for barley samples, and B. L. Jones for the sample of *T. monococcum*. P. R. Shewry and J.-C. Autran are visiting scientists in receipt of NATO postdoctoral research fellowships. Reference to a company or product name by the Department is only for information and does not imply approval or recommendation to the exclusion of others that may also be suitable.

Received 2 April; accepted 21 May 1980.

1. Harlan, J. R. in *Origins of Agriculture* (ed. Reed, C. A.) 357–383 (Mouton, The Hague, 1977).
2. Konzak, C. F. *Adv. Genet.* **19**, 407–582 (1977).
3. Smith, D. B. & Flavell, R. B. *Biochem. Genet.* **12**, 243–256 (1974).
4. Miflin, B. J. & Shewry, P. R. in *Seed protein Improvement in Cereals and Grain Legumes*, 137–158 (International Atomic Energy Agency, Vienna, 1979).
5. Kasarda, D. D., Bernardin, J. E. & Nimmo, C. C. in *Advances in Cereal Science and Technology* Vol. 1 (ed. Pomeranz, Y.) 158–236 American Association of Cereal Chemists, St Paul, Minnesota, 1976).
6. Shewry, P. R., Ellis, J. R. S., Pratt, H. M., Miflin, B. J. *J. Sci. Fd Agric.* **29**, 433–441 (1978).
7. Wrigley, C. W. & Shepherd, K. W. *Ann. N.Y. Acad. Sci.* **209**, 154–162 (1973).
8. Mecham, D. K., Kasarda, D. D. & Qualset, C. O. *Biochem. Genet.* **16**, 831–853 (1978).
9. Bietz, J. A., Huebner, F. R., Sanderson, J. E. & Wall, J. S. *Cereal Chem.* **54**, 1070–1083 (1977).
10. Autran, J. C., Lew, E. J.-L., Nimmo, C. C. & Kasarda, D. D. *Nature* **282**, 527–529 (1979).
11. Bietz, J. A., Paulis, J. W. & Wall, J. S. *Cereal Chem.* **56**, 327–332 (1979).
12. Shewry, P. R., Field, J. M., Kirkman, M. A., Faulks, A.J. & Miflin, B. J. *J. exp. Bot.* **31** (in the press).
13. Booth, M. R. & Ewart, J. A. D. *Biochim. biophys. Acta* **181**, 226–233 (1969).
14. Charbonnier, L. *Biochim. biophys. Acta* **359**, 142–151 (1974).
15. Edman, P. & Begg, G. *Eur. J. Biochem.* **1**, 80–91 (1967).

16. Pisano, J. J., Bronzert, T. J. & Brewer, H. B. Jr *Analyt. Biochem.* **45,** 43-59 (1972).
17. Kulbe, K. D. *Analyt. Biochem.* **59,** 564–573 (1974).
18. Jeppson, J.-O. & Sjoquist, J. *Analyt. Biochem.* **18,** 264–269 (1967).
19. Bhown, A. S., Mole, J. E., Weissinger, A. & Bennett, J. C. *J. Chromatogr.* **148,** 532–535 (1978).
20. Kimura, M. *Scient. Am.* **241** (5), 98–126 (1979).
21. Kasarda, D. D., Da Roza, D. A. & Ohms, J. I. *Biochim. biophys Acta* **351,** 290–294 (1974).
22. Patey, A. L., Evans, D. J., Tiplady, R., Byfield, P. G. H. & Matthews, E. W. *Lancet* **ii,** 718 (1975).
23. Bietz, J. A. *Cereal Chem.* (in the press).
24. Shewry, P. R., March, J. M. & Miflin, B. J. *Phytochemistry* (in the press).
25. Schmitt, J. M. & Svendsen, I. *Carlsberg Res. Commun.* (in the press).
26. Shepherd, K. W. *Proc. 3rd Int. Wheat Genet. Symp.* (eds Finlay, K. W. & Shepherd, K. W.) 86–96 (Australian Acad. Sci., Canberra, 1968).
27. Kasarda, D. D., Bernardin, J. E. & Qualset, C. O. *Proc. natn. Acad. Sci. U.S.A.* **73,** 3646–3650 (1976).
28. Mitrofanova, O. P. *Tsitologiya i Genetika*–10 (3), 244–247 (1976).
29. Shepherd, K. W. in *Proc. 4th Int. Wheat Genet. Symp.* (eds Sears, E. R. & Sears, L. M. S.) 745–760 (Agric. exp. Station, University of Missouri, Columbia, 1973).
30. Shewry, P. R. *et al. Heredity* **44,** 383–389 (1980).

Structure of *S. platensis* [2Fe-2S] ferredoxin and evolution of chloroplast-type ferredoxins

Keiichi Fukuyama*, Toshiharu Hase†, Satoshi Matsumoto*, Tomitake Tsukihara*, Yukiteru Katsube*, Nobuo Tanaka‡, Masao Kakudo‡, Keishiro Wada† & Hiroshi Matsubara†

* Faculty of Engineering, Tottori University, Tottori 680, Japan
† Department of Biology, Faculty of Science, Osaka University, Toyonaka, Osaka 560, Japan
‡ Institute for Protein Research, Osaka University, Suita, Osaka 565, Japan

Ferredoxins are iron–sulphur proteins with either one or two [4Fe-4S] clusters or one [2Fe-2S] cluster and they function as electron carriers in diverse metabolic systems. Extensive comparative studies on the primary structures of ferredoxins with low oxidation–reduction potentials from a wide variety of organisms have provided information on the structure–function and evolutionary relationships of these proteins[1,2]. In addition, the three-dimensional structure of *Peptococcus aerogenes* 2[4Fe-4S] ferredoxin has been elucidated[3]. However, nothing is known about the three-dimensional structure of [2Fe-2S] ferredoxins such as those of chloroplasts. Here we report the three-dimensional structure of a [2Fe-2S] ferredoxin of *Spirulina platensis*, a blue-green alga, determined by X-ray crystallography at 2.5 Å resolution, and discuss the characteristic features of the molecule in relation to the molecular evolution of ferredoxins of this class.

We will give only a brief description of our study, because full details of the analytical procedures and crystal structure of ferredoxin will be reported elsewhere. The crystals were orthorhombic with a space group C222$_1$ of $a = 62.32$, $b = 28.51$, $c = 108.08$ Å and $Z = 8$. Intensity data, including both reflections of each Friedel pair, were collected for native and uranium derivative crystals on a Rigaku four-circle diffractometer with Ni-filtered CuKα radiation by an ω scan procedure. After correction for absorption[4] and radiation damage, the intensities of equivalent reflections were averaged. The heavy-atom parameters[5] were refined by the F_{HLE} method[6] with empirically determined values of the real/imaginary scattering ratio to give an R value ($R = \sum |F_{\mathrm{HLE}} - f_{\mathrm{H}}| / \sum |F_{\mathrm{HLE}}|$) of 0.398 for 1,956 reflections (55% of total reflections). The best phase angle was calculated by the single isomorphous replacement method[7] coupled with the anomalous dispersion method[8], where the anomalous dispersion effect of the two iron atoms was taken into account. The mean figure of merit at 2.5 Å resolution was 0.58 for 2,182 reflections (61% of total reflections). A Kendrew-type skeletal model was built up using a Richards box[9] on the basis of the best electron density map. The molecular structure is shown in Fig. 1.

The sulphur atoms of Cys 41 and Cys 46 coordinate to one iron atom, and those of Cys 49 and Cys 79 to the other iron atom[5]. The coordination geometry around each iron atom is tetrahedral, judging from the electron density distribution around the atoms. The cluster is located near the molecular surface and is mainly surrounded by hydrophobic residues, leaving only one side, the sulphur atoms of Cys 41 and Cys 46, exposed to the solvent. In *P. aerogenes* ferredoxin and *Chromatium* HiPIP, electron transfer was suggested to be achieved through aromatic side chains in close contact with the [4Fe-4S] cluster[3,10]. However, in *S. platensis* ferredoxin there are no invariant aromatic side chains in close contact with the [2Fe-2S] cluster. An alternative possibility is that electron transfer may occur via the orbitals of cysteinyl sulphur atoms, as these residues are directly bonded to the cluster and two of them are located outside the molecule, as described above. Comparison of the amino acid sequences of various chloroplast-type ferredoxins[2] shows that several ferredoxins, particularly those of higher plants, have deletions at positions 10 and 14 and, in this case, proline at position 11. The segment of residues 9–14 in *S. platensis* ferredoxin without the two deletions corresponds to the loop at the end of the antiparallel β-sheet. The overall structure of this region is probably very similar in the two types of ferredoxin, because the segment in ferredoxin without the two residues may take a 3_{10} turn by forming a hydrogen bond between the CO of residue 9 and NH of residue 13. In other words, the change in chain length of this region merely shifts the nature of turn without causing any major structural variation.

Figure 2 shows variations in the 26-amino acid sequence of chloroplast-type ferredoxins[2]. The substitution frequencies of amino acids among 26 chloroplast-type ferredoxins are plotted against the distances between each α-carbon atom and the cluster, and Fig. 3 demonstrates that the carbon atoms distant from the cluster have higher substitution frequencies.

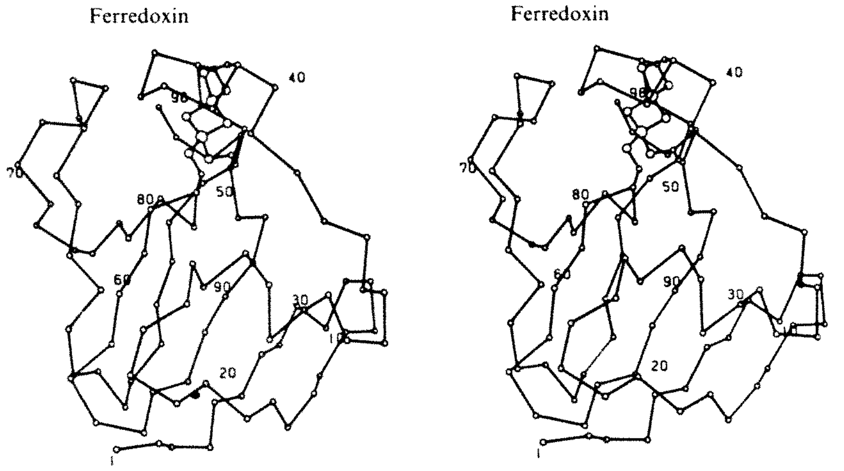

Fig. 1 The polypeptide chain of *S. platensis* ferredoxin shown by stereo pair drawing. The cluster is located at the top of the molecule. Residues 3–9 and 14–20 form an antiparallel β-sheet, and residues 5–8 and 87–89 form a parallel β-sheet. A short helical segment occurs at residues 25–31. There is a relatively large cavity in the interior of the molecule surrounded by the β-sheets and helix. The heavy-atom binding site is at Asp 36.

0028–0836/80/310522—03$01.00

There are 22 invariant and 14 variant positions, defining a variant position as a site occupied by more than 6 different amino acid residues in various ferredoxins. Structurally and functionally essential portions of the molecule must be occupied by invariant residues. For example, the four cysteine residues, Cys 41, Cys 46, Cys 49 and Cys 79, binding the two iron atoms are invariant and are most important in electron transfer function. The sites of the other invariant residues in the three-dimensional structure of *S. platensis* ferredoxin are shown in Fig. 4. As can be seen, most of the invariant residues are around the [2Fe-2S] cluster. The segments from Pro 38 to Cys 49 and from Thr 78 to Ala 81 must be important in stabilizing the cluster cavity. Note also that the segment from residues 65 to 69 consists almost entirely of invariant and semi-invariant residues (that is, chemically similar amino acid residues) located near the cluster. These observations suggest that invariant and semi-invariant residues surround the cluster cavity, making an evolutionarily conserved environment for the cluster in all the widely divergent ferredoxins isolated from various organisms, including blue-green algae and higher plants, which diverged more than 15 billion years ago. Some of the invariant glycine residues are located at the corners of the main chain: Gly 13, Gly 56 and Gly 74 must be necessary for chain folding.

```
1                 10                  20
A T Y K V T L I N E A E G I N E T I D C D D D T Y
- D F N T K V K T K D D   T K K K V K V S E G K R
  S   Q I H F V S - E T   L D H E L T   E P   S T
  A   M   V   L     P S   - T R V F E   P A   E F
  I                   Q     E N I   Q   A     Q
                            Q Q               A
                            P A               V
                            A V
                              I
                              F

        30                  40                  50
I L D A A E E A G L D L P Y S C R A G A C S T C A
V I E H G S D K A V E I   S     Q     S     S   T
L     Q       T   I V     L                     L
      V       S   Y       F
      I       E   -
              Q
              V
              L

                  60                  70
G T I T S G T I D Q S D Q S F L D D D Q I E A G Y
  K V K D   R A N E D E G A     E E S   Q K K   F
    L E T   D V   - E               E   V D R   W
      A E   S L                     G   M Q S
      V A   E                           L G E
      I V   P                             A Q
      L     A                             L G
            F

        80                  90                99
V L T C V A Y P T S D C T I K T H Q E E G L Y -
I M     H   I A K G N G V   S     K   D K V T G
        A   F   R     A     E     A   S D I S A
        I       E     V     Q     V   Q N   A
                A     I     A           S   V
                V     L     V           E   L
                            M           A   F
                            L               -
```

Fig. 2 The amino acid sequence of *S. platensis* ferredoxin[2,11] and the distribution of various amino acid residues present in chloroplast-type ferredoxins. The sequence of *S. platensis* ferredoxin (top row) is shown by the one-letter code. The different amino acid residues found in the sequences of 25 other chloroplast-type ferredoxins are shown below the sequence. –, Represents a deletion.

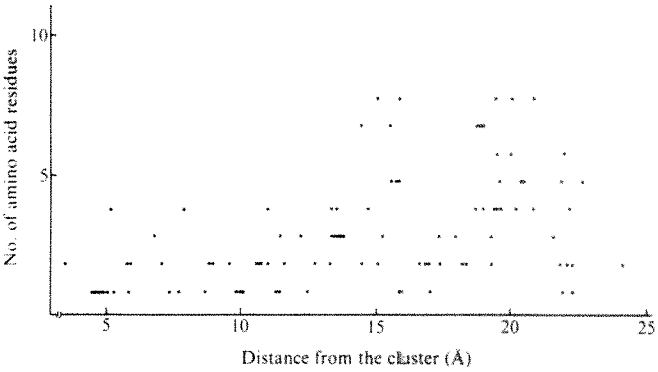

Fig. 3 The relationship between the number of amino acids substituted in 26 chloroplast-type ferredoxins and the distances between each α-carbon atom and cluster.

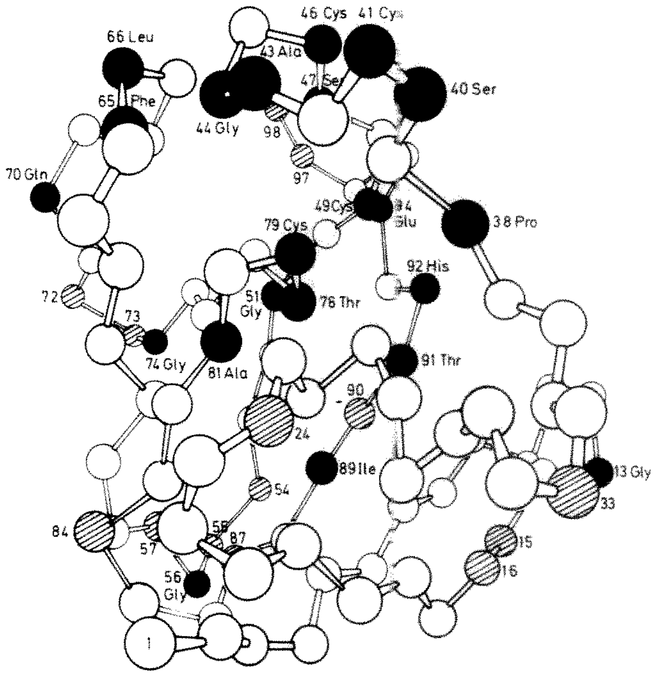

Fig. 4 The distribution of invariant and variant positions in ferredoxin sequences in the three-dimensional structure of *S. platensis* ferredoxin. ● And ▨ represent invariant and variant positions, respectively. The [2Fe-2S] cluster is not shown.

There is no remarkable feature about the distribution of variant positions in the primary structure, except that they are not near the functionally important cysteine residues. However, as shown in Fig. 4, it is obvious that they occur in the lower part and on the surface of the three-dimensional structure, producing a remarkable compartmentation between variant and invariant positions in the molecule. We have given a brief account of the relationship between the three-dimensional structure and variation in the amino acid residues in terms of evolution based on preliminary results on the structure[2].

Received 27 March; accepted 27 May 1980.

1. Yasunobu, K. T. & Tanaka, M. in *Iron-Sulfur Proteins* Vol. 2 (ed. Lovenberg, W.) 29–123 (Academic, New York, 1973).
2. Matsubara, H., Hase, T., Wakabayashi, S. & Wada, K. in *Evolution of Protein Structure and Function* (eds Sigman, D. S. & Brazier, M. A. B.) (Academic, New York, in the press).
3. Adman, E. T., Sieker, L. C. & Jensen, L. H. *J. biol. Chem.* **248**, 3987–3996 (1973).
4. North, A. C. T., Phillips, D. C. & Mathews, F. S. *Acta crystallogr.* **A24**, 351–359 (1968).
5. Tsukihara, T. *et al. J. Biochem., Tokyo* **84**, 1645–1647 (1978).
6. Singh, A. K. & Ramaseshan, S. *Acta crystallogr.* **21**, 279–280 (1966).

7. Blow, D. M. & Rossmann, M. G. *Acta crystallogr.* **14,** 1195–1202 (1961).
8. Matthews, B. W. *Acta crystallogr.* **20,** 82–86 (1966).
9. Richards, F. M. *J. molec. Biol.* **37,** 225–230 (1968).
10. Carter, C. W. Jr, Kraut, J., Freer, S. T. & Alden, R. A. *J. biol. Chem.* **249,** 6339–6346 (1974).
11. Wada, K., Hase, T., Tokunaga, H. & Matsubara, H. *FEBS Lett.* **55,** 102–104 (1975).

Prevalence of amber suppressor-containing coliforms in the natural environment

Bonnie Marshall & Stuart B. Levy

Departments of Molecular Biology and Microbiology and of Medicine,
Tufts University School of Medicine, Boston, Massachusetts 02111

Amber suppressible genes have been introduced into vectors[1,2] and proposed for use in recombinant DNA studies. Such genes can be expressed only in a host bacterium with amber suppressors. To assess the biological containment of this kind of mutation we have now examined the frequency of bacteria with amber suppressors in faecal samples from humans and animals in different environments. This approach allowed us to evaluate the number of individuals in an environment bearing bacteria with amber suppressor mutations and the frequency of these bacteria within the faecal samples of each individual. Of all individuals sampled 30.5% contained detectable levels of bacteria with amber suppressor activity. In >75% of these samples, the level of suppressor-containing bacteria was <10%, about half of which were <1%. Most of these were *Escherichia coli*: however, *Citrobacter* and *Klebsiella* were also found. In three samples, essentially all coliforms had suppressor activity. Excluding these three samples, the estimated frequency of amber suppressors among faecal coliforms was 1.5%; however, if the data from these individuals were included, the overall frequency among faecal samples could be as high as 10%. By itself, the finding suggests that amber suppressor mutations in recombinant DNA vectors may not offer as great a safety feature as originally considered. These data, however, must be considered together with the known low sensitivity of wild-type *E. coli* to laboratory phages[3,4] and their low recipient ability for some plasmids.

To perform these studies we required a genetic vector which could be introduced into wild-type host cells. Different phages proved unsuccessful. Because *inc*P1 plasmids have a wide host range, we chose this as a vector for our study. We were greatly aided by the availability of plasmid pLM2 (ref. 5) (developed by Leonard Mindich) which contains amber suppressible mutations[6] in tetracycline and ampicillin resistance determinants while encoding a wild-type kanamycin resistance gene.

Samples of intestinal coliforms were obtained from five populations: hospital patients, laboratory workers, urban residents, rural residents and farm animals. A fresh faecal swab (Culturette; Scientific) was obtained from each donor, inoculated on to a MacConkey agar plate (Mac) and diluted by two-dimensional spreading on to four quadrants of the plates. These 'master' plates were then incubated at 37 °C overnight and refrigerated at 4 °C or tested immediately.

For mating studies with these coliforms, two *E. coli* strains were used as donors of plasmid pLM2: Ca274[6] bearing pLM2 (from L. Mindich)[5] and D15–12, a bile-salt sensitive, 'rough' *E. coli* produced in our laboratory by mating pLM2 into our host *E. coli* DO-19. The use of minimal agar eliminated the auxotrophic Ca274 from matings, while D15–12 was removed due to its death on the bile-salt-containing Mac agar.

The scheme for identification of endogenous suppressor-containing bacteria was as follows: a lawn of the donor organisms (Ca274 or D15–12) was inoculated on to a non-selective nutrient plate. The master plate, containing colonies of coliforms from each faecal sample, was replica-plated[7] on to the lawn of donor bacteria. After overnight incubation, the 'mating' plate was replica-plated on to media (minimal media for mating with Ca274; Mac agar for mating with D15–12) which would not allow the donor organism to grow and which contained either kanamycin (Kan) ($40\ \mu g\ ml^{-1}$) or ampicillin (Amp) ($50\ \mu g\ ml^{-1}$) + tetracycline (Tet) ($10\ \mu g\ ml^{-1}$) + Kan ($40\ \mu g\ ml^{-1}$).

The Kan replica plate assessed the efficiency of transfer of pLM2 to the wild-type coliforms; the Amp–Tet–Kan replica plate identified which of the recipient bacteria carried a suppressor mutation. Initially the master plate was replica-plated on to Mac+Kan ($40\ \mu g\ ml^{-1}$) and on to Mac+Tet ($10\ \mu g\ ml^{-1}$) + Amp ($30\ \mu g\ ml^{-1}$) + Kan ($40\ \mu g\ ml^{-1}$) to identify endogenous coliforms with resistance to Kan and/or resistance to Tet + Amp + Kan. Faecal samples bearing large numbers of bacteria resistant to Kan or a combination of Tet–Amp–Kan were excluded from analysis. pLM2 mating using either Ca274 or D15–12 showed 100% transfer efficiency of plasmid when known, good recipients were used in this replica-plating method. The observed frequency of transfer of pLM2 from both hosts was similar. Thus, the presence of any naturally occurring auxotrophic coliforms, which could have been missed in the Ca274 matings, was presumably small. The frequency of auxotrophic wild-type *E. coli* has been recently reported at about 9% (ref. 4).

Bacterial colonies, positive (Su^+) and negative (Su^-) for suppressor activity, were picked from the master plate, purified and retested by the plate method with the same or an alternative donor organism to confirm the presence or absence of amber suppression. Furthermore, some of the identified suppressor strains containing pLM2 were isolated and used to mate pLM2 into DO-11, an Su^-, Nal^R strain (this laboratory) or into a Su^+, streptomycin-resistant B40 (*supD*) strain. In all tests the intactness of the amber mutations on the plasmid was confirmed, with the exception of those few in which the presence of lytic phage prevented conjugation.

Faecal samples from 190 individuals from the five populations were tested. Of these, 30.5% had Su^+ bacteria present, all among the lactose fermenters. Biotyping (Analytab, API 20E) of 36 Su^+ isolates identified 33 as *E. coli*, 2 as *Citrobacter freundii* and 1 as *Klebsiella pneumoniae*. Most (>75%) of the faecal samples containing Su^+ bacteria showed them at a frequency of < 10%; in about 30% of samples, Su^+ bacteria occurred even

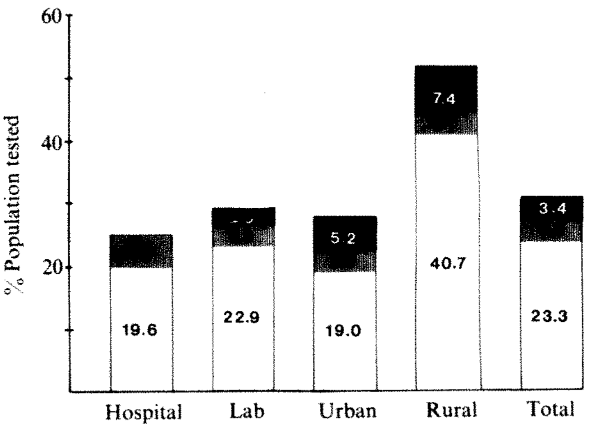

Fig. 1 Frequency of suppressor coliforms in faecal samples of four different human populations. The percentage of all samples containing any suppressor bacteria is represented by the whole bar. Frequencies (f) of suppressor occurrence within individual samples are shown by bar subdivisions as follows: open, $0 < f < 10\%$; hatched, $10 \leq f < 50\%$; closed, $f \geq 50\%$. The number of individuals sampled from each population was: hospital, 56; laboratory, 35; urban, 58; rural, 27.

0028–0836/80/310524—02$01.00

more rarely (<1.0%). Six samples showed a high level (>50%) of bacteria with suppressor activity (Fig. 1). Of note, we found three samples (from a laboratory worker and two urban dwellers) in which ~100% of the bacteria bore amber suppressors. Over 95% of the bacteria on these plates were recipients of the plasmid and Su$^+$.

The frequency of Su$^+$ bacteria in faecal samples from males and females showed equal distribution both overall and within environments. Su$^+$ bacteria occurrence, however, was twice as common in the human rural population as in humans tested in the other three environments. Fourteen non-human faecal samples were also tested (six fowl, five cows, one fly, one goat, one kitten). Of these, four (28.6%) showed the presence of Su$^+$ bacteria (at levels of <10%). This is in keeping with the frequency found in samples from the total human population.

The frequency of Su$^+$ bacteria among the entire pool of faecal coliforms tested was estimated by dividing the approximately $3.5–5 \times 10^3$ Su$^+$ bacteria identified by the estimated $3.5–5 \times 10^4$ transconjugants on the 190 plates examined. This calculation gave an estimated frequency of Su$^+$ *E. coli* of ~10%. This figure, however, is elevated considerably by the three individuals whose samples were essentially all Su$^+$. By excluding these individuals, the estimated frequency drops to roughly 1.5%.

The colonies that were not recipients of plasmid pLM2 obviously could not be evaluated for suppressor activity; however, there is no evidence to indicate that Su$^+$ bacteria have a different recipient ability from Su$^-$ bacteria. Furthermore, the ability of the faecal bacterial colonies to mate with the test organism, in the conditions described, was generally high. In 40% of the samples, 90% or more of the colonies accepted pLM2, allowing a relatively complete examination of the available flora. In only 15% of the faecal samples were less than 20% of the total colonies able to receive the plasmid; in all cases, at least 10 colonies per sample were evaluable.

Our data show that lactose-fermenting bacteria with amber suppressor activity are not uncommon in nature, and seem to be more frequent than has been previously recorded. All were lactose fermenters, *E. coli* being predominant. Using the same plasmid, Robeson *et al.*[4] found a level of about 0.4% suppressor-containing bacteria in 443 independently isolated wild-type *E. coli* from faecal and non-faecal sources. Our study, which examined whole faecal flora of different individuals, gave an estimated frequency of 1.5% in the majority of faecal samples. This value does not differ greatly from previous estimates[4]; however, the finding of 3 in 190 individuals with large amounts of Su$^+$ bacteria suggests that a much larger pool of these bacteria may exist in nature.

Given this frequency of Su$^+$ bacteria, the amber suppressor mutations in themselves, while providing some biological containment, may not be as effective as previously believed. The real effectiveness, however, must be considered in relationship to the actual ability of the mutant vector to propagate in wild-type coliforms. We and others have noted that some plasmids are poorly maintained in wild-type coliforms. In the case of λ vectors, the probability of vector rescue is greatly diminished because of the very low susceptibility of wild-type *E. coli* to this phage[3]. As an indication, we tested 27 isolates of our suppressor-containing coliforms with λ *vir*. None could be productively infected. Thus the degree of biological containment achieved by the introduction of suppressor mutations is greatly dependent on the choice of phage or plasmid vector used.

This study was supported by NIH contract no. NO1AI72529. We thank Toni Keller and Stanley Miller for help with the analyses.

Received 5 November 1979; accepted 23 April 1980

1. Blattner, F. R. *et al. Science* **196**, 161–169 (1977)
2. Enquist, L., Tiemeier, D., Leder, P., Weisberg, R. & Sternberg, N. *Nature* **259**, 596–598 (1976)
3. Leder, P., Tiemeier, D. & Enquist, L. *Science* **196**, 175–177 (1977)
4. Robeson, J. P., Goldschmidt, R. M. & Curtiss, R. III *Nature* **283**, 104–106 (1980).
5. Mindich, L., Cohen, J. & Weisburd, M. *J. Bact.* **126**, 177–182 (1976).
6. Russell, R. L. *et al. J. molec. Biol.* **47**, 1–13 (1970)
7. Lederberg, J. & Lederberg, E. M. *J. Bact.* **63**, 399–406 (1952).

DNA cloning in *Streptomyces*: resistance genes from antibiotic-producing species

C. J. Thompson, J. M. Ward & D. A. Hopwood

John Innes Institute, Colney Lane, Norwich NR4 7UH, UK

The biochemical and morphological differentiation of actinomycetes makes them academically and economically interesting. Their secondary metabolites provide the majority of medically and agriculturally important antibiotics[1] (streptomycete genes may also be the primary source of clinically important antibiotic resistance[2]); their complex morphological developmental cycle involves a series of changes from vegetative mycelial growth to spore formation[3]. Recombinant DNA technology would add a powerful new dimension to the analysis of these various aspects of actinomycete biology and would also facilitate the development of industrial strains with increased antibiotic yield, or capable of making new antibiotics[4]. For most of these purposes, cloning of genes within and between actinomycetes is required to study the expression of particular genes in genetic backgrounds defined by mutations of the characters under study. To achieve this, we have now developed a method for molecular cloning involving the transfer of genes between unrelated streptomycetes.

For initial interspecific cloning experiments we chose *Streptomyces lividans* strain 66 (ref. 5) as host, since no restriction-modification systems are known in this strain and because a potential plasmid vector (SLP1.2) was available for it; all cleavage sites for the restriction endonucleases *Bam*HI and *Pst*I lie in a dispensable region of SLP1.2(ref. 6). Into these sites we attempted to insert resistance genes from two antibiotic-producing streptomycetes. *Streptomyces fradiae*, which makes neomycin, contains a neomycin phosphotransferase (APH) and a neomycin acetyltransferase (AAC) (ref. 7 and J. Davies, personal communication). *Streptomyces azureus*, which makes thiostrepton, contains a ribosomal RNA methylase capable of protecting ribosomes from binding thiostrepton[8].

Foreign DNA was inserted into the vector in two ways. The first approach used ligation of *Mbo*I genomic DNA fragments, of length 2–20 kilobase pairs, into the *Bam*HI site of SLP1.2 (ref. 9). *Mbo*I, which recognizes a sequence of only four base pairs (GATC), generates the same single-stranded termini (GATC) as *Bam*HI (recognition sequence GGATCC). The numerous *Mbo*I sites expected in *Streptomyces* chromosomal DNA (about 1 per kilobase pair; unpublished data) allowed us to generate a suitably random population of donor fragments by partial digestion with *Mbo*I (about 10% of the sites were cleaved). This seemed advisable as we knew nothing about the positions of restriction enzyme targets within genes or promotors, or about possible fragment size selection during ligation and transformation. The second approach used double digestion of SLP1.2 with *Bam*HI and *Pst*I to excise a 2.6-kilobase pair sequence of non-essential DNA and generate non-homologous single-stranded ends (one from the *Bam*HI and the other from a *Pst*I site). Recircularization required the insertion of a segment of DNA having corresponding termini. Such fragments were generated by partially cleaving donor chromosomal DNA with *Mbo*I to 5–28 kilobase pairs and then completely with *Pst*I (giving an average of one *Pst*I cut per *Mbo*I fragment).

Ligation mixtures containing SLP1.2 and fragments of *S. fradiae* or *S. azureus* total genomic DNA were transformed into *S. lividans* protoplasts. The original procedure[10] was modified to increase the transformation efficiency approximately 20-fold. Transformation was indicated by the appearance of 'pocks' (circular zones of sporulation inhibition associated with plasmid transfer, sometimes called the *ltz* (*lethal zygosis*) phenotype[11] in the lawn of *S. lividans* growth arising from the regenerated

0028-0836/80/310525—03$01.00

Table 1 Properties of the six recombinant plasmids

Strain	Plasmid	Size kilobase pairs		Method of construction		Presence of restriction fragment F	Site at vector–insertion junctions		Enzyme specified
		Plasmid	Insertion	Vector cleavage	Donor DNA cleavage		J1	J2	
M180	SLP1.2	14.4	0	—	—	+	—	—	None
TC7	pIJ1	24.8	13.0	*Pst*I/*Bam*HI	*Pst*I/*Mbo*I	—	Not *Bam*HI	*Pst*I	AAC
TC8	pIJ2	17.8	3.4	*Bam*HI	*Mbo*I	+	*Bam*HI	*Bam*HI	APH
TC9	pIJ3	22.1	10.3	*Pst*I/*Bam*HI	*Pst*I/*Mbo*I	—	Not *Bam*HI	*Pst*I	APH
TC10	pIJ4	23.4	11.6	*Pst*I/*Bam*HI	*Pst*I/*Mbo*I	—	Not *Bam*HI	*Pst*I	AAC
TC11	pIJ5	19.0	4.6	*Bam*HI	*Mbo*I	+	Not *Bam*HI	Not *Bam*HI	23S rRNA methylase
TC14	pIJ6	21.3	6.9	*Bam*HI	*Mbo*I	+	*Bam*HI	*Bam*HI	23S rRNA methylase

The recombinant plasmids were constructed by inserting genomic fragments containing genes for antibiotic resistance enzymes into SLP1.2. Neomycin resistance, due to AAC or APH, was cloned from *S. fradiae* (a variant of ATCC 10745 selected for high level resistance to neomycin and provided by Dr J. Davies); thiostrepton resistance (23S ribosomal RNA methylase) was cloned from *S. azureus* ATCC 14921. pIJ1, pIJ3 and pIJ4 were generated from *Pst*I and *Bam*HI cleaved SLP1.2 ligated to fragments of donor DNA double digested with *Mbo*I and *Pst*I; they therefore do not contain the small *Pst*I fragment F of SLP1.2 (see Fig. 3). pIJ2, pIJ5 and pIJ6 were constructed by ligation of SLP1.2 cleaved with *Bam*HI to *Mbo*I fragments of donor DNA. Plasmid and insert sizes (relative to the *Hin*dIII fragments of bacteriophage λ: 23.5, 9.59, 6.76, 4.44, 2.28, 1.94 and 0.58 kilobase pairs) were determined from the combined molecular weights of fragments in *Bam*HI/*Hin*dIII double digests, allowing for the presence or absence of fragment H (see Fig. 3). Insertion of DNA fragments having *Mbo*I termini into the *Bam*HI site of SLP1.2 reconstituted a *Bam*HI site in four out of nine hybrid junctions (J1 and J2 in Fig. 3) as deduced from the presence of fragments D and/or E (Fig. 3) in *Bam*HI/*Hin*dIII double digests (reconstitution was expected on random grounds in about one-third of junctions since one-half of each hexanucleotide junction contains half the original *Bam*HI sequence of the vector and the other half, coming from an *Mbo*I site in 73% G+C DNA, has a 36.5% (73% × 0.5) probability of having *Bam*HI specificity). The expected reconstitution of the *Pst*I site at J2 in plasmids pIJ1, pIJ3 and pIJ4 was confirmed by the presence of restriction fragment G (Fig. 3).

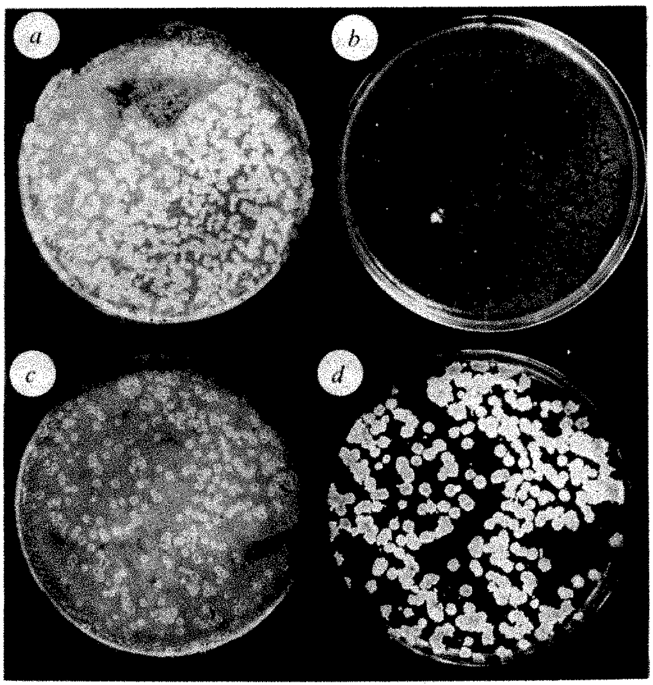

Fig. 1 The isolation of a clone carrying drug resistance. *S. azureus* genomic DNA (2.5 μg) was partially cleaved with *Mbo*I into fragments of 2–20 kilobase pairs; SLP1.2 (0.5 μg) was cleaved with *Bam*HI. Vector and genomic fragments were mixed and ligated (4 h at 10 °C followed by 72 h at 4 °C in ligation salts which contained 66 mM Tris-HCl (pH 7.5), 1 mM EDTA, 10 mM $MgCl_2$, 10 mM 2-mercaptoethanol and 0.1 mM ATP) at a total DNA concentration of 40 μg ml^{-1} with T4 DNA ligase (prepared according to ref. 16). Ligation products were introduced to 3×10^9 *S. lividans* strain 66 protoplasts (haemocytometer counts) by a modification (unpublished results) of the PEG-mediated transformation procedure[10]. These protoplasts gave rise to 5×10^7 colonies and 4×10^4 pocks (see *a*) after regeneration on 20 plates of R2 agar[17] containing 0.5% Difco yeast extract (R2 YE). When these lawns were replica-plated to R2 YE plates containing 50 μg ml^{-1} thiostrepton, two spots of drug resistant growth appeared (one is shown in *b*). After purification of this strain, its plasmid DNA was isolated by CsCl–ethidium bromide centrifugation[18] and used to re-transform *S. lividans* protoplasts. Non-selected regeneration (*c*) followed by replication to thiostrepton (*d*) demonstrated 100% correlation between pocks (*c*) and thiostrepton-resistant growth (*d*).

protoplast population (Fig. 1). When such lawns were replicated to plates containing antibiotic (50 μg ml^{-1} thiostrepton, or 1 μg ml^{-1} neomycin), patches of growth appeared corresponding to certain pocks on the regeneration plates (2 thiostrepton-resistant out of 40,000 pocks in an experiment with *Mbo*I-generated fragments, 2 neomycin-resistant out of 10,000 pocks in a similar experiment, and 3 neomycin-resistant out of 10,000 pocks when the donor DNA was cleaved with *Mbo*I and *Pst*I). The drug resistance and ltz phenotypes of these clones were transferred coincidentally at high frequency (10–100%) in matings with genetically marked *S. lividans* derivatives, indicating that they contained drug resistance genes inserted into SLP1.2. This was confirmed by transformation using the CCC plasmid DNA which could be isolated from each clone; the plasmids conferred drug resistance (Fig. 1) on all (>95%) transformants (that is, pocks).

Agarose gel electrophoresis of the hybrid plasmids revealed that each was larger than SLP1.2 (Fig. 2). *Hin*dIII digestion of each plasmid yielded SLP1.2 fragments B and C, as expected (Fig. 3). *Hin*dIII fragment A, which contained the cloning sites, was, however, invariably increased in size (Fig. 2). Since the inserted fragments came from DNA which had been only partially digested with *Mbo*I, they could not be excised in one piece with *Mbo*I. Moreover, ligation of *Streptomyces* (73% G+C) *Mbo*I fragments into a *Bam*HI site should alter the sequence at about two-thirds of the *Bam*HI–*Mbo*I junctions to eliminate the *Bam*HI site. The fact that a *Bam*HI recognition site was found at four out of nine recombinant junctions (Table 1) confirmed this prediction, and will allow the precise removal of the neomycin-(APH) and thiostrepton-resistance genes from the recombinant plasmids pIJ2 and pIJ6 for recloning purposes. The increased size of *Hin*dIII fragment A was used to calculate the amount of inserted DNA in each clone (Table 1). The sizes of the inserts (4–13 kilobase pairs) agreed with the molecular weight range of the donor DNA fragments.

Interspecific gene transfer was confirmed biochemically. The four neomycin-resistant clones were assayed for APH and AAC activities; two contained APH and two AAC. Extracts from both thiostrepton-resistant clones were found to contain thiostrepton-resistant ribosomes and the expected ribosomal RNA methylase activity. Thus the availability of *S. lividans* clones containing the ribosomal RNA methylase of *S. azureus* confirmed its potential to confer thiostrepton resistance on the producing organism[8]. In the case of neomycin resistance, the *S. lividans* clones established that the presence of either of the two neomycin modifying enzymes of *S. fradiae* is sufficient to give

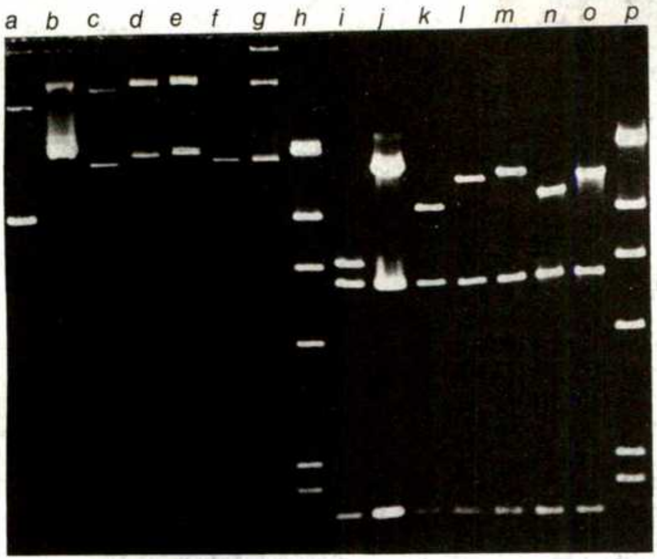

Fig. 2 Agarose gel electrophoresis of recombinant plasmids and their cleavage fragments produced by *Hin*dIII. The DNA species were separated by electrophoresis in 0.8% agarose using a Tris-acetate buffer[19] for 15 h at 1 V cm^{-1}. *h* and *p*, bacteriophage λ DNA cleaved with *Hin*dIII; *a*, the parent SLP1.2 plasmid and *b–g*, the recombinant plasmids PIJ 1–6 respectively, uncleaved (the fastest migrating band in each track is the CCC plasmid species); *i*, SLP1.2 and *j–o*, pIJ1-6 respectively, cleaved with *Hin*dIII. Note the indistinguishable sizes of the two smaller *Hin*dIII fragments in SLP1.2 and the series of recombinant plasmids and the increased size of the largest fragment in each recombinant.

resistance to neomycin. Comparable clones promise to be valuable in understanding the resistance mechanisms of other antibiotic-producing actinomycetes and perhaps the origins of clinically important drug resistance genes[2].

The results, in conjunction with those of Bibb *et al.*[12] on the cloning of methylenomycin resistance from *S. coelicolor* into *S. coelicolor* and *S. lividans*, and our unpublished results showing that two randomly chosen genes for amino acid biosynthesis could be cloned from the chromosome of *S. coelicolor* A3(2) on to the SCP2* plasmid of that strain, indicate that molecular cloning in streptomycetes on existing plasmid vectors is quite practicable. We feel that our cloning of three genes conferring resistance, by known mechanisms, to stable and readily available antibiotics augurs well for the further development of cloning vectors for streptomycetes. Possible resistance enzymes for many aminoglycosides[7], macrolides[13], chloramphenicol[14] and other antibiotics are available in the actinomycetes. It should therefore be relatively straightforward to build a streptomycete vector bearing more than one resistance gene in order to: select for the presence of the vector[15], detect clones by insertional inactivation[15], and achieve high level expression of cloned genes (highly efficient promoters for some of these genes are being sought among mutant strains showing increased drug resistance). Such a vector would facilitate, for example, the cloning of genes involved in antibiotic biosynthesis or differentiation, on which this laboratory is now embarked.

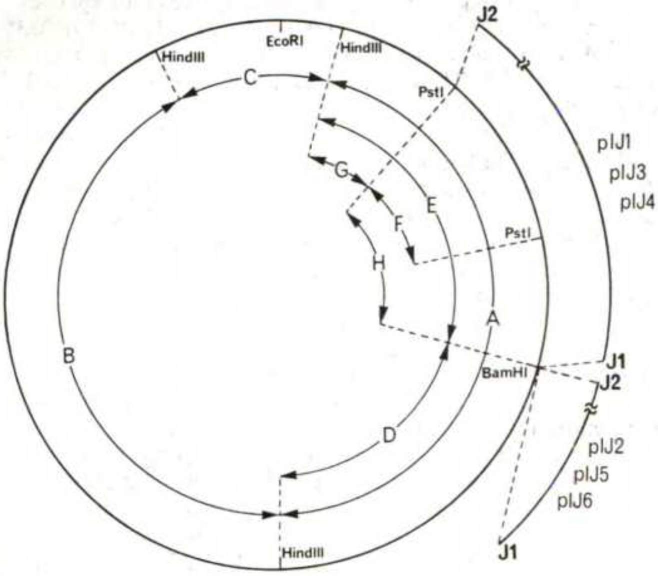

Fig. 3 Restriction map of the SLP1.2 plasmid for enzymes *Eco*RI, *Hin*dIII, *Pst*I and *Bam*HI[6] (continuous circle) and positions of insertions in recombinant plasmids pIJ1-6 (Table 1).

We thank Dr Eric Cundliffe for the *S. azureus* strain and the RNA methylase assays, Dr Ken-ichi Komatsu for the assays of AAC and APH, Drs Keith Chater, Julian Davies and Tobias Kieser for helpful discussions, and the National Research Development Corporation for financial support.

Received 20 March; accepted 21 May 1980.

1. Bérdy, J. *Adv. appl. Microbiol.* **8,** 309–406 (1974).
2. Benveniste, R. & Davies, J. *Proc. natn. Acad. Sci. U.S.A.* **70,** 2276–2280 (1973).
3. Chater, K. F. & Merrick, M. J. in *Developmental Biology of Prokaryotes* (ed. Parish, J. H.) 93–114 (Blackwell, Oxford, 1979).
4. Hopwood, D. A. & Chater, K. F. *Phil. Trans. R. Soc.* B **290,** 313–328.
5. Lomovskaya, N. D., Mkrtumian, N. M., Gostimskaya, N. L. & Danilenko, V. N. *J. Virol.* **9,** 258–262 (1972).
6. Bibb, M. J., Ward, J. M. & Hopwood. D. A. *Devl ind. Microbiol.* (in the press).
7. Davies, J. & Smith, D. I. *A. Rev. Microbiol.* **32,** 469–518 (1978).
8. Cundliffe, E. *Nature* **272,** 792–795 (1978).
9. Delinas, R. E., Myers, P. A. & Roberts, R. J. *J. molec. Biol.* **114,** 169–179 (1977).
10. Bibb, M. J., Ward, J. M. & Hopwood, D. A. *Nature* **274,** 398–400 (1978).
11. Hopwood, D. A., Bibb, M. J., Ward, J. M. & Westpheling, J. in *Plasmids of Medical, Environmental and Commercial Importance* (eds Timmis, K. N. & Pühler, A.) 245–258 (Elsevier, Amsterdam, 1979).
12. Bibb, M. J., Schottel, J. L. & Cohen, S. N. *Nature* **284,** 526–531 (1980).
13. Graham, M. Y. & Weisblum, B. *J. Bact.* **137,** 1464–1467 (1979).
14. Shaw, W. V. & Hopwood, D. A. *J. gen. Microbiol.* **94,** 159–166 (1976).
15. Bolivar, F. *et al. Gene* **2,** 95–113 (1977).
16. Murray, N. E., Bruce, S. A. & Murray, K. *J. molec. Biol.* **132,** 439–505 (1979).
17. Okanishi, M., Suzuki, K. & Umezawa, H. *J. gen. Microbiol.* **80,** 389–400 (1974).
18. Bibb, M. J., Freeman, R. F. & Hopwood, D. A. *Molec. gen. Genet.* **154,** 155–166 (1977).
19. Barnes, N. M. *Science* **195,** 393–394 (1979).

DNA cloning in *Streptomyces*: a bifunctional replicon comprising pBR322 inserted into a *Streptomyces* phage

J. E. Suarez & K. F. Chater

John Innes Institute, Colney Lane, Norwich NR4 7UH, UK

The Gram-positive, mycelial, differentiating streptomycetes are responsible for the production of many important antibiotics. The availability of gene cloning systems in this microbial group would have many industrial applications[1] besides allowing more penetrating study of the genetics of *Streptomyces coelicolor* A3(2) (which, as the best understood streptomycete genetically, serves as a model for much other *Streptomyces* genetics)[2]. Recent successes[3,4] (see previous paper[4]) in introducing *Streptomyces* DNA into *S. coelicolor* and *Streptomyces lividans* on plasmid vectors would be nicely complemented by the availability of *Streptomyces* bacteriophage vectors (discussed in ref. 5): for example, many phages have wide and easily defined host ranges; heat-inducible prophages might be used to give high copy number of cloned DNA; efficient phage promoters might be used to increase gene expression; there may be differential stabilities for particular DNA sequences cloned in plasmids *vis-à-vis* phages; selective insertion of DNA, utilizing packaging constraints, may be possible with phages; and *in situ* hybridization[6] of radioactive probes to DNA in plaques is likely to be simple. We describe here the use of the moderately wide host range temperate phage, ΦC31[7], for this purpose.

Although ΦC31 DNA (39 kilobases) is not known to have single targets for any restriction enzymes, it possesses six *Eco*RI sites[5] which might be used for inserting DNA. Viable deletion mutants have been obtained[5] that should allow the insertion of fragments of foreign DNA without interfering with packaging of DNA into maturing phage particles. DNA of ΦC31 efficiently transfects *Streptomyces* protoplasts in the presence of polyethylene glycol[8]. The particular phage strain chosen was ΦC31*cts*Δ23, which has about 8% (3.25 kilobases) less DNA than the wild-type ΦC31 (J.E.S. and K.F.C., unpublished observations). The small *Escherichia coli* plasmid pBR322 (4.362 kilobases)[9,10], which has single *Eco*RI, *Bam*HI and *Pst*I sites, was selected as the DNA for insertion.

The ΦC31*cts*Δ23 vector DNA was treated[11] with T4 ligase to close its cohesive ends covalently[5,12], precipitated with ethanol and partially cleaved with *Eco*RI to give an average of about one cut per molecule. After a second ethanol precipitation, the DNA was ligated in the presence of a 25-fold molar excess of completely *Eco*RI-cleaved pBR322, and the DNA mixture was used to transfect *S. lividans* protoplasts[8]. Of 1,500 plaques obtained with a sample of DNA mixture containing 100 ng ΦC31*cts*Δ23 DNA (about 30-fold fewer plaques than expected for 100 ng ΦC31 *cts* DNA in a normal transfection)[8] one hybridized to ^{32}P-labelled pBR322 probe DNA in a filter–hybridization test[6].

DNA was isolated from the purified presumed hybrid phage and analysed by digestion with restriction enzymes (Fig. 1). An *Eco*RI fragment of 4.36 kilobases, present in the hybrid DNA but not in DNA of ΦC31*cts*Δ23, co-migrated with *Eco*RI-cleaved pBR322. Single sites for *Bam*HI and *Pst*I, absent from the control DNA, were present in the hybrid DNA, and were both within the novel *Eco*RI fragment (not shown). In digestions with single enzymes, the smaller *Bam*HI fragment was 10.8 kilobases, and the smaller *Pst*I 7.4 kilobases. These data were consistent with insertion of pBR322 into ΦC31*cts*Δ23 in the position and orientation shown in Fig. 2.

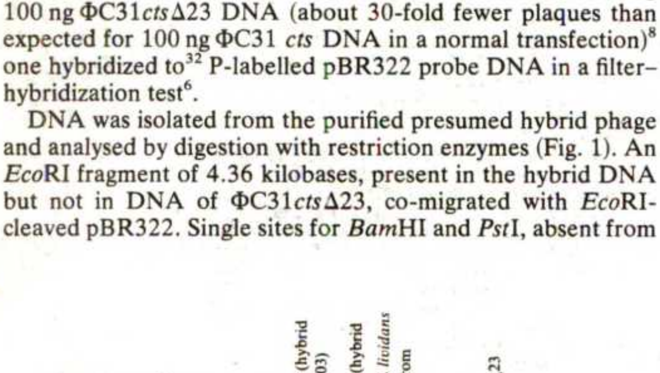
DNA
λ
ϕC31 *cts*Δ23
ϕC31*cts*Δ23/pBR322 (hybrid from initial transfection of *S.lividans*)
pBR322
ϕC31*cts*Δ23/pBR322 (hybrid plasmid from *E.coli* 803)
ϕC31*cts*Δ23/pBR322 (hybrid after transfection of *S. lividans* with hybrid plasmid from *E coli* 803)
λ
scheme for ϕC31 *cts*Δ23 and hybrid DNA
Enzyme
*Sal*PI
*Eco*RI
*Bam*HI
*Sal*PI
*Eco*RI
*Eco*RI
*Eco*RI
*Eco*RI
*Bam*HI
*Sal*PI
*Sal*PI
*Eco*RI
fragment
size (kb)
A
13.38
(A')
(12.15)
B
9.23
pBR322
4.36
C²³
3.37
D
3.37
E
3.11
F
2.94
G
1.78
a
b
c
d
e
f
g
h
i
j
k

Fig. 1 Restriction enzyme analysis of DNA of ΦC31 derivatives using electrophoresis in 1% agarose gels. Tracks *a* and *k* are molecular size standards of λ DNA treated with *Sal*PI (ref. 13). Phage DNA was prepared by conventional procedures (ref. 16). Note that the DNA in tracks *c*, *d* and *e* is indistinguishable from that in tracks *i*, *j* and *h*, but that (as expected) in the plasmid form of the hybrid DNA (track *g*), *Eco*RI fragment A' (the fusion product of *Eco*RI fragments B and F, the cohesive ends of the phage DNA[5]) completely replaces B and F. Fragment C^{23} (3.4 kilobases (kb)) is the reduced form present in ΦC31*cts*Δ 23, of the wild-type fragment C (6.6 kilobases, absent from this gel) (ref. 5).

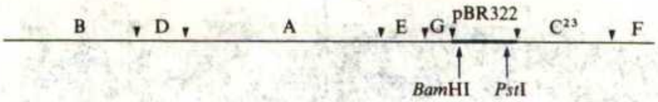

Fig. 2 Structure deduced for ΦC31*cts*Δ23–pBR322 hybrid DNA from data in Fig. 1, based on the *Eco*RI restriction map of ΦC31 DNA given in ref. 17. Letters above the map are *Eco*RI fragment designations.

Wild-type ΦC31 DNA contains no sites for the *Pst*I isoschizomer *Sal*PI present in *Streptomyces albus* P: consequently, ΦC31 is not restricted by *S. albus* P[13]. However, phage from the plaque containing pBR322 sequence homology was restricted and modified by *S. albus* P: its efficiency of plating on *S. albus* P was 20-fold lower (data not shown) when the previous host was *S. lividans* than when it was *S. albus* P (using *S. lividans* as a standard host). A similar level of restriction by *S. albus* P was previously seen with phage R4, which has one *Sal*PI target site in its DNA[14]. Presumably, introduction of the *Pst*I (=*Sal*PI) site of pBR322 into ΦC31 was responsible for the observed restriction. This property provided a supplementary way of identifying the hybrid clone.

The *Eco*RI site of pBR322 is not within a region needed for plasmid replication or expression of its tetracycline or ampicillin resistance genes in *E. coli*. Therefore, assuming that the ΦC31DNA would be largely unexpressed in *E. coli*, the hybrid molecule should replicate in *E. coli* as a plasmid and express both drug resistances. This was found to be the case: very similar efficiencies of transformation[11] of a *recA* derivative of *E. coli* 803 (*metB hsdS*) to tetracycline resistance were obtained with supercoiled pBR322 DNA and ligated or non-ligated hybrid DNA. (The similarity between the efficiencies with ligated and non-ligated DNA probably reflects the high stability of hydrogen bonding between the cohesive ends of ΦC31 DNA[5,12].) The colonies obtained were all Met$^-$ and resistant to both tetracycline (25 μg ml^{-1}) and ampicillin (200 μg ml^{-1}) when tested by replica plating. Plasmid DNA isolated from nine colonies transformed with hybrid DNA gave an *Eco*RI digestion pattern which was distinguishable from that obtained with the original hybrid DNA isolated from phage particles only by the expected covalent joining of the cohesive ends of the phage DNA (Fig. 1). (Plasmid DNA isolated from two of the *E. coli* colonies transformed with pBR322 DNA was indistinguishable from pBR322 using *Eco*RI digestion.)

We next tested whether *S. lividans* protoplasts could be transfected by the hybrid plasmid DNA isolated from *E. coli*. About 250 ng hybrid plasmid DNA gave 1,100 plaques—a frequency 10–100-fold lower than that obtained with DNA isolated from the hybrid phage. DNA from phages obtained from five of these plaques was indistinguishable by restriction enzyme analysis from the DNA of the original hybrid (Fig. 1).

The data reported here demonstrate the following: (1) the plaque hybridization technique[6] is applicable to the *Streptomyces* phage ΦC31; (2) pBR322 DNA can be inserted into ΦC31*cts*Δ23 DNA at an *Eco*RI site 6.35 kilobases from one end of the molecule without obvious effects on the ability of the phage to form plaques, proving the feasibility of using this phage as a DNA cloning vector and providing single dispensible *Bam*HI and *Pst*I target sites which will be important in the future use of derivatives of the hybrid as cloning vectors;(3) the presence of the *Pst*I (= *Sal*PI) site of pBR322 in the hybrid phage causes it to be restricted by *S. albus* P; (4) DNA of the ΦC31*cts*Δ23–pBR322 hybrid can easily be transformed into *E. coli* (even without ligation of the phage cohesive ends), and maintained there without any evidence of structural instability during subculture for at least 30 cell generations; (5) the supercoiled covalently closed circular DNA isolated from *E. coli* transfects *S. lividans* protoplasts at least moderately efficiently, suggesting the absence of a severe restriction barrier (which might have operated on DNA last propagated in *E. coli*); (6) the pBR322 sequence is stably inherited during propagation of the hybrid molecule as a phage in *S. lividans*.

The ability of the hybrid DNA to inhabit either *Streptomyces* or *E. coli* will be invaluable in introducing some of the powerful genetic techniques (such as transposon mutagenesis)[15] available in *E. coli* into the study of *Streptomyces* genetics. It may also be possible to turn to advantage the absence of packaging constraints on the size of the molecule when it is replicating in the plasmid mode, *vis-à-vis* the presence of such constraints during its growth as a phage.

Dr A. G. Hepburn provided not only extensive technical advice but also labelled and unlabelled pBR322 DNA. We thank Professor D. A. Hopwood and Dr C. J. Thompson for invaluable comments on the manuscript, and Celia Bruton for technical assistance. J.E.S., on leave from the University of Oviedo, Spain, was the recipient of a grant from the Vicente Canada Blanch Foundation.

Received 19 March; accepted 21 May 1980.

1. Hopwood, D. A. & Chater, K. F. *Phil. Trans. R. Soc.* **B290**, 313–328 (1980).
2. Hopwood, D. A., Chater, K. F., Dowding, J. E. & Vivian, A. *Bact. Rev.* **37**, 371–405 (1973).
3. Bibb, M. J., Schottel, J. L. & Cohen, S. N. *Nature* **284**, 526–531 (1980).
4. Thompson, C. J., Ward, J. M. & Hopwood, D. A. *Nature* **286**, 525–527 (1980).
5. Chater, K. F. *Devl ind. Microbiol.* (in the press).
6. Benton, W. D. & Davis, R. W. *Science* **196**, 180–182 (1977).
8. Lomovskaya, N. D., Mkrtumian, N. M., Gostimskaya, N. L. & Danilenko, V. N. *J. Virol.* **9**, 258–262 (1972).
8. Suarez, J. E. & Chater, K. F. *J. Bact.* **142**, 8–14 (1980).
9. Sutcliffe, J. G. *Nucleic Acids Res.* **5**, 2721–2728 (1978).
10. Bolivar, F. *et al. Gene* **2**, 95–113 (1977).
11. Hepburn, A. G. & Hindley, J. *J. biochem. biophys. Meth.* **1**, 299–308 (1979).
12. Sladkova, I. A., Lomovskaya, N. D. & Chinenova, T. A. *Genetika* **13**, 342–344 (1977).
13. Chater, K. F. *Nucleic Acids Res.* **4**, 1989–1998 (1977).
14. Chater, K. F. & Carter, A. T. *J. gen. Microbiol.* **109**, 181–185 (1978).
15. Kleckner, N., Roth, J. & Botstein, D. *J. molec. Biol.* **116**, 125–159 (1977).
16. Chater, K. F. & Wilde, L. C. *J. Bact.* **128**, 644–650 (1976).
17. Lomovskaya, N. D., Chater, K. F. & Mkrtumian, N. M. *Microbiol. Rev.* (in the press).

Novobiocin inhibition of simian virus 40 DNA replication

Howard J. Edenberg

Department of Biochemistry, Indiana University School of Medicine,
Indianapolis, Indiana 46223

Supercoiling in eukaryotic cells can be explained by the packaging of DNA into nucleosomes in the presence of nicking–closing enzymes[1]. This does not, however, rule out the presence of a DNA gyrase. DNA gyrase[2] is involved in the introduction and maintenance of supercoiling in prokaryotic cells[3–6] and in DNA replication in *Escherichia coli*[4,6,7]. Novobiocin and coumermycin-A_1 inhibit prokaryotic DNA replication[4,7–11] by inhibiting the subunit of the gyrase responsible for its ATPase and energy transduction activities[3,4,12–14]. The inhibition of DNA synthesis in a mammalian cell[15] and in rat liver mitochondria[16] by novobiocin suggests that a gyrase required for initiation of replication is inhibited. Because the presence of a gyrase in eukaryotic cells would be of great interest, I have examined this question in a well characterized model system, the replication of simian virus 40 in its host (monkey) cell. The results demonstrate here that novobiocin and coumermycin A_1 inhibit SV40 DNA synthesis in mammalian cells and inhibit DNA polymerase α, the replicative DNA polymerase in this system[17,18]. Novobiocin, but not coumermycin A_1, reduces the degree of supercoiling of DNA pulse-labelled in its presence, probably through its inhibition of protein synthesis. Thus the inhibition of SV40 DNA synthesis by novobiocin does not alone prove the involvement of a DNA gyrase.

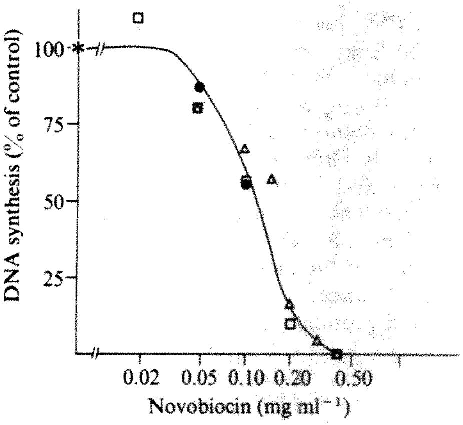

Fig. 1 Novobiocin inhibition of SV40 DNA synthesis in intact cells. CV-1 cells were grown to confluence in minimal essential medium (MEM) with 10% fetal calf serum (FCS), infected with SV40, and incubated in MEM with 2% FCS as previously described[20]. Novobiocin (Boehringer) was added from a stock solution of 10 mg ml^{-1} in 2.0 mM Tris-HCl, *p*H 7.5, as noted. Radioactive labelling was terminated by removal of medium, two rinses with phosphate buffered saline, and extraction of viral DNA by the method of Hirt[19]. □, Novobiocin was added 20 h after infection, [^{3}H]dT (1.8 μCi ml^{-1}) was added 75 min later, and incubation was continued for a further 24 h. △, Novobiocin was added 18.5 h after infection, [^{14}C]dT (0.08 μCi ml^{-1}) was added 90 min later and incubation was for a further 25 h. ●, At 39 h after infection, the medium was replaced with fresh medium containing 2% FCS and 12.5 mM HEPES (*p*H 7.1); 2 h later novobiocin was added, and 120 min after drug addition [^{3}H]dT (12 μCi ml^{-1}) was added for a 30-min pulse.

The effect of novobiocin on SV40 DNA synthesis was studied by examining the incorporation of radioactive label into viral DNA (selectively extracted from the cells by the method of Hirt[19] about 40 h after infection). As shown in Fig. 1, novobiocin inhibits SV40 DNA replication in a dose-dependent manner; 50% inhibition is achieved by ~0.1–0.2 mg ml^{-1} novobiocin. Inhibition of DNA synthesis by novobiocin is rapid (the steady-state level is reached within 90 min) and reversible. The concentration of novobiocin required to inhibit SV40 replication is about 100 times greater than that required to inhibit DNA synthesis in *E. coli*[7,9].

Since the inhibition of processes in two different systems by the same drug does not necessarily imply that the same target enzyme is involved in both systems, I tested the effect of novobiocin on the replicative DNA polymerase. We have previously shown that DNA polymerase α is responsible for SV40 DNA synthesis[17,18]. DNA polymerase α, partially purified from the host monkey cells, was tested in a standard *in vitro* assay[17] and as shown in Fig. 2 was 50% inhibited by ~0.2 mg ml^{-1} novobiocin, a concentration similar to that which inhibits replication in cells. This inhibition would suffice to explain the inhibition of SV40 DNA synthesis. Since the substrate in these studies consists of short linear segments of DNA which are extensively nicked and gapped, this inhibition cannot be related to a need to relieve supercoiling. DNA polymerase γ is also inhibited (50% at about 0.6 mg ml^{-1}); DNA polymerase β is not inhibited (data not shown). These results confirm reports that similar concentrations of novobiocin inhibit a crude DNA polymerase α of rat brain[21] and that high levels inhibit a human 7S DNA polymerase[22], but do not significantly inhibit DNA polymerase β[21,22].

Closed circular SV40 DNA made during a 30–40 min pulse in novobiocin-inhibited cells (0.1 mg ml^{-1} and above) has a greater density in CsCl–ethidium bromide density gradients than does SV40 DNA from control cells (Fig. 3), indicating that it is less negatively supercoiled[23,24]. This was confirmed by examining the dependence of sedimentation rate on ethidium bromide

0028–0836/80/310529—03$01.00

concentration[23-25]; the minimum sedimentation rate of SV40 DNA extracted from control cells occurred at about 2 μg ml^{-1} ethidium bromide, while that of SV40 DNA made in the presence of 0.1–0.2 mg ml^{-1} novobiocin occurred at about 1.0–1.5 μg ml^{-1}. Novobiocin itself does not bind to DNA[8], and would not directly alter the supercoiling. DNA made during long labelling periods in the presence of novobiocin is indistinguishable from that made in control cells (data not shown). At these levels of novobiocin, protein synthesis is also inhibited (data not shown) and the change in supercoiling could be a result merely of less packaging of the DNA into nucleosomes due to this inhibition of protein synthesis.

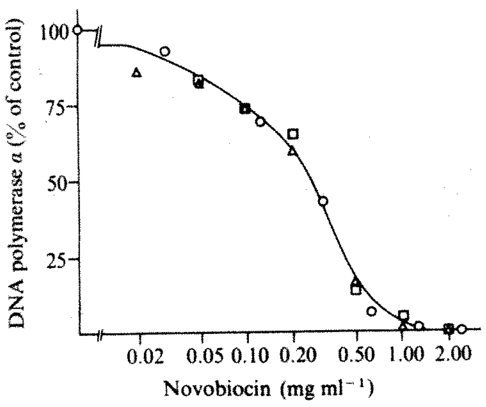

Fig. 2 Novobiocin inhibition of DNA polymerase *α in vitro*. DNA polymerase *α* assays were conducted as previously described[17]; the reaction mixtures contained (per 0.1 ml) 50 μg activated DNA and 15 μg bovine serum albumin, in 0.05 M Tris–HCl *p*H 8.5, 7.5 mM $MgCl_2$, all four dNTPs at either 15 μM (○, △) or 25 μM (□); and [^{3}H]dTTP (2 μCi). Two different preparations of DNA polymerase *α* were used, one partially purified through DEAE cellulose as previously described[17] (○) and an independent preparation purified in a similar manner and then further purified through phosphocellulose[26] (△, □). Both preparations were shown to be sensitive to *N*-ethyl maleimide, and resistant to dideoxy-TTP[17,18,27]. Incorporation was normalized to the value from reactions lacking drugs; 100% represents 235 pmol (○), 340 pmol (△), or 180 pmol (□) of dTTP incorporated in 30 min.

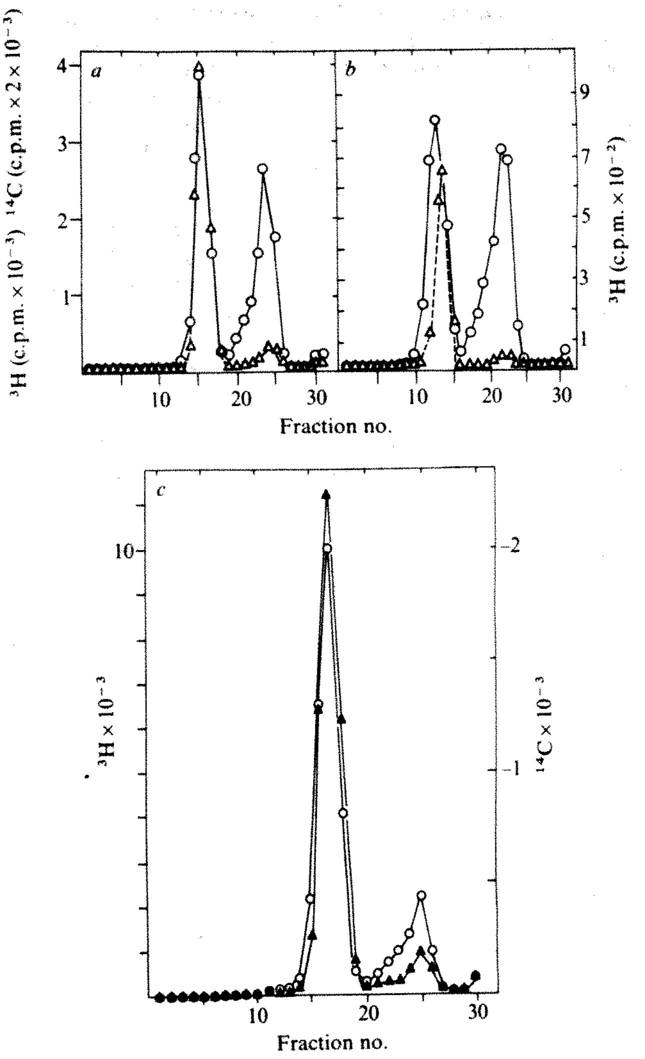

Fig. 3 Ethidium bromide–caesium chloride equilibrium gradients. Control SV40 DNA was isolated by the method of Hirt[19] from infected cells incubated with [^{14}C]dT (0.08 μCi ml^{-1}) from 22 to 45 h post-infection (△). Pulse-labelled DNA was isolated in the same manner at 40 h post infection (○). *a*, Cells were incubated for 20 min with [^{3}H]dT (25 μCi ml^{-1}), in the absence of drug. *b*, Cells were incubated for 2 h with 0.2 mg ml^{-1} novobiocin, and then [^{3}H]dT (25 μCi ml^{-1}) was added for 35 min. *c*, Cells were incubated for 2 h with 0.005 mg ml^{-1} coumermycin-A_1 and then [^{3}H]dT (25 μCi ml^{-1}) was added for 40 min. The Hirt supernates were extracted with chloroform/isoamyl alcohol (24 : 1), aliquots of ^{14}C-DNA (control) (△) were mixed with the ^{3}H-DNA (pulse) (○) from control or drug-treated cells, and each was adjusted to a refractive index of 1.388 with CsCl, buffer (0.01 M Tris–HCl *p*H 8.0, 0.01 M NaCl, 0.001 M EDTA) and ethidium bromide (0.27 mg ml^{-1} final concentration). Centrifugation was for 42 h at 38,000 r.p.m., 20 °C in a Beckman 50Ti rotor. Fractions were collected, carrier DNA was added, and the DNA precipitated with HCl and filtered through glass fibre filters, all as previously described[20]. For *a* and *b*, ^{14}C scales are the same, ^{3}H scales differ. Density decreases from left to right.

To clarify this situation, I examined the effects of coumermycin-A_1 (refs 10, 11) on SV40 DNA synthesis. Coumermycin-A_1 lyses monkey cells at concentrations above 0.01 mg ml^{-1}; at slightly lower concentrations it inhibits SV40 DNA replication, and at slightly higher concentrations inhibits DNA polymerase *α* (50% at about 0.03 mg ml^{-1}) and *γ* (50% at 0.2 mg ml^{-1}). Coumermycin-A_1, however, inhibits DNA replication without significantly altering the supercoiling of SV40 DNA, as tested both with equilibrium density gradients (Fig. 3*c*) and sedimentation rate measurements in the presence of ethidium bromide. These comparative data reinforce the suggestion that the difference in supercoiling seen with novobiocin is a secondary effect of the drug.

After submission of this manuscript, the presence of type II DNA topoisomerases in eukaryotic cells was reported[28]; no gyrase activity was reported. These topoisomerases are reported to be sensitive to high levels of novobiocin[28], and the authors relied on the previously reported sensitivity of replication to high levels of novobiocin[15] to argue that these topoisomerases might be the target enzymes. These conclusions are premature, since the data presented here demonstrate that the effects of novobiocin and coumermycin-A_1 on SV40 DNA synthesis can be explained as the results of inhibiting DNA polymerase *α* and protein synthesis. The results presented here provide no direct evidence for participation of a DNA gyrase in SV40 DNA replication, although they do not rule out the possibility.

This research was supported by a USPHS grant R01 GM 25681.

Received 20 February; accepted 26 May 1980.

1. Germond, J. E., Hirt, B., Oudet, P., Gross-Bellard, M. & Chambon, P. *Proc. natn. Acad. Sci. U.S.A.* **72**, 1843–1847 (1975).
2. Gellert, M., Mizuuchi, K., O'Dea, M. H. & Nash, H. A. *Proc. natn. Acad. Sci. U.S.A.* **73**, 3872–3876 (1976).
3. Gellert, M., O'Dea, M. H., Itoh, T. & Tomizawa, J.-I. *Proc. natn. Acad. Sci. U.S.A.* **73**, 4474–4478 (1976).

4. Cozzarelli, N. R. *Science* **207,** 953–960 (1980).
5. Gellert, M., Mizuuchi, K., O'Dea, M. H., Itoh, T. & Tomizawa, J.-I. *Proc. natn. Acad. Sci. U.S.A.* **74,** 4772–4776 (1977).
6. Drlica, K. & Snyder, M. *J. molec. Biol.* **120,** 145–154 (1978).
7. Staudenbauer, W. L. *J. molec. Biol.* **96,** 201–205 (1975).
8. Smith, D. H. & Davis, B. D. *Biochem. biophys. Res. Commun.* **18,** 796–800 (1965).
9. Cozzarelli, N. R. *A. Rev. Biochem.* **46,** 641–668 (1977).
10. Ryan, M. J. *Biochemistry* **15,** 3769–3777 (1976).
11. Ryan, M. J. & Wells, R. D. *Biochemistry* **15,** 3778–3782 (1976).
12. Higgins, N. P., Peebles, C. L., Sugino, A. & Cozzarelli, N. R. *Proc. natn. Acad. Sci. U.S.A.* **75,** 1773–1778 (1978).
13. Sugino, A., Higgins, N. P., Brown, P. O., Peebles, C. L. & Cozzarelli, N. R. *Proc. natn. Acad. Sci. U.S.A.* **75,** 4838–4842 (1978).
14. Mizuuchi, K., O'Dea, M. H. & Gellert, M. *Proc. natn. Acad. Sci. U.S.A.* **75,** 5960–5963 (1978).
15. Mattern, M. R. & Painter, R. B. *Biochim. biophys. Acta* **563,** 306–312 (1979).
16. Castora, F. J. & Simpson, M. V. *J. biol. Chem* **254,** 11193–11195 (1979).
17. Edenberg, H. J., Anderson, S. & DePamphilis, M. L. *J. biol. Chem.* **253,** 3273–3280 (1978).
18. De Pamphilis, M. L. *et al. Cold Spring Harb. Symp. quant. Biol.* **43,** 679–692 (1979).
19. Hirt, B. *J. molec. Biol.* **26,** 365–369 (1967).
20. Edenberg, H. J. *Nucleic Acids Res.* **8,** 573–586 (1980).
21. Sung, S. C. *Biochim. biophys. Acta* **361,** 115–117 (1974).
22. DePhilip, R. M., Lynch, W. E. & Lieberman, I. *Cancer Res.* **37,** 702–704 (1977).
23. Gray, H. B. Jr, Upholt, W. B. & Vinograd, J. *J. molec. Biol.* **62,** 1–19 (1971).
24. Bauer, W. & Vinograd, J. in *Basic Principles in Nucleic Acid Chemistry* Vol 2 (ed. Ts'O, P. O. P.) 265–303 (Academic, New York, 1974).
25. Upholt, W. B., Gray, H. B. Jr & Vinograd, J. *J. molec. Biol.* **61,** 21–28 (1971).
26. Fisher, P. A. & Korn, D. *J. biol. Chem.* **252,** 6528–6535 (1977).
27. Fisher, P. A., Wang, T. S.-F. & Korn, D. *J. biol. Chem* **254,** 6128–6137 (1979).
28. Liu, L. F., Liu, C.-C. & Alberts, B. M. *Cell* **19,** 697–707 (1980).

Identification of integrated hepatitis B virus DNA and expression of viral RNA in an HBsAg-producing human hepatocellular carcinoma cell line

Prasanta R. Chakraborty, Nelson Ruiz-Opazo, Daniel Shouval* and David A. Shafritz

Departments of Medicine and Cell Biology and the Liver Research Center, Albert Einstein College of Medicine, 1300 Morris Park Avenue, Bronx, New York 10461

Alexander and co-workers[1] have developed a tissue culture cell line (PLC/PRF/5) from a primary hepatocellular carcinoma of a Mozambican male with a positive serum for hepatitis B virus surface antigen (HBsAg). This cell line produces and secretes HBsAg but no other known viral protein[1–3]. PLC/PRF/5 therefore contains at least part of the hepatitis B virus (HBV) genome in functional form. The 42-nm, spherical Dane particle in human serum is thought to represent the complete infectious agent of HBV[4]. The core of this particle contains circular double-stranded DNA in which one strand is 'nicked' (complete but not covalently closed) and the other strand is incomplete (lacking 15–45% of its sequence complement)[4,5]. Four proteins have been associated with the HBsAg, core antigen (HBcAg), e antigen and a viral DNA polymerase[4]. Several groups have now cloned Dane particle DNA in *Escherichia coli*[6–10], and both restriction maps and a complete DNA sequence have been determined. Various studies suggest that there is sequence heterogeneity in Dane particle DNA isolated from patients expressing the same or different viral subtypes, as well as sequence variation in different clones of Dane particle DNA obtained from a given individual[10,11]. Other studies[12,13] have reported HBV DNA sequences in DNA from liver cancer tissue. In none of these cases was viral DNA reported to be integrated into the host cell genome. With the improvement in techniques for characterizing viral DNA molecules, we have begun to analyse HBV genes and their expression in the PLC/PRF/5 cell line by molecular hybridization of cellular DNA and RNA to cloned ^{32}P-labelled plasmid HBV DNA. We now present evidence in PLC/PRF/5 cells for integration of HBV DNA into the host genome and expression of three RNA molecules containing HBV-specific sequences. These findings are consistent with observations in several animal virus models in which integrated viral DNA is found during oncogenic transformation.

HBV DNA contains a unique *Eco*RI site which was used for insertion of HBV sequences. Therefore, treatment of cloned recombinant λ phage or plasmid pA01 DNAs containing the complete sequence of fully double-stranded Dane particle DNA (3,250–3,300 base pairs) with *Eco*RI should release the entire sequence of HBV DNA as a single fragment, which can be identified by agarose slab gel electrophoresis, nitrocellulose filter transfer and hybridization to an appropriate ^{32}P-labelled HBV probe (Southern blot)[14]. Figure 1 shows the autoradiograph of a Southern blot of recombinant λ HBV DNA, λ HBV DNA digested with *Eco*RI and λ HBV DNA digested with *Eco*RI followed by a second restriction endonuclease to generate additional HBV fragments. *Eco*RI generates a single HBV fragment of ~3,250 base pairs (lane *b*), *Eco*RI followed by *Bam*HI generates two fragments of ~1,900 and 1,400 base pairs (lane *c*), *Eco*RI plus *Bgl*II generates three fragments of ~2,250, 700 and 100 base pairs (lane *d*), *Eco*RI plus *Hin*cII yields four fragments of ~1,800, 800, 450 and 200 base pairs (lane *e*) and *Eco*RI plus *Hin*dII (lane *f*) generates one 3,250-base pair fragment as found with *Eco*RI alone (that is, the HBV sequence in recombinant λ phage DNA contains no *Hin*dIII restriction site). In each case, the total length of HBV restriction fragments is approximately 3,250 base pairs. For reasons which are unclear, in lane *e* the hydrization signal for the 1,800 base pair band was weak and this band reproduced poorly on the photograph. For subsequent studies, restriction enzymes *Eco*RI and *Hin*dIII were used.

Figure 2 shows the autoradiograph of a Southern blot of PLC/PRF/5 DNA digested with either *Eco*RI or *Hin*dIII, using

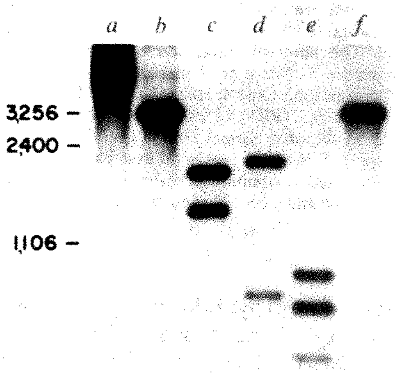

Fig. 1 Restriction enzyme analysis of cloned λ HBV DNA. Recombinant (5 μg) λ HBV DNA was digested with 5 units of *Eco*RI restriction endonuclease. Digested material (1 μg) was further digested with 1 unit of *Bam*HI, *Bgl*II, *Hin*cII or *Hin*dIII, respectively. All digestions were carried out in appropriate buffers at 38°C for 6–12 h. Aliquots (1 μg) of each digested sample were placed on a separate lane of a 0.8% agarose slab gel and electrophoresis carried out in Peacock and Dingman buffer[31] at 50 V for 5–6 h. After electrophoresis, the DNA fragments were transferred to nitrocellulose paper and the paper was hybridized with nick-translated ^{32}P-labelled pA01 HBV probe as described by Southern[15]. Nick-translation was carried out according to a modified procedure of Rigby *et al.*, using *E. coli* DNA polymerase I. Both ^{32}P-dATP and ^{32}P-dCTP (specific activity 300–800 Ci mmole^{-1}) were included in the reaction to obtain uniform labelling of high specific activity ($1-2\times10^8$ per DNA). After hybridization, the nitrocellulose paper was exposed overnight on Kodak XR-5 film for autoradiography. Lane *a*, undigested λ HBV DNA, lane *b*, λ HBV DNA + *Eco*RI; lane *c*, λ HBV DNA + *Eco*RI + *Bam*HI; lane *d*, λ HBV DNA + *Eco*RI + *Bgl*II; lane *e*, λ HBV DNA + *Eco*RI + *Hin*cII; lane *f*, λ HBV DNA + *Eco*RI + *Hin*dIII. The position of restriction fragments of plasmid pBR322 run on a separate lane are shown on the left.

---

*Permanent address: Hadassah University Hospital, Jerusalem, Israel.

0028–0836/80/310531—03$01.00

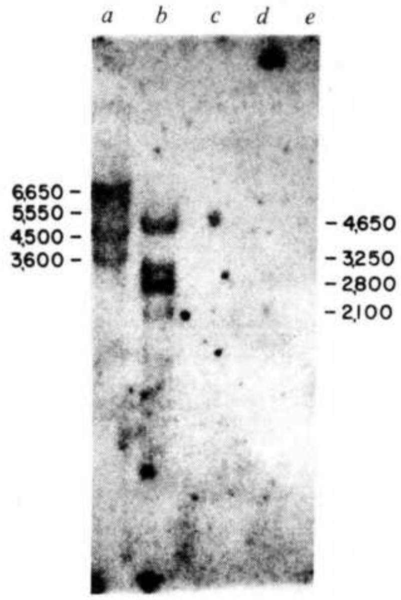

Fig. 2 Restriction enzyme analysis of total DNA from PLC/PRF/5 cells. PLC/PRF/5 cells were grown to confluence in monolayer culture using Eagle's minimal essential medium supplemented with glutamine, non-essential amino acids, 10% heat-activated fetal calf serum, penicillin, streptomycin and Fungizone. Trypsinized cells were lysed with detergent according to the procedure of Innis and Miller[33], nuclei were pelleted by centrifugation at 5,000*g* for 5 min, and DNA and nuclear RNA were obtained by SDS-phenol extraction followed by ethanol precipitation. Nuclear DNA was purified further by ribonuclease A digestion, followed by SDS-proteinase K treatment and phenol/chloroform/isoamyl alcohol extraction. DNAs from other tissues were purified essentially as described above, except that the starting material was total nucleic acids. Aliquots of 20 μg of each DNA sample were digested with *Eco*RI or *Hin*dIII in appropriate digestion buffer. To ensure complete digestion, 20 units of restriction endonuclease were used and incubation was at 37 °C. After 12 h of incubation, 20 additional units of fresh enzyme were added and incubation continued for an additional 12 h. Electrophoresis of these samples, their subsequent transfer to nitrocellulose paper and hybridization to ^{32}P-labelled pA01 HBV DNA were as described in Fig. 1 legend. The autoradiograph was developed by exposing the nitrocellulose paper for 5–7 days on Kodak XR-5 film using intensifying screens (Picker Corporation). Lane *a*, *Hin*dIII-digested PLC/PRF/5 DNA; lane *b*, *Eco*RI-digested PLC/PRF/5 DNA; lane *c*, *Eco*RI-digested rat liver DNA; lane *d*, *Eco*RI-digested normal human liver DNA; lane *e*, *Eco*RI-digested salmon sperm DNA. The length (in base pairs) of specific labelled fragments was determined by comparison with restriction enzyme fragments of plasmid pBR322 used as standards.

^{32}P-labelled HBV DNA as hybridization probe (specific activity 2×10^8 c.p.m. per μg). Lane *a* shows four HBV restriction fragments with *Hin*dIII of sequence length ~6,650, 5,550, 4,500 and 3,600 base pairs, respectively. The 5,550-base pair fragment reproduces poorly on this photograph but is present on all autoradiographs of this material. Lane *b* shows four HBV restriction bands with *Eco*RI, ranging from 2,100–2,200 to 4,650 base pairs. *Eco*RI-digested rat liver DNA (lane *c*), normal human liver DNA (lane *d*) and salmon sperm DNA (lane *e*) show no bands hybridizing with ^{32}P-HBV DNA. As one fragment with *Eco*RI and four fragments with *Hin*dIII are larger than cloned full-length double-stranded Dane particle DNA, these results suggest that HBV DNA sequences are integrated into PLC/PRF/5 cell line DNA. The possibility cannot be excluded that host or other virus-related sequences are associated with extrachromosomal HBV DNA to produce some of these bands. However, as *Hin*dIII recognizes no internal cleavage site in HBV DNA, the presence of four large fragments with this enzyme strongly favours integration of viral DNA sequences. The band migrating at 3,250 base pairs after *Eco*RI digestion (lane *b*) could represent a small amount of extrachromosomal (non-integrated) HBV DNA, and the 6,650-base pair band after *Hin*dIII treatment (lane *a*) could represent a dimer or circular concatomer of HBV DNA. Further studies will be necessary to characterize these bands fully.

The number and size of HBV restriction fragments suggest that more than one, but only a few, discrete host integration sites are involved. Although the lengths of fragments generated with *Hin*dIII are larger than those obtained with *Eco*RI, a more precise comparison cannot be made. This is especially true as HBV DNA integrated into different sites may contain deletions or rearrangements affecting the restriction pattern, and Dane particles from the original patient are not available for comparison.

To study viral RNA expression in this cell line, total cytoplasmic and nuclear RNAs were isolated and separated into poly(A)$^+$ and poly(A)$^-$ fractions. RNA samples were applied to denaturing glyoxal slab gels, blotted to diazobenzyloxymethyl (DBM)-cellulose paper and HBV sequences identified by hybridization with ^{32}P-HBV probe[15]. As shown in Fig. 3, total cytoplasmic poly(A)$^+$ RNA (lanes *a* and *a'*) reveals two bands containing virus sequences, 21.5S (3,050 nucleotides) and 19.5S (2,500 nucleotides). Total nuclear RNA (lane *b*) shows three bands of 27S, 21.5S and 19.5S (the migration of all components in this fraction is retarded slightly by the presence of high molecular weight nuclear RNA). The 21.5S and 19.5S bands in nuclear RNA probably represent the same components as found in the cytoplasm. Cytoplasmic poly(A)$^-$ RNA (lane *d*) also shows a 27S band (4,700 nucleotides). Hybridisable material in the nuclear fraction is alkaline labile (lane *c*), ruling out the possibility of DNA contamination, and poly(A)$^+$ RNA from normal human liver (lane *e*) shows no distinct radioactive bands, demonstrating the specificity of our HBV probe.

The biological activity and function of these viral RNAs are unknown. The presence of a poly(A)tail in the 21.5S and 19.5S RNA species suggests that they represent specific viral mRNAs. It has been reported that this cell line produces HBsAg[1–3], and a recent DNA sequencing study of Dane particle DNA proposes a

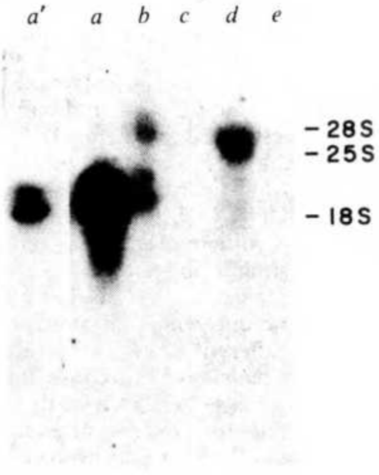

Fig. 3 Identification of RNA molecules containing HBV sequences in PLC/PRF/5 cells. Nuclei and cytoplasm from 2×10^8 PLC/PRF/5 cells were prepared as described in Fig. 2 legend. Isolated nuclei were resuspended and lysed in 50 mM Tris-HCl *p*H 7.5, 2 mM NaEDTA, 150 mM NaCl and 1% SDS. Nuclear RNA and DNA were isolated by phenol/chloroform/isoamyl alcohol extraction and nuclear RNA was recovered by repeated differential salt precipitation. Total cytoplasmic RNA was isolated from the post-nuclear supernatant fraction by SDS/phenol/chloroform/isoamyl alcohol extraction followed by ethanol precipitation. Total cytoplasmic RNA was fractionated further into poly(A)$^+$ and poly(A)$^-$ RNA by oligo(dT)-cellulose column chromatography. 15–60 μg of RNA was denatured by a glyoxal procedure[34] and electrophoresed on an agarose slab gel in Peacock–Dingman buffer[31] for 5–6 h at 50 V. RNA was blotted to DBM paper[16] and hybridized to nick-translated ^{32}P-labelled PA01 HBV DNA. After hybridization, the DBM paper was exposed on Kodak XR-5 film for autoradiography using intensifying screens. Lanes *a*–*e* were exposed for 3 days. Lane *a'* is lane *a* of the same gel exposed to autoradiography for only 17 h. Lane *a*, 15 μg of cytoplasmic poly(A)$^+$ RNA; lane *b*, 50 μg of total nuclear RNA; lane *c*, 50 μg of alkali-treated total nuclear RNA; lane *d*, 60 μg of cytoplasmic poly(A)$^-$ RNA; lane *e*, 20 μg of cytoplasmic poly(A)$^+$ RNA from normal human liver. The position of 18S, 25S and 28S ribosomal RNA markers determined in separate lanes is shown to the right.

892-base pair region as coding for this protein[9]; it is therefore surprising to find no viral RNA in the cytoplasm close to 1,000 nucleotides. Most probably, either the 21.5S or the 19.5S $\text{poly}(A^+)$ viral RNA codes for HBsAg. The finished polypeptide (molecular weight 25,000) may be derived by post-translational processing of a larger precursor. As the PLC/PRF/5 cell line produces only one known viral protein (HBsAg), the role of the other two viral specific RNAs remains unclear. These RNAs may code for nonstructural proteins which do not become incorporated into the mature virion, as observed in other systems after viral infection[16].

At present, the major evidence linking HBV to hepatocellular carcinoma is epidemiological[17]. A variety of virus–cell interactions have been described in oncogenic transformation and/or persistent viral infection in cultured cells, so the PLC/PRF/5 line provides an excellent model for studying these phenomena as related to HBV gene expression. The ability of these cells to grow rapidly in tissue culture as well as in soft agar[18], and to produce tumours in athymic *nu*/*nu* mice[19] (our unpublished observations), indicates a malignant phenotype. However, in considering the relationship between the presence of viral genes and tumorigenicity, it is important to remember that transformation may result from altered cellular gene expression rather than the function of HBV genes. Therefore, the mere presence of integrated HBV genes with limited expression of HBV proteins does not prove viral oncogenicity, although these findings are consistent with observations in other systems[19–23]. In spite of this limitation, evaluation of HBV genes and their expression in PLC/PRF/5 cells provides the first opportunity of studying the biology and pathobiology of HBV infection at the molecular level.

In the present study, viral DNA is transcribed into three specific RNAs. Although the function of these RNAs has not been determined, two are $\text{poly}(A)^+$ (21.5S and 19.5S) and presumably represent cytoplasmic viral mRNAs. The third viral RNA is $\text{poly}(A)^-$, is found in both the nucleus and the cytoplasm, and is larger than full-length Dane particle DNA. This suggests that the 27S RNA is derived by co-transcription of host and viral sequences from an integrated viral transcription unit, or that the full genome of hepatitis B virus in the cell is larger than that observed in Dane particles. Although other explanations are possible, evidence suggesting synthesis of small amounts of rapidly sedimenting RNA, containing viral and host sequences in molecules of larger apparent size than the viral genome, has been reported during integration of SV40 viral DNA[24–28]. In the present case, this material has been identified as a specific RNA molecule (27S or 4,700 nucleotides on agarose gel electrophoresis in strongly denaturing conditions) and represents a significant portion of viral sequences in both the nucleus and cytoplasm. The exact nature and role of 27S HBV RNA, as well as the other viral RNAs, remain to be determined.

After this manuscript was submitted, Marion *et al.*[28] reported similar findings of integrated HBV-DNA in the PLC/PRF/5 cell line.

We thank Dr J. Summers[30] for providing recombinant λ phage and pA01 HBV DNA, Dr I. Millman for PLC/PRF/5 cells and Dr Probir Sarkar for advice. Research was supported in part by NIH grant AM 17702, American Cancer Society Institutional grant IN-28U and the Sara Chait Memorial Foundation. D.S. is the recipient of an NIH John E. Fogarty International Fellowship. These studies represent part of a thesis by N. R.-O. to be submitted to the Sue Golding Graduate Division, Albert Einstein College of Medicine, in partial fulfillment of the requirements for the degree of D.Phil.

Received 27 February; accepted 27 May 1980.

1. Macnab, M., Alexander, J. J., Lecatsas, G., Bey, E. M. & Urbanowicz, J. M. *Br. J. Cancer* **34,** 509–515 (1976).
2. Marion, P. L., Salazar, F. H., Alexander, J. J. & Robinson, W. S. *J. Virol.* **32,** 796–802 (1979).
3. Skelly, J., Copeland, J. A., Howard, C. R. & Zuckerman, A. J. *Nature* **282,** 617–618 (1979).
4. Robinson, W. S. *A. Rev. Microbiol.* **31,** 357–377 (1977).
5. Summers, J., O'Connell, A. & Millman, I. *Proc. natn. Acad. Sci. U.S.A.* **72,** 4597–4601 (1975).
6. Burrell, C. J., Mackay, P., Greenaway, P. J., Hofschneider, P. H. & Murray, K. *Nature* **279,** 43–47 (1979).
7. Charnay, P., Pourcel, C., Louise, A., Fritsch, A. & Tiollais, P. *Proc. natn. Acad. Sci. U.S.A.* **76,** 2222–2226 (1979).
8. Sninsky, J. J., Siddiqui, A., Robinson, W. & Cohen, S. N. *Nature* **279,** 346–348 (1979).
9. Valenzuela, P. *et al. Nature* **280,** 815–819 (1979).
10. Pasek, M. *et al. Nature* **282,** 575–579 (1979).
11. Siddiqui, A., Sattler, F. & Robinson, W. S. *Proc. natn. Acad. Sci. U.S.A.* **76,** 4664–4668 (1979).
12. Lutwick, L. I. & Robinson, W. S. *J. Virol.* **21,** 96–104 (1977).
13. Summers, J. *et al. J. med. Virol.* **2,** 207–214 (1978).
14. Southern, E. M. *J. molec. Biol.* **98,** 503–517 (1975).
15. Alwine, J. C., Kemp, D. J. & Stark, G. R. *Proc. natn. Acad. Sci. U.S.A.* **74,** 5350–5354 (1977).
16. Tooze, J. *Molecular Biology of Tumor Viruses* Pt 2 (Cold Spring Harbor Laboratory, New York, 1979).
17. Szmuness, W. *Prog. med. Virol.* **24,** 40–69 (1978).
18. Alexander, J., Macnab, G. & Sanders, R. *Perspectives Virol.* **10,** 103–120 (1978).
19. Desmyter, J., Roy, M. B., Bradburne, A. F. & Alexander, J. J. in *Viral Hepatitis* (eds Vyas, G. N., Cohen, S. N. & Schmid, R.) Ch. 44 (Franklin Institute Press, Philadelphia, 1978).
20. Varmus, H. E., Guntaka, R. V., Deng, C. T. & Bishop, J. M. *Cold Spring Harb. Symp. quant. Biol.* **39,** 987–996 (1974).
21. Steffen, D. & Weinberg, R. A. *Cell* **15,** 1003–1010 (1978).
22. Botchan, M., Topp, W. & Sambrook, J. *Cell* **9,** 269–287 (1976).
23. Flint, J. *Cell* **10,** 156–166 (1977).
24. Lindberg, U. & Darnell, J. E. *Proc. natn. Acad. Sci. U.S.A.* **65,** 1089–1096 (1970).
25. Tonegawa, S., Walter, G., Bernardini, A. & Dulbecco, R. *Cold Spring Harb. Sym. quant. Biol.* **35,** 823–831 (1970).
26. Acheson, N. H., Buetti, E., Scherrer, K. & Weil, R. *Proc. natn. Acad. Sci. U.S.A.* **68,** 2231–2235 (1971).
27. Rozenblatt, S. & Winocour, E. *Virology* **50,** 558–566 (1972).
28. Wall, R. & Darnell, J. E. in *The Biology of DNA Tumor Viruses* (ed. Schiminovich, S.) 191–199 (Plenum, New York, 1976).
29. Marion, *et al. J. Virol.* **33,** 795–806 (1980).
30. Cummmings, I. W. *et al. Proc. natn. Acad. Sci. U.S.A.* **77,** 1842–1846 (1980).
31. Dingman, C. W. & Peacock, A. C. *Biochemistry* **7,** 659–667 (1968).
32. Rigby, P. W., Dickmann, M. A., Rhodes, C. & Berg, P. *J. molec. Biol.* **113,** 237–251 (1977).
33. Innis, M. & Miller, D. *J. biol. Chem.* **254,** 9148–9154 (1979).
34. McMaster, G. K. & Carmichael, G. G. *Proc. natn. Acad. Sci. U.S.A.* **74,** 4835–4838 (1977).

Presence of integrated hepatitis B virus DNA sequences in cellular DNA of human hepatocellular carcinoma

Christian Brechot*‡, Christine Pourcel*, Anne Louise*, Bernadette Rain† & Pierre Tiollais*

* Unité de Recombinaison et Expression Génétique (INSERM U.163),
Institut Pasteur, 28 rue du Dr Roux–75015 Paris, France
† Laboratoire d'Anatomapathologie (Service du Pr Ette.M),
CHU Treichville–Abidjan, Côte d'Ivoire

Hepatitis B virus (HBV) may be one of the agents involved in the aetiology of human primary liver cancer[1]. This hypothesis is supported by (1) the similarity between the geographical distribution of chronic carriers of the viral surface antigen (HBsAg) and that of hepatocellular carcinoma (HCC); (2) the increase in the prevalence of HBV markers in serum of patients with primary liver cancer when compared with the general population[1]; (3) the observation that HBV infection precedes the development of the tumour[1]. Moreover, these epidemiological indications of an association between HBV infection and hepatocellular carcinoma are supported by the detection of HBV markers such as HBsAg[2,3] or viral DNA sequences, although in a non-integrated form[4,5] in tumour tissue. To study the relationship between HBV and primary liver cancer further, we looked for the presence of free or integrated viral DNA in tumour tissue of human hepatocellular carcinomas and in a HBsAg-producing human hepatoma cell line[6]. Using the blot-transfer hybridization technique and cloned HBV DNA as a probe, we have now demonstrated that the viral DNA is integrated in the cellular genome both in tumour tissue and in a hepatoma cell line.

Tumoral tissue was an autopsy sample obtained from a 53 yr old man who lived in the savanna in the Ivory Coast (Ethnie Bete). HBsAg (subtype undetectable) and Anti-HBc were present in the serum (as tested by radioimmunoassay: AusRIA-II and Corab, Abbott Laboratories). HBV e

---

‡ Present address: Unité de Recherches de Physiopathologie Hépatique (INSERM U.24), Hôpital Beaujon, Clichy, France.

0028–0836/80/310533—03$01.00

antigen (tested by immunodiffusion) and anti-HBsAg (tested by radioimmunoassay: Ausab-Abbott Laboratories) were absent from the serum. Immunofluorescence, using anti-HBsAg and anti HBcAg labelled with fluoresceine isothiocyanate[7], was negative in the tumour tissue. Normal liver tissue from this patient was not available.

The cellular DNA was extracted as described in Fig. 1 legend. Non-digested DNA and restriction fragments were analysed by agarose gel electrophoresis (Fig. 1*a*). We chose the restriction endonucleases *Eco*RI and *Hin*dIII because *Eco*RI cleaves the HBV genome once and *Hin*dIII does not cut any of the HBV genomes so far cloned[8,9]. Cloned P-labelled HBV DNA was used as a probe to detect viral sequences[8]. As shown in Fig. 1*a*, hybridization of non-digested cellular DNA with the HBV probe occurred only in the high molecular weight (MW) DNA. Hybridization of the *Hin*dIII restriction fragments revealed the existence of five bands (Fig. 1*a*). Three bands corresponded to DNA fragments which migrated more slowly than the HBV genome and had MWs of 25,000, 19,000 and 12,000 respectively. Two bands of weaker intensity were located at the position of DNA fragments of MWs 3,200 and 2,400. Hybridization of the *Eco*RI restriction fragments revealed the presence of several bands (Fig. 1*a*). Three bands corresponded to DNA fragments of respective MWs 14,000, 8,000 and 6,500. Another particularly intense band was located at the position of the HBV genome. A similar pattern was observed with DNA extracted from tumour tissue of two other patients (Ivory Coast) with hepatocellular carcinoma (data not shown). No hybridization signal was observed with DNA extracted from a normal liver as a control (data not shown).

We analysed in the same way DNA from the hepatoma cell line PLC/PRF/5 (a generous gift from Dr J. Alexander) which was derived from a human hepatocellular carcinoma and which produced HBsAg (subtype ad)[10]. At the 100th passage, HBsAg was produced in the supernatant at a concentration of 50 ng ml^{-1}. Hybridization of non-digested cellular DNA occurred only in high molecular weight DNA (Fig. 1*b*). Analysis of *Hin*dIII restriction fragments revealed the presence of five bands of MWs 24,000, 17,000, 12,000, 6,500 and 4,200, respectively. Analysis of *Eco*RI restriction fragments revealed the presence of eight bands; one of these was intense and corresponded to a DNA fragment of MW 3,000 (Fig. 1*b*). The DNA pattern was identical at the 100th and 140th passages.

Taken together, these results demonstrate the integration of HBV DNA sequences in the cellular DNA of both the tumour tissue and the cell line. Our results differ from those of another study of human tumour tissue in which only free viral DNA was detected[4,5]. However, our results obtained with the cell line PLC/PRF/5 are in agreement with those observed recently by Marion *et al.*[11], although the number and size of the restriction DNA fragments are different. The presence of several sharply delineated bands in the *Hin*dIII pattern of the tumour tissue (Fig. 1*a*) suggests the existence of a limited number of integration sites in the cellular DNA. These results are consistent either with the development of the liver tumour from one clone with several integration sites or with its development from a few clones each having particular integration sites. The difference in intensity of the bands could reflect a variability of the number of viral genomes or of the viral DNA length in the different integration sites. The very intense band located at the same position as that of HBV genome in the *Eco*RI pattern of the tumour tissue is not present in the non-digested DNA pattern. This result is consistent with the presence of two or more whole viral genomes inserted in tandem head-to-tail. The presence of a very small quantity of free viral DNA cannot be ruled out by our experiments.

The presence of integrated HBV DNA sequences in both the human hepatocellular carcinomas and in the cell line reinforce the interest of these two results. Indeed, the Alexander cell line produces HBsAg, possesses characteristics of malignancy[6] and induces tumours in mice that are similar to human hepatoma[12]. Demonstration of the integration of HBV genome in cellular DNA is an additional argument for HBV as a factor in human hepatocellular carcinoma. Until now, integration of viral DNA in the genome of human tumours has only been confirmed for Epstein–Barr virus in Burkitt's lymphoma and some nasopharyngeal carcinomas[13]. Our observation is another example of such a relationship between a DNA virus and human cancer. However, the demonstration of integrated HBV DNA sequences is not sufficient to assert the role of HBV in the onset of human primary liver cancer. Additional studies should compare the pattern observed in non-tumorous and tumorous liver cells.

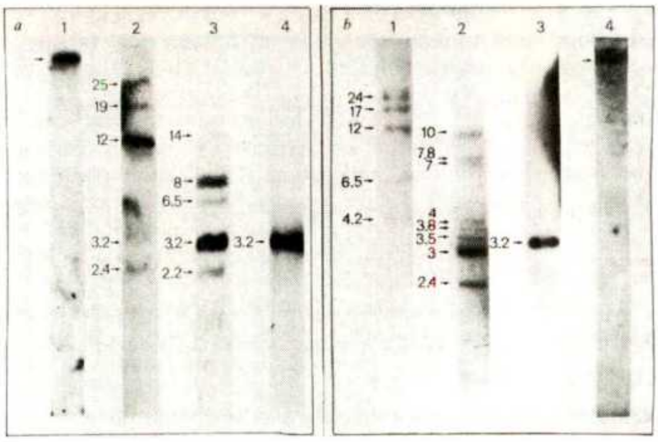

Fig. 1 The liver tumorous tissue is a postmortem sample obtained 6 h after death and kept frozen in liquid N_2. Tissue was pulverised in liquid N_2, then transferred into lysis buffer (Tris-HCl 10 mM, *p*H 7.8, NaCl 10 mM, SDS 0.5%, EDTA 10 mM) and digested with 500 μg ml^{-1} of Pronase (Boehringer) at 37 °C for 2 h. DNA was extracted with phenol/chloroform, dialysed, treated with 100 μg ml^{-1} of RNase A (Boehringer) and dialysed. Cellular DNA of the cell line was extracted by the same procedure using the same lysis buffer. The extracted DNA had an average MW of 100×10^6. Digestion with restriction endonucleases *Eco*RI (Biolabs) and *Hin*dIII (Biolabs) was carried out at 37 °C for 8 h using 2 units of the enzyme for 1 μg of DNA and the appropriate reaction mixtures. Digestion products were precipitated with ethanol, dissolved in electrophoresis buffer (Tris-HCl, *p*H 7.8, 40 mM, sodium acetate 5 mM, EDTA 10 mM) and 0.2% agarose beads[14]. Electrophoresis was carried out in 0.8% agarose gels for restricted DNA and 0.4% gels for non-digested DNA using horizontal slabs of 20 cm long and 0.5 cm thick at 1 V cm^{-1} for 24 h. DNA was then transferred to nitrocellulose filter by a modification of the Southern technique described by Wahl *et al.*[15]. The filter was hybridized using cloned HBV DNA[8] as a probe and the nick-translation procedure[16]. [α-^{32}P]dCTP (Amersham, 2,000 Ci mmol^{-1} and [α-^{32}P]dTTP (Amersham, 2,000 Ci mmol^{-1}) were used and the probe yielded a specific activity of 4×10^8 c.p.m. per μg. The hybridization procedure used dextran sulphate as described by Wahl *et al.*[15]; 5×10^6 c.p.m. of probe was added to each filter. The nitrocellulose filter was autoradiographed with preflashed Kodak X-Omat R film in the presence of a Dupont Lightning Plus screen. *a*, Tumour tissue: lane 1, 30 μg of non-digested cellular DNA; lane 2, 80 μg of cellular DNA digested with *Hin*dIII; lane 3, 80 μg of cellular DNA digested with *Eco*RI; lane 4, 30 μg of cellular DNA from normal liver cells mixed with 10 pg of cloned HBV DNA. *b*, Cell line PLC/PRF/5: lane 1, 20 μg of cellular DNA digested with *Hin*dIII; lane 2, 20 μg of cellular DNA digested with *Eco*RI; lane 3, 10 pg of cloned HBV DNA; lane 4, 20 μg of non-digested cellular DNA. Cloned HBV DNA digested with *Bam*HI and λplac5cI857S7 DNA digested with *Hin*dIII were used as molecular weight markers.

We thank Professors Attia, Beda, Loubienes and Drs Carsuzaa, Condat and Soubeyran for providing autopsy samples, Professor Benhamou and Mr Roland Nageotte for helpful discussion, and Miss Michelle Fonck for technical assistance.

Received 24 March; accepted 5 June 1980.

1. Kew, M. C. in *Viral Hepatitis* (eds Vyas G. N., Cohen, S. N. & Schmid, R.) 439–450 (Franklin Institute Press, Philadelphia, 1978).
2. Goudeau, A. *et al. Int. J. Cancer* **24,** 421–429 (1979).
3. Thung, S. N., Gerber, M. A., Sarno, E. & Popper, H. *Lab. Invest.* **41,** 101–105 (1979).
4. Summers, J. *et al. J. med. Virol.* **2,** 207–214 (1978).
5. London, W. T. in *Viral Hepatitis* (eds Vyas, G. N., Cohen, S. N. & Schmid, R.) 455–458 (Franklin Institute Press, Philadelphia, 1978).
6. Alexander, J. J., Bey, E., Geddes, E. & Lecatsas, G. *S. Afr. med. J.* **50,** 2124–2128 (1976).
7. Brechot, C. *et al. Digest. Dis. Sci.* (in the press).
8. Charnay, P., Pourcel, C., Louise, A., Fritsch, A. & Tiollais, P. *Proc. natn. Acad. Sci. U.S.A.* **76,** 2222–2226 (1979).

9. Sninsky, J. J., Siddiqui, A., Robinson, W. S. & Cohen, S. N. *Nature* **279**, 346–348 (1979).
10. Alexander, J. J., Macnab, G. & Saunders, R. in *Perspectives Virol.* **10**, 103–120 (1978).
11. Marion, P. L., Salazar, F. H., Alexander, J. J. & Robinson, W. S. *J. Virol.* **33**, 795–806 (1980).
12. Desmyter, J., Ray, M. B., Bradburne, A. F. & Alexander, J. J. in *Viral Hepatitis* (eds Vyas, G. N., Cohen, S. N. & Schmid, R.) 459–463 (Franklin Institute Press, Philadelphia, 1978).
13. Kaschka-Dierich, C., Falk, L., Bjursell, G., Adams, A. & Lindhal, T. *Int. J. Cancer* **20**, 173–180 (1977).
14. Schaffner, W., Gross, K., Telford, J. & Birnstiel, M. *Cell* **8**, 471–478 (1976).
15. Wahl, G. M., Stern, M. & Stark, G. R. *Proc. natn. Acad. Sci. U.S.A.* **76**, 3683–3687 (1979).
16. Weinstock, R., Sweet, R., Weiss, M., Cedar, H. & Axel, R. *Proc. natn. Acad. Sci. U.S.A.* **75**, 1299–1303 (1978).

Integration of hepatitis B virus sequences and their expression in a human hepatoma cell

Jeffrey C. Edman, Patrick Gray, Pablo Valenzuela, Leslie B. Rall & William J. Rutter

Department of Biochemistry and Biophysics, University of California, San Francisco, California 94143

Hepatitis derived from hepatitis B virus (HBV) infection is endemic throughout the world, but it is particularly prevalent in Asia and Africa[1]. In these areas, demographic studies show a strong coincidence between HBV infection (assayed by HBV antigenic markers) and the incidence of primary liver cancer. On these grounds, a causal link between HBV infection and primary hepatocellular cancer has been proposed[2–5]. Recently, a human hepatoma cell line (PLC/PRF/5; Alexander cells) has been shown to produce hepatitis B surface antigen (HBsAg)[6]. We show here that the Alexander cell line contains at least six (four complete and two partial) hepatitis B viral genomes integrated into high molecular weight host DNA. An analysis using specific probes to fragments of the HBV genome suggests that integration of the virus in most cases occurs at the nicked cohesive end region of the virus. Expression of viral sequences using Northern blots demonstrates the presence of RNA transcripts specific for the surface antigen sequences of HBV DNA and the absence of detectable transcripts corresponding to the hepatitis B core antigen.

The study of the possible role of HBV in cell transformation has been hampered by the lack of an *in vitro* system for propagation of the virus. However, with the Alexander cell, which is derived from a hepatoma obtained from a male individual from Mozambique, HBsAg accumulates in the media as characteristic 22-nm particles[6,7]. The HBsAg of Alexander cells is identical to that isolated from HBV carriers and contains the unglycosylated and glycosylated forms of HBsAg protein (molecular weights (MWs) 25,000 and 29,000, respectively)[8,9]. In contrast, the Alexander cells do not produce hepatitis B core antigen (HBcAg; MW 19,000[8]), the cryptic HBeAg[10] or free virus (Dane particles)[11]. The presence of the endogenous Dane particle DNA polymerase that fills in the partially single-stranded region of HBV DNA to generate a double-stranded circular structure with cohesive ends[12] has not been tested. These cells show typical epithelial cell growth and exhibit many of the functions of liver cells. They also induce HBsAg-positive tumours in nude mice[13].

We have examined the physical state and expression of the HBV sequences in Alexander cells using the techniques developed by Southern for DNA analysis[14], 'Northern' blots for RNA analysis[15] and nick-translated cloned HBV sequences as probes[16]. Figure 1 shows the hybridization with the cloned HBV DNA probe to *Hin*dIII, *Eco*RI and *Hin*dIII–*Eco*RI digestions of high molecular weight DNA prepared from Alexander cells. The autoradiograph shows the presence of several large DNA fragments that hybridize with the probe. *Hin*dIII digestion (lane 2) yields at least six hybridizing bands, ranging from 4.2 to >30 kilobases. The unit length in all six is greater than that of the HBV DNA (3.2 kilobases). As there are no *Hin*dIII sites in any of the cloned HBV sequences reported, the data suggest at least six different sites for the integration of HBV DNA into host cell DNA. There is no detectable free viral DNA at 3.2 kilobases; this is consistent with the lack of virus production of these cells. This pattern of hybridization is observed in Alexander cells after many passages in tissue culture and also in recloned populations of the cells. Thus, the multiplicity of bands does not reflect cell heterogeneity.

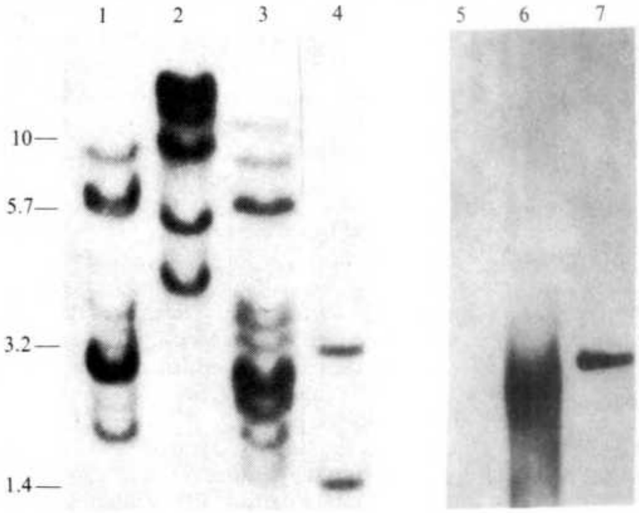

Fig. 1 Hybridization of ^{32}P-labelled HBV DNA probe to *Eco*RI (lane 1), *Hin*dIII (lane 2) and *Hin*dIII-*Eco*RI (lane 3) digests of Alexander cell DNA; standards were derived from cloned HBV DNA (lane 4, 3,200 and 1,400 base pairs), *Eco*RI-digested normal human liver DNA (lane 5), *Eco*RI-digested chronic hepatitic liver DNA (lane 6) and Dane particle DNA made double stranded by endogenous DNA polymerase reaction (lane 7). DNA was prepared from Alexander cells by suspending 0.5 ml of packed cells in 5 ml of 10 mM Tris-HCl (*p*H 7.4), 10 mM NaCl and 2 mM EDTA-Na_2. SDS and proteinase K were then added slowly to 2.5% and 0.1%, respectively. The solution was incubated for 18-24 h at 37 °C, extracted once with phenol, once with chloroform/isoamyl alcohol (24 : 1) and precipitated with two volumes of ethanol. The precipitate was resuspended in 5 ml of the same buffer, RNase A and RNase T1 added to 40 $\mu g\ ml^{-1}$ and 10 $\mu g\ ml^{-1}$, respectively, and digested for 1 h at 37 °C. The phenol and chloroform/isoamyl alcohol extractions were repeated, and the DNA precipitated with ethanol and resuspended in 10 mM Tris-HCl, *p*H 7.4, and 1 mM EDTA. DNA from liver samples was prepared in an identical manner except the tissue was homogenized briefly with a Teflon homogenizer before the addition of SDS and proteinase K. Dane DNA was made completely double stranded and extracted according to Landers *et al.*[12]. Restriction enzyme (New England Biolabs) digests were carried out according to the manufacturer's instructions. Completion of digests was monitored by addition of 1 μg of λ DNA to a small fraction of the digest and digested DNA was precipitated with ethanol. The samples were run on 1% agarose gels. DNA was transferred to nitrocellulose filters according to Southern[14] and hybridized to nick-translated[23] HBV probe in the presence of 10% dextran sulphate[24]. Numbers on the left-hand side indicate the fragment sizes in kilobase pairs.

*Eco*RI digestion (Fig. 1, lane 1) produces a series of 10 bands ranging from 2.4 to 9.5 kilobases with a particularly intense band at 3.0 kilobases. As HBV DNA contains a single *Eco*RI site, it is expected that *Eco*RI digestion would give twice as many hybridizing fragments as *Hin*dIII-restricted DNA. Ten rather than twelve bands were observed. This discrepancy may be the result of overlap of bands at the 3.0 kilobase band, as an analysis using a more highly resolving gel system shows that there are multiple bands in this region (data not shown). Figure 1 also shows the results of a similar analysis of HBV viral DNA (lane 7), normal human liver DNA (lane 5) and DNA from the liver of a chronic hepatitis patient (lane 6). No hybridization signal was detected in the DNA from normal liver; thus, there are no sequences closely related to HBV DNA in the normal human genome. Hybridization characteristic of free viral DNA was detected from the DNA of a chronic hepatitic liver.

0028–0836/80/310535—04$01.00

To determine the fraction of HBV information retained in each of the six integrated viral sites, we hybridized Alexander DNA with fragments of HBV DNA. Cloned HBV DNA was digested with a combination of restriction enzymes to yield a series of fragments each representing roughly one-sixth of the viral genome. Figure 2*a* and *b* show the source of these fragments and their positions within the viral genome. These fragments were purified by polyacrylamide gel electrophoresis, individually nick translated and hybridized with *Hin*dIII-digested Alexander DNA. Autoradiographs of these hybridization reactions are presented in Fig. 3*a* and summarized in Fig. 2*c*. *Hin*dIII digestion generates the six fragments which presumably contain full-length integrated HBV sequences. Four of the bands (30, 27, 18 and 5.7 kilobases) hybridize with all the probes; thus, each contains a major fraction of the HBV genome. However, the 10-kilobase band *Hin*dIII fragment does not hybridize with the *Bgl* 3 probe (see Fig. 2 legend) and the 4.2 kilobase *Hin*dIII fragment does not hybridize with the *Bgl* 3 and *Bgl* 2 probes and therefore contain partial HBV genomes. The absent sequences of both partial genomes are in the region of the core antigen gene. The apparent deletion of HBV information in the 10- and 4.2-kilobase fragments could also be explained by the presence of additional *Hin*dIII sites in these two integrated copies. This would generate an additional *Hin*dIII fragment hybridizing to the apparently deleted regions. No such fragments were detected.

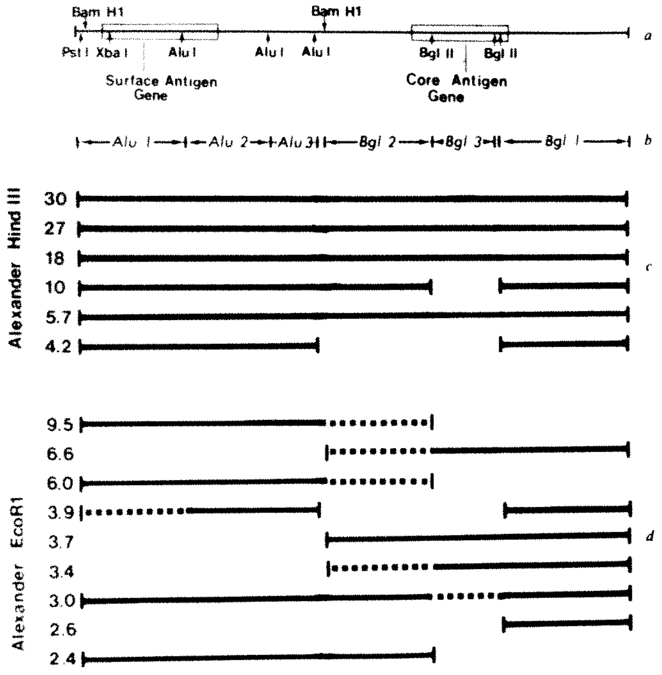

Fig. 2 Source of HBV DNA fragment probes and summary of hybridization to Alexander cell DNA digests. *a*, Restriction map of cloned HBV DNA linearized by *Eco*RI[16]; *b*, fragment probes used in the hybridization reactions. Cloned HBV DNA was digested with *Bam*H*I* and *Eco*RI, and the 1,800- and 1,400-base pair fragments purified by agarose gel electrophoresis and electroelution. The 1,800-base pair fragment was digested with *Bgl*II to yield fragments *Bgl* 1–*Bgl* 3 and the 1,400-base pair fragment with *Alu*I to yield *Alu* 1–*Alu* 3. Fragments derived from these digests were purified by polyacrylamide gel electrophoresis and individually nick translated. The sizes of the various fragments (in base pairs) are: *Alu* 1, 714; *Alu* 2, 344; *Alu* 3, 242; *Bgl* 1, 789; *Bgl* 2, 584; *Bgl* 3, 421. *c*, Summary of hybridization of fragment probes to *Hin*dIII-digested Alexander cell DNA. The sizes (in base pairs) of *Hin*dIII fragments hybridizing to the entire HBV probe are given on the left. A solid bar represents a positive hybridization result and absence of a bar represents no hybridization to the same regions as shown in *a* and *b*. For example, the 10-kilobase *Hin*dIII fragment of Alexander cell DNA does not hybridize to the *Bgl* 3 probe. *d*, Summary of hybridization of fragment probes to *Eco*RI-digested Alexander cell DNA. As in *c*, *Eco*RI fragment size is given on the left. A solid bar represents strong hybridization, a dashed bar weak hybridization. Two patterns of hybridization are evident. The 9.5-, 6.0-, and 2.4-kilobase bands hybridize from the *Eco*RI site through the surface antigen gene with the *Bgl*2 region and the 6.6-, 3.7- and 3.4-kilobase bands hybridize from the *Eco*RI site through the core gene into *Bgl*2. Anomalous hybridization is observed in the 3.9-, 3.0- and 2.4-kilobase bands.

The orientation of HBV DNA sequences within the Alexander genomic DNA has been studied by hybridizing the specific probes to *Eco*RI-digested Alexander DNA (Fig. 3*b*). As there is a single *Eco*RI site in the viral genome and assuming that integration is not random with respect to the virus, two patterns of hybridization should be observed, one hybridizing to fragments of HBV from the HBV *Eco*RI site clockwise to the region of integration, and the other pattern going counterclockwise. As summarized in Fig. 2*d* , two such patterns are obtained. One hybridizes from the *Eco*RI site through the surface antigen gene to a region approximately 1,600 base pairs from the *Eco*RI site; the other hybridizes approximately 1,600 base pairs in the opposite direction. Thus, *Eco*RI cleavage essentially bisects the integrated genome. This places the integration site in the region of the cohesive end region of Dane DNA[17]. There are three exceptions to this general pattern. One is the 3.9 kilobase fragment that hybridizes to both sides of the *Eco*RI site in one of the integrated regions. Another exception is the 2.6 kilobase band hybridizing only to a small region of HBV. This probably arises from the integration of a partial HBV genome. Finally, the 3.0 kilobase band apparently hybridizes with all regions of the genome. The hybridization intensity varies with different probes and is particularly weak with the *Bgl* 3 probe. The width of the band also varies, being nearly resolved into two bands using *Alu* 1 as a probe and appearing as a single band using *Bgl* 1. As this band may be resolved into three bands, it is possible that the anomalous hybridization in this region is due to a multiplicity of bands representing a combination of fragments having the two hybridization patterns. Other possible explanations are tandem integration of the virus or the loss of an *Eco*RI site in one of the viral copies coupled with the presence of *Eco*RI sites flanking the viral sequences.

The orientation of HBV integration may be responsible for the selective pattern of HBV gene expression in these cells. An analysis of the expression of HBV was carried out by hybridization of HBV probes to poly (A)-enriched Alexander cell RNA fractionated into size classes by electrophoresis in denaturing conditions[18]. This RNA was transferred to diazotized paper as described by Alwine *et al*[18]. and then hybridized with cloned HBV DNA probe (Fig. 4). The predominant hybridization signal is a high molecular weight RNA approximately the size of 18S ribosomal RNA(~2,000 bases). This band hybridizes specifically to the *Alu* 1 fragment (see Fig. 2 legend) of the HBV genome that contains the surface antigen gene but includes 300 base pairs 5′ to the gene (the *Bgl* A probe, see Fig. 4 legend) and 700 base pairs 3′ to the gene (the *Bgl* B probe). This major transcript does not hybridize to the *Bgl* 1, *Bgl* 2 or *Bgl* 3 probes, demonstrating the absence of core antigen-specific transcripts. These studies suggest that at least 1,500 base pairs of the HBV genome hybridize to the transcript. As this is smaller than the total transcript, additional sequences may be contributed by transcription of sequences of the Alexander genomic DNA and/or by poly (A) addition. HBV probes also hybridized to larger and smaller RNA sequences than the major transcript. This hybridization is HBV-specific as negligible background is observed in the hybridization of HBV DNA to uninfected liver RNA (data not shown). The HBV-related RNA which is larger than the major transcript is obviously of considerable significance because it must represent either a precursor to the approximately 2,000-base major transcript or an independent transcript(s). The lower molecular weight material probably represents processing or degradation of the major transcript, as is seen in other systems.

Others have previously investigated the question of HBV integration into the host cell genome. Summers *et al.*[19] studied a series of six hepatomas using nick-translated HBV DNA. They concluded that some of the tumours contained HBV DNA but that none contained integrated virus. Marion *et al.*[20] have recently reported the integration of HBV in Alexander cells. They detected only three *Hin*dIII fragments hybridizing to total

HBV probe, roughly corresponding to the lower three bands found in Fig. 1, lane 2. The source of this discrepancy is uncertain; however, it is not a result of partial cleavage by restriction enzymes in our experiments. The present experiments demonstrate that HBV sequences are integrated into a minimum of six different sites in Alexander cell DNA. The results suggest that the nicked cohesive end region of HBV DNA coincides with the region of integration of at least several of the HBV fragments. A circular structure with terminally redundant ends has been suggested as the precursor to integration in retroviruses, known integrating viruses[21,22]. Such a structure could be formed in HBV by repair of the nicked region with the endogenous polymerase activity, resulting in a structure that contains a terminally redundant sequence.

Integration of HBV in a malignant cell does not imply that the virus is the oncogenic agent. However, viral transformation is usually associated with the integration of viral sequences into host chromosomal DNA. If HBV is an oncogenic virus, the transformation event producing the Alexander cell might have involved the gene product HBsAg or be some function of the integration of HBV. Analysis of the integration of HBV in other hepatomas, as well as efforts to obtain the expression of the HBsAg gene in mammalian cells, may help to clarify this issue. However, the putative role of HBV in transformation itself will be greatly facilitated by the development of an *in vitro* cell system that is capable of propagation and integration of the virus.

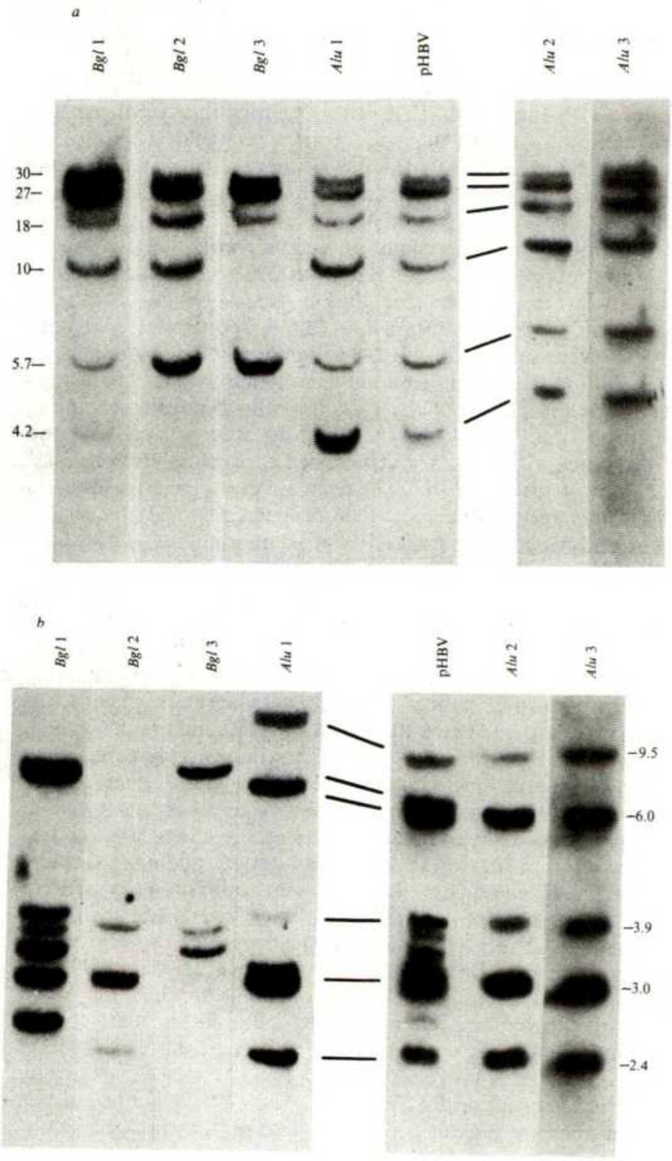

Fig. 3 Hybridization of *Hin*dIII (*a*) and *Eco*RI (*b*) digests of Alexander DNA with probes representing fragments of HBV DNA. Digestion products were run on 0.8% agarose gels and blotted to nitrocellulose filters. Individual lanes were cut out and hybridized to probes derived from cloned HBV DNA. The various probes are described in Fig. 2*a*,*b*. pHBV represents probe prepared from the entire HBV sequence. These hybridizations are summarized in Fig. 2*c*,*d*. Fragment sizes are indicated in kilobase pairs.

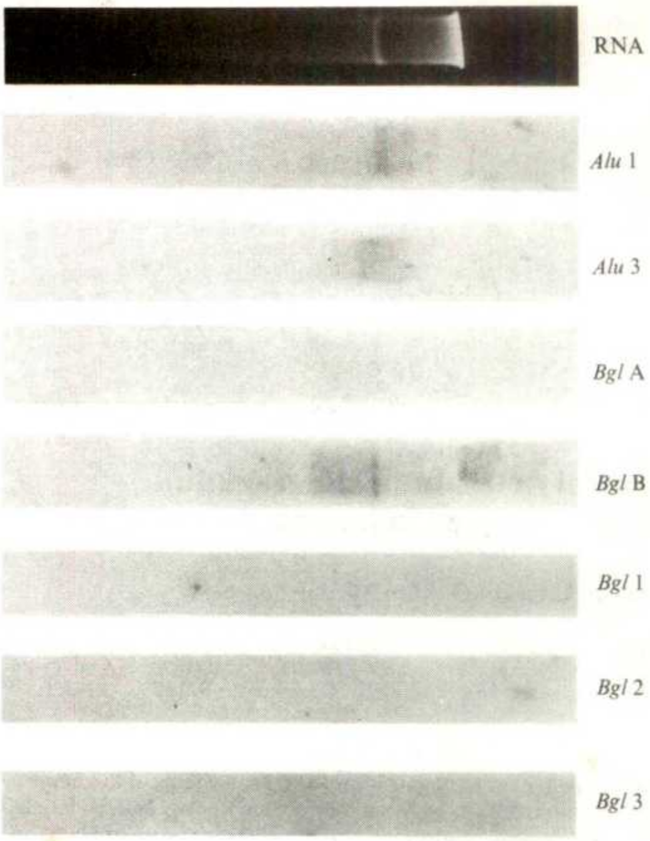

Fig. 4 Hybridization of poly(A)-enriched Alexander cell RNA with ^{32}P-cloned HBV DNA fragments. RNA was isolated from Alexander cells by the method of Chirgwin *et al.*[25] and passed once over oligo(dT)-cellulose. This RNA was run on a methyl mercury agarose gel and transferred to diazotized paper as described by Alwine *et al.*[15]. Individual lanes were cut out and hybridized to the various probes as shown in Fig. 2*b*. In addition, two other probes were used: *Bgl* A was derived from *Bgl* 1 and represents a 100-base pair fragment adjacent to the *Eco*RI site, and *Bgl* B is derived from *Bgl* 2, being 100-base pairs from the *Bam*HI site. RNA lane shows an ethidium bromide stain of the gel before transfer.

We thank Drs J. Birnbaum, M. Hilleman, R. Hirschman and A. Tytell for the initial supply of Alexander cells and Dane particle preparations, Dr E. Smuckler for human hepatitic liver, Dr H. M. Goodman for helpful discussion, and L. Spector for preparation of the manuscript. P.G. is a fellow of the Damon Runyon–Walter Winchell Cancer Fund. This research was supported by a grant from Merck Sharpe & Dohme Research Laboratories.

Received 20 March; accepted 18 June 1980.

1. Zuckerman, A. J. *J. Tox. envir. Hlth* **5**, 275–280 (1979).
2. Zuckerman, A. J. *Human Viral Hepatitis*, 2nd edn (North-Holland/American Elsevier, Amsterdam, 1975).
3. Vogel, C. L., Anthony, P. P., Sadikali, F., Barker, L. F. & Peterson, M. R. *J. natn. Cancer Inst.* **48**, 1583–1588 (1972).
4. Larouze, B. *et al. Lancet* **ii**, 534–538 (1976).
5. Okuda, K. & Nakashima, T. *Prog. Liver Dis.* **6**, 639–650 (1979).
6. McNab, G., Alexander, J., Lecatsas, G., Bey, E. & Urbanowicz, J. M. *Br. J. Cancer* **34**, 509–515 (1976).
7. Alexander, J. J., Beym E., Geddes, E. & Lecatsas, G. *S. Afr. med. J.* **50**, 2124–2128 (1976).
8. Gerin, J. L. & Shih, J. W. K. *Viral Hepatitis* (eds Vyas, G. N., Cohen, S. N. & Schmid, R.) 147–153 (Franklin Institute Press, Philadelphia, 1978).
9. Skelly, J., Copeland, J. A., Howard, C. R. &. Zuckerman, A. J. *Nature* **282**, 617–618 (1979).
10. Takahashi, K. *et al. J. Immun.* **122**, 275–279 (1979).
11. Dodd, R. Y. *et al.* in *Viral Hepatitis* (eds Vyas, G. N., Cohen, S. N. & Schmid, R.) 722 (Franklin Institute Press, Philadelphia, 1978).

12. Landers, T. A., Greenberg, H. B. & Robinson, W. S. *J. Virol.* **23,** 368–376 (1977).
13. Desmyter, J., Ray, M. B., Bradburne, A. F. & Alexander, J. in *Viral Hepatitis* (eds Vyas, G. N., Cohen, S. N. & Schmid, R.) 459–463 (Franklin Institute Press, Philadelphia, 1978).
14. Southern, E. M. *J. molec. Biol.* **98,** 503–517 (1975).
15. Alwine, J. C., Kemp, D. J. & Stark, G. R. *Proc. natn. Acad. Sci. U.S.A.* **74,** 5350–5354 (1977).
16. Valenzuela, P. *et al. Nature* **280,** 815–819 (1979).
17. Charnay, P., Pourcel, C., Louise, A., Fritsch, A. & Tiollais, P. *Proc. natn. Acad. Sci. U.S.A.* **76,** 2222–2226 (1979).
18. Bailey, J. M. & Davidson, N. *Analyt. Biochem.* **70,** 75–83 (1976).
19. Summers, J. *et al. J. med. Virol.* **2,** 207–214 (1978).
20. Marion, P. L., Salazar, F. H., Alexander, J. J. & Robinson, W. S. *J. Virol.* **33,** 795–806 (1980).
21. Tronick, S. R. *et al. Proc. natn. Acad. Sci. U.S.A.* **76,** 6314–6318 (1979).
22. Shank, P. R. *et al. Cell* **1,** 1383–1410 (1978).
23. Rigby, P. W. J., Dieckman, M., Rhodes, C. & Berg, P. *J. molec. Biol.* **113,** 237–251 (1977).
24. Wahl, G. M., Stern, M. & Stark, G. R. *Proc. natn. Acad. Sci. U.S.A.* **76,** 3683–3687 (1979).
25. Chirgwin, J. M., Przybyla, A. E., MacDonald, R. J. & Rutter, W. J. *Biochemistry* **18,** 5294–5299 (1979).

Partial deletion of the α-globin structural gene in human α-thalassaemia

Stuart H. Orkin & Alan Michelson

Division of Hematology-Oncology, Children's Hospital Medical Center, Sidney Farber Cancer Institute, Department of Pediatrics, Harvard Medical School, Boston, Massachusetts 02115

Defective synthesis of specific polypeptide chains of haemoglobins is the hallmark of human disorders known collectively as the thalassaemia syndromes[1]. Genetic lesions intimately linked to or within the globin genes are responsible for these conditions. Recently, the molecular basis of several forms of thalassaemia has been clarified by examination of the organization and structure of globin genes. Gene mapping studies using the gel blotting technique of Southern[2] have revealed an array of deletions involving globin structural genes in thalassaemias[3–12] and nucleotide sequencing has identified a point mutation responsible for thalassaemia in one individual[13]. In most α-thalassaemias, deletion of entire α-globin structural genes has been observed[3,4]. In specific forms of β-thalassaemia in which δ-globin chain expression is affected ($\delta\beta$-thalassaemia, $\gamma\delta\beta$-thalassaemia and hereditary persistance of fetal haemoglobin syndrome), various deletions within the cluster of closely linked γ-, δ- and β-globin genes occur[5–9]. In some Asian Indian individuals with β°-thalassaemia, an internal deletion in the DNA involving the 3′-portion of the β-globin gene has been described[10–12]. Lastly, in one Chinese patient with β°-thalassaemia, a nonsense mutation within the β-sequence has been identified[13]. We now report a new genetic lesion present in some individuals with α-thalassaemia: an extensive deletion of the 5′ portion of the α-globin structural gene. This defect has been characterized by DNA sequence analysis of cloned α-thalassaemia genes.

In normal humans the α-globin structural genes are duplicated and closely linked[14]. By gel blotting experiments these genes have been localized to a 22.5 kilobase fragment of genomic DNA generated by the restriction enzyme *Eco*RI. In α-thalassaemic DNA samples, several different alleles of the normal complex are observed. These include *Eco*RI fragments of 22.5, 18–20 and 2.6 kilobases in length[15,16]. The 22.5-kilobase fragment, grossly normal by restriction mapping, contains two structural genes, one of which is presumed to be functionally abnormal on the basis of its presence in some individuals with HbH disease α-thalassaemia, a condition in which only one functional α-globin gene exists. The 18–20-kilobase fragment contains a single α-gene that most commonly arises due to non-homologous crossing-over within the region of the duplicated structural genes. We focus here on the 2.6-kilobase fragment, identified only in several individuals with HbH disease originating from the Mediterranean basin. On the basis of DNA–DNA hybridization[15,16], this fragment seemed to contain at most a single α-globin structural sequence. To characterize this novel restriction fragment in detail, we have cloned it in bacteriophage λ vectors from two unrelated individuals with α-thalassaemia and analysed its structure by restriction mapping and DNA sequencing.

The α-specific 2.6-kilobase fragments were cloned from these two individuals by different strategies. The lymphocyte DNA of patient 1 (HbH disease genotype: 18–20 kilobases/2.6 kilobases[15]) was digested with *Eco*RI and fragments of 2.2–2.8 kilobases were isolated by preparative agarose gel electrophoresis. This enriched DNA fraction was ligated to the outer arms of phage λgtWES (ref. 17) and packaged *in vitro* into viable phage[18], and recombinants were screened by the plaque assay method of Benton and Davis[19] using total $(\alpha+\beta)$ ^{32}P-labelled globin cDNA as probe. Positive phages were then rescreened using nick-translated DNA from the plasmid α-cDNA clone JW101[20]. Among approximately 3×10^5 recombinants, one α-globin-specific phage was isolated. Analysis of its DNA indicated that, in addition to a 2.6-kilobase fragment, at least two other DNA fragments in the 2–3-kilobase size range were present. The 2.6-kilobase fragment was recloned in λ Charon 16A (ref. 21) free of these other human fragments. This phage was designated $\lambda\alpha$T1(2.6). A 'library' of the lymphocyte DNA of patient 2 (HbH disease genotype: 22.5 kilobases/2.6 kilobases) was prepared in λCharon 4A (ref. 21) by the procedure of Kemp *et al.*[22]. Screening of this library constructed from partial *Eco*RI* digestion fragments yielded several α-specific phage containing the 2.6-kilobase fragment. From one such isolate the 2.6-kilobase fragment was subcloned in λ Charon 16A and designated $\lambda\alpha$T2(2.6).

Gel blotting of these recombinant phage with α-globin probes specific for sequences either 5′ or 3′ to the *Hin*dIII site normally present at the codons for amino acids 90/91 of the α-sequence[14,23] demonstrated that coding sequences from both regions were present in the 2.6-kilobase *Eco*RI fragment (Fig. 1). Additional restriction mapping immediately raised questions regarding the nature of the cloned globin gene. For example, cleavage sites for *Mbo*II and *Taq*I located normally in the α-sequence within the 5′-untranslated region and at the codons for amino acids 46/47 (ref. 23), respectively, were not present in the anticipated positions 5′ to the intragenic *Hin*dIII site (Fig. 2). *Taq*I and *Mbo*II sites located approximately 55 and 170 base pairs 3′ to the *Hin*dIII site were located within what was found to be an intervening sequence of approximately 150 base pairs within the cloned α-thalassaemia gene (see below and Fig. 2). The presence of these latter restriction sites in this α-globin gene is in accord with recent findings regarding intervening sequences of cloned normal human α-genes[24]. In agreement with our previous mapping of genomic DNA, *Bam*HI and *Hpa*I[15], as well as *Sac*I and *Bgl*II, did not cut the 2.6-kilobase fragment.

To determine the nature of the cloned globin gene and to localize the lesion responsible for thalassaemia in this instance, DNA sequencing was carried out using the chemical degradation method of Maxam and Gilbert[25]. The sequencing strategy and a partial sequence of the gene from approximately −170 to +60 base pairs relative to the intragenic *Hin*dIII site are shown in Figs 2–4. The nucleotide sequence predicts the correct α-globin amino acid sequence from amino acids 57 to 99. An intervening sequence, the initial portion of which is shown, interrupts the coding sequence after codon 99, as is the case in the mouse α-globin gene[26] and probably also the normal human α-globin genes[24]. There is an abrupt loss of the α-globin coding sequence 5′ to codon 57 (Figs 3, 4). The DNA sequence of this region does not encode any globin-like polypeptide. In fact, it contains a termination codon (UGA) at the position expected for codon 48. Gel blotting experiments (not shown) did not reveal any hybridizable α-globin sequences 5′ to the *Hin*fI site depicted in Fig. 2, therefore indicating that the missing 5′ portion of the α-sequence is not contained within the cloned 2.6-kilobase fragment. Additional DNA sequencing, to be reported elsewhere, has revealed a complete α-globin sequence for codons 100–141 following the intervening sequence as well

0028-0836/80/310538—03$01.00

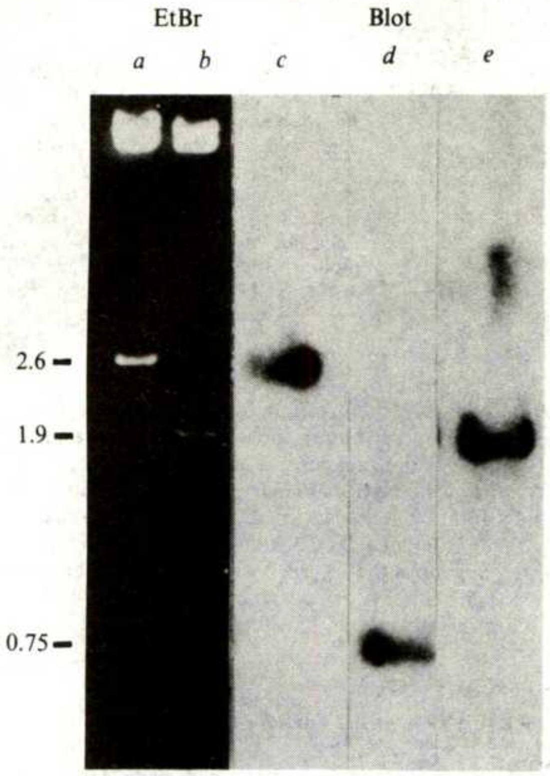

Fig. 1 Gel blotting of $\lambda\alpha$T1(2.6) DNA with 5'- and 3'-specific α-probes. Recombinant phage DNA (0.5 μg) was digested with *Eco*RI alone (lanes *a,c*) or *Eco*RI + *Hin*dIII (lanes *b, d, e*) and electrophoresed in 1% agarose. Ethidium bromide (EtBr) staining of the DNA is shown in lanes *a,b*. Lanes *c,d,e* represent hybridization to 5' + 3'-specific, 5'-specific and 3'-specific α-globin DNA probes, respectively. 5' + 3'-specific probe was prepared by nick translation of plasmid JW101 DNA[20]. Probes specific for α-sequences 5' and 3' to the intragenic *Hin*dIII site were prepared from JW101 DNA digested with *Hin*dIII, as described by Embury *et al.*[4]. The sizes of fragments resulting from digestion of the cloned segment are shown in kilobases. Gel blotting of $\lambda\alpha$T2(2.6) DNA yielded identical results.

as the presence of a 3'-untranslated region exhibiting several scattered single nucleotide changes from the published normal mRNA sequence[23]. Whether these changes reflect previously unrecognized sequence polymorphisms within α-globin genes or sequence divergence from normal in these α-thalassaemia genes is uncertain at present. Thus, the striking feature of the structure of the α-globin gene present in the 2.6-kilobase fragment is the absence of the 5'-untranslated region and codons 1–56.

Two observations show this structurally abnormal globin gene is not an artefact of cloning. First, the identical deletion has been observed in the fragment cloned from unrelated individuals by different cloning strategies. Furthermore, several independent recombinant phages with the same structure of the 2.6-kilobase fragment have been isolated from the library constructed from the DNA of patient 2. The precise reproducibility with which this fragment has been isolated argues strongly against its accidental creation during the cloning procedures. Second, in gel blotting experiments, the 2.6-kilobase *Eco*RI fragment of genomic DNA of these patients hybridizes in the presence of a vast excess of unlabelled JW101 DNA with probe prepared from the portion of the 2.6-kilobase fragment 5' to the intragenic *Hin*dIII site (not shown). Thus, sequences 5' to codon 57 in the cloned fragment reside in the same location in genomic DNA.

The 2.6-kilobase fragment, therefore, seems to have arisen by a deletion originating 5' to a normal α-globin gene. In theory, a large insertion of DNA within the coding segment of the gene might have occurred. In this case, the missing 5' portion of the α-gene would be located elsewhere in the genome and be represented in gel blotting experiments as an additional restriction fragment. As analysis of genomic DNA of individuals with the 2.6-kilobase *Eco*RI fragment has not revealed such additional hybridizing bands[15,16], a deletion rather than an insertion of DNA is the likely origin of this structurally abnormal globin gene. Note that this is the first partially deleted globin gene in which the deletion terminates within the coding region. In the partial deletion of δ-globin sequences in one form of $\delta\beta$-thalassaemia[6] and of β-sequences in β°-thalassaemia[10–12] the deletions end within the large intervening sequences. On the basis of its distance from the 3' *Eco*RI site[14,15] and the presence of specific restriction sites in its 3'-flanking region (for example, extragenic *Xba*I site[27]), the α-globin sequence of the 2.6-kilobase fragment is probably derived from the 3'-α-globin gene of the normal duplicated complex.

By gene cloning, Lauer *et al.*[24] have determined the arrangement of α-like globin genes in normal human DNA as

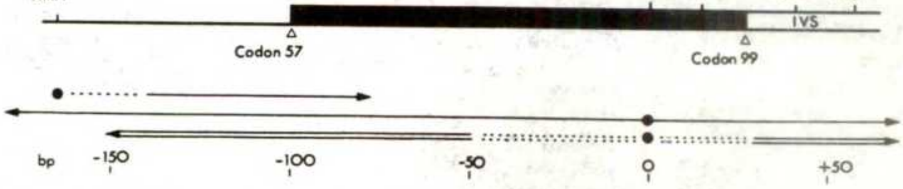

Fig. 2 Restriction map of the 2.6-kilobase cloned fragment and the strategy for DNA sequencing. The map of the cloned 2.6-kilobase fragment of $\lambda\alpha$T1(2.6) (upper portion) was constructed from the results of gel blotting and partial restriction mapping by the method of Smith and Birnstiel[28] after end-labelling of the *Hin*dIII site. The expanded segment below indicates the region of the cloned insert that was sequenced by the method of Maxam and Gilbert[25]. The solid dots indicate the fragment ends that were labelled. Single arrows indicate fragments labelled at the 5' end with [^{32}P-γ]ATP by polynucleotide kinase[25]. Double arrows indicate fragments that were 3' labelled with [^{32}P-α]dNTPs by the action of the Klenow fragment of *Escherichia coli* DNA polymerase. The solid portions of these arrows indicate those regions for which unequivocal sequences for each fragment were obtained. HdIII = *Hin*dIII; MbII = *Mbo*II; IVS = intervening sequence. The filled boxed regions indicate globin coding regions. The open boxed area represents the nearly 150-base pair intervening sequence present in the cloned gene. 3'-Untranslated sequences are shown by the cross-hatched area. The cloned fragment is orientated with its 5' end to the left.

```
Cloned Gene   TGGAATCTTAGCACTTTGGGAGGCCAAGGTGGGATGGTCACTTGAGCCTGGGAGTTCAAGACCAGCCTA
                                                                               GGCCACGGCAAGAAGGTG
α-Globin      LeuSerPheProThrThrLysThrTyrPheProHisPheAspLeuSerHisGlySerAlaGlnValLysGlyHisGlyLysLysVal
                                                         48                             57
α-mRNA        CUGUCCUUCCCCACCACCAAGACCUACUUCCCGGACUUCGACCUGAGCCACGGCUCUGCCCAGGUUAAGGGCCACGGCAAGAAGGUG


Cloned Gene   GCCGACGCGCTGACCAACGCCGTGGCGCACGTGGACGACATGCCCAACGCGCTGTCCGCCCTGAGCGACCTGCACGCGCACAAGCTT
α-Globin      AlaAspAlaLeuThrAsnAlaValAlaHisValAspAspMetProAsnAlaLeuSerAlaLeuSerAspLeuHisAlaHisLysLeu
                                                                                           90
α-Globin      GCCGACGCGCUGACCAACGCCGUGGCGCACGUGGACGACAUGCCCAACGCGCUGUCCGCCCUGAGCGACCUGCACGCGCACAAGCUU


                                        GTGAGCGGCGGGCCGGGAGCGATCTGGGTCGAGGGG....
Cloned Gene   CGGGTGGACCCGGTCAACTTCAAG ----- Intervening Sequence -------
α-Globin      ArgValAspProValAsnPheLysLeuLeuSerHisCysLeuLeuValThrLeuAlaAla....
                                   99
α-mRNA        CGGGUGGACCCGGUCAACUUCAAGCUCCUAAGCCACUGCCUGCUGGUGACCCUGGCCGCC....
```

Fig. 3 Partial nucleotide sequence of the 2.6-kilobase fragment. The nucleotide sequence of the portion of the cloned insert shown at the bottom of Fig. 2 is compared here with the amino acid and nucleotide sequences of normal α-globin and α-globin mRNA[23]. The underlined segment 5′ to the position of codon 57 does not resemble normal α- or other globin sequences. The nucleotide sequence of $\lambda\alpha$T2(2.6) was identical in the region shown here.

5′-ζ2-ζ1-$\psi\alpha$1-α2-α1-3′ where ζ1 and ζ2 are embryonic α-like genes, $\psi\alpha$1 a non-functional α-like gene, and α1 and α2 the normal adult α-genes. Restriction maps of the ζ and $\psi\alpha$1 genes and their flanking regions do not resemble the pattern of sites within our 2.6-kilobase fragments at their 5′ ends. This suggests that the 5′ extent of the deletion responsible for the creation of the 2.6-kilobase fragment lies beyond the region mapped by Lauer *et al.*[24] and therefore more than 25–30 kilobase upstream from the region of the normal α-globin genes. If this is the case, homozygosity for the 2.6-kilobase allele would result in defective embryonic haemoglobin synthesis. This lethal form of thalassaemia might go undetected due to the early time at which fetal loss would occur. The true incidence of the thalassaemia gene studied here among Mediterranean individuals is not known. As we identified this gene in 6 unrelated individuals with HbH disease among 12 cases initially analysed[15], it cannot be exceedingly rare. We should anticipate, therefore, the discovery of fetal wastage due to homozygosity for this α-thalassaemia gene in populations in which it is prevalent rather than a hydrops fetalis phenotype[1], the consequence of deletion of the adult α-globin structural genes without simultaneous deletion of embryonic α-like genes.

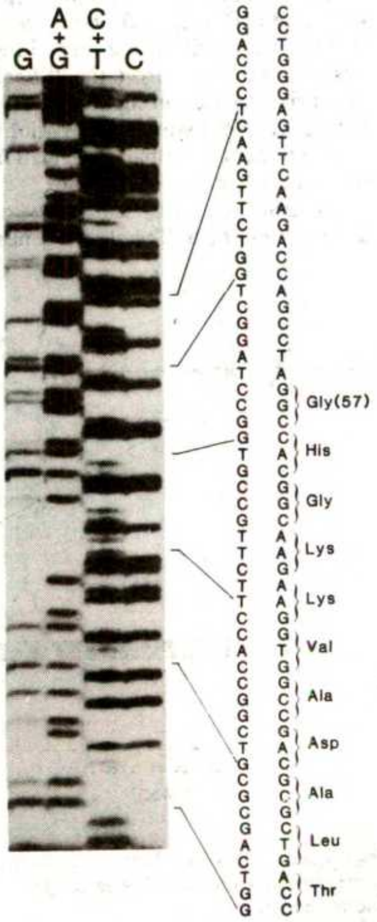
G
A + G
C + T
C
GGACCCTCAAGTTCTGGTCGGATCCGGTGCCGTTCTTCCACCGGCTGCGCGACTGG
CCTGGGAGTTCAAGACCAGCCTAGGCCACGGCAAGAAGGTGGCCGACGCGCTGACC
Gly(57)
His
Gly
Lys
Lys
Val
Ala
Asp
Ala
Leu
Thr

Fig. 4 Sequencing gel of the region containing the deletion in $\lambda\alpha$T1(2.6). The 0.75-kilobase *Eco*RI/*Hin*dIII fragment of $\lambda\alpha$T1(2.6) (Fig. 1) was 5′ labelled at the *Hin*dIII site and subjected to the chemical degradation reactions of Maxam and Gilbert[25]. The products were electrophoresed in a 0.38-mm thick 20% urea-acrylamide slab at 2,000 V for 24 h.

We thank Dr David G. Nathan for his continued support and encouragement and J. Lauer and T. Maniatis for a preprint of ref. 24. S.H.O. is the recipient of a Research Career Development Award of the National Heart, Lung, and Blood Institute-NIH and a grant from the National Foundation March of Dimes. *Note added in proof*: The 3′-untranslated region of the α-thalassaemia gene is that of the normal α1 gene. Therefore, the α-thalassaemia gene is derived from α1 and the normal α-globin genes differ in sequence in that region.

Received 2 April; accepted 16 May 1980.

1. Weatherall, D. J. & Clegg, J. B. *Cell* **16,** 467–479 (1979).
2. Southern, E. M. *J. molec. Biol.* **98,** 503–517 (1975).
3. Orkin, S. H. *et al. New Engl. J. Med.* **299,** 166–172 (1978).
4. Embury, S., Lebo, R., Dozy, A. & Kan, Y. W. *J. clin. Invest.* **63,** 1307–1310 (1979).
5. Mears, J. G. *et al. Proc. natn. Acad. Sci. U.S.A.* **75,** 1222–1226 (1978).
6. Fritsch, E. F., Lawn, R. M. & Maniatis, T. *Nature* **279,** 598–603 (1979).
7. Orkin, S. H., Alter, B. P. & Altay, C. *J. clin. Invest.* **64,** 866–869 (1979).
8. Ottolenghi, S. *et al. Nature* **278,** 654 (1979).
9. Van der Ploeg, L. H. T., Koning, A., Oort, M., Roos, D., Bernini, L. & Flavell, R. A. *Nature* **283,** 637–642 (1980).
10. Flavell, R. A., Bernards, R., Kooter, J. M. & deBoer, E. *Nucleic Acids Res.* **6,** 2749–2760 (1979).
11. Orkin, S. H., Old, J. M., Weatherall, D. J. & Nathan, D. G. *Proc. natn. Acad. Sci. U.S.A.* **76,** 2400–2404 (1979).
12. Orkin, S. H., Kolodner, R., Michelson, A. & Husson, R. *Proc. natn. Acad. Sci. U.S.A.* (in the press).
13. Chang, J. C. & Kan, Y. W. *Proc. natn. Acad. Sci. U.S.A.* **76,** 2886–2889 (1979).
14. Orkin, S. H. *Proc. natn. Acad. Sci. U.S.A.* **75,** 5950–5954 (1978).
15. Orkin, S. H. *et al. Cell* **17,** 33–42 (1979).
16. Kan, Y. W. *et al. Blood* **54,** 1434–1438 (1979).
17. Tilghman, S. *et al. Proc. natn. Acad. Sci. U.S.A.* **74,** 4406–4410 (1977).
18. Blattner, F. *et al. Science* **202,** 1279–1284 (1978).
19. Benton, W. D. & Davis, R. W. *Science* **196,** 180–182 (1977).
20. Wilson, J. T. *et al. Nucleic Acids Res.* **5,** 563–581 (1978).
21. Blattner, F. R. *et al. Science* **196,** 161–169 (1977).
22. Kemp, D. J., Cory, S. & Adams, J. M. *Proc. natn. Acad. Sci. U.S.A.* **76,** 4627–4631 (1979).
23. Wilson, J. T. *et al. J. biol. Chem.* **255,** 2807–2815 (1980).
24. Lauer, J., Shen, C-K. J. & Maniatis, T. *Cell* **20,** 119–130 (1980).
25. Maxam, A. & Gilbert, W. *Meth. Enzym.* (in the press).
26. Nishioka, Y. & Leder, P. *Cell* **18,** 875–882 (1979).
27. Goossens, M. *et al. Proc. natn. Acad. Sci. U.S.A.* **77,** 518–521 (1980).
28. Smith, H. O. & Birnstiel, M. L. *Nucleic Acids Res.* **3,** 2387–2398 (1976).

Errata

In the letter 'Mantle composition derived from the composition of lherozites' by S. Maaloe and R. Steel, *Nature* **285,** 321–322, the first line of paragraph 6 was omitted; it should read 'The composition of the mantle generating abyssal tholeiite'.

In the article 'Sequence of retrovirus provirus resembles that of bacterial transposable elements' by Shimotono *et al.*, *Nature* **285,** 550–554, in Fig. 2 legend it should read 'Labelled termini are indicated by (⊢)' not (–) as shown. In Fig. 4 legend lines 21 and 22 should be omitted.

In the News and Views article 'Extra-pituitary actions of LHRH and its agonists' by Richard M. Sharpe, *Nature* **286,** 12–14, line 9 on page 14 should be replaced by 'LHRH has taught most of us to regard'

BOOK REVIEWS

Plants, politics and empires

A.H. Bunting

Science and Colonial Expansion: The Role of the British Royal Botanic Gardens. By L.H. Brockway. Pp.215. (Academic: New York and London, 1979.) $21, £12.

THE author offers this book as an account of "botanical imperialism" and a historical-anthropological analysis of the role of the Royal Botanic Gardens, Kew, in the expansion of the British Empire. Her purpose is to demonstrate that nineteenth-century Kew was a "control centre", the directors of which conspired with the Government to press the botanical resources of the Earth, and of Latin America in particular, into the service of British imperialism and the expansion of colonial rule, especially in Asia. Since she sees no redeeming facets in imperialism and colonialism, the tone of the book is overwhelmingly critical; and since both her objectives and her raw materials are restricted in scope, her presentation is out of balance. The broad sweep of Kew's immense contribution to pure and applied botany, the foundations of which were laid in the nineteenth century, hardly emerges.

About half of the book is devoted to setting the stage. An introduction, and a brief and superficial chapter on the political and economic history of the British Empire, are followed by an essay on the diffusion of domesticated plants around the world, which is offered as the primary reason for the growth of human population since 1492.

Two chapters on the growth and organization of science in Britain in the eighteenth and nineteenth centuries in general (including its social and personal links with government), and on the evolution of Kew and the overseas botanic gardens in particular, make much of class distinction and patronage; and so it is the more unfortunate that the Darwin-Wedgwood connection did not lead the author to ponder the relative roles of the Lunar and the Royal Societies. The special train which brought Wickham's 70,000 rubber seeds from Liverpool becomes an example of the power of authority serving imperial interest.

The next three chapters, on quinine, rubber and sisal, the core of the book, are followed by a final ten pages containing a curious miscellany — the Crystal Palace as a symbol of the common interests of feudal landowners and the new industrialists (because Paxton had learnt to build glasshouses at Chatsworth), leading on to the Palm House as a symbol of Kew's overseas role, a résumé of the history of British plant exploration and the growth of plantation industries, followed by some concluding remarks on the social function of science.

Taken as a whole, the book resembles, in structure, ideas and language, an unpolished and somewhat immature PhD thesis. It is a library study, supplemented by visits to Brazil and to Kew. Most of the references are to secondary sources, mostly from the social sciences, often written 100 years or more after the observations or events they review. A good deal of the biological comment is gauche — among much else, *Stylosanthes* is cited as a forage grass; the seed dispersal mechanism of *Hevea* cannot by itself explain the small density of trees of this genus in the Amazonian forest; *Ficus elastica* is not a vine; the significance of the monocarpic habit of *Agave* is misunderstood; and the nature of taxonomic work and the rules of priority in botanical nomenclature are misrepresented. If the biology is so unprofessional (and, moreover, written in a mixture of colloquial American and the metalanguage of an unfamiliar profession), what is the biological reader to think of the historical, economic and political material?

In fact the historical material about Kew, and the details of the transfers of plant materials in the eighteenth and nineteenth centuries, seem to be accurate enough. Much of it will be sufficiently unfamiliar to be interesting to non-specialists. The interpretation of history is something else. It makes much of smuggling and other knavish activities (though the circumstances in which Linnaeus' herbarium was transferred to Britain have escaped the author's censorious eye), and of the "conversion of knowledge to profit and power" by the British in support of imperialism. Thus *Cinchona* plantations were established in the Nilgiris, with seeds and plants spirited out of the Andean countries, to aid control of malaria in the Indian Army in the aftermath of the Mutiny. Quinine then made it easier for the British to bring their families to live in India and so to widen the social gulf between British and Indians. Kew organized the smuggling of rubber out of Brazil — though J.W. Purseglove (*Tropical Crops, Dicotyledons* p.149. Longman: London, 1968) firmly rebuts this gloss on the events — for British military, industrial, commercial and other imperialist purposes. Kew is castigated for publishing, as scientific and technical information, secrets of the botany and processing of sisal which enabled Germany to obtain materials of a Mexican plant from a supplier in Florida in order to build a sisal industry in German East Africa which fell into Britain's lap when Tanganyika was mandated to her after the First World War.

The transfer of economic plant materials from one country to another is consistently treated as expropriation. While unique artefacts, or mineral resources, can be expropriated, genetic resources are by their nature renewable. Transferred plant materials can of course be used to produce improved varieties and build plantation industries which may bring far greater advantages to foreigners than to the people of their countries of origin. This is but one of the many harsh features of the uneven development of nations. Plant resources can be expropriated only where they are also eradicated in their country of origin, as the Dutch attempted to do with the clove tree early in the seventeenth century.

The cynic could comment here that many plant species and varieties are at present unlikely to be saved for posterity unless they are in part expropriated, since they are at severe and increasing risk in their native lands.

Many people today share the author's uncompromisingly critical attitude towards conquest, the oppression of man by man, imperialism in general (including neocolonialism and the multinational companies), and British imperialism in particular, and look askance at the

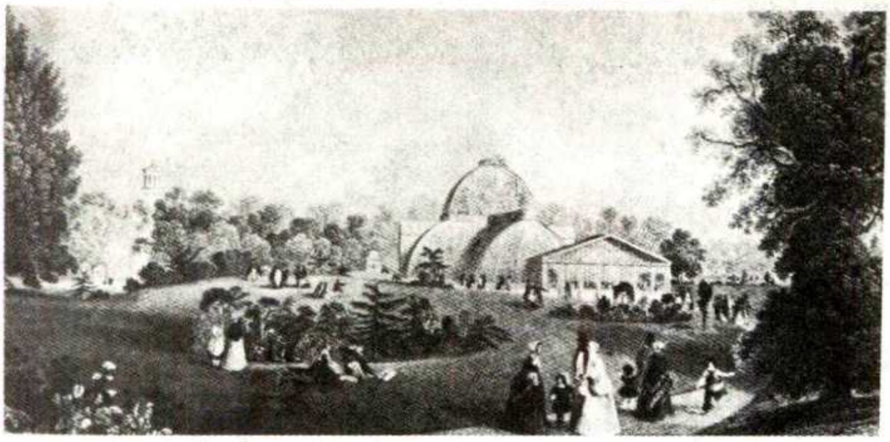

Kew Gardens in the 1850s, showing the newly constructed Palm House

arrogant self-righteousness of some nineteenth-century attitudes towards Britain's civilizing role among the lesser nations. We can well imagine that the destruction of indigenous weaving and metal industries in India, by imports from Britain, helped to provide a cheap labour force for plantation industries in India (and later elsewhere in tropical Asia) when none was available in tropical America. Indeed this was advanced in the early 1830s as an argument for establishing a tea industry in India (*Tea Cultivation, India*. House of Commons Papers 63, 1839).

To most, however, this will seem an unduly eclectic view. Rubber provides a significant part of the economic basis for political independence in Malaysia and Indonesia; Indian quinine in its time saved many lives throughout the world; sisal has brought foreign exchange and some employment to Tanzania; and Kew continues to provide valued services, including third-country quarantine, for many developing countries.

Perhaps even more important are the personal and professional links, which include Kew and the Linnean Society, which hold together the large and active community of pure and applied botanists throughout the Commonwealth.

All in all, then, an unsatisfactory book; and in view of the great potential interest of its theme, a disappointing one. □

A.H. Bunting, formerly Professor of Agricultural Botany, is Professor of Agricultural Development Overseas in the University of Reading, UK.

Krylov and the genesis of statistical physics

Michael Berry

Works on the Foundations of Statistical Physics. By N.S. Krylov. Pp.283. (Princeton University Press: Princeton and Guildford, UK, 1980.) Hardback $19.50, £10.80; paperback $7.50, £4.15.

RECENT YEARS have seen real progress towards answering fundamental questions in statistical mechanics, thanks largely to the Russian school led by Kolmogorov and Sinai. Their work was stimulated by the thorough and imaginative studies of N.S. Krylov, who died in 1947 at the tragically early age of 29. With the publication of this book, Krylov's works are at last available to English-speaking readers.

Krylov emphasized the importance of explaining how systems relax to equilibrium, and indeed regarded this as the central problem of statistical mechanics. He shows that a sufficient condition for relaxation is that the system's dynamics possess the property of mixing, which means that an initial patch of phase space (i.e. a group of systems) eventually spreads to cover the whole energetically available region in filamentary fashion (whilst preserving its area). Most previous work had concentrated on ergodicity, namely the property that a point in phase space (i.e. a single system) eventually passes arbitrarily close to every energetically available phase point. Ergodicity is a weaker property than mixing, and does not guarantee statistical behaviour. Krylov traced the source of mixing (at least for systems of colliding hard spheres) to instability of trajectories, i.e. the exponential divergence of neighbouring orbits. He employed this idea in an approximate calculation of relaxation times. Subsequent research has abundantly confirmed that this type of instability is indeed the source of unpredictable behaviour in causal systems.

The book is not easy to read, because Krylov's repetitious style of writing makes it hard to hold the thread of his complex argument. Nevertheless, this is an important document, which should be studied by anybody seriously interested in statistical mechanics. A valuable feature of this book is an appendix by Sinai, outlining recent developments of Krylov's ideas. □

Michael Berry is Professor of Physics at the University of Bristol, UK.

Developments in plant molecular biology

Martin R. Hartley and R. John Ellis

Nucleic Acids in Plants. By T.C. Hall and J.W. Davies. Vol.I pp.261, Vol.II pp.237. (CRC: Boca Raton, Florida/Blackwell Scientific: Oxford, 1980.) Vol. I $64.95, £48.75; Vol. II $59.95, £44.75.

THESE two volumes represent the only comprehensive treatise so far published in the area of plant nucleic acids, and reflect the upsurge in interest and the exciting new developments that have recently taken place in plant molecular biology. The aim of the books is to provide a detailed and critical appraisal of selected topics which include many current research interests in plant nucleic acids, as well as some related aspects of protein synthesis and genetic manipulation. The title "Nucleic Acids *in* Plants" has allowed the inclusion of contributions on viral, viroid and plasmid nucleic acids, which together with a chapter on gene manipulation by sexual and somatic cell techniques occupy Vol.II.

Volume I deals with nucleic acids found in 'healthy' plants, with articles on nuclear genome organization (Walbot and Goldberg), chloroplast DNA (Tewari), RNA polymerases (Becker), tRNAs (Weil), rRNA (Leaver) and mRNA (Hall). The styles of these chapters vary considerably, from epic literature reviews to more personal accounts. For example, Weil's 33-page article cites 432 references, while Tewari's 65-page contribution cites only 62 and relies largely on the author's own data. All of the articles are authoritative and are mostly easily readable, although by the very nature of some of the topics under discussion it has not always been possible to avoid a catalogue approach. Particularly impressive are Walbot and Goldberg's description of the intricacies of DNA reassociation kinetics in an intelligible fashion, and Becker's critical and reasoned account of plant RNA polymerases, in which he dispels many myths, including those about the action of plant growth substances at the transcriptional level. Most articles contain fairly detailed sections on methodology, where advice is offered on the merits and limitations of different techniques. Although these sections are not sufficiently detailed to enable the reader to repeat experiments, they do provide valuable first-hand information of a kind which is not usually given in original papers or reviews, and therefore they should prove extremely useful for researchers entering the field. As is inevitable in such books, the reviews are out of date by up to two years, especially in the field of mRNA and chloroplast DNA where little of the recent cloning work is analysed.

Volume II contains chapters on plant DNA viruses (Hull), monopartite plant viruses (Zaitlin), multipartite and satellite plant viruses (Lane), the translation of plant viral RNA (Davies), viroids (Dickson), the crown gall phenomenon (Schell) and plant gene manipulation (Bingham). All are useful summaries of the state of the art at the time of writing, which varied from 1976 to 1978 judging from the references. Studies on plant viruses have not had the same impact on biology as have studies on bacteriophages and animal viruses, but several of the chapters stress their potential importance for improvements in agriculture. However the overall impression given is that plant virology is poorly developed compared to its bacterial and animal counterparts; these articles show that there is a long way to go before such studies lead to major improvements in agriculture by direct genetic manipulation. Thus the chapter by Hull is entitled "The DNA of Plant DNA Viruses" but most of the detailed information is confined to cauliflower mosaic DNA. That by Bingham discusses the various methods proposed for the genetic manipulation of crop plants from a plant breeder's point of view, and correctly stresses the severe nature of the problems to be overcome. His case is not helped by the fact that the work referred to on p.218 on the expression of foreign DNA in cultured plant cells has not stood the acid test of reproducibility in other laboratories. The contributions by Zaitlin, Lane and Davies contain much detailed information on the isolation, characterization, synthesis and translation of plant viral RNAs. These chapters will be especially useful to those entering the field.

The message stands out clearly that much more work of high quality is what plant virology needs before its full potential can be realized, and the latter volume should contribute towards this goal by informing and interesting young research workers. In this respect it is to be regretted that each slim book is so highly priced; 19p a page will deter many people from purchasing two useful volumes. □

Martin R. Hartley and R. John Ellis are Lecturer and Professor respectively in the Department of Biological Sciences at the University of Warwick, UK.

Catalytic chemistry of palladium

M.W. Roberts

Palladium Catalyzed Oxidation of Hydrocarbons. By P.M. Henry. Pp.407. (Reidel: Dordrecht, The Netherlands, Boston and London, 1980.) Dfl. 125, $65.

IT IS perhaps surprising to someone not closely involved with the field that a book of over 400 pages can be entirely devoted to how palladium catalyses homogeneously the oxidation of hydrocarbons. However, a quick glance at this book left me in no doubt that it contains a wealth of interesting chemistry and that the idea is entirely justified. The book is aimed at three groups of people: (1) the industrialist interested in catalysis; (2) organic chemists interested in synthetic aspects; and (3) physical chemists interested in mechanistic aspects. The author is ideally suited to tackle such a task, being currently in a university post but having spent some 15 years in industry.

The book is divided into seven chapters. The author, however, having decided that there will be mainly two groups of readers — first, those largely interested in preparative chemistry, and second, those interested in both preparative and mechanistic aspects — has separated mechanistic discussions from the purely descriptive sections. Being mainly interested in heterogeneously catalysed reactions, I found this helpful.

In the first chapter we are led gently through a historical account, then some aspects of the basic inorganic chemistry of palladium in its various valence states — Pd(0), Pd(I) and Pd(III) — are described, followed by a discussion of the organometallic chemistry of palladium and finally catalysis. The two basic catalytic mechanisms considered are: (1) oxidation-addition or its reverse, reduction-elimination; and (2) the insertion reaction or its reverse.

Chapter 2 deals exclusively with the oxidation of monoolefines leading to the formation of aldehydes and ketones, esters and ethers. Over half of the book is devoted to the first two chapters, while the remaining five deal with the reaction of dienes and polyenes, π-allyl complexes, reactions of acetylenes, reactions of aromatic compounds and what are termed "miscellaneous reactions".

An excellent bibliography of approximately 40 pages lists 1124 references largely taken from papers published during the past decade. Among the references there is a good sprinkling of patents reported, reflecting the author's links with the industrial application of palladium catalytic chemistry.

There is a great deal of information in this book which will cater for a wide cross-section of chemists. The detail is impressive and indicative of the author's close involvement with the subject. I found it perhaps unusual to have a blend of detailed preparative chemistry intertwined with mechanistic argument, but possibly physical chemists are unfamiliar with this approach! The author set out to "give a survey of both the range and utility of the (homogeneous) catalytic chemistry of palladium and to discuss the basic reaction paths . . .". This, I believe, he has accomplished satisfactorily. In addition there is much of benefit in this book for those interested in heterogeneous catalysis (and its possible relationship with homogeneous systems); however, what is difficult for the non-specialist to ascertain is how much of the mechanistic discussion is 'established fact' and how much 'interesting speculation'. □

M.W. Roberts is Professor of Physical Chemistry at University College, Cardiff, UK.

Alone; the story of South American mammals

R.J.G. Savage

Splendid Isolation: The Curious History of South American Mammals. By G.G. Simpson. Pp.256. (Yale University Press: New Haven and London, 1980.) $17.50, £11.05.

FIFTY years ago Dr G. G. Simpson escaped death from revolutionaries in Argentina and undaunted carried on to lead a fossil-hunting expedition into distant Patagonia. He has returned many times to South America and has devoted a large portion of his long and very active scientific career to studying South American fossil mammals. In 1934 Simpson published a narrative of that first expedition; his deservedly popular book *Attending Marvels* (Macmillan: New York) vividly portrays the excitement of fossil hunting and the fascination of those bleak Patagonian landscapes. In *Splendid Isolation* he now addresses a wide readership with, as he subtitles the book, the curious history of South American mammals.

The book begins with chapters on the history of discovery from the time when Darwin found fossils there in 1832, on where and how fossil mammals occur, and on stratigraphical stages and mammal ages. For almost all of the past 60 million years the South American continent has been isolated without land connections anywhere — neither to Antarctica or Africa, nor to Central or North America. A land link was only re-established within the past 5 million years. Thus throughout almost the entire Cenozoic era it was in splendid isolation, receiving only periodic mammal invasions by waif dispersal from some other continent(s). The history of the faunas is retailed in three phases: the earliest faunas of the Palaeocene and Eocene have just three basic stocks (the marsupials, xenarthrans and condylarths); in the second phase during the Oligocene and Miocene, we witness the addition of rodents and primates; and the third phase begins in the early Pliocene (as defined by Simpson) with the build-up to the great American interchange of mammal faunas north-south across the continents. The book finishes with a summary chapter and a note on the restoration of extinct animals.

The book is highly factual and, as we would expect of the doyen, highly accurate and up-to-date with the latest fossil discoveries. But the facts are too often dry and indigestible. Accounts of each family with descriptions of their dental characteristics do not make easy reading, the more so as few are adequately illustrated. Indeed the illustrations are almost totally limited to elemental reconstructions — all without scale. The Plio-Pleistocene and Recent faunas are very summarily treated; much of the space here is devoted to etymological discourse. Simpson's penchant for both logodaedaly and sesquipedality are evident throughout. There are no photographs, no skeletal reconstructions and only one palaeogeographical map — and that of the mid-Cretaceous. Palaeogeography is a subject to which the author has himself made signal contributions, yet it is all but ignored in this book; it merits space only in the last three pages. Considering the tremendous impact of plate tectonics theory over the past decade, much could have been said, if only in summary, about the continent's history and its relationships to adjacent regions during the past 80 million years. The author tells us his first and second phase colonizations were waif dispersals. The centre(s) of origin of waifs has been the subject of copious debate; Simpson, fairly but very briefly, disposes of the arguments on the grounds that we have too few facts to come to definitive conclusions. The third phase colonization is certainly better documented, but Simpson refuses to be drawn into the current debates on palaeogeographical models, dispersal or vicariance — the latter originating with a Venezuelan biologist. Many scientists feel such models are useful in that they offer a challenge to discover adequate evidence to test a hypothesis. With the immense knowledge and unique experience Simpson possesses, we would all appreciate and profit from having his palaeogeographical interpretation. For without this, the history is as Hamlet without the Prince of Denmark. The task may be, to use Simpson's words, Herculean, but it is hardly Sisyphean.

There is no recent work with which *Splendid Isolation* can readily be compared. Patterson and Pascual's brilliant essay review of 1972, "The Fossil Mammal Fauna of South America" (In *Evolution, Mammals and Southern Continents*, edited by A. Keast *et al.* State University of New York Press: Albany), is still indispensable to the serious student. Yet, while the balance of topics treated in *Splendid Isolation* is sometimes too light and sometimes too heavy, there is much a student will find interesting in this curious history.

R.J.G. Savage is Reader in Vertebrate Palaeontology at the University of Bristol, UK.

Suspending time: a guide for biologists

David E. Pegg

Low Temperature Preservation in Medicine and Biology. Edited by M.J. Ashwood-Smith and J. Farrant. Pp.323. (Pitman Medical: Tunbridge Wells, UK/University Park Press: Baltimore, 1980.) £17.50, $39.50.

WHEN Polge, Smith and Parkes made the discovery, in 1948, that glycerol would enable avian spermatozoa to survive freezing at −79°C, they could scarcely have anticipated the impact their observation was to have in medicine and biology. The special value of preserving viable cells in the deep-frozen state is that this essentially suspends time: chemical reactions are arrested and even the recrystallization of ice is prevented at the generally used storage temperature of −196°C, the boiling point of nitrogen. Then, only ionizing radiation can produce damage, but as Ashwood-Smith points out in this book, it would take 32,000 years to accumulate a dose of 600 rads! The cryobiologists' trick then is to cool cells to, and recover them from, −196°C without damage. Although the conditions necessary to achieve this differ widely from cell to cell, remarkable successes have been achieved: nowadays, innumerable scientists and technicians in fields as disparate as clinical blood banking, animal husbandry, immunology, reference culture collection of bacterial, fungal, animal and plant cells, and entomology use cryopreservation as a tool in their daily work, perhaps with little knowledge of the principles upon which the techniques are based. This book sets out to provide a guide for such workers.

Farrant opens the book with a delightfully clear elementary explanation of mechanisms of freezing injury and cryoprotection. Ashwood-Smith then describes current techniques for the preservation of tissue culture cells and some mammalian tissues, and Polge, truly one of the founders of cryobiology, contributes an excellent chapter on the development of techniques for the cryopreservation of spermatozoa — full of practical detail, but also interestingly reflective on the way in which this field has developed. Whittingham gives excellent guidance from his wide personal experience of the low temperature preservation of early embryos of many mammals. The chapters on haematological applications, by Rowe and Schaefer, are essentially practical and detailed, while Knight provides an admirable critical account of work on the preservation of leukocytes, emphasizing the difficulties of obtaining valid measurements of post-thaw recovery. The chapters on protozoa and helminth parasites by James, on micro-organisms by Ashwood-Smith and on plant cells by Morris are all clear and packed with practical advice, while the contribution by Ring on the cryobiology of insects and their cells is particularly fascinating and goes beyond practical preservation to describe the fascinatingly varied adaptations found in insects that survive the extremely low temperatures occurring in Arctic regions. The book concludes with a chapter of general practical guidance.

Without doubt, this will prove to be a valuable text: it is not, however, as comprehensive as its title might suggest. Low temperatures, but without freezing, are widely used in medicine and biology for the short-term preservation of cells, tissues and organs, most importantly perhaps of blood cells for transfusion and of tissues and organs for transplantation. None of this is dealt with. Moreover the excellent introductory chapter could, I believe, usefully be supplemented by a more detailed discussion of theoretical cryobiology to help the reader digest the mass of 'cookbook' detail found in the subsequent chapters. Also, the balance of contributors seems a little strange in that it does not reflect the major contribution of workers in the USA during the past 20 years. Finally, the chapter on practical aspects would be much improved by the inclusion of greater detail of the actual equipment and procedures being discussed. (The thermocouple table on p.290 differs from the current BSI and NBS standards.) These are relatively small details, however, and the editors can be congratulated on a most useful compilation: perhaps they will consider widening the scope of future editions.

David E. Pegg is head of the MRC Medical Cryobiology Group in the Department of Surgery, University of Cambridge, UK.

nature

7 August 1980

Towards a more competent Civil Service

The narrow issue of how much scientists working in the British Civil Service should be paid during 1980 will no doubt be settled by this week's arbitration hearing, to which the Civil Service Department has been driven by the Institution of Professional Civil Servants (see *Nature*, 24 July). The outcome, no doubt, will be a compromise between the government's offer and the claim by the IPCS — and a further setback for the system of "pay research" by which salaries are determined. The more serious questions of how, and on what terms, scientists should be recruited to the Civil Service will however remain unasked. As a result, scientists in the public service will continue to be treated as a group apart while the public service and thus the British government will continue to be less effective than it could and should be. It is a scandal that so little attention has been paid, since the publication in 1968 of the report of the Fulton Commission on the organization of the Civil Service, to these important issues.

Traditionally, as the whole world knows, the British Civil Service has been a happy and largely successful hunting ground for gifted generalists, able to turn their attention from the administration of bits and pieces of the British Empire to the administration of, say, the publicly supported schools. It is customary to suppose that in the nineteenth century the system worked splendidly, although with hindsight it is clear that for every brilliant administrator of India thrown up by the system there was a small army of dull pecksniffs guiding the growth of the public service in unimaginative directions. How could it be otherwise, given the traditional method of recruitment into the Administrative Civil Service? Although in the twentieth century the Administrative Class has replenished its ranks with graduates from well connected universities, Oxford and Cambridge in particular, rather than from the sons of well connected families (as in the nineteenth century), the principle is unchanged. It is to take a man (or now, mercifully, a woman) of high intelligence but without particular expertise, and to let him learn the craft of public service on the job in one ministry after another, with spells of duty rarely spanning more than three years. Within the service, frequency of movement is a mark of success, with the result that the high fliers, as they are called, begin and end as generalists — intelligent, to be sure, but almost proud of having no expert knowledge of the fields of the public service they administer. Recognizing, however, that the public service increasingly requires expert knowledge in many different fields, the Administrative Civil Service has built up separate cadres of specialists — scientists and engineers but also economists and architects, for example.

The Fulton Commission was born of a suspicion that this system was increasingly an anachronism. The suspicion was confirmed by the commission's analysis. Its conclusion that generalists, sometimes rudely but properly called amateurs, had outlived their usefulness to society as public servants was understandably unpalatable to those primarily concerned. In the circumstances, it is something to be grateful for that the least radical of the Fulton Commission's recommendations have indeed been followed. The Administrative Civil Service now looks less eagerly to the products of Oxbridge courses in classics or history for its new recruits. Responsibility for recruitment has been transferred from the Treasury to the newly created Civil Service Department, while steps have been taken, as Fulton asked, to make it easier for people with experience of other walks of life to join the Civil Service in mid-career. (Even so, the flux of people into and out of the public service is not nearly as great as Fulton hoped.) Under these arrangements, there is of course no reason why scientists or people with other specialist backgrounds should not compete for places in the Administrative Civil Service alongside those with other kinds of degrees. Understandably, the numbers of those prepared to ape the generalists at such an early stage in their careers as scientists is small and likely to remain so.

The Fulton Commission acknowledged that this was likely to be the case, for which reason (among others) it urged that there should be a merger of the Science and Administrative classes. Since 1968, British governments have stolidly declined to follow this proposal. Administration, they say, no doubt on the advice of the administrators, is in itself a special skill, distinct from other kinds of skills. The one concession to the Fulton view to have been made in the past decade is a scheme by means of which scientist within the public service can apply for a transfer to the Administrative Branch. Again, understandably, the volume of transfers is a trickle. More seriously, the habits of the public administration are unchanged — those who enter the Administrative Civil Service from some other part of the public service do so on terms spelled out by the administrators.

The result, increasingly apparent, is that the British government is denied the kind of advice and administration that circumstances now demand. The record of simple administrative errors stemming from innocence of technical matters grows with the passage of the months. It is not so long since the renegotiation by the Home Office of the international allocation of broadcasting frequencies robbed the BBC of facilities now plainly essential to its social function. More recently, the British government has been allowed to dither about the payment of the second promised tranche of £25 million to the semiconductor company INMOS (*Nature*, 5 June), apparently in ignorance of the nature of technical development in novel fields. (In the end, as the Prime Minister announced last week, the National Enterprise Board has been allowed to meet its moral obligation.) Unhappily, such conspicuous errors are almost by definition relatively minor. The influence of an ill-informed administration on the evolution of more substantial policies is harder to pin down. The chopping and changing in British energy policy over the past two decades, however, clearly carries the marks of technical innocence. So does the apparent assumption by several government departments that funds for research and development, or education, can be turned off and on as water from a tap. The truth is that, in such fields, uncertainty is more damaging than mere shortage of funds. But elsewhere, again apparently from lack of technical knowledge, the Civil Service conspires with the government to attempt to make water run uphill. How else is it possible to explain the devotion of successive governments (but not the present) to regional policies intended to share such prosperity as the country continues to enjoy more equitably between different parts of the country? The objective, of course, is admirable, but the results have been at best meagre, as economists have been saying all along.

It would of course be wrong to think that maladministration of this kind would vanish if more of the administration of the government's affairs were shouldered by scientists and other specialists. Scientists and other specialists do not have a monopoly of wisdom, and there is also something in the administrators' claim that good judgement in public administration comes with experience. This, however, is merely an argument in favour of the Fulton Commission's proposal that there should be a thorough merging of the scientific and the administrative Civil Services. While many scientists within the public service would no doubt wish to follow the public interest and their own in the pursuit of research and development, others would be able to contribute more effectively than is at present

0028-0836/80/320545-02$01.00

possible to the routine work of the public service, preventing the howlers which are at present perpetrated by the generalists and helping also to ensure that major issues of public policy are dealt with in a manner that is technically sound and, with luck, imaginative as well. One unconvenanted benefit would be that the hosts of advisory committees which at present litter Whitehall could be reduced in number — one of the present government's ambitions. Perhaps the first British Prime Minister who happens to be a scientist might take up the shamefully neglected cause of making the British Civil Service more competent.

Radiation standards not yet for changing

The chequered history (see page 550) of the report on low-level ionizing radiation, published last week by the US National Academy of Sciences, should not detract from its value. The report was commissioned by the Environmental Protection Agency and has been prepared by the academy's Committee on the Biological Effects of Ionizing Radiation. It is popularly known as BEIR III to distinguish it from an earlier report in 1972 and from the first draft of this document (released just over a year ago before all the members of the committee had had their say). The issues with which it deals are of great importance, not merely for regulatory agencies such as the Environmental Protection Agency, for those concerned with industrial health and safety (not only in the nuclear industry) but also for the public at large, rightly concerned that there should be a judicious assessment of the potential hazards of ionizing radiation, especially that produced by the nuclear industry. The public importance of the topic has of course been keenly appreciated for the past quarter of a century, with the result that attempts to calculate the hazards of radiation have been made by national governments, independent organizations such as national academies and even by the United Nations. The particular value of BEIR III stems from that feature for which it is likely to be most criticized — for by including the opinions of members of the committee dissenting on scientific grounds from the main report, it serves to dramatize the uncertainties that persist in this difficult field.

The abiding difficulty in the estimation of the consequences of radiation exposure is that of extrapolating downwards, from the often tragic experience of people who happened to be living in Hiroshima and Nagasaki in 1945, those who were treated with X rays for a variety of diseases such as rheumatoid arthritis or ankylosing spondylitis in the 1930s or those who worked as radiographers before the hazards of radiation were fully appreciated, to the rest of us, whose organs receive 100 mrem a year (in round numbers) from natural and unnatural causes — cosmic rays, natural radioactivity such as potassium-40, visits to the orthopaedics people, airline travel and the like. Hitherto, most serious studies of how the extrapolation should be carried out have been based on the assumption that the risk of damage is proportional to the dose of radiation. (The days have long since gone when it was permissible to talk of a "threshold" dose below which radiation entailed no risk of damage.) BEIR III breaks new ground by flirting seriously with the notion that the relationship between the risk of damage and the dose of radiation that produces it may not be linear after all, but rather quadratic, at least where the induction of some kinds of cancers is concerned. (On the genetic consequences of radiation exposure, BEIR III follows earlier studies in affirming that only the linear extrapolation is prudent in the present state of knowledge or, rather, ignorance.) This is why the report has engendered controversy among its authors even before publication.

Superficially, it is true, even to entertain the possibility that the rate of induction of some kind of cancer may be proportional not to D (where D is dose) but to $\alpha + \beta D + \gamma D^2$ (where α is the spontaneous rate, and β and γ are constants to be adjusted to fit the data) looks like a way of resurrecting the threshold hypothesis. For if γ is positive, extrapolation downwards from large to small D will suggest that the risk of harm by small doses of radiation, such as those attributable to krypton-85 in the atmosphere, for example, will be disproportionately less than those attributable to large doses.

The argument of BEIR III by way of justification is plausible but not conclusive. To their credit, the authors have acknowledged this to be the case. The conjecture that to cause a cancer it may be necessary to break the same DNA molecule at two places (not just one) before natural repair mechanisms have had time to do their work is modestly advanced, with as full a list of the objections as anybody could ask for. The experimental data bearing on this point which are marshalled by the report are impressive, but derive mostly from animal studies. The document acknowledges that the information available about the causation of human cancer is not "robust" enough to distinguish between the possible dose–response models, although there is some reason to think that skin cancer does not turn up at low doses of radiation, that the relationship between leukaemia induction and radiation dose among the Japanese bomb survivors is adequately represented by a quadratic relationship but that the risk of breast cancer is linearly related to the dose of radiation.

Inevitably, a quadratic rather than a linear relationship implies that the risk of cancer induction after exposure to small doses of radiation is reduced. BEIR III includes comparisons of the calculated risks based on the two assumptions which suggest that the risk of cancer induction after exposure to, say, 10 rads of ionizing radiation will be halved if the relationship between risk and dose is quadratic, not linear. Superficially, that represents a substantial change, for which reason it is relevant that the earlier calculations (like those of BEIR III) are accompanied by large (and unavoidable) errors; the new estimates, based on the quadratic assumption, do not lie all that far outside the errors of earlier calculations. A more serious difficulty (to which one of the dissenters, Professor Edward Radford, draws attention) is the element of arbitrariness in the way in which BEIR III had to calculate the parameters in its quadratic relationship between risk and dose from a few clumps of data relating to high acute exposures.

How, then, should the regulatory agencies respond to BEIR III? Some, no doubt, will be tempted to say that present regulations for occupational exposure to radiation might safely be relaxed, although not by very much. It will be a mistake, however, if BEIR III is taken as a licence for such a step. For the report itself is properly so hedged about with qualifications (and packed with interesting but complicated evidence to suggest how sensitivity to radiation may vary with age, sex and genetic constitution) that it cannot be regarded as the last work on the subject. Accordingly, the regulatory agencies should for the time being stick to the assumptions on which their calculations have hitherto been based while setting out more energetically to test the interesting proposal put forward by BEIR III. Perhaps the most conspicuous omission from the report is the committee's own assessment of the work that needs to be done more adequately to underpin its argument and conclusion. It is, however, plain that much can be done to test the conclusions of BEIR III. Animal experiments designed to test the risk of specific kinds of tumours after exposure to radiation could help to distinguish between the linear and quadratic hypotheses. BEIR III itself makes much of the results of the classic epidemiological study by Court-Brown and Doll on the incidence of tumours of people treated with X rays for ankylosing spondylitis. It is too much to ask that the regulatory agencies and the nuclear industries throughout the world should apply the same care to the study of the health of the only substantial group now exposed to relatively large doses of radiation—those occupationally exposed in nuclear plants?

Congress turns sour on technology fund

Washington

As part of a general effort to cut the foreign aid budget, Congress is threatening to veto the major US contribution to the new international fund for science and technology in developing countries which was set up following last year's United Nations Conference on Science and Technology for Development (UNCSTD).

The House of Representatives Appropriations Committee last week recommended the elimination from the 1981 budget request of a $10 million contribution which the Carter administration had proposed for the new fund. The committee also proposed changing the foreign aid bill so as to prevent any of the $130 million allocated to the United Nations Development Programme — the agency handling the fund — being used for this purpose.

UNDP officials hope that these recommendations will be rejected when the full House debates the foreign aid bill. Otherwise they fear that withdrawal of the US contribution could put the whole fund in jeopardy. This, they warn, would have repurcussions for relationships between the US and the many countries — particularly in Africa — which have already submitted project proposals to the fund on the understanding that adequate support has been promised.

Delegates to the UNCSTD conference in Vienna last August agreed to the fund as an interim measure. Initially the developing countries had proposed a more ambitious scheme for a $2,000 million to $4,000 million annual tax on technology transfers from the developed nations, but this was quickly rejected as unrealistic.

Promises were, however, made to explore the long-term prospects for such a scheme. Meanwhile a two-year interim fund was proposed under the auspices of the UNDP, with an initial target set at $250 million, of which the US indicated it would be prepared to cover 20 to 25 per cent.

In practice, even this target turned out optimistic. At a meeting in New York in March, total pledges of $36 million were made, primarily by Austria, Denmark, Norway, Sweden, The Netherlands and the US. (The UK made it clear in Vienna that it was not prepared to contribute: France and Germany are still negotiating conditions under which they may give up to $9 million more.)

Even though the total was less than had been hoped for, the UNDP decided that enough had been raised to get the fund off the ground. With the support of the UN General Assembly, the fund officially became operational in May. UNDP has already received over 550 applications from the governments of developing countries, and 70 projects have been selected as candidates for funding.

One African country has approached the UNDP for joint funding of a new metallurgical research institute, and another eight are already including possible support from the UNDP in schemes to integrate science and technology policies into their five-year economic plans.

UNDP officials argue that for the US to withdraw its proposed contribution — given its central role in engineering the Vienna compromise and steering attention away from the more far-reaching third world demands — would not only prejudice the future of the fund itself, but would also cast a cloud over all future negotiations on overseas aid.

The proposed $10 million US contribution has already been endorsed by the science committees and the foreign affairs committees in both the House and the Senate. Indeed some congressmen say they would have been prepared the support the $15 million contribution which President Carter had proposed in his original January request.

Despite this support, however, the appropriations committees are proving harder to convince. Commenting on its proposal that the US should not contribute to the fund, the House Appropriations Committee says that it took the action because the Administration had failed to provide adequate information on the activities of the fund.

This information is now being hastily provided, in the hope that at least some members of the Appropriations Committee can be persuaded to change their position. But the UNDP contribution has also become tied up with the conflict between the Congress and the Administration over the latter's plan to set up an Institute for Scientific and Technical Cooperation (ISTC) as a focus for research relevant to developing countries.

Last year Congress accepted the ISTC proposal in principle, but the appropriations committees failed to allocate funds after a bitter fight over the form that the institute should take, and its relationship to existing scientific and technological programmes in the Agency for International Development.

This year the Administration has again put forward the ISTC for funding. But despite plans to reduce its scope it seems increasingly unlikely that the institute will get off the ground.

Such a failure, embittered as it would be by the disputes which there have been between the Administration and Congress about overseas aid and the growing hostility of Congress towards multilateral aid programmes, imply that supporters of the UNDP have an uphill task ahead of them.

David Dickson

Compromise for Finniston?

On the principle that ministers cannot go on holiday until parliament has seen that their desks are clear, the British government was earlier this week preparing its much-delayed response to the report of the Finniston Committee on engineering education. The response will lose some friends and make some enemies, but is otherwise likely to be a compromise.

The central issue to have become apparent since the committee's report was published earlier this year is whether responsibility for the education of professional engineers, including the accreditation of university and other courses, the definition of professional standards and the certification of those claiming them, should rest with a new public body to be called the British Engineering Authority.

The Finniston Committee argued that there should be such a body, which would inevitably take over from the separate engineering institutions many of their existing educational and professional responsibilities. The committee also asked that such a body should be statutory, responsible to the minister responsible for industry — for the time being Sir Keith Joseph, Secretary of State for Industry. Only by such a device, the committee argued, could the reorganization of engineering education and qualification be carried out in such a way that industry could take notice. The committee also recognized that even the British government has, on paper at least, a long purse.

Since the publication of the report in February, the Department of Industry has invited comments from no fewer than 400 interested parties, most of whom have apparently replied. Many respondents, the Confederation of British Industries and the Committee of Vice-Chancellors and Principals for example, have however disappointed members of the Finniston Committee by warning the government against the notion that the engineering profession should be regulated directly by the government. This advice is likely to be the more influential because those who offer it also welcome structural changes in engineering education and qualification.

The favourite compromise seems to be that there should indeed be a new authority responsible for engineering education, but that it should be set up as an autonomous institution by the Privy Council, not by the government as such. To begin with, there should be a measure of direct financial help from the British government, but in the long run it might be appropriate that support should be channelled through bodies such as the University Grants Committee.

0028-0836/80/320547-01$01.00

Radioactive waste

Windscale leak

The scathing report last week from the British Nuclear Inspectorate on the latest radioactive leak from the Windscale reprocessing plant raises familiar issues. Yet again, it seems, a substantial leakage of radioactivity, 100,000 curies this time, has arisen from relatively minor design faults and sheer human frailty.

One of the benefits of the arrangement under which the Nuclear Installations Inspectorate works directly to the Health and Safety Executive is, however, that its full report (Health and Safety Executive, £1.25) has now been made public. It emerges that the inspectors had seriously considered prosecuting British Nuclear Fuels Limited, or members of the senior staff at Windscale, for breaches of the operating licence. Instead, the inspectors have asked the company (which is state-owned) to take remedial action and plainly hope that publication of their report will be a more effective safeguard for the future. BNFL has duly eaten humble pie, with a statement reading like the public confessions common in China during the Cultural Revolution.

The chronology of this latest incident at Windscale begins in 1955 when a plant was built for bleeding off small quantities of highly active liquid waste from the reprocessing line as part of the research programme then under way at Harwell to glassify highly active waste. The UK Atomic Energy Authority (then the operator of Windscale) erected building 701 which contained a 1,400-litre stainless steel tank in which active waste could be aged for an appropriate length of time, and a device for transferring some of this material into 20-litre shielded flasks for transport to Harwell. There were arrangements for returning waste from the building to the main processing line, principally from a small 70-litre sump in the floor of the building.

After the last consignment of waste to Harwell in 1958, Building 701 seems to have fallen out of use and out of mind. For some years, workmen at Windscale followed the standard operating procedure of emptying the sump at regular intervals, but during the 1970s the practice had become irregular. BNFL told the inspectors that they assumed that the liquid collecting in the sump was not radioactive, but probably consisted of rainwater leaking through the roof of the building and of condensation inside. The inspectors complain that BNFL should have considered the chance that active waste was splashing over the movable vanes used in a valve arrangement to divert the stream of active waste in one direction or another.

Attemps to empty that sump during the 1970s were not always successful, now it seems because one of the two outlet lines had been mistakenly cut and blanked off in 1971. Curiosity about the level of liquid in the sump could not reliably be satisfied — the pointer on the face of the instrument recording the liquid level can apparently turn full circle and then keep on turning, so an over-full sump may seem nearly empty.

The leak was discovered during a survey of the Windscale site in 1978, and recognized to consist of fission products only two years old in March 1979 when the nuclear inspectors were informed. The inspectors say that for several years the sump had been overflowing and that radioactive material had found its way through the stainless steel cladding lining the bottom of the building to soak through the concrete foundation to the ground beneath.

The penance required from BNFL includes the reinstrumentation of building 701, its isolation and, eventually, its decontamination, the monitoring of radioactivity in the ground beneath the plant (where most of the activity is some three metres beneath the surface) and preparation for the physical isolation of the activity or even the removal of the contaminated soil.

Both parties to the investigation agree that nobody has been exposed to a significant radiation dose because of the leak.

European biotechnology

EEC proposals

The European Commission's proposals for the regulation of genetic manipulation, once widely feared for their restrictiveness, have turned out to be comparatively tame. The commission's "recommendation", submitted to the Council of Ministers this week, requires merely that experiments in genetic manipulation should be registered nationally. The proposals are thus much less constraining than the directive proposed in 1978 and later withdrawn.

A "recommendation" carries no legal force but, if agreed by ministers, has a certain moral force among the nine member states. Last week's recommendation argues that while hazards are now thought to be "non-existent or small" it would nevertheless be prudent to register experiments centrally in case so far undetected "long-term effects" exist. To deal with commercial objections about confidentiality, notification would be restricted to "the portion of the experimental protocol which is required for the evaluation of safety".

Compulsory notification already exists in the United Kingdom, and may do so in Germany if a proposed law on genetic engineering re-emerges after the October election. Elsewhere it is voluntary.

The commission would also set up a committee of experts, mandated by member states, to examine at least once a year the need for harmonization of regulations and to consider emerging knowledge of hazards. **Robert Walgate**

IWC whaling quotas

Politics wins out

The recent 32nd annual meeting of the International Whaling Commission (IWC) closed after a week of political struggle between those nations seeking a ban on commercial whaling (led by France, the Netherlands and the United States) and those, mainly the whaling nations (Canada, Chile, Iceland, Japan, South Korea, Peru, South Africa, Spain and the Soviet Union),arguing that such a ban could not be justified.

Any hope of a total moratorium was crushed at the beginning of the meeting, and for most of the week it looked as if agreement on quotas might never be reached. On the final day of the meeting, however, quotas were eventually agreed — 13,753 whales of all species can be taken in 1981–82 compared with 15,883 in 1980–81. The alternative of no agreement at all might have led to the demise of the whaling commission and a free-for-all, which would have been an even greater blow to the conservationists.

The purpose of the IWC's annual meetings is to reach agreement on the management of whale stocks for the next year based on the advice of its scientific committee. One of the problems is that the monitoring and prediction of whale population dynamics is fraught with difficulties, allowing interested parties to interpret the statistics as they wish.

The task of the IWC's scientific committee, which met a few weeks before the commission's main meeting, is to formulate a basis on which catch quotas can be set. It does this by estimating the current population of individual whale stocks and the ideal population which could be supported in the absence of interference by man. A population slightly below the ideal level will replace itself more rapidly than one at the ideal level because of increased resources per whale. The aim is to maintain populations at the level which shows the greatest replacement rate and hence gives the maximum sustainable yield (MSY). Under the IWC's new management procedure, a target yield, which provides guidance for setting catch quotas, is set at 90 per cent of MSY. The management procedure also stipulates that all catching should stop on any stock which falls to 10 per cent below the level at which it produces the MSY.

Estimated stock sizes and MSY and recommended catch limits

North Pacific, Western Division

	Males (11+)	*Females (10+)*
1910 stock × 10^3	157.9	175.0
1981 stock × 10^3	66.5	124.6
1981/1910	42.1%	71.2%
MSY level × 10^3	88.3	131.1
1981% MSY level	75.3	95.0
Catch limits	0	405

0028-0836/80/320548-02$01.00

The ideal population can be estimated only by knowing the current population and its rate of change. Almost all the data on the status of current stocks have come from whaling ships which have been providing information on the basis of catch per unit effort. This works on the principle that the difficulty of finding and catching a whale is inversely proportional to the total number of whales available. Changes from year to year in making a catch will reflect change in the population size and hence allow estimates of ideal population to be made.

IWC whaling quotas

North Atlantic	1980/81	1981/82		1980/81	1981/82
Sperm	273	130	*S. Hemisphere*		
Minke	2,543	2,554	Bryde's	264	264
Sei	100	100	Sperm	580	300
Fin	624	701	Minke	8,102	6,718
North Pacific			*Others*		
Bryde's	479	529	Bowhead	18	17
Sperm	1,350	890	Humpback	10	10
Minke	1,361	1,361			
Gray	179	179	Totals	15,883	13,753

Catch per unit effort, however, is not a reliable measurement on which to base calculations of population because it varies considerably with different whaling techniques. When allowances for handling time were recently taken into account, it was found that the depletion of population was being seriously underestimated.

One new way of modelling populations which overcomes some of the difficulties with catch per unit effort was proposed by John Beddington and J G Cooke of the University of York at the recent scientific committee meeting. It has already been applied to sperm whale stocks in the North Pacific with some success. The Beddington and Cooke model uses the fact that whaling distorts the distribution of length in populations as the basis for calculations of current and ideal populations (whaling ships tend to catch big animals leaving smaller ones behind). By examining the current length distribution of the catch and the change over recent years and by knowing the size of the catch, the current population and hence the ideal population can be calculated. This technique works well for species of whale, such as the sperm whale, which vary considerably in length.

One difficulty with the management procedure is that it only works well for species which have already been depleted where the catch is a fair proportion of the current population. The minke whale, for example, the most heavily exploited species, cannot be managed easily because its numbers are actually on the increase. Sperm whales also present problems, because unlike all other species, they are polygamous. Only large males over 25 years of age can hold harems so the damage to the sperm whale population of taking only the largest whales could be greater than at first suspected.

The deliberations of the scientific committee probably did not affect the outcome of the recent meeting as much as might have been expected. In spite of Beddington and Cooke's new evidence on sperm whales, which led the scientific committee to recommend that they should not be killed in the North Pacific, a quota of 890 was awarded to Japan. Some concession to the scientific evidence was made, however, by banning the killing of female sperm whales and all males over 45 feet long. Two other seriously endangered species also failed to get total protection: the humpback whale of the North Atlantic — Eskimoes in Greenland will be able to kill 10 next year — and the bowhead whale in the Bering sea where a small quota has been set for the benefit of Eskimoes in Alaska.

Judy Redfearn

More Soviet psychiatry

Physicist held

Vladimir Kislik, nuclear physicist, long-term refusnik and member of the European Physical Society, has been committed to a Kiev mental ward, apparently to prevent him from meeting western visitors to the city. Although this means of repression has of recent years been used against a number of political dissidents, including geneticist Zhores Medvedev and mathematician Leonid Plyushch, this is the first time that it has been used against a Soviet scientist who simply wishes to emigrate to Israel.

Kislik applied for an exit visa in 1972, but was refused on the grounds of access to state secrets while at his previous job at the Chelyabinsk Nuclear Reactor Plant. Following his application, he was dismissed from his research post at the Institute of Physics of the Ukrainian Academy of Sciences and since then has had to work as a bus-ticket seller, nightwatchman and the like. He attempted, however, to keep up his scientific reading and to organize a scientific seminar for other refusniks in his own home. In June 1976, however, he was beaten up by security police and threatened that he must close his seminar — or else face a criminal charge of black market activities. Meanwhile his name "disappeared" from the Soviet bibliographies and from references to the papers which he had published in his professional capacity.

He did, however, have one unpublished paper on the "Absorption of Helium by Irradiated Samples of Austenitic Steels". Before his dismissal from the institute, this research had been cleared for open publication. Kislik managed to send the paper by hand to the United States, where in 1977 it appeared in the *Journal of Nuclear Materials*

Shortly afterwards, an article appeared in the local evening paper *Vechernyi Kiev*, accusing Kislik of being a foreign agent and of smuggling out nuclear secrets. At the end of 1979, the accusation was revived, and he was informed by the Kiev Public Prosecutor, Ignatiev, that a file had been opened against him under Article 136 of the Ukrainian Penal Code "Violation of Authors' and Inventors' Rights" — in other words, plagiarism.

Since October 1979, Jewish emigration from Kiev has virtually ceased and routine police harassment of long-term refusniks has intensified. In April 1980, Kislik was prevented from travelling to Moscow for the refusniks' International Symposium on Collective Phenomena. One of the western visitors to the symposium, Professor Paul Kessler of the Collège de France, later visited Kislik in Kiev. After the visit, Professor Kessler reports, he was attacked by four strangers in plain clothes who gave him an "intentionally not too heavy" beating, which, he believes, was meant simply to intimidate him. A few weeks later, Kislik managed to make contact with some American geneticists who were attending a meeting in Kiev — an event which, some of his friends believe, was not unconnected with the latest harassment.

On 25 June, Kislik was picked up in the street and taken to the police station for an identity parade in connection with an alleged theft. On 4 July, he was arrested for alleged hooliganism and given 15 days detention. When this term was up, and he was not released, he threatened to go on hunger strike. The next day, 19 July, he was transferred to a psychiatric ward in the Pavlov hospital. Ironically, and to a certain extent in support of Soviet claims that Jews (as opposed to "Zionists") suffer no discrimination in the Soviet Union, the doctor in charge of the case is a certain Naum Lifshits.

Vera Rich

0028-0836/80/320549-02$01.00

Neuroscience

Snyder's pad

Washington

The Johns Hopkins Medical School in Baltimore has joined the growing ranks of United States research universities in announcing its intention to set up a new department devoted to neuroscience. This will be the first new department to have been established at the medical school for twenty years. Under the direction of the new department's chairman, Dr Solomon H. Snyder, who will become the medical school's first professor of neuroscience, its research will be concerned with the chemical and pharmacological aspects of brain function. Dr Snyder, joint winner of the 1978 Albert Lasker Basic Medical Research Award for his work on the actions of neurotransmitters and, in particular, on the functioning of opiate drugs, is this year's president of the American Society of Neurosciences.

The proposal to set up the department was made by an *ad hoc* group appointed by the medical school last autumn. The committee said that there were "compelling academic grounds" for a new department and pointed out that although knowledge in the field of neuroscience dovetailed with that in other disciplines, there was now a common body of knowledge and methodological approaches shared by people trained and working in neuroscience.

Bringing together the neurological aspects of various traditional disciplines into a single department will have organizational as well as academic advantages. According to Dr Steven Muller, president of Johns Hopkins University, "although Hopkins has universally recognized strength in several areas of neuroscience, the School of Medicine now needs the cohesive focus in neurobiology so necessary for the development of exciting and rigorous teaching programmes for medical students and for predoctoral and postdoctoral students in neuroscience".

One of the immediate research interests of the new department will be a study of effects of Huntingdon's disease on enzyme activity in the brain. This will form part of a nine-project research programme on the disease which last week received a grant of $1.8 million from the National Institute of Neurological and Communicative Disorders and Stroke.

David Dickson

Byelorussian graduates

Missing out

Young Byelorussian graduates are failing to take up their appointed posts in the Soviet national economy, according to a recent survey by the Byelorussian SSR State Committee for Labour.

According to Soviet practice, all young persons completing higher education must work for a prescribed period (usually three years), in whatever post the relevant ministry assigns to them. These posts can be anywhere in the Soviet Union, not necessarily in their own home republic. In Byelorussia, however, the system seems to have broken down. In 1978, says the survey, over 3,000 newly qualified specialists — just under 5% of the total — failed to turn up at their appointed enterprises.

In all, out of the 120,000 persons holding higher qualifications in agriculture 41,000 are now working in non-agricultural jobs, 10,000 with teaching qualifications are not teaching and 13,000 university and technical college graduates are working in branches of industry, building and transport unrelated to their education. Over 25% of the young specialists who have graduated in the past four years are now doing jobs which require no higher qualifications.

The ministries themselves, it appears, are partly to blame. A spokesman for the Byelorussian State Committee for Labour explained that many ministries distribute their young graduates at random, often switching them from the job for which they were originally destined letting them go off and find work for themselves, or terminating their assigned job earlier than scheduled. An increasing number of departments are refusing to employ graduates along the lines for which they have been trained. Cases of patronage and "protection" are also said to account for an unspecified number of graduates failing to fulfil their "civil obligations" of directed work.

Nor surprisingly, the professional skill of management workers in Byelorussian industry and agriculture is also said to be "rather low" and causing "great concern."

Vera Rich

Radiation risks

Twice lucky?

Washington

After a year of intense internal debate, the US National Academy of Science has issued a report revising its earlier estimates of the health risks of low-level radiation, and indicating that these may be lower than it had previously suggested.

In particular, academy scientists have qualified their support for the linear "no threshold" model for predicting dose–response relationships at low levels of radiation. They now say that, given all the uncertainties involved, a linear quadratic relationship is more likely to be realistic and that the linear hypothesis should be considered merely to define the upper limits of risk.

The report, which was prepared by the Academy's Committee on the Biological Effects of Ionizing Radiation (the BEIR Committee) and was commissioned by the Environmental Protection Agency, does not recommend specific exposure levels. But its findings are likely to reduce pressure on the agency to develop more stringent regulations.

The committee's conclusions, however, are still under fire. The chariman of the subcommittee on somatic effects, Dr Edward Radford, claims that support for the linear hypothesis was downgraded on the basis of a biased selection of data, giving too much weight to laboratory studies and not enough to epidemiological evidence. Another committee member, Dr Harald Rossi claims that the committee has not gone far enough in its revisions, and that the dangers are still being overstated.

The BEIR Committee first gave its support to the linear hypothesis in its initial report, published in 1972. Given the many uncertainties surrounding attempts to estimate the effects of low-level radiation, and in particular the impossibility of providing conclusive statistical evidence based solely on epidemiological studies, the committee proposed the linear hypothesis as a basis for regulation.

Since then, it has been used as the basis for standard setting by the EPA. But it has been challenged by the nuclear industry, which claims that it provides an unrealistic assessment of the health risks of nuclea power, and thus could lead to overly-restrictive legislation.

The BEIR committee came out with a revised version of its report last spring. It again endorsed the linear dose–response relationship as a basis for regulation and provided estimates of the several hundred additional cancer deaths per million population that would result from continuous exposure to one rad of radiation.

Publication of the report, however, brought into the open a fierce debate which had until then taken place within the committee over how much weight to give to

0028-0836/80/320550-02$01.00

different types of evidence — and the appropriate dose–response models which could threfore be justified.

Five members of the committee issued a dissenting statement, claiming that insufficient weight had been given to radiobiological data and that accepting the linear hypothesis as a basis for regulation, would result in regulations which would hinder the development of nuclear energy and the use of radiation in medicine.

When it became clear that additional members of the committee also had reservations, academy president Dr Philip Handler decided that the controversial section should be rewritten. The revised report was published in Washington last week, with dissenting statements from Drs Radford and Rossi.

The new report goes some way to establishing a compromise on what the academy calls the "ideological differences" between committee members over methods for estimating numerical risk values for cancer induction.

Whereas previously, for example, the committee had used data on general cancer incidence taken from survivors of the Nagasaki atomic bomb explosion, the new report gives this data less prominence than the cancer mortality data on survivors in both Hiroshima and Nagasaki, which suggests a more quadratic dose–response relationship at low radiation levels.

Similary, rather than giving estimates of predicted increased cancer mortality and morbidity based directly on the linear hypothesis for the effects of low LET (linear energy transfer) radiation — primarily X-rays and gamma rays — the new report presents a range of risk estimates based on linear, linear-quadratic and quadratic models. And it adds that the linear-quadratic is "most consistent with existing human epidemiological studies and radio-biological data and knowledge".

Dr Radford took no part in the rewriting process. He remains critical of the final results, claiming that the report ignores much new data in support of the linear hypothesis, with the consequent risk of understating the dangers of radiation.

Dr Rossi, too, remains dissatisfied. He claims that his own work and that of others on the effects of radiation on plant cells suggests that the linar hypothesis overstates the dangers. And that even though its prominence has been downplayed, it is still likely to be used in standard setting, to the disadvantage of the nuclear industry.

David Dickson

Calculations and measurements

What follows is a summary of the definitions in BEIR III relating to the somatic effects of ionizing radiation. The terms of reference of the study, set by the US Environmental Protection Agency, include an explicit reference to nonlinear effects. The report therefore includes a discussion of the small-scale effects of the interaction of radiation with matter along the following lines.

Radiation dose (D) is a quantity of energy deposited in matter; the unit is the rad (equivalent to 100 ergs of absorbed energy per gramme), soon to be replaced by the SI equivalent of the gray (or Gy), with 1 Gy = 100 rad. Charged particles (e.g. α particles) or uncharged and indirectly ionizing particles (e.g. X rays) differ from each other in the rate of "linear energy transfer" (LET) along their tracks; for a given particle, the LET is also a function of energy. The LET is low (a few keV per μm) for cosmic-ray μ-musons, high for α-particles.

Concerned as it is with nonlinear effects, BEIR III needs to introduce a microscopic analogue of the macroscopic dose D called "specific energy" z and intended as a measure of energy deposition by radiation in sub-cellular structures such as cell nuclei.

The deposition of energy along the track of a particle is not uniform on such a scale, because the interactions of radiation with matter entail interactions with discrete entities in the irradiated matter. Thus although (with appropriate units) the average value of z (written $\bar{z}$) must equal D, the microscopic intensity of energy deposition can vary dramatically with different kinds of radiation.

The report goes on to consider (but does not eventually adopt as an assumption) the proposition that for radiation to cause somatic damage, two "sublesions" must occur within some small range (say 1 μm) in a cell and within some specified interval of time. Then the frequency of "lesions" (E) will be $K(\overline{z^2})$ where K is a constant. Moreover, the mean square microscopic dose will be related to the macroscopic dose (D) by $\overline{z^2} = wD + D^2$ where w is a constant determined unambiguously by the statistical properties of z for the type of radiation concerned.

One consequence of this argument is that even the assumption that it takes *two* sublesions ("hits") within some microscopic region leads to a dose-effect relationship in which the risk of damage is of the form $\beta D + \gamma D^2$, but in that case β and γ should be related to each other by the statistical properties of the radiation concerned, whence the relative biological effectiveness of high-LET and low-LET radiation should be calculable.

With this said, BEIR III says that wherever possible empirical data have been fitted to curves with the form $(a_0 + \alpha_1 D + \alpha_2 D^2)$ exp $(-\beta_1 D - \beta_2 D^2)$ where all the constants are positive, a_0 represents the spontaneous rate of some effect and the exponential term (significant only at high doses) takes account of competition from cell death.

BEIR III includes a discussion of using human epidemiological data as a means of determining dose–response relationships empirically. Apart from familiar problems of bias (people exposed to diagnostic X-rays may be especially prone to cancer, for example), the report draws attention to the retrospective character of most epidemiological studies, the problems occasioned by the long latency period for cancer induction, the distinction between mortality and morbidity (and the possibility that the latter may be under-reported), differences of susceptibility between different genetic groups.

Numerical calculations of cancer caused by radiation yields rates per million people assumed to be taken from a population represented by life-tables for the United States population in the period 1969 – 71.

The BEIR report uses two alternative models for calculating the "excess" effects of radiation. Absolute risks from radiation exposure are represented by constant probabilities of cancer formation, or of death therefrom, for each year of life after the lapse of the latency period. Relative risks are calculated on the assumption that the effect of radiation exposure is to increase the formation of cancer, or of cancer mortality, in proportion to the spontaneous rate at the age at which the damage becomes apparent.

Like previous analyses of the consequences of radiation exposure, BEIR III leans heavily on data gathered over the years from the populations of Hiroshima and Nagasaki, but again it breaks new ground by seeking to separate the effects of gamma and neutron doses at the two explosions. The two explosions differed in that at Nagasaki the explosion exposed the population to much smaller neutron doses than that at Hiroshima.

To make the calculations of risk explicit, BEIR III considers three separate cases of radiation exposure: (a) a single exposure of a population represented by the US life-tables to 10 rad of low-LET radiation; (b) a continuous lifetime exposure at a rate of 1 rad per year; and (c) a pattern of exposure to 1 rad a year at ages chosen so as to simulate occupational exposure to radiation.

Different assumptions give very different results. Spontaneous cancer mortality for the standard US population is calculated at 16.38 per cent, and the consequences of a single exposure of the whole population to a dose of 10 rad turns out to be an extra 766 deaths (0.47 per cent) on the absolute risk calculation and an extra 2,255 deaths (1.4 per cent) on the relative risk basis, on the assumption that the dose-effect relationship is represented by a quadratic function including a linear term.

BEIR III is so far distributed in typescript form, but will be available in book form from the National Academy of Sciences later in 1980.

0028-0836/80/320551-01$01.00

Alternative energy

Europe stirs

In Britain and France, there are now signs that governments are prepared to back alternative energy sources with real money. Last week, M Andre Giraud, the French industry minister, announced a 50 per cent increase of the solar energy budget. Hard on his heels, the UK government will announce this week a plan to spend £6.5 million on geothermal and wind energy projects.

With the latest increase, the French solar energy budget will amount to an annual £21 million. The *Commissariat à l'energie solaire* (Comes) estimates that France may produce 7.5 to 9 million tonnes of oil equivalent (mtoe) from biomass by 1990, more than 10 million mtoe by 2000 and ultimately 30 mtoe.

In 1990, solar heating is expected to provide 1.3 to 1.5 mtoe, geothermal energy 0.8 to 1 mtoe, and "*microcentrales*" (small solar power stations) 0.4 to 0.5 mtoe. Together with biomass, these sources will furnish 5 per cent of French energy needs compared with 1 per cent now.

Biomass is the centre of the French programme and forest wastes, used for methanol production and rural energy needs, its chief element. There is also a plan to use agricultural wastes and, in the process, to develop fermenters and distilleries which can be exported to Third World countries. There are somewhat pious hopes that these countries, using local biomass, would then re-export liquid and gaseous energy products to France, thus ultimately reducing French dependence on OPEC countries.

In Comes's vision, French agriculture would also be transformed, with more acreage devoted to energy crops and some 60,000 to 80,000 jobs created.

In Britain, the Department of Energy has recently estimated that some 8 per cent of Britain's energy requirements could come from biomass (including 2–3 per cent from burning domestic rubbish), while only two years ago the estimates were about 0.5 per cent. These estimates are however arrived at differently from the French, and represent a large number of small contributions from the energy-efficient use of farm and industrial waste, and finding sites for energy crops.

The major UK commitment announced by the Department of Energy this week is to geothermal "hot rocks" by means of a £7.2 million, three-year research programme at the Camborne School of Mines in Cornwall. The United Kingdom will provide £6 million and the European Commission £1.3 million for the project, which is intended to demonstrate the feasibility of a 30 MW (thermal) generator involving paired wells, 6,500 ft deep, and 2 million m^2 of fractured rock surface. The project is "complementary" to that at Los Alamos in the United States, using explosive fracturing rather than high water pressure to create the surface, project leader Dr A W Batchelor said this week. The entire land area of the United Kingdom could be exploited for geothermal energy production, said Batchelor, producing electrical energy at 10 per cent efficiency, if commercial drillings could be constructed to reach 7,000 to 8,000 metres depth. (Current deepest North Sea wells are 6,000 metres.)

A further grant of £450,000 goes to Dr Peter Musgrove of the University of Reading to develop a 25-metre diameter, 130 kW vertical axis windmill, the prototype of a 2–3 MW device. The North of Scotland Hydroelectric Board is showing great interest in wind energy, which is increasingly seen as the most advanced of the alternative sources in the United Kingdom.

In Germany, a question in the Bundestag last week led to the publication of figures which showed a decrease in the non-nuclear energy research programme for the first time since 1972. By 1979, spending in the programme had reached £164 million but it fell to £148 million this year. Within the decrease however, — alternative energy research managed to score a rise from £20 million (1979) to £25 million (1980). This year's budget includes £14 million on solar, £6 million on wind and £4 million on geothermal energy. Comparable figures for the Department of Energy in the United Kingdom are £1.7 million on solar, £1 million on wind and £2.1 million on geothermal.

Robert Walgate

Alternative technology

Water play

Villagers from two very different developing countries, Kenya and Nepal, are to benefit from the results of a project to improve the efficiency of watermills used to grind corn. The project has been stimulated by Jean Gimpel, a European historian of science and technology, who says that several international agencies are taking an interest.

Vertical axis watermills appear to be in common use in hilly regions of many developing countries (and can even be found in some industrialized countries). They have traditionally been used to grind corn for small communities of farmers. M. Gimpel, whose cause is the revival of traditional technologies in rural areas, first interested the Nepalese in modernizing traditional watermills by taking to Nepal a model of a watermill of improved design. Last year, the Research Centre for Applied Science and Technology (RECAST) at the University of Kirtiput set up a project to build a prototype mill in the Kathmandu valley under the supervision of Mr C. B. Joshi. M. Gimpel says that the Agricultural Development Bank of Nepal has been sufficiently impressed with the project to have distributed models of the prototype to all its branches. The bank has also set up a loan scheme for millers who want to improve their own mills.

The RECAST watermill succeeds chiefly by using well designed bucket-shaped vanes which can accept the full impulse of the water. Replacing the pin mounting of the turbine shaft with ball bearings also increases efficiency, as does enclosing the water feed to the mill in a covered chute. Gimpel and Joshi say that all the work can be done with local skills, mainly the carpenter's who can carve new paddles to the specified design.

Mr Joshi has compared the performance of the improved and traditional mills and says that the modified watermill is 80 per cent more efficient. The power output is increased by 81 per cent, the speed by 48 per cent and the productivity by 50 per cent.

The improvements also include a millstone cover to prevent loss of flour during grinding, a system for collecting the flour to save time and wastage in brushing the flour off the stone and electric light generated by a small dynamo driven by a bicycle wheel.

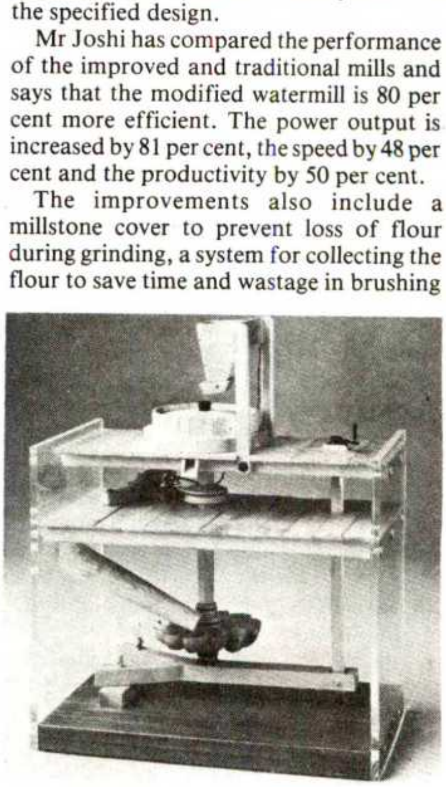

Although the improvements cost money, Mr Joshi estimates that the extra costs should be repaid more than three times within a year. He also says that the increased power output of the mills could be used to drive other machines — rice dehuskers, trip hammers and bellows and circular saws or lathes. He foresees small industries based around the mills, rather similar to the industrial complexes of eighteenth century England.

The Kenyan government, which has taken up the project since seeing models of the Nepalese mill at the United Nations conference on Technical Cooperation between Developing Countries in Nairobi in May, is hoping to have a small complex of several full-scale improved mills operating near Nairobi for next year's international conference on renewable energy.

Judy Redfearn

0028-0836/80/320552-02$01.00

Pre-Pleistocene climates

from Samuel M. Savin

ATTEMPTS to reconstruct the history of the world's climate and to understand its changes are among the oldest of geological problems. While enormous progress has been made in recent years, especially in understanding Cenozoic (0 to 65 Myr) climates, it is sobering to read Lyell's[1] 1837 summary of paleoclimatology and to realize for how long geologists have been struggling with similar climatic questions. One problem which continues to create difficulties is the host of variables which can be summarized under the term climate (e.g. average and seasonal variation of temperature, average and seasonal distribution of rainfall, aridity, wind, etc.) while only one, or a very few, are manifested in any single type of deposit. Furthermore, many of these climatic variables can only be documented in a qualitative or semi-quantitative fashion.

An exception to this state of affairs is the climate of the past million years or so. A great deal is now known[2] about the nature of glacial and interglacial stages and the timing of each. It has been possible to develop testable hypotheses of the causes of glacial-interglacial fluctuations and to develop models of glacial-stage atmospheric circulation[3].

Further back in time interpretation of climate becomes increasingly difficult. At a recent symposium on Pre-Pleistocene Climates*, J. Imbrie (Brown University) pointed to recent advances in Pleistocene climatology. Two types of models which are likely to prove especially useful are Global Circulation Models (GCM's) and models which can be thought of as sensitivity studies, designed to test the sensitivity of the climate to proposed changes in some controlling variable (e.g. insolation, atmospheric chemistry, continental and oceanic geometry, etc.). GCM's have been applied to the study of atmospheric circulation 18,000 years ago[3] with promising results. L. Gates (Oregon State University) discussed the kinds of geologic information needed if GCM's as well as simplified models are to be applied to the study of Mesozoic and Paleozoic climates.

Geologic information becomes increasingly generalized and climatic models must become correspondingly less detailed as we proceed backward in time. Pre-Jurassic deep sea sediments have been entirely swallowed up in subduction zones so the record of marine climate is found only in those continental shelf sediments that have survived erosion or metamorphism — a scattered record at best. However, so little is known about the climates of Paleozoic and Precambrian times that even a small amount of climatic data may answer key questions. For some parts of geologic history zero-dimensional climatic models, yielding average global temperatures, can be most useful. In earliest geologic time, for example, J. Pollack (NASA-Ames Research Center) noted that almost any acceptable theory of solar energy production yields solar output only 70 or 80 percent of the modern value. The geologic evidence, however, suggests that temperatures during at least much of the early Precambrian were as warm as, or warmer than today's. Any interpretation of the mechanisms controlling Precambrian climate must resolve this dilemma.

Deep sea sediments, when they are available, provide the most readily interpretable climatic information. The two most common approaches to obtaining paleoclimatic information from deep sea sediments are those based on paleontology and those based on oxygen isotope analyses. Haq (Woods Hole Oceanographic Institute) demonstrated his method of identifying acme events, or peak periods of environmentally (including climatologically) induced floral and faunal migration. Identifying such events involves obtaining fossil census data covering a broad geographical area. The unwieldy census data is reduced into a manageable number of factors, the dominance of each of which is presumed to be environmentally controlled. The migration of the factors through space and time is then interpreted in terms of variations in environmental conditions.

Oxygen isotopes have permitted detailed interpretation of surface and bottom water temperature history throughout the Cenozoic. While there is some debate, especially for the late Cenozoic, as to the extent to which isotopic variations reflect temperature change and the extent to which they reflect the growth and retreat of continental ice, isotopic fluctuations can be correlated remarkably well from place to place and clearly reflect climatic variations. Berger (Scripps Institute of Oceanography) characterized the Cenozoic isotopic record as showing step-like transitions from one state to another and attempted to discriminate between externally forced climatic changes and those generated internally within the earth-ocean-atmosphere system. He suggested, as did Thierstein (Scripps), that a number of events including the terminal Cretaceous extinction event and the rapid growth of Antarctic ice in mid-Miocene time belong to the latter class. Moore and Pisias (University of Rhode Island) examined the Cenozoic isotopic record, concentrating on variability rather than absolute values of temperatures. Using this annual approach they were able to show that the climate is substantially more variable at some times than others. Highly variable climates may turn out to be characteristic of less stable climatic systems, easily shifted from one state to another. The oxygen isotopic compositions of pre-Cretaceous fossils have frequently been altered by diagenetic processes. As pointed out by Savin, and by Hallam (University of Birmingham) the isotope record adds little, if anything, to our understanding of Jurassic climates. Uncertainties in the interpretation of the isotopic data are as large as or larger than uncertainties in non-isotopic estimates of Jurassic temperatures. Perhaps surprisingly, isotopes, especially of cherts, promise to be useful in providing constraints on early Precambrian temperatures. While the uncertainties in the isotopic temperature are indeed large, they are smaller than uncertainties in temperatures estimated by other means.

Samuel M. Savin is in the Department of Geological Sciences, Case Western Reserve University, Cleveland.

---

*The symposium was held on May 22, 1980 in Toronto at the Annual Meeting of the American Geophysical Union and was part of a study by the Geophysics Study Committee of the National Research Council. The aims of the symposium and study are to summarize the status of Pre-Pleistocene climatology and to identify key areas for future research. A final report will be published by the National Academy of Sciences in 1981.

0028-0836/80/320553-02$01.00

In assembling the climatic record on the continents it seems difficult to avoid the anecdotal approach. Terrestrial deposits are widely scattered and are subject to local variations in climate. Climatic variables other than temperature are far more important in affecting terrestrial deposits than marine. However, in spite of these difficulties, Wolfe (US Geological Survey) was able to show that Cenozoic climatic changes derived from North American plant fossils parallelled those of the North Atlantic from planktonic foraminifera. Eugster (Johns Hopkins University) showed a climatic reinterpretation of the Eocene Green River evaporites suggesting a climate similar to that of Holocene Southeastern California. Van Houten (Princeton University) assembled data on ancient laterites and calcretes from which he was able to draw consistent conclusions about climatic zonations. Crowell (University of California, Santa Barbara) assembled and critically evaluated evidence for Paleozoic and Precambrian glaciations. He offered a hypothetical series of plate reconstructions for Precambrian glacial stages not based on geophysical constraints but drawn so as to cluster glaciated regions in polar areas. Uncertainties in the paleomagnetic data are sufficient to permit considerable freedom in choice of continental positions. While lagging behind our knowledge of oceanic climates, knowledge of terrestrial climates is becoming more complete and techniques for obtaining that knowledge are becoming more sophisticated.

The oceans carry a significant amount of heat, and hence changes in oceanic circulation can be expected to have affected climate. Berggren (Woods Hole) presented a correlation between the climate of the past 200 Myr and the opening and closing of oceanic gateways (or barriers to circulation). At the time of the Eocene-Oligocene boundary there is a correlation between the opening of the Greenland-Norwegian Sea to the Arctic, the breaching of the Rio Grande Rise and the possible initial opening of the Drake Passage on the one hand and the marked cooling of oceanic bottom water and terrestrial climates on the other. He also pointed to a correlation between the elevation of the Isthmus of Panama 3 Myr ago and the onset of Northern Hemisphere continental glaciation.

In a field as complex and wide ranging as the history of climate throughout the history of the earth it is not surprising that the extent of our knowledge so often seems small. However, it was apparent at the symposium that great strides have been made in the past 15 years in pre-Pleistocene paleoclimatology, not only in the acquisition of climatic knowledge but in the development of new tools and techniques. □

---

1. Lyell, C. *Principles of Geology* (1837).
2. CLIMAP Project Members *Science* **191**, 1131 (1976).
3. Gates, W.L. *Science* **191**, 1138 (1976).

Towards a submarine hydrology

from Marcus G. Langseth

The excitement generated by the discovery of hydrothermal fields at the axes of the Galapagos and the East Pacific rises notwithstanding, seawater movement within the crust also dominates geothermal heat transfer in the older and colder midoceanic ridge flanks. The pore fluids involved in this circulation system are at low temperature (usually less than 50°C at the top of the crust) and flow rates are slow (centimeters per year). If the high temperature hydrothermal zones at ridge axes are analagous to volcanic and geothermal zones such as Iceland, the low temperature circulation on the ridge flanks may be likened to groundwater movement. The phenomena of submarine hydrology may have little intrinsic glamour but their scientific and practical importance is nevertheless great. Several groups, particularly in the United States, are busily exploring ridge-flank thermal regimes and the past two years have seen some interesting and puzzling developments. Many of these emerged at the last three meetings of the American Geological Union.

The evidence that cold bottom-water circulates below the seafloor consists of temperature gradient measurements which show that temperatures at the base of the sedimentary layer are much less than those expected if the crust were in conductive equilibrium with the lithosphere. Anomalously low crustal temperatures are usually found where the sedimentary cover is thin (less than 200 meters) and where there are frequent exposures of the igneous oceanic basement. The inference is that bottom-water enters the igneous crust at these exposures and moves laterally below the sediments through a basement made permeable by extensive fracturing, thus carrying away much of the geothermal heat. It has been assumed that this circulation is driven by geothermal heat so that it is a kind of channelized convection, but recent observations have brought this simple model into question.

These observations were made on the flanks of the Mid-Indian Ocean Ridge by the Lamont-Doherty group late in 1977. They involve lines of closely-spaced temperature gradient measurements made with a temperature probe two to five meters long which is lowered into the sediments as it is towed over the bottom by a surface ship. Sonic reflection profiles over the same area throw light on the structure of the sediments. The heat-flow variations suggest that there is cellular convection in the crust and that some of the discharge and recharge may take place through the sedimentary cover. A group from the University of Washington, in a joint study with the Pacific Geoscience Centre in Canada, has made similar studies on the Juan de Fuca and Explorer ridges and found evidence for cellular convection and for the penetration of cold seawater beneath the sediments for distances of up to fifteen km from the nearest outcrops. Another survey on the flank of the Mid-Atlantic Ridge east of Brazil by the Lamont-Doherty group indicates that the crust is cooled up to twenty km from basement exposures requiring lateral flow rates in the range of 10^{-9} to 10^{-8}m/sec.

Particular attention has been paid to the two Low Heat-Flow areas of the Eastern Pacific, discovered in 1963, by Von Herzen and Uyeda in the Guatemala Basin southwest of Central America and at the equator southest of Hawaii. The areas are covered by thick pelagic sediments, 300m or more thick, yet their average heat-flow is less than one-third of the mean heat-flow from the earth. A Woods Hole group has now studied the Equatorial Low Heat-Flow Zone and found thermal evidence for an upward flow of porewater through the sedimentary blanket. The highest heat fluxes coincide with areas of rough basement which seem to focus the water flow.

Earlier this year, a Lamont-Doherty group made a detailed survey in the Guatemala Basin. Seismic profiling surveys showed a 400 m sedimentary blanket periodically broken by north-east trending ridges protruding through the cover and associated with fracture zones spaced 40 to 50 km apart. A line of temperature gradient measurements between two of the ridges shows anomalously low gradients even though the entire area between exposures is thickly sedimented. It appears that the basement in the Guatemala Basin is being 'ventilated' by this regularly spaced set of ridges.

During this survey, measurements of porewater pressure within the sediments were made by Dallas Abbott of the Lamont-Doherty Observatory. Anomalously, pore pressures are less than hydrostatic in sediments five meters below the seafloor and are accompanied by low

---

Marcus G. Langseth is in the Lamont-Doherty Geological Observatory, New York.

0028-0836/80/320554-02$01.00

temperature gradients. Abbott explained that these are exactly the circumstances that would be expected if there were a downward flow of porewater. She suggested that the low temperature in the thick sediments of the Guatemala Basin may indicate a slow drawdown of seawater through the sedimentary cover that reemerges at the ridges.

Whether the flow through the sediments is, however, significant is controversial. Nonlinearities of temperature profiles on the ridge flanks have been repeatedly observed. The Lamont-Doherty group, on the basis of their 1977 survey, attributed these to water flow through the sediments. At most stations temperature gradients decrease with depth, implying upward flow.

The flow rates are surprisingly high, tens of centimeters per year. Even if the permeability of sediments is among the higher values found in the samples, pressure gradients of the same order of magnitude as the hydrostatic are needed to drive the flows. The pressures cannot be achieved by thermal stresses associated with thermal convection but three possibilities remain: 1) the *in situ* permeability is much higher than laboratory measurements indicate; 2) there are unknown sources of pressure in the oceanic crust; or 3) the non-linear temperature profiles may have another explanation. Nonlinearity in temperature profiles can stem from many phenomena; for example an increase in conductivity with depth, changes in the bottomwater temperature and heat generation in the sediments. The present data are insufficient to decide between alternative explanations and as a consequence, there is much interest in other approaches demonstrating significant flow of sedimentary interstitial water.

Chemical gradients in sedimentary porewater will also vary with depth if the flow rates are of the same magnitude as the ionic diffusion rates. A combined University of Rhode Island and Woods Hole study, reported at the June 1979 American Geophysical Union Conference, found calcium-depth profiles in sediments in the Galapagos Hydrothermal Mounds field consistent with an upward flux of 0.3 to 15 cm yr^{-1}; whereas, profiles in an adjacent low heat-flow zone show seawater concentrations of calcium consistent with downward advection of water. However, sediments in this area are only about 20-30 m thick.

Porewaters from DSDP cores provide chemical profiles across thick sedimentary layers and a consistent pattern is emerging from measurements made by geochemists at the Scripps Institute, Lamont-Doherty Observatory and the University of Rhode Island. Sediments in older areas of the ocean show chemical gradients that preclude water flow through the sediments at thermally significant rates. However, in ridge flank areas, chemical gradients in the sediments are small or nonexistent, so vertical advection may be possible. The chemistry of interstitial waters promises to be one of the clearest means to detect water advection, particularly when coupled with temperature profiles.

The other means of investigating possible subseafloor flows is by *in situ* pore pressure measurements. The measurements of Abbott in the Guatemala Basin were the first such experiments attempted in deep-sea sediments. The measurements are difficult to carry out but initial results are repeatable and show significant pressure anomalies. Further tests of this new technique are planned.

Deep-sea drilling on the Costa Rica Rift during DSDP-IPOD Leg 69 showed there was a substantial drop in excess pressure across a 260 m thick sedimentary layer. One hole drilled through the sediments and into the basement showed a drawdown of water of about one meter per hour which persisted for at least 60 days. Pore pressures at the bottom of this hole estimated from extrapolation of pulse tests were nearly twenty bars below hydrostatic. Anomalously low pressures below the sediments may be a widespread phenomenon, as they have already been reported at two sites in the Mid-Atlantic Ridge on Legs 37 and 46 and Leg 60 in the Mariana Trough.

There are a number of ways by which the low pressures may be produced. They include; a fossil low pressure, perhaps from the lowered sea level of the last ice age; alteration reactions in the basement that cause a volume decrease and large-scale thermal convection with the low pressure field centred below the sediments. The possibility that the low pressures result from intrabasement reactions suggests that inward flow of water at outcrops can occur without discharge, a result that would agree with seafloor heat-flow observations.

The proposal that Challenger be available for an additional two years of Deep Sea Drilling could allow new data to be obtained on the hydrology of the oceanic crust. Particularly important will be pressure measurements in holes that penetrate through sediments into igneous basement. These measurements can be made with a packer, a tool that seals the annulus between the hole wall and the pipe, allowing bottom-hole pressures and *in situ* permeabilities to be determined. Temperature and porewater chemistry observations in the sediments and in the bottom of holes that penetrate basement will add the third dimension to the seafloor distributions provided by conventional seafloor methods.

One of the most promising approaches to the problems discussed here would be to use the Challenger to reenter existing holes. These holes are in thermal equilibrium and the experiments using the packer could be efficiently done in a predrilled hole. A sufficient number of reentry holes in both the ridge flank and in older seafloor exist to permit a variety of thermal and sedimentary environments to be sampled.

The questions about the extent and magnitude of circulation in the suboceanic crust have great relevance to problems of nuclear waste disposal in the deep seabed. The US Department of Energy is considering the burial of waste in durable cannisters within sediments such as the abyssal clays of the Northern Pacific which are assumed to be impermeable. Incomplete knowledge of the driving forces and extent of water circulation in the crust and sediments makes these assumptions questionable. However, should it turn out that low pressures in the oceanic crust are not associated with circulation that returns seawater to the ocean, then long-term disposal may become a possiblity. □

Membrane protein distributors

from M.J. Geisow

ON theoretical as well as experimental grounds, lipid vesicles have long been considered the likely carriers of proteins between the membranes of the cell. Rothman and Fine (*Proc. natn. Acad. Sci. U.S.A.* **77**, 780; 1980) have now demonstrated that a trans-bilayer glycoprotein, the small G protein of Vesicular Stomatitis Virus (VSV) is inserted into the membrane of coated vesicles during its migration to the surface of CHO cells. Furthermore — and of wide importance for studies of the transport of proteins synthesised on rough endoplasmic reticulum (RER) — intracellular transit of G from RER to the Golgi apparatus in which terminal sugars are added also takes place in clathrin-coated vesicles.

The character of the clathrin coat and its self-assembly in the plasma membrane may provide a basis for the specificity required in a membrane protein transport system. As early as the 1960's, Friend and Farquhar (*J. Cell. Biol.* **35**, 369; 1967) suggested that coated vesicles conveyed material to apical regions of the plasma membrane in rat vas deferens epithelial cells. The vesicles were seen in close association with the Golgi apparatus and cytochemical observations suggested that they might also transport lytic enzymes to lysosomes but supporting biochemical evidence was lacking until the experiments of Rothman and Fine.

Their choice of a viral protein to track the route of membrane proteins was a simplifying one as G is the only glycoprotein synthesised in CHO cells following VSV infection. In just the same way as native membrane glycoproteins, G

M.J. Geisow is in the National Institute for Medical Research, Mill Hill, London.

0028-0836/80/320555-02$01.00

is glycosylated in the endoplasmic reticulum and hexamannose units of the core oligosaccharide are replaced by terminal sugars in the Golgi apparatus. The pre-Golgi form of G is distinguishable from the post-Golgi processed protein by its sensitivity to endoglycosidase H (Endo H).

Coated vesicles purified from a large pool of VSV-infected cells contained G as well as the characteristic spectrum of vesicle polypeptides and G could be co-precipitated with clathrin using monospecific anticlathrin. Newly-synthesized G was detectable by pulse-chase labelling, in this case carrier vesicles derived from bovine brain allowed isolation of a small number containing radiolabelled G. A kinetic study of the transport of G in the vesicles was then possible, using Endo H to determine the amount of Golgi-processed protein.

It was clear that G was present in coated vesicles in transit to the plasma membrane since the vesicle fraction never contained more than 20% of the pool of labelled protein. More importantly, the specific activity of labelled G in the vesicles rose twice during the chase, showing the transport of first the Endo-H sensitive (pre-Golgi) glycoprotein and then the transport of the Endo-H resistant glycoprotein. The clearance of the post-Golgi form of G from the vesicles coincided with the appearance of G on the cell surface (55% of the label in 65 min).

G was demonstrated to be actually present within the coated vesicle membrane by uncoating vesicles containing ^{3}H-mannose-labelled G on metrizamide gradients. A single ^{3}H-labelled polypeptide corresponding to G floated up with the CV lipid vesicle fraction.

Coated vesicles are known to 'shuttle' rapidly within cells and short transit times are certainly in keeping with their functions as a transport system. The presumed cycling time of coated vesicles is much faster than the observed time for the total transport of pulse-labelled VSV G protein suggesting that many trips are made by the same vesicles or at least certain of their components. The difficulty of depleting some endocytic receptors which are known to be internalized in coated vesicles again suggests that they are re-used.

Of course, the recognition of the identity of the carriers still leaves open the question of how a given protein arrives at the appropriate cellular membrane, but at least this sorting problem has been brought nearer to the compass of current experiment. □

Adhesion of pathogenic microorganisms

from Mary Lindley

MICROORGANISMS that enter the internal tracts of the body and come to rest on mucous membranes would seem to need a firm anchorage before invading or discharging their toxins into the underlying epithelium. Otherwise they would surely be swept away by the muscular activity of the tract or by the fluid passing through. Nevertheless, a link between adhesion and pathogenicity was recognised only slowly. The first clear evidence of the significance of bacterial adhesion came during the 1970s when veterinary scientists showed that certain strains of *Escherichia coli* must produce not only toxins but also an antigen, designated K88, in order to cause diarrhoea in piglets. Recognised by the ability to agglutinate red blood cells, K88 and the similar K99, produced by strains infecting calves and lambs, are hair-like fimbriae (also known as pili but unrelated to sex pili), which mediate adhesion to the intestinal mucosa. Analogous plasmid-encoded fimbriae, designated colonisation factor I and II (CFA/I and /II), have been described in certain *E.coli* from cases of human diarrhoea.

Thus a similar picture has begun to emerge for human diarrhoea, although the pace of work is hampered by the difficulty of finding a suitable system to study. At a recent symposium on adhesion and pathogenicity* D.C.A. Candy (Institute of Child Health, London) reported tests of adhesion of *E.coli* to human buccal epithelial cells and intestinal cells. This work has confirmed that CFA/I is important in adhesion to human small intestine. Investigation of an outbreak of acute diarrhoea in infants has lead to the isolation of a strain of *E.coli* producing a colonisation factor resembling CFA/II. There are also signs that some infants with protracted diarrhoea may be more prone than others to adhesion by *E.coli*, in the same way that some but not all piglets develop diarrhoea in response to *E.coli* carrying K88.

Apart from CFA/I and/II, strains of *E.coli* causing diarrhoea in man may carry antigens of a different sort — type 1 fimbriae (also known as common fimbriae). M.M. Levine and his colleagues (University of Maryland School of Medicine, Baltimore) are looking for a combination of all three that could form the basis of vaccine against infant and travellers' diarrhoea, analogous to that already used successfully for piglets. He suggested that a vaccine would probably include antigens such as CFA/I and/II plus type 1 fimbriae of perhaps three different antigenic varieties. The immediate task is to find antigens common to a sufficient variety of bacterial strains to provide a broad spectrum of protective antibodies when used as a vaccine.

Studies of *Neisseria gonorrhoeae* adhering to buccal epithelial cells, described by E.C. Tramont (Walter Reed Army Medical Center, Washington DC) have shown that fimbriae are the principal antigens mediating adhesion, again making them the obvious target for prophylaxis. Human antibodies against these fimbriae can be found in genital secretions from naturally occurring cases of gonorrhoea, albeit needed in very large amounts to block adhesion *in vitro*. One possible approach to prevention could be immunization to produce protective antibodies against fimbriae. The other approach discussed by Tramont would be to inhibit adhesion competitively by bathing the site of infection in fimbriae. Tramont believes that any vaccine against gonorrhoea will have to be applied locally to give the best possible results.

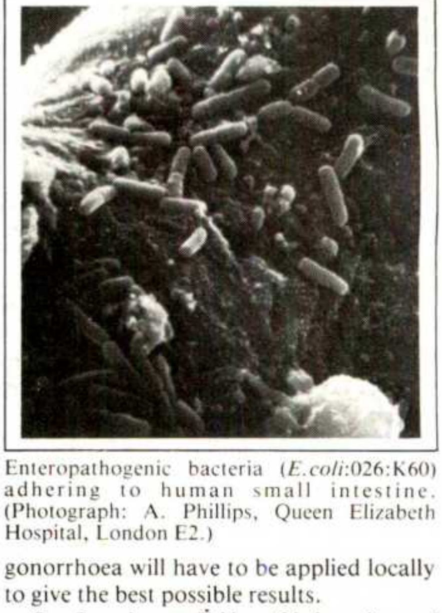

Enteropathogenic bacteria (*E.coli*:026:K60) adhering to human small intestine. (Photograph: A. Phillips, Queen Elizabeth Hospital, London E2.)

C. Svanborg Édén (University of Göteborg, Sweden) thinks that fimbriae also mediate the adhesion of those intestinal *E.coli* that infect the urinary tract. She has found that the extent of adhesion seems to be related to virulence, which is greatest in strains causing acute pyelonephritis, intermediate in those causing acute cystitis, and low in those producing no symptoms although they are detectable in the urine. Susceptibility to infection also seems to vary, and this, she suggested, may be associated with the density of receptors on the host cells. Candidates for those receptors are glycolipids related to globoside, which inhibit the adhesion of *E.coli* to urinary

Mary Lindley is an assistant editor of Nature.

---

*A symposium on Adhesion and Microorganism Pathogenicity was held on 13-15 May at the Ciba Foundation in London. It was organised by Dr Katherine Elliott and the proceedings will be published by Pitman Medical.

0028-0836/80/320556-02$01.00

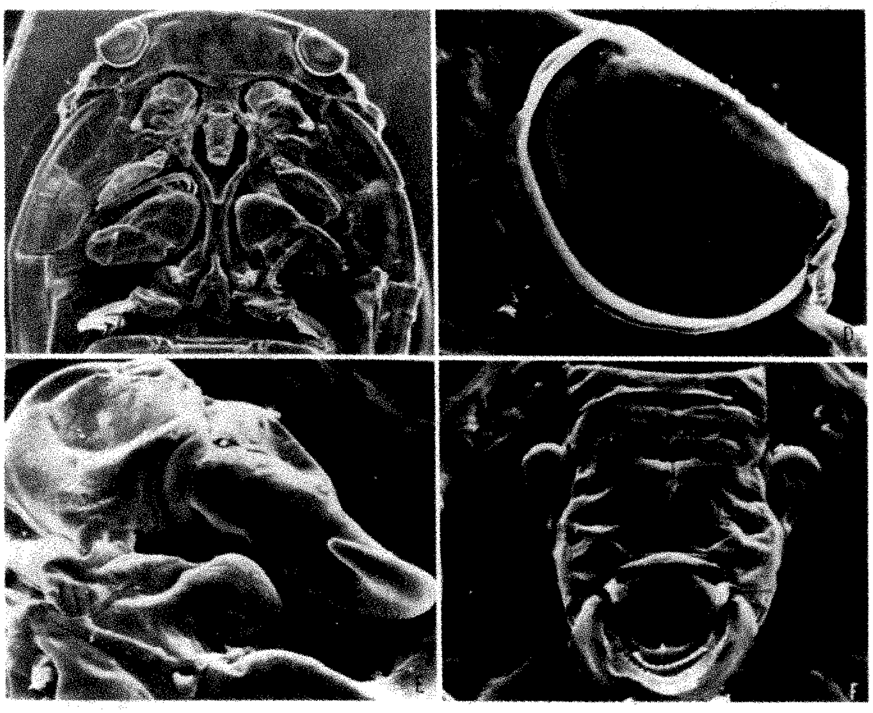

Caligus coryphaenae Steenstrup and Lütken, female: top left, cephalon, ventral (30X); top right, frontal lunule (200X); bottom left, second antenna (200X); bottom right, a happy mouth tube (280X).

from R.J. Roberts

A recent Smithsonian Contribution to Zoology* by Cressey & Cressey has made a major contribution to resolving many of the problems of copepod taxonomy. There are more than a 1,000 known copepod species with very wide ranging structural diversity and the same hallowed, often inaccurate, drawings have appeared in text after text. The copepods are parasites of the economically important mackerel and tuna fish groups and when they occur in large numbers they can be a source of significant financial loss.

The scanning electron microscope pictures from the report, reproduced alongside, show various features of a parasite of the tunny. The bottom right-hand plate, which they designate "the happy mouthtube" shows something that parasitologists have long suspected — that copepods enjoy life even if their hosts do not. □

R.J. Roberts is Director of the Institute of Aquaculture, University of Stirling, Scotland.

*Roger Cressey & Hilary Boyle Cressey *Parasitic Copepods of Mackerel- and Tuna-like Fishes (Scombridae) of the World* Smithsonian Contributions to Zoology 311 (Smithsonian Institution Press, City of Washington, 1980).

tract epithelium, whereas other glycolipids and monosaccharides do not.

N. Sharon (Weizmann Institute, Rehovoth) reminded the symposium that bacterial adhesion may be inhibited by simple sugars, particularly mannose in the case of various strains of *E.coli* and salmonella. This has suggested that mannose or mannose-like residues on the host cell form part of the receptor for the bacteria which attach to them. There is considerable evidence, said Sharon, that many strains of bacteria contain a lectin-like substance, specific for mannose, which may take the form of fimbriae or flagella or may be embedded in the outer membrane. (Adhesion mediated by CFA/I and/II, K88 and K99 is insensitive to mannose, while that due to type 1 fimbriae is sensitive.) He said there is good reason to believe that the mannose-sensitive attachment plays a role in pathogenicity, and he has found that α methyl-D-mannoside diminishes infection of the urinary tract of mice by virulent strains of *E.coli*.

Adhesion, often of a more transitory nature, is an obligatory step in the infection of cells by mycoplasma. S. Razin (Hebrew University of Jerusalem), describing work done in conjunction with W. Bredt (University of Freiburg), said that adhesion, chiefly in the respiratory tract, enables toxic products of mycoplasma metabolism, such as ammonia and hydrogen peroxide, to reach concentrations sufficient to damage the cells. He said that sialic acid residues form the receptors of the cells, while the binding sites on the mycoplasma are apparently membrane proteins. Adhesion seems to depend on the metabolic state of the mycoplasma, with the electrochemical ion gradient across the membrane also being influential.

Another parasite, the protozoan responsible for amoebic dysentery, has come under closer scrutiny as a health problem of the developing world. The trophozoite stage of *Entamoeba histolytica* begins the infectious process by adhering to intestinal epithelial cells, and from there can penetrate into the circulation, adhering to red blood cells and phagocytosing them. D. Mirelman (Weizmann Institute) reported that a lectin found in the trophozoite is apparently involved in the adhesion. He thinks the lectin is separate from the amoeba's toxin, for the two activities can be demonstrated in different fractions obtained from the trophozoite.

For the merozoite stage of the malaria parasite, adhesion to red blood cells is an essential part of the cycle of invasion, multiplication, release and reinvasion that produces characteristic symptoms of anaemia and fever in the host. Adhesion seems to be mediated by specific receptor molecules on merozoite and red cell — evidence includes the specificity of each species of merozoite for either young or old red cells of certain host species and for a particular blood group antigen. R.J. Howard (National Institute of Allergy and Infectious Diseases, Bethesda), discussing work with *Plasmodium vivax* and *Plasmodium knowlesii*, pointed out that characterization of the molecules involved in recognition is hampered because the morphological changes occurring during the cycle are likely to affect the receptors.

D.F.H. Wallach (Tufts-New England Medical Center, Boston) recalled that after invasion, a merozoite matures and multiplies within a vacuole. At the same time the host red cell's cytoskeleton is destroyed and its surface membrane is altered by modification of component proteins and insertion of others synthesised by the parasite. The new proteins are immunogenic in the host, and two of them are involved in protective immunity and have antigenic features common to several species of *Plasmodium* that cause malaria in mammals. This lack of species specificity should make such proteins an attractive target in the search for a vaccine against malaria.

Although the details of adhesion and its relationship to pathogenicity are likely to be hard won, the potential rewards in terms of prevention and treatment of disease are clearly considerable. Vaccines are an obvious outcome to hope for, but other approaches are possible. E.H. Beachey (University of Tennessee College of Medicine, Memphis) reported that small, sublethal concentrations of various antibiotics can disrupt the adhesion of some *E.coli* and *Streptococcus pyogenes*. Especially effective are antibiotics that act on the ribosomes or the cell wall, and Beachey presumes that they interfere with the synthesis or assembly of the fimbriae. This suggests the possibility of combating bacteria with doses of antibiotics sufficient to prevent adhesion but not necessarily to kill them; such low doses would avoid problems of toxicity. As the details of adhesion become better understood, more such relationships should emerge. □

0028-0836/80/320557-01$01.00

Virus crystallography comes of age

from Stephen C. Harrison

VIRUS particles are simple paradigms for all sorts of sub-cellular assemblies, and detailed views of their organization have long been sought. X-ray diffraction studies of virus crystals began at almost the same time as crystallographic investigation of small proteins[1], and a certain mystique of the 'ultimate' in large unit cells grew up around them. The reports in *Nature* by Abad-Zapatero *el al.* [2] of Southern Bean Mosaic Virus (SBMV) at 2.8 Å resolution and by Unge *el al.*[3] of Satellite Tobacco Necrosis Virus (STNV) at 4 Å resolution follow by less than two years the publication of 2.8 Å resolution structures of Tobacco Mosaic Virus (TMV) disk[4] and of Tomato Bushy Stunt Virus (TBSV)[5]: 'virus crystallography' is no longer a vague promise, and several striking results emerge from comparison of the structures at hand.

All these efforts have relied on some recent advances in technique — particularly in computing. Rossman and Blow[6] observed almost 20 years ago that non-crystallographic symmetry in structures such as viruses could enormously facilitate solution of the X-ray phase problem, but only in the last five years have algorithms, machines and programs been available to carry out the lengthy iterative calculations[7]. In principle, these iterations should converge from any initial approximation to the phases; in practice, however, experimental errors in observed structure amplitudes and approximations in the computational scheme require a non-random starting point. The work on TMV disk, TBSV and SBMV have all relied on the standard method of isomorphous replacement to provide this start. The STNV solution is rather more daring, using isomorphous phases to 10 Å and phase extension stepwise to 4Å by non-crystallographic symmetry averaging. A more conventional computation was also perfomed, using initial SIR phases to 4 Å, and the reported agreement between this and the phase-extension calculation is excellent. It is difficult to assess the accuracy of a 4 Å map from density alone, since the shape of features depends on local conformation, and a more complete measure of the success of phase extension will be recognition of polypeptide chain and residues when the STNV structure is carried to 3 Å or beyond.

The coat subunit of a spherical virus assembles into a regular, icosahedrally symmetric shell and the shell is a package for nucleic acid[8]. Moreover, in most structures the same subunit is found in several conformationally distinct positions, genetic economy requiring a larger coat than can be constructed from just sixty (i.e. one icosahedral quota). These architectural conditions demand a way of incorporating nucleic acid that adapts an inherently nonrepeating structure (the loops and stems of folded RNA) to a regular surface lattice. In structures with more than 60 subunits, they further demand a subunit that can adopt alternative bonding arrangements and hence also a mechanism for avoiding ambiguity.

In TMV, which has been resolved at 4 Å by diffraction from orientated gels[9], three nucleotides are bound into a groove-like site on each subunit. The coat is an 'unwinding protein' and imposes its own helical order on the RNA backbone. One might imagine by analogy that each protein subunit of a spherical virus could bind to an exact length of nucleic acid. If the binding sites were located on a part of the protein fixed in the surface lattice, the RNA would be piecewise icosahedrally ordered, and portions of it would be visible in a suitable electron density map. This model can be ruled out in TBSV and apparently now in SBMV, where no clear RNA-related features appear. In both cases, however, a significant portion of the protein subunit (about 60 residues) is also invisible in the map, implying absence of a unique spatial relationship to the rest of the chain. This portion lies at the N-terminus, and it is a plausible candidate for a nucleic-acid binding sequence. If so, we can imagine two RNA packing modes that might interact with a flexibly-linked binding domain: (1) Viral RNA *in situ* could have a more or less defined tertiary structure, requiring binding regions on the protein loosely tethered to the rest of the subunit, in order to seek out appropriate sites on a non-icosahedrally-symmetric nucleic-acid structure; (2) RNA stems and loops could be compactly but essentially randomly close-packed in the particle (some 60 to 70% of the RNA in such viruses is probably in double-helical stems[10]), again requiring flexibly-linked protein regions for interaction with appropriate RNA structures or sequences. Crystallographic structure determination necessarily yields an average over the operations of the space group, and in SBMV and TBSV, a unique RNA structure would be blurred by the high symmetry of the lattice postion on which the particle lies. In STNV, the asymmetric unit comprises an entire particle, and Unge *et al.* point out that

Subunits and their arrangement in SBMV and TBSV. The SBMV subunit (upper left) has an N-terminal arm and a single, folded domain, homologous to the S-domain of TBSV (upper right); 180 subunits pack to form a T = 3 viral shell. The arms of 60 of the subunits (positions denoted C) are ordered as shown by heavy lines in the central diagram. The actual folding of an ordered arm is along an inside edge of the S-domain with a loop around the particle threefold axis (see diagram in lower right-hand corner). Three such loops embrace, and the 60 ordered arms form a connected framework. The arms of subunits in positions denoted A and B are not regularly ordered in SBMV or TBSV (lower left). The cylindrical projections in the central diagram represent P-domain dimers in TBSV; they are, of course, absent in SBMV.

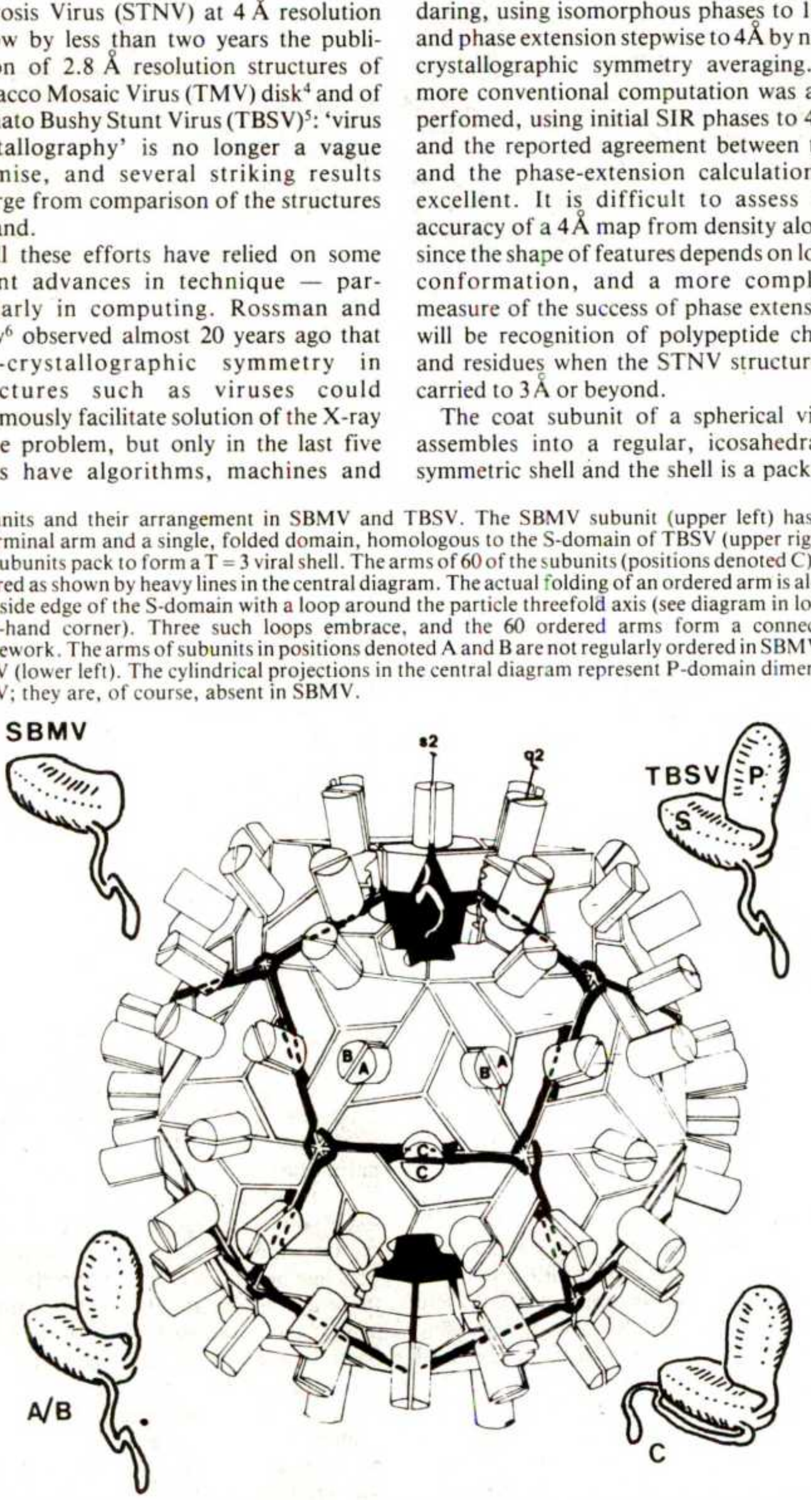

Stephen C. Harrison is Professor of Biochemistry at Harvard University.

0028-0836/80/320558-02$01.00

crystallographic symmetry alone does not exclude determination of RNA configuration. Such a determination would require not only a unique RNA conformation, but also sufficient asymmetry imposed thereby on the shell that consistent orientations appeared throughout the crystal. The present map is ambiguous on that point, but a high degree of order does not appear likely.

The N-terminal 15 residues cannot be traced, and the general appearance of internal density is not immediately recognizable as a single structure. It is useful in this connection to recall that the uniqueness of the secondary structure has not been established for viral RNA, although the correlation of nuclease sites and predicted single-stranded regions in 'flower diagrams' of the MS2 sequence suggest a general regularity[11]. In any one stock of virus, a given RNA molecule is likely to differ from the mean sequence at a number of positions[12]. Moreover, the compactness of the configuration in the virus appears to be imposed by the shell, rather than by its own sequence, since RNA of the size of the genomes in these viruses has a much larger radius of gyration under conditions of physiological ionic strength than that of the cavity into which it is packed[13]. Indeed, the degree of compaction is striking: from figures given by Unge *et al.*, the volume available to STNV RNA implies an inner cavity with space for about 1.2 g H_2O per g RNA; the packing of TBSV RNA is comparably tight. A model of more or less random close packing of roughly parallel RNA stems is appealing, since very efficient packaging can be achieved without any significant demands on RNA structure or sequence. But it will not be simple to prove such a picture.

The most surprising of recent results is probably the similarity of the SBMV subunit to the S-domain of TBSV. Various evolutionary speculations can be made, but from the point of view of assembly and its control, there are two more immediate conclusions that should be emphasized. The first is the identical way in which these two T = 3 structures solve the ambiguity problem alluded to above. A portion of the polypeptide chain, just N-terminal to the compact domain(s), is ordered on sixty subunits and disordered on the remaining 120. The sixty ordered arms effectively serve as an internal, T = 1 framework: they interdigitate around icosahedral twofolds. This scaffold, formed by a flexibly linked part of the subunit chain determines the size and curvature of the particle. The choice between alternative bonding patterns at interfaces that must so adapt is dictated by the symmetry and geometry of the network of arms. One might imagine cases where the network would be formed of a distinct protein — could this be the case with cores in bacteriophage head assembly[14] or VP2 and VP3 in polyoma and SV40[15]? The second direct conclusion that emerges from comparison of TBSV and SBMV is the significance of modularity in the design of assembling subunits. In SBMV as seen in the paper of Abad-Zapatero *et al.*, the subunit has three functional parts: an unseen (RNA-binding?) N-terminal piece, the framework-like arm (including sequences in the intertwined β-annulus), and the major folded domain. In TBSV, there is an additional folded domain (the P-domain). Clearly the P-domain is not essential for particle stability, since it is missing in SBMV. It does appear to be a strong twofold 'clamp', and the hinge between it and the S-domain is required for subunits to conserve these two fold interactions while still adapting to the T = 3 surface lattice.

With these advances now at hand, what about the crystallography of other viruses and large assemblies? SBMV and TBSV show quite dramatically that the spatial arrangement of modules in a subunit protein is characteristic of the assembly, but not necessarily of the isolated polypeptide; the remarkable interdigitation of N-terminal arms could not have been anticipated (or even seen) in the structure of the subunit alone. The possible consequences for those who would like to visualize a ribosome, for example, are sobering: high-resolution structures of large assemblies may not readily be constructed from structures of component parts. There is, however, a converse advantage of flexibly-linked modules: in cases where function is a property of a particular module of a large protein, proteolytic dissection and piecewise crystallization is a fruitful and helpful strategy. This is the case, for example, with influenza virus haemagglutinin[16] and may well be appropriate for the presumptive RNA-binding, N-terminal portions of SBMV or TBSV. □

---

1. Bernal, J. & Fankuchen, I. *Nature* **139**, 923 (1939).
2. Abad-Zapatero, C., Abdel-Meguid, S., Johnson, J, Leslie, A., Rayment, I., Rossmann, M., Suck, D. & Tsukihara, T. *Nature* **286**, 33 (1980).
3. Unge, T., Liljas, L., Strandberg, B., Vaara, T., Kannan, K., Fridborg, K., Nordman, C. & Lenj, P. *Nature* **285**, 373 (1980).
4. Bloomer, A. C., Champness, J. N., Bricogne, G., Staden, R. & Klug, A. *Nature* **276**, 362 (1978).
5. Harrison, S. C., Olsen, A. J., Schutt, C. E., Winkler, F. K. & Bricogne, G. *Nature* **276**, 368 (1978).
6. Rossman, M. G. & Blow, D. *Acta Cryst.* **16**, 39 (1978).
7. Bricogne, G. *Acta Cryst.* **A30**, 395 (1974). *Acta Cryst.* **A32**, 832 (1976)
8. Caspar, D. L. D. & Klug, A. *Cold Spring Harb. Symp. quant. Biol.* **27**, 1 (1962).
9. Stubbs, G., Warren, S. & Holmes, K. C. *Nature* **267**, 216 (1977).
10. Witz, J. & Strazielle, C. in *Subunits in Biological Systems*, **B** (ed. Fasman, G. & Timashaff, S., Dekkar, New York.)
11. Fiers, W. *et al. Nature* **260**, 500 (1976).
12. Domingo, E., Sabo, D., Taniguchi, T. & Weissmann, C. *Cell* **13**, 735 (1978).
13. Gesteland, R. & Boedtker, H. *J. mol. Biol.* **8**, 496 (1975).
14. Casjens, S. & King, J. *Rev. Biochem.* **44**, 555 (1975).
15. Murakami, W. T. & Schaffhausen, B. in *Molecular Studies in Viral Neoplasia 25th M. P. Anderson Symposium*, (Williams & Willians, Baltimore, 1974).
16. Wilson I. A., Skehel, J. J. & Wiley, D. C. in *Structure and Variation in Influenza Virus* (ed. Laver G & Air, G.) (Elsevier/North-Holland, New York, 1980)

Open-ended fusion systems

from R. F. Post

JAPAN, among all of the highly industrialized nations, is the most dependent on imported energy. Japan is also a nation that owes its advanced technology both its present economic strength and its hopes for future economic growth. Given these circumstances it is not surprising that nuclear fusion research has been singled out for special attention by the Japanese government. Fusion, for which the primary fuel is heavy hydrogen, extractable at low cost from water, would be an extremely attractive long-term energy source. It is against this backdrop that a specialized scientific meeting dealing with a particular approach to fusion, so-called open-ended magnetic confinement systems was convened in Japan in April.*

Open-ended fusion systems are a class of fusion 'magnetic bottles' in which the field lines of the externally-generated magnetic field (needed to confine the hot fusion plasma) enter at one end of the bottle and exit from the other end. Open-ended magnetic bottles are in contrast to ones such as the tokamak, where the field lines remain entirely within the doughnut-shaped confinement chamber.

R. F. Post is Deputy Associate Director for Physics in the Magnetic Fusion Division of the Lawrence Livermore National Laboratory, University of California.

An example of an open-ended system is the simple mirror machine, in which the field lines form a tubular bundle constricted at both ends (the mirrors). The charged particles of a fusion plasma, once trapped between the mirrors, continue to gyrate back and forth along the field lines, being repeatedly reflected by magnetic mirrors in the same way that charged particles are trapped, between the north and south magnetic poles, in the Van Allen radiation belts that surround the earth.

Present interest in the mirror approach to fusion power stems in part from an inherent advantage that some kinds of mirror fields possess in their ability to suppress the so-called MHD or fluid-like turbulences in magnetically confined plasmas. From this property derives the remarkable ability of specially-shaped mirror fields (called 'magnetic wells') to stably confine very high plasma pressures for a given magnetic field intensity. To this inherent advantage has recently been added a new feature — the tandem mirror idea — an idea that shows promise of greatly improving the economic prospects of mirror fusion systems relative to older mirror approaches. The tandem mirror

---

The 'International Symposium on Physics in Open-Ended Fusion Systems' was held at the new University of Tsukuba, Japan in April 1980.

0028-0836/80/320559-02$01.00

consists of two small conventional mirror cells located at each end of a large central confinement chamber around which is wound a simple solenoidal magnet coil. The hot plasmas in these end cells create positive electric potentials that act to electrostatically 'plug' the end leakage of charged particles from the central cell far more effectively than is possible with a single mirror at each end acting alone. Though invented in the USSR and, independently, in the US about four years ago, the first tandem mirror device to be constructed and operated (Gamma-6; 1978) was built at Tsukuba University, Japan, preceding the larger experiment (TMX; 1979) brought on line at the Lawrence Livermore Laboratory.

The scientific validity of the tandem mirror idea for enhancing mirror confinement was made clear in papers by Kawabe (Tsukuba) and Grubb and Drake (Lawrence Livermore Laboratory) who described experiments in the Tsukuba Gamma-6 and Livermore TMX experiments, respectively. Work in progress (TMX) includes more detailed measurements of particle and energy transport, the role of microinstabilities and their suppression, and the study of plasma pressure limits as determined by MHD effects. Baldwin (Livermore) then described recent developments in tandem mirror theory, including the important new idea (originated by Baldwin and Logan) of the thermal barrier. In a tandem mirror, a thermal barrier is a specially designed cell that, through the generation of a locally-negative potential region, can act to thermally isolate the end plug from the central cell. Thermal isolation then would permit the heating of plug electrons to higher temperatures than those of the central cell, with resultant increased plug potential at lowered plug plasma density — a major economic advantage.

The use of radiofrequency fields to enhance the confinement of open-ended systems has been a major topic in fusion research in Japan for many years. Pioneered at Nagoya under the direction of K. Takayama, this work led to the construction at Nagoya of a large mirror-cusp device, RFC-XX. Itatani (Nagoya) described preliminary results with this machine, in which enhancement of confinement of moderate temperature plasmas by factors of 5 or more (over the confinement observed with r.f. turned off) were seen. Whether good confinement of higher temperature plasmas can be achieved is not yet resolved. RFC-XX however appears to be the most advanced facility for the study of such questions in any fusion laboratory.

An important sub-class of mirror systems are those where the phenomenon of field-reversal is invoked to improve confinement. In a field-reversed mirror — a form of the so-called "compact toroid" configuration — the internal diamagnetic currents of the mirror-trapped plasma are made to be sufficiently intense to reverse the direction of the magnetic field near the axis within the plasma, thus closing the magnetic lines on themselves within the plasma interior and thereby inhibiting plasma losses through the mirrors. Interest in such configurations, which dates back many years to related systems (such as the electron ring ASTRON of Christofilos), comes from their geometric simplicity and, especially, from their extremely efficient use of the external field. The field-reversed mirror shares with the tandem mirror the generic idea that properties of the plasma are used to improve its own confinement. The Symposium provided a forum for the discussion of most of the FRM work now in progress, including, for example, work at the Los Alamos Laboratory on field-reversed configurations produced by a coaxial gun (Sherwood; Los Alamos) and field-reversed electron rings (Fleischmann; Cornell).

Some of the most unusual mirror devices were described in the papers concerning work at Novosibirsk (Ryutov, Koidan). In addition to the AMBAL tandem mirror, now under construction, there are two other mirror devices: PSP-2, a device in which mirror confinement is enhanced by electrically-induced plasma rotation, and GOL-1, a device using multiple mirror cells and operating at very high plasma density. Both of the latter innovative devices owe much in their origin to the former Director of the Novosibirsk fusion group, G. I. Budker, who died July 4, 1977.

Judging from the lively discussion at the conference, and from the enthusiasm of the participants, interest in open-ended systems is increasing not only in Japan but world wide. In the case of the Japanese effort, it seems equally clear that their contributions to research on open-ended magnetic fusion systems will become increasingly important over the next few years. ☐

100 years ago

PHYSICS WITHOUT APPARATUS

It is almost a proverb in science that some of the greatest discoveries have been made by the most simple means. It is equally true that almost all the more important facts and laws of the physical sciences can be illustrated and explained by the help of experiments made without special or expensive apparatus, and requiring only the familiar objects of common life for their performance. The greatest exponents of popular science — and amongst them notably Faraday — delighted in impromptu devices of this kind. It is indeed surprising how throughout the whole range of natural philosophy the hand of the master can turn to account the very simplest and rudest of apparatus. A silver spoon, a pair of spectacle lenses, a tumbler of water, and a few sheets of paper suffice to illustrate half the laws of geometrical optics. A few pieces of sealing-wax, some flannel, silk, writing paper, pins, and glass tumblers will carry the clever experimenter a long way into the phenomena of electricity. These are things which any person can procure, and which any person can be taught to use. But their right use depends on the possession of accurate scientific knowledge and a clear understanding of *what* the various experiments are to prove. In fact the art of experiment and the science of inductive reasoning are the essential qualifications necessary to make *Physics without apparatus* profitable.

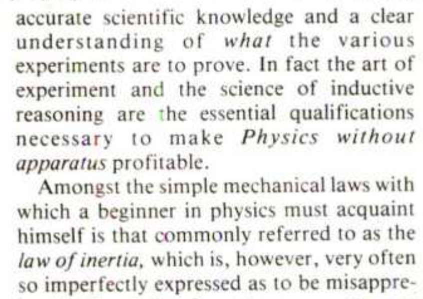

Amongst the simple mechanical laws with which a beginner in physics must acquaint himself is that commonly referred to as the *law of inertia*, which is, however, very often so imperfectly expressed as to be misapprehended. It requires force to move matter, not because matter is inherently lazy or sluggish, but because it possesses *mass*. The greater the mass of matter in a ball, the harder work is it to send it rolling. Force is also required to stop matter that is moving, the reason again being that a mass moving under the impulse of an impressed force possesses a certain moving energy which cannot be at once reduced to nothing. In either case — either to move a mass or to alter the motion of a mass — force must be employed and energy expended. Of this law of inertia many examples might be given: and there are many curious facts which this law serves to explain. Some of the most striking of these are those in which the effect of sudden forces is different from that which might have been expected. In Fig. 1 we give an illustration of an experiment of this nature. A wooden rod — say a broomstick — has a couple of needles fixed into its ends, and it is then supported upon two wineglasses resting upon two chairs. If a heavy poker is now brought down very violently upon the middle of the stick it will break in two without the needles or the glasses being broken. A feeble or indecisive blow will fail to do this, and will break the glasses or the needles, or both. Here the moving energy of the heavy mass, the poker, is suddenly transferred to the middle of the stick, so suddenly that it is broken asunder before the thrust has *time* to reach the fragile supports. From *Nature* 22 5 August, 320 & 321, 1880.

0028-0836/80/320560-01$01.00

REVIEW ARTICLE

New findings in methane-utilizing bacteria highlight their importance in the biosphere and their commercial potential

I. J. Higgins, D. J. Best & R. C. Hammond
Biological Laboratory, University of Kent, Canterbury, Kent CT2 7NJ, UK

Recent results, showing that the ubiquitous methane-utilizing bacteria (methanotrophs) can partially oxidize and, in some cases, extensively metabolize complex organic compounds, call for a reappraisal of their role in the cycling of elements in the biosphere. Possible environmental implications and opportunities for industrial exploitation are discussed.

ABOUT half of the substantial, but not precisely known, proportion of total organic carbon degraded by anaerobic microflora is converted to methane. The amount of the hydrocarbon released into the atmosphere, however, represents only about 0.5% of total carbon turnover[1]. The disparity between this figure and the large amounts of methane produced by the methanogenic bacteria is due mainly to the activities of aerobic methane-utilizing microorganisms (methanotrophs), situated between the anaerobic sediments responsible for methane production and the atmosphere, and partly to the microbial oxidation of methane anaerobically. On this basis alone, organisms responsible for the oxidation of methane are therefore of major importance in the carbon cycle and much current research effort is being devoted to an understanding of their physiology and biochemistry. Our present knowledge has been comprehensively reviewed in recent years[2–6] and our purpose here is not to reiterate this information but rather to survey important new findings implicating methane-oxidizing bacteria in transformations of substances which are not their growth substrates, particularly multi-carbon compounds, and to highlight possible consequences and applications of these microbial activities.

The ubiquity of methane-utilizing bacteria is attested to by the variety of sources from which various workers have been able to isolate them[7]. The many strains isolated in the last 15 years are predominatly aerobic Gram-negative bacteria, growing only on methane or, in some cases, on methanol or dimethyl ether. They can be divided into two distinct groups (types I and II) based on the morphology of their internal membranes and the nature of their carbon assimilation pathways. In recent years, however, facultative methane-oxidizing bacteria, apparently similar to type II obligate methanotrophs, have been isolated[8,9] and some yeasts have been implicated in methane oxidation[10]. Evidence for the involvement of fungi and algae in this process is more equivocal. Although microbial utilization of methane is primarily an aerobic process, it has been shown recently that some species can oxidize it anaerobically. In particular, energy for growth can be obtained by coupling methane oxidation to carbon dioxide with sulphate reduction to hydrogen sulphide[11]. A small amount of methane oxidation may also be accomplished by methanogens[12].

Mechanisms of methane oxidation

In the current context we are particularly concerned with the aerobic, obligate methanotrophs because of recent advances in our understanding of the mechanisms of methane oxidation in these bacteria. It has been known for many years that these microorganisms oxidize methane to carbon dioxide by a route involving successive two-electron oxidation steps via methanol, formaldehyde and formate. Carbon is incorporated into cell material at the oxidation level of formaldehyde by type I species, which use the ribulose monophosphate pathway (Quayle cycle), and in type II species, using the serine pathway, as formaldehyde and carbon dioxide[2–6]. Both groups of bacteria can grow only on a restricted range of reduced C_1 compounds and, in their selectiveness resemble the so-called obligate autotrophs. Nevertheless, it has long been known that such bacteria, either as washed suspensions or in culture, will partially oxidize simple substrate analogues, such as ethane, propane and butane, to the corresponding alcohols, aldehydes and fatty acids[13]. This was presumed to reflect some lack of specificity in the enzymes involved in methane oxidation. Subsequently, it was shown that carbon monoxide, ammonia and ethene are also oxidized[14–16]. However, there is now known to be a surprisingly vast range of multi-carbon compounds, often not closely related to the natural substrates, which are oxidized by methanotrophs[17–19]. Although this capacity varies between species, the following types of compound are oxidized by washed cell suspensions: long-chain alkanes (up to at least hexadecane), alkenes, aromatic and alicyclic hydrocarbons, phenols, long-chain and alicyclic alcohols, pyridine, multi-ring compounds and chlorinated aromatic hydrocarbons. In each case only a limited number of products (sometimes only one) are formed as a result of this unexpected activity, showing that there is, nevertheless, some mechanistic specificity. In some cases the products are simply hydroxylated derivatives, suggesting that a reaction analogous to the oxidation of methane to methanol has occurred. Commonly, there is further oxidation of these hydroxylated compounds to yield aldehydes and carboxylic acids. Many of these biotransformations have been shown to occur in both the presence and absence of methane[17].

'Fortuitous metabolism'?

These activities have been described as 'fortuitous metabolism' (ref. 18), implying that they are merely due to the lack of specificity of oxidative enzymes, whose primary function is to effect the oxidation of methane to carbon dioxide. Such extraordinary lack of enzyme specificity would be extremely unusual if it were entirely fortuitous and we argue here that this phenomenon has developed and been retained because of its survival value to these species. It may well also be of environmental importance and could prove of commercial value, as evidenced by the recent filing of a number of patents on this subject[20–26].

We now have some understanding of the enzymological basis of this lack of specificity and it mainly reflects the properties of enzymes initiating methane oxidation, methane monooxygenases (MMOs). In common with some other

0028-0836/80/320561—04$01.00

monooxygenases, these enzymes have proved difficult to purify but oxygenase involvement was clearly indicated by the ^{18}O-incorporation experiments described by Higgins and Quayle[27]. Subsequently, cell-free activities were studied in a number of species, but substantial purification has been reported in only two, *Methylococcus capsulatus* (Bath) and *Methylosinus trichosporium* OB3b. The system seems to be best characterized in the former species and there is some uncertainty concerning the true nature of the system in the latter[3,4]. There is evidence, however, that growth, and perhaps storage conditions, may markedly affect the characteristics of the enzyme of *M. trichosporium*[28]. Since the first report of cell-free MMO activity by Ribbons and Michalover[29], several workers have reported that such activities are not totally specific for methane, higher gaseous alkanes, alkenes, ammonia and carbon monoxide also being oxidized[30–33]. The range of substrates for MMOs was dramatically extended by Colby *et al.*[34], who showed that cell-free extracts of *M. capsulatus* (Bath) oxidized a wide range of hydrocarbons and related compounds. It has since been shown that enzymes from other species are also relatively nonspecific, but in some cases the specificity is more restricted[18]. Although these findings account for the ability of whole organisms of some methanotrophs to introduce an oxygen atom into many compounds, they do not explain the further oxidation of some of these initial products to, for example, aldehydes and carboxylic acids. These further oxidation processes for simple analogues of methane no doubt reflect lack of absolute specificity of the methanol- and formaldehyde-oxidizing enzyme systems. In the case of more complex hydroxylated products, recent evidence suggests the involvement of other enzymes with no known roles in C_1 metabolism. For example, a number of species contain a broad-specificity, secondary alcohol dehydrogenase[35]. It was thought that intact cells of *M. capsulatus* (Bath) had a rather limited oxidizing capacity[18] but it is now known to be more extensive (H. Dalton, personal communication).

Transformations effected by *M. trichosporium*

Recent work in our laboratory has revealed not only that intact *M. trichosporium* can effect the partial oxidation of a relatively wide range of hydrophobic organic compounds but also that the transformations, in some cases, involve more extensive or even non-oxidative metabolism[17]. Examples of transformations observed are shown in Table 1. With the exception of benzoic acid formation from toluene, the simple oxidation reactions are due entirely to MMO activity. The formation of benzoic acid from toluene and of other acids and aldehydes shown involves MMOs plus other oxidoreductase enzymes. Dechlorination of substituted aromatic compounds and shifts in the positions of ring substituents may be manifestations of the different mechanisms of action of MMOs or may involve other enzyme activities. Debromination reactions have also been reported[36].

Two cases are shown in which dechlorination is associated with covalent attachment of a methyl or alkanoate group to an aromatic ring. We currently have no understanding of these reactions but it is conceivable that they are, in part, due to the lack of specificity of MMOs and they may indicate some type of free radical mechanism[37], or involve other enzyme activities.

In the current context, two of these examples are of special importance, namely the transformations of ethylbenzene and 1-phenylheptane. In each case, products arise as a result of side-chain oxidation and degradation. With the former compound, α-oxidation must be involved, whereas in the latter, the degradation process probably involves β-oxidation. In addition, recent experiments with 1-[^{14}C]-n-hexadecane also suggest that *M. trichosporium* can slowly degrade long-chain alkanes; after incubation with washed cell suspensions in rigidly aseptic conditions, about 5% of the radioactivity was recovered in carbon dioxide (D.J.B., unpublished data).

Although it is well known that most methanotrophs require methane or some other reduced C_1 compounds for growth, the question arises of whether they can obtain supplementary carbon and/or energy from other sources. Clearly, ω-oxidation of alkanes, followed by further oxidation to fatty acids which are subsequently β-oxidized will yield reducing equivalents, which might be used for energy transduction, and acetate for possible incorporation into cell material. Radiolabelling experiments have shown that products of oxidation of several gaseous alkanes and also acetate, the product of β-oxidation, are incorporated into cell material by methanotrophs[38–41]. The findings of Wadzinski and Ribbons[39], using *Methanomonas methanooxidans*, are of particular interest. Acetate, present in the medium during growth on methane, greatly increased the growth yield and it was incorporated into cell material, especially into amino acids, as well as, in part, being oxidized to carbon dioxide by a tricarboxylic acid cycle.

Possible evolutionary reasons for the lack of specificity of methane monooxygenases

A wide range of hydrocarbons and related compounds are continually released into the environment in substantial amounts. They are natural products present in most living organisms, they arise by seepage from subterranean oil and gas deposits and are pollutants due to man's activities. There are also many hydrocarbon derivatives that are xenobiotic products of the chemical industry. Despite controversy concerning specific compounds regarded as pollutants, most hydrocarbons and hydrocarbon-like materials currently turned over in the biosphere are not novel but have been substantial components of the carbon cycle throughout most of evolutionary history. It follows, therefore, that such compounds have always been present in the environment of methanotrophs. As methane is invariably present in their natural habitats, it is not surprising that many of them have developed an obligate requirement for C_1 compounds for growth. These organisms are not in direct competition for survival with heterotrophs. They are, however, in competition with each other for available methane and it is probable that any mechanisms which might develop and enable them to utilize ancillary carbon and/or energy sources would generally be of selective value either to supplement their metabolism or facilitate survival under severe methane limitation.

Although some of the simple oxidation reactions catalysed by methanotrophs and by their MMO activities are of no obvious survival value, for example, the epoxidation of propene, others seem to be responsible for initiating useful metabolism. We would argue, therefore, that there has been selection pressure for the development of broad-specificity MMOs and other oxidoreductases. This selection pressure must be sufficient to outweigh any disadvantage of such lack of specificity. These disadvantages include truly fortuitous oxidations yielding neither energy nor products of value to these bacteria. Indeed, in these conditions, reducing equivalents would be wasted, as MMO requires a source of reducing power, which may be derived from the further oxidation of methanol, its analogues or storage polymers. In addition, some products may prove toxic. Because it is clear that these oxidations occur in the presence of

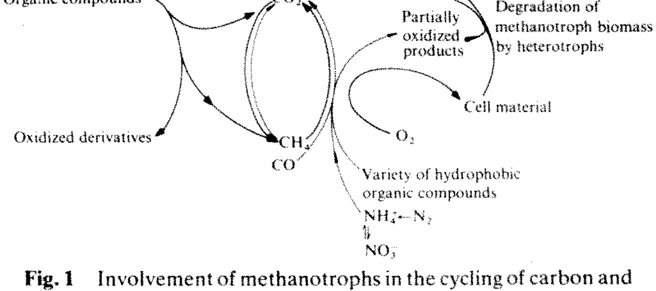

Fig. 1 Involvement of methanotrophs in the cycling of carbon and nitrogen in the biosphere.

Table 1 Examples of biotransformations effected by resting whole organism suspensions of *Methylosinus trichosporium* OB3b

Type of reaction	Compound	Products
Oxidation	$CH_3CH=CH_2$ Propene	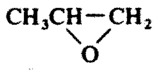$CH_3CH{-}CH_2$ (O bridge) Propene oxide
	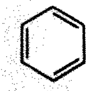 Benzene	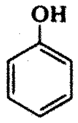 Phenol
	$CH_3(CH_2)_{14}CH_3$ Hexadecane	$CH_3(CH_2)_{14}CH_2OH$ Hexadecan-1-ol
	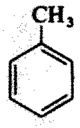 Toluene	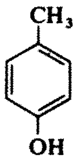 *p*-Hydroxy-toluene 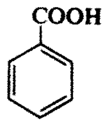 Benzoic acid
Oxidation and degradation	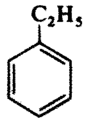 Ethyl benzene	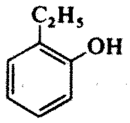 *o*-Hydroxy-ethylbenzene 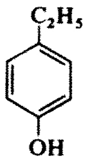 *p*-Hydroxy-ethylbenzene
		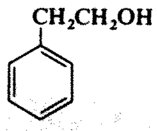 2-Phenylethanol
		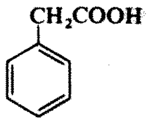 Phenyl acetic acid 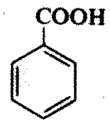 Benzoic acid
	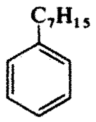 1-Phenylheptane	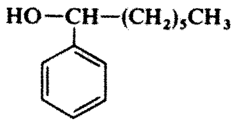 1-Hydroxy-1-phenylheptane 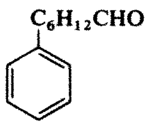 1-Phenyl-heptan-7-al 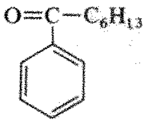 1-Oxo-1-phenylheptane 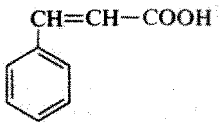 Cinnamic acid 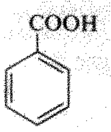 Benzoic acid
Oxidation and dechlorination	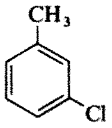 *m*-Chlorotoluene	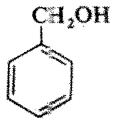 Benzyl alcohol 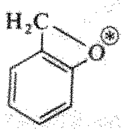 Benzyl epoxide[*]
Oxidation, dechlorination and condensation	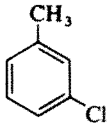 *m*-Chlorotoluene	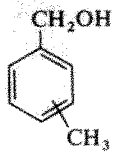 *m*- or *p*-methyl benzyl alcohol
Oxidation and condensation	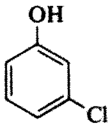 *m*-Chlorophenol	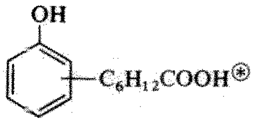 An hydroxyphenylheptanoic acid[*]
Oxidation and rearrangement	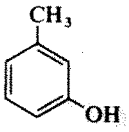 *m*-Cresol	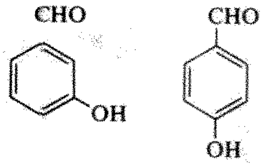 *m*- and *p*-hydroxybenzaldehyde
	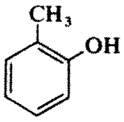 *o*-Cresol	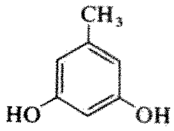 5 Methyl-1,3-benzene diol

---

* Tentative identification.

methane, disadvantages may also arise through competition between methane and other potential substrates for the active site. At first sight, an equally plausible explanation for lack of specificity would not involve evolutionary arguments but would be dictated by some mechanistic requirements of MMO. However, there is substantial evidence against this view. For example, the MMO of one species, *Pseudomonas methanica*, shows greater specificity than those of other species[18] and higher alkane monooxygenases that have been investigated are relatively specific. On the balance of the evidence, therefore, many of these metabolic activities are probably not fortuitous and instead have substantial metabolic significance.

It has generally been accepted that heterotrophic organisms are responsible for mineralization of hydrocarbons, their derivatives and related xenobiotics[42]. If these recently discovered, extensive metabolic activities of some species of the ubiquitous methanotrophs prove to be widespread amongst the group, it is likely that they play a significant part in the mineralization of complex, organic material, in addition to their already documented, major role in the carbon cycle. Methanotrophs are also involved in the nitrogen cycle, being able to fix atmospheric nitrogen, oxidize ammonia and reduce nitrite[3].

It is clear from this discussion that methanotrophs are important in the biosphere (Fig. 1), yet only 15 years ago they were regarded, even by most microbiologists, as obscure, uncooperative, perhaps unimportant microorganisms, as evidenced by the fact that, before 1970, only three species had been isolated and well authenticated[7]. Today, in spite of the efforts of many research groups and the isolation of some 200 strains of methanotrophs, their significance is still not widely recognized, and this fact, in part, provoked the writing of this article.

Some of the oxidative biotransformations catalysed are difficult and/or expensive to effect by conventional chemical means. The whole organism activities are relatively stable and many products are either not further degraded or are degraded only slowly. It is therefore possible that some of these species will prove valuable as industrial catalysts, exploiting intact bacteria or enzymes derived therefrom[20–26].

Two important recent developments may facilitate such industrial exploitation. First, genetic manipulation of these strains is proving possible[43] and second, using cell-free preparations, processes may be devised in which reducing equivalents for the MMOs are supplied electrochemically, thereby dispensing with any requirement for expensive pyridine nucleotide coenzymes[44–46].

We thank Mr D. Scott for helpful discussion and the SRC and ICI Limited for financial support.

1. Ehhalt, D. H. in *Microbial Production and Utilization of Gases* (eds Schegel, H. G., Gottschalk, G. & Pfennig, N.) 13–22 (Erich Goltze, Göttingen, 1976).
2. Quayle, J. R. & Ferenci, T. *Microbiol. Rev.* **42,** 251–273 (1978).
3. Wolfe, R. S. & Higgins, I. J. *Int. Rev. Biochem. microbial Biochem.* **21,** 268–353 (1979).
4. Colby, J., Dalton, H. & Whittenbury, R. *A. Rev. Microbiol.* **33,** 481–517 (1979).
5. Higgins, I. J. in *Diversity of Bacterial Respiratory Systems* (ed. Knowles, C. J.) (CRC Press, Boca Raton, in the press).
6. Higgins, I. J. & Hammond, R. C. in *Biochemistry of Microbial Degradation* (ed. Gibson, D. T.) (Dekker, New York, in the press).
7. Quayle, J. R. *Adv. microbial Physiol.* **7,** 119–203 (1972).
8. Patt, T. E., Cole, G. C., Bland, J. & Hanson, R. S. *J. Bact.* **120,** 955–964 (1974).
9. Patel, R. N., Hou, C. T. & Felix, A. *J. Bact.* **136,** 352–358 (1978).
10. Wolf, H. J. & Hanson, R. S. *J. gen. Microbiol.* **114,** 187–194 (1979).
11. Panganiban, A. T., Patt, T. E., Hart, W. & Hanson, R. S. *Appl. envir. Microbiol.* **37,** 303–309 (1979).
12. Zehnzer, A. J. B. & Brock, T. D. *J. Bact.* **137,** 420–432 (1979).
13. Foster, J. W. & Davis, R. H. *J. Bact.* **91,** 1924–1931 (1966).
14. Hubley, J. H., Mitton, J. R. & Wilkinson, J. F. *Archs Microbiol.* **96,** 365–368 (1974).
15. O'Neill, J. G. & Wilkinson, J. F. *J. gen. Microbiol.* **100,** 407–412 (1977).
16. de Bont. J. A. M. & Mulder, E. G. *J. gen. Microbiol.* **83,** 113–121 (1974).
17. Higgins, I. J. *et al. Biochem. biophys. Res. Commun.* **89,** 671–677 (1979).
18. Stirling, D. I. & Dalton, H. *FEMS Microbiol. Lett.* **5,** 315–318 (1979).
19. Hou, C. T., Patel, R. N., Laskin, A. I. & Barnabe, N. *Appl. envir. Microbiol.* **38,** 127–134 (1979).
20. Dalton, H. *UK Patent Application* No. 27886 (1977).
21. Higgins, I. J. *UK Patent Application* No. 19712 (1978); No. 2024205A (1980).
22. Higgins, I. J. *UK Patent Application* No. 35123 (1978); No. 2024205A (1980).
23. Higgins, I. J. *UK Patent Application* No. 7908357 (1979).
24. Hou, C. T., Patel, R. N. & Laskin, A. I. *UK Patent Application* No. 7913054 (1979).
25. Hou, C. T., Patel, R. N. & Laskin, A. I. *UK Patent Application* No. 7913062 (1979).
26. Hou, C. T., Patel, R. N. & Laskin, A. I. *UK Patent Application* No. 7913063 (1979).
27. Higgins, I. J. & Quayle, J. R. *Biochem. J.* **118,** 210–218 (1970).
28. Brannan, J., Scott, D. & Higgins, I. J. *Proc. 3rd Int. Symp. microbial Growth on C_1 Compounds* (in the press).
29. Ribbons, D. W. & Michalover, J. L. *FEBS Lett.* **11,** 41–44 (1970).
30. Tonge, G. M., Harrison, D. E. F. & Higgins, I. J. *Biochem. J.* **161,** 333–344 (1977).
31. Ferenci, T. *FEBS Lett.* **41,** 94–98 (1974).
32. Ferenci, T., Strøm, T. & Quayle, J. R. *J. gen. Microbiol.* **91,** 79–91 (1975).
33. Ribbons, D. W. *J. Bact.* **122,** 1351–1363 (1975).
34. Colby, J., Stirling, D. I. & Dalton, H. *Biochem. J.* **165,** 395–402 (1977).
35. Hou, C. T., Patel, R., Laskin, A. J., Barnabe, N. & Marczak, I. *Appl. envir. Microbiol.* **38,** 135–142 (1979).
36. Stirling, D. I. & Dalton, H. *J. gen. Microbiol.* **116,** 277–283 (1980).
37. Hutchinson, D. W., Whittenbury, R. & Dalton, H. *J. theor. Biol.* **58,** 325–335 (1976).
38. Leadbetter, E. R. & Foster, J. W. *Archs Mikrobiol.* **35,** 92–104 (1960).
39. Wadzinski, A. M. & Ribbons, D. W. *J. Bact.* **123,** 380–381 (1975).
40. Patel, R. N., Hoare, S. L. & Hoare, D. S. *Antonie van Leeuwenhoek* **45,** 499–511 (1979).
41. Eccleston, M. & Kelly, D. P. *J. gen. Microbiol.* **75,** 211–221 (1973).
42. Higgins, I. J. & Gilbert, P. D. in *The Oil Industry and Microbial Ecosystems* (eds Chater, K. W. A. & Sommerville, H. J.) 80–117 (Institute of Petroleum, London, 1978).
43. Warner, P. J., Higgins, I. J. & Drozd, J. W. *FEMS microbiol. Lett.* **7,** 181–185 (1980).
44. Higgins, I. J. & Hill, H. A. O. *UK Patent Application* No. 2033428 (1980).
45. Higgins, I. J. *et al.* in *Hydrocarbons in Biotechnology* (eds Harrison, D. E. F., Higgins, I. J. & Watkinson, R. J.) (Institute of Petroleum, London, in the press).
46. Cass, A. E. G. *et al. Nature* **285,** 673–674 (1980).

ARTICLES

Anorthositic magmas and the origin of proterozoic anorthosite massifs

Robert A. Wiebe

Department of Geology, Franklin and Marshall College, PO Box 3003, Lancaster, Pennsylvania 17604

Many anorthositic plutons of the Nain complex were formed from highly feldspathic parental magmas, which were probably generated by melting or factional crystallization of tholeiite at 15–22 kbar. Their existence suggests a high geothermal gradient and thick continental crust during the mid-Proterozoic.

PROTEROZOIC anorthosite massifs have long presented three major problems to geologists interested in crustal evolution: (1) what were the parental magmas of the anorthosite intrusions[1]; (2) what is the tectonic significance of the broad belts of these intrusions; and (3) why were most of these complexes emplaced during a restricted interval of the Proterozoic[2]? Solution of the first problem is probably an essential precursor to solving the other two. This article summarizes new evidence for the existence of a suite of highly feldspathic magmas parental to anorthositic rocks in Labrador.

The bulk composition of anorthosite massifs is generally much more feldspar-rich than any known magmas[3]. Has fractional crystallization of plagioclase from normal basaltic or andesitic magmas produced these highly feldspathic plutons, or have

0028-0836/80/320564—04$01.00

these plutons been formed by unusually feldspathic magmas? If basaltic magmas were parental, complementary mafic and ultramafic intrusions must also formed. Gravity surveys indicate that many of these complexes lack hidden mafic and ultramafic bodies[4,5], and even where such mafic intrusions are apparently associated[6], it has not been shown that they are comagmatic with the anorthosites. If andesitic or other intermediate magmas were parental, then complementary plutons of mafic and granitic rocks should be present. Large volumes of granite are commonly associated with anorthosites, but it is not clear that they are comagmatic with the anorthosites. Many granites seem to have been formed from separate melts generated from continental crust[7,8]. The alternative to a 'normal' parental magma is an unusual, highly feldspathic magma. Although several works have suggested parental magmas of this type on the basis of extensive field study[9,10], the evidence has not been sufficient to establish a consensus that such feldspathic magmas did indeed exist and were parental to massif anorthosites. However, recent studies of three anorthositic plutons in the Nain complex of Labrador, outlined below, provide clear evidence that each of these plutons had a distinct, recognizable anorthositic parental magma. These anorthositic magmas together with high-alumina basalts[11,12] indicate that a highly feldspathic magma series was responsible for the formation of the Nain and probably other Proterozoic anorthosite complexes.

Nain complex

The Nain complex is a typical Proterozoic anorthosite massif of area ~15,000 km^2 located along the coast of Labrador. It is ideal for study because it lacks later deformation and metamorphism and because contact relations are well displayed in coastal outcrops. Nearly half of the complex consists of anorthositic intrusions (colour index = 0–20); as many as 20 major anorthositic plutons may be present. Some are highly differentiated and layered; others are homogeneous and massive. Most have average plagioclase compositions between An_{70} and An_{40}. Minor amounts of gabbroic and troctolitic rocks are present[11,13]. Minor ferrodioritic rocks represent late stage differentiates of the anorthosites and mafic intrusions[14]. Somewhat less than half of the Nain complex consists of granite, most of which approaches minimum-melt composition and does not seem to be comagmatic with the anorthosites[15].

Field evidence for anorthositic magmas

Two anorthositic plutons in Nain have fine-grained anorthositic margins. (Strictly, the intrusions should be termed leuconorite because they have colour indices[16] in the range 10–18). One of the chilled margins represents a gradation in average plagioclase grain-size from 3 cm about 5 m in from the contact to 2 mm at the contact with country rock. The other chilled zone shows less variation and is less abrupt. These fine-grained rocks are compositionally equivalent to the coarse-grained anorthositic rocks with which they are associated. Plagioclase in all rocks is characteristically subhedral to euhedral with weak normal and oscillatory zoning. Mafic phase are orthopyroxene and inverted pigeonite with minor ilmenite, magnetite and apatite. The mineralogy suggests that the parental magma must have been relatively dry.

Fine-grained anorthositic dykes are associated with a third intrusion. They were injected into and preserved within a highly refractory xenolith of basic granulite[8]. Average grain size in many of the anorthositic dykes is 1–2 mm while the associated anorthosite has plagioclase in the range 1–7 cm.

The highly feldspathic and relatively dry magmas proposed here could exist only at high temperatures, and such temperatures are indicated by field relations along contact zones. Where anorthosite has intruded quartzofeldspathic gneisses, there is abundant evidence that the gneisses have been partially melted within 10–20 m of the contact. Granitic melt has locally mixed with anorthositic magma or crystal mush along some contacts, and locally derived granitic veins have cut or mixed with dykes emanating from the anorthosite. Hypidiomorphic textures are common in banded gneisses near the contact. Euhedral overgrowths occur on corroded plagioclase, and interstitial areas of alkali feldspar include small euhedral crystals of quartz and biotite. In contrast to these textures, gneisses farther from the anorthosites have allotriomorphic granular textures. Berg[17] has estimated that the depth of emplacement in this area was equivalent to a pressure of about 4 Kbar and that the country rock may have been only 200–300 °C before emplacement. An anhydrous magma, which was as feldspathic as the chilled rocks, must have had a liquidus temperature of ~1,300 °C. If the magma were emplaced at the temperature, the contact zone would have adjusted rapidly[18] to ~800 °C, well below the solidus of the feldspathic magma and above the beginning of melting of the gneisses.

Not all contacts of anorthosites with country rock are characterized by chilled feldspathic margins and remobilized gneiss. Most other contact zones can be explained by emplacement of plagioclase-rich crystal mush with mafic interstitial liquid and by processes of crystal–liquid fractionation along the contact.

Table 1 Major and trace-element compositions and norms of proposed parental magmas of three anorthositic plutons of the Nain complex

Specimen	Kheovik Island*	Tunungayualok Island†	Uivakh Peninsula‡
SiO_2	53.30	54.82	55.58
TiO_2	0.28	0.94	0.77
Al_2O_3	24.84	22.28	21.21
Fe_2O_3	1.13	0.26	0.06
FeO	2.30	5.16	6.31
MnO	0.05	0.08	0.08
MgO	2.87	2.05	1.37
CaO	10.42	9.13	8.23
Na_2O	4.33	4.31	4.84
K_2O	0.41	0.84	1.25
P_2O_5	0.07	0.13	0.30
Mg/Mg + Fe(Tot)	0.61	0.40	0.28
Norm (mol % An)	54.8	50.0	42.7
Rb	dl§	11	24
Sr	642	579	590
Ba	222	490	696
Zr	116	155	183
V	21	68	44
Ni	29	10	2
Weight norms			
Qz	—	1.68	0.46
Or	2.43	5.33	7.36
Ab + An	83.76	75.19	73.41
Di	3.32	4.76	5.53
Hy	7.33	10.56	10.98
Ol	0.83	—	—
Mag	1.63	0.38	0.09
Ilm	0.53	1.79	1.47
Ap	016	0.31	0.70

All analyses determined by X-ray fluorescence; recalculated to 100% anhydrous.

* Composition represents the average of 17 analyses of coarse-grained rocks from the interior of the pluton. This composition is very similar to that obtained for fine-grained anorthositic rocks within a chilled contact zone. These latter compositions were not used because of minor contamination by granitic melt in the contact zone.

† Composition represents the average of 17 analyses of coarse-grained rocks. This composition is very similar to that obtained for fine-grained anorthositic dykes related to this pluton[8].

‡ Composition is based on the average of two nearly identical relatively fined-grained samples within 50 m of the intrusive contact. (REEs for two samples are listed in Table 3.)

§ Less than detection limit.

Geochemical evidence for anorthositic magmas

The chilled margins and dykes each have chemical compositions which are nearly identical to the compositions of the coarse-grained, homogeneous and massive anorthositic intrusions with which they are associated. One can thus argue that the average compositions of these intrusions must approximate their parental magmas. Estimates of the compositions of these parental magmas (Table 1) are based on the compositions of the chilled rocks or on averages of samples from the interior of the pluton. These three magmas are all highly aluminous ($Al_2O_3 = 21$–25%) with SiO_2 between 53% and 56%. Each has a distinct Mg/Mg+Fe which varies with normative anorthite. Incompatible elements (such as, K, P, Rb, Ba and Zr) all increase as anorthite decreases. Normative colour index (wt %) varies from ~14 for the most calcic magma to ~19 for the most sodic.

Figure 1 and Table 2 present rare-earth element (REE) data for one intrusion and its associated fine-grained dykes. All analysed rocks contain approximately the same amount of plagioclase (roughly 80–90%).[8] The remarkably constant REE content of the fine-grained dykes contrasts strongly with the variation shown by the coarse-grained rocks. The average REE content of the coarse-grained rocks approximates the REE abundance in the dykes. The similarity in REEs (as well as major and other trace elements[8]) between dykes and coarse-grained rocks strongly supports the other data which indicate that the parental magma of this intrusion was anorthositic and similar in composition to the dykes.

REEs have also been determined for rocks which approximate compositions of the parental magmas of the other two intrusions (Table 3). Two values for each pluton have been averaged and plotted on the same diagram with the average REEs of dykes related to the first pluton (Fig. 2). These REE patterns and abundances are taken to be characteristic of the magmas which have produced these three anorthositic plutons. All three have a similar light REE enrichment with a small positive Eu-anomaly. The magma with highest An (Kheovik) has the lowest REEs, and the magma with lowest An (Uivakh) has the highest REEs. There does not seem to be a systematic variation in the size of the Eu-anomaly and the Eu-anomalies are much smaller than most reported for anorthosites. Although the small positive Eu-anomalies might be interpreted as being due to minor feldspar accumulation[19], field relations preclude that interpretation for these rocks. Except for slight depletion in heavy REEs, the REE abundances of these anorthositic rocks fall within the range of values for Hawaiian basalts[20]. In terms of REEs and major elements these anorthositic rocks closely resemble anorthosite parental magmas estimated by Simmons and Hanson[21].

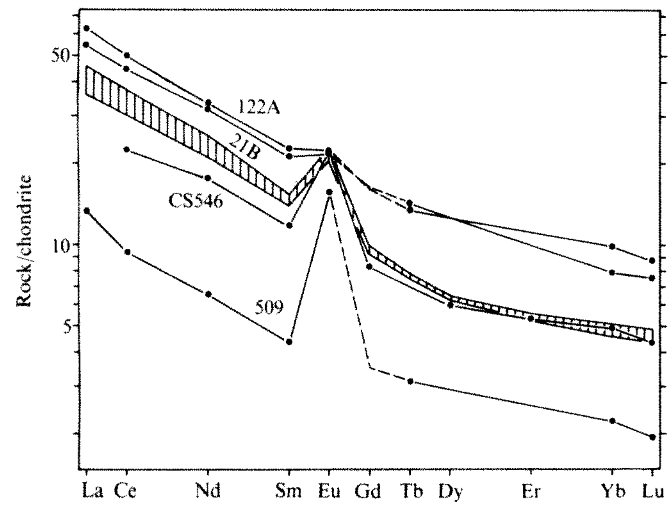

Fig. 1 Chondrite-normalized REEs from coarse-grained anorthositic rocks and fine-grained dykes related to the Tunungayualok Island intrusion. Analyses are listed in Table 2. Vertically ruled pattern shows the complete range of REEs in the fine-grained dykes.

Table 2 REEs in rocks related to the Tunungayualok Island intrusion

	Dykes				Coarse-grained rocks			
Spec	500B*	715B*	718A*	500D†	122A†	218†	509†	CS546*
La				14.9	20.8	18.2	4.44	
Ce	31.0	26.1	32.7	29.5	44.9	39.3	8.24	19.8
Nd	14.0	13.2	15.1	12.6	20.0	19.0	3.95	10.6
Sm	2.60	2.55	2.76	2.54	4.10	3.86	0.788	2.14
Eu	1.57	1.54	1.41	1.54	1.54	1.51	1.09	1.53
Gd	2.32	2.33	2.45					2.07
Tb				0.35	0.64	0.67	0.146	
Dy	1.97	2.05	2.03					1.88
Er	1.04	1.12	1.06					1.07
Yb	0.922	1.03	0.920	0.955	1.98	1.58	0.445	0.985
Lu				0.153	0.299	0.258	0.066	0.147

* Isotope dilution analyses by E. C. Simmons

† Instrumental neutron activation analysis (INAA) by R.A.W.

Origin of anorthositic magmas

Highly feldspathic magmas provide an immediate explanation for the existence of the Proterozoic anorthosite massifs. However, the source and genesis of these magmas remain significant problems. The fact that An and Mg/Mg+Fe vary sympathetically suggests that these magmas were in equilibrium with both plagioclase and pyroxene and that they therefore represent cotectic compositions. Available experimental data suggest that an appropriate cotectic with at least 75–80% plagioclase is present at pressures in the range 15–22 kbar in olivine-free tholeiitic compositions[22,23]. If they represent partial melts, their highly feldspathic compositions suggest that feldspar was in the source area and that a high proportion of the feldspar was melted. Light REE enrichment and small positive Eu-anomalies also suggest major melting of feldspar[21]. A pure feldspar source (for example, Archean anorthosite) is extremely unlikely because of the sympathetic variation of Mg/Mg+Fe with normative An in the three magmas. Direct derivation by partial melting of the mantle seems unlikely because of the low Mg/Mg+Fe (ref. 21).

Alternatively, the feldspathic magmas reported here may have been derived by fractional crystallization from tholeiitic magma[24]. Possible distribution coefficients for REEs[21] indicate that fractional crystallization of clinopyroxene could lead to a magma enriched in light REEs and depleted in heavy REEs, and develop a positive Eu anomaly from a liquid initially lacking one. Cotectic crystallization of plagioclase would also increase REEs and could be responsible for the smaller Eu of the Uivakh magma. Proterozoic dykes which cut the Nain complex have recently been found to carry megacrysts of high-Al orthopyroxene and cumulate nodules of plagioclase and two

Table 3 REEs in rocks of the Kheovik Island and Uivakh Peninsula intrusions

	Kheovik Island		Uivakh Peninsula	
Spec	777	779	856	857
La	9.03	10.17	23.54	23.09
Ce	19.96	21.40	51.43	50.74
Nd	8.9	11.1	32.1	28.2
Sm	1.86	1.72	5.14	5.44
Eu	0.88	0.92	2.12	2.19
Tb	0.226	0.206	0.732	0.835
Yb	0.550	0.644	1.71	2.03
Lu	0.064	0.100	0.254	0.318

All analyses were determined by INAA at the NASA Johnson Space Center in Houston.

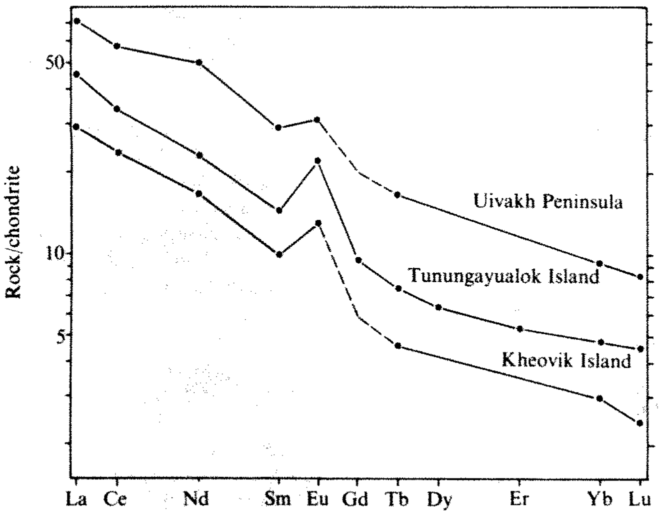

Fig. 2 Chondrite-normalized REEs of proposed partental magmas for three anorthositic plutons of the Nain complex. Values for the Kheovik Island and Uivakh Peninsula plutons are averages of analyses in Table 3. Values for the Tunungayualok Island intrusion are averages of the four analysed fine-grained dykes.

pyroxenes. The composition of these minerals suggest that they would represent lower crustal cumulates responsible for the fractionation from basaltic to anorthositic magma.

If these magmas have been generated from tholeiitic compositions, the need for a feldspar-rich cotectic suggests a tectonic environment characterized by a relatively high geothermal gradient and thick crust. An intracontinental rift zone might provide conditions necessary to generate these anorthositic magmas, and recent workers have argued that the Proterozoic anorthosite massifs have developed in such an environment[2,17,24].

Conclusions

The anorthositic magmas proposed here are documented by chilled margins and fine-grained dykes. They have compositions essentially identical to the coarse-grained, massive, homogeneous anorthositic intrusions with which they are associated. Although only three different magmas have been documented so far in Nain, it seems highly probable the many other similar but distinct plutons of massive anorthositic rocks will prove to have crystallized from other batches of feldspathic magma. There is also abundant evidence that high Al basaltic magmas make volumetrically significant contributions to the anorthosite complexes[11,12,24].

The anorthositic rocks within the Proterozoic complexes, therefore, seem to have been generated by magmas ranging in composition from high-Al basalt[11,24] to the highly feldspathic magmas reported here. These magmas define an entirely new association which is clearly distinct from previously known basaltic and calc-alkaline series. This unique magma association implies that unique tectonic and thermal settings are responsible for the generation of the Proterozoic anorthosite massifs. If most of these massifs prove to have ages in a restricted time period (for example 1,400–1,500 Myr), as present evidence suggests[24], then the conditions necessary to generate that magma series must have been most common in that period. Recognition that unusually feldspathic magmas are involved in anorthosite genesis should aid in evaluating how tectonic style, crustal thickness, and the geothermal gradient evolved in Proterozoic time.

This work was supported by NSF grants EAR 73–00667 A02 and EAR 75–14423 A01.

Received 21 February; accepted 5 June 1980.

1. Buddington, A. F. *Geol. Soc. Am. Mem.* **132,** 477–488 (1972).
2. Bridgewater, D. & Windley, B. F. *Spec. Publ. geol. Soc. S. Afr.* **3,** 307–317 (1973).
3. Isachsen, Y. W. *N.Y. St. Mus. Sci. Serv. Mem.* **18,** 435–445 (1970).
4. Simmons, G. *Bull. geol. Soc. Am.* **75,** 81–98 (1964).
5. Stephenson, R. & Thomas, M. D. *Can. J. Earth Sci.* **16,** 24–37 (1979).
6. Keary, P. & Thomas, M. D. *Geol. Ass. Can. Abstr.* **4,** 60 (1979).
7. Hubbard, F. H. & Whitley, J. E. *Nature* **271,** 439–440 (1978).
8. Wiebe, R. A. *Am. J. Sci.* **279,** 394–410 (1979).
9. Buddington, A. F. *Geol. Soc. Am. Mem.* **7** (1939).
10. Osborne, F. F. *Trans. R. Soc. Can. 3rd Ser., sect. 4,* **43,** 85–112 (1949).
11. Morse, S. A. *Geol. Soc. Am. Mem.* **112** (1969).
12. Berg. J. G. *Univ. Massachusetts Geol. Dept. Contr.* **13,** 107–119 (1974).
13. Planansky, G. A. *Univ. Massachusetts Geol. Dept. Contr.* **1,** 83–89 (1973).
14. Wiebe, R. A. *J. Petrol.* **20,** 239–269 (1979).
15. Wiebe, R. A. *Can. J. Earth Sci.* **15,** 1326–1340 (1978).
16. Streckeisen, A. *Earth Sci. Rev.* **12,** 1–33 (1976).
17. Berg. J. H. *J. Petrol.* **18,** 399–430 (1977).
18. Jaeger, J. C. in *Basalts,* 530–536 (Interscience, New York, 1968).
19. Philpotts, J. A. & Schnetzler, C. C. *Geochim. cosmochim Acta* **34,** 307–322 (1970).
20. Schilling, J. G. & Winchester, J. W. *Contr. Miner. Petrol.* **23,** 27–37 (1969).
21. Simmons, E. C. & Hanson, G. N. *Contr. Miner. Petrol.* **66,** 119–135 (1978).
22. Emslie, R. F. *Yb. Carnegie Inst. Washington* **69,** 148–155 (1971).
23. Green, T. H. *Can. J. Earth Sci.* **6,** 427–440 (1969).
24. Emslie, R. F. *Precamb. Res.* **7,** 61–98 (1978).

High-salt d(CpGpCpG), a left-handed Z′ DNA double helix

Horace Drew, Tsunehiro Takano, Shoji Tanaka, Keiichi Itakura* & Richard E. Dickerson

Division of Chemistry and Chemical Engineering, California Institute of Technology, Pasadena, California 91125
*City of Hope National Medical Center, Duarte, California 91010

*The DNA tetramer d(CpGpCpG) or CGCG crystallizes from high-salt solution as a left-handed double helix, the Z′ helix. Its structure differs from that of the other known left-handed helix, Z-DNA, by a C1′-*exo *sugar pucker at deoxyguanosines rather than C3′-*endo, *and these represent two alternative solutions to the same steric constraint arising from the* syn *glycosyl bond orientation. The apparent molecular basis for the Z to Z′ transition in going from intermediate to high salt is substitution of a bound anion for water at guanine amino groups, and consequent charge repulsion of anions and backbone phosphates.*

THE predominance of right-handed DNA helices of the A and B families was called into question recently by the discovery[1] that the double-helical DNA hexamer d(CpGpCpGpCpG) is a left-handed helix, and one in which the repeating unit is two base pairs rather than a single step. This 'Z helix' has since been found to explain the X-ray patterns from certain fibres with alternating purine–pyrimidine sequences[2]. We now report that the high-salt form of the tetramer d(CpGpCpG) (hereafter to be termed CGCG) also adopts a left-handed conformation, similar to but not identical with the Z helix.

We, like Wang[1], chose alternating CG oligomers of DNA for study because it has been known for some time[3–6] that

0028–0836/80/320567—07$01.00

alternating poly (dC-dG) undergoes a reversible, salt-induced conformation change with a midpoint at about 0.7 M MgCl$_2$ or 2.5 M NaCl (essentially the same ionic strengths); the exact nature of this change has been a matter of interest. We have reported that such a transition with a change in ionic strength of the surrounding medium can also be observed with the tetramer CGCG in the crystalline state itself[7]. Hexagonal crystals of a low-salt form can be grown by diffusion of ethanol into aqueous solutions of CGCG (for experimental details as well as crystallographic survey data, see ref. 7). High-salt crystals are grown by vapour diffusion from solutions containing DNA, MgCl$_2$ and 2-methyl-2,4-pentanediol (MPD). The hexagonal low-salt crystals that form initially in this latter method crack into smaller blocks as the MgCl$_2$ concentration approaches 1 M. These blocks and the crystals that nucleate subsequently show the orthorhombic X-ray pattern of the high-salt form. Conversely, high-salt crystals that are placed in a more dilute solution convert immediately from the orthorhombic to a slightly disordered version of the hexagonal X-ray pattern[7]. Although the diffraction intensity distribution is quite different in the two forms, the transition is apparently small enough to be accommodated within the crystal lattice packing. Unit cell dimensions suggest that the transition involves a shifting of the double helices relative to one another along the *c* axis, with the lateral packing of helices being relatively unaffected, as in Fig. 3 of ref. 7. The structure of the high-salt form is now known and is the subject of the present article.

Structure analysis

Crystallization data and preliminary X-ray survey results have already been reported[7]. High-salt crystals are orthorhombic, space group C222$_1$, with cell dimensions $a = 19.50$ Å, $b = 31.27$ Å, $c = 64.67$ Å, and with one CGCG double helix (two CGCG monomer strands) per crystallographic asymmetric unit. The empirical formula of $C_{38}N_{16}O_{22}H_{46}P_3$ per strand leads to a molecular weight of 1,172, and the measured crystal density of 1.6 g cm^{-3} indicates that the crystals are only 49% DNA by weight. The structure was solved by the method of single isomorphous replacement. Diffusion of various ions and complexes into pre-grown CGCG crystals failed to produce a usable isomorphous derivative. Instead, two covalent heavy atom derivatives were prepared by *de novo* synthesis of the tetramer, with 5-bromocytosine in place of one of the cytosines at the first or third position, using the triester synthesis[8]. The derivative with bromine at the third position (3Br-CGCG) crystallized isomorphously with the native compound, whereas that with bromine at the first position (1Br-CGCG) did not. In the light of the final structure, we now can see that insertion of bromine at the beginning of the molecule interferes with stacking of adjacent double helices up the *c* axis, whereas 3Br-CGCG has no such impediment to stacking. Single isomorphous replacement phases[9] calculated from the 3Br derivative yielded a mean figure of merit of 0.42 to a resolution of 2.7 Å. These phases were used to calculate a 'best' or least r.m.s. error electron density map[10]. A Kendrew wire model served as the starting point for Jack–Levitt refinement[11]. The completed structure consists of 158 non-hydrogen DNA atoms and 86 ordered solvent atoms per asymmetric unit. The current residual error or *R* factor for 1,900 reflections ($>2\sigma$) to a resolution of 1.5 Å (beyond which the pattern fades rapidly) is 19.9%.

The CGCG double helix

As shown in Fig. 1, two CGCG strands in the high-salt crystals form a short left-handed antiparallel double helix with Watson–Crick base pairing. As in the Z helix reported for the CGCGCG hexamer[1], cytosines retain their customary *anti* orientation about the C–N glycosyl bond, with the sugar ring turned away from the O2 carbonyl oxygen of the cytosine ring, and guanines adopt an unusual *syn* conformation with the sugar ring bent towards the guanine N3 ring nitrogen. The sugar–phosphate backbone therefore has a zigzag path, with two steps along the chain as the true helical repeat. The helical rotation between repeating units or pairs of base pair steps is −60°. The minor

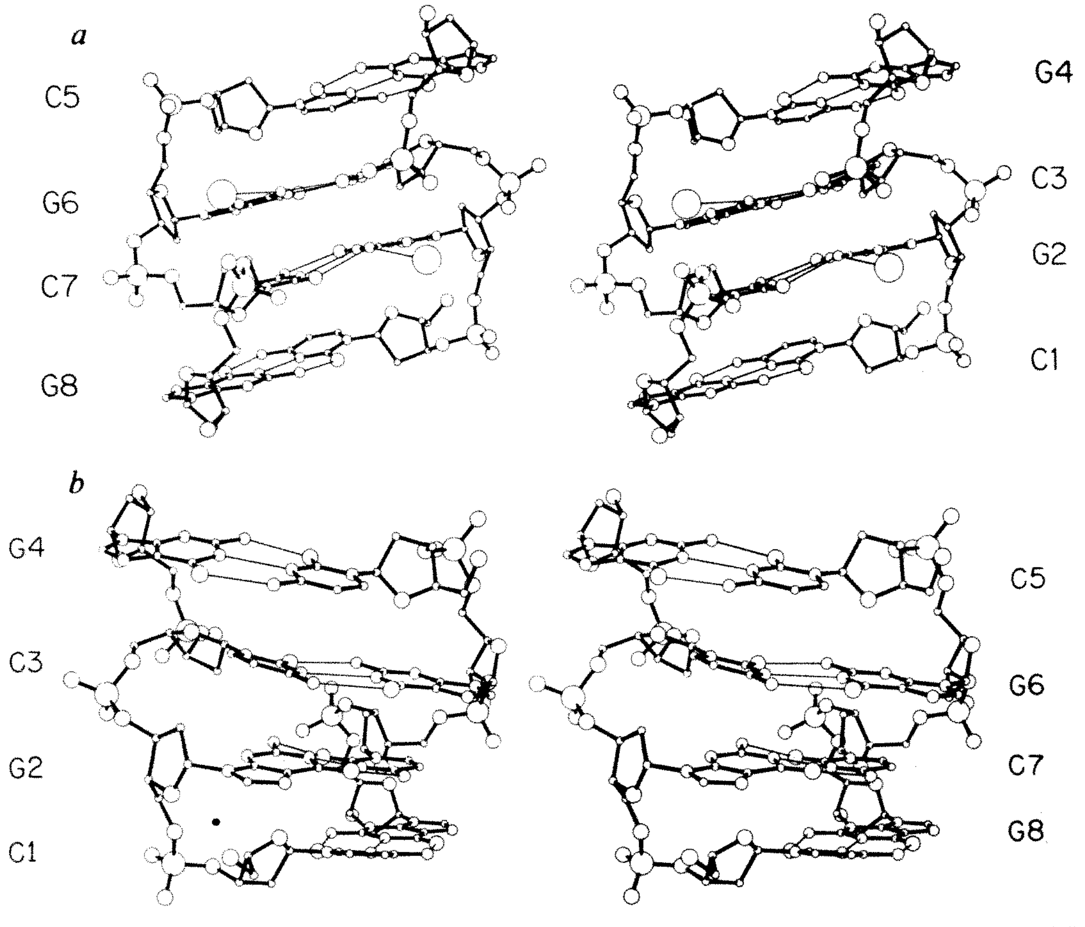

Fig. 1 Stereo pair drawings of the high-salt CGCG double helix. Cytosine and guanine bases are labelled C1 to G8 to the left and right of the two stereo images. Two chloride ions are shown in *a* as large spheres coordinated to the N2 amides of guanosines G2 and G6. Other spheres in order of decreasing radius represent P, O, N and C. The phosphorus atoms along the backbone are referred to as P2, P3 and P4 in one strand and P6, P7 and P8 in the other. *a*, View into the minor groove, down the approximate 2-fold axis. *b*, Oblique view from the outside, in the direction that would correspond to the major groove in the right-handed helices.

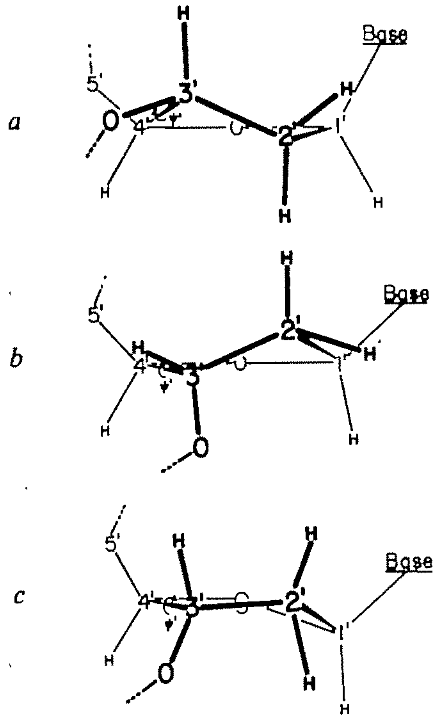

Fig. 2 Deoxyribose ring conformations: *a*, C3'-*endo*; *b*, C2'-*endo*; *c*, C1'-*exo*. The value of the C4'–C3' torsion angle ψ' is clearly defined by the positions of atoms O3' (attached to C3') and C5', and is 82° (*a*), 144° (*b*), and 120° (*c*) for the conformations drawn here.

groove containing the guanine amino and cytosine carbonyl groups (Fig. 1*a*) is the only true groove in the helix, because what corresponds formally to the major groove with guanine carbonyl and cytosine amino groups (Fig. 1*b*) is pushed out to the surface of the helix so that it is not a groove at all. The *syn–anti* alternation of glycosyl bonds may limit all such zigzag left-handed helices to alternating purine–pyrimidine sequences, because placing a pyrimidine base in the *syn* conformation brings its O2 carbonyl oxygen close enough to the O1' oxygen of deoxyribose to disturb their first hydration shells and permit dipole–dipole repulsion.

The low-salt CGCGCG hexamer[1] and the present high-salt CGCG tetramer differ slightly in the tilt of base planes to the helix axis and base repeat spacing along the helix axis. In the hexamer the bases are tilted 7° away from perpendicularity to the helix axis and the average rise per residue along the axis is 3.7 Å. In the tetramer the base plane tilt is 9° and the average rise per residue is 3.8 Å. These differences are associated with a more fundamental change in sugar conformation at deoxyguanosine. In the hexamer the sugar pucker is C2'-*endo* at cytosines and C3'-*endo* at guanines. The tetramer also has C2'-*endo* sugars at cytosines, but at guanines the conformation is C1'-*exo*. This latter is a conformational variant of C2'-*endo*, and quite distinct from C3'-*endo* (Fig. 2). Hence, to a crude first approximation, the sugar pucker is repetitive along the CGCG chain rather than alternating as in CGCGCG.

The evidence for sugar pucker comes less from direct observation of the rings themselves than from the geometry of the backbone chain. As the X-ray data for the tetramer do not extend to atomic resolution, every atom in the deoxyribose ring cannot be resolved and positioned accurately from electron density alone. A better guide to sugar puckering is the torsional angle about the C4'–C3' bond in the five-membered ring (ψ' in Fig. 2). The X-ray results allow this angle to be specified with considerable accuracy, as the C5'-C4'-C3'-O3' linkage is an extended chain with well resolved atoms. This torsional angle is directly related to the sugar pucker as shown in Fig. 2: ~82° for the C3'-*endo* configuration, 144° for C2'-*endo* and an intermediate 120° for C1'-*exo* (ref. 12). In the CGCG structure it averages 141±4° for the four cytosine positions, and 122±1° for three of the four guanines; at one of the 3'-terminal guanines, G8, the final O3' oxygen is disordered, so its ψ' value of 141° is not representative of the ideal helical structure.

The C1'-*exo* conformation can be regarded as a slightly 'bent' C2'-*endo*, and this deformation can be seen from the tetramer structure to arise from a close contact between the N3 nitrogen atom of a guanine ring and the C2' atom in the sugar ring that is in *syn* orientation to it. This distance averages 3.1±0.1 Å in the crystal, with a C1'-*exo* pucker. Forcing the ring back into a C2'-*endo* conformation would push these atoms 0.4 Å closer together, leading to an unacceptably short non-bonded contact. The observed tetramer backbone, therefore, represents the best that can be done using a repetitive C2'-*endo*-like sugar pucker, in the presence of alternating *syn* and *anti* glycosyl bonds. The alternation of 2'-*endo* and 3'-*endo* present in the CGCGCG hexamer[1] represents a different solution to the same steric problem.

We have termed our structure the Z' helix because it differs from the Z helix to about the same degree, if in a different way, as the A' helix with 12 base pairs per turn[13,14] does from the A helix with 11 (ref. 15). Transitions between both pairs, A to A' and Z to Z', can be induced by changes in salt concentration. A similar salt-induced transition is observed between the two principal members of the third family of helices, B with 10 base pairs per turn and C with 9⅓ (refs 16–18). From this viewpoint it might have been more consistent for the C helix to be termed the B', but consistency in an evolving scientific nomenclature is a goal scarcely to be hoped for.

Unlike CGCGCG, the molecular helix axis in CGCG does not coincide with a crystallographic axis, and the molecules are not stacked in such a way as to simulate a continuous helix. In Fig. 3, the two molecules are related by a 2-fold axis normal to the plane of the paper through the centre of the diagram. Horizontal 2-fold axes above and below these molecules also relate them to other molecules not shown at the top and bottom of Fig. 3. An elongated solvent peak of eight electrons occupancy extends between positions 3.5 Å away from the N2 amino groups of guanines G4 on the two molecules shown, and the distance from the amino group suggests that this is a partial-occupancy, disordered chloride site rather than water. At the other end of each molecule, the amino group of guanine G8 is coordinated to a water molecule at 2.7 Å distance rather than to Cl$^-$, and a network of solvent molecules crosses each horizontal 2-fold axis to connect to another molecule not shown. Each molecular helix

Table 1 Comparison of left-handed DNA helices

Helix	Z'	Z
Where found	High-salt CGCG	Low-salt CGCGCG
Repeating units per turn	6 07±0.31	6
Lateral crystal packing diameter*	18.4 Å	18.1 Å
Rise per repeat	7.61±0.11 Å	7 43 Å†
Base pair tilt to helix axis	9°	7°
Rotation per repeating unit	−59.4±3.1°	−60°
Glycosyl torsion angle (χ)		
Deoxycytidine	*anti* (23°)	*anti* (21°, 32°)‡
Deoxyguanosine	*syn* (−106°)	*syn* (−112°, −118°)‡
Sugar pucker (ψ')		
Deoxycytidine	C2'-*endo* (141°)	C2'-*endo* (138°, 147°)‡
Deoxyguanosine	C1'-*exo* (122°)	C3'-*endo*§ (99°, 94°)‡
Distance of P from axis		
d(CpG)	6.0±0.3 Å	6 9 Å
d(GpC)	8.2±0.4 Å	8.0 Å
P–P distance across helix		
d(CpG)	11.4 and 12 1 Å	12.5 Å
d(GpC)	16 5 Å	15 Å
Ref.	This work	1

As the repeating unit in each helix is two consecutive bases, C and G, all helix parameters given have been expressed in terms of this repeat, rather than individual bases. Idealized parameters for the Z' helix have been obtained using a helix-building program provided by John Rosenberg.

* $d = 0.5\,(a^2+b^2)^{\frac{1}{2}}$, where *a* and *b* are crystal cell dimensions.

† *c*/6, where *c* is the cell dimension along the helix axis.

‡ Variants Z_I and Z_{II}, respectively[27]

§ Reported as C3'-*endo*, but with torsion angles closer to C2'-*exo* (ref 12)

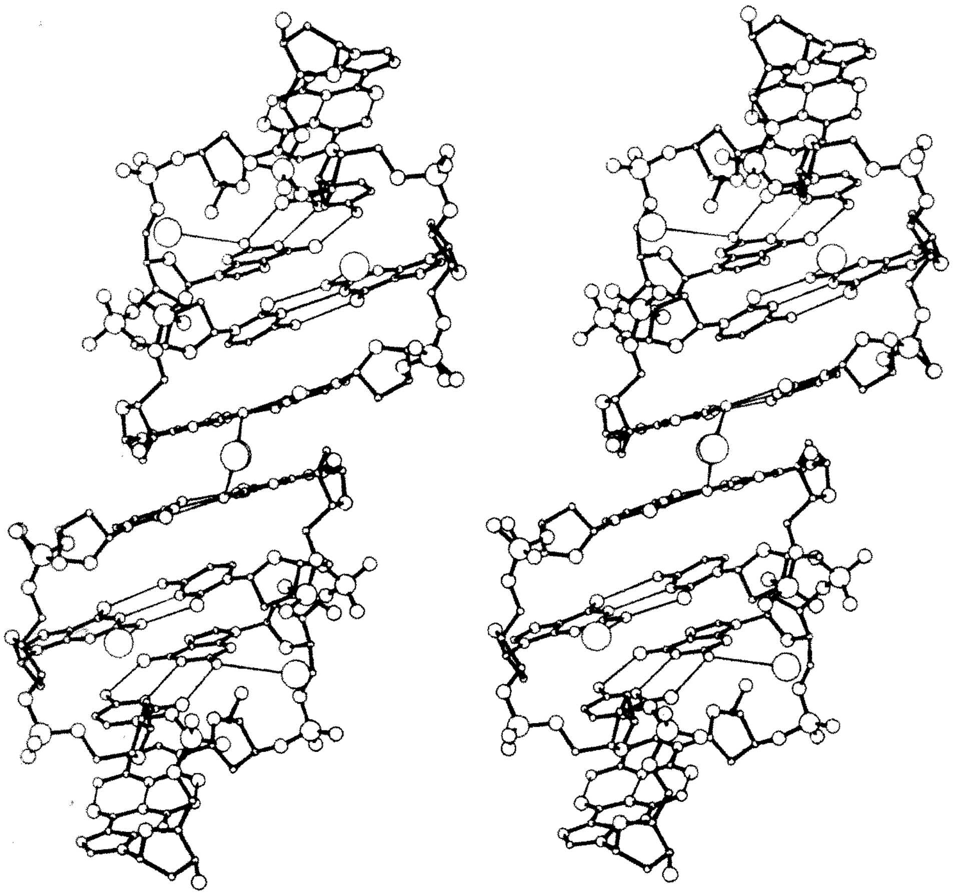

Fig. 3 Stereo drawing of stacking of neighbouring molecules along the *c* axis (vertical). These two molecules are related by a crystallographic 2-fold axis normal to the plane of the drawing through the central bridging chloride ion (large circle). This ion is actually a cigar-shaped peak elongated vertically from one guanine plane to the other, and could represent statistical occupancy of two sterically exclusive coordination positions to the two G4 guanine rings.

axis is tilted 14.3° away from the crystallographic *c* axis, which is vertical in Fig. 3.

In addition to this mismatch of molecular helix axes, the two molecules shown are not stacked in a way that continues the helical twist. For this to be true, the lower two base pairs of the top molecule in Fig. 3 should be rotated by −60° relative to the upper two base pairs of the bottom molecule. The observed rotation is only −30°, and the reason for this smaller rotation is that it maximizes base pair overlap between molecules. The absence of linking phosphate groups permits this more favourable stacking with base pairs almost eclipsing one another, whereas within a helix the GpC base stacking involves a 32° twist. The combination of a 60° helical twist within each molecule and a 30° non-helical twist between molecules turns the *c* axis into a pseudo-4_3 screw axis, leading to a strengthening of $(0, 0, l)$ reflections with $l = 4n$ and weakening of the others, as was noted from the first survey X-ray photographs[7]. The molecular packing is exactly as was predicted in Fig. 7 of ref. 7, except that the lateral 2-fold axes run between molecules rather than through the molecular centres. The 2-fold symmetry of the two halves of any one molecule is only approximate.

The idealized Z′ helix

To establish the helix axis and other helical parameters as shown in Table 1, the rotational and translational parameters that best mapped the first CG half of the molecule onto the second half had to be found analytically. As with CGCGCG, there are six repeating units per turn of ideal continuous helix. The rise per repeat and the tilt of base planes to the helix axis are both slightly greater in CGCG than in CGCGCG, but the most conspicuous differences are the deoxyguanosine sugar puckering, mentioned earlier, and the phosphate separation distances listed in Table 1.

Figure 4 shows three CGCG molecules stacked on top of one another with their helix axes coincident and with −60° rotation between them to simulate one complete turn of Z′ helix. Although each molecule is correct as observed, this idealized arrangement of them has no relationship to the actual molecular packing in the crystals. Zigzag lines connect the phosphorus atoms, including missing phosphates necessary to turn the three molecules into a continuous helix. As was noted for the Z helix, each cytosine deoxyribose ring has its oxygen atom packed against a guanine ring one step farther along the chain. Each base plane in Fig. 4 is puckered or twisted, and the observed deformations imply a steric repulsion by this close-packed sugar oxygen. A careful examination of Fig. 2 of ref. 1 reveals a similar apparent repulsion between guanine rings and deoxyribose oxygens in the Z helix, and this may be a characteristic feature of these left-handed zigzag structures.

Ion binding and helix conformational change

CGCGCG was crystallized from low-salt conditions and CGCG from high salt. The explanation for their observed difference in backbone conformation, and also for the salt dependence of the transition, may lie in the presence of bound chloride ions in the CGCG structure. DNA itself is a polyanion; if one assumes a charge of −3 on each CGCG strand and the observed crystal packing, then the crystals are 2.0 M in negative charges which must be neutralized by cations. By comparison, crystals of CGCGCG with an assumed −5 charge per strand and the published cell constants[1] are 2.6 M in negative charge, which sets a lower limit on the compensating cationic charge molarity.

Table 2 Solvent binding to base amino groups in CGCG

Base no.	N-to-solvent distance (Å)	Refined total electrons	Probable identity
Minor groove:	N2 of guanines		
G2	3.6	16	Cl^-
G4	3.5	8	Cl^-
G6	3.2	11	Cl^-
G8	2.7	5	H_2O
Major groove:	N4 of cytosines		
C1	—	—	—
C3	3.1	4	H_2O or Cl^-?
C5	3.2	7	Cl^-
C7	3.6	8	Cl^-

Although CGCGCG was crystallized from low-salt solution conditions, it is by no means in a low-salt or low-ionic strength environment within the crystals themselves, and this may be significant for the helix conformation in the crystal. CGCGCG might better be described as an intermediate salt structure.

As mentioned earlier, high-salt CGCG has additional chloride anions bound within the crystal structure, and these are listed in Table 2. In the minor groove, two sites of occupancy 16 and 11 electrons are found 3.6 Å and 3.2 Å away from the N2 amino groups of guanines G2 and G6 (Fig. 1*a*). An elongated 8-electron peak bridges N2 amino groups of guanines G4 on adjacent molecules as depicted in Fig. 3. Two more partial-occupancy chloride sites are coordinated to amino group N4 of cytosines C5 and C7 on the 'major groove' surface of the molecule. Hence, allowing for partial occupancy and other possible minor sites, we estimate that there are approximately four bound chlorides per double-stranded helix or two per monomer. This leads to a total negative charge molarity from DNA plus chloride of 3.7 M, which again places a lower limit on compensating cation molarity.

The phosphate group connecting bases G6 and C7 in CGCG is rotated out and away from the narrow groove relative to its position in CGCGCG, in a manner which suggests electrostatic repulsion between it and the chloride bound to G6 (Fig. 1*a*). The phosphate connecting G2 and C3 is rotated away from the chloride bound to G2 in a similar manner, and together these account for the 1.5 Å increase in GpC phosphate separation in the Z′ helix shown in Table 1. By contrast, in CGCGCG the phosphate and the guanine N2 amino groups are actually bridged by a hydrogen-bonding water molecule, as shown schematically in the left half of Fig. 5. This difference in phosphate position is sufficient to account for the increase in torsion angle ψ' from 82° in CGCGCG to 122° in CGCG, and the change in sugar conformation at guanine from C3′-*endo* to C1′-*exo*. It is significant that Pohl and Jovin[3] did not see a salt-induced conformational change in either poly(dI-dC) or poly(dA-dT), both of which lack the N2 amino group in the minor groove. Patel's observation that poly(dI-dC) shows only a single phosphorus NMR resonance[19] rather than the two found with poly(dG-dC)[20] indicates that the (dI-dC) polymer is not already in a zigzag left-handed helix in the conditions examined. It may be that the loss of the solvent interaction in Fig. 5 tips a delicate free energy balance in favour of a right-handed helix.

This is the first single-crystal study of an alteration in double-helix geometry produced by binding of ions, but not the first time that such mechanisms have been invoked to explain transitions monitored by circular dichroism or other methods. Both the A to A′ transition[13,14] and the B to C[16-19] may involve specific ion binding, and there may be a certain amount of parallelism in the behaviour of the three principal families of nucleic acid double helices: A, B and Z.

Why a left-handed helix at all?

To date, X-ray, circular dichroism, laser raman and/or NMR evidence has been found for a salt- or alcohol-induced transition that probably involves a right- to left-handed helix change, with poly(dG-dC) (ref. 3) and poly(dI-Br^{5}dC) (ref. 20), but not with

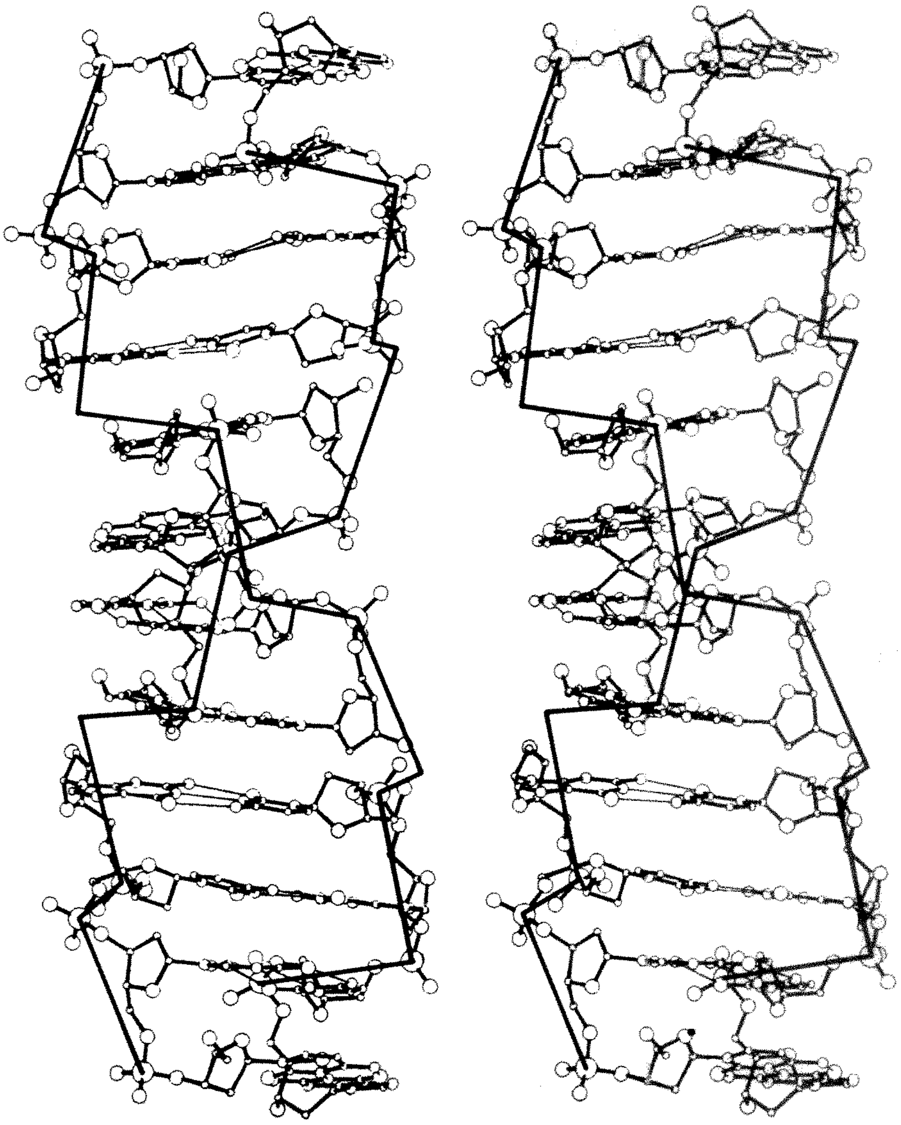

Fig. 4 Stereo view of stacking of three CGCG molecules on top of one another in such a way as to simulate a continuous 6-fold Z′ helix. Zigzag lines connect the phosphate backbone of an ideal helix, including the absent phosphates between molecules. The base plane normal is tilted 9° to the helix axis. The nearest phosphates on opposite strands are only 8.1 Å apart across the minor groove. The 'major groove' is pushed to the outside of the helix and is not a groove at all. Base plane puckering is such as to suggest steric repulsion by adjacent cytosine deoxyribose oxygen atoms. This is an isometric drawing with the viewing point at infinity; previous stereo figures have been perspective drawings with a finite viewing distance.

Table 3 Nucleic acid double-helix geometry

Family	A		B		Z	
Helix sense	Right		Right		Left	
Glycosyl bonds	*anti*		*anti*		*syn/anti*	
Sugar pucker	C3′-*endo*		C3′-*exo* (or C2′-*endo*)		Alternating	
Helix	A	A′	B	C	Z	Z′
Bases per turn	11	12	10.4–10*	$9\frac{1}{3}$	12	12
Rotation per base	32.7°	30°	34.6°–36°	38.6°	−60°/2	−60°/2
Pitch (Å)	30.9	36	33.8	31	44.6	45.7
Rise per base (Å)	2.8	3.0	3.38	3.31	7.43/2	7.61/2
Lateral packing diameter (Å)	23	23	19.3	19.2	18.1	18.4
Base tilt	16°–19°	10°	−6°	−8°	−7°	−9°
Refs						
Conformation	15	13, 14	15	16, 18	1	This work
Transformations within family	13, 14, 17		16–18, 29, 30		7, this work	
Transformation from B family	16, 21, 28		—		3–7, 20	

*Fibre diffraction experiments indicate 10 base pairs per turn, but solution measurements[31] and theoretical calculations[32] favour a slightly larger non-integral value. The entire B–C family probably represents a continuum of rotation angles in the range 34°–39°.

poly(dI-dC) itself, poly(dA-dT), poly(dA-Br^{5}dU), poly(dA-I^{5}dU), the ribonucleic acid poly(rG-rC), or any sequence lacking a purine/pyrimidine alternation[3,20]. It is not difficult to see why zigzag left-handed helices might be limited to such alternating sequences: the steric repulsion mentioned earlier between cytosine and a *syn* deoxyribose ring may be sufficient. However, why should even poly(dG-dC) adopt a left-handed geometry in preference to a right-handed helix of the A or B families, and why the apparent discrimination between various possible alternating sequences?

Properties of the six principal helices in the three helix families are compared in Table 3, and their known interconversions are schematized in Fig. 6. The three sectors of the circle about the B helix represent the three ways of bringing about transitions: lowering the humidity of fibres or films, increasing the alcohol concentration, or raising the ionic strength by increasing the salt concentration. Transitions within one family seem to be salt dependent and may even involve specific ion binding. This is certainly true for anion binding in the Z to Z′ transition, as the X-ray results have demonstrated. Ivanov[17] has also observed a correlation between the relative abilities of alkali metal cations to induce the B to C transition, the radii of the hydrated cations and the width of the minor groove as the helix winds down from 10 base pairs per turn to $9\frac{1}{3}$. Little information is available about the A to A′ transition in DNA, but in RNA the transition is salt induced. All these interconversions within families are probably non-cooperative as they occur gradually over a reasonably broad range of conditions.

The transitions between the B helix and A or Z families are sharper and are cooperative in nature[4,21]. This is not surprising, because a major change in backbone conformation at one point along the helix will make it easier for neighbouring regions to adopt the same changes, and for the transformation to propagate along the helix. Only the B to C conversion is appreciably temperature sensitive: with a ΔH° of −10 kcal, the C form is increasingly favoured as the temperature falls[22,23]. In contrast, the B to A and B to Z transitions are essentially isoenthalpic and independent of temperature[3,21].

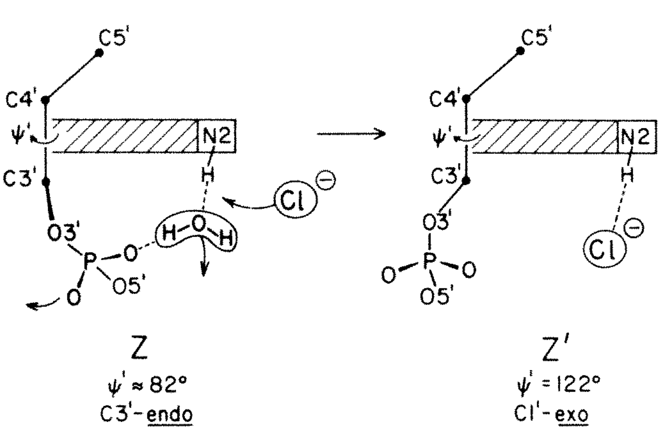

Fig. 5 Interactions between deoxyguanosine O3′ phosphate and N2 amino group in the Z helix of low-salt CGCGCG (left) and Z′ helix of high-salt CGCG (right). In CGCGCG the two groups are bridged by a water molecule, whereas in CGCG the phosphate is repelled by a bound chloride. This can account for the observed increase in ψ′ (the C4′–C3′ torsion angle) from 82° in CGCGCG to 122° in CGCG, and the change in sugar pucker from C3′-*endo* to C1′-*exo*.

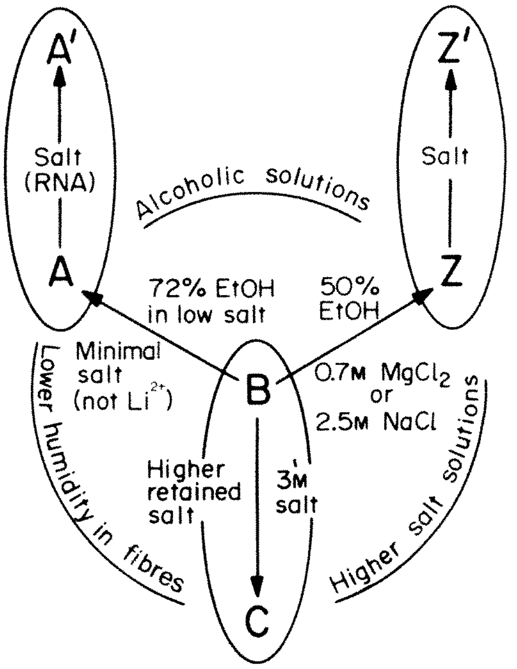

Fig. 6 Families of double helices and transitions between them. Transitions between members of one family, within oval outlines, are influenced by salt concentration. Transitions between families can be brought about by changing relative humidity and salt content in fibres or films, or changing ionic strength or solvent polarity in solution. Critical salt and ethanol concentrations, from refs. 3, 6, 17, are expressed as midpoints rather than endpoints of transitions. The B to Z transition, involving a change in helix sense, may be restricted only to certain alternating purine/pyrimidine sequences.

Ions in high-salt conditions could be imagined to have any of three roles in effecting helix transformations: (1) specific binding to DNA, (2) charge-cloud screening of phosphate–phosphate backbone repulsions, or (3) a general lowering of activity of water molecules because of hydration of ions. Phosphate screening has been invoked to explain both the B to Z and the B to C transitions[1,3,17], but this seems unlikely for two reasons. Although phosphate groups on different helix strands are closer together in the Z or C helices than in the B, they are fully as close in A and Z. If the screening argument were valid, the A helix should be stabilized by high-salt conditions. In fact, it seems to be the form of choice only in minimal salt conditions, whether in fibres or in solution. Moreover, the B to Z conversion is favoured both by alcohol and by salt, and these have opposite effects on phosphate repulsions: salt diminishes the repulsion by charge-cloud screening, but alcohol increases the strength of negative charge repulsion by lowering the dielectric constant of the surrounding medium. Manning[24] has also pointed out that, because of the phenomenon of charge condensation along a polyelectrolyte, the local ion concentration around a polyelectrolyte charge and its degree of neutralization do not follow a simple law of mass action; the phosphate charges in DNA may be largely neutralized by even a small excess of cations, as recent ^{23}Na NMR experiments have shown[25].

The one effect that is shared by the drying of fibres, increasing salt concentration and increasing the amounts of such solvents a ethanol, isopropanol or dioxane, is a general lowering of the activity or effective concentration of water molecules. Each treatment, in a sense, is a kind of local dehydration of the polymer. If one regards the B form as most stabilized by interactions with water molecules, whether specific or nonspecific, and the A and Z forms as less involved with water, then all of the inter-family transitions in Fig. 6 become consistent. Although achieved by different means, they have a common result. This interpretation would also explain why both the 'low-salt' hexamer and the high-salt tetramer of CG adopt a Z conformation in the crystal, because the water activity is lowered by both the high DNA concentration and the high cation concentration required for charge neutrality. The act of crystallization is a process of concentration for both DNA and ions.

As Fig. 6 suggests, the left-handed Z helix family actually seems to be the conformation of choice when water activity is lowered, but only if the base sequence permits its adoption. At present, this seems to require an alternating purine/pyrimidine sequence, or even poly(dG-dC). Is this preference for the Z helix sufficiently strong to produce it even if adjacent regions of DNA are of sequences that cannot adopt the Z conformation? More information is needed from crystal structure analyses of related double helices. Data have been collected in this laboratory by Drew and Wing[26] on a self-complementary DNA dodecamer with the sequence CGCGAATTCGCG, having adjacent Z-compatible and Z-incompatible segments. Other dodecamers are being synthesized with sequences that, hopefully, will exhibit classical B or C helix structures. These, and other carefully chosen sequence variants, should greatly assist the unravelling of the importance of solvent and other factors in stabilizing different helical types, the significance of the new left-handed structures and their ability to influence the conformation of neighbouring sequences that cannot adopt the Z or Z′ configuration.

We thank Michael Becker and Peter Dervan for many productive discussions of helix structure. This is contribution no. 6198 from the Norman W. Church Laboratory of Chemical Biology. This work was carried out with the support of NIH Grants GM-12121 and GM-24393, and NSF Grant PCM79-13959. H.D. was the recipient of a NIH Predoctoral Traineeship.

Received 1 April; accepted 19 June 1980.

1. Wang, A. H.-J. *et al. Nature* **282,** 680–686 (1979).
2. Arnott, S., Chandrasekaran, R., Birdsall, D. L., Leslie, A. G. W. & Ratliff, R. L. *Nature* **283,** 743–745 (1980).
3. Pohl, F. M. & Jovin, T. M. *J. Molec. Biol.* **67,** 375–396 (1972).
4. Pohl, F. M., Jovin, T. M., Baehr, W. & Holbrook, J. J. *Proc. natn. Acad. Sci. U.S.A.* **69,** 3805–3809 (1972).
5. Pohl, F. M., Ranade, A. & Stockburger, M. *Biochim. biophys Acta* **335,** 85–92 (1973).
6. Pohl, F. M. *Nature* **260,** 365–366 (1976).
7. Drew, H. R., Dickerson, R. E. & Itakura, K. *J. molec. Biol.* **125,** 535–543 (1978).
8. Itakura, K., Katagiri, N., Bahl, C. P., Wightman, R. H. & Narang, S. A. *J. Am. chem. Soc.* **97,** 7327–7332 (1975).
9. Dickerson, R. E., Weinzierl, J. E. & Palmer, R. A. *Acta crystallogr.* **B24,** 997–1003 (1968).
10. Dickerson, R. E., Kendrew, J. C. & Strandberg, B. E. *Acta crystallogr.* **14,** 1188–1195 (1961).
11. Jack, A. & Levitt, M. *Acta crystallogr.* **A34,** 931–935 (1978).
12. Levitt, M. & Warshel, A. *J. Am. chem. Soc.* **100,** 2607–2613 (1978).
13. Arnott, S., Fuller, W., Hodgson, A. & Prutton, I. *Nature* **220,** 561–564 (1968).
14. Arnott, S., Hukins, D. W. L., Dover, S. D., Fuller, W. & Hodgson, A. R. *J. molec. Biol.* **81,** 107–122 (1973).
15. Arnott, S. & Hukins, D. W. L. *Biochem. biophys. Res. Commun.* **47,** 1504–1509 (1972).
16. Marvin, D. A., Spencer, M., Wilkins, M. H. F. & Hamilton, L. D. *J. molec. Biol.* **3,** 547–565 (1961).
17. Ivanov, V. I., Minchenkova, L. E., Schyolkina, A. K. & Poletayev, A. I. *Biopolymers* **12,** 89–110 (1973).
18. Arnott, S. & Selsing, E. *J. molec. Biol.* **98,** 265–269 (1975).
19. Patel, D. in *Nucleic Acid Geometry and Dynamics* (ed. Sarma, R. H.) 185–231 (Pergamon, New York, 1980).
20. Patel, D. J., Canuel, L. L. & Pohl, R. M. *Proc. natn. Acad. Sci. U.S.A.* **76,** 2508–2511 (1979).
21. Ivanov, V. I., Minchenkova, L. E., Minyat, E. E., Frank-Kamenetskii, M. D. & Schyolkina, A. K. *J. molec. Biol.* **87,** 817–833 (1974).
22. Brahms, S., Brahms, J. & Van Holde, K. E. *Proc. natn. Acad. Sci. U.S.A.* **73,** 3453–3457 (1976).
23. Chan, A., Kilkuskie, R. & Hanlon, S. *Biochemistry* **18,** 84–91 (1979).
24. Manning, G. S. *Q. Rev. Biophys.* **11,** 179–246 (1978).
25. Anderson, C. F., Record, M. T. Jr & Hart, P. A. *Biophys. Chem.* **7,** 301–316 (1978).
26. Wing, R. M., Drew, H., Tanaka, S., Itakura, K. & Dickerson, R. E., in preparation.
27. Wang, A. H.-J. *et al. Science* (submitted).
28. Tunis-Schneider, M. J. & Maestre, M. F. *J. molec. Biol.* **52,** 521–541 (1970).
29. Hanlon, S., Brudino, S., Wu, T. T. & Wolf, B. *Biochemistry* **14,** 1648–1660 (1975).
30. Wolf, B. & Hanlon, S. *Biochemistry* **14,** 1661–1670 (1975).
31. Wang, J. C. *Proc. natn. Acad. Sci. U.S.A.* **76,** 200–203 (1979).
32. Levitt, M. *Proc. natn. Acad. Sci. U.S.A.* **75,** 640–644 (1978).

Helical periodicity of DNA determined by enzyme digestion

D. Rhodes & A. Klug

MRC Laboratory of Molecular Biology, Hills Road, Cambridge CB2 2QH, UK

The periodicity of DNA has been determined by binding short, stiff pieces of DNA to a flat surface and using DNase I to probe the accessibility of the phosphodiester bonds. We have found that the distance between successive DNase I cutting sites is 10.6 ± 0.1 bases for the DNA immobilized on three different surfaces. We identify this value with the number of base pairs per turn of the DNA double helix in solution.

FOR many years it was assumed that the B form of DNA, observed in X-ray diffraction patterns from fibres at high humidity, represented the structure of DNA in solution [1-3]. The B form has 10 base pairs per turn of the helix, but recent studies have suggested a value close to 10.5 (refs 4, 5). However, the disagreement persists[6]. We describe here a new approach to the problem of the helical repeat of free DNA, which gives results of high precision.

An accurate determination of the helical periodicity of DNA in solution is required to follow in detail the folding of DNA from solution into nucleosomes, the elementary building blocks of chromatin. We have postulated[4] a change in the DNA periodicity when nucleosomes are formed, in order to reconcile the model of a nucleosome core derived from X-ray crystallographic studies, where the DNA in each nucleosome is wound into about two turns of a superhelix, with measurements of the superhelicity on closed, circular DNA extracted from SV40 chromatin, which showed a change of linkage number nearer one[7].

Our approach is based on that used previously to probe the helical periodicity of DNA on the nucleosome[8-11]. The action of DNase I (and some other nucleases) on chromatin or on nucleosome cores is to produce, after denaturation of the DNA, a set of single-stranded fragments differing in size by about 10 bases. Presumably the enzyme tends to attack the regions of the DNA backbone which are well exposed, and so will produce a spectrum of fragment sizes, which will repeat with approximately the periodicity of the DNA double helix. Liu and Wang[12] found a similar distribution of DNase I fragments when studying DNA interacting with gyrase, and also observed it in the case of DNA bound to hydroxylapatite. This work, together with the development by Lutter[9] of a high resolution gel electrophoresis

0028-0836/80/320573—06$01.00

system capable of resolving random sequence DNA fragments differing in size by a single nucleotide, stimulated the experiments described in this article.

A double-stranded DNA fragment, nominally 140 base pairs long, has been immobilized on a flat, inorganic surface, then lightly digested with DNase I and the fragments produced separated by the denaturing, high resolution gel system. The distance between successive DNase I cutting 'sites', that is the distance between neighbouring groups of accessible phosphodiester bonds, is found to be 10.6 ± 0.1 bases. Because of the simple geometry of the experiment, and because the same value is found for the DNA bound to three different inorganic surfaces, we believe that the measured distance between DNase I cutting sites directly reflects the helical periodicity of DNA free in solution.

Design of the experiment

The idea behind the experiment is that if a straight, stiff piece of DNA lies on an atomically flat surface, the access of the enzyme to one side of the DNA helix is hindered in a uniform way along its length (Fig. 1). Only the most exposed phosphodiester bonds will be accessible to the enzyme, and these will recur with the periodicity of the double helix (Fig. 2*b*). The distance between the sites of attack of the nuclease gives the helical repeat directly. In the absence of a hindering surface all phosphodiester bonds are equally accessible and no 'image' of the periodicity is seen.

There are two methods for measuring the periodicity of the nuclease cutting sites. The first is to use a piece of DNA of defined length and incorporate a radioactive label at, say, the 5' terminus. Then the length of a single-stranded fragment produced by the nuclease action gives the position of cutting from the 5' end, and the intensity of the band on the autoradiograph gives essentially the frequency of cutting at that site. A kinetic analysis of the cutting rate can be made[8]. For this method to work, all the DNA molecules must lie in the same azimuthal orientation relative to the surface, and this assumption is justified by the results. The second method, which does not require a fixed length of DNA and is independent of the orientation of the molecule, is to introduce the label after the nuclease digestion, but this gives less total information (see below).

As a source of short, random sequence, double helical DNA pieces of defined length, we have used '140-base pair DNA' extracted from nucleosome cores, actually 148 ± 2 bases long. The persistence length of DNA is about 600 Å, so this DNA behaves like stiff rods[13,14].

To immobilize the DNA on the surface, that is to stop it rolling about, inorganic crystals were chosen which naturally formed flat surfaces, and where divalent cations were present or could be supplied. To exclude the possibility of a particular surface imposing a particular periodicity on the DNA by epitaxial action, experiments were performed with three different materials having different surface structures, namely calcium phosphate, magnesium phosphate and mica. To minimize interactions between the DNA molecules, fine crystalline dispersions were used so that the binding surface areas were very large in comparison with the concentration of DNA.

Materials and methods

Double helical DNA was extracted with water-saturated phenol/chloroform (1 : 1 v/v) from preparations of nucleosome cores[8], precipitated twice with ethanol and the precipitate dissolved in 20 mM Tris-HCl, *p*H 8.0, and 20 mM NaCl. The length distribution of the single strands ranged from 146 to 150 bases with an average of 148 bases.

The 5' termini of the 140-base pair DNA were labelled with ^{32}P by incubating with [γ-^{32}P]ATP (Amersham) and T4 polynucleotide kinase (Boehringer) essentially as described by Lutter[8,9]. The efficiency of labelling was not less than 50%. When DNA was digested with DNase I before end-labelling, the DNase I fragments were labelled with ^{32}P as described elsewhere[8]. To be able to quantify the binding of ^{32}P-labelled DNA to a surface, the excess [γ-^{32}P]ATP was separated from the labelled DNA fragment on a non-denaturing, 6% polyacrylamide gel[8].

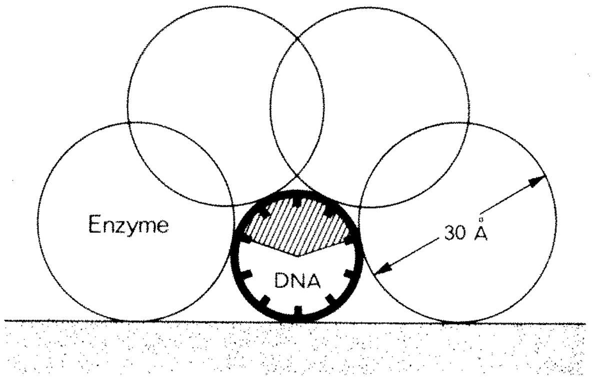

Fig. 1 Schematic drawing of the accessibility of an enzyme to DNA lying on a flat surface. The surface restricts a spherical enzyme with a diameter of 30 Å to a maximum of four accessible phosphodiester bonds. (DNase I, if spherical, would be larger than shown and have even less access to the DNA.)

The calcium phosphate and magnesium phosphate surfaces were prepared by mixing potassium phosphate with either $CaCl_2$ or $MgCl_2$ to a final concentration of 40 mM potassium phosphate and 25 mM $CaCl_2$ or 25 mM $MgCl_2$ in 50 mM Tris-HCl, *p*H 8.0. Magnesium phosphate readily forms platelet-like crystals whereas calcium phosphate forms a polycrystalline precipitate. The mica surface was prepared by grinding up mica sheets, washing and resuspending the powder at 0.2 g ml^{-1}, in 50 mM KCl, 8 mM $MgCl_2$ and 20 mM Tris-HCl, *p*H 8.0. Similar conditions were used to bind DNA to mica for electron microscopy[15].

A typical experiment consisted of adding 5 μg ^{32}P-5'-end-labelled 140-base pair DNA to 50 μl of a suspension of calcium phosphate or magnesium phosphate or mica, and leaving for 1–2 h at room temperature. The extent of binding can be monitored by pelleting the suspension and measuring the radioactivity in the pellet.

Incubations with DNase I (Worthington) were carried out in conditions where all the DNA was bound to the surface. In the experiments using calcium or magnesium phosphate, 10 U DNase I was used at 37 °C for 5–20 s, but with mica only 0.5 U DNase I was needed to obtain the same extent of digestion. Incubations were stopped by adding EDTA in excess of the divalent cation. The DNA was extracted with chloroform/isoamyl alcohol (24 : 1 v/v) and precipitated twice with ethanol. DNase I digests of the parent nucleosome cores, which were used as size markers, were carried out as reported elsewhere[9].

Samples of both DNase I-digested 140-base pair DNA and nucleosomes were fractionated by 6–10% denaturing high resolution gel electrophoresis, which is capable of resolving random sequence DNA fragments that differ in size by only one base[9].

Experiments with 140-base pair DNA

The results of a typical experiment where the 5'-end-labelled 140-base pair DNA preparation was bound to calcium phosphate, magnesium phosphate and mica, and then digested with DNase I are shown in Fig. 3, lanes a–c. In the autoradiograph a pattern of fine bands can be seen, which represent single-stranded DNA fragments differing in size by only one base. The intensities of the fine bands vary sinusoidally, showing broad maxima at regular intervals, about 10 bases apart.

The 'ladder' formed by the broad bands or maxima is an image of one side of the DNA structure as seen by the nuclease. A group of successive phosphodiester bonds, which are accessible to DNase I, give in the autoradiograph a set of intense fine bands. This set of fine bands, if unresolved, would give a broad band, or envelope, whose centre corresponds to a local maximum in the frequency of cutting on the DNA. We call this a 'site'[9].

The distance between DNase I cutting sites can be obtained by simply counting the number of fine peaks between the maxima, corresponding to sites, and then dividing by the number of sites traversed. In Fig. 4 the number of fine peaks between sites S3 and S9 is 63, giving a value of $^{63}/_{6} = 10.5$ bases. A more objective analysis of the densitometer tracings using Fourier methods, described later, gives 10.6 ± 0.1 bases as the distance between consecutive DNase I cutting sites.

Note that the absolute lengths of the fragments, which are determined by including known length markers in the gel separation (Fig. 3, lane N), and which locate the sites with respect to the 5′ end, have no role in this determination.

Interpretation of the DNase I cutting pattern

We have interpreted the above results as if most of the DNA molecules lie in the same azimuthal orientation on the surface, and also as if both DNA strands were being cut at exactly the same distance from each respective 5′ terminus.

The simplicity of the DNase I pattern in Figs 3 and 4, which show maxima with halfwidths of 4–5 bases and about 10 bases apart, suggests that these assumptions are valid. After allowing for the distribution of DNA lengths present in the original preparation[9], the width of the DNase I cutting site is only about 2 bases. This is what one might expect when the access of a molecule, with a minimum diameter of 30 Å, to the DNA helix is hindered by a flat, backing surface (Fig. 1). Moreover, as either or both of the two 5′ termini in a molecule are labelled at random, what is observed is the composite frequency of cutting on the two strands of the double helix. The two strands must be cut in a symmetrical fashion to give rise to such a clean pattern. This means that the two ^{32}P-labelled 5′ termini bear the same relationship to the binding surface, which is geometrically equivalent to saying that the unique dyad through the centre of the DNA molecule lies perpendicular to the surface (Fig. 2*b*). If this were not the case and the orientations of the molecules were random, then each 5′ end of the two strands in a molecule would give rise to its own series of bands, but displaced with respect to each other. The maxima in the cutting pattern would then be much broader than we have observed.

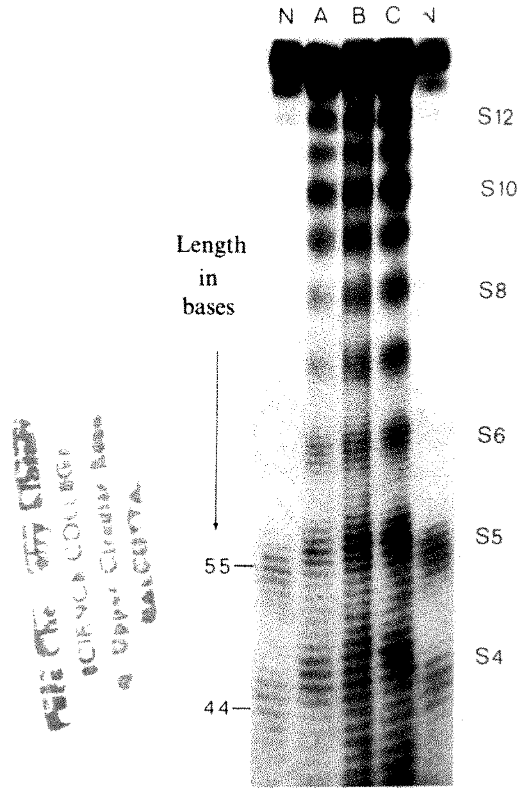

Fig. 3 Autoradiograph of DNA fragments from electrophoresis in a high resolution, denaturing gel made with 8% acrylamide and 1.35% methylene-bis-acrylamide. Lanes A, B and C contain DNA from DNase I digests of/the ^{32}P-end-labelled 140-base pair DNA preparation bound to calcium phosphate (A), mica (B) and magnesium phosphate (C). Lane N contains DNA from DNase I digests of ^{32}P-end-labelled nucleosome cores. Broad bands in lanes A, B and C, corresponding to sites of DNase I attack, are labelled S4 to S12, while the absolute fragment length in bases is indicated for lane N on the left.

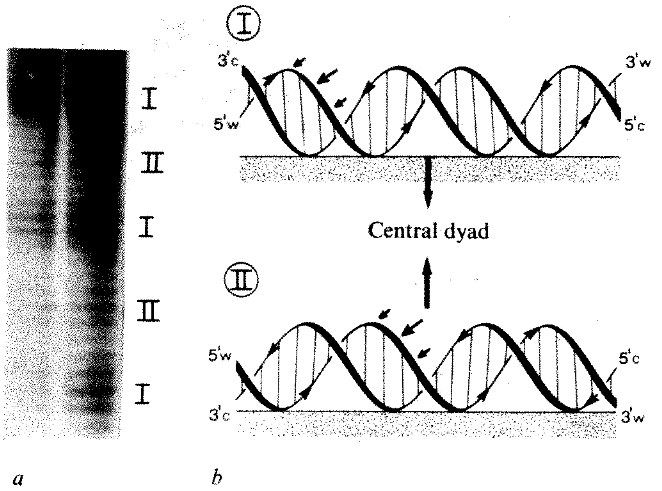

Fig. 2 Two settings of DNA on the surface. *a*, Autoradiograph from a region of a denaturing, high resolution gel electrophoresis of a sample showing two patterns of band maxima, I and II, displaced relative to each other by five bases. *b*, Schematic drawing of the two possible azimuthal orientations of a DNA molecule bound symmetrically to a surface. Setting I represents the major azimuth of the DNA, giving rise to the DNase I fragments as also observed in Fig. 3, lanes A, B and C. Setting II represents the minor azimuth of the DNA, giving rise to a set of DNase I fragments which migrate halfway between the major set of DNase I fragments. The piece of DNA in II is rotated through 180° with respect to I. A site of DNase I cutting is represented by three arrows. (This site need not occur at the most exposed position, furthest from the surface, as the enzyme need not cut at the site of binding.)

Although the results speak for themselves, it seems at first sight unlikely that all the DNA molecules would lie down in the same orientation. While clearly the bulk of the energy of binding to the surface comes from the phosphates along the length of the molecule, these would be indifferent to the orientation adopted. However, the binding of the ends of the molecule depends on the particular orientation and presumably it is the need to balance this interaction at the two ends which decides the symmetrical orientation adopted.

Further reassurance that the DNA molecules dispose themselves symmetrically on the surface comes from some experiments where a second, fainter pattern of bands can be seen lying halfway between those in the normal pattern, also repeating about every 10 bases (Fig. 2*a*). We believe the second pattern comes from DNA molecules which have rotated through 180° with respect to the first setting, so that the 5′ termini are still symmetrically disposed, and the central dyad is still perpendicular to the surface. This rotation would give an apparent translation of half of the periodicity, about 5 bases (Fig. 2*b*, I, II). When the second setting is present, never at more than about 30%, then counting between maxima becomes more difficult, but the Fourier analysis still gives the same value of 10.6 bases. That it is the ends which determine the particular orientation is made clear by an experiment in which the 140-base pair DNA preparation was treated with nuclease S1, which would remove any bases projecting at the 5′ end. This treatment results in both settings I and II appearing with equal proportion.

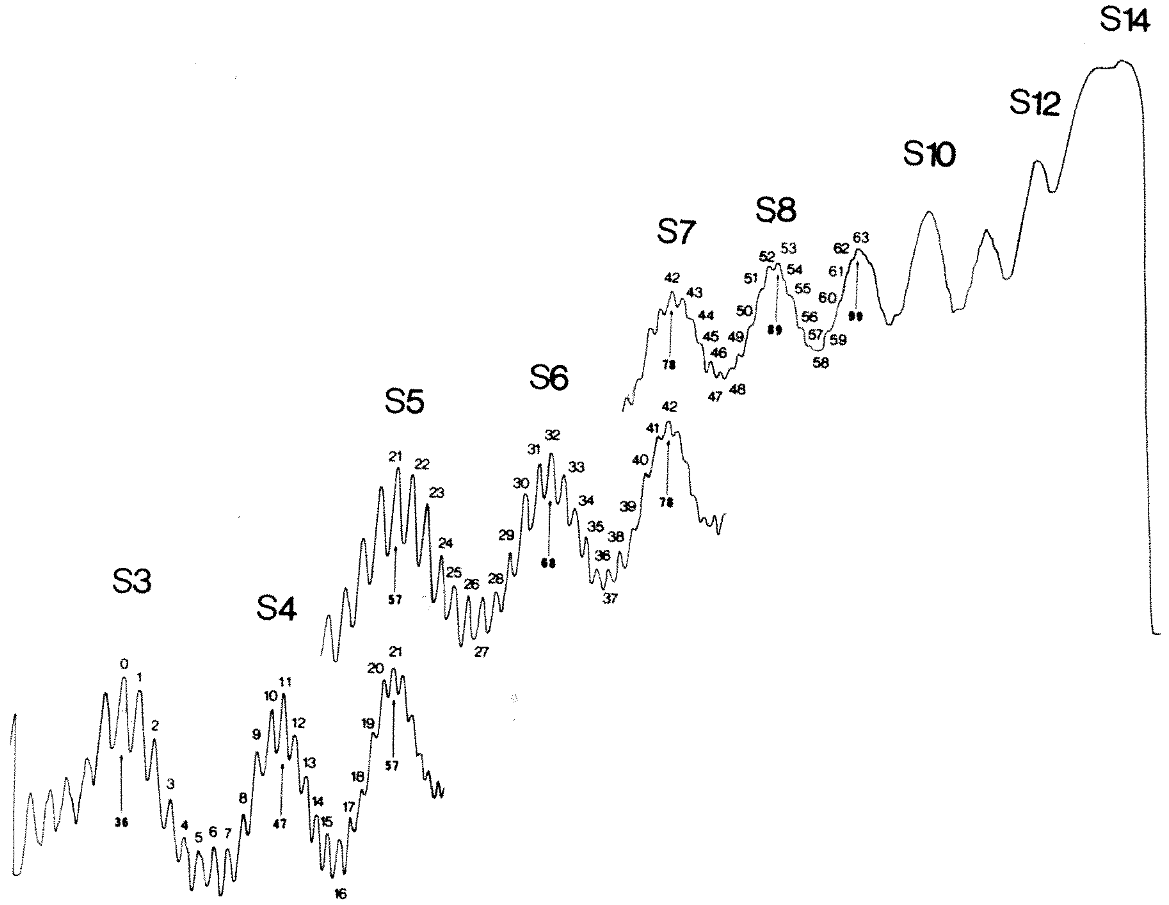

Fig. 4 Densitometer tracings of autoradiographs from the high resolution gel in Fig. 3, lane A (S5–S14), and of the same sample electrophoresed for a shorter time (S3–S5). The fine peaks, which are produced by DNA fragments differing in size by one base, have been numbered from 0 to 63 over the five bands from S3 to S9. The absolute fragment length in bases is indicated under the broad peaks in the densitometer tracing.

Probability of DNase I cutting at the sites

The probability of cutting at each site on the 140-base pair DNA can be found by cutting out the broad bands from the gels and measuring the radioactivity in each. However, the percentage of radioactivity in a band must be corrected for any cutting which might have occurred between that site and the labelled 5′ end[8].

The result is shown in Fig. 5. The probabilities of cutting at each of the 13 sites are approximately equal, but there is a clear tendency for an alternation between successive sites. This is to be expected, as in a DNA helix with a screw of 10.6 bases, there is almost an exact integral repeat after two turns. This local alternation in cutting frequency can indeed be seen directly in Figs 3 and 4, in the region of sites S9 and S13. Apart from this small modulation, analysis of Fig. 5 shows that all sites are essentially equivalent and cut at random, again justifying one of the assumptions behind the experiment.

Fourier analysis of the cutting frequency

The gel patterns may be analysed by Fourier transformation, which is more objective and accurate than simply counting the number of fine peaks between maxima, corresponding to sites. Moreover, it is the only method applicable when there are superimposed patterns with different periodicities or, what is more germane (see below), several patterns with the same periodicity but different starting points.

A Fourier transformation program applied to the amplitudes of the fine peaks in a densitometer tracing of an autoradiograph of a high resolution•gel produces a frequency spectrum of the periodicity (ies) present. The results of the method applied to such densitometer tracings as given in Fig. 4 are shown in Fig. 6. The breadth of the central maximum and the side lobes are just what would be expected from the limited length of pattern used in the analysis, in this case five repeats. The good agreement with the theoretical function expected (of the form $\sin 2\pi NX/2\pi NX$ where N is the number of bases and X the periodicity in 'reciprocal bases') indicates that a single waveform is making up the DNase I patterns of Figs 3 and 4.

The frequency spectra given by the experiments with the 140-base pair DNA bound to the three surfaces agree well with each other. The mid-points at half height are: calcium phosphate, 10.58 bases; magnesium phosphate, 10.6 bases; and mica, 10.62 bases. These values coincide well within the experimental error, which we estimate is 0.1 base. We conclude that the distance between DNase I cutting sites reflects a property of the DNA structure that is conserved when the DNA is bound to different inorganic surfaces.

Experiments with DNA of different lengths

To eliminate the possibility that the helical periodicity of 10.6 bases per turn of DNA found above could somehow depend on the particular length or end distribution of DNA used, we have also investigated a preparation of nominally 200-base pair DNA pieces extracted from nucleosomes (rather than from nucleosome cores). This contains a range of sizes, from 140 to 240 base pairs. With such a wide distribution of lengths, the external 5′ end-labelling technique loses its simplicity. The radioactive label is now introduced after the nuclease treatment, to label the new 5′ ends of the fragments produced ('internal labelling').

The result of such an experiment is shown in Fig. 7, together with that of a 140-base pair DNA preparation treated in the same way. A pattern of bands with intensity maxima at about

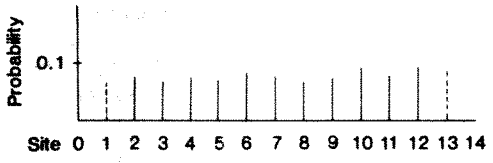

Fig. 5 The normalized probability of DNase I cutting at each site on the 140-base pair DNA fragment bound to calcium phosphate. S1 and S13 are shown dashed as these values are less accurate than the values at the other sites. The diagram is for the early stages of digestion, when the average number of cuts per single strand is 0.98.

every 10 bases is seen, but this has a higher background than the patterns shown in Fig. 3. The difference between the two experiments is that in Fig. 3 and Fig. 7, channel A, the only fragments seen are those beginning at the ^{32}P-labelled 5′ end and ending at a DNase I cut, whilst in the case of the '200-base pair DNA' (Fig. 7, lane D) all the fragments produced by DNase I are seen because the ^{32}P label was introduced after incubation with the enzyme. The pattern obtained by internal labelling does not depend on the azimuthal orientation of the DNA molecules. The first experiment gives a direct map of the cutting sites, whereas the second gives the autocorrelation function containing a superposition of similar patterns, all with different starting points.

Thus in Fig. 7, lane D the gel scans do not show a clear sinusoidal pattern, so direct counting of peaks between maxima is more difficult. The Fourier method gives a frequency of cutting of 10.8 ± 0.3 bases (not shown). This value is, however, less reliable than that given by the external 5′-end-labelling method, because it is weighted by the shorter fragments which occur in greater number than the long ones, whereas in the 'external' method all fragments occur in equal proportions (in the early stages of digestion). Even the 140-base pair DNA piece, of defined length, gives a less accurate value when the internal cuts, rather than original 5′ ends are labelled. However, in the gel, the ladder of band maxima from the 200-base pair DNA (Fig. 7, lane D) lines up well with that of the 140-base pair DNA (Fig. 7, lane E), showing that the periodicity of DNase I cutting is independent of the length of DNA used.

In these two patterns, each fragment is produced from two DNase I cuts. Thus, the distance between neighbouring DNase I cutting sites can be obtained simply by dividing the absolute length of a fragment (hitherto not required) by the fragment number (Fig. 7). This method gives a periodicity of DNase I cutting of 10.6 bases, in agreement with the results obtained from the external labelling experiment.

Consistency of absolute size of fragments and the periodicity

The ladder of broad bands produced from DNase I fragments labelled after digestion (Fig. 7, lanes D or E), lies nearly halfway between the ladder of DNase I fragments produced from the 5′-end-labelled 140-base pair DNA preparation (Fig. 7, lane A). This tells us that, for this particular length of DNA, the origin of the series of DNase I cutting sites is 4.5 bases away from its 5′ terminus (compare 2*b*, I). This value, together with the values of the absolute lengths of the fragments found in the experiment shown in Figs 3 and 4, provides a check on the helical periodicity. For instance, the centre of site S5 is at 57.3 bases (Fig. 4), which would give the origin of DNase I cutting at 57.3–5 × 10.6 = 4.3 bases, from the 5′ end, in very good agreement with the independently measured value.

Other measurements of the helical periodicity of DNA

It has long been recognized that crystal packing tends to produce an integral number of base pairs per turn of a helix, permitting repeated regular contacts along the fibre length[16].

Prompted, in part, by the issue raised by us[4], Wang used a novel method to determine the helical repeat of DNA in solution[5]. This makes use of the effects of oligonucleotide insertions on the superhelicity of closed, circular DNA. He found a value of 10.4 bases per turn, which is close to the value of 10.6 bases we have found. Theoretical calculations by Levitt have suggested that straight DNA free in solution is most stable with 10.6 base pairs per helical turn rather than 10 (ref. 17).

The DNA fibres have been re-investigated by Zimmerman and Pfeiffer[6] who concluded, from X-ray diffraction studies, that highly swollen fibres still had the 10 base pairs per turn of the

Fig. 6 Frequency spectrum of DNase I cutting patterns computed by Fourier transformation. ^{32}P-end-labelled 140-base pair DNA fragment bound to: ▲, calcium phosphate; ■, magnesium phosphate; and ●, mica. In each case the mid-point at half height of the main peak occurs at 10.6 bases. 107 points (53 bases) were used in the analysis for all three surfaces.

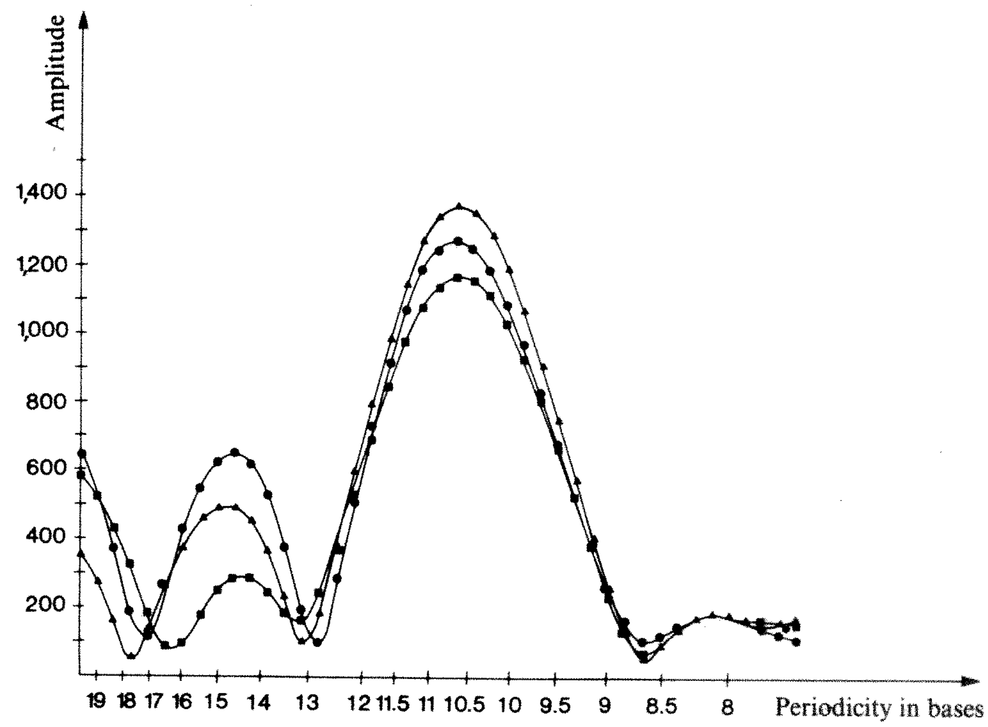

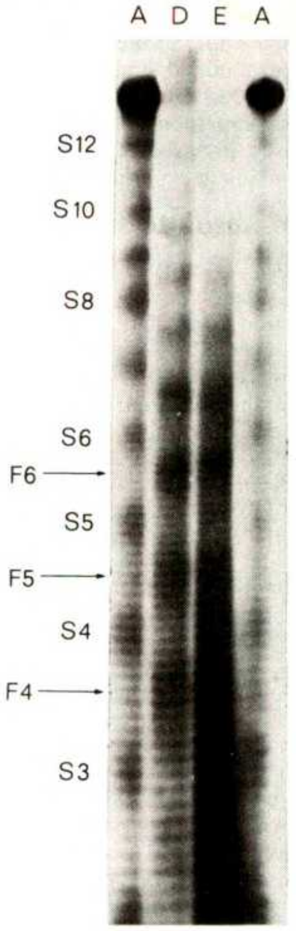

Fig. 7 Autoradiograph from a high resolution, denaturing gel made with 8% acrylamide and 1.35% methylene-bis-acrylamide. Lane A contains DNA from DNase I digests of the ^{32}P-end-labelled 140-base pair DNA preparation (external label). Lane D contains DNA fragments from DNase I digests of the 200-base pair DNA preparation, labelled after digestion (internal label). Lane E contains DNA fragments from DNase I digests of the 140-base pair DNA preparation, labelled after digestion. Broad bands in lane A corresponding to DNase I sites are labelled S3 and S12, while F4 to F6 indicate the DNase I fragments in lanes D and E. In all three experiments the DNA was bound to calcium phosphate.

helix. In our laboratory, J. T. Finch and L. C. Lutter (unpublished) have carried out X-ray studies on partially oriented gels of short stiff pieces of DNA, 150–300 base pairs long, in which the interparticle centre-to-centre distance was about 30 Å, but still found a helical repeat of 10 base pairs . Clearly these results disagree with our finding of 10.6 base pairs per turn of the DNA helix in solution. We can only conclude that in these gels or fibres of DNA, the molecules still interact, however weakly, through several layers of water and influence each other to produce an integral screw. It is relevant that structuring of water on the surface of clays appears to decay with a distance of about 10 Å (ref. 18).

Other measurements of the helical repeat are less reliable. Circular dichroism measurements and small angle X-ray scattering of DNA in solution have been used but the results are questionable because of the complexity of the data[19,20]. Griffith[21], from an electron microscope study, has reported a pitch of 10.5 base pairs, but in view of the systematic study by Vollenweider *et al.*[22] on the effects of dehydration during sample preparation, it is unlikely that the measurements made by Griffith referred to DNA in the B form.

Finally, it is known that the helical periodicity of DNA in solution is influenced, to some extent, by cation type and concentration, and temperature[23,24], but the effects on our results would amount to changes of not more than 0.1 base pair. In our experiments the cations and the ionic strength have been somewhat different, for the DNA bound to the three different inorganic surfaces, but nevertheless the same helical repeat was obtained.

Relationship to the DNA in nucleosome cores

The knowledge of the helical periodicity of DNA in solution is not only of intrinsic interest, but has important implications for the supercoiling of DNA in chromatin. To resolve the linkage number paradox, referred to in the introduction, we[4] suggested that the helical periodicity of DNA changes from 10.4–10.7 base pairs in solution to about 10 in the nucleosome. The value of 10.6 base pairs we have found for the helical periodicity of DNA in solution agrees with this prediction. However, the prediction was dependent on taking the value of 10 base pairs per turn for DNA wrapped on the nucleosome core, the value then given by Noll[25] from his DNase I digestion studies.

Ironically however, more accurate measurements show that the average distance between DNase I cutting sites on the DNA in nuclei[26] and on the nucleosome[9] is about 10.4 bases, rather than 10. Nevertheless, as pointed out in ref. 26, the periodicity of DNase I cutting, although closely related to the structural periodicity, need not be the same. This is because of the geometry of the nucleosome structure, where all the cutting sites on the DNA do not offer the same environment to the enzyme. In fact, it was concluded by Prunell *et al.*[26] that DNase I fragments from nucleosome DNA, that are multimers of 10.4 bases, could have been produced from a helical repeat of 10 base pairs. This question will be further discussed elsewhere (L. C. Lutter and A. K., in preparation).

In contrast to the case of DNA on the nucleosome, the geometry of our experiment, with the DNA lying on a flat surface, is simple. The accessibility of each turn of the double helix to the enzyme should remain constant along the length of the DNA fragment. This is confirmed by the result that the probability of cutting at successive sites is essentially the same (Fig. 5), quite unlike the results for DNA on the nucleosome[8]. We therefore conclude that the distance between DNase I cutting sites, on DNA immobilized on a surface, directly reflects the helical periodicity. Moreover, because we have found the same value of 10.6 ± 0.1 bases for three different surfaces with different atomic geometry, we identify this value with the number of base pairs per turn of the DNA double helix in solution.

We thank Drs P. J. G. Butler and R. A. Crowther for helpful discussions, and Dr. Crowther for writing the Fourier transformation program.

Received 27 February; accepted 28 May 1980.

1. Watson, J. D. & Crick, F. H. C. *Nature* **171,** 737–738 (1953).
2. Langridge, R., *et al. J. molec. Biol.* **2,** 38–64 (1960).
3. Arnott, S. & Hunkins, D. W. L. *Biochem. Biophys. Res. Commun.* **47,** 1504–1507 (1972).
4. Finch, J. T. *et al. Nature* **269,** 29–36 (1977).
5. Wang, J. C. *Proc. natn. Acad. Sci. U.S.A.* **76,** 200–203 (1979).
6. Zimmerman, S. B. & Pheiffer, B. H. *Proc. natn. Acad. Sci. U.S.A.* **76,** 2703–2707 (1979).
7. Germond, J. E., Hirt, B., Oudet, P., Gross-Bellard, M. & Chambon, P. *Proc. natn. Acad. Sci. U.S.A.* **72,** 1843–1847 (1975).
8. Lutter, L. C. *J. molec. Biol.* **124,** 391–420 (1978).
9. Lutter, L. C. *Nucleic Acids Res.* **6,** 41–56 (1979).
10. Simpson, R. T. & Whitock, J. P. Jr *Cell* **9,** 347–353 (1976).
11. Noll, M. *J. molec. Biol.* **116,** 49–71 (1977).
12. Liu, L. F. & Wang, J. C. *Cell* **15,** 979–984 (1978).
13. Hays, J. B., Mager, M. E. & Zimm, B. H. *Biopolymers* **8,** 531–536 (1969).
14. Kovacic, R. T. & van Holde, K. E. *Biochemistry* **16,** 1490–1498 (1977).
15. Portmann, R. & Koller, Th. *Proc. 6th Eur. Congr. Electron Microscopy*, Jerusalem, Vol. II, 546–547 (1976).
16. Dover, S. D. *J. molec. Biol.* **110,** 699–700 (1977).
17. Levitt, M. *Proc. natn. Acad. Sci. U.S.A.* **75,** 640–644 (1978).
18. Olejnik, S. & White, J. W. *Nature phys. Sci.* **236,** 15–16 (1972).
19. Chan, A., Kilkuskie, R. & Hanlon, S. *Biochemistry* **18,** 84–91 (1979).
20. Bram, S. *J. molec. Biol.* **58,** 277–288 (1971).
21. Griffith, J. D. *Science* **201,** 525–527 (1978).
22. Vollenweider, H. J., James, A. & Szybalski, W. *Proc. natn. Acad. Sci. U.S.A.* **75,** 710–714 (1978).
23. Wang, J. C. *J. molec. Biol.* **43,** 25–39 (1969).
24. Anderson, P. & Bever, W. *Biochemistry* **17,** 594–601 (1978).
25. Noll, M. *Nucleic Acids Res.* **1,** 1573–1579 (1974).
26. Prunell, A. *et al. Science* **204,** 855–858 (1979).

LETTERS

The complex radio galaxy 4C47.51 (1919+479)

J. G. Robertson

Netherlands Foundation for Radio Astronomy, PO Box 2, 7990 AA Dwingeloo, The Netherlands

An observation of the source 1919+479 with the Westerbork Synthesis Radio Telescope (WSRT) at $\lambda = 21$ cm has shown it to have a remarkable morphology, probably that of a very unusual and very large wide angle tail radio galaxy. It is situated in a cluster of galaxies at an estimated redshift of ~0.1. Although distortions of the morphology of radio sources caused by a cluster environment are well known, for example in producing normal head–tail and wide angle tail sources, the observed structure of 1919+479 is shown here to differ in several respects from previously known cluster sources.

1919+479 was included in a study[1,2] of 4C sources situated in the direction of Zwicky clusters of galaxies, in which observations at 2,695 MHz with the NRAO 300-ft telescope and the three-element interferometer (operated as a synthesis instrument) were presented. The former showed that the overall size was about 8 arc min, the latter showed a component coincident with the associated optical galaxy, and two other hot-spots. The Zwicky cluster in this case was Zw1916.8+4855 (which is of exceptionally large angular extent, nearly 20°, ref. 3). However, inspection of the optical field has shown that the galaxy identified with 1919+479 is almost certainly situated in a background cluster (see below).

The present observation was made in July 1979, at which time the WSRT consisted of 13 available telescopes along a 1.3 km east–west line. Details of the telescope and standard data reduction procedures are given elsewhere[4]. One 12 h observation was sufficient to obtain data on baselines from 36 m to 1,296 m with an increment of 36 m. This resulted in a grating ring radius of 20×27 arc min ($\alpha \times \delta$) and, with the usual tapered illumination of the aperture, a synthesized beam of 26×35 arc s. After Fourier transformation of the data, the CLEAN algorithm[5] was applied, and the resulting total intensity map is shown in Fig. 1. The noise level in this map is 0.48 mJy per beam area. The map has been corrected for the attenuation due to the primary beam of the individual telescopes; however, this is only 7% at most for the emission from 1919+479.

The galaxy previously proposed[2] as the optical identification is marked in Fig. 1. The radio structure is clearly very unusual. The diffuse region labelled F exhibits an approximately constant opening angle of ~47°, but is abruptly cut off at its far end in a straight line perpendicular to the ridge line. Connecting this component to the galaxy at C is a jet or tail which has two sharp bends. Between C and D the jet is unresolved, but in region E it has a half-power width of ~20 arc s. The western lobe of the source includes the bright component B and a 'tail' A. Although in gross morphology the lobe BA resembles an independent head–tail galaxy, and has no detectable emission connecting it with the eastern complex, it is almost certainly part of the same source. This is because inspection of the Palomar Sky Survey reveals no galaxy of $m_R \lesssim 18$ in the region of hot-spot B or its northern extension. Identification with a galaxy fainter than this limit would imply an unrealistically large size (≳4 Mpc) for the lobe. Moreover, the map of polarized intensity (prepared from the present WSRT observation) shows that the emission from region B is ~12% polarized, in contrast to the low degrees of polarization normally found near the parent object (for example, ~1% for component C). The 'head' B is also clearly extended both along the head–tail axis and perpendicular to it (the latter at region B1), unlike normal head–tail sources. Finally, the integrated flux densities of the two lobes are similar (see below). If this interpretation is correct, 1919+479 is a very unusual wide angle tail galaxy.

Of the three components shown in the NRAO interferometer map[2], two are confirmed by the present observation (B and C), while the third, located to the south-west of the weak source south of the apex of component F, is not confirmed.

No measured redshift is available for the galaxy identified with 1919+479. However, if the galaxy is assumed to have an absolute magnitude of $M_p = -21.7$ ($H_0 = 75$ km s^{-1} Mpc^{-1}), typical of the galaxies associated with wide angle tailed radio sources in clusters[6], then its apparent magnitude (on the PSS red plate) of ~14 mag implies a redshift of ~0.1. Using this estimate, the projected extent of both lobes is ~700 kpc. This places 1919+479 among the largest known cluster sources. The integrated flux densities are $S_{1412} = 0.47 \pm 0.03$ Jy and 0.61 ± 0.03 Jy for the eastern and western lobes respectively, giving a total luminosity at 1.4 GHz of 1.6×10^{24} W Hz^{-1} sr^{-1}, typical of tailed or complex sources. Integration of the contour diagram from the NRAO 300-ft observation[2] shows that $S_{2695} = 0.57 \pm 0.03$ Jy, giving a spectral index $\alpha_{1.4}^{2.7} = 1.0 \pm 0.1$ ($S \propto \nu^{-\alpha}$). The equipartition magnetic field[7] in component F is ~1.7 μG and the minimum energy density in relativistic particles and magnetic field is $\sim 2 \times 10^{-13}$ erg cm^{-3} (taking the emitting volume as a cone). If this component is confined by thermal pressure of a hot intracluster medium (ICM), then $nT \gtrsim 280$ cm^{-3} K, where n is the number density of protons in the ICM, and T is its temperature. In the diffuse component A the equipartition field is ~2.2 μG and the minimum value of nT required to confine the component laterally is ~660 cm^{-3} K. These values are typical of large diffuse radio source lobes (irrespective of whether or not the source is located in a cluster of galaxies)[8-10].

On the Palomar Sky Survey red plate the galaxy identified with 1919+479 is seen to be surrounded by a group or cluster of galaxies: there are five galaxies within 1 arc min and about 10 within 3 arc min. They are 2–3 magnitudes fainter than the radio source identification, consistent with their being typical cluster galaxies at a redshift of ~0.1, while the identified galaxy is the

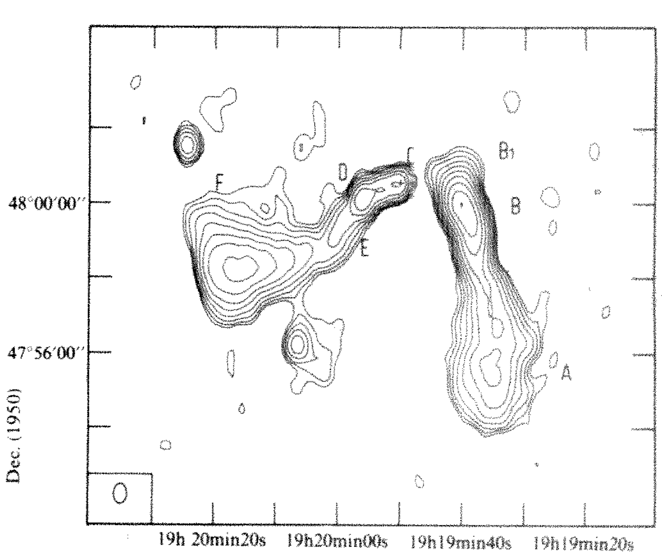

Fig. 1 Total intensity distribution of 1919+479 at 1412 MHz. The contour levels (logarithmically spaced) are 0.9, 1.5, 2.5, 4.2, 7.0, 11.5, 19.5, 32.5, 54.0 and 90 mJy per beam area. Letters identify components of the source discussed in the text; +, the position of the associated galaxy. The inset ellipse represents the half-power beam.

0028-0836/80/320579—02$01.00

dominant member of the cluster. The total extent of the cluster is difficult to determine because of the low galactic latitude (15.2°, that is well below the latitude for completeness of the Abell catalogue[11]) and because of possible confusion with fainter members of the overlying very extended Zwicky cluster. However, there are ~55 possible members within a radius of 15 arc min (the Abell radius for a cluster of redshift ~0.1). The cluster could, therefore, be as rich as Abell's[11] richness class 0 or perhaps 1, but further optical observations will be required to examine the cluster membership of the various galaxies. Radial velocity information from measured redshifts of the galaxies is also needed for more detailed modelling of the interaction of the radio source with the surrounding medium. The two small diameter radio sources to the north and south of component F have no optical identifications on the PSS.

In comparison with other complex extended sources, 1919+479 has a large size (unless the adopted redshift is a serious overestimate). With lobe sizes of ~700 kpc and an overall extent of ~1.2 Mpc, this source would considerably exceed the size of previously known large cluster sources such as IC711 (550 kpc, ref. 12), 1709+397 (460 kpc, ref. 13) or even the regions of diffuse emission in Abell 2256 (~650 kpc, ref. 8) or the Coma cluster (~450 kpc, ref. 14). Only the giant radiogalaxies such as 3C236 (~4 Mpc, ref. 15) and 3C326 (1.7 Mpc, ref. 9), which are not situated in clusters, significantly exceed the estimated size of 1919+479. The gap in the emission between the galaxy at C and the nearest part of component B/B1 is also large, although not exceptionally so. Its length is ~140 kpc, much larger than the gaps of 3–10 kpc commonly found near the heads of head–tail galaxies[16,17], and greater than that in wide angle tail sources such as 3C465 (25 kpc, ref. 18) but of the same order as the gap between the nuclear source and the western component of 1200+519 (~90 kpc, ref. 13) if the wide angle tail interpretation of the latter source is adopted. A further similarity between these two sources is the existence of a continuous tail or jet of emission extending from the galaxy to the second lobe. The physical processes responsible for the morphology of these two sources may therefore be similar, although it should be noted that the overall size of 1200+519 is only 220 kpc, and neither of its lobes is individually exceptional.

To return to the morphology of 1919+479, there are several interesting relations between the two lobes. First, a line passing through hot-spot D and the galaxy also passes perpendicularly through a noticeable protrusion B1 in the western lobe. (This feature is well above the noise level and is seen very distinctly in a map made with no tapering of the observations in the aperture plane.) This line is likely to be the axis of recent activity. Moreover, an extension of the ridge line in the triangular component F passes through the peak of the hot-spot B and is parallel to the line DCBI. This would be consistent with simultaneous ejection of the material which has given rise to the prominent components F and B, and with projected motion of the galaxy in an approximately northward direction being responsible for the overall wide angle tail morphology. The clearest problem which this source poses to interpretation within present models is the formation of the uniformly diverging region F, with its termination along a straight line. Projection effects may play a part in the appearance of this component, but for them to be a major influence the long axis of the component must lie almost along the line of sight, which would imply an extremely large physical size. An unusual three-dimensional structure seems unavoidable. Another interesting feature is the one-sided jet CDE. The presence of a surrounding medium (presumably an intracluster medium) would seem to be essential to explain the observed morphology, but making detailed models of this source will be possible only after observations at other frequencies become available, enabling the spectral index and polarization properties to be examined in detail, and after a reliable redshift is found from optical observations.

The Westerbork Synthesis Radio Telescope is operated by the Netherlands Foundation for Radio Astronomy with the financial support of the Netherlands Organization for the Advancement of Pure Research (ZWO). I thank Dr R. D. Ekers, Dr R. G. Strom and Professor Dr H. van der Laan for comments, Dr J. O. Burns for pointing out that 1919+479 lies in a background cluster, and R. Windhorst for assistance in the preparation of overlays for optical examination of the field.

Received 13 February; accepted 3 June 1980.

1. Burns, J. O. *Astr. J.* **83,** 1143 (1978).
2. Burns, J. O. & Owen, F. N. *Astr. J.* **84,** 1478 (1979).
3. Zwicky, F. & Herzog, E. *Catalogue of Galaxies and of Clusters of Galaxies* Vol. III (California Institute of Technology 1966).
4. Högbom, J. A. & Brouw, W. N. *Astr. Astrophys.* **33,** 289 (1974).
5. Högbom, J. A. *Astr. Astrophys. Suppl.* **15,** 417 (1974).
6. Valentijn, E. A. *Astr. Astrophys.* **78,** 367 (1979).
7. Pacholczyk, A. G. *Radio Astrophysics* (Freeman, San Francisco, 1970).
8. Bridle, A. H., Fomalont, E. B., Miley, G. K. & Valentijn, E. A. *Astr. Astrophys.* **80,** 201 (1979).
9. Willis, A. G. & Strom, R. G. *Astr. Astrophys.* **62,** 375 (1978).
10. Ekers, R. D., Fanti, R., Lari, C. & Ulrich, M-H. *Astr. Astrophys.* **69,** 253 (1978).
11. Abell, G. O. *Astrophys. J. Suppl.* **3,** 211 (1958).
12. Wilson, A. S. & Vallée, J. P. *Astr. Astrophys.* **58,** 79 (1977).
13. Miley, G. K. & Harris, D. E. *Astr. Astrophys.* **61,** L23 (1977).
14. Valentijn, E. A. *Astr. Astrophys.* **68,** 449 (1978).
15. Strom, R. G. & Willis, A. G. *Astr. Astrophys.* **85,** 36 (1980).
16. Downes, A. *Mon. Not. R. astr. Soc.* **190,** 261 (1980).
17. Owen, F. N., Burns, J O. & Rudnick, L. *Astrophys. J. Lett* **226,** L119 (1978).
18. van Breugel, W. J. M. *Astr. Astrophys.* (in the press).

IUE observations of the atmospheric eclipsing binary system ζ Aurigae

Robert D. Chapman

Laboratory for Astronomy and Solar Physics, NASA-Goddard Space Flight Center, Greenbelt, Maryland 20771

ζ Aurigae is an eclipsing binary star system with a property shared by only a few other systems. It consists of two stars in orbit around one another: a cool supergiant star (spectral type *K2* II) and a hot main sequence (spectral type *B8* V) star. The supergiant star is nearly 200 times larger than the Sun, while the main sequence star is only about seven times larger than the Sun. The Earth lies in the orbital plane of the two stars, and thus they periodically eclipse one another. When the relatively small *B* star goes into eclipse behind the cool supergiant star, its light passes through extended outer gaseous layers—the outer atmosphere—of the cool star. Thus the *B* star is an astrophysical light source which serves as a probe of the atmosphere of the *K* star. The eclipses, which occur every 972 days, have been well studied at visible wavelengths[1,2]. We report here IUE observations of the ζ Aur stellar system carried out between September 1979 and January 1980. A preliminary look at the data shows the advantage of UV observations of the system. There is strong evidence for cool, outflowing material near the primary star and hotter material farther from the primary perhaps in a shockwave. The onset of the atmospheric phase of the eclipse of the system—difficult to predict because of the irregularities of the supergiant atmosphere—began between 15 September and 1 November 1979.

As the *B* star goes into eclipse behind the *K* star, one wishes to study spectral lines produced by absorption of the *B*-star photospheric light by the *K*-star atmosphere. At roughly 4,300 Å the two stars are equally bright, and thus at this and longer wavelengths the photospheric light of the *K* star makes interpretation difficult. However, at UV wavelengths the *K* star is much fainter than the *B* star, and interpretation of the observations is greatly simplified. In the IUE case, with spectra in the wavelength range 1,200–3,200 Å, the *K*-star continuum is negligible, and we can observe spectral lines produced by the extended *K*-star atmosphere with no contamination from the *K*-star photospheric spectrum, throughout the entire wavelength range.

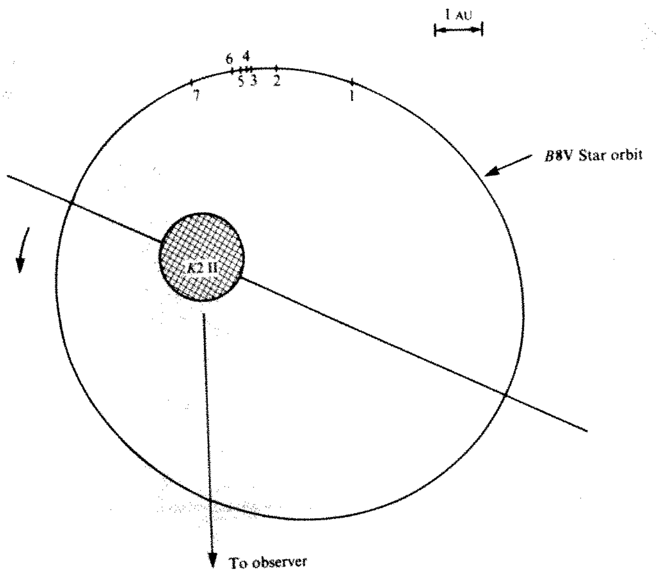

Fig. 1 Schematic diagram of the ζ Aur system.

Spectra have been obtained when the *B* star was as the positions numbered in Fig. 1. The 1979 dates of the observations are: (1) 15 September; (2) 1 November; (3) 13 November; (4) 15 November; 18 November; (6) 22 November and (7) 16 December.

The spectrum obtained on 15 September, a pure absorption spectrum, looks very similar to the spectrum of the *B*7 + *B*8 star 64 Orionis, supplied by D. S. Leckrone (see Fig. 2). The major differences between the ζ Aur spectrum and the 64 Ori spectrum is the presence of very strong multi-component absorption lines of Si II (1,260 Å, 1,264 Å), Si IV (1,394 Å, 1,403 Å), C IV (1,548 Å and 1,551 Å), and the presence of Mg II resonance doublet (2,795 Å and 2,802 Å) with strong P Cygni profiles.

The profile of the Mg II doublet Fig. 3 shows the classical P Cygni shape, indicative of an expanding shell. The absorption component of each line appears to show a reversed profile, characteristic of the strongest solar lines such as the Ca II, *H* and *K* lines. However, the appearance is undoubtedly due to two absorption lines being present, probably because of a double shell. This conclusion is supported by the spectra taken during the total phase of the eclipse. If the peak in the absorption line were chromospheric emission from the *K* star—as one finds in the case of the reversed Ca II-line profiles—then that central emission should remain visible during total eclipse even after the continuum and the absorption lines have vanished. In fact, the central emission is not present and, therefore, it must have been continuum showing between two partially resolved absorption lines.

The spectra obtained between 1 and 18 November show a large number of absorption lines not present in the 15 September spectrum. The absorption lines increase in number and strength during the time period (Fig. 4). The 1 November spectrum has been studied in some detail, and a large fraction of the absorption lines have been identified. Ionic spectra which have changed from 15 September to 1 November, showing that they arise from an extended atmosphere or dense wind region surrounding the *K* star include Al II, Al III, Cr II, Mn II, Fe II, Ni II and Ca II. This wavelength region includes the resonance lines of many of these ions. The majority of the lines correspond to lines observed in the UV solar emission line spectrum from Skylab[3,4]. The C IV, Si IV and Mg II lines observed in the 15 September spectrum are also visible in the 1 November spectrum but are very little changed in appearance. We conclude that the high ionization potential lines are formed far from the *K* star, whereas the group of low-ionization-potential lines which show significant changes are formed in cool plasma nearer to the *K* star: probably a cool wind. These cool wind lines seem to be shifted longward relative to the centre of mass of the binary system. Thus, the outflow must be dynamically influenced by the *B* star.

The high ionizations potential lines are typified by the C IV lines (Fig. 5). Each of the C IV lines consists of a narrow line, near the rest wavelength, and a longward shifted broad line. If one looks at the entire sequence of C IV lines, the narrow lines clearly remain unchanged, whereas the broad lines increase in strength into the eclipse. I believe that the narrow, constant line is probably interstellar, while the broad line is formed near the *B* star, perhaps in a shockwave produced by the *B* star moving supersonically through the *K*-star wind. Highly turbulent motion in the shockwave can account for the breadth of the absorption line.

On 22 November the *B*-star continuum had disappeared, and an emission line spectrum was present. The emission lines, which include C II, Si II, Si III, Si IV, S II, Mn II, Fe II, Ni II, correspond closely to the absorption lines observed in earlier

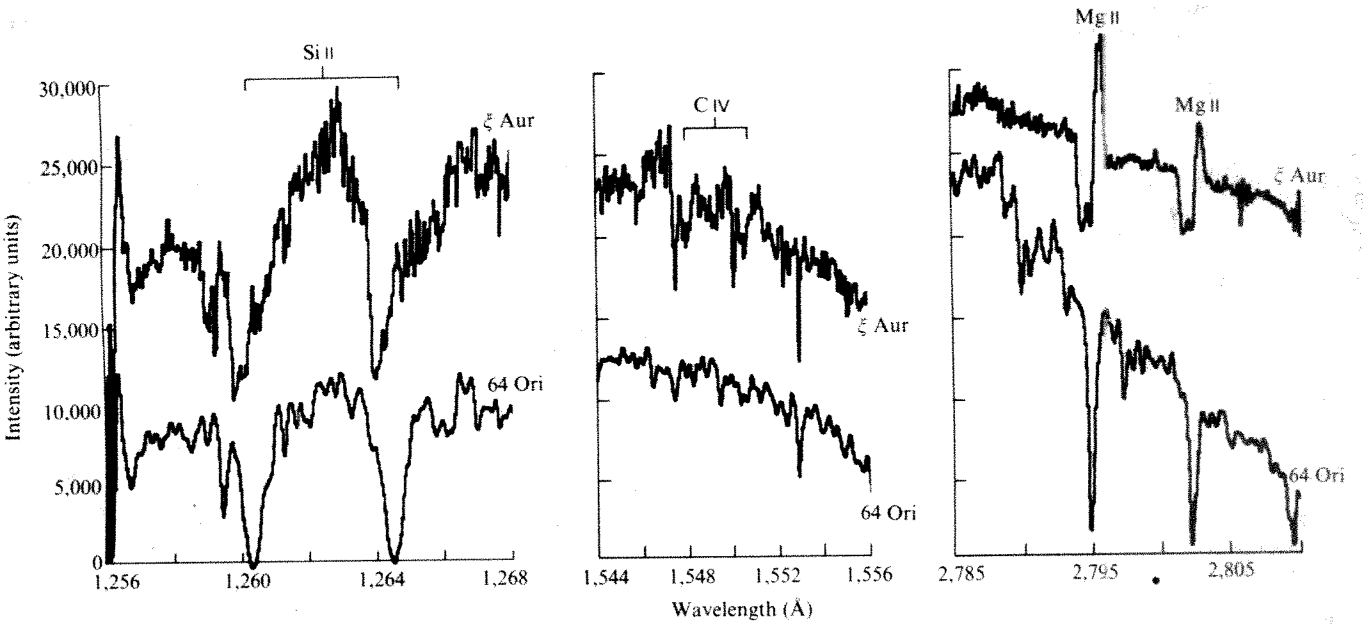

Fig. 2 Comparison between spectra of ζ Aur and the single *B*8 V star 64 Ori.

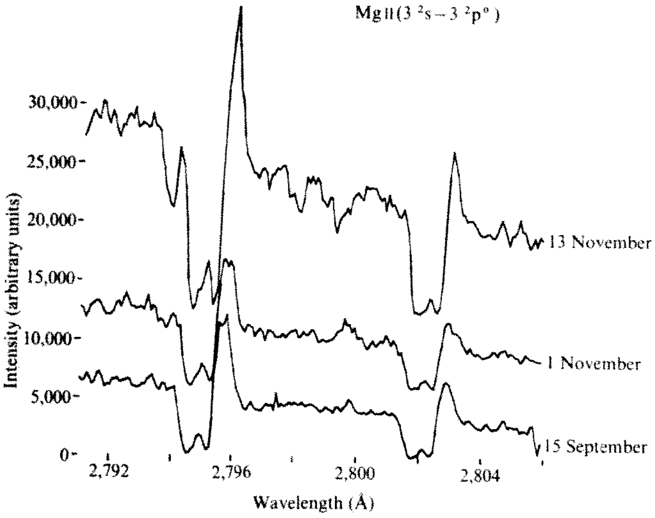

Fig. 3 The Mg II resonance doublet lines show strong P Cygni profiles. The appearances of the lines change very little with time, as can be seen from these three samples. The amplitude increase on 13 November is an exposure effect. On 22 November, the continuum level was too faint to record, and only the emission remained.

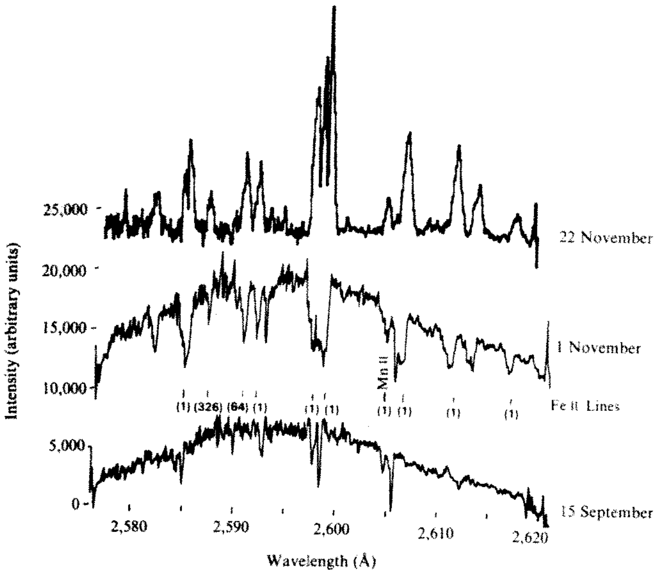

Fig. 4 Three exposures showing the region of the Fe II resonance lines. Between 1 and 22 November 1979, the absorption lines continue to increase in width. Multiplet number is indicated on figure.

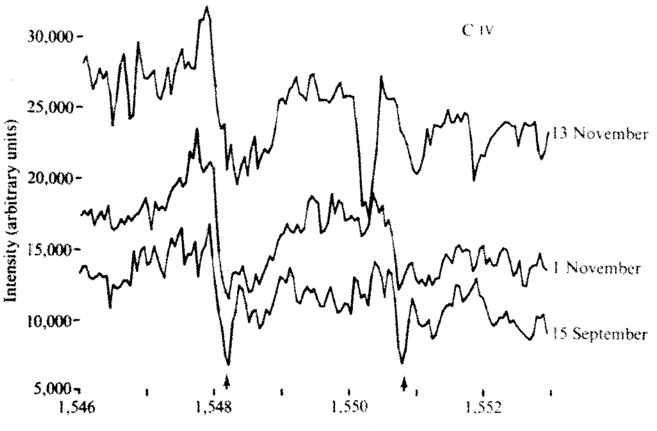

Fig. 5 The spectrum region of the C IV resonance lines. Each line seems to consist of a shortward feature and a longward feature. The longward feature is broader and shallower than the shortward. By 13 November, the features have blended together. Arrow marks laboratory wavelength.

spectra. We have searched for intercombination lines that have been observed in many stellar shell spectra, particularly in the low ionization stages of oxygen. None were found. The density of the material is therefore quite high, probably in excess of $10^{12}\,\mathrm{cm}^{-3}$.

We are now embarking on a more thorough study of the ζ Aur data, including additional observations during total eclipse and egress. Full details will be published elsewhere.

We thank the project scientist and observatory administrator for the opportunity to carry out this project, and the resident astronomers and staff of the IUE observatory at the NASA-Goddard Space Flight Center for practical assistance.

Received 15 January; accepted 18 April 1980.

1. Wilson, O. C. in *Stars and Stellar Systems* Vol. 6 (ed. Greenstein, J. L.) 436–464 (University of Chicago Press, 1960).
2. Wright, K. O. in *Vistas in Astronomy* Vol. 12, 147–182 (Pergamon, New York, 1970).
3. Doschek, G. A., Feldman, J. & Cohen, L. *Astrophys. J. Suppl.* **33**, 101–111 (1977).
4. Cohen, L., Feldman, J. & Doschek, G. A. *Astrophys. J. Suppl.* **37**, 393–405 (1978).

IR observation of a persistent meteor train

M. A. Hapgood

Department of Physics, University of Southampton,
Southampton SO9 5NH, UK

A long-lived (>32 min) persistent meteor train has been observed with a low light television camera which was sensitive only to radiation between wavelengths of 700 and 900 nm. The peak emission from the train was about 2×10^{17} photons $\mathrm{s}^{-1}\,\mathrm{m}^{-1}$ and the meteor which produced the train had a magnitude corrected to the zenith of about −6. It is suggested here that this IR emission arises from the excitation of the atmospheric band of molecular oxygen ($b^1\Sigma_g \rightarrow X^3\Sigma_g$) by the sodium catalytic process, a process which Baggaley[1–3] has previously proposed to be responsible for the visible radiation from persistent meteor trains.

The persistent train was recorded between 01.30 and 02.02 UT on 19 September 1979 from the Jungfraujoch Observatory in the Swiss Alps (46°33′N, 7°59′E, 3,570 m). The train was observed with an image isocon television camera used in integration mode to image structure in the near IR airglow. A picture was produced every half second and was recorded on a time lapse video tape recorder. A camera tube with a photocathode having an extended red (S-25) photocathode spectral response was used and a Schott RG715 filter was placed over the front of the camera lens to eliminate visible light. Thus the effective spectral region of the camera was confined to a region between 700 and 900 nm as shown in Fig. 1 (obtained by combining manufacturers' specifications).

The meteor which produced the train appeared at 01.30.14 (±1 s) UT. The luminous trail started outside the field of view, entered at the upper edge (elevation 17°) and ended in the middle of the field (elevation 12°). The range of the meteor from the camera may be estimated at 300 ± 50 km. As the meteor travelled 2.9° in 0.5 s at the estimated range of 300 km the velocity $v \gtrsim 30\,\mathrm{km\,s}^{-1}$. Comparing the brightness of the meteor with Jupiter recorded under similar conditions gave m_v of −3 for the brightest part, which was at an elevation of 14°. Using the correction given by Lovell[4], the magnitude of the meteor adjusted to the zenith was about −6.

The train which persisted after the passage of the meteor originated from a part of the meteor trail at elevations between 14.0 and 14.5°. Taking the range as 300 km it follows that the train lay between 15 and 20 km above the end height of the meteor. Assuming that the end height lay between 70 and 80 km suggests that the train lay at heights between 85 and 100 km.

During the period of observation the persistent train moved eastwards across the field of view. The upper and middle parts of the train moved very rapidly. By 02.02 UT they were 18° east of the original azimuth which indicates a drift velocity of 50 ± 10 m s^{-1}. The lower part of the train became drawn out behind the main body of the train and parallel to the drift direction. The drift velocity of the trailing edge of the train was estimated to be about 20 m s^{-1}. Thus there was considerable wind shear at the lower end of the train. This shear and the comparatively high velocity above it suggest that the train lay well above the mesopause and confirm the range of heights deduced from elevation measurements.

The brightness of the train was estimated by comparison with field stars of spectral class A. At the beginning, the brightest part of the train was comparable to a star of magnitude +5 but by the end of the period of observation it was barely visible above the limiting magnitude +7. To convert stellar magnitudes into photon emission rates we assume that the stars radiate as black bodies. Thus in our spectral passband a fifth magnitude star of class A_0 gives a photon flux at the camera of 2×10^8 m^{-2} s^{-1}. As we used a fairly narrow spectral passband, we neglect the differences between the spectra of the stars and the train and take the photon flux from the train to be 2×10^8 m^{-2} s^{-1} at the camera. This flux came from a portion of the persistent train which corresponded to a single resolution element in the picture (about 0.2° of angular extent, equivalent to 1 km at the estimated range of 300 km). By assuming that the meteor train was at right angles to the line of sight we obtain a line emission rate from the persistent train of 2×10^{17} photons s^{-1} m^{-1}. This estimate will be seriously in error only if the meteor were travelling in a direction close to the line of sight. This seems unlikely as the meteor train was of significant angular extent (>6°).

The depth of the Earth's shadow[5] in the region of the train at the time of observation was about 1,000 km so the light was generated in the train rather than being scattered sunlight. The light from such self luminous trains is thought to be generated by a cyclic chemical process first suggested by Chapman[6,7]:

$$O_3 + M \rightarrow MO + O_2 \qquad (1)$$

$$O + MO \rightarrow M + O_2 \qquad (2)$$

Metal atoms (M) released by the meteoroid catalyse the conversion of atomic oxygen and ozone to diatomic oxygen. If the reactions are sufficiently exothermic the products may be in excited states and emit photons as they decay to their ground states. The process may continue almost indefinitely as the metal atoms are recycled and the energy is extracted from the atmosphere. Baggaley has studied the case of sodium[1-3] for which both reactions have high rates[8]: a significant proportion of the sodium atoms produced by reaction (2) are in the excited ^2P state which decays by D line emission. Baggaley[3] estimated the production rate for the ^2P state from data on the sodium nightglow and found that to produce a clearly visible persistent train (one emitting $>5\times10^{15}$ photons s^{-1} m^{-1}) a meteor of $m_v > -2$ is required. Because almost all persistent trains (>96%) are produced by meteors brighter than $m_v \sim -2$ Baggaley concludes that the visible light emission from persistent trains can be explained solely by this process—the sodium catalytic process.

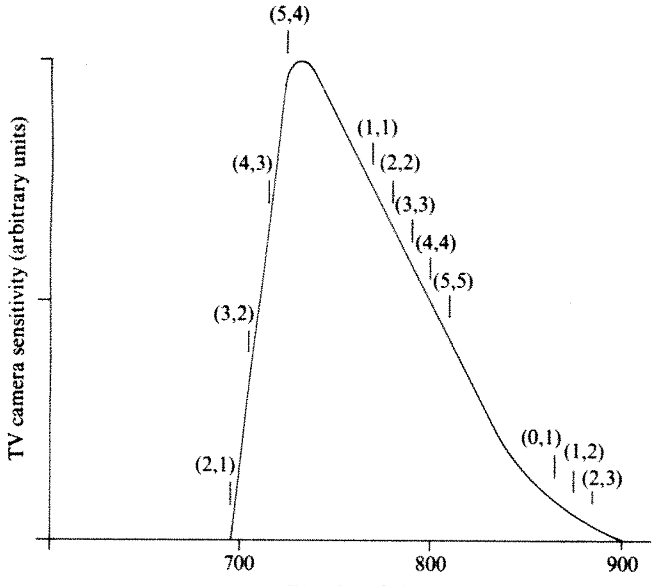

Fig. 1 The effective spectral response of the television camera and the positions of the vibrational bands of the atmospheric system of O_2.

The present radiation detected from the persistent train cannot be sodium light. We therefore consider whether the oxygen molecules in reactions (1) and (2) may be produced in excited states. The $b^1\Sigma_g$ state of molecular oxygen, in the absence of quenching, decays to the ground state emitting radiation in a band between 700 and 900 nm, as shown in Fig. 1. (The (1,0) and (0,0) bands are not shown as these connect with the vibrational ground state of O_2 and so are lost to a ground-based observer by absorption in the atmosphere.) The transition is foribdden for electric dipole radiation and so it has a long radiative lieftime of 12 s (ref. 9). The quenching of O_2 ($b^1\Sigma_g$) proceeds mainly by collision with N_2 and has a rate constant[9] $K = 2\times10^{-21}$ m^3 s^{-1}. This leads to significant quenching[10] only at heights below 85–90 km. It follows that the molecular oxygen emissions will not be quenched at the heights of the train reported here.

The production of O_2 ($b^1\Sigma_g$) is permitted in reactions involving many elements but because of the high reaction rates, the most favourable case is sodium. If we study reaction (2) for sodium, we find that, with an energy[1] for the reaction of 2.5 ± 0.2 eV, there are four variations of the basic reaction which are energetically and spin allowed:

	energy required	
$NaO\,(X^2\pi) + O\,(^3P) \rightarrow Na\,(^2S) + O_2(X^3\Sigma)$	0 eV	(3a)
$Na\,(^2S) + O_2(a^1\Delta)$	0.98 eV	(3b)
$Na\,(^2S) + O_2(b^1\Sigma)$	1.63 eV	(3c)
$Na\,(^2P) + O_2(X^3\Sigma)$	2.09 eV	(3d)

For reactions (3b) and (3c) the energy required is that needed to excite the lowest vibrational level ($v = 0$) in the upper electronic state. The total energy available from the reaction is much more than this so the higher vibrational levels may be excited (up to $v = 5$ for the $b^1\Sigma_g$ state). Reaction (3d) produces the sodium D line emission discussed by Baggaley and reaction (3c) produces molecular oxygen emission in the near IR. If the reaction were to take branch (3c) as often as (3d) we may expect a photon emission rate from molecular oxygen comparable to the photon emission rate from sodium. This gives an emission rate[3] of 5×10^{15} photons s^{-1} m^{-1} for a $m_v \sim -2$ meteor which extrapolates to 2×10^{17} photons s^{-1} m^{-1} for a meteor of $m_v \sim -6$. This is in good agreement with the emission rate from the train reported here. Thus the near IR emission from the persistent train may be explained in terms of the sodium catalytic process.

I thank M. J. Taylor for help wth the observations and Miss P. Rothwell for valuable discussions. The use of the Hochalpine Forschungsstation Jungfraujoch during September 1979 is gratefully acknowledged.

Received 31 March; accepted 13 June 1980.

1. Baggaley, W. J. *Bull. astr. Insts Csl.* **27**, 244–246 (1976).
2. Baggaley, W. J. *Nature* **257**, 567–568 (1975).
3. Baggaley, W. J. *The Observatory* **98**, 8–11 (1978).
4. Lovell, A. C. B. *Meteor Astronomy*, 131 (Oxford University Press, 1954).
5. Colin, L. & Myers, M. A. *Computed Times of Sunrise and Sunset in the Ionosphere* (NASA TM X-1233, 1966).
6. Chapman, S. in *The Aurora and Airglow* (eds Armstrong, E. B. & Dalgarno, A.) 204–205 (Pergamon, Oxford, 1955).
7. Chapman, S. *J. geophys. Res.* **64**, 2064–2065 (1959).
8. Kolb, C. E. & Elgin, J. B. *Nature* **263**, 488–490 (1976).
9. Zipf E. C. *Can. J. Chem.* **47**, 1863–1870 (1969).
10. Baggaley, W. J. *Bull. astr. Insts Csl.* **28**, 356–359 (1977).

Photoelectrochemical conversion using reaction-centre electrodes

A. Frederick Janzen
Photochemical Research Associates, Inc., London, Ontario,
Canada N6E 2V2

Michael Seibert*
Solar Energy Research Institute, Golden, Colorado 80401

Recent reports have demonstrated the possibility of using photoactive, biological membrane components in photoelectrochemical cells[1]. Such systems have produced small photovoltages and photocurrents. The present studies in our laboratories have led to the attachment of a much simpler biological complex, the bacterial photosynthetic reaction centre isolated from *Rhodopseudomonas sphaeroides*, directly onto an SnO_2 electrode. The light-induced, primary-charge-separation processes which occur across the reaction-centre macromolecule have been coupled to the electrode, and in a two-electrode configuration photovoltages of 70 mV and photocurrents of 0.3 μA cm^{-2} have been observed in an external circuit. The phenomena are not due to Dember effects, and 'reactor-centre electrodes' may serve as a model system for future photovoltaic devices.

Photoelectrochemical cells have used chloroplast membranes[2], chloroplasts[3,4], photosystem-I particles[5], purple-membrane fragments containing bacteriorhodopsin[6,7], and bacterial reaction centres[8]. In most cases, the biological component was incorporated into liposomes or bilayer lipid membranes, and in some cases the stability was enhanced by using polymers or lipid-impregnated filters. Because the interiors of liposomes are inaccessible to contemporary electrodes, definitive electrochemical studies are very difficult. Lipid bilayers often trap solvents and have small working surfaces. Furthermore, the geometry necessitated by lipid bilayer systems (two half-cells separated by the bilayer) would be quite cumbersome in a solar energy conversion device. In contrast, chloroplast membranes[2,3] have been deposited directly onto the surface of an electrode, thus forming a simpler photoelectrochemical cell.

Bacterial reaction-centre complexes are the simplest biological units that carry out the primary photochemistry of photosynthesis. They have been isolated from photosynthetic bacterial membranes and are relatively stable at high concentration in room temperature and light conditions. A reaction centre[9] is an 80,000–100,000 molecular weight complex containing three protein subunits and six chlorophyllous chromophores, and it carries out a multistep charge separation process with a quantum efficiency of one. In the case of *Rhodopseudomonas sphaeroides* reaction centres, 15.2% of the incident solar energy (air mass 1.2) is available as the chemical potential of charge separation at the level at which the bacteriochlorophyll dimer donor ($BChl_2$) is oxidized and the iron/quinone acceptor (X) is reduced[10]. This estimate assumes that the sample is of sufficient optical density to absorb all incident light between 380 and 865 nm. Several investigators[11,12] have suggested that reaction centres might be deposited onto electrodes as model systems for future solar energy conversion devices. The first successful direct electrical coupling of an isolated photosynthetic reaction centre to an electrode is described here.

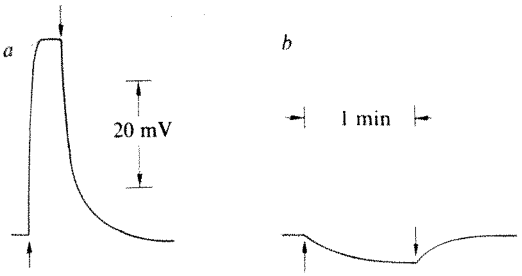

Fig. 1 The open-circuit photovoltage produced by a reaction-centre-coated, SnO_2 electrode exposed to red light (~40 mW cm^{-2}) in an electrochemical cell. *a*, Freshly-coated electrode. The electrode acts as a photocathode since the midpoint potential of the X acceptor in the reaction centre is more oxidizing than the flat-band potential of SnO_2. The kinetics of the photovoltage can vary with the sample. *b*, Autoclaved electrode. Upward and downward arrows indicate light on and light off, respectively. The photovoltage produced by an uncoated, SnO_2 electrode in these conditions was <1 mV.

Using the method of Dutton *et al.*[13] we isolated reaction-centre complexes from the purple, non-sulphur photosynthetic bacterium *Rhodopseudomonas sphaeroides* R-26 (a mutant strain of ATH 2.4.1 lacking highly unsaturated carotenoids). The complexes were suspended in 10 mM Tris-HCl buffer (*p*H = 8.0) at a concentration of 266 μM. Reaction centres were transferred to working electrode surfaces by dipping the electrodes into the concentrated, reaction-centre suspension. Excess liquid was removed from the lower part of the electrodes and the electrodes were dried in the dark. Platinum electrodes were platinized using standard methods, and SnO_2-coated glass was from Corning Glass Works. The experimental cell consisted of a working electrode and either a platinized platinum or SnO_2 counter electrode. The electrolyte was 0.1 M Na_2SO_4 and 0.05 M hydroquinone in water or Tricine buffer (*p*H = 7.1). The light source was a tungsten lamp (Unitron Instruments), and the light passed through both a Corning CS2-62 red filter, which cuts off light below 600 nm, and a 7-cm water filter. Photovoltages and photocurrents were measured in the external circuit with a Keithley Instrument Model 177 multimeter, using various load resistors connected in parallel or series with the meter. Absorbance spectra were obtained with a Cary 219 spectrophotometer. Action spectra were measured at very low light intensity using a tungsten light source focused through a 0.25-m Bausch and Lomb monochromator (6-nm bandwidth). The reciprocal of the quantum flux necessary to elicit a 10-μV response across a 10-kΩ resistor was plotted as a function of the wavelength.

Platinized platinum was the first working electrode material we investigated. Table 1*a* presents the photovoltages and photocurrents obtained when reaction-centre complexes were dried as a thin film on this surface. Small open-circuit photovoltages and short-circuit photocurrents were observed routinely, and the photoeffects lasted for at least several days. If these phenomena were due to the light-induced charge separation associated with the primary processes of photosynthesis, electrodes coated with inactive reaction centres would not be expected to produce photo-induced voltages and currents. Autoclaved reaction-centre-coated platinum electrodes (Table 1*b*) exhibit photoeffects of the same order as unautoclaved

Table 1 Photoeffects in reaction-centre-coated, platinized platinum electrodes

Working electrode condition	Open-circuit photovoltage (mV)	Short-circuit photocurrent (μA)
a. Freshly coated electrode	2.1	1.07
b. Autoclaved electrode	3.65	0.32

The total irradiated area of the electrode was about 0.25 cm^2 in each case.

---

* To whom correspondence should be addressed.

electrodes, indicating that biologically active electron transfer is not involved. Dember effects[1] could account for the phenomena shown in Table 1.

The absence of any coupling of the primary charge separation to the electrode could be due to rapid back reactions from the electrode to the oxidized reaction centres or to quenching of excitation by energy transfer from excited reaction centres to the metal[14]. If this is the case, the use of semiconductor electrode materials might overcome the problem. Consequently, we made reaction-centre electrodes using SnO_2-coated glass. Figure 1*a* shows that a reaction-centre-coated SnO_2 electrode can typically generate an open-circuit photovoltage of 37 mV. The maximum value observed thus far is 70 mV. A maximum photovoltage of about 495 mV is possible (the difference between the midpoint redox potential of the $BChl_2$ primary donor, +450 mV, and that of the X acceptor, −45 mV, because $BChl_2$ and X are located on opposite sides of the reaction-centre molecule). Mismatching of the energy levels of the reaction-centre molecules with the energy levels of the SnO_2, charge recombination within the reaction-centre film, and a lack of reaction-centre orientation could account for the small photovoltages. Typical short-circuit photocurrents observed are $\sim 0.3\ \mu A\ cm^{-2}$. The residual photovoltage after autoclaving indicated in Fig. 1*b* is probably due to a Dember effect.

If electrons pumped across the reaction centre during the primary photoact of photosynthesis do equilibrate with the electrode, the action spectrum of the photocurrent measured in the external circuit should correspond to the absorbance spectrum of the reaction centres. Figure 2 compares the solution absorbance spectrum, the absorbance spectrum of a thin reaction-centre film, and the action spectrum of the photocurrent. The absorbance spectrum of the film is distorted with respect to the solution spectrum due to the effects of light scattering. The action spectrum, however, follows the solution spectrum closely. The peaks in the spectra at around 800 and 860 nm are due to bacteriochlorophyll absorption, while the peak at 760 nm is due to bacteriopheophytin absorption. The quantum yield (absorbed photons) for the production of electrons by 800-nm photons was 0.002.

We conclude that charge separation generated across the reaction-centre molecule as a result of the primary photochemistry of photosynthesis can be electrically coupled directly to semiconductor electrode materials (although inefficiently yet). Such reaction-centre electrodes can be used in a photoelectrochemical cell to generate photovoltages and photocurrents in an external circuit. Similar results have been obtained using electrodes on which chlorophyll or chlorophyll analogues have been deposited[15–18]. These electrodes may lead to new methods of probing the primary photochemistry of photosynthesis and may also serve as model systems for future inorganic or organic photoelectrochemical devices.

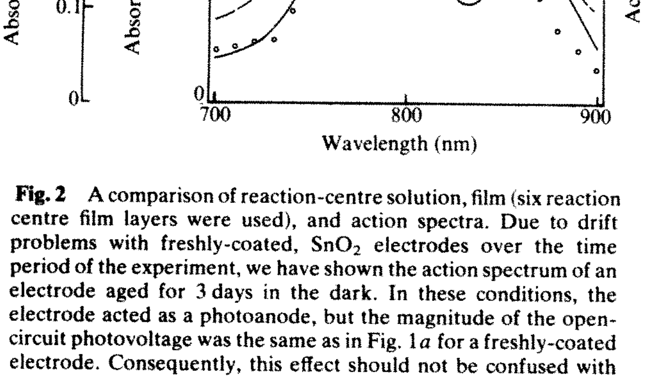

Fig. 2 A comparison of reaction-centre solution, film (six reaction centre film layers were used), and action spectra. Due to drift problems with freshly-coated, SnO_2 electrodes over the time period of the experiment, we have shown the action spectrum of an electrode aged for 3 days in the dark. In these conditions, the electrode acted as a photoanode, but the magnitude of the open-circuit photovoltage was the same as in Fig. 1*a* for a freshly-coated electrode. Consequently, this effect should not be confused with the small photoanodic effects of autoclaved electrodes (Fig. 1*b*). The action spectra of freshly-coated electrodes show the same peaks as aged electrodes, but the relative peak heights are distorted. The action spectra of autoclaved electrodes have no peaks in the 700–900 nm range.

We thank J. R. Bolton and J. C. Grosskreutz for their encouragement and A. J. Nozik for his suggested improvements of this manuscript. This work was supported in part by the US Department of Energy, contract EG-77-C-01-4042.

Received 21 February; accepted 28 May 1980.

1. Bolton, J. R. & Hall, D. O. *Ann. Rev. Energy* **4,** 349–497 (1979).
2. Allen, M. J. in *Living Systems as Energy Converters* (eds Buvet, R. *et al.*) 271–274 (Elsevier, Amsterdam, 1977).
3. Ochiai, H. *et al. Agric. biol. Chem.* **43,** 181–183 (1979).
4. Haehnel, W. *et al. Z. Naturforsch.* C **23,** 392–401 (1978).
5. Gross, E. L. *et al. Photochem. Photobiol.* **28,** 249–256 (1978).
6. Skulachev, V. P. *FEBS Lett.* **64,** 23 (1976).
7. Packer, L. *et al.* in *Living Systems as Energy Converters* (eds Buvet, R. *et al.*) 119–128 (Elsevier, Amsterdam, 1977).
8. Drachev, L. A. *et al. FEBS Lett.* **50,** 219 (1975).
9. Seibert, M. in *Current Topics in Bioenergetics* (eds Sanadi, D. R. & Vernon, L. P.) 39–73 (Academic, New York, 1978).
10. Seibert, M. & Janzen, A. F. *Proc. 2nd Miami int. Conf. Alternative Energy Sources* (in the press).
11. Clayton, R. *Brookhaven Symp. on Biology* **28,** 1–15 (1977).
12. Seibert, M. *et al. AIChE Symp. Ser., No. 181,* **74,** 42–46 (1978).
13. Dutton, P. L. *et al. FEBS Lett.* **60,** 275–280 (1975).
14. Gerischer, H. & Willig, F. in *Topics in Current Chemistry* (eds Davison, A. *et al.*) 31–84 (Springer, Berlin, 1976).
15. Mountz, J. M. & Tien, H. Ti, *Photochem. Photobiol.* **28,** 395–400 (1978).
16. Miyasaka, R. *et al. J. Am. chem. Soc.* **100,** 6657–6665 (1978); *Nature* **277,** 638–640 (1979).
17. Janzen, A. F. & Bolton, J. R. *J. Am. chem. Soc.* **101,** 6337–6341 (1979).
18. Wasielewski, M. *Abst. 3rd Solar Photochemistry Research Conf.* 76–80 (1979).

Cross-polarization ^{13}C NMR spectroscopy of whole soils

P. F. Barron*, M. A. Wilson†, J. F. Stephens*, B. A. Cornell‡ & K. R. Tate§

* CSIRO Fuel Geoscience Unit, North Ryde, New South Wales, 2113 Australia
† CSIRO Division of Process Technology, North Ryde, New South Wales, 2113 Australia
‡ CSIRO Division of Food Research, North Ryde, New South Wales, 2113 Australia
§ DSIR Soil Bureau, Lower Hutt, New Zealand

The ideal tool for the analysis of soil organic matter would enable structural group analysis to be performed on whole soil samples in a non-destructive manner. However, up till now, there have been no adequate techniques available to characterize the structure of amorphous humic compounds in the solid state. Moreover, it has not been possible to dissolve all the organic material from the soil and obtain soluble material for analysis without chemical alteration during solvent extraction or pyrolysis. Although conventional NMR spectra of amorphous solids reveal no structural information due to large dipolar interactions, the use of high power cross-polarization (CP) techniques[1] has overcome difficulties in obtaining ^{13}C NMR spectra of solids to the extent that spectra can be obtained in much shorter times and organic functional groups partly resolved. We now report the first recorded ^{13}C NMR spectra of whole soils and show that this technique has the potential for structural analysis of organic matter in solid soil samples.

Although the ^{13}C cross-polarization technique has been well documented[1,2], a brief description is necessary here. Its major advantages over conventional ^{13}C NMR are a reduction of the time required to obtain a usable spectrum which, in turn, is better resolved owing to the elimination of heteronuclear dipolar broadening. The increased sensitivity to ^{13}C is achieved in two stages: the first by the transfer of polarization from the more polarized and more abundant ^1H spins to the ^{13}C spins. The maximum possible enhancement due to this effect is given by the ratio of the two gyromagnetic ratios, $\gamma_H/\gamma_{^{13}C}$, which is about 4. The second, and more significant, contribution results from the ^{13}C spin–lattice relaxation now occurring at the spin–lattice relaxation rate of the proton population which, in general, is an order of magnitude faster than the conventional ^{13}C rate. Thus the frequency with which data may be accumulated is greatly increased. In the presence of the high power heteronuclear decoupling field, the remaining line widths of the order of 0.2–2 kHz are due predominantly to residual ^{13}C chemical shift anisotropy (CSA)[2] and are not removed by the CP technique. However, the reduction in line widths is sufficient to allow partial resolution of many of the ^{13}C resonances from different functional groups with amorphous solids. The ^{13}C technique is used in the present study to determine the relative abundance of different functional groups in the organic matter in a range of soils.

To obtain this information, a number of experimental conditions must be satisfied. For example, it must be established that all carbon types approach the same degree of polarization enhancement during the CP process. This requirement is satisfied if the proton population is assumed to relax with a uniform spin temperature according to a single time constant, $T_{1\rho}$, as a result of spin-diffusion. Although the efficacy of spin-diffusion is quite short range on the time scale of the relaxation rates encountered in the soils studied here, this assumption has been widely used in the interpretation of spectra obtained from closely related coal samples which possess similar proton relaxation rates[3,4]. A second consideration is the r_{CH}^{-6} (where r_{CH} is the internuclear distance between carbon and hydrogen) dependence of the cross-polarization rate. Clearly the non-protonated carbons will cross-polarize at a slower rate than protonated carbons[3,4], setting a lower limit to the contact time used to achieve adequate cross-polarization. Finally, the delay between repeating the pulse sequence must be sufficiently long to allow for the spin–lattice relaxation of the proton population.

Unfortunately, as the polarization enhancement to which the ^{13}C spin system is approaching decreases with length of contact at the rate of the ^1H $T_{1\rho}$, over-allowance in the choice of contact time will lead to reduced enhancement and increased accumulation time. Also, over-allowance in the choice of pulse repetition time will lead to increased accumulation time. Because soils have low carbon contents (<25%), both the contact and pulse repetition times must be optimised for maximum time efficiency as well as equal response of different carbon types to the CP process.

To estimate the optimum conditions for this study, Maungatua silt loam, details of which are shown in Table 1, was examined using a range of contact and recycle times. Recycle times of 0.5–2 s resulted in no apparent differences in the total signal or those parts of the signal pertaining to specific carbon types, indicating that spin–lattice relaxation is very efficient for all carbon types ($T_1 < 0.1$ s). The ^{13}C–^1H contact time was varied from 0.25 to 2 ms with maximum enhancement occurring in the range 0.5–1 ms. No change in relative enhancement of different carbon types was evident for contact times greater than 0.5 ms. Hence, cross-polarization rates are fast and the ^1H $T_{1\rho}$ is short (<10 ms), as has been found in coals[3,4]. Thus the spectrum of Maungatua soil could be semiquantitatively interpreted using a contact time of about 1 ms and a recycle time as short as 0.5 s. All other soils were examined using a single contact of 1 ms duration with a recycle time of 1 s except for Taupo C horizon clay where a recycle time of 0.5 s was used due to the low carbon content.

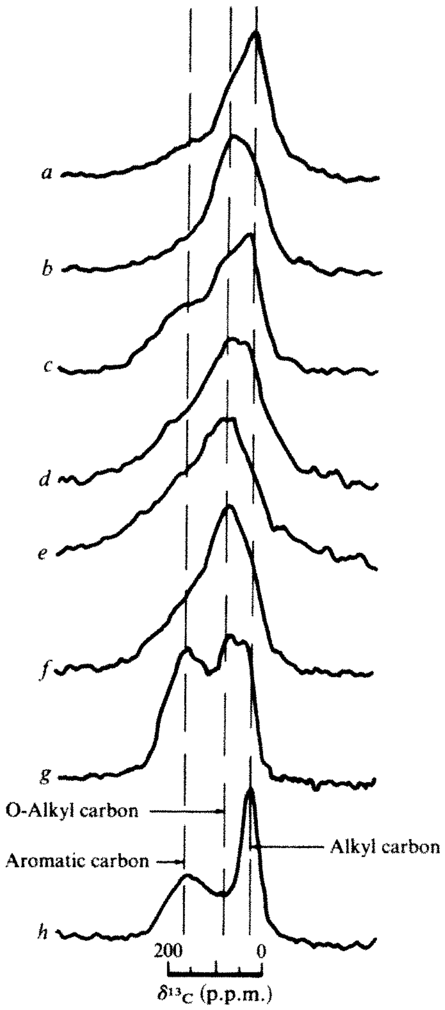

Fig. 1 CP-NMR spectra of soils and coals obtained with a Bruker CXP-100 spectrometer operating at 22.63 MHz for ^{13}C and a Bruker z-22v ^{13}C-[^1H] double resonance probe. ^1H irradiation fields of 28 and 7 G for ^{13}C and ^1H respectively were used to satisfy the Hartmann–Hahn condition[2] necessary for cross-polarization. The number of free induction decays collected ranged from 2×10^4 to 2×10^5. *a*, Maungatua humic silt loam. *b*, McKerrow fine sandy loam A_1 (clay-size fraction <0.02 μm, 23% organic matter) isolated by ultrasonic dispersion of soil in water and subsequent separation into sand-, silt- and clay-size material. *c*, Te Kopuru sand B_h horizon. *d*, Te Kopuru sand A horizon. *e*, Taupo C horizon clay concentrate (<0.2 μm, 6.3% organic matter). Conditions of isolation have been described elsewhere[6]. *f*, Taupo B horizon clay concentrate (<0.2 μm, 13.2% organic matter). Conditions of isolation have been described elsewhere[6]. *g*, Yallourn coal (woody brown coal). *h*, Wandoan coal (sub-bituminous black coal).

Table 1 Properties of Maungatua humic silt loam

New Zealand classification[5]	Podzolized upland yellow-brown earth	
Horizon	A_1	
%C	22.1	
Cation exchange capacity *me*%	39.0	
Total exchangeable bases *me*%	1.1	
Parent material	Thick schist over comminuted schist	
Vegetation dominants	Canopy:	
	Chionochloa rigida	35%
	Dracophyllum longifolium	35%
	Celmisia coriacea	15%
	Ground layer:	
	Astelia linearis	
	Celmisia gracilenta	
	Cladonia aggregata	

Figure 1 shows typical spectra of soils and soil fractions, together with spectra of brown and black sub-bituminous coals for comparison. Details of the other soils used in these experiments have been reported previously[5–7]. ^{13}C CP spectra of coals normally consist of a relatively sharp resonance due to alkyl carbons and a broader, unsymmetrical peak to lower field, due to aromatic carbons[3,4]. The spectrum of Wandoan coal (Fig. 1*h*) is typical of this. The Yallourn xylitic brown coal spectrum (Fig. 1*g*) exhibits an additional resonance indicative of carbons α- to oxygen in ethers and alcohols (O-alkyl), and is also obviously more aromatic. In contrast, in Maungatua soil (Fig. 1*a*), the dominant carbon type is alkyl with a significant amount of O-alkyl carbon also present. The aromatic carbon content seems much lower than in either coal. Figure 1*c*, *d* show the spectra obtained from the B_h and A horizons of the Te Kopuru sand. The B_h horizon of Te Kopuru sand is clearly more aromatic than the Maungatua soil and is also possibly slightly more aromatic than the A horizon of Te Kopuru sand. Similarly, more of the aliphatic carbon in the A horizon is bound to oxygen than in the B_h horizon. Thus, the chemical structure of the soil organic matter may vary with profile depth as well as soil type.

Humic and fulvic extracts of soils usually contain carboxylic acid carbon[8–14] but no distinct signals were obtained downfield of the aromatic carbon signal. It is possible that the signal is hidden by the large chemical shift anisotropies of aromatic and carboxylic carbons[1]. The use of the 'magic angle spinning' technique (MAS)[2], which removes the CSA broadening, in conjunction with the CP process should clarify this point. The brown coal spectrum exhibits a shoulder on the low field side of the aromatic signal which is possibly due to carboxylic carbon.

In the soils with low carbon content, we were able to obtain spectra by physically separating the carbon-rich clay fractions. As found for the Maungatua soil, the clay fraction of the A horizon of McKerrow fine sandy loam (Fig. 1*b*) is highly aliphatic, but it is also apparent that more of the aliphatic carbon is bound to oxygen. We have also obtained spectra from the $<0.2\ \mu m$ clay fractions of the B and C horizons of Taupo sandy soil (a vitric andosol developed on pumice) (Fig. 1*e*). The C horizon fraction contained only 6% carbon and required 2×10^5 scans at 0.5 s pulse repetition to obtain the spectrum. At the field strength used (21.1 kG) the technique is probably limited to soils or soil fractions of about this carbon content or greater.

Early workers believed that humic substances were highly aromatic polycyclic materials[13]. However, recent workers have proposed different structures. Schnitzer has suggested that humic materials are highly substituted monocyclic materials in which some of the substituents are polymethylene chains of fatty acids[14]. Other workers[9–12] have suggested that humic materials are more aliphatic than previously thought. Grant[15] has shown that polymethylene can comprise as much as 30% of the organic matter in a particular soil, while Anderson and Russell[16] have offered evidence which suggests that polymaleic acid-like polymers may be important constituents of humic substances. In the soils we have investigated, our results indicate the variation in the nature of the organic matter present, from highly aliphatic to moderately aromatic.

We are continuing our studies of soil organic matter by the ^{13}C CP technique with the aim of correlating the variation in structure with soil forming factors, in particular, vegetation. The combination of the 'magic angle spinning' technique with the CP process will provide more detailed and quantitative information.

We thank R. Tyler and N. Russell for coal samples and Drs A. Campbell and K. Goh for some of the soil samples. Support to P.F.B. was provided under the National Energy Research, Development and Demonstration program administered by the Commonwealth Department of National Development.

Received 31 March; accepted 2 June 1980.

1. Pines, A., Gibby, M. G. & Waugh, J. S. *Phys. Lett.* **15,** 373–376 (1972); *J. chem. Phys.* **59,** 569–590 (1973).
2. Mehring, M. *High Resolution NMR Spectroscopy in Solids* (Springer, Berlin, 1976).
3. Vanderhart, D. L. & Retcofsky, H. L. *Fuel* **55,** 202–204 (1976).
4. Bartuska, V. J., Marciel, G. E., Schaefer, J. & Stejskal, E. O. *Fuel* **56,** 345–358 (1977).
5. Molloy, L. F. & Blakemore, L. C. *N.Z.J. Sci.* **17,** 233–255 (1974).
6. Campbell, A. S., Young, A., Livingstone, L., Wilson, M. A. & Walker, T. W. *Soil Sci.* **123,** 362–366 (1977).
7. New Zealand Soil Bureau, *N.Z. Soil Bur. Bull.* **26,** 1–27 (1968).
8. Wilson, M. A., Jones, A. J. & Williamson, B. *Nature* **276,** 487–489 (1978).
9. Wilson, M. A. & Goh, K. M. *J. Soil Sci.* **28,** 645–652 (1977).
10. Ogner, G. *Soil Biol. Biochem.* **11,** 1058 (1979).
11. Ludemann, H. D., Lentz, H. & Vila, J. F. *Biochem. Biophys. Res. Commun.* **72,** 1063–1070 (1976).
12. Newman, R. H., Tate, K. R., Barron, P. F. & Wilson, M. A. *J. Soil Sci.* (in the press).
13. Kononova, M. M. *Soil Organic Matter* 2nd edn, 73–78 (Pergamon, Oxford, 1966).
14. Schnitzer, M. & Khan, S. U. *Soil Organic Matter* (Elsevier, New York, 1978).
15. Grant, D. *Nature* **270,** 709–710 (1977).
16. Anderson, H. A. & Russell, J. D. *Nature* **260,** 597 (1976).

0028–0836/80/320587—02$01.00

Harmattan dust deposition in northern Nigeria

Grant McTainsh

School of Earth Sciences, Macquarie University, North Ryde,
New South Wales 2113, Australia

Studies of atmospheric dust deposits originating from Africa, within Atlantic Ocean sediments[1,2], have provided useful indirect information on Quaternary environments, but dust studies in Africa are rare. Here Harmattan dust deposition measurements at Kano, northern Nigeria during the 1978–79 season are reported. A relation between dust deposition, visibility, solar radiation and wind speed is defined, which deteriorates during the latter half of the Harmattan season. A probable explanation of this deterioration is the local remobilization of existing dust.

The dust is thought to originate from the Faya Largeau area in the Chad Basin[3] (Fig. 1). From there the dust plume travels WSW at an altitude[4] of 600–900 m reducing visibility, relative humidity, solar radiation and temperatures along its path. The Harmattan season extends from October to April though it may vary considerably from year to year.

The dust collection technique was designed to measure the amount of Harmattan dust falling onto the ground from suspension in the atmosphere. A dust trap was set up 9 m above ground level on the roof of a building on the campus of Bayero University, Kano, isolated from local soil dust movements. The trap was a basin of distilled water 20 cm deep exposing a water surface of 0.27 m^2 for collecting dust. Water level was maintained daily 10 cm below the top. To prevent bird contamination of the dust trap a second basin was kept full for birds to use. The dust laden water was evaporated in laboratory ovens weekly and the residue weighed. Collections were made during three Harmattan seasons, 1976–79.

Casual observations during the Harmattan season suggest a close association between visibility and dust deposition but the

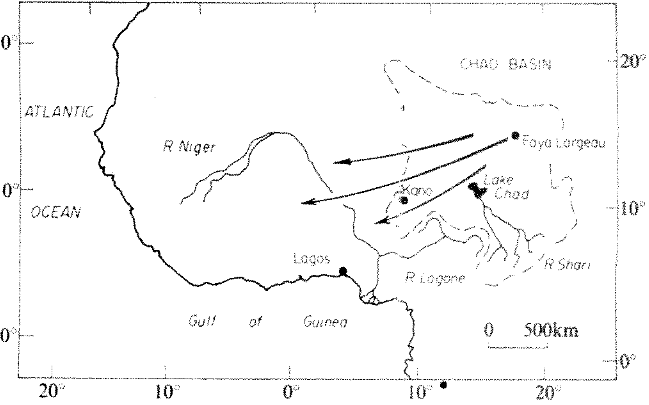

Fig. 1 The Harmattan wind in West Africa.

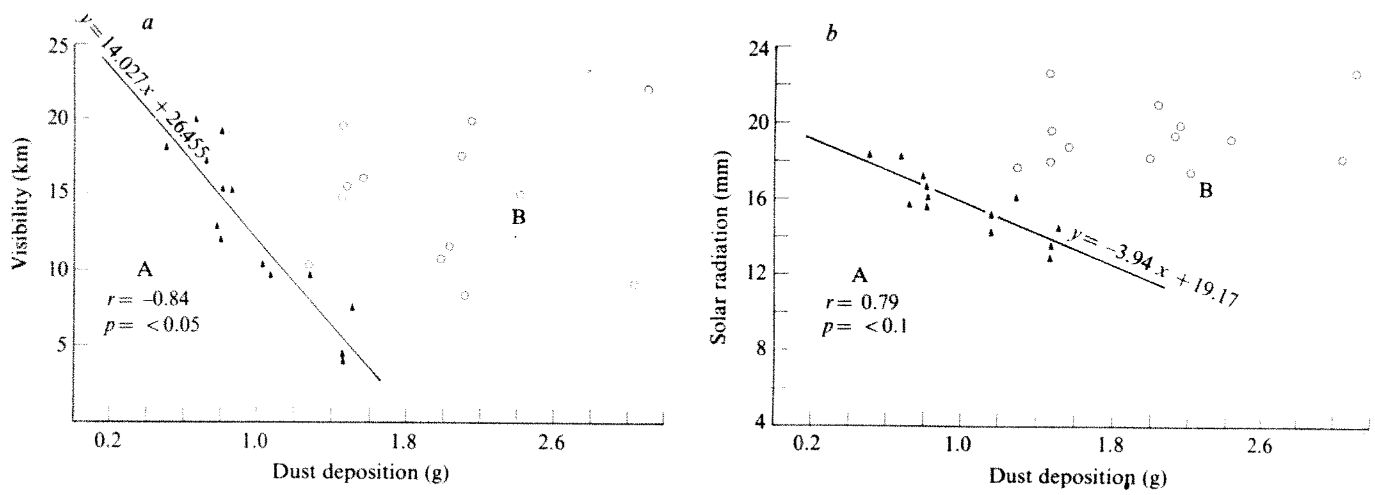

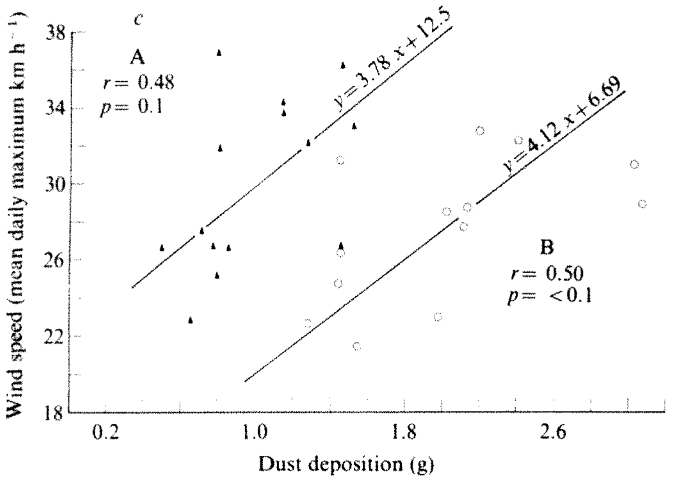

Fig. 2 *a*, The relation of visibility to Harmattan dust deposition—weekly mass of dust settling over 0.27 m of distilled water (see text); *b*, the relation of solar radiation to Harmattan dust deposition; *c*, the relation of wind speed to Harmattan dust deposition. ▲, Time period A (October–January); ○, time period B (January–April). *r* is the correlation coefficient and *p* is the significance level found in a test of the hypothesis $r = 0$ against $r \neq 0$.

monitored rates indicate a more complex relationship. During the first part of the season periods of low visibility are associated with high dust deposition. As the season progresses measured deposition was far greater than observed visibility would suggest. Data on visibility, solar radiation (Gunn Bellani) and wind speed obtained from Kano International Airport were averaged over each of the 28 weekly dust measurement periods of the 1978–79 season. Relationships with deposition are shown in Fig. 2.

The data consistently fell into two time periods, here termed A (12 October–12 January) and B (13 January–27 April). During A a close relation emerges between visibility and deposition and between solar radiation and deposition ($r = -0.84$ and -0.79 respectively, Fig. 2*a*, *b*). During B these relations deteriorate to statistical insignificance. The relation of wind speed to deposition remains at a lower but stable level throughout the season ($r = 0.48$ and 0.50, Fig. 2*c*).

A probable explanation of these differences is local remobilization and secondary deposition of the dust during B, increasing the measured deposition and upsetting the expected relationships with visibility and solar radiation. As the remobilized dust is not derived from high altitudes the expected relations with visibility and solar radiation are disrupted, whereas during A primary deposition is dominant.

Wind speed data support this view. During A, increases in Harmattan wind speed are accompanied by greater dust deposition. During B the amount of dust deposited is higher than wind speed might suggest (Fig 2*c*) as wind is remobilizing and redepositing dust.

The start of the Harmattan season coincides with the end of the wet season so that during A tall grasses abound and relative humidity levels are high thus minimizing dust remobilization. As the grasses die off, relative humidity decreases and the total amount of deposited dust increases, conditions become conducive to remobilization and secondary deposition. This process might be accentuated by grass burning during the latter part of the dry season adding coarser particles to the measured deposition. These particles may have relatively little influence on visibility.

Therefore, measured dust deposition rates during B (after mid January) overestimate the Harmattan dust influx. The visibility–deposition regression line (Fig. 2*a*) is taken to indicate primary Harmattan dust deposition. Visibility data for each week during B are used to predict the expected deposition for each week. The difference between expected and measured deposition I assume to be secondary deposition.

When the corrected data are derived, total Harmattan dust deposition at Kano during 1978–79 is 99.1 g m^{-2}. This figure represents a reduction in total measured deposition of 41.7% which is the amount of secondary deposition. Based on measured dust bulk density of 0.85 g cm^{-3} the 1978–79 Harmattan dust influx represents a layer of dust 0.116 mm thick.

Harmattan dust deposition measurements made by Bromfield[5] in the same area during 1969–72 amount to 22.6 g m^{-2} which is far lower than rates given here, and surprising during a time of drought. Bromfield collected dust in a dry deposition gauge (B.S. 1747 Part 1 1961) which can seriously underestimate deposition[6].

Published[7] dust accumulation rates measured on land vary from 6.6 to 20,100 mm kyr^{-1} which could in part reflect different collection and calibration techniques. A standardized method for monitoring dust is urgently needed.

With respect to historic fluctuations in dust deposition, the visibility–dust deposition relation defined here could be used to estimate dust deposition over the period for which meteorological data are available, thus providing a sensitive index of environmental change in historic times within the Sahel.

I thank Innocent Ukenna for help with the dust collections and note the recent and tragic death of Dr M. P. S. Collins of the Bayero University Harmattan Research Group. Thanks go to Bayero University for financial aid and Martin Williams for discussion.

Received 24 March; accepted 3 June 1980.

1. Parkin, D. W. & Shackleton, N. J. *Nature* **245**, 455–457 (1973).
2. Parmenter, C. & Folger, D. W. *Science* **185**, 695–697 (1974).
3. Hamilton, R. A. & Archbold, J. W. *Q. Jl R. met. Soc.* **71**, 231–265 (1945).
4. Kalu, A. E. in *Saharan Dust* (ed. Morales, C.) 95–118 (Wiley, New York, 1979).
5. Bromfield, A. R. *J. agric. Sci.* **83**, 423–425 (1974).
6. Cadle, R. D. *The Measurement of Airborne Particles* (Wiley, New York, 1975).
7. Goudie, A. S. *J. Arid Envir.* **1**, 291–310 (1978).

Coupled effects of atmospheric N_2O and O_3 on the Earth's climate

Wei-Chyung Wang & Nien Dak Sze

Atmospheric and Environmental Research, Inc., 872 Massachusetts Avenue, Cambridge, Massachusetts 02139

Increased application of nitrogen fertilizer[1] could perturb the atmospheric nitrogen cycle and might lead to a possible increase[2-6] in atmospheric N_2O. N_2O plays an important role in stratospheric chemistry[7-9] as well as in the global radiation budget[10-12]. Recent studies[13-15] suggest that perturbation of local ozone could also significantly affect the global climate. Here we show that a doubling in the present day N_2O level might significantly perturb the distribution of O_3 and HNO_3, and that the associated climatic feedbacks from O_3 and HNO_3 perturbations could contribute as much as 0.23 K warming of the surface temperature, in addition to 0.44 K directly caused by N_2O doubling.

Nitric oxide (NO) is formed in the stratosphere mainly by the reaction of $O(^1D)$ with N_2O (refs 7–9),

$$O(^1D) + N_2O \rightarrow 2NO \qquad (1)$$

and may serve as a catalyst for O_3 removal[16,17] mainly by

$$NO + O_3 \rightarrow NO_2 + O_2 \qquad (2)$$

and

$$NO_2 + O \rightarrow NO + O_2. \qquad (3)$$

In the lower stratosphere ($z < 30$ km), NO and NO_2 may, however, couple with stratospheric odd hydrogen (HO_x) and odd chlorine (ClX) mainly through reactions

$$NO + HO_2 \rightarrow OH + NO_2 \qquad (4a)$$

$$NO_2 + OH + M \rightarrow HNO_3 + M \qquad (4b)$$

$$NO + ClO \rightarrow Cl + NO_2 \qquad (5a)$$

and

$$NO_2 + ClO + M \rightarrow ClNO_3 + M \qquad (5b)$$

Note that while addition of NO may enhance O_3 removal through reactions (2) and (3), it may reduce the efficiency of both the HO_x cycle ($OH + O_3 \rightarrow HO_2 + O_2$; $HO_2 + O_3 \rightarrow OH + 2O_2$) and the ClX cycle ($Cl + O_3 \rightarrow ClO + O_2$; $ClO + O \rightarrow Cl + O_2$) as sinks for O_3, particularly in the region below 30 km. Thus, an increase in stratospheric NO (or N_2O) may lead to O_3 depletion in the upper stratosphere and to O_3 increase in the lower stratosphere and upper troposphere. (For reviews of current understanding of stratospheric chemistry see refs 18–22).

Table 1 Calculated surface temperature change ΔT_s(K) caused by a doubling of the present day atmospheric N_2O abundance, 320 p.p.b.v.

Case	Model	ΔT_s(K)
A	N_2O	0.44
B	$N_2O + O_3$	0.62
C	$N_2O + O_3 + HNO_3$	0.67

Case A considers the sole effect due to N_2O increase. Case B includes the additional effect of O_3 perturbation (Fig. 2). Case C represents the combined effect associated with N_2O increase, including the feedbacks from perturbation to O_3, HNO_3 and NO_2. The effect of NO_2 increase is mainly to increase the absorption of solar radiation in the atmosphere[24], with possible greenhouse effect as it has IR bands[30]. However, the calculated surface cooling due to the associated NO_2 increase is small, ~0.01 K. For the constant cloud temperature parameterization[26] with ice-albedo feedback[27], the calculated surface temperature change should be multiplied by a factor of 2.

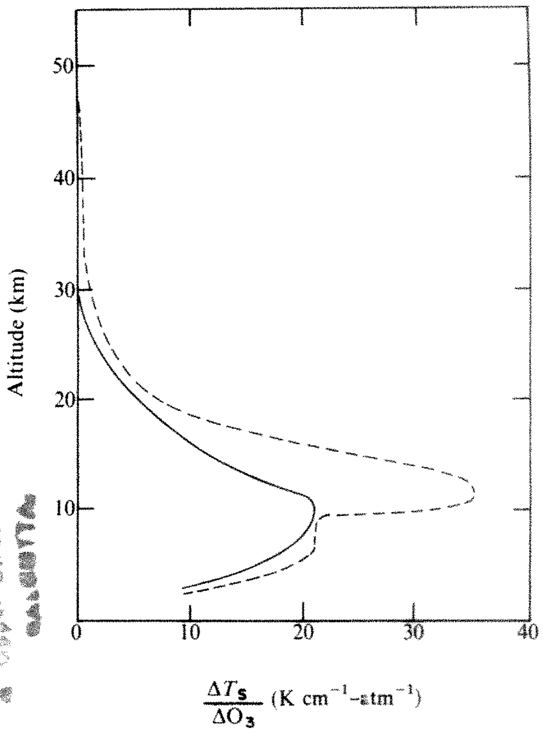

Fig. 1 Sensitivity of surface temperature change ΔT_s(K) to changes in local O_3 amount for mid-latitude (solid line) and tropical atmospheres (dashed line) (after ref. 15).

Besides its dominant role in the stratospheric chemistry, N_2O has strong IR absorption bands at 4.5, 7.78 and 17 μm, and thus contributes to the 'greenhouse effect'. Calculations[10-12] indicate that an increase in the atmospheric N_2O abundance due to the increased application of nitrogen fertilizer[2-6] might directly influence the troposphere climate.

We consider here some of the indirect climatic effects that might be associated with the compositional changes caused by N_2O increase. For instance, because of the strong photochemical coupling between N_2O, O_3 and other trace species, changes in atmospheric N_2O may perturb the O_3 distribution which also has an important role in maintaining the stratospheric thermal structure and the Earth–troposphere radiative energy balance[13-15,23]. Figure 1 shows the calculated sensitivity[15] of surface temperature T_s to changes of local O_3. Note that the maximum sensitivity occurs at around 12 km.

Furthermore, because N_2O is the precursor (reaction (1)) to stratospheric NO_x (NO, NO_2, HNO_3, NO_3, N_2O_5, $ClNO_3$), changes in N_2O would cause similar changes in HNO_3 and NO_2. Note that HNO_3 has IR absorption bands[13] at 5.9, 7.5, 11.3 and 21.8 μm while NO_2, primarily absorbs solar radiation in the UV and visible[24]. Consequently, changes in HNO_3 and NO_2 may also affect the global radiation budget. The combined climatic effects to be expected from a large increase of N_2O are therefore due, in part, to direct greenhouse effect of N_2O as discussed by Wang *et al.*[10] and, in part, to the perturbation of atmospheric chemical composition (for example, O_3, HNO_3 and NO_2) caused by the interaction of N_2O with other trace species.

Figure 2 shows the calculated changes in the vertical thermal structure and the O_3 profile resulted from a doubling of the present day atmospheric N_2O abundance, 320 p.p.b.v. (parts per 10^9 by volume). Note that while the calculated perturbation to column O_3 amount is relatively small (~2% increase), the changes in local O_3 amount are relatively large, up to ~+18% at 12 km and −19% at 38 km. The increase in O_3 below ~26 km is

0028-0836/80/320589—02$01.00

mainly attributed to the strong coupling between NO_x, HO_x and ClX while the decrease above 28 km to reactions (2) and (3). The calculated changes in O_3 profile (Fig. 2) are sensitive to the choice of diffusion coefficients and the stratospheric OH concentrations which are uncertain by at least a factor of 2 or 3. In view of such large uncertainties, the quantitative aspect of the results presented in Fig. 2 should be taken with caution. The calculated changes of the column abundance of HNO_3 and NO_2 resulted from a N_2O doubling are +85% and +75% respectively. These results, on the other hand, are relatively model independent.

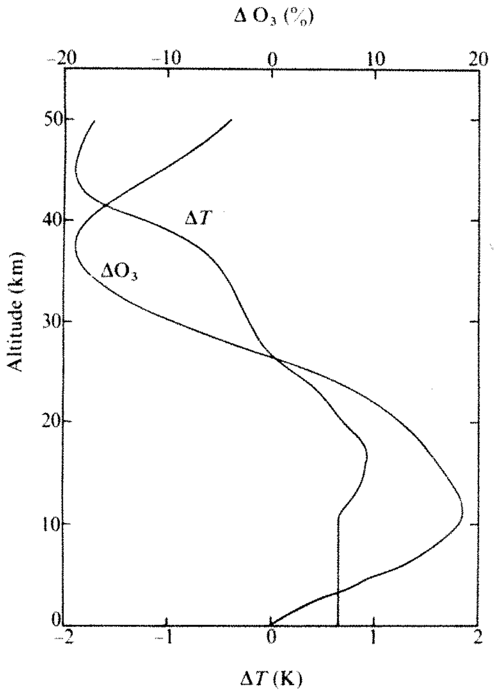

Fig. 2 The calculated changes in thermal structure and O_3 profile due to a doubling of present day N_2O abundance of 320 p.p.b.v. The calculations were based on iterative runs between the one-dimensional radiative-convective model[10] and the one-dimensional photochemical-diffusive model[25]. In the one-dimensional radiative-convective model, we used: (1) 6.5 K km^{-1} as the critical lapse rate[23]; (2) constant relative humidity parameterization[23]; (3) constant cloud altitude parameterization[26]; and (4) fixed surface albedo[27] (that is, no ice-albedo feedback). In the one-dimensional photochemical-diffusive model, transport was treated by using the expedient concept of eddy diffusion with the diffusion coefficients taken from ref. 28. The rate data for the oxygen-hydrogen-nitrogen-chlorine chemistry were taken from ref. 22. The stratospheric H_2O mixing ratio f_{H_2O} was assumed to be constant with altitude and with f_{H_2O} set equal to 4.5 p.p.m.v. (ref. 22). The mixing ratio of ClX at 50 km was 2.2 p.p.b.v., which corresponds to the contributions of various known chlorocarbons to the present stratospheric chlorine level.

The combined climatic effects of the changes in N_2O, O_3, HNO_3 and NO_2 are to decrease the temperature above ~26 km and to increase below. The stratospheric cooling is mainly associated with the local O_3 depletion because the solar radiative heating is reduced. Note that the decrease in solar heating is partially compensated by a warming effect associated with the absorption of upwelling thermal emission from a higher tropospheric temperature of about 0.67 K. The warming effect, however, seems less effective at higher altitude, as reflected by the feature that the calculated maximum cooling occurs at considerable higher altitudes than the region where O_3 depletion peaks. On the other hand, the stratospheric warming with temperature increase up to 1 K can be attributed to the increases in both the local O_3 and the solar radiation reaching the region as a result of O_3 reduction in the upper stratosphere.

Table 1 shows the computed surface temperature change ΔT_s associated with N_2O doubling. In contrast to the partial surface cooling effect caused by the CFMs-induced O_3 perturbation[15,29], the effect of the N_2O-O_3 coupling provides a significant positive feedback and increases the surface temperature from 0.44 K (case A) to 0.62 K(case B). The 30% enhancement in ΔT_s is mainly caused by the calculated increases of O_3 in the lower stratosphere and upper troposphere, a region where the response of T_s to O_3 changes is maximum, as shown in Fig. 1. The associated increase in HNO_3 produces an additional positive feedback effect and increases the surface temperature further, to 0.67 K (case C). The combined climatic effect seems quite significant when compared with the one-dimensional model predicted[27] 2 K global surface warming due to a doubling of the present day atmospheric CO_2 concentration.

Note however, that the foregoing calculations are based on one-dimensional models in which uncertainties are large. The sources of uncertainties may arise from: (1) the inadequacies[31] in the basic formulation of one-dimensional models; (2) the treatment of humidity, clouds and the use of critical lapse rate to approximate the vertical transport of heat by atmospheric motions[22], (3) the complexity of the stratospheric chemical reactions where those involving peroxy(HO_2) are particularly not well understood[20,21], and (4) the lack of present knowledge of the atmospheric N_2O cycle. Thus, the present uncertainties make it difficult to quantify the errors associated with the calculated climatic effect due to N_2O increase. Presumably some of the uncertainties discussed here may be narrowed when more atmospheric data and sophisticated models become available. Nevertheless, it seems clear that should we study the climatic effect due to a change of atmospheric 'greenhouse' material (such as N_2O) which can also influence the atmospheric chemical composition, feedback from compositional changes should be considered.

W.C.W. thanks J. E. Hansen and A. A. Lacis who initiated and participated in the development of the one-dimensional radiative-convective model. We also thank F. M. Luther for the NO_2 absorption data. This work was supported by grant NAS1-15943 from NASA Langley Research Center and by the Chemical Manufacturers Association.

Received 17 March; accepted 2 June 1980.

1. Burns, K. C. & Hardy, R. W. F. *Nitrogen Fixation in Bacteria and Higher Plants* (Springer, New York, 1975).
2. Crutzen, P. J. *Geophys. Res. Lett.* **3**, 169–172 (1976).
3. McElroy, M. B., Elkins, J. W., Wofsy, S. C. & Yung, Y. L. *Rev. Geophys. Space Phys.* **14**, 143–150 (1976).
4. Liu, S. C., Cicerone, R. J., Donahue, T. M. & Chameides, W. L. *Geophys. Res. Lett.* **3**, 157–160 (1976).
5. Sze, N. D. & Rice, H. *Geophys. Res. Lett.* **3**, 343–346 (1976).
6. Johnston, H. S. *J. geophys. Res.* **82**, 1767–1772 (1977).
7. Nicolet, M. & Vergison, E. *Aeron. Acta* **90**, 1–26 (1971).
8. McElroy, M. B. & McConnell, J. C. *J. atmos. Sci.* **28**, 1095–1098 (1971).
9. Crutzen, P. J. *J. geophys. Res.* **76**, 7311–7327 (1971).
10. Wang, W. C., Yung, Y. L., Lacis, A. A., Mo, T. & Hansen, J. E. *Science* **194**, 685–690 (1976).
11. Yung, Y. L., Wang, W. C. & Lacis, A. A. *Geophys. Res. Lett.* **3**, 619–621 (1976).
12. Donner, L. & Ramanathan, V. *J. atmos. Sci.* **37**, 119–124 (1980).
13. Ramanathan, V. & Dickinson, R. E. *J. atmos. Sci.* **36**, 1084–1104 (1979).
14. Fishman, J., Ramanathan, V., Crutzen, P. J. & Liu, S. C. *Nature* **282**, 818–820 (1979).
15. Wang, W. C., Pinto, J. P. & Yung, Y. L. *J. atmos. Sci.* **37**, 333–338 (1980).
16. Crutzen, P. J. *Q. Jl R. met. Soc.* **96**, 320–325 (1970).
17. Johnston, H. S. *Science* **173**, 517–522 (1971).
18. Nicolet, M. *Rev. Geophys. Space Phys.* **13**, 593–636 (1975).
19. Johnston, H. S. & Pokolske, J. *Rev. Geophys. Space Phys.* **16**, 491–520 (1978).
20. Logan, J. A., Prather, M. J., Wofsy, S. C. & McElroy, M. B. *Phil. Trans. R. Soc.* **A290**, 187–234 (1978).
21. Thrush, B. A. *Nature* **276**, 345–348 (1978).
22. Hudson, R. D. & Reed, E. I. (eds) *The Stratosphere: Present and Future* (NASA Publ. 1049, 1979).
23. Manabe, S. & Wetherald, R. T. *J. atmos. Sci.* **24**, 241–259 (1967).
24. Luther, F. M. *J. appl. Met.* **15**, 479–481 (1976).
25. Sze, N. D. & Wu, M. F. *atmos. Envir.* **10**, 1117–1125 (1976).
26. Cess, R. D. *J. atmos. Sci.* **33**, 1831–1843 (1976).
27. Wang, W. C. & Stone, P. H. *J. atmos. Sci.* **37**, 545–552 (1980).
28. Wofsy, S. C. *A. Rev. Earth planet. Sci.* **4**, 441–469 (1976).
29. Ramanathan, V. *Science* **190**, 50–52 (1975).
30. McClatchey, R. A. *SPIE*, **195**, 2–6 (1979).
31. Tuck, A. F. *Phil. Trans. R. Soc.* **A290**, 477–494 (1979).

Plio-Pleistocene reversal of displacement on the North Anatolian fault zone

P. L. Hancock & A. A. Barka

Department of Geology, University of Bristol, Queen's Building,
University Walk, Bristol BS8 1TR, UK

Fault plane solutions[1] and the offset of geomorphic and man-made features[2–4] show that present-day displacements on the North Anatolian fault zone are right-lateral (Fig. 1). The present analysis of some of the mesoscopic faults and joints cutting Upper Neogene–Lower Pleistocene continental sediments in intermontane basins between Cerkes and Erbaa indicates that there was left-lateral motion on the fault zone during part of its neotectonic evolution. The structures include conjugate reverse faults striking north-west, conjugate normal faults and joints striking north-east, and conjugate vertical joints enclosing an acute angle about a north-east trending bisector (Figs 2 and 3).

The ~1,200 km arc of the North Anatolian fault zone is generally interpreted as an early Neogene intracontinental transform boundary separating the Black Sea and Anatolian plates[2,5] (Fig. 1*a*). As part of a study of neotectonic structures associated with the fault zone, we have surveyed fractures of mesoscopic scale cutting Neogene–Quaternary continental sediments in five intermontane basins between Cerkes and Erbaa (Fig. 1*b*). The basins are situated astride or adjacent to fault breaks which developed during six westwards migrating, large magnitude earthquakes. The aim of investigating the mesofractures was to infer directions of compression and extension related to shear along the fault zone. Other studies of mesofractures have demonstrated their value in the kinematic analysis of major fault zones[6,7].

Although Neogene–Quaternary successions are different in each basin, those older than the late Pleistocene are regarded as belonging to the Pontus Formation[8] or its lateral equivalents. The ~500 m Lower Pontus Formation (Upper Miocene–Lower Pliocene) comprises lacustrine gravels, sands and clays passing laterally and upwards into fluviatile sediments. The 300 m Upper Pontus Formation (Upper Pliocene–Lower Pleistocene) also consists of fluvio-lacustrine sediments but passes laterally into colluvium in the Cerkes region. Unlike the mainly marine Neogene successions bordering the Aegean, the minor divisions of the Pontus Formation have not been dated precisely; the continental sediments have yielded few fossils of biostratigraphical value.

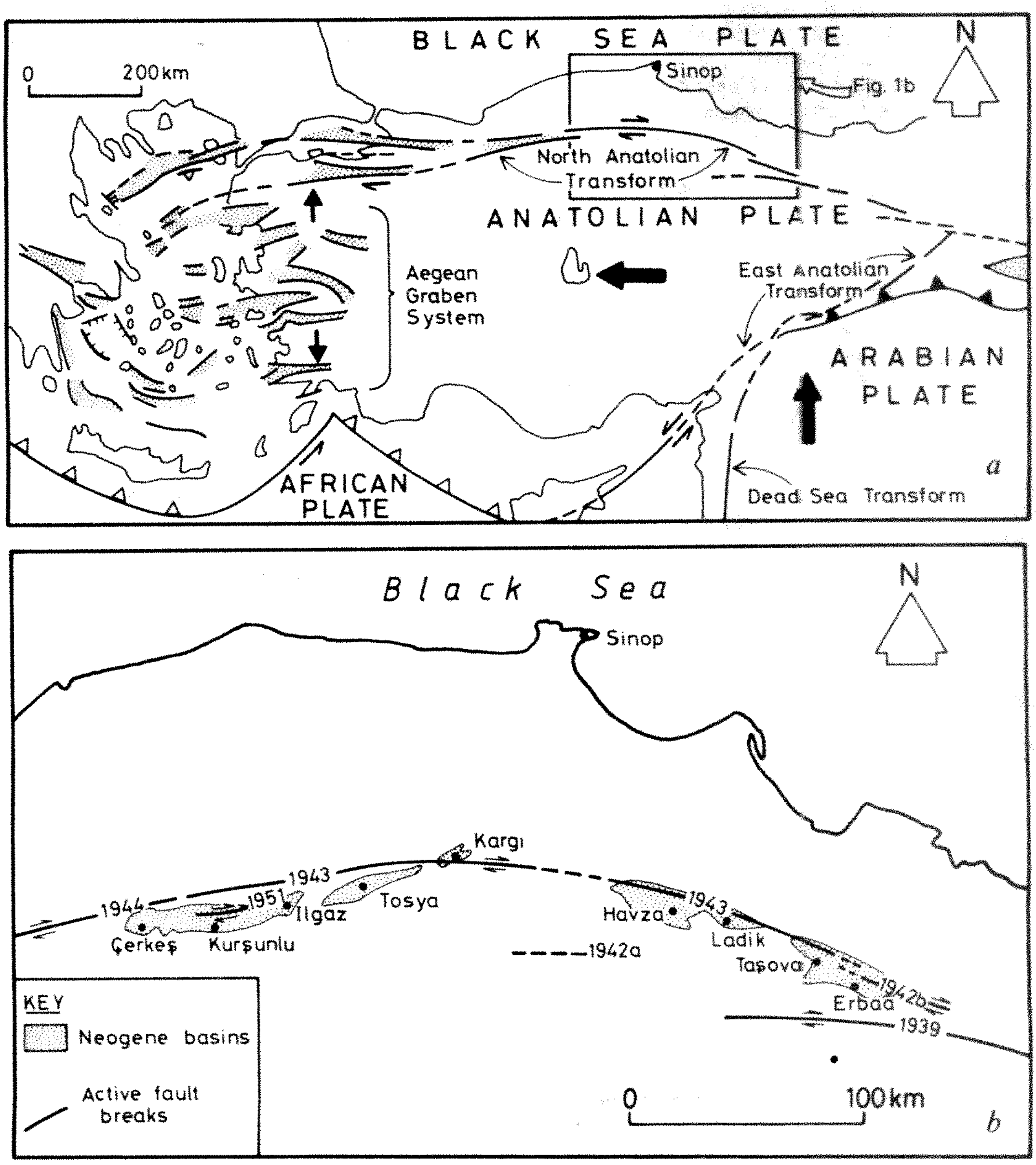

Fig. 1 *a*, Plate setting of the studied segment of the North Anatolian transform fault zone (after ref. 2). *b*, Locations of the sampled Neogene basins. The traces of active fault breaks generated during six large magnitude earthquakes are also shown.

0028-0836/80/320591—04$01.00

Table 1 Principal directions of compression or extension inferred from the analysed mesofractures

Basin		Reverse mesofaults Analysed fractures	σ_1	Normal mesofaults Analysed fractures	σ_3	Steeply inclined joints Analysed fractures	σ_3	Vertical joints Analysed fractures	σ_3	Trend of fault zone
Cerkes–Kursunlu–Ilgaz	West	Single fault set	087–267	Single fault set	320–140	Conjugate shear joints	351–171	Single set of extension joints	324–144	080
	Centre	Conjugate faults	065–245	Conjugate faults	330–150			Conjugate shear joints	343–163	078
	East	Single fault set	042–222	Conjugate faults	287–107	Conjugate shear joints	299–119	Conjugate shear joints	303–123	069
Tosya				Conjugate faults	318–138	Conjugate shear joints	312–132	Conjugate shear joints	331–151	079
Kargi				Conjugate faults	335–155	Conjugate shear joints	345–165	Conjugate shear joints	337–157	090
Havza–Ladik								Conjugate shear joints	336–156	110
Tasova–Erbaa				Conjugate faults	325–145			Conjugate shear joints	344–164	120
Number of analysed fractures		20		65		65		380		

σ_1 (maximum principal stress direction) and σ_3 (minimum principal stress direction) are given as horizontal projections of those directions.

Where growth faults and/or contemporaneous (intrasequence) erosion surfaces truncate fault planes, it is possible to distinguish between synsedimentary and post-sedimentary faults. However, because the movements responsible for generating the fractures were approximately identical during basin filling and later tectonism, the distinction between the two categories of faults is of less kinematic significance than in rocks where the time interval between deposition and subsequent tectonism is longer. Synsedimentary and post-sedimentary faults occur throughout the Pontus Formation and it is not possible to recognize horizons corresponding to particular tectonic events. Both faults and joints are less frequent in the Upper Pontus Formation.

The structures sampled during the full survey of mesoscopic-scale fractures are either joints (85%) or faults (15%). The latter are rarely greater than 20 m^2 in area and show displacements generally not exceeding 2 m. The orientations of 1941 mesofractures at 142 localities were measured. Twenty-seven per cent of these fractures are interpreted as being related to left-lateral shear. Figure 2 shows the morphology of some of them, of which 14% are faults and 86% are joints. At each sample locality, the sediments are horizontal or uniformly dipping and orientation data were collected from small, structurally homogeneous domains of 15 m^2 area. Because the majority of analysed faults cut horizontal sediments and show vertical offsets, and because the intersects between conjugate faults are

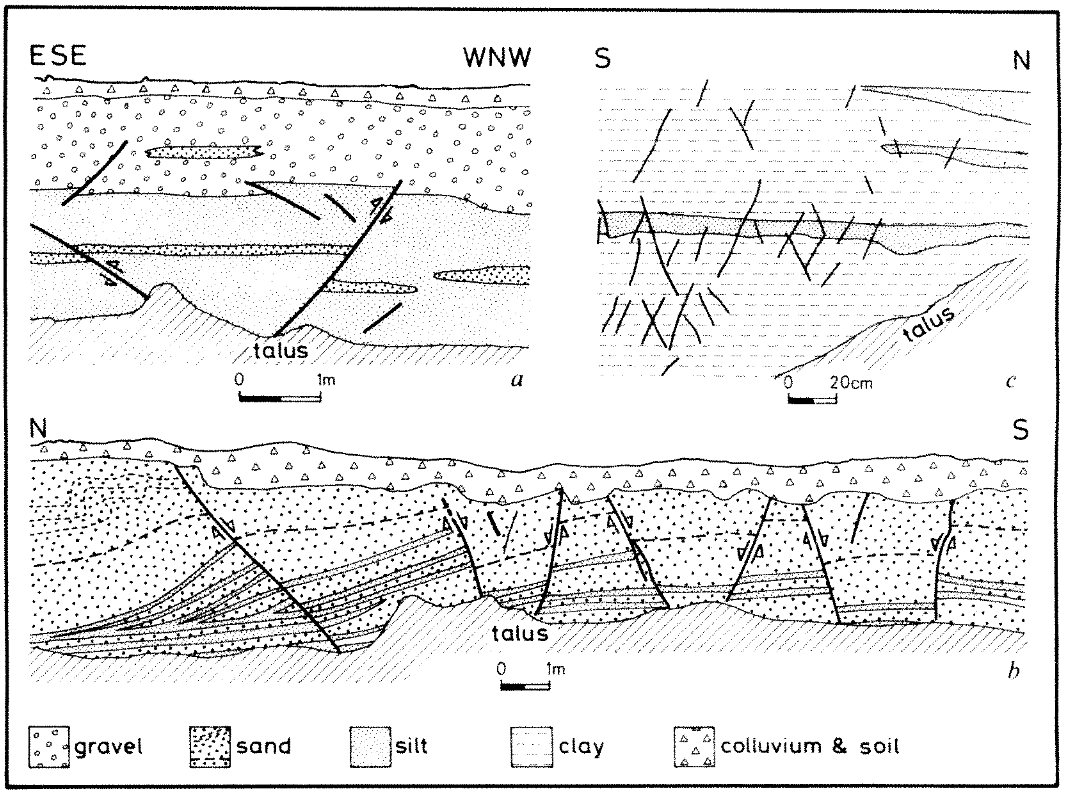

Fig. 2 Sketches from photographs of the analysed structures. *a*, Conjugate reverse mesofaults displacing gravels, sands and silts in the Lower Pontus Formation about 5 km west of Kursunlu. *b*, Conjugate normal mesofaults displacing cross-bedded sands and silts in the Lower Pontus Formation at Kursunlu. Synsedimentary folds are exposed at the north end of the section. *c*, Conjugate normal shear joints cutting silts interbedded with clays in the Lower Pontus Formation about 3 km south-east of Tosya.

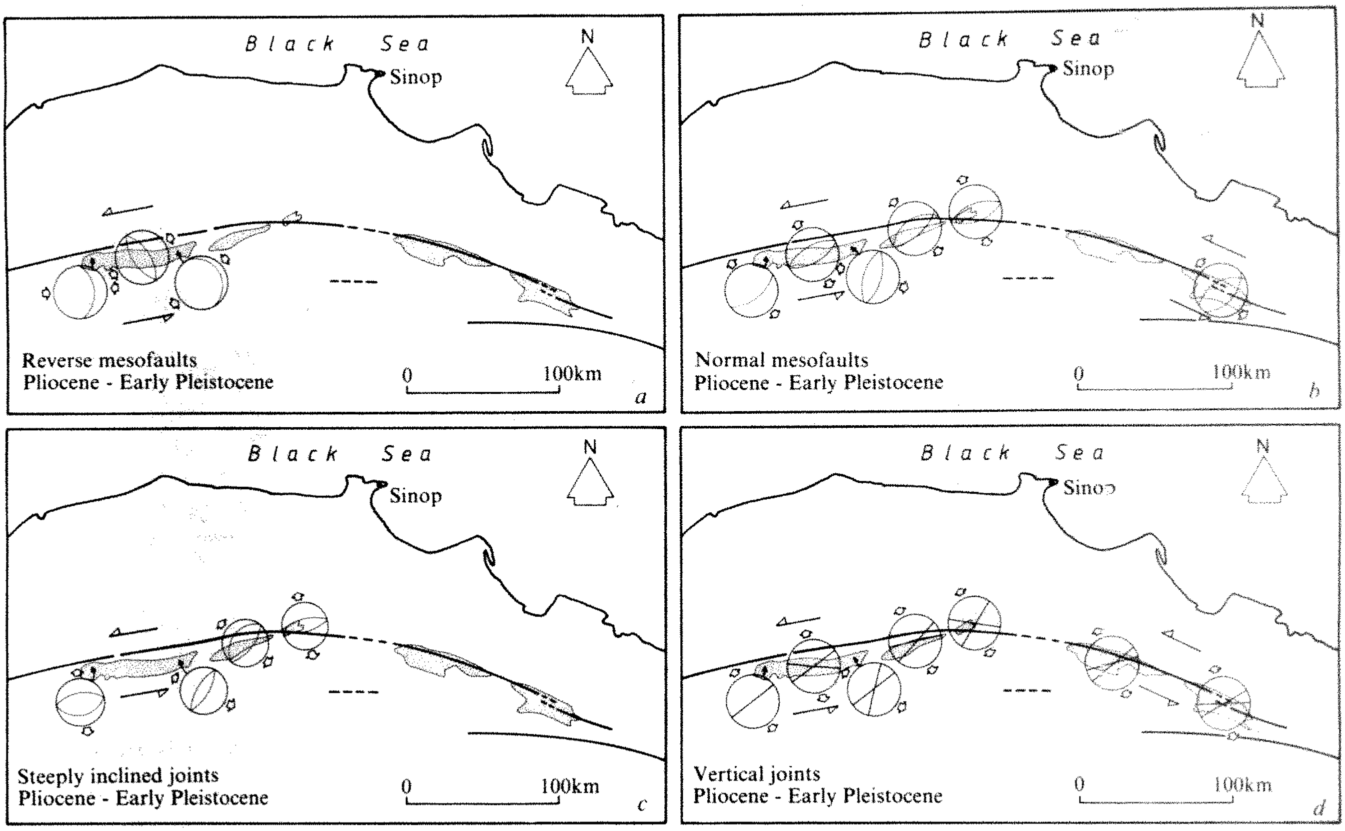

Fig. 3 Mean cyclographic traces of mesofracture sets of Pliocene–early Pleistocene age and from which a left-lateral sense of displacement on the North Anatolian fault zone may be inferred. Stereograms are lower-hemisphere Lambert plots of sets in either horizontal sediments or tilted sediments imagined to be restored to the horizontal. Pairs of arrows immediately outside each plot show horizontal directions of compression or extension inferred from the fractures, and believed to be related to the influence of left-lateral shear along the fault zone. See Fig. 1*b* for names of basins and dates of earthquake fault breaks. *a*, Reverse mesofaults. *b*, Normal mesofaults. *c*, Steeply inclined joints. *d*, Vertical joints.

horizontal or gently plunging, we conclude that displacements were dominantly dip-slip, either reverse or normal.

The fractures were analysed by determining the mean orientations of sets, field relationships being used to decide whether they are conjugate. Although conjugate faults are not present at all localities, it was possible to allocate single fault sets to an appropriate system by comparing their geometry with that of parallel joints belonging to conjugate sets. Approximate orientations of principal stress directions (Table 1) were determined from geometrical analysis of conjugate sets or single extension fracture sets. It was not possible to use the more precise technique of analysing striations on failure surfaces to determine either the orientations of principal strain axes[9] or stress axes[10] because only 11% of the faults are striated, and because many of the analysed structures are joints, which by definition cannot be lineated. It was unrealistic to determine the orientations of strain axes because, to get any regional meaning from them, an areal knowledge of the total slip on each set is required; unless the total slip on both conjugate sets is equal, the preferential development of one set rotates the X and Z axes. There was no evidence for more than one episode of displacement on any fault which is probably due to the mesoscale nature of the fractures. The determination of stress directions from conjugate shears is valid theoretically only when the fractures cut mechanically isotropic rocks. However, as field studies[6,11] demonstrate, many rock masses contain numerous sets of symmetrically arranged mesofractures, and hence as Couples[12] states "... the ordered orientations of fractures indicate that the formation of one crack, and even the formation of many fractures, does not appreciably alter the orientation of the causative stresses, otherwise, the ordering would not be obtained".

The ~27% of mesofractures from which it is possible to infer that there was some left-lateral shear on the North Anatolian fault zone belong to four categories: reverse mesofaults; normal mesofaults; steeply inclined joints; and vertical joints (Fig. 3). Whereas fractures related to right-lateral shear are abundant in both the Pontus Formation and the overlying Upper Pleistocene–Holocene sediments, those related to left-lateral shear are restricted to the Pontus Formation. The number of localities at which mesofractures related to different shear regimes intersect each other is limited. Most of those interpreted as being related to left-lateral shear are cut by those related to right-lateral shear.

North-west trending reverse mesofaults are the least abundant fractures (Fig. 3*a*), being observed only in the Cerkes–Kursunlu–Ilgaz basin where they are relatively common in the Lower Pontus Formation in the region of Kursunlu (Fig. 2*a*). Normal mesofaults (Figs 2*b* and 3*b*) strike between NNE and ENE. They are equally abundant in both the Upper and Lower Pontus Formations, but as Fig. 3*b* shows, they are restricted to the western basins with the exception of Tasova–Erbaa. Figure 3*c* shows the distribution of joint sets at mean inclinations between 50 and 74°. These fractures, which are commonly parallel or subparallel to nearby normal mesofaults, are interpreted as conjugate normal shear joints (Fig. 2*c*). Their distribution is restricted to the three western basins in which they are more abundant in the Lower Pontus Formation. Vertical joints are common in both divisions of the Pontus Formation in the three western basins, but are restricted to the Lower Pontus Formation in the two eastern basins. Except for the western subarea of the Cerkes–Kursunlu–Ilgaz basin, where the system is represented by a single set of extension fractures, the vertical joints form conjugate sets (Fig. 3*d*). They enclose a mean dihedral angle which is 41°, suggesting that they are mainly surfaces in the shear–extension fracture transition.

Although mesofractures in Neogene basins external to the fault zone were not sampled in detail, a reconnaissance survey suggests that they are significantly less abundant than within the basins associated with the fault zone. Thus, we believe that the neotectonic mesofractures described above are restricted to the fault zone and are not part of a regional system.

The restriction of mesofractures related to left-lateral shear to sediments of the Pontus Formation, together with the observation that both synsedimentary and post-sedimentary structures are represented, suggests that the movements responsible for their generation occurred, possibly intermittently, during the late Miocene–early Pleistocene interval but did not continue after that. The greater abundance of the fractures in the west (79% of analysed surfaces) may indicate that left-lateral shear was more along the western part of the fault zone.

The difficulty of dating divisions of the Pontus Formation prevents the recognition of individual phases of compression or extension. The attitudes and displacement senses on the mesofractures are consistent with their development as secondary structures within a zone along which there was left-lateral displacement, a sense of shear which is the reverse of that along the North Anatolian fault zone at present.

A comprehensive explanation for the inference that there was some left-lateral shear on the fault zone is beyond the scope of this letter. Left-lateral shear may have been a consequence of either or both: a reversal of motion, possibly related to reversals detected in the Aegean region[13]; or the effect of local mechanical constraints caused by, for example, anti-Riedel[14] overlaps of faults.

Fieldwork was funded by M.T.A. of Ankara and A.A.B. acknowledges that institute for a post-graduate award. We thank Nicholas Ambraseys for his comments about the North Anatolian fault zone and his advice. Jean Bees drafted the figures.

Received 28 February; accepted 12 June 1980.

1. McKenzie, D. P. *Geophys. J. R. astr. Soc.* **30,** 109–185 (1972).
2. Şengör, A. M. C. *J. geol. Soc. Lond.* **136,** 269–282 (1979).
3. Allen, C. R. *Contr. No. 1577, Div. Geol. Sci., Calif. Inst. Tech.* 1–32 (1969).
4. Ambraseys, N. N. *Tectonophysics* **9,** 143–165 (1970).
5. Dewey, J. F., Pitman, W. C., Ryan, W. B. F. & Bonnin, J. *Bull. geol. Soc. Am.* **84,** 3137–3180 (1973).
6. Hancock, P. L. & Kadhi, A. *J. geol. Soc. Lond.* **135,** 339–347 (1978).
7. Hancock, P. L. & Atiya, M. S. *J. Struct. Geol.* **1,** 143–153 (1979).
8. Irrlitz, W. *Beih. geol. Jb.* **120,** 1–111 (1972).
9. Mercier, J.-L., Vergely, P. & Delibassis, N. *Tectonophysics* **19,** 315–332 (1973).
10. Angelier, J. *Tectonophysics* **56,** T17–T26 (1979).
11. Stearns, D. W. & Friedman, M. *Mem. Am. Ass. petrol. Geol.* **16,** 82–106 (1972).
12. Couples, G. in *Stress in the Earth* (ed. Wyss, M.) 113–133 (Birkhauser, Basel, 1977).
13. Mercier, J. *Bull. Soc. geol. Fr. 7 Ser.* **19,** 663–672 (1977).
14. Tchalenko, J. S. & Berberian, M. *Bull. geol. Soc. Am.* **86,** 703–709 (1975).

Sr isotopic geochemistry of voluminous rhyolitic ignimbrites and related rocks, Batopilas area, western Mexico

Marvin A. Lanphere*, K. L. Cameron† & Maryellen Cameron†

* US Geological Survey, Menlo Park, California 94025
† Board of Earth Sciences, University of California, Santa Cruz, California 95064

The middle Tertiary ignimbrites of the Sierra Madre Occidental of western Mexico form the largest continuous rhyolitic province in the world. Minor amounts of intermediate lavas occur interlayered with the ignimbrites, and Sr isotope data on the complete range in rock compositions must be considered when evaluating hypotheses for the origin of the rhyolites. Initial ^{87}Sr/^{86}Sr ratios of andesites, dacites and rhyolites from the Batopilas region of western Chihuahua lie in the range 0.7042–0.7050, showing no systematic variation with rock composition. The data reported here support a crystal fractionation hypothesis for the origin for the voluminous rhyolitic ignimbrites.

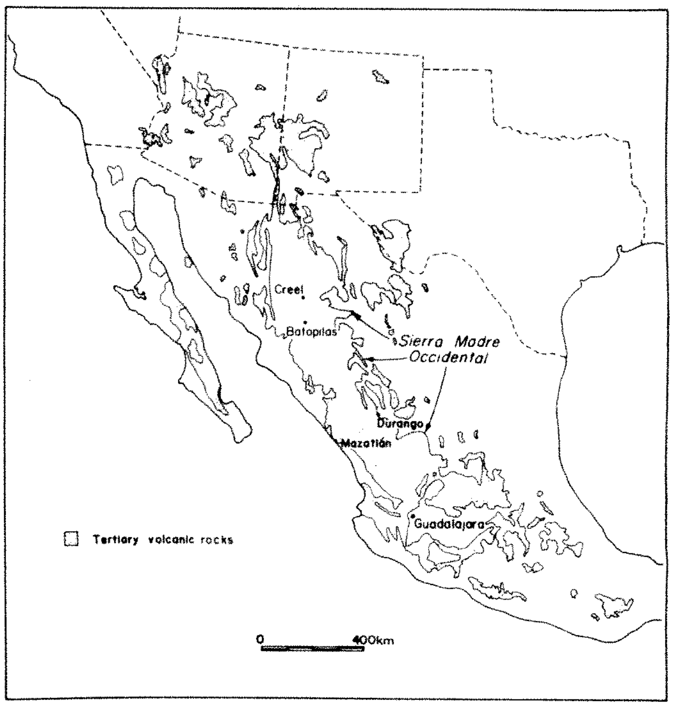

Fig. 1 Distribution of Tertiary volcanic rocks in Mexico and the adjacent US.

A high volcanic plateau, the Sierra Madre Occidental, parallels the west coast of Mexico for 1,200 km (Fig. 1). The plateau is capped by a thick section of middle Tertiary extrusive rocks, predominantly rhyolitic ignimbrites (ash-flow tuffs), referred to informally here as the Upper Volcanic sequence. These ignimbrites, most of which were erupted between 34 and 27 Myr ago, cover at least 200,000 km^2 in western Mexico and have an average thickness[1–3] approaching 1,000 m. An eastward-dipping subduction zone was active off the west coast of Mexico when these rocks were erupted[4]. The volcanic deposits occur as a belt parallel to the western continental margin (Fig. 1), suggesting that they represent a middle Tertiary magmatic arc associated with that subduction[5]. The Sierra Madre Occidental contains a larger volume of rhyolitic rocks than do better known ignimbrite provinces such as the Central Andes (>70,000 km^3, ref. 6), North Island, New Zealand (>15,000 km^3, ref. 7) and Central America (>10,000 km^3, ref. 8). The total original volume of rhyolitic ignimbrites in the western US may have exceeded that of Mexico, but much of that has now been removed by erosion or covered by more recent deposits.

Most of the samples described here are from the Batopilas region of western Chihuahua (Fig. 1). Data on a few samples of rhyolite from the Creel area (Fig. 1), about 100 km north of Batopilas, are also reported. The Upper Volcanic sequence near Batopilas was erupted ~30 Myr ago[3]. More than 80% of the sequence is composed of rhyolitic ignimbrites, but rhyolitic, dacitic and andesitic lava flows occur interlayered with the ignimbrites. The andesite-to-rhyolite series is calc-alkalic and contains ~1% K_2O at $SiO_2 = 60\%$ (refs 3, 5); the ignimbrites typically contain 71–75% SiO_2 and 0.5–1.5% normative corundum. The present study compared the Sr isotopic compositions of the voluminous rhyolites with those of the associated intermediate lavas. The only previously published Sr isotopic data on rocks of the Upper Volcanic sequence were on eight samples of rhyolite collected along a transect between Durango and Mazatlan (Fig. 1), some 400 km south of the Batopilas area, and three samples from near Cuauhtemoc, ~175 km north-east of Batopilas[9]. The initial ^{87}Sr/^{86}Sr ratios of these samples range from 0.7033 to 0.7062.

Rb and Sr concentrations were determined by X-ray fluorescence. The uncertainties in concentration measurements are estimated to be ~3% based on replicate analyses of USGS rock standards. Sr isotopic composition was measured on samples dissolved in HF and $HClO_4$; Sr was separated using ion-

Table 1 Rb, Sr and Sr isotopic compositions of samples from the Upper Volcanic sequence of the Sierra Madre Occidental, western Chihuahua, Mexico

Sample no.	Rock type or mineral	SiO_2 (wt %)	Rb* (p.p.m.)	Sr* (p.p.m.)	$^{87}Rb/^{86}Sr$	$(^{87}Sr/^{86}Sr)$† Measured	$(^{87}Sr/^{86}Sr)$‡ Initial
Batopilas area							
MX-7526	Lava	60.5	72	437	0.476	0.70491 ± 17	0.70471 ± 17
MXU-7616	Lava	61.0	86	468	0.531	0.70497 ± 17	0.70474 ± 17
MX-7528	Lava	62.4	65	392	0.480	0.70468 ± 20	0.70448 ± 20
MXB-7714	Lava	64.5	244	418	1.69	0.70538 ± 19	0.70466 ± 19
MXY-7618	Lava	65.2	79	402	0.568	0.70495 ± 9	0.70471 ± 9
MX-7530	Lava	67.6	136	319	1.23	0.7053 ± 3	0.7048 ± 3
MX-7530	Plagioclase	—	—	—	—	0.70485 ± 25	—
M-172	Ignimbrite§	71.5	139	373	1.08	0.70545 ± 20	0.70499 ± 20
MXU-7615	Ignimbrite	72.1	133	196	1.96	0.70519 ± 14	0.70435 ± 14
MX-7522	Ignimbrite	73.5	87	252	0.999	0.7052 ± 2	0.7048 ± 2
MX-7522	Plagioclase	—	—	—	—	0.70475 ± 20	—
M-161	Ignimbrite	74.7	179	160	3.24	0.70623 ± 16	0.70485 ± 16
M-220	Lava	74.9	114	164	2.01	0.70505 ± 29	0.70419 ± 29
MXY-7617	Lava	75.4	133	143	2.69	0.70563 ± 17	0.70448 ± 17
MX-7504	Ignimbrite	76.2	267	94	8.22	0.7081 ± 3.5	0.7046 ± 3.5
MX-7504	Plagioclase	—	—	—	—	0.7051 ± 2.5	—
Creel area							
M-205‖	Lava	73.0	164	295	1.61	0.70812 ± 10	0.70743 ± 10
M-276	Lava	76.2	170	197	2.50	0.70660 ± 11	0.70554 ± 21
M-103	Lava	76.3	118	157	2.17	0.7071 ± 2	0.7063 ± 2

* Rb and Sr concentrations measured by X-ray fluorescence.

† $^{86}Sr/^{88}Sr$ ratios normalized to a value of 0.1194. $^{87}Sr/^{86}Sr$ ratios adjusted to a value of 0.71014 for NBS $SrCO_3$ standard. Analyses were made at US Geological Survey, Menlo Park.

‡ Corrections to measured $^{87}Sr/^{86}Sr$ ratios due to addition of radiogenic ^{87}Sr are based on K–Ar ages, ref. 3.

§ All ignimbrites are whole rock samples.

‖ 40 km south of Creel.

exchange chromatography. Mass spectrometry was done with an automated 30.48-cm-radius 90°-sector single-collector instrument using a triple-filament source and digital data acquisition. A typical Sr-composition determination consists of 24–36 measurements of each mass. The uncertainties in isotopic composition (Table 1) are standard deviations of analytical precision.

The initial $^{87}Sr/^{86}Sr$ ratios for 13 samples of andesitic to rhyolitic rocks of the Upper Volcanic sequence from the Batopilas area range from 0.7042 to 0.7050 (Table 1). There is no systematic variation in initial ratios with SiO_2 content (Fig. 2), Sr content or Rb/Sr ratio. The Pearson correlation coefficient, r, between the initial $^{87}Sr/^{86}Sr$ ratio and SiO_2 content, Rb content, and Rb/Sr ratio are −0.20, 0.05, and −0.15, respectively. The correlation coefficient between initial $^{87}Sr/^{86}Sr$ ratio and Sr content is 0.40 (Fig. 3). However, the null hypothesis that these two variables are linearly related is rejected at the 5% level of significance. That is, there is no significant correlation between the $^{87}Sr/^{86}Sr$ ratio and the Sr content of the analysed samples. Upper Volcanic rhyolites from Creel are more radiogenic than those from Batopilas, with initial ratios ranging from 0.7055 to 0.7074 (Table 1). Initial ratios reported by McDowell *et al.*[9] for eight samples of rhyolite from the Durango-Mazatlan area range from 0.7033 to 0.7062.

Rocks of the Upper Volcanic sequence from the Sierra Madre Occidental have somewhat higher $^{87}Sr/^{86}Sr$ ratios than Quaternary andesites of the Trans-Mexico volcanic belt (0.7036–0.7043, ref. 10). The ignimbrites from Mexico are similar in Sr isotopic characteristics to Cenozoic ignimbrites from Nevada[11] and Central America[12] but are less radiogenic than ignimbrites from Chile[13]. The middle Tertiary andesite-to-rhyolite series of the San Juan Mountains volcanic field of Colorado, shows an increase in initial $^{87}Sr/^{86}Sr$ ratio from about 0.7054 to 0.7070 with increasing SiO_2 content[14]. This increase was interpreted[14] to reflect interaction of the silicic magmas with Precambrian upper crust enriched in radiogenic Sr. In contrast to the San Juan ignimbrites, there is no evidence in the Sr isotopic data that the Batopilas rhyolites interacted with radiogenic crust. The nature of the crust beneath the region is uncertain, but Anderson and Silver[15] reported that the southern limit of the Precambrian craton probably lies about 200 km to the north. McKee *et al.*[16] reached a similar conclusion for the origin of early Miocene (21–27 Myr old) rhyolitic ash-flow tuffs in the northwestern part of the Great Basin, US. Initial $^{87}Sr/^{86}Sr$ ratios ranging from 0.7042 to 0.7062 were interpreted to reflect only small amounts of contamination of mantle-derived magmas by crustal material.

The Sr isotopic data reported here support the fractional crystallization model proposed recently by Cameron *et al.*[17] for the origin of the Batopilas rhyolites. The rare-earth element patterns of the ignimbrites can be modelled closely using associated andesites and dacites as parents (K.L.C. and G. N. Hanson, unpublished data). The fractionating assemblage was dominated by plagioclase (>60%) and contained ~10% magnetite with the remaining phases being pyroxene and/or hornblende. The ultimate parent was probably a basaltic magma of mantle origin. Th–Sr variations within the andesite to rhyolite series are inconsistent with a hypothesis that the series were derived by different degrees of melting of similar crustal sources (M.C., K.L.C. and W. C. Bagby, unpublished data). The rhyolites of the Sierra Madre Occidental are heterogeneous isotopically as shown by a comparison of the Batopilas and Creel data (Table 1) and the analyses reported by McDowell *et al.*[9]. Some of the silicic magmas may have interacted with radiogenic

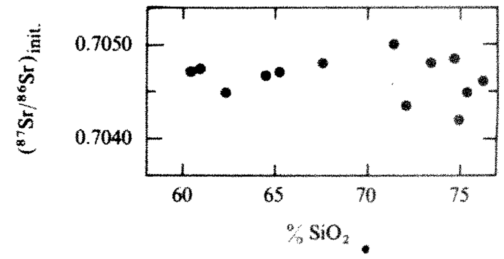

Fig. 2 Initial $^{87}Sr/^{86}Sr$ ratio plotted against SiO_2 content for rocks in the Upper Volcanic sequence of the Batopilas area.

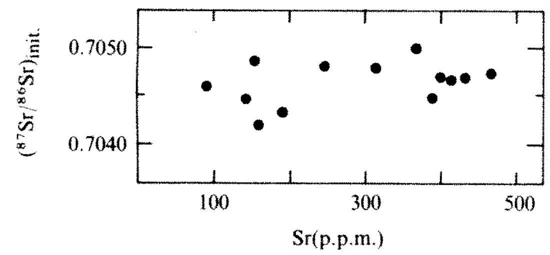

Fig. 3 Initial $^{87}Sr/^{86}Sr$ ratio plotted against Sr content for rocks in the Upper Volcanic sequence of the Batopilas area.

crust. Nevertheless, the Sr isotope data from the Batopilas region establish that no such interaction was required to produce the voluminous rhyolitic ignimbrites of the Sierra Madre Occidental.

Fieldwork was supported by NSF Grant EAR 77-09006. We also acknowledge partial support from the Donors of the Petroleum Research Fund, administered by the American Chemical Society. We thank W. C. Bagby for several of the samples, and A. L. Berry for making the Sr isotopic measurements at the laboratories of the US Geological Survey in Menlo Park.

Received 29 February; accepted 28 May 1980.

1. McDowell, F. W. & Clabaugh, S. E. *Geol. Soc. Am. Spec. Pap.* **180,** 113–124 (1979).
2. Swanson, E. R., Keizer, R. P., Lyons, J. I. & Clabaugh, S. E. *Bull. geol. Soc. Am.* **89,** 1000–1012 (1978).
3. Bagby, W. C. thesis, Univ. California, Santa Cruz (1979).
4. Atwater, T. & Molnar, P. *Stanford Univ. Publ. Geol. Sci.* **13,** 136–148 (1973).
5. Cameron, K. L., Cameron, M., Bagby, W. C., Moll, E. J. & Drake, R. E. *Geology* **8,** 87–91 (1980).
6. Pichler, H. & Zeil, W. *Bull. Volcanol.* **35,** 424–452 (1972).
7. Ewart, A. & Stipp, J. J. *Geochim. Cosmochim. Acta* **32,** 699–736 (1968).
8. Pushkar, P., McBirney, A. R., & Kudo, A. M. *Bull. Volcanol.* **35,** 265–294 (1972).
9. McDowell, F. W., Duex, T. W., Henry, C. D. & Long, L. E. *U.S. Geol. Surv. Open-File Rep.* **78–701,** 289–291 (1978).
10. Moorbath, S., Thorpe, R. S. & Gibson, I. L. *Nature* **271,** 437–438 (1978).
11. Noble, D. C., Hedge, C. E., McKee, E. H. & Korringa, M. K. *Bull. geol. Soc. Am.* **84,** 1393–1405 (1973).
12. Pushkar, P., McBirney, A. R. & Kudo, A. M. *Bull. Volcanol.* **35,** 265–294 (1972).
13. Thorpe, R. S., Francis, P. W. & Moorbath, S. *Earth planet. Sci. Lett.* **42,** 359–367 (1979).
14. Lipman, P. W., Doe, B. R., Hedge, C. E. & Steven, T. A. *Bull. geol. Soc. Am.* **89,** 59–82 (1978).
15. Anderson, T. H. & Silver, L. T. *Geol. Soc. Am. Abstr. Prog.* **7,** 141 (1975).
16. McKee, E. H., Noble, D. C., Hedge, C. E. & Bonham, H. F. *U.S. Geol. Surv. Prof. Pap.* **800–D,** D99–D102 (1972).
17. Cameron, K. L., Cameron, Maryellen & Bagby, W. C. *Geol. Soc. Am. Abstr. Prog.* **11,** 397 (1979).

Ancient Archaean supracrustal rocks from the Limpopo Mobile Belt

Peter C. Horrocks

Department of Geology, University of the Witwatersrand,
Jan Smuts Avenue, Johannesburg 2001, South Africa

A preliminary study has been made to establish pressure, temperature and water activity parameters for the high-grade metamorphism of the early Archaean supracrustal rocks exposed in the Limpopo Mobile Belt near Messina, South Africa. The results reported here indicate that a significant orogenic crustal thickness up to ~30 km was developed before ~3,100 Myr ago in the region.

The high-grade and poly-deformed supracrustal gneisses studied occur south-east of Messina in the Central Zone[1] of the Limpopo Mobile Belt (Fig. 1). They are thought to have been deposited at least partly on a sialic basement made up of the ~3,800 Myr old Sand River Gneisses[2], which are cut by 3,570 Myr old tholeiitic dykes[2] that have not been recognized in the supracrustal gneisses. The supracrustal gneisses were intruded by the anorthositic, gabbroic and peridotitic gneisses of the Messina layered intrusion[3] probably ~3,270 Myr ago (J. M. Barton Jr, work in preparation). Subsequently, an important event of igneous and metamorphic activity affected all of these rocks ~3,150 Myr ago[4], and a second suite of ~3,060 Myr old tholeiitic dykes were intruded[2].

The supracrustal gneisses are predominantly quartzo-feldspathic, but contain numerous interlayers and lenses of pyroxenitic amphibolite, quartzite, magnetite quartzite, garnet–cordierite gneiss, calc-silicate gneiss and marble. The mafic lithologies commonly preserve othopyroxene + clinopyroxene + amphibole + plagioclase + quartz + magnetite ± garnet assemblages, and frequently show prograde metamorphic textures in which orthopyroxene has replaced and overgrown amphibole, while some localities show coexisting clinopyroxene and garnet. Kelyphitic coronas predominatly made up of plagioclase are developed around the garnet in lithologies with abundant amphibole, and in some samples, the garnet is almost completely replaced, or remains only as a few scattered optically continuous remnants in the centres of these reaction coronas. Thus, these kelyphitic textures are thought to be the result of retrograde processes (ref. 5, and P.C.H., in preparation), and not due to a second prograde metamorphism as has been described for previously metamorphosed rocks with a resulting low water partial pressure[6]. The metapelitic lithologies contain garnet + cordierite + biotite + sillimanite (±kyanite) + plagioclase + quartz ± K-feldspar ± amphibole ± orthopyroxene. The garnet is commonly distinctly zoned with more inclusion-filled cores, which are more pyrope-rich, overgrown by thin more almandine-rich and inclusion-poor rims (work in preparation). Some localities preserve kyanite overgrown by sillimanite[7–9].

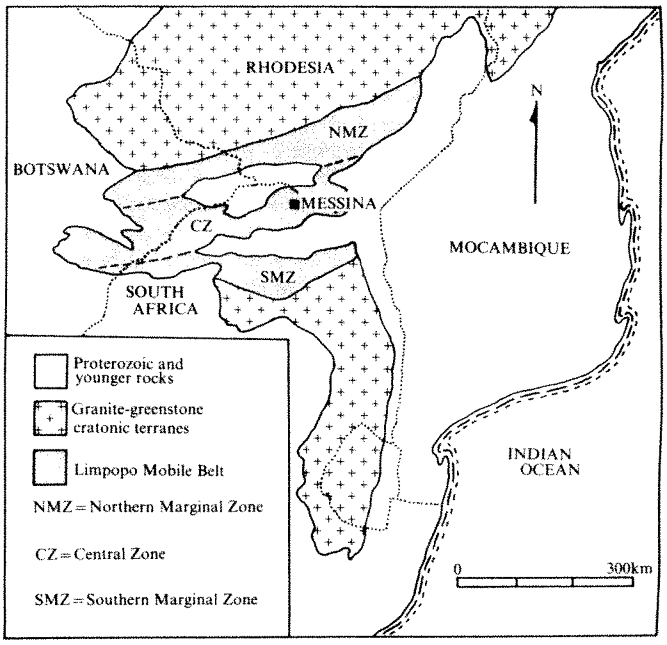
RHODESIA
NMZ
BOTSWANA
MESSINA
CZ
SMZ
SOUTH AFRICA
MOCAMBIQUE
N
INDIAN OCEAN
0
300km
Proterozoic and younger rocks
Granite-greenstone cratonic terranes
Limpopo Mobile Belt
NMZ = Northern Marginal Zone
CZ = Central Zone
SMZ = Southern Marginal Zone

Fig. 1 A simplified geological map of part of southern Africa showing the location of Messina and the Limpopo Mobile Belt.

Peraluminous and magnesia-rich rocks within these metapelitic gneisses consist of corundum + spinel + sapphirine + cordierite + garnet + phlogopite ± orthopyroxene ± gedrite, and these undersaturated assemblages apparently represent metamorphic residua after the extraction of minimum melt granitic anatectic liquids[10,11]. Symplectitic coronas about garnet are developed in places where the garnet is replaced by an intergrowth of radial orthopyroxene grains in plagioclase (Fig. 2). This garnet is relatively unzoned, and it is not obvious whether this reaction is prograde or retrograde. However, some samples preserve only spherical 'knots' comprising myrmekitic orthopyroxene grains in plagioclase suggesting the complete breakdown and

0028–0836/80/320596—04$01.00

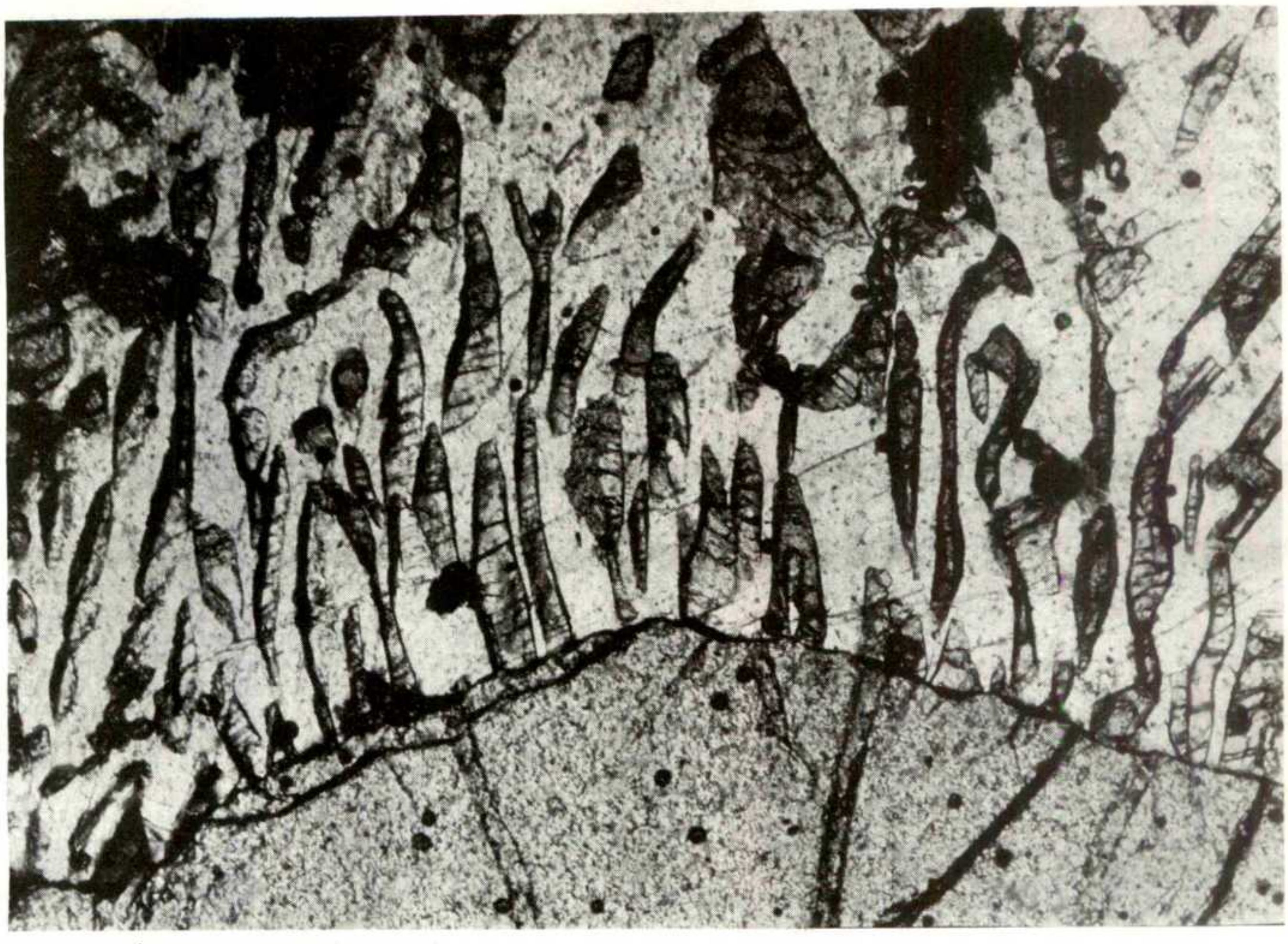

Fig. 2 A photomicrograph of the garnet–orthopyroxene–plagioclase symplectite. Note the worm-like orthopyroxene grains in the plagioclase which radiate out from the garnet porphyroblast. Scale bar, 0.5 mm.

Table 1 Temperature, pressure and water activity estimates for the supracrustal rocks near Messina, Limpopo Belt

Equilibria Coexisting minerals	(1) & (2) opx + cpx	(3) opx + gar-rim	(4) cpx + gar-rim	(5) gar-rim + biot	(6) gar-rim + cord	(7) opx + cpx + hble + qz
Refs	12–14	12, 14, 16, 21	15–17	18, 19	16, 18	23
Mafic rock samples						
27	890 ± 50	660 ± 50 6.3 ± 3	690 ± 50 at 6 kbar	—	—	0.10 ± 0.01
X21395	870 ± 50	—	—	—	—	0.06 ± 0.01
X21399	870 ± 50	665 ± 50 5.5 ± 3	690 ± 50 at 6 kbar	—	—	0.03 ± 0.01
Pelitic samples						
21-7-F	—	—	—	755 ± 50 at 6 kbar	630 ± 50 7 ± 1.5	—
21-7-G	—	—	—	730 ± 50 at 6 kbar	750 ± 50 6.5 ± 1.5	—
Symplectite						
2-8-10B	—	680 ± 50 5.6 ± 3	— —	640 ± 50 at 6 kbar	— —	— —
Sapphirine rocks						
2-8-12	—	—	—	640 ± 50 at 6 kbar	610 ± 50 8.1 ± 1.5	— —
11-8	—	780 ± 50 at 6 kbar	—	655 ± 50 at 6 kbar	590 ± 50 8.2 ± 1.5	—

See text for details of the equilibria used, and a discussion on the errors. Temperatures are in °C; pressures in kbar; water activities are expressed as a fraction between 0 and 1 for equilibrium 7 only. biot, biotite; cord, cordierite; cpx, clinopyroxene; gar, garnet; hble, hornblende; opx, orthopyroxene; qz, quartz.

replacement of garnet probably by a retrograde process similar to that which is thought to have produced the kelyphitic coronas.

Electron microprobe analyses of the above mineral assemblages mean that several thermodynamic techniques can be used to estimate some of the pressure, temperature and water activity parameters of the high-grade metamorphism these rocks have experienced. The analytical technique used natural and synthetic standards, and was routinely able to repeat known international standards typically to within 2% for all relevant elements. Temperature estimates have been calculated using the following equilibria:

$$\underset{\text{opx}}{Mg_2Si_2O_6} = \underset{\text{cpx}}{Mg_2Si_2O_6} \tag{1}$$

$$\underset{\text{cpx}}{CaMgSi_2O_6} + \underset{\text{opx}}{Mg_2Si_2O_6} = \underset{\text{opx}}{CaMgSi_2O_6} + \underset{\text{cpx}}{Mg_2Si_2O_6} \tag{2}$$

$$\underset{\text{garnet}}{Mg_3Al_2Si_3O_{12}} + \underset{\text{opx}}{3CaMgSi_2O_6} = \underset{\text{garnet}}{Ca_3Al_2Si_3O_{12}} + \underset{\text{opx}}{3Mg_2Si_2O_6} \tag{3}$$

$$\underset{\text{garnet}}{Mg_3Al_2Si_3O_{12}} + \underset{\text{cpx}}{3CaFeSi_2O_6} = \underset{\text{garnet}}{Fe_3Al_2Si_3O_{12}} + \underset{\text{cpx}}{3CaMgSi_2O_6} \tag{4}$$

$$\underset{\text{garnet}}{Fe_3Al_2Si_3O_{12}} + \underset{\text{biotite}}{KMg_3AlSi_3O_{10}(OH)_2} = \underset{\text{garnet}}{Mg_3Al_2Si_3O_{12}} + \underset{\text{biotite}}{KFe_3AlSi_3O_{10}(OH)_2} \tag{5}$$

$$\underset{\text{cordierite}}{3Fe_2Al_4Si_5O_{18}} + \underset{\text{garnet}}{2Mg_3Al_2Si_3O_{12}} = \underset{\text{cordierite}}{3Mg_2Al_4Si_5O_{18}} + \underset{\text{garnet}}{2Fe_3Al_2Si_3O_{12}} \tag{6}$$

The geothermometers derived from these equilibria[12–19] are based on experimental data and calculated values are typically within 50 °C of the experimental condition. Thus the maximum practical resolution of these techniques is probably about ±50°C and about ±100 °C at worst. Fe^{3+} was estimated in pyroxene and garnet by a stoichiometric method[20] and was found to cause generally a lowering of the temperature estimates by not more than 50 °C in most cases, and usually much less than 50 °C. Pressure estimates were made from equilibria (3) and (6), and these geobarometers[12,16,21], also based on experimental data, have given more inconsistent results[22], mainly due to the problems surrounding Al solution in pyroxene. At worst, these barometers reproduce the experimental values to within 5 kbar (ref. 12) and to within 1.5 kbar (ref. 16) for the garnet–cordierite equilibrium. Typically, the best resolution for practical purposes is probably limited to ±3 kbar (ref. 21). The water activity was calculated using equilibrium (7) (S. Richardson, personal communication) in the mafic lithologies:

$$\underset{\text{tremolite}}{Ca_2Mg_5Si_8O_{22}(OH)_2} = \underset{\text{diopside}}{2CaMgSi_2O_6} + \underset{\text{enstatite}}{3MgSiO_3} + SiO_2 + H_2O \tag{7}$$

together with certain thermodynamic approximations[23] based on hydrothermal equilibrium data. The results from these calculations are summarized in Table 1 and Fig. 3.

The P–T field thus suggested for the supracrustal rocks in the region (Fig. 3) supports the petrographical evidence of this study and that of other studies in the region[7–9], particularly with regard to the association of enstatite + kyanite + quartz[7], sillimanite overgrowths on kyanite[7–9], prograde othopyroxene replacement of amphibole (that is, granulite facies metamorphism), retrograde kelyphitic coronas about garnet in the mafic rocks, and the garnet zonation in the pelitic rocks. The early phase of this metamorphism which produced the orthopyroxene-bearing assemblages in the mafic rocks, and the pyrope-rich garnet and corundum in the pelitic rocks (work in preparation), was characterized by temperatures in excess of 800 °C and probably pressures up to 10 kbar (Fig. 3). Water activities in the mafic rocks were low, with H_2O making up ≤10% of the fluid present during the high-grade phase of the metamorphism. CO_2 was probably the most abundant fluid present during this time, based on a comparison with a study of liquid inclusions in granulites from southern Norway[24]. A subsequent retrogression to a lower temperature–pressure regime is recorded by the development of the kelyphitic rims about garnet in the mafic lithologies, the almandine-rich garnet overgrowths and the spinel + sapphirine + cordierite association (work in preparation) in the pelitic rocks, and probably also the production of the symplectitic textures about garnet (Fig. 2). Here, pressures of between 5 and 7 kbar were attained at temperatures of ~600–700 °C (Fig. 3).

The early phase of this metamorphism suggests that the supracrustal stratigraphy, deposited sometime between 3,570-Myr ago and the emplacement of the Messina layered intrusion ~3,270 Myr ago, was subjected to rapid burial to depths probably greater than 30 km into regions of the lower crust either by subsidence or tectonic means. An earlier study of an enstatite + kyanite + quartz association from Zimbabwe[7] also suggested pressures in excess of 10 kbar and temperatures close to 950 °C with the enstatite having an Al_2O_3 content of over 5.5%. These data suggest that this metamorphism reflects an average geothermal gradient during the peak of the metamorphic event of less than about 30 °C km^{-1} in the lower regions of the crust. This compares favourably with other suggested Archaean geotherms[25–28]. The metamorphic and igneous activity about 3,150 Myr ago, which reset the Rb–Sr isotopic ratios in the rocks of the Messina layered intrusion[3] probably reflects the peak of this phase of the metamorphism. Subsequent orogenic events occurred during the interval from ~3,100 Myr ago to ~2,400 Myr ago[4] during which minimum melt granitic anatectic liquids were extracted[29] and intense polyphase deformation was imposed on the lithologies[9]. Although temperature and pressure data currently available do not provide sufficient evidence in themselves, these events could probably represent a continous progression of tectonism and metamorphism[8,9] during the

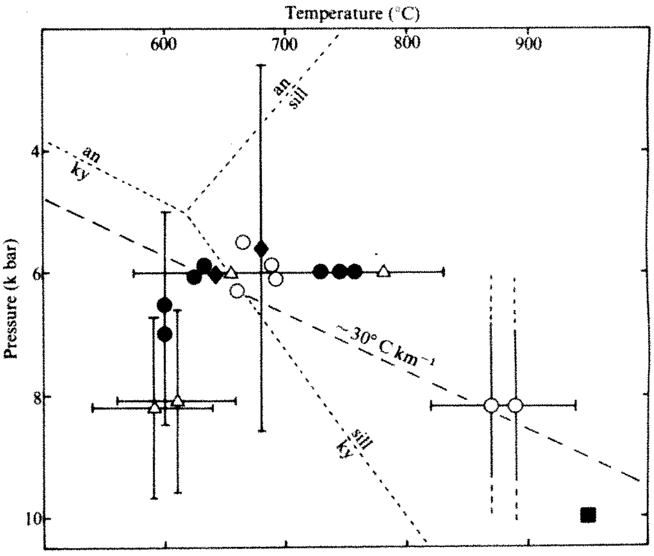

Fig. 3 A pressure–temperature diagram showing the results given in Table 1: ○, mafic rocks; ●, pelitic lithologies; △, sapphirine-bearing samples; ◆, symplectite sample; ■, enstatite + kyanite + quartz[7] association discussed in the text. an, andalusite; ky, kyanite; and sill, sillimanite.

erosional and/or tectonic excavation of the supracrustal rocks and the resulting pressure and temperature changes. The exhumation of these gneisses would cause waning pressures at maintained temperatures, probably adiabatically, and may explain the retrogression as manifest by the kelyphitic textures and garnet zonation. The end of high-grade metamorphism and the onset of comparative tectonic stability are evidenced by a fabric-free dolerite dyke of ~2,200 Myr in age[30]. This ancient basement-supracrustal event of high-grade metamorphism may not predate the development of the greenstone–grandodiorite–tonalite terrains which comprise much of the Earth's shield areas, but perhaps represents a contemporaneous development at lower crustal levels now only exposed in limited zones of the ancient shields. The geometry of these zones (or 'belts') is probably superimposed, and not a result of the intrinsic metamorphic history.

This work was sponsored by the South African Council for Scientific and Industrial Research, and is Contribution No. 56 in South Africa's contribution to the International Geodynamics Project. I thank T. N. Clifford, W. Schreyer, A. B. Thompson, D. J. Ellis, R. E. P. Fripp, J. M. Barton Jr and M. K. Watkeys for criticisms.

Received 12 February; accepted 3 June 1980.

1. Cox, K. G. *et al. Phil. Trans. R. Soc.* **A257,** 71–218 (1965).
2. Barton, J. M. Jr, Fripp, R. E. P. & Ryan, B. *Nature* **267,** 487–490 (1977).
3. Barton, J. M. Jr, Fripp, R. E. P., Horrocks, P. C. & McLean, N. *Am. J. Sci.* **279,** 1108–1134 (1979).
4. Barton, J. M. Jr & Ryan, B. *Botswana geol. Surv. Bull.* **12,** 183–200 (1977).
5. Leyreloup, A., Lasnier, B. & Marchand, J. *Pétrologie* **1,** 43–55 (1975).
6. De Wit, M. J. & Strong, D. F. *J. Geol.* **83,** 609–627 (1975).
7. Chinner, G. A. & Sweatman, T. R. *Miner. Mag.* **36,** 1052–1060 (1968).
8. Light, M. P. R., Broderick, T. J. & Watkeys, M. K. *Botswana geol. Surv. Bull.* **12,** 61–74 (1977).
9. Light, M. P. R. & Watkeys, M. K. *Ann. Rhodesian geol. Surv.* **III,** 35–40 (1978).
10. Clifford, T. N., McIver, J. R. & Stumpfl, E. F. *Miner. Mag.* **40,** 347–356 (1975).
11. Lal, R. K., Ackermand, D., Seifert, F. & Halder, S. K. *Contr. Miner. Petrol.* **67,** 169–187 (1978).
12. Wood, B. J. & Banno, S. *Contr. Miner. Petrol.* **42,** 109–124 (1973).
13. Wells, P. R. A. *Contr. Miner. Petrol.* **62,** 129–140 (1977).
14. Powell, R. *Phil. Trans. R. Soc.* **A288,** 457–469 (1978).
15. Raheim, A. & Green, D. H. *Contr. Miner. Petrol.* **48,** 179–203 (1974).
16. Wells, P. R. A. *J. Petrol.* **20,** 187–226 (1979).
17. Ellis, D. J. & Green, D. H. *Contr. Miner. Petrol.* **71,** 13–22 (1979).
18. Thompson, A. B. *Am. J. Sci.* **276,** 425–454 (1976).
19. Ferry, J. M. & Spear, F. S. *Contr. Miner. Petrol.* **66,** 113–117 (1978).
20. Ryburn, R. J., Raheim, A. & Green, D. H. *Lithos* **9,** 161–164 (1975).
21. Wood, B. J. *Contr. Miner. Petrol.* **46,** 1–15 (1974).
22. O'Hara, M. J. & Yarwood, G. *Phil. Trans. R. Soc.* **A288,** 441–456 (1978).
23. Fisher, J. R. & Zen, E.-An. *Am. J. Sci.* **270,** 297–314 (1971).
24. Touret, J. *Lithos* **4,** 423–436 (1971).
25. Burke, K. & Kidd, W. S. F. *Nature* **272,** 240–241 (1978).
26. Drury, S. A. *Nature* **274,** 720–721 (1978).
27. England, P. C. *Nature* **277,** 556–558 (1979).
28. Bickle, M. J. *Earth planet. Sci. Lett.* **40,** 301–323 (1978).
29. McCarthy, T. S. thesis, Univ. Witwatersrand (1977).
30. Barton, J. M. Jr *Precamb. Res.* **9,** 57–80 (1979).

Evidence for pre-Devensian glaciation in the northeastern Lake District

J. Boardman

Department of Humanities, Brighton Polytechnic, Falmer, Brighton, East Sussex BN1 9PH, UK

In the northeastern English Lake District two major till units occur. The upper unweathered unit is clearly the product of late-Devensian glaciation[1]. The lower till has undergone severe humid temperate chemical weathering and contains palaeosol features. It must pre-date the Ipswichian interglacial[2]. Pre-Devensian weathering profiles of an interglacial character have not previously been described in northern England. There has been scant previous evidence for a pre-Devensian glaciation of north-west England[3,4]. No date has been assigned to 'Early Scottish' till which has been located around Carlisle. Till in Low Furness is recorded beneath 'interglacial beds', but this was described in the nineteenth century and cannot be relocated[1,3]. It has generally been accepted that erosion during the Devensian effectively removed pre-existing deposits and it has been assumed that the landforms of the Lake District, including the major erosional features, are the product of the last glaciation[5,6]. I show here that, in the Vale of Threlkeld, this is not the case.

In the valleys of Mosedale and Thornsgill Beck, two south bank tributaries of the Glenderamackin (Fig. 1), 10 km east of Keswick, a sequence of glacigenic, glacifluvial and periglacial deposits overlie thinly-cleaved mudstones of Ordovician Skiddaw Group[7]. The surface tills form drumlins and till hummocks, and glacifluvial sands and gravels locally form kames. All these features are considered to be of late Devensian age[1]. The Mosedale Beck valley was eroded by high meltwater discharges released by the corrie glacier at Wolf Crags which last developed in Younger Dryas time[4]. In places, such as on Threlkeld Common, stone-banked solifluction lobes disturb the till and these are probably of Younger Dryas age.

The recently discovered succession in the area[2] reveals weathered till at the base, overlain by fresh unweathered till or unweathered sands and gravels. Four representative sites are considered in Fig. 2.

At Carel Gully and site D, yellowish-brown weathered till is overlain by a grey till which incorporates, at its base, lenses of the weathered material. At two sites, D and N, a weathering profile exists—the severely weathered till grading down into fresh till. In the weathered till manganese staining is frequent, clasts are soft and friable, and surface textures on quartz grains, examined by scanning electron microscopy, indicate severe chemical weathering and an absence of glacial processes (P. Wilson, personal communication). At site E, the weathered till unit is dissected by a channel which is filled with similarly weathered sands and gravels. This in turn is overlain by coarse unweathered gravels which form a terrace fragment of Younger Dryas age.

At N, the upper part of the site is obscured but it is probable that unweathered Devensian material completes the sequence, as it is exposed at nearby sites. In places, a gleyed horizon is developed in a silty clay band at the base of the severely weathered till. The dominant colour is orange (7.5YR 6/8) but it contains many irregular mottles of low chroma (5Y 7/1). In thin section these are seen to be iron-depleted areas (albans). Channels and chambers reflect biological activity[8], and in some cases, are lined with translocated clay and silty clay. Gleying, translocation of clay, and biological activity are characteristic of the B horizon of certain soils.

The chief characteristics of the weathered till in the area are: (1) high proportion of soft and friable clasts that can be crushed by hand; (2) typical bright yellowish-brown (10YR 6/6) clast colour and yellowish-brown (10YR 5/8) matrix colour which differ from greenish-grey (7.5GY 5/1) and dark grey (N 3/0) respectively of the fresh materials; (3) low silt and clay percentages, 13 and 7% for the weathered till samples, in contrast to values of 23 and 20% for unweathered equivalents; (4) clay mineral suites dominated by illite and vermiculite which are typical of many weathering products of acid igneous rock types (R. Merriman, personal communication).

The weathering profile is interpreted as having formed in a period of protracted weathering on a stable land surface such as is typical of a vegetated temperate interglacial environment.

The sequence of events can be summarized as: (1) deposition of the lower till and glacifluvial sands and gravels; (2) severe chemical weathering under humid temperate conditions; (3) deposition of the upper till incorporating lenses of the pre-existing weathered till unit; (4) deposition of terrace gravels in Mosedale and corrie glaciation at Wolf Crags.

0028–0836/80/320599—02$01.00

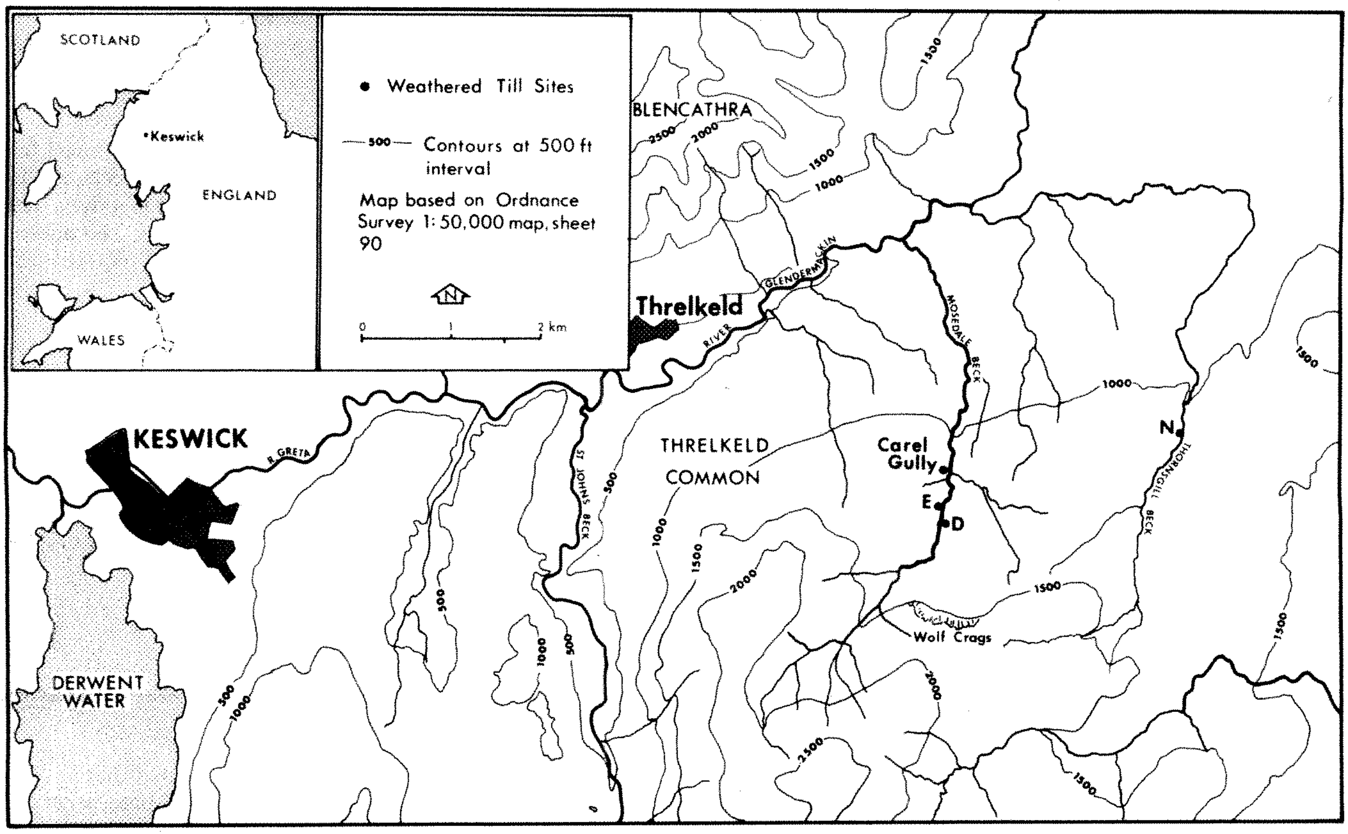

Fig. 1 Location of sites.

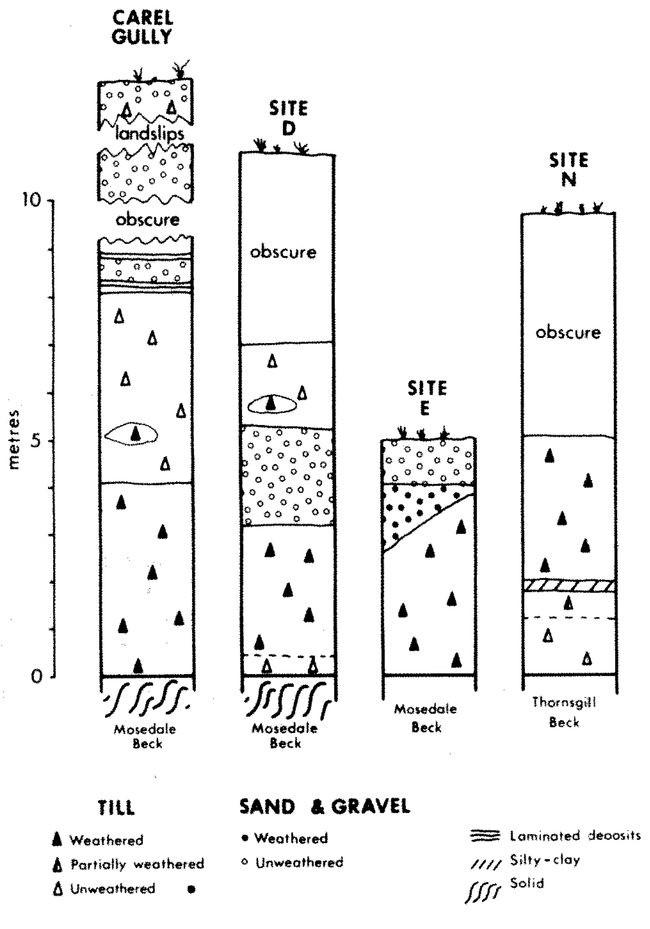

Fig. 2 Stratigraphy of sites.

With reference to the established British Quaternary stratigraphy[9], the upper till and associated glacial landforms is Devensian, the weathering profile is most likely to be Ipswichian, and the weathered till unit is probably Wolstonian. Till of that age has been described from East Yorkshire and Lincolnshire[10], and a possible Wolstonian till containing Lake District erratics occurs in the Peak District[11]. However, in the Lake District, a maximum age cannot be assigned to the till: it may be of greater antiquity.

Preservation of unconsolidated sediments beneath till is rare in highland Britain, and in the northeastern Lake District seems to be the result of irregular bedrock topography. The survival of deposits at several sites suggests that Devensian erosion had a limited impact on the Vale of Threlkeld. Classic glacial features in the area such as the truncated spurs of Blencathra (Fig. 1) are therefore likely to be pre-Devensian in age. By implication, other major glacial troughs in the Lake District may also have been in existence at the onset of the last glaciation.

I thank Dr P. Bullock for advice on pedological aspects and Dr J. Catt for comments, Mr J. Rose, who discovered the weathered till in Mosedale, for discussions and comments. Mr S. Frampton drew the diagrams. The Central Research Fund, University of London, financed the cutting of thin sections.

Received 1 May; accepted 18 June 1980.

1. Evans, W. B. & Arthurton, R. S. in *A Correlation of Quaternary Deposits in the British Isles* (eds Mitchell, G. F. *et al.*) (Geological Society of London, 1973).
2. Boardman, J. *Proc. Cumbs geol. Soc.* **4,** 33–44 (1979).
3. Huddart, D., Tooley, M. J. & Carter, P. A. in *The Quaternary History of the Irish Sea* (eds Kidson, C. & Tooley, M. J.) (Seel House, Liverpool, 1977).
4. Pennington, W. in *The Geology of the Lake District* (ed. Moseley, F.) (Yorkshire Geological Society, 1978).
5. King, C. A. M. *The Geomorphology of the British Isles: Northern England* (Methuen, London, 1976).
6. Moseley, F. in *The Geology of the Lake District* (ed. Moseley, F.) (Yorkshire Geological Society, 1978).
7. Jackson, D. in *The Geology of the Lake District* (ed. Moseley, F.) (Yorkshire Geological Society, 1978).
8. Brewer, R. *Fabric and Mineral Analysis of Soils* (Krieger, New York, 1976).
9. Mitchell, G. F. *et al.* (eds) *A Correlation of Quaternary Deposits in the British Isles* (Geological Society of London, 1973).
10. Madgett, P. A. & Catt, J. A. *Proc. Yorks. geol. Soc.* **42,** 55–108 (1978).
11. Burek, C. in *Limestones and Caves of the Peak District* (ed. Ford, T. D.) (Geo. Abstracts, 1977).

Gene frequency changes and adaptation in marine cockles

Elizabeth Gosling

Zoology Department, University College, Galway, Ireland

When closely related species overlap geographically, a change of character state may occur in one species which is directly attributable to the presence in the same environment of an ecologically similar species[1,2]. Most reports of this phenomenon—called character displacement—have been concerned with divergence, rather than convergence, in morphologial characters between species in the zone of sympatry. There has been only one report on genetic displacement at the allelic level[3]. In this, Murphy observed a divergence in allele frequency at a leucine aminopeptidase locus in sympatric species of marine limpets which he interpreted as allelic accommodation in response to interspecific competition[3]. I report here a study of two closely related species of cockles, *Cerastoderma edule* and *Cerastoderma glaucum*, in which *C. glaucum* exhibits a convergence in allele frequency at the phosphoglucomutase (Pgm) locus when it is found intermixed with *C. edule*.

In the British Isles, *C. edule* is widely distributed intertidally whereas *C. glaucum* is found in stagnant saline pools isolated from tidal influences[4,5]. However, occasionally the two species are found together intertidally, apparently occupying identical ecological niches[6]. The two species are morphologically very similar and were separated using the characteristics outlined by Boyden[7]—shell shape, ligament length, shape of ribs, digestive gland coloration and internal shell pigmentation.

Pgm is coded at a single locus with three electrophoretic alleles, Pgm^A, Pgm^B and Pgm^C, present in *C. glaucum* and Pgm^C, Pgm^D, Pgm^E and Pgm^F present in *C. edule*. The allele Pgm^C is common to both species (Fig. 1). Because of the different electrophoretic mobilities of Pgm allozymes in *C. glaucum* and *C. edule*, the Pgm system can therefore be used in conjunction with morphological characteristics to separate the two species. In this study, unispecific samples of *C. edule* were collected from the intertidal region of the shore whereas all unispecific samples of *C. glaucum* were taken from stagnant saline pools where the cockles were permanently submerged. Table 1 presents allele frequency data in two unispecific populations of *C. edule* and *C. glaucum*. To date, all unispecific populations of either species from Irish and British sites exhibit little geographical variation in allele frequency at this locus (unpublished results). In addition to the above samples, mixed populations of the two species were collected intertidally from two Irish sites (Keeraunnagark and Shannon Estuary) and two British sites (the Fleet, Dorset, and Hullbridge Ferry, Essex). At these sites, *C. glaucum* experiences quite different environmental conditions from the lagoon habitat, such as exposure to air, exposure to wave action and tidal amplitude. In the case of each mixed population, an attempt was made to collect unispecific populations of *C. glaucum* and *C. edule* from sites situated close to the mixed population. The results of the Pgm allozyme analyses of these samples are shown in Fig.2. In some cases (see Fig. 2 *c*, *d*), it was not possible to collect unispecific samples from sites which were geographically close to a mixed population. However, the result was the same for each *Cerastoderma* assemblage, that is, allele frequency in *C. glaucum* was consistently nearer to that of *C. edule* in mixed populations of the two species by a statistically significant ($P<0.05$) amount. Allele frequency in *C. edule* from unispecific populations, or from populations where it was mixed with *C. glaucum*, showed no significant ($P>0.05$) difference.

Table 1 *Pgm* allele frequencies in allopatric populations of *C. edule* and *C. glaucum* from W. Ireland

		Allele frequency							
	N	*A*	*B*	*C*	*D*	*E*	*F*	χ^2	
C. edule Shannon Estuary	80	—	—	0.09	0.34	0.54	0.03	2.43	NS
C. glaucum Carna, Galway	95	0.0	0.68	0.32	—	—	—	2.81	NS

N, no. of individuals analysed. χ^2, Goodness-of-fit of observed to expected frequencies from Hardy–Weinberg equilibrium. NS, not significant, $P>0.05$.

Cross-fertilization can be ruled out as an explanation for the observed convergence in allele frequency. First, no Pgm enzyme genotypes indicative of hybridization were observed. Second, hybridization between these species is, in any case, unlikely. Although individuals with apparently intermediate morphological characteristics occur in mixed populations and cross-fertilization can take place in the laboratory[7,8], attempts[8] to rear hybrid larvae have met with little success. In general, attempts have been less successful between species originating from mixed populations than between species taken from different geographical locations[8]. In addition, displacement in spawning times occurs in mixed populations[9], thereby ensuring effective reproductive isolation between the two species.

The results of the present study suggest that the genetic displacement, that is, the change in allele frequency which occurs only when *C. glaucum* coexists with *C. edule*, is a genetic consequence of adaptation to the intertidal habitat. Previous reports[3,10-12] have implicated interspecific competition as the cause of character displacement in the zone of sympatry. There is no evidence in the literature to suggest that the two cockle species compete in the zone of contact. If interspecific competition is occurring, one might expect the observed difference in

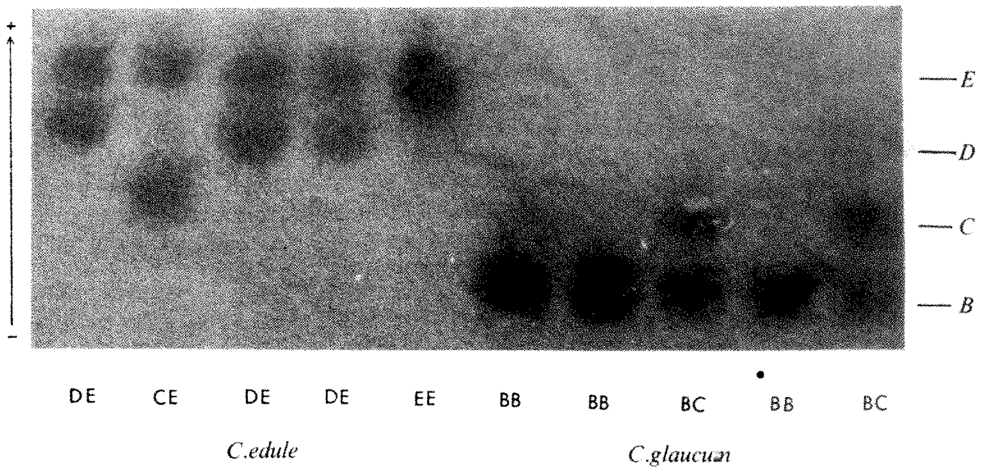

Fig. 1 *Pgm* alleles in *C. edule* and *C. glaucum*. Mixed samples of *C. edule* and *C. glaucum* together with unispecific samples of *C. edule* were collected from the intertidal region of the shore; unispecific samples of *C. glaucum* were collected from non-tidal lagoon sites. A portion of the foot was excised from living individuals and homogenized manually in approximately two volumes of 50 mM Tris-HCl buffer, *p*H 7.8 (1:1w/v). Electrophoresis was carried out at 2 °C in horizontal starch gel (Connaught) using the Tris/EDTA/maleic buffer system, *p*H 7.4, of Spencer *et al.*[13]. Gels were run for 14–16 h at 6.5 V cm^{-1}. Sliced gels were stained for Pgm using the paper overlay method described by Scopes[14].

0028–0836/80/320601—02$01.00

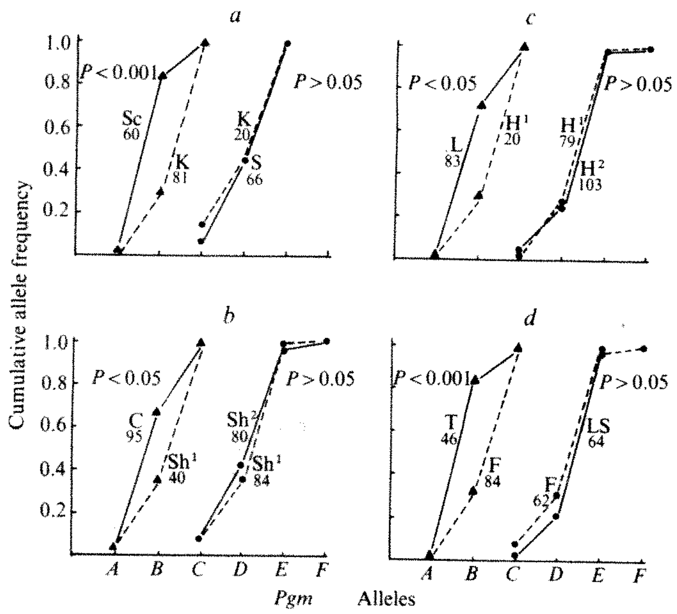

Fig. 2 Cumulative frequency of *Pgm* alleles in allopatric (———) and sympatric (– – – –) populations of *C. glaucum* (▲) and *C. edule* (●). Samples were collected from four habitats that supported mixed populations of *C. glaucum* and *C. edule* and in each case a unispecific populations of *C. glaucum* and *C. edule* was collected from a site situated as close as possible to the mixed population. Results for each *Cerastoderma* assemblage are presented separately in *a*, *b*, *c* and *d*. *P* was derived from a two-tailed Kolmogorov–Smirnov two-sample test of the H_0 that the distribution of alleles in allopatric and sympatric populations of *C. edule* and *C. glaucum* are identical. *a*, S: Silverstrand, Galway; K: Keeraunnagark, Galway; Sc: Screebe, Galway. *b*, C: Carna, Galway; Sh^1, Sh^2: Shannon Estuary, Limerick. *c*, L: Lady's Island, Wexford; H^1, H^2: Hullbridge Ferry, Essex, UK. *d*, T: Tacumshin, Wexford; F: The Fleet, Dorset, England; LS: Leigh-on-Sea, Essex. Numbers beneath each site abbreviation indicate size of sample.

allele frequency to vary depending on the proportions of *C. glaucum* and *C. edule* present in mixed samples. This was not the case, as is evident from Fig. 2*a* and *c*, where the ratio of *C. glaucum* to *C. edule* in the two samples was 4 : 1 and 1 : 4 respectively. In the sample from Fleet, Dorset, individuals of *C. glaucum* were not actually intermixed with *C. edule* but were separated from them by a geographical distance of about 0.5 km. However, *C. glaucum* shows the characteristic shift in allele frequency which indicates that sympatry of the two species is not necessary to produce this effect.

We conclude that, although character divergence or convergence in sympatry can occur in response to interspecific competition there must also be occasions, for example in this study, when it occurs for reasons not directly connected with the presence of another species.

I thank N. P. Wilkins and J. McKay for useful discussions and the following people who helped in the collection of samples: D. McGrath, B. Healy, G. O'Sullivan, A. Beaumont, G. Pickett, B. Dawson and D. Seaward. This work was supported by a grant from the National Board of Science and Technology, Ireland.

Received 11 February; accepted 3 June 1980.

1. Grant, P. R. *Biol. J. Linn. Soc.* **4,** 39–68 (1972).
2. Grant, P. R. *Evol. Biol.* **8,** 237–337 (1975).
3. Murphy, P. G. *Nature* **261,** 228–230 (1976).
4. Boyden, C. R. & Russell, P. J. C. *J. Anim. Ecol.* **41,** 719–734 (1972).
5. Kingston, P. F. *Mar. Biol.* **28,** 317–323 (1974).
6. Brock, V. *Mar. Biol.* **54,** 149–156 (1979).
7. Boyden, C. R. *J. mar. biol. Ass. U.K.* **51,** 605–622 (1971).
8. Kingston, P. F. *Nature* **243,** 360 (1973).
9. Rygg, B. *Sarsia* **43,** 65–80 (1970).
10. Fenchel, T. *Oecologia Berl.* **20,** 19–32 (1975).
11. Dunham, A. E., Smith, G. R. & Taylor, J. N. *Evolution* **33,** 877–896 (1979).
12. Schindel, D. E. & Gould, S. J. *Paleobiology* **3,** 259–269 (1977).
13. Spencer, N., Hopkinson, D. A. & Harris, H. *Nature* **204,** 742–745 (1964).
14. Scopes, R. K. *Biochem. J.* **107,** 139–150 (1968).
15. Siegel, S. *Nonparametric Statistics for the Behavioural Sciences*, 127–136 (McGraw-Hill, New York, 1956).

Juvenile hormone mimics the photoperiodic apterization of the alate gynopara of aphid, *Aphis fabae*

Jim Hardie

Agricultural Research Council Insect Physiology Group,
Department of Zoology and Applied Entomology,
Imperial College, London SW7 2AZ, UK

Extensive investigations of the environmental factors influencing the alate–apterous dimorphism of the summer, parthenogenetic, virginoparous generations of aphids have shown that crowding has a major influence on the development of the alate morph, although temperature and nutrition are also important[1,2]. These factors may act prenatally, postnatally or both, depending on the species. However, the physiological control of this dimorphism within the individual has not been elucidated. As the apterous adult and the larvae share certain morphological features[3] it has been suggested that the hormone controlling larval–adult metamorphosis, juvenile hormone (JH), also influences development of apteriform characteristics[4,5]. Indirect evidence from measurements of corpus allatum (CA) volumes and CA nuclei were believed to support this theory[6] and early experiments with topically applied JH extracts and analogues seemed to divert alate development towards the apterous condition[2,5]. Attempts to obtain more direct evidence have been negative or inconclusive[6]. Recently, Lees[7] has questioned this hypothesis, citing the following evidence: (1) examination of more extreme forms produced by topical application of JH mimics to middle instar alatae shows them to be developing towards a fifth instar, supernumerary larva (that is juvenilization) rather than towards an apterous morph (that is apterization); (2) in an autumn, short-day-induced alate morph of *Aphis fabae*, namely the gynopara (see below), authentic apterization can be effected by postnatal exposure to long photoperiods, the first larval instar being most sensitive to this treatment. By contrast, it was the late second and the third instars that were most sensitive to juvenilization following topical application of JH analogues. It is shown here that larger doses of a more active hormone (JH1) will closely mimic the photoperiodic apterization of these gynoparae but that apterization is not due to the neotenic action of JH. Evidence is also presented suggesting that the alate-apterous dimorphism in summer, long-day generations is not controlled by JH.

In many host-alternating aphid species a separate alate, viviparous morph is produced in response to short days and gives birth to the sexual females (the oviparae). In *Aphis fabae* these gynoparae (Fig. 1*a*) are morphologically very similar to the alate virginoparae but may differ in the number of secondary rhinaria (placoid sensilla) on the antennae[8]. The major differences between the two alates lie in their behaviour [8] and in the morph of their progeny.

In the experiments described below, *A. fabae* [from a clone originally isolated in 1946 (ref. 9)] were reared on germinating tick beans (*Vicia faba*) at 15 °C. Long day (LD) conditions were 16 h light : 8 h dark and short day (SD) conditions 12 h light : 12 h dark. When progeny of an apterous virginopara from an LD stock culture are reared in isolation in SD conditions they develop as apterous adults and their progeny, that is the second generation in SD, are mainly alate gynoparae but include a few late-born males and apterous virginoparae. If only the progeny born before the appearance of the males are reared at a density of between 1 and 10 per germinating bean in SD conditions then 99.8% (1,140 in 1,142) develop as gynoparae. Initially the germinating beans are 1–1.5 cm tall.

As mentioned earlier, the development of the adult alate gynopara of *A. fabae* also depends on the postnatal environ-

0028–0836/80/320602—03$01.00

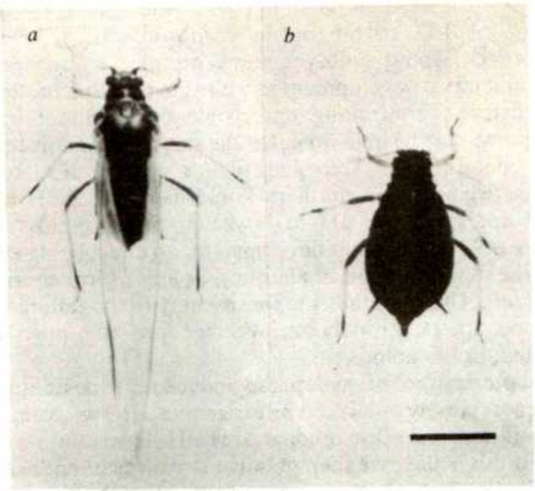

Fig. 1 *a*, The alate gynopara of *Aphis fabae* which produces sexual females (oviparae). *b*, A presumptive gynopara which has been completely apterized by topical application of 0.1 μg JH1 during the first instar. This aphid was reared in short-day conditions; similar apterae are produced when presumptive gynoparae are reared from the first instar in long-day conditions. As far as is known they are morphologically identical to apterous virginoparae. Scale bar, 1 mm.

ment[7]. If presumptive gynoparae complete larval development in LD conditions after transfer from SD during the first or early second instar a number develop into adult apterae or alate/apterous intermediates, that is apterization occurs. In extreme cases this is complete and the adult morph is identical to the apterous virginopara (see Fig. 1*b*). The proportion of adults showing various degrees of apterization is maximal if transfer to LD is effected during the first 24 h of postnatal development and decreases with the age of transfer (Fig. 2).

Lees[7] has previously shown that by examination of fifth instar (normally adult) individuals it is possible to distinguish the more extreme forms of juvenilized alate gynoparae induced by treatment with JH mimics juvenilization and presumptive gynoparae which have been diverted along an apterous developmental pathway by postnatal exposure to LD (apterization). Less extreme apterized and juvenilized alate fifth instar individuals—those designated as 25% morphological effect—are difficult to distinguish. This category is, however, rare in the LD, 'authentic' apterization (12 of 1,017 insects transferred to LD between days 1 and 4 of postnatal development) and so when observed in the following JH experiments it was assumed to be an indication of juvenilization rather than apterization.

It was found that photoperiodic apterization could in fact be mimicked by JH (Figs 1*b*, 2). JH1 (0.1 μg, Calbiochem) in 0.1 μl acetone was applied topically to the abdomen of presumptive gynoparae, postnatal development continuing in SD conditions. The numbers of insects showing apterous characters was less than that obtained by transfer to LD conditions at the same stage of development except on the fourth day after birth. However, the response profile was similar in both apterizing treatments. Presumptive gynopara controls either, untreated or treated with 0.1 μl of acetone, and reared in SD at <10 per bean were almost all alate adults (0.2% of individuals showed apterous characters).

JH-treated insects that were not apterized often showed juvenilization are the second and third instars, an observation for the degree of juvenility the total effect was calculated after Lees[7] (Fig. 3). The developmental stages most sensitive to juvenilizations are the second and their instars, an observation also reported by Lees[7]. Thus the apterizing effects and the juvenilizing effects of JH treatment show different sensitivity profiles, a finding which indicates that separate target sites exist and that apterization is not due to the neotenic action of JH.

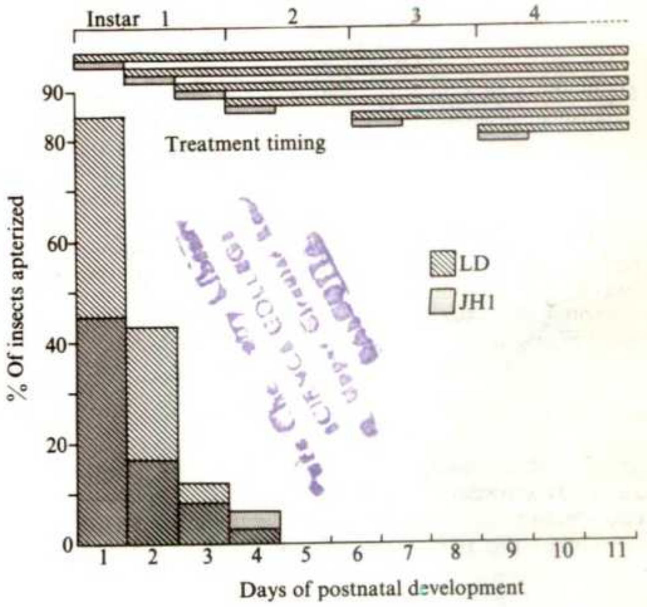

Fig. 2. The percentage of presumptive gynoparae which showed some degree of apterization when either transferred to LD conditions (hatched) or treated with a single application of 0.1 μg JH1 (stippled) at different stages during postnatal development. The JH-treated insects were reared in SD conditions throughout development. All insects were reared with an initial population of 10 per germinating bean but due to the increased mortality in JH-treated individuals there was often less than 10 for much of development. Number of insects tested in the LD treatment were: day 1, 193; day 2, 148; day 3, 143; day 4, 94; first day of the third instar, 61; first day of the fourth instar, 102. Only the survivors of the JH treatment could be scored and survival depended on the age when treated. Survivors per number treated were: day 1, 67/210; day 2, 24/454; day 3, 37/389; day 4, 77/103; first day of the third instar, 65/70; first day of the fourth instar, 102/104. Of controls dosed on day 1 with 0.1 μl acetone and reared in SD 27/30 survived; all survivors were alate gynoparae. Of untreated controls reared in SD 99.8% (971/973) were alate when reared at a density of between 2 and 10 individuals per germinating bean while 100% (142/142) were alate when reared at one per bean. These alatae are induced by the pre- and postnatal SD treatment, not by crowding.

Table 1 The apterizing effects of 0.1 μg JH1 on presumptive gynoparae less than 24 h after birth, compared with the alatizing effect of crowding. Development continued in SD conditions

Crowding intensity	Control survival	Experimental survival	% Insects showing apterization Controls	JH-treated
a Relatively uncrowded (10 aphids per germinating bean)	(404/410) = 98.5%	(67/210) = 31.9%*	0.5%	44.8%
b Crowded (200 aphids per bean stipule)	(166/250) = 66.4%	(13/250) = 5.2%	0%	0%

The crowding intensity was increased in *b* compared with *a* not only by increasing the number of aphids in the colony but also by using a bean stipule (growing tip removed). These plants showed retarded growth during the experiments when compared with the germinating beans. The increase in density of crowding leads to a decreased survival in both control and experimental animals. Control animals are untreated.

* These values are the same as those of day 1, JH-treated insects in Fig. 2.

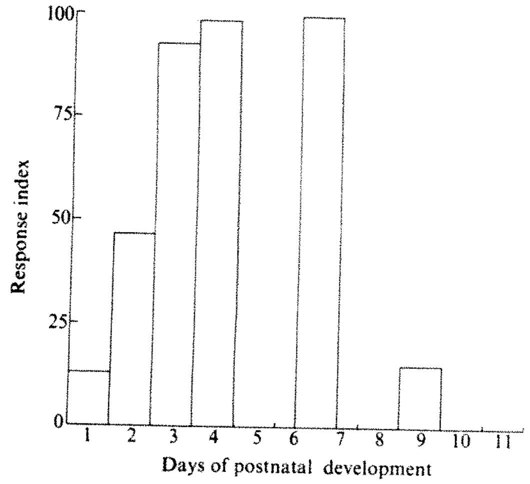

Fig. 3 The total degree of juvenilization exhibited by aphids that were not apterized by JH treatment in Fig. 2. The response index was calculated after Lees[7], each insect being assigned to one of five groups of 'morphological effect' namely 0, 25, 50, 75 and 100%. 0% was a normal alate while 100% was a fifth instar supernumerary nymph, the other groups falling between these extremes. The response index was calculated as $\Sigma(\% \, ME \times n)/N$; ME, morphological effect; n, number showing this grade of response; and N, total number of individuals. Due to the different mortalities and apterization caused by the treatments the N varied as follows: day 1, 37; day 2, 20; day 3, 34; day 4, 72; first day of the third instar, 65; first day of the fourth instar, 102.

In LD, virginoparous aphid generations wing production is induced by crowded conditions, postnatal crowding being a predominant factor in *A. fabae*[10]. It was therefore of interest to test whether the LD apterization of presumptive gynoparae observed in relatively uncrowded conditions (10 per germinating bean) could be opposed by the alatizing effect of crowding. In one experiment where day 1 presumptive gynoparae were crowded on to a single bean stipule (growing tip removed) and transferred to LD, 100% (126 of 126) of the adult survivors were alatae, in a second experiment 88% (83 of 94) were alatae. In uncrowded conditions only 15% (28 of 193) were alatae (Fig. 2). Thus the apterization induced by LD could be cancelled out by crowding.

Experiments were also designed to test the effectiveness of apterization by exogenous JH against the alatizing effect of crowding. Fifty first-day presumptive gynoparae were treated with 0.1 μg of JH1 and placed on a bean stipule with 50 first-day control aphids marked by the removal of the left antenna. After leaving these insects to settle overnight a further 100 first-day larvae with the right antenna removed were added to the same stipule to act as an additional crowding agent. This crowded colony was allowed to develop in SD conditions and scored for alate/apterousness in the fourth or fifth instar. Due to the large residual effects of the JH1 during the larval instars most sensitive to juvenilization, the fifth instar individuals, in these experiments, were all supernumerary nymphs. However, alate individuals could easily be distinguished from apterized insects. Table 1 summarizes the results of five such experiments (*b*) in comparison with a similar uncrowded series (*a*). It can be seen that the increase in intensity of crowding decreases the survival of both control and JH-treated individuals but all survivors in the crowded JH-treated experiments were alatae while 45% were apterized in uncrowded experiments. Control experiments showed there to be no differential mortality between alate and apterous morphs. Thus the apterization of alate gynoparae induced by either LD or JH treatment may be cancelled out by crowding.

Recent examination of the role of JH in controlling aphid polymorphism, as investigated by topical application of JH or analogues, indicates that in addition to influencing larval–adult metamorphosis it has a possible role in the embryonic determination of LD parthenogenetic morphs as opposed to oviparae[11,12]. Aphid embryogenesis occurs paedogenetically throughout larval development as well as in the adult mother, so that JH levels controlling embryonic development in LD virginoparae may be high except at the stage when adult characters are determined. According to this view both alate and apterous virginoparous mothers would have raised JH levels. Topical application of JH to larvae of these aphids would influence only larval–adult development, no effect being expected on the determination of alatiform or apteriform characters of the adult. This hypothesis is consistent with the failure of JH to induce aptera production, whether pre- or postnatally controlled, in LD aphids[6,12].

The apterization of gynoparae induced by postnatal LD treatment is closely mimicked by exogenous JH, suggesting that LD conditions increase endogenous JH levels in *A. fabae* larvae. If this is the case then putative low titres of endogenous JH induced by SD exposure would promote both wing development and the embryonic development of oviparae. Both LD- and JH-induced apterization involves a switch in embryonic development from oviparae to parthenogenetic viviparae (ref. 7 and unpublished results). The observation that crowding can cancel out the apterization induced by either LD or JH points to the existence of a separate factor which controls the alate–apterous dimorphism in LD, virginoparous aphids.

I thank Professors A. D. Lees and B. Johnson for advice and Professor J. S. Kennedy for comments on the manuscript.

Received 14 November 1979; accepted 2 June 1980.

1. Hille Ris Lambers, D. *A. Rev. Ent.* **11**, 47–78 (1966).
2. Lees, A. D. *Adv. Insect physiol.* **3**, 207–277 (1966).
3. Kennedy, J. S. & Stroyan, H. L. G. *A. Rev. Ent.* **4**, 139–160 (1959).
4. Johnson, B. *Ent. exp. appl.* **2**, 82–99 (1959).
5. Lees, A. D. in *Insect Polymorphism* (ed. Kennedy, J. S.) 68–78 (Roy. Ent. Soc., London, 1961).
6. Hales, D. F. in *Phase and Caste Determination in Insects. Endocrine Aspects* (ed. Luscher, M.) 105–115 (Pergamon, Oxford, 1976).
7. Lees, A. D. *Nature* **267**, 46–48 (1977).
8. Kennedy, J. S. & Booth, C. O. *Ann. appl. Biol.* **41**, 88–106 (1954).
9. Kennedy, J. S. & Booth, C. O. *Ann. appl. Biol.* **38**, 25–64 (1950).
10. Shaw, M. J. P. *Ann. appl. Biol.* **65**, 191–196 (1970).
11. Mittler, T. E., Nassar, S. G. & Staal, G. B. *J. Insect Physiol.* **22**, 1717–1725 (1976).
12. Lees, A. D. in *Comparative Endocrinology* (eds Gaillard, P. J. & Boer, H. H.) 165–167 (Elsevier, Amsterdam, 1978).

Two distinct patterns of visual evoked response asymmetry in human albinism

W. M. Carroll, B. S. Jay, W. I. McDonald & A. M. Halliday

The National Hospital for Nervous Diseases, Queen Square, London
WC1 3BG and Moorfields Eye Hospital, City Road,
London EC1, UK

Results are presented which confirm that in human albinos each cerebral hemisphere receives a predominantly monocular input from the contralateral eye, giving rise to an asymmetry of the visual evoked potential (VEP) to whole-field stimulation which is similar to that for stimulation of the temporal half-field in the same individual. The further finding of two distinct, and in some respects opposite, types of topographical asymmetry raises the possibility that there are two anatomically distinct variants in the retinocortical projection in human albinism, as there are in the Siamese cat.

Albinism is associated with a peculiar anatomical anomaly of the visual pathways resulting from a misrouting of the retinogeniculate projections. In the extensively studied Siamese cat, not only is the whole of the temporal half-field of each eye projected to the opposite hemisphere, but also up to 20° of the nasal half-field. Each hemisphere therefore receives a predominantly monocular input from the contralateral eye, with only the more peripheral parts of the nasal field represented

0028–0836/80/320604—03$01.00

ipsilaterally[1]. A similar anomaly appears to be associated with albinism in all the mammalian species so far studied, including albino rats, guinea pigs, rabbits, and mink[2–7]. There is now also evidence for a similar anomaly in man[8].

The misrouting of the retinocortical projection results in a partial disorganization of the normal cortical retinotopic representation in the contralateral occipital lobes, and it appears from anatomical and electrophysiological studies in Siamese cats that the visual system deals with the abnormal projection from the nasal field of the contralateral eye in two distinct ways. In one, the 'Boston' pattern, the anomalous central 20° of the nasal field has a separate representation in V1 and V2 (areas 17 and 18) interpolated on either side of the 17/18 border, so that the representation of the fixation point or the area centralis is shifted away from the common border of areas 17 and 18 by the abnormal input[9]. In the other variant, the 'mid-Western' pattern, the area centralis is still positioned, as in the normal cat, at the 17/18 border, and the abnormal input from the contralateral temporal hemiretina overlies it, so that mirror-symmetrical points to either side of the fixation point go to almost identical positions on the cortex, rather as the homologous points from homonymous half-fields in each eye converge in the normal cat[10]. A further feature of the mid-Western pattern is the 'suppression' or reduced number of cortical units in the area of cortex receiving the abnormal input. There has been some evidence suggesting that in some cases both types of anomaly may co-exist in the same individual[11].

Creel *et al.* have recorded the visual evoked potential in human albinos and report that up to 70% of individuals have an abnormal response with evidence of missing components from the hemisphere receiving the uncrossed visual pathway[12–14]. Since pattern reversal VEPs have proved particularly consistent in normal healthy subjects, and the responses from each half-field show a characteristic asymmetry in all normal individuals[15,16], we have recorded the VEPs in 15 human albinos to reversal of a black-and-white checkerboard pattern of 50′ checks, using a multi-channel montage to examine in detail the topographical distribution of the response over the back of the head. Three had X-linked, and five had autosomal recessive ocular albinism and seven were oculocutaneous albinos (tyrosinase positive in six). The visual acuities were 6/36 or worse bilaterally in nine subjects and the remainder had best monocular acuities of between 6/9 and 6/24. No differences were found in the size of the central nasal and temporal visual fields and all but three had varying degrees of pendular or jerk nystagmus when the eyes were in the primary position. In all, the nystagmus diminished considerably during VEP recording. Recordings where fixation (monitored throughout) was judged inadequate or nystagmus excessive or which were not reproducible were rejected.

All the monocular responses to a circular stimulus of 16 degree radius showed a marked asymmetry which clearly distinguished them from those of normal subjects (Fig. 1). This whole-field response asymmetry invariably resembled the asymmetry produced by stimulation of the temporal half-field in the same eye. However, two quite distinct, and in some respects opposite, types of asymmetry were encountered in the albino group. In five subjects the $\overline{\text{P100}}$ component (major positivity) was ipsilateral to the stimulated eye or temporal half-field, being similar in distribution to the $\overline{\text{P100}}$ of the temporal half-field response of the normally pigmented subject. In nine others the distribution of the $\overline{\text{P100}}$ was the reverse of that found in normal subjects with this component appearing in the channels contralateral to the stimulated eye. One individual showed a mixture of the two patterns, the $\overline{\text{P100}}$ being ipsilateral for the left eye responses and contralateral for the right eye responses. In both groups of subjects the $\overline{\text{P100}}$ to nasal half-field stimulation showed an almost identical distribution to that for the temporal half-field and whole-field responses from the same eye. In general, the amplitude of the nasal field $\overline{\text{P100}}$ was smaller than the temporal field $\overline{\text{P100}}$, this difference being most marked in the first group of five subjects. There was, however, no

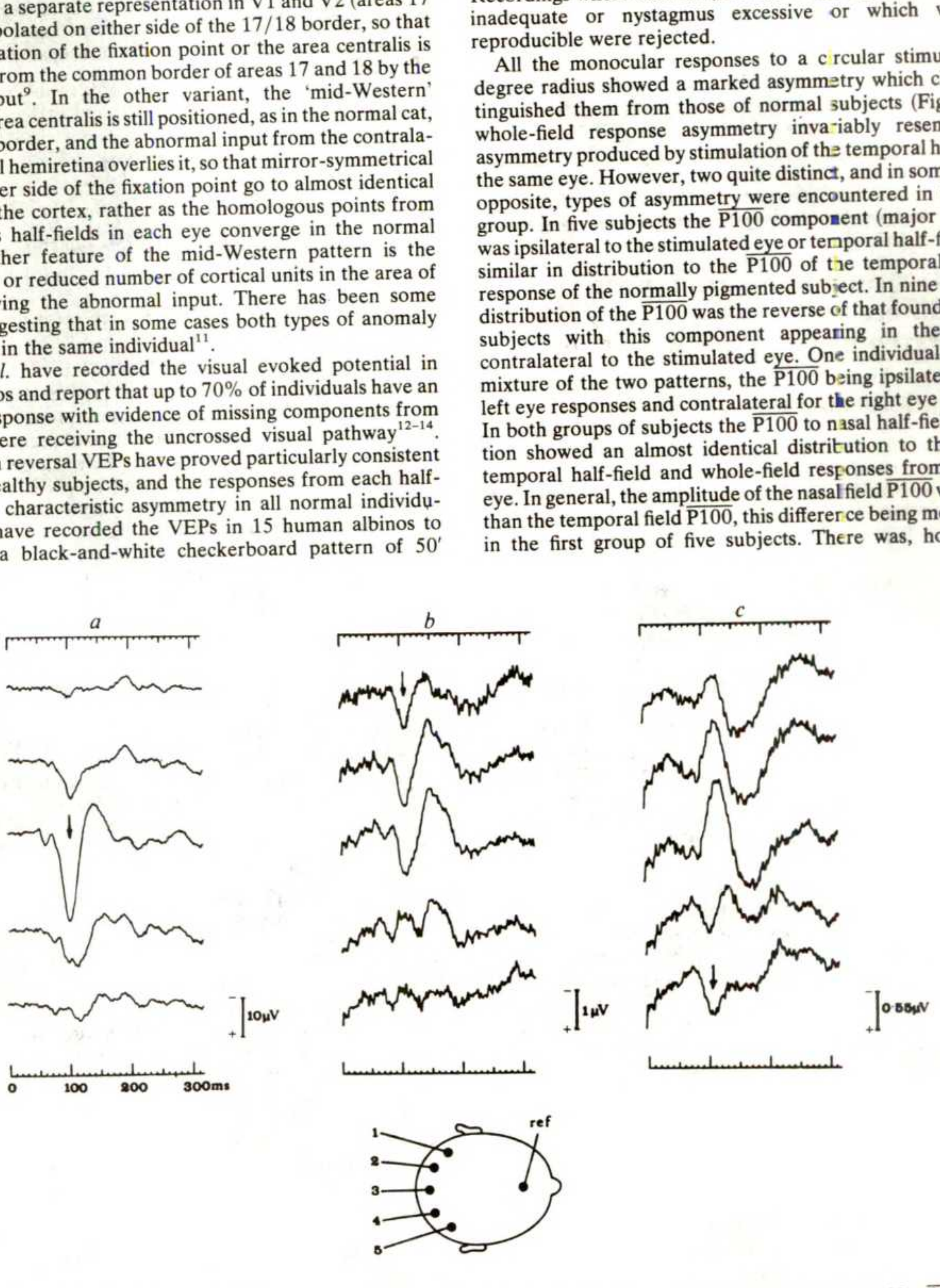

Fig. 1 Left eye whole-field (16 deg radius) VEPs from: *a*, a normal subject; *b*, the grand average of the 5 albino subjects with a $\overline{\text{P100}}$ (arrow) distribution ipsilateral to the stimulated left eye and *c*, the grand average of the 9 albino subjects with a contralateral $\overline{\text{P100}}$ (arrow) distribution. Note in the normal subject the larger amplitude and symmetrical distribution of the $\overline{\text{P100}}$ about the midline. The midline electrode of the transverse chain of 5 is situated 5 cm above the inion.

obvious association between the various types of albinism and the two patterns of VEP asymmetry. The mean amplitude of the VEPs to all fields of stimulation in the albinos was significantly smaller than in the normal population, in line with the lowered visual acuity characteristic of this group.

Received 21 April; accepted 18 June 1980.

1. Guillery, R. W. *Brain Res.* **14,** 739–741 (1969).
2. Guillery, R. W. *Brain Res.* **33,** 482–485 (1971).
3. Cunningham, T. J. & Lund, R. D. *Brain Res.* **34,** 394–398 (1971).
4. Creel, D. J. & Giolli, R. A. *Expl Neurol.* **36,** 411–425 (1972).
5. Sanderson, K. J. *Anat. Rec.* **172,** 398 (1972).
6. Guillery, R. W. & Kaas, J. H. *Science* **180,** 1287–1289 (1973).
7. Giolli, R. A. & Guthrie, M. D. *J. comp. Neurol.* **136,** 99–125 (1969).
8. Guillery, R. W., Okoro, A. N. & Witkop, C. J. *Brain Res.* **96,** 373–377 (1975).
9. Hubel, D. H. & Wiesel, T. N. *J. Physiol., Lond.* **218,** 33–62 (1971).
10. Kaas, J. H. & Guillery, R. W., *Brain Res.* **59,** 61–95 (1973).
11. Cooper, M. L., Blasdel, G. G. & Pettigrew, J. D. *Assoc. Res. Vision Ophthalmol. Abstr.*, 216 (1978).
12. Creel, D. J., Witkop, C. J. & King, R. A. *Inv. Ophthalm.* **13,** 430–440 (1974).
13. Creel, D. J., O'Donnell, F. E. & Witkop, C. J. *Science* **201,** 931–933 (1978).
14. Creel, D. J. *J. Biomed. Engng* **1,** 100–104 (1979).
15. Barrett, G., Blumhardt, L. D., Halliday, A. M., Halliday, E. & Kriss, A. *Nature* **261,** 253–255 (1976).
16. Blumhardt, L. D. & Halliday, A. M. *Expl Brain Res.* **36,** 53–69 (1979).

Ethyl β-carboline-3-carboxylate shows differential benzodiazepine receptor interaction

Mogens Nielsen & Claus Bræstrup*

Psychopharmacological Research Laboratory, St Hans Mental Hospital, Department E, DK-4000 Roskilde, Denmark
* Research Laboratories, A/S Ferrosan, Sydmarken 1-5, DK 2860 Soeborg, Denmark

High-affinity binding of ^{3}H-diazepam and ^{3}H-flunitrazepam has provided evidence for the presence of benzodiazepine receptors on brain neurones[1–6]. Pharmacological evidence showing a clear correlation between receptor affinity and *in vivo* pharmacological potency for several benzodiazepines[7] and a link between benzodiazepine receptors and GABA (γ-aminobutyric acid) receptors at the molecular level[8,9], indicates that these receptors are relevant to the pharmacological and clinical effects of benzodiazepines. In searching for possible endogeneous ligands for benzodiazepine receptors we have recently isolated ethyl β-carboline-3-carboxylate (β-CCE) from human urine and brain, and shown that β-CCE has a higher affinity than diazepam for brain benzodiazepine receptors[10]. β-CCE itself is probably not present in the brain, but may be closely related to an endogenous benzodiazepine receptor ligand[10]. We report here that β-CCE, in contrast to benzodiazepines, can distinguish clearly between benzodiazepine receptors in cerebellum and hippocampus. This result strongly indicates that benzodiazepine receptors are not a single class of non-interacting entities. It has not been possible to determine whether two distinct receptors are present and/or whether true negative cooperativity exists among hippocampal, but not cerebellar, benzodiazepine receptors.

Purification of human urine, including treatment with hot ethanol, yielded 1.78 mg β-CCE[10], which was stored in 50% ethanol at 0–4 °C for more than 2 months without loss of activity. Its identity was confirmed by *de novo* synthesis and crucial experiments were repeated with synthetic material (A/S Ferrosan). Crude membrane fractions from different brain regions were prepared by homogenization by an Ultra Turrax homogenizer in 10 vol of ice-cold 25 mM potassium phosphate buffer, *p*H 7.1, followed by dilution to 100 v/w original tissue. Aliquots of 500 μl were used directly in binding experiments. β-CCE test solution (25 μl) was added to assays just before ^{3}H-flunitrazepam (25 μl, 87 Ci mmol^{-1}, NEN) and samples were incubated at 0 °C for 40 min. Specific ^{3}H-flunitrazepam binding was estimated by conventional filtration techniques[2] using 3×10^{-6} M diazepam to assess nonspecific binding.

The first indication that β-CCE did not interact like a simple competitive inhibitor on a single class of benzodiazepine receptor came from Scatchard analysis of ^{3}H-flunitrazepam binding to rat forebrain. These plots were curvilinear in the presence of β-CCE[10] whereas plots without β-CCE never (>200 experiments) exhibited curvatures. A regional study on rat brain revealed that the curvature was most pronounced in the hippocampus and that no curvature was detected in cerebellum (Fig. 1). Other brain regions, such as frontal cortex, occipital cortex, striatum, hypothalamus and thalamus all exhibited curvilinear Scatchard plots for ^{3}H-flunitrazepam in the presence of β-CCE (data not shown).

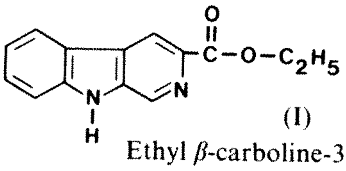
(I)

Ethyl β-carboline-3-carboxylate
(3-carboethoxy-9H-pyrido [3,4-b] indole; β-CCE)

Fig. 1 Ethyl β-carboline-3-carboxylate (3-carboethoxy-9H-pyrido[3,4-b]indole; β-CCE).

Benzodiazepine receptors can exist in several conformations which exhibit different affinities. Various proportions of alternative conformational states in different brain areas might account for the observed difference between cerebellum and hippocampus. Mixed type inhibition by β-CCE, however, was consistently seen in hippocampal synaptosomal membranes which had been prepared in various ways known to favour different conformational states—for example, membranes prepared in sucrose[2]; in membranes washed five times (Tris-citrate)[11]; in washed membranes which were 'activated' by 3×10^{-5} M GABA[8,11,12]; in membranes treated with Triton X-100 (0.1%)[13]; in partially heat-inactivated membranes (Tris-HCl; 15 min at 60 °C)[14]; in crude membranes prepared in a physiological buffer (122 mM NaCl, 4.8 mM KCl, 0.97 mM $CaCl_2$, 1.2 mM $MgSO_4$, 16 mM phosphate, 1 mM ascorbic acid, 11 mM glucose) and in crude membranes activated by 30 mM potassium iodide[15] (data not shown). These data indicate that curvilinear Scatchard plots were not dependent on any previously described conformational heterogeneity.

Besides the induction by β-CCE of curvilinear Scatchard analysis, hippocampal benzodiazepine receptor binding differed from cerebellar binding in the displacement potency of β-CCE for ^{3}H-flunitrazepam. The IC_{50} value for β-CCE, which is the concentration displacing 50% of specific ^{3}H-flunitrazepam binding, was only 0.36 ng ml^{-1} (range 0.22–0.57 ng ml^{-1}, Hill coefficient 0.95 ± 0.02, mean ± s.e.m., $n=4$) in cerebellum compared with 2.7 ng ml^{-1} (range 1.7–3.6 ng ml^{-1}, Hill coefficient 0.75 ± 0.04, mean ± s.e.m., $n=4$) in hippocampus (Fig. 2). β-CCE was more potent in displacing ^{3}H-flunitrazepam in cerebellum than in hippocampus irrespective of the membrane preparation used (see above, data not shown). Furthermore, cerebellar and hippocampal tissue from mouse and pig exhibited about the same difference in affinity for β-CCE as did rat brain tissue (data not shown).

The almost sevenfold higher affinity of β-CCE for cerebellar than for hippocampal ^{3}H-flunitrazepam binding does not unequivocally show that β-CCE possesses higher affinity for cerebellar receptors because IC_{50} values depend on the K_D value for the ^{3}H-ligand. The K_D value for ^{3}H-flunitrazepam binding was, however, quite similar in cerebellum ($K_D = 1.40\pm0.08$ nM; mean ± s.e.m., $n=10$) and hippocampus ($K_D = 1.34\pm0.04$ nM; mean ± s.e.m., $n=16$), excluding regional differences in the affinity for ^{3}H-flunitrazepam as a major contributor to the observed regional differences.

0028–0836/80/320606—02$01.00

The present results clearly show that benzodiazepine receptors in cerebellum and hippocampus are not identical. One interpretation would be that one class of receptor is most abundant or exclusively present in cerebellum and that this class exhibits high affinity for β-CCE. Two or more classes of receptors are present in hippocampus; at least one of them exhibits reduced affinity for β-CCE. The observation of Hill coefficients below unity is compatible with the presence of more than one receptor species in the hippocampus with different affinities. The possible occurrence of receptor heterogeneity in the central nervous system was proposed, based on experimental evidence showing biphasic dissociation curves[14], polyphasic heat inactivation curves[14] and flat ^{3}H-diazepam displacement curves with Hill coefficient below unity for some new triazolopyridazines[14]. Furthermore, curvilinear Scatchard plots for ^{3}H-diazepam were found in the brain of lower vertebrates[16]. Direct evidence for benzodiazepine receptor heterogeneity in hippocampus has been obtained in photoaffinity labelling experiments using ^{3}H-flunitrazepam. SDS-electrophoresis of these irreversibly radiolabelled receptors showed two molecular species with different molecular weights (MWs) (W. Sieghart and M. Karobath, personal communication).

An alternative explanation for the present results that is compatible with both the curvlinear Scatchard analysis and the Hill coefficients below unity would be that benzodiazepine receptors in hippocampus, in contrast to cerebellar receptors, exhibit true negative cooperativity. Solubilization of benzodiazepine receptors reveals MWs of either 50,000 (ref. 17), 200,000 (ref. 18) or 110,000 (C.B. *et al.*, unpublished), depending on the procedures applied, indicating the possible presence of dimers or tetramers. Receptors composed of polymer subunits in hippocampus might possess mutually interacting sites, so that binding of β-CCE (but not of a benzodiazepine) to one site decreases the affinity of the adjacent receptor site for benzodiazepines. Apparent negative cooperativity has previously been observed for the interaction of a neurotransmitter agonist with receptors identified by labelled antagonists[19,20]. It is tempting to speculate that β-CCE is an 'agonist' to 'antagonistic sites' labelled by benzodiazepines. Studies of several drug receptors show that GTP changes the affinity of agonist binding to antagonist sites[21,22]. We found no effects of GTP (10^{-5}–10^{-4} M) on the affinity of β-CCE in hippocampus or cerebellum (data not shown), indicating that any cooperative interaction is not dependent on GTP-dependent coupling of the benzodiazepine receptor to adenylate cyclase.

Much work has gone into developing benzodiazepine derivatives with more selective pharmacological actions. Clinically available benzodiazepines apparently always exhibit anxiolytic, hypnotic and anticonvulsant properties in accordance with their lack of selectivity for any particular class of benzodiazepine receptors. New classes of drugs, such as triazolopyridazines[23] and derivatives of β-carboline-3-carboxylic acid, may interact preferentially with particular classes of receptor and exhibit new profiles of action.

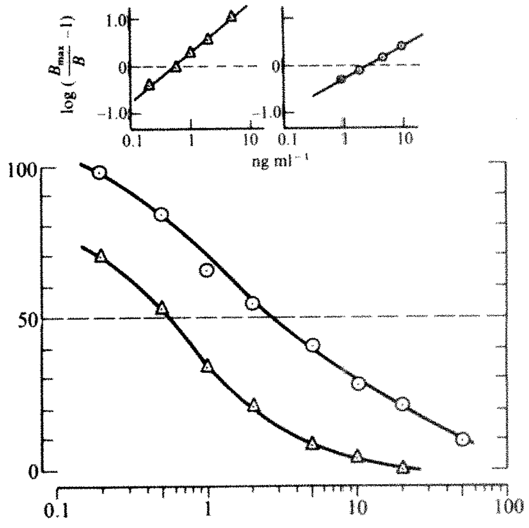

Fig. 3 Inhibition of ^{3}H-flunitrazepam binding (1 nM) to crude membrane fractions of rat hippocampus (○) and cerebellum (△) by increasing concentrations of ethyl β-carboline-3-carboxylate (0.2–50 ng ml^{-1}) added in duplicate. Total binding in hippocampus and cerebellum was 16,200 and 11,600 c.p.m. per assay, respectively. Nonspecific binding was 6–11% of total binding. Plots are representative of four separate experiments. Inset: Hill plots of the above data. Hill coefficients were 0.95±0.02 and 0.75±0.04 (mean±s.e.m. of 4 values) for cerebellum and hippocampus, respectively.

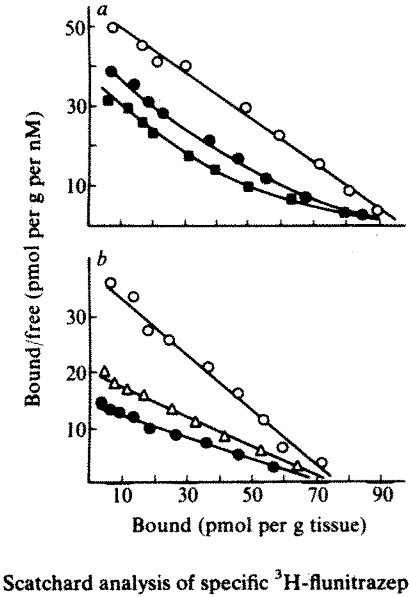

Fig. 2 *a*, Scatchard analysis of specific ^{3}H-flunitrazepam binding in rat hippocampus. Crude membrane fractions (2 mg original tissue per assay) were incubated with ^{3}H-flunitrazepam (0.2–20 nM) in duplicate as described in the text. Blanks contained 3×10^{-6} M diazepam. Control (no addition of inhibitor), ○; addition of ethyl β-carboline-3-carboxylate, ● (0.56 ng ml^{-1}) and ■ (1.1 ng ml^{-1}). The results are from a single experiment which was repeated three times with very similar results. *b*, Scatchard plot of ^{3}H-flunitrazepam binding in rat cerebellum estimated as described in *a*. Control (no addition of inhibitor) ○; addition of ethyl β-carboline-3-carboxylate △ (0.28 ng ml^{-1}) and ● (0.56 ng ml^{-1}). The experiment was repeated three times with similar results.

Received 17 March; accepted 2 June 1980.

1. Squires, R. F. & Bræstrup, C. *Nature* **266**, 732–734 (1977).
2. Bræstrup, C. & Squires, R. F. *Proc. natn. Acad. Sci. U.S.A.* **74**, 3805–3809 (1977).
3. Möhler, H. & Okada, T. *Science* **198**, 849–851 (1977).
4. Mackerer, C. R., Kochman, R. L., Bierschenck, A. & Bremner, S. S. *J. Pharmac. exp. Ther.* **206**, 405–413 (1978).
5. Speth, R. C., Wastek, G. J., Johnson, P. C. & Yamamura, H. I. *Life Sci.* **22**, 859–866 (1978).
6. Bræstrup, C., Nielsen, M., Biggio, G. & Squires, R. F. *Neurosci. Lett.* **13**, 219–224 (1979).
7. Bræstrup, C. & Squires, R. F. *Eur. J. Pharmac.* **48**, 263–270 (1978).
8. Tallman, J. F., Thomas, J. W. & Gallager, D. W. *Nature* **274**, 383–385 (1978).
9. Guidotti, A., Toffano, G. & Costa, E. *Nature* **275**, 553–555 (1978).
10. Bræstrup, C., Nielsen, M. & Olsen, C.-E. *Proc. natn. Acad. Sci. U.S.A.* **77**, 2288–2292 (1980).
11. Bræstrup, C., Nielsen, M., Krogsgaard-Larsen, P. & Falch, E. *Nature* **280**, 331–333 (1979).
12. Karobath, M. & Sperk, G. *Proc. natn. Acad. Sci. U.S.A.* **76**, 1004–1006 (1979).
13. Beaumont, K., Chilton, W. S., Yamamura, H. I. & Enna, S. J. *Brain Res.* **148**, 153–162 (1978).
14. Squires, R. F. *et al. Pharmac. Biochem. Behav.* **10**, 825–830 (1979).
15. Costa, T., Rodbard, D. & Pert, C. B. *Nature* **277**, 315–317 (1979).
16. Nielsen, M., Bræstrup, C. & Squires, R. F. *Brain Res.* **141**, 342–346 (1978).
17. Battersby, M. K., Richards, J. G. & Möhler, H. *Eur. J. Pharmac.* **57**, 277–278 (1979).
18. Tallman, J. F. *et al.* in *Receptors for Neurotransmitters and Peptide Hormones* (eds Pepeu, G., Kuhar, J. & Enna, S. J.) 277–283 (Raven, New York, 1980).
19. Birdsall, N. J. M., Burgen, A. S. V. & Hulme, E. C. *Molec. Pharmac.* **14**, 723–736 (1978).
20. Bradbury, A. F., Smith, D. G., Snell, C. R., Birdsall, N. J. M. & Hulme, E. C. *Nature* **260**, 793–795 (1976).
21. Lefkowitz, R. J., Mullikin, D. & Caron, M. G. *J. biol. Chem.* **251**, 4686–4692 (1976).
22. Creese, I., Usdin, T. & Snyder, S. H. *Nature* **278**, 577–578 (1979).
23. Lippa, A. S. *et al. Brain Res. Bull.* **5**, Suppl. 2 (in the press).

Adrenal corticoids regulate sensitivity of noradrenaline receptor-coupled adenylate cyclase in brain

Philip L. Mobley & Fridolin Sulser

Psychopharmacology Research Center, Tennessee Neuropsychiatric Institute, 1501 Murfreesboro Road, Nashville, Tennessee 37217

Considerable evidence indicates that alterations in the availability of noradrenaline (NA) at postsynaptic sites can cause compensatory changes in the NA stimulated cyclic AMP generating system in various brain regions. Thus, an increased responsiveness to NA has been reported in the limbic forebrain and cortex following reserpine or 6-hydroxydopamine[1-3]. Conversely, manipulations which increase the availability of NA at receptor sites (monoamine oxidase (MAO) inhibitors, electroconvulsive treatment (ECT), tricyclic antidepressants) cause a decrease in responsiveness[4-6]. This up and down-regulation of central noradrenergic sensitivity is generally linked to changes of the density of β-adrenergic receptors[7-10]. The findings that psychotropic drugs which can either precipitate (reserpine) or alleviate (tricyclic antidepressants, MAO inhibitors and also ECT) depressive states cause opposite changes in the NA receptor-coupled adenylate cyclase system in brain have provided the basis for a revised catecholamine hypothesis of affective disorders[11]. It has also been suggested that the pituitary adrenal axis may have a role in mood disorders[12]. Since manipulation of the levels of corticosterone through bilateral adrenalectomy can alter the sensitivity of catecholamine-sensitive adenylate cyclase systems in preparations from liver[13,14] and adipose tissue[15], we have tried to determine if corticosterone could regulate the NA receptor-coupled adenylate cyclase system in brain tissue. We now report that adrenal corticoids can alter the sensitivity of this system to NA.

Male Sprague–Dawley rats weighing 200–250 g were used for all experiments. Animals were anaesthetized with ether and the adrenal glands removed bilaterally. In sham-operated rats, the glands were located but not removed. All animals were given free access to both tap water and 3% saline as it has been demonstrated that adrenalectomized animals develop a salt taste and are thus able to regulate their own salt intake[16]. Animals had free access to a standard laboratory diet (Purina) and were maintained in standard laboratory conditions (12 h light-dark cycle). Two weeks following surgery, the animals were decapitated, the brains rapidly removed and the frontal cortex dissected. For studies of the NA-sensitive adenylate cyclase system, the cortex was sliced in one plane at 0.3-mm intervals and tissue slices were incubated in Krebs-Ringer bicarbonate buffer (pH 7.4, 37°C) as previously described[17]. The cyclic AMP response to NA was established by exposing the tissue slices to the agonist for 10 min. Following aspiration of the buffer solution, the slices were frozen in liquid nitrogen and homogenized in 0.3 M perchloric acid. Cyclic AMP was isolated by ion exchange chromatography as previously described[17] and measured by the protein binding assay of Gilman[18]. The effect of adrenalectomy on β-adrenergic receptors in the frontal cortex was assessed with ^{3}H-dihydroalprenolol (DHA) based on the method of Bylund and Snyder[19]. Binding curves were determined over a ligand concentration range of 0.3 to 14 nM in a final volume of 1 ml. Nonspecific binding was determined in the presence of 10 μM (±)-propranolol. The dissociation constant (K_d) and maximum binding (B_{max}) values were determined by Scatchard analysis[20]. Protein was assayed by the method of Lowry *et al.*[21]. The significance of the data was evaluated by the 2-tailed Student *t*-test. Drugs were obtained as follows: noradrenaline HCl, isoprenaline HCl, corticosterone, protein kinase from beef heart, cyclic AMP (Sigma) ^{3}H-cyclic AMP and ^{3}H-dihydroalprenolol (both NEN).

Two weeks following bilateral adrenalectomy the NA-induced cyclic AMP accumulation was significantly higher in slices from the rat frontal cortex as compared with the cyclic AMP accumulation in cortical slices from sham-operated rats. Dose–response curves comparing responses in tissue from adrenalectomized and sham-operated animals suggest that this change in sensitivity to NA is due to a shift in the maximum responsiveness of the system (Fig. 1). Significant differences in cyclic AMP accumulation occurred at NA concentrations of 100 and 1,000 μM (68% and 44% respectively). No significant changes in the EC$_{50}$ values were observed. In addition, bilateral adrenalectomy appeared not to have any effects on basal levels of cyclic AMP (Table 1).

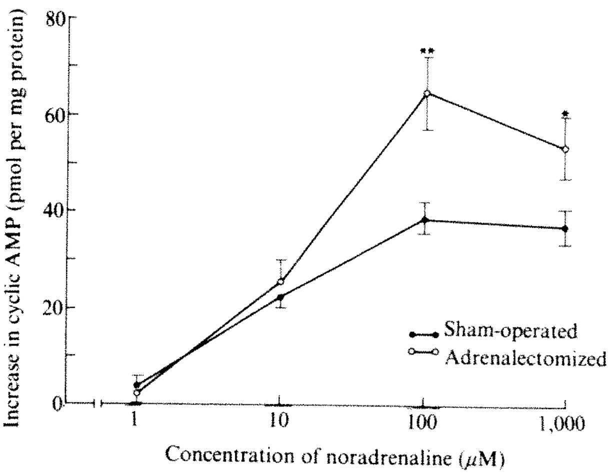

Fig. 1 Effect of adrenalectomy on the noradrenaline-induced increase in cyclic AMP accumulation in slices of rat frontal cortex. Slices of the frontal cortex from either sham-operated or adrenalectomized rats (2 weeks post-operative) were exposed to varying concentrations of noradrenaline for 10 min. The increase in cyclic AMP represents agonist-stimulated cyclic AMP levels minus basal levels (15.5 ± 1.8 and 13.1 ± 1.8 pmol cyclic AMP per mg protein in tissue from sham-operated and adrenalectomized animals respectively). Each point represents the mean of 13 to 16 samples ± s.e.m obtained in four separate experiments. EC$_{50}$ values were calculated to be 7.0 ± 2.2 (n = 4) and 12.0 ± 2.5 (n = 4) μM in tissue from sham-operated and adrenalectomized animals respectively. * $P < 0.05$, ** $P < 0.01$, as compared with sham-operated animals.

Corticosterone (10 mg per kg) administered to adrenalectomized rats for 5 days before death completely abolished the difference in sensitivity to NA (Table 1). Similar treatment elicited only a slight nonsignificant lowering of the accumulation of cyclic AMP in sham-operated rats. Again, no significant changes were observed in basal levels of cyclic AMP with any of these treatments. Also, bilateral demedullation did not produce significant changes in the sensitivity of the system to NA. The results indicate that the observed change in sensitivity to NA after bilateral adrenalectomy is a consequence of the removal of the adrenal corticosteroids.

Although the cyclic AMP accumulation elicited by NA was significantly altered following adrenalectomy, no significant changes were observed in the response to maximally effective concentrations (10 μM) of isoprenaline: 27.6 (s.e.m., 4.2, *n*, 18) and 22.5 (s.e.m., 2.6, *n*, 18) pmol cyclic AMP per mg protein in slices from sham-operated and adrenalectomized animals respectively. Only slight, nonsignificant changes occurred in the B_{max} value for specific ^{3}H-DHA binding. In tissue from sham-

0028-0836/80/320608—02$01.00

Table 1 Effect of corticosterone on adrenalectomy induced change in sensitivity of the noradrenaline sensitive adenylate cyclase system in frontal cortex

	Cyclic AMP response to noradrenaline (100 μM) (pmol per mg protein ±s.e.m.)	
	Minus corticosterone	Plus corticosterone
Sham-operated	48.8±4.8	40.0±3.2
Adrenalectomized	68.7±4.1*	37.1±1.9†

Corticosterone (10 mg per kg) or vehicle (corn oil) were administered subcutaneously to adrenalectomized and sham-operated rats for 5 days preceding death (injections started 9 days post-operation). The cyclic AMP response to 100 μM noradrenaline equals the agonist-stimulated level minus the basal level. Basal levels in pmol per mg protein ±s.e.m. were as follows: sham-vehicle, 14.5±1.1; sham-corticosterone, 16.6±1.4; adrenalectomy-vehicle, 14.7±1.1, adrenalectomy-corticosterone, 13.2±1.0. Each value represents the mean of 8 samples for basal levels and 12 samples for agonist-stimulated levels.

* $P<0.01$, as compared with sham-operated rats not receiving corticosterone.

† $P<0.001$, as compared with adrenalectomized rats not receiving corticosterone.

operated rats B_{max} was 244 fmol per mg protein (s.e.m., 24; *n*, 6) versus 276 fmol per mg protein (s.e.m., 24; *n*, 6) in tissue from adrenalectomized rats. Also, no significant changes in K_d values were found: 2.59 nM (s.e.m., 0.08; *n*, 6) and 2.83 nM (s.e.m., 0.08; *n*, 6) for sham-operated and adrenalectomized animals respectively.

In the liver, it has been demonstrated that the enhanced cyclic AMP response after adrenalectomy is associated with an increase in the number of β-adrenergic receptors[22]. The results of the present studies suggest that the altered cyclic AMP response to NA in cortical slices following bilateral adrenalectomy is mainly a consequence of changes in a non-β-receptor-mediated portion of the adrenergic cyclic AMP generating system.

Interestingly, it has been reported that chronic stress can decrease the sensitivity of this system[23]. Since chronic stress and antidepressant treatments both produce subsensitivity of the NA receptor-coupled adenylate cyclase system, Stone[24] has proposed subsensitivity to NA as a link between adaptation to stress and antidepressant therapy. Although it can be concluded from the present studies that alterations in the level of adrenal steroids can either directly or indirectly alter the sensitivity of the NA receptor-coupled adenylate cyclase system in brain tissue, both the molecular mechanisms accounting for the observed sensitivity changes and the role of the hypothalamus–pituitary–adrenal axis in affective disorders remain topics for further study.

This study was supported by USPHS grant MH-29228, a Fellowship by Hoffmann-La Roche (P.L.M.) and by the Tennessee Department of Mental Health and Mental Retardation.

Received 21 January; accepted 9 June 1980.

1. Palmer, G. C. *Neuropharmacology* **11,** 145–149 (1972).
2. Vetulani, J., Stawarz, R. J. & Sulser, F. *J. Neurochem.* **27,** 661–666 (1976).
3. Kalisker, A., Rutledge, C. H. O. & Perkins, J. P. *Molec. Pharmac.* **9,** 619–629 (1973).
4. Vetulani, J. & Sulser, F. *Nature* **257,** 495–496 (1975).
5. Vetulani, J., Stawarz, R. J., Dingell, J. V. & Sulser, F. *Naunyn-Schmiedebergs Archs Pharmak.* **293,** 109–114 (1976).
6. Frazer, A. *et al. J. Pharmac. exp. Ther.* **206,** 311–319 (1978).
7. Sporn, J. R., Harden, T. K., Wolfe, B. B. & Molinoff, P. B. *Science* **194,** 624–626 (1976).
8. Banerjee, S. P., Kung, L. S., Riggi, S. J. & Chanda, S. K. *Nature* **268,** 455–456 (1977).
9. Bergstrom, D. A. & Kellar, K. J. *Nature* **278,** 464–466 (1979).
10. Gillespie, D. D., Manier, D. H. & Sulser, F. *Comm. Psychopharmac.* **3,** 191–195 (1979).
11. Sulser, F. *Pharmakopsychiatrie* **11,** 43–52 (1978).
12. Carroll, B. J. & Mendels, J. in *Hormones, Behavior, and Psychopathology* (ed. Sachar, E. J.) 193–224 (Raven, New York, 1976).
13. Bitensky, M. W., Russell, V. & Blanco, M. *Endocrinology* **86,** 154–159 (1970).
14. Leray, F., Chambant, A. -M., Perrenond, M. -L. & Hanoune, J. *Eur. J. Biochem.* **38,** 185-192 (1973).
15. Exton, J. H. *et al. J. biol. Chem.* **247,** 3579–3588 (1972).
16. Richter, C. P. *Am. J. Physiol.* **115,** 155–161 (1936).
17. Blumberg, J. B., Vetulani, J., Stawarz, R. J. & Sulser, F. *Eur. J. Pharmac.* **37,** 357–366 (1976).
18. Gilman, A. G. *Proc. natn. Acad. Sci. U.S.A.* **67,** 305–312 (1970).
19. Bylund, D. B. & Snyder, S. H. *Molec. Pharmac.* **12,** 568–580 (1976).
20. Scatchard, G. *Ann. N.Y. Acad. Sci.* **51,** 660–672 (1949).
21. Lowry, O. H., Rosebrough, N. J., Farr, A. L. & Randall, R. J. *J. biol. Chem.* **193,** 265–275 (1951).
22. Wolfe, B. B., Harden, T. K. & Molinoff, P. B. *Proc. natn. Acad. Sci. U.S.A.* **73,** 1343-1347 (1976).
23. Stone, E. A. *J. Neurochem.* **32,** 1335–1337 (1979).
24. Stone, E. A. *Res. Commun. Psychol. Psychiat. Behav.* **4,** 241–255 (1979).

Suppression of *in vitro* lymphocyte reactivity by cyclosporin A: existence of a population of drug-resistant cytotoxic lymphocytes

T. Horsburgh*, P. Wood & L. Brent

Department of Immunology, St Mary's Hospital Medical School,
London W2 1PG, UK

Cyclosporin A (CS-A) is an unusual endecapeptide isolated from the fungi *Cylindrocarpon lucidum* Booth and *Trichoderma polysporum*[1]. It is a potent immunosuppressive drug that prevents rejection of kidney[2–4] and heart[5,6] allografts whilst having a low myelotoxicity[7]. Its mode of action is still unclear but its main target appears to be the T lymphocyte[8]. The mixed lymphocyte reaction (MLR) and cell-mediated lymphocytoxicity (CML) used here are generally regarded as *in vitro* correlates of allograft rejection[9]. Our data show that CS-A is a powerful inhibitor of MLR reactivity, regardless of whether the cells were obtained from normal or presensitized donors; that the CML of lymph node cells is likewise totally inhibited if the drug is added early during cell culture; and that, by contrast, the cytotoxic response of spleen cells from presensitized but not from normal mice is only partially inhibited, even with a tenfold increase in dose. It is therefore suggested that there exists a population of cytotoxic spleen cells that is relatively resistant to the action of this drug.

Cyclosporin A (CS-A) was added at different times after initiation of MLR between CBA ($H-2^k$) responder cells and irradiated BALB/c ($H-2^d$) or DBA/2 ($H-2^d$) splenic stimulator cells (Fig. 1). The presence of CS-A from the beginning of culture caused almost complete inhibition of ^3H-thymidine (^3H-Tdr) incorporation. Addition of the drug at later times was also effective in inhibiting further proliferative responses. (All experiments were done at least twice, with closely similar results.)

Inhibition of MLR was dose-dependent (Fig. 2). At an initial concentration of either 0.125 or 0.25 $\mu g\ ml^{-1}$, CS-A severely inhibited the primary MLR response whereas lower concentrations, 0.05 and 0.01 $\mu g\ ml^{-1}$ (the latter not shown), were far less effective. MLR cultures of lymph node cells from mice presensitized *in vivo* one month before, by either a skin graft or via allogeneic spleen cells injected intraperitoneally, showed a similar response to the drug. Here the untreated control cells from presensitized donors produced an earlier though lower peak in the MLR. Depression of MLR after *in vivo* presensitization has previously been described by Cooley[10], who suggested that it was brought about by either a redistribution of subpopulations of lymphocytes in the animal or the elimination, during culture, of some of the stimulator cells by preformed cytotoxic cells. In our experiments the presensitized cells gave normal primary MLR responses to third-party spleen cells (C57B1, $H-2^b$) and these cultures were similarly inhibited by the same concentrations of CS-A (not shown).

---

* Present address: Department of Surgery, Leicester General Hospital, Leicester, UK.

0028–0836/80/320609—03$01.00

The same range of CS-A concentrations also impaired the generation of cytotoxic lymphocytes from cultures of both normal and presensitized spleen and lymph node cells (Fig. 3). Thus, cytotoxicity after 5 days of culture was abolished when CS-A was added on day 0. Whereas addition of the drug on day 1, and to a lesser extent on day 2, partially inhibited cytotoxicity, such an effect was no longer demonstrable when the drug was added on day 3. Similar results were obtained when the cells were cultured for 6 rather than 5 days, indicating an early and lasting impairment of the capacity to produce cytotoxic cells. Addition of CS-A at later times affected the cytotoxic response of normal cells more strongly than that of presensitized cells and this probably reflects the more rapid development of cytotoxic cells in the latter[11]. Ethanol, the CS-A solvent, did not affect CML responses at the appropriate concentration; nor was the drug directly cytotoxic as judged by the low background of radioactivity released by ^{51}Cr-labelled target cells when incubated with the drug at 1 μg ml^{-1}. However, when cytotoxic cells were assayed in the presence of 1 μg ml^{-1} CS-A, ^{51}Cr release was reduced from a control value of 68.3% to 34 ± 3%. This suggests that mature cytotoxic lymphocytes are susceptible to the action of CS-A but that they are less vulnerable than MLR and/or CML precursor cells. It is unlikely that CML suppression was due to retention of the drug, because addition of CS-A to control CML cultures on day 5, followed by 30 min incubation and two washes, had no effect on the level of cytotoxicity.

The action of CS-A on the generation of cytotoxic cells, too, was dose-dependent (Fig. 4). CML cultures derived from normal spleen cells incubated with 0.06 μg ml^{-1} or more showed little or no cytotoxicity. Higher doses (0.125 μg ml^{-1}) were required to obtain significant inhibition of cytotoxicity when using cells from presensitized donors, and even a tenfold increase (1 μg ml^{-1}) failed to suppress the response completely, despite the fact that at this higher concentration the response of presensitized lymph node cells had been abolished (see Fig. 3). This, together with the sharp break in the curve for presensitized cells of Fig. 4, strongly suggests that there are at least two subpopulations of cytotoxic lymphocytes, with differing sensitivities to the drug. That preformed cytotoxic cells are less susceptible to CS-A suppression has already been shown above and it is therefore to be assumed that the drug-resistant subpopulation consists of preformed cytotoxic cells present in the spleens of mice sensitized *in vivo*. We have not, however, looked directly for the presence of cytotoxic effector cells in the spleens of *in vivo* sensitized mice, and others[12] have failed to find them 4 weeks after skin graft sensitization, albeit in a different strain combination. It should also be said that while it is reasonable to assume that the cells inhibited at the proliferative stage of MLR are cytotoxic precursors, we cannot exclude the possibility that an entirely different subpopulation of cells, such as T helper lymphocytes, is involved.

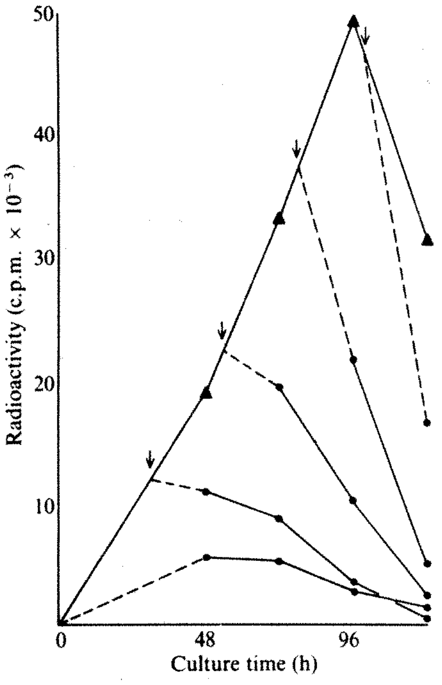

Fig. 1 MLR of mouse spleen cells after addition of CS-A at various times after beginning of culture. MLR's were performed in microtest plates, with each well containing 5×10^5 CBA responder cells and 5×10^5 irradiated (2000R) BALB/c stimulator cells in 0.2 ml RPMI 1640 medium, supplemented with 10% fetal calf serum, 2 mM glutamine, 3×10^{-5} M 2-mercaptoethanol, 24 mM sodium bicarbonate, penicillin (1 iu per ml) and streptomycin (1 μg ml^{-1}). The cells were incubated at 37 °C in a humidified atmosphere of 5% CO_2: 95% air and pulsed with 1 μCi ^{3}H-Tdr at 370 mCi mmol^{-1} 18 h before the cells were collected. CS-A was dissolved in ethanol and added to the cultures at different times (indicated by arrows) to give a final concentration of 1 μg ml^{-1} of CS-A and 0.5% ethanol. The addition of ethanol only did not affect the MLR (data not shown). ▲, Control; ●, experimental curves after addition of CS-A; broken lines, postulate of curves after addition of CS-A.

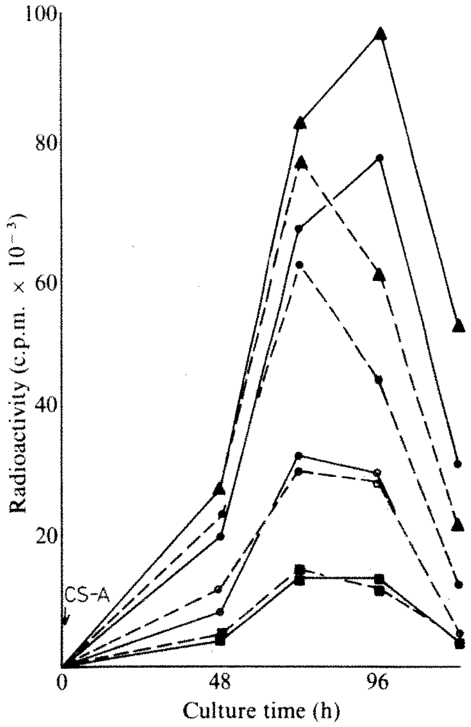

Fig. 2 Addition of different doses of CS-A to cultures of normal or presensitized CBA lymph node cells and DBA/2 stimulator spleen cells. CS-A was added at the beginning of culture. For conditions of culture, see legend to Fig. 1. Solid lines, normal cells; broken lines, presensitized cells; ▲, controls; ●, 0.05 μg ml^{-1}; ○, 0.125 μg ml^{-1}; ■, 0.25 μg ml^{-1}.

These results suggest that higher concentrations of CS-A would be required *in vivo* to suppress T-dependent immune responses in presensitized animals, and preliminary results of skin grafting experiments are consistent with this prediction.

Our MLR data confirm the reports of others[13,14] who have shown that CS-A suppresses the response of lymphocytes to mitogens such as phytohaemagglutinin and to histocompatibility antigens in MLR. We have shown, further, that the drug is a potent inhibitor of CML provided that it is added in the first 48 h of culture. The similarity between the concentration of CS-A required to inhibit CML and MLR suggests that the suppression of CML is brought about, essentially, by inhibition of the proliferative responses required for the generation of cytotoxic cells; it also provides an explanation for the residual cytotoxic activity in presensitized spleen CML's.

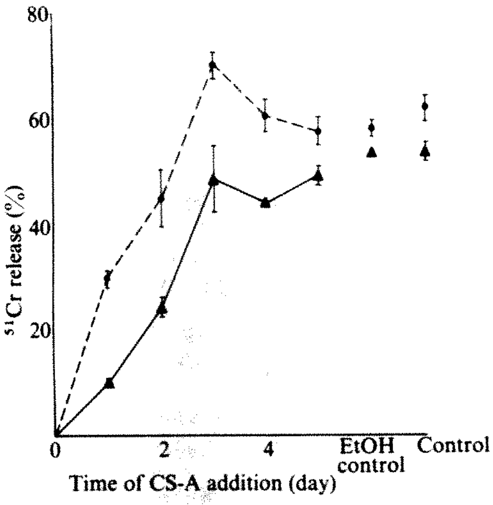

Fig. 3 Addition of CS-A at different times during the course of CML culture between normal or presensitized CBA lymph node cells and DBA/2 stimulator spleen cells: effect on generation of cytotoxicity. CBA responder cells were incubated with irradiated DBA/2 stimulator spleen cells in a ratio of either 1:2 or 2:1 in 10 ml RPMI medium supplemented as described in the legend to Fig. 1, at a total concentration of $3.75\times10^6\,\text{ml}^{-1}$. CS-A was dissolved in ethanol and added either at the beginning of the culture or during the course of the next 5 d, to a final concentration of 1 μg ml^{-1}. The 25 ml flasks were incubated upright at 37°C in a humidified atmosphere of 5% CO_2:95% air. The cells were collected after 5 d and tested for cytotoxicity in a 4 h ^{51}Cr release assay. Equal volumes (100 μl) of effector cells (at $4\times10^6\,\text{ml}^{-1}$) and ^{51}Cr-labelled PY815 mastocytoma target cells (at $10^5\,\text{ml}^{-1}$) were incubated in microtest plates for 4 h at 37 °C. The plates were spun at 200*g* for 5 min, and 100 μl of supernatant from each well was counted. Cytotoxicity (%) was calculated according to the formula:

$$\left(\frac{\text{Test}-\text{background}}{\text{Total release}-\text{background}}\right)\times 100\ \text{(c.p.m.)}$$

Background release of radioactivity from the target cells was never more than 10% and usually less than 5% of the total amount incorporated. ▲, Normal; ●, presensitized. Error bars indicate ±1 s.e.m.

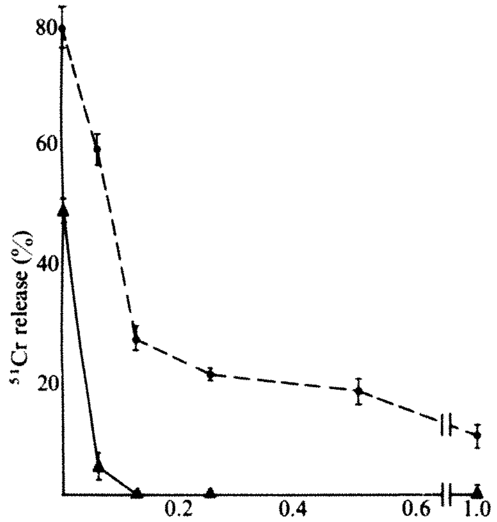

Fig. 4 Addition of different doses of CS-A to CML cultures of either 25×10^6 normal or presensitized CBA spleen cells and 12.5×10^6 DBA/2 stimulator spleen cells: effect on generation of cytotoxicity. CS-A was added at the beginning of culture. For other details, see legend to Fig. 3. Cytoxicity assays were carried out after 5 d of culture. ▲, Normal; ●, presensitized. Error bars indicate ±1 s.e.m.

CS-A may therefore not be an ideal agent for the reversal of rejection crises in clinical transplantation or in the treatment of presensitized graft recipients.

We thank Miss G. Kalsi for technical assistance and J. F. Borel, Sandoz Ltd, Basle for a gift of cyclosporin A. This work was supported by the Medical Research Council.

Received 28 March; accepted 6 June 1980.

1. Dreyfuss, M. *et al. Eur. J. appl. Microbiol.* **3,** 125–133 (1976).
2. Calne, R. Y. & White, D. J. G. *IRCS J. med. Sci.* **5,** 595 (1977).
3. Greene, C. J. & Allison, A. C. *Lancet* **i,** 1182–1183 (1978).
4. Calne, R. Y. *et al. Lancet* **ii,** 1323–1327 (1978).
5. Calne, R. Y. *et al. Lancet* **i,** 1183–1185 (1978).
6. Jamieson, S. W. *et al. Lancet* **i,** 545 (1979).
7. Borel, J. F., Feurer, C., Gubler, H. U. & Stahelin, H. *Agents Actions* **6,** 468–475 (1976).
8. Brent, L. *Transplantn Proc.* **12,** 234–243 (1980).
9. Häyry, P., Andersson, L. C., Nordling, S. & Virolainen, H. *Transplantn Rev.* **12,** 91–140 (1972).
10. Cooley, M. A. *Scand. J. Immun.* **7,** 371–380 (1978).
11. Kuperman, O. J. & Bach, F. J. *Scand. J. Immun.* **6,** 161–172 (1977).
12. Simpson, E., O'Hopp, S. & Wunderlich, J. *Transplantation* **18,** 374–377 (1974).
13. Leoni, P., Garcia, R. C. & Allison, A. C. *J. clin. Lab. Immun.* **1,** 67–72 (1978).
14. White, D. J. G., Plumb, A. M., Pawelec, G. & Brons, G. *Transplantation* **27,** 55–58 (1979).

Endotoxin-induced uveitis in rats as a model for human disease

J. T. Rosenbaum, H. O. McDevitt, R. B. Guss & P. R. Egbert

Department of Medicine, Stanford University School of Medicine,
Stanford University Medical Center, Stanford, California 94305

Acute anterior uveitis is a relatively common disease of uncertain aetiology. Its association with a wide variety of systemic disorders including ankylosing spondylitis, Reiter's syndrome, Behçet's disease, juvenile rheumatoid arthritis, psoriatic arthritis, inflammatory bowel disease and sarcoidosis and the prevalence of the HLA antigen B27 (ref. 1) in cases without associated disease have been noted but not explained. In general, animal models for uveitis have not clarified the mechanism of human disease. Most require direct intravitreal injection[2] or repeated immunizations with retinal or uveal antigens[3]. Uveitis does occur in adjuvant arthritis, a syndrome that can be produced in rats by the systemic injection of peptidoglycan from the cell wall of a variety of Gram-positive bacteria[4]. The disease, which was initially described following the injection of mycobacteria in mineral oil, has many similarities to Reiter's syndrome[5], including the development of eye pathology in as many as 40% of the animals[6]. As Reiter's syndrome is associated with enteric Gram-negative infections such as *Shigella*, *Salmonella* and *Yersinia*, we sought to produce an arthritis in rats by injecting killed Gram-negative bacteria. Although we have not observed clinical arthritis in these animals, careful histological study has shown the near-universal appearance of uveitis. The studies described below indicate that the eye disease is due to a portion of the bacterial cell wall known as endotoxin or lipopolysaccharide (LPS).

The typical eye histology produced is shown in Fig. 1. This response could be produced by 1 mg of *Escherichia coli*, *Klebsiella* or *Shigella* but not by 1 mg of *Staphylococcus* or by 0.1 mg of *E. coli.* The different response following Gram-negative as opposed to Gram-positive bacteria encouraged us to assess the reaction to endotoxin alone.

In Lewis rats, we were able to induce uveitis by intravenous or intraperitoneal (i.p.) injections of LPS as well as LPS by the footpad route (f.p.). Comparable abnormal histology was also noted when the source of LPS was extracted from *Shigella flexneri* or *Shigella sonnei* by the Westphal method. Preliminary studies show that the lipid A portion of LPS as obtained by acid hydrolysis and solubilized by coupling to bovine serum albumin[8] could itself induce uveitis.

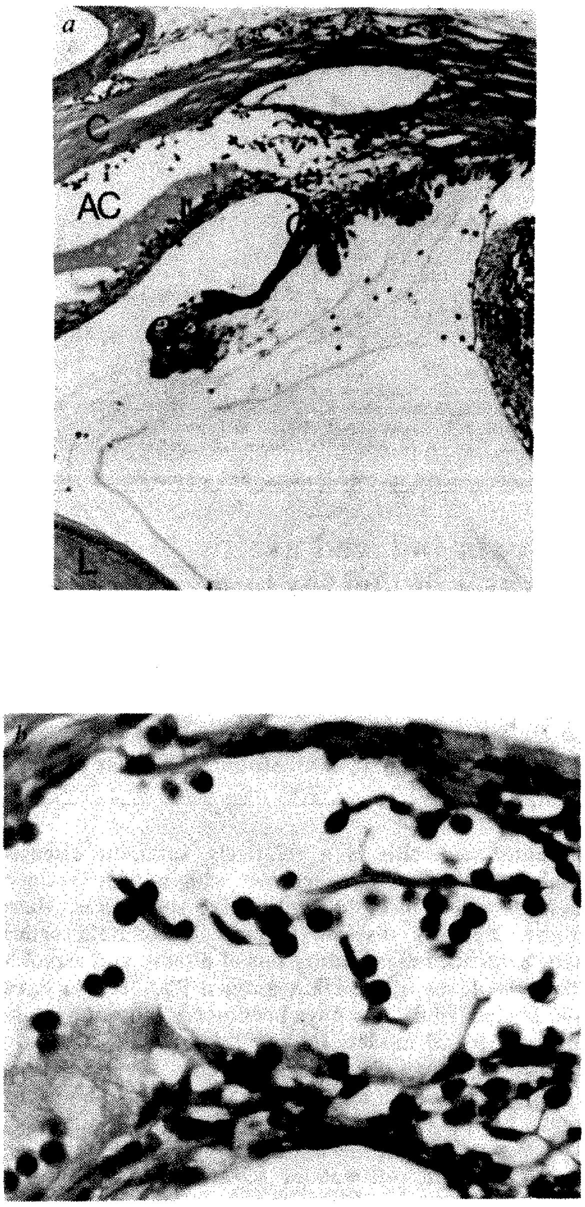

Fig. 1 The top photomicrograph shows many inflammatory cells near the iris (I), anterior chamber (AC) and ciliary body (CB) of a rat eye. A marked proteinaceous exudate is present in the anterior chamber adjacent to the iris. The cornea (C), retina (R) and lens (L) are also labelled for orientation. The photomicrograph below is a higher-power view showing that the infiltrating cells are both polymorphonuclear leukocytes and mononuclear cells. Lewis rats (~250 g), usually 4-6 months old, were used. Bacteria were grown overnight in thioglycollate broth, killed with formalin, washed three times with saline, and lyophilized. Bacteria included *E. coli, Klebsiella, S. sonnei* and *S. aureus*, coagulase positive. Bacteria were injected with 0.1 cm^3 of a mineral oil suspension asceptically into the footpad of a rat that had been lightly anaesthetized with ether. Eyes were obtained 48 h later, after the animal had been killed with ether and exsanguination. Eyes were fixed in 10% neutral buffered formalin and stained with haematoxylin and eosin. Eye pathology was evaluated by two of us (R.G. and P.E.) without knowledge of the treatment received. Eyes were considered to demonstrate uveitis only if a representative cross-section contained five or more inflammatory cells, either polymorphonuclear leukocytes or lymphocytes, in the anterior chamber, posterior chamber or vitreous. In most abnormal eyes a proteinaceous exudate was also apparent. This definition of disease permitted complete concordance by the two observers.

A dose–response curve showed that no detectable changes were present 48 h after 10 μg of *E. coli* LPS injected f.p. but that 50 μg f.p. or 300 μg i.p. produced reactions comparable to that following 100 μg. A dose of LPS sufficient to produce eye disease induced no significant abnormalities in the heart, lung, liver, kidney, spleen, skin, intestine or marrow as judged by light microscopy.

Eyes studied 1 h after an injection of 100 μg LPS f.p. showed no significant abnormality but by 4 h, cells were beginning to accumulate. The disorder was maximal around 48 h, was still present, although declining, 96 h after the injection, and could not be detected 1 week after the injection. When LPS was administered twice over a 3-week period, the disease recurred, but multiple doses of LPS over several weeks tended to abolish or markedly diminish the disease.

In total, bilateral uveitis was seen in all 23 animals 48 h after either 1 mg of lyophilized Gram-negative bacteria or 100 μg LPS given by a variety of routes, in a variety of strains and from a variety of sources (see Table 1). Although a contaminating substance cannot be completely discounted, the reaction seems to be due to endotoxin, in particular the lipid A portion of endotoxin, as argued by its appearance after various Gram-negative bacteria but not after *Staphylococcus aureus* injection and by its occurrence following injection of LPS from different sources.

The absence of cellular abnormalities in other tissues is surprising but it might be predicted from the work of other investigators who have noted that doses of LPS sufficient to cause death (approximately 5 mg in a rat) produce relatively little histological change[9]. The amelioration of disease after repeated injections is reminiscent of the phenomenon of tolerance to endotoxic shock[10].

The concept that bacterial products might induce uveitis is not a novel one. Woods first described 'poisons' from bacteria "which have a definite action upon the uveal tract in the eye" (ref. 11). Others have used live bacteria, primarily streptococcus, and succeeded in producing uveal changes in a minority of rabbits at variable times after injection[12]. For a time, elimination of potential foci of infection such as tonsils or carious teeth was in vogue as a method for treating uveitis[13]. Attention focused specifically on endotoxin when Ayo reported a 'toxic ocular reaction' in rabbits that was ascribed to 'Shwartzman toxins' (ref. 14). This response could include an iridocyclitis but disappeared within 24 h and specifically could not be produced in rats[15]. A change in ocular vascular permeability following intravenous endotoxin had been noted within 1 h in the rabbit[16]. Others have reported that intravenous endotoxin produces an aqueous cellular response in less than 5% of rabbits, although cells in the uvea are common[17].

Endotoxin-induced disease differs markedly from the eye findings in adjuvant arthritis in that the reaction occurs within 24 h of the immunization whereas eye findings in adjuvant disease never occur before 8 days after injection and are maximal at 10–15 days[6]. Eye disease occurs in only a minority of susceptible animals in adjuvant disease[6], but seems to be near universal in rats after LPS injection.

Circumstantial evidence suggests that this model might have relevance for human disease. The most obvious link is with Crohn's disease and ulcerative colitis. In both of these, circulating endotoxaemia may develop with active disease[18].

In Reiter's syndrome a variety of Gram-negative dysenteries may provoke arthritis and uveitis[7]. In Behçet's syndrome, bowel pathology could conceivably account for a source of endotoxaemia. As endotoxin is known to release lysozyme[19], the elevated lysozyme levels seen in Crohn's disease[20], ulcerative colitis[20] and Behçet's disease[21] as well as in sarcoidosis could be related to endotoxin or a stimulus with endotoxin-like activity. Because uveitis in man is closely linked to the HLA antigen B27 (ref. 22), an important advantage of a rat as opposed to a rabbit model, is that the role of the major histocompatibility complex (MHC) can be explored. The variety of strains susceptible to endotoxin-induced uveitis suggests that the effects of LPS are

Table 1 Variety of strains susceptible to endotoxin-induced uveitis

Strain	No. injected with LPS/ no. with uveitis	No. of controls/ no. with uveitis
Lewis	3/3	3/0
Wistar–Lewis	2/2	2/0
Wistar	1/1	
Lea-X	1/1	
BC	1/1	
Fischer	1/1	
Buffalo	2/2	2/0
Sprague–Dawley	2/2	2/0
Long Evans	2/2	2/0
ACI	2/2	1/0
Totals	17/17	12/0

Male rats (200–250 g) were injected in the footpad with *E. coli* LPS 055 (Difco) after light ether anaesthesia. The dose was 100 μg in 0.1 cm^3 of saline. Control rats with the exception of the Lewis rats were given an injection of sterile saline alone. Eyes were removed 48 h after injection. Methods for histology and criteria for uveitis were identical to that used following the injection of whole bacteria. Disease was bilateral in all cases.

not restricted by the MHC. However, if the claimed cross-reaction between *Klebsiella* and HLA-B27 is confirmed[23,24], B27-positive individuals might be predisposed to endotoxaemia through either mimicry or a receptor[25] phenomenon for a *Klebsiella* product. This putative cross-reaction with a Gram-negative bacteria might explain the frequency with which *Klebsiella* is found in the stool of ankylosing spondylitis patients before a flare of uveitis[26].

An alternative explanation for the relationship between the MHC and uveitis is that LPS is only one of several factors responsible for disease in man, with a second factor being determined by an immune response gene within the MHC. For example, intravitreal injection of endotoxin can predispose the eye to immune complex deposition[27] and preliminary evidence in our laboratory suggests that systemic endotoxin might also facilitate immune complex deposition in the eye. Such a dual causality model would account for both the observed MHC association and the lack of strain restriction for the endotoxin effects.

Current work in our laboratory is aimed at establishing the mechanism of disease in the animal model, testing the possible relevance of the animal disease to uveitis in man, and exploring the potential role of endotoxin in the induction of arthritis and immune complex uveitis.

We thank Ms Bonnie Paschal and Ms Priscilla Hendricks for technical assistance, and Dr Jon C. Ross for interpreting slides of organs other than the eye. *Shigella* strains were from Dr John Shively, *E. coli* LPS from Drs Stuart Koretz and Samuel Strober, and Lewis rats from Simonsen Laboratories, Microbiological Associates or the breeding colony of Dr Irving Weissman.

Received 26 December 1979; accepted 3 June 1980.

1. Brewerton, D. A., Caffrey, M., Nicholls, A., Waters, D. & James, D. C. O. *Lancet* **ii,** 994–996 (1973).
2. Gamble, C. N., Aronson, S. B. & Brescia, F. B. *Archs Ophthal.* **84,** 321–330 (1970).
3. Wacker, W. B., Donoso, L. A., Kaslow, C. M., Yankeelov, J. A. & Organisciak, D. T. *J. Immun.* **119,** 1948–1958 (1977).
4. Kohashi, O., Pearson, C. M., Watanabe, Y., Kotani, S. & Koga, T. *J. Immun.* **116,** 1635–1639 (1976).
5. Pearson, C. M., Waksman, B. H. & Sharp, J. T. *J. exp. Med.* **113,** 485–510 (1961).
6. Waksman, B. H. & Bullington, S. J. *Archs Ophthal., N.Y.* **64,** 751–761 (1960).
7. Calin, A. & Fries, J. F. *Ann. int. Med.* **84,** 564–566 (1976).
8. Rietschel, E. T. & Galanos, C. *Infect. Immun.* **15,** 34–49 (1977).
9. Thomas, L. *A. Rev. Physiol.* **16,** 467–490 (1954).
10. Griesman, S. E. & Hornick, R. B. *Trans. Am. clin. clim. Ass.* **56,** 43–50 (1975).
11. Woods, A. C. *Archs Ophthal.* **45,** 451–464 (1916).
12. Berens, C., Angevine, M., Guy, L. & Rothbard, S. *Am. J. Ophthal.* **21,** 1315–1329 (1938).
13. Rosenow, E. C. & Nickel, A. C. *Am. J. Ophthal.* **15,** 1–18 (1932).
14. Ayo, C. *Proc. Soc. exp. Biol.* **47,** 500–501 (1941).
15. Ayo, C. *J. Immun.* **47,** 113–125 (1943).
16. Howes, E. L., McKay, D. G. & Aronson, S. B. *Lab. Invest.* **24,** 217–228 (1971).
17. Levene, R. Z. & Breinin, G. M. *Archs Ophthal.* **61,** 568–577 (1969).
18. Aoki, K. *Acta med. okayama* **32,** 147–158 (1978).
19. Weissman, G. & Thomas, L. *J. exp. Med.* **116,** 433–450 (1962).
20. Peeters, T. L., Vantrappen, G. & Geboes, K. *Gut* **17,** 300–305 (1976).
21. Hayasaka, S., Hara, S. & Mizuno, K. *Albrecht v. Graefes Arch. Ophthal.* **203,** 139–144 (1977).
22. Dausset, J. & Svejgaard, A. *HLA and Disease* (INSERM, Paris, 1976).
23. Ebringer, A., Cowling, P., Ngwa Suh, N., James, D. C. O. & Ebringer, R. W. *HLA and Disease*, 27 (INSERM, Paris, 1976).
24. Seager, K., Bashir, H. V., Geczy, A. F., Edmonds, J. & De Vere-Tyndall, A. *Nature* **277,** 68–70 (1979).
25. Geczy, A. F., Alexander, K., Bushir, H. V. & Edmonds, J. *Nature* **283,** 782–784 (1980).
26. Ebringer, R., Cadwell, D. & Ebringer, A. *Br. med. J.* **1,** 383 (1979).
27. Gamble, C. N., Aronson, S. B. & Brescia, F. B. *Archs Ophthal.* **84,** 331–334 (1970).

Elution of herpes simplex virus-specific cytotoxic antibodies from squamous cell carcinoma of uterine cervix

Pradeep Seth & N. Balachandran

Department of Microbiology,
All India Institute of Medical Sciences,
Ansari nagar, New Delhi-16, India

There is evidence that carcinoma of the cervix uteri is associated with infection with herpes simplex virus type 2 (HSV-2), and although indirect evidence suggests an aetiological relationship[1–6], this remains controversial[7–9]. One facet of the problem is that complement-dependent cytotoxic antibodies to HSV-2-infected cells have been undetectable or found only in low titre in sera from patients with progressive cervical cancer whereas higher titres have been found where cervical lesions are less advanced[10,11]. Indeed, cytotoxic antibody titres have been found to rise during the follow-up period after successful treatment[11]. Absorption of these antibodies by the tumour cells has been proposed as a possible reason for low HSV-2 cytolytic reactivity in patients with progressing cervical cancer[10]. This explanation assumes the presence of HSV-2-specific antigen(s) on the tumour cells. We now provide support for this assumption with evidence that absorbed HSV-2-specific antibodies can be eluted from cervical cancer tissue.

Elution of bound immunoglobulin from freshly removed tissues from six patients with cervical cancer, stage I (five patients with squamous cell carcinoma, one with adenocarcinoma), one patient with ovarian cancer, two patients with uterine fibroids, three patients with squamous cell carcinoma of the skin and from three normal uterine cervices was achieved by treatment with 15% NaCl (*p*H 7.4) at 37 °C (ref. 12). The protein content of the eluates was estimated[13] and the class of immunoglobulin present was determined by polyacrylamide gel electrophoresis using purified human serum IgM, IgG and IgA as markers. Although the eluates from all tissues contained proteins, IgG was the only detectable immunoglobulin eluted from all squamous cell carcinoma tissues as well as cervical adenocarcinoma tissues (Table 1). Tissues from uterine fibroids and normal cervix failed to yield any immunoglobulin by the technique used. The nature of other protein(s) present in the eluates was not determined.

Complement-dependent cytolytic activity of the eluate was assayed on ^{51}Cr-labelled BHK-21 cells infected 22–24 h previously with HSV-1 or HSV-2, at a multiplicity of infection of 3–5 plaque forming units (PFU) per cell[14]. The eluate (0.1 ml) was diluted 1:5 in Tris-buffered saline, *p*H 7.2, mixed with 5×10^4 cells and incubated at 37 °C for 60 min. Then, 0.2 ml of fresh guinea pig complement diluted 1:10 was added and the mixture was incubated at 37 °C for another 90 min. The cytolysis was stopped by adding 2 ml of cold Tris-diluent to each tube, which was then centrifuged at 600*g* for 3 min at 4 °C. Aliquots (1 ml) of the supernatant were transferred to another tube and counted for radioactivity in a Packard automatic γ spectrometer. Each test included: labelled cells only, which were frozen and thawed in distilled water for maximum ^{51}Cr release, cells with eluate alone to control for eluate toxicity, and cells

Table 1 Complement-dependent antibody-mediated lysis of infected (HSV, vaccinia) and uninfected BHK-21 cells by the eluates from cancer and normal tissues

Tissue processed				Lysis by the eluate* of ^{51}Cr-labelled BHK-21 cells					
Source	Weight (g)	Protein conc. of eluate (ng ml^{-1})	Class of Ig present in eluate	Virus infecting BHK-21 cells	Maximum release control (c.p.m.)	Spontaneous release control (c.p.m.)	Eluate toxicity control (c.p.m.)†	Test release (c.p.m.)	% Specific release‡
Squamous cell cancer of cervix stage I	2.045	300	IgG	HSV-1	2,365	278	139	1,655	66
				HSV-2	2,476	369	147	2,471	100
				Vaccinia	3,565	581	350	397	0
				None	3,972	307	152	187	0
Squamous cell cancer of cervix stage I	1.80	111	IgG	HSV-1	2,365	278	172	487	10
				HSV-2	2,476	369	185	685	15
				Vaccinia	3,565	581	337	382	0
				None	3,972	307	147	182	0
Squamous cell cancer of cervix, stage I	1.40	83	IgG	HSV-1	2,365	278	181	491	10
				HSV-2	2,476	369	177	643	13
				Vaccinia	3,565	581	386	453	0
				None	3,972	307	175	208	0
Squamous cell cancer of cervix, stage I	0.630	233	IgG	HSV-1	1,973	205	114	346	8
				HSV-2	1,791	211	127	371	10
				Vaccinia	3,565	581	275	346	0
				None	3,972	307	182	211	0
Squamous cell cancer of cervix, stage I	2.255	620	IgG	HSV-1	1,973	205	121	435	13
				HSV-2	1,791	211	113	451	15
				Vaccinia	3,565	581	285	369	0
				None	3,972	307	197	218	0
Squamous cell cancer of skin	1.90	120	IgG	HSV-1	2,789	383	211	219	0
				HSV-2	2,561	367	207	251	0
				Vaccinia	2,856	309	259	281	0
				None	3,331	218	101	123	0
Squamous cell cancer of skin	2.35	185	IgG	HSV-1	2,789	383	195	238	0
				HSV-2	2,561	367	219	227	0
				Vaccinia	2,856	309	272	285	0
				None	3,331	218	111	139	0
Squamous cell cancer of skin	2.13	163	IgG	HSV-1	2,789	383	203	213	0
				HSV-2	2,561	367	189	256	0
				Vaccinia	2,856	309	223	249	0
				None	3,331	218	137	148	0
Adenocarcinoma of cervix, stage I	2.125	244	IgG	HSV-1	2,365	278	141	173	0
				HSV-2	2,476	369	163	210	0
				Vaccinia	3,565	581	277	381	0
				None	3,972	307	161	201	0
Ovarian carcinoma	1.95	ND	ND	HSV-1	1,973	205	179	191	0
				HSV-2	1,791	211	151	177	0
				Vaccinia	3,565	581	309	403	0
				None	3,972	307	153	192	0
Fibroid uterus	4.010	540	Nil	HSV-1	2,365	278	143	201	0
				HSV-2	2,476	369	147	258	0
				Vaccinia	3,565	581	367	411	0
				None	3,972	307	148	207	0
Fibroid uterus	1.41	140	Nil	HSV-1	2,365	278	137	161	0
				HSV-2	2,476	369	151	207	0
				Vaccinia	3,565	581	352	275	0
				none	3,972	307	129	192	0
Normal cervix	1.13	540	Nil	HSV-1	1,973	205	127	141	0
				HSV-2	1,791	211	146	179	0
				Vaccinia	3,565	581	321	238	0
				None	3,972	307	208	222	0
Normal cervix	2.22	80	Nil	HSV-1	1,973	205	141	159	0
				HSV-2	1,791	211	110	143	0
				Vaccinia	3,565	581	357	259	0
				None	3,972	307	179	215	0
Normal cervix	1.85	190	Nil	HSV-1	1,973	205	136	147	0
				HSV-2	1,791	211	161	169	0
				Vaccinia	3,565	581	283	197	0
				None	3,972	307	182	229	0

Each tissue was minced finely and passed through a 60-wire mesh screen to obtain a cell suspension. It was washed 15 times with 10-ml volumes of phosphate-buffered saline (0.025 M PBS, *p*H 7.4) and the UV absorbance of the supernatant after the 15th wash was checked at 280 nm wavelength in a spectrometer. No further washing was done if *A* was less than 0.025. When it was more, additional washings were given until *A* was less than 0.025. The pellet was then suspended in 5 ml of 15% NaCl (*p*H 7.4) and incubated at 37 °C for 2 h. After that, it was centrifuged at 10,000*g* for 10 min, and the sediment was re-extracted with 15% NaCl. The supernatants of both extractions were pooled and dialysed against 500 ml of PBS for 24 h with two changes of buffer. It was then centrifuged at 36,000*g* for 1 h and the supernatant was collected and concentrated 10-fold by vacuum dialysis. It was centrifuged at 5,000*g* for 30 min and the clear supernatant was taken as eluate for further testing as described in the text. ND, Not done.

* A 1 : 5 dilution of the eluate was tested.

$$‡\ \%\ \text{Specific release} = \frac{\text{test release (c.p.m.)} - \text{spontaneous release (c.p.m.)}}{\text{maximum release (c.p.m.)} - \text{spontaneous release (c.p.m.)}} \times 100.$$

† Values of eluate toxicity controls are always less than spontaneous release control. In cases where the values of the former are greater than the latter, the eluate is too toxic to be tested.

with complement alone as a control for spontaneous ^{51}Cr release. All test systems, including controls, were carried out in duplicate and their c.p.m. were averaged. The cytolytic antibody activity was expressed as the per cent specific release of ^{51}Cr according to the formula[15]

$$\%\ \text{Specific release} = \left(\frac{^{51}\text{Cr release in the presence of eluate and compement} - \text{spontaneous release}}{\text{Maximum release} - \text{spontaneous release}} \right) \times 100$$

The eluates from cervical squamous cell carcinoma produced 8–66% lysis of HSV-1 infected cells and 10–100% lysis of HSV-2-infected cells (see Table 1). The cytolytic pattern of the eluates suggests the presence of antibody activity to cross-reacting antigens of HSV-1 and HSV-2. However, the cytolytic activity was more pronounced against HSV-2-infected cells. Specificity of the antibody activity was established by the failure of the eluates to lyse vaccinia-infected BHK-21 cells[16] or uninfected BHK-21 cells. Moreover, eluates from other tumour tissues as well as normal healthy cervix did not show any cytolytic activity against infected or uninfected BHK-21 cells.

Each tissue was also tested for the presence of virus. A portion of tissue was ground in a homogenizer and 0.1 ml of the homogenate was inoculated onto two stationary cultures of Vero cells grown in Eagle's minimum essential medium (MEM) supplemented with 5% calf serum. The cultures were incubated at 37 °C and observed for 14 days. None of the homogenates produced a cytopathic effect suggestive of HSV. Furthermore, three tissues from squamous cell carcinoma of the cervix, three tissues from squamous cell carcinoma of the skin, one tissue each from adenocarcinoma of the cervix, uterine fibroid and normal cervix were minced separately into 1-mm^3 explants and co-cultivated with monolayers of Vero cells which were then fed with MEM containing 20% fetal calf serum[17]. The cultures were observed for 8 weeks for cytopathic effects before they were discarded. No virus was recovered on co-cultivation.

These data indicate the presence of HSV-specific antigens on the tumour cells of squamous cell carcinoma of the uterine cervix in the absence of apparent infection of these cells by the virus. However, latent or abortive infection of the tumour tissue by HSV cannot be definitely excluded, even though no HSV was isolated from any cervical cancer tissues.

Evidently, HSV-specific cytotoxic antibodies had been absorbed from the blood of the patients with cervical cancer *in vivo* by HSV-specific antigens present on the tumour cells. This absorption seems to be specific for squamous cell carcinoma of the cervix, as HSV-specific immunoglobulins could not be eluted from squamous cell carcinoma of the skin. The absorbed antibody may be either functioning as blocking antibody in tumour enhancement[18] or involved in the cell-mediated destruction of the tumour cells[19]. Furthermore, the absence of HSV-specific antigens in tissues from squamous cell carcinoma of the skin, ovarian carcinoma and uterine fibroids strongly suggests a role of HSV in the aetiology of squamous cell carcinoma of the uterine cervix.

On the basis of the present data, it is difficult to understand how the low titres of HSV-cytolytic antibodies in the sera of patients with progressing cancer of the cervix could arise from absorption of antibodies by the tumour cells[10]. However, the presence of circulating immune complexes in the sera of patients with cervical cancer[20] might interfere with the assay of cytolytic antibodies by the ^{51}Cr-release test, and absorption of antibodies by the tumour cells may account for depletion of only a small portion of cytolytic antibodies from the circulation.

These results, although obtained using only a few patients, are nevertheless striking. As no infective virus could be detected or reactivated, it is tempting to suggest that the virus-specific IgG is adsorbed to virus-specified determinants on the neoplastic cells.

We thank Drs V. L. Bhargava, S. Kumar and D. Ghosh for the clinical material and Drs L. N. Mohapatra, S. Balaya and R. Kumar for their advice.

Received 9 April; accepted 13 June 1980.

1. Nahmias, A. J. *et al. Am. J. Epidemiol.* **91,** 547–552 (1970).
2. Rawls, W. E. *et al. Cancer Res.* **33,** 1477–1482 (1973).
3. Seth, P. *et al. Int. J. Cancer* **33,** 708–714 (1978).
4. Frenkel, N. *et al. Proc. natn. Acad. Sci. U.S.A.* **69,** 3784–3789 (1972).
5. Aurelian, L. *et al. Science* **174,** 704–707 (1971).
6. Abrahim, A. N. *et al. Proc. Soc. exp. Biol. Med.* **152,** 343–347 (1976).
7. Zur Hausen, H. *Biochim. biophys. Acta* **417,** 25–53 (1975).
8. Melnick, J. L. & Adam, E. *Prog. exp. Tumour Res.* **21,** 49–69 (1978).
9. Nahmias, A. J. & Sawanabori, S. *Prog. exp. Tumour Res.* **21,** 117–139 (1978).
10. Christenson, B. *Int. J. Cancer* **20,** 694–701 (1977).
11. Thiry, L. *et al. Am. J. Epidemiol.* **100,** 251–261 (1974).
12. Gupta, R. K. & Morton, D. L. *Cancer Res.* **35,** 58–62 (1975).
13. Lowry, O. H. *et al. J. biol. Chem.* **193,** 265–275 (1951)
14. McClung, H. *et al. Am. J. Epidemiol.* **104,** 181–191 (1976).
15. Brunner, K. T. *et al. Immunology* **14,** 181–196 (1968).
16. Balachandran, N. *et al. J. gen. Virol.* **45,** 65–72 (1979).
17. Bastian, F. O. *et al. Science* **178,** 306–307 (1972).
18. Moller, G. *Nature* **204,** 846–847 (1964).
19. Witz, I. P. *Adv. Cancer Res.* **25,** 95–148 (1978).
20. Seth, P. *et al. Clin. exp. Immun.* **38,** 77–82 (1979).

How many types of erythroleukaemia are induced by retroviruses in mice?

Rita Anand & Richard Steeves*

Albert Einstein College of Medicine, 1300 Morris Park Avenue, Bronx,
New York 10461

Erythroleukaemia, until now defined by morphological criteria, has been observed in mice infected with several distinct virological entities, including the polycythaemia-inducing strains of Friend virus complex (FV-P)[1,2], the anaemia-inducing strains of Friend[3] and Rauscher[4,5] virus complex (FV-A and RV-A, respectively) and various helper-independent virus isolates derived from the FV-A[6] or RV-A[7] complexes. Whereas erythroleukaemia develops rapidly (within 2–3 weeks) in mice infected with any strain of FV or RV, the helper-independent virus alone is pathogenic in mice only if they are infected neonatally[6,7]. We now describe how two biological markers can be used to distinguish among the otherwise confusing array of virus-induced erythroleukaemias in mice. The evidence suggests that there are three different classes of this disease: (1) those (S^+E^+) from which both defective spleen focus-forming virus (SFFV) and erythropoietin-independent, erythroid colony-forming units (CFU-EI) can be recovered, (2) those (S^+E^-) from which only SFFV (but not CFU-EI) can be recovered, and (3) those (S^-E^-) from which neither SFFV nor CFU-EI can be recovered. There is a consistent association between the type of virus used to induce the erythroleukaemia and the class of the disease induced.

Since Friend's isolation of a virus that rapidly induced "a disease having the character of a leukaemia" (ref. 8), there have been many reports on Friend virus, some containing different interpretations of the disease induced by this virus[3,9,10], others describing different host responses to different strains of the virus[11,12], and still others describing different isolations of similar viruses which induce diseases similar to that induced by Friend virus[6,7,13–16]. About a decade ago a defective virus in Friend[17,18] and Rauscher[19] virus preparations was discovered which has the capacity to induce macroscopic spleen foci[20,21] and sometimes polycythaemia[12] in susceptible strains of mice. Clearer knowledge of the virus came from Troxler and colleagues[6,22–24], who analysed single cell clones inoculated with FV-P or with FV-A, and developed from each type of infected clone SFFV-infected non-producer cell lines that were free of detectable helper virus. When they used different helper viruses to rescue infectious pseudotypes of SFFV, they found that the haematocrit response of infected hosts was associated with the origin of SFFV (from FV-P- or FV-A-infected cells) rather than with that of its helper virus[24].

---

* Present address: Division of Radiation Oncology, University of Wisconsin, 600 Highland Avenue, Madison, Wisconsin 53792.

Table 1 Three host response patterns to erythroleukaemia-inducing retroviruses

Virus strain	Recovery of SFFV ($\times 10^3$ FFU ml^{-1})	Recovery of CFU-EI (per 10^5 spleen cells)
FV-P (Lilly)	52.0	620
FV-P (Axelrad)	78.4	371
FV-P (Mirand)	0.2	85
FV-A (Dmochowski)	0.5	0
RV-A (Rauscher)	3.5	0
F-MuLV$_{201}$	0	0
RV-A variant (Fredrickson)	0	0

Abbreviations: CFU-EI, erythropoietin-independent, erythroid colony-forming unit; FV-P, polycythaemia-inducing strain of Friend virus complex; FV-A, anaemia-inducing strain of Friend virus complex; F-MuLV$_{201}$, clone 201 of a helper-independent murine leukaemia virus (MuLV) that was isolated from FV-A[24]; RV-A, anaemia-inducing strain of Rauscher virus complex; RV-A variant, helper-independent MuLV isolated from RV-A that lacks spleen focus-forming virus (SFFV)[7]. Virus complexes (the first five strains) considered to contain SFFV were diluted 10^{-1} from stock (10% w/v spleen homogenates) and injected intravenously into young adult BALB/c mice. Two weeks later their spleens were collected and assayed for SFFV by the spleen focus assay[20] and for CFU-EI according to the method of Liao and Axelrad[27]. Helper-independent MuLVs (the last two strains) considered to lack SFFV were not diluted from stock, but were injected intraperitoneally into suckling BALB/c mice within 48 h of birth. Three to four weeks later their spleens were collected and assayed as described above.

However, the pathology of erythroid leukaemias and dyscrasias in mice has not been well defined, and there has been little agreement among the morphological descriptions of virus-induced diseases of this sort. For example some investigators have described the diseases induced by the same viruses as erythroblastosis[9,10,25,26] or simply erythrocytopoietic disease[13]. In a search for non-morphological criteria that could be used to define erythroid leukaemias, we compared several different virus strains according to their capacity to initiate SFFV replication and/or the production of CFU-EI[27] in BALB/c mice. The results of this comparison, summarized in Table 1, show that by 3 weeks after infection the diseases induced could be divided into three categories on the basis of the recovery from splenic tissues of: both SFFV and CFU-EI (S^+E^+); SFFV but not CFU-EI (S^+E^-); neither SFFV nor CFU-EI (S^-E^-).

Let us now correlate these classes of erythroid leukaemia with the viruses used to induce them. Because of previous reports[12,27] it was not surprising that all strains of FV-P would induce S^+E^+ leukaemias. (On the basis of this clear association we would predict that the recently discovered, cloned, murine sarcoma virus[28] that induces an S^+E^+ erythroid cell proliferation might also induce polycythaemia.) The presence of SFFV in FV-A-infected mice was also not surprising, for earlier conflicting reports on this finding[12,29] were recently settled by the elegant cloning experiments of Troxler *et al.*[24]. However, the absence of CFU-EI among SFFV-positive leukaemia cells of FV-A-infected mice was significant.

Could the lack of CFU-EI in FV-A-infected mice be attributed to the lower titres of SFFV usually encountered in FV-A stocks[30]? Probably not, as the recovery of SFFV from mice infected with a low dose of FV-P (Mirand) was 10-fold lower than that of FV-A-infected mice (Table 1), although CFU-EI were only recovered from the former. Also, Steinheider *et al.*[31] failed to recover CFU-EI from FV-A-infected DBA/2 mice given an amount of SFFV 'comparable' to that given to CFU-EI-positive, FV-P-infected mice, although the actual dose of SFFV in the infecting inoculum was not stated. In the present study (data not shown) CFU-EI were readily detected in mice after infection with FV-P diluted almost to the end point for SFFV. Therefore, it seems that CFU-EI are not an expression of SFFV infection *per se*, but of erythropoietin-independent erythroid precursors destined to contribute to the development of polycythaemia. Their apparent absence after FV-A infection is in keeping with the failure of infected hosts to develop polycythaemia; this provides another qualitative distinction (in addition to the haematocrit response) between FV-A and FV-P.

The last (S^-E^-) class of leukaemias, like the first two classes, is distinctly erythroid in nature[22,32], and disease can be induced almost as rapidly (within 3–4 weeks of infection). Unlike the first two classes, the S^-E^- leukaemias develop only if the recipient mice have been inoculated with virus neonatally, probably due to the lack of immunodepressive SFFV in the viral inocula. This absence of SFFV was clearly shown for F-MuLV clone 201 by transfection experiments with molecularly cloned viral DNA[33]. Even though mice infected neonatally with F-MuLV$_{201}$ or with the Fredrickson variant of RV-A[7] did not yield SFFV or CFU-EI (Table 1), they did develop erythroid leukaemia, as tested by cytological examination of blood smears or splenic imprints.

Other candidate viral agents that might induce S^-E^- leukaemias are Dawson's F-MuLV variant[16] and Kirsten's MuLV[14]. Unfortunately, the former was not available to us, and samples of the latter failed to induce disease in our mice. There are other examples of murine viruses, apparently lacking SFFV, with the capacity to induce leukaemia[34]. These agents should all be examined and compared with the prototype strain, F-MuLV$_{201}$, by both biological and biochemical means.

It is curious that F-MuLV$_{201}$, isolated from FV-A and regularly collected from the spleens of infected mice only 3 weeks post-infection, should induce erythroid leukaemia, whereas F-MuLV originally isolated from the Friend or Rauscher virus complexes induced lymphoid leukaemias[35–37]. The latter viruses were obtained from lymphomatous lymph nodes and spleen 3–4 months post-infection, so it is possible that differences in the passage histories of these viruses altered their tissue tropism. Alternatively, there may be a genetic difference between erythrotropic and lymphotropic forms of F-MuLV in Friend and Rauscher virus stocks. One way to test the latter possibility might be to compare the pathogenic properties of erythrotropic and lymphotropic MuLV pseudotypes of polycythaemia-inducing and anaemia-inducing strains of SFFV. Such a study, recently made by Troxler *et al.*[24] with erythrotropic F-MuLV$_{201}$ and lymphotropic Moloney MuLV, failed to show any effect of the pseudotyping helper virus on the haematocrit response of mice to either polycythaemia-inducing SFFV or anaemia-inducing SFFV. More studies are needed to clarify the pathogenic roles of helper virus and defective virus in the induction of erythroleukaemia.

We thank Dr Frank Lilly for helpful discussions and Mrs Ida Shapiro and Mr Vernon Grant for secretarial and technical assistance, respectively. This investigation was supported by NCI grant CA-19873.

Received 12 March; accepted 5 June 1980.

1. Stephenson, J. R., Axelrad, A. A. & McLeod, D. L. *J. natn. Cancer Inst.* **48,** 531–539 (1972).
2. Steeves, R. A. *J. natn. Cancer Inst.* **54,** 289–297 (1975).
3. Zajdela, R. *Bull. Cancer* **49,** 351–373 (1962).
4. Siegel, B. V., Weaver, W. J. & Koler, R. D. *Nature* **201,** 1042–1043 (1964).
5. Cox, K. O. & Keast, D. *J. natn. Cancer Inst.* **50,** 941–946 (1973).
6. Troxler, D. H. & Scolnick, E. M. *Virology* **85,** 17–27 (1978).
7. Weitz-Hamburger, A. *et al. Cancer Res.* **33,** 104–111 (1973).
8. Friend, C. *J. exp. med.* **105,** 307–318 (1957).
9. Metcalf, D., Furth, J. & Buffett, R. F. *Cancer Res.* **19,** 52–59 (1959).
10. Tambourin, P. & Wendling, F. *Nature new Biol.* **234,** 230–233 (1971).
11. Fieldsteel, A. H., Dawson, P. J. & Bostick, W. L. *Cancer Res.* **23,** 355–362 (1963).
12. Mirand, E. A. *et al. Proc. Soc. exp. Biol. Med.* **127,** 900–904 (1968).
13. Rauscher, F. J. *J. natn. Cancer Inst.* **29,** 515–543 (1962).
14. Kirsten, W. H. & Mayer, L. A. *J. natn. Cancer Inst.* **39,** 311–335 (1967).
15. Pope, J. H. *Aust. J. exp. Biol. med. Sci.* **41,** 349–362 (1962).
16. Dawson, P. J., Dresler, S. L. & Fieldsteel, A. H. *Cancer Res.* **39,** 1611–1615 (1979).
17. Fieldsteel, A. H., Kurahara, C. & Dawson, P. J. *Nature* **223,** 1274 (1969).
18. Eckner, R. J. & Steeves, R. A. *Nature new Biol.* **229,** 241–243 (1971).
19. Bentvelzen, P., Aarssen, A. M. & Brinkhof, J. *Nature new Biol.* **239,** 122–123 (1972).

20. Axelrad, A. A. & Steeves, R. A. *Virology* **24,** 513–518 (1964).
21. Pluznik, D. H. & Sachs, L. *J. natn. Cancer Inst.* **35,** 535–546 (1964).
22. Troxler, D. H. *et al. Virology* **76,** 602–615 (1977).
23. Troxler, D. H. *et al. Proc. natn. Acad. Sci. U.S.A.* **74,** 4671–4675 (1977).
24. Troxler, D. H. *et al. Virology* **102,** 28–45 (1980).
25. Boiron, M. *et al. J. natn. Cancer Inst.* **35,** 865–884 (1965).
26. Dunn, T. B. & Green, A. W. *J. natn. Cancer Inst.* **36,** 987–1001 (1966).
27. Liao, S. K. & Axelrad, A. A. *Int. J. Cancer* **15,** 467–482 (1975).
28. Ostertag, W. *et al. J. Virol.* **33,** 573–582 (1980).
29. Golde, D. W. *et al. Proc. natn. Acad. Sci. U.S.A.* **76,** 962–966 (1979).
30. Mirand, E. A. in *Regulation of Erythropoiesis* (eds Gordon, A. S., Condorelli, M. & Peschle, C.) 333–341 (Il Ponte, Milan, 1971).
31. Steinheider, G., Seidel, H. J. & Kreja, L. *Experientia* **35,** 1173–1175 (1979).
32. Morse, B. *et al. Blood* **51,** 623–632 (1978).
33. Oliff, A. I. *et al. J. Virol.* **33,** 475–486 (1980).
34. Sher, C. D., Scolnick, E. M. & Siegler, R. *Nature* **256,** 225–226 (1975).
35. Dawson, R. J., Rose, W. M. & Fieldsteel, A. H. *Br. J. Cancer* **20,** 114–121 (1966).
36. Steeves, R. A. *et al. J. natn. Cancer Inst.* **46,** 1209–1217 (1971).
37. Ishimoto, A. & Maeda, M. *J. natn. Cancer Inst.* **44,** 361–368 (1970).

New regulators of melanin biosynthesis and the autodestruction of melanoma cells

John Pawelek*, Ann Körner, Alan Bergstrom & Jean Bologna

Department of Dermatology, Yale University School of Medicine,
New Haven, Connecticut 06510

The hues of mammalian skin and hair vary from white to jet black. Silvers has recently catalogued over 130 different coat colour mutations at more than 50 genetic loci in the house mouse (*Mus musculus*), a useful model for study[1]. Some of these loci govern differentiation of melanocytes and their migration from the neural crest region during embryogenesis[2]. Others, however, involve expression of genes for melanin synthesis within the pigment cell, such as *c*-locus mutations, where animals are phenotypically albino. *c*-locus albinism is presumably due to a deficiency of active tyrosinase, the enzyme catalysing the initial steps in the melanin synthetic pathway. It has generally been assumed that the only regulated steps in this pathway are those governed by tyrosinase, since *in vitro*, melanin is spontaneously formed from dopa quinone (Fig. 1). However, Logan and Weatherhead have provided evidence for post-tyrosinase inhibition of melanogenesis by melatonin in hair follicles of Siberian hamsters[5], as do our studies with various mutants of Cloudman mouse melanoma cells, suggesting the involvement of a second regulatory site. We describe here three new factors which control melanin synthesis that we have partially purified from Cloudman cells: (1) dopachrome conversion factor (DCF), which accelerates the conversion of dopachrome to 5,6-dihydroxyindole (see ref. 6 for detailed description); (2) 5,6-dihydroxindole conversion factor, which catalyses the conversion of 5,6-dihydroxyindole to melanin and is active only when cells are exposed to melanotropin (MSH), and (3) 5,6-dihydroxyindole blocking factor, which restricts melanogenesis at 5,6-dihydroxyindole. This third factor appears to protect cells from the cytotoxic effects of melanin precursors, and it is removed when the cells are exposed to MSH. Discovery of the factors indicates that regulation of the melanin biosynthetic pathway is more complex than previously supposed.

DCF has recently been described[6]. In brief, it was first discovered by the observation that extracts of amelanotic melanoma cells rapidly converted dopachrome to a colourless compound. A factor was subsequently isolated that catalysed the conversion of dopachrome to 5,6-dihydroxyindole-2-carboxylic acid followed by a spontaneous decarboxylation to 5,6-dihydroxyindole. DCF reacts specifically with dopachrome, having no effect on tyrosine or dopa. DCF was found in two different mouse melanomas (B16 and Cloudman S91), the hamster melanoma of Greene[7], and mushrooms. It was absent from Friend erythroleukaemia cells, neuroblastoma cells, myeloma cells, and L-cell fibroblasts. Serial dilutions of melanoma cell extracts showed that equal amounts of DCF were present in cells whether or not they had been exposed to MSH. All three factors were observed in experiments described below. Extracts of control cells or MSH-treated cells were mixed with dopachrome. In each case there was a rapid decrease in absorbance at 475 nm due to DCF activity compared with the slow, spontaneous decrease in the buffer blank (Fig. 2*a*). (Note that this figure shows the DCF reaction in extracts of control cells. The extent and magnitude of the reactions were the same in extracts of MSH-treated cells.) Following the DCF reaction, the samples containing extracts of control cells remained colourless for at least 24 h. However, samples containing extracts of MSH-treated cells turned dark rapidly as melanochrome (absorbing at 540 nm) and then melanin were formed (Fig. 2*b*). Melanin production in reactions with extracts of MSH-treated cells was faster than that occurring spontaneously in the reactions containing only buffer and dopachrome.

These experiments were extended using 5,6-dihydroxyindole rather than dopachrome as a substrate. Extracts of control or MSH-treated cells were mixed with 5,6-dihydroxyindole for 3 h at 30°C. The following points were evident: (1) there was a slow, spontaneous conversion of 5,6-dihydroxyindole to melanin in tubes containing buffer only; (2) melanin production was prevented by extracts of control cells; and (3) melanin production was accelerated by extracts of MSH-treated cells. After 24 h the tube containing buffer had turned black due to spontaneous melanin formation while the tubes containing extract of control cells remained colourless (data not shown).

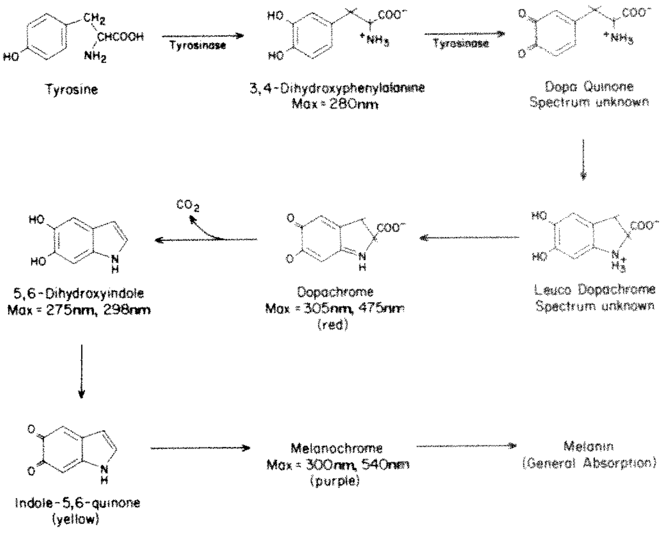

Fig. 1 Stages in the oxidation of tyrosine to melanin, modified slightly from the scheme of Mason and Raper[3]. Note that while this scheme depicts melanin biosynthesis as a polymerization of indole-5,6-quinone alone, it has been shown that mammalian melanins are heteropolymers, containing many different combinations of the precursors shown[4].

Samples were removed from the tubes and analysed for 5,6-dihydroxyindole content by HPLC (Fig. 3). The 5,6-dihydroxyindole peaks (arrows) were integrated and the results are as follows. Panel *a* shows the 5,6-dihydroxyindole content of a mixture of buffer and indole that was kept on ice for 3 h. Panel *b* shows 5,6-dihydroxyindole from the same mixture that was incubated for 3 h at 30 °C (89% of the sample in *a*). Panel *c* shows the 5,6-dihydroxyindole content of an incubated mixture

---

* To whom requests for reprints should be sent.

0028–0836/80/320617—03$01.00

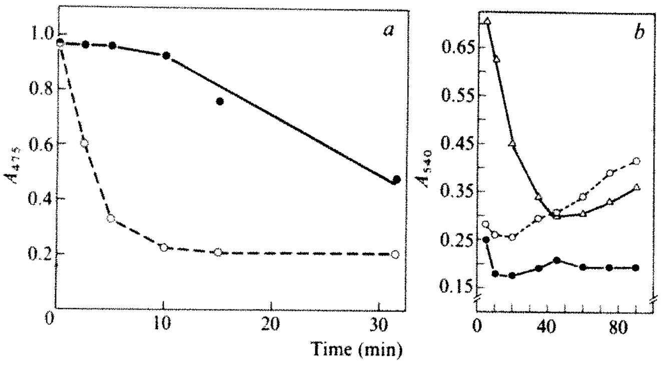

Fig. 2 Effects of cell extracts on dopachrome. Extracts were prepared from an MSH-responsive cell line (PSI-mel-1 (ref. 8)) by the following procedure. Cells were collected with EDTA (1 mM) in isotonic saline, spun for 10 min at 2,000*g*, and lysed with 5 vol ice-cold Triton X-100 (0.5%) in sodium phosphate buffer (50 mM, *p*H6.8). The lysate was then centrifuged (30,000*g*, 15 min) and the pellet containing melanin and cellular debris was discarded. Protein content of the supernatant fraction was determined by the method of Bradford[9]. Such extracts were prepared from control cells and cells that had been exposed to MSH (2×10^{-7} M) for 3 days (isobutylmethyl xanthine was not used in this experiment). The extracts (0.1 ml, 0.4 mg protein) were mixed with 0.2 ml dopachrome which had been diluted for absorbance measurements. Panel *a* shows a decrease in absorbance due to dopachrome at 475 nm after different incubation periods at room temperature with extracts from control cells (solid line: buffer; dotted line: cell extract). The disappearance in absorbance with time was due to the action of DCF which was present in equal amounts in extracts of both control and MSH-treated cells[6]. Panel *b* shows the changes in absorbance at 540 nm with time. The initial decreases were due to DCF activity since dopachrome shows some absorbance at 540 nm. Increases in absorbance at 540 nm were due to melanin synthesis which could be readily detected by the eye. Dopachrome solution was prepared by mixing a solution of dopa with Ag_2O and filtering[10]. ●, Control cell extract; ○, MSH-treated cell extract; △, buffer blank.

of indole and control cell extract (98% of the sample in *a*). Panel *d* shows the 5,6-dihydroxyindole content in the incubated mixture of indole and MSH-treated cell extract (5.7% of the sample in *a*). Thus direct measurements of the 5,6-dihydroxyindole content of the tubes confirmed what was visually apparent: melanin synthesis from 5,6-dihydroxyindole was prevented by control cell extracts and accelerated by MSH-treated cell extracts. These experiments demonstrate the existence of both a 5,6-dihydroxyindole conversion factor and a blocking factor. MSH treatment removes the blocking factor and allows for expression of the conversion factor.

It has been known for some time that melanin precursors can be cytotoxic[12–15]. Because MSH increases tyrosinase levels one would predict that, in the presence of MSH, the rate of production of melanin precursors is also increased. This has been shown to be the case in culture as cells exposed to MSH are much more susceptible to the toxic effects of tyrosine and dopa than control cells[14].

If it were true that only tyrosinase activity were affected by MSH, then the toxicity of melanin precursors distal to dopa quinone should not be influenced by the presence or absence of MSH. We show below that this is not the case. We have found that the toxic effects of dopachrome are markedly increased when the target cells have been treated with MSH (Fig. 4). (Note in Fig. 4 legend that 3-methylisobutylxanthine was used to potentiate the MSH effect.) The effects were quite striking when observed with the phase microscope. After only 1 h exposure to dopachrome (10^{-4}M), cells preincubated with MSH began to lyse. In contrast, cells exposed during this same time to either control culture medium, or medium containing MSH, dopa plus MSH, or dopachrome alone still appeared healthy. About fivefold less dopachrome was sufficient for 50% killing when the cells were exposed to MSH compared to when they were not exposed to the hormone. Addition of dibutyryl-cyclic-AMP (10^{-3} M) also increased the sensitivity to dopachrome, indicating that the cellular response was likely to be cyclic-AMP mediated (data not shown). The dose–response studies shown in Fig. 4 were done in parallel with an amelanotic variant cell line[8] that showed a very weak response to MSH in terms of pigment production. The 'non-responsive' line was only slightly sensitized by MSH to the toxicity of dopachrome. Extracts of the amelanotic line contained 5,6-dihydroxyindole blocking factor and no 5,6-dihydroxyindole conversion factor activity whether or not the cells were exposed to MSH (data not shown). We feel that the most likely explanation for the increased sensitivity of MSH-activated cells to dopachrome is the removal of the 5,6-dihydroxyindole blocking factor and the expression of active 5,6-dihydroxyindole conversion factor. We realize, however, that our evidence is only circumstantial and that more experiments are necessary to prove these points.

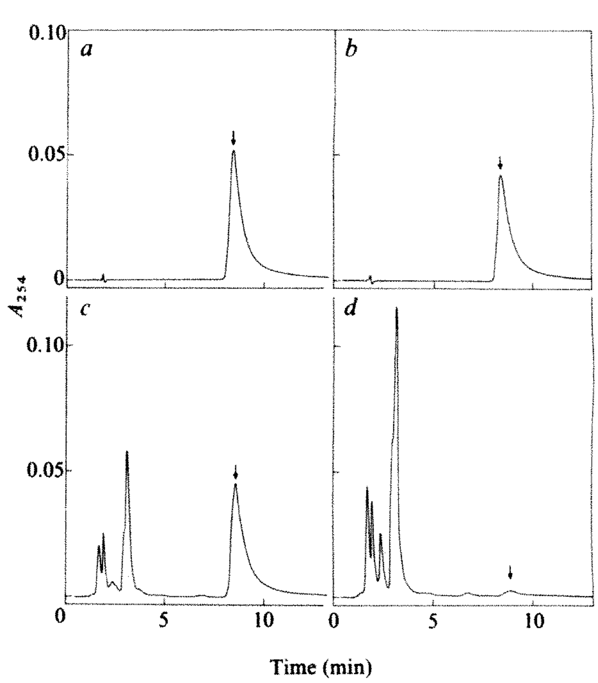

Fig. 3 Effects of extracts prepared from control- and MSH-treated cells on 5,6-dihydroxyindole as analysed by HPLC. Experimental design is outlined in the legend to Fig. 2. 5,6-dihydroxyindole (3.5×10^{-4} M) was used instead of dopachrome. Protein concentrations in the undiluted cell extracts were 7 mg ml^{-1}. The reaction mixes were adjusted to 100 µl with sodium phosphate (0.05 M, *p*H6.8), incubated in a shaking water bath at 30 °C for 3 h and aliquots (20 µl) from the tubes were analysed for 5,6-dihydroxyindole content. An Altex Molel 330 Isocractic liquid chromatograph equipped with a Model 110A pump and a 20-µl sample loop was used. Absorbance of the eluent was monitored at 254 nm with an 8-µl Analytical Optical Unit. Experiments were performed with an Ultrasil ODS Column (Altex Instruments, Inc.), 0.46 cm internal diameter × 25 cm. The column was packed with octadecyl-silica particles of 10 µm average diameter. The mobile phase was methanol/sodium phosphate (50 mM, *p*H 6.5) 1:9. Flow rate was maintained at 1.8 ml min^{-1}. 5,6-dihydroxyindole eluted at about 8.4 min (arrows). The indole was synthesized as described by Axelrod and Lerner[11] and stored in crystalline form in N_2 at −20 °C. Before each experiment, appropriate amounts of 5,6-dihydroxyindole were dissolved in degassed buffer (sodium phosphate, 0.05M, *p*H6.5). *a*, Indole plus buffer, 3 h in ice; *b*, indole plus buffer, 3 h at 30 °C; *c*, indole plus control cell extract (50 µl), 3 h at 30 °C; *d*, indole plus extract (50 µl) of MSH-treated cells, 3 h at 30 °C. Material that eluted between 1 and 4 min was from the cell extracts alone and did not change during the 3-h incubation period.

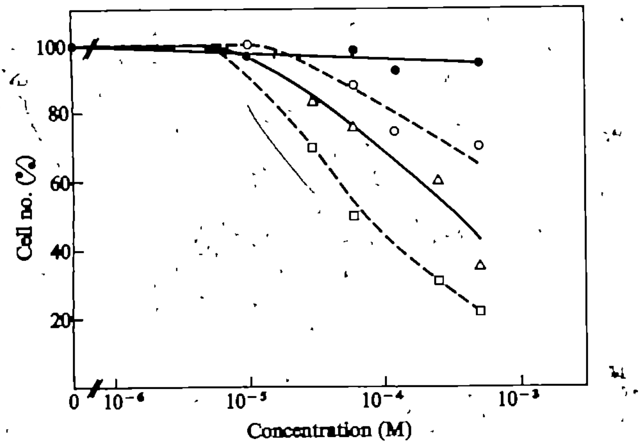

Fig. 4 Effects of MSH on the toxicity of dopa and dopachrome against Cloudman S91 mouse melanoma cells. Cells (10^5) from an MSH-responsive line (PSI-mel-1 (ref. 8)) were cultured in monolayer for two days either in plain culture medium or in medium supplemented with MSH (2×10^{-7} M) and methylisobutylxanthine (MIX 5×10^{-5} M). Two days later the cells were given fresh medium containing dopa or dopachrome as indicated. After 2.5 h, the dopa and dopachrome were removed and the cells were given fresh medium. The next day the cells were collected with EDTA (1 mM) in isotonic saline, and counted in a Coulter counter. Dopachrome was prepared as above by oxidizing dopa with Ag_2O. Control cultures received either buffer that had been mixed with Ag_2O and filtered, or buffer only (sodium phosphate, 0.05 M pH 6.8). The control cell numbers were similar in each case. Values represent the averages from quadruplicate cultures and the variation was less than ±10%. The experiments were repeated several times with similar results. MIX, a phosphodiesterase inhibitor, was used to potentiate the MSH effect. At the concentration used (5×10^{-5} M) MIX had no effect by itself. ●, Dopa; ○, dopa+MSH; △, dopachrome; □, dopachrome+MSH.

The relevance of the three factors to mammalian melanogenesis remains to be demonstrated. There are, however, numerous reports of skin and coat colour regulation which might be explained by the actions of one or more of these factors. Three examples are tyrosinase-positive albinism in humans[16], the annual pelage colour cycle in the Siberian hamster[5], and in general the wide variation in mammalian coat colours[1]. Also, the MSH-mediated sensitization of melanoma cells to dopachrome shown in Fig. 4 is likely to be explained by the factors we have described and is of relevance to the establishment of a rational therapy for human melanoma. The first step towards a full understanding of the physiological role of these factors is the elucidation of their molecular structures, a goal that we are now pursuing.

We thank Karen Vane and Marilyn Murray for providing cells, Dr Aaron B. Lerner for 5,6-dihydroxyindole, and Drs Saul Lande and Gisela Moellmann for helpful discussions. Supported by grants from the USPHS and The American Cancer Society.

Received 5 February, accepted 5 June 1980

1. Silvers, W K The Coat Colors of Mice A Model for Mammalian Gene Action and Interaction (Springer, Berlin, 1979)
2 Rawles, M E Physiol Rev. 28, 383–408 (1948)
3 Mason, H S Adv Enzym 16, 105–184 (1955)
4 Hempel, K in Structure and Control of the Melanocyte (eds Della Porta, G & Muhlbock, O) 162–175 (Springer, Berlin, 1966)
5. Logan, A & Weatherhead, B J invest Derm 71, 295–298 (1978)
6 Korner, A & Pawelek, J. J. invest Derm (in the press)
7 Greene, H S N Cancer Res 18, 122–125 (1958).
8 Pawelek, J. et al Proc natn Acad Sci U S A 72, 951–955 (1975)
9 Bradford, M Analyt Biochem 72, 248–254 (1976).
10 Mason H. S J biol Chem. 172, 83–99 (1948)
11 Axelrod, J. & Lerner, A B Biochim biophys Acta 71, 650–655 (1963).
12. Lerner, A B Am J Med 51, 141–148 (1971)
13 Pawelek, J J invest. Derm 66, 201–209 (1976)
14. Pawelek, J & Lerner, A B Nature 276, 627–628 (1978)
15 Wick, M M J. invest Derm. 74, 63–65 (1980).
16 King, R A , Olds, D P & Witkop, C J. Pigment Cell 4, 16–20 (1979)

Transformation-specific secreted phosphoproteins

Donald R. Senger*, Dyann F. Wirth† & Richard O. Hynes

Department of Biology and Center for Cancer Research,
Massachusetts Institute of Technology, Cambridge,
Massachusetts 02139

We have previously shown that transformed mammalian cells secrete two classes of transformation-specific proteins of molecular weight (MW) about 60,000 (ref. 1). Secretion of both classes of proteins occurs regardless of the transforming agent and is temperature-sensitive in a cell line which is temperature-sensitive for the transformed phenotype (ts B77 Rat 1; see ref. 1). One of the classes consists of non-phosphorylated polypeptides. The proteins of this class, derived from transformed mouse, rat and hamster lines, are all antigenically related to one another. The second class of transformation-specific secreted proteins is antigenically distinct from the first class, that is, it is not precipitated by antiserum which recognizes the non-phosphorylated class. This second class comprises major phosphoproteins also in the 60,000 MW range[1]. These major phosphoproteins were found to be secreted by transformed hamster, rat, mouse and rabbit cells. We now report that these transformation-specific phosphoproteins are all antigenically related, regardless of the transforming agent. The phosphoproteins are synthesized by the cells, phosphorylated intracellularly and subsequently released into the culture medium. These transformed cells also secrete protein kinase activities capable of phosphorylating the transformation-specific phosphoproteins *in vitro*. The major sites of *in vivo* and *in vitro* phosphorylation seem to be identical.

Antiserum was raised to the purified phosphoproteins secreted by B77 Rat 1 cells. $^{32}PO_4$-labelled conditioned media from several cell lines were immunoprecipitated with this antiserum. Figure 1 shows that the transformation-dependent phosphoproteins derived from the various species are, in fact, all antigenically related. The size and degree of heterogeneity of the phosphoproteins vary (Fig. 1) and seem to be dependent on the species from which the transformed cell line was derived rather than on the transforming agent[1]. There are several possible explanations for the apparent size differences and heterogeneity. The various phosphoproteins may have identical amino acid sequences but differ in degree of phosphorylation or proteolytic processing. Alternatively, the phosphoproteins may have similar but not identical primary structure. In any event, all show transformation sensitivity, and rat phosphoprotein antigens are present among the phosphoproteins of the other species.

In order to establish that the transformation-specific phosphoproteins are synthesized by the cells and do not arise by phosphorylation of serum proteins, the antiserum raised against the ts B77 Rat 1 (34 °C) phosphoproteins was preabsorbed with fetal calf serum (in which cells were cultured). This preabsorption did not alter the extent or specificity of the immunoprecipitation of the phosphoproteins of MW 62,000 (62K) (not shown). In addition, when the ts B77 Rat 1 cells (34 °C) were cultured and labelled with $^{32}PO_4$ in the absence of serum, the same amounts of 62K phosphoproteins were found in the conditioned medium (not shown). These results indicate that the 62 K phosphoproteins

---

Present addresses: *Department of Pathology, Beth Israel Hospital, Boston, Massachusetts 02215 †Biological Laboratories, Harvard University, Cambridge, Massachusetts 02138 are not fetal calf serum proteins that are simply phosphorylated by the cells.

To obtain further evidence that the phosphoproteins are synthesized by the cell, ts B77 Rat 1 cells (34 °C, transformed phenotype) were preincubated in the presence and absence of cycloheximide and then labelled with $^{32}PO_4$ in the continued presence or absence of the drug. As shown in Fig. 2, cycloheximide treatment abolishes secretion of the 62K phosphoproteins, indicating that protein synthesis is required for their phosphorylation and release from the cells.

The cell-associated forms of the B77 Rat 1 phosphoproteins were identified by immune precipitation of ^{32}P-labelled cellular lysates. Figure 3 shows the results of such an experiment, which also shows the specificity of the antiserum. From among the very large number of phosphoproteins present in cell lysates (Fig. 3, track *g*) the antiserum bound only three proteins, all of MW about 62,000 (Fig. 3, track *d*). These intracellular 62K proteins have mobilities identical with those found in the conditioned medium after a chase (Fig. 3, track *f*). We were unable to chase completely the radioactivity in the 62K proteins from cell lysates, presumably because of the difficulty encountered in chasing phosphate pools[2]. However, proportional amounts of pulse lysate and chase medium were found to contain identical quantities of 62K proteins (compare Fig. 3, tracks *d* and *f*), suggesting efficient secretion of the phosphoproteins synthesized during the pulse. Furthermore, the ratios of the different phosphate-labelled bands are the same in the pulse-labelled cells and the chase medium. These results indicate that all the 62K phosphoproteins are phosphorylated intracellularly and subsequently secreted into the culture medium in parallel.

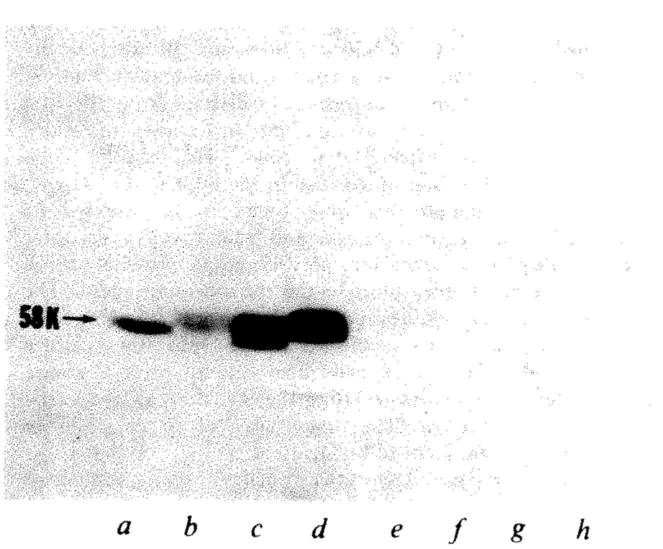

Fig. 1 ^{32}P-labelled conditioned media from various transformed cell lines were immunoprecipitated with antibody to the 62K transformation-specific secreted proteins from B77 Rat 1 cells. Cells and culture conditions, metabolic labelling with ^{32}P-orthophosphate, immunoprecipitation, SDS-polyacrylamide (7.5%) gel electrophoresis and autoradiography were as previously described[1]. Antiserum was prepared as follows. ts B77 Rat cells were grown to confluence at 34 C in roller bottles, washed three times with serum-free medium and incubated overnight with serum-free medium (200 ml per roller bottle). Conditioned medium (1,800 ml) was spun at 10,000 r.p.m. for 10 min and passed over a water-washed DE-11 cellulose (Whatman) column (100 ml). The DE-11 cellulose had been pre-swollen in acid and base as recommended by Whatman and washed extensively with distilled water before loading. Virtually 100% of the transformation-dependent 62K phosphoprotein in the conditioned medium bound to the column (there actually seem to be several transformation-dependent phosphoproteins all with similar mobility corresponding to a MW of 62,000; see track *d* above and track *f* of Fig. 3). The loaded column was then washed with 1,000 ml of 0.25 M NaCl; this step removed contaminants without eluting the 62K phosphoproteins. The 62K phosphoproteins were eluted from the column with 0.5 M NaCl and concentrated by vacuum dialysis against phosphate-buffered saline. This antigen preparation was analysed by SDS-polyacrylamide gel electrophoresis, and it was determined that 90% of the protein had mobility identical to that of the 62K phosphoproteins. The remainder consisted of several other species in very low concentration. The 58K–62K transformation-dependent, non-phosphorylated proteins, which we have described previously[1], were not present in the antigen preparation because they do not bind to DE-11 at the ionic strength used here (our unpublished data). The rabbit was injected the first time (at eight dorsal sites) with 1 mg of 62K phosphoprotein in complete Freund's adjuvant. Three weeks later the injections were repeated with 1 mg protein and incomplete Freund's adjuvant. Antibody was present in serum 2 weeks later. The specificity of the antiserum is indicated in Fig 3. *a*, Immune serum, NIL.8-HSV (hamster); *b*, immune serum, py3T3 (mouse); *c*, immune serum, Moloney MSV-MuLV SIRC (rabbit); *d*, immune serum, ts B77 Rat 1 (34 °C) (rat); *e*–*h*, preimmune serum, media as in *a*–*d*.

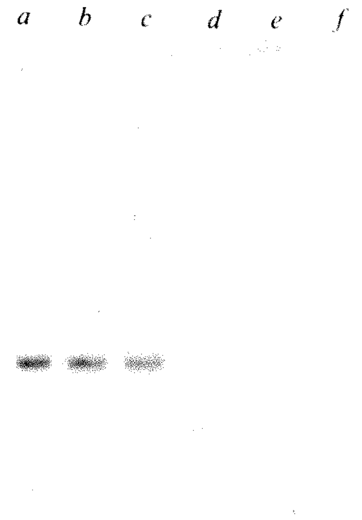

Fig. 2 Protein synthesis is required for secretion of the transformation-specific 62K phosphoproteins by ts B77 Rat 1 (34 C) cells. *a*–*c*, Media from control cells labelled for 1 h with ^{32}P-orthophosphate; *d*–*f*, media from cells preincubated with cycloheximide (20 μg ml^{-1}) for 1 h before labelling for 1 h. The prominent band in tracks *a*–*c* corresponds to a MW of 62,000.

The phosphoproteins secreted specifically by transformed cells can be phosphorylated *in vitro* by incubating the conditioned media with [γ-^{32}P]ATP. The *in vitro* labelled phosphoproteins are precipitable with the antiserum which recognizes the *in vivo* labelled form (not shown). Furthermore,

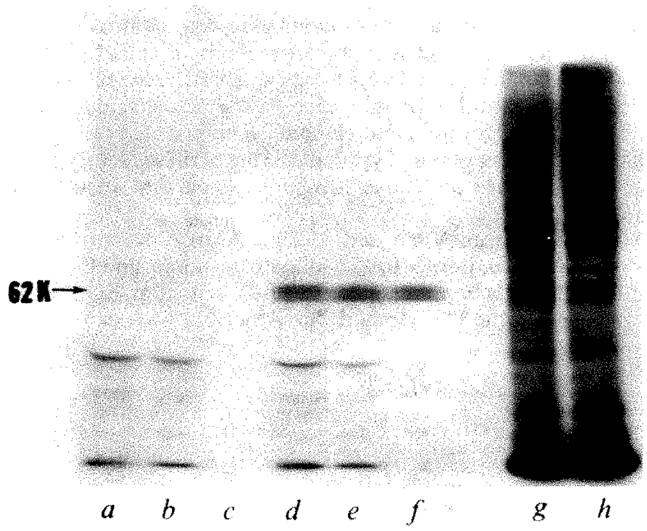

Fig. 3 ^{32}P-orthophosphate-labelled ts B77 Rat 1 (34 C, transformed phenotype) cell lysates and chase medium were immunoprecipitated with antibody to the 62K transformation-specific phosphoproteins. *a*, Preimmune serum, cell lysate, 45 min label; *b*, preimmune serum, cell lysate, 45 min label, 45 min chase; *c*, preimmune serum, equivalent amount of chase medium; *d*, immune serum, cell lysate, 45 min label; *e*, immune serum, cell lysate, 45 min label, 45 min chase; *f*, immune serum, equivalent amount of chase medium; *g*, total cell lysate, 45 min label, 1/10th the volume used in *d*; *h*, total cell lysate, 45 min label, 45 min chase, 1/10th the volume used in *e*.

a comparison of the phosphopeptides generated by partial proteolysis of the *in vitro* and *in vivo* labelled 62K phosphoproteins indicates that the major *in vitro* and *in vivo* sites of phosphorylation are likely to be identical (see Fig. 4).

Identical levels of *in vitro* phosphorylation of the 62K phosphoproteins (ts B77 Rat 1, 34 °C) were observed in serum-free conditioned medium and in conditioned medium containing 5% fetal calf serum (not shown). This result indicates that the protein kinase activity is secreted by the cells and is not a serum protein. We also found that conditioned medium from ts B77 Rat 1 cells (34 °C) can phosphorylate histones in the presence of ^{32}P-ATP, whereas unconditioned medium does not have this phosphorylating activity, again indicating secretion of protein kinase by the cells (data not shown). We have found that the phosphorylating activity secreted by B77 Rat 1 cells and ts B77 Rat 1 cells can be equally inactivated by preincubation at 41 °C. This suggests that the phosphorylating activity does not contain the lesion responsible for the temperature-sensitive phenotype of the ts B77 Rat 1 cells.

Experiments with serum from tumour-bearing animals[3,4] have suggested that the transformation-specific phosphoproteins described here are antigenically distinct from pp60^{src}, the 60,000-MW phosphoprotein encoded by the *src* gene of avian sarcoma virus. Serum active against the endogenous *sarc* gene protein of both avian and mammalian cells[5] also failed to precipitate the secreted phosphoproteins.

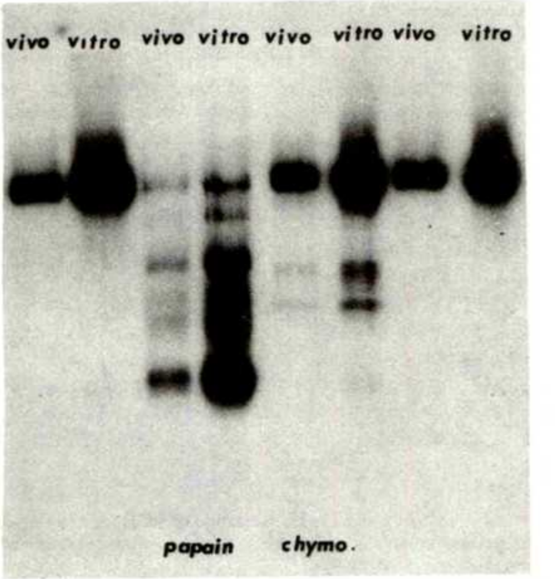

Fig. 4 Partial proteolysis of the 62K phosphoproteins from ts B77 Rat 1 (34 °C) cells labelled *in vivo* with ^{32}P-orthophosphate or *in vitro* with [γ-^{32}P]ATP. Total labelled conditioned medium, labelled *in vivo* or *in vitro* as previously described[1], was electrophoresed on a 7.5% preparative slab gel. The 62K phosphoprotein band containing all the 62K species was cut from the dried preparative gel, rehydrated in Laemmli stacking gel buffer[8] and electrophoresed on a 12.5% Laemmli gel with 250 μg papain or 50 μg chymotrypsin (chymo.), or no additions. 'vivo' 62K ^{32}P-labelled proteins from the media of cells labelled *in vivo* with $^{32}PO_4$; 'vitro', 62K proteins from the media of unlabelled cells, 62K proteins subsequently labelled *in vitro* with [γ-^{32}P]ATP.

In addition, the transformation-specific phosphoproteins are unable to phosphorylate IgG in immune precipitates, an activity which is characteristic of pp60^{src} and pp60^{sarc} (refs 4–7). However, incubations of [γ-^{32}P]ATP and washed 62K phosphoprotein immunoprecipitates did result in ^{32}P labelling of the 62K phosphoprotein itself. Whether this represents autophosphorylation or phosphorylation by a separate kinase activity in the immunoprecipitate is not known.

To summarize, the phosphoproteins described here are closely correlated with the transformed phenotype. In cells which are temperature-sensitive for transformation, secretion of the phosphoproteins is temperature-dependent. The phosphoproteins are synthesized by the cells and are not derived by phosphorylation of serum proteins. These transformation-dependent phosphoproteins are common to all mammals for which we have so far obtained transformed cell lines—hamster, rat, mouse and rabbit. Because of their antigenic relatedness, it seems likely that the transformation-specific phosphoproteins secreted by the various cell lines have a common function. Their close correlation with transformation suggests that they may be involved in the maintenance of some aspect of the transformed state.

We thank Carl Bryant and Antonia Destree for technical assistance, Naomi Foster for photography, Dr P. W. Robbins for his interest and helpful suggestions, and all those who provided the cells and antisera used in these studies. This work was supported by grants from the NIH, NCI (RO1 CA 17007 to R.O.H. and PO1 CA 14051 to S.E. Luria) and from the American Cancer Society (VC 258). R.O.H. is the recipient of an NCI Research Career Development Award.

Received 11 February; accepted 24 April 1980.

1. Senger, D. R., Wirth, D. F. & Hynes, R. O. *Cell* **16,** 885–893 (1979).
2. Hauschka, P. *Meth. Cell Biol.* **7,** 361–462 (1973).
3. Purchio, A. F., Erikson, E., Brugge, J. S. & Erikson, R. L. *Proc. natn. Acad. Sci. U.S.A.* **75,** 1567–1571 (1978).
4. Levinson, A. D., Oppermann, H., Levintow, L., Varmus, H. & Bishop, J. *Cell* **15,** 561–572 (1978).
5. Oppermann, J., Levinson, A. C., Varmus, H. E., Levintow, L. & Bishop, J. M. *Proc. natn. Acad. Sci. U.S.A.* **76,** 1804–1808 (1979).
6. Collett, M. S. & Erikson, R. L. *Proc. natn. Acad. Sci. U.S.A.* **75,** 2021–2024 (1978).
7. Collett, M. S., Erikson, E., Purchio, A. F., Brugge, J. S. & Erikson, R. L. *Proc. natn. Acad. Sci. U.S.A.* **76,** 3159–3163 (1979).
8. Laemmli, U. K. *Nature* **227,** 680–685 (1970).

Evidence that a developmentally regulated glycoprotein is target of adhesion-blocking Fab in reaggregating *Dictyostelium*

Claudia Steinemann & Roger W. Parish

Department of Cytology, Plant Biology Institute, University of Zürich,
Zollikerstrasse 107, CH 8008 Zürich, Switzerland

The target site of adhesion-blocking Fab in aggregating *Dictyostelium discoideum* cells is a plasma membrane glycoprotein of approximate molecular weight 82,000 (refs 1–3), which is no longer synthesized after aggregation, and disappears from the plasma membrane[4,5]. However, since cell adhesion remains important during later stages of differentiation[6–8], presumably another protein(s) takes over its function. One candidate is a glycoprotein (molecular weight 95,000) whose synthesis commences at the tip stage and continues until the completion of development[5,8]. Both proteins are strongly antigenic[4]. When pseudoplasmodia ('slugs', a late developmental stage) are disaggregated and replated, the cells recapitulate the previous sequence of morphological changes much more quickly than before[6–8], although the glycoprotein of molecular weight 82,000 is not resynthesized during reaggregation[4,8]. We report here that monovalent antibody (Fab) directed against slug plasma membranes inhibits reaggregation by binding to the glycoprotein of molecular weight 95,000 which thus seems to be involved in cell adhesion.

Antisera against slug plasma membranes contained antibodies specific for a number of proteins (Fig. 1*a*). Apart from actin, the major antigen in the membrane was a glycoprotein of molecular weight 95,000 (ref. 4, Fig. 1*a*). This antigen could be extracted from the plasma membrane with butanol and was the major antigen in the butanol extract (Fig. 1*b*). Radioactive

0028–0836/80/320621—03$01.00

acetate and glucosamine were incorporated into this glycoprotein from the tip stage until late culmination[5] (Fig. 1*c*, *d*). The glycoprotein was not present in the plasma membrane of amoebae or aggregating cells[4,5].

When slug cells were disaggregated and the single cells shaken in buffer, aggregates had already formed after 45 min (Fig. 2*a*). Reaggregation was inhibited when Fab directed against slug plasma membrane was present (Fig. 2*b*). Fab directed against plasma membranes from vegetative or early aggregation cells had no effect on reaggregation (Fig. 2*d*). When a butanol extract from slug plasma membrane was incubated with the anti-slug Fab, reaggregation was no longer inhibited (Fig. 2*c*). Hence, antigens in the butanol extract were evidently competing with cells for adhesion-blocking Fab.

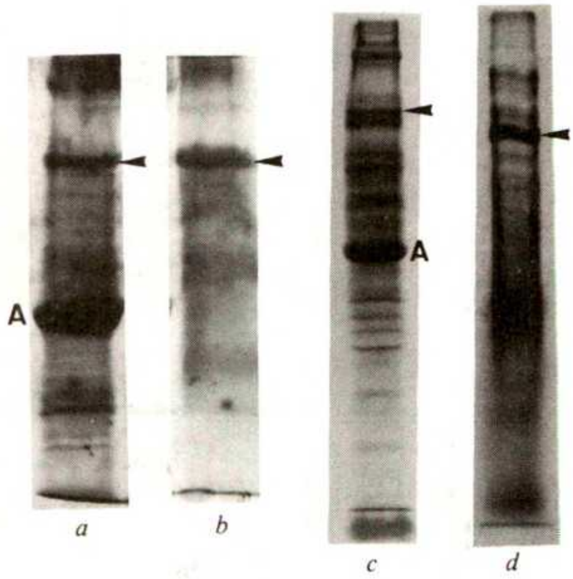

Fig. 1 The plasma membrane of slug cells: antigens and proteins incorporating L-[1 − ^{14}C]fucose and [1 − ^{14}C]acetate. Growth of *D. discoideum* NC-4 (wild type) cells, labelling of cultures with isotopes, plasma membrane isolation, SDS-polyacrylamide gel electrophoresis, autoradiography, preparation of antisera and detection of antigens on gels were performed as described previously[4,5,9]. Plasma membranes were injected into rabbits in Freunds Complete Adjuvant; injection in saline resulted in a low titre of antibody directed against the antigen of molecular weight 95,000, (indicated by the arrow). *a*, Antigens in total slug plasma membrane; SDS-polyacrylamide gels were incubated with antisera raised against slug plasma membranes. (A = actin; molecular weight 42,000.) *b*, Antigens in the butanol extract of slug plasma membranes; SDS-polyacrylamide gels incubated with antisera as in *a*. *c*, Autoradiograph of SDS-polyacrylamide gel of slug plasma membrane after labelling from the tip stage with [1 − ^{14}C]acetate. *d*, Autoradiograph of plasma membrane from early slug stage after labelling from mid-aggregation with L-[1 − ^{14}C]fucose.

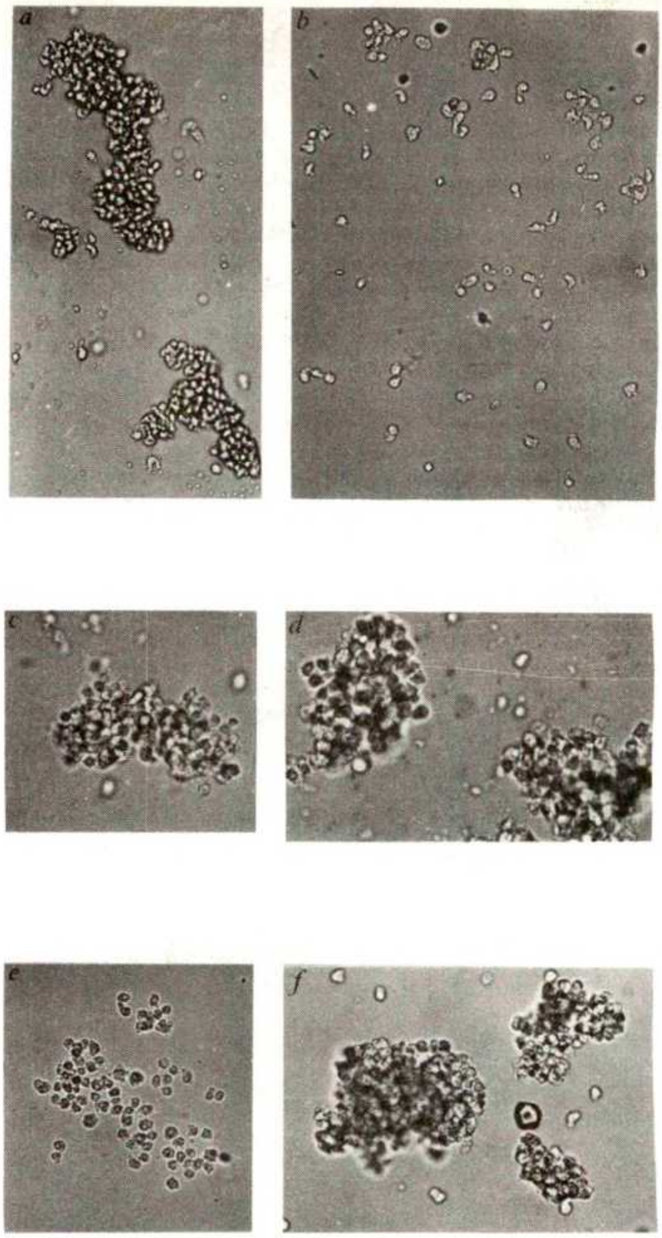

Fig. 2 The effects of Fab on the reaggregation of disaggregated slug cells. Fab was purified as described previously[9]. Reaggregation was assayed by incubating disaggregated slug cells[8] (2×10^7 cells ml^{-1}) in a roller culture (40 r.p.m., Multipurpose Rotator, Scientific Industries) in 20 mM KCl, 24 mM $MgCl_2$ and 10 mM EDTA in 0.05 M Sørensens phosphate buffer (*p*H 6.5). Fab was added to give a final concentration of 1 mg protein ml^{-1}. Removal of Fab specific for the antigen of molecular weight 95,000 was accomplished in the following way. Plasma membranes were isolated from vegetative cells (3.6×10^9) and extracted with butanol. The extract (1.1 mg protein in 370 µl) was electrophoresed on SDS slab gels (18 lanes). The region corresponding to the antigen of molecular weight 95,000 was cut out and SDS removed by shaking the gel pieces in 25% isopropanol/10% acetic acid solution for 20 h, changing the solution once. The gel pieces were then washed with 15 mM Na phosphate buffer (*p*H 6.8) for 3 h with one change of buffer. The slices were shaken for 6 h with 200 µg Fab in 2.0 ml PDF solution (20 mM KCl, 25 mM $MgCl_2$ in 0.05 M Sørensens phosphate buffer, *p*H 6.5). The PDF solution containing Fab which had not bound to the antigen in the gel was removed and the gel shaken overnight in 2.0 ml PDF solution to further remove any non-specifically bound Fab. The two PDF solutions were combined (4.0 ml) and concentrated by vacuum dialysis (final volume 0.20 ml). Hence, a Fab fraction was obtained from which the Fab binding to the antigen of molecular weight 95,000 had been at least partially removed. As controls, Fab was incubated with other regions of the gel. Cells were photographed after 45 min in the roller culture. *a*, Control; *b*, anti-slug Fab; *c*, anti-slug Fab plus proteins extracted from slug plasma membranes using butanol; *d*, Fab (against aggregation competent cells); *e*, anti-slug Fab remaining after incubation with a gel slice from the region of the gel corresponding to molecular weights 80,000–90,000; *f*, anti-slug Fab after removal of Fab specifically binding to the antigen of molecular weight 95,000.

We determined whether the antigen of molecular weight 95,000 was involved in cell adhesion by cutting the antigen from SDS gels and using the gel slices to remove the specific Fab from the total Fab[9]. The remaining Fab (more than 98% of total Fab) was subsequently unable to inhibit reaggregation (Fig. 2*f*). Preincubation of anti-slug Fab with another region of the gel (such as the region representing molecular weights 80,000–90,000) did not prevent Fab inhibiting reaggregation (Fig. 2*e*).

Anti-slug Fab was also incubated with aggregation-competent cells to remove any Fab directed against contact sites for the protein of molecular weight 82,000 that might be present. The remaining Fab still inhibited reaggregation of disaggregated slug cells. Hence the results were not due to contamination with Fab against this antigen. The anti-slug Fab did not block the EDTA-resistant adhesion of aggregation-competent cells or the EDTA-sensitive adhesion of vegetative cells. (Fab against aggregation-competent cells did, however, block the adhesion of these cells.)

Recently, Geltosky *et al.*[10] described a glycoprotein of molecular weight 150,000, present on the surface of vegetative *D. discoideum* cells, whose concentration increased during the first 10 h of development. Fab directed against this protein blocked the ability of aggregation-competent cells to reaggregate. However, the synthesis of such a glycoprotein was not detected in labelling experiments[5]. (A glycoprotein of molecular weight 155,000 was synthesized later, between early aggregation and culmination[5].) One explanation for this discrepancy would be that the glycoprotein described by Geltosky *et al.*[10] is stored in the cytoplasm of vegetative cells and transported to the cell surface during early development. It may bind to one of the glycoproteins of molecular weights 82,000 or 95,000 on adjacent cells. In our plasma membrane preparations no proteins with molecular weights of approximately 150,000 were markedly antigenic. Hence, our Fab contained few, if any, molecules directed against the glycoprotein of Geltosky *et al.*[10]. When the region of the gel corresponding to a molecular weight of 150,000 was preincubated with anti-slug Fab, the remaining Fab still inhibited aggregation.

Our results suggest that the antigen of molecular weight 95,000 is involved in cell adhesion, although we cannot be absolutely sure that it is not another protein running at around that region on gels that is responsible. However, we consider this unlikely as butanol extracts contained no other detectable proteins which ran so near to this antigen as to be included in the gel slice. The possibility that binding of Fab to the antigen of molecular weight 95,000 indirectly inhibits reaggregation by selective steric impairment of another set of molecules cannot be excluded.

The plasma membrane glycoproteins involved in cell adhesion during the early developmental stages of both *D. discoideum* (molecular weight 82,000)[2] and *Polysphondylium pallidum*[11] (molecular weight 71,000)[9] are no longer synthesized when aggregation is complete and are subsequently lost from the cells[4,5,8,9]. This may be related to the sorting out of pre-spore and pre-stalk cells that occurs during the post-aggregation phase[12–16]. The glycoprotein of molecular weight 95,000 of *D. discoideum*, for example, may be restricted to one cell type or occur at different concentrations on the two types. We are using immunofluorescence to check these possiblities. The glycoprotein of molecular weight 150,000 apparently does not disappear from the plasma membrane during differentiation[10]. However, it may be part of a second type of adhesion which is not involved in sorting out. Alternatively, a change in only one component of an adhesion system may be sufficient to induce sorting out.

We thank Dr C. R. Parish for providing the antisera. This work was supported by the Schweizerische Nationalfonds zur Förderung der wissenschaftlichen Forschung (grant no. 3.421–0.78).

Pure Chemistry Library
SCIENCE COLLEGE
92 Upper Circular Road
CALCUTTA.

Received 18 February; accepted 5 June 1980.

1. Beug, H., Katz, F. & Gerisch, G. *J. Cell Biol.* **56,** 647–658 (1973).
2. Müller, K. & Gerisch, G. *Nature* **274,** 445–449 (1978).
3. Müller, K., Gerisch, G., Fromme, I., Mayer, M. & Tsugita, A. *Eur. J. Biochem.* **99,** 419–426 (1979).
4. Parish, R. W., Schmidlin, S. & Parish, C. R. *FEBS Lett.* **95,** 366–370 (1978).
5. Parish, R. W. & Schmidlin, S. *FEBS Lett.* **98,** 251–256 (1979).
6. Newell, P., Longlands, M. & Sussman, M. *J. molec. Biol.* **58,** 541–554 (1971).
7. Soll, D. R. *Devl Biol.* **47,** 292–302 (1975).
8. Parish, R. W. & Schmidlin, S. *FEBS Lett.* **99,** 270–274 (1979).
9. Steinemann, C., Hintermann, R. & Parish, R. W. *FEBS Lett.* **108,** 379–384 (1979).
10. Geltosky, J. E., Weseman, J., Bakke, A. & Lerner, R. A. *Cell* **18,** 391–398 (1979).
11. Bozzaro, S. & Gerisch, G. *J. molec. Biol.* **120,** 265–279 (1978).
12. Takeuchi, I. *Devl Biol.* **8,** 1–26 (1973).
13. Francis, D. & O'Day, D. *J. exp. Zool.* **176,** 265–272 (1971).
14. Müller, U. & Hohl, H. R. *Differentiation* **1,** 265–272 (1973).
15. Forman, D. & Garrod, D. R. *J. Embryol. exp. Morphol.* **40,** 229–243 (1977).
16. Durston, A. J. & Vork, F. *J. Cell Sci.* **36,** 261–279 (1979).

Modulation of brain polyphosphoinositide metabolism by ACTH-sensitive protein phosphorylation

J. Jolles, H. Zwiers, C. J. van Dongen, P. Schotman, K. W. A. Wirtz* & W. H. Gispen

Division of Molecular Neurobiology, Rudolf Magnus Institute for Pharmacology and Laboratory for Physiological Chemistry, Medical Faculty, Institute of Molecular Biology, State University of Utrecht
*Laboratory of Biochemistry, State University of Utrecht, Padualaan 8, Utrecht, The Netherlands

Phosphorylation of membrane components is thought to be an important process in membrane function[1]. Phosphorylated proteins[2] and a special class of phospholipids, the (poly)phosphoinositides (poly PI)[3], are implicated in the regulation of membrane permeability and synaptic transmission in neurones. For many years, protein phosphorylation and poly PI metabolism have been studied in parallel without knowledge of their possible interaction. We report here that the ACTH-sensitive protein kinase/B-50 protein complex which we recently isolated in soluble form from rat brain synaptosomal plasma membranes[4,5] has lipid phosphorylating activity. Exogenously added phosphatidylinositol 4-phosphate (DPI) is phosphorylated to phosphatidylinositol 4,5-diphosphate (TPI), and this DPI-kinase activity is dependent on the state of phosphorylation of the protein kinase/B-50 protein complex. The results imply that phosphorylation of protein may affect the metabolism of (poly)PI in brain cell membranes.

Effects of peptide hormones on phosphatidylinositol (PI) metabolism in cell membranes of peripheral tissues have been obtained[6–8]. Similarly, corticotropin (ACTH) is known to affect (poly)PI metabolism in membrane fractions from rat brain[9]. An enhanced metabolism of TPI was also found in response to cholinergic and noradrenergic receptor stimulation[10] and after the influx of Ca^{2+} into the cell[11]. With respect to the phosphorylation of proteins, we found that ACTH exerts a dose- and structure-dependent inhibitory effect on the *in vitro* phosphorylation of specific proteins in synaptosomal plasma membranes[4]. The ACTH-sensitive protein kinase (molecular weight 71,000; isoelectric point 5.5) and one of its substrate proteins (B-50; molecular weight 48,000; isoelectric point 4.5) were isolated and the phosphorylation of the B-50 protein was found to be Ca^{2+}-dependent[5].

The protein kinase/B-50 complex used in the present study was obtained from a Triton–KCl solubilized synaptosomal plasma membrane fraction and subjected to further purification by DEAE-cellulose chromatography and ammonium sulphate precipitation (ASP) as described before (see legend to Fig. 1). The ASP fraction has been characterized by SDS–polyacrylamide slab gel electrophoresis: the position of B-50 and its protein kinase are indicated in Fig. 1*a*. Upon incubation of this ASP fraction with [γ-^{32}P]ATP only the B-50 protein became labelled (Fig. 1*b*). Interestingly, addition of DPI to the ASP fraction in the phosphorylation medium produced [^{32}P]TPI as shown by autoradiography after thin layer chromatography of the lipid extract (Fig. 1*c*).

When the eluate of the DEAE–cellulose column was assayed for B-50 protein and DPI-kinase activity, it was found that the two activities cochromatographed, suggesting a possible relationship (J.J. *et al.*, in preparation). Confirming previous results[6], incubation of the ASP fraction in the presence of $ACTH_{1-24}$ resulted in a dose-dependent inhibition of B-50 phosphorylation (Table 1). Concomitantly, the phosphorylation

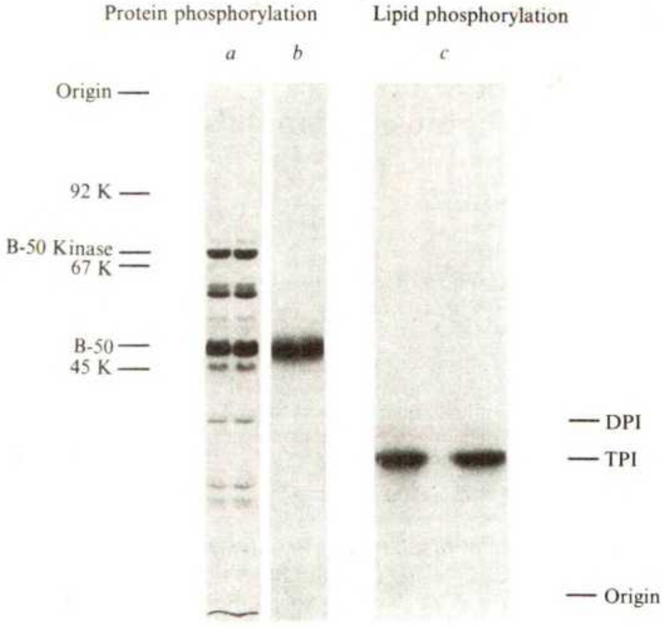

Fig. 1 *a*, Gel staining pattern showing the position of the protein bands, and *b*, autoradiogram showing the endogenous phosphorylation profile of the $ASP_{55-80\%}$ fraction. Each track contains 6 μg of total ASP protein. The position of molecular weight marker proteins, and of B-50 and B-50 kinase is indicated. *c*, Autoradiogram after extraction and thin layer chromatography of ASP fraction incubated with exogenous DPI. The position of DPI and TPI is indicated. Each lane shows the results of duplicate determinations. The ACTH-sensitive protein kinase and its protein substrate, the B-50 protein, were isolated as described by Zwiers *et al.*[5,6]. Briefly, a crude synaptosomal plasma membrane fraction was prepared from rat brain. The membrane-bound B-50 protein kinase activity was solubilized with 0.5% Triton X-100 with 75 mM KCl in 6 mM Tris, 0.1 mM dithiothreitol (*p*H 8.1) and the solubilized proteins separated by DEAE-cellulose chromatography. The proteins were eluted with a salt gradient in 10 mM Tris, 1 mM $CaCl_2$, 0.1 mM dithiothreitol, *p*H 7.4 (buffer A). The eluate fractions containing the peak of B-50 protein and B-50 phosphorylating activity were pooled and subjected to 55% ammonium sulphate saturation. After separation of the precipitated proteins by centrifugation the supernatant was saturated to 80% with ammonium sulphate and the precipitate collected by centrifugation. This $ASP_{55-80\%}$ fraction was dissolved in 400 μl buffer A and dialysed overnight against 1 l of buffer A. The phosphorylation assay was performed in the following conditions: 50 mM Na acetate, 10 mM Mg acetate, 1 mM Ca acetate (*p*H 6.5), 7.5 μM ATP, 2 μCi [γ-^{32}P]ATP (~3,000 Ci $mmol^{-1}$, Amersham), 7.5 μl ASP fraction, 40 μM DPI (disodium salt, Sigma) in a final volume of 25 μl. The enzyme fraction was routinely preincubated for 5 min before the incubation was started by the addition of DPI and ATP. Buffer with or without $ACTH_{1-24}$ was added 15 s before the ATP and incubation continued for 15 min unless indicated otherwise. Protein phosphorylation and lipid phosphorylation assays were always run in parallel. The protein phosphorylation reaction was terminated by the addition of a denaturating solution and the proteins were separated by SDS–polyacrylamide gel electrophoresis. After staining with Fast Green FCF and autoradiography the labelled protein bands were cut from the gel and measured for radioactivity by liquid scintillation counting[4,5]. The lipid phosphorylation reaction was terminated by the addition of ice-cold chloroform/methanol/13 N HCl solution (200 : 100 : 0.75 v/v). Carrier poly PI were added and an acid extraction was carried out. The lipid extract was separated by one-dimensional high performance thin layer chromatography (HPTLC) on precoated HPTLC plates (Merck) impregnated with 1% K oxalate. After lipid staining and autoradiography the labelled lipids were scraped from the plate and counted for radioactivity in a liquid scintillation counter[8,12]. All experiments were performed at least three times.

of exogenously added DPI to TPI was stimulated (+35% and +149% at 10 μM and 100 μM ACTH respectively). Because similar ACTH effects have been obtained with brain synaptosomal membrane fractions[4,12], it seems very probable that the enzymes responsive to the peptide in synaptosomal plasma membranes are present in the ASP fraction. The correlation between inhibited B-50 phosphorylation and stimulated TPI formation suggests that the state of B-50 phosphorylation may affect the DPI kinase activity (see ref. 13 for a recent review on the regulation of enzymatic activity by phosphorylation). To test this hypothesis the ASP fraction was preincubated with [γ-^{32}P]ATP for various periods of time, and DPI kinase activity was measured after this B-50 prephosphorylation period. As Fig. 2*a* shows, the extent of B-50 protein phosphorylation increased with time up to 40 min but DPI kinase activity diminished with increasing B-50 phosphorylation, providing additional evidence for a direct relationship between B-50 protein and DPI phosphorylation. It appears that the formation of TPI is especially affected by the final 30% of the protein phosphorylation; more insight into the exact molecular mechanisms involved is needed to appreciate the significance of this finding more fully. To eliminate the possibility that the decreased formation of TPI is due to enzyme breakdown during the phosphorylation period,

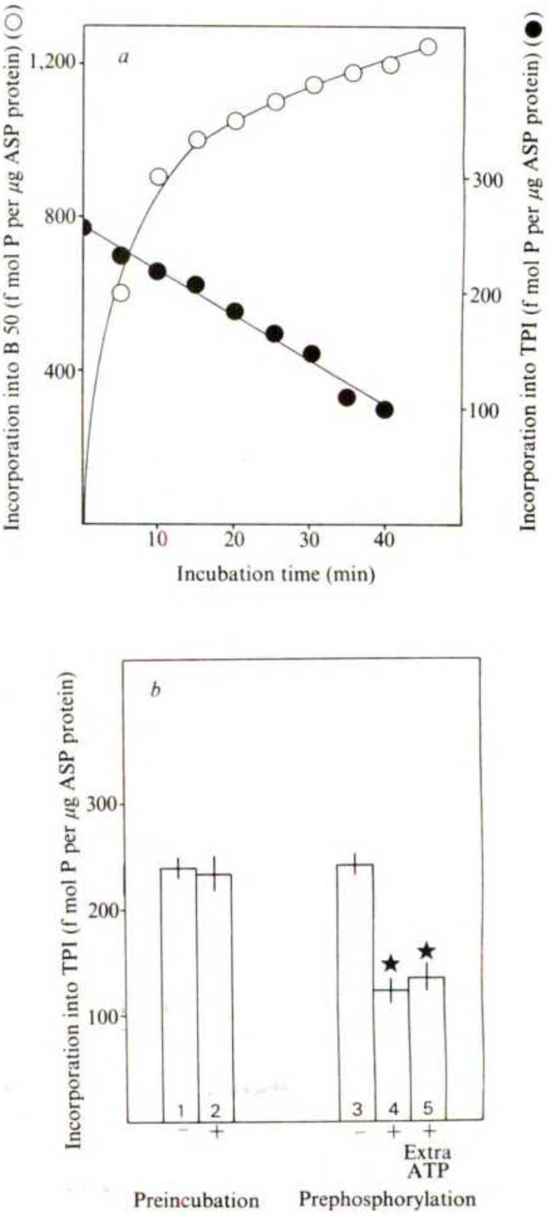

Fig. 2 *a*, The effect of B-50 prephosphorylation on TPI formation. Incubations were performed as described in the legend to Fig. 1, with the following modifications: ASP fractions were incubated in the absence of DPI for 5–45 min (○). Exogenous DPI was added to the ASP fraction after the various prephosphorylation time periods (0–40 min) and incubation continued for another 5 min. The amount of TPI formation in these 5 min periods (0–5, 5–10 min etc.) was measured (●). *b*, The effect of B-50 prephosphorylation on TPI formation: influence of preincubation and ATP. ASP fractions were incubated for 15 min in the presence of ATP and DPI as indicated in the legend to Fig. 1 (group 1 and 3). Group 2 was preincubated for 30 min before addition of DPI and ATP. Group 4 was preincubated for 30 min in the presence of ATP before DPI was added and the incubation continued for another 15 min. Group 5 was treated like group 4 but extra ATP containing 2 μCi [γ-^{32}P]ATP was added together with the DPI to give a final concentration of 15 μM ATP.

TPI formation was measured with and without 30 min preincubation in the absence of ATP. As Fig. 2*b* shows, preincubation had no effect. Furthermore, the decreased TPI formation seemed not to be related to exhaustion of ATP during the prephosphorylation, as the amount of labelled lipid was significantly depressed even after the addition of extra ATP (Fig. 2b). These results are in line with those obtained with ACTH (Table 1 and refs 4, 5, 12): there seems to be an inverse relationship between B-50 phosphorylation and TPI formation. Therefore, and in view of the studies on enzyme phosphorylation[13], we propose that the effect of ACTH on TPI production is secondary to the effect on protein phosphorylation: the peptide inhibits the B-50 kinase[4], and the B-50 substrate protein in its non-phosphorylated form, stimulates TPI formation. It awaits further experimentation to determine whether the B-50 protein is a regulatory factor of the DPI-kinase or the kinase itself.

Table 1 The effect of $ACTH_{1-24}$ on B-50 phosphorylation and TPI formation

Treatment	Incorporation (f mol P per µg ASP protein) B-50	Increase (%)	TPI	Increase (%)
No addition	994.9±8.0		180.0±9.1	
$ACTH_{1-24}$ (10 µM)	517.3±21.2	−48†	242.2±16.2	+35*
$ACTH_{1-24}$ (100 µM)	308.4±25.4	−69†	448.4±30.0	+149†

Incubations were performed as described in the legend to Fig. 1. Values represent mean ± s.e.m. ($n = 5$). Differences were tested with Student's t-test.

* $P < 0.01$.

† $P < 0.001$.

Interestingly, Takai *et al.*[14,15] recently demonstrated that the activity of a Ca^{2+}-dependent protein kinase is linked to PI and its breakdown product 1,2-diacylglycerol, suggesting that a functional relation exists between protein phosphorylation and phosphatidylinositol metabolism. DPI and especially TPI are very potent chelators of Ca^{2+} and Mg^{2+} (refs 3, 16); they interact strongly with proteins and, due to their very negative headgroup which contains three (DPI) or five (TPI) negative charges, these lipids may carry the negative potential of the membrane[17,18]. Thus a change in the relative amounts of the phosphoinositides PI/DPI/TPI in the membrane may affect the conformation of membrane proteins and change the amount of Ca^{2+} and Mg^{2+} bound to the membrane. Both protein phosphorylation[1,2] and (poly)PI metabolism[3] are implicated in the regulation of membrane permeability and synaptic transmission in neurones. The results obtained in the present study suggest that the phosphorylation of a quantitatively minor membrane protein (B-50 protein), may bring about profound changes in membrane characteristics by changing the content of poly PIs. The demonstration that ACTH influences this process may suggest new avenues for investigating the biochemical mechanisms underlying agonist–effector cell membrane interactions.

Received 14 March; accepted 27 May 1980.

1. Williams, M. & Rodnight, R. in *Progress in Neurobiology* Vol. 8 (eds Kerkut, G. A., Phillis, J. W.) 183–250 (Pergamon, Oxford, 1977).
2. Greengard, P. *Science* **199,** 146–152 (1978).
3. Michell, R. H. *Biochim. biophys. Acta* **415,** 81–148 (1975).
4. Zwiers, H., Wiegant, V. M., Schotman, P. & Gispen, W. H. *Neurochem. Res.* **3,** 455–463 (1978).
5. Zwiers, H., Tonnaer, J., Wiegant, V. M., Schotman, P. & Gispen, W. H., *J. Neurochem.* **33,** 247–256 (1979).
6. Zwiers, H., Schotman, P. & Gispen, W. H. *J. Neurochem.* **34,** 1689–1699 (1980).
7. Kirk, C. J., Verrinder, T. R. & Hems, D. A. *FEBS Lett.* **83,** 267–271 (1977); *Biochem. Soc. Trans.* **6,** 1031–1033 (1978).
8. Farese, R. V., Sabir, A. M. & Vandor, S. L. *J. biol. Chem.* **254,** 6842–6844 (1979).
9. Jolles, J., Wirtz, K. W. A., Schotman, P. & Gispen, W. H. *FEBS Lett.* **105,** 110–114 (1979).
10. Abdel Ladif, A. A., Green, K. & Smith, J. P. *J. Neurochem.* **32,** 225–228 (1979).
11. Griffin, H. D. & Hawthorne, J. N. *Biochem. J.* **176,** 541–552 (1978).
12. Jolles, J., Dekker, A., Schotman, P., Wirtz, K. W. A. & Gispen, W. H. *Brain Res. Bull.* (in the press).
13. Krebs, E. G. & Beavo, J. A. *A. Rev. Biochem.* **48,** 923–959 (1979).
14. Takai, Y. *et al. J. biol. Chem.* **254,** 3692–3695 (1979).
15. Takai, Y., Kishimoto, A., Kikkawa, U., Mori, T. & Nishizuka, Y. *Biochem. biophys. Res. Commun.* **91,** 1218–1224 (1979).
16. Hawthorne, J. N. & Kai, H. in *Handbook of Neurochemistry* Vol. 3 (ed. Lajtha, A.) 491–508 (Plenum, New York, 1970).
17. Torda, C. *Neurobiology* **3,** 10–28 (1973).
18. Torda, C. *Int. Rev. Neurobiol.* **16,** 1–66 (1974).

Chemically induced myotonia in amphibia

A. H. Bretag, S. R. Dawe & A. G. Moskwa

South Australian Institute of Technology, North Terrace, Adelaide, South Australia, Australia

Frogs and toads treated with high doses of anthracene-9-carboxylic acid (A-9-C) develop prolonged muscular contractions and 'divebomber' electromyograms characteristic of myotonia. Hitherto, myotonia has been considered peculiar to homeotherms where it is associated with several hereditable diseases and can be induced by specific treatments, most of which seem to act by decreasing membrane chloride conductance[1]. Our work indicates that myotonia can be induced in amphibia by similar means. We offer possible reasons why others have missed seeing myotonia in amphibia.

Toads, *Bufo marinus,* weighing about 120 g and frogs, *Littoria aurea,* of 30–60 g were kept at room temperatures of 20–25 °C and injected subcutaneously with A-9-C (167 mg per kg as a 10 mg ml^{-1} solution neutralized with NaOH). Myotonic behaviour could then be observed in the toads within half an hour. In the frogs it took a number of hours to develop. If jumping was provoked it resulted in one or a few normal jumps followed by jumps with severe extensor spasm on landing. This often caused the animal to freeze in a bizarre attitude for some seconds (Fig. 1), before slowly relaxing and then resuming a normal squatting position. Continued provocation to jump eventually resulted in a return to normal. After rest for half an hour, however, the whole cycle could be repeated. This kind of response could be obtained for 2 or 3 days following the injection of A-9-C after which jumping behaviour gradually returned to normal over the next few days.

Library
SCIENCE COLLEGE,
Upper Circular Road
CALCUTTA.

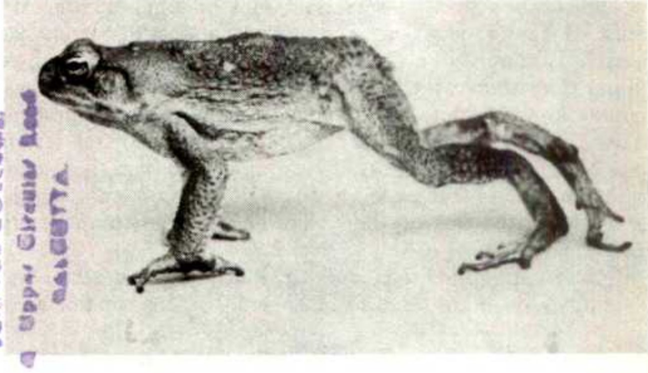

Fig. 1 An A-9-C treated toad, still immobile and stiff-legged, ~3s after landing from a jump. We have occasionally seen these animals overbalance on landing to become supported on their forelegs and snout with their hind legs extended above them. By contrast, untreated toads jump, land and resume their normal squatting position within half a second.

While animals were displaying myotonic behaviour, audio electromyograms could be recorded from leg muscles with frequent 'divebomber' bursts of activity in response to slight movements of the concentric recording needle. After exercise 'warm up', divebomber sounds were virtually eliminated.

Sartorius muscles, *in vitro,* could also be made to produce myotonic contractions (Fig. 2*a*) in response to A-9-C at concentrations comparable to those expected to pertain in the *in vivo* experiments. Similar results could be obtained using 4,

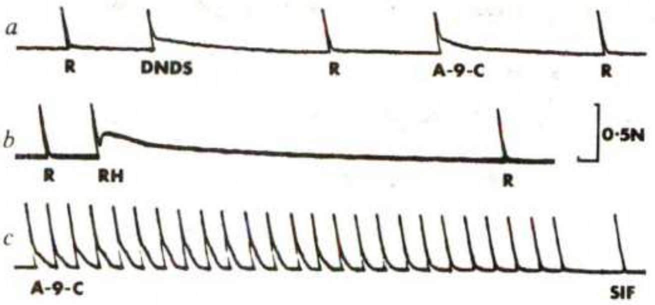

Fig. 2 Isometric tension records from isolated frog and toad sartorius muscles bathed at room temperature (20 °C) in Ringer solution[2] (R) and synthetic interstitial fluid[3] (SIF), respectively. Muscles were allowed to equilibrate in particular solutions for 10 min before stimulation with a train of three, just supramaximal, 1 ms pulses[4] at 225 Hz. *a*, Frog sartorius muscle in control solution (R) and with the addition of DNDS (2mmol l^{-1}) and A-9-C (2.25 mmol l^{-1}) showing that normal relaxation is interrupted and prolonged by these agents. Time scale, 1 s. *b*, Frog sartorius muscle. Response in control solution (R) compared with response in a chloride-free solution (RH) made by substituting appropriate quantities of sodium 3,5-diacetamido-2,4,6-triiodobenzoate (Hypaque, Winthrop) for sodium chloride, and potassium and calcium sulphate for their chlorides. Cationic activities were maintained constant[5]. Time scale, 1 s. *c*, Toad sartorius muscle. Record of contractions resulting from stimulation at 5 s intervals in the presence of A-9-C (2.25 mmol l^{-1}). After about 20 such stimuli the prolonged relaxation returns to normal, as illustrated in the final contraction of the record which was initiated 10 min after washout of the A-9-C with SIF. Time scale, 5 s.

4'-dinitro-2, 2'stilbenedisulphonic acid (DNDS, Fig. 2*a*), furosemide (not shown) or a chloride-free bathing solution (Fig. 2*b*). Muscles were stimulated only once every 10 min as 'warm up' was rapidly produced by more frequent stimuli (Fig. 2*c*). Typical myotonic after-discharges of action potentials could be found in A-9-C treated toad sartorius muscle fibres following constant current stimulation (Fig. 3). An increase in input resistance was observed in these A-9-C treated fibres.

The effects we have observed in amphibian muscle suggest a reduced membrane leakage conductance and, as in mammalian muscle[1], are most likely to be low chloride-conductance myotonia. Consistent with this interpretation, A-9-C is the most potent known chloride conductance blocker in mammalian muscle[6] while DNDS and furosemide are similarly potent blockers of anion transport in red blood cells[7] and the kidney respectively[8]. In our experiments their action cannot be distinguished from that of a low chloride solution (compare Fig. 2*a*, *b*).

Induced myotonia has not previously been described in amphibia and there seem to be several reasons for this apart from the possibility of species differences. First, the doses of A-9-C that we have used are considerably higher than those used by others[9] and the long delay before significant behavioural effects appear in frogs may have caused slight myotonia to be overlooked. Second, since exercise quickly produces 'warm up', myotonia is best seen if the animals are closely confined for half an hour before testing.

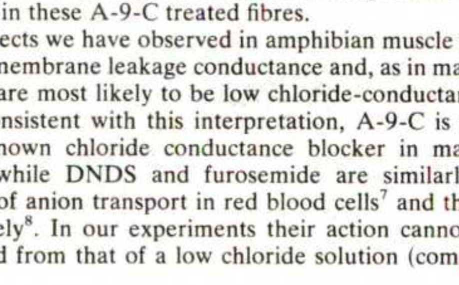

Fig. 3 Intracellular 3M KCl microelectrode recording of a myotonic after-discharge of action potentials in a single fibre of toad sartorius muscle bathed in SIF containing A-9-C (2.25 mmol l^{-1}) at 20 °C. The fibre was stimulated by the constant current pulse shown in the upper trace delivered through a second microelectrode (2M K citrate) inserted close to the voltage recording electrode.

We thank the Muscular Dystrophy Association of S.A. and the Research Committee of the South Australian Institute of Technology for support.

Received 3 March; accepted 2 June 1980.

1. Bryant, S. H. in *Pathogenesis of Human Muscular Dystrophies: Proceedings of the Fifth International Scientific Conference of the Muscular Dystrophy Association* (ed. Rowland, L. P.) 715–728 (Excerpta Medica, Amsterdam, 1977).
2. Adrian, R. H. *J. Physiol., Lond.* **133,** 631–658 (1956).
3. Bretag, A. H. *Life Sci.* **8,** 319–329 (1969).
4. Rüdel, R. & Senges, J. *Naunyn-Schmiedebergs Arch. Pharmac.* **274,** 337–347 (1972).
5. Bretag, A. H. in *Basic Research in Myology: Proceedings of the Second International Congress on Muscle Diseases*, Pt 1 (ed. Kakulas, B. A.) 641–646 (Excerpta Medica, Amsterdam, 1973).
6. Palade, P. T. & Barchi, R. L. *J. gen. Physiol.* **69,** 879–896 (1977).
7. Barzilay, M. & Cabantchik, Z. I. *Biophys. J.* **21,** 11a (1978).
8. Burg, M., Stoner, L., Cardinal, J. & Green, N. *Am. J. Physiol.* **225,** 119–124 (1973).
9. Bryant, S. H. & Morales-Aguilera, A. *J. Physiol., Lond.* **219,** 367–383 (1971).

Control of tension development in scallop muscle fibres with foreign regulatory light chains

R. M. Simmons & A. G. Szent-Györgyi

Department of Physiology, University College London, Gower Street,
London WC1E 6BT, UK, and Department of Biology,
Brandeis University, Waltham, Massachusetts 02154

We have shown previously that chemically skinned fibre bundles from scallop muscle can be desensitized to the action of calcium by the removal of the regulatory light chains of myosin and that sensitivity can be restored by the re-addition of scallop light chains[1]. We have now confirmed these results and extended our observations to fibre bundles from which one or both of the regulatory light chains per myosin have been removed (by treatment with EDTA at 7 and 25 °C, respectively) and replaced by the corresponding light chains from other species. In the case of a double substitution—where both light chains were replaced—sensitivity was restored completely by light chains from other molluscs and from gizzard muscle; for a single substitution there was restoration of sensitivity by all the light chains tested.

The tension response of a chemically skinned fibre bundle to an activation–relaxation sequence is shown in Fig. 1*a*. There was no tension development in relaxing solution ($[Ca^{2+}] < 10^{-10}$ M) and maximal development in activating solution ($[Ca^{2+}] = 10^{-4.8}$ M). Treatment with EDTA at 25 °C removed both regulatory light chains, as shown in other preparations by urea gel electrophoresis, and tension development was maximal in relaxing solution as well as in activating solution (Fig. 1*b*). Thus, the fibre bundle was no longer sensitive to calcium, in the sense that regulatory control had been completely lost.

Fully desensitized fibre bundles were exposed to light chains from the same and other species, tested for their sensitivity to calcium and analysed for light chain content by urea (and in some cases SDS) gel electrophoresis. The results are summarized in Table 1. In most cases, two light chains per myosin were successfully combined. Preparations treated with light chains from the scallop and other molluscan species (spisula, mercenaria and loligo) showed a complete restoration of sensitivity towards calcium (Fig. 1*c*). Sensitivity was also restored by the combination of chicken gizzard light chains (Fig. 1*d*), but rabbit skeletal, bovine cardiac and lobster tail muscle light chains had little or no effect (Fig. 1*e*). Some fibre bundles which

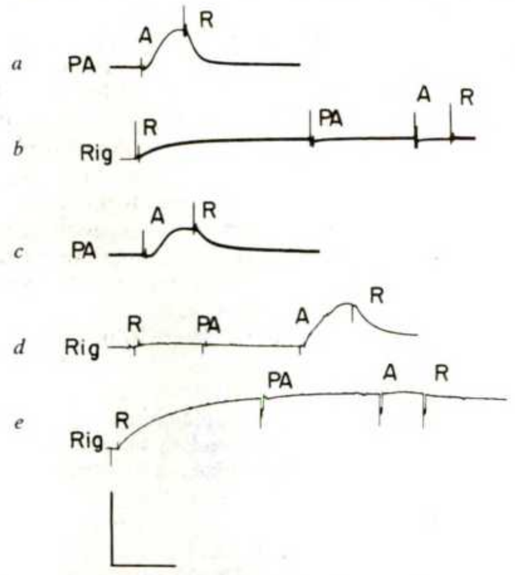

Fig. 1 Double-substitution experiments. Tension responses of skinned fibre bundles to activation–relaxation sequences; effects of complete removal of scallop regulatory light chains and of replacement by light chains from the scallop and other species. *a–c*, Same fibre bundle; *a*, before EDTA treatment; *b*, desensitized by treatment with EDTA at 25 °C (control); *c*, resensitized with scallop light chains; *d*, complete substitution of scallop light chains by gizzard light chains; *e*, complete substitution by lobster light chains. Fibre bundles were from the striated adductor muscle of *Placopecten magellanicus*. Removal and addition of light chains were as described in Table 1 legend. Symbols for solutions: PA, pre-activating (a relaxing solution with low [EGTA] to increase rate of tension development in activating solution); A, activating; R, relaxing; Rig, rigor. Solutions[6] (concentrations in mM unless stated): PA; EGTA 0.1, HDTA 29.9, $[Ca^{2+}] \sim 10^{-8}$ M. A; CaEGTA 30, $[Ca^{2+}] = 10^{-4.8}$M. R, Rig; EGTA 30, $[Ca^{2+}] < 10^{-10}$ M. PA, R, A; phosphocreatine 19, [MgATP] = 5, creatine kinase 1–2 mg ml^{-1}. All solutions; $[Mg^{2+}] = 1$, trimethylamino ethanesulphonic acid 100, *p*H 7.0, I 0.2 M, 20 °C. Scales: *a–c*, tension 100 mg, time 1 min; *d*, *e*, tension 84 mg, time 41 s. Tension was close to zero at the start of the records.

had been treated with cardiac and rabbit skeletal light chains produced less tension than normal both in the presence and absence of calcium. This inhibition was particularly pronounced after long incubations with light chains and no inhibition was observed when the same fibre bundle was tested before and after the addition of light chains, when full combination was achieved after incubation for 1 h.

Although it was comparatively simple to remove both scallop light chains per myosin, it proved difficult to remove exactly one light chain per myosin (by treatment with EDTA at 7 °C, which is successful with myofibrillar preparations[2–4]). Different preparations and slightly different procedures resulted in from 0.7 to 0.9 light chains remaining. These fibre bundles did not show a complete loss of sensitivity towards calcium, that is, the tension developed in activating solution was greater than that in relaxing solution (control fibre bundles in Fig. 2*a* and Table 2). This result is difficult to interpret quantitatively because light chain removal may not have been homogeneous throughout a bundle, so that some myosin molecules may have remained with both light chains intact. The addition of non-molluscan light chains to such fibre bundles resulted in the combination on average of more than one foreign light chain per myosin and there was a considerable variation in the amount combined (range 1.26–1.60 light chains per myosin). All the light chains tested gave a considerable restoration of sensitivity towards calcium (Fig. 2*b* and Table 2) and it is likely that the restoration was mainly due to the combination of foreign light chains to myosin molecules with a single remaining scallop light chain. The degree of restoration of sensitivity for rabbit skeletal and cardiac light chains is surprisingly high; the gel results show that a substantial number of myosin molecules must have become doubly substituted, and these molecules would have remained desensitized (Table 1). It is possible that the inhibition of tension development observed for double substitutions by these light chains reduced their contribution, resulting in an overestimate of sensitivity. Double substitution by lobster light chains had no inhibitory effect and it is noticeable that the degree of restoration of sensitivity in the single substitution experiments with lobster light chains was less than for cardiac or rabbit skeletal light chains. The full restoration of sensitivity by gizzard light chains was to be expected as these light chains confer sensitivity on their own (Table 1).

These results confirm ATPase measurements in scallop myofibrils; when both scallop light chains have been removed, sensitivity can be wholly restored by the combination of light chains from molluscan species and from vertebrate smooth muscle, but not with light chains from vertebrate skeletal, cardiac or lobster muscle[5]. They also confirm that sensitivity is restored in the case of a single remaining scallop light chain following the combination of light chains that do not themselves confer sensitivity towards calcium[3,4].

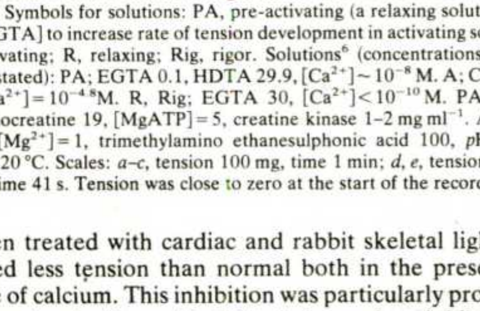

Fig. 2 Single-substitution experiments. Effect on tension development of removal of a single scallop regulatory light chain and replacement by a non-molluscan light chain. *a*, Single remaining scallop light chain (control); *b*, single substitution by cardiac light chains. Solutions as described in Fig. 1 legend. Scales: *a*, tension 50 mg, time 1 min; *b*, tension 50 mg, time 43 s.

Table 1 Regulatory light chain content and calcium dependence of tension development in double-substitution experiments

Source of added regulatory light chain	No. of fibre bundles	% Sensitivity (mean±s.d.)	Regulatory light chains per myosin (mean ± s.d.)
Control	15	0	0
Scallop striated	7	89 ± 18	1.66 ± 0.35
Spisula	2	100	1.76
Loligo syphon retractor	2	98	2.14
Mercenaria	3	95 ± 3	1.77 ± 0.10
Bovine cardiac	4	14 ± 28*	1.74 ± 0.12
Rabbit striated	9	5 ± 6	1.84 ± 0.45
Lobster tail	4	3 ± 2	1.65 ± 0.46
Chicken gizzard	6	92 ± 5	2.05 ± 0.30

Sensitivity of tension development (second column) was obtained from the ratio of the extra tension developed in activating solution (compared with the tension in relaxing solution) to the total tension developed in activating solution and expressed as a percentage. Fibre bundles were chemically skinned with 1% Brij 35 in 50 mM KCl, 5 mM EGTA, 5 mM $MgCl_2$, 5 mM ATP and 20 mM imidazole-HCl, *p*H 7.0, usually at 18–20 °C for 0.5–1 h. Light chains were removed by a 0.5–3-h incubation at 25–27 °C with 10 mM EDTA in 40 mM KCl and 20 mM imidazole-HCl, *p*H 7.0. Fibre bundles were combined with light chains by a 1–3-h incubation with 0.5 ml 0.1% light chain in 50 mM KCl, 5 mM $MgCl_2$, 5 mM EGTA and 20 mM imidazole-HCl, *p*H 7.0, in the presence of 1 mM freshly prepared dithiothreitol. Incubation at 4 °C gave the most reproducible results for tension measurements. Light chains were prepared as described previously[4]. Scallop, mercenaria and spisula light chain contents were determined by urea–acrylamide gel electrophoresis; lobster, loligo, rabbit skeletal, cardiac and gizzard light chain contents were obtained from 14–15% SDS-acrylamide gel electrophoresis in phosphate. Fibre bundles were rinsed with water and freeze-dried. Sample buffer (70 µl) was added to the dried fibre bundles and incubated for 3 min in boiling water (SDS gels) or for 2 h at 37 °C (urea gels). Although the fibre bundles did not dissolve completely in the sample buffer, the light chains dissociated fully and repeated incubation with new sample buffer did not extract additional light chains. Aliquots (50 µl) of the samples were applied on tube gels. Gels were stained with acid fast green and analysed densitometrically. Densities obtained with light chains were corrected for molecular weights and stain uptake. Regulatory light chain content per myosin was obtained from the density ratios of the regulatory and essential light chain bands. The two essential light chains of myosin are not removed by EDTA treatment[2], so a ratio of 1 corresponds to 2 regulatory light chains per myosin.

* Three of the fibre bundles gave low tensions.

Table 2 Regulatory light chain content and calcium dependence of tension development in single-substitution experiments

Source of added regulatory light chain	No. of fibre bundles	% Sensitivity (mean ± s.d.)	Scallop regulatory light chains per myosin (mean ± s.d.)	Foreign light chains per myosin (mean ± s.d.)
Control	7	43 ± 21	0.78 ± 0.07	
Bovine cardiac	6	96 ± 3		1.35 ± 0.08
Rabbit striated	6	88 ± 8		1.47 ± 0.11
Lobster tail	6	73 ± 17		1.33 ± 0.09
Chicken gizzard	6	98 ± 3		1.52 ± 0.12

Methods used were similar to those given in Table 1 legend except that incubation in EDTA solution was at 7 °C.

These experiments were performed at the Marine Biological Laboratory, Woods Hole and at University College London. The work was supported by PHS grant AM 15963 and a Muscular Dystrophy Association grant to A.G.S.-G. and a Programme Grant from the MRC to R.M.S. We thank the Wellcome Trust for a travel grant to R.M.S.

Received 23 November; accepted 16 June 1980.

1. Simmons, R. M. & Szent-Györgyi, A. G. *Nature* **273**, 62–64 (1978).
2. Chantler, P. D. & Szent-Györgyi, A. G. *J. molec. Biol.* **138**, 473–492 (1980).
3. Kendrick-Jones, J. *Nature* **249**, 631–634 (1974).
4. Kendrick-Jones, J., Szentkiralyi, E. M. & Szent-Györgyi, A. G. *J. molec. Biol.* **104**, 747–775 (1976).
5. Chantler, P. D., Sellers, J. R. & Szent-Györgyi, A. G. *Biophys. J.* **25**, 92a (1979).
6. Moisescu, D. G. *Nature* **262**, 610–613 (1976).

Formation of helical filaments by copolymerization of two types of 'straight' flagellins

Ritsu Kamiya & Sho Asakura

Institute of Molecular Biology, School of Science, Nagoya University, Nagoya 464, Japan

Shigeru Yamaguchi

Department of Biology, School of Education, Waseda University, Tokyo 160, Japan

Bacterial flagella undergo transition between several discrete types of left-handed and right-handed helical structures when exposed to acidic[1] or alkaline *p*H[2], or to mechanical force[3]. Calladine[4] and ourselves[5] have presented models to explain such polymorphism, assuming that protein subunits (flagellin) in a flagellum can be transformed into two conformations (L- and R-states) depending on the species of flagellin and on the environmental conditions. An obvious prediction from these 'two-state' models is that there should be two types of straight flagella (L- and R-types) that are made up exclusively of flagellins in either the L-state or the R-state. We have shown that straight flagella from two species of mutants, *Salmonella* SJ814 (ref. 6) and *Escherichia coli* hag 177 (ref. 7), are closely similar to the predicted R- and L-types, respectively[5]. Recently we have isolated 10 strains of straight-flagellar mutants of *Salmonella*. We show here that their flagella can also be classified into the L- and the R-types, and that copolymerization of flagellins from two heterologous types (L and R) makes discrete types of helical filaments, whereas that of homologous pairs of flagellins (L and L, or R and R) makes only straight filaments.

Ten mutant strains with a straight-flagellar phenotype (SJW 1655–SJW1664) were isolated from SJW1103, which produces normal flagella with the antigenicity of i in phase 1 and is nonflagellate in phase 2 (S.Y., in preparation). All of them are spontaneous mutants selected on semi-solid agar plates. Flagella from these mutants were examined by electron microscopy and optical diffraction, after they had been detached from the cell body and partially purified by differential centrifugation. It was found that the diffraction pattern of the SJW1655 flagella was significantly different from those of the other nine species. Most notably, the *z*-coordinate of the near-equatorial layer-line (the reflection from 11 near-longitudinal rows of subunits[6]) was as large as 1/400 $Å^{-1}$ in SJW1655, whereas it was about threefold smaller in the rest of the mutants (Fig. 1). As the diffraction pattern of the SJW1655 flagella was closely similar to that of *Salmonella* SJ814 flagella[6], we considered these two types of flagella to be homologous forms. The twisting of the near-longitudinal rows of subunits in the SJW1655 flagella, obtained from 34 measurements, was 7.8 ± 0.8° at the surface of the flagellum. This value was in good agreement with the twisting predicted for the R-type straight flagella[5]. On the other hand, the diffraction patterns of the other nine kinds of straight flagella were similar to that of *E. coli* hag177 flagella[7], which have been considered to be L-type[5], in that the spacing of the near-equatorial layer-line was about 1,500 Å. Measurements of this spacing in 31 diffraction patterns of SJW1660 flagella indicated that the near-longitudinal rows of subunits in this kind of flagella were inclined at an angle of 3.4 ± 1.0° with respect to the filament axis. Also, the other species of flagella (about 10 measurements for each) had mean values of twisting of between 2.0° and 3.4°, agreeing with the value predicted for the L-type[5]. From these results, we considered that flagella from strains SJW1656 to SJW1664 belonged to the L-type.

Flagellins from two R-type mutants (SJ814 and SJW1655) and two L-type mutants (SJW1658 and SJW1660) were mixed pairwise in all possible combinations at various protein ratios, and polymerized by the addition of fragmented flagella[8]. It was

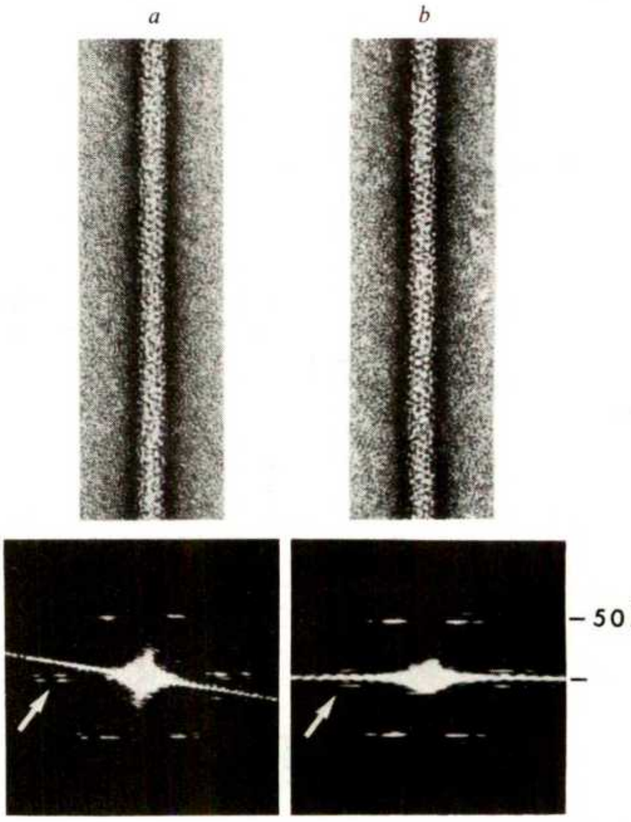

Fig. 1 Electron micrographs and optical diffraction patterns of the two types of straight flagella. *a*, The L-type from SJW1660; *b*, the R-type from SJW1655. Flagellar specimens were negatively stained with 1% uranylacetate. The diameter of the flagellum is about 200 Å. In the diffraction pattern, the near-equatorial layer-line is arrowed. Other mutants (SJW1656–SJW1659, SJW1661–SJW1664) gave diffraction patterns closely similar to that of *a*.

0028-0836/80/320628—03$01.00

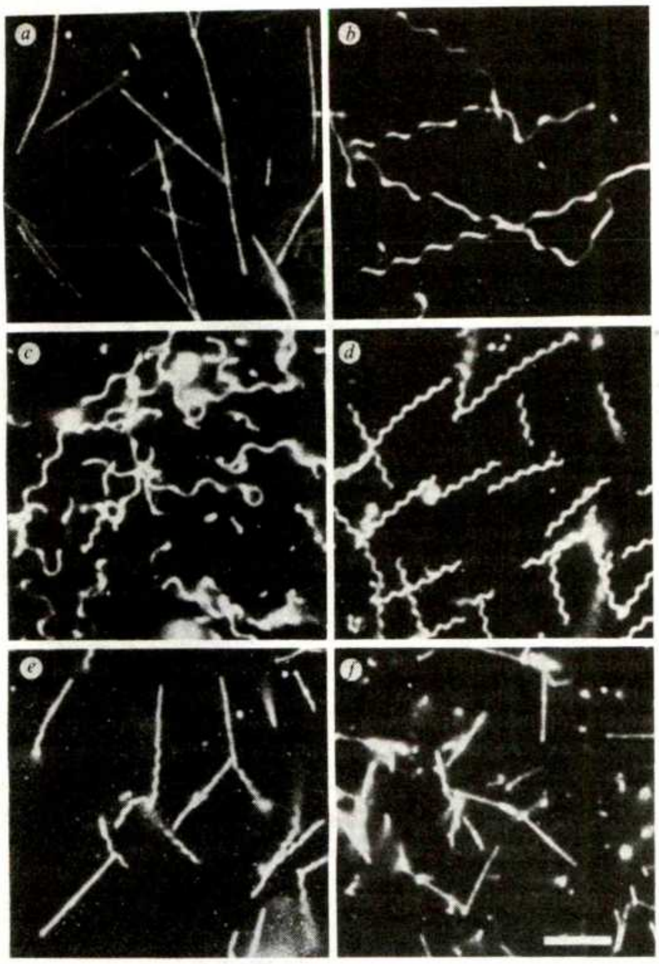

Fig. 2 The products of copolymerization of flagellins from SJW1660 (L-type) and SJW1655 (R-type) at various mixing ratios. The protein ratio of the R-type flagellin to the total monomers was: *a*, 0%; *b*, 10%; *c*, 25%; *d*, 50%; *e*, 90%; *f*, 100%. The two kinds of monomeric flagellins were prepared by the method of S.A. and Iino[8] to give a concentration of 5.0 mg protein ml^{-1} in 0.15 M NaCl. After they had been mixed at various ratios, 1/20 to 1/8 volume of fragmented flagella from SJW1655 (5.0 mg ml^{-1}) was added to each mixture as nuclei for polymerization. It took about 2 days for almost all the flagellin monomers to be polymerized. Essentially the same results were obtained when fragmented flagella from SJW1660 were used as the polymerization nuclei. The SJW1665 flagellin polymerized much more slowly than the SJW1660 flagellin, and for unknown reasons, it was difficult to obtain long polymers of the SJW1655 flagellin. All the photographs were taken with a dark-field microscope with an intense light source[1] after the specimens had been diluted to about 0.03 mg ml^{-1} with 10 mM sodium phosphate buffer (*p*H 7.0). Scale bar, 5 μm.

found that when homologous pairs of flagellins (L and L, or R and R) were mixed, the products were always straight filaments, irrespective of the mixing ratio. However, when heterologous combinations of flagellins (L and R) were mixed, the products assumed various helical forms (Fig. 2). As in the previous experiments of copolymerization using flagellins from SJ814 and from a wild-type strain[8], helical shapes assumed by the products were discrete. It was the frequency of appearance of a helical form that depended on the mixing ratio of the two kinds of flagellins. The frequency of a helical form depended also on the species of the two types of flagellins used. When the ratio of the R-type flagellin was less than 25% of the total monomers, in the copolymerization of the SJW1660 and the SJW1655 flagellins, the products were mostly left-handed helices, including a form resembling the wild-type flagella (normal form). As the ratio of the R-type flagellin was increased, several types of right-handed helices appeared, including the so-called curly type. We have observed seven types of helical forms in these copolymerization experiments besides the two types of straight flagella. Morphological analyses of these helices will be reported elsewhere.

As the antigenicity of the SJ814 flagellin (1, 2) was different from that of the other kinds of flagellins used (i), we could prove that the polymers formed in the mixture of the SJ814 and one of the other species of flagellins were actually copolymers, by showing that all of them could be labelled with either anti-1, 2 or anti-i antibody (Fig. 3). The distribution of the antibodies along a filament showed a strong gradient, corresponding to the different rate of polymerization of the two kinds of flagellins. Such a gradient has frequently been observed in previous studies of copolymerization[8,9], and may explain the simultaneous occurrence of several types of helices in a single copolymer. We are now examining the distribution of the antibodies at a substructural level in heterologous copolymers such as shown in Fig. 3*a*, to see whether or not the two types of flagellin molecules are arranged with regularity. Although we have not come to a definite conclusion due to the limited resolution of electron micrographs, our impression has been that the substructural distribution is rather random. If this is found to be the case, we should assume that the flagellin molecules from either the L- or the R-type of straight flagella can be transformed into both L- and R-forms once they are incorporated into a copolymer, and that a flagellar filament has an inherent ability to organize itself into a uniform helix. At any rate, our demonstration that two types of flagellins from straight flagella copolymerize into helical

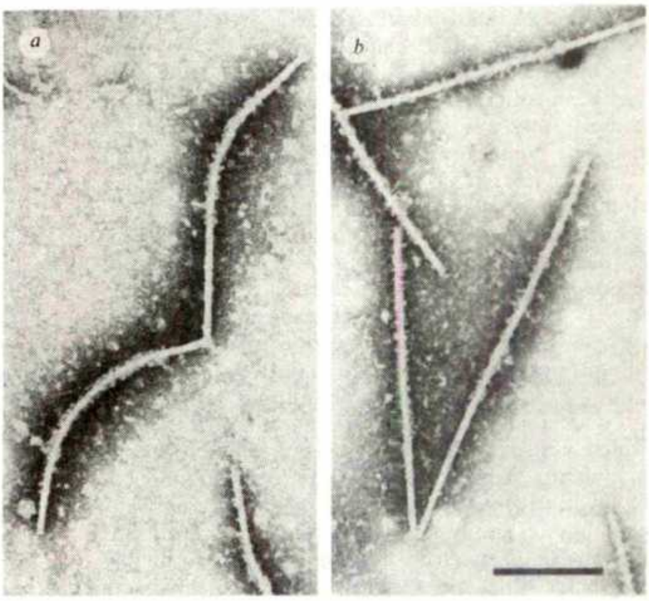

Fig. 3 Antibody staining of copolymers. Flagellins used are: *a*, SJ814 (R-type, antigenicity 1, 2) and SJW1660 (L-type, antigenicity i); *b*, SJ814 and SJW1655 (R-type, antigenicity i). Note that the filaments are curved in *a*, whereas they are straight in *b*. In each case, 1 : 1 mixture of the two kinds of flagellins (5.0 mg ml^{-1}) was polymerized by the addition of 1/2 volume of fragmented flagella from SJ814 (5.0 mg ml^{-1}). After being adsorbed onto electron microscope grids, the specimens were treated with anti-i antibody and negatively stained with 0.5% phosphotungstate (*p*H 7.0). In both of the photographs, the V-shaped portions with no antibodies attached correspond to the fragments of the SJ814 flagella used as the nuclei of polymerization. In *a*, the density of antibodies rapidly decreases along the length towards the tip, indicating that the SJW1660 flagellin was incorporated much faster than the SJ814 flagellin. When these specimens were reacted with anti-1, 2 antibody instead of anti-i, whole lengths of filaments were labelled, with density distributions complementary to these photographs (data not shown). Scale bar, 0.2 μm.

filaments should provide strong support for the idea that flagellar polymorphism arises as the consequence of dimorphic transition of the flagellin molecules.

Received 18 April; accepted 3 June 1980.

1. Kamiya, R. & Asakura, S. *J. molec. Biol.* **106,** 167–186 (1976).
2. Kamiya, R. & Asakura, S. *J. molec. Biol.* **108,** 513–518 (1977).
3. Macnab, R. M. & Ornston, M. K. *J. molec. Biol.* **112,** 1–30 (1977).
4. Calladine, C. R. *J. molec. Biol.* **118,** 457–479 (1978).
5. Kamiya, R., Asakura, S., Wakabayashi, K. & Namba, K. *J. molec. Biol.* **131,** 725–742 (1979).
6. O'Brien, E. J. & Bennett, P. M. *J. molec. Biol.* **70,** 132–152 (1972).
7. Kondoh, H. & Yanagida, M. *J. molec. Biol.* **96,** 641–652 (1975).
8. Asakura, S. & Iino, T. *J. molec. Biol.* **64,** 251–268 (1972).
9. Kuroda, H. *Biochim. biophys. Acta* **285,** 253–267 (1972).

A conformational isomer of bovine pancreatic trypsin inhibitor protein produced by refolding

D. J. States, C. M. Dobson, M. Karplus & T. E. Creighton*

Department of Chemistry, Harvard University, 12 Oxford Street,
Cambridge, Massachusetts 02138
* Medical Research Council Laboratory of Molecular Biology,
Hills Road, Cambridge CB2 2QH, UK

Refolding of the bovine pancreatic trypsin inhibitor protein (BPTI) after reduction of its three cysteine disulphide linkages can occur when the reduced protein is placed in a suitable oxidizing medium (ref. 1 and refs therein). The refolding process has been studied by trapping chemically intermediates which contain only one or two disulphide bonds (ref. 1 and refs therein). We report here that during structural studies of these intermediates by NMR, we have found that complete re-oxidation of the protein results in substantial quantities of a metastable folded species which is identical to native BPTI in its covalent bonding (including the disulphide bonds) but possesses a somewhat different conformation. The existence of such a species is supported by circular dichroism measurements on refolded BPTI[2]. This novel form of BPTI is of considerable interest because it can be used to provide information about the folding mechanism and conformational stability of the protein.

Figure 1 shows ^{1}H NMR spectra of native BPTI and of BPTI which was reduced and re-oxidized fully as described in detail elsewhere[3]. The overall appearance of the spectrum of the re-oxidized material is similar to that of the native protein, but examination shows that two species are present. One of these has an NMR spectrum indistinguishable from that of native BPTI; the other has a slightly different spectrum and is a new species formed in the refolding process. Samples of BPTI were reduced and refolded in various conditions (using oxidized dithiothreitol rather than glutathione as the oxidizing agent and varying the *p*H, ionic composition and temperature of the refolding environment). In every case a mixture of two products was obtained and the novel species had the same NMR spectrum. It seems, therefore, that a conformational isomer exists which has a structure independent of the specific folding conditions, although the amount of the isomer produced does depend on them. In particular, more isomer was observed when refolding was carried out with slower rates of disulphide formation and at lower temperatures; the ratio of the isomer to native BPTI varied from 2.3 at 5 °C to 0.7 at 35 °C in the conditions described in Fig. 1 legend.

The NMR spectra of samples of the refolded material remained essentially constant when samples were left in solution for days at room temperature. Warming the solution to 37 °C for several minutes resulted in the disappearance of the resonances

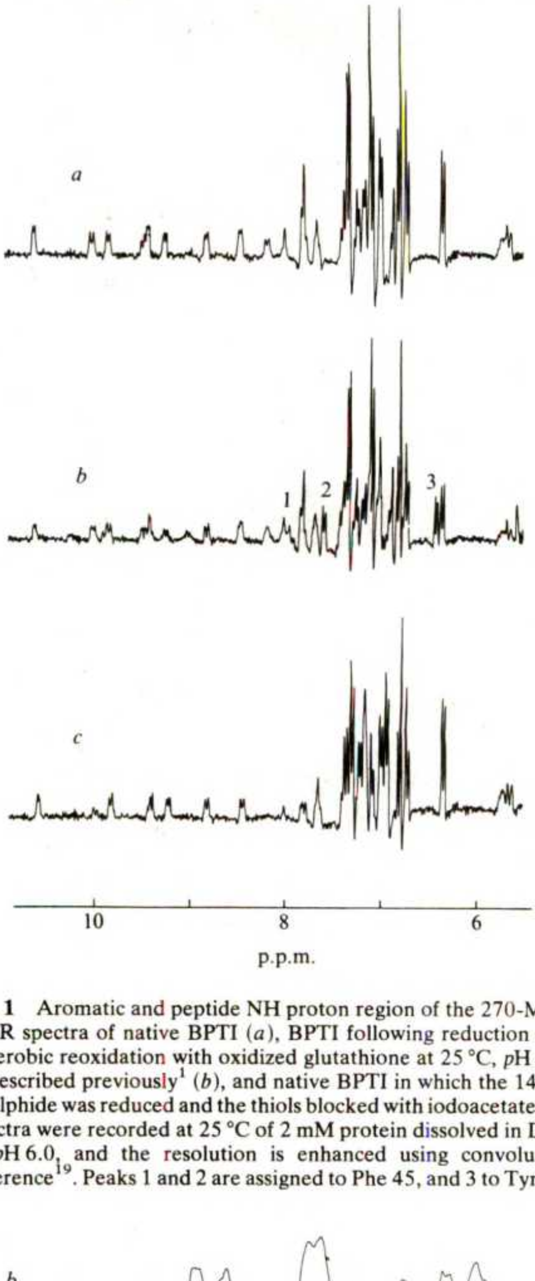

Fig. 1 Aromatic and peptide NH proton region of the 270-MHz NMR spectra of native BPTI (*a*), BPTI following reduction and anaerobic reoxidation with oxidized glutathione at 25 °C, *p*H 8.7, as described previously[1] (*b*), and native BPTI in which the 14–38 disulphide was reduced and the thiols blocked with iodoacetate (*c*). Spectra were recorded at 25 °C of 2 mM protein dissolved in D_2O at *p*H 6.0, and the resolution is enhanced using convolution difference[19]. Peaks 1 and 2 are assigned to Phe 45, and 3 to Tyr 23.

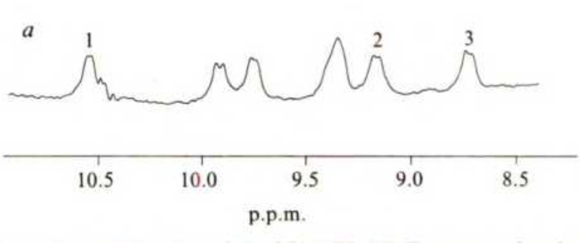

Fig. 2 Low field region of the 270-MHz NMR spectra of native BPTI (*a*) and BPTI refolded (*b*) as described in Fig. 1 legend. Spectrum *c* is a difference spectrum in which a fraction of *a* was subtracted from *b* to reveal the spectrum of isomeric BPTI. Peaks 1, 2 and 3 are from the peptide NH protons of Tyr 23, Tyr 21 and Gln 31, respectively[9].

0028–0836/80/320630—03$01.00

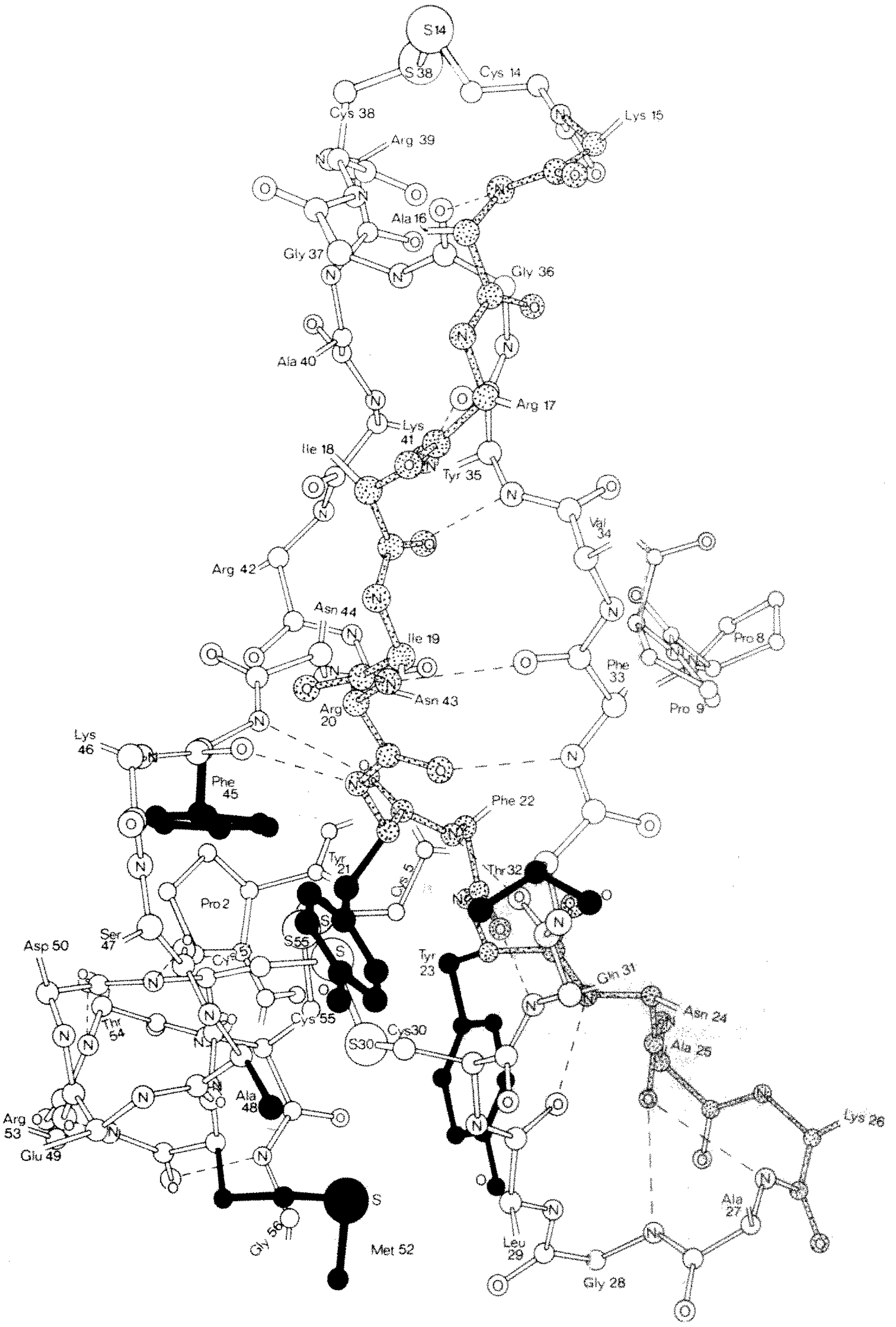

Fig. 3 Part of the crystal structure[12] of native BPTI showing the region of the protein where conformational differences exist in the metastable form. Side chains of residues whose resonances have been observed to have the largest chemical shift differences between the native and isomeric BPTI are shown in dark shading. The lightly stippled backbone is that portion which is threaded through the loop generated by the 30–51 disulphide bond.

of the isomer and an increase in the intensity of the resonances of the native protein. By following the intensities of resonances of the two species, the conversion of the isomer to the native species was found to proceed at a rate of $(3.5\pm0.7)\times10^{-5}\,s^{-1}$ at 37 °C and *p*H 6.0. Measurement of the temperature dependence of the rate gave an activation energy of 55 ± 10 kcal mol^{-1}.

It is clear from these data that the refolding of BPTI results in a significant and sometimes dominant amount of a metastable species with a different NMR spectrum, and therefore a different conformation, from native BPTI. That the conversion of the metastable species to the native species takes place in conditions in which rearrangement of disulphide bonds cannot occur shows that the same disulphide bonds are present as in the native species, as had also been shown by peptide analysis[4]. Comparison of the two NMR spectra shows further that the basic structural arrangement of the native BPTI is not lost in the new species. Of particular importance is a comparison of the proton resonances of the aromatic and methyl groups, which have all been assigned in the spectrum of native BPTI[5–7]. Most of these resonances have the same positions (to ±0.02 p.p.m.) in the two spectra, indicating that much of the protein conformation is essentially the same in the two species. Significant differences (shifts up to ±0.1 p.p.m.) are found for the resonances of Tyr 21, Tyr 23 and Phe 45 in the aromatic region and of Thr 32, Ala 48 and Met 52 in the methyl region. Further information comes from the resonances of the peptide NH hydrogens which exchange slowly with solvent. In the spectrum of isomeric BPTI there are resonances within 0.05 p.p.m. of resonances in the spectrum of native BPTI for 7 out of the 10 protons whose exchange rates[9,11] are less than $10^{-3}\,min^{-1}$ at 22 °C and *p*H 6.5. Three peaks, assigned to Tyr 21, Tyr 23 and Gln 31, have chemical shift values which differ in the two spectra by more than 0.1 p.p.m. (Fig. 2). The distinctive chemical shifts and long exchange rates of these protons have been attributed to their role in internal hydrogen bonding[10,11]; most of the resonances arise from the β-sheet secondary structure, which passes through the entire molecule (see Fig. 3). The conservation in number and near conservation of chemical shifts of these NH resonances in the two spectra indicate, therefore, that the hydrogen bonding network of native BPTI is intact in the isomeric species. In particular, it has been established[12] in native BPTI that the polypeptide chain passes through a loop produced by the existence of the 30–51 disulphide bond (Fig. 3), and the NMR data exclude the possibility that the protein chain is incorrectly 'threaded' in the isomer.

All the residues whose resonances are perturbed are rather close together, in the portion of the molecule (native structure) surrounding the 30–51 and 5–55 disulphide bonds, which are near to each other (Fig. 3). The major conformational differences between native and metastable BPTI therefore lie in this part of the structure.

It is useful to compare this conclusion with the results[5] from studies of a derivative of BPTI with one of the disulphide bonds, 14–38, reduced. The spectrum of this species is shown in Fig. 1*c*. There are no large shifts in any of the resonances and those with small shifts arise from residues in the part of the molecule near to the broken 14–38 bond, notably Thr 11 and Tyr 35. There are negligible shifts in the resonances perturbed in the isomeric BPTI, indicating that the conformations of the isomeric BPTI and the 14–38 reduced species are altered in different regions of the structure.

The simplest explanation for the existence of the isomer would be that it is a normal intermediate in the final step of the refolding process; that is, when the last disulphide bond (14–38) is formed, the isomeric conformation is produced which then goes on to generate slowly the native conformation. This possibility is unlikely because a significant proportion of BPTI in the native conformation is formed when refolding (which takes only minutes) is carried out at temperatures so low (<25 °C) that the metastable isomeric species converts to the native species only over a period of days. Thus, it is more likely that the two forms of folded BPTI arise from alternative parallel pathways. Further, it has been found that re-oxidation of the 14–38 reduced species results in BPTI with a spectrum identical to that of the native species, so that it is unlikely that the conformational differences between the isomers arise in the formation of the 14–38 bond.

To investigate possible origins of the alternative pathway in earlier parts of the refolding reaction, the one- and two-disulphide bond intermediates have been examined. The conformations of these, other than the one with only the 14–38 bond in the reduced state, are significantly different from that of native BPTI, with a much less well defined globular structure, particularly in the one-disulphide species. This is in essential agreement with conclusions from immunochemical analysis of these intermediates[13]. It seems possible, therefore, that the conformational isomer arises from the same disulphide bond formation sequence as native BPTI but has a difference in structure which arises because of the stability of this difference in an early intermediate. This could be due to the existence of a *cis* rather than the *trans* conformer found for all four proline residues in native BPTI (Pro 2 is close to the region of the observed structural changes)[14,15], a different conformation around the 30–51 or 5–55 disulphide bond, or some other difference in a main-chain or side-chain dihedral angle. The formation of the 14–38 bond, or some earlier step, could then 'lock in' the conformational difference. Alternatively, the two different folded species could result from pathways in which the sequences of disulphide bond formation are different. For example, in the initial stages of folding several pathways are known to exist and to result in the formation of different two-disulphide species, which then rearrange to the 30–51, 5–55 species before complete refolding. It is interesting in view of the results reported here that the relative stabilities of different two-disulphide species have been found to be temperature dependent (T.E.C., unpublished results).

The present results are of significance for an understanding of the mechanism of protein folding and for the analysis of the determinants of protein conformation. Of primary interest is the demonstration that two similar globular structures can exist; even in a protein as small as BPTI a specific structure can be formed during folding that is not at the free energy minimum[16,17]. Further, the activation energy for the transition from the metastable to the native species is high; it is of the order of the highest activation energies measured for exchange of the backbone amide hydrogens of native BPTI[10]. This suggests that, although the conformational difference between the two species is localized, the transition involves a significant disruption of the structure. If the specific element that distinguishes the two structures is a dihedral angle rotation, conformational constraints would have to be the source of the high activation energy. This is analogous to the tyrosine and phenylalanine ring 'flips' for which the observed activation energies of up to 25 kcal mol^{-1} are much larger than the internal rotation barrier[7,18].

It will be of considerable interest to use the existence of this conformational isomer to elucidate the structural and dynamic aspects of folding transitions in proteins.

We thank Bayer AG for a gift of BPTI (Trasylol). The NMR experiments were carried out at the NMR Facility for Biomolecular Research, Francis Bitter National Magnet Laboratory, Massachusetts Institute of Technology. The NMR Facility is supported by grant RR0995 from the Division of Research Resources of the NIH, and by the NSF under contract C-670. This work is also supported in part by grants GM26272 and EY00062 from the NIH.

Received 18 February; accepted 5 June 1980.

1. Creighton, T. E. *Prog. Biophys. molec. Biol.* **33,** 231–298 (1978).
2. Kosen P. thesis, Harvard Univ. (1978).
3. Creighton, T. E. *J. molec. Biol.* **113,** 275–293 (1977).
4. Creighton, T. E. *J. molec. Biol.* **87,** 563–577 (1974).
5. Snyder, G. H., Rowan, R., Karplus, S. & Sykes, B. D. *Biochemistry* **14,** 3765–3777 (1976).
6. Wüthrich, K., Wagner, G., Richarz, R. & Perkins, S. J. *Biochemistry* **17,** 2253–2263 (1978).
7. Wagner, G., De Marco, A. & Wüthrich, K. *Biophys. Struct. Mechanism* **2,** 139–158 (1976).
8. Marinetti, T. D., Snyder, G. H. & Sykes, B. D. *Biochemistry* **15,** 4600–4608 (1976).
9. Wüthrich, K. & Wagner, G. *J. molec. Biol.* **130,** 1–18 (1979).
10. Hilton, B. D. & Woodward, C. K. *Biochemistry* **17,** 3325–3332 (1978).
11. Richarz, R., Sehr, P., Wagner, G. & Wüthrich, K. *J. molec. Biol.* **130,** 19–30 (1979).
12. Deisenhofer, J. & Steigemann, W. *Acta crystallogr.* **B31,** 238–250 (1975).
13. Creighton, T. E., Kalef, E. & Arnon, R. *J. molec. Biol.* **123,** 129–147 (1978).
14. Brandts, J. F., Halvorson, H. R. & Brennan, M. *Biochemistry* **14,** 4953–4963 (1975).
15. Cook, K. H., Schmid, F. X. & Baldwin, R. L. *Proc. natn. Acad. Sci. U.S.A.* **76,** 6157–6161 (1979).
16. Goldberg, M. in *Dynamic Aspects of Conformation Changes in Biological Macromolecules* (ed. Sadron, C.) 57 (Reidel, Dortrecht, 1973).
17. Anfinsen, C. B. *Science* **181,** 223–230 (1973).
18. Gelin, B. R. & Karplus, M. *Proc. natn. Acad. Sci. U.S.A.* **72,** 2002–2006 (1975).
19. Campbell, I. D., Dobson, C. M., Williams, R. J. P. & Xavier, A. V. *J. magn. Res.* **11,** 172–181 (1973).

A diffusion–collision–adhesion model for the kinetics of myoglobin refolding

F. E. Cohen*, M. J. E. Sternberg & D. C. Phillips

Laboratory of Molecular Biophysics, Department of Zoology,
South Parks Road, Oxford OX1 3PS, UK

I. D. Kuntz & P. A. Kollman

Department of Pharmaceutical Chemistry, School of Pharmacy,
University of California, San Francisco, California 94143

There are two distinct experimental and theoretical problems of protein folding: the thermodynamic issue of characterizing the folded state, and the kinetic question of the path between the unfolded and native states[1]. Here we consider the second question and present a diffusion–collision–adhesion model for the folding of the α-helical protein myoglobin. In particular, we consider the fast refolding species of the unfolded state and ignore the slow transition between unfolded states that has been attributed to proline isomerization[2].

---

* Present address: Department of Pharmaceutical Chemistry, School of Pharmacy, University of California, San Francisco, California.

Baldwin[3] and Karplus and Weaver[4,5] have considered the experimental and theoretical evidence as to the probable rate-limiting step during (fast) folding. They agree that the formation of a local structure by a random search is unlikely to act as a nucleus for subsequent rapid folding. Instead, they opt for intermediate control in which the relative stabilities of the intermediates determine the pathway(s) and the rate of folding. Local structures (for example, α-helices) of transient stability diffuse together, collide and then adhere (pair) together. There is no requirement for an obligatory intermediate and folding may proceed along several paths. The intermediates for myoglobin are assemblies of α-helices as suggested by Ptitsyn and Rashin[6].

Rate constants for the steps are derived from the model of Karplus and Weaver[4,5]: collision, not adhesion, is the rate-limiting step. Detailed stereochemical information about helix packing in myoglobin is taken from the work of Richards and co-workers[7,8]. The folding follows intermediate control, shows the cooperative behaviour that has been observed experimentally[9,10], and we find several paths linking the unfolded and native states. A second calculation considers N-terminal folding that may occur during biosynthesis[11,12]. In our model, apomyoglobin is considered as six fluctuating α-helices (ABEFGH). Initially, pairs of α-helices collide to form a cluster. Each cluster can grow by docking either with one other α-helix or with another cluster that contains two or more α-helices. We allow only the five strongest helix/helix interactions (AH, BE, BG, GH, FH)[7] that are observed in the folded myoglobin. This implies that the interactions that are dominant in the final structure are important in the folding pathway and that incorrect helix pairings do not significantly interfere with the rate of formation of native intermediates.

In the model of Karplus and Weaver[4,5], the time required for the interaction of two helices is

$$\tau = \frac{1}{\beta}\left(\frac{l\Delta V}{DA}\right) \tag{1}$$

where l is the characteristic length, ΔV is the volume of finite diffusion space, D is a diffusion coefficient ($\sim 1\times10^{10}$ Å^2 s^{-1}), A is the area of the target surface and β is the fraction of time that both segments are helical when they collide.

To calculate rate constants for the condensation of two helices, we assume that ΔV is the space between two concentric spheres. The outer radius is determined by

$$r_{ij}^{\mathrm{ext}} = 1.5H + 3.3C \tag{2}$$

where i and j are the residues central to the helix–helix interaction[7], and H and C are the number of residues between i and j in helical and coiled conformations, respectively. The inner radius, r_{ij}^{pack}, is taken as the length of the segment which is mutually perpendicular to the axes of the interacting helices[7,8].

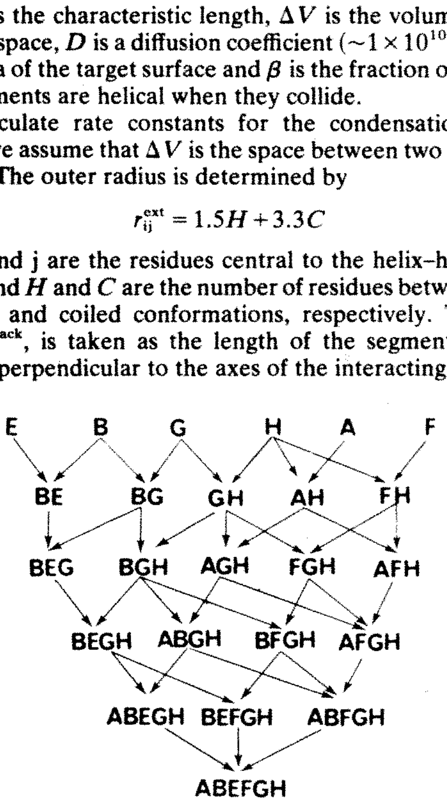

Fig. 1 Possible folding paths for myoglobin. Only the addition of single helices to preformed clusters is depicted. Condensations between preformed clusters, for example, BE + GH → BEGH, are omitted for the sake of clarity.

Table 1 Parameters for the diffusion–collision equation

Interaction	Average potential contact area loss on association* $A = (A_i + A_j)/2$(Å^2)	r_{ij}^{pack} (Å)	r_{uj}^{ext} (Å)
G111-H135	185	10.5	25.05 (17.55‡, 19.05§, 17.55‖)
A10-H134	170	8.5	189.3 (95.3†, 26.0§, 118.2‖, 142.05¶, 15.2§¶)
B25-E65	145	7.5	50.70 (43.20§, 24.00§‖¶)
F90-H142	125	8.5	66.90 (54.15‡, 12.90¶)
B28-G110	155	8.5	120.00 (45.45†, 112.50¶, 12.9‡¶ 89.40‖¶)

* From Richmond and Richards[7].

‡ AH formed; † BE formed; § BG formed; ‖ FH formed; ¶ GH formed.

If the target area for the interaction is the average of the potential accessible areas lost when the two helices pack (A_i and A_j)[7], then equation (1) becomes

$$\tau = \frac{\frac{1}{2}(r_{ij}^{\mathrm{ext}} + r_{ij}^{\mathrm{pack}}) \times \frac{4}{3}\pi((r_{ij}^{\mathrm{ext}})^3 - (r_{ij}^{\mathrm{pack}})^3)}{\beta 10^{10} \frac{1}{2}(A_i + A_j)} \tag{3}$$

Clearly, r_{ij}^{ext} is a function of the degree and nature of the condensation of the molecule. For example, the volume of diffusion space available for the FH interaction is decreased if GH has been formed (see Table 1).

In our model, α-helices that have correctly paired do not dissociate. Clearly, proteins denature and so a helix–helix pair can dissociate. However, in conditions where the folded structure is stable, dissociation will be slower than association. If the stability of the native structure is indicative of the stability of various intermediates, dissociation is probably negligible. Moreover, the rate of dissociation is a complex function of the solvent and temperature that remains undefined.

The only adjustable constant in this anlysis is ρ, the probability that a potential helical segment will be helical when it interacts. For a pair of fluctuating helices, $\beta = \rho^2$; for one fluctuating helix packing against a solid cluster, $\beta = \rho$; and for two solid clusters packing, $\beta = 1$. In the two simulations that follow, $\rho = 0.002$. Smaller values of ρ decrease the cooperativity of the folding transition and larger values decrease the lag time for renaturation. Changes in ρ had little effect on which intermediates were observed, although the half lives of these species were affected.

In our model of myoglobin, there are 24 states (see Fig. 1). There exists a matrix of 24 × 24 second order rate constants which define a system of simultaneous second order differential equations. As a closed form solution to this problem does not exist in general, the rate equations are solved iteratively with time steps of 25 μs. Figure 2*a* shows the exponential behaviour of the concentration of the final state. The concentration begins to level off after 2 ms and slowly goes to completion. Two intermediate states are significantly (>5%) populated: FGH and ABFGH. The lag phase, although noticeable, is small. This is undoubtedly because the initial steps in this simulation overwhelmingly favour products. In the refolding of ribonuclease A in 50% methanol at temperatures less than −20 °C, a lag in the absorbance change due to the burial of tyrosine residues is observed. The lag lasts approximately 100 s at *p*H 6.0, −25 °C (A. L. Fink and B. Lustig, personal communication).

In an attempt to simulate biosynthesis, the initial concentrations of the isolated helices were repeated. Thus, the concentration of H was 0.0 until the concentration of G reached 1.0. The rate of synthesis was such that a myoglobin chain was made in 1.2 s. BE is the first intermediate to appear, followed by the production of BEG, BEGH and then the native state (see Fig. 2*b*).

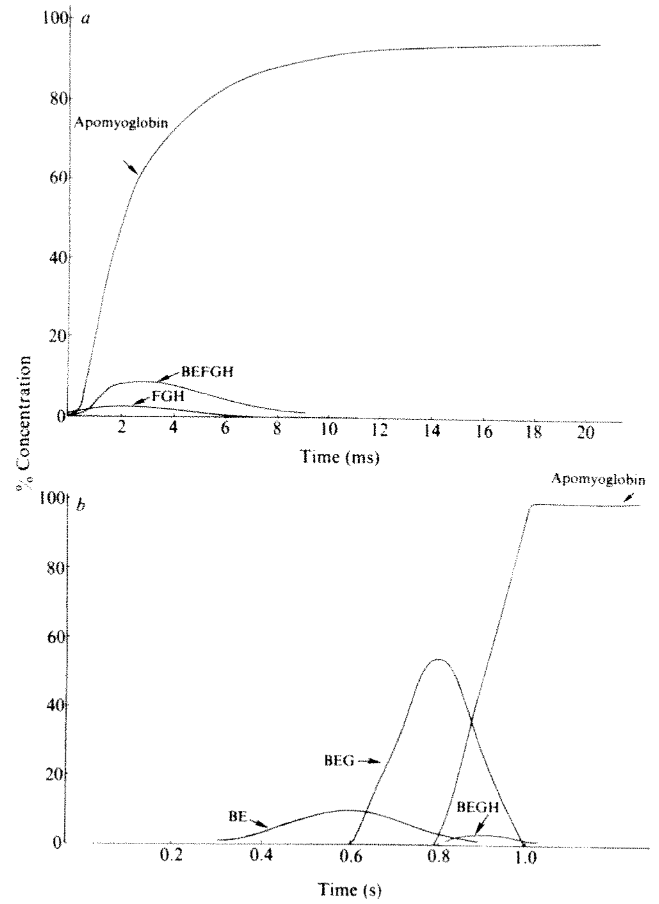

Fig. 2 *a*, Simulated renaturation kinetics of apomyoglobin as a function of time. The concentrations of intermediates which are significant are also plotted. *b*, Simulated folding kinetics of apomyoglobin during biosynthesis. The time taken to synthesize a helical segment is 0.2 s.

In these two simulations, two distinct sets of intermediates were significantly populated. Thus, we suggest that folding can occur through many alternative pathways which ultimately converge to the native structure. Cooperativity results from the decrease in the volume of diffusion space as a function of molecular organization. In principle, the intermediates of renaturation could be trapped and identified in a stop-flow experiment. Alternatively, the sites of helix–helix interaction could be chemically blocked to inhibit the completion of the folding and the intermediates created could then be characterized. Studies by Zabin and co-workers suggest that intermediates in biosynthesis could be characterized by immunological probes[12].

This model assumes that no mismatched pairs of hydrophobic patches on the surface of the α-helices are stabilized. A more realistic assumption would be that mismatched helix–helix pairs could tautomerize to a correct pairing. These tautomerizations would have low activation barriers, as the individual helical conformations have been stabilized and the volume of diffusion space is reduced. This tautomerization mechanism might explain Creighton's finding[1] that there is an obligatory mismatched disulphide bridge on the pathway joining the unfolded and native states of pancreatic trypsin inhibitor.

Received 14 March; accepted 9 June 1980.

1. Creighton, T. E. *Prog. Biophys. molec. Biol.* **33,** 231–297 (1978).
2. Brandts, J. F., Halvorson, H. R. & Brennan, M. *Biochemistry* **14,** 4953–4963 (1975).
3. Baldwin, R. L. *Protein Folding* (ed. Jaenicke, R.) (Elsevier, Amsterdam, 1980).
4. Karplus, M. & Weaver, D. L. *Nature* **260,** 404–406 (1976).
5. Karplus, M. & Weaver, D. L. *Biopolymers* **18,** 1421–1437 (1979).
6. Ptitsyn, O. B. & Rashin, A. A. *Biophys. Chem.* **3,** 1–20 (1975).
7. Richmond, T. J. & Richards, F. M. *J. molec. Biol.* **119,** 537–555 (1978).
8. Cohen, F. E., Richmond, T. J. & Richards, F. M. *J. molec. Biol.* **132,** 275–288 (1979).
9. Shen, L. L. & Hermans, J. *Biochemistry* **11,** 1836–1841 (1972).
10. Shen, L. L. & Hermans, J. *Biochemistry* **11,** 1845–1849 (1972).
11. Phillips, D. C. *Proc. natn. Acad. Sci. U.S.A.* **57,** 484–495 (1967).
12. Hamlin, J. & Zabin, I. *Proc. natn. Acad. Sci. U.S.A.* **69,** 412–416 (1972).

Rescue of a splicing defective mutant by insertion of an heterologous intron

Peter Gruss & George Khoury

Laboratory of Molecular Virology, National Cancer Institute,
National Institutes of Health, Bethesda, Maryland 20205

It is now widely accepted that the primary transcripts of many eukaryotic genes contain intervening sequences (introns)[1-3]. These introns, which vary considerably in length, have been found in both coding and noncoding regions[4-15]. They are removed from the primary transcript in one or more steps by a process called RNA splicing[16]. The role of RNA splicing, the size and position of introns and the signals which modulate the splicing process are under intense investigation. These studies have been greatly facilitated by the use of viral mutants or viral–eukaryotic recombinant molecules. The SV40 system has been of particular value in elucidating certain genetic elements which are critically involved in the splicing process[17-21]. Further insight into the biological significance of the splicing process has come from a mutant from which precisely one intron has been removed (intron-minus mutant, d1-2350). This deletion mutant has the potential to circumvent the need for splicing. However, the inability of d1-2350 to accumulate late viral transcripts indicates that splicing is a requirement for the biogenesis of stable mRNA[22]. This finding is supported by studies using the mouse β^{maj} globin gene inserted into SV40. The inserted portions contained either the complete globin gene[23] or a segment encompassing the intron plus the entire 3′ end of the gene[24]. As polyadenylation is known to precede splicing[2,3], the possibility exists that every transcript possesses sequences near the 3′ end that are directly involved in the splicing process. We report here that, to test this possibility as well as to pursue the question of whether the splicing event and/or defined sequences in the intron are required for the biogenesis of mRNAs, we inserted an isolated intron lacking its own genomic 5′ and 3′ ends into the intron-minus mutant previously described. The experimental protocol provided for obtaining both possible orientations of the insert relative to the late genomic region. Investigation of the transcriptional products indicated that stable mRNA was produced only by the mutant containing the intron in the sense orientation.

There are, however, a few reported examples of abundant unspliced cytoplasmic mRNA. These include the histone mRNAs[38] (which also differ from most other eukaryotic transcripts in having an abbreviated or absent 3′-polyadenylation signal) and the messenger for adenovirus polypeptide IX[39]. Whether these examples are fundamentally different from the majority of eukaryotic genes studied thus far, or if there is a special category of unspliced stable transcripts remains to be determined.

The *in vitro* construction of the recombinants is outlined in Fig. 1. An *Eco*RI fragment containing the entire chromosomal portion of the mouse β^{maj} globin gene[15,25] was cloned at the *Eco*RI site in pBR322. This DNA was cleaved with *Hin*dII and a fragment 573 nucleotides long was isolated by gel electrophoresis. This fragment represents the small intron (intron *1*) of mouse β^{maj} globin chromosomal DNA plus some flanking sequences, but lacks the 5′- and 3′-terminal sequences of the β^{maj} globin gene. An enzyme which conveniently cuts at a single site present in the late region of the intron-minus mutant (d1-2350) is *Hpa*II. This recipient site is located in the leader region of d1-2350, 221 nucleotides upstream from the donor splice junction[22,26], for the SV40 16S mRNA. The cleavage of d1-2350 DNA with *Hpa*II thus results in a linearized DNA containing 'sticky' *Hpa*II ends. To obtain efficient ligation of the globin intron fragment harbouring 'blunt' *Hin*dII termini to the linearized DNA, the *Hin*dII ends were converted to *Hpa*II ends by the addition of synthetic oligonucleotides (linkers)[27]. Liga-

0028-0836/80/320634—04$01.00

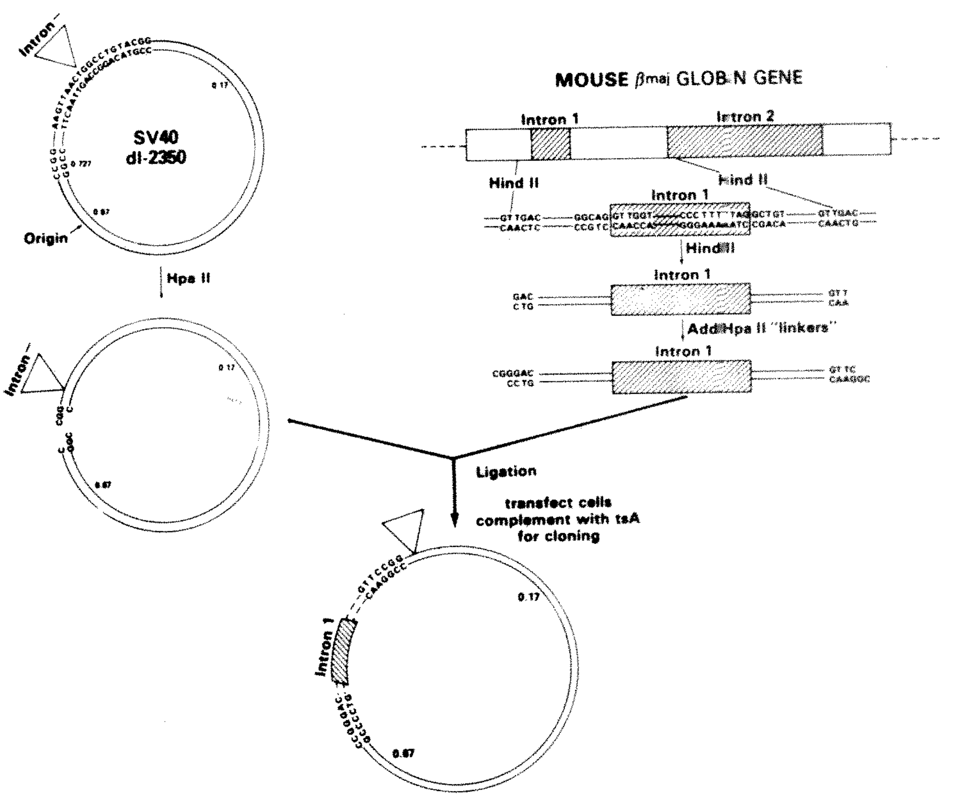

Fig. 1 Insertion of mouse $\beta^{\rm maj}$ globin intron *1* into SV40 d1-2350. Plasmid DNA (pBR322) containing the active mouse $\beta^{\rm maj}$ globin gene[15,25] insert was cleaved with *Hin*dII and a fragment of 573 nucleotides representing the entire intron *1* plus some flanking sequences was purified. This DNA (10 μg) was blunt-end ligated to 2.5 μg of *Hpa*II decamer linkers (CCGGATCCGG from Collaborative Research) in conditions exactly as described by Maniatis *et al.*[27]. The DNA containing *Hpa*II linkers was purified away from unligated linkers by gel electrophoresis and subsequently cleaved with *Hpa*II. A second electrophoresis step was used to purify the DNA containing sticky *Hpa*II ends. In parallel, SV40 d1-2350 DNA (4.5 μg) was reacted with *Hpa*II, extracted with phenol and dialysed. The globin fragment containing *Hpa*II ends (1.2 μg) was ligated to d1-2350 DNA (4.5 μg) in a total volume of 100 μl in a buffer (50 mM Tris-HCl *p*H 7.8, 10 mM $MgCl_2$, 20 mM dithiothreitol, 60 μM ATP) using 2 units T4 DNA ligase (Biolabs). The reaction mix was incubated for 1 h at 15 °C, then further reacted for 16 h at 4 °C. The ligated recombinants were separated from unligated material by agarose gel electrophoresis. Purified recombinant DNA was used in an infectious centre assay[40] and complemented with SV40 tsA. Many plaques were picked and used to grow viral stocks in secondary African green monkey kidney cells[40].

tion was subsequently carried out using a twofold molar excess of globin DNA over the d1-2350 recipient DNA. As *Hpa*II termini were present on every end, the insertion of the globin intron can occur in both possible orientations relative to the late transcription unit. The ligated DNA products were transfected into secondary AGMK cells using the facilitating agent DEAE-dextran[28,29]. We used tsA, a helper virus defective in early gene function at non-permissive temperature (40 °C)[30], to complement the ligated DNA product by providing the missing gene functions for the late viral structural proteins VP2, VP3 and VP1. The decision to use tsA rather than tsB (which is temperature sensitive for VP1) was based on three critical points: (1) As tsA provides an intact late region, it non-selectively complements all mutants defective in late function(s). The tsA mutant should be capable of complementing our ligated recombinant molecules, even if no stable mRNA or protein is produced after insertion of an intact intron. (2) Regardless of the orientation of the inserted globin intron relative to the late transcription unit, tsA should complement the recombinant molecule. (3) The chromosomal $\beta^{\rm maj}$ globin DNA fragment providing the intron also contains some flanking sequences from the globin gene. Close inspection of these sequences[24] reveals the presence of six ATG triplets. Should these triplets serve at the RNA level as translation initiation codons, they would produce proteins which differ from VP1, and would not complement tsB.

With the help of tsA, many clones were obtained and screened for the presence of globin DNA sequences (see Fig. 2). A plasmid carrying the entire mouse $\beta^{\rm maj}$ globin gene was cleaved with *Sac*I and the two resulting fragments were separated on an agarose gel and subsequently transferred to nitrocellulose filter paper[31]. The filter was cut into small (3 mm) strips and hybridized to ^{32}P-labelled DNA from cloned recombinants. As an example (Fig. 2*a*, *c*, *d*), three mutant clones hybridize exclusively to the small (1.15 kilobase) fragment representing intron *1* and the 5′ region of the $\beta^{\rm maj}$ globin gene. One cloned mutant (Fig. 2*b*) seems not to contain a globin-specific insert.

The entire DNA sequence of SV40[32,33] and mouse $\beta^{\rm maj}$ globin is known. Thus, our physical characterization of cloned recombinant DNA could be limited to a few restriction endonucleases so as to determine the orientation of the insert. A combination of cleavage by *endo R Ava*II and *endo R Bam*HI, and subsequent size determinations of the fragments by polyacrylamide gel electrophoresis, allows an identification of the orientation of the inserted globin intron relative to the late transcription unit (data not shown). Two classes of recombinants were obtained and are schematically outlined in Fig. 3. In the case of the recombinant d1-2350-I, the globin intron is inserted in the sense direction, whereas in d1-2350-II the intron is orientated in the antisense direction.

The structure of the recombinant molecules suggests that even after the removal of the intron by a potential splicing reaction, a stable transcript should retain a total of 456 nucleotides (intron flanking sequences) derived from the mouse $\beta^{\rm maj}$ globin gene. Thus, an mRNA from the recombinant template is expected to increase in size by this amount relative to 16S mRNA transcribed from the tsA helper template. Should unspliced recombinant mRNA be present, the size increase would be 456 + 116 = 572 nucleotides. To identify such a hybrid mRNA and to distinguish between spliced and unspliced transcripts, cytoplasmic polyadenylated RNA was prepared from AGMK cells infected with the recombinants containing the

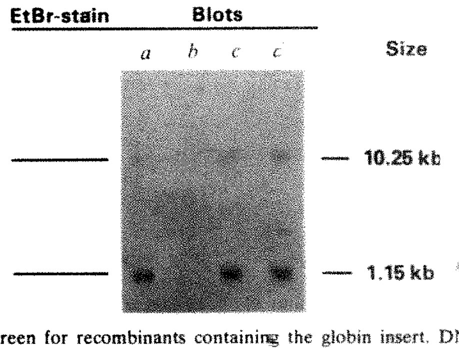

Fig. 2 Screen for recombinants containing the globin insert. DNA was prepared from a plasmid containing the entire mouse $\beta^{\rm maj}$ globin gene. This DNA was cleaved with *Sac*I, an enzyme generating two fragments. The smaller fragment (1.15 kilobases (kb)) represents the 5′-end portion (including intron *1*) of the gene, the larger fragment (10.25 kilobases) contains the sequences of the 3′ end. This cleaved DNA (20 μg) was electrophoresed into an 1.4% agarose gel (in 0.04 M Tris *p*H 7.8, 0.005 M sodium acetate, 0.001 M EDTA) and subsequently blotted on to a nitrocellulose filter paper[31]. The filter paper was cut into strips 3 mm wide. Each strip was hybridized to a ^{32}P-labelled DNA preparation obtained from cells infected with the different mutant stocks[35]. Mutants *a*, *c* and *d* contain the globin-specific insert, whereas mutant *b* does not have any detectable globin-specific sequences. EtBr, Ethidium bromide.

intron in either the sense or the antisense direction. Aliquots of both RNA preparations were electrophoresed in duplicate through an agarose gel containing methyl mercury hydroxide and subsequently transferred to diazotized benzyloxymethyl (DBM) paper[34]. One track of each preparation was hybridized to ^{32}P-labelled SV40 DNA; the second track was hybridized to ^{32}P-labelled mouse β^{maj} globin DNA. Figure 4 presents the results. In the right-hand panel of the gel, RNA from the two recombinants (d1-2350-I and d1-2350-II) was hybridized to ^{32}P-labelled SV40 DNA. In both tracks two bands appear in similar positions. These positions are identical to those for the 16S and 19S mRNAs of the SV40 control (not shown). Thus, these classes apparently represent RNA derived from the tsA helper genome. In the track containing RNA from the recombinant which has the globin intron in the sense direction, an additional band (2,050 nucleotides) appears. This class of mRNA is 450 nucleotides larger than 16S mRNA. In addition to SV40 homologous sequences, this class of RNA alone also has sequences which are homologous to mouse β^{maj} globin DNA (Fig. 4, left panel). These observations indicate that the insertion of an intron in the sense direction is sufficient for activation of a late spliced SV40-containing mRNA. It seems that mouse β^{maj} globin intron *1* and its flanking nucleotides are functional as a splice signal in heterologous genes even in the absence of its original 5′- and 3′-genomic end.

Split genes, containing introns which are not represented in their terminally processed RNA, are unique to eukaryotes. The precise removal of the intron takes place at the RNA level[1–3]. It has been suggested that the splicing mechanism is required not only for the removal of the intron but also for stabilization of the RNA[17,18,22,23]. In the present study we have examined directly the role of an isolated globin gene intron and its flanking nucleotides inserted into a previously constructed SV40 mutant lacking precisely the intervening sequence of 16S mRNA (intron-minus mutant d1-2350)[22]. A principal experimental difference between this study and previous reports[23] is the rescue of stable SV40 RNA from the splicing defective mutant d1-2350 by insertion of an intron derived from a heterologous gene. As an intron source we selected a restriction enzyme fragment from the mouse β^{maj} globin gene[15,25], representing the entire intron *1* plus some flanking sequences. However, the 5′- and 3′-terminal sequences of the globin gene are not retained. Construction of the mutant involves insertion of globin gene intron *1* into the late region (0.72 map unit) of d1-2350. The site of insertion is 221 nucleotides upstream from the original splice junction for 16S mRNA. Thus, the location of the inserted intron differs from the original position of the intron for 16S RNA. Although the experimental protocol for the insertion allowed ligation in both possible orientations relative to the late transcription unit, only the presence of an intron in the sense direction rescued stable mRNA. This confirms the earlier observation by Hamer and Leder that the polarity of a genomic fragment consisting of the 3′ end and large β^{maj} globin intron, relative to the SV40 transcription unit, was critical to the splicing of the hybrid mRNAs[23]. A correctly orientated intron can be removed in a splicing process, as indicated by the size of the resultant chimaeric RNA. It should be emphasized, however, that some mouse flanking sequences for globin intron *1* are preserved in these recombinant molecules and may be required for efficient splicing. Recent studies have suggested that small nuclear RNA (snRNA) molecules may serve as a 'guide' or strut in aligning pre-mRNA sites for splicing[35,36].

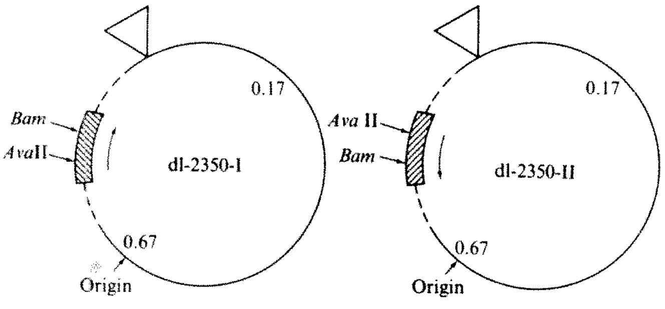

Fig. 3 Physical map of the recombinant DNA. For the establishment of a physical map, we concentrated on a determination of the orientation of the insert relative to the late transcription unit. A combination of *Ava*II and *Bam*HI endonucleases enabled us to determine the orientation by sizing the fragments. Both possible classes of recombinant give rise to six specific fragments, using these particular enzymes. Four out of those six fragments were expected to be identical (1,580, 1,006, 519 and 185 base pairs). The size of the remaining two fragments in the case of d1-2350-I (sense direction) was 867 and 710 base pairs, whereas the insert in the antisense direction (d1-2350-II) yielded two fragments of 987 and 590 base pairs. The analysis was carried out using 4% polyacrylamide gels (acrylamide = bis, 20 : 1) for electrophoresis in a 0.04 M Tris *p*H 7.8, 0.02 M sodium acetate, 0.001 M EDTA buffer.

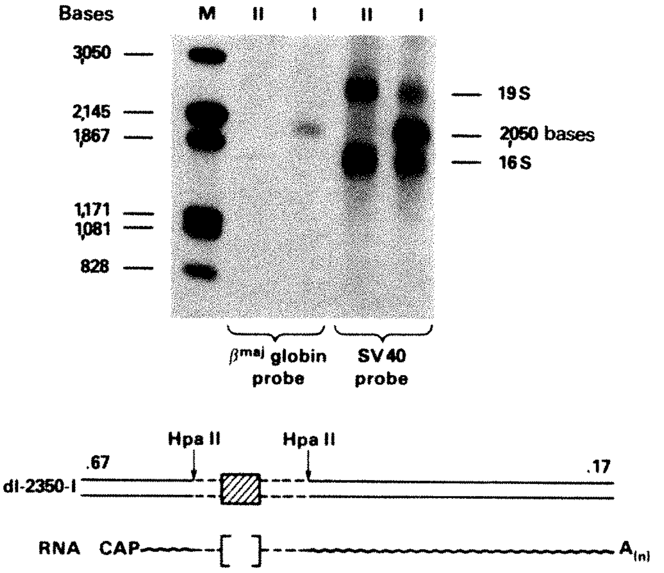

Fig. 4 RNA analysis. Cytoplasmic RNA from the recombinants was prepared 48 h after infection of secondary AGMK cells with 10 plaque-forming units per cell. Cells were treated with 0.5% NP40, 0.14 M NaCl, 0.01 M Tris *p*H 7.5 and 0.0015 M $MgCl_2$ (ref. 41). Poly(A)-containing RNA was selected by chromatography on an oligo(dT)–cellulose column. Aliquots of the RNA preparations from d1-2350-I (sense insert) and d1-2350-II (antisense insert) were electrophoresed in a 1.2% agarose gel containing methyl mercury hydroxide. Electrophoresis and subsequent transfer of the RNA to DBM paper were as described by Alwine *et al.*[34]. The resulting imprints were preincubated and hybridized with 200,000 c.p.m. of either a ^{32}P-labelled SV40 DNA or a ^{32}P-labelled plasmid DNA containing the entire mouse β^{maj} globin gene. Both probes were made by nick translation and had a specific activity of 10^8 c.p.m. per μg DNA. As a size marker, ^{32}P-labelled restriction enzyme fragments of the indicated sizes were electrophoresed in a parallel track. The bottom portion of the figure outlines an interpretation of the data (the transcript deriving from the recombinant d1-2350-I, sense insert).

The globin sequences flanking the inserted intron contain six ATG triplets, which are potential candidates for translational initiation in each reading frame. All precede the actual AUG triplet for initiation of VP1 translation. Attempts to clone these recombinant molecules using tsB in parallel experiments did not result in any plaques containing the recombinants. This observation confirms the data of others[37] suggesting that the first available AUG is in most cases preferentially used as the initiation signal for translation. Therefore, VP1 cannot be produced in amounts sufficient to complement SV40-tsB.

The flanking sequences which are preserved do not contain either the 5′ or 3′ end of the globin gene. Thus, it seems unlikely that either end specific to a particular mRNA is directly involved in splicing. Furthermore, the lack of obvious homology between SV40 and globin 5′ or 3′ ends suggests that no similar sequence is likely to be provided by SV40. The comparison of SV40 late introns with globin intron *1* did not show extensive homology, with the exception of consensus sequences at the splice junctions. Nevertheless, the insertion of the globin intron resulted in the reconstitution of stable RNA. This experimental result provides strong support for the idea that the splicing event is coupled to the stability of the RNA. Accordingly, defined intron sequences seem less likely to be involved in a positive transcriptional regulation event. Thus, while the polarity of the intron is critical to its function, the species of origin and the relative position in the mRNA are not. These observations suggest that introns represent functional elements in the generation of certain stable mRNAs.

We thank P. Leder for providing the cloned mouse β^{mai} globin gene, M. König and J. Duvall for technical assistance, and C.-J. Lai, J. Alwine, R. Dhar, S. Segal and B. Dunn for helpful discussions. P. G. is a recipient of a grant of Deutsche Forschungsgemeinschaft.

Received 3 April; accepted 16 May 1980.

1. Tilghman, S. M., Curtis, P. J., Tiemeier, D. C., Leder, P. & Weissmann, C. *Proc. natn. Acad. Sci U.S.A.* **75,** 1309–1313 (1978).
2. Lai, C.-J., Dhar, R. & Khoury, G. *Cell* **14,** 971–982 (1978).
3. Blanchard, J. M., Weber, J., Jelinek, W. & Darnell, J. E. *Proc. natn. Acad. Sci. U.S.A.* **75,** 5344–5348 (1978).
4. Lindenmaier, W. *et al. Proc. natn. Acad. Sci. U.S.A.* **76,** 6196–6200 (1979).
5. Cordell, B. *et al. Cell* **18,** 533–543 (1979).
6. Dugaiczyk, A. *et al. Proc. natn. Acad. Sci. U.S.A.* **76,** 2253–2257 (1979).
7. Lomedico, P. *et al. Cell* **18,** 545–558 (1979).
8. Busslinger, P., Portman, R. & Birnstiel, M. *Nucleic Acids Res.* **6,** 2997–3008 (1979).
9. Cochet, M. *et al. Nature* **282,** 567–574 (1979).
10. Van Ooyen, A., Vanden Berg, J., Mantei, N. & Weissmann, C. *Science* **206,** 337–344 (1979).
11. Gannon, F. *et al. Nature* **278,** 428–434 (1979).
12. Lai, E. C. *et al. Cell* **18,** 829–842 (1979).
13. Tiemeier, D. C. *et al. Cell* **14,** 237–245 (1978).
14. Leder, A. *et al. Proc. natn. Acad. Sci. U.S.A.* **75,** 6185–6191 (1978).
15. Tilghman, S. *et al. Proc. natn. Acad. Sci. U.S.A.* **74,** 4406–4410 (1977).
16. Berget, S. M., Moore, C. & Sharp, P. C. *Proc. natn. Acad. Sci. U.S.A.* **74,** 3171–3175 (1977).
17. Lai, C.-J. & Khoury, G. *Proc. natn. Acad. Sci. U.S.A.* **76,** 71–75 (1979).
18. Khoury, G., Gruss, P., Dhar, R. & Lai, C.-J. *Cell* **18,** 85–92 (1979).
19. Breathnach, R., Benoist, C., O'Hare, K., Gannon, F. & Chambon, D. *Proc. natn. Acad. Sci. U.S.A.* **75,** 4853–5847 (1978).
20. Seif, I., Khoury, G. & Dhar, R. *Nucleic Acids Res.* **6,** 3387–3398 (1979).
21. Benoist, C., O'Hare, K., Breathnach, R. & Chambon, P. *Nucleic Acids Res.* **8,** 127–142 (1980).
22. Gruss, P., Lai, C.-J., Dhar, R. & Khoury, G. *Proc. natn. Acad. Sci. U.S.A.* **76,** 4317–4321 (1979).
23. Hamer, D. H. & Leder, P. *Cell* **18,** 1299–1302 (1979).
24. Hamer, D. H. & Leder, P. *Nature* **281,** 35–40 (1979).
25. Konkel, D. A., Tilghman, S. M. & Leder, P. *Cell* **15,** 1125–1132 (1978).
26. Ghosh, P. K. *et al. J. biol. Chem.* **253,** 3643–3647 (1978).
27. Maniatis, T. *et al. Cell,* **15,** 687–701 (1978).
28. McCutchon, J. H. & Pagano, J. S. *J. natn. Cancer Inst.* **41,** 351–357 (1968).
29. Lai, C.-J. & Nathans, D. *Virology* **60,** 466–475 (1974).
30. Tegtmeyer, P. & Ozer, H. L. *J. Virol.* **8,** 516–524 (1971).
31. Southern, E. M. *J. molec. Biol.* **98,** 503–517 (1975).
32. Reddy, V. B. *et al. Science* **200,** 494–502 (1978).
33. Fiers, W. *et al. Nature* **273,** 113–120 (1978).
34. Alwine, J. C., Kemp, D. J. & Stark, G. R. *Proc. natn. Acad. Sci. U.S.A.* **74,** 5350–5354 (1977).
35. Murray, V. & Holliday, R. *FEBS Lett.* **106,** 5–7 (1979).
36. Lerner, M. R., Boyle, J. A., Mount, S. M., Wolin, S. L. & Steitz, J. A. *Nature* **283,** 220–224 (1980).
37. Kozak, M. *Cell,* **15,** 1109–1123 (1978).
38. Brockman, W. W. & Nathans, D. *Proc. natn. Acad. Sci. U.S.A.* **71,** 942–946 (1974).
39. Penman, S. *J. molec. Biol.* **17,** 117–130 (1966).
40. Schaffner, W., Kunz, Daetwyler, H., Telford, J., Smith, H. O. & Birnstiel, M. L. *Cell* **14,** 655–671 (1978).
41. Aleström, P., Akusjärvi, G., Perricaudet, M., Mathews, M. B., Klessign, D. F. & Pettersson, U. *Cell* **19,** 671–681 (1980).

Theoretical analysis of transitions between B- and Z-conformations in torsionally stressed DNA

Craig J. Benham

Department of Mathematics, University of Kentucky, Lexington, Kentucky 40506

Recently, a new structure called Z-DNA has been proposed for alternating poly(dG-dC)·poly(dG-dC) sequences based on crystallographic analysis of the hexanucleotide[1]. The Z-form is a left-handed double helix containing 12 base pairs per turn. In contrast, the Watson–Crick B-form helix is thought to have 10.4 pairs per turn of right-handed helix[2,3,8]. A cooperative, salt-induced conformational transition has been observed in poly(dG-dC)·poly(dG-dC)[4], which has been interpreted as being between the B-form (low salt) and the Z-form (high salt)[1]. We now analyse the possibility that such transitions could occur in susceptible sequences in physiological conditions as a consequence of the torsional stresses imposed by superhelicity. As *in vivo* DNA commonly occurs in a negatively supercoiled, hence underwound, state, these transitions could serve important biological functions. Both thermodynamic and statistical mechanical theories of stress-induced two-state transitions have been developed previously[5,6]. Here we apply these theories to transitions between the B-form and the Z-form in regions of appropriate base sequence. Assuming that the unstressed duplex is entirely B-form, we show that when the molecule is constrained to be underwound, susceptible regions may transform to the Z-form, thereby absorbing most of the torsional deformation. Interestingly, this transition is relatively independent of temperature.

Consider a linear segment containing N base pairs, of which N_Z sequential pairs may undergo the B–Z transition. Let this segment be twisted by q turns away from its unstressed (hence totally B-form) shape. This torsional deformation will be partitioned between local transitions to the Z-form and smooth twisting in both the B- and Z-form regions so as to minimize the total conformational free energy involved. Denote the number of base pairs per helix repeat in the unstressed B-form by $A_B = 10.4$ and in the Z-form by $A_Z = -12$ (the negative sign deriving from the presumed opposite handedness of the two forms). Let τ_B (and τ_Z) denote the twist rate at which the B-form (and Z-form) regions are deformed away from their unstressed shape. If n bases occur in the Z-form, then

$$\tau_B = 2\pi[q + (n/A) - (n\tau_Z/2\pi)]/(N - n) \qquad (1)$$

where $1/A = 1/A_B - 1/A_Z$. The conformational free energy associated to this torsionally deformed structure is given by

$$F(n, \tau_Z) = a + bn + \frac{nC_Z\tau_Z^2}{2} + \frac{C_B}{2(N-n)}\left[2\pi\left(q + \frac{n}{A}\right) - n\tau_Z\right]^2 \qquad (2)$$

Here, C_Z and C_B are the torsional stiffnesses of the Z- and the B-form structures, b is the free energy required to change one base pair from B to Z and a is the extra free energy needed to initiate the transition in a region. Although C_Z is not known, it is reasonable to assume that $C_Z \simeq C_B$. Stable conformations occur at those values of n and τ_Z which minimize the free energy of equation (2)[5]. It follows that the segment must be underwound

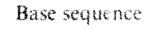

Fig. 1 The probability of being in the B-form is computed for a sequence of $N = 80$ base pairs, of which $N_Z = 8$ consecutive pairs are susceptible to transition to the Z-form. For clarity, the transition profiles of a sequence of 40 base pairs containing the susceptible region are plotted at various values of the torsional deformation q. First, when $q = 0$ all base pairs are in the B-form with probability 1. The other four curves are for $q = -0.38m$, $m = 1, 4$. As the amount of negative torsional deformation increases, so does the probability of susceptible pairs transforming to Z-form. The parameters used in this calculation are $T = 298$ K, $\sigma = 1.36 \times 10^{-6}$, $s = 3.86$. For intermediate values of q (before the transition is complete) the statistical mechanical calculation gives $\tau_B = \tau_Z = -0.4$ deg per base pair. The transition profiles calculated at $T = 353$ K are virtually identical to those shown here. These results agree well with those from the thermodynamic analysis.

0028–0836/80/320637—02$01.00

by $q < -bNA/4\pi^2 C_B$ before stable regions of Z-structure occur. When q satisfies this condition, unique non-zero values of n and τ_Z exist which minimize the conformational free energy[5]. These are

$$n = -qA - (bNA^2/4\pi^2 C_B) \tag{3}$$

$$\tau_B = \tau_Z = -bA/2\pi C_B \tag{4}$$

where $0 < n < N_Z$. (If the segment is sufficiently underwound that $n = N_Z$, then $\tau_z = \tau_B$ is found from equation (1). To illustrate these results we use values $C_B = 8.5 \times 10^{-12}$ erg base pair rad^{-2} and $b = 0.8$ kcal mol^{-1} from the literature[4,7]. Then a segment must be underwound by 0.33 deg per base pair before the onset of transition to structures containing stable Z-form regions. When deformed beyond this threshold, enough susceptible base pairs switch to Z-structure for the twist rates to be maintained at $\tau_B = \tau_Z = -0.33$ deg per base pair. Only when the segment is so underwound that all susceptible sequences are in the Z-form do τ_B and τ_Z decrease below -0.33 deg per base pair.

To augment the above treatment we apply the statistical mechanical theory of two state transitions in torsionally stressed DNA[6] to the present problem. This renders computable the transition probability profiles of specific base sequences, which more accurately reflect the fluctuational character of these transitions.

The partition function for this transition is[6]

$$Z = \sum_{n=0}^{N_Z} \left[I_n \sum_{r_n} (s^n \sigma^\gamma) \right] \tag{5}$$

where r_n enumerates all states containing n Z-form base pairs, s is the equilibrium constant for a susceptible base pair, σ is the cooperativity factor and γ is the number of beginnings of sequences of base pairs in the Z-form. Also,

$$I_0 = \exp(-2\pi^2 q^2 C_B \beta / N), \tag{6a}$$

$$I_n = \left(\frac{2\pi(N-n)}{NnC_B\beta} \right)^{1/2} \exp\left(\frac{-2\pi^2 C_B \beta (q + n/A)^2}{N} \right), \quad 0 < n \leq N_Z \tag{6b}$$

From this partition function one can determine transition profiles, the expected value of τ_B and other equilibrium properties of the system as described in ref. 6. Figure 1 shows the results of a sample calculation carried out on a sequence of 80 base pairs, of which 8 were susceptible to the transition. Note that because the enthalpy of the B–Z transformation is zero[4], this two-state transition is not thermal in character, but rather depends primarily on the imposed torsional deformation q.

We have presented two theoretical analyses of transitions between B-form and Z-form in torsionally stressed DNA. In this initial formulation the possible role of local denaturation (perhaps necessary at the junction between B-form and Z-form regions, for example) has not been considered. A three-state treatment of this problem will be presented elsewhere. Despite lack of precise knowledge of several important parameters (torsional stiffness C_Z, cooperativity factor σ), the present analysis predicts that B–Z transitions could occur in response to the torsional deformations consequent on (negative) DNA superhelicity. In principle, it is possible that similar transitions also occur between other conformational states of the DNA. It has been suggested that stress-induced conformational transitions at defined sequences may serve diverse regulatory functions by altering the accessibility of the bases[5].

Received 25 February; accepted 19 May 1980.

1. Wang, A. *et al. Nature* **282**, 680–686 (1979).
2. Wang, J. *Proc. natn. Acad. Sci. U.S.A.* **76**, 200–204 (1979).
3. Levitt, M. *Proc. natn. Acad. Sci. U.S.A.* **75**, 640–644 (1978).
4. Pohl, F. & Jovin, T. *J. molec. Biol.* **67**, 375–396 (1972).
5. Benham, C. *Proc. natn. Acad. Sci. U.S.A.* **76**, 3870–3874 (1979).
6. Benham, C. *J. chem. Phys.* **72**, 3633–3639 (1980).
7. Barkley, M. & Zimm, B. *J. chem. Phys.* **70**, 2991–3007 (1979).
8. Crick, F., Wang, J. & Bauer, W. *J. molec. Biol.* **129**, 449–461 (1979).

Metarhodopsin I/metarhodopsin II transition triggers light-induced change in calcium binding at rod disk membranes

U. B. Kaupp, P. P. M. Schnetkamp & W. Junge

Universität Osnabrück, Schwerpunkt Biophysik, Postfach 4469,
D-4500 Osnabrück, FRG

The hypothesis of Yoshikami and Hagins[1] that calcium ions act as diffusible transmitter molecules between the photochemistry of rhodopsin and the subsequent electrical events at the outer plasma membrane of rods initiated many investigations on light-stimulated calcium release in vertebrate photoreceptor cells (see refs 2, 3). Although it now seems firmly established that light has some effect on the redistribution of calcium in various disk preparations[2,4,5], reconstituted systems[6,7] and intact rod outer segments[3,8], the physiological significance remained unclear. We previously reported a rapid, light-triggered calcium release from binding sites at the disk membrane in the presence of calcium ionophore A23187 (refs 3, 8). However, there is no evidence for rapid calcium release into the cytosol in the absence of ionophore. On fragmentation of intact rod outer segments, calcium release due to a light-regulated change of calcium binding appeared almost completely abolished[3,8]. We describe here experiments with sonicated rod outer segments in which the previously observed loss of the calcium release capacity has been prevented. Calcium release in sonicated disks in the presence of A23187 kinetically follows the metarhodopsin I/metarhodopsin II transition ($\tau_{1/2} = 10$ ms, activation energy $E_A = 34$ kcal mol^{-1}), suggesting that calcium release is triggered by this photochemical transition.

Intact cattle rod outer segments have been isolated according to Schnetkamp *et al.*[9]. Disk vesicles were obtained by sonication of intact rod outer segments in a medium containing sucrose, 600 mM; Ficoll 400, 5% v/v; HEPES, pH 7.0 2 mM, for 30 s at 40 W. The suspension also contained about 3–4 μM of free calcium introduced by the stock suspension of rod outer segments.

Inhibition of calcium release can be prevented by keeping the ionic strength of the final suspension medium below 5 mM of 1:1 electrolyte, irrespective of the fragmentation procedure (lysis or sonication) and the fragmentation conditions (for example, high or low ionic strength). We conclude that the apparent abolition of the release capacity in fragmented rods is caused by regulation of calcium binding by cations other than calcium which had no access to the site of calcium release in both rods with a leaky and an intact plasma membrane.

Rapid calcium release was followed by means of kinetic flash spectrophotometry with the calcium indicator arsenazo (III). Details on working with arsenazo (III) and the principle and instrumentation of flash spectrophotometry have been reviewed elsewhere[3,10]. In a suspension of sonicated disks buffered with only 2 mM HEPES at pH 6.8, pH measurements with the pH indicators bromcresol purple and Mg-arsenazo (III) (ref. 11) demonstrated that the total proton buffering capacity (membranes and HEPES) is sufficient to suppress light-induced pH changes which might give rise to pH-induced absorption changes of arsenazo (III) (not shown). To obtain kinetically undistorted recordings of calcium release in sonicated material at higher time resolution (Fig. 1*a*), signals due to the intrinsic photochemistry of arsenazo (III) (ref. 3) have been recorded separately and subtracted from the superimposed calcium-indicating signals by means of a signal averager with a data reduction program (Nicolet 1072). The signal-to-noise ratio was improved by sampling of signals over several repetitions from one cuvette.

0028–0836/80/320638—03$01.00

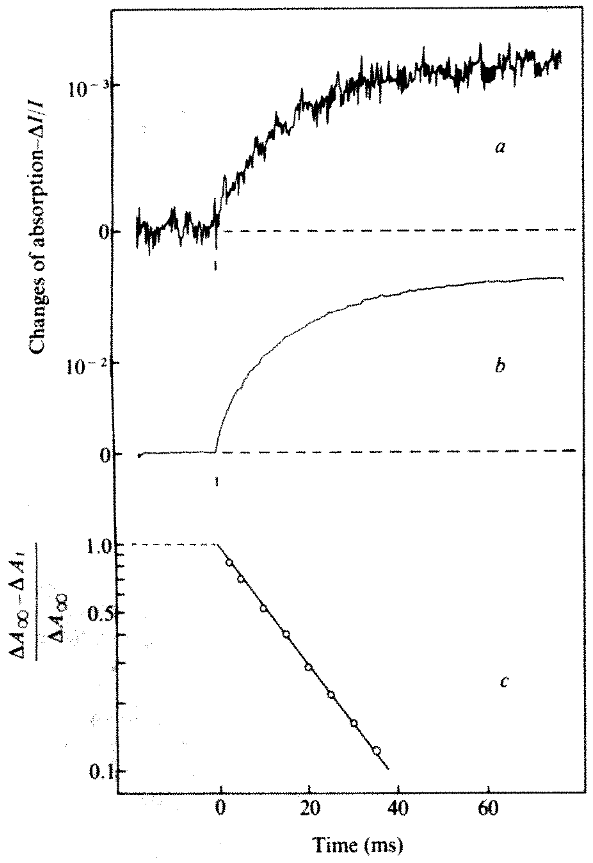

Fig. 1 Time course of the light-induced absorption changes at: *a*, 655 nm and *b*, 382 nm after excitation of sonicated rod outer segments by a flash at $t = 0$ in the presence of arsenazo (III) and A23187. Signals were obtained by averaging from one sample over 16 repetitions for *a* and four repetitions for *b* at a frequency of 0.5 Hz. The optical bandwidth of the measuring beam was 16 nm, the electrical integration time 200 μs. Further conditions as in Fig. 2. *c*, Semilogarithmic plot of the calcium-indicating absorption change from part *a*.

The half-rise time of flash-induced calcium release in the presence of equal amounts of A23187 (10 μM) depends on the structural integrity of rod outer segments (Fig. 2). In intact rod outer segments, calcium release occurs more slowly ($\tau_{1/2}$ = 300 ms) than in sonicated disk vesicles ($\tau_{1/2}$ = 10 ms). Unlike its kinetics, the stoichiometry of calcium released/rhodopsin bleached is comparable in both preparations (~0.4 calcium/rhodopsin*). Light-triggered calcium release in sonicated material is depicted in Fig. 1*a* at a higher time resolution. A semilogarithmic plot of the absorption changes from Fig. 1*a* reveals that the time course of calcium release can be described by a single first order reaction (Fig. 1*c*). Concomitantly in intact rod outer segments and sonicated suspensions the metarhodopsin I/metarhodopsin II transition has been recorded at 382 nm. A half-rise time of about 10 ms at 20 °C and at *p*H 7 was observed for both preparations. The time course of this photochemical transition is shown for sonicated disk vesicles in Fig. 1*b*. From inspection of Fig. 1 it is evident that the time course of rapid calcium release in sonicated rods in these conditions closely parallels that of the metarhodopsin I/metarhodopsin II transition.

To determine the energy of activation for both processes, the temperature dependence of the respective rate constants has been investigated in similar conditions (Fig. 3). Rate constants have been calculated from overall half-rise times according to $1/\tau_{1/2} = \mathrm{k}(\ln 2)^{-1}$. The metarhodopsin I/metarhodopsin II transition exhibits *p*H- and temperature-dependent biphasic kinetic behaviour (ref. 12 and our unpublished observation) and therefore two ways of analysing the data have been adopted. First, the overall rate constants of the metarhodopsin I/metarhodopsin II transition are shown in Fig. 3 (closed circles). They match reasonably well with the calcium release data (triangles). If only the rate constant of the slower kinetic component is considered (Fig. 3, open circles) the correspondence, especially for higher temperatures, is even better. This is due to the temperature dependence of the relative amplitudes of the two kinetic phases of the metarhodopsin I/metarhodopsin II transition which favours the rapid component at higher temperatures[12]. Notwithstanding this subtlety of a biphasic kinetic behaviour of the metarhodopsin I/metarhodopsin II transition, it is obvious from Fig. 3 that both reactions have a similar activation energy of about 34 kcal mol^{-1}.

The similarity of activation energies and time constants of both reactions strongly suggests that the calcium release system is intimately coupled to the metarhodopsin I/metarhodopsin II transition. In agreement with this notion is the linear relationship between metarhodopsin II formation and the amount of calcium release reported earlier[3,8].

The rapid rise time of the calcium-indicating absorption changes in sonicated vesicles probably reflects the actual time required for the trigger step to occur. The diffusion time of calcium ions from binding sites through the suspending medium to an indicator molecule[13] as well as the relaxation time of complex formation between arsenazo (III) and calcium[14] are too short to contribute significantly to the time course of the calcium-monitoring absorption changes. The mechanism underlying the slower kinetics in intact rod outer segments probably involves an additional reaction step and will be considered elsewhere[15], but from the present study it is obvious that in the presence of 10 μM A23187 the kinetics of calcium release are not rate limited by the ionophore.

For the actual release step two distinct mechanisms may be considered. In the first model, calcium is bound directly to rhodopsin and released during the metarhodopsin I/metarhodopsin II transition due to a change of the electrostatic interaction between calcium and its coordination groups at the rhodopsin molecule. This change could involve spatial separation of chelating groups accompanying conformational changes

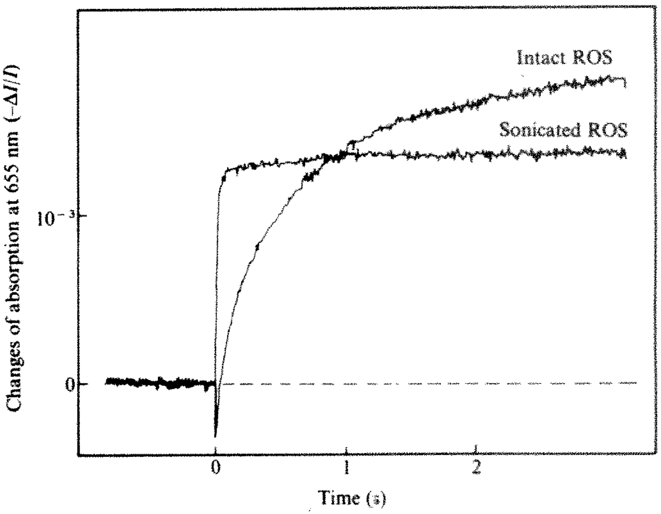

Fig. 2 Time course of the light-induced absorption changes at 655 nm after excitation of intact and sonicated rod outer segments (ROS) by a flash at $t = 0$ in the presence of arsenazo (III) and ionophore A23187. Suspension medium contained: sucrose, 600 mM; HEPES, 2 mM; Tris, 0·5 mM at *p*H 7.0; arsenazo (III), 30 μM; A23187, 10 μM; free calcium concentration 3–4 μM and rhodopsin, 3.5 μM. Fraction of rhodopsin bleached/flash about 4%. Cuvette path length 10 mm. Temperature, 20 °C. Excitation wavelength, 530 nm; half duration of excitation flash 10 ns. Signals were obtained by averaging from one sample over four repetitions at a frequency of 0.1 Hz.

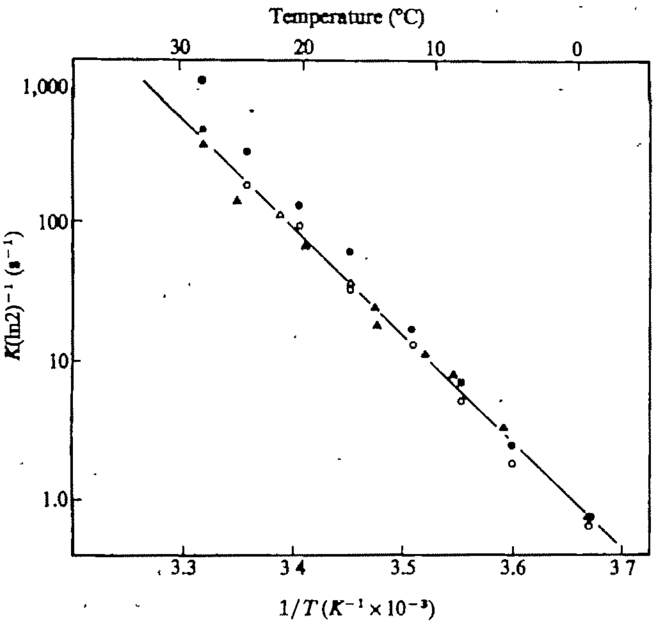

Fig. 3 Arrhenius plot of the temperature dependence of the calcium release (△), the metarhodopsin I/metarhodopsin II transition (●), and the slow component of the metarhodopsin I/metarhodopsin II transition (○) in sonicated rod outer segments. Further conditions as in Fig. 2.

within rhodopsin. In the second model, a reorientation of molecular dipoles within the rhodopsin molecule or rapid proton uptake[16] could decrease an interfacial potential at the disk membrane. According to $K_D = K_D^0 \exp(-2e\varphi/kT)$ the apparent binding constant K_D of calcium binding sites (not necessarily on rhodopsin) is dependent on the surface potential φ(K_D^0 = binding constant in the absence of any interfacial potential). Consequently any change of an interfacial potential will result in a redistribution of calcium bound to the membrane.

It is difficult to decide between the models outlined above. The close correlation between calcium release and the metarhodopsin I/metarhodospin II transition could be interpreted in favour of the first model. However, the fact that rapid calcium release is completely abolished when rod outer segments are dissolved in either nonylglucose (gift of Dr W. J. de Grip, Nijmegen) or Triton X-100 (not shown) would be difficult to explain if calcium were directly bound to rhodopsin. A more detailed account of the interrelationship between calcium release, rapid proton uptake and interfacial potentials will be published elsewhere[15].

This work was financially supported by the Deutsche Forschungsgemeinschaft.

Received 21 February, accepted 19 May 1980

1 Yoshikami, S. & Hagins, W. A Biophys J Abstr. 16, 35a (1971)

2. Smith, H G., Fager, R S & Litman, B J Biochemistry 16, 1399–1405 (1977)

3. Kaupp, U. B., Schnetkamp, P P M & Junge, W. in *Detection and Measurement of Free Ca^{2+} in Cells* (eds Ashley, C C & Campbell, A K.) 287–308 (Elsevier, Amsterdam, 1979)

4. Shevchenko, T F. *Biophysics* 21, 327–330 (1976).

5. Smith, H G., Jr & Bauer, P J. *Biochemistry* 18, 5067–5073 (1979)

6 O'Brien, D., Zumbulyadis, N , Michaels, F M & Ott, R A. *Proc natn. Acad Sci U S A* 74, 5222–5226 (1977).

7. Hubbell, W L , Fung, K -K , Hong, K & Chen, Y S in *Vertebrate Photoreception* (eds Barlow, H B & Fatt, P) 41–59 (Academic, London, 1977).

8 Kaupp, U B., Schnetkamp, P P M & Junge, W. *Biochim biophys Acta* 582, 390–403 (1979)

9 Schnetkamp, P P. M , Klompmakers, A. A & Daemen, F J M *Biochim biophys Acta* 582, 379–389 (1979).

10. Junge, W in *Chemistry and Biochemistry of Plant Pigments* Vol. II (ed Goodwin, T W) 233–333 (Academic, London, 1976)

11 Russell, J T & Martonosi, A N *Biochim biophys Acta* 544, 413–429 (1978)

12. Hoffman, W., Siebert, F., Hofmann, K. P & Kreutz, W *Biochim biophys Acta* 503, 450–461 (1978).

13. Kaupp, U B thesis, Univ Berlin (1979)

14. Scarpa, A., Brinley, F. J. Jr & Dubyak, G. *Biochemistry* 17, 1378–1386 (1978)

15. Kaupp, U. B , Schnetkamp, P P. M & Junge, W. (in preparation)

16 Emrich, H. M. *Z. Naturforsch* B26, 352–356 (1971)

A novel conformation of valinomycin in its barium complex

S. Devarajan, C. M. K. Nair, K. R. K. Easwaran & M. Vijayan

Molecular Biophysics Unit, Indian Institute of Science,
Bangalore–560 012, India

Knowledge of the molecular mechanisms involved in ionophore-mediated cation transport would be valuable for understanding many essential functions of biological membranes[1–3]. Cations are transported in several stages, such as formation of the ionophore–cation complex, diffusion across the cell membrane and subsequent release of the cation. Several conformational rearrangements are involved in this process, and so a detailed understanding of all the conformational possibilities of the ionophore seems to be essential for elucidating the molecular mechanism of ion transport. We are carrying out spectroscopic and crystallographic studies to explore the possible conformational stages of ionophores by complexing them, in different solvents, with cations of various sizes and charges. We report here a novel conformation of the ionophore valinomycin in its barium complex. It can be described as an extended depsipeptide chain, without internal hydrogen bonds, wound in the form of an ellipse with the two barium ions located at the foci.

Spectroscopic studies in solution (for example, circular dichroism (CD) spectra shown in Fig. 1) carried out by us indicated that the conformation of valinomycin in its barium complex was different from those in uncomplexed valinomycin and its complex with monovalent cations. Barium perchlorate and barium thiocyanate were used to investigate complexation

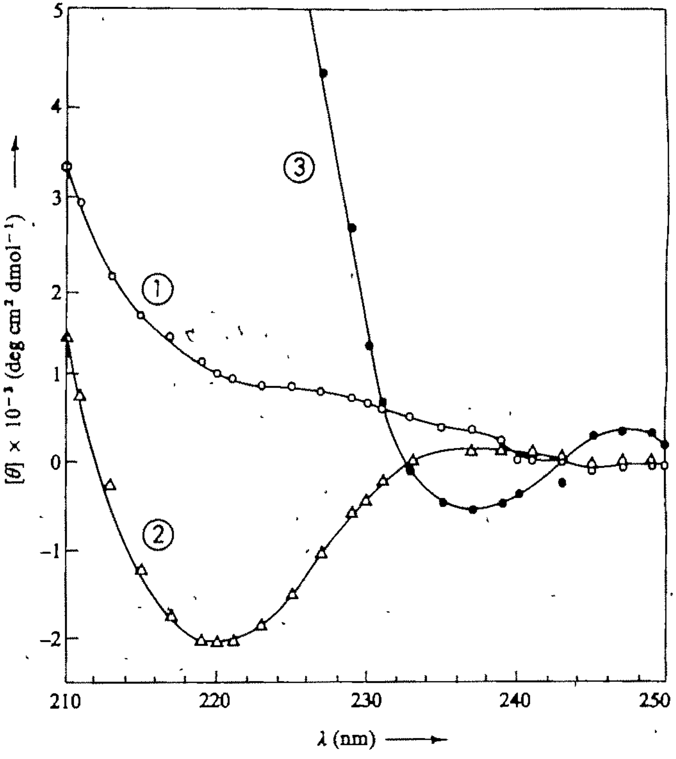

Fig. 1 CD spectra in acetonitrile of free valinomycin (○), its 1:2 barium perchlorate complex (△) and its 1.1 potassium perchlorate complex (●). The concentration of valinomycin was 29 mM (○, △) and 9 mM (●). In the potassium perchlorate complex the molar ellipticity, [θ], continuously increases with decrease in λ with a [θ] value of 25,000 deg cm^2 per dmol at λ = 210 nm.

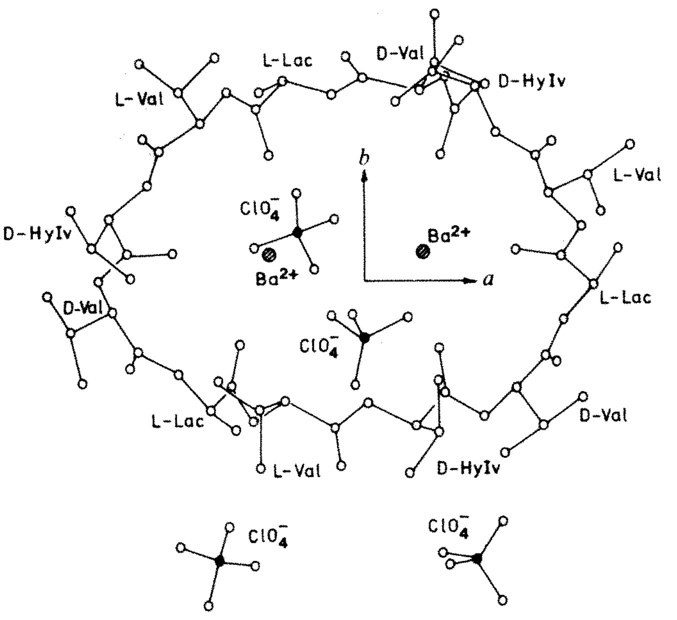

Fig. 2 The location of the valinomycin molecule, the barium ions and the perchlorate groups as viewed along the *c* axis in the crystals of a 1 : 2 valinomycin–barium perchlorate complex.

of valinomycin with Ba^{2+}. CD data on the titration of barium perchlorate with the ionophore in acetonitrile indicated valinomycin–Ba^{2+} complexes with 2 : 1, 1 : 1 and 1 : 2 stoichiometries, although the conformation of the molecule stabilized only at high salt concentrations (S.D. and K.R.K.E., in preparation). CD could not be used with barium thiocyanate because of the high UV absorption of the thiocyanate group. However, proton NMR indicated a stable 1 : 2 valinomycin–barium thiocyanate complex, although the titration curve based on NMR data for the thiocyanate salt was different from that for the perchlorate salt (S.D. *et al.*, in preparation). Thus, it seemed that valinomycin could form 1 : 2 complexes with barium perchlorate as well as barium thiocyanate and we decided to attempt X-ray crystallographic studies on these complexes.

Complexes (1 : 2) of valinomycin with barium perchlorate and barium thiocyanate were crystallized by slow evaporation of slightly aqueous acetonitrile solutions containing the respective components in molar proportions. The crystals were mounted in thin-walled glass capillaries together with the solvent. X-ray diffraction photographs showed that the valinomycin–barium perchlorate complex crystallizes in the orthorhombic space group $P2_12_12_1$ with $a = 28.304$ Å, $b = 16.938$ Å, $c = 19.543$ Å and $z = 4$, whereas the thiocyanate complex crystallizes in the monoclinic space group C2 with $a = 29.48$ Å, $b = 16.49$ Å, $c = 19.92$ Å, $\beta = 111.4°$ and $z = 4$. X-ray intensity data from both the crystals were collected on a computer controlled four-circle CAD-4 diffractometer using graphite monochromatized MoKα radiation to a maximum Bragg angle of 23°. The structure of the barium perchlorate complex was subsequently determined by the heavy atom method and refined by the block-diagonal structure factor least squares technique to an R value of 0.13 for 3,504 observed reflections ($I > 2\sigma(I)$). So far, the two barium ions and all the non-hydrogen atoms belonging to the valinomycin molecule, the four perchlorate groups and four water molecules have been located.

The location of the barium ions, the valinomycin molecule and the perchlorate ions in the crystal structure is shown in Fig. 2. The main-chain dihedral angles[4] in the valinomycin molecule correspond approximately to those for an extended chain. The molecule can be described as an extended depsipeptide chain, with no internal hydrogen bond, wound in the form of an ellipse with the barium ions located at the foci. Three consecutive amide carbonyl groups coordinate to one of the barium ions whereas the remaining three consecutive amide carbonyl groups coordinate to the other barium ion. The coordination of the cation is completed by perchlorate and water oxygens. The conformation of valinomycin observed in the structure is totally different from those found in the crystal structures of uncomplexed valinomycin[5,6] and its potassium complex[7]. It is also different from the conformations unambiguously characterized so far in solution studies[1-3].

We thank the University Grants Commission and the Department of Science and Technology, India, for financial assistance, and Dr A. M. Shaik for help with data collection. The atomic coordinates have been deposited in the Crystallographic Data Bank, University Chemical Laboratory, Lensfield Road, Cambridge, UK.

Received 3 March; accepted 5 June 1980.

1. Ovchinnikov, Yu. A., Ivanov, V. T. & Shkrob, A. M. in *Membrane Active Complexes* (Elsevier, Amsterdam, 1974).
2. Pressman, B. C. *A. Rev. Biochem.* **45,** 501–530 (1976).
3. Ovchinnikov, Yu. A. *Eur. J. Biochem.* **94,** 321–336 (1979).
4. Ramachandran, G. N. & Sasisekharan, V. in *Advances in Protein Chemistry* (eds Anfinson, C. B. *et al.*) 284–437 (Academic, New York, 1968).
5. Karle, I. L. *J. Am. chem. Soc.* **97,** 4379–4386 (1975).
6. Smith, G. D. *et al. J. Am. chem. Soc.* **97,** 7242–7247 (1975).
7. Neupert-Laves, K. & Dobler, M. *Helv. chim. Acta* **58,** 432–442 (1975).

Circular polarization observed in bioluminescence

Hans Wynberg*, E. W. Meijer*, J. C. Hummelen*, H. P. J. M. Dekkers†, P. H. Schippers† & A. D. Carlson‡

* Department of Organic Chemistry, University of Groningen, The Netherlands
† Department of Theoretical Organic Chemistry, University of Leiden, The Netherlands
‡ Department of Neurobiology & Behavior State University of New York at Stony Brook, Stony Brook, New York 11790

While investigating circular polarization in luminescence[1,2], and having found it in chemiluminescence[3,4], we have studied bioluminescence because it is such a widespread and dramatic natural phenomenon[5,6]. We report here that left and right lanterns of live larvae of the fireflies, *Photuris lucicrescens* and *Photuris versicolor*, emit circularly polarized light of opposite sense.

Firefly larvae (Fig. 1) were gathered in the US and sent by airmail to The Netherlands. They were alive up to and during most of the experiments. In our first attempts to detect polarization of luminescence, we measured the total light emission from both lanterns of the larvae. The results were puzzling and disappointing; vanishingly small circular polarization was observed, with only a few exceptions. To our surprise, we noted—fortuitously—that measurements of the light emission from the left or right lanterns separately gave more constant and encouraging results. During the latter experiments one important fact was established. By shifting and rotating the lanterns through many angles and positions with respect to the optical axis of the apparatus, we found that orientational artefacts could not be the origin of the circular polarization subsequently measured. Whereas in these early experiments we used excised lanterns rigidly mounted in a cell, in the later experiments we preferred to attach entire larvae with fine wire to a holder. The holder was positioned in front of a diaphragm so that one lantern only was fixed onto the optical axis of the apparatus. Continuous bioluminescence, lasting from several minutes to an hour, was achieved by feeding the larvae with a concentrated solution of racemic amphetamine hydrochloride in water. Luminescence usually began 5–30 min after the addition of amphetamine. Measurements were then made immediately.

The circular polarization of luminescence was measured as the anisotropy factor or g_{lum} factor $(I_L - I_R)/\frac{1}{2}(I_L + I_R)$. The difference in the numbers of left and right circularly polarized

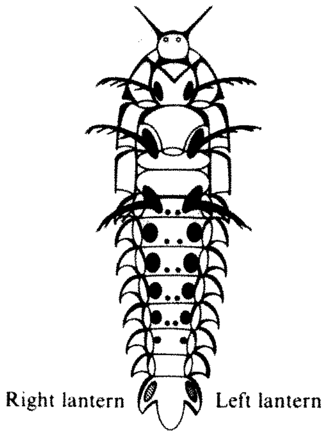

Fig. 1 Sketch of the firefly larva (ventral view). The shaded spots at the bottom represent the lanterns.

photons emitted, $I_L - I_R$, was modulated at a frequency of 50 kHz and detected as alternating photocurrent; the average luminescence $\frac{1}{2}(I_L + I_R)$ was measured as direct photocurrent[1,2,7-9]. Measurements of circular polarization of bioluminescence (CPBL) of 16 firefly larvae lanterns are shown in Fig. 2, revealing that the left and right lanterns emit polarized light of opposite sense. Within each group there is a considerable variation in the total light emission and values of g for the individual lanterns. In these experiments, the construction of the sample holder prevented a detailed investigation of orientational effects. However, on the basis of results of earlier experiments, we believe that neither position effects nor those due to linear polarization could have decisively affected our result.

What is the origin of the CPBL, and what is the origin of the difference in handedness shown by the left and right lanterns? According to the accepted mechanism of firefly bioluminescence mediated by luciferin, an achiral emitting state, III* (see Fig. 3), is involved[5,10-13]. This achiral excited state, by itself, offers no possibility of explaining the CPBL. It may be argued however, that the true excited state consists of a complex between the achiral III* and the enzyme luciferase. Such a chiral excited state complex should, in principle, be capable of emitting circularly polarized light[3,4]. A second explanation would invoke a circularly dichroic medium capable of partially absorbing the emitted light. Neither of these two modes can explain why the left and right lanterns emit polarized light of opposite sense, unless enantiomeric enzymes, active sites or membranes are proposed. In the absence of any evidence for enantiomeric structures, we are forced to conclude that the CPBL of opposite sense must, at least in part, be based on a macroscopic phenomenon rather than on molecular chirality.

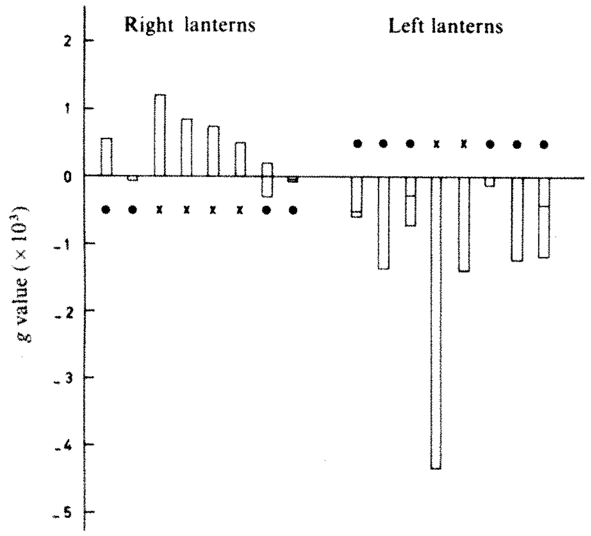

Fig. 2 Results of measurements of circular polarization of bioluminescence of firefly larvae lanterns with sufficiently high emission intensity. The height of each bar represents the g value for an individual lantern of *Photuris lucicrescens* (X) or *Photuris versicolor* (●). Superimposed bars refer to the effect of orientational changes (see text). The circular polarization is measured at the peak of the emission band at a wavelength of 540 nm using a spectral bandwidth of 40 nm. The r.m.s. noise level corresponds with $g \leq 5 \times 10^{-4}$.

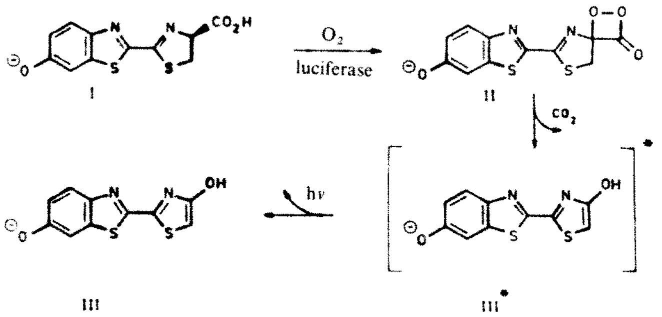

Fig. 3 Schematic mechanism of luciferin/luciferase bioluminescence. Oxygenation of luciferin (I) yields the intermediate II which in turn releases CO_2, resulting in the production of III (or, by H^+-abstraction, the enol dianion) in an electronically excited state. This state emits a quantum of light as it goes to its electronic ground state.

We propose the following hypothesis. The light from a bioluminescent emitter may be (partially) plane polarized due to anisotropy of an absorbing medium or, more likely, by inhomogeneous formation of excited states due to local molecular organization within a photocyte[14]. This plane polarized light will become elliptically polarized when it passes through a linearly birefringent medium. Orientated biopolymers can serve as such a medium. On a macroscopic scale the larvae, like many living organisms, have a symmetry plane dividing the lanterns. In this sense the lanterns are enantiomeric, even though their constituent molecules are of the same chirality; they may be viewed as macroscopic meso-structures. It is reasonable to assume that this macroscopic mirror image relationship holds on the level of the membrane structure and orientation of the emitters. This will result in circularly polarized light of opposite sense. The emitters from one lantern emit partially plane polarized light making angle $+X°$ with the fast axis of its linear birefringent medium. The result is ellipticity of one sense $(+Y)$. The mirror image relationship of the emitters in the other lantern results in partially plane polarized light with angle $-X°$ with respect to the fast axis of its linear birefringent medium. This must result in ellipticity of opposite sense $(-Y)$. We may expect, then, that the meso-orientated lanterns in any bioluminescent organism will emit circularly polarized light of opposite handedness, provided the chirality on the molecular level does not exceed the effect. The results described above suggest experiments dealing with the linear polarization of firefly larvae bioluminescence. Such experiments are planned.

Received 29 February; accepted 13 June 1980.

1. Dekkers, H. P. J. M. & Closs, L. E. *J. Am. chem. Soc.* **98,** 2210–2219 (1976).
2. Emeis, C. A. & Oosterhoff, L. J. *Chem. Phys. Lett.* **1,** 129–132 (1967).
3. Wynberg, H. & Numan, H. *J. Am. chem. Soc.* **99,** 603–605 (1977).
4. Wynberg, H., Numan, H. & Dekkers, H. P. J. M. *J. Am. chem. Soc.* **99,** 3870–3871 (1977).
5. McCapra, F. *Acct. chem. Res.* **9,** 201–208 (1976).
6. Badcock, J. R. & Merrett, N. R. *Nat. envir. Res. Coun. New. Jers.* **5,** 4 (1972).
7. Gafni, A. & Steinberg, I. Z. *Photochem. Photobiol.* **15,** 93–96 (1972).
8. Luk, C. L. & Richardson, F. S. *J. Am. chem. Soc.* **96,** 2006–2009 (1974).
9. Steinberg, I. Z. in *Biochemical Fluorescence* Vol. I (eds Chen, R. F. & Edelhoch, H.) 79–113 (Dekker, New York, 1976).
10. Koo, J.-Y., Smidt, S. P. & Schuster, G. B. *Proc. natn. Acad. Sci. U.S.A.* **75,** 30–33 (1978).
11. White, E. H., Midno, J. A. & Umbreit, M. *J. Am. chem. Soc.* **97,** 198–200 (1975).
12. McElroy, W. D. & Deluca, M. in *Bioluminescence in Action* (ed. Herring, P.) 109–127 (Academic, London, 1978).
13. McCapra, F. in *Bioluminescence in Action* (ed. Herring, P.) 49–73 (Academic, London, 1978).
14. Wampler, J. E. in *Bioluminescence in Action* (ed. Herring, P.) 9–48 (Academic, London, 1978).

BOOK REVIEWS

Fuel for the 'back-end' debate

Ian Smart

Nuclear Nonproliferation: The Spent Fuel Problem. Edited by Frederick C. Williams and David A. Deese. Pp.221. (Pergamon: New York and Oxford, 1980.) $30, £15.

THE 'back end' of the commercial nuclear fuel cycle, covering what happens to fuel material after its irradiation and withdrawal from power reactors, has had more attention and words lavished on it since 1976 than, arguably, it deserves. It contributes a trivial proportion to the cost of nuclear electricity. It offers more technical choices, and fewer imperatives, than earlier stages in the cycle. And, while no one doubts that plutonium from spent power reactor fuel can be used in nuclear explosives, the danger of that particular route to nuclear proliferation, in relation to others, has frequently been exaggerated. Yet the floods of emotion and typescript continue to rise around the fuel cycle's back end: around nuclear waste management, around reprocessing and the recycling of its products, and around the handling of spent fuel itself.

Reasons for this almost obsessive concern are obvious: the prospect of a so-called 'plutonium economy', based on exploiting back-end opportunities, is genuinely arresting. On the one hand, the consequential introduction of commercial fast breeder reactors is seen by some as a necessary graduation from nuclear infancy, but by others as a leap into economically uncharted and technically dangerous obscurity. On the other hand the issue of nuclear weapons proliferation raised by widespread commercial separation of plutonium is quantitatively, even if not qualitatively, new. And, to cap it all, any discussion of the back end, with or without reprocessing, touches the problem of nuclear waste, management of which provokes more environmental fears — together with more complacency, superstition and reciprocal condescension — than any other topic in the nuclear debate. One may regret that so much time is spent in writing or reading about the back end, at the risk of ignoring what may be more pressing difficulties in the rational and safe development of nuclear power, but one cannot be surprised.

The pathetically familiar polarization of the back-end debate is well illustrated by conflicting images of spent reactor fuel itself: on one side the image of spent fuel as a 'plutonium mine' of immediately valuable fissile material, to be extracted and exploited for good or ill, on the other the image of it as merely one form of nuclear waste, to be buried away out of sight and reach as quickly as possible. Both views are caricatures, justifiable only by ignoring the time factor. In the main, spent fuel is currently a nuisance, encumbering storage ponds at reactor sites and imposing additional costs on utilities. Yet the reactors concerned have extracted less than 1% of the energy potentially available in the uranium originally mined. The rest remains locked up in the spent fuel, as plutonium and depleted uranium, or in the tails at enrichment plants, to be extracted only if and when fast breeder reactors are commercially feasible and widely available. That day may not come, and spent fuel may remain a radioactive nuisance. Meanwhile, however, to treat it as nothing but waste would be like refining crude oil merely to extract bitumen for roads, and then setting fire to all that remained because the internal combustion engine was not yet ready for commercial service. Today's burden may be tomorrow's scarce resource.

One merit of this book is that it studiously avoids caricaturing spent fuel as either immediate gold or permanent dross. Although it starts from the premise, espoused by the Carter administration, that commercial reprocessing is currently uneconomic and politically undesirable, it acknowledges that circumstances may change, and that the ways in which spent fuel is handled today must not preclude using its plutonium content in the future. From there, it moves to the judgement that, to ease pressure on storage at reactors while also preventing an allegedly dangerous increase in the volume and distribution of reprocessed plutonium, more ambitious provision must be made for away-from-reactor (AFR) storage, which could usefully be under some kind of international control. The task it then sets itself is to explore the manner in which an international spent fuel storage arrangement might be set up in different regions of the world.

So far, so good. Whether or not too much time has recently been spent in agonizing over the back end, nothing like enough careful thought has yet been given to how, in the real world, international or multinational arrangements might reduce the fears of proliferation, environmental damage or public rejection which surround various stages of the fuel cycle. It is encouraging, therefore, to find that "a working group of fifteen scholars and professionals, representing a diversity of academic levels, professions, experience, and nationalities, met biweekly over the course of a year" at Harvard, and that here we have 11 of their papers, dealing not only with politics, technology and economics at a general level but also with five major world regions. Marvin Miller shows that, although more development is needed, there are technical methods of storing spent oxide fuel safely (and retrievably) for at least 25 years. Boyce Greer and Mark Dalzell outline an ingenious economic model which suggests that all except the largest reactor-operating countries might well save a lot of money during that period by sending their spent fuel for storage in large international facilities, even at a considerable distance. The editors, David Deese and Frederick Williams, provide an introductory discussion of the political options available and of the political criteria which are likely to determine the location of any international spent fuel store, and reach the sensible conclusion that the right approach to building an international regime is a gradual and incremental one, serving energy as well as non-proliferation concerns and eschewing dramatic or, above all, unilateral, policy excursions. And Tariq Osman Hyder adds a crucial warning that no such regime will be created unless developing as well as developed countries are convinced in advance of its equity. A foundation of realism and feasibility seems to have been laid.

Thereafter, unfortunately, everything slides downhill. The papers on political prospects in specific regions, clearly drafted as essays for a biweekly seminar, are altogether slighter contributions, uneven in technique and quality and sometimes uncertain on fact. All are ultimately pessimistic. Melvyn Nathanson, while offering the eccentric thought that the USSR might store spent fuel from outside Comecon, regards internationally controlled storage arrangements as irrelevant to Eastern Europe. Onkar Marwah sees none but the remotest prospect of Indian Ocean countries subscribing to such an arrangement, and then only if a regional store on a remote French or Australian island accepted nothing but fuel from a few fully safeguarded plants. Victoria Johnson and Carlos Astiz are driven back to suggesting Paraguay or Uruguay as the only possible hosts for a Latin American store. Richard Broinowski is hardly more optimistic about Asia and the Middle East, and Robert Gallucci even less encouraging, if that is possible, about Western Europe. At the end, therefore, the editors, concluding sadly that there is little chance of rational economic arguments overriding "the centrifugal forces of international politics", leave one asking whether the dinner was worth the detour.

It may be because their surveys of regional politics so depressed them that the editors and authors found no reason even to consider some of the most obtrusive problems in working towards international or multinational fuel cycle arrangements. There is no discussion here of the criteria which should govern the release of spent fuel from international custody. There is almost nothing about institutional form or organization: how rights, responsibilities, costs or authority might be pooled, distributed or devolved. These are glaring omissions, which inevitably detract from the book's value. They might nevertheless be justified if the political prospects were as impenetrably gloomy as here indicated. The hard fact, however, is that the political analyses in the volume often verge on the simplistic, and are forced, moreover, towards pessimism by questionable underlying assumptions: that international arrangements for spent fuel storage must, for example, be addressed in isolation from other fuel cycle functions, or that membership of any multinational fuel cycle institution must be drawn from a single geographical region. Above all, those responsible for the study have steered so far away from the Scylla of believing that political obstacles will vanish in the face of an intellectually coherent scenario that they have fallen victim to the Charybdis of equating the politically difficult with the palpably impossible.

The authors are to be praised for venturing into turbulent waters which it may be politically essential for governments to explore thoroughly during the next few years, and for setting up some preliminary aids to navigation. At the end of the day, however, their courage seems to have failed, because they have judged the icebergs of politics to be immutable. It is not necessary, and it may not be wise, to assume that national policies must be as unalterable, or diplomacy always as impotent, as their conclusions would suggest. □

Ian Smart is an independent adviser on international energy affairs, and was Chairman of the International Consultative Group on Nuclear Energy (1977–80).

Learning from the Arctic peoples

John Ebling

The Human Biology of Circumpolar Populations. International Biological Programme 21. Edited by F.A. Milan. Pp.367. (Cambridge University Press: Cambridge, 1980.) £35, $75.

THE Arctic regions were the last major environment to be conquered by *Homo sapiens*. The radiation of human beings into colder climes northwards and southwards from the tropics probably started about half a million years ago and extended into western and central Europe under conditions of great cold during the Pleistocene. At the end of the Old Stone Age, the use of clothing enabled the human hunters to follow the retreating ice of the Third Würm Glaciation into the Eurasiatic land mass and finally to move into the New World. What adaptations were involved? In general, the physiological differences between modern circumpolar peoples and those more favoured climatically are not striking. They may, perhaps, show an earlier onset of cold vasodilation and have uniformly warmer fingers, but their eyes differ little, even though they are exposed to continuous low temperatures, blowing snow in winter and high ultraviolet radiation in spring. In the far Arctic, people survive mainly on protein, without any obvious source of essential vitamins, and generate necessary glucose from amino acids. The polyunsaturated fats from seal and whale oils keep plasma cholesterol and heart disease at enviably low levels.

The Human Biology of Circumpolar Populations is an admirably edited source book with contributions from Canada, the USA, Denmark, Norway, Finland, France and the USSR. The chapters deal in turn with the demography, genetics, craniofacial features, ophthalmology, anthropometry, nutrition, physiology and behaviour of the 16 indigenous Arctic peoples, ranging from the Lapps of Scandinavia to the Eskimos of Greenland and including the lesser known Siberian groups and the Ainu.

The publication of such a book, and the special studies of the International Biological Programme which went into its making, are timely. The circumpolar peoples are changing. Alcoholism, leading to accidents, violence and other social disorders, is on the increase. There is much that our society needs to learn from them before they are destroyed by contact with us. □

John Ebling is Professor of Zoology in the University of Sheffield, UK.

Ecological view of marine animal diseases

R.J. Roberts

Diseases of Marine Animals. Vol.1. Edited by O. Kinne. Pp. 466. (Wiley: Chichester, UK, and New York, 1980.) £25, $73.15.

BECAUSE of the span of our knowledge, and the complexity of the subject, pathology books are nowadays generally multi-author volumes which deal with a single species (usually human beings) or even a single organ system. Comparative pathology texts are few and generally relate to specifically defined groups of economic significance such as domesticated animals or teleost fish. Only a brave, or naive, person would attempt to write a textbook covering the diseases of virtually the entire animal kingdom in so far as it inhabits the marine environment. Surprisingly this brave man is not Otto Kinne, whose name appears as editor on the cover of this first volume in a series of four, but one G.H. Lauckner who has apparently been responsible for the entire content of all four volumes apart from the two very general introductory chapters. He appears to have received less than adequate credit for this mammoth task.

Dr Kinne is a distinguished marine ecologist and in the foreword to this first volume he gives his view that disease is primarily an ecological phenomenon. This is a very different attitude to that of the majority of comparative pathologists and, I suspect, of commercial aquaculturists and fishery biologists as well. It is true, however, that marine ecologists have too often focused exclusively on holistic ecosystem properties and food-web interrelations in ignorance of the impact of diseases on populations. It is a stated aim of this series to synthesize all of the information available to allow the ecological significance of diseases in the marine environment to be appreciated.

This first volume covers the lower invertebrates, ranging from the Protozoa to the Gastropoda. These are the groups covered by the smallest amount of published literature in comparative pathology, and thus for many of them the scarcity of documentation is perforce out of all relation to their importance to the marine ecologist. This is no fault of Dr Lauckner's but it does impede the objective of helping biologists to give disease its appropriate place within the marine ecological model.

Since very few of the invertebrates covered in this volume are cultured, or even fished, the economic incentive for the detailed scientific study of their diseases has been absent. Most of the records of such diseases are one-off observations rather than systematic studies and often even Dr Lauckner is unable to do more than detail the paucity of available information.

Although the book is well produced and beautifully printed, most pathologists (though not, I suspect, parasitologists) would jib at the extensive use of line drawings rather than photomicrographs in all but a very limited number of instances.

The gathering together of such a mass of information, often related only by its ecosystem, and its synthesis into a review of this magnitude indicates great determination. As a source of information for scholars of a wide range of subjects it will be invaluable. I doubt, however, if it will substitute for a specific monograph on any of the groups covered. It is neither specialized enough nor complete. I do expect, though, that the complete series will find its place in any library attempting to cover the field of marine biology. □

R.J. Roberts is Director of the Institute of Aquaculture at the University of Stirling, UK.

An 'axiomatic' approach to quantum mechanics

J.L. Martin

Quantum Mechanics. By A. Böhm. Pp. 522. (Springer: Heidelberg and New York, 1979.) DM 58, $31.90.

IN WRITING about quantum mechanics, where does an author begin? There are several possibilities. He may struggle through the historical development of the subject, with all its gropings and false starts — excellent in its place, but not in a standard text. He may begin with elementary physical examples, and using a judicious mixture of assertion, intuition, correspondence principle and Ehrenfest's theorem — uncluttered with too much mathematics — attempt to lead the reader into a 'feel' for the subject. Or he may adopt an 'axiomatic' approach: 'Here are the rules; where do they lead?'. The trouble with this last option is that the reader who is looking for enlightenment may have to journey for too long in the dark before the dawn of what it is all about.

This is an 'axiomatic' book, and I would hazard the opinion that it is not for the physicist — not even for the theoretical physicist — but for the mathematician who is already familiar with the basic structure of quantum mechanics. Moreover, the selection of topics obviously reflects the author's personal interests to a degree; thus I find it difficult to recommend the book as a text, as the coverage is so uneven. It may well be useful to anyone with an interest in the mathematical aspects of quantum mechanics, developed from a particularly algebraic point of view. (The very first mention of a physical system, p.10, runs: "The mathematical image of a physical system is an operator *-algebra in a linear scalar-product space $\mathscr{H}$". This sets the tone of the book as a whole.) The reader who wishes to learn to use quantum mechanics as a tool will be disappointed; a glance at the problems at the end of each chapter will confirm this. Compare them, for example, with those in classics such as Schiff (*Quantum Mechanics.* McGraw-Hill: New York, 1968).

In reading the book, I felt I was listening to the lectures. The presentation in parts was too discursive and rambling for my taste: after all, the reader can re-read the text if he needs to, and writing a book is a golden opportunity to tighten up a lecture style into something more terse and tidy, in which the wood can be seen in spite of the trees.

There are many small and usually unimportant misprints which betray a lack of care at the proof-reading stage — "communication relations" (p.41); in the index under "Selection rules", "hydrogen bomb" should surely be "hydrogen atom". And by the way, the Argand diagram was not introduced to help us understand the scattering amplitude. Jean Robert Argand did his work in 1806! □

J.L. Martin is Reader in Physics at King's College, University of London, UK.

Controversial view of primate evolution

R. D. Martin

Evolutionary History of the Primates. By Frederick S. Szalay and Eric Delson. Pp.580. (Academic: New York and London, 1980.) $48, £31.20.

THERE has been a great proliferation of research into the evolutionary radiation of the primates over the past 15 years. Reanalysis of the evidence has benefited from new palaeontological work, from a virtual explosion of new information on living primates (notably including biochemical data) and, above all, from reassessment of the methods used to infer phylogenetic relationships. As primate palaeontologists, Frederick Szalay and Eric Delson have both made significant contributions in the first of these areas, and *Evolutionary History of the Primates* is accordingly an authoritative and competent guide to the great array of recognized primate fossils.

A brief introduction includes, among other things, a handy chronological catalogue of known primate fossil sites and a simple outline of primate molar tooth morphology. The methods used for inferring evolutionary relationships, which owe much to Hennig, are touched upon; but this all-important aspect should have been discussed in full detail, especially since the authors themselves admit to a divergence of opinion. The bulk of the book consists of a systematic survey of primate groups, with notes on extant forms and extensive, well-illustrated descriptions of the fossils. In this respect, the book will undoubtedly serve as a valuable reference source and its usefulness is enhanced by a selective bibliography and a glossary of terms. Numerous good-quality scaled photographs combine to make this the most comprehensive primate fossil guide available to date, and it is to be recommended to anyone with an interest in primate evolution.

A sharp distinction must be drawn, however, between the mere description of fossil primate material and its interpretation within a comprehensive evolutionary framework. A severe limitation of this book lies in the exclusion of virtually all information other than that derivable from teeth and bones. It is particularly surprising that there is barely a reference to the evolution of the primate brain, since endocasts are now available to document fundamental features in numerous fossil primate species. In their introduction the authors accept that the reliability of phylogenetic inferences increases with the scope of the data analysed, yet they ignore or even discount out-of-hand much relevant information (e.g. immunological data) derived from living primates. A proper synthesis of both palaeontological and neontological data must be achieved before maximal accuracy can be expected.

The rationale underlying the classificatory scheme used in the book is also inadequately explained. In places, new taxonomic groupings have been established as direct concomitants of the authors' personal hypotheses regarding evolutionary affinities, whereas elsewhere this strict Hennigian approach has not been followed. Some innovations have much to commend them; others will generate little but confusion. It is probably a wise move to erect a separate suborder Plesiadapiformes to accommodate *Plesiadapis* and its apparent relatives, thus emphasizing the enormous morphological gulf between these early Tertiary forms and the "primates of modern aspect" (Simons). Indeed, it is by no means certain that the plesiadapiforms exhibit anything other than convergent dental and basicranial similarities to the more obvious primates.

On the other hand, there are several taxonomic changes which could well have been omitted without in the least detracting from the authors' provisional evolutionary hypotheses. Szalay and Delson do not combine all of the primates of modern aspect (their "euprimates") into a formal taxonomic category, despite abundant evidence that this is a monophyletic grouping, so it is difficult to see why other classificatory novelties were required. Two examples illustrate the problems. Firstly, in line with a few other authors, the lemur family Cheirogaleidae has been moved from the superfamily Lemuroidea (containing all the other Malagasy lemurs) to join the Lorisidae in the superfamily Lorisoidea. Szalay's interpretation of certain morphological evidence, which is shared by some but has been disputed by others (and which is in direct conflict with available biochemical evidence), suggests a recent common ancestry for cheirogaleids and lorisids. Whether or not this hypothesis proves to be tenable in the long term, the immediate practical outcome of the taxonomic upheaval is that the term 'lorisoid', which has had a distinct and useful meaning for decades, has been rendered ambiguous. According to which classification one now follows, the word 'lorisoid' may or may not subsume the mouse lemurs and their relatives. Similarly, Szalay and Delson have reduced the marmoset and tamarin group from family level to the tribe Callitrichini and have lumped them together with *Callimico* and the Cebinae *(Cebus + Saimiri +* conjectured fossil relatives) into the family Cebidae. This drastic modification is based on Rosenberger's tenuous interpretation of minor dental and cranial features as "shared derived characters" linking marmosets and tamarins to cebines and is once again in conflict with immunological evidence. Henceforth, to the confusion of many involved in research upon marmosets and tamarins, the term 'cebid' might denote *either* 'all New World monkeys other than marmosets and tamarins' (this being the almost universally accepted meaning to date) *or* 'marmosets, tarmarins, *Callimico* and cebines'.

Must we pay the price of such linguistic confusion as provisional hypotheses are generated in the pursuit of a more scientific understanding of primate evolutionary history? □

R. D. Martin is Reader in Physical Anthropology at University College, and Visiting Professor in Zoology at Birkbeck College, University of London, UK.

Conformation of saturated heterocycles

A.R. Katritzky

The Conformational Analysis of Heterocyclic Compounds. By Frank Riddell. Pp. 153. (Academic: London and New York, 1980.) £17, $39.50.

THIS SMALL book will be of considerable help not only to organic and physical chemists, but also to workers in biochemistry and in other biological areas who need to understand something of the conformational analysis of saturated heterocycles. The first two chapters set the scene by summarizing the fundamental concepts on which conformational analysis is based, and then by picking out and emphasizing the differences which characterize the treatment of saturated heterocycles as compared with their carbocyclic analogues.

The remaining two-thirds of the book is organized into five chapters dealing with (1) 4- and 5-membered rings, (2) 6-membered oxygen-containing rings, (3) 6-membered nitrogen-containing rings, (4) 6-membered rings containing sulphur or phosphorus, and (5) 7-membered and larger rings. To treat this variety of topics within 150 pages, the author must of course be selective: he has rightly chosen to discuss the most important and fundamental ring systems, and thus little attention is paid to polycyclic derivatives. He has wisely decided to describe, clearly and in some detail, a smaller number of compounds rather than to attempt an encyclopaedic treatment which could have degenerated into mere lists.

The work has obviously been a labour of love; the proof-reading has been carried out excellently, the diagrams are well drawn and clear, and the book has an authoritative ring about it. Further, the subject has not been without its controversial features and on the whole the author deals fairly with these aspects. □

A.R. Katritzky is at present Professor of Organic Chemistry and Dean of the School of Chemical Sciences at the University of East Anglia, UK, but will be taking up a new appointment as Kenan Professor of Organic Chemistry at the University of Florida, Gainesville, in September 1980.

Soviet physics

A. J. Leggett

Soviet Scientific Reviews. Section A: Physics Reviews Vol. 1. Edited by I.M. Khalatnikov. Pp.305. (Harwood: Chur, Switzerland, 1979.) Dfl.125, $67.75.

THIS book is one of a new series which is intended to bring to English-speaking physicists some of the highlights of current research in the Soviet Union. This first volume contains six review articles which concentrate primarily on advances made by Soviet physicists in papers published in 1977, although reference is made to earlier, and contemporary non-Soviet, work as appropriate. The reviews fall conveniently into three groups of two papers each: Belavin (on instantons) and Zakharov and Manakov (on solitons) concentrate on mathematical developments in field theory, particularly the use of algebraic geometry, and make little if any reference to experiment; the papers by Volovik (superfluid ^{3}He) and Ivlev (nonequilibrium phenomena in superconductors) are largely theoretical but refer to relevant experiments from time to time; while those by Pokrovskii and Timofeev (exciton condensation in semiconductors) and Borovik-Romanov and co-workers (spin waves in antiferromagnets) are mainly experimental in content.

These reviews are definitely not of the type which could usefully be picked up by a non-specialist as an introduction to the subject in question. They will probably be most useful to those who, while not actively enough involved in a particular area of research to wish to spend a lot of time reading the original Soviet literature, are nevertheless close enough to it to want to keep up with important developments in some detail. For them, this book may play the role as regards Soviet physics that occasional lectures and the 'grapevine' play for much of non-Soviet research. However, although the editor states that he has tried to include "those fields in which Soviet physics is pursuing a direction of its own" it is not clear in most cases that a review covering non-Soviet (or all) work in the area would necessarily be very different in style or emphasis — which perhaps goes to show that the communication gap is not all that serious after all!

The translation is mostly of a high standard, but I hope that in future volumes the series editors will allow more time for proof-reading and also do something about the type-face used; in the present volume the symbols for italic vee and Greek nu are almost indistinguishable, which leads on occasion (e.g. p.261) to extreme confusion. □

A. J. Leggett is Professor of Theoretical Physics at the University of Sussex, Brighton, U.K.

nature

14 August 1980

Open season for nuclear diplomatists

The world's nuclear diplomatists are in for a long hot summer. Many of them, still recovering from the meeting of the UN Committee on Disarmament which ended only a week ago, will have been back in Geneva on Monday for the Second Review Conference of the Non-Proliferation Treaty, which is planned to last four weeks. Once that is over, many of the same people will be off to Vienna for the annual General Conference of the International Atomic Energy Agency (IAEA), which on past form is likely to be much occupied with the adequacy (and the cost) of the international nuclear safeguards system. This year, however, two weeks in Vienna will not for many be sufficient — they may have to stay on for the first meeting of the new Committee on Assurance of Supply, the body whose existence was decreed in June by the Board of Governors of the IAEA, whose composition and agenda are not yet decided but which could play a crucial part in helping to bolster up the Non-Proliferation Treaty. What, it is natural to ask, will this bout of activity accomplish? Will the families of the diplomatists who will thus be giving up vacations think their sacrifice has been worthwhile?

As always, it is too soon to say, but the prospects for the weeks ahead should be clarified by what happens in Geneva between now and 5 September. Inevitably, the NPT conference will be a quarrelsome affair. Many harsh things will be said, especially by non-nuclear parties to the treaty (see *Nature,* 12 June). Some will complain that the three nuclear powers which have signed the NPT (the Soviet Union, the United Kingdom and the United States) have done too little to implement their promise to negotiate measures of strategic disarmament. If Salt II were not in limbo, the nuclear powers might have been able to reply convincingly. The best they have to offer now is the tripartite report on the negotiations towards a Comprehensive Test-Ban Treaty, submitted to the Committee on Disarmament at the end of July. Plainly, there has been some progress, but a cheerful interim statement is no substitute for a treaty. That is what the non-nuclear parties to the NPT will be saying. The same states will complain that too little has been done, both by the nuclear powers and those signatories of the NPT in a position technologically to do so, to foster the development of civil nuclear power elsewhere. The nuclear powers are no doubt hoping to blunt the edge of this complaint by referring to the meeting planned for Vienna at the end of September. They must expect to have to make some promises about the scope and speed of those proceedings. But the test by which the success of the Review Conference should be judged is that of whether the non-nuclear signatories of the NPT leave Geneva having been persuaded that non-proliferation has come to stay — or at least that the present regime will last for another five years.

It is therefore important that, in at least two respects this second conference will not be much occupied with two of the issues that perplexed the first, in 1975. Then, the non-nuclear signatories of the treaty were still grumbling about its discriminatory character. Is it not an outrage, they were inclined to ask, that safeguards should be rigorously applied to non-nuclear states but not to the real black sheep, the nuclear powers themselves? The treaty has not changed in the past five years, but it does appear that all parties to the treaty have come to accept that it must be discriminatory in this narrow sense. It cannot be otherwise unless and until the nuclear powers have agreed to forsake nuclear weapons altogether. With the fate of Salt II in mind, few at Geneva will be asking for that moon now. The vigour with which they would have complained at discrimination will no doubt be diverted into the more legitimate complaint that the nuclear powers, having dragooned and cajoled non-nuclear powers into signature of the treaty, have then chosen to impose separately agreed restrictions on international trade in nuclear equipment even when the would-be recipients have signed the NPT and come to safeguards agreements with the IAEA.

The other bone of contention which has been resolved in the past five years is the issue of peaceful nuclear explosions. Largely at the insistence in the 1960s of countries such as Brazil and India (which, ironically, is not a signatory of the treaty), the NPT requires that the nuclear powers should provide, through the IAEA, peaceful nuclear explosions to those non-nuclear powers able to persuade the IAEA that they have a need of them. Mercifully, the suspicion that peaceful nuclear explosions would be an economic blessing in disguise is fast melting away. Only in the Soviet Union, where as many as eight of the 28 nuclear explosions in 1979 may have been "peaceful", does enthusiasm persist. The government of India, which used the PNE argument to justify its nuclear explosion in May 1974, has not thought it worthwhile repeating its indiscretion. The nuclear powers need not expect a drubbing at Geneva because they have not been trudging the world for the past decade, offering to blow out harbours and other holes in the ground for all and sundry.

For small mercies, the nuclear powers will no doubt be grateful. What can they say on the major issues they will be confronted with? By now, fortunately, there is enough experience of the NPT for its true nature to be widely understood. The treaty itself is no more a guarantee that anxiety about nuclear proliferation can be banished than was Prohibition a guarantee against alcoholism. From the start, the principle underlying the treaty has been that of a bargain between the nuclear and non-nuclear powers. The nuclear powers would work towards strategic arms control, the non-nuclear powers would meanwhile not embark on military programmes. The bargain is, of course, not comprehensive. China, France and India remain outside the treaty, as do a great many supposedly non-nuclear powers that are presumed to have an interest in nuclear weapons — Pakistan, Brazil, Argentina, Egypt, Israel and South Africa, for example. Worse still, some of the signatories of the NPT are rightly regarded with suspicion. Is it possible that countries such as Libya or Iraq, dutiful signatories of the NPT, have it in mind that they can use the benefits of access to nuclear technology which the treaty offers so as to build up a stock of fissile material and then simply give notice, as the NPT allows, that they are withdrawing from its provisions and its safeguards? In such circumstances, it is wisest that even the staunchest supporters of the NPT should recognize its weaknesses. The only realistic objective is somehow to contain the pace of nuclear proliferation — which, paradoxically, requires that the NPT system should be robust enough to survive the emergence of the next nuclear power, whichever it may be. At the same time, it is essential that states not yet party to the treaty should be provided not merely with a sense of pressure from the non-proliferators but also that they should be given incentives in due course to sign on the dotted line.

This is the sense in which the meeting of the Committee on the Assurance of Supply at the end of September may be crucial. Unlike the review conference of the NPT, the committee will in principle bring together all members of the IAEA, France and China among them — although nobody knows as yet which will turn up. This broadening of the scope of discussions about proliferation is greatly to be welcomed. The committee's most

0028-0836/80/330647-02$01.00

urgent task is to restore the confidence of the non-nuclear states in the willingness of potential suppliers to sell nuclear equipment and raw materials. President Carter's unilateral out-of-the-blue non-proliferation policy of 1967, and the tactless US Nuclear Non-Proliferation Act of 1968, has been the chief but not the only offender. The US Administration's difficulty in living with the Act it has sponsored in Congress (see *Nature*, 31 July) should be a sign to people elsewhere that there is no future in an agreement among suppliers to trade only with states that have accepted full IAEA safeguards. The government of France would not even consider such a proposal. The best hope for the CAS meeting is to devise incentives that will persuade states outside the NPT system that it would be in their best interests to join the club. An international convention to regulate the nuclear business on a multilateral basis, however desirable, is probably for similar reasons unattainable. Uranium banks under international auspices, or internationally managed reprocessing plants, offer more scope for imaginative negotiation. And is it too much to ask that the nuclear powers and the nuclear suppliers can use the two months ahead to repeat the message they were trumpeting a quarter of a century ago — that nuclear power is indeed a way of helping forward economic development in all kinds of states? One of the other circumstances that have changed in the past five years is that non-nuclear states are now in a mood again to believe the message.

The question remains of what the nuclear powers will have to report at the review conference about progress towards strategic disarmament. Last month's report to the Committee on Disarmament shows that the Comprehensive Test-Ban negotiations have made substantial headway toward verification. If the treaty is signed, there will be arrangements for the exchange of seismic data, a committee of "experts" to assess them and procedures for dealing with challenges raised by one party or another. So much has been agreed. So why not sign the treaty right away? That is what some non-nuclear powers will be asking in Geneva in the next few weeks. In doing so, they will enormously underestimate the problems with which the three nuclear powers are grappling. States such as the Soviet Union and the United States are considering, apparently in good faith, binding themselves to forswear the further development of nuclear weapons, thus ensuring that, in the course of time, weapons now considered central to their security will be built less confidently than at present — and are doing this while there remains no assurance that China and France would follow suit. It is a huge political enterprise — and one that may not succeed. To have travelled so far along such an unpromising road is creditable.

Putting Finniston's cart before the horse

The British government's response to the Finniston report on engineering education is best described as frivolous. That may have been inevitable. The report was commissioned by a Labour government with an earnest conviction that governments have a duty to ensure that social institutions of all kinds are well suited to their purpose. Sir Monty Finniston and his colleagues on the committee of inquiry, set up in 1978, responded with gusto to the implicit invitation to reconstruct the whole pattern of engineering education. They were nothing if not radical. They set out to diminish the influence of the engineering institutions by proposing that there should be a new body, called the British Engineering Authority, to be responsible both for the certification of professional engineers and the validation of engineering courses, in universities and elsewhere in higher education. The committee also asked for changes in the educational system itself; engineering students would follow courses much like those now available, but with more work experience, but a minority would stay on for an extra year and come away with a higher qualification. The underlying objective of the Finniston Committee was to enhance the reputation of engineers in British society as a whole, whence (in part) the proposals that the state should pay larger stipends to engineering students than to others, that public authorities should not let contracts without insisting that only registered engineers are employed on them, and that properly registered engineers should be entitled by statute to regular periods of sabbatical leave (admittedly in the good cause of continuing education). Looking back over the past two years, and at the host of these fondly conceived but now stillborn proposals, the committee will no doubt rue its bad luck. It has fallen to a non-interventionist government, and to the most zealously non-interventionist minister of that government (Sir Keith Joseph) to respond.

An engineering authority of some kind will indeed come about, but not yet and not in the form the Finniston Committee asked for. Certainly it will not be the body "with teeth" that Sir Monty Finniston and his colleagues have been asking for since their report was published. Instead, the Privy Council (which can grant Royal Charters and thus legitimize the activities of non-governmental public bodies, universities for example) will be asked to set it up. The government will appoint the first slate of members, and help with petty cash for the first year or two. After that the authority will be expected to make its own way in the world, persuading universities that it is in their interests to have their courses validated by the new organization, qualified engineers that they had better be registered under the new rules (still to be written) than with the existing engineering institutions and employers that the new certificate of registration is a worthwhile professional qualification. The prospect is daunting. There is a high chance that the new authority will be no more successful than the Council of Engineering Institutions, set up for similar purposes by the engineering institutions themselves (and which, apparently, will continue to exist, no doubt sniping from the wings from time to time). Many will say that it would have been better not to have had an engineering authority at all than to have so willingly courted the chance of failure. And that is the sense in which the government's decision is frivolous. For whatever the faults of the Finniston proposals, and there are several, the new arrangements are certain to be regarded — as was the Finniston Committee itself — as the best hope for the improvement of the engineering profession. Once the new authority exists, it will for a time at least tend to stifle other instruments of change.

This is a sad solution to have been wrought from the widespread recognition, in the past few years, that something should be done to change the pattern of engineering education and professional recognition. The explanation seems to be that first Finniston and now the government have put the cart before the horse. The most urgent need is for a more imaginative experiment in engineering education in the universities, and for level-headed evaluation of the consequences. Everybody accepts that intending engineers, like intending doctors, profit from first-hand knowledge of the problems with which they will have to deal in later life. There is, however, no assurance that the pattern of four-year courses now being tried out in English universities (and which Finniston endorsed) will be a substantial improvement on the present. To the extent that these courses will continue to skimp on basic science, the result may well be engineers whose education is more expensive but who are no better fitted for the needs of modern industry. For the truth is that a profession such as engineering should be a cadre of people with very different backgrounds and skills. The objective would have been better served if the government had encouraged the universities, through the existing machinery of the University Grants Committee, to develop courses that differ among each other but which collectively mightyield the diversity the profession needs. The trouble is, of course, that such a development would require extra funds for the universities. This is hardly the time to be asking for more.

Another violation of NIH guidelines

Washington

Cross-contamination between vials containing viruses being transported from Britain to California may have caused a San Diego scientist inadvertently to carry out experiments prohibited under the National Institutes of Health's guidelines for recombinant DNA research. This, at least, is the "working hypothesis" which Dr Samuel I. Kennedy, of the University of California at San Diego, offered last week to explain what may prove to be the third violation of the guidelines.

Dr Kennedy, who moved to California from the University of Warwick in 1977, has been studying the activity of several arboviruses. In particular, he has been looking at the ways in which virus reproduction is inhibited by naturally produced "defective interfering particles" containing only a fragment of the virus genetic material. Earlier this year, Dr Kennedy and his research assistants cloned what they thought were subgenomic fragments of the Sindbis virus, a cause of fever and skin rash carried by mosquitoes in parts of Africa, India and Australia.

Following "confusing" results of attempts to characterize the nucleotide sequences in the resultant recombinant DNA produced in disabled *Escherichia coli*, the cloned material was sent to the Public Health Laboratories in Berkeley for analysis. There it was discovered that the cloned fragments appeared to have derived not from Sindbis virus but from Semliki Forest virus, another arbovirus being studied in Kennedy's laboratory.

This raised difficulties, for although the Sindbis virus has been classified by the Center for Disease Control (CDC) as a Class 2 agent — which under the NIH guidelines could be cloned under P2 physical containment conditions — the classification of the Semliki virus was ambiguous.

Until recently, the Semliki virus, known primarily as a cause of headaches and fever, was considered even safer to work with than Sindbis virus. Three years ago, however, a German research worker died after being infected by a wild-type strain of the virus. As a result of this incident, CDC is considering classifying the Semliki Forest virus as C3, although subject to certain qualifications.

At the end of last month, NIH announced changes in their guidelines to allow viruses in this class to be cloned under P3 containment conditions. However, at the time when Dr Kennedy's experiments were carried out, the cloning of C3 agents was prohibited.

As soon as the university suspected that the NIH guidelines might have been violated, both the Institutional Biosafety Committee and the NIH's Office of Recombinant DNA Activities (ORDA) were informed. ORDA is now carrying out an investigation, and will eventually make recommendations to NIH Director Dr Donald Fredrickson on what action should be taken.

The ORDA investigation seems likely to concentrate on three aspects. First, how could the confusion between the two types of virus have occurred and was this the result of cross-contamination during transit from research laboratories in Britain?

Second, ORDA must determine what classification it would have given to the Semliki Forest virus if a cloning application had been made at the beginning of the year. Approval as a Class 2 agent would have permitted the experiment; approval as Class 3 would have disallowed it. This problem is complicated by the fact that CDC classification of arboviruses is under revision. A European scientist was told by NIH earlier this year that although the Semliki virus would probably be considered to fall within Class 3, in certain geographic locations and conditions of use it might be considered C2, permitting cloning under P2 containment.

Finally, ORDA will be looking closely at the procedures followed by Dr Kennedy and the university once a violation of the guidelines was suspected. Dr Kennedy stopped work on the cloned fragments, and informed the Institutional Biohazard Committee of the apparent mix-up, as soon as the results of the laboratory tests were received at the end of last month. Some of his graduates students, however, had previously approached the head of the biology department, Dr Donald Helinski, expressing concern about preliminary results and taking a different view of the actions that ought to be taken.

Both university and NIH officials stress that there was no public hazard involved. "We were not even cloning the entire genetic information in the virus" says Kennedy, pointing out that even if it was Semliki virus, the guidelines allow this to be safely cloned under the P3 containment conditions that were in fact used.

The biggest impact of the incident is likely to be on public perception of how the guidelines are working. Since the NIH guidelines were introduced in 1976, there have been two reported violations. In one a scientist from the Harvard Medical School carried out experiments without the necessary prior clearance from NIH. In the other, San Francisco scientists conducted experiments with a plasmid vector before it had been officially approved.

David Dickson

Small beer for scientists

Scientists working for the British Civil Service are unlikely to be satisfied by the outcome of the arbitration on salary scales for 1980, which was completed last week. After the arbitration award was made known, Mr William McCall, General Secretary of the Institution of Professional Civil Servants (IPCS), said that the outcome was disgraceful and that "if this is what the system now in force for settling the pay of scientists in the Civil Service produces, then the system will have to be changed".

There have been several bones of contention between the IPCS and the Civil Service Department since the first offer of salaries for 1980. The department's proposals (see *Nature*, 24 July) were especially mean to the higher grades of the scientific Civil Service — those in the grade of Senior Principal Scientific Officer were, for example, offered no increase except the annual increments to which they were contractually entitled.

The IPCS has complained consistently that the device of pay research for relating the salaries of higher civil servants to those of comparable groups of workers in the private sector undermines the principle that scientists within the Civil Service should be paid the same as other civil servants of comparable rank and that, in any case, the data on salaries earned by scientists in the private sector are insufficient as an accurate foundation for pay research.

The Civil Service Arbitration Tribunal appears to have gone only a little way to meet these protests. The salaries of Senior Principal Scientific Officers will after all be increased by 3.2 per cent in 1980 compared with 1979, taking the maximum salary in this grade to £16,250 a year, compared with the claim by the union for £18,248.

The salaries of Principal Scientific Officers, which ranged from £8,613 to £11,343 at the beginning of the year, are to be increased to between £9,690 and £12,540, figures which are increased by between 1.5 per cent and 4.1 per cent as a result of the tribunal's intervention.

Scientific Officers, earlier in the year earning between £6,332 and £8,705, are now to receive salaries increased by between 20 per cent (at the bottom of the scale) and 10 per cent (at the top). The salaries of lower grades will be increased by proportions not very different from the rate of inflation.

Even so, this will not go far to meet the complaint that the salaries of scientists in the Civil Service are less than those of people of similar rank — Principal Scientific Officers will, for example, be paid £1,260 a year less than Administrative Officers.

The reason why the arbitration tribunal made this new award are not known, and may never be, although a report on the issue will be published next month.

0028-0836/80/330649-01$01.00

Nuclear Iraq

Perrin protests

Anxieties about French nuclear collaboration with Iraq have now burst into the open. Last week, the grand old man of nuclear power in France, Francis Perrin, contradicted his government's statements about the supply of a research reactor and highly enriched uranium to Iraq, in a deal to exchange oil for technology. "It cannot be said", Perrin argued in an interview with *France-Soir*, "that the provision of this reactor will not enable a country like Iraq to produce an atomic weapon in a few years' time".

Without addressing the question directly, however, the French government had earlier insisted that its cooperation with Iraq is directed to "perfectly legitimate ends", and that the agreement is also covered by guarantees. The government said it was "astonished" at the accusations that had been made against it, and asked by what principle Iraq's right to nuclear power could be refused.

Perrin, who was president of the Commissariat à l'Energie Atomique from 1951, and who was confirmed in that post by President de Gaulle in 1960, does not believe that nuclear peace and war can be separated so neatly. He believes it unlikely that Iraq would directly divert any part of the 11-kg charge of 93 per cent uranium-235 to be supplied by France, for this would fly directly in the face of too many international agreements. "But evidently, if Iraq trains personnel with this reactor, they could prepare plutonium by irradiating [unenriched] uranium." This plutonium might be prepared initially for research; then, when they had enough plutonium and technicians, they could break their agreement (under the Non-Proliferation Treaty, which Iraq signed in 1969) not to build weapons.

The controls of the International Atomic Energy Agency — which requires monthly flow-sheets of fissile materials belonging to NPT signatories, and whose inspectors make regular visits to their nuclear establishments — are effective, says Perrin, but a country can always decide to reject them.

Iraq already has a small Soviet reactor, using 80 per cent enriched fuel, under IAEA safeguards. The details of the new French reactor have not yet been received at the IAEA, but the safeguards provisions require that they should arrive more than six months before the reactor is charged with fuel. Charging is, however, unlikely before the end of 1981, the date set before Iraq's chief nuclear expert, Yihya al Meshad, was murdered in Paris on 13 June. It is, however, known that the reactor will be based on the French 50-MW thermal reactor Osiris at Orsay, which takes a charge of 9½ kg of 93 per cent uranium-235. Osirak, the Iraqi version, is planned to be slightly bigger — 70 MW with an 11-kg charge.

Italy is also supplying nuclear facilities to Iraq in exchange for oil, including an isotope laboratory with a hot cell which in principle could be used for reprocessing and plutonium separation but, says the Italian government, it is much too small to have a bearing on weapons production.

President Saddam Hussein of Iraq has rejected all speculation that Iraq may be building a weapon, and has pointed out that Israel is generally regarded as already having the bomb, and has never signed the NPT. "Other countries" said an IAEA spokesman "have been less cooperative than Iraq".

President Hussein, with a $75,000 million five-year plan, also dreams of a technological transformation of his country, and recognizes that Iraq's principal need is technically trained manpower. He believes that Osirak will contribute to such a pool. Now that Iraq is increasingly turning from its East European and Soviet partners towards OECD countries for technology, it may be wise to take Hussein seriously.

Troubled seer

Robert Walgate

Remote sensing

Going private?

Washington

Fierce arguments have been generated in Washington by plans under discussion in the Carter Administration to create a fully operational system from the remote-sensing satellites developed by the National Aeronautics and Space Administration.

Few challenge the idea that responsibility for remote sensing should eventually pass to the private sector, but there is disagreement about the pace at which the transfer should occur and the degree of control which the federal government should retain.

Responsibility for coordinating the transfer from NASA to the private sector has been given to the National Oceanic and Atmospheric Administration (NAOO). The NAOO proposes a two-stage process, involving an initial stage for developing the sensor technology, that would extend to the end of the decade, before a fully operational system would be available for private use.

Several companies, keen to establish themselves in a potentially lucrative market, argue that this time scale is unnecessarily slow. In particular, executives from the Comsat Corporation, which has already successfully taken over responsibility for telecommunications satellites, are arguing that it could start doing the same for remote sensing by 1983.

The temptation to use telecommunications as a model for successful commercial exploitation is strong, but remote sensing is likely to have a rougher ride. The market is undeveloped and heterogeneous.

Thus at a Senate hearing two weeks ago, a spokesman for the National Governors Association said that the remote-sensing system "should be considered in the same context as census, cartographic, geological and meteorological data which are provided as a public service of the federal government".

Aware of this public responsibility, NOAA is considering two ways of allowing federal agencies to buy data under guaranteed purchase contracts. One would transfer responsibility for this entirely to a private corporation, the other would set up a new "for-profit" corporation with both privately and publicly appointed members.

The cost of remote sensing is another problem. According to NOAA administrator Dr Richard Rank, the remote sensing system will probably not be self-financing until the end of the century, and thus will rely on subsidy for the foreseeable future.

But there will still be a temptation to maximize returns, even in the early stages, and state governments are worried that high prices could discourage potential state and local government users from even exploring the potential usefulness of Landsat data, particularly if — as NOAA has suggested — experimental data during the interim period are priced the same as operational data.

Excessive pricing could also have important international implications. Some countries could complain that they are unable to afford information about their own natural resources which can be bought on the open market by multinational mining corporations. The State Department accepts the principle that prices should be consistent for both domestic and foreign users, but warns that price increases should be gradual so that foreign users can adjust to them.

Present users are, however, more concerned at the quality of the service. NASA now has two Landsat satellites in orbit, but both are having problems which have restricted the amount of data being received. Unexpected difficulties have also arisen in the next satellite, Landsat D,

0028-0836/80/330650-02$01.00

scheduled to be launched in 1982. Development of the instrument called a "thematic mapper", and intended to provide direct information on crop differentiation, is so much delayed that Landsat D may have to be launched without it.

The delays in both technical plans and administrative arrangements have created inevitable frustrations. Those who have already experienced the benefits of remote sensing technology are keen to exploit it as rapidly as possible, and are already hinting that they may look to other countries — such as France and Japan — as an alternative source of remote sensing services. Moreover, some members of Congress claim that the delays reflect a general lack of imagination in the White House about the US space effort.

NOAA is at present working out the details of the transition plan in preparation for its submission as part of the 1982 budget request early next year. It seems more likely to include only limited private involvement — perhaps restricted to processing and marketing the data produced by federally operated satellites.

David Dickson

Lords committee

Dumping ahead

The House of Lords Select Committee on Science and Technology embarked on its summer break last week with the promise of a new inquiry in October into the disposal of hazardous waste. The inquiry will be the committee's second quick investigation — the report of the first, on electric vehicles, is due to be published at the beginning of September. A longer investigation of forestry in the United Kingdom will continue until the end of the year.

The suggestion of an inquiry into hazardous waste disposal came from Basildon District Council in Essex, where a large proportion of Britain's toxic industrial waste is dumped. When the House of Commons Select Committee on the Environment declined to take the matter up because of other commitments, the Lords committee stepped in, believing the topic to fit well into its remit of investigating areas of science and technology of public concern.

The worry of Basildon District and Essex County Councils is that there is no coherent national policy for hazardous waste disposal, largely because the relevant section of Part II of the 1974 Control of Pollution Act has never been implemented. The councils also believe that Essex has become a main centre for hazardous waste disposal by historical accident rather than for good practical reasons.

Dumping at Pitsea

The government has laid down guidelines for dealing with the disposal of hazardous waste but no regulations as to who should be responsible for arranging disposal. The 1974 Act says that local authorities should take that responsibility and should inform the Secretary of State for the Environment of the arrangements they have made. The Act empowers the Department of the Environment to bring these and other provisions (affecting water quality, for example) into force when it chooses. So far it has chosen not to do so, allegedly on the grounds of cost. Redland Purle, Britain's largest waste disposal company, owns the country's largest dump at Pitsea in Essex. The council has power to monitor the sites and has taken measures to restrict the quantities dumped, but it would take other local authorities to take some of the load.

The Lords committee will no doubt be looking at the institutional arrangements for coping with hazardous waste. It also intends to investigate the basis for some of the technical arrangements, for example the criteria used for choosing suitable sites and deciding what can be dumped where. The Select Committee hopes the inquiry can come to grips with new methods of disposal and suggest how more use could be quickly made of them.

Judy Redfearn

Energy alternatives

German plans

A West German commission on "future nuclear energy politics", set up two years ago by the Bundestag to resolve the nuclear question, has reached its eagerly awaited conclusions. They are equivocal.

West Germany should shelve a final "decision" on nuclear power until 1990, says the commission. But in the meantime the country should build as many reactors as it needs, provided it makes due effort on the development of coal, conservation and renewable sources.

The all-party parliamentary commission, consisting of seven members of the Bundestag and eight technical experts from industry, environmental groups and the trades unions, considers that it will be impossible to judge — for ten years — whether nuclear energy should be expanded in Germany. The growth rate of electricity consumption, the effectiveness of conservation measures and the impact of renewable energy are too uncertain to make commitments to any particular source.

The commission does however spell out its demands for immediate and increased government powers to enforce energy conservation — the abolition of mileage rates for business cars, an energy tax, more bicycle paths and tighter controls on insulation standards in new homes and factories. The commission also asks for an "energy service" to provide, free of charge, an infrared survey of buildings to show where the heat leaks out. These and other measures have been described by the Christian Democratic Union, the main opposition party, as introducing "a totalitarian energy conservation state".

Elsewhere, the recommendations have been seen as vague and offering all things to all men — especially with the recommendation that reactors should be built if energy demand requires them. The major nuclear construction company in Germany, Kraftwerk-Union, has argued that it will be running out of work in 1983 — it has lost its contract for four reactors in Iran, and there is doubt as to whether Brazil will take up its full option for eight. Thus some suggest that a construction programme of one or two reactors a year over the next decade, a programme similar in its scale to the British, is quite consistent with the commission's view.

At the same time, the report has bee interpreted by environmentalists as recom mending a further delay in the country' nuclear development. (Germany now h five power reactors above 500 MW electri in total 15 reactors produce about 9 GW It is not surprising that the commission h been represented in the German press a man wearing two badges, one say "nuclear no thanks" and the ot "nuclear power — yes please".

The forthcoming October gen

0028-0836/80/330651-02$01.00

election may have played some part in the commission's equivocation: there has been an understanding among the parties that nuclear power should not be an election issue. The debate on the report was eclipsed the same day by another on Chancellor Schmidt's visit to Moscow.

The commission also recommended that it should reconstitute itself after the election, to complete its task. It was set up in December 1978 after a lengthy debate on the future of the Kalkar 300 MW prototype fast breeder, now under construction. It was decided then to construct Kalkar, but not to charge it with plutonium until expert advice had been received on Germany's need for a "plutonium economy". The nuclear energy futures commission was set up to provide that advice, but (beginning work in 1979) it decided that there was not time before the election for such a broad investigation. Hence the fast breeder is not mentioned in the commission's recommendations.

The result is that Germany remains without a strong federal lead on nuclear power. It will remain so until the majority of the ruling coalition — only ten in the present Bundestag — cannot be threatened by the strong minority in the coalition which will always vote against nuclear development.

The election is thus critical for nuclear energy, despite the parties' intention to keep it out of the limelight. A number of decisions await a nuclear majority, not the least of them the location of intermediate storage facilities for spent fuel. The CDU Prime Minister of West Saxony, Herr Albrecht, where the Gorleben salt-dome offers a potential long-term geological store, is hoping to give hospitality to the waste after the election. Other current battles (against environmentalist opposition) such as that to increase the density of spent fuel storage, by a factor of four, on reactor sites, by inserting cadmium sheets between the rods to absorb neutrons, may be more easily won if a federal government is returned which can give a more definite "yes" to nuclear power.

Robert Walgate

Pesticide safety

No numbers

Washington

Stepping out of line with the fashionable wisdom — at least among congressional egislators — a little-noticed report from he National Academy of Sciences has ome out with some harsh words about the angers of squeezing data on the health ffects of agricultural pesticides into a neat ost-benefit mould.

The report was prepared by a committee the academy's Environmental Studies Board as a follow-up to earlier studies by the Environmental Protection Agency (EPA). In general it supports the agency's concern that environmental regulations should be as explicit, and as well quantified, possible.

It also points out, however, that in attempting to produce legally defensible decisions, agency administrators often underplay the uncertainties and qualifications that surround scientific assessments of risks and benefits, particularly of human morbidity and mortality data. Here, the report says, quantification is carried to "unwarranted extremes".

According to the committee, present understanding of cancer development "does not permit us to draw reliable numerical inferences from the kind of laboratory data normally available about the effects of pesticides and other compounds on the development of cancers in humans".

There is therefore a danger, it says, not only of overestimating risk by the use of too conservative assumptions, but also of underestimating it by neglecting potentially important factors. "We say the error can go either way" said committee chairman Professor Robert Dorfmann of Harvard University's department of economics.

The committee therefore recommends that the EPA abandons its attempts to produce numerical estimates of the impact of pesticide use on human health except where reliable epidemiological data are available. Instead, it proposes the use of "a carcinogenic activity indicator" as a measure of relative carcinogenicity of chemical compounds. This would be based on the results of laboratory bioassays.

In addition, to underscore the uncertainties in risk evaluation, two figures are proposed for every risk estimate. One would be a measure of "most probable" risk, conveying the analyst's best judgement of the level that would be realized in assumed conditions. The other would be a "maximum plausible" estimate taken as the upper limit of a 90 per cent confidence interval.

The EPA has made no official comment on the report. The agency is involved in reviewing its procedures for weighing the risks and benefits of pesticides in the light of recent administrative changes.

Its review could be influenced by an unintended consequence of the new report. As part of its analysis, the committee carried out a detailed review of chlorobenzilate, using its recommended procedures to produce its own assessment of the risks and benefits. Comparing its evaluation with that obtained by the EPA in 1976, it concluded that not only had worst-case estimates of exposures used to assess health risks been highly improbable, but also that the economic benefits of using the pesticide — particularly the costs of not using it — had been wildly overestimated.

When a draft version of the rep circulated last year, these discre were seized on by the Environ Defense Fund (EDF) to challen EPA's decision to allow limited us pesticide. However, an admini court in Washington has since rul the EDF had no legal standing to ta in EPA's rule-making proc Nevertheless, this could have sig impact on rule-making in the agenc in the past many of the restricti pesticide use have followed ch from the EDF and other s environmentalist groups.

David D

Russian plate tectonics

Drift of change

"Plate tectonics" and "cont drift" have been dirty words to or Soviet geophysics for many ye orthodoxy being, in this case, lai not by Party doctrine but by the p views of Academician Belouso acknowledged head of the geophysical establishment. Rather themselves be shut off fro international scientific community, the Soviet biologists in Lysenko Soviet geophysicists have become a inventing semantic variants s "ocean-floor movement" under they can discuss the proscribed ide

These strategies have been used, most part, strictly within the ac community, and it was only on ext rare occasions that any mention wa of such concepts in the general pres such was the announcement that ow crustal movements the BAM Baikal Mainline railway, would be completed, 50 cm longer than ori planned.)

Now, however, an official of the Academy of Science's Instit Archaelogy has given what amoun press conference on continental d though without mentioning an troversial terms. Describing a new the lithosphere under thw world prepared by the Institute, the explained to a TASS corresponde "the lithosphere is thinnest in the ce the oceans where median oceanic pass" and that "it is precisely in thos that the lithosphere is formed."

Information on the thicknes structure of the lithosphere und oceans is therefore "important for many theoretical problems", in par for understanding the process of for of our planet".

Ve

Vietnam in space

Queue-jumping

The recent 8-day sojourn of Vietnamese cosmonaut Pham Tuam aboard the Salyut-6 space station marked a significant change in the Comecon Interkosmos joint space programme. For the first time the non-Soviet participant came from a developing and non-aligned country — a point which both the Soviet and Vietnamese press agencies stressed at the expense of comment on the scientific content.

Phan Tuam's flight, moreover, meant a change in the projected running order of participation, which, most Baikonur watchers had accepted, was related to the size of the contribution the various countries had made to the earlier unmanned stage of the Interkosmos programme (the Interkosmos satellites and Vertikal high-altitude probes). In effect, this meant that the European nations of the bloc would go first, with Cuba and Mongolia bringing up the rear. Vietnam, which joined Comecon in summer 1978, long after all the other members had their cosmonaut candidates installed at the Gagarin space centre, seemed destined for the final place in the programme.

However, with four countries still to go (Romania, and the three non-European members), Vietnam was unexpectedly advanced three places. Both TASS and VNA stressed unequivocally that that there were political implications in this move. Whatever the reason for the changed schedule, however, the interesting question remains: what, precisely could Vietnam contribute to the space programme?

It would be incorrect to suggest that the developing members of Comecon — Cuba, Mongolia and Vietnam — have nothing to offer the Interkosmos programme, or at the most can offer only sites for tracking stations. As early as 1978, the Polish cosmonaut Miroslaw Hermaszewski said that Cuba and Mongolia were working on their experimental programmes for when their turns came. (At that time, Vietnam had still not joined the Interkosmos programme.) Pham Tuam's programme, as reported to date, corresponds remarkably well with those of the other non-Soviet cosmonauts.

First, and inevitably, came the medical programme, the testing of cardiovascular and lung functions under zero gravity. Then, equally routine, experiments on semiconductor crystal growth — in this case, gallium phosphide and a triple bismuth-antimony-tellurium compound. These experiments use a Soviet furnace aboard Salyut-6, but the test capsules come from the non-Soviet participant, which also provides a suitable symbolic name for the project — Morava for Czechoslovakia, Berolina for East Germany and so on. This time, it was Halong, after a gulf in Vietnam.

Not surprisingly, the regular photographic and visual observations carried out from Salyut were given a Vietnamese slant. Silting up of the river mouths, and the effect this has on fish feeding habits, observations of tidal flooding and erosion, and hydrological surveys of the Mekong and Red River Basins were especially stressed. And, most Vietnamese of all, Pham Tuam had taken along samples of azola water ferns, fast-growing, nitrogen-rich plants which are traditionally used as fertilizers for the growing rice crop, and which could prove useful aboard future permanent space stations.

Comecon doctrine concerning its third world projects (including its own three "developing" members) firmly eschew the concept of "aid". All such undertakings are termed "cooperation" projects, although recent bilateral scientific-technological cooperation deals signed between Vietnam and, for example, Czechoslovakia and East Germany consist largely of the European partner providing experts and know-how, and Vietnam reciprocating with raw materials. Nevertheless, no attempt has been made, as far as Interkosmos is concerned, to present the joint Soviet-Vietnamese flight as a partnership of technological equals. While by no means a passenger, Pham Tuam characterized his role rather as a harbinger of things to come. "It is a new demonstration of the effective cooperation within the socialist community", he said before embarking, which "will also demonstrate the abilities of the Vietnamese people".

Vera Rich

Shuttle for orbit

The US National Aeronautics and Space Administration has screwed up its courage and settled on a launching date for the first orbiting version of the space shuttle — March 1981. The decision was taken at the end of last month and in the face of the setback a few days earlier when a fire damaged a shuttle engine during a test firing in Mississippi.

The decision follows a week-long review of the recent ups and downs of the development of the shuttle, and has apparently been taken in the belief that only a tight schedule will sufficiently concentrate the minds of those involved in putting the first shuttle (called Columbia) into an Earth orbit.

The timetable now agreed would move Columbia from the building it now occupies at Cape Canaveral to the shed in which it will be mated with the solid fuel boosters on 23 November. Thereafter it will be mounted on its launch pad and the main engines of the shuttle will be fired for a period of 20 seconds some time in February. Thereafter, there will be five weeks to the final launch date.

Although anxiety persists about the tiles intended to provide thermal shielding for the shuttle, it has apparently been decided not to encumber the first flight with the "tile repair kit" intended to enable the crew of the shuttle craft to replace damaged tiles in flight.

Airport noise

London's out

The Noise Advisory Council (NAC) has provided some timely ammunition for the opponents of the plan to build the third London Airport at Stansted in Essex. Last week, hard on the heels of the formal application for permission to develop the airport by the British Airport Authority, the council announced that the Stansted site will be marginally more of a noise nuisance than the other five sites on the airport authority's short-list.

The application for development permission has gone to the Essex County Council. There will be a public inquiry on the proposals, probably early next year. That will be the second occasion on which the people of Stansted have been divided into hawks and doves.

Choosing a site for London's third airport has already taken 27 years. The chief problem has been that cost-benefit analyses yield equivocal results even when they themselves, like the Roskill Commission of 1968–70, cost more than £2 million. Uncertainty about the growth of demand for air travel has also taken the steam out of what seemed to be an urgent problem ten years ago.

According to NAC, Maplin, situated on the north of the Thames estuary, would disturb nearby residents least but would require the removal of a Ministry of Defence establishment — which might create environmental problems of its own — and the building of new road and rail links into London. It would also disrupt local bird life. Stansted, an inland site north of London, would be the cheapest site to develop — it already has a small airport, which could be extended, and good links with London, but it is situated near several small towns. The NAC report estimates that 17,000 people would find aircraft noise a nuisance if a two-runway airport were built.

Estimates of annoyance caused by aircraft noise are themselves equivocal. The Noise Advisory Council quotes values of the Noise-Number Index, calculated in such a way as to correlate with surveys of the extent to which people are annoyed by aircraft movements. One difficulty in using this index as a basis for assessing the impact of new airports is that the calibration has been based on surveys at established airports, such as Heathrow, where residents have to some degree become accustomed to aircraft noise after long exposure. Further difficulties stem from uncertainty about flight paths, the noisiness of future aircraft and the future volume of air traffic.

The NAC report says that the noise dis-

0028-0836/80/330653-02$01.00

advantage of Stansted over the other sites, excluding Maplin, is only marginal. But it recommends that if Stansted is chosen, local residents should be compensated either in the form of noise insulation or by grants to enable them to move house. It further adds that Stansted could be justified on environmental grounds only if it reduced the total environmental impact of London's airports, especially Heathrow, where about one and a half million people live within the contour of noise annoyance. Hitherto, the case for a third airport has been to absorb increases in demand for air travel rather than to take pressure off existing airports.

The airports authority's proposal for Stansted is for a one-runway airport capable of handling 15 million passengers a year — considerably smaller than a previous proposal thrown out in 1965–66 to build an airport for 100 million passengers a year. One of the additional attractions of the Stansted site is that the existing airport could be enlarged gradually to meet changes in demand.

Judy Redfearn

Polish water

Much and little

Last month's floods, which produced emergency conditions in 22 out of the 49 provinces of Poland and caused a massive loss of crops, especially hay, potatoes and sugar beet, have focused attention once again on the paradox of Poland's water supply. Ranking only twenty-second in Europe in *per capita* water index (1,700 m^3 a year compared with the European average of 4,800 m^3 a year), Poland is nevertheless subject to periodic inundations after which the water runs off uselessly into the Baltic. At best, Poland can store only 5 per cent of the water it receives from natural precipitation and incoming rivers. (Bulgaria, Czechoslovakia and the Soviet Union, by contrast, store 12-15 per cent.) Along Poland's largest river, the Vistula, there is no storage capacity whatsoever.

To remedy this, the Central Committee of the Polish United Workers' Party adopted on 16 June 1978 a resolution calling for a multi-disciplinary development and management programme for the Vistula. "Program-Wisla", as it is called, got off the ground very rapidly, at least on the theoretical and planning side. Polish geographers, hydrographers, economists, agriculturalists and ecologists produced imaginative plans which include hydroelectric stations, irrigation works, the improvement of navigation channels, the construction of retaining walls and some 34 or 35 dams along the navigable course of the river between Oswiecim (Auschwitz) and Gdansk. The whole scheme, which is intended to raise Poland's water storage capacity to 20 per cent, as well as benefiting agriculture, industry and the human environment, is scheduled for completion by the end of the century.

So vast an enterprise, say the planners, is nevertheless beyond the capacity of Poland alone, and there will be major scope for international cooperation. But before the Vistula is confined by the engineers into what will be, in effect, a series of basins, the water must be of acceptable purity, since once the natural scour is eliminated, the ecologists agree that the river would not regenerate itself. The Vistula (like Poland's other major river, the Odra) has no water of class I or II purity anywhere in its course, while one-third of its total length is polluted beyond the limit of toleration. Purification and regeneration of the river is the first priority of Program-Wisla.

The problem, however, is far from simple. The headwaters of the Vistula are subject to natural "pollution" by mineral salts leached out of the soil of Silesia. The river flows through the Silesian industrial belt and the Cracow-Nowa Huta conurbation, with its vast steel mills, and past the open-cast sulphur mines at Tarnobrzeg. It picks up its largest tributary, the Bug, already heavily polluted by the Soviet pulp and paper industry, passes through Warsaw, whose sewerage arrangements are, to say the least, antiquated, through Plock with its mushrooming petrochemical plant and finally arrives in the Bay of Gdansk where pollution is so heavy that water-sports are prohibited.

There are nevertheless some bright spots in this picture. The Tarnobrzeg mines, in particular, are managed on strict ecological principles, with recultivation of the land section by section as soon as the sulphur is stripped. Water control there, say the mine engineers, has to prevent seepage from the river to the mine rather than the reverse. The Bug, the one part of the Vistula basin not entirely under Polish control, has just been made the subject of a special Polish-Soviet cooperation agreement. And week after week, the Polish media stress the emphasis being given to anti-pollution measures, effluent treatment and the introduction of closed cycle technology under the aegis of Program-Wisla.

Such technology or the exchange of know-how could well be a fruitful field for international cooperation, both within and outside the Comecon bloc. But Polish experts have hitherto been cool at the prospect of Western cooperation, feeling that their prospective partners have been more interested in selling existing standard equipment than providing know-how specifically tailored to Polish circumstances. Since the Polish economy suffers from a chronic lack of hard currency, this is a major problem. The latest negotiations, between Poland and the United Kingdom, seem to be taking a different and — from the Polish point of view — a more promising course. It is understood that before any concrete proposals are put forward from the British side, a small investigative team will visit Poland in the autumn to make an on-the-spot assessment.

Vera Rich

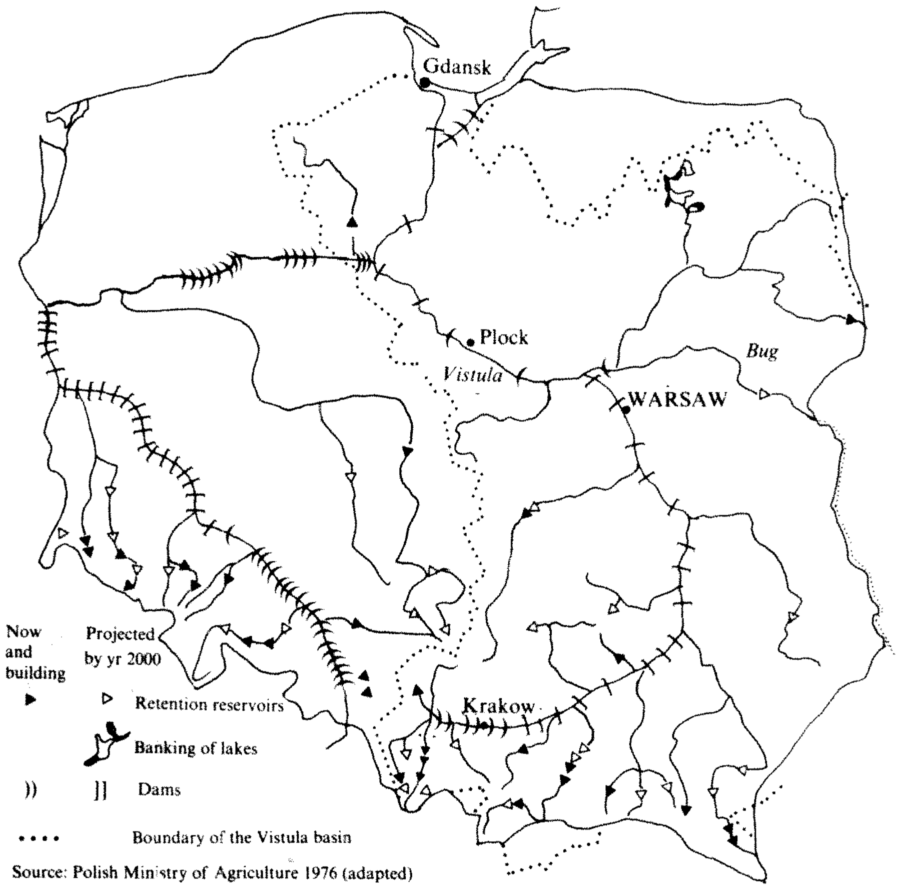

Source: Polish Ministry of Agriculture 1976 (adapted)

0028-0836/80/330654-01$01.00

The cooling Earth

from Henry N. Pollack

WHAT can the exhaust of the Earth's heat engine tell about its internal workings and fuel? The exhaust is the heat lost from the Earth's interior, and the internal workings are the manner by which heat is transported upward from the deep interior. The fuel is thought to be principally nuclear, comprising the radioactive isotopes present in varying trace concentrations throughout the Earth.

Let us look first at the exhaust. The measurement of the heat flux over the Earth's surface is an endeavour of the last two decades, and the global survey is still only half complete. However, an important empirical rule, that heat flow varies inversely with crustal age, has enabled estimates of the heat flow to be made for the unsurveyed areas of the globe. At the present time the Earth seems to be discharging about 40 × 10^{12}W (ref. 1-3).

Does the engine run smoothly, or does it race, or idle on occasion? How characteristic of recent Earth history is the present-day heat loss? Because the heat loss is strongly correlated with the age of the ocean floor, which in turn is related to oceanic crustal accretion rates that are known to be variable, it is likely that the heat flow has fluctuated in the past. Sprague and Pollack[4] have reconstructed the age distribution of oceanic and continental crust over the past 180 Myr and conclude that the heat loss has ranged between 39 and 52 × 10^{12}W, with an average of 43 × 10^{12}W, slightly higher than the present-day value.

The internal workings of the Earth engine are only weakly constrained by knowledge of the heat loss alone. The planetary thermal history models of 20 years ago were principally conductive models, in accord with the then prevailing view of an Earth without global scale horizontal movements. However, even before mobility became accepted in the 1970s, Tozer[5] argued that thermally-activated solid-state creep would, in response to thermally induced buoyancy, lead to large scale mobility within the Earth. The temperature dependent creep serves as a thermostat, with convection relieving the Earth of excessive heat by transporting it to the uppermost mantle where it makes the final journey to the surface by conduction through the upper horizontal boundary layer of the convection. This upper boundary layer comprises the plates of the lithosphere.

While the concept of solid-state thermal convection in planetary interiors is clear enough, a complete mathematical description of the process is difficult. The patterns of the Earth's topography, heat flow, gravity, and plate velocites provide surface constraints, but even so the broad features of the convection remain elusive. However, simpler quantitative treatments, which yield certain general characteristics of the convection system have recently been exploited[6-9]; collectively they are referred to as 'parameterized' thermal history models. At the heart of these analyses is the assumption, suggested by both theory and experiments, that the heat loss from a convecting system depends on the temperature difference driving the convection (the so-called Nusselt number — Rayleigh number relationship). The models yield the history of such properties as the mean temperature and viscosity of the mantle and the mean velocity and radial heat flux of the convective circulation over the lifetime of the Earth. The calculations all explicitly require the specification of the variation with time of the Earth's internal heat production, and thus a link is forged to the Earth's nuclear fuel and its characteristic rate of decay.

The existence of nuclear fuel in the Earth has been known ever since the discovery of radioactivity in rocks in the early part of this century. However, the abundance and blend of the fuel has been a subject of some debate. The principal heat-producing isotopes are ^{238}U, ^{235}U, ^{232}Th and ^{40}K, with respective half-lives of 4.47, 0.70, 14.0, and 1.25 billion years. Their abundances in the crust of the Earth are comparatively well known, and recognized to be significant enrichments over any possible primordial concentrations throughout the bulk of the Earth.

What then can be said of the primordial abundances of each of the principal isotopes? It was first pointed out in the 1950s that if the Earth had an isotopic endowment similar to that of the chondritic meteorites then the internal heat production would be just about adequate to supply the surface heat flow. However, the 'chondritic coincidence' as this near equilibrium between heat production and loss came to be known, was not without some inconsistencies as well. In particular, the relative proportions of U, Th, and K in chondrites are rather different from that in terrestrial rocks. If the primitive Earth were indeed chondritic, most of the uranium apparently now resides in the crust, while most of the potassium must be elsewhere, presumably deeper within the Earth. Wasserburg *et al.*[10] proposed an alternative primordial isotopic endowment which reflected the K:U:Th ratios found in the crust of the Earth. *Yet a third approach has recently been put forward by Sleep*[11] and by Stacey[12] *who use the abundance of* ^{40}Ar, a decay product of ^{40}K, *to estimate* the K abundance of the Earth. *Their* calculations *indicate a K:U ratio* even smaller than the model of Wasserburg *et al.* The significance of the K:U ratio resides in the much longer *half-life* of ^{238}U (the dominant uranium isotope) compared to that of ^{40}K. *An* Earth thermally evolving under the influence of *long lived uranium* and thorium has a slow and *steady* releas of heat, with a decrease by only a factor o two or so during it's lifetime. potassium dominated thermal evolutio such as would derive from the chondri mix, is characterized by a more vigor early history *and an eight-fold decreas internal heat production over the Ear* history. *Thus the thermal and tect history of the Earth is closely tied to blend of the radio-active fuel.*

Now come the new family of p meterized thermal history models, and t tell a disquieting story, at least as far deducing something of the Eart primitive chemistry from the present-d heat loss. It appears that the heat lo derives not only from radiogenic heat, but also in part from 'initial' heat, the energy residual from the accretion of the planet and settling out of the metallic core. The

---

Henry N. Pollack is [illegible] *Geological Sciences,* [illegible]

1. Sclater, J. G., Jaupart, C. & Galson, D. *Rev. Geophys. Space Phys.* **18** 269 (1980).
2. Davies, G. F. *Rev. Geophys. Space Phys.* **18**, in the press.
3. Chapman, D. S. & Pollack, H. N., *EOS Trans. Am. Geophys. Un.* **61**, 383 (1980).
4. Sprague, D. & Pollack, H. N. *Nature* **285**, 393 (1980).
5. Tozer, D. C. *Phil. Trans. R. Soc.* **258**, 252 (1965).
6. Sharpe, H. N. & Peltier, W. R. *Geophys. J. R. astr. Soc.* **59** 171 (1979).
7. Schubert, G., Stevenson, D. & Cassen, P. *J. geophys. Res.* **85**, 2531 (1980).
8. Davies, G. F. *J. geophys. Res.* **85**, 2517 (1980).
9. Turcotte, D. L., Cook, F. A. & Williams, R. J. *Proc. Lunar Planet. Sci. Conf.*, **10** (1979).
10. Wasserburg, G. J., MacDonald, G. J. F., Hoyle F. & Fowler, W. A. *Science* **143**, 465 (1964).
11. Sleep, N. H. *J. Geol.* **87**, 671 (1979).
12. Stacey, F. D. *Phys. Earth Planet. Int.* **22**, 89 (1980).

0028-0836/80/330655-02$01.00

calculated fraction of the present-day heat loss attributable to the initial heat appears to be highly model dependent; Schubert *et al.*[7] estimate that at least 15-35% of the heat flow is non-radiogenic, while Sharpe and Peltier[6] contend that it is not essential to invoke *any* radiogenic heat to understand the main thermal features of the Earth. Initial heat alone may be adequate to drive the Earth engine. Schubert *et al.* emphasize that while the amount of the non-radiogenic heat loss may be reasonably debated, a significant contribution to the total heat flow is unavoidable.

Some generalities do emerge from all the new thermal histories: 1) the Earth is and has been cooling, albeit very slowly, at a rate probably no greater then 100° C per billion years (the quintessential energy storage device!), 2) the cooling has been accompanied by a stiffening of the mantle and a slowing of the convective circulation, 3) the upper boundary layer of the convection, that part of the circulation moving horizontally at the Earth's surface and comprising the lithospheric plates, has thickened over the Earth's history. But if through these models we have learned a little of the functioning of the Earth's engine, it seems we know less than we thought about the Earth's primitive chemistry. The engine apparently will run on nearly any blend of fuel, and the thermal energy exhausted reveals little of the internal chemistry. The principal sources of geochemical insight, alas, must continue to be the continental and oceanic crustal rocks, salted with occasional bits of the mantle, and the much smaller collection of extraterrestrial samples; less help appears to be forthcoming from the Earth's heat than a generation of earth scientists had hoped for. □

The collagen gene family

from Ellen Solomon

COLLAGEN proteins occur as a family of molecules with closely related structures but varying tissue distributions. At least nine different genes code for protein with collagens unique features of a repeating pattern (every third amino acid is glycine) and large amounts of the unusual amino acids hydroxyproline and hydroxylysine.

The total number of genes in the family may be as high as fifteen or sixteen if some of the less well characterized chains are included, as well as the A,B,C, chains of Clq, and if some of the observed heterogeneity in sequence is due to different gene loci. These genes have almost certainly evolved by duplication and divergence of a common ancestral sequence, but nothing is yet known of their linkage. cDNA and genomic clones have been isolated from the chick proα_2(I) chain (Lehrach *et al. Proc. natn. Acad. Sci. U.S.A.* 75, 5417; 1978; Sobel *et al. Proc. natn. Acad. Sci. U.S.A.* **75**, 5846; 1978; Vogeli *et al. Nucleic Acid Res.* **8**, 1823; 1980). Based on clones panning 55 Kb of the chick genome, de rombrugghe (National Institutes of ealth) estimates that the proα_2(I) gene vers 40 Kb and that there are more than) intervening non-coding sequences that ary in size from 60-70 to 3-4,000 bp. These orkers have analysed six coding regions in ree separate regions of the helical portion f the molecule; five of these are 54 bp (18 mino acids). They propose that the helical ortion of the collagen gene arose by duplication and divergence of a 54 bp equence and that these regions diverged by the insertion or deletion of units of 9 bp — the basic (Gly-X-Y) repeat of collagen. Boedtker and colleagues (Harvard University) have analysed the codon usage for the amino acids in the α_1(I) and α_2(I) chains of Type I collagen and find that the usage differs significantly between the chains. Genomic clones of the sheep proα_2(I) have also been isolated (Schafer *et al. Nucleic Acids Res* **8**, 2241; 1980, and show at least 17 intervening sequences in 60% of the 3′ portion of the gene. Non-coding sequences are 300 to 1,600 bp, while the coding regions are 250 bp or less. Somatic cell genetic studies using species-specific DNA probes should soon clarify the location of some of the collagen genes and their possible synteney, if not linkage.

Haemoglobins (Weissman, Yale University), histones (Zweidler, Institute for Cancer Research, Philadelphia) and heat shock proteins (McCarthy, University of California, San Francisco) were discussed as representatives of rather different types of gene families, in regard to linkage and co-ordinate expression. Until the genetic map of the collagen genes is known it is obviously not possible to know if, as a family, it resembles any of these others. By analogy with the non-linked α and β genes, and the linked $\beta\cdot\delta\cdot\gamma$ genes of haemoglobin, will the proα_1(I) and proα_2(I) genes of collagen be unlinked and the proα_2(I,II,III,IV,) linked? Alternatively, will all the "collagenes" form a linked cluster as with the histones, or be scattered throughout the genome as with the actin, ubulin, and heat shock genes of Drosophila? As yet there is no information to whether any of the collagen genes exist in multiple copies.

There [illegible] inherited connective tissue diseases are likely to involve defects in col[illegible]es, such as Marfan's Synd[illegible]eogenesis imperfecta and [illegible]ards their understanding ap[illegible] these diseases have eluded definition at the molecular level, largely because of the extreme difficulty of the protein chemistry. It was agreed that current DNA technology should be applied to defining these diseases, bearing in mind that in most cases there is no direct evidence for collagen gene involvement. It is not reasonable to clone collagen genes from individuals with connective tissue disorders without direct evidence that these genes are actually involved as the primary defect. A more general approach is needed whereby collagen gene mutations can be detected. One suggestion was to screen as many different patients as possible, with different diseases, by restriction mapping and Southern blots using collagen probes, and where appropriate tissue biopsies are available, by S1 mapping. Using these two techniques some types of mutations in the collagen genes could be detected. For results from either of these techniques to be meaningful, however, a great deal of data is needed regarding the degree of variation in these genes in the normal population. A second approach discussed at length was that of linkage analysis within families using the collagen gene probes and restriction site polymorphisms, as done by Kan and Dozy, for sickle cell anaemia (*Lancet* ii 910; 1978). The collagen diseases are rare, extremely heterogeneous, both clinically and genetically, and probably often represent new mutations. They are unlikely to have evolved by selection, as have some of the haemoglobinopathies, and it was therefore emphasised that each family would have to be screened with a set of restriction enzymes to find an appropriate polymorphism. The purpose of this type of analysis would be both to identify affected fetuses by prenatal diagnosis, and also to indicate the involvement of a collagen gene defect in those diseases.

Also discussed was the complexity of the genetics of a protein with as many enzymatic post-translational modifications as collagen. For example, mutations in different modification enzymes could lead to the same disease phenotype, and different mutations in the same enzyme could give dominant or recessive modes of inheritance.

The extensive post-translational modifications of collagen and proteoglycans, including removal of signal sequences, hydroxylation, glycosylation, disulfide bond formation, triple helix formation, and procollagen to collagen conversion was an important topic. Different types of collagen are modified to different extents and individual types of collagen show a degree of heterogeneity in their particular modification. Among the questions regarding modification, therefore, is to what degree individual primary amino acid sequences determine the position and extent of, say hydroxylation

---

A conference on 'Gene families of collagens and other proteins' was held from April 27-May 2, 1980 at CMDNJ — Rutgers Medical School. The organisers were D. J. Prockop and P. C. Champe.

Ellen Solomon is Head of the Somatic Cell Genetics Laboratory at the Imperial Cancer Research Fund Laboratories, London.

0028-0836/80/330656-02$01.00

and glycosylation, and whether there are tissue-specific enzymes for each of the different types of collagen. As yet there is no direct evidence for such enzymes (Kivirikko, University of Oulu, Finland). This may well be due to the difficulty in assaying many of these enzymes. The need exists for more rapid and specific assays for each enzyme including electrophoretic separation techniques, and immunological or colourometric detection. The questions of tissue-specific forms of the enzymes, genetic map location, possible linkage of groups of these enzymes, linkage to the collagen genes, and control of expression could be approached if less cumbersome assays could be developed.

A final major topic was the extracellular matrix (collagen, fibronectin, proteoglycans, fibrin) and the cytoskeleton (actin, microtubules, intermediate filaments). Through much information exists on structural differences between individual members of the gene families (collagen, actin, tubulin, keratin) the funtional significance of these differences is not at all clear. Certain common functional domains can, however, be identified. For example, the collagen cross-linking regions and collagenase cleavage site are strongly conserved in collagen Types I. II and III. Other macromolecules are associated with collagen fibres, and may have specific interactions with the collagen and each other. The most clearly defined system is that of cartelage proteoglycan, where the proteoglycan combines with hyaluronic acid and link protein to form large aggregate structures (Muir, Kennedy Institute of Rheumatology, London). It is anticipated that collagen will also be incorporated into such multimeric structures. Fibronectin has a number of separate functional domains that allow it to bind to collagen proteoglycan and the cell (Vaheri, Helsinki University). Martin (National Institutes of Health) reported that proteins analagous to fibronectin but specific for chondrocytes (chondronectin) and epithelial cell (laminin) have been discovered. These bind specifically to these cells and their collagens. Such interactions may explain the role of the tissue specific collagens. □

Assembly of immunoglobulin heavy chain genes

from H. V. Molgaard

IT has been clear ever since it became possible to compare the amino acid sequences of immunoglobulin molecules that they pose two formidable problems for genetics. The first is the extreme variability of the N terminal portions (V regions) of the chains, which make up the antigen-recognition site. The second is how one of a very large number of V regions can come to be associated with one of a very small number of the constant regions (C regions) which mediate the effector functions of the molecule in the elimination of antigen.

It was the occurrence of a very variable sequence joined to a relatively constant sequence that led Dreyer and Bennet to propose that the V and C genes are separately encoded in the genome[1] — a proposal which was confirmed by the first DNA sequence studies on mouse light chains. Those studies showed that a large but limited set of V genes exists at some distance from the C gene in the germline DNA. During the maturation of an antibody-producing B cell, one of the V genes is brought into the proximity of the C gene. As it has turned out, this translocation also provides at least a partial explanation for antibody diversity, since it has proved that the V region is itself constructed from two genes: the V gene and one of four J genes adjacent to the C gene on the germline DNA. V genes seem able to combine at random with one of the J genes, the exact site of the junction varying slightly and coinciding with hypervariable region 3 on the light chain[2].

DNA sequence analysis has now been extended to the mouse heavy chain genes, which are of particular interest because of the evidence that each V gene may be translocated more than once in the course of ontogeny. Unlike the light chains, for which there is only one C region gene for each set of V regions, each heavy chain V gene (V_H gene) may be expressed with any of eight different heavy chain constant genes (C_H genes), C_μ, C_γ, $C_{\gamma 1a}$, $C_{\gamma 2b}$, $C_{\gamma 3}$, C_α, C_ε, C_δ, which define the heavy chains as μ, γ, α etc and the different classes of antibody molecule, IgM, IgG, and so on. All V_H regions are expressed first in μ chains, but the same V_H sequence may later be expressed as part of a γ chain or an α or an ε chain. The mechanism of this phenomenon, the heavy chain switch is therefore a mystery peculiar to the heavy chain genes. DNA sequencing has shed some important light on this mystery; but it has also shown that the V regions of the heavy chain genes have a more complex structure than their light-chain partners.

The V_H region is encoded by three genes.

Hybridisation of germ line DNA with V_H probes has shown that there are at least 50 and probably many more V_H genes, arranged in tandem arrays[3–5] and separated by an unknown length of DNA from a cluster of C genes[6].

Comparison between the DNA sequence of a germ line V_H gene and the corresponding rearranged sequence expressed in a myeloma have in two different cases — a V sequence expressed in an α chain[7] and another expressed in a γ_{2b} chain[8] — shown that the germ line V_H segment ends at the sequence coding for the third hypervariable region before the end of the expressed V_H sequence. This suggested, by analogy with the light chain genes, that the missing sequences should be found in J segments near a C gene. Since $C\mu$ is the first C gene to be expressed in B-cell ontogeny, the J segments were sought and found near the $C\mu$ gene in a cluster of four, 8kb upstream from $C\mu$. However, the J segments still do not account for all of the third hypervariable region. This has lend to the suggestion that the missing residues are separately encoded in yet another set of gene segments, the 'D' or 'diversity' segments, the existence of which had already been predicted on the basis of the amino acid sequence data[9,10].

It remains controversial whether heavy chain diversity is fully accounted for by random combination of V,D and J segments and codon variation at the joins of these segments or whether further diversity arises out of point mutations at the other two hypervariable regions during the differentiation of the B lymphocyte.

Mechanism of V gene rearrangement

With the availability of data from both light and heavy chain germ line gene segments it is possible to generalise about the mechanism of V-J segment translocation. In both cases it involves deletion of the intervening DNA[4,11] and in both cases two short conserved sequences occur in the sequences 3′ to the V segment and 5′ to the J segment close to the point of recombination.

At the germ line V_H and J_H segments which are rearranged and expressed in the S107 myeloma the two conserved sequences are arranged[7] as shown below. One strand is shown folded back on itself to illustrate that the J_H segment conserved sequences are almost inverse complements of the V_H segment sequences. Comparison of these sequences at all the known light and heavy chain V segments shows that they can all be derived from the heptamer CACAGTG and the nonamer ACAAAAACC with usually only one or two base changes. Similarly the conserved sequences at all the J segments derive from CACTGTG and GGTTTTTGT.

Another striking feature of these

residue 101 **Asp**	non coding sequences
5′ V_H segment . . . GAT	GCA$\overline{\text{CACAGTG}}$ — 23 nucleotides — $\overline{\text{ACACAAACC}}$
3′ J_H segment . . . CAT	C $\overline{\text{GTGTCAG}}$ — 22 nucleotides — $\overline{\text{TGATTTTGA}}$
residue 107 **Tyr**	non coding sequences

H.V. Molgaard is in the Biophysics Department of University of London King's College

0028-0836/80/330657-03$01.00

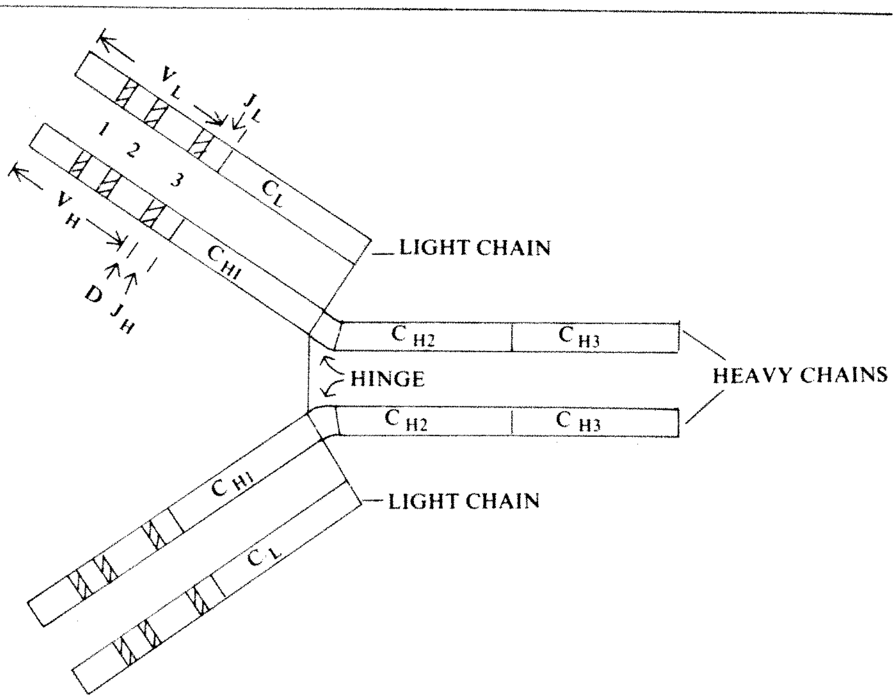

Fig. 1 Schematic diagram of an IgG antibody molecule. C_{H1}, C_{H2}, C_{H3} and C_L are the the heavy (H) and light (L) chain constant region domains — these are regions 100-125 amino acids long within the chains which show some homology with each other in amino acid sequence and secondary structure. The parts of the light chain V region coded by the V_L and J_L gene segments are shown as are the sections of the heavy chain V region coded by the V_H, D and J_H gene segments. The hypervariable regions 1,2,3 determine the antigen recognition and binding site. The C regions mediate the effector functions involved in the elimination of antigen.

conserved sequences is that the length of the random sequence separating the heptamer and nonamer is highly conserved. At the heavy chain V and J segments the separating sequences vary from 21 to 24 base pairs (bp) in length. In contrast, in the two light chain families, the κ and λ chains, the spacers at the V segments differ from those at the J segments. The spacers at the V_{κ} segments are 11 or 12 bp long while the spacers at the J_{κ} segments are 21-24 bp long. Conversely at the V_{λ} segments the spacer is 22 or 23 bp while at the J_{λ} segments a 12 bp spacer occurs.

Spacer lengths of 11-12 and 21-24 bp correspond closely to one and two turns of the double helix, and mean that the heptamer and nonamer form a nearly continuous sequence around the double helix interrupted by one or two complete turns. Since in light chain V-J recombination, a one turn spaced heptamer and nonamer and a conserved sequence interupted by two turns occur at the two recombining segments Early *et al.*[7] and Sakano *et al.*[8] propose that two different but closely related joining proteins recognise the one and two turn spaced sequences and that these proteins form a complex within which the cutting and joining of the DNA takes place. As it is likely that the heavy chain V and J segments recombine first with a D segment this model predicts that the D segments should be flanked by these conserved sequences interrupted by one turn. It would also rule out recombination within the V and J segments. Early *et al.*[7] argue against a mechanism involving the previously proposed stem structures[11,12] which can be formed between these inverse complementary sequences flanking the V and J segments on the grounds that such structures are unlikely to form spontaneously between such widely separated segments of DNA and that they do not account for the conservation of the spacer sequences.

These sequence homologies between the light and heavy chains suggest that, whatever the recombination mechanism, it is the same for both light and heavy chain genes. As the two light chain families and the heavy chain family are each on different chromosomes recombination between families is prevented.

The mechanism of the heavy chain class switch

A further important implication of the germ line organisation of the heavy chain genes can be drawn from the discovery that the J segments which are expressed in α and γ_{2b} heavy chains of myeloma proteins are next to the $C\mu$ gene in the germ line: this establishes that the translocation of V_H and C_H gene segments to give complete α and γ_{2b} chain genes must have been preceded by the recombination of a V_H segment with a J_H segment at the C_{μ} gene. The second recombination event, the heavy chain switch, occurs between a complete $V_H J_H$–C_{μ} gene and, for example, either a C_{α} or a $C_{\gamma 2}$ gene which is still in a germ line context. In addition to the recombined $V_H D J_H$ segments, a considerable portion of the J_H-C_{μ} intron is translocated, giving a new intron in the expressed α or γ gene whose sequences originate partly from the J_H-C_{μ} intron[13,14,6 & 8].

In the hope of identifying specific signals in the DNA sequence which could mediate the heavy chain switch, Sakano *et al.*[8] have identified the sites in the J_H-C_{μ} intron and in the sequences 5′ to the germ line $C_{\gamma 2b}$ gene where the recombination event which gave a complete expressed γ2b gene had occurred, and have sequenced the DNA around these sites. Two short sequences, TCCTGG and AGA, occur at equivalent positions 5′ to the two sites and could be the signals for the μ to γ2b switch. However, these sequences do not occur at the μ to α[8] and μ to γ_1[13] switch sites, both of which lie in a region of tandemly repeated sequences in the J_H-C_{μ} intron. It seems that the switch sites are different for the different class switches and may even vary within one type of class switch[15]. The recombination sites involved in the class switch need not be unique as long as they do not create signals which terminate transcription or destroy the signals required for the splicing event which removes the intron containing these sites.

It is possible that the homologies in the flanking sequences of the different C_H genes are a consequence of their evolutionary history. Each C region consists of three or four (depending on the heavy chain class) partly homologous domains thought to have evolved by tandem duplication from a common sequence coding for a single domain. Homologies in the flanking sequences might then have been conserved if they had come to acquire a role in the recombination events leading to class switches. If indeed the three domains of each C region derive from the same gene, then weaker sequence homologies might be expected in the

1. Dreyer, W.J. & Bennett, J.C. *Proc. natn. Acad. Sci. U.S.A.* **54**, 864 (1965).
2. For a review, see Dunnick, W. *Nature* **281**, 253 (1979).
3. Rabbitts, T.H., Matthyssens, G., & Hamlyn, P.H. *Nature* **284**, 238 (1980).
4. Cory, S. & Adams, J. *Cell* **19**, 37 (1980).
5. Kemp, D.J., Cory, S., & Adams, J. *Proc. natn. Acad. Sci. U.S.A.* **76**, 4627 (1979).
6. Maki, R., Traunecker, A., Sakano, H., Roeder, W., & Tonegawa, S. *Proc. natn. Acad. Sci. U.S.A.* **77**, 2142 (1980).
7. Early, P., Huang, H., Davis, M., Calame, K., & Hood, L. *Cell* **19**, 981 (1980).
8. Sakano, H., Maki, R., Kurosawa, Y., Roeder, W., & Tonegawa, S. *Nature* **286**, 676 (1980).
9. Rao, D.N., Rudikoff, S., Krutsch, H., & Potter, M. *Proc. natn. Acad. Sci. U.S.A.* **76**, 2890 (1979).
10. Schilling, J., Clevinger, B., Davie, J.M., & Hood, L. *Nature* **283**, 35 (1980).
11. Sakano, H., Hüppi, K., Heinrich, G., & Tonegawa, S. *Nature* **280**, 288 (1979).
12. Max, E.E., Seidman, J.G., & Leder, P. *Proc. natn. Acad. Sci. U.S.A.* **76**, 3450 (1979).
13. Kataoka, T., Kawakami, T., Takahashi, N., & Honjo, T. *Proc. natn. Acad. Sci. U.S.A.* **77**, 919 (1980).
14. Davis, M.M. *et al. Nature* **283**, 733 (1980).
15. Dunnick, W., Rabbits, T.H., & Milstein, C. *Nature* **286**, 669 (1980).
16. Rabbitts, T.H., Foster, A., Dunnick, W., & Bentley, D.L. *Nature* **283**, 351 (1980).
17. Coleclough, C., Cooper, D., & Perry, R.P. *Proc. natn. Acad. Sci. U.S.A.* **77**, 1422 (1980).
18. Cory, S., Jackson, J., & Adams, J.M. *Nature* **285**, 450 (1980).
19. Honjo, T. & Kataoka, T. *Proc. natn. Acad. Sci. U.S.A.* **75**, 2140 (1978).
20. Yaoita, Y. & Honjo, T. *Nature* in the press.
21. Yoshida, T.H., Imai, H.T., & Potter, M. *J. natn. Cancer Inst.* **41**, 1083 (1968).
22. Joho, R. & Weissman, I.L. *Nature* **284**, 179 (1980).

0028-0836/80/330658 03$01.00

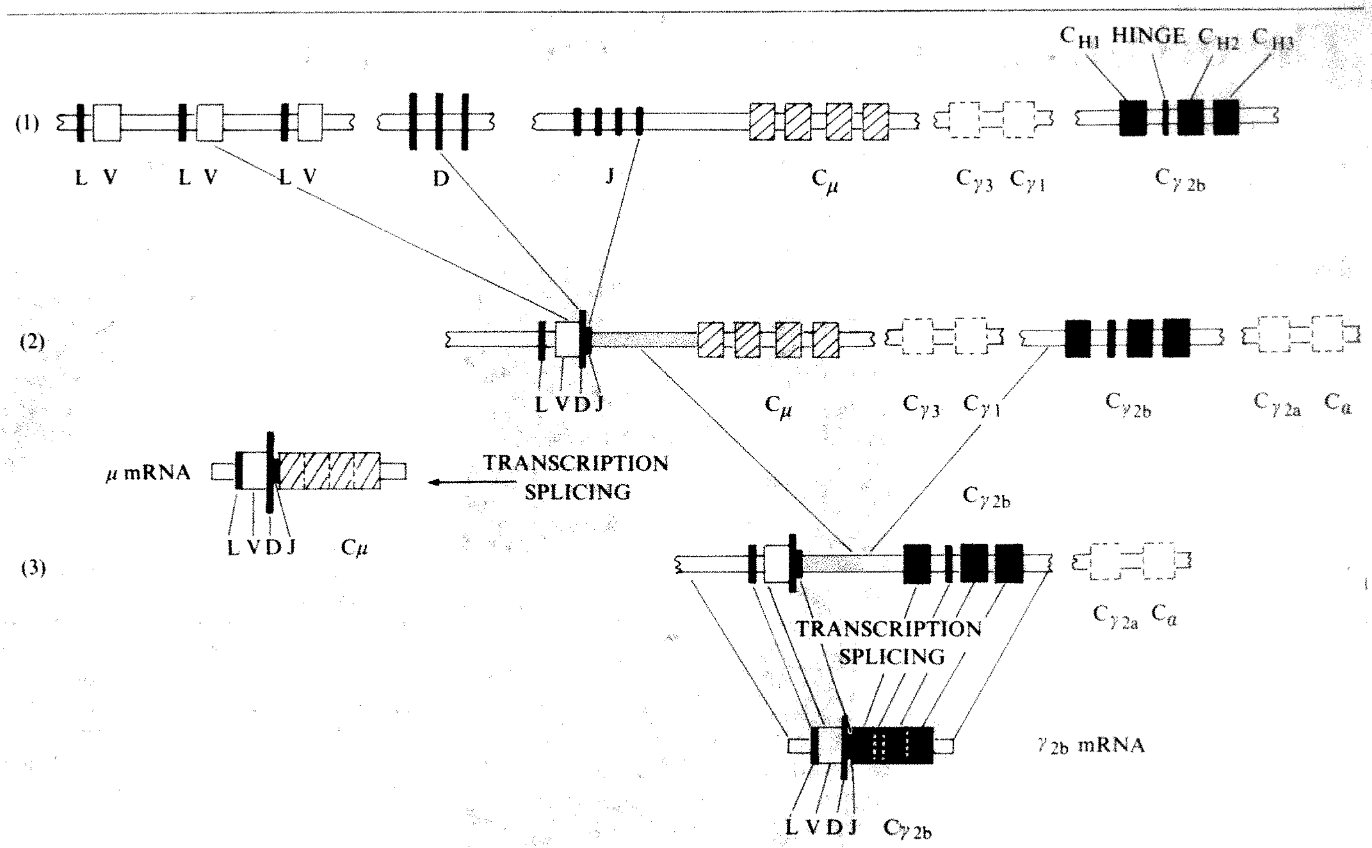

Fig. 2 Recombination events leading to a complete γ2b gene. (1) The germ line DNA before rearrangement. These is a cluster of at least 50 genes (each with a short leader sequence L) coding for part of the variable (V) region, a cluster of D gene segments coding for most of the third hypervariable region and some distance away there are 4 J segments which complete the Vregion coding sequence. The J segments lie about 8kb from the C_μ gene which lies at the start of a cluster containing all the C region genes. The C region gene sequences are interrupted by non-coding sequences to give a series of exons which coincide with the domains and the hinge region in the C region amino acid sequence (2) In the first translocation event one of each of the V, D and J segments are recombined to give a complete μ chain transcription unit. The transcript is a copy of the gene as shown but the non-coding sequences (introns) are removed by splicing events which lead to a continuous coding sequence in the μ m-RNA. (3) A second translocation event, the heavy chain switch, deletes the C_μ, $C_{\gamma 3}$ and $C_{\gamma 1}$ gene segments and places the VDJ segment and part of the J-C_μ intron near the $C_{\gamma 2b}$ gene. Following transcription the introns are removed by splicing leading to a continuous coding sequence in the γ2b mRNA.

intervening sequences that have been found between constant region domains. Such homologies have in fact been found in an investigation of a deletion mutant in a myeloma cell line. An illegitimate recombination event or class switch has led in this case to the deletion of an exon coding for the first domain in $C_{\gamma 1}$ (ref. 16). That the region of tandemly repeated sequences in and near the switch region is a particularly good site for recombination is illustrated by the spontaneous deletions which occur in this region, on cloning or propogation in *E. Coli* and which have prevented several groups from isolating complete DNA fragments containing these C_μ flanking sequences[8,14].

The heavy chain switch involves deletion of C_H gene segments.

The overwhelming evidence of a number of experiments by different groups in which cloned constant region probes have been used to probe the DNA of many different plasmacytomas is that the expression of a constant region class other than μ involves deletion of other constant region genes including C_μ in a way which is consistent with a C_H gene order μ–γ_3–γ_1–γ_{2b}–γ_{2a}–α (δ and ε have not yet been studied) and a model in which the genes preceding the expressed gene are deleted[4,16–18]. Some controversy remains however as to whether the deletions occur only on one chromosome or on both. Honjo and Kataoka[19], who were the first to find evidence for the deletion model, concluded on the basis of DNA hybridization kinetics that deletion was confined to one allele. Yaoita and Honjo[20] have now produced stronger evidence for deletion on only one allele by analysing a IgG_{2b} secreting myeloma induced in an F_1 hybrid of C57BL and BALB/c mice. A judicious choice of restriction enzymes enabled them to distinguish the two alleles and to show that the C_μ and $C_{\gamma 1}$ genes of the expressed allele are deleted and the expressed $C_{\gamma 2b}$ gene is rearranged, while the unexpressed alleles C_μ, C_{γ_1} and $C_{\gamma 2b}$ are unchanged. They did find two unexpected rearrangements in the 5′ flanking sequences of the unexpressed C_μ allele and in the 3′ flanking sequences of the unexpressed $C_{\gamma 1}$ gene.

However, in the numerous myelomas analysed by the other groups deletions and rearrangements often occur on both alleles. Unexpected rearrangements such as the rearrangement of both C_α alleles in some IgG_{2a} expressing tumours has led Coleclough *et al.*[17] to propose a stochastic model in which, after the first translocation which creates the complete μ gene, deletion events may occur within the C_H cluster on both alleles, only some of which expose a V_H gene to a second C_H gene leading to a heavy chain switch. Other deletions may have no effect on expression or may limit the options for further switching.

It should be borne in mind that all these studies have been carried out with mouse plasmacytomas which are known to show chromosomal abnormalities, are of unknown ploidy, being perhaps mostly hypo tetraploid[21] and have been maintained in culture much longer than the life time of a normal diploid B-cell. Some of the events observed in the myelomas may not occur or may be infrequent in normal cells. In an isolated study of a mixed population of normal B cells Joho and Weissman[22] produced evidence consistent with rearrangement occurring on only one C_κ allele. The question has been raised, however, of whether the technique they used has sufficient resolution to detect cells with both chromosomes rearranged if those cells are in a minority. The events on the second allele are important as only one allele is expressed (allelic exclusion).

With the question of allelic exclusion, molecular immunologists are drawn into the issue of how events occurring on one chromosome might affect those occurring on another; and thus into fields of enquiry even thornier than those they have so successfully tackled in the last five years. □

The origins of marine bioluminescence

from Frank McCapra and Russell Hart

THE astonishment of seeing bright light issuing from living organisms is sometimes reflected in the view that the light must have a unique biochemical origin. Yet a timely reminder of the wide variety of the chemical systems involved has been provided by the recent observations of Dunlap, Hastings and Shimomura (*Proc. natn. Acad. Sci. U.S.A.* **77**, 1394; 1980). They have demonstrated that although two distantly related organisms, the dinoflagellate *Pyrocystis lunula* and the euphausiid shrimp *Meganyctiphanes norvegica* have the same novel luminescent reactant or luciferin this molecule has no structural similarity to the luciferins identified in more than 20 other organisms.

The luminescent reaction in most organisms occurs by the action of a luciferase upon a luciferin. The similarities in the luciferins and luciferases in different organisms can be traced both by seeing if a light emitting cross-reaction is possible between the chemicals extracted from each of them and by elucidating the chemical structure of the luciferins themselves.

Experiments of this type have shown that although there is no simple pattern of distribution of particular luciferins and luciferases among the light emitting organisms one molecule does appear again and again. This 'coelenterate-type' luciferin (luciferin 1, see Fig. 1) either in the free state, protein-bound or as a simple derivative, has been found in a variety of coelenterates and in such unrelated animals as shrimp, squid and fish (see Table 1). This widespread distribution may best be explained if the luciferin derives from a common origin in the food chain.

A second luciferin (luciferin 2, see Fig. 1), *'Cypridina* luciferin' has a similar structure to coelenterate luciferin sharing the same imidazopyrazine nucleus and producing light by an identical chemical mechanism (McCapra *Accounts Chem. Res.* **9**, 206; 1976) but it has no amino acids in common with luciferin 1 and must have a separate origin. No single food source could be responsible for the appearance of both luciferins in higher organisms. Luciferin 2 is also widely distributed in a variety of organisms (see Table 2), again suggesting a food chain origin. This is supported by the finding that several luminescent fish, e.g. *Apogon* and *Parapriacanthus* (Johnson *et.al. Proc. natn. Acad. Sci. U.S.A.* **47**, 486; 1961) have been caught with large numbers of *Cypridina* in the gut and the luciferin of these predators is identical to that of the food organism.

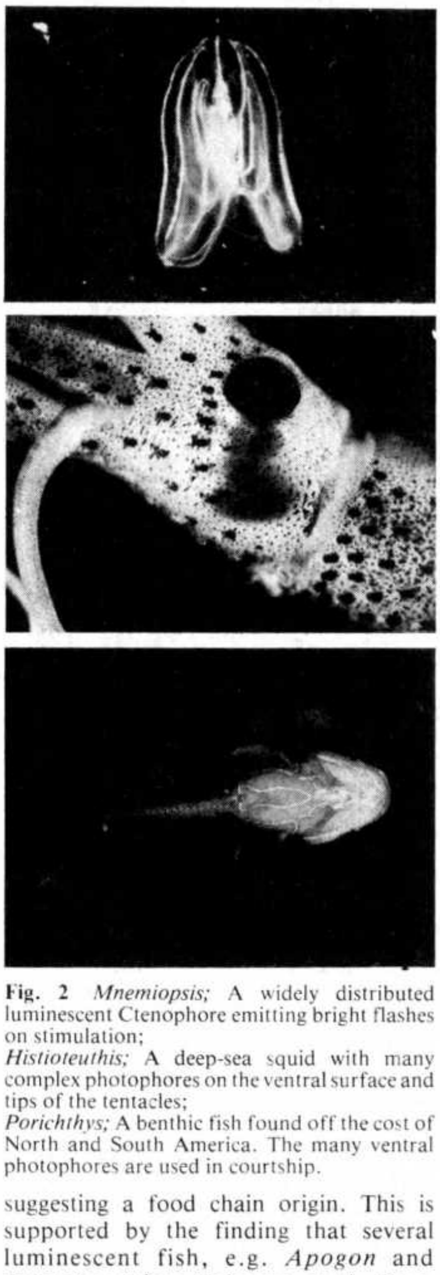

Fig. 2 *Mnemiopsis;* A widely distributed luminescent Ctenophore emitting bright flashes on stimulation;
Histioteuthis; A deep-sea squid with many complex photophores on the ventral surface and tips of the tentacles;
Porichthys; A benthic fish found off the cost of North and South America. The many ventral photophores are used in courtship.

More direct evidence that the *Cypridina* luciferin is derived from *Cypridina* comes from the work done by Tsuji and his collaborators (*Mol. Cell. Biochem.*, **9**, 3; 1975) with the midshipman fish *Poricthys notatus* collected in two separate locations off the western coast of the US. The fish collected in Puget Sound are 'dark' although possessing the large number of highly developed photophores of the southern (Californian) luminescent fish. The only way in which luminescence could be induced in the 'dark' fish was either by injection or ingestion of *Cypridina* luciferin, demonstrating a direct link between food source and light emission.

It may be that the Puget Sound area merely lacks the required, as yet unidentified, food organism containing the luciferin or a precursor. The complexity of the photophores, the nature of the transport involved and the response to administered luciferin nevertheless suggest caution in accepting this simple view. For example it is extremely unlikely that the ingested enzyme (luciferase) could survive proteolysis in the gut. In addition the endogenous luciferase in either the dark or luminous fish differs in several significant aspects from *Cypridina* luciferase.

Doubts about a food source as the sole origin of luciferin do indeed arise. For example luciferin is notoriously unstable with a lifetime in solution of a few days at most. Yet *Poricthys* luminescence, once developed by administration of small amounts of luciferin persists for up to seven months. It should be noted however that coelenterate-type luciferin is often found as a sulphate derivative, which is considerably more stable (Hori, Nakano & Cormier *Biochim. Biophys. Acta* **256**, 638; 1972). If a similar derivative exists for *Cypridina* luciferin then this would reduce the force of this objection.

Other luminous organisms (Table 3) have luciferins and bioluminescent systems with nothing in common with each other or the coelenterates.

Frank McCapra and Russell Hart are in the School of Molecular Sciences, University of Sussex.

Fig. 1 (1) Coelenterate-type luciferin, (2) *Cypridina* luciferin, (3) amino pyrazine which can condense with (4) p-hydroxyphenylpyruvic acid to produce (1).

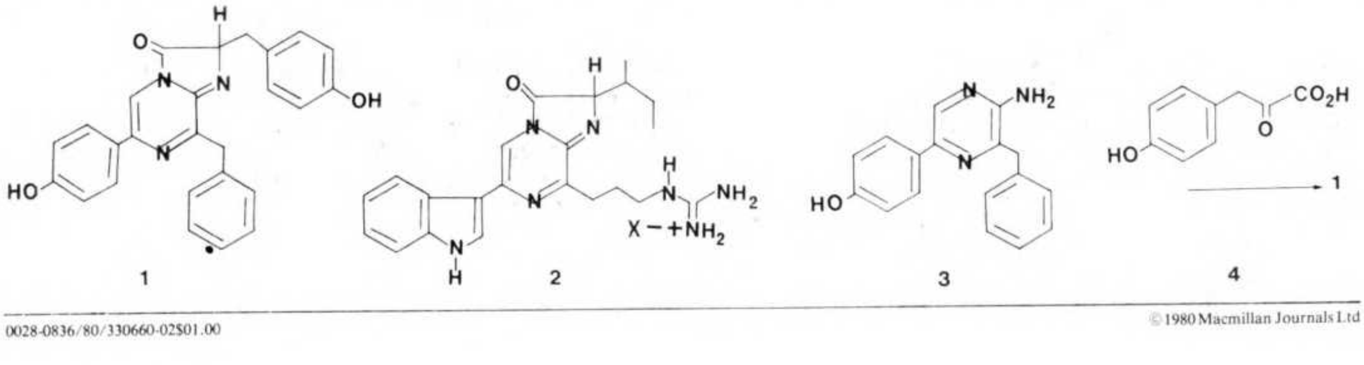

1 2 3 4

0028-0836/80/330660-02$01.00

There is no doubt that bioluminescence arose anew many times in evolutionary history. This is shown by the markedly different structures found for the luciferins. The ubiquity of coelenterate-type luciferin does suggest a single source in this case, but may obscure several instances of *de novo* synthesis. No direct experiments have been done to settle the matter, nor do we know very much about the genetic mechanisms controlling the generation of luciferin and luciferase. Some problems are already raised by the need to explain (in genetic terms) the simultaneous appearance of luciferin and luciferase in the same organism. These will be compounded if it is necessary to account for their separate appearance in unrelated organisms.

A possibility is that food sources contain peptide material capable of elaboration by the luminescent organisms. Such sources may or may not be luminescent. By analogy with the firefly, it may be that degradation of the product of the reaction or of the less stable luciferin gives rise to the amino pyrazine which may then condense with p-hydroxyphenylpyruvic acid (see Fig. 1) following a known synthesis. It is clear that no single origin can be demonstrated, and establishing the actual blend of mechanisms will require both direct feeding experiments using labelled precursors, and some insight into the genetic mechanisms controlling the whole phenomenon. □

Table 1: Organisms with Coelenterate-type luciferin 1

Anthozoa	
Sea pansy	*Renilla spp.*[a]
Sea pen	*Ptilosarcus guerneyi*[a]
	Stylatula elongata[a]
Sea cactus	*Cavernularia obesa*[a]
	Acanthoptilum gracile[a]
Hydrozoa	
Jellyfish	*Aequorea forskalea*[a]
Hydroid	*Obelia geniculata*[a]
Ctenophore	
	Mnemiopsis leidyi[a]
	Beroe sp.[a]
Mollusca	
Teuthoidean squid	*Watasenia scintillans*[b]
	Eucleoteuthis luminosa[b]
	Chiroteuthis imperator[b]
	Onychoteuthis banksi borealijaponica[b]
Sepioidean squid	*Sepiolina nipponensis*[b]
Pisces	
Myctophid fish	*Diaphus spp.*[b]
	Neoscopelus microchir[b]
Stomiatoidean fish	*Argyropelecus hemigymnus*[b]
	Yarella illustris[b]
Crustacea	
Decapod shrimp	*Acanthephyra spp.*[a]
	Oplophorus spinosus[b]
	Heterocarpus spp.[b]
	Systellaspis spp.[b]
	Sergestes spp.[b]
Mysidacean shrimp	*Gnathophausia spp.*[b]
Copepod	*Pleuromamma piseckí*[c]

(*a*) After Cormier in *Bioluminescence in Action p.75* (ed. Herring (Academic Press, London, 1978)
(*b*) After Shimomura, Inoue, Johnson & Haneda (*Comp. Biochem. Physiol.* **65B**, 435; 1980).
(*c*) Hart, Herring & McCapra.

Table 2: Organisms with *Cypridina* luciferin 2

Ostracod crustacean	*Cypridina spp.*
Teleost fish	*Poricthys notatus*
Cardinal fish	*Apogon ellioti*
Sweeper fish	*Parapriacanthus ransonneti*

Table 3: Organisms with other luciferins

Bacteria	*Photobacterium phosphoreum*
Dinoflagellate	*Pyrocystis lunula*
Euphausiid shrimp	*Meganictyphanes norvegica*
Boring Clam	*Pholas dactylus*

A new dimension for particle detectors

from David J. Miller

THE trouble with modern particle physics experiments is that you need to detect all kinds of particles at the same time. Not so long ago there were groups of ten or so physicists who did important programmes of research with nothing much more than a dozen neutron counters, or five spark chambers and a magnet. But storage-ring physics is different. As Cashmore (Oxford) told us on the first day of the Uppsala meeting*, the PETRA e^+e^- collider at Hamburg only produces 20 collisions per intersection region per day with strongly interacting particles (hadrons) in the final state. At such rates each event must be made to give up every scrap of information that can be measured. We don't want to see just the charged tracks. We want to see which of them are pions, kaons, protons, muons or electrons. All of the γ-rays must be converted. Neutrons and long lived K^0 must be made to interact. Neutrinos will escape, of course, but it is very important that they should be the only particles to escape so that their missing energy and momentum can be inferred from the measured particles.

The new director designate of CERN, Schopper (Hamburg), told us about the plans to build a first stage 'stripped down' LEP (large electron-positron) machine in Geneva by 1986. If this goes ahead, the first proposals for detectors will be asked for in 1981.

The detectors now working at other storage-ring machines provide prototypes for many of the ideas presented at the meeting. They are constructed like Russian babuschka dolls. Around the beam-pipe is nested a sequence of different devices, each fitted tightly over the next with the minimum of lost volume and without any chinks for particles to escape. Closest to the pipe there is often a multiwire proportional chamber and usually a cylinder of scintillation-counters. These establish the position of charged tracks coming out into the detector and, even more important, they establish the starting time. The time of flight of a particle from the pipe to an outer ring of counters, one or two metres away, is measurably different for pions, kaons and protons below about 2 GeV/c. At present, times can be measured to about 200 picoseconds, though considerably better particle identification could be made if 50 picosecond resolution were possible. Schemes for doing this were presented, but it was not obvious that any marked improvement can be made which will be as reliable, compact and robust as scintillators. Strand (Brookhaven, US) reported an elegant technique for making hodoscopes of 1 mm scintillating fibres, though this offers the advantage of good resolution at high particle fluxes rather than an improvement in timing.

The next shell of the detector is usually a tracking-chamber. At LEP it will have to be able to resolve up to 50 charged particles, many of them bunched in 'jets'. The present chambers working at PETRA (Hamburg) seem only just good enough for the job, though one of them, in the JADE detector, is more ambitious than the others. It uses fewer drift-cells and lets the electrons from a track drift further than in the conventional chambers. This, or the even more ambitious TPC (the time-projection-chamber at Stanford, built by a Berkeley group and reported at the meeting by Nygren), seemed to be the model people were taking for the LEP detector. Position resolution of 100 microns should be possible — though present detectors only achieve around 200 microns — and tracks only 5 mm apart will need to be resolved. Separating close tracks is where TPC and JADE win over the conventional chambers. But these two 'pictorial drift chamber' techniques also give many more samplings of the ionisation on a track and that can also be used to provide π/K/proton identification below 1.5 GeV/c and, in principle, from 3.5 to about 40 GeV/c by measuring the 'relativistic rise' in ionisation. There was more controversy over the measurement of the

---

*An international meeting on experimentation at LEP was held in Uppsala, Sweden from the 16th to the 20th of June 1980.

0028-0836/80/330661-02$01.00

relativistic rise than over any other topic. Allison (Oxford) claims that the ISIS device is now achieving the predicted resolution in ionisation measurement, but there were many others who have made similar measurements and, as Lehraus (CERN) has observed, can only come within a factor of $\sqrt{2}$ of the goal. Such a factor is crucial when the effect is only a 10% change is energy-loss and one expects around ± 4% uncertainty in measurements.

An alternative to relativistic-rise measurements is to use c̄erenkov radiation to separate π, K and proton. TASSO at PETRA, as described by Leconte, has two large slices of c̄erenkov counters which penetrate through the outer part of the detector and cover 20% of 4π solid-angle. There is a layer of aerogel counters with refractive index 1.023 and outside it two layers of atmospheric-pressure gas counters. This is an impressive and complex piece of instrumentation, yet it still leaves gaps — momenta at which π, K and proton cannot be separated. A recurrent call from speakers was for even lighter aerogel — a gossamer-like clear plastic — and groups at Saclay and Lund claimed that they will get the refractive index of aerogel down to 1.006 well before LEP is built. The disadvantage of the c̄erenkov approach to particle identification is that it seriously impedes the other kinds of measurement which, in a general purpose detector, come outside the tracking chamber. A radical idea from Ypsilantis (Ecole Polytechnique) may overcome this by using concentric spherical c̄erenkov detectors in which particles would produce ring images whose size would give the particle type and whose position would give the direction. Successful tests have been made on the detection of c̄erenkov light by large-area gas counters, but a list of formidable technical problems still has to be solved before a ring-imaging central detector can be proposed for LEP.

In the central region only charged tracks are measured. But a great deal of energy goes into the neutrals; π^0s and γ-rays or neutrons and long-lived K^0s. To catch the neutrals 'calorimeters' are used. These are dense arrays of heavy material and counters in which a fraction of the energy from an interacting neutral particle is converted into analogue signals which are summed to give a measurement of the energy. For electromagnetic showers the requirement is a high value of the atomic number Z, since γ-ray conversion and electron bremsstrahlung are proportional to Z^2. The most precise energy measurements are those made with sodium iodide crystals and a number of specialised detectors ('crystal balls') have been used for γ-ray spectroscopy with a small tracking chamber surrounded by hundreds of closely packed crystals. One such device may be needed at LEP because there are a number of very important single-γ decays which should be looked for, such as $e^+e^- \rightarrow$ (Higgs + γ) at the Z^0 peak, or the cascading γ decays of the "toponium" family — an expected heavy analogue of the well-established ψ/J "charmonium" family in which the $\psi\ (3.7) \rightarrow \gamma\chi$ processes have given useful information on quark binding. Less-specialised electromagnetic calorimeters will need similar energy resolution to the present lead plus liquid argon or lead scintillator systems, and better spatial resolution than all but the best of present detectors. Lots of new ideas for electromagnetic calorimetry were presented, including a plea by the author for the merits of solid argon, based on work by an École Polytechnique-UCL collaboration. The new suggestion which was best received was the 'Time Projection Quantameter' — a drift-chamber filled with perforated lead sheets. It could not — nor could other gas-filled calorimeters — match the energy-precision of lead-glass or lead plus argon but it has good spatial resolution and may be easier to run than some of the other devices. For neutrons and long-lived kaons a much thicker and coarser calorimeter is needed because the absorption length for strongly interacting particles (hadrons) is much longer than for electrons and γ-rays. Some of the present detectors incorporate hadron calorimeters outside the electromagnetic calorimeter and there was considerable discussion of these techniques. The best material to use is probably uranium, which amplifies and feeds back the energy normally lost as slow neutrons, but in many cases people are happy to use the segmented iron return yoke of the track-chamber magnet. It was surprising to many of us that with a conventional solenoid around the central detector and with a hadron calorimeter of uranium plus scintillator, charged hadron energies above 10 GeV/c might be better measured in the calorimeter than in the tracking chamber.

Solenoid magnets remain popular. There is a strong school of thought which advocates conventional, large-radius, low-field solenoids, rather than small superconducting ones. For specialised detectors the 'open solenoid', as used by the DELCO detector at Stanford, can allow particles out into c̄erenkov counters without interacting, but experience with the PETRA detectors shows that one radiation-length of coil does not interfere too badly with the performance of a subsequent electromagnetic calorimeter.

One intriguing development reported at the meeting may turn out to be important in many other fields as well as in high energy physics. Kunz (Stanford University) described his 'emulating processor', a small cheap home-made microprocessor which has similar internal architecture to Stanford's large IBM computer. This allows it to execute programs which have been compiled on the IBM and so take away a large part of the 'number crunching' load from the central laboratory machine. One Stanford experiment now claims to have more computing power than two or three of the major international laboratories put together. Among other powerful electronic techniques which can now be considered there was considerable interest in 'flash analogue to digital converters' — devices developed for television purposes which sample an analogue level at a rate of more than 40 MHZ. They are expensive at the moment and, as an alternative, the TPC group made a strong defence of their charge-coupled shift-register technique for doing the same kind of job. They claim it costs only $30 per channel including the analogue to digital converter. When the data has been digitised it must be checked. Do all these 'hits' constitute a track? How much energy did the calorimeter catch? It may be that the advances in hard-wired or field-programmable microprocessor logic will play a larger part in improvements of the instrumentation at LEP, compared with PETRA, than any advances in the detectors themselves. LEP will have 25 microseconds between bunch-crossings so it will be possible, according to Waloschek (Hamburg), to apply ~ 50,000 separate series and parallel tests on the data from one event before deciding whether to record it; and if there is a bank of emulating processors standing by it could then be possible to run through the complete analysis on the spot. A totally different approach to decision-making logic was suggested by Julia Thompson (Pittsburg) who has been experimenting with a holographic technique which might go well with fibre-optic data transmission.

Techniques already exist for doing many of the things that need doing at LEP and there is a community of high energy physicists from all over the world who are eager to get started. The teams are likely to be of a hundred or so per experiment. There will not be much that a ten-man-team could do by themselves, but since the equipment is so modular it is clear that small groups from many separate institutions will contribute their own pieces to the whole and, with the spread of remote-access computer systems, much of the analysis will still be done in universities hundreds of miles away from LEP itself. ☐

100 years ago

In a recent paper to the Belgian Academy (*Bull.*, No. 5) Abbé Spée contends that the spectral line D3, with wave-length about 588, observed in the chromosphere and protuberances, and assigned to a hypothetical body, helium, which some suppose to have a still more simple molecular constitution than hydrogen, probably belongs in reality to this gas. As to its non-reversibility, he considers that at a very small distance from the chromosphere the solar hydrogen may be so far cooled as to be comparable to that which we manipulate, and so, unable to extinguish waves which it can no longer produce, just as a stretched cord loses the property of vibrating in sympathy if its tension have been altered.

From *Nature* **22**, 12 August, 350, 1880.

David J. Miller is in the Department of Physics and Astronomy, University College, London.

0028-0836/80/330662-02$01.00

Nature Vol. 286 14 August 1980

REVIEW ARTICLE

The ontogeny of the neural crest in avian embryo chimaeras

Nicole M. Le Douarin

Institut d'Embryologie du CNRS et du Collège de France, 49bis, avenue de la Belle-Gabrielle, 94130 Nogent-sur-Marne, France

The migration and subsequent development of autonomic ganglion cell precursors can be followed in suitably constructed chimaeric quail–chick embryos, thanks to the distinctive structures of quail and chick interphase nuclei. The decisive role of environmental factors arising from non-neuronal tissues on the chemical differentiation of neurones was demonstrated together with the lability of their phenotype during ontogeny.

EMBRYONIC development involves extensive movements of cells to achieve histogenesis and modelling of the body. With a few exceptions, such movements are extremely difficult to follow precisely by classical embryological methods. In fixed tissues, migrating cells, if they can be identified at all, can usually only be recognized in favourable situations, as for example when they are just leaving their site of origin. Since the expression of a particular differentiated phenotype generally occurs only after cell migration has taken place, the cells rapidly become indistinguishable from the equally undifferentiated surrounding tissues. The construction of embryonic 'fate maps' thus involves marking presumptive migrating cells so that their movements can be followed during ontogeny. This type of study, from which fundamental data on the formation and the fate of the germ layers have been obtained[1,2], entails differential labelling of relatively large tissue areas with rather crude methods, such as the application of vital dyes or small marking particles to specified embryonic regions. To investigate the migratory behaviour of individual cells, more precise means had to be found. One important way of achieving such refinement has been the use of techniques for combining early embryonic cells of different genotype. Such chimaeras develop normally and can be used to trace cell lineages through characteristic genetic markers.

In recent years, cell migration, cell derivation and cell–cell interactions during ontogeny of the avian embryo have become better understood, through the development of such a marking technique based on differences of the nuclear structure in two species of birds—the chick (*Gallus gallus*) and the quail (*Coturnix coturnix japonica*).

The quail–chick marking technique

The presence in all embryonic and adult cell types of the quail of a large amount of heterochromatin associated with the nucleolus was first described in 1969, and this characteristic was proposed as a cell-marking technique in combinations of embryonic cells from the quail and the chick[3]. Taxonomically, the two birds are closely related, but they differ significantly in the duration of their incubation period (16 days for the quail, 21 days for the chick) and their size at birth: the newly hatched chick weighs about three times as much as the quail. However, as shown by the tables of development of the two species[4,5], the chronology of development and also the size of the embryo differ only slightly during the first half of the incubation period, when the most decisive events of embryogenesis occur. Quail and chick cells can readily be recognized in sectioned material with the Feulgen–Rossenbeck stain or in the electron microscope after the routine uranyl acetate-lead citrate staining procedure. In undifferentiated cells, characterized by a high proliferation rate, the nucleolus is enlarged and made up of intimately associated DNA- and RNA-containing structures[6]. In most differentiated cell types, the nucleolus is formed of a compact mass (sometimes 2 or 3) of heterochromatin, distinct from the nucleolar RNP, which occur as 'satellites' in contact with the heterochromatin. The structure of the nucleolus thus varies somewhat according to the cell type considered and the degree of differentiation reached. Nevertheless, the differences in their structures in quail and chicken cells are always conspicuous enough to make them easy to identify[6].

Quail–chick chimaeras can be constructed either *in vivo* or in culture. In the latter case, interactions between cell types from each species can be analysed in the course of a definite histogenetic process. Organotypic culture *in vitro* or grafting of the combined tissues on the avian chorioallantoic membrane (CAM) provides suitable conditions for these kinds of experiment[7,8]. The quail–chick system has also been applied to cell culture for recognition of nuclei in heterokaryons after acridine-orange staining[9]. However the domain in which it has so far been the most profitable is in the analysis of chimaeric embryos constructed *in ovo* by implanting quail cells into chick, or vice versa.

This method has been applied in my laboratory to study the ontogeny of two systems that involve extensive cell migrations in the embryo, the neural crest and the haemopoietic organs.

Migration pattern and fate of neural crest cells

The neural crest is a transitory structure of the vertebrate embryo arising from the lateral ridges of the nervous primordium and giving rise, among other cell types, to the neurones and supporting cells of the peripheral nervous system (sensory ganglia of the head and the rachis and autonomic sympathetic and parasympathetic ganglia), to the melanocytes and to mesenchymal derivatives in the head. As the elements derived from the neural crest are dispersed in various locations, the neural crest cells have to migrate throughout the developing body before reaching the embryonic rudiment in which they differentiate. This structure is, in many ways, an attractive model for the study of certain developmental problems and the fate of its cells has been widely investigated. Although they yielded much important information, the experimental techniques used by earlier workers for investigating differentiating capabilities of crest cells (excision and electrocauterization of the neural anlage, and various cell labelling techniques: see refs 6, 10, 11) did not provide a complete and detailed picture of the migration pattern and the developmental fate of the whole population derived from the crest. The application of the quail–chick marker to this problem brought additional information on the role of the neural crest in the construction of the head in higher

0028-0836/80/330663—07$01.00

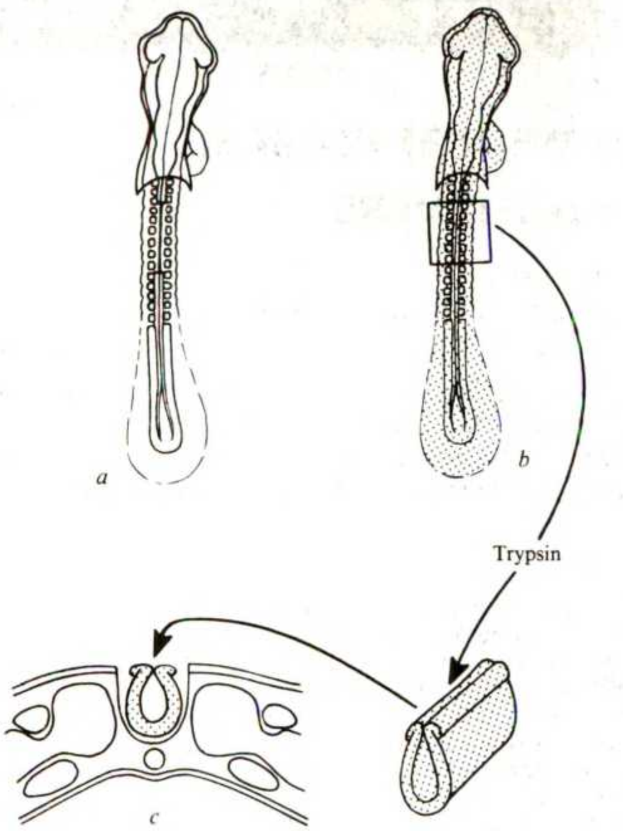

Fig. 1 Schematic representation of the isotopic-isochronic grafting technique of neural primordium between quail and chick embryos. *a*, Chick host embryo following the removal of the neural anlage from somite 4 to somite 10. *b*, Quail donor embryo from which the corresponding fragment of the neural tube + neural fold is isolated by enzymatic digestion. *c*, Graft of the quail neural primordium into the chick embryo.

vertebrates[12-16] and allowed new crest derivatives to be identified[17-19]. The method used, derived from that described by Weston[20], involved (1) surgical removal of a defined region of the neural primordium in a host embryo before the onset of crest cell migration at this level; and (2) its replacement by the strictly equivalent neural area originating from a donor embryo of the alternative species, at the same developmental stage (that is, isotopic and isochronic grafts) (Fig. 1). Since the graft is correctly positioned in the host, it develops normally in the chimaera (Fig. 2). Furthermore, the regulation processes that often follow extirpation of embryonic territories do not take place in the chimaera since the empty space is occupied by an equivalent structure originating from the donor embryo. Immunological mechanisms do not function during embryonic life and tissues of the two species are thus tolerated by each other. In the cephalic region, where the neural fold is larger than in the trunk, selective substitution of pieces of the neural crest alone can be carried out[12,13]. Migration of crest cells is followed on serial sections of the host embryos at various developmental stages. Recognition of the phenotype displayed by the grafted cells requires identification of both nuclear characteristics and an appropriate differentiation marker in the same cell. Electron microscopy can sometimes do this but, more often, the successive application of a cytochemical method (for example Falck's technique to evidence catecholamines[21]) and the Feulgen–Rossenbeck stain on the same section, have to be used.

Differentiation of the peripheral nervous system

Cells originating from the neural crest differentiate into constituents of two major neuronal systems: the sensory and the autonomic. Considerable interest has been focused in recent years on the development of autonomic nerve cells and particularly on their chemical differentiation in terms of neurotransmitter synthesis. In complementary approaches the migratory behaviour and capabilities for differentiation of the presumptive autonomic neuroblasts have been studied by means of transplantation experiments *in vivo*, and the stability of neurotransmitter synthesis in developing autonomic neurones has been examined *in vitro*.

Although the ganglia of the autonomic nervous system and the adrenomedullary cells have long been recognized to be of neural crest origin, the migration pathways followed by their precursor cells were controversial (see ref. 22). By using the quail–chick chimaera system, we investigated their origin in normal development in the avian embryo. Isotopic and isochronic grafts of small fragments (corresponding to a length of 4–6 somites) of quail neural primordium into chick embryos (and vice versa) were systematically carried out along the whole length of the neural axis. The migrating neural crest cells were thereafter observed on serial sections of the host trunk (in the sympathetic chain and the adrenal medulla) and digestive tract (in the enteric and intravisceral ganglia). A correspondence could be established between the level of the graft and the definitive location of ganglion cells. In this way, the fate map of the autonomic cell precursors could be established (Fig. 3).

One of the striking observations made during these experiments was the finding that in the cervico-dorsal region (between somites 7 and 28) neural crest cell migration was strictly confined to the dorsal mesenchyme derived from the somites and the intermediate cell mass. Except for the melanocytes and for the Schwann cells that followed the nerve bundles to the periphery, neural crest derivatives were restricted to the sensory and sympathetic chain ganglia, the aortic and adrenal plexuses and the adrenomedullary paraganglia. No ganglion cell precursors penetrated the dorsal mesentery to contribute to either the ganglion of Remak or the enteric plexuses. In contrast, isotopic grafts carried out at the vagal (from somites 1 to 7) and lumbosacral (behind the 28th somite pair) levels of the neural primordium resulted in colonization of both the dorsal mesenchyme and the splanchnopleure. The myenteric plexuses are derived mainly from the crest at the level of somites 1–7; the contribution of the lumbosacral crest is restricted to the ganglion of Remak and to some ganglion cells of the post-umbilical gut. Crest cells continue to migrate ventrally from the vagal region between the 7- and 14-somite stages (approximately) and become incorporated into the mesodermal wall of the fore-gut, where they subsequently undergo a long cranio-caudal migration. Penetration of the hind-gut by either vagal or lumbo-sacral crest cells does not occur before days 7 to 8 of incubation[22,23].

The neural crest can therefore be divided into several different axial regions with respect to the development of the autonomic nervous system. One (level of somites 1–7) gives rise

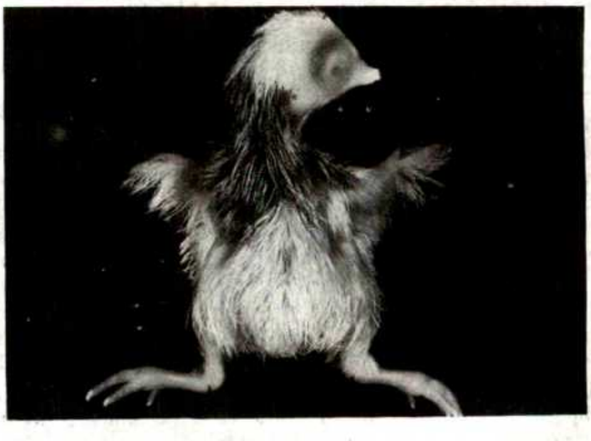

Fig. 2 Transverse pigmented stripe resulting when a fragment of a quail neural tube was grafted into a White Leghorn chick embryo.

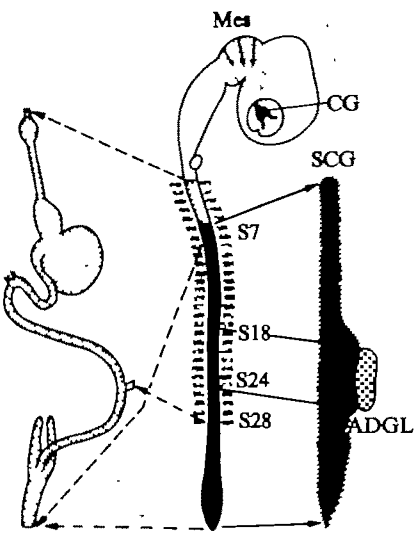

Fig. 3 Diagram showing the origin of adrenomedullary cells and autonomic ganglion cells. The spinal neural crest caudal to the level of the fifth somite gives rise to the ganglia of the orthosympathetic chain. The adrenomedullary cells originate from the spinal neural crest between the level of somites 18–24. The vagal neural crest (somites 1–7) gives rise to the parasympathetic enteric ganglia of the pre-umbilical region, the ganglia of the post-umbilical gut originating from both the vagal and lumbosacral neural crest. The ganglion of Remak is derived from the lumbosacral neural crest (posterior to the 28th somite level). Ciliary ganglion (CG) is derived from the mesencephalic neural crest. ADGL, adrenal gland; Mes., mesencephalon; SCG, superior cervical ganglion.

to the enteric ganglia of the gut. Another (somites 7–28) is the precursor of sympathoblasts of the trunk (within this area, the 'adrenomedullary' level of the crest contributes to the adrenal glands) and, finally, there are two regions from which both enteric and sympathetic ganglion cells arise (somites 5–7 and behind the 28th pair of somites). Next, neural primordia were transplanted heterotopically between quail and chick embryos, as shown in Fig. 4. This was to find out whether the migratory behaviour and phenotypic expression of crest cells from these regions were irreversibly fixed before migration and if experimental rearrangement of the axial levels of the neural crest would lead to developmental disturbances in the distribution and development of crest cell derivatives. Analysis of the resulting chimaeras showed that the neural crest cells of the adrenomedullary region, grafted at the vagal level, were able to colonize the gut (which they never do in normal development) and give rise to functional cholinergic enteric ganglia; second, neural crest cells from the quail mesencephalon or rhombencephalon, grafted at the chick adrenomedullary level, produced adrenergic sympathetic ganglia, populated the adrenal gland and differentiated into adrenomedullary-like cells[24,25]. This indicated that the migratory behaviour of the crest cells depends on the pathways available when they leave the neural primordium rather than on some specificity related to their origin in the neural axis. The vagal and the adrenomedullary regions of the embryo provide preferential pathways leading crest cells to the gut and to the suprarenal gland, respectively. In addition, the phenotypic expression of the crest cell population is regulated by environmental factors which elicit either cholinergic or adrenergic cell differentiation, irrespective of their fate in normal development. Furthermore, the potentialities for giving rise to cholinergic parasympathetic cells, adrenergic sympathetic ganglia and adrenomedullary paraganglia are not restricted to the areas identified in the isotopic-isochronic experiments, but are present in the entire crest.

Two questions thus arise. First, do the environmental signals for differentiation act on neural crest cells during their migration or after they have reached their definitive location? And second, when do the developing autonomic neurones become irreversibly differentiated into adrenergic or cholinergic cells?

When is the chemical differentiation of the autonomic neurone precursor determined?

To determine if chemical differentiation occurs before migration, we investigated the kind of transmitter synthesized by neurones when their extraintestinal migratory phase was eliminated. Since neural crest cells reach the hind gut only at 7 to 8 days of incubation, the colorectum remains totally aneural if it is removed from the embryo before this stage and grown on the CAM. When such an aneural rectum was associated with trunk neural crest for 10 to 12 days on the CAM, the crest cells migrated into it and differentiated into Auerbach's and Meissner's plexuses, in which catecholamine (CA)-containing cells were never observed. In contrast, significant levels of choline acetyltransferase (CAT) and acetylcholinesterase (AchE) activities were present in the explants[7,26]. Thus the induction of cholinergic metabolism does not depend on environmental signals received by autonomic neurone precursor cells during migration.

In contrast, the expression of the adrenergic phenotype in sympathoblasts does seem to be influenced by developmental cues during the dorso-ventral migration of the neural crest cells. By associating the neural crest with various trunk structures, Cohen[27] and Norr[28] reached the conclusion that the crest cells receive differentiating signals on their route and that the notochord, ventral neural tube and somitic mesenchyme are of decisive importance in promoting CA-synthesis in crest neuroblasts.

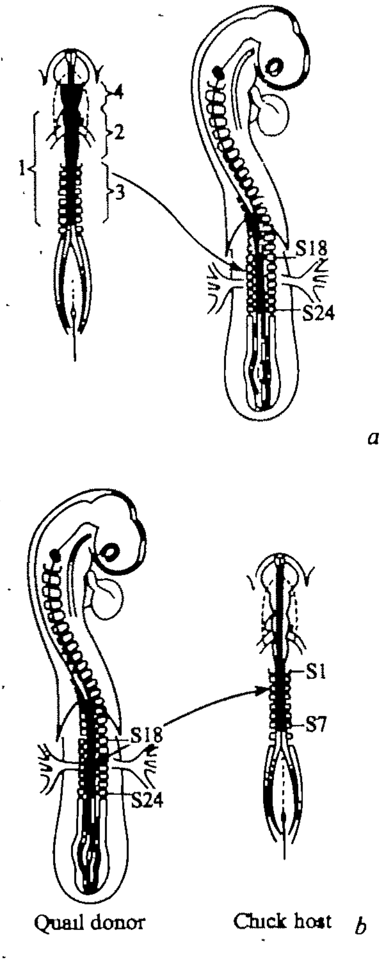

Fig. 4 Heterotopic grafts of quail neural primordium into the chick embryo. *a*, The quail primordium is removed from the mesencephalon; the anterior rhombencephalon or at the vagal level and grafted into the adrenomedullary region. *b*, The neural tissue is taken at the adrenomedullary level and grafted at the vagal level.

	Enteric ganglia	CAT activity	Adrenergic ganglia
Quail NC 1 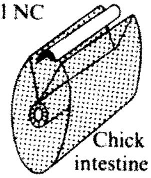 Chick intestine	+	+	–
Quail NC+NT 2 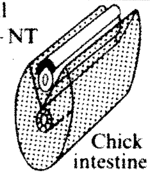 Chick intestine	+	Not determined /	–
Quail NC+NT 3 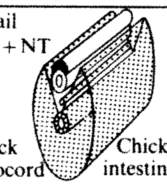 Chick notocord Chick intestine	+	Not determined /	+

Fig. 5 Association of the aneural colorectum of a 5-day chick embryo with various dorsal trunk structures of 2-day embryos: (1) chick intestine + quail neural crest (NC). (2) chick intestine + quail neural crest and neural tube (NT). (3) chick intestine + quail neural crest/neural tube and chick notochord. CAT, choline acetyltransferase. Cholinergic ganglia develop in all cases. Adrenergic ganglia differentiate only in explants containing the notochord.

It is striking that the first CA-containing neuroblasts appear in the somitic mesenchyme (in fact in the sclerotomal part of the somite) in the immediate vicinity of the notochord and of the dorsal aorta. We therefore decided to reinvestigate the respective roles of each of these dorsal trunk structures (neural tube, notochord and somitic mesenchyme) in sympathoblast differentiation. When trunk neural primordium was isolated and inserted in aneural gut wall mesenchyme (Fig. 5), the neural crest gave rise to enteric plexuses; but in spite of the presence of the neural tube in the explants, no CA-containing cells could be detected in the ganglia. The result was therefore similar to the differentiation observed when the neural crest alone was associated with the gut[26]. In contrast, the inclusion of the notochord in the tissue associations resulted in the development of cholinergic myenteric plexuses and also in the formation of a series of adrenergic ganglia, located in the wall of the gut and characterized by the greenish fluorescence of CA. It is therefore clear that among the dorsal trunk structures, the notochord is of decisive importance in eliciting adrenergic differentiation in sympathoblasts, since, in its presence, adrenergic cells develop in the splanchnopleural gut mesenchyme, which normally supports only cholinergic differentiation. Moreover, this finding is in contradiction with the conclusions previously reached by Cohen[27] that the somite was the only structure of the embryo able to provide a convenient mesenchymal environment for adrenergic differentiation of crest-derived neuroblasts. In fact, culture experiments (unpublished) show that both the notochord and the sclerotomal part of the somitic mesenchyme are equally able to induce CA metabolism in the crest neuroblasts. This accounts perfectly for the distribution of the adrenergic cells in the trunk structures of the early embryo.

A recent observation made by Cochard *et al.*[29] in the rat embryo supports the notion that notochord induces the adrenergic phenotype. Both tyrosine hydroxylase and CA first appear at 11.5 days of gestation in the sympathetic ganglia of the trunk. But, in addition, cells with an adrenergic phenotype are transiently detectable in the gut wall from day 11.5 to about day 14.5. Thus CA differentiation in these cells may have been induced by interactions with the somite-notochord-neural tube environment during their dorso-ventral migration towards the gut. The resulting adrenergic phenotype is expressed for a time after cells have left the dorsal trunk structures and while they are pursuing their migration in the gut, but it cannot be maintained in the gut, either because of the lack of appropriate stimulation, or because other factors intervene.

Lability of transmitter phenotype in developing autonomic neurones

If the neurotransmitter phenotype of neural crest cells is selected by the tissue environment during early development what is the stability of the chemical differentiation in the developing autonomic neurones? We have investigated this by attempting to change the fate of already differentiating ganglion cells.

Cholinergic ciliary ganglion from 4.5–6 day quail embryos were incubated and implanted into the dorsal trunk environment of a 2-day chick host at the level of somites 18 to 24, the idea being to subject the maturing cholinergic cells to the adrenergic signals normally operating from day 3 to 4 on the precursors of sympathoblasts and adrenomedullary cells (Fig. 6). The ciliary ganglion, which normally never contains adrenergic cells at any stage, exhibited cholinergic activity at the time of grafting[30–33]. Examination of the host embryos at 8 to 10 days showed that, irrespective of its age when grafted, the ciliary ganglion never remained intact at the site of implantation. Quail cells were found dispersed in the host trunk structures, but not randomly: they were always localized exclusively in normal sites of neural crest cell arrest and participated in the formation of various host crest derivatives, that is sympathetic ganglia, aortic and adrenal plexuses, adrenomedullary cords, ganglion of Remak and enteric plexuses. However, quail cells were virtually never found in the host sensory ganglia; in contrast, the Schwann cells of the rachidian nerve were mostly of the quail type at the site of the graft.

The ability of cells of a differentiating ganglion to migrate anew when grafted into the microenvironment which normally sustains crest cell migration is remarkable enough. However, the result obtained by treating the sections with the combined FIF–Feulgen–Rossenbeck techniques was even more striking: the quail cells which had homed to the sympathetic ganglia, the aortic and adrenal plexuses and the suprarenal gland exhibited the bright greenish fluorescence of CA (Fig. 7). In electron microscopy, most of the quail cells of the suprarenal gland, recognizable by their large DNA-rich nucleolus, were also seen to contain the electron-dense secretory granules characteristic of adrenomedullary cells.

Although in some cases sympathetic chain ganglia in the host were found to be totally (or mainly) made up of quail cells, grafted and host cells were usually intermingled. The possibility that the fluorescence observed in the quail cells resulted merely from an uptake of CA released by host sympathoblasts was ruled out by experiments in which the host neural crest was removed before the graft of the quail parasympathetic ganglion. In this case, adrenergic nervous structures entirely made up of quail cells developed at the site of the operation and showed the same CA fluorescence as in the previous series[33].

The cells of the ciliary ganglion which colonized the splanchnopleure and became localized in the host Remak and enteric ganglia were not CA-positive after FIF treatment, and presumably developed as cholinergic cells.

In recent (unpublished) experiments, pieces of ciliary ganglia taken from quail embryos as old as 9 days of incubation were similarly grafted into 2-day chick embryos. Quail cells were found in the same locations in the host structures as in the previously described experiments except that their migration was practically restricted to the dorsal trunk and generally did not penetrate the dorsal mesentery. Many quail cells were found with CA fluorescence in the sympathetic host ganglia in the adrenal gland and in the aortic plexuses.

We are currently examining in detail the ability of the grafted cells to proliferate in a young host. Merely from the extent of quail cell distribution in the 8-day host following the graft of a 4.5-to 6-day-old ciliary ganglion, it is clear that their number is higher than the total number of neurones of the mature ciliary ganglion. Detailed counts of the number of quail cells labelled one hour after ^{3}H-thymidine injection at various intervals after grafting, show that many mitoses occur both during the migration of ciliary ganglion cells and after their stabilization in host structures. Numerous quail neurones and adrenomedullary cells are labelled with ^{3}H-thymidine at all stages up to 9 days of incubation of the host. These observations are in agreement with the recent findings[34] that developing sympathoblasts, actually synthesizing CA, divide until late in development.

Such proliferative potential is not maintained as long in the cholinergic ciliary ganglion since, according to the work of Landmesser and Pilar[31], mitotic activity has virtually stopped in chick neuroblasts at stage 25 (4.5 to 5 days of incubation), while the definitive number of neurones, after physiological cell death has occurred, is reached around day 12. Therefore, transplantation of a cholinergic ganglion into a younger host changes its developmental program profoundly enough to modify not only its chemical differentiation but also the number of cell cycles that the neuroblasts undergo before reaching maturity.

In summary, our results demonstrate that CA synthetic ability exists in cells of developing cholinergic ganglia; although not expressed in normal development, it can be elicited by the dorsal trunk structures and the adrenal gland environment.

Since all our experiments deal with the transplantation, not of single cells but of a population, our results do not allow us to state that the appearance of CA-producing cells results from the conversion of initially cholinergic cells. It may well be that the ciliary ganglion, even as late as 9 days of incubation, contains a pool of still undifferentiated neuroblasts which may be destined to disappear later on in normal development. It should nevertheless be emphasized that the capacity for a developing autonomic neurone to change its transmitter metabolism in response to environmental influences has been indisputably demonstrated by experiments *in vitro*[35–38].

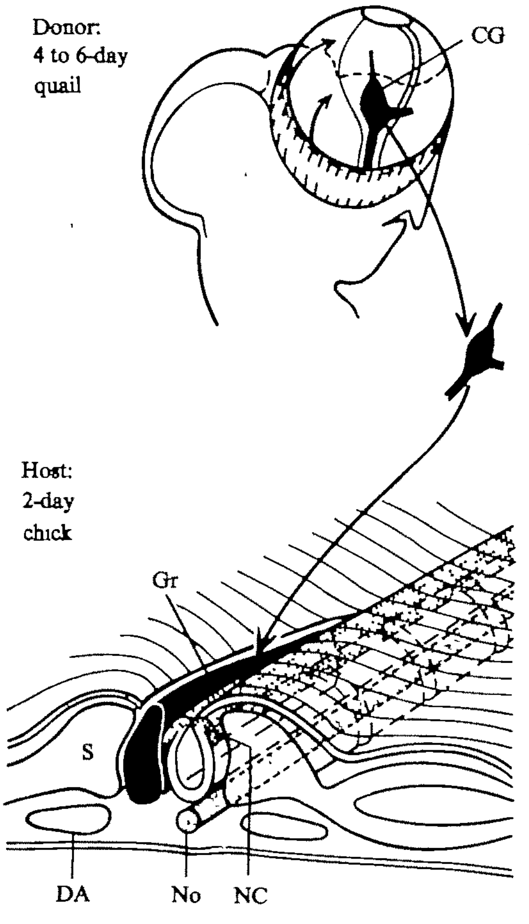

Fig. 6 Experimental design for back-transplantation of differentiating cholinergic ganglia from 4- to 6-day quail donor embryos into 2-day chick hosts. The ciliary ganglion (CG) is dissected and inserted either whole or in pieces into a slit made between the neural primordium and the somites (S). DA, dorsal aorta; Gr, graft; NC, neural crest; No, notochord.

Manipulation of the fluid environment in which dissociated post-mitotic neurones from the newborn rat superior cervical ganglion are growing has been shown to influence the choice of transmitters and the type of synapse they make. These elegant experiments (reviewed by Patterson[39]) have revealed the existence of a soluble factor mediating the conversion of an adrenergic to a cholinergic phenotype Moreover, during the switch in transmitter metabolism in culture, neurones with both adrenergic and cholinergic functions have been identified in single-cell cultures[40,41].

Although cell physiology may be profoundly altered by culture conditions, the results obtained *in vitro* are important in defining the mechanisms regulating autonomic nervous system development *in vivo*, particularly in two respects. First, the discovery that a change in transmitter synthesis can occur in post-mitotic nerve cells and the demonstration of dual-function neurones in culture strengthen the view that in the transplantation experiments *in vivo*, the environment imposes the choice of phenotypic expression on bipotential neuroblasts. The alternative hypothesis, that the microenvironment merely selects from a mixed population of committed adrenergic and cholinergic neuroblasts, becomes more unlikely. If the dual-function neurones detected in culture represent a transitional state between the adrenergic and the cholinergic condition, it seems probable that a similar process takes place in reverse when the cholinergic ciliary ganglion cells become adrenergic after back-transplantation into a younger host. Second, the demonstration that cholinergic differentiation can be triggered *in vitro* by a factor of non-neuronal cell origin suggests that an analogous mechanism might operate *in vivo*. In particular our experiments suggest that adrenergic differentiation is regulated by 'factors' produced by cells of the notochord or by the sclerotomal part of the somite and released into the extracellular matrix. Alternatively, an integral membrane component of the somitic mesenchyme might influence crest cell differentiation through intimate cell–cell contacts. The developmental relationships between sclerotomal and neural crest cells during ontogenesis support such a hypothesis but, experiments involving cultures of neural crest *in vitro*, to be described below, show that such cell–cell contacts are not necessary for eliciting CA metabolism in the developing sympathoblasts.

Developmental capabilities of neural crest cells *in vitro*

From their study of the *in vitro* differentiation of crest cells in the absence of any other tissue of the embryo, Greenberg and Schrier[42] reported CAT activity in mesencephalic neural crest cells after 7 days in culture and Cohen[43] described the appearance of adrenergic cells in trunk crest cultures. In both cases, the total neural anlage was explanted for 48 hours and, after the migration of crest cells had taken place, the neural tube was mechanically removed. This technique cannot avoid possible contamination of the crest cultures by central neurones or possible influence of the neural tube itself on peripheral neuroblast differentiation[44]. Therefore our approach has been to excise neural crest from quail embryos, at both mesencephalic and truncal levels, by a microsurgical procedure that leaves the neural tube in place. Cultures of pure crest explants from each region underwent morphological differentiation and were able to synthesize both ACh and CA. Although the amount of neurotransmitter synthesized could be increased by co-culturing with a variety of embryonic tissues, the ratio of ACh to CA formed in a given culture was markedly dependent on the composition of the liquid medium. In particular, horse serum was found to favour ACh synthesis, whilst fetal calf serum preferentially enhanced CA production. These studies, together with those of other workers[42,43], strongly suggest that direct intercellular contact with non-neural tissue is not essential for inducing neurotransmitter synthesis.

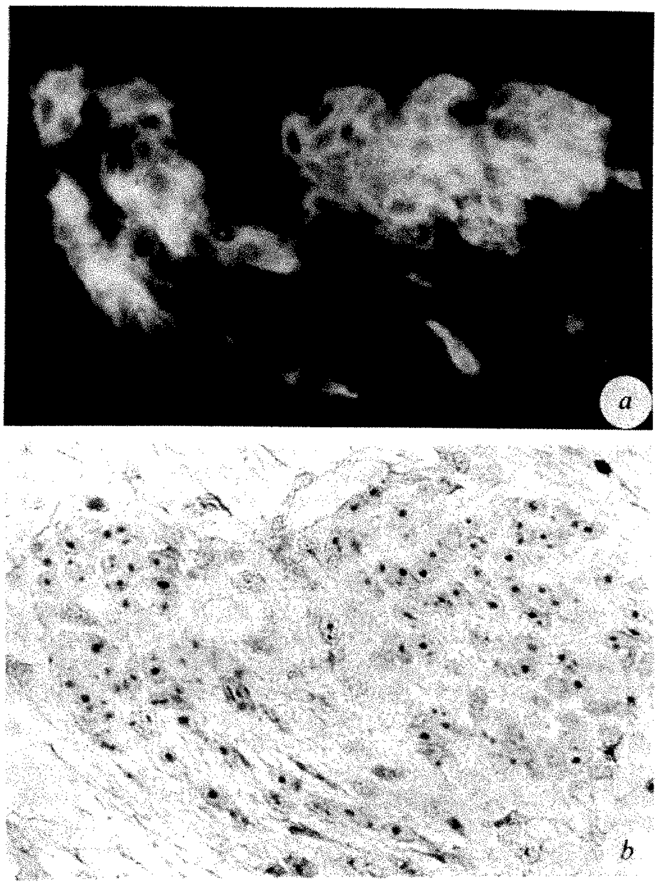

Fig. 7 Result of the experiment of back-transplantation of a quail autonomic ganglion into a 2-day chick embryo (as represented in Fig. 6). Transverse section of the host at 7 days of incubation at the level of the sympathetic ganglia. *a*, CA-containing cells shown after application of Falck's technique. *b*, Post-staining of the same section with the Feulgen reaction shows that the fluorescent cells originate from the grafted ciliary ganglion since they have the nuclear marker. ×460.

The choice between the cholinergic and the adrenergic pathways made *in vivo* by future neuroblasts could thus be the result of selective induction by soluble factors encountered at the opportune moment. If such an interpretation is correct, one has to assume that differentiating factors for both ACh and CA synthesis are present in the culture medium. They might be provided by the serum and/or by the embryo extract. Another possibility is that neuroblast precursors have the ability to synthesize neurotransmitters while still in the neural primordium; the role of environmental cues would then be limited to stabilizing and enhancing the appropriate phenotype.

As far as the adrenergic system is concerned, a number of histochemical studies have shown that the earliest detectable appearance of tyrosine hydroxylase and of CA synthesis in presumptive sympathoblasts coincides with their aggregation into the primary sympathetic chain[29,45,46]. This suggests that the first of the above mentioned alternatives is correct and that an inductive event occurs during the crest cells' dorso-ventral migration which gives them a bias towards the adrenergic pathway. On the other hand, recent results from our laboratory cast serious doubt on the applicability of this hypothesis to cholinergic differentiation[47]. We were, in fact, able to show that mesencephalic crest, excised from quail embryos of 8–12 somites (when the crest appears as an actively migrating sheet of cells under the ectoderm[44]) is able to convert ^{3}H-choline to ^{3}H-ACh and that this transformation is due to CAT. Furthermore, this activity can also be detected at an even earlier stage (5–7 somites), when migration is just beginning. In other words, mesencephalic crest cells already contain a cholinergic system when they start to migrate. We cannot yet say whether all or only some of the crest cells are involved. However, if we assume that the early cholinergic differentiation concerns the presumptive parasympathetic neuroblast (the ciliary ganglion is derived from the mesencephalic crest[13,48]), the obvious implication is that no inductive stimulus is necessary once the latter have reached their definitive site, and cholinergic maturation involves consolidation and augmentation of already acquired properties. There is one clear case in which external cues have been shown to stabilize synthesis of a particular kind of transmitter and decrease the lability of neuronal chemical differentiation: Walicke *et al.*[49] have shown that the chemical differentiation of sympathetic neurones is stabilized by neuronal activity itself.

Conclusions

In our laboratory and elsewhere quail–chick chimaeras have proved most useful in the investigation of the early stages of the differentiation of the nervous system[48,50,51]. We have already identified some new derivatives of the neural crest and analysed certain aspects of the development of the autonomic nervous system; comparison of the *in vivo* transplantation and *in vitro* culture experiments has been particularly fruitful.

Future experiments will explore the developmental relationships which may exist between the neuroblasts that give rise to the sensory neurones of the dorsal root ganglia and those which become autonomic cells. It would be of great interest to know when the commitment of these different cell types occurs and whether the choice in this case also, remains labile for a while. The relationships between the glial satellite cells of the ganglia and the neural cell lines will also be examined. Furthermore the chemical differentiation of the peripheral neurones needs to be reconsidered in terms of neurotransmitters other than just ACh and CA and including neuropeptides.

Note that the chimaeric cell labelling technique has also been of great value in analysing many other aspects of embryonic development such as the ontogeny of the haemopoietic system[52–59], the development of the kidney[60,61] and limb[62–67] and the early movements of cells in gastrulation[68,69].

This work was supported by the CNRS, the Délégation Générale à la Recherche Scientifique et Technique and by a Research Grant from the US National Institutes of Health (5 R01 DE04257-03).

1. Vogt, W. *Arch. Entw. Mech.* **106,** 542–610 (1925).
2. Pasteels, J. *Archs Biol.* **48,** 381–488 (1937).
3. Le Douarin, N. *Bull. Biol. Fr. Belg.* **103,** 435–452 (1969).
4. Hamburger, V. & Hamilton, H. L. *J. Morph.* **88,** 49–92 (1951).
5. Zacchei, A. M. *Archs Anat.* **66,** 36–62 (1961).
6. Le Douarin, N. *Expl Cell Res.* **77,** 459–468 (1973); *Devl Biol.* **30,** 217–222 (1973); *Med. Biol.* **52,** 281–319 (1974); *Ciba Fdn Symp.* **40,** 71–101 (1976).
7. Smith, J., Cochard, P. & Le Douarin, N. M. *Cell Different.* **6,** 199–216 (1977).
8. Jotereau, F. V. & Le Douarin, N. M. *Devl. Biol.* **63,** 253–265 (1978).
9. Le Douarin, N. M. & Rival, J. M. *Devl. Biol.* **47,** 215–221 (1975).
10. Hörstadius, S. in *The Neural Crest: Its Properties and Derivatives in the Light of Experimental Research*, 111 (Oxford University Press, London, 1950).
11. Weston, J. A. *Adv. Morphogenesis* **8,** 41–114 (1970).
12. Johnston, M. C., Bhakdinaronk, A. & Reid, Y. C. in *Oral Sensation and Perception: Development in the Fetus and Infant* (ed. Bosma, J. F.) (U.S. Govt. Printing Office, Washington, 1974).
13. Noden, D. M. *Devl. Biol.* **67,** 296–312 (1978); **67,** 313–329 (1978); in *The Specificity of Embryological Interactions* (ed. Garrod, D.), 4–49 (Chapman and Hall, London, 1978).
14. Le Lièvre, C. *J. Embryol. exp. Morph.* **31,** 453–477 (1974); **47,** 17–37 (1978).
15. Le Lièvre, C. & Le Douarin, N. *J. Embryol. exp. Morph.* **34,** 124–154 (1975).
16. Le Douarin, N. & Le Lièvre, C. in *Birth Defects* (*Excerpta Medica Intern. Congr. Ser.* no. 432), (eds Littlefield, J. W. & de Grouchy, J.) 141–153 (1978).
17. Le Douarin, N. & Le Lièvre, C. *C.r. hebd. Séanc. Acad. Sci., Paris* **270,** 2857–2860 (1970).
18. Le Douarin, N., Le Lièvre, C. & Fontaine, J. *C.r. hebd. Séanc. Acad. Sci., Paris* **275,** 583–586 (1972).
19. Le Douarin, N. M. in *Gut Hormones* (ed. Bloom, S. R.) 49–56 (Churchill Livingstone, Edinburgh, 1978).
20. Weston, J. A. *Devl. Biol.* **6,** 279–310 (1963).
21. Falck, B. *Acta physiol. scand.* **56,** Suppl. 197, 1–25 (1962).
22. Le Douarin, N. & Teillet, M. A. *J. Embryol. exp. Morph.* **30,** 31–48 (1973).
23. Teillet, M. A. *W. Roux'Arch. dev. Biol.* **184,** 251–268 (1978).
24. Le Douarin, N. & Teillet, M. A. *Devl. Biol.* **41,** 162–184 (1974).
25. Le Douarin, N. M., Renaud, D., Teillet, M. A. & Le Douarin, G. H. *Proc. natn. Acad. Sci. U.S.A.* **72,** 728–732 (1975).
26. Teillet, M. A., Cochard, P. & Le Douarin, N. M. *Zoon* **6,** 115–122 (1978).
27. Cohen, A. M. *J. exp. Zool.* **179,** 167–182 (1972).
28. Norr, S. C. *Devl. Biol.* **34,** 16–38 (1973).
29. Cochard, P., Goldstein, M. & Black, I. *Proc. natn. Acad. Sci. U.S.A.* **75,** 2986–2990 (1978).
30. Landmesser, L. & Pilar, G. *J. Physiol., Lond.* **222,** 691–713 (1972).
31. Landmesser, L. & Pilar, G. *Fedn Proc.* **37,** 2016–2022 (1978).

32. Chiappinelli, V., Giacobini, E., Pilar, G. & Uchimura, H. *J. Physiol., Lond.* **257**, 749–767 (1976).
33. Le Douarin, N. M., Teillet, M. A., Ziller, C. & Smith, J. *Proc. natn. Acad. Sci. U.S.A.* **75**, 2030–2034 (1978).
34. Rothman, T. P., Gershon, M. D. & Holtzer, H. *Devl. Biol.* **65**, 322–341 (1978).
35. Patterson, P. H. & Chun, L. L. Y. *Proc. natn. Acad. Sci. U.S.A.* **71**, 3607–3610 (1974).
36. Patterson, P. H. & Chun, L. L. Y. *Devl. Biol.* **56**, 263–280 (1977).
37. Burton, H. & Bunge, R. P. *Brain Res.* **97**, 157–162 (1975).
38. Johnson, M. *et al. Nature* **262**, 308–310 (1976).
39. Patterson, P. H. *A. Rev. Neurosci.* **1**, 1–17 (1978).
40. Furshpan, E. J., MacLeish, P. R., O'Lague, P. H. & Potter, D. D. *Proc. natn. Acad. Sci. U.S.A.* **73**, 4225–4229 (1976).
41. Landis, S. C. *Proc. natn. Acad. Sci. U.S.A.* **73**, 4220–4224 (1976).
42. Greenberg, J. H. & Schrier, B. K. *Devl. Biol.* **61**, 86–93 (1977).
43. Cohen, A. M. *Proc. natn. Acad. Sci. U.S.A.* **74**, 2899–2903 (1977).
44. Ziller, C., Smith, J., Fauquet, M. & Le Douarin, N. M. *Prog. Brain Res.* **51**, 59–74 (1979).
45. Enemar, A., Falck, B. & Håkanson, R. *Devl. Biol.* **11**, 268–283 (1965).
46. Teitelman, G., Baker, H., Joh, T. H. & Reis, D. J. *Proc. natn. Acad. Sci. U.S.A.* **76**, 509–513 (1979).
47. Smith, J., Fauquet, M., Ziller, C. & Le Douarin, N. *Nature* **282**, 853–855 (1979).
48. Narayanan, C. H. & Narayanan, Y. *J. Embryol. exp. Morph.* **47**, 137–148.
49. Walicke, P. A., Campenot, R. B. & Patterson, P. H. *Proc. natn. Acad. Sci. U.S.A.* **74**, 5767–5771 (1977).
50. Saxod, R. *Devl. Biol.* **32**, 167–178 (1973).
51. Narayanan, C. H. & Narayanan, Y. *J. Embryol. exp. Morph.* **43**, 85–105 (1978).
52. Jotereau, F. V. & Le Douarin, N. M. *Devl. Biol.* **63**, 253–265 (1978).
53. Houssaint, E., Belo, M. & Le Douarin, N. *Devl. Biol.* **53**, 250–264 (1976).
54. Le Douarin, N. in *Differentiation of Normal and Neoplastic Hematopoietic Cells* 5–31 (Cold Spring Harbor Laboratory, New York, 1978); in *Mechanisms of Cell Change* (eds Ebert, J. E. & Okada, T. S.) 293–326 (Wiley, New York, 1979).
55. Le Douarin, N. & Jotereau, F. *Nature new Biol.* **246**, 25 (1973); *J. exp. Med.* **142**, 17–40 (1975).
56. Dieterlen-Lièvre, F. *J. Embryol. exp. Morph.* **33**, 607–619 (1975).
57. Martin, C., Beaupain, D. & Dieterlen-Lièvre, F. *Cell Differentiation* **7**, 115–130 (1978).
58. Beaupain, D., Martin, C. & Dieterlen-Lièvre, F. *Blood* **53**, 212–225 (1979).
59. Kahn, A. J. & Simmons, D. J. *Nature* **258**, 325–327 (1975).
60. Gumpel-Pinot, M., Martin, C. & Croisille, Y. *C.r. hebd. Séanc. Acad. Sci., Paris* **272**, 737–739 (1971).
61. Martin, C. *J. Embryol. exp. Morph.* **35**, 485–498 (1976).
62. Gumpel-Pinot, M. *C.r. hebd. Séanc. Acad. Sci., Paris* **279**, 1305–1308 (1974).
63. Christ, B., Jacob, H. J. & Jacob, M. *Experientia* **30**, 1446–1449 (1974); 1449–1451 (1974); **34**, 241–242; 514–516 (1978).
64. Chevallier, A. *J. Embryol. exp. Morph.* **42**, 275–292 (1977); *W. Roux's Archiv.* **184**, 57–73 (1978); *J. Embryol. exp. Morph.* **49**, 73–88 (1979).
65. Chevallier, A. J., Kieny, M., Mauger, A. & Sengel, P. in *Vertebrate Limb and Somite Morphogenesis* (eds Ede, D. A., Hinchliffe, J. R. & Balls, M.) 421–432 (Cambridge University Press, 1977).
66. Dhouailly, D. & Kieny, M. *Devl. Biol.* **28**, 162–175 (1972).
67. Kieny, M. in *Vertebrate Limb and Somite Morphogenesis* (eds Ede, D. A., Hinchliffe, J. R. & Balls, M.) 87–103 (Cambridge University Press, 1977).
68. Kieny, M. & Pautou, M. P. *W. Roux's Archiv.* **179**, 327–338 (1976); **183**, 177–191 (1977).
69. Saunders, J. W., Gasseling, M. T. & Errick, J. E. *Devl. Biol.* **50**, 16–25 (1976).
70. Vakaet, L. *C.r. hebd. Séanc. Acad. Sci., Paris* **167**, 781–783 (1973); 1053–1055 (1973); *Année. Biol.* **13**, 35–41 (1974).
71. Hornbruch, A., Summerbell, D. & Wolpert, L. *J. Embryol. exp. Morph.* **51**, 51–62 (1979).

ARTICLES

An immunoglobulin deletion mutant with implications for the heavy-chain switch and RNA splicing

W. Dunnick, T. H. Rabbitts & C. Milstein

MRC Laboratory of Molecular Biology, Hills Road, Cambridge CB2 2QH, UK

The IF2 immunoglobulin mutant is a DNA deletion of one coding segment and large sections of the flanking intervening sequences. The deletion results in a new splicing pattern and starts in a DNA region containing tandemly repeated sequences which may carry heavy-chain class switch signals.

IF2 WAS the first structurally defined deletion mutant of eukaryotic cells growing in tissue culture[1]. It was isolated as a spontaneous mutant secreting an immunoglobulin of altered isoelectric point[2]. Its phenotype was defined by sequence analysis[1], mRNA size[3] and mRNA sequence[4] as due to an internal deletion of the $\gamma 1$ heavy chain of the parental myeloma protein secreted by the cell line P3 (a line of the tumour MOPC 21 (ref. 5) adapted to tissue culture[6]). Internal deletions of immunoglobulin heavy chains are characteristic of a myeloma-like disease, the human heavy-chain disease (HCD)[7,8], and IF2 represents an analogous example in the mouse. We show here that the genetic origin of the protein deletion is a large deletion at the DNA level. The deletion involves at least 5.5 kilobases, including an entire segment of coding sequence (exon) and parts of the intervening sequences (introns). The consequence is a new phenotype resulting from the splicing of two exons not normally ligated together, demonstrating the importance of colinearity of splicing points.

The segments of DNA at which the deletion begins and ends have been studied in detail. The present study leads us to conclude that those points are relevant to an important event taking place during maturation of the immune response, the heavy-chain switch. For this reason, experiments are also described to explore further the correlation between the IF2 deletion and the class switch.

The IF2 mutation is a DNA deletion in the heavy-chain gene

The constant (C) region of the $\gamma 1$ heavy chain (the subclass secreted by P3 and its mutant IF2) is divided into three domains of primary and tertiary structure homology, designated CH1, CH2 and CH3 from the amino- to the carboxy-terminal end. Between the CH1 and the CH2 domains there is a segment, the hinge region, of about 13 amino acids, which includes all the inter-chain disulphide bridges. The IF2 protein deletion encompasses exactly the CH1 domain. The gene for the Cγ1 region contains four segments of DNA coding for each of the domains and the hinge (exons) separated by intervening sequences (introns)[9,10]. As the exons are spliced together, the CH1 protein deletion could be the result of either a DNA deletion of part or all of the CH1 exon, or the result of another

0028–0836/80/330669—07$01

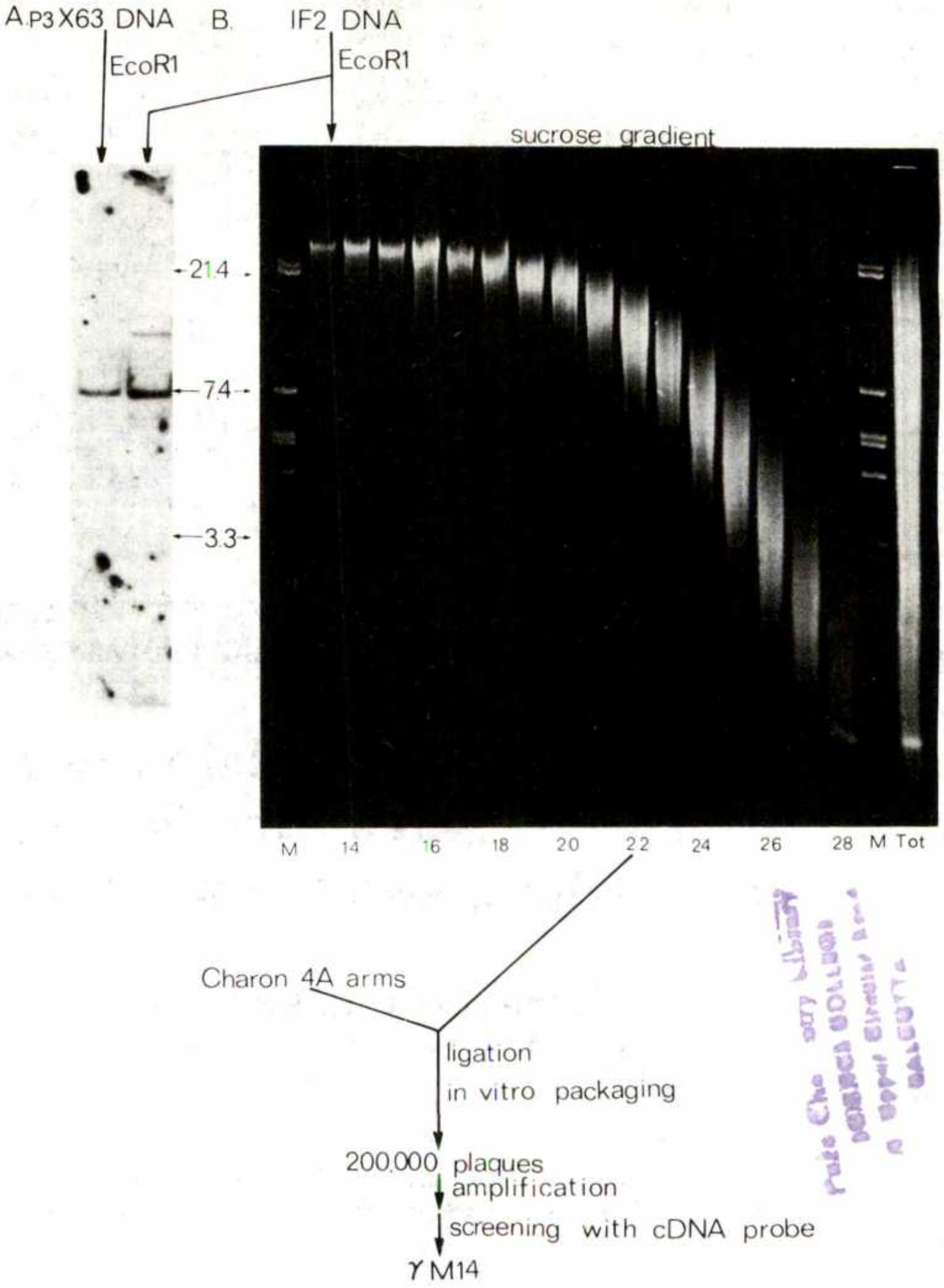

[illegible] Library
[illegible] COLLEGE
[illegible] Upper Circular Road
CALCUTTA

Fig. 1 Isolation of a recombinant DNA clone containing γ1 coding sequences from IF2 cells. *a*, Identification of *Eco*RI fragments containing γ1 sequences. High molecular weight DNA from P3-X63 cells (left) or IF2 cells (right) was digested with *Eco*RI, using as an internal control the digestion pattern of phage λ DNA. The digested mouse DNAs were fractionated on a 0.8% agarose gel and transferred by blotting onto nitrocellulose filters[40]. The filters were pretreated and hybridized in 1×SSC, 0.9% dextran sulphate to nick-translated pγ1/A5 (ref. 4) DNA as previously described[11,41,42]. The filters were washed[11] and autoradiographed for 14 days at −70 °C, using preflashed film and tungstate intensifying screens[43]. *b*, Partial purification and cloning of the IF2 mutant gene. High molecular weight DNA (600 μg) from IF2 cells was digested with *Eco*RI, extracted with phenol and precipitated with ethanol. The sample, dissolved in 0.25 ml 50 mM NaCl, 20 mM EDTA, was fractionated on a 10–30% sucrose gradient containing 1 M NaCl, 1 mM EDTA, 10 mM Tris (*p*H 7.5) in the SW27 rotor (25,000 r.p.m., 23 h, 20 °C). The gradient was fractionated into 39 fractions, and aliquots of fractions 13–28 were analysed on a 0.8% agarose gel, using *Eco*RI-digested λ DNA (M) as size markers. Also present on the gel was *Eco*-RI-digested IF2 DNA which had not been fractionated on a sucrose gradient (Tot). The DNA was visualized by ethidium bromide staining. Charon 4A DNA[12] was digested with *Eco*RI and the left- and right-hand fragments (19.8 and 10.8 kilobases) were purified on sucrose gradients as described above. About 4 μg of these Charon 4A 'arms' were ligated to 4 μg of fraction 22 of the *Eco*RI-digested, fractionated IF2 DNA (above), and the resulting DNA was packaged into phage particles *in vitro*[44–46]. The packaged DNA was used to transfect *E. coli* strain 803 suII⁺suIII⁺; about 200,000 plaques were generated. The top agar containing these plaques was scraped into culture media, and a phage stock was prepared[44]. After this amplification process, about 400,000 plaques were screened by the Benton–Davis procedure[47]. Hybridization to nick-translated pγ1/A5 was in 6×SSC (no dextran sulphate). Positively hybridizing plaques were repurified twice as individual plaques. Three resulting plaques which hybridized to pγ1/A5 were designated γM1, γM5 and γM14.

event leading to the incorrect splicing of the V-region exon to the hinge exon. To investigate these two alternatives, we have studied the structure of the IF2 DNA.

The γ1 genes of IF2 cells and of the clone P3-X63 from the parental cell line were compared by the Southern filter hybridization technique, using as a probe the cloned IF2 heavy-chain cDNA[4]. Two fragments hybridize to the cDNA probe in *Eco*RI-digested P3-X63 DNA: a 6.8-kilobase fragment which contains the γ1 wild-type constant-region coding sequences[9,10], and a 20-kilobase fragment which has been assigned to the γ2a coding sequences[11] (Fig. 1*a*). In addition to these fragments, the cDNA clone hybridizes to more fragments in *Eco*RI-digested IF2 DNA, a 15-kilobase fragment and weakly to a 6-kilobase fragment (which we designate the 6.0 RI fragment). We have partially purified the 15-kilobase fragment by sucrose gradient fractionation after *Eco*RI digestion (Fig. 1*b*). The enriched fraction was ligated into the λ vector Charon 4A (ref. 12) and packaged *in vitro*, and about 200,000 plaques were amplified and 400,000 plaques screened. Three clones which hybridized to the cDNA clone were purified and grown in bulk for analysis. The three clones seemed to be similar, in that their restriction patterns after *Eco*RI digestion were identical (not shown). One (γM14) was analysed extensively.

A restriction map of γM14 was constructed using single and double digests with *Eco*RI, *Bam*HI, *Hin*dIII, *Xba*I and *Kpn*I (Fig. 2*a*). The IF2 DNA insert includes four *Eco*RI fragments. Therefore, the γM14 clone seems to be a product of partial *Eco*RI digestion, in spite of the fact that the IF2 DNA was apparently digested to completion, as shown by the digestion of an internal control phage λ DNA. We have isolated an independent, but identical clone by a second *Eco*RI digestion of IF2 DNA and screening of Charon 4A clones prepared from unfractionated IF2 DNA. Thus, it is very unlikely that the four *Eco*RI fragments came together by random re-ligation.

Southern hybridization analysis showed that the IF2 heavy-chain cDNA hybridized to the 6.0 RI fragment and to two *Pst*I fragments of about 1.8 and 1.6 kilobases from γM14 DNA. More extensive restriction enzyme and Southern hybridization analysis (which will be discussed below) located the two *Pst*I fragments within the 6.0 RI fragment (Fig. 2*b*). These two *Pst*I fragments were isolated and partially sequenced by a combination of the dideoxy method on phage M13 subclones[13,14] and the Maxam–Gilbert method on a pBR322 subclone[15] (see Fig. 2*b* legend). These sequences demonstrated that the two *Pst*I fragments contained the γ1 hinge, CH2 and CH3 coding sequences and appropriate introns arranged as shown in Fig. 2*b*. Part of these sequences, including the hinge exon and about 80 nucleotides to the left of the hinge exon (that is, in the intervening sequence towards the V region), are shown in Fig. 2*c*. The sequence derived from the γM14 clone agrees with that of the Cγ1 gene[9,10] throughout the hinge exon and for the first 46 nucleotides to the left of the hinge coding sequence (with a single A for G discrepancy). Forty-six nucleotides into the intervening sequence, the two sequences diverge completely.

The nucleotide sequences presented in Fig. 2*c* and others we have completed (Fig. 2*b*) demonstrate that the γM14 recombinant clone contains γ1 coding sequences. They also indicate that the γ1 gene included in γM14, when compared with the parental γ1 gene, has been altered in the intervening sequence between the CH1 and hinge exons. To determine the extent of this change, we have constructed a detailed restriction map of the IF2 γ1 gene and compared this with the published restriction sites in the normal γ1 gene[9,10]. As expected from the sequences described above, the restriction sites (compare Fig. 3*a* and *b*) lying to the right of the hinge correspond to those previously mapped in the wild-type gene[9,10]. On the other hand, those to the left do not correspond at all to the sites to the left of the hinge in the γ1 gene. In particular, the enzyme sites for *Bam*HI, *Xba*I, *Sac*I and *Hin*cII, which cut in the γ1 CH1 exon, or just to its left, are missing or altered. These differences correlate with the loss of CH1 from the IF2 heavy chain[1]. The restriction mapping data indicate that a deletion removes the whole of the CH1 exon, at least 3 kilobases of the intron to its left, and 0.3 (85%) of the intron to its right.

The V region of P3 cells and IF2 cells are identical[1]. Therefore, the IF2 deletion must begin in the V–CH1 intervening sequence (after the V-region exon). The deletion results in the direct splicing of the V exon to the hinge exon. Insofar as can be estimated by gross yields of mRNA[3], the IF2 cell splices the V exon to the hinge exon as efficiently as P3 cells splice V to CH1 and CH1 to the hinge. Thus, only the linear order of exons seems to determine which exons are joined together, as has been suggested by the sequences of junction regions. These results argue against a multiplicity of splicing enzymes, for the splicing machinery seems to be able to join any exon–intron boundary to any intron–exon boundary. As the same V region can be spliced with different C regions (the class switch), the argument of a single enzyme specificity applies to all heavy chains.

The fact that 85% of the CH1-hinge intron and at least 5 kilobases (see below) of the V–CH1 intron have been deleted without affecting splicing capability provides evidence against the importance of internal intron sequences in splicing. This also

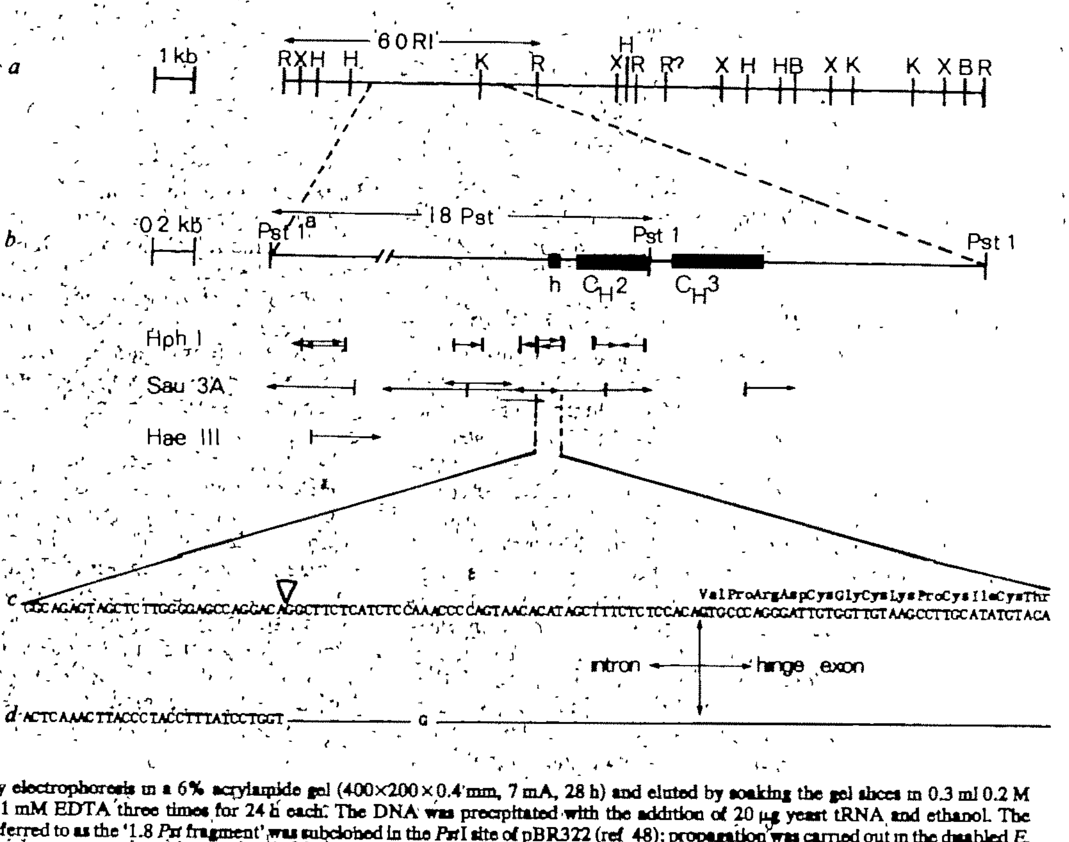
a
1 kb
6 0 RI
R X H H
K
R
H
X R R?
X H H B X K
K X B R
b
0 2 kb
Pst 1
a
1 8 Pst
Pst 1
Pst 1
h
C_H2
C_H3
Hph I
Sau 3A
Hae III
c
Val Pro Arg Asp Cys Gly Cys Lys Pro Cys Ile Cys Thr
GGCAGAGTAGCTCTTGGGGAGCCAGGACAGGCTTCTCATCTCCAAACCCCAGTAACACATAGCTTTCTCTCCACAGTGCCCAGGGATTGTGGTTGTAAGCCTTGCATATGTACA
intron
hinge exon
d
ACTCAAACTTACCCTACCTTTATCCTGGT
G

Fig. 2 Restriction analyses and sequencing of the recombinant clone γM14 *a*, **Restriction map of γM14.** This map was constructed from the restriction pattern of single and double digests of γM14 DNA, and single digests of *Eco*RI fragments eluted from agarose gels. The 0 7-kilobase *Eco*RI fragment could not be unambiguously placed, although partial *Eco*RI digestion of γM14 DNA suggested its position to be between the 3 0- and 6.8-kilobase *Eco*RI fragments. The 6.0-kilobase *Eco*RI fragment (hereafter referred to as '6 0 RI fragment') hybridized to the pγ1/A5 probe. The γM14 clone is a product of partial *Eco*RI digestion of IF2 DNA; a small amount of the 6.0 RI fragment (total digestion product) can be seen in Southern hybridization filters (Fig. 1*a*) R, *Eco*RI; K, *Kpn*I; B, *Bam*HI; X, *Xba*I, H, *Hin*dIII. *b*, **Sequencing strategy.** Two *Pst*I fragments from γM14 (about 1 8 and 1.6 kilobases) hybridized to pγ1/A5 in a Southern filter hybridization experiment (not shown). These fragments were prepared by electrophoresis in a 6% acrylamide gel (400×200×0.4 mm, 7 mA, 28 h) and eluted by soaking the gel slices in 0.3 ml 0.2 M sodium acetate, 0.5% SDS and 0.1 mM EDTA three times for 24 h each. The DNA was precipitated with the addition of 20 µg yeast tRNA and ethanol. The 1.8-kilobase fragment, hereafter referred to as the '1.8 *Pst* fragment' was subcloned in the *Pst*I site of pBR322 (ref 48); propagation was carried out in the disabled *E. coli* strain MRC-1 (GMAG issue number 2–5). Some *Hph*I fragments were prepared from this plasmid (designated pγ1/IF2P.1.8) and sequenced by the method of Maxam and Gilbert[15]. Strand separation was accomplished by hybridization to appropriate single-stranded M13 DNA (see below and ref. 49). The 1.8- and 1 6-kilobase *Pst*I fragments were cut with *Sau*3A, and the subfragments were ligated into the *Bam*HI site of a derivative of M13mp2 containing a single *Bam*HI site[30] and an amber mutation (G. Winter, unpublished). The ligated DNAs were used to transform *E. coli* JM101 (ref 50) and DNA samples from white plaques were sequenced using the dideoxy method[13,14] The fragments sequenced are shown in the lower part of Fig 2*a* Each arrow represents sequences obtained from an independent clone. A 1,200-base pair *Hae*III fragment from pγ1/IF2P.1.8 was purified on a 6% acrylamide gel, and about 0.5 µg of this fragment was cloned in the *Eco*RI site of M13mp2 using synthetic *Eco*RI linkers[14]. DNA from a white plaque was sequenced by the dideoxy method[13,14] Note the break in the 1.8 *Pst* fragment, which we estimate to be 400 base pairs. The sequence derived is shown fully in Fig. 4. *c*, **Sequences near the hinge coding region.** The sequence of the hinge coding region (with amino acid sequence) and of the adjacent intervening sequence is shown. The intron between the hinge and CH2, the CH2 exon and part of the 3′-untranslated region of γM14 have also been sequenced and correspond to the published γ1 sequences from newborn mouse DNA[10] and from the MOPC 21 myeloma DNA[9]. The following differences were noted (using the numbering system of Honjo *et al.*[10]): residues 800–801, we find three Ts rather than two[10]; residues 804–805, we find three Cs rather than two[10]; residues 809–811, we find four Cs rather than three[10], residue 828, we find C rather than A[10], residues 843–844, we find three Cs rather than two[10], residue 1,754, we find T rather than C[10], residue 1,821, we find G rather than C[10] *d*, **The sequence of the γ1 germ-line gene[9] near the hinge coding region.** The line indicates concordance with the γM14 sequence.

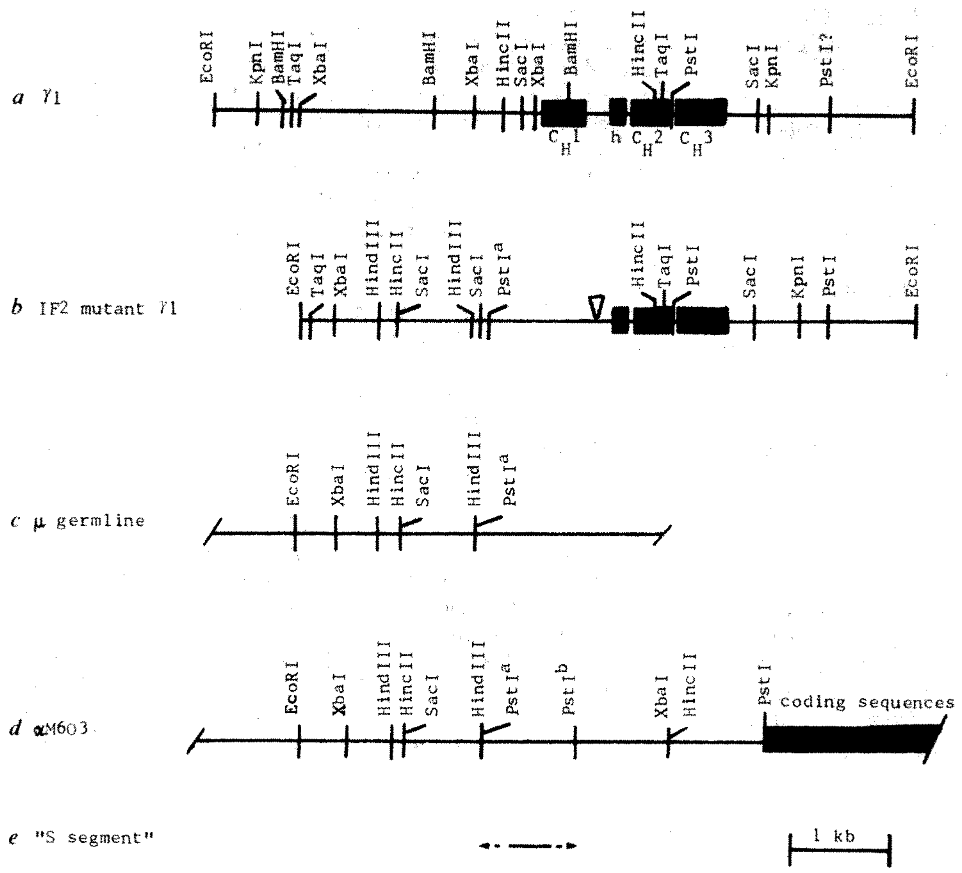

Fig. 3 Restriction maps of various DNA segments associated with mouse heavy-chain genes. The restriction maps shown are the wild-type P3 γ1 gene[9,10] (*a*), the IF2 mutant γ1 gene (*b*), a segment of the Cμ gene[24,30] (*c*) and the α gene of M603 myeloma cells[24] (*d*). The restriction map of the IF2 γ1 gene was constructed from Southern filter hybridization data of digests of γM14 DNA, and from restriction analysis of the isolated 6.0 RI fragment. The α gene from M603 cells is known to have introns; we do not show them in *d*. *e* Shows the region in which the switch leading to the M603 α gene took place (the S segment).

introduces severe constraints on models implicating secondary structure of introns in splicing events, and highlights the importance of intron sequences near the splicing points[16–18].

The IF2 deletion and human HCD proteins

IF2 is analogous to HCD proteins where the deletion involves a single exon[7,8]. In other HCD proteins, deletions involve part or all of the V region in addition to the CH1 domain[7]. The amino terminus of HCD proteins may or may not be recognizable as V region. Still other HCD protein deletions do not involve the V–C junction at all; in some cases, only the hinge is deleted, in others CH3 is apparently missing[7]. The HCD proteins are thus a heterogeneous group, and are probably the result of several different types of mutation. Some are likely to be the result of nonsense mutations[1,7], and mutations in RNA splicing signals have been hypothesized to be involved in HCD protein variants[19]. We have shown that one such protein, the IF2 heavy chain, is the result of a DNA deletion. Below we propose that others, especially those centering on the V–C junction, will also reflect deletions at the gene level. Many of these deletions may result from errors in the recognition of class switch signals.

The heavy-chain switch

Early in the immune response, the dominant heavy-chain class is μ; later the dominant class becomes γ or perhaps α. This switch pattern in whole animals can also be demonstrated in single cells or in clones of single cells, although the exact sequence and restrictions of the class switch are somewhat controversial[20–23]. It is now believed that the molecular events in commitment to a single VH gene and in the class switch are as follows: a single VH gene is first expressed by an integration event to a putative JH fragment associated with Cμ (ref. 24), an event analogous to the one observed in the joining of VL and JL in light chains[25–28], for the putative signal sequences adjacent to VH genes are homologous to those in VL genes[29]. This leads to VHCμ expression. The class switch requires a second, different form of rearrangement, involving a different segment of DNA believed to lie in the intervening sequence between VH and Cμ (refs 11, 24, 30). Recent hybridization analysis of DNA from cells making various classes of heavy chains[11,31,32] support the hypothesis proposed by Honjo and Kataoka[33] that the class switch occurs by deletion events involving the exons and introns of all CH genes between the expressed V region and the new CH gene to be expressed.

Davis and colleagues[24] have presented evidence that in an α myeloma about half of the intron between VH and Cα is derived from the germ-line μ gene; the other half is derived from the germ-line Cα gene. The position of this sequence change occurs between the sites labelled *Pst*I^a and *Pst*I^b in Fig. 3*c*, *d*, as *Pst*I^a and all sites to the left are found in the Cμ gene, whereas *Pst*I^b and all sites to the right of *Pst*I^b are found in the germ-line Cα gene[24]. A similar situation has been described in an expressed γ1 gene[30]. In both cases, the switch seems to have taken place within the DNA segment designated S in Fig. 3*e*. It is reasonable to suggest this region as being crucial in the heavy-chain switch.

The S segment in γM14 DNA

The restriction map of the IF2 gene to the left of the deletion boundary (Fig. 3*b*) corresponds to a part of the germ-line Cμ gene and the homologous part of the expressed α M603 gene (Fig. 3*c*, *d*). In other words, the intron fragment of the Cμ germ-line gene which is retained during the deletion leading to the class switch is part of the γM14 DNA we have cloned. We were therefore in a position to study the sequences which may be involved in the heavy-chain switch.

Part of the γM14 sequence which contains the 'S segment' is shown in Fig. 4. Immediately at the site of the IF2 deletion (at the bottom of Fig. 4), tandemly repeated homologous sequences begin. The repeat unit is 49 base pairs long and is repeated

10 1/3 times. No two of the repeated sequences are identical, varying from each other by 1 to 14 residues. This set is preceded by 11 unrelated nucleotides and then by a second set of repeats of a basic unit beginning with GGGGT followed by two to four GAGCT pentanucleotides. Towards the left (the V region), the repeat drifts away from the basic unit and the number of GAGCT subunits becomes more variable. There is a total of about 38 repeats of such elements with an average content of two to three GAGCT subunits. The divergence is such that no significant homology is retained within 100 bases of *Pst*I*.

In a general sense, tandemly repeated sequences would be ideal for promotion of DNA deletions like those that take place in the heavy-chain switch. A simple hypothesis could then be that each heavy-chain C gene is preceded by homologous S segments containing tandemly repeated units. Recombination by pairing between the repeats (for example, from a μ gene and a γ gene) would result in deletion of all the sequences between them. This hypothesis predicts (1) the presence of at least one S segment for each C region in the germ line, and (2) the loss of one germ-line S segment for each CH gene lost during a switching event. To test this hypothesis we have used the 1.8 *Pst* fragment, which also contains the γ1 hinge and CH2 coding sequences, as a probe for the S segment in *Eco*RI-digested kidney and myeloma DNAs (Fig. 5). The *Eco*RI fragments containing the γ2a (ref. 11), γ2b (ref. 34) and γ1 (refs 9, 10) coding sequences, which hybridize to the γ1 coding sequences in 1.8 *Pst*, are detected in kidney DNA (slot 6). In addition, at least five *Eco*RI fragments from kidney DNA hybridize to the 1.8 *Pst* fragment (bands a, b, d, e, f) but not to the γ1 coding sequences (results not shown, see also ref. 9). This result agrees with prediction (1) of multiple germ-line S segments. In agreement with prediction (2), at least three of these fragments are lost as one follows the expression of heavy chains These are b, a and d as one follows the expected progression kidney-μ-γ1-γ2b-γ2a-α

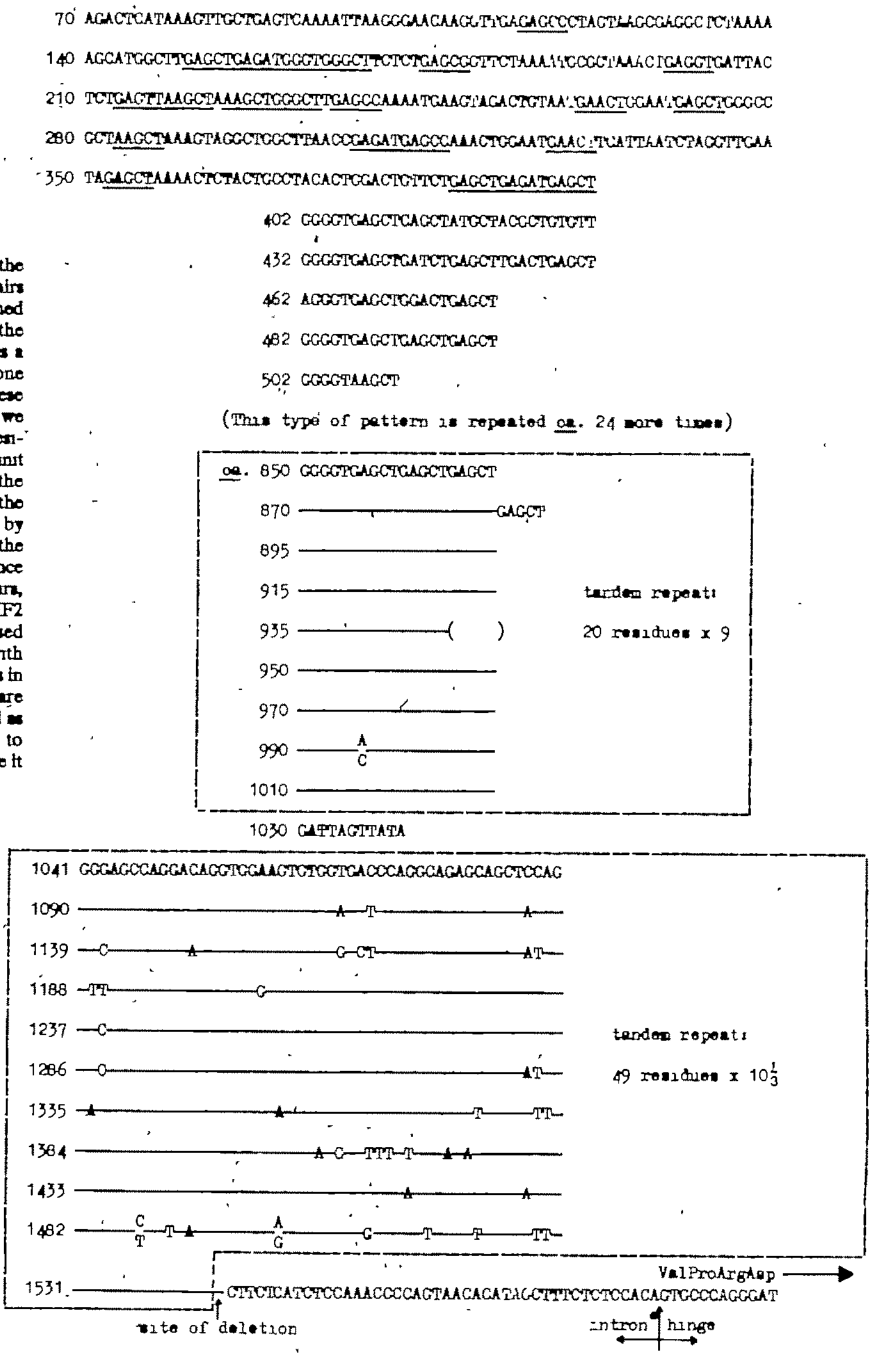
70 AGACTCATAAAGTTGCTGAGTCAAAATTAAGGGAACAAGCTTGAGAGCCCTACTAAGCCGAGCCTCTAAAA
140 AGCATGGCTTGAGCTGAGATGGGTGGGCTTCTCTGAGCCGTTCTAAAATCCGCTAAACTGAGGTGATTAC
210 TCTGAGTTAAGCTAAAGCTGGGCTTGAGCCAAAATGAAGTAGACTGTAATGAACTGGAATGAGCTGCGCC
280 GCTAAGCTAAAGTAGGCTGGCTTAACCGAGATGAGCCAAACTGGAATGAACTTCATTAATCTAGGTTGAA
350 TAGAGCTAAAACTCTACTGCCTACACTGGACTGTTCTGAGCTGAGATGAGCT
402 GGGGTGAGCTCAGCTATGCTACCCTGTGTT
432 GGGGTGAGCTGATCTGAGCTTGACTGAGCT
462 AGGGTGAGCTGGACTGAGCT
482 GGGGTGAGCTGAGCTGAGCT
502 GGGGTAAGCT
(This type of pattern is repeated ca. 24 more times)
ca. 850 GGGGTGAGCTGAGCTGAGCT
870
GAGCT
895
915
935
( )
950
970
990
A
C
1010
tandem repeat:
20 residues x 9
1030 GATTAGTTATA
1041 GGGAGCCAGGACAGGTGGAAGTCTGGTGACCCAGGCAGAGCAGCTCCAG
1090
A T A
1139
C A G CT AT
1188
TT G
1237
C
1286
C AT
1335
A A T TT
1384
A C TTT T A A
1433
A A
1482
C T T A A G G T T TT
1531
tandem repeat:
49 residues x 10 1/3
ValProArgAsp
CTTCTCATCTCCAAACCCCAGTAACACATAGCTTTCTCTCCACAGTGCCCAGGGAT
site of deletion
intron
hinge

Fig. 4 Tandemly repeated sequences near the site of the IF2 deletion. The numbers indicate the distance in base pairs from *Pst*I* (Figs 2*b*, 3) In residues 70–401, the underlined nucleotides show homology (80% or more) to the pentanucleotide GAGCT In residues 402–511, there is a repetitive pattern beginning with GGGGT followed by one to five GAGCTs, or some close derivative of it These patterns can be seen on the upper half of sequencing gels; we estimate that this pattern is repeated 24 more times (residues 511–850). In residues 850–1,029, this repetitive unit has become more or less exact, except for variations in the number of GAGCT pentanucleotides To emphasize the more exact repeat unit, residues 850–1,029 are enclosed by dotted lines, and solid lines indicate concordance with the sequence at the top line of the box After a short sequence (residues 1,030–1,040), a new tandem repeat appears, extending from residues 1,041 to 1,545 (the site of the IF2 deletion). Again, the repeated sequences are enclosed within dotted lines and solid lines indicate concordance with the sequence at the top line of the box. The repeated units in residues 402–1,040 and those in residues 1,041–1,545 are apparently unrelated. These sequences were determined as described in Fig. 2. As the sequence from residues 444 to 1,040 was determined on one DNA strand only, we judge it to be 95% accurate

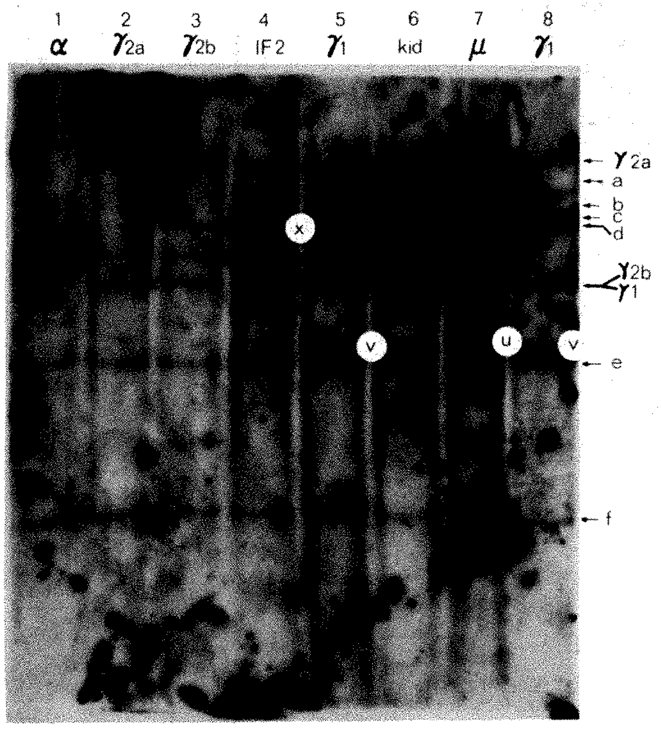

Fig. 5 Arrangement and rearrangement of tandemly repeated and associated sequences in DNA from myelomas secreting various classes of immunoglobulin. DNAs from kidney cells and various myelomas were digested with *Eco*RI and analysed by the Southern filter hybridization technique[11]. Hybridization to pγ1/IF2P.1.8 was in 6×SSC (no dextran sulphate). Slot 1, MOPC 315 DNA (α heavy-chain producer); slot 2, P1 DNA (γ2a heavy-chain producer); slot 3, MPC 11 DNA (γ2b heavy-chain producer); slot 4, IF2 DNA (γ1 mutant heavy-chain producer); slot 5, X63 DNA (γ1 heavy-chain producer); slot 6, kidney DNA; slot 7, MOPC 104E DNA (μ heavy-chain producer); slot 8, NSII/1 DNA (γ1 heavy-chain producer; the NSII/1 heavy chain is smaller than the parental X63 γ1 heavy chain; the nature of the defect is not known[35]. All DNAs were prepared from tissue culture cells except for 104E (slot 7) which was from ascites cells. Infiltration by lymphoid and non-lymphoid tissue could account for minor contaminants. Bands labelled γ1, γ2b and γ2a contain coding sequences which cross-hybridize to the cDNA clone pγ/A5 (see also ref. 11).

Note that in the γ2b producer (slot 3), the γ2b band has, albeit slightly, shifted position. The switch to γ2b production deletes theγ1 gene[11,31–33]. The γ2b sequences may be rearranged to give an *Eco*RI fragment of a slightly different size. This band and all others in the γ2b/γ1 position are different from band z present in the γ2a producer (slot 2). Band z does not hybridize to the γ1 cDNA sequences (data not shown); we presume that this contains the rearranged S segment.

(refs 11, 30–32). In addition, for most of the myelomas tested, new fragments hybridizing to the noncoding part of the 1.8 *Pst* probe can be identified (bands u, v, y and z). This is presumably the result of sequence rearrangement in the environment of S segments during the switch. To describe it schematically, let us take the sequence A-B-C-B-D-B-E. Deletion of B-C would yield A-B-D-B-E, and would involve a change in two fragments containing B. A-B-C and C-B-D are lost, D-B-E is retained, and a new fragment, A-B-D, is formed. Specifically, we suggest that bands u, v, y and z are the rearranged forms of S present when μ, γ1, γ2b and γ2a (respectively) are expressed. We have not rigorously shown that u and v are different, but we have shown that the z component of γ2a and γ2b are indeed different. The latter cross-hybridizes with the γ1 coding sequences whereas the former does not (results not shown, see also ref. 9). This highlights the shortcomings of this type of analysis. Fragments may exist which are not detected (too large or too small) or are hidden under other hybridizing fragments. For example, we have no good candidates for the Cγ3 and Cα germ-line S

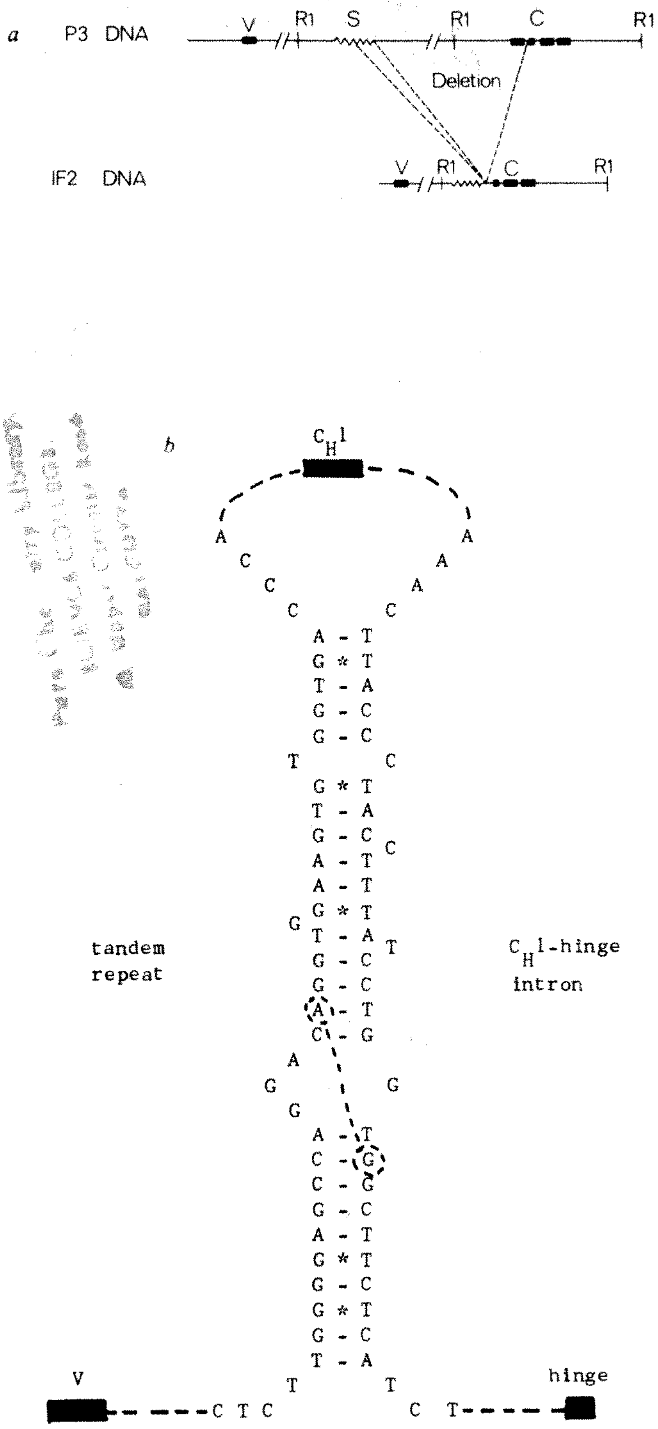

Fig. 6 *a*, Generation of the IF2 mutant. The hypothesized structures of P3 γ1 gene and of IF2 γ1 gene are shown, with coding sequences in darkened boxes and the S segment in a zig-zag line. The dotted lines denote the extent of the IF2 deletion, which could begin in the S segment or at its right end. *b*, A putative hairpin loop at the site of the IF2 deletion. The left-hand side of this structure below the circled A was constructed using the sequence of the IF2 gene to the left of the deletion (Fig. 4, residues 1,525–1,543). The left-hand side above the circled A was constructed from the consensus sequence of the 49-base tandem repeat (which is represented by residues 1,054–1,073, Fig. 4). The right-hand side comes from the Cγ1 sequence[10] near the site of the IF2 deletion (see also Fig. 2*d*). Ligation of the circled A and G would result in the sequence at the site of the deletion in the IF2 gene (Fig. 2) and deletion of the sequences above these two residues. G+T base pairs are shown by an asterisk; in the other DNA strand (not shown) these would be unpaired A+C.

segments. On the other hand, there are other components (for example, band c) for which we find no good explanation. Two germ-line fragments (e and f) hybridizing to the 1.8 *Pst* fragment, but not to the $\gamma 1$ cDNA clone, persist even in the α producer. These fragments may correspond to the other heavy chains ε and/or δ, to a hitherto unidentified heavy chain, or to repeats of a similar sequence unrelated to immunoglobulins.

From the experiment shown in Fig. 5, the minimium size of the IF2 deletion can be calculated. IF2 DNA (slot 4) shows two new bands, x and w, and lacks the rearranged band v. Band x is the product of partial *Eco*RI digestion we have cloned. Presumably, the IF2 deletion resulted in fusion of band v and the $\gamma 1$ coding sequences to yield band w (the 6.0 RI fragment). Thus, the size of the IF2 deletion is 5.5 kilobases [6.8 kilobases ($\gamma 1$ coding sequences) + 4.7 kilobases (band v) − 6.0 kilobases (band w)], asssuming no *Eco*RI fragments between band v and the fragment containing the $\gamma 1$ coding sequences.

We would like to argue that the signals for the class switch are based on the tandem repeats described above. As we have discussed, the switch occurs in or near the S fragment, which is mostly composed of these tandem repeats. Further evidence for involvement of the tandem repeats is provided by a comparison of the work of Kataoka *et al.*[30] and the one described here. Based on the restriction maps shown in Fig. 3, one can locate in their work an S segment which included the putative switch point. A close inspection of their sequence shows the presence of four sequential pseudo-repeats homologous to the 49-base pair repeat shown in Fig. 4 (starting 14 residues from the putative switch point). Preceding these sequences is a long sequence about 10% of which is GAGCT.

The difference between the sequences described by us and those described by Katoaka *et al.*[30] could have trivial sources, such as drift during tumour propagation. The difference could be a consequence of the deletion which gave rise to IF2. We prefer a third alternative, which is that these differences are a consequence of the switch process itself. The precise point of the switch could vary along the extended tandemly repeated sequences in both the donor gene (for example, μ) and the acceptor gene (for example, γ)[24,30]. Therefore, two rearranged $\gamma 1$ genes could have different S sequences, depending on how the donor and acceptor S sequences aligned, and where the recombinational event took place. Also, the S sequences in $\gamma 1$ genes might vary depending on whether or not the V regions went through a VH–C$\gamma 3$ intermediate.

HCD proteins in general, and IF2 in particular, have been implicated with DNA rearrangements for several years. Specifically, it has been proposed that signals for DNA rearrangements were duplicated along with primordial CH domains during the evolution of modern CH genes[35]. The signals preceding each CH gene retained their function while those between CH domains drifted. Some HCD deletions could result from the illegitimate use of the ancestral homologue within a single CH gene, as opposed to legitimate use of switch signals between CH genes.

With this in mind, we searched for homology between S-segment sequences, which we believe to be the switch signals, and sequences in the normal $\gamma 1$ gene[9,10]. This search resulted in a hairpin loop structure at the site of the deletion (Fig. 6). This hypothetical structure was formed between a consensus sequence of the 49-base repeat and the sequence of the $\gamma 1$ germ-line gene at the site of the deletion. The sequence of the IF2 $\gamma 1$ gene at the deletion results from the ligation of the circled A and G (see also Fig. 2*c*). The sequences above these two residues would represent the deletion. Such hairpin loop structures can only be speculative. The free energy of the structure shown in Fig. 6*b* is +3.4 kcal mol^{-1} (refs 36, 37), corresponding to a melting temperature of 30 °C. This value can be compared with those of similar structures. For example, the proposed hairpin structure for κ V–J joining[27,28] has a free energy of about −19 kcal mol^{-1} ($T_m = 67$ °C). Obviously, for a low frequency event such as a mutation, one expects relatively unstable structures.

In conclusion, we suggest that the deletion which gave rise to the IF2 mutant, and also the deletions for similar HCD proteins[5], were the result of illegitimate use of switch signals. Whether the proposed hairpin loop formation, or other mechanisms such as sister chromatid exchange[38], represent a model for the physiological switch remains to be seen.

We thank A. R. MacLeod for DNA ligase, G. Winter for the M13mp2 vector containing the *Bam*HI site and amber mutation, F. Blattner for phage Charon 4A, and S. Brenner for the bacterial strain MRC-1. W.D. was a fellow of the Jane Coffin Childs Memorial Fund, and this work was supported in part by a grant from that fund.

After submission of our article, we received a copy of manuscript by Sakano *et al.* (see accompanying article[39]). Our sequence (Fig. 4) up to residue 448 is identical (except for nine bases) to their sequence of the germ-line Cμ gene between residues 1,114 and 1,490. After residue 448, however, the two sequences differ drastically. It seems, therefore, that in the P3 lineage the switch from the Cμ gene occurred to the right of this point. Apparently, in the three cases so far described, the switch has taken place at three different sites. Furthermore, tandemly repeated units in the sequences of Sakano *et al.*, Kataoka *et al.* and ourselves are in the same polarity, implicating homologous pairing rather than hairpin loop formation in the DNA exchange mechanism associated with the switch.

Received 7 May; accepted 25 June 1980.

1. Adetugbo, K., Milstein, C. & Secher, D. S. *Nature* **265,** 299–304 (1977).
2. Cotton, R. G. H., Secher, D. S. & Milstein, C. *Eur. J. Immun.* **3,** 135–140 (1973).
3. Cowan, N. J., Secher, D. S. & Milstein, C. *Eur. J. Biochem.* **61,** 355–368 (1976).
4. Dunnick, W., Rabbitts, T. H. & Milstein, C. *Nucleic Acids Res.* **8,** 1475–1484 (1980).
5. Potter, M. in *Methods in Cancer Research* Vol. 2 (ed. Burch, H.) 105–132 (Academic, New York, 1967).
6. Horibata, K. & Harris, A. W. *Expl Cell Res.* **60,** 61–77 (1970).
7. Franklin, E. C. & Frangione, B. in *Contemporary Topics in Molecular Immunology* (ed. Inman, F. P.) 89–126 (Plenum, New York, 1975).
8. Franklin, E. C. *J. Immun.* **121,** 2582–2583 (1978).
9. Sakano, H. *et al. Nature* **277,** 627–633 (1979).
10. Honjo, T. *et al. Cell* **18,** 559–568 (1979).
11. Rabbitts, T. H. *et al. Nature* **283,** 351–356 (1980).
12. Blattner, F. R. *et al. Science* **196,** 161–169 (1977).
13. Schreier, P. G. & Cortese, R. *J. molec. Biol.* **129,** 169–172 (1979).
14. Sanger, F. *et al. J. molec. Biol.* (submitted).
15. Maxam, A. & Gilbert, W. *Proc. natn. Acad. Sci. U.S.A.* **74,** 560–564 (1977).
16. Lerner, M. R. *et al. Nature* **283,** 220–224 (1980).
17. Catterall, J. F. *et al. Nature* **257,** 510–513 (1978).
18. Breathnach, R. *et al. Proc. natn. Acad. Sci. U.S.A.* **75,** 4953–4857 (1978).
19. Frangione, B. & Franklin, E. C. *Nature* **281,** 600–602 (1979).
20. Pernis, B., Forni, L. & Luizzati, A. L. *Cold Spring Harb. Symp. quant. Biol.* **41,** 175–183 (1976).
21. Wang, A. C. *et al. Proc. natn. Acad. Sci. U.S.A.* **66,** 337-343 (1970).
22. Sledge, C. *et al. Proc. natn. Acad. Sci. U.S.A.* **73,** 923–927 (1976).
23. Gearhart, P. J. *Nature* **269,** 812–813 (1977).
24. Davis, M. M. *et al. Nature* **283,** 733–739 (1980).
25. Bernard, O., Hozumi, N. & Tonegawa, S. *Cell* **15,** 1133–1144 (1978).
26. Seidman, J. G. & Leder, P. *Nature* **276,** 790–795 (1978).
27. Sakano, H. *et al. Nature* **280,** 288–294 (1979).
28. Max, E. E., Seidman, J. G. & Leder, P. *Proc. natn. Acad. Sci. U.S.A.* **76,** 3450–4354 (1979).
29. Rabbitts, T. H. & Matthyssens, G. *Proc. natn. Acad. Sci. U.S.A.* (submitted).
30. Kataoka, T. *et al. Proc. natn. Acad. Sci. U.S.A.* **77,** 919–923 (1980).
31. Cory, S. & Adams, J. M. *Cell* **19,** 37–52 (1980).
32. Coleclough, C., Cooper, D. & Perry, R. P. *Proc. natn. Acad. Sci. U.S.A.* **77,** 1422–1426 (1980).
33. Honjo, T. & Kataoka, T. *Proc. natn. Acad. Sci. U.S.A.* **75,** 2140–2144 (1978).
34. Yamawaki-Kataoka, Y. *et al. Nature* **283,** 786–789 (1980).
35. Milstein, C. *et al.* in *Cellular Selection and Regulation in the Immune Response* (ed. Edelman, G. M.) 245–264 (Raven, New York, 1974).
36. Wang, J. C. in *DNA Synthesis, Present and Future* (eds Molineux, I. & Kohrijama, M.) 347–366 (Plenum, New York, 1978).
37. Tinoco, I. *et al. Nature new Biol.* **246,** 40–41 (1973).
38. Rabbitts, T. H., Hamlyn, P. H. & Matthyssens, G. & Roe, B. *Can. J. Biochem.* **58,** 176–187 (1980).
39. Sakano, H., Maki, R., Kurosawa, Y., Roeder, W. & Tonegawa, S. *Nature* **286,** 676–683 (1980).
40. Southern, E. M. *J. molec. Biol.* **98,** 503–517 (1975).
41. Wahl, G. M., Stern, M. & Stark, G. R. *Proc. natn. Acad. Sci. U.S.A.* **76,** 3683–3687 (1979).
42. Jeffreys, A. J. & Flavell, R. A. *Cell* **12,** 429–439 (1977).
43. Laskey, R. A. & Mills, A. D. *FEBS Lett.* **82,** 314–316 (1979).
44. Maniatis, T. *et al. Cell* **15,** 687–701 (1978).
45. Hohn, B. & Murray, K. *Proc. natn. Acad. Sci. U.S.A.* **74,** 3259–3263 (1977).
46. Blattner, F. R. *et al. Science* **202,** 1279–1280 (1978).
47. Benton, W. D. & Davis, R. W. *Science* **196,** 180–182 (1977).
48. Bolivary, F. *et al. Gene* **2,** 95–113 (1977).
49. Baralle, F. E., Shoulders, C. C. & Proudfoot, N. J. *Cell* (in the press).
50. Messing, J. *et al. Proc. natn. Acad. Sci. U.S.A.* **74,** 3642–3646 (1977).
51. Cowan, N. J., Secher, D. S. & Milstein, C. *J. molec. Biol.* **90,** 691–701 (1974).

Nature Vol. 286 14 August 1980

Two types of somatic recombination are necessary for the generation of complete immunoglobulin heavy-chain genes

Hitoshi Sakano, Richard Maki, Yoshikazu Kurosawa, William Roeder & Susumu Tonegawa

Basel Institute for Immunology, 487 Grenzacherstrasse, Postfach CH 4005, Basel 5, Switzerland

At least two types of somatic recombination are necessary for the generation of a complete immunoglobulin γ2b gene from germ-line DNA sequences. The first type of recombination consists of the assembly of three separate DNA segments, each encoding a different part of the variable region. The second type of recombination replaces the exons coding for the constant region of the μ chain with those coding for the same region of the γ2b chain. The DNA sequencing studies suggest that the two types of recombination operate by different mechanisms.

COMPLETE, active immunoglobulin genes are created by somatic recombination that occurs during the differentiation of lymphocyte precursor cells[1–3]. The organization of the gene sequences before and after somatic recombination has been studied extensively for both λ- and κ-type light chains in the mouse[4–10]. These studies established that in the embryonic genome, the major portion of the conventionally defined variable (V) region is encoded in a DNA segment (V DNA) that is located some distance away from a DNA segment (J DNA) coding for the rest of the V region. The J DNA segment has been mapped a few kilobases upstream of (that is, 5′ side, with respect to the direction of transcription) the single-copy DNA segment (C DNA) coding for the constant (C) region. In the myeloma cells in which the light-chain gene in question is active, the V DNA segment and the J DNA segment are contiguous as a consequence of a recombination that apparently accompanies deletion of the DNA sequence occurring between the V and J DNA segments in the germ-line genome[7]. The entire region of the chromosome containing the V DNA segment, J DNA segment, J–C intron and C DNA segment is transcribed into a single RNA molecule from which a mature messenger RNA is generated by RNA splicing[11,12]. The V–J joining step is considered to be a key event in the activation of the immunoglobulin gene. It may also contribute to the increase of the organism's capacity to synthesize a large number of different antibodies[7,13–15].

As the heavy-chain polypeptide is also composed of a V and C region, one might assume that what has been established at the DNA level for the light chains would also be true for heavy chains. However, the expression of heavy chains has some features which make it considerably more complex than that of light chains. For instance, unlike the light chains, there are in the mouse at least eight different C regions, each of which seems to share the same set of V regions, that is, a given V gene can be expressed with more than one heavy-chain class or subclass. In addition, it seems that, as the lymphocytes differentiate, the C region of the heavy chain synthesized switches from one class to another without alteration of the V region[16–18].

Recently, we reported on the structure of the complete γ2b gene isolated from a myeloma, MOPC141, an IgG2b secretor[19]. These studies showed that, unlike the light-chain genes, at least two recombinations are necessary to generate the heavy-chain gene. One of them occurs at or near the 3′ end of the V DNA segment and in the vicinity of the J DNA segment. In contrast to the light-chain genes, where the J DNA segments are located in the 5′-flanking regions of their respective C genes, in the heavy-chain gene system the J DNA used for the MOPC141 γ2b gene does not lie in the 5′-flanking region of the germ-line Cγ2b gene, but is located in the 5′-flanking region of the germ-line Cμ gene. This recombination between V DNA and J DNA near the Cμ gene probably allowed the μ gene to be activated in the precursor B cells to MOPC141 myeloma. The second recombination occurs between a pair of sites, one located between the J DNA segment and the Cμ gene and the other in the 5′-flanking sequence of the Cγ2b gene, and replaces the Cμ-coding exons with the Cγ2b exons. This recombination is referred to as 'switch recombination', for it seems to be a key event preceding the heavy-chain switch. A similar gene structure was also observed for a complete α-chain gene[20] and for a γ1-chain gene[21].

We report here on the two types of recombination, studied by DNA sequencing. The sequences around the V–J joining and the switch recombination sites have different features, suggesting that at least two distinct enzyme systems are involved in the generation of the active immunoglobulin γ2b gene. In addition, sequence analysis of the V DNA of MOPC141 and its germ-line components, the embryonic V DNA and J DNA, revealed that the third hypervariable region is encoded in a separate DNA segment(s) in the germ-line genome.

Mouse DNA inserts in the DNA clones used in this study are listed in Fig. 1. The homology among these DNA fragments has been determined by heteroduplex analysis and restriction enzyme mapping. The coding regions were mapped by R-loop analysis using mRNAs from MOPC141 (γ2b) or MOPC104E (μ). Isolation and electron microscopic characterization of clones M141–P21 (complete γ2b), MEP203 (embryonic J plus Cμ) and MEP3 (embryonic Cγ2b) have been described elsewhere[19]. The isolation of the embryonic V-gene clone, PJ14, is described below.

Identification of J DNA for MOPC141

We have previously identified the putative V–J joining site on the complete γ2b gene clone (M141–P21) and on an embryonic Cμ gene clone (MEP203) by heteroduplex analysis and R-loop mapping[19]. The electron microscopic studies indicated that the putative J DNA for the MOPC141 heavy-chain gene lies 3.6 kilobases 5′ to the Cγ2b gene on M141–P21 and 5 kilobases 5′ to the Cμ gene on MEP203. To analyse the structural features of heavy-chain V–J joining sites, we determined the nucleotide sequences of the appropriate regions of M141–P21 and MEP203. Although the amino acid sequence of the MOPC141 heavy chain is unknown, identification of the J DNA segment coding for this chain was possible because J-peptide sequences are highly conserved. As shown in Fig. 2, M141–P21 carries a DNA sequence in the vicinity of the putative V–J joining sites which can encode a peptide that is identical to the J peptides of

0028-0836/80/330676—08$01.00

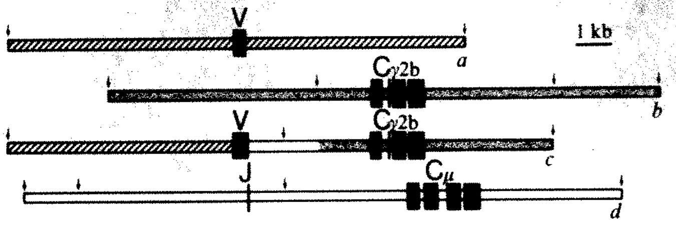

Fig. 1 Mouse DNA inserts in the clones used in the study. Embryonic V_{M141} gene clone PJ14 (*a*), embryonic Cγ2b gene clone MEP3 (*b*), complete γ2b gene clone M141–P21 (abbreviated to M141) (*c*) and embryonic Cμ gene clone MEP203 (*d*) are shown. Arrows indicate *Eco*RI cleavage sites. Filled boxes are exons identified by R-loop mapping. The regions of homology among the four DNA clones as determined by heteroduplex analysis are indicated by bars of different types of shading.

MOPC21 and MOPC173 heavy chains (see Table 1). We also analysed the MEP203 insert to determine whether the same J DNA segment is present in the expected position. Our previous study on clones MEP203 and M141–P21 suggested that the J_{M141} DNA segment and the sequence that follows this segment are derived from a region 5′ to the Cμ gene. In fact, the sequence of MEP203 showed that the J DNA segment and its 3′ noncoding sequence found on M141–P21 are also present in the region about 5 kilobases 5′ to the Cμ gene on MEP203 (Fig. 2). Comparison of these two J_{M141} DNA sequences, one on M141–P21 and the other on MEP203, indicates that the germ-line J_{M141} DNA can encode the M141 J peptide starting with the second nucleotide of the Leu codon at position 112.

In γ2b heavy-chain peptides, the boundary of V and C regions has been thought to be around Ala 126 (ref. 22). The J_{M141} DNA segment can fully encode Ser 125, but only partially Ala 126. We found a triplet, GGT, instead of the Ala codon GCN. Because, in almost all cases studied thus far, an intron starts with the doublet GT (ref. 23), we tentatively conclude that the coding of the J_{M141} DNA ends with the first letter G in the triplet GGT.

Four heavy-chain J DNA segments around 8 kilobases 5′ to the germ-line Cμ gene

Previous studies showed that most, if not all, κ-light-chain J DNAs are tightly linked[7,13]. To examine whether the same applies to the heavy-chain J DNA segments, we isolated DNA clones containing the rearranged V gene from myelomas MOPC603, MOPC315, HOPC8 and MOPC173 and analysed the heteroduplexes formed between each of these DNA clones and the embryonic μ DNA clone MEP203. It is expected that the divergency point observed on a Y-shaped heteroduplex molecule corresponds to the J DNA segment used for expression in the respective myeloma cells. In this way, we mapped four different J DNA segments in the region 5′ to the Cμ gene, at 1.1 (MOPC173-II J), 1.6 (HOPC8-II J), 1.9 (MOPC315 J) and 2.2 (MOPC603 J) kilobases, 5′ to the *Eco*RI site located 3.5 kilobases from Cμ DNA on MEP203. As MEP203 carries a 3-kilobase deletion at 1.5 kilobases 5′ to the Cμ gene (see below), the *Eco*RI site is 6.5 kilobases from the Cμ gene on the mouse chromosome. Using μ-chain mRNA from MOPC104E in R-loop analysis, we also identified the J_{M104E} DNA segment at 2.3 kilobases 5′ to the *Eco*RI site (data not shown). As the MOPC104E μ chain and the MOPC603 α chain seem to have the same J peptide (Table 1), this J DNA segment is probably the same as that detected by heteroduplex analysis using the MOPC603-derived V-gene clone.

Figures 3*Aa* and 4 show the restriction map and the DNA sequence of the 1.5-kilobase J-rich region, respectively. So far, 22 heavy chains have been sequenced in the J-peptide regions. They can be classified into four different groups according to the amino acid sequences of the J peptides (Table 1). Comparison of these J-peptide sequences with the DNA sequence allowed identification of the corresponding four J DNA segments. These four segments can account for all heavy-chain J peptides sequenced so far (see Table 1) and, therefore, seem to encode the J peptides of all different classes or subclasses. We designate these J DNAs as J_{H1}, J_{H2}, J_{H3} and J_{H4} from 5′ towards 3′. No additional J-like DNA sequence has been observed in the 1.5-kilobase region sequenced thus far. There is one unexpressed J DNA, Jκ3 (ref. 7), in a κ-light-chain gene, and there may also be some in the heavy-chain gene.

Isolation of the germ-line V-gene clone for the MOPC141 heavy chain

To determine the recombination site on the germ-line V gene, we attempted to identify and clone the *Eco*RI DNA fragment carrying the germ-line V gene for the MOPC141 heavy chain. First, we analysed embryonic DNA by Southern hybridization using the V DNA probe purified from M141–P21. This probe is a 257-base pair *Ava*II–*Hga*I fragment encoding residues 9–94 of the M141 heavy chain (Fig. 3*Ab*). In the *Eco*RI digest of mouse embryo DNA, about 10 hybridizable bands were detected (data not shown). Detection of 5–10 bands by a single V-gene probe has previously been reported for both κ light chains[5,9] and heavy chains[24–26]. This is due to cross-hybridization among a subset of germ-line V genes that have presumably diverged more recently. As the length of the 5′-noncoding region of the V_H gene on M141–P21 is 6.5 kilobases, the size of the *Eco*RI fragment carrying the germ-line V_H DNA for the M141 heavy chain should be larger than 6.5 kilobases. We separated the *Eco*RI digest of embryonic DNA on a preparative agarose gel, eluted the DNA from the 6.5–23-kilobase region and used it for DNA cloning. Using the V-region probe, we isolated some 30 clones from 2 separate experiments and classified them into 5 different types according to the size of the *Eco*RI insert. Heteroduplex molecules formed between the clones of each type and M141–P21, a complete γ2b gene clone, were examined by electron microscopy.

Although the *Eco*RI inserts of these clones were all hybridizable with the V-gene probe, only the clones containing a 14-kilobase insert formed Y-shaped heteroduplex molecules with M141–P21, in which the homology extended from the 5′ *Eco*RI end to a site 6.9 kilobases away from it. R-loop analysis using the MOPC141 γ2b mRNA indicated that the V-coding DNA segments map at or around the heteroduplex fork point. We further analysed one of these 14-kilobase clones, PJ14, by restriction mapping and DNA sequencing. Evidence that the 14-kilobase clone contains the germ-line V gene for the MOPC141 γ2b chain is obtained from restriction enzyme maps. The cleavage sites for *Bam*HI, *Kpn*I, *Xba*I, *Sac*I and *Hin*dIII in the 5′-flanking region of the V gene on M141–P21 were all found at the corresponding positions on the embryonic V-gene clone, PJ14 (data not shown).

The third hypervariable region is encoded separately

The DNA sequences around the V-coding regions of PJ14 and M141–P21 are shown in Fig. 2. The sequences include a 46-base pair exon presumably coding for the hydrophobic signal peptide, an 81-base pair intron, the entire V-gene exon and the 3′-flanking regions. As in all κ- and λ-chain genes studied so far (refs 4, 6, 8 and G. Heinrich, unpublished results), the V coding begins with the residue at position −4 within the signal peptide. Also, as in the light-chain genes, the coding by the embryonic clone PJ14 ends prematurely with Ser 97, whereas that of the myeloma clone, as mentioned above, continues up to Ser 125. In the 0.6-kilobase stretch of DNA starting with the *Hin*dIII site in the 5′-noncoding region and ending with the Ser 97 codon, the

Table 1 Amino acid sequences of mouse immunoglobulin heavy chains around the carboxyl ends of the V_H regions

Myeloma	End of V	HV3	J	J DNA
M104E	··· YYCAR	DY	d W Y F D V W G A G T T V T V S S	
J558	··· YYCAR	D	r Y – – – – – – – – – – – – – – –	
T15	··· YYCAR	DYYGS	s Y – – – – – – – – – – – – – – –	
M603	··· YYCAR	NYYGST	– – – – – – – – – – – – – – – –	
M167	··· YYCTR	DADYGDSYF	g – – – – – – – – – – – – – – –	J_{H1}
T601	··· YYCAR	LGYY	g – – – – – – – – – – – – – – –	
S107	··· YYCAR	DYYGS	s Y – – – – – – – – – – – – – – –	
H8	··· YYCAR	DYYGN	s Y – – – – – – – – – – – – – – –	
M511	··· YYCAR	DGDYGS	s Y – – – – – – – – – – – – – – –	
M315	··· YYCAG	DNDHL	Y F D Y W G Q G T T L T V S S	
X24	··· YYCAR	LGYYG	– – – – – – – – – – – – – – –	
Hdex4	··· YYCAR	DK	n – – – – – – – – – – – – – –	J_{H2}
Hdex5	··· YYCAR	DS	n – – – – – – – – – – – – – –	
A4	··· YYCTT		s W F A Y W G W G T L V T V S A	
E109	··· HYCTT		g – – – – – – – – – – – – – –	
U61	··· YYCTT		g – – – – – – – – – – – – – –	
A47N	··· YYCST		g – – – – – – – – – – P – – –	J_{H3}
X44	··· YYCAR	LHYYGYA	– – – – – – – – – – – – – – –	
J539	··· YYCAR	LHYYGYN	– – – – – – – – – – – – – – –	
M141	··· YYCAS	VSIYYYGRSDKYFT	l D Y W G W G T S V T V S S	
M21	··· YYCAR	HGNYPW	Y A M – – – – – – – – – – – – –	J_{H4}
M173	··· YYCAR	SP	Y Y A M – – – – – – – – – – – – –	

Amino acid sequences of 22 mouse heavy chains[27,32,34–40] for residues 90–113 (numbering is after Kabat *et al.*[22]) are shown by one-letter codes[41]. According to the J-region peptides, the chains are classified into four groups. The amino acid sequence of the MOPC141 γ2b chain was deduced from the nucleotide sequences determined in this study. The first amino acid residues in the J peptides are shown in small letters whenever the first letters of their codons are not included in the corresponding J DNA segments.

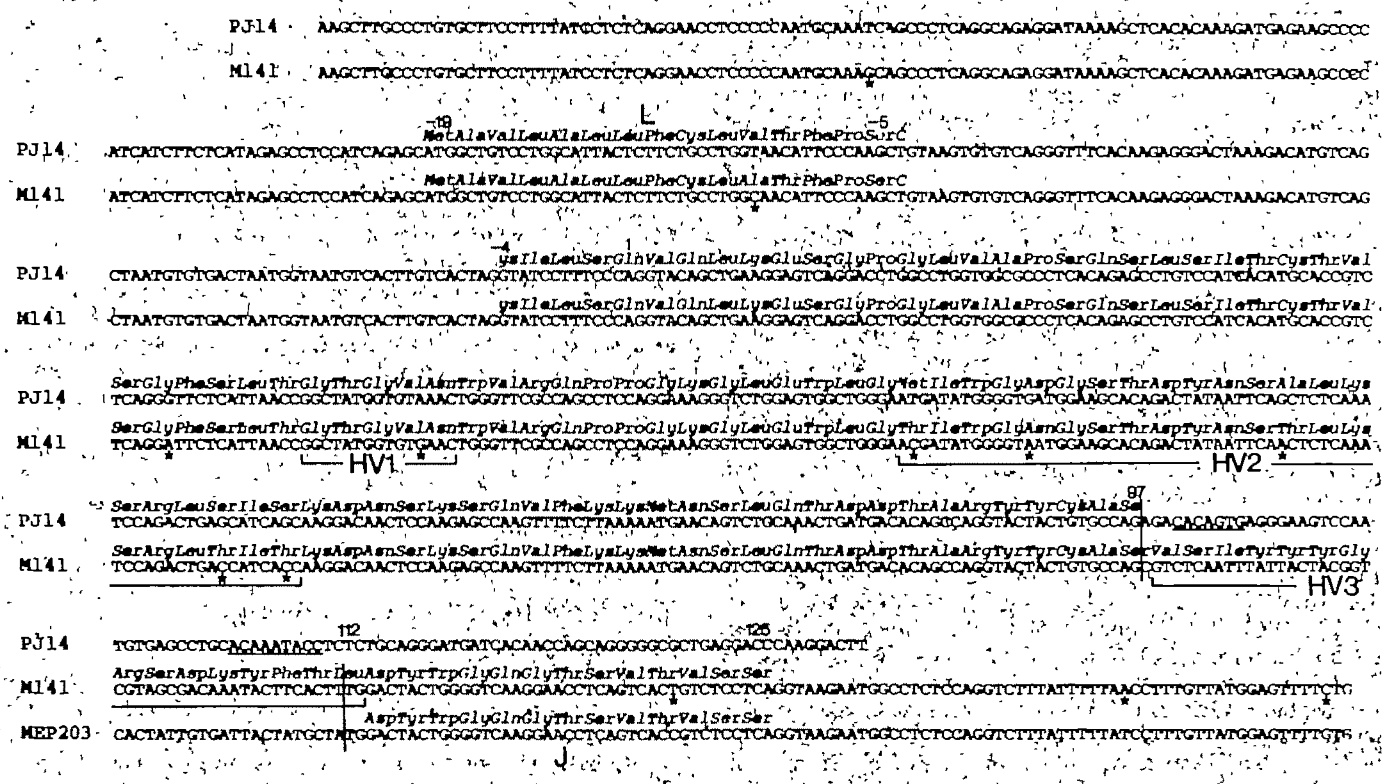

Fig. 2 Nucleotide sequences of MOPC141 V_H DNA (M141), its embryonic V_H DNA (PJ14) and the embryonic J DNA (J_4) coding for the J peptide of the MOPC141 γ2b chain (MEP203). Sequencing strategy is shown in Fig. 3A. Sequence determination was carried out according to the method of Maxam and Gilbert[43]. The amino acid sequence of the complete MOPC141 V region predicted by the nucleotide sequence of clone M141 is shown in italics. The amino acid sequences predicted by the germ-line V DNA segment in clone PJ14 and the J_4 DNA segment in clone MEP203 are also shown. The nucleotide differences observed between the two clones, M141 and PJ14, are shown by asterisks. Vertical lines indicate the possible recombination sites. The two conserved sequences in the 3′-flanking region of the embryonic V DNA are underlined. HV1, HV2 and HV3 designate the three hypervariable regions.

sequences of the two DNA clones differ in 9 base pairs. Of these differences, 6 are within the first and the second hypervariable (HV) regions. Similar, limited, single-base differences have previously been observed in the hypervariable regions of a germ-line V gene and its somatic variants for the light chains of both λ and κ types and were taken as direct evidence for somatic diversification of antibody genes[6]. Three other differences may be a consequence of the similar somatic mechanism or may have occurred during the propagation of the myeloma cells.

Figure 2 also shows the DNA sequence around the J_{M141} DNA segment of the embryonic clone MEP203. As described before, coding begins within the Leu 112 triplet and ends with the Ser 125 triplet. It thus seems that the 14-residue peptide comprising the third hypervariable region (HV3) beginning with Val 98 and ending with Thr 111 is encoded in neither the germ-line V gene nor the J DNA segment. This situation is in contrast to that of light-chain genes previously studied[6–8], in which no such coding gap was observed. We suggest that the third hypervariable region of this heavy chain is encoded in one or more discrete DNA segments (D DNA segments for 'diversity'[27]) that lie elsewhere in the germ-line genome. The V, D and J DNA segments must be assembled by recombination to generate the complete V gene present in the myeloma cells.

The exact joining ends of V and J DNA segments are unfixed

Close examination of the amino acid sequences around the third hypervariable region and the nucleotide sequences around the 3′ end of the germ-line V_H gene and around the 5′ end of the J_H DNA segments suggest several interesting features of the DNA joining events. As previously suggested for the light-chain J DNA segments[7,13–15], the exact 5′ boundary of J_H DNA segments seems to be unfixed (Table 1). For instance, in the case of J_{H4}, the coding of the MOPC141 γ2b chain begins with the second base of the Leu 112 triplet UUG as indicated in Fig. 2. In contrast, coding of the MOPC21 γ1 chain and the MOPC173 γ2a chain by the same J_{H4} DNA segment seems to start with a Tyr triplet UAU and another Tyr triplet UAC, respectively. The first letters of the two Tyr triplets are 7 and 10 bases ahead (5′ side) of the first base used for the coding of the MOPC141 J region. Similar examples for J_{H1}, J_{H2} and J_{H3} are indicated in Fig. 4 and Table 1.

The DNA sequence of the clone PJ14 demonstrated that coding by the germ-line V_{M141} gene ends with the second letter of the Ser 97 codon AGC (Fig. 2). As shown in Table 1, the amino acid sequences immediately preceding Ser 97 are highly conserved among various V regions. Particularly noteworthy is

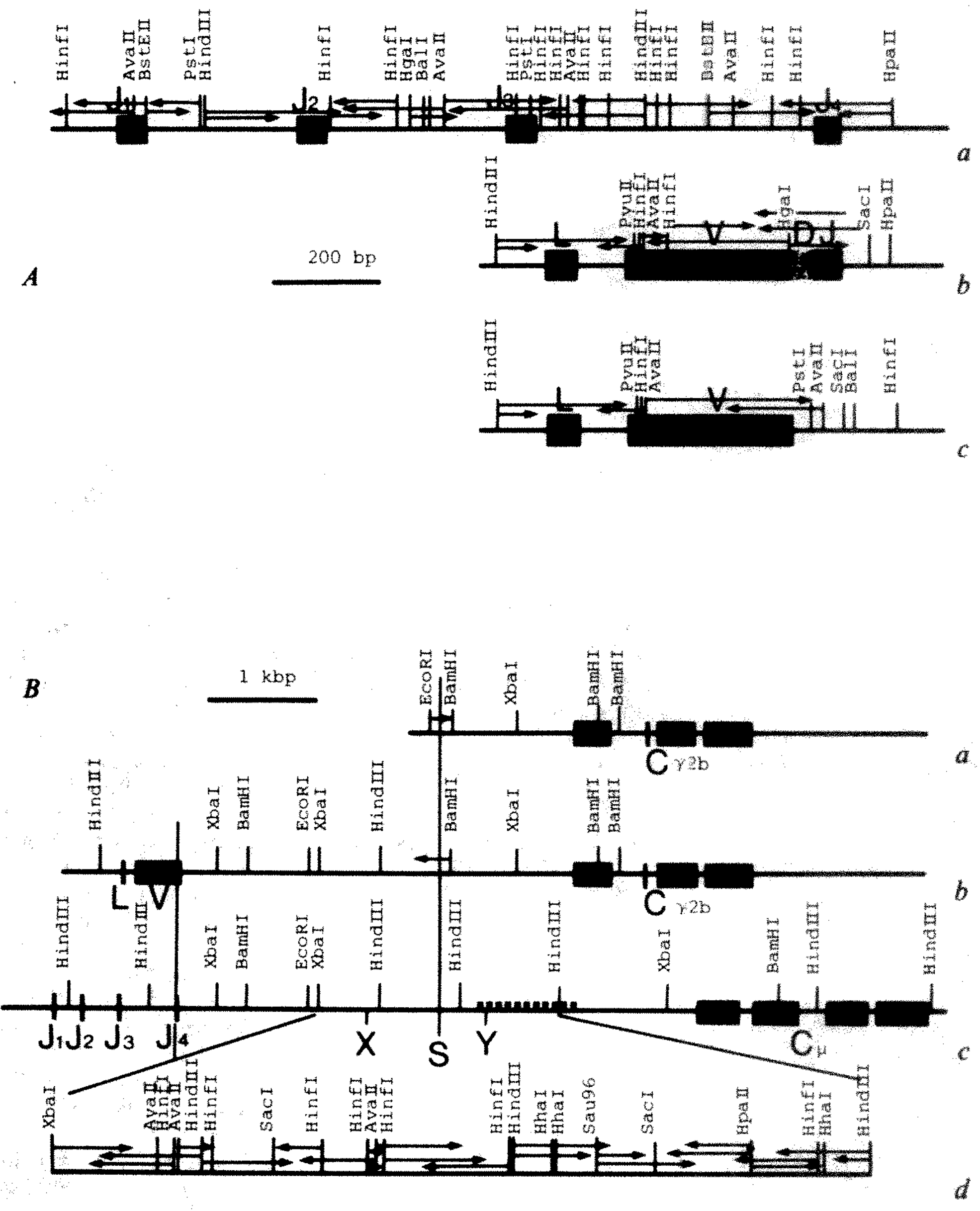

Fig. 3 Restriction enzyme cleavage maps of part of the mouse DNA inserts in clones MEP 203 (*Aa*, *Bc*, *Bd*), MEP3 (*Ba*), M141–P21 (*Ab*, *Bb*) and PJ14 (*Ac*). Cleavage sites were determined by the end-labelling method of Smith and Birnstiel[42], by the separation of single and double digests of DNA fragments by various restriction enzymes, and/or by DNA sequence determination. Horizontal arrows indicate the extent and direction of sequence determination. The filled boxes are exons identified by R-loop mapping and/or DNA sequencing. Vertical line S in *B* indicates the switch recombination sites for MOPC141 heavy-chain genes. X and Y in *Bc* are sequences similar to the Sμ(γ2b) sequence. Four J DNA segments, J_1, J_2, J_3 and J_4, were identified by heteroduplex analysis of rearranged V-gene clones isolated from MOPC603, MOPC315, HOPC8 and MOPC173, respectively. The J DNA segment for MOPC104E was identified as J_1 by R-loop mapping with μmRNA of MOPC104E. The region of clone MEP203, composed of repetitions of CTGAG or sequences closely related to it, is indicated by a broken line in *Bc*. bp, base pairs; kbp, kilobase pairs.

```
                                                            J1   TyrTrpTyrPheAspValTrpGlyAlaGlyThrThrValThrValSerSer
GGTGCCTTAAGGCAGGATATGGAGAGAGTTTTAGTATAGGAACAGAGGCAGAACAGAGACTGTGCTACTGGTACTTCGATGTCTGGGGCGCAGGGACCACGGTCACCGTTTCCTCAGGTA   120
                                                           S107 M603 M167

AGCTGGCTTTTTTCTTTCTGCACATTCCATTCTGAAACGGGAAAAGATATTCTCAGATCTCCCCATGTCAGGCCATCTGCCACACTCTGCATGCTGCAGAAGCTTTTCTGTAAGGATAGG   240

GTCTTCACTCCCAGGAAAAGAGGCAGTCAGAGGCTAGCTGCCTGTGGAACAGTGACAATCATGGAAAATAGGCATTTACATTGTTAGGCTACATGGGTAGATGGGTTTTTGTACACCCAC   360
                     J2 TyrPheAspTyrTrpGlyGlnGlyThrThrLeuThrValSerSer
TAAAGGGGTCTATGATAGTGTGACTACTTTGACTACTGGGGCCAAGGCACCACTCTCACAGTCTCCTCAGGTGAGTCCTTAAAACCTCTCTCTTCTATTCAGCTTAGATAGATTTTACTG   480
                      M315

CATTTGTTGGGGGGGAAATGTGTGTATCTGAATTTCAGGTCATGAAGGACTAGGGACACCTTGGGAGTCAGAAAGGGTCATTGGGGGCCCTGGCTGACGCAGACAGACATCCTCAGCTCC   600

CAGACCTCATGGCCAGAGATTTATAGAGATCCTGGCCAGCATTGCCGCTAGGTCCCTCTCTTCTATGCTTTCTTTGTCCCTCACTGGCCTCCATCTGAGATAATCCTGGAGCCCTAGCCA   720
                                         J3 AlaTrpPheAlaTyrTrpGlyGlnGlyThrLeuValThrValSerAla
AGGATCATTTATTGTCAGAGGTCTAATCATTGTTGTCACAATGTGCCTGGTTTGCTTACTGGGGCCAAGGGACTCTGGTCACTGTCTCTGCAGGTGAGTCCTAACTTCTCCCATTCTAAA   840
                                         H8-II A4    J539

TGCATGTTGGGGGGATTCTGAGCCTTCAGGACCAAGATTCTCTGCAAACGGGAATCAAGATTCAACCCCTTTGTCCCAAAGTTGAGACATGGGTCTGGGTCAGGGACTCTCTGCCTGCTG   960

GTCTGTGGTGATATTAGAACTGAAGTATGATGAAGGATCTGCCAGAACTGAAGCTTGAAGTCTGAGGCAGAATCTTGTCCAGGGTCTATCGGACTCTTGTGAGAATTAGGGGCTGACAGT  1080

TGATGGTGACAATTTCAGGGTCAGTGACTGTCAGGTTTCTCTGAGGTGAGGCTGGAATATAGGTCACCTTGAAGACTAAAGAGGGGTCCAGGGGCTTTTCTGCACAGGCAGGGAACAGAA  1200

TGTGGAACAATGACTTGAATGGTTGATTCTTGTGTGACACCAAGAATTGGCATAATGTCTGAGTTGCCCAAGGGTGATCTTAGCTAGACTCTGGGGTTTTTGTCGGGTACAGAGGAAAAA  1320
           J4 TyrTyrAlaMetAspTyrTrpGlyGlnGlyThrSerValThrValSerSer
CCCACTATTGTGATTACTATGCTATGGACTACTGGGGTCAAGGAACCTCAGTCACCGTCTCCTCAGGTAAGAATGGCCTCTCCAGGTCTTTATTTTTAACCTTTGTTATGGAGTTTTCTG  1440
            M173 M21  M141
                 M173-II
```

Fig. 4 Nucleotide sequence of the 1.4-kilobase region of the embryonic clone MEP203 containing four J_H DNA segments. The sequencing strategy is shown in Fig. 3*Aa*. The J_H DNA segments are referred to as J_1, J_2, J_3 and J_4 from 5′ to 3′. The amino acid sequences encoded by these J DNA segments are shown in italics. The sequences closely related to the palindromic heptamer, CACTGTG, and present in front of every J DNA segment, are underlined. The vertical lines indicate determined (solid lines) or predicted (broken lines) sites where coding by the J DNA segments begin in the various heavy-chain genes present in the indicated myelomas. The sites were determined by comparing the J DNA sequences with the sequences of the rearranged V DNA cloned from the respective myeloma. (See Fig. 2 for the M141 γ2b chain gene. The others are based on unpublished sequence data.) We have identified, isolated and sequenced two rearranged V genes, one from HOPC8 and the other from MOPC173. The V regions encoded by these rearranged V genes are different from the published ones, and are therefore referred to as H8-II and M173-II. It is not clear whether these V genes are part of the active heavy-chain genes of the respective myelomas. The putative sites for the heavy-chain genes of S107, M167, M315, A4, J539, M173 and M21 were deduced by comparing the J-peptide amino acid sequence of each heavy chain with the DNA sequence of the corresponding J DNA segment (Table 1).

the universal Cys at position 95. Tyr 93, Tyr 94, Ala 96 and Arg 97 are also well conserved. We therefore believe that the coding by most, if not all, germ-line V genes ends in the immediate vicinity of the 97th triplet. If so, coding gaps of various lengths exist in the majority of the cases listed in Table 1. As suggested above, these residues must be encoded elsewhere in the genome. The gaps in the heavy chains of four myelomas, A4, E109, U61 and A47N, are the shortest: only the first letter of Gly 98 is unaccounted for. Similarly, only several more bases are necessary to code for the HV3 of the J558 α chain. Previous studies on κ-chain genes indicated that the 3′ end of a given germ-line V gene may not be precisely fixed and could shift within a range of several nucleotides[7]. If the same applies to the heavy-chain genes, the heavy chains with shorter HV3, such as those of A4, E109, U61 and J558, could be fully encoded by the respective germ-line V gene and the J DNA segment. It thus seems that in some cases the germ-line V DNA segment directly joins with the J DNA segment, as is the case in the light-chain genes. However, it is also possible that the assembly of the V_H always occurs in two steps, but that in some cases the D segments are very short or do not even contribute to protein encoding at all.

In either case, by modulation of the joining sites and by various combinations of these DNA segments, diversity could be generated in the third hypervariable region of heavy-chain molecules. However, the location and number of the D DNA segments in the germ-line genome are unknown. They may be at the 3′ end of each of the multiple germ-line V genes or clustered between the V DNA segments and the J DNA segments. In either case we assume that the order of the V, D and J DNA segments in the germ-line genome is the same as in the completely assembled V genes, so that successive joining of the three types of DNA segments is possible by the looping-out of the intervening spacers.

Sequence characteristics around the V and J joining sites

We have previously reported that the five Jκ DNA segments and the one Jλ DNA segment are preceded by two blocks of short, conserved sequences: a palindromic hexamer interrupted by an AT base pair at the centre of symmetry, CACTGTG, and a nanomer, GGTTTTTGT (ref. 7). Similar sequences are also present 5′ to all four J_H DNA segments, although deviation from the basic sequences seems to be slightly higher for the J_H segments than for the J_L segments (Table 2). We also reported previously that germ-line Vκ and Vλ DNA clones contain inverted complements of the nanomer and heptamer in the 3′-noncoding regions. As shown in Fig. 2 and summarized in Table 2, the same or similar sequences are also present in the equivalent positions of the germ-line V_{H141} gene clone. Based on the fact that these sequences are highly conserved, we propose that they constitute recognition signals for the putative recombinase. The finding of similar sequences near the heavy-chain gene DNA segments strengthens the validity of this hypothesis.

In the case of J_{H3}, two sequences, CACAATG and CAATGTG, are closely related to the basic heptamer sequence, CACTGTG. Similarly, two sequences, TATTGTG and TACTATG, are present near the 5′ end of J_{H4} (Fig. 4). In these cases it is not clear which of the two sequences constitutes part of the proposed recognition signal.

The presence of the closely related conserved sequences in the corresponding positions of both light- and heavy-chain germ-line V genes and their J DNA segments suggests that all recombination events necessary for the generation of complete, somatic V genes are carried out by the same or a similar mechanism. We predict that the similar recognition sequences are also present on both sides of the D DNA segments.

An additional feature of the conserved signal sequences is the striking regularity in the length of the spacer between the heptamer and the nanomer. As summarized in Table 2, in almost all cases the spacers are 12 or 23 base pairs long. One exception is one of the two alternative cases of J_{H4}, where the spacer is 31 base pairs long. As a DNA double helix completes a turn every 10.4 base pairs[21], the above indicates that the internal boundaries of the heptamer and the nanomer of a given DNA segment are orientated in nearly the same direction relative to the axis of the helix, regardless of the length of the spacer. The spacers of all $V\kappa$ segments correspond to one turn, and those of $V\lambda_I$ and $V\lambda_{II}$ to two turns. The spacer of V_{M141} is two turns long. All $J\kappa$ spacers are two turns whereas the $J\lambda_I$ spacer is one turn. All spacers of the four J_H segments are two turns. The 31-base pair spacer, one of the two alternative spacers of J_{H4}, could be considered as an exceptional three turns. It should be emphasized that although the lengths of the spacers are conserved in a given type of gene segment, their sequences have diverged widely.

A model of the joining enzymes

The above mentioned features around the joining sites suggest some predictions about the nature of the recombinases. In both λ and κ light-chain V–J joinings, one partner in the recombination displays the heptamer and nanomer one turn of the helix apart from the recombinase, and the other displays these sequences two turns apart. We predict that the recombinase contains two DNA-binding proteins: one recognizing the heptamer and nanomer one turn apart, and the other recognizing them two turns apart. As the two partners carry essentially identical recognition sequences, the two DNA-binding proteins would be structurally closely related.

The germ-line V_{M141} gene and all J_H segments show the recognition sequences separated by two-turn spacers. If the D segment contains recognition sequences with one-turn spacers on each side, then V–D and D–J joinings would be mediated by recombinases having components equivalent to those acting on the light-chain genes. In this way, all recombinations leading to the assembly of immunoglobulin V genes would follow a one-turn/two-turn spacer rule.

The two recombinase components hold the two recombining partners together and cut and rejoin the strands in the vicinity of the heptamers. As the recognition sequences of one partner are complementary to those of the other, it is possible that intrastrand base pairing occurs, however transiently, in the enzyme–DNA complex and facilitates the ligation reaction.

This rule prohibits some unwanted recombinations, such as those between $V\lambda$ and $J\kappa$, and $V\kappa$ and $J\lambda$. However, some other unwanted recombinations, such as those between V_H and $J\lambda$, D and $J\kappa$, and $V\lambda$ and $V\kappa$, could occur. This may be the reason that the three gene families are distributed in three different chromosomes.

Table 2 The two conserved blocks of sequences near the V–J or V–D–J joining sites

J DNA segments	Nanomers		Heptamers	Ref(s)
$J\kappa1$	GGTTTTTGT	23	CACTGTG	7, 13
$J\kappa2$	AGTTTTTGT	23	CAGTGTG	7, 13
$J\kappa3$	GGGTTTTGT	21	CACTGTA	7, 13
$J\kappa4$	GGTTTTTGT	24	CACTGTG	7, 13
$J\kappa5$	GGTTTTTGT	23	CACTGTG	7, 13
$J\lambda I$	GGTTTTTGC	12	CACAGTG	6
J_{H1}	AGTTTTAGT	22	GACTGTG	*
J_{H2}	GGTTTTTGT	23	TAGTGTG	*
J_{H3}	ATTTATTGT	21	CACAATG	*
		23	CAATGTG	*
J_{H4}	GGTTTTTGT	22	TATTGTG	*
		31	TACTATG	*
Basic sequence	GGTTTTTGT		CACTGTG	
V DNA segments	**Heptamers**		**Nanomers**	**Ref.**
$V\kappa21C$	CACAGTG	11	ACAAAAACC	7
$V\kappa21B$	CACAGTG	12	ACAAAAACC	†
VK41	CACAGTG	12	ACATAAACC	8
VK2	CACAGTG	12	ACATAAACC	5
$V\lambda_I$	CACAATG	22	TCAAGAACA	6
$V\lambda_{II}$	CACAATG	23	ACAAGAACA	4
V_{H141}	CACAGTG	23	ACAAATACC	*
Basic sequence	CACAGTG		ACAAAAACC	

Two blocks of conserved sequences found in the 5′-flanking region of J DNA segments and in the 3′-flanking region of embryonic V DNA segments are compared. The numbers between the two types of sequences indicate the distance between them in base pairs. The bases different from those of the basic sequences in the corresponding positions are underlined. The refs from which the sequences were taken are listed (* this paper; † G. Heinrich, personal communication).

The switch recombination sites for the complete γ2b gene of MOPC141

Our previous electron microscopic studies[19] demonstrated that the complete γ2b gene clone M141–P21 shows some homology to the germ-line Cμ gene clone MEP203 and some to the germ-line Cγ2b gene clone MEP3. As shown in Fig. 1, the homology between clone M141–P21 and MEP203 is 2.4 kilobases long and extends, on M141–P21, from the 3′ end of the V DNA segment to a site 1.2 kilobases 5′ to the Cγ2b gene, and, on MEP203, from the J_4 DNA segment to a site 2.5 kilobases 5′ to the Cμ gene. The remaining part of the 3.6-kilobase V–Cγ2b intron of the complete γ2b gene and the sequence that follows this part are entirely homologous to the germ-line Cγ2b gene clone. The restriction enzyme maps of the three DNA clones shown in Fig. 3*B* confirm the results of the electron microscopic studies. Thus, the cleavage sites present in the first 2.2-kilobase portion of the V–Cγ2b intron are also present at the corresponding positions of the germ-line Cμ gene clone, whereas the cleavage sites located in the rest of the intron and the DNA stretch that follows are also found in the corresponding regions of the germ-line Cγ2b gene clone. The maps show that switch recombination occurs between a pair of sites, one located within the 750-base pair *Hin*dIII–*Hin*dIII segment of the germ-line Cμ gene clone and the other within the 200-base pair *Eco*RI–*Bam*HI segment of the germ-line $C\gamma_{2b}$ gene clone, and generates the 650-base pair *Hin*dIII–*Bam*HI segment present in the complete γ2b gene clone (see Fig. 3*B*).

To understand this novel somatic event better, we determined the nucleotide sequences around the switch recombination sites (Fig. 5*a*). As expected, the 5′ portion of the M141–P21 sequence is the same as the sequence of the germ-line Cμ gene clone, MEP203, whereas the 3′ portion is identical to the sequence of the germ-line Cγ2b gene clone, MEP3. The exact μ–γ2b switch recombination sites are indicated by a vertical line in Fig. 5*a*. We propose to refer to the μ–γ2b switch sites on the germ-line Cμ gene and the germ-line Cγ2b gene as Sμ(γ2b) and Sγ2b(μ), respectively.

Sequences around the μ–γ2b switch sites

Are there any characteristic sequences around the μ–γ2b switch sites that might be considered as part of the recognition signal for the recombinase? As shown in Fig. 5*a*, two short blocks of sequences, $\begin{matrix}\text{TCCTGG}\\ \text{AGGACC}\end{matrix}$ and $\begin{matrix}\text{AGA}\\ \text{TCT}\end{matrix}$, present in front of (towards the 5′ side of) Sμ(γ2b) are also present near the Sγ2b(μ) site in the equivalent positions. The two sets of sequences are in the same orientation relative to the direction of transcription, and thus, differ from those sequences conserved near the V–J joining sites not only in the sequence content but also in the relative

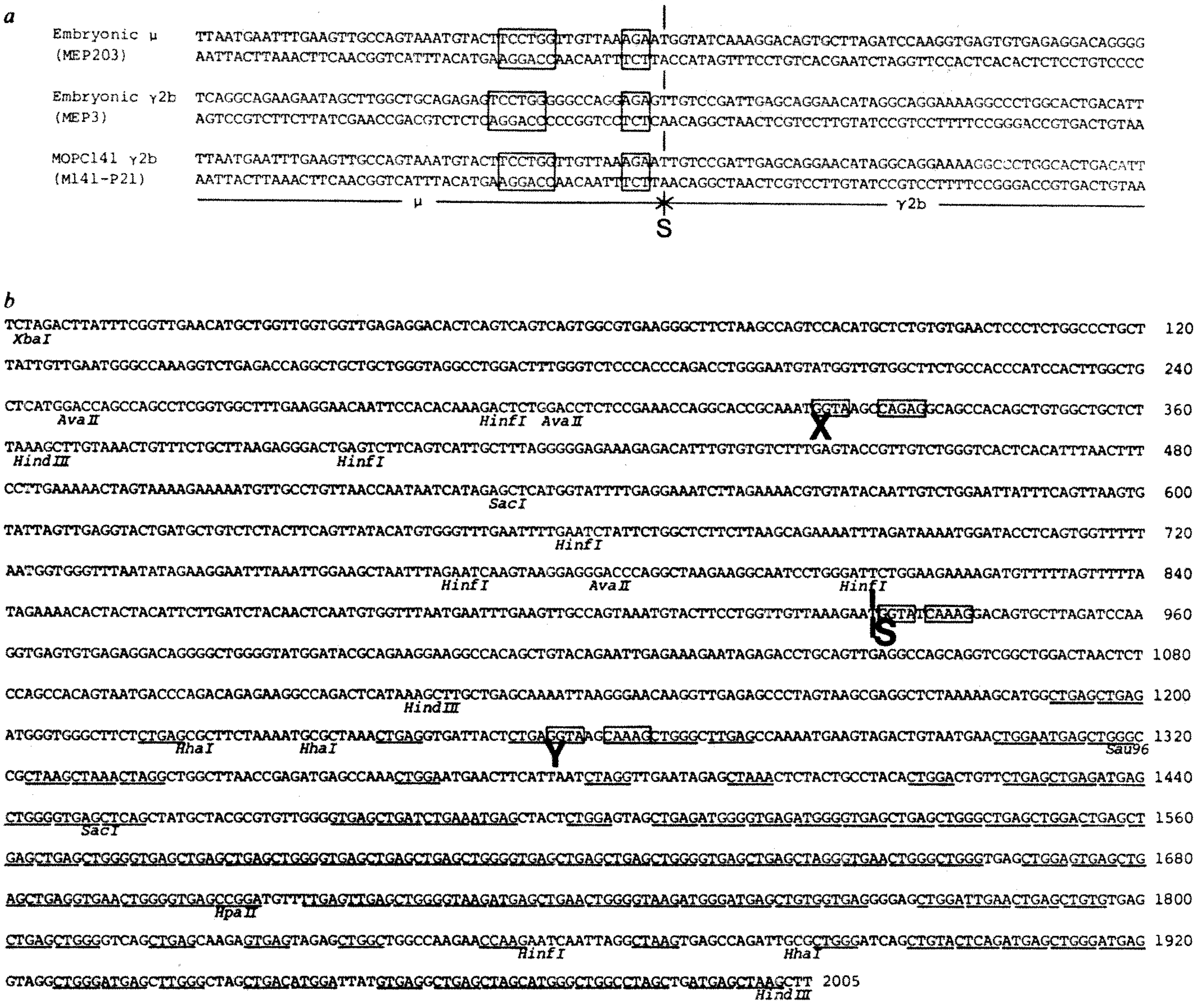

Fig. 5 *a*, Nucleotide sequences around the μ(γ2b) switch recombination sites in clones MEP203, MEP3 and M141–P21. Sequencing strategy is shown in Fig. 3*B*. The recombination sites are indicated by the vertical line designated by S. The two blocks of sequences commonly present in the 5′ side of the recombination sites of the embryonic μ and γ2b gene clones are in boxes. *b*, The nucleotide sequence of 5′-flanking region of Cμ DNA surrounding the switch recombination site for M141 γ2b gene. The 1.8-kilobase *Xba*I–*Hin*dIII segment (Fig. 3*Bd*) was sequenced according to the strategy shown in Fig. 3*Bd*. Two regions (X and Y) homologous to the M141 γ2b switch site (S) are indicated and common sequences GGTA and CAPuG are in boxes. Pentameric sequence CTGAG or its related sequences are underlined.

orientation. Although it is not clear whether these sequences are indeed recognized by the recombinase, the results suggest that the enzymatic mechanism for the μ–γ2b switch recombination is quite different from that for V–J joining.

Sequences of the 5′-flanking region of the germ-line Cμ gene

Recently, Davis *et al.*[20] isolated a complete α heavy-chain gene clone from MOPC603 that carries both V_H and Cα genes. Heteroduplex analysis of this clone against the germ-line Cα and Cμ gene clones suggested that the complete α heavy-chain gene is also generated by a switch recombination that involves the 5′-flanking region of the germ-line Cμ gene. The Sμ(α) site was mapped between the two *Hin*dIII sites at 2.2 and 1.3 kilobases, respectively, from the Cμ gene (see Fig. 3*Bc*). Thus, the μ–α and μ–γ2b switch recombinations seem to use different sites in the 5′-flanking region of the germ-line Cμ gene. This suggests that there may be several different switch sites in this region, possibly one at least for each of the six heavy-chain classes or subclasses, with the possible exception of the δ chain. (The behaviour of B cells suggests that μ–δ switches probably do not occur[29,30].)

We therefore extensively sequenced the 5′-noncoding region of the germ-line Cμ gene clone, MEP203. Fig. 3*Bd* shows the restriction map of the 2.2-kilobase region preceding the Cμ gene, and its complete nucleotide sequence is shown in Fig. 5*b*. We searched for sequences that had a resemblance to those found near the Sμ(γ2b) site and found two, which are referred to as X and Y and are located, respectively, around 0.6 kilobases upstream and 0.3 kilobases downstream of the Sμ(γ2b) site (Fig 5*b*). All three sequences share a tetranucleotide, GGTA, and a pentanucleotide, CAPuAG. However, the two sequences, TCCTGG and AGA, commonly present in the regions 5′ to the Sμ(γ2b) and Sγ2b(μ) sites, are absent in the vicinities of X and Y. It is premature to predict that X and Y are indicative of switch recombination sites. Cloning and sequence analysis of complete heavy-chain genes of various classes and subclasses will clarify the matter. (Recently, we learned that the Y sequence is indeed used for the recombination of the γ1 gene sequenced by Kataoka *et al.*[21] (N. Takahashi and T. Honjo, personal communication).)

In the 0.8-kilobase region extending from the 5′ side of the Y sequence to the *Hin*dIII site, a pentameric sequence, CTGAG, or its close variants are repeated in tandem. As the Sμ(α) site reported by Davis *et al.*[20] falls within this region, involvement of the repeated sequence in the μ–α switch recombination can be invoked. Indeed, our recent DNA sequencing study on the germ-line Cα gene clone indicates that the same pentameric sequences are prominent in the region where the Cα(μ) site had been mapped by Davis *et al.* (H.S., unpublished observations).

Clone MEP203 carries a deletion of about 3 kilobases which seems to have occurred during the cloning or subsequent propagation of the clone in *Escherichia coli.* Restriction enzyme maps of several independent Cμ gene clones isolated by our laboratory and another laboratory[20] suggest that most clones carry deletions of various lengths that map between the two *Hin*dIII sites surrounding the Y sequence. As shown in Fig. 5*b*, this is the region where the pentameric sequences are repeated. Our recent DNA sequencing studies on two independent Cμ gene clones carrying different deletions confirmed that these deletions occur within the pentamer-rich regions.

The two types of somatic recombination

The present studies deal with two types of somatic recombination required for the generation of complete heavy-chain genes, namely V–D–J or V–J joining and switch recombination. The two types of recombination are clearly different in several aspects, although they both occur somatically during lymphocyte differentiation. Although V–D–J or V–J joining should precede the synthesis of the free μ chain detected in pre-B cells[31], switch recombination almost certainly occurs after these cells mature to small B cells bearing complete IgM molecules on the cell surface. V–D–J or V–J joining takes place at the margins of two protein-encoding DNA segments and generates complete V genes. In contrast, switch recombination occurs in the sequences located away from the protein-encoding DNA segments and in effect replaces the Cμ exons of the complete μ-chain gene with exons coding for the C regions of other heavy-chain classes or sub-classes, except, perhaps, for the δ class.

In V–D–J or V–J joining, the recombinant DNAs are to be translated in the recombined regions. This imposes certain restrictions on the precise cutting and joining sites because the encoded polypeptide chains would have to fold properly to be able to function as immunoglobulin subunits. Indeed, this type of recombination seems to occur within a short (several base pairs) region adjacent to the conserved palindromic heptamer present at the margin of every V and J DNA segment studied to date. However, the recombination site does not seem to be unique in a given gene segment and this flexibility, however limited, seems to have been exploited during evolution to increase the genetic capacity of the organism's antibody repertoire. Switch recombination can *a priori* occur anywhere within the 7.5-kilobase intron separating the J DNA segments and the Cμ exons, and anywhere within a several-kilobase region located 5′ to the respective C exon of other classes, as long as the transcription unit on the recombined DNA can encompass the V and C exons and the transcript can be processed properly to the mature mRNA. This suggests that switch recombination sites may be scattered widely in these regions. Indeed, the Sμ(γ2b) site for the MOPC141 γ2b chain and the Sμ(α) site for the MOPC603 α chain are at least 500 base pairs apart. Furthermore, our recent studies demonstrated that in the *Eco*RI digests of various myeloma DNA, the sizes of the DNA fragments detected by the 3-kilobase *Xba*I–*Xba*I fragment carrying the switch region (see Fig. 3*Bc*) are diverse, even among those myelomas secreting the heavy chains of the same class or subclass (R.M., unpublished observations). This suggests that one or both switch recombination sites are not class or subclass specific.

We previously proposed that the V–J joining can be considered as a reversal of an ancient, accidental insertion of an IS-like DNA element carrying invertedly repeated sequences at the margins[7]. In contrast, the evolution of immunoglobulin chains suggests that the C exons of various heavy-chain classes or subclasses arose by duplication of ancient Cμ exons and their flanking sequences[44]. The switch recombination sites have probably arisen from these duplicated flanking sequences by making use of the sequence homology among them. Whether the switch to various classes or subclasses is actively controlled at the level of the DNA recombinations remains to be determined.

Early *et al.*[33] have independently reported the analysis of M603 α heavy-chain V DNA and its germ-line V DNA and J DNA. They found that the 18-base pair D DNA segment in M603 V DNA is not accounted for by either germ-line V DNA or J DNA. They also identified two heavy-chain J DNAs by nucleotide sequencing that correspond to our J_{H1} and J_{H2}. Our determined or predicted joining sites on J_{H1} DNA for M603, M167 and S107 heavy-chain genes are in agreement with their direct sequencing of cDNAs for heavy-chain mRNAs prepared from respective myelomas.

We thank Dr Michael Potter for myelomas and Ms L. Sultzman, Mr G. Dastoornikoo, Ms L. Gibson, Mrs P. Riegert and Mr A. Traunecker for technical assistance.

Received 5 May; accepted 23 June 1980.

1. Hozumi, N. & Tonegawa, S. *Proc. natn. Acad. Sci. U.S.A.* **73,** 3628–3632 (1976).
2. Tonegawa, S., Hozumi, N., Matthyssens, G. & Schuller, R. *Cold Spring. Harb. Symp. quant. Biol.* **41,** 877–889 (1976).
3. Brack, C., Hirama, M., Schuller, R. & Tonegawa, S. *Cell* **15,** 1–14 (1978).
4. Tonegawa, S. *et al. Proc. natn. Acad. Sci. U.S.A.* **74,** 3171–3175 (1978).
5. Seidman, J. G. *et al. Proc. natn. Acad. Sci. U.S.A.* **75,** 3881–3885 (1978).
6. Bernard, O., Hozumi, N. & Tonegawa, S. *Cell* **15,** 1133–1144 (1978).
7. Sakano, H., Hüppi, K., Heinrich, G. & Tonegawa, S. *Nature* **280,** 288–294 (1979).
8. Seidman, J. G., Max, E. E. & Leder, P. *Nature* **280,** 370–375 (1979).
9. Lenhard-Schuller, R., Hohn, B., Brack, C., Hirama, M. & Tonegawa, S. *Proc. natn. Acad. Sci. U.S.A.* **74,** 4709–4713 (1978).
10. Seidman, J. G. & Leder, P. *Nature* **276,** 790–795 (1978).
11. Gilmore-Herbert, M. & Wall, R. *Proc. natn. Acad. Sci. U.S.A.* **75,** 342–345 (1978).
12. Schibler, U., Marcu, K. B. & Perry, R. P. *Cell* **15,** 1495–1509 (1978).
13. Max, E. E., Seidman, J. G. & Leder, P. *Proc. natn. Acad. Sci. U.S.A.* **76,** 3450–3454 (1979).
14. Weigert, M., Gatmaitan, L., Loh, E., Schilling, J. & Hood, L. *Nature* **276,** 785–790 (1978).
15. Weigert, M. *et al. Nature* **283,** 497–499 (1980).
16. Pernis, B., Forni, L. & Amante, L. *Ann. N.Y. Acad. Sci.* **190,** 420–431 (1971).
17. Pernis, B., Forni, L. & Luzzati, A. L. *Cold Spring Harb. Symp. quant. Biol.* **41,** 175–183 (1976).
18. Cooper, M. D., Kearney, J. F., Lydyard, P. M., Grossi, C. E. & Lawton, A. R. *Cold Spring Harb. Symp. quant. Biol.* **41,** 139–145 (1976).
19. Maki, R., Traunecker, A., Sakano, H., Roeder, W. & Tonegawa, S. *Proc. natn. Acad. Sci. U.S.A.* **77** (in the press).
20. Davis, M. M. *et al. Nature* **283,** 733–739 (1980).
21. Kataoka, T., Kawakami, T., Takahashi, N. & Honjo, T. *Proc. natn. Acad. Sci. U.S.A.* **77,** 919–923 (1980).
22. Kabat, E. A., Wu, T. T. & Bilofsky, H. in *Sequences of Immunoglobulin Chains* (NIH, Bethesda, 1979).
23. Breathnack, R., Benoist, C., O'Hare, K., Cannon, F. & Chambon, P. *Proc. natn. Acad. Sci. U.S.A.* **75,** 4853–4857 (1978).
24. Rabbitts, T. H., Matthyssens, G. & Hamlyn, P. H. *Nature* **284,** 238–243 (1980).
25. Davis, M., Early, P., Calame, K., Livant, D. & Hood, L. in *Eucaryotic Gene Regulation* (eds Axel, R., Maniatis, T. & Fox, C. F.) 393–406 (ICN–UCLA Symp., Academic, New York, 1979).
26. Cory, S. & Adams, J. M. *Cell,* **19,** 37–51 (1980).
27. Schilling, J., Clevinger, B., Davie, J. M. & Hood, L. *Nature* **283,** 35–40 (1980).
28. Wang, J. C. *Proc. natn. Acad. Sci. U.S.A.* **76,** 200–203 (1979).
29. Salsano, P., Froland, S. S., Natvig, J. B. & Michaelsen, T. E. *Scand. J. Immun.* **3,** 841–846 (1974).
30. Fu, S. M., Winchester, R. J. & Kunkel, H. G. *J. Immun.* **114,** 250–261 (1975).
31. Burrows, P., LeJeune, M. & Kearney, J. F. *Nature* **280,** 838–840 (1974).
32. Rao, D. N., Rudikoff, S., Krutzsch, H. & Potter, M. *Proc. natn. Acad. Sci. U.S.A.* **76,** 2890–2894 (1979).
33. Early, P. *et al. Cell* **19,** 981–992 (1980).
34. Kehry, M., Sibley, C., Fuhrman, J., Schilling, J. & Hood, L. *Proc. natn. Acad. Sci. U.S.A.* **76,** 2932–2936 (1979).
35. Vrana, M., Rukikoff, S. & Potter, M. *Proc. natn. Acad. Sci. U.S.A.* **75,** 1957–1961 (1978).
36. Francis, S. H., Leslie, R. G. Q., Hood, L. & Eisen, H. N. *Proc. natn. Acad. Sci. U.S.A.* **71,** 1123–1127 (1974).
37. Milstein, C., Adetugbo, K., Cowan, N. J. & Secker, D. S. *Prog. Immun.* **2,** 157–168 (1974).
38. Bourgeois, A., Fougereau, M. & Depreval, C. *Eur. J. Biochem.* **24,** 446–455 (1972).
39. Rudikoff, S. & Potter, M. *Proc. natn. Acad. Sci. U.S.A.* **73,** 2109–2112 (1976).
40. Rudikoff, S. & Potter, M. *Biochemistry* **13,** 4033–4038 (1974).
41. IUPAC–IUB Commission *J. Biochem.* **113,** 1 (1969).
42. Smith, H. O. & Birnstiel, M. L. *Nucleic Acids Res.* **3,** 2387–2398 (1976).
43. Maxam, A. & Gilbert, W. *Proc. natn. Acad. Sci. U.S.A.* **74,** 560–564 (1978).
44. Hill, R. L., Delaney, R., Fellows, R. E. Jr & Lebovitz, H. E. *Proc. natn. Acad. Sci. U.S.A.* **56,** 1762–1769 (1966).

The cDNA for the β-subunit of human chorionic gonadotropin suggests evolution of a gene by readthrough into the 3′-untranslated region

John C. Fiddes & Howard M. Goodman

Howard Hughes Medical Institute Laboratory, Department of Biochemistry and Biophysics,
University of California, San Francisco, California 94143

A 579-base pair approximately full-length cDNA which codes for the 145-amino acid long β-subunit of human chorionic gonadotropin (HCG) has been cloned in the plasmid vector pBR322 and its complete nucleotide sequence determined. A hydrophobic presequence of 20 amino acids can be identified from the nucleotide sequence. The amino acid sequence of the β-subunit is known to be related to those of the β-subunits of the other glycoprotein hormones LH, FSH and TSH, but the β-subunit of HCG is unique in that it contains a C-terminal extension of about 30 amino acids which has no homologous counterpart in the other three hormones. Analysis of the βHCG cDNA nucleotide sequence suggests that this extension may have arisen by the loss of the termination codon of an ancestral β-like gene so that most of what was previously the 3′-untranslated region now codes for protein. The β-subunit of HCG terminates with the codon UAA located 16 bases before the poly(A) in the sequence AAUAAA. This sequence is believed to be a recognition signal involved in either polyadenylation or processing and therefore has a dual role in this gene, serving both a coding and a regulatory function.

HUMAN chorionic gonadotropin (HCG) is a member of a group of four glycoprotein hormones which are functionally and structurally related. The other three hormones in the group, luteinizing hormone (LH), follicle-stimulating hormone (FSH) and thyroid-stimulating hormone (TSH), are synthesized in the anterior pituitary, whereas chorionic gonadotropin is synthesized in large amounts by the placenta. The level of HCG reaches a maximum about 10–12 weeks after conception and declines towards the end of pregnancy. The hormone functions to stimulate the corpus luteum to produce steroid hormones which are essential for the maintenance of pregnancy (for reviews see refs 1, 2). An antigen which is immunologically similar to HCG is also produced by many tumour tissues and transformed cell lines[3] as well as by certain bacterial strains[4].

All four hormones are glycosylated and consist of an α- and a β-subunit[5]. The same α-subunit is common to all four hormones and in the case of humans is 92 amino acids long[6–11], whereas the β-subunits have sequences unique to each hormone and confer biological specificity.

Comparison of the β-subunits reveals that they are all related. In the human the β-subunits of HCG, LH, FSH and TSH are 145, 115, 118 and 112 amino acids long, respectively[7,12–16]. The β-subunit of HCG is thus about 30 amino acids longer than those of the other three hormones. The highest level of homology observed (82%) is between the β-subunits of HCG and LH, the homologies between all other pairs of β-subunits ranging from about 30 to 40%. Alignment of the β-subunit amino acid sequences shows that the extra 30 amino acids of the HCG β-subunit form a C-terminal extension that is unique to HCG and thus has no homologous counterpart in the other three β-subunits.[7] The function of this extension is not known.

We have described previously the isolation by cloning in the plasmid vector pBR322 of a 621-base pair cDNA fragment, synthesized from first trimester placental mRNA, which codes for the entire α-subunit[17]. The results obtained when this cDNA fragment is used to hybridize to human genomic DNA digested with various restriction enzymes imply that the α-subunit is coded for by a single gene (ref. 17 and unpublished results).

The present report describes the isolation, also from first trimester placental mRNA, of a 579-base pair cDNA fragment which codes for the 145 amino acids of the β-subunit of HCG and for a previously unknown 20 amino acid-long presequence. Examination of the sequence of the β HCG cDNA reveals that the C-terminal extension has probably arisen by the loss of a termination codon in an ancestral β-like gene so that the 3′-untranslated region now codes for amino acids. The sequence AAUAAA (ref. 18) in the β-subunit of HCG has the dual function of containing the termination codon (UAA) of the gene and a possible recognition site for polyadenylation or processing of the mRNA.

Cloning of the cDNA for the β-subunit of HCG

First trimester placental polyadenylated RNA has been shown previously[17,19–22] by *in vitro* translation and immunoprecipitation of the products to be an enriched source of the mRNAs coding for both subunits of HCG. However, there seems to be an excess of α over β mRNA; this finding correlates with the excess of free α-subunit polypeptide over the β-subunit in the placenta[23].

The cDNA for the α-subunit of HCG was identified previously on the basis of restriction enzyme analysis. Total first trimester placental cDNA was digested with a variety of restriction endonucleases and the products were visualized by electrophoresis on 5% polyacrylamide gels. Prominent restriction enzyme fragments were observed and it was assumed that these arose by digestion of the major cDNA species, the α-subunit of HCG. Recombinant plasmids were therefore screened by restriction enzyme digestion of their DNA and those containing fragments which corresponded in size to those observed in total cDNA were considered potential α HCG recombinants. Sequence analysis confirmed the identity of one such recombinant.

This approach, however, has the disadvantage that there is no positive correlation between prominent restriction enzyme fragments and a particular mRNA species until DNA sequences have been determined. Potential recombinants for the β HCG cDNA were, in fact, isolated in this way but were found by sequencing not to code for the β-subunit.

A more direct approach is to use the known amino acid sequence of a protein to predict the existence of a restriction enzyme site in the gene. Most restriction enzymes do not have recognition sequences which are uniquely determined by certain

0028-0836/80/330684—04$01.00

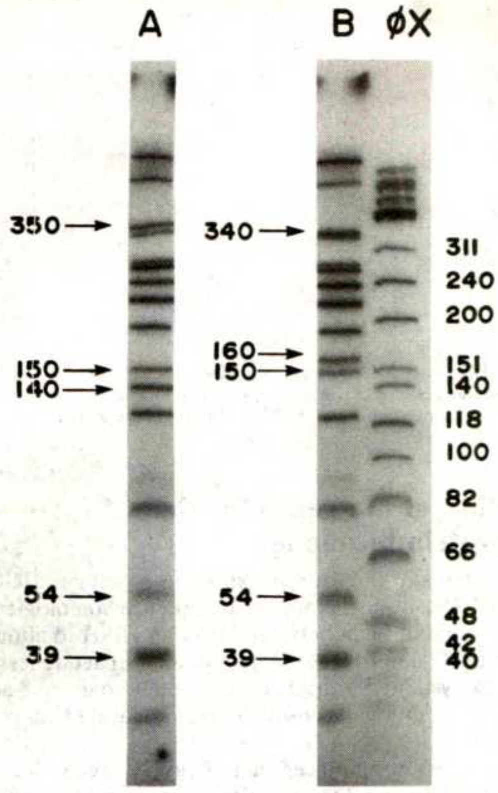

Fig. 1 Restriction enzyme analysis with *Sau*96I of the two recombinants between pBR322 and the cDNA of the β-subunit of HCG. The recombinants were obtained from first trimster placental cDNA in the size range of 500–700 base pairs using the approach of adding synthetic *Hin*dIII oligonucleotide linkers to the cDNA. Experimental details were as described previously[17] with the exception that strain RRI was used in place of χ1776. All experiments conformed with the NIH Guidelines for Recombinant DNA Research. Overnight cultures in L broth (3 ml each) were grown for 72 recombinants and the cells were pelleted. Cleared lysates were made using lysozyme, EDTA and Triton[48] and were dialysed extensively against 0.3 M NaCl, 10 mM Tris-Cl, *p*H 8.0, and 1 mM EDTA before precipation with ethanol. Each plasmid DNA preparation was then resuspended in 10 µl H_2O and 1 µl of the DNA was digested at 37 °C for 30 min with 1 unit of *Sau*96I (Biolabs) in a 5 µl reaction containing 50 mM NaCl, 6 mM Tris-Cl, *p*H 7.5, 6 mM $MgCl_2$ and 1 mM dithiothreitol. The sample was then used directly to resuspend 1 µCi of [α-^{32}P]dGTP which had been evaporated to dryness and 0.5 units of DNA polymerase I (Klenow modification) were added before incubation at room temperature for 15 min (ref. 26). The sample was then electrophoresed directly on a 0.3-mm thick 5% polyacrylamide gel until the bromphenol blue marker dye was about 5 cm from the bottom of the gel. The gel was then soaked for 15 min in 10% acetic acid to elute free [α-^{32}P]dGTP and was exposed overnight to X-omat R film at −70° C with an intensifying screen. Lanes A and B show autoradiographs of the *Sau*96I digests of the two pBR322–β HCG recombinants. The sizes of the fragments corresponding to the β HCG cDNA are indicated (see text). The third lane is a *Hin*fI digest of ΦX174 RF DNA used as size markers.

amino acid pairs, but two enzymes, *Asu*I (ref. 24) and *Sau*96I (ref. 25), are particularly useful because they recognize the sequence GGNCC. As glycine is coded for by the four codons GGN and proline by the four codons CCN, every Gly-Pro dipeptide must be represented by an *Sau*96I site in the corresponding gene. Other groups of amino acids may also be coded for by sequences containing *Sau*96I sites, as the sequence GGNCC may be translated in two other reading frames.

As there are Gly-Pro dipeptides at positions 102 and 103 and positions 136 and 137 in the β-subunit of HCG[7,12,13], the corresponding gene must have *Sau*96I sites 102 base pairs apart. Within this 102 base pairs of DNA, at amino acid positions 104–106 and 122–124, are the sequences Lys-Asp-His and Lys-Ala-Pro, respectively, which, with the appropriate codon choice, would also correspond to *Sau*96I sites. These restriction enzyme sites would result in the 102-base pair fragment being divided into pieces 9, 54 and 39 base pairs long.

Double-stranded cDNA was synthesized from first trimester placental RNA as described before (ref. 17 and Fig. 1 legend) and fragments in the size range of 500–700 base pairs were recovered from a preparative 5% polyacrylamide gel and cloned into the unique *Hin*dIII site of pBR322. Small-scale DNA preparations were made from 72 such recombinants and the DNAs digested with *Sau*96I. The resulting DNA fragments from the recombinant plasmids were labelled at their termini with [α-^{32}P]dGTP using DNA polymerase I (ref. 26 and Fig. 1) and analysed on 5% polyacrylamide gels.

Two of the recombinants were observed to have *Sau*96I fragments 54 and 39 base pairs long (Fig. 1) and were thus considered potential β HCG clones. The 9-base pair fragment would not be observed on a 5% polyacrylamide gel. In addition to these fragments, a 150-base pair fragment is common to both recombinants. A fragment of this size is compatible with the amino acid sequence for the β-subunit of HCG, as the sequence Pro-Ala-Leu at positions 50–52 could be coded for by a nucleotide sequence containing *Sau*96I site, which is about 150 bases from the *Sau*96I site corresponding to the Gly-Pro dipeptide at positions 102–103.

The other *Sau*96I fragments, 350 and 140 base pairs long in the case of A and 340 and 160 in the case of B, were shown by combined *Hin*dIII and *Sau*96I digestion (data not shown) to be terminal fragments containing pBR322 sequences in addition to cloned sequences. The two recombinants were thus considered potential candidates for containing β HCG cDNA sequences and seem to represent slightly different lengths of copying of the same mRNA species.

DNA sequence analysis of the β HCG cDNA

Both potential β HCG recombinants were positively identified by DNA sequence analysis. The plasmid DNAs were digested with *Hin*dIII, labelled with polynucleotide kinase and [γ-^{32}P]ATP, and the 5′-terminal *Hin*dIII–*Sau*96I fragments sequenced. Subsequently, the complete sequence of recombinant A, which is about 10–20 nucleotides longer than B at the 5′ end, was determined. Both the chemical method of Maxam and Gilbert[27] and the chain-termination method of Maat and Smith[28] were used, because both methods used the same 5′-terminally labelled double-stranded DNA fragments. The sequence was determined on both strands of the DNA to ensure accuracy.

The complete sequence of recombinant A, designated pBR322-cβHCG, is presented in Fig. 2. The cDNA is 579-base pairs long, of which 40 represent the poly(A) sequence. All 145 codons which correspond exactly to known amino acid sequence of β HCG can be identified[7,12,13].

A hydrophobic presequence of 18–29 amino acids, which is processed to generate the mature polypeptide, is observed in secretory proteins (see ref. 29 for a compilation of presequences). The α-subunit of HCG has a 24 amino acid-long presequence[17,30], but no information is available on the presequence of the β-subunit. If the sequence preceding the serine codon at position 1 in β HCG is read in triplets towards the 5′ end, potential ATG initiation codons are observed at positions −18 and −20 (see Fig. 2). No other ATG codons are observed between this position and the 5′ end of the cloned cDNA in this or the other two reading frames. It has been proposed, on the basis of examining the 5′-untranslated sequences of 22 eukaryotic mRNA species, that the initiator methionine codon is the AUG located closest to the 5′ end of the mRNA[31]. Two exceptions to this rule have been observed with the mRNAs for the VP1 in the virus SV40[32,33] and for bovine preproparathyroid hormone[34], but in both cases it has been proposed that the AUG triplet in the 5′-untranslated region is masked by secondary structure. The β-subunit of HCG can thus be predicted to have a presequence 20 amino acids long, but the existence of a larger presequence (greater than 28 amino acids long) cannot be definitely ruled out because there are no termination codons in phase in the part of the 5′ untranslated region which has been cloned. Characteristically, the presequence of β HCG is hydrophobic, with the somewhat unusual structure of seven consecutive leucine residues at positions −8 to −14.

The nucleotide sequence of the β HCG cDNA has a very high G+C content (G 28.0%, C 38.0%, A 16.3%, T 17.6%) when compared with total human DNA (G 19.5%, C 19.8%, A 30.9%, T 29.6%). A similar bias towards a high G + C content is also observed in the human cDNAs for insulin^{35} and chorionic somatomammotropin (ref. 36 and E. Tischer, J.C.F. and H.M.G., unpublished data), but is not so noticeable in growth hormone^{37}, the α-subunit of HCG^{17} or β-globin$^{38-40}$.

Consistent with the high G+C content of β HCG cDNA is the very considerable bias towards codons ending in G or C (G 31.9%, C 50.6%, A 7.2%, T 10.2%). A compilation of the nucleotides present in the third codon position of the known human cDNA sequences is given in Fig. 3. The high incidence of codons ending in G and C seems to be a common feature of human genes even with growth hormone, β-globin and α HCG, which do not have a marked overall high level of G and C. These data are consistent with the observation^{41} that codon choice is species specific and, if this has a role in modulating translation, may present difficulties in obtaining high levels of expression of human genes in other cell types.

```
                               -20
                               met glu met phe gln gly leu leu leu
AGACAAGGCAGGGGACGCACCAAGG      ATG GAG ATG TTC CAG GGG CTG CTG CTG
1                                  30

    -10                                         1
leu leu leu leu ser met gly gly thr trp ala ser lys glu pro leu
TTG CTG CTG CTG AGC ATG GGC GGG ACA TGG GCA TCC AAG GAG CCG CTT
        60                                      90

                10                                      20
arg pro arg cys arg pro ile asn ala thr leu ala val glu lys glu
CGG CCA CGG TGC CGC CCC ATC AAT GCC ACC CTG GCT GTG GAG AAG GAG
 HaeIII                 120

                                30
gly cys pro val cys ile thr val asn thr thr ile cys ala gly tyr
GGC TGC CCC GTG TGC ATC ACC GTC AAC ACC ACC ATC TGT GCC GGC TAC
150                                     180

        40                                      50
cys pro thr met thr arg val leu gln gly val leu pro ala leu pro
TGC CCC ACC ATG ACC CGC GTG CTG CAG GGG GTC CTG CCG GCC CTG CCT
            210                 PstI     Sau96I   HaeIII/Sau96I

                            60
gln val val cys asn tyr arg asp val arg phe glu ser ile arg leu
CAG GTG GTG TGC AAC TAC CGC GAT GTG CGC TTC GAG TCC ATC CGG CTC
                                270          TaqI/HinfI

70                                      80
pro gly cys pro arg gly val asn pro val val ser tyr ala val ala
CCT GGC TGC CCG CGC GGC GTG AAC CCC GTG GTC TCC TAC GCC GTG GCT
        300                                     330

                90                                      100
leu ser cys gln cys ala leu cys arg arg ser thr thr asp cys gly
CTC AGC TGT CAA TGT GCA CTC TGC CGC CGC AGC ACC ACT GAC TGC GGG
  PvuII                 360

                                110
gly pro lys asp his pro leu thr cys asp asp pro arg phe gln asp
GGT CCC AAG GAC CAC CCC TTG ACC TGT GAT GAC CCC CGC TTC CAG GAC
Sau96I     Sau96I                        420                 Hin

        120                                     130
ser ser ser ser lys ala pro pro pro ser leu pro ser pro ser arg
TCC TCT TCC TCA AAG GCC CCT CCC CCC AGC CTT CCA AGC CCA TCC CGA
fI                  HaeIII/Sau96I                      480   Hin

                        140                     145
leu pro gly pro ser asp thr pro ile leu pro gln 0C
CTC CCG GGG CCC TCG GAC ACC CCG ATC CTC CCA CAA TAA AGGCTTCTCAAT
fI/SmaI/Sau96I/HaeIII           MboI                      530

CCGC[A]40
 539
```

Fig. 2 Nucleotide sequence of the 579-base pair cDNA fragment coding for the β-subunit of HCG. The amino acid sequence of the 145-amino acid long protein^{7,12,13} is shown as well as the 20-amino acid long presequence deduced from the nucleotide sequence. Nucleotides are numbered below the sequence and amino acids above the sequence. Only those restriction enzyme sites used in the sequence analysis are indicated. The AAUAAA sequence at the 3′ end of the coding region is marked.

cDNA	Base A	T	G	C
hαCG	25	28	29	35
hβCG	12	17	53	84
hGH	31	29	65	93
hCS	17	17	60	75
hInsulin	14	8	43	45
hβGlobin	10	40	53	45

Fig. 3 Frequency of third position codon choices in the known human cDNA sequences; β HCG, α HCG^{17}, growth hormone (HGH)^{37}, chorionic somatomammotropin (HCS)^{36}, insulin^{35} and β-globin$^{37-39}$.

Evolution of the genes for the glycoprotein hormones

The β-subunits of the four glycoprotein hormones HCG, LH, FSH and TSH all show amino acid sequence homologies which range from about 30% between HCG and FSH to about 80% between HCG and LH. Alignment of all four sequences shows that the 12 cysteine residues are completely conserved and that there is an additional conserved region located at positions 34–38 in β HCG.

A much less pronounced homology between the α- and β-subunits of bovine TSH has also been proposed by Pierce^{42}, leading to the suggestion that all glycoprotein hormones genes evolved from a common ancester which subsequently diverged to generate α and β sequences. This amino acid sequence homology can also be detected between α and β HCG and is presented in Fig. 4. The alignment used here differs somewhat in the N-terminal region from that proposed from bovine TSH and can now also be extended to include the presequences. Overall, the homology is very low (16% not including the deletions and insertions), but there is still a very noticeable conservation of the cysteine residues, with 6 of the 12 being maintained between the α and β-subunits.

Figure 4 also shows the alignment of the coding nucleotide sequences for the α- and β-subunits of HCG based on the same alignment as used with the amino acid sequences. Overall, the homology level is still very low (31%), but there are certain areas which are considerably more closely related, especially in the regions of the cysteine residues. The observed similarity between the sequences does not merely reflect a similar bias in base composition between the two species, for the base composition of the α cDNA (G 20.0%, C 24.5%, A 26.6%, T 29.0%) is very different from that of the β cDNA (G 28.0%, C 38.0%, A 16.3%, T 17.6%).

The nucleotide sequence data therefore tend to confirm the proposal that the α and β genes are related and thus probably have evolved from a common ancester, as the homology previously detected at the amino acid level is somewhat more apparent when the nucleotide sequences are considered. In this respect, therefore, the glycoprotein hormone genes may be similar to the globin genes, which are also assumed to have evolved from a common precursor^{43} into an α gene and a family of several β-like genes.

Readthrough into the 3′-untranslated region

The 3′-untranslated region of the β HCG mRNA is only 16 bases long and is thus remarkably short when compared with other eukaryotic mRNA species (see Fig. 2). The termination codon UAA is located in the sequence AAUAAA, which is found in the 3′-untranslated regions of all polyadenylated eukaryotic cellular mRNAs^{18} at about 15–20 bases from the poly(A). The lack of this sequence in some non-polyadenylated plant viral mRNAs^{44} led to the proposal that the AAUAAA is involved in the process of polyadenylation[45]. However, there is an exception to this, as the genomic RNAs of several picornoviruses are polyadenylated but do not have the AAUAAA sequence[46]. Thus, it may be that in the case of the cellular mRNAs this sequence acts as a signal in the processing of a larger precursor mRNA molecule as well as being involved in polyadenylation. In β HCG mRNA, this sequence therefore has a dual overlapping function, as it codes for the last codon, CAA (Gln), and for the terminator (UAA), in addition to the proposed regulatory function.

The alignment of the β-subunit amino acid sequences shows that the β-subunit of HCG has a C-terminal extension of about 30 amino acids which has no homologous counterpart in the other three. As the β HCG mRNA has such an unusually short 3′-untranslated region, it can be proposed that the β-subunit of HCG evolved from a common β-subunit ancester by some readthrough event so that the 3′-untranslated sequence became a coding region. This could have arisen by changes such as point or frameshift mutations or by an alteration of the splicing pattern of the precursor mRNA. Verification of this proposal will require sequence analysis of the genes for the other three β-subunits so that homologies between their 3′-untranslated regions and the C-terminal extension of β HCG can be investigated.

A similar observation has also been made with the abnormal human α-haemoglobin Constant Spring, which has a 31-amino acid C-terminal extension when compared with normal α-globin[47]. Sequence analysis of normal human α-globin cDNA showed that the carboxy-terminal amino acids of α-globin Constant Spring could be coded for by the 3′-untranslated region with a termination codon located in the same position as in β HCG[39].

The availability of cloned cDNA sequences for both subunits of HCG should facilitate further investigation of the structure and regulation of the gonadotropin genes. Hybridization probes can be generated to investigate the cellular genes to determine whether any linkage exists between the related genes and to examine the synthesis of HCG in the placenta, transformed cells and, possibly, bacteria.

J.C.F. was the recipient of a postdoctoral fellowship from the Anna Fuller Foundation. H.M.G. is an investigator of the Howard Hughes Medical Institute. The work was supported by grant (no. CA 14026) to H.M.G. We thank H. Martinez and S. Bock for the computer analysis of the DNA sequence, R.A. Hallewell for discussions, J.P. Thirion for assistance in screening some of the cDNA recombinants, members of the Department of Obstetrics and Gynecology at UCSF for assistance in obtaining placental material and B. McCabe for typing the manuscript. Avian myeloblastosis virus reverse transcriptase was from the NCI.

```
                            met glu met phe gln
                β CG        ATG GAG ATG TTC CAG ... ... ... ...
                            *** **      * *
                α CG        ATG GAT TAC TAC AGA AAA TAT GCA GCT
                            met asp tyr tyr arg lys tyr ala ala

    gly leu leu leu leu leu leu leu ser met gly gly thr trp ala
... GGG CTG CTG CTG TTG CTG CTG CTG AGC ATG GGC GGG ACA TGG GCA
        ***  *      ***   *  **  *           *           *  **
ATC TTT CTG GTC ACA TTG TCG GTG TTT CTG CAT GTT CTC CAT TCC GCT
ile phe leu val thr leu ser val phe leu his val leu his ser ala

ser lys glu pro leu arg pro arg cys arg pro ile asn ala thr leu
TCC AAG GAG CCG CTT CGG CCA CGG TGC CGC CCC ATC AAT GCC ACC CTG
 *   *  * * * *   *  *  ***     ***     *        *    *  *   *
CCT GAT GTG CAG GAT TGC CCA GAA TGC ACG CTA CAG GAA AAC CCA TTC
pro asp val gln asp cys pro glu cys thr leu gln glu asn pro phe

ala val glu lys glu gly cys pro val cys ile thr val asn thr thr
GCT GTG GAG AAG GAG GGC TGC CCC GTG TGC ATC ACC GTC AAC ACC ACC
         **   *     **    * **   *
TTC TCC CAG CCG ... GGT GCC CCA ATA CTT CAG ... ... ... ... ...
phe ser gln pro     gly ala pro ile leu gln

ile cys ala gly tyr cys pro thr met thr arg val leu gln gly val
ATC TGT GCC GGC TAC TGC CCC ACC ATG ACC CGC GTG CTG CAG GGG GTC
    **      *** * * ***   *  *   *   *              *
... TGC ATG GGC TGC TGC TTC TCT AGA GCA TAT CCC ACT CCA CTA AGG
    cys met gly cys cys phe ser arg ala tyr pro thr pro leu arg

leu pro ala leu pro gln val val cys asn tyr arg asp val arg phe
CTG CCG GCC CTG CCT CAG GTG GTG TGC AAC TAC CGC GAT GTG CGC TTC
     *       *        * **          ***  *   *      * *  *
TCC AAG AAG ACG ATG TTG GTC CAA AAG AAC GTC ACC TCA GAG TCC ACT
ser lys lys thr met leu val gln lys asn val thr ser glu ser thr

glu ser ile arg leu pro gly cys pro aro gly val asn pro val val
GAG TCC ATC CGG CTC CCT GGC TGC CCG CGC GGC GTG AAC CCC GTG GTC
     *   *           *       *   *   *      **  *        *   **
TGC TGT GTA GCT AAA TCA TAT AAC AGG GTC ACA GTA ATG GGG GGT TTC
cys cys val ala lys sor tyr asn arg val thr val met gly gly phe

ser tyr ala val ala leu ser cys gln cys ala leu cys arg arg ser
TCC TAC GCC GTG GCT CTC AGC TGT CAA TGT GCA CTC TGC CGC CGC AGC
         *                  **  **  **          **            *
AAA GTG GAG AAC CAC ACG GCG TGC CAC TGC AGT ACT TGT TAT TAT CAC
lys val glu asn his thr ala cys his cys ser thr cys tyr tyr his

thr thr asp
ACC ACT GAC
*    **  *
AAA TCT TAA
lys ser OC
```

Fig. 4 Alignment of the amino acid and nucleotide sequences of the coding regions of the α (lower lines) and β (upper lines) subunits of HCG. To maximize the homologies, one insertion of five codons, and two deletions of one and six codons have been proposed in the α sequence. The overall sequence homologies are 16.1% and 31.0% for the amino acids and nucleotides, respectively These values do not take into account the deletions and insertions Only the region of the β HCG coding sequence which has a homologous counterpart in the α-subunit (amino acids −20 to 99) is shown

Received 8 April, accepted 2 June 1980

1 Canfield, R E, Birken, S, Morse, J H & Morgan, F J in *Peptide Hormones* (ed Parsons, J A) 299–315 (University Park Press, Baltimore, 1976)
2 Bahl, O P *Fedn Proc* **36**, 2119–2127 (1977)
3 Acevedo, H F, Slifkin, M, Pouchet, G R & Rakhshan, M in *Detection and Prevention of Cancer* Part 2, Vol 1 (ed. Nieburgs, H E) 937–963 (Dekker, New York, 1978).
4 Maruo, T, Cohen, H, Segal, S J & Koide, S S *Proc natn Acad Sci U.S.A* **76**, 6622–6626 (1979)
5 Swaminathan, N & Bahl, O P *Biochem biophys Res Commun* **40**, 422–427 (1970)
6 Bellisario, R, Carlsen, R B. & Bahl, O P *J biol Chem* **248**, 6796–6809 (1973)
7 Morgan, F J, Birken, S & Canfield, R. E. *J. biol Chem* **250**, 5247–5258 (1975)
8 Sairam, M R, Papkoff, H & Li, C. H *Biochem biophys Res Commun* **48**, 530–537 (1972)
9. Inagami, T., Murakami, K, Puett, D, Stockell-Hartree, A & Nureddin, A *Biochem J* **126**, 441–442 (1971)
10. Shome, B & Parlow, A F *J clin Endocr Metab* **39**, 169–202 (1974)
11 Rathnam, P & Saxena, B B *J biol Chem* **250**, 6735–6746 (1975)
12 Keutmann, H T & Williams, R M *J biol Chem* **252**, 5393–5397 (1977)
13 Birken, S & Canfield, R E *J biol. Chem* **252**, 5386–5392 (1977)
14 Saxena, B. B & Rathnam, P *J biol Chem* **251**, 993–1005 (1976)
15 Sairam, R M & Li, C H *Biochem biophys Res Commun* **54**, 426–431 (1973)
16 Shome, B & Parlow, A F *J clin Endocr Metab* **39**, 203–205 (1974)
17 Fiddes, J C, & Goodman, H M. *Nature* **281**, 351–356 (1979)
18. Proudfoot, N. J & Brownlee, G. G *Nature* **263**, 211–214 (1976)
19. Landefeld, T D, McWilliams, D R & Boime, I *Biochem biophys Res Commun* **72**, 381–390 (1976).
20 Daniels-McQueen, S *et al. J biol Chem* **253**, 7109–7114 (1978)
21 Chatterjee, M, Baliga, S & Munro, H. *J biol. Chem* **251**, 2945–2951 (1976)
22 Chatterjee, M Munro, H N *Biochem biophys Res Commun* **77**, 426–433 (1977)
23. Franchimont, P., Gaspard, V, Reuter, A & Heynen, G *Clin. Endocr* **1**, 315–316, (1973)
24 Hughes, S G, Bruce, T & Murray, K (in preparation)
25 Sussenbach, J S, Steenbergh, P H, Rost, J A, van Leeuwen, W J & van Embden, J D A *Nucleic Acids Res* **5**, 1153–1163 (1978).
26 Drouin, J. *J. molec. Biol* (in the press).
27. Maxam, A. M & Gilbert, W. *Proc. natn Acad. Sci. U S A* **74**, 560–564 (1977)
28. Maat, J. & Smith, A J H *Nucleic Acids Res* **5**, 4537–4545 (1978).
29. Habener, J F. *et al Proc. natn Acad Sci U S A* **75**, 2616–2620 (1978)
30 Birken, S., Fetherston, J, Desmond, J, Canfield, R & Boime, I. *Biochem. biophys Res Commun.* **85**, 1247–1253 (1978)
31 Kozak, M *Cell* **15**, 1109–1123 (1978)
32 Ghosh, P K *et al J. biol Chem* **253**, 3643–3647 (1978).
33 Haegeman, G & Fiers, W *Nucleic Acids Res* **5**, 2359–2371 (1978)
34. Kronenberg, H M. *et al Proc natn Acad Sci U S A* **76**, 4981–4985 (1979)
35 Bell, G I *et al Nature* **282**, 525–527 (1979)
36 Shine, J, Seeburg, P H, Martial, J A, Baxter, J D & Goodman, H M *Nature* **270**, 494–499 (1977)
37 Martial, J A, Hallewell, R A, Baxter, J D. & Goodman, H M *Science* **206**, 602–607 (1979)
38. Marotta, C A., Wilson, J T, Forget, B G & Weissman, S M *J biol Chem* **252**, 5040–5053 (1977)
39 Proudfoot, N J & Longley, J I *Cell* **9**, 733–746 (1976)
40 Chang, J. C., Temple, G F, Poon, R F, Neumann, K H & Kan, Y W *Proc natn Acad Sci U S A* **74**, 5145–5149 (1977).
41. Grantham, R, Gautier, C., Gouy, M, Mercier, R & Pavé, A *Nucleic Acids Res* **8**, r49–r62 (1980)
42 Pierce, J G, Liao, T. H & Carlsen, R B. in *Hormonal Proteins and Peptides* Vol. 1 (ed Li, C H) (Academic, New York, 1973)
43 Ingram, V. M *Haemoglobins in Genetics and Evolution* (Columbia University Press, New York, 1963)
44 Briand, J. P., Jonard, G., Guilley, H, Richards, K D. & Hirth, L *Eur J Biochem* **72**, 453–463 (1977)
45 Porter, A G., Merregaert, J, van Emmelo, J & Fiers, W *Eur J Biochem* **87**, 551–561 (1978)
46 Porter, A. G *et al Nature* **276**, 298–301 (1978)
47 Clegg, J B, Weatherall, D J & Milner, P F. *Nature* **234**, 337–340 (1971)
48. Katz, L, Kingsbury, D T & Helinski, D. R. *J Bact* **114**, 577–591 (1973)

LETTERS

No IR burst from the X-ray rapid burster MXB1730–335

S. Sato, K. Kawara, Y. Kobayashi, T. Maihara & H. Okuda

Department of Physics, Kyoto University, Kyoto 606, Japan

J. Jugaku

Tokyo Astronomical Observatory, Mitaka, Tokyo 181, Japan

The X-ray rapid burster MXB1730–335, discovered by Lewin *et al.*[1] has been identified with a compact globular cluster embedded in the midst of the galactic plane and named[2] Liller 1. It has an extremely large interstellar extinction ($A_v = 11$ mag) from which Liller[2] and Kleinmann *et al.*[4] derived its distance as 10 kpc. Kulkarni *et al.*[3] detected IR bursts in the globular cluster, six times during their 2.5 h observing time on 4–5 April 1979 using a 1-m telescope at Kavalur[3]. The burst power emitted in *H*-band was estimated to be $1.6\text{–}2.3 \times 10^{30}$ W. Stimulated by this report, we monitored MXB1730–335 using a multi-band IR photometer for about 10 h during April and August 1979. In the latter period, although the X-ray bursts were very active, no coincident IR and X-ray burst could be detected. We show here that this conflicts with previous results by Kulkarni *et al.*[3] and Jones *et al.*[5].

The source was observed on 20–22 April 1979 at *H*-, *K*- and *L*-bands using a multi-colour photometer attached to the 1-m IR telescope at the Agematsu IR Observatory of Kyoto University. During the monitoring time, ~4 h in three days, we could not detect any change of flux exceeding the statistical fluctuations; 2.7×10^{-17} W cm^{-2} μm^{-1} at the *H*-band, 1.8×10^{-17} W cm^{-2} μm^{-1} at the *K*-band and 3×10^{-17} W cm^{-2} μm^{-1} at the *L*-band.

The X-ray satellite HAKUCHO, launched in February 1979, registered a revival of X-ray burst activity from early August 1979. We again attempted to monitor this in the near-IR using the 61-cm telescope of the University of Hawaii on Mauna Kea where we were conducting a deep IR survey in the galactic plane. The observations were performed with a multi-colour photometer built for the survey. The photometer can monitor four colours: *I*(0.82 μm), *H*(1.61 μm), *K*(2.21 μm) and *L*(3.61 μm) bands simultaneously, using beam splitters in conjunction with a Si-photodiode (*I*-band) and three independent InSb photovoltaic detectors (*H*-, *K*- and *L*-bands). The time constant of the lock-in-amplifier was set at 0.3 s. The beam was wobbled in N–S direction with a beam throw of 1.5 arc min at ~10 Hz.

Table 2 Upper limits to the IR flux changes in association with the X-ray burst event at 12 August 06.38.27 (UT)

	Upper limits	
Band	Observed (W cm^{-2} μm^{-1})	Corrected for interstellar extinction (W cm^{-2} μm^{-1})
I (0.82 μm)	1×10^{-17}	1×10^{-15}
H (1.61 μm)	1×10^{-17}	6×10^{-17}
K (2.21 μm)	4×10^{-18}	1×10^{-17}
L (3.61 μm)	2×10^{-17}	3×10^{-17}

No bursts were observed within the statistical fluctuation of the signals in any channel during the observing time of 6 h during 9, 10 and 12 August 1979. The details of the observations in April and August are summarized in Table 1; γ Sgr was chosen as a calibration star.

During the period in August, HAKUCHO was observing X-ray bursts almost every 20 or 30 min (ref. 6). From statistical considerations, therefore, it is improbable that an X-ray burst did not occur during our IR observations which lasted 6 h. However, the observations of HAKUCHO and that of the IR monitoring missed each other most of the time. Only in the following event was an X-ray burst accompanied by an IR observation.

An X-ray burst associated with IR bursts:

Onset time:	06.38.27 UT 12 August 1979
Burst duration:	126 s
X-ray burst flux:	1.3×10^{-15} W cm^{-2} (3–10 keV)

(Observation by HAKUCHO[6])

As the X-ray observation was interrupted, its end time was not observed but this is undoubtedly one of the typical X-ray bursts of the so-called 'trapezoidal' form[6]. Figure 1 shows the IR raw data in *H*- and *K*-bands recorded on strip charts in the corresponding time of the X-ray burst event. The X-ray burst profile is also shown for comparison[6].

We can find no change in the IR flux which is larger than statistical fluctuations before or after the onset of the X-ray burst. The r.m.s. fluctuations of the signals are 7×10^{-17} W cm^{-2} μm^{-1} and 2×10^{-17} W cm^{-2} μm^{-1} for *H*- and *K*-bands, respectively. Slight depressions labelled 'adj' were accidentally caused by the pointing adjustment of the telescope.

To improve the statistics, we integrated the observed fluxes of the source in its steady state before the onset of the burst and during on-burst time, from which upper limits for changes of the flux level can be estimated; the results are given in Table 2

Table 1 Journal of observations

Date (1979)	Time (UT)	Duration (min)	Bands	Beam (arc s)	Observatory
20 April	19.41–20.20	20	*K*	40ϕ	Agematsu
21 April	17.47–20.10	136	*H*, *K*, *L*	60ϕ	Agematsu
22 April	18.30–20.10	86	*H*, *K*, *H*	60ϕ	Agematsu
		Total: 242 = 4 h 02 min			
	Photometry:	$H(6.6^{\mathrm{mag}})$ $K(5.8^{\mathrm{mag}})$ $L(6.2^{\mathrm{mag}})$		Beam size: 50 arc s^2 ϕ	
9 August	09.49–10.49	55	*I*, *H*, *K*, *L*	60×20	Mauna Kea
11 August	06.12–10.31	90	*I*, *H*, *K*, *L*	60×20	Mauna Kea
12 August	06.14–10.00	226	*I*, *H*, *K*, *L*	60×20	Mauna Kea
		Total: 372 = 6 h 12 min			
	Photometry:	$I(9.5^{\mathrm{mag}})$, $H(6.2^{\mathrm{mag}})$, $K(5.4^{\mathrm{mag}})$, $L(5.6^{\mathrm{mag}})$		Beam size: 60×20 arc s^2	

0028–0836/80/330688—02$01.00

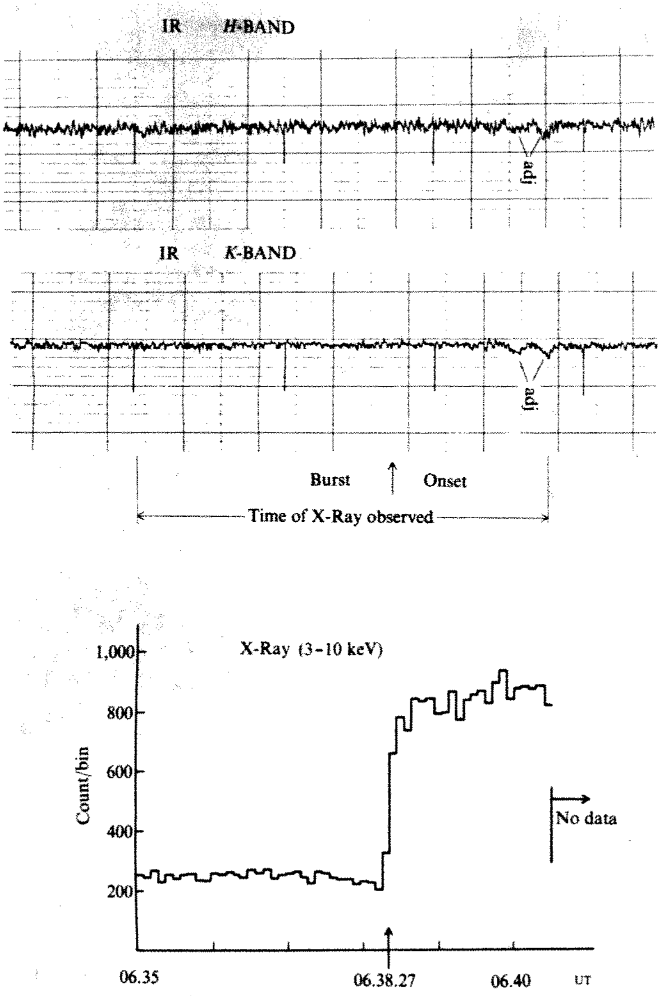

Fig. 1 IR observational data at *H*-and *K*-bands in correspondance with the X-ray burst event on 12 August 1979.

corrected for the interstellar extinction assuming $A_K = 1.1$ mag (ref. 4).

The intrinsic fluxes thus obtained for *K*- and *L*-bands are substantially smaller than the X-ray flux of 1.3×10^{-15} W cm^{-2} (3–10 keV) of the order of 10^{-2}. Assuming a distance of 10 kpc for the source, we estimate the upper limit to the energy release in the IR region to be of the order of 10^{29} W in a band width of 1 μm. This is more than one order of magnitude smaller than that detected by Kulkarni *et al.*[3]. Recently, Jones *et al.*[5] have announced another detection of IR bursts in the globular cluster on 5 September 1979, about a month later than our observations. Its energy release in *K*-band was estimated to be 2.2×10^{30} W, compatible with the previous results obtained by Kulkarni *et al.*[3].

The positive detections by Kulkarni *et al.*[3] and by Jones *et al.*[5] apparently disagree with our negative results. This may be attributable to difference in Types of the X-ray bursts. In fact Kulkarni *et al.* assumed their IR bursts to be associated with Type 1 X-ray bursts, while the X-ray bursts observed by the HAKUCHO were exclusively Type II bursts[6].

The IR bursts so far observed are not accompanied by X-ray data. We need to make simultaneous observations in the X-ray and IR regions for confirmation of their exact concurrence, or their relationship to the burst Type. If they occur simultaneously, the emission should be of nonthermal origin; which means that magnetic field would be strongly coupled with the emission mechanism. Polarimetric observations would give data about such a mechanism and about the energy spectrum.

We thank the HAKUCHO group for their encouragement and collaboration, also Dr J. T. Jefferies, director of the Mauna Kea Observatory, for permission to use the 61-cm telescope on Mauna Kea. Our work at the Mauna Kea Observatory was partly supported by the Asahi Press Science Foundation.

Received 23 April; accepted 2 June 1980.

1. Lewin, W. H. G. *et al. Astrophys. J. Lett.* **207**, L95–L99 (1976).
2. Liller, W. *Astrophys. J. Lett.* **213**, L21–L23 (1977).
3. Kulkarni, P. V., Ashok, N. M., Apparao, K. M. V. & Chitre, S. M. *Nature* **280**, 819–820 (1979).
4. Kleinmann, D. E., Kleinmann, S. G. & Wright, E. L. *Astrophys. J. Lett.* **210**, L83–86 (1976).
5. Jones, A. W. *et al. Nature* **283**, 550–551 (1980).
6. Inoue, H. *et al. Nature* **283**, 358–360 (1980).

The IR variability of SS433

A. B. Giles*, A. R. King*, R. F. Jameson*,
M. R. Sherrington*, J. H. Hough†, J. A. Bailey†
& E. C. Cunningham†

*Astronomy Department, University of Leicester, Leicester LE1 7RH, UK
†Hatfield Polytechnic Observatory, Bayfordbury House, Hertford SG13 8LD, UK

We report here the results of a one-year monitoring programme of SS433 at IR and visual wavelengths. The most striking feature of these observations is the near constancy of the IR colours while the source's flux varies over a range of ~1.2 mag. There is no evidence for the 13.1-day period first reported in radial-velocity measurements by Crampton *et al.*[1]. However, it seems possible that an 11.8-day period is present.

SS433 remains an object of great interest because of the presence of enormously Doppler-shifted emission lines swinging back and forth across its spectrum[3–5]. (Suggested models are given in refs 6, 7 and comprehensive reviews of the spectroscopic data in refs 8, 9.) The work reported here is not directly connected with the emission-line phenomena but provides

Table 1 *JHK* Photometry of SS433

JD	$J \pm \Delta J$		$H \pm \Delta H$		$K \pm \Delta K$	
3942.369	9.73	0.04	9.10	0.02	8.45	0.02
3944.392			8.79	0.04	8.12	0.02
3945.367	9.41	0.04	8.75	0.02	8.12	0.02
3973.351	9.38	0.02	8.62	0.03	8.05	0.02
3978.359	9.26	0.02	8.51	0.03	7.94	0.02
4007.674	9.59	0.10	8.69	0.03	8.01	0.04
4012.676	9.35	0.02	8.65	0.03	7.99	0.02
4014.660	9.18	0.02	8.46	0.02	7.91	0.01
4015.640	9.25	0.02				
4019.080	9.57	0.05	8.77	0.05	8.17	0.05
4021.030	9.00	0.05	8.27	0.05	7.72	0.05
4023.070	8.79	0.05	8.01	0.05	7.47	0.05
4023.140	9.08	0.07	8.45	0.07	7.73	0.07
4024.010	9.35	0.07	8.68	0.07	7.88	0.07
4024.030	9.34	0.05	8.78	0.05	7.78	0.05
4025.080	8.95	0.07	8.20	0.07	7.28	0.07
4096.375	8.64	0.03	7.84	0.02	7.23	0.03
4097.458	9.23	0.04	8.51	0.04	7.76	0.04
4098.396	9.51	0.03	8.79	0.04	8.16	0.04
4099.375	9.76	0.03	9.11	0.02	8.32	0.03
4100.542	9.68	0.02	8.99	0.02	8.35	0.02
4101.563	9.54	0.02	8.74	0.02	8.13	0.02
4104.375	8.98	0.02	8.17	0.02	7.45	0.02
4107.500	9.04	0.02	8.22	0.02	7.41	0.02
4108.479	8.95	0.02	8.11	0.02	7.41	0.02
4109.458	9.12	0.02	8.32	0.02	7.67	0.02
4149.417	9.49	0.02	8.66	0.01	7.99	0.02
4150.375	9.20	0.01	8.43	0.01	7.73	0.02
4151.438	9.05	0.01	8.24	0.01	7.63	0.01
4152.344	8.76	0.02	7.93	0.01	7.26	0.01
4153.396	8.75	0.03	7.82	0.02	7.20	0.01
4157.396	9.43	0.04	8.50	0.03	7.96	0.04
4188.736	9.92	0.01	8.92	0.01	8.19	0.01
4189.713	9.28	0.01	8.48	0.01	7.84	0.01
4296.350	9.26	0.04	8.54	0.02	7.95	0.02
4354.258	9.09	0.01	8.48	0.01	7.86	0.01
4354.383	9.08	0.01	8.41	0.01	7.80	0.01
4355.385	9.17	0.01	8.49	0.01	7.89	0.01

0028–0836/80/330689—03$01.00

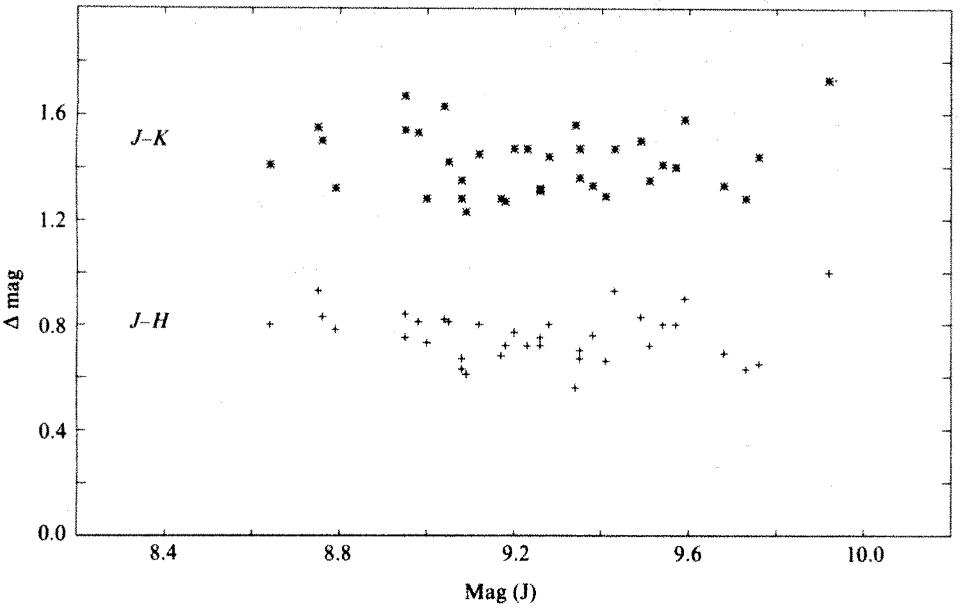

Fig. 1 *J-K* (*) and *J-H* (+) colours plotted against *J* magnitude for SS433.

additional information about the nature of the underlying binary system. The variability of the source has been studied at several wavelengths[2,10-14] and the radial velocity period of 13.1 days first reported by Crampton *et al.*[1] has now also been detected in the Hα line-to-continuum ratios[15]. A spectroscopic modulation of 13 days has also been reported by Liller *et al.*[16].

We have observed SS433 between April 1979 and May 1980 with various instruments, mostly from the Cabezon Observatory, Tenerife, using the 1.5-m IR flux collector. At Tenerife, most of the data were obtained at *VJHK* with the Leicester photometer or Hatfield polarimeter/photometer, which use the same InSb Dewar and photon counting systems. Additional *V* points were obtained at Tenerife with the RGO travelling optical polarimeter/photometer. Further *JHK* data were obtained at the AAT in Australia and at Ukirt in Hawaii. This collection of data has been supplemented with other published data[17,18].

All these data are presented in Tables 1–3 but here we mainly confine our discussion to the more abundant data in Table 1. The *JHK* measurements have been combined to produce Fig. 1 which shows the remarkable constancy of the IR colours. This is just as expected for free–free emission[18-20].

The *J* data in Table 1 have been folded at trial periods in the range 0.1–50 days using the technique of Bopp *et al.*[21] to find the most likely period. This method is appropriate to a small sample of data containing large and irregular gaps in temporal coverage.

Table 2 *V* Photometry of SS433

JD	*V*	±Δ*V*
4007.674	13.64	0.08
4012.676	13.86	0.03
4014.660	13.59	0.02
4101.563	14.24	0.02
4103.375	13.67	0.02
4107.500	13.55	0.02
4108.479	13.86	0.02
4109.458	13.95	0.02
4131.396	14.00	0.02
4132.382	13.98	0.04
4133.344	13.95	0.03
4134.354	14.01	0.02
4139.350	13.78	0.03
4140.350	13.71	0.03
4141.351	14.00	0.02
4142.344	14.12	0.02
4143.354	14.13	0.02
4149.417	14.60	0.10
4150.375	14.46	0.08
4151.438	14.37	0.07
4152.344	14.04	0.05

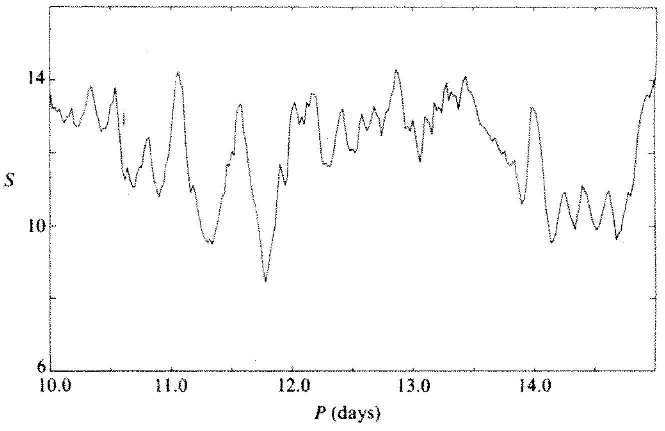

Fig. 2 An analysis of the *J* data for periodicities (Bopp *et al.*[21]). Sharp dips indicate periods of interest and the vertical scale is logarithmic ($S = \Sigma \Delta M$).

The results are shown in Fig. 2, and there is no indication of a 13.1-day period. This may be confirmed by folding the data at this period; no reasonable light curve results.

Originally Giles[22] reported smooth *JHK* light curves for a period of 11.8 ± 0.05 days, possessing two minima, the broader one being used to define the ephemeris

$$1979 \text{ August } 14.26(\pm 0.5)\ \text{UT} + 11.8E$$

This ephemeris was used to predict the occurrence of the possible narrow 'eclipse' feature[22] which was then apparently

Table 3 *B*, *I* Photometry of SS433

JD	*B*	±Δ*B*
4012.676	15.42	0.06
4014.660	15.20	0.04
4015.640	15.27	0.04
4150.375	16.18	0.22
4151.438	16.03	0.18
4152.344	15.70	0.25
JD	*I*	±Δ*I*
4096.375	9.26	0.30
4097.458	10.16	0.20
4098.396	10.76	0.40

confirmed by several subsequent observations at UKIRT in Hawaii. Further points obtained at the AAT in early 1980 also apparently confirm this feature, in phase although the width and depth are undefined and probably variable. The dip around 11.8 days from the Bopp analysis of Fig. 2 naturally produces a reasonable light curve when the data are folded at this period. Figure 3 shows the resulting *J* light curve. The apparent smoothness of this curve is somewhat less than that evident for the first attempt[22] now that more points have been added. SS433 may well have some variability over long time scales in addition to that caused by any binary period modulation.

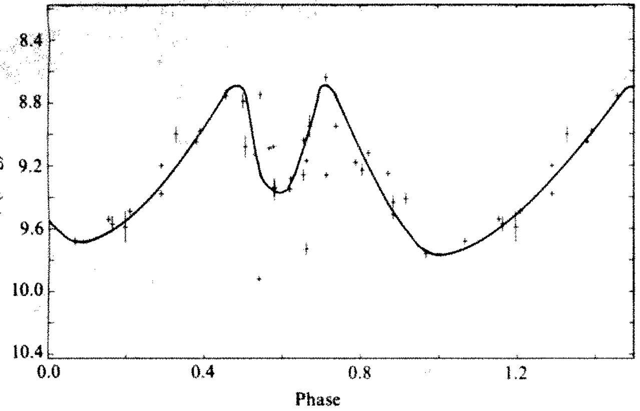

Fig. 3 *J* light curves for the data folded at 11.8 days.

We note that the photometry by Glass (personal communication) agrees with our range of intensity and colour variation but is not entirely consistent with our possible period. Such differences may prove important when a much larger data base is available if they can be related to the 164-day period. It is clearly important that the existence or otherwise of this 11.8-day period should be demonstrated over the coming summer. This will best be achieved by ~3 weeks of complete coverage rather than by folding irregularly spaced short data sets. The limited optical data we have obtained shows no periodicity so we are unable to comment on the 6.45/12.9-day period reported by Kemp *et al.*[23] or the 12.8-day period of Gladyshev *et al.*[24].

Given the unprecedented nature of SS433 it does not seem inconceivable that the source should have two periods, only one or even neither of which is a true orbital period. SS433 will clearly repay further detailed photometric study. Observations of any modulation in the X-ray flux or low-energy cutoff would be of special interest.

We thank D. J. Axon and D. A. Allen for use of their data and I. S. Glass for communicating his results and helpful discussion. We thank the SRC for funding.

Received 29 April; accepted 5 June 1980.

1. Crampton, D., Cowley, A. P. & Hutchings, J. B. *Astrophys. J. Lett.* **235,** L131 (1980).
2. Clark, D. H. & Murdin, P. *Nature* **276, 44** (1978).
3. Margon, B. *et al. Astrophys. J. Lett.* **230,** L41 (1979).
4. Liebert, J., Angel, J. R. P., Hege, E. K., Martin, P. G. & Blair, W. P. *Nature* **279,** 384 (1979).
5. Margon, B., Ford, H. C., Grandi, S. A. & Stone, R. P. S. *Astrophys. J. Lett.* **233,** L63 (1979).
6. Fabian, A. C. & Rees, M. J. *Mon. Not. R. astr. Soc.* **187,** 13P (1979).
7. Abell, G. O. & Margon, B. *Nature* **279,** 701 (1979).
8. Murdin, P., Clark, D. H. & Martin, P. G. RGO Preprint (1980).
9. Margon, B. in *Galactic X-ray Sources* (Proc. Nato Summer School, in the press).
10. Clark, D. H., Green, A. J. & Caswell, J. L. *Austr. J. Phys. Astrophys. Suppl.* **37,** 75 (1975).
11. Gottlieb, E. W. & Liller, W. IAU Circ. No. 3354 (1979).
12. McGraw, J., Starrfield, S., Angel, R. & Carleton, N. *IAU Circ.* No. 3363 (1979).
13. Leibowitz, E. M., Mazeh, T. & Sternberg, A. *IAU Circ.* No. 3414 (1979).
14. Glass, I. S. *IAU Circ.* No. 3363 (1979).
15. Margon, B., Grandi, S. A. & Downes, R. A. UCLA Preprint No. 85 (1980).
16. Liller, W., *et al. Bull. Am. astr. Soc.* **11,** 732 (1979).
17. Impey, C. D. *IAU Circ.* No. 3379 (1979).
18. Wynn-Williams, C. G. & Becklin, E. E. *Nature* **282,** 810 (1979).
19. Giles, A. B., King, A. R., Cooke, B. A., McHardy, I. M. & Lawrence, A. *Nature* **281,** 282 (1979).
20. Allen, D. A. *Nature* **281,** 284 (1979).
21. Bopp, B. W., Evans, D. S., Laing, J. D. & Deeming, T. J. *Mon. Not. R. astr. Soc.* **147,** 355 (1970).
22. Giles, A. B. *IAU Circ.* No. 3419 (1979).
23. Kemp, J. C., Barbour, M. S., Arbabi, M., Leibowitz, E. M. & Mazeh, T. *Astrophys. J. Lett.* **238,** L26 (1980).
24. Gladyshev, S. A., Kurochkin, N. E., Novikov, I. D. & Cherepashchuk, A. M. *Astr. Circ.* No. 1086 (1979).

0028–0836/80/330691—03$01.00

Ultrasonic imaging in scanning electron microscopy

G. S. Cargill III*

Cavendish Laboratory, Madingley Road, Cambridge CB3 0HE, UK

A new type of microscopy is described here which uses a focused, modulated electron beam to generate ultrasonic waves at the front surface of a specimen and a piezoelectric transducer to detect these waves at the rear surface. The transducer output is used to form a scanned, magnified image of the specimen. A unique feature of this technique is that image contrast comes primarily from spatial variations in thermal and elastic properties. Images of integrated circuits have been obtained with ~4 μm resolution. In thin film specimens 0.1 μm resolution should be possible.

This mode of ultrasonic imaging in scanning electron microscopy is called electron-acoustic microscopy in analogy with photoacoustic microscopy[1–5] in which a laser is similarly used to generate acoustic or ultrasonic waves by thermoelastic expansion. An advantage of electron-acoustic microscopy is that the electron beam can be focused to a much smaller spot than is possible with visible light; and with proper attention to problems of electron beam spreading within the specimen, this can lead to improved spatial resolution. Although the present experiments have used 6 MHz beam chopping and 1 μm spot size, GHz chopping[6] could be used with a more finely focused electron beam to obtain ~0.1 μm resolution in thin film specimens. Only slight modifications to a commercial scanning electron microscope are needed to chop the electron beam at MHz rates. Secondary electron images can be recorded as well as electron-acoustic images, permitting easy comparisons of microscopic features revealed by the two different techniques. Electron-acoustic images can be viewed at normal SEM scan rates.

Table 1 Contributions of beam spreading d_S and of thermal diffusion d_T to the effective source diameter D*

	Au	Cu	Al	Si
d_S	0.7	1.4	4.8	5.5
d_T	2.5	2.5	2.1	1.6
D	2.8	3.0	5.3	5.8

* A 30 keV incident electron beam of diameter $d_B = 1$ μm is chopped at $\omega/2\pi = 6$MHz for thick specimens of Au, Cu, Al, and Si. All values are given in micrometres.

Major components of the electron-acoustic microscope are indicated in Fig. 1. Electrostatic deflection plates were located below the second condenser lens of a Stereoscan S4-10 SEM. Sinusoidal and d.c. voltages on the deflection plates were adjusted to produce square-wave beam current. Lenses were adjusted for maximum peak current at the specimen, typically 10 μA, with a 1.2 mm final aperture and 30 kV accelerating voltage. In most cases a 12 mm diameter, x-cut quartz 6-MHz transducer crystal was bonded with 'Durofix' cement to the bottom surface of a threaded metal plug, as in Fig. 1*b*, and the specimen to be examined was bonded onto the top of the plug and connected to earth through it. The transducer output, after amplification, rectification and black level suppression, controlled the intensity of the display cathode-ray tube.

Electron-acoustic images obtained with the beam striking either an aluminium plug (Fig. 1*b*) or the upper electrode of the transducer (Fig. 1*c*) consisted of irregular arrangements of bright and dark patches of about 0.5 mm size, which moved

---

* Present address: IBM Thomas J. Watson Research Center, Yorktown Heights, New York, 10598.

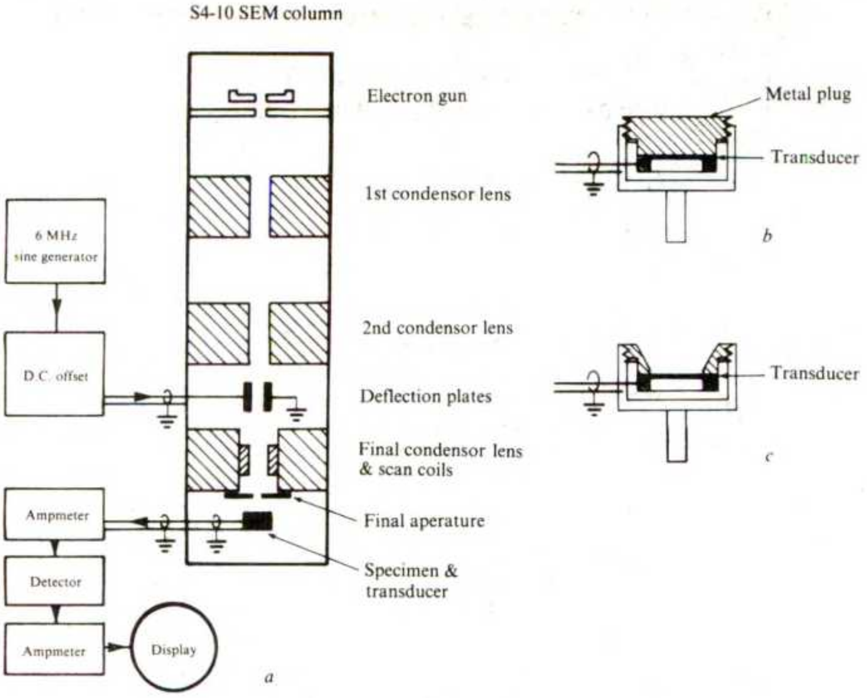

Fig. 1 Major components of the electron-acoustic microscope (*a*); and cross-section sketches of the transducer assembly, with the crystal bonded to the bottom of a metal plug (*b*), and without the metal plug (*c*).

about as the frequency was swept ±25 kHz. This contrast must have resulted from interferences involving reflected acoustic waves. Because the instantaneous transducer output is proportional to the average normal compression of the crystal, considerable cancellation is expected to occur for either of these arrangements.

Using a plug made from Invar, a low thermal expansion ($\alpha < 2 \times 10^{-6}$) alloy, instead of Al ($\alpha = 23 \times 10^{-6}$), greatly reduced the signal strength. A composite Invar-Al plug was also examined; electron-acoustic and secondary electron micrographs are shown in Fig. 2*a*. In the electron-acoustic micrograph the Invar is dark and the Al is covered with bright patches. These results are consistent with the contrast between Invar and Al being caused primarily by the larger thermal expansion of Al.

Electron-acoustic and secondary electron micrographs of Fig. 2*b* show a small area of an integrated circuit chip. In both micrographs the Al conductor lines are bright and the Si substrate, partially covered with silica, is dark. The contrast in parts of the secondary electron image is due to variations of the thickness of the silica, but this contrast is not so visible in regions covered by conductor lines. However, in the electron-acoustic image the brightness of the conductors and of the substrate is reduced over steps in the silica.

The resolution of such electron-acoustic micrographs is essentially the diameter of the region in which elastic waves are produced by periodic electron beam heating and is determined by (1) the incident beam diameter d_B, (2) the extent of beam spreading in the specimen d_S, and (3) the thermal diffusion length d_T. For the present experiments $d_B \simeq 1$ μm, including degradation caused by beam chopping. The penetration and spreading of the electron beam depend on accelerating voltage and on specimen composition and thickness. Values of d_S in Table 1 are estimates for thick specimens calculated with the simplified energy loss expression[7]

$$d_S(\mu\text{m}) = E_0^{1.43}/10\rho \tag{1}$$

where ρ is the density (g cm^{-3}) and E_0 is the incident electron energy (keV). Together, d_B and d_S determine the size of the region of energy disposition. Thermal diffusion further enlarges the source size by about the thermal diffusion length $d_T = (2K/\rho C\omega)^{1/2}$, where K is the thermal conductivity, C is the specific heat, and $\omega/2\pi$ is the frequency[8]. Values of d_T for several materials are given in Table 1, together with resulting estimates of total effective source diameters

$$D = (d_B^2 + d_S^2 + d_T^2)^{1/2} \tag{2}$$

This form of summation is commonly used in electron optics to estimate the effective beam diameter resulting from various lens aberrations (see, for example, equation 11 in ref. 9). For our

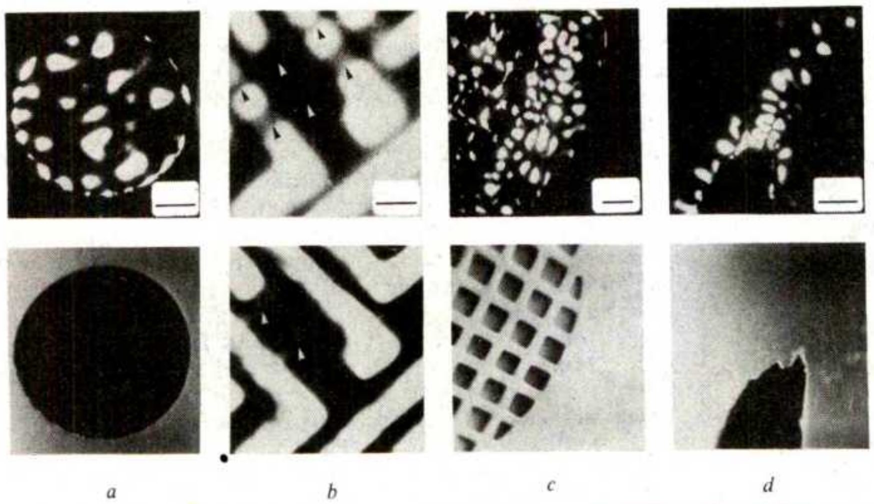

Fig. 2 Electron-acoustic (top) and secondary electron (bottom) micrographs: *a*, Al rod in Invar plug, scale bar, 0.5 mm; *b*, integrated circuit chip (arrows indicate steps in silica), scale bar, 10 μm; *c*, Cu grid on Cu plug, scale bar, 0.1 mm; *d*, hole in Al plug, scale bar, 0.5 mm.

experimental conditions, electron-acoustic micrographs are, therefore, expected to have resolutions of 3–6 μm, that is, much smaller than the wavelength $\lambda \approx 1$ mm, for longitudinal acoustic waves.

Contrast in electron-acoustic images involves both generation and propagation of ultrasonic waves. For simple cases of elastic wave generation by transient surface heating, White has shown that the stress amplitude for a given absorbed power density is proportional to $\zeta = B\alpha(K\rho C)^{-1/2}$, where B is the bulk modulus[8]. Values of ζ for Invar (<1.0), Al (3.1), and Si (1.1) (in units of 10^7 dyn s$^{1/2}$ cal^{-1}) are qualitatively consistent with contrast in electron-acoustic images of Fig. 2*a*,*b*.

Although contrast for flat, homogeneous specimens seems to depend mainly on ζ, under some circumstances other factors are also important. Thermoelastic expansions produced by the chopped electron beam are more effective in producing ultrasonic signals when they are well matched to the frequency and spatial characteristics of normal vibrational modes of the material being examined. For example, flexural modes of the 13-μm thick Cu grid in Fig. 2*c* are more efficiently excited than are vibrations in the copper plug to which the grid is glued. Although acoustic signals passing from the grid through the plug to the transducer are somewhat attenuated in the glue bond, the average signal from the grid is stronger than that from the plug. The bright spots on the electron-acoustic image are the antinodes of the 6-MHz normal mode pattern.

An example of contrast from subsurface features is shown in Fig. 2*d*. The specimen was a 6-mm high Al plug with a 1.6-mm diameter hole intersecting its upper surface at 6.5°. Only the exit hole is visible in the secondary-electron image. However, in the electron-acoustic image a collection of bright spots of high acoustic signal strength follow the course of the hole until it reaches a depth $z \approx 0.1$ mm below the surface, about 20 times the source depth $D_z = (d_S^2 + d_T^2)^{1/2}$. The magnitude of thermoelastic expansion will not be affected by subsurface features which are well below this source depth. The subsurface hole is seen in the electron-acoustic image mainly through its effect on the propagation and interference of ultrasound. However, sensitivity to subsurface features at depths $z \gg D_z$ is expected to be poor in the present experiments, because the acoustical wavelength λ is much larger than the source diameter D, producing a strongly diverging acoustic wave. Subsurface sensitivity and resolution should be improved by using a much higher frequency so that $\lambda \ll D$.

These results indicate that electron-acoustic microscopy can be used to examine some thermal and elastic properties of solids on a truly microscopic scale. This capability should be particularly useful in studies of defects and inhomogeneities in amorphous solids and in investigations of biological materials. Examination of specimens which are susceptible to electron beam damage may require using lower accelerating voltages and coating specimens with thin, electron opaque films.

Support from the SRC and from Churchill College is acknowledged. Dr W. C. Nixon provided guidance on electron beam deflection methods. Dr G. J. Curtis, AERE Harwell, provided advice and equipment for detecting ultrasonic signals. I thank Drs L. M. Brown and A. Howie for valuable suggestions.

Note added in proof: Examples of lower resolution electron-acoustic images at 100 kHz have recently been reported[10].

Received 16 June; accepted 11 July 1980.

1. von Gutfeld, R. J. & Melcher, R. L. *Appl. Phys. Lett.* **30,** 257–259 (1977).
2. Wickramasinghe, H. K., Bray, R. C., Jipson, V., Quate, C. F. & Salcedo, J. R. *Appl. Phys. Lett.* **33,** 923–925 (1978).
3. Luukkala, M. & Penttinen, A. *Electron. Lett.* **15,** 325–326 (1979).
4. Rosencwaig, A. & Busse, G. *Appl. Phys. Lett.* **36,** 725–727 (1980).
5. Rosencwaig, A. *J. appl. Phys.* **51,** 2210–2211 (1980).
6. Menzel, E. & Kubalek, E. *SEM/1979/I, SEM Inc.*, AMF O'Hare, 305–317.
7. Reimer, L. *SEM/1979/II, SEM Inc., AMF O'Hare*, 111–124.
8. White, R. M. *J. appl. Phys.* **34,** 3559–3567 (1963).
9. Oatley, C. W., Nixon, W. C. & Pease, R. F. W. *Adv. Electron. Electron Phys.* **21,** 181–247 (1965).
10. Brandis, E. & Rosencwaig, A. *Appl. Phys. Lett.* **37,** 98–100 (1980).

Polymerization of phosphazene crystal by plasma-exposure

Yoshihito Osada*†, Masafumi Hashidzume†, Eishun Tsuchida‡ & Alexis T. Bell§

†Department of Chemistry, College of Liberal Arts and Science, Ibaraki University, Mito 310, Japan
‡Department of Polymer Chemistry, Waseda University, Tokyo 160, Japan
§Department of Chemical Engineering, University of California, Berkeley, California 94720

Attempts to polymerize hexachlorocyclotriphosphazene $(PNCl_2)_3$ by high-energy irradiation methods in the solid state have failed to give a significant amount of the polymer. We report here that $(PNCl_2)_3$ crystals can be polymerized quite easily when exposed to a low-pressure radio-frequency plasma. The polymerization takes place almost simultaneously with the plasma-exposure. The monomer conversion increases with the plasma power as well as plasma-duration. The product is a white, rubber-like material having a similar appearance to the elastomer obtained by thermal polymerization. The IR spectrum shows the same backbone structure as that obtained by thermal polymerization. It has also been found that post-polymerization takes place at elevated temperatures following a brief exposure (1–5 min) of plasma onto phosphazene crystals.

During the past decade, the chemistry of poly(phosphazene) has undergone significant development, following the demonstration that $(PNCl_2)_3$ could be polymerized thermally to a soluble high polymer[1] and the chlorine atoms substituted by various organic groups[2]. The presence of phosphorous and nitrogen in the backbone of these polymers causes the wide range of physical and chemical properties and their high temperature resistance[3].

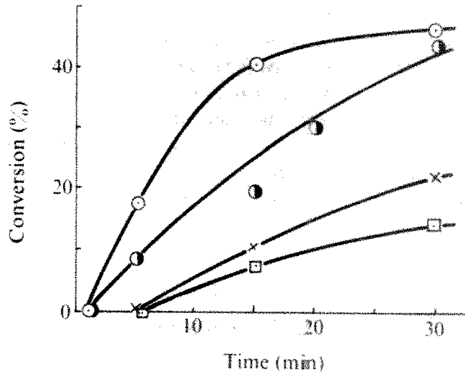

Fig. 1 Monomer conversion versus plasma duration for the polymerization of $(PNCl_2)_3$ at different power levels. Plasma power: ⊙, 110W, ◑, 90W; ×, 70W; ⊡, 50W. The plasma was sustained at 0.1 torr and room temperature.

$(PNCl_2)_3$ is usually polymerized by heating the molten monomer *in vacuo* at temperatures of 250–300 °C for 1–2 days (ref. 4). Below these temperatures, monomer conversions of only a few per cent conversion per day are observed. An attempt[5] to polymerize this cyclic compound in the solid state by γ-radiation has failed to give any significant amount of polymer at dosages, up to 10^6–10^8 rad. Irradiation by 4-MeV electrons with a dose of 10^9 rad at −70, 25 and 120 °C *in vacuo* gave only 1–2% of an insoluble product, in spite of the high dose[6]. The only example of solid-state polymerization of $(PNCl_2)_3$ is that observed using 50 keV X-ray radiation[7]. A maximum of 10% conversion of the monomer to an elastomeric polymer was

---

* To whom correspondences and reprint requests should be addressed.

0028-0836/80/330693—02$01.00

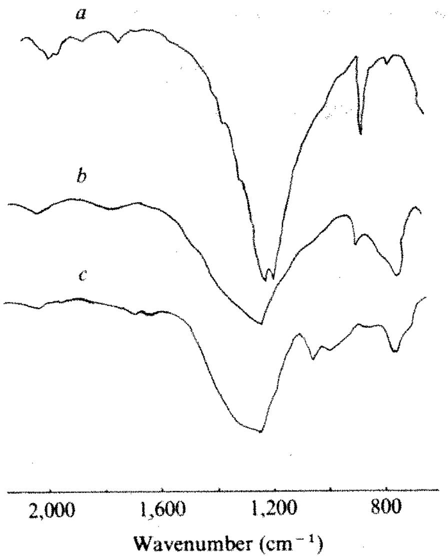

Fig. 2 IR spectra of (PNCl$_2$)$_3$ (*a*) and polymers obtained by thermal polymerization (260 °C, 15 h) (*b*), and plasma exposed polymerization (110W, 30 min) (*c*).

observed when the monomer was maintained near the melting point (114 °C) and irradiated for 40 h at a dose rate of 1.2 Mrad h^{-1}.

We have now found that (PNCl$_2$)$_3$ crystals can be polymerized quite easily when exposed to the effects of a low-pressure radio-frequency plasma. Plasma exposure was carried out on sublimed (PNCl$_2$)$_3$ crystals (Nippon Seika Chemistry Incorporated) placed in a glass ampule which was inserted between a pair of parallel-plate electrodes connected to an RFG-200 radio-frequency generator (Samco International Incorporated), operating at 13.56 MHz. The ampule was evacuated and a room temperature glow discharge was initiated in the phosphazene vapour remaining in the ampule. Following plasma-exposure, the samples were washed thoroughly with *n*-hexane to remove any unpolymerized material.

The polymerization of phosphazene takes place quite rapidly on plasma exposure, and the monomer conversion increases with the plasma power as well as the plasma-duration (Fig. 1). An oily product is formed in the very initial stage of the polymerization. The final product, however, is a white, rubber-like material having a similar appearance to the elastomer obtained by thermal polymerization. Figure 2 shows IR spectra of the phosphazene polymers obtained by plasma exposure and thermal polymerization, and demonstrates that the same backbone structure is obtained by both polymerization methods. Cross-linking might occur through labile chlorine atoms during the plasma exposure, because the observed chlorine content in the polymer decreased slightly, relative to that in the monomer, and a new absorption band attributed to P–O bond appeared near 1,040 cm^{-1}. Postpolymerization has been found to occur at elevated temperatures following a brief exposure of the phosphazene crystals. As shown in Fig. 3, (PNCl$_2$)$_3$ exposed to a plasma for 1 or 5 min undergoes postpolymerization up to certain level at 180 or 220 °C, whereas no polymerization takes place in these conditions for (PNCl$_2$)$_3$ without plasma exposure.

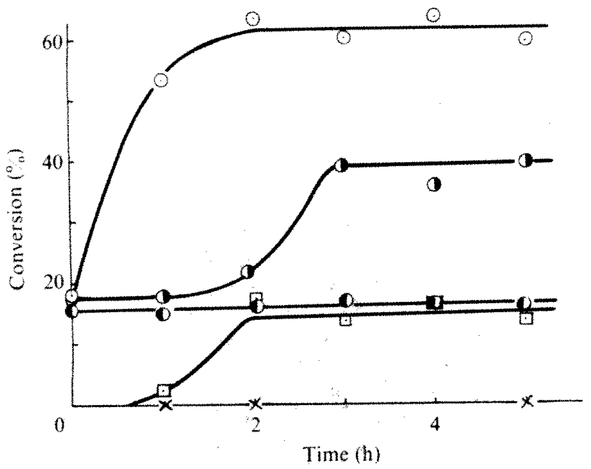

Fig. 3 The effect of time on the postpolymerization of (PNCl$_2$)$_3$. Plasma power, 110W; plasma duration and temperature of postpolymerization: ○, 5 min, 220 °C; ◑, 5 min. 180 °C; ◐, 5 min, 140°C; ⊡, 1 min, 180°C; ×, no plasma, 220 °C.

A mechanism for the polymerization of (PNCl$_2$)$_3$ under the effects of a low-pressure plasma has not yet been determined. Thermal polymerization is considered to be a minor component, however, as extensive polymerization takes place when the gas temperature in the plasma was maintained below 160 °C or the phosphazene crystals were kept at temperatures as low as −20 °C.

This research was supported in part by a Grant-in Aid from the Ministry of Education, Japan, grant 455351 (1979).

Received 24 March; accepted 26 June 1980.

1. Allcock, H. R. & Kugel, R. L. *J. Am. chem. Soc.* **87**, 4216 (1965).
2. Allcock, H. R., Kugel, R. L. & Valan, K. J. *Inorg. Chem.* **5**, 1709 (1966).
3. Tate, D. P. *J. Polym. Sci.* **C48**, 33 (1974).
4. Allcock, H. R. *Science* **193**, 1214 (1976).
5. Manley, T. R. *Nature* **184**, 899 (1959).
6. Spindler, M. W. & Vale, R. L. *Macromolec. Chem.* **43**, 237 (1961).
7. Caglioti, V., Cordischi, D. & Mele, A. *Nature* **195**, 492 (1962).

Configuration at C-24 in steranes and sterols

J. R. Maxwell, A. S. Mackenzie & J. K. Volkman

Organic Geochemistry Unit, University of Bristol, School of Chemistry, Cantock's Close, Bristol BS8 1TS, UK

Most marine and terrestrial organisms and aquatic sediments contain sterols with an alkyl group at C-24. Assignment of the configuration at this position has important biosynthetic, taxonomic and geochemical implications[1–3]; for example, it is required to elucidate biosynthetic pathways responsible for alkylation[1,2], and to reveal sources of sterols in species where there is no *de novo* synthesis[4,5] and in recent sediments[3,6]. Similarly, routine separation of the C-24 isomers of steranes in sedimentary rocks (formed from sterols present at the time of deposition) should provide information on the nature of the contributing organisms and the isomerization reactions thought to occur in steranes with increasing depth of burial and the associated temperature rise[7,8]. Using an extension of gas chromatographic (GC) methods applied previously to the separation of stereoisomers of acyclic isoprenoid acids[9] and alkanes[10], we report here (1) the complete separation of (24*R*)-24-methyl-5α-cholestane (I) from its C-24 isomer (II in Fig. 1), the partial separation of (24*R*)- and (24*S*)-24-ethyl-5α-cholestane (III and IV), (2) the application of these separations to a study of the C-24 configuration in the steranes of a sedimentary rock and a petroleum and in those from reduction of the sterols of a marine coccolithophorid, and (3) similar separations of the corresponding 3β-OH saturated C$_{28}$ and C$_{29}$ alcohols as acetates (stanol acetates).

To date, assignment of the C-24 configuration in steroidal compounds has relied on X-ray crystallography[3,6], differences in melting points[11], optical rotation measurements[12,13] or chemical shifts in ^{1}H nuclear magnetic resonance (NMR) spectra[14]. These

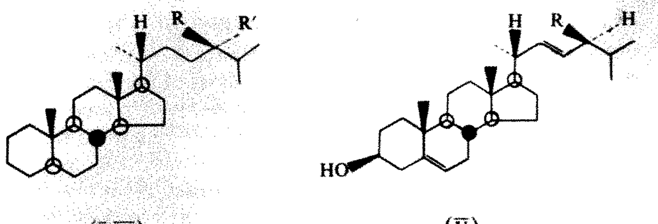

(I-IV) (V)

Fig. 1 Structural formulae of C-24 alkylated steranes (I–IV) and major free sterol of *E. huxleyi* (V). (I), R = CH_3; R' = H. (II), R = H;R^1 = CH_3. (III), R = C_2H_5; R^1 = H. (IV), R = H; R^1 = C_2H_5.

methods typically require a few milligrammes of the isolated compound and their application to studies of the components of small quantities of complex mixtures is limited.

Chromatographic separation of C-24 isomers of sterols or steranes has proved difficult[15–17]. The only report describes partial separation of milligramme quantities of (24*R*)-24-methyl-5α-cholestane (I) and its 24*S* isomer (II) on alumina[18]. In these conditions, previous separation of coeluting steranes is required[7]. Figure 2*a* shows the partial chromatogram of a 50:50 mixture (quantitated accurately by spiking with 5α- and 5β-cholestane) of (24*R*)- and (24*S*)-methyl-5α-cholestanes ((I) and (II)) obtained with a Carlo Erba Fractovap (series 2151) chromatograph fitted with a 100 m × 0.24 mm glass column, roughened and deactivated by the barium carbonate technique of Grob *et al.*[19], and coated statically[20] with a dichloromethane

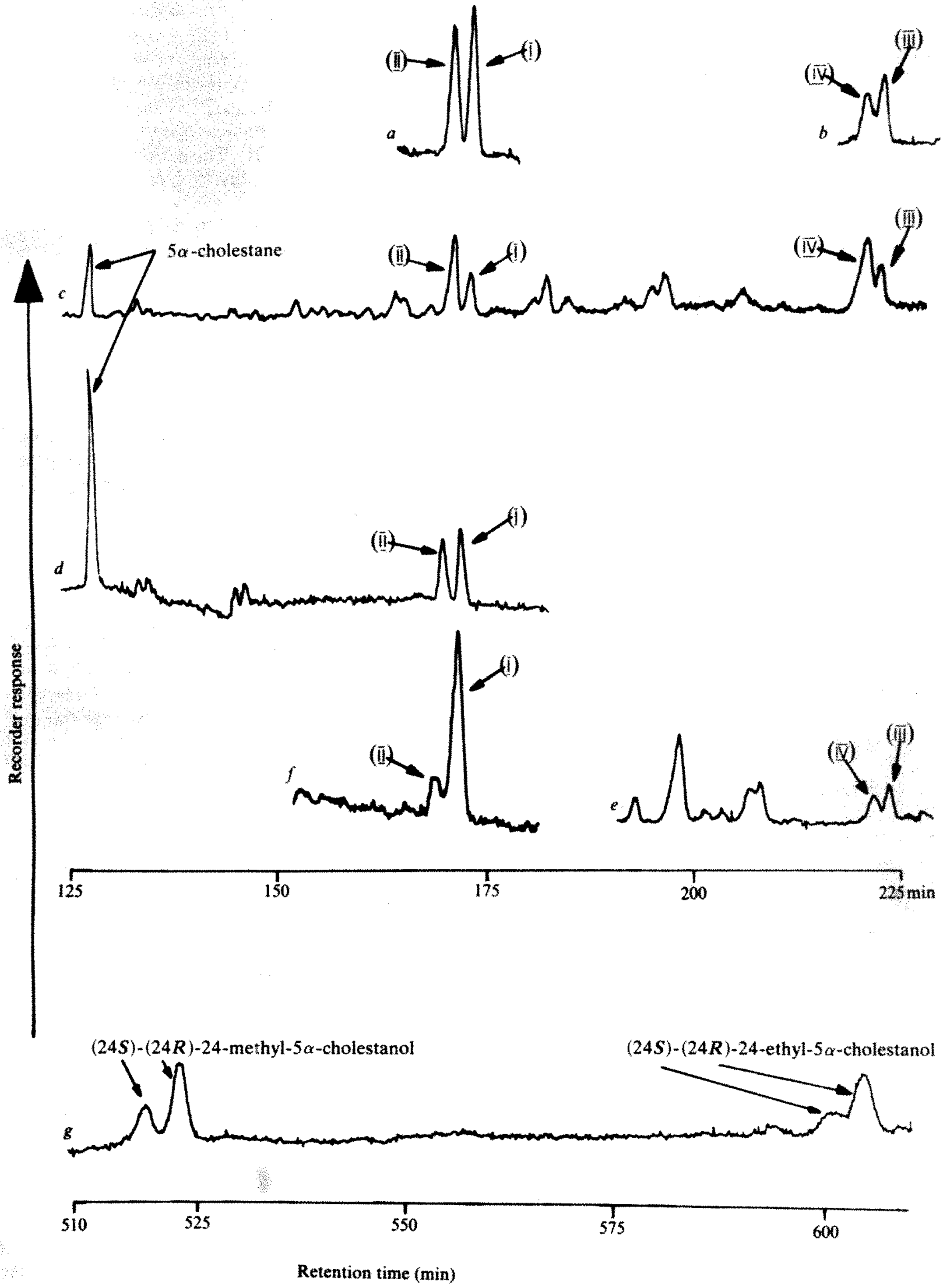

Fig. 2 Partial gas chromatograms of: *a*, 50:50 mixture of (24*R*)- and (24*S*)-24-methyl-5α-cholestanes; *b*, 50:50 mixture of (24*R*)- and (24*S*)-24-ethyl-5α-cholestanes; *c*, Green River shale branched and cyclic alkanes; *d*, thiourea adduct of Rozel Point crude oil branched and cyclic alkanes; *e*, thiourea non-adduct of Rozel Point crude oil branched and cyclic alkanes; *f*, steranes from reduction of the free desmethylsterols of *E. huxleyi*; and *g*, 5α-stanols (as acetates) from a recent sediment. (For conditions, see text.)

solution of diethylene glycol succinate (DEGS) and polyethylene glycol succinate (PEGS) (75:25; wt:wt) to produce a 0.06 µm film; H_2 was the carrier gas (2.3 kg cm^{-2} back pressure ~7.5 cm^3 min^{-1}); the oven was programmed from 40 to 160 °C at 4 °C min^{-1} and then maintained at 160 °C. Figure 2*b* shows partial separation of a 50:50 mixture of (24*R*)- and (24*S*)-24-ethyl-5α-cholestane ((III) and (IV)) (quantitated as above) in the same conditions. Elution orders were established in both cases by co-injection, with (II) and (IV) respectively, and amounts injected were 5–15 ng of each component. Although both standard mixtures comprise equal amounts of the two isomers, the peak heights are not equal. This is most apparent for the ethylcholestanes (Fig. 2*b*) where there is a contribution to the second eluting 24*R* isomer peak from the first eluting 24*S* isomer. The areas of the two methylcholestane peaks are equal so the first eluting 24*S* isomer peak is slightly broader (Fig. 2*a*).

The method has been used to separate the steranes in samples of the Green River shale (Colorado, Eocene) and Rozel Point crude oil (Utah, unknown age), as the C-24 stereochemistry of certain steranes has been assigned previously by ^{1}H NMR[7]. Steranes whose nuclear and C-20 stereochemistry differs from that of the presumed precursor sterols have been reported from sedimentary rocks and petroleum[7,8,17], but discussion is limited here to those which are isomeric at C-24 and which have the same configuration as the original sterols at all other chiral centres (that is, 5α, 8β, 9α, 14α, 17α(H), 20*R*). GC analysis of the branched and cyclic alkane fraction from the shale sample indicated a 75:25 mixture of (24*S*)-24-methyl-5α-cholestane (II) and the 24*R*-isomer (I), and a 75:25 mixture of the 24*S* C_{29} sterane (IV) and its C-24 isomer (III; Fig. 2*c*). These ratios are the same as those obtained independently by ^{1}H NMR[7]. The branched and cyclic alkane fraction of the crude oil was too complex for analysis without further fractionation and was subjected to thiourea adduction (twice)[21]. As expected[22], the 24-ethyl-5α-cholestanes were essentially not adducted, whereas 24-methyl-5α-cholestanes were almost completely adducted. GC analysis of the adduct and non-adduct showed, as determined previously by ^{1}H NMR, the 24-methyl- and 24-ethyl-5α-cholestanes to be present in 50:50 mixtures of 24*R* abnd 24*S* epimers (Fig. 2*d*, *e*) when compared with the mixtures of the standards. Adduction of the standards revealed no detectable fractionation at C-24.

Thiourea adduction is required for the analysis of the steranes of most shales and oils. The non-adduct is, however, sometimes too complex for direct GC analysis of the C-24 configuration in 24-ethyl-5α-cholestanes and problems of co-elution with other components are occasionally encountered in evaluation of the 24-methyl-5α-cholestanes in the adduct. Analysis of the 24-methyl-5α-cholestanes (in conditions of partial separation) from a suite of Toarcian shales from the Paris Basin shows a preference for the (24*S*) isomer (60:40 in favour of 24*S*) in samples with a mild thermal history, which is lost on increased burial depth[8]. The preservation of a preference for 24*S* components in those shales with a mild thermal history may relate to the sterols of the source organisms. Most algae and fungi seem to produce 24β (24*S* where the side chain is saturated) sterols, whilst most higher plant sterols are 24α[1,2]. However, there are exceptions and plants can contain both configurations[23,24].

The C-24 stereochemistry in sterols is related to alkylation reaction mechanisms[1,24]. Biosynthetic, taxonomic, and marine studies would clearly benefit from a routine method of separating C-24 isomers and which could be applied to the small quantities of complex mixtures commonly encountered. Hydrogenolysis/hydrogenation of two sterols, (24*S*)-24-methylcholesta-5,22E-dien-3β-ol and (24*R*)-24-ethylcholesta-5,22E-dien-3β-ol, by bubbling H_2 through a suspension of the sample (~50 µg) and PtO_2 (1 mg) in glacial acetic acid (5 cm^3) containing perchloric acid (1 drop) produced (after 4 h) yields of ~60% of sterane. The 5α-stanol acetate (~20%) and the free 5α-stanol (~20%) were also produced, but no unreacted sterol was recovered. GC analysis of the steranes showed evidence of a small extent of isomerization during the reaction, and a ratio of 4.2-4.5:1 of the two C-24 isomers in favour of the original configuration was observed. This minor extent of isomerization has already been noted by ^{1}H NMR analysis of the products of hydrogenation of certain sterols[25]. No isomerization was detected when sterols with no side chain double bond were hydrogenolysed/hydrogenated.

The technique of analysis of the steranes resulting from hydrogenolysis/hydrogenation has been applied to the study of the major free sterol of the microscopic marine coccolithophorid, *Emiliania huxleyi*, family Gephyrocapsaceae[26]. This ubiquitous marine alga[27,28] has given rise to extensive calcium carbonate (coccolith) deposits in many deep-sea areas, including the Black Sea[29]. It is remarkable in that it biosynthesizes a novel carotenoid, 19′-hexanoyloxyfucoxanthin[30] and C_{37}–C_{39} straight chain alkenes and alkenones which are abundant in many sediments[31,32]. Gas chromatographic/mass spectrometric analysis of the free desmethylsterol fraction as the TMSi ethers, using conditions described previously[6], showed 24-methylcholesta-5,22E-dien-3β-ol as the major component. The fraction was hydrogenolysed/hydrogenated as above and similar products and yields were obtained. Without purification, the products were analysed by GC on DEGS/PEGS and (24*R*)-24-methylcholestane and (24*S*)-24-methylcholestane were found to be present in the ratio 4.3:1 (Fig. 2*f*). The major free sterol of *E. huxleyi* is, therefore, (24*S*)-24-methylcholesta-5,22*E*-dien-3β-ol (V that is, 24α).

The latter isomer is the same as that produced by the diatoms, *Phaeodactylum tricornutum*[5] and *Nitzschia closterium*[33], and it is interesting that the fatty acid composition of *E. huxleyi* is also similar to those of the diatoms[34]. Phytoflagellate[34] *Ochromonas* spp. (Chrysophyceae) produce sterols with the opposite C-24 configuration to that in *E. huxleyi*[1,11] and such differences may be useful in the classification of many such microscopic algae, which can be difficult[26].

Attempts to avoid the reduction step and extend the method to the direct examination of steroidal alcohols have been partly successful. Partial separations of C_{28} and C_{29} stanol acetate isomeric pairs were obtained (Fig. 2*g*) after elution times ~9–10 h (conditions as above, but programming from 40° to −190 °C at 4 °C min^{-1}), but no separation of $\Delta^{5,22}$ steryl acetates isomeric at C-24 has been achieved.

The examples described show clearly the value of the technique in (1) the study of the sterane distributions of sedimentary rocks, and (2) structural studies of sterols in organisms. These preliminary results also suggest that the approach will be useful in assigning the input sources of sterols in sediments. Many of these samples contain complex mixtures with varying degrees and positions of unsaturation, and fractionation by argentation thin layer chromatography[35] before reduction should prove useful. Definition of the sources of sedimentary sterols also requires routine determination of the C-24 configuration of sterols biosynthesized and/or incorporated by a variety of individual organisms and the GC approach should allow rapid screening of small quantities of complex mixtures.

We thank NERC (GR3/2951 and GR3/3758) for GC/MS facilities, Drs L. J. Mulheirn and G. Ryback for donating steranes and Rozel Point alkane fraction, Mr P. A. Comet for the stanol acetate mixture, and Dr A. M. K. Wardroper for helpful discussions. A.S.M. also thanks the SRC for a Studentship and J.K.V. gratefully acknowledges support from NERC (GR3/3419).

Received 1 May; accepted 13 June 1980.

1. Goad, L. J., Lenton, J. R., Knapp, F. F. & Goodwin, T. W. *Lipids* **9**, 582–595 (1974).
2. Patterson, G. W. *Lipids* **6**, 120–127 (1971).
3. Lee, C., Gagosian, R. B. & Farrington, J. W. *Org. Geochem.* **2**, 103–113 (1980).
4. Nes, W. R. *Lipids* **9**, 596–612 (1974).
5. Rubinstein, I. & Goad, L. J. *Phytochemistry* **13**, 485–487 (1974).
6. Wardroper, A. M. K., Maxwell, J. R. & Morris, R. J. *Steroids* **32**, 203–221 (1978).
7. Mulheirn, L. J. & Ryback, G. *Nature* **256**, 301–302 (1975).
8. Mackenzie, A. S., Patience, R. L., Maxwell, J. R., Vandenbroucke, M. & Durand, B. *Geochim. cosmochim. Acta* (in the press).
9. Ackman, R. G., Cox, R. E., Eglinton, G., Hooper, S. N. & Maxwell, J. R. *J. chromatogr. Sci.* **10**, 392–401 (1972).

10. Patience, R. L., Rowland, S. J. & Maxwell, J. R. *Geochim. cosmochim. Acta* **42,** 1871–1875 (1978).
11. Gershengorn, M. C. *et al. Biochemistry* **7,** 1698–1706 (1968).
12. Bernstein, S. & Wallis, E. S. *J. org. Chem.* **2,** 341–345 (1938).
13. Lenfant, M., Lecompte, M. F. & Farrugia, G. *Phytochemistry* **9,** 2529–2535 (1970).
14. Rubinstein, I., Goad, L. J., Clague, A. D. H. & Mulheirn, L. J. *Phytochemistry* **15,** 195–200 (1976).
15. Anderson, R. A., Brooks, C. J. W. & Knights, B. A. *J. Chromatogr.* **75,** 247–259 (1973).
16. Brooks, C. J. W., Henderson, W. & Steel, G. *Biochim. biophys. Acta* **296,** 431–445 (1973).
17. Seifert, W. K. & Moldowan, J. M. *Geochim. cosmochim. Acta* **43,** 77–96 (1979).
18. Ryback, G. *J. Chromatogr.* **116,** 207–210 (1976).
19. Grob, K., Grob, G. & Grob, K. Jr *Chromatographia* **10,** 181–187 (1977).
20. Bouche, J. & Verzele, M. *J. Gas Chromatogr.* **6,** 501–505 (1968).
21. Murphy, M. T. J., McCormick, A. & Eglinton, G. *Science* **157,** 1040–1042 (1967).
22. Mulheirn, L. J. & Ryback, G. in *Advances in Organic Geochemistry 1975* (eds Campos, R. and Goni, J.) 173–192 (ENADIMSA, 1977).
23. Mulheirn, L. J. *Tetrahedron Lett.* 3175–3178 (1973).
24. Nes, W. R. *et al. Lipids* **12,** 511–527 (1977).
25. Thompson, M. J., Dutky, S. R., Patterson, G. W. & Gooden, E. L. *Phytochemistry* **11,** 1781–1790 (1972).
26. Parke, M. & Dixon, P. S. *J. mar. Biol. Ass. U.K.* **56,** 527–594 (1976).
27. McIntyre, A. & Bé, A. W. H. *Deep Sea Res.* **14,** 561–597 (1967).
28. Okada, H. & Honjo, S. *Deep Sea Res.* **20,** 355–374 (1973).
29. Bukry, D. in *The Black Sea—Geology, Chemistry and Biology* (eds Degens, E. T. & Ross, D. A.) 353–363 (AAPG Memoir 20, 1974).
30. Arpin, N., Svec, W. A. & Liaaen-Jensen, S. *Phytochemistry* **15,** 529–532 (1976).
31. Volkman, J. K., Eglinton, G., Corner, E. D. S. & Sargent, J. R. in *Advances in Organic Geochemistry 1979* (eds Douglas, A. G. & Maxwell, J. R.) (Pergamon, Oxford, in the press).
32. De Leeuw, J. W., v.d. Meer, F. W. & Rijpstra, W. I. C. in *Advances in Organic Geochemistry 1979* (eds Douglas, A. G. & Maxwell, J. R.) (Pergamon, Oxford, in the press).
33. Orcutt, D. M. & Patterson, G. W. *Comp. Biochem. Physiol.* **50B,** 579–583 (1975).
34. Chuecas, L. & Riley, J. P. *J. mar. Biol. Ass. U.K.* **49,** 97–116 (1969).
35. Morris, L. J. *J. Lipid Res.* **7,** 717–732 (1966).
36. Ling, N. C., Hale, R. L. & Djerassi, C. *J. Am. Chem. Soc.* **92,** 5281–5282 (1970).

Thermoluminescence dating of volcanic plagioclases

G. Guérin & G. Valladas

Centre des Faibles Radioactivités Laboratoire mixte CNRS-CEA,
91190 Gif-sur-Yvette, France

Thermoluminescence (TL) is a well-established archaeological dating[1] technique but the most common mineral in volcanic rocks, plagioclase feldspar, is affected by 'anomalous fading' which prevents its use for dating lava flows. We describe here how the α contribution to annual dose rate is calculated. Plagioclase ages are compared with those obtained by ^{14}C, K–Ar and TL dating on quartz. Our samples come from the Chaîne des Puys (Massif Central, France). We conclude that TL is a promising tool for dating continental lava flows in the range 3,000–300,000 yr BP.

The intensity of light emitted during thermal stimulation of a mineral is related to the radiation dose it has accumulated since its last heating (palaeodose). A basic assumption that the electronic trapping states responsible for the TL emission are stable. A routine check, the 'plateau' test, consists of plotting the ratio of the natural TL to the increment of TL induced by a laboratory-added radiation dose (artificial TL, ATL) against temperature; a constant value must be reached above a certain temperature. However, as shown by Wintle[2], most volcanic plagioclases do not have a plateau in the usual temperature range of study (620–720 K). Thus, the maximum ages obtained by TL are too small by as much as an order of magnitude. This effect was attributed to a spurious loss of electrons from their traps in the 620–720 K temperature region where the mean life of charge carriers should be larger than 10^5 yr. Bailiff's[3] has made promising attempts to avoid anomalous fading using phototransfer.

The study of high temperature TL emission (700–1,000 K) of plagioclases is restricted to the UV spectrum because having to cut off the black-body thermal emission necessitates using a thick glass UV filter. In such conditions, we have already suggested[4] that glow peaks might be unaffected by anomalous fading.

Figure 1*Aa* shows the natural TL glow curve of a Labrador aliquot (from Olby flow); Fig. 1*Ab* is the glow curve obtained when a 16 krad dose is added to another aliquot of the same weight. The ratio of the natural TL to the increment of TL induced by the added dose is plotted in Fig. 1*B*. There is no plateau but a tendency for stabilization above 850 K which indicates the onset of a region of different behaviour. As already described for quartz[5], we try to eliminate the lower temperature TL emission by preheating. Figure 1*C* shows the plateau test in different conditions of preheating. Figure 1*Cc* (850 K, for 1 min) is rather flat which indicates that the remaining glow peak is a constant function of temperature.

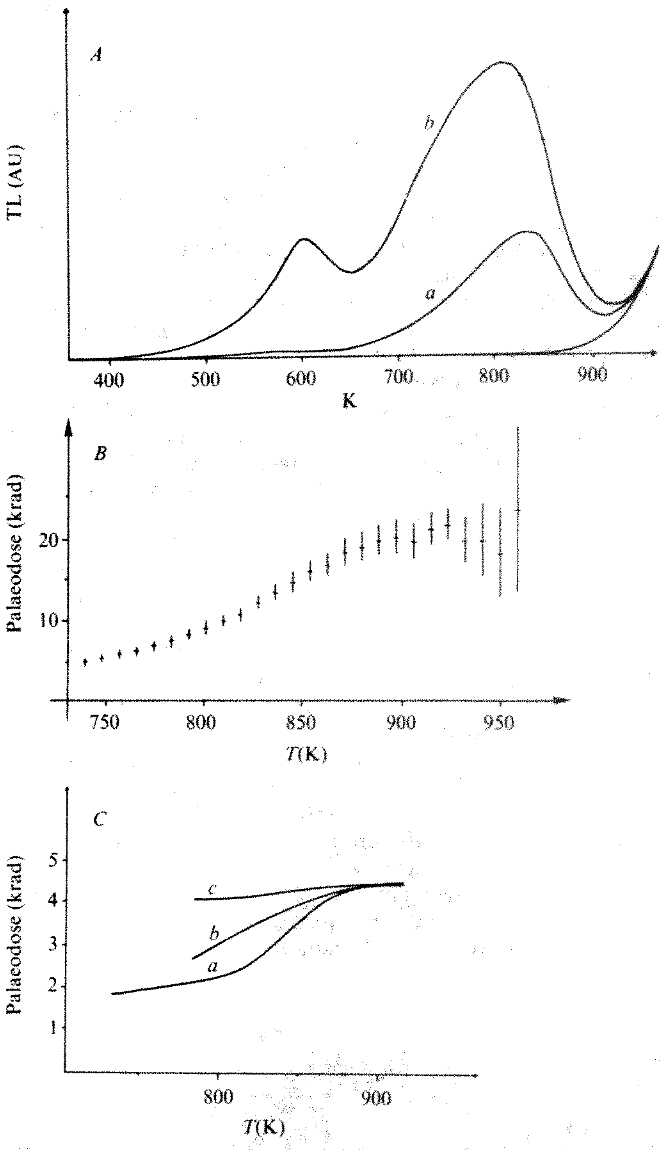

Fig. 1 *A*, TL glow curves of Olby Labrador: *a*, TLN; *b*, TLN+16 K. *B*, Plateau test of Olby plagioclase. *C*, Plateau curves for Saint-Saturnin preheated plagioclase: *a*, 1 min 735 K; *b*, 1 min 781 K; *c*, 1 min 832 K.

Wintle[2] has pointed out that anomalous fading mainly occurs soon after the sample has received an artificial radiation dose. To check for short-term fading we determined the apparent dose remaining after one year of storage of a lava sample from the Olby flow which had been previously heated to 960 K for 4 h, cooled and γ irradiated at 7.395 ± 187 rad at low dose rate. The apparent measured dose 7.238 ± 293 rad agrees with the deposited dose.

In such conditions there was no evidence of short-term fading; although these two arguments usually allow a mineral to be used for TL dating, they cannot be assumed on a geological time scale. Therefore, we studied lava flows of known age from the Chaîne des Puys (Massif Central, France)[6].

0028–0836/80/330697—03$01.00

Table 1 *a*, U, Th and K content of the plagioclase samples; *b*, radiation properties of the plagioclase samples

a	U (p.p.m.)	Th (p.p.m.)	K_2O (%)	*b*	Palaeodose (krad)	Supralinearity (krad)	D_α (mrad yr^{-1})	D_β (mrad yr^{-1})	D_γ (mrad yr^{-1})
St Saturnin	1.70	6.18	1.75	St Saturnin	4.57 ± 0.36	0.60	249.8	161.9	87.1
Laschamp	1.77	9.10	2.14	Laschamp	15.6 ± 1.20	0.40	177.1	193.5	108.2
Puy Laschamp	1.90	6.85	1.78		15.6 ± 1.20	2.30	212.5	165.0	91.9
Olby	2.40	8.83	2.02	Olby	20.20 ± 1.60	0.50	219.4	198.1	114.4
Egaules	1.08	7.20	1.51	Egaules	20.15 ± 1.00	2.70	65.6	136.3	77.9
Montgreleix	1.73	6.28	1.63	Montgreleix	61.50 ± 4.90	9.60	126.8	154.4	85.6
Mazoires	2.00	7.00	1.59	Mazoires	79.50 ± 8.10	Negligible	115.2	153.4	89.8

TL measurements were done on plagioclases ranging from andesine to labrador, carefully extracted from the lava by gentle crushing, and separated by sieving heavy liquid and magnetic techniques. We selected a grain size of 80–125 μm to remove finer microlites and to keep only the microphenocrysts. TL glows were measured with a glass filter (325 nm) which allows a maximum temperature of 1,100 K. The heating rate is generally 5 Ks^{-1} to 10 $K s^{-1}$, artificial irradiations were carried out with a ^{137}Cs γ source (4.02 rad s^{-1}). After preheating, usually at 830 K for 1 min, the plagioclases all presented a single glow peak around 920 K (5 $K s^{-1}$, heating rate).

The palaeodose is obtained by comparing natural TL with artificial TL, a supralinearity correction is included which results from a non-linear initial increase of the TL signal as a function of the dose (saturation curve). This correction is estimated from the second glow. Annual β and γ dose rates are computed from U–Th and K contents, measured by γ-ray spectrometry with a Ge–Li detector (Table 1*a*), using Bell's data[7]. There is no grain size correction for β radiation from K because the internal K content measured with an EDAX electron-microprobe does not substantially differ from the average K content of the lava. The very small correction, <1% of the total dose, for the β radiation from U and Th families, is neglected. Because of the very high efficiency of α particles in the production of TL in plagioclases (about five times higher than quartz), the α contribution to the annual dose rate is important even when using a grain size of 100 μm. Indeed, the TL induced by α radiation may reach one-third of the total TL as shown in Table 1*b* where the palaeodose, supralinearity correction, and the annual dose rates for α, β and γ radiation are given.

α-dosimetry present problems mainly because of the short average range of α particles in matter. We must, therefore, know the repartition of the α emitters in the middle where the plagioclase is naturally irradiated. With a resolution of several microns, comparable with the range of α particles, fission track mapping can represent U distribution in the lava. As seen in Fig. 2 microphenocrysts of plagioclase and olivine near 100 μm have a low U content. Hence the average U or Th concentration of the total lava does not accurately represent the actual concentration seen by the feldspar. As Th and U are strongly linked from a geochemical point of view, we can assume that their distributions are not very different. Thus, a single figure will relate the concentration of U in the plagioclase to the concentration of U or Th of the total rock, for example N_0, the ratio of the peripheral fission track density to the mean density of tracks in the thin section.

In the lava, a plagioclase grain is submitted to an omnidirectional flux of α particles of various energies. To simulate this flux, we used calibrated laboratory α sources and vibrated the plagioclase grains so that they were irradiated in many positions. For each α particle, omnidirectional experimental α flux was related to the equivalent γ dose which would have produced the same TL; this is termed $\chi(E)$. Up to an energy of 9 MeV, $\chi(E)$ can be fitted by a straight line cutting the χ energy axis at 500 keV. The energy spectrum of α particles from U and Th families, when they are in secular equilibrium (which is checked by our spectrometry measurements) leads to global factors $\hat{\chi}_U$ and $\hat{\chi}_{Th}$ which relate the natural omnidirectional flux to the equivalent γ dose:

$$\hat{\chi}_{U(Th)} = \frac{\int_0^{E_{\max}} \chi(E) \frac{dn}{dE}_{U(Th)} dE}{\int_0^{E_{\max}} \frac{dn}{dE}_{U(Th)} dE}$$

Note that, while assuming $\chi(E)$ to be linear, $\hat{\chi}_U$ is very close to

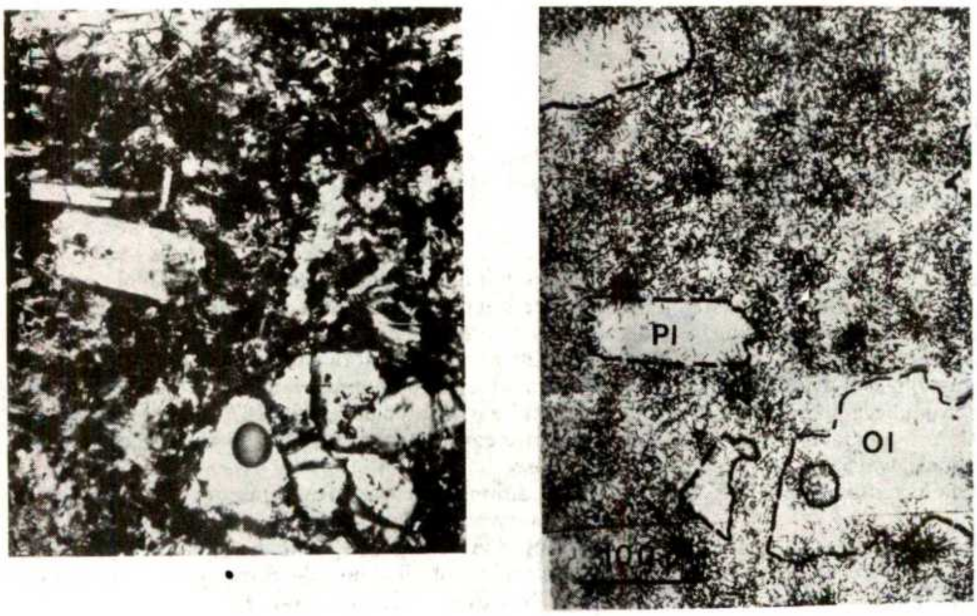

Fig. 2 Photograph of the thin section of St-Saturnin basalt and its fission track mapping. Ol, Olivine; Pl, plagioclase (Labrador).

χ(3.06 MeV) and $\hat{\chi}_{\mathrm{Th}}$ to χ (3.40 MeV). Then the contribution to the dose of α particles external to the grain can be written:

$$D = N_0(\hat{\chi}_{\mathrm{Th}}\phi_{\mathrm{Th}} + \hat{\chi}_{\mathrm{U}}\phi_{\mathrm{U}})$$

where $\hat{\chi}_{\mathrm{U}}$ and $\hat{\chi}_{\mathrm{Th}}$ do not differ much. ϕ_{Th} and ϕ_{U} are the omnidirectional fluxes, respectively, due to Th and U determinated for the total rock. Moreover, we do take into account the U (or Th) generally present inside the grain (<0.2 p.p.m.). The internal contribution to the dose can be written with a similar formula to that of the external α dose but the value of χ is obtained using a grain size of a few micrometres (fine grains technique)[12]. In general, the internal α dose rate contribution approximately represents 25% of the α dose (8% of the total annual dose rate).

Table 2 TL dated plagioclase samples compared with conventional techniques

	TL	Conventional	
St Saturnin	8,980 ± 1,150	7,880 ± 350	^{14}C*
		8,100 ± 1,100	TL (clay)†
Olby	37,300 ± 3,500	42,000 ± 3,000	TL (Q)‡
		39,000 ± 6,000	U-Th§
Laschamp	31,900 ± 2,850	34,300 ± 3,000	TL (Q)‡
	32,500 ± 3,100		
Egaules	69,580 ± 6,500	75,000 ± 7,500	K–Ar‖
Montgreleix	163,300 ± 14,500	175,000 ± 13,000	K–Ar‖
Mazoires	215,800 ± 20,500	242,000 ± 10,000	K–Ar‖

* Revised from Pelletier *et al.*[8] using a 5,730 yr half life for ^{14}C.
† Revised from Huxtable and Aitken[9].
‡ Revised from Valladas[10] TL dating on quartz, with revised calibration of reference sources.
§ Revised from Condomines[11].
‖ Revised from Gillot (unpublished work) K–Ar dating on mesostase; Egaules age is an upper limit.

Finally, the estimation of the α dose rate is carried out with an accuracy not much better than 20%.

When crushing the rock the plagioclases are fragmented which leads to an overestimate of χ and an underestimate of the age. For example, if 30% of the 100 μm plagioclases had an initial size of 200 μm, the age obtained would be 4% too low[13]. This correction has not been applied to the present data.

Our first results are shown in Table 2, and compared with the ages obtained using more conventional techniques. The agreement of TL dated plagioclases is good and indicates that within our experimental error, ±8%, there are no major systematic errors.

We conclude that high-temperature TL emission is not systematically affected by either anomalous fading or by thermal fading and can be used for dating volcanic flows. As saturation doses of plagioclases are around 400 krad, TL allows dating continental volcanics from 3,000 to 300,000 yr BP.

Received 28 January; accepted 5 June 1980.

1. Aitken, M. J., Zimmermann, D. W. & Fleming, S. J. *Nature* **219**, 442–445 (1968).
2. Wintle, A. G. *Nature* **245**, 143–144 (1973).
3. Bailiff, I. K. *Nature* **264**, 531–533 (1976).
4. Valladas, G. & Valladas, H. *Proc. 18th int. Symp. Archaeometry*, Bonn (1978).
5. Valladas, G. *Proc. 18th int. Symp. Archaeometry*, Bonn (1978).
6. Gillot, P. Y. *et al. Earth planet. Sci. Lett.* **42**, 444–450 (1979).
7. Bell, W. T. *Archaeometry* **19**, 99–100 (1977).
8. Pelletier, H., Delibrias, G., Labeyrie, J., Perquis, M. T. & Rudel, A. *C.r. Acad. Sci. hebd Séance, Paris* **214**, 2221–2222 (1959).
9. Huxtable, J. & Aitken, M. J. *Nature* **275**, 207–209 (1978).
10. Valladas, G. *et al. A Specialist Seminar on TL Dating*, Oxford 1978, PACT 165–173 (Council of Europe, Strasbourg, 1978).
11. Condomines, M. *Nature* **276**, 257–258 (1978).
12. Zimmerman, D. W. *Archaeometry* **13**, 29–52 (1971).
13. Bell, W. T. *Ancient TL* No. 2 (in the press).

Palaeomagnetism of beach ridges in South Australia and the Milankovitch theory of ice ages

Mart Idnurm

Bureau of Mineral Resources, Canberra ACT 2601, Australia

Peter J. Cook

Research School of Earth Sciences, Australian National University, Canberra ACT 2600, Australia

Although the Pleistocene glaciations continue to attract new explanations[1–3], an early explanation in terms of secular variations of the Earth's orbital elements, the Milankovitch theory[4], has recently gained considerable support[5,6]. This theory predicts insolation variations with periodicities of ~20,000, 40,000 and 100,000 yr. Its popularity is attributable mostly to deep-sea sediment information on variations of the glaciation-sensitive ^{16}O/^{18}O isotopic ratio and the increasingly convincing match of those variations to the Milankovitch climatic curves[7–9]. Independently, land-based evidence is accumulating in favour of the Milankovitch theory from raised coral terrace[10], loess[11], and pollen studies[12]. We discuss here evidence for the Milankovitch theory from a South Australian sea-level record.

In the south-east corner of South Australia, a beach ridge sequence extends approximately parallel to the present-day coast line for some 250 km. It is best developed between Robe, on the coast, and Naracoorte, 100 km inland, where eight ridge systems containing 13 well defined parallel beach ridges occur (Fig. 1). The sequence ranges in altitude from near sea level at Robe to ~100 m at Naracoorte. To the east of Naracoorte the ridges become progressively less well defined but remain recognizable for a further 200 km inland. Offshore from Robe there are at least two more beach ridges representing low sea levels[13]. Detailed drilling of the Robe–Naracoorte sequence[14] has revealed that the ridges are composed of cross-bedded calcarenite, with the lower part of the sequence deposited in beach or near-beach conditions and the upper part in aeolian conditions. In general, the stratigraphy is consistent with a prograding coastal sequence developed on a slowly uplifted region, the beach ridges representing successive high sea-level stands. Sprigg[13,15,16] has argued that the Robe–Naracoorte sequence and the Milankovitch insolation curves are in good agreement, assuming that the sea-level variations were caused by melting of glaciers during periods of high insolation at critical northern latitudes. Sprigg's comparisons have, however, lacked a time scale based on biostratigraphic or absolute ages. We now date the sequence by polarity reversal, and use this age to test the Milankovitch theory.

Ten of the best preserved ridges were hand sampled between Robe and Naracoorte (Fig. 1). The material was fine- to medium-grained calcarenite composed of a framework of fine abraded biogenic material, quartz, and rare feldspar grains, all coated to varying degrees with iron oxides. Opaque grains, particularly iron sesquioxides, were rare. The cement varied from sparite to microsparite. The sediments ranged from semi-consolidated to well consolidated and their colour varied from yellow to pale reddish brown. Obvious pedogenic modifications, such as colour mottling or pronounced calcretization, were avoided during sampling. Except for the initial work, when a Digico spinner magnetometer was used, all measurements were made with an ScT cryogenic magnetometer. Thermal demagnetization, usually at 50 °C increments, was used to analyse the remanence. Magnetic susceptibilities were determined between heatings to monitor mineralogical changes.

0028–0836/80/330699—04$01.00

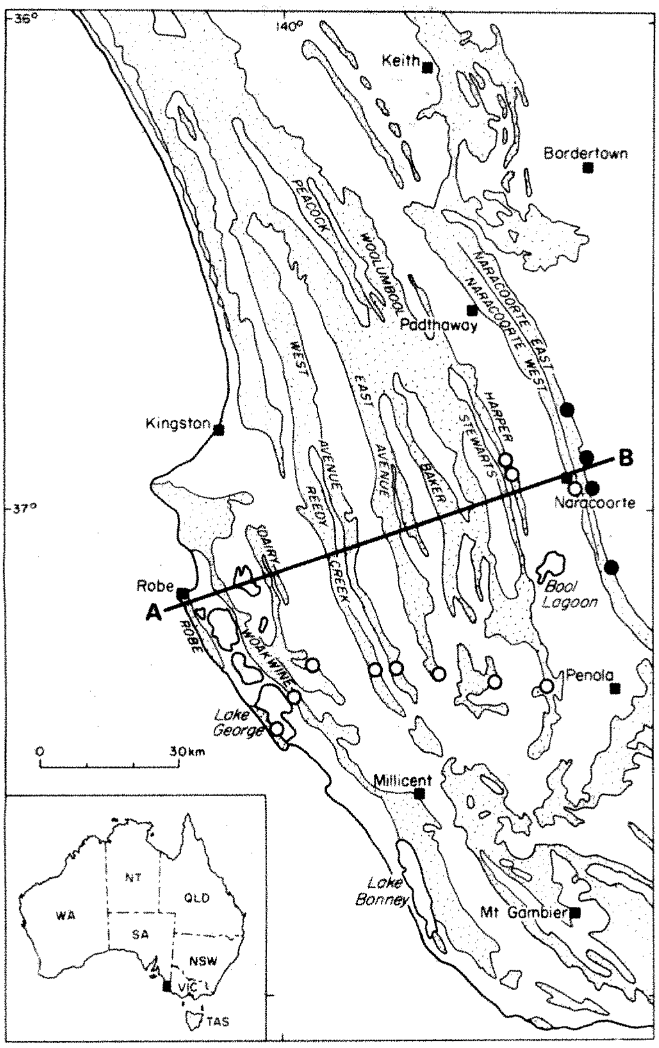

Fig. 1 The beach ridge sequence in southeastern South Australia. Open symbols indicate sampling sites with normal polarity, closed symbols indicate reversed polarity sites.

The NRM intensities ranged from 0.5 to 5 mA m^{-1}. Generally two components of magnetization were observed: a relatively low blocking temperature component which was interpreted as partly a laboratory-storage effect and partly a recent-field effect, and a harder component that exhibited normal polarity for all samples (20) collected between Robe and the West Naracoorte ridge system, and reversed polarity at the East Naracoorte ridge system (Fig. 1). Figure 2 shows thermal demagnetization behaviour of samples collected from ridges adjacent to the polarity reversal. This polarity reversal marks the 720,000 yr Brunhes–Matuyama boundary[17] and provides, for the first time, an age constraint for the ridge sequence. The presence of reversed polarity at the East Naracoorte ridge system was confirmed by sampling at different localities across the ridge and along the ridge axis (nine samples).

The measurements were complicated by an increase in magnetic susceptibility during heatings. This increase was associated with the generation of spurious moments and eventually led to a pronounced magnetic viscosity. In specimens where the onset of the spurious moments was delayed, a third stable magnetization component of very low intensity (0.1–0.2 mA m^{-1}) and high blocking temperature could be isolated. This component showed random directions between different specimens prepared from the same sample.

The most likely origin for the primary remanence is chemical, resulting from processes such as dehydration of iron oxyhydroxides and graingrowth of haematite beyond the critical superparamagnetic grain volume[18]. A detrital origin for the remanence (DRM) is inconsistent with the high-energy beach-aeolian depositional environment of the sediments. A post-depositional origin (PDR) seems unlikely because the filling of pore space by the calcite cement would have displaced and misoriented any aligned grains in the matrix. The authigenic haematite occurs as pigment in the cement and as coatings on the surfaces of framework grains, and is related to the processes of reddening of dune sands. The hard component of remanence, characterized by random directions, apparently results from the rare unaligned detrital iron sesquioxide grains in the sediments. While acknowledging that pedogenic processes could overprint and, if sufficiently intense, destroy any Matuyama magnetic epoch remanence, we believe that the intermediate blocking temperature component represents the primary chemical remanence in the samples collected. The absence of obvious pedogenic modifications, such as colour mottling, in the material selected for palaeomagnetic work, suggests that such processes are not significant. The effects of continued graingrowth, post-dating the Brunhes–Matuyama reversal, are more subtle and remain problematic.

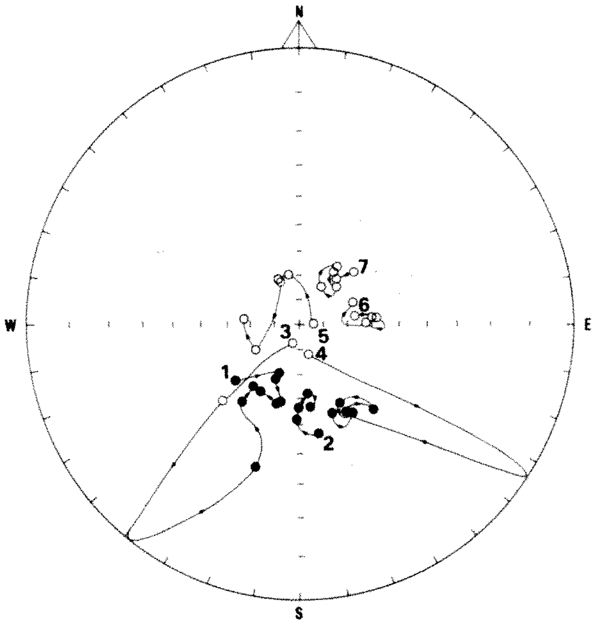

Fig. 2 Remanence directions in beach ridges adjacent to the Brunhes–Matuyama reversal boundary. The diagram shows thermal demagnetization behaviour of seven samples at 100 °C increments commencing from NRM. The arrows indicate directions of increasing heat treatments. Solid symbols correspond to positive inclinations, open symbols to negative inclinations. Samples 1–4 are from two different sites in ridge system 9; samples 5 and 6 are from ridge system 8; and sample 7 is from ridge 7b.

There was probably a time lag between ridge formation and the acquisition of chemical remanence. This time lag would have to be added to the Brunhes–Matuyama reversal date to obtain the true age of deposition. In Victoria, siliceous dunes redden down to 2 m depth within 20,000 yr of deposition. However, more calcareous dunes seem to take significantly longer, possibly of the order of 30,000 yr, for reddening to the same depth (ref. 19 and J. Bowler, personal communication). Bearing in mind that chemical remanence is likely to be acquired before the final stage of reddening has been reached, we may expect the time lag between dune formation and acquisition of chemical remanence to be <30,000 yr. Assuming a remanence acquisition time lag of 30,000 yr, and a depositional time of 30,000 yr for the ridge systems (the average value estimated from the secondary ridge

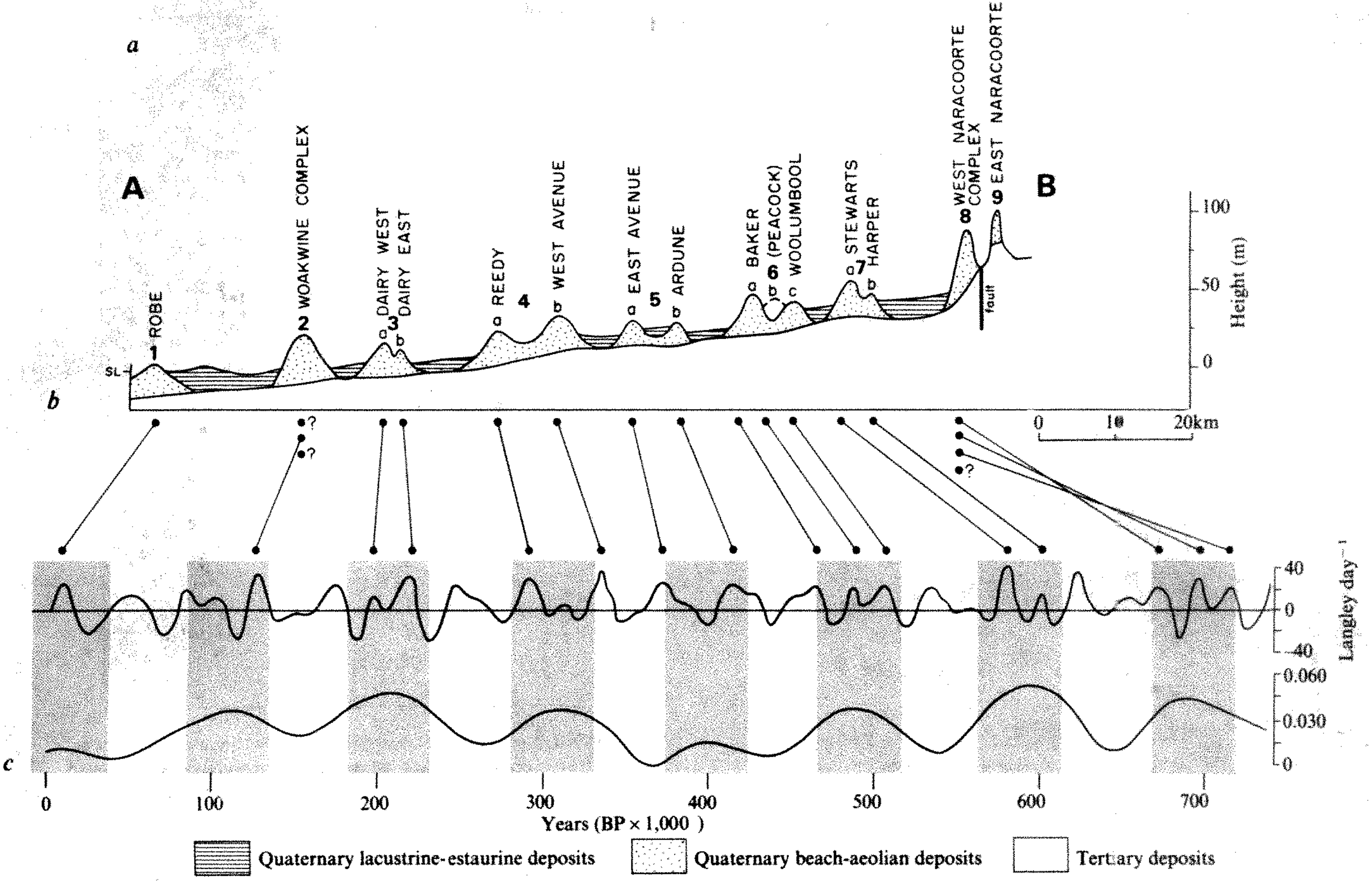

Fig. 3 *a*, Section AB of Fig. 1 through the beach ridges. Ridges 2 and 8 are compound dunes. The Peacock Ridge, which is not intercepted by the line AB, is shown by the broken outline. *b*, Summer insolation in langleys day^{-1} at latitude 65° N relative to the 1950 AD values (after ref. 20). The stippled intervals indicate interpreted interglacial phases of the (approximately) 100,000-yr climatic cycle. Tentative correlations between ridges and insolation maxima are shown by interconnecting lines. *c*, Variations in orbital eccentricity (after ref. 20).

spacings by linear interpolation between the centre points of the ridge systems which are assumed as a first approximation to be 100,000 yr apart), the mean age of the West Naracoorte ridge system is estimated as 665,000–735,000 yr, depending on the exact location of the Brunhes–Matuyama boundary between those two ridge systems. From the surface expression of the ridges (Fig. 3) and from subsurface drilling information[14], eight high sea-level ridge systems are recognized between Robe and Naracoorte where the sequence seems best differentiated. Assuming that no major ridge systems are telescoped (that the uplift has been continuous, though not necessarily at an absolutely constant rate), the average periodicity of the major ridge systems is obtained as 95,000–105,000 yr (~100,000 yr). A dominant 100,000-yr cyclicity has been found in other climatic records[7,11,12]. Most of the ridge systems contain more than one dune, suggesting the possibility of shorter-period changes in the sea-level record.

A tentative interpretation of the raised beach ridges in terms of Berger's[20] modified Milankovitch insolation curves for latitude 65° N, and the dominant 100,000-yr cyclicity, is shown in Fig. 3. The interpretation is based on the assumptions that the ridges form only during high sea-level stands and that these occur at a particular phase of the 100,000-yr cycle. It also has to satisfy two time constraints: an interglacial (ridge-forming) phase at present, and at 700,000 yr BP (during the deposition of the West Naracoorte complex). The interglacial phases for the sequence are then derived as shown by the stippling in Fig. 3. Note first that the interglacial phases coincide with high-orbital eccentricities. This agrees with the oxygen isotope results[7], but contradicts the Milankovitch theory that predicts eccentricity dependence in the opposite sense[20], and finds only a minor eccentricity contribution to climatic variation. Second, with the exceptions discussed below there is a one-to-one correlation between the ridges and principal insolation maxima belonging to the 100,000-yr interglacial phases. Third, the subsidiary ridge spacings agree qualitatively with the time intervals between the insolation maxima: the narrow (3 km average) spacings correspond to 20,000 yr intervals and the wide (7 km average) spacings, to 40,000 yr intervals (we assume here, in common with other sea-level studies[21–23], a relatively constant rate of tectonic uplift).

Problems with correlation occur in the West Naracoorte and Woakwine complexes, both of which are composed of superimposed dunes[14,15]. At West Naracoorte where the dunes are stacked against a fault pediment, some doubt exists over the presence of a fourth dune. At Woakwine correlation is possible with only the oldest of the three insolation peaks of the 85,000–135,000-yr interglacial phase: evidence from elsewhere[21–23] indicates that the high sea-level stands that would correspond to the two youngest peaks of the interglacial phase were well below the first stand. The superposition of Woakwine dunes, indicating repeated transgressions, cannot, therefore, be explained by the Milankovitch theory. Aharon *et al.*[24] have recently considered evidence for a non-Milankovitch sea-level high at 120,000 yr that seems to have reached the earliest high mark, and have proposed an Antarctic ice-surge[25] as the explanation.

Finally, we note the relevance of the present results to geoidal sea-level changes. The geodetic sea level contains regional irregularities that are subject to change, and any significant geoidal variation would modify the interpretation of sea levels in terms of glacio-eustatic changes[26]. Although, with the exceptions noted above, the present results are consistent with Milankovitch's predictions of climatic variation and do not require geoidal changes to be invoked, this does not rule out significant geoidal changes that occur in phase with Milankovitch glacio-eustatic changes, nor major geoidal changes with periods in excess of 700,000 yr.

We conclude that the South Australian ridge sequence contains components related to the Earth's orbital elements. Except for the dominance of the 100,000-yr component and its phase relative to the eccentricity variations, the ridge evidence is consistent with the Milankovitch theory.

We thank P. Aharon, J. M. A. Chappell, D. Denham, M. W. McElhinny and P. Wellman for comments. M.I. publishes with the permission of the Director, Bureau of Mineral Resources.

Note added in proof: Recent geochronological results (D. A. Schwebel, personal communication) confirm the interpreted age of the Woakwine complex.

Received 21 April; accepted 12 June 1980.

1. McCrea, W. H. *Nature* **255**, 607–609 (1975).
2. Öpik, E. J. *Ir. Astr. J.* **12**, 253–276 (1976).
3. Bray, J. R. *Nature* **260**, 414–415 (1976).
4. Milankovitch, M. in *Handbuch der Geophysik* (eds Koppen, W. & Geiger, R.) Vol 9 (1938).
5. Mason, B. J. *Quat. J. R. met. Soc.* **102**, 473–499 (1976).
6. Kukla, G. *Nature* **261**, 11 (1976).
7. Hays, J. D., Imbrie, J. & Shackleton, N. J. *Science* **194**, 1121–1132 (1976).
8. Berger, A. L. *Nature* **269**, 44–45 (1977).
9. Kominz, M. A., Heath, G. R., Ku, T.-L. & Pisias, N. G. *Earth planet. Sci. Lett.* **45**, 394–410 (1979).
10. Chappell, J. *Quat. Res.* **3**, 221–236 (1973).
11. Kukla, E. *Geol. För. Stockh. Förh.* **92**, 148–180 (1970).
12. Ruddiman, W. F. & McIntyre, A. *Geol. Soc. Am. Mem.* **145**, 111–146 (1976).
13. Sprigg, R. C. *Sed. Geol.* **22**, 53–96 (1979).
14. Cook, P. J. *et al. BMR J. Aust. Geol. Geophys.* **2**, 81–88 (1977).
15. Sprigg, R. C. *Geol. Surv. S. Aust. Bull.* **29** (1952).
16. Sprigg, R. C. *18th int. Geol. Congr. Proc.* **13**, 226–237 (1952).
17. McDougall, I. in *The Earth: Its Origin, Structure and Evolution* (ed. McElhinny, M. W.) 543–566 (Academic, London, 1979).
18. Haigh, G. *Phil. Mag.* **3**, 267–286 (1958).
19. Price, W. A. *Bull. geol. Soc. Am.* **73**, 1281–1289 (1962).
20. Berger, A. L. *Quat. Res.* **9**, 139–167 (1978).
21. Mesolella, K. J., Matthews, R. K., Broecker, W. S. & Thurber, D. L. *J. Geol.* **77**, 250–274 (1969).
22. Veeh, H. H. & Chappell, J. *Science* **167**, 862–865 (1970).
23. Chappell, J. & Veeh, H. H. *Bull. geol. Soc. Am.* **89**, 356–368 (1978).
24. Aharon, P., Chappell, J. & Compston, W. *Nature* **283**, 649–651 (1980).
25. Wilson, R. T. *Nature* **201**, 147–149 (1964).
26. Mörner, N.-A. *J. Geol.* **84**, 123–151 (1976).

Quaternary temperatures and precipitation for the north-west coast of North America

C. J. Heusser*, L. E. Heusser*† & S. S. Streeter†

* Department of Biology, New York University, Box 608, Tuxedo, New York 10987
† Lamont-Doherty Geological Observatory of Columbia University, Palisades, New York 10964

Palynologists utilize present-day pollen rain to interpret the climatic setting of pollen records from Quaternary deposits. Analogues are sought which relate the present with the past. Because climatic conditions at mid-latitudes during the Quaternary were diverse, often ranging from a tundra type at one extreme to a closed forest type at the other, a modern data set should cover the extremes of vegetation and climate expected during this time. For interpreting climatic parameters from Quaternary pollen in land and marine cores, we calculated a pair of regression equations relating modern pollen rain from the Pacific coastal forest and tundra to mean July temperature and mean annual precipitation at a series of sites from the Aleutian Islands to northern California. We describe here how application of these equations to Quaternary pollen profiles from western Washington enabled us to quantify temperature and precipitation over the past ~80,000 yr.

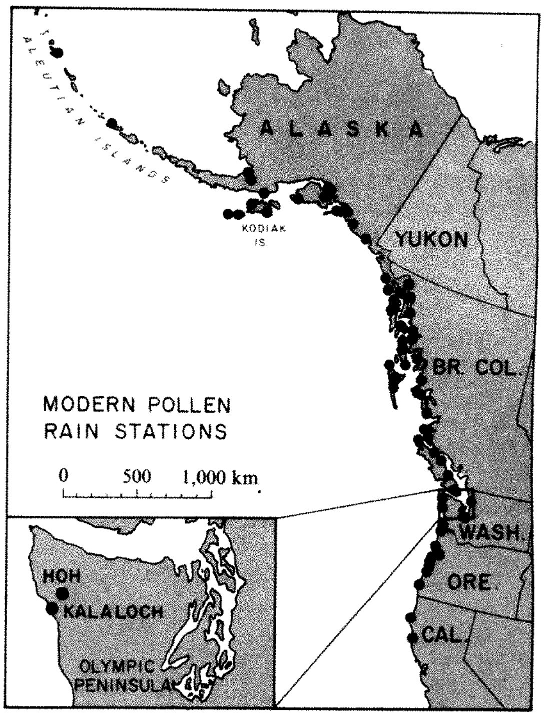

Fig. 1 Distribution of 59 composite sites on the north-west coast of North America showing where modern surface pollen was collected and the location of fossil pollen sites.

Temperate coniferous forest is the outstanding arboreal vegetation along >4,000 km of the north-west coast of North America between northern California and southwestern Alaska (36–61° N)[1,2]. In western Washington and southwestern British Columbia its leading constituents, western hemlock, Sitka spruce, and western red cedar, grow to their greatest proportions. Douglas fir and alder are widely distributed throughout this region chiefly because of disturbance. Southward into California, Douglas fir, pine and redwood rise in proportion in the communities, and a broadleaf sclerophyllous element, consisting notably of oak, tanoak, chinquapin and madrone, enters at the drier inland and southern limits of the forest. Northwestward in Alaska, the hemlock, spruce and cedar become mixed with other species, for example, mountain hemlock, Pacific silver fir and Alaska yellow cedar, which are montane-subalpine to the south. Lowland forest communities increasingly give way to muskeg and, at the same time, lose their complexity, so that on Kodiak Island and on the adjacent Alaska Peninsula, Sitka spruce alone forms the edge of the forest. Beyond this, westward to the Aleutian Islands, the forest is replaced by tundra, at first through an ecotone of shrubby alder and willow.

Optimum conditions of the maritime climate of Washington and British Columbia cause the long growing season and richness of coniferous species that are characteristic of the Pacific coastal forest in this region. Precipitation annually averages near 3,000 mm but decreases to 2,000 mm or less towards the interior; mean July temperature is ~14 °C on the coast and ~15 °C inland[3–7]. Precipitation is heaviest in southeastern Alaska–British Columbia and falls off to less than 1,000 mm in California and southwestern Alaska. July temperatures of 8–10 °C in coastal tundra rise by ~6° to ~16 °C in California.

Modern pollen rain data are for surface samples from 178 sites at <100 m in elevation located between Attu, furthest west of the Aleutian Islands in Alaska, and the vicinity of San Francisco in California. Data from the sites were consolidated in the form of 59 composite records (Fig. 1). This averaging process ensures that site data represent the broad features of the pollen rain[8]. Surface samples were mostly collected, and analysed by one of us (C.J.H.) to avoid inconsistencies in identification. Thirteen numerically important taxa selected for multivariate statistical analysis from 67 different kinds of pollen identified are pine, spruce, western hemlock, mountain hemlock, fir, Douglas fir, redwood, alder, birch, oak, grass, sedge and composite. Pollen values, percentages of the sum of the 13 taxa at each site, were row normalized and *Q*-mode, rotated principal components (factor) analysed[9]. Four resultant pollen factors, which are basically monotypic and account for 93% of the data, are western hemlock, alder, grass and pine. Although pollen rain has many sources of variation[8,10], the vegetation of the north-west coast as it varies geographically is the dominant control underlying the distribution of the pollen factors.

A stepwise regression relating the four factors to mean July temperature and annual precipitation yielded a pair of transfer functions (Table 1). Temperature and precipitation data used in calculating the equations were interpolated from 10-yr averages (1968–77) of records from 43 meteorological stations located near sea level between Attu and San Francisco[3-7]. The western hemlock and pine factors were found to be significant predictors of precipitation, and these along with the grass factor predicted temperature. Alder predicted neither variable at the 5% level of significance. The temperature and precipitation equations, respectively, have standard errors of 13% (1.1 °C) and 19% (620 mm) of the observed ranges. Plotting observed values against predicted values of temperature and precipitation show the residuals to be distributed normally.

The regression equations were applied to fossil pollen percentages (Fig. 1) obtained from a core taken in a bog in the Hoh River valley of western Washington and from a section of biogenic and alluvial sediments exposed in a seacliff some 23 km away near Kalaloch[11,12]. Pollen derived from the Hoh–Kalaloch sediments provides a continuous data base for the past ~80,000 yr. Chronostratigraphy is based on 14 ^{14}C dates reaching ~16,000 yr BP in the Hoh core and 14 ^{14}C dates extending from ~16,000 to >47,000 yr BP in the Kalaloch section.

The resulting curve of mean July temperature for the western Washington coast over the period of record shows a range from ~10 to 15 °C (Fig. 2). The modern mean of 14.5 °C differs from our best estimate of the actual mean by 0.3 °C. The high frequency fluctuations in the Kalaloch values, which partly reflect changes in rates of sedimentation in a fluvio-lacustrine complex, display two relatively warm intervals at ~60,000 and ~30,000 yr BP and the most protracted cold interval during the late Pleistocene. This latter, beginning ~28,000 yr BP and continuing until ~13,000 yr BP, was abruptly terminated by a rapid temperature increase of 3 °C. Amelioration continued until ~8,000 yr BP when temperature reached a maximum for all the time represented by the curve. Subsequent cooling after 8,000 yr BP seems to have been replaced only recently by a warming trend that continues to the present.

Application of the regression equation for mean annual precipitation to the Hoh-Kalaloch pollen data resulted in a curve with a range 1,300–2,400 mm (Fig. 2). The modern annual total is 600 mm less than that measured nearby but is within the error of estimation. Principal features of the curve are the direct relationship shown with temperature during the Pleistocene and the inverse relationship during the Holocene. The pervasive, relatively moist intervals, mostly between 2,000 and 2,400 mm, of the first 50,000 yr of record were replaced ~28,000 yr BP by an extended dry interval. Except for a brief peak in precipitation of 2,200 mm at ~18,000 yr BP, values were on the whole between ~1,300 and 1,600 mm. At the close of the Pleistocene, precipitation increased synchronously with temperature, reaching a maximum of >2,400 mm. It then decreased, as abruptly as it had increased, to a minimum of ~1,500 mm at ~8,000 yr BP which coincides with the time of the Holocene temperature maximum. Conditions of dryness and warmth ended relatively rapidly, and precipitation since has remained between ~2,200 and 2,300 mm except for a very recent drying trend.

Table 1 Transfer function equations for the north-west coast of North America

Variable (factors)		Regression coefficient
Equation NWNA-1 (July temperature)		
X_4	grass	−5.00737
X_1	western hemlock	−3.40429
X_3^2	pine × pine	−7.62694
X_3	pine	−6.34598
Intercept		15.02636
Equation NWNA-1 (Annual precipitation)		
X_1	western hemlock	1,216.99829
X_3	pine	−735.70166
Intercept		1,152.01180

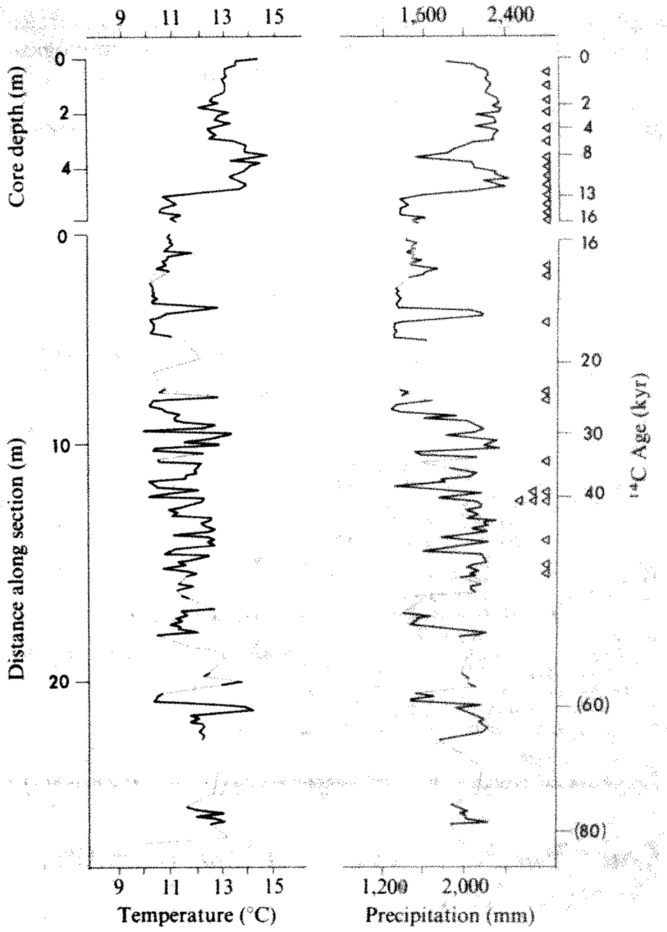

Fig. 2 Mean July temperature and annual precipitation for the past ~80,000 yr represented by the Hoh bog core (upper portion) and Kalaloch seacliff section (lower portion) in western Washington. Arrows indicate ^{14}C-dated levels; bracketed ages shown are estimates from finite ^{14}C ages and the rate of sedimentation. Dotted portions of the curves indicate samples with communalities of <0.5 which thus do not correspond strongly to the surface data set.

These results extend the application of multivariate statistics to North American Pleistocene pollen records earlier than the late-glacial. Transfer functions applied to pollen data previously yielded temperature estimates for the past 15,000 yr in Minnesota[13] and the past 5,500 yr in the Northwest Territories of Canada[14,15]. The curves generated by our data refine trends recorded for the Pacific slope of Washington on semi-quantitative grounds[16] and compare well with records of sea-surface temperature and oxygen isotope stratigraphy of the nearby continental rise[17,18]. The differences between Holocene interglacial and Pleistocene glacial modes generally agree with models of North Pacific region[19,20]. The glaciation periods during the Pleistocene were cold and relatively dry with ameliorated moist episodes intervening. During the Holocene, coolness was associated with greater precipitation, and intervals of warmth were drier. This suggests that the prevailing mechanism controlling climate on the north-west coast during the present interglaciation contrasts with the mechanism in effect during glaciation.

We thank R. F. Black and W. L. Coonrad for Alaskan surface samples, F. D. Manning for British Columbia meteorological data, and W. F. Ruddiman and J. T. Andrews for critical reviews. This work was supported by NSF grants DEB-7612561 A01 and DEB-7910505. An expanded version of this paper will be presented elsewhere.

Received 16 April; accepted 11 June 1980.

1. Waring, R. H. & Franklin, J. F. *Science* **204**, 1380–1386 (1979).
2. Heusser, C. J. *Am. Geogr. Soc. Spec. Pub.* 35 (American Geographical Society, 1960).
3. United States Department of Commerce Climatological Data Alaska *Annual Summary* (1968–77).
4. Canada Department of Transport *Canad. weath. Rev.* 6–15 (1968–77).
5. United States Department of Commerce Climatological Data Washington *Annual Summary* (1968–77).
6. United States Department of Commerce Climatological Data Oregon *Annual Summary* (1968–77).
7. United States Department of Commerce Climatological Data California *Annual Summary* (1968–77).
8. Webb III, T., Laseski, R. A. & Bernabo, J. C. *Ecology* **59**, 1151–1163 (1978).
9. Imbrie, J. & Kipp, N. G. in *Late Cenozoic Glacial Ages* (ed. Turekian, K. K.) 71–181 (Yale University Press, New Haven, 1971).
10. Wright Jr, H. E. *Quat. Res.* **6**, 581–596 (1976).
11. Heusser, C. J. *Quat. Res.* **2**, 189–201 (1972).
12. Heusser, C. J. *Bull. geol. Soc. Am.* **85**, 1547–1560 (1974).
13. Webb III, T. & Bryson, R. A. *Quat. Res.* **2**, 70–115 (1972).
14. Kay, P. A. *Quat. Res.* **11**, 125–140 (1979).
15. Andrews, J. T., Mode, W. N. & Davis, P. T. *Arctic Alpine Res.* **12**, 41–64 (1980).
16. Heusser, C. J. *Quat. Res.* **8**, 282–306 (1977).
17. Heusser, L. E., Shackleton, N. J., Moore, T. C. & Balsam, W. L. *Geol. Soc. Am. Abstr. Prog.* **7**, 1113–1114 (1975).
18. Heusser, L. E. & Shackleton, N. J. *Science* **204**, 837–839 (1979).
19. Gates, W. L. *Science* **191**, 1138–1144 (1976).
20. Manabe, S. & Hahn, D. G. *J. geophys. Res.* **82**, 3889–3911 (1977).

Goat Paddock cryptoexplosion crater, Western Australia

J. E. Harms*, D. J. Milton†, John Ferguson‡, D. J. Gilbert*, W. K. Harris§ & Bruce Goleby||

* Broken Hill Proprietary Company Limited, 140 William St, Melbourne, Victoria 3001, Australia.
† US Geological Survey, MS 928, Reston, Virginia 22092
‡ Bureau of Mineral Resources, Geology & Geophysics, PO Box 378, Canberra City, ACT 2601, Australia
§ South Australia Dept Mines, PO Box 151, Eastwood, South Australia 5063, Australia
|| Research School of Earth Sciences, Australian National University, Canberra, ACT 2600, Australia

Goat Paddock, a crater slightly over 5 km in diameter (18°20′ S, 126°40′E), lies at the north edge of the King Leopold Range/Mueller Range junction in the Kimberley district, Western Australia (Fig. 1). It was noted as a geological anomaly in 1964 during regional mapping by the Bureau of Mineral Resources, Geology and Geophysics and the Geological Survey of Western Australia. The possibility of its being a meteorite impact crater has been discussed[1], although this suggestion was subsequently ignored[2]. Two holes were drilled by a mining corporation in 1972 to test whether kimberlite underlay the structure. Here we report the findings of five days of reconnaissance in August 1979 which established that Goat Paddock is a cryptoexplosion crater containing shocked rocks and an unusually well exposed set of structural features.

Goat Paddock is a circular plain bounded for most of its circumference by steep cliffs 100–150 m high (Fig. 2). To the north, the rim has been eroded, opening a broad connection with the valley of the O'Donnell River. To the south and east, the ground is higher and more rugged, so that a raised rim is not evident. The circularity of the rim is reduced by erosion and by the presence of remnants of crater fill within the wall. Its topography is clearly unusual but not immediately suggestive of a crater.

The two drill holes, one at the centre and one about 1,250 m north-east of the centre, penetrated 211 and 212 m of lacustrine sediments before entering brecciated sandstone. The nearly equal depths suggest the absence of a central peak, which might have been expected as the critical diameter for the transition from simple to complex terrestrial cryptoexplosion craters is 2–3 km in sedimentary strata and about 4 km in crystalline rocks[3]. The fine-grained nature of the mudstone at the base of the crater fill, immediately above untransported breccia in both drill holes does, however, suggest that there may be a moat in the outer crater floor that acted as a trap for coarse debris. The small depth/diameter ratio is closer to those of larger, complex craters than to those of smaller, simple craters[3].

The canyons eroded into and through the walls of Goat Paddock offer some of the best exposures of the upper rim wall and rim flank of any cryptoexplosion crater in the World (Fig. 2). Nearly everywhere in the walls, bedrock has been upturned from its regional dip of 15° NNW to dip away from the crater. Dips reach the vertical near the crater lip and are overturned to the horizontal or inverted outward dips on the rim flank. In some sections, the rim flank appears to be composed of moderately dipping and presumably overturned imbricate plates a hundred metres or so across which are separated by screens of breccia. Intensely disturbed rock reaches as far as 800 m from the present rim crest. At one locality, a fault surface with a dip of 75° towards the crater and with striations pitching 75° separates undisturbed sandstone from overturned sandstone (Fig. 2*b*). The sense of motion on the fault was not determined: it may be either a thrust fault or a normal fault produced by slumping of the rim into the crater. On the south rim, no overturned flap is

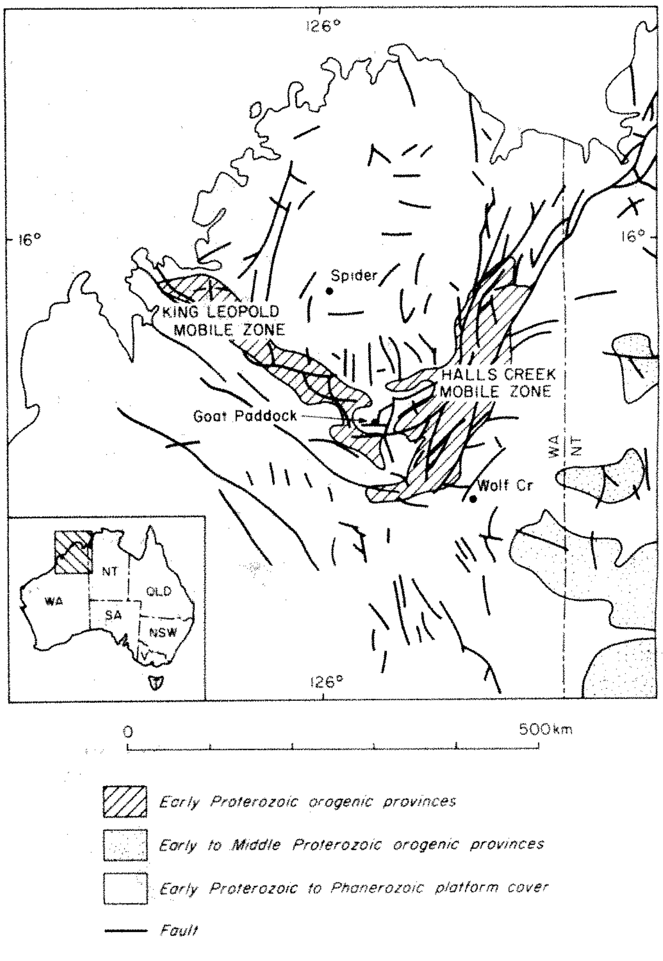
126°
16°
16°
Spider
KING LEOPOLD MOBILE ZONE
HALLS CREEK MOBILE ZONE
Goat Paddock
WA
NT
Wolf Cr
NT
WA
QLD
SA
NSW
V
126°
0
500km
Early Proterozoic orogenic provinces
Early to Middle Proterozoic orogenic provinces
Early Proterozoic to Phanerozoic platform cover
Fault
Cryptoexplosion structure

Fig. 1 Locality map of a portion of northwestern Australia showing main tectonic features and cryptoexplosion structures.

0028–0836/80/330704—03$01.00

apparent, but the autochthonous rock is deformed into at least one open anticline (Fig. 2*c*).

The disturbed beds show a high degree of fracturing everywhere and grade into breccia inside and particularly outside the rim crest. At many breccia occurrences, attitudes of the larger clasts are close to those of nearby coherent bedrock, and the lithologies are the same, showing that little mixing or long-distance transport has taken place. On the south rim, a series of ridges ~20 m high have fractured bedrock at the base and breccia at the top. No fallout (air-sorted debris) was found on the rim, and we are uncertain whether the breccia at high levels on the rim includes throwout (debris ejected ballistically).

The true crater wall (at the edge of the upturned beds) has a slope of 35°, locally reaching 50° or more. A breccia of unoriented clasts, tentatively interpreted as autochthonous breccia is usually immediately adjacent. This generally grades over a short distance into breccia having a roughly oriented texture, which is apparently talus. Above this breccia is a well-cemented conglomerate with rounded clasts and distinct bedding. The transition is locally gradational, but more commonly conglomerate dipping 20° discordantly overlies talus dipping 35°. The conglomerate, in turn, grades into grit, interbedded grit and siltstone, and finally the mudstone of the crater floor.

Conglomerate (and breccia) occurs not only within the crater bowl but also in depressions outside the crater rim. Some of these depressions appear to be crescentic troughs concentric with the rim. In one section the entire series of overturned plates seems to be displaced outwards to produce a double rim crest, with the gap between the outer edge of upturned bedrock and the inner edge of the displaced plates filled by breccia and conglomerate (Fig. 2*b*). Other conglomerate bodies appear to be approximately radial rather than concentric, and some of the gorges seem to be exhumed from conglomerate rather than freshly eroded through bedrock. Radial conglomerate bodies may occupy zones opened during the cratering process or they may simply fill pre-cratering valleys. The local topography at the time of the cratering event was probably no less rugged than the present topography and should have affected the details of the crater form.

The level of fill within the crater is close to that of a break in slope of the original crater wall, which may be a junction of the steep wall with the gently sloping outer crater floor or with a bench between the steep wall and floor. Thus, although around most of the circumference early crater fill laps onto the wall or is concealed by fans formed during the present erosion cycle, at several points overturned bedrock crops out as far as a 350 m from the base of the cliff. A small patch of melt breccia was found in one creek between the base of the wall and the innermost bedrock outcrop (Fig. 2c). The substrate is not exposed, but apparently slopes gently, as the larger melted clasts are approximately horizontal.

The central drill hole penetrated 19 m and the northeastern hole 5 m below the crater floor. Core recovery was poor, probably because of abundant incoherent rock flour, but recovered core shows sandstone with well-developed shatter cones or with a rhombic shatter fracturing. A few fragments with poorly developed shatter cones were also found in the breccia at the crater wall. Shock features in quartz (cleavage, planar features, basal deformation lamellae, plastic deformation, reduced birefringence) are abundant in clasts from breccia outcrops. These features culminate in the melt breccia which contains, besides clasts of various lower degrees of shock, twisted sheets of vesicular silica glass, now largely recrystallized to fine-grained quartz. To date, coesite or stishovite have not been found.

More than 20 pollen or spore species were identified in a sample of sediment from a depth of 139 m in one of the drill holes. The assemblage is dominated by proteaceous-like grains. Despite differences, there are sufficient species in common to indicate a correlation with the *Malvacipollis diversus* zone of Stover and Partridge[4] in southeastern Australia and therefore a probable early Eocene age. This is supported by a very low frequency of *Nothofagidites* spp. and the association of species such as *Latrobosporites amplus* (Stanley), *Proteacidites leightonii* Stover, *P. confragosus* Harris, and *Triporopollenites ambiguus* Stover.

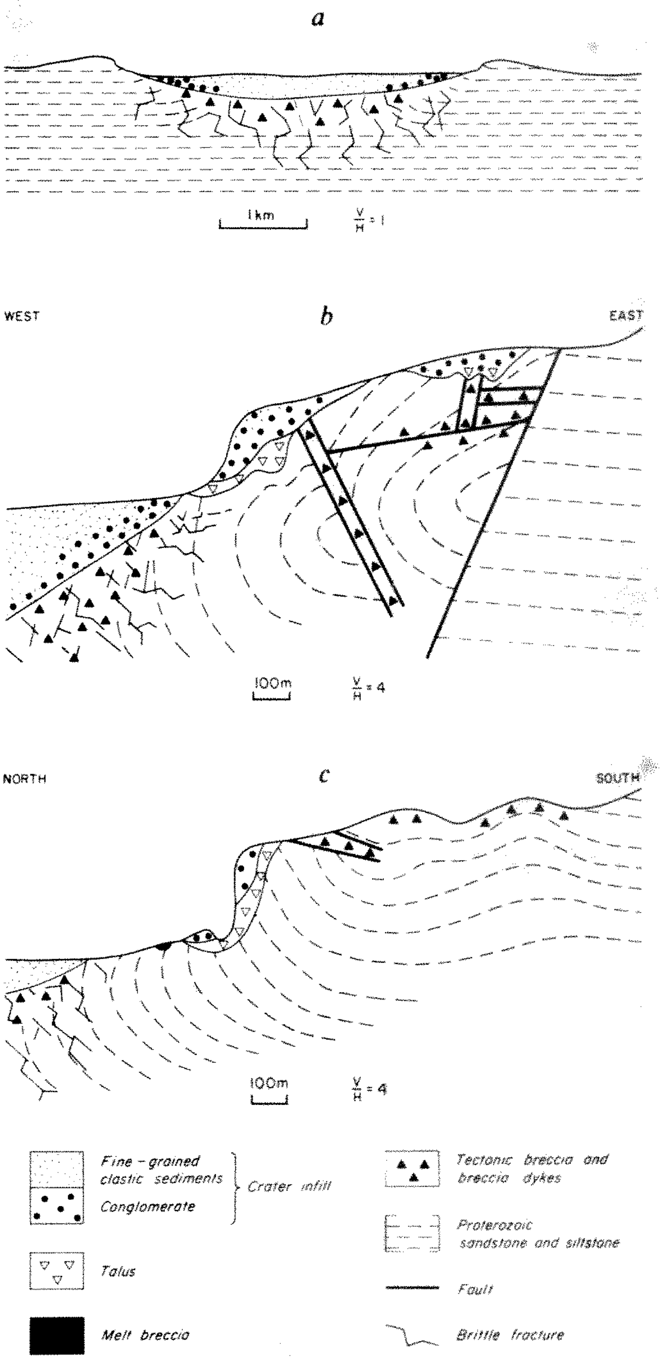

Fig. 2 Cross-sections of Goat Paddock Crater. *a*, Generalized structure; *b*, section along gorge eroded through east wall; *c*, section through south wall. Sections are based on photographs and sketches, and are hypothetical below the level of the crater floor.

The orientation of remanent magnetism in the melt breccia is normal and not significantly different from that of the present local field, but samples have not been magnetically cleaned. An Eocene orientation should be recognizable but could have been lost during weathering.

Goat Paddock is clearly a cryptoexplosion crater, of a type generally attributed to meteorite impact. Nevertheless, in the absence of meteoritic material, hypotheses of endogenous origin are defensible. The 875 m diameter Wolf Creek Crater[5,6], which is only 160 km to the south-east, is associated with oxidized meteoritic iron, although the association could be coincidental[7]. Wolf Creek seems to be less eroded than Goat Paddock, so an age as old as Eocene and a paired relationship seems unlikely although not impossible. About the same distance north-west of Goat Paddock is another cryptoexplosion structure, known as 'The Spider' (Fig. 1), which we have also briefly examined. Disturbed and shatter-coned strata occupy an area about 5 km in diameter. The structure resembles that of central uplifts of other cryptoexplosion structures and is apparently exposed at a level considerably below an original crater floor. The depth of erosion indicates an age greater than that of Goat Paddock. The Spider and probably Wolf Creek are in tectonically stable blocks, but Goat Paddock lies near the intersection of the King Leopold and Halls Creek Mobile Zone (Fig. 1), which have been intermittently active through geological time. Adjacent to the King Leopold Mobile Zone is a major province of salic alkaline igneous intrusion[8,9] dated as early Miocene[10]; this province, and an area adjacent to the Halls Creek Mobile Zone, have also recently been identified as areas of major kimberlite intrusion of unknown age.

J.E.H. and D.J.G. publish with permission of The Broken Hill Proprietary Company Limited. D.J.M. publishes with permission of the director, United States Geological Survey and J.F. with permission of the director, Bureau of Mineral Resources, Geology & Geophysics. D.J.M. is supported by the NASA Planetology Program.

Received 9 April; accepted 17 June 1980.

1. Roberts, H. G., Halligan, R. & Playford, P. E. *Rec. Bur. Miner. Resour. Geol. Geophys., Aust.* 1965/156 (1965).
2. *Bur. Miner. Resour. Geol. Geophys., Aust.* (1:250 000 Geological Series—Explanatory Notes Mt Ramsay, 1968).
3. Grieve, R. A. F. & Robertson, P. B. *Icarus* **38,** 212–229 (1979).
4. Stover, L. E. & Partridge, A. D. *Proc. R. Soc. Vict.* **85,** 237–286 (1973).
5. Guppy, D. J. & Matheson, R. S. *J. Geol.* **58,** 30 (1950).
6. Fudali, R. F. *J. Geol.* **87,** 55–67 (1979).
7. McCall, G. J. H. *Ann. N.Y. Acad. Sci.* **123,** 970–988 (1965).
8. Prider, R. T. *J. geol. Soc. Aust.* **6**, 2, 71–118 (1960).
9. Derrick, G. M. & Gellatly, D. C. *Bull. Bur. Miner. Resour. Geol. Geophys.* **125,** 103–119 (1972).
10. Wellman, P. *J. geol. Soc. Aust.* **19,** 471–474 (1973).

Did Iapetus start to open during the Cambrian?

R. Anderton

Department of Applied Geology, University of Strathclyde,
Glasgow G1 1XJ, UK

The geological evolution of the British Isles during the Lower Palaeozoic was dominated by the presence of the Iapetus Ocean. Although the timing of the major events in its later history are reasonably well known, its pre-Ordovician evolution is far less clear because of the absence of rocks of that age in the area of the Iapetus suture. To deduce the early history of the Ocean, circumstantial evidence from rocks originally deposited on the adjacent continental crust is needed. Petrographical evidence, from such rocks in the Dalradian, is discussed here and implies that Iapetus had still not opened by ~670 Myr ago. A dramatic increase in tectonic instability after this date, culminating in the extrusion of the Lower Cambrian Tayvallich Volcanics, is considered to date the continental rupture that led to the formation of Iapetus. This view is in contrast to the assumption that continental break-up must have preceded the earliest Dalradian sedimentation[1] and that the red-bed fluvio-lacustrine sediments of the Torridon Group, dated at ~810 Myr, could be a consequence of this initial rifting[2].

The Dalradian Supergroup contains a virtually continuous record of largely marine deposition from the late Precambrian (sedimentation starting at least 700 Myr and possibly as long as 800 Myr ago) until the Cambrian or possibly Lower Ordovician. Within this sequence are several psammite formations that are largely composed of mineralogically mature quartzofeldspathic detritus that tells one little about its source area. However, within the middle Dalradian (Argyll Group) Jura Quartzite are occasional rounded pebbles of what was, before Caledonian metamorphism, ferruginous chert or jasper[3]. These show a range of textures typical of the oolitic and banded facies of the Proterozoic cherty iron-formations found in early Proterozoic shelf sequences. Furthermore, they are very similar to pebbles described from the Applecross Formation of the Torridon Group[4] which is known from palaeocurrent and radiometric evidence to have been derived from an area to the north-west of the present Scottish mainland[5]. The mineralogical maturity and absence of all but these very stable clasts, probably recycled from older conglomerates, suggests that the Jura Quartzite source area consisted largely of Proterozoic sedimentary rocks, with only minor first cycle input from the Archean basement. The Scottish 'Torridonian' together with the Eriksfjord Formation[6] and the Ketilidian sediments[7] of South Greenland may just be remnants of what was, in late Proterozoic times, a more extensive sedimentary cover over the now exposed Archean basement.

The similarity between the Dalradian and some of the Torridon Group pebbles, together with evidence of a clastic input from a northwesterly direction into some Argyll Group turbidite basins[8], suggests a northwesterly, largely sedimentary source for Argyll Group psammites. This source must have lain in the area of the present Scotland–Greenland continental margins although it may have stretched even further to the north-west (Fig. 1*a*).

Most lower Dalradian Appin and Grampian Group coarse-grained sediments are also composed of mineralogically mature quartzofeldspathic detritus without distinctive clasts[9] that could similarly have been derived from a largely sedimentary source area lying to the north-west throughout the late Proterozoic. The position of the Moine metasediments in this palaeogeographical picture is, however, as unclear as the status of the Moine itself. The ~750 Myr ages from Moine pegmatites have been interpreted as either the date of a 'Morarian' orogenic event[10] or Grenvillian ages partially reset by Caledonian metamorphism[11]. The lack of petrographical evidence for a nearby orogenic belt in the Appin and Grampian Groups, whose deposition probably spans the period of the Morarian event, is more consistent with the latter hypothesis. However, if the timing of the Morarian event is confirmed, its significant tectonometamorphic effects may have only been felt at depth with its palaeogeographical impact being restricted to mild uplift and erosion of the low grade top of its metasedimentary pile.

The hypothesis of a northwesterly, largely sedimentary, source could well apply to all the Dalradian Grampian, Appin and Argyll Group coarse-grained sediments except for one, the Port Askaig Tillite. This lies at the base of the Argyll Group stratigraphically below the Jura Quartzite and is correlated with the Varangian or Eocambrian tillite found throughout the Caledonian belt and dated in Finmark[12] at ~670 Myr. It contains a suite of granite clasts throughout its outcrop from Banff to Connemara, quite unlike anything found in the other psammites, and must have been derived from a largely igneous and metamorphic source[13,14]. If the area to the north-west was blanketed by Proterozoic sediments at this time, a southeasterly source is required for the Tillite as previously suggested by Howarth[14] and Spencer[15]. This is consistent with the direction of ice-pushed folds from the Tillite in Argyll[13], Donegal[14] and elsewhere in the Caledonian belt[15]. The Midland Valley landmass, which may have acted as a southeasterly source for the Southern Highlands Group[16] during the Cambrian (Fig. 1*c*) and was probably of the right composition to supply granite and quartzite clasts, would not have been large enough to nourish the extensive and persistent glaciers of Port Askaig Tillite times. Rather, the glacier source most probably lay in a more extensive area further to the south-east which, on petrographical grounds, could have been in northern continental Europe[15] (Fig. 1*b*). It is, therefore, most unlikely that there could have been an ocean basin between this presumed source and the present Dalradian outcrop at this time.

0028-0836/80/330706—03$01.00

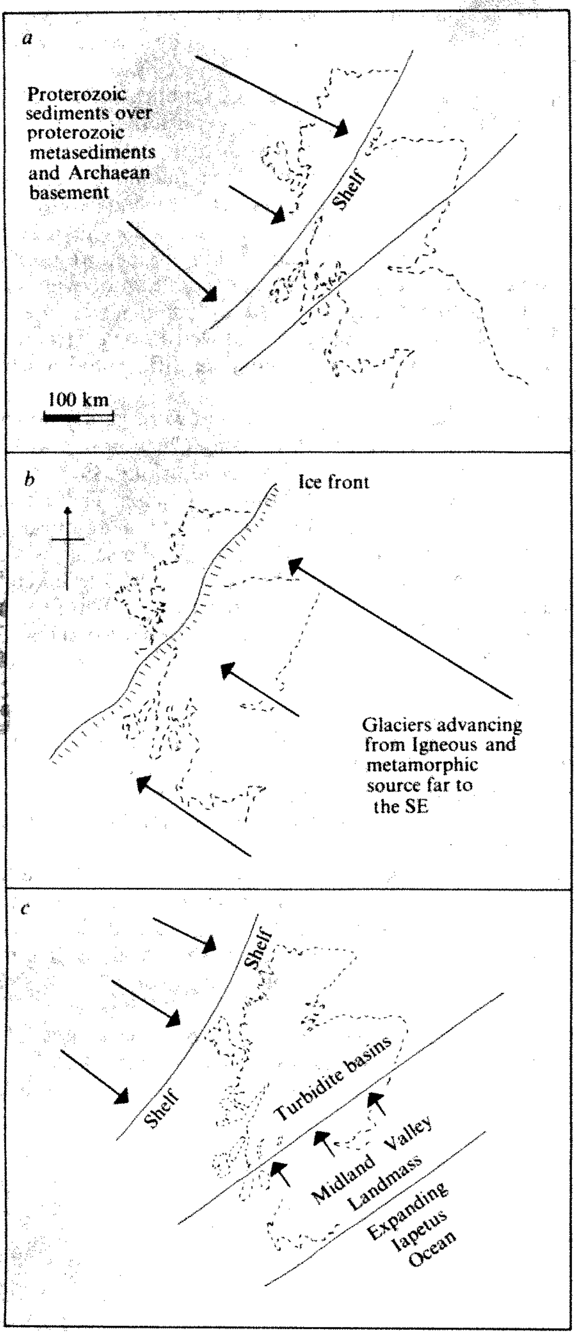
a
Proterozoic sediments over proterozoic metasediments and Archaean basement
Shelf
100 km
b
Ice front
Glaciers advancing from Igneous and metamorphic source far to the SE
c
Shelf
Shelf
Turbidite basins
Midland Valley Landmass
Expanding Iapetus Ocean

Fig. 1 Location of source areas during Dalradian times, arrows show suggested directions of main sediment influx into the Dalradian depositional area for: *a*, most of Grampian Appin and Argyll Group times; *b*, Port Askaig Tillite times; and *c*, Southern Highland Group times. Position of palaeogeographical elements drawn very schematically with respect to present rock outcrops and without any correction for tectonic shortening. Ice front drawn for one instant in time, the ice limit may have lain far to the north-west.

If Iapetus had not opened by Port Askaig Tillite times, when did it open? Before the deposition of the Tillite, there is little evidence for tectonic instability. Broad, differential subsidence can account for thickness and regional facies variations. However, after the Tillite, major syndepositional faults exerted an increasing control over sedimentation. Rapid subsidence along these faults produced turbidite basins with steep, unstable slopes as exemplified by the Scarba Conglomerate/Easdale Slates[8], Crinan Grits (A. K. Barraclough, personal communication) and Tayvallich Limestone[17]. Finally, eruption of the tholeiitic Tayvallich lavas and intrusion of sills[18] marked the peak of tectonic instability and crustal tension. The rapid basin subsidence is considered to be a precursor of rifting due to regional crustal tension with the lavas signifying the final break. An alternative hypothesis is that the tectonism and volcanism relate to back-arc spreading following the initiation of subduction. Both are considered feasible by Graham and Bradbury[19] on petrochemical grounds, but the latter is rejected here because of the petrographical evidence discussed above.

The precise dating of the suggested rifting is not possible because of the minimal fossil and radiometric control on Dalradian events. However, the base of the Cambrian probably lies not far below the Tayvallich Volcanics[20] and the Argyll Group turbidite basins range from roughly the middle of the Vendian or Eocambrian, say 640 Myr ago, onwards. A period of crustal tension leading to increasing tectonic instability after 640 Myr, culminating in volcanism and final continental break-up around 600 Myr, is therefore indicated. This is in close agreement with an end Proterozoic/Lower Cambrian age for rifting in Newfoundland, suggested originally by Bird and Dewey[21], on the basis of the stratigraphic relationships of a suite of lavas correlated with the subsequently dated ~605 Myr old Long Range Dykes[22]. This leaves only ~90 Myr for ocean expansion, about the same as the time available for closure, if subduction started in the Lower Ordovician as suggested by evidence from the Ballantrae ophiolite[23] and final (probably diachronous[24]) closure took place during the late Silurian to early Devonian[25]. At, say, a total spreading rate of 4 cm yr^{-1} this would still produce an ocean 3,600 km across, as wide as is required by available faunal[26] and palaeomagnetic[27] evidence from the Ordovician. However, the existence of well defined trilobite provinces in Britain does require the existence of an effective barrier by the late Lower Cambrian[28], possibly only 20 Myr after the suggested rifting. A faster spreading rate may, therefore, be indicated.

The hypothesis of a late opening for Iapetus has, if correct, several implications. (1) The existence and location of the area of Dalradian sedimentation were unrelated, at least in its early stages, to Iapetus. The Dalradian developed in an ensialic crustal environment[16]. (2) Continental rifting subsequently took place to the south-east of the Dalradian basin in an area of more brittle crust. There is, therefore, no stratigraphic mirror image of the Dalradian to the south-east of Iapetus, although because of the possible oblique opening and closing of the Ocean, this cannot be demonstrated until the relative positions of northern and southern Britain during the late Proterozoic are known. This uncertainty also makes it difficult to relate the evidence for late Proterozoic subduction in Anglesey, which may be more closely related to the evolution of a southerly Cadomian Ocean[29], to the Dalradian picture. (3) The direct stratigraphic evidence for the timing of rifting, such as plateau lavas, fluvial facies and salt, is not visible in the British part of the Caledonian belt, although it may be buried beneath younger rocks near the suture or have been thrust under the Dalradian during its collision with the Midland Valley microcontinent during the Grampian orogeny[30]. The presently exposed Dalradian rocks were deposited at least 100 km (possibly several hundred kilometres after allowance for tectonic shortening) away from the rifted continental edge, in a pre-existing marine basin well away from the more obvious effects of continental rupture.

Received 1 April; accepted 12 June 1980.

1. Dewey, J. F. *Nature* **222,** 124–129 (1969).
2. Stewart, A. D. *Geol. Soc. Lond. Spec. Rep.* **6,** 43–51 (1975).
3. Anderton, R. *Scott. J. Geol.* (in the press).
4. Williams, G. E. *Mem. Am. Ass. petrol. Geol.* **12,** 609–629 (1969).
5. Allen, P., Sutton, J. & Watson, J. V. *J. geol. Soc. Lond.* **130,** 85–91 (1974).
6. Emeleus, C. H. & Upton, B. G. J. in *Geology of Greenland* (eds Escher, A. & Watt, W. S.) 152–181 (Geological Survey, Greenland, 1976).
7. Allaart, J. H. in *Geology of Greenland* (eds Escher, A. & Watt, W. S.) 120–151 (Geological Survey, Greenland, 1976).
8. Anderton, R. in *The Caledonides of the British Isles Reviewed* (eds Harris, A. L., Holland, C. H. & Leake, B. E.) 483–488 (Scottish Academic, Edinburgh, 1980).
9. Hinkman, A. H. *Scott. J. Geol.* **11,** 117–142 (1975).
10. van Breeman, O., Halliday, A. N., Johnson, M. R. W. & Bowes, D. R. *Geol. J. Spec. Issue* **10,** 81–106 (1978).
11. Brewer, M. S., Brook, M. & Powell, D. in *The Caledonides of the British Isles Reviewed* (eds Harris, A. L., Holland, C. H. & Leake, B. E.) 129–137 (Scottish Academic, Edinburgh, 1980).

12. Pringle, I. R. *Geol. Mag.* **109,** 465–472 (1973).
13. Spencer, A. M. *Mem. geol. Soc. Lond.* **6** (1971).
14. Howarth, R. J. *Proc. R. Ir. Acad.* **71B,** 1–35 (1971).
15. Spencer, A. M. *Geol. J. Spec. Issue* **6,** 217–240 (1975).
16. Harris, A. L., Baldwin, C. T., Bradbury, H. J., Johnson, H. D. & Smith, R. A. *Geol. J. Spec. Issue* **10,** 115–138 (1978).
17. Knill, J. L. in *The British Caledonides* (eds Johnson, M. R. W. & Stewart, F. H.) 99–121 (Oliver & Boyd, Edinburgh, 1963).
18. Graham, C. M. *J. geol. Soc. Lond.* **132,** 61–84 (1976).
19. Graham, C. M. & Bradbury, H. J. *Geol. Mag.* (in the press).
20. Downie, C., Lister, T. R., Harris, A. L. & Fettes, D. J. *Rep. Inst. geol. Sci.* 71/9 (1971).
21. Bird, J. M. & Dewey, J. F. *Bull. geol. Soc. Am.* **81,** 1031–60 (1970).
22. Stukas, V. & Reynolds, P. H. *Earth planet. Sci. Lett.* **22,** 256–266 (1974).
23. Church, W. R. & Gayer, R. A. *Geol. Mag.* **110,** 497–592 (1973).
24. Phillips, W. E. A., Stillman, C. J. & Murphy, T. *J. geol. Soc. Lond.* **132,** 579–609 (1976).
25. McKerrow, W. S. & Ziegler, A. M. *Nature phys. Sci.* **240,** 92–94 (1972).
26. McKerrow, W. S. & Cocks, L. R. M. *Nature* **263,** 304–306 (1976).
27. Piper, J. D. A. *Scott, J. Geol.* **14,** 93–107 (1978).
28. Cowie, J. & McNamara, K. J. *Palaeontology* **21,** 615–634 (1978).
29. Anderton, R., Bridges, P. H., Leeder, M. R. & Sellwood, B. W. *A Dynamic Stratigraphy of the British Isles* (George Allen & Unwin, London, 1979).
30. Longman, C. D., Bluck, B. J. & van Breemen, O. *Nature* **280,** 578–581 (1979).

Equilibrated Nd–unequilibrated Sr isotopes in mantle xenoliths

E. Jagoutz*, R. W. Carlson & G. W. Lugmair

Scripps Institution of Oceanography and Chemistry Department,
University of California, San Diego, La Jolla, California 92093

Isotopic analyses of mantle xenoliths transported to the surface by alkali basalt eruptions complement data obtained from studying basic magmas. These xenoliths also enable mantle characteristics to be examined before they have been affected by the fractionation processes which occur during magma genesis. The data on ultramafic nodules demonstrate Sr isotopic disequilibrium between mineral phases within a single xenolith[1–5]. This suggests that isotopic disequilibrium on a grain-size scale may be important in determining the isotopic composition of melts derived from the mantle. However, recent work on carefully cleaned mineral separates from alpine peridotites[6] and ultramafic nodules[2] has shown that, in many cases, the highly radiogenic $^{87}Sr/^{86}Sr$ found in minerals with low Sr concentrations (olivine, orthopyroxene) can be considerably reduced by leaching the sample in dilute acids before analysis. To investigate the nature of isotopic disequilibria between minerals of lherzolitic nodules, we report here a combined study of the Nd and Sr isotopic composition of two spinel lherzolites from New Mexico and Arizona. These samples were selected from a large number of ultramafic xenoliths for which major and trace element compositions had been determined[7]. The two nodules measured represent two end members of a distinct group of nodules which have major element compositions that would make them suitable parent materials for basaltic melts. These two nodules show no obvious signs of metasomatic alteration or re-equilibration under more than one pressure and temperature regime. Interstitial glass does not occur in either nodule investigated. Hence, the Nd and Sr isotopic composition of these nodules and constituent minerals were expected to provide important constraints on the nature of basalt source regions in the mantle in general, and, in particular, that underlying the American South-West.

Sample KH-1 is a spinel lherzolite from Kilbourne Hole, New Mexico, a recent maar-type volcano in the Rio Grande Rift. Major and trace element compositions of KH-1 were reported by Jagoutz *et al.*[7]. This sample is characterized by considerable depletion of the light rare earth elements (LREE), but still has relatively high Ca and Al abundances (2.45 and 1.89 wt % respectively)[7]. KH-1 is coarse granular in texture and, based on petrographical and chemical evidence, was defined as 'primitive'. From sample KH-1, carefully separated and cleaned clinopyroxene (cpx) and orthopyroxene (opx) separates, as well as a leached whole rock (WR) aliquot and its surface leachant, were measured.

Sample SC-1 is from the recent, xenolith-laden, alkalic magmas of San Carlos, Arizona. As reported[7], SC-1 has an almost flat relative REE pattern with many other refractory elements also in nearly unfractionated 'chondritic' relative abundances. From this sample, an acid leached whole rock aliquot and two cpx separates were analysed. The first cpx separate was subjected to the acid leaching procedure used for KH-1 mineral separates. The second cpx aliquot was more harshly etched to investigate possible zoning which may be reflected in the isotopic composition, as well as to determine the effect on the acid treatment on possible differential leaching of ^{87}Sr.

The two samples were very friable and were gently crushed and sieved to a grain size of 0.1–0.3 mm. Clean grains without visible inclusions were separated by handpicking. For the opx separate of KH-1, only grains >2 mm were taken. These grains were then washed in warm 2M HCl for 20 min in an ultrasonic bath. After a 5-min treatment with 5% HF, the samples were crushed and a fraction between 100 and 200 mesh was taken for final handpicking under a binocular microscope. This separate was leached for 5 min in 5% HF and then again washed in warm 2M HCl, followed by an ultrasonic treatment in warm 2M HCl for 20 min.

The KH-1 whole rock leach was produced by leaching an aliquant (0.9779 g) of powdered (<200 mesh) bulk rock in 2M HCl for 20 min. The HCl solution was then filtered. Weight loss in this procedure (57.9 mg) is not representative of the actual amount of material which went into solution due to the loss of a very fine-grained fraction during filtering.

Two SC-1 cpx separates were prepared by the method described above. One cpx fraction (26.8 mg) was further treated for 45 min in concentrated HF and $HClO_4$ in an ultrasonic bath. After this etching, the sample was washed with high purity water. The etching solution plus the water wash were evaporated and processed as sample 'SC-1 cpx etch'. The remaining cpx (19.3 mg) was dissolved to become sample 'SC-1 cpx residue'. Weight loss during this procedure was 7.5 mg (28%) and is believed to have been completely retained in the etch solution.

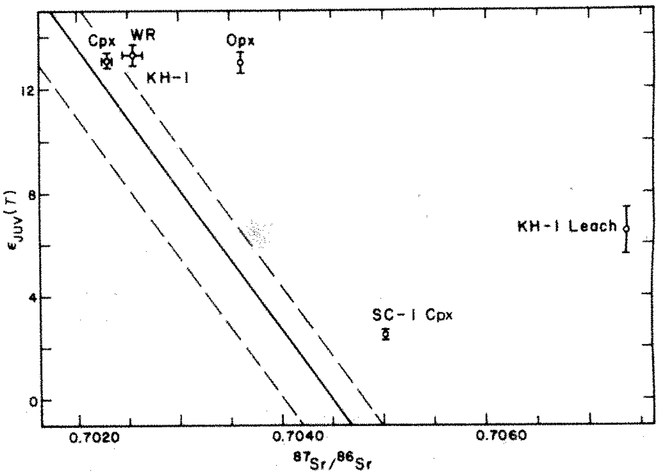

Fig. 1 $\varepsilon_{JUV}(T)$ plotted against $^{87}Sr/^{86}Sr$. $\varepsilon_{JUV}(T)$, expressed in parts per 10^4, is the fractional deviation of $^{143}Nd/^{144}Nd$ in samples from that existing in a chondritic reference reservoir. The Sr–Nd trend line observed for young basaltic rocks and the approximate range of values (dashed lines) about this trend are adopted from O'Nions *et al.*[16] and DePaolo and Wasserburg[17]. Note the observed Nd isotopic equilibration, but Sr disequilibrium in the minerals of KH-1 and the offset of the SC-1 cpx point to higher $^{87}Sr/^{86}Sr$ than found for the basalts.

---

* Permanent address: Max-Planck Institut für Chemie, Abteilung Kosmochemie, Saarstrasse 23, 6500 Mainz, FRG.

0028–0836/80/330708—03$01.00

Table 1 Analytical results

Sample	Weight (mg)	[Sm] (p.p.m.)	[Nd] (p.p.m.)	$^{147}Sm/^{144}Nd$*	$^{87}Sr/^{86}Sr$†‡	$^{143}Nd/^{144}Nd$‡§	$\varepsilon_{JUV}(T)$‖
KH-1 cpx	107.6	1.42	2.71	0.3171	0.70229 ± 6	0.513308 ± 15	13.1 ± 0.3
KH-1 opx	730.7	0.0230	0.0249	0.5578	0.70361 ± 4	0.513301 ± 21	13.0 ± 0.4
KH-1 WR	299.1	0.242	0.456	0.3208	0.70255 ± 9	0.513319 ± 21	13.3 ± 0.4
KH-1 'Leach'				0.1918	0.70736 ± 3	0.512971 ± 48	6.5 ± 0.9
SC-1 cpx	56.3	3.66	10.3	0.2150	0.70501 ± 4	0.512764 ± 11	2.5 ± 0.2
SC 1 WR	327.7	0.680	1.89	0.2174		0.512763 ± 24	2.5 ± 0.5
'SC-1 cpx etch'	'7.5'				0.70488 ± 3		
'SC-1 cpx residue'	19.3				0.70498 ± 4		

Cpx, clinopyroxene; opx, orthopyroxene; WR, whole rock.

* Uncertainty ≈ 0.1%.

† Sr fractionation corrected to $^{86}Sr/^{88}Sr = 0.1194$; values measured for NBS 987 Sr show a total range of ±0.01% about $^{87}Sr/^{86}Sr = 0.71014$.

‡ Errors correspond to last digits and represent 95% C.L.

§ Nd measured as NdO^+ fractionation corrected to $^{148}NdO/^{144}NdO = 0.242436$ ($^{148}Nd/^{144}Nd = 0.241572$).

‖ Ref. 15.

Procedures for dissolution, chemical separation, and isotopic analysis have been reported previously[8,9]. Samples were totally spiked after dissolution for Sm and Nd concentration determination. Only the etched cpx separate and its leach from SC-1 were spiked for Sr concentration measurement. Blanks for Sm, Nd and Sr for the chemical procedures used were 8, 50 and 300 pg respectively.

Nd and Sr isotopic results and Sm and Nd concentrations are presented in Table 1. Distinct differences are apparent in the $^{143}Nd/^{144}Nd$ of samples SC-1 and KH-1. However, minerals within a single sample have Nd isotopic compositions which agree within analytical uncertainty. This is dramatically demonstrated in the case of KH-1 where a large spread in $^{147}Sm/^{144}Nd$ was measured for opx and cpx. On the other hand, despite the careful pretreatment of the samples, $^{87}Sr/^{86}Sr$ in KH-1 is considerably higher in opx than in cpx.

The observed equilibrium for Nd between cpx, opx (and the whole rock) of KH-1 demonstrates that Nd was in diffusive equilibrium at the time of the nodule's eruption on to the surface. These findings are similar to those reported by other workers[16–18] who found cpx and garnet to be in Nd isotopic equilibrium in garnet lherzolite xenoliths at the time of their inclusion in South African kimberlites. On the other hand, in KH-1, the measured Sr fractions derived from the different mineral separates are not isotopically equilibrated.

Possible explanations for the observed differences in $^{87}Sr/^{86}Sr$ in KH-1 could be: (1) Sr diffusion in the mantle is much slower than that of Nd; (2) radiogenic growth of ^{87}Sr since the last time of Nd equilibration; (3) residual contamination of the measured mineral phases not removed by the leaching procedure; (4) (partial) equilibration with a fluid enriched in ^{87}Sr.

Although there is no direct experimental evidence for a difference between the diffusivity of Nd and Sr, some inferences could be drawn from the diffusive behaviour of M^{3+} and M^{2+} ions and the influence of ionic radii on diffusivity in silicate melts[13]. These data suggest the importance of charge in influencing diffusivity and imply that Nd should diffuse slower than Sr. The evidence above implies that, at least in the case of KH-1, the measured differences in $^{87}Sr/^{86}Sr$ were introduced after, or at the time of, the last equilibration of the Nd system. Because of the high precision obtained in the Nd isotopic measurements and the large spread in $^{147}Sm/^{144}Nd$ between opx and cpx, an upper limit of 8 Myr can be set for the time of the last Nd equilibration. If this also records the time of the last complete Sr equilibration, then taking the extreme limit of no ^{87}Rb decay in cpx ($^{87}Rb/^{86}Sr = 0$) an $^{87}Rb/^{86}Sr = 11.6$ would be required in opx to produce the measured differences in $^{87}Sr/^{86}Sr$ between the mineral separates within the 8 Myr upper limit imposed by the Nd equilibration. This ratio is 50–100 times the actual value measured for opx from other ultramafic nodules[1,3–5]. Therefore, it seems very unlikely that the observed Sr disequilibrium is the result of *in situ* radiogenic growth of ^{87}Sr within the minerals.

Results for the surface leach of the KH-1 whole rock sample show the presence of an HCl soluble surface coating with $^{87}Sr/^{86}Sr = 0.70736$. Nd in this surface leach was very low in concentration ($<10^{-8}$g Nd per g of bulk rock) with $^{143}Nd/^{144}Nd = 0.51297$ corresponding to $\varepsilon_{JUV}(T) = +6.5$. Two sources for this radiogenic Sr component can be proposed: (1) surface contaminant deposited from the vapour phase of the host basalts in the Kilbourne Hole area. However, the observed $^{87}Sr/^{86}Sr$ in the leach is considerably higher than found for the basalts in the area[1]; (2) deposition on to the minerals of salts contained in the groundwater of the area. This is supported by the similarity in $^{87}Sr/^{86}Sr$ measured for this surface wash and that found for caliche from the Rio Grande Rift (E. Padovani, personal communication). Therefore, it follows that the disequilibrium found for $^{87}Sr/^{86}Sr$ in the minerals from KH-1 may be due to incomplete removal of this surface contaminant, or possibly even a small degree of diffusion of this Sr contaminant into the mineral grains. The effect of this contaminant would be much more pronounced for minerals with low Sr content such as opx (and olivine), but would have little effect on cpx due to its high Sr content. On the other hand, the leaching experiment performed on SC-1 cpx does not indicate the presence of any residual contaminant after the initial acid washings. However, note that, due to the very high Sr concentration of SC-1 cpx (126 p.p.m.), this experiment may not be very sensitive towards detecting residual contamination. In addition, there is no evidence from this experiment to indicate preferential leaching of ^{87}Sr by the various acid treatments.

Although the exact cause of the observed mineral Sr isotopic disequilibrium is not tightly constrained by the data presented here, it is apparent from this and previous work[10–12] that Nd isotopic equilibration between major mantle minerals (cpx, opx, garnet) is achieved on time scales which are much shorter than predicted from experimental subsolidus diffusion data.

Figure 1 displays the isotopic results as $\varepsilon_{JUV}(T)$ plotted against $^{87}Sr/^{86}Sr$. This figure and the major element data[7] indicate that KH-1, with $\varepsilon_{JUV}(T) = 13.1$, is a suitable parent material from which a magma similar in composition to mid-ocean ridge basalts could be derived. If KH-1 is representative of LREE-depleted primitive nodules in this area, then the results provide evidence for the existence of oceanic-type mantle underlying the Rio Grande Rift. A similar conclusion was reached by Reid and Woods[14], based on a major element comparison for nodules from the same area with those found at Salt Lake Crater, Hawaii.

The Sm–Nd model ages of SC-1 and KH-1 (T_{ICE}) of 814 ± 157 and 819 ± 26 Myr, respectively, are in reasonably good agreement. One explanation for this concordance is that the source for these two samples was initially depleted in incompatible elements close to 800 Myr ago from a primordial reservoir with 'chondritic' relative REE abundances. If the group of 'primitive' nodules, of which KH-1 and SC-1 are only two examples, do represent mantle samples which have rather uncomplicated differentiation histories, then these nodules can provide important constraints on the nature of the mantle. Of particular interest is that this group of nodules shows very similar major element compositions, yet has highly variable abundances of the incompatible elements. As all the radiometric systems also belong to the group of incompatible elements, the large variability in the degree of depletion of these elements in 'primitive' nodules such as KH-1 and SC-1 has profound implications for the interpretation of the isotopic data. In particular, the similar major element compositions of SC-1 and KH-1 clearly show that incompatible element mobilization can be accomplished without significant depletion in the basaltic component (that is, CaO, Al_2O_3). Therefore, the isotopic data presented here for KH-1 suggest that mantle with 'undepleted' abundances of CaO and Al_2O_3 can have Nd and Sr isotopic composition similar to that assumed for the 'depleted' oceanic mantle.

We thank H.-G. Stosch for treating the SC-1 clinopyroxenes with appropriate harshness and for many beneficial discussions. Irene Spellman typed the manuscript for which we are grateful. This work was supported by NASA grant NGL 05-009-150.

Received 14 January; accepted 16 June 1980.

1. Stueber, A. M. & Ikramuddin, J. *Geochim. cosmochim. Acta* **38**, 207–216 (1974).
2. Basu, A. R. & Murthy, V. R. *Earth planet. Sci. Lett.* **35**, 239–246 (1977).
3. Burwell, A. D. M. *Earth planet. Sci. Lett.* **28**, 69–78 (1975).
4. Kudo, A. M., Brookins, D. G. & Laughlin, A. W. *Earth planet. Sci. Lett.* **15**, 291–295 (1972).
5. Dasch, E. J. & Green, D. H. *Am. J. Sci.* **275**, 461–469 (1975).
6. Menzies, M. & Murthy, V. R. *Earth planet. Sci. Lett.* **38**, 346–354 (1978).
7. Jagoutz, E. *et al. Proc. 10th Lunar planet. Sci. Conf.* 2031–2050 (1979).
8. Lugmair, G. W., Scheinin, N. B. & Marti, K. *Proc. 6th Lunar Sci. Conf.* 1419–1429 (1975).
9. Stosch, H. G., Carlson, R. W. & Lugmair, G. W. *Earth planet. Sci. Lett.* **47**, 263–271 (1980).
10. O-Nions, R. K., Carter, S. R., Evensen, N. M. & Hamilton, P. J. *EOS* **59**, 399 (1979).
11. Allégre, C. J. & Shimizu, N. *EOS* **59**, 399 (1979).
12. Basu, A. R. & Tatsumoto, M. *Science* **205**, 398–401 (19791.
13. Magaritz, M. & Hofmann, A. W. *Geochim. cosmochim. Acta* **42**, 847–858 (1978).
14. Reid, J. B. & Woods, G. A. *Earth planet. Sci. Lett.* **41**, 303–316 (1978).
15. Lugmair, G. W., Marti, K., Kurtz, J. P. & Scheinin, N. B. *Proc. 7th Lunar Sci. Conf.* 2009–2033 (1976).
16. O'Nions, R. K., Hamilton, P. J. & Evensen, N. M. *Earth planet. Sci. Lett.* **34**, 13–22 (1977).
17. DePaolo, D. J. & Wasserburg, G. J. *Geophys. Res. Lett.* **4**, 465–468 (1977).

Effects of biotic and abiotic elicitors on phytoalexin metabolism in soybean

P. Moesta & H. Grisebach

Department of Biochemistry, Biologisches Institut II der Universität, Schänzlestr. 1, D-7800 Freiburg, FRG

Elicitors induce accumulation of phytoalexins in plants[1]. Recently Yoshikawa[2] concluded that biotic and abiotic elicitors act by different mechanisms. Thus a biotic elicitor, such as the cell walls of *Phytophthora megasperma* var. sojae, stimulated glyceollin synthesis in soybean cotyledons but had no significant effect on glyceollin degradation. In contrast, the abiotic elicitor $HgCl_2$ had only a slight effect on the biosynthetic activity but strongly inhibited glyceollin degradation. Here we report results which are contrary to Yoshikawa's conclusion.

Yoshikawa estimated biosynthetic activity by pulse-labelling with ^{14}C-L-phenylalanine. It is, however, not known whether uptake of this compound was influenced by elicitor treatment. For measurement of glyceollin degrading activity, cotyledons were incubated with glyceollin. The drawback of this method is that externally supplied glyceollin could be converted differently than the glyceollin in the internal pool. Because of the importance of elicitors in phytoalexin research[1], we have reinvestigated the effect of a biotic and an abiotic elicitor on glyceollin synthesis and conversion in soybean cotyledons by pulse-labelling with $^{14}CO_2$. By using high pressure liquid chromatography (HPLC) for separation of products, it was also possible to determine rate of synthesis and conversion of 3,6α,9-trihydroxypterocarpan, a precursor of glyceollin[3].

Figure 1 shows the accumulation of glyceollin (containing the three isomers[6,7]) and trihydroxypterocarpan (THP) after induction with the glucan from *P. megasperma*[5] or $HgCl_2$ as elicitor. Induction with glucan results in somewhat faster and higher accumulation of both compounds compared to the induction with $HgCl_2$. In the latter case glyceollin accumulation levels off earlier than THP accumulation. Controls with sterile cut cotyledons, treated only with buffer, contained only very small amounts of both compounds (<1 μg per g fresh weight) which could not be quantitated.

The integrated curves for the rates of synthesis of glyceollin and THP after induction with either elicitor (Fig. 2) show no significant differences between the effects of the biotic and abiotic elicitor. In both cases the rate of THP synthesis is higher than that of glyceollin synthesis. Half-times of conversion were

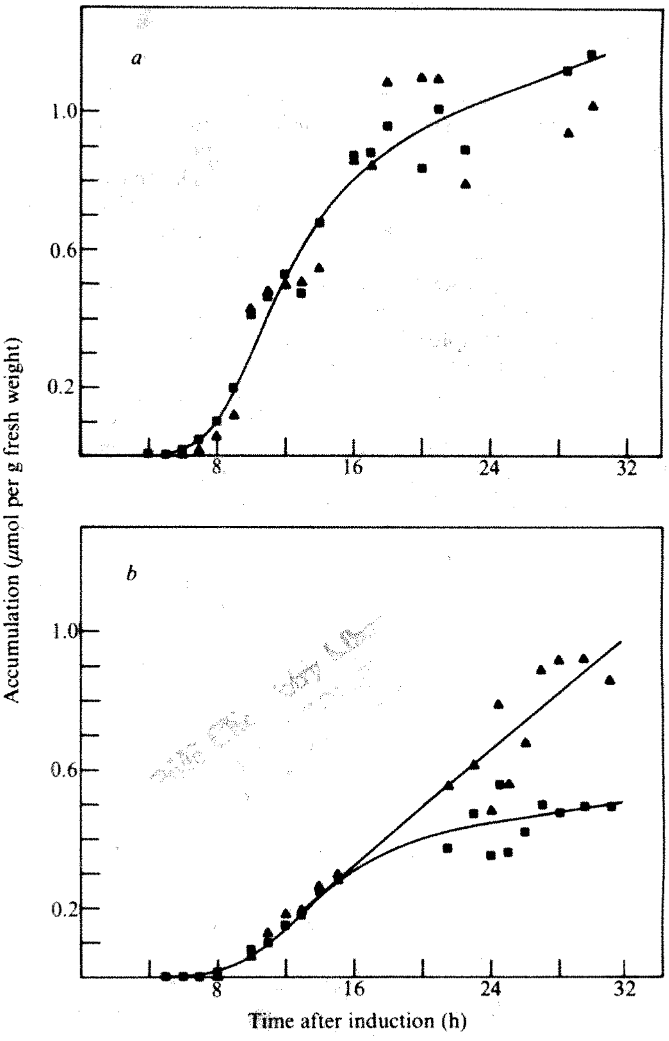

Fig. 1 Effect of glucan from *P. megasperma* and of mercuric chloride on accumulation of glyceollin (■) and trihydroxypterocarpan (▲) in soybean cotyledons. Detached cotyledons from 5-day-old seedlings of the soybean [Glycine max (L.) Merr.] cultivar Harosoy 63 were wounded as described by Ayers *et al.*[4], except that wounds were made on the lower surface of the cotyledons. An aliquot (100 μl) of an elicitor solution (*a*, biotic elicitor: heat-solubilized mycelial wall of *P. megasperma* var. sojae[5] (glucan), 300 μg glucose-equivalents ml^{-1}; *b*, abiotic elicitor: 1.5 mM $HgCl_2$) was placed on wounded areas of each of 20 cotyledons, and these were incubated on moist filter paper in Petri dishes at 30 °C in the dark. Both elicitors were used in concentrations optimal for glyceollin accumulation. At the times indicated, the cotyledons were extracted with 100 ml of 60% ethanol by vacuum infiltration for 30 min, then the ethanol was removed under reduced pressure, the remaining solution was extracted with 100 ml of ethylacetate and the organic phase dried over Na_2SO_4. After removing the solvent under reduced pressure, each sample was chromatographed on Sephadex LH-20 (30 × 2.5 cm) in methanol. Separation of glyceollin, 3,6α-9-trihydroxypterocarpan and minor isoflavonoid components was then achieved by HPLC as described by Zähringer *et al.*[3]. The pterocarpan components were quantitated with a Waters Modul 730 using an extinction coefficient of 10.000 (ref. 4).

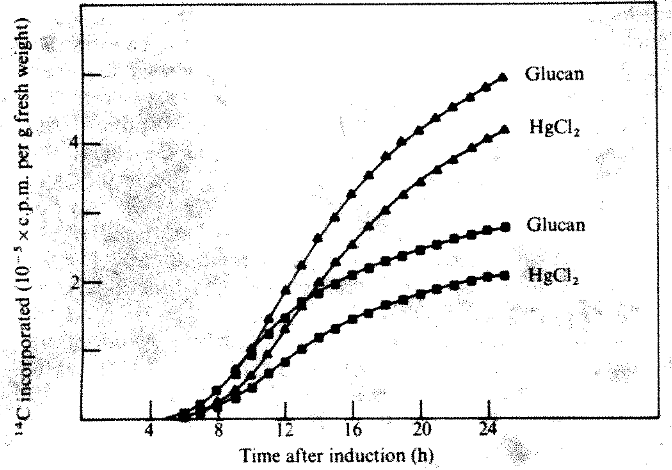

Fig. 2 Synthetic activity for glyceollin (■) and trihydroxyperocarpan (▲) production after treatment with glucan or mercuric chloride. Each set of 20 cotyledons was incubated in a 800-ml capacity gas-tight chamber with 100 μCi $^{14}CO_2$ (53.5 mCi mmol^{-1}) under illumination (Osram L 40 W/25, 9,500 lx) for 1 h before sampling. Radioactivity of the components was determined in the efflux of HPLC column with a Beckman Model LS-335 scintillation spectrometer using a toluene scintillation fluid. Radioactivity of glyceollin and THP (in c.p.m. per g fresh weight) was plotted against time after induction. For better comparison with the data obtained for accumulation, the curves were graphically integrated. Estimation of degradation activity (data not shown): 20 Petri dishes, each with 20 cotyledons, were transferred 8 h after induction with the elicitors into a 35 l chamber and were incubated under illumination with 1 mCi $^{14}CO_2$ (53.5 mCi mmol^{-1}) for 5 h. The pulse was followed by a chase phase (with illumination), in which $^{14}CO_2$ was replaced by air blown through the chamber. Twenty samples were analysed between 20 and 50 h after induction for radioactivity as described above.

obtained from pulse-chase experiments. Straight lines on semilogarithmic plots were obtained by linear regression analysis from which the following half-times were estimated: glyceollin (glucan) 112 ± 63 h; glyceollin ($HgCl_2$) 89 ± 53 h; THP (glucan) 39 ± 8 h; THP ($HgCl_2$) 36 ± 13 h. Determination of half-times in the controls was not possible due to the very low amounts of glyceollin and THP.

These results are not in agreement with Yoshikawa's conclusion[2] that biotic and abiotic elicitors have a diverse mode of action, at least in soybean cotyledons. Rates of synthesis of glyceollin and of its precursor trihydroxypterocarpan, as well as rates of conversion, are very similar with the two types of elicitors. From the relatively long half-time of conversion of glyceollin, one can conclude that accumulation of glyceollin isomers results mainly, if not exclusively, from stimulation of their synthesis by the elicitors. The rate of conversion of THP very probably represents its transformation to the 2-prenyl derivative, a potential precursor of glyceollin[3].

Our results are in agreement with the suggestion of Hargreaves[8] that mercuric chloride causes the production or release of constitutive phytoalexin elicitors. Such elicitors would be expected to have the same mode of action as externally supplied biotic elicitors.

This work was supported by Deutsche Forschungsgemeinschaft (SFB 46). P.M. thanks the Studienstiftung des Deutschen Volkes for a stipend.

Received 19 May; accepted 16 June 1980.

1. Albersheim, P. & Valent, B. S. *J. Cell Biol.* **78,** 627–648 (1978).
2. Yoshikawa, M. *Nature* **275,** 546–547 (1978).
3. Zähringer, U., Ebel, J., Mulheirn, L. J., Lyne, R. L. & Grisebach, H. *FEBS Lett.* **101,** 90–92 (1979).
4. Ayers, A. R., Ebel, J., Finelli, F., Berger, N. & Albersheim, P. *Plant Physiol.* **57,** 751–759 (1976).
5. Ayers, A. R., Ebel, J., Valent, B. & Albersheim, P. *Plant Physiol.* **57,** 760–765 (1976).
6. Lyne, R. L., Mulheirn, L. J. & Leworthy, D. P. *J.C.S. Chem. Comm.* 497–498 (1976).
7. Lyne, R. L. & Mulheirn, L. J. *Tetrahedron Lett.* 3127–3128 (1978).
8. Hargreaves, J. A. *Physiol. Plant Pathol.* **15,** 279–287 (1979).

Precocenes induce effect of juvenile hormone excess in *Locusta migratoria*

S. Fridman-Cohen & M. P. Pener*

Department of Zoology, The Hebrew University, Jerusalem, Israel

Precocene I and II (PI and PII)[1] and synthetic analogues[2–4] induce symptoms of permanent juvenile hormone (JH) deficiency in certain hemipteroid[1,5,6] and orthopteroid[7–11] insects. Younger nymphs treated with precocenes moult to precocious prothetelic nymph–adult intermediates, termed adultiforms[8], whereas treatment of older nymphs (too late for obtaining morphogenetic response) or of adults results in lack of oocyte development. The precocenes act as 'anti-allatins', causing atrophy of the corpora allata (CA)[8,12–14]. Recent findings suggest that the CA specifically metabolize precocenes to cytotoxic 3,4-epoxy-recocenes, possibly due to the epixidases present therein for JH biosynthesis; the accumulating precocene-epoxide seems to poison the glands[15,16]. This theory is supported by the claim that active CA are required for the effect of PII in *Oncopeltus*[6,17]. We demonstrate here that 7-ethoxy-PII ('Precocene III' = PIII), or PII itself, applied to last instar *Locusta* nymphs, induce an effect strictly typical of that of JH excess, in spite of eventually exerting the conventional anti-allatin effect. Our findings provide strong circumstantial evidence that supposedly inactive CA of these nymphs are temporarily activated by the precocenes, resulting in an outburst of JH biosynthesis before the glands are inhibited or destroyed.

Crowded nymphs of *Locusta migratoria migratorioides*, kept in routine conditions used in our laboratory[8], were used for the experiments. PIII (ZR 3623, Zoecon) topically applied in acetone to 0–27-h-old fifth (last) instar nymphs caused a portion of them to moult to metathetelic adultoids, that is, to sixth (supernumerary) instar nymphs with some adult characteristics, or to sixth instar nymph–adult intermediates (Fig. 1, AD). These adultoids were morphologically similar to those obtained after implantation of extra CA into early fifth instar nymphs[18,19]. Some adultoids even exhibited an extra (sixth) moult, although they died in its course, being unable to shed off the exuvium. Another portion of the fifth instar nymphs treated moulted to 'imperfect adults' (Joly's[18] 'imago imparfait'). These are adults with curled or twisted wings which occasionally (5–10%) also occur among normal locusts (controls, C in Fig. 2), usually due to external disturbances during adult emergence and/or expansion of the wings. Imperfect adults are obtained, however, much more frequently after implantation of extra CA, presumably mostly due to internal disturbances; their presence in relatively large numbers indicates a slight metathetelic effect[18]. The third portion of the nymphs moulted to morphogenetically normal adults.

With increasing doses of PIII the number of metathetelic individuals increased (Fig. 2), up to a maximum (10 adultoids and 6 imperfect adults out of 23 nymphs treated) at 50 μg per nymph. Further increase of the dose, however, resulted in a decrease of the metathetelic forms. At 500 μg per nymph metathetely disappeared; with regard to morphogenesis (but not for other effects, see below) the results were similar to those obtained in acetone treated controls. Were PIII a JH analogue, increasing doses would have eventually resulted in 100% adultoids. As a reverse trend was observed, PIII would not seem to act as a JH analogue in spite of inducing the effect of JH excess at lower doses.

The duration of the fifth instar was not distinctly affected by the dose when subsequent adultoids or imperfect adults were obtained; the respective averages for these two categories were

---

* To whom correspondence should be addressed.

0028–0836/80/330711—03$01.00

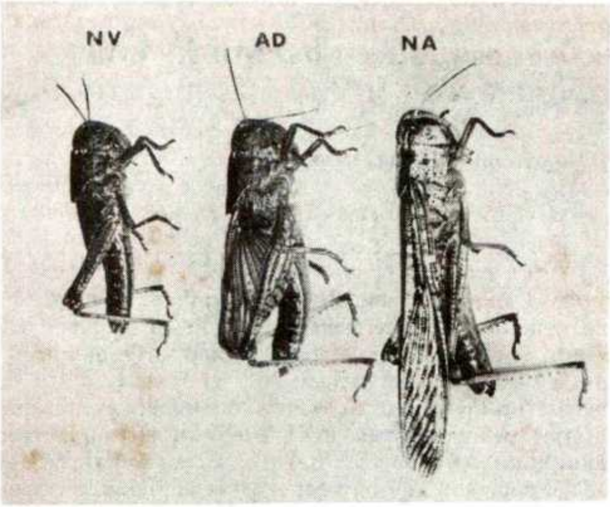

Fig. 1 Sixth instar metathetelic adultoid (AD) of *Locusta migratoria* obtained after topical application of 7-ethoxy-precocene II ('precocene III') to 0–27-h-old fifth (last) instar nymphs, in comparison with normal acetone-treated fifth instar nymph (NV) and normal (sixth instar) adult (NA).

189 (range 122–242) h and 228 (122–315) h. For morphogenetically normal adults the overall value was 245 (187–357) h, but here some dose-dependent trend was observed; with increasing doses the average duration of the fifth instar increased from 220 (187–286) h (25 or 50 μg PIII per nymph) to 275 (215–357) h (500 μg PIII). Morphogenetically normal acetone-treated controls gave 258 (215–311) h. Metathetely seems to be correlated, therefore, with shorter duration of the previous instar.

The same locusts from which Fig. 2 was obtained were maintained for 23–37 days after moult to adults or adultoids. The colour of all survivors was then recorded and the locusts were dissected; the state of the oocytes was noted in females and the CA were examined in both sexes. Lack of vitellogenetic oocytes, absence of yellow colour and atrophied CA indicated an anti-allatin effect (see ref. 8). Vitellogenetic oocytes and presence of yellow colour were sufficient for recognizing functional CA in imperfect or morphogenetically normal adults. Adultoids, however, especially with dominating larval features, often did not show signs of sexual maturation (see also ref. 18); in these cases conclusions were limited to the results of the examination of the CA. Dose–response data (Fig. 3) yielded the customary sigmoid curve, revealing that PIII did induce the conventional anti-allatin effect of the precocenes, in spite of exerting the metathetelic effect. Interestingly, 50 μg PIII per nymph, the dose which induced maximum methathetely (Fig. 2), was the closest to ED_{50} (50% of locusts with non-functional CA) for the anti-allatin effect (Fig. 3).

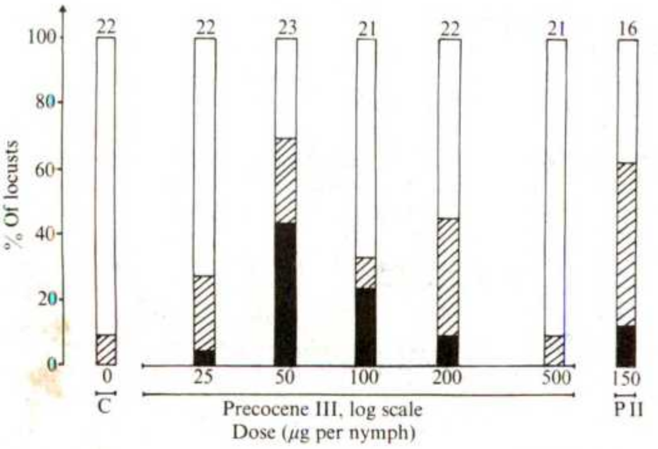

Fig. 2 Dose–response of precocene induced metathetely. 'C', acetone-treated controls: 'Precocene III' treatment with 7-ethoxy-precocene II: 'PII' treatment with precocene II. Each column represents a single experimental group. Number of locusts in each group after the next (from fifth to sixth instar) moult (constituting 100% for the ordinate) is noted on the top of each column. Mortality during the fifth instar did not exceed two locusts in any group. Filled area sixth instar adultoids; hatched area; sixth instar imperfect adults; unshaded area; sixth instar morphogenetically normal adults.

A single experiment with PII (Calbiochem) revealed that the double effect, induction of metathetely (PII, Fig. 2) and anti-allatin action (PII, Fig. 3), is not confined to PIII. Studies of dose–response relationships of PII with regard to both effects are under way.

Only JH or bioanalogues are known to induce metathetely. Since precocenes do not seem to act as JH analogues (see above), the metathetely observed by us is presumably a result of endogenous JH excess. The CA are the only known source of endogenous JH in *Locusta* and JH titre in the haemolymph is undetectable or very low in early last instar nymphs[20–22]. Thus, in accord with conventional concepts, *in situ* CA seem to be rather inactive at this time (although transplanted necessarily denervated CA may show activity, see refs 20, 23). At present the sole feasible explanation for metathetely seems to be, therefore, that PIII (and PII) directly or indirectly activates the nymphs' own CA resulting in an outburst of JH biosynthesis and release. Activated CA, however, presumably rapidly metabolize the precocenes to cytotoxic precocene-epoxides which then inhibit or destroy the glands[15,16]. Thus, precocene-induced CA activation is probably very temporary. More active CA may destroy themselves more quickly, leaving less time for JH biosynthesis. If so, with increasing doses the balance would be gradually shifted to produce less JH and more precocene-epoxide, resulting in decrease of metathetely and increase of anti-allatin effect. This reasoning exactly fits our results, including the eventual complete loss of the effect of JH excess at high doses.

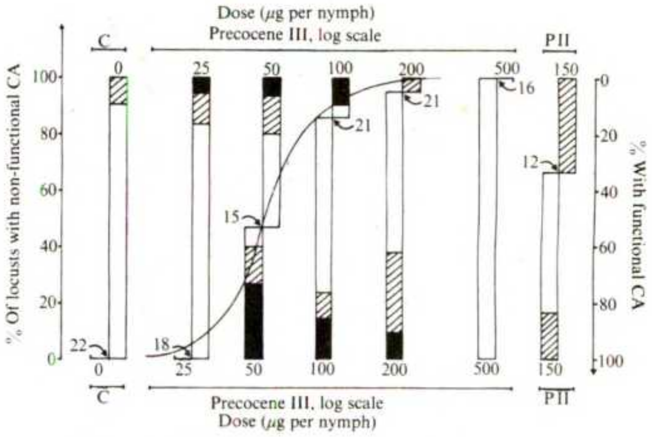

Fig. 3 Dose–response relationships of the anti-allatin effect of precocenes. Number of locusts at the examination of the anti-allatin effect (23–37 days after moult to sixth instar adultoids or adults) is noted with arrows at the meeting point of rising and hanging columns for the same dose and substance. Locusts were the same as used for Fig. 2, except for some which died (naturally, accidentally or during extra moult of some adultoids) or were lost between examination of metathetely (Fig. 2) and of anti-allatin effect. The sigmoid curve is the dose–response curve for the anti-allatin effect of 7-ethoxy-precocene II ('Precocene III'). Abbreviations and shading as in Fig. 2.

None of the adultoids or adults turned green in the present experiments. Green colour is caused by JH in *Locusta* nymphs[18,19,23], but its absence can easily be explained if precocene-induced CA activation is indeed temporary. The timing of susceptibility of the integument to JH may differ for morphogenetic and for colour effects, or alternatively, a longer lasting or continuous JH titre (but a low one, as normal solitary nymphs are mostly green without morphogenetic disturbances) may be needed for green colour induction. Both explanations can be reconciled with previous experimental findings and theoretical considerations[18,21]. If this is so, precocene-induced temporary activation of the CA may occur in other stages too, but it may not become overt. In younger instars no metathetely would be discernible and a short outburst of JH excess may be just as insufficient for inducing green colour as in last instar nymphs. Moreover, if our interpretation of the results is correct (on the basis of present knowledge of insect endocrinology no other explanation can be offered without wild speculation), differences in susceptibility of different species, or of different instars of the same species, differences in effectiveness of different methods of administration (such as topical application and residual coating methods) and eventually possible development of precocenes to insect control agents, may all be related to precocene-induced activation of the CA.

We thank Dr G. B. Staal of Zoecon Corporation for a gift of precocene III, Mr Y. Toren for keeping the locust cultures and Mr P. Amitai for taking the photograph of Fig. 1 and drawing the other figures. This research was supported by a grant from the US–Israel Binational Science Foundation (BSF), Jerusalem, Israel.

Received 10 April; accepted 2 July 1980.

1. Bowers, W. S., Ohta, T., Cleere, J. X. & Marsella, P. A. *Science* **193**, 542–547 (1976).
2. Bowers, W. S. *Pontificae Academiae Scientiarum Scripta Varia* **41**, 129–156 (1977).
3. Ohta, T. & Bowers, W. S. *Chem. pharmac. Bull.* **25**, 2788–2789 (1977).
4. Brooks, G. T., Hamnett, A. F., Jennings, R. C., Ottridge, A. P. & Pratt, G. E. *Proc. 1979 British Crop Protection Conference—Pests and Diseases*, 273–279 (1979).
5. Tarrant, C. A. & Cupp, E. W. *Trans. R. Soc. trop. Med. Hyg.* **72**, 666–668 (1978).
6. Unnithan, G. C. & Nair, K. K. *Ann. ent. Soc. Am.* **72**, 38–40 (1979).
7. Pener, M. P. & Orshan, L. *Israel J. Zool.* **26**, 262–263 (1977).
8. Pener, M. P., Orshan, L. & De Wilde, J. *Nature* **272**, 350–353 (1978).
9. Němec, V., Chen, T. T. & Wyatt, G. R. *Acta ent. bohemoslov.* **75**, 285–286 (1978).
10. Pedersen, L.-E. K. *Gen. comp. Endocr.* **36**, 502–509 (1978).
11. Chênevert, R., Paquin, R. & Perron, J.-M. *Naturaliste Can.* **105**, 425–427 (1978).
12. Unnithan, G. C., Nair, K. K. & Bowers, W. S. *J. Insect Physiol.* **23**, 1081–1094 (1977).
13. Schooneveld, H. *Experientia* **35**, 363–364 (1979).
14. Schooneveld, H. *Cell Tissue Res.* **203**, 25–33 (1979).
15. Brooks, G. T., Pratt, G. E. & Jennings, R. C. *Nature* **281**, 570–572 (1979).
16. Pratt, G. E., Jennings, R. C., Hamnett, A. F. & Brooks, G. T. *Nature* **284**, 320–323 (1980).
17. Masner, P., Bowers, W. S., Kälin, M. & Mühle, T. *Gen. comp. Endocr.* **37**, 156–166 (1979).
18. Joly, L. thesis, Univ. Strasbourg (1960).
19. Staal, G. B. *Publ. Fonds Landbouw Export Bur. 1916–1918* No 40, 1–125 (1961).
20. Johnson, R. A. & Hill, L. *J. Insect Physiol.* **19**, 1921–1932 (1973).
21. Joly, L., Hoffmann, J. & Joly, P. *Acrida* **6**, 33–42 (1977).
22. Huibregtse-Minderhoud, L. thesis, Univ. Utrecht (1979).
23. Joly, P. *Ann. Soc. ent. Fr.* **3**, 601–608 (1967).

Killed *Listeria monocytogenes* vaccine is protective in C3H/HeJ mice without addition of adjuvants

Hans van Dijk, Frans M. A. Hofhuis, Els M. J. J. Berns, Cees van der Meer & Jan M. Willers

Immunology Section of the Laboratory of Microbiology, State University, Catharijnesingel 59, 3511 GG Utrecht, The Netherlands

Resistance of mice to the facultative intracellular parasite *Listeria monocytogenes* involves cellular immunity[1], as it can be transferred passively with viable lymphoid cells[2] but not with serum. Induction of protective immunity can only be achieved by vaccination with sublethal numbers of viable listeria[3,4] or with dead listeria in combination with certain adjuvants[5,6]. Killed listeria vaccines as such are not protective. Effective adjuvants are lipopolysaccharide (LPS)[5], dextran sulphate (molecular weight 500,000) and suramin[6], whereas Freund's complete adjuvant is ineffective[6]. All these polyanionic substances have a shortlived deleterious effect on macrophage function[5–7]. It seems necessary for their adjuvant activity that they be present during the induction of immunity, most probably resulting in incomplete degradation of the dead listeria within the macrophage. During the effector phase, however, the adjuvants need to be virtually absent[8,9], so that macrophages are unhampered in eliminating the infective bacteria of an eliciting listeria injection. We describe here our finding that LPS-nonresponder C3H/HeJ mice, unlike H–2 identical C3HeB/FeJ or H–2 unrelated mice, can develop resistance to a lethal dose of viable *L. monocytogenes* on a single injection with dead listeria vaccine without any adjuvant added. This suggests that the C3H/HeJ mouse has some kind of 'intrinsic adjuvant'. If present, such an intrinsic adjuvant would, in analogy to the effective adjuvants[5–7], probably be a polyanionic substance. By means of protamin precipitation[10], we have found evidence for the presence of such a substance in the serum of C3H/HeJ mice.

C3H/HeJ (H–2^k), C3HeB/FeJ (H–2^k) and BALB/c (H–2^d) mice, aged 10–14 weeks, received 10^8 heat-killed listeria or a control saline injection. The dose of 10^8 listeria was shown to be optimally protective if injected in combination with adjuvant[6]. Seven days later, protective immunity was tested by injection of $20 \times LD_{50}$ of live listeria and subsequent daily inspection of the animals for two weeks (LD_{50} = the dose resulting in 50% death of unimmunized BALB/c mice in similar conditions). None of the saline-injected mice, except for one C3H/HeJ mouse, survived the challenge with viable listeria (Table 1). Vaccinated C3H/HeJ mice, however, in contrast to BALB/c and even to H–2 identical C3HeB/FeJ mice, were significantly protected against the lethal challenge.

In view of the current ideas about the development of resistance towards intracellular parasites[6,7], our results suggest the C3H/HeJ mouse to bear a kind of intrinsic adjuvant. This adjuvant might be cell-linked, perhaps identical to the macrophage defect[11]. According to this hypothesis, defective macrophage processing would result in incomplete degradation of immunogenic elements of the dead vaccine, promoting the induction of protective immunity. During the effector phase, however, the macrophage defect of the C3H/HeJ mouse could be corrected by lymphokine production[12]. Another explanation of our findings might be that the intrinsic adjuvant of the C3H/HeJ mouse is not cell (macrophage) linked, but that it is, for instance, a soluble serum factor. As the effective adjuvants are polyanionic substances, the serum of C3H/HeJ mice was investigated for such a substance by protamin sulphate precipitation[10], and the C3H/HeJ mouse was compared with the C3HeB/FeJ and the BALB/c mouse. As Table 2 shows, a 'protamin precipitable factor' (PPF) was indeed present in C3H/HeJ serum. PPF was also found in C3HeB/FeJ and BALB/c serum, but in substantially lower concentrations.

It is possible that there is no relationship between the relatively high PPF level, the macrophage defect and other errors of the C3H/HeJ mouse, such as a defect in the early classical complement system[14], most probably residing in the C_{3b} or C_{4b} inactivator system[15]. An interesting alternative explanation is, however, that there is a relationship or even identity between the abnormalities of the C3H/HeJ mouse. In that construction,

Table 1 Resistance of the mouse strains to a lethal listeria infection after injection with a dead vaccine

Mouse (sub)strain	Injection	
	Vaccine	Saline
C3H/HeJ	24/30	1/30
C3HeB/FeJ	2/30	0/30
BALB/c	0/30	0/30

Groups of five male C3H/HeJ, C3HeB/FeJ and BALB/c mice were injected intraperitoneally with 10^8 heat-killed (60 min, 56 °C) listeria or saline. Seven days later, the animals were challenged intraperitoneally with live ($20 \times LD_{50}$) listeria. The numbers of survivors on the numbers of mice challenged were recorded for 2 weeks. Results of six such experiments are summarized above.

0028-0836/80/330713—02$01.00

Table 2 Serum levels of protamin precipitable factor

Mouse (sub)strains	PPF serum level (units ml^{-1})	*P* value (Student's *t*-test)
C3H/HeJ	291 ± 32	
C3HeB/FeJ	133 ± 20	<0.0005 (two-sided)
BALB/c	68 ± 4	$\ll 0.0001$

Groups of 20 male C3H/HeJ, C3HeB/FeJ and BALB/c mice were bled for individual sera by retro-orbital puncture at 11.30 p.m. To 20 μl of serial dilutions of these sera, 2 ml Veronal-buffered saline, *p*H 7.4, containing 0.15 mM Ca^{2+} and 0.5 mM Mg^{2+} (VSB^{++})[13] and 250 μg protamin sulphate, dissolved in 25 μl of VSB^{++}, were added. The mixture was incubated at room temperature for 20 min, whereafter the turbidity was determined by measuring the E_{450} against a serum blanco. As found for heparin, which was used as reference, a linear relationship between the serum concentration and the turbidity was observed. PPF concentrations have been expressed in equivalents of heparin units.

PPF would resemble heparin in more than one respect: heparin is easily precipitated by protamin, it is an inhibitor of several enzyme activities[16], most probably also within the macrophage into which it is easily incorporated[17]. Moreover, it mimics the effects of the C_{3b} inactivator system in preventing C_{3b}-B complex formation[18]. The identity and activities of PPF will be subject of further study.

Whatever the case, our observations on the development of protective immunity on injection with a dead listeria vaccine and on the high PPF levels in the C3H/HeJ mouse are expected to bring new insights in both the acquisition of resistance to intracellular parasites and the defect(s) of the C3H/HeJ mouse.

Received 21 April; accepted 18 June 1980.

1. Mackaness, M. B. *J. exp. Med.* **116,** 381–406 (1962).
2. Mackaness, M. B. *J. exp. Med.* **129,** 973–992 (1969).
3. Hasenclever, H. F. & Karakawa, W. W. *J. Bact.* **74,** 584–586 (1957).
4. Kerckhaert, J. A. M., Hofhuis, F. M. A. & Willers, J. M. N. *Immunology* **32,** 1027–1032 (1977).
5. Rodriguez, G. E., McClatchy, J. K. & Campbell, P. A. *Infect. Immun.* **10,** 1163–1169 (1974).
6. Van der Meer, C., Hofhuis, F. M. A. & Willers, J. M. N. *Nature* **269,** 594–595 (1977).
7. Willers, J. M. N. *et al. Antonie van Leeuwenhoek* **45,** 41–48 (1979).
8. Hahn, H. *Infect. Immun.* **10,** 1105–1109 (1974).
9. Hahn, H. & Bierther, M. *Infect. Immun.* **10,** 1110–1119 (1974).
10. Graham, D. T., Pomeroy, A. R. & Smythe, D. B. *Thromb. Haemostasis* (*Stutig.*) **41,** 583–589 (1979).
11. Ruco, L. P. & Meltzer, M. S. *J. Immun.* **120,** 329–334 (1978).
12. Vogel, S. N. & Rosenstreich, D. L. *J. Immun.* **123,** 2842–2850 (1979).
13. Mayer, M. M. in *Experimental Immunochemistry* 2nd edn (eds Kabat, E. A. & Mayer, M. M.) 133 (Thomas, Springfield, 1961).
14. Hoffmann, M. K. *J. Immun.* **121,** 619–621 (1978).
15. Van Dijk, H., Van Heuven-Nolsen, D., Rademaker, P. M., Bloksma, N. & Willers, J. M. *Cell Immun.* **51,** 402–407 (1980).
16. Jaques, L. B. *Science* **206,** 528–533 (1979).
17. Mahadoo, J. & Jaques, L. B. *Med. Hypoth.* **5,** 835–842 (1979).
18. Weiler, J. M., Yurt, R. W. & Austen, K. F. *J. Immun.* **120,** 1802 (1978).

Mechanism of origin of complete hydatidiform moles

Patricia A. Jacobs*, Carola M. Wilson*, Joyce A. Sprenkle†, Neil B. Rosenshein‡ & Barbara R. Migeon†

* Department of Anatomy and Reproductive Biology, University of Hawaii School of Medicine, Honolulu, Hawaii 96822
† Departments of Pediatrics and ‡ Gynecology and Obstetrics, Johns Hopkins University, Baltimore, Maryland 21210

Complete or 'true' hydatidiform mole, an abnormality of human gestation, is characterized by hydropic degeneration of all placental villi, marked hypertrophy of the trophoblast, absence of a fetus and a propensity to become malignant. The chromosome constitution of complete moles is usually 46,XX[1,2], and Kajii *et al.* reported that the entire genome in seven out of seven cases was paternal in origin, with all centromere markers homozygous for paternal heteromorphisms[3]. These observations, since confirmed[4,5], can be explained by the fertilization of an 'empty' egg—no effective genome—by either a haploid sperm that then duplicates without cytokinesis, to restore the diploid number, or by a diploid sperm resulting from failure of the second meiotic division. We report here a study of a series of complete moles that shows the first alternative to be correct in the majority of cases.

Diploidization of the sperm would result in an entirely homozygous conceptus, while fertilization with a diploid sperm would give rise to heterozygosity for some of those genes heterozygous in the father and situated distal to the points of exchange. As all chromosome heteromorphisms are situated at or very near the centromere they cannot be used alone to distinguish between the two mechanisms of origin. We therefore studied the phosphoglucomutase$_1$ (PGM_1) genotypes, as well as both C and Q-band chromosome heteromorphisms of an unselected series of complete moles and their parents from Baltimore and Hawaii.

PGM_1 has two common alleles with gene frequencies of approximately 0.76 and 0.24 (ref. 6). The locus is on the short arm of chromosome 1 and maximum likelihood estimates suggest that in males it is 50 centimorgans from the centromeric heteromorphic band at q12 (ref. 7). We restricted our analyses of non-centromeric markers to PGM_1 because that is the only locus available to us (1) with a genotype that can be determined reliably in both parental blood and fetal tissue; (2) with a high frequency of parental heterozygosity; and (3) which is situated sufficiently far from the centromere to ensure frequent recombination with it.

Results for 24 moles are shown in Table 1. In 20 cases successful chromosome studies were completed on cells cultured from the mole and both parents, and in a further 4 from mole and mother alone. Twenty-one moles had a 46,XX constitution, one had an additional medium-sized chromosome in the few cells we could analyse, one had a variable count with a mode at 85,XXXX and one was 46,XY. Cultures from nine 46,XX moles were treated with 5-bromodeoxyuridine (BUdR) and the cells were stained with acridine-orange to investigate X-chromosome allocycly[8]. All nine moles had a single allocyclic X in more than 96% of metaphases examined and were thus indistinguishable from cells from normal females.

In 22 moles the centromeric heteromorphisms in all informative chromosomes appeared homozygous and clearly of paternal origin. The PGM_1 genotype of the mole and both parents was determined for 14 of these 22 moles and in a further 3 cases for the mole alone. In all 17 cases, including 6 in which the father was known to be heterozygous, the mole was homozygous. Based on gene frequencies, it can be estimated that, if the moles originated from a diploid sperm resulting from failure of the second meiotic division, 6.2 of the 17 tested moles would be heterozygous at the PGM_1 locus as would 4.0 of the 6 in which the father is known to be heterozygous. The absence of heterozygosity at the PGM_1 locus is significant both for the total number of moles tested ($P<0.001$) and for the offspring of known heterozygous fathers ($P<0.01$) and is therefore strongly supportive of a haploid sperm origin for most of the 46,XX moles.

Yamashita *et al.*[9] reported the HLA specificities of 13 moles and their parents and in 11 informative matings the moles showed no heterozygosity. However, the maximum likelihood estimate for the distance of the HLA loci from the centromere of chromosome 6 in males is only 8 centimorgans (B. J. B. Keats, personal communication). Thus HLA is an inefficient locus for determining the exact origin of 46,XX moles and in a series of 11 the expectation of heterozygosity, given an origin by failure of meiosis II leading to a diploid sperm, is only 1.8, not significantly different from the zero observed. Lawler *et al.*[10] tested five different loci in parents and moles and found the mole to be

Table 1 Cytogenetic and PGM$_1$ observations on 24 complete moles

No.	Chromosome constitution		Chromosome heteromorphisms* Chromosome no.										PGM$_1$† type
			1	3	4	9	13	14	15	16	21	22	
K456	46,XX	Pat		aa	aa		ab		ab			ab	
		Mat	—	bc	ab	—	cd	—	bb	—	—	cc	—
		Mole		aa	aa		aa		aa			aa	
K487	46,XX	Pat	—								—	—	
		Mat	ab	—	—	—	—	—	—	—	aa	ab	—
		Mole	cc								bb	cc	
K513	46,XX	Pat		ab		ab	ab			aa			
		Mat	—	ac	—	aa	cd	—	—	ab	—	—	—
		Mole		bb		bb	aa			aa			
K515	85,XXXX	Pat		aa									
		Mat	—	bb	—	—	—	—	—	—	—	—	—
		Mole		aaaa									
K739	46,XX	Pat		ab		ab	ab	aa	aa				
		Mat	—	cc	—	ac	cd	ab	bb	—	—	—	—
		Mole		ac		bc	ac	ab	ab				
K901	46,XX	Pat	aa	ab		aa	ab	aa	ab	aa	ab	aa	1-1
		Mat	bb	cd	—	ab	ac	ab	ab	bb	ac	ab	1-1
		Mole	aa	aa		aa	bb	aa	aa	aa	bb	aa	1-1
K1040	46,XX	Pat	aa				ab		ab	ab	ab		1-1
		Mat	bc	—	—	—	cd	—	aa	aa	ac	—	1-2
		Mole	aa				aa		aa	aa	bb		1-1
K1064	46,XX	Pat	—	—		—			—			—	—
		Mat	aa	ab	—	aa	—	—	ab	—	—	ab	—
		Mole	bb	cc		bb			cc			aa	1-1
K1200	46,XX	Pat		—			—	—			—	—	—
		Mat	—	ab	—	—	ab	ab	—	—	aa	ab	1-2
		Mole		aa			aa	aa			bb	cc	1-1
K1248	46,XX	Pat		ab			ab	aa	ab		ab	ab	1-2
		Mat	—	ac	—	—	ac	ab	bb	—	ac	ab	1-1
		Mole		aa			aa	aa	aa		aa	aa	1-1
K1250	47,XX,+C	Pat			ab		ab		ab				1-1
		Mat	—	—	bb	—	cd	—	cd	—	—	—	1-2
		Mole			aa		aa		aa				1-1
K1359	46,XX	Pat		aa	aa		ab				ab	aa	1-1
		Mat	—	ab	bc	—	bc	—	—	—	ab	ab	1-2
		Mole		aa	aa		aa				aa	aa	1-1
S22	46,XX	Pat	ab		ab		ab		aa	ab	ab	ab	
		Mat	aa	—	aa	—	aa	—	bc	cc	aa	bb	—
		Mole	aa		aa		aa		aa	aa	aa	aa	
S26	46,XX	Pat		ab	ab		ab	ab	aa	ab		ab	1-1
		Mat	—	bc	ab	—	bc	cc	ab	ac	—	ab	2-2
		Mole		aa	aa		aa	aa	aa	aa		aa	1-1
S28	46,XX	Pat		ab			ab	ab	aa		aa	ab	1-2
		Mat	—	ac	—	—	cd	ac	ab	—	ab	ac	1-1
		Mole		aa			aa	aa	aa		aa	bb	2-2
S30	46,XX	Pat		ab			ab	ab	ab		ab		1-2
		Mat	—	ac	—	—	ac	ac	aa	—	aa	—	1-1
		Mole		bb			bb	bb	aa		aa		1-1
S31	46,XX	Pat		ab			ab	ab	ab		ab	aa	1-1
		Mat	—	ac	—	—	ac	aa	aa	—	ab	bc	1-2
		Mole		aa			aa	bb	bb		aa	aa	1-1
S32	46,XX	Pat		aa				ab				ab	1-2
		Mat	—	ab	—	—	—	aa	—	—	—	ac	1-1
		Mole		aa				bb				aa	2-2
S35	46,XX	Pat		—			—		—		—	—	—
		Mat	—	ab	—	—	ab	—	ab	—	ab	ab	2-2
		Mole		cc			cc		cc		cc	cc	1-1
S39	46,XX	Pat		ab			ab		ab		ab	aa	1-2
		Mat	—	ac	—	—	ac	—	cd	—	aa	ab	1-2
		Mole		aa			aa		aa		aa	aa	2-2
S40	46,XX	Pat		ab	ab		ab		ab		ab	ab	1-1
		Mat	—	ac	ab	—	bc	—	cc	—	aa	aa	1-2
		Mole		bb	aa		aa		aa		aa	aa	1-1
S41	46,XY	Pat	ab				ab			aa		ab	1-2
		Mat	aa	—	—	—	ab	—	—	ab	—	ab	1-1
		Mole	ab				aa			aa		aa	1-1
S45	46,XX	Pat		aa			aa	ab	ab			ab	1-1
		Mat	—	bb	—	—	ab	cc	bb	—	—	ac	1-1
		Mole		aa			aa	aa	bb			aa	1-1
S46	46,XX	Pat		aa			ab	ab	ab		aa	ab	1-2
		Mat	—	ab	—	—	cd	aa	cc	—	ab	ab	1-2
		Mole		aa			aa	aa	aa		aa	ag	2-2

* Heteromorphisms of chromosomes 3, 4, 13, 14, 15, 21 and 22 were studied on Q-banded preparations[12] while those of chromosomes 1, 9 and 16 were studied on C-banded slides[13]; a, b and c are symbols and do not represent specific heteromorphisms.

† PGM$_1$ genotyping was carried out on parental red cells, molar tissue and cultured fibroblasts by cellulose acetate electrophoresis[14]. In each case, the result from molar tissue assay was confirmed in cultured cells derived from the specimen.

homozygous in 18 informative tests in which the father was heterozygous. However the distribution of the 18 tests among the loci examined is not given and, as the centromere distance is not shown for many of the loci, it is not possible to determine the significance of their data, although they support a haploid origin.

Two atypical moles in our series are worthy of comment. In one, a 46,XX mole (K739), many of the centromeric heteromorphisms appeared heterozygous and comparison with the parental chromosomes showed this mole to be the product of a normal conception containing both a paternal and a maternal genome. We could not determine the origin of the single 46,XY mole (S41) because the centromeric heteromorphisms and PGM_1 observations were compatible with either a normal conception or fusion of two sperm with an empty egg, although they excluded fertilization by a diploid sperm. Observations on a 46,XY mole have been reported that suggest a paternal origin resulting from the fertilization of an empty egg by either two haploid sperm or a diploid sperm that arose by failure of the first meiotic division[11].

The observation that there are at least three mechanisms of origin for complete moles, each with different genetic implications, is important in the formulation of a hypothesis to explain the propensity of complete moles to undergo malignant transformation. It would be interesting to know whether such a propensity is a property of all three types of complete moles or whether it is restricted to, or more prevalent in, any one class.

We thank Tai Do and David Hilbert for PGM_1 assays, and Aileen Matsuyama and Irene Buchanan for culturing moles. This work was supported by grants HD 07879 and HD 05465 from NIH.

Received 4 May; accepted 13 June 1980.

1. Vassilakos, P., Riotton, G. & Kajii, T. *Am. J. Obstet. Gynec.* **127,** 167–170 (1977).
2. Szulman, A. E. & Surti, U. *Am. J. Obstet. Gynec.* **132,** 20–27 (1978).
3. Kajii, T. & Ohama, K. *Nature* **268,** 633–634 (1977).
4. Jacobs, P. A., Hassold, T. J., Matsuyama, A. M. & Newlands, I. M. *Lancet* **ii,** 49 (1978).
5. Wake, N., Takagi, N. & Sasaki, M. *J. natn. Cancer Inst.* 51–57 (1978).
6. Cavalli-Sforza, L. L. & Bodmer, W. F. *The Genetics of Human Populations* (Freeman, San Francisco, 1971).
7. Rao, D. C., Keats, B. J. B., Lalouel, J. M., Morton, N. E. & Yee, S. *Am. J. Hum. Genet.* **31,** 680–696 (1979).
8. Dutrillaux, B., Laurent, C., Couturier, J. & Lejeune, J. *C.r.hebd. Séanc. Acad. Sci. Paris* **276,** 3179–3181. (1973).
9. Yamashita, K., Wake, N., Araki, T., Ichinoe, K. & Makoto, K. *Am. J. Obstet. Gynec.* **135,** 597–600 (1979).
10. Lawler, S. D. *et al. Lancet* **ii,** 580 (1979).
11. Surti, U., Szulman, A. E. & O'Brien, S. *Hum. Genet.* **51,** 153–156 (1979).
12. Matsuura, J. S., Mayer M. & Jacobs, P. A. *Hum. Genet.* **52,** 203–210 (1979).
13. Sumner, A. T. *Expl Cell Res.* **75,** 304–306 (1972).
14. Sonneborn, H. H. *Humangenetik* **17,** 49–55 (1972).

Bone-forming cell line derived from embryonal carcinoma cells

J. F. Nicolas, J. Gaillard, H. Jakob & F. Jacob

Unité de Génétique cellulaire du Collège de France et de
l'Institut Pasteur, 25 rue du Dr Roux, 75724 Paris Cedex 15, France

The use of established cell lines of various types has provided information on the properties of certain stem cells and on the conditions of their differentiation. No bone-forming cell line has so far been described. We report here the isolation, from *in vitro* differentiating teratocarcinoma cells[1], of a line which, on subcutaneous injection into syngeneic mice, gives rise to ossicles. The appearance of ossicles is preceded by the formation of a cartilaginous matrix, thus reproducing what has been described as endochondral differentiation[2]. The ossicles obtained are rapidly colonized by host marrow, are non-malignant and stop growing 2 weeks after injection of the cells. In certain conditions, however, osteosarcomas, chondroosteosarcomas and fibrosarcomas can be obtained. From these tumours, cell lines have been isolated which retain *in vitro* the properties of the cells found in the tumour.

Cell line 3/A/1D-1 was isolated from differentiated cultures of the embryonal carcinoma line PCC3/A/1 after *in vitro* differentiation[1]. These cells have a pseudo-epithelial appearance, are contact-inhibited and aligned at confluency. In electron micrographs, numerous intracisternal virus-like A particles, but no C particles, can be seen.

Two weeks after subcutaneous injection of 2×10^6 cells into 129/Sv mice, an ossicle is formed at the injection site in 50% (45/91) of the mice. The formation of these tumours has been followed by histological examination (Fig. 1*a–f*). The initial step seems to correspond to the development of primitive mesenchymal cells (Fig. 1*a*) which, after 2 weeks, give rise to chondroblasts and chondrocytes (Fig. 1*b*,*c*). These cells show the typical transformation that is observed in endochondral ossification, with mineral deposits near the surface of the hypertrophied chondrocytes and in the peripheral matrix (Fig. 1*c*,*d*). Then, foci of haematopoiesis and typical marrow appear inside the bone cavity (Fig. 1*e*,*f*). Marrow smears show classical bone marrow cells, including erythrocytic and granulocytic cells as well as megakaryocytes. The ossicles thus obtained are benign tumours; they stop growing 2–3 weeks after injection of the cells and some ossicles have been observed for 1 yr without further changes. However, within 2–4 months, fibrosarcomas frequently appear (20 out of 42 129/Sv mice observed during 6 months). These tumours develop independently of whether or not the mice form ossicles. Thus, between the 20 mice presenting fibrosarcomas, only 10 had previously developed an ossicle. Three independent fibrosarcomas were transplanted 5 to 10 times in 129/Sv. In some of these tumours, bone cells could be observed.

The manner in which the cells were injected was of importance for further development of the tumours. When subcutaneous lesions were provoked by scratching, the percentage of ossicles formed increased from 50 to 100% (41/41). Furthermore, in most cases malignant osteosarcomas and/or fibroosteosarcomas developed (Fig. 1*g*,*h*). In certain species, such as rabbit and rat, various treatments[3,4] or inert substances[5,6] are known to cause subcutaneous development of ossicles. Therefore the origin of the different elements found in ossicles formed upon injection of 3/A/1 D-1 cells was studied. First, no ossicle was ever observed in control 129/Sv mice injected with medium alone, with or without subcutaneous lesions (0/18). Therefore, the mere production of lesions is not sufficient to induce ossicle formation in mice. Second, mice from strains other than 129/Sv were injected with 3/A/1 D-1 cells. Whatever their major histocompatibility (H-2) haplotype, none developed any ossicles (0 out of 42 allogeneic injections). Even mice bearing an H-2^b haplotype (as do 129/Sv) were negative. The injection and the presence of the cells for only a few days (before allogeneic rejection) are insufficient for the development of ossicles.

To reduce the possibilities of a contribution by the host, 3/A/1 D-1 cells were injected into the eye of 129/Sv mice. In every case, the development of bone tissue could be observed. As in the case of subcutaneous injections, the process began by the appearance of mesenchymal cells, rapidly followed by chondrocytes and osteoblast cells. However, no bone marrow could be observed in these conditions.

A direct study of the origin of the different elements of the ossicles was then carried out. After injection of 3/A/1 D-1 cells into (129/Sv × C57BL)F_1 mice, marrow-containing ossicles were formed at the site of injection. The origin of the marrow cells present in such H-2^{bc}/H-2^k hybrids was studied by cytotoxicity tests with anti-H-2 sera. Bone marrow cells were found to respond to both anti-H-2.2 (which detects private specificity 2 of H-2^b) and anti-H-2.32 (which detects private specificity 32 of H-2^k) sera (Fig. 2). Thus, the majority of bone marrow cells appear to be of host origin. To study stromal cells[8,9], 3/A/1 D-1 cells were injected into (129/Sv × Rb 163)F_1 mice which carry a metacentric chromosome (9-19) as marker. The bone cavities of the ossicles obtained were flushed and the cells put in culture. Karyotype analysis of epithelial and pseudofibroblastic cells 18

0028–0836/80/330716—03$01.00

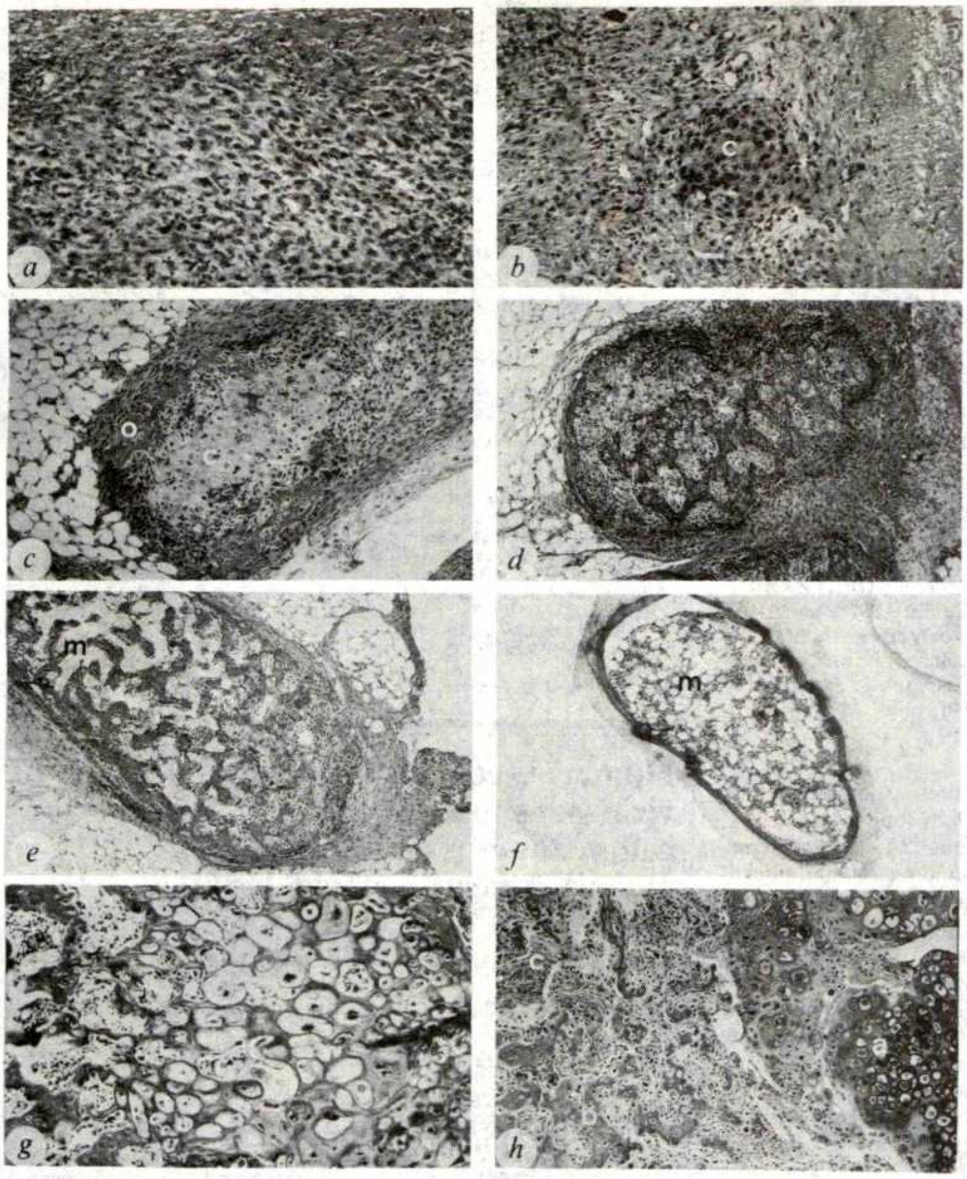

Fig. 1 Types of tumours obtained by subcutaneous injection of 3/A/1 D–1 cells. *a–f*: Ossicle formation. Detectable tumours appear 9–14 days after subcutaneous injection of cells. Final ossicle (as shown in *f*) is found 2–3 weeks after injection. *a–e* Illustrate earlier aspects of tumours dissected shortly after their appearance. *a*, Primitive mesoblast (12-day old tumour); *b*, precartilaginous nodule (10-day old tumour); *c*, ossification (o) at the periphery of cartilage (c) (10-day old tumour); *d*, trabeculation of the bone (13-day old tumour); *e*, formation of medullar cavity (14-day old tumour); *f*, mature ossicle with marrow (transversal section, 60-day old tumour); *g*, *h*, malignant proliferation; *g*, abnormal cartilage (45-day old tumour); *h*, osteochondrosarcoma. a, cartilage; b, trabecular bone; e, mesenchyme (90-day old tumour). Cell line 3/A/1 D–1 was isolated from embryonal carcinoma cell line PCC3/A/1 after *in vitro* differentiation[1,7]. 2×10^6 PCC3/A/1 cells were plated on tissue culture Petri dishes (Falcon, diameter 10 cm) and kept at confluency. 25 days later, various types of mesodermal derivatives were apparent. The cells were dissociated with 0.05% trypsin and replated at different densities. One week later the culture medium was replaced for three days by a medium enriched in KCl (1 M final), a treatment found to kill selectively embryonal carcinoma cells. After several weeks, surviving differentiated cells stopped growing. Two months later some clones began to multiply. One of these was isolated and recloned. It was called 3/A/1 D–1. The cells were cultivated in Dulbecco's modified Eagle medium (DMEM) with 15% fetal calf serum (Gibco). Cells were maintained at high density (not below 10^4 cm^{-2}) and replated every 2 days after mild treatment with trypsin (0.05%). To obtain benign bone formation (F), 10^6 to 5×10^6 cells were injected subcutaneously into mice (in a total volume of 0.5 ml of DMEM). Tumours appeared not later than 2 weeks after injection, in 50% of injected mice. No delayed appearance of bone was observed in the negative mice. To obtain malignant growth (*g*, *h*), lesions have to be provoked by scratching at the time of cell injection. In this case, 100% of the mice present an irregular ossicle after 2 weeks. In the majority of cases, this ossicle continued to grow (*g*, *h*) and was found to be transplantable.

Table 1 Origin of osteosarcomas and fibrosarcomas obtained in F_1 (129×C57BL) as shown by reinjection into parental mice

	No. of mice developing tumours		
	No. of mice injected		
	F_1 H-2^{bc}/H-2^k	129/Sv H-2^{bc}/H-2^{bc}	C57BL H-2^k/H-2^k
Osteosarcoma			
1903	2/2	2/2	0/2
1860	2/2	2/2	0/2
1969	3/3	3/3	0/3
2055	2/2	2/2	0/0
Fibrosarcoma			
1738	2/2	2/2	0/2

The tumours were dissected and dissociated by mincing with scissors in DMEM + 1% fetal calf serum. They were reinjected subcutaneously or subcutaneously and intraperitoneally using a needle of 0.8 mm diameter. The injected mice were males approximately 8 weeks old.

days after the beginning of the culture showed the presence of both host cells (39 chromosomes, 1 metacentric and 78 chromosomes, 2 metacentrics) and 3/A/1 D–1 cells (75 chromosomes, no metacentric) (Fig. 3). The latter cells behave like established cells and continue to proliferate when femoral marrow control cultures have stopped growing. A cell line (3/A/1 D–1 M) has been re-isolated from these cultures. After subcutaneous injection of such cells into 129/Sv mice, a typical ossicle colonized by marrow cells is formed. Osteosarcomas, however, have never developed from these ossicles. Similar behaviour has been observed with a 10-month old ossicle of a 129/Sv mouse. Thus, even long after the formation of the ossicle, cells derived from 3/A/1 D–1 that conserve certain of their properties can be isolated among stromal cells of the bone.

The origin of the bone cells found after injection of 3/A/1 D–1 cells into a mouse cannot be studied directly in the ossicles formed. However, it can be reasonably assumed that the osteochondrosarcomas that are frequently formed when lesions are provoked at the site of injection have the same origin as the bone cells of ossicles. Thus, we have investigated the origin of osteochondrosarcomas obtained in (129/Sv×C57BL)F_1 mice. If derived from F_1 mice, these tumours should be rejected by

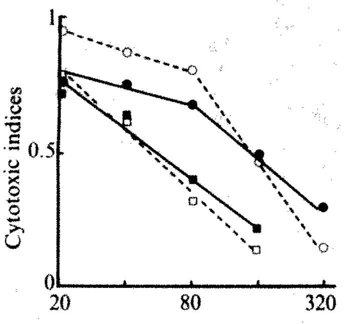

Fig. 2 Origin of ossicle marrow cells found in F_1 mice: cytotoxic effect of anti-H-2^b and anti-H-2^k sera. Cytotoxicity experiments were carried out as described in Artzt *et al.*[10]. Cell viability was estimated by trypan blue exclusion. Marrow cells from the ossicle were obtained by flushing the bone cavity with DMEM+5% immunoglobulin precipitated treated serum (IPT, Gibco). The cells were centrifuged, washed and red blood cells were lysed with a solution of ammonium chloride (0.87% in H_2O). After one additional centrifugation, cells were finally resuspended in Hank's+4% IPT at 10^6 cells ml^{-1}. The anti-H-2^b serum (B10D2×A)F_1 anti-B10A (2R) recognizes only private specificity 2. The anti-H-2^k serum (B10A×A) anti-B10K recognizes only private specificity 32. These two sera are a gift of Dr D. Schreffler. ●, Anti-32 serum and ■, anti-2 serum on ossicle marrow cells; ○, anti-32 serum and □, anti-2 serum on lymph node cells.

129/Sv and C57BL mice. However two tumours obtained in F_1 could be successfully transplanted in 129/Sv (but not in C57BL mice (Table 1). In several transplantations (5 to 15 transfers), these tumours retained their osteochondrosarcoma nature. Cells of one of these tumour lines have been established in culture (3/A/1 D-1 T°). The cells are not contact-inhibited; they have an aneuploid karyotype different from that of 3/A/1 D-1 (Fig. 3). Electron microscopic analysis reveals the presence of A-type virus particles (like in 3/A/1 D-1). When injected into mice, these cells always produce osteochondrosarcomas, even after conversion into the ascitic form.

A similar analysis was done with some of the fibrosarcomas which develop when 3/A/1 D-1 cells are injected without scratching. Like the osteosarcomas, these tumours are derived from injected cells (Table 1).

In conclusion, when injected into compatible mice, 3/A/1 D-1 cells induce the formation of a structure very similar to normal bone and/or osteochondrosarcomas. All the available evidence supports the hypothesis that the bone cells are formed directly from 3/A/1 D-1 cells. Although not completely excluded, the alternative hypothesis, that is, that 3/A/1 D-1 cells induce host cells to differentiate into bone, seems unlikely.

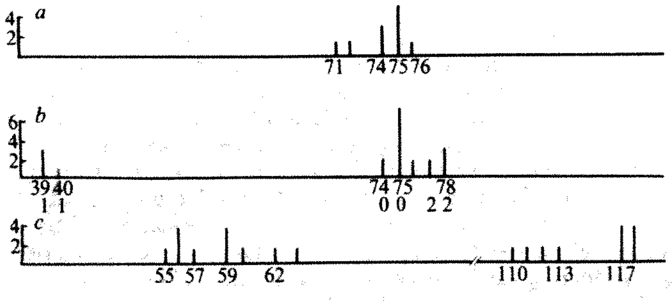

Fig. 3 Karyotype analysis of 3/A/1 D-1 (*a*), of stromal cells from ossicles obtained in (129/Sv×Rb 163)F_1 after 18 days in culture (*b*), and of 3/A/1 D-1 T° cells (osteochondrosarcoma cells) (*c*). Mitotic figures were obtained as described in Rothfels and Siminovitch[11]. Rb 163 refers to strain Rb(9-19) 163 Harwell, carrying a robertsonian fusion of chromosomes 9 and 19. The number of such metacentric chromosomes is given under the number of chromosomes (lower part).

The host, however, contributes to the marrow cells which populate the ossicle. In certain conditions, malignant cells can be selected *in vivo* from such tumours. These cells may (osteochondrosarcoma) or may not (fibrosarcoma) express chondrocyte and bone potentialities. They probably derive from pre-existing variants of the cloned cells and are selected in unknown conditions. All these cell lines provide valuable model systems for the study of normal and abnormal behaviour of osteogenic cells.

This work was supported by grants from the Centre National de la Recherche Scientifique (LA 269), the Délégation Générale à la Recherche Scientifique et Technique, the Institut National de la Santé et de la Recherche Médicale and the André Meyer Foundation.

Received 12 March; accepted 25 June 1980.

1. Nicolas, J. F., Avner, P., Gaillard, J., Guénet, J. L., Jakob, H. & Jacob, F. *Cancer Res.* **36,** 4224–4231 (1976).
2. Pritchard, J. J. in *Differentiation and Growth of Cells in Vertebrate Tissues* (ed. Goldspink, G.) 101–128 (Chapman & Hall, London, 1974).
3. Bridges, J. B. *Int. Rev. Cyt.* **8,** 253–278 (1959).
4. Wlodavski, K., Kobus, M. & Luczak, M. *Nature* **281,** 386–387 (1979).
5. Reddi, A. H. & Anderson, W. A. *J. Cell Biol.* **69,** 557–572 (1976).
6. Urist, M. R., Mikulski, A. & Lietze, A. *Proc. natn. Acad. Sci. U.S.A.* **70,** 1828–1832 (1979).
7. Nicolas, J. F., Dubois, Ph., Jakob, H., Gaillard, J. & Jacob, F. *Annls Microbiol. Inst. Pasteur, Paris* **126A,** 3–22 (1975).
8. Friedenstein, A. J. & Chailakhyan, R. F. *Transplantation* **17,** 331–340 (1974).
9. Cline, M. J. & Golde, D. W. *Nature* **277,** 177–181 (1979).
10. Artzt, K. *et al. Proc. natn. Acad. Sci. U.S.A.* **70,** 2988–2992 (1973).
11. Rothfels, K. H. & Siminovich, L. *Stain Technol.* **33,** 73–77 (1958).

Human T-cell cultures from virus-sensitized donors can mediate virus-specific and HLA-restricted cell lysis

K. K. Sethi, I. Stroehmann* & H. Brandis

Institut für Med. Mikrobiologie und Immunologie, Universität Bonn, 5300 Bonn-Venusberg, FRG

Human cells infected with viruses such as herpes simplex virus (HSV) or Epstein–Barr virus (EBV) become susceptible to the lytic action of a distinct population of lymphocytes termed natural killer (NK) cells present in the blood of normal (sero-negative) and sero-positive individuals[1,2]. Although NK cells probably represent a subset within the T-cell lineage[3,4], they are apparently not restricted in their lytic activity by the major histocompatibility complex (MHC) determinants as are most cytotoxic T lymphocytes (CTLs; ref. 5), but can potentially lyse a variety of unrelated virus-infected[6] or uninfected cultured cells[4,7]. In studies with murine models, it has been demonstrated that HSV[8,9] or murine cytomegalovirus (MCMV) specific[10,11] CTLs show the phenomenon of H-2 restriction initially described by Doherty and Zinkernagel with the LCM virus system[12], which is that the CTLs and targets must share H-2K or H-2D products. However, studies in man have not demonstrated the existence of HSV- or human cytomegalovirus (HCMV)-specific CTLs showing HLA (human analogue of mouse H-2) restriction in their lytic activity towards virally infected targets. We demonstrate here that T cells from the peripheral blood of patients recently cured of HSV or HCMV infections, when triggered *in vitro* with specific antigen and grown as long-term cultures in the presence of T-cell growth factor (TCGF), can mediate virus-specific and HLA-restricted lysis of virus-infected targets. We believe this to provide the first evidence that HLA-restricted and virus-specific T-cell mediated cytotoxicity can be demonstrated in human–HSV and HCMV systems. These HSV- or HCMV-specific CTLs could be important in limiting the *in vivo* spread of the respective viruses and/or in the pathogenesis of the disease caused by them.

---

* Medizinische Klinik, Immunologische Abteilung, Universität Bonn, FRG.

0028-0836/80/330718—03$01.00

Table 1 Lytic activity of long-term cultures of T cells derived from individuals sensitized to HSV, HCMV or EBV towards HSV- or HCMV-infected HLA-matched or unmatched targets

Effector T cells Donors (HLA)	Seropositive for:†	Target cell donor (HLA)*	Per cent lysis of targets infected with HSV-1 50:1	HSV-1 20:1	HCMV 50:1	HCMV 20:1	Uninfected 50:1	Uninfected 20:1
Ar (A2, 32/B5, 15)	HSV-1	Autologous	42	29	16	1	2	0
		Ru (A2, 3/B15, 40)	37	24	10	0	3	0
		Sr (A1, 2/B8, 15)	40	30	12	1	2	2
		Se (A1, 9/B8, 12)	12	5	10	1	2	0
		Me (A3, 11/B7, 35)	9	5	10	2	2	0
Ru (A2, 3/B15, 40)	HSV-1	Autologous	56	25	6	3	2	0
		Ar (A2, 32/B5, 15)	39	22	9	2	0	1
		Pk (A2, w32/B15, 17)	45	27	10	1	2	0
		Se (A1, 9/B8, 12)	15	3	4	2	3	1
		Ss (A1, 29/B8, 12)	18	4	13	1	6	0
Se (A1, 9/B8, 12)	HSV-1	Autologous	39	21	4	0	3	0
		Sr (A1, 2/B8, 15)	36	26	6	1	2	0
		Ss (A1, 29/B8, 12)	32	20	9	1	2	0
		Ar (A2, 32/B5, 15)	15	3	19	2	3	
		Ru (A2, 3/B15, 40)	9	2	10	1	2	0
Ki (A2, w24/B5, 7)	HCMV	Ar (A2, 32/B5, 45)	8	0	42	26	3	0
		Tr (A2, 3/B7, 40)	5	1	36	19	2	0
		Se (A1, 9/B8, 12)	6	0	10	2	2	0
		Ss (A1, 29/B8, 15)	12	0	9	3	1	0
Nn (A2, w24/B15, w44)	HCMV	Autologous	5	0	49	29	4	0
		Ar (A2, 32/B5, 15)	9	1	35	21	3	0
		Se (A1, 9/B8, 12)	8	0	11	2	0	0
		Ss (A1, 29/B8, 12)	16	3	8	4	0	0
Tr (A2, 3/B7, 40)	HCMV	Autologous	9	0	51	28	2	0
		Ru (A2, 3/B15, 40)	6	0	43	23	5	0
		Me (A3, 11/B7, 35)	8	1	46	29	3	0
		Se (A1, 9/B8, 12)	4	1	12	3	2	0
Me (A3, 11/B7, 35)	EBV	Autologous	8	2	9	1	0	0
		Tr (A2, 3/B7, 35)	9	1	12	2	2	0
Nk (A1, 2/B15, 38)	EBV	Autologous	6	1	8	1	1	0

Data are presented for eight blood donors; three of them (Ar, Ru, Se) had very recent (15 days–2 months) histories of herpes labialis; three (Ki, Nn, Tr) had recovered from recent (1–2 months) CMV pneumonitis and two (Me, Nk) were hospitalized for infectious mononucleosis. PBLs from heparinized blood of each donor were isolated on Ficoll–Hypaque (Lymphoprep; Nyco) gradients[13]. Washed PBL suspensions were prepared in growth medium (GM) containing RPMI 1640 (Flow), 20% heat-inactivated human serum (sero-negative for HSV, CMV and EBV), 25 mM HEPES buffer, 200 mM glutamine, 5×10^{-5}M 2-mercaptoethanol and antibiotics Aliquots (5 ml) of 10×10^6 fresh or cryopreserved PBLs sensitized to each particular virus were mixed with UV-ray inactivated samples (0, 1 μl) of specific virus (10^6 plaque-forming units (PFU) of HSV-1 strain Thea, 10^6 PFU of MCMV strain AD 169 or 100 μl of EBV obtained as stock virus from Dr Roggendorf, University of Munich). After 5 days at 37 °C in a humidified atmosphere with 5% CO_2, T cells were separated from stimulated PBLs as previously described[14,15]. Briefly, washed suspension (10^7 cells ml^{-1}) was added to equal volumes of 2% washed SRBC and normal human serum pre-absorbed with SRBC. After centrifugation at 50g for 5 min, the mixture was layered on Ficoll–Hypaque, incubated at 4 °C for 30 min and then centrifuged for 30 min at 200g. Rosetting cells, that is, the T-cell enriched population, were sedimented with SRBC which were subsequently lysed by hypotonic shock and the remaining cells suspended in GM. These stimulated T cells were maintained in long-term cultures by seeding 10^5 cells in individual wells of 24-well Costra tissue culture dishes with GM plus 20% TCGF (1.5 ml $well^{-1}$). TCGF was prepared as described elsewhere[16,17]. Briefly, PBL (5×10^6 ml^{-1}) from normal donors were cultured with PHA (1 μg ml^{-1}) in a total volume of 5 ml GM. After 48 h at 37 °C, the cell-free supernatant was filtered (0.22 μm Millipore filter) and stored (−20 °C) until required. T cells maintained in TCGF had increased in density after 5–7 days and were split at 1×10^4 cells ml^{-1} in fresh GM–TCGF. On days 15–45, the cells were washed and used as effectors in cytotoxicity assays. As targets, secondary human skin monolayer cultures from HLA-typed individuals were prepared in 25-cm flasks and inoculated with 5 PFU per cell of HSV or MCMV. After virus adsorption (37 °C for 1 h), the monolayers were washed and fed with GM containing 100 μCi $Na_2{}^{51}CrO_4$. Mock-infected cultures were incubated with ^{51}Cr as usual. After 4 h (HSV-infected) or 8 h (HCMV-infected) monolayers were disaggregated by 0.25% trypsin, washed and suspended in GM. Aliquots (100μl; 10^4 cells) of test targets were mixed in round-bottomed plastic tubes with 100 μl ($2-5\times10^5$ cells) of appropriate effectors. After centrifugation (50g for 10 min) the tubes were incubated for 4 h at 37 °C. The tubes were recentrifuged (400g for 10 min) in the cold and, from each tube, 100 μl of supernatant was collected and counted in a γ counter. The results are expressed as % specific ^{51}Cr release according to the formula: $100\times(E-S)/(M-S)$, where E = release in test, S = spontaneous release in medium alone, M = maximum radioactivity releasable in c.p.m. in 1% Triton. During the 4-h assay period the leakage of ^{51}Cr from HSV- or CMV-infected or uninfected targets in the presence of medium alone ranged from 8–12% of detergent-releasable counts. Since standard errors of triplicates seldom exceeded 3% they are omitted from the data.

* HLA-A/B antigens shared with effectors are underlined.

† Patients sensitized to HSV were negative for HCMV and vice versa.

Heparinized blood was obtained from selected donors sensitized to HSV-1 (three subjects), HCMV (three subjects) and EBV (two subjects). Peripheral blood mononuclear leukocytes (PBL) were purified over Ficoll–Hypaque density gradients by centrifugation[13]. Freshly isolated or cryopreserved PBL samples from sensitized donors were stimulated with specific antigen for 5 days *in vitro*. The activated T cells were separated by rosetting with sheep red blood cells (SRBC) as described previously[14,15]. T cells collected from each individual were maintained in long-term proliferating cultures using TCGF obtained as 48-h supernatant from phytohaemagglutinin (PHA; Wellcome)-stimulated normal PBL[16,17]. After 20–45 days of *in vitro* culture, the proliferating T cells of each donor were tested for lytic activity against selected panels of HSV or HCMV infected targets in a 4-h ^{51}Cr release assay (all attempts to detect the presence of immunoglobulin-producing cells in these cultures failed). In initial experiments, target cells were prepared by stimulating normal PBL from individual donors for 4 days with PHA (T blasts). The T blasts were then infected with virus and simultaneously labelled with ^{51}Cr. However, when the effectors were titrated against such targets, the level of spontaneous ^{51}Cr release was very high (up to 25%). Because of this drawback (although it had no significant influence on the interpretation of the results), human skin fibroblast cultures were established from HLA typed individuals by a standard procedure[18], infected with HSV-1 or HCMV, labelled with ^{51}Cr and then used as targets.

Table 1 shows that long-term T-cell cultures originating from three HSV sensitized individuals (Ar, Ru, Se) exerted reproducibly strong lytic activity towards HSV-infected but not

HCMV-infected autologous or HLA-A/B related fibroblast targets when assayed at an effector-to-target cell ratio of 50 : 1. Conversely, cultured T cells from three donors (Ki, Nn, Tr) sensitized to HCMV exerted a high level of lytic activity towards HCMV- but not HSV-infected autologous or HLA-A/B-matched targets. Freshly isolated PBL from sensitized donors or those stimulated *in vitro* with specific antigen for 5 days showed lytic activity towards virus-infected targets but this was not HLA restricted (data not shown). Apparently, for the generation of virus-specific and HLA-restricted secondary CTLs, the growth of specific antigen-triggered CTL precursors in nonspecific TCGF was mandatory. Controls, in identical conditions, proliferating long-term T-cell cultures from two donors sensitized to EBV showed no preferential HLA-restricted lysis of HSV- or HCMV-infected targets; these T cells, however, could lyse EBV-infected autologous or HLA-matched B blasts to very high levels (unpublished data). Generally, T cells from normal donors (seronegative for HSV and HCMV) were difficult to maintain in continuous cultures. However, T cells from two selected sero-negative donors could be established as long-term cultures but these, although highly efficient in mediating nonspecific lysis of targets, showed no evidence of virus specificity and HLA restriction (data not shown).

It is obvious (Table 1) that both HSV- and HCMV-sensitized T-cell cultures could mediate low but significant levels of cytotoxicity against homologous virus-infected and HLA-A/B-different (unmatched) targets. However, the amounts of ^{51}Cr released in these instances are no greater than the values when the same effectors were titrated against heterologous virus-infected targets. In separate experiments (data not shown), blocking attempts with cold HSV-infected or HCMV-infected HLA-matched fibroblasts gave a reduction in cytotoxicity against specific targets, which paralleled that ascribed to virus-specific CTLs; the amount of ^{51}Cr released due to NK cell activity being unchanged.

The above observations imply that even though the bulk of lytic activity exerted by long-term cultured T cells from HSV- or HCMV-sensitized donors was virus-specific and HLA-restricted, they also sometimes display significant nonspecific NK-cell-like activity. From the data it can be visualized that lowering the E : T cell ratio to 20 : 1 tended to eliminate the nonspecific lysis of targets and thereby gave generally low but exclusively virus-specific and HLA-restricted lytic values. We are now attempting to clone the long-term cultures of T cells containing potentially virus-specific and HLA-restricted CTLs in an attempt to study in detail the role of HLA-A and/or -B specificities in the recognition phenomenon.

In human–viral systems, HLA restriction of CTL-mediated cytotoxicity has been previously reported to occur only against influenza[19,20] and measles[21,22] virus infected cells. The issues of specificity and HLA restriction in the EBV system is still unresolved[23,24]. The cytotoxicity data presented here have revealed HLA restriction of lysis mediated by secondary HSV- or HCMV-specific long-term T-cell cultures. However, because of the small number of sensitized donors used for establishing virus-specific T-cell cultures, one might question whether the HLA-restricted lysis mediated by them is a general phenomenon or, as in the case of the influenza virus system[25], donors carrying certain HLA gene product(s) lack the ability to generate virus-specific CTLs. This aspect is under investigation. Some data have been obtained (K.K.S., manuscript submitted), which suggest that for the *in vitro* generation of secondary HSV or HCMV-specific CTLs, human Ia-like HLA/D antigens have an essential role. The precise reason(s) for the failure to demonstrate the presence of virus-specific and HLA-restricted CTLs in *in vivo* situations during primary or secondary infections remains unclear; it is probably not due to the lack of development of CTL precursors during primary virus infections. In this connection, it has been shown in the mouse–HSV model[26] that the generation of CTLs is prevented by suppressor cells which can be eliminated by treatment of animals with cyclophosphamide.

Received 15 April; accepted 18 June 1980.

1. Ching, C. & Lopez, C. *Infect. Immun.* **26,** 49–56 (1979).
2. Blazar, B., Patarroyo, M., Klein, E. & Klein, G. *J. exp. Med.* **151,** 614–627 (1980).
3. West, W. H., Cannon, G. B., Kay, H. D., Bonnard, G. D. & Herbermann, R. B. *J. Immun.* **48,** 355–361 (1977).
4. Bakacs, T., Gergely, P. & Klein, E. *Cell. Immun.* **32,** 317–328 (1977).
5. Doherty, P. C., Blanden, R. V. & Zinkernagel, R. M. *Transplantn Rev.* **29,** 89–124 (1976).
6. Santoli, D., Trinchieri, G. & Lief, F. S. *J. Immun.* **121,** 526–538 (1978).
7. Kall, M., Koren, H. S. *Cell. Immun.* **40,** 58–68 (1978).
8. Sethi, K. K. & Brandis, H. *Z. Immunforsch. exp. Ther.* **150,** 162–173 (1977).
9. Pfizenmaier, K., Starzinski-Powitz, A., Röllinghoff, M. & Wagner, H. *Nature* **256,** 630–632 (1977).
10. Quinnan, G. V., Manischewitz, J. E. & Ennis, F. A. *Nature* **273,** 541–543 (1978).
11. Sethi, K. K. & Brandis, H. *Archs Virol.* **60,** 227–238 (1979).
12. Zinkernagel, R. M. & Doherty, P. C. *Nature* **248,** 701–702 (1974).
13. Bøyum, A. *Scand. J. clin. Lab. Invest.* **21,** 31–50 (1968).
14. Lay, W. H., Mendes, N. F., Bianco, C. & Nussenzweig, V. *Nature* **230,** 531–532 (1971).
15. Chess, L., MacDermott, R. P. & Schlossmann, S. F. *J. Immun.* **113,** 1113–1121 (1974).
16. Morgan, D. A., Ruscetti, F. W. & Gallo, R. C. *Science* **193,** 1007–1008 (1976).
17. Strausser, J. L. & Rosenberg, S. A. *J. Immun.* **121,** 1491–1495 (1978).
18. Therkelsen, A. J. *Acta path. microbiol. scand.* **61,** 317 (1964).
19. McMichael, A. J., Ting, A., Zweerink, H. J. & Askonas, B. A. *Nature* **270,** 524–526 (1977).
20. Biddison, W. E. & Shaw, S. *J. Immun.* **122,** 1705–1709 (1979).
21. Kreth, H. W., terMeulen, V. & Ecker, G. *Med. Microbiol. Immun.* **165,** 203–214 (1979).
22. Wright, L. L. & Levy, N. L. *J. Immun.* **122,** 2379–2387 (1979).
23. Lipinski, M. *et al. J. exp. Med.* **150,** 1310–1322 (1979).
24. Rickinson, A. B., Wallace, L. E. & Epstein, M. A. *Nature* **283,** 865–867 (1980).
25. McMichael, A. *J. exp. Med.* **148,** 1458–1467 (1978).
26. Pfizenmaier, K., Jung, H., Starzinski-Powitz, A., Röllinghoff, M. & Wagner, M. *J. Immun.* **119,** 939–944 (1977).

IgM-autoantibodies against isologous erythrocytes also react with isologous IgG(Fc)

David A. Cunliffe & K. O. Cox

School of Biological Sciences, Flinders University of South Australia,
Bedford Park, South Australia 5042, Australia

The mechanisms by which the adaptive immune system of animals discriminate between foreign and self components are not known. It is generally believed that antibodies are produced only in response to foreign agents. However, against this axiom there is mounting evidence that normal animals produce autoantibodies against a variety of self components[1–6]. In two murine model systems, a high proportion of IgM-producing cells secrete autoantibodies. In one model, the autoantibodies are specific for isologous mouse IgG(Fc)[5] and in the other, the autoantibodies are specific for antigens revealed on the surface of mouse erythrocytes (RBC) by proteolytic enzymes[6]. The function of these two autoimmune responses is a mystery. Here we show that the two responses are related. The lysis of mouse RBC, modified with bromelain (brom), by IgM autoantibodies was completely inhibited by isologous IgG(Fc), and antibodies against mouse IgG(Fc) formed precipitin bands with solubilized membranes from mouse RBC. We conclude that mouse RBC membranes and IgG(Fc) have at least one antigenic determinant in common and that this determinant is the target for autoimmune responses in normal mice.

Plaque-forming cell (PFC) assays of mouse spleen cells secreting antibodies were performed by the liquid monolayer system of Cunningham and Szenberg[7]. The methods for modifying RBC with brom and for estimating the haemolytic activity of sera for mouse brom RBC have been described elsewhere[8]. The low levels of circulating IgM directed against mouse brom RBC in normal mice were increased by injections of lipopolysaccharide (LPS), an established polyclonal B cell activator[9].

The possibility of an antigenic relationship between mouse IgG and mouse brom RBC was first noted in an assay for the haemolysis of mouse brom RBC. Antisera against mouse brom RBC were collected from mice 4 days after an intraperitoneal injection of 40 μg of LPS. Incubation of the antisera with mouse IgG before adding the target RBC reduced its haemolytic titre from 512 to less than 2 (Table 1). The inhibition of haemolysis

0028–0836/80/330720—03$01.00

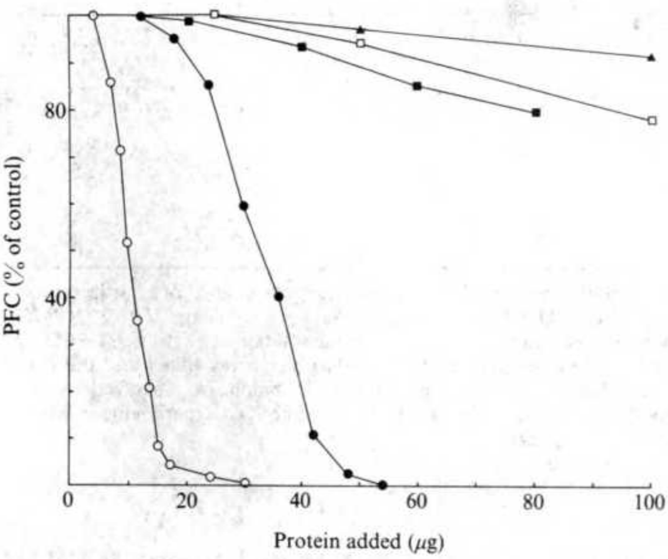

Fig. 1 The inhibition of PFC by isologous IgG(Fc). The effect of IgG on PFC directed against three target RBC, mouse brom RBC, sheep RBC and rat RBC, was measured. To lyse mouse brom RBC, spleens were collected from normal mice while for the latter targets spleens were collected from mice 4 days after an intraperitoneal injection with either 0.2 ml 6% sheep or rat RBC. The PFC assay was performed using a reaction mixture with a final volume of 200 μl[8]. Rabbit serum was used as the complement source for all assays. PFC against mouse brom RBC; ●, +IgG; ○, +IgG(Fc); ■, +IgG(Fab); PFC against sheep RBC: □, +IgG; PFC against rat RBC: ▲, +IgG. The 100% values were 9,000 PFC/spleen against mouse brom RBC; 88,000 PFC/spleen against sheep RBC and 34,000 PFC/spleen against rat RBC.

Table 1 Inhibition by mouse IgG of the haemolysis of mouse brom RBC

Antibody source	Target RBC	Protein added Identity	Amount (μg)	Haemolytic titre
Mouse anti-rat RBC sera	Rat RBC	—	—	128
		Mouse IgG	50	128
Mouse anti-sheep RBC sera	Sheep RBC	—	—	512
		Mouse IgG	50	256
Mouse anti-mouse brom RBC sera	Mouse brom RBC	—	—	512
		Mouse IgG	50	<2
IgM fraction of mouse anti-mouse brom RBC	Mouse brom RBC	—	—	1,024
		Mouse IgG	50	<2
		Rabbit IgG	100	256
		Guinea pig IgG	100	512
		Human IgG	100	1,024
		Mouse IgG_1	50	<2
		Mouse IgG_{2A}	50	<2
		Mouse IgG_{2B}	50	<2
		Mouse IgG(Fc)	20	<2
		Mouse IgG(Fab)	100	256

The antisera specific for mouse brom RBC, sheep RBC and rat RBC were collected from groups of five mice, 4 days after mice in each group had been injected intraperitoneally with 40 μg LPS or 0.2 ml 6% sheep RBC or 0.2 ml 6% rat RBC. The IgM fraction was prepared from 10 ml of mouse anti-mouse brom RBC sera by $(NH_4)_2SO_4$ precipitation, followed by chromatography on sepharose 6B. The IgG component of the fraction was then further reduced by passage through a protein A-sepharose CL-4B column[14]. The mouse IgG subclasses and fractions of IgG from mice, guinea pigs, rabbits and humans were each prepared from individual pools of sera (10 ml) using protein A-sepharose CL-4B (ref. 14). The Fab and Fc fragments were prepared by papain digestion of serum IgG (ref. 15). Undigested IgG was removed by chromatography on sephadex G100 and the Fab and Fc fragments separated using protein A-sepharose CL-4B. The assays were performed by incubating 50 μl of the required antibody source with 50 μl of PBS containing the appropriate IgG for 30 min at 37 °C. After the addition of 5 μl of 10% RBC as indicated and 10 μl of rabbit serum (source of complement), the incubation was continued for a further 30 min at 37 °C. The haemolytic titre was recorded as the final dilution in which complete lysis of the RBC occurred.

was not due to an anticomplement effect because the haemolytic activity of mouse antisera directed against either rat or sheep RBC was not inhibited by preincubation with mouse IgG (Table 1). The failure of the IgG in the antiserum to inhibit the haemolytic activity against mouse brom RBC is puzzling. The concentration of IgG relative to that of specific antibody may be critical.

The inhibition, by mouse IgG, of haemolysis of mouse brom RBC was further examined using an IgM fraction prepared from the sera with specificity for mouse brom RBC. The IgG content of the fraction was reduced by affinity chromatography. Table 1 shows that the haemolytic activity against mouse brom RBC was inhibited by isologous IgG of various subclasses and by IgG(Fc) but not by IgG(Fab) or by heterologous IgG. These results are compatible with the reactivity of mouse IgM antibodies specific for isologous IgG[5,10].

Mouse IgG was also used to inhibit antibodies against mouse brom RBC secreted by cells in a PFC assay (Fig. 1). The effector cells were prepared from the spleens of normal mice. The inhibition was not due to a cytotoxic or anticomplement effect because PFC assays using sheep or rat RBC as targets for spleen cells from mice immunized with either RBC type were relatively insensitive to the addition of mouse IgG. Again it was shown that IgG(Fc), rather than IgG(Fab), inhibited plaque formation.

The results presented in Fig. 2 provide direct evidence of at least one antigenic determinant being common to both mouse RBC membranes and IgG(Fc). Triton-soluble extracts of membranes prepared from either normal or brom-modified RBC[11] contained a component that reacted with rabbit antiserum specific for mouse IgG(Fc). Significantly, there was no line of precipitation between an antiserum specific for mouse IgG(Fab) and the two membrane preparations. Thus it seems very unlikely that the precipitin band between RBC membranes and anti-IgG(Fc) was due to the non-specific association of IgG with the RBC.

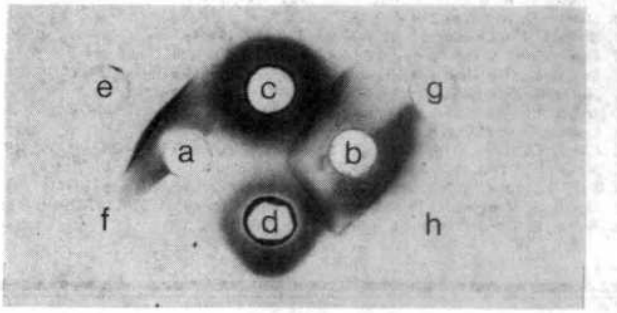

Fig. 2 Immunological cross-reactivity between mouse IgG(Fc) and mouse RBC membrane proteins. The wells contained *a*, rabbit anti-mouse IgG(Fab); *b*, rabbit anti-mouse IgG(Fc); *c* and *d*, triton soluble extracts of membranes from normal and brom RBC respectively; *e* and *g*, mouse IgG(Fab); *f* and *h*, mouse IgG(Fc). Dr P. L. Ey provided the specific sera. The method of triton-solubilization of RBC membranes has been described elsewhere[11]. The immunodiffusion was performed in 1% (wt/v) agarose which also contained 1% (v/v) Triton X 100 and 1% (wt/v) NaCl. The gels were stained using Coomassie Blue[16].

The biological significance of the autoimmune responses against determinant(s) common to IgG(Fc) and mouse RBC membranes is not shown by these results. One question that arises is whether both IgG molecules and RBC elicit autoantibodies. It is possible, for example, that the primary stimulus for autoantibody production is the IgG molecule and that the autoantibodies cross-react with structures in the membranes of RBC. Thus, there may be no physiological role for the autoimmune response against RBC. If the autoimmunity is primarily against IgG(Fc), its biological role could be important in terms of functioning of immune responses. Dresser[4,5] has proposed that IgM antibodies specific for IgG antibodies could play a role in reacting with IgG–antigen complexes and serve to amplify the initiation of the complement cascade. However, this explanation does not account for the extremely high proportion of Ig-secreting cells from the peritoneal cavity of normal mice that are specific for mouse brom RBC. Following a short-term culture, the number of cells producing antibody against mouse brom RBC can represent up to 85% of the Ig-secreting cells present[6,12]. It is possible that B cells in the peritoneal cavity undergo some hormonal and/or antigenic influence before being distributed throughout the body. For example, antigens present in the peritoneal cavity to which early B cells may respond could generate diversity of B cells by some, at present, unknown mechanism. Dresser[5] has already suggested that the high level of IgM anti-IgG(Fc) secreting cells in the spleen may be involved in generating diversity. Similarly Möller and her colleagues[13] have proposed recently that IgM antibodies against IgG(Fc) may be involved in stimulating the immune system non-specifically to generate and maintain an adequate repertoire of B cells. Experimental support for any of these suggestions would change our concept of the development and functioning of adaptive immune responses.

Received 31 March; accepted 26 June 1980.

1. Talal, N. (ed.) *Autoimmunity* (Academic, New York, 1977).
2. Arend, P. & Nijssen, J. *Nature* **269,** 255–277 (1977).
3. Cunningham, A. J. *Transplantn Rev.* **31,** 23 (1976).
4. Dresser, D. W. & Popham, A. M. *Nature* **264,** 552–554 (1976).
5. Dresser, D. W. *Nature* **274,** 480–483 (1978).
6. Steele, E. J. & Cunningham, A. J. *Nature* **274,** 483–484 (1978).
7. Cunningham, A. J. & Szenberg, A. *Immunology* **14,** 599–600 (1968).
8. Cox, K. O., Baddams, H. & Evans, A. *Aust. J. exp. Biol. Med. Sci.* **55,** 27–37 (1977).
9. Möller, G. *Transplantn Rev.* **23,** 126–137 (1975).
10. Izui, S., Eisenberg, R. A. & Dixon, F. J. *J. Immunol.* **122,** 2096–2102 (1979).
11. Cunliffe, D. A. & Cox, K. O. *Molec. Immunol.* **16,** 427–433 (1979).
12. Cox, K. O., Evans, D. A., Brooks, D. & Cunliffe, D. A. *Immunology* **38,** 355–365 (1979).
13. Möller, E., Ström, H. & Al-Balaghi, S. *Scand. J. Immunol.* (in the press).
14. Ey, P. L., Prowse, S. J., & Jenkin, C. R. *Immunochemistry* **15,** 429–436 (1978).
15. Gorini, G., Medgyesi, G. A. & Doria, G. J. *Immunology* **103,** 1132–1142 (1969).
16. Weeke, B. *Scand. J. Immunol.* 2, Suppl. **1,** 1–35 (1973).

A binding site on mast cells and basophils for the anti-allergic drug cromolyn

Nachman Mazurek, Gilad Berger & Israel Pecht

Department of Chemical Immunology, The Weizmann Institute of Science, Rehovot, Israel

Calcium permeability of basophil and mast cell membranes is stimulated on allergen binding to its specific membrane-bound IgE[1–3]. This entry of Ca^{2+} ions into the cell triggers the degranulation and secretion process[4]. Disodium cromoglycate (cromolyn DSCG), the disodium salt of 1,3-bis(-2-carboxychromon-5-yloxy)-2-hydroxypropane, inhibits the degranulation and release of anaphylactic mediators, and has found wide application in the treatment of allergic bronchial asthma[5–7]. Accumulated evidence indicates that this inhibition takes place by blocking the calcium uptake[8,9]. To localize its site of action, the drug has been covalently conjugated to fluorescent polyacrylamide and polyglutaraldehyde beads (0.7 and 0.2 μm in diameter, respectively)[10]. We show here that these drug–bead conjugates (DBC) do prevent the drug penetrating into the cell without reducing its ability to inhibit histamine release (Table 1). Furthermore, we show a specific Ca^{2+}-dependent binding of the DBC to the membranes of rat peritoneal mast cells (RPMC) and basophils.

Table 1 Inhibition of histamine release from rat peritoneal mast cells by DSCG and DBC

DSCG	Beads	DBC	% Release
—	—	—	3*
—	—	—	35
200 μM	—	—	6
—	10^7–10^8 ml^{-1}	—	34
—	—	10^7–10^8 ml^{-1}†	8

Inhibition of histamine release after preincubation of sensitized mast cells[14] with DSCG or DBC before antigen challenge. 2×10^5 RPMC were preincubated for 5 min in Tyrode solution at 37 °C with DSCG or DBC. Then antigen (ovalbumin 40 μg ml^{-1}) was added and the cells incubated for an additional 10 min. Histamine was assayed by the method of Shore[15]. Results are the mean of two experiments in which each is a duplicate.

* Spontaneous release.

† Drug/DBC ≈ 10^6–10^{10} molecules per bead.

Figure 1 shows the visualization and localization of DSCG binding sites on mast cells using image intensified fluorescence microscopy. The representative fluorescence histograms obtained by fluorescence-activated cell sorter (FACS) analysis of cells stained with DBC are shown in Fig. 2. When rat basophilic leukaemia cells are incubated with DBC, areas of bright fluorescence are clearly observed over the whole cell surface (Fig. 1), and 97% of the cells are stained (Fig. 2, Table 2).

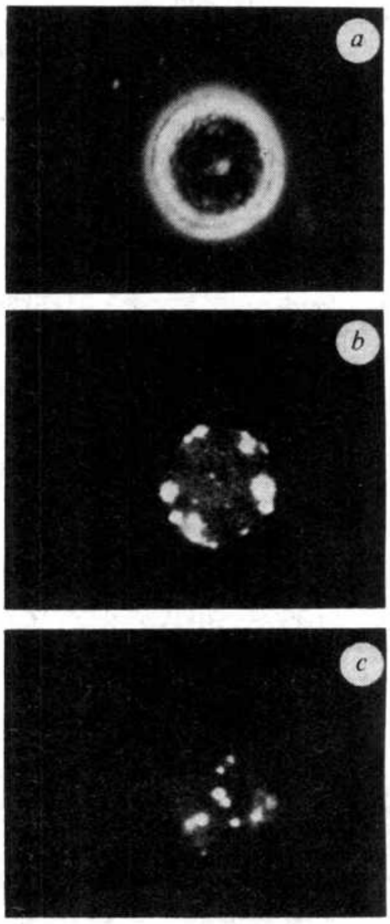

Fig. 1 Fluorescence and phase micrographs of the labelled cells were taken from a TV screen that projects an intensified image of the cells[16]. Rat basophil leukaemia cells (RBL-2H3) were incubated with 50 μg ml^{-1} of DBC in Tyrode solution (NaCl 137.0 mM, KCl 2.7 mM, NaH_2PO_4 0.4 mM, HEPES 10 mM, glucose 5 mM, $CaCl_2$ 1.8 mM, $MgCl_2$ 1.0 mM, BSA 2%) at 25 °C for 30 min. *a*, The phase mode; *b* and *c* are both in the fluorescence mode, but at different focal depths.

The possibility of DSCG acting in the extracellular fluid was excluded by the following experiment: when DSCG and Ca^{2+} ions were added to sensitized RPMC, and the cells were sedimented and resuspended in a fresh medium and exposed to antigen, inhibition of histamine release was still maintained.

Specificity of DBC binding to the cells was examined using two approaches (Table 2). One group of controls was concerned with excluding nonspecific binding of beads free of the drug. Nonspecific binding due to the extra electrostatic charges of the drug's carboxylates was tested using beads to which glutamate had been covalently conjugated. Trypsinization of mast cells (resulting in removal of membrane proteins) significantly reduced the binding of the conjugated beads. Another group of controls was concerned with the target cells' specificity of binding of DBC. BW5147 AKR/J thymoma cells and the P-815 BALB/c mastocytoma cell line, which do not secrete histamine, were not stained with DBC. Competitive inhibition of binding was found between the conjugated drug and DSCG (Fig. 2, Table 2). DSCG prevents ^{45}Ca uptake by mast cells[8,9]. When RPMC are incubated with DBC in a Ca^{2+}-free medium, a drastic reduction of staining is observed (Fig. 2, Table 2). The phenomena reported here all demonstrate strict calcium dependence. That combined with our observation that cromoglycate forms complexes with Ca^{2+} in solvents of low polarity[11,12], leads us to suggest that the cromoglycate–Ca^{2+} complex binds to a specific site on the cell membrane, possibly the calcium 'gates'. For the formation of this specific ternary complex, both the cromone nucleus of the drug and its Ca^{2+}-chelating capacity are considered to be essential.

Table 2 DBC staining monitored by the FACS

Cells	Beads	Treatment	% Cells stained
RPMC	—	Regular	5
RPMC	Free beads	Regular	8
RPMC	DBC	Regular	71
		Competition by:	
RPMC	DBC (1)	Preincubation with DSCG (5×10^{-3} M)	33
RPMC	DBC (2)	Co-incubation with DSCG (10^{-2} M)	19
RPMC	DBC	Ca^{2+}-free medium	6
RPMC	DBC	Preincubation with trypsin	30
RPMC	Beads conjugated to glutamate	Regular	20
RBL-2H3	—	Regular	7
RBL-2H3	Free beads	Regular	20
RBL-2H3	DBC	Regular	97
RBL-2H3	DBC	Preincubation with DSCG	32
RBL-2H3	DBC	Ca^{2+}-free medium	40
Lymphocytes	—	Regular	14
Lymphocytes	Free beads	Regular	18
Lymphocytes	DBC	Regular	14
P-815	—	Regular	4
P-815	Free beads	Regular	4
P-815	DBC	Regular	4

Each sample contained 10^6 cells incubated with DBC (10^7–10^8 beads ml^{-1}) in Tyrode solution for 30 min at room temperature. The RBL-2H3 cells were incubated in Tyrode containing 2% bovine serum albumin (BSA). Trypsinization of cells was carried out with a 0.25% trypsin solution for 30 min at 37 °C. Preincubation with DSCG was carried out at room temperature. As controls for staining other cells we used the BW5147 AKR/J thymoma cells for lymphocytes and also the P-815 BALB/c mastocytoma.

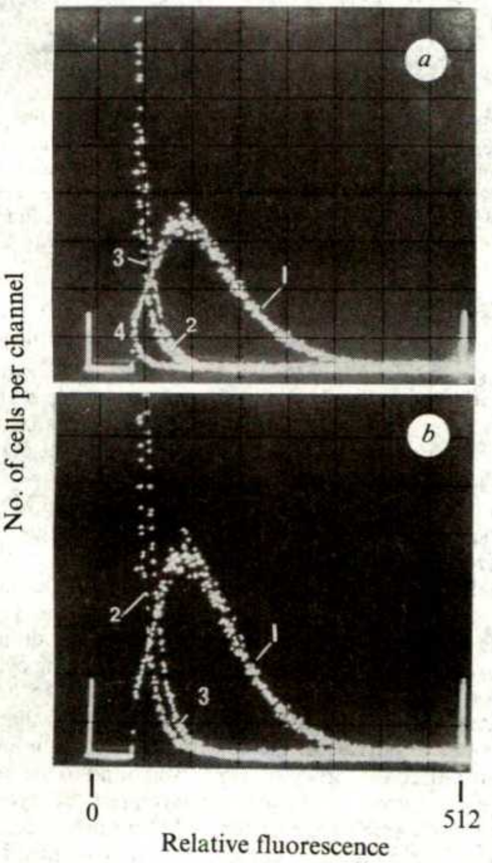

Fig. 2 Fluorescence histograms representative of rat basophilic leukaemia secreting cells (RBL-2H3) labelled with drug–tetramethyl rhodamine isothiocyanate polyglutaraldehyde bead conjugates were obtained by a fluorescence-activated cell sorter (FACS-II, Becton-Dickinson)[13]. The 400-mW, 514.5-nm line from an argon ion laser (Model 164, Spectra-Physics) intersects the stream just below the nozzle so that the cells are illuminated while they are in the fluid jet. The 580-nm large-pass filter (Dictric Optics) and the 590-nm long-pass filter (No. 2-73 Corning Glass Works) improved the red colour separation. Only living cells in the size range of 14 μm were analysed, that is, FACS was size-gated to exclude small cells (as lymphocytes) and smaller-appearing dead cells. The cells were treated as for fluorescence microscopy. *a*, Four histograms are shown: 1, specific binding of DBC; 2, cells with DBC in a Ca^{2+}-free medium; 3, cells in the presence of drug-free beads; 4, auto-fluorescence of the cells. *b*, Competitive inhibition exerted by the addition of free DSCG (see Table 2) causes a shift towards low fluorescence which resembles that due to the nonspecific staining (2), compared with the specific binding curve (1).

We thank Drs A. Rembaum and S. Margel for the supply of microsphere beads, Mr A. Petrank for the operation of the FACS II, Dr C. Geller-Bernstein for advice, Dr J. Schlessinger for help with the intensified microscopy, and Dr H. Metzger for the 2H3 cell line.

Received 6 February; accepted 21 May 1980.

1. Foreman, J. C., Hallet, M. B. & Mongar, J. L. *J. Physiol., Lond.* **271,** 193–214 (1977).
2. Foreman, J. C. & Mongar, J. L. *J. Physiol., Lond.* **239,** 381–391 (1974).
3. Orr, T. S. C. & Allison, A. C. *Nature* **236,** 350–351 (1972).
4. Foreman, J. C., Mongar, J. L. & Gomperts, B. D. *Nature* **245,** 249–251 (1973).
5. Cox, J. S. G. *Nature* **216,** 1328–1329 (1967).
6. Kusner, E. J., Dubnick, B. & Herzig, D. J. *J. Pharmac. exp. Ther.* **184,** 41–46 (1973).
7. Thomson, D. S. & Evans, D. P. *Clin. exp. Immun.* **13,** 537–544 (1973).
8. Foreman, J. C. & Garland, L. G. *Br. med. J.* **1,** 820–821 (1976).
9. Spataro, A. C. & Bosmann, H. B. *Chem. Pharmac.* **25,** 505–510 (1976).
10. Margel, S., Zisblatt, S. & Rembaum, A. J. *Immun. Meth.* **28,** 341–353 (1979).
11. Spitzer, J. C. *Int. Archs Allergy appl. Immun.* **60,** 356–358 (1979).
12. Mazurek, N., Geller-Bernstein, C. & Pecht, I. *FEBS Lett.* **111,** 194–196 (1980).
13. Bonner, W. A., Hullet, H. R., Sweet, R. G. & Herzenberg, L. A. *Rev. scient. Instrum.* **43,** 404–409 (1972).
14. Foreman, J. C. & Mongar, J. L. *J. Physiol., Lond.* **224,** 753–769 (1972).
15. Shore, A. P., Burkhalter, A. & Cohn, H. V. *J. Pharm. exp. Ther.* **127,** 182–186 (1959).
16. Schlessinger, J., Shechter, Y., Willingham, M. C. & Pastan, I. *Proc. natn. Acad. Sci. U.S.A.* **75,** 2659–2663 (1978).

Asymmetric F_c receptor distribution on human PMN oriented in a chemotactic gradient

Robert J. Walter, Richard D. Berlin & Janet M. Oliver

Department of Physiology, University of Connecticut Health Center, Farmington, Connecticut 06032

Phagocytosis of antibody-coated particles and immune complexes by polymorphonuclear leukocytes (PMN) and macrophages is initiated by binding to F_c receptors[1–3]. While it appears that subsequent ingestion requires receptor–F_c interactions to occur along the entire periphery of the particle[4], the distribution of F_c receptors over the leukocyte surface is unknown. We show here that during chemotaxis the F_c receptors of human neutrophils are localized to the cell's leading edge. This restricted receptor topography coincides with cell orientation and does not require net forward movement of PMN. Thus, F_c receptors are located in precisely that region of the cell most likely to first encounter opsonized particles.

IgG-opsonized sheep erythrocytes were used as F_c receptor probes. Since we found that aldehyde fixation (paraformaldehyde, formalin, or glutaraldehyde) destroyed or drastically altered F_c receptor activity, opsonized erythrocytes were bound to living cells. Incubation conditions were selected to minimize the redistribution and internalization of F_c receptor complexes[5].

Human PMN were allowed to settle on to coverslips which were then inverted on to a chemotaxis chamber consisting of an elevated bridge between two parallel wells[6]. One well of the chamber was filled with 10^{-7} M *N*-formyl-methionyl-leucyl phenylalanine (FMLP) and the other well with Hank's balanced salt solution. A concentration gradient of the chemoattractant was thus established across the bridge. After 10–15 min, when cell orientation had occurred, coverslips were floated off the chambers with buffer, and opsonized erythrocytes at a 5% haematocrit were placed on the coverslip for 15–60 seconds at 37 °C. Unbound erythrocytes were rinsed off and the PMN fixed with 2% glutaraldehyde. Most of the PMN (>80%) in these preparations bound one or more erythrocytes. We showed previously[5] that little redistribution and no internalization of particle–receptor complexes occurs during this brief period of incubation at 37 °C.

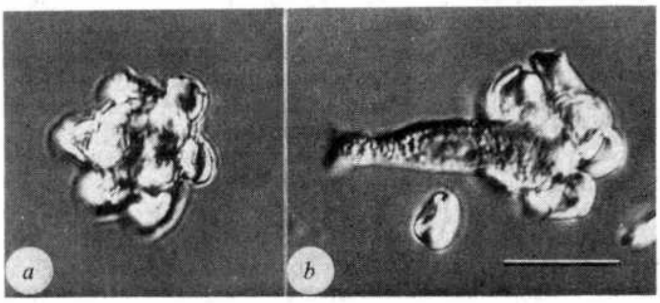

Fig. 1 Human PMN obtained by venipuncture were separated from heparinized whole blood by allowing erythrocytes to sediment at 1 × *g* in 1.25% dextran (pyrogen-free). The leukocyte-rich plasma was drawn off, 1 ml aliquots layered on to 0.5 ml of Lymphocyte Separation Medium (Bionetics), and the gradient centrifuged in a Brinkmann–Eppendorf centrifuge for 1 min. The resulting pellet was rinsed once in Hank's balanced salt solution and contaminating erythrocytes lysed by hypotonic shock. In the final leukocyte suspension, more than 95% of the cells were PMN and the remainder were eosinophils. *a*, After settling on to glass coverslips, PMN were usually rounded or somewhat flattened. Opsonized erythrocytes bind more or less uniformly over their exposed cell surface. *b*, PMN in a gradient of FMLP for 10–15 min are oriented and motile. The nucleus is localized in the bulge of cytoplasm that marks the anterior pole. Frequently, one or more lobes of the nucleus may extend posteriorly toward the trailing uropod. In the incubation conditions used here, opsonized erythrocytes bind avidly and almost exclusively to the anterior portion of the oriented PMN. (Scale bar, 10 μm.)

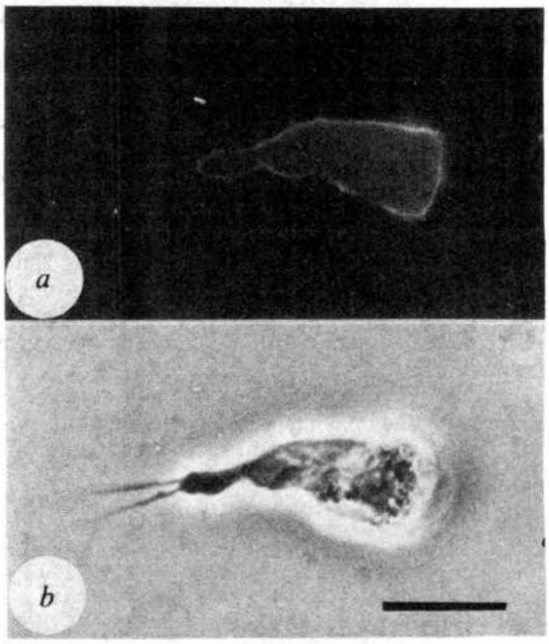

Fig. 2 PMN oriented in an FMLP gradient, fixed in 2% paraformaldehyde, and then labelled with fluorescein–Con A (25 μg ml^{-1}). *a*, Con A binding is essentially uniform except for a slight enhancement in the anterior region of the oriented cell. *b*, Phase contrast micrograph of the same PMN. Two long retraction fibres are evident posteriorly. (Scale bar, 10 μm.)

The rounded or somewhat flattened non-oriented PMN (seen in the absence of FMLP) bound opsonized erythrocytes more or less uniformly about their circumference (Fig. 1*a*). Oriented PMN are elongated with the nucleus localized in a bulge near the anterior pole of the cell (Fig. 1*b*) pointing toward the well containing FMLP. A fine membrane ruffle (lamellipodium, protopod) may form the actual leading edge while a long cytoplasmic uropod trails behind the cell. More than 98% of oriented PMN that bound opsonized erythrocytes displayed them only over the anterior portion of the cell. In the few remaining cells (<2%), opsonized erythrocytes were also bound to the extreme tip of the trailing uropod. The marked asymmetry of erythrocyte binding to the leading edge of the cell is probably due to the preferential distribution of receptors, although it is possible that receptors in this region have a higher apparent affinity.

Under the conditions described above, PMN were oriented and actively motile at rates exceeding 35 μm min^{-1} along the gradient (as seen by time-lapse videotape). If calcium- and magnesium-free media containing 2 mM EDTA were used throughout the experiment, PMN became oriented with respect to the gradient but did not actually move over the substrate[6,7]. Nevertheless, opsonized erythrocytes still bound only to the anterior pole of these oriented PMN.

F_c receptor asymmetry occurs without obligatory, parallel redistribution of other receptors. Thus, on oriented, paraformaldehyde-fixed PMN, fluorescein–concanavalin A (Con A) binds over the entire cell and shows only a slight increase in fluorescence intensity at the anterior pole (Fig. 2*a*, *b*). This apparent enhancement may, in fact, be caused by increased cell thickness and/or folding of plasma membrane in this region.

The mechanism for the establishment of asymmetric F_c receptor activity is not yet understood. It seems possible that coincident with cell orientation, specialized plasma membrane

0028-0836/80/330724—02$01.00

domains may be set up possibly through direct or indirect cytoskeletal interactions. Microfilaments accumulate in the anterior portion of oriented PMN[8] while centrioles along with the bulk of the microtubules are probably posterior to the nucleus[9]. This cytoskeletal architecture might directly affect the local composition of the plasma membrane[7,9,10]. Accordingly, F_c receptors might be enriched in the anterior portion of the PMN. Alternatively, local (perhaps cytoskeleton-related) changes in the lipid composition of the membrane or in membrane surface tension[11] might afford regions of minimum free energy to certain classes of molecules (such as F_c receptors). In either case, Con A distribution may appear relatively unaffected by these PMN membrane domains due to the heterogeneity of the Con A binding sites.

The chief function of the PMN is to seek out and ingest invading microorganisms. This function may be facilitated by restricting the topography of F_c receptors in the membrane during chemotaxis. In particular, the movement of F_c receptors to the leading edge as the phagocyte changes orientation ensures their localization in that part of the membrane most likely to first encounter opsonized particles.

This work was supported by NIH grant nos GM 07185 to R.J.W., CA 15544 to R.D.B., and ES 01106 and grant no BC 179 from the American Cancer Society to J.M.O.

Received 14 April; accepted 28 May 1980.

1. Rabinovitch, M. in *Mononuclear Phagocytes* (ed. van Furth, R.) 299–315 (Blackwell, Philadelphia, 1970).
2. Griffin, J. A. & Griffin, F. M. Jr *J. exp. Med.* **150,** 653–675 (1979).
3. Huber, H. & Fudenberg, H. H. *Ser. Haemat.* **3** part 2, 160–175 (1970).
4. Griffin, F. M. Jr, Griffin, J. A., Leider, J. E. & Silverstein, S. C. *J. exp. Med.* **142,** 1263–1282 (1975).
5. Walter, R. J., Berlin, R. D., Pfeiffer, J. R. & Oliver, J. M. *J. Cell Biol.* **86,** 199–211 (1980).
6. Zigmond, S. H. *J. Cell Biol.* **75,** 606–616 (1977).
7. Marasco, W. A., Becker, E. L. & Oliver, J. M. *Am. J. Path.* **98,** 749–768 (1980).
8. Oliver, J. M., Krawiec, J. A. & Becker, E. L. *J. reticuloend. Soc.* **24,** 697–704 (1978).
9. Bessis, M. & DeBoisfleury, A. *Blood Cells* **2,** 365–410 (1976).
10. Ash, J. F., Louvard, D. & Singer, S. J. *Proc. natn. Acad. Sci. U.S.A.* **74,** 5584–5588 (1977).
11. Greenspan, H. P. *J. theor.Biol.* **70,** 125–134 (1978).

Receptors for concanavalin A cluster at the front of polarized neutrophils

D. L. Weinbaum, J. A. Sullivan & G. L. Mandell

Department of Medicine, Box 385, University of Virginia School of Medicine, Charlottesville, Virginia 22908

Polymorphonuclear neutrophils (PMN) can recognize, engulf and kill microorganisms and are thus an important host defence against infection. The initial encounter between a microbe and the neutrophil takes place at the neutrophil surface. Receptors, including those for the Fc end of the immunoglobulin G (ref. 1), the C3b component of complement[2], formyl peptides[3] and plant lectins[4] have been identified on the surface of neutrophils. We have now examined the surface pattern and arrangement of receptors for the plant lectin concanavalin A (Con A) to determine if the surface receptor array varied with the functional state of the neutrophil. We found that receptors for Con A clustered at the front of polarized neutrophils.

Human PMN were obtained by gravity sedimentation of whole heparinized blood (10 units ml^{-1})[5] or by the formation of monolayers from freshly clotted blood. Cells obtained by the former approach were washed twice and resuspended in Hanks' balanced salt solution. Monolayers were prepared by incubating fresh blood on carefully cleaned glass coverslips at 37 °C for 30 min. The clot that formed was washed off gently, leaving monolayers consisting of 90–95% PMN. Fluorescein- or rhodamine-labelled Con A (10 μg ml^{-1}) was added to live cells and the cells fixed in either 2% glutaraldehyde or 4% paraformaldehyde in phosphate-buffered saline. They were then examined and photographed with a Zeiss Axiomat photomicroscope under phase contrast or fluorescence illumination. Neutrophils were considered polarized if they had a morphologically defined front (leading edge) and tail. Polarized PMN that migrated in a gradient of chemotactic substances were considered orientated. Each experiment was repeated at least three times, and in all cases 50 mM D-mannose blocked Con A binding.

PMN in suspension are spherical (Fig. 1*a*) with no discernible front or tail. When they were incubated with fluorescein-labelled Con A for 15 min and then examined live or fixed in suspension, a uniform surface pattern of fluorescence was observed (Fig. 1*b*)[6]. When PMN in suspension were fixed before the addition of Con A, the fluorescein-labelled lectin was again distributed uniformly. Thus, receptor sites for Con A were distributed uniformly over the surface of the nonpolarized PMN in suspension (Table 1).

We next examined receptor location on polarized but non-orientated PMN. PMN in suspension became polarized when incubated with the chemotactically active peptide *N*-formyl-L-methionyl-L-phenylalanine (10^{-6} M)[7]. Such polarized neutrophils were incubated for 15 min with fluorescein-labelled Con A and all the lectin accumulated at the tail. With prior fixation to immobilize receptor sites, there was marked accumulation of fluorescence at the leading edge in 23 ± 1.73% PMN: we call this pattern a 'headlight' (Table 1).

When cells were allowed to move across coverslips after the addition of Con A, the label moved to the tail, forming bright fluorescent buttons or 'tail lights' as described by Ryan *et al.*[4] (Fig. 1*c*, *d*). However, when polarized cells moving over coverslips were fixed to immobilize receptor sites before the addition of Con A, the headlight pattern was seen on 69.9 ± 3.1% PMN. In other experiments, PMN were orientated towards *N*-formyl-L-methionyl-L-phenylalanine (10^{-6} M) in an agarose chemotaxis system[8]. Addition of fluorescein-labelled

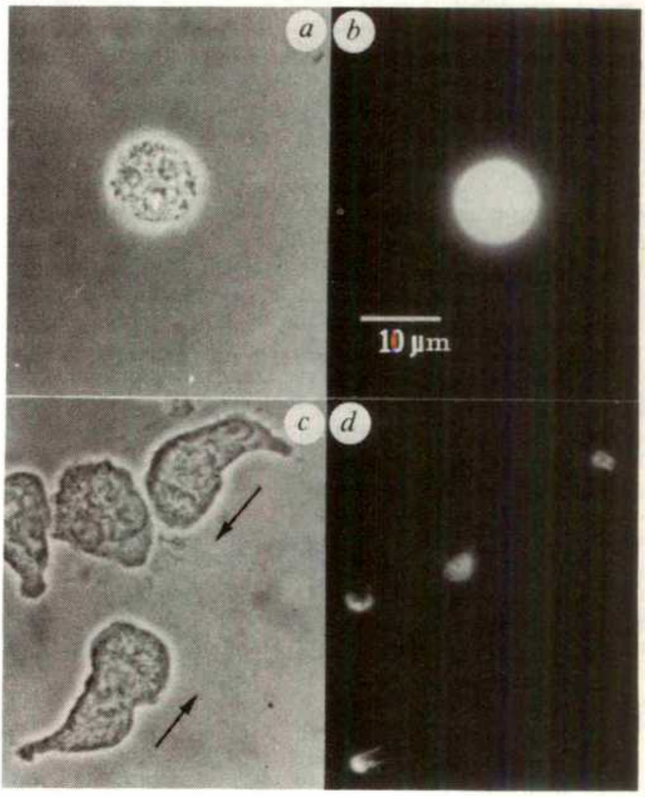

Fig. 1 Binding of fluorescein-labelled Con A to neutrophils. Each set of photographs consists of phase contrast and fluorescence micrographs of the same field. Arrows indicate direction of migration. *a*, *b*, Cells in suspension incubated with 10 μg ml^{-1} Con A and then fixed. Binding is uniform. *c*, *d*, Live neutrophils moving on a monolayer 15 min after addition of Con A. The lectin has accumulated at the tail and thus tail lights were seen.

0028-0836/80/330725—02$01.00

Table 1 Per cent of PMN with indicated distribution of fluorescein-Con A

	Head	Tail	Uniform
Nonpolarized in suspension	0	0	91.4 ± 1.2* ($n = 5$)
Polarized in suspension			
Fixed before Con A	23.0 ± 1.7	0	77.1 ± 1.7 ($n = 3$)
Fixed after Con A	0	90.8 ± 1.7	9.2 ± 1.7 ($n = 5$)
Polarized on monolayer			
Fixed before Con A	69.9 ± 3.1	0	30.3 ± 3.2 ($n = 8$)
Fixed after Con A	0	91.7 ± 2.3	8.3 ± 2.3 ($n = 3$)
Polarized and orientated on monolayer			
Fixed before Con A	76.9 ± 2.6	0	22.8 ± 2.5 ($n = 20$)
Fixed after Con A	0	91.0 ± 1.5	9.0 ± 1.5 ($n = 3$)

Each experiment represented counts of 100 neutrophils. n Is the number of times the experiment was carried out on different days. Results are expressed as the mean ± s.e.m.

* Remainder showed irregular clumping of fluorescence.

Con A after fixation revealed binding sites localized at the leading edge of $76.9 \pm 2.6\%$ PMN (Fig. 2*a–d* and Table 1).

To determine whether new Con A-binding sites were available after bound sites had been swept to the tail, a monolayer of PMN labelled with fluorescein-Con A was incubated for 15 min to enable the lectin to move to the tail. After fixation, rhodamine-labelled Con A was added. Binding sites were revealed by the formation of new headlight areas of red fluorescence (Fig. 2*e*).

Incubation of PMN with colchicine (10^{-4} M), which interferes with microtubular function[6], did not prevent the formation of head- or tail lights. However, incubation with cytochalasin B ($5\ \mu g\ ml^{-1}$), a microfilament poison[9], prevented polarization and abolished head and tail light formation. Nonpolarized PMN in suspension or on monolayers did not cap Con A receptors unless the microtubular system was first disrupted[6,10] but, as reported here, polarized neutrophils clustered unbound Con A receptors at the leading edge and spontaneously capped bound receptors at the tail.

Oliver *et al.*[11] observed a uniform pattern of microfilaments redistribute to polar aggregation when associated with Con A capping in diamide-treated nonpolarized PMN. Berlin *et al.*[12] have shown that Con A–receptor complexes aggregated in the region of pseudopod formation in phagocytosing PMN. Immunofluorescent staining has shown the pseudopods to be enriched in microfilaments[12,13]. The lamellapodium or leading edge of polarized PMN is also enriched in microfilaments[14]. This, together with our finding that cytochalasin abolished headlight formation, suggests that microfilaments are associated with receptor clustering at the leading edge.

Both Con A and certain piliated strains of *Escherichia coli* bind to mannose-sensitive receptor sites on the neutrophil surface[15,16]. This implies that their binding sites may be identical. Piliated, but not non-piliated, *E. coli* are ingested by PMN in the absence of serum opsonins[15,17]. Thus, these receptors may be important in the recognition and subsequent ingestion of microbes. We are attempting to localize complement (C3b) and immunoglobulin (Fc) receptors on polarized PMN, but we have been unable to find a fixative that maintains cellular morphology without destroying the receptor sites.

Thus, polarized PMN move with a leading edge studded with Con A receptors and when these receptors are bound, the receptor–lectin complex moves to the tail. New unbound receptors seem to be generated or uncovered at the leading edge. The array of receptors at the leading edge of the neutrophil may be important for its ability to function as an efficient phagocyte.

We thank Lillian Robertson and Joyce Henderson for their assistance with this manuscript. This work was supported in part by NIH grants AI 09504 and T32AI 07046.

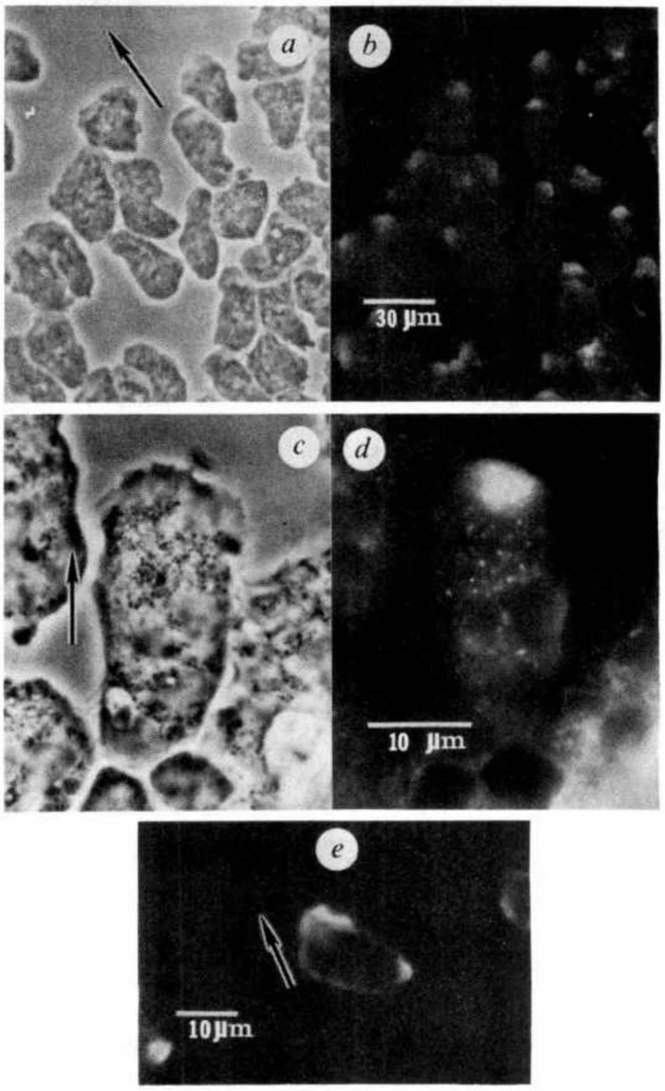

Fig. 2 Each set of photographs consists of phase contrast and fluorescence micrographs of the same field. Arrows indicate direction of migration. *a*, *b*, Neutrophils migrating in a gradient of the chemotactic peptide *N*-formyl-L-methionyl-L-phenylalanine under agarose for 30 min. Con A was added after fixation. A bright accumulation of Con A at the leading edge in a headlight pattern was seen on the oriented cells. *c*, *d*, A high power view of this phenomenon showing that Con A receptors are most dense at the leading edge. In *b* and *d* the punctate appearance of fluorescence inside the cell, not associated with the headlight, represents nonspecific granular fluorescence that is not blocked by 50 mM D-mannose. *e*, Neutrophils were incubated with Con A on a monolayer for 15 min and then fixed. Fluorescein-Con A (green in original) accumulated at the tail as in Fig. 1*d*. Rhodamine-labelled Con A was then added. Rhodamine-Con A (red in original) bound to the leading edge. Thus, the cell fluoresced in two colours, red at the leading edge and green at the tail. This indicated that new binding sites for Con A were available. These may be newly uncovered or regenerated sites.

Received 8 April; accepted 26 June 1980.

1. Messner, R. P. & Jelinek, J. *J. clin. Invest.* **49,** 2165–2171 (1970).
2. Ehlenberger, A. G. & Nussenzweig, V. *J. exp. Med.* **145,** 357–371 (1977).
3. Williams, L. T., Snyderman, R., Pike, M. C. & Lefkowitz, R. J. *Proc. natn. Acad. Sci. U.S.A.* **74,** 1204–1208 (1977).
4. Ryan, G. B., Borysenko, J. Z. & Karnovsky, M. J. *J. Cell Biol.* **62,** 351–365 (1974).
5. Nelson, R. D., Quie, P. G. & Simmons, R. L. *J. Immun.* **115,** 1650–1656 (1975).
6. Oliver, J. M. & Zurier, R. B. *J. clin. Invest.* **57,** 1239–1247 (1976).
7. Smith, C. W., Hollers, J. C., Patrick, R. A. & Hassett, C. *J. clin. Invest.* **63,** 221–229 (1979).
8. Nelson, R. D., Fiegel, V. D. & Simmons, R. L. *J. Immun.* **117,** 1676–1683 (1976).
9. Hartwig, J. H. & Stossel, T. P. *J. Cell Biol.* **71,** 295–303 (1976).

10. Albertini, D. F., Berlin, R. D. & Oliver, J. M. *J. Cell Sci.* **26,** 57–75 (1977).
11. Oliver, J. M., Lalchandani, R. & Becker, E. L. *J. reticuloendothelial Soc.* **21,** 359–364 (1977).
12. Berlin, R. D. & Oliver, J. M. *J. Cell Biol.* **77,** 789–804 (1978).
13. Stendahl, O. I., Hartwig, J. H., Brotschi, E. A. & Stossel, T. P. *J. Cell Biol.* **84,** 215–224 (1980).
14. Boyles, J. & Bainton, D. F. *J. Cell Biol.* **82,** 347–368 (1979).
15. Bar-Shavit, Z., Ofek, I., Goldman, R., Mirelman, D. & Sharon, N. *Biochem. biophys. Res. Commun.* **78,** 455–460 (1977).
16. Bittiger, H. & Schnebli, H. P. *Concanavalin A as a Tool* (Wiley, New York, 1976).
17. Silverblatt, F. J., Dreyer, J. S. & Schauer, S. *Infect. Immun.* **24,** 218–223 (1979).

Topographical distribution of coated pits

J. R. Pfeiffer, J. M. Oliver & R. D. Berlin

Department of Physiology, University of Connecticut Health Center, Farmington, Connecticut 06032

The internalization of a wide range of biologically significant macromolecules, particularly low density lipoproteins (LDL) and proteins such as α_2-macroglobulin and epidermal growth factor, occurs primarily through characteristic, bristle-coated indentations of the cell surface known as coated pits[1–4]. Current interest has focused on the topographical relationship between surface receptors for these ligands and the coated pits[2]. We establish here that coated pits are themselves distributed non-randomly on the J774.2 mouse macrophage cell surface. Morphometric and statistical analyses of cell profiles in electron micrographs indicate two levels of asymmetry: in all cells, pits are clustered; after colchicine treatment they accumulate over a microvillous protuberance that develops at one pole of the cell. This topographical heterogeneity suggests a new level at which cellular responses to growth substances and hormones may be regulated.

Coated pits were defined as regions of membrane indentation approximately 0.3 μm long and underlain by a fuzzy coat which in favourable micrographs appeared as periodic spikes or bristles (Fig. 1). They frequently occupied the bases of microvilli and were characteristically separated by a clear space from the adjacent cytoplasm. To determine their distribution, a cell was first selected and photographed at ×8,900. Pits with openings to the medium were then located by searching the entire perimeter of the cell at a magnification of ×160,000. Their approximate positions were marked on a sketch which guided subsequent identification of pits on the low magnification micrograph of the same cell (Fig. 2*a*, arrows). A sonic digitizer was used to determine the length between pits and the total cell circumference from these micrographs.

Untreated J774.2 macrophages[5] that were grown in Dulbecco's modified Eagle medium with 20% horse serum, fixed in suspension and processed for electron microscopy as before [6–8], maintained a rounded shape. Cell profiles were thus selected at random except that each one contained a portion of the cell nucleus. In these untreated cells, the average distance between pits in two separate experiments involving 37 pits on 12 cells and 45 pits on 10 cells was, respectively, 24.2 μm and 18.6 μm. Assuming the thickness of the section to be 70 nm and the cell-surface area to be roughly 1,500 μm^2, this corresponds to a surface density of approximately 0.35 pits per μm^2 or approximately 500 coated pits per cell.

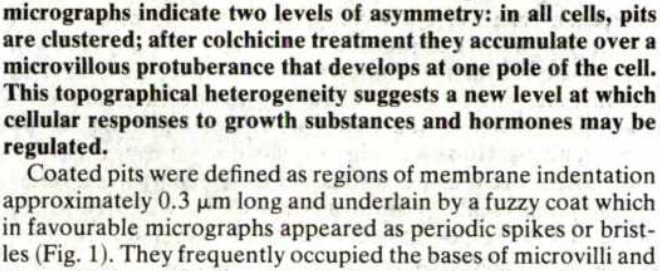

Fig. 1 The ultrastructure of coated pits. The left frame illustrates the typical thickened membrane and bristled cytoplasmic face of coated pits. The right frame demonstrates the clear zone between coated pits and the adjacent cytoplasm. Scale bar, 0.1 μm.

Table 1 Statistical analysis of coated pit distribution

Rejection of randomness hypothesis test		Untreated macrophages	Colchicine-treated protuberant macrophages
Basic quadrat* χ^2 analysis	Quadrats 6 or 10 μm	NS	$P<0.05$
Basic quadrat* χ^2 analysis	Quadrat 3.6 μm	$P<0.01$	
Variance/mean* ratio analysis		NS	$P<0.001$
Eberhardt statistic†		$P<0.01$	$P<0.005$
Contiguous quadrats‡		$P<0.005$	$P<0.005$

* These are essentially comparisons of the observed distribution of coated pits with a theoretical Poisson distribution into quadrats. Quadrats are equal-length segments along the surface profile scored for numbers of pits. The theoretical distribution is based on the mean number of pits per quadrat. In our experiments, 37–38 pits were distributed along 600–900 μm of profile, in quadrats 3.6, 6 and 10 μm long. For the basic quadrat, χ^2-test is used, and for the variance/mean ratio analysis, $t=(\text{variance/mean})-1/(2/n-1)^{1/2}$. Both tests are insensitive to fine-grained non-randomness and are affected somewhat by the choice of quadrat size.

† In this analysis a series of random points (taken from a table of random numbers) was placed on the extended profile and a distance X_i measured from the random point to the nearest pit. The Eberhardt statistic

$$A=m\sum_{i=1}^{m}X_i^2\Big/\sum_{i=1}^{m}X_i^2$$

where m = number of random points used, was then computed, and its critical values taken from the table of Hines and Hines[9]. This is a sensitive test for non-randomness, particularly for clustering over small dimensions.

‡ This quadrat analysis is based on the hierarchal design of Greig-Smith[10]. It allows analysis at various dimensional levels, systematically 'searching' for a quadrat size that reveals non-randomness. The modification of Mead[11] allows analysis over a series of scales. NS, not significant.

After colchicine treatment (2 μM, 30–45 min), greater than 80% of J774.2 cells developed a bulge or protuberance that was bordered by microvillous membrane and was frequently separated from the cell body by a constricted neck region[6,8]. In these cells, analysis of randomly selected profiles yielded 14.7 μm between pits (one experiment; 37 pits on 11 cells). Analyses of profiles that displayed both the protuberance and cell body of the same cell gave 15.3 μm and 11.6 μm between pits (two experiments involving 63 pits on 12 cells and 80 pits on 11 cells, respectively). This corresponds to an average linear density of around 0.53 pits per μm^2 in colchicine-treated macrophages. As the mean pit densities on randomly chosen profiles and profiles of clearly protuberant cells are so similar, selection of protuberant profiles for subsequent studies does not introduce counting bias. The 50% increase pit density after colchicine (0.53 compared with 0.35 pits per μm^2) is unexplained but may reflect the decreased pinocytosis observed previously[8] in colchicine-treated J774.2 macrophages.

Are coated pits distributed randomly? To answer this question the consecutive distances between pits were measured on 10–12 profiles from the untreated and colchicine-treated samples in each of two experiments. The perimeters were connected end to end by joining them at a point taken midway along the greatest inter-pit distance on each profile. This provided one continuous sample of pit distribution. A variety of statistical tests for randomness were then applied.

0028–0836/80/330727—03$01.00

The distribution of pits on untreated, rounded cells was first examined statistically by dividing the total profile length into consecutive sections or quadrats of equal length, determining the number of pits in each quadrat and calculating the proportion of quadrats with different numbers of pits (0, 1, 2, 3). This was compared by χ^2-test with a theoretical Poisson distribution based on the mean number of pits per quadrat, or by *t*-test using the method of variance/mean ratio. When the quadrat size was chosen to be 6 µm of profile, a random surface distribution of coated pits on rounded cells was indicated (that is, the statistical hypothesis that the sample is random is not rejected by these tests). When the quadrat was reduced to 3.6 µm the pit distribution appeared non-random (Table 1). This difference in statistical significance dependent on the length of quadrat suggested that the nonrandomness was based on the presence of clusters of pits. To test this, we used published methods of mathematical ecology in which nonrandomness of populations may be analysed at several scales without bias. These methods are based either on nearest-neighbour analysis, by examining the variance of distances from random points to pits along the profile[9], or by an hierarchical quadrat analysis in which the variance at each level of complexity (scale) in relation to the next is directly examined[10,11]. The results of these more refined tests, also summarized in Table 1, reinforce the simpler analysis indicating that coated pits are distributed non-randomly.

In contrast to the subtle clustering of pits on untreated cells, coated pits along profiles from colchicine-treated cells showed a non-random distribution by even the simplest statistical tests (Table 1). Furthermore, from inspection of the electron micrographs of protuberant cells (for example, Fig. 2*a*), it was suggested that coated pits were relatively more numerous in the protuberance than in the cell body. A procedure was therefore developed to combine data from different profiles so as to emphasize common topographical features. A radial grid was placed over the cell with its centre across the 'neck' region separating the protuberance from the cell body. The same grid was placed over a diagrammatic cell (Fig. 2*b*). Every coated pit from successful cell profiles was transferred into 1 of the 12 segments of the generalized profiles to build up a cumulative distribution pattern. The results of two such experiments are shown in Fig. 2*c* and *d*. Few coated pits are found on the 'body', whereas both 'head' and 'neck' regions are significantly enriched for coated pits. It can be seen from Table 2 that the linear density in the head is approximately five times that of the cell body. An eight-fold higher density of coated pits exists in the neck than in the cell body. This increased pit density in the protuberance and concomitant depletion of pits over the body surface is reminiscent of the capping of concanavalin A–receptor complexes on protuberant leukocytes[6-8,12] or the segregation of surface immunoglobulin into the uropod of lymphocytes[13].

The mechanism by which coated pits are clustered and capped is unclear. The distances between pits are too great for clustering due to ligand bridging of pits. Direct connections between pits and microfilaments that could pull them are also not necessarily involved. We have shown before that segregation of surface markers can probably occur without direct connections of the segregating species with microfilaments[6,8,12,14]. In addition, coated pits are characteristically underlain by a clear zone that seems to lack microfilaments, although at some point microfilaments may still be involved in the internalization of coated pits[15]. Based on our previous work on the segregation of membrane ligand–receptor complexes[6,8,12,14], we propose that pits (or their molecular precursors) probably move by diffusion or by inclusion in membrane flow to overlie the neck and protuberance where they are trapped by local alterations in membrane structure, the latter perhaps being stabilized by microfilaments. However, other explanations are not excluded.

Table 2 Distribution and regional linear density of coated pits on profiles of J774.2 macrophages

Region	% Total pits	Linear density	
		Pits per µm of profile	Relative density
Expt 1			
Control			
Whole perimeter	100	0.0413	1.00
Colchicine-treated			
Whole perimeter	100	0.0654	1.58
Head	28	0.0734	1.78
Neck	56	0.1562	3.78
Body	16	0.0187	0.45
Expt 2			
Control			
Whole perimeter		0.0595	1.00
Colchicine-treated			
Whole perimeter	100	0.0862	1.45
Head	36	0.1225	2.06
Neck	53	0.1870	3.14
Body	11	0.0238	0.40

We emphasize that the existence of such topographical variation may represent a critical mechanism by which cells can modulate their responses to growth substances and hormones. Several investigators have stressed the inherently random distribution of membrane receptors of hormones that are internalized through coated pits[1-4]. It follows that the clustering of pits on rounded cells and particularly their redistribution following colchicine may place coated pits at a variable distance from membrane receptors and so may alter the cellular response to ligands that bind these receptors. For example, topographical phenomena may underlie the potentiation by colchicine of DNA synthesis induced in serum-starved, quiescent fibroblasts by epidermal growth factor, fibroblast growth factor, insulin and other hormones[16,17]

We thank Dr Robert Rippey for discussions on statistics. This work was supported in part by NIH grants CA185544 and grant

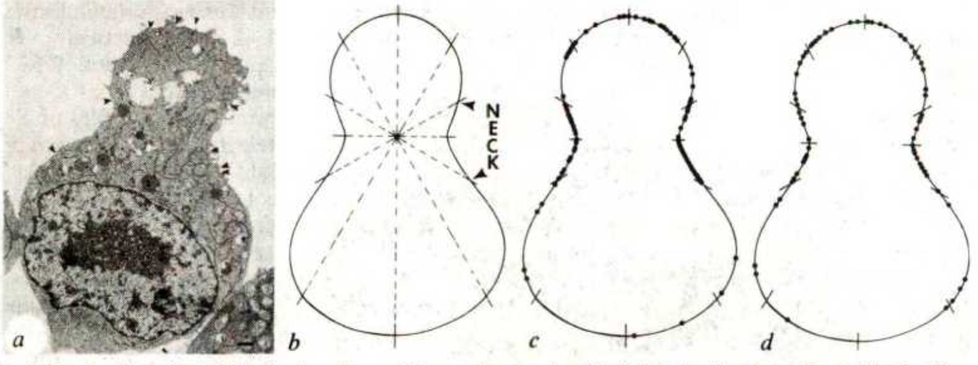

Fig. 2 The topography of coated pits on protuberant cells. Coated pits were first identified on electron micrographs of thin sections through protuberant cells (arrows, *a*). A radial grid was then placed over the profile with its centre at the midpoint of a line across the narrowest 'neck' region between cell body and protuberance and radii fanning out every 30° above and below the line. An identical grid was placed over a diagrammatic cell (*b*) whose 'head' and 'body' profiles were drawn in proportion to their average lengths on the individual cell profiles. This device allowed the ready transfer of pit distribution from the original cell profile to the generalized cell. The four segments referred to as 'neck' are marked: segments above these are the 'head' and segments below the 'body'. *c*, *d* Show the cumulative pit distributions from two separate experiments that analysed 12 (*c*) and 11 (*d*) profiles of colchicine-treated protuberant cells. The diagrams were built up of 63 and 80 pits, respectively. Scale bar 1 µm. Obviously, an analogous diagram for untreated symmetrical cells cannot be constructed because there is no common morphological feature by which to orientate the different profiles.

BC-179 from the American Cancer Society. J.M.O. holds a Faculty Research Award from the American Cancer Society.

Received 11 March; accepted 6 June 1980.

1. Anderson, R. G. W., Goldstein, J. L. & Brown, M. S. *Proc. natn. Acad. Sci. U.S.A.* **73,** 2434–2438 (1976).
2. Goldstein, J. L., Anderson, R. G. W. & Brown, M. S. *Nature* **279,** 679–684 (1979).
3. Gordon, G., Carpenter, J-L., Cohen, S. & Orci, L. *Proc. natn. Acad. Sci. U.S.A.* **75,** 5025–5029 (1978).
4. Willingham, M. C., Maxfield, F. R. & Pastan, T. H. *J. Cell Biol.* **82,** 614–625 (1979).
5. Ralph, P. & Nakoinz, I. *Nature* **257,** 393–394 (1975).
6. Albertini, D. F., Berlin, R. D. & Oliver, J. M. *J. Cell Sci.* **26,** 57–75 (1977).
7. Oliver, J. M., Albertini, D. F. & Berlin, R. D. *J. Cell Biol.* **71,** 921–932 (1976).
8. Walter, R., Berlin, R. D., Pfeiffer, J. R. & Oliver, J. M. *J. Cell Biol.* **86,** 199–211 (1980).
9. Hines, W. G. S. & O'Hara-Hines, R. J. *Biometrika* **66,** 73–79 (1979).
10. Greig-Smith, P. *Ann. Bot. N.S.* **16,** 293–316 (1953).
11. Mead, R. *Biometrics* **30,** 295–307 (1974).
12. Oliver, J. M. & Berlin, R. D. *Symp. Soc. exp. Biol.* **23,** 277–298 (1979).
13. Schreiner, G. F., Braun, J. & Unanue, E. R. *J. exp. Med.* **144,** 1683–1688 (1976).
14. Berlin, R. D. & Oliver, J. M. *J. Cell Biol.* **77,** 789–804 (1979).
15. Salisbury, J. L., Condeelis, J. S. & Satir, P. *J. Cell Biol.* **83,** 72a (1979).
16. Friedkin, M., Legg, A. & Rozengurt, E. *Proc. natn. Acad. Sci. U.S.A.* **76,** 3909–3913 (1979).
17. Otto, A. M., Zumbe, A., Gibson, L., Kubler, A-M. & de Asua, L. J. *Proc. natn. Acad. Sci. U.S.A.* **76,** 6435–6438 (1979).

Insulin and antibodies against insulin receptor cap on the membrane of cultured human lymphocytes

Joseph Schlessinger*

Department of Chemical Immunology, The Weizmann Institute of Science, Rehovot, Israel

Emmanuel Van Obberghen & C. Ronald Kahn

Section on Cellular and Molecular Physiology, Diabetes Branch, National Institute of Arthritis, Metabolism and Infectious Diseases, NIH, Bethesda, Maryland 20205

When insulin interacts with its target cells, it binds to a specific membrane receptor and triggers a chain of events which stimulate many physiological responses[1,2]. Although the mechanism of insulin action remains uncertain[2-4], electron microscopy has suggested that unoccupied insulin receptors appear in clusters of two to six molecules and that insulin becomes internalized after binding to them[5,6]. Insulin receptors on 3T3 fibroblasts labelled with rhodamine–insulin (R-insulin) are diffusely distributed and mobile on the cell surface, with a lateral diffusion coefficient $D \sim (3\text{–}5) \times 10^{-10}$ cm^2 s^{-1}. At 37°C, hormone–receptor complexes aggregate into immobile patches which are soon endocytosed[7,8]. A new tool for such studies has been provided by the discovery of autoantibodies to the insulin receptor in the sera of certain patients with insulin-resistant diabetes[9]. These antibodies stimulate various physiological responses normally mediated by insulin[10-14]. Both the bivalent antibodies $(\mathrm{Fab'})_2$ and the monovalent Fab′ block insulin binding, but only the bivalent antibodies are biologically active[14], Fab′ acting as a competitive antagonist[14]. Similarly, antibodies raised against purified insulin receptors can mimic insulin[15], suggesting that microaggregation of receptors could be involved in the action of this hormone[14,16]. We now report that at 37°C both R-insulin and the rhodamine-labelled antibodies against insulin receptors form a single cap on one pole of the cell. Cells which were first treated at 37°C with fluorescein–insulin (F-insulin, at partial receptor occupancy), fixed with formaldehyde and then treated with either R–insulin or rhodamine-labelled anti-receptor antibodies, showed overlapping caps of the two markers. These experiments demonstrate directly the aggregation of insulin receptors and suggest either that insulin receptors are multivalent towards the hormone or that the unoccupied receptors migrate together with the occupied ones in the formation of caps.

When IM-9 lymphocytes were incubated with R–insulin (50 ng ml^{-1}) for 90 min at 4°C, the hormone appeared diffusely distributed over the cell surface. If these cells were subsequently incubated at 37°C, the labelled hormone–receptor complexes clustered within 15 min and formed a single cap on one pole of the cell. Similar caps were observed when lymphocytes were incubated for 30 min at 37 °C with R-insulin (50 ng ml^{-1}) without preincubation at 4 °C (Fig. 1*a*, *b*). Insulin-induced capping occurred in approximately 60% of lymphocytes, the rest showing weak diffuse or patchy staining. Pretreatment of cells with 10^{-2} M sodium azide for 30 min at 37 °C inhibited capping, and R-insulin formed visible patches over the cell surface (Fig. 2*a*, *b*). Capping was not affected by preincubation for 30 min at 37 °C with 10^{-5} M colchicine, a microtubule-disrupting agent, concanavalin A (Con A, 20 μg ml^{-1}), which inhibits capping and mobility of various other antigens on the membrane of lymphocytes, or 10^{-4} M cycloheximide, which inhibits protein synthesis.

When lymphocytes were labelled with 50 μg ml^{-1} of rhodamine-labelled autoantibodies against insulin receptors, similar results were obtained. At 37 °C, the antibodies induced a single cap on one pole of the cell (Fig. 1*c*, *d*). As with R-insulin, when cells were preincubated with sodium azide, patches were seen, instead of a single cap (Fig. 2*e*, *f*). Binding of anti-receptor antibody and R-insulin was specific. If the cells were incubated with 0.4 μg ml^{-1} of native insulin with either R-insulin (Fig. 2*c*, *d*) or rhodamine-labelled anti-receptor antibodies, a weak diffuse fluorescence was observed. This reflects nonspecific interactions between the antibodies and the cell surface and is similar to the pattern observed when lymphocytes are incubated with equivalent amounts of IgG fraction of normal human antibodies (data not shown).

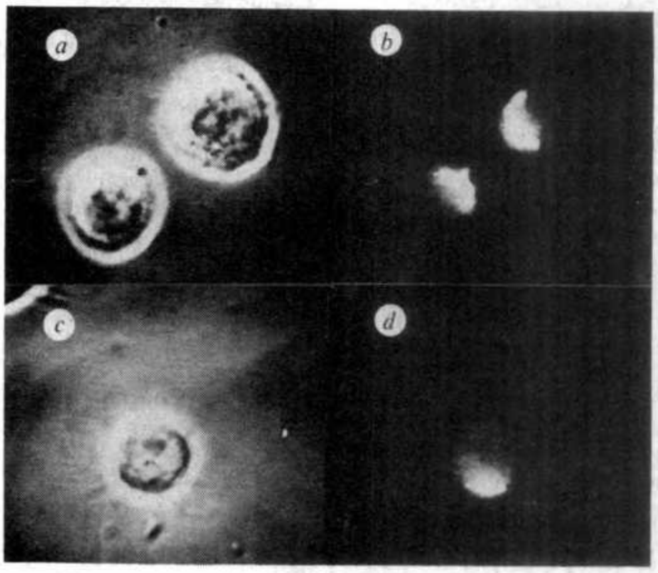

Fig. 1 The distribution of R-insulin and rhodamine-labelled autoantibodies against insulin receptors on IM-9 lumphocytes. Lymphocytes suspended in Hank's balanced salt solution (BSS) containing 1 mg ml^{-1} bovine serum albumin (2×10^6 cells ml^{-1}) were incubated with either 50 ng ml^{-1} R-insulin or 50 μg ml^{-1} of rhodamine-labelled autoantibodies against the receptors isolated from insulin-resistant diabetics for 30 min at 37 °C. After the incubation, the cells were washed twice with Hank's BSS, fixed with 1% formaldehyde for 10 min at 23 °C, washed twice more and mounted on microscope slides for microscopic observation. The fluorescence and the phase micrographs of the IM-9 lymphocytes were taken with a Polaroid camera from a television screen that projects the intensified image of these cells. Full details about this system were previously reported[8,28]. *a*, Phase; *b*, fluorescence micrographs of the same field of cells labelled with R-insulin. *c*, Phase; *d*, fluorescence micrographs of the same field of cells labelled with rhodamine-conjugated antibodies against insulin receptor. ×1,900.

---

* To whom correspondence should be addressed.

0028-0836/80/330729—03$01.00

Table 1 The distribution of R-insulin and other reagents on the cell surface

Expt	Reagents	Cell distribution	% Cells	Presence of co-caps
I	*a* F-insulin (5 ng ml^{-1})	Caps	55 ± 6	Yes
	b R-insulin (150 ng ml^{-1})	Caps	49 ± 8	
II	*a* F-insulin (5 ng ml^{-1})	Caps	58 ± 7	Yes
	b R-anti-insulin receptor (50 μg ml^{-1})	Caps	52 ± 6	
III	*a* F-insulin (150 ng ml^{-1})	Caps	62 ± 6	No
	b R-insulin (150 ng ml^{-1})	Diffuse background		
IV	*a* Insulin (150 ng ml^{-1})	—		
	b R-insulin (150 ng ml^{-1})	Diffuse background		
V	*a* R-insulin (150 ng ml^{-1})	Caps	50 ± 8	No
	b Fluorescein–lipopolysaccharide	Diffuse	100	
VI	*a* R-insulin (150 ng ml^{-1})	Caps	62 ± 11	No
	b Fluorescein–Con A	Diffuse	100	

In all the experiments the IM-9 lymphocytes were first incubated for 30 min at 37 °C with reagent *a*, washed with PBS, fixed with formaldehyde and after additional washing labelled with reagent *b* for 30 min at 23 °C. The values are the average of four different experiments.

Double-label experiments were carried out to examine whether insulin and antibody-induced receptor capping affect only the occupied receptors or produce a more general effect. Lymphocytes were incubated with F-insulin (5 ng ml^{-1}) for 30 min at 37 °C. (At this concentration 20–30% of receptors are occupied.) Cells were then washed twice in phosphate-buffered saline (PBS), fixed with 3% formaldehyde for 10 min at 23 °C and incubated for a further 30 min at 23 °C with a near-saturating concentration of R-insulin (150 ng ml^{-1}). The two markers seemed to be distributed in a single cap (Fig. 3, Table 1). When cells were labelled with saturating concentrations of either F-insulin (200 ng ml^{-1}) or native insulin (0.4 μg ml^{-1}), fixed and labelled with R-insulin, only background fluorescence was observed, in the spectral range of rhodamine. We have previously reported that hormone binding was not affected and that receptor clustering was inhibited by mild fixation with formaldehyde[8].

A similar experiment was carried out with F-insulin and rhodamine-labelled anti-receptor antibodies. The cells were first incubated with F-insulin (5 ng ml^{-1}, 20–30% receptors occupied), washed, fixed and labelled with rhodamine anti-receptor antibodies (50 μg ml^{-1}). As before, F-insulin and rhodamine-labelled anti-receptor antibodies appeared in the same domain. Interestingly, in all these experiments, only 50–60% of cells were capped. We do not know the reason for this. It is difficult to evaluate the pattern of the diffusely labelled cells because the nonspecific fluorescence appeared in a similar pattern.

Although occupied insulin receptors may cause co-capping of unoccupied receptors, insulin-induced receptor capping does not affect the general distribution of other membrane components. IM-9 lymphocytes were labelled with R-insulin (50 ng ml^{-1}), fixed with 3% formaldehyde and incubated for 20 min at 23 °C with fluorescein–Con A (20 μg ml^{-1}). In contrast to a single cap of R-insulin observed on 62% of lymphocytes, nearly 100% of the cells showed uniform distribution of fluorescein–ConA. Results were similar when cells were labelled with R-insulin, fixed and labelled with a fluorescein-labelled lipopolysaccharide (50 μg ml^{-1}). This molecule is embedded artificially in the lipid matrix of the membrane of various cell types[17]. In this experiment, R-insulin appeared in caps on 50% of the cells, whereas nearly 100% of the cells showed uniform distribution of fluorescein-labelled lipopolysaccharide.

Thus, insulin or antibodies against its receptors form patches and caps of insulin receptors on the membrane of IM-9 lymphocytes. This provides further evidence that insulin receptors can diffuse[8] laterally in the plane of the membrane of IM-9 lymphocytes, and that insulin or antibodies against its receptors redistribute their receptors on the cell membrane. Our data also demonstrate that insulin or antibodies against insulin receptors bind to the same domain on the cell surface, as revealed by fluorescence microscopy, and that insulin receptors are operationally multivalent towards the hormone molecule. This operationally multivalent species could also be pictured as an oligomer of monovalent recognition subunits.

It is difficult to explain how a small, presumably monovalent molecule such as insulin can induce receptor clustering, although other polypeptides such as epidermal growth factor[8],

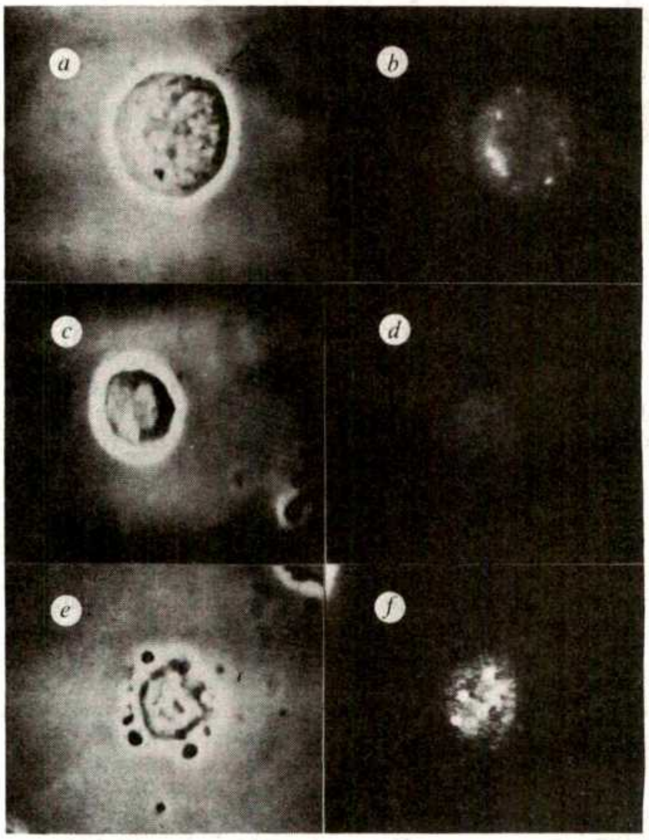

Fig. 2 Sodium azide inhibits the formation of caps of insulin or antibodies against insulin receptor on IM-9 lymphocytes. *a*, Phase; *b*, fluorescence micrographs of the same field of IM-9 lymphocytes preincubated with 10^{-2} M of sodium azide for 30 min at 37 °C and then for an additional 30 min with R-insulin. The cells were washed with PBS, fixed with formaldehyde and mounted on microscope slides for microscopic observation. *c*, Phase; *d*, fluorescence micrographs of the same field of IM-9 lymphocytes which were incubated with 0.4 μg ml^{-1} native insulin together with 50 ng ml^{-1} R-insulin. The weak diffuse fluorescence reflects the nonspecific binding of the fluorescent hormone. *e*, Phase; *f*, fluorescence micrographs of the same field of cells preincubated with 10^{-2} M of sodium azide for 30 min at 37 °C and then for additional 30 min with 50 μg ml^{-1} of rhodamine-labelled antibodies against insulin receptor. The cells were washed, fixed and mounted for microscopic observation. × 1,900.

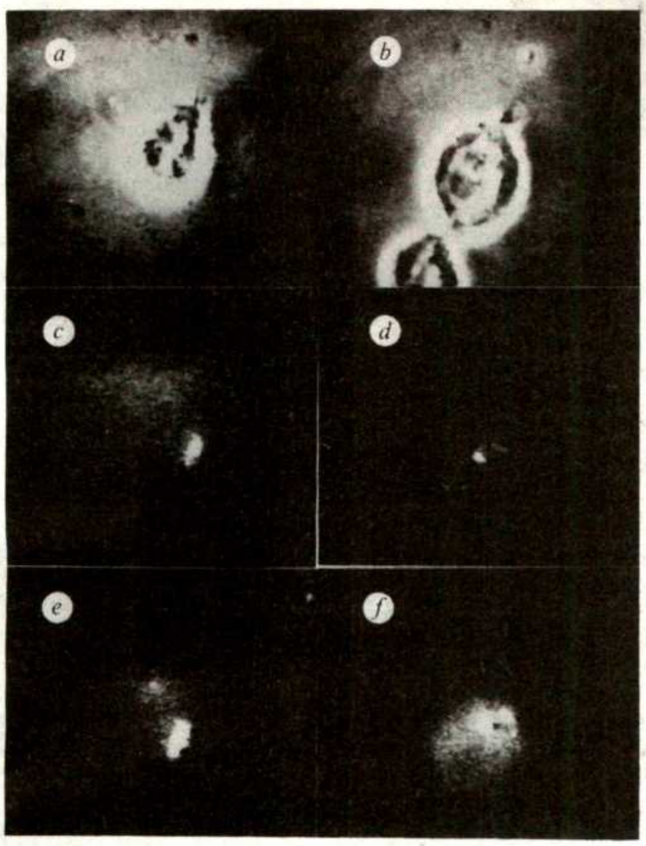

Fig. 3 Co-capping of F-insulin and R-insulin on IM-9 lymphocytes. IM-9 lymphocytes were incubated with 5 ng ml^{-1} F-insulin for 30 min at 37 °C; at this concentration 20–30% of the receptors are occupied. The cells were washed, fixed with 3% formaldehyde for 10 min at 23 °C and then incubated for an additional 30 min at 23 °C with 100 ng ml^{-1} of R-insulin. *a*, *b* and *c* are micrographs of one cell and *d*, *e* and *f* are micrographs of a second cell. *a* Is phase, *b* and *c* are fluorescence micrographs of F-insulin and R-insulin, respectively. *d*, Phase; *e* and *f* are fluorescence micrographs of F-insulin and R-insulin, respectively. ×1,900.

nerve growth factor[18] and enkephalin[19] can also induce receptor clustering. For insulin, a simple mechanism would be self-aggregation on the cell surface, for insulin dimerizes and aggregates in solution at concentrations above 10^{-6} M and its local concentration on the cell membrane is about 10^{-6} M (ref. 16). On the other hand, if surface aggregation is a biologically important process, it must differ from aggregation in solution because several insulins do not aggregate in solution, but are biologically active[14]. A more plausible mechanism is that hormone binding induces a conformational transition in the receptor molecules that increases the binding affinity between mobile receptors. Our finding that partial occupancy of insulin receptors leads to co-capping of unoccupied receptors can be interpreted in two ways. One explanation is that the receptor molecules are multivalent towards the hormone. At low levels of receptor occupancy, one or more binding sites of each multimer is occupied, and as they cap, they bring with them the unoccupied receptors. The second possibility is that the receptor molecules are independent, but the conformational transition induced in them by the binding of insulin enhances the interactions between neighbouring receptors, leading to the migration of unoccupied receptors together with the occupied one. Both explanations, however, imply that the receptor molecule is operationally multivalent towards the hormone, which is consistent with the negative cooperativity exhibited by insulin binding to its membrane receptors in IM-9 lymphocytes[20]. Hormone-induced microaggregation of multivalent receptors could be the mechanism of negative cooperativity. It is not known whether insulin receptors cluster in coated areas of the plasma membrane, as do α_2-macroglobulin and epidermal growth factor[21,22], and the biological significance of hormone-induced receptor capping is unclear. At physiological concentrations, insulin does not induce microscopically visible receptor caps or patches, but microaggregation of receptors is likely at such concentrations. Other data suggest that microaggregation of receptors is an important step in the chain of events leading to the bioactivity of insulin and epidermal growth factor[14–16]. The larger microscopically visible caps are induced at concentrations of insulin in which it 'down-regulates' its membrane receptors. Indeed, we have found a good correlation between the extent of insulin-induced receptor loss (down-regulation) and the amount of IM-9 lymphocytes which cap (unpublished results). Furthermore, both processes depend on hormone concentration, time and temperature. This suggests a possible physiological role to insulin-induced receptor capping.

J.S. acknowledges support by grants from NIH (CA-25820) and from the US-Israel Binational Science Foundation.

Received 24 March; accepted 23 June 1980.

1. Czech, M. P. *A. Rev. Biochem.* **46,** 359 (1979).
2. Kahn, C. R. *J. Cell Biol.* **70,** 261–286 (1976).
3. Terris, S. & Steiner, D. F. *J. biol. Chem.* **250,** 8389–8398 (1975).
4. Godfine, I. D., Smith, G. J., Wong, K. Y. & Jones, A. L. *Proc. natn. Acad. Sci. U.S.A.* **74,** 1368–1372 (1977).
5. Jarett, L. & Smith, R. M. *J. supramolec. Struct.* **6,** 45–59 (1977).
6. Gorden, P., Carpentier, J. -L., Freychet, P., LeCam, A. & Orci, L. *Science* **200,** 782–785 (1978).
7. Schlessinger, J., Shechter, Y., Cuatrecasas, Y., Willingham, M. C. & Pastan, I. *Proc. natn. Acad. Sci. U.S.A.* **75,** 5353–5357 (1978).
8. Schlessinger, J., Shechter, Y., Willingham, M. C. & Pastan, I. *Proc. natn. Acad. Sci. U.S.A.* **75,** 2659–2663 (1978).
9. Flier, J., Kahn, C. R., Roth, J. & Bar, R. S. *Science* **190,** 63–65 (1975).
10. Kahn, C. R., Baird, K. L., Flier, J. S. & Jarrett, D. B. *J clin. Invest.* **60,** 1094–1106 (1977).
11. Kasuga, M. *et al. J. clin. Endocr. Metab.* **47,** 66–77 (1978).
12. Lawrence, J. C., Larner, J., Kahn, C. R. & Roth, J. *Molec. cell. Biochem.* **22,** 153–157 (1978).
13. Van Obberghen, E. *et al. Nature* **280,** 500–502 (1979).
14. Kahn, C. R., Baird, K. L., Jarrett, D. B. & Flier, F. S. *Proc. natn. Acad. Sci. U.S.A.* **75,** 4209–4213 (1978).
15. Jacobs, S., Chang, K. J. & Cuatrecasas, P. *Science* **200,** 1283–1284 (1978).
16. Schlessinger, J. in *Physical Chemical Aspects of Cell Surface Events in Cellular Regulation* (eds C. Delisi & R. Blumenthal) 89–111 (Elsevier, New York, 1979).
17. Wolf, D. E. thesis, Cornell Univ. (1979).
18. Levi, A., Shechter, Y., Neufeld, E. J. & Schlessinger, J. *Proc. natn. Acad. Sci. U.S.A.* (in the press).
19. Hazum, E., Chang, K. -J. & Cuatrecasas, P. *Science* **206,** 1077–1079 (1979).
20. De Meyts, P., Bianco, A. R. & Roth, J. *J. biol. Chem.* **251,** 1877–1888 (1976).
21. Maxfield, F. R., Schlessinger, J., Shechter, Y., Pastan, I. & Willingham, M. C. *Cell* **14,** 805–811 (1978).
22. Gorden, P., Carpentier, J.-L., Cohen, S. & Orci, L. *Proc. natn. Acad. Sci. U.S.A.* **75,** 5025–5029 (1978).

Myosin from fetal hearts contains the skeletal muscle embryonic light chain

Robert G. Whalen & Susan M. Sell

Département de Biologie Moléculaire, Institut Pasteur,
25 rue du Dr Roux, 75724 Paris, France

The contractile proteins of adult skeletal and cardiac muscle tissue are very similar. Some of these proteins are identical in amino acid sequence[1,2] or differ only slightly[3]. Various structural studies have shown that the heavy and light chains of myosin are also homologous in skeletal and cardiac muscles[4–11]. In developing skeletal muscles, certain myosin subunits are present which are not found in the corresponding adult muscle[7,10–13]. Whether fetal cardiac muscle also contains myosin subunits homologous to these early forms is not known. We now report that ventricular myosin of fetal rats has a light chain polypeptide corresponding to the skeletal muscle embryonic light chain[11]. This result provides further evidence that a form of myosin light chain, not detectable in adult skeletal or ventricular myosin, is characteristic of the early stages of striated muscle development[14].

Myosin purified from 20-day embryonic rat ventricles by Sepharose or DEAE-cellulose chromatography[11] contains three components of the same molecular weight as adult myosin (Fig. 1*a*), but also has a band of approximate molecular weight (MW) 26,000 (Fig. 1*b*). Two-dimensional gel analysis of adult

0028–0836/80/330731—03$01.00

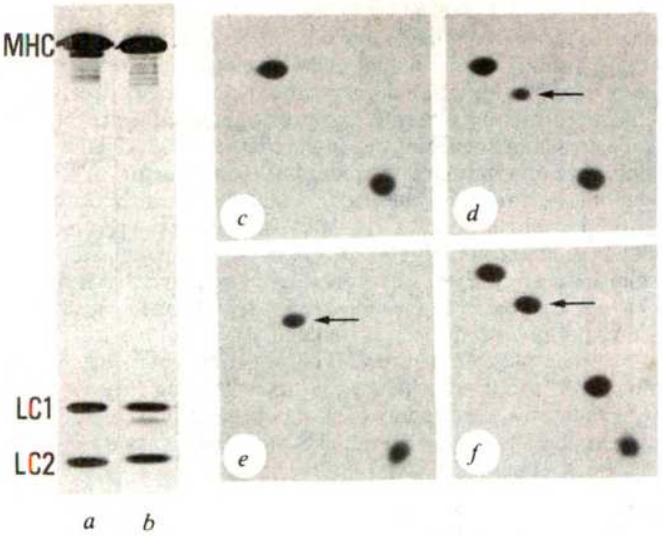

Fig. 1 Gel electrophoresis of various myosin samples. Myosins were extracted and purified from adult rat heart ventricles, 20-day fetal rat heart ventricles and fused L6 myotube cultures as previously described[11]. The final step in the purification procedure for the preparations shown here was chromatography on Sepharose 2B in the presence of 1 mM ATP[11]. *a*, Adult cardiac myosin and *b*, embryonic cardiac myosin were analysed on one-dimensional SDS gels. The positions of light chains (LC1 and LC2) and heavy chain (MHC) are indicated. Two-dimensional gel analysis of myosin light chains[11] was performed on *c*, adult cardiac myosin, *d*, embryo cardiac myosin, *e*, L6 myosin and *f*, a mixture of L6 and embryo cardiac myosin. Only the light chain region is shown. About 15 μg of each myosin were loaded on the gels. The arrows in *d–f* indicate the $\mathrm{LC1_{emb}}$ protein.

and embryonic cardiac myosin light chains (Fig. 1*c*,*d*) clearly revealed two and three components respectively. Myosin from the myogenic rat cell line L6 is composed of two light chains, an LC2 protein of the fast skeletal type plus the embryonic light chain $\mathrm{LC1_{emb}}$ described previously[11]. Co-electrophoresis of embryonic cardiac myosin with L6 myosin showed that the third light chain component in the cardiac preparation corresponded to $\mathrm{LC1_{emb}}$ as determined by their co-migration (Fig. 1*e*,*f*). No fast-type light chains were detected in the embryonic cardiac myosin, as suggested previously[15]. The earlier result may have been due to contamination of the embryonic myofibrillar preparations by histones, as shown elsewhere[16,17].

The possibility that cardiac and L6 embryonic light chain are identical is supported by the following results. During partial proteolysis of SDS-denatured myosin using *Staphylococcus aureus* protease, $\mathrm{LC1_{emb}}$ is converted to a polypeptide of approximately 23,000 MW, whereas LC1 light chains of adult fast, slow and cardiac myosin are relatively resistant[7]. We have verified that this 23,000-MW species is not derived from the heavy chain at these levels of degradation by comparing the cleavage pattern of isolated L6 myosin heavy chain with that of the whole molecule (heavy and light chains; not shown). As Fig. 2 shows, cardiac $\mathrm{LC1_{emb}}$ is degraded to a polypeptide of the same molecular weight as that derived from the L6 embryonic light chain (Fig. 2*a*,*b*). The resistance of the adult cardiac LC1 to *S. aureus* protease (Fig. 2*c*) also suggests that it is not directly related to $\mathrm{LC1_{emb}}$.

The ratios of the various cardiac myosin light chains were determined by densitometry of the stained bands on one-dimensional SDS gels. Adult myosin contains LC1 and LC2 in a ratio of $1.16 \pm 0.08:1 (n = 5)$, which after correction for their respective molecular weights (22,000 and 20,000 (ref. 9)) is close to the expected 1:1 stoichiometry. Densitometry of embryonic cardiac myosin reveals that the ratio of $\mathrm{LC1} + \mathrm{LC1_{emb}}$ to LC2 is $1.19 \pm 0.08 : 1 (n = 4)$. $\mathrm{LC1_{emb}}$ represents about 25% of the total LC1-type light chain in this myosin.

The myosin heavy chain of embryonic cardiac myosin was examined by partial proteolytic cleavage after denaturation by SDS[7,18]. The pattern of degradation is very similar to that of adult cardiac myosin after treatment with *S. aureus* protease (Fig. 2*b*,*c*). The one-dimensional analysis of patterns obtained after cleavage by chymotrypsin or papain also reveals extensive similarity (results not shown). However, two-dimensional analysis after chymotryptic degradation reveals several quantitative differences. For example, some minor polypeptides in the adult myosin pattern (Fig. 3*a*) are major species in the embryonic pattern (Fig. 3*c*); they are indicated in Fig. 3*b* by arrows in the gel containing a mixture of the two reactions. Other polypeptides are major in the adult and minor in the embryonic preparation. No detectable amounts of any adult fast or embryonic skeletal myosin heavy chain isozymes are seen in the cleavage patterns of embryonic cardiac myosin (Fig. 2*a*,*b*, and ref. 7). The quantitative differences seen in the embryonic and adult patterns may mean that these preparations are mixtures of two or more isozymes, the ratios of which are different. This possibility is consistent with results of electrophoresis of native intact myosins[19] which reveals three rat ventricular myosin isozymes (V_1, V_2 and V_3). V_3 is predominant in 18-day embryos (J. F. Y. Hoh, personal communication) while V_1 is the major form in the adult[19]. It is therefore possible that the heavy chain isozyme we find in embryonic heart tissue corresponds to that of V_3 myosin. Interestingly, a V_3 isozyme reappears in large amounts in hypertrophic hearts[20].

We have demonstrated a novel form of myosin light chain in embryonic skeletal muscle[11], and the results presented here reveal an identical, or at least very similar, protein in embryonic rat ventricular myosin. Because the two-dimensional gel technique is capable of high resolution, co-migration of these two proteins is suggestive of identity. The presence of a cleavage site

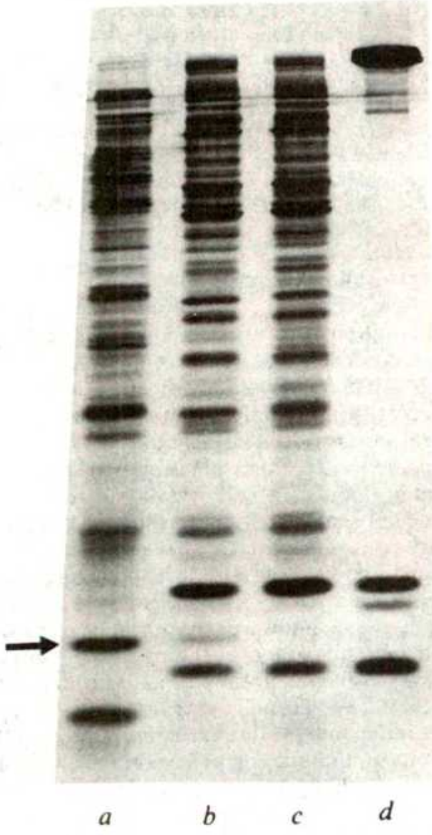

Fig. 2 Partial proteolysis of skeletal and cardiac $\mathrm{LC1_{emb}}$ by *S. aureus* protease. About 16 μg of myosin was treated with *S. aureus* protease in the presence of SDS as described previously[7] and then analysed on a one-dimensional SDS gel. Results are shown for the treatment of *a*, L6 myosin, *b*, embryo cardiac myosin and *c*, adult cardiac myosin. *d*, Untreated embryo cardiac myosin shows the positions of various intact light chains. The $\mathrm{LC1_{emb}}$-derived fragment is indicated by an arrow.

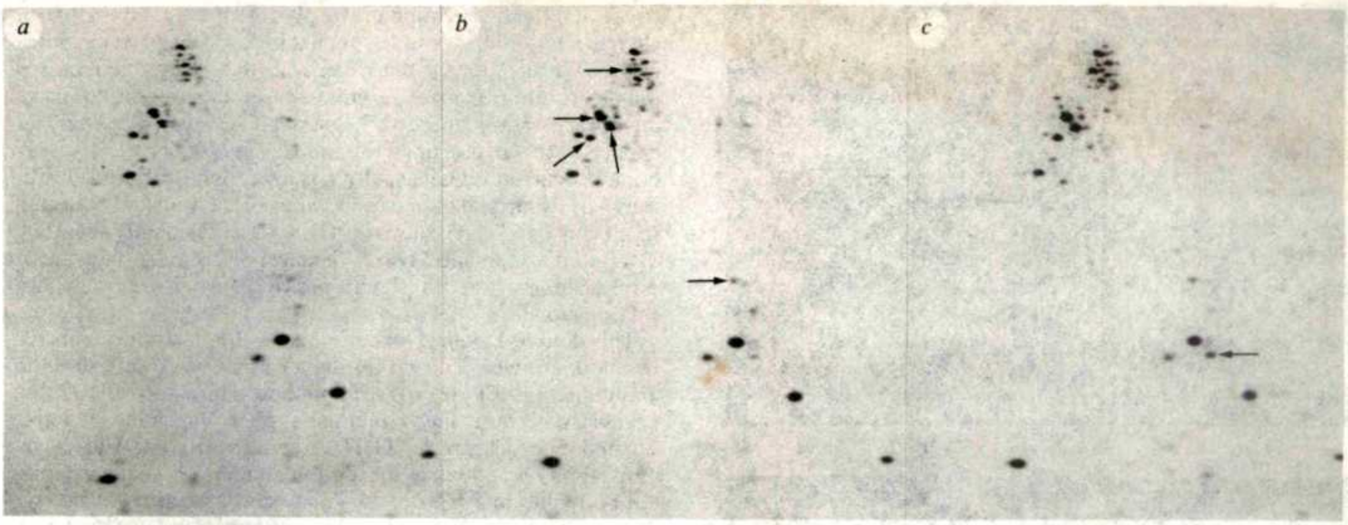

Fig. 3 Polypeptide maps of adult and embryo cardiac myosin heavy chains. The partial chymotryptic cleavage reactions were carried out as described for two-dimensional gel analysis[7] except that the final myosin concentration was only 1 mg ml^{-1}. About 60 μg were loaded on the gels containing *a*, adult and *c*, embryonic myosin cleavage products. Gel *b*, contained about 30 μg of each of the adult and embryonic cleavage products. The arrows in *b*, indicate polypeptides that are major in the embryonic myosin map *c*, and minor in the adult map *a*. The arrow in *c* indicates the intact LC1_{emb} protein. Two-dimensional gels were run as described[11] except that the isoelectric focusing gel was 21 cm long and the second dimension slab gel was 19 cm high, composed of a 4-cm stacking gel and 15-cm separation gel. The gels are presented with the basic *p*H range to the left.

for *S. aureus* protease in both the skeletal and cardiac proteins is also consistent with this possibility. The LC1_{emb} light chain is not found in adult ventricular myosin (shown here) nor in adult skeletal muscle[11]. While we cannot rule out that LC1_{emb} might be a major component of some adult myosin, it seems to be present in skeletal and ventricular myosin only at the early stages of development. The relative stoichiometry of the LC1 and LC2 components in fetal cardiac myosin is the same as in adult myosin, although LC1_{emb} partially replaces the adult cardiac LC1 at the early stages.

The similarity of the ventricular heavy chain isozymes found at 20 days *in utero* with those of the adult could be interpreted in several ways. Conceivably a distinct embryonic form is never present in developing myocytes. Alternatively, cardiac tissue could be much more developed biochemically at this stage than skeletal muscle, and an embryonic form may already have been replaced by the adult forms. Even though myocytes are still proliferating in the perinatal period, these dividing cells are biochemically differentiated[21]. In contrast to the heavy chain, the light chains have not attained the adult phenotype by 20 days of gestation. If the absence of a distinct embryonic heavy chain at this time is simply due to rapid turnover of such a form, then the situation is the inverse of developing skeletal muscle in which LC1_{emb} disappears more rapidly than embryonic heavy chain[7,14,22].

We thank Dr K. Schwartz for helpful discussions and Professor F. Gros for support and encouragement. This laboratory is supported by the CNRS, DGRST, INSERM, CEA and the Muscular Dystrophy Association of America.

Received 23 January; accepted 21 May 1980.

1. Mak, A. S., Lewis, W. G. & Smillie, L. B. *FEBS Lett.* **105,** 232–234 (1979).
2. Wilkinson, J. M. *Eur. J. Biochem.* **103,** 179–188 (1980).
3. Vandekerckhove, J. & Weber, K. *Differentiation* **14,** 123–133 (1979).
4. Streter, F. A., Balint, M. & Gergely, J. *Devl Biol.* **46,** 317–325 (1975).
5. Brevet, A. & Whalen, R. G. *Biochimie* **60,** 459–466 (1978).
6. Flink, I. L., Rader, J. H. & Morkin, E. *J. biol. Chem.* **254,** 3105–3110 (1979).
7. Whalen, R. G., Schwartz, K., Bouveret, P., Sell, S. M. & Gros, F. *Proc natn. Acad. Sci. U.S.A.* **76,** 5197–5201 (1979).
8. Weeds, A. G. *FEBS Lett.* **59,** 203–208 (1975).
9. Weeds, A. G. *Eur. J. Biochem.* **66,** 157–173 (1976).
10. Huszar, G. *Nature new Biol.* **240,** 260–264 (1972).
11. Whalen, R. G., Butler-Browne, G. S. & Gros, F. *J. molec. Biol.* **126,** 415–431 (1978).
12. Hoh, J. F. Y. & Yeoh, G. P. S. *Nature* **280,** 321–322 (1979).
13. Rushbrook, J. I. & Stracher, A. *Proc. natn. Acad. Sci. U.S.A.* **76,** 4331–4334 (1979).
14. Whalen, R. G. in *Plasticity of Muscle* (ed. Pette, D.) 177–191 (Walter de Gruyter, Berlin, 1980).
15. Pelloni-Mueller, G., Ermini, M. & Jenny, E. *FEBS Lett.* **67,** 68–74 (1976).
16. Dabrowska, R., Sosinski, J. & Drabikowski, W. *FEBS Lett.* **79,** 295–300 (1978).
17. Pette, D., Vrbova, G. & Whalen, R. G. *Pflügers Arch. ges Physiol.* **369,** 85–89 (1979).
18. Cleveland, D. W., Fischer, S. G., Kirschner, M. W. & Laemmli, U.K. *J. biol. Chem.* **252,** 1102–1106 (1977).
19. Hoh, J. F. Y., McGrath, P. A. & Hale, P. T. *J. molec. cell. Cardiol.* **10,** 1053–1076 (1978).
20. Lompré, A.-M., *et al.*, *Nature* **282,** 105–107 (1979).
21. Claycomb, W. C. *Expl Cell Res.* **118,** 111–114 (1979).
22. Whalen, R. G., Butler-Browne, G. S., Sell, S. & Gros, F. *Biochimie* **61,** 625–632 (1979).

Coexistence of α-fetoprotein, albumin and transferrin immunoreactivity in neurones of the developing mouse brain

C. Dominique Toran-Allerand

Center for Reproductive Sciences (IISHR) and Department of Neurology, Columbia University, College of Physicians & Surgeons, 630 West 168th Street, New York, New York 10032

α-Fetoprotein (AFP), a major fetal plasma protein, is present at high levels (mg ml^{-1}) throughout development and at extremely low levels (ng ml^{-1}) in the normal adult (see refs 1,2). Unlike that of most other species, rat and mouse AFP bind oestrogens with a high afinity[3]. This aroused speculation regarding its involvement in the growth and differentiation of oestrogen target tissues[4]. Extracellular sequestration of maternal oestrogens through binding to AFP is generally assumed to protect the female rodent brain from excessive oestrogenization (masculinization) from the high oestrogen levels present during the critical period for sexual differentiation[5]. There is an intracellular pool of AFP of unknown function in brain cytosol of fetal and neonatal rats[6] and mice[7]. Its intraneuronal localization has been confirmed within the central and peripheral nervous systems of the developing rat[8,9] and human fetus[10] by immunoperoxidase cytochemistry. Other major plasma binding proteins such as albumin[9,10] and prealbumin[10] but not transferrin[9,10] have also been localized within neurones of the developing rat and human brain. As part of a continuing ontogenetic study, I present here the first evidence, derived by single- and double-label immunofluorescence, for the intraneuronal localization and coexistence of immunoreactive AFP, albumin and transferrin within the same neurones of the late fetal and postnatal mouse brain. These observations may be relevant to the process of sexual differentiation of the brain, and the mechanism of transport of hormones and other growth-promoting substances into neurones during development.

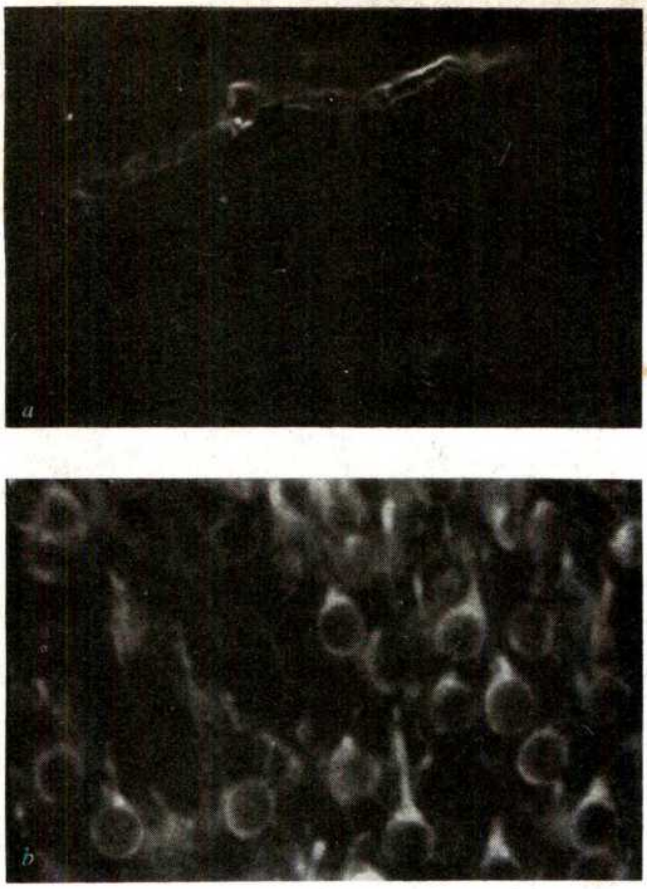

Fig. 1 *a*, Immunofluorescent staining of the newborn male mouse hypothalamus with the non-immune IgG control. Note the total absence of cellular fluorescence and the localization of the staining to a blood vessel only. This section was adjacent to the one in Fig. 2*b* × 100. Detailed methods for Figs 1 and 2 are given in the text. *b*, Immunofluorescent localization of mouse AFP in immature neurones of the 18-day fetal female mouse cerebral cortex. Note the cytoplasmic immunoreactivity with extension into the primary neuronal processes. × 175.

Brains from sexed 18-day fetal, newborn, 8-day post-natal and adult mice were immersed in ice-cold ethanol/acetic acid[11] without stirring for 24 h, dehydrated, cleared and embedded according to the method of Sainte-Marie[12], and processed for single- or double-label immunofluorescence. Demonstration of antigen localization was carried out by incubations of 3–4-μm serial coronal sections with purified goat antibodies to mouse AFP, the γ-globulin (IgG) fraction of rabbit antiserum to mouse albumin either unlabelled or conjugated to fluorescein isothiocyanate (FITC) (Cappel), or goat antiserum to mouse transferrin (Cappel) for 48 h at 4 °C. After washing in phosphate-buffered saline (PBS) (*p*H 7.4), antibody binding was visualized either by the direct method (FITC-conjugated anti-mouse albumin) or indirectly by adding goat anti-rabbit or rabbit anti-goat IgG conjugated to either (FITC) (green) or tetramethyl rhodamine isothiocyanate (TRITC) (red) (Cappel) for 24 h at 4 °C. The sections were then washed in PBS (*p*H 7.6), mounted in Gelvatol and examined with a Zeiss microscope equipped with both fluorescein and rhodamine optics, and epi-illumination.

Controls included: (1) non-immune goat and rabbit sera; (2) absorption (neutralization) of AFP antibodies by newborn mouse serum (high AFP levels); (3) absorption with purified mouse albumin or mouse transferrin (Cappel); (4) the fluorochrome conjugates alone, and (5) newborn mouse liver, a site of AFP, albumin and transferrin synthesis, as a positive control. These showed no fluorescence except for the liver, which confirmed the localization of the plasma proteins to the parenchymal cells. Furthermore, to distinguish the specific intracellular localization of the plasma proteins from their passive uptake, resulting from experimentally induced alterations in cell membrane permeability[13,14], parallel sections were always exposed to antiserum to mouse IgG (Cappel)[13]. IgG immunoreactivity was usually localized only to blood vessels (Fig. 1*a*). Neuronal fluorescence was generally absent, although small clusters of IgG-staining cells were occasionally seen only in regions of obvious tissue damage. Cells were considered AFP-, albumin- or transferrin-positive only if they were also IgG-negative.

The double-labelling experiments (AFP–albumin; transferrin-albumin) were carried out by a combined direct (albumin) and indirect (AFP; transferrin) method. This approach became necessary because the sequential application of the two conjugated fluorochromes (TRITC–rabbit anti-goat; FITC–goat anti-rabbit) resulted in the double staining of each primary antibody due to apparent conjugate cross-reactivity. The conjugated fluorochromes themselves, however, did not detect the inappropriate antibody nor did they stain the tissue in the absence of antibody. The double labelling experiments consisted of sequential applications on the same tissue section of the goat antibodies (AFP or transferrin), TRITC–rabbit anti-goat IgG and FITC–rabbit anti-mouse albumin IgG, each for the time periods described above. Double-label detection of AFP and transferrin was not possible because of their shared species of origin (goat).

Intracellular localization of all three plasma proteins was observed only in the brains of the 18-day fetal, newborn and 8-day postnatal mice. The adult brains exhibited no fluorescence. Specific fluorescence was observed in cell groups throughout the developing brains of both sexes and seemed to be localized to neurones only. Large numbers of post-mitotic neuroblasts and immature neurones exhibited bright, specific intracytoplasmic fluorescence which often extended into primary processes, initial dendritic segments and axons (Figs 1, 2). Neuronal nuclei did not fluoresce. AFP-, albumin- and transferrin-containing neurones were widely distributed in diverse regions, including the cerebral cortex (Fig. 1*b*), septum, basal ganglia, hippocampus, brain stem (Fig. 2*a*), hypothalamus (Fig. 2*b*), cerebellum and medulla. The numbers of fluorescing neurones in any given region increased with its developmental stage. This was exemplified quite strikingly in the cerebral cortex, where the numbers and topographic distribution of fluorescing neurones were closely correlated with differentiation of the cortical layers. In the hypothalamus, preoptic area and the amygdala, however, certain nuclear regions known from ^{3}H-oestradiol autoradiography to contain oestradiol receptors were rendered anatomically distinctive by the complete or almost complete and bilaterally symmetrical absence of fluorescence. These regions include the medial preoptic area, the suprachiasmatic, arcuate, ventromedial and ventral premamillary nuclei of the hypothalamus, and the medial and cortical amygdaloid nuclei and will be described elsewhere (in preparation). Specific fluorescence was also seen in the epithelial cells of the choroid plexus, in the meninges, in blood vessels, to varying degrees in the apical portions of ependymal cells, and in the extracellular space of the developing brains. Fluorescence of the extracellular space, however, decreased significantly between birth and the 8th postnatal day and was totally absent from the adult brain.

Double-labelling experiments demonstrated that all neurones which exhibited fluorescence for either AFP or transferrin (red) also contained albumin (green). Although the lack of suitable antibodies precluded any direct comparisons of AFP and transferrin localization, the topographic distribution of albumin-containing cells in serial sections suggests that all three proteins are in the same neurone.

This is the first demonstration of AFP, albumin and transferrin immunoreactivity in the developing mouse brain and of their coexistence within the same neurones. These observations also confirm that the AFP in mouse brain cytosol is intraneuronal[7].

Furthermore, transferrin has not previously been localized intraneuronally, its specific absence, rather, being noted[9,10]. Because of the inadequacy of the blood-brain barrier at the ages studied, the intraneuronal coexistence of the three plasma proteins makes it seem more likely that they have been taken up by endocytosis from the cerebrospinal fluid and blood[10] than synthesized locally. This hypothesis is supported by the observed immunoreactivity of blood vessels, choroid plexus epithelium and the extracellular space. To investigate the alternative possibility, however, we are now determining whether or not AFP is synthesized in developing neurones by carrying out *in situ* and solution hybridizations to the messenger RNA with a cloned chromosomal DNA probe specific for AFP.

The discrete intracytoplasmic localization of AFP, albumin and transferrin raises questions regarding their possible active and essential role in neuronal differentiation and development. As binders of a variety of hormones and other biologically active substances, these three plasma proteins may mediate or modulate their intraneuronal transport. It has been proposed, for example, that at low steroid concentrations cellular entry of oestrogen into the immature rat uterus may be a carrier-mediated event in contrast to the diffusion seen with high levels[15]. Moreover, the essential role of albumin in the active transport of thyroid hormones into rat hepatocytes in culture has been demonstrated[16]. Incorporation of albumin (but not of other proteins) into the nutrient medium of cultured chick sensory ganglia, furthermore, significantly enhanced the biological activity of nerve growth factor (NGF) by doing more than merely preventing its adsorption to glassware[17].

The intraneuronal localization of the oestrophilic AFP has important implications for the process of sexual differentiation of the rodent brain. Its intracellular presence forces one to reconsider the generally held concept that the female rodent brain is protected from exposure to maternal oestrogens by the extracellular AFP[5]. On the contrary, neuronal uptake (perhaps by endocytosis) of such oestrogen-binding proteins as AFP and albumin must bring oestradiol into the cell. Intracellular dissociation of the protein–oestradiol complex, resulting from the greater affinity of oestradiol for its receptor, could liberate the steroid for subsequent association with its cytoplasmic receptors. Such a mechanism might thus provide certain neurones of both sexes with the intracellular source of oestradiol of non-androgen origin previously postulated as necessary for the induction of both male and female patterns of neural differentiation[18,19].

This phenomenon, however, need not be limited to the particular proteins described here. In those species (birds, humans) whose AFP has little or no oestrogenic affinity[1,2], other binding proteins, including albumin, may serve the same functions by similar mechanisms. Its possible active role in the transport of thyroid hormones and NGF-like substances, among others, as well as its capacity to bind oestrogens, renders albumin also of considerable potential importance to the development of the central nervous system. Furthermore, the intraneuronal localization of albumin makes it imperative that antisera raised to bovine serum albumin-conjugated antigens be pre-absorbed with albumin before use in immunocytochemical studies of developing central nervous system tissue both *in situ* and in cultures exposed to serum-containing medium.

The significance of the intraneuronal localization of transferrin is unknown. That transferrin *per se* may mediate important developmental functions, however, is suggested by recent *in vitro* observations[20] that transferrin (90% iron-free) is essential for neuronal differentiation and survival in serum-free medium.

The cellular uptake of plasma proteins during development may not be unique to the brain. Preliminary studies (unpublished observations) suggest that immunoreactive AFP, albumin and transferrin are also localized within cells of the neonatal adenohypophysis. Their presence in other hormonal target tissues remains to be determined.

I thank Dr E. Ruoslahti (La Jolla Cancer Research Foundation) for the gift of the antibodies to mouse AFP, Dr G. Godman for the Gelvatol, Drs H. Jalanko (City of Hope), A. Etgen and A.-J. Silverman for helpful discussions, Dr C. Paden for photographic assistance and Mrs G. Katzauer for sectioning the tissues. This study was supported in part by grants from NIH (HD-08364), NSF (BNS 77-0859), the WT Grant Foundation, and the March of Dimes Birth Defects Foundation. C.D.T.-A. is in receipt of a NIMH Research Scientist Development Award (MH-00192).

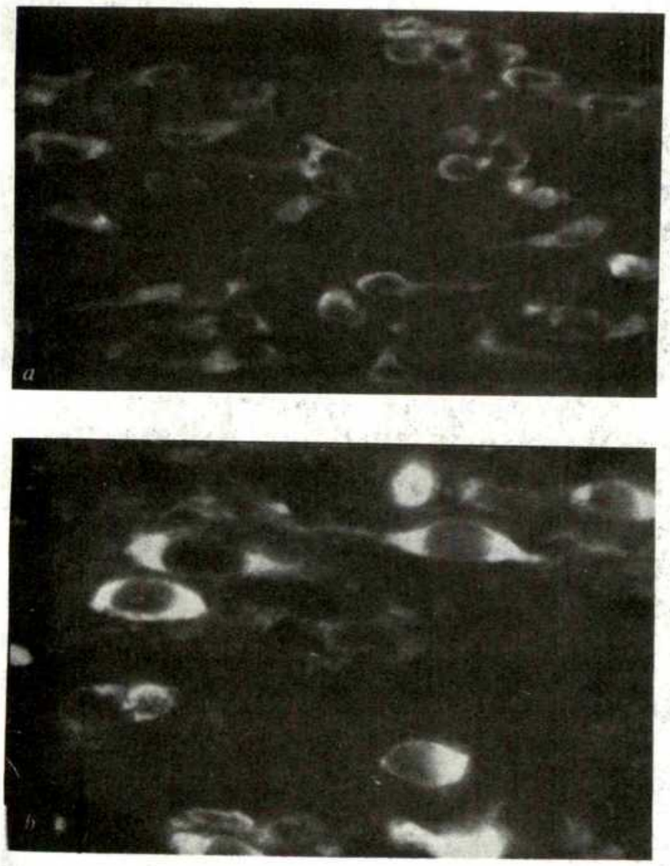

Fig. 2 *a*, Immunofluorescent localization of mouse albumin in neurones of the 8-day female mouse midbrain. ×100. *b*, Immunofluorescent localization of mouse transferrin in neurones of the newborn male mouse hypothalamus. ×175.

Received 13 March; accepted 14 May 1980.

1. Ruoslahti, E. & Engvall, E. *Scand. J. Immun.* Suppl. **6,** 1–17 (1978).
2. Ruoslahti, E. & Seppälä, M. *Adv. Cancer Res.* **29,** 275–346 (1979).
3. Nunez, E. A., Benassayag, C. Savu, L., Vallette, G. & Jayle, M. F. *Ann. Biol. anim. Biochem. Biophys.* **16,** 491–501 (1976).
4. Nunez, E. A., Benassayag, C., Savu, L. & Delorme, J. in *Carcino-Embryonic Proteins* Vol. I, (ed. Lehmann, F.-G.) (Elsevier, Amsterdam, 1979).
5. Plapinger, L. & McEwen, B. S. *Endocrinology* **93,** 1119–1128 (1973).
6. McEwen, B. S., Plapinger, L., Chaptal, C., Gerlach, J. & Wallach, G. *Brain Res.* **96,** 400–407 (1975).
7. Attardi, B. & Ruoslahti, E. *Nature* **263,** 685–687 (1976).
8. Benno, R. H. & Williams, T. H. *Brain Res.* **142,** 182–186 (1978).
9. Trojan, J. & Uriel, J. *C. r. hebd. Séanc. Acad. Sci. Paris* D**289,** 1157–1160 (1979).
10. Møllgård, K., Jacobsen, M., Jacobsen, G. K., Clausen, P. P. & Saunders, N. R. *Neurosci. Lett.* **14,** 85–90 (1979).
11. Hamashima, Y., Harter, J. G. & Coons, A. H. *J. Cell Biol.* **20,** 271–279 (1964).
12. Sainte-Marie, G. *J. Histochem. Cytochem.* **10,** 250–256 (1962).
13. Engelhardt, N. V., Goussev, A. I., Shipova, L. Ja. & Abelev, G. I. *Int. J. Cancer* **7,** 198–206 (1971).
14. Guillouzo, A. *et al. J. Histochem. Cytochem.* **26,** 948–959 (1978).
15. Milgrom, E., Atger, M. & Baulieu, E. E. *Biochim. biophys. Acta* **320,** 267–283 (1973).
16. Krenning, E. P., Docter, R., Bernard, H. F., Visser, T. J. & Hennemann, G. *FEBS Lett.* **107,** 227–230 (1979).
17. Stach, R. W., Garian, N. & Olender, E. J. *J. Neurochem.* **33,** 257–261 (1979).
18. Toran-Allerand, C. D. *Brain Res.* **106,** 407–412 (1976); **189,** 413–427 (1980).
19. Döhler, K.-D. & Hancke, J. L. in *Hormones and Brain Development* (eds Dörner, G. & Kawakami, M.) 153–157 (Elsevier, Amsterdam, 1978).
20. Bottenstein, J. E., Skaper, S. D., Varon, S. S. & Sato, G. H. *Expl Cell Res.* **125,** 183–190 (1980).

Glial cells in the enteric nervous system contain glial fibrillary acidic protein

Kristjan R. Jessen & Rhona Mirsky

Department of Anatomy and MRC Neuroimmunology Project, Department of Zoology, University College London, Gower Street, London, WC1E 6BT, UK

The complex nervous networks found throughout the mammalian gut—the enteric nervous system—are histologically, ultrastructurally, and, to some extent, functionally—similar to the central nervous system[1-3]. The glial cells of the small enteric ganglia are generally classified as Schwann or satellite cells, since they are found in the peripheral nervous system, possess nuclei which ultrastructurally resemble those of Schwann cells and are derived from the neural crest[4,5]. However, it has been argued that these cells resemble astrocytes of the central nervous system with respect to gross and fine structure, and their relationship with the enteric neurones and their processes[1,6]. In immunohistochemical studies of these cells, both in frozen sections of gut wall and in tissue culture preparations of the enteric plexuses, we found evidence that the enteric glial cells are rich in glial fibrillary acidic protein (GFAP), a protein associated with the 100 Å glial intermediate filaments[7], and hitherto believed to be specific to astrocytes of the central nervous system only[8,9].

Figure 1 illustrates the immunofluorescence seen when frozen sections through ganglia of the rat myenteric plexus, cerebellum and sympathetic ganglia were treated with antisera raised against human GFAP; similar results were obtained with three different antisera[9,10]. As shown in Fig. 1*b*, the antisera reacted strongly with the glial cells in the myenteric ganglia, the immunofluorescence characteristically surrounding the neuronal cell bodies, which were always unstained. The glial staining was of similar intensity to that of astrocytes in frozen sections from the central nervous system (Fig. 1*b*, *d*). No staining was found in the Schwann cells, satellite cells, neurones or axons in sections from other autonomic ganglia with any of the three antisera (Fig. 1*c*). However, Yen and Fields have recently found evidence that a minority of peripheral glial cells in adult rat sciatic nerve sections also contain GFAP immunoreactivity using the same antisera as we used here (personal communication).

It has been demonstrated that astrocytes of the central nervous system maintain their glial filaments when grown in tissue culture and show striking, filamentous GFAP immunofluorescence on treatment with GFAP antisera[11]. It was therefore interesting to see whether enteric glial cells in culture also exhibited GFAP immunoreactivity. Explant cultures of the myenteric plexus were obtained from the proximal colon of 7–14-day-old rats as described elsewhere[12]. We have suggested that one of the cell types in such cultures, identifiable on the basis of occurrence, morphology and interaction with other cells, may be the enteric glial cells[12]. When cultures of the plexus, maintained *in vitro* for 7–10 days, were treated with the GFAP antisera, it was found that most of these putative glial cells showed bright, filamentous immunofluorescence, very similar to that seen in astrocytes in tissue culture (Fig. 2). Other flat cells, fibroblast-like in morphology, were unstained, as were the neuronal cell bodies and their processes. As with astrocytes in culture[13], the morphology of the cells showing GFAP immunofluorescence was quite varied. Many, however, had tapering processes and in most cells part of the cell body flattened out, forming often extensive, thin membraneous expansions.

To establish conclusively that the glial cells in the enteric plexuses contained GFAP, we compared the distribution of GFAP immunofluorescence with that of neurofilament (NF)

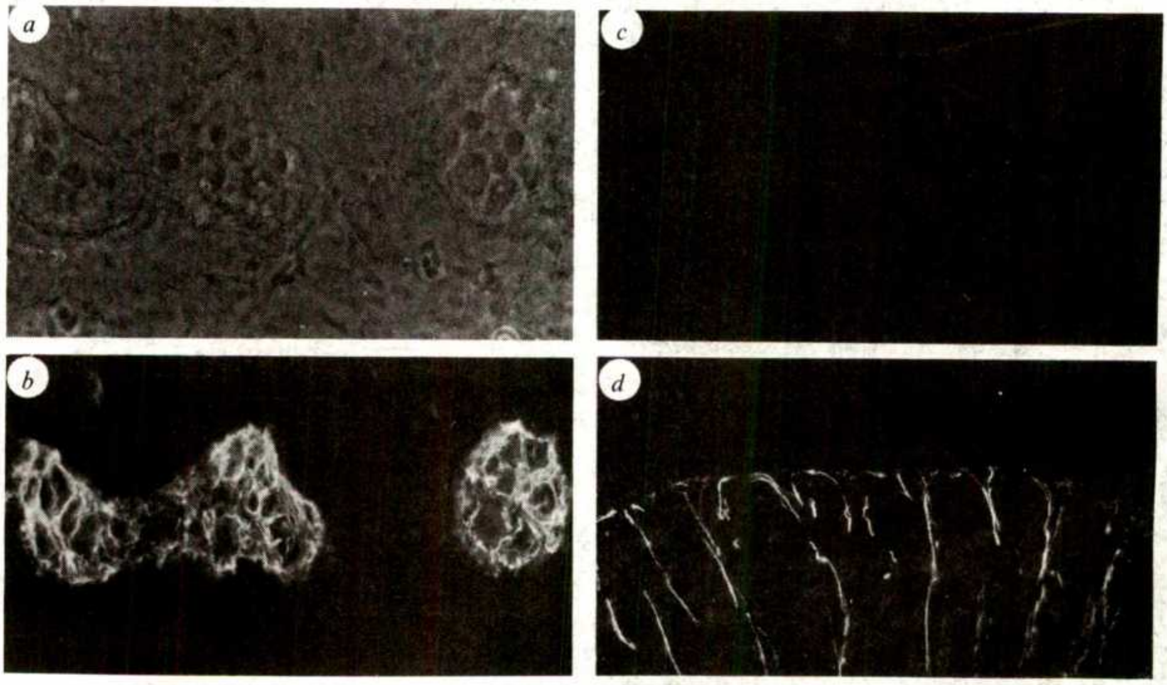

Fig. 1 GFAP immunofluorescence in frozen sections of *a* and *b*, rat colon, *c*, dorsal root ganglion, and *d*, cerebellum. 10 μm sections were left overnight at 4 °C, then incubated overnight at 4 °C with rabbit anti-human GFAP serum (1 : 1000), followed by goat anti-rabbit IgG conjugated to rhodamine (G anti-RIg-Rd) for 30 min at room temperature. They were viewed with *a*, phase contrast or (*b*–*d*), fluorescence optics, using a Zeiss Universal microscope. Only the glial cells in the myenteric plexus are labelled in *b*; the neurones in the plexus and the circular and longitudinal muscle are all unlabelled. No immunofluorescence is seen in any of the dorsal root ganglion cells *c* while the cerebellum shows typical GFAP labelling in processes of Bergmann astrocytes *d* (*a*, *b*, *c* ×300; *d* ×200). The antiserum donated by Drs D. Dahl and A. Bignami has been extensively characterized in a number of studies, which have shown that it specifically stains astrocytes both in tissue sections and cultures and does not stain other cells in nervous or non-nervous tissues[8,9,11,13,16]. The antisera donated by Dr R. Pruss were prepared from human GFAP as described by Drs D. Dahl and A. Bignami[9]. Extensive testing of these antisera on tissue sections and cultures revealed that the staining properties of both antisera are identical to those of the Dahl and Bignami antiserum (R. Pruss, personal communication).

0028-0836/80/330736—02$01.00

immunofluorescence. The NF antiserum was prepared against the 155,000 molecular weight subunit of neurofilament protein[14]. The distribution of NF immunofluorescence in the rat myenteric plexus and sympathetic ganglia is illustrated in Fig. 3. In ganglia of the plexus (Fig. 3*a*) the NF antiserum typically revealed the neuronal cell bodies. No fluorescence was present in the glial cells surrounding the neurones, so that the NF staining pattern was the converse of that seen with the GFAP antisera. In the superior cervical ganglion (Fig. 3*b*) the most prominent sites of NF immunoreactivity were the axons of transversely cut axon bundles. Staining was also seen in the cell bodies of most neurones although the intensity varied markedly between cells and only a few of them stained as intensely as did the axons. All these structures were completely unstained when treated with GFAP antisera. Thus, the pattern of NF immunofluorescence in both tissues is completely different from that of GFAP immunofluorescence, from which we conclude that the immunoreactivity observed in these tissues following treatment with GFAP antisera resides in glial cells and not in neurones.

GFAP is the major protein of the 100 Å filaments found in astrocytes; the GFAP-containing filaments are one of five different, but related classes of intermediate filaments that can be distinguished both by immunological and biochemical methods. The others are neurofilaments, found in central and peripheral nervous systems, desmin filaments, present in muscle cells, keratin filaments in epithelial cells and vimentin filaments, the only filament type that has a wide distribution among different types of cells[15]. GFAP-containing filaments have so far been found exclusively in astrocytes of the central nervous system and have often been used as a cell-type specific marker for astrocytes[7–9,11,13]. However, our results indicate that under appropriate conditions, GFAP can be expressed by glial cells in the peripheral nervous system. The enteric glial cells, like astrocytes, express GFAP both *in situ* and in culture. It has previously been noted that although the enteric glial cells have some of the morphological characteristics of Schwann cells they also show notable structural similarities with astrocytes[1,5,6]. Like astrocytes, the enteric glial cells carry extensive branching and irregular processes which mingle with neuronal processes in a dense synaptic neuropil, they possess glycogen granules and contain a very large number of glial filaments, arranged in a manner similar to that seen in astrocytes. The results described in this paper demonstrate that these enteric glial cells are different from typical Schwann cells and satellite cells not only in structural but also in some biochemical features. More work is needed to determine whether these cells should be classified as modified Schwann or satellite cells, adapted to suit a complex, integrative nervous system, or whether they are sufficiently different from other peripheral glial cells to warrant consideration as a separate class of glial cells.

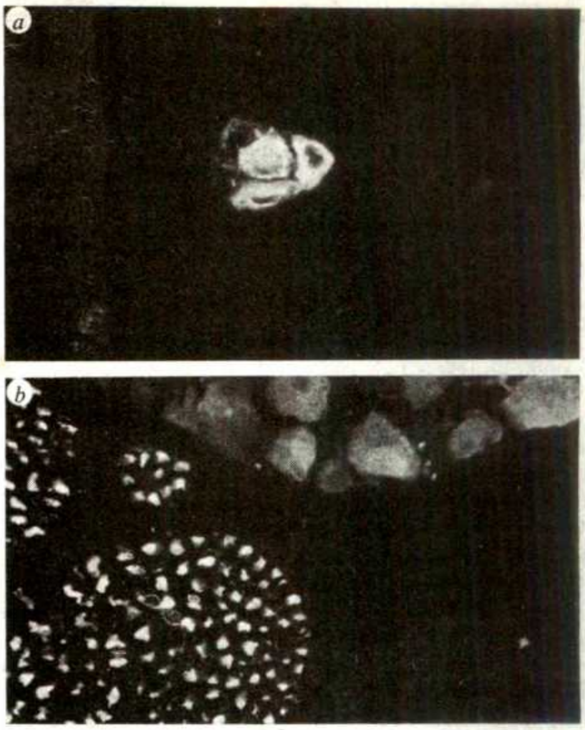

Fig. 3 Neurofilament immunofluorescence in frozen sections of *a*, rat colon and *b*, dorsal root ganglion. 10μm sections were left overnight at 4 °C and then stained overnight with rabbit anti-NF (1:400), followed by G anti-RIg-Rd for 30 min at room temperature. They were then viewed with fluorescence optics as described in Fig. 1. Three neuronal cell bodies in the myenteric plexus are clearly stained with the NF antibodies (*a*). The glial cells surrounding them, in contrast to Fig. 1 *b*, are unlabelled. Neuronal labelling is seen in both cell bodies and axons in the dorsal root ganglion (*b*). In both *a* and *b* there is a clear difference in the pattern of staining between the NF antiserum and the GFAP antiserum staining seen in Fig. 1 (×430).

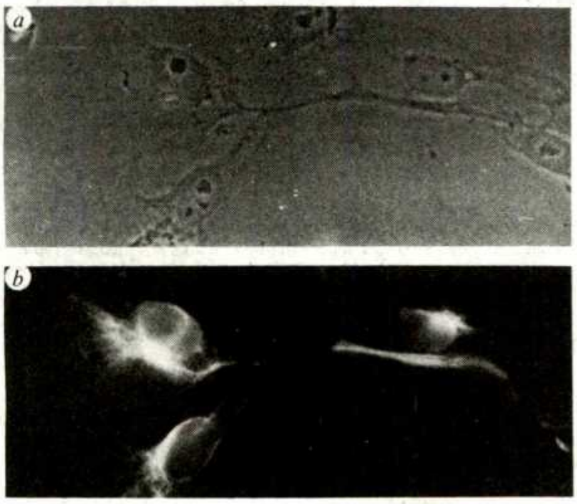

Fig. 2 GFAP immunofluorescence in explant culture from the proximal colon of 15-d-old rat. *a* Represents a phase contrast view of the same field as shown in *b* where fluorescence optics are used (see Fig. 1). Cultures were fixed with 5% acetic acid in ethanol at −20 °C for 10 min, incubated with rabbit anti-human GFAP (1:100) for 30 min at room temperature, followed by G anti-RIg-Rd for 30 min at room temperature. Flat cells in the culture are stained in a filamentous pattern similar to GFAP staining of cultured astrocytes (×640).

We would like to thank Professor Geoffrey Burnstock for generous provision of materials and laboratory facilities, Drs R. Pruss, D. Dahl and A. Bignami for gifts of the three antisera raised against human GFAP, and Dr B. H. Anderton for the NF antiserum. K.R.J. was supported by the Mental Health Foundation.

Received 13 March; accepted 6 June 1980.

1. Gabella, G. *J. Anat.* **111,** 69-97 (1972).
2. Wood, J. D. *Physiol. Rev.* **55,** 307–324 (1975).
3. Wood, J. D. in *Integrative Functions of the Autonomic Nervous System* (eds Brooks, C. M., Koizumi, K. & Sato, A.) 177–193 (Elsevier, Amsterdam, 1979).
4. Schofield, G. C. in *Handbook of Physiology* Vol 4 (ed. Code, G. F.) 1579–1627 (Williams and Wilkins, Baltimore, 1968).
5. Cook, R. D. & Burnstock, G. *J. Neurocytol.* **5,** 195–206 (1976).
6. Gabella, G. *Zeitschrift für Naturforschung,* **26b,** 244–245 (1971).
7. Schachner, M., Hedley-Whyte, E. T., Hsu, D. W., Schoonmaker, G. & Bignami, A. *J. Cell Biol.* **75,** 67–73 (1973).
8. Bignami, A., Eng, L. F., Dahl, D. & Uyeda, C. T. *Brain Res.* **43,** 429–435 (1972).
9. Dahl, D. & Bignami, A. *Brain Res.* **116,** 150–157 (1976).
10. Pruss, R. *Nature* **280,** 688–690 (1979).
11. Antanitus, D. S., Choi, B. H. & Lapham, L. W. *Brain Res.* **89,** 363–367 (1975).
12. Jessen, K. R., McConnell, J. D., Purves, R. D., Burnstock, G. & Chamley-Campbell, J. *Brain Res.* **152,** 573–579 (1978).
13. Raff, M. C. *et al. Brain Res.* **174,** 283–308 (1979).
14. Anderton, B. H., Thorpe, R., Cohen, J., Selvendran, S. & Woodhams, P. J. *Neurocytol.* (in the press).
15. Lazarides, E. *Nature* **283,** 249–256 (1980).
16. Ludwin, S. K., Kosek, J. C. & Eng, L. F. *J. comp. Neurol.* **165,** 197–208 (1976).

Monoclonal anti-acetylcholine receptor antibodies can cause experimental myasthenia

David P. Richman*, Christopher M. Gomez*, Phillip W. Berman†, Steven A. Burres*, Frank W. Fitch* & Barry G. W. Arnason*

*The University of Chicago, Chicago, Illinois 60637
†The Salk Institute, San Diego, California 92212

Myasthenia gravis (MG) is a disease which occurs as a consequence of an autoimmune response directed against the nicotinic acetylcholine receptor (AChR) of the myoneural junction[1-3]. Antisera raised against complex antigens such as AChR comprise a mixture of antibodies reactive with various determinants on the antigen molecule. The antibodies against any single determinant may be of several immunoglobulin classes and idiotypes. Antibodies produced by cloned lymphocyte–myeloma hybridoma cell lines have provided a way of analysing the diverse components making up a polyclonal antiserum[4] and assessing the relative contribution made by each to the overall immune reaction *in vivo*[5,6]. We have applied this technique to the investigation of the autoimmune response in MG. We demonstrate here that certain monoclonal anti-*Torpedo* AChR antibodies, when injected intravenously into normal rats, induce an acute myasthenic syndrome. Thus binding of a single molecular species of antibody reactive with a single antigenic determinant can result in all of the manifestations of an autoimmune disease.

Hybridoma cell lines producing anti-AChR antibody were obtained and partially characterized as described elsewhere[7,8]. A Lewis rat (Microbiological Associates) was immunized with AChR purified from the electroplax of *Torpedo californica*. Spleen cells from this animal were fused with the mouse myeloma cell line P3-X63-Ag8 (provided by Dr C. Milstein). Proliferating hybridomas were screened for production of anti-AChR antibody by a haemagglutination assay (HA) using sheep erythrocytes coated with *Torpedo* AChR (ref. 8).

The binding properties of the hybridoma antibodies have been partially characterized by assessing changes in HA titre when AChR-coated red cells were preincubated with cholinergic ligands. Antibodies from the independently isolated, cloned, hybrid cell lines fall into four groups (1) blockable by α-bungarotoxin; (2) partially blockable by cholinergic ligands; (3) titres increased in the presence of some nicotinic ligands; (4) titres unaffected by any cholinergic ligand or by α-bungarotoxin[8]. The heavy chain class (Table 1) of each antibody was determined by radial immunodiffusion with antisera (provided by Dr Hervé Bazin)[9]. Immunoglobulin-enriched culture supernatant preparations from each hybridoma and from P3-X63-Ag8 were injected intravenously into individual young female Lewis rats (Fig. 1). Animals were examined every 12 h. At either 48 or 72 h the animals underwent *in vivo* measurement of the evoked muscle responses of the gastrocnemius muscle to repetitive sciatic nerve stimulation and *in vitro* measurement of minature endplate potentials (m.e.p.ps) from the diaphragm[10]. All m.e.p.p. amplitudes were corrected to a resting potential of 85 mV. Input resistances ranged from 4 to 15 MΩ. At 48 or 72 h tissues were taken for histological study and blood samples were obtained for serum antibody titre determination by both HA and radioimmunoassay[11].

Two of six antibodies tested (56I and 73G) produced both the clinical and electrophysiological manifestations of myasthenia in injected animals (Fig. 1, Table 1). Injection of similar amounts of antibody (as determined by both antibody titre and immunoglobulin concentration) from the other anti-AChR producing hybridomas or from the myeloma line alone was ineffective. Decrementing evoked muscle responses to repetitive nerve stimulation and diminished amplitude of m.e.p.p. correlated with clinical disease (Table 1). Of five animals tested with clinical signs of myasthenia, four demonstrated decrement of 10% or more. None of 10 animals injected with other antibodies or with the myeloma protein exhibited decrement. The m.e.p.p. amplitudes of 6 of 8 animals injected with antibodies 56I or 73G were lower than any of the values for the 10 animals injected with the other antibodies or myeloma protein. The means of the two groups differed significantly [0.55 ± 0.02 compared with 0.70 ± 0.02 mV (mean ± s.e.m.), $P < 0.001$][12].

Frozen sections of muscle were obtained from several sites. Mononuclear cell infiltrates were located selectively in the regions of endplates of animals injected with antibodies 56I or 73G (Fig. 2*a*). In these areas numerous fibres were undergoing necrosis with frank invasion by mononuclear cells. In sections stained for cholinesterase activity, many cholinesterase-reactive regions were separated from the underlying fibres; the cholinesterase staining was sometimes diffuse and lacked detail (Fig. 2*b*). Frequently mononuclear cells were interposed between the muscle fibres and the cholinesterase-reactive regions (Fig. 2*c*). Serial sections stained for acid phosphatase demonstrated that the infiltrating mononuclear cells were macrophages. No histological abnormalities were found in animals injected with the other antibodies or the myeloma protein.

The syndrome produced here by injection of a hybridoma supernatant fraction containing monoclonal anti–AChR antibody is indistinguishable from the acute phase of rat experimental autoimmune myasthenia gravis (EAMG)[13] or from the disease produced by injection of syngeneic immune serum[14]. The fact that preparations from some anti-AChR producing clones, and from the myeloma line alone, produced no effects suggests that it is not other factors present in the culture supernatants that are responsible for the observed findings. This is the first demonstration, to our knowledge, of the production of

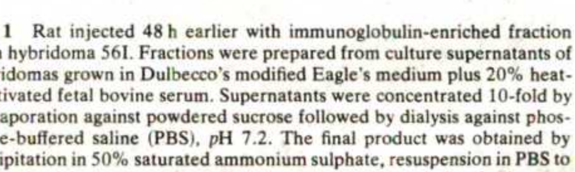

Fig. 1 Rat injected 48 h earlier with immunoglobulin-enriched fraction from hybridoma 56I. Fractions were prepared from culture supernatants of hybridomas grown in Dulbecco's modified Eagle's medium plus 20% heat-inactivated fetal bovine serum. Supernatants were concentrated 10-fold by pervaporation against powdered sucrose followed by dialysis against phosphate-buffered saline (PBS), *p*H 7.2. The final product was obtained by precipitation in 50% saturated ammonium sulphate, resuspension in PBS to ~5% of original volume, and dialysis against PBS. A similar faction was prepared using supernatants from cultures of the myeloma line P3-X63-Ag8. Approximately 1 ml (40–100 mg of protein of 56I and 73G, up to 250 mg of the other antibodies) of each preparation was injected into normal rats. Agar gel electrophoresis followed by densitometric scanning indicated that all preparations consisted of 85–90% albumin and 10–15% immunoglobulin. Isoelectric focusing of the material (performed by David Mattson) revealed 8–12 immunoglobulin bands, 6 of which were those of the myeloma protein. Clinical disease had a similar time course in animals receiving either of the two myasthenia-inducing antibodies and correlated with dose of antibody injected and with serum titre at time of death. Extremity weakness was noted 18–24 h after injection; this worsened over the next 24–36 h. In more severely affected animals susceptibility to fatigue was such that, after one or two steps, the animals lurched to either side. Some showed almost no power in flexion or extension of upper extremity digits so that the front paws remained cupped. Weight loss in these animals, possibly caused by weakness of neck extensors and muscles of mastication, averaged 17 g over the 3-day period of observation. Consistently observed were dried porphyrin secretions crusting the eyelids, nares, and periorbital fur. Weakness was reversed temporarily by intraperitoneal edrophonium chloride.

0028-0836/80/330738—02$01.00

a defined pathological syndrome by an immune reaction mediated by monoclonal antibody. Since the antibody is monoclonal it is presumed to bind to a single determinant on the AChR molecule, to express a single set of idiotypic determinants, and to be of a single immunoglobulin class. It must have, therefore, a single set of effector functions, for example, interaction with complement, interaction with macrophages. These characteristics are sufficient, in the cases of antibodies 56I and 73G, to induce myasthenia.

Data are not yet available to explain the failure of some of the anti-AChR antibodies to induce myasthenia. Since the antibodies were raised against AChR from *Torpedo californica* electroplax, it is most likely that the ineffective antibodies simply do not cross-react with rat junctional AChR (preliminary data seem to support this explanation). Other possible explanations may include a requirement for binding to a particular portion of the AChR molecule.

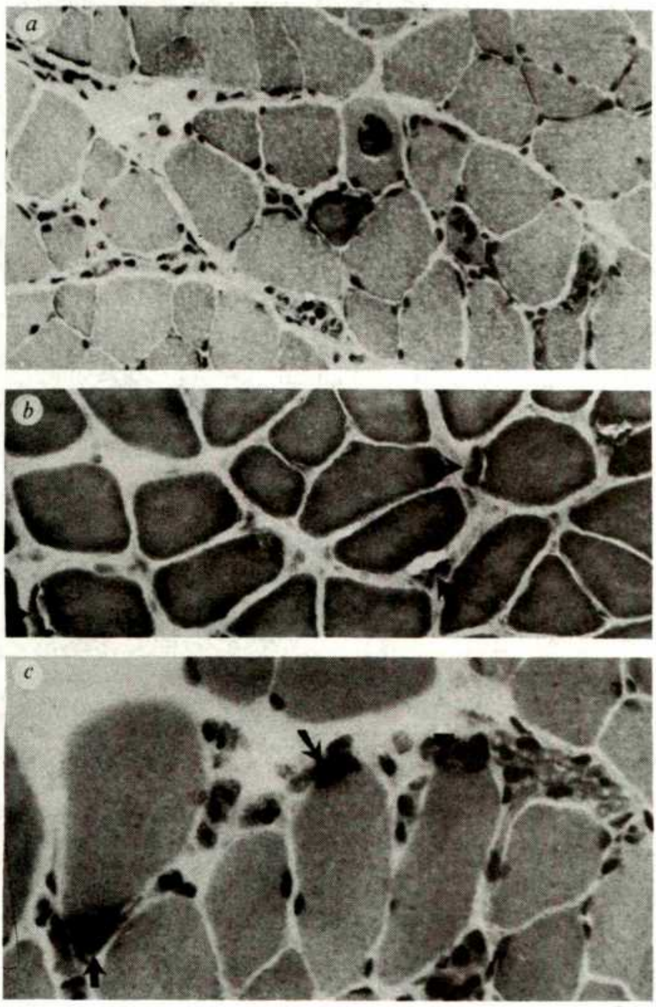

Fig. 2 Forelimb extensor muscle specimens from an animal injected 48 h earlier with antibody 56I. Fresh tissue was quick frozen, sectioned (9-μm), and stained with haematoxylin and eosin (*a*), or for cholinesterase activity by either a modification of the Karnovsky method[22] (*b*) or by α-naphthyl acetate esterase[23] (*c*). Some sections were also stained for acid phosphatase activity[24] (not shown). Mononuclear cell invasion, along with presence of necrotic fibres, is seen in a region shown, on serial section, to contain many end plates (*a*). Several cholinesterase-reactive regions (arrows) are separated from their muscle fibres (*b*). Direct observation identified these regions as cholinesterase-reactive by their distinctive brown gold colour. Invasion of cholinesterase-reactive regions (arrows) by mononuclear cells is seen along with disintegration of one region (arrow head) identified under direct observation by the distinctive dark red colour obtained with this technique (*c*). *a*, ×135, *b*, *c*, ×90.

Table 1 Effects of monoclonal anti-AChR antibodies

Hybridoma antibody (Class) [Specificity pattern]*	Disease score†	Amount injected (nmol)‡	Serum HA titre ($\log_2$)§	% Decrement at 5 Hz‖	m.e.p.p. amplitude (mV)
56I (IgG2b)	3	4.8	16	20	0.49**
[2]	3	3.6	11 (0.12)	26	0.50**
	2	1.8	ND	10	0.63
	0	1.0	10 (0.06)	incr.	0.51**
73G (IgG2b)	3	3.6	14 (0.08)	13	0.58**
[3]	3	3.6	13 (0.12)	incr.	0.64
	3	2.4	14 (0.09)	ND	0.53**
	0	0.5	10 (0.05)	3	0.56**
60D (IgG2a)	0	1.8¶	17	incr.	0.71
[1]	0	0.2¶	11	1	0.63
62J (IgG2a)	0	2.2	16 (0.69)	incr.	0.65
[2]	0	2.2	ND	incr.	0.64
57L (IgM)	0	5.1	14 (0.03)	1	0.66
[2]	0	5.1	6 (0.04)	incr.	0.77
77F (IgM)	0	2.3	13 (0.12)	incr.	0.72
[4]	0	2.3	4	incr.	0.81
P3-X63-Ag8	0	0	0	incr.	0.80
(IgGl)	0	0	0	incr.	0.64

* Defined by effect of cholinergic ligands on HA titre[8]: 1, blockable by α-bungarotoxin; 2, partially blockable by cholinergic ligands; 3, increased titre in presence of nicotinic ligands; 4, unaffected by cholinergic ligands.

† 0, no clinical findings; 1, forelimb weakness; 2, weakness of all extremities and abnormal gait; 3, unable to support own weight.

‡ As determined by radioimmunoassay with ^{125}I-α-bungarotoxin-labelled AChR.

§ Values in parentheses are results, in nmol ml^{-1}, by radioimmunoassay.

‖ incr. increment.

ND, not done.

¶ As determined by radioimmunoassay with ^{3}H-AChR (ref. 11), since the binding of this antibody is blocked by α-bungarotoxin.

** $P < 0.01$ when compared with mean of 60D, 62J, 57L, 77F, P3-X63-Ag8.

Mere binding of antibody to AChR is probably not sufficient to induce the syndrome. Various studies have suggested requirements for cross-linking of AChRs by antibody and for complement fixation[15-20]. Such antibody effector functions are primarily determined by heavy chain class or subclass. Both myasthenia-inducing antibodies, 56I and 73G, are of subclass IgG2b and should, therefore, be capable of diffusing into muscle, binding macrophages and fixing complement[21].

The observations reported here establish that a single antibody species, in an otherwise normal organism, can lead to a severe immunologically mediated disorder. Loss of regulation of a single immunocyte clone may be sufficient, therefore, to cause an autoimmune syndrome.

This research was supported in part by grants from the NIH (NS 15462, NS 13546, NS 05715, A 19268), the Muscular Dystrophy Association of America and the Myasthenia Gravis Foundation Inc.

Received 7 December 1979; accepted 21 May 1980.

1. Drachman, D. B. *New Engl. J. Med.* **298,** 136–142 (1978).
2. Heidman, T. & Changeux, J-P. *A. Rev. Biochem.* **49,** 313–356 (1978).
3. Lindstorm, J. *J. supramolec. Struct.* **4,** 389–403 (1976).
4. Kohler, G. & Milstein, C. *Nature* **256,** 495–497 (1975).
5. McKearn, T. J., Sarmiento, M., Weiss, A., Stuart, I. P. & Fitch, F. W. *Curr. Topics Microbiol. Immun.* **81,** 61–65 (1978).
6. Koproski, H. *et al. Curr. Topics Microbiol. Immun.* **81,** 8–19 (1978).
7. Gomez, C. M. *et al. Fedn Proc.* **38,** 1421 (1979).
8. Gomez, C. M. *et al. Biochem. biophys. Res. Commun.* **88,** 575–582 (1979).
9. Bazin, H., Beckers, A. & Querinjean, P. *Eur. J. Immun.* **4,** 44–48 (1974).
10. Burres, S. A., Richman, D. P., Crayton, J. W. & Arnason, B. G. W. *Muscle Nerve* **2,** 186–190 (1979).
11. Berman, P. W. & Patrick, J. *J. exp. Med.* (in the press).
12. Burres, S. A., Crayton, J. W. Gomez, C. M. & Richman, D. P. (in preparation).
13. Lindstrom, J. M., Einarson, B., Lennon, V. A. & Seybold, M. E. *J. exp. Med.* **144,** 726–727 (1976).
14. Lindstrom, J. M., Engel, A. G., Seybold, M. E., Lennon, V. A. & Lambert, E. H. *J. exp. Med.* **144,** 739–753 (1976).
15. Kao, I. & Drachman, D. B. *Science* **196,** 527–529 (1977).
16. Heinemann, S., Bevan, S., Kullberg, R., Lindstrom, J. & Rice, J. *Proc. natn. Acad. Sci. U.S.A.* **74,** 3090–3095 (1977).
17. Anuyl, R., Appel, S. H. & Narahoshi, T. *Nature* **267,** 262–263 (1977).
18. Drachman, D. B., Angus, C. W., Adams, R-N., Michelson, J. D. & Hoffman, G. J. *New Engl. J. Med.* **298,** 1116–1122 (1978).
19. Toyka, K. V. *et al. New Engl. J. Med.* **296,** 125–131 (1977).
20. Lennon, V. A., Seybold, M. E., Lindstrom, J. M., Cochrane, C. & Ulevitch, R. *J. exp. Med.* **147,** 973–983 (1978).
21. Medgyesi, G. A., Fust, G., Gergley, J. & Bazin H. *Immunochemistry* **15,** 125–129 (1978).
22. Namba, T., Nakamura, T. & Grob, D. *Am. J. clin. Path.* **47,** 75–77 (1967).
23. Engel, A., Tsujibata, M., Lindstrom, J. & Lennon, V. *Ann. N.Y. Acad. Sci.* **274,** 60–67 (1975).
24. Yam, L. T., Li, C. Y. & Crosby, W. H. *Am. J. clin. Path.* **55,** 283–290 (1971).

Physicochemical and immunological characterization of an HCG-like substance from human pituitary glands

S. Matsuura*, M. Ohashi*, H. C. Chen*||,
R. C. Shownkeen†, A. Stockell Hartree†,
L. E. Reichert Jr‡, V. C. Stevens§ & J. E. Powell§

* Endocrinology and Reproduction Research Branch, National Institute of Child Health and Human Development, National Institutes of Health, Bethesda, Maryland 20205
† Department of Biochemistry Annex, 5 Shaftesbury Road, University of Cambridge, Cambridge CB2 2BW, UK
‡ Department of Biochemistry, Albany Medical College, Albany, New York 12208
§ Division of Reproductive Biology, College of Medicine, The Ohio State University, Columbus, Ohio 43210

Human chorionic gonadotropin (HCG), or an HCG-like substance (HCG′), has been reported to be produced more widely in human than merely by placental tissue and by certain tumours[1,2]. It has been difficult to detect low levels of HCG in the presence of human luteinizing hormone (LH) because the two are structurally similar and react similarly in most assays. Each is composed of two glycoprotein subunits (α and β), and the major difference between the hormones is an extra 35 amino acid residue at the carboxyl terminal of HCG β-subunit[3]. The availability of a radioimmunoassay using antibodies directed towards this sequence made possible the distinction of HCG′ from LH in extracts of urine from normal postmenopausal women and in pooled human pituitaries[4,5]. Although the existence of HCG′ in either urinary extracts or pituitary fractions has been investigated extensively, on the basis of immunological, biological and physicochemical characteristics typical of HCG, the possibility that some proteases mimic the biological and immunological activities of HCG[6,7] must be carefully considered. We describe here a series of isolation procedures, including a specific immunoaffinity chromatographic step and isoelectrofocusing, which not only separate HCG′ from LH but also eliminate the effect of protease contamination. Furthermore, analyses of our purest HCG′ have revealed that its isoelectric points, molecular size and immunological and biological activities are similar to those of HCG but distinct from those of LH.

Peptides corresponding to the carboxyl terminal sequence of HCG β-subunit are denoted here as s12, s30, s35 and t23 (refs 1, 8, 9). The numbers indicate the number of residues in the peptide (counting back from residue 145, the carboxyl terminal glutamine); s denotes synthetic and t denotes isolation from a tryptic digest of the β-subunit. A specific radioimmunoassay based on an antiserum to s35[9] was used to measure HCG′ in eluents of ion exchange chromatographs. Alternative antisera are specified in Figs 1 and 2 legends. Other assays used were an *in vitro* bioassay based on stimulation of testosterone production by mouse interstitial cells[10] and a radioligand receptor assay using rat testis homogenates[11]. The adsorbent for immunoaffinity column chromatography was prepared as follows. The γ-globulin fraction from a well characterized antiserum (H114)[8] raised in rabbits against s30 was fractionated on a column of Sepharose 4B which had been covalently linked[12] to s12. After washing the column with 0.01 M Na, K-PO_4 and 0.15 M NaCl, *p*H 7.4 (PBS), the adsorbed antibodies were eluted with 0.1 M citrate buffer, *p*H 2.2. After dialysis and concentration by ultrafiltration, they were coupled[12] to Sepharose 4B. This immunoabsorbent preparation was able to bind 102 μg of HCG (lot CR119) per ml of gel sediment.

The starting material for purification of HCG′ was the freeze-dried follicle-stimulating hormone (FSH)-containing fraction CM-1 which had been isolated by a standard procedure from pooled acetone-dried human pituitaries[13]. Specific radioimmunoassay revealed that HCG′ was concentrated in this fraction, from which most of the LH had been removed. Further purification of FSH yielded an FSH-free side-fraction (designated DE-1) which was unadsorbed on DEAE-cellulose chromatography in 0.02 M potassium phosphate buffer at *p*H 7 (ref. 13) and which was eightfold more potent in HCG′ than fraction CM-1. A small portion of fraction DE-1 (in the above phosphate buffer containing 0.2 M NaCl, 0.37 mM $CaCl_2$ and 0.37 mM $MnCl_2$) was fractionated on a column of concanavalin A–Sepharose. Less than 5% of immunoactive HCG′ was unadsorbed. The bulk of the recoverable HCG′ was apparently glycosylated as it could be eluted with 1 M α-methyl-D-glucopyranoside. Chromatography of DE-1 on Sephadex G-100 yielded a fraction (Seph-2B) in which HCG′-specific immunoactivity was increased a further twofold to a potency 1% as active as highly purified HCG (lot CR119). The peak elution volume of the immunoactivity suggested a molecular size larger than that of LH and similar to that of HCG. Fraction Seph-2B was obtained in a yield of about 1.6 mg per 1,000 pituitaries.

Immunoaffinity chromatography was used for further purification of HCG′. Fraction Seph-2B (1.5 mg) was applied to a column (0.9 × 10 cm) of Sepharose 4B linked to purified

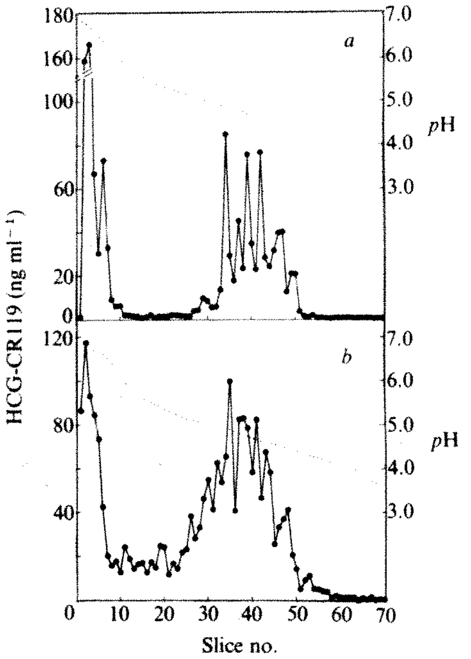

Fig. 1 Isoelectric focusing of fraction Aff-2. This was carried out with cylindrical gels in 6-mm i.d. Pyrex tubes[17]. Carrier ampholytes with *p*I ranges 2–4 (Accurate 42902) and 4–6 (LKB 1809-116) were each diluted to 4% (w/v) in 0.04 M L-histidine buffer, *p*H 7.74. Equal volumes were mixed to make a stock ampholyte solution. Polymerization mixture (2.35 ml per tube) contained 1% ampholytes, 5% acrylamide and 15% *N,N*′-diallyltartardiamide. Polymerization was started by addition of 0.015% (w/v) $K_2S_2O_8$, 5×10^{-4}% (w/v) riboflavin and 0.05% (v/v) *N,N,N*′,*N*′-tetramethylethylenediamine. The catholyte was 0.1 M L-histidine, *p*H 7.74, and the anolyte was 0.1 M formic acid, *p*H 2.29. HCG (CR119), 5.45 μg, (*a*) and pituitary fraction Aff-2, whose immunoactivity approximated to 10 μg of HCG-CR119 (*b*), were each dissolved in 100 μl of 30% sucrose and applied to the gel. The electrofocusing was carried out at 200 V for 18 h. The *p*H gradient along the gels was measured by an automated procedure[17]. Gels were sectioned into 1-mm slices which were each extracted at 4 °C with 1 ml 0.05 M phosphate buffer, *p*H 7.4, containing 0.1% bovine serum albumin (BSA). Each extract was radioimmunoassayed using anti-HCG serum H80[1] (●—●), and major peaks were also bioassayed by measuring testosterone production *in vitro*.

|| To whom reprint requests should be addressed.

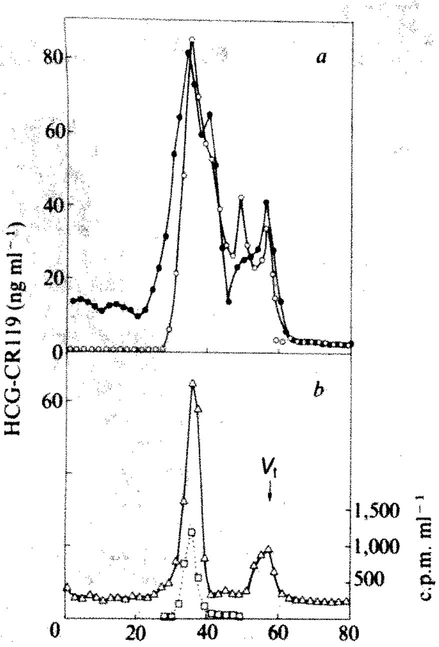

Fig. 2 Gel chromatography on Sephacryl S200 of material in the pooled major peak slices of Fig. 1*b*. A column of Sephacryl S200 (0.9 × 200 cm) was equilibrated with 0.05 M NH_4HCO_3, *p*H 7.8, containing 0.1% BSA. Slices numbered 28–52 were pooled and extracted (as in Fig. 1 legend). The extract was desalted on a column of Sephadex G-25 (equilibrated with the above buffer) and freeze-dried. This material, plus a trace of ^{125}I-iodo-HCG, was dissolved in 2 ml of the buffer and applied to the Sephacryl column. The flow rate was 15 ml h^{-1}; 2-ml fractions were collected. These were tested by radioimmunoassays using anti-HCG serum H80[1] (●—●) and anti-t23 serum H93[1] (○—○), as well as by a radioligand receptor assay (△—△) using rat testis homogenate[11]. The elution of ^{125}I-iodo-HCG was monitored by its radioactivity (□···□). The total column volume is indicated by V_t.

antibodies to s30 and equilibrated with the PBS buffer. The column was washed thoroughly with buffer and water, and adsorbed material (fraction Aff-2) was eluted with 1 M NH_4OH, neutralized with 1 M acetic acid and freeze-dried. This immunoaffinity procedure permits the separation of HCG′ from LH and other substances by binding HCG′ to the purified immunoabsorbent specific to the unique carboxyl terminal peptide of HCG β-subunit. Furthermore, this step should, we believe, eliminate possible pitfalls arising from contaminant proteases which have been reported to simulate HCG activities measuring displacement of ^{125}I-iodo-HCG, stimulation of steroid production or augmentation of adenylate cyclase activity[6,7].

To ascertain whether Aff-2 has physicochemical and immunological characteristics peculiar to HCG and biological activities typical of HCG, the following investigations were carried out. Fraction Aff-2 and purified HCG (batch CR119) were compared in isoelectrofocusing experiments (Fig. 1). Aff-2 contained components within the pI' range 4.4–5.1 (Fig. 1*b*), which is similar to the range for HCG as found by us (Fig. 1*a*) and by others[14]. This is further evidence that human pituitaries contain an HCG-like substance. When immunoreactive peaks were tested by the *in vitro* bioassay[10], all were active in proportion to their immunoactivity. Using a single HCG (CR119) standard we obtained ratios of biological to immunological activities ranging from 0.3 to 0.6. The same range of ratios was obtained for HCG (CR119) in a parallel experiment. Reported pI' values for LH are between *p*H 7 and 9 (ref. 5). The nature of the higher pI' component which appears in both patterns is not known; it was not always detected in separate experiments carried out in the same conditions. If HCG′ is a precursor of LH[4] it is possible that the latter is formed during our experimental procedures and that it appears as the higher pI' component in pattern *b*. Differences in sialic acid content of the various components, which are thought to be responsible for the electrophoretic heterogeneity of HCG[14], may also account for that of HCG′.

To establish whether the acidic components of Aff-2 after electrofocusing had a molecular size similar to that of HCG, the acidic fractions (pI' 4.4–5.1; Fig. 1*b*) were pooled, desalted, freeze-dried, mixed with a trace amount of ^{125}I-iodo-HCG and chromatographed on Sephacryl S200. Chromatogram patterns were revealed by means of two radioimmunoassays and a radioligand receptor assay for HCG (Fig. 2). Each pattern contained a major peak, comprising 73–79% of total activity recovered, and the three peak maxima (corresponding to fractions 34 and 35) were each coincident with the maximum for radioiodinated HCG. Thus, most of the recovered HCG′ with pI' 4.4–5.1 not only exhibited biological activity but also had a molecular size similar to that of intact HCG.

In conclusion, we have demonstrated that the substance purified from human pituitaries by Sephadex G-100 gel filtration followed by immunoaffinity chromatography using purified antibodies specific to the unique carboxyl terminal peptide of the HCG β-subunit, possesses pI' values within the same range as HCG and that the respective acidic components are biologically active in stimulating mouse interstitial cells to produce testosterone. The majority of these acidic components have the molecular size of HCG as revealed by gel chromatography. These data provide further evidence that an HCG-like substance is present in human pituitary extracts which differs from LH in its physicochemical and immunological characteristics. Furthermore, the HCG-like substance found in urinary extracts of postmenopausal women[4] and a patient with Klinefelter's syndrome[1] could originate from the pituitary. Our data also suggest that pituitary HCG′ is glycosylated and thus is different from the non-glycosylated HCG-like substance reported in very low concentrations in many normal tissues[2,15]. However, there was no indication that the gonadotropic activity detected in the latter case was not due to proteases. Although it is possible that pituitaries of pregnant women or patients with neoplasm containing HCG or HCG′ accidentally contaminate the pool of pituitary collection, the detection of HCG′ in pituitary glands and in urinary concentrates[4,5] all from postmenopausal women thought not to secrete HCG, provides strong support that the normal pituitary gland contains HCG′. Larger quantities of highly purified pituitary HCG′ will be required to determine whether it is identical to placental HCG or whether it is an immunologically related substance, possibly a precursor of LH[4] (which is known to have some sequence differences in its β-subunit when compared with the same portion of HCG[16]).

We thank Drs K. J. Catt, E. F. Hartree, G. D. Hodgen and G. T. Ross for helpful suggestions and the MRC for human pituitaries and for a grant in support of this work.

Received 4 February; accepted 21 May 1980.

1. Chen, H. C. *et al. Proc. natn. Acad. Sci. U.S.A.* **73,** 2885–2889 (1976).
2. Braunstein, G. D., Kamdar, V., Rasor, J., Swaminathan, N. & Wade, M. E. *J. clin. Endocr. Metab.* **49,** 917–925 (1979).
3. Morgan, F. J., Birken, S. & Canfield, R. E. *J. biol. Chem.* **250,** 5247–5258 (1975).
4. Chen, H. C., Matsuura, S., Hodgen, G. D. & Ross, G. T. in *Novel Aspects of Reproductive Physiology* (eds Spilman, C. H. & Wilks, J. W.) 289–308 (Spectrum, New York, 1978).
5. Robertson, D. M. *et al. Acta endocr.* **89,** 492–505 (1978).
6. Richert, N. D. & Ryan, R. J. *Proc. natn. Acad. Sci. U.S.A.* **74,** 4857–4861 (1977).
7. Maruo, T., Segal, S. L. & Koide, S. S. *Endocrinology* **104,** 932–939 (1979).
8. Matsuura, S., Ohashi, M., Chen, H. C. & Hodgen, G. D. *Endocrinology* **104,** 396–401 (1979).
9. Stevens, V. C. in *Proc. V int. Congr. Endocr.* Vol 1 (ed. James, V. H. T.) 379–385 (Excerpta Medica, Amsterdam, 1976).
10. Van Damme, M. P., Robertson, D. M. & Diczfalusy, E. *Acta endocr.* **77,** 655–671 (1974).
11. Catt, K. J., Dufau, M. L. & Tsuruhara, T. *J. clin. Endocr. Metab.* **34,** 123–132 (1972).
12. March, S. C., Parikh, I. & Cuatrecasas, P. *Analyt. Biochem.* **60,** 149–152 (1974).
13. Stockell Hartree, A. *Meth. Enzym.* **37,** 380–389 (1975).
14. Merz, W. E., Hilgenfeldt, U., Brossmer, R. & Rehberger, G. *Hoppe-Seyler's Z. physiol. Chem.* **355,** 1046–1050 (1974).
15. Yoshimoto, Y., Wolfsen, A. R., Hirose, F. & Odell, W. D. *Am. J. Obstet. Gynec.* **134,** 729–733 (1979).
16. Keutmann, H. T., Williams, R. M. & Ryan, R. J. *Biochem. biophys. Res. Commun.* **90,** 842–848 (1979).
17. Chrambach, A., Jovin, T. M., Svendsen, P. J. & Rodbard, D. *Meth. Protein Sep.* **2,** 27–144 (1976).

MATTERS ARISING

Does the C-terminal tetrapeptide of gastrin and CCK exist as an entity?

IT was reported by Rehfeld *et al.*[1] that the COOH-terminal tetrapeptide (Trp-Met-Asp-Phe-NH_2, abbreviated to G4 or CCK4), which is common to gastrin and cholecystokinin (CCK), exists in free form in pancreatic nerves, and may control islet hormone release. This report extends previous studies from the same group in which G4 was said to occur in pyloric antral mucosa in concentrations up to twice those of heptadecapeptide gastrin (G17), and in intestine and brain in concentrations considerably higher than those of the 33-residue form of CCK (CCK33) or its COOH-terminal octapeptide (CCK8). In these studies, particular importance was attached to the observation that after gel filtration of tissue extracts, a peak of material eluted in the position of G4 and reacted in radioimmunoassays using antisera specific for the COOH-terminus of gastrin and CCK. However, recent studies in our laboratory cast doubt on the interpretation of these data, and suggest instead that free G4 does not exist in significant amounts in pancreas or gut.

We have raised a rabbit antiserum to G4 conjugated through its NH_2-terminal amino group to thyroglobulin by glutaraldehyde. When used in radioimmunoassays with an ^{125}I-CCK8 label, this antiserum reacts almost equally with G4, G17 and CCK8, and can detect 10–20 pmol l^{-1} of G4. This system offers a clear advantage for the estimation of G4 over the one used by Rehfeld *et al.*, because in the latter system G4 has a 30-fold lower immunochemical potency than CCK8 and CCK33. To estimate the true molar concentration of G4, it was, in effect, necessary for Rehfeld *et al.* to multiply the peak of activity eluting in the position of G4 by 30 compared with the other peaks. There is an obvious disadvantage in this method, for errors are also greatly magnified. Such a correction is unnecessary, of course, when G4, CCK8 and G17 and the other principal forms of CCK and gastrin have equal immunoreactivity. We have found that when hog pancreas is extracted according to the method of Rehfeld *et al.*, the total concentration of immunoreactivity measured with the G4 antiserum was 3.5 ± 0.8 pmol per g (mean, ± s.e., $n = 4$; G4 standard). Closely similar estimates (2.1 ± 0.4 pmol per g) were obtained with a second radioimmunoassay system using an antibody (L48, CCK8 standard) that, like Rehfeld's, reacts about 50 times less well with G4 than with CCK8. Fractionation on Sephadex G-50 indicated that over 80% of immunoreactivity in the extracts had the properties of CCK8. These data indicate that G4 cannot occur in more than trace amounts in pancreas. However, when synthetic G4 was added to the tissue early in the extraction procedure in amounts comparable to those reported by Rehfeld *et al.*, the peptide was recovered in a yield of 73 ± 6%. In parallel studies we have also failed to confirm the presence of G4 in hog, rat or human antral mucosal extracts, which according to Rehfeld *et al.* contain G4 at about 15 nmol per g; instead, we have consistently found a major peak of immunoreactivity corresponding to G17, confirming numerous previous studies.

We conclude from our work that free G4 does not occur in significant amounts in pancreas or gut. The high concentrations of G4 reported by Rehfeld *et al.* reflect the fact that a minor component of gastrin–CCK immunoreactivity is interpreted as G4 and estimates of its molar concentration corrected to allow for the low potency of G4 in the assay system. This correction might conceivably be justified if G4 was proven to exist naturally by isolation and full chemical characterization; this has not been the case. Until the material described by Rehfeld *et al.* in pancreas and elsewhere is isolated and characterized, its true concentration in these tissues cannot be determined. The issues raised here serve to emphasize the very great caution that needs to be exercised in identifying and determining substances by gel filtration and radioimmunoassay, when the material in question has not been isolated.

G. J. DOCKRAY
R. A. GREGORY

Department of Physiology,
University of Liverpool,
Brownlow Hill,
PO Box 147,
Liverpool L69 3BX, UK

1. Rehfeld, J. F. *et al. Nature* **284,** 33–38 (1980).

REHFELD *ET AL.* REPLY—First, we note that the total CCK immunoreactivity in pancreatic extracts measured by the G4 antiserum, 3.5 pmol per g, is of the same order of magnitude as that reported by us[1] (6.8 pmol equiv. CCK8 per g). It is interesting also that the L48 antiserum, which reacts less well with G4, measures lower concentrations (2.1 pmol per g) than the G4 antiserum, suggesting that G/CCK4 is indeed present in the pancreas.

Second, Dockray has previously reported[2] that the mammalian brain contains significant amounts of a third immunoreactive component (BP III) with a size corresponding to G/CCK4 or G/CCK6. He measured this BP III peak by four different C-terminal specific antisera (including our ab. 2716). Using CCK8 as standard, the BP III peak constituted 12% of the CCK8-like peak in hog, 31% in dog and 18% in rat cerebral cortex (Table 2 in ref. 2). The BP III peak should be easily measurable by the new G4 antiserum. We are surprised that Dockray has not discussed these earlier results in the light of his new assay findings.

Third, we can only speculate on the reason for the discrepancy between our data (supported by Dockray's earlier data[2]) and those of Dockray and Gregory. (1) Microheterogeneity of the natural tetrapeptide (in analogy with the microheterogeneity of CCK octapeptide[3]) might explain[4,5] the failure of the new assay to measure G/CCK4-like material. (2) Several samples of synthetic G4 received by us from other laboratories have been found to be grossly impure, and even the purest contain minor impurities—might the new G4 antiserum of Dockray and Gregory have specificity for these impurities? (3) In the raising of antibodies, we question the use of G4 conjugates prepared by means of glutaraldehyde. The presence in G4 of N-terminal Trp complicates the normal reaction with aldehydes, and we would anticipate that conjugation would be through a carboline rather than the terminal amino group. If this is so, the specificity of antibodies raised to such conjugates might be abnormal.

In conclusion, we consider the evidence to be in favour of the presence of a tetrapeptide in brain, gut and pancreas, but final confirmation must come from isolation and sequence work.

J. F. REHFELD
L.-I. LARSSON
N. R. GOLTERMANN
T. W. SCHWARTZ

Institute of Medical Biochemistry,
University of Aarhus, Denmark

J. J. HOLST
S. L. JENSEN

Institute of Medical
Physiology (c), and
Department of Surgery (c),
University of Copenhagen,

J. S. MORLEY

Imperial Chemical
Industries Ltd,
Alderley Park,
Cheshire, UK

1. Rehfeld, J. F. *et al. Nature* **284,** 33–38 (1980).
2. Dockray, G. J. *Nature* **264,** 568–570 (1976).
3. Dockray, G. J., Gregory, R. A., Harris, J. I., Hutchison, J. B. & Runswick, M. J. *Nature* **274,** 711–713 (1978).
4. Rehfeld, J. F. in *Hormone Receptors in Digestion and Nutrition* (eds Rosselin, G., Fromageot, P. & Bonfils, S.) 45–53 (Elsevier, Amsterdam, 1979).
5. Rehfeld, J. F. & Morley, J. S. in preparation.

0028–0836/80/330742—01$01.00

BOOK REVIEWS

Most orthodox heresy: Jensen on IQ myths

Steve Blinkhorn

Bias in Mental Testing. By Arthur R. Jensen. Pp.800. (Methuen: London/Free Press: New York, 1980.) £15, $29.95.

CONSPIRACY theory ranks high in popularity among theories of psychological testing. According to this view, psychometricians, whether wittingly or not, have succeeded in constructing devices which systematically and unwarrantably discriminate against non-whites, lower social classes and possibly females. There is a popular belief that intelligence (mental ability, scholastic aptitude, mental maturity and so on) tests are constructed using scholastic achievement in a white middle-class educational system as a criterion and that devious means are adopted to force scores to a normal distribution. Accordingly, such tests are inappropriate for non-whites, for working, rather than middle-class, individuals and so on. The appropriate action is therefore either not to use them at all or to correct the inherent bias by using lower cut-off scores for, or adding a constant to the scores of, the disadvantaged groups.

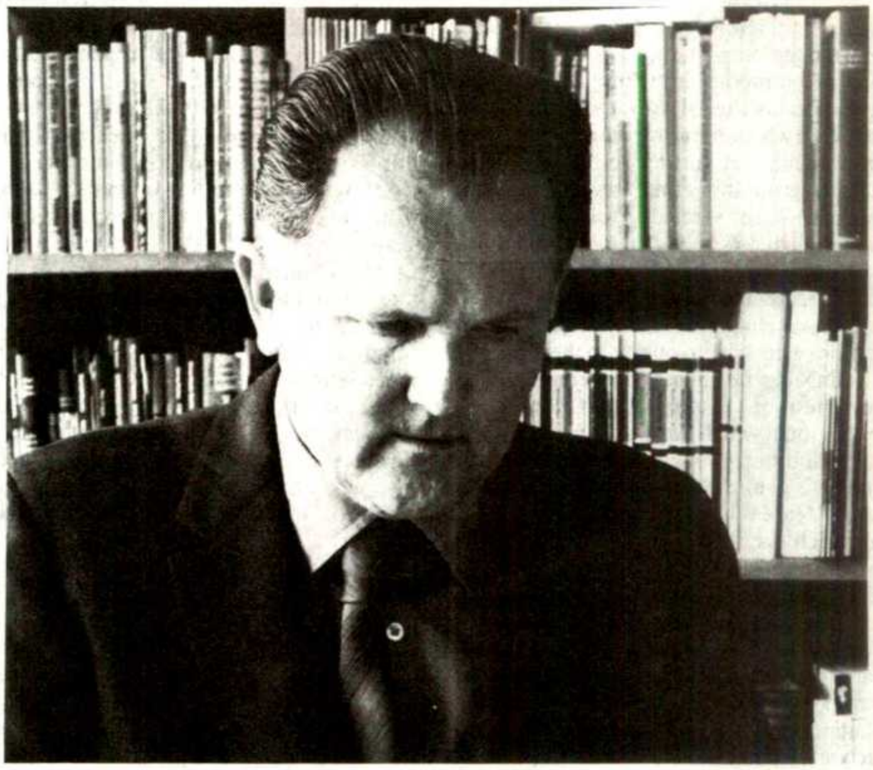
Arthur Jensen, "scholarly and dispassionate".

Added impetus to the propagation of this point of view has come in the aftermath of the Burt affair, and phrases such as "the IQ myth" and "the new assault on equality" have gained currency. One of the few topics on which most psychologists (and not only psychologists) seem to feel entitled to pronounce is the validity or otherwise of so-called IQ tests. Sadly, such pronouncements do not always benefit from the technical competence and sense of history which make for an informed judgement. There is a notion abroad that what tests measure and how fairly they discriminate can be determined by inspection, the implication being that psychometricians are peculiarly insensitive to what is patently obvious or deliberately, and for the worst of motives, disingenuous in the pursuit of their craft.

The whole question of inherent bias in mental tests has been brought to a new crisis point by a series of court judgements which have handed down verdicts as to whether or not particular tests are biased. The notorious 15 IQ points difference between mean scores of blacks and whites in the USA gives the topic social, moral and political importance. If this difference is the result of test bias, then something ought to be done about the tests. If, on the other hand, the tests merely reflect a true difference, however caused, then no amount of advanced psychometrics will save an unhappy state of affairs.

Jensen's description of how, as a student, he "came to believe that nearly all standard IQ tests were grossly biased against virtually everyone but the white middle class" is an unexpected entrée to a book which amasses an overwhelming weight of evidence to the contrary. He then proceeds to spend nearly half the book developing the statistical and methodological basis for an examination of test bias. There is implicit in his treatment of classical test theory a criticism of the standard of public debate on test bias. Too many psychologists are either ignorant of, or dismiss as statistical conjuring tricks, elementary procedures such as correcting correlation coefficients for restriction of range or for attenuation by unreliability, or regard predictive validity coefficient of the usual magnitude (0.3 to 0.5) as hopelessly small and indicative of little utility. On the assumption that all interested parties were thoroughly acquainted with basic psychometrics, the book could have been half its actual length.

On the question of bias itself, Jensen is remarkably up to date with the current state of theory and practice. The distinction between bias (a statistical concept and a matter of fact) and unfairness (which involves a value judgement) is well made, and the fact that different definitions of fairness conflict when made operational in terms of the practical use of tests is driven home. The kernel of Jensen's thesis is to be found in Chapters 10 and 11, in which the empirical evidence of test bias (1) in predicting occupational and educational success and (2) in the internal structure of tests, is reviewed. Much of this material is counter-intuitive. It is not the case that for a given test score blacks perform better at work or at school. On the contrary, using prediction equations based on white groups may disadvantage the whites, in that blacks have to do as well or better on the tests to do as well on the task. Nor does the notion that verbal tests yield lower scores for blacks than do non-verbal tests, stand up to scrutiny. Finally, there is no evidence from the internal structure of tests that they are measuring something different in the different racial and social groups.

In short, Jensen provides methods for detecting bias, collates a large amount of empirical evidence and justly concludes that there is no substantial, replicable evidence of inherent bias in commonly used tests where native-born English speakers are concerned. He also disposes of several widespread myths about tests, such as the so-called Pygmalion (teacher expectancy) effect. There is a willingness evident in the psychological community to accept criticisms of psychometric techniques on blatantly *ad hoc* grounds, and a supreme unwillingness to pay attention to the large body of empirical evidence which supports the utility of tests, in particular in cutting across social and ethnic groupings and revealing talent where it is least expected (which, after all, was the original reason for their introduction).

Jensen has neither time nor patience for the overuse and misuse of tests, however. His last chapter is an indictment of malpractice which ought to be required reading for all those who actually enjoy using tests or like to treat IQ as the criterion of personal worth *par excellence*.

Undoubtedly many will feel that by restricting himself to a rather technical brief Jensen is missing the point. The abstractness for which test constructors often strive, they may point out, is itself a cultural variable, highly prized and cultivated in the white middle-class. The format of tests reinforces certain values (accuracy at speed, seeking to generalize, solution of problems in the abstract rather than the concrete) which may be dominant in white middle-class culture.

There follow from this two questions. Is it the case that the kinds of abstract reasoning abilities implicated in, say, Spearman's view of intelligence can be consistently assessed? Is it the case that an individual's capacity to deal effectively with his world depends on such skills? If the answer to the first is affirmative, as Jensen claims and by and large demonstrates, the answer to the second is by no means an obvious yes. Wechsler has defined intelligence as "the capacity of an individual to understand the world about him and his resourcefulness to cope with its challenges". Such a view clearly involves the nature of the world in which an individual exists, and non-intellective characteristics of the individual as important elements in the determination of intelligence.

Now, tests constructed in line with the views of both Spearman and Wechsler intercorrelate highly. This is hardly surprising, given the importance placed in Western society on intellectual skills, for we live in a society where some social security forms demand a higher level of reading skill than the *Times*. But the distinction needs to be maintained, not least because whilst a given level of intelligence in Spearman's terms may imply capacity to cope with the business of living, the reverse need not be true. One wonders whether the high value placed on intelligence in our society is a universal feature, not so much in remote tribes as in ancient Egypt and Rome, or to choose a more immediate instance, in China during the cultural revolution. That is to say, could we choose to organize our society so that differences in intelligence are unimportant, and if so would that kind of society be successful, stable and desirable?

If, as Jensen shows, the accusation of test bias is unfounded, then the truth of the matter is that differences in achievement reflect the extent to which society demands the abilities assessed by the tests. Whether these demands are proper, necessary and fair is entirely open to question, but fiddling test scores to make racial differences vanish is as unworthy as the exaltation of IQ as the sole criterion of personal worth. It neither promotes the interests of those in sympathy with whom it is done nor protects them against the failure it makes more likely. It makes as much sense as subtracting 8 IQ points from the scores of myopics, on the grounds that this is the mean difference between myopics and non-myopics, and clearly myopics are advantaged in that their condition makes them read more books and play less football.

There is a widespread notion that since tests necessarily involve specific tasks, IQ is merely a matter of specific learned skills of a particular kind. Yet such evidence as there is suggests that coaching in specific skills has little transfer value. The point of intelligence testing is not whether an individual can solve problems having a certain logical structure, but whether he can identify the logical structure and find strategies to solve them. Many tasks can be made easier by making their structure more patent and immediately concrete: much of the recent work critical of Piaget has adopted this approach. Such studies point to ways of bringing a wider range of performances within the capacity of the individual, and have immediate relevance to education and training. Their relevance to the study of intelligence, seen as a high-level ability to detect the structure of problems and organize lower-level strategies towards a solution, is however seriously in doubt.

This book is informative, refreshing and a valuable contribution to the literature; its worth as a compendium can hardly be overrated, and it may well find a role as a textbook of psychometrics for the clarity of its exposition of classical test theory. Its scholarly and dispassionate tone will come as a surprise to those who know of Jensen only as a leading figure in anti-test demonology, however out of sympathy they may be with its content.

Steve Blinkhorn is a Senior Lecturer in Psychology at Hatfield Polytechnic, UK.

Understanding nuclear astrophysics

Bernard Pagel

An Introduction to Nuclear Astrophysics. By Jean Audouze and Sylvie Vauclair. Pp.168. (Reidel: 1980.) Hardback Dfl.75, $39.50; paperback Dfl.40, $19.95.

SINCE the 1920s, the development of astrophysics has been closely associated with advances in nuclear physics which have led to our current understanding of stellar energy sources, stellar evolution, nucleosynthesis and nuclear cosmochronology, and to continuing attempts to understand the distribution of the chemical elements in the light of ideas about cosmology and the evolution of galaxies.

These topics are engagingly presented by two well-known French astronomers in this book, which is written at a level suited to first-year undergraduates, but will also be appreciated by graduate students and others desiring an up-to-date introduction to the subject. Succinct descriptions of the basic interactions of physics and of the observable Universe are followed by outlines of big-bang cosmology, stellar evolution and the abundances of the elements in the Solar System, stars and cosmic rays. The remainder of the book gives somewhat more detailed accounts of specific theoretical topics: nuclear reactions and the various nucleosynthesis processes currently considered significant, Solar System and galactic nuclear time-scales and the chemical evolution of galaxies. A brief concluding chapter sketches historical developments and a few outstanding problems.

By far the strongest feature of this book is the nuclear physics, which is carefully and clearly described at the appropriate level. Other aspects are more sketchily treated. This does not matter too much for the observational part, which is adequate as a background to the theory apart from occasional minor infelicities such as a reference to quasars as having "the same optical properties as the stars". A more serious gap is the lack of a coherent account of the non-nuclear aspects of stellar structure and evolution, which makes it difficult for the reader to envisage the context in which the nuclear reactions operate. The chapter on nuclear chronologies and the origin of the Solar System is especially good, but the one on chemical evolution of galaxies shows signs of over-hasty preparation and proof-reading — some equations (including one credited to myself!) are either nonsensical as written or inconsistent with the accompanying text; inconsistent and undefined symbols also occur. (There are also a few minor errors of fact here: the abundance ratio N/O is not as high in the Magellanic Clouds as in the solar neighbourhood and the simple model of galactic chemical evolution does not predict that we should see stars with *literally* zero metal abundance.) The English is generally adequate, though noticeably less than perfect. Finally, prospective purchasers should be warned that I have come across a copy (not my review copy) that is misbound, with several pages in the wrong order.

In short, a curate's egg of a book in which the largely excellent intentions of the authors have been frustrated by insufficient attention to detail at different stages of production. The broad sweep of the subject is well presented, though, the illustrations are good and a useful set of references is given, so that on balance this is a welcome and useful book. ☐

Bernard Pagel is a Deputy Chief Scientific Officer at the Royal Greenwich Observatory and Visiting Professor of Astronomy at the University of Sussex.

Bring Your Library Up-To-Date With This ANS Edition...

R. Sher and S. Untermyer II
MONOGRAPH

The Detection of Fissionable Materials by Nondestructive Means

298 pages — 6″ × 9″
Hardbound $49.00

American Nuclear Society
555 North Kensington Avenue
La Grange Park, IL 60525 USA

Please take my order for ____ book(s).
☐ Payment in full enclosed.
☐ Bill me and I accept postage and handling charges.

Name ____
Organization ____
Street ____
City ____
State ____ **Zip** ____

Circle No. 01 on Reader Enquiry Card.

Number 3 in the *Enzymes* dynasty

Athel Cornish-Bowden

Enzymes. Third edition. By Malcolm Dixon and Edwin C. Webb. Pp. 1116. (Longman: London/Academic: New York, 1979.) £25, $49.50.

WHEN THE first edition of this book was reviewed in *Nature* (**182**, 969-970; 1958) it was described as "one of the finest books that has appeared on the topic of enzymes". Two editions and 22 years later this is still true; there have been other excellent books on enzymes, but none with the breadth of this one. Despite the long period since the second edition appeared in 1963, the new edition resembles its predecessors surprisingly closely and has essentially the same organization of material. The authors have included an astonishing amount of useful information in what is still a single volume. This is especially remarkable in view of the amount of space they have devoted, mistakenly in my view, to the Enzyme Commission's classification system for enzymes. More than 300 pages are given over to a description of its principles and a virtually complete list of known enzymes. Surely a better use could have been found for this space.

Another section of questionable usefulness, one that must surely have added substantially to the price of the book, is the "Atlas" of crystalline enzymes, which consists of 25 pages of reproductions of photomicrographs. As this is now relegated to close to the back of the book it would seem that the authors recognize that readers no longer gasp in wonderment at the knowledge that enzymes can be crystallized.

In other respects the authors have displayed an admirable sense of what is worth including and what is not. The early chapters are concerned with practical matters and include much useful advice without becoming enmired in experimental detail of no general interest. The discussion of steady-state enzyme kinetics is especially good and almost justifies purchase of the book by itself. Rather oddly, it is not all in one place but is divided between Chapters 4 and 8, which account for about a quarter of the book. Obviously there are some points of detail where one might quarrel with the treatment, but in general it is balanced and thorough. These two chapters also contain an account of transient-state kinetics, but one senses that this is not a major interest of the authors. The other chapters, concerned with specificity, mechanisms, cofactors, protein structure, protein biosynthesis and enzyme biology, are also of a high standard. Of these, protein biosynthesis is perhaps one topic that might have been omitted, not because of any lack of importance, but because it has developed into a subject rather separate from general enzymology and I doubt whether its devotees will look for an account of it in a book about enzymes.

Finally, a word about production. I was pleased to be sent a copy of the American edition for review, as this is soberly and robustly bound. By contrast, the British publishers should be ashamed of their covers, which are not only ugly but are also far too flimsy for a book of 1100 pages. ☐

Athel Cornish-Bowden is a Lecturer in Biochemistry at the University of Birmingham.

Scientific terms by numbers

Alan Isaacs

Longman Dictionary of Scientific Usage. By A. Godman and E.M.F. Payne. Pp.684. (Longman: 1980.) Flexi £4.35, $14.95.

FOR THE casual user of a scientific dictionary — someone who needs to look up the meaning or spelling of a word from time to time — this is not the book to buy. To find the meaning of a word in this dictionary you have first to read the instructions, then you have to look in the index for a two-letter set code that will identify the field of science of the word and for a three-figure number to find the position of the word in the set. Memorizing both the set code and the number, you then search the body of the book for the appropriate set. The alleged advantage of this cumbersome system is that the book is designed specifically for the non-native speaker of English who will benefit from the thesaurus-like arrangement in which terms that are "closely related in meaning or subject area" are grouped together. Even if foreign learners have more patience and perseverance than native speakers, this system has its dangers. If you look up *free electron* in this dictionary you will be directed from the index to the section on radio terms (code NM). There you will be told that it is "an electron in a crystal which [*sic*] is free to move under the influence of an electric field". The user, if he relies on this dictionary, will never know that free electrons also exist in gases. This example highlights the hazards of this kind of coding.

In general, though, the definitions appear to be clear and accurate, and there are plenty of useful collocations and cross-references to help the foreign learner (once he has mastered the meaning of the cross-referencing arrows pointing East, North and South). It is such a shame that most compilers of dictionaries for non-native speakers feel obliged to clutter their books with redundant information (the new *Chambers Universal Learners' Dictionary* is a notable exception). Will a foreign scientist or student really be helped by seeing An or H against a word? Even if he looks in the front matter, where he will learn that the former denotes a non-gradable antonym and the latter a hyponym, will he be any the wiser? If I were a foreign scientist I would want a dictionary that tells me what I want to know simply, by having the information available in its alphabetical place. I am not sure that I would want to be confused with coded answers to questions that I am never likely to ask. Hyponym indeed! □

Alan Isaacs, a former teacher of scientific English to foreign students, is editor of the Penguin Dictionary of Science *and* Longman's New Dictionary of Physics, *and science editor of* Collins English Dictionary.

RNP particles and the virus club

B.S. Cox

Viruses and Plasmids in Fungi. Edited by Paul A. Lemke. Pp.680. (Dekker: 1979.) SFr.110, $55.

MANY fungi harbour ribonucleoprotein particles consisting of a spherical or polyhedral capsid-like structure 35 ± 10 nm in diameter, containing one or more molecules of double-stranded RNA. The particles are rather reminiscent of reovirus.

They are a remarkable group of objects. In the first place, it appears to be quite impossible to infect any fungus with them. The lengths to which numbers of mycovirologists have gone to demonstrate this rather fundamental property of a virus have been extraordinary, both for the man-hours spent and the total lack of success. Secondly, without exception, they are symptomless. Of course it is rather difficult to connect the symptoms of a disease with a virus if one cannot infect the host with it; and the energetically-researched "La France disease" of cultivated mushrooms may indeed be caused by the two or more 'viruses' associated with it. On the other hand, of course, the disease may cause the viruses. 'Virus' is often found, apparently, in healthy mushrooms.

Not all of the *ds*RNAs of fungi are without phenotypic effects. Cytoplasmically inherited *ds*RNAs produce the 'killer' toxins of many species of yeast and of the smut fungus, *Ustilago maydis.* They also apparently cause the fascinating non-pathogenic variant of *Endothia parasitica.* This blight has deprived two generations of Americans of their native chestnuts for the Thanksgiving stuffing. The hypovirulence of the variant is invasive and suppressive, and can be used not only to limit the spread of the cankers caused by virulent strains on *Castanea* but actually to depress the virulence of the pathogen itself.

Cryptic or not, these RNP particles of fungi are curiosities. They are extremely widespread, occurring in all major groups of fungus including water moulds. They form a strikingly homogeneous group of organelles. Homogeneity, universality and non-infectionness suggest a very ancient common origin, but how have they been maintained? Is it possible for a non-essential, wholly cryptic self-replicating particle to survive in such a specialized environment without the means of spreading by infection? The killer (M) *ds*RNA of yeast depends for its maintenance on 30 nuclear genes: one mutation and it's gone. How does it survive? The L-*ds*RNA has not been found to depend on any nuclear genes. Why not? Do the *ds*RNAs do something useful, or is the killer/immunity property a self-selecting mechanism? If so, do all fungi possess it?

Although neither answers to these questions nor, indeed, the questions, are to be found in this book, there are two clear and succinct reviews of the genetics and molecular biology of the RNP particles of yeast, *Ustilago* and *Endothia.* There are also excellent accounts, sometimes commendably brief, of an assortment of non-RNP particles, DNA plasmids, bacterial or rickettsia-like structures and even a couple of cytoplasmically-inherited conditions with no particle to call their own (senescence in *Podospora* and meiotic failure in *Coprinus*). For the rest, there are detailed, rather self-indulgent articles cataloguing biophysical and ultrastructural studies of RNPs, speculations about their life-histories, a methods paper without protocols, many more or less indistinguishable electron micrographs and many a discussion about what these RNPs should be called. The general opinion is that they should be awarded the accolade 'virus', perhaps by broadening the category of admissible members. I can't help feeling that this obsession with joining the club has rather diverted attention and effort away from the problem of what they really are. Much of the repetitive material about functionless particles could have been condensed into a single review article (Chapter II covers all the ground) and perhaps some space given to the many other cytoplasmically-inherited determinants of fungi which have phenotypes but no physical basis yet identified. Visibility in the electron microscope is not the only passport to respectability.

The book is a little out of date but is, nevertheless, for some topics, a very useful source. □

B.S. Cox is a Lecturer in Botany at Oxford University.

Jewish genetics

Kurt Hirschhorn

Genetic Disorders among the Jewish People. By R.M. Goodman. Pp.493. (Johns Hopkins University Press: 1979.) $32.50, £17.50.

THE genetics of the Jewish people have received a great deal of attention over the past few years. This is primarily due to the virtually unequalled opportunity created by the population dynamics of the state of Israel. Previously isolated groups of Jews have been immigrating to Israel, where they continue a certain degree of inbreeding and are beginning to outbreed with other Jewish groups. Driven by the tradition of Israeli research on human genetics, particularly under the leadership of the late Drs E. Goldschmidt and C. Sheba, a new and large generation of human geneticists has been quick to take advantage of this temporary opportunity.

Three recent publications summarizing these data as well as studies done outside Israel have been *The Genetics of the Jews* by A.E. Mourant, A.C. Kopec and K. Domaniewska-Sobczak (Clarendon: 1978), *Genetic Diseases Among Ashkenazi Jews* edited by R.M. Goodman and A.G. Motulsky (Raven: 1979) and the book reviewed here. The first of these is primarily a tabular accumulation of gene frequencies in various Jewish groups and contains much useful data, while the second represents the proceedings of a symposium with many excellent reviews.

This present book is a *tour de force* which pulls together a mass of reports and develops a comprehensive description of the status of these studies. One could argue with some details such as interpretations of ancient history and the inclusion of a number of genetic diseases found in Jews with "Jewish genetic diseases", and there are occasional lapses in clarity. None of these criticisms should detract from the fact that this is a major and useful book for all human geneticists as well as students of Judaism. This is a field which is applicable to genetic centres wherever Jewish patients may appear and which is certain to grow over the next 20 years. The book also provides a general model for genetic studies in populations, and is therefore recommended for a wide audience. □

Kurt Hirschhorn is Professor and Chairman of the Department of Pediatrics at Mount Sinai Medical Center, New York.

nature

21 August 1980

Directive 59 and European defence

The Democratic convention last week was perhaps needlessly enlivened by the curious affair of Mr Edmund Muskie's claimed innocence of the most recent alleged shift in United States strategic policy — the increased emphasis now to be given to military targets in the disposition of American nuclear warheads. Several questions arise, but are unlikely to be answered in the near future, if at all. Did President Carter let slip news of the instruction to the US military on which the new strategy is based — called Directive 59 — in order to impress the impending convention or to take the wind out of Mr Reagan's sails, thus robbing the Secretary of Defense, Dr Harold Brown, of the place in the history books that he might have earned by making a public speech on the subject? (Dr Brown will indeed have made such a speech on 20 August.) Did Mr Muskie have to complain about not knowing of Directive 59 because his officials at the Department of State had not had time to tell him? And did he complain in the terms he used — more sorrow than anger — because of the rumours current earlier in the week that the Secretary rather than the President might end up as the Democratic Party's nominee for the election in November? In this quiet season of the year, these questions will excite attention for weeks to come. There is a danger that the more important question of what Directive 59 really means may be overlooked.

The first thing to say about Directive 59 is that it is not so much an order to the troops as an acknowledgement of what the tropps have been doing, and are prepared to do. Many years have passed since the Department of Defence sought to demonstrate to Congress and the world that the great megatonnage in the warheads of Soviet missiles was more than made up for by the versatility of Multiply-Independent Re-entry Vehicles or independently targeted warheads, MIRVs for short. Since then, both sides of the equation have become larger, and their difference no easier to calculate. For at least a decade, however, the United States has made no secret of its wish to be so well equipped with accurate and separately manoeuvrable warheads that it can reasonably hope to attack crucial military targets, not just cities full of mere people. With the MX missile, and others of the same generation now in prospect, the US military (and their Soviet counterparts) should soon be able to deliver on that promise. Directive 59 is therefore largely an acknowledgement in public of what the Pentagon has been saying about its aspirations since the early 1970s. It should be acknowledged that half a decade has yet to pass before US Strategic Air Commands will be so well equipped that they can do what the US President now says they must do — to be prepared to fight strategic nuclear wars by matching their opponents' strength tit-for-tat while keeping enough in reserve to be able to deliver a final devastating assault. The commanders, however, are not running for election.

For those with long memories — historically, so to speak — there is an ironical circularity in this state of affairs. A quarter of a century ago, when the American Atlas and Titan rockets were still being tested, while the Soviet strategic armoury was dependent on subsonic aircraft for delivery, and when what was called the Cold War was at its height, a number of honest men (the late Sir John Slessor prominent among them) developed the theory of "graduated deterrence". The idea was that the world would be a safer place if the West, at least, was able to match its retaliation more or less exactly with whatever attacks might come its way. The objective was to find some way of managing the escalation of a strategic nuclear war so that it could stop short of the ultimate catastrophe, mutual and virtually total destruction of the two sides in a conflict. The concept was to many people preferable to that of deterrence based on all-out retaliation at the first sign of a strategic attack, but even on paper there were snags. To many Europeans, the most obvious flaw in the theory was that controlled escalation of a strategic conflict would make it possible for the United States to lose its nerve half-way along, with the result that the United States guarantee of Western Europe would be diminished. The most serious argument against the theory of graduated deterrence, at least in the nuclear stages of a strategic conflict, was, however, technical; the missiles of the 1950s were simply not accurate enough to match the need. What has happened now, after a quarter of a century, is that it will soon be technically possible to follow a strategy of graduated deterrence.

What will be the consequences? Again the 1950s are instructive, and it is no surprise that Dr Harold Brown thought it wise to send a message of reassurance to the other NATO governments once Mr Carter had let Directive 59 out of the bag. The new strategic doctrine, Dr Brown said, is but a stage in the evolution of United States strategic policy. This is no more than he said at the meeting of the NATO Nuclear Planning Group at Bodo in Norway last June, and what he is likely to repeat when the same group meets again in November. Other NATO governments appear to have accepted this to be the truth, but they have not yet had time to work out the implications of the new development. The overriding question in their minds will be the question that preoccupied them in the 1950s — will the graduated deterrence strengthen or weaken the United States guarantee of Europe?

The calculation is far from easy, and is best accomplished by successive approximations starting from the assumption that both the American and Soviet strategic forces are capable only of the mass destruction of their opponents' cities. Although the North Atlantic Treaty, like the Warsaw Pact, is a solemn declaration of the superpowers' commitments to their allies, it is only a piece of paper. Nobody supposes that a strategic conflict in Europe would evoke an automatic response in Washington or Warsaw — people pressing buttons without turning over in their minds the prospect that their own people were about to be destroyed. In other words, even with the strategic balance of the 1950s and early 1960s, there was a chance that Europe might be left to its own devices and other people's missiles. The crucial question is whether Directive 59, old hat though it may be, increases or diminishes that chance.

First — this is what Dr Brown has been implying — it will be easier for the United States to honour its commitment to its allies if it can respond to a strategic threat by measures that are more specific than all-out retaliation. If, at the first sign of strategic trouble in Europe, somebody in Washington is faced with the choice of doing nothing or of setting in train an all-out nuclear exchange, he (or she?) is more likely to do nothing than if the choice were between inaction and some more calculated response. In this sense, Directive 59 should be a reassurance to the Western European members of NATO that their powerful ally will be more likely to stir a finger. By the same test, however, the controlled escalation of a nuclear conflict inevitably offers more opportunities for the United States (or, for that matter, the Soviet Union) to lose its resolution. Now, as was apparent in the 1950s, graduated deterrence cuts both ways. The strategic umbrella is broader, but there are more holes in it.

The immediate question (for when the US election has been held) is whether Western European governments will be more conscious of their increased security or of the increased opportunities for the United States to pull out from a European battlefield. Their perceptions will be determined by political and

0028-0836/80/340747-02$01.00

not military calculations. Will a more bellicose president (Mr Reagan) also be more isolationist? Would President Carter, if re-elected, be able to balance his apparently incorrigible unawareness of the European consequences of his domestic pronouncements (such as that about Directive 59) with the flexible and imaginative view of Salt II, Salt III and the other matters at the root of European security to keep the confidence of his NATO allies? Time, no doubt, will tell.

Until that issue is resolved, there are bound to be hankerings in Western Europe after the position adopted by the French a quarter of a century ago, when the Gaullist doctrine of independence was evolving. The French position is quite clear, and has been consistent from the start. In the last resort, the argument goes, even the most solemn guarantees are likely to be abrogated. It makes no sense to think that the people of the United States will knowingly sacrifice themselves for the sake of France. On the other hand, France can safeguard its own future by acquiring an independent nuclear force able to inflict damage on potential adversaries that is more or less proportional to its own potential value as a prize. The British case for the retention of an independent deterrent, much rehearsed when the British government decided three weeks ago to adopt the Trident system of nuclear submarines as its next-generation nuclear deterrent, is subtly different. The objective, that argument runs, is to influence the perceptions not of allies but of adversaries: if it should be thought by others — however mistakenly — that the United States might, in a tight corner, leave Europe to its own devices, the result might be a conflict that would otherwise be deterred. The West German government, denied both these options by its solemn declaration within the Western European Union that it would never become a nuclear power, is understandably (and rightly) more concerned with the threat from Soviet medium-range missiles across the Eastern frontier and would like faster progress with Salt III.

What, in these uncertain circumstances, is to be done? The conventional advice is to wait until after the American election (and then perhaps to wait until a new Administration is installed). That is a counsel of defeat. It is in the best interests of NATO, but would also serve the good cause of diminishing the risk of strategic conflict, if the three principal European states were to use the forthcoming period of uncertainty to decide among themselves what they want for European security. The British and French justifications of their independent nuclear forces are not so different that they could not be reconciled, while both are consistent with a NATO agreement with the Warsaw Pact on medium-range missiles (Salt III). Conventionally, again, it is supposed that an Anglo-French deterrent is unthinkable and that Salt III must wait on Salt II coming out of limbo (which in turn must wait on Afghanistan and, again, the election). But this is not a time for making decisions that must of necessity occupy most of the 1980s. President Carter's announcement of Directive 59, domestically, is an opportunity to begin that process.

What price the price of crude petroleum?

The recession in the industrialized countries of the West is now also beginning to hurt the oil-producing states. In the past few weeks, production in many OPEC states has declined as consumption in many industrialized states has stagnated or even fallen marginally. Some producers are now trimming back the premiuns they have been in the habit of adding to the prices on which they have been settling at the periodic OPEC price fixings, with the result that the prices charged for refined products, especially petrol or gasoline, have themselves fallen by a per cent or so. Meanwhile, the Rotterdam spot market (which is not physically in Rotterdam but rather is the name for a system by which oil traders sell tankerfuls of oil to each other while the ships are still at sea) has seen the price of crude oil fall back and the volume offered for sale by the oil-producing states shrink to a trickle. Understandably, if prices are falling, the oil producers prefer to leave their petroleum in the ground. Only some of the oil producers, Iran most conspicuously, will be embarrassed if, for a time, oil revenues noticeably shrink. But the emerging slump in the demand for oil differs in many important ways from previous occasions in the recent past, 1976 for example, when there seemed to be a surplus of crude oil. It is also an opportunity for the oil-consuming states of the industrialized West to put their own pricing policies for oil in order.

There is some evidence that the present slackening of demand for oil reflects not merely the economic recession in the West but the beginning of an underlying trend towards reduced oil consumption. That this should be happening is merely a sign that increased prices bring lower consumption, the sort of thing that Adam Smith was saying 200 years ago. The only surprise is that it has taken seven years, since the first dramatic increases of the price of oil in the autumn of 1973, for consumers to make arrangements to manage with less. Ironically, in this the first stage of the recession, high interest rates will be a brake on the pace at which new capital developments might help to accelerate the conversion of industrial plant and commercial buildings to more efficient ways of using energy. It may be some small comfort for everybody concerned that, if this recession follows the standard pattern, there will come a time when interest rates are low again. On present form, however, even if present trends persist, it will be a decade or so before the industrialized West's dependence on imported OPEC oil has lessened to the point at which the consumers will be able to look the suppliers in the eye and argue about the price of oil.

In the meantime, there are other steps that could and should be taken, the chief of which is to bring about a greater of harmony between the oil pricing policies of the consumer states. For governments appear still be divided on the objectives of their oil pricing policy: they see higher prices as a means of encouraging conservation, but they differ in the degree to which they wish to protect their electors from reality. The worst offender is the United States, where Congress has stolidly declined to let the Administration take steps to let the price of oil rise towards the international price of crude. (Is that another issue that will be more easily decided when the presidential election has been run?) One result is that the pressures towards conservation are not as strong as they might have been. Another is that energy-intensive industries in the United States are blessed with a commercial advantage over their competitors elsewhere which is widely considered to be unfair. In the past few weeks, there have been rumblings from the European chemical industry that European governments will not be able indefinitely to ignore. Yet they appear to be unwilling to follow the sensible course of harmonizing their systems for taxing oil so as to ensure that, at least within Europe, nobody has an unfair advantage. The European Commission's proposals to this end were given short shrift earlier this year. In Europe, perhaps the worst offender is the British government, which rigidly follows OPEC prices in trading North Sea oil without apparently appreciating the strategic benefits that would flow from a slightly lower price.

Further ahead, the overriding need is for a mechanism resembling a free market that would serve as a means of fixing a realistic price for oil and, ultimately, for other fuels. The notion that oil importers that are also oil producers (chiefly the United Kingdom and the United States) might deliberately use part of their production to increase the volume of crude oil traded on the Rotterdam market (see *Nature*, 3 July) could not fail to have some influence on future OPEC prices. The attempts now being made to organize a future market in crude petroleum, great though the technical difficulties may be, could be an influence of the same kind. The trouble, as always, is that Western oil producers are unwilling to sacrifice any part of their security of supply for the benefits (to them as well as others) of lower prices.

0028-0836/80/340748-02$01.00

Columbia and Yale at odds about Felig

An unhappy scandal has rocked the departments of medicine at Columbia University and Yale University, has led to the resignation of the newly appointed chairman of the department of medicine at Columbia, Dr Philip Felig and has again raised accusations of plagiarism in the scientific literature.

The trouble, regarded as a tragedy for all concerned by members of the department of medicine at Columbia, was first reported by the *New York Times* last week. What follows is a chronology of the events of the past few years.

In December 1978, Dr Felig, then at the department of internal medicine at Yale, was sent by the *New England Journal of Medicine* a paper which had been submitted by Dr Jesse Roth from the National Institutes of Health with Dr Helena Wachslicht-Rodbard as co-author. The paper, entitled "Insulin binding in *anorexia nervosa*", was sent to Dr Felig as a referee and eventually returned to the *New England Journal of Medicine* where it was published in April 1979.

Early in 1979, Felig and his associate of five or six years, Dr Vijay Soman, submitted to the *American Journal of Medicine* a paper with essentially the same title as that of Roth, which was sent by the Editor to a group of referees which included Dr Roth.

The authors of the original paper recognized that some portions of the text of the Felig-Soman paper were identical with their own original and that an equation which became the basis for their own statistical analysis of their data was similarly identical. Dr Wachslicht-Rodbard protested to the Editor of the *American Journal of Medicine* and later Roth protested to Felig, as a result of which Felig offered to withdraw the abstract of the paper already submitted to that year's FASEB meeting in Atlantic City, to reprimand Dr Soman, to amend his paper so as to acknowledge Roth's priority and to arrange that the paper should not be published until after Roth's had appeared, which was in April 1979 (*New England Journal of Medicine* **300**, 882).

Meanwhile, Roth's colleague at NIH had written to Felig and to the Dean of Medicine at Yale suggesting that much of the data which was the basis for the collaboration between Dr Soman and Dr Felig might be suspect and asking for an audit of the laboratory's work. Even though Dr Felig had at the outset denied the possibility that there might be irregularities in his laboratory, he agreed to an audit and, according to Dr Roth, not to publish his paper until the audit had been completed. In the event, the audit was long delayed and Soman and Felig's paper was published in January 1980 (*American Journal of Medicine* **68**, 66). Only by February 1980 had the independent audit been carried out, revealing discrepancies between raw data and published accounts thereof. Whereupon Dr Soman admitted "fudging" data.

During this period, a Columbia search committee was seeking a new chairman for the department of medicine. In the autumn of 1979, the search committee interviewed Dr Felig, decided to offer him the post and had completed negotiations with him for his removal from Yale to Columbia at the turn of the year. Since then, Dr Felig has been making periodic visits to Columbia, where he began work full-time at the beginning of the academic year in mid-June, having by then moved to New York.

People at Columbia say that they do not dispute Dr Felig's explanation that the alleged plagiarism in the article submitted to the *American Journal of Medicine* may have arisen because Dr Soman had kept a copy of the article sent to Dr Felig for review and passed on to him. Equally, they say, Dr Felig may have submitted his referee's report to the *New England Journal of Medicine* on the basis of a draft prepared by Dr Soman. They emphasize that there are no grounds for disputing Dr Felig's statement that he was unaware of similarities between his paper to the *American Journal of Medicine* and the paper submitted to the *New England Journal of Medicine.*

The audit in February 1980 of the data compiled in Dr Felig's laboratory prompted a second and again external audit by Dr Jerrold Olefsky of the University of Colorado. By then, Dr Felig had asked that Dr Soman should write a letter declaring that he alone was responsible for such similarities as there may have been between the Roth paper and that submitted by Felig and Soman to the *American Journal of Medicine* and Soman was dismissed. The independent audit disclosed that of more than a dozen papers submitted in recent years from Dr Felig's laboratory involving collaboration with Dr Soman at least eight were under a cloud and that six were unsupported by raw data gathered in the usual way in laboratory notebooks.

In February 1980, however, Dr Felig had proposed that Dr Soman should be appointed as assistant professor in the department of medicine at Columbia University without, people at Columbia now say, disclosing that Dr Soman's work was under a cloud. Although the dean of the medical school, Dr Donald F. Tapley, was informed of the outcome of the second independent audit of the Felig paper in March this year, it is now said that Dr Tapley did not inform his colleagues at Columbia until July, when word of the alleged plagiarism had been spread about and when Columbia, with Dr Felig already in post as chairman of the department of medicine, set up an *ad hoc* committee to look into the affair. During the early summer of this year, Dr Felig was at pains to deal with the consequences of the two independent audits.

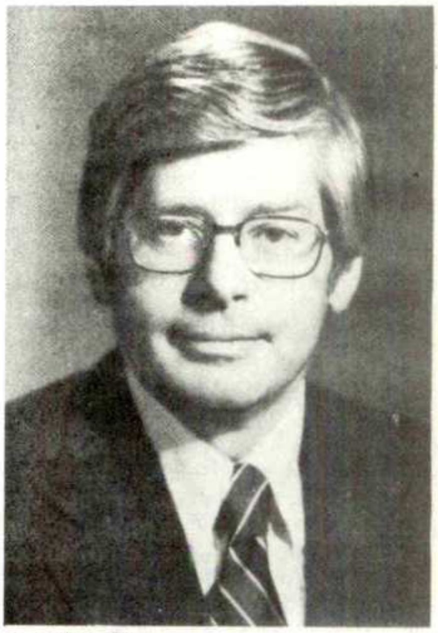
Dr Philip Felig

One of the papers concerned in the investigation — Soman, V. and Felig, P. "Regulation of the glucagon receptor by physiological hyperglucagonaemia" — was published in *Nature* (**272**, 829; 1978), and Dr Felig wrote to the Editor to say that it had not been possible to find the original data and that "until further data are available, the hormone binding data contained in that publication must be considered questionable". (Dr Felig had also written to the editors of several other journals in similar terms but a retraction in respect of another paper will appear in the current issue of the journal *Diabetes.*) Dr Felig was told by *Nature,* in May, that in Dr Soman's interest it would be best if a retraction in respect of the *Nature* paper appeared only when the position had been cleared up.

In the event, the *ad hoc* committee at Columbia took the view that Dr Felig was at fault in not having been able to recognize similarities between the paper which he signed and submitted to the *American Journal of Medicine* and that which he had, a few weeks earlier, been asked to review; for having delayed for as much as nine months before seeing that an audit of his laboratory's data had been carried out; and for not volunteering to his academic colleagues at Columbia the trouble he had encountered at Yale. Faced with this complaint, Dr Felig resigned from Columbia at the end of last month.

Yale takes a quite different view of what has happened. On the telephone this week,

0028-0836/80/340749-02$01.00

Dr Robert W. Berliner said that Columbia had made a gigantic mistake. He said that the alleged plagiarism consisted of a sentence or two and an equation that is not nearly as special as is claimed. People at Yale, indeed, suspect that Dr Felig is the victim of a misunderstanding. He has been invited to return to Yale and has apparently agreed to do so. This week, Dr Felig was on vacation. Dr Roth, while sympathetic to the predicament in which Dr Felig initially found himself, expressed the view that it was careless of Dr Felig to go ahead with publication before the audit had been completed.

School computing

Money to spend

The British government's £9 million programme to promote the use of computers in schools is getting off to a slow start because of delays in appointing a director. To avoid the possibility of losing some of the money if it is not spent before next March, the Department of Education and Science (DES), which is putting up the funds, has already had to award some grants. About £500,000 of the £1 million set aside for this financial year has been either awarded or earmarked for projects which are as yet planned only in outline. The allocation of larger sums for projects which will define the emphasis of the four-year programme will have to wait for the new director whose appointment is expected to be announced in September.

The present programme has grown out of a plan of the previous Labour government to spend £12 million on developing the educational value of microcomputers. None of that money was spent, however, because of the change of government in April last year. After more than a year of deliberation, the present Conservative government announced last March that it was to renew the programme by spending £9 million over the next four years: £1 million is to be spent before March 1981 and £2.7 million is to be spent in each of the remaining three years. When it is fully underway, the programme is to be administered by the Council for Educational Technology for the United Kingdom.

The DES has yet to decide on the overall objectives of the programme because to do so it needs the advice of the director as well as a recently appointed advisory committee of civil servants, teachers and representatives of educational organizations. The advisory committee gave the matter some thought at its first meeting at the end of July. All members were agreed that the programme should aim to improve the use of computers in schools but there was a difference of opinion on what should be the long-term objectives of computer education. Some members believe that the aim should be to acquaint most school leavers with computers and their uses: others believe that the aim should be to give pupils a grounding in programming and computer technology. Members plan to resolve the issue at the committee's next meeting in September.

Much of the work on computers in schools has been done by the Council for Educational Technology for the United Kingdom, which will administer the current programme when it gets under way. Other groups, which will no doubt be looking for funds, include Micro and Mini Computer Users in Secondary Education, a voluntary organization which is building up a library of software and guidance notes for teachers, and the Schools Council. The Schools Council hopes to receive grants to extend its existing work on compiling software and course notes on several subjects central to the school curriculum. Some of the packages it has already produced are designed to be of use in teaching history, economics, geography and even home heating, as well as chemistry, physics and biology.

Only about one hundred schools in Britain own their own computer and it is unlikely that much of the £9 million will be spent directly on increasing that number. One major constraint on the work funded under the programme will be that it should lead to results or suggestions for computer use which are within the financial limits of local education authorities.

Judy Redfearn

Soviet environment

Old hands back

Environmental protection is now a major feature of Soviet planning, and Moscow radio recently took to task Western newspapers (including the *Guardian*) which, it said, reported only the negative aspects of Soviet ecology. In response, the commentator drew specific attention to a speech of Academician N.P. Dubinin, delivered at this year's plenary meeting of the Soviet Academy of Sciences, and which was later published in the *Vestnik* of the Academy.

Academician Dubinin is a leading Soviet geneticist, whose work, notably his book *Evolutionary Genetics* had been suppressed during the Lysenko period. His address to the academy, entitled *Genetics and its significance for Mankind* covered a whole range of topics from plant-breeding to genetic engineering. Nearly half his speech, however, was devoted specifically to the genetic aspects of pollution, which, he explained, make up an important section of the Soviet Union's "Man and biosphere" programme, which is the responsibility of a special environmental Interdisciplinary Council of the State Committee of the USSR on science and technology.

In his speech, Dubinin stressed that much of the work in this field was taking place within the framework of the United States – USSR collaboration programme. By stressing the collaborative aspect, he was thus able to quote exclusively from US sources on the genetic hazards of pollution by mutagens, or to attribute to American authors the more pessimistic viewpoint that "at the present time science does not have at its disposal the means of solving this exceptionally complex problem". On the other hand he attributes to Soviet authors a "highly promising express test scheme" for studying the frequency of genetic mutation, tests based on leukocyte cultures and a method for determining gene and chromosome mutations in embryo mouse cells. The American J. V. Neel, however, receives due credit for his improved monitoring programme for observing the increase of mutations due to the Hiroshima and Nagasaki bombs.

In a speech intended to review the positive aspects of Soviet genetics, open criticism of past policy would clearly be out of place. There were, however, one or two, interesting allusions to the Lysenko aberration. In speaking of the "adaptive norm", Dubinin specifically cited his own (erstwhile banned) work of 1948, and stressed the importance of establishing whether or not unfavourable genetic changes had occurred over the last 20 to 30 years. Soviet genetics, it should be recalled was effectively restored only in 1963 – 64. In a speech which the Soviet media singled out as the proper and positive way to report environmental genetics, such low-key criticisms, it appears, are quite in order.

Vera Rich

Frogs to eat

The edible frog (*Rana esculenta*), the basis of a number of French recipes for gourmets, is one of the species widespread on the mainland of Europe which have established themselves only with difficulty in the United Kingdom. The photograph is taken from a Nature Conservancy Council booklet, *Wildlife Introductions to Great Britain,* which is the report of a working party of the UK Committee for International Nature Conservation. The edible frog is apparently now established only in the counties of Norfolk and Sussex.

0028-0836/80/340750-02$01.00

Interferon production

Japan now

International agreements for the manufacture of interferon appear to be catching on. Last week, the Wellcome Foundation Limited (whose sole shareholder is the British foundation known as the Wellcome Trust) announced an agreement with the Sumitomo Chemical Company of Japan that will in due course enable the Japanese company to use Wellcome technology for manufacturing lymphoblastoid interferon.

The project, which is thought to be potentially worth several million pounds to the British company, will first of all involve clinical trials in Japan based on interferon supplied by Wellcome. Thereafter, the Japanese company will decide whether or not to go ahead with the building of a plant for producing interferon commercially, using the techniques developed at the Wellcome Foundation over the past few years.

Broadly speaking, the technique is to infect a culture of lymphoblastoid cells with Sendai virus, which stimulates interferon production, and to extract lymphoblastoid interferon on chromatography columns loaded with antibodies against the type of interferon being produced.

So far there has been no opportunity to decide whether the recently announced technique for raising monoclonal antibodies against interferon (Secher, D. S. and Burke, D. C., *Nature,* **285,** 446; 1980) will make this process efficient.

The cost of interferon plants of this kind is likely to be of the order of £5 million. It is thought that the production of interferon by the Wellcome Foundation now exceeds the total production of Finland, hitherto the chief source of interferon. For those drug houses manufacturing interferon from tissue cultures, the overriding question for the future must be whether cloning techniques will lead to more efficient and cheaper manufacture.

If it is possible to obtain as many as a hundred molecules of interferon from a bacterium such as *Escherichia coli* carrying an interferon gene, the capital costs of the manufacturing plants required to produce a given amount of interferon will be reduced at least in proportion to the ratio of the generation times of bacteria and cells in culture — 20 minutes to three days, or a factor of a hundred. Drug houses using tissue culture techniques (which are thought to include Roche and Merck as well as Wellcome) appear however to be counting on the length of the period of clinical investigation of cloned interferon that would be needed before these could be put on the market.

As things are, there is no direct evidence that cloned interferon is equivalent to that from tissue culture and in any case the multiplicity of interferon molecules now being identified will need to be distinguished from each other physiologically and clinically, a process thought by the existing manufacturers to require five years or so.

Although the agreement with the Sumitomo Chemical Company has been formally signed, there are some grounds for anxiety that the arrangement may be frustrated by difficulties in Japan about the widespread use of whatever materials the Wellcome Foundation's Japanese partner eventually seeks to put on the market.

Occupational safety

Cuts ahead

Britain's Health and Safety Executive (HSE) is expecting difficulty in cutting its coat according to its cloth. In its latest annual report, published earlier this week, the HSE says that the government's plan to set its 1981-83 grant at 6% below the grant for 1979-80 will mean a reduction in the amount of work it can carry out.

Most of the savings will be made on staff, probably by reducing numbers from 4200 to 3800, and on internal office costs. But, says the report, some of its work of direct relevance to employers and workers, in particular that of the Factory Inspectorate, is bound to suffer. The research budget is also expected to come off particularly badly, with cuts of 18 per cent or about £2.2 million expected for the main research and development budget.

The main fear of John Locke, Director of the HSE, is that its work will become more reactive, dealing only with problems retrospectively. Such a move would be contrary to the policy of anticipating problems adopted by the executive since its creation in 1974.

Locke regards the anticipation of problems through extensive visits to workplaces and an active research programme a priority, even above some of the daily demands on the executive's time. In the report, he says that longer term work on problems with no immediate obvious effects on employers and workers, especially those of occupational exposure to chemicals, noise and radiation, must continue even if cuts have to be made elsewhere. Such a policy would be in line with the changing emphasis of the executive's work over recent years from accidents at work to longer term health problems.

The plan is to make most of the cuts in the research budget fall in those areas, commonly involving standard testing, where industry could be persuaded to step in with funds. Hence, the HSE hopes that industry will make up for the £1.6 million reduction in the research division's direct support to the inspectorates by arranging for its own tests to be done. Industry is also to be encouraged to pay for and conduct some of the work done under three of the executive's major current research projects; a study on the toxic effects of low levels of isocyanates, a study on mortality in the rubber industry and a project at Porton Down to study the dispersal of heavy gas clouds. To avoid industry totally controlling studies on its own problems, the HSE still intends to be responsible for designing and monitoring research projects. Industry, however, will be encouraged to provide its own data for them or to pay for research that is done independently.

One of the executive's problems in defining a coherent programme of future work is that with the increasing public awareness of health and safety issues, largely fostered by its previous work, increasing demands are constantly being made on its resources and new problems are brought to its attention. One of the major areas in which it will be stepping up its work is nuclear safety to cope with the government's plans to increase the nuclear power programme and to build a pressurized water reactor. Additional resources are to be put into the Nuclear Installations Inspectorate and almost all the work on fast reactor safety is to cease so that resources can be transferred to studies of PWR design. Work will also increase on toxic chemicals and major hazards, both of which are part of EEC programmes of research.

In a plea for kinder cuts by the government, the report argues that a major reduction in its services could lead to increased expenditure elsewhere, especially in the health services and sickness pay. It says that if further cuts, beyond 6% are planned then the Health and Safety Commission, the body to which the executive is responsible, would look to the government for suggestions as to which areas of its work it should reduce.

The executive does have some statistics to support its case. The number of fatal accidents for those industries covered by the executive throughout its five year life, fell from 651 in 1974 to 544 in 1979. Non-fatal accidents have also dropped by about 25% over the period.

Judy Redfearn

Graduate students

Places sought

Demand from new British graduates for research grants is surprisingly buoyant this year. Half-way through the short season during which the research councils make awards, the Science Research Council at least is modestly encouraged by the volume of applications, which is well up on that of last year.

Part of the explanation is the relaxation of the rules for the awards in the gift of the SRC Engineering Board. For the second year, awards of engineering studentships both for research and for advanced study (usually leading to an MSc degree) are being made on the principle of "first come,

0028-0836/80/340751-02$01.00

first served".

Now that word of the new regulations has percolated to the universities, the Engineering Board's objective of increasing the amount of postgraduate study seems well on the way to being achieved. The Engineering Board has set itself a target for this year of 435 research studentships and 535 advanced course studentships, and gives the impression of being prepared to spend more in future years if only it can attract suitable applicants.

In science subjects, where the rules are unchanged, the target for the award-making season is virtually the same as last year — 769 research studentships and 435 advanced course studentships. These awards are made on the nomination of university and polytechnic departments on the basis of quota allocations by the various subject committees of the Science Research Council. Even so, there is some evidence that the volume of applications is greater than in 1979.

The parallel operation of these two systems is likely to throw an interesting light on the workings of the quota system. Although (outside engineering) the quotas are fixed by the SRC subject committees after a necessarily subjective estimate of the capacity of individual departments to provide training in research, many of those who wish to see a further concentration of research support on departments with high reputations have regarded the quota system as an impediment to change. Would-be engineering research students are in the circumstances more free to decide where to settle, for which reason a comparison of the distribution of research students in science and engineering will be of some interest when the award-making process is over.

Applications for postgraduate awards have also increased under the SRC's scheme for Cooperative Awards for Science and Engineering (CASE) although a relaxation of the rules may again have helped. CASE studentships involve research projects worked out in partnership by a university department and an industrial company, which in previous years have had to be approved by the SRC before a student award can be made. For the first time this year, university departments have been allowed to nominate a student while seeking approval for a project, although an award remains conditional on the students' performance in the degree examinations.

The target for CASE studentships this year is 760, but clearly the SRC would again spend more if there were a sustained demand. It is, however, something of a surprise that the council has been able to build up to 700 awards a year in less than a decade of CASE studentships.

The apparent buoyancy of demand for postgraduate awards is somewhat at odds with reports that many new graduates are this year more anxious to find permanent jobs than to remain in research. By the end of the summer, it is also possible that much of the demand may have melted away. One of the hazards of the process is that awards offered are not always taken up, sometimes because applications are made in duplicate. The SRC's record of this kind is that of a husband and wife who each made sixteen separate applications.

NPT review conference

Smooth start

The Second Review Conference of the Non-Proliferation Treaty (NPT) got off to a smooth and predictable start in Geneva last week. From the opening declarations which delegates to the conference were making in the first six working days, it is plain that the non-nuclear weapons states which are parties to the treaty will be urging that the nuclear powers have made too little progress too slowly towards strategic disarmament, and that the restrictions imposed on trade in nuclear materials in recent years are both a violation of the treaty and discriminatory against developing countries.

Delegates from nuclear weapons states are however heartened that these protests have been couched in moderate language. For their part, the nuclear weapons states (the Soviet Union, the United Kingdom and the United States) have been making much of the report on the comprehensive test-ban negotiations submitted to the Committee on Disarmament at the end of July and of the Committee on Assurance of Supply set up under the International Atomic Energy Agency and due to hold its first meeting at the end of September.

Procedural matters appear to have caused so far the few anxieties that have flitted across delegates' minds at Geneva. As planned by the preparatory conferences, however, the Iraqi delegate was in the end appointed charman of the conference. It has been agreed that most of the work will be done by two committees which met for the first time on Tuesday and which are concerned respectively with progress towards disarmament and security of supply.

Work on the drafting of the conference report will begin next week, and although everybody seems reconciled to the notion that the report will refer to the discontents of the non-nuclear powers, it was hoped last week that a consensus document would be agreed.

For the most part the nuclear powers presented a united front in their formal speeches, drawing attention to the need to strengthen the NPT system and to the detailed character of the report on the comprehensive test-ban negotiations. At one point, however, the Soviet delegate did seek to embarrass the United States by pointing out that Salt II would by now have been ratified had it not been for the United States Congress.

The discontents of the non-nuclear powers, expressed in several of the formal statements, were eloquently put by Mr Domingo Siazon, the leader of the Philippine delegation, who argued forcefully that restrictions on the supply of nuclear materials devised in the past few years by nuclear suppliers were a violation of the NPT, and that signatories of the treaty such as the Philippines, having signed in good faith, had every reason to expect that the nuclear powers would honour their undertaking to provide nuclear materials, fuel and equipment, without discrimination.

It is planned that the review conference will end on 5 September.

Windmill power

UK gets wind

Windmills seem to be on the march in Britain. Officials at the Central Electricity Generating Board (CEGB) will embark this summer on the choice of a site for a large windmill which the board plans to order in 1983 and commission by 1985.

The decision to buy a windmill, announced last week, seems to indicate that the board has decided to take wind power seriously. It is the first piece of alternative energy technology to be bought by the board, Britain's sole electricity utility, on a commercial basis. The early announcement of the plan is intended to stimulate British industry to develop an improved machine by 1983.

The CEGB's plan is to choose a site where other windmills could be built later to assess the characteristics of windmill arrays. It is prepared to spend about £10 million on building ten 1-MW machines. The first windmill will be a 1-MW machine, probably of horizontal axis, with a blade span of no less than 200 ft suspended 150 ft above ground. While industry is busy working on new designs to compete for the order, the CEGB will be gaining operating experience on a smaller 100-kW machine which it hopes to buy as soon as possible.

The apparent sudden interest in wind power has been stimulated by recent developments in the United States. Hamilton Standard, an American company which has pioneered wind-turbine technology, has recently claimed to have designed a windmill which could bring down the cost of wind-generated electricity to as little as 1–2 pence per kWh. Previous best estimates of cost have been about 3–4 pence per kWh.

Undoubtedly, these low estimated costs have stimulated interest in wind power within the CEGB. It is too soon to know what part windmills will eventually play in the pattern of the CEGB's electricity generation. Intermittent generation is an obvious problem unless pumped storage is available. The CEGB says that the chief contribution will be in saving fuel.

Costs of generating electricity from

0028-0836/80/340752-02$01.00

power stations now being built range from 2.28 pence per kWh (nuclear) to 3.59 pence per kWh (coal). If, because of intermittent generation, windmills do not reduce the total need for installed capacity, however, the cost of wind-generated power should be compared with the costs of fuel in conventional stations, 0.61 pence per kWh (nuclear) and 2.30 pence per kWh (coal).

Hamilton Standard claims to have applied some of the principles involved in building helicopters to the design of a flexible windmill capable of bending in the wind and responding to wind coming from different directions. Until now, most windmill designs have assumed the need for a large rigid structure capable of standing up in gales and for very strong rigid sails to withstand opposing gravitational forces. Hamilton Standard is now saying that a bendy windmill can withstand considerable forces and can be built more cheaply because less material is needed.

A cheaper windmill could also operate economically in wind speeds of only 6 m s^{-1} to operate effectively. The ability to respond more sensitively to variations in wind direction also suggests that a flexible design of windmill might be successful in relatively low wind speeds.

In the light of these considerations, the CEGB says that it will be looking at flat inland sites, probably in the east of England, as well as hilltop sites for its first big windmills. A low inland site would have the added advantage of causing less environmental trouble than a hilltop in the rural areas of Scotland or Wales.

Judy Redfearn

Nuclear generation costs compared

The report of the Central Electricity Generating Board (CEGB) for the year to the end of March 1980 includes a detailed analysis of the costs of generating electricity from power stations of different types which is likely to be much quoted in the months ahead, when plans are being laid for the further development of the British nuclear power programme. The figures now published represent a departure from previous practice in that the assumptions on which they are based are stated more explicitly than in the past, with allowance being made for elements of cost such as the interest paid during the period of construction and the cost of decommissioning the stations concerned.

During the past year, the cost of nuclear power generated from the first generation of British "Magnox" stations was less than that of electricity from coal or oil. The costs for the past year are shown in the accompanying Table 1.

Part of the reason why the nuclear costs turn out to be so advantageous is that the initial capital costs of the Magnox stations, built between the late 1950s and the late 1960s, are much lower than present-day replacement costs would be. Although the same is true of the capital costs of conventional power stations, the fact that nuclear capital costs represent a greater proportion of the total implies that the figures are not a reliable guide to the costs of building new power stations of the same types.

One surprising feature of the CEGB's operations during 1979–80 is that the load factors of the nuclear stations were more or less the same as those of conventional stations. Electricity generated by the nuclear plant amounted to 70 per cent of net capacity, compared with 69 per cent for coal-fired stations and 77 per cent for oil-fired stations. Originally, it was intended that the nuclear plant in the British generating system should be run at virtually full capacity; the board says that the lower load factors now being obtained from the nuclear power stations reflect their increased age. The costs of electricity generation are obtained by dividing the total cost of operation by the amount of electricity generated and thus increase as load factors decline.

Table 2 Costs for Hinkley B (AGR) and Drax (coal-fired)

	Hinkley Point B p/kW h	Drax first half p/k W h
Capital charges and provision for decommissioning	0.37	0.12
Interest during construction	0.18	0.04
Inclusive fuel costs	0.55	1.25
Other costs of operation	0.16	0.09
Research	0.07	0.01
Training	0.02	0.01
Total	**1.35**	**1.52**

The CEGB's annual report also provides costs on a comparable basis for two of its newest power stations — the Advanced Gas-Cooled Reactor station (the first of its type to be commissioned) and the newly-completed Drax coal-fired power station. The figures are shown in Table 2. The load factors for the AGR station (Hinkley Point B) and Drax were 55 per cent and 74 per cent respectively. The poor availability of the AGR reflects the difficulties in bringing this station into operation. It may seem remarkable that, in the circumstances, the cost of electricity generated is not much greater than that from the older Magnox station.

Mainly because of inflation, the CEGB expects nuclear costs to rise. The net cost of electricity from the three AGR stations soon to be commissioned (Dungeness B, Hartlepool and Heysham I) are estimated at 2.62 pence per kWh, 2.28 pence per kWh and 2.31 pence per kWh respectively. The increase is largely attributable to increased capital costs, three times as great as those for Hinkley Point B. At the same time, the board estimates that the cost of conventional electricity will have increased still further, with oil-fired plant producing electricity at a cost of more than 6 pence per kWh and the second half of the coal-fired Drax station producing electricity at 3.59 pence per kWh.

For the first time, the CEGB also provides figures to show the basis on which future investment decisions are being made. The principle is that of discounted cash flow in which future costs are represented by a present cost using a discount rate of 5 per cent per annum. The board also makes the assumption that the price of coal will increase at an average rate of 2 per cent a year at least until the end of the century and notes that the cost of building generating plants of all kinds has recently been increasing faster than inflation. The calculations now published, and summarized in Table 3, show that a nuclear generating plant has potential advantages over a coal-fired plant both in generating electricity more cheaply and in its effect on the economics of the generating systems as a whole — assuming that nuclear plants would displace less efficient plants, the Net Effective Cost of nuclear generating capacity becomes negative, implying a net saving for each power station built.

Table 3 Overall comparison of costs for nuclear and coal-fired stations

	Nuclear p/k W h	Coal-fired p/kW h
Capital charges at station and provision for decommissioning*	1.39	0.76
Interest during construction*		
Inclusive fuel costs	0.61	2.38
Other costs of operation	0.22	0.21
Generation costs	2.22	3.35
Less fuel saving from displacing less efficient plant	2.68	3.02
	—0.46	+0.33

Table 1 Costs of power generation by Magnox, coal-fired and oil-fired stations in 1979-80

	Nuclear (Magnox) p/kW h	Coal-fired p/kW h	Oil-fired p/kW h
Capital charges and provision for decommissioning	0.34	0.09	0.14
Interest during construction	0.06	0.02	0.02
Inclusive fuel costs	0.60	1.29	1.61
Other costs of operation	0.26	0.14	0.14
Research	0.03	0.01	0.01
Training	0.01	0.01	0.01
Total	**1.30**	**1.56**	**1.93**

0028-0836/80/340753-02$01.00

CORRESPONDENCE

Nuclear facts

SIR — The letter which you published on 10th July under the heading "Nuclear Protest" from three correspondents from Edinburgh Science for People, contains several misleading statements.

It is wrong to claim that trade union rights are "denied" in the nuclear power industry. Many of the staff in the industry who belong to trades union are very active in participating in debates about nuclear issues within their movement and in promoting the case for nuclear power development. They are presumably best able to judge their own conditions of employment; your correspondents should take account of their views and of those of the trade union leaders who speak for them.

It is incorrect to describe the UKAEA Constabulary as "an armed secret police force". There is nothing secret about them. They are sworn in as special constables. They are individually responsible for their actions and their powers are more circumscribed than those of the ordinary civil police. The AEA Constabulary are responsible to the Secretary of State for Energy through the Chairman of the Authority, and their functions have been reported to and debated by Parliament.

It is impossible to claim that the civil application of nuclear energy to commercial electricity generation has led to weapons proliferation; all of the existing nuclear weapons states found ways of implementing their political decision to have such weapons which did not start from a nuclear power programme.

This exchange of letters seems to me to substantiate the need identified in your editorial (19 June) for professional people, in universities, industry and government, to resolve their points of disagreement. We should at least be able to start with a correct statement of the facts before debating the political aspects of nuclear power development.

L. E. J. ROBERTS

AERE Harwell,
Oxon, UK

Geological sport

SIR— The Geological Olympics are over for another four years. The 26th International Geological Congress held on 7–17 July in Paris had the feel of an Olympic Marathon, with well over 2,500 talks in nine working days. Anybody attending each day deserved an Olympic medal for endurance, for on some days they had to make an agonizing choice between eighteen simultaneous sessions on such diverse topics as Ophiolites, Cambrian Stratigraphy, Geophysics of the Lithosphere and Upper Mantle, Applied Geochemistry, History of Tectonics pre 1922, Coal and Magnetic Stratigraphy and Ocean Floor Reconstruction.

What was the delegate likely to encounter? There was always the chance of "meeting old friends and hearing old papers" but in fact there was plenty of new research "on display". The problem was the way in which it was displayed. Having sat through approximately 2,000 slides (16 papers/day × 6.5 days × 20 slides/paper = 2,080 slides), I can honestly say that probably only one half of them were legible. The rest might well have not been shown — indeed, some speakers even apologized with the standard "If you could see the relevant points, you would notice. . .".

Why are some slides so atrocious at conferences? Admittedly some were superb — large lettering, good use of colours. Others, regrettably, were just unintelligible. The slide of a table photographed directly from a journal, itself produced by offset-litho techniques is a good example. In these cases, the printing has probably been reproduced three or four times with an inevitable reduction in definition each time. The result is a blur from row 1, a sigh from the back and another author loses his audience's concentration. Maybe the time has come for "pre-talk screening" of slides to take place and rejection of those considered of dubious quality.

Apart from poor visual aids, the conference was a tremendous success. The sight of two German scientists actively discussing manganese nodules in English at a conference in France under a session chairman from Hawaii confirms that the occasion had an international flavour. But I wonder how many tribal groups (geochemists, geophysicists, petrologists, etc.) actually strayed outside their own compounds during the fortnight and how many merely "flew in" for the relevant day's papers.

Those who took this second course will have undoubtedly missed some of the more worthwhile aspects of the gathering — although no doubt pressing commitments elsewhere are partly to blame for brief visits. Maybe the Earth Scientists of today are becoming too specialized and hence, as chemists become geochemists, physicists geophysicists etc., the ability to understand broad based geology is declining.

S.J. WAKEFIELD

Dept. of Oceanography,
University College,
Swansea, UK

2,4,5-T dispute

SIR—Now that I have returned to the UK I have seen your editorial of 17 July and without complaining about the snide reference to me (no doubt prompted by your reluctance to publish the piece you requested me to write on the cancer issues) you have still got the 2,4,5-T issue wrong. I have no idea where you got the figure of 100 tons for the quantity of herbicide-based materials imported. As far as I know it is nearer 160 tons. *Nature* should (as in the back part of the magazine) abandon prejudice and support quite reasonable and sane crusades to protect people.

CLIVE JENKINS

Association of Scientific Technical
and Managerial Staffs, London, UK

The source of the figures quoted in the leading article to which Mr Jenkins refers is as follows. Customs and Excise give imports of 2,4,5-T into the United Kingdom in 1979 as 116 tonnes. Use of the material in the United Kingdom in 1979 was given as 58 tonnes in an answer to a Parliamentary Question on 20 June. The difference is accounted for by re-exports. Mr Jenkins has been informed of the source of the figures used but insists that his letter should be published. The article of his own to which Mr Jenkins refers was invited in March but not published because, in the judgement of the editorial staff of *Nature*, it dealt with a different aspect of the problem from that originally defined.

Editor, *Nature*

Misciting latest

SIR—In their News and Views article "*Just so stories and cautionary tales*" *(Nature,* 31 July)[1], Robert May and Miranda Robertson quote our study[2] where we point out that W. D. Hamilton's paper *The genetical evolution of social behaviour*[3] is frequently miscited as *The genetical theory of social behaviour.* Although the recent trend to miscite the paper can be traced back to E. O. Wilson's *Sociobiology, the New Synthesis*[4], the mutation has occurred independently at least three times and is an easy one to make for those familiar with Sir Ronald Fisher's *The Genetical Theory of Natural Selection*[5].

Similarly, misciting Wilson's book as *Sociobiology, the Modern Synthesis,* as May and Robertson did, is easy to do for anyone who has read Sir Julian Huxley's *Evolution, the Modern Synthesis*[6].

PAUL HARVEY
JON SEGER

School of Biological Sciences University of Sussex, Falmer, UK and Department of Biology, Harvard University, Cambridge, Massachusetts

1. *Nature* **286**, 327–329 (1980).
2. *New Scientist* **87**, 50–51 (1980).
3. *J. theor. Biol.* 7, 1–52 (1964).
4. Harvard University Press (1975).
5. Clarendon, Oxford (1930).
6. Harper, New York (1942).

Distance measured

SIR, — Bougault and Treuil in their *Nature* article (17 July) fail to inform us whether their distances are nautical or statute "mille passum" — there is a difference of 11.5 chains between these units, equivalent to 10,000 yr of seafloor spreading. Confusion could be avoided, and precision improved, by quoting distances in the traditional leagues of Columbus, Champlain and the imperturbable Captain Nemo.

PAUL MOHR

Department of Geology,
University College Galway,
Galway, Ireland

Filter tips

SIR—Dr Zeki's red filter described in your article (*Nature,* 31 July, p.435) is really excellent for use in photographing fluorescent DNA bands on agarose gels. One of the most important factors for a contrast filter is the absence of fluorescence of the filter itself. Conventional red filters usually emit fairly strong fluorescence when hit by a strong UV ray from a transilluminator, and this fluorescence makes for a somewhat bright background and an unclear photograph. We have been using a UV filter in front of a conventional red filter, to cut UV light and thus to minimize the self-fluorescence of the red filter. In this manner a satisfactory photograph can be obtained. It is important to use a good UV filter, however, because some emit a weak fluorescence.

Comparison of Dr Zeki's filter with our double filter showed the former to be superior. Dr Zeki's filter is completely free of intrinsic fluorescence. My thanks to Dr Owen for his helpful observation.

TAKESHI UOZUMI

Department of Agricultural Chemistry,
The University of Tokyo, Japan

0028-0836/80/340754-01$01.00

NEWS AND VIEWS

Neutrino weight watching

from A. De Rújula and S.L. Glashow

IN the past few months, there has been a great deal of excitement about neutrinos, chiefly because of two sets of experiments which have been reported. One experiment, due to F.W. Reines and his group at the University of California (Irvine), based on measurements of neutrinos from a nuclear reactor, has been interpreted as evidence for neutrinos whose mass is not identical with zero. The same conclusion is suggested by very preliminary results from a neutrino experiment at CERN. To the extent that both these experiments suggest that there may be interconversion between the three known species of neutrinos, the conclusions would help to account for the measured deficit of neutrinos from the sun. The interpretation of the experiments so far reported is however both uncertain and controversial. Plainly we are in for a period of lively argument; the hope must be that people will now design the experiments that must and should be carried out to settle this intriguing issue.

Pauli, in 1932, postulated the existence of neutrinos (and antineutrinos) in order to explain why beta rays, unlike alpha and gamma rays, are not monoenergetic. Nuclear beta decay releases a fixed amount of energy shared between two light particles, an electron and an antineutrino (so that $n \rightarrow p + e^- + \bar{\nu}$). Pauli's particles were not however 'seen' until 1957, when Cowan and Reines showed that antineutrinos emitted by a nuclear reactor produce positrons in a remote detector ($\bar{\nu} + p \rightarrow e^+ + n$).

The muon (μ) is a charged particle much like the electron, but heavier. It is produced together with a neutrino in the decay of a pion by a process much like nuclear beta decay. In 1962, we learned that neutrinos produced with muons (ν_μ) are distinct from those produced with electrons (ν_e) for a beam of 'muon neutrinos' arising from decaying pions was seen to produce muons in a detector, but never electrons. Today, the electron is known to have an even heavier charged sibling called tau (τ). It, too, seems to have its own kind of neutrino (ν_τ).

Experimental study of tritium beta decay a decade ago demonstrated that the mass of the electron neutrino may be zero and must be very small, less than 60 eV/c^2 or 10^{-31} grams[1]. The mass is at least four orders of magnitude less than that of the electron. Perhaps all three kinds of neutrinos are exactly massless — what could be simpler and more elegant? The trouble is that this kind of reasoning once led us astray with space reflection, time inversion and charge conjugation, which have turned out not to be symmetries at all. Nature will find her own way to elegance. We dare not frame laws of nature that have no logical necessity. Conservation of energy and of electric charge are well founded. Many other 'laws' are suspect. Protons may not live forever, and neutrino masses may be merely very small.

Indeed a recent report from the Institute for Theoretical and Experimental Physics in Moscow suggests that the mass of the electron neutrino is not zero[2]. Again, the beta decay of tritium was studied, because it is the least energetic of all beta decays and hence the one most sensitive to neutrino masses. According to the authors, "the results perhaps give an evidence for the existence of the non-zero neutrino mass" in the range 14 to 40 eV/c^2. This cautious conclusion reflects the great difficulty of the analysis of the experimental results, for the effects of such neutrino masses on the observed energy of the electrons are of the same order of magnitude as the atomic or molecular corrections that must be made. Astrophysicists must nevertheless be delighted by the Soviet result, since they have a problem that neutrino masses of a few eV or tens of eV may solve. There is more mass in our universe, it seems[3], than can be accounted for in known forms of matter. This 'missing mass problem' recurs at various scales of length — the universe as a whole; in the dynamics of clusters, groups and pairs of galaxies; and in the massive, extended and non-luminous halos that most galaxies are known to have. May this missing mass be in the form of neutrinos?

Cosmological black-body radiation is interpreted as a relic of and evidence for the primordial big bang. As well as the observed electromagnetic radiation, it must include neutrinos. Hundreds of neutrinos, on the average, must inhabit each cubic centimeter of the universe. Should the heaviest neutrino have a mass of between 5 to 50 eV/c^2, these relic neutrinos would *in toto* outweigh the stars. They would provide the missing mass, and they could bind to galaxies to form their halos. The mass in our universe would consist mostly of neutrinos, which are so weakly interacting that they may be detected only by their collective gravitational effects.

Non-zero neutrino masses imply a new phenomenon called neutrino oscillation, or neutrino mixing. Bruno Pontecorvo[4], in 1968, showed that massive neutrinos might change their identities in flight. A particle which is born as an electron neutrino in a beta decay may periodically behave as if it were a muon neutrino or a tau neutrino. Suppose that there are three kinds of neutrinos and that they are not massless. Call them ν_H, ν_M, and ν_L: the heaviest, the middleweight, and the lightweight. The crucial point is that ν_e need not be one of *these* neutrinos. Its wave function may be a linear combination of the three, with the muon neutrino and the tau neutrino being orthogonal combinations of the same three. On this picture, neutrinos arising from nuclear beta decay are born as electron neutrinos but, as time passes, their ν_H, ν_M, and ν_L components evolve differently. As the linear combination changes, the beam becomes a mixture of electron neutrinos, muon neutrinos and tau neutrinos. There will be oscillations of neutrino identity with frequencies that are determined by the differences between the masses of the neutrinos. These oscillations can lead to a variety of novel observable effects.

Electron neutrinos should be copiously

A. De Rújula is at CERN, Geneva and S.L. Glashow is Professor of Physics at the Lyman Laboratory, Harvard University.

---

1. Bergkvist, K.E. *Proc. Topical Conf. Weak Interactions* CERN 69-7 p.91 (1969).
2. Lyubimov, V.A., Novikov, E.G., Nozik, V.Z., Tretyakov, E.F., & Kosik, V.S. (unpublished).
3. For a review, see: Faber, S.M. & Gallagher, J.S. *Ann. Rev. Astron. Astrophys.* **17**, 135 (1979). A more recent discussion is found in Schramm, R & Steigman, G., Gravity Foundation Prize Essay, 1980 (unpublished).
4. Pontecorvo, B *Sov. Phys. JETP* **26**, 984 (1968).
5. For a review, see: Bahcall, J.N., *Rev. Mod. Phys.* **50**, 881 (1978).
6. Reines, F., Sobel, H.W., & Pasierb, E. (unpublished).
7. Feynman, R., & Vogel, P. (unpublished).
8. For a review, see Wachsmuth, H., CERN-EP/79-115C (1979). For an interpretation of these results in terms of neutrino oscillations, see De Rújula, A., Lusignoli, M., Maiani, L., Petkov, S.T., & Petronzio, R *Nuclear Physics* **B168**, 54 (1980).

0028-0836/80/340755-02$01.00

produced by the mechanisms that power the sun.[5] These solar neutrinos have been detected on Earth when they transmute chlorine atoms to argon atoms. The observed flux of solar neutrinos appears to be too small by a factor of about three when compared with theoretical expectations. There are two popular explanations for this 'solar neutrino problem'. One stems from the observation that the chlorine experiment is sensitive to only a small minority of the solar neutrinos, the most energetic. These arise from a rare solar nuclear reaction, for which the calculation of the solar flux may be wrong. Accordingly, it is necessary to repeat the experiment with a detector sensitive to a broader range of neutrino energies. Many tons of such exotic and costly materials as gallium or indium are needed for this. But the phenomenon of neutrino oscillations could provide a more intriguing resolution of the solar neutrino problem. With maximal neutrino mixing, the solar neutrinos may have become an equal mix of the three neutrino species by the time they have reached the Earth. Since the method of detection of solar neutrinos is sensitive only to electron neutrinos, the apparent flux is thereby reduced to one-third. This explanation of the solar neutrino deficit requires neutrinos to have masses of at least 10^{-6} eV and to mix to a considerable extent.

Several recent ground-based experiments point in the direction (but do not amount to a compelling proof) of neutrino oscillations. Two of these tentative sets of results must be regarded as teasers for the more precise experiments that can and must be done.

Electron antineutrinos ($\bar{\nu}_e$) from a reactor were observed in a deuterium (d) detector eleven meters away[6]. Two reactions induced by the antineutrinos were studied, $\bar{\nu}_e + d \rightarrow n + n + e^+$ and $\bar{\nu} + d \rightarrow n + p + \bar{\nu}$. The first is a conventional 'charged current' weak interaction to which only electron antineutrinos can contribute. Other antineutrinos can make only μ^+ or τ^+, for which there is not enough energy. Thus, the first reaction would be inhibited by neutrino oscillations. The second reaction is a 'neutral current' weak interaction characteristic of the now accepted electroweak theory. It is unaffected by neutrino oscillations because the neutral currents involve all neutrino species equally. The ratio of the number of charged-current events to the number of neutral-current events is therefore sensitive to the existence of neutrino oscillations but relatively insensitive to the poorly-known flux of antineutrinos from the reactor.

Reines *et al.*[6] measured this ratio and find that it is about half of what one would expect with no neutrino oscillations. This suggests considerable neutrino mixing and neutrino mass splittings of at least 0.5 eV. The statistics of the effect are not yet convincing, however, and the authors cautiously conclude "... that further experimentation with $\bar{\nu}_e$ at reactors ... would be helpful in elucidating the effect here observed, as well as experiments at accelerators and with cosmic rays." The interpretation of this experiment has been criticized by Feynman and Vogel[7], who have pointed out a possible inconsistency between the deuterium experiment and an earlier hydrogen experiment by the same group done under similar experimental conditions. When this inconsistency is taken into account, the evidence for neutrino oscillations becomes less than convincing. The controversy is alive, and a revised version of the Reines *et al.* manuscript is in circulation.

The second set of data comes from an accelerator experiment at CERN with a beam of neutrinos expected to consist of equal numbers of electron and muon neutrinos. These neutrinos are very energetic, so that the muon neutrinos may interact in the detector to make muons just as readily as the electron neutrinos may interact to make electrons. If there are no neutrino oscillations, one should therefore see equal numbers of electrons and muons in the detector. The same should be true if there are oscillations connecting electron and muon neutrinos, since as many ν_e become ν_μ as ν_μ become ν_e. The Big European Bubble Chamber, sitting in this neutrino beam, has so far observed about 20 neutrino-induced events[8]. Only half as many electrons as muons were seen, but the statistics are clearly limited. If the observations are significant, however, a possible explanation is that electron neutrinos mix with tau neutrinos. This could explain the apparent systematic deficit of the electron neutrino component in the CERN experiment, in that of Reines *et al.* and in the solar neutrino experiment.

There are thus several suggestive experimental indications that neutrinos have mass and do oscillate. None of the experiments is beyond question. Yet, such results would fit quite well into current theoretical developments concerning the synthesis of the strong, weak and electromagnetic interactions. All of these 'grand unified theories' *predict* that baryon number is violated, so that all nuclear matter ultimately decays. Many of than also *demand* that neutrinos have mass, but say nothing of what these masses are. Particle theorists may not know quite what they are doing, but they do feel they are on the right track. Positive results from proton-decay experiments and from neutrino-oscillation experiments will tell us much about the nature of the underlying theory. For example, a model with neutrino masses involves seven more measurable parameters than a model with massless neutrinos. We need these hints. Moreover, proton-decay and neutrino-oscillation experiments do not depend upon the construction of ever larger accelerators. The high-energy frontier is certainly of fundamental importance, but there is still much to be learned at lesser energies. □

Esoteric DNA?

from Mervyn J. Turner and John S. Cordingley

ONE of the more esoteric areas within the field of mitochondrial DNA research has been the study of kinetoplast DNA (kDNA). Protozoa of the order Kinetoplastida, which includes the causative agents of the leishmaniases and trypanosomiases, characteristically contain a single large mitochondrion within which is found the kinetoplast, a disc-shaped mass of tightly packed DNA spatially associated with the basal body of the flagellum. Electron microscopy of spread kDNA shows a complex network of two kinds of interconnected DNA circles. The size of the smaller 'minicircle' component is species specific, varying between 700 and 2,300 base pairs, with each network containing about 10,000 minicircles. Each network also contains up to 50 copies of a larger 'maxicircle' component of up to 35 kilobase pairs. RNA transcripts of the maxicircle can be readily detected and this is one of several pieces of evidence suggesting that maxicircle DNA is equivalent to the mitochondrial DNA of other eukaryotes.

There is no similar consensus on the function (if any) of the minicircles. A number of laboratories have suggested from hybridisation kinetics and restriction endonuclease digestion that the minicircles within each network are heterogeneous with respect to sequence. Using cloned minicircles from *Trypanosoma brucei*, Donelson *et al.* (*Plasmid* **2**, 572; 1979) extended these data to show about 25% sequence homology between *T. brucei* minicircles. Chen and Donelson (*Proc. natn. Acad. Sci. U.S.A.* 77, 2445; 1980) now report the complete sequences of two cloned *T. brucei* minicircles, each of about 1,000 base pairs. The two molecules share about 12% homology within a nearly continuous stretch, and another 15% scattered randomly throughout the rest of the two sequences, thus confirming the prediction of about 25% homology.

Does this bring us any closer to an understanding of the function of the

---

Mervyn J. Turner and John S. Cordingley are in the MRC Biochemical Parasitology Unit, The Molteno Institute, Cambridge.

0028-0836/80/340756-02$01.00

minicircle? Fouts and Wolstenholme (*Nucl. Acids Res.* **6**, 3785; 1979) found an RNA transcript of 240 bases from minicircles of *Crithidia acanthocephali*, but as yet no such transcript has been found in *T. brucei*. Intriguingly, there are potential coding transcripts of comparable size in each minicircle sequence, and in each case such potential transcripts begin within the 12% of continuous sequence homology. Circumstantial evidence suggests that this 12% homology is conserved within all minicircles of *T. brucei*, since it has been reported that the restriction endonulease Taq 1 cleaves all *T. brucei* minicircles and a recognition sequence for this enzyme is found within the 12% homology (the only Taq 1 site in one of the kDNA sequences). There are no obvious origins of replication in the kDNA sequences, which are characterised by a distinct lack of palindromes and inverted repeats. Outside the 12% continuous homology, the sequences are remarkably A-T rich (77%), perhaps analogous to the high A-T content in non-coding regions of other mitochondrial genomes.

These data leave open the question of minicircle function. Possible suggested functions for the kinetoplast, some more far-fetched than others, have included a structural role at the base of the flagellum; a means of segregating maxicircles equally at division; a repository of transposons; and an involvement in the control of antigenic variation or other gene expression.

Minicircles have many features in common with satellite and repetitive DNA in other systems. In addition to the presence of multiple copies, they possess a buoyant density distinct from the nuclear DNA and show internal repeats and sequence divergence. This feature is particularly obvious in *T. cruzi* minicircles, which appear to comprise four tandem repeats of a related sequence (Leon *et al. Biochem. Biophys. Acta* **607**, 221;1980). Thus, having no demonstrated phenotypic effect, one may speculate that minicircles are an example of mitochondrial parasitic DNA! □

Can genes choose habitats?

from J.S. Jones

ALTHOUGH the history of evolutionary genetics is largely a tale of attempts to explain genetic variation there is no consensus of opinion as to the evolutionary forces involved. One possibility is that variation is promoted by the complexity of the environment; if one allele is favoured in one microhabitat and its alternatives in others, then natural selection within the population could maintain genetic variation.

There are a number of convincing instances of an association between the genetic diversity of a population and the ecological complexity of its habitat. In the genus *Drosophila*, for example, species living in the complex environment of a tropical forest have up to ten times as many chromosome inversions as those living in simpler habitats such as deserts or offshore islands[1]. Again, studies of populations of *Drosophila willistoni* show there is a clear relationship between the extent of chromosome polymorphism and the floral diversity of the environment[2].

Since the first attempts to provide a theoretical basis for these effects were made by Levene[3], many mathematical models of natural selection in heterogenous environments[4] have been put forward. In a recent paper, however, Maynard Smith and Hoekstra[5] show that most of these models are limited in their usefulness; only under certain very specific conditions of the relative fitness of each allele in each ecological riche can they maintain polymorphism. They therefore have little more value as a general explanation of genetic variation than do the older theories in which heterozygotes have an overall advantage over homozygotes[6].

However, models of natural selection in complex environments become much more powerful if individuals of different genotypes are able to select the niche in which they are most fit[7]. Habitat choices linked to genetic differences have now been found for a variety of genetic polymorphisms.

The early experiments of Kettlewell in which melanic and non-melanic *Biston betularia* were released into a barrel painted with black and white stripes showed that the moths chose resting sites against which they were best camouflaged. This kind of experiment has now been extended to other species and to natural populations[8]. *Anolis* lizards in the Caribbean show a polymorphism related to camouflage in which the different morphs choose the appropriate habitat; unstriped individuals spend most of their time on the ground, while those with stripes prefer to live in the bushes in which they are best concealed[9]. Taylor and Powell[10], working in the Sierra Nevada mountains of California in a locality which has a mosaic of woodland and open habitats, marked *D. persimilis* captured from the various habitats with fluorescent dusts. When they released them into the wild the flies showed a strong tendency to return to a habitat similar to the one in which they were first captured. This behaviour is associated with local differences in the frequencies of chromosome inversions.

Habitat selection is also involved in the chromosomal variation of the mosquito *Anopheles arabiensis*[11]; in Nigeria mosquitos possessing certain inversions are more likely to rest indoors (and hence to bite humans) than are others from the same population with a different chromosome constitution. However, not all inversion polymorphisms involve habitat selection. Atkinson and Miller[12] find no evidence that *D. subobscura* from particular habitats tend to return to them. This contrasts with *D. persimilis* but may be related to the evolutionary inflexibility of *subobscura*'s inversion polymorphism, which shows few geographic or temporal trends.

Nearly all animals are highly variable for the genes controlling soluble enzymes. Remarkably, there is now evidence that individuals with different genotypes for certain enzymes may select a habitat which increases their fitness. The freshwater isopod *Asellus aquaticus* lives on decaying leaves and is polymorphic at an amylase locus. Homozygotes for one of the amylase alleles select willow when given a choice between willow and beech in the laboratory to a much greater extent than do the other genotypes[13]. This is reflected in local differences in gene frequency in ponds containing both types of leaf. The alcohol dehydrogenase polymorphism of *D. melanogaster* is the most extensively studied of all enzyme polymorphisms. When larvae are placed at a junction between medium containing 17% ethanol and medium without ethanol, those homozygous for the Adh^{F} allele tend to move onto the alcohol medium; Adh^{S} homozygotes show no habitat preference[14]. This behaviour is related to the higher activity of Adh^{F} in metabolising ethanol and to the selective advantage conferred on flies bearing this allele when faced with an alcohol stress[15]. Clearly, a general tendency for animals of different enzyme genotype to select the ecological niche to which they are biochemically most suited might help to answer the vexed question of why there is so much molecular polymorphism in natural populations.

The theory of sympatric speciation — that a single species may split into two reproductively isolated populations

---

J.S. Jones is in the Department of Genetics and Biometry, University College, London.

1. Spieth, H.T. & Heed, W.B. *Annu. Rev. Ecol. Syst.* **3**, 269 (1972).
2. DaCunha, A.B. & Dobzhansky, Th. *Evolution* **8**, 119 (1954).
3. Levene, H. *Am. Nat.* **87**, 331 (1953).
4. Ewing, E.P. *Am. Nat.* **114**, 197 (1979).
5. Maynard Smith, J. & Hoekstra, R. *Genet. Res.* **35**, 45 (1980).
6. Lewontin, R.C., Ginzburg, L.R. & Tuljapurkar, S.D. *Genetics* **88**, 149 (1978).
7. Taylor C.E. *Genetics* **83**, 887 (1976).
8. Boardman, M., Askew, R.R. & Cook, L.M. *J. Zool.* **172**, 343 (1974).
9. Schoener, T.W. & Schoener, A. *Evolution* **30**, 650 (1976).
10. Taylor, C.E. & Powell, J.R. *Oecologia* **37**, 69 (1978).
11. Coluzzi, M., Sabatini, A., Petrarca, V. & Dideco, M.A. *Nature* **266**, 832 (1977).
12. Atkinson, W.D. & Miller, J.A. *Heredity* **44**, 193 (1980).
13. Christensen, B. *Hereditas* **87**, 21 (1977).
14. Cavener, D., Behav. *Genetics* **9**, 359 (1979).
15. Clarke, B. *Genetics* **79**, 101 (1975).
16. Bush, G.L. *A. Rev. Ecol. Syst.* **6**, 339 (1975).

0028-0836/80/340757-02$01.00

without complete geographic isolation — has been put forward and discredited so often that Mayr has compared it to the Hydra which grew nine heads whenever one was struck off. Habitat selection might, nevertheless, lead to the genetic division of a population if the different genotypes mate within the micro-habitats which they have chosen. The most convincing examples of this are found in insects which parasitise plants and which have strong host-plant fidelity[16]. In Wisconsin the introduced hawthorn fly *Rhagoletis pomonella* showed a sudden — and presumably genetic — habitat extension to apples in 1864 and to cherries in 1960. These populations are now partially reproductively isolated from each other so that at least the early stages of speciation have been completed. How widespread this mechanism is remains to be seen.

Most new ideas in evolutionary biology can be traced directly to the writings of Charles Darwin and habitat selection is no exception. In the *Origin of Species* he wrote: "The more diversified the descendents from any one species become . . ., by so much will they be better able to seize on many and widely diversified places in the polity of nature and so be enabled to increase in numbers." With evidence that choice behaviour may play a part even in molecular evolution, Darwin's suggestion is at last receiving the attention which it deserves. □

Switching on the muscle genes

from Harriet Harris

THE differentiation of muscle fibres from precursor myoblasts is accompanied by particularly striking changes in cellular morphology and function. Myoblasts are developmentally committed cells, but mononucleate and lacking the biochemical and structural attributes of muscle. Myofibre differentiation proceeds by fusion of myoblasts into long, multinucleate myotubes, and this is accompanied by pronounced changes in the pattern of protein synthesis, most notably a several hundred-fold increase (Devlin & Emerson *Cell* **13**, 599; 1978) in the synthesis of actin, myosin and other myofilament proteins which assemble into sarcomeres. After some days, cultured myotubes are contractile and resemble terminally differentiated muscle fibres.

A central question concerning the mechanism of differentiation in this, or any, system, is how, and at what level are changes in gene expression regulated? Are the changes in protein synthesis a direct reflection of changes in the transcription of genomic DNA into RNA, or are there additional controls at the post-transcriptional level, that is, the processing of nuclear RNA into cytoplasmic messenger and its translation into protein? The answer may not be simple: multiple modes of regulation are indicated for muscle by a quantitative study by Devling and Emerson (*op. cit.*) on the pattern of post-fusion protein synthesis. Interestingly, expression of the major muscle proteins myosin (heavy and light chains), troponin and tropomyosin appears to be coordinately regulated, but a number of other muscle-specific, but mainly unidentified polypeptides exhibit different patterns of expression. Actin and myosin synthesis have, however, attracted the most attention and in the past, both transcriptional and post-transcriptional control mechanisms have been invoked to account for the immense proliferation of muscle myosin on cell fusion. More recent biochemical work (Strohman *et al. Cell* **10**, 265; 1977) and *in situ* hybridization experiments (John *et al. Cell* **12**, 501; 1977) on myosin mRNA show that, although some myosin message is present in prefusion myoblasts, the amount is greatly amplified in myotubes. This argues against the existance of a pool of stored message, but is consistent with either an increase in transcription on fusion, or an increase in the stability of message, as proposed by Buckingham *et al.* (*Proc. natn. Acad. Sci. U.S.A.* **71**, 1466; 1974).

An account of a much broader attack on the whole area of gene expression in muscle differentiation is given in two recent papers from Gros' laboratory at the Institut Pasteur (Affara *et al. J. mol. Biol.* **141**, 441; 1980; Affara *et al. J. mol. Biol.* **141**, 459; 1980). These describe experiments to monitor changes occurring during differentiation in the widest possible range of gene products, at three levels: in the nuclear RNA (nRNA), that is, at the level of transcription, in the cytoplasmic mRNA population and in the pattern of polypeptides synthesized. Cultured cells representing three different stages in mammalian myogenesis were employed in this study: an undifferentiated mouse embryonal carcinoma cell line, a mouse teratocarcinoma-derived myoblast cell line and myotubes formed *in vitro*. To compare the complexity of transcribed sequences at each stage of differentiation, Affara *et al.* hybridized excess total nRNA from each type of cell (undifferentiated, myoblast and myotube) to single-copy mouse DNA. The committed cells (myoblast and myotube) showed a 30% increase in the extent of hybridization over the carcinoma cells, implying that new DNA sequences are transcribed at this stage. The cytoplasmic mRNA (polysomal, poly A-containing mRNA) populations at each stage of differentiation were compared by hybridization experiments using complementary DNA (cDNA) probes for the mRNA from each cell type. It was thus shown that, although most mRNA sequences found in undifferentiated cells are still present in myoblasts and myotubes, at each stage in differentiation a new set of mRNAs enters the polysomes. Is the appearance of these messages under transcriptional control? cDNA probes enriched for myotube-specific sequences, or those common only to myoblasts and myotubes, were used to search for these sequences in nRNA. The results suggest that RNA found specifically in the polysomes of differentiated cells is absent from the nRNA of undifferentiated cells, implying that, in these cells, the corresponding genes are not transcribed. This conclusion was supported by testing the susceptibility of common and myotube mRNA-specific sequences in chromatin to nuclease attack; unexpressed genes are expected to show greater resistance than those transcribed (Weintraub & Groudine *Science* **193**, 848; 1976). Such an increased resistance was indeed found for myotube-specific genes in carcinoma cell chromatin, but not in myotube chromatin. It thus appears that the presence of new messages in the polysomes of myoblasts and myotubes is regulated at the level of trascription. However, because some RNA sequences common to myoblasts and myotubes, and present in similar amounts in the nuclei of both show increased abundance in myotube cytoplasm, the authors suggest that post-transcriptional factors may modulate the quantities of some polysomal mRNAs.

The next question addressed by Affara *et al.* is whether the new group of mRNAs which appear in the cytoplasm of myotubes are indeed translated, and whether they code for identifiable, muscle-specific proteins. The set of myotube-specific messages was purified by a hybridization technique and translated *in vitro*. Many of the polypeptides produced correspond to new proteins synthesized by myotubes *in vivo*. These included, most rewardingly, myosin light chains, muscle actin and troponin as major components, thus confirming that the expression of these proteins is regulated by the appearance of specific, new messages at cell fusion.

There are still some flaws in the experimental system of Affara and colleagues. Limitations in analytical

---

Harriet Harris is in the MRC Laboratory of Molecular Biology, Cambridge.

0028-0836/80/340758-02$01.00

technique (the cDNA probes are not pure; certain messages may not be efficiently translated *in vitro*) make it difficult to trace the expression of any particular gene from transcription to translation with any confidence. An increase in experimental resolution will be required to distinguish the relative contributions of transcription and message stability to the rate of synthesis of specific proteins. A further criticism concerns the validity of the teratocarcinoma cell line as a model for normal muscle development. Although most of the identified muscle-specific polypeptides produced by the myotubes were characteristic of fast skeletal muscle, the authors also noted production of embryonic myosin light chain and slow muscle troponin C, which implies that there are aberrations in the regulatory mechanisms of these cells. However, it is to be hoped that the experimental approach outlined in these papers will lay the foundations for a more detailed understanding of the mechanisms of myogenesis. ☐

Multiphoton ionization interference effects

from Peter Knight

DIFFERENCES between results and theory in multiphoton ionization experiments seem to have been resolved by a recent experiment of the Saclay group (Morellec *et al. Phys Rev. Lett.* **44**, 1394; 1980).

The ionization of atoms by the simultaneous absorption of several photons from an intense laser field has been the subject of intensive investigation recently, spurred on in part by the potential application to isotope separation. However, experiments and theory have been disagreeing by up to four orders of magnitude (*Nature* **270**, 561; 1977) even for the simplest example of non-resonant two-photon ionization of a simple alkali such as caesium. Calculations employing second-order perturbation theory all agree in predicting a deep interference minimum in the two-photon ionization cross-section of caesium at photon energies between 2.3 and 2.6 eV arising from cancellations of 6p and 7p intermediate state contributions. Experiments of Van der Wiel and colleagues (*J. Phys.* **B 8**, 1617; 1975) saw no such minimum, and their observed cross-sections were four orders of magnitude greater than expected from theory. Several attempts have since been made to explain this anomaly and the experiment of Morellec *et al.* seem to have resolved the problem by using a very much more intense laser than that of Van der Wiel.

Most workers in the field have suspected that an explanation of the discrepancy between theory and experiment was connected with the presence of a small number of alkali dimer molecules in the atomic beam target. To find the interference minimum is difficult experimentally: the atomic cross-section is (obviously) very small. On the other hand caesium molecules can ionize and produce a detector signal very easily in the wavelength range where the predicted atomic minimum should occur, since they possess many intermediate levels at the appropriate energies and can be reasonantly ionized. The molecules are in fact so easy to ionize that they can dominate the ionization rate even if their concentration is very low (a few percent) of the atomic concentration. Van der Wiel and his coworker did attempt to isolate and eliminate molecular contributions yet still found their anomalously high cross-sections survived.

The Saclay group have now attacked the dimer problem in two ways. First, they work at much higher intensities than Van der Wiel using a three-stage oscillator-amplifier dye laser pumped by the second-harmonic of a ruby laser. Their experiments could then be carried out using laser intensities of 10^{10} W/cm^2 compared with 10^5 W/cm^2 of Van der Wiel. Under such circumstances the resonant molecular ionization signal is saturated and is proportional to the intensity whereas the unsaturated atomic signal depends quadratically on the laser intensity and is easily distinguished from the molecular background. Secondly, the Saclay group performed their experiment with and without a caesium atomic beam superheater which efficiently dissociates dimers, and clearly see a reduction in the molecular component by more than an order of magnitude when the superheater is used. Using these two improvements together results in the atomic signal dominating the unwanted molecular signal in the 10-20 GW/cm^2 laser intensity range.

Two-photon ionization cross-section of Cs atoms as a function of photon energy and laser wavelength (from Morellec *et al. Phys Rev. Lett.* **44**, 1396; 1980). Triangles: experimental points of Van der Wiel normalized to new photoionization cross-sections; circles: experimental points of Morellec *et al.*; curves *a*, *b* and *c* are perturbative calculations noted in the text; curve *d* is a theoretical result incorporating laser bandwidths in a simple model of Armstrong and Eberly.

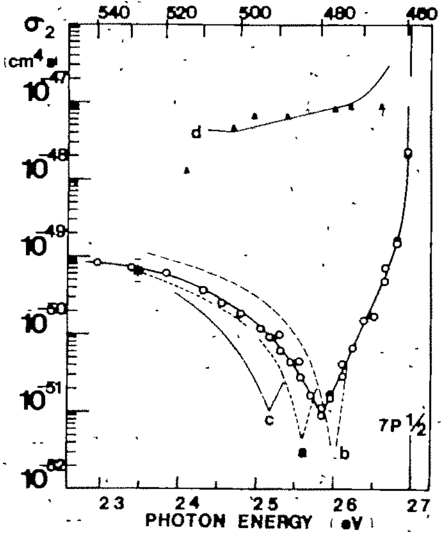

The Saclay results for the ionization count are converted into a value for the two-photon generalized cross-section σ_2 taking into account well-known multimode coherence effects. Their results for σ_2 are shown in the figure and compared with earlier results of Van der Wiel and various theroetical values. It is clear that the expected ionization minimum has been observed, with a reduction by two orders of magnitude in σ_2 in going from photon energies of 2.3 to 2.58 eV, and then a huge increase as the photon energy approaches the 7p$_{1/2}$ intermediate-state resonance. Curves *a*, *b* and *c* are all derived from second-order perturbation theory using different atomic calculational methods: curve *a* is due to Bebb (*Phys. Rev.* **149**, 26; 1966), curve *b* to Teague *et al.* (*Phys. Rev.* **A14**, 1057; 1976) and *c* to Rachman *et al.* (*Phys. Lett.* **68A**, 433; 1978). These second-order perturbative theories are in quite good agreement with each other and with the Saclay data, and disagree with the data of Van der Wiel *et al.* Curve *d* in the figure, due to Armstrong and Eberly (*J. Phys.* **B12**, L291; 1979), although agreeing with Van der Wiel's data, disagrees with the new results and the second-order theoretical results. Curve *d* is obtained by incorporating laser fluctuations into the ionization dynamics in a first approximation using a phase-diffusion model of the laser bandwidth. This clearly exaggerates the laser bandwidth in the wings of the laser line and over-emphasises fluctuations in a way anticipated by Armstrong and Eberly who are currently working on improved laser-bandwidth models. The conclusion is that for the system studied by the Saclay group, second-order perturbation theory is adequate, that the interference minimum is observed once precautions are taken to eliminate molecular background, and that the earlier experiments at lower intensity were probably limited by this molecular background. It looks as if the non-resonant multiphoton ionization of simple atoms is now fairly well understood. ☐

Peter Knight is in the Optics Section, Blackett Laboratory, Imperial College, London.

0028-0836/80/340759-01$01.00

The source of cells for regeneration

from J.M.W. Slack

A solution to the long standing problem of the source of cells for regeneration has been brought nearer by recent studies on planaria and the amphibian limb. The experiments use two techniques: X radiation doses which can inhibit cell division and regeneration without killing the tissues, and markers which allow the fate of cell populations to be followed.

Both planaria and the limb undergo 'epimorphic' regeneration in which a blastema consisting of cells which are visibly undifferentiated and indistinguishable from one another is formed at the wound site. The blastema cells first proliferate and then differentiate to reform the missing body part containing several different cell types.

The key questions are:— (1) Is the blastema formed (a) from cells drawn from all parts of the body, or (b) from tissues local to the wound? (2) Is the regenerate formed (a) by the *de novo* differentiation of reserve cells, or (b) by dedifferentiation and redifferentiation of functional tissue cells? (3) Is the blastema (a) a mixture of cells pre-committed to differentiate into particular cell types, or (b) composed of similar pluripotent cells able to become any of the cell types in the regenerate?

Although the questions are logically independent the discussion usually becomes polarised into an argument of 'neoblasts *versus* metaplasia'. 'Neoblast' is a term often used to indicate small basophilic cells present in planaria and other organisms, or sometimes in a special sense to indicate mobile pluripotential cells reserved for regeneration. 'Metaplasia' is the dedifferentiation of functional cells followed by redifferentiation of the cells or their progeny into a different histological type — for example transformation from myotube to chondrocyte. The 'neoblast *versus* metaplasia' argument thus corresponds to options 1a, 2a and 3b *versus* options 1b, 2b and 3b. Although the controversy has become fixed in this dichotomy, it must be remembered that other combinations of answers to the three questions are also possible.

J.M.W. Slack is in the Imperial Cancer Research Fund Laboratories, Mill Hill, London.

Planaria can regenerate from either an anterior or a posterior cut surface and contain scattered small basophilic cells which have been called neoblasts by many authors. Early experiments[1] showed that regeneration could be prevented by X-irradiation, but if the worm contained an unirradiated portion (either a shielded region or an unirradiated graft) then it could regenerate fully, even when the healthy portion was some distance from the level of amputation. The time taken for regeneration to begin increases with this distance and correlates with migration of the neoblasts through the intervening tissue.

This showed that a blastema can be formed from migratory cells and is capable of forming all the tissues of the regenerate. However, it did not exclude the possibility that the migratory cells were formed by dedifferentiation, or that in unirradiated worms differentiated tissues local to the wound can also contribute to the blastema. Indeed, histological and electron microscopic studies suggest that local dedifferentiation does occur[2].

Now studies have been published[3–6] on the regeneration of a strain of planaria which are naturally occurring mosaics: the somatic cells are triploid, the cells of the male germ line are diploid and the cells of the female germ line are hexaploid. Regeneration from the gonadless regions gives rise to worms whose somatic tissues consist wholly of triploid cells, whilst regeneration from a cut surface through the gonadal region gives rise to blastemas and regenererates containing some diploid and/or hexaploid cells. Of particular significance is that myotubes with diploid nuclei were found in the muscle of the regerated pharynx[6]. If germ cells and their precursors are accepted as *bona fide* differentiated cells then metaplasia has clearly occurred by the sequence: germ cell→ blastema cell→ muscle cell. However, it could be argued that the germ cells are a special case because in other circumstances they may exhibit pluripotency without passing through a sexual cycle, for example in mammalian teratocarcinoma. This objection might be overcome by building up stocks of worms whose somatic tissues are of an unusual ploidy so that metaplasia between different somatic tissues can be looked for.

Many species of urodele amphibia will regenerate limbs after amputation. The limb contains no small basophilic cells and the histology of the blastema suggests formation by dedifferentiation of muscle, cartilage and connective tissue. Amputation through a small X-irradiated region does not result in regeneration even when the remainder of the limb and the rest of the animal is unirradiated[7] so, in contrast to the planaria, it seems that a blastema cannot be formed without the participation of tissues local to the wound.

Recently studies on metaplasia have been carried out using axolotl tissues labelled by tritiated thymidine and triploidy[8–10] or pigmentation and allogenic differences leading to graft rejection[11,12]. Grafts of a particular marked tissue into an X-irradiated limb followed by amputation of the limb through the graft leads to the formation of a regenerate wholly composed of graft-derived cells, confirmed by the retention of the marker in the various cell types. The irradiated background tissue is necessary because although it does not contribute any cells to the regenerate it does contribute pattern information without which few structures are formed from a small graft[13].

The results are summarised in the Table below. It is clear that there is extensive metaplasia between the different internal tissues, which are all derived from the mesoderm of the embryo. However, epidermis never contributes to the internal tissues and vice versa, indicating the existence of a lineage restriction between tissues of different embryological origin.

So although there may be some restrictions on the possible interconversions, there is now good evidence from both planaria and the amphibian limb that some functional cell types can dedifferentiate and that their progeny can appear in the regenerate as different histological types. These results should be taken seriously by those who advocate theories of cellular differentiation based on irreversible events such as the chemical modification or rearrangement of DNA. □

Cell types found in regenerates formed from grafts of particular tissues.

	Grafted Tissue				
	ectodermally derived	mesodermally derived			
cell types in regenerate:	epidermis	dermis	muscle	cartilage	nerve (sheath)
epidermal	+	—	—	—	—
myotube	—	+	+	?	+
chondrocyte	—	+	+	+	+

•

+ marked cells are present, — marked cells absent,? conflict of results between laboratories.

1. Wolff, E. in *Regeneration* (ed. Rudnick, D.) 53-84 (Ronald Press Co., New York, 1962).
2. Hay, E.D. in *The Stability of the Differentiated State* (Springer-Verlag, Berlin/Heidelberg, 1978).
3. Gregmigni, V. & Puccinelli, I. *J. Exp. Zool.* **199**, 57 (1977).
4. Gregmigni, V., Miceli, C. & Puccinelli, I. *J. Embryol. Exp. Morph.* **55**, 53 (1980).
5. Gregmigni, V., Miceli, C. & Picano, E. *J. Embryol. Exp. Morph.* **55**, 65 (1980).
6. Gregmigni, V. & Miceli, C. *Wilhelm Roux's Archives* **188**, 107 (1980).
7. Butler, E.G. & O'Brien, J.P. *Anat. Rec.* **84**, 407 (1942).
8. Steen, T.P. *J. Exp. Zool.* **167**, 49 (1968).
9. Namewirth, M. *Dev. Biol.* **41**, 42 (1974).
10. Dunis, D.A. & Namenwirth, M. *Dev. Biol.* **36**, 97 (1977).
11. Wallace, H. *J. Embryol. Exp. Morph.* **28**, 419 (1972)
12. Maden, M. & Wallance *H. Acta Embryol Exp.* **2**, 77 (1975).
13. Maden, M. *J. Embryol. Exp. Morph.* **50**, 325 (1979).

0028-0836/80/340760-01$01.00

A glacial relict mollusc

from B. Coles and B. Colville*

THE mollusc *Vertigo genesii* (Gredler), thought to be extinct in Britain, has been found living in the Upper Teesdale National Reserve. *V. genesii* has a scattered distribution in Boreal and Arctic Europe where it lives in base-rich flushes of montane character[3,4] and is common in British deposits of late-glacial age (12,500 — 10,000 BP)[5,6].

The Upper Teesdale National Nature Reserve, UK, is well known for its exceptional flora, including a relict arctic-alpine element.[1] A similar faunal element has not been recognised although the Reserve contains invertebrates of rare occurrence in Britain.[2] The specimens were found, alive, in tufts of *Carex demissa* Hornem. (agg.) in the open parts of base-rich flushes on Widdybank Fell (450 m) in May 1979; their presence was confirmed in July of the same year. Mollusca associated with *V. genesii* were:— *Lymnaea truncatula* L., *Succinea pfeifferi* (Rossmässler) and *Nesovitrea hammonis* (Ström). Plants present were:— *Armeria maritima* Willd., *Plantago maritima* L., *Juncus triglumis L., Kobresia simpliciuscula* (Wahlen.), *Carex demissa* Hornem. (agg.), *C. panicea* L. and *Equisetum variegatum* Web. & Mohr. *Minuartia stricta* Hiern (which is probably the most notable plant of the Teesdale flushes, Teesdale being its only station outside the arctic circle) was not found at this site but the flush is otherwise typical of areas in Upper Teesdale where an arctic-alpine flora occurs. The occurrence of *V. genesii* in Upper Teesdale and its association with the relict arctic-alpine flora agrees well with the European distribution of the species. It is noteworthy that the associated Mollusca in Upper Teesdale were also common associates of *V. genesii* in the late-glacial.

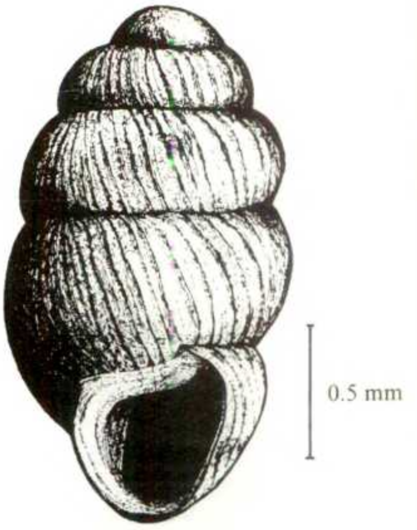

Vertigo genesii

---

1. For a summary of the natural history of Upper Teesdale see:— Clapham, A.R. Ed., Upper Teesdale, Collins, London (1978).
2. See Coulson, J.N. in chapter 8 of ref. 1.
3. Ehrmann, P. Die Tierwelt Mitteleuropas II, Weichtiere, Molusca, Quelle & Meyer, Leipzing (1933).
4. Zilch, A. and Jaeckel, S.G.H. Ergänzung Tierwelt Mitteleuropas Weichtiere, Mollusca, Quelle & Meyer, Leipzig (1962).
5. Kerney, M.P. Late-glacial deposits on the chalk of South-East England, Phil. Trans. Ser. B **246**, 203-254 (1963).
6. Kernev M.P. Brown, E.H. and Chandler, T.J. The Late-glacial and Post-glacial history of the chalk escarpment near Brook, Kent, Phil. Trans. Ser. B **248**, 135-204 (1964).

We would like to thank the Nature Conservancy Council and in particular J. P. Doody, for permission to do work in Upper Teesdale National Nature Reserve.

**Author's address: 27 Dove St., York.*

Sign, symbol and syntax in the language of apes

from Brendan O. McGonigle

TERRACE'S[1] recent criticism of evidence suggesting that apes can master "the conversational, semantic, or syntactic organization of language" has intensified a controversy spanning a century of speculation by primatologists. In the 19th century, several determined attempts were made to teach apes to talk but they were largely unsuccessful, only a few words being mastered by some animals. Later, Yerkes[2] identified part of the problem as the medium of communication. Apes would not mimic what they heard; instead their powers of imitation were heavily dependent on vision. Impressed by their intelligence, especially as a result of Köhler's now classic studies of insightful behaviour by chimpanzees[3], Yerkes suggested that apes "might be taught to use their fingers, somewhat as does the deaf and dumb person, and thus helped to acquire a simple, non-vocal 'sign language' ".

More than 40 years later this suggestion was put to the test[4] when a young chimpanzee, Washoe, was trained by the Gardners on a form of manual-visual communication claimed to be a version of American sign language (ASL). By the third year of the project, Washoe had acquired a stable repertoire of some 85 signs of which a number were used in two sign combinations in a manner compatible with that reported for children[5]. In addition, Washoe invented a number of signs of her own. A striking case was *bib* whose ASL equivalent was not known to her trainers when it was first introduced (appropriately) by the chimp. In later tests the Gardners monitored Washoe's capacity to answer 'wh' questions (who, what, where, whose) the production of which constitutes the first evidence that children have grammatical competence[5]. With various simplification procedures for analysing their data (now contentious) the Gardners found that the question frames exerted a very high control over the replies as indexed by the grammatical appropriateness of the answers. In carrying out the tests the Gardners relied on productive (making the chimp formulate a reply in terms not given in the question) rather than comprehension tests which "effectively eliminates the problem of clever Hans cueing".

Despite its apparent scientific rigour, the work has had its critics. In a recent attack, Seidenberg and Petitto[6] claim that Washoe's signing does not resemble signing in ASL in any important way. Instead, they allege that a large proportion of ape signs can be interpreted without any special knowledge of apes or ASL and form part of a repertoire of unlearnt gestures. These authors also challenge the Gardners' method of simplifying or reducing the replies of Washoe to 'wh' questions before reporting them. Amongst those deleted were signs which were repetitious of those in a question and signs which were repeated during a reply. The effect is to trim a response such as *you me you out me* to *you me* thus giving the utterance a more humanlike form — a possibly serious distortion in their view. By contrast, children in the early stages of language acquisition "typically produce utterances which are reduced relative to the corresponding adult forms, leading to the characterization of their speech as telegraphic".

Terrace and his associates have also found evidence for redundancy in the signing of their chimpanzee Nim, trained like Washoe in what is in fact Pidgin Sign English (PSE). Some utterances contained as many as 16 signs issued in "a striking, redundant, recursive string". In analysing the relationship between 2, 3, and 4 sign combinations, moreover, Terrace has found a major difference between Nim and children. When making longer utterances the child deletes repeated elements and expands on the information given in the shorter utterance. By contrast Nim's additions to the two sign utterances tended to be redundant, for example, "play me", "play me Nim" or repetitious, for example, "eat Nim eat". Terrace suggests that the purpose of three sign combinations by Nim is to add emphasis rather than convey new information.

The really significant findings in the report by Terrace *et al.* which

Brendan O. McGonigle is in the Department of Psychology, University of Edinburgh, Scotland.

0028-0836/80/340761-02$01.00

indicate that Nim has little language ability are the following. (i) An increase in vocabulary to 125 signs during the course of the training programme did not result in a related expansion in the mean length of utterance (MLU). This remained fairly stable over the course of the programme. (ii) There was little originality in Nim's utterances. A high percentage (87%) were classifiable as 'adjacent' (i.e. following the teacher's utterance without a definite pause) and a large percentage of these (~ 40%) were either imitations or 'reductions' (containing some of the utterances of the teacher and nothing else). (iii) Nim showed little evidence of the 'turn-taking' strategy which characterizes human conversation. Instead a large majority of his signs overlapped with those of his teachers — most of them interruptions which could not be construed as attempts to 'take the floor'.

To check that Nim was not an atypical case, Terrace *et al.* have analysed two films of Washoe which also include signing behaviour by Ally (Nim's full brother) and Koko, a gorilla[7]. Their analysis shows they claim that "Washoe's utterances were adjacent and imitative of her teachers' utterances . . . ninety-two percent of Ally's, and all of Koko's, signs were signed by the teacher immediately before Ally and Koko signed".

The Gardners hotly deny that Terrace's analysis is accurate, claiming instead that single frame and slow-play analyses misrepresent and distort the record. They also draw attention to the fact that Washoe frequently signed to herself when she was unaware of an observer, or when looking at pictures in magazines[4]. As things stand it will be some time before the technical and the statistical issues raised by Terrace's analysis can be resolved.

One conclusion which does emerge, however, is that where there is suspicion that some of an ape's signs are merely imitative of an earlier use in the same test by the teacher, the use of syntactic criteria including word order may reduce the danger of 'over-attribution' by the experimenter. To use these criteria it would be necessary to establish that the constituents of any utterance had particular meanings when presented in isolation, that signs in different linear combinations had different meanings, and that each order structure is not specific to a unique combination of signs. So far none of the chimpanzee language projects appear to have met all of these criteria — at least within the same study. Premack[8], who trained a chimp, Sarah, using an artificial language based on plastic symbols claims that "chimps can be taught word order but only with explicit training . . . ". He found no evidence that Sarah could produce structural innovations, although he claims she converted the trainer's (production) order of symbols and "produced sentences by systematic rearrangement . . .". On this latter point, however, he offers no evidence. As for word understanding, the use of too few alternatives in the tests employed frequently leads to ambiguity as to what the chimp has understood. (For instance, the preposition *on* was taught in isolation such that word order was always a simple clue to the subject-object relationship specified. It would not have been had this preposition been contrasted with *under*).

Stronger evidence for grammatical competence comes from Project Lana[9] where chimps have been trained to use lexigrams from a language called Yerkish. A computer monitors the productions of the subject — achieved by depressing keys — which must conform to the rules of a correlational grammar before any requests can be honoured, e.g. *Please machine give chow period*. The words *please* and *period* are fixed features of the sentence frame to enable the computer to determine the beginning and the end of an utterance. Examination of the performance of the subject Lana over one month of training revealed that she composed on her keyboard "76 strings of 6 lexigrams that were grammatical sentences and that did not figure in any training programme, whereas during the same period she produced only 71, 6-lexigram strings that were ungrammatical"[10]. Clearly there is evidence here of innovation. However, the analysis did not include consideration of the communicative or the contextual appropriateness of these grammatical strings and it seems likely that not all of the constituent lexigrams in the strings carried an independent meaning for Lana. For example, *please* is an invariant feature of a sentence frame necessary to get the computer to accept a message. It is improbable, as Seidenberg and Petitto[6] point out, that the appropriate depression of this key suggests that the ape has a sense of politesse. More recent work on this project has shown, furthermore, that apes begin to use individual lexigrams as referents for objects and actions after they are able to produce ordered sequences of them to produce food. The apparent ordering of signs must be rigorously analysed to determine the extent to which the sequences are controlled simply by lexical order rules independent of their (constituent) meaning.

Issues of syntax apart, it seems pertinent to ask what apes tutored in these various 'languages' have revealed about their mentation which could not be inferred from other aspects of their behaviour. The results thus far are ambivalent. On the one hand the content of ape language merely reaffirms the narrow incentive range within which the chimp seems to operate in laboratory situations. His favourite words seem to be those which invite the listener to donate food or drink, or which command attention (although this pattern may change when more work is carried out with mature subjects). On the other hand, the restrictions on semantic role which Terrace describes in the case of Nim (indexed by a marked restriction on the range of agents and beneficiaries, e.g. NIM, me, you and the names of other animates) are symptomatic perhaps of an egocentric form of thought — a characteristic of early stages of child development according to Piaget — not easily revealed by non-verbal tests. The response of apes to attempts to teach them the spatio-temporal conventions for reference to objects and events outside the immediate context of utterance should provide further important clues to the cognitive resources available to these enigmatic primates. □

---

1. Terrace, H.S., Petitto, L.A., Sanders, D.J. & Bever, T.G. *Science* **206**, 891 (1979).
2. Yerkes, R.M. *Almost Human* (Jonathan Cape, New York, 1925).
3. Köhler, W. *The Mentality of Apes* (Liveright, New York, 1925).
4. Gardner, B.T. & Gardner, R.A. *J. exp. Psychol.* **104** 244 (1975).
5. Brown, R. *A First Language: the Early Stages* (George Allen and Unwin, London, 1973).
6. Seidenberg, M.S. & Petitto, L.A. *Cognition*, 7, 177 (1979).
7. Patterson, F. *Brain and Language* **5**, 72 (1978).
8. Premack, D. *Intelligence in Ape and Man* (Lawrence Erlbaum Associates, Hillsdale, N.J., 1976).
9. Rumbaugh, D.M. *Language Learning by a Chimpanzee: The Lana Project* (Academic Press, New York, 1977).
10. Von Glasenberg, In *Language Learning by a Chimpanzee* (Ed. Rumbaugh, D.M.) (Academic Press, New York, 1977).

100 years ago

HUMAN HYBERNATION

In the *Transactions* of the Royal Society Dr. W. Oliver has recorded the history of an extraordinary sleeping person named Samuel Chilton of Tinsbury, near Bath, who on May 13 1694, being then 'of robust habit of body, not fat, but fleshy, and a dark brown hair," happened, without any visible cause or evident sign, to fall into a very profound sleep, out of which no art used by those who were near him could rouse him until after a month's time; then he rose of himself, put on his clothes, and went about his business of husbandry as usual; slept, could eat and drink as before, but spoke not one word till about a month after. In 1696, on the 9th of April, this youth fell off to sleep again, and although a heroic apothecary, Mr. Gibbs, bled him, blistered him, and scarified him, he slept on for seventeen weeks, waking up on August 7, not knowing he had slept above a night, and unable to be persuaded he had lain so long, until going out into the fields he found everybody busy getting in the harvest, and then remembered very well that when he fell asleep they were sowing of the barley and oats which he now saw ripe and ready to be cut down. For six weeks of this sleep he had fasted, but after he awoke he went to work in his ordinary way, and continued to work until August 17, 1697, when, after complaining of shivering and cold in his back, and vomiting once or twice, he fell into one of his long sleeps once more. So he lay sleeping until November 19, when he awoke, said he "felt very well, thank God," ate some bread and cheese, and dropping off still another time, slept on until the end of January, 1698, and "then waked perfectly well, not remembering anything that happened all this while."

REVIEW ARTICLE

Nucleosome assembly

Ronald A. Laskey & William C. Earnshaw
MRC Laboratory of Molecular Biology, Hills Road, Cambridge CB2 2QH, UK

Histones and DNA can spontaneously associate to form the nucleosome subunits of eukaryotic chromatin, but two proteins which occur in the eukaryotic nucleus can facilitate nucleosome assembly and greatly extend the conditions which permit assembly to occur. Recently several laboratories have reported new experimental systems which help to analyse, reconstruct and exploit the cellular mechanisms of chromatin assembly.

IN eukaryotic nuclei DNA is packaged into regularly repeating nucleoprotein units called nucleosomes. The structure of the nucleosome has been reviewed extensively[1–4] and the major features of the prevailing model[5] are summarized in Fig. 1. Two structural domains have been distinguished by nuclease digestion, a protected nucleosome core and an exposed linker DNA segment of variable length. The nucleosome core consists of 146 base pairs of DNA coiled around a central histone octamer containing two each of the histones H2A, H2B, H3 and H4. Histone H1 associates with a further 20 base pairs of DNA adjoining the core, to complete two full superhelical turns of 80 base pairs each around the histone octamer[6,7]. In addition to this simple repeating structure chromatin possesses a complex range of local variations in the distribution of nonhistone proteins[8,9].

Studies of chromatin assembly have been directed both at determining the pathway of nucleosome assembly and also at analysing the functional significance of variations in chromatin structure. Chromatin assembly by dialysis against gradients of salt under nonphysiological conditions (starting at >1 M NaCl) has produced information about nucleosome structure, but attempts to attach biological significance to the assembled structures have been repeatedly confused by artefacts (reviewed in refs. 2–4).

Recently several new experimental systems for assembling nucleosome cores or nucleosomes at physiological ionic strength have been described. They fall into three classes: (1) self-assembly systems[10,11] in which histones and DNA associate without assembly factors; (2) factor mediated assembly systems in which assembly is facilitated by purified assembly factors[12,13]; and (3) unfractionated cell homogenates[14–16] which attempt to mimic the cellular processes and which can be fractionated further to elucidate the cellular mechanisms of chromatin assembly. All three classes will be considered here, together with investigations of assembly of replicating chromatin in intact cells. At present only the unfractionated cell homogenates have been able to reconstitute the physiological spacing between adjacent nucleosomes.

Self-assembly of the nucleosome core

Histones and DNA contain the morphogenetic information required to assemble a nucleosome core. This has been clearly demonstrated by the reconstitution of nucleosome cores by salt gradient dialysis from approximately 1 M NaCl (refs 17–21).

Although the capacity for self assembly was readily demonstrated at unphysiological salt concentrations, it has only recently been observed at ionic strengths close to physiological. Ruiz-Carrillo *et al.*[10] renatured core histones into H3/H4 tetramers and H2A/H2B dimers by prolonged dialysis and slowly pumped the histones into an excess of DNA at 0.2 M NaCl. The product was shown to be authentic nucleosome cores[10] (Fig. 2). If histone H1 was included a precipitate formed. This could be redissolved by dialysing the precipitate to lower salt concentrations (10–30 mM). In a second study by Stein *et al.*[11] the core histones and DNA were mixed more abruptly. A precipitate formed, but redissolved during 16 h at 37 °C, to reveal substantial formation of nucleosome cores. In both cases excess histones caused irreversible precipitation.

Although these two assembly procedures[10,11] are limited in the conditions which yield soluble products rather than insoluble precipitates, they clearly establish the principle that nucleosome cores can self-assemble from histones and DNA in the absence of other factors.

Nuclear proteins which facilitate nucleosome core assembly *in vitro*

Two proteins from the eukaryotic nucleus allow nucleosome core assembly to proceed rapidly *in vitro* without precipitation. One appears to interact with DNA and the other with histones. They are respectively DNA topoisomerase I (nicking-closing enzyme)[13] and nucleoplasmin, an acidic thermostable protein which was originally isolated from *Xenopus* eggs[12].

The assembly pathway mediated by DNA topoisomerase I involves making a complex between topoisomerase I and DNA and then adding histones[13]. Approximately one topoisomerase I molecule is required for each nucleosome assembled, corresponding to 20 times more of the enzyme than would relax the same weight of supercoiled DNA. Assembly is inhibited when the weight of histones exceeds the weight of DNA. It is not clear yet if topoisomerase I acts by decreasing the electrostatic attraction between DNA and histones (see below) or by performing some additional function such as providing a swivel. DNA topoisomerase I occurs at substantial concentrations in the chromatin of a wide range of eukaryotes. Its properties and distribution have been reviewed elsewhere[22].

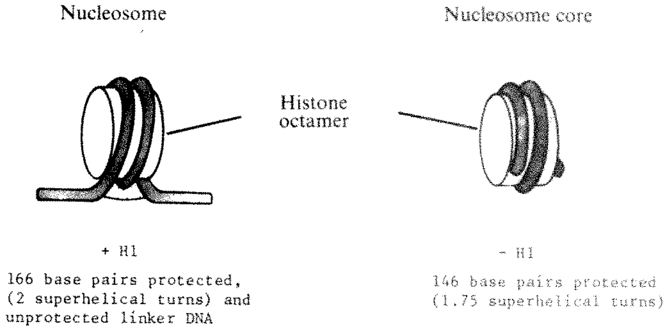
Nucleosome
Nucleosome core
Histone octamer
+ H1
166 base pairs protected, (2 superhelical turns) and unprotected linker DNA
- H1
146 base pairs protected (1.75 superhelical turns)

Fig. 1 A model for the structure of the nucleosome[5,6] and nucleosome core[5], in which DNA is wrapped around the surface of a flat protein cylinder consisting of two each of histones H2A, H2B, H3 and H4 (refs 1–4).

0028-0836/80/340763—05$01.00

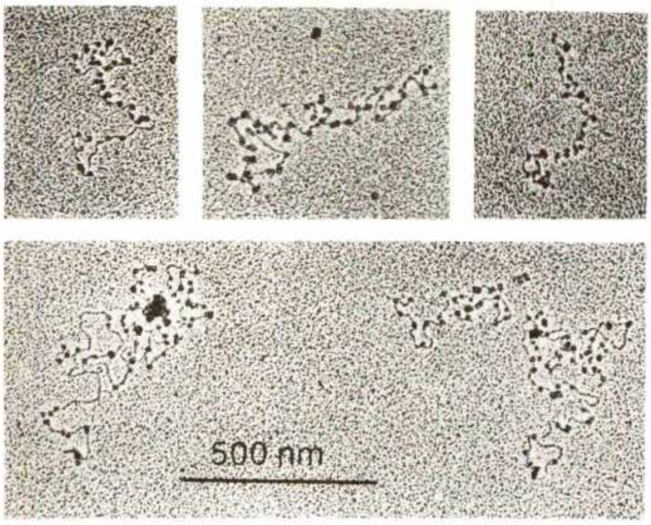

Fig. 2 Electron micrograph of nucleosome cores assembled by very slowly pumping core histones (without H1) into excess DNA at physiological ionic strength. Reproduced with permission from ref. 10.

Fractionation of a cell-free nucleosome assembly system[14] from eggs of *Xenopus laevis* led to the identification and purification of an acidic, thermostable protein which facilitates nucleosome core assembly *in vitro* when histones and DNA are rapidly mixed[12]. The protein is rich in potentially charged amino acids (notably 30% Asx + Glx)[23]. It is phosphorylated[24,25] and it has an isoelectric point of 5 (ref. 26). In solution it is an unusual multimer, a pentamer of the $M_r = 29{,}000$–$30{,}000$ subunits, and this pentamer is active in nucleosome core assembly[27]. The protein does not bind detectably to DNA or nucleohistone[27] but it does bind histones *in vitro*[12,27]. Its activity is independent of DNA topoisomerase[12,23,27], and the properties of the protein, which itself has no associated topoisomerase activity, are strikingly different from known DNA topoisomerases[22]. Unlike DNA topoisomerase I it can mediate nucleosome core assembly in the presence of excess histones[12,27].

Recently this protein has been shown to be the most abundant protein in the *Xenopus* oocyte nucleus, occurring at about 5 mg ml^{-1} and representing 7.5–10% of the total nuclear protein[24–26]. It is localized in the nucleoplasm[24–26] and using a combination of immunofluorescence and immunoprecipitation, Krohne and Franke have shown that this, or a conserved, antigenetically related protein, occurs at substantial concentrations in the nucleoplasm of a wide range of vertebrate cell types[25] (Fig. 3). The probable reason why it had not been observed in nuclei previously is rapid leakage from nuclei in aqueous isolation buffers[24–26]. Thus it was first discovered in total homogenates of cells in meiotic metaphase[12]. With the agreement of Krohne and Franke we propose to call this protein 'nucleoplasmin' reflecting its unusual intracellular location.

Although it is not clear if nucleoplasmin is tightly bound to the histone pool of *Xenopus* oocytes[24,25] its ability to bind histones *in vitro* led to the suggestion that it assembles nucleosomes *in vitro* both by neutralizing electrostatic repulsion between histones thus promoting histone:histone interactions, and also by acting as a 'molecular chaperone' which competes against the strong electrostatic attraction between histones and DNA, thus minimizing nonspecific insoluble aggregates[12,27].

These interpretations are consistent with the observations of Stein *et al.*[11] that polyglutamic and polyaspartic acids can also greatly facilitate nucleosome core assembly when used in the conditions described for nucleoplasmin. In additon Stein *et al.*[11] showed that polyglutamic acid causes histones to associate to form stable octamers in the absence of DNA and at physiological ionic strength. These observations may partly explain the mechanism of nucleosome core assembly by nucleoplasmin *in vitro*.

Although nucleoplasmin assembles nucleosome cores *in vitro*, the possibility that *in vivo* it performs a wider role of mediating between the many highly charged components of the nucleus deserves investigation.

The methods for assembling nucleosome cores *in vitro* at physiological ionic strength are summarized in Table 1. From a comparison of the methods the following principles emerge. First the steric information for self-assembling a nucleosome core resides in histones and DNA themselves. Second nonspecific electrostatic interactions between histones and DNA or between histones and nucleosomes[28,29] can result in insolubility of the product. This problem can be minimized by careful control of the experimental conditions, but it is accentuated by the presence of histone H1 or excess free histones. Third, the problem of solubility can be avoided by using 'assembly factors'. Fourth, these may act in different ways. Thus DNA topoisomerase interacts with DNA permitting subsequent ordered interaction with histones while nucleoplasmin and polyglutamic acid or polyaspartic acid appear to promote histone:histone interactions and do not interact directly with DNA. The simplest unifying hypothesis appears to be that the assembly factors described so far act *in vitro* by competing against or masking the strong electrostatic interaction between histones and DNA thus allowing self assembly to occur without aggregation and precipitation. Although it is possible that the assembly factors are recycled there is no evidence that they act truly catalytically or that they contribute steric specificity to the assembly pathways.

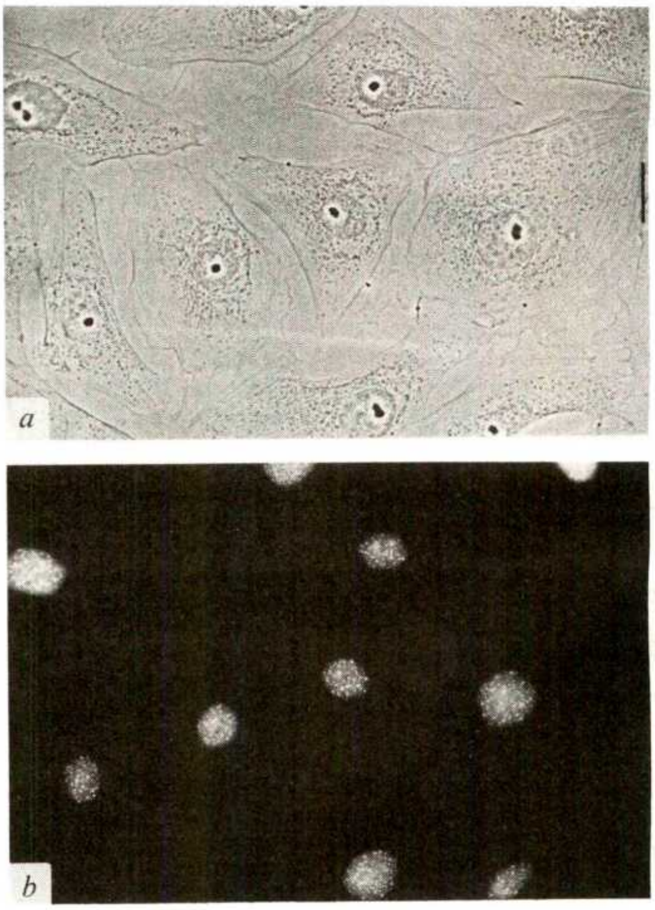

Fig. 3 Phase contrast (*a*) and immunofluorescence microscopy (*b*) of rat kangaroo cells incubated with antiserum raised against nucleoplasmin from oocyte nuclei of *Xenopus laevis*. The cells all show a strong and specific staining of their nuclei. Scale bars, 20 μm. Photograph supplied by G. Krohne and W. Franke (see refs 24 and 25).

Table 1 Methods for assembling nucleosome cores *in vitro* using purified reagents at physiological ionic strength

Method	Normal location	Approximate weight ratios	Time to completion	Product characterization†	Reference to method
Without assembly factors:					
(1) slow pumped addition of histones to excess DNA		1 DNA ≤1 core histones	2–5 h*	*A–E*	10
(2) rapid mixing		1 DNA ≤1 core histones	16 h (precipitates and redissolves slowly)	*A–C*	11
With assembly factors:					
Factor	Normal location				
(1) DNA topoisomerase I	Chromatin (eukaryotes)	1 DNA ≤1 core histones 0.4 topoisomerase I	<1 h	*A–D*	13
(2) Nucleoplasmin	Nucleoplasm (amphibians, birds, mammals, possibly elsewhere)	1 DNA 2 core histones 3–4 nucleoplasmin	<1 h	*A–C*	12
				D–E	27
(3) Polyglutamic acid	Synthetic	1 DNA 2 core histones 3–4 polyglutamic acid	~5 min	*A* and *F*	11

* Precipitates when histone H 1 is present.

† Key to product characterisation: *A*, Electron microscopy; *B*, supercoiling; *C*, sedimentation; *D*, digestion by micrococcal nuclease; *E*, digestion by DNase I; *F*, protein cross-linking

Cellular mechanism of nucleosome assembly

There is no direct evidence yet that either DNA topoisomerase I or nucleoplasmin is involved in the cellular mechanism of nucleosome assembly. However, the following observations are consistent with their involvement. First, both proteins occur in the nucleus at concentrations sufficient to assemble nucleosome cores *in vitro*. Second, when naked DNA is introduced into *Xenopus* oocyte nuclei or into eggs which are in meiotic metaphase it is rapidly relaxed by high concentrations of topoisomerase before it is assembled into nucleosomes[14,30]. Third, eggs of *Xenopus laevis* contain a large histone pool, sufficient for 20,000 diploid nuclei[31,32] and of the assembly methods described above only nucleoplasmin (or polyglutamic and aspartic acid) allows nucleosome assembly and chromatin solubility in the presence of excess histones[10,11]. Fourth, the endogenous histones in *Xenopus* egg homogenates exhibit anomalous charge properties, adsorbing to positively charged but not negatively charged resins at neutral *p*H suggesting that they are bound in a complex with a net negative charge. Purified nucleoplasmin mimics this effect when mixed with histones[27]. Finally, the rate of nucleosome core assembly by purified nucleoplasmin is similar to the rate in unfractionated homogenates and is sufficient to account for the rapid rate of nucleosome assembly in the early *Xenopus* embryo[27].

Recent work of Nelson *et al.*[16] suggests that *Drosophila* embryos may contain yet another nucleosome assembly factor. Although it has not yet been characterized, it seems to differ in some of its properties from either nucleoplasmin or DNA topoisomerase I. It will be interesting to see if it is related to a polypeptide, 'X', which Worcel *et al.*[33] observed associated with nascent nucleosomes in cultured *Drosophila* cells. In the same study[33] newly replicated DNA was observed to associate stably with H3 and H4 2–10 min before it associated stably with H2A and H2B and 10–20 min before it associated with H-1. A similar sequence of events has been deduced for mouse hepatoma cells[34] and replicating SV40 chromatin[35]. Ruiz-Carrillo *et al.*[10] have shown that a similar sequence of additions can be used to assemble nucleosomes *in vitro*. While this sequence of histone depositions may be widespread, it is not clear if it is essential *in vivo*. Thus the time course of histone depositions described by Worcel *et al.* is unlikely in early *Drosophila* embryos where the entire interphase of the cell cycle lasts only 3.4 min[36,37] shorter than the lag between depositions of different histones observed by Worcel *et al.* From *in vitro* studies there is evidence that nucleosomes can be assembled by interaction of DNA with either preformed histone octamers[11,29] or dissociated dimers and tetramers[10]. It is possible that the multiple nucleosome assembly pathways *in vitro* reflect multiple alternative pathways in the cell, which would not be surprising if the problem of assembling nucleosome cores correctly involves simply limiting electrostatic interactions between histones and DNA to localized regions, nucleosomes, and preventing indiscriminate electrostatic cross-linking leading to precipitation.

An aspect of nucleosome assembly *in vivo* which we have not considered above is the role of transient post-translational histone modifications seen in newly synthesized histones[38–40]. Since nucleosome cores can be assembled efficiently *in vitro* from unmodified histones (Table 1) it is tempting to speculate that the modifications might have an alternative role such as specifying the periodicity between adjacent nucleosomes in chromatin.

Assembly of regularly spaced chains of nucleosomes

Nucleosome cores are not distributed randomly along DNA, but are spaced at regular intervals of approximately 200 base pairs[41,42]. The average length of the linker DNA varies between different cell types so that the nucleosome repeat length ranges from about 160 base pairs in fungi and rabbit cortical neurones to 241 in sea urchin sperm[43–47].

However none of the purified *in vitro* assembly systems listed in Table 1 has reproduced the native spacing. They either space nucleosomes randomly or at intervals which are shorter than those from the parent native chromatin[10,13,27]. In contrast, as seen in Fig. 4, the unfractionated cell-free assembly system from *Xenopus* eggs spaces nucleosomes regularly at about 195 base pairs[14] and the same has recently been shown for an unfractionated assembly system from *Drosophila* embryos[16]. The mechanism which specifies the length of the internucleosome linker is unexplained but some models can be firmly eliminated. First, the correct spacing does not arise by copying the spacing on a parental molecule. It can arise *de novo* on naked DNA[14,16] (Fig. 4). Second, it does not require DNA replication or the discontinuous synthesis of Okazaki fragments since it can occur in the absence of DNA replication[14]. Third, it is unlikely to arise from a conserved periodic signal in DNA since spacing is observed on reconstituted prokaryotic templates (ref. 16 and W.C.E. unpublished observation) which are not naturally assembled into nucleosomes. On the other hand, it seems possible that it may be mediated by transient nucleosome sliding since it occurs in circumstances where assembly appears to be non-cooperative[14], suggesting that a mechanism must exist for correctly aligning randomly deposited nucleosomes. So far correct inter-nucleosome spacing has only been observed in assembly systems which use an endogenous stored histone pool, namely egg extracts from *Xenopus* and *Drosophila*[14,16]. Woodland[48] has shown that the stored histones of *Xenopus* eggs have secondary modifications characteristic of newly-synthesized histones in somatic cells, which raises the possibility that the transient histone modifications may be the missing ingredient required to achieve correct spacing in purified assembly systems. This hypothesis can be tested, and with the emergence of evidence suggesting that nucleosomes have specific phase-relationships with some DNA sequences[49–55] there is an obvious need to develop purified assembly systems which position nucleosomes precisely on DNA.

Relationship of nucleosome assembly to DNA replication

Nucleosomes persist in the region of replication forks and both daughter DNA duplexes are rapidly converted to nucleosomes[56–60]. By labelling nascent histones with dense amino acids and ^{3}H-lysine, Leffak *et al.*[61] have shown that parental histone octamers segregate conservatively to one of the daughter duplexes and that groups of parental nucleosomes segregate together. There is disagreement, however, over the site of assembly of new nucleosomes. Studies in which newly replicated chromatin is density-labelled by dense thymidine analogues, then fixed in formaldehyde and separated from bulk chromatin on the basis of its greater density have repeatedly suggested that new histones associate with unreplicated DNA[62–64]. In contrast, studies which have fractionated nascent chromatin from bulk chromatin by sedimentation avoiding the use of dense thymidine analogues or formaldehyde fixation have suggested that new histones are deposited at or near the replication fork[33,35]. Additional support for the view that new nucleosomes form on newly replicated DNA comes from experiments in which protein synthesis is inhibited by cycloheximide[65]. Here putative replication forks can be observed in which one of the daughter duplexes is fully assembled into nucleosomes while the other appears to be naked DNA. This suggests that parental nucleosomes pass to one of the daughter duplexes leaving the other as the site for new nucleosome formation. One of the two newly synthesized strands (the lagging strand) at a replication fork is synthesized discontinuously in Okazaki fragments (reviewed in ref. 66), and Seidman, Levine and Weintraub[67] have argued that this strand is probably the site of new nucleosome formation (Fig. 5). Although the discontinuous synthesis of DNA is not necessary to specify the spacing between adjacent nucleosomes (see above), a more attractive possibility is that the repeating nucleosome structure of chromatin may specify the periodicity of Okazaki fragments with replication proceeding by unfolding one parental nucleosome at a time[68].

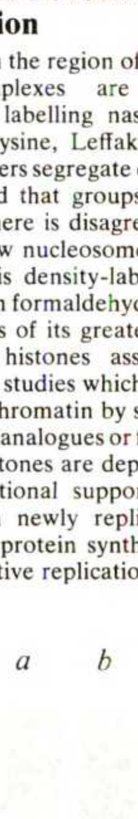

Fig. 4 Assembly of regularly spaced chains of nucleosomes by incubating ^{32}P DNA in homogenized eggs of *Xenopus laevis* (as in ref. 14). *a*, The chromatin assembled *in vitro* was cleaved with micrococcal nuclease deproteinized and electrophoresed in a 1.7% agarose gel. *b*, DNA fragments cleaved from rat-liver nuclei by micrococcal nuclease and ^{32}P-labelled by nick translation were electrophoresed on the same gel to show nucleosome spacing at 195 base pairs.

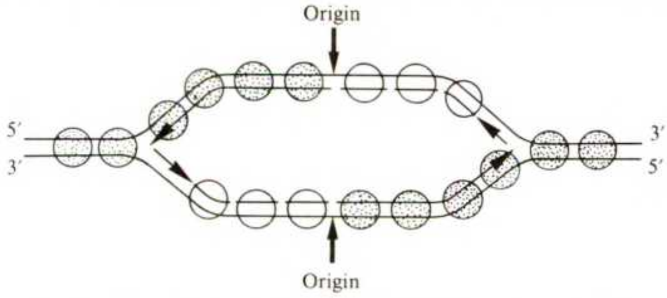

Fig. 5 A model for segregation of nucleosomes at replication forks proposed in ref. 67. Parental nucleosomes (stippled) segregate conservatively to the daughter DNA duplex containing the continuously synthesized strand, while new nucleosomes (unstippled) are assembled on the daughter duplex which is synthesized discontinuously in Okazaki fragments. Arrows indicate the direction of DNA strand growth. While this model is attractive, it is still opposed by some studies (see text).

Assembly of transcriptionally active nucleosomes

Digestion with nucleases indicates that transcriptionally active regions of chromatin are organized into nucleosome-like structures but that these have a different conformation from bulk chromatin (reviewed in refs 2–4). Regions of chromatin which code for RNA in a particular cell type are selectively sensitive to digestion by DNase I[69,70] or DNase II[71]. The degree of DNase I sensitivity is the same whether the gene is transcribed occasionally or frequently[72] suggesting that this altered conformation is a property of all genes which are competent to be transcribed. The boundaries of DNase I sensitive regions are precise[54,73] and the active conformation appears to correspond to elevated levels of two non-histone proteins HMG 14 and HMG 17[74,75] of the 'high mobility group'[76]. Furthermore Weisbrod and Weintraub[75] have shown that these two proteins can restore DNase I sensitivity to salt-washed chromatin or nucleosome cores[77], indicating that the nucleosomes from which they were eluted contain an additional structural peculiarity apart from HMG 14 and 17. This could either be the presence of an additional modification or factor specifying the sites to which HMG 14 and 17 should bind, or alternatively the lack of a normal nucleosome component which competes with HMG 14 and 17 for occupation of a site within the nucleosome.

How does such a structure originate? Weintraub has shown that the DNase I sensitive structure arises within 3 min of replication of that region of DNA, suggesting that the decision to assemble potentially active or inactive chromatin occurs at the time of DNA replication[60]. Therefore our understanding of the differentiation of somatic cells would be substantially enhanced by a knowledge of the mechanisms which assemble newly replicated DNA into transcriptionally competent nucleosomes and of the regulatory mechanisms which rigorously select specific regions of the genome for assembly into the active conformation. The *in vitro* nucleosome assembly systems which have been reviewed here are ideally suited for investigating these questions.

We thank C. Dingwall, J. Gurdon, R. Harland, A. Klug, J. Thomas, and S. Weisbrod for comments on the manuscript.

1. Kornberg, R. D. *A. Rev. Biochem.* **46,** 931–954 (1977).
2. Felsenfeld, G. *Nature* **271,** 115–122 (1978).
3. Chambon, P. *Cold Spring Harb. Symp. quant. Biol.* **42,** 1209–1234 (1978).
4. Lilley, D. M. J. & Pardon, J. F *A. Rev. Genet.* **13,** 197–233 (1979).
5. Finch, J. T. *et al. Nature* **269,** 29–36 (1977).
6. Thoma, F., Koller, Th. & Klug, A. *J. Cell biol.* **83,** 403–427 (1979).
7. Simpson, R. T. *Biochemistry* **17,** 5524–5531 (1978).
8. Mayfield, J. E., Serunian, L. A., Silver, L. M. & Elgin, S. C. R. *Cell* **14,** 539–544 (1978).
9. Elgin, S. C. R. & Weintraub, H. *A. Rev. Biochem.* **44,** 725–774 (1975).
10. Ruiz-Carrillo, A., Jorcano, J. L., Eder, G. & Lurtz, R. *Proc. natn. Acad. Sci. U.S.A.* **76,** 3284–3288 (1979).
11. Stein, A., Whitlock, J. P. & Bina, M. *Proc. natn. Acad. Sci. U.S.A.* **76,** 5000–5004 (1979).
12. Laskey, R. A., Honda, B. M., Mills, A. D. & Finch, J. T. *Nature* **275,** 416–420 (1978).
13. Germond, J. E., Rouviere-Yaniv, J., Yaniv, M. & Brutlag, D. *Proc. natn. Acad. Sci. U.S.A.* **76,** 3779–3783 (1979).
14. Laskey, R. A., Mills, A. D. & Morris, N. R. *Cell* **10,** 237–243 (1977).
15. Baldi, M. I., Mattoccia, E. & Tocchini-Valentini, G. P. *Proc. natn. Acad. Sci. U.S.A.* **75,** 4873–4876 (1978).
16. Nelson, T., Hsieh, T-S. & Brutlag, D. *Proc. natn. Acad. Sci. U.S.A.* **76,** 5510–5514 (1979).
17. Axel, R., Melchior, W., Sollner-Webb, B. & Felsenfeld, G. *Proc. natn. Acad. Sci. U.S.A.* **71,** 4101–4105 (1974).
18. Oudet, P., Gross-Bellard, M. & Chambon, P. *Cell* **4,** 281–300 (1975).
19. Germond, J. E., Hirt, B., Oudet, P., Gross-Bellard, M. & Chambon, P. *Proc. natn. Acad. Sci. U.S.A.* **72,** 1843–1847 (1975).
20. Camerini-Otero, R. D., Sollner-Webb, B. & Felsenfeld, G. *Cell* **8,** 333–347 (1976).
21. Steinmetz, M., Streeck, R. E. & Zachau, H. G., *Eur. J. Biochem.* **83,** 615–628 (1978).
22. Champoux, J. J. *A. Rev. Biochem.* **47,** 449–479 (1978).
23. Laskey, R. A., Honda, B. M., Mills, A. D., Harland, R. M. & Earnshaw, W. C. in *Eukaryotic Gene Regulation, ICN-UCLA Symposium* 14 (eds Maniatis, T., Axel, R. & Fox, C. F. 551–559) (Academic, New York, 1979).
24. Krohne, G. & Franke, W. *Proc. natn. Acad. Sci. U.S.A.* **77,** 1034–1038 (1980).
25. Krohne, G. & Franke, W. *Expl. Cell Res.* (in the press).
26. Mills, A. D., Laskey, R. A., Black, P. & De Robertis, E. M. *J. molec. Biol.* **139,** 561–568 (1980).
27. Earnshaw, W. C., Honda, B. M., Laskey, R. A. & Thomas, J. O. *Cell* (in the press).
28. Voordouw, G. & Eisenberg, H. *Nature* **273,** 446–448 (1978).
29. Stein, A. *J. molec. Biol.* **130,** 103–104
30. Wyllie, A. H., Laskey, R. A., Finch, J. & Gurdon, J. B. *Devl. Biol.* **64,** 178–188 (1978).
31. Adamson, E. D. & Woodland, H. R. *J. molec. Biol.* **88,** 263–285 (1974).
32. Woodland, H. R. & Adamson, E. D. *Devl. Biol.* **57,** 118–135 (1977).
33. Worcel, A., Han, S. & Wong, M. L. *Cell* **15,** 969–977 (1978).
34. Senshu, T., Fukada, M. & Ohashi, M. *J. Biochem.* (*Japan*) **84,** 985–988 (1978).
35. Cremisi, C., Chestier, A. & Yaniv, M. *Cell* **12,** 947–951 (1977).
36. Rabinowitz, M. *J. Morphol.* **69,** 1–49 (1941).
37. Blumenthal, A. B., Kriegstein, H. J. & Hogness, D. S. *Cold Spring Harb. Symp. quant. Biol.* **38,** 205–233 (1973).
38. Louie, A. J. & Dixon, G. H. *Proc. natn. Acad. Sci. U.S.A.* **69,** 1975–1979 (1972).
39. Ruiz-Carrillo, A., Wangh, L. J. & Allfrey, V. *Science* **190,** 117–128 (1975).
40. Jackson, V., Shires, A., Tanphaichitr, N. & Chalkley, R. *J. molec. Biol.* **104,** 471–483 (1976).
41. Hewish, D. R. & Burgoyne, L. A. *Biochem. biophys. Res. Commun.* **52,** 504–510 (1973).
42. Noll, M., *Nature* **251,** 249–251 (1974).
43. Morris, N. R., *Cell* **9,** 627–632 (1976).
44. Noll, M., *Cell* **8,** 349–355 (1976).
45. Thomas, J. O. & Thompson, R. J. *Cell* **10,** 633–640 (1977).
46. Compton, J. L., Bellard, M. & Chambon, P. *Proc. natn. Acad. Sci. U.S.A.* **73,** 4382–4386 (1976).
47. Spadafora, C., Bellard, M., Compton, J. L. & Chambon, P. *FEBS Lett.* **69,** 281–285 (1976).
48. Woodland, H. R. *Devl Biol.* **68,** 360–370 (1979).
49. Ponder, B. A. J. & Crawford, L. V. *Cell* **11,** 35–49 (1977).
50. Varshavsky, A. J., Sundin, O. & Bohn, M. *Cell* **16,** 453–466 (1979).
51. Waldeck, W., Föhring, B., Chowdhury, K. Gruss, P. & Sauer, G., *Proc. natn. Acad. Sci. U.S.A.* **75,** 5964–5968 (1978).
52. Scott, W. A. & Wigmore, D. J. *Cell* **15,** 1511–1518 (1978).
53. Wittig, B. & Wittig, S. *Cell* **18,** 1173–1183 (1979).
54. Wu, C., Bingham, P. M., Livak, K. J., Holmgren, R. & Elgin, S. C. R. *Cell* **16,** 797–806 (1979).
55. Musich, P. R., Maio, J. J. & Brown, F. L. *J. molec. Biol.* **117,** 637–655 (1977).
56. Seale, R. L. *Nature* **225,** 247–249 (1975).
57. Seale, R. L. *Cold Spring Harb. Symp. quant. Biol.* **42,** 433–438 (1978).
58. McKnight, S. L. & Miller, O. L. Jr *Cell* **12,** 795–804 (1977).
59. Levy, A. & Jakob, K. M. *Cell* **14,** 259–267 (1978).
60. Weintraub, H. *Nucleic Acids Res.* **7,** 781–792 (1979).
61. Leffak, M., Grainger, R. & Weintraub, H. *Cell* **12,** 837–845 (1977).
62. Seale, R. L. *Cell* **9,** 423–429 (1976).
63. Hancock, R. *Proc. natn. Acad. Sci. U.S.A.* **75,** 2130–2134 (1978).
64. Jackson, V., Granner, D. & Chalkley, R. *Proc. natn. Acad. Sci. U.S.A.* **73,** 2266–2269 (1976).
65. Riley, D. & Weintraub, H. *Proc. natn. Acad. Sci. U.S.A.* **76,** 328–332 (1979).
66. Hand, R. *Cell* **15,** 317–325 (1978).
67. Seidman, M. M., Levine, A. J. & Weintraub, H. *Cell* **18,** 439–449 (1979).
68. Kornberg, R. D. *Science* **184,** 868–871 (1974).
69. Garel, A. & Axel, R., *Proc. natn. Acad. Sci. U.S.A.* **73,** 3966–3970 (1976).
70. Weintraub, H. & Groudine, M. *Science* **93,** 848–853 (1976).
71. Gottesfeld, J. M., Bagi, G., Berg, B. & Bonner, J. *Biochemistry* **15,** 2472–2483 (1976).
72. Garel, A., Zolan, M. & Axel, R. *Proc. natn. Acad. Sci. U.S.A.* **74,** 4867–4871 (1977).
73. Flint, S. J. & Weintraub, H. M. *Cell* **12,** 783–794 (1977).
74. Levy, W. B. & Dixon, G. *Nucleic Acids Res.* **5,** 4155–4163 (1978).
75. Weisbrod, S. & Weintraub, H. *Proc. natn. Acad. Sci. U.S.A.* **76,** 630–634 (1979).
76. Goodwin, G. H., Walker, J. M. & Johns, E. W. in *The Cell Nucleus* Vol. 6 (ed. Busch, H.) pp. 181–219 (1978).
77. Weisbrod, S., Groudine, M. & Weintraub, H. *Cell* **19,** 289–301 (1980).

ARTICLES

An Archaean sub-seafloor geothermal system, 'calc-alkali' trends, and massive sulphide genesis

P. J. MacGeehan* & W. H. MacLean

Abitibi Project, Department of Geological Sciences, McGill University, 3450 University Street, Montreal, Quebec, Canada H3A 2A7

Archaean Noranda-type exhalative massive sulphide ores were formed by sub-seafloor geothermal activity which leached mafic constituents and ore metals from iron-rich bimodal (basalt–rhyolite) tholeiites and converted them to hydrothermally altered greenschist facies 'intermediate' rocks of apparent calc-alkaline affinity.

A MAJOR problem in the study of Archaean and younger greenstone belts is the identification of the primary geochemistry of volcanic rocks that have been subjected to extensive rock–water interaction. The rocks, mostly fine grained basalts exhibiting greenschist facies mineralogy, are normally classified on the basis of chemical composition and normative mineralogy on the assumption that rock–water interaction was largely an isochemical process. This hypothesis apparently succeeds in large parts of the greenstone belts where the volcanic rocks were only weakly hydrated during halmyrolysis and burial metamorphism, but, in some areas, sub-seafloor geothermal activity contemporaneous with volcanism produced more intense rock–water interaction with higher water-to-rock ratios. It is in these areas of intense hydrothermal alteration, seafloor exhalative activity and associated massive sulphide mineralization, that the primary petrological and chemical identity of the volcanic rocks has been radically changed, causing them to be incorrectly identified using standard geochemical rock classification schemes.

The nature of this problem became evident during research in the Matagami, Quebec Archaean volcanic centre and mining district in the Abitibi greenstone belt, where sulphide ores are associated with several thick domal accumulations of rhyolite

---

* Present address: Department of Geological Sciences, Queen's University, Kingston, Ontario, Canada K7L 3N6.

0028-0836/80/340767—05$01.00

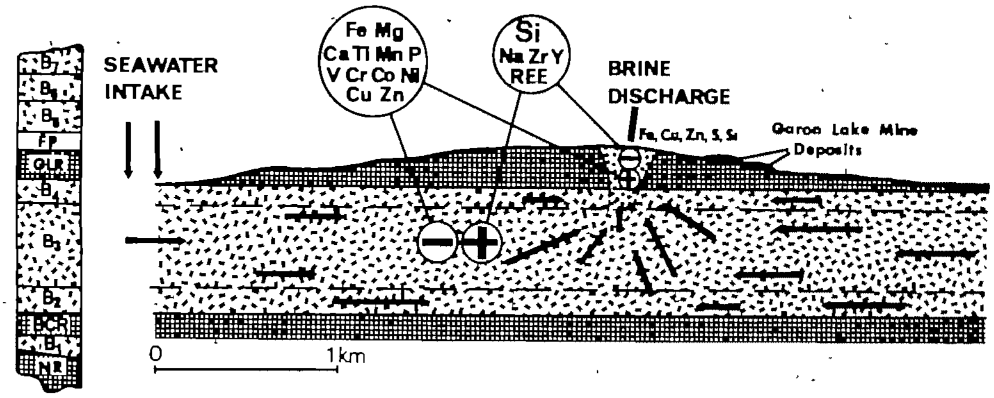

Fig. 1 Volcanic stratigraphy and diagrammatic vertical section through the Garon Lake geothermal system. B_1–B_7, basalts; FP, andesite, GLR, Garon Lake rhyolite; BCR, Bell Channel rhyolite; NR, Norita rhyolite. The pattern with circles denotes intensely chloritized Garon Lake rhyolite.

interbedded with iron-rich pillowed basalt flows. These rocks were formerly described as 'calc-alkaline'[1] owing to the predominance of rocks of 'intermediate' chemical composition (andesite–dacite–rhyolite). These show a large scatter rather than a systematic alkali-enrichment on an AFM plot, a feature characteristic of many mineralized Archaean volcanic centres[2–5]. However, they are now known to constitute a hydrothermally altered bimodal basalt–rhyolite suite of clear tholeiitic affinity[6]. Their apparent 'calc-alkaline' traits reflect a hydrothermal overprint caused by rock–water interaction during sub-sea floor geothermal activity as a modified seawater brine intensely spilitized, silicified and leached metals from large volumes of iron-rich tholeiitic basalt before discharging through overlying rhyolite to deposit massive sulphides on the sea floor.

In this article we examine the petrography and geochemistry of the rock–water interaction in the Garon Lake geothermal system at Matagami, and compare and contrast the trends produced with recognized igneous fractionation trends.

The Garon Lake geothermal system

The Garon Lake geothermal system developed within a 500-m thick sequence of tholeiitic pillowed basalt (units B_2–B_4) after extrusion of the Garon Lake rhyolite (Fig. 1). The basalts are underlain by the Bell Channel rhyolite, thus the reservoir rocks of the system are confined to a narrow, well-defined stratigraphic interval in which the individual flow-units have been mapped in detail and followed along strike for several kilometres. The basalts are intruded by contemporaneous gabbro sills of very similar mineralogical and chemical composition, several of which may have been lateral feeders to the pillowed flows. The geological setting, petrology and primary geochemistry of the units have been discussed elsewhere[6,7], where they were shown to form part of a bimodal basalt–rhyolite suite of tholeiitic affinity.

Most of the volcanic rocks have been hydrothermally altered to some degree: the basalts are intensely spilitized and silicified, whereas the domal parts of the Garon Lake rhyolite are pervasively chloritized and transected by zones of disseminated sulphide mineralization. Earlier studies have shown that this alteration accompanied sub-seafloor geothermal activity which began while the volcanic rocks and contemporaneous intrusions were still hot, and terminated before the extrusion of volcanic rocks overlying the Garon Lake rhyolite[7,8]. At the time when the geothermal system was active, seawater was convected through basalt from intake zones at the periphery of the rhyolite and then discharged through permeable zones (now alteration pipes) in the rhyolite dome. The exhalative massive sulphide lenses at the Garon Lake mine formed down slope from the western alteration pipe[9]. The geothermal system had a lateral extent >5 km (Fig. 1), indicating that >10 km^3 of volcanic rock were subjected to hydrothermal alteration.

Rock–water interaction

The reservoir rocks are bleached and mottled pillowed basalts that would almost invariably be called 'andesite' in the field. Two main stages of hydrothermal alteration can be recognized petrographically: (1) an early and minor stage of dominantly destructive (argillic) alteration that accompanied localized convective fluid movement in water-bearing basalt bordering some of the contemporaneous gabbro sills[8]; and (2) a later and

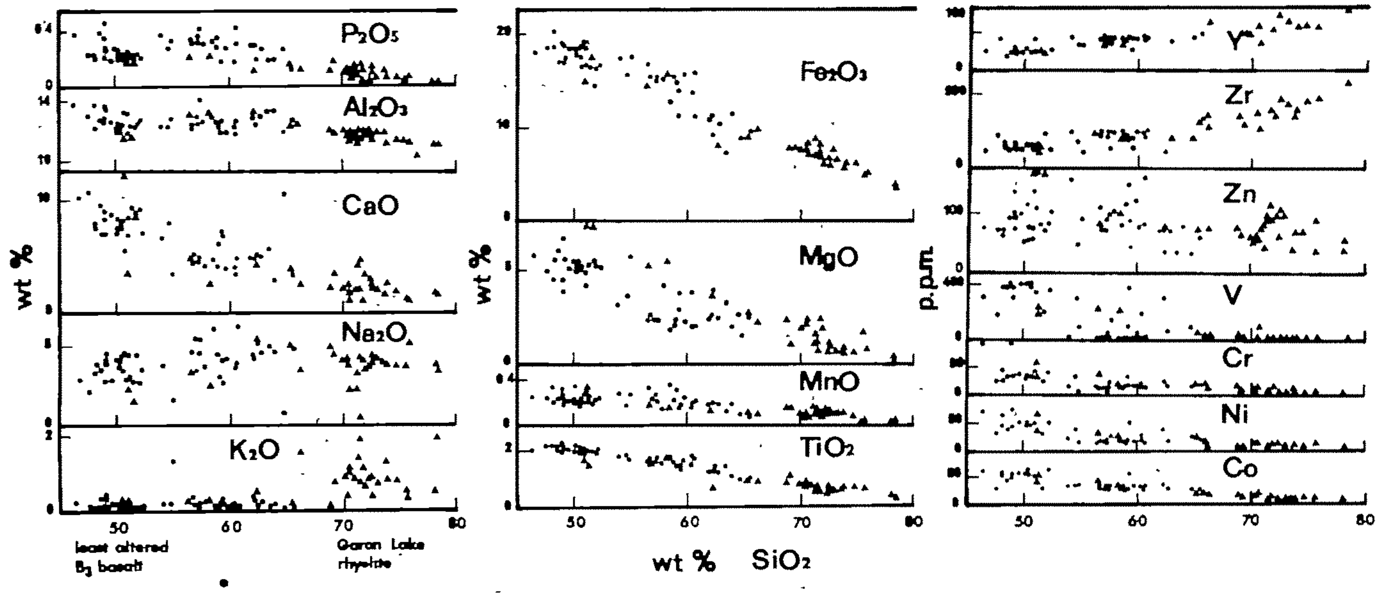

Fig. 2 Plot of major and trace elements against SiO_2 for the B_3 basalt and Garon Lake rhyolite units. Alteration produces the continuum of data. ●, B_3 basalt samples; ▲, Garon Lake rhyolite samples. Total iron as Fe_2O_3.

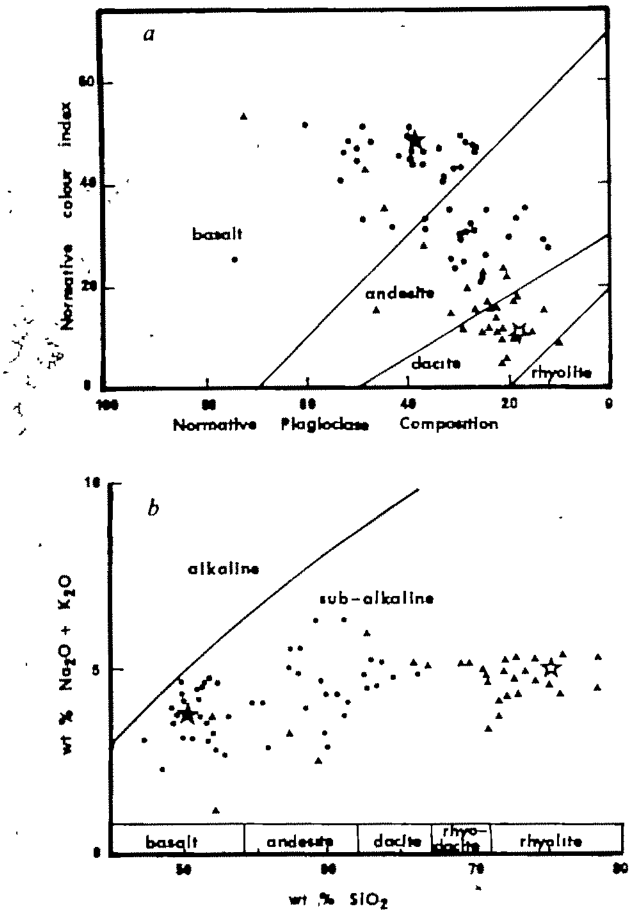

Fig. 3 *a*, Normative CI against normative An[15] *b*, Total alkalies against SiO_2; the rock classification based on SiO_2 content is after Gélinas *et al.*[3], although those by Spitz and Darling[4] and Jolly[16] are very similar. The mean composition of least altered samples are: ★, B_3 basalt; and ☆, Garon Lake rhyolite.

widespread stage of intense spilitization that accompanied large-scale convective circulation of fluid after the reservoir rocks were sealed from above by the Garon Lake rhyolite (Fig. 1).

Spilitization is localized around pervasive quartz–epidote-filled veinlets and cylindrical pipes (alteration patches[10]) which transect the basalt section. These structures form an interconnecting network interpreted as conduits of concentrated fluid flow at the time the geothermal system was active. Whereas the smaller veinlets have a random orientation, the larger veinlets and pipes are invariably orientated parallel to stratigraphy, indicating a dominantly horizontal vector of fluid movement within the reservoir rocks (Fig. 1).

The basalt around the quartz–epidote structures has been intensely bleached and silicified to light grey and grey-green domains up to one or several metres in diameter. Although the igneous fabric was almost entirely preserved in these domains the mineral assemblages were drastically changed: plagioclase phenocrysts and laths were replaced by single crystals of inclusion-free albite that commonly retain original twin planes, pyroxene was replaced by actinolite (twin planes, exsolution lamellae and subophitic textures partly preserved), and ulvospinel first crystallized ilmenite in trelliswork patterns but was then partly replaced by actinolite and sphene. With advanced spilitization, epidote, magnetite, ilmenite and sphene were replaced by quartz, albite, minor chlorite and rutile, the latter as needles preserving the outline of former ilmenite grains. This intense spilitization grades outward to a zone of weak but pervasive hydration where basalt has a uniformly dark green colour and a more or less constant chemical composition. Here, the pyroxene is pseudomorphed by dark green actinolite, plagioclase is saussuritized, and the groundmass consists of ulvospinel granules and sodic plagioclase crystallites in a chloritic, devitrified glass matrix.

Overall, the mineralogical changes in the basalts were accompanied by significant decreases in colour index and increases in hardness so that they now frequently resemble andesites and dacites in the field. The role of quartz is particularly important. While not a primary phase or a product of isochemical devitrification of basaltic glass, quartz increases significantly with increasing degree of alteration.

The Garon Lake rhyolite (dacite in some classification schemes[6,11,15]) is devitrified quartzo-feldspathic and generally spherulitic acid glass that contains up to 20% inverted β-quartz and sodic plagioclase phenocrysts and rare granophyre fragments[6–8]. Zones of intense chloritization that constitute the alteration pipes are mineralized with chalcopyrite and pyrite (Fig. 1). The direct replacement of rhyolite glass (~75% SiO_2) by massive chlorite (~35% SiO_2) proceeded without obvious volume change; β-quartz phenocrysts were corroded and plagioclase grains were either partly corroded or entirely replaced by granulose quartz plus chlorite or massive chlorite.

Geochemical changes

Intense spilitization of the reservoir rocks was accompanied by major chemical adjustments, the most important being the significantly higher SiO_2 content of altered samples. Unaltered or least altered samples of the chilled rims and cores

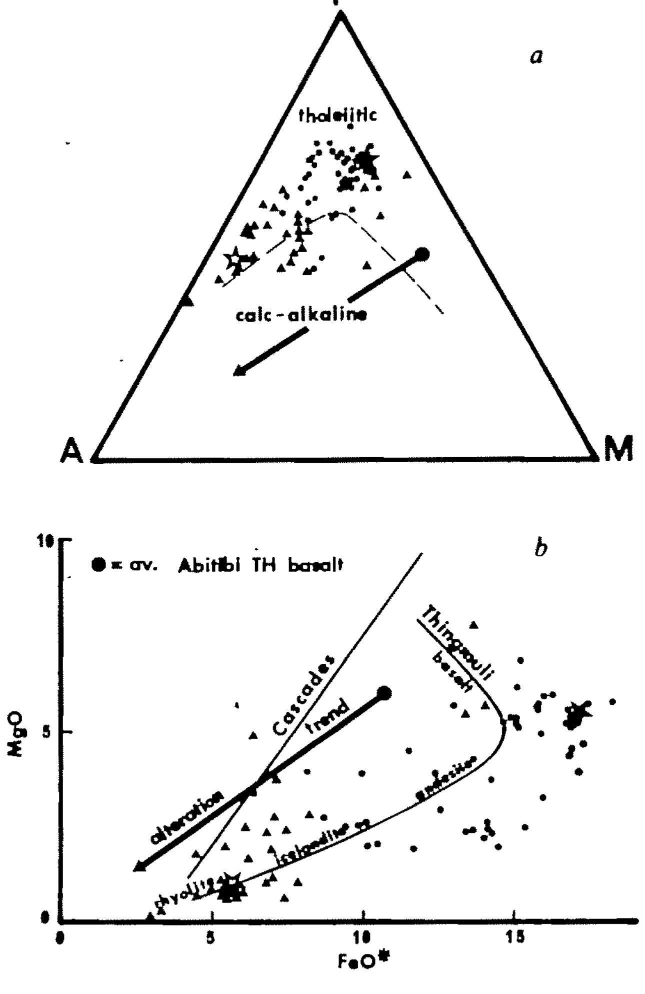

Fig. 4 *a*, AFM plot. The dividing line is after Irvine and Baragar[15]. *b*, MgO against FeO* (total iron as FeO) The Thingmuli[17] (tholeiitic) and Cascades (calc-alkaline) trends are shown. A plot, ●, of the mean composition of basalts from the Abitibi greenstone belt[18] shows how alteration would move them into the calc-alkaline field.

of pillows lie in the compositional range 48–52% SiO_2, but hydrothermally altered samples show a progressive increase in SiO_2 to 65% in the B_3 unit and up to 75% in B_4 (ref. 8). Increases in SiO_2 in B_3 (Fig. 2) are accompanied by: (1) a linear depletion in FeO*, MgO, CaO, TiO_2, P_2O_5, V, Cr, Mn, Co, Ni, Cu, Zn and Cd, reflecting their dissolution during breakdown and reconstitution of the mafic minerals and plagioclase; (2) a significant increase in Na accompanying the albitization of plagioclase; and (3) comparable increases in Zr, Y and REE by factors of up to three. K_2O, which probably had a very low initial content, remains low in the altered rocks. Although scatter is considerable, the ratios of depleted elements (FeO*/MgO, FeO*/TiO_2, and so on) remained essentially constant and identical to the igneous ratios, indicating that their dissolution was a congruent, non-selective process. Hydrothermal alteration in the remaining basalt flows (units B_2 and B_4) was very similar, although changes in the intensity of silicification, in the Na_2O/SiO_2 enrichment, and in the behaviour of P_2O_5 and Al_2O_3 did occur with stratigraphic height within the geothermal system[7,8].

Two lines of evidence, the petrographic observation of the pseudomorphic replacement of the igneous rock fabric and the immobile behaviour of Al_2O_3 (Fig. 2), indicate that rock–water interaction was essentially a constant volume process. The incremental enrichment in SiO_2 and Na_2O was therefore accompanied by the active congruent dissolution and transport of FeO*, MgO, CaO, TiO_2 and the trace elements listed above, because only SiO_2, CaO and Al_2O_3 (quartz and epidote) were later precipitated in the hydrothermal conduits[10]. This alteration accompanied an increase in the temperature of the fluid. The precipitation of silica in the central part of the geothermal system occurred around the critical point of the brine ($T \sim 400\,°C$; $P < 0.75$ kbar)[12–14], where SiO_2 solubility decreases rapidly with rising temperatures while that of most other components continues to increase. Similarly, as the metal-charged brine rose through the rhyolite to the sea floor it cooled, leached silica from rhyolite, and precipitated most of the elements dissolved from the underlying reservoir rocks as minerals in the alteration pipe and massive sulphides on the sea floor (Fig. 2).

Significance of the alteration trends

Rock–water interaction during sub-seafloor geothermal activity caused the congruent dissolution of many major and trace elements from basalt, their transport by fluid, and their later precipitation in similar ratios in rhyolite approaching the discharge points of the system. Cumulatively, this resulted in the compositional gap of the bimodal basalt–rhyolite suite being spanned by a continuum of altered rock compositions (Fig. 2). Using as an example only one basalt flow from the reservoir and the overlying Garon Lake rhyolite (Figs 2–6), the geochemistry of the hydrothermally altered rocks seems to be indistinguishable from the spectrum of intermediate igneous rock compositions. Hydrothermally altered basalt and rhyolite samples span the field through andesite and dacite on a normative colour index versus normative plagioclase composition diagram (Fig. 3a) used to classify volcanic rock types[15], and classification systems based on SiO_2 content[3,4,16] (see Fig. 3b).

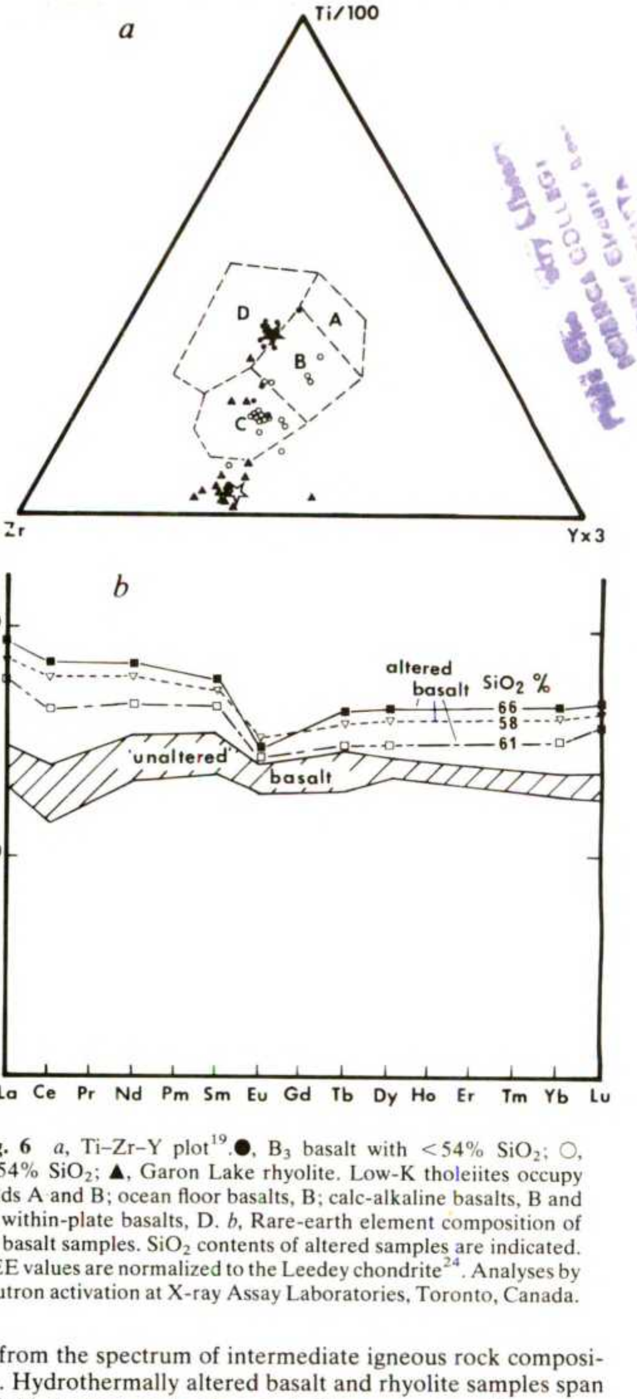

Fig. 6 *a*, Ti–Zr–Y plot[19]. ●, B_3 basalt with <54% SiO_2; ○, >54% SiO_2; ▲, Garon Lake rhyolite. Low-K tholeiites occupy fields A and B; ocean floor basalts, B; calc-alkaline basalts, B and C; within-plate basalts, D. *b*, Rare-earth element composition of B_3 basalt samples. SiO_2 contents of altered samples are indicated. REE values are normalized to the Leedey chondrite[24]. Analyses by neutron activation at X-ray Assay Laboratories, Toronto, Canada.

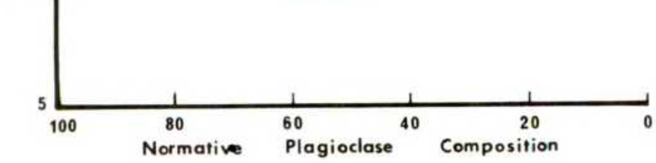

Fig. 5 Comparision of Al_2O_3 with normative An[15].

Furthermore, as rock–water interaction involved the net substitution of salic (SiO_2, Na_2O, and so on) for basic (FeO*, MgO, CaO, TiO_2, and so on) components, the resulting chemical alteration patterns resemble igneous fractionation trends. For example, most major and trace elements show a variation typical of volcanic rock suites when plotted against a fractionation index (for example, SiO_2, Fig. 2; differentiation index and solidification index plots show similar patterns). However, despite Na metasomatism during spilitization of basalt, altered samples remain in the sub-alkaline field on an alkali–silica plot (Fig. 3b). The resemblance with a fractionation trend is also seen on an AFM plot, widely used to distinguish tholeiitic from calc-alkaline rocks; the least altered basalt samples lie close to the FM join and altered samples extend towards the alkali corner (Fig. 4a). The resemblance is maintained in plots not involving the alkalis, for example, FeO* versus MgO (Fig. 4b), where, despite the scatter, the alteration parallels the later stages of the Thingmuli tholeiitic trend[17]. There is no evidence of iron enrichment, however, and the resemblance to a tholeiitic trend is dictated by the high initial FeO*/MgO of this basalt which precludes a calc-alkaline association. This would not have been so in most Archaean centres where the basalts generally have much lower FeO*/MgO ratios (see Fig. 4 for plots of average Abitibi basalt[18]). In its essential characteristics (alkali enrichment with depletion of mafic oxides) the alteration mimics a calc-alkaline fractionation trend, and would easily be confused for one in many mineralized volcanic centres. This apparent calc-alkaline affinity is indicated on many other major element plots except that of Al_2O_3 against normative plagioclase composition (Fig. 5) where the low mobility of Al_2O_3 during alteration confines the data to the tholeiitic field.

The whole trace element suite was also mobile during alteration: V, Cr, Co, Ni, Cu, Zn and Cd decreased, and Zr, Y and REE increased with increasing SiO_2 content (Figs 2–6). A plot of the 'immobile' elements Ti, Zr and Y (Fig. 6*a*) shows how mobile they have been. The negative correlation of Ti for Zr and Y that can be seen in Fig. 2 produces a continuum of points between the original basalt and rhyolite on Fig. 6*a*. This diagram has been used successfully to distinguish the tectonic setting of modern basalts ($<54\%$ SiO_2)[19], and the correlations made there have been frequently used to classify older rocks[20–23]. Most samples from the reservoir rocks of the geothermal system with less than 54% SiO_2 do plot in a small area of Fig. 6*a*, but the tendency of the altered rocks to move to the calc-alkaline field is apparent. Plots with Cr, Co and Ni yield similar results. The REE are also mobile but retain the flat profile (Fig. 6*b*) typical of fractionated tholeiites, lacking the characteristic strong LREE enrichment and high La/Yb ratios of calc-alkaline rocks. Rather than being immobile, these elements actually provide a good monitor of progressive alteration in a single flow.

Conclusions

Intense rock–water interaction in the Garon Lake sub-seafloor geothermal system accompanied spilitization of volcanic rocks and contemporaneous high-level gabbro sills. Massive chemical exchange occurred in and adjacent to zones of dynamic flow of seawater-derived brine; essentially isochemical hydration occurred where flow was sluggish or stagnant. Hydrothermal alteration preserved volcanic features (pillow selvages, amygdules, hyaloclastite-filled interstices) and pseudomorphed igneous fabric as it converted bimodal basalt–rhyolite tholeiites to rocks that are petrographically indistinguishable from metamorphosed andesites and dacites. The major and trace element geochemistry of the altered rocks are 'intermediate' in character and show calc-alkaline affinity on most discrimination diagrams.

The predominance of these 'intermediate' rocks at Matagami and in other mineralized volcanic centres in the Archaean of Canada, led to the original assumption that exhalative massive sulphide ores of the Noranda type were associated with 'calc-alkaline' volcanic rocks, and, by inference, with active volcanism along consuming plate boundaries[1,4,25]. It is now evident that these conclusions may be in error. Rather than denoting a tectonic setting, these 'intermediate' 'calc-alkaline' volcanic rocks may in fact reflect the geochemical imprint of sub-seafloor geothermal activity that generated important ore deposits.

This work was supported by a Quebec Government FCAC grant 649 and NSERC grant A7719. We thank R. F. Martin, A. J. Hynes, G. R. Webber, D. Francis, K. St. Seymour, C. J. Hodgson and T. H. Pearce for helpful comments.

Received 8 May, accepted 5 June 1980

1 Descarreaux, J *CIM Bull* 6, 61–69 (1973)
2 Allard, G O *Quebec Dept Nat Resour, Miner Dep Rep DP-368* (1976)
3 Gélinas, L *et al* in *Volcanic Regimes in Canada* (eds Baragar, W R A, Coleman, L C & Hall, J. M) Spec. Pap 16, 265–295 (Geological Association of Canada, 1977)
4 Spitz, G & Darling, R *Can J Earth Sci* 12, 1820–1849 (1975)
5 Boswick, A E & Sousa, G. *Precamb Res.* 6, 235–248 (1978)
6. MacGeehan, P. J & MacLean, W H *Nature* 283, 153–157 (1980)
7 MacGeehan, P J. thesis, McGill Univ, Montreal (1979).
8. MacGeehan, P J *Can J Earth Sci* 15, 551–570 (1978)
9. MacLean, W H & MacGeehan, P J *IREM/MERI Case Hist* 76–1, (McGill University, Montreal, 1976)
10 Harrigan, D B & MacLean, W. H *Can J Earth Sci* 13, 500–511 (1976)
11 Streckeisen, A *Geology* 7, 331–335 (1979)
12. Kennedy, G C. *Econ Geol* 45, 629–653 (1950)
13 Sourirajan, S & Kennedy, G C *Am J Sci.* 260, 115–141 (1962)
14 Spooner, E. T C. & Fyfe, W S *Contr Miner Petrol* 42, 287–304 (1973)
15 Irvine, T N & Baragar, W R A *Can J Earth Sci* 8, 523–548 (1971)
16. Jolly, W T in *Volcanic Regimes in Canada* (eds Baragar, W R A, Coleman, L C & Hall, J M) Spec Pap 16, 311–330 (Geological Association of Canada, 1977)
17 Carmichael, I S E *J Petrol* 5, 435–460 (1964)
18 Goodwin, A M. in *Volcanic Regimes in Canada* (eds Baragar, W R A, Coleman, L C & Hall, J M) Spec Pap 16, 205–241 (Geological Association of Canada, 1977)
19 Pearce, J A & Cann, J R *Earth planet Sci Lett* 19, 290–300 (1973)
20 Morrison, M A *Earth planet Sci Lett* 39, 407–416 (1978)
21 Davies, J F, Grant, R W E & Whitehead, R E S *Can J Earth Sci* 16, 305–311 (1979)
22 Winchester, J A & Floyd, P A *Earth planet Sci Lett.* 28, 459–469 (1976)
23 Smith, R E & Smith, S E *Earth planet Sci Lett* 32, 114–120 (1976).
24. Nakamura, N. *Geochim cosmochim Acta* 38, 757–775 (1974)
25. Sangster, D F & Scott, S D in *Handbook of Strata-Bound and Stratiform Ore Deposits* Vol 6 (ed Wolf K H) 129–222 (Elsevier, Amsterdam, 1976)

Antigenic drift between the haemagglutinin of the Hong Kong influenza strains A/Aichi/2/68 and A/Victoria/3/75

Martine Verhoeyen, Rongxiang Fang, Willy Min Jou, René Devos,
Danny Huylebroeck, Eric Saman & Walter Fiers

Laboratory of Molecular Biology, State University of Ghent, Ledeganckstraat 35, B-9000 Ghent, Belgium

A DNA copy of the gene coding for the influenza A/Aichi/2/68 haemagglutinin protein was cloned in the plasmid pBR322 and the complete nucleotide sequence determined. Comparison of this primary structure and the deduced amino acid sequence with the haemagglutinin gene and protein of strains belonging to the same (H3) subtype and to different subtypes, of both human (H2) and avian (Hav1) origin, documents further at the molecular level the two independent modes of antigenic variation of the virus—drift and shift.

THE ability of type A influenza strains to change their antigenic properties is a major obstacle to controlling the viral disease by vaccination, and the virus continues to be an important cause of illness in the human population. Two types of change have been recognized: antigenic 'drift' seems to be the result of a certain number of local alterations in the viral surface proteins (thought

0028-0836/80/340771—06$01.00

to be selected under the pressure of the immune system), whereas antigenic 'shift' is a radical change of the antigenic properties of the surface protein, leading to the emergence of new pandemic strains. The origin of these pandemic strains is unknown, but it has been speculated that they result from a recombination event between a human virus and an influenza strain from an animal reservoir[1].

Type A influenza viruses have a negative-stranded RNA genome consisting of eight distinct RNA segments[2–4]. The two surface antigens, haemagglutinin and neuraminidase, are glycoproteins and have been assigned to viral RNAs 4 and 5 or 6 (depending on the strain), respectively[2,3]. We have recently determined the primary structure of the haemagglutinin gene from the relatively recent human influenza strain A/Victoria/3/75 (H3N2), starting from cloned DNA[5] and using fast DNA sequencing techniques. Compared with RNA and protein sequencing methods, this approach has the advantage of much greater speed and accuracy and avoids special problems, such as those encountered during the sequencing of hydrophobic regions of polypeptides.

We describe here the cloning and elucidation of the structure of the haemagglutinin gene of A/Aichi/2/68, which formed the beginning of the so-called Hong Kong (H3N2) period. The gene sequence and deduced amino acid sequence are compared with those of our previously reported Victoria strain[5], with an intermediate H3N2 isolate, A/Memphis/102/72 (this haemagglutinin was sequenced as cloned DNA[6] and except for a small hydrophobic region also as protein[7,8]), with amino acid data from monoclonal variants[9] and field strains[10], with the gene sequence of A/Japan/305/57 (H2N2)[11], which occurred at the start of the 1957–67 influenza wave, and with the fowl plague haemagglutinin gene (Hav1)[12].

Cloning the A/Aichi/2/68 haemagglutinin gene

The high yielder, recombinant strain X31, which carries the haemagglutinin and neuraminidase genes of A/Aichi/2/68, was used as the RNA source in our study. Double-stranded (ds) DNA copies of the haemagglutinin genetic information were synthesized and cloned essentially as described previously for the haemagglutinin gene of the A/Victoria/3/75 strain[5]. The major steps of the procedure are briefly summarized as follows: the mixture of eight negative-stranded X31 virion RNA segments was polyadenylated at the 3′ end[13], converted into dsDNA copies, sized on a 1.5% agarose gel and the material corresponding to full-length haemagglutinin dsDNA recovered form *Escherichia coli* K12 HB101 (refs 5, 14). Thirty-nine dTTP and annealed to oligo(dA)-tailed plasmid pBR322 in the *Pst*I restriction site, and the resulting hybrid was used to transform *Escherichia coli* K12 HB101 (refs 5, 14). Thirty-nine tetracycline-resistant colonies were obtained. When hybridized[15] to a ^{32}P-labelled gene 4 RNA probe, four of the clones showed positive hybridization. One plasmid (pXHA14) containing an insert of approximately 1,860 base pairs (including the A · T tails used for cloning) was chosen for further characterization.

Nucleotide sequence of pXHA14

The insert in plasmid pXHA14 was characterized by restriction mapping according to Smith and Birnstiel[16]. Subsequently, fragments were prepared by digestion with the appropriate restriction enzymes, 5′-terminally labelled, and sequenced according to the method of Maxam and Gilbert[17]. The nucleotide sequence is shown in Fig. 1 as the coding information or complement of the viral RNA. As the structure is highly homologous to the previously determined Victoria haemagglutinin gene (Fig. 1), we did not systematically attempt to read both strands. Nevertheless, more than half of the sequence was confirmed by analysis of both strands.

As expected from the cloning strategy used[5,14,18] (initiating second DNA strand synthesis starting from a terminal hairpin of the first DNA strand, followed by S_1 nuclease treatment), a small portion of the haemagglutinin genetic information corresponding to the 3′ end of the cDNA is missing from the clone. As we started from negative-stranded influenza RNA, this region corresponds to the 3′ end of the coding information (beyond the arrow in Fig. 1). Because two other strains belonging to the same subtype have been shown to share exactly the same 3′-noncoding sequence[5,6], we did not attempt to complete this sequence for the Aichi strain. Assuming identity in this region, 27 nucleotides would be missing from the pXHA14 plasmid, compared with 24 nucleotides missing from plasmid pVHA14, which contains the Victoria haemagglutinin information[5]. Taking into account an additional 27 base pairs at the 3′ end of the influenza-specific information in pXHA14, the total length of the Aichi haemagglutinin RNA is 1,765 nucleotides: 29 nucleotides precede the signal for the AUG translation initiation codon, the translated region extends over 1,698 nucleotides (specifying 566 amino acids), and the (presumed) 3′-terminal noncoding stretch comprises 38 nucleotides (including the signal for the UGA terminator).

The detailed organization of the haemagglutinin RNAs belonging to the Hong Kong (H3) subtype (Victoria[5], Memphis[6–8], Aichi) seems to be identical except for the insertion of three nucleotides (specifying an asparagine residue at position 8′ of the HA1) in the relatively recent Victoria/3/75 strain (Figs 1, 2). The haemagglutinin RNA from another human subtype (H2)[11] and from an avian subtype (fowl plague)[12] are of comparable length.

The protein sequence

The haemagglutinin is synthesized as a single polypeptide chain which is subsequently modified by glycosylation and post-translational processing. The latter involves removal of an NH_2-terminal signal peptide[19] and proteolytic cleavage into HA1 and HA2 to yield mature haemagglutinin and infective virus[20,21]. Assuming that the Aichi sequence also starts with the NH_2-terminal blocking group pyroglutamic acid, as found in the Memphis H3 strain[22] (a blocked amino terminus of the HA1 is a general characteristic of H3 human strains and of two putative progenitor animal strains[23–25]), the signal sequence would be 16 amino acids long, as in Victoria[5] and Memphis[6,22]. Within the H3 subtype, the length and hydrophobic character of the signal peptide seem to be maintained, but the exact sequence is not (Figs 1, 2). There is no variation between the positions of cysteine residues in H3 strains. Also, the sequence of the Japan and fowl plague strain can easily be aligned according to the cysteines, allowing for a minimum number of insertions/deletions between strains[5,26]. It is therefore to be expected that the disulphide bonding pattern is the same between these three subtypes and probably in all influenza A haemagglutinins, thus giving the haemagglutinin molecules a very similar three-dimensional conformation. The disulphide bonds have recently been determined for the A/Memphis/102/72 strain[27].

As in the other H3 strains Victoria and Memphis and also in the H2 Japan strain, the region excised from between HA1 and HA2 consists of a single arginine residue; this situation contrasts with fowl plague haemagglutinin, where six residues are removed[12,28]. A second hydrophobic sequence, at the NH_2 terminus of the HA2, which may have a role in interaction with and penetration of the cell membrane during infection, is highly conserved in all influenza A strains examined so far, even in a single B-type strain, and also in the NH_2 terminus of the F1 subunit of Sendai virus[25]. Near the C terminus of HA2 there is a third hydrophobic region (amino acids 185–210 of HA2 in Fig. 1), which is involved in anchoring the haemagglutinin in the lipid viral envelope. The precise functioning of the signal interrupting the translocation of membrane proteins ('stop-transfer' sequence[29]) remains to be established. However, in contrast to the signal sequence, this stop-transfer sequence seems to be constant within the H3 subtype in at least three different field strains.

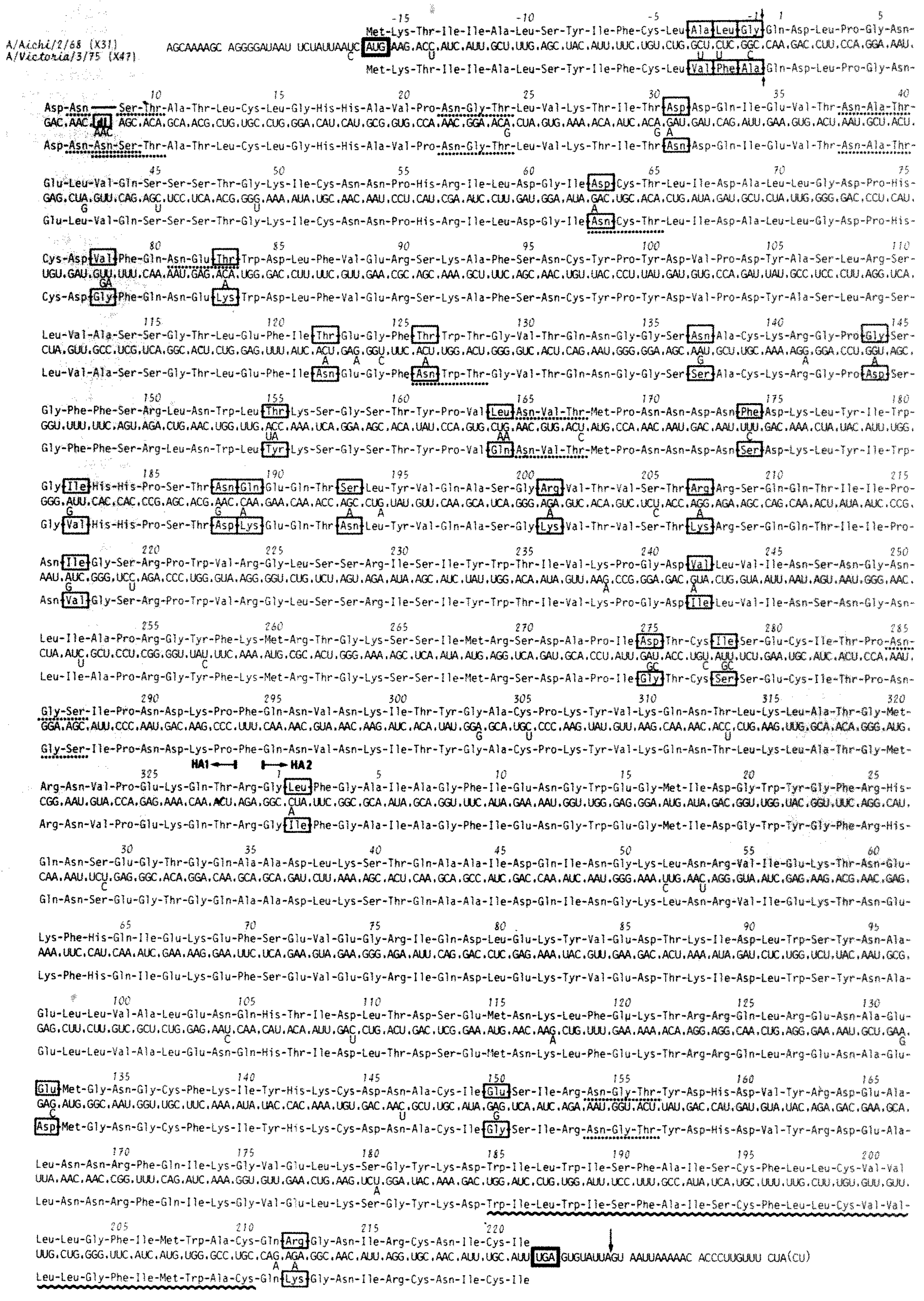

Fig. 1 Comparison of the haemagglutinin genes and deduced amino acid sequence of influenza strains A/Aichi/2/68 and A/Victoria/3/75. The nucleotide sequence of the Aichi gene is shown as the complementary viral RNA (coding strand); only the substitutions in the Victoria gene[5] are given. The Aichi nucleotide sequence is derived from cloned DNA; however, the sequence shown from the 3′ end up to the vertical arrow was missing from the cloned DNA and is assumed to be identical to the same region in Victoria (see text). The initiation and termination codons are shown in heavy boxes. Differences between amino acid sequences are shown in light boxes. Potential glycosylation sites are indicated by dotted lines. The wavy line indicates the hydrophobic region of HA2 that is embedded in the lipid membrane of the virion.

The percentage of homology in the HA1 portion is modest but usually in the same range between each two strains belonging to a different subtype (between 34 and 37%), whereas the homology is higher in HA2 (H3:H2, 50%; H3:Hav1, 66%; H2:Hav1, 52%). The fact that the HA2 is much more similar between H3 and Hav1 than between two human strains (H3 and H2) whereas the HA1 varies to approximately the same extent demonstrates how difficult it is to define the evolutionary relationship between different pandemic strains. The fraction conserved in all three subtypes (taking Aichi as the H3 prototype) is only 21% in HA1, but 42% in HA2. These values illustrate the importance of the HA1 portion to the antigenic variability of the influenza haemagglutinin.

Comparison of H3 strains: genetic drift

The nucleotide sequence of the haemagglutinin gene and the deduced amino acid sequence of the protein of the Aichi/68 and Victoria/75 strains are compared in Fig. 1. There are 67 nucleotide differences (3.8%): an insertion in the Victoria gene of three nucleotides close to the NH_2 terminus of the HA1 (coding for an extra asparagine residue) and 64 nucleotide substitutions. Of these latter changes, 63 occur in the coding region: 34 are silent nucleotide substitutions and the other 29 changes cause 28 amino acid differences (there is one case, at position 155 of the HA1, of two nucleotide changes resulting in a single amino acid change). Thus, in total there are 29 amino acid differences (including one insertion) or a 5.1% amino acid divergence accumulated over a 7-yr period (1968–75). By comparing maps of soluble tryptic peptides and amino acid composition data from nine strains isolated between 1968 and 1977 with the amino acid sequence of the A/Memphis/102/72 strain, Laver and collaborators[10] found a minimum (only soluble peptides were examined) of 20 amino acid changes occurring during that period. Another conclusion was that once a residue had changed, it did not change again in the later variants, except for a few apparent reversions to the original amino acid (apparent because there is a no reason to believe that prototypes of successive epidemics as isolated from nature form a direct genealogical lineage). The same observations are made when the complete amino acid sequence of the three H3 haemagglutinin molecules, Victoria/75 (ref. 5), Memphis/72 (refs 6–8) and Aichi/68, are compared (Fig. 2). Again, a likely explanation for the apparent reversions is that, for example, the Memphis strain is not the parent of the Victoria strain. Also, at the level of silent mutation, the same phenomenon of an occasional apparent reversion is observed (not shown).

As expected, most amino acid changes were found in the HA1 part of the protein (Fig. 2, Table 1); indeed, the antigenic character is thought to reside largely, if not entirely, in this section[30–32]. Over the 1968–75 period of antigenic drift, 22 (6.7%) of the amino acids have changed in HA1 whereas only 4 (1.8%) have been replaced in HA2. Comparing all three H3 subtypes (Fig. 2), 27 variable residues are observed in HA1 and 5 in HA2. Note that there is some clustering of the amino acid changes in the middle third (amino acids 110–226) of the HA1 in the three strains examined. A similar differential variability between both subchains of the haemagglutinin molecule has been observed by Laver and colleagues[10]. Variants have been isolated which are resistant to monoclonal antiserum, and the haemagglutinins of these have probably changed at only a single amino acid position[9]. As these variants are still neutralized by total antiserum against the parent virus, it seems very likely that a more profound change (of at least two amino acids) would be required to generate a new field strain capable of overcoming the immunity of the population.

Taking into account the number of different natural variants that have been isolated and the number of epidemics reported during the period considered[33,34], it is reasonable to assume that a not unimportant fraction of the 22 differences in HA1 observed between Aichi/68 and Victoria/75 (probably at least one-third and possibly up to two-thirds or even more, that is, 7–15 amino acids or more) have played a part in the antigenic variability. Also, if one considers the relative abundance of differences between HA1 and HA2 to reflect the antigenic variability within HA1 above the background of tolerable mutation rates, a value of 16 residues is obtained. However, these changes may be clustered in several 'antigenic sites' (each comprising a limited number of amino acids involved in the reaction with the antibody[9,35]) or they may influence the way the antigenic site is presented to the antibody by conformational changes. Thus, the analysis of amino acid sequences in a limited number of natural strains is not in itself sufficient for a delineation of antigenic sites.

Another approach is the analysis of variants selected with monoclonal antibodies. The Hong Kong variants studied by Laver and colleagues[19] have amino acid changes at positions 54, 143, 205 and a fourth one in the region 217–224 of the HA1 (the latter two changes were observed in the variants selected with the same monoclonal antibody). There are no amino acid changes around residue 54 in the three strains compared in Fig. 2, but a change of both the adjacent residue 53 and amino acid 54 (but to a different amino acid from that in the monoclonal variant) have been described[10]. Again, the amino acids next to residue 143, residues 144 (Fig. 2) and 145 (ref. 10), have been found to change in field strains. Natural changes around the third variant (205) are at positions 207 (Fig. 2 and ref. 10) and 208 (ref. 10). Thus, from all cases where a direct comparison is possible, in only one instance was an amino acid change found in the same position in a monoclonal antibody-selected variant and in a field strain (residue 54), and even then the residue by which it was replaced was completely different (to a lysine and a serine, respectively), suggesting that the immunological selection in nature works differently from that in the laboratory model experiments. The reason for this (systematic) discrepancy is unknown, although it is quite clear that the immunological pressure in an infected immune individual is very different from the selection pressure working in a murine monoclonal hybridoma to select laboratory variants.

Most of the amino acid changes in these H3 haemagglutinins have been acquired by single base substitutions and are rela-

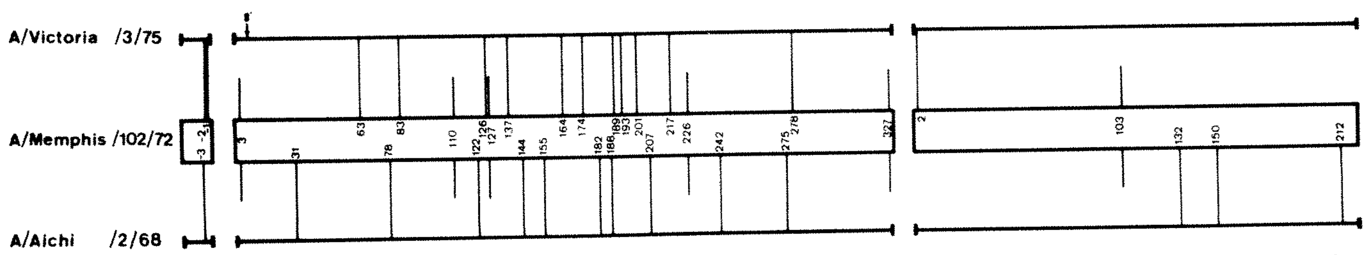

Fig. 2 Differences between the amino acid sequence of three H3 haemagglutinins derived from the virus strains A/Aichi/2/68 (the present paper), A/Memphis/102/72 (ref. 6) and A/Victoria/3/75 (ref. 5). The Memphis sequence used here is the complete one obtained by Sleigh *et al.*[6], rather than the one obtained by Ward and Dopheide[7,8], which lacks the hydrophobic region close to the C-terminus of the HA2. Apart from this, both sequences are essentially the same. Each difference is indicated by its number in the signal sequence (S), HA1 and HA2 portions of the molecule, respectively, and by a line connecting the strains involved. Two small lines at the same position in the Memphis strain indicate non-identity with either Aichi or Victoria (apparent reversions; see text).

Table 1 Variation observed among three H3 haemagglutinins

	Nucleotide changes leading to an amino acid change			Silent nucleotide changes		Total of nucleotide changes	
Comparison	No. of changes	% Nucleotide changes	% Amino acid changes	No. of changes	% Nucleotide changes	No. of changes	% Nucleotide changes
Aichi-Memphis	16 (4)	1.6 (0.6)	4.6 (1.8)	14 (9)	1.4 (1.4)	30 (13)	3.0 (2.0)
Memphis-Victoria	16 (2)	1.6 (0.3)	5.2 (0.9)	13 (3)	1.3 (0.4)	32 (5)	3.2 (0.8)
Aichi-Victoria	22 (4)	2.2 (0.6)	6.7 (1.8)	23 (10)	2.3 (1.5)	48 (14)	4.9 (2.1)
Total variable sites	27 (5)	2.7 (0.8)	8.2 (2.3)	24 (11)	2.4 (1.7)	54 (16)	5.5 (2.4)

The HA1 and HA2 regions are considered separately; the values for HA2 are given in parentheses. For the HA1 region the total number of nucleotides and amino acids is 984 and 328, respectively. The AAC insertion (asparagine residue 8') in the Victoria strain has been taken into account only in columns 3 (% amino acid changes) and 6 and 7 (total of nucleotide changes). The HA2 region comprises 663 nucleotides and 221 amino acids in all strains.

tively frequently observed interchanges between proteins in general[36]. Apart from this relationship directly determined by the genetic code, chemically, the substitutions are often of a conservative nature: Gly↔Ala; Ile↔Val; Leu↔Phe; Leu↔Ile; Glu↔Asp; Arg↔Lys. There is one amino acid change (Thr→Tyr) which is both infrequently observed and of a chemically drastic nature. Whether this latter change (at position 155 of HA1) is antigenically important is not known. Not surprisingly, it is the only change caused by two nucleotide substitutions.

Glycosylation sites

All potential glycosylation sites (known to be at Asn-X-Ser or Asn-X-Thr sequences) of the Aichi haemagglutinin are identical to the sites in A/Memphis/102/72, and these glycosylation sites have recently been directly confirmed[7,8]. Thus, it is probable that the glycosylation pattern has remained constant during the period 1968–72. However, one site (position 81 in HA1) disappears and two potential new sites (at positions 63 and 126) are created in Victoria relative to the 1968 prototype (and Memphis/72). Thus, the pattern of glycosylation in the HA1 is not invariable within the H3 subtype. The effect (if any) of this variation on the antigenic properties remains to be established. Note that the positions of the glycosylation sites are rather variable between different subtypes, except at position 154 of the HA2 chain, which has been conserved in all influenza A strains examined so far[5–8,11,12].

Further considerations

Not only nucleotide substitutions leading to an amino acid change but also silent mutations occur somewhat more frequently in the sequence coding for HA1 (2.3%) than in that coding for HA2 (1.5%) (Table 1). This enhanced value is statistically significant at the 5% level as tested by χ^2 analysis. If this trend is consolidated by more data, the question arises as to the meaning of this higher variability in HA1 independent of selection pressure at the protein level. It could perhaps be interpreted as base changes selected as a function of the preservation of a defined secondary structure in the viral RNA that has been more disturbed by nucleotide changes causing amino acid replacements in HA1 than HA2. A well defined secondary (and tertiary) structure may be important in the formation of the nucleoprotein complex or for packaging the eight RNAs in a molar ratio in the particle. Another case where the importance of secondary structure in the genome of RNA viruses has been well documented involves the RNA phages, where it has been shown that the number of base changes between RNA phages is 2.5 times lower in double-stranded regions than in single-stranded regions[37].

If one considers the actual number of silent and non-silent single base changes in the 61 codons for the 20 amino acids in the HA1 and the HA2 coding sequence and compares these values with those that would be expected assuming that single base replacements are acquired on a random basis, the differences are quite striking. According to this assumption, 25.5% of the substitutions would be expected to be neutral and 74.5% would cause an amino acid change[38]. In reality, one finds in the HA1: silent changes, 23; non-silent changes, 20; non-silent changes expected taking the silent ones as the 25.5% value, 67. In the HA2 region these values are: silent changes, 10; non-silent changes, 4; non-silent changes expected, 29. This means that in HA1, 70% of the potentially non-silent mutations would be selected against; this percentage is even higher (86%) in HA2. A similar comparison between RNA phages leads to a value of 93% (ref. 37). All these deviations from randomness are statistically meaningful at the 0.1% level (χ^2 test). Although these estimates are not very accurate (it is not valid to assume an equal probability for a nucleotide to change in any direction), they are, nevertheless, a relative measure of the selection pressure to maintain the amino acid sequence in a molecule or its subregions.

Considering the nature of the nucleotide substitutions, transitions are much more frequent than transversions: of the 64 single-base substitutions between Aichi and Victoria, 49 are transitions and only 15 are transversions. Similarly, comparison of nucleotide sequences from two RNA bacteriophages, MS2 and R17, reveals 29 transitions and 5 transversions[37]. Even in the (at least at first approximation) neutral third-letter position of fourfold degenerate codons, 12 out of 15 changes are transitions between the influenza strains, and all 11 changes are transitions in the comparison between the two phages. It is quite possible that these transitions arise during replication by the formation of G · U instead of the normal G · C or A · U interactions[37].

Finally, it is too early to understand the basis of drift from the sequence information available for the haemagglutinins of natural H3N2 strains and of variants selected by monoclonal antibodies. The three-dimensional structure of the X31 haemagglutinin will probably soon be solved[39], especially as the primary amino acid sequence is now available for reference. This may then, in combination with the available and forthcoming sequence information, provide a solid framework for understanding the variability of the virus within a subtype, the mechanism of antigenic drift and the number and distribution of antigenic sites on the haemagglutinin molecule.

We thank Dr J. Skehel for a gift of X31 RNA and W. Kuziel for help with the manuscript. This research was supported by grants from the Fonds voor Kollektief Fundamenteel Onderzoek and the Gekoncerteerde Akties of the Belgian Ministry of Science. D. H. thanks the IWONL and M.V. thanks the NFWO for fellowships.

Received 16 April; accepted 17 June 1980.

1. Laver, W. G. & Webster, R. G. *Br. med. Bull.* **35,** 29–33 (1979).
2. Palese, P. & Schulman, J. L. *Proc. natn. Acad. Sci. U.S.A.* **73,** 2142–2146 (1976).
3. Scholtissek, C., Harms, E., Rohde, W., Orlich, M. & Rott, R. *Virology* **74,** 332–344 (1976).
4. McGeoch, D. J., Fellner, P. & Newton, C. *Proc. natn. Acad. Sci. U.S.A.* **73,** 3045–3049 (1976).
5. Min Jou, W. *et al. Cell* **19,** 683–696 (1980).
6. Sleigh, M. J., Both, G. W., Brownlee, G. G., Bender, V. J. & Moss, B. A. in *Structure and Variation in Influenza Virus* (eds Laver, W. G. & Air, G. M.) 69–79 (Elsevier, Amsterdam, 1980).
7. Ward, C. W. & Dopheide, T. A. in *Structure and Variation in Influenza Virus* (eds Laver, W. G. & Air, G. M.) 27–38 (Elsevier, Amsterdam, 1980).
8. Dopheide, T. A. & Ward, C. W. in *Structure and Variation in Influenza Virus* (eds Laver, W. G. & Air, G. M.) 21–26 (Elsevier, Amsterdam, 1980).

9. Laver, W. G. *et al. Virology* **98,** 226–237 (1979).
10. Laver, W. G., Air, G. M., Dopheide, T. A. & Ward, C. W. *Nature* **283,** 454–457 (1980).
11. Gething, M.-J., Bye, J., Skehel, J. & Waterfield, M. in *Structure and Variation in Influenza Virus* (eds Laver, W. G. & Air, G. M.) 1–10 (Elsevier, Amsterdam, 1980).
12. Porter, A. G. *et al. Nature* **282,** 471–477 (1979).
13. Devos, R., Gillis, E. & Fiers, W. *Eur. J. Biochem.* **62,** 401–410 (1976).
14. Devos, R., van Emmelo, J., Contreras, R. & Fiers, W. *J. molec. Biol.* **128,** 595–619 (1979).
15. Grunstein, M. & Hogness, D. S. *Proc. natn. Acad. Sci. U.S.A.* **72,** 3961–3965 (1975).
16. Smith, H. O. & Birnstiel, M. L. *Nucleic Acids Res.* **3,** 2387–2398 (1976).
17. Maxam, A. M. & Gilbert, W. *Proc. natn. Acad. Sci. U.S.A.* **74,** 560–564 (1977).
18. Efstratiadis, A., Kafatos, F. C. & Maniatis, T. *Cell* **10,** 571–585 (1977).
19. McCauley, J. *et al. FEBS Lett.* **108,** 422–426 (1979).
20. Lazarowitz, S. G. & Choppin, P. W. *Virology* **68,** 440–454 (1975).
21. Klenk, H.-D., Rott, R., Orlich, M. & Blödorn, J. *Virology* **68,** 426–439 (1975).
22. Ward, C. W. & Dopheide, T. A. *Virology* **103,** 37–53 (1980).
23. Laver, W. G. & Webster, R. G. *Virology* **81,** 482–485 (1977).
24. Ward, C. W. & Dopheide, T. A. *Br. med. Bull.* **35,** 51–56 (1979).
25. Waterfield, M. D., Espelic, K., Elder, K. & Skehel, J. J. *Br. med. Bull.* **35,** 57–63 (1979).
26. Brownlee, G. G. in *Structure and Variation in Influenza Virus* (eds Laver, W. G. & Air, G. M.) 385–390 (Elsevier, Amsterdam, 1980).
27. Dopheide, T. A. & Ward, C. W. *FEBS Lett.* **110,** 181–183 (1980).
28. Klenk, H.-D. in *Structure and Variation in Influenza Virus* (eds Laver, W. G. & Air, G. M.) 213–222 (Elsevier, Amsterdam, 1980).
29. Blobel, G. *et al. Soc. exp. Biol. Symp.* **33,** 9–36 (1979).
30. Jackson, D. C., Dopheide, T. A., Russell, R. J., White, D. O. & Ward, C. W. *Virology* **93,** 458–465 (1979).
31. Jackson, D. C., Russell, R. J., Ward, C. W. & Dopheide, T. A. *Virology* **89,** 199–205 (1978).
32. Potter, C. W. & Oxford, J. S. *Br. med. Bull.* **35,** 69–75 (1979).
33. Pereira, M. S. in *Influenza Virus, Vaccines and Strategy* (ed. Selby, P.) 25–31 (Academic, London, 1976).
34. Pereira, M. S. *Br. med. Bull.* **35,** 9–14 (1979).
35. Atassi, M. Z. & Smith, J. A. *Immunochemistry* **15,** 609–610 (1978).
36. Dayhoff, M. O., Schwartz, R. M. & Orcutt, B. C. in *Atlas of Protein Sequence and Structure* Vol. 5, Suppl. 3 (ed. Dayhoff, M. O.) 345–352 (The National Biomedical Research Foundation, Silver Springs, Maryland, 1978).
37. Min Jou, W. & Fiers, W. *J. molec. Biol.* **106,** 1047–1060 (1976).
38. Jukes, T. H. & King, J. L. *Nature* **281,** 605–606 (1979).
39. Wilson, I. A., Skehel, J. J. & Wiley, D. C. in *Structure and Variation in Influenza Virus* (eds Laver, W. G. & Air, G. M.) 339–348 (Elsevier, Amsterdam, 1980).

RNA splicing generates a variant light chain from an aberrantly rearranged κ gene

Edmund Choi*, Michael Kuehl† & Randolph Wall*

* Molecular Biology Institute and Department of Microbiology and Immunology, UCLA School of Medicine, Los Angeles, California 90024
† Department of Microbiology, University of Virginia School of Medicine, Charlottesville, Virginia 22908

Both C_κ regions in MPC 11 cells are rearranged into active transcription units, one producing a normal κ chain and the other an internally deleted κ fragment lacking a V region. The gene coding for the κ fragment mRNA is aberrantly rearranged and lacks a site for $V \rightarrow C_\kappa$ splicing. An alternative splicing event which deletes the V region from the nuclear RNA precursor generates the κ fragment mRNA.

IMMUNOGLOBULIN light-chain variable (V) and constant (C) regions are rearranged in the formation of active genes (that is, transcription units)[1-4]. These somatic rearrangements join a specific germ-line V region with a J region while retaining the intervening sequence (intron) separating the J and C regions in germ-line DNA[1-4]. Some myeloma cells also contain C regions arranged differently from either the germ-line pattern or the pattern in the active transcription unit producing immunoglobulin light chains[5,6]. The detailed structure of such rearranged C regions has not been determined. These presumably aberrant DNA arrangements have been proposed to be the mechanism for allelic exclusion in immunoglobulin-producing cells. However, it has not been shown whether or not such aberrantly rearranged C regions are transcribed. Indeed, the relationship of DNA rearrangements to the activation of immunoglobulin genes for transcription remains to be resolved.

Immunoglobulin messenger RNAs, like virtually every eukaryotic mRNA now studied, are processed from larger nuclear RNA precursors by RNA splicing[7-10]. It seems that RNA splicing may be an obligatory step for the generation of stable mRNA[11-13]. One clue to the signals possibly used in RNA splicing has emerged from the nucleotide sequencing of cloned eukaryotic genes containing introns. All eukaryotic genes now studied (including several immunoglobulin light- and heavy-chain genes, with one notable exception) have the characteristic nucleotides 5′-/*GT*-intron-*AG*/-3′ at the junctures between introns and exons (summarized in ref. 14). Compilation of subsequent sequences has shown that the 5′ (upstream) and 3′ (downstream) ends of introns approximate to the following consensus or 'optimal' splice sites[14-16]

5′-exon-AG/$\underline{\mathit{GT}}$AAGTA——intron——
——TTTTYTTTTTTCTTNC$\underline{\mathit{AG}}$/G-exon-3′

These upstream and downstream splice sites flanking an intron presumably must be brought together for RNA splicing to occur. One of the abundant, small nuclear RNA (snRNA) species called U-1 (ref. 17) is exactly complementary to these 'optimal' sequences at RNA splicing sites. A mechanism for RNA splicing has been proposed in which U-1 snRNA is the recognition component of the nuclear RNA splicing enzyme complex and hybridizes with both ends of an intron so as to align them in exact register for RNA splicing[15,16]. However, the significance of these presumptive signals and the molecular mechanisms of RNA splicing remain to be elucidated.

We have approached these questions by investigating how cloned MPC 11 myeloma cells simultaneously produce both a normal κ light-chain containing precursor, P, V, J and C_κ regions, and a variant κ light-chain fragment containing *P* and C_κ regions but lacking V and J regions[18,19]. Combining nuclear RNA and DNA mapping approaches, we find that the two κ mRNAs in MPC 11 cells are independently transcribed from two separate transcription units with rearranged C_κ regions. Aberrant rearrangement of one C_κ region in MPC 11 cells generates the transcription unit for the κ fragment light chain. The nuclear RNA transcript of this aberrantly rearranged C_κ region undergoes an unusual RNA splicing step which generates the κ fragment mRNA. The detailed structure of this variant MPC 11 C_κ gene is presented in the accompanying article[20].

MPC 11 cells contain two rearranged C_κ regions

The expression of two different κ light chains in MPC 11 cells suggests that there must be two differently rearranged C_κ regions. This prediction was confirmed by Southern mapping[21] of the C_κ regions in *Bam*HI-cleaved DNA from MPC 11 (clone 45.6) and spleen cells. Hybridization with a cloned cDNA probe (pL21-5, 22) which contains the C_κ region reveals that 45.6 cells contain strongly hybridizing fragments of 3.0 and 7.7 kilobases (Fig. 1). Spleen DNA which has non-rearranged C_κ regions contains a single C_κ band at 14 kilobases. Weakly hybridizing fragments of 5.1, 5.5 and 5.7 kilobases, present in all the cell lines and spleen DNA, are probably due to a small amount ($\simeq$50 nucleotides) of MOPC 21 V-region sequences in the pL21-5 probe[22] which react with MOPC 21 and related V regions in the DNA. The MOPC 21 V-region does not cross-hybridize with either the MPC 11 or MOPC 321 V regions (E.C., unpublished results).

0028-0836/80/340776—04$01.00

To determine which C_κ restriction fragments correspond to the normal and fragment MPC 11 light chains, we examined a variant (clone NP.2) which expresses only the κ fragment but not the normal light chain. In contrast to those of 45.6 cells, the *Bam*HI digests of NP.2 cells reveal only a single strongly hybridizing fragment of 3.0 kilobases. As this is the only C_κ fragment in NP.2 cells, it must represent the rearranged C_κ region which encodes the κ fragment chain. Apparently, the 7.7 *Bam*HI fragment represents the C_κ region which encodes the normal κ light chain in MPC 11 cells, because the loss of normal light-chain expression in NP.2 cells is correlated with the loss of this fragment. Thus, the loss of normal light-chain expression in the NP.2 variant clone, which was isolated from MPC 11 cells by nitrosoguanidine mutagenesis, seems to be due to the deletion of the rearranged C_κ region coding for this chain.

Nuclear RNA species derived from the normal and fragment genes

Previous results from our laboratory[23] and from Schibler *et al.*[9] revealed multiple κ light-chain nuclear RNA species in MPC 11 cells. To distinguish between the nuclear RNA processing pathways for normal κ and the κ fragment mRNAs, we compared the κ nuclear RNA species in wild-type MPC 11 45.6 cells making both κ chains with those in the NP.2 variant line which synthesized only the C_κ fragment chains.

Polyadenylated nuclear RNA was fractionated on methyl mercury hydroxide gels, transferred onto diazophenylthioether (DPT) paper ('RNA blots', ref. 24) and hybridized with nick-translated C_κ-gene probe (Fig. 2, panel *a*). The 45.6 cells contain five distinct C_κ nuclear RNA species: 6.5, 5.6, 3.6, 1.2 and 0.8 kilobases. The 1.2- and 0.8-kilobase species represent the normal κ light-chain and κ fragment mRNAs, respectively[9,23]. These κ nuclear RNA species are in approximate agreement with those previously reported[9,23] except that the largest band is here resolved into 6.5- and 5.6-kilobase species. When the C_κ-gene probe was hybridized to nuclear RNA from NP.2 cells, only the 3.6- and 0.8-kilobase species were seen (Fig. 2, panel *a*).

These findings outline the two different κ light-chain RNA processing pathways in MPC 11 cells. No larger κ nuclear RNA species are detected either by RNA blots or in brief pulse-labelling experiments (E. C., M. K. and R. W., unpublished results). Although it is not formally proven here, we presume that the polyadenylated 6.5- and 3.6-kilobase species represent the primary transcripts for the κ light-chain and κ fragment mRNAs, respectively. The definition of the sequences in these presumptive primary transcripts provides a means of further defining the structures of the two active κ transcription units in MPC 11 cells.

To characterize these κ transcripts further, we isolated two specific restriction fragments of the C_κ-gene clone[2,3] (see Fig. 2, inset). One contains a portion of the intron between the J regions and C_κ region (designated IS), the other fragment encompasses the entire J-region cluster (designated J; see Fig. 2, inset). The intron probe hybridized to the 6.5- and 5.6-kilobase precursors in 45.6 cells (Fig. 2, panel *b*). It also hybridized to the 3.6-kilobase species in both 45.6 and NP.2 cells, indicating that this nuclear RNA species contains sequences from the $J \rightarrow C_\kappa$ intron in normal κ light-chain transcription units. As expected, this probe did not hybridize with either the 1.2- or the 0.8-kilobase mRNA species.

We next determined which nuclear RNA species contained J-region sequences. As expected, the restriction fragment containing all five known κ J regions hybridized with the 6.5-, 5.6- and 1.2-kilobase κ RNAs in 45.6 cells (Fig. 2, panel *c*). In contrast, the 3.6- and 0.8-kilobase κ species in 45.6 or NP.2 cells did not hybridize with the J probe (Fig. 2, panel *c*), suggesting that the transcription unit for the κ fragment does not contain J regions.

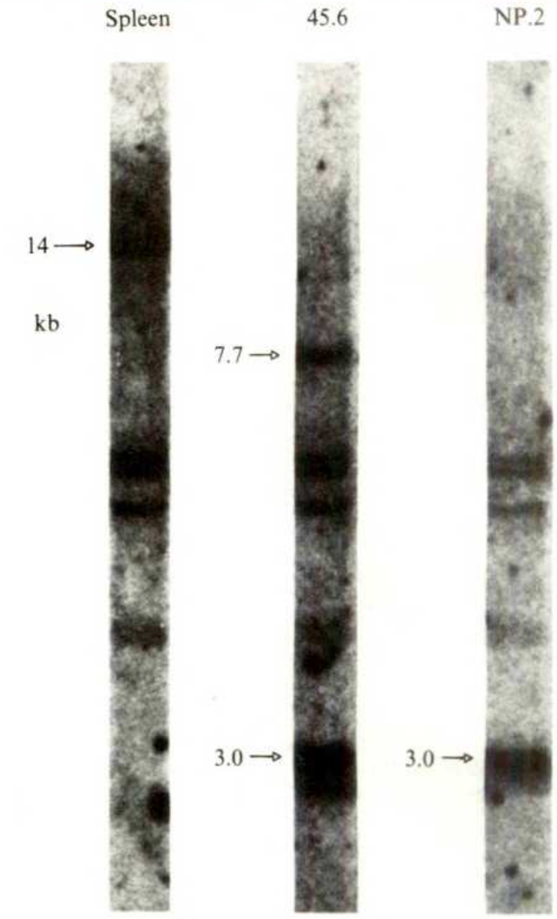

Fig. 1 Southern hybridization analysis of the κ constant region specific *Bam*HI DNA fragments of spleen and MPC 11 wild-type and variant plasmacytomas. Fragments generated by *Bam*HI digestion of BALB/c spleen, MPC 11 clone 456, and MPC 11 clone NP.2 DNAs were fractionated by electrophoresis in 0.75% gels, alkali denatured, neutralized and transferred to nitrocellulose filters[21]. The filters were hybridized to 0.2 μg of nick-translated ^{32}P-labelled pL21-5 plasmid DNA (1.5×10^8 c.p.m. per μg) and subjected to autoradiography. The pL21-5 cDNA plasmid probe contains approximately 550 nucleotides of MOPC 21 κ mRNA sequence, including all the 3'-untranslated, constant region and J-region sequences as well as 50 nucleotides of MOPC 21 V-region sequences[22]. Fragment lengths were determined by comparison with ethidium bromide-stained *Eco*RI and *Hin*dIII fragments of phage λ phage DNA. Lane *a*, spleen DNA; lane *b*, MPC 11 clone 45.6; lane *c*, MPC 11 clone NP.2 DNA.

It has previously been shown that the MPC 11 κ fragment mRNA contains a MOPC 321-like hydrophobic precursor (P) region linked to the C_κ region[19]. To determine if the nuclear RNA precursor to the C_κ fragment mRNA also contains the MOPC 321 V region, we hybridized a nick-translated restriction fragment containing the V region of MOPC 321 to nuclear RNA from 45.6 and NP.2 cells. Only the 3.6-kilobase species in both cell lines contains a V region which hybridizes with the MOPC 321 variable region (Fig. 2, panel *d*). This probe did not hybridize to the 6.5- or 5.6-kilobase RNA precursors in 45.6 cells, establishing that there are no MOPC 321 V-region sequences on the precursors to the normal κ light chain of MPC 11 cells.

The two independent κ nuclear RNA processing pathways are clearly defined by these results. Those RNA precursors in the normal κ light-chain processing pathway are identified by the presence of J-region sequences, and those in the κ fragment pathway are distinguished by the presence of MOPC 321 V-region sequences.

The processing pathway for the full-length κ mRNA is

$$6.5 \text{ kilobases} \rightarrow 5.6 \text{ kilobases} \xrightarrow[\text{splice}]{V\rightarrow C_\kappa} \rightarrow 1.2\text{-kilobase mRNA}$$

In the transcription unit for the normal MPC 11 κ light chain, the V region is joined to J_4 and contains a 3.5-kilobase intron separating the joined V+J from the C_κ region[3,4]. This intron is removed in the processing step from the 5.6-kilobase nuclear RNA to the 1.2-kilobase mRNA, apparently with another

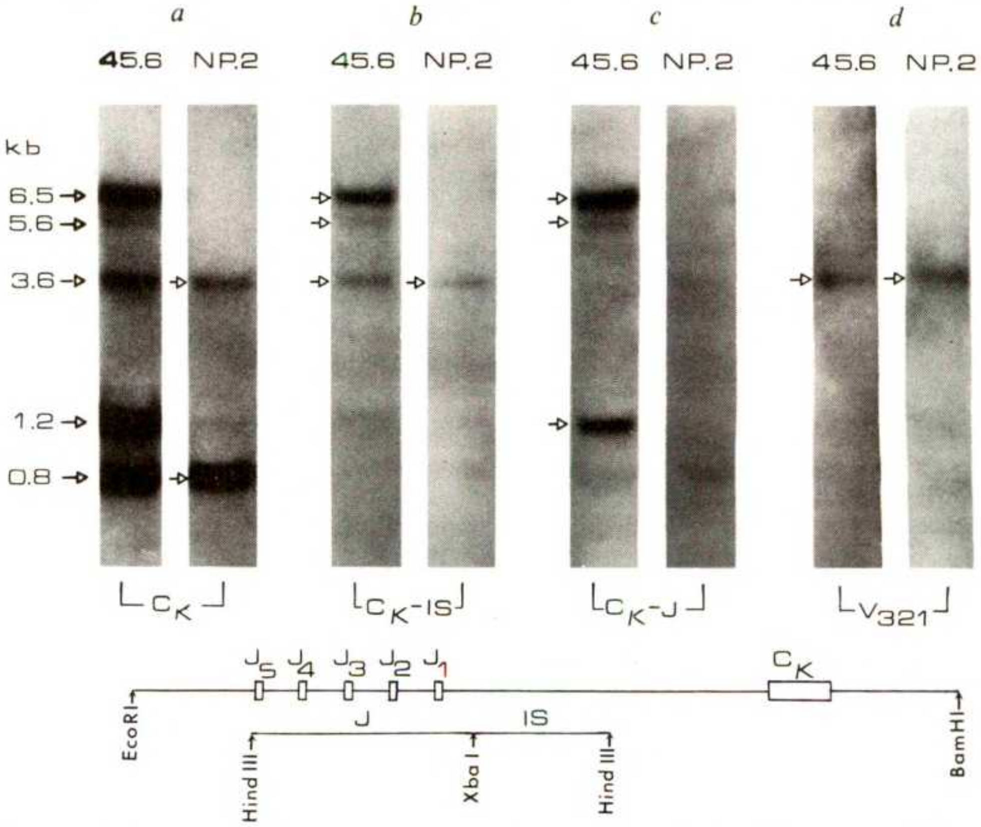

Fig. 2 Analysis of nuclear RNA species in 45.6 and NP.2 cells. Nuclear RNA was prepared from detergent-washed nuclei[31]. Poly(A)$^+$ nuclear RNA was fractionated on 1% agarose gels containing 5.0 mM methyl mercury hydroxide[32]. Nuclear RNA was loaded at 20 μg per lane. All operations involving methyl mercury hydroxide were carried out using appropriate safety measures. The RNA transfer was carried out as described by Wahl *et al.*[33] except that DPT paper was used instead of diazobenzyloxymethyl paper. Following transfer, the DPT paper was hybridized with nick-translated probes and washed in conditions described by Wahl *et al.*[33]. The restriction fragments used for nick translation were isolated from agarose gels[23]. The specific activities of the ^{32}P-labelled probes ranged from 7×10^7 to 2×10^8 c.p.m. per μg; $2-3\times10^6$ c.p.m. were hybridized to each lane. The following probes were each hybridized to a pair of lanes containing the nuclear RNA from 45.6 and NP.2 cells. Panel *a*, C_κ embryo genome clone. The 6.5-kilobase *XbaI–Hin*dIII restriction fragment[3] from the C_κ clone is outlined in the inset below the RNA lanes. Panel *b*, intervening sequence probe. A 1.1-kilobase *XbaI–Hind*III restriction fragment designated IS in the C_κ embryo gene was used. Panel *c*, J-region probe. A 1.7-kilobase *Hin*dIII/*Xba*I restriction fragment designated J in the diagram was used. panel *d*, 321 variable region probe. An *Ava*I restriction fragment containing the 321 variable region was isolated from a recombinant cDNA clone. Filters in panels *b*, *c* and *d* rehybridized with the C_κ embryonic probe used in lane *a* showed that all the κ nuclear species were present on these filters (data not shown). The following mouse rRNAs were used to calculate the sizes of hybridized nuclear RNA bands 45s(14.1 kilobases), 32s (6.6 kilobases), 28s (5.2 kilobases) and 18s (2.1 kilobases)[34].

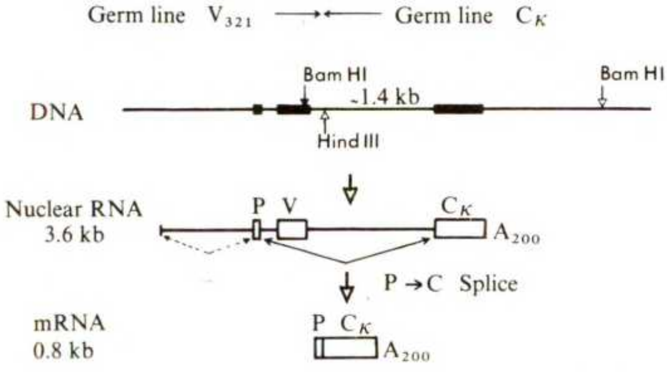

Fig. 3 The transcription unit and nuclear RNA processing pathway for the MPC 11 C_κ fragment mRNA. Polyadenylation of the 3.6-kilobase nuclear RNA precedes RNA splicing. Other details of the model are discussed in the text.

undefined intron amounting to approximately 1 kilobase. This V→C_κ splicing event may proceed throught a rapidly labelled intermediate of approximately 2.1 kilobases which is readily detected in pulse-labelling experiments[23] but not in RNA blots, as the latter technique primarily detects stable species of nuclear RNA.

The processing pathway for the κ fragment mRNA seems to be

$$3.6\ \text{kilobases} \xrightarrow{\text{P}\rightarrow\text{C}_\kappa\ \text{splice}} \rightarrow 0.8\text{-kilobase mRNA}$$

Because the 3.6-kilobase nuclear RNA precursor lacks a J region and the germ-line MOPC 321 V region lacks an upstream splice site, this V region cannot be spliced to the C_κ region. The κ fragment chain lacks the last three carboxy-terminal amino acids of the MOPC 321 P region[18,19]. This suggests that the normal splicing site at the 3′ end of the P region is spliced to the site at the 5′ side of the C_κ region, thereby generating the fragment light-chain mRNA (Fig. 3). It is not known if the P region is alternatively spliced to the 5′ end of the 321 V-region gene. The RNA product of such a splice, removing only approximately 0.2 kilobases, would probably not be distinguished in RNA blots. Moreover, the product RNA might be rapidly degraded in the nucleus. The efficiency of P→C_κ splicing is not known. However, it is likely that this unusual splice occurs at a comparatively high frequency, because the 3.6-kilobase RNA species and the κ-fragment mRNA comprise, respectively, some 20% of the κ RNA in the nucleus and cytoplasm of 45.6 cells. The P→C_κ splice removes approximately 2 kilobases. An additional splice removing approximately 0.8 kilobases also apparently occurs in the generation of the κ fragment mRNA. This splice presumably involves 5′-untranslated leader sequences (Fig. 3).

Structure of the κ fragment transcription unit

The fragment transcription unit apparently contains P, V and C regions, but lacks J regions. Moreover, it contains the intervening sequence up to 1.1 kilobases from the 5′ side of the C_κ region (that is, sequences homologous to the *Xba*I*Hin*dIII fragment; Fig. 2, inset). A model consistent with these results would predict that the embryonic MOPC 321 V region is joined to a point in the intervening sequence preceding the embryonic C_κ gene (including the *Hin*dIII site 1.1 kilobases from the C_κ region), such that the J regions are deleted. The presence of the fragment κ gene on a 3.0-kilobase *Bam*HI restriction fragment allows us to localize the rearrangement further. A *Bam*HI restriction site is located 1.2 kilobases 3′ to the embryonic C_κ gene[2,3]. The sequences flanking the 3′ end of the C_κ gene are conserved during the somatic rearrangement of the DNA to form the active immunoglobulin gene[2,3,6]. Assuming that the C_κ gene amounts to 0.5 kilobases (including the contiguous 3′-untranslated region), the *Bam*HI site 5′ to the C_κ gene is approximately 1.4 kilobases away. No *Bam*HI site exists in this region in the embryonic C_κ gene[2,3]. Therefore, this *Bam*HI site must have originated on the 3′ end of the rearranged MOPC 321 V region[2]. A likely *Bam*HI site is found at amino acid 96 in the germ-line MOPC 321 variable region[2]. This would place the rearranged 321 V region approximately 1.4 kilobases away from the C_κ region (Fig. 3). This predicted arrangement of the MPC 11 κ fragment transcription unit has been confirmed by direct nucleotide sequence by Seidman and Leder[20].

Discussion

These results clearly show that both C_κ alleles can be rearranged into concomitantly active transcription units. However, with regard to allelic exclusion, it should be noted that these MPC 11 cells produce only a single functional secreted κ chain. Because the aberrant rearrangement which generates the κ fragment occurs by recombination between homologous germ-line DNA sequences[20], it is likely that other immunoglobulin-producing cells will also express V regions joined at this intervening sequence site. Certainly, the demonstration that such rearranged C_κ genes are transcribed suggests that the activation of immunoglobulin C_κ genes for transcription does not necessarily result from the normal V→J joining event. Recent findings indicate that in certain myeloma cell lines, an unrearranged C_κ gene is apparently transcribed concomitantly with the rearranged C_κ gene which generates mRNA[25]. This suggests that DNA rearrangement may not initiate the transcription of an immunoglobulin gene but may rather generate a complete transcription unit bounded by an initiation site for transcription (contributed by the V-region segment) and a poly(A) addition site (contributed by the C-region segment). These two elements may be sufficient to delineate a transcription unit capable of producing a stable, polyadenylated primary transcript which can be processed to immunoglobulin mRNA.

The MPC 11 κ fragment mRNA contains two exons (P, C_κ) which are not normally spliced together in immunoglobulin mRNA. Such shuffling of exons presumably does not occur very frequently in normal mRNA splicing. However, RNA splicing can apparently bypass a mutant splicing site provided that the RNA precursor contains other introns with functional splicing sites. In such precursors, as in the MPC 11 κ fragment, such an event could result in the deletion of a complete exon.

This seems to be the most likely explanation for the large number of immunoglobulin heavy-chain deletion variants which have lost internal domains or the hinge region[26,27]. A particularly striking example of such a heavy chain deletion variant is the IF2, γ_1 chain, which lacks the C_H1 domain and has the V_H region joined directly to the hinge[28]. A γ_1 heavy-chain gene which may resemble the IF2 variant gene has been cloned from MOPC 21 myeloma tumour DNA[29]. This MOPC 21 γ_1 clone is identical in nucleotide sequence to another γ_1 gene clone from embryo DNA[30] except that the trinucleotide, GTG, which directly follows the C_H1 domain, is deleted[29,30]. Presumably, RNA transcripts of this MOPC 21 γ_1 gene lack a functional splice site at the C_H1/intron juncture and would be expected to splice the V_H region to the hinge, producing an internally deleted variant chain like IF2. Future studies on immunoglobulin deletion variants should serve to define further the signals and steps in RNA splicing.

These studies were supported by NIH research grants AI13410, CA12900 and AI12525. E. C. was supported by NIH Training Grant CA 09056. DPT paper was developed by Brian Seed, C_κ embryo clone was made available to us by P. Leder, and the MOPC 321 cDNA clone was from S. Tonegawa.

Received 4 April; accepted 18 June 1980.

1. Brack, C., Hirama, M., Lenhard-Schuller, R. & Tonegawa, S. *Cell* **15**, 1–14 (1978).
2. Sakano, H., Hüppi, K., Heinrich, G. & Tonegawa, S. *Nature* **280**, 288–294 (1979).
3. Max, E. E., Seidman, J. G. & Leder, P. *Proc. natn. Acad. Sci. U.S. A.* **76**, 3450–3454 (1979).
4. Seidman, J. G., Max, E. E. & Leder, P. *Nature* **280**, 370–375 (1979).
5. Lenhard-Schuller, R., Hohn,, B., Brack, C., Hirama, M. & Tonegawa, S. *Proc. natn. Acad. Sci. U.S.A.* **75**, 4709–4713 (1978).
6. Seidman, J. G. & Leder, P. *Nature* **276**, 790–795 (1978).
7. Gilmore-Hebert, M. & Wall, R. *Proc. natn. Acad. Sci. U.S.A.* **75**, 342–345 (1978).
8. Gilmore-Hebert, M. & Wall, R. *J. molec. Biol.* **135**, 879–891 (1979).
9. Schibler, U., Marcu, K. B. & Perry, R. P. *Cell* **15**, 1495–1509 (1978).
10. Perry, R. P., Kelley, D. E. & Schibler, U. *Proc. natn. Acad. Sci. U.S.A.* **76**, 3678–3682 (1979).
11. Gruss, R., Lai, C-J, Dahr, R. & Khoury, G. *Proc. natn. Acad. Sci. U.S.A.* **76**, 4317–4321 (1979).
12. Hamer, D. H. & Leder, P. *Cell* **18**, 1299–1302 (1979).
13. Berg, P. in *Mobilization and Reassembly of Genetic Information* (eds Scott, W. A., Schultz, J., Werner, R. & Joseph, D. R.) (Academic, New York, in the press).
14. Seif, I., Khoury, G. & Dhar, R. *Nucleic Acids Res.* **6**, 3387–3398 (1979).
15. Rogers, J. H. & Wall, R. *Proc. natn. Acad. Sci. U.S.A.* **77**, 1877–1879 (1980).
16. Lerner, M. R., Boyle, J. A., Mount, S. M., Wolin, S. L. & Steitz, J. A. *Nature* **283**, 220–224 (1980).
17. Ro-Choi, T. S. & Henning, D. *J. biol. Chem.* **252**, 3814–3820 (1979).
18. Kuehl, W. M. *et al. Cell* **5**, 139–147 (1975).
19. Rose, S. M., Kuehl, W. M. & Smith, G. P. *Cell* **12**, 453–462 (1977).
20. Seidman, J. G. & Leder, P. *Nature* **286**, 779–783 (1980).
21. Southern, E. M. *J. molec. Biol.* **98**, 503–517 (1975).
22. Wall, R. *et al. Nucleic Acids Res.* **5**, 3113–3128 (1978).
23. Komaromy, M. Clarke, P., Choi, E., Kuehl, M. & Wall, R. in *Eukaryotic Gene Regulation* Vol. 14 (eds Axel, R., Maniatis, T. & Fox, C. F.) 421–431 (Academic, New York, 1979).
24. Alwine, J. C., Kemp, D. J. & Stark, G. R. *Proc. natn. Acad. Sci. U.S.A.* **74**, 5350–5354 (1977).
25. Perry, R. P. *et al.*, *Proc. natn. Acad. Sci. U.S.A.* **77**, 1937–1941 (1980).
26. Franklin, E. C. & Frangione, B. in *Contemporary Topics in Molecular Immunology* (ed. Inman, F. P.) 89–126 (Plenum, New York, 1975).
27. Franklin, E. C., Prelli, F. & Frangione, B. *Proc. natn. Acad. Sci. U.S.A.* **76**, 452–456 (1978).
28. Adetugbo, K. *J. biol. Chem.* **253**, 6076–6080 (1978).
29. Sakano, H. *et al. Nature* **277**, 627–633 (1979).
30. Honjo, T. *et al. Cell* **18**, 559–568 (1979).
31. Fedoroff, N., Wellauer, P. K. & Wall, R. *Cell* **10**, 597–610 (1977).
32. Bailey, J. M. & Davidson, N. *Analyt. Biochem.* **70**, 75–85 (1976).
33. Wahl, G. M., Stern, M. & Stark, G. R. *Proc. natn. Acad. Sci. U.S.A.* **76**, 3683–3687 (1979).
34. Wellauer, P. K., Dawid, I. B., Kelley, D. E. & Perry, R. P. *J. molec. Biol.* **89**, 397–407 (1974).

A mutant immunoglobulin light chain is formed by aberrant DNA- and RNA-splicing events

J. G. Seidman & Philip Leder

Laboratory of Molecular Genetics, National Institute of Child Health and Human Development, National Institutes of Health, Bethesda, Maryland 20205

A mutant immunoglobulin gene has been formed by an abnormal (non V/J) recombination event such that abnormal RNA splicing is required to form a mutant light chain. The structure of the gene suggests that the small palindrome thought to be involved in V/J joining also provides the basis for this abnormal DNA recombination and that the absence of a J segment and RNA splice signal allows an abnormal RNA splicing reaction to occur.

THE generation of antibody diversity depends on a specialized form of genetic recombination that operates in somatic cells during lymphocyte differentiation[1–4]. The combinational power of joining one of several hundred variable region genes to one of the four J-region segments encoded close to the constant-region gene creates literally thousands of unique genetic possibilities[5–9]. Recent DNA cloning and nucleotide sequences analyses have revealed many of the molecular details of this

0028–0836/80/340779—05$01.00

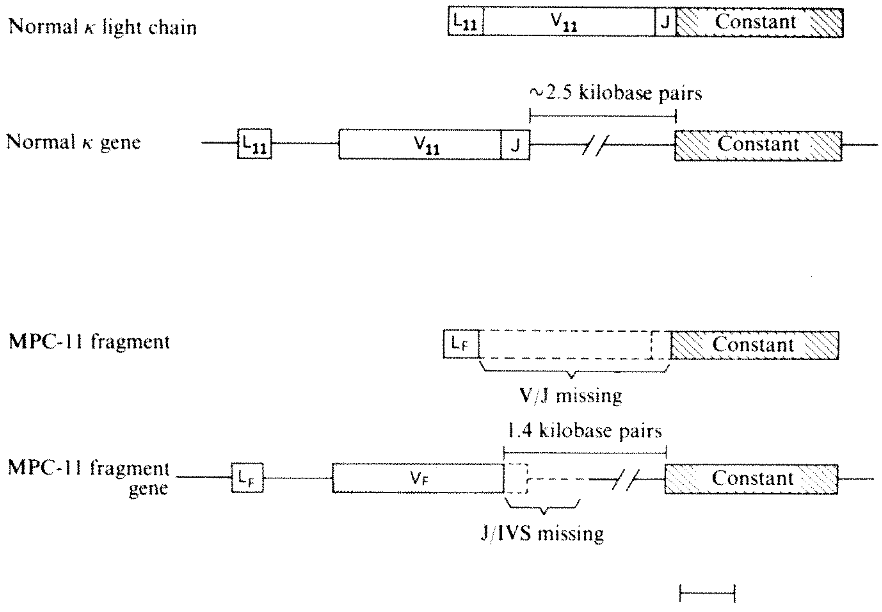

Fig. 1 The structure of the MPC-11 light chains and their genes. The MPC-11 cell synthesizes two κ light chains—a normal κ light chain and the MPC-11 fragment. We presume that the normal κ light chain is encoded by a normal κ gene, while the MPC-11 fragment is encoded by the MPC-11 fragment gene. The leader of the MPC-11 normal κ light chain (L_{11}) and the leader of the MPC-11 fragment (L_F) do not have the same amino acid sequence[12,13]. The amino acid sequence of L_F is identical to the leader of the MOPC-321 light chain[12,13]. Scale bar, 0.1 kilobase pairs.

process, including a plausible molecular basis for the special recombination event[8,9]. They also provide an accurate picture of an active κ immunoglobulin gene[7]. In its final form, the κ light-chain gene consists of three separate coding elements separated by two intervening sequences of DNA. Obviously, the formation of a light chain requires both DNA- and RNA-splicing reactions.

Kuehl and Scharff[10] have described an immunoglobulin-producing cell that is relevant to both these processes. They showed that the cell line MPC-11 produced two light chains, one apparently normal and the other, a lower molecular-weight fragment, at first thought to contain only constant region sequences. Further studies showed that a derivative of this cell line had lost its ability to produce normal light chains, but that it continued to produce the fragment. In addition, the fragment was encoded in a shorter-than-normal mRNA species[11]. These studies led to the conclusion that there must be two independently active κ genes in MPC-11 cells and that (at least in this instance) the process of allelic exclusion that affects most antibody-producing cells had been circumvented[10]. Subsequent amino acid sequence determinations[12,13] on an *in vitro* synthesized fragment precursor showed that it consisted of a hydrophobic leader sequence joined directly to the κ constant region and that the sequence corresponding to the variable region (the joined V and J segments) was completely lacking (Fig. 1). Moreover, the hydrophobic leader sequence of the fragment was different from that of the intact light chain produced by MPC-11. Instead, it corresponded to a sequence associated with the VK21 subgroup of κ light chains[12,14], an observation that strengthened the notion that each MPC-11 light chain corresponded to a separately expressed allele.

While the simplest explanation for these observations might have been that both chromosomal genes underwent V/J recombination in MPC-11 and that one, the fragment gene, suffered a subsequent deletion of the separately encoded V/J segment, this is not the case. While it might also seem possible that the rearranged gene arose from the normally rearranged gene by a subsequent deletion, this is ruled out by our finding that the normally rearranged chromosome has lost (by deletion associated with V/J recombination) the V-region genes corresponding to those used to form the fragment gene (J.S. and P.L., unpublished data). Since we also found that the fragment gene lacks all J regions, neither gene could serve as precursor for the other and both, therefore, appear to have been derived from independent, allelic germ-line chromosomes. Using DNA cloning, direct sequence analysis and *in situ* hybridization, we show that both alleles have indeed undergone rearrangement in the MPC-11 cell line, but that the fragment gene has undergone a recombination event that has joined its V region to a site close to the κ constant region, but not associated with any J segment. This joining has apparently been guided by the same palindromic sequence (CACAGTG) that occurs adjacent to all V and J segments thus far sequenced, for the recombination has occurred at the only instance of this palindrome between the J regions and the κ constant-region gene (E. Max, unpublished). Since the J region normally provides the RNA splice site at the 5′ end of the intervening sequence between the variable and constant regions, its absence in the fragment gene must prevent the normal RNA splice from occurring. Thus the fragment mRNA must be formed by an aberrant RNA splice involving the hydrophobic leader segment skipping its normal splicing partner, the V segment, and being joined directly to the C region. The nucleotide sequence suggests a mechanism for the aberrant DNA splicing event that involves homologous rather than normal V/J recombination.

In an accompanying study, Choi, Kuehl and Wall[15] show how this mutant gene generates mRNA precursors that follow the required aberrant RNA splicing pathway and that their structure can be reconciled with the structure of the mutant gene described here.

Restriction fragments containing the constant region gene in MPC-11 DNA

Confirmation of the prediction[10] that MPC-11 cells encode two separate and active κ constant-region genes was obtained from *in situ* hybridization experiments in which all the restriction fragments that encode κ constant regions could be identified (Fig. 2). If two constant region genes are present in MPC-11 DNA and have undergone somatic rearrangement, one would expect to find two new restriction fragments each containing a constant region, neither of which should be identical to the fragments observed in embryonic DNA. Cleavage of MPC-11 DNA with the restriction enzyme *Bam*HI produces two such fragments, one 7.7 and the other 3.0 kilobase pairs in length (Fig. 2). The presence of two non-germ-line genes in MPC-11 DNA does not, however, prove that both of these genes are involved in the synthesis of the two light chains expressed in MPC-11 cells. Nor does it allow us to identify the fragment responsible for mutant light-chain production. Other plasmacytoma cells have been shown to contain several non-germ-line genes other than the one which is expressed as a light-chain polypeptide (ref. 7 and E. Max, S. P. Kwan, J. G. S. and P. L., unpublished results). The assignment of the two *Bam*HI restriction fragments to the normal and fragment light-chain genes can be made by taking advantage of several cell lines derived by Scharff and co-workers from MPC-11 that continue to produce the fragment peptide but no longer produce the normal MPC-11 light chain.

One of these cell lines, NP2, yields DNA containing only the 3-kilobase pair *Bam*HI constant-region containing fragment (Fig. 2). Presumably the 7.7-kilobase pair fragment missing in NP2 but present in the parental line encodes the normal MPC-11 light chain, while the 3.0-kilobase pair *Bam*HI fragment must encode the fragment polypeptide. Apparently the NP2 cells have suffered a deletion of the normal MPC-11 light-chain gene and this deletion accounts for their inability to synthesize this light chain. Interestingly, another cell line, B47L3NP, has also lost the ability to produce the normal MPC-11 light chain, but has retained the 7.7-kilobase pair *Bam*HI fragment (Fig. 2). Obviously the mechanism by which this gene is inactivated is not accounted for by a major deletion, making it a fruitful subject for further investigation.

The MPC-11 fragment gene consists of a variable region and constant region without a J segment

To determine the genetic mechanism that led to the formation of the fragment peptide, we isolated the MPC-11 *Eco*RI DNA fragment that encodes the rearranged fragment gene using preparative agarose gel electrophoresis[17]. The proper fragment, about 20 kilobase pairs long, could be identified because it yielded the expected 3.0-kilobase pair *Bam*HI fragment (Fig. 2). The fragment was cloned in λ vector CH4A, identified and further purified using standard recombinant DNA techniques[18].

SCIENCE COLLEGE
Upper Circular Road
CALCUTTA

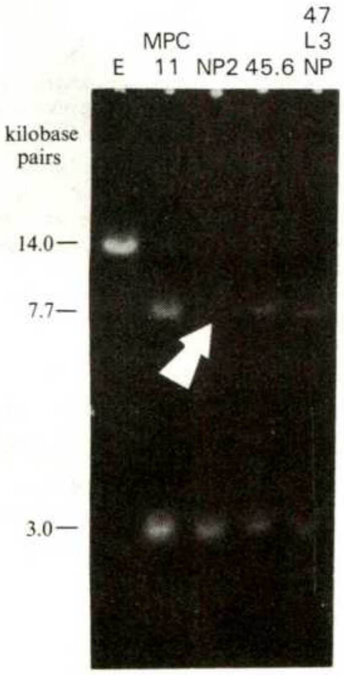

Fig. 2 The constant region containing fragments in DNA derived from embryonic light chain producing and non-producing cells. The DNA from 14-day-old BALB/c embryos (E), MPC-11 and NP2 myeloma tumours, and the 45.6 and B47L3NP (47L3NP) cell lines was restricted with *Bam*HI nuclease, and fractionated on an agarose gel, blotted onto nitrocellulose filters and hybridized to ^{32}P-labelled constant region probes as described previously[6,16]. The B47L3NP cell line was derived from 45.6 and no longer secretes a normal κ light chain. NP2 was originally derived from MPC-11 cells as a cell that does not secrete normal MPC-11 light chain, and has since been carried as a myeloma. The constant region probe hybridizes to one fragment of embryonic DNA (14.0 kilobase pairs) but two fragments of MPC-11 DNA (7.7 and 3.0 kilobase pairs). The arrow indicates the absence of the 7.7-kilobase pair fragment in NP2 DNA; we presume that this fragment encodes the MPC-11 normal κ light chain. The 3.0-kilobase pair *Bam*HI fragment derives from the MPC-11 fragment gene.

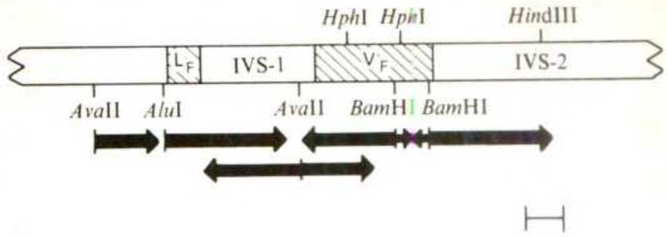

Fig. 3 The restriction fragments used to determine the nucleotide sequence of the MPC-11 fragment gene. A 20-kilobase pair constant region containing *Eco*RI fragment was cloned from MPC-11 DNA into Charon 4A (CH4A MPC-11 fragments) using the procedures described previously[6]. This phage contained a 5-kilobase pair *Hin*dIII fragment that hybridized to the 2.8-kilobase pair *Hin*dIII fragment derived from embryonic DNA that contained all of the κ J-region segments and 1.0 kilobase pairs of intervening sequence[8]. The 5-kilobase pair *Hin*dIII fragment was subcloned into pBR322 (pBR322–MPC-11 fragment) as previously described[8]. Three *Bam*HI fragments (1.8, 0.6 and 0.1 kilobase pairs) were excised from this plasmid and subjected to the nucleotide sequencing procedures described by Maxam and Gilbert[19]. The arrows indicate the orientation of the sequences determined and the approximate length of the sequence obtained from each restriction fragment. Scale bar: 0.1 kilobase pairs.

Preliminary restriction mapping and hybridization experiments indicated that the fragment gene did not contain any of the κ J-region segments (data not shown). That is, the cloned MPC-11 fragment gene did not hybridize to restriction fragments containing several κ J regions, and it did not contain the *Xba*I, *Sac*I or *Bgl*II restriction sites that are about 1,000 base pairs to the 3′ side of the κ J regions (refs 8, 9, and our unpublished results). Thus, it seemed that the MPC-11 fragment gene was formed by a recombination event that occurred about 1,400 base pairs from the κ constant region at a position that contained no J-region genes.

These conclusions could be confirmed and further details revealed by direct sequence determination. Accordingly, an appropriate *Hin*dIII fragment was sub-cloned from the hybrid phage into pBR322 and the sequence of the relevant region determined using the chemical degradation procedure of Maxam and Gilbert[19] according to the strategy outlined in Fig. 3. The complete sequence of the segment, translated in accordance with the genetic code is shown in Fig. 4.

The fact that the hydrophobic leader segment identified by our sequence was in agreement with the amino acid sequence determined on the fragment peptide[12,13], confirmed that we had cloned the correct gene. But the sequence also revealed that the aberrant recombination event that formed the fragment gene had brought in an unexpected, cryptic V-region coding sequence that was not expressed in the fragment polypeptide. In contrast to the situation in normal light-chain genes, the V-region sequence was not adjacent to a J segment.

The MPC-11 fragment gene was formed by an unusual recombination event

Normally a κ light-chain gene is formed by a recombination event that joins one of many κ variable-region genes to one of four J regions to create a gene with the structure indicated in Fig. 1 (normal κ gene). The structure of the MPC-11 fragment gene (Figs 1, 4) is unusual. As noted above, this gene has no J region and lacks part of its intervening sequence. It is, therefore, unlikely that this gene was formed by the site-specific recombination events that normally join V and J segments. Clearly

```
                10        20        30        40        50        60        70        80        90
                 |         |         |         |         |         |         |         |         |
  0   ACATGTGATGTTCTAGTAAATTTTCTGCTAACACCAACTTCCTCTGGGTGGGTGAAACAGGGGCAGGTGCACATGGAGAAACAGTACATATACTCTGCTG

100   ATTTGCATATGAAATAATTTTATAACAGCCTGGCXXXXXCTGCGATGGAGACAGACACACTCCTGCTATGGGTGCTXCTGCTCTGGGTTCCAGGTGAGGG
                                                INIGluThrAspThrLeuLeuLeuTrpValValLeuLeuTrpValPro

200   CGTCAGAAGTGCCGAGAGAAACCTCTGTGGACATCATGATTTTGCATGCCTATGGGTTCATAAACACTATAATTAATGCACTGTAATTGGTTATTGTTTC

300   CTGGAGACCCCTTCATTTACCTGGATGTCTAATAGTGATGTCCGCAAGTATTCTTGATATTTTTGTTGAAAGGTXXXCTCTGCTGGGAAGGCTTTTATAC

400   ATAAATAACAATAGTCTGTGTGTTTATCATTCCAGGTTCCACAGGTGACATTGTGCTGACCCAATCTCCGGCTTCTTTGGCTGTGTCTCTAGGGCAGAGG
                                        GlySerThrGlyAspIleValLeuThrGlnSerProAlaSerLeuAlaValSerLeuGlyGlnArg

500   GCCACCATATCCTGCAGAGCCAGTGAAAGTGTTGATAGTTATGGCAATAGTTTTATGCACTGGTACCAGCAGAAACCAGGACAGCCACCCAAACTCCTCA
      AlaThrIleSerCysArgAlaSerGluSerValAspSerTyrGlyAsnSerPheMetHisTrpTyrGlnGlnLysProGlyGlnProProLysLeuLeuI

600   TCTATCGTGCATCCAACCTAGAATCTGGGATCCCTGCCAGGTTCAGTGGCAGTGGGTCTAGGACAGXXXXXXCCCTCACCATTAATCCTGTGGAGGCTGA
      leTyrArgAlaSerAsnLeuGluSerGlyIleProAlaArgPheSerGlySerGlySerArgThrAspPheThrLeuThrIleAsnProValGluAlaAs

700   TGATGTTGCAACCTATTACTGTCAGCAAAGTAATGAGGATCCGCACAGTGATAGGAACAGAGCCACTAATCTGAAGAGAACAGAGATGTGACAGACTACA
      pAspValAlaThrTyrTyrCysGlnGlnSerAsnGluAsp

800   CTAATGTGTGAAAAACAAGGAAAGGGGTGACTT
```

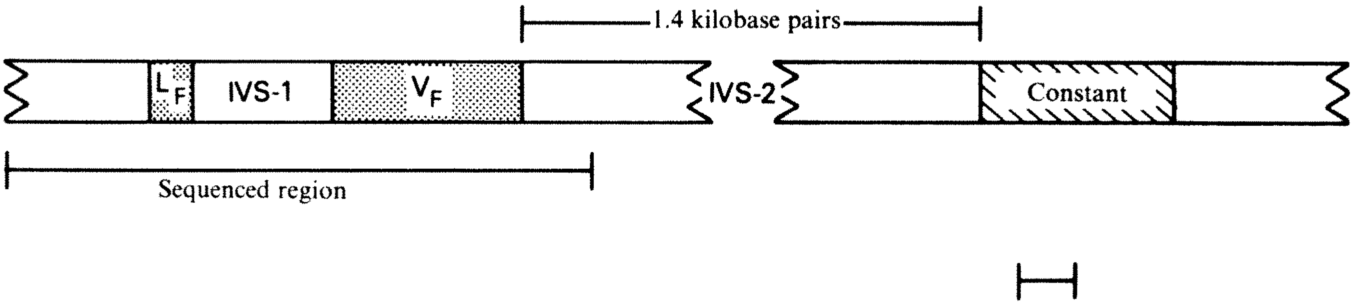

Fig. 4 The nucleotide sequence of the MPC-11 fragment gene. The nucleotide sequence was determined as described in Fig. 3. The portion of the gene that has been sequenced is indicated in the diagram. The leader corresponds to the first amino acid coding block and the variable region to the second coding block. The line over the sequence at the 3′ end of the variable region corresponds to the homologous segment found in several κ variable regions and the κ intervening sequence. Scale bar, 0.1 kilobase pairs.

one of the germ-line precursors of this gene must have been the germ-line κ constant-region gene. The fragment containing this gene has been cloned and much of its nucleotide sequence has been determined (refs 8, 9 and E. Max, unpublished data). The 3′ end of the MPC-11 fragment gene is identical in sequence to a region about 1.4 kilobase pairs 5′ from the K constant-region coding sequence. The other germ-line precursor of MPC-11 fragment gene must be the κ variable-region gene we see here in rearranged form (Fig. 4). From the amino acid translation of its nucleotide sequence, it is clear that this variable region gene is a member of the BALB/c $V_\kappa 21$ subgroup[20]. In fact, one of the proteins that falls into this subgroup but is derived from NZB mice ($V_\kappa 21$ C) has an amino acid sequence identical to the variable-region gene found in the MPC-11 fragment gene[21]. It seems that the MPC-11 fragment gene derived its variable region from one member of the BALB/c $V_\kappa 21$ subgroup.

How was this $V_\kappa 21$ variable region gene brought to within 1.4 kilobase pairs of the κ constant-region gene into a region that lacks J segments? We and others[8,9] have suggested that normal V/J gene recombination involves the recognition of a palindromic sequence ($\mathrm{CAC}^{\mathrm{A}}/_{\mathrm{T}}\mathrm{GTG}$) that is found immediately to the 5′ side of all J regions and to the 3′ side of all V regions thus far sequenced[7-9,22,23]. This V/J joining event does not take place by homologous recombination because these palindromic sequences are removed from both the variable and the J region during recombination. Homologous recombination would have preserved one copy of the homologous sequence. The sequence CACAGTG occurs only once between the J- and C-region genes and this is exactly at the site of the recombination event that formed the fragment gene (see below); the palindrome has been preserved in the MPC-11 fragment gene (Fig. 5).

Homology between the germ-line V- and C-region segments, in fact, extends beyond the V/J palindrome. As noted above, the 2.5-kilobase pair intervening sequence that separates the germ-line κ constant-region gene from the J-region segments contains the palindromic CACAGTG only once at a position about 1.4 kilobase pairs from the C-region gene. By aligning the recombined fragment gene sequence and the germline J/C segment, the point of divergence between the two sequences identifies the point of recombination. When the two sequences were aligned we realized that the recombination event must have taken place within 15 base pairs of the 3′ end of the $V_\kappa 21$C variable region gene at a point 1.4 kilobase pairs from the C-region gene. The sequence 5′-CACAGTGATA-3′ (or a sequence that differs by only a single nucleotide) has been found at the 3′ side of the three κ variable-region genes that have thus far been characterized[7,22]. This sequence is also found at the 3′ side of the variable-region gene found in the MPC-11 fragment gene and has also been located at the recombination site in the germ-line J/C fragment. Thus it seems that this fragment gene was formed by homologous recombination taking advantage of

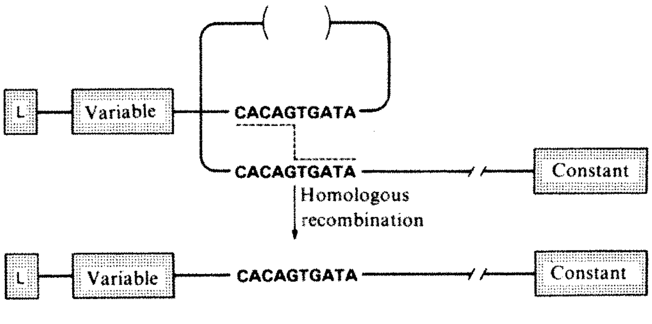

Fig. 5 A model for the homologous recombination event that formed the MPC-11 fragment gene. The data that suggest that this recombination is intrachromosomal and occurs on the non-rearranged chromosome will be presented elsewhere[25].

Fig. 6 The two possible splicing modes for RNA transcripts of the MPC-11 fragment gene. By analogy to a normal light-chain gene, the MPC-11 fragment gene must have three of the four normal splice signals (+); the missing splice signal (−) is due to the lack of a J-region gene. These three splice signals could be used in two different modes, to generate two different mRNAs.

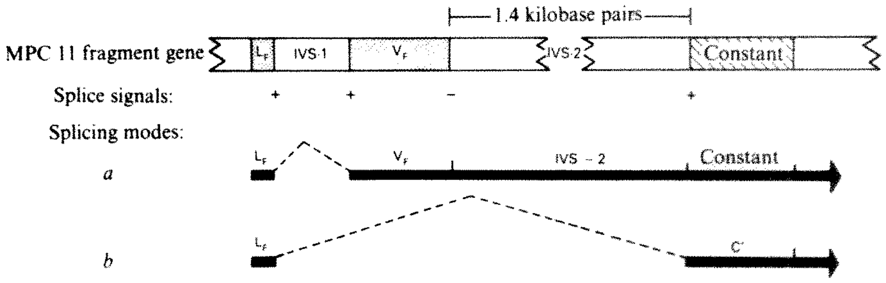

sequences that are found on both the germ-line variable-region and κ constant-region/J-region intervening sequences. The event is shown diagrammatically in Fig. 5. This finding further suggests that this position might behave as a hot spot for aberrant light-chain gene formation. Indeed, similar genes may account for short mRNA species seen in a number of plasmacytoma cell lines[24].

Forbidden splicing of the precursor RNA is required to form the fragment peptide

A comparison of the structures of the fragment peptide and its corresponding gene presents something of a paradox in that the V-region sequence is present in the gene, but absent in the fragment polypeptide (Fig. 1). Normally, the V-region coding sequence is joined to a J segment that must contribute, in addition to a 13-codon long segment of DNA, a signal for RNA splicing so that the V/J segment can be joined to the constant-region sequence in the mature mRNA. In the case of the fragment gene, there is no J segment and therefore apparently no signal for joining V and C regions into a continuous mRNA. The theoretical splicing alternatives for the fragment gene transcript are shown diagrammatically in Fig. 6. A normal splice pair exists between the leader and V-region segments (Fig. 6*a*), but this splice would lead to the formation of leader-variable region peptides coupled to the translation product derived from the intervening sequence. No such peptides have been sought or found. The only way the mRNA corresponding to the fragment peptide could be formed is by joining the leader sequence directly to the constant-region sequence (Fig. 6*b*), skipping the normal leader/V splice. Formation of the fragment peptide must, therefore, involve not only an abnormal DNA recombination event but also an abnormal RNA splice.

Ordinarily an RNA splice that produces a mutant protein would be expected to be quite rare. Errors in splicing occurring in even a small proportion of splice segments would seem disadvantageous in a large gene containing many splice junctions since they would seriously reduce the yield of normal mRNA. Evidently some feature of the transcript must specify the splicing order, assuring that proper donors and acceptors are matched and joined. The fragment light chain gene evidently lacks this control. The simple notion that processing can only occur by splicing next to adjacent donors and acceptors is ruled out by this mutant gene, because the existence of the MPC-11 fragment proves that the constant region competes successfully with the variable region for joining to the leader sequence (fragment mRNAs constitute roughly 20% of normal mRNA levels[11]). On the other hand, it is possible to imagine that forbidden splices occur only when there is an imbalance between donors and acceptors. That is, perhaps a preference for adjacent donor/acceptor joining normally reduces the availability of unmatched partners and provides sufficient specificity to guide normal splicing. The difficulty with this notion, while accounting quite well for the events that occur in this mutant light-chain gene, is that it does not satisfactorily account for the variation in splicing observed in several viral mRNA precursors in which alternative splice pathways are frequently used[26–28].

Violation of allelic exclusion: activation of light-chain promoters

Kuehl and Scharff and their co-workers[10] concluded that, in contrast to the usual situation in antibody-producing cells, two genes must be active in the MPC-11 cell. The basis by which allelic exclusion is avoided in MPC-11 can be discerned by taking into account the structure of these genes and the recent observation by Perry *et al.*[24] that both constant-region genes, germ line and rearranged, are actively transcribed in many plasmacytomas. Most antibody-producing cells contain only one gene that has undergone V/J recombination so as to produce a normal light chain. Notwithstanding the fact that both genes are transcribed, only the properly rearranged one will produce a light-chain product. In the case of MPC-11, one normal light-chain gene has presumably been formed (Fig. 2), but the fragment gene, though abnormally formed, is actively transcribed and has sufficient elements of structure so as to produce a mutant light chain. This observation, taken together with those of Perry *et al.*[24], suggest to us that a higher order of control activates regions of a chromosome and that promoters that happen to fall within this region will be actively transcribed. For example, all V-region sequences might carry their own promoters which remain inactive until moved into an open region of a B-cell chromosome. Such a region obviously surrounds the C-region locus. The availability of many cloned V-region segments suggests that the existence of multiple, independent V-region promoters can be tested experimentally.

We thank Drs Michael Kuehl and Matthew Scharff for their gifts of cells used in these studies and for their helpful advice, Barbara Norman and Marion Nau for their participation in these studies and Terri Broderick for her assistance in the preparation of the manuscript.

Received 4 April; accepted 5 May 1980.

1. Dreyer, W. J. & Bennett, J. C. *Proc. natn. Acad. Sci. U.S.A.* **54,** 861–868 (1965).
2. Hozumi, N. & Tonegawa, S. *Proc. natn. Acad. Sci. U.S.A.* **73,** 3628–3632 (1976).
3. Rabbitts, T. H. & Forster, A. *Cell* **13,** 319–327 (1978).
4. Seidman, J. G. *et al. Proc. natn. Acad. Sci. U.S.A.* **75,** 3881–3885 (1978).
5. Brack, G., Hirama, M., Lenhard-Schuller, R. & Tonegawa, S. *Cell* **15,** 1–14 (1978).
6. Seidman, J. G. & Leder, P. *Nature* **276,** 790–795 (1978).
7. Seidman, J. G., Max, E. E. & Leder, P. *Nature* **280,** 370–375 (1979).
8. Max, E. E., Seidman, J. G. & Leder, P. *Proc. natn. Acad. Sci. U.S.A.* **76,** 3450–3454 (1979).
9. Sakano, H., Hüppi, K., Heinrich, G. & Tonegawa, S. *Nature* **280,** 288–294 (1979).
10. Kuehl, W. M. & Scharff, M. D. *J. molec. Biol.* **89,** 409–421 (1974).
11. Kuehl, W. M. *et al. Cell* **5,** 139–147 (1975).
12. Rose, S. M., Kuehl, W. M. & Smith, G. P. *Cell* **12,** 453–462 (1977).
13. Burstein, Y. & Schechter, I. *Proc. natn. Acad. Sci. U.S.A.* **74,** 716–720 (1977).
14. Burstein, Y. & Schechter, I. *Biochem. J.* **157,** 145–151 (1976).
15. Choi, E., Kuehl, M. & Wall, R. *Nature* **286,** 776–779 (1980).
16. Southern, E. M. *J. molec. Biol.* **98,** 503–517 (1975).
17. Polsky, F., Edgell, M., Seidman, J. & Leder, P. *Analyt. Biochem.* **87,** 397–410 (1978).
18. Tiemeier, D., Tilghman, S. & Leder, P. *Gene* **2,** 173–191 (1977).
19. Maxam, A. & Gilbert, W. *Proc. natn. Acad. Sci. U.S.A.* **74,** 560–564 (1977).
20. McKean, D., Potter, M. & Hood, L. *Biochemistry* **12,** 794–759 (1973).
21. Weigert, M., Gatmaitan, L., Loh, E., Schilling, J. & Hood, J. *Nature* **276,** 785–790 (1978).
22. Seidman, J. G., Leder, A., Nau, M., Norman, B. & Leder, P. *Science* **202,** 11–17 (1978).
23. Bernard, O., Hozumi, N. & Tonegawa, S. *Cell* **15,** 1133–1144 (1978).
24. Perry, R. P. *et al. Proc. natn. Acad. Sci. U.S.A.* (in the press).
25. Seidman, J. *et al. Proc. natn. Acad. Sci. U.S.A.* (in the press).
26. Berk, A. & Sharp, P. A. *Cell* **14,** 695–711 (1978). •
27. Kitchingman, G. R., Lai, S. P. & Westphal, H. *Proc. natn. Acad. Sci. U.S.A.* **74,** 4392–4395 (1977).
28. Gelinas, R. E. & Roberts, R. J. *Cell* **11,** 533–544 (1977).

LETTERS

γ-Ray burst observations from the UCB/LASL experiment on ISEE-3

W. D. Evans, R. W. Klebesadel, J. G. Laros & J. Terrell

University of California, Los Alamos Scientific Laboratory,
Los Alamos, New Mexico 87545

S. R. Kane

Space Sciences Laboratory, University of California,
Berkeley, California

Since the discovery of the intense bursts of γ rays by Klebesadel *et al.*[1] in 1973, little progress has been made in the identification of the sources of the bursts. The initial observations provided directions to several sources with sufficient accuracy to establish the approximate isotropic distribution of the sources[2], but not to provide a basis for association with any known objects. γ-ray burst astronomy entered a new phase in 1976 with the launch of Helios 2 and Solrad 11 containing the first experiments designed expressly for that purpose[3,4]. It then became possible to derive several error boxes that were very narrow in one dimension[3,5]. Using these data it was determined that the bursts are not associated with any type of object that has previously been recognized as a high energy astrophysical source—for example, X-ray sources. In 1978 a true interplanetary network of burst detectors was established with the launch of instruments on Pioneer Venus Orbiter[6], ISEE 3[7-9] and Venera 11 and 12[10,11]. With baseline separations that can exceed 1 AU, this network provides a basis for the location of the γ burst sources with an accuracy sufficient for optical identifications. We briefly describe here one of these instruments, a joint Berkeley/Los Alamos experiment on the ISEE 3 spacecraft, and present some initial results from that experiment. These results are currently being combined with those from the other experiments to obtain accurate burst locations to be reported elsewhere.

The University of California X-Ray Spectrometer[7] was originally designed to monitor solar emission continuously over the energy range 4.8–14 keV (1.2 cm^2 Xe/CO$_2$ proportional counter) and 12–1,264 keV (22 cm^2 NaI(Tl) scintillation detector). Additional electronic instrumentation, provided by the Los Alamos Scientific Laboratory (LASL), was later incorporated into the experiment to record the data from the intense, short lived γ-bursts at a very high rate and with good timing accuracy. This addition consisted of a data handling system that accepts photon counts from the higher energy PHA channels of the scintillation detector and monitors the counting rate for rapid increases that indicate either a γ burst or a solar flare. When a transient event of either origin occurs, high time resolution data are accumulated in a 36 kbit solid state memory for later transmission at a much reduced rate. During a γ burst the summed counting rate from six PHA channels covering the energy range 136–1,264 keV is recorded at the highest time resolution. For counting rates below 1,365 s^{-1} the accumulations are made over fixed intervals of 11.72 ms. At higher rates the operation automatically changes to a 'time-to-spill' mode wherein the resolution improves linearly with counting rate to an ultimate 0.24 ms, while the statistical significance of each accumulation remains constant. Six-channel energy spectra covering the same 136–1,264 keV range are accumulated simultaneously at a factor of 12 coarser time resolution. None of the bursts observed to date have challenged the counting rate capacity or ultimate time resolution of the instrument. (The extremely intense 5 March 1979 event was largely blocked by the spacecraft.)

The ISEE 3 spacecraft was launched in August 1978 and was placed into a heliocentric orbit so that it remains approximately on the Earth–Sun line (at the inner Lagrangian point) at a geocentric distance of 0.01 AU (5 light s). Between launch and 19 April 1979, 12 γ bursts, each confirmed by other instruments, have been detected and recorded by the UCB/LASL experiment. Bursts known to have occurred on 24 November 1978 and 13 January 1979 were missed due to incomplete (~90%) satellite tracking coverage. Virtually all spurious events that we have seen here were caused by statistical fluctuations in the background counting rate, as opposed to cosmic ray-induced noise or other non-statistical sources. These spurious events can occur as frequently as ~1 per day, depending on the trigger criteria in effect. As the criteria are selectable by command, we have sacrificed some sensitivity to eliminate the spurious events during most of the mission. Table 1 lists the dates and times of the confirmed γ burst events and their approximate peak intensities (defined as the highest 0.14 s wide time-history bin) and total integrated fluxes. The latter two quantities have not been corrected for detector efficiency or spacecraft shielding and scattering. Thus, the intensity entries in Table 1 are useful only as a very rough guide and as an indication of the sensitivity and dynamic range of the instrument. For example, it can be inferred that the sensitivity limit of the instrument is ~2 photons cm^{-2} ($\leq 10^{-6}$ erg cm^{-2}). Of course, more intense bursts might be missed because of their spectra, directions, or time histories.

Figure 1 shows samples of the temporal and spectral data obtained so far. We do not discuss the singular event of 5 March 1979 as it has been treated extensively elsewhere (see, for example, refs 12–14). The 4 November 1978 event (Fig. 1), though unusually intense, exhibits most of the classical γ-burst characteristics such as fast rise and fall times, multiple peaked structure, and near background rates between peaks. As can be seen qualitatively in Fig. 1*Ab*, a χ^2 analysis of the spectral information showed no evidence for spectral variability, to within the statistical uncertainties. In view of the complex time history, this spectral constancy above 130 keV seems surprising, and must bear critically on the emission mechanism for this burst. The Apollo 16 γ burst[15-17] and others[4] also featured complex structures combined with no detectable spectral variability. Finally, an intriguing pattern can be seen in the time history of this event. Namely, the bulk of the emission is concentrated in three double peaks, with ~9 s between doublets and with the components of the doublets separated in time by amounts proportional to their intensities. While we make no claims regarding the significance of this possible pattern, we point it out as the type of information that can be extracted from continuous, high time resolution γ-burst data records. Clearly, the short-lived nature of the bursts means that a collection of

Table 1 γ bursts observed by the UCB/LASL experiment on ISEE 3

Date	Time (UT)	Intensity (photons cm^{-2} s^{-1})	Flux (photons cm^{-2})
14 September 1978	16.42.08	*	*
18 September 1978	19.49.33	7	7.5
21 September 1978	03.55.56	9.2	7.5
19 October 1978	18.26.46	2.8	7.5
4 November 1978	16.17.49	29	80
15 November 1978	21.07.25	2.5	3
19 November 1978	09.26.58	28	65
5 March 1979	15.52.05	74	16
7 March 1979	22.18.51	6.5	27
31 March 1979	21.09.36	3	2.8
18 April 1979	07.41.02	8.8	9.3
19 April 1979	16.13.43	3.8	7.8

* Data were lost during the intense part of the burst.

0028-0836/80/340784—03$01.00

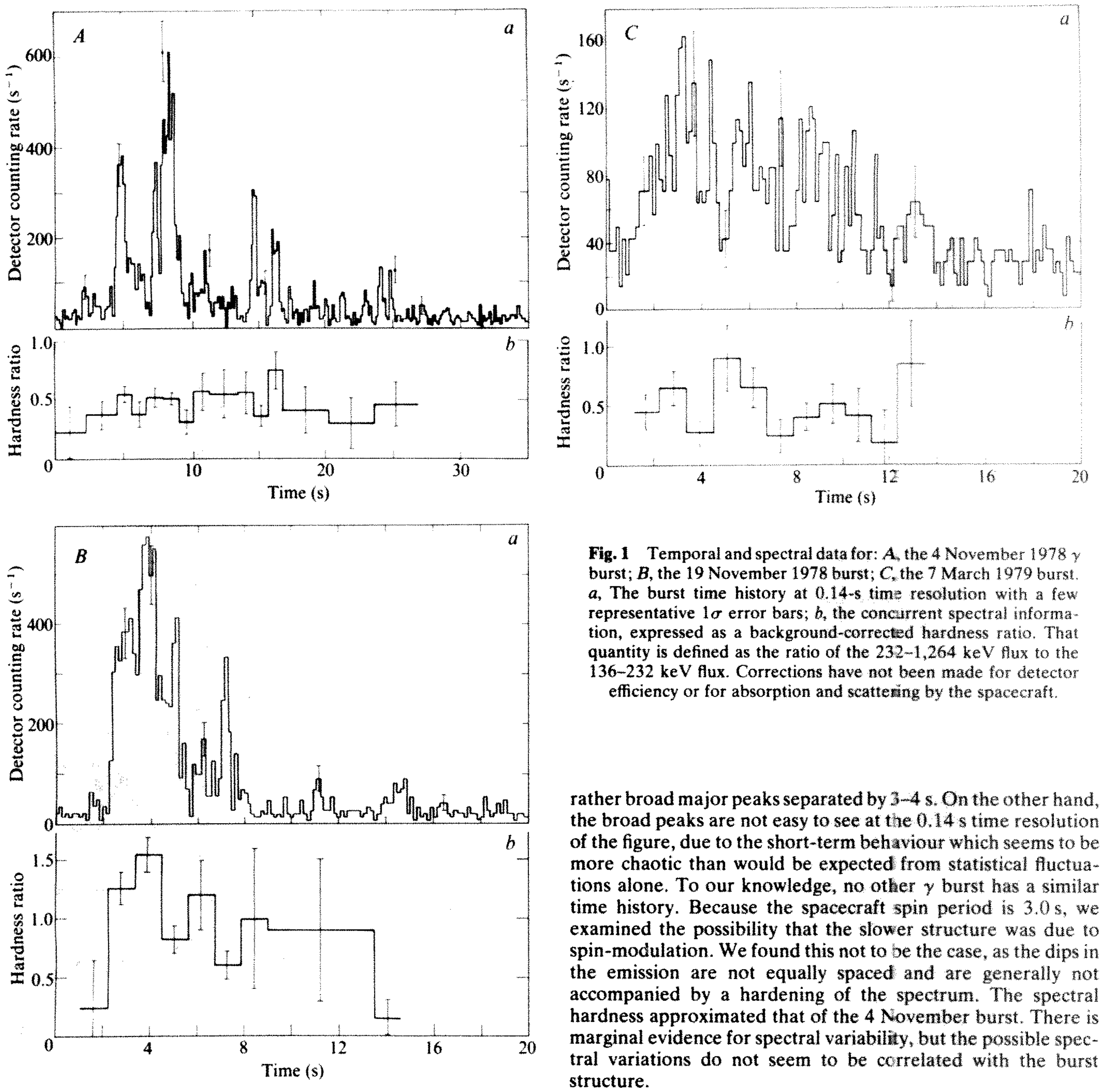

Fig. 1 Temporal and spectral data for: *A*, the 4 November 1978 γ burst; *B*, the 19 November 1978 burst; *C*, the 7 March 1979 burst. *a*, The burst time history at 0.14-s time resolution with a few representative 1σ error bars; *b*, the concurrent spectral information, expressed as a background-corrected hardness ratio. That quantity is defined as the ratio of the 232–1,264 keV flux to the 136–232 keV flux. Corrections have not been made for detector efficiency or for absorption and scattering by the spacecraft.

such information is needed before the significance of this or other possible patterns can be assessed.

The 19 November 1978 burst (Fig. 1*B*) was also one of the most intense ever recorded. As pointed out by Evans *et al.*[6], its time history is atypical in that after the initial sharp rise the counting rate remained at a very high level for an unusually long time. Alternatively, the initial 3 s of the burst might appear to consist of a blend of several sharp peaks that are atypically close together. Also, the average spectrum of the burst is unusually hard, as can be seen by comparing Fig. 1*B* with Fig. 1*A* and *C*. Finally, there is clear evidence for spectral variability correlated with the burst structure. Although the counting statistics do not allow a precise correlation, there is no doubt that the sharp spikes seen in Fig. 1*Aa* at ~5 and at ~7 s have softer spectra than the early part of the burst, and this is probably true also for the spikes at 11 and 14 s. Of course, the spectral hardness may simply be decreasing monotonically.

The 7 March 1979 burst (Fig. 1*C*), though not particularly intense at any given instant, had a fairly large total flux and an unusual time history. It is possible to discern in Fig. 1*Ca* several rather broad major peaks separated by 3–4 s. On the other hand, the broad peaks are not easy to see at the 0.14 s time resolution of the figure, due to the short-term behaviour which seems to be more chaotic than would be expected from statistical fluctuations alone. To our knowledge, no other γ burst has a similar time history. Because the spacecraft spin period is 3.0 s, we examined the possibility that the slower structure was due to spin-modulation. We found this not to be the case, as the dips in the emission are not equally spaced and are generally not accompanied by a hardening of the spectrum. The spectral hardness approximated that of the 4 November burst. There is marginal evidence for spectral variability, but the possible spectral variations do not seem to be correlated with the burst structure.

To obtain a more quantitative comparison of the burst time histories, a Fourier analysis program was carried out. The methods used were not entirely the standard techniques, but have been used or discussed previously[14,18,19]. Each time series consisted of 35.86 s of data in 3,060 time bins each 11.72 ms wide. The data were subjected only to linear detrending; no grouping or smoothing was used. The spectra were examined up to the Nyquist frequency of 42.67 Hz, but only te region below 8 Hz is shown in Fig. 2, since there is little significant higher frequency information. The results generally confirm our previous qualitative statements on the burst time histories, and also point out some less obvious features. The power spectra of the two November 1978 events both show significant peaks in the 0.1–1 Hz region, indicating a degree of regularity in their time histories. One curious pattern that was pointed out above in the 4 November 1978 burst, probably produced the spectral peak at 0.1 Hz. The 0.3 Hz spectral peak is most likely due to the ~3 s separation of the spikes seen in Fig. 1*A* at 2, 5, 8, 11, and 14 s. Also, further examination of the 19 November time history shows that the several count rate peaks are separated by ~1.1 s or a multiple thereof, giving rise to the 0.9 Hz spectral peak. The very broad peak below 0.3 Hz reflects the duration of the main part of the γ burst, but may also be due in part to the widely separated counting spikes near the end of the burst. On the other hand, the power spectrum of the 7 March 1979 event approximates that of white noise due to counting fluctuations, except for the low-frequency power below ~0.5 Hz. Thus, the chaotic appearance of the 7 March time history (Fig. 1*Ca*) is either not statistically significant, or contributes only a small amount of power spread approximately uniformly over a broad frequency band. The spiky appearance of this spectrum is due mainly to the greatly magnified vertical scale relative to the other power spectra shown. Of the three bursts, only the 19 November event clearly shows excess power at higher frequencies, even beyond 8 Hz. This high frequency power undoubtedly results from the sharp counting rate transitions evident, though not optimally displayed, in Fig. 1*B*.

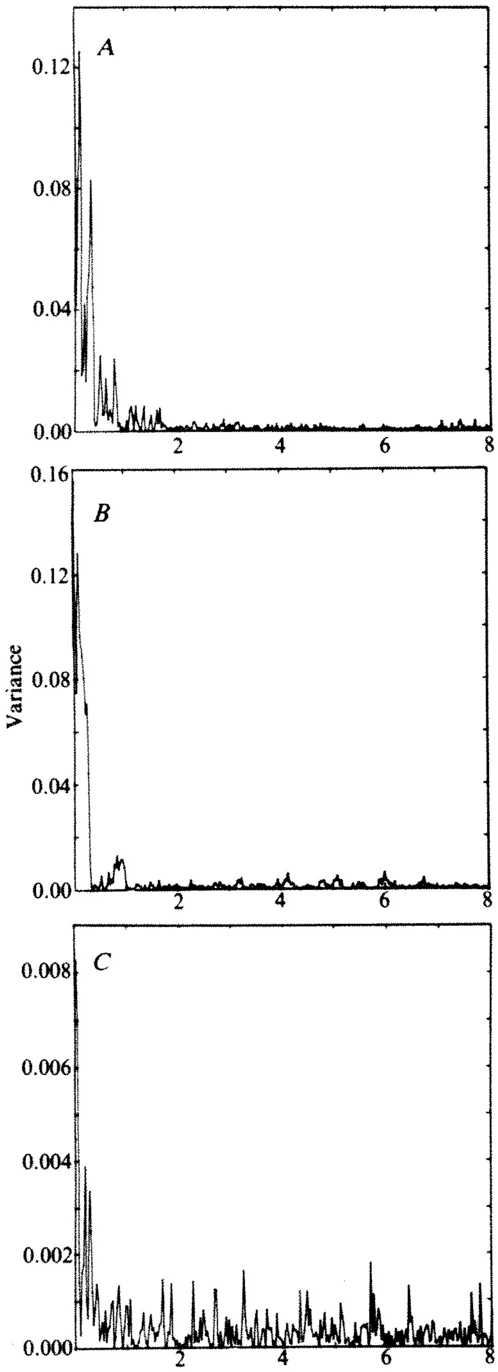

Fig. 2 Power spectra for the three γ-ray bursts shown in Fig. 1. *A*, 4 November 1978; *B*, 19 November 1978; *C*, 7 March 1979. The ordinate is variance per Fourier harmonic. Each time series consisted of 3,060 accumulations at time intervals of 11.72 ms for a total time of 35.86 s. The data have been detrended before analysis in each case. No grouping or smoothing has been used. Only the lower portion of the frequency spectrum, up to 8 Hz, is shown (the Nyquist frequency is 42.67 Hz).

This temporal and spectral information from the UCB/LASL γ burst experiment on ISEE 3 indicates that the three bursts studied had comparable integrated fluxes, but showed significant differences in their power spectra as well as in the qualitative appearances of their time histories. There are also important differences in their average energy spectra, and in their degree of spectral variability. Thus, the present examples show that the γ-burst phenomenon is diverse, and that the sources of the bursts constitute either a very loose class or possibly more than one class of objects. This fact must be taken into account in analyses, for example, the interpretation of log N/log S curves, which assume a 'standard' γ burst object.

We thank Earl Tech and other members of the data analysis section of the LASL high altitude physics group for assistance, and Bill Aiello and Henry Primbsch for their work on the experiment hardware. This research was supported by NASA under contract NAS5-22307 and by the US Department of Energy.

Received 15 January; accepted 16 June 1980.

1. Klebesadel, R. W., Strong, I. B. & Olson, R. A. *Astrophys. J. Lett.* **182,** L85 (1973).
2. Strong, I. B., Klebesadel, R. W. & Olson, R. A. *Astrophys. J. Lett.* **188,** L1 (1974).
3. Cline, T. L. *et al. Astrophys. J. Lett.* **229,** L47 (1979).
4. Laros, J. G., Evans, W. D., Klebesadel, R. W., Olson, R. A. & Spalding, R. E. *Nature* **267,** 131 (1977).
5. Cline, T. L. *et al. Astrophys. J. Lett.* **232,** L1 (1979).
6. Evans, W. D. *et al. Science* **205,** 119 (1979).
7. Anderson, K. A. *et al. IEEE Trans. Geosci. Elect.* **GE-16,** 157 (1978).
8. Hovestadt, D. *et al. IEEE Trans. Geosci. Elect.* **GE-16,** 166 (1978).
9. Cline, T. L., Gloeckler, G., Hovestadt, D. & Teegarden, B. J. *IEEE Trans. Geosci. Elect.* **GE-16,** 173 (1978).
10. Chambon, G. *et al. Proc. 1979 COSPAR Conf.* (in the press).
11. Mazets, E. P. *et al. Astr. Zhurnal-Pis'ma* **5,** 163 (1979).
12. Evans, W. D. *et al. Astrophys. J. Lett.* **237,** L7 (1980).
13. Cline, T. L. *et al. Astrophys. J. Lett.* **237,** L1 (1980).
14. Terrell, J., Evans, W. D., Klebesadel, R. W. & Laros, J. G. *Nature* **285,** 383 (1980).
15. Metzger, A. E., Parker, R. H., Gilman, D., Peterson, L. E. & Trombka, J. I. *Astrophys. J. Lett.* **194,** L19 (1974).
16. Trombka, J. I. *et al. Astrophys. J. Lett.* **194,** L27 (1974).
17. Gilman, D., Metzger, A. E., Parker, R. H., Evans, L. G. & Trombka, J. I. *Astrophys. J.* **236,** 951 (1980).
18. Terrell, J. & Olsen, K. H. *Astrophys. J.* **161,** 399–413 (1970).
19. Terrell, N. J. *Astrophys. J. Lett.* **174,** L35–L41 (1972).

A high sensitivity determination of the hard X-ray spectrum of Sco X-1

R. E. Rothschild, D. E. Gruber, F. K. Knight, P. L. Nolan & Y. Soong

Center for Astrophysics and Space Sciences, University of California at San Diego, La Jolla, California 92093

A. M. Levine, F. A. Primini, W. A. Wheaton* & W. H. G. Lewin

Department of Physics and Center for Space Research, Massachusetts Institute of Technology, Cambridge, Massachusetts 02139

The results of hard X-ray observations of Sco X-1 by HEAO 1 and OSO 7 are reported here. We have found that the X-ray spectrum between 20 and 70 keV is consistent with thermal bremsstrahlung from a hot plasma[1] at a temperature of 5.15 ± 0.05 keV. Observations with the instruments of HEAO 1 on 6–7 September 1978, and with those of OSO 7 during 1972, have not confirmed reports[2] that the bremsstrahlung spectrum is accompanied by an extra component at energies greater than 40 keV—indeed, our observations yield a two-standard deviation upper limit to the flux in this region of 6.4×10^{-6} photons cm^{-2} s^{-1} keV^{-1}.

---

* Present address: Jet Propulsion Laboratory, Pasadena, California.

0028-0836/80/340786—03$01.00

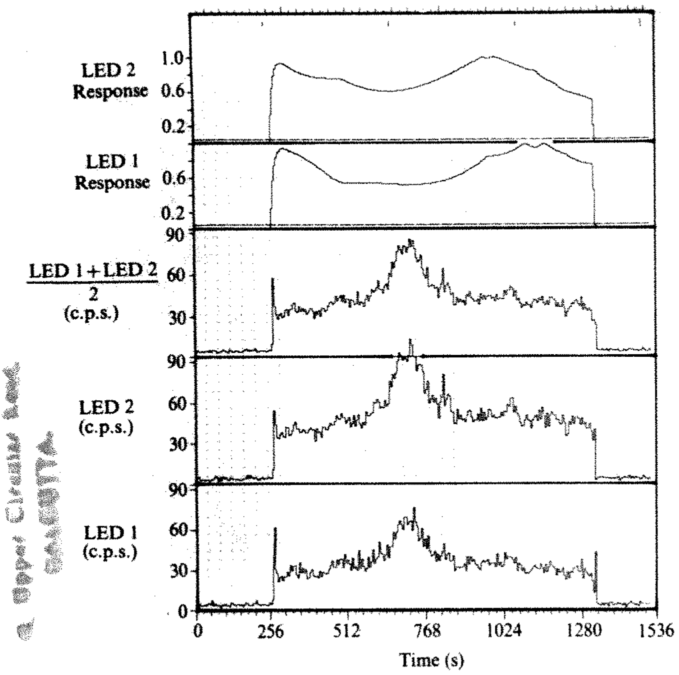

Fig. 1 The aspect-corrected counting rates for the two low energy detectors (LED) aboard HEAO 1 during one 17-min exposure to Sco X-1 on 7 September 1978 covering the energy range 20–220 keV. Also shown is the mean of the two sets of rates and the collimator response to Sco X-1 for each detector. Time 0.000 corresponds to 1 h 8 min 22 s UT. c.p.s., counts per second.

The UCSD/MIT high energy X-ray and low energy γ-ray instrument[3] aboard HEAO 1 consisted of seven NaI(Tl)/CsI(Na) phoswich scintillation detectors covering various energy ranges from 10 keV to 10 MeV that were actively shielded by 4–10 cm of CsI. Two of these detectors, of $\approx 100\ \mathrm{cm}^2$ each, sensitive over the range 20–220 keV, were collimated by Sn/Cu slats to 1.5° × 20° FWHM. An observation of Sco X-1 was conducted on 6–7 September 1978 by alternating between source and background regions separated by 2° with 17-min segments for each. This length of time was chosen to sample uniformly, on the average, regions of different particle-induced background due to varying cosmic-ray cutoff throughout the orbit. In this way an important systematic uncertainty in background subtraction could be minimized.

The HEAO 1 observation provided 17 separate exposures to Sco X-1; of these, one displayed pronounced variability, that is an X-ray flare which is shown in Fig. 1. In addition to the 2-min flaring by a factor of ≈ 2, this exposure differs from the others by having about twice the average intensity off the flare of the others. As spectral shape may vary with intensity[1], the exposure containing the flare was not included in the accumulation of the mean spectrum. It was, instead, studied in detail for spectral changes during this period of both enhanced intensity and activity.

The net counts spectrum was fitted by folding various analytical models through the instrumental response, which included photopeak efficiency, non-linear pulse height to energy conversion, resolution, and K-escape effects, to form a model counts spectrum. This was then compared with the net counts spectrum, and best-fit parameters were determined by minimizing χ^2. Spectrum dependent efficiencies were calculated and divided into the net counts spectrum to form the inferred mean incident photon spectrum, which is shown in Fig. 2.

The mean spectrum was fit by both a thermal bremsstrahlung model, including a Gaunt factor, and the same model modified to account for Compton interactions in a hot, fully ionized cloud surrounding the X-ray source[4]. The resultant best-fit temperatures were 5.15 ± 0.05 keV and 3.24 ± 0.05 keV, respectively, and the latter fit was insensitive to optical depth to electron scattering in the range $\tau = 5$–20. The best-fit temperatures are in agreement with earlier results at lower energies[1,4]. The inferred mean incident flux and the best-fit ($kT = 5.15$ keV) thermal bremsstrahlung model are shown in Fig. 2 together with the inferred flux from the flare alone. An attempt was then made to test for the presence of a high energy excess in the mean spectrum with respect to either thermal model. Assuming a power law form for the excess ($\mathrm{d}N/\mathrm{d}E \propto E^{-1}$), none was detected at 95% confidence and the 2σ upper limit to any excess is 6.4×10^{-6} photons $\mathrm{cm}^{-2}\ \mathrm{s}^{-1}\ \mathrm{keV}^{-1}$, or 0.56 μJy, in the range 72–222 keV.

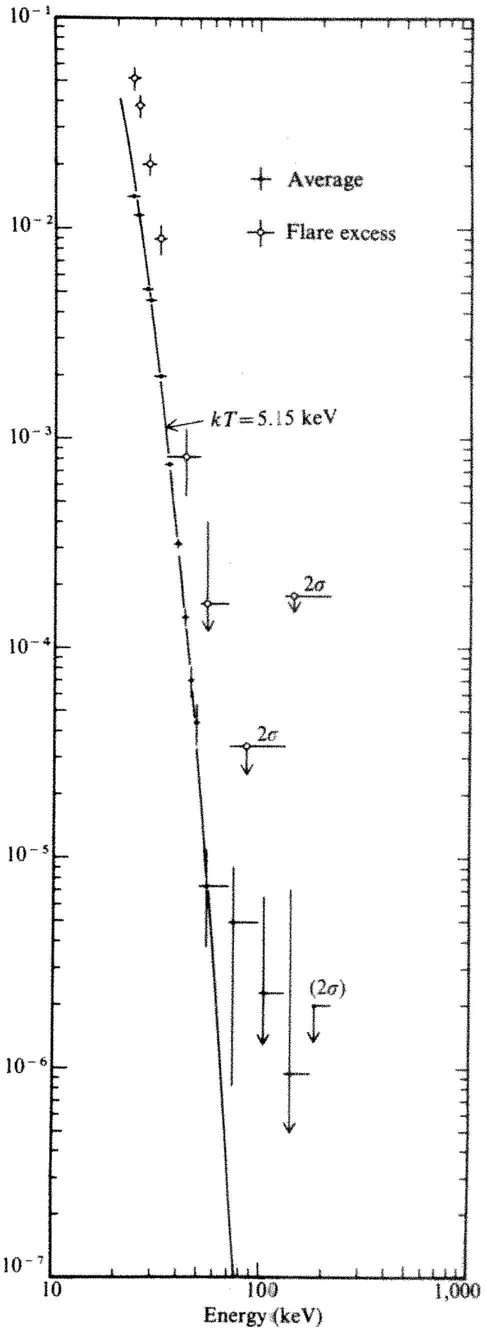

Fig. 2 The inferred incident spectrum of Sco X-1 from 20 to 220 keV from the observations by the HEAO 1 satellite beginning on 6 September 1978. ●, The flux averaged over the entire 12-h observation with the exception of one 17-min interval that contained a flare of 2-min duration (see Fig. 1). ○, The flux from the flare alone with the remainder of the 17-min exposure used as background. All error bars are 1σ unless otherwise noted.

The study of the flare exposure was divided into the flare alone (from 655 to 778 s in Fig. 1) and the remainder of the exposure (from 256 to 655 s and 778 to 1,331 s in Fig. 1). The spectrum of the flare alone, which is also shown in Fig. 2, is the net flux above the remainder of this exposure, and can be compared to the mean spectrum of the other exposures to determine if the same process could have caused both spectra. Acceptable fits to the flare alone are possible with best-fit values for kT of 6.1 ± 0.5 keV and 3.5 ± 0.5 keV for the two thermal models, respectively, or with a power law index of 6.6 ± 0.2. The narrow energy range over which the flare was observed, however, precludes the selection of one model over another, but the data are consistent with a thermal origin for the flare. No evidence for a high energy excess above the thermal model was seen in the flare, with the 2σ upper limit being 1.4×10^{-4} photons cm^{-2} s^{-1} keV^{-1}, or 11 μJy, from 52 to 222 keV.

For the remainder of the flare exposure, the best-fit values for kT of this enhanced activity were 4.9 ± 0.2 and 3.1 ± 0.1 keV, respectively, for the two thermal models mentioned above and the 2σ upper limit to any excess flux was 3.4×10^{-5} photons cm^{-2} s^{-1} keV^{-1}, or 3.1 μJy, from 72 to 222 keV.

The UCSD OSO 7 SKYMAP[5] contains 280 s of live time to Sco X-1 from scanning in mid (May–June) and late (November–December) 1972. These data come from a 64 cm^2 NaI(Tl) detector sensitive from 5 to 500 keV, that was actively shielded by CsI(Na) and had a field of view of 6.5° FWHM. This observation differs from that of HEAO 1 in that data were accumulated over two 18-day periods separated by six months, and thus represents more of a long-term average compared with the brief observation by HEAO 1.

The OSO 7 observation of Sco X-1 was fitted in a similar manner. The fitting process yielded a best-fit temperature of 6.5 ± 0.5 keV for the thermal bremsstrahlung model and 3.2 ± 0.2 keV for the Compton modified thermal model. The ≈ 1.5 keV higher temperature as compared to the HEAO 1 result is consistent with the range of temperatures reported over the past several years for Sco X-1 (ref. 1). As in the HEAO 1 measurements, no excess above the thermal spectrum was observed, and the 2σ upper limit to the flux from 60 to 208 keV was 6.2×10^{-5} photons cm^{-2} s^{-1} keV^{-1}, or 5.4 μJy.

Over the past decade and a half, only four observations claim 3σ or greater excesses above a thermal model with fluxes of a few 10^{-4} photons cm^{-2} s^{-1} keV^{-1} in the 50–100 keV range[6-9]. All four of these have systematic uncertainties, such as possible source confusion, varying background counting rates, and broad instrumental resolution, that reduce the significance of their results. If, indeed, this excess is time variable, however, the magnitude of the change must be more than an order of magnitude at 100 keV.

Models of the Sco X-1 binary system generally include mass flow onto a compact object surrounded by an accretion disk. Both thermal bremsstrahlung[10] and power law[11] spectral shapes have been predicted for the X-ray data. The observed temperature for thermal models will not be a true measure of the plasma temperature as various proposed processes might alter the spectral shape. A high-temperature plasma ($kT \approx 75$ keV) could be degraded by Compton interactions to form a spectrum with a lower measured temperature[12]. On the other hand, an intense soft X-ray flux ($kT \approx 3$ keV) impinging on the plasma material could undergo Compton scattering to higher energies with either a resultant higher measured temperature[4] or possibly the appearance of a high energy excess[10] or both. The absence of an observed high energy excess indicates that the mean free path for inverse Compton scattering must be either so low that the scattered flux is below instrument sensitivity, or so high that the reprocessed spectrum resembles an exponential of higher measured temperature. A third possibility is that kT is not high enough to scatter photons to greater than 40 keV.

The nature of the collapsed object powering the X-ray emission in Sco X-1 is uncertain. The minimum mean luminosity of this observation is 1.3×10^{36} erg s^{-1}, using 270 pc as a minimum distance[13]. This places it near the limiting luminosity for spherical accretion onto a white dwarf[14]. Add to this the factor of 5 overall increase in the flare, and it seems quite unlikely that spherical accretion onto a white dwarf could be responsible. On the other hand, accretion onto a neutron star could easily generate such luminosity. Non-spherical accretion onto white dwarfs, however, can also generate luminosities in the 10^{37} erg s^{-1} range that may be observable[1] (N. D. Kylafis, personal communication), and, therefore, allow the white dwarf hypothesis.

We thank R. M. Pelling, J. L. Matteson, W. A. Baity, H. Hudson, B. Dennis, M. Coe and N. Kylafis for their discussions, and R. Pegg and G. Huszar for computer support. This work was supported by NASA contract NAS-8-27974.

Received 10 April; accepted 26 June 1980.

1. Miyamoto, C. & Matsuoka, M. *Space Sci. Rev.* **20,** 687–755 (1977).
2. Agrawal, P. C. *et al. Astrophys. Space Sci.* **10,** 500–507 (1971).
3. Matteson, J. L. *Proc. AIAA 16th Aerospace Sci. Meet.* Huntsville, Alabama, paper 78-35 (1978).
4. Lamb, P. & Sanford, P. W. *Mon. Not. R. astr. Soc.* **188,** 555–563 (1979).
5. Rothschild, R. E., Baity, W. A., Mushotzky, R. F., Wheaton, W. A. & Peterson, L. E. (*COSPAR*) *X-Ray Astronomy* (eds Baity, W. A. & Peterson, L. E.) 369–372 (Pergamon, Oxford, 1979).
6. Haymes, R. C., Harnden, Jr, F. R., Johnson III, W. N. & Prichard, H. M. *Astrophys. J. Lett.* **172,** L47–49 (1972).
7. Riegler, G. R., Boldt, E. & Serlemitsos, P. *Nature* **226,** 1041–1043 (1970).
8. Peterson, L. E. & Jacobson, A. S. *Astrophys. J.* **145,** 962–965 (1966).
9. Greenhill, J. G., Coe, M. J., Bell-Burnell, S. J., Strong, K. T. & Carpenter, G. F. *Mon. Not. R. astr. Soc.* **189,** 563–570 (1979).
10. Shakura, N. I. *Soviet Astr.* **16,** 756–762 (1973).
11. Pringle, J. E. & Rees, M. J. *Astr. Astrophys.* **21,** 1–9 (1972).
12. Kylafis, N. D. & Lamb, D. Q. *Astrophys. J. Lett.* **228,** L105–110 (1979).
13. Bahcall, J. N. *Physics and Astrophysics of Neutron Stars and Black Holes* (eds Giacconi, R. and Ruffini, R.) 63–110 (North-Holland, Amsterdam, 1978).
14. Kylafis, N. D. thesis, Univ. Illinois (1978).

Solar-flare produced ^{3}He in lunar samples

M. N. Rao & T. R. Venkatesan

Physical Research Laboratory, Ahmedabad 380 009, India

Lunar rocks and soils undergo long-term irradiation by solar and galactic cosmic rays (SCR and GCR) leading to compositionally-distinct spallation spectra for noble gases[1,2] and leaving behind fossil records characteristic of different irradiation features. Because the SCR effects are restricted to the first few millimetres of rocks and soils in contrast to GCR, various studies based on solar flare tracks[3,4], thermoluminescence[5], and radionuclides[3,6] over the past decade have aimed to decipher these fossil records bearing the imprints of the low (SCR) and high (GCR) energy irradiation phenomena. These studies have greatly helped our understanding of the energy spectra and fluxes of charged particles streaming out of the Sun. We have already reported quantitative studies, aimed at isolating the SCR and GCR produced Ne and Ar isotopes in several lunar soils and rocks[1,2] and have calculated their solar flare exposure ages which agree with the 'surface' exposure ages based on ^{26}Al and particle track studies[3]. We describe here, for the first time, using ^{3}He in samples from three different depths of lunar rocks, a method for deducing the absolute SCR (flare) proton fluxes in the past few million years which compare favourably with those derived from ^{26}Al and ^{53}Mn studies[3,6] of other lunar samples.

When a large crater is formed on the surface of the Moon, deeply buried rocks are excavated to the surface. During such shock events, rocks could be either completely or partially degassed of their noble gas. The helium in a heavily shocked rock is considered to have completely degassed. As the earlier ^{3}He history in this rock was completely erased out at the time it was brought to the lunar surface by the shock event, its subsequent irradiation on the lunar surface results in equal exposure times to SCR and GCR. If $m(^{3}\mathrm{He})$ is the measured spallogenic ^{3}He content per g of the rock with a simple history, we have

$$m(^3\text{He}) = (P_g + P_s)T$$

where P_g and P_s are the GCR and SCR ^{3}He production rates respectively. Choosing a deep interior sample (R3) from a rock, such that $P_s = 0$, means that $m(^3\text{He}) = P_g T$. As P_g is known, T for R3 can be calculated. Samples close to the top surface (R1) will contain a mixture of SCR, GCR, SW (solar wind) components of ^{3}He and intermediate samples (R2) deeper than 3–4 mm from the top surface will contain only GCR and SCR produced ^{3}He. The ^{3}He in R1 sample is corrected for solar wind contribution using the measured ^{4}He content and a ^{3}He/^{4}He ratio of 3.6×10^{-4} as found in several bulk lunar soils[7]. The corrected ^{3}He in R1 represents the SCR + GCR production.

In the case of rocks with a simple history, the SCR proton flux is deduced as follows. Assuming (1) T (GCR) = T (SCR) and (2) the diffusion losses, if any, are same for both GCR and SCR produced ^{3}He, we can calculate T (GCR) from R3 which is equal to $m(^3\text{He})/P_g$ as shown above. T will decrease if there is any gas loss and irrespective of such losses, $m(^3\text{He})/T$ will give the true production rate. Using the calculated T, we compute the total SCR + GCR production rates, $(P_s + P_g = m(^3\text{He})/T)$ for other samples (R1 and R2) and plot these values against depth as shown in Fig. 1. Then, using assumed SCR fluxes and the known GCR flux, we calculate the combined production profiles for various depths in the rock and match the production profiles with the data points. The SCR parameters that fit best to the data points describe quantitatively the SCR flux to which this rock was exposed.

We measured He, Ne, Ar contents in six samples from known depths of two well documented rocks 61016 and 64435. Using the analytical methods described elsewhere[2] we could resolve quantitatively the SW, SCR and GCR components for the ^{21}Ne and ^{38}Ar in these samples. Using the production rates of Hohenberg *et al.*[8], we calculated their SCR and GCR ages (Table 1) and the results obtained by both ^{21}Ne and ^{38}Ar methods show agreement within experimental errors. The measured ^{40}Ar contents are much less compared with the expected ^{40}Ar from ^{40}K decay during 3,100–3,400 Myr after solidification[9]. We attribute the loss of ^{40}Ar (about 90%) to the shock event at the time of South Ray crater formation that excavated the rocks from lunar interior. During the same event more than 99% of the radiogenic ^{4}He was also lost. Thus the assumption that T (GCR = T (SCR) can be applied to the rock samples from 61016 and 64435.

Table 1 GCR and SCR ages of lunar rocks

Rock	^{21}Ne age (Myr) SCR	^{21}Ne age (Myr) GCR	^{38}Ar age (Myr) SCR	^{38}Ar age (Myr) GCR
61016*	1.3 ± 0.2	4.0 ± 0.3	1.7 ± 0.2	3.7 ± 0.3
64435	0.6 ± 0.1	1.2 ± 0.2	0.8 ± 0.2	1.4 ± 0.2

R1, R2 and R3 samples of 61016 are taken from 0.3–2 mm; 4–7 mm and 16–18 mm depths whereas another set of R1, R2 and R3 samples of 64435 are taken from 0.2–1.5 mm; 4.5–7.5 mm and 7.5–9.0 mm depths, respectively.

* See ref. 2.

As pointed out earlier, the T (GCR) obtained from $m(^3\text{He})/P_g$ represents the apparent age of the rock and it will be lower than the true value if there are ^{3}He losses. Helium may sometimes be lost by diffusion and this source of gas loss is discussed below. To study the depth dependence of ^{3}He diffusion, we consider the R2 and R3 results of rock 64435. The observed ^{3}He contents are $(0.44 \pm 0.02) \times 10^{-8}$ and $(0.43 \pm 0.03) \times 10^{-8}$ cm^3 STP g^{-1} respectively and they do not show much variation as a function of depth. Further, a study of ^{3}He/^{21}Ne and ^{3}He/^{38}Ar ratios in these samples may throw light on the diffusion pattern of ^{3}He relative to other cosmogenic isotopes of Ne and Ar. The ratio of the ^{3}He (SCR + GCR)/^{21}Ne (SCR + GCR) in different samples of rocks 61016 and 64435 range from 3.5 to 4.0. The near-constancy of the observed ^{3}He/^{21}Ne ratios suggest that the depth-dependent diffusion effects are not significant in these samples. Similar observations are made by studying ^{3}He/^{38}Ar ratios in these samples from rocks 61016 and 64435. In this context, note that ^{3}He losses were observed in some feldspar-bearing lunar[10] rocks and meteorites[11]. It is not clear whether these losses are due to diffusion or to shock effects. For example, Heymann *et al.*[11] showed that in meteorites such as Shergotty and Zagami, even though feldspar-rich, the ^{3}He was almost quantitatively retained. In Sera de Mage also, no loss of ^{3}He in big feldspar grains was observed. This suggests that shock effects have an important role in affecting ^{3}He losses in some of these samples. However, even if there are minor diffusion losses, this method holds good as long as the losses are not depth-dependent.

As we do not have the deepest samples where P_s is almost zero, we adopt the following procedure to deduce the SCR proton fluxes from our studies. We calculate the theoretical ^{3}He production profile as a function of depth for combined SCR + GCR production per Myr, using the Reedy–Arnold model[12] and a SCR proton flux of J ($E > 10$ MeV) = 70 p cm^{-2} s^{-1} and $R_0 =$ 100 MV (ref. 6) and a GCR flux of 1.7 p cm^{-2} s^{-1}. The production cross-sections are taken from ref. 13. Figure 1*a* represents this theoretical profile. Using the SCR + GCR combined production rate for the 61016–R3 sample at a depth of 5.1 g cm^{-2}, we calculate T (GCR) for 61016 to be (1.6 ± 0.1) Myr. This agrees with the SCR ages based on ^{21}Ne and ^{38}Ar (see Table 1) and the surface age of 1.5 Myr based on particle track studies[3]. Then we use this T (GCR) to find the $m(^3\text{He})/T$ for the R1 sample of 61016. The observed R3 value is normalized so as to fall on curves *a* or *b* in Fig. 1 and the other data points are scaled accordingly. These values are plotted in Fig. 1. Similarly in case of 64435–R3 sample, using the (SCR + GCR) ^{3}He production rate at the corresponding depth, we calculate the T (GCR) for rock 64435 which turns out to be (0.55 ± 0.10) Myr. This agrees with the SCR ages based on ^{21}Ne and ^{38}Ar within the error limits (see Table 1). We plot the $m(^3\text{He})/T$ values for the R2 and R1 samples in Fig. 1 as a function of depth as described above. Within the error limits, all the points of rocks 61016 and 64435 seem to fit curve Fig. 1*a*.

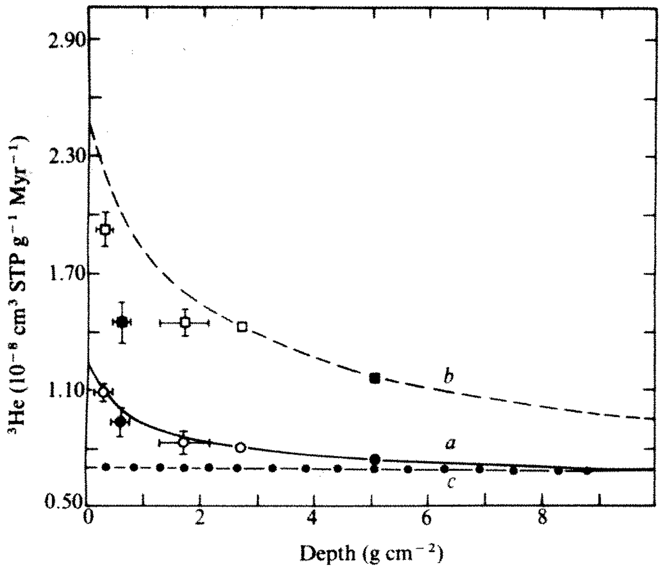

Fig. 1 Production profiles of (SCR + GCR) ^{3}He as a function of depth in lunar rocks 64435 (□, ○) and 61016 (■, ●). The deepest points (R3) of 64435 (at 2.7 g cm^{-2}) and of 61016 (at 5.1 g cm^{-2}) are normalized to fall on curves *a* or *b*. The other R1 and R2 points are scaled accordingly. The normalizing points are shown without error bars. The solid curve *a* is generated from the SCR proton flux given by Kohl *et al.*[6] and the dashed curve *b* is generated from the SCR flux given by Bhandari *et al.*[3]. Curve *c* represents the depth profile[12] for GCR production of ^{3}He using the particle flux mentioned for proton energies above 1 GeV. ^{3}He in R2 sample of 61016 could not be measured due to power failure.

We can then check how these data points, using the same procedure, fit to a different SCR proton flux of J ($E > 10$ MeV) = 125 p cm^{-2} s^{-1} and $R_0 = 150$ MV, deduced by Bhandari *et al.*[3] for the same rocks based on ^{26}Al studies. The combined (SCR + GCR) ^{3}He production profile calculated for this SCR flux is shown by Fig. 1*b*. The T (SCR) calculated for this flux for 61016 turns out to be 1.0 Myr and for 64435, 0.3 Myr which are smaller than the surface exposure ages of 1.5 Myr and 0.5 Myr respectively, deduced by track studies[3]. Using the normalization procedure, for R3 points of rocks 61016 and 64435, we calculate the other R1 and R2 points with the new (SCR + GCR) ^{3}He production rates and plot the points as a function of depth in Fig. 1.

The fit of the data points to curve *b* is clearly less satisfactory than to curve *a*. This shows that the ^{3}He production profile generated using a SCR proton flux of J ($E > 10$ MeV) = 70 p cm^{-2} s^{-1} and $R_0 = 100$ MV (ref. 6) seems to fit the data points better. The erosion, solid angle and so on, corrections for these samples are expected to be minor. Further experiments are in progress using well-documented samples to understand this discrepancy in the fluxes as well as to find the suitability of this method to determine the solar flare exposure ages of lunar samples in time scales >10 Myr where the radioactivity methods using ^{26}Al and ^{53}Mn are inapplicable because of saturation effects.

We thank Professors D. Lal and N. Bhandari for valuable discussions during this work which is carried out under Lunar Science Proposal Nos. SL-9191 and SL-9095, and J. T. Padia for assistance.

Received 19 March; accepted 26 June 1980.

1. Bhai, N. B., Gopalan, K., Goswami, J. N., Rao, M. N. & Venkatesan, T. R. *Proc. 9th Lunar planet. Sci. Conf.* 1629–1645 (1978).
2. Rao, M. N., Venkatesan, T. R., Goswami, J. N., Nautiyal, C. M. & Padia, J. T. *Proc. 10th Lunar planet. Sci. Conf.* 1547–1564 (1979).
3. Bhandari, N., Bhattacharya, S. K. & Padia, J. T. *Proc. 7th Lunar Sci. Conf.* 513–523 (1976).
4. Arrhenius, G. *et al. Proc. 2nd Lunar Sci. Conf.* 2583–2589 (1971).
5. Hoyt, H. P., Jr, Walker, R. M. & Zimmerman, D. W. *Proc. 4th Lunar Sci. Conf.* 2489–2502 (1973).
6. Kohl, C. P., Murrell, M. T., Russ III, G. P. & Arnold, J. R. *Proc. 9th Lunar planet. Sci. Conf.* 2299–2310 (1978).
7. Eberhardt, P. *et al. Proc. 3rd Lunar Sci. Conf.* 1821–1856 (1972).
8. Hohenberg, C. M., Marti, K., Podosek, F. A., Reedy, R. C. & Shirck, J. R. *Proc. 9th Lunar planet. Sci Conf.* 2311–2344 (1978).
9. Stettler, A., Eberhardt, P., Geiss, J., Grogler, N. & Maurer, P. *Proc. 4th Lunar Sci. Conf.* 1865–1888 (1973).
10. Lugmair, G. W., Marti, K., Kurtz, J. P. & Scheinin, N. B. *Proc. 7th Lunar Sci. Conf.* 2009–2033 (1976).
11. Heymann, D., Mazor, E. & Anders, E. *Geochim. cosmochim. Acta* **32**, 1241–1268 (1968).
12. Reedy, R. C. & Arnold, J. R. *J. geophys. Res.* **77**, 537–555 (1972).
13. Walton, J. R., Heymann, D., Yaniv, A., Edgerley, D. & Rowe, M. W. *J. geophys. Res.* **81**, 5689–5699 (1976).

Excitation of the Na D-doublet of the nightglow

D. R. Bates & P. C. Ojha

Department of Applied Mathematics and Theoretical Physics,
Queen's University Belfast, Belfast BT7 1NN, UK

We infer from the absolute intensity of the nocturnal D-doublet emission, the abundance of free Na and other relevant information that there is very little possibility of an alternative to Chapman's theory[1] that the excited Na atoms involved are released by NaO–O collisions. The nature of the collision process is discussed here. We point out that a remarkably high branching ratio for the reaction path leading to excited (rather than normal) sodium is necessary. A high branching ratio is explained by considering the symmetry properties of the correlated electronic states.

In 1939 Chapman[1] proposed the oxidation–reduction cycle:

$$\mathrm{Na + O_3} \xrightarrow{k_1} \mathrm{NaO + O_2} \qquad (1)$$

$$\mathrm{NaO + O}\begin{cases} \xrightarrow{fk_2} \mathrm{Na(^2P) + O_2} & (2a)\\ \xrightarrow[(1-f)k_2]{} \mathrm{Na(^2S) + O_2} & (2b)\end{cases}$$

Thermochemical studies[2] have removed doubts over whether process (2a) is exothermic.

The case against the possibility of invoking another chemiluminescent cycle may be seen to be virtually conclusive: thus rocket measurements[3] show that the emission comes from near the 90-km level and lidar measurements[4] show that the number density n(Na) in this region is around 4×10^3 cm^{-3}, so that even with a rate coefficient as fast as 2.5×10^{-10} cm^3 s^{-1} and a 10-km thick layer, the typical nightglow intensity[5] of 100 R would necessitate the number density of the reactant being some 1×10^8 cm^{-3}; ozone is almost certainly the only atmospheric constituent which readily reacts with or excites atomic sodium and which may have such a high nocturnal abundance near 90 km; and, if it is accepted that process (1) must be involved, then so almost certainly must process (2) because of the lack of another reducing process which meets the double requirement of being at least as effective in the atmospheric region concerned and of being sufficiently exothermic. Furthermore, interferometric measurements on D-line profiles[6] reveal that the Na(^{2}P) atoms have a kinetic energy of 0.046 eV which suggests that they arise from a chemical process like process (2a) rather than from dissociative recombination involving NaO$^+$ or NaO$_2^+$ produced from incoming Na$^+$ ions as has been conjectured[7].

An understanding of the nature of processes (1) and (2) came when Kolb and Elgin[8] suggested that both are of the electron-jump type. From the ionization potentials of Na and NaO and the electron affinities of O$_3$ and O they calculated the crossing distances r_X for the {Na–O$_3$} : {Na$^+$–O$_3^-$} and {NaO–O} : {NaO$^+$–O$^-$} covalent–ionic potential pairs. Assuming the cross-sections to be πr_X^2, they deduced the rate coefficients. The values of r_X are 4.5 Å and 2.3 Å respectively (the latter being smaller than originally[8] obtained due to the use of what should be a better[9] estimate of the ionization potential of NaO); the corresponding rate coefficients at 200 K are

$$k_1 = 3.4 \times 10^{-10}\ \mathrm{cm^3\ s^{-1}}, \qquad k_2 = 1.0 \times 10^{-10}\ \mathrm{cm^3\ s^{-1}} \qquad (3)$$

Note, however, that processes (1) and (2) are not of the class typified by

$$\mathrm{K + I_2 \rightarrow KI + I} \qquad (4)$$

to which the electron-jump model is commonly applied[10,11]. A key feature of process (4) is that the I$_2^-$ formed in a vertical transition at the crossing is so highly excited vibrationally that it dissociates readily leaving the I$^-$ and K$^+$ ions bound together by their Coulomb attraction and leaving the I atom free. In the case of processes (1) and (2), there is little vibrational excitation in a vertical transition and, moreover, the product molecules are not produced directly from oppositely charged fragments. The mechanism is that, while the reactants are on the ionic potential surface, they make a hard collision which excites internal energy and thereby makes an exothermic channel more likely to be followed than reversal through the entrance channel. For process (1), the fission of the collision complex occurs along {NaO$^+$–O$_2^-$} : {NaO–O$_2$} and for process (2), along {Na$^+$–O$_2^-$} : {Na–O$_2$}, where the {NaO$^+$–O$_2^-$} and {Na$^+$–O$_2^-$} potential surfaces are for the same electronic states as the {Na$^+$–O$_3^-$} and {NaO$^+$–O$^-$} potential surfaces, respectively.

Oxidation and reduction proceeds rapidly enough to maintain chemical equilibrium between Na and NaO and it is convenient to express the D-doublet photon emission rate as

$$E(5{,}893) = fk_1 n(\mathrm{Na}) n(\mathrm{O_3}) \qquad (5)$$

0028–0836/80/340790—02$01.00

Table 1 Symmetry properties of the Na–O correlated molecular states

Row	Fragments	Correlated molecular states*
(*a*)	$NaO(X^2\Pi)+O(^3P)$	$^2A'(3), ^4A'(3), ^2A''(3), ^4A''(3)$
(*b*)	$NaO^+(X^3\Sigma^-)+O^-(^2P)$	$^2A'(1), ^4A'(1), ^2A''(2), ^4A''(2)$
(*c*)	$Na^+(^1S)+O_2^-(X^2\Pi_g)$	$^2A'(1), ^2A''(1)$
(*d*)†	$Na^+(^1S)+O_2^-(^4\Sigma_g^+, ^4\Delta_g)$	$^4A'(2), ^4A''(1)$
(*e*)	$Na(^2S)+O_2(X^3\Sigma_g^-)$	$^2A''(1), ^4A''(1)$
(*f*)	$Na(^2S)+O_2(a^1\Delta_g)$	$^2A'(1), ^2A''(1)$
(*g*)	$Na(^2S)+O_2(b^1\Sigma_g^+)$	$^2A'(1)$
(*h*)	$Na(^2P)+O_2(X^3\Sigma_g^-)$	$^2A'(1), ^4A'(1), ^2A''(2), ^4A''(2)$

* Following the standard notation[18], A′ indicates a state whose eigenfunction is symmetrical with respect to the plane and A″ one whose eigenfunction is anti-symmetrical while the numeral in brackets is the number of such states.

† Only the two lowest[18] suitable states of O_2^- are displayed.

the number densities on the right being better determined than the other number densities concerned. Kolb and Elgin[8] did not discuss the factors which control the branching ratio *f* but commented that a value between 10^{-1} and 10^{-2} would apparently be required to account for the nightglow. Recent data requires that *f* be not greatly below unity.

Stellar occultation measurements by Reigler and others[12,13] show that near the Equator $n(O_3)$ is some 1×10^8 cm^{-3} or less between 85 and 90 km rising to $\sim2\times10^8$ cm^{-3} at 95 km. Real variations occur and considerable uncertainty remains. Measurements[14] (31 °N, February) on the 110.8 GHz O_3 rotational line give 5×10^8 cm^{-3} at 80 km falling to about 1×10^8 cm^{-3} at 85 km; indirect deduction[15] from satellite data (20 °N, June) on the intensity of the (9, 3) hydroxyl band give 6×10^8 cm^{-3} between 80 and 85 km and 3×10^8 cm^{-3} at 90 km. Atmospheric model calculations[13] give a nocturnal distribution with a broad maximum of around 2×10^8 cm^{-3} in the 85–95 km region. Simultaneous lidar measurements on n(Na) and photometer measurements on the intensity I(5,893) of the D-doublet have been carried out at São José dos Campos (23 °S)[16]. The inference was drawn that the peak photon emission rate was at 88 km, where n(Na) was 3×10^3 cm^{-3}, and had the value 1×10^2 cm^{-3} s^{-1}. To reproduce this, it may be seen from process (5) that, with k_1 as in process (3), *f* would have to be about 0.3 even if $n(O_3)$ were as great as 3×10^8 cm^{-3}. Later lidar and photometer measurements[17] lead to compatible values. We need to examine whether *f* for process (2) can indeed be as high as required for the nightglow.

Parting along $\{Na^+–O_2^-\}:\{Na–O_2\}$ may yield either

$$Na(^2P)+O_2(X^3\Sigma_g^-) \tag{6}$$

or

$$Na(^2S)+O_2^*(X^3\Sigma_g^-, b^1\Sigma_g^+ \text{ or } a^1\Delta_g) \tag{7}$$

the asterisk indicating possible vibrational excitation. The crossings giving rise to reaction products (6) are at a greater separation than the numerous crossings giving rise to reaction products (7) and these latter are not readily traversed as is evident from the large[18] cross-section (34–38 Å^2) for the quenching process

$$Na(^2P)+O_2 \rightarrow Na(^2S)+O_2^*(X^3\Sigma_g^-, b^1\Sigma_g^+ \text{ or } a^1\Delta_g) \tag{8}$$

Furthermore, compared with the channels yielding products (6), the many relatively exothermic channels yielding products (7) are very strongly favoured statistically. Thus, it might seem that *f* must be minute.

However, consider the symmetry properties of the correlated molecular states concerned. Referring to Table 1, species $^4A'$ appears in reactant row (*a*), the product row (*h*) and the intermediate ionic rows (*b*) and (*d*) the last of which involves excited O_2^-, but does not appear in the product rows (*e*) to (*g*). Because the species does not change during an encounter, it follows that the simple electron-jump model gives the statistical weight ratio of 1/3 for *f* the branching ratio. Although the closeness of the fragments at the crossings may affect the quantitative predictions of the model regarding k_2 (which is not of critical importance) and *f*, there is certainly no reason to doubt that the branching ratio is as high as Chapman's theory demands.

D.R.B. thanks Professors T. M. Donahue and M. Nicolet for correspondence on the nocturnal ozone abundance.

Received 2 May; accepted 26 June 1980.

1. Chapman, S. *Astrophys. J.* **90,** 309–316 (1939).
2. Hildenbrand, D. L. & Murad, E. *J. chem. Phys.* **53,** 3403–3408 (1970).
3. Greer, R. G. H. & Best, G. T. *Planet. Space Sci.* **15,** 1857–1881 (1967).
4. Sandford, M. C. W. & Gibson, A. J. *J. atmos. terr. Phys.* **32,** 1423–1430 (1970).
5. Hunten, D. M. in *The Radiating Atmosphere* (ed. McCormac, B. M.) 3–16 (Reidel, Dordrecht, 1971).
6. Sipler, D. P. & Biondi, M. D. *Planet. Space Sci.* **26,** 65–73 (1978).
7. Sechrist, C. F. *EOS* **57,** 972 (1976).
8. Kolb, C. E. & Elgin, J. B. *Nature* **263,** 488–489 (1976).
9. O'Hare, P. A. G. & Wahl, A. C. *J. chem. Phys.* **56,** 4516–4525 (1971).
10. Herschbach, D. R. *Adv. Chem. Phys.* **10,** 319–392 (1966).
11. Gislason, E. A. in *Alkali Halide Vapors* (eds Davidovits, R. & McFadden, C. L.) 415–440 (Academic, New York, 1979).
12. Reigler, G. R., Drake, J. F., Liu, S. C. & Cicerone, R. J. *J. geophys. Res.* **81,** 4997–5001 (1976).
13. Reigler, G. R. *et al. Geophys. Res. Lett.* **4,** 145–148 (1977).
14. Penfield, H., Litvak, M. M., Gottlieb, C. A. & Lilley, A. E. *J. geophys. Res.* **81,** 6115–6120 (1976).
15. Frederick, J. E., Rusch, D. W. & Liu, S. C. *J. geophys. Res.* **83,** 2441–2445 (1978).
16. Clemesha, B. R., Kirchhoff, V. W. J. H. & Simonich, D. M. *J. geophys. Res.* **83,** 2499–2503 (1978).
17. Kirchhoff, V. W. J. H., Clemesha, B. R. & Simonich, D. M. *J. geophys. Res.* **84,** 1323–1327 (1979).
18. Grice, R., *Adv. Chem. Phys.* **30,** 247–312 (1975).
19. Krauss, M., Neumann, D., Wahl, A. C., Das, G. & Zemke, W. *Phys. Rev.* A7, 69–77 (1973).
20. Herzberg, G. *Electronic Spectra of Polyatomic Molecules,* 10 (Van Nostrand, Princeton, 1966).

Physicochemical speciation of lead in drinking water

Roy M. Harrison & Duncan P. H. Laxen

Department of Environmental Sciences, University of Lancaster,
Lancaster LA1 4YQ

Recent studies have highlighted the importance of drinking water as a route of human exposure to lead[1,2]. Whilst there are ample data on lead concentrations in drinking water[3], little is known of its physical and chemical forms (physicochemical speciation)[4]. Such information is important as the speciation of ingested lead influences the efficiency of absorption from the gastrointestinal tract[5]. Knowledge of speciation should also provide a fuller understanding of the factors controlling the solubility of lead in potable waters[6] and hence assist in devising the most cost-effective means of plumbosolvency control. We have determined experimentally the speciation of lead in three different tapwaters and report here diverse forms of dissolved and particle-associated lead, dependent primarily on the chemical matrix of the raw water.

Based on calculations of equilibrium solubilities, the Water Research Centre has predicted that basic lead carbonate, $2PbCO_3.Pb(OH)_2$ is the most stable insoluble lead compound to be formed in the conditions pertaining to most potable waters in Britain[6]. We have analysed the off-white surface deposit from inside a lead water pipe using X-ray powder diffraction and confirm this to be basic lead carbonate. However, as the Water Research Centre indicated[6], higher concentrations of lead can occur in potable waters than would be predicted by equilibrium of free lead ions with basic lead carbonate. The formation of ion pairs, or organic complexes of lead, or the presence of lead in insoluble particulate form in the water were all suggested as possible means by which these enhanced concentrations might occur, although no experimental measurements were made.

A range of techniques suitable for metal speciation exist, all of which essentially classify the species according to some operationally defined association[7]. We have recently developed a

Table 1 Analysis of tapwater samples

Sample	Alkalinity (μg ml^{-1} as $CaCO_3$)	pH	Organic carbon (μg ml^{-1})	Specific conductance (μS)
Lancaster University	21	7.5	9.4	130
Bentham	20	6.8	1.6	92
Glasgow	4	6.7	8.0	42

speciation scheme for freshwaters, which combines several established techniques[8]. It is based principally on a size fractionation of the metal species. Briefly, samples were collected in polythene bottles and filtered as soon as possible (in parallel, not in series) through Nuclepore filters under pressure in Amicon stirred cells. In two cases filtration was started within 2 h of collection, whilst with the Glasgow sample filtration was unavoidably delayed for 24 h. Nuclepore filters were selected as they have inherently better size discrimination properties than membrane filters and suffer lesser contamination and adsorption problems. Both filter and filtration apparatus were pretreated with a $Ca(NO_3)_2$ solution to minimize adsorption losses[9]. They were rinsed with deionized double-distilled water to remove excess $Ca(NO_3)_2$ and then with a portion of sample before filtration. Recovery tests with pre-filtered samples of tapwater and riverwater, as well as with a synthetic river water, using filters of 0.015–12 μm pore size showed recovery to be independent of filter pore size. Mean recoveries were as follows: Pb, 86%; Cu, 94%; Fe, 101%; Mn, 100%. A fuller discussion of the significance of these adsorption tests is given elsewhere[8]. Note, however, that if, as is likely, adsorption is independent of filter pore size then adsorption losses will only affect the quantification of the smallest size fraction, as the others are calculated by difference and are hence independent of adsorption losses. Contamination during filtration was very low: Pb, <0.1 ng ml^{-1}; Cu, <0.1 ng ml^{-1}; Fe, <0.5 ng ml^{-1}; Mn, <0.05 ng ml^{-1}.

The total metal concentrations in each filtrate were determined by flameless atomic absorption for Fe and Mn, and by anodic stripping voltammetry (ASV) for Pb and Cu following UV-ray acid digestion. A standard additions calibration was applied in all cases. As a measure of the ASV-labile concentration at the natural pH of the sample, ASV analyses were performed on the 1-μm filtrate at a hanging mercury drop electrode, using CO_2 in nitrogen as a buffer. A titration procedure was used to indicate the extent and strength of any complexation and the slope of the titration curve after saturation of the complexation capacity was used to quantify the labile response.

Labile metals were also defined by their uptake on Chelex 100 exchange resin. A 48-h batch technique was employed, using 2 ml of resin in the calcium form per 60 ml of sample in a polythene bottle. This provided a measure of metal complexes with slower dissociation kinetics. Finally, UV-ray irradiation (1 kW Hanovia lamp) was used to destroy organic matter and so release metals previously associated with the organics in a non-ASV-labile form. The increase in labile metal following UV-ray irradiation is a measure of the metals strongly bound with organic matter[7]. This procedure has, however, proved to be inapplicable for most freshwaters, there being a loss rather than gain of ASV-labile metal, due probably to uptake onto hydrous ferric oxide precipitated during the irradiation[8]. It still, nevertheless, provides qualitative information on the nature of the ASV-labile metal.

Particular care has been exercised in the evaluation of the ASV-labile results, due to recently recognized limitations of the method[10,11]. However, interpretation of the data is strengthened by a consistency between the results derived from each of the techniques. Finally, note that in common with all speciation studies, the results might to some unknown extent reflect artefacts of the various handling operations, starting with the sampling itself.

Three tapwater samples were analysed. These included two morning first draw waters, from Glasgow (Scotland) and Bentham (North Yorkshire). The former came from a house with lead-lined tank and lead piping, the latter from a house with copper piping internally, but a lead service pipe. Both waters were of rather low alkalinity and pH (Table 1) and could be described as aggressive in respect of plumbosolvency. The other sample was from the University of Lancaster (copper piping with high-lead soldered capillary joints) and was taken after a thorough flushing of the pipes.

The results are presented in Table 2. Copper has been included, as its speciation behaviour usually differs from that of lead, the latter forming predominantly inorganic species, the former organic[12]. As a substantial proportion of the lead appeared in the colloidal size fractions, the elements iron and manganese were also analysed, as these elements can exist in waters as colloidal hydrous oxide particles or coatings, as well as in association with organic macromolecules[13]. The colloidal hydrous oxides are effective at adsorbing metals from waters and show a particularly strong affinity for lead[14]. The University tapwater sample had a total lead concentration of only 3.3 ng ml^{-1}, the major proportion of which, 76%, was filterable (<0.015 μm). This filterable lead was however not ASV-labile, and hence cannot exist as Pb^{2+}. The water supply is a mixture of moorland surface water and River Lune water and has a substantial organic content (Table 1). Titration of the tapwater sample with lead showed further ability to complex lead as indicated by the ASV signal until the complexation capacity had been exceeded. This complexation capacity was lost following UV-ray irradiation of the sample, which destroys organic matter. The major portion of the lead is, therefore, probably present as non-labile low molecular weight organic complexes, although some may also exist as non-labile inorganic species.

In the Bentham tapwater, which is derived from spring waters and is of low organic content, 53% of the lead and 33% of the copper were associated with colloidal particles of 0.015–1.0 μm. A significant fraction of the lead (19%) was in the particulate size range 1–12 μm. This may have been due to basic lead carbonate which precipitates as rather large particles (unpublished results). The size distribution of the lead in the colloidal size range parallels that of iron rather closely. The mole ratio Pb/Fe is $\sim$0.2 in all three fractions between 0.015 and 1.0 μm. This is consistent with the lead occurring in association with hydrous oxides of iron, either by ion-exchange, by specific adsorption or by co-precipitation. The Chelex-labile copper corresponds closely to the ASV-labile metal, whilst for lead more metal is Chelex-labile. This additional labile metal must, furthermore, be due in some way to release from the colloidal metal fraction. It is either a result of weak lead complexation with organic macromolecules or a slow release from the hydrous oxides due to the disturbed equilibrium in the presence of the Chelex resin. There was no apparent complexation capacity for additional lead during titration of the sample, and UV-ray irradiation did not cause a change in the peak potential of the ASV lead signal, adding weight to the suggestion that inorganic species of lead predominate in this water.

The Glasgow sample, abstracted originally from Loch Katrine, contained the highest concentration of total lead, 372 ng ml^{-1}, and the highest percentage of ASV-labile lead, 63%. Again a high proportion (71%) of lead was associated with the colloidal size fractions, although in contrast to the Bentham water most of this colloidal lead (75%) was in the small size range 0.015–0.08 μm. Note that a significant proportion of this colloidal lead must contribute to the ASV and Chelex-labile lead. During titration of the sample with additional lead a separate lead signal at a more anodic potential developed after $\sim$800 ng ml^{-1} of lead had been added. This is indicative of complexation of the ASV-labile metal in the original sample[15]. After UV-ray irradiation of the sample the original ASV signal disappeared to be replaced by a more anodic peak. It seems that a large proportion of the lead in this sample (63%) existed as ASV-labile organic complexes, a major portion being of high molecular weight (0.015 μm is equivalent to a molecular weight of ~300,000). In the case of copper in the raw sample, ASV-labile metal could not be distinguished. Copper forms stronger complexes with organics than lead and its complexation is often non-ASV-labile[12], as seems to be the case with this sample.

In the three waters examined there is apparently little or no free ionic lead. A significant portion of the lead exists in the colloidal size fractions, associated with hydrous iron oxides or organic macromolecules depending on the composition of the water. There is some particulate lead in the 1–12 μm size range, which may be metal precipitate, or may be associated with clay minerals, but little or no lead in larger particles, >12 μm. This would suggest that the lead in the samples examined is not a result of particles flaking off the basic lead carbonate lining of the lead water pipes.

Plumbosolvency is clearly not a simple equilibrium between solid basic lead carbonate and dissolved Pb^{2+} ions and ion pairs. It depends rather on the adsorption and complexation capacity of the hydrous oxides and organic complexing agents such as humic acids. Techniques of plumbosolvency control depend on an increase in the sample *p*H and hardness/alkalinity[6,16]. The lead concentration is, however, not always reduced to the extent predicted by theoretical calculations of equilibrium solubility[6,16] and the complex lead speciation in real tapwaters, as indicated by our results, may account for this result. The reduction in plumbosolvency achieved by *p*H and hardness/alkalinity control may be a function of a decrease in the rate of lead dissolution and/or the effect of competing cations such as Ca^{2+} for adsorption, ion-exchange and complexation sites, in addition to the anticipated decrease in equilibrium solubility.

One option that has been considered for reduction of lead levels in drinking water is the use of chelating resin at the consumer's tap[6]. Our results demonstrate that this measure is likely to have a limited effectiveness, as a substantial fraction of the lead will probably be in a non-ion-exchangeable form.

The health implications of our findings are uncertain. However, at *p*H 1–2 in the acidified samples, all lead is ASV-labile (Table 2) and is probably present as free metal ions. Hence at the *p*H of the stomach, tapwater lead will also take this form and hence may well be more available for absorption than the lead bound in foodstuffs. This may explain the high effectiveness of removal of lead piping in reducing blood lead levels in the study previously cited[2].

Table 2 Results of speciation study

a, Lancaster University tapwater, well flushed

Size fraction (μm)	Metal concentration ($ng\ ml^{-1}$ (%))			
	Pb	Cu	Fe	Mn
>12	—	2 (8)	17 (9)	1.4 (16)
1.0–12	—	—	—	—
0.4–1.0	—	—	—	—
0.08–0.4	0.8 (24)	3 (12)	173 (87)	2.7 (30)
0.015–0.08			—	—
<0.015	2.5 (76)	19 (79)	8 (4)	4.8 (54)
Total	3.3	24	198	8.9
ASV-labile*	<0.2 (<6)	1 (4)	NA	NA

b, Bentham tapwater, first flush

Size fraction (μm)	Metal concentration ($ng\ ml^{-1}$ (%))			
	Pb	Cu	Fe	Mn
>12	—	—	51 (30)	11.1 (53)
1.0–12	16 (19)	12 (3)	51 (30)	—
0.4–1.0	14 (17)	40 (11)	16 (10)	—
0.08–0.4	22 (26)	42 (12)	34 (20)	0.8 (4)
0.015–0.08	8 (10)	36 (10)	10 (6)	1.8 (9)
<0.015	24 (29)	228 (64)	6 (4)	7.1 (34)
Total	84	358	168	20.8
ASV-labile*	20 (24)	231 (65)	NA	NA
Chelex-labile*	39 (46)	224 (63)	20 (12)	7.3 (36)
Acid ASV-labile†	87 (104)	360 (101)	NA	NA

c, Glasgow tapwater, first flush

Size fraction (μm)	Metal concentration ($ng\ ml^{-1}$ (%))			
	Pb	Cu	Fe	Mn
>12	3 (1)	0.1 (<1)	1.8 (3)	0.3 (7)
1.0–12	49 (13)	1.7 (8)	20.1 (35)	2.1 (47)
0.4–1.0	7 (2)	0.9 (4)	2.4 (4)	0.2 (4)
0.08–0.4	59 (16)	1.9 (8)	6.1 (11)	0.4 (9)
0.015–0.08	198 (53)	9.5 (42)	18.0 (31)	0.3 (7)
<0.015	56 (15)	8.3 (37)	9.0 (16)	1.2 (27)
Total	372	22.4	57.4	4.5
ASV-labile*	236 (63)	NA	NA	NA
Chelex-labile*	207 (56)	9.8 (44)	5.9 (10)	1.1 (24)
Acid ASV-labile†	382 (103)	22.4 (100)	NA	NA

* 1-μm filtrate.
† Unfiltered sample 0.5% HNO_3.
NA, Not available.

We thank Dr M. R. Moore and Mr A. Britten for assistance in providing the Glasgow tapwater sample.

Received 6 May; accepted 2 July 1980.

1. Department of Health and Social Security *Lead and Health* (HMSO, London, 1980).
2. Thomas, H. F., Elwood, P. C., Welsby, E. & St Leger, A. S. *Nature* **282**, 712 (1979).
3. Department of the Environment *Pollution Paper* No. 12 (HMSO, London, 1977).
4. *Health Hazards from Drinking-Water* (WHO, Copenhagen, 1978).
5. Chamberlain, A. C. *et al. UKAEA Rep.* AERE-R9198 (HMSO, London, 1978).
6. Water Research Centre *Tech. Rep. TR43* (Water Research Centre, Medmenham, 1977).
7. Florence T. M. & Batley, G. E. *Talanta* **24**, 151 (1977).
8. Laxen, D. P. H. & Harrison, R. M. (in preparation).
9. Nürnberg, H. W., Valenta, P., Mart, L., Raspor, B. & Sipus, L. *Z. analyt. Chem.* **282**, 357 (1976).
10. Brezonik, P. L., Brauner, P. A. & Stumm, W. *Water Res.* **10**, 605 (1976).
11. Shuman, M. S. & Michael, L. C. *Analyt. Chem.* **50**, 2104 (1978).
12. Ernst, R., Allen, H. E. & Mancy, K. H. *Wat. Res.* **9**, 969 (1975).
13. Mill, A. J. B. *Envir. Techn. Lett.* **1**, 97 (1980).
14. Bacso, J., Szalay, A. & Kiss, K. *Sci. Tot. Envir.* **9**, 271 (1978).
15. O'Shea, T. & Mancy, K. H. *Analyt. Chem.* **48**, 1603 (1976).
16. Akers, C. J. & Fellows, R. *Envir. Hlth* **87**, 148 (1979).

Measurements of $CHFCl_2$ in background tropospheric air

S. A. Penkett*, N. J. D. Prosser*, R. A. Rasmussen† & M. A. K. Khalil†

* Environmental and Medical Sciences Division, AERE Harwell, Oxon OX11 0RA, UK
† Oregon Graduate Center, Beaverton, Oregon.

The likely impact of fluorocarbons on the Earth's ozone layer has recently been reviewed in two major reports[1,2] which, although showing difference of emphasis, both concluded that uncontrolled emissions of F11 ($CFCl_3$) and F12 (CF_2Cl_2) would lead to a substantial reduction in the level of ozone in the Earth's ozone shield (13–16%). The effect of F11 and F12 on ozone would be considerably reduced if they were removed on a large scale by some mechanism which operated in the troposphere. Such a mechanism has been proposed for F11, which involves conversion to F21 ($CHFCl_2$) on the surface of aerosols suspended in the atmosphere[3]. Crescentini and Bruner[4] have recently reported measurements of the F21 concentration that were of sufficient magnitude to suggest that tropospheric removal of F11 was occurring on a scale greater than stratospheric removal. We report here data which refute this suggestion by showing that the level of F21 in the clean background troposphere is virtually unmeasurable.

Several attempts have been made to measure the concentration of F21 in the atmosphere. It was first detected by Rasmussen[5] using a gas chromatograph/mass spectrometer (GC/MS) combination, and he quoted a value of ~10 p.p.t.v. (1 p.p.t.v. = 1 part in 10^{12} by volume). Singh *et al.*[6] reported F21

0028–0836/80/340793—03$01.00

background concentrations of 14.9 ± 4.9 p.p.t.v. as preliminary data for a clean site in Yosemite National Park, California. Subsequently, their more extensive global measurements[7] in the Northern and Southern Hemispheres concluded a tropospheric average of 5 ± 3 p.p.t.v. However, they felt that the lack of a significant interhemispheric gradient for an anthropogenic compound with such a short atmospheric lifetime implied that it was probably an artefact of analysis, although they were unable to determine its source. Measurements in their studies were made using a gas chromatograph equipped with an electron capture detector (GC/ECD). F21 is a difficult species to measure and measurements made with the electron capture detector are not the most reliable as the detector is nonspecific. Glasgow *et al.*[8] reviewed the artefact problems associated with these early F21 measurements. Crescentini and Bruner[4] have shown that a species is present in air which has a mass spectrum identical to that of F21, and they estimate its concentration to be as high as 20 p.p.t.v. in air collected in central Italy. If this were the case for the well-mixed troposphere, then decomposition of F11 to F21 could represent a very substantial sink for F11. The present measurements using a GC/MS combination suggest that the level of F21 in the background troposphere is probably well below 1 p.p.t.

A Hewlett-Packard 5710 gas chromatograph and a VG micromass 16F mass spectrometer combination were used to make the measurements on concentrated air samples. Two concentration techniques were used, both based on collection of liquid air and subsequent removal of the major permanent gases at liquid nitrogen temperature. In one method the oxygen and nitrogen were removed by a stream of pure helium and carbonyl sulphide was used as an internal standard to estimate the effective volume injected (see ref. 9 where xenon was used for a similar purpose). The other method relied on carefully trapping a known volume of liquid air (~3 ml), then pumping away the oxygen/nitrogen excess. Alternatively, a small volume of gaseous air was injected into the cryotrap. Tests with a standard showed that a 95% recovery of material could be achieved by this method. The concentrated samples were then injected into a 3-m OV101 column held at 30 °C, using helium as a carrier gas. COS was measured using mass 60 and F21 was measured using masses 67, 69 and 102. Because of the extremely low concentrations of F21 that were present, this was generally done using the single ion mode. Attempts to measure all three ions simultaneously resulted in rather poor signal-to-noise ratios. A typical chromatogram that resulted for mass 67 in the single ion mode is shown in Fig. 1. Chromatograms for masses 69 and 102 showed similar peak separation and signal-to-noise ratios. The peak ascribed to F21 in Fig. 1 had an identical retention time as an F21 standard, also a linear response to F21 concentrations between 100 p.p.t.v.and 10 p.p.b.v. (1 p.p.b.v. = 1 part in 10^9 by volume) was shown by the instrument. These latter standards were injected in 10-ml syringes so that the mass of F21 entering the detector at the 100 p.p.t. level was actually lower than that injected in the concentrated air samples, which typically contained the equivalent of 2 litres of air.

All of the data collected in this programme of F21 measurements are shown in Table 1. The first 14 results are values of the F21 concentration in the ambient air at Harwell, five of which used one technique for quantitative estimation and nine used another. The average value of the 14 estimations is 1.6 p.p.t.v. with $\sigma = 0.7$ p.p.t.v. There is no significant difference in the two groups of data obtained by the two techniques (1.8 ± 0.5 p.p.t.v. and 1.5 ± 0.7 p.p.t.v.), and this gives us confidence that our average of 1.6 p.p.t.v. is correct. The possibility that some compound other than F21 is being measured is not very high, as the results obtained using masses 69 and 102 are almost identical to those obtained using mass 67. Chloroethane, which contains a peak at *m/e* 67 in its mass spectrum, was observed to co-elute with F21 in this study; however, chloroethane does not have *m/e* peaks at 69 and 102.

Estimates of the F21 concentration in air samples from other locations are also shown in Table 1. Samples 16–19 represent particularly clean air samples, and there the average falls to 0.08 p.p.t. Whether this number is significantly different from the noise level (~0.05 p.p.t.v.) is not possible to tell with the present experimental system. The numbers can be taken to indicate that the F21 concentration in the background troposphere is well below 1 p.p.t.v.

Tests have been made for contamination and decay in the containers used to bring the air to Harwell. Samples 15–18 were contained in aluminium cans with metal-bellows valves. There was no evidence for any decay in a similar can filled with Harwell air on 21 March 1979 and analysed on 21 May 1979 and 13 June 1979. Sample 19 was contained in a stainless steel can, but there is no reason to suspect decay in this system. Previous tests by one of us (R.A.R.) also showed that no growth of F21 occurred over a two-week period.

Our value for F21 in rural air in Southern England (1.6 p.p.t.v.) is substantially lower than previously reported estimates at other locations[4–7]. Rasmussen[10] has since revised his estimate of F21 concentrations originally reported (~10 p.p.t.v.) and now considers a value of 1.5 p.p.t.v. to be more likely. The data of Singh *et al.*[6,7] were all obtained by GC/ECD and the chances of overestimation are quite large. A major problem in the analysis of F21 is to devise a column that will give complete separation of F21 from other neighbouring compounds. Rasmussen in his early work observed that chloroethane (C_2H_5Cl, boiling point, 12.7°C) had a retention time similar to F21 (boiling point, 8.9 °C) in the conditions of analysis used with an SP 2100 column and temperature programming. Singh *et al.*'s[11] elution of F21 (boiling point, 8.9 °C) before CH_3Br (boiling point, 3.5 °C) on a DC 200 column substrate is inconsistent with the elution sequence of materials with increasing boiling points on that type of column. Additionally, the separation of F21 from CH_3I (boiling point, 43 °C) on 0.5% SP 1000 Carbopack B column has presented difficulties[12]. This leaves only Crescentini and Bruner's[4] high value to be accounted for. Assuming that they may have been sampling polluted air, we collected air samples in the area between Liverpool and

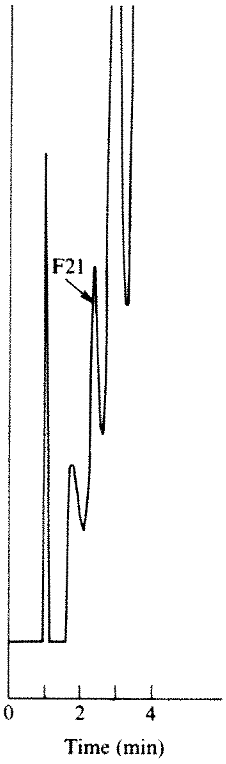

Fig. 1 F21 ambient air stored between 21 March and 21 May 1979; 2.6 p.p.t.v. at *m/e* 67. The sample size was 730 ml.

Table 1 Results of F21 measurement programme at Harwell

No.	Date	Sample	Vol. (ml)	F21 (p.p.t.v.)	Mass no.	Comments
1	7 November 1978	OA.1		1.9	67	COS used as internal standard
2		OA.2		2.6	67	
3		OA.3		2.2	67	
4	8 November 1978	OA.4		1.7	67	
5		OA.5		1.0	67	
6	13 March 1979	OA.6	3 mlLA	1.1	67	Known volume of liquid air
7		OA.7	3 mlLA	1.1	69	
8	14 March 1979	OA.8	3 ml LA	1.9	102	
9		OA.9	3 ml LA	2.3	102	
10		OA.10	3 mlLA	1.9	67	
11	21 May 1979	OA.11		1.1	67	
12		OA.12		0.5	67	
13		OA.13		0.6	67	
14	13 June 1979	OA.14		2.8	67	
15	14 March 1979	Longview Al Plant (PNW)	3 ml LA	1.9	67	
16		Tasmania	3 ml LA	—	102	
17		Tasmania	3 ml LA	0.2	102	
18		Background PNW	3 ml LA	0.07	67	
19	15 March 1979	South Pole	3 ml LA	0.1	67	
20	21 May 1979	OA stored 21 March 1979	3 ml LA	2.6	67	
21			1 ml LA	2.6	67	
22	13 June 1979		1 ml LA	2.0	67	
23	12 June 1979	Northwich	100 ml A	4.2	67	100 ml of gaseous air injected into cryotrap
24		Northwich	100 ml A	13	67	
25		Runcorn	100 ml A	37	67	
26		Runcorn	100 ml A	34	67	
27		OA	100 ml A	—	67	

OA, Outside air; LA, liquid air; A, air; PNW, Pacific North West; Al, aluminium.

Manchester. When measured using mass 67, samples 23–26 showed elevated levels of F21 with values between 4 and 37 p.p.t.v. Unfortunately these values were not confirmed by measuring masses 69 and 102, and samples collected more recently in this area show only very low F21 levels (~1.5 p.p.t.v.). Whilst it is thus quite feasible that Crescentini and Bruner were sampling F21 in polluted air, there still remains some doubt that concentrations as high as 20 p.p.t.v. occur.

If the only sink for F11 in the troposphere involved F21 production, then a lifetime for F11 could be derived from a knowledge of the relative F11/F21 concentrations and the rate of decay of F21. In the troposphere, the most likely sink for F21 is reaction with OH radicals, so:

$$\mathrm{CCl_3F\ (F11)} \rightarrow \mathrm{CHCl_2F\ (F21)} \xrightarrow{[\mathrm{OH}]} \text{products}$$

and

$$\tau(\mathrm{F11}) \sim \frac{[\mathrm{F11}]}{[\mathrm{F21}]}\,\tau(\mathrm{F21})$$

This simplified equation yields a τ(F11) of 200–300 yr. The concentrations of F11 and F21 were taken to be 165 p.p.t.v. and 1.6 p.p.t.v., respectively. $\tau(\mathrm{F21}) \sim \{\bar{K}[\overline{\mathrm{OH}}]\}^{-1}$ is between 2 and 3 yr based on the reaction rate constant of F21 with OH of $1.5 \times 10^{-12} \exp(-1{,}184/T)$ cm^3 molecule^{-1} s^{-1} (ref. 13) at the average temperature of 260 K with mean OH densities in the range $0.6\text{–}1 \times 10^6$ molecules cm^{-3} (ref. 14). This equation for τ(F11) is approximately valid when F11 and F21 are in a steady state. We calculated the lifetime of F11 using more complex expressions without the steady-state assumption, but the results were not significantly different. Furthermore, we used the average of the highest observed concentrations of F21 (1.6 p.p.t.v.). Our other measurements imply that, in fact, the global concentration of F21 is probably well below this value (~0.1 p.p.t.v.), which would in turn imply that such a conversion of F11→F21 is much less significant than calculated above. Therefore, our measurements show that the lifetime of F11 due to its possible conversion to F21 is much longer than that derived from stratospheric photolysis[15], which is ~50 yr. For this tropospheric removal process of F11 to be equivalent to stratospheric photolysis, a background F21 concentration of 6 p.p.t.v. would be required; a dominant tropospheric removal process would need a level exceeding 10 p.p.t.v.

In the discussion above, we have considered the extreme case where all the observed atmospheric burden of F21 results from destruction of F11. In fact, all or part of the atmospheric burden may be due to other sources which include direct industrial emissions[8] and volcanic emissions[16,17].

Definite statements can be made only if more data are collected on the atmospheric concentrations of F21 in the background atmosphere, which would also justify more detailed theoretical treatments than discussed in this study. Our present experimental results show that non-urban F21 concentrations range from ~0.1 to 2.5 p.p.t.v., indicating that even if there are environmental processes which destroy F11, converting it to F21, they would not be a significant global, tropospheric sink for F11.

We thank Dr R. G. Derwent for helpful discussions and Steve Crawford and Bob Dalluge for laboratory assistance. This work was funded by the Chemical Manufacturers Association and the UK Department of the Environment. The samples 23–26 were obtained with help from ICI Ltd. Support from the NSF, grants ATM 7806628 and DPP 77-23468, is gratefully acknowledged.

Received 27 May; accepted 3 July 1980.

1. *Chlorofluorocarbons and their Effects on Stratospheric Ozone* (Pollut. Pap. No. 15, HMSO, London, 1979).
2. *Stratospheric Ozone, Depletion by Halocarbons, Chemistry and Transport* (National Academy of Sciences, Washington, DC, 1979).
3. Ausloos, P., Rebbert, E. R. & Glasgow, L. C. *Natn. Bur. Stand. J. Res.* **82,** 1 (1977).
4. Crescentini, G. & Bruner, F. *Nature* **279,** 311 (1979).
5. Rasmussen, R. A. *EPA Rep.* *R0804033-01 (1976).
6. Singh, H. B., Salas, L., Shigeishi, H. & Crawford, A. *Atmos. Envir.* **11,** 819 (1977).
7. Singh, H. B., Salas, L., Shigeishi, H. & Scribner, E. *Science* **203,** 899 (1979).
8. Glasgow, L. C., Jesson, J. P. & Ward, R. B. *Atmos. Envir.* **12,** 692 (1978).
9. Rasmussen, R. A., Penkett, S. A. & Prosser, N. *Nature* **277,** 549 (1979).
10. Rasmussen, R. A. *Atmospheric Measurement of $CHFCL_2$* (F21, Final Rep. No. 78-60, Chemical Manufacturers Association, London, 1979).
11. Singh, H. B., Salas, L. J., Shigeishi, H. & Smith, A. H. *Fate of Halogenated Compounds in the Atmosphere Interim Rep.* No. PB 278-198 to EPA, 19 (1978).
12. Bruner, F., Bertoni, G. & Crescentini, G. *J. Chromatogr.* **167,** 399 (1978).
13. DeMore, W. B. *Chemical Kinetics and Photochemical Data for Use in Stratospheric Modelling Evaluation Numbers* (Jet Propulsion Laboratory, Pasadena, 1979).
14. Volz, A., Ehhalt, D. H., Derwent, R. G. & Khedim, A. *Ber. der Kernforsch.* No. 1604 (1979).
15. Derwent, R. G. & Eggleton, A. E. J. *Harwell Rep. AERE R 9112* (HMSO, London, 1978).
16. Stoiber, R. E., Leggett, D. C., Jenkins, T. F., Murrmann, R. P. & Rose, W. I. *Bull. geol. Soc. Am.* **82,** 2299 (1971).
17. Graedel, T. E. *Chemical Compounds in the Atmosphere* (Academic, New York, 1978).

A climatically responsive tree-ring record from *Widdringtonia cedarbergensis*, Cape Province, South Africa

Peter W. Dunwiddie

Quaternary Research Center, University of Washington, Seattle, Washington 98195

Valmore C. LaMarche Jr

Laboratory of Tree-Ring Research, University of Arizona, Tucson, Arizona 85721

The use of dated tree-ring series to reconstruct past climate has received much attention in recent years[1,2]. The development of long and climatically responsive chronologies in many areas of the Southern Hemisphere is an important step towards better understanding past environments in these areas[3,4], but little dendrochronologically related work of any sort has been done on the African continent[5–11], and most of this has consisted primarily of ring counts to estimate ages. We report here on the development and climatic interpretation of the first dated annual ring-width index chronology from Africa south of the Sahara.

Tree-ring samples were collected from a large number of sites in South Africa[12] as part of a broader-scale effort to reconstruct climatic variability in the Southern Hemisphere. The results of reconnaissance sampling, combined with previous experience elsewhere, led us to concentrate on conifers in the genera *Podocarpus* (Podocarpaceae) and *Widdringtonia* (Cupressaceae) in western and southern Cape Province. One species, *W. cedarbergensis*, seemed to offer particular promise by virtue of its apparent great age, its tree-ring properties, and its occurrence in marginal habitats of the Cedarberg Mountains.

The Die Bos site, which provided the tree-ring samples on which this analysis is based, is located in the rocky Cedarberg Mountains about 200 km north of Cape Town. It is one of the largest remaining stands of *W. cedarbergensis*, whose numbers have been greatly reduced by woodcutting and wild fires. Scattered *Protea* (sp.) trees and shrubs are the main associates on this sparsely vegetated site. The climate in the Cedarberg is moderately warm in summer and cold in winter, and the area receives between 300 and 900 mm of precipitation per year, mainly in winter.

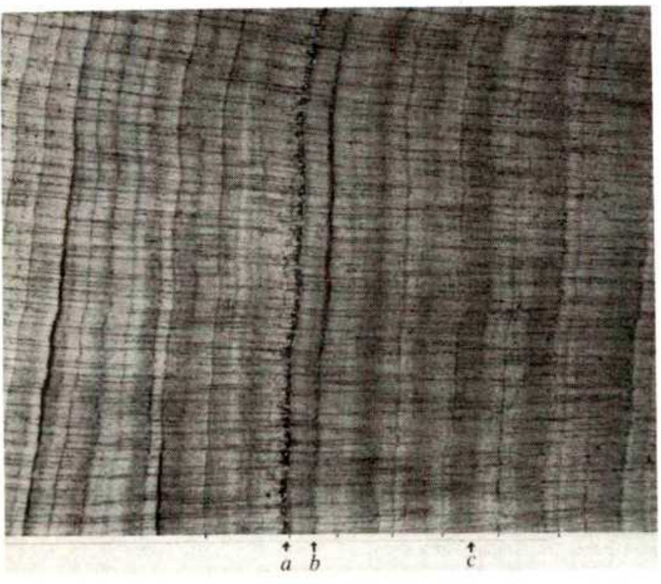

Fig. 1 Detail of growth rings in *W. cedarbergensis*. *a*, Frost ring in earlywood of 1787; •*b*, resin band in centre of 1786 ring; *c*, intra-annual band in latewood of 1783 ring. Rings following 1787 have clearer latewood terminations than do earlier ones.

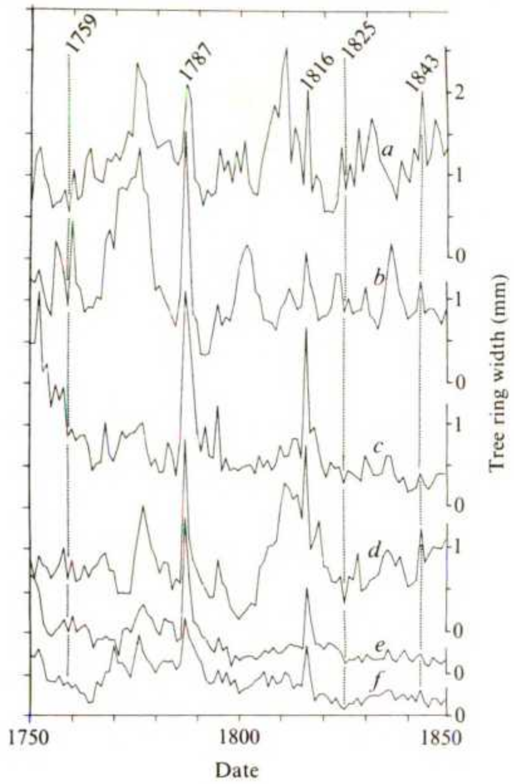

Fig. 2 Portions of ring-width plots for six trees from the Die Bos site illustrating crossdating in the period 1750–1850.

Our sample includes 58 increment cores from 28 living trees up to 12 m tall and 150 cm in diameter. These are supplemented by cross-sectional disks from 19 dead trees and stumps. Lobate growth is uncommon in this material, as is the wedging out of individual rings. Circuit uniformity is generally good, with ring-width patterns being similar on various radii of the same tree. However, several growth features make cross-dating unlike that in most other species (Fig. 1). Many rings lack an abrupt termination of latewood growth, and may have several false bands within the latewood, making determination of the precise ring boundary difficult. Resin-filled bands of cells occur in some rings that may appear as sharper, more distinct lines than the true boundary. The 'signature' rings commonly used by dendrochronologists to crossdate specimens (rings that are relatively narrow on many trees in a site) are not common. Rather, unusually wide rings (Fig. 2), which in some cases (1787, 1816) exhibit characteristic frost damage in the earlywood are more reliable dating checks. These frost rings (Fig. 1) are unusual because trees of most species are not susceptible to such damage after they reach several centimetres in diameter. At Die Bos, mature trees are found with frost rings that date consistently between trees. It is not known why these rings are often relatively wide as well. Figure 2 also illustrates the wide variation in growth rates and sensitivities found in trees at this site. Some, like trees *c* and *e*, are relatively slow-growing, but have several extremely wide rings. Others, such as *a* and *b*, have many relatively wide rings, some of which crossdate with other trees. There is little doubt that the rings dated in this chronology are annual, for several reasons. First, the extreme seasonality of the

0028-0836/80/340796—02$01.00

Mediterranean-type climate is likely to limit growth to a single growing season each year. Second, locally absent ('missing') rings are infrequent, and relatively few rings in any specimen are ambiguous; false bands can usually be clearly differentiated from the annual rings by careful inspection and crossdating.

The site chronology beginning in AD 1564 (Fig. 3) was developed by standard methods[1] after all suitable samples were dated. It represents the average of ring-width index series from 52 radii on a total of 32 trees, an unusually large sample size. An analysis of variance[1] based on data for the 1892–1976 subperiod showed that 29% of the total sample variance is retained by the site chronology, indicating a fairly high degree of ring-width variation in common between different radii and different trees. Presumably, this reflects a fair degree of common response to year-to-year variations in the local environment, including climate.

A climatic response function[1] was computed to evaluate the nature of the climatic 'signal' contained in the site chronology (Fig. 4). It is based on comparison, using multivariate analytical methods, of monthly climatological data from a nearby station with the annual ring-width index during the period 1931–60. The climatic variables used are the monthly average daily maximum temperature and the total monthly precipitation during each month in an 18-month climatic interval beginning in spring (October) of the year preceding initiation of ring growth, and ending in autumn (March) of the calendar year following the year in which growth begins. That is, this interval includes the past and present growing seasons. The growing season for this species probably includes the period October through March. Previous ring-width index was not used in generating the response function shown here, but incorporating previous growth in the analysis produces very similar results.

The response function results show a high degree of correlation of tree growth with climatic factors; 73% of the year-to-year variability in ring-width index can be explained by departures from normal temperature and precipitation during the 18-month interval preceding and concurrent with the growing season. However, the response is complex, with opposite responses to the same variables occurring in different seasons of the year. A dominant feature is the positive response to precipitation of the previous and current spring and early summer (September or October to December). Coupled with a negative response to higher than normal temperatures in the previous and current early summer (November–December), this suggests that one component of the relationship is a negative response of tree growth to spring and early summer drought. However, in some months, a negative response to precipitation and positive response to temperature also occur. We can tentatively interpret the long tree-ring chronology (Fig. 3) as a record of spring and early summer moisture availability, but other chronologies from a greater diversity of habitats and a broader geographic area must be developed, studied, and compared to understand better the climatic history of southwestern South Africa over the past several hundred years. For example, the occurrence of frost rings in most trees following the extremely large volcanic eruption of Tambora at 8 °S in 1815 may suggest a dust veil effect on temperatures of interest to climatologists.

Dendrochronological study of *W. cedarbergensis* can also provide a fire frequency record. Several charred disks from the Die Bos site have an outer ring dated 1872, and some living trees exhibit a marked growth surge beginning the next year, suggesting a release effect following fire. A marked resin band in the ring for 1771, along which many specimens split, may be the result of an earlier fire. Fire-scarred living trees are unusual in this resinous, flammable species; trees are generally either killed or left unscarred by fire.

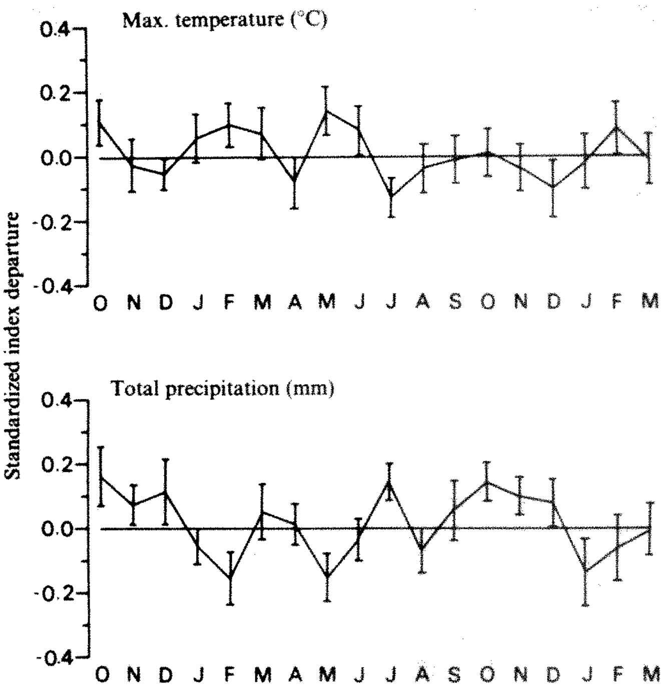

Fig. 4 Climatic response function for the Die Bos *Widdringtonia cedarbergensis* chronology. Based on combined climatological data from Clanwilliam, Calvinia, and Langgevens, Cape Province, 1931–60.

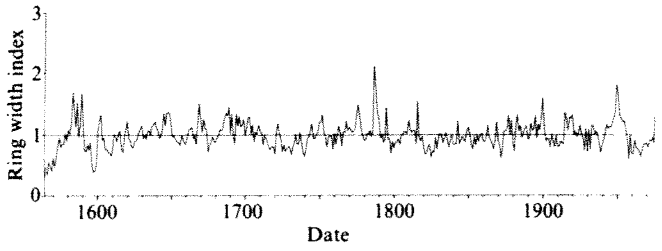

Fig. 3 Site chronology of average ring-width indices, Die Bos, Cape Province.

There is potential for development of much longer tree-ring chronologies than that presented here. Dead wood decays slowly in this semi-arid environment, especially in rock crevices or overhanging rock shelters, and wood from stumps, logs, and remnants can be cross-dated with living material. Ring-width plots for trees *a* and *d* (Fig. 2) illustrate the matching of such 'floating' series with growth records of living trees at the site.

This analysis illustrates the potential for development and climatic interpretation of long tree-ring records from southern Africa. In addition to study of ring-width variability, other approaches such as analysis of stable isotopic composition may yield further information. Some of this material has already been supplied for isotopic analysis.

We thank F. Kruger, A. Lamb, and F. Hanekome for support and field assistance, E. Ashton for selected climatological data from copies of the South African Weather Bureau's magnetic tapes. This research was supported by the Climate Dynamics Program, Division of Atmospheric Sciences, NSF.

Received 11 April; accepted 5 May 1980.

1. Fritts, H. C. *Tree-Rings and Climate* (Academic, London, 1976).
2. LaMarche, V. C. Jr *Nature* **276**, 334–38 (1978).
3. Dunwiddie, P. W. *N.Z.J. Bot.* **17**, 251–66 (1979).
4. Ogden, J. *Aust. J. Ecol.* **3**, 339–56 (1978).
5. Walter, V. H. *Naturwissenschaften* **28**, 607–12 (1940).
6. Guy, G. L. *Proc. Trans. Rhod. Sci. Ass.* **54**, 68–84 (1970).
7. Storry, J. G. *S. Afr. J. Sci.* **71**, 248 (1975).
8. Hall, M. *Ann. Natal Mus.* **22**, 693–703 (1976).
9. Curtis, B. A., Tyson, P. D. & Dyer, T. G. J. *S. Afr. J. Sci.* **74**, 92–95 (1978).
10. Lilly, M. A. *An assessment of the dendrochronoloical potential of indigenous species of trees in South Africa*, Occ. Paper No. 18 (Dept Geogr. & envir. Stud., Univ. of Witwatersrand, Johannesburg, 1977).
11. Munaut, A. V., Berger, A. J., Guiot, J. & Mathieu, L. *Evolution des Atmosphères Planétaires et Climatologie de la Terre* (Centre National d'Etudes Spatiales, Nice, 1978).
12. LaMarche, V. C. Jr, Holmes, R. L., Dunwiddie, P. W. & Drew, L. G. *Laboratory of Tree-Ring Research Chronology Series 5*, Vol. 5 (University of Arizona, Tucson, 1979).

Organic matter fluxes from sediment traps in the equatorial Atlantic Ocean

Stuart G. Wakeham, John W. Farrington, Robert B. Gagosian, Cindy Lee, Hein DeBaar, Gale E. Nigrelli, Bruce W. Tripp, Steven O. Smith & Nelson M. Frew

Department of Chemistry, Woods Hole Oceanographic Institution, Woods Hole, Massachusetts 02543

The vertical flux of particulate organic matter to the ocean floor is controlled by complex remineralization and transport processes. Rapidly sinking, large (>32 μm) particles may account for most of the vertical mass flux[1-3]. Experiments involving collection of sedimenting particles in traps deployed at varying depths in the water column provide a way of assessing these processes directly[2-12]. Measurement of organic carbon content of trap material may lead to a general understanding of the flux of particulate organic matter to the sea floor[3,8-10]. However, details of the transport and transformation phenomena involving sinking particulate organic material can be elucidated only by determining distributions of specific organic compounds associated with the particles[11,12]. We report here direct flux measurements and composition of lipids obtained by organic geochemical studies of particulate material collected in a deep-sea moored sediment trap experiment in the equatorial Atlantic Ocean.

The PARFLUX E station was located on the Demerara abyssal plain (5,288 m) ~750 km from the Guyana coast at 13°30.2′ N, 54°00.1′ W. Four sediment traps were placed along a fixed mooring at depths of 389, 988, 3,755 and 5,068 m, and recovered after 98 days (November 1977–February 1978). The water column had a weak oxygen minimum between 200 and 400 m, and the main thermocline was located at 300 m. No significant nepheloid layer was reported[7]. Sodium azide was added to each trap before emplacement and diffused into the collection cup[13] during the experiment to retard bacterial spoilage of the trapped material.

Particulate samples were wet sieved and split with a rotary splitter[3]. Aliquots were taken for geological[3], elemental and isotopic[7], and organic geochemical (present) studies. About one-sixteenth of each sample (0.03–0.4 g sediment depending on availability) was extracted with toluene/methanol (1:1). Amino acids present in this extract were partitioned into saturated salt solution, while the remaining lipids were partitioned into hexane. The hydrolysed amino acids were analysed by a modification of the fluorescence technique of Hill *et al.*[14]. An aliquot of the hexane-soluble lipids (0.5–5 mg of lipid) was hydrolysed for total fatty acid analysis. A second aliquot (0.4–4 mg) was separated into constituent organic compound classes by adsorption chromatography (Merck silica gel 60, 5% deactivated with water) by elution with a series of solvents of increasing polarity (ranging from hexane, toluene in hexane, increasing proportions of ethyl acetate in hexane, ethyl acetate, to methanol).

The molecular composition of compound classes collected (given in Table 1) was determined by glass capillary gas chromatography (GC) (Carlo Erba 2150 and 4160, and Hewlett Packard 5710 and 5840 chromatographs; 15–25 m × 0.3 mm i.d. columns, deactivated by persilylation and coated with SE-52[15]) and capillary gas chromatography/mass spectrometry (GC/MS) (Finnigan 3200 and 1015 SL). Electron impact and isobutane- or methane-chemical ionization spectra were obtained, depending on the compound class. Fatty acids were analysed as methyl esters[16], and fatty alcohols and sterols as acetate derivatives[17]. Wax esters, steryl esters, and triacylglycerols were analysed intact by capillary GC and GC/MS. Compounds were identified where possible by comparison with GC retention times and mass spectra of authentic standards. Concentrations of hexane-soluble lipids were estimated by weighing an aliquot on an electrobalance; concentrations for compound classes are sums of individual compounds determined by gas chromatography. Laboratory blanks were carried through the entire workup and were generally significantly lower than samples. We cannot estimate sampling variability as single samples were collected, but analytical precision for each compound class is better than ±20%.

Organic geochemical results for PARFLUX E sediment trap samples are given in Table 1 as total amounts of material in each trap and as mass fluxes at the depths sampled. The major compositional features of the lipid classes analysed are summarized in Table 2. Further details of compound distributions will be given elsewhere.

Particles <1 mm in size accounted for most of the particulate flux at all depths sampled. The amount of material <1 mm varies little with depth in the water column. Honjo[3] found these particles to be amorphous aggregates of organic matter composed of foraminiferal tests, radiolarian skeletons, small pteropod shells, and faecal pellets. Only in the 389 m trap were particles >1 mm important, these including larger faecal pellets and some intact zooplankton[3].

Bulk organic matter flux decreased rapidly with increasing depth in the mesopelagic zone (389 and 988 m traps), stabilizing in the bathypelagic layer (3,755 and 5,068 m samples). Organic carbon comprised ~50% of the organic matter in the mesopelagic samples and ~35% at the two deeper depths. Of the organic carbon fixed in the euphotic zone at this location[3] (200 mg m^{-2} day^{-1}), ~4–6% reached the mesopelagic traps. Only ~1% arrived in the deep traps. These observations are consistent with a rapid turnover of bulk organic matter in the upper portion of the water column, with a small and highly fractionated amount reaching the sea floor.

Lipids were rapidly depleted in the upper 1,000 m of the water column. Unlike bulk organic matter and organic carbon, lipid fluxes decreased throughout the water column. Lipids became a proportionally smaller fraction of the organic flux (15% at 389 m and 2% at 5,068 m), indicating that they were consumed preferentially compared with other components of the overall organic pool.

Fluxes for specific organic compound classes followed three trends (Table 1): (1) a rapid decrease with depth (hydrocarbons, fatty acids, wax esters, steroid ketones, and lipid-associated amino acids); (2) a rapid decrease between 389 and 988 m followed by a slight flux increase in the 3,755 m trap (free fatty alcohols); (3) a maximum flux at 988 m (free sterols, steryl esters, triacylglycerols). Major aspects of our observations are outlined below and in the tables.

Hydrocarbons of planktonic origin (n-C_{17}, C_{19}, and a lesser amount of pristane) dominated all four traps. Long-chain (C_{25}–C_{31}) hydrocarbons were also present at lower abundances at all depths, indicating long-range transport of continentally derived material. Sterenes were detected, primarily in the 389 and 988 m samples, where they were more abundant than alkanes in the same carbon range. This suggests active microbial transformations of organic matter in or on sinking particles and a relatively fast biogeochemical formation for sterenes[18]. We cannot, however, rule out a planktonic source for these cyclic hydrocarbons.

The flux of total fatty acids (free + esterified) decreased 60-fold with increasing depth. Free fatty acids, a minor fraction of the total acid pool, showed a smaller decrease. The fatty acid composition of the particulates reflects a planktonic source. Recycling and sinking of particles resulted in rapid degradation of all fatty acid moieties, unsaturated compounds being lost more rapidly than saturated ones (for example, saturated/unsaturated acids = 5 and 60 at 389 and 5,068 m respectively). Branched-chain fatty acids, potential markers of microbial contribution[19-22], were minor constituents, and their relative abundance did not increase with depth.

0028-0836/80/340798—03$01.00

Table 1 Organic geochemical results for PARFLUX E sediment traps

Depth of 1.5 m^2 trap (m)	Sample designation	Particle size	Particulate matter[*]	Organic matter[†]	Organic carbon[†]	Hexane-soluble lipids[‡]	Hydrocarbons[§]	Total fatty acids[§]	Free fatty acids[§]	Wax esters[§]	Steroid ketones[§]	Amino acids (Lipid fraction)[§]	Free fatty alcohols[§]	Free sterols[§]	Steryl esters[§]	Triacylglycerols[§]
									Amount of material per trap							
			(g)			(mg)	(µg)									
389	E6	<1 mm	6.6	1.4	0.7	225	1,200	39,100	4,100	770	4,720	300	20,500	19,100	170	390
	E2	>1 mm	3.6	0.6	0.3	70	250	16,500	2,600	530	130	90	4,100	7,400	60	90
988	E3	<1 mm	6.7	1.2	0.5	170	1,120	17,400	470	180	3,300	43	1,800	31,400	2,300	2,100
	E1	>1 mm	0.5	0.1	0.04	20	170	5,100	—[‖]	20	20	3.2	980	3,360	200	110
3,755	E4	<1 mm	6.8	0.7	0.2	25	140	1,280	—[‖]	16	530	13	6,300	900	8	17
5,068	E5	<1 mm	6.9	0.7	0.2	13	97	910	200	49	590	14	760	550	9	12
									Fluxes							
			(mg m^{-2} day^{-1})			(µg m^{-2} day^{-1})										
389	E6	<1 mm	45.1	9.7	4.7	1,530	8.2	270	27.9	5.3	32.1	2.0	140	130	1.2	2.6
	E2	>1 mm	24.2	3.9	2.0	470	1.7	110	17.8	3.6	0.9	0.6	30	50	0.4	0.6
988	E3	<1 mm	45.9	7.9	3.7	1,160	7.6	120	3.2	1.2	22.4	0.3	12	214	15.9	14.3
	E1	>1 mm	3.3	0.7	0.3	130	1.2	35	—[‖]	0.1	0.1	0.02	7	23	1.3	0.7
3,755	E4	<1 mm	46.4	4.8	1.7	170	1.0	8.7	—[‖]	0.1	3.6	0.1	43	6	0.06	0.12
5,068	E5	<1 mm	47.0	4.9	1.7	85	0.7	6.2	1.4	0.3	4.0	0.1	5	4	0.06	0.08

[*] Weight calculated from weighing replicate aliquots of splits[3].
[†] Data from ref. 3.
[‡] Gravimetric determination.
[§] Determined by GC or HPLC (amino acids).
[‖] Not detectable relative to blank.

Unsaturated wax esters (for example, $C_{34:1}/C_{34:0} = 40$ at 389 m) dominated the wax ester flux. The composition was indicative of a zooplankton origin[23,24]. Degradation of unsaturated wax esters appeared faster than loss of saturated analogues. However, even at 5,068 m depth, unsaturated compounds dominated the wax ester distribution ($C_{34:1}/C_{34:0} = 15$).

Steroid ketones (stanones + stenones) exhibited a gradual flux decrease with increasing depth. The major ketone in each sample was cholest-4-en-3-one, representing 60% of the ketone flux into the mesopelagic traps and about 35% into the deeper traps. *In situ* production of steroid ketones, possibly through microbial transformations of sterols, may have occurred as the particles sank. The gradual flux decrease of ketones compared to sterols (see below) could be due to differing degradation rates.

Amino acids associated with the lipid fraction in the mesopelagic traps were similar in composition to the protein amino acid composition of plankton. Such distributions were also found in suspended particulate matter filtered from seawater in the Pacific[25]. In contrast, only glutamic acid, aspartic acid, alanine, serine and glycine were detected in the deeper traps. These are the major amino acids in bacterial cell walls[26] and may reflect bacterial input.

Free fatty alcohols of 14, 16 and 18 carbon atoms were associated with particles in all four traps. Only about 10% of the alcohols in the 389 m trap were found in the 988 m trap. On the other hand, we observed a significant enrichment of fatty alcohols at 3,755 m. The several compounds responsible for this increase remain unidentified at present, but they are neither straight-chained molecules nor phytol.

The free sterol flux maximized at 988 m, where cholest-5-en-3β-ol accounted for 95% of the sterol composition. In contrast, at 389, 3,755 and 5,068 m, a wide range of planktonic sterols were present.

Steryl ester fluxes and molecular distributions correlate well with free sterols, although the relative flux increase at 988 m over 389 m was about an order of magnitude greater for the esters. In the 389 m sample, steryl esters were composed of a range of sterols (Table 2) and primarily $C_{16:0}$ and $C_{18:0}$ fatty acids. However, esters of cholest-5-en-3β-ol predominated at 988 m.

Triacylglycerols in the 389 m trap were composed primarily of $C_{18:0}$, $C_{18:1}$ and $C_{16:0}$ fatty acids, resulting in a C_{45}-C_{63} carbon range. Polyunsaturated fatty acid moieties ($C_{22:6}$ and $C_{20:5}$) were more abundant in the 988 m sample than saturated or monounsaturated acids.

Our results suggest that significant alteration of organic compounds produced by phytoplankton and zooplankton[21,23,24,27–29] in the upper water column takes place even before the particles reached the shallowest trap. For example, *n*-C_{17}, C_{19}, and pristane were depleted relative to other alkanes in the 389 m trap compared with freshly sampled indigenous zooplankton collected at 300 m at the PARFLUX E site (our analyses). Unsaturated fatty acids and wax esters in this trap were apparently degraded more rapidly than saturated acids and esters. On the other hand, sterenes and steroid ketones were generally absent from the plankton lipid but were abundant in the trap samples.

Details of food web dynamics, microbial transformations and biochemical reactions in the open ocean are poorly understood. However, it is apparent that many of the organic compounds we analysed are consumed (recycled and/or remineralized) in the mesopelagic layer in this part of the ocean. Only a few per cent of these compounds are associated with particles reaching the bathypelagic zone. Nevertheless, alterations of the composition of extractable organic matter on the sinking particles occur throughout the water column and significant amounts of labile organic material reach the sea floor. Many of the compositional changes we observed take place below the ~300 m depth below which Menzel[30] thought most organic compounds were refractory.

We cannot preclude that vertically migrating zooplankton were not entrapped in the mesopelagic sediment traps. However, it is unlikely that the flux maxima at 988 m for sterols, steryl esters, and triacylglycerols are due to such entrapment. Only in the 389 m trap did particles >1 mm contribute

Table 2 Composition of lipid classes in PARFLUX E sediment traps

Compound class	Range	Compound distribution
Hydrocarbons	C_{15}–C_{32}	n-C_{17}, C_{19} dominate all depths, CPI_{23-29} = 1.2–1.4 sterenes (such as, cholest-2-ene, 3,5-cholestadiene) abundant
Fatty acids	C_{14}–C_{26}	$C_{16:0}$*, $C_{18:1}$, $C_{18:0}$ dominate all depths†
		$C_{20:5}$, $C_{22:6}$—10–20% of total acids in mesopelagic traps, 1–2% in bathypelagic traps
		Iso, anteiso C_{15}, C_{17} minor (<2%) at all depths
Wax esters	C_{26}–C_{44}	$C_{34:1}$, $C_{32:1}$ dominate all depths (~75% of total wax ester at 389 m; ~50% at 988 and 5,026 m, 25% at 3,755 m depth)
		Fatty acids. C_{14}–C_{26}; $C_{16:0}$, $C_{22:0}$, $C_{18:1}$ major
		Fatty alcohols: C_{14}–C_{26}; $C_{16:0}$, $C_{18:1}$, $C_{16:1}$, $C_{18:0}$ major
Steroid ketones	—	Cholest-4-en-3-one dominates (>60% of total ketones in mesopelagic traps, ~35% in bathypelagic traps)
Amino acids	—	Typical planktonic amino acids in upper traps
(extractable)		Glutamic acid, aspartic acid, alanine, serine, glycine only in deeper traps suggesting bacterial input (?)
Free fatty alcohols	C_{12}–C_{24}	$C_{16:0}$, $C_{18:1}$, $C_{18:0}$, $C_{16:1}$ dominate
Free sterols	—	Cholest-5-en-3β-ol dominant sterol at all depths (95% of sterol distribution at 988 m; 20–50% in other depths)
		Cholesta-5,22(E)-dien-3β-ol, 24-methylcholesta-5,22(E)-dien-3β-ol, 4,23,24-trimethyl-5α-cholest-22-en-3β-ol abundant
Steryl esters	—	Fatty acids. 389 m $C_{16:0}$, $C_{18:0}$ major 988 m $C_{16:0}$, $C_{14:0}$, $C_{18:0}$, $C_{18:1}$ major
		Sterols: 389 m cholest-5-en-3β-ol (60%), cholesta-5,22(E)-dien-3β-ol, 24-methylcholesta-5,22(E)-dien-3β-ol, 5α-cholestan-3β-ol. 988 m cholest-5-en-3β-ol (85%), 5α-cholestan-3β-ol, cholesta-5,22(E)-dien-3β-ol
Triacylglycerols	C_{45}–C_{57}‡	C_{51}, C_{53}, C_{55}, C_{57} compounds predominate
		Fatty acids: 389 m $C_{18:0}$, $C_{18:1}$, $C_{16:0}$ major 988 m $C_{22:6}$, $C_{20:5}$ also dominant

* Shorthand notation denotes number of carbon atoms: number of double bonds.

† For each category, compounds are listed in order of decreasing relative abundances.

‡ Total carbon number (acyl carbons + glycerol carbons).

significantly to the flux of organic compounds (Table 1). Furthermore, at 988 m the individual molecular constituents of the sterol, steryl ester, and triacylglycerol fractions were vastly different compared with both shallower and deeper samples (Table 2). Two hypotheses may be proposed to account for these maxima. First, differences in biological communities populating this region of the water column may be responsible for the different inputs of these organic compound classes at depth compared to shallower than 389 m. Alternatively, organic matter produced in the euphotic zone may be compartmentalized and transported through 389 m, followed by the release of these compounds below the 389 m trap.

Our interpretations are constrained by the limited data set—a single set of samples from one location in the World's ocean. In addition, our lipid analyses account for only ~15–20% of the total organic flux. However, we are pursuing a better understanding of the cycling of organic matter in the oceans by continuing detailed organic analyses of particulate matter collected in sediment traps in both open ocean (North central Pacific) and coastal (Peru upwelling, Panama Basin, and coastal California) areas. Interpretation of all sediment trap results are complicated by questions of differential settling rates, resuspension of bottom sediments and horizontal transport processes, trapping efficiencies, and the potential for chemical and biochemical reactions after particles have been intercepted.

Several authors have focused on the measurement of total organic carbon associated with particles caught in sediment traps[2–5,8–10]. Our results, however, show for the first time that while total organic carbon fluxes in the deep ocean decrease only slightly throughout the water column, the composition of portions of this material changes dramatically. These changes reflect processes acting on the particles during transport through the water column, and they are important to the composition of the organic matter being deposited at the sediment–water interface.

This research was supported by contract NOOO14-79C-0071 from the Office of Naval Research and grants OCE 78-26084, OCE 78-26180, and OCE 77-27004 from the National Science Foundation. We thank Susumu Honjo, Peter G. Brewer and Derek W. Spencer for sediment trap samples, and Carl O. Erba for analytical assistance and S. Henrichs, D. Repeta, J. Hunt and S. Honjo for valuable comments. Woods Hole Oceanographic Institution contribution No. 4569.

Received 19 March, accepted 9 June 1980

1 McCave, I N. *Deep-Sea Res* **22**, 491–502 (1975)
2 Honjo, S *J mar Res* **36**, 469–492 (1978)
3 Honjo, S *J mar Res* **38**, 53–97 (1980)
4. Berger, W H & Soutar, A *Science* **156**, 1495–1497 (1967)
5 Wiebe, P H, Boyd, S H & Winget, C *J mar Res* **34**, 341–354 (1976)
6 Spencer, D. W *et al J mar Res* **36**, 493–523 (1978)
7 Brewer, P G, Nozaki, Y, Spencer, D W & Fleer, A P *J mar Res* (in the press)
8 Knauer, G A, Martin, J H & Bruland, K W *Deep-Sea Res* **26**, 97–108 (1979)
9 Hinga, K R, Sieburth, J McN & Heath, J R *J. mar Res* **37**, 557–579 (1979)
10 Deuser, W. G & Ross, E H *Nature* **283**, 364–365 (1980).
11 Crisp, P T, Brenner, S, Venkatesan, M I, Ruth, E & Kaplan, I R *Geochim cosmochim. Acta* **43**, 1791–1801 (1979)
12 Prahl, F. G & Carpenter, R *Geochim cosmochim Acta* **43**, 1959–1972 (1979)
13 Honjo, S & Connell, J F *Tech Rept*, 79–80 (Woods Hole Oceanographic Institution, 1979)
14 Hill, D W, Walters, F H, Wilson, T D & Stuart, J D *Analyt Chem* **51**, 1338–1341 (1979)
15. Grob, K, Grob, G & Grob, K Jr *H R C & C C* **2**, 31–35 (1979), **2**, 677–678 (1979)
16 Metcalf, L D & Schmitz, A A *Analyt Chem* **33**, 363–364 (1963)
17 Galli, G & Paoletti, E G *Lipids* **2**, 72–75 (1967)
18 Gagosian, R B & Farrington, J W *Geochim cosmochim Acta* **42**, 1091–1101 (1978)
19 Lee, R F & Parker, P. L. *Science* **152**, 649–650 (1966)
20. Cooper, W J & Blumer, M *Deep-Sea Res* **15**, 535–540 (1968)
21 Oliver, J D & Colwell, R R *Int J Syst. Bact* **23**, 442–458 (1973)
22 Perry, G J., Volkman, J K, Johns, R B. & Bauer, J H Jr *Geochim cosmochim Acta* **43**, 1715–1725 (1979)
23. Nevenzel, J C *Lipids* **5**, 308–319 (1970)
24 Sargent, J R, Lee, R F & Nevenzel, J C in *Chemistry and Biochemistry of Natural Waxes* (ed Kolattukudy, P E) 49–91 (Elsevier, New York, 1976)
25 Sassen, R J & Mague, T H *Mar Chem.* **6**, 215–231 (1978)
26 Salton, M R J *Microbial Cell Walls* (Wiley, New York, 1961)
27 Goad, L J in *Marine Natural Products Chemical and Biological Perspectives* Vol 2 (ed Scheuer, P J.) 76–172 (Academic, London, 1976)
28 Sargent, J R in *Biochemical and Biophysical Perspectives in Marine Biology* (eds Malins, D C & Sargent, J R.) 149–212 (Academic, London, 1976)
29 Schmitz, F J in *Marine Natural Products Chemical and Biological Perspectives* Vol 1 (ed Scheuer, P. J.) 241–297 (Academic, New York, 1973)
30 Menzel, D W in *The Sea*, Vol 5 (ed Goldberg, E D) 659–678 (Wiley, New York, 1974).

First age-diagnostic fossils from the central part of the North Greenland foldbelt

Finn Surlyk*, John Malcolm Hurst† & Merete Bjerreskov‡

*Geologisk Museum, Øster Voldgade 5, 1350 København K, Denmark
†Grønlands Geologiske Undersøgelse, Øster Voldgade 10, 1350 København K, Denmark
‡Institut for Historisk Geologi og Palaeontologi, Øster Voldgade 10, 1350 København K, Denmark

The discovery of Lower Llandovery (Silurian) graptolites in Peary Land, near the top of the sequence in the central part of the North Greenland foldbelt, shows that the rocks in this sequence are mostly pre-Silurian. It also permits correlation of the lithostratigraphic units in the central foldbelt[1] with those on the margin[2] and on the unfolded platform to the south[3,4]. This places constraints on the timing of the Innuitian orogeny in North Greenland.

A 600 km long east–west trending Palaeozoic foldbelt forms the Arctic coastal area of North Greenland[3] (Fig. 1). The foldbelt continues to the west as the Innuitian mobile belt of the Canadian Arctic islands[5]. In Greenland the belt is up to 100 km wide and the degree of deformation and metamorphism increases from south to north[1]. The folded sequence includes Upper Precambrian to Lower Palaeozoic rocks of a northern clastic trough and the adjacent part of a southern carbonate platform.

The evolution of the platform–trough system started in the late Precambrian with the development of an incipient east–west trending trough. Faulting and subsidence continued through Cambrian, Ordovician and Silurian times. The trough was formed by rifting and the southern margin was controlled by major faults. The northern margin is not known in Greenland as it was probably situated under the present Arctic Ocean. The trough expanded in several episodes by southwards shift of the southern margin to new fault systems. During this process, the older fault systems became intrabasinal and largely inactive (Fig. 2).

The first Precambrian?–Cambrian phase of trough fill mainly comprised turbidites, dark mudstones, light lime mudstones and resedimented conglomerates (quartzite and Paradisfjeld Groups; Fig. 3) reflecting the incipient nature of the rift. Subsequently, Cambrian turbidite sedimentation reflects deeper water and a greater differentiation of shelf and trough. Transport was both lateral from south and north and longitudinal from the east. At the end of this phase turbidite sedimentation was punctuated by several episodes of conglomeratic gravity flows initiated on the platform margin and upper slope. The turbidites and conglomerates represent the Polkorridoren Group[1] and formation A (ref. 2) (Fig. 3).

The supply of coarser clastics dramatically decreased in the latest Cambrian, and the Ordovician was characterized by slow deposition of black mudstones and cherts, (bulk of the Sydgletscher Group[1] and formation B (ref. 2)) probably in a deeply submerged narrow rift. Thick resedimented conglomerates derived from the margin of the carbonate platform and the upper slope were deposited along the southern margins of the trough.

The transition from Ordovician to Silurian was marked by a new phase of turbidite sedimentation and a sequence several kilometres thick was deposited in the trough during the Silurian (formation C (ref. 2) and 'Un-named Silurian flysch formation'[4]). Silurian turbidites from eastern Peary Land to Hall Land (Fig. 1) were transported longitudinally from the east.

Contemporaneously, a variety of shallow marine limestones and dolomites with minor intercalations of terrigenous clastics were deposited on the platform to the south (Figs 2 and 3).

During the Llandovery–Wenlock transition the platform margin collapsed. The position of the new border fault is not precisely known, but in the Peary Land area the onlapping turbidite sequence can be followed several hundred kilometres to the south[6].

Silurian turbidite sedimentation was periodically interrupted by deposition of resedimented conglomerates derived from the upper slope and platform margin. The youngest preserved deposits of the North Greenland trough are turbidites and chert conglomerates.

Subsequently, orogenic deformation of the sequence is assumed to be of Devonian–early Carboniferous age[3]. Foldbelt strike is east–west parallel to the strike of the platform trough boundary. The southern margin of the foldbelt (Fig. 1) roughly coincides with this boundary and three major tectonic zones are recognizable in the Peary Land region. The platform carbonates are mainly undeformed whilst the trough clastics adjacent to the platform are folded. Northwards deformation increases and in Johannes V. Jensen Land the trough sediments are metamorphosed to amphibolite facies along the northern coast[1].

In the past, three independent stratigraphies have been put forward for each of these zones. To the south a comprehensive scheme covers the generally richly fossiliferous carbonates[3,4,7–9]. The overlying Silurian turbidite sequence is lithologically monotonous and poorly fossiliferous and has not received the same detailed study. However, three formations can be recognized, comprising a basal mainly shaly unit of Llandovery to Wenlock age, a middle sandy turbidite unit of Wenlock age and an upper conglomerate unit of Wenlock age (Fig. 3).

The sequence of the foldbelt margin was subdivided into three formations[2]. These include formation A, a sandy turbidite sequence capped by a major resedimented conglomerate unit. This is overlain by formation B, mainly a mudstone and chert sequence with wedges of resedimented conglomerate. Finally, formation C is the basal part of a major sandy turbidite unit. There are a few sporadic biostratigraphic dates from these sequences but there is no comprehensive zonation. Formation A is bioturbated in several horizons and it is underlain by units containing abundant trace fossils. The base of formation B contains graptolites of earliest Ordovician (early Canadian) age[10]. Consequently, formation A is probably Cambrian age throughout. Formation B has yielded graptolite faunas from the lower half indicating an early to middle Ordovician age. The graptolites *Climacograptus miserabilis* Elles & Wood and *Orthograptus* sp., resembling *O. quadrimucronatus* (Hall) indicating a late Ordovician (Cincinnatian) age, have been

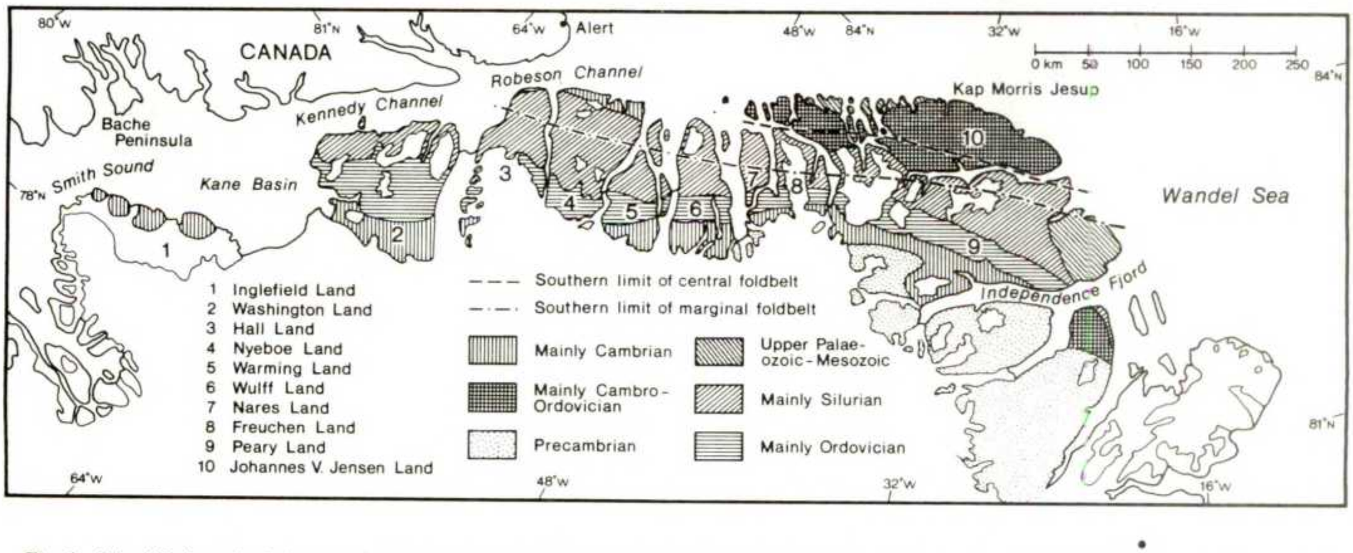

Fig. 1 Simplified geological map of North Greenland. Based on refs 3, 8 and unpublished observations. The southern limit of the central foldbelt corresponds to the Harder Fjord fault. The southern limit of the marginal foldbelt roughly corresponds to the Navarana Fjord fault.

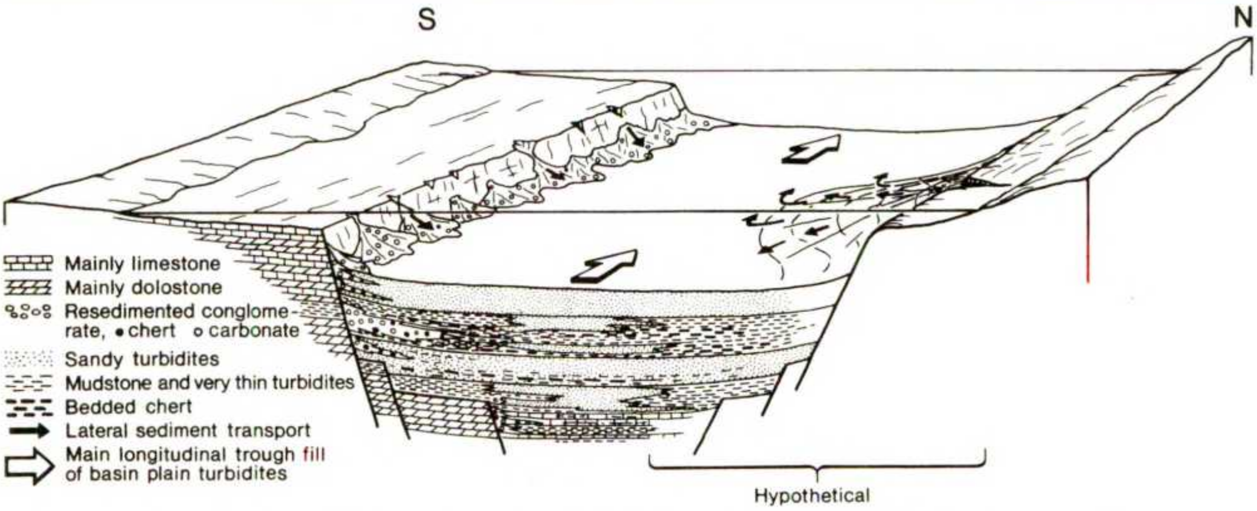
S
N
Mainly limestone
Mainly dolostone
Resedimented conglomerate, • chert ○ carbonate
Sandy turbidites
Mudstone and very thin turbidites
Bedded chert
Lateral sediment transport
Main longitudinal trough fill of basin plain turbidites
Hypothetical

Fig. 2 Tectonic sedimentological setting of the early Palaeozoic rift in Peary Land, in late Silurian time.

obtained from the top of formation B. Formation boundaries are diachronous particularly between formations B and C, which fall within the Upper Ordovician to Lower Silurian range.

Until now, no age-diagnostic fossils have been obtained from the central part of the foldbelt, but unidentifiable graptolite fragments were reported from the upper part of the sequence[1]. The first lithostratigraphic scheme for this area[11] was subsequently revised[1] and comprises three groups subdivided into informal formations (Fig. 3). A fourth group was recognized[12] in 1979. These comprise from below: an un-named quartzite group, and the Paradisfjeld, Polkorridoren and Sydgletscher Groups[12]. Previously, correlation between the three independent stratigraphic schemes of the central foldbelt, foldbelt margin and unfolded carbonates and clastics to the south was speculative. This was due to lack of faunas and to lateral facies changes.

Two formations were recognized in the Polkorridoren Group[1], of which the upper characteristic turbidite unit was tentatively correlated with formation C of the foldbelt margin and the Silurian turbidites of the unfolded areas to the south[3]. This correlation was based primarily on lithological resemblance. By implication the overlying Sydgletscher Group was assumed to be of late Silurian to Devonian age[2,3]. This group which is more than 1 km thick is divided into five formations[1,12]. An assemblage of graptolites was found 142 m above the base of the penultimate formation, termed upper Sydgletscher shales (3d)[1]. These graptolites, the first age-diagnostic fossils derived from the central part of the foldbelt (Fig. 4), provide a correlation link with areas to the south, considerably revising earlier schemes.

The graptolites appear as flattened carbon films with inconspicuous thecal structures and some are tectonically compressed. The material comprises about 10 incomplete biserial and 15 monoserial fragments. Three specimens can be referred to *Climacograptus rectangularis* (M'Coy)? and four monoserial fragments to *Atavograptus* aff. *atavus* Jones (Fig. 4). *C. rectangularis* has generally been reported from the *atavus* to *cyphus* Zones of the Lower Llandovery[13] and recently at least up to the *triangulatus* Zone[14]. *A. atavus sensu lato* has been reported from the *atavus* to *magnus* Zones[13]. However, *A.* aff. *atavus* is very similar to specimens described from the *atavus* Zone of Bornholm[15] and the sample is probably referable to a stratigraphical level around the *atavus–cyphus* Zones in the Lower Llandovery.

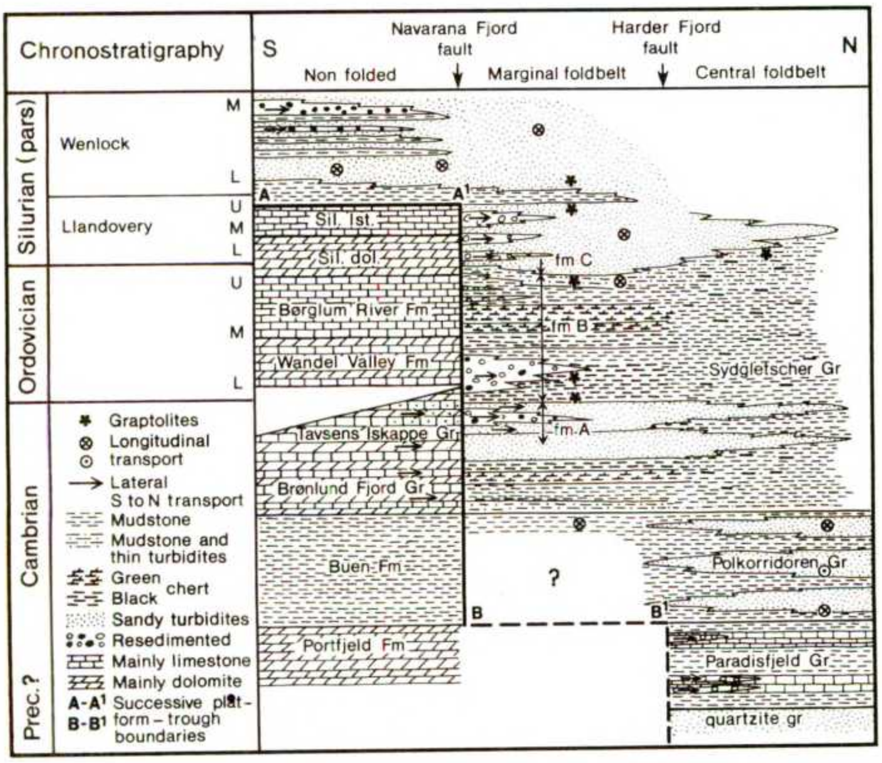

Fig. 3 Stratigraphy and facies distribution of a north–south transect through the Lower Palaeozoic carbonate platform–clastic trough system of Peary land. Based on refs 1, 4, 22 and unpublished observations.

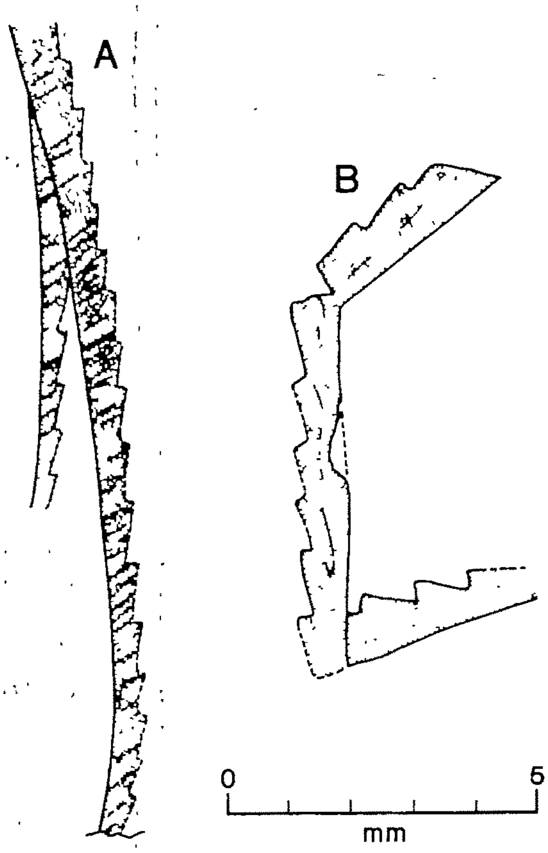

Fig. 4 First age diagnostic fossils from the central North Greenland foldbelt. *a*, *Atavograptus* aff. *atavus* (Jones). Two proximal fragments. *b*, *Atavograptus* aff. *atavus*. One distal fragment. Both specimens are from the upper Sydgletscher shales. MGUH 15077 and MGUH 15078. GGU sample 230273.

This indicates the bulk of the Sydgletscher Group is of pre-Lower Llandovery, *atavus* Zone age, and thus mainly of Ordovician age and that it is broadly contemporaneous with formation B of the foldbelt margin (Fig. 3). The correlation between the Sydgletscher Group and formation B is strongly supported by lithological evidence as both units are characterized by black cherts and mudstones. The graptolite-bearing formation is overlain by a several hundred metres thick formation consisting of extremely thick turbidite beds. Individual beds are structureless and reach thicknesses of 30 m suggesting a rapid depositional rate for the formation.

This formation is the youngest rock unit of the central foldbelt and it is unlikely to be much younger than early Llandovery.

The three stratigraphic schemes used to describe the trough sediments of the central foldbelt, foldbelt margin and unfolded area can now be combined into a single stratigraphic scheme (Fig. 3). The scheme which is informal, shows the main facies types and their spatial distribution. A formal comprehensive stratigraphy will be published elsewhere.

In spite of the new biostratigraphic data, it is still difficult to date precisely the orogenesis. The youngest folded rocks within the central foldbelt are of Llandovery or only slightly younger age. Towards the south and west in the marginal parts of the foldbelt, the top part of the Silurian turbidite sequence yields graptolites of Ludlow (late Silurian) age (our unpublished observations). The presence of earliest Devonian has been suggested for a single locality in western Hall Land on the basis of one specimen of the graptolite *Monograptus* cf. *aequabilis*[16]. It was recently reidentified by Jaeger (personal communication) as *Monograptus* cf. *transgrediens* Perner and probably of Pridoli (latest Silurian) age. The graptolite bed was overlain by strata containing alleged Devonian vertebrates[17] assigned a Devonian age partly on the basis of the underlying graptolites. There is thus no evidence of Devonian rocks in North Greenland.

In eastern Peary Land the folded sequences are overlain with angular unconformity by Upper Pennsylvanian and younger rocks[3,18–20]. Reliable isotopic ages have not yet been obtained. Therefore, the diastrophism can only be loosely dated as Devonian to early Pennsylvanian. Comparison with Arctic Canada fails to yield more definitive evidence regarding time of diastrophism. In Ellesmere Island the most extensive and intensive deformation in the history of the Innuitian mobile belt commences not later than middle Devonian and was completed before the late early Pennsylvanian[21].

We thank P. R. Dawes, J. D. Friderichsen, N. Henriksen, A. K. Higgins and J. S. Peel for criticisms. This work is published with the permission of the director of the Geological Survey of Greenland.

Received 5 May, accepted 26 June 1980.

1 Dawes, P. R. & Soper, N. J. *Mem. Am. Ass. petrol. Geol.* **19**, 117–134 (1973)
2 Dawes P. R. & Soper, N. J. *Rapp. Grønl. geol. Unders.* **93**, 1–40 (1979)
3 Dawes, P. R. in *Geology of Greenland* (eds Escher, A. & Watt, W. S.), 248–303 (Geological Survey of Greenland, Copenhagen, 1976)
4 Christie, R. L. & Peel, J. S. *Rapp. Grønl. geol. Unders.* **82**, 1–48 (1977)
5 Trettin, H. P. *et al. Geol. Ass. Can. Spec. Pap.* 11, 83–179 (1972)
6 Peel, J. S. *Rapp. Grønl. geol. Unders.* (in the press)
7. Troelsen, J. C. *Meddr Grønland* **149**, 1–29 (1949)
8 Dawes, P. R. *Bull. geol. Soc. Denmark* **20**, 197–239 (1971)
9 Jepsen, H. F. *Meddr Grønland* **192**, 1–42 (1971)
10. Bjerreskov, M. & Poulsen, V. *Rapp. Grønl. geol. Unders.* **55**, 10–14 (1973)
11 Fränkl, E. *Meddr Grønland* **103**, 1–61 (1955).
12 Soper, N. J. *et al. Rapp. Grønl. geol. Unders.* (in the press)
13 Hutt, J. *Palaeontogr. Soc. (Monogr.)*, pt 2, 1–59 (1975)
14 Lenz, A. C. *Acta Palaeont. Pol.* **24**, 137–153 (1979)
15 Bjerreskov, M. *Fossils and Strata* **8**, 1–94 (1975)
16 Berry, W. B. N. *et al. Rapp. Grønl. geol. Unders.* **65**, 11–13 (1974).
17 Bendix-Almgreen, S. E. & Peel, J. S. *Rapp. Grønl. geol. Unders.* **65**, 13–16 (1974)
18 Troelsen, J. C. in *Geology* (eds Winther, P. C. *et al.*) 6–8 (1950)
19 Petryk, A. A. *Rapp. Grønl. geol. Unders.* **85**, 16–21 (1977)
20. Håkansson, E. *Rapp. Grønl. geol. Unders.* **88**, 73–83 (1979)
21 Trettin, H. P. & Balkwill, H. R. *Can. J. Earth Sci.* **16**, 749–769 (1979).
22 Ineson, J. & Peel, J. S. *Rapp. Grønl. geol. Unders.* (in the press)

Structure of supernumerary limbs

M. Maden

The National Institute for Medical Research, Mill Hill,
London NW7 1AA, UK

The generation of supernumerary limbs by rotation of amphibian limb buds or regeneration blastemas is a phenomenon well known to embryologists[1,2]. The recent revival of interest in this aspect of limb morphogenesis has been largely due to the stimulus provided by the polar coordinate model for control of limb outgrowth and pattern[3] and subsequent efforts to test its validity. The geometrical rules postulated in the polar coordinate model make precise predictions about the handedness of supernumerary limbs. Following antero-posterior (AP) or dorso-ventral (DV) inversions, they should be of the same handedness as the stump, whether single or in pairs, but after inversion of both axes (APDV) pairs should be of opposite handedness[3]. It is surprising, therefore, that the structure of supernumerary limbs has never been studied in sufficient detail to report whether they really are normal limbs, for only the skeletal elements are examined in cleared whole mounts (see Fig. 1). This only allows an assessment of the AP axis, and to determine the dorsal and ventral surfaces (and hence the handedness), the curvature of the digits is noted. I therefore decided to study the muscle patterns of all types of supernumeraries, and report here that, contrary to expectation, the majority of APDV supernumeraries are not normal limbs but are mirror-image duplications in the dorso-ventral axis, that is, either double-dorsal or double-ventral. This presents problems for contemporary models of pattern formation in the limb, and issues a warning to those who use supernumerary limbs as an experimental tool to investigate other areas of developmental biology.

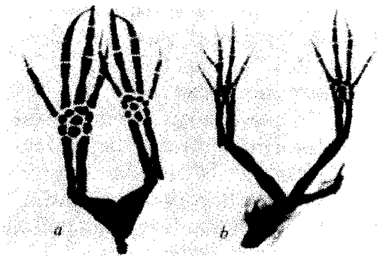

Fig. 1 *a*, Supernumerary limb generated by grafting a left blastema to a right stump. On the left is the right graft, on the right the perfect right-hand supernumerary limb which appeared at the posterior pole of the stump and bifurcates in the stylopodium. *b*, Supernumerary limb generated by rotating a right blastema 180° and replacing it on the same stump. On the right is the graft, on the left the supernumerary which appeared at the dorsal pole of the stump and bifurcated in the stylopodium. The similarity between this supernumerary and that in *a* is striking and it would normally have been identified as a left limb. In fact, on sectioning it was discovered to be double-ventral in structure (see Figs 2*c*, 3*e*). Victoria blue staining.

The experiments were carried out on young *Ambystoma mexicanum*, 80–140 mm long, whose limbs had been amputated through the mid-stylopodium level. At the late cone/early palette stage, blastemas were cut off and either placed on the contralateral stump (AP or DV inversions) or replaced upside down on the same stump (APDV rotations). Such grafted blastemas continue their own development into normal limbs as well as participating in the generation of supernumerary limbs at the graft–stump boundary. When they had fully developed, the muscle patterns of 20 of these grafts were examined and they revealed a completely normal anatomy[4]. The most characteristic features of normal limbs are to be found at the carpal and digit level, where the dorsal extensors have separated into four crescent-shaped muscles, the extensores digitorum breves (Fig. 2*a*). The flexors, comprised of about 16 separate muscles[4], form a large mass of tissue on the ventral surface of the hand which in the digits, splits into four semi-circles of muscle (Fig. 2*a*). A three-dimensional reconstruction of the normal muscle pattern (Fig. 3*a*) shows that the sparser dorsal muscles terminate in the metacarpals (tendons travel distally to the tips of the digits) whereas the ventral muscles themselves extend right to the last phalanx.

The first series consisted of 11 limbs whose AP axis had been reversed, yielding a total of 12 supernumeraries. Ten limbs developed single supernumeraries, all at the posterior side of the host limb (Fig. 1*a*), and one a double supernumerary (Table 1). It is interesting that this striking bias towards the production of supernumeraries at the posterior pole after upper arm inversions is also apparent from other studies[5,6], but it disappears when blastemas from the lower arm are inverted. All the supernumeraries produced in this series were perfect limbs whose digits curved ventrally and from an examination of the skeletal structure (Fig. 1*a*) would be considered normal limbs. Analysis of the muscle patterns of each of these 12 supernumeraries confirmed that they were indeed completely normal (Fig. 3*b*, Table 1) and that all were of stump handedness.

The second series comprised seven limbs whose DV axis had been reversed. This yielded a total of 10 supernumeraries, 4 single and 3 double (Table 1). These were more equally distributed between the two poles than in the previous series–55% dorsal, 45% ventral. One was slightly displaced in the antero-dorsal quadrant. Apart from their position, these supernumeraries were in every respect identical to those in the first series and an analysis of the muscle pattern confirmed that they were completely normal limbs (Fig. 3*c*, Table 1). Again, they were all of stump handedness.

The third series comprised 12 blastemas rotated 180° (APDV). These were a group of limbs from a previous series[7] and were selected for analysis here because of a good separation of graft and supernumerary(ies). For instance, the example shown in Fig. 1*b* bifurcates in the humerus. Eight limbs had single supernumeraries and four had double supernumeraries, making 16 in all, whose position of origin was random (Table 1). These all looked normal when stained with Victoria blue (Fig. 1*b*) although in some cases their digits did not curve. An analysis of their muscle patterns revealed that 5 of the 16 (Table 1) had at the carpal level separate crescent-shaped extensores digitorum breves both dorsally and ventrally (Fig. 2*b*), terminating at the metacarpals. These limbs had no ventral flexor muscles extending to the tips of the digits and were thus identified as double-dorsal limbs. The three-dimensional reconstructions supported this conclusion (Fig. 3*d*). A further six supernumeraries had an uncharacteristically excessive amount of muscle on their dorsal surfaces which did not separate into small crescent-shaped elements (Fig. 2*c*). Instead of the dorsal muscles terminating in the metacarpals, they continued to the end of the digits and, together with the normal ventral muscles, formed thick circles of muscle surrounding each digit (Fig. 2*c*). These limbs were thus identified as double-ventral (Fig. 3*e*, Table 1). The third category of APDV supernumeraries contained five limbs which were completely normal (Fig. 2*d*, Table 1).

Thus, the AP and DV supernumeraries examined here were normal in every respect and were of stump handedness as had been previously supposed. In contrast, the APDV supernumeraries had an equal chance of being double-dorsal, double-

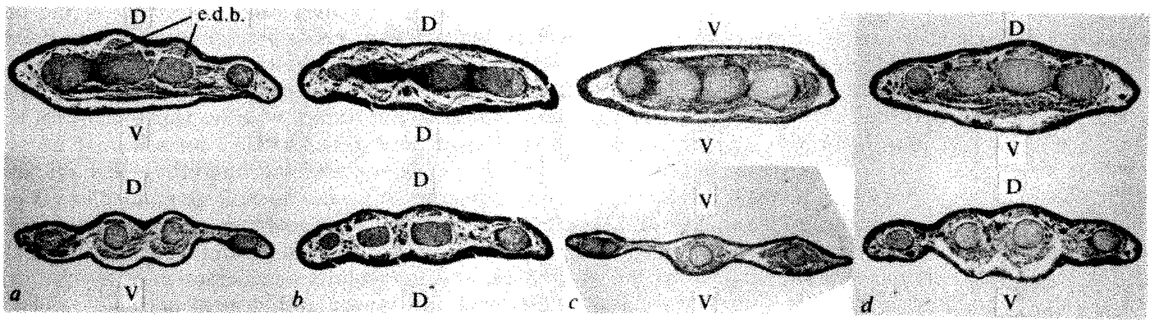

Fig. 2 Sections through the carpal/metacarpal level (upper sections) and distal metacarpal level (lower sections) of various types of limb. Stained with haematoxylin and eosin. The dorsal (D) and ventral (V) surfaces are marked. *a*, A limb which developed from a grafted blastema. This shows completely normal muscle patterns[4]. In the upper section note that the first (left) and fourth (right) digit extensors have already terminated, leaving only those of the second and third digits (e.d.b.). These are crescent-shaped and sit on the flat tops of the basal carpals. The ventral flexor muscles extend right across the hand and are composed of about 16 separate muscles[4]. The lower section through the digits shows the ventral muscles separated into large semi-circles. ×175. *b*, An APDV supernumerary. Clearly, the muscle patterns have mirror-image symmetry, as small, crescent-shaped muscles appear at the top and bottom of the limb. This is a double-dorsal limb, the three-dimensional reconstruction of which is shown in Fig. 3*d*. Note also that, particularly in the lower section, the cartilages seem to be mirror-images—both surfaces of the middle two elements are flat-topped. ×168. *c*, Another type of APDV supernumerary. As in *b* the muscles are mirror-images and in the digits they form complete circles of muscle around the phalanges. This is a double-ventral limb, the three-dimensional reconstruction of which is shown in Fig. 3*e*. Again, particularly in the upper section, the carpals appear mirror-images. ×120. *d*, Another type of APDV supernumerary. This, in contrast to the previous two, was a completely normal limb (compare with *a*). ×190.

Table 1 The number, position (relative to stump axes) and structure of supernumeraries generated by AP, DV or APDV rotation of blastemas

	AP supernumeraries				DV supernumeraries				APDV supernumeraries			
	Supernumerary 1		Supernumerary 2		Supernumerary 1		Supernumerary 2		Supernumerary 1		Supernumerary 2	
No.	Position	Structure	Position	Structure	Position	Structure	Position	Structure	Position	Structure	Position	Structure
1	P	Normal	—	—	V	Normal	—	—	PD	Double D	—	—
2	P	Normal	—	—	AD	Normal	—	—	AV	Double D	—	—
3	P	Normal	—	—	D	Normal	—	—	D	Normal	—	—
4	P	Normal	—	—	D	Normal	—	—	D	Normal	—	—
5	A	Normal	P	Normal	D	Normal	V	Normal	D	Double D	—	—
6	P	Normal	—	—	D	Normal	V	Normal	D	Double V	—	—
7	P	Normal	—	—	D	Normal	V	Normal	AD	Double D	—	—
8	P	Normal	—	—	—	—	—	—	V	Double V	—	—
9	P	Normal	—	—	—	—	—	—	AV	Double D	P	Double V
10	P	Normal	—	—	—	—	—	—	D	Normal	V	Normal
11	P	Normal	—	—	—	—	—	—	A	Double V	V	Double V
12	—	—	—	—	—	—	—	—	P	Normal	D	Double V

P, posterior; A, anterior; D, dorsal; V, ventral; AD, antero-dorsal quadrant; AV, antero-ventral quadrant; PD, postero-dorsal quadrant.

ventral or normal. As emphasized above, only well separated, four-digit supernumeraries were selected for study and the typical hypomorphic structures produced in any series of rotations—spikes, fused supernumeraries or ones with fewer digits than normal—were ignored. These are clearly abnormal in the AP axis and perhaps also in the DV axis. Furthermore, it may well be that other classes of APDV supernumeraries will be found, those appearing at frequencies of less than 1 in 16, and this possibility is now being investigated. Nevertheless, the generation of mirror-image limbs has two significant implications for theories of pattern formation. First, it adds to the growing body of results which present severe difficulties for the polar coordinate model and is contrary to the prediction that pairs of APDV supernumeraries should be of opposite handedness. The concept of handedness is meaningless when applied to mirror-image limbs, and pairs were not even of opposite mirroring (Table 1). The only other model which attempts to describe the generation of supernumerary limbs in such detail is the serial threshold model[8], which ascribes the formation of mirror-image limbs to different rates of intercalation in each of the three axes. However, theories based solely on local cell–cell interactions cannot, at their present stage of development, provide a satisfactory explanation for the appearance of APDV supernumeraries because, whatever their structure, there will always be large areas of gross discrepancy either between the supernumerary and the stump or between the supernumerary and the blastema. This problem is not solved by the discovery of mirror-image limbs because a double-dorsal limb at, say, the dorsal pole of the stump will abut directly on to the ventral pole of the rotated blastema. This should, according to local intercalation rules, generate more supernumeraries *ad infinitum*. Clearly, such simplistic descriptions cannot explain these phenomena and new models must be devised which incorporate more global field constraints.

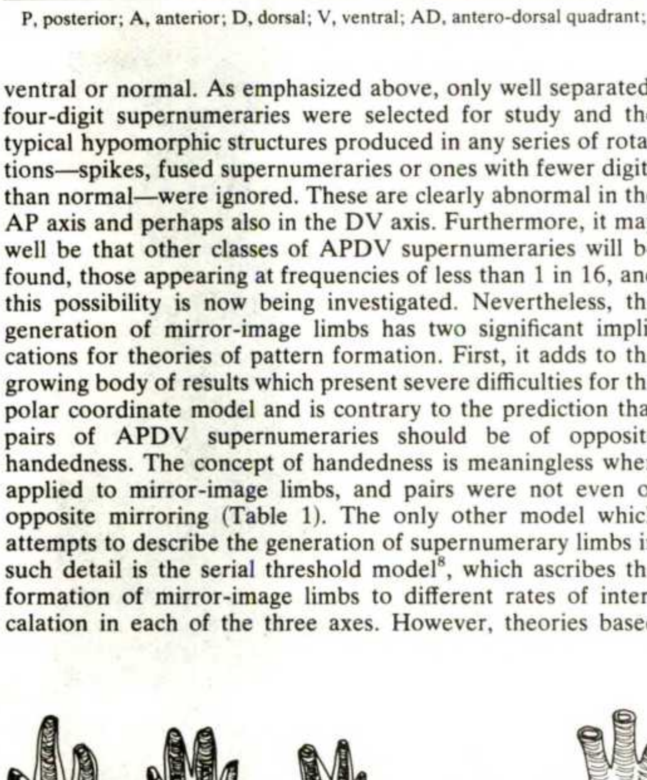

Fig. 3 Three-dimensional reconstructions of muscle patterns from serial sections of various limbs. Every 10th section was drawn with a camera lucida. These drawings were then projected 1 cm apart on to another piece of paper and the surface configurations of the muscles were then drawn. Each reconstruction drawn above is to the same scale to show the variation in proximo-distal extent of muscles. They are all viewed from the dorsal (extensor) surface with flexors underneath and all have a break in the wrist to help visualize their internal structure. *a*, Grafted limb. The blastema, grafted at the late cone/early palette stage, develops into a normal limb despite having at least one axis inverted relative to the stump. The dorsal extensor muscles (dotted) terminate at the carpal/metacarpal level whereas the ventral flexor muscles (cross-hatched) continue to the ends of the digits. This is the normal muscle pattern in the axolotl forelimb[4]. *b*, An AP supernumerary limb. This shows the same features as *a*—short extensors (dotted), long flexors (cross-hatched). *c*, A DV supernumerary limb showing normal muscle patterns as in *a* and *b*. *d*, An APDV supernumerary. In this case, the ventral muscles (clear) do not extend to the tips of the digits, but form a mirror-image pattern of the dorsal muscles (dotted) and terminate at the carpal/metacarpal level. This is a double-dorsal limb, the histology of which is shown in Fig. 2*b*. *e*, An APDV supernumerary. Here both dorsal (cross-hatched) and ventral muscles are much more profuse; they continue to the tips of the digits and form complete circles of muscle. This is a double-ventral limb, the histology of which is shown in Fig. 2*c*.

These present results also suggest that deterministic models be replaced by those with a more probabilistic nature, however unsatisfying this may be. The polar coordinate model is a highly deterministic model in which the cells can only show one particular behaviour following one particular experimental interference. The result is a strict series of predictions. This is clearly not the case for APDV supernumeraries; each class of structure—double-dorsal, double-ventral or normal—had an equal chance of appearing. This probabilistic concept has been considered previously in connection with the induction of supernumeraries at angles of rotation other than 180° (ref. 7). Further work has revealed a frequency distribution in which the angle of rotation is directly related to the likelihood of supernumerary induction[9].

It is to be hoped that this finding of mirror-image supernumeraries is a universal phenomenon in both regeneration and development. In support of this, I have carried out 180° rotations of developing limb buds in *Rana temporaria* and nearly all of the supernumeraries so generated were double posterior in structure. This may indicate that the plane in which APDV supernumeraries are duplicated is species dependent, but that the general principle remains the same. If this is so, it has implications for the other developing system commonly studied, the chick limb bud. It means that a graft of the zone of polarizing activity (ZPA) in normal dorso-ventral orientation (equivalent to an AP inversion) should generate a different type of reduplicate from a ZPA graft with reversed dorso-ventral orientation (equivalent to an APDV rotation). How current models of ZPA activity can cope with this situation remains to be seen.

I thank Katriye Mustafa for technical assistance in all aspects of this work.

Received 12 March; accepted 20 June 1980.

1. Abeloos, M. & Lecamp, M. *C. r. hebd. Séanc. Acad. Sci., Paris* **192,** 639–641 (1931).
2. Harrison, R. G. *J. exp. Zool.* **32,** 1–136 (1921).
3. French, V., Bryant, P. J. & Bryant, S. V. *Science* **193,** 969–981 (1976).
4. Grim, M. & Carlson, B. M. *Z. Anat. Entwickl.-Gesch.* **145,** 137–184 (1974).
5. Tank, P. W. *Devl Biol.* **62,** 143–161 (1978).
6. Wallace, H. & Watson, A. *J. Embryol. exp. Morph.* **49,** 243–258 (1979).
7. Maden, M. & Turner, N. *Nature* **273,** 232–235 (1978).
8. Slack, J. M. W. *J. theor. Biol.* **82,** 105–140 (1980).
9. Turner, N. & Maden, M. (submitted).

A one-dimensional pattern in the cellular slime mould *Polysphondylium pallidum*

F. W. Spiegel & E. C. Cox

Department of Biology, Princeton University, Princeton, New Jersey 08544

The cellular slime mould *Polysphondylium pallidum* has a fruiting body with whorls of branches spaced at regular intervals along the stalk (Fig. 1). The spacing between successive whorls is quite regular and under genetic control[1]. Because stalk cell number per interval correlates strongly with interval length, we have studied the influence of ploidy on the distance between whorls to determine if cell counting could account for the spacing. It is known that diploid spores and amoebae of *Dictyostelium discoideum* and *Polysphondylium violaceum* are roughly twice the size of their haploid parents[2,3], and we find that stalk cells in *P. pallidum* follow the same pattern. Our results show that the number of stalk cells between successive whorls in haploids is approximately twice the number in diploids, while the spacing remains the same. This clearly indicates that spacing is not achieved by a cell counting mechanism. Instead, it appears to depend on distance.

Cells were grown and diploids were constructed by previously published methods[3] using genetically marked parent strains. In every case diploid clones were shown to segregate the appropriate recessive genetic markers. Two- to three-day-old fruiting bodies cultured on water agar in the presence of activated charcoal were either photographed directly (Fig. 1) or trapped under a cover slip for photography at higher magnification (Fig. 2). Figure 1 compares developing and mature diploid fruiting bodies to the two haploid parents. It is quite clear that whorl spacing in diploids is very similar to that in haploids. Quantitative measurements of large numbers of sorocarps bear out this impression: spacing in five independently isolated diploids is indistinguishable from the haploid parents (Table 1).

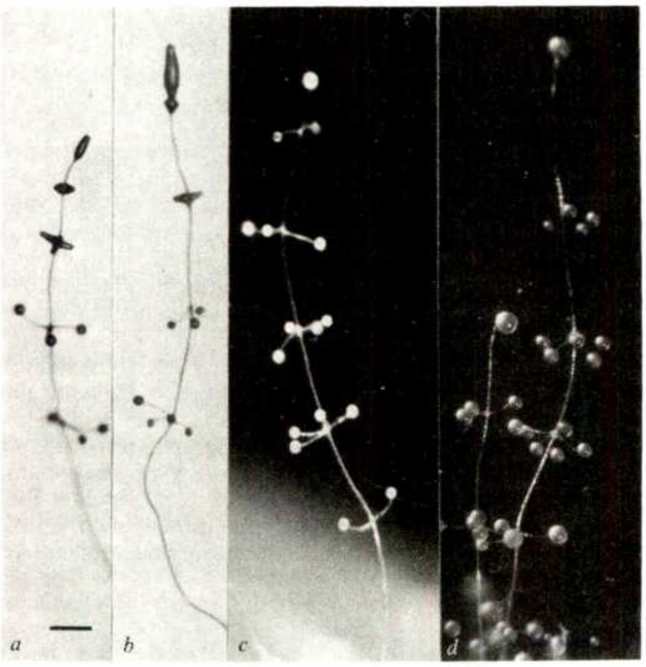

Fig. 1 Comparison of haploid and diploid *Polysphondylium pallidum* fruiting bodies. *a*, Culminating sorogen of haploid PN519; *b*, culminating sorogen of diploid 95a; *c*, mature sorocarp of haploid PN525; *d*, mature sorocarp of diploid 95a. The larger sori in *d* are the result of absorption of water in humid culture conditions. Scale bar, 100 μm.

The most striking feature of whorl spacing in diploid sorocarps is that spacing does not depend on a cell counting mechanism. This conclusion follows from the results shown in Fig. 2 and Table 1. It is qualitatively evident from Fig. 2 that the number of cells between whorls is larger in the two haploid parents than in diploid progeny, even though the distance between whorls is very similar. This impression is borne out by the detailed quantitative measurements summarized in Table 1. The average number of cells per interval in the haploid strains PN519 and PN525 is almost exactly twice the number in the diploid isolates 95a to 95e, while the cell length is approximately one half. The size and shape of diploid spores, shown clustered about the stalks in Fig. 2, bears the same relationship to haploid spore shape in *P. pallidum* as it does in *D. discoideum* and *P. violaceum*[2,3].

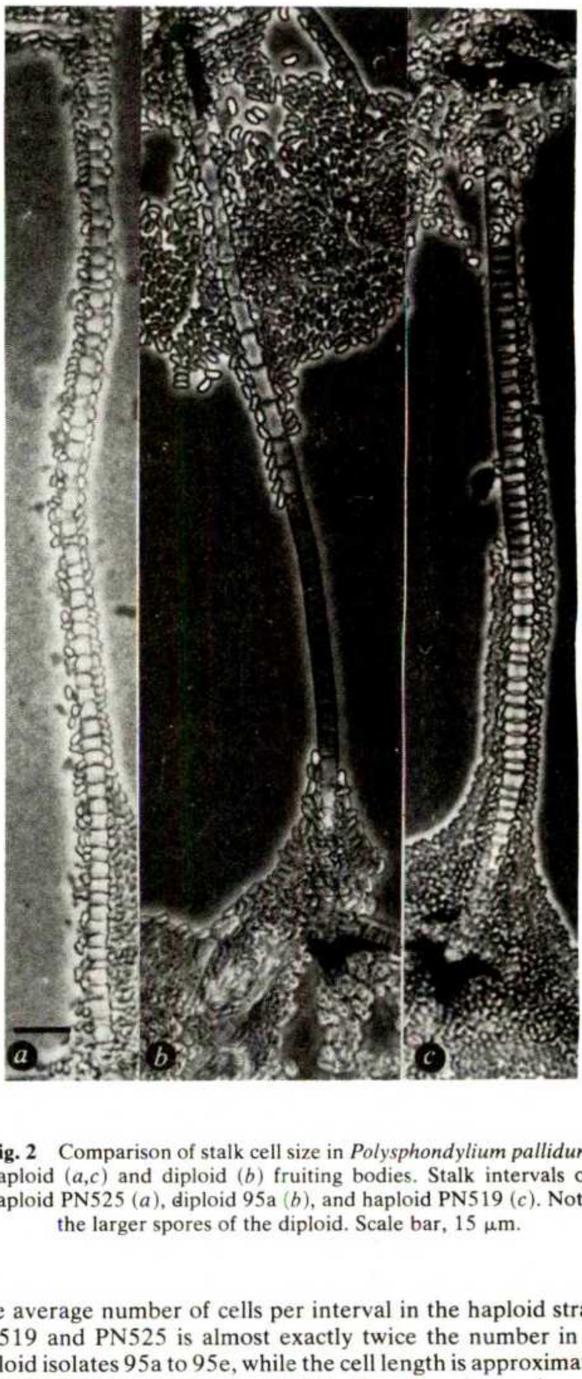

Fig. 2 Comparison of stalk cell size in *Polysphondylium pallidum* haploid (*a*,*c*) and diploid (*b*) fruiting bodies. Stalk intervals of haploid PN525 (*a*), diploid 95a (*b*), and haploid PN519 (*c*). Note the larger spores of the diploid. Scale bar, 15 μm.

These results thus eliminate one simple hypothesis that is *a priori* appealing, and suggest that whorl spacing depends on

0028–0836/80/340806—02$01.00

some mechanism other than cell counting. They are reminiscent of the effect of increasing ploidy on cell number in amphibians, where animals maintain their size and shape by using fewer, larger cells[4]. *P. pallidum* is unlike many higher plants, however, which tend to become proportionately larger following an increase in ploidy[5,6], and unlike bristle spacing along *Drosophila melanogaster* basitarsi, where spacing mechanisms seem to depend on the number of cells in normal diploid and intersex triploids[7].

Table 1 Interval length between whorls and cell number per interval in haploid and diploid strains of *P. pallidum*

Strain	Ploidy	Average interval length (μm)	Average cell number/interval	Average cell length/interval (μm)
PN519	*n*	374 (110)	45.7 (18.5)	8.7 (2.2)
PN525	*n*	354 (79)	40.4 (14.0)	9.5 (2.7)
95a	2*n*	350 (99)	18.4 (8.1)	20.7 (5.8)
95b	2*n*	319 (100)	20.5 (8.0)	16.7 (4.7)
95c	2*n*	349 (87)	21.4 (9.7)	18.1 (5.3)
95d	2*n*	358 (97)	20.5 (7.5)	18.8 (5.3)
95e	2*n*	304 (91)	18.8 (8.3)	17.4 (4.8)

Comparison of interval length between whorls, stalk cell number per interval, and stalk cell length between haploid and diploid strains of *P. pallidum*. A minimum of 100 intervals on a minimum of 20 sorocarps was counted for each strain. Diploids 95a–e were constructed from the parents PN519 and PN525[3]. Values shown in parentheses represent ± s.d.

The developmental history of each whorl in *P. pallidum* is complex. Stalk cells are laid down apically as the sorogen ascends the elongating stalk. At regular intervals masses containing variable numbers of cells pinch off basally from the ascending sorogen (this may be seen clearly in Fig. 1*a*). These cells differentiate into whorls with varying numbers of arms, each arm bearing a terminal sorus of spores[8,9]. The timing of these events clearly determines the spacing frequency. We have determined[1] that the control of spacing in *P. pallidum* is as well defined as heterocyst spacing in the prokaryote *Anabaena cylindricata*[10], even though the distances over which the spacing mechanism must operate are roughly an order of magnitude larger in *P. pallidum*, because spacing mutants can be isolated in *P. pallidum* (our unpublished data). Since a facile genetic system is available[11], and because the spacing may be altered by physiological manipulation[9,12], it may be possible to analyse in some detail the genetic and physical basis for whorl spacing in this simple eukaryote.

We thank David Francis for supplying the genetic stocks used in this study. This work was supported in part by a grant to the Biology Department by the Whitehall Foundation and by USPHS grants AI09392 and CA09167.

Received 28 March; accepted 11 July 1980.

1. Spiegel, F. W. & Cox, E. C. (in preparation).
2. Sussman, M. & Sussman, R. R. *J. gen. Microbiol.* **28,** 417–429 (1962).
3. Warren, A. J., Warren, W. D. & Cox, E. C. *Genetics* **83,** 25–47 (1976).
4. Fankhauser, G. in *Analysis of Development* (eds Willier, B. H. Weiss, A. & Hamburger, V.) 126–150 (Saunders, Philadelphia, 1955).
5. Darlington, C. D. *Chromosome Botany and the Origins of Cultivated Plants*, 3rd edn (Allen and Unwin, London, 1973).
6. Stebbins, G. L. *Chromosomal Evolution in Higher Plants* (Addison-Wesley, Reading, Massachusetts, 1971).
7. Held, L. I. Jr *Wilhelm Roux Arch. EntwMech. Org.* **187,** 105–127 (1979).
8. Bonner, J. T. *The Cellular Slime Molds* (Princeton University Press, 1967).
9. Harper, R. A. *Bull. Torrey Bot. Club* **59,** 49–84 (1932).
10. Wilcox, M. *Nature* **228,** 686–687 (1970).
11. Francis, D. W. *Differentiation* **15,** 187–193 (1970).
12. Raper, K. B. in *The Fungi* (eds Ainsworth, G. C., Sparrow, F. K. & Sussman, A. S.) 9–36 (Academic, New York, 1973).

0028–0836/80/340807—04$01.00

Induction of abnormal development and differentiation in cultured mammary glands by cyclic adenine nucleotide and prostaglandins

Frederick V. Schaefer, R. Philip Custer & Sam Sorof

Institute for Cancer Research, Fox Chase Cancer Center, Philadelphia, Pennsylvania 19111

Squamous (epidermoid) metaplasia is a common abnormality of development and differentiation, in which various epithelia are replaced by cells resembling those of the epidermis. The metaplastic cells differentiate into flattened cells that frequently form keratotic flakes and whorls. The cells may regress, remain benignly squamous, or progress to epidermoid carcinoma[1]. Squamous metaplasias have previously been brought about by mechanical injury[2], vitamin A deficiency[3,4] and chemical carcinogens[5–7]. In search of the physiological mediators of abnormal development and differentiation in oncogenesis, we have now discovered that the combination of dibutyryl cyclic AMP, prostaglandins (PGs) E_1, E_2 and B_1, and papaverine (Pap) induces squamous metaplasia with keratin production in the epithelium of cultured mammary glands. The three inducers may act synergistically to elevate the level of intracellular cyclic adenine nucleotide. Removal of these inducers causes the regression of the metaplastic cells. Retinoid does not block the induction of this squamous metaplasia, even though retinoid has previously prevented and reversed the squamous metaplasias caused by vitamin A deficiency or chemical carcinogens in other organs[4,8]. The findings suggest that cyclic adenine nucleotide and the PGs may mediate the squamous metaplasias present in many abnormal, transformed and malignant tissues, and possibly also the normal development and differentiation of epithelia into keratin-producing, stratified squamous cells, as in skin.

The mouse mammary gland can now be manipulated to undergo three courses of development and differentiation *in vitro*. First, normal development and differentiation of mouse mammary glands can be induced in culture[7,9,10]. The glands of hormonally primed female BALB/c mice, 3 to 4 weeks old, consist mainly of ducts with numerous terminal buds. When cultured in serum-free medium containing insulin (I), prolactin (P), aldosterone (A) and hydrocortisone (H), the glands develop lobuloalveoli[7,9,10] and produce casein[11]. Removal of all hormones except I (regression medium) brings about alveolar involution[7,10]. Such mammary glands exhibit no metaplasia (series 1 and 2, Table 1). Subsequent incubation with epidermal growth factor and IPAH induces a second lobuloalveolar development, which can again be involuted in the regression medium[12]. All these processes resemble those that normally occur *in vivo*.

Second, the epithelial cells of the cultured mammary glands can also be transformed by chemical carcinogens, as evidenced by the production of nodule-like alveolar lesions that have escaped the hormonal controls of alveolar development[7,13–15]. The transformed glands are dysplastic, metaplastic[7,15] and tumorigenic[14]. In contrast, chemically analogous noncarcinogens have little or no transforming activity[7,16]. Retinoid can prevent, suppress and apparently reverse the transformations caused by procarcinogens[15,17], which require metabolic activation to become reactive, but not the transformations brought about by many activated carcinogens[17].

A third course of development and differentiation is reported here. The combination of three agents (dibutyryl cyclic AMP, specific PGs and Pap) induces an extensive stratified squamous cell metaplasia with keratin production in cultured mammary glands (Fig. 1). Fresh whole mammary glands of hormonally

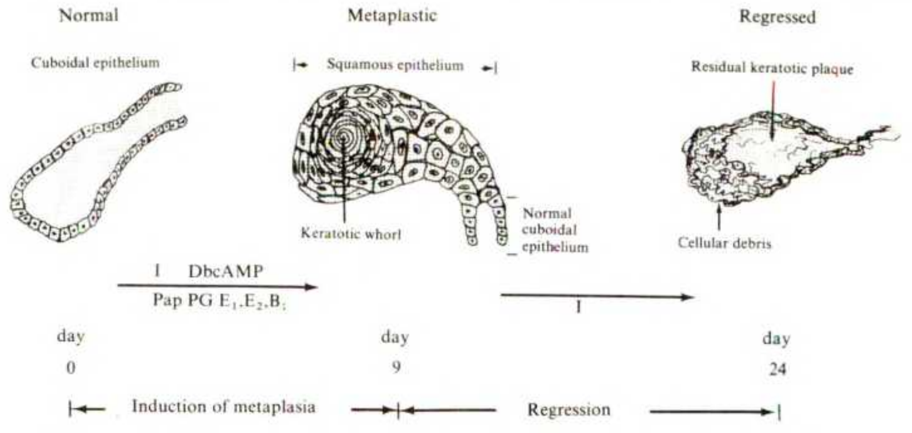

Fig. 1 Abnormal development, differentiation and involution in mouse mammary glands in culture: induction of squamous metaplasia and keratin production by cyclic adenine nucleotide, PGs and Pap. The serum-free whole organ culture system has been described[7,9,10]. Female BALB/c mice, 3–4 weeks old, were primed by subcutaneous injections of β-oestradiol (1 μg) and progesterone (1 mg) for 9 consecutive days. On the day following the last injection (day 0), mice were killed and their entire second thoracic mammary glands were excised and floated in medium on Dacron rafts in 95% O_2 and 5% CO_2 atmosphere. Serum-free keratinizing medium consisted of Waymouth MB752/1 medium (1 ml per gland), 350 $\mu g\,ml^{-1}$ L-glutamine, 35 $\mu g\,ml^{-1}$ penicillin G, and the supplements, dibutyryl cyclic AMP (DbcAMP) (10^{-4} M), Pap (10^{-6} M), (both Sigma), and I (5 $\mu g\,ml^{-1}$ (Calbiochem). 'Enhancing medium' consisted of the keratinizing medium with additions of PGE_1, PGE_2 and PGB_1 (each 5 $\mu g\,ml^{-1}$) (Upjohn). On day 9, the mammary glands exhibited extensive squamous metaplasia and deposits of keratin. Maintenance of the glands for an additional 15 days (days 9–24) in 'regression medium', containing I (5 $\mu g\,ml^{-1}$) as the only supplement, caused the metaplastic foci to involute. Media were renewed every 2 or 3 days as required. Glands were coded, fixed, sectioned at 5 μm, and stained with haematoxylin and eosin for histological analysis, and by Masson's trichrome method for histochemical detection of keratin (bright red colour).

primed BALB/c mice were cultured for 9 days in serum-free 'keratinizing medium', containing dibutyryl cyclic AMP (10^{-4} M), Pap (10^{-6} M) as a phosphodiesterase inhibitor[18], and I (5 $\mu g\,ml^{-1}$). Most (62%) of the mammary glands developed a few foci of epidermoid metaplasia (intensity grade 1) that often differentiated to form keratin (series 3, Table 1). Further, when this medium was supplemented with a mixture of PGE_1, PGE_2 and PGB_1, each at 5 $\mu g\,ml^{-1}$ (enhancing medium) in series 4, there was considerable enhancement of the ability of dibutyryl cyclic AMP to induce the squamous development and differentiation of the epithelium that lined both the mammary ducts and alveoli (Fig. 2*a*,*b*). Virtually all glands (99%) contained numerous foci of metaplasia with central cornification and keratin plaques (intensity grade 4). Mitotic figures were present in both the metaplastic and normal epithelial cells. All three PGs were necessary for maximal effect. Lowering the concentration of each PG to 1 $\mu g\,ml^{-1}$ still invoked the epidermoid metaplasia in all glands, although the foci were fewer and smaller (grade 1–2, not shown). The addition of a mixture of PGF_1 and $PGF_{2\alpha}$, each at 5 $\mu g\,ml^{-1}$, to the keratinizing or enhancing medium did not augment the effect (series 5).

The induction of the epidermoid metaplasia specifically required the presence of cyclic adenine nucleotide. Dibutyryl cyclic GMP at the same concentration (10^{-4} M), or sodium butyrate (cleavage product of dibutyryl cyclic AMP) at twice that concentration, failed to replace the dibutyryl cyclic AMP of enhancing medium (11% and 0% frequencies, respectively; series 6 and 7). Cyclic AMP or 5' AMP had little activity compared to the more lipophilic dibutyryl cyclic AMP; they required the three PGs to reach the level of activity exhibited by the dibutyryl cyclic AMP without PG in keratinizing medium (series 8 and 9). Omission of both dibutyryl cyclic AMP and Pap from enhancing medium caused complete loss of activity in the control series 10 (Fig. 2*c*). A modified enhancing medium lacking only dibutyryl cyclic AMP was partially active (30%, intensity grade 1), presumably because of an inhibition of degradation of endogenous cyclic AMP by Pap (series 11). Comparison of results of series 7 and 11 indicates that the presence of sodium butyrate was mildly inhibitory. The high frequency (100%) and intensity (grade 4) of metaplasia following deletion of Pap from enhancing medium are consistent with the presence of only a low level of endogenous cyclic AMP phosphodiesterase activity in the glands (series 12). The use of IPAH medium or the omission of all supplements except I (regression medium) resulted in no metaplasia (series 1 and 2). Mammary glands of mice not hormonally primed yielded an intermediate level of squamous metaplasia in enhancing medium (each of 26 glands, intensity grade 2).

Table 1 Induction of epidermoid metaplasia in cultured mammary glands

			Metaplastic glands	
Series	Treatment*	No. of glands	Frequency† %	Intensity grade‡
1	I+P+A+H	30	0	0
2	I	30	0	0
3	Dibutyryl cyclic AMP+Pap+I (keratinizing)	31	62	1
4	Dibutyryl cyclic AMP+Pap+I+PGE_1, E_2, B_1 (enhancing)	114	99	4
5	Dibutyryl cyclic AMP+Pap+I+PGE_1, E_2, B_1, $F_{1\alpha}$, $F_{2\alpha}$	34	100	4
6	Dibutyryl cyclic GMP+Pap+I+PGE_1, E_2, B_1	27	11	1
7	Sodium butyrate+Pap +I+PGE_1, E_2, B_1	16	0	0
8	Cyclic AMP+I+ PGE_1, E_2, B_1	21	52	1
9	5'AMP+I+PGE_1, E_2, B_1	28	68	1
10	PGE_1, E_2, B_1+I (control)	46	0	0
11	Pap+PGE_1, E_2, B_1+I	27	30	1
12	Dibutyryl cyclic AMP+I+PGE_1, E_2, B_1	18	100	4

*Whole mammary glands from hormonally primed mice were incubated for 9 d in serum-free medium containing the listed supplements at the following concentrations: dibutyryl cyclic AMP, dibutyryl cyclic GMP, cyclic AMP, and 5' adenylic acid (5' AMP), each at 10^{-4} M; Pap at 10^{-6} M; PGs, I, P, A, and H, each at 5 $\mu g\,ml^{-1}$; and sodium butyrate at 2×10^{-4} M.

†Per cent of multiple of glands with foci of stratified squamous epithelial cells and keratin deposits.

‡Intensity of metaplasia on a scale of 1–4: grade 0, no epidermoid metaplasia; grade 1, minimal epidermoid change. Foci were sparsely distributed and poorly developed. Grades 2 and 3, intermediate grades quantitatively approaching 1 and 4, respectively. Grade 4, well developed foci of epidermoid metaplasia involving the lining of most major ducts and distal ductules. Differentiation of squamous epithelium was partial to complete, the latter forming keratin plaques.

The abnormally developed and differentiated epidermoid cells involuted following the removal of the dibutyryl cyclic AMP, Pap and PGs (Fig. 1). Incubation of the metaplastic glands for an additional 15 days (days 9–24) in the regression medium caused complete involution of both the epidermoid and cuboidal (normal secretory) epithelia, leaving behind a residue of keratin plaques (Fig. 2*d*).

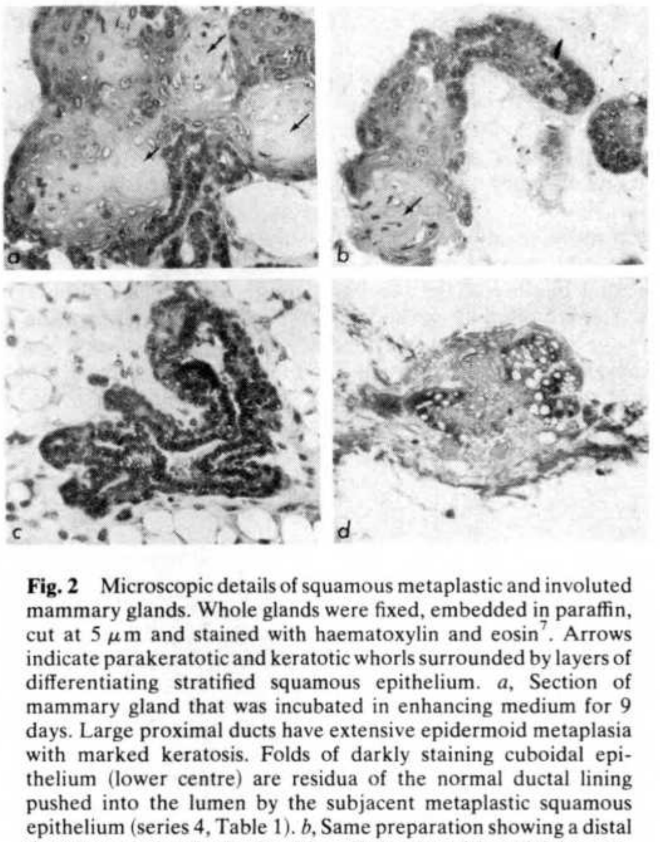

Fig. 2 Microscopic details of squamous metaplastic and involuted mammary glands. Whole glands were fixed, embedded in paraffin, cut at 5 μm and stained with haematoxylin and eosin[7]. Arrows indicate parakeratotic and keratotic whorls surrounded by layers of differentiating stratified squamous epithelium. *a*, Section of mammary gland that was incubated in enhancing medium for 9 days. Large proximal ducts have extensive epidermoid metaplasia with marked keratosis. Folds of darkly staining cuboidal epithelium (lower centre) are residua of the normal ductal lining pushed into the lumen by the subjacent metaplastic squamous epithelium (series 4, Table 1). *b*, Same preparation showing a distal ductule and alveolar buds with well developed keratinizing epidermoid metaplasia. Normal-appearing cuboidal cells are admixed above and to the right (series 4, Table 1). *c*, Section of a control gland that was incubated in the absence of dibutyryl cyclic AMP and Pap in medium containing I and PGE_1, PGE_2 and PGB_1 for 9 days. The appearance is like that of the primed gland at day 0. The ductal system is developed, but there is no lobuloalveolar growth. The epithelium is of the normal cuboidal type and shows no epidermoid metaplasia (series 10, Table 1). *d*, Section of a gland that was incubated in enhancing medium for 9 days, and then kept in regression medium for 15 days. A distal alveolar lobule that was partially metaplastic has involuted, leaving a residue of vacuolated secretory cells and a central plaque of keratin. All squamous cells have disappeared.

The induction of the metaplasia was not blocked by retinoid. The presence of 2-retinylidene-5,5-dimethyl-1,3-cyclohexanedione (retinylidene dimedone) at 10^{-5}, 10^{-7} or 10^{-9} M for 9 days failed to prevent the squamous metaplasia and keratin production brought about by enhancing medium (all 100%, not shown). This retinoid was chosen because it prevents, suppresses and apparently reverses the transformations of the cultured mammary glands caused by procarcinogens[15,17]. The failure of the retinoid to prevent squamous metaplasia in the present study is in marked contrast to the preventions and reversals of squamous metaplasias arising from vitamin A deficiency[3,4] and chemical carcinogens[5–7] in other systems. If these agents are effective in a common pathway, this difference suggests that the cyclic nucleotide, PGs and Pap act at stages after those of vitamin A deficiency and chemical carcinogens. Alternatively, separate pathways may be involved.

The present findings provide the initial indication of the identities of the possible physiological inducers of epidermoid metaplasia. Cyclic adenine nucleotide, certain PGs and Pap specifically and reversibly induce this abnormal development and differentiation in the epithelial cells of cultured mammary glands, endowing them with characteristics of skin. The common denominator among the inducers may be that they act synergistically to elevate the level of intracellular cyclic adenine nucleotide in three ways: first, by the exogenous entry of dibutyryl cyclic AMP, second, by the stimulation of the synthesis of cyclic AMP due to the actions of the PGs on adenyl cyclase[19,20], and third, through an inhibition by Pap of the phosphodiesterase-mediated degradation of the nucleotide[18].

The normal course of lobuloalveolar development and differentiation (casein production) impeded the abnormal course of squamous metaplastic development and differentiation (keratin production). Prior induction of the normal course in whole mammary glands cultured in medium containing IPAH markedly reduces the subsequent induction of the metaplasia in enhancing medium (F.V.S., R.P.C. and S.S., unpublished). Conversely, agents that elevate the intracellular level of cyclic AMP have recently been reported to inhibit the production of α-lactalbumin and casein by mammary glands in fragment culture[21].

The possibility arises that cyclic AMP and PGE_1 and PGE_2 may be the mediators of the squamous metaplasias that occur in many abnormal, transformed and malignant tissues, including mammary glands, of animals and humans[1,7,8,22–26]. Agents that elevate the level of intracellular cyclic AMP have been variously reported either to stimulate or to inhibit the growth of cells of mammary gland[27], epidermis[28] and other organs[28,29]. Further, several types of normal differentiation have previously been elicited by these same inducers in cell cultures of fibroblasts[30–32], skeletal muscle[33], melanoma[34] and other systems[19,20,29]. In addition, the production of keratohyaline granules is stimulated in cultures of human skin by theophylline, an inhibitor of the phosphodiesterase degradation of cyclic AMP[35] and keratin filaments are present in the cytoskeletons of epithelial cells in many organs[36]. It accordingly seems reasonable to investigate whether cyclic adenine nucleotide and specific PGs are the physiological mediators of the normal and abnormal development and differentiation of epithelia into enhanced keratin-producing, stratified squamous cells, as in skin and other organs.

We thank Dr W. Thomas London for critical discussions, Mrs Dovile Cooper for assistance, Mrs Ruth Bender for histological preparations, the Upjohn Company for a gift of PGs and Dr Michael B. Sporn for a gift of retinylidene dimedone, which was synthesized by Drs Nancy Acton and Arnold Brossi. This study was supported in part by NIH grants CA-21522, CA-05945, CA-06927 and RR-05539, and an appropriation from the Commonwealth of Pennsylvania.

Received 14 March; accepted 26 June 1980.

1. Anderson, W. A. D. & Kissane, J. M. in *Pathology* Vol. 1, 7th edn, 84–85 (Mosby, St. Louis, 1977).
2. McDowell, E. M., Becci, P. J., Schurch, W. & Trump, B. F. *J. natn. Cancer Inst.* **62,** 995–1008 (1979).
3. Wolbach, S. B. & Howe, P. R. *J. exp. Med.* **42,** 753–777 (1925).
4. Marchok, A. C., Cone, M. V. & Nettesheim, P. *Lab. Invest.* **33,** 451–460 (1975).
5. Lasnitski, I. *Br. J. Cancer* **5,** 345–352 (1951).
6. Harris, C. C. *et al. J. natn. Cancer Inst.* **48,** 743–761 (1972).
7. Tonelli, Q. J., Custer, R. P. & Sorof, S. *Cancer Res.* **39,** 1784–1792 (1979).
8. Sporn, M. B., Dunlop, N. M., Newton, D. L. & Smith, J. M. *Fedn Proc.* **35,** 1332–1338 (1976).
9. Ichinose, R. R. & Nandi, S. *J. Endocr.* **35,** 331–340 (1966).
10. Wood, B. G., Washburn, L. L., Mukherjee, A. S. & Banerjee, M. R. *J. Endocr.* **65,** 1–6 (1975).
11. Terry, P. M., Ball, E. M., Ganguly, R. & Banerjee, M. R. *J. immun. Meth.* **9,** 123–134 (1975).
12. Tonelli, Q. J. & Sorof, S. *Nature* **285,** 250–252 (1980).
13. Banerjee, M. R., Wood, B. G. & Washburn, L. L. *J. natn. Cancer Inst.* **53,** 1387–1393 (1974).
14. Telang, N. T., Banerjee, M. R., Iyer, A. P. & Kundu, A. B. *Proc. natn. Acad. Sci. U.S.A.* **76,** 5886–5890 (1979).
15. Dickens, M. S., Custer, R. P. & Sorof, S. *Proc. natn. Acad. Sci. U.S.A.* **76,** 5891–5895 (1979).
16. Kundu, A. B., Telang, N. T. & Banerjee, M. R. *J. natn. Cancer Inst.* **61,** 465–469 (1978).
17. Dickens, M. S. & Sorof, S. *Nature* **285,** 581–584 (1980).
18. Prasad, K. N. & Kumar, S. in *Control of Proliferation in Animal Cells* (eds Clarkson, B. & Baserga, R.) 581 (Cold Spring Harbor Laboratory, New York, 1974).
19. Samuelsson, B., Granström, E., Green, K., Hamberg, M. & Hammarström, S. *A. Rev. Biochem.* **44,** 669–695 (1975).
20. Samuelsson, B. *et al. A. Rev. Biochem.* **47,** 997–1029 (1978).
21. Perry, J. W. & Oka, T. *Proc. natn. Acad. Sci. U.S.A.* **77,** 2093–2097 (1980).

22. Pasternack, J. G. & Wirth, J. E. *Am. J. Path.* **12,** 423–437 (1936).
23. Deringer, M. K. *J. natn. Cancer Inst.* **22,** 995–1002 (1959).
24. Huvos, A. G., Lucas, J. C. & Foote, F. W. *N. Y. St. J. Med.* **73,** 1078–1082 (1973).
25. Medina, D. *J. natn. Cancer Inst.* **53,** 213–221 (1974).
26. Hassan, M. O. & Olaizola, M. Y. *Archs Path. Lab. Med.* **103,** 624–630 (1979).
27. Taylor-Papadimitriou, J., Purkis, P. & Fentiman, I. S. *J. cell. Physiol.* **102,** 317–321 (1980).
28. Green, H. *Cell* **15,** 801–811 (1978).
29. Friedman, D. L. *Physiol. Rev.* **56,** 652–708 (1976).
30. Johnson, G. S., Friedman, R. M. & Pastan, I. *Proc. natn. Acad. Sci. U.S.A.* **68,** 425–429 (1971).
31. Hsie, A. W. & Puck, T. T. *Proc. natn. Acad. Sci. U.S.A.* **68,** 358–361 (1971).
32. Sheppard, J. R. *Proc. natn. Acad. Sci. U.S.A.* **68,** 1316–1320 (1971).
33. Aw, E. J., Holt, P. G. & Simons, P. J. *Expl Cell Res.* **83,** 436–438 (1973).
34. Johnson, G. S. & Pastan, I. *Nature new Biol.* **237,** 269–270 (1972).
35. Chopra, D. *Br. J. Derm.* **96,** 255–262 (1977).
36. Sun, T.-T., Shih, C. & Green, H. *Proc. natn. Acad. Sci. U.S.A.* **76,** 2813–2817 (1979).

Specific binding of ^{3}H-substance P to rat brain membranes

M. R. Hanley*, B. E. B. Sandberg*, C. M. Lee*, L. L. Iversen*, D. E. Brundish† & R. Wade†

* MRC Neurochemical Pharmacology Unit, Department of Pharmacology, University of Cambridge Medical School, Hills Road, Cambridge CB2 2QD, UK
† Ciba-Geigy Pharmaceuticals Division, Horsham, West Sussex RH12 4AB, UK

The undecapeptide substance P is a putative neurotransmitter in the mammalian central nervous system (CNS), and may be associated with pain fibres in the spinal cord[1,2]. Radiolabelled derivatives of other neuropeptides havd been used to demonstrate specific interactions with receptor sites on brain membranes[3–6], and this approach has now been explored with substance P. We have now prepared [4-^{3}H-Phe^8]-substance P and we find that it binds reversibly to a saturable population of sites in rat brain particulate fractions. Scatchard analysis of concentration-dependent saturation of binding indicates a single population of non-interacting sites with a high affinity ($K_d = 0.38$ nM) and a low density ($B_{max} = 27.2$ fmol per mg protein). Kinetic analyses indicate an apparent dissociation equilibrium constant of 0.46 nM. A variety of neurotransmitter amines and amino acids, and other peptides do not compete at the substance P sites, but structurally related peptides or shorter C-terminal fragments of substance P are active. The rank order of potency of these substance P-related peptides agrees with that reported for their effects in depolarizing spinal cord neurones[7]. The regional distribution of the specific binding sites for ^{3}H-substance P parallels that of substance P immunoreactivity, being high in the hypothalamus and low in the cerebellum and cerebral cortex. The characteristics of the ^{3}H-substance P binding sites are consistent with those expected for substance P receptors.

^{3}H-labelled substance P was prepared by reductive deiodination of the protected peptide [Boc-Arg^1,Lys(Boc)^3, Phe(I)^8]-substance P with tritium as similarly described for corticotropin-(1-24)-tetracosapeptide[8]. The solid-phase synthesis of the precursor peptide and the tritiation and purification of the radiolabelled substance P will be reported in detail elsewhere. The specific activity of the final product was 23 Ci mmol^{-1}, based on quantitative amino acid analysis and confirmed by radioimmunoassay. The purity was assessed by TLC in three different solvent systems, by isocratic and gradient-elution reverse-phase HPLC in three systems, and by measurements of the immunoreactivity of serially diluted samples against C-terminal sequence- and N-terminal sequence-directed[9] antisera. By all techniques, the purity was $\geq$90%, and the major contaminant was substance P sulphoxide, in which the C-terminal methionine residue was oxidized[10]. Aliquots of ^{3}H-substance P were stored at a concentration of 0.25 mM in 0.01 M HCl in glass vials under liquid nitrogen. For use, samples were diluted to 25 μM with 0.1 M HCl containing 1 mg ml^{-1} bovine serum albumin (BSA; recrystallized, Sigma). In these conditions, the labelled peptide could be stored at −20 °C for up to 10 days, with repeated freezing and thawing, and accumulated <5% of ^{3}H-substance P sulphoxide and negligible amounts of other labelled products. On the guinea pig ileum, ^{3}H-substance P had contractile activity equipotent with that of synthetic unlabelled substance P.

^{3}H-substance P was rapidly degraded when incubated at 37 °C with a crude synaptic membrane preparation from rat brain (see Fig. 1 legend for procedure). For this reason, all incubations included the peptidase inhibitors bacitracin (300 μg ml^{-1}), phenylmethylsulphonyl fluoride (0.1 mM), and *p*-chloromercuribenzoate (0.1 mM), and the incubations were performed at 4 °C. ^{3}H-substance P was stable to enzymatic digestion in these conditions as determined by HPLC analyses of acid extracts of membrane-bound radioactivity after various intervals (5–60 min). Control experiments indicated that none of these additions interfered with ^{3}H-substance P binding.

At low concentrations of ^{3}H-substance P(<1 nM), 50–60% of the total binding of the labelled peptide to brain membranes could be inhibited by the addition of 10μM unlabelled peptide. The specific component of binding, defined in this way, was saturable, whereas the nonspecific binding (in the presence of 10μM substance P) was linearly dependent on ligand concentration (Fig. 1*a*). The specific and nonspecific components were both linearly dependent on the amount of tissue present in the

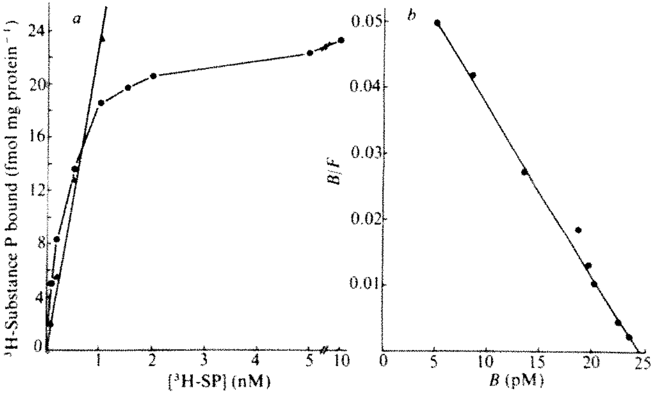

Fig. 1 *a*, Concentration dependence of specific (circles) and nonspecific (triangles) ^{3}H-substance P binding to rat brain membrane fractions. Whole brains minus cerebral cortex and cerebellum were dissected on ice from adult male Sprague–Dawley rats and homogenized in 10 vol ice-cold 10% sucrose/20 mM HEPES (*p*H 7.4) with a Teflon–glass homogenizer. The homogenate was centrifuged at 1,000*g* (5 min, 4 °C) to remove cellular debris. The supernatant was centrifuged at 11,000*g* (20 min, 4 °C) to prepare a crude mitochondrial pellet. The pellet was lysed by resuspension in 10 vol of ice-cold 5 mM HEPES (*p*H 8.1). The lysate was centrifuged at 100,000*g* (30 min, 4 °C). The resulting pellet was resuspended with a Teflon–glass homogenizer in 5 vol of 20 mM HEPES (*p*H 7.4) and stored frozen at −20 °C. For binding assays, 50 μl of the thawed membrane suspension were added to 430 μl of incubation medium (20 mM HEPES *p*H 7.4 containing 0.5% recrystallized BSA, 300 μg ml^{-1} bacitracin, 0.1 mM phenylmethylsulphonyl fluoride, 0.1 mM *p*-chloromercuribenzoate) in small plastic tubes kept on ice. The tubes were preincubated for 60 min before further additions. Drug, radiolabel and blank additions were made in 10-μl aliquots so that the final volume was 500 μl. Nonspecific binding was defined by adding substance P to a final concentration of 10 μM. In all cases, total and nonspecific binding determinations were made in triplicate. The ^{3}H-substance P was diluted from a 25 μM stock solution with incubation medium. Incubations were performed for 20 min on ice, and were terminated by dilution with 2.5 ml of ice-cold 20 mM HEPES/1% BSA (HEPES/BSA). Membrane-bound ^{3}H-substance P was measured by rapid filtration of the diluted samples through Millipore EGWP (0.2 μm) filters pre-equilibrated with ice-cold HEPES/BSA for 3h. Filters were rinsed with 3 × 2.5 ml of ice-cold HEPES/BSA. Filtration and rinsing were completed in <1 min. Filters were clarified by the addition of 4 ml ethoxyethanol and counted by the addition of 10 ml toluene scintillant. The data points are the means of triplicates in a single experiment. These results have been replicated in four separate experiments by the same technique. In three additional experiments using a centrifugation assay to measure binding, the specific binding data were reproduced, but nonspecific binding represented a greater proportion of the total (70–80%). *b*, Scatchard plot of the specific binding data in *a*.

0028-0836/80/340810—03$01.00

incubation. A Scatchard analysis (Fig. 1*b*) of the saturation curve for specific binding yielded a single straight line from which the density of the sites (B_{max}) was 27.2 fmol per mg protein and the dissociation constant (K_d) was calculated as 0.38 nM. Addition of a large molar excess of unlabelled substance P to membranes previously incubated with ^3H-substance P led to an exponential decay of specific binding (Fig. 2*b*). These data, when analysed by a semi-log plot, gave a straight line with a slope of $-0.15\ min^{-1}$, corresponding to a half time of dissociation of 4.6 min, and a dissociation rate constant (k_{off}) of $2.5\times10^{-3}\ M^{-1}\ s^{-1}$ (Fig. 2*b*). The time course for association of 2 nM ^3H-substance P reached a plateau for nonspecific sites at 2 min (data not shown) and for specific sites at 10 min (Fig. 2*a*). Plotting these data according to a first-order reaction gave a straight line with a slope of 0.47. The association rate constant (k_{on}) determined from the slope was $5.4\times10^6\ M^{-1}\ s^{-1}$. Using the equation $K_d = k_{off}/k_{on}$, an equilibrium dissociation constant of 0.46 nM was calculated, in good agreement with that determined from saturation data.

Table 1 Inhibition of specific ^3H-substance P binding to rat brain membranes by related peptides

Peptide	Rat brain binding inhibition IC_{50}(nM)*	Relative potency	Rat spinal cord depolarization (ref. 7) (relative potency)
Substance P (SP)	3	1.0	1.0
SP_{2-11}	10	0.3	0.6–0.9
SP_{3-11}	36	0.08	0.4–1.0
SP_{4-11}	64	0.05	0.8–1.0
SP_{5-11}	6	0.5	2–12
SP_{6-11}†	1.8	1.7	5–12
SP_{7-11}	220	0.01	<0.02
SP free acid	100	0.03	ND
Eledoisin	11	0.3	ND
Physalaemin	1.6	1.9	ND

* Determined from Hill plots of inhibition of binding of 2 nM ^3H-substance P. Data were generated from the means of triplicates of at least three separate experiments. For experiments with C-terminal fragments of substance P, 1 mM puromycin was added to the incubation medium to protect against aminopeptidase degradation. All peptides were commercial products (Peninsula) and were checked for purity by HPLC.

† Pyroglutamyl N-terminal form. Negative at 10 μM: angiotensin II and III, apamin, bombesin, bradykinin, α-bungarotoxin, carnosine, cholecystokinin-8 (non-sulphated), cholecystokinin-33, leucine-enkephalin, methionine-enkephalin, β-endorphin, β-lipotropin, neurotensin, SQ-20881, thyrotropin-releasing hormone, vasoactive intestinal peptide, vasopressin. Negative at 100 μM: aspartic acid, baclofen, capsaicin, carbamylcholine, dopamine, γ-aminobutyric acid, glutamic acid, glycine, histamine, serotonin, noradrenaline.

The sites were inhibited by structurally related analogues and by C-terminal fragments of substance P but not by a range of other neurotransmitters or peptides (Table 1). The rank order of potencies for a series of C-terminal fragments of substance P was hexapeptide > substance P > heptapeptide > decapeptide > nonapeptide > octapeptide > pentapeptide. Physalaemin and eledoisin, naturally-occurring substance P-related peptides[11], were also effective in competing for specific sites. Substance P free acid, in which the C-terminal methionine amide is replaced by a methionine, was about 30 times less active than substance P. Baclofen, a putative susbstance P antagonist[7], had no effect on ^3H-substance P binding. The IC_{50} for nonradioactive substance P (against 2 nM ^3H-substance P) was 3 nM, corresponding to an apparent K_d of 0.48 nM, in close agreement with both kinetic and equilibrium measurements of the dissociation constant.

A preliminary survey of the regional distribution of ^3H-substance P binding in rat brain was performed, using a single radioligand concentration (2 nM). ^3H-substance P binding sites were unevenly distributed among rat brain regions (Table 2). The density of specific sites was highest in substance P-rich areas such as hypothalamus and midbrain, and lowest in cerebral cortex and cerebellum, which contain only small amounts of substance P[12].

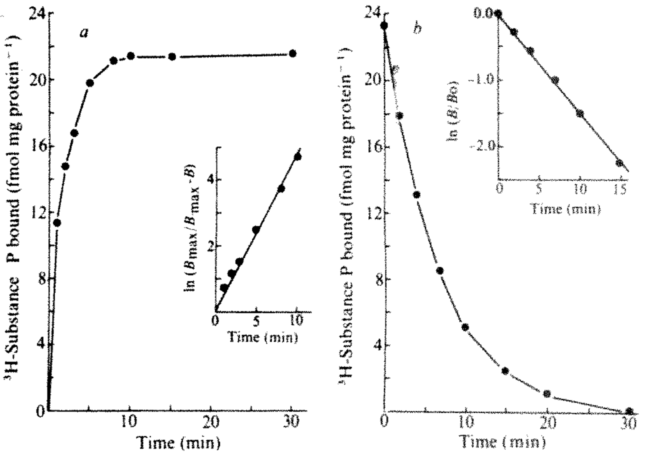

Fig. 2 *a*, Time course of specific ^3H-substance P binding at 4 °C. 2 nM ^3H-substance P was incubated with rat brain membrane fractions, and total and nonspecific binding were determined at the indicated intervals to generate the specific binding. The points are the means of triplicates in three separate experiments. Insert: Linearization of the time course curve for calculation of k_{on} as described elsewhere[6]. *b*, Dissociation time course of specific ^3H-substance P binding at 4 °C. 2 nM ^3H-substance P was incubated on ice for 20 min with rat membrane fractions. Substance P was then added to a final concentration of 10 μM at time zero. Samples of total and nonspecific binding were filtered at the indicated intervals afterwards. The results are the means of triplicates in three separate experiments. Insert: Linearization of the dissociation curve for calculation of k_{off} as described elsewhere[6].

The structural specificity of the high affinity binding sites in rat brain resembles that determined by measurements of the biological activity of substance P and related peptides[13]. Most studies have focused on the actions of substance P on peripheral tissues, but Otsuka and Konishi[7] examined the potencies of substance P and shorter fragments in depolarizing motor neurones after bath application to newborn rat spinal cord, and their results (summarized in Table 1) are in agreement with the present binding data. In particular, it is noteworthy that the hexapeptide fragment is more potent than the native peptide, both in its activity on spinal cord and in inhibiting ^3H-substance P binding, whereas the C-terminal pentapeptide fragment shows a marked reduction in activity. Piercey and Einspahr[14] have also shown a marked reduction in activity of the C-terminal pentapeptide electrophysiologically on dorsal horn neurones.

Table 2 Regional distribution of specific ^3H-substance P binding to rat brain membrane fractions

Region	Binding (fmol per mg protein)
Brainstem	15±5
Cerebellum	6±3
Hypothalamus	36±9
Midbrain	29±6
Striatum	17±4
Temporal cortex	4±2

Individual regions were dissected on ice and crude mitochondrial fraction membranes prepared as in Fig. 1. The specific binding of 2 nM ^3H-substance P was determined using membrane fractions stored frozen at −20 °C as described in Fig. 1 legend. The protein content was determined by the Lowry technique. The results are means ±s.e.m. for triplicate measurements of total and nonspecific binding in four separate experiments. In preliminary experiments substance P-displaceable binding was observed in the cerebellum, cerebral cortex and hippocampus that could also be inhibited by angiotensin II and SQ-20881 (0.1–10 μM), unlike the binding in other regions or in total brain (minus cerebellum and cortex). The nature of this unselective peptide-binding site is not known, but the incubation medium was routinely supplemented with 10 μM angiotensin II to eliminate its contribution.

Although data for the substance P-related peptides physalaemin and eledoisin are not available for rat spinal cord, these substances are approximately equipotent with substance P in a number of other test systems[13,15], and they had a similar potency to substance P in the binding assay. Removal of the C-terminal amide in substance P free acid greatly reduces biological potency in a number of test systems[13,16], and was also found markedly to reduce potency in the binding assay.

Although there have been other published reports of high-affinity binding of radioactively labelled substance P derivatives to brain membrane preparations[17,18], we believe that the present results reflect most closely the known biological activity of substance P. Thus, Nakata *et al.*[17] described the binding of ^{3}H-substance P to rabbit brain membrane preparations, but observed no antagonism by physalaemin. Furthermore, we have been unable to replicate their measurement technique as we observe large amounts of ^{3}H-substance P binding to the type of membrane filters used by these authors, even in the absence of tissue. From the present results, it seems unlikely that the specific binding of ^{3}H-substance P could have reached equilibrium during the 1 min incubation period at 0 °C used by these authors. Mayer *et al.*[18] studied the binding of [^{125}I-Tyr^8]-substance P to a synaptic vesicle fraction from rat brain. Although the labelled peptide exhibited high affinity binding ($K_d = 0.32$ nM), and the regional distribution of binding sites in brain resembled that of endogenous substance P[19], the specificity of this binding bore little relation to biological activity, since C-terminal fragments of substance P inhibited binding only at micromolar concentrations, and physalaemin enhanced rather than inhibited binding of the labelled analogue. Putney *et al.*[20] and Jensen and Gardner[21] have described the use of ^{125}I-physalaemin to label substance P receptors in dispersed parotid acinar cells and dispersed pancreatic acinar cells respectively. In each case, the authors described specific high-affinity binding sites that were present in unusually low density. It is interesting that the density of ^{3}H-substance P sites in rat brain is lower than that seen for many conventional amine or amino acid neurotransmitter receptor sites[22], but is similar to the values reported for other brain peptide-binding sites[3-5].

The characteristics and regional distribution of the high affinity binding sites for ^{3}H-substance P described here are in close correspondence with those expected for substance P receptors in the CNS. The radioligand binding assay offers an important new tool for investigating the occurrence and pharmacological properties of such substance P receptors.

M.R.H. is a Fellow of the Helen Hay Whitney Foundation. C.M.L. is a Li Po Chun Scholar.

Received 28 April; accepted 23 June 1980.

1. Cuello, A. C. *et al.* in *Centrally Acting Peptides* (ed. Hughes, J.) 135–156 (Macmillan, London, 1978).
2. Piercey, M. F., Einspahr, F. J., Dobby, P. J. K., Schroeder, L. A. & Hollister, R. P. *Brain Res.* **186,** 421–434 (1980).
3. Moody, T. W., Pert, C. B., Rivier, J. & Brown, M. R. *Proc. natn. Acad. Sci. U.S.A.* **75,** 5372–5376 (1978).
4. Sirett, N. E., McLean, A. J., Bray, J. J. & Hubbard, J. I. *Brain Res.* **122,** 299–312 (1977).
5. Taylor, D. P. & Pert, C. B. *Proc. natn. Acad. Sci. U.S.A.* **76,** 660–664 (1979).
6. Kitabgi, P. *et al. Proc. natn. Acad. Sci. U.S.A.* **74,** 1846–1850 (1977).
7. Otsuka, M. & Konishi, S. *Cold Spring Harb. Symp. quant. Biol.* **40,** 135–143 (1976).
8. Brundish, D. E. & Wade, R. J. *Chem. Soc. Perkin Trans.* I, 2186–2189 (1973).
9. Lee, C. M., Emson, P. C. & Iversen, L. L. *Life Sci.* (in the press).
10. Floor, E. & Leeman, S. *Analyt. Biochem.* **101,** 498–503 (1980).
11. Bertaccini, G. *Pharmac. Rev.* **28,** 127–177 (1976).
12. Kanazawa, I. & Jessell, T. *Brain Res.* **117,** 362–367 (1976).
13. Bury, R. W. & Mashford, M. L. *Aust. J. exp. Biol. med. Sci.* **55,** 671–735 (1977).
14. Piercey, M. F. & Einspahr, F. J. *Brain Res.* **187,** 481–486 (1980).
15. Erspamer, G. F., Erspamer, V. & Piccinelli, D. *Naunyn-Schmiedebergs Archs Pharmak.* **311,** 61–65 (1980).
16. Couture, R., Fournier, A., Magnan, J., St. Pierre, S. & Regoli, D. *Can. J. Physiol. Pharmac.* **57,** 1427–1436 (1979).
17. Nakata, Y., Kusaka, Y., Segawa, T., Yajima, H. & Kitagawa, K. *Life Sci.* **22,** 259–268 (1978).
18. Mayer, N., Lembeck, F., Saria, A. & Gamse, R. *Naunyn-Schmiedebergs Archs Pharmak.* **306,** 45–51 (1979).
19. Saria, A., Mayer, N., Lembeck, F. & Pabst, M. *Naunyn-Schmiedebergs Archs Pharmak.* **311,** 151–157 (1980).
20. Putney, J., Van De Walle, C. & Wheeler, C. *J. Physiol., Lond.* **301,** 205–212 (1980).
21. Jensen, R. T. & Gardner, J. D. *Proc. natn. Acad. Sci. U.S.A.* **76,** 5679–5683 (1979).
22. Snyder, S. H. & Bennett, J. P. *A. Rev. Physiol.* **38,** 153–175 (1976).

β-Endorphin alters luteinizing hormone secretion via the amygdala but not the hypothalamus

N. Parvizi & F. Ellendorff

Institut für Tierzucht und Tierverhalten, FAL, Mariensee, 3057
Neustadt 1, FRG

Morphine and enkephalins are able to alter pituitary hormone secretion[1-3]. It has been postulated that they do not act directly at the pituitary[4], but rather that the hypothalamus is the site at which inhibition or stimulation of pituitary hormone secretion is initiated[4]. On the other hand, endogenous opiates have been located in distinctly different neuronal regions, including areas outside the hypothalamus[5]. The effects of β-endorphin on plasma luteinizing hormone (LH) levels have not been explored, and the present experiments attempt to elucidate the contribution and the possible site of action of β-endorphin in the control of LH secretion. The results show that β-endorphin inhibits pituitary LH secretion if applied into the amygdala but not when given into the hypothalamus.

Stainless steel guide tubings (22 gauge) containing inner 28-gauge tubing were implanted bilaterally in the basolateral

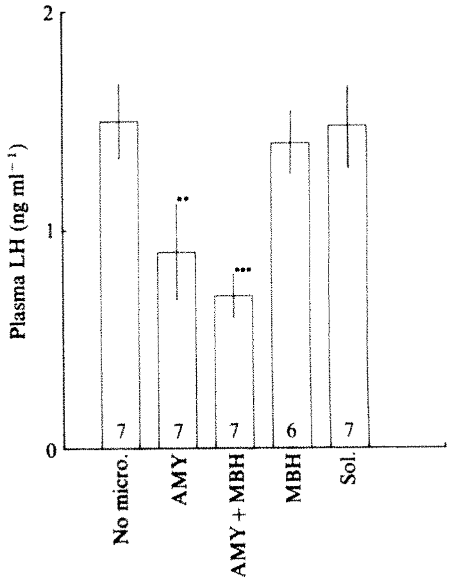

Fig. 1 Decrease of plasma LH levels 100–180 min after microinjection of 30 ng β-endorphin into the amygdala (AMY) or mediobasal hypothalamus (MBH) and amygdala of ovariectomized miniature pigs. 'No micro', control blood sampling without any treatment; 'Sol.', microinjection of 1 μl of 0.7% saline. Numbers in the bars represent the number of animals. For statistical analysis the period of sampling was divided into three blocks each of nine successive samples taken at 10-min intervals. The mean LH value for each animal within each block was calculated. A one-way analysis of variance was then carried out to detect differences among mean LH values of treatments and time blocks. ** $P \leq 0.01$; *** $P \leq 0.001$; $\bar{x} \pm$ s.e.m.

0028-0836/80/340812—02$01.00

hypothalamus and amygdala of seven adult, ovariectomized miniature pigs. The tips of the tubing ended 3 mm above the desired depth. Two weeks later and 5 days before the beginning of the experiment, a silastic catheter was placed in the external jugular vein. During the recovery period, the animals were familiarized with the manipulations of the implant. The experiment was designed so that each animal served as its own control. A control period preceded the treatment on each experimental day. Saline (solvent), 1 µl, β-endorphin (Serva cat. no. 52558), 30 ng, were microinjected on 4 different days at 3-day intervals into either the basolateral hypothalamus or amygdala, or simultaneously into the two tissues. The sequence of treatment was randomly assigned for each animal. Microinjections were given through a 28-gauge tubing connected to a Hamilton syringe as described[6,7]. Blood samples (2 ml) were collected at 10-min intervals from 90 min before to 180 min after microinjection. On one day, blood samples were taken without any treatment. Thus, a double control system allowed us to consider the animals as a group and individually. Plasma LH was estimated by radioimmunoassay[8].

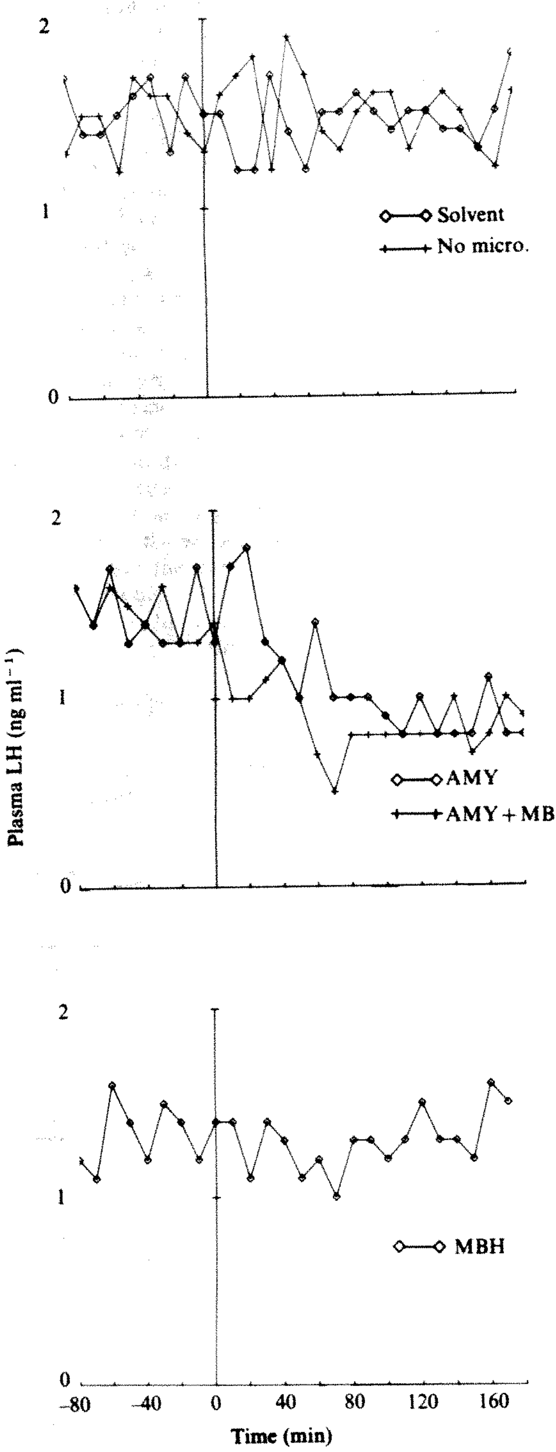

Fig. 2 Point by point presentation of plasma LH levels before and after microinjection of 30 ng β-endorphin into the mediobasal hypothalamus (MBH), amygdala (AMY) or both tissues. 'Solvent' indicates microinjection of 1 µl 0.7% saline into the hypothalamus and amygdala at time 0; 'No micro' indicates control blood sampling without any microinjection; each point represents seven (AMY, control or solvent) or six (MBH, AMY + MBH) animals. For clarity the s.e.m. values are omitted.

Histological verification at the end of the experiment indicated that in six out of seven animals the tips of the tubing were located in the basolateral hypothalamus, and in all seven animals the tips were within the amygdala. Microinjection of β-endorphin into the basolateral hypothalamus had no significant effect on LH secretion, but microinjection into the amygdala of the same animals decreased plasma LH levels significantly ($P \leq 0.01$; for statistical analysis see Fig. 1 legend). The onset of inhibition occurred within 60 min of microinjection (Fig. 2). The simultaneous microinjection of β-endorphin into the hypothalamus and amygdala resulted in a decrease in plasma LH levels similar to that seen with microinjection into the amygdala alone (Fig. 2). This would be expected if β-endorphin were priming the hypothalamus to incoming signals.

The application of other substances, such as steroids[6,7,9] or catecholamines[9], directly into the basolateral hypothalamus causes dramatic changes in LH secretion. Hence the absence of any changes in plasma LH after β-endorphin microinjection into the hypothalamus was unexpected. It suggests, among other possibilities, that hypothalamic LH-releasing hormone (LH-RH) secreting cells are not directly sensitive to β-endorphin and that β-endorphin-induced changes in LH originate from extra-hypothalamic neurones, thereby in some way inhibiting LH-RH. Thus, the high number of β-endorphin receptors in the hypothalamus[10] must be involved in mechanisms not related to LH-RH secretion. The amygdala, on the other hand, must now be considered as one site where β-endorphins, among other substances, induce changes that eventually result in altered LH-RH discharge and thus inhibition of pituitary LH secretion. Although we do not know how this is brought about, the amygdala has been identified as a preferred site of endogenous opiate accumulation[5,10]. However, the effect on plasma LH that we have observed is probably only one effect of amygdala-β-endorphin interplay. For example, it is known that the amygdala and β-endorphin[12,13], as well as LH-RH[14,15], are involved in controlling a wide range of behavioural patterns.

This work was supported by the Deutsche Forschungsgemeinschaft. We thank Mrs A. Schulte-Derne and Miss R. Duensing for assistance.

Received 24 January; accepted 18 June 1980.

1. Dupont, A., Cusan, L., Garon, M., Labrie, F. & Li, C. H. *Proc. natn. Acad. Sci. U.S.A.* **74,** 358–359 (1977).
2. Ieiri, T., Chen, H. T. & Meites, J. *Neuroendocrinology* **29,** 288–292 (1979).
3. Bruni, J. F., van Vugt, D., Marshall, S. & Meites, J. *Life Sci.* **21,** 471–466 (1977).
4. Meites, J., Bruni, J. F., van Vugt, D. A. & Smith, A. F. *Life Sci.* **24,** 1325–1336 (1979).
5. Bloom, F., Ballenberg, E., Rossier, J., Ling, N. & Guillemin, R. *Proc. natn. Acad. Sci. U.S.A.* **75,** 1591–1595 (1978).
6. Parvizi, N. & Ellendorff, F. *Nature* **256,** 59–60 (1975).
7. Parvizi, N., Elsaesser, F., Smidt, D. & Ellendorff, F. *Endocrinology* **101,** 1078–1087 (1977).
8. Pomerantz, D. K., Ellendorff, F., Elsaesser, F., König, A. & Smidt, D. *Endocrinology* **94,** 330–335 (1974).
9. Parivzi, N. & Ellendorff, F. *Brain Res.* **148,** 521–525 (1978); *J. Steroid Biochem.* **12,** 331–335 (1980).
10. Uhl, G. R., Childers, S. R. & Synder, S. H. in *Frontiers in Neuroendocrinology* Vol. 5 (eds Ganong, W. F. & Martini L.) 289–328 (Raven, New York, 1978).
11. Eleftherious, B. G. (ed.) *The Neurobiology of the Amygdala* (Plenum, New York, 1972).
12. Bloom, F., Segal, D. & Guillemin, R. *Science* **194,** 630–632 (1976).
13. Tache, Y., Lis, M. & Collu, R. *Life Sci.* **21,** 841–846 (1977).
14. Moss, R. L. & McCann, S. M. *Science* **181,** 177–179 (1973).
15. Pfaff, D. W. *Science* **182,** 1148–1149 (1973).

Genetic alteration of nerve membrane excitability in temperature-sensitive paralytic mutants of *Drosophila melanogaster*

Chun-Fang Wu*†‡ & Barry Ganetzky*§

* Division of Biology, California Institute of Technology, Pasadena, California 91125
† Department of Zoology, University of Iowa, Iowa City, Iowa 52242
§ Laboratory of Genetics, University of Wisconsin, Madison, Wisconsin 53706

Single mutations that disrupt basic physiological processes such as axonal conduction and synaptic transmission provide one means to study the membrane components and mechanisms that underlie these processes[1–8]. Temperature-sensitive paralytic mutants of *Drosophila melanogaster* which behave normally at a permissive temperature (23–25 °C) but become paralysed at a restrictive temperature (usually 29–37 °C) have been utilized in such studies. An example is *nap*^{ts} (no action potential, temperature-sensitive), a recessive second-chromosome mutation that causes paralysis of larvae and adults at 37 °C. Electrophysiological recordings have demonstrated that *nap*^{ts} specifically affects a component of axonal membranes[5]. Here we show that axonal conduction in *nap*^{ts} larvae is abnormally sensitive to tetrodotoxin (TTX), a specific blocker of voltage-sensitive sodium channels[9], and that the refractory period of action potentials differs from wild type, consistent with the idea that *nap*^{ts} alters the function of sodium channels. It is further shown that *para*^{ts} (paralysed, temperature-sensitive), a recessive *X*-linked mutation[1], also specifically disrupts axonal conduction and that the two mutations affect functionally related membrane components. Identification of other mutants defective in associated components of nerve membranes is made feasible by using techniques described here.

The TTX sensitivity of nerve conduction was measured in both mutant and normal (Canton-S) larvae. The postsynaptic excitatory junctional potentials (e.j.ps) were recorded intracellularly from medioventral longitudinal muscles in the larval neuromuscular preparation[5,10]. In *Drosophila*[10] and other dipteran[13,14] larvae, these muscles are innervated by two multiterminal axons with multiple branches and lack regenerative action potentials under physiological conditions[10]. Blockage of axonal conduction causes the loss of the evoked e.j.p. For the *nap*^{ts} larva shown in Fig. 1*a*, 5nM TTX has diminished the e.j.p. appreciably and at 10 nM the e.j.p. is completely gone. Axonal conduction but not synaptic transmission is blocked because a graded postsynaptic potential with short latency distinct from the normal e.j.p. can be evoked by electrotonically depolarizing the nerve terminal with high intensity stimuli[5,11,12]. The wild-type e.j.p. is only slightly affected by 10 nM TTX, diminishing at 20 nM TTX, and finally disappearing at 40 mM TTX, at which point a graded response can be evoked electrotonically (Fig. 1*b*).

In any given larva, we found little variation in the dose of TTX required to block the e.j.p. in different body segments. For the different *nap*^{ts} larvae tested, the effective concentration ranged from 5–15 nM (9.8 ± 4.4 nM; $\bar{x} \pm$ S.D.; $n = 11$ larvae). For wild type the range was 20–65 nM (40.3 ± 11.1 nM; $n = 9$ larvae). The difference in TTX sensitivity was confirmed by direct recording of nerve compound action potential. This result also indicates that *nap*^{ts} affects the TTX sensitivity of both the sensory and motor axons in the nerve bundle.

The observed difference in TTX sensitivity is not a consequence of differences in genetic background other than the *nap*^{ts} mutation responsible for the paralytic phenotype. By using a translocation which inserts the *nap*$^{+}$ locus into the *Y* chromosome[5], the TTX sensitivity of *X*/*Y*; *nap*^{ts}/*nap*^{ts} and *X*/*Ynap*$^{+}$; *nap*^{ts}/*nap*^{ts} larvae were compared. These larvae are essentially identical in genetic background, but the former have the behavioural phenotype of *nap*^{ts} whereas the latter are *nap*$^{+}$. The e.j.p. in these control larvae was blocked at a TTX concentration of 32.5 ± 10.9 nM ($n = 4$ larvae), comparable to the effective dose for Canton-S (40.3 ± 11.1 nM).

The altered TTX sensitivity is consistent with the idea that *nap*^{ts} alters the function or number of sodium channels[5]. Biochemical analysis of nerve membrane properties in *Drosophila* has begun[7,15] and can provide independent evidence. Preliminary results from competible, saturable binding of ^{3}H-TTX to a crude particulate fraction prepared from adult heads indicate different binding properties between normal and *nap*^{ts} extracts[15].

A possible alteration in the density and/or kinetics of voltage-dependent ionic channels in *nap*^{ts} is also suggested by an abnormal refractory period of the compound action potential. The axonal refractory period is determined by the kinetics of activation of sodium and potassium channels and the inactivation of sodium channels[16]. For each axon in a nerve bundle there is a definite refractory period during which a second stimulus cannot elicit another propagated response. The second compound action potential gradually recovers as the interval between two stimuli increases, because an increasing number of axons are again able to generate a propagated response (Fig. 2*a*). The second response recovers more rapidly in control than in *nap*^{ts} larvae even though the stimulus strength relative to the threshold is the same. We defined $\tau_{1/2}$ as the interval between stimuli needed to obtain a second response with amplitude 50% of the first. The $\tau_{1/2}$ decreases for both mutant and control larvae as the stimulus intensity increases (Fig. 2*b*). However, at almost every relative stimulus strength, the mutant requires a longer interval for recovery than does the control. The minimum $\tau_{1/2}$ is

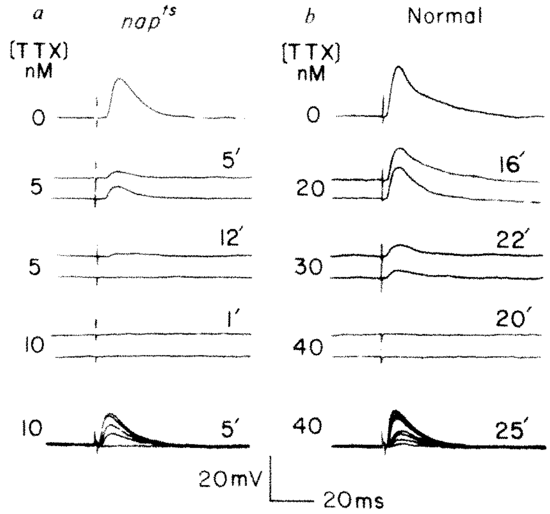

Fig. 1 Continuous recordings (23 °C) from ventrolateral longitudinal muscles in the mutant *nap*^{ts} and the normal (Canton-S) larvae showing e.j.ps at different TTX concentrations shown to the left of each trace. Segmental nerve bundles were severed close to the ventral ganglion and stimulated (0.2 ms duration) via a glass suction electrode. E.j.ps were recorded intracellularly using glass microelectrodes filled with 3M KCl (30–60 mΩ). TTX was added to the bath solution to change concentrations in increments of 5–10 nM. Solutions were mixed and enough time allowed for equilibration. Traces were made at different times after change of TTX concentration as marked on the right of each trace. *a*, *nap*^{ts} larva. At 5 nM TTX, the e.j.p. is almost entirely blocked within 12 min. Synaptic transmission is not affected by TTX because graded potentials (bottom trace, superimposed recordings) can still be evoked electrotonically by strong stimuli (1.0 ms duration) even at 10 nM TTX when active conduction is blocked. *b*, Normal larva. The e.j.p. is lost only after 25 min in 40 nM TTX. At this point graded responses could be evoked electrotonically. The bath solution[5,10] contains 0.8 mM Ca^{2+}.

---

‡ To whom correspondence should be addressed at University of Iowa.

0028-0836/80/340814—03$01.00

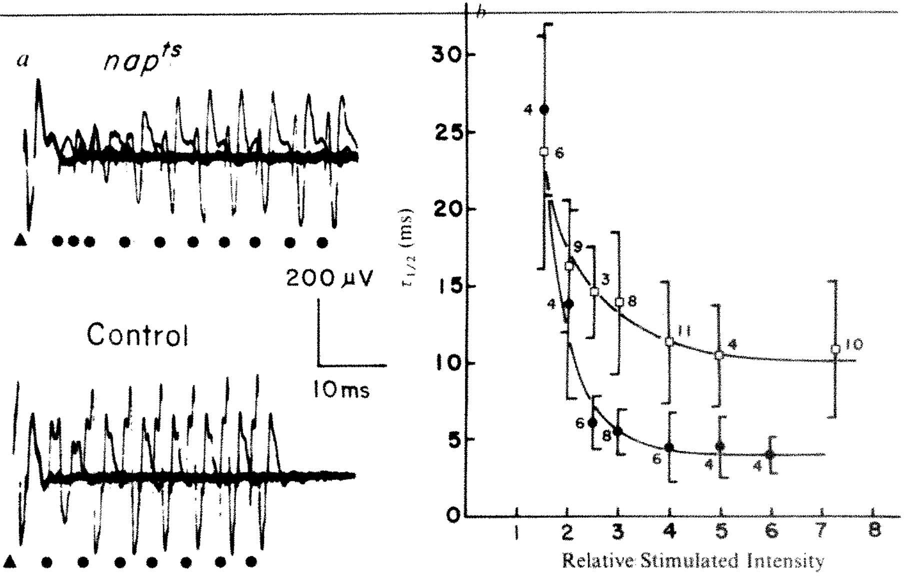

Fig. 2 *a*, Compound action potentials of *nap*^{ts} and control larvae at 23 °C showing refractory period. The segmental nerve bundles were cut close to the ganglion and stimulated at the cut end with a suction electrode. A second suction electrode drew up a loop of nerve near the distal end and recorded the response[5]. Responses to twin stimuli with increasing interval between them are superimposed. In *nap*^{ts} larva the second response attains complete recovery after an interval of 20–25 ms following the first stimulus. Stimulus intensity was 4 V; threshold was 1 V; stimulus duration was 0.2 ms. For control larvae the second response has recovered within 10 ms following the first stimulus. Stimulus intensity was 5.2 V; threshold was 1.3 V; stimulus duration was 0.2 ms. In these superimposed traces triangles mark the first stimuli and dots mark the second stimuli. *b*, Refractory period of compound action potential for *nap*^{ts} (□) and control (●) larvae at different stimulus intensities determined from experiments like those shown in Fig. 2*a*. The interval ($\tau_{1/2}$) between stimuli necessary to produce a second response with an amplitude 50% of the first response was determined at different stimulus intensities relative to threshold. $\tau_{1/2}$ decreases as the stimulus intensity increases. The minimum attainable $\rho_{1/2}$ is more than twice as long in *nap*^{ts} larvae as in control larvae. Each point represents an average from the number of nerves indicated. Error bars represent standard deviation.

about 4 ms in control larvae but is close to 10 ms in the mutant. This suggests that in *nap*^{ts} each axon contributing to the compound action potential has a longer than normal refractory period. Another less likely possibility is that *nap*^{ts} has a specific effect only on those axons with a short refractory period.

These effects of *nap*^{ts} on nerve conduction at permissive temperatures are unlikely to be due to a defect in a passive electrical property of excitable membranes such as increase in leakage conductance. Computer simulations of active conduction in a Hodgkin-Huxley model axon[16] of the size found in *Drosophila* showed that the observed increase in refractory period and the conduction block at the restrictive temperature cannot be accounted for solely by an increase in leakage conductance (Joyner and Wu, unpublished data).

If *nap*^{ts} does affect the sodium channel, it will be of interest to identify other mutations with similar properties. Of eight other temperature-sensitive paralytic mutants on the *X* and second chromosomes that we recently examined, only *para*^{ts} shows behavioural and physiological phenotypes like those of *nap*^{ts}. Adult *para*^{ts} flies show rapid reversible paralysis at 29 °C (ref. 1). Simultaneous recording of the e.j.p. and nerve compound action potential indicates that the e.j.p. and compound action potential disappear at 37 °C but return when temperature is lowered (Fig. 3). In normal larvae, the e.j.p. and the compound action potential persist up to at least 40 °C (ref. 5). Synaptic transmission is not blocked in *para*^{ts} larvae because a graded e.j.p. could still be elicited electrotonically after failure of active conduction. Therefore, *para*^{ts}, like *nap*^{ts}, specifically blocks axonal conduction at high temperature, as originally suggested by Siddiqi[17].

The *nap*^{ts} and *para*^{ts} gene products may share a related function because the double mutant is lethal even at temperatures permissive for each single mutant as shown in Table 1. A comparison of progeny classes 2 or 3 with 1 indicates that *nap*^{ts} or *para*^{ts} can cause a slight reduction in viability. However, the striking result is the complete failure to recover any double mutant progeny at all (class 4). The same is true for other *para* alleles in combination with *nap*^{ts} (Ganetzky and Wu, unpublished data). The lethality appears specific for the combination of *para* with *nap*, since other *X*-linked temperature-sensitive paralytic mutants show no such synergistic interaction with *nap*^{ts}.

In other examples of synthetic lethality in *Drosophila*, it has been possible to demonstrate at the biochemical level that the mutations involved have related functions[18]. If *nap*^{ts} is shown to disrupt the assembly or function of sodium channels, a similar defect for *para*^{ts} might be indicated. However, the two mutants do not appear to act identically because at room temperature *para*^{ts}, unlike *nap*^{ts}, did not appear to differ significantly from wild type in TTX sensitivity or refractory period. One interesting possibility is that sodium channels are comprised of at least two different protein subunits—one altered by *nap*^{ts} and the other by *para*^{ts}.

Whether or not this notion proves correct, it is certainly the case that the gene products specified by the *nap* and *para* loci play essential roles in membrane excitability. By utilizing genetic and physiological techniques, it should be possible to identify other genes in *Drosophila* that control primary events of excitability in the nervous system. Moreover, we wish to emphasize that analysis of double mutants, as in the case of *nap*^{ts} and *para*^{ts}, can reveal functional relationships between gene products in excitable membranes that would be difficult to detect in any other way.

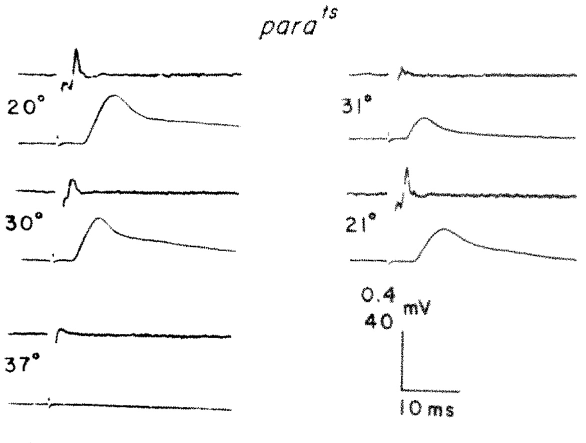

Fig. 3 Continuous recording of compound action potential and evoked e.j.p. from a *para*^{ts} larva at various temperatures. The e.j.p. (bottom trace in each panel) was recorded intracellularly from the same ventrolateral longitudinal muscle fibre. The compound action potential (top traces) was recorded from the nerve bundle containing the motor axons innervating the impaled muscle fibre. As the temperature is raised from 20° to 37 °C, both the e.j.p. and the compound action potential disappear (left). They reappear when the temperature is lowered back to 21 °C (right). The calcium concentration in bath solution was 0.8 mM.

Table 1 Progeny resulting from cross of $\frac{para^+}{Y}\,\frac{nap^{ts}}{nap^{ts}}$ ♂♂ × $\frac{para^{ts}}{para^{ts}}\,\frac{Cy}{nap^{ts}}$ ♀♀ at 23 °C

♀♀		♂♂	
$\frac{para^+}{para^{ts}}\,\frac{Cy}{nap^{ts}}$	$\frac{para^+}{para^{ts}}\,\frac{nap^{ts}}{nap^{ts}}$	$\frac{para^{ts}}{Y}\,\frac{Cy}{nap^{ts}}$	$\frac{para^{ts}}{Y}\,\frac{nap^{ts}}{nap^{ts}}$
2144	1270	1872	0

Cy (Curly) is a dominant wing marker located on a multiply inverted chromosome that does not undergo genetic exchange with its nap^{ts} bearing homologue. The *Cy* chromosome carries a normal allele of nap^{ts}. Four classes of progeny are expected to emerge from the above cross with equal frequencies. The four classes are distinguishable by sex and wing phenotype. Because both nap^{ts} and $para^{ts}$ are recessive, only the last class of progeny among the four is mutant for both $para^{ts}$ and nap^{ts}.

We thank S. Benzer for support and encouragement, L. Kauvar and R. Joyner for allowing us to cite work in progress and our colleagues especially M. Tanouye for comments on the manuscript. Work supported at various times by NSF grant PCM 73-01972 to S. B., Jane Coffin Childs Postdoctoral Fellowship and USPHS grant NS 15390 to B. G., and USPHS grant NS 15350 and NS 15797 to C.-F. W.

Received 28 May; accepted 16 June 1980.

1. Suzuki, D. T., Grigliatti, T. & Williamson, R. *Proc. natn. Acad. Sci. U.S.A.* **68,** 890–893 (1971).
2. Grigliatti, T. A., Hall, L., Rosenbluth, R. & Suzuki, D. *Mol. gen. Genet.* **120,** 107–114 (1973).
3. Ikeda, K., Ozawa, S. & Hagiwara, S. *Nature* **259,** 489–491 (1976).
4. Siddiqi, O. & Benzer, S. *Proc. natn. Acad. Sci. U.S.A.* **73,** 3253–3257 (1976).
5. Wu, C.-F., Ganetzky, B., Jan, L. Y., Jan, Y.-N. & Benzer, S. *Proc. natn. Acad. Sci. U.S.A.* **75,** 4047–4051 (1978).
6. Poodry, C. A. & Edgar, L. *J. Cell Biol.* **81,** 520–527 (1979).
7. Gitschier, J., Strichartz, G. R. & Hall, L. M. *Biochem. biophys. Acta* **595,** 291–303 (1980).
8. West, G. J. & Catterall, W. A. *Proc. natn. Acad. Sci. U.S.A.* **76,** 4136–4140 (1979).
9. Narahashi, T. *Physiol. Rev.* **54,** 813–889 (1974).
10. Jan, L. Y. & Jan, Y.-N. *J. Physiol. Lond.* **262,** 189–214 (1976).
11. Katz, B. & Miledi, R. *Proc. R. Soc. Lond.* **B167,** 23–38 (1967).
12. Jan, Y.-N., Jan, L. Y. & Dennis, M. J. *Proc. R. Soc Lond.* **B198,** 87–108 (1977).
13. Hardie, J. *J. Insect Physiol.* **22,** 661–668 (1976).
14. Hardie, J. & Osborne, M. P. *Comp. Biochem. Physiol.* **57A,** 59–66 (1977).
15. Kauvar, L. M. *CalTech Biol. ann. Report,* 154 (1979).
16. Hodgkin, A. L. & Huxley, A. F. *J. Physiol. Lond.* **117,** 500–544 (1952).
17. Siddiqi, O. in *Regulation of Growth and Differentiated Function in Eukaryotic Cells* (ed. Talwar, G. P.) 541–549 (Raven, New York, 1975).
18. Lucchesi, J. C. *Genetics* **59,** 37–44 (1968).

Non-uniform Ca^{2+} buffer distribution in a nerve cell body

D. Tillotson & A. L. F. Gorman

Department of Physiology, Boston University School of Medicine,
80 E. Concord Street, Boston, Massachusetts 02118

In nerve cells, Ca^{2+} influx through voltage-dependent channels in the membrane causes a transient rise in the intracellular, free Ca^{2+} concentration[1-3]. Such changes have been shown to be important for the release of transmitter at the axon terminal[3,4] and for the control of the movement of ions through channels in the soma membrane[5,6]. The transient behaviour of the rise in Ca^{2+} concentration can, in part, be explained by the presence of sequestering systems in the cell which tend to limit the magnitude and duration of changes in internal Ca^{2+} (refs 7–10). It is possible that systems involved in buffering changes in internal Ca^{2+} are not distributed uniformly throughout the cell. This is particularly likely in the cell body, where a significant portion of the cytoplasm is occupied by the nucleus, whose buffering capacity may differ from that of other cellular regions. We report here that in the soma of a molluscan pacemaker neurone, the machinery responsible for short-term buffering of Ca^{2+} ions is localized near the inner surface of the plasma membrane.

The pacemaker neurone R-15 in the abdominal ganglion of *Aplysia californica* was used, and experiments were carried out in artificial seawater which contained (in mM) 500 NaCl, 10 KCl, 10 $CaCl_2$, 50 $MgCl_2$ and 10 Tris at *p*H 7.7, and at a temperature of 16 °C. In some experiments, Na^+ was completely replaced by Tris. The procedures for iontophoretic injection of ions or pressure injection of purified arsenazo(III), voltage clamping the soma membrane and monitoring changes in intracellular Ca^{2+} with differential absorbance micro-spectrophotometry were similar to those described previously[11,12].

The experimental design is shown in Fig. 1*a*. Arsenazo(III) was injected and its intracellular concentration (about 200 µM) was determined using a small light-accepting probe (~150 µm diameter) which was about half the cell diameter. Starting near the inner membrane surface, an electrode containing 0.2 M $CaCl_2$ was advanced through the cytoplasm in 20-µm increments in a neurone clamped at a holding potential of about −40 mV, and absorbance changes associated with small test Ca^{2+} injections were measured at each increment. A fourth electrode containing 0.5 M EGTA was used to inject EGTA iontophoretically into the cell. The small light-accepting probe, used previously[11,12] for measuring absorbance changes produced by Ca^{2+} injection from a microelectrode, has the disadvantage that

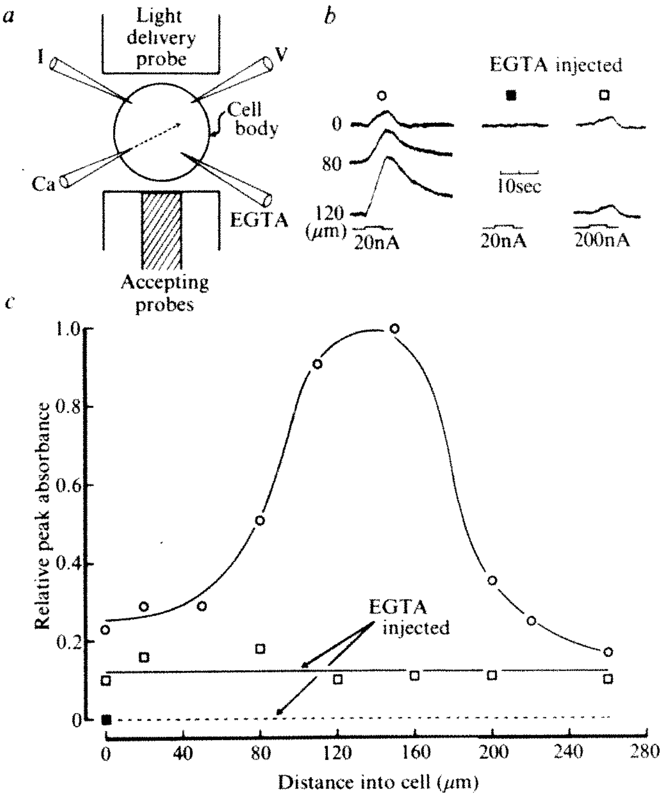

Fig. 1 Effects of Ca^{2+} injections at various distances in the soma cytoplasm on the free, intracellular Ca^{2+} concentration measured with arsenazo(III). *a* Shows the experimental arrangement. The nerve cell soma (cell body) was impaled with voltage (V), current (I), Ca^{2+} injection (Ca) and EGTA injection (EGTA) electrodes and positioned between a pair of fibre optic probes. Large and small (hatched lines) light-accepting probes are shown. *b* Shows the differential absorbance changes at 660–690 nm during Ca^{2+} injections for 5 s (20 or 200 nA) at the indicated distances into the cytoplasm from the cell membrane before (left column) and after injection of EGTA for 5 min (200 nA) (middle and right columns). The arsenazo(III) was 98.6% pure and its intracellular concentration was estimated to be about 200 µM. *c* Shows a plot of the normalized absorbance changes produced by Ca^{2+} injections (5 s, 20 nA) at various distances into the cell from the membrane before (open circles) and after (closed square) EGTA injection. The open squares plot the absorbance changes produced by a 10-fold increase in Ca^{2+} injection intensity (5 s, 200 nA) after EGTA injection. All data are from the same cell.

0028-0836/80/340816—02$01.00

part of the cytoplasm and the plasma membrane are not directly in the light path. With all other factors equivalent, a test Ca^{2+} injection just outside the light path will produce a distorted absorbance signal, with slower rising kinetics and a reduced peak amplitude relative to those produced by an identical injection within the light path. To examine the localization of the Ca^{2+} buffer system, we replaced the small light-accepting probe (after injection of arsenazo(III)) with a probe of 400 μm diameter, which was larger than the average cell diameter (~300 μm), thus rendering all points inside the cell equivalent. This system was tested experimentally using a 300-μm diameter droplet of solution (containing 300 mM KCl and 0.2 mM arsenazo(III) and buffered to a *p*H of 7.3 with 100 mM MOPS) in place of the neurone and injecting Ca^{2+} at different distances within the droplet. The changes in absorbance produced by Ca^{2+} injections were identical at all points within the droplet even at short times (within a few seconds of the injection), when elementary diffusion considerations dictate that the injected Ca^{2+} cannot have equilibrated throughout the droplet. This indicates that the sensitivity of the measurement system does not depend significantly on the position at which the injection is made. The use of a larger light probe, however, results in the transmission of a significant fraction of the incident light around the cell and hence severely limits our ability to quantify absorbance changes in terms of changes in internal Ca^{2+} concentration[12,13], although changes in the relative peak absorbance and in the kinetics of the absorbance can be determined.

Dye absorbance changes associated with small test Ca^{2+} injections (20 nA, 5 s) at different points in the cytoplasm are shown in the first column in Fig. 1*b* and a full set of measurements from the same cell are plotted in Fig. 1*c*. The amplitude of the absorbance signal is taken as an index of the buffering capacity of a region of the cytoplasm near the electrode tip. As the Ca^{2+} microelectrode was advanced into the centre of the cell, the amplitude of the absorbance signal increased and its kinetics decreased, indicating a diminution of buffering strength relative to the cell boundary, but as the electrode tip was moved towards the opposite membrane, the signal amplitude and kinetics returned to control values. Similar results were found in three other cells. The results from all four cells suggest that there may be a cytoplasmic layer near the cell membrane (0–50 μm) which has a different buffering capacity from that found in the centre of the cell.

To control for the possibility that the apparent Ca^{2+} buffering localization at the cell boundary is caused by a peculiarity of the absorbance recording arrangement, the Ca^{2+} chelating agent EGTA was injected iontophoretically into the cell for 5 min at 100 nA. An injection of this duration and intensity is more than sufficient to abolish all absorbance changes in cell R-15 produced by Ca^{2+} influx into the cytoplasm from the external medium during 0.5 s voltage-clamp pulses to all positive membrane potentials. We reasoned that a high internal EGTA concentration, if uniformly distributed throughout the cytoplasm, would render the whole cell equivalent with respect to buffering capacity, and that in these conditions Ca^{2+} injections at various distances through the soma would give absorbance changes of equal amplitude. The localization experiment was repeated after EGTA injection using a 10-fold greater injection current (200 nA, 5 s), because the previous injection level produced no measurable change in absorbance. The predicted result of equivalent intracellular buffering is shown in Fig. 1*b* and *c*. We conclude, therefore, that in normal circumstances the capacity to buffer Ca^{2+} is differentially distributed in the soma, being greatest in a cytoplasmic layer near the cell plasma membrane.

In most cells, buffering of intracellular Ca^{2+} is thought to be controlled by both sequestration by internal organelles and extrusion by systems in the plasma membrane[7–9]. In nerve cells, a membrane-bound Na–Ca exchange system has been suggested as playing a significant part in the maintenance of intracellular Ca^{2+} levels[14] and could explain the observed buffering localization, as Ca^{2+} near the membrane, and hence near the Na–Ca exchange sites, would be extruded more quickly than Ca^{2+} in the cell interior. To test for this possibility, we examined the effect of removal of extracellular Na^+ on the absorbance change associated with Ca^{2+} injection near the inner membrane surface. Removal of external Na^+ should stop the exchange process[1,14], but it had no significant effect on the amplitude or time course of the absorbance change. This result agrees with previous findings from molluscan neurones[15] and suggests that short-term Ca^{2+} buffering may not depend on the Na^+-dependent transport of Ca^{2+} out of the cell. However, the situation with Ca^{2+} influx through the plasma membrane may be entirely different and membrane extrusion systems may be very much more important.

In nerve cells, changes in the total internal Ca^{2+} concentration are caused primarily by influx from the external medium, and evidence from squid axon suggests that the rise in free intracellular Ca^{2+} concentration is confined to the cell periphery[1,16]. The localization of the machinery responsible for Ca^{2+} removal near the inner membrane surface may provide a physical basis for this confinement. It is well known that the nuclear membrane is freely permeable to large molecules and that the cytoplasm is continuous between the nuclear and non-nuclear regions of the cell; the localization of the buffer at the cell periphery therefore suggests that the buffering apparatus may be attached to some structural element in the cytoplasm. The identity of the systems responsible for this localization is uncertain, but could include membrane sites and cytoplasmic proteins which bind Ca^{2+}, and those intracellular organelles (such as mitochondria, endoplasmic reticulum) which sequester Ca^{2+} near the membrane.

This work was supported by USPHS grant NS11429.

Received 26 March; accepted 18 June 1980.

1. Baker, P. F., Hodgkin, A. L. & Ridgway, E. B. *J. Physiol., Lond.* **218,** 709–755 (1971).
2. Stinnakre, J. & Tauc, L. *Nature new Biol.* **242,** 113–115 (1973).
3. Llinás, R., Steinberg, I. Z. & Walton, K. *Proc. natn. Acad. Sci. U.S.A.* **73,** 2918–2922 (1976).
4. Katz, B. & Miledi, R. *J. Physiol., Lond.* **192,** 407–436 (1967).
5. Meech, R. W. *A. Rev. Biophys. Bioengng* **7,** 1–8 (1978).
6. Tillotson, D. *Proc. natn. Acad. Sci. U.S.A.* **76,** 1497–1500 (1979).
7. Baker, P. F. *Ann. N.Y. Acad. Sci.* **307,** 250–268 (1978).
8. Blaustein, M. P., Ratzlaff, R. W. & Kendrick, N. K. *Ann. N.Y. Acad. Sci.* **307,** 195–212 (1978).
9. Brinley, F. J. Jr *A. Rev. Biophys. Bioengng* **7,** 363–392 (1978).
10. Meech, R. W. & Thomas, R. C. *J. Physiol., Lond.* **298,** 111–129 (1980).
11. Thomas, M. V. & Gorman, A. L. F. *Science* **196,** 531–533 (1977).
12. Gorman, A. L. F. & Thomas, M. V. *J. Physiol., Lond.* **275,** 357–376 (1978).
13. Thomas, M. V. *Biophys. J.* **25,** 541–548 (1979).
14. Blaustein, M. P. & Hodgkin, A. L. *J. Physiol., Lond.* **200,** 497–528 (1969).
15. Meech, R. W. & Thomas, R. C. *J. Physiol., Lond.* **265,** 867–879 (1977).
16. Mullins, L. J. & Requena, J. *J. gen. Physiol.* **74,** 393–413 (1979).

Ouabain stimulation of noradrenaline transport in guinea pig heart

Virendra K. Sharma, Lorelle A. Pottick & Shailesh P. Banerjee

Department of Pharmacology and Toxicology, University of Rochester School of Medicine and Dentistry, Rochester, New York 14642

Cardiac glycosides such as ouabain inhibit Na^+-dependent high-affinity noradrenaline uptake in sympathetic nerve terminals by interacting with $(Na^+ + K^+)$ATPase located in the neuronal membrane[1–3]. It has been suggested that the augmentation of noradrenaline concentration at the neuromuscular junctions following the inhibition of its uptake may contribute to the ouabain-induced cardiac arrhythmia seen with toxic doses of the drug[4,5]. Although it is generally accepted that the biochemical basis for the pharmacological response of cardiac glycosides must involve specific interaction of this class of drugs with the cardiac cell membrane Na^+, K^+-exchange pump, the precise molecular mechanism for the improvement of muscle performance by ouabain is controversial[6,7]. Many investigators

claim that cardiac glycosides increase myocardial force of contraction by inhibiting $(Na^+ + K^+)$ATPase[8-10]. According to this hypothesis, such an inhibition might increase the intracellular concentration of Na^+, which may augment the activity of the transmembrane Na^+, Ca^{2+}-exchange pump described by several workers[11-14]. We have found that ouabain stimulates Na^+-dependent transport of noradrenaline by guinea pig heart sympathetic nerve terminals.

There is increasing evidence that low doses of cardiac glycosides increase the contractility of the myocardium and stimulate the active transmembranous transport of monovalent cations[15-18]. Such a conclusion has been vigorously challenged by Michael and co-workers[19,20]. It is possible that the stimulation of cation transport by cardiac glycosides may be observed in intact cells as opposed to broken cell membrane preparations. Thus, Michael and his co-workers[19,20], who used an isolated purified enzyme system, were unable to observe any stimulation of $(Na^+ + K^+)$ATPase activity by ouabain. We decided to investigate this possibility by examining the effects of different concentrations of ouabain on Na^+-dependent noradrenaline transport in sympathetic nerve terminals of cardiac muscle. If the noradrenaline uptake system is tightly coupled to $(Na^+ + K^+)$ATPase[1-5], and low doses of ouabain can stimulate cation transport[15-18], then these low concentrations of this cardiac glycoside must increase velocity of Na^+-dependent noradrenaline uptake into the cardiac sympathetic nerve terminals.

The Na^+-dependent $[^3H]$noradrenaline uptake in guinea pig heart slices was measured as described previously[2,5]. The effect of several concentrations of ouabain on Na^+-dependent $[^3H]$noradrenaline uptake is shown in Table 1. Although 1×10^{-10} M ouabain produced a small stimulation of the Na^+-dependent $[^3H]$noradrenaline uptake, 1×10^{-9} M and 5×10^{-10} M increased the initial velocity of $[^3H]$noradrenaline transport into the cardiac sympathetic nerve terminals by about 28% and 63%, respectively. When the concentration of ouabain was raised to 5×10^{-9} M, a significant inhibition of uptake was observed. Several experiments with different concentrations of ouabain (between 2×10^{-10} M and 8×10^{-10} M) indicated that maximal stimulation of Na^+-dependent $[^3H]$noradrenaline uptake is seen at 5×10^{-10} M ouabain.

Table 1 Effect of different concentrations of ouabain on high-affinity noradrenaline uptake in guinea pig heart slices

Concentration of ouabain (pM)	Specific $[^3H]$noradrenaline uptake (pmol g^{-1} h^{-1})*
0	83.8 ± 2
1	77.1 ± 1
50	79.1 ± 6
100	96.6 ± 7
500	136.7 ± 3‡
1000	107.8 ± 6†
5000	37.2 ± 4†

Male guinea pigs were killed by a blow on the head. Ventricle of the heart was removed immediately and placed in modified Krebs solution (4 °C) and cleared of extraneous tissues as described previously. Modified Krebs solution had the following composition (mM): NaCl, 118; KCl, 4.7; $CaCl_2$, 2.5; $MgCl_2$, 0.54; $NaHCO_3$, 25; NaH_2PO_4, 1; and glucose, 11. EDTA (20 $\mu g\ ml^{-1}$), ascorbic acid (200 $\mu g\ ml^{-1}$) and nialamide (1.25×10^{-5} M), were added to retard the spontaneous oxidation of noradrenaline. Ventricle slices were prepared with a Stadie–Riggs tissue microtome. The slices were weighed and immersed in 10 ml beakers containing 3.8 ml of Krebs solution. All data were obtained from triplicate slices and each experiment was repeated at least once more. Varying concentrations of ouabain (0.1 ml volume) and 26 nM $[^3H]$noradrenaline were added and the slices were shaken in a Dubnoff metabolic incubator at 37 °C in an atmosphere of 95% O_2 and 5% CO_2 for 10 min. Preliminary experiments indicated that the rate of $[^3H]$noradrenaline uptake remained linear for at least 10 min when the weight of the slices was between 20 and 40 mg. Nonspecific accumulation of radioactivity or blanks was routinely determined in triplicate by parallel incubation at 4 °C for 10 min. After incubation, slices were rinsed three times with ice-cold Krebs solution, blotted on filter paper, and placed in 1 ml of ice-cold 0.4 N perchloric acid. Tissues were extracted in the acid for 21 h at 4 °C and this was followed by centrifugation at 3,000g for 10 min in a Sorvall centrifuge (Model GLC-2). An aliquot (0.5 ml) of each sample was transferred to a vial containing 9.5 ml of Scintiverse (Fisher) and counted in a Packard Tri-Carb liquid scintillation spectrometer (Model 3380) at 30% efficiency as determined with internal standards. Tissue/medium ratios for $[^3H]$noradrenaline uptake were calculated as (c.p.m. per g wet weight tissue)/(c.p.m. per ml of medium). Results shown are averages of four experiments and each experiment was run in triplicate.

* Mean ±s.e.m.

† $P < 0.01$ compared with control.

‡ $P < 0.001$ compared with control.

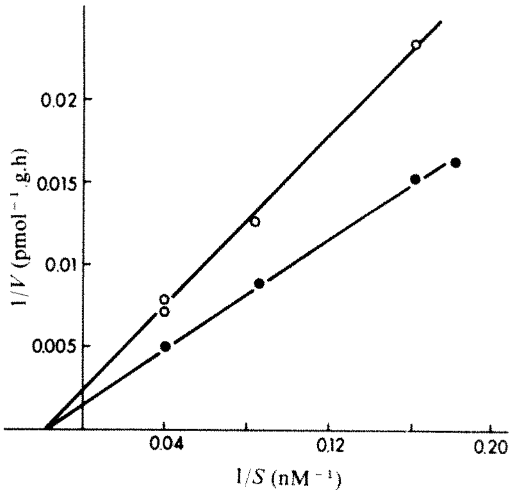

Fig. 1 Reciprocal plots of initial velocity of high-affinity noradrenaline uptake in guinea pig heart slices either in the presence (●) or absence (○) of 0.5 nM ouabain. Each point represents the mean of four determinations. Slopes and intercepts of the lines were determined by the method of least squares.

This increase of $[^3H]$noradrenaline uptake in sympathetic nerve terminals by ouabain may be due to an enhancement of the maximal velocity or apparent affinity of the uptake system for noradrenaline. The biochemical mechanism for the augmentation of $[^3H]$noradrenaline uptake in guinea pig slices by ouabain was evaluated by kinetic analysis. Results shown in Fig. 1 indicate that the maximal velocity (V_{max}) for $[^3H]$noradrenaline uptake into the nerve endings of guinea pig heart slices is 444 pmol per g tissue per h, with the apparent affinity constant (K_m) for noradrenaline being 5.6×10^{-8} M. The presence of 5×10^{-10} M ouabain increased the maximal velocity for $[^3H]$noradrenaline uptake to 667 pmol per g tissue per h without altering the K_m for the neurotransmitter (Fig. 1). These results indicate that ouabain may stimulate $[^3H]$noradrenaline uptake in cardiac sympathetic nerve terminals by increasing the V_{max} without affecting K_m.

There are several implications arising from this observation of stimulation of Na^+-dependent noradrenaline transport in guinea pig heart sympathetic nerve terminals by ouabain. First, there is some controversy on the involvement of $(Na^+ + K^+)$ATPase in the transport for noradrenaline[21]. Recent evidence from several laboratories indicates an intimate relationship between these two transport systems[1-5]. For example, ouabain has been found to show identical species sensitivity for the inhibition of $(Na^+ + K^+)$ATPase and noradrenaline uptake in heart and spleen slices[1-3]. Again, in regenerating sympathetic nerve terminals, ouabain binding sites appear before noradrenaline uptake systems can be detected[5]. As the low concentration of ouabain that is known to stimulate the Na^+, K^+-exchange pump[15-18] activates noradrenaline uptake (Table 1), these two transport systems must be coupled. Second, there is some dispute regarding the mechanism by which ouabain alters the level of noradrenaline at the neuromuscular junction. It has been suggested that ouabain may stimulate release of noradrenaline from sympathetic nerve terminals without affecting the uptake mechanism[22,23]. As ouabain cannot stimulate noradrenaline uptake by augmenting the release of accumulated noradrenaline, there has to be some direct effect of ouabain on high-affinity noradrenaline uptake mechanisms.

In conclusion, this report describes for the first time a stimulation of Na^+-dependent noradrenaline uptake in myocardial sympathetic nerve terminals by ouabain. Since ouabain selectively interacts with cell surface $(Na^+ + K^+)$ATPase, the results of this report provide further insight into the relationship between the monovalent cation transport pump and the noradrenaline uptake system.

This work was supported in part by grant HL-18185 from NIH.

Received 17 January; accepted 18 June 1980.

1. Sharma, V. K. & Banerjee, S. P. *Fedn Proc.* **35,** 405A (1976).
2. Sharma, V. K. & Banerjee, S. P. *Eur. J. Pharmac.* **41,** 417–429 (1977).
3. Stickney, J. L. *Res. Commun. chem. Path. Pharmac.* **14,** 227–235 (1976).
4. Sharma, V. K. & Banerjee, S. P. *Molec. Pharmac.* **13,** 796–804 (1977).
5. Sharma, V. K. & Banerjee, S. P. *Molec. Pharmac.* **15,** 35–42 (1979).
6. Schwartz, A., Lindenmayer, G. & Allen, J. C. *Pharmac. Rev.* **27,** 3–134 (1975).
7. Godfraind, T. *Biochem. Pharmac.* **24,** 823–827 (1975).
8. Besch, H. R., Jr., Allen, J. C., Glick, G. & Schwartz, A. *J. Pharmac. exp. Ther.* **171,** 1–12 (1970).
9. Akera, T., Larsen, F. S. & Brody, T. M. *J. Pharmac. exp. Ther.* **173,** 145–151 (1970).
10. Langer, G. A. *Circulation* **46,** 180–187 (1972).
11. Baker, P. F. *Prog. biophys. mol. Biol.* **24,** 177–223 (1972).
12. Langer, G. A. *A. Rev. Physiol.* **35,** 55–86 (1973).
13. Reuter, H. *Circulation Res.* **34,** 599–605 (1974).
14. Brading, A. F. *Phil. Trans. R. Soc.* B **265,** 35–46 (1973).
15. Ghysel-Burton, J. & Godfraind, T. *Br. J. Pharmac.* **66,** 175–184 (1979).
16. Cohen, I., Daut, J. & Noble, D. *J. Physiol., Lond.* **260,** 55–74 (1976).
17. Blood, B. E. *J. Physiol., Lond.* **251,** 69P (1975).
18. Blood, B. E. & Noble, D. *J. Physiol., Lond.* **266,** 76A (1977).
19. Michael, L., Pitts, B. J. R. & Schwartz, A. *Science* **200,** 1287–1289 (1978).
20. Michael, L. H., Schwartz, A. & Wallick, E. T. *Molec. Pharmac.* **16,** 135–146 (1979).
21. White, T. D. & Keen, P. *Molec. Pharmac.* **7,** 40–45 (1971).
22. Garcia, A. G. & Kirpekar, S. M. *Br. J. Pharmac.* **47,** 729–747 (1973).
23. Paton, D. M. *Br. J. Pharmac.* **49,** 614–627 (1973).

Removal of sialic acid from cardiac sarcolemma does not affect contractile function in electrically stimulated guinea pig left atria

S. E. Harding & J. Halliday

Department of Pharmacology, King's College, London WC2R 2LS, UK

Calcium is essential for the maintenance of contraction in the heart, and it has been suggested that the glycoprotein matrix on the external surface of cardiac cells is a critical factor in the supply of 'activator' calcium to the beating heart[1]. Sialic acid residues are important calcium-binding sites in the matrix and treatment with neuraminidase, an enzyme which cleaves sialic acid from oligosaccharide chains, has been reported to abolish spontaneous contraction in cultured heart cells, without causing general breakdown in the plasma membrane[2,3]. However, we report here that in intact, electrically stimulated guinea pig atrial preparations, neuraminidase treatment produces no significant changes in resting tension or force of contraction. It is also without effect on the response to calcium removal and replacement, and inotropic or toxic concentrations of cardiac glycosides. In these experiments, up to 79% of the total tissue sialic acid was removed, and electron microscopy studies showed that this removal was accompanied by marked reduction of lanthanum binding to the sarcolemma. We therefore conclude that the calcium-binding sialic acid residues in the external matrix of the cardiac cells are of little importance in the maintenance of contractile function in these intact atrial preparations.

In preliminary determinations of the total sialic acid content of guinea pig heart, by incubation of the tissue in 0.05 M H_2SO_4 at 80 °C for 1 h (a modification of the method of Bers[4]), the content in nmol sialic acid per mg wet weight was 1.64 ± 0.12 for atria ($n = 6$) and 1.49 ± 0.14 (s.e.m.) for ventricles ($n = 4$). Although these values are not significantly different, the time course of sialic acid release by neuraminidase was found to be much slower in ventricles than in atria. By method (1) (see Table 1 legend), neuraminidase treatment freed 79% of total sialic acid from the atria within 5 h, whereas the corresponding release from ventricles was only 24%. We therefore decided to use atria in all further experiments.

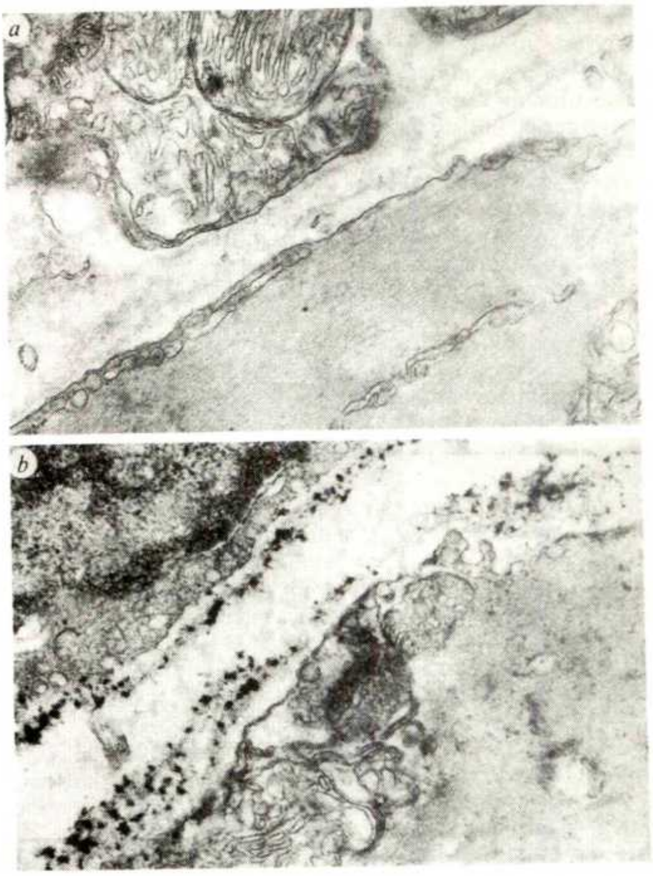

Fig. 1 Electron micrographs of neuraminidase-treated (*a*) and control (*b*) guinea pig left atria. Fixation and lanthanum staining were as described in the text. Note the heavy deposits of lanthanum on the external matrix of control cells, and their absence in neuraminidase-treated atria. ×30,000.

For the experiments in which the force of contraction was monitored, two methods were used for the incubation of the tissue with neuraminidase (see Table 1 legend). The first, in which the atrial strip was detached from the electrodes and incubated in a concentrated enzyme solution, had the advantage that all the neuraminidase-sensitive sialic acid, 1.30 ± 0.06 nmol per mg wet weight ($n = 5$), was removed in the 5-h period (the mean percentage difference between the amount released at 5 h and that at 6 h was $2.4 \pm 1.5\%$, and was not significant). This lack of further release was not due to deterioration of the enzyme, because the 5-h incubation medium was as effective as fresh neuraminidase solution in releasing sialic acid from *N*-acetylneuramin-lactose (from bovine colostrum, Sigma). The second method, in which the enzyme was added to the Krebs solution in the organ bath, enabled the force of contraction and resting tension to be monitored throughout the incubation. However, the sialic acid content of the bath could not be measured directly with this method because the volume of dilution was too great; parallel incubations in small volumes, but with the same ratio of enzyme to Krebs, were required to estimate the release. The amount released by this procedure was 1.07 ± 0.04 nmol sialic acid per mg wet weight ($n = 5$). This represents 65% of the total (82% of the neuraminidase-sensitive) sialic acid content, which is less than that achieved with method (1), but still higher than the 61% removal shown to cause disruption of the external matrix of cultured heart cells[3].

Electron microscopy studies were done to confirm visually that neuraminidase treatment was removing sialic acid residues from the external matrix. Tissues were exposed to concentrated neuraminidase (1 unit ml^{-1}) for 5 h, then transferred to HEPES buffer, composition (mM) 133 NaCl, 3.6 KCl, 1.0 $CaCl_2$, 0.3

$MgCl_2$, 16.0 glucose, 3.0 HEPES (*p*H 7.1), containing 5 mM $LaCl_3$ for 2 h. The temperature was maintained at 37 °C and the solutions were continuously bubbled with 100% O_2. Control tissues were exposed to the acetate buffer alone (see Table 1 legend) during the first 5 h. The tissues were fixed as described in ref. 3.

Preliminary results showed that in neuraminidase-treated tissues, lanthanum binding is greatly reduced in all areas (Fig. 1*a*). Control tissues, however, demonstrate the normal pattern of lanthanum binding described by other workers[3]; that is, large accumulations of lanthanum at the external matrix of the sarcolemma (Fig. 1*b*). This finding supports the biochemical data suggesting that neuraminidase treatment of whole atria is effective in removing at least part of the glycocalyx.

As may be seen in Table 1, the force of contraction of the control atrial preparations declines over the time course of these experiments. This is a well reported phenomenon, termed 'ageing', which Carrier *et al.* have suggested[5] is due to a decrease in calcium binding at the external surface of the sarcolemma; however, sialic acid removal neither enhanced nor attenuated this fall in force, casting some doubt on this hypothesis. In addition, sialic acid removal did not alter the resting tension, indicating that the capacity of the heart to relax was unchanged, and implying that the systems involved in the maintenance of low intracellular calcium between beats had not been affected.

We were particularly interested in the effect of neuraminidase treatment on the response to ouabain, as several reports have suggested that positive inotropic concentrations of cardiac glycosides increase external calcium binding. Ouabain, for example, increased both the density of the negative charges on the cardiac membrane[6] and the amount of La^{3+}-displaceable calcium bound to this surface[7]. We found, however, that neuraminidase treatment had no effect on either the positive inotropic response to 0.2 μM ouabain or the maximum rise in force evoked by a higher concentration. The toxicity of ouabain was assessed by the time to onset of arrhythmias after administration of a toxic concentration, and the rise in resting tension 30 min after this administration. Neither parameter was altered by sialic acid removal (see Table 1).

In the experiments with cultured heart cells, it was reported that neuraminidase treatment increased the amount of ^{45}Ca taken up[2], and the speed of uptake and washout[8]. This observation suggested that the external matrix might in some way regulate calcium entry to or exit from the cell. We therefore examined the effect of neuraminidase on the rate of fall in force of atrial preparations after removal of calcium from the bathing medium, and the subsequent rise on calcium replacement. The method, and the procedure for calculating half-times, are given in Table 2 legend. No differences in rates of decline and recovery of force of contraction between control and neuraminidase-treated preparations could be detected; a slight decrease was seen in the time taken for the force to fall, but the control also showed this change. It was possible to resolve the fall in force after calcium removal into two exponential decay processes[9], and therefore, in case there had been opposing changes in the two processes that were not apparent in the overall half-times, each curve was analysed, and the intercept on the ordinate and the half-life calculated for both the fast and slow decays. Once again, there was no significant difference between control and neuraminidase-treated preparations, indicating that there had been no change in the rate of loss of calcium from, or return of calcium to, those pools associated with maintenance of contraction.

Table 2 Effects of neuraminidase treatment on rates of decrease or recovery of force with calcium removal or replacement, respectively

	Half-time (s) for decrease in force of contraction following Ca^{2+} removal		Half-time (s) for increase in force of contraction following Ca^{2+} replacement	
	Before 5 h incubation	After 5 h incubation	Before 5 h incubation	After 5 h incubation
Control (*n* = 6)	22.9 ± 2.7	16.4 ± 1.1	45.5 ± 3.1	57.5 ± 6.9
Neuraminidase-treated (*n* = 6)	21.3 ± 2.2	18.2 ± 1.1	57.4 ± 4.9	58.3 ± 5.8

Method (2) (see Table 1 legend) was used for neuraminidase treatment of the atrial strip. For calcium removal, the organ bath was drained, then washed through with prewarmed, pre-oxygenated, calcium-free Krebs (calcium not osmotically replaced). Half-time for the decrease in force of contraction was taken as the time for the force to decrease to 50% of that immediately before draining the bath. After 2 min, calcium was re-introduced by injection of 100 mM $CaCl_2$ solution to give a bath concentration of 2.5 mM. Half-time for recovery was the time to reach ½(max-min) force, where max = maximum force of contraction attained within 10 min of calcium replacement, and min = force immediately before replacement. This procedure was repeated three times before and three times after neuraminidase treatment. All values are mean ± s.e.m.

In our experiments, therefore, removal of a large proportion of sialic acid from the membrane had no detectable effect on the function of the intact myocardium. These results are difficult to reconcile with those obtained in cultured cells, where spontaneous beating ceased and calcium exchangeability rose after neuraminidase treatment[2]. A possible explanation for this difference is that the culturing of the cells, which includes trypsin

Table 1 Effect of neuraminidase treatment on resting tension and force of contraction and response to ouabain in guinea pig atria

			Response to ouabain			
	Force of contraction after incubation (%)*	Decrease in resting tension during incubation (%)*	Increase in force of contraction with 0.2 μM ouabain (%)†	Maximum increase in force with ouabain (%)†	Time to onset of arrhythmias after addition of 1 μM ouabain (min)	Increase in resting tension with 1 μM ouabain (%)†
Method (1) (*n* = 4)						
Control	13.5 ± 7.1	—	173 ± 10.3	218 ± 37.0	—	—
Neuraminidase-treated	18.5 ± 5.3	—	163 ± 22.1	292 ± 19.8	—	—
Method (2) (*n* = 8)						
Control	41.9 ± 4.3	28.5 ± 14.2	157 ± 7.2	204 ± 8.9	11.8 ± 4.2	7.5 ± 3.4
Neuraminidase-treated	46.8 ± 2.7	43.0 ± 14.2	153 ± 5.5	211 ± 11.6	18.8 ± 4.5	10.2 ± 6.1

Left atria were halved and mounted in contact with platinum electrodes in a 10-ml organ bath containing Krebs (119 mM NaCl, 4.7 mM KCl, 0.94 mM $MgSO_4.7H_2O$, 1.2 mM KH_2PO_4, 25 mM $NaHCO_3$, 11 mM glucose, 2.5 mM $CaCl_2$) bubbled with 95% O_2/5% CO_2, and stimulated at 3 Hz, 500 μs, supramaximal voltage. In method (1) the tissue was then unhooked from the electrode and placed in 1 ml acetate buffer (50 mM Na acetate, 154 mM NaCl, 9 mM $CaCl_2$, 5 mM KOH and 100 mM Tris-HCl, *p*H 7.4) containing 1 unit ml^{-1} neuraminidase (Behringwerke: 1 unit will split off 1 μmol *N*-acetylneuraminic acid from human α_1-acid glycoprotein in 1 min at 37 °C and *p*H 5.5), and bubbled with 100% O_2. Aliquots (0.2 ml) of the incubation medium were assayed for free sialic acid by the Warren method[10]. After 5 h, when all the neuraminidase-sensitive sialic acid had been split off, the preparation was removed, resuspended in the organ bath and stimulation restarted. After a period of equilibration, ouabain was added to the bath to a concentration of 0.2 μM and the positive inotropic effect allowed to develop for 30 min. In method (2) neuraminidase was added directly to the organ bath to give a concentration of 0.1 units ml^{-1}, and the tissue kept beating throughout the incubation. Parallel experiments using smaller volumes were done to estimate release of sialic acid by this method. After 5 h the neuraminidase was removed by washing the tissue six times with Krebs solution; ouabain was then added to a bath concentration of 0.2 μM as before. After 30 min the concentration was raised to 1 μM and the force of contraction and resting tension were monitored for a further 30 min. The time to onset of arrhythmias and increase in resting tension were taken as indices of ouabain toxicity. Control tissues were treated similarly to test ones, except that neuraminidase was omitted from the acetate buffer. All values given are the mean ± s.e.m. No neuraminidase-treated values differ significantly from control ($P < 0.05$).

* Expressed as a percentage of that immediately before incubation with neuraminidase.

† Expressed as a percentage of that immediately before addition of ouabain.

digestion, may have in some way increased the susceptibility of the matrix to disruption by sialic acid removal. Alternatively, it is just possible that similar changes in calcium permeability did occur in our preparations, but that the reserve capacity of the calcium-sequestering systems of the cell was sufficient to compensate for the extra influx.

The cessation of beating in the neuraminidase-treated, cultured cells might not be due to failure of contraction mechanisms as such, but to a disturbance of pacemaker mechanisms; this could explain why our preparations, which were electrically stimulated, continued to beat after a similar treatment. However, preliminary experiments with spontaneously beating right atria have shown that contractile activity is maintained throughout 5 h incubation in concentrated neuraminidase (1 unit ml^{-1}) at 37 °C. It therefore seems unlikely that sialic acid removal results in a disruption of pacemaker mechanisms.

We have thus shown that treatment of guinea pig atria with neuraminidase can remove up to 79% of tissue sialic acid and strip lanthanum-binding sites from the external sarcolemma. This disruption of the external glycocalyx, however, has no detectable effect on the force of contraction of electrically stimulated atria or the response of these atria to ouabain or calcium-free media. It seems, therefore, that the contribution of the sialic acid residues in the external glycoprotein matrix to contractile function in the guinea pig atrium is negligible.

We wish to thank Mr G. Morgan and Miss K. Bugg for the electron microscope studies, and Drs I. K. M. Morton and J. Littleton for their helpful discussion. S.H. is an MRC student.

Received 15 February; accepted 16 June 1980.

1. Langer, G. A. *Am. J. Physiol.* **235**, H461–H468 (1978).
2. Langer, G. A., Frank, J. S. & Nudd, L. M. *Am. J. Physiol.* **237**, H239–H246 (1979).
3. Frank, J. S. Langer, G. A. Nudd, L. M. & Seraydarian, K. *Circulation Res.* **41**, 702–714 (1977).
4. Bers, D. M. *Biochim. biophys. Acta* **555**, 131–146 (1979).
5. Carrier, G. O., Lullman, H., Neubauer, L. & Peters, T. *J. molec. cell. Cardiol.* **6**, 333–347 (1974).
6. Hungerford, R. T. *et al. Fedn Proc.* **38**, 372 (1979).
7. Nayler, W. G. *J. molec. cell. Cardiol.* **5**, 101–110 (1973).
8. Langer, G. A., Frank, J. S., Nudd, L. M. & Seraydarian, K. *Science* **193**, 1013–1015 (1976).
9. Riggs, D. S. *The Mathematical Approach to Physiological Problems* (MIT Press, London, 1963).
10. Warren L. *J. biol. Chem.* **234**, 1971–1975 (1959).

Covalent linking of photoreactive insulin to adipocytes produces a prolonged signal

Dietrich Brandenburg, Cornelia Diaconescu, Derek Saunders & Peter Thamm

Deutsches Wollforschungsinstitut, Veltmanplatz 8,
D-5100 Aachen, FRG

The first step of insulin's many cellular functions is specific binding to receptors on the plasma membrane of target cells. The subsequent molecular basis of insulin action, particularly the coupling mechanism(s) involved in transmitting the biological message, remains largely unknown[1]. Our approach to the problem centres on the application of a series of well characterized photo-insulins carrying an aryl–azido or nitro–aryl–azido group in positions A1, B1, B2 or B29 (refs 2–4). Specific binding to membrane components could be demonstrated with B1-, B29- (ref. 5) and A1-photo-insulins[6] as well as a B2-derivative[7]. We now report that lipogenesis is increased to, and maintained at, near-maximal levels for several hours after photoinduced covalent binding of B2- (2-nitro,4-azidophenylacetyl)-des-Phe^{B1}-insulin (Napa-DP-insulin[3]) to living adipocytes.

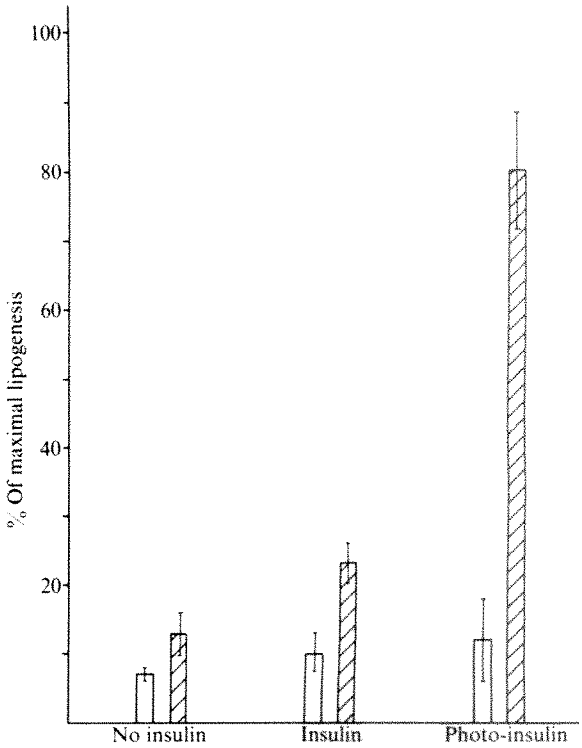

Fig. 1 Effect of covalent binding of photolabelled insulin on lipogenesis in adipocytes. Experiments were carried out with irradiation (▨) and without irradiation (☐) with the indicated preincubations. Per cent values (height of columns) are the ratios of basal lipogenesis (c.p.m. without added insulin) to maximal response (c.p.m. at 10 ng insulin per ml) and represent averages from three independent experiments. Adipocytes were prepared[13] from epididymal fat tissue of four Sprague–Dawley rats (130–160 g) and resuspended in 90 ml of Krebs–Ringer–HEPES buffer, *p*H 7.4, containing 1% bovine serum albumin[14]. Three lots of 25 ml (2–4 × 10^5 cells per ml) were transferred to thermostatted (37 °C) Millipore ultrafiltration chambers (47 mm internal diameter) equipped with boiled Millipore-MF-filters (8 μm pore size) and Teflon-coated stirrer bars. All subsequent operations up to the irradiation period were carried out in light of long wavelength (λ 500 nm). No addition was made to the first chamber (blank). Insulin (monocomponent pork, Novo; 14 pmol ml^{-1}) was added to the second chamber and Napa-DP-insulin (14 pmol ml^{-1}) to the third. The suspensions were equilibrated under slow ~100 r.p.m.) stirring for 5 min. Each chamber was then irradiated from above for 1 min with a Philips HPK 125 W/L UV lamp equipped with a black glass filter (UVW-55, Hanau Wertheim). The lamp was 8 cm from the surface of the stirred adipocyte suspension. After irradiation, the Millipore chambers were sealed. Warm (37 °C) Krebs–Ringer–HEPES buffer (300 ml) was run through in a constant volume washing procedure at a flow rate of 10 ml min^{-1}. After washing, 1-ml aliquots (quadruplicates) of the suspensions were used in a lipogenesis assay according to ref. 8. The incubation time was 2 h. Control experiments were carried out as above, but without irradiation.

A fat cell assay[8] was used to determine the biological effects of Napa-DP-insulin. Adipocytes were first incubated with Napa-DP-insulin (80 ng ml^{-1}) to obtain a receptor occupancy of more than 90% (ref. 9). The photoreactive group was activated by short exposure to UV light of wavelengths 300–400 nm. Cells were then washed for 30 min by a mild constant-volume procedure which diluted the insulin concentration by 1 : 3 × 10^4. The wash period was sufficient to allow for dissociation of the non-covalently bound insulins from the receptor. These adipocytes were then used in a standard lipogenesis assay to determine the effect of prebound and added insulin. In control experiments, adipocytes were incubated in the dark or under UV light with or without unmodified insulin.

It was important to find conditions of activation which would not damage the adipocytes. Appropriate experiments in which

0028–0836/80/340821—02$01.00

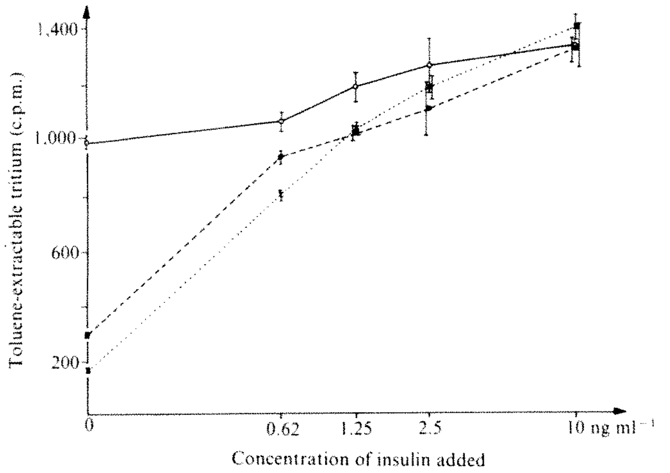

Fig. 2 Insulin-stimulated incorporation of tritium from D-[2-^{3}H] glucose into toluene-extractable lipids of isolated rat fat cells after the following pretreatment: curve 1 (· · · · ·), irradiation only; curve 2 (– – – – –), preincubation with insulin (14 pmol ml^{-1}) + irradiation; curve 3 (———), preincubation with Napa-DP-insulin (14 pmol ml^{-1}) + irradiation.

adipocytes were irradiated for various periods showed that there was no appreciable loss in lipogenic viability after 1 min of irradiation. This represents twice the half life of the photo-label in the same conditions, an activation of about 75% (ref. 4).

Adipocytes preincubated with high concentrations of insulin and subsequently washed gave basal values which were only slightly higher than normal (Fig. 1), and to a somewhat greater extent in the case of Napa-DP-insulin. Adipocytes responded normally to increasing concentrations of insulin in the subsequent lipogenesis assay (data not shown). The higher basal values may be related to the memory effect described by Gliemann[10].

Irradiation of adipocytes which had been preincubated with insulin caused basal lipogenesis to increase from 11 to 23% (Fig. 1). However, the concentration dependence and maximal stimulation in the lipogenesis assay were similar to those of cells preincubated without insulin (see curves 1 and 2 in Fig. 2). A considerable increase in basal lipogenesis was observed after irradiation of adipocytes preincubated with photoreactive insulin (Fig. 1 and Fig. 2, curve 3). This amounted to 75% of the maximal stimulation in two experiments and to 90% in a third. The difference between the experiments was probably due to small uncontrollable variations in the conditions of irradiation.

The addition of progressively higher concentrations of insulin to the medium resulted in a further incorporation of tritium into lipids until maximal response was reached. In all three experiments, the maximal stimulation of lipogenesis in adipocytes preincubated with or without insulin or Napa-DP-insulin was identical within experimental error. Maintenance of normal insulin sensitivity in the latter case indicates that the adipocytes were still fully viable and that the effects were not due to specific damage through photo-sensitization.

Our study demonstrates that photoreactive insulin can be activated without interfering with the viability of isolated adipocytes. Furthermore, covalent binding indeed generates a biological response. This response lasts for a considerable period. The photo-insulin-treated cells are handled for a period of 0.75 h (washing and pipetting) before the 2-h incubation with ^{3}H-glucose, so that the covalent hormone–receptor complex must be functional over at least 2.75 h. However, it is not inconceivable that the complexes are functional as long as they are intact.

Specific covalent binding of insulins with photoreactive groups at the N-terminus of the B-chain to cell membrane preparations has been demonstrated[6,7,11]. Therefore, we deduce that the effect we observed was due to specific linkage to the adipocyte receptor. It is interesting that the N-terminus of the B-chain has previously not been included in the putative receptor-binding region of the hormone[12]. The irreversible complex that is formed is obviously able to elicit the subsequent events of glucose transport and metabolism. Experiments are under way to determine whether a given population of covalently bound hormone–receptor complexes has the same ability to stimulate lipogenesis and glucose transport as the same population of noncovalently linked hormone–receptor complexes.

This work was supported by Sonderforschungsbereich 113 Diabetesforschung Düsseldorf.

Received 7 March; accepted 24 June 1980.

1. Czech, M. P. *A. Rev. Biochem.* **46,** 359–384 (1977).
2. Thamm, P. & Brandenburg, D. in *Peptides 1978–Proc. 15th Eur. Peptide Symp.*, Poland (eds Siemion, Z. & Kupryszewski, G.) 639–642 (Wroclaw University Press, Poland, 1979).
3. Thamm, P., Saunders, D. & Brandenburg, D. in *Proc. 2nd int. Insulin Symp.*, Aachen (eds Brandenburg, D. & Wollmer, A.) 309–316 (De Gruyter, Berlin, 1980).
4. Saunders, D., Thamm, P. & Brandenburg, D. in *Proc. 2nd int. Insulin Symp.*, Aachen (eds Brandenburg, D. & Wollmer, A.) 317–325 (De Gruyter, Berlin, 1980).
5. Wisher, M. H. *et al. Diabetologia* **15,** 282 (1978).
6. Wisher, M. H. *et al. Biochem. biophys. Res. Commun.* **92,** 492–498 (1980).
7. Kühn, L., Meyer, H., Rutschmann, M. & Thamm, P. *FEBS Lett.* **113,** 189–192 (1980).
8. Moody, A. J., Stan, M. A., Stan, M. & Gliemann, J. *Horm. Metab. Res.* **6,** 12–16 (1974).
9. Gammeltoft, S. & Gliemann, J. *Biochim. biophys. Acta* **320,** 16–32 (1973).
10. Gliemann, J., Gammeltoft, S. & Vinten, J. *J. biol. Chem.* **250,** 3368–3374 (1975).
11. Yip, C. C., Yeung, C. W. T. & Moule, M. L., *Biochemistry* **19,** 70–76 (1980).
12. Pullen, R. A. *et al. Nature* **259,** 369–373 (1976).
13. Rodbell, M. *J. biol. Chem.* **239,** 375–380 (1964).
14. Gliemann, J. & Vinten, J. *J. Physiol., Lond.* **236,** 499–516 (1974).

A monomeric insulin from the porcupine (*Hystrix cristata*), an Old World hystricomorph

R. Horuk*, T. L. Blundell*, N. R. Lazarus†, R. W. J. Neville†, D. Stone‡ & A. Wollmer§

* Laboratory of Molecular Biology, Department of Crystallography,
† Biochemical Research Department, The Wellcome Foundation Ltd,
† Biochemical Research Department, The Wellcome Foundation Ltd., Temple Hill, Dartford, Kent DA1 5AH, UK
‡ Protein Chemistry R&D, Wellcome Research Laboratories, Langley Court, Beckenham, Kent, UK
§ Fachgebiet Struktur und Funktion der Proteine, Abteilung Physiologische Chemie, Rheinisch-Westfälische Technische Hochschule, D-5100 Aachen, FRG

The insulins of New World hystricomorph rodents exhibit many novel amino acid changes in primary structure when compared with other mammalian insulins[1–3]. These changes give rise to unusual properties (low potency, failure to self-associate[4–6]) not shared by other naturally-occurring insulins. We report here on the primary structure, zinc-binding properties and circular dichroism (CD) of porcupine insulin (*Hystrix cristata*), the first Old World hystricomorph insulin to be investigated, and discuss the changes in primary structure of the hormone in relation to its properties. Residue B_{22} is strongly implicated as being responsible for the unusual properties of porcupine insulin.

Porcupine insulin differs at seven residues from bovine insulin (Fig. 1) and is unable to bind zinc (Fig. 2). Such behaviour has been noted only in hagfish[7], guinea pig[4] and casiragua[6] insulins. These latter insulins lack the zinc-coordinating B_{10} His together with several other residues on the dimer–dimer interface of bovine insulin which have been implicated in zinc binding and hexamer formation[8]. As these residues are conserved in porcupine insulin, an alternative explanation is required to account for its failure to bind zinc.

The CD spectrum of porcupine insulin shows concentration independence in both the near and far UV (Fig. 3). The intensity of the tyrosyl CD band of bovine insulin at 275 nm has been shown to be dependent on concentration and has been largely

	1	2	3	4	5	6	7	8	9	10	11	12	13	14	15	16	17	18	19	20	21	22	23	24	25	26	27	28	29	30
A Chain																														
Bovine	Gly	Ile	Val	Glu	Gln	Cys	Cys	Ala	Ser	Val	Cys	Ser	Leu	Tyr	Gln	Leu	Glu	Asn	Tyr	Cys	Asn									
Porcupine				Asp				Thr	Gly								Gln													
B Chain																														
Bovine	Phe	Val	Asn	Gln	His	Leu	Cys	Gly	Ser	His	Leu	Val	Glu	Ala	Leu	Tyr	Leu	Val	Cys	Gly	Glu	Arg	Gly	Phe	Phe	Tyr	Thr	Pro	Lys	Ala
Porcupine																					Asn	Asp					Arg			

Fig. 1 Comparison of the primary structures of bovine and porcupine.

assigned to perturbation of the tyrosines at B$_{26}$ and B$_{16}$, which become buried as the hormone dimerizes (W. Strassbürger, J. Fleischauer and A.W., unpublished results). Because these residues are conserved in porcupine insulin, one would expect a concentration dependence at 275 nm if dimerization occurred. Therefore, the lack of concentration dependence is further proof of the inability of porcupine insulin to dimerize. As porcupine insulin is monomeric, its CD spectrum is compared with that of monomeric bovine insulin (that is, at concentrations below 10^{-6}M). The CD spectra of the two insulins can be seen to be more similar at 275 nm (Fig. 4). However, the positive band at 196 nm in bovine insulin is blue-shifted to 193 nm in porcupine insulin and is reduced in ellipticity. The negative extremum found at 208 nm in bovine insulin also shows reduced ellipticity in porcupine insulin. The ellipticity of the bands at 196 and 208 nm are dependent on backbone conformation rather than on side-chain chromophores and have been largely assigned to α-helix. These data suggest that at *p*H 8.4 the tertiary structures of porcupine and bovine insulins are different. On acidification to *p*H 2, the CD spectrum of porcupine insulin more closely resembles that of bovine insulin measured at neutral *p*H; at 275 nm the two spectra are almost indistinguishable, although differences at 196 nm are still apparent (Fig. 4). The acidification of porcupine insulin seeks to alter its tertiary structure towards a more 'bovine-like' insulin conformation.

We explain these observations as follows. In bovine and most other insulins the conformation of the hormone may be stabilized by a complementarity of charge betwen B$_{22}$ Arg guianidinium group and A$_{21}$ Asn carboxylate[8]. Both enzymatic cleavage of the A$_{21}$ Asn (ref. 9) and substitution of the B$_{22}$ Arg (ref. 10) result in a modification of the tertiary structure of the hormone and affect its ability to aggregate[5,9,10]. The substitution B$_{22}$ Arg by Asp in porcupine insulin (Fig. 1) will bring two negative charges into close proximity unless there is a change of conformation, which may also result in a loss of zinc binding and self-association. At low *p*H, protonation of either B$_{22}$ Asp or the A$_{21}$ α-carboxylate may remove charge–charge repulsion and allow a close approach of the B$_{22}$–A$_{21}$ residues, resulting in the change of tertiary structure of porcupine insulin towards the conformation of the bovine molecule. A similar mechanism has been suggested for the effect of acidification of guinea pig insulin[11].

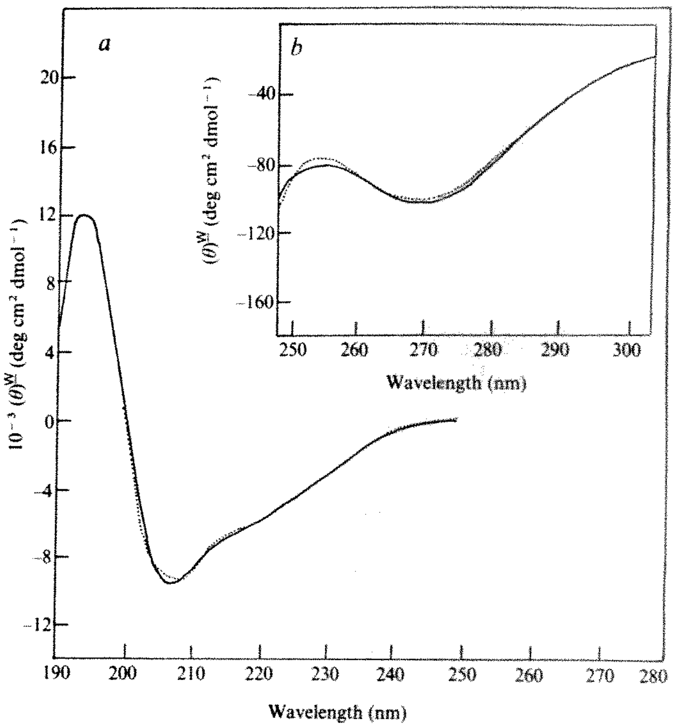

Fig. 3 Circular dichroism spectrum of porcupine insulin as a function of concentration. ——, 4×10^{-5}M porcupine insulin; · · · ·, 4×10^{-6}M porcupine insulin in 0.025 M Tris buffer, *p*H 8.4, zinc free. Bovine insulin has a concentration-dependent CD spectrum at both 222 nm and 275 nm (ref. 5).

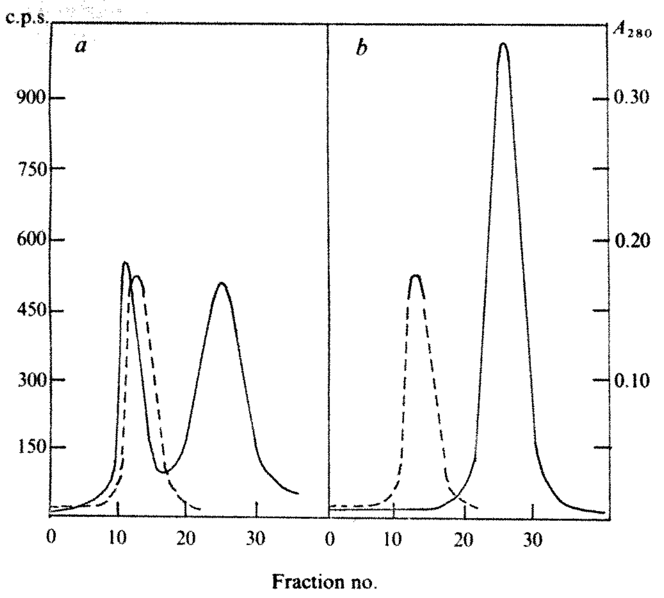

Fig. 2 The formation of ^{65}Zn–insulin complexes by bovine (*a*) and porcupine (*b*) insulins and their separation from free ^{65}Zn ions on a Sephadex G-25 column (1.5 × 30 cm) at *p*H 7.4 in a Veronal buffer[4], 3 ml fraction volumes collected. – – –, Insulin; ——, ^{65}Zn.

The affinity of binding of porcupine insulin to rat liver plasma membrane insulin receptors and its ability to stimulate the conversion of [3-^{3}H]glucose into lipid by isolated rat fat cells were determined. The most notable property of porcupine insulin revealed by these assays, apart from the decrease in biological potency of the hormone, was the discrepancy between the receptor binding affinity, 25%, and the biological activity, 4%, of the hormone (both relative to bovine insulin). Similar discrepancies have been found in hagfish insulin[12] and in several

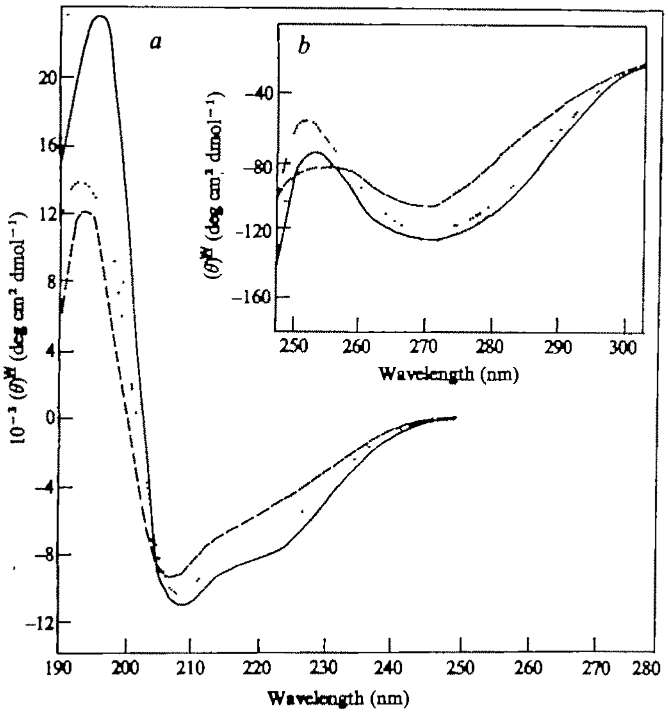

Fig. 4 Circular dichroism spectrum of porcupine insulin at *p*H 2.0 and 8.4 and of bovine insulin at *p*H 7.8. – – –, Porcupine insulin 4×10^{-5}M, *p*H 8.4; · · · ·, porcupine insulin 4×10^{-5}M, *p*H 2.0; ——, bovine insulin 4×10^{-6}M, *p*H 7.8. All are in 0.025M Tris buffer at the *p*H indicated, zinc free.

insulin analogues[13]. We are unable to detect a common factor between these insulins and cannot explain the discrepancy. The decrease in potency of porcupine insulin is probably due to the substitution of the B_{22} Arg, because this is the only residue not conserved in the putative receptor binding site proposed by Pullen *et al.*[14]. A similar substitution, B_{22} Arg to Asp, arises in guinea pig insulin and has been cited by Zimmerman *et al.*[15] as being responsible for the low potency of this insulin. A recently synthesized analogue of bovine insulin substituted only at B_{22} Arg to Asp has been reported to have a reduced potency (K. Yueh-ting, personal communication).

Other substitutions in the sequence of porcupine insulin which might also contribute to its decrease in binding affinity are at A_4 Glu to Asp, B_{21} Glu to Asn, and B_{27} Thr to Arg, all of which lie on the periphery of the receptor binding region of the hormone[14]. Note also that hagfish insulin, which also has a substitution at B_{21} Glu (Glu to Val), has a greatly reduced potency[12]. This insulin has conserved all the residues involved in receptor binding and has a nearly identical conformation to that of bovine insulin[16]. Thus, it is likely that the substitution at B_{21} makes an important contribution to the decrease in potency of porcupine insulin.

Examination of the primary structure of four New World hystricomorph insulins reveals no one amino acid substitution that is characteristic of this suborder[3]. All the insulins share the property of low potency (blood glucose lowering, or [3-^{3}H]glucose conversion into lipid) when compared with bovine or porcine insulin. Scrutiny of the porcupine insulin sequence also fails to show any characteristic amino acid substitutions. Low potency persists. We speculate that hystricomorph rodents, both New and Old World[17], have low-potency insulins because of a common evolutionary pressure. This pressure has resulted in a reduction of the role of insulin as a modifier of glucose metabolism, as well as a change in the insulin receptor[3]. We speculate that another function of insulin has been consequently upgraded. One such function could be its mitogenic activity.

We thank Professor S. Gombe for organizing the collection of porcupine pancreas, and Drs A. J. B. Haigh and D. G. Rae (Wellcome Kenya Ltd) for maintaining contact and successfully preserving and despatching the glands. R.H. thanks the SRC for a CASE Studentship.

Received 28 February, accepted 9 June 1980

1. Blundell, T L & Wood, S P. *Nature* **257**, 197–203 (1975)
2 Smith, L F *Diabetes* 21, Suppl 2, 457–460 (1972)
3 Horuk, R *et al* *Nature* **279**, 439–440 (1979)
4 Zimmerman, A E, Kells, D I L & Yip, C C *Biochem biophys Res Commun* **46**, 2127–2133 (1972)
5 Wood, S P, Blundell, T L, Wollmer, A, Lazarus, N R & Neville, R W J *Eur J. Biochem* **55**, 531–542 (1975)
6 Horuk, R *et al* in *Hormones and Cell Regulation* (eds Dumont, J E & Nunez, J) (Elsevier, Amsterdam, in the press)
7 Peterson, J D, Steiner, D. F., Emdin, S O & Falkmer, S *J biol Chem* **250**, 5183–5191 (1975)
8 Blundell, T L, Hodgkin, D C, Dodson, G G. & Mercola, D *Adv Protein Chem* **26**, 279–402 (1972)
9 Goldman, J. & Carpenter, F H *Biochemistry* 13, 4566–4574 (1974)
10 Zimmerman, A E. & Yip, C. C *J. biol Chem* **249**, 4021–4025 (1974)
11 Wood, S P thesis, Univ Sussex (1976)
12 Emdin, S O, Gammeltoft, S & Gliemann, J *J biol Chem* **252**, 602–608 (1977)
13 Sonksen, P H *Nature* **282**, 11–12 (1979)
14 Pullen, R. A. *et al* *Nature* **259**, 369–373 (1976)
15 Zimmerman, A E, Moule, M L & Yip, C. C *J biol Chem* **249**, 4026–4029 (1974)
16 Cutfield, J F *et al* *J molec Biol* **132**, 85–100 (1979)
17 Wood, A E. in *The Biology of Hystricomorph Rodents* (eds Rowlands, I W & Weir, B J) 21–51 (Academic, London, 1974).

Crystal structure of a ribosomal component at 2.6 Å resolution

Marie Leijonmarck, Stig Eriksson & Anders Liljas

Institute of Molecular Biology, Uppsala University, Box 562,
S-751 22 Uppsala, Sweden

Structural information about the ribosomes has been sought in many ways[1,2]. It is known that the 50S subunit of *Escherichia coli* ribosomes contains four copies of the ribosomal protein L7/L12 (refs 3–7) in a unique region[8,9]. A complex can be isolated consisting of those four copies bound to another ribosomal protein, L10 (refs 10–13). L7/L12 aggregates into elongated dimers in solution[14,15]. Ribosomes deprived of L7/L12 have a reduced affinity for supernatant factors such as EF-Tu and EF-G and almost no capacity for factor-dependent GTP hydrolysis[16–18]. The sequence of the 120 amino acid residues in L7/L12 from *E. coli* has been determined[19], and two domains of L7/L12 (residues 1–36 and 53–120, respectively) have been crystallized separately[20]. We now report the first crystal structure of a ribosomal component, a C-terminal fragment (CTF) of the protein L7/L12 from *E. coli*, determined to 2.6 Å resolution. The CTF has a compact, plum-shaped tertiary structure with a high content of secondary structure. The three α-helices and three β-strands in CTF account for 32% α-helix and 14% β-structure in the intact L7/L12 protein. A binding site for anions shows some resemblance to the known nucleotide binding site in many proteins.

Ribosomes, subunits, the protein L7/L12 and its fragments were obtained as described earlier[11,20]. The crystallization of CTF started with a solution containing 0.2 M citrate *p*H 3, 10 mM $MgSO_4$, 0.8 M $(NH_4)_2SO_4$ and 2–10 mg ml⁻¹ protein. Crystals were obtained in hanging drops at 20 °C by vapour diffusion against 4 M $(NH_4)_2SO_4$. These bipyramidal crystals grew to a maximum length of about 0.4 mm over a period of 1–2 months. Before use the crystals were washed in 4 M $(NH_4)_2SO_4$. Native data were collected on a crystal in 4 M $(NH_4)_2SO_4$ at *p*H 4.2. Two heavy atom derivatives were used: 2 mM *p*-chloromercuribenzene sulphonic acid (PCMBS) at *p*H 5.2 and 1 mM $KAu(CN)_2$ at *p*H 4.2. They were soaked for 3 days. These crystals belong to the space group $P4_32_12$ with cell dimensions $a = b = 54.7$ Å and $c = 42.5$ Å and contain one molecule of CTF (molecular weight ≈ 6,900) per asymmetric unit. X-ray intensities were collected at +4 °C on a Philips-Stoe computer-controlled 4-circle diffractometer[21]. The 2,218 independent reflections in the 2.6-Å resolution sphere were collected on one native crystal. For the heavy atom derivatives, Friedel pairs were measured at ±2θ in blocks of 100 reflections. Data were cor-

0028-0836/80/340824—03$01.00

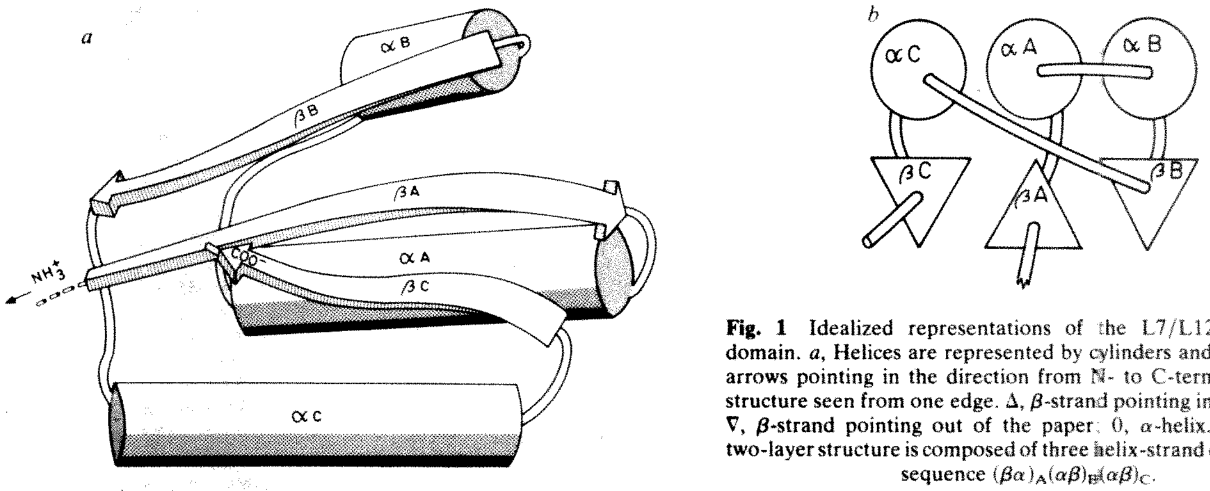

Fig. 1 Idealized representations of the L7/L12 C-terminal domain. *a*, Helices are represented by cylinders and β-strands as arrows pointing in the direction from N- to C-terminus. *b*, The structure seen from one edge. Δ, β-strand pointing into the paper; ∇, β-strand pointing out of the paper. 0, α-helix. This simple two-layer structure is composed of three helix-strand couples in the sequence $(\beta\alpha)_A(\alpha\beta)_B(\alpha\beta)_C$.

rected for Lorentz-polarization effects and for radiation damage and a semi-empirical absorption correction was applied[22].

The heavy atom positions were determined from three-dimensional difference Patterson functions, calculated with coefficients including the anomalous scattering[23]. The Patterson map of the PCMBS derivative was interpretable in terms of a single PCMBS site with the Hg atom as well as the S atom on the crystallographic 2-fold axis. The major site of the gold derivative was obvious from the Patterson map, whereas minor sites were derived from cross-phased difference Fourier maps. With phase angles in the two enantiomorphic space groups derived from the PCMBS derivative alone, two difference Fouriers of the gold cyanide derivatives were calculated. The clear difference in peak height showed the space group to be $P4_32_12$. The final state of the least squares refinement is shown in Table 1. Using the phase angles obtained, a 'best' native Fourier[24] was calculated.

The electron density map shows a clear distinction between solvent and protein. The protein part was interpreted as a single continuous polypeptide chain. A unique alignment could be made of the amino acid sequence (residues 53–120) with regard to the chain tracing. Rough coordinates were measured from the map as a guideline for the model building on a Vector General 3404 graphical display unit. The program package FRODO by Jones[25] was used.

The C-terminal fragment of L7/L12 is a plum-shaped molecule of approximate dimensions 20×20×35 Å. It is composed of three α-helices and three β-strands, all lying roughly along the long axis of the molecule (Fig. 1). The three helices form one layer and the antiparallel β-strands form a second layer with the usual twist[26]. We have found no other protein containing this simple arrangement of secondary structure elements.

L7/L12 has a high proportion of charged residues. Nevertheless, all the residues between the two layers of secondary structure are hydrocarbon side chains (Fig. 2). These residues are never exchanged for polar residues in any of the three known sequences (Fig. 3).

A surprisingly large surface area on the β-sheet side of the CTF molecule is composed of only hydrophobic side chains (Ile 57, Ala 61, Leu 78, Ala 90, Pro 91 and Ala 93). This hydrophobic surface may ultimately be found to be a surface for contact of CTF with other regions of the L7/L12 polypeptide or for other proteins[27]. The hydrophobic surface of CTF is lined by acidic residues, Asp 55, Glu 82, Asp 85, Glu 96 and Glu 118 and the C-terminal carboxyl group.

CTF obviously has a compact domain structure. This agrees well with the following observations: the spontaneous cleavage[20] seems to have occurred where the polypeptide enters into the domain; limited proteolysis experiments also yield a very similar fragment[27]; a comparison of the L7/L12 sequences from three species shows that the region just before residue 53 is hydrophilic, highly variable and has frequent deletions[5].

CTF has about 38 residues (56%) in α-helices and 17 residues (25%) in β-strands, 32% and 14%, respectively, of the 120 residues in L7/L12. A high helical content for L7/L12 has been observed by many investigators from circular dichroism (CD) spectra[3,28–31]. Two groups have observed 10–20% β-structure[3,31] by analysis of the entire far-UV region of the CD spectrum. With so much β-structure in CTF, there would be

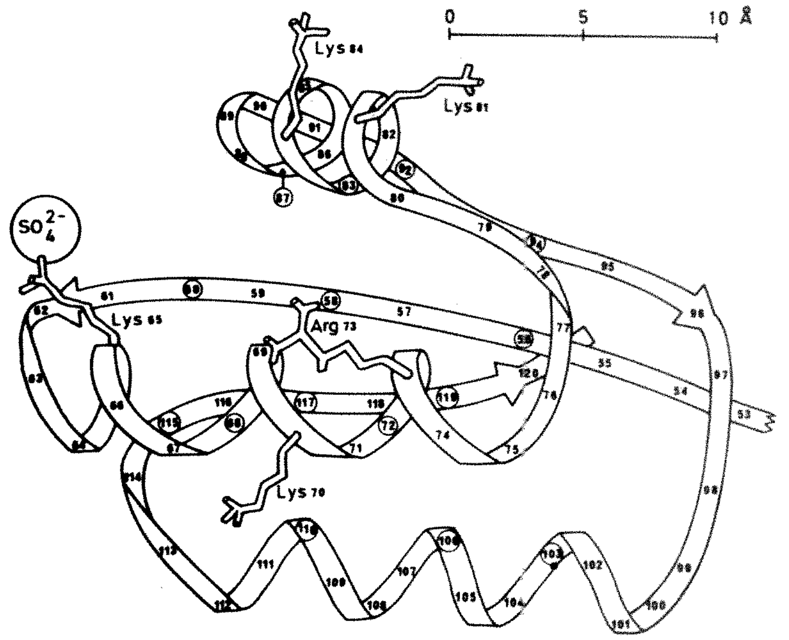

Fig. 2 The structure of the L7/L12 C-terminal domain shown as a ribbon. The approximate location of each residue is indicated. This view of the molecule is opposite to the one in Fig. 1. The residues pointing into the hydrophobic core are in circles. This side of the molecule has five basic residues specially indicated here, without counter ions from the protein. A very significant electron density, best interpreted as a bound sulphate ion, is observed near Gly 62. This binding has some similarities to the nucleotide binding family of proteins.

little, if any, β-structure in the N-terminal part of the L7/L12 protein.

Several predictions of the secondary and tertiary structure of L7/L12 have been made[32-35], all inconsistent with the CTF structure in Fig. 2. For example, Ptitsyn *et al.*[32] predicted the three α-helices but missed the three β-strands. All other attempts overestimated the α-helical content. Even when the occurrence of β-structure was considered (ref. 35 and Argos and A.L., unpublished work), a correct assignment of the β-strand was impossible.

An unusual feature of L7/L12 is its resistance to complete denaturation, for which one domain of the protein seems to be responsible[29,31]. As this contains the β-structure it must be the C-terminal domain. Two reasons for this stability must be the high amount of residues in secondary structure and the extremely hydrophobic interior. A domain with this stability would be unlikely to adopt different conformations in ribosomes, solution or crystals. Several observations suggest that the C-terminal domains of the four L7/L12 molecules are located at the tip of one of the protruberances on the 50S particle[8,27].

A globular electron density, best explained as a sulphate, is located near the turn between the β_A-strand and the α_A-helix. This site is analogous to that found in a large family of enzymes that bind nucleotides or other anions at the junction between the C-terminal side of a β-strand and the N-terminal of a helix[36]. The sulphate ion is bound close to residues Ala 61, Gly 62 and Lys 65, all three being conserved in the three known sequences (Fig. 3).

The protein L7/L12 must be present for optimal function of the ribosome[16,37]. One of the functions of the protein is to mediate the EF-Tu- and EF-G-dependent GTP hydrolysis[18]. The complete C-terminal domain seems to be required for this function[38,39]. Several pieces of evidence[27] make it tempting to believe that the EF-Tu molecule is bound to the ribosome with phosphates of the GTP molecule at the anion binding site of the L7/L12 C-terminal domain.

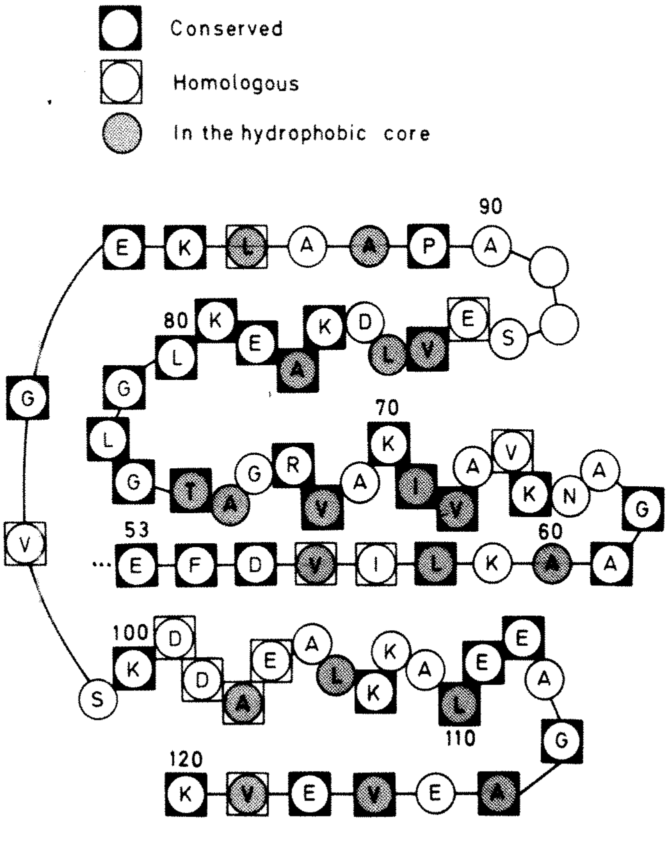

Fig. 3 The C-terminal amino acid sequence[19] arranged into the various secondary structure elements. Amino acids in helices are in a wavy arrangement without connecting lines, and residues in β-strands are connected with horizontal lines. Invariant and homologous residues between the three complete sequences known[5] are enclosed in shaded or light boxes. The shaded circles indicate residues being part of the hydrophobic core. The two empty circles before residue 90 indicate that the sequence from *Bacillus subtilis* has two more residues in this region. The one-letter code for amino acids is used[40].

Table 1 Heavy atom parameters and some refinement statistics

Derivative	Site*	x	y	z	M	B	R_K	$\langle F_H\rangle/\langle E\rangle$
PCMBS	Hg	0.113	0.113	ND	40.	13.1	0.09	2.6
	S	0.026	0.026	ND	9.4	7.2		
	Cl(1)	0.097	0.132	0.104	13.6	7.1		
	Cl(2)	0.148	0.122	0.265	13.3	8.3		
	Cl(3)	0.136	0.084	0.205	9.0	−2.7		
$KAu(CN)_2$	Au(1)	0.423	0.257	0.415	44.7	15.8	0.12	1.6
	Au(2)	0.413	0.259	0.495	24.4	25.9		
	Au(3)	0.285	−0.012	0.168	19.8	45.5		
	Au(4)	0.170	0.433	0.248	11.4	52.1		
	Au(5)	0.073	0.418	0.518	6.7	11.9		

Mean figure of merit = 0.72. B = isotropic temperature factor (Å^2); $R_K = \Sigma|F_{PH,o} - F_{PH,c}|/\Sigma|F_{PH,o}|$; $\langle F_H\rangle/\langle E\rangle$ = the average heavy atom structure factor/the average lack-of-closure error; M = occupancy in electrons on an approximate absolute scale; ND, parameter not refined.

* Indicated atom used for form factor calculation.

We thank Professor C. G. Kurland for stimulating collaboration and encouragement, Professor C. I. Brändén, Dr D. Donner, Dr T. A. Jones, Dr I. Pettersson, Professor B. Strandberg and Dr B.-O. Söderberg for valuable discussions, help, suggestions and support, and B. Karlsson and B. Wiklund for technical assistance. This work has been supported by the Swedish Natural Science Research Council, Knut and Alice Wallenberg's Foundation and the Magnus Bergvall Foundation.

Received 14 April; accepted 20 June 1980.

1. Kurland, C. G. *A. Rev. Biochem.* **46,** 173–200 (1977).
2. Garrett, R. A. *Int. Rev. Biochem.* **25,** 121–177 (1979).
3. Möller, W., Castleman, H. & Terhorst, C. P. *FEBS Lett.* **8,** 192–196 (1970).
4. Möller, W. in *Ribosomes* (eds Nomura, M., Tissières, A. & Lengyel, P.) 711–731 (Cold Spring Harbor, New York, 1974).
5. Matheson, A. T., Möller, W., Amons, R. & Yaguchi, M. in *Ribosomes* (eds Chambliss, G. *et al.*) 297–332 (University Park, Baltimore, 1979).
6. Hardy, S. J. S. *Molec. gen. Genet.* **140,** 253–274 (1975).
7. Subramanian, A. R. *J. molec. Biol.* **95,** 1–8 (1975).
8. Strycharz, W. A., Nomura, M. & Lake, J. A. *J. molec. Biol.* **126,** 123–140 (1978).
9. Boublik, M., Hellmann, W. & Roth, H. E. *J. molec. Biol.* **107,** 479–490 (1976).
10. Pettersson, I., Hardy, S. J. S. & Liljas, A. *FEBS Lett.* **64,** 135–138 (1976).
11. Pettersson, I. & Liljas, A. *FEBS Lett.* **98,** 139–144 (1979).
12. Pettersson, I. *Nucleic Acids Res.* **6,** 2637–2646 (1979).
13. Gudkov, A. T., Tumanova, L. G., Gongadze, G. M. & Bushuev, V. N. *FEBS Lett.* **109,** 34–38 (1980).
14. Wong, K.-P. & Paradies, H. H. *Biochem. biophys. Res. Commun.* **61,** 178–184 (1974).
15. Österberg, R., Sjöberg, B., Liljas, A. & Pettersson, I. *FEBS Lett.* **66,** 48–51 (1976).
16. Hamel, E., Koka, M. & Nakamoto, T. *J. biol. Chem.* **247,** 805–814 (1972).
17. Sander, G., Marsh, R. C. & Parmeggiani, A. *Biochem. biophys. Res. Commun.* **47,** 866–873 (1972).
18. Koteliansky, V. E., Domogatsky, S. P., Gudkov, A. T. & Spirin, A. S. *FEBS Lett.* **73,** 6–11 (1977).
19. Terhorst, C., Möller, W., Laursen, R. & Wittmann-Leibold, B. *Eur. J. Biochem.* **34,** 138–152 (1973).
20. Liljas, A., Eriksson, S., Donner, D. & Kurland, C. G. *FEBS Lett.* **88,** 300–304 (1978).
21. Söderberg, B. O., Holmgren, A. & Brändén, C. I. *J. molec. Biol.* **90,** 143–152 (1974).
22. North, A. C. T., Phillips, D. C. & Mathews, F. S. *Acta crystallogr.* **A24,** 351–359 (1968).
23. Matthews, B. W. *Acta crystallogr.* **20,** 82–86 (1966).
24. Blow, D. M. & Crick, F. H. C. *Acta crystallogr.* **12,** 794–802 (1959).
25. Jones, T. A. *J. appl. Crystallogr.* **11,** 268–272 (1978).
26. Chothia, C. *J. molec. Biol.* **75,** 295–302 (1973).
27. Leijonmarck, M., Pettersson, I. & Liljas, A. *7th Aharon Katzir-Katchalsky Conf.* (in the press).
28. Dzionara, M. *FEBS Lett.* **8,** 197–200 (1970).
29. Boublik, M., Visentin, L. P., Weissbach, H. & Brot, N. *Archs Biochem. Biophys.* **198,** 53–59 (1979).
30. Gudkov, A. T., Khechinashvili, N. N. & Bushuev, V. N. *Eur. J. Biochem.* **90,** 313–318 (1978).
31. Luer, C. A. & Wong, K.-P. *Biochemistry* **19,** 178–183 (1980).
32. Ptitsyn, D. B., Denesyuk, A. I., Finkelstein, A. V. & Lim, V. I. *FEBS Lett.* **34,** 55–57 (1973).
33. Wittmann-Liebold, B., Robinson, S. M. L. & Dzionara, M. *FEBS Lett.* **81,** 204–213 (1977).
34. Gudkov, A. T., Behlke, J., Vtiurin, N. N. & Lim, V. I. *FEBS Lett.* **82,** 125–129 (1977).
35. Luer, C. A. & Wong, K.-P. *Biochemistry* **18,** 2019–2027 (1979).
36. Rossmann, M. G. & Argos, P. *Molec. cell. Biochem.* **21,** 161–182 (1978).
37. Pettersson, I. & Kurland, C. G. *Proc. natn. Acad. Sci. U.S.A.* (in the press).
38. Agthoven, A. J., Maassen, J. A., Schrier, P. I. & Möller, W. *Biochem. biophys. Res. Commun.* **64,** 1184–1191 (1975).
39. Koteliansky, V. E., Domogatsky, S. P. & Gudkov, A. T. *Eur. J. Biochem.* **90,** 319–323 (1978).
40. Dayhoff, M. O. in *Atlas of Protein Sequence and Structure* (National Biomedical Research Foundation, Silver Spring, Maryland, 1972).

BOOK REVIEWS

The growing pains of Robert Oppenheimer

Rudolf Peierls

Frank Oppenheimer

Robert Oppenheimer, 1926 or 1927 — "the young researcher whose professors had doubts about his scientific future . . .".

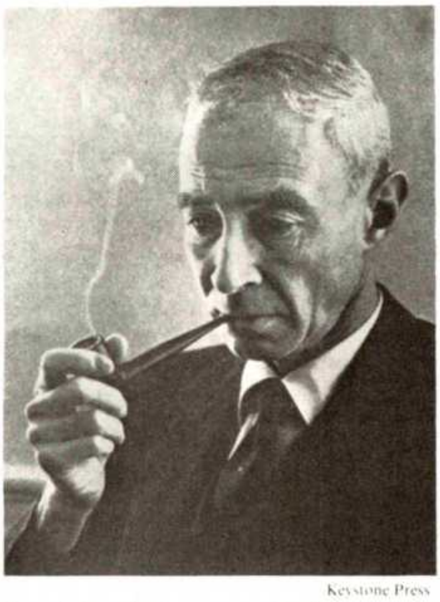

Keystone Press

Oppenheimer in later years, after his success as director of Los Alamos and the ordeal of the "Oppenheimer Trials".

Robert Oppenheimer: Letters and Recollections. Edited by Alice Kimball Smith and Charles Weiner. Pp.250. (Harvard University Press: 1980.) $20, £12.

ROBERT Oppenheimer was one of the most famous scientists of his time, not so much for his contributions to theoretical physics, although these were substantial enough, but as mentor of a large number of successful theoreticians, and above all for his direction of the Los Alamos Laboratory at which the atom bomb was developed and produced during the Second World War.

The impressions he made on superficial acquaintance were very different at different times and on different occasions, and sometimes appeared hard to reconcile. The shy and introverted young boy and student became the successful director of a vast enterprise, successful very largely by his skill in dealing with people. The young researcher, whose professors had doubts about his scientific future because he had difficulty in expressing himself in writing, became famous for always finding the *mot juste* to sum up a situation. His lightning speed of understanding, which often produced the answer or a comment before his questioner had completed half his explanation, would on occasions make him miss the point of an important new idea, and he could meet presentations of such ideas by young colleagues with withering criticism. The ivory-tower scholar who did not know or care much about public affairs found his social conscience in the late 1930s by taking an interest in liberal and left-wing groups (an interest which formed part of the accusations in the security hearings against him), and later became a national figure in the debates about international relations and defence policy.

The present volume traces the development of this complex personality. The editors, Alice Kimball Smith and Charles Weiner are singularly well qualified for their task. Mrs. Smith was at Los Alamos from the start until the end of the War, and therefore well acquainted with the atmosphere of the place and with many of its members. She later made a study of the part played by scientists in the post-war period in influencing legislation towards civilian control of atomic energy. Dr Weiner is a physicist concerned with recent scientific history, who has recorded interviews with many distinguished physicists.

In describing themselves as editors of Oppenheimer's letters and recollections, they do not really do justice to their work. The letters are supplemented, where there are gaps, not only by passages of Oppenheimer's recollections taken from later interviews, but also by comments from friends, colleagues and pupils, painstakingly collected and sensitively evaluated. In many places the editors' comments, based on this material, are more informative than the letters. They not only identify many of the people and events referred to in the letters, but also summarize events and developments not mentioned in the letters or which took place in periods from which no letters have survived. The book is therefore really intermediate between edited correspondence and a serious biography.

The young Oppenheimer was not the type to keep copies of his letters, and not many of the recipients preserved them. The fact that there remain enough letters from the pre-War period to provide a clear picture of Oppenheimer's attitudes and development during that time is largely due to the few friends who kept the letters and made them available. One of these is Herbert W. Smith, his English teacher in the Ethical Culture School; letters to him are most numerous of any of the correspondents. In the earlier part Oppenheimer sends him essays and verse; his evident desire for approval makes Smith a kind of father figure.

Almost as numerous are the letters to Oppenheimer's brother, Frank, in which the elder brother gives much advice and exhortation, and shows great warmth and affection, though sounding a little patronizing at times. Amongst other sizeable collections of letters are those to Francis Ferguson, whom he first met in his final year at the Ethical Culture School and with whom a close and sometimes tempestuous friendship developed. Of a later period, the physicist George Uhlenbeck, who was a close friend, preserved many interesting letters.

The first three chapters are based on these letters and a few others, supplemented by other information collected by the editors. From his home background we follow Robert to the Ethical Culture School, where he was an excellent scholar in all subjects, and where his interest in science was first aroused through mineralogy. After leaving school and after a year's convalescence from dysentery contracted during a trip to Europe, he visited New Mexico in the summer with his teacher, Herbert Smith. This was the beginning of his deep attachment to the south-west. In 1922, aged 17, he entered Harvard. He spread his studies over a wide range of subjects, mostly on the literary side but including chemistry, in which he graduated in 1925, and some physics. The number and diversity of courses, and the amount of reading he managed, must have meant hard work; at the same time he learned to make contact with people and form friendships.

In his final year at Harvard an important influence was Percy Bridgman, in whose laboratory Oppenheimer did some experimental work, and his decision to go for postgraduate study in physics probably owed much to Bridgman. He decided to go to Cambridge. His studies there did not work out too well. He was not accepted to work under Rutherford, as he had hoped, but did some experimental research under J.J. Thomson, which did not make much progress. However, he had the chance at Cambridge of meeting many distinguished people, including Niels Bohr and other theoreticians, and it became clear to him then that he wanted to do theoretical work. During the Cambridge period he had times of very deep depression and unhappiness, but he was able to deal with his own disturbed state more effectively than any doctors he consulted.

After a year at Cambridge he moved to Göttingen, a congenial environment, to work with Max Born. This was the exciting time when quantum mechanics emerged, and the beginning of Oppenheimer's passionate devotion to theoretical physics, and also of his constructive contributions to the subject. He qualified in one year for a PhD, and returned to the United States in 1927. After a semester at Harvard and one at the California Institute of Technology, he spent another year in Europe, visiting Ehrenfest, Kramers and Pauli. Then he moved to California, holding appointments at Caltech and Berkeley, dividing his time between the two places. He liked this arrangement because at Caltech there were many theoreticians from whom he could learn, while at Berkeley he was practically the only modern theoretical physicist, and thus could contribute more to teaching and research. This unusual arrangement continued until he became involved with atomic energy in 1942. It was here that he started to gather a group of graduate students, who usually followed his annual migration — and that he developed his power as a teacher and leader in research. It was in the California years that he first became concerned with the world around him and with politics. It was in that period that he got married.

He was now an established and respected member of the physics community, as expressed in his election to the National Academy in 1941.

In 1942, when work on the atomic bomb was becoming a serious project, he was asked to take charge of work on fast-neutron fission, which was related to the problems of design and performance of a bomb. The period from this time until the end of the War is dealt with in Chapter 4. Here the task of the editors changes. It is no longer a question of searching out the few surviving letters and filling gaps, but rather to select, from amongst the voluminous files of official correspondence, the letters which are most informative of Oppenheimer's attitude and ways.

In coordinating the experimental and theoretical work carried out in different universities, he immediately showed his characteristic ability for summarizing, for stating the main issues clearly and for formulating questions. It soon became clear that efficiency demanded that this work be concentrated in a single centre, and he became involved in the planning of the new laboratory and the selection of a site. At some stage General Groves, head of the 'Manhattan District' (the code name for the atomic weapons project), decided to appoint Oppenheimer the director of the new laboratory. This was a daring decision, considering that Oppenheimer was a theoretician, not experienced in administration and had the reputation of being rather disorganized in practical matters. Yet the decision was amply justified by its success. Chapter 4 helps to understand why. In addition to his lucidity in recognizing and expressing the main issues, Oppenheimer managed to deal with people in a manner which made them feel that they were respected, and gave them the confidence that their views and their needs were taken into account. The letters give examples of the many large and small problems that the director had to handle, and the pressure under which he was working. One of the surprising facts is how much mutual respect, and indeed affection, developed between Oppenheimer and Groves, in spite of the enormous disparity between their personalities.

Chapter 5 covers the three months from the end of the War to Oppenheimer's departure from Los Alamos. The letters are now concerned with post-War plans for Oppenheimer, positions for the staff of Los Alamos and the organization of atomic-energy research, and reflect the burden of responsibility that scientists carried because of their work on the bomb. The last document by Oppenheimer is his speech at Los Alamos, in which he discusses the future of international relations and the idea of international control of atomic energy.

The editors decided, wisely, to terminate the collection of letters at this point, since from then on the glare of publicity which fell on him, the great volume of correspondence and his membership of numerous official committees, changed the style of his letters, which tended to become more official and more guarded. They do not give the kind of insight which makes the letters reproduced in the book such fascinating reading. The book therefore does not, except in a brief résumé, deal with the post-Los Alamos Oppenheimer, with his directorship of the Institute for Advanced Study in Princeton or with the security hearings usually called the "Oppenheimer Trials", but there are other sources to cover these matters. However, the period it does cover, the growth of an unusually gifted and sensitive person to maturity, and to his success in a gruelling job, is of absorbing interest. ☐

Sir Rudolf Peierls is Emeritus Wykeham Professor of Physics at the University of Oxford. He spent 18 months at Los Alamos working under Oppenheimer.

Pluto, the unique planet

J. Veverka

The Planet Pluto. By A. J. Whyte. Pp. 147. (Pergamon: 1980.) $17.50, £8.75.

FIFTY years have passed since the discovery of Pluto on February 18, 1930, but until recently the planet's physical properties were still subject to much debate. The discovery of a satellite by Christy and Harrington in 1978 made it possible to determine the mass of the planet, and recent speckle interferometry by Arnold, Boksenberg and Sargent produced the first good measurement of the radius. Finally we can say something about Pluto's mean density and composition.

Within half a century our conception of Pluto has changed from that of a rocky body, about the size of Earth, to an icy double-planet so tiny that it is dwarfed by such satellites as Ganymede and Titan. Latest data indicate that the planet is only some 1,500 km in radius (slightly smaller than our Moon, but three times bigger than the largest asteroid). Its companion, Charon, a relative giant, is almost half the size of the primary (our Moon is only a quarter as big as Earth). The average density of Pluto is probably less than 1.5 g cm^{-3}, indicating a predominantly icy constitution. It is still uncertain whether

Pluto does or does not have an atmosphere, but methane frost on its surface was discovered in 1976 by Cruikshank, Pilcher and Morrison.

Whyte's *The Planet Pluto* is one of two very timely recent books about this unique world. Both can be recommended highly. The second book is W. G. Hoyt's *Planets X and Pluto* (University of Arizona Press), a well-documented, readable account of the discovery and subsequent studies of the planet, based largely on Lowell Observatory records.

Whyte's book is a succinct, thorough summary of our growing knowledge of Pluto. Results are given more or less chronologically without critical comment. This type of presentation has its advantages, but there are occasions where one wishes the author had allowed himself to be more critical. Obvious examples involve Kiladze's numerology, Brady's planet, certain very noisy spectra over-interpreted in fantastic fashions and pedantic models of the planet's interior calculated before the mass or size of Pluto were known.

There are only occasional typos and the odd trivial error, and few important references are omitted. Most notably, no mention is made of such important papers as those of Seidlemann *et al.* (*Publs astr. Soc. Pacif.* **84**, 858) and Goldreich and Ward (*Publs astr. Soc. Pacif.* **84**, 737) which appeared in 1972 and demonstrated that Brady's huge trans-Neptunian planet is an impossibility. The references are up to date until July 1979, and thus do not include some important new results such as the speckle determination of the radius of Pluto by Arnold and his colleagues.

In spite of its high price, the book is recommended heartily to anyone interested in Pluto. It is hoped that it will make a contribution to a much-needed re-evaluation of Pluto's importance to our understanding of the Solar System. Perhaps more astronomers will see fit to observe the planet with the techniques now available while it is near perihelion during the next two decades. Pluto has emerged as a unique body in our Solar System and as such is worthy of closer study, and especially of direct exploration by spacecraft. Opportunities exist to fly-by Jupiter — and have another look at Io — and arrive at Pluto before the end of the century. ☐

J. Veverka is at the Laboratory for Planetary Studies, Cornell University, New York.

End of a chapter in population genetics

Alan Robertson

Mathematical Population Genetics. Biomathematics Vol. 9. By W.J. Ewens. Pp.322. (Springer-Verlag: 1980.) DM 59, $33.10.

SINCE the rediscovery of Mendelian segregation, the combinatorial properties of the phenomenon have been fascinating to the mathematician (as indeed they were to Mendel himself). What Ewens calls the "golden age" of mathematical population genetics was dominated by Fisher, Haldane and Wright, the first two with professional training and the latter an inspired amateur. For a time, the theory was far ahead of the relevant evidence but the emergence of new experimental techniques (gel electrophoresis, amino-acid sequencing of proteins and, more recently, DNA sequencing) has not only provided a large body of data, though mostly concerned with protein evolution, but has also stimulated new conceptual approaches, such as the misnamed 'non-Darwinian evolution', and a great deal of sophisticated mathematics. For instance, our view of the basis of mutation at individual loci is quite altered — we think no longer of 'forward' and 'back' mutation but of an infinite progression which almost never retraces its path and which has led to an 'infinite allele' theory of some elegance.

Many recent theoretical papers seem to have been written for mathematicians rather than biologists. Ewens does an excellent job of presenting the different contributions, many from himself or his students. Aimed at the graduate or research student, two threads are neatly interwoven throughout. Having first presented the theoretical approach to a topic, he ends with his own view of its present biological status. The book deals mainly with the statistics of genes in populations and less than 15 pages are concerned with quantitative genetics. Its value to the reader obviously depends on the latter's mathematical level. I have certainly found it useful and stimulating — an indication not only of my mathematics but that I share the author's prejudices.

Perhaps, too, this volume marks the end of a chapter — of a theory of evolution in terms of the substitution of single mutations. Papers dealing with the mathematical properties of systems of tandemly repeated loci have already appeared (though none are referred to here), and current issues of *Cell* and *PNAS* are full of discussions of transposable sequences, a new kind of genetic polymorphism, arising from a novel source of variation. ☐

Alan Robertson is Professor at the Institute of Genetics, University of Edinburgh.

The potential of peat

Hamish Anderson

Peat: Industrial Chemistry and Technology. By Charles H. Fuchsman. Pp.279. (Academic: 1980.) $28, £15.80.

AT A time when many countries, faced with ever-declining supplies and resources of basic raw materials, are currently re-assessing the potential of alternative sources of energy and of feedstocks for the chemical industry, the appearance of Dr Fuchsman's book is particularly welcome and opportune. Indeed, this publication constitutes the first real attempt in the English language to collect and collate information on the chemistry and technology of an industry which, until now, has centred largely in eastern and northern Europe. Based on data judiciously selected from over 450 references, including many from Soviet publications not readily accessible to Western scientists, the author presents a most readable and concise review of the nature of organic components in peat and of the alternative technologies available for converting these components into commercially useful and value-added products.

Following a general introduction on the nature and distribution of peat resources and the history of peat utilization for industrial purposes, Chapter 2 presents a somewhat superficial account of the classification and chemical characterization of different bog and peat types, as a result of which the complicated and often ambiguous terminology and nomenclature may trouble the non-specialist. It is also surprising that sapropel, a material now widely used in the USSR, is considered to be of little importance to chemical technology.

The extraction of peat with organic solvents is dealt with in considerable detail in Chapters 3–5, which help to clarify a murky area of the peat research effort. The chemistry and utilization of peat carbohydrates and hydrolysates of peat polysaccharides are comprehensively covered in Chapters 6–8, followed by an account of the hydrolytic production of furfural, lactic and glycolic acids and other sugar by-products. A further use of these hydrolysates is the indirect production of proteins and fats by the culture of yeasts — a process which has a long and honourable

The second edition of the *Glossary of Geology*, edited by Robert L. Bates and Julia A. Jackson, has been published by the American Geological Institute, Falls Church, Vermont. The updated *Glossary* includes 36,000 terms, compared to 33,000 in the 1972 edition, and is available from the AGI, price $60.

history in peat technology.

In a book which deals largely with the subject from an industrial viewpoint, it is surprising to find that the longest section (Chapter 12) is devoted to a review of the occurrence and structural chemistry of humic acids and lignin. By contrast, Chapters 13–15 provide a most valuable account of the theory and practice of peat carbonization, specifications for coke and related products, and the production and utilization of distillates and gases from peat pyrolysis.

Chapter 16 on chemical methods of peat analysis is perhaps the weakest in the entire book. In a work containing such an extensive and well-documented bibliography up to, and including, 1978, it is surprising to be presented with many analytical methods which are out of date. Thus much stress is placed on the use of paper chromatography for the estimation of components of hydrolysates, disregarding modern liquid and gas chromatographic techniques for the analysis of waxes, steroids, terpenes, phenols, sugars and amino acids. Automated flow analysis methods are not mentioned. The concluding three chapters deal with the scale of peat processing operations, economic and social implications, environmental impact and pollution control.

Overall, Charles Fuchsman's book fills an important gap in existing literature and will be widely welcomed not only by specialists in the field concerned but by all those engaged in peat research and development. □

Hamish Anderson is a Principal Scientific Officer at the Macaulay Institute for Soil Research, Aberdeen.

Art of the insoluble

R. H. Pain

Hydrophobic Interactions. By A. Ben-Naim. Pp.311. (Plenum: 1980.) $32.50, £20.48.

MEDAWAR has reminded us that the pursuit of science is the art of the soluble. This book is about the art of the insoluble.

To judge by the number of monographs recently published on the subject, interest in the hydrophobic effect and its involvement in the stabilization of biological structures is at a high point.

Kauzmann in 1959 (*Adv. Protein Chem.* **14**, 1) drew attention to the fact that the association of non-polar groups in an aqueous medium exhibits thermodynamic properties which can only be explained in terms of changes in the entropy of the solvent. Such groups, which are present on many biological molecules, come together not so much due to mutual attraction as to a mutual distaste for water. These concepts have been developed by several groups to provide a valuable tool with which biochemists can rationalize a wide range of interactions. What may be called the thermodynamic approach to hydrophobic interactions is widely accepted and remains useful because of the still limited understanding of the structure of water. The beauty of thermodynamics in such a situation lies in its ability to handle phenomena quantitatively without having to make any assumptions as to mechanism, and some of the workers in this field have vigorously eschewed any attempt to taint the purity of the approach by considering molecular mechanisms. The frustration which this kind of treatment apparently induces in biochemists is well illustrated by widespread references in the literature to 'water structures' and 'icebergs', and indeed there is much that we want and need to know about the details of the hydrophobic interaction.

DON'T MISS THE
Grand Tour!

Last year at Jupiter. They are already nearing Saturn. Then it's on to Uranus, and Neptune, and possibly Pluto. Voyager photos are amazing, data from onboard experiments revolutionary. And full coverage of the tour can now be yours, along with features on nearly every other body in this solar system. So keep up with science - by subscribing to Planetary Astronomy.

Published bi-monthly by the James-Mims Observatory, Inc., a non-profit corporation. Subscriptions are $5.00/yr., $9.50/2 yrs. (US), $7.00/yr., $13.50/2 yrs. (Canada, Mexico) $8.50/yr., $16.00/2 yrs Other countries).

PLANETARY ASTRONOMY
P.O. Box 15854 Dept. N
Baton Rouge,• LA 70895

Circle No. 04 on Reader Enquiry Card.

The monograph by Ben-Naim attempts to steer a course somewhere in between the thermodynamic and the molecular-structure approaches. It is not in any sense a review, as the limited and selective list of references indicates, but an account of the author's own attempts over a period of years to tackle the problem of hydrophobicity. The first impression is one of clarity in his treatment of the subject. He leads the reader patiently, if at times paternally, through the development of his argument in a way which is refreshing and helpful. The argument is clarified by a series of diagrams which enable the model-orientated reader to grasp the significance of the equations. Frequent "Comment" paragraphs provide summary, objective assessment of the previous sections. It is, surprisingly, these comments which first make for a sense of unease, for the general impression conveyed is that more experimental data are required to test the theory or that the theory being developed does not relate to real and highly complex macromolecular systems.

The author begins by drawing a useful distinction between the *direct* parts of the interaction between two particles in solution and the *indirect* part which comprises the hydrophobic interaction. His approach is based on that of statistical mechanics and he sets out to describe the interaction in terms of association rather than solubility. The contrasts with the thermodynamic approach are marked, in that the familiar description of the hydrophobic interaction in terms of characteristic changes in entropy and heat capacity is absent. In fact, consideration of these does not appear until three-quarters of the way through the book. The treatment progresses through discussion of the interaction between two simple particles to interaction between many solute particles, with particular emphasis on the non-additivity or cooperative aspects. The final chapter concerns the temperature and pressure dependence of hydrophobic interactions. Statistical mechanical derivations are assigned to appendices in order to make the text more readable. Various kinds of experiments are described, although some of these, such as those involving the association of carboxylic acids, are notoriously difficult to interpret in terms of the hydrophobic contribution.

This book is unlikely to be of value to the biochemist. Little light is shed on the four fundamental questions raised in the preface as to the nature and role of hydrophobic interactions — these are still best answered by intuitions and prejudices based largely on the thermodynamic approach. The book is a useful contribution for the hydrophobic buff, summarizing the application of the statistical mechanical approach. For my money, though, further understanding of the hydrophobic interaction will only come as we learn more about the behaviour of the solvent at the molecular level. □

R. H. Pain is Professor of Physical Biochemistry at the University of Newcastle upon Tyne.

nature

28 August 1980

Plagiarism, piracy and principles

How honest is the scientific community? Is it, as the story books would have us believe, that every single member of the scientific community is a knight in shining armour, dedicated only to the pursuit of truth and indifferent to where the pursuit will lead? Or may it be, as some would say, that the scientific community is by and large no more honest or dishonest than any other group of professional people in which personal rivalry and ambition cannot be ignored? Might it even be that scientists are if anything less honest, more venial, than the professional groups with which they invite comparison? There is a sense in which these questions and others like them are strictly meaningless. The scientific community is at best a loose aggregation of people with often very different interests, working in laboratories of very different character with techniques that differ profoundly from each other. In some circumstances, scientists work alone, perhaps even in isolation. In others they are members of large teams of people, united by a common interest yet constantly (and understandably) on the look-out to ensure that no one person derives an advantage from the collaboration that cannot be justified by his own contribution to it. There are some who argue that in such circumstances even the notion of a scientific community makes no sense. But there is also a sense in which, from time to time, such questions cannot be avoided. In the past few months, they have been made inescapable by the discovery of cases of widespread plagiarism in the scientific literature, by the latest well-publicized case in which experimental data were as much a product of people's imagination as of laboratory measurement and by the general fear that when times are hard and budgets being reduced in many areas, standards are bound in any case to be at risk.

What is the truth? It is prudent first of all to recognize that recent scandals, however spectacular, are neither as great a slur on the reputation of scientists as many outsiders would like to think nor as novel as many scientists would pretend. There is a tendency among professional scientists reading for the first time tales of large-scale plagiarism (see *Nature*, 12 June and 31 July) to huff and puff, turn red in the face and utter some solemn declaration that something, almost anything, must be done to defend the fair name of science. This tendency should be resisted. It is too often forgotten that the misdemeanours of the present are often mere shadows of the misdemeanours of the past. The seventeenth century, after all, was riven with controversies about whose idea belonged to whom, and people such as Robert Hooke found it sensible to conceal notions such as *ut tensio si vis* in anagrams.

In the days when the importance of data gathered from the real world as the foundation of all theory was not widely appreciated, the theft of ideas pure and simple was easier but also potentially more damaging than at present. In a small part, the conventions by which the scientific profession now regulates itself derive from from the bad experiences of these early days. The object of the convention is to give truth an overwhelming advantage over falsehood, originality a powerful edge on repetitiveness and to make it possible that people whose contributions to the stream of discovery are very different are nevertheless able to work easily alongside each other. The scientific community should count itself lucky that these conventions are now so deeply ingrained, so widely respected and so infrequently dishonoured.

It is always something of a tragedy when the conventions are broken, especially if for personal gain or for the sake of personal esteem, but it is also important that when they are found to be broken, the scientific community should not get on its high horse and over-righteously pursue the transgressors. Especially because the conventions of the profession are so widely known, and because it is so widely understood that the penalty of being found out may be the end of a career, it is only charitable to acknowledge that a deliberate breach of the conventions may be a sign of something pathological, or of insupportable stress. The profession should, in other words, be more compassionate than is often at present the case towards those who fall foul of the conventions and are expelled.

None of this implies that the conventions themselves should be made less strict. On the contrary, there are some respects in which they need to be made tighter. But it is crucial that the scientific community should clearly understand the purposes that the conventions are meant to service. In this connection, even the most primitive of the conventions — that which outlaws falsehood — is not, as some would have it, a matter of morality in some high-minded sense; rather, it has a practical purpose. The scientific community, like any other branch of scholarship, hangs together because of a common interest in a common pool of knowledge. A person who announces the results of experiments showing that water will run uphill, or that chewing-gum becomes superconducting at the temperature of liquid oxygen, or who merely decides to make his way in the world by synthesizing data that confirm some widely held theory, is potentially misleading all his colleagues, wasting their time and diminishing their chance of making a substantial contribution to understanding. Falsehood is thus an impediment to the progress of science as whole, and small falsehoods may have a disproportionately great effect. Whether those who utter falsehoods are immoral in some wider sense is hardly relevant.

But what is a falsehood? The word is not synonymous with the opposite of truth. There is no shame in publishing in the literature an observation which turns out to be incorrect, perhaps because of some instrumental defect or conceptual flaw. Similarly, an entirely wrong-headed theory, the "luminerferous aether", for example, is not an offence against the conventions of the community provided that it is argued on grounds which are explicit, and accessible to all. (From this derives the subconvention that original publications should contain the details needed to repeat an experiment or to reconstruct an argument.) Popper would say that the discovery of untruths of this kind is not merely a chore but the essence of science. Falsehood is different, for it requires of the perpetrator the wish to deceive. Falsehood cannot as easily be rooted out. Telling one from the other without the lapse of time would inevitably entail the impossible task of assessing individual honesty. By convention, it is supposed that everybody is honest — how else could it be? How true is that assumption?

The second primitive convention, common to the whole of scholarship, is that credit must be given where it is due. The objective is not merely that scientists should enjoy that faint glow of pride that follows from discovery or authorship (which is nevertheless a justifiable reward in a profession where other rewards are few and far between) but that it should be possible for others to reconstruct the origins of new ideas, putting them in a wider intellectual context and making them intelligible. But failure to acknowledge sources adequately and generously is also bound to cause personal offence — people are human, after all — which can seriously damage the free exchange of data and ideas.

These, as they must be, are high ideals. How well are they kept? The recent flurry of plagiarism is not a good guide to present

0028-0836/80/350831-02$01 00

standards, if only because plagiarism is so easily detected and demonstrated. Plagiarists are either fools or desperate people. Concocting false data, cooking the books, is a more private matter and therefore harder to detect. Many heads of busy laboratories will be alarmed to think what may be happening without their knowledge — and will no doubt come to the conclusion that their only safeguard is to be directly involved in their own research, not merely as leaders but as colleagues of those who do the work. Even so, clearcut transgressions are likely to be rare. Less flagrant misdemeanours, or complaints thereof, are much more common. A helpful referee may find that his constructive comments become the gist of somebody else's publication. A member of a coordinated research programme may find that the contributions he has made to the planning of an enterprise turn up in the literature without his knowledge. Or references to important contributions to some field may be skimped for the sake of a false impression of originality. There is a lot of this about.

Remedies are unfortunately not easily devised. In the old days (half a century ago) it was the common practice for the head of a laboratory to take responsibility for everything that happened in it or was published from it. Grand old men used to terrorize their juniors yet give their work the stamp of authenticity. To turn back the clock would be impossible and would solve nothing, for even grand old men are capable of falsehood. Yet there is something in the view that the standards of behaviour would be improved if only laboratories as units engaged more freely and openly in discussions of their collective work. Falsehood is necessarily a private matter; open discussion must help to show it up — or even show that falsehood is unnecessary. It is only proper to record that many of the best laboratories are among the most willing to talk domestically. It would also help if external pressures on individual scientists could be abated. The competition for grants, promotion and kudos is the driving force. The need to publish derives from that. There is at least a chance that these pressures would abate substantially if the methods of financing research were only subtly changed. Shifting the balance of decision from external agencies to laboratories themselves would be certain to help. Is this the constructive course to follow after the disclosures of the past few weeks?

Pesticides in developing countries

Many years have passed since the argument about the future of the environment in which people live was sharply polarized, dividing those who considered that the surface of the Earth is a robust place and those who argued that, on the contrary, quite small changes affecting the ecological balance might have catastrophic consequences. Mercifully, these discussions are now conducted more moderately. Both sides in the old argument seem to have decided that everybody's interest will be served if consensus rather can conflict can be built around environmental problems. Unfortunately, however, it seems that old habits die hard. From time to time, vestiges of the sharp divisions of the 1960s crop up in public statements and in the newspapers. One of the citadels of the extreme environmentalists appears to be the journal called *New Internationalist*, published by no less an organization than Oxfam, widely respected for the way in which it has tackled problems in developing countries with energy, compassion and imagination which are rare even for the most dedicated voluntary organizations.

New Internationalist is, however, over-imaginative in the way it tackles problems of the environment in developing countries. Thus, in the July 1980 issue of the journal, an article by the editorial staff of the journal which appears under the heading "Peddling pesticide" begins with the declaration that "until DDT was banned as a proven cancer-causing agent it was the penicillin of pesticides . . .". The article goes on to argue that the chemical companies, disconcerted to have been "caught pushing poisons", stopped manufacturing DDT in developed countries but set about selling their manufactured stocks in countries overseas. The objective of the article is to argue that the multinational chemical companies are using the developing world as an outlet for sales that would otherwise be frustrated and asks that Western governments should put a stop to their wicked ways. The argument thus brings together two important elements of the demonology of the extreme environmental movement of a decade ago — big business in general, and international business in particular, and pesticides in general, DDT in particular. Nobody quite understands where these demons have sprung from but no doubt they have their roots in a variety of improper practices in the past. For there is no doubt that at many periods in the past century developing countries have been exploited unfairly by business interests from overseas. Similarly, it is beyond dispute that DDT and the other organochlorine pesticides were used indiscriminately and perhaps irresponsibly soon after their introduction — although it appears that most of the damage that followed was in North America, where agriculture is intensive, and not in the developing countries. None of this, however, excuses what *New Internationalist* has to say about DDT, especially because what the developing countries need to know most urgently is more complicated.

The truth is that DDT is not a poison in any reasonable meaning of that word. Its acute toxicity to people is low, which is why it was widely used, a quarter of a century ago, for the control of mosquito populations in the areas of the world where malaria is endemic. Similarly, the evidence that DDT is "cancer-causing" is ambiguous in the ordinary meaning of those words. It is true that high doses of DDT fed to laboratory animals will induce cancer, as indeed they provoke disturbances of liver function. But there is no evidence that the use of DDT has in the past caused damage to people when used with suitable precautions and in circumstances that are appropriate. The more toxic organochlorine pesticides are more damaging to animal life, but even they have not been taken off the market in most industrialized countries because of the damage they might do to people — rather they have been controlled and sometimes banned for fear of what they might do to wildlife populations.

In developing countries, circumstances are different. It may be regrettable but it is true that many governments in developing countries are less squeamish about wildlife populations than are the governments (and the electorates) of industrialized countries. *New Internationalist* would be fighting a good cause if it sought to alert them to the importance of a balanced wildlife population and to the importance of refraining from needlessly disturbing the natural ecology. In due course, many such governments would no doubt follow industrialized states in controlling DDT for fear of unwanted effects on the wildlife population. But for many of these governments there is a more urgent reason why powerful pesticides such as DDT should be used with discrimination. The original enthusiasm for the use of DDT in controlling malaria has evaporated now that problems of insecticide resistance have become natural restraints on what can be accomplished. Similarly, in the industrialized countries which practise intensive agriculture, the United States and Western Europe in particular, there are growing dangers that the uncontrolled use of pesticides may serve chiefly to stimulate the emergence of resistant insects. The difficulty is that such problems cannot be solved simply by taking one, or even several, offending chemicals off the market — somehow, instead, their use has to be planned imaginatively. Is not this the point that *New Internationalist* and its parent organization should be seeking to establish?

0028-0836/80/350832-01$01.00

Uranium exposure limits in dispute

A new dispute has arisen between epidemiologists and health physicists over the interpretation of data on the health effects of low levels of ionizing radiation, the subject of a recent report from the National Academy of Sciences (*Nature* 7 August p. 550).

This time the disagreement centres on whether current exposure limits to the radioactive gas radon and its decay products may present an unnecessarily high risk of lung cancer to the 7,000 uranium miners currently employed in the United States.

And the precise shape of the low-level dose–response curve has been given a new significance by growing concern about the possible health risk to the general public from radon-emitting building materials, since radon's precursor, radium-226, is a trace element contained in most rocks and soil.

In the light of epidemiological evidence on occupational exposures that has been accumulated since the current standards were set in 1971, the National Institute of Occupational Safety and Health (NIOSH) has suggested to the Department of Labor that permitted exposure limits for uranium miners should be significantly reduced.

However, the International Council for Radiological Protection (ICRP) argues that no change is needed. In a set of new recommendations currently being circulated to its members, the ICRP says that on the basis of dosimetric techniques applied to models of the lung, the current exposure limits appear to be adequate.

Mining companies — already facing a tight economic squeeze because of a virtual collapse in the international market for uranium ore — are using the ICRP's arguments to press the department not to reduce the limits. A move to reduce the limits could mean that mining companies would have to install expensive ventilation equipment.

Research in the 1950s and 1960s confirmed an abnormally high incidence of lung cancer among uranium miners. The cause was identified as radon and its alpha-emitting decay products — known as radon daughters — which become attached to air particles and can lodge in miners' lungs. The Department of the Interior introduced in 1971 an exposure limit of 4 working level months (WLM) a year, with a ceiling airborne concentration not to exceed 1.0 WL. (One working level (WL) is defined as a radon daughter concentration in one litre of air resulting in the emission of 1.3×10^5 MeV of potential alpha energy).

Since then, evidence from epidemiological studies in Canada, Sweden, Czechoslovakia and the United States, suggests, according to a report put together by a NIOSH study group, that the full effects of radon exposure may have been underestimated, and that "there appears to be no margin of safety associated with the present standard".

The working group point out that triggering doses may be substantially lower than the cumulative doses associated with a particular incidence of lung cancer, since the radiation absorbed after the triggering dose may have been biologically redundant. In addition, the contribution of smoking to lung cancer among miners may have been overestimated in previous work. Some studies appear to show a higher rate of lung cancer among miners who do not smoke than among those who do — perhaps because cigarette smoking creates a thicker layer of mucus which may provide some protection against alpha emissions.

In submitting the report to the Department of Labor's Mine Safety and Health Administration (MSHA) Dr Anthony Robbins, Director of NIOSH, says that the apparent excess risk of lung cancer among those who might accumulate 120 WLM over a working lifetime — perhaps twice previous estimates — was a cause for major public health concern.

"On the basis of the study group's report, we feel that the present MSHA standard of 4 WLM per year does not provide an adequate degree of protection for underground miners exposed to radiation when it is evaluated over their exposure lifetime," Dr Robbins says.

NIOSH officials met with MSHA at the beginning of this month, and agreed that there is enough scientific evidence to support a possible revision of the regulation.

The department has already been petitioned to reduce permitted exposure levels by Ralph Nader's Health Resources Group and the Oil Chemical and Atomic Workers, a labour union to which many of the uranium miners belong. The two organizations are demanding that the maximum allowed radiation be reduced from 4 to 0.7 WLM per year.

However, the department is being urged by the industry to take into account the ICRP regulations suggesting little need for change. The ICRP proposals, agreed in draft form at a meeting of the commission in Brighton, UK earlier this year, describe two different ways of estimating what might be considerd a safe exposure level.

Using epidemiological techniques based essentially on the same data as those analysed by the NIOSH working group, ICRP suggest that a safe limit would be between 2 and 10 WLM per year.

However, the ICRP also makes estimates based on a dosimetric analysis of the expected effect on the lung of a given amount of radiation, and in particular to that region of the lung particularly susceptible to alpha emission.

The latter approach, according to the ICRP, leads to a recommended exposure limit of 5–8 WLM per year based on a regular lung dose, or 9–14 WLM per year based on a mean lung dose. And given the variability in the epidemiological data, ICRP suggests that a figure of 5 WLM should be used as the basis for regulation — adding that for uranium miners already exposed to additional gamma radiation, this limit would tend to be reduced by 20 per cent for radon daughters alone, bringing it in line with the current US standard.

Ironically this conculsion is somewhat in conflict with the judgement of the National Academy of Sciences' Committee on the Biological Effects of Ionizing Radiation (BEIR), which last month moved closer to ICRP's position that for a different type of low level radiation (that resulting from X rays and gamma rays) a linear dose–response model may overstate the dangers.

In its comments on the dangers from alpha emission and other sources of high-LET (linear energy transfer) radiation, however, the BEIR committee drew heavily on the epidemiological studies of uranium miners and others to conclude that "the application of the linear hypothesis is less likely to lead to overestimates of risk and may, in fact, lead to underestimates".

David Dickson

High-altitude research

Reflated hopes

A threat to halt the launching of large scientific balloons from two sites in Australia may yet be averted if a proposal to update equipment and share running costs is accepted by the five countries which regularly use them. The continuation of the facilities is particularly important for astronomers from Australia, the United States, Britain, Germany and Japan who want to send balloon-borne payloads to high altitudes to study X-ray and UV sources in the Southern Hemisphere near the Galactic Centre.

The Australian government has threatened to close the facilities at Mildura, Victoria and Alice Springs in the Northern Territory because it says that it is heavily subsidizing foreign astronomers whose governments do not pay an economic fee. The United States is the only country that currently contributes to running costs: it pays a third, Australia making up the remaining two thirds. Other users of the facility currently pay about £10,000–11,000 for a launch and nothing towards basic running costs.

0028-0836/80/350833-02$01.00

Britain, Germany and Japan have each been launching on average two to three balloons per year. Australia started searching for alternative funds four years ago when Britain was the main foreign user apart from the United States. An attempt then to get Britain to pay one third of the running costs, about £50,000, failed with Britain's Science Research Council pleading poverty.

The current threat to close the facilities unless outside funds are found quickly seems likely to produce results. Britain and the United States have agreed to accept a proposal, put by Professor Vic Hopper of Melbourne University during recent visits to both countries, to share running costs between the five principal users and to update some of the out-dated equipment.

The new proposal appeals to Britain in particular because the cost would be shared by more countries, Germany and Japan having become regular users of the facilities over the past four years. The plan would also allow user countries to up-date equipment by providing their own. Hence the United States and Germany might consider providing a better launch truck for heavier balloons and Britain would be willing to provide an improved kilobit telemetry link from its now abandoned Skylark rocket programme. Professor Hopper left for Germany and Japan last week to discuss his ideas there.

Britain seems to have come round to the view that it can hardly refuse Professor Hopper's proposal, especially if the United States, Germany and Japan also agree to cooperate. Compared to the cost of other collaborative projects with Australia, such as the Anglo-Australian telescope, the cost would be almost insignificant. In the interests of international collaboration, at least, it would probably be worth it.

Judy Redfearn

Nuclear reactors

Czech closure

In a sudden policy about-face, the Czechoslovak Nuclear Energy Commission has admitted that the country's first nuclear power station at Jaslovske Bohunice had to be closed down permanently after a major incident a few years ago. Speaking on Prague Radio, Milos Drahny, a senior official of the Commission admitted that a serious defect had damaged the 440-MW No. 1 generating set at the country's first VVER-440 light-water nuclear power station.

This admission follows almost two years of semi-official denials backed up by glowing accounts in the media of the benefits which the station was bringing to the Czechoslovak national economy (a claimed 2 million MW generated in 1979). As recently as 17 July 1980, Prague TV carried a news item reporting the completion of "summer maintenance work" on the No. 1 set.

The closure of the station was first reported in November 1978 in Document 22 of the Charter 77 movement. This document reported two accidents. The first, on 5 January 1976, was due to an obstruction in the safety valve of a fuel cell (probably due to human error), leading to an escape of radioactive coolant (CO_2) and the death of two workers who could not be evacuated in time, since one of the emergency exits had been locked as part of an anti-pilfering campaign. The second accident, on 24 February 1977, was due to human error in the loading of a fuel cell, producing a rupture in the primary circuit and extensive contamination in the primary and secondary circuits. Activated steam was voided into the atmosphere, and there was an escape of liquid into a nearby stream, which had to be fenced off temporarily.

The public discussion which the Chartists had hoped to evoke never materialized. The authorities took the stance that there was no accident. But the total absence of sound data (workers at the plant who had been at risk in the first accident were not even allowed to know the extra dosage they had absorbed) caused rumours to proliferate. By 1979, it was widely believed that the liquid spilled from the second accident had got as far as the Danube — an allegation which the Chartists themselves have never either supported or denied, and which on the face of it would be very difficult to substantiate since the Danube Commission deals only with pollution caused by ships and there is, to date, no overall monitoring system for the river.

Document 22 in its concluding paragraphs called for a moratorium in the Czechoslovak nuclear energy programme until the public had been informed of, and had had a chance to consider, the hazards involved. But with the authorities firmly committed, like all Comecon countries, to nuclear power, construction went on apace; the No. 2 set at Jaslovske Bohunice is now undergoing acceptance trials, the Dukovany station is under construction and work on the Mochovce station has been started.

Nevertheless, and without any reference to Document 22, the Czech and Slovak media have from time to time appeared to be answering the Chartists on specific issues. One of the main criticisms made in Document 22 was of the psychological and physical health of the staff at Jaslovske Bohunice. The majority of workers, said the Chartists, were willing to work dangerously long hours without proper safety precautions in return for high pay and consoling themselves with alcohol and petty pilfering. Official releases countered this with descriptions of health and safety regulations, and the careful psychological monitoring of prospective employees. Other articles stressed safety precautions and contingency plans for antipollution measures in the event of any serious radiation leaks.

Drahny's belated announcement that such an accident has, in fact, already occurred, will come as no great surprise to the Czechs and Slovaks, accustomed as they are to the rewriting of the past. They may be intrigued, however, by the timing of the announcement, which came a few days before the anniversary of the 1968 Soviet intervention.

Vera Rich

Space telescope

Edinburgh's bid

Britain's Science Research Council (SRC) is to put in a bid to the European Space Agency (ESA) to house the European space telescope coordinating facility at the Royal Observatory, Edinburgh. Bids are also expected from the European Southern Observatory at Garching, West Germany, at least one astronomical institute in France and possibly one each in Spain and Italy. ESA plans to decide on a site early next year.

European scientists will receive at least 15 per cent of observing time on the space telescope — a joint ESA–US National Aeronautics and Space Administration (NASA) project — due for launch aboard the space shuttle in late 1983, roughly in proportion to ESA's contribution to its capital cost. The task of the European Coordinating Facility (ECF) will be to receive data from NASA's Space Telescope Science Institute, and to analyse and disseminate them to European users of the space telescope, within a matter of days of receipt of the data in the United States. But bigger plans are afoot for the ECF. It will be designed to handle all data produced by the space telescope; ESA is currently negotiating with NASA to receive data

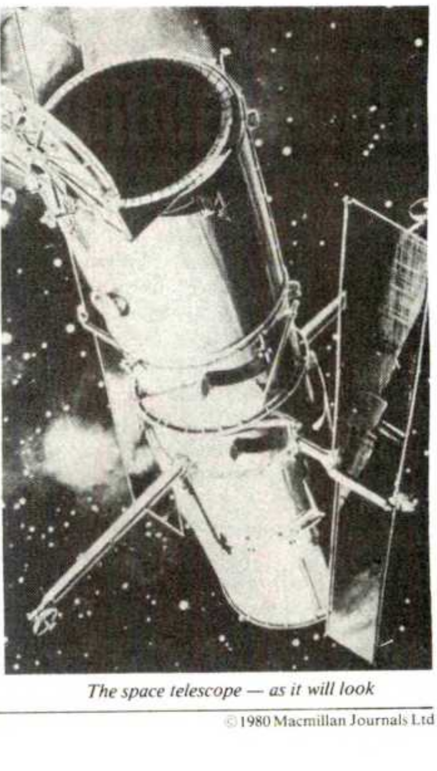

The space telescope — as it will look

0028-0836/80/350834-02$01.00

which are not initially allocated to European astronomers when exclusive rights to it have expired after one year.

The SRC believes that its proposal stands a good chance of success because it would use Britain's Starlink facility which already employs highly sophisticated methods of image processing to analyse data from ground-based telescopes. The Royal Observatory in Edinburgh houses one of Starlink's six nodes. European astronomers would be able to access space telescope data quickly by travelling to Edinburgh or only slightly more slowly at one of the sites of the five other nodes, three of which are within easy reach of London, the other two being in Manchester and Cambridge. One of the main reasons for choosing Edinburgh rather than any of the five other institutes housing a node is that from next October, Dr Malcolm Longair will be director of the Edinburgh observatory. He has been closely involved in the space telescope programme since its inception.

To cope with the enormous increase in data, however, facilities at the Royal Observatory would need to be expanded, particularly by enhancing the existing image processing unit and building a special unit to cope with the data.

ESA plans to pay about £66,000 towards the capital cost of the facility, about £33,000 per year towards running costs and the salaries of seven staff. The host institution will be expected to find the rest of the cost from its own pocket.

The SRC estimates that to build the facility at Edinburgh, it would have to provide about £250,000 and pay for an extra five staff.

Judy Redfearn

German workforce

Ten years on

Microcircuits and other new technologies likely to be adopted in the 1980s in West Germany will result in the loss of 1.8 million jobs in some low-skill sectors, and a gain of 1.9 million in other higher-skill occupations, says a new forecast commissioned by three Federal German ministries.

This massive shift in employment will require government policy "specifically shaped to counteract what will be an increasing tendency towards conflict in the community" says the report, prepared by Mackintosh Consultants Ltd of the UK and Prognos AG of Basle.

The German government has described the report as a brilliant study and awarded the teams a prize for their efforts. Mackintosh Consultants reviewed probable technical developments by making studies in the UK, Japan, Germany and the USA; and Prognos AG looked at social and economic factors, including union and management attitudes affecting their introduction in the current decade. Both studies were detailed and sectional, dividing the economy into at least 50 sections and jobs into 26 categories, all of which were looked at individually (see table).

The study identified 15 sensitive sectors of the German economy where the pressure to innovate was great, but the ability to respond small. Prominent among them were the chemical industry and refineries, where the price of imported oil will require conversion to new feedstocks; but conversion will require massive investment in new capital equipment, new skills in the workforce and possibly new locations for industry to meet the distribution requirements of new raw materials.

Jobs directly connected with the introduction of the new technologies — such as installation, and the repair and maintenance of what may initially be unreliable (because untested) technologies — would increase during the 1980s by 471,000. But typically the qualifications required in the new jobs will be far in excess of the jobs being eliminated: spotting if a cherry is on a cake requires less education than spotting the fault in the device which detects cherries on cakes.

The area in which most jobs would be lost is in the operation of processing plants, largely through the introduction of microprocessors to handle decision-making on production lines. Here, the report estimates, there will be 396,000 fewer jobs in 1990 than there were in 1977. "Assembly", categorized separately in the study, would also lose 323,000 jobs, through reductions in numbers of components and the automatic assembly of, for example, television sets.

The Bundesministerium für Forschung und Technologie (BMFT) have estimated the range of unemployment which might follow from the Mackintosh-Prognos scenario, given different conditions of economic growth and government and industrial investment. At a pessimistic level of 2 per cent annual growth in gross national product (compared to the Mackintosh–Prognos estimate of 2.9 per cent), investment would be expected to be low, and unemployment would rise from 1.03 million this year to 2.23 million in 1985 and 2.4 million in 1990. It would fall again to 1.44 million in 1995, the BMFT estimate.

Mackintosh's project director for the study, Mr Tom Jacobs, said last week the likely speed of innovation would be great in the next decade but would need great social change. Hence, says the report, Germany must develop "a high level of social communication and willingness to support common objectives, which is only possible if based upon a high level of overall understanding of where the community's best interests lie. Thus, the management of social learning processes becomes a central task in politics."

Robert Walgate

Economically active persons classified by type of activity in FRG for 1977 and 1990

Field of activity	Economically active persons (thousands) 1977	1990	Change: 1990 compared to 1977 (%)
1 Mainly management functions	922	1,104	19.7
2 Office work	3,863	3,611	−6.5
3 Entertainment, publishing	125	152	21.6
4 Education	897	1,076	20.0
5 Cleaning operations	872	1,002	14.9
6 Installation, repair and maintenance of machinery	2,224	2,695	21.2
7 Specialized consulting, R&D	1,171	1,604	37.0
8 General supply services	2,343	2,150	−8.2
9 Special supply services	498	470	−5.6
10 Assemblers and assistants	2,467	2,144	−13.1
11 Rail transport	199	165	−17.1
12 Road and sea transport	748	797	6.6
13 Operating processing plants	1,396	1,000	−28.4
14 Special tasks in manufacture of metal products	780	801	2.7
15 Special tasks in construction	1,371	1,095	−20.1
16 Special tasks in food, beverages, tobacco	501	531	6.0
17 Special tasks in agriculture	1,610	1,372	−14.8
18 Special tasks in mining	151	132	−12.6
19 Special tasks in manufacture of clothing	200	200	0
20 Special tasks in printing	151	104	−31.1
21 Transmission of information	176	157	−10.8
22 Health services	727	917	26.1
23 Legal advice, business consultancy	126	158	25.4
24 Security functions	927	1,120	20.8
25 Test, measurement	376	371	−1.3
26 Others	100	64	−36.0
Total	**24,921**	**24,992**	0.3

Environmental carcinogens

Nitrite safe?

The US processed-meat industry received a welcome reprieve last week when the Food and Drug Administration (FDA) and the Department of Agriculture (USDA) announced that there was "insufficient evidence" to label sodium nitrite — a widely used meat preservative — a carcinogen.

Two years ago results of experiments contracted by the FDA to Dr Paul M. Newberne, Professor of Nutrition and Food Sciences at the Massachusetts

0028-0836/80/350835-02$01.00

Institute of Technology (MIT) suggested that nitrite produced cancer in the lymphatic system of laboratory rats.

Almost 13 per cent of 1,350 test animals in the study were said to have developed lymphomas, compared with only 5.75 per cent of the 573 not being fed nitrites.

The FDA had proposed a phased withdrawal of nitrites, but at the same time had announced that the MIT study was to be placed in the public record "so that the process of external scientific scrutiny can commence". As well as gathering comments from their own scientists, the FDA and the USDA commissioned a Washington-based contract research group, Universities Associated for Research and Education in Pathology, to review the 50,000 tissue slides taken by Dr Newberne of his 2,000 test animals.

Last week the two agencies announced that the review of the slides revealed insufficient evidence to support Dr Newberne's conclusions that nitrites increased the risk of cancer in the lymphatic system. The review group said that it found fewer of the slides indicated the presence of cancer than Dr Newberne had concluded, and the agency scientists agreed.

Some of the supposed lymphomas were noncancerous, the group said, and some were histiocytic sarcomas, which have no known human counterpart.

On the basis of this reassessment of Dr Newberne's data, the two agencies announced that they were dropping plans to phase out the use of nitrites.

However, the statement emphasized that steps are still being taken to reduce the level of nitrites in food because of concern that, through the effects of cooking or digestion with other chemicals, nitrites can form nitrosamines, known potent carcinogens.

Following last week's announcement, the FDA has also asked the National Academy of Sciences to review and evaluate all available scientific data about nitrites, and to analyse possible alternative preservatives for use in the meat and poultry industries.

The decision not to impose a ban on nitrites was widely welcomed by food industry officials, where nitrites are used not only to prevent the spread of botulism, but also to give meat the red colouring favoured by US consumers. The industry had complained that there was no alternative agent with equivalent taste, texture and handling characteristics, and had previously claimed that a ban might destroy the US pig industry, over 70 per cent of whose products are processed with the use of nitrites.

When his research results were reported two years ago, Dr Newberne urged that they should be confirmed by other research workers before any ban was introduced. Last week he was on vacation, unable to comment on the review group's critique of his research techniques.

David Dickson

Energy conservation

UK forecasts

The UK Atomic Energy Authority (UKAEA) has dismissed as "uneconomic and risky" proposals for an aggressive policy on energy conservation put forward by the International Institute for Environment and Development (IIED) 15 months ago.

That "low energy stategy" placed too much emphasis on conservation and too little on the expansion of indigenous fuel supplies say the UKAEA. Furthermore, the strategy leads to a shortfall in oil and gas supplies of up to 108 million tonnes of coal equivalent in the year 2025, say the authority, overestimates the savings possible in the domestic sector, and is inconsistent in its projections of sectional and overall economic growth.

What no doubt stuck in the authority's throat was the claim in the IIED report that electricity output can be met by building only 6 GW of nuclear capacity in the first quarter of next century, so that nuclear power would become "a peripheral issue", and that the fast breeder "could be shelved indefinitely". (In contrast, the UK government has since announced a 15-GW nuclear construction programme over the decade beginning 1982.) Thus the authority wish to argue that energy demand, and particularly electricity demand, will remain more buoyant than the IIED calculate.

Gerald Leach, principal author of the IIED report, last week admitted that the low energy strategy could lead to an oil and gas shortfall in 2025, in so far as it was possible to calculate that distance into the future, but said that it would be very easy to make good the shortfall by, for example, increased coal production for which his estimate for the year 2025 had been more conservative even than the 170 million tonne target set for the year 2000 by the National Coal Board.

In domestic conservation, the level of savings depended greatly on the assumed price ratio between gas and electricity as a function of time, said Leach. "Everyone is crashing out of electricity now", and electricity prices will increase further as coal and oil become more expensive. So if cheap nuclear electricity does come on line in the UK in the 1990s it may be too late.

On the other hand, argue the UKAEA, the assumption in the low energy strategy that real incomes in 2025 will be 3 times those of today, and that electricity prices relative to gas will be 2.4 times cheaper than today, are incompatible with the assumption that domestic electricity use will decline. The greater heat gains available from electric heat pumps and their quietness, compared with gas-driven heat pumps, will lead to their preferential adoption, say the authority; and the IIED have ignored a likely trend to greater size in domestic appliances. UK refrigerators average 5–6 cubic ft, whereas American ones average 12 cubic ft.

But potentially the most damning criticism in the UKAEA reply is that the IIED report is inconsistent. One of its most attractive conclusions was that high growth was possible alongside a reduction in energy use; but the assumed growth rate is not matched by the sectional estimates from which energy use is derived.

The IIED report, in its high growth case, assumes 2.94% annual growth in gross domestic product and the growth of non-energy manufacturing industry at only 2.19%. But that implies, the UKAEA point out, that the other sectors (which are mainly service industries) grow faster than 2.94%, whereas the IIED figures show much lower growth in the measures used (for example, floor area for the commercial and institutional sector).

Leach's reply to this is that he assumes, on the basis of many interviews and studies, that the monetary productivity of a given unit in the service sector will increase. For example, the £/m^2 generated in office work will increase through the introduction of microcircuitry.

Robert Walgate

Soviet space

Salyut women

Although Soviet planners decided in 1976 not to recruit any more women to follow Valentina Tereshkova into space as a pilot, they also announced that women would still be eligible to serve aboard space stations as doctors, astronomers or stewardesses. None has yet done so but it seems as if a welcome is now being prepared aboard Salyut.

Until now, the Salyut stations have been somewhat cramped, and, according to an unattributed talk on Moscow radio last month, "quite hard and difficult even for men". Now, however, Salyut-type stations have "more acceptable" conditions for joint work by both men and women. In the near future, stations will have separate cabins, rest rooms and showers.

Salyut 6 already has an experimental shower cabinet, in which the cosmonaut is sluiced by a stream of water drops borne by an airflow. In the future the beads of water which remain in the shower cabinet instead of passing on to the recycling system will be dealt with by the newest aid to space hygiene, a special towelling drying-bag.

One on-board luxury the would-be citizeness-cosmonaut still cannot expect is the traditional bunch of flowers on Women's Day (8 March). Soviet space biologists announced last month that they were abandoning attempts to grow flowers in space, for lack of positive results, and they were now concentrating their attention on radishes, cucumbers and carrots, which could form an important addition to the cosmonauts' diet.

Vera Rich

0028-0836/80/350836-02$01.00

NEWS AND VIEWS

Lamarckist revival in immunology

From R.B. Taylor

DARWIN'S concept of natural selection has gained almost universal acceptance. Along with it most biologists also tacitly accept Weissmann's doctrine of the inviolability of the germ-plasm, and so reject the possibility that acquired characteristics could be inherited. The old controversy on this last point has recently been re-opened by E. J. Steele. In his book (*Somatic selection and adaptive evolution*, Williams-Wallace, Toronto-London, 1979) he assembles evidence that acquired characteristics may be inherited, and suggests how this might occur. His proposal is based on Temin's protovirus and provirus hypotheses for the evolutionary origin and biological role of the C-type RNA viruses (*J. Nat. Cancer Inst.* **46**; *Science* **192**, 1975). These viruses can transduce genetic information from one somatic cell to another by capturing intracellular RNA sequences (e.g. messenger RNA) and infecting other cells where the RNA is copied by reverse transcriptase into DNA capable of being integrated into the genome. It would require only that such information be transduced into germ-cell DNA for inheritance of acquired characteristics to become conceivable — as indeed was suggested by Temin. If somatic mutations are capable of being selected by environmental pressures (as is widely accepted for the lymphocytes of the immune system) then this would increase the probability of their being transmitted to the germ-line and fixed as heritable characteristics.

This neo-Lamarckist hypothesis has recently received experimental support in a paper by Gorczynski and Steele, (*Proc. Nat. Acad. Sci. U.S.A.* **77**, 2871; 1980) who make the startling claim that neonatally induced immunological tolerance to MHC (major histocompatibility, or transplantation) antigens can be genetically transmitted to the offspring through at least two generations.

The experiment consisted first in the induction of tolerance in *male* mice of the CBA strain by the classical procedure of neonatal injection of lymphoid and bone marrow cells from a hybrid donor strain bearing foreign MHC antigens: (CBA × A)F_1 (Billingham *et al. Phil. Trans. R. Soc. B* **239**, 357; 1956). The neonatal injection was followed by regular further injections: a procedure known to induce a state of chimaerism. When they reached adulthood these tolerant males were mated with normal females. Some of the offspring from this first mating were killed and examined for tolerance by testing the ability of their spleen cells to mount a cytotoxic (CTL) response *in vitro* against target cells of the donor strain. Others were allowed to survive and were mated either with each other, or with normal CBA mice to give a second generation. These, and their first generation parents, were likewise examined for tolerance by CTL assay. Both generations, neither of which had been intentionally exposed to the tolerogen, showed a wide range of response, from normal down to undetectable. The important point is that a high proportion of them (50–60% of the 1st generation and 20–40% of the 2nd generation) gave responses significantly below those given by control CBA mice. Specificity was demonstrated by the fact that the mice responded normally to a 3rd party strain: C57B1/6J.

Such a remarkable result must be questioned very closely — both as to its technical adequacy, and as to the interpretation given to it. The CTL assay used in the experiment is a standard procedure and does not demand any major technical innovations. Although most of the results depend on one-point assays, the same degree of hyporesponsiveness was seen even at a fourfold higher concentration of attacker cells. One might ask for more controls to show that the inherited patterns of response were really dependent on the initial induction of tolerance, and not on a tendency of some CBA males to throw hyporesponsive liters. One might also ask that the tests *in vitro* should be supported by evidence of graft tolerance *in vivo*.

The further interpretation leaves even more room for questions. We must ask (a) *what*, in terms of phenotype, was transmitted; and (b) *how* was it transmitted? To answer the first question we need to define immunological tolerance in its various guises, and ask to which of these (if any) the Gorczynski-Steele phenomenon belongs.

In its broadest operational sense tolerance means a state of specific unresponsiveness, which includes states of significant hyporesponsiveness such as were found in many of the mice claimed to have inherited tolerance. It can exist in T cells or B cells or both. Underlying the condition of tolerance may be any of a variety of mechanisms which fall into two categories: those in which active suppression by suppressor lymphocytes has been demonstrated, and those in which it has not, and which are assumed therefore to be due to irreversible 'deletion' of competent cells. This distinction is important because although somatic selection could act to favour a mutant with positive function (suppression) it could not act on a loss mutant. The usual test for distingushing between deletion and suppression is to make a cell mixture in order to see if the tolerant cells will be able to prevent the normal cells from responding. However, this test could not necessarily be used to establish that suppressive mechanisms are operating in the mice with inherited tolerance. This is because it would not detect suppressor cells whose action was to *prevent the development* of competent cells from stem cells. It is this kind of cell which has recently been detected (by a different test) in mice which would otherwise be thought to have a deletion-type of tolerance (Gorczynski and MacRae *J. Immunol* **122**, 737 & 747; 1979).

The agents of active suppression have been identified both as suppressor T cells and as free antibodies. In both cases, there is now evidence that they may carry specificity for the variable regions (idiotypes) on the antigen receptors of the cells they suppress. The situation becomes even more complex when we consider artificially-induced tolerance to MHC antigens, because the tolerance-inducing inoculum usually contains cells capable of reacting against the host. This they can do either by the unexpected, but now well established ability of F_1 hybrid cells to recognise parental strain MHC antigens (Shearer, *et al., Cold Spring Harbour Symp*, **41**, 511; 1976); or by means of an anti-idiotypic response against the

---

R.B. Taylor is in the Department of Pathology, The Medical School, University of Bristol, UK.

0028-0836/80/350837-02$01 00

receptors by which the parent recognises the foreign antigens in the F_1 (Ramseier & Lindenmann *Pathol. Microbiol.* **34,** 379; 1969). This latter mechanism can suppress the parental cells so as to produce what amounts to a phenotypic state of tolerance (Binz *et al. Nature* **246,** 146; 1973). Thus a state of tolerance can involve any of a wide variety of different mechanisms, all of which may represent facets of the way self-tolerance is maintained. At least some of the positive suppressor mechanisms however seem to be specially stimulated after induction of tolerance by artificial means. This is important because it is clear that natural self-tolerance is not inherited; if it were one would expect to see it in the homozygous offspring of an $F_1 \times$ parent mating. In fact however such mice do not tolerate the foreign F_1 antigens any better than their homozygous, non-tolerant parent.

It is possible however that Gorczynski's and Steele's mice have inherited, not their fathers' suppressive mechanisms, but the antigen to which the fathers have been made tolerant. Very large numbers of donor cells were injected at regular intervals throughout the fathers' lives, so genes specifying donor antigens could as easily be imagined to have found their way into the germ-line as somatically mutated paternal genes. In that case such genes would be expressed in a proportion of the offspring and would be recognised and tolerated as 'self'. This possibility is mentioned by Gorczinski and Steele.

This brings us to the second of our two questions: was the information actually transmitted in the DNA of germ cells, or did it go by some less direct route? The fact that fewer of the second generation mice were tolerant than the first argues that the characteristic was not fixed in the germ line, and thus would require some special proviso for it to be accepted as inheritance in the DNA. In place of this, some other routes bear consideration. Could tolerance have been transmitted via a regulatory antibody or lymphocyte, or an antigen-bearing stem cell, in the seminal plasma? There is no precendent for such a route. In addition it would require the mothers to become tolerant, which seems highly unlikely in view of the known difficulty of inducing tolerance to MHC antigens in the adult animal.

Another possibility, by which one might escape frontal challenge to Weissmann's dogma, is that the information could be carried across the generations by viruses as such, without requiring violation of germ-line DNA. There are indeed a number of instances in which virus infection both *in vitro,* and *in vivo* has been associated with the appearance of unexpected (or 'alien') MHC specificities. But whether the virus actually transduces the MHC-specific information (as would be necessary if this were to explain the inheritance of tolerance) or whether it merely triggers some predetermined change in the structure of the MHC molecules is not known. In any case there is as yet no good evidence from this or any other source for viral transduction *in vivo.* Furthermore, for viral infection to serve as an explanation it would have to be strictly limited to the venereal route, otherwise tolerance would have been expected to appear in some control mice in the same animal house.

Yet another possibility (A. Müllbacher, personal communication) depends on the already-mentioned capacity of F_1 hybrids to make a response to the parent. Thus if the tolerogenic inoculum of F_1 lymphoid cells were making such a response to the CBA host, it might have the effect of selecting against the CBA-type among developing germ cells, and thus favour any mutations bearing A strain antigens. These mutations could then be perpetuated by normal inheritance, and there would be no need for a special viral transduction mechanism. Once again, however, there is no precedent for this type of selection.

In answer to our second question, then, it is not easy to offer an alternative mechanism for the transmission of tolerance which is any more credible than the Lamarckian one favoured by Gorczynski and Steele. Clearly, the basic result must be repeated in other laboratories. It will be important to establish mendelian inheritance through further generations, and to characterize the tolerant state. In addition one would expect from the point of view of survival value in evolution, that immune responsiveness as well as non-responsivenes would prove to be heritable. ☐

Solar luminosity variations

from Ronald L. Gilliland

THE solar luminosity is the primary force driving the earth's atmospheric circulation and it is probable that variations in the solar constant of as little as 0.3% would have a measurable effect on the climate. In a recent paper, Dearborn and Blake (*Astrophys. J.* **237,** 616; 1980) describe the effects on the solar luminosity of varying the efficiency of convection and they briefly discuss mechanisms which could produce such changes. One such mechanism is a fluctuation in the average properties of the convection cells seen near the solar surface. At the depth where the luminosity is quite sensitive to the convective efficiency the number of cells is $\sim 10^3$. If the properties of individual cells are allowed to vary by 10%, then stochastic variations of $\sim 0.3\%$ in the total flux could occur. An alternative mechanism for inducing changes of convective efficiency is interaction with the cyclic variation of magnetic field strength associated with the 11 year solar sunspot cycle.

To examine the significance of the Dearborn and Blake study it is necessary to briefly describe the solar convection zone. The sun has a convective region extending to a depth of some 200,000 km or $\sim 30\%$ by radius. As over most of this region convection is very efficient and capable of carrying a much larger flux than is actually present, changes in the convective efficiency will have little effect on the luminosity. In the outer 3,000 km the convective efficiency begins to drop. Here a significant part of the flux is carried by radiative transfer and changes in the convective flux are readily induced by small changes in the convective efficiency. Dearborn and Blake have adopted the standard approach of modeling the very complex phenomena of turbulent convection with a simple 'mixing length' theory in which the size of convective cells at any given level is given by the assumed mixing length. It is the assumed mixing length which Dearborn and Blake alter to bring about a change of convective efficiency. They find that quite small changes in the mixing length parameter on timescales of days to $\sim 10^3$ years can lead to significant luminosity variations. These results are interesting and provocative since they show that solar luminosity variations are theoretically plausible on these timescales. However, quantitative predictions cannot be made as there is no physical connection between the proposed mechanisms leading to convective efficiency variations and modeling of them.

The solar models which show luminosity changes in response to a forced variation of convective efficiency also show radius variation. Sofia *et al.* (*Science* **204,** 1306; 1979) argue that measurements of solar radius variations can be used as a proxy measure of luminosity changes. The use of radius variations as a proxy depends on the theoretical determination of the relative change of radius with respect to luminosity (defined as $W = \frac{\Delta R/R}{\Delta S/S}$, R = solar radius, S = solar constant) resulting from assumed changes in convective efficiency. This would be very useful since historical records of the solar radius (from transit timings of the sun crossing the meridian, eclipse observations, and timings of Mercury transits) extend back a few hundred years. Unfortunately, direct monitoring of the solar luminosity has been carried out only for parts of this century and there is insufficient data for long-term correlations with climate.

The early claim by Sofia *et al.* that radius

Ronald L. Gilliland is a visitor in the High Altitude Observatory of the National Center for Atmospheric Research, US.

0028-0836/80/350838-02$01.00

Devonian trilobites

from R. A. Fortey

In a recent publication*, Eldredge and Branisa describe a whole series of beautifully preserved trilobites from Devonian rocks in Bolivia, including a number of genera and species new to science.

The trilobites are an extinct group of arthropods that flourished from the Cambrian to Permian periods (about 600—250 Myr BP). Unlike many invertebrate fossils, they have a complex and varied morphology, and rapid changes have occurred in virtually all parts of the exo-skeleton. They are therefore an ideal group to use as tests of the different theories for reconstructing phylogeny. The visual system in particular is very sophisticated and there are complex shufflings in the arrangement and numbers of lenses. The specimens described by Eldredge and Branisa are remarkable for their well-preserved muscle impressions and they have been able to record speciation within a geographically and taxonomically limited group. Of particular interest is their demonstration of the number of specific variations that can be played on a relatively few morphological themes — a product of one of the rapid 'radiations' that happened from time to time during the long history of the trilobites. □

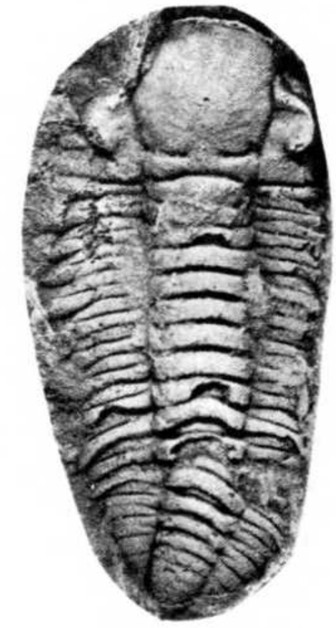

Andinacaste legrandi. Sora Sora, Bolivia. Dorsal view of cast of a complete individual × 3.

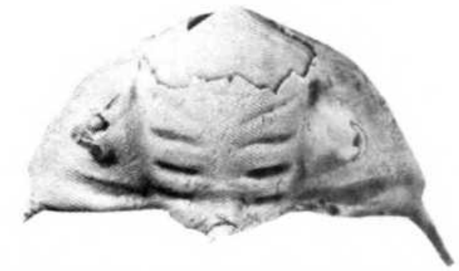

Bainella (Bainella) 'acacia'. Pebble Island, Falkland Islands. Dorsal view of cephalon × 1.

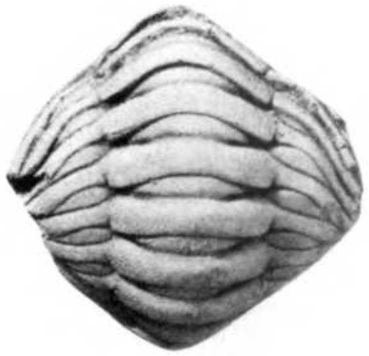

Phacopina. Belén region, Bolivia. Dorsal view of portion of thorax × 3.

R.A. Fortey is in the Department of Palaeontology, British Museum of Natural History, London.

---

*Niles Eldredge & Leonardo Branisa *Calmoniid Trilobites of the Lower Devonian Scaphiocoelia zone of Bolivia, with remarks on related species* Bulletin of the America Museum of Natural History **165**, 2; 1980.

---

variations could be used as a means of determining luminosity changes has encountered several problems. First of all, similar calculations conducted by different groups have found widely discrepant values for W. (Dearborn and Blake found $W = 5 \times 10^{-3}$. Sofia *et al.* found $W = 7.5 \times 10^{-2}$. In my own studies I have found $W = 8.5 \times 10^{-4}$. This is a total spread of × 100!) The numerical discrepancies are related to a much more fundamental problem. The mixing length theory does not model the turbulent convective flow in a time-dependent deterministic sense (feedback with variations of individual cells or the magnetic field can not be included). The mixing length is a free parameter which is normally adjusted in order for the calculation to match time-averaged global observed conditions (for example, radius and luminosity). While the mixing length theories may adequately describe time-independent global structure, results of perturbations within the mixing length theory framework do not necessarily have any relation to actual physical processes. The mixing length theory does not adequately describe the detailed structure of the outer 3,000 km of the solar convection zone (where the changes in question arise). Indeed different versions of mixing length theory exist which give observationally indistinguishable solar models, but quite different structures in the outer 3,000 km which are so important for this problem. Using mixing length theory to determine more than rough qualitative estimates for the relative radius and luminosity variations is highly questionable.

In order to predict reliable quantitative results for solar radius and luminosity variations it will be necessary to directly incorporate the causal mechanisms. For the stochastic variation mechanism a deterministic hydrodynamic model of convection in multiple dimensions is required. To follow the effects of a variable magnetic field one must couple the full 3-dimensional hydrodynamic treatment of convection with an equation to determine the magnetic field. One must thus solve the non-linear astrophysical dynamo problem (see Moffat, H.K. *Nature* **285**, 16; 1980). This is a very difficult problem — reliable quantitative results are unlikely to be found in the near future.

While past measurements of solar luminosity and radius variations have not been highly significant, our ability to make precise measurements may be expected to improve in the near future. The Solar Maximum Mission launched February 14, 1980 should provide measurements of the solar luminosity with an absolute accuracy of 0.1% and a relative precision 0.02% over a planned period of 1-2 years. Preliminary results indicate that the quoted precision will be achieved and that statistically significant variations are occurring. Willson *et al.* (*Science* **207**, 179; 1980) have claimed direct detection of a 0.4% luminosity increase over a 2.4 year period with two rocket flights. A change of this magnitude occurring periodically over a few years or as part of a longer trend would have probable climatological significance. SMM and future satellite missions should allow us to know whether or not solar luminosity variations are taking place. The High Altitude Observatory is sponsoring a solar diameter measuring project based on transit timings which should be capable of detecting monotonic radius changes to < 0.01% over a baseline of a few years. Simultaneous radius and luminosity determinations are of importance in developing and checking theoretical models of solar variations. Thus, while current theoretical models of solar variations can be viewed as little more than suggestive, the day is near when direct observational determinations of such changes can be made, which in turn should help the development of realistic models. □

0028-0836/80/350839-02$01.00

Pseudogenes

from Nick Proudfoot

A new and unexpected discovery has now come from the molecular analysis of gene families that code for globin. Studies from a variety of mammalian species reveal that in each case more gene sequences are present in the genome than are necessary to encode the known globin polypeptides. Sequence analysis of these extra globin genes shows that they have a variety of nucleotide changes that would result in either aberrant or absent polypeptide formation. The term 'pseudogene' — defined as a region of DNA that displays significant homology to a functional gene but has mutations that prevent its expression — has been coined for these aberrant genes.

The first example of a eukaryotic pseudogene was described by Jacq, Miller and Brownlee (*Cell* **12**, 109; 1977) for the Xenopus 5S gene system. These and further studies (Miller *et al.* *Cell* **13**, 717; 1978) revealed that the 5S gene was directly adjacent to an almost but not quite faithful 5S gene copy. No pseudogene 5S RNA has ever been detected *in vivo*. More recently extra genes which may be pseudogenes have been found in the rabbit (Hardison *et al.* *Cell* **18**, 1285; 1979) and human β-globin gene clusters (Fritsch *et al.* *Cell* **19**, 959; 1980) and human α-globin gene cluster (Lauer *et al.* *Cell* **20**, 119, 1980).

During a recent meeting entitled "Haemoglobin Switching" at Airlie House, Virginia, US the β-like gene families of human, rabbit, mouse, sheep and goat and α-like gene families of human and mouse were described in some detail. In each case more genes were detected than expected and evidence was presented suggesting that most of these extra genes are, in fact, pseudogenes. As recently published from the laboratories of Phillip Leder and Oliver Smithies (Nishioka *et al.* *Proc. natn. Acad. Sci. U.S.A.* **77**, 2806; 1980; Vanin *et al.* *Nature* **286**, 222; 1980), Nishioka and Vanin described a mouse α-globin gene that has various frame shift mutations which are in turn followed by in-phase termination codons. As a result no α-globin-like polypeptides can be produced. The gene has a further remarkable feature — both introns are precisely excised so that it resembles a somewhat mutated α-globin messenger RNA.

Both speakers suggested possible mechanisms to explain how such an 'intronless' gene could have arisen. A favourite model is that messenger RNA or its reverse transcript somehow upsets the replicative process, even though the presence of globin mRNA or reverse transcriptase in germline cells has yet to be demonstrated. During replication of a globin gene, messenger RNA or complementary DNA might base pair with the gene sequence and loop out the two introns. Subsequent repair of such hybrids could result in intron excission. Another, perhaps more plausible, model is that the enzymes involved in splicing out introns from precursor RNA might also be capable of splicing DNA in an analogous manner. Presumably such DNA splicing would have to be a freak occurrence, or no intron would be safe. Nishioka described a second mouse α-like globin gene that appears to be a candidate for pseudogene status. Although both introns are present, several base changes in the gene would alter amino acids thought essential for globin function. Furthermore, the normal termination codon is mutated so that translation of the mRNA would continue into the 3′ noncoding region. Such a mutation has been found to be the cause of a rare genetic disorder in man — haemoglobin Constant Spring (Clegg *et al.* *Nature* **234**, 337; 1971).

Two pseudogenes of the goat were described by Lingrel in a β-globin gene family (Zingrel, Haynes, Schon, Clearly & Gallagher, unpublished).One gene has several terminator codons close to the start of the gene that would prevent the expression of globin. The other has a variety of base changes that would alter amino acids essential to globin function. There are also β-like globin pseudogenes in positions between embryonic and adult globin genes in mouse and rabbit. Hutchinson described the mouse β-pseudogene which appears to have completely lost its 5′ side so that the first β-like sequence detectable is at around amino acid position 75. Beyond this the sequence is clearly β-like and the second intron is in place. However, short deletions and additions of sequence together with terminator sequences indicate that this gene is inactive (Jahn, Hutchinson, Phillips, Weaver, Haigwood, Voliva & Edgell *Cell* in the press). In contrast to the mouse gene the rabbit β-pseudogene as described by Hardison has β-like sequence corresponding to all regions of the adult β gene except for its 3′ noncoding sequence which is barely identifiable. Again a deletion of one nucleotide close to the beginning of the gene coding sequence quickly puts any translation product from this gene out of phase (Lucy & Maniatis *Cell* in the press). Finally, a human α-globin pseudogene was described (Proudfoot & Maniatis *Cell* in the press), again between the embryonic and adult α-like genes. This gene is 70-80% homologous to the adult α-globin gene throughout its sequence but has a deletion of 20 nucleotides in the middle of the gene that puts the amino acid sequence out of phase.

An interesting feature of the last four pseudogenes is that they lack the putative intron splicing signals found at the beginning and end of all introns (Breathnach *et al.* *Proc. natn. Acad. Sci. U.S.A.* **75**, 4853; 1978; Lerner *et al.* *Nature* **283**, 220; 1980). It therefore seems unlikely that any transcripts produced by these genes could be spliced correctly. Two further features of the globin pseudogenes described should be mentioned. First, most of them, in addition to mutations that would directly affect translation into globin polypeptides, have potential transcription mutations. For instance, the intronless mouse α-globin and the second goat β-globin psuedogenes lack the putative promoter signal or 'Hogness Box' PyATApu (M. Goldberg, Doctoral Thesis, Stanford University), while the human α-globin and the same goat β-globin pseudogenes lack the putative polyadenylation signal AATAAA (Proudfoot & Brownlee *Nature* **263**, 211; 1976). Second, in each case where the complete linkage arrangement of the particular globin gene cluster has been established (human α and β, rabbit β, mouse β) a pseudogene is found between the embryonic or fetal and adult globin genes.

Can any function be ascribed to pseudogenes? Vanin *et al.* postulate that pseudogenes might restrict gene expression by using up the transcriptional apparatus of the cell in futile pseudogene transcription. Perhaps the presence of a pseudogene next to each adult globin gene is related to such a regulatory process. Alternatively, globin pseudogenes could be the source of new gene products if translated in one of the two other coding frames or if translation includes intron sequences which are unspliced. However, so far no new protein product has been suggested or identified for these pseudogenes.

It may be better to consider pseudogenes as relics of evolution. Globin genes probably evolved by duplication. After the initial duplication event each member of a pair could diverge and useful sequence variations would be selected. Presumably, first α and β and then embryonic and fetal globin genes were produced in this manner. Mutations that restrict expression of the genes could also occur. In an extreme case, such as a promoter mutation, it is possible that one gene might be completely switched off. There would be then no selective advantage in the switched-off gene remaining globin-like so the whole gene sequence might be expected to gradually drift from the original sequence. In another case a mutation might only partially inactive the gene resulting in low level expression. Human δ-globin and mouse β-minor globin genes might be living examples of such an evolutionary process. Finally, it is possible that certain gene mutations such as a frame shift might not

---

N.J. Proudfoot is a Senior Research Fellow in Biology at the California Institute of Technology, Pasadena, California, U.S.A.

0028-0836/80/350840-02$01.00

only incapacitate the gene but result in the expression of a new protein detrimental to the whole animal. Although such mutant genes might be expected to rapidly disappear from the population, further inactivating mutations might occur that could then allow these genes to become fixed in the population. There is, in any case, no reason to believe that pseudogenes *per se* have any function although, of course, new genes could evolve from them.

The molecular analysis of globin genes is probably more advanced than any other mammalian gene system at this time. It seems likely that when other gene families are equally well characterized new pseudogenes will be identified. Indeed, extrapolating from the situation in globin, one in four gene sequences may be pseudogenes. Put in simple terms this suggests that one quarter of our genes might be dead. □

Volcanic ash southern style

from Ian Smalley

WITH the eruptions of Mt. St Helens still making the headlines in the northern hemisphere this was a good time to have a conference* on volcanic ash deposits (alias tephras) in New Zealand. It might be noted that the St Helens eruption has produced about 1 km^3 of ash but the last eruption of the Taupo volcano in the mid North Island of New Zealand produced about 24 km^3, possibly all in about 15 minutes through a vent 100 m wide.

P. Froggatt (Victoria University, Wellington) reviewed the tephras from Taupo. There have been 8 major rhyolitic eruptions during the past 10,000 years. Their stratigraphy and distribution is well understood and provides useful marker beds over most of the North Island. A source vent for each eruption has now been established. The most useful and widespread marker bed is the Taupo pumice (1,820 yrs BP) which erupted from within Lake Taupo at Horomatangi Reefs. The stratigraphy and nature of the Taupo pumice have now been revised and show a variety of eruptive mechanisms. The last phase of the eruptions was the most voluminous and destructive, being a series of pyroclastic flows which swept radially outward over all topography for more than 60 km. Reconstruction of the eruptive history of this ignimbrite has important implications for older eruptions such as the Kawakawa tephra (20,000 yrs BP) and the older welded ignimbrites.

P. Kamp (Waikato University) discussed the Pleistocene tephras in Hawkes Bay and their implications for Quaternary events. The tephras provide an absolute time-scale for the Kidnappers Group sedimentary succession, the deposition of which was predominantly glacio-eustatically controlled and which matches the standard deep-sea chronostratigraphy (core V28–238). The correlation of Pleistocene tephras elsewhere in New Zealand with Kidnappers tephras may enable events on land to be tied into the sea-level chronology. Nine discrete rhyolitic tephras, which Kamp has named informally A to I, occur in the 350 m thick Kidnappers Group succession.

V. Neall (Massey University) offered some comparisons between the volcanoes in the Cascade Range in the Western United States (including Mt. St. Helens) and Mt Egmont in New Zealand. The geological setting of each volcano and its relationship to non-volcanic rocks provides useful comparisons, particularly with respect to control of pyroclastic flow and lahar mudflow distribution. Frequency of tephra eruptions in Holocene times varies from 1 per 100–200 years at St. Helens (based on the last 4,000 years record), to 1 per 250–350 years at Egmont, 1 per 500–1,000 years at Rainier and 1 per 800 years at Shasta. The Egmont tephra succession displays a remarkably uniform mineralogy in marked contrast to tephras within the last 500 years. Pyroclastic flows from Egmont have been as frequent as those produced from St Helens and Shasta, but are much less in volume.

A. Palmer (Victoria University, Wellington) considered the occurrence of airfall tephra in the loess of the Wairarapa, at the southern end of the North Island. The 20,000 yr BP Kawakawa tephra occurs as a pinkish white 5–10 cm band of coarse silt to fine sand-sized glass and pumice fragments and is consistently found at two thirds the depth of the top (Ohakean) loess unit. The tephra influences bulk density and water contents for at least 50 cm above the primary airfall material and similar bulk density and water content variations within the older loesses probably indicate volcanic ash. Some further observations on loess were provided by N. Kennedy (DSIR Soil Bureau, Rotorua) but he was concerned with what has come to be known as 'tephric' loess. Some problems are arising in the more northerly parts of the North Island with a redeposited tephra material which might be classed as a loess. According to Kennedy tephric loess is deposited during arid climatic periods and is always found sandwiched between tephras of 15,000–20,000 yrs BP. Thus the period 15–20,000 BP is regarded as cold and arid. In the Rotorua basin the average rate of accumulation during that critical period was 0.3 cm/yr.

D. Seward (N.Z. Inst. Nuclear Sci.) reported on progress in fission track dating of tephra deposits. Tephras represent time planes within both marine and continental sediments and are most suitable for stratigraphic chronology and correlation. Glass was the first material used for fission track dating of tephras but most glasses have undergone varying amounts of annealing and this has reduced the size and density of the spotaneous fission tracks, and produced a 'young' age. The most suitable mineral in the tephras is zircon. The Tertiary-Quaternary sequences in New Zealand contain sufficient tephras for a tight time scale to be realised throughout. However, because of error limits the fission track ages of individual tephras must be closely analysed before tephras from one sequence can be absolutely correlated with those from another. C. Vucetich (Victoria University, Wellington) offered some Quaternary tephra correlations, from c.40,000 yrs BP to c.300,000 yrs BP. The chronology was based on two fission track dates for zircons by B. Kohn: Puketirau tephra (Tirau) 0.22 ± 0.03 Myr and Omokoroa tephra (Tauranga) 0.36 ± 0.04 Myr and indirect dating per c.120,000 yr marine transgression.

D. Lowe (Waikato University) demonstrated the usefulness of tephra layers preserved in peats. The recent identification of more than twelve unweathered and unmixed thin discrete air-fall tephras in piston cores from shallow peaty lakes near Hamilton have provided a stratigraphic record of late Pleistocene (post-Kawakawa tephra) and Holocene tephra deposits in the Waikato region. Identification of the tephras was greatly aided by using X-radiography techniques and these are being actively developed by the Waikato group, with particular possibilities seen in the techniques of xeroradiography which utilises a reusable photo receptor plate instead of conventional X-ray film.

The situation may appear hazardous but like the farmers persistently cultivating the slopes of Etna the scientists find rich results are derived from volcanic ash. The scale of New Zealand vulcanism in the past has been colossal with the Taupo eruptions judged by G.P.L. Walker to have been perhaps among the largest ever. The enormous spread of volcanic material in New Zealand means that the datable volcanic events in the north can offer useful stratigraphic indicators even down into the glaciated south. □

Ian Smalley is in the Soil Bureau, Department of Scientific and Industrial Research, Lower Hutt, New Zealand.

*Tephra Workshop meeting, held at Victoria University, Wellington, on 30 June and 1 July 1980. Organised by C. Vucetich, R. Howarth and P. Froggatt; proceedings to be published by the Geology Department, Victoria University.

0028-0836/80/350841-01$01.00

Strategies of drug resistance in herpes simplex

from H. J. Field and G. K. Darby

ALTHOUGH effective anti-viral drugs are only just being developed it already seems likely that viruses have diverse strategies of drug resistance. Foremost among the anti-viral drugs is acyclovir (ACV)*, a nucleoside analogue which has shown great promise particularly against herpes simplex virus (HSV) infection. A wealth of encouraging results already exist for animal model systems [1-8], and clinical trials in man are now underway in Britain and the US.

Workers at Burroughs Wellcome first showed that two virus specified enzymes are involved in the mechanism of action of this compound[9-11]. Firstly ACV is 'activated' in infected cells by conversion to its triphosphate, the initial step in this process being carried out by the virus-coded enzyme, thymidine kinase (TK). For the drug to block the multiplication of the virus, the ACV-triphosphate must then interact with a second virus-coded enzyme, DNA polymerase[9,12].

Elion and her colleagues[9] showed that a virus unable to induce thymidine kinase was resistant to the drug. It also seemed that a second class of resistant virus — one with an altered DNA polymerase function — was theoretically possible. Investigations of resistant viruses generated by passage of HSV in the presence of the drug[13] suggested that resistance could indeed arise in this way, although initially it was only observed in TK$^-$ viruses. Evidence that mutations in the DNA polymerase gene of HSV could confer resistance to ACV was provided independently by Coen and Schaffer [14] and Schnipper and Crumpacker[15]. In both cases viruses were investigated in which exposure to phosphonoacetic acid (PAA) — a compound acting predominantly at the level of DNA polymerase[16] — had produced PAA resistance. The TK$^+$ viruses selected for resistance to PAA had also frequently acquired resistance to ACV, and it was concluded that the most likely location for this second ACV-resistance locus was the polymerase gene. Both groups also observed that selection of resistant strains in the presence of ACV generally yielded TK-deficient viruses although Coen and Schaffer[14] described one strain which appeared in addition, to have acquired resistance at the polymerase locus.

Is ACV resistance likely to become a clinical problem in man? To answer this we must look at the biological properties of resistant viruses. TK$^-$ viruses arise readily in tissue culture in actively dividing cells where TK is a non-essential virus function. Evidence is accumulating, however, that such viruses are attenuated in animal model systems, particularly in their interactions with the nervous systems[13, 17-21]. This may make their establishment *in vivo* unlikely and may also explain the lack of reports of such isolates from animals undergoing treatment with ACV.

In contrast with the frequent isolation of TK-deficient viruses, the change to resistance at the DNA polymerase locus occurs much less readily[13-15]. Since in this case the enzyme function is essential for virus replication, there must be considerable constraints on structural alterations. Nevertheless, studies on PAA-resistant viruses[22] and a TK$^+$, ACV-resistant virus[13] suggest that these viruses may not be attenuated as much as TK-deficient strains and may therefore be more of a problem. It is interesting in this context that a study by Hirano *et al.* last year[23] revealed that resistant strains of HSV isolated from patients treated with Idoxuridine were TK$^+$, leading the authors to speculate that these were DNA polymerase mutants. This contrasts with the TK$^-$ phenotype commonly associated with Idoxuridine resistance generated *in vitro*.

In the next few months information should become available on isolates obtained from humans treated with ACV. The *in vitro* work to date suggests that the analysis of such isolates will be complex and may well reveal unexpected strategies employed by HSV to outwit the nucleoside chemist. ☐

**9-(2-Hydroxyethoxymethyl) guanine, also known as acycloguanosine.*

1. Pavan-Langston, D., Campbell, R & Lass, J. *Am. J. Ophthalmol.* **86**, 618 (1978).
2. Kaufman, H. E., Varnell, E. D. Centifanto, Y. M. & Rheinstrom, S. D., *Antimicrobial Agents & Chemother.* **14**, 842 (1978).
3. Bauer, D. J., Collins, P., Tucker Jr., W. E. & Macklin, A. W. *Brit. J. Ophthalmol.* **63**,429 (1979).
4. Shiota, H., Inoue, S. & Yamane, S. *Brit. J. Ophthalmol.* **63**, 425 (1979).
5. Falcon, M. G. & Jones, B. R. *Brit. J. Ophthalmol.* **63**,422 (1979).
6. Field, H. J., Bell, S. E., Elion, G. B., Nash, A. A. & Wildy, P. *Antimicrob. Agents & Chemother.* **15**, 554 (1979).
7. Park, N. H., Pavan-Langston, D., McLean, S. L. & Albert, D. M. *Antimicrob. Agents & Chemother.* **15**, 775 (1979).
8. Klein, R. J., Friedman-Kien, A. E. & De Stefano, E. *Antimicrob. Agents & Chemother.* **15**, 723 (1979).
9. Elion, G. B., Furman, P. A., de Miranda, P., Beauchamp, L. & Schaeffer, H. J. *Proc. natn. Acad. Sci. U.S.A.* **74**, 5716 (1977).
10. Fyfe, J. A., Keller, P. M., Furman, P. A. Miller, R. L. & Elion, G. B. *J. biol. Chem.* **253**, 8721 (1978).
11. Furman, P. A., St. Clair, M. H. Fyfe, J. A., Rideout, J. L., Keller, P. M. & Elion, G. B. *J. Virol.* **32**, 72 (1979).
12. Schaeffer, H. J., Beauchamp, L., de Miranda, P., Elion, G. B., Bauer, D. J. & Collins, P. *Nature* **272**, 583 (1978).
13. Field, H. J. & Darby, G. *Antimicrob. Agents & Chemother.* **17**, 209 (1980).
14. Coen, D. M. & Schaffer, P. A. *Proc. natn. Acad. Sci. U.S.A.* **77**, 2265 (1980).
15. Schnipper, L. E. & Crumpacker, C. S. *Proc. natn. Acad. Sci. U.S.A.* **77**, 2270 (1980).
16. Honess, R. W. & Watson, D. H. *J. Virol.* **21**, 584 (1977).
17. Marcialis, M. A., La Colla, P., Schjivo, M. L., Flore, O., Firinu, A. & Loddo, B. *Experientia* **31**, 502 (1975).
18. Field, H. J. & Wildy, P. *J. Hyg. Camb.* **81**, 267 (1978).
19. Tenser, R. B., Miller, R. L. & Rapp, F. *Science* **205**, 915 (1979).
20. Tenser, R. B. & Dunstan, M. E. *Virol.* **99**, 417 (1979).
21. Klein, R. J., De Stefano, E., Brady, E. & Friedman-Kien, A. E. *Arch. Virol.* In the press.
22. Klein, R. J. & Friedman-Kien, A. E. *Antimicrob. Agents & Chemother.* **7**, 289 (1975).
23. Hirano, A., Yumura, K., Kurimura, T., Katsumoto, T., Moriyama, H. & Manabe, R. *Acta Virol.* **23**, 226 (1979.

H.J. Field and G.K. Darby are in the Division of Virology, Department of Pathology, University of Cambridge.

Primeval galaxies and the X-ray background

from Beatrice M. Tinsley

YOUNG galaxies must have been spectacular objects, with very high rates of star formation and associated bright stars, supernovae, optical nebulosities and X-ray sources. Some years ago, Partridge and Peebles noted that primeval galaxies might be detectable not only as individual objects (*Astrophys. J.* **147**, 868; 1967) but also as a source of diffuse background radiation at wavelengths from ultraviolet to infrared. (*Astrophys. J.* **148**; 1968). The search for primeval galaxies began with those papers and continuing into the present has branched into X-ray astronomy.

Most of the effort has focussed on individual primeval galaxies, with optical searches for them and theoretical models for their properties in all parts of the electromagnetic spectrum, (for a review see Sunyaev *et al. Comments Astrophys.* **7**, 183; 1978; Meier & Sunyaev *Scientific American* Nov. 1979 and Tinsley *Phil. Trans. R. Soc.* **296**, 303; 1980). Galaxies have been found in deep counts that have much bluer colors and probably higher rates of star formation than their nearby descendents (Bruzual & Kron *Astrophys. J.* in the press), but it is not know whether these are young or luminous enough to quality as *bona fide* primeval galaxies.

Searching for the integrated background light of young galaxies has proved to be an extremely difficult task at optical wavelengths because the diffuse extragalactic

Beatrice M. Tinsley is Professor of Astronomy at Yale University.

0028-0836/80/350842-02$01.00

light is fainter than the zodiacal light and probably fainter than scattered starlight in our own galaxy. Thus the latest observational efforts (Spinrad & Stone, *Astrophys. J.* **226**, 609; 1978; Dube *et al.* *Astrophys J.* **232**, 333, 1979) have succeeded only in setting readily understandable upper limits to the integrated light of primeval galaxies.

A new idea is that young galaxies might be detectable in the X-ray background — a well-established isotropic radiation that may or may not be simply a superposition of quasars and other known X-ray sources (see Rees in *Objects of High Redshift* IAU Symposium **92**, ed. Abell & Peebles, 1980). Some astronomers have been tempted to account for the X-ray background by thermal bremsstrahlung from a hot intergalactic medium, perhaps dense enough to close the universe, but this is unsatisfactory because the energy required to heat the gas would be excessively high (Field & Perrenod *Astrophys. J.* **215**, 717; 1977). However, thermal bremsstrahlung is a possibility if the emitting gas is very highly clumped, and this is where young galaxies enter the picture: two papers by Tanaka and Ikeuchi (*Prog. Theor. Phys.* **62**, 393; 1979) and Bookbinder *et al.* (*Astrophys. J.* **237**, 647; 1980) consider the radiation from gas heated by supernovae in primeval galaxies. The supernovae would heat the gas to a temperature of about 100 keV, implying that its thermal X-ray emission could explain the spectrum of the background (at energies of about 2 - 50 keV) if most of the active phase of star formation in galaxies occurred rather recently in cosmic time, at redshifts less than 2.

The difficult question is whether young galaxies can supply enough X-rays to account for a significant fraction of the background intensity. Bookbinder *et al.* conclude that they can, but the point is debatable. Their ingenious approach is to estimate the X-ray emission of each young galaxy by relating its supernova production to the mass of metals produced by exploding stars; the mass of metals can then be estimated in turn from the quantity of metal-rich stars now remaining in each galaxy. The present luminosities and colours of galaxies are the observable quantities used to indicate the mass of metal-rich stars, and an uncertain factor in the calculation is the ratio of this mass to total galactic luminosity. Bookbinder *et al.* find that the emitted X-rays are sufficient if the mass-to-luminosity ratio is 90 solar units. This number is uncomfortably high, since, as the authors note, observed mass-to-luminosity ratios of the metal-rich parts of galaxies are typically about 10. Nevertheless, Bookbinder *et al.* feel that, within the uncertainties, hot has being driven from young galaxies could contribute signficantly to the background near 50 keV.

This would be a very satisfying result, both accounting for the X-ray background and implying that primeval galaxies have been found. It should be noted, however, that the predicted X-ray intensity depends on the square of the mass-to-luminosity ratio of metal-rich stars, so with the plausible value of 10 for that ratio the young galaxies contribute only 1% of the X-ray background. A similar result was obtained by Tanaka and Ikeuchi (loc. cit.), who scaled their result to the mean density of galactic stars in the universe, and found with a plausible density that young galaxies contributed about 1% of the X-ray background at 10 keV. A significantly higher contribution would require more supernovae in young galaxies than estimated by either set of authors, which does not seem very likely since Bookbinder *et al.'s* supernovae even accounted for the known metals in intergalactic space. It therefore seems most plausible that gas heated in young galaxies makes a negligible contribution to the X-ray background.

Primeval galaxies may also be bright in X-rays from other sources. For example, Bookbinder *et al.* consider the possibility of large populations of stellar X-ray sources, analogous to the famous Cygnus X-1 (black hole) system in our own galaxy. However, stellar and other possible diffuse sources in primeval galaxies probably do not contribute a significant part of the background, since they could not account for its spectrum over a significant energy range.

We seem to be back to the question of whether primeval galaxies can ever be found. Individual sources may be a more promising avenue of discovery than any integrated background radiation, because they can always be studied further for predicted signatures of young galaxies. As noted above, some faint blue galaxies have been found that are viable candidates for very young objects, and it would be most exciting to study these in all possible detail, including high resolution imagery with the coming Space Telescope. □

Noisy chaos

from N. MacDonald

IN experiments in hydrodynamics the onset of turbulence (see *Nature* **283**, 431; 1980) is frequently preceded by a sequence of bifurcations from one periodic mode to another of doubled period. This has caused renewed interest in those mathematical models characterised by a similar series of solutions with period doubling, followed by the onset of non-periodic 'chaotic' behaviour as some parameter of the model is varied.

Perhaps the best known deterministic physical model with a chaotic solution is that of Lorenz (*Nature* **271**, 305; 1978) for flows in a horizontal layer of liquid across which a temperature gradient is maintained. In Lorenz' own calculations chaos comes about, as the Rayleigh number *R* is raised, by a sudden transition from a simple periodic flow. However, Robbins recently has shown (*S.I.A.M.J.App.Math.* **36**, 457; 1979) that as one lowers *R* to approach the chaotic region from the other direction, there is a sequence of bifurcations of this kind.

In a much simpler category of models employing one-dimensional maps (May *Nature* **261**, 459; 1976) such as

$$X_{n+1} = \lambda X_n(1 - X_n) \qquad (1)$$

the multiple bifurcations are through solutions of period 2, 4, . . 2^N, . . as one increases λ. The transition values λ_N accumulate in a regular manner towards a limiting value λ_C at which a non-periodic solution first occurs. Models of this type, are commonly used to study the population dynamics of insects which have one distinct generation each year, and one such model has recently been applied to populations of annual plants (Watkinson *J. theor. Biol*, **83**, 345; 1980). Difference equations such as (1) also have a somewhat subtle connection with differential equation models such as that of Lorenz.

There are difficulties in interpreting experimental data by means of any purely deterministic model with non-periodic, and apparently randomly fluctuating, solutions. This is perhaps most readily seen when a model such as (1) is used to describe population dynamics. The reproductive rate λ is liable to change from year to year because of random environmental influences. How can one expecte to unscramble these effects from those of deterministic chaos for a fixed λ? Again, in any physical model with such delicately poised dynamics it would be wise to allow for the perturbing effects of thermal fluctuations by including an additional random force term.

Rather little attention seems to have been paid to this difficulty, but in a recent paper Crutchfield and Hubermann (*Phys. Lett.* **A77**, 407, 1980) have studied the equation

$$X_{n+1} = X_n(1 - X_n) + N\sigma, \qquad (2)$$

in which $N\sigma$ is a Gaussian random number with zero mean and standard deviation σ. They have also studied the effect of a random force term added to a model of an anharmonic oscillator with a periodic forcing term. Several authors (*Nature* **274**, 847; 1978) have studied chaos in deterministic models of this type, and Crutchfield and Hubermann have previously shown (*Phys. Rev. Lett.* **43**, 1743; 1979) that multiple bifurcations occur in their particular version. They have characterised the chaotic solutions in

N. MacDonald is in the Department of Natural Philosophy, University of Glasgow.

0028-0836/80/350843-02$01.00

terms of a frequency spectrum containing a number of strong spikes on top of a broad distribution of frequencies. As one moves across the chaotic region, away from the critical parameter value that ends the period-doubling sequence, these spikes merge in pairs, simplifying the spectrum. Eventually only the broad band remains, the solution giving way to a simple periodic solution. The authors mention that Lorenz, in unpublished work, has established a similar structure of the solutions of model (1).

The strikingly simple qualitative result now obtained by Crutchfield and Hubermann is that, both in model (2) and in the noisily forced oscillator, the effect of the noise term is to remove the later stages of the bifurcation sequence of chaotic solutions. As the amplitude of the noise term is increased, this bifurcation gap widens.

The authors believe that this result should be capable of experimental test in situations in which the noise level can be controlled. Their anharmonic oscillator model was originally devised for application to solid state systems where anharmonic degrees of freedom can couple to a periodic field. Superionic conductors are an example of such a system. They are (Boyce & Hubermann *Phys. Rep.* **51**, 189; 1979) solids which display ionic conductivities many orders of magnitude greater than those of normal salts. They can be characterised by the presence of a rigid lattice of one type of ion in which another type of ion can move freely. The diffusion coefficients are very dependent on temperature, and for this reason Crutchfield and Hubermann suggest that superionic conductors may be particularly suitable for controlled variation of the noise term to test for the bifurcation gap. □

Cystic fibrosis

from Leighton Dann

UNTIL a few years ago, the genetic disease cystic fibrosis (CF) was considered to be a childhood disease as most patients succumbed at an early age. With the use of modern drugs the prognosis has been much improved and patients commonly reach adulthood. Thus CF has graduated from the paediatric clinic and entered general medicine.

This changing pattern provided the focus for much of the 8th International Congress on the disease held recently in Toronto*, with sessions on progression with age, and on genetics, diagnosis and screening.

The basic defect, as yet unidentified, primarily affects exocrine glands and so various bodily functions are impaired. Bronchopulmonary disease remains the greatest problem, and successful treatment and control of infection is a major goal of research. Several delegates discussed alternatives to antibiotic therapy, and H.V. Reynolds (Yale University New Haven) reported the use of immunoprophylaxis. Much of the work has concentrated on the bacterium *Pseudomonas aeroginosa* as it is so prevalent and so highly pathogenic in CF lung infection, particularly in the later stages of the disease. Although he showed that immunization with a multivalent lipopolysaccharide vaccine boosted existing titres of antibodies against the organism in the blood, no effect was noted in the lungs of patients. As with antibiotic therapies, serum values of drugs or antibodies bear little relation to local concentrations in the lungs. Reynolds felt that although this method of treatment was of no value to the patient who is already infected, early immunization, before infection with *P. aeroginosa,* might prove beneficial. He also suggested that other antigens should be studied, for example exotoxin A and several high molecular-weight cell wall polysaccharides.

A most promising therapeutic application of the chelating agent EDTA was proposed by R.E. Wood (Case Western Reserve University, Cleveland). He and his colleagues found that incorporation of EDTA into the culture medium retarded the growth of *P. aeroginosa* due to sequestration of divalent metal ions, particularly magnesium. There was also marked synergism shown between EDTA and many commonly used antibiotics. Preliminary experiments on animals show that EDTA does not affect mucociliary transport at the concentrations needed to arrest growth of bacteria and may therefore prove safe for use in the human lung.

Another major problem of CF is pancreatic insufficiency. Although it may be controlled by administration of pancreatic extracts, large and often increasing amounts must be given as the disease progresses. A new form of enzyme supplement, Pancrease, (manufactured by Johnson & Johnson, Slough, UK) was discussed by R. Dinwiddie (Hospital for Sick Children, London) A. M. Weber (Hospital Ste-Justine, Montreal) and D. J. Holsclaw and H. Keith (Hahnemann Hospital, Philadelphia).

Pancrease consists of enteric coated microspheres of pancreatic enzymes in a gelatin capsule, and passes intact through the stomach to the intestine. With this mode of administration fat absorption is greatly improved and patients have access to a more normal diet as well as being able to take fewer tablets each day (about 6 instead of about 30). Similarly, better food absorption was reported by D.J. Cameron (Hospital for Sick Children, London) and E. Rossi (Childrens Hospital, University of Berne) if cimetidine is used as an adjunct to pancreatic supplements. This drug lowers gastric acid output and so higher concentrations of enzymes reach the intestine intact.

Early diagnosis is of paramount importance for good prognosis, and much effort was focussed on newer methods of detection, especially those potentially amenable to mass screening or to antenatal diagnosis. R.B. Ellio (University of Auckland) described his test for immunoreactive trypsin in newborns. Because the pancreatic ducts are blocked, trypsin leaks into the blood and is present in high concentrations in affected babies. Great interest was shown in this test, as it is done on dried blood spots and could therefore be incorporated into existing screening programmes for phenylketonuria.

J. Lieberman (Veterans Administrations Medical Centre, Sepulveda, California) described an assay which detects a specific IgM-binding fructose-specific lectin in CF serum. He suggested that this test could prove useful in detecting heterozygote carriers of the CF gene, as the lectin is present in the blood of parents of affected children. The connection between this lectin and the CF factor (a highly basic small protein found in many body fluids) remains to be elucidated.

J.C. Manson (Western General Hospital, Edinburgh) reported the production of antiserum in mice using CF factor isolated from serum by isoelectric focusing. Preliminary results with the antiserum are highly succesful but its availability is limited. This method has potential as a screening test for homozygotes not only in newborns but also antenatally, for amniotic fluid from an affected fetus contains CF factor. In another approach to antenatal diagnosis, reported by L.G. Dann (Queen Charlotte's Hospital, London), an arginine esterase assay is used on cultured amniotic fluid cells. However lack of suitable samples is hampering validation of the method.

While delegates were optimistic that the outlook for patients with CF would continue to improve, it was clear that a better understanding of the disease and in particular, the basic defect, was needed before CF became truly a treatable disease. The work in progress presented at the congress encourage the hope that by the time of the next congress, in Britain in 1984, much of this will have been achieved. □

Leighton Dann is in Queen Charlotte's Maternity Hospital, London.

*The Conference was held on 26th-30th May 1980 in the Royal York Hotel, Toronto and was organized by the Canadian Cystic Fibrosis Foundation.

0028-0836/80/350844-01$01.00

ARTICLES

Free calcium in heart muscle at rest and during contraction measured with Ca^{2+}-sensitive microelectrodes

Eduardo Marban, Timothy J. Rink*, Richard W. Tsien & Roger Y. Tsien*

Department of Physiology, Yale University School of Medicine, New Haven, Connecticut 06510
* Physiological Laboratory, University of Cambridge, Cambridge CB2 3EG, UK

Direct measurements of free Ca^{2+} in heart cells are needed for an understanding of the regulation of contractility. We developed and used Ca^{2+}-sensitive microelectrodes with fine tips, stable properties and ample sensitivity to free Ca^{2+} in the sub-micromolar range. In quiescent ventricular muscle, measurements which passed tests for electrode sealing and cell viability gave a mean free Ca^{2+} concentration of 0.26 μM. During contractures, we recorded Ca^{2+} transients rising as high as 10 μM. In studying the effects of catecholamines on free Ca^{2+} and force, we found evidence that adrenaline can reduce myofibrillar Ca^{2+} sensitivity in intact heart muscle.

ALTHOUGH it is widely believed that a rise in intracellular calcium activates contraction in heart muscle, the level of free Ca^{2+} at rest or during activity remains quantitatively uncertain. The strength of contraction can be widely varied by ions, hormones or drugs. It is often not clear, however, whether such inotropic agents act by changing the amount of activator Ca^{2+} or by modifying the Ca^{2+}-responsiveness of the contractile machinery. Direct measurements of free Ca^{2+} in cardiac muscle are obviously desirable. Recently, the Ca^{2+}-sensitive photoprotein aequorin has been used to record Ca^{2+}-related signals from various cardiac preparations[1-3]. The technique is well suited for monitoring changes in Ca^{2+} during twitch contractions, and has already provided much useful information about inotropic effects. However, as the investigators are careful to point out, the method has certain limitations. The light signals do not easily give absolute values of free Ca^{2+} because of various uncertainties, including interference from intracellular Mg^{2+} or H^+. A large number of cells must be injected with aequorin, resting levels can apparently not be detected, and light signals during twitches must be signal-averaged to overcome noise. Ca^{2+}-sensitive microelectrodes[4-6] offer another approach with different advantages and limitations, which may complement optical techniques using aequorin or other Ca^{2+}-indicators. In the first attempts at applying Ca^{2+}-electrodes to cardiac tissue, investigators[7,8] used sheep Purkinje fibres because the cells in this preparation are large enough (40–50 μm diameter) to tolerate electrode tip diameters of ≥ 1 μm. To be useful in the smaller cells of working heart muscle itself (10–15 μm diameter), Ca^{2+}-electrodes must have tips of sub-micrometre size, while retaining stable properties and ample resolution down to 10^{-7} M free Ca^{2+} or lower. These requirements are fulfilled by the Ca^{2+}-sensitive microelectrodes which we have made with a new Ca^{2+}-sensor. The electrodes enabled us to measure intracellular free Ca^{2+} in ventricular muscle, both at rest and during contractures.

Unbranched papillary muscles, 0.4–0.8 mm in diameter and 2–4 mm long, were isolated from right ventricles of 8–12-week-old ferrets (*Mustela putorius furo*). Ferrets were chosen because their hearts usually contain two or more robust preparations with suitable geometry for force measurements[9]. Muscles were placed in a chamber for superfusion with oxygenated Tyrode solution containing (in mM): 150 NaCl, 4 KCl, 1.8 $CaCl_2$, 0.5 $MgCl_2$, 5 glucose and 10 Tris HCl buffer (pH 7.2–7.4). The preparation was mounted with one end fixed and the other end attached to a force transducer. To reduce movements which would tend to dislodge the electrodes, the muscle was carefully positioned on a pedestal, with resting length well below that giving peak developed twitch force. Suitable high input impedance electrometers (WP Instruments) recorded signals from the Ca^{2+}-sensitive microelectrode (V_{CaE}) and a conventional microelectrode filled with 3 M KCl (V_m). Bath potential was defined as zero for both electrodes; the bath was earthed by an agar bridge containing 3 M KCl. The preparation was first penetrated by the conventional microelectrode, usually during continuous stimulation of twitch contractions. After a stable V_m impalement had been obtained, stimulation was discontinued and the preparation was impaled by the Ca^{2+}-electrode at a second site several cell lengths away from the V_m impalement. V_{CaE}, V_m and their difference ($V_{CaE} - V_m = V_{diff}$) were recorded along with contractile force on a chart recorder and a magnetic tape recorder. V_{diff} is a measure of free Ca^{2+} inside the cell.

Electrode construction and characteristics

Micropipettes were pulled from thin-walled, borosilicate tubing to a size that gave resistances of 8–12 MΩ if filled with 3 M KCl. The pipettes were baked dry at 200 °C, siliconized with tributylchlorosilane vapour, and back-filled under pressure with the pCa 7 buffer solution described in Fig. 1 legend. The electrodes were then bevelled until the resistance dropped to about 40% of the original value, giving a sharp tip with an outer diameter of about 0.5 μm. Next, a 10–50-μm column of the Ca^{2+}-sensor, dissolved in tetrahydrofuran, was sucked into the tip of the electrode. This sensor, a modification of the polyvinylchloride (PVC) macroelectrode membrane of Ammann *et al.*[10], consisted of 10% (w/w) neutral Ca^{2+}-ligand, *N,N'* - di(11 - ethoxycarbonyl)undecyl - *N,N'*,4,5 - tetramethyl-3,6-dioxaoctane-1,8-diamide, 8% tetraphenylarsonium tetrakis (p-biphenylyl)borate, 10% PVC and 72% (o-nitrophenyl)octyl-ether. The tetrahydrofuran, used to reduce viscosity, evaporated away in a few minutes, leaving a PVC gel impregnated with the other sensor components in the tip of the electrode.

This new PVC-gelled sensor offers various advantages over previous Ca^{2+}-sensitive microelectrode compositions. (1) Mechanical stability is much improved over liquid sensors; the

0028–0836/80/350845—06$01.00

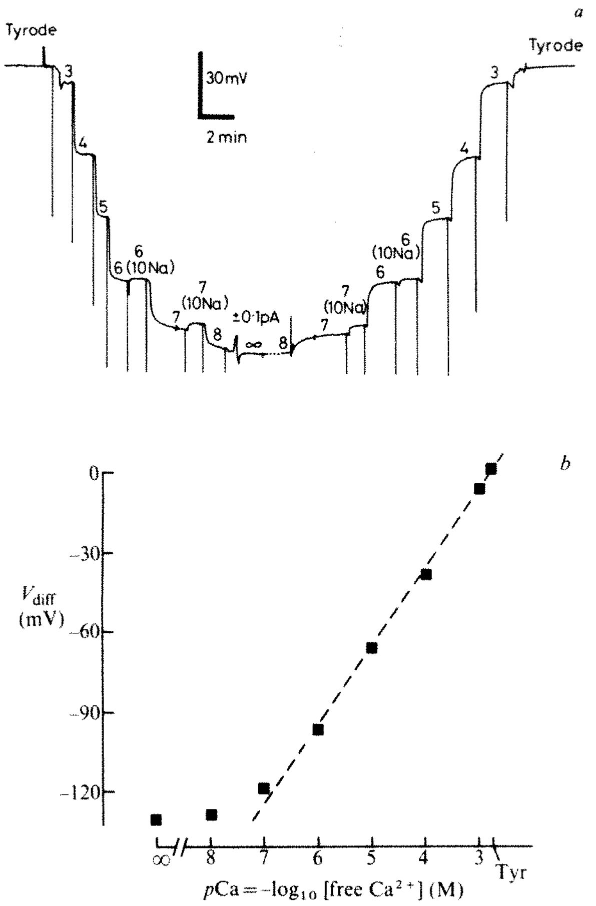

Fig. 1 Calibration plots for a Ca^{2+}-electrode with a bevelled tip of outer diameter ~0.5 μm. *a*, Calibration recording taken after a 5-h impalement of a ventricular cell. The e.m.f. of the Ca^{2+}-electrode was measured against a 3 M KCl reference electrode. The different test solutions are designated by their pCa values except for the initial solution which was the Tyrode solution containing 1.8 mM Ca^{2+}. The pCa 3 solution had 1 mM $CaCl_2$, 98 mM KCl and 10 mM K-MOPS, pH 7.3. The pCa 4, 5, 6, 7 and 8 solutions had 10 mM Ca-ligand (NTA, NTA, HEEDTA, EGTA, and EGTA, respectively), 5 mM $CaCl_2$, 90 mM KCl, 10 mM H^+ buffer (MOPS, Tris, HEPES, MOPS and HEPES) titrated with KOH to pH 7.39, 8.42, 7.70, 7.29 and 7.80. The 'pCa ∞' solution had 10 mM EGTA, no added Ca^{2+} and pH 7.6. The 'pCa 6 (10 Na)' and 'pCa 7 (10 Na)' solutions were the pCa 6 and 7 solutions to which 10 mM NaCl were added. '±0.1 pA' denotes current pulses to test the electrode resistance, $\sim 7\times10^{10}\,\Omega$. During the solution changes, the electrometer was switched into a standby mode for a few seconds. This was responsible for the electronic artefacts, a sharp downward spike followed by linear negative drift. *b*, Plot of the collected data from four calibration series including those shown in *a*, first descending, then ascending Ca^{2+} concentrations, before and after impalement. The potentials, V_{diff}, were read off the calibration recordings just before the next solution change. The zero of the scale was defined as the potential in 1.8 mM Ca^{2+} Tyrode in the first calibration run. The height of the symbols shows the full range (±1.5 mV) of potentials recorded in each buffer during the four calibrations. The dashed line indicates the theoretical (Nernst) slope, 29.5 mV per pCa unit at 24 °C.

PVC gel very seldom backs up or escapes from the tip. (2) Electrode response is increased at low Ca^{2+} levels, giving greater resolution between 10^{-6} M and 10^{-7} M free Ca^{2+} than previously achieved in fine microelectrodes suitable for use in small cells. (3) Electrode lifetime and stability are greatly increased. These electrodes retain their responsiveness over periods of 8–36 h. Use of the electrodes is often limited not by ageing, but rather by blunting of the tip with repeated penetrations.

The performance of the electrodes at low Ca^{2+} showed quantitative variations even when they were constructed in similar fashion from the same batch of sensor. Therefore, each electrode was individually tested by exposing it to a series of calibrating solutions (see Fig. 1 legend), following a procedure described elsewhere[11]. The calibrating solutions are designated by their free Ca^{2+} concentration, $[Ca^{2+}]$, given in units of pCa ($= -\log_{10}[Ca^{2+}]$). This convention was chosen instead of a Debye–Hückel activity scale so as to conform with (1) chemical measurements of Ca^{2+}-chelator dissociation constants[12], which are given in units of concentration, and (2) previous studies using aequorin or skinned fibres. The pCa scale can be readily converted into $-\log_{10}(Ca^{2+}$ activity) on a Debye–Hückel scale by adding a constant correction. This is possible because the KCl in the calibrating solutions keeps the Ca^{2+} activity coefficient nearly constant for $[Ca^{2+}] < 1$ mM. If, for example, one uses a Ca^{2+} activity coefficient of 0.36 (see refs 10, 13), our pCa 7 solution would be assigned a value of 7.44 for $-\log_{10}(Ca^{2+}$ activity).

Figure 1 shows the calibration of a fine, bevelled, PVC-sensor electrode. The response is nernstian down to 10^{-6} M, with some 24 mV between 10^{-6} and 10^{-7} M, and 10 mV below 10^{-7}, against a background of ~125 mM K^+. This is the best performance yet reported for a Ca^{2+} electrode with a sub-micrometre tip. At low Ca^{2+} levels, the electrodes have a small response to intracellular levels of Na^+ (refs 14–16). Figure 1*a* shows that 10 mM Na^+ increases the electrode potential by 1 mV at pCa 6 and 4 mV at pCa 7, so at intracellular resting Ca^{2+} levels, Na^+ interference needs to be taken into account. As with previous neutral ligand Ca^{2+} sensors[11,17], interference from Mg^{2+} and H^+ can be neglected. Even in Ca^{2+}-free solutions containing EGTA, increasing free Mg^{2+} from 0 to 5 mM (higher than estimated intracellular levels[18,19]) produces only 1–3 mV increase in electrode potential, and changing pH from 7.6 to 6.6 gives only 0–2 mV. At higher Ca^{2+} levels, ≥0.1 μM, interfering cations have even less effect. The influence of temperature must also be considered, as the calibrations were normally done at room temperature whereas the experiments were carried out at 35–37 °C. In separate experiments, calibrations were made at

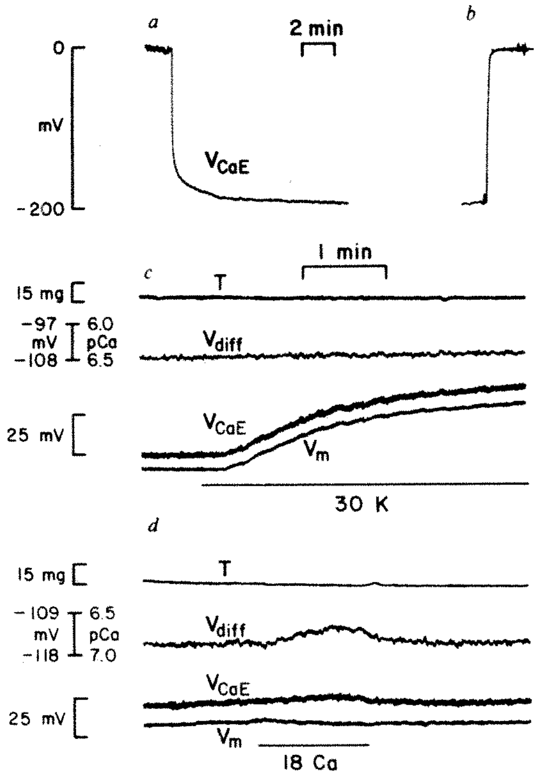

Fig. 2 Measurements of intracellular free Ca^{2+} and tests of their validity. *a*, Ca^{2+}-electrode signal (V_{CaE}) during impalement of a ferret papillary muscle. *b*, V_{CaE} during withdrawal of the same electrode after 3 h continuous intracellular recording. *c*, Common-mode rejection test in another preparation, using K^+-depolarization below the contractile threshold as a test signal. In this panel and subsequent ones, $V_{diff} (= V_{CaE} - V_m)$ is given on an absolute vertical scale, but the vertical positions of the V_{CaE} and V_m traces are arbitrary. At the beginning of *c*, $V_{CaE} = -200$ mV and $V_m = -92$ mV. *d*, Ca_0 elevation test in a third preparation. At beginning of record, $V_{CaE} = -196$ mV and $V_m = -81$ mV.

Table 1 Free Ca^{2+} concentration in unstimulated muscles

Preparation	Ca^{2+} electrode no.	Penetration no.	Test(s)	*p*Ca
Y22-2	26	3	18Ca, 30K	6.3
Y24-3	8	2	18Ca	6.7
		4	18Ca	6.4
Y25-3L	17	1	18Ca	6.6
		2	18Ca, 16K	6.4
	19a	1	18Ca	6.5
		4	18Ca, 16K	7.0
Y26-1	0	1	18Ca	6.7
	13	1	18Ca	6.9
Y29-1	7	1	18Ca, 30K	6.6
		6	18Ca, 30K	6.5
Y30-1	19b	2	30K	6.5
			Mean ± s.e.m.	6.59 ± 0.06

Intracellular *p*Ca values were determined by comparing V_{diff} levels, taken while muscles were bathed in 1.8 mM Ca^{2+}, 4 mM K^+ Tyrode solution, with electrode calibrations, carried out immediately after withdrawal from the muscle. Impalements satisfied quantitative criteria described in the text for electrode stability, sealing-in and cell viability. During tests of common-mode rejection using 16 or 30 mM K_o, $(\Delta V_{diff}/\Delta V_m)$ ranged between 0.98 and 1.07.

both 21 and 37 °C, using Ca^{2+} buffer compositions adjusted for temperature according to data from ref. 12. Raising the temperature merely scaled the response of the electromotive force (e.m.f.) by the ratio of absolute temperatures, in accord with the Nernst equation. For values of e.m.f. obtained in resting cells, the temperature correction amounts to about 3 mV, opposite and approximately equal to the magnitude of the sodium correction. The response time of the electrodes is many seconds at micromolar levels of Ca^{2+}, so they are not expected to follow transients during single twitches. Attention was therefore focused on 'resting' levels and slow changes during maintained contractures.

Intracellular measurements in resting muscles

Figure 2 illustrates electrode recordings during penetration and withdrawal, along with some tests of the validity of intracellular measurements. Figure 2*a* shows V_{CaE} during impalement of a cell with a Ca^{2+}-sensitive microelectrode. V_{CaE} undergoes a rapid negative deflection due in part to the membrane potential, and a slower negative-going change which can be attributed to sealing-in of the electrode and its sluggish response at low free Ca^{2+}. Figure 2*b* shows V_{CaE} during withdrawal of the Ca^{2+} electrode after a continuous 3-h impalement. The main point is the comparison between steady e.m.f.s measured at the beginning and end of the intracellular recording. The steady levels measured in the tissue agree extremely well, as do the levels in the external solution, indicating the absence of significant d.c. drift.

If $(V_{CaE} - V_m)$ is to be taken as a measure of intracellular free Ca^{2+}, it is necessary to consider the seal around the tip of the Ca^{2+} electrode and the viability of the impaled cell. Two types of test were applied to screen out defective impalements. One test uses changes in external potassium concentration (K_o) to vary the membrane potential over the range below contractile threshold. If the Ca^{2+}-electrode records from a cell which retains its normal resting potential, it should respond to a moderate elevation of K_o with a voltage change (ΔV_{CaE}) which closely matches the depolarization measured elsewhere in the preparation by the conventional microelectrode (ΔV_m). This is the case in Fig. 2*c* during a depolarization produced by 30 mM K_o. The quality of the common-mode rejection is also evident on the V_{diff} trace, which remains quite steady. Measurement of contractile force (*T*) confirmed that this level of depolarization was insufficient to activate tension.

In another test of impalement quality, the extracellular calcium concentration (Ca_o) was elevated, as shown in Fig. 2*d*. If the seal around the electrode tip was poor, or if the cell was otherwise damaged, one would expect a large V_{CaE} signal, as was sometimes seen. If, on the other hand, the tip was well sealed within a viable cell, one would expect only a modest change in V_{CaE}. In the experiment illustrated in Fig. 2*d*, a 10-fold increase of Ca_o produced little change in V_m and only a small positive-going deflection in V_{CaE}. The maximal change in V_{diff} was 4 mV, corresponding to $\Delta p\mathrm{Ca} = 0.22$, but there was no measurable development of force.

In these experiments and others, measurements of free Ca^{2+} in unstimulated muscles were examined according to various criteria to decide whether or not the impalements were acceptable. (1) Electrode stability was assessed in each case by comparing pre-impalement and post-impalement calibrations. The measurement was rejected unless the responses to *p*Ca 6 agreed to within 10 mV. (2) The quality of the seal around the Ca^{2+}-electrode tip and the viability of the impaled cell were checked by one or both of the following tests. First, exposure to 18 mM Ca_o (as in Fig. 2*c*): measurements were rejected if V_{diff} changed by more than 10 mV. Second, exposure to 16 or 30 mM

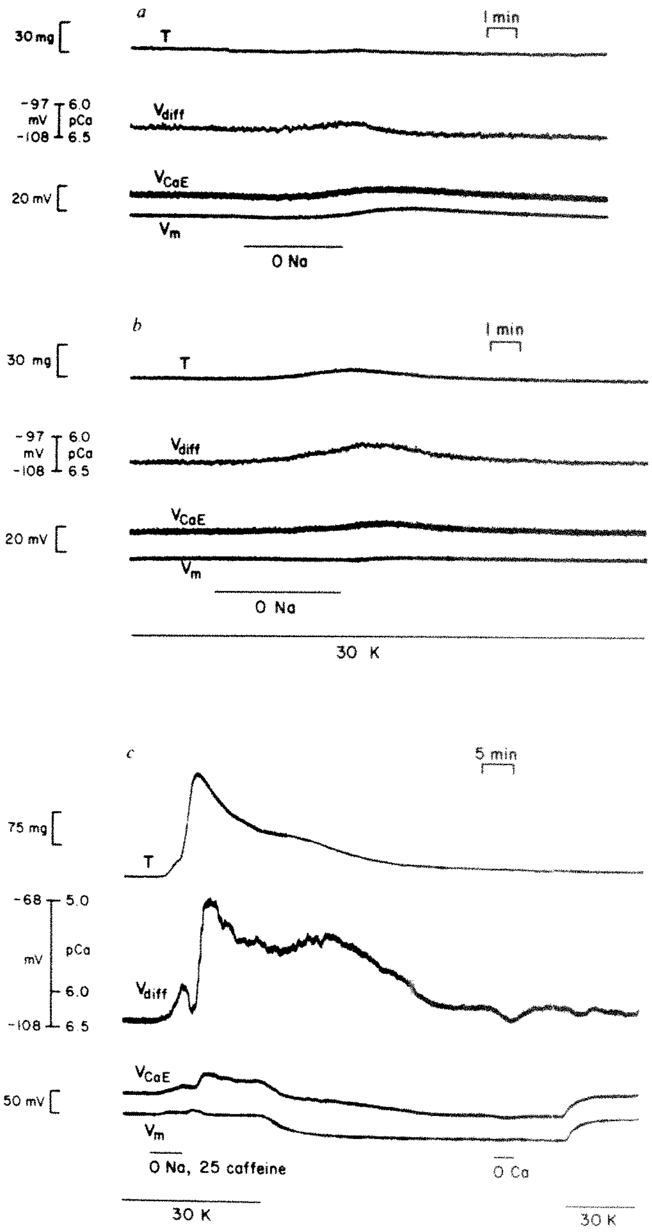

Fig. 3 Changes in free Ca^{2+} and force in response to a series of zero Na^+ challenges during continuous V_{CaE} and V_m impalements. *a*, Exposure to 0 Na(choline) in the presence of 4 mM K_o. V_m was −92 mV at beginning of record. *b*, 0 Na(choline) exposure in the presence of 30 mM K_o. V_m was −48 mV at beginning of record. *c*, Exposure to 0 Na(choline), 25 mM caffeine in the presence of 30 mM K_o. K_o was reduced from 30 to 4 mM and later restored to 30 mM as a test of whether both electrodes would respond equally to an imposed membrane potential change. Exposure to nominally Ca^{2+}-free solution was used to check continued responsiveness of V_{CaE}.

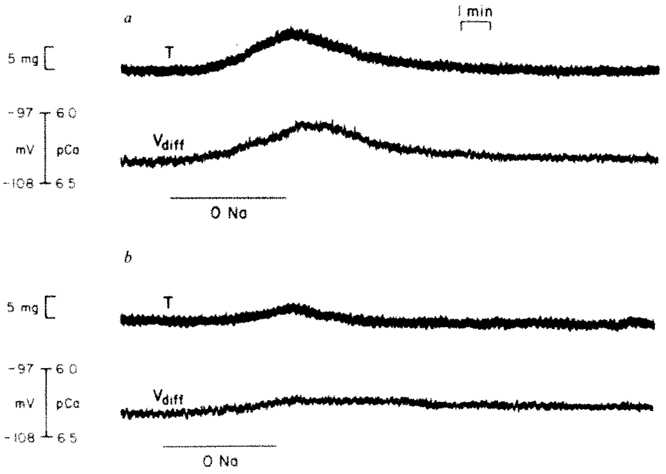

Fig. 4 Effect of isoprenaline (3 μM) on Ca^{2+} and force signals produced by Na^+ withdrawal in the presence of 30 mM K_o. Relative to control (*a*), Ca^{2+} and force transients were both attenuated by the catecholamine (*b*) and showed partial recovery towards their original amplitudes when a third 0 Na(choline) challenge was applied 25 min after removing the drug (records not shown). Records in *a* are taken from the same run as those in Fig. 3*b*.

K_o (see Fig. 2*d*): measurements were rejected if ΔV_{CaE} and ΔV_m differed by more than 10%. From a large number of attempts, 12 measurements were considered acceptable by these criteria (Table 1). The average resting level in *p*Ca units was 6.59 ± 0.06 (mean ± s.e.m.), or 0.26 μM. In the same series of measurements, the average resting potential in 4 mM K_o was −84.7 ± 1.7 mV.

Calcium transients during contractures

How does the free Ca^{2+} in unstimulated muscles compare with the level needed to activate the contractile proteins? One indication comes from the above-mentioned test of raising extracellular Ca^{2+} from 1.8 to 18 mM. Although any resulting large rises in intracellular Ca^{2+} were discarded due to the likelihood that gross penetration damage had occurred, small increases (as in Fig. 2*c*) were nevertheless observed even in five runs where independent tests with 16 or 30 mM K_o indicated good electrode sealing (Table 1). In those runs, raising extracellular Ca^{2+} 10-fold gave a peak increase of 1.2–2.6-fold in intracellular Ca^{2+}, but no measurable force ever developed. This suggests that resting levels were safely below the threshold for Ca^{2+}-activated force development in the conditions of our experiments. Such a conclusion may not hold at longer sarcomere lengths, corresponding to the peak of the length–tension relationship[20–22], where the myofibrils are known to be more sensitive to Ca^{2+} (refs 23, 24).

The relationship between free Ca^{2+} and force was studied further during sodium-removal contractures. Figure 3 shows records from a continuous Ca^{2+}-electrode impalement illustrating the responses to progressively stronger contracture challenges. Figure 3*a* shows the effect of replacing extracellular Na^+ with choline in the presence of 4 mM K_o. Here, Na^+ removal elicited an apparent 40% rise in free Ca^{2+}, but only a barely detectable increase in force. (Because the presumed fall in intracellular Na^+ would have depressed V_{diff} by 1 to 2 millivolts, the true rise in Ca^{2+} would have been slightly more than 40%). In Fig. 3*b* the stimulus for increasing intracellular Ca^{2+} was strengthened by partially depolarizing the preparation with 30 mM K_o before Na^+ removal, a procedure known to enhance Na^+-free contractures. In this case, the intracellular Ca^{2+} rose to a peak of almost 1 μM. (1 μM Ca^{2+} is high enough for changes in intracellular Na^+ to have a negligible effect on the electrodes.) Finally, in Fig. 3*c*, the contracture challenge was further augmented by including 25 mM caffeine in the Na^+-free solution. This produced a much larger force transient, and a Ca^{2+} signal which reached a peak of 10 μM. To demonstrate that the V_{CaE} signal was not due to dislodgment of the Ca^{2+} electrode, K_o was changed. Both V_{CaE} and V_m display similar hyperpolarizations during reduction of K_o from 30 to 4 mM, as well as the corresponding subsequent depolarization when 30 mM K_o was restored. The quality of the common-mode rejection, seen at higher amplification on V_{diff}, argues that the Ca^{2+}-electrode remained well sealed within a viable cell. The three parts of the experiment demonstrate the feasibility of recording both small and large calcium transients during varying degrees of contractile activation.

Relaxant effects of catecholamines

The advantages of the Ca^{2+}-electrode approach encouraged us to study the regulatory effects of catecholamines on excitation–contraction coupling. Stimulation of β-adrenoreceptors by adrenaline or isoprenaline not only increases developed force during a twitch (the positive inotropic effect) but also abbreviates the twitch and accelerates relaxation. These 'relaxant effects' (refs 25–29) are important in allowing adequate time for diastolic filling when the heart rate increases, as with exercise. A closely related relaxant phenomenon can be seen during contractures when exposure to adrenaline or isoprenaline reduces the force evoked by K^+-induced depolarization[25–27] or Na^+ withdrawal[26]. Two possible mechanisms involving cyclic AMP[28–30] have been suggested by studies of subcellular fractions or of skinned or hyperpermeable preparations. First, cyclic AMP may increase Ca^{2+} uptake by the sarcoplasmic reticulum[31,32] and, second, it may decrease the Ca^{2+} sensitivity of the myofibrils by promoting phosphorylation of a regulatory protein such as troponin-I[33–36]. Contracture experiments with Ca^{2+}-electrodes offer the possibility of seeing whether either or both

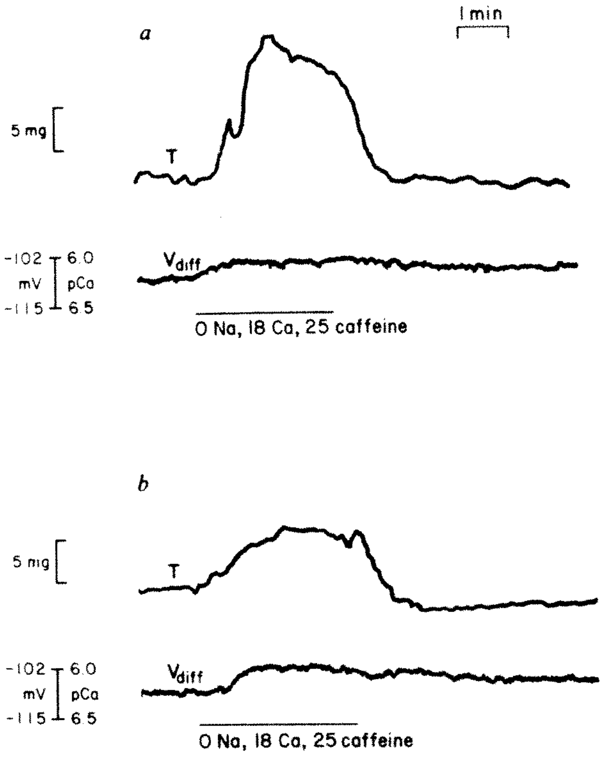

Fig. 5 Effect of adrenaline on Ca^{2+} and force signals evoked by caffeine-containing contracture solution. Horizontal bars indicate period of superfusion with 0 Na(choline), 18 mM Ca, 25 mM caffeine. 30 mM K_o present throughout. *a*, Control; *b*, 10 μM adrenaline (7 min). Contracture force returned to within 25% of control when the challenge was repeated after 20 min superfusion with adrenaline-free solution containing 1 μM propranolol but the Ca^{2+}-electrode was unfortunately dislodged by the contracture. The force records are unusually noisy in this figure because a force transducer with low sensitivity and low compliance was used in the hope of minimizing preparation movement.

mechanisms operate in intact cardiac muscle. Figure 4 shows Ca^{2+} and force signals during Na^+-withdrawal contractures: Fig. 4*a* is the response to Na^+-free solution before drug treatment, and Fig. 4*b* is the response in the presence of 3 μM isoprenaline. Both the force transient and the Ca^{2+} transient were reduced by the catecholamine (and showed partial recovery when the drug was removed). Similar results were obtained in an experiment using 10 μM isoprenaline. Because the Ca^{2+} transients, as well as force, were attentuated, these observations are consistent with enhancement of Ca^{2+} uptake by the sarcoplasmic reticulum as the predominant relaxing mechanism, although other possibilities are not excluded.

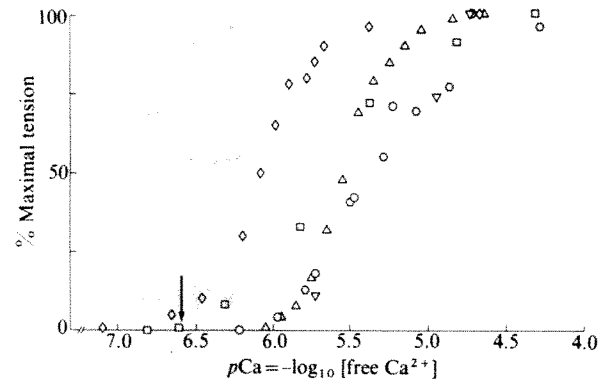

Fig. 6 Calcium requirements for cardiac myofibrillar activation, taken from published work on skinned or hyperpermeable preparations of mammalian cardiac muscle. All data have been adjusted along the horizontal axis so that recalculated *p*Ca values conform with Ca-EGTA binding constants given in ref. 12. The same binding constants were used in preparing calibration buffers for the Ca^{2+}-electrodes[11] and give log (effective stability constant for Ca-EGTA at *p*H 7.0) = 6.42. This value is in close agreement with the value (6.40) determined by Allen *et al.*[42]. ◇, Solaro *et al.*[43], Fig. 3, triangles. ○, Fabiato and Fabiato[44], Fig. 7, inverted triangles. ∘ , Kerrick and Donaldson[45], Fig. 1, filled triangles. □, Endo and Kitizawa[46], Fig. 7. ▽, McClellan and Winegrad[35], Fig. 9, open circles. △, Hibberd and Jewell[24], Fig. 1, filled circles. The arrow denotes the mean *p*Ca (6.59 ± 0.06) in quiescent myocardium as determined in this study.

Any reduction of myofibrillar Ca^{2+} sensitivity could best be seen if the Ca^{2+} transient were not reduced. To this end, caffeine was included in the contracture solution to inhibit Ca^{2+} uptake by the sarcoplasmic reticulum and promote net release[37]. As Fig. 5*a*, *b* illustrates, adrenaline treatment actually increased the Ca^{2+} transient during a 0 Na^+/18 Ca^{2+}/25 caffeine challenge. However, the contracture force was reduced, as expected if the contractile machinery were less responsive to a given level of Ca^{2+}. This result was confirmed in each of two additional experiments using 10 μM adrenaline. These observations provide evidence that adrenergic regulation of myofibrillar Ca^{2+} sensitivity, first proposed on the basis of biochemical studies, can indeed occur in intact cardiac muscle.

Discussion

Our experiments show that Ca^{2+}-sensitive microelectrodes can be made sharp enough and selective enough to measure free Ca^{2+} inside relatively small mammalian cells. The bevelled tips of these electrodes are sufficiently fine for impalements to be maintained with no greater difficulty than those of ordinary voltage-recording microelectrodes, despite the strong contractility of cardiac ventricular muscle. The nearly logarithmic response of the Ca^{2+}-electrode to free Ca^{2+} makes it possible to quantify intracellular Ca^{2+} levels both at rest and during contraction, with only slight interference from other ions. Limitations of this technique include the rather slow speed of response at the low intracellular Ca^{2+} levels, and the requirement for simultaneous measurement of membrane potential. Also, a Ca^{2+}-electrode takes a point sample which could be unrepresentative of Ca^{2+} concentrations elsewhere. Gradients inside one small ventricular cell are unlikely to persist over the time scale examined in the present work, but we have seen marked variations in the pattern of Ca^{2+} responses in different cells in the same papillary muscle. Thus it is not surprising that the tension recorded from the whole muscle often fails to track the Ca^{2+} transient, which was always measured in a single superficial cell. When studying modifications of contractile responses, we have assumed that physiological or pharmacological interventions have qualitatively similar effects on all the cells.

Our mean resting level of free Ca^{2+}, 0.26 μM (*p*Ca 6.59) in ferret ventricular muscle, is somewhat lower than that reported by Coray *et al.*[38], 0.36 μM in sheep myocardium, but higher than results of Uhm *et al.*[39], 0.12 μM in rabbit ventricular muscle. Over the critical range 0.1–1.0 μM free Ca^{2+}, the liquid sensor electrodes of those workers had a smaller response (5–9 mV)[8,38] than the PVC-gelled electrodes of the present study (18–24 mV), so that any small errors in estimates of the membrane potential or of interference from other ions would have less influence on our values for *p*Ca. Although the present measurements are not limited by electrode sensitivity to Ca^{2+}, all microelectrode recordings are susceptible to artefacts from impalement damage. We have accepted only those measurements which passed above-mentioned criteria for good electrode sealing and cell viability, but some residual perturbation by penetration damage cannot be excluded.

It is interesting to compare Ca^{2+} levels measured in intact fibres with levels which produce tension in 'skinned' or 'hyperpermeable' mammalian ventricular preparations, where Ca-EGTA buffers are applied directly to the contractile apparatus. Figure 6 shows *p*Ca-tension relationships from six published reports, adjusted for a standardized Ca-EGTA dissociation constant. Our resting value of *p*Ca 6.59 (vertical arrow) is at, or in most cases well below, the apparent threshold for Ca^{2+}-activated force. Moreover, the peak Ca^{2+} readings in the series of challenges shown in Fig. 3 are *p*Ca 6.3, 6.1 and 5.0. Reading off from the main cluster of *p*Ca-tension relationships for skinned fibres, we would expect barely detectable, small and near-maximal tensions, respectively, and indeed, the observed peak tensions were ~0, 9 and 240 mg. This agreement should be viewed with caution because of the microelectrode sampling problem discussed above and because skinned fibre *p*Ca-tension relationships can be markedly influenced by temperature[40,41], solution composition[35], sarcomere length[23,24] and perhaps, method of skinning and source of tissue. The effects of adrenergic compounds on Ca^{2+} transients and contractures were also in qualitative agreement with results from subcellular fractions[31–34,36] or hyperpermeable preparations[35]. Working with intact muscle, we found evidence that catecholamines may modify myofibrillar Ca^{2+} sensitivity and reduce peak Ca^{2+} elicited by sodium removal. These results illustrate how Ca^{2+} electrodes could be useful in future studies on the regulation of cardiac contractility.

This work was supported by the USPHS and the SRC. T.J.R. received travel grants from the Royal Society and Wellcome Trust. We thank Professor W. Simon for (*o*-nitrophenyl)octylether and Drs C. J. Cohen, W. K. Chandler and R. C. Thomas for helpful comments.

Note added in proof: Lee, Uhm and Dresdner[47] have just described Ca^{2+}-electrode measurements in rabbit ventricular muscle. Their Ca^{2+} values incorporate a calculated activity coefficient of 0.32 and are based on an effective stability constant for Ca-EGTA of $10^{6.76}\,M^{-1}$ at *p*H 7.0 rather than $10^{6.42}\,M^{-1}$ as in our work. Multiplication by 6.84 corrects their data to our units of free Ca^{2+} concentration and brings their value of 38 nM Ca^{2+} activity in resting cells to 260 nM free Ca^{2+} concentration, in fortuitously exact agreement with our results. O'Doherty *et al.*[48] have recently reported another sensor composition which appears to have comparable performance to the mixture used here.

Received 6 May; accepted 7 July 1980.

1. Allen, D. G. & Blinks, J. R. *Nature* **273,** 509–513 (1978).
2. Allen, D. G. & Kurihara, S. *J. Physiol., Lond.* **292,** 68P–69P (1979).
3. Wier, W. G. *Science* **207,** 1085–1087 (1980).
4. Oehme, M., Kessler, M. & Simon, W. *Chimia, Aarau* **30,** 204–206 (1976).
5. Brown, H. M., Pemberton, J. P. & Owen, J. D. *Analytica chim. Acta* **85,** 261–276 (1976).
6. Christoffersen, G. R. J. & Simonsen, L. *Acta physiol. Scand* **101,** 492–494 (1977).
7. Isenberg, G. & Dahl, G. *Pflügers Arch. ges. Physiol.* **373,** R9 (1978).
8. Sokol, J. H., Lee, C. O. & Lupo, F. J. *Biophys. J.* **25,** 143a (1979).
9. Chapman, R. A. & Léoty, C. *J. Physiol., Lond.* **256,** 287–314 (1976).
10. Ammann, D., Güggi, M., Pretsch, E. & Simon, W. *Analyt. Lett.* **8,** 709–720 (1975).
11. Tsien, R. Y. & Rink, T. J. *Biochim. Biophys. Acta* **599,** 623–638 (1980).
12. Martell, A. E. & Smith, R. M. *Critical Stability Constants* Vol. 1 (Plenum, New York, 1974).
13. Craggs, A., Moody, G. J. & Thomas, J. D. R. *Analyst* **104,** 412–418 (1979).
14. Ellis, D. *J. Physiol., Lond.* **273,** 211–240 (1977).
15. Lee, C. O. & Fozzard, H. A. *J. gen. Physiol.* **65,** 695–708 (1975).
16. Cohen, C. J. & Fozzard, H. A. (in preparation).
17. Rink, T. J., Tsien, R. Y. & Warner, A. E. *Nature* **283,** 658–660 (1980).
18. Polimeni, P. I. & Page, E. *Circulation Res.* **33,** 367–374 (1973).
19. Fabiato, A. & Fabiato, F. *J. Physiol., Paris* **75,** 463–505 (1979).
20. Matsubara, I. & Millman, B. M. *J. molec. Biol.* **82,** 527–536 (1974).
21. Moss, R. L., Sollins, M. R. & Julian, F. J. *Nature* **260,** 619–621 (1976).
22. Lappé, D. L. & Lakatta, E. G. *Science* **207,** 1369–1371 (1980).
23. Fabiato, A. & Fabiato, F. *J. gen. Physiol.* **72,** 667–699 (1978).
24. Hibberd, M. G. & Jewell, B. R. *J. Physiol., Lond.* **290,** 30P–31P (1979).
25. Kavaler, F. & Morad, M. *Circulation Res.* **18,** 492–501 (1966).
26. Graham, J. A. & Lamb, J. F. *J. Physiol., Lond.* **197,** 479–509 (1968).
27. Morad, M. & Rolett, E. L. *J. Physiol., Lond.* **224,** 537–558 (1972).
28. Meinertz, T., Nawrath, H. & Scholz, J. *Naunyn-Schmiedebergs Archs Pharmak.* **293,** 129–137 (1976).
29. McAfee, D. A., Whiting, G. J. & Siegel, B. *J. molec. cell. Cardiol.* **10,** 705–716 (1978).
30. Tsien, R. W. *Adv. Cyclic Nucleotide Res.* **8,** 363–420 (1977).
31. Kirchberger, M., Tada, M. & Katz, A. M. *J. biol. Chem.* **249,** 6166–6173 (1974).
32. LaRaia, R. J. & Morkin, E. *Circulation Res.* **35,** 298–306 (1974).
33. Ray, K. & England, P. *FEBS Lett.* **70,** 11–17 (1976).
34. Cole, H., Frearson, N., Moir, A., Perry, S. J. & Solaro, R. J. *Recent Adv. Stud. cardiac Struct. Metab.* **11,** 111–119 (1978).
35. McClellan, G. B. & Winegrad, S. *J. gen. Physiol.* **72,** 737–764 (1978).
36. Holroyde, M. J., Howe, E. & Solaro, R. J. *Biochim. biophys. Acta* **586,** 63–69 (1979).
37. Weber, A. & Herz, R. *J. gen. Physiol.* **52,** 750–759 (1968).
38. Coray, A., Fry, C. H., Hess, P., McGuigan, J. S. & Weingart, R. *J. Physiol., Lond.* **305,** 60P–61P (1980).
39. Uhm, D. Y., Lee, C. O. & Dresdner, K. *Fedn Proc.* **39,** 967 (1980).
40. Brandt, P. W. & Hibberd, M. G. *J. Physiol., Lond.* **258,** 76P (1976).
41. Lindley, B. D. & Godt, R. E. *Fedn Proc.* **39,** 580 (1980).
42. Allen, D. G., Blinks, J. R. & Prendergast, F. *Science* **195,** 996–998 (1977).
43. Solaro, R. J., Wise, R. M., Shiner, J. S. & Briggs, F. N. *Circulation Res.* **34,** 525–530 (1974).
44. Fabiato, A. & Fabiato, F. *J. Physiol., Lond.* **249,** 469–495 (1975).
45. Kerrick, W. G. L. & Donaldson, S. K. B. *Pflügers Arch. ges. Physiol.* **358,** 195–201 (1975).
46. Endo, M. & Kitizawa, T. in *Biophysical Aspects of Cardiac Muscle* (ed. Morad, M.) (Academic, New York, 1978).
47. Lee, D. O., Uhm, D. Y. & Dresdner, K. *Science* **209,** 699–701 (1980).
48. O'Doherty, J. O., Youmans, S. J., Armstrong, W. McD. & Start, R. J. *Science* **209,** 510–513 (1980).

Deletion of immunoglobulin heavy chain genes from expressed allelic chromosome

Yoshio Yaoita* & Tasuku Honjo*

Department of Physiological Chemistry and Nutrition, Faculty of Medicine, University of Tokyo, Tokyo 113, Japan

We have studied the organization of immunoglobulin heavy-chain genes in a γ2b-chain (BALB/c allotype)-producing myeloma BKC F_1 #15 induced in a F_1 mouse between C57BL and BALB/c. Southern blot hybridization studies using cloned μ, γ1 and γ2b-chain genes as probes demonstrate that the μ- and γ1-chain genes of the expressed chromosome are deleted while these genes of the unexpressed chromosome are retained. The γ2b-chain gene of the expressed allele is rearranged while that gene of the unexpressed allele seems unchanged, as do the γ2a-chain genes. These results support the allelic deletion mechanism in heavy-chain class switch and the order of H chain genes.

DREYER and Bennett[1] proposed a model that a variable region (V) and a constant region (C) of the immunoglobulin polypeptide chain are encoded by two separate genes in the germ-line, which are eventually brought together by somatic recombination. Recent isolation and characterization of immunoglobulin light (L)- and heavy (H)-chain genes have convincingly borne out the predictions of the Dreyer–Bennett hypothesis[2–11]. Analyses of L-chain genes have demonstrated that the V–C recombination takes place between a germ-line V_L gene and a J_L region that is a few thousand nucleotides away from the C_L gene[12,13]. It is believed that the intervening sequence separating the J and C genes is removed at the RNA level by splicing[14].

Possible mechanisms have been proposed to account for the V–C recombination, which can be classified into deletion, copy-insertion, excision–insertion and inversion models[15–19]. A model for the immunoglobulin gene organization and reorganization should explain such unique phenomena known in lymphocytes as allelic exclusion and class switch. In a given lymphocyte a C_H gene of one allele is expressed and that of the other allele is suppressed (allelic exclusion). A V_H-region sequence is successively joined with different C_H-region sequences during differentiation of a lymphocyte (class switch).

Previously we showed that the copy numbers of the specific C_H genes in myeloma DNA were reduced depending on the class or subclass of the C_H gene expressed in the myeloma[20]. Our data indicate that the DNA segment located between a V_H gene and the C_H gene expressed is excised out of the chromosome to recombine the two genes. Such recombination seemed to occur only on one of the two allelic chromosomes. We have also proposed that H-chain genes are aligned on one chromosome in the order: V_H genes, unknown spacer, μ, γ3, γ1, γ2b, γ2a and α (ref. 20). Such alignment, together with successive deletion, can explain the class-switch phenomenon. This model is called the allelic deletion model. The deletion of C_H genes, in accord with the above order of the C_H genes, was recently confirmed by Rabbitts *et al.*[21]. The deletion of the DNA segment located between two adjoining sequences was also confirmed in the κ-type L-chain gene by Sakano *et al.*[12].

Elsewhere we have reported cloning of the rearranged γ1-chain gene from a γ1 chain-producing myeloma MC 101 and compared its structure with H-chain genes cloned from newborn mouse DNA[22]. Such analyses indicate that the rearranged γ1-chain gene contains at its 5′ flanking region a newly introduced segment that was located originally at the 5′ flanking region of the μ-chain gene in newborn mouse DNA. The recombination site is not the putative J region but a novel region called *S* region. These results are in agreement with the prediction of the deletion model, although they do not necessarily prove the model.

In this report we describe direct evidence that the deletion of the specific H-chain genes takes place only on the expressed chromosome using a myeloma induced in a F_1 mouse between C57BL and BALB/c which have different allotypes in the H-chain C regions.

Probes and restriction maps of the μ-, γ1- and γ2b-chain genes

We have already cloned the *Eco*RI fragments containing the γ1-, γ2b and μ-chain genes from newborn mouse DNA and determined their nucleotide sequences[4,8,9,22–24]. We used the 1.2-kilobase pair *Hin*dIII fragment of the cloned μ-chain gene,

---

*Present address: Department of Genetics, Osaka University School of Medicine, Osaka 530, Japan.

0028-0836/80/350850—04$01.00

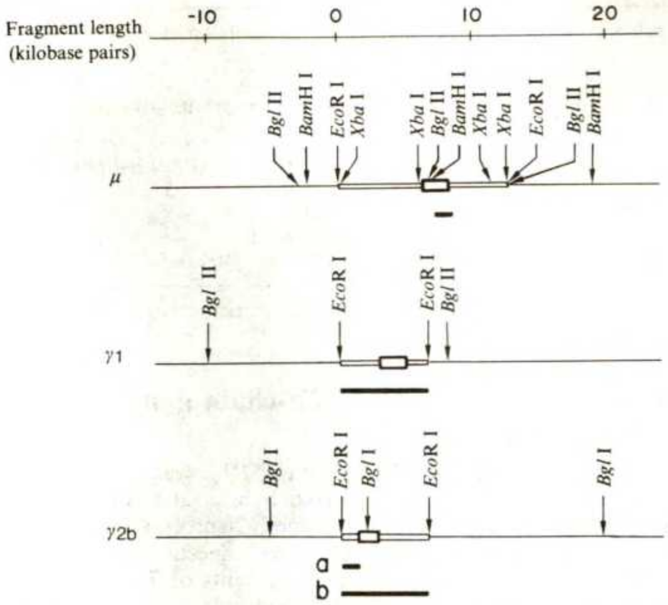

Fig. 1 Restriction enzyme cleavage sites around the μ-, $\gamma 1$- and $\gamma 2b$-chain genes. DNA is displayed from left to right with the direction of transcription. Narrower rectangles show the cloned DNA fragments. Wider rectangles show locations of structural genes. DNA fragments used for probes are indicated by horizontal bars below the restriction maps. μ-chain gene probe, 1.2-kilobase pair *Hin*dIII fragment that contains the CH3 and CH4 domains of the μ-chain gene clone[21]; $\gamma 1$-chain probe, 6.6-kilobase pair *Eco*RI fragment containing the $\gamma 1$-chain gene[8]; $\gamma 2b$-chain gene probe a, 1.35-kilobase pair, *Bam*HI fragment (5′ fragment) of the $\gamma 2b$-chain gene clone[22]; $\gamma 2b$-chain gene probe b, 6.6-kilobase pair *Eco*RI fragment containing the $\gamma 2b$-chain gene[22].

the cloned *Eco*RI fragment (6.6 kilobase pairs) of the $\gamma 1$-chain gene, the cloned $\gamma 2b$-chain gene and the 1.35-kilobase pair *Bam*HI fragment of the cloned $\gamma 2b$-chain gene as probes for hybridization (Fig. 1). Although the whole $\gamma 2b$-chain gene clone ($\gamma 2b$ probe b) has extensive homology with the $\gamma 2a$-chain gene[23,25], the 1.35-kilobase pair *Bam*HI fragment ($\gamma 2b$ probe a), which corresponds to the 5′ fragment of the cloned $\gamma 2b$-chain gene, does not cross-hybridize with the $\gamma 2a$-chain gene under the stringent washing conditions used in the present study. Detailed maps of restriction endonuclease cleavage sites within these clones have been determined[8,22–24]. We have determined the restriction sites of *Bgl*II adjacent to the cloned $\gamma 1$-chain gene fragment by digestion of mouse DNA with several combinations of two restriction enzymes, followed by Southern blot hybridization of the restriction DNA fragments. Similarly, we have determined the restriction sites of *Bgl* I adjacent to the cloned $\gamma 2b$-chain gene fragment and the sites of *Bam*HI and *Bgl* II adjacent to the cloned μ-chain gene fragment. These restriction sites were confirmed by Southern blot hybridization using the 5′ or 3′ fragment of the cloned DNA as a probe. Figure 1 summarizes the results of these analyses and the known sites of restriction endonucleases used in the present study. The fragments used for probes are also shown.

Allelic deletion of the μ- and $\gamma 1$-chain genes

To prove the deletion of the C_H gene from one chromosome, it is essential to distinguish the C_H genes on different chromosomes. BALB/c and C57BL mice have different allotypes in H-chain C regions[26], suggesting that their C_H genes may have different nucleotide sequences. We searched for restriction endonucleases that produce the C_H-gene fragments of different lengths between BALB/c and C57BL alleles. Among restriction endonucleases tested (*Pvu*II, *Bam*HI, *Eco*RI, *Hin*dIII, *Sma*I, *Pst*I, *Kpn*I, *Xba*I *Bgl*II) we found that *Bgl*II can distinguish the $\gamma 1$-chain genes of BALB/c and C57BL alleles. As for the $\gamma 2b$-chain gene, we have tested *Xho*I, *Ava*I, *Sal*I, *Xba*I, *Bgl*II, *Bam*HI, *Bst*EII and *Bgl*I, and found that *Xho*I or *Bgl*I digestion produces different $\gamma 2b$-chain gene fragments between BALB/c and C57BL DNAs. The μ-chain genes of C57BL and BALB/c alleles were distinguished by digestion with *Xba*I, *Eco*RI or *Kpn*I, while digestion with *Bam*HI or *Bgl* II did not distinguish the two alleles.

Only a few myelomas are available, which were induced in the F_1 mouse between BALB/c and C57BL (ref. 27). BKC F_1 #15, that produces the $\gamma 2b$-chain protein with the BALB/c allotype, is suitable for our purpose since the allelic deletion model predicts the deletion of the $\gamma 1$- and μ-chain genes from the BALB/c chromosome of this myeloma.

When BALB/c and C57BL DNAs were digested with *Xba*I, blotted and hybridized with the μ-chain probe, they produced the 4.8 and 2.8-kilobase pair bands, respectively (Fig. 2*a*, lanes 1

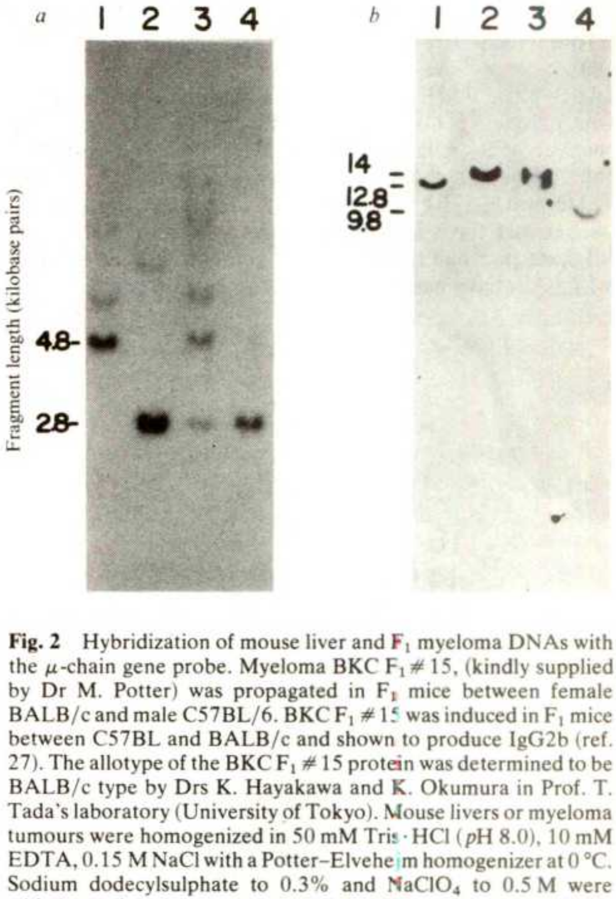

Fig. 2 Hybridization of mouse liver and F_1 myeloma DNAs with the μ-chain gene probe. Myeloma BKC F_1 #15, (kindly supplied by Dr M. Potter) was propagated in F_1 mice between female BALB/c and male C57BL/6. BKC F_1 #15 was induced in F_1 mice between C57BL and BALB/c and shown to produce IgG2b (ref. 27). The allotype of the BKC F_1 #15 protein was determined to be BALB/c type by Drs K. Hayakawa and K. Okumura in Prof. T. Tada's laboratory (University of Tokyo). Mouse livers or myeloma tumours were homogenized in 50 mM Tris · HCl (*p*H 8.0), 10 mM EDTA, 0.15 M NaCl with a Potter–Elvehjem homogenizer at 0 °C. Sodium dodecylsulphate to 0.3% and $NaClO_4$ to 0.5 M were added to a whole homogenate. The homogenate was extracted with 0.5 vol. each of water-saturated phenol and a chloroform–isoamyl alcohol mixture (24 : 1). The water phase was separated by centrifugation, dialysed against 0.1 × SSC (0.015 M NaCl, 0.0015 M Na citrate) for 24 h digested with RNase (100 $\mu g\ ml^{-1}$) in a dialysis bag for 24 h at room temperature and then extracted with phenol. After dialysis against 0.1 × SSC for 48 h, 1.27 g of CsCl was added to 1 ml of the water phase. After centrifugation at 30,000 r.p.m. for 48 h, fractions with high viscosity were collected and dialysed against 0.1 × SSC for 48 h. DNAs (5 μg each) were digested with *a*, *Xba*I or *b*, *Eco*RI, electrophoresed in 0.5% agarose gels (Sigma type I) and transferred to nitrocellulose filters (Schleicher and Schuell) according to the method of Southern[32]. DNA fixed on filters was hybridized with the μ-chain gene probe as described previously[8]. The probe DNA was labelled with [α-^{32}P]TTP (Amersham) by nick translation[33]. The specific activity of the probe was 200 c.p.m. pg^{-1}. After hybridization, filters were rinsed with 2 × SSC and then washed in 0.1 × SSC plus 0.1% SDS (four times) for 40 min each at 67 °C. Filters were finally rinsed with 2 × SSC, dried and exposed to X-ray film using a DuPont Cronex lightening plus intensifier screen at −80 °C. Origins of DNA used are: lanes 1, BALB/c liver; lanes 2, C57BL/6 liver; lanes 3, F_1 mouse liver; lanes 4, BKC F_1 #15 myeloma.

and 2). BKC F_1 #15 DNA, when digested with *Xba*I, yielded only the μ-chain gene fragment of the C57BL allele while F_1 mouse DNA contained the μ-chain gene fragments of both BALB/c and C57BL alleles (Fig. 2*a*, lanes 3 and 4). Faint bands larger than 6 kilobase pairs are due to contamination of other *Hin*dIII fragments of the μ-chain gene clone to the 1.2-kilobase pair *Hin*dIII fragment used as a probe (see Fig. 1) because these faint bands disappeared when the recloned 1.2-kilobase pair *Hin*dIII fragment was used as a probe. It is worth noting that a faint band (at 6.1 kilobase pairs) of the BALB/c chromosome is also absent from the F_1 myeloma DNA. The μ-chain gene of the C57BL allele in BKC F_1 #15 appeared to be unchanged at its 3′ distal region since DNAs of C57BL and BKC F_1 #15 produced identical μ-chain gene fragments of 12- and 8.5-kilobase pairs when digested with *Bam*HI and *Bgl* II, respectively (ref. 28 and see Fig. 1). However, the 5′ region flanking the μ-chain gene of the C57BL allele in BKC F_1 #15 is rearranged because the μ-chain gene fragment (9.8-kilobase pairs) in *Eco*RI-digested BKC F_1 #15 DNA was smaller than the band (14-kilobase pairs) observed in *Eco*RI-digested C57BL DNA (Fig. 2*b*, lanes 2 and 4).

BALB/c and C57BL DNAs, when digested with *Bgl*II, yielded the γ1-chain gene fragments of 18- and 14.5-kilobase pairs, respectively (Fig. 3, lanes 1 and 2). Naturally, F_1-mouse DNA contained the γ1-chain gene fragments derived from both BALB/c and C57BL alleles. It is evident that BKC F_1 #15 DNA has lost the γ1-chain gene of the BALB/c allele (the 18-kilobase pair band), whereas the gene on the C57BL allele (the 14.5-kilobase pair band) seems to remain intact (Fig. 3, lane 4).

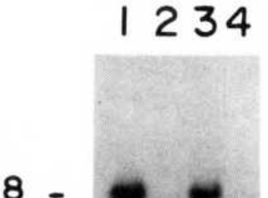

Fig. 3 Hybridization of mouse liver and F_1 myeloma DNAs with the γ1-chain gene probe. DNAs (30 μg each) were digested with *Bgl*II and hybridized as described in the legend to Fig. 2 with the [α-^{32}P]-labelled γ1-chain gene probe. Origins of DNA used are: lane 1, BALB/c liver; lane 2, C57BL/6 liver; lane 3, F_1 mouse liver; lane 4, BKC F_1 #15 myeloma.

Table 1 Restriction fragments of immunoglobulin H-chain genes in mouse liver and myeloma

Origin of DNA	Size of restriction DNA fragments (kilobase pairs)			
	μ (*Xba*I)	γ1 (*Bgl*II)	γ2b (*Bgl*I)	γ2a (*Eco*RI)
BALB/c liver	4.8	18.0	7.5	23.0
C57BL liver	2.8	14.5	9.5	23.0
F_1 liver	4.8+2.8	18+14.5	–	–
BKC F_1 #15	2.8	14.5	9.5 and 6.5	23.0

The results of Figs 2–4 are summarized. Restriction enzymes used are shown in parentheses.

Rearrangement of the γ2b-chain gene of the expressed allele

The γ2b-chain gene in BKC F_1 #15 DNA was analysed by digestion with *Bgl* I and Southern blot hybridization using the 5′ fragment of the cloned γ2b-chain gene (γ2b probe a) as a probe. As shown in Fig. 4 (lanes 1 and 2), *Bgl* I digestion of BALB/c and C57BL DNAs produced the fragments of 7.5- and 9.5-kilobase pairs respectively, which hybridized with the γ2b chain probe a. BKC F_1 #15 DNA, when digested with *Bgl* I, yielded the γ2b-chain gene fragments of 6.5- and 9.5-kilobase pairs (Fig. 4*a*, lane 4). The results indicate that the 5′ region of the γ2b-chain gene on the BALB/c allele was rearranged, while that gene on the C57BL allele seems to remain unchanged in BKC F_1 #15 DNA. However, we do not exclude the possibility that the γ2b-chain gene on the C57BL allele may have undergone some rearrangements which we did not detect. We also found that the 3′ region flanking to the γ2b-chain gene of the BALB/c allele is rearranged in BKC F_1 #15 DNA when the 3′-portion probe of the γ2b-chain gene was used[28].

Presence of the γ2a-chain genes

Both BALB/c and C57BL DNAs, when digested with *Eco*RI, produced the 6.6- and 23-kilobase pair fragments hybridizing to the γ2b-gene probe b which cross-hybridizes with the γ2a-chain gene (Fig. 4*b*, lanes 1 and 2). The 6.6-kilobase pair fragment corresponds to the cloned γ2b-chain gene and the 23-kilobase pair fragment was identified as the γ2a-chain gene fragment[21]. F_1-mouse and BKC F_1 #15 DNA contained the γ2a-chain gene fragment (23-kilobase pairs) (Fig. 4*b*, lanes 3 and 4). The γ2a-chain gene seems to be intact in BKC F_1 #15 although we cannot exclude the possibility that the γ2a-chain gene contains an undetected rearrangement.

Organization of immunoglobulin H-chain genes in BKC F_1 #15 myeloma

Restriction DNA fragments of the μ-, γ1-, γ2b- and γ2a-chain genes in BALB/c mice, C57BL mice, F_1 mice and BKC F_1 #15 myeloma are listed in Table 1. It is evident that BKC F_1 #15 has lost the μ- and γ1-chain genes of the BALB/c chromosome and contains the rearranged γ2b-chain gene of the BALB/c chromosome. This myeloma contains the μ-, γ1- and γ2b-chain genes of the C57BL chromosome. BKC F_1 #15 contains the γ2a-chain gene although we did not distinguish two alleles. These results are in agreement with the prediction of the allelic deletion model. Nevertheless, we found an unexpected rearrangement at the 5′ region flanking the μ-chain gene of the C57BL chromosome that is unexpressed in BKC F_1 #15. The two chromosomes of BKC F_1 #15 are schematically represented in Fig. 5.

Unexpected rearrangements in BKC F_1 #15

Although the deletion profile of C_H genes in BKC F_1 #15 DNA is as predicted by the allelic deletion model, we found two unexpected rearrangements in BKC F_1 #DNA; one in the 5′

region flanking the μ-chain gene of the unexpressed chromosome (Fig. 2*b*, lane 4) and the other in the 3′ region flanking to the γ2b-chain gene of the expressed chromosome[28].

It is possible that rearrangement in the 5′ region flanking the μ-chain gene of the C57BL allele is related to the mechanism to suppress the H chain genes on the C57BL chromosome. It may be relevant to this assumption that the 5′ region flanking the μ-chain gene is proposed to contain the putative J region and the *S* region that is important to class-switch recombination[22].

It is difficult to understand why the rearrangement in the 3′ region flanking the γ2b-chain gene of the expressed chromosome is necessary to express the γ2b-chain gene. It may be possible that the 3′ rearrangement of the C_H gene takes place so that the class switch stops at this particular gene. Otherwise, a V_H gene together with a J region moves farther down to a C_H gene remaining at the 3′ side of the expressed gene.

Deletion of C_H genes in other myelomas

Rabbitts *et al.*[21] reported that C_H genes, which are located 5′ to the expressed C_H gene, are absent from both chromosomes in several myelomas induced in BALB/c mice. We also observed similar deletion from both chromosomes and found that the expressed C_H genes are rearranged in different manners between homologous chromosomes in these myelomas[28]. The results may suggest that C_H gene deletion, which accompanies the rearrangement of the expressed C_H genes, takes place successively, but not simultaneously, in the allelic chromosomes. Several forms of rearranged κ-type L-chain genes were isolated from κ-chain-producing myelomas[29,30].

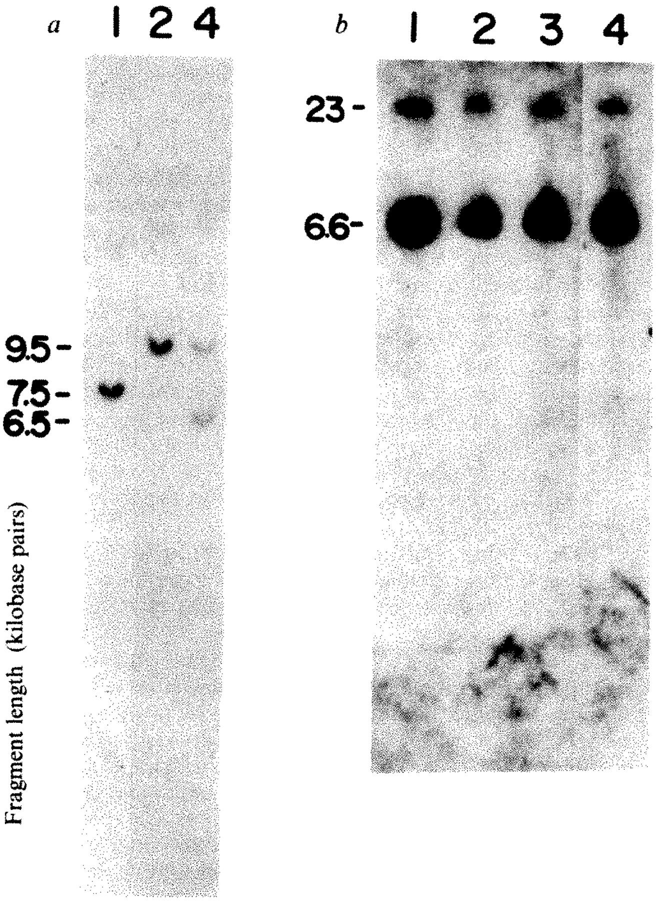

Fig. 4 Hybridization of mouse liver and F_1 myeloma DNAs with the γ2b-chain gene probes. DNAs were digested with *a*, *Bgl*I or *b*, *Eco*RI, and hybridized as described in the legend to Fig. 2 with [α-^{32}P]-labelled probes indicated. The γ2b probes a and b were used in *a* and *b* respectively. Origins of DNA used are: lanes 1, BALB/c liver; lanes 2, C57BL/6 liver; lanes 3, F_1 mouse liver; lanes 4, BKC F_1 #15 myeloma.

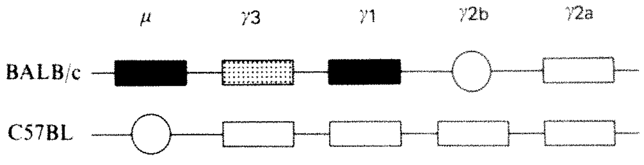

Fig. 5 Schematic representation of C_H genes in BKC F_1 #15. Each line shows one chromosome derived from each parent. The order of C_H genes is as proposed before[20]. Open and closed rectangles indicate 'intact' and deleted genes, respectively. (The word 'intact' simply means that the change is not detected in the present study.) Circles indicate rearranged genes. The γ3-chain gene, which was not determined in the present study, is assumed to be deleted from the BALB/c chromosome and indicated by a dotted rectangle.

However, we cannot exclude the possibility that such rearrangements could be secondary mutations in myelomas. We are quite aware of the fact that chromosomal anomalies are rather frequent in myeloma cells[29]. Nonetheless, the perfect agreement of the C_H-gene deletion profile (the order and allelic chromosome) with the prediction of the allelic deletion model is something more than accidental coincidence. Seidman and Leder[5] reported that only one member of an allelic pair of L-chain genes is rearranged in κ-chain-producing myelomas, MOPC 149 and MOPC 41. Studies on differentiated B lymphocytes are necessary to determine whether or not the case of BKC F_1 #15 is universal and directly applicable to normal lymphocytes.

We are grateful to Dr Y. Mano for continuous encouragement, Drs T. Tada, K. Okumura and K. Hayakawa for stimulating discussions and determination of the allotype of the BKC F_1 #15 protein and Drs Y. Suzuki and M. Obinata for critical reading of the manuscript, also to our colleagues for helping us to maintain tumour-bearing animals. This investigation was supported in part by grants from the Ministry of Education, Science and Culture.

Received 12 February; accepted 6 June 1980.

1. Dreyer, W. J. & Bennett, J. C. *Proc. natn. Acad. Sci. U.S.A.* **54,** 864–869 (1965).
2. Tonegawa, S., Brack, C., Hozumi, N. & Schuller, R. *Proc. natn. Acad. Sci. U.S.A.* **74,** 3518–3522 (1977).
3. Brack, C., Hirama, M., Lenhard-Schuller, R. & Tonegawa, S. *Cell* **15,** 1–14 (1978).
4. Honjo, T. in *Immunology '78* (eds Yamamura, Y. & Tada, T.) 75–82 (Nakayama-shoten, Tokyo, 1978).
5. Seidman, J. G. & Leder, P. *Nature* **276,** 790–795 (1978).
6. Seidman, J. G. *et al. Proc. natn. Acad. Sci. U.S.A.* **75,** 3881–3885 (1978).
7. Early, P. W., Davis, M. M., Kaback, D. B., Davidson, N. & Hood, L. *Proc. natn. Acad. Sci. U.S.A.* **76,** 857–861 (1979).
8. Honjo, T. *et al. Cell* **18,** 559–568 (1979).
9. Kataoka, T., Yamawaki-Kataoka, Y., Yamagishi, H. & Honjo, T. *Proc. natn. Acad. Sci. U.S.A.* **76,** 4240–4244 (1979).
10. Kemp, D. J., Cory, S. & Adams, J. M. *Proc. natn. Acad. Sci. U.S.A.* **76,** 4627–4631 (1979).
11. Sakano, H. *et al. Nature* **277,** 627–633 (1979).
12. Sakano, H., Hüppi, K., Heinrich, G. & Tonegawa, S. *Nature* **280,** 288–294 (1979).
13. Max, E. E., Seidman, J. G. & Leder, P. *Proc. natn. Acad. Sci. U.S.A.* **76,** 3450–3454 (1979).
14. Rabbitts, T. H. *Nature* **275,** 291–296 (1978).
15. Dreyer, W. J., Gray, W. R. & Hood, L. *Cold Spring Harb. Symp. quant. Biol.* **32,** 353–367 (1968).
16. Gally, J. A. & Edelman, G. M. *Nature* **227,** 341–342 (1970).
17. Kabat, D. *Science* **175,** 134–140 (1972).
18. Sledge, C., Fair, D. S., Black, B., Kruegar, R. G. & Hood, L. *Proc. natn. Acad. Sci. U.S.A.* **73,** 923–927 (1976).
19. Tonegawa, S., Hozumi, N., Matthyssens, G. & Schuller, R. *Cold Spring Harb. Symp. quant. Biol.* **41,** 877–889 (1976).
20. Honjo, T. & Kataoka, T. *Proc. natn. Acad. Sci. U.S.A.* **75,** 2140–2144 (1978).
21. Rabbitts, T. H., Forster, A., Dunnick, W. & Bentley, D. L. *Nature* **283,** 351–356 (1980).
22. Kataoka, T., Kawakami, T., Takahashi, N. & Honjo, T. *Proc. natn. Acad. Sci. U.S.A.* **177,** 919–923 (1980).
23. Yamawaki-Kataoka, Y., Kataoka, T., Takahashi, N., Obata, M. & Honjo, T. *Nature* **283,** 786–789 (1980).
24. Kawakami, T. Takahashi, N. & Honjo, T. *Nucleic Acids Res.* (submitted).
25. Yamawaki-Kataoka, Y. *et al. Biochemistry* **18,** 490–494 (1979).
26. Lieberman, R. *Springer Seminars in Immunopath.* **1,** 7–30 (1978).
27. Sibinovic, K. H., Potter, M., D'Hoostelaere, L., Kobe, B. & Wax, J. *Catalogue of Plasmacytomas and Other Tumors of the Lymphoreticular System,* third edn (Litton Bionetics, Maryland 1976).
28. Yaoita, Y. & Honjo, T. *Biomed. Res.* **1,** 164–175 (1980).
29. Lenhard-Schuller, R., Hohn, B., Brack, C., Hirama, M. & Tonegawa, S. *Proc. natn. Acad. Sci. U.S.A.* **75,** 4709–4713 (1978).
30. Steinmetz, M., Zachau, H. G. & Mach, B. *Nucleic Acid Res.* **6,** 3213–3229 (1979).
31. Yoshida, T. H., Imai, H. T. & Potter, M. *J. natn. Cancer Inst.* **41,** 1083–1095 (1968).
32. Southern, E. M. *J. molec. Biol.* **98,** 503–517 (1975).
33. Maniatis, T., Jeffreys, A. & Kleid, D. G. *Proc. natn. Acad. Sci. U.S.A.* **72,** 1184–1188 (1975).

The 5′ ends of *Drosophila* heat shock genes in chromatin are hypersensitive to DNase I

Carl Wu

Society of Fellows, Harvard University, and The Biological Laboratories, Harvard University, 16 Divinity Avenue, Cambridge, Massachusetts 02138

Many specific sites in Drosophila *chromatin are hypersensitive to DNase I. The positions of such sites were mapped along the regions of the genome coding for two heat shock proteins. Such sites lie at the 5′ ends of heat shock genes and may function as elements for recognition by molecules which regulate gene activity.*

EUKARYOTIC DNA is packaged as chromatin, a complex of protein and DNA within the cell nucleus (see ref. 1 for review). How might this compaction affect the expression of genetic information? Recently, in a study of the chromatin structure at specific regions in the *Drosophila* genome, we reported that certain localized sites were exquisitely sensitive to the nucleolytic enzyme DNase I (ref. 2). By digesting native chromatin gently with DNase I, electrophoresing the DNA on agarose gels and visualizing specific regions by hybridization with a cloned probe[3], we could show that each of five *Drosophila* loci displayed a unique set of preferred cleavages[2]. This preference did not appear on naked DNA, nor in the cleavage pattern of the entire genome[2]. Here, I map such DNase I-sensitive sites near the genes for two heat-inducible polypeptides in *Drosophila melanogaster.*

Mapping DNase I-sensitive sites

I mapped the positions of DNase I-sensitive sites by a novel indirect end-labelling technique that displays the partial digestion products. After gentle treatment of chromatin in nuclei with DNase I, the purified DNA is cleaved completely with a rarely cutting restriction enzyme, electrophoresed and blotted on to nitrocellulose in a typical Southern transfer[3]. The blot is then probed with a short cloned ^{32}P-labelled DNA segment that abuts a chosen restriction cut; the lengths of the labelled subfragments greater than the probe length define the distance between the restriction cut and the partial DNase I cuts.

This technique was applied to the genes for two heat shock proteins in *D. melanogaster* (Oregon R) embryos and in cultured cells [Schneider line 2 (ref. 4)] derived from such embryos. In *Drosophila*, an elevation in temperature from 25 °C to near 37 °C rapidly activates a small number of specific genes, and sharply reduces pre-existing gene activity (see ref. 5 for review). Cytologically, new puff sites appear in the salivary gland polytene chromosomes[6,7]. The heat-induced messenger RNAs direct the synthesis of new polypeptides, the heat shock proteins[8–14], present in all tissues tested as well as in some cell lines.

The most abundant heat-induced product is a 70,000 molecular weight heat shock protein, hsp 70. There are five copies of the uninterrupted 2.2-kilobase pair hsp 70 coding sequence, two at the cytogenetic locus *87A* and three at *87C* (refs 15–25). The five copies of the coding region and an adjoining 0·3-kilobase pair 5′-noncoding region are closely conserved; however, the sequences near the 5′ terminus diverge somewhat between the genes at the two loci, reflected in characteristic restriction site differences[20,24]. At *87A*, the two genes lie head to head, an inverted repeat around a central spacer[25]. At *87C*, a single hsp 70 gene lies at a distance, not yet determined, from an array of two (or three, in a variant) tandem copies organized in a direct repeat[19–23].

Figure 1*a* shows the partial DNase I cuts in Schneider cell chromatin upstream from the internal *Bam* site common to all five hsp 70 gene copies; the fragmentation pattern is aligned following the left to right, 5′ to 3′ convention. The *Bam* digest alone, on purified DNA, is shown in Fig. 1*a*, lane 2. Fragments obtained in low yield in this and subsequent similar digests are due either to cross-reaction with partially homologous sequences[24] or to polymorphism in the organization of the sequences adjacent to the hsp 70 coding region. (Populational polymorphism in these cultured cells is not surprising. Schneider initiated the line with explants from several hundred embryos[4]; the subcultures used here have to my knowledge never been cloned.) Increasing extents of partial DNase I cleavage on chromatin (Fig. 1*a*, lanes 3–5) reveal preferred cuts at two adjacent sites which span about 150 and 90 base pairs, flanking and extending through the 5′ end of the hsp 70 coding region. The control DNase I cleavage on naked DNA reveals a fairly uniform fragmentation pattern (Fig. 1*a*, lanes 7, 8). Although some sequence specificity[26] can be seen, this effect is minor (see also Fig. 4 of ref. 2). Hypersensitivity to DNase I must, therefore, primarily be a function of chromatin structure.

To show that no sensitive regions lie near the internal *Bam* site, I mapped the cuts upstream from an internal *Sal* site close to the hsp 70 3′ end (Fig. 1*b*, lane 2). Consistent with the previous *Bam* map, preferred cuts are localized at the 5′ end of the hsp 70 coding region, overlapping the *Sal* restriction cut characteristic of the two genes at locus *87A*. A number of preferred cuts are also observed upstream from the 5′ regions for the gene copies at locus *87C*. Some of these sites may map to the region at *87C* containing repeated sequences responsible for the heat-induced, nontranslated RNA of unknown function[17,27]. The locations of the 5′ ends of these RNAs have not been determined.

Downstream from the internal *Bam* site (Fig. 2), no sensitivity in the hsp 70 coding sequence can be detected near the common 3′ *Sal* site, but other sensitive sites are found past the hsp 70 messenger sequence (Fig. 2, lane 4). As two (or in a variant, three) of the hsp 70 gene copies at *87C* are organized in a direct repeat[19–23], the 5′ sensitivity in a distal gene copy would map downstream from its preceding partner (2.0–2.1 kilobase pairs from the internal *Bam* site, expected from the tandem hsp 70 map in ref. 21). No known genes occur near the two other sensitive sites. Only three out of five *Bam* fragments are selectively lost on DNase I digestion (Fig. 2, lane 5), so two hsp 70 gene copies must lack preferred cleavages downstream from their 3′ ends for at least 1 and 3 kilobase pairs, respectively. The minor DNase I cleavages which characteristically occur very close to the 5′ sensitive regions (Figs 1–3) coincide with positions of micrococcal nuclease cleavage (data not shown), and might reflect sensitivity of the linker regions between specifically

0028–0836/80/350854—07$01.00

placed nucleosomes[1] adjacent to the hypersensitive sites (see below).

5′ Sensitivity for individual hsp 70 genes

Are the 5′ sensitive regions common to all gene copies of hsp 70? I exploited the restriction site differences between the genes at *87A* and *87C* to display selectively locus-specific DNase I cuts. By digesting with both *Sal* and *Bgl*I in the experiment shown in Fig. 3*a*, all fragments from *87A* can be of no greater length than the 1.7-kilobase pair *Sal–Bgl*I segment. Thus, any longer partial fragments must be from *87C*. Figure 3*a*, lanes 2–4, show that the 5′ sensitive sites are present for the three gene copies at *87C*. It is likely that this sensitivity is a sum of three individual contributions; otherwise, some of the *87C* restriction fragments should be disproportionately retained on DNase I cleavage (Fig. 3, lane 4).

Similarly, digesting with *Pst* (Fig. 3*b*) ensures that all hsp 70 fragments from *87C* can be of no greater length than the 1.1-kilobase pair *Pst* fragment. Thus, any longer partial fragments must be from *87A*. The preferred cuts about 1.3 kilobase pairs upstream from the reference *Pst* site (Fig. 3*b*, lane 3) indicate 5′ sensitivity for the two hsp 70 gene copies at *87A*. Both must possess a 5′ sensitive site, from the identical rates at which the two smallest *Bam* fragments disappear on DNase I digestion in Fig. 1*a* (these two fragments are specifically reduced by a *Bam* plus *Bgl*I digest not shown, to the 0.8-kilobase pair

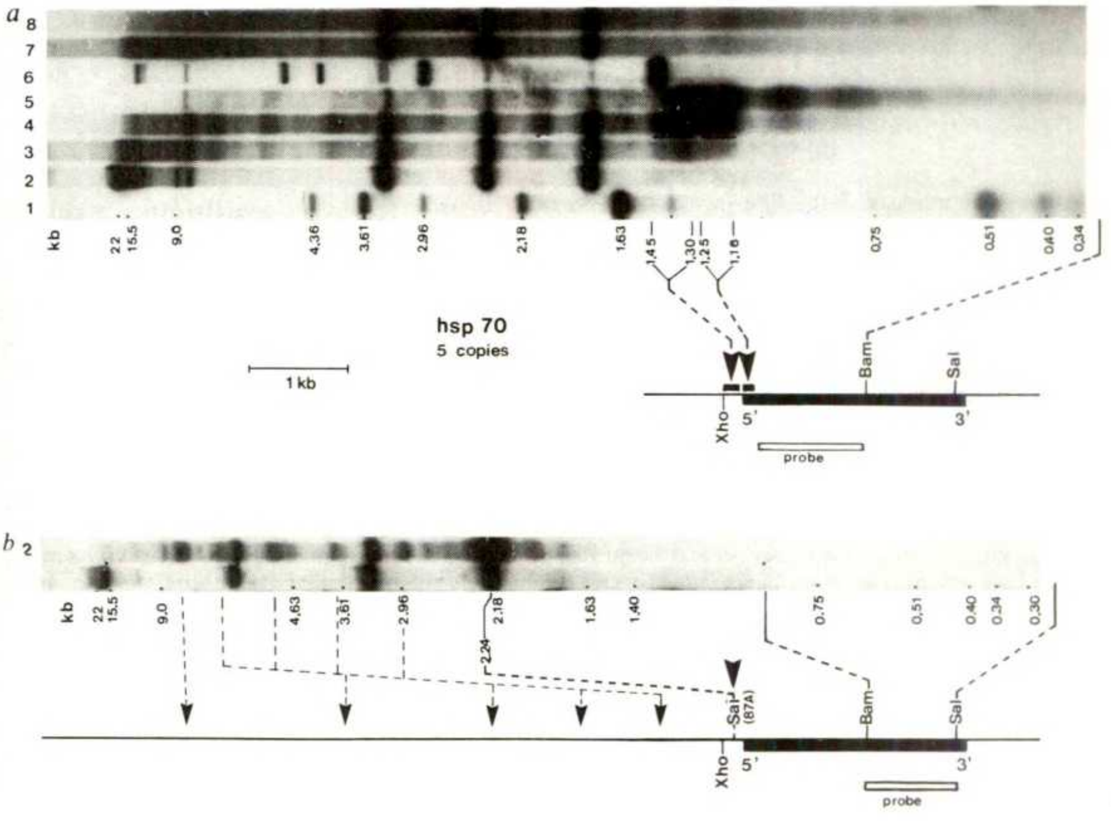

Fig. 1 Autoradiograms showing the partial DNase I cuts in Schneider cell chromatin upstream from the internal *Bam* site (*a*) and the 3′ *Sal* site (*b*) common to all hsp 70 gene copies. ***a***, Nuclei were purified from *Drosophila* Schneider line 2 tissue culture cells as described elsewhere[2], except that the final centrifugal spin was through 1.5 M sucrose. The nuclear pellet was rinsed once before resuspension at about 3×10^8 nuclei per ml in digestion buffer[2] (60 mM KCl, 15 mM NaCl, 15 mM Tris-HCl, *p*H 7.4, 0.5 mM dithiothreitol, 0.25 M sucrose, 3 mM $MgCl_2$, 0.05 mM $CaCl_2$). Various amounts of DNase I (Worthington) were added to aliquots of nuclei and digestion proceeded for 3 min at 25 °C. The reaction was terminated by the addition of EDTA and SDS to 12.5 mM and 0.5%, respectively, and the DNA was purified by immediate organic extractions. RNA was removed by RNase A and T1 digestion, the RNases by proteinase K digestion and the protease by repeated organic extractions as described in ref. 2. The DNA was precipitated in ethanol and redissolved at a concentration of 1 or 2 mg ml^{-1} in 10 mM Tris-HCl *p*H 7.4, 5 mM NaCl and 1 mM EDTA. Secondary *Bam*HI restriction digestions were carried out according to manufacturer's directions (New England Biolabs). The digestions were terminated as above, and the DNA samples in 10% glycerol, 5% Ficoll and marker dyes were electrophoresed on a 1.3% agarose gel, 30 cm long, in a Tris-acetate buffer system[41]. The upper half of the gel containing the large DNA fragments was immersed in 0.1 M HCl for 15 min to facilitate transfer of the DNA out of the agarose gel[42]. The DNA was denatured, neutralized and blotted on to nitrocellulose essentially according to Southern[3]. The nitrocellulose filter was rinsed in 9×SSC (1×SSC is 0.15 M NaCl, 0.015 M Na citrate, *p*H 7.0), 0.9 M NH_4 acetate, dried and baked under vacuum for 3 h at 75 °C. The filter was presoaked in 5× Denhardt's solution[43] (1× Denhardt's solution is 0.02% Ficoll, 0.02% bovine serum albumin, 0.02% polyvinylpyrollidone), 5× SSC, 50 mM Na phosphate, *p*H 7.0, and 0.25 mg ml^{-1} denatured salmon sperm DNA for 8 h at 67 °C and hybridized for 8 h at 67 °C in a slit chamber to plasmid pPW232.1 (ref. 17), labelled with ^{32}P by nick translation as described elsewhere[2] to a specific activity of about 1×10^8 d.p.m. per μg DNA. The hybridization mixture contained 5× Denhardt's solution, 5×SSC, 20 mM Na phosphate *p*H 7.0, 0.5 mg ml^{-1} denatured salmon sperm DNA, 0.1% SDS and 10% dextran sulphate to accelerate the hybridization reaction[42], and about 0.3 μg labelled plasmid DNA per 40 ml hybridization solution. After hybridization, the filter was washed twice in 5× Denhardt's solution, 3×SSC, 25 mM Na phosphate *p*H 7.0, 0.25% SDS and at least thrice in 0.1×SSC, 0.1% SDS, each round for 20–30 min at 67 °C. Autoradiography was on Kodak XR5 film. For later blots, the background noise could be reduced by doubling the concentration of Denhardt's solution at all stages and similarly for SDS in the primary wash. pPW232.1 (ref. 17), the cloned probe segment, is homologous to the 1.1-kilobase pair (kb) *Pst* fragment in Fig. 3 representing approximately the 5′ half of the hsp 70 coding region, indicated on the restriction map by the open bar. The lanes indicate: 1, marker DNA fragments from pBR322 (ref. 44), cut with *Pst*I; *Hin*fI; *Pst*I/*Sal*I; *Pst*I/*Eco*RI; *Pst*I/*Ava*I, and other recombinant plasmid fragments homologous to pBR322 sized at 9.0, 15.5 and 22 kilobase pairs. On a gel of this agarose content (1.3%), a linear relationship between log fragment length and mobility is obtained in the region bounded by the 0.75- and 3.61-kilobase pair markers; the resolution is about 30 base pairs for fragments not overexposed. 2, *Bam* digest on Schneider cell DNA, purified directly from whole cells. An identical pattern is observed with purified DNA from isolated nuclei incubated in digestion buffer without DNase I. 3–5, Partial DNase I digests on chromatin at a final DNase I concentration of 1, 2 and 4 units ml^{-1}, respectively. Only the major regions of preferential DNase I cleavage are indicated by the arrows on the hsp 70 restriction map, aligned beneath the autoradiogram. The filled bars directly under the arrows indicate the measured span of hypersensitivity, taken from the lines drawn on the autoradiogram adjacent to lane 4. 6, *Bam* plus *Xho* digest on Schneider cell DNA. The reaction did not go to completion. 7, 8, Partial DNase I digests on naked DNA. DNA at 0.4 mg ml^{-1} was digested with DNase I at 0.1 and 0.3 units ml^{-1}, respectively, for 1 min at 25 °C before secondary *Bam* cleavage. These two digestion points were picked from a series for purposes of comparison against the chromatin digests in lanes 4 and 5 because of their approximately equivalent overall extents of DNase I cleavage, monitored by gel electrophoresis and ethidium bromide staining after DNase I cleavage (data not shown). ***b***, See legend to *a* for a description of materials and methods. *Sal* was used for the secondary cleavage; the DNA fragments were sized on a 1.2% agarose gel; pPW229.1 (ref. 17), the cloned probe, is homologous to the *Bam–Sal* fragment representing approximately the 3′ half of the hsp 70 coding region. The lanes indicate: 1, *Sal* digest on Schneider cell DNA. The 2.24-kilobase pair *Sal* fragment is due to the hsp 70 gene copies at *87A*. 2, Partial DNase I digest on chromatin, as in *a*, lane 4. The hsp 70 gene copies at *87A* are reduced to the 2.24-kilobase pair *Sal* fragment or shorter fragments, so all longer fragments must be due to DNase I cleavage upstream from the hsp 70 coding regions at *87C*. The more prominently cleaved sites are indicated by the arrows over the restriction map at about 3.0, 3.8, 4.7, 6.1 and 8.0 kilobase pairs from the 3′ *sal* site. Interestingly, the preferred cuts about 3 kilobase pairs upstream from the 3′ *Sal* reference site map to a common region of homology upstream from the hsp 70 coding region; what Moran *et al.*[20] refer to as the x element. See text for discussion of the other sensitive sites.

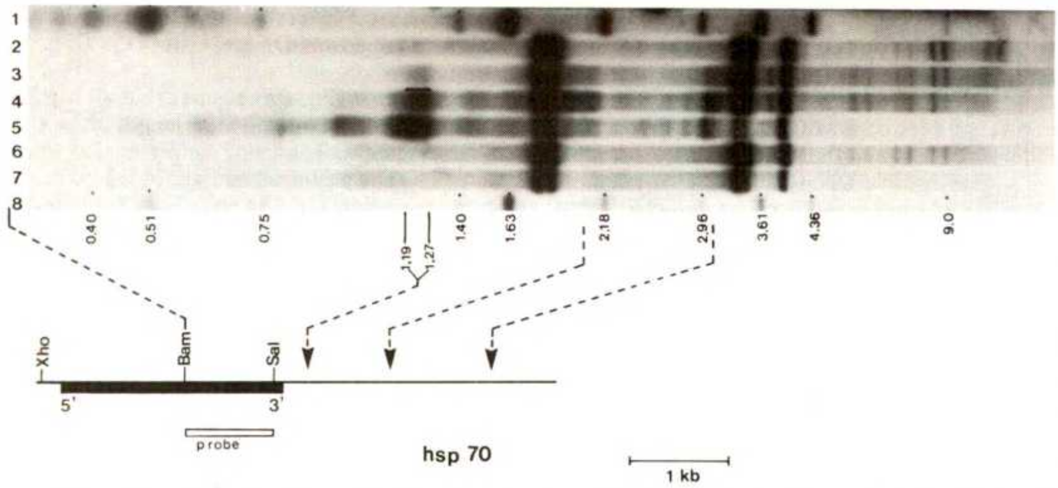

Fig. 2 Autoradiogram showing the partial DNase I cuts in Schneider cell chromatin downstream from the central *Bam* site common to all hsp 70 gene copies. *Bam*HI was used for the secondary cleavage; the DNA fragments were sized on a 1.3% agarose gel; pPW229.1 (ref. 17) was the labelled probe. The lanes indicate: 1, 8, Marker DNA fragments. 2, *Bam* digest on Schneider cell DNA. 3–5, Partial DNase I digests on chromatin at a final DNase I concentration of 1, 2 and 4 units ml^{-1}, respectively. The hypersensitive sites in lane 4 are indicated by arrows over their mapped positions on the hsp 70 restriction map at about 1.2, 2.1 and 3.1 kilobase pairs from the central *Bam* site. The second and fifth largest *Bam* fragments seen in lane 5 are not selectively lost on DNase I digestion. From densitometry of these fragments in lanes 2 and 5, they are about half as sensitive to DNase I as the other three *Bam* fragments (data not shown). See text for discussion. 6, 7, Partial DNase I digests on naked DNA, as in Fig. 1*a*, lanes 7, 8.

fragment characteristic of the *87A* hsp 70 sequences). In summary, the data indicate that a 5′ sensitive structure is present for most or all of the hsp 70 gene copies.

The other set of preferred DNase I cuts in Fig. 3*b*, lane 3, is likely to be wholly a result of the inversely repeated arrangement[25] of the hsp 70 genes at *87A*. Its interpretation is complicated by the variable length of the spacer region between these two genes[25], reflected in the *Pst* restriction pattern. Assuming that the 2.6–2.9-kilobase pair fragments are derived from the most abundant variant *Pst* segment, their display would be accounted for by the probe reacting with partial DNase I fragments from both ends of this 4.0-kilobase pair *Pst* segment. The two slightly longer and more sharply defined minor daughter fragments remain mysterious; they may be due partly to local DNase I sequence preference, shown in the control naked DNA digest (Fig. 3*b*, lane 5).

DNase I sensitivity of the active hsp 70 sequences

The 5′ sensitivity described so far is present before induction. Figure 4*a* shows the state of hsp 70 chromatin before and after 15 min of heat shock at 35 °C. Essentially the whole of the active hsp 70 coding sequence becomes sensitive to DNase I[28], but with a magnitude less than the 5′ sensitivity, which is still partially retained (Fig. 4*c*, lanes 4, 6). Curiously, some of the normally sensitive sites upstream from the hsp 70 5′ ends seem to lose definition with heat shock.

As a control, the DNA blot shown in Fig. 4*a* was immediately reprobed with another cloned segment not related to the heat shock genes, pDm4 (ref. 29), locus *62F*; the previous label was not removed. Densitometry (Fig. 4*c*), of the resulting blot in Fig. 4*b* shows that all hsp 70 restriction fragments are selectively

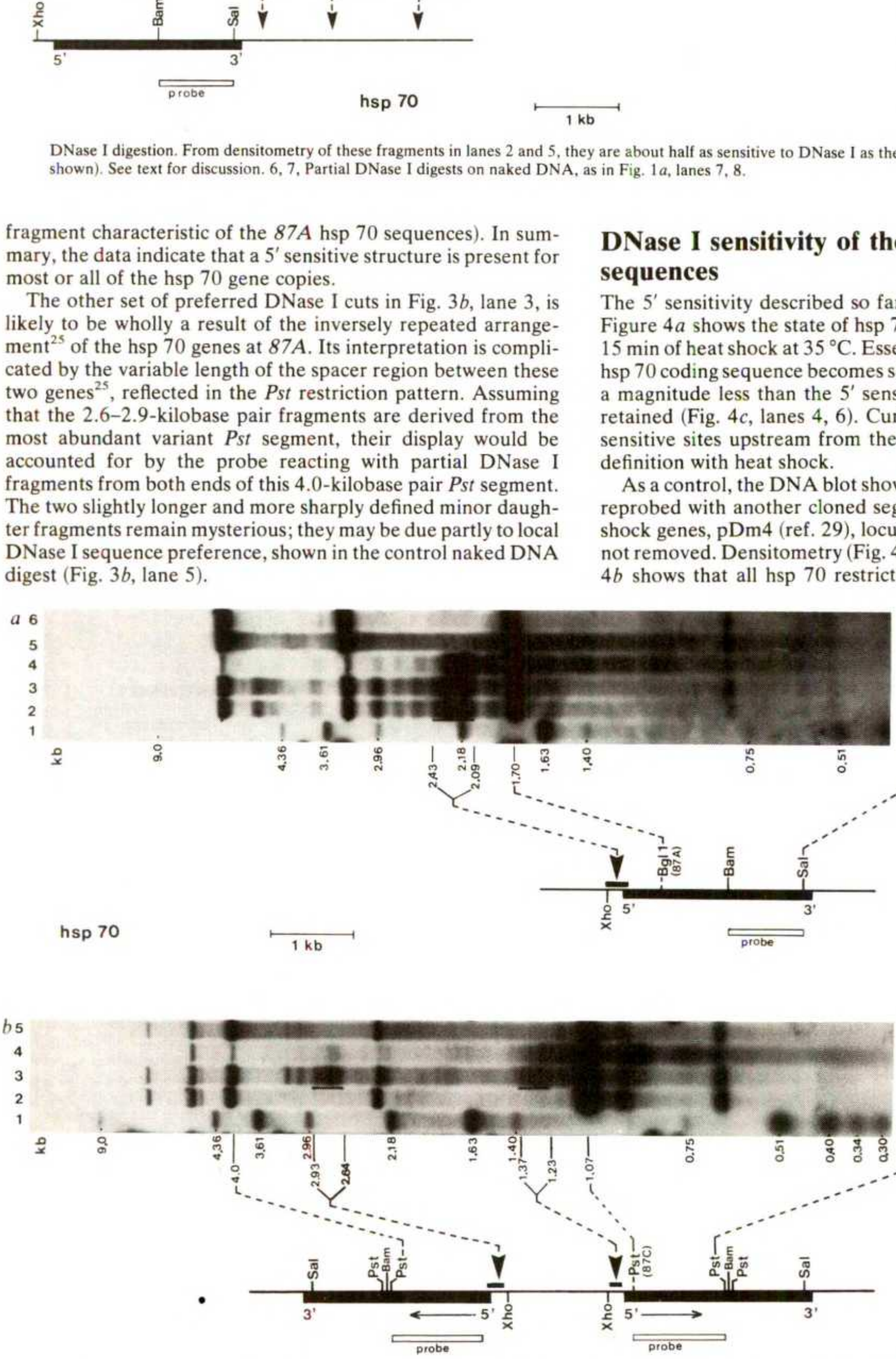

Fig. 3 *a*, Autoradiogram showing *87C* locus-specific DNase I cuts in Schneider cell chromatin upstream from the hsp 70 3′ *Sal* site. *Sal*I and *Bgl*I were used for the secondary cleavage; the DNA fragments were sized on a 1.2% agarose gel; pPW229.1 (ref. 17) was the labelled probe. The lanes indicate: 1, Marker DNA fragments. 6, *Sal* plus *Bgl*I digest on Schneider cell DNA. 2–4, Partial DNase I digests on chromatin from two separate experiments, using a final DNase I concentration of 8 units ml^{-1}, and 2 and 4 units ml^{-1}, respectively. 5, Partial DNase I digest on naked DNA, as in Fig. 1*a*, lane 7. *b*, Autoradiogram showing 87*A* locus-specific DNase I cuts in Schneider cell chromating upstream from a central *Pst* site in the hsp 70 coding region. *Pst*I was used for secondary cleavage; the DNA fragments were sized on a 1.3% agarose gel, and pPW232.1 (ref. 17) was the labelled probe. Only the restriction map for the 4.0-kilobase pair *Pst* fragment is shown, redrawn from the map of clone 122, from ref. 25. See text for discussion. The lanes indicate: 1, Marker DNA fragments. 2, *Pst* digest on Schneider cell DNA. 3, 4, Partial DNase I digests on chromatin at a final DNase I concentration of 2 and 4 units ml^{-1}, respectively. 5, Partial DNase I digest on naked DNA, as in Fig. 1*a*, lane 7.

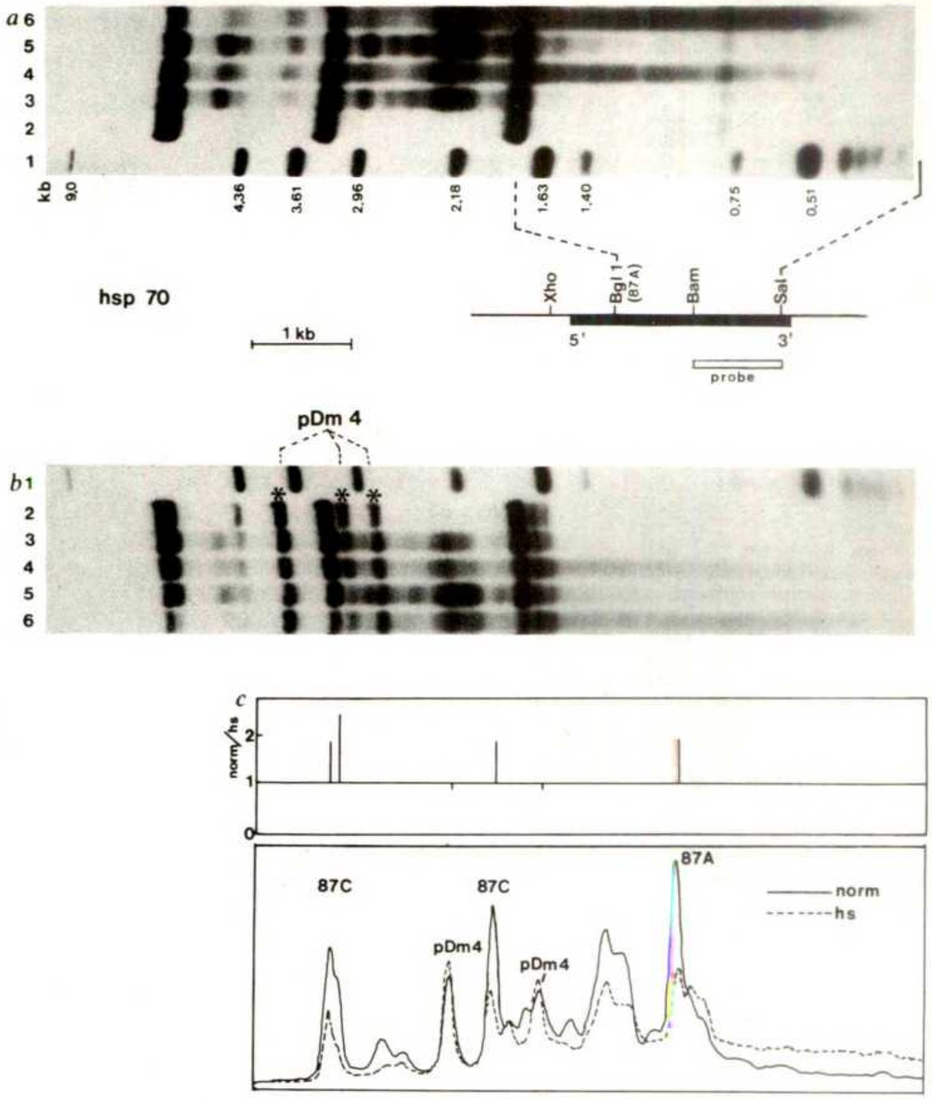

Fig. 4 *a*, Autoradiogram showing the state of hsp 70 chromatin before and after heat shock induction. *Sal*I and *Bgl*I were used for secondary cleavage; the DNA fragments were sized in a 0.8% agarose gel, and pPW229.1 (ref. 17) was the labelled probe. The lanes indicate: 1, Marker DNA fragments. 2, *Sal* plus *Bgl*I digest on Schneider cell DNA. DNA from heat-induced cells gave an identical pattern (data not shown). 3, 5, Partial DNase I digests on uninduced Schneider cell chromatin at a final DNase I concentration of 6 and 8 units ml^{-1}, respectively. 4, 6, Partial DNase I digests on chromatin in Schneider cells heat shocked at 35 °C for 15 min, as described elsewhere[28]. The two digestion points (final DNase I concentrations of 2 and 4 units ml^{-1}, respectively) were chosen out of a series for comparison against those in lanes 3 and 5 because of their close equivalence to the latter in overall extents of DNase I cleavage. They were monitored by gel electrophoresis and ethidium bromide staining (data not shown) and by reprobing this DNA blot with a cloned *Drosophila* DNA segment not involved in the heat shock response (see *b*). *b*, Autoradiogram showing the state of the chromatin at sequences homologous to pDm4 (ref. 29) before and after heat shock induction. The DNA blot in *a* was immediately reprobed with labelled pDm4 without removal of the previous label. See legend to *a* for key to the lanes. Both pDm4- and pPW299.1-specific fragments are displayed. The most prominent fragments labelled by pDm4 are indicated by asterisks. *c*, A densitometric scan of lanes 5 and 6 in *b*. The ratios of the peak heights between normal (norm) and heat shocked (hs) conditions for the pPW229.1- and two pDm4-specific fragments are schematically displayed over the scan.

digested after heat shock, whereas the pDm4 fragments are not. This indicates that most or all of the five gene copies of hsp 70 are in the active chromatin conformation, consistent with the finding that transcription occurs at both *87A* and 87*C* loci after heat shock[17,24].

Hsp 83 chromatin

The sequences for the 83,000 dalton heat shock protein, hsp 83, reside at the cytogenetic locus *63BC* (ref. 24). From a *Sal* restriction site within the single-copy coding sequence[24], partial DNase I cleavages upstream and downstream in a region extending about 40 kilobase pairs were mapped (Fig. 5*a*, *b*). A cluster of preferred cuts lie about 2.3–3.2 kilobase pairs upstream from the internal *Sal* site, and two clusters are observed starting from about 1.8 kilobase pairs downstream. No preferred cuts lie near the internal *Sal* site (data not shown). Holmgren and Meselson (manuscript in preparation) have recently mapped the 5′ terminus of a precursor to the hsp 83 mRNA to about 160 base pairs downstream from the *Eco*RI site indicated in Fig. 5. Thus, a DNase I-hypersensitive region overlaps or is very near the sequences complementary to the 5′ end of this RNA. No known genes occur at the clusters of preferred cuts downstream from the hsp 83 sequence. A low level of hsp 83 RNA is produced in normal conditions in Schneider cells (R. Holmgren and M. Meselson, in preparation). This would account for the slight sensitivity to DNase I shown by sequences homologous to RNA in Fig. 5. Previous single DNase I digests at this locus show that at 35 °C these sequences become more DNase I sensitive[30].

Nucleosome arrangement near DNase I-sensitive regions

The basic structural unit of eukaryotic chromatin is the nucleosome, composed of about 200 base pairs of DNA, of which 140 base pairs is wrapped around a core of histones (see ref. 1 for review). Analysis of the nucleosome organization of the hsp 70 genes has been complicated by the multiplicity of the gene copies. In Fig. 6, I map the partial micrococcal nuclease cuts upstream from the *Sal* site in the single-copy hsp 83 coding region; this nuclease preferentially cleaves the linker or spacer DNA between nucleosome cores.

The specific cuts made by micrococcal nuclease in chromatin (Fig. 6, lanes 2–5) reveal a striking degree of order in nucleosomal arrangement, in spite of the sequence specificity shown by the enzyme on naked DNA[31] (Fig. 6, lanes 7–9). Each of the three DNase I-hypersensitive sites near the 5′ end of the gene for hsp 83 is flanked by distinctive micrococcal nuclease cuts. The relative intensity and 100–110-base pair interval between the flanking cuts suggest a deviant structure at these regions. Further upstream, eight specific cuts are evident, beyond which nonlinear mobility of the DNA fragments and special sensitivity of some sequences make interpretation of the pattern difficult. However, the data show sufficiently that those eight nucleosomes are positioned specifically on the DNA[32–35] (but see ref. 36), and furthermore, that the spacing between adjacent nucleosome cores is irregular (suggested from previous general studies; see ref. 1), determined probably by the local DNA sequence[34]. Downstream from the region of DNase I

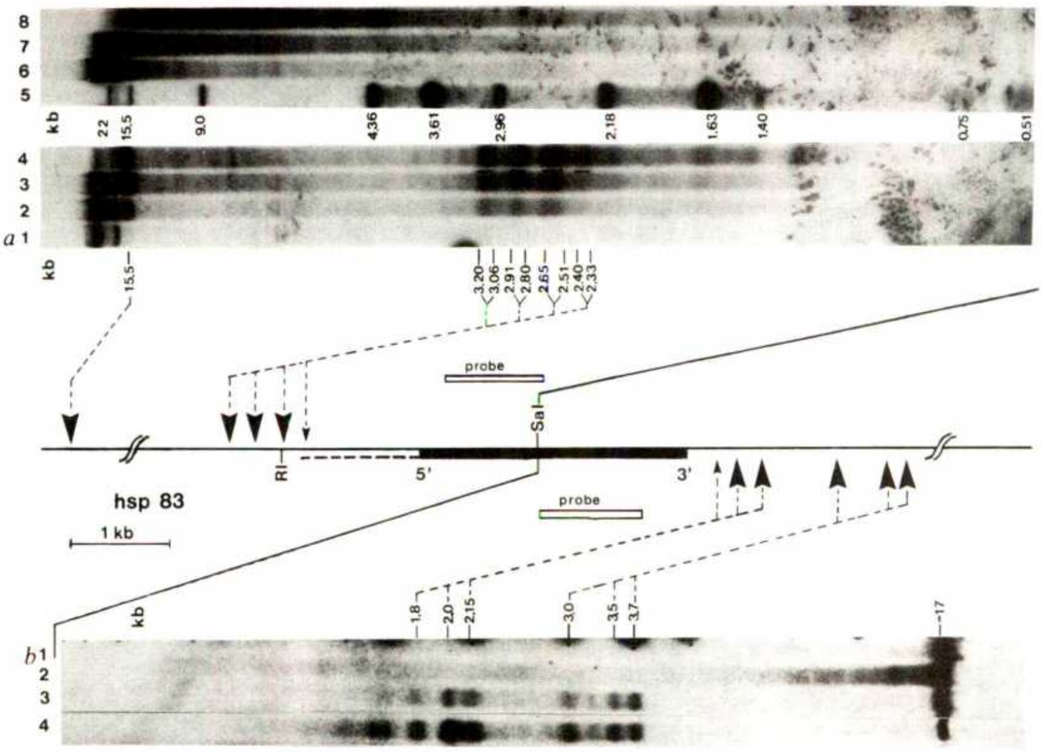

Fig. 5 *a*, Autoradiogram showing the partial DNase I cuts in Schneider cell chromatin upstream from the *Sal* site in the hsp 83 coding region (redrawn from Holmgren *et al.*[24]). The position of the *Eco*RI site was determined on a DNA blot not shown here. The filled bar depicts the location of the coding region downstream from the single intervening sequence in this split gene (R. Holmgren and M. Meselson, in preparation). *Sal*I was used for secondary cleavage; the DNA fragments (10 μg per track) were sized on a 1% agarose gel, and the labelled probe was a subclone from pPW244 (ref. 24) containing the *Pst* segment representing approximately the 5′ half of the hsp 83 coding region. This probe extends through the internal *Sal* site by about 50 base pairs (see restriction map) but the small extra segment barely, if at all, labels the cleavages downstream. The lanes indicate: 1, *Sal*I digest on Schneider cell DNA. A minor polymorphism at the external *Sal* site, or cross-reaction with a partially homologous fragment is observed. 2–4, Partial DNase I digests on chromatin at a final DNase I concentration of 0.5, 1 and 2 units ml^{-1}, respectively. Only the more prominent cleavages are noted by the arrows on the restriction map. 5, Marker DNA fragments. 6–8, Partial DNase I digests on naked DNA. DNase I at a concentration of 0.025, 0.05 and 0.1 unit ml^{-1}, respectively, was reacted with the DNA at 0.4 mg ml^{-1} in digestion buffer for 1 min at 25 °C. *b*, Autoradiogram showing the partial DNase I cuts in Schneider cell chromatin downstream from the *Sal* site in the hsp 83 coding region[24]. *Sal*I was used for secondary cleavage; the DNA fragments were sized on a 0.8% agarose gel; the cloned probe was a *Sal–Hae*II fragment gel-purified after cleavage from pPW244, representing approximately the 3′ half of the hsp 83 coding region[24]. A Du Pont Lightning Plus intensifying screen was used for this film exposure. The lanes indicate: 1, *Sal*I digest of Schneider cell DNA. 2, Partial DNase I digest of naked DNA, as in *a*, lane 6. 3, 4, Partial DNase I digests on chromatin, at a final DNase I concentration of 6 and 8 units ml^{-1}, respectively. This experiment was separate from that in *a*, lanes 3, 4, but the overall extents of cleavage are comparable. Only the more prominent cleavages are indicated by arrows on the restriction map.

hypersensitivity, the micrococcal nuclease cuts are less discrete, except for a cut 1.2 kilobase pairs from the *Sal* reference site. Such disperse cuts[28,30] would be expected for the slightly active hsp 83 gene at 25 °C. On further activation at 35 °C, the fragment pattern in Fig. 6 remains essentially similar (data not shown).

Comparison of hypersensitivity in cultured cells and embryos

Figure 7 shows a comparison of hypersensitive sites in chromatin from Schneider line 2 cells and from 6–18-h *D. melanogaster* (Oregon R) embryos. The 5′ sensitivity in the hsp 70 and hsp 83 genes (denoted by asterisks in Fig. 7*a*, *b*) is essentially the same for both materials, in spite of the populational polymorphism in external restriction sites shown largely by the Oregon R DNA. Intriguingly, several randomly selected regions not involved in the heat shock response [pDm4 (ref. 29), locus *62F*, and pPW100 (ref. 2), loci *57BC*, *83C*] reveal sensitive sites (denoted by asterisks in Fig. 7*c*, *d*) in the cell line, but not in Oregon R embryos. This result suggests that some hypersensitive sites in chromatin are not omnipresent, but perhaps limited to certain cell types or to particular stages in development.

An element for recognition?

The two *Drosophila* genes examined at three chromosomal loci exhibit a DNase I-sensitive chromatin structure at the 5′

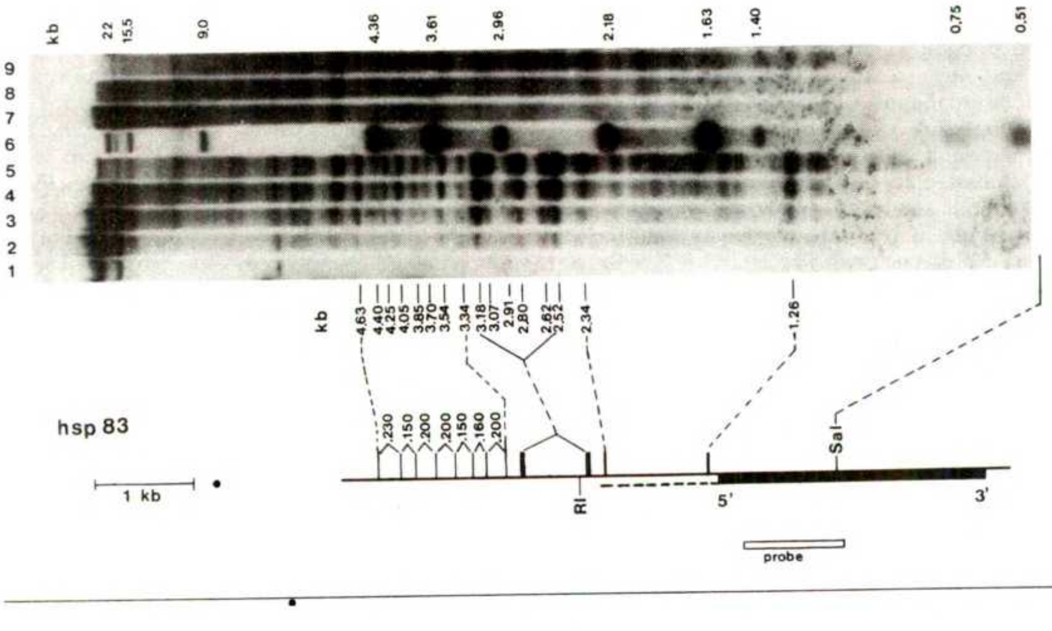

Fig. 6 Autoradiogram showing the partial micrococcal nuclease cuts in Schneider cell chromatin upstream from the *Sal* site in the hsp 83 coding region; produced as in Fig. 5*a*. The lanes indicate: 1, *Sal*I digest on Schneider cell DNA. 2–5, Partial micrococcal nuclease (Worthington) digests on chromatin at a final nuclease concentration of 0.75, 1.5, 3.0, 6.0 units ml^{-1}, respectively, at 25 °C for 3 min. 6, Marker DNA fragments. 7–9, Partial micrococcal nuclease digests on naked DNA at a final nuclease concentration of 1.25, 2.5 and 5 units ml^{-1}, respectively, at 25 °C for 1 min.

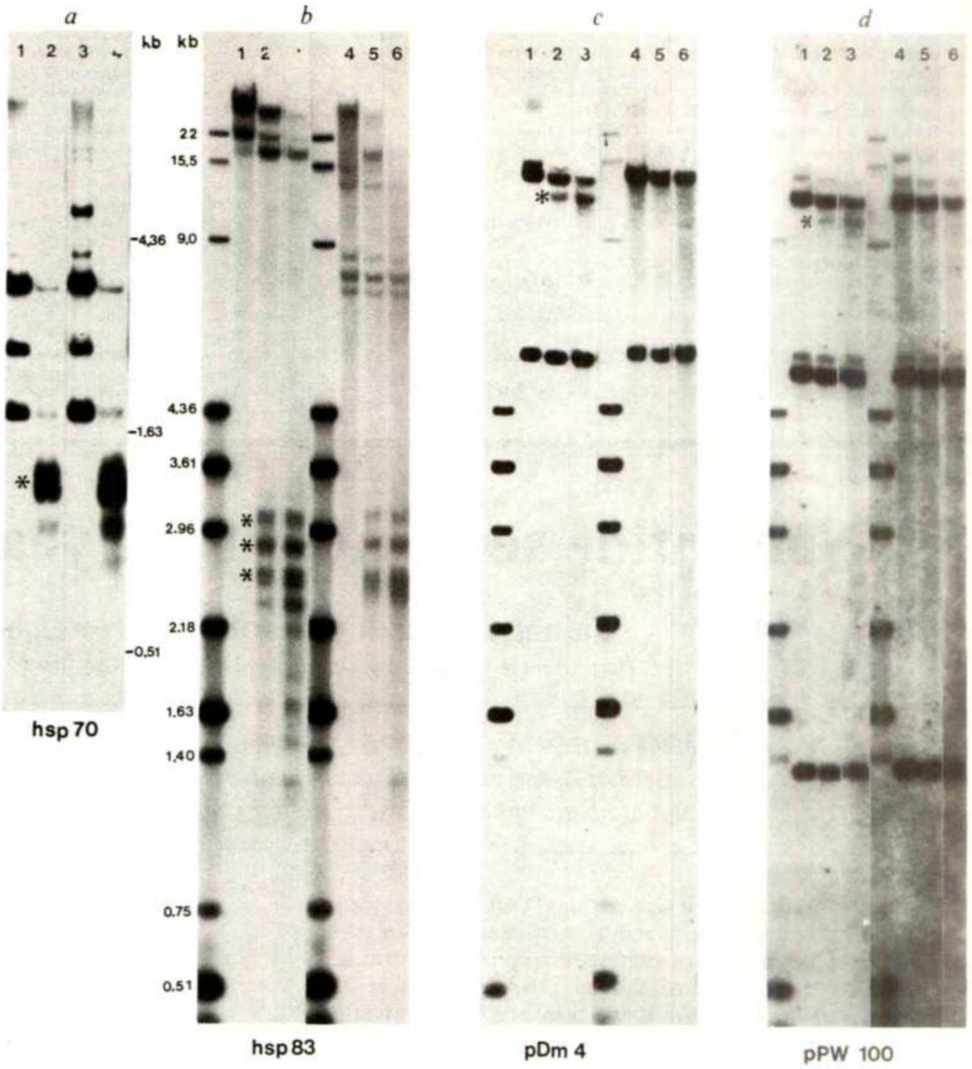

Fig. 7 Autoradiographic comparison of DNase I-hypersensitive sites at chromosomal regions homologous to four cloned segments, between Oregon R embryos and Schneider line 2 cells. Nuclei from 6–18-h embryos were isolated as described elsewhere[2]. The rest of the experiment was essentially as described in Fig. 1 legend. *a*, The hsp 70 region. DNA fragments were sized on a 1.1% agarose gel; *Bam*HI was used for secondary cleavage and the blot was probed with pPW232.1 (ref. 17). The lanes indicate: 1, 3, *Bam*HI digest of Schneider cell and Oregon R DNA, respectively. 2, 4, Partial DNase I digests of Schneider cell (8 units ml^{-1}) and Oregon R (6 units ml^{-1}) chromatin, respectively. ***b***, The hsp 83 region. DNA fragments were sized on a 0.8% agarose gel; *Sal*I was used for secondary cleavage; the blot was probed as in Fig. 5*a*. The lanes indicate: 1, 4, *Sal*I digest of Schneider cell and Oregon R DNA respectively. 2, 3, Partial DNase I digests (6 and 8 units ml^{-1}, respectively) of Schneider cell chromatin. 5, 6, Partial DNase I digests (2 units ml^{-1} in two separate experiments) of Oregon R chromatin. ***c***, ***b*** was reprobed with labelled pDm4 (ref. 34), without removal of the previous label. ***d***, ***c*** was reprobed with labelled pPW100 (ref. 2), without removal of the previous labels.

terminus of the coding sequence before activation. This 5′ sensitivity may reflect a specially exposed or structurally modified stretch of eukaryotic DNA for recognition by regulatory molecules. The other sites adjacent to the hsp coding regions may be indicative of the 5′ termini of unknown or yet unmapped transcription units, as in the repeated sequence elements at locus *87C* (refs 17, 27), or they may reflect other chromosomal functions. The findings documented here, although unique to eukaryotic gene structure, have a precedent in the structure of viral chromatin; the origin of replication (and transcription) of SV40 and polyoma virus has been shown to be in a preferentially nuclease-susceptible conformation[37–39].

What might be the basis of this unique sensitivity? A special DNA sequence at these regions could bind other macromolecules such as specific proteins that cause the sensitivity and align neighbouring nucleosomes specifically on the DNA, or the sequence may possess a peculiar base order that renders it sensitive when the DNA in the region is coiled and supercoiled in nucleosomes and higher order structures. The molecular basis notwithstanding, a new regulatory feature in relation to prokaryotic models of gene control appears: an element for recognition at the 5′ end of a gene based on an exposed chromatin structure that defines its potential for activation, this potential being realized on induction, perhaps according to the bacterial paradigm of specific activators and repressors. Such a two-stage model of eukaryotic gene regulation has some implications for developmental biology. Specifically, the hypersensitive sites observed in tissue culture cell chromatin but not in embryonic chromatin might suggest that a developmentally regulated gene (as opposed to the heat shock genes) possess a 5′ exposed structure only in the appropriate cell type or developmental stage. Sites of DNase I hypersensitivity have recently been observed in the chicken[40], and Weintraub and colleagues (personal communication) have detected tissue-specific hypersensitive sites for the chick globin gene. Will the various developmental systems currently amenable to molecular analysis yield data consistent with this view of gene regulation?

I thank Walter Gilbert for a crucial discussion on mapping hypersensitive sites and for suggesting the particular form of end-labelling used here. I also thank Robert Holmgren, Rick Morimoto and Matthew Meselson for continual communication, discussion and permission to quote research data before publication, Sarah Elgin, in whose laboratory part of the work with *Drosophila* embryos was performed, R. Holmgren, R. Morimoto, P. Bingham, J. Jack and M. Meselson for gifts of cloned DNA, many colleagues for discussions, Harold Weintraub for a prepublication manuscript, the Harvard Society of Fellows for a Junior Fellowship and W. Gilbert for critical comments on this manuscript, research facilities and support. This work was funded by NIH grant GM21514-06 to W. Gilbert.

Received 24 April; accepted 19 June 1980.

1. Felsenfeld, G. *Nature* **271**, 115–122 (1978).
2. Wu, C., Bingham, P. M., Livak, K. J., Holmgren, R. & Elgin, S. C. R. *Cell* **16**, 797–806 (1979).
3. Southern, E. M. *J. molec. Biol.* **98**, 503–517 (1975).
4. Schneider, I. *J. Embryol. exp. Morph.* **27**, 353–365 (1972).
5. Ashburner, M. & Bonner, J. J. *Cell* **17**, 214–254 (1979).
6. Ritossa, F. *Experientia* **18**, 571–573 (1962).
7. Ashburner, M. *Chromosoma* **31**, 356–376 (1970).
8. Tissieres, A., Mitchell, H. K. & Tracy, U. M. *J. molec. Biol.* **84**, 389–398 (1974).
9. McKenzie, S. L., Henikoff, S. & Meselson, M. *Proc. natn. Acad. Sci. U.S.A.* **72**, 1117–1121 (1975).
10. Spradling, A., Penman, S. & Pardue, M. L. *Cell* **4**, 395–404 (1975).

11. Lewis, M., Helmsing, P. J. & Ashburner, M. *Proc. natn. Acad. Sci. U.S.A.* **72,** 3604–3608 (1975).
12. Spradling, A., Pardue, M. L. & Penman, S. *J. molec. Biol.* **109,** 559–587 (1977).
13. McKenzie, S. L. & Meselson, M. *J. molec. Biol.* **117,** 279–283 (1977).
14. Mirault, M. E., Goldschmidt-Clermont, M., Moran, L., Arrigo, A. P. & Tissieres, A. *Cold Spring Harb. Symp. quant. Biol.* **42,** 819–829 (1978).
15. Henikoff, S. & Meselson, M. *Cell* **12,** 441–451 (1977).
16. Ish-Horowicz, D., Holden, J. J. &. Gehring, W. J. *Cell* **12,** 643–652 (1977).
17. Livak, K. J., Freund, R., Schweber, M., Wensink, P. C. & Meselson, M. *Proc. natn. Acad. Sci. U.S.A.* **75,** 5613–5617 (1978).
18. Schedl, P. *et al. Cell* **14,** 921–929 (1978).
19. Craig, E. A., McCarthy, B. J. & Wadsworth, S. C. *Cell* **16,** 575–588 (1979).
20. Moran, L. *et al. Cell* **17,** 1–8 (1979).
21. Artavanis-Tsakonas, S., Schedl, P., Mirault, M. E., Moran, L. & Lis, J. *Cell* **17,** 9–18 (1979).
22. Mirault, M. E., Goldschmidt-Clermont, M., Artavanis-Tsakonas, S. & Schedl, P. *Proc. natn. Acad. Sci. U.S.A.* **76,** 5254–5258 (1979).
23. Ish-Horowicz, D., Pinchin, S. M., Schedl, P., Artavanis-Tsakonas, S. & Mirault, M. E. *Cell* **18,** 1351–1358 (1979).
24. Holmgren, R., Livak, K., Morimoto, R., Freund, R. & Meselson, M. *Cell* **18,** 1359–1370 (1979).
25. Goldschmidt-Clermont, M. *Nucleic Acids Res.* **8,** 235–251 (1980).
26. Bernardi, A., Gaillard, C. & Bernardi, G. *Eur. J. Biochem.* **52,** 451–457 (1975).
27. Lis, J. T., Prestidge, L. & Hogness, D. S. *Cell* **14,** 901–919 (1978).
28. Wu, C., Wong, Y. C. & Elgin, S. C. R. *Cell* **16,** 807–814 (1979).
29. Wensink, P. C., Finnegan, D. J., Donelson, J. E. & Hogness, D. S. *Cell* **3,** 315–325 (1974).
30. Wu, C. thesis, Harvard Univ. (1979).
31. Anfinsen, C. B., Cuatrecasas, P. & Taniuchi, H. in *The Enzymes Vol.* IV, 3rd edn (ed. Boyer, P. D.) 177–199 (Academic, New York, 1971).
32. Ponder, B. A. & Crawford, C. V. *Cell* **11,** 35–49 (1977).
33. Musich, P. R., Maio, J. J. & Brown, F. L. *J. molec. Biol.* **117,** 657–677 (1977).
34. Chao, M. V., Gralla, J. & Martinson, H. G. *Biochemistry* **8,** 1068–1074 (1979).
35. Wittig, B. & Wittig, S. *Cell* **18,** 1173–1183 (1979).
36. Fittler, F. & Zachau, H. G. *Nucleic Acids Res.* **7,** 1–13 (1979).
37. Scott, W. A. & Wigmore, D. J. *Cell* **15,** 1511–1518 (1978).
38. Varshavsky, A. J., Sundin, O. & Bohn, M. *Cell* **16,** 453–466 (1979).
39. Waldeck, W., Fohring, B., Chowdhury, K., Gruss, P. & Sauer, G. *Proc. natn. Acad. Sci. U.S.A.* **75,** 5964–5968 (1978).
40. Kuo, M. T., Mandel, J. L. & Chambon, P. *Nucleic Acids Res.* **7,** 2105–2113 (1979).
41. Hayward, G. S. & Smith, M. G. *J. molec. Biol.* **63,** 383–395 (1972).
42. Wahl, G. M., Stern, M. & Stark, G. R. *Proc. natn. Acad. Sci. U.S.A.* **76,** 3683–3687 (1979).
43. Denhardt, D. *Biochem. biophys. Res. Commun.* **23,** 641–646 (1966).
44. Sutcliffe, J. G. *Nucleic Acids Res.* **5,** 2721–2728 (1978).

Nucleotide sequence of the yeast plasmid

James L. Hartley & John E. Donelson
Department of Biochemistry, University of Iowa, Iowa City, Iowa 52242

The nucleotide sequence of the yeast DNA plasmid (2μ circle) from Saccharomyces cerevisiae *strain A364A D5 has been determined. The plasmid contains 6,318 base pairs, including two identical inverted repeats of 599 base pairs. Possible functions are suggested, and attributes of an improved vector for cloning foreign DNAs in yeast are discussed.*

THE yeast plasmid (2μ circle) is a circular DNA molecule with a contour length of about 2 μm (about 6 kilobases) that is present in about 70 copies per cell of most yeast strains and constitutes about 3% of the total yeast cellular DNA[1-3]. Its most distinguishing structural feature is the presence of two inverted repeat (IR) sequences of about 600 base pairs that are separated by a large unique region (about 2.7 kilobases) and a small unique region (about 2.3 kilobases)[3-8]. In yeast cells reciprocal recombination between the inverted repeats produces a mixture of two sequence forms (A and B) of the yeast plasmid that differ in the orientation of one unique region relative to the other[3-9]. When the yeast plasmid is cloned in *Escherichia coli* using recombinant DNA techniques this reciprocal recombination does not occur.

Two observations suggest that the yeast plasmid is located, at least some of the time, in the yeast nucleus. First, the plasmid can be isolated in a condensed nucleosome form with which histones are associated, similar to yeast nuclear chromatin[10,11]. Second, its replication occurs only during the S phase, each molecule is replicated only once, and replication is regulated by the same genes that control the initiation and completion of nuclear DNA replication[12,13]. There is no evidence that the yeast plasmid is capable of integrating into chromosomal DNA.

The biological function of the yeast plasmid is not known. However, portions of the plasmid are transcribed *in vivo* into polyadenylated mRNAs which have been mapped relative to restriction enzyme fragments of the DNA[14]. The poly(A)-containing RNAs direct the synthesis of protein in *in vitro* translation experiments. Plasmid-specific proteins have been detected when the plasmid has been introduced into *E. coli* minicell-producing strains[3,15,16]. Yeast strains have been isolated which do not have any plasmid sequences present, but possess normal growth properties in laboratory conditions[17,18].

Recently the yeast plasmid has acquired increased significance as an efficient vector for yeast transformation[19-24]. Experiments with chimaeric DNAs containing all or part of the yeast plasmid indicate that maximum transformation stability is obtained when one of the two inverted repeats is present[25], suggesting that the replication origin of the plasmid may be within this sequence. Thus the yeast plasmid is an attractive system for the study of eukaryotic gene control and chromosomal replication.

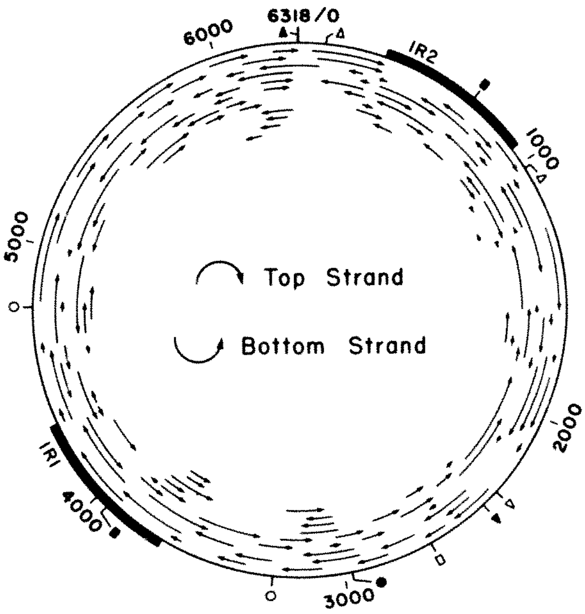

Fig. 1 Map of the yeast plasmid (form A) and the sub-sequences used to derive the sequence. Arrows indicate the location and extent of each subsequence, clockwise for the top strand, counter-clockwise for the bottom strand. Thick lines represent the inverted repeats IR1 and IR2. Restriction enzyme cleavage sites shown are *Eco*RI (▲), *Hin*dIII (△), *Xba*I (■), *Pst*I (□), *Hpa*I (●) and *Ava*I (○).

We report here the sequence of the yeast plasmid. The boundaries of the inverted repeats are defined and potential protein coding regions are identified. The location of the origin of replication and the function of one of the protein coding regions are discussed. Improvements in the cloning of foreign DNAs in yeast are suggested.

0028–0836/80/350860—06$01.00

Source of the sequence

For the sequence determinations, the yeast plasmid was recovered from the recombinant plasmid p82-6B. This is a plasmid which was found in a library of random yeast strain A364A D5 DNA fragments cloned in the *E. coli* plasmid pMB9 (ref. 26) by the poly(dA)·poly(T) tailing technique[27]. It was initially identified by screening individual colonies in the library for the presence of yeast plasmid sequences by the Grunstein and Hogness procedure[28] and subsequently shown to contain about 1.5 copies of the yeast plasmid (E. Gubbins, K. Chen and J.E.D., unpublished data). The 1.5 copies probably arose from a yeast plasmid dimer that was tailed with poly(dA) at random internal single-strand nicks or double-strand scissions during the poly(dA) addition such that part of the dimeric sequence was removed during the cloning procedure.

The circular yeast plasmid (form A) contains two *Eco*RI sites, one in each of the two unique regions, such that *Eco*RI digestion generates two fragments of 3.9 and 2.4 kilobases (ref. 5). The initial sequencing strategy was to determine the sequence of these two fragments individually and then identify and sequence restriction fragments which would overlap the two *Eco*RI sites. As the sequencing progressed, it became convenient to subclone a 4.1 kilobase *Hin*dIII fragment that contained the entire 3.9-kilobase *Eco*RI fragment and hence possessed an *Eco*RI site near each end. Thus the sequence of the 2.4-kilobase *Eco*RI fragment was obtained using the fragment recovered directly from p82-6B, and the rest of the sequence was largely obtained from the cloned 4.1-kilobase *Hin*dIII fragment subcloned in pBR322. Both plasmids were completely stable when maintained in the *recA E. coli* strain HB101.

The sequence of the plasmid was obtained by collecting sequence data from as many 3′-terminally labelled *Hpa*II-, *Sau*3AI-, *Taq*I-, and *Hin*fI-fragments as could be strand separated[29] or digested with a second restriction enzyme to separate the labelled ends. In practice, about three-quarters of the fragments could be separated into two distinct strands on a strand separation gel. Overlapping sub-sequences were identified by computer analysis[30] or by inspection. Restriction sites found during this process were used for subsequent sequencing runs to fill gaps or to increase coverage of both strands. The individual sequences (about 140 in all) were each read at least three times. All changes and corrections were made on a computer file to minimize clerical error.

Features of the sequence

Figure 1 shows a map of the restriction fragments used to obtain the sequence data and Fig. 2 shows the complete sequence. The inverted repeats are designated IR1 and IR2 according to the nomenclature of Hollenberg[16]. Of the 6,318 base pairs, 61% are dA+dT, close to the dA+dT content of yeast chromosomal DNA (about 64%) and much lower than the value for mitochondrial DNA of 79% (ref. 3). The sequence is numbered taking nucleotide 1 as the G of the *Eco*RI site nearest IR2. The inverted repeats are 599 base pairs long, extending from 341 through to 939 (IR2) and from 3,714 to 4,312 (IR1). The unique regions are therefore 2,774 and 2,346 base pairs long. The sequence contains previously mapped sites for the restriction enzymes *Eco*RI (1; 2,407), *Pst*I (2,652), *Hin*dIII (105; 1,017; 2,331), *Hin*cII (217; 2,964), *Hpa*I (2,964; subset of *Hin*cII sites), *Ava*I (3,258; 4,764) and *Xba*I (703; 3,945). In addition, sites for *Pvu*I (1,755; 2,729), *Pvu*II (2,029; 2,133), *Bal*I (264), *Bcl*I (304) and *Cla*I (6,284) are predicted. Sites for the enzymes *Bam*HI, *Kpn*I, *Sal*I, *Sst*I, *Sst*II, *Xho*I, *Bgl*I and *Bgl*II do not appear in the sequence. A total of 87% of the plasmid was sequenced on both strands and at least one overlap was obtained for all restriction sites used in sequencing. The sequence of the region 1–1,022 has been reported previously by another laboratory[32] and differs from that presented here at eight positions.

The inverted repeats are the most prominent feature of the plasmid. Their sequences were determined separately and found to be completely homologous. The IR boundaries are not marked by any striking symmetry features. However, a remarkable concentration of symmetry elements occurs near the centres of the IRs, at 640–761 and 3,892–4,013. In these 122-base pair regions are found a 13-base pair direct repeat and a dyad symmetry (abc—c′b′a′) of 16 base pairs, both contained within an imperfect dyad symmetry of 49 base pairs. These regions can be drawn as two alternative stem and loop structures (Fig. 3) which would have thermodynamic stabilities of the order of −50 kcal mol^{-1} when calculated by rules derived from oligoribonucleotide studies[33]. The longest run of alternating purines/pyrimidines found in the plasmid is located at 564–581 and 4,072–4,089. It has been proposed that these might form left-handed helical structures *in vivo*[34]. Possible implications for these features are discussed below.

A second concentration of symmetry elements is found in the large unique region. About 5.5 copies of a sequence of 62–63 base pairs arranged as direct tandem repeats are found between positions 2,960 and 3,302 (Fig. 2). Five repeats, 2,987–3,048, 3,049–3,111, 3,112–3,173, 3,174–3,235 and 3,236–3,297, share 78–97% (average 90%) homology with a consensus sequence

5′-TTTTTPuPyAGAACAAAAATGCAACGCGAGAGCG

CTAATTTT$\frac{\text{A}}{\text{T}}$CAAACAAAGAATCTGAGCTTCA-3′.

Two sets of two of these repeats, 2,975–3,098 and 3,099–3,223, can be aligned to give tandem copies of 124 base pairs which share 97% homology. In addition, this area is rich in dyad symmetries, including a perfect dyad at 2,987–3,002 and 3,236–3,251. The significance of these symmetries is not known. They appear to be dispensible to the plasmid, however, since deletions in this area are seen in natural isolates[5]. No large alphabetic palindromes (abc—cba) were found in the yeast plasmid.

The sequence was examined for potential protein-coding regions, that is, regions starting with an ATG codon and terminating with any of the stop codons. Three such long open translation reading frames were found, ‘Able’ (423 codons, molecular weight (MW) 48,625; 5,570–520; top strand; reading frame 2), ‘Baker’ (373 codons, 43,235 MW; 2,008–890; bottom strand; reading frame 3) and ‘Charlie’ (296 codons, MW 33,199; 5,198–4,311; bottom strand; reading frame 2) as shown in Fig. 4. All three coding regions terminate within inverted repeats, although ‘Baker’ ends just inside the IR1 boundary. ‘Able’ terminates with TAA, ‘Baker’ with TAG and ‘Charlie’ with TGA. Proteins of MW 20,000 and less could be encoded by other regions. Overlapping coding regions such as are seen in several circular viral genomes[35–37] are not found in the yeast plasmid.

Homology between the yeast plasmid and the bacterial cloning vector pBR322 has been reported[38] on the basis of hybridization experiments. Computer comparisons of the two DNAs under various homology requirements did not reveal any extensive identities. The longest perfect homology is 13 base pairs.

Discussion

The sequence of the yeast plasmid can be inspected from the standpoint of (1) its utilization as a vector for cloning foreign DNA fragments, and (2) its existence as a eukaryotic ‘minichromosome’ organized by histones into nucleosomes, and containing an origin of replication and one or more genes with attendant regulatory elements. Two conclusions regarding the plasmid's *in vivo* functions can be drawn from the sequence and from the work of other investigators: the location of the origin of replication and the identification of the gene product which mediates the interconversion of forms A and B. Both conclusions concern the use of the yeast plasmid as a cloning vehicle.

Several lines of evidence support the suggestion that the origin of replication of the yeast plasmid is near the *Xba*I site in IR1 (position 3,945). First, the regions surrounding the *Xba*I

```
        10         20         30         40         50         60         70         80         90        100        110        120        130        140        150
GAATTCTGAA CCAGTCCTAA AACGAGTAAA TAGGACCGGC AATTCTTCAA GCAATAAACA GGAATACCAA TTATTAAAAG ATAACTTAGT CAGATCGTAC AATAAAGCTT TGAAGAAAAA TGCGCCTTAT TCAATCTTTG CTATAAAAAA
CTTAAGACTT GGTCAGGATT TTGCTCATTT ATCCTGGCCG TTAAGAAGTT CGTTATTTGT CCTTATGGTT AATAATTTTC TATTGAATCA GTCTAGCATG TTATTTCGAA ACTTCTTTTT ACGCGGAATA AGTTAGAAAC GATATTTTTT

       160        170        180        190        200        210        220        230        240        250        260        270        280        290        300
TGGCCCAAAA TCTCACATTG GAAGACATTT GATGACCTCA TTTCTTTCAA TGAAGGGCCT AACGGAGTTG ACTAATGTTG TGGGAAATTG GAGCGATAAG CGTGCTTCTG CCGTGGCCAG GACAACGTAT ACTCATCAGA TAACAGCAAT
ACCGGGTTTT AGAGTGTAAC CTTCTGTAAA CTACTGGAGT AAAGAAAGTT ACTTCCCGGA TTGCCTCAAC TGATTACAAC ACCCTTTAAC CTCGCTATTC GCACGAAGAC GGCACCGGTC CTGTTGCATA TGAGTAGTCT ATTGTCGTTA

       310        320        330        340        350        360        370        380        390        400        410        420        430        440        450
ACCTGATCAC TACTTCGCAC TAGTTTCTCG GTACTATGCA TATGATCCAA TATCAAAGGA AATGATAGCA TTGAAGGATG AGACTAATCC AATTGAGGAG TGGCAGCATA TAGAACAGCT AAAGGGTAGT GCTGAAGGAA GCATACGATA
TGGACTAGTG ATGAAGCGTG ATCAAAGAGC CATGATACGT ATACTAGGTT ATAGTTTCCT TTACTATCGT AACTTCCTAC TCTGATTAGG TTAACTCCTC ACCGTCGTAT ATCTTGTCGA TTTCCCATCA CGACTTCCTT CGTATGCTAT
                                            └→IR2

       460        470        480        490        500        510        520        530        540        550        560        570        580        590        600
CCCCGCATGG AATGGGATAA TATCACAGGA GGTACTAGAC TACCTTTCAT CCTACATAAA TAGACGCATA TAAGTACGCA TTTAAGCATA AACACGCACT ATGCCGTTCT TCTCATGTAT ATATATATAC AGGCAACACG CAGATATAGG
GGGGCGTACC TTACCCTATT ATAGTGTCCT CCATGATCTG ATGGAAAGTA GGATGTATTT ATCTGCGTAT ATTCATGCGT AAATTCGTAT TTGTGCGTGA TACGGCAAGA AGAGTACATA TATATATATG TCCGTTGTGC GTCTATATCC

                                                                           ①
       610        620        630        640        650        660        670        680        690        700        710        720        730        740        750
TGCGACGTGA ACAGTGAGCT GTATGTGCGC AGCTCGCGTT GCATTTTCGG AAGCGCTCGT TTTCGGAAAC GCTTTGAAGT TCCTATTCCG AAGTTCCTAT TCTCTAGAAA GTATAGGAAC TTCAGAGCGC TTTTGAAAAC CAAAAGCGCT
ACGCTGCACT TGTCACTCGA CATACACGCG TCGAGCGCAA CGTAAAAGCC TTCGCGAGCA AAAGCCTTTG CGAAACTTCA AGGATAAGGC TTCAAGGATA AGAGATCTTT CATATCCTTG AAGTCTCGCG AAAACTTTTG GTTTTCGCGA
                                                                                     ③          ③                                    ②                    ②

       760        770        780        790        800        810        820        830        840        850        860        870        880        890        900
CTGAAGACGC ACTTTCAAAA AACCAAAAAC GCACCGGACT GTAACGAGCT ACTAAAATAT TGCGAATACC GCTTCCACAA ACATTGCTCA AAAGTATCTC TTTGCTATAT ATCTCTGTGC TATATCCCTA TATAACCTAC CCATCCACCT
GACTTCTGCG TGAAAGTTTT TTGGTTTTTG CGTGGCCTGA CATTGCTCGA TGATTTTATA ACGCTTATGG CGAAGGTGTT TGTAACGAGT TTTCATAGAG AAACGATATA TAGAGACACG ATATAGGGAT ATATTGGATG GGTAGGTGGA

       910        920        930        940        950        960        970        980        990       1000       1010       1020       1030       1040       1050
TTCGCTCCTT GAACTTGCAT CTAAACTCGA CCTCTACATC AACAGGCTTC CAATGCTCTT CAAATTTTAC TGTCAAGTAG ACCCATACGG CTGTAATATG CTGCTCTTCA TAATGTAAGC TTATCTTTAT CGAATCGTGT GAAAAACTAC
AAGCGAGGAA CTTGAACGTA GATTTGAGCT GGAGATGTAG TTGTCCGAAG GTTACGAGAA GTTTAAAATG ACAGTTCATC TGGGTATGCC GACATTATAC GACGAGAAGT ATTACATTCG AATAGAAATA GCTTAGCACA CTTTTTGATG
                                   IR2←┘

      1060       1070       1080       1090       1100       1110       1120       1130       1140       1150       1160       1170       1180       1190       1200
TACCGCGATA AACCTTTACG GTTCCCTGAG ATTGAATTAG TTCCTTTAGT ATATGATACA AGACACTTTT GAACTTTGTA CGACGAATTT TGAGGTTCGC CATCCTCTGG CTATTTCCAA TTATCCTGTC GGCTATTATC TCCGCCTCAG
ATGGCGCTAT TTGGAAATGC CAAGGGACTC TAACTTAATC AAGGAAATCA TATACTATGT TCTGTGAAAA CTTGAAACAT GCTGCTTAAA ACTCCAAGCG GTAGGAGACC GATAAAGGTT AATAGGACAG CCGATAATAG AGGCGGAGTC

      1210       1220       1230       1240       1250       1260       1270       1280       1290       1300       1310       1320       1330       1340       1350
TTTGATCTTC CGCTTCAGAC TGCCATTTTT CACATAATGA ATCTATTTCA CCCCACAATC CTTCATCCGC CTCCGCATCT TGTTCCGTTA AACTATTGAC TTCATGTTGT ACATTGTTTA GTTCACGAGA AGGGTCCTCT TCAGGCGGTA
AAACTAGAAG GCGAAGTCTG ACGGTAAAAA GTGTATTACT TAGATAAAGT GGGGTGTTAG GAAGTAGGCG GAGGCGTAGA ACAAGGCAAT TTGATAACTG AAGTACAACA TGTAACAAAT CAAGTGCTCT TCCCAGGAGA AGTCCGCCAT

      1360       1370       1380       1390       1400       1410       1420       1430       1440       1450       1460       1470       1480       1490       1500
GCTCCTGATC TCCTATATGA CCTTTATCCT GTTCTCTTTC CACAAACTTA GAAATGTATT CATGAATTAT GGAGCACCTA ATAACATTCT TCAAGGCGGA GAAGTTTGGG CCAGATGCCC AATATGCTTG ACATGAAAAC GTGAGAATGA
CGAGGACTAG AGGATATACT GGAAATAGGA CAAGAGAAAG GTGTTTGAAT CTTTACATAA GTACTTAATA CCTCGTGGAT TATTGTAAGA AGTTCCGCCT CTTCAAACCC GGTCTACGGG TTATACGAAC TGTACTTTTG CACTCTTACT

      1510       1520       1530       1540       1550       1560       1570       1580       1590       1600       1610       1620       1630       1640       1650
ATTTAGTATT ATTGTGATAT TCTGAGGCAA TTTTATTATA ATCTCGAAGA TAAGAGAAGA ATGCAGTGAC CTTTGTATTG ACAAATGGAG ATTCCATGTA TCTAAAAAAT ACGCCTTTAG GCCTTCTGAT ACCCTTTCCC CTGCGGTTTA
TAAATCATAA TAACACTATA AGACTCCGTT AAAATAATAT TAGAGCTTCT ATTCTCTTCT TACGTCACTG GAAACATAAC TGTTTACCTC TAAGGTACAT AGATTTTTTA TGCGGAAATC CGGAAGACTA TGGGAAAGGG GACGCCAAAT

      1660       1670       1680       1690       1700       1710       1720       1730       1740       1750       1760       1770       1780       1790       1800
GCGTGCCTTT TACATTAATA TCTAAACCCT CTCCGATGGT GGCCTTTAAC TGACTAATAA ATGCAACCGA TATAAACTGT GATAATTCTG GGTGATTTAT GATTCGATCG ACAATTGTAT TGTACACTAG TGCAGGATCA GGCCAATCCA
CGCACGGAAA ATGTAATTAT AGATTTGGGA GAGGCTACCA CCGGAAATTG ACTGATTATT TACGTTGGCT ATATTTGACA CTATTAAGAC CCACTAAATA CTAAGCTAGC TGTTAACATA ACATGTGATC ACGTCCTAGT CCGGTTAGGT

      1810       1820       1830       1840       1850       1860       1870       1880       1890       1900       1910       1920       1930       1940       1950
GTTCTTTTTC AATTACCGGT GTGTCGTCTG TATTCAGTAC ATGTCCAACA AATGCAAATG CTAACGTTTT GTATTTCTTA TAATTGTCAG GAACTGGAAA AGTCCCCCTT GTCGTCTCGA TTACACACCT ACTTTCATCG TACACCATAG
CAAGAAAAAG TTAATGGCCA CACAGCAGAC ATAAGTCATG TACAGGTTGT TTACGTTTAC GATTGCAAAA CATAAAGAAT ATTAACAGTC CTTGACCTTT TCAGGGGGAA CAGCAGAGCT AATGTGTGGA TGAAAGTAGC ATGTGGTATC

      1960       1970       1980       1990       2000       2010       2020       2030       2040       2050       2060       2070       2080       2090       2100
GTTGGAAGTG CTGCATAATA CATTGCTTAA TACAAGCAAG CAGTCTCTCG CCATTCATAT TTCAGTTATT TTCCATTACA GCTGATGTCA TTGTATATCA GCGCTGTAAA AATCTATCTG TTACAGAAGG TTTTCGCGGT TTTTATAAAC
CAACCTTCAC GACGTATTAT GTAACGAATT ATGTTCGTTC GTCAGAGAGC GGTAAGTATA AAGTCAATAA AAGGTAATGT CGACTACAGT AACATATAGT CGCGACATTT TTAGATAGAC AATGTCTTCC AAAAGCGCCA AAAATATTTG

      2110       2120       2130       2140       2150       2160       2170       2180       2190       2200       2210       2220       2230       2240       2250
AAAACTTTCG TTACGAAATC GAGCAATCAC CCCAGCTGCG TATTTGGAAA TTCGGGAAAA AGTAGAGCAA CGCGAGTTGC ATTTTTTACA CCATAATGCA TGATTAACTT CGAGAAGGGA TTAAGGCTAA TTTCACTAGT ATGTTTCAAA
TTTTGAAAGC AATGCTTTAG CTCGTTAGTG GGGTCGACGC ATAAACCTTT AAGCCCTTTT TCATCTCGTT GCGCTCAACG TAAAAAATGT GGTATTACGT ACTAATTGAA GCTCTTCCCT AATTCCGATT AAAGTGATCA TACAAAGTTT

      2260       2270       2280       2290       2300       2310       2320       2330       2340       2350       2360       2370       2380       2390       2400
AACCTCAATC TGTCCATTGA ATGCCTTATA AAACAGCTAT AGATTGCATA GAAGAGTTAG CTACTCAATG CTTTTTGTCA AAGCTTACTG ATGATGATGT GTCTACTTTC AGGCGGGTCT GTAGTAAGGA GAATGACATT ATAAAGCTGG
TTGGAGTTAG ACAGGTAACT TACGGAATAT TTTGTCGATA TCTAACGTAT CTTCTCAATC GATGAGTTAC GAAAAACAGT TTCGAATGAC TACTACTACA CAGATGAAAG TCCGCCCAGA CATCATTCCT CTTACTGTAA TATTTCGACC

      2410       2420       2430       2440       2450       2460       2470       2480       2490       2500       2510       2520       2530       2540       2550
CACTTAGAAT TCCACGGACT ATAGACTATA CTAGTATACT CCGTCTACTG TACGATACAC TTCCGCTCAG GTCCTTGTCC TTTAACGAGG CCTTACCACT CTTTTGTTAC TCTATTGATC CAGCTCAGCA AAGGCAGTGT GATCTAAGAT
GTGAATCTTA AGGTGCCTGA TATCTGATAT GATCATATGA GGCAGATGAC ATGCTATGTG AAGGCGAGTC CAGGAACAGG AAATTGCTCC GGAATGGTGA GAAAACAATG AGATAACTAG GTCGAGTCGT TTCCGTCACA CTAGATTCTA

      2560       2570       2580       2590       2600       2610       2620       2630       2640       2650       2660       2670       2680       2690       2700
TCTATCTTCG CGATGTAGTA AAACTAGCTA GACCGAGAAA GAGACTAGAA ATGCAAAAGG CACTTCTACA ATGGCTGCCA TCATTATTAT CCGATGTGAC GCTGCAGCTT CTCAATGATA TTCGAATACG CTTTGAGGAG ATACAGCCTA
AGATAGAAGC GCTACATCAT TTTGATCGAT CTGGCTCTTT CTCTGATCTT TACGTTTTCC GTGAAGATGT TACCGACGGT AGTAATAATA GGCTACACTG CGACGTCGAA GAGTTACTAT AAGCTTATGC GAAACTCCTC TATGTCGGAT

      2710       2720       2730       2740       2750       2760       2770       2780       2790       2800       2810       2820       2830       2840       2850
ATATCCGACA AACTGTTTTA CAGATTTACG ATCGTACTTG TTACCCATCA TTGAATTTTG AACATCCGAA CCTGGGAGTT TTCCCTGAAA CAGATAGTAT ATTTGAACCT GTATAATAAT ATATAGTCTA GCGCTTTACG GAAGACAATG
TATAGGCTGT TTGACAAAAT GTCTAAATGC TAGCATGAAC AATGGGTAGT AACTTAAAAC TTGTAGGCTT GGACCCTCAA AAGGGACTTT GTCTATCATA TAAACTTGGA CATATTATTA TATATCAGAT CGCGAAATGC CTTCTGTTAC

                                                                                                                                                          ⑤
      2860       2870       2880       2890       2900       2910       2920       2930       2940       2950       2960       2970       2980       2990       3000
TATGTATTTC GGTTCCTGGA GAAACTATTG CATCTATTGC ATAGGTAATC TTGCACGTCG CATCCCCGGT TCATTTTCTG CGTTTCCATC TTGCACTTCA ATAGCATATC TTTGTTAACG AAGCATCTGT GCTTCATTTT GTAGAACAAA
ATACATAAAG CCAAGGACCT CTTTGATAAC GTAGATAACG TATCCATTAG AACGTGCAGC GTAGGGGCCA AGTAAAAGAC GCAAAGGTAG AACGTGAAGT TATCGTATAG AAACAATTGC TTCGTAGACA CGAAGTAAAA CATCTTGTTT
                                                                                                                                      ④

⑤     3010       3020       3030       3040       3050       3060       3070       3080       3090       3100       3110       3120       3130       3140       3150
AATGCAACGC GAGAGCGCTA ATTTTTCAAA CAAAGAATCT GAGCTGCATT TTTACAGAAC AGAAATGCAA CGCGAAAGCG CTATTTTACC AACGAAGAAT CTGTGCTTCA TTTTTGTAAA ACAAAAATGC AACGCGAGAG CGCTAATTTT
TTACGTTGCG CTCTCGCGAT TAAAAAGTTT GTTTCTTAGA CTCGACGTAA AAATGTCTTG TCTTTACGTT GCGCTTTCGC GATAAAATGG TTGCTTCTTA GACACGAAGT AAAAACATTT TGTTTTTACG TTGCGCTCTC GCGATTAAAA
                        ④                                                    ④

                                                                                                ⑤
      3160       3170       3180       3190       3200       3210       3220       3230       3240       3250       3260       3270       3280       3290       3300
TCAAACAAAG AATCTGAGCT GCATTTTTAC AGAACAGAAA TGCAACGCGA GAGCGCTATT TTACCAACAA AGAATCTATA CTTCTTTTTT GTTCTACAAA AATGCATCCC GAGAGCGCTA TTTTTCTAAC AAAGCATCTT AGATTACTTT
AGTTTGTTTC TTAGACTCGA CGTAAAAATG TCTTGTCTTT ACGTTGCGCT CTCGCGATAA AATGGTTGTT TCTTAGATAT GAAGAAAAAA CAAGATGTTT TTACGTAGGG CTCTCGCGAT AAAAAGATTG TTTCGTAGAA TCTAATGAAA
  ④                                                         ④                                                                    ④

      3310       3320       3330       3340       3350       3360       3370       3380       3390       3400       3410       3420       3430       3440       3450
TTTTCTCCTT TGTGCGCTCT ATAATGCAGT CTCTTGATAA CTTTTTGCAC TGTAGGTCCG TTAAGGTTAG AAGAAGGCTA CTTTGGTGTC TATTTTCTCT TCCATAAAAA AAGCCTGACT CCACTTCCCG CGTTTACTGA TTACTAGCGA
AAAAGAGGAA ACACGCGAGA TATTACGTCA GAGAACTATT GAAAAACGTG ACATCCAGGC AATTCCAATC TTCTTCCGAT GAAACCACAG ATAAAAGAGA AGGTATTTTT TTCGGACTGA GGTGAAGGGC GCAAATGACT AATGATCGCT

④     3460       3470       3480       3490       3500       3510       3520       3530       3540       3550       3560       3570       3580       3590       3600
AGCTGCGGGT GCATTTTTTC AAGATAAAGG CATCCCCGAT TATATTCTAT ACCGATGTGG ATTGCGCATA CTTTGTGAAC AGAAAGTGAT AGCGTTGATG ATTCTTCATT GGTCAGAAAA TTATGAACGG TTTCTTCTAT TTTGTCTCTA
TCGACGCCCA CGTAAAAAAG TTCTATTTCC GTAGGGGCTA ATATAAGATA TGGCTACACC TAACGCGTAT GAAACACTTG TCTTTCACTA TCGCAACTAC TAAGAAGTAA CCAGTCTTTT AATACTTGCC AAAGAAGATA AAACAGAGAT

      3610       3620       3630       3640       3650       3660       3670       3680       3690       3700       3710       3720       3730       3740       3750
TATACTACGT ATAGGAAATG TTTACATTTT CGTATTGTTT TCGATTCACT CTATGAATAG TTCTTACTAC AATTTTTTTG TCTAAAGAGT AATACTAGAG ATAAACATAA AAAATGTAGA GGTCGAGTTT AGATGCAAGT TCAAGGAGCG
ATATGATGCA TATCCTTTAC AAATGTAAAA GCATAACAAA AGCTAAGTGA GATACTTATC AAGAATGATG TTAAAAAAAC AGATTTCTCA TTATGATCTC TATTTGTATT TTTTACATCT CCAGCTCAAA TCTACGTTCA AGTTCCTCGC
                                                                                                                 └→IR1

      3760       3770       3780       3790       3800       3810       3820       3830       3840       3850       3860       3870       3880       3890       3900
AAAGGTGGAT GGGTAGGTTA TATAGGGATA TAGCACAGAG ATATATAGCA AAGAGATACT TTTGAGCAAT GTTTGTGGAA GCGGTATTCG CAATATTTTA GTAGCTCGTT ACAGTCCGGT GCGTTTTTGG TTTTTTGAAA GTGCGTCTTC
TTTCCACCTA CCCATCCAAT ATATCCCTAT ATCGTGTCTC TATATATCGT TTCTCTATGA AAACTCGTTA CAAACACCTT CGCCATAAGC GTTATAAAAT CATCGAGCAA TGTCAGGCCA CGCAAAAACC AAAAAACTTT CACGCAGAAG

                                          ①
      3910       3920       3930       3940       3950       3960       3970       3980       3990       4000       4010       4020       4030       4040       4050
AGAGCGCTTT TGGTTTTCAA AAGCGCTCTG AAGTTCCTAT ACTTTCTAGA GAATAGGAAC TTCGGAATAG GAACTTCAAA GCGTTTCCGA AAACGAGCGC TTCCGAAAAT GCAACGCGAG CTGCGCACAT ACAGCTCACT GTTCACGTCG
TCTCGCGAAA ACCAAAAGTT TTCGCGAGAC TTCAAGGATA TGAAAGATCT CTTATCCTTG AAGCCTTATC CTTGAAGTTT CGCAAAGGCT TTTGCTCGCG AAGGCTTTTA CGTTGCGCTC GACGCGTGTA TGTCGAGTGA CAAGTGCAGC
    ②                  ②                                  ③                  ③

      4060       4070       4080       4090       4100       4110       4120       4130       4140       4150       4160       4170       4180       4190       4200
CACCTATATC TGCGTGTTGC CTGTATATAT ATATACATGA GAAGAACGGC ATAGTGCGTG TTTATGCTTA AATGCGTACT TATATGCGTC TATTTATGTA GGATGAAAGG TAGTCTAGTA CCTCCTGTGA TATTATCCCA TTCCATGCGG
GTGGATATAG ACGCACAACG GACATATATA TATATGTACT CTTCTTGCCG TATCACGCAC AAATACGAAT TTACGCATGA ATATACGCAG ATAAATACAT CCTACTTTCC ATCAGATCAT GGAGGACACT ATAATAGGGT AAGGTACGCC

      4210       4220       4230       4240       4250       4260       4270       4280       4290       4300       4310       4320       4330       4340       4350
GGTATCGTAT GCTTCCTTCA GCACTACCCT TTAGCTGTTC TATATGCTGC CACTCCTCAA TTGGATTAGT CTCATCCTTC AATGCTATCA TTTCCTTTGA TATTGGATCA TACCCTAGAA GTATTACGTG ATTTTCTGCC CCTTACCCTC
CCATAGCATA CGAAGGAAGT CGTGATGGGA AATCGACAAG ATATACGACG GTGAGGAGTT AACCTAATCA GAGTAGGAAG TTACGATAGT AAAGGAAACT ATAACCTAGT ATGGGATCTT CATAATGCAC TAAAAGACGG GGAATGGGAG
                                                                                                            IR1←┘

      4360       4370       4380       4390       4400       4410       4420       4430       4440       4450       4460       4470       4480       4490       4500
GTTGCTACTC TCCTTTTTTT CGTGGGAACC GCTTTAGGGC CCTCAGTGAT GGTGTTTTGT AATTTATATG CTCCTCTTGC ATTTGTGTCT CTACTTCTTG TTCGCCTGGA GGGAACTTCT TCATTTGTAT TAGCATGGTT CACTTCAGTC
CAACGATGAG AGGAAAAAAA GCACCCTTGG CGAAATCCCG GGAGTCACTA CCACAAAACA TTAAATATAC GAGGAGAACG TAAACACAGA GATGAAGAAC AAGCGGACCT CCCTTGAAGA AGTAAACATA ATCGTACCAA GTGAAGTCAG

      4510       4520       4530       4540       4550       4560       4570       4580       4590       4600       4610       4620       4630       4640       4650
CTTCCTTCCA ACTCACTCTT TTTTTGCTGT AAACGATTCT CTGCCGCCAG TTCATTGAAA CTATTGAATA TATCCTTTAG AGATTCCGGG ATGAATAAAT CACCTATTAA AGCAGCTTGA CGATCTGGTG GAACTAAAGT AAGCAATTGG
GAAGGAAGGT TGAGTGAGAA AAAAACGACA TTTGCTAAGA GACGGCGGTC AAGTAACTTT GATAACTTAT ATAGGAAATC TCTAAGGCCC TACTTATTTA GTGGATAATT TCGTCGAACT GCTAGACCAC CTTGATTTCA TTCGTTAACC

      4660       4670       4680       4690       4700       4710       4720       4730       4740       4750       4760       4770       4780       4790       4800
GTAACGACGC TTACGAGCTT CATAACATCT TCTTCCGTTG GAGCTGGTGG GACTAATAAC TGTGTACAAT CCATTTTTCT CATGAGCATT TCGGTAGCTC TCTTCTTGTC TTTCTCGGGC AATCTTCCTA TTATTATAGC AATAGATTTG
CATTGCTGCG AATGCTCGAA GTATTGTAGA AGAAGGCAAC CTCGACCACC CTGATTATTG ACACATGTTA GGTAAAAAGA GTACTCGTAA AGCCATCGAG AGAAGAACAG AAAGAGCCCG TTAGAAGGAT AATAATATCG TTATCTAAAC

      4810       4820       4830       4840       4850       4860       4870       4880       4890       4900       4910       4920       4930       4940       4950
TATAGTTGCT TTCTATTGTC TAACAGCTTG TTATTCTGTA GCATCAAATC TATGGCAGCC TGACTTGCTT CTTGTGAAGA GAGCATACCA TTTCCAATCG AATCAAACCT TTCCTTAACC ATCTTCGCAG CAGGCAAAAT TACCTCAGCA
ATATCAACGA AAGATAACAG ATTGTCGAAC AATAAGACAT CGTAGTTTAG ATACCGTCGG ACTGAACGAA GAACACTTCT CTCGTATGGT AAAGGTTAGC TTAGTTTGGA AAGGAATTGG TAGAAGCGTC GTCCGTTTTA ATGGAGTCGT

      4960       4970       4980       4990       5000       5010       5020       5030       5040       5050       5060       5070       5080       5090       5100
CTGGAGTCAG AAGATACGCT GGAATCTTCT GCGCTAGAAT CAAGACCATA CGGCCTACCG GTTGTGAGAG ATTCCATGGG CCTTATGACA TATCCTGGAA AGAGTAGCTC ATCAGACTTA CGTTTACTCT CTATATCAAT ATCTACATCA
GACCTCAGTC TTCTATGCGA CCTTAGAAGA CGCGATCTTA GTTCTGGTAT GCCGGATGGC CAACACTCTC TAAGGTACCC GGAATACTGT ATAGGACCTT TCTCATCGAG TAGTCTGAAT GCAAATGAGA GATATAGTTA TAGATGTAGT

      5110       5120       5130       5140       5150       5160       5170       5180       5190       5200       5210       5220       5230       5240       5250
GGAGCAATCA TTTCAATAAA CAGCCGACAT ACATCCCAGA CGCTATAAGC TGTACGTGCT TTTACCGTCA GATTCTTGGC TGTTTCAATG TCGTCCATTT TGGTTTTCTT TTACCAGTAT TGTTCGTTTG ATAATGTATT CTTGCTTATT
CCTCGTTAGT AAAGTTATTT GTCGGCTGTA TGTAGGGTCT GCGATATTCG ACATGCACGA AAATGGCAGT CTAAGAACCG ACAAAGTTAC AGCAGGTAAA ACCAAAAGAA AATGGTCATA ACAAGCAAAC TATTACATAA GAACGAATAA

      5260       5270   •   5280       5290       5300       5310       5320       5330       5340       5350       5360       5370       5380       5390       5400
ACATTATAAA ATCTGTGCAG ATCACATGTC AAAACAACTT TTTATCACAA GATAGTACCG CAAAACGAAC CTGCGGGCCG TCTAAAAATT AAGGAAAAGC AGCAAAGGTG CATTTTTAAA ATATGAAATG AAGATACCGC AGTACCAATT
TGTAATATTT TAGACACGTC TAGTGTACAG TTTTGTTGAA AAATAGTGTT CTATCATGGC GTTTTGCTTG GACGCCCGGC AGATTTTTAA TTCCTTTTCG TCGTTTCCAC GTAAAAATTT TATACTTTAC TTCTATGGCG TCATGGTTAA

      5410       5420       5430       5440       5450       5460       5470       5480       5490       5500       5510       5520       5530       5540       5550
ATTTTCGCAG TACAAATAAT GCGCGGCCGG TGCATTTTTC GAAAGAACGC GAGACAAACA GGACAATTAA AGTTAGTTTT TCGAGTTAGC GTGTTTGAAT ACTGCAAGAT ACAAGATAAA TAGAGTAGTT GAAACTAGAT ATCAATTGCA
TAAAAGCGTC ATGTTTATTA CGCGCCGGCC ACGTAAAAAG CTTTCTTGCG CTCTGTTTGT CCTGTTAATT TCAATCAAAA AGCTCAATCG CACAAACTTA TGACGTTCTA TGTTCTATTT ATCTCATCAA CTTTGATCTA TAGTTAACGT
```

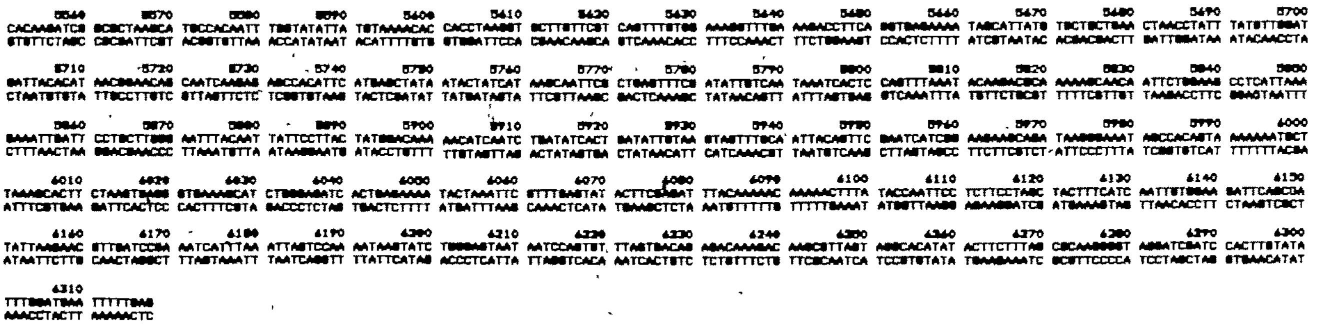

Fig. 2 Sequence of the yeast plasmid. Boundaries of IR1 (3,714–4,312) and IR2 (341–939) are shown. Symmetry elements are identified by number: 1, regions which can be drawn as stem and loop structures (Fig. 3); 2, longest dyad symmetries (abc–c'b'a') in the sequence; 3, perfect direct repeats; 4, direct tandem repeats of 62–63 bp, or portions thereof; 5, dyad symmetries associated with these repeats. Sequences were determined by the method of Maxam and Gilbert[29]. Restriction fragments were labelled using repair synthesis of DNA polymerase I (10 units of enzyme in 100 μl of 70 mM Tris–HCl, *p*H 8.0, 70 mM NaCl, 10 mM $MgCl_2$, incubated at 4 °C for 10 min with [α-^{32}P]dNTP and 5–15 pmol of each restriction fragment). Sequencing gels were 0.4 mm thick, 6% (90×30 cm) or 20% (43×43 cm) polyacrylamide/urea gels run warm[42].

sites in both IR1 and IR2 contain extensive elements of symmetry which can be drawn as large secondary structures (Fig. 3). Such structures are highly significant statistically (data not shown) and have been found near the origins of replication of many genomes[39–41]. Second, J. Broach and J. Hicks (J. Broach, personal communication) have cloned various pieces of the yeast plasmid and shown that vectors which contain IR1 can successfully transform [cir°] yeast (strains which lack endogenous 2μ circles), whereas vectors containing only IR2 cannot. Third, deletion mapping by Broach and Hicks indicates that about 100 base pairs of the large unique region adjacent to IR1 is an essential part of the origin. Since IR1 and IR2 are precisely identical, the involvement of this unique segment presumably determines which inverted repeat will be used for the origin. Examination of translation reading frames of the plasmid (Fig. 4) shows that this is the only segment next to an inverted repeat that is not part of a potential protein coding region. It is possible that this segment (from around position 3,600 to within IR1) is transcribed to yield the RNA primer for initiation of replication. Since electron microscopic examination of replicating yeast plasmid molecules suggests that a second origin, presumably within IR2, is used at least some of the time (C. Newlon, personal communication), this primer may contain some inverted repeat component.

The yeast plasmid sequence contains three regions which could code for proteins of MWs 33,000, 43,000 and 48,000 (Fig. 4). The location of these are in general agreement with the results of previous studies[14–16]. Observations of Guerineau and co-workers[22,23] suggest a function for one of these regions. They constructed vectors containing the entire yeast plasmid in which the coding region 'Able' was interrupted by the insertion of a piece of bacterial DNA. Such vectors successfully transformed [cir°] yeast, but no recombination between the inverted repeats was seen, that is, cells transformed with form A vectors maintained the chimaeric DNAs as form A for long periods[23]. In contrast, [cir⁺] strains (which contain endogenous yeast plasmid) rapidly interconverted forms A and B, such that only a mixture of the two forms was detected[22]. Broach and Hicks have made similar observations (J. Broach, personal communication). A diffusible product of coding region 'Able' is thus implicated as mediating the form interconversion process. This gene product and its substrate, the inverted repeats of the 2μ circle, represent

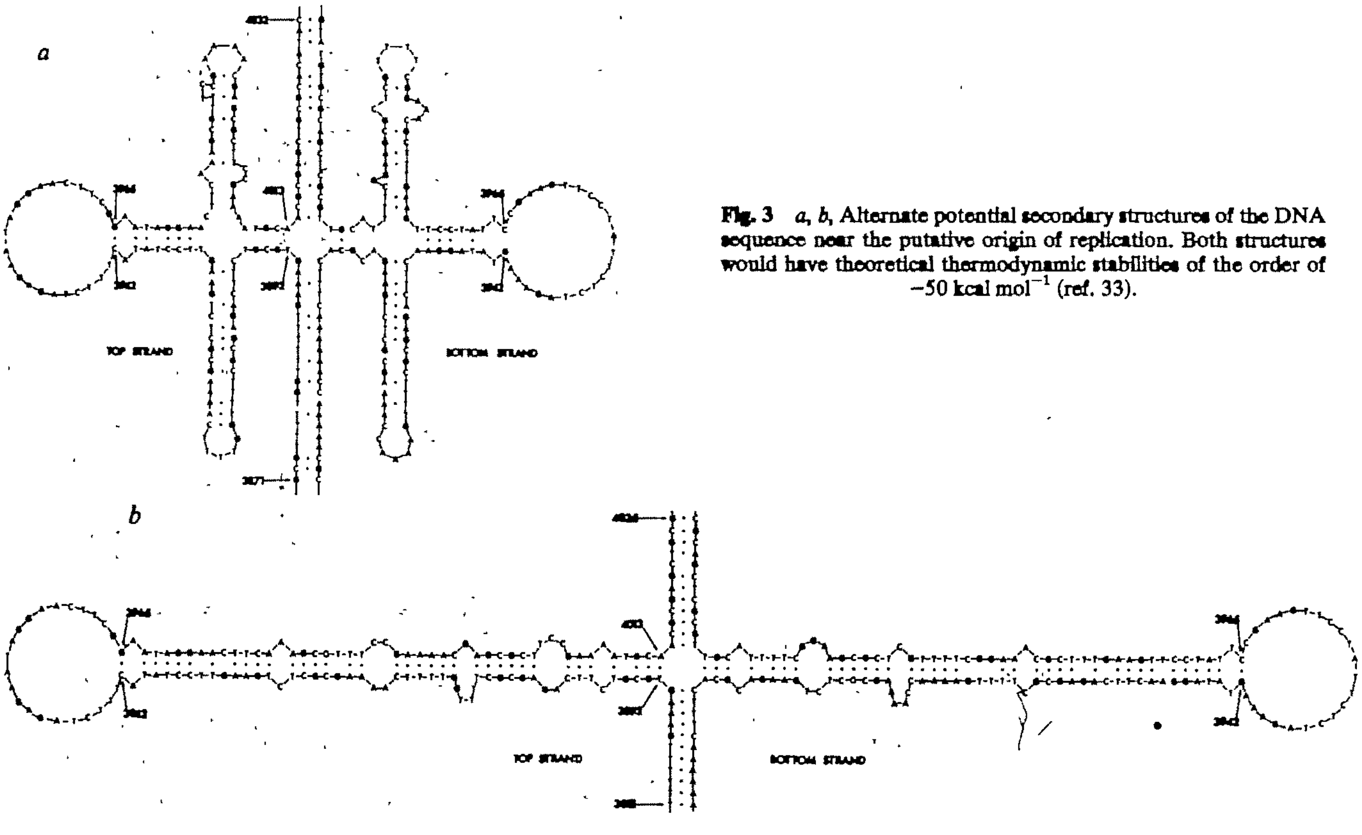

Fig. 3 *a*, *b*, Alternate potential secondary structures of the DNA sequence near the putative origin of replication. Both structures would have theoretical thermodynamic stabilities of the order of −50 kcal mol^{-1} (ref. 33).

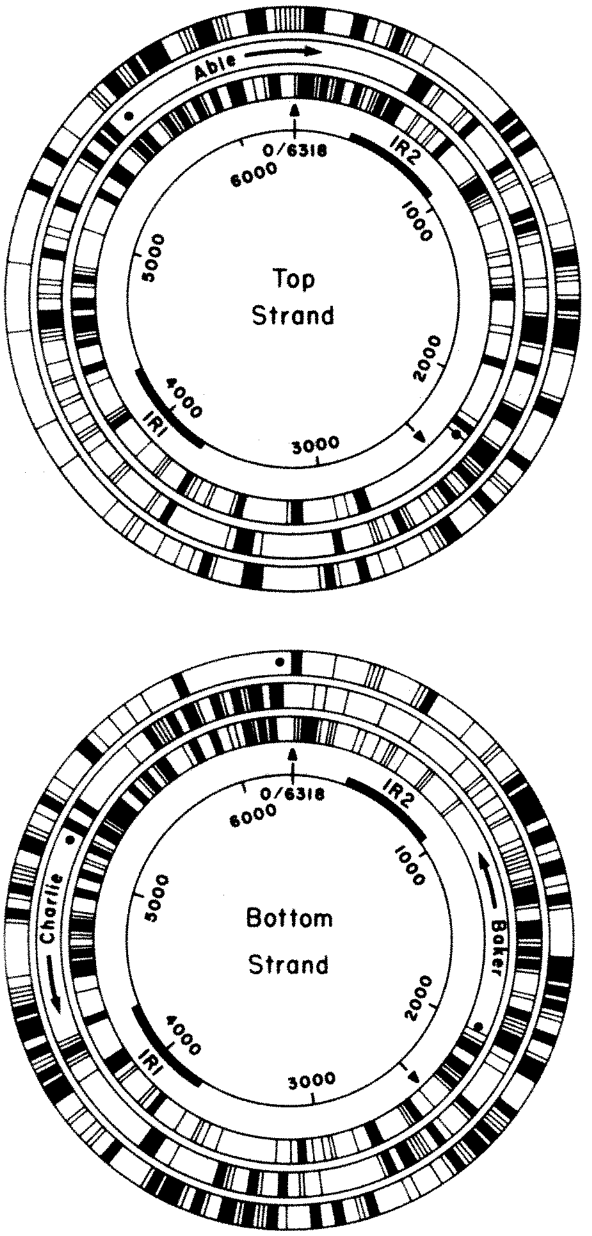

Fig. 4 Approximate positions of stop codons in the different reading frames of the yeast plasmid. TAA codons are represented by blocks (■), while TAG and TGA codons are shown as lines. Start codon positions for 'Able' and 'Baker', and 'Charlie' and two other large open reading frames are indicated by dots (●). The outer, middle and inner rings correspond to reading frames 1, 2 and 3, respectively. For the top strand reading frames 1, 2 and 3 begin with the codons GAA (positions 1–3), AAT (2–4) and ATT (3–5), while for the bottom strand reading frames 1, 2 and 3 begin with codons CTC (6,318–6,316), TCA (6,317–6,315) and CAA (6,316–6,314). Triangles indicate *Eco*RI cleavage sites.

a unique opportunity to study eukaryotic recombination at the molecular level.

A second observation of Gerbaud *et al.*[22] has implications for the construction of yeast transformation vectors. They determined the levels of expression of a yeast gene (*ura3*) inserted at two different points in their vector. It was found that the *ura3* activity per transformed cell was three times higher when the gene was inserted at the *Eco*RI site within coding region 'Able' than when it was carried within the bacterial plasmid segment of the vector. Since the 'Able' product is apparently actively expressed in yeast (above) it is reasonable to suppose that the higher expression was due to efficient transcription utilizing the 'Able' promoter or other transcriptional signals.

In view of these considerations, some attributes of a vector–host system for the transformation of yeast may be suggested. The host should be [cir^{+}] since high transformation frequency and reasonable stability are obtained[19,22]. The vector should contain the origin of replication but should not contain the entire yeast plasmid, since Toh-e *et al.* have shown that increased stability results from this arrangement when the host is [cir^{+}] (ref. 25). The vector should also contain coding region 'Able' for the insertion of foreign DNA to be expressed in the yeast host. The sequence indicates that the small *Ava*I fragment of the form B plasmid would have all these properties. This 2,945 base pair fragment would contain the origin of replication and the entire 'Able' coding region, as well as segments flanking both ends of 'Able'. Within the 'Able' sector there are single sites for the restriction enzymes *Eco*RI, *Hin*dIII, *Bal*I, *Bcl*I and *Cla*I which might be suitable for expression of foreign genes. In combination with a suitable selection marker(s) the resultant plasmid should possess improved properties for cloning foreign DNAs in yeast.

The sequence of the yeast plasmid may improve the usefulness of yeast for DNA cloning experiments. In addition, the sequence provides a starting point for further investigations of such functions as replication, recombination and gene control in a well characterized eukaryotic genetic system.

Copies of the sequence with a complete listing of all restriction sites are available on request.

We thank B. Nichols and P. Moynihan for help in sequencing experiments, T. Gregori for technical assistance, P. Gyllstrom for computer help, L. Korn for his computer program, J. Broach for communicating results before publication, and C. Newlon for critical readings of the manuscript. This work was supported by grant GM21696. Recombinant DNA experiments adhered to NIH guidelines (P2+EK1).

Received 1 May; accepted 26 June 1980.

1. Clark-Walker, G. D. & Miklos, G. L. G. *Eur. J. Biochem.* **41**, 359–365 (1974).
2. Bak, A., Christiansen, C. & Christiansen, G. *Biochim. biophys. Acta* **269**, 527–530 (1972).
3. Gubbins, E. J., Newlon, C. S., Kann, M. D. & Donelson, J. E. *Gene* **1**, 185–207 (1977).
4. Livingston, D. M. & Klein, H. L. *J. Bact.* **129**, 472–481 (1977).
5. Cameron, J. R., Phillipsen, P. & Davis, R. W. *Nucleic Acids Res.* **4**, 1429–1448 (1977).
6. Guerineau, M., Grandchamp, C. & Slonimski, P. P. *Proc. natn. Acad. Sci. U.S.A.* **73**, 3030–3034 (1976).
7. Hollenberg, C. P., Degelmann, A., Kustermann-Kuhn, B. & Royer, H. D. *Proc. natn. Acad. Sci. U.S.A.* **73**, 2072–2076 (1976).
8. Beggs, J. D., Guerineau, M. & Atkins, J. F. *Molec. gen. Genet.* **148**, 287–294 (1976).
9. Bell, L. & Byers, B. *Proc. natn. Acad. Sci. U.S.A.* **76**, 3445–3449 (1979).
10. Nelson, R. G. & Fangman, W. L. *Proc. natn. Acad. Sci. U.S.A.* **76**, 6515–6519 (1979).
11. Livingston, D. M. & Hahne, S. *Proc. natn. Acad. Sci. U.S.A.* **76**, 3727–3731 (1979).
12. Zakian, V. A., Brewer, B. J. & Fangman, W. L. *Cell* **17**, 923–934 (1979).
13. Livingston, D. M. & Kupfer, D. M. *J. molec. Biol.* **116**, 249–260 (1977).
14. Broach, J. R., Atkins, J. F., McGill, C. & Chow, L. *Cell* **16**, 827–839 (1979).
15. Hollenberg, C. P., Kustermann-Kuhn, B. & Royer, H. D. *Gene* **1**, 33–47 (1976).
16. Hollenberg, C. P. *Molec. gen. Genet.* **162**, 23–34 (1978).
17. Livingston, D. M. *Genetics* **86**, 73–84 (1977).
18. Tabak, H. F. *FEBS Lett.* **84**, 67–70 (1977).
19. Beggs, J. D. *Nature* **275**, 104–109 (1978).
20. Hicks, J. B., Hinnen, A. H. & Fink, G. R. *Cold Spring Harb. Symp. quant. Biol.* **43**, 1305–1314 (1978).
21. Struhl, K., Stinchcomb, D. T., Scherer, S. & Davis, R. W. *Proc. natn. Acad. Sci. U.S.A.* **76**, 1035–1039 (1979).
22. Gerbaud, C. *et al. Gene* **5**, 233–253 (1979).
23. Blanc, H., Gerbaud, C., Slonimski, P. P. & Guerineau, M. *Molec. gen. Genet.* **176**, 335–342 (1979).
24. Beggs, J. D., Van den Berg, J., Van Ooyen, A. & Weissmann, C. *Nature* **283**, 835–840 (1980).
25. Toh-e, A., Guerry-Kopecko, P. & Wickner, R. B. *J. Bact.* **141**, 413–416 (1980).
26. Bolivar, F., Rodriguez, R. L., Betlach, M. C. & Boyer, H. W. *Gene* **2**, 75–93 (1977).
27. Roychoudhury, R., Jay, E. & Wu, R. *Nucleic Acids Res.* **3**, 863–877 (1976).
28. Grunstein, M. & Hogness, D. S. *Proc. natn. Acad. Sci. U.S.A.* **72**, 3961–3965 (1975).
29. Maxam, A. M. & Gilbert, W. *Proc. natn. Acad. Sci. U.S.A.* **74**, 560–564 (1977).
30. Korn, L. J., Queen, C. L. & Wegman, M. N. *Proc. natn. Acad. Sci. U.S.A.* **74**, 4401–4405 (1977).
31. Mahler, H. R. & Cordes, E. H. *Biological Chemistry* 2nd edn (Harper and Row, New York, 1971).
32. Hindley, J. & Phear, G. A. *Nucleic Acids Res.* **7**, 361–375 (1979).
33. Tinoco, I. *et al. Nature new Biol.* **246**, 40–41 (1973).
34. Arnott, S., Chandrasekaran, R., Birdsall, D. L., Leslie, A. G. W. & Ratliff, R. L. *Nature* **283**, 743–745 (1980).
35. Soeda, E., Arrand, J. R., Smolar, N., Walsh, J. E. & Griffin, B. E. *Nature* **283**, 445–453 (1980).
36. Sanger, F. *et al. Nature* **265**, 687–695 (1977).
37. Fiers, W. *et al. Nature* **273**, 113–119 (1978).
38. Strathern, J. N., Newlon, C. S., Herskowitz, I. & Hicks, J. B. *Cell* **18**, 309–319 (1979).
39. Crews, S., Ojala, D., Posakony, J., Nishiguchi, J. & Attardi, G. *Nature* **277**, 192–198 (1979).
40. Benz, E. W., Reinberg, D., Vicuna, R. & Hurwitz, J. *J. biol. Chem.* **255**, 1096–1106 (1980).
41. Shortle, D. & Nathans, D. *J. molec. Biol.* **131**, 801–817 (1979).
42. Sanger, F. & Coulson, A. R. *FEBS Lett.* **87**, 107–110 (1978).

Addendum from J. Hindley, T. C. Elleman & G. A. Phear

Department of Biochemistry, University of Bristol,
Bristol BS8 1TD, UK

The accompanying article by Hartley and Donelson presents the sequence of the type A yeast plasmid recovered from *Saccharomyces cerevisiae* strain A364A D5 by cloning into pMB9. We have independently determined about 63% of the type A plasmid sequence from pJDB 71 (ref. 1; a hybrid constructed by inserting the 2μ plasmid from *S. cerevisiae* strain DR19/8T into the *Eco*RI site of pMB9), using a different approach and have compared the two sets of data. This is of interest for two reasons. First, Hartley and Donelson used the Maxam–Gilbert procedure whereas we have relied entirely on the dideoxynucleotide chain termination procedure using single-stranded templates generated by cloning restriction fragments into linearized phage M13mp2 RF-DNA and subsequently isolating the single-stranded recombinant phages[2]. The sequence comparison was made over a total of 4,004 nucleotides comprising sequences totalling 3,053 nucleotides from the larger and 951 nucleotides from the smaller unique regions of the plasmid. Both sets of data were in complete agreement. This result therefore completely validates the reliability of the newer sequencing procedures used in this work. Neither during propagation of the hybrid plasmid nor in the subsequent M13 cloning and primed syntheses is there any evidence of rearrangements or deletions of sequences.

Second, the data imply that the unique regions in the plasmid, bounded by the inverted repeats, are fully conserved in two unrelated strains of yeast. This identity includes a sequence of 863 nucleotides extending from the *Eco*RI site at position 2,407 to position 3,270. This region contains a set of 6.5 direct tandem repeats of 62–63 residues and in two other plasmid isolates (Scp 2 and Scp 3)[3], which contain deletions of about 130 and 220 base pairs respectively, the mapping data puts both these deletions within the region of tandemly repeated sequences. The available data therefore suggests that, apart from this deletable region, the unique regions of the plasmid are strongly conserved. Differences are found however when the inverted repeat regions are compared. All these seem to be single base changes and occur in regions outside the possible reading frames suggested by Hartley and Donelson (see ref. 4).

1. Beggs, J. D. *Nature* **275,** 104–109 (1978).
2. Sanger, F., Coulson, A. R., Barrell, B. G., Smith, A. J. H. & Roe, B. A. *J. molec. Biol.* (in the press).
3. Cameron, J. R., Phillipsen, P. & Davis, R. W. *Nucleic Acids Res.* **4,** 1429–1448 (1977).
4. Hindley, J. & Phear, G. A. *Nucleic Acids Res.* **7,** 361–375 (1979).

LETTERS

The double quasar 0957+561 as a gravitational lens: further VLA observations

P. E. Greenfield & B. F. Burke

Department of Physics, Massachusetts Institute of Technology,
Cambridge, Massachusetts 02139

D. H. Roberts

Brandeis University, Waltham, Massachusetts 02254

The twin quasars 0957+561 A,B, separated by only 6 arc s on the sky, have been shown to have nearly identical redshifts ($z_e \simeq 1.41$, $z_a \simeq 1.39$) by Walsh *et al.*[1], who suggested that they were the double image of a single object, split by the gravitational refraction of an unseen massive intervening object. Further optical spectroscopy[2] has confirmed the remarkable similarities of the emission and absorption spectra of the two quasars, and strengthened the case for a gravitational lens model. Radio maps at 6 cm made with the Cambridge 5-km telescope[3] and with the VLA[4] showed that, in addition to two unresolved sources coincident with the optical quasars, there were extended regions of radio emission, apparently associated with the north (A) quasar which greatly complicated the gravitational lens hypothesis. We now report a full 12-h synthesis made at the VLA at 6-cm wavelength[5] which confirmed the earlier maps and showed additional features at lower flux levels. In particular, this map revealed two small radio 'jets', one close to each of the quasars. The absence of corresponding second images of either of these jets near the other quasar was used to rule out models in which the gravitator was located near the midpoint of the line between A and B (ref. 5).

The lens hypothesis was boosted by the discovery[6,7] that the field of 0957+561 was overlaid by a rich cluster of galaxies at $z \simeq 0.39$. Furthermore, the nucleus of the brightest member of the cluster (designated G1) lay ~1 arc s north of the B quasar, very near the position of the B radio jet. Young *et al.*[7] presented models for gravitational imaging of the underlying object quasar, invoking both the properties of an extended gravitator (G1) and the existence of an additional source of bending (the cluster as a whole) and were able to account for most of the observed features. The B jet, however, remained difficult to understand as part of the gravitational image of the quasar and its extended radio emission. The present results clarify the nature of the B radio jet, and further strengthen the gravitational lens interpretation of the double quasar.

The observations consist of a full 12-h synthesis made at 6 cm on the Very Large Array of the National Radio Astronomy Observatory during 22–23 February 1980. A total of 22 antennas were functioning, with baselines ranging between 45 m and 22.4 km. Observing conditions were ideal, and the data were of significantly higher quality than those obtained in October 1979[5]. The performance of the array was monitored by frequent observations of the nearby point source 1031+567 and the flux scale was set by assuming the 4,885 MHz flux density of 3C286 to be 7.41 Jy. Editing, gridding, and Fourier transformation of the data were carried out using the standard VLA data reduction procedures. The resulting 'dirty' map was processed with the modified CLEAN algorithm of Clark[8]. The clean map, shown in Fig. 1, has a resolution of 0.66 by 0.41 arc s FWHM, and a dynamic range (map peak/r.m.s. noise) of ~200 : 1.

The significant feature of Fig. 1 is the resolution of the B jet into a point source (which we now denote G) of 2.3 ± 0.2 mJy flux, located 1.06 ± 0.02 arc s N and 0.15 ± 0.02 arc s E of the B quasar. The position and flux of G are consistent with our previous observations[5]. An optical photograph of the field, made on the University of Hawaii 2.2-m telescope by Stockton[9], puts the optical nucleus of G1 0.99 ± 0.03 arc s N and 0.19 ± 0.03 arc s E of the B quasar, or 0.08 ± 0.05 arc s SE of the radio position. Thus, the optical nucleus of G1 and the radio source G are coincident within the small uncertainties. The simplest interpretation is that G is a compact radio source in the nucleus of G1 and is not part of the gravitational image. If this is so, the 5 GHz power of G is $P_{5000} = 1.1 \times 10^{-23}$ WHz^{-1} sr^{-1} ($q_0 = 1/2$, $H_0 = 50$ km s^{-1} Mpc^{-1}, spectral index assumed to be 0.25). Although little is known about the compact radio structure of cD galaxies selected without regard for their low-frequency properties, G is comparable to the central components of 3CR radio galaxies[10]. Although there is at least one other interpretation (see below), the fact that G is not significantly north of the nucleus of G1 removes the last strong objection to the gravitational lens explanation of 0957+561.

0028–0836/80/350865—02$01.00

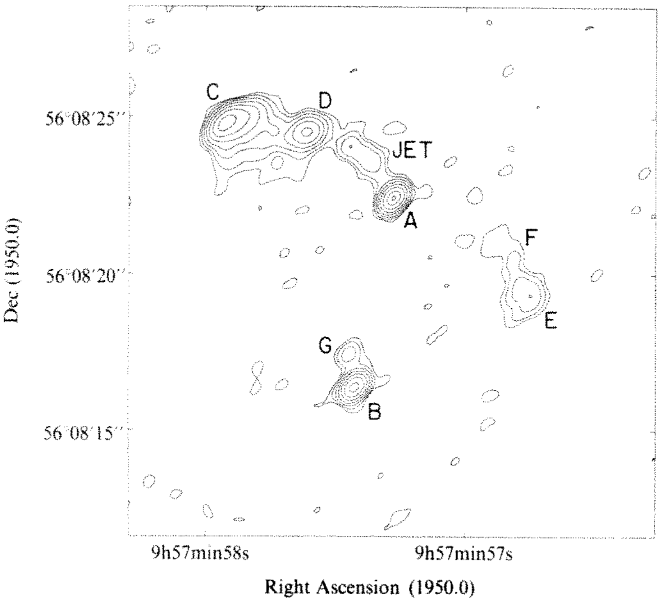

Fig. 1 The double quasar 0957+561 A,B, mapped at λ6 cm by the VLA on 22–23 February 1980. The point sources A and B are coincident with the optical quasars, and the small source G lies very close to the nucleus of the intervening galaxy G1 which is apparently forming the double image. The contour levels are 1, 2, 4, 8, 16, 32, 64 and 95% of the peak flux of 35.9 mJy.

We now consider how well the details of the gravitational imaging are understood, what further data may be needed, and what more can be learned from the double quasar. The important features to be accounted for are: (1) the near-equality of the fluxes of A and B despite their very different separations from G1; (2) the absence of second images of any of the extended radio emission; (3) the lack of resolution of the B image by the VLA or by existing VLBI observations; and (4) the fact that the nucleus of G1 lies slightly (0.4 arc s) off the line between A and B. Young *et al.*[7] have suggested that the first two points are consequences of the existence of a caustic for an extended gravitational lens. In their picture, the B image is formed very close to the caustic and is, therefore, anomalously amplified, while the extended emission lies beyond the caustic so no second images are formed. This model has the additional consequence that the B image must itself be multiple. The VLBI observations of Porcas *et al.*[11] and Haschick *et al.*[12] show the existence of compact components in both A and B, but have insufficient dynamic range to give useful details of their brightness distributions. The high dynamic range of the observations presented here enable us to constrain a possible double nature of B. There is no evidence for a broadening of B relative to A at a level of 5% of the beamwidth. Thus, if two images B and B′ are of equal intensity ($I = I'$), their separation $\delta\theta$ is less than 0.16 arc s. We are, therefore, unable to rule out model 'c' of Young *et al.* in which $I/I' = 1.45$ and $\delta\theta = 0.15$ arc s.

Young *et al.* have emphasized that the cluster as a whole may play an important role in forming the image, and they attribute property (4) above to the effect of the cluster. As a result of the cluster, one of their models results in the observed B image plus a very faint B′ image nearly coincident with G1. This may be the correct interpretation of the small radio source G. If in fact G is north of the nucleus of G1, G cannot be the third image B′. In addition, note that the absence of second images of the extended emission must be used to constrain the role of the cluster, and Young *et al.* did not consider the radio data in constructing their models.

Improved VLBI experiments currently underway will constrain models in which B is double with separation less than the 0.16 arc s detectable in the current VLA data. In addition, measurement of the time delay between the arrival of the A and B images will help ascertain the importance of the cluster in the image formation. The differential delay, expected to be of the order of months in the absence of the cluster, could be multiplied by a factor of the order of 5 by the effect of the cluster[7]. In principle, this sensitive probe of the cluster could yield information on any 'hidden' mass in the cluster[5]. The intensity ratio $I_A/I_B = 1.23 \pm 0.02$ in the data presented here, while it was 1.32 ± 0.02 in October 1979 (ref. 5), so there seems to be measurable variability in the underlying quasar, making a time-delay measurement feasible. Finally, we note that cD galaxies such as G1 can have double or multiple nuclei, and hence may have appreciable non-radial refraction effects. Thus it may not be necessary to invoke strong bending due to the cluster in order to understand the slight misalignment of A–G1–B.

The National Radio Astronomy Observatory is operated by Associated Universities, Inc. under contract with the NSF. The research at the Massachusetts Institute of Technology was supported by a grant from the NSF.

Received 6 June; accepted 3 July 1980.

1. Walsh, D., Carswell, R. F. & Weymann, R. J. *Nature* **279,** 381–384 (1979).
2. Weymann, R. J. *et al. Astrophys. J. Lett.* **233,** L43–L46 (1979).
3. Pooley, G. G. *et al. Nature* **280,** 461–464 (1979).
4. Roberts, D. H., Greenfield, P. E. & Burke, B. F. *Science* **205,** 894–896 (1979).
5. Greenfield, P. E., Roberts, D. H. & Burke, B. F. *Science* **208,** 495–497 (1980).
6. Gunn, J. E. *et al. IAU Circ.* No. 3431 (1979).
7. Young, P. J. *et al. Astrophys. J.* (in the press).
8. Clark, B. G. *Astr. Astrophys.* (in the press).
9. Stockton, A. (submitted).
10. Hine, R. G. & Longair, M. S. *Mon. Not. R. astr. Soc.* **188,** 111–130 (1979).
11. Porcas, R. W. *et al. Nature* **282,** 385–389 (1979).
12. Haschick, A. D. *et al.* (submitted).

Optical spectroscopy of interplanetary dust collected in the Earth's stratosphere

P. Fraundorf, R. I. Patel, J. Shirck* & R. M. Walker

McDonnell Center for the Space Sciences, Washington University,
St Louis, Missouri 63130

J. J. Freeman

Corporate Research Department Monsanto Company,
800 N. Lindbergh Blvd, St Louis, Missouri 63166

A new class of extraterrestrial material has recently become available for study: interplanetary dust particles (2–30 μm in size) collected in the atmosphere at 20-km altitude by inertial impactors mounted on NASA U-2 aircraft in the programme of sampling initiated by Brownlee *et al.*[1]. The extraterrestrial nature of a compositionally 'chondritic' subset of these particles has been verified by measurements of the elemental and isotopic abundances of noble gases[2,3]. We report here the first optical absorption spectra of these interplanetary dust particles (IDPs). We show that absorption features in the visible at ~9,800 cm^{-1} and in the IR at ~1,000 cm^{-1} are present in spectra of these particles. An ~1,000 cm^{-1} feature is present in optical spectra of meteorites, comet dust and interstellar dust, although its cause in the latter two is a subject of some debate[4,5]. Future experimental work on these laboratory samples promises to shed light on the alternatives, at least for particles in the Solar System dust cloud.

Particle handling techniques are described elsewhere[6]. After removal from collectors supplied by Brownlee, particles were individually cleaned of the silicone oil collecting medium by immersion in a running stream of hexanes. They were mounted and characterized briefly by optical microscopy, scanning electron microscopy and energy dispersive X-ray analysis before

---

* Present address: 3M Center, Building 201-3E, St Paul, Minnesota 55133.

0028-0836/80/350866—03$01.00

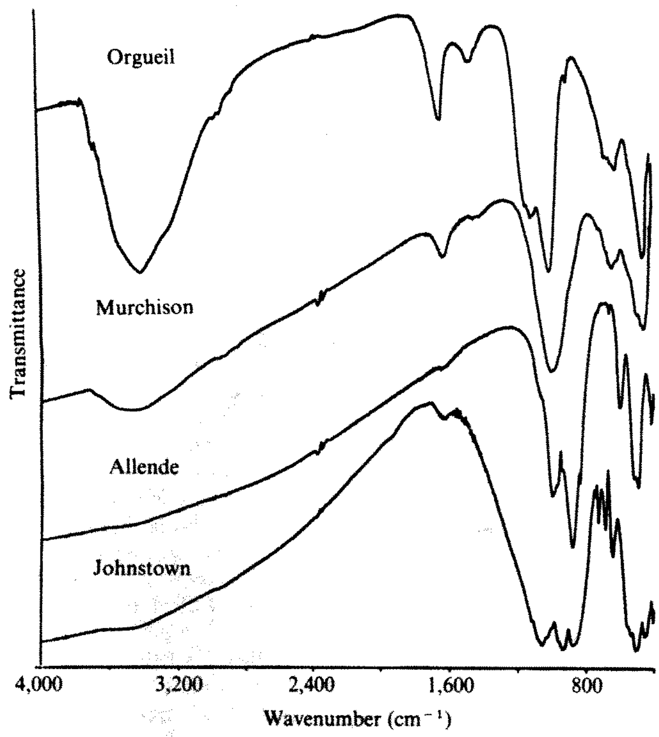

Fig. 1 IR transmission spectra of different meteorites at room temperature. The samples were prepared by mechanically grinding a 1-mg sample with 100 mg of KBr and forming a clear pressed pellet by the standard IR-KBr pellet preparation technique. A commercial Nicolet 7199 FTIR spectrometer equipped with a globar source and mercury–cadmium–telluride detector was used to record the IR specta.

being crushed and mounted for the measurement of optical properties using Fourier transform spectroscopic methods.

Absorption spectra of meteoritic materials in the mid-IR show a wealth of detail. Figure 1 shows room temperature (25 °C) IR spectra from several different meteorites between 4,000 and 400 cm^{-1} obtained using large (10^{-3} g) samples. Similar spectra have been published previously[4]. The structured absorption feature centred near ~1,000 cm^{-1} is probably due to Si–O stretch bands of meteoritic silicates. The spectra of these samples were then recorded at near liquid nitrogen temperature (−196 °C) to simulate the lower temperatures found in space. Figure 2 compares the low temperature (−168 °C) and room temperature spectra of the Orgueil meteorite. At low temperature, the weaker bands become sharper and better resolved, but the distinguishing spectral features are not significantly altered.

An IR spectrum of pieces from three IDPs (total sample ~10^{-9} g) is shown in Fig. 3*a*. A broad feature in the region 1,300–800 cm^{-1} is clearly present. Figure 3*b* shows a comparison spectrum of small particles from the Orgueil meteorite taken under similar circumstances. Possible causes for the IDP feature include mafic silicates[4] and carbonaceous material[5] which are known to be present in these particles[7–9].

Figure 4 shows the visible/near IR spectra of several carbonaceous meteorites, and of a sample composed of five crushed IDPs (total sample ~3×10^{-9} g). The well studied feature centred at ~9,800 cm^{-1} in the meteoritic spectra is due to crystal field transitions of iron[10]. Comparisons of the IDP and the carbonaceous chondrite spectra show that the absorption spectra are different, in spite of the similarities in elemental abundances of the two classes of object[7]. A weak iron crystal field absorption band is present in the IDP spectrum.

A prominent ~1,000 cm^{-1} feature is a commonly observed feature of dust found in different astrophysical settings[4]. Although it may never be possible to establish definitively the nature of the material (or materials) responsible for such an absorption in interstellar dust, it seems likely that the problem

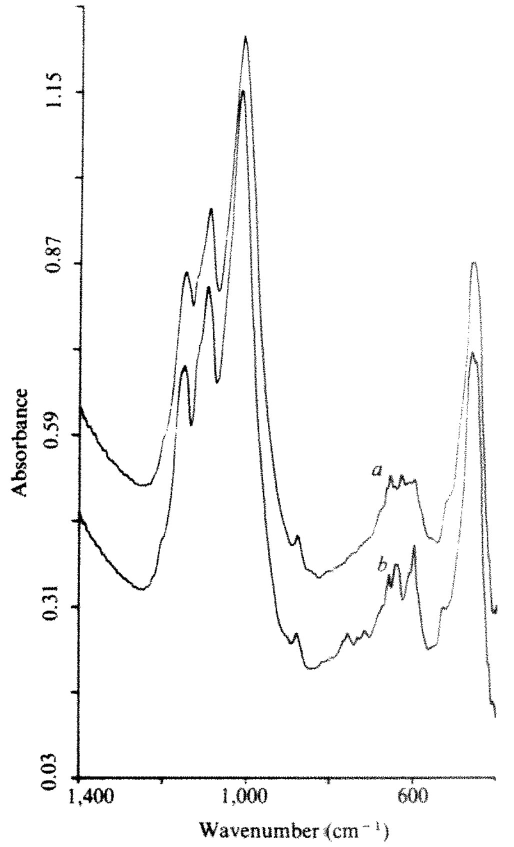

Fig. 2 IR transmission spectra of the Orgueil meteorite: *a*, at room temperature (25 °C); *b*, at −168 °C.

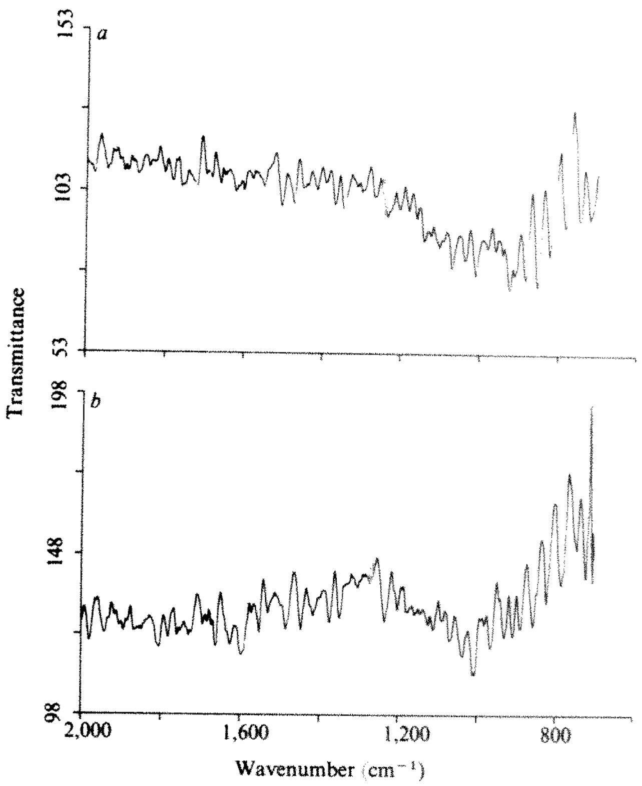

Fig. 3 IR transmission spectra of: *a*, IDPs; *b*, a particle from the matrix of Orgueil. Spectra were acquired by crushing the particles onto a thin (~100 μm) freshly cleaved KBr plate using a glass slide and centering them in a 50 μm aperture[11]. The sample mount was then placed in a 4× beam condenser using an *f*/1 KBr lens and aligned by adjusting the sample position until the detector signal was maximized. Spectra were obtained by 20,000 time averaged scans with 8 cm^{-1} resolution.

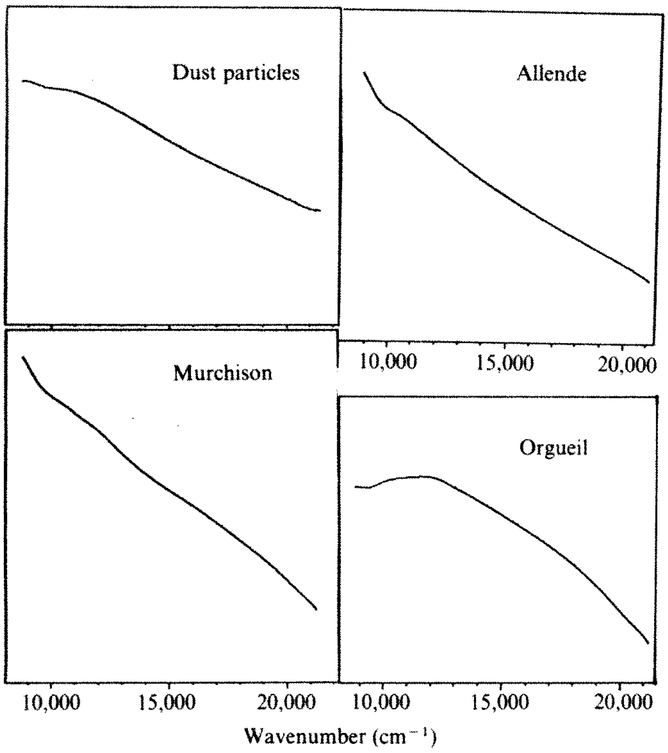

Fig. 4 Visible/near-IR spectra of powdered samples from IDPs and several carbonaceous chondrites. Ordinate values are proportional to the ratio of light transmitted through the sample and light transmitted through a blank. The spectra were obtained using the solar FTS at the Kitt Peak National Observatory. The instrument is a dual beam FTS having input and output focal lengths of 2.9 and 2.3 m, respectively. The beam splitter was silver on quartz and an entrance aperture (*f*/50) of 4 mm was used. Transmission measurements were made on powdered samples which were immersed in silicone oil and sandwiched between glass slides, separated by spacers. Illumination was provided by a 150 W tungsten–halogen lamp.

can be solved for interplanetary dust. Although the collected IDPs have certainly experienced some thermal alteration during deceleration in the Earth's atmosphere, the particles seem to retain absorption features found in cosmic dust. Work is in progress to separate, or at least remove selectively, the various constituents of the IDPs to evaluate separately their contribution to the absorption. A severe constraint is posed by the small size of the particles and their present rarity. The particles are also known to differ considerably in their mineral assemblages from one particle to the next[9]. Fourier transform spectroscopy on individual particles may prove to be an important future technique for the nondestructive classification of particles according to type.

We thank Dr J. Brault for assistance at the Kitt Peak National Observatory, Drs C. Anderson, D. Huppler and D. W. Vidrine of Nicolet Instrument Corporation for their help, and particularly Dr D. Brownlee who made IDPs available for this study, and G. Flynn for helpful discussions. This work was supported by NASA grant NGL 26-008-065.

Received 12 May; accepted 26 June 1980.

1. Brownlee, D. E., Tomandl, D. A. & Olszweski, E. *Proc. 8th Lunar Sci. Conf.*, 149–160 (1977).
2. Rajan, R. S. *et al. Nature* **267**, 133–134 (1977).
3. Hudson, B., Flynn, G. J., Fraundorf, P., Hohenberg, C. M. & Shirck, J. *Science* (submitted).
4. Knacke, R. F. in *Protostars and Planets* (ed. Gehrels, T.) 112–133 (University of Arizona Press, 1978); *Nature* **269**, 132–133 (1977).
5. Hoyle, F. & Wickramasinghe, N. C. *Nature* **268**, 614–616 (1977).
6. Flynn, G. J., Fraundorf, P., Shirck, J. & Walker, R. M. *Proc. 9th Lunar Sci. Conf.* 1187–1208 (1978).
7. Brownlee, D. E. in *Protostars and Planets* (ed. Gehrels, T.) 134–152 (University of Arizona Press, 1978).
8. Fraundorf, P. & Shirck, J. *Proc. 10th Lunar Sci. Conf.* 951–976 (1979).
9. Fraundorf, P. thesis, Washington Univ. (1980).
10. Gaffey, M. J. & McCord, T. B. in *Comets, Asteroids and Meteorites* (ed. Delsemme, A. H.) 199–218 (The University of Toledo Press, 1977).
11. Cournoyer, R., Shearer, J. C. & Anderson, D. H. *Analyt. Chem.* **49**, 2275–2277 (1977).

Solar variability and climatic change during the current millennium

Minze Stuiver

Departments of Geological Sciences and Zoology, Quaternary Research Center, University of Washington, Seattle, Washington 98195

Claims of a Sun–weather relationship[1] can only be evaluated properly when the history of solar change is known in detail. The most obvious feature of solar variability is the change over time in the number of sunspots on the visible half of the Sun. A less visible indicator of solar change is the ^{14}C content of tree rings. The atmospheric ^{14}C levels derived from tree ring measurements can be tied to the Sun's modulation of the cosmic ray flux in the vicinity of the Earth, and thus provide a history of solar change.[2] We report here a comparison of climate records with the record of solar change obtained from atmospheric ^{14}C variations. This yielded 'negative' results, that is, a relationship between the climatic time series and the ^{14}C derived record of solar change could not be confirmed.

The modulation of the cosmic ray flux (and the associated atmospheric ^{14}C production rate Q in atoms s^{-1} cm^{-2} of the Earth's surface) by the Sun occurs through changes in the magnetic shielding properties of the solar wind. However, this is not the only cause of atmospheric ^{14}C change. The Earth's geomagnetic field also influences the pathways of the charged particles that constitute cosmic radiation. Both solar modulation and longer-term geomagnetic field changes have to be taken into account when decoding the atmospheric ^{14}C signal. A carbon reservoir model[2,3] that describes terrestrial carbon exchange between the atmosphere, ocean and biosphere can be used to calculate from the atmospheric record the production rate changes ΔQ_M. In carbon reservoir modelling, the long-term trend in the atmospheric ^{14}C attributed to Earth geomagnetic dipole changes is removed by deducting the sinusoidal approximation given by Houtermans[4]. The remaining ^{14}C variations are used to calculate the ^{14}C production rate changes ΔQ_M around the steady state value of 1.57 atoms cm^{-2} s^{-1} from the model. The magnitude of the ΔQ_M changes caused by solar modulation depends on the Earth's geomagnetic field intensity because the average global ^{14}C production becomes less sensitive to solar modulation when the Earth's geomagnetic field increases[5,6]. The ΔQ_M values given here are normalized to the present-day Earth's geomagnetic field intensity by using the correction factor $[M(0)/M(t)]^{0.63}$ derived from data given by O'Brien. The magnetic field changes were obtained from data given by Barton *et al.*[7].

Climate-related changes in carbon reservoir exchange rates may also cause atmospheric ^{14}C levels to change. The calculated record of ^{14}C production rate changes (ΔQ_M) may, therefore, contain 'fictitious' rate changes that are not related to solar modulation, but to climate changes. The contribution to the ΔQ_M record of such fictitious ΔQ_M changes is difficult to evaluate, but it can be argued that climate variability is not a dominant factor in producing century-type atmospheric ^{14}C variations[2,8].

The changes in calculated ^{14}C production rates generally agree with the evidence for solar change obtained from historical observations of sunspot number and aurorae. For instance, there are three intervals in the post AD 1200 sunspot record where visual sunspot observations are lacking (the Wolf, Spörer and Maunder minima). For each interval of reported low incidence of sunspots, the ΔQ_M record reaches a maximum. There is also covariance between ^{14}C production rate changes and sunspot numbers for the eighteenth and nineteenth centuries[2].

When discussing the ^{14}C changes, note that the standard deviation in the ^{14}C measuremens is ~1.5–2 ‰. This corresponds to an average standard deviation in the calculated

0028-0836/80/350868—04$01.00

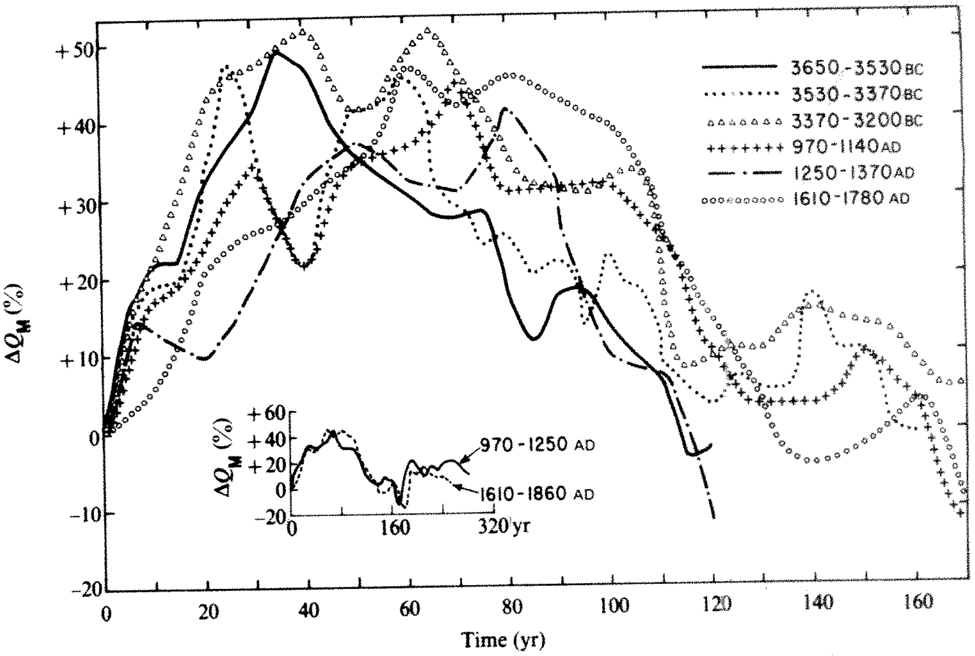

Fig. 1 ^{14}C-production rate changes ΔQ_M of solar oscillatory modes that are similar to the Maunder minimum mode. The ΔQ_M values are the increases over the preceding lowest ^{14}C production rate. The ^{14}C production rate changes were normalized on the present-day Earth geomagnetic field intensity (see text).

ΔQ_M values of ~4%. It is possible to recognize many similarities within the stated precision in the ^{14}C pattern. The ^{14}C production rate changes are, therefore, not random fluctuations.

Two of the ΔQ_M oscillations in the current millennium are, within the experimental error, copies of each other. These are the variations encountered between AD 970 and 1250, and between AD 1610 and the end of the nineteenth centry (see Fig. 1). The similarity of the Fig. 1 curves implies that the 'grand medieval maximum' of the twelfth century[9] has the same level of solar activity as the AD 1740–1840 interval. The Sun switches near AD 1250 to the quiet Wolf minimum, whereas the Sun is still active after AD 1890. The agreement between the curves terminates, therefore, after 280 yr.

The close correspondence of some of the ^{14}C record puts limitations on the theories of solar dynamo behaviour. Dynamo theories may include the possibility that the envelope of the solar cycle, and the associated magnetic field in interplanetary space, is inherently unpredictable[10]. The repetitive pattern seen in the ^{14}C record argues against this interpretation.

Many of the oscillations are similar to the late seventeenth century Maunder minimum pattern. The ΔQ_M oscillations between AD 970 and 1100, AD 1250 and 1370, and AD 1610 and 1750 all have the same magnitude, approximate duration and shape (Fig. 1). The geomagnetically normalized ΔQ_M variations, calculated from a ^{14}C record[11] between 3650 and 3300 BC are also given in Fig. 1. The 3650–3520 BC, 3530–3370 BC, and the 3370–3260 BC oscillations again have similar magnitudes and duration. The times necessary to reach the maximum production rate change are different. This rise-time is 40 yr for the BC oscillations and 50–70 yr for the more recent ones.

Three of the four major oscillations of the current millennium are of the Maunder minimum type, lasting 120–140 yr. The remaining oscillation is the Spörer minimum, lasting nearly twice as long (240 yr). The Spörer oscillatory mode is seen less frequently than the Maunder mode. The ^{14}C record given by Suess[12] suggests that the preceding Spörer mode occurred as long ago as 700 BC.

A spectral analysis of the post-AD 730 record yields the curve in Fig. 2*a*. The probability of exceeding, in a random distribution, the peak sizes with periods of about 130 and 200 yr are, respectively, 1.4 and 4.9 ‰.

The so-called 'Little Ice Age' in Europe in the seventeenth century is sometimes attributed to the solar changes that took place during the Maunder minimum[9]. If indeed the Sun does influence climate in this manner, then there should be many more Little Ice Ages because the solar Maunder mode is quite prevalent. One would then also like to postulate a cooling of double duration for the less frequent double Maunder (Spörer) mode. In fact, with four major oscillations during a millennium, it would be conceivable that 40-odd little ice ages existed during the current Interglacial. Furthermore, one would expect similarities in climatic response for certain periods, such as the AD 970–1250, and the AD 1610–1890 intervals.

Figure 3 shows the solar-related ΔQ_M record compared with eight climate records. Two of these are based on oxygen-isotope ratio measurements in ice cores. The derivation of the ages of

Table 1 Correlation coefficients r derived from cross-correlating the ^{14}C production rate record given in Fig. 3 (ΔQ_M curve) with the climate records listed below

Fig. 2	Locality	r	r_{max}	Δt (yr)	r_{max}	Δt (yr)
a	Oxygen isotopes ice core, Devon island[14]	+0.08			+0.25 (5%)	50
b	Oxygen isotopes ice core, Camp Century, Greenland[15]	−0.19	−0.43 (3.5%)	−30	+0.33 (19%)	90
c	Oxygen isotopes ice core, Crete, Greenland[16]	−0.01			−0.26 (5%)	50
d	Tree ring width, Lapland[17]	−0.01	−0.33 (6%)	−90	+0.36 (3%)	50
e	Winter severity index, Russia[18]	−0.14	−0.43 (1.6%)	−30		
f	Tree ring density, Lauenen, Switzerland[19]	+0.05	−0.31 (10%)	−90		
g	Winter severity index, UK[18]	−0.03				
h	Mean annual temperature, UK[18]	−0.06				
i	Deuterium isotopes tree rings, White Mountains, Nevada[20]	−0.11				
j	Tree ring width, White Mountains, Nevada[21]	−0.32	−0.32 (5%)	0	−0.32 (5%)	0

The r_{max} values are obtained by assuming (1) climate lags the ΔQ_M curve (Δt positive) or (2) climate-influencing variables precede the Q changes (Δt negative). The probabilities of exceeding the listed r values in a random series are given in parentheses. r_{max} values are only listed for time lags of 100 yr or less.

the Camp Century core (Fig. 3*b*) and Devon Island (Fig. 3*a*) are mainly based on ice flow dynamics. The time scale of all other curves is based on either tree ring counting or historic dating. Ages determined in this manner should be considered more accurate than those assigned to the oxygen isotope curves.

The climate curves in Fig. 3 were constructed from available records that are listed in Table 1. These records give information on regional climate only. They are used for a comparison with the solar record because other, more representative, indicators of global climate are not available over such a long interval.

A downward move of the climatic parameters in Fig. 3 implies in all instances a colder environment. The solar ΔQ_{M} record is plotted on an inverse scale, mainly to facilitate a visual investigation of a possible relationship between reduced solar activity (higher ^{14}C production rates) and colder climate.

Conclusions that can be drawn from the comparisons made in Fig. 3 are:

(1) The detailed work of Schweingruber *et al.* on tree ring density[19] does not agree with contemporaneity of the Maunder minimum and the climatic cooling of the seventeenth century that is often referred to as the Little Ice Age. The tree-ring density record points to an extended cold episode between AD 1570 and 1640. This interval coincides with the period of high solar activity (low ΔQ_{M} values) between the Spörer and the Maunder minimum. Several of the other climate records given in Fig. 3 also have a tendency towards colder weather during this interval of high solar activity.

(2) During the Sun's switch to the less active Spörer and Maunder minimum modes, Russia especially experienced colder winters.

Correlation coefficients derived from cross-correlating the climate and solar curves are small in nearly all cases. These coefficients r are given in Table 1, which also lists the oxygen isotope record of Crete, Greenland[16] and a Lapland tree-ring width series[17], not shown in Fig. 3, for which the r values are both -0.01. The White Mountains' ring width data cross-correlate with the solar record at the 5 % significance level. The other correlation coefficients indicate a complete absence of a direct relationship between the solar Q and climate curves.

By assuming a time lag between climate and the solar curves, it is possible to obtain larger correlation coefficients for several of the time series listed in Table 1. There are two possibilities: either climate lags the solar curve (Δt positive) or the solar properties that possibly influence climate precede the Q changes (Δt negative). Table 1 lists those Δt values ($|\Delta t \leq 100$ yr) for which r reaches a maximum value $r_{\max}$.

Because the Q record has substantial autocorrelation (it takes a 50-yr lag for the autocorrelation coefficient to approach zero) the normal test of significance is no longer applicable. Autocorrelation reduces the number of independent observations used in interpreting the derived cross-correlation coefficients. The effective number N of independent observations were calculated for each time lag according to the procedures discussed by Quenouille[22]. The number N was subsequently used in deriving the probabilities of exceeding the Table 1 $r_{\max}$ values.

Table 1 lists nine climate series of different regions (series *h* is partially derived from series *g* and has not been included in the following discussion). One hundred and eighty-nine comparisons were made by lagging the data up to 100 yr (21 comparisons with the Q record for each climate series). In a

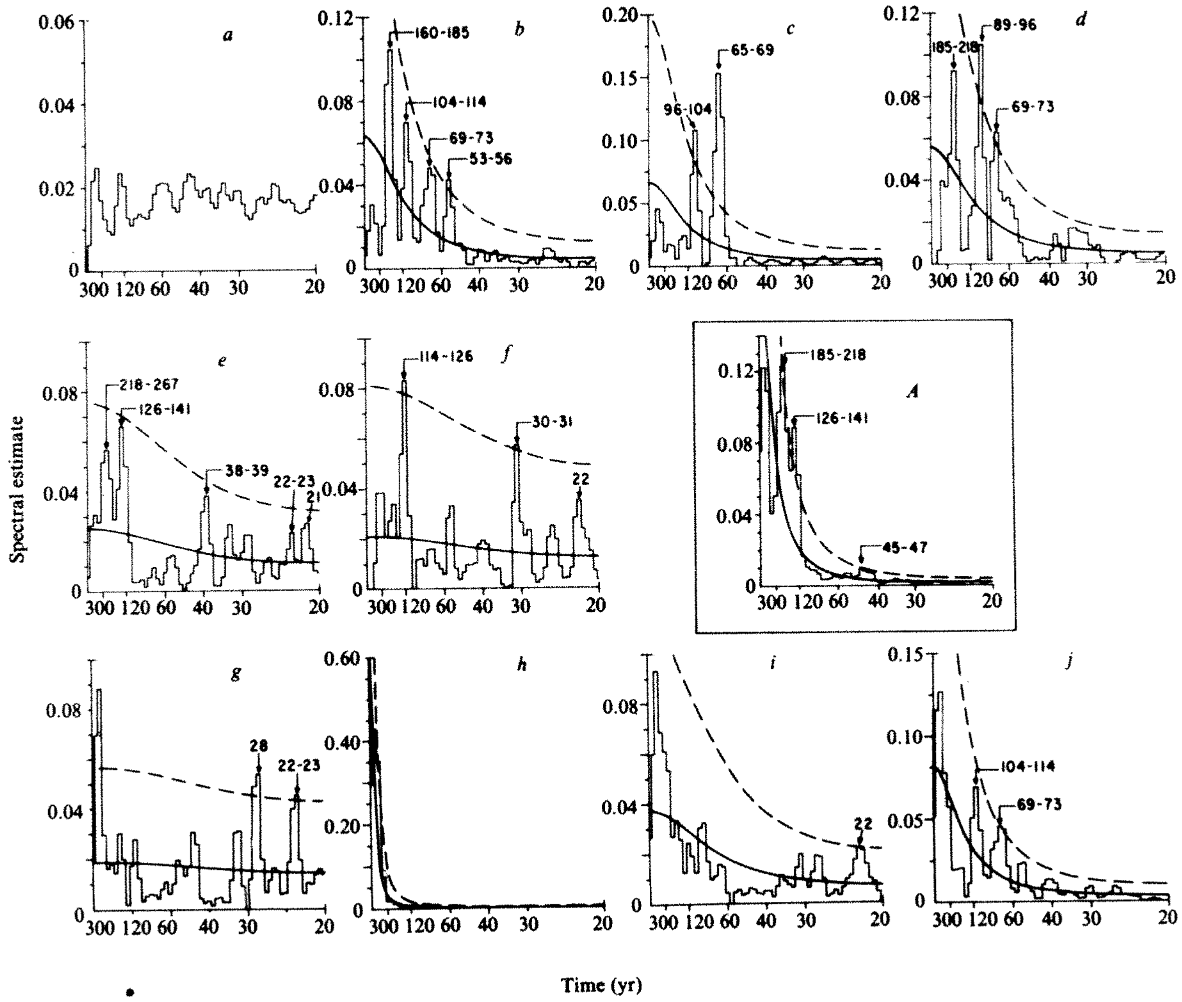

Fig. 2 Spectral distribution of the post-700 AD ^{14}C production rate record (curve *A*) and climate records (curves *a*–*j*). The various climate records are described in Table 1. The dashed line gives the 2σ confidence limit whereas the solid line gives the red noise continuum[13].

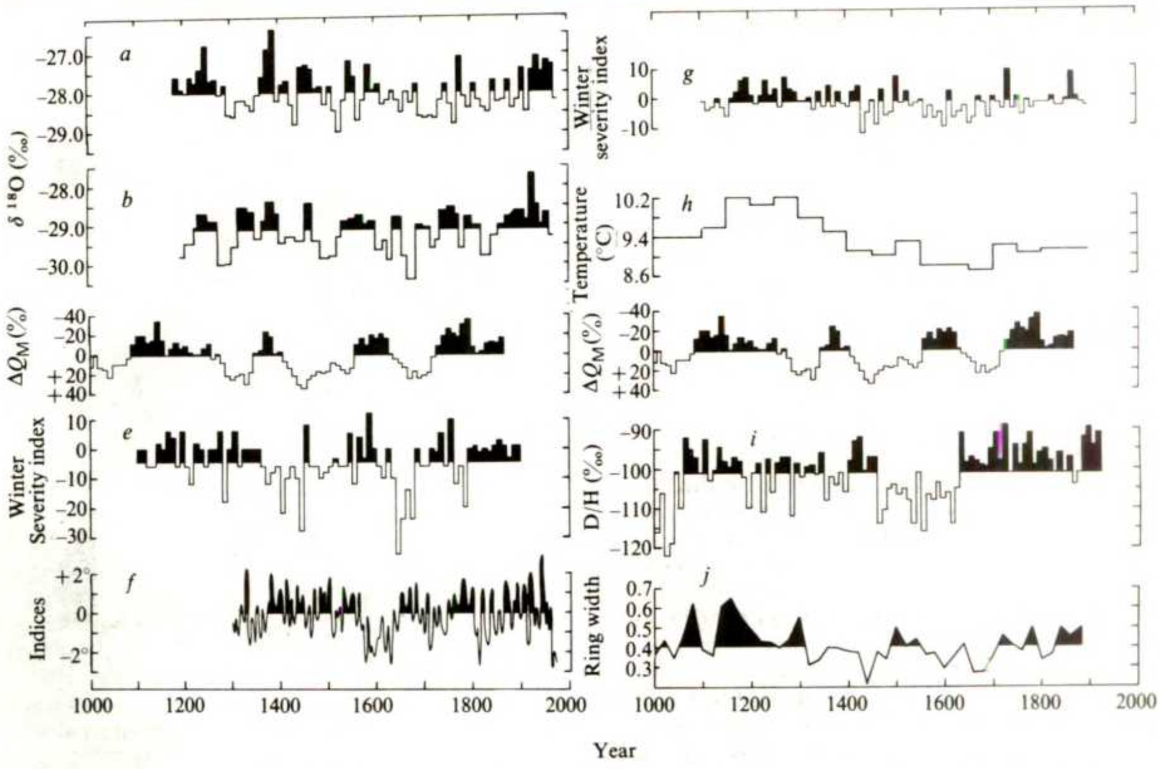

Fig. 3 A comparison of climate and ^{14}C production rate records. The various climate records are described in Table 1.

comparison of non-related time series, the distribution of correlation coefficients should be 1, 9, 51 and 128 for, respectively, the 0–0.3%, 0.3–5%, 5–32% and 32–100% probability intervals. The Q and climate comparisons yield a distribution of 0, 12, 50 and 127 correlation coefficients for the intervals listed above. The combined lagged climate records therefore do not cross-correlate with the Q record beyond random statistics.

Another approach to the investigation of a Sun–weather relationship is to look for common periodicities in the solar related ΔQ_M record and the climate records. The climate records contain several periodicities (Fig. 2). The closest agreement in spectral distribution between the solar related ^{14}C (curve A) and climate records is obtained for the Russian winter severity index (curve e). The spectra of other high-latitude regions, such as Camp Century, Greenland (curve b) and Lapland (curve d) also partially agree. On the other hand, the climate spectra also have several periodicities that are not present in the ^{14}C derived solar record. One of these periods, near 70 yr, is found in four climate records. Note that the 22-yr cycle, already discussed by Epstein and Yapp for the D/H record (curve i) is also present in the winter severity indices of England and Russia (curves g and e), and the Swiss tree-ring record (curve f). The 22-yr cycle is absent in the ^{14}C production record (curve A) but this is due to a lack of sensitivity for the faster oscillations (a rapid decadal production rate change is attenuated more, and results in atmospheric ^{14}C variations of a few per mil only).

Earlier studies of the ^{14}C and climate record[9,23–25] suggested a direct relationship between the solar modulated atmospheric ^{14}C levels and climate. These studies did not take into account the variable time lag between the atmospheric ^{14}C levels and the ^{14}C production rate changes. The precision of the ^{14}C record used in those investigations also did not allow for a detailed study of a phase shift between solar input function and climate. The high precision ^{14}C measurements reported here do not support a statistically significant relationship between the combined regional climate and ^{14}C time series.

Many factors influence local climate change, and a solar influence on climate can perhaps be expected in a few areas only. The Camp Century and Russian climate records demonstrate on the basis of the statistical analysis a climate solar relationship (albeit 30 yr out of phase). A selective comparison of solar and climate records, however, can only be justified if a mechanism can be found that explains the postulated increased sensitivity to solar changes of these areas. Perhaps jet stream oscillations that seem to relate to the 11-yr solar cycle[27] may provide some answers in this direction.

The length of the records discussed above does not allow for the investigation of a solar–climate relationship with periodicities of the order of millennia[26]. Sun–weather effects may still also be tied to other parameters of solar change, such as the umbra–penumbra ratios discussed by Hoyt[28].

This work was supported by the NSF Climate Dynamics Program grant ATM 7821608. P. M. Quay calculated ^{14}C production rates through carbon reservoir modelling and P. Reimer developed the computer program for spectral analysis.

Received 6 May; accepted 3 July 1980.

1. Pittock, A. B. *Rev. Geophys. Space Phys.* **16,** 400–420 (1978).
2. Stuiver, M. & Quay, P. D. *Science* **207,** 11–19 (1980).
3. Oeschger, H., Siegenthaler, U., Schotterer, U. & Gugelman, A. *Tellus* **27,** 168–192 (1975).
4. Houtermans, J. C. thesis, Univ. Bern (1971).
5. Lingenfelter, R. E. & Ramaty, R. in *Proc. 12th Nobel Symp.* (ed. Olsson, I. U.) 513–535 (Wiley, New York, 1970).
6. O'Brien, K. *J. geophys. Res.* **84,** 423–431 (1979).
7. Barton, C. E., Merrill, R. T. & Barbetti, M. *Phys. Earth planet. Inter.* **20,** 96–110 (1979).
8. Stuiver, M. and Quay, P. D *Radiocarbon* **22** (in the press).
9. Eddy, J. A. *Climatic Change* **1,** 173 (1977).
10. Gilman, P. A. *Abstr. Conf. The Ancient Sun* (NSF/NASA/NCAR, Boulder, 1979).
11. De Jong, A. F. M., Mook, W. G. & Becker. B. *Nature* **280,** 48–49 (1979).
12. Suess, H. E. *Radiocarbon* (in the press).
13. Mitchell, J. M. *et al. Tech. Not.* No. 79, 33–79 (World Meteorological Organization, No. 195, TP 100, Geneva, 1966).
14. Paterson, W. S. B. *et al. Nature* **266,** 508–511 (1977).
15. Johnson, S. J., Dansgaard, W., Clausen, H. B. & Langway, C. C. *Nature* **227,** 482–483 (1970).
16. Dansgaard, W. *et al. Nature* **225,** 24–28 (1975).
17. Sirén, G. *Commun. Inst. For. Fenn. Hels.* **54,** 2 (1961).
18. Lamb, H. H. *Climate: Present, Past and Future* Vol. 2 (Methuen, 1977).
19. Schweingruber, F. H., Braeker, O. U. & Schaer, E. in *Evolution of Planetary Atmospheres and Climatology*, 369–372 (Centre National d'Etudes Spatialis, Toulouse, 1976).
20. Epstein, S. and Yapp, C. J. *Earth planet. Sci. Lett.* **30,** 252–261 (1976).
21. LaMarche, V. C. *Science* **183,** 1043–1048 (1974).
22. Quenouille, M. H. *Associated Measurements* Vol. 68 (Butterworths, London, 1952).
23. Siscoe, G. L. *Nature* **276,** 348–352 (1978).
24. Damon, P. E. *Met. Monogr.* **8,** 106–111 (1968).
25. Suess, H. E. *Met. Monogr.* **8,** 146–150 (1968).
26. Denton, G. H. & Karlen, W. *Quat. Res.* **3,** 155–205 (1973).
27. Nastrom, G. D. *J. geophys. Res.* **85,** No. C1, 443–452 (1980).
28. Hoyt, D. V. *Climatic Change* **2,** 79–92 (1979).

Modern climate–tree-growth relationships and climatic reconstruction in sub-Arctic Alaska

Harriet L. Garfinkel & Linda B. Brubaker

College of Forest Resources, University of Washington, Seattle, Washington 98195

Statistical comparisons between tree-ring width sequences and climatic records provide a means of identifying climatic limitations on tree growth and allow the reconstruction of past climates. This information is especially important in the North American sub-Arctic where climate–growth relationships are poorly understood and instrumental weather records are very short, typically less than 75 yr. Dendroclimatic reconstructions before 1900 are essential for estimating a realistic range of high latitude climatic variation, because twentieth century climate is now thought to be somewhat anomalous[1]. While some dendroclimatic studies have been carried out in the sub-Arctic[2–8], none has made full use of current multivariate statistical techniques. This study, as part of a multidisciplinary investigation of treeline fluctuations in the Brooks Range of Alaska, uses ring-width sequences of white spruce (*Picea glauca* [Moench] Voss) to define climatic limitations on radial growth at treeline and to reconstruct past climatic variables for Fairbanks, Alaska. Multiple regression techniques were used to analyse climate–growth relationships and the results suggest important modifications to the theory that growth at treeline is limited primarily by summer temperature[2,8,9]. For example, we have found that radial growth is directly related to summer and autumn temperature and precipitation during certain months, but is inversely related to winter–spring temperature. The same ring-width sequences were used to reconstruct average May–July temperature at Fairbanks, Alaska, for the period 1829–1930. This reconstruction, which more than doubles the length of the existing climatic record, was verified by statistically comparing it to independent instrumental data. It indicates that the Fairbanks area has been warmer in the twentieth century than in the nineteenth century during these months. As the longest annual record of temperature from northern Alaska, this reconstruction provides quantitative evidence for a climatic warming similar to that occurring throughout large portions of the Northern Hemisphere during the past 100 yr (refs 10–12).

Fourteen ring-width chronologies were obtained according to standard dendrochronological techniques[13] from sites (67–68° N, 153–155° W) within continuous forest and treeline environments in the Walker Lake–Alatna River valley area of the Brooks Range. Each chronology represents the average of age-standardized ring widths[14] of two increment cores from each of 15 or more trees. To examine climate–growth relationships, the chronology of each site was used as the dependent variable in a stepwise multiple regression analysis with monthly climatic data from the Interior Basin climatic division[16] within which the sites are located. This analysis, termed response function analysis by Fritts *et al.*[17], defines the correlations of radial growth with monthly temperature and precipitation during and preceding the actual growing season. Months before the growth season are included in the analysis because climatic conditions during this period can affect growth during the subsequent summer[15]. The growth variance accounted for by temperature and precipitation in the 14 analyses ranges from 11.2 to 54.7% and averages 36.0%.

The basic form of the response function was similar at all sites and these results are summarized in Fig. 1. This set of climate–growth correlations suggests physiological processes which limit growth in the sub-Arctic. In addition to the expected positive correlation with current summer temperature, growth exhibits a strong positive correlation with previous autumn temperature and negative correlations with previous summer, winter and spring temperatures. The positive response of growth to current summer temperature suggests that warm temperatures can increase rates of net photosynthesis and enhance growth in treeline environments during the growing season. The prominent positive correlation with previous autumn temperature suggests that warm autumn temperatures lead to increased photosynthesis after the end of the growing season, resulting in greater reserves of carbohydrates for the next year. Note that this correlation exists for periods after growth has ceased in the preceding summer, suggesting that photosynthates are put into reserve rather than used for late-season growth. In fact, climatic conditions that hasten the cessation of growth during one summer may actually promote increased growth during the next. This hypothesis is consistent with the negative correlation of growth at all sites with previous July temperature, as low temperatures near the end of the growing season can cause early termination of growth[18,19].

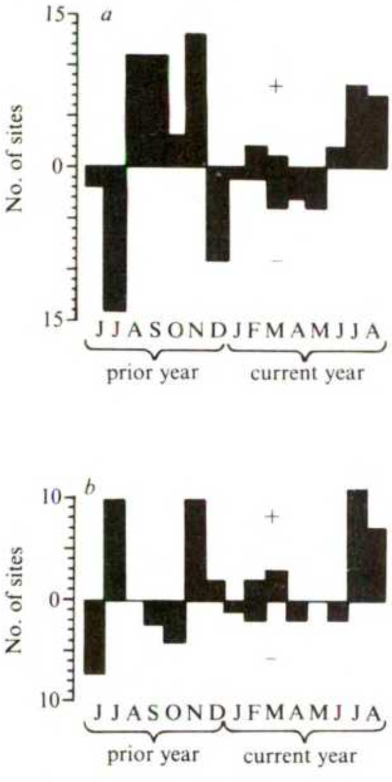

Fig. 1 Response function summary for: *a*, temperature; and *b*, precipitation. The vertical scale represents the number of sites exhibiting significant ($P < 0.05$) positive (upper half of scale) or negative (lower half of scale) correlation with each climatic variable. The climatic variables are mean monthly temperature and total monthly precipitation for the June before the growth season through August of the current year.

The negative correlation of growth with winter–spring temperature may reflect the adverse effects of winter desiccation[19–21]. Thawing of foliage precedes thawing of the stem and soil during periods of above average temperature. As a result, transpiration is activated while water uptake is inhibited, leading to severe water stress. Coupled with this is an increase in respiration which, if prolonged, will lead to death of foliage[23].

While precipitation during certain months is strongly correlated with growth, the responses do not follow clear seasonal trends and are not as easy to interpret as the temperature responses. The water relations of high latitude trees, particularly during the dormant months, has not been studied extensively, making evaluation of these responses difficult. However, the positive correlation for current summer months suggests that internal water stress can limit photosynthesis at sub-Arctic treeline sites when temperatures are high. Relationships of this

0028–0836/80/350872—03$01.00

type are commonly found on arid or semi-arid sites where moisture stress limits growth[15]. The south flank of the Brooks Range is, in fact, a dry environment, as it receives an average of only 332 mm of precipitation per year[16].

These response function results suggest that ring-width sequences from Interior Alaska contain significant climatic information and can be used to reconstruct past climatic fluctuations. Dendroclimatic reconstruction is a multistep process developed over the past decade by Fritts and others[6,17,24]. In this study, principal component analysis was performed on the tree-ring chronologies to concentrate the information present in the data into a small number of variables (eigenvectors) and to satisfy the statistical assumption that regression variables are linearly independent.

Annual values (amplitudes) associated with the first five eigenvectors served as the tree-growth data set in the reconstruction procedure. Numerical relationships between these amplitudes and selected Fairbanks climatic variables[16] were defined by stepwise multiple regression analysis in a process termed calibration. Fairbanks, though nearly 400 km south-east of the study area, has the longest climatic record in the Interior Basin Climatic Division. In each regression equation, the monthly temperature or precipitation measurements were expressed in terms of the tree-growth eigenvector amplitudes for the period 1931–74. Climatic variables were reconstructed by entering eigenvector amplitudes for the period 1828–1932 into the regression equations. Finally, the reconstructions were verified by statistically testing their similarity to Fairbanks instrumental records for 1906–30 which had been withheld from the calibration. Reconstructions of May, June and July temperature passed ($P<0.05$) two, three and four of the four verification tests respectively. The individual reconstructions of these months were averaged for a simplified reconstruction of early growth season temperature which passed three of the tests. February temperature and December precipitation each passed one of the verification tests, lending some validity to these reconstructions. However, this is not considered sufficient verification for climatic interpretation. These results, along with the R^2 values for the corresponding calibration equations are presented in Table 1.

Table 1 Calibration and verification statistics

Climatic variable	R^2	Correlation	Sign test	Product mean	Reduction of error	No. of tests passed
February temperature	0.394	—	—	*	—	1
May temperature	0.654	*	—	*	—	2
June temperature	0.628	†	*	*	—	3
July temperature	0.475	†	*	*	‡	4
December precipitation	0.369	—	—	*	—	1
Average of reconstructed May–July temperature		†	*	*	—	3

—, Not significant; *, significant at $P<0.05$; †, significant at $P<0.01$; ‡, no significance test available; positive value considered significant (H. C. Fritts, personal communication).

The agreement between instrumental climatic data and the values predicted by the regression equation for the calibration period is reflected in the R^2 value. This statistic can be interpreted as the percentage of the climatic variance accounted for by the tree-ring data. The regression model included the amplitudes of the first five tree-ring eigenvectors, which account for 90.8% of the tree-growth variance as independent variables in the regression. Eigenvectors beyond five account for little variance individually and are assumed to represent random variation. Additional predictive power was gained by lagging these amplitudes 2 yr behind and 1 yr ahead of the climatic data for 20 possible independent variables (five eigenvectors at four lags). The final regression equation is

$$y_t = (b_1)(x_{1,t}) + (b_2)(x_{2,t}) + \cdots + (b_{20})(x_{20,t})$$

where y_t is the predicted value of mean monthly temperature or total monthly precipitation for $t = 1932$–72. (Here, if June–August represent the growing season of year t, the preceding nine months are also considered to be in year t, even though September to December are actually part of the preceding calendar year.) b_i Is the regression coefficient for the amplitude $i = 1, 20$, and $x_{i,t}$ is the amplitude value for $i = 1, 20$ and $t = 1932$–72. Again, the 20 coefficients for year t correspond to the amplitudes of eigenvectors 1–5 for years $t-1$, t, $t+1$ and $t+2$. In the stepwise multiple regression, only those variables with an F ratio >1 were used as predictors in the final equation. Four verification tests were performed on each reconstruction to evaluate the correspondence of reconstructed values with actual climatic data. (1) The correlation test is a standard measure of the predictability between reconstructed and actual climatic data before the calibration period. (2) The sign test is a nonparametric procedure which counts the number of agreements and disagreements in sign changes between adjacent years in the two series. (3) The product mean assesses both the sign and the magnitude of the departures from the calibration period averages. (4) The reduction of error (RE) is a very rigorous test of association between a series of actual values and their estimates. It compares the sum of squares of the differences between the reconstructed and actual data with the sum of squares of differences between the actual data and their mean. The degrees of freedom used to test the significance of the correlation and product mean tests were adjusted downward to correct for serial correlation present in the reconstructed and instrumental time series[28]. These tests are described in detail elsewhere[15].

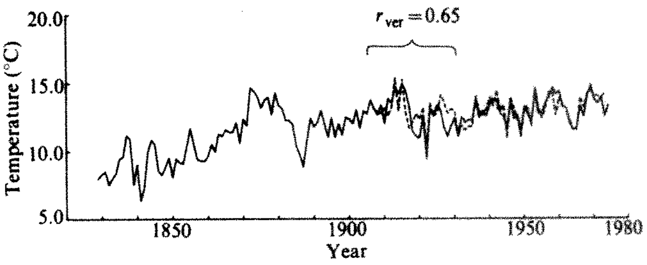

Fig. 2 Climatic reconstructions (———) and Fairbanks weather station data (------) for mean May–July temperature. r_{ver} Is the correlation between the reconstructed and instrumental values for the verification period (1906–30).

The reconstruction of average May–July temperature (Fig. 2) indicates that the twentieth century has been approximately 2.1 °C warmer than the nineteenth century during these months.

This reconstructed warming episode is consistent with our knowledge of treeline fluctuations in Alaska. In the study area, healthy seedlings are presently abundant above the treeline, and upper elevation stands of white spruce are apparently not greatly stressed. These findings indicate a current advance of treeline, already noted in other parts of Alaska[25,26], and Scandinavia[27]. The expansion of the boreal forest, coupled with the warming trend reconstructed for the past 100 yr, is evidence of the widespread warming which has been observed in other areas of the Northern Hemisphere during this period[10–12]. The magnitude of the climatic warming also supports the finding that climatic fluctuations at northern latitudes tend to be more pronounced than simultaneous variations in temperate regions[10,11].

This study demonstrates the usefulness of Alaskan tree-ring sequences and climatic records for dendroclimatic reconstruction. In particular, climatic data from distant stations may be used successfully, so that sampling need not be restricted to those few areas near meteorological stations with long records. Our reconstructions can be extended at least 200 yr by the collection of longer chronologies from the Brooks Range. Refinement of the statistical models will give additional months of temperature and precipitation to the reconstructed data set producing a more complete view of past climatic fluctuations in northern Alaska.

We thank G. Goldstein, T. Hinckley, R. Reanier, R. Stettler, M. Thomashow and F. Ugolini for helpful comments. This research was supported by NSF grant DP 76-23041.

Received 7 March; accepted 13 June 1980.

1. Bryson, R. A. & Hare, F. K. in *Climates of North America* Vol. II (ed. Landsberg, H. E.) (Elsevier, New York, 1974).
2. Giddings, J. L. Jr *Dendrochronology in Northern Alaska* (University of Arizona Press, Tucson, 1941).
3. Giddings, J. L. Jr *Tree Ring Bull.* **9**, 26–32 (1943).
4. Haugen, R. K. *Science* **158**, 773–775 (1967).
5. Haugen, R. K. & Brown, J. E. *Proc. 3rd Int. Conf. on Permafrost*, 393–398 (1978).
6. Stockton, C. W. & Fritts, H. C. *Wat. Res. Bull.* **9**, 1006–1027 (1973).
7. Blasing, T. J. & Fritts, H. C. in *Climate of the Arctic* (eds Weller, G. & Bowling, S. A.) 45–58 (University of Alaska Press, Fairbanks, 1975).
8. Kay, P. A. *Arctic Alp. Res.* **10**, 133–138 (1978).
9. Mikola, P. in *Tree Growth* (ed. Kozlowski, T. T.) (Ronald, New York, 1962).
10. Mitchell, J. M. Jr *Ann. N.Y. Acad. Sci.* **95**, 235–50 (1961).

11. Lamb, H. H. *Climate: Present, Past and Future* (Methuen, London, 1972).
12. LeRoy, L. E. *Times of Feast, Times of Famine* (Doubleday, New York, 1971).
13. Stokes, M. A. & Smiley, T. L. *An Introduction to Tree-Ring Dating* (University of Chicago Press, Chicago, 1968).
14. Fritts, H. C., Mosimann, J. E. & Bottorff, C. P. *Tree-Ring Bull.* **29,** 15–20 (1969).
15. Fritts, H. C. *Tree Rings and Climate* (Academic, London, 1976).
16. US Environmental Data Service. *Climatological Data: Alaska* (1977).
17. Fritts, H. C., Blasing, T. J., Hayden, B. P. & Kutzbach, J. E. *J. appl. Met.* **10,** 845–864 (1971).
18. Bamberg, S., Schwarz, W. & Tranquillini, W. *Ecology* **48,** 264–269 (1967).
19. Billings, W. D. & Mooney, H. A. *Biol. Rev.* **43,** 481–529 (1968).
20. Sakai, A. *Ecology* **51,** 657–664 (1970).
21. Tranquillini, W. in *The Water Relations of Plants* (eds Rutter, A. J. & Whithead, F. H.) 153–167 (Blackwell, London, 1963).
22. Tranquillini, W. in *Water and Plant Life: Problems and Modern Approaches* (eds Lange, O. S., Kappen, L. & Schulze, E. D.) 473–491 (Springer, Berlin, 1976).
23. Levitt, J. *Responses of Plants to Environmental Stresses* (Academic, New York, 1972).
24. Fritts, H. C., Lofgren, G. R. & Gordon, G. A. *Quat. Res.* **12,** 18–46 (1979).
25. Griggs, R. F. *Science* **85,** 251–255 (1937).
26. Haugen, R. K. *Abstr. Int. Ass. Quat. Res.* VII, 197 (1965).
27. Hustich, I. *Fennia* **82,** 1–25 (1958).
28. Dawdy, D. R. & Matalas, N. C. in *Handbook of Applied Hydrology* (ed. Chow, V. T.) 87 (McGraw-Hill, New York, 1964).

Observations of dilatancy-induced polarization anomalies and earthquake prediction

Stuart Crampin[*], Russ Evans[*], Balamir Üçer[†], Mark Doyle[*][‡], J. Peter Davis[*][§], Galia V. Yegorkina[||] & Alistair Miller[*][¶]

[*] Institute of Geological Sciences, Murchison House, West Mains Road, Edinburgh EH9 3LA, UK
[†] Kandilli Observatory, Çengelköy, Istanbul, Turkey
[‡] Department of Geophysics, University of Edinburgh, James Clerk Maxwell Building, Edinburgh EH9 3JZ, UK

Much of the search for earthquake prediction schemes has centred on the expectation that rocks in the impending source area will show dilatancy: the opening of cracks at high stress-levels. Recent developments in the theory of seismic wave propagation in cracked media[1] demonstrate that shear-wave splitting will occur in seismic-wave propagation through cracked structures, when the cracks have any overall alignment. This splitting causes polarization anomalies in the seismograms, and it has been suggested[1] that dilatancy, induced by the build-up of stress before earthquakes, might be recognized and monitored by analysis of these anomalies. We present here new observations which support this hypothesis.

The crust and upper mantle of the Earth are thoroughly permeated by cracks. Sedimentary rocks contain joints and fractures, which can lead to pronounced seismic velocity-anisotropy in shallow beds[2,3]. Igneous rocks in the crust, and possibly the crystalline upper-mantle[4], contain microcracks within grains and along grain boundaries[5]. These various cracks are essentially closed and transparent to seismic waves under high isotropic confining-pressure and low pore-pressure[4]. The primary action of non-hydrostatic stress on rock will be to modify the existing lines of weakness (cracks) in the rock, and the effects will depend on whether the cracks are initially open or closed, and on the relative confining and pore-pressures. At low ambient-stress and low pore-pressure, systems of open cracks may be differentially closed[6], and at high ambient-stress, systems of closed cracks may be differentially opened, if the pore pressure and non-lithostatic stresses are sufficiently high. The term 'dilatancy' is used here to cover both these differential processes, in addition to the usual meaning of the opening of fresh cracks under high local stress-levels. This differential opening of existing cracks may occur over substantial distances, and is probably the direct cause of many of the precursory phenomena, which are sometimes observed hundreds of kilometres from impending epicentres[7]. Laboratory experiments demonstrate that, in stressed rock-samples, existing cracks[6] and newly opened cracks[8–10] both take up pronounced alignments, and certainly all stress-induced dilatancy in the Earth will open cracks in preferred directions. Note that there is now a hypothesis that gas at high pore-pressure may exist at deep levels in seismic regions[11], so that dilatancy cracks could be gas filled even in the upper mantle.

The wavelengths of seismic waves are so much greater than the likely dimensions of any stress-induced cracks, that the velocity variations of seismic waves propagating through a dilatancy zone of aligned cracks can be modelled by propagation through purely-elastic anisotropic media[1]. Theoretical and numerical calculations demonstrate[1,12,13] that, except in a few specific symmetry-directions, anisotropy writes a characteristic signature into the polarization of the shear wavetrain. This signature is a distinctive feature of seismic waves propagating through anisotropic media and will persist for any following isotropic-segments of the path. A plane shear-wave splits on entry into a dilatancy zone into two orthogonally-polarized phases, which are not, in general, parallel to either the vertical or horizontal directions (curved wavefronts show more complicated effects). These split waves travel with different velocities, and result in the shear-wave particle-motion being resolvable into nearly-orthogonally polarized components[1,13]. The arrival of these 'split' shear-waves may be identified by abrupt changes in direction (anomalies) of the particle motion, when plotted in polarization diagrams[1]. The time delay between the phases may be estimated from suitable rotated seismograms, or more directly from polarization diagrams. This delay is proportional to the degree of differential shear-wave anisotropy, and the length of the path through the anisotropic rock, which for long paths will be the dimensions of the dilatancy zone. Consequently, the delay is not very sensitive to small errors in epicentral location or focal depth. However, it is sensitive even to quite weak crack-anisotropy[1], and seems to be a way of monitoring the whole dilatancy episode from initiation of the stress-induced cracking, through the possible influx of water[14], to the conclusion of the earthquake sequence. An example of the sensitivity is that saturation of dry cracks by water would approximately double the differential shear-wave anisotropy for about half of all directions of propagation through any given system of cracks[1]. This should be recognizable on the seismograms, and may help to resolve whether cracks are gas filled at depth in the crust, and whether the influx of water is an essential part of the source process. Thus, if they can be observed, shear-wave polarization-anomalies could lead to a better understanding of the whole earthquake source-process.

We believe that such anomalies have now been observed. For several years, delays between shear-wave arrivals on pairs of unrotated horizontal-component seismograms have been recorded[15] on arrays of three-component seismometers in seismic regions in Armenia, and Fergana, USSR. The delays were observed on between 5 and 10% of all seismograms from local and regional events at all azimuths and at distances up to 450 km. These delays were interpreted[15] as being due to shear-wave splitting caused by anisotropy directly induced by the build-up of stress before an earthquake. Recently, the magnitudes of these delays have been shown to vary before large earthquakes, and to be correlated with the directions of nearby geological faults[16]. However, we consider that anisotropy due to crack dilatancy is likely to dominate any anisotropy directly induced by stress in the Earth.

Gupta[17] probably observed similar anomalies to those of Yegorkina *et al.*[15] from several series of earthquakes in Nevada, US, at distances of >100 km from a single three-component seismic station. However, the small range of azimuths did not allow any convincing interpretation[18], and Gupta was misled

---

Present addresses: § Department of Geological & Geophysical Sciences, Princeton University, Princeton, New Jersey 08540; || Institute of Physics of the Earth, Bolshaya Grouzinskaya 10, Moscow 123810, USSR; ¶ Overseas Development Administration, Eland House, Stag Place, London SW1E 5DH, UK.

0028–0836/80/350874—04$01.00

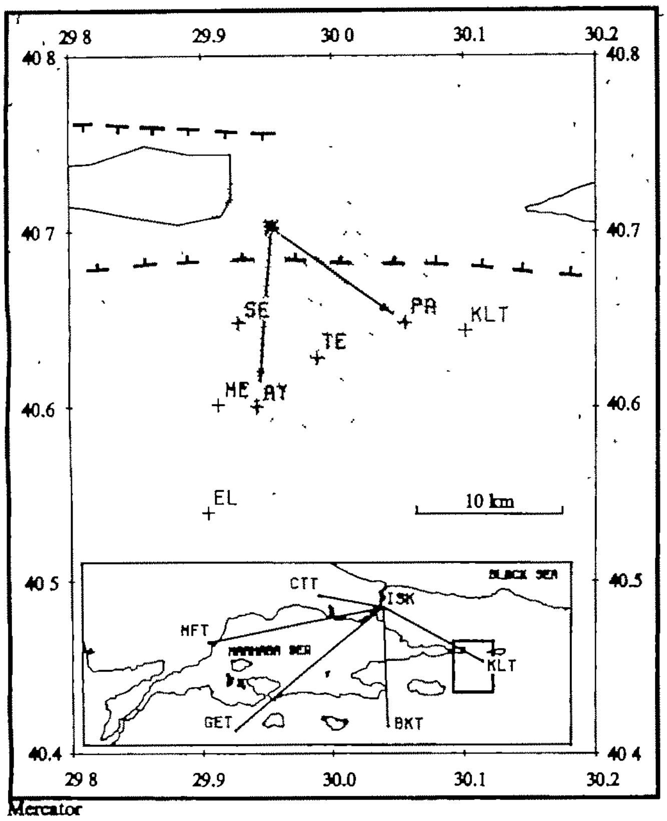

Fig. 1 Map showing the TDPNET three-component stations, with inset of MARNET stations. Most of the local earthquakes occurred within the shaded area, and the epicentre of the earthquake used for Fig. 2 is marked by an asterisk. The heavy dashed line shows the approximate lines of the Northern Anatolian Fault, which in this area appears to be a graben structure.

into seeking shear-waves split only into SV and SH components, when the seismic traces clearly did not display such polarizations. Gupta's observations will be discussed in detail elsewhere.

Similar delays have been observed on records from a small closely-spaced network in Turkey, TDPNET (Fig. 1), of three-component seismometers specifically designed to monitor polarization anomalies. A centre of low-magnitude seismic activity was identified near the Northern Anatolian Fault from MARNET records (MARNET is a radio-linked seismic network spanning the Marmara Sea, Turkey). A collaborative project between the Institute of Geological Sciences and Kandilli Observatory deployed TDPNET over the swarm activity for eight weeks during the summer of 1979. High-quality recordings were obtained from several hundred small earthquakes at epicentral distances of <20 km, and depths between 8 and 15 km. The analogue magnetic-tape records were digitized at 100 samples s^{-1}, and display impulsive P- and S-wave arrivals very suitable for polarization analysis. A few records show shear waves arriving at different times on the unrotated horizontal-seismograms from events at all azimuths, similar to the observations of Yegorkina *et al.*[15,16]. The majority, however, show shear waves arriving at the same time on both horizontal traces, and display shear-wave splitting only when plotted in polarization diagrams.

Figure 2 shows examples of both types of record from the same earthquake at different stations. The seismograms are typical of the data set: almost every shear wavetrain with sufficient signal-to-noise ratio (several hundred examples) shows shear-wave splitting in polarization diagrams, and a few show splitting in the unrotated horizontal-seismograms, as in the observations of Yegorkina *et al.* Figure 2*a* shows separate shear-wave arrivals on the two horizontal-components, despite the azimuth to the epicentre being 40° from the instrument orientations: the shear arrival on the east-west component is about 0.2 s later than the arrival on the north-south. Figure 2*b* shows shear waves arriving simultaneously on both horizontal components. Splitting is not easily identified on the original or the rotated seismograms, but is clearly visible in the horizontal projection of the polarization diagrams.

The horizontal polarizations diagrams show abrupt changes in the direction of the particle motion. We interpret these anomalies as the arrival of phases with different linear polarizations due to shear-wave splitting in propagation through anisotropic material. Any other explanation is untenable: the anomalies cannot be caused by isotropic discontinuities, because no isotropic structure can split shear waves propagating in almost all directions; and it is unlikely to be a source effect, when the sources are small and the P-wave arrivals comparatively simple. There are very few previous studies of short-period particle-motion so it is difficult to know what sort of phenomena to expect. Local and regional earthquakes that we have examined in a region of low seismicity (Scotland) have elliptical shear-motion without the characteristic abrupt turning points of the TDPNET records. Orthogonal changes in polarization are sometimes observed in local and regional events, when there is a mixture of Rayleigh and Love surface-waves present. However, this cannot account for orthogonal polarizations in the first half-second following the initial shear-arrival, particularly when the paths are direct rays with little possibility of head-wave, channel-wave, or surface-wave interactions. We consider that some form of anisotropy must be the cause of the split shear-arrivals.

We suggest that dilatancy is the only possible explanation of this anisotropy. Stress on cracked rock (all crustal rocks are heavily cracked[2-5], although many of these cracks may be initially sealed) causes the cracks to open and close anisotropically[6], and such dilatant structures are expected to cause shear-wave splitting[1]. Dilatancy is the only possible explanation of anisotropy, which can have such large, if not dominating, effects in such otherwise heterogeneous regions as Turkey and Armenia. A demonstration that the delays between the shear waves vary with time (stress) would confirm our interpretation.

Clearly, such splitting is not easy to analyse. However, some conclusions can be drawn from the existing data: many of the shear waves in the TDPNET records (Fig. 2*a*) and Armenia[15] do not split parallel to SH or SV, but into more general orientations. This supports the hypothesis that the splitting is not caused by isotropic conversions. It also suggests that the dilatancy is unlikely to consist of horizontal cracking as suggested by Wang[19], which would result in transverse isotropy and splitting only into SH or SV components.

Figure 2 shows several abrupt changes in direction of the shear-wave polarizations. These may be due to complicated local structure, but may also be due to a curved wavefront propagating through a structure with comparatively strong anisotropy. The group-velocity vector is not, in general, parallel to the phase-velocity vector in anisotropic media[12]. Consequently, the map of the positions reached by the energy of two shear-waves radiating from a point in a given time, the wave surface, may be extremely complicated, with three-dimensional cusps, ridges, and multiple points. Cusps, in particular, are very common features of shear-wave energy propagation in anything other than very weak anisotropy. Rays propagating in directions within a cusp may have four shear-wave arrivals, with different velocities, different polarizations, and wavefronts which are not parallel. The density of cracks in Earth structures is large enough to produce strong anisotropy: the only detailed field measurements of velocity anisotropy known to us[2] were interpreted[3] as due to two sets of intersecting cracks, each with crack density of the order of 0.2. The large crack densities were due to large dimensions and aspect ratios. Thus, some crack anisotropy in the Earth is strong enough to produce complicated wave-surfaces containing cusps, and this is preferred explanation for the several abrupt changes of polarization in Fig. 2.

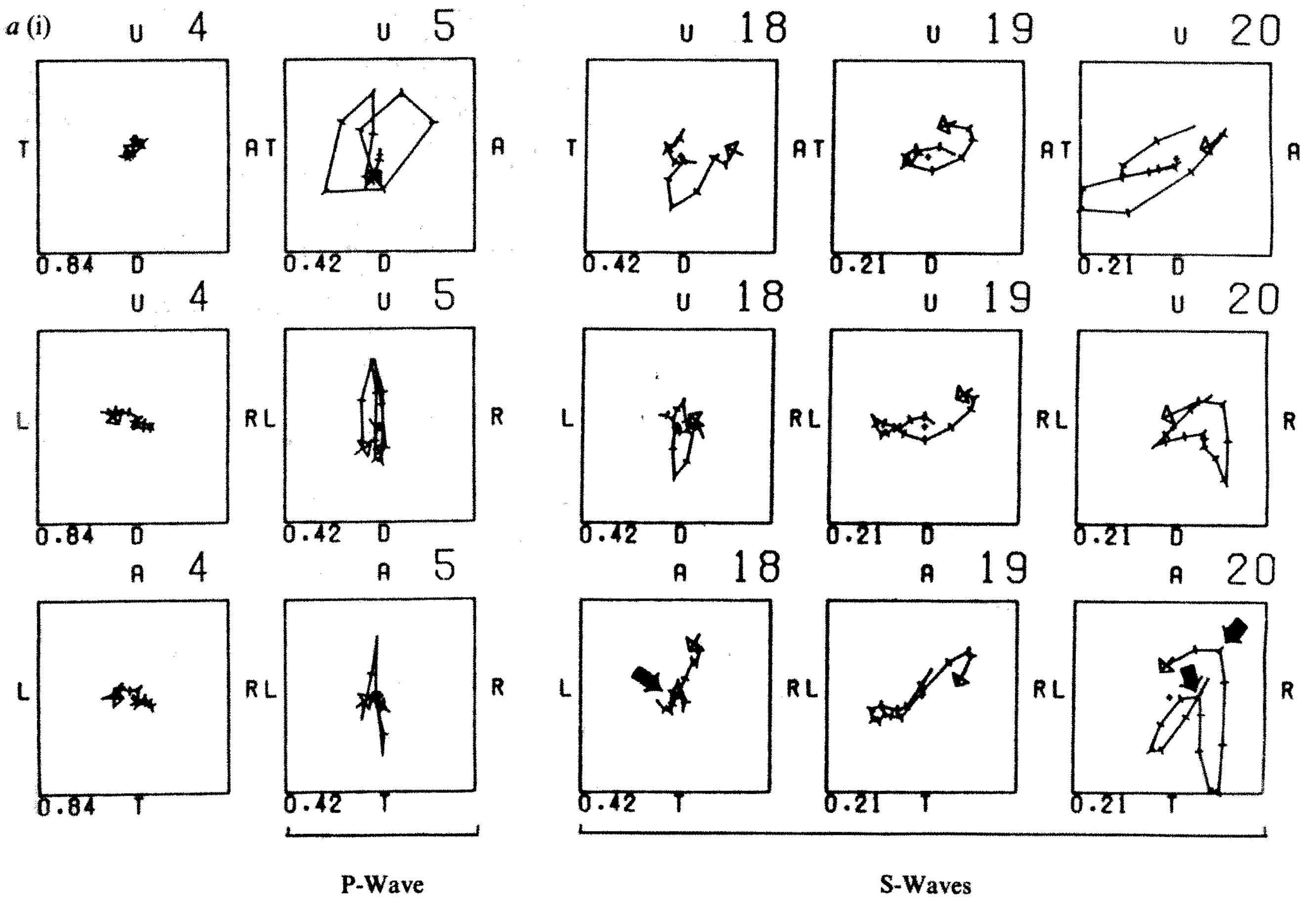

a (i)
U 4
U 5
U 18
U 19
U 20
T
AT
A
0.84 D
0.42 D
0.21 D
L
RL
R
A 4
A 5
A 18
A 19
A 20
0.84 T
0.42 T
0.21 T
P-Wave
S-Waves

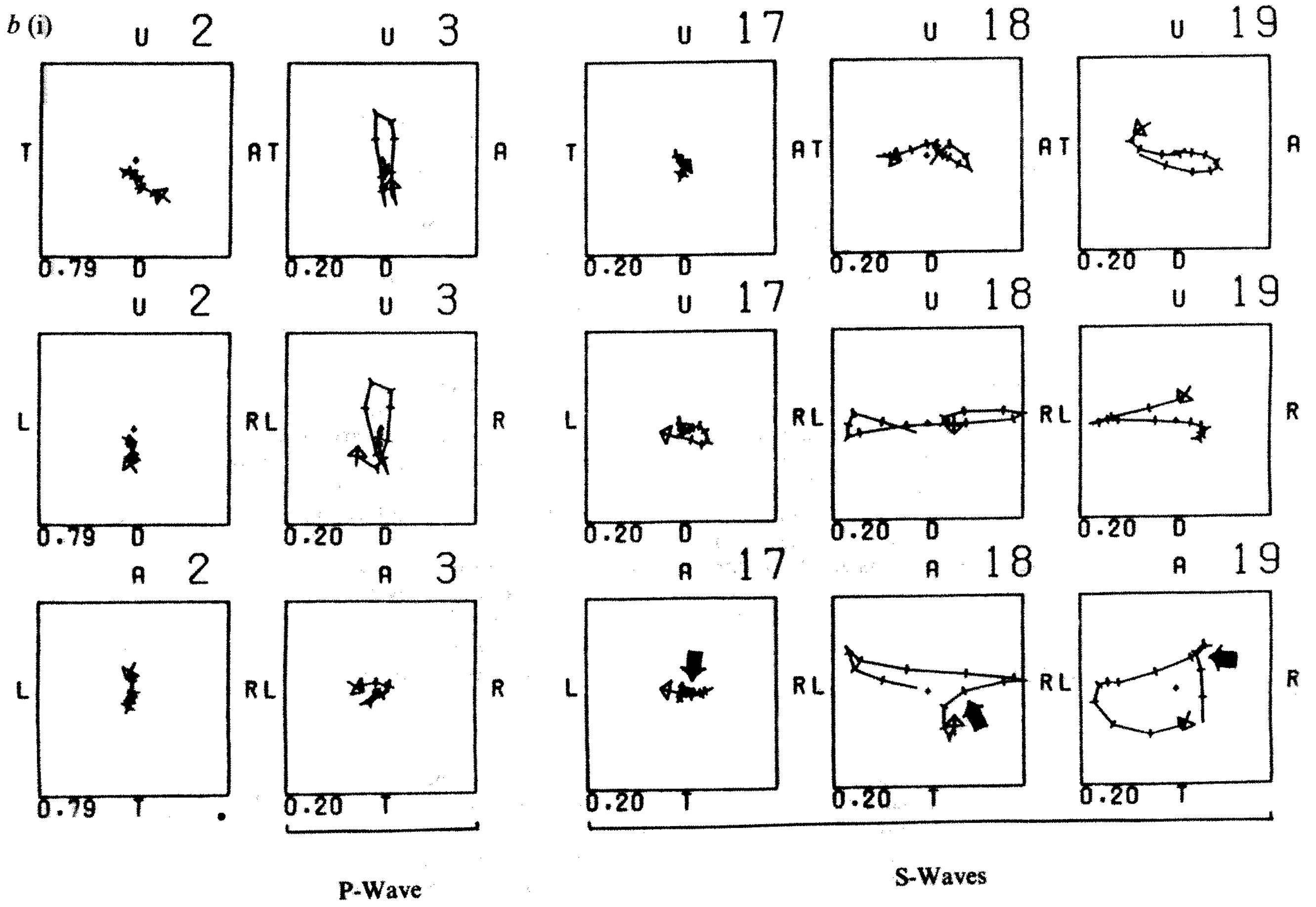

b (i)
U 2
U 3
U 17
U 18
U 19
T
AT
A
0.79 D
0.20 D
L
RL
R
A 2
A 3
A 17
A 18
A 19
0.79 T
0.20 T
P-Wave
S-Waves

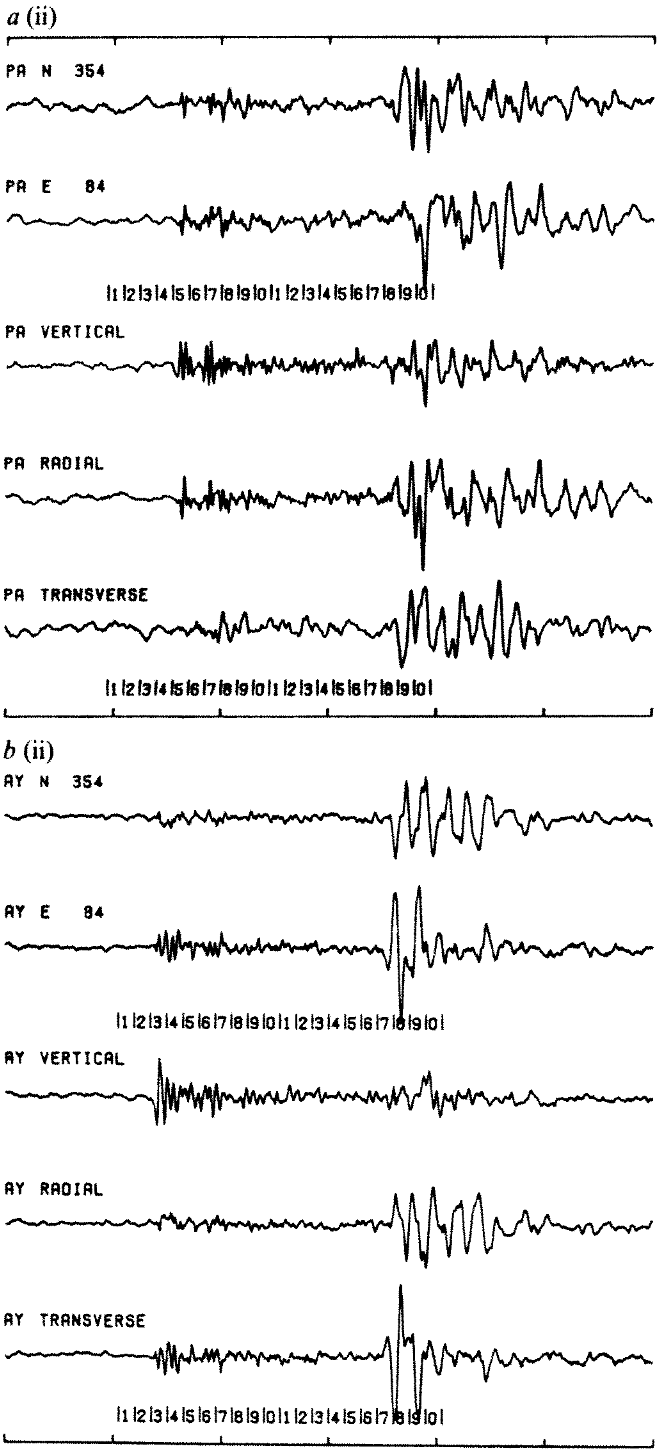

Fig. 2 Examples of seismograms and polarization diagrams for a small earthquake on 15 September 1979 with epicentre 40°42′10″ N, 29°57′13″ E, depth 13 km, and magnitude $M_L = 1.5$. The seismograms are, from the top: unrotated horizontals N 354° E and N 84° E, vertical, and rotated radial and transverse components. The numbered polarization-diagrams for P- and S-wave arrivals are the projections of the particle motion on to three orthogonal-planes for the correspondingly numbered 0.15-s time-windows marked either side of the rotated traces. Directions: U, up; D, down; T, towards; A, away from the source. L, left; R, right in the direction of the station. Each set of three diagrams has been normalized and the relative multiplication factor is marked at the bottom left of each diagram. The heavy arrows on the horizontal projection of the S waves mark the first S-wave arrival, and the subsequent arrivals of phases with different polarizations. Cross bars marked on the polarization diagrams at every 1/100 s, allow delays to be estimated. *a*, Seismograms at PA: hypocentral distance 17 km; azimuth of arrival N 305° E. *b*, Seismograms at AY: hypocentral distance 18 km; azimuth of arrival N 5° E.

Our comparatively simple hypothesis of extensive dilatancy links several previously unrelated earthquake phenomena, and seems to be present to the several seismic regions of North Anatolia, Armenia, Fergana, and possibly Nevada. Our suggestion that stress in the Earth can be monitored by examining shear wavetrains in polarization diagrams would be very important for earthquake prediction studies. All previous precursors, including V_P/V_S anomalies[1], are probably indirect effects of this dilatancy, and seem to occur unpredictably. The TDP experiment suggests that polarization anomalies may occur in almost all shear wavetrains propagating through dilatancy zones, and might be generally available for estimating changes in the Earth's stress.

We thank Dr J. C. Savage for helpful comments. This research has been supported by various organizations, but mostly by the Natural Environment Research Council and Kandilli Observatory. This letter is published with the approval of the director of the Institute of Geological Sciences.

Received 16 May; accepted 2 July 1980.

1. Crampin, S. *Geophys. J. R. astr. Soc.* **53,** 467–496 (1978).
2. Bamford, D. & Nunn, K. R. *Geophys. Prosp.* **27,** 322–338 (1979).
3. Crampin, S., McGonigle, R. & Bamford, D. *Geophysics* **45,** 345–360 (1980).
4. Brace, W. F. *Flow and Fracture in Rocks* (eds Heard, H. C., Borg, I. Y., Carter, N. L. & Raleigh, C. B.) (*Geophys. Monogr.*, 16, AGU, Washington, 1972).
5. Simmons, G. & Richter, D. *Physics and Chemistry of Minerals and Rocks*, 105–137 (ed. Strens, R. G. J.) (Wiley, New York, 1976).
6. Nur, A. & Simmons, G. *J. geophys. Res.* **74,** 6667–6674 (1969).
7. Dobrovolsky, I. P., Zubkov, S. I. & Miachkin, V. I. *Pure appl. Geophys.* **117,** 1025–1044 (1979).
8. Brace, W. F., Paulding, B. W. & Scholz, C. *J. geophys. Res.* **71,** 3939–3953 (1966).
9. Gupta, I. N. *Bull. seism. Soc. Am.* **63,** 1157–1161 (1973).
10. Hadley, K. *J. geophys. Res.* **80,** 4845–4850 (1975).
11. Gold, T. *J. petrol. Geol.* **1,** 3–19 (1979).
12. Crampin, S. *Geophys. J. R. astr. Soc.* **49,** 9–27 (1977).
13. Keith, C. M. & Crampin, S. *Geophys. J. R. astr. Soc.* **49,** 181–243 (1977).
14. Myachkin, V. I., Brace, W. F., Sobolev, G. A. & Dieterich, J. H. *Pure appl. Geophys.* **113,** 169–181 (1975).
15. Yegorkina, G. V., Rakitov, V. A., Garetovskaya, I. V. & Yegorova, L. M. *Izv. Akad. Nauk. SSSR*, *Fiz. Zemli*, *No. 8*, 43–55 (in Russian), 554–562 (English edition) (1977).
16. Volvovsky, I. S., Egorkina, G. V. & Popov, E. A. *Pap. Workshop on Modern Methods of Registration and Interpretation of Seismic Observations*, Yalta (1979).
17. Gupta, I. N. *Science* **182,** 1129–1132 (1973); *Bull. seis. Soc. Am.*, **64,** 1997–2001 (1974); **65,** 425–437 (1975).
18. Ryall, A. & Savage, W. U. *Bull. seism. Soc. Am.* **64,** 1943–1951 (1974).
19. Wang, C.-Y. *Nature* **251,** 405–406 (1974).

Tritium in the deep North Atlantic Ocean

William J. Jenkins & Peter B. Rhines

Woods Hole Oceanographic Institution, Woods Hole,
Massachusetts 02543

A distinct core of tritium (from nuclear weapons testing in the atmosphere) marks the southward flowing jet of the deep western boundary current of the North Atlantic circulation at 30 °N latitude. The concentrations, of the order of 0.5–1.0 TU (1 tritium unit = 1 ^{3}H atom per 10 ^{8}H atoms), indicate a roughly 10-fold dilution of source waters in the far north. This thin jet, 50 km in width, carries water into subtropical regions which, until recently, were free of anthropogenic tritium. It underlies the more extensive distributions of tritium found in more rapidly renewed waters above the permanent thermocline.

The deep waters of the world's oceans have descended from the sea surface in a very few regions of the far northern and southern Atlantic. Stable density stratification constrains the actual sinking processes to be locally intense and variable, but the great mass of deep ocean is such that the replenishment process proceeds on a time scale of centuries. This planetary-scale thermohaline convection thus provides a long time-constant for many aspects of the ocean–atmosphere system.

Both climatic change and the dispersal of pollutants and trace chemicals in the biosphere are influenced by the slow overturning of the sea.

Observations[1-5] (Fig. 1*a*) and theory[6-7] suggest that the deep and abyssal flow proceeds initially equatorwards, away from the sources of sinking water, along concentrated paths lying near western continental or topographic boundaries. A complementary poleward and upward circulation occurs, apparently, as a broad, weak flow in the interior of the ocean basins. The combination of this circulation with turbulent exchange between boundary current and interior establishes the large-scale gradients of chemical properties, such as the saline tongue[8] in Fig. 1*a*. The flow at this temperature horizon (1.9 °C) is traceable to both Arctic and Antarctic sinking regions.

The decisive influence of boundary currents on the global distributions of trace material has motivated an observational programme, described elsewhere[9], at a site where the deep boundary current is particularly well defined, Fig. 1*b*. In this programme current meters, CTD profilers, XBT probes and, by chance, visitation, drifting surface- and deep floats were used to examine the core of the current, and its relationship with the basin-wide circulation.

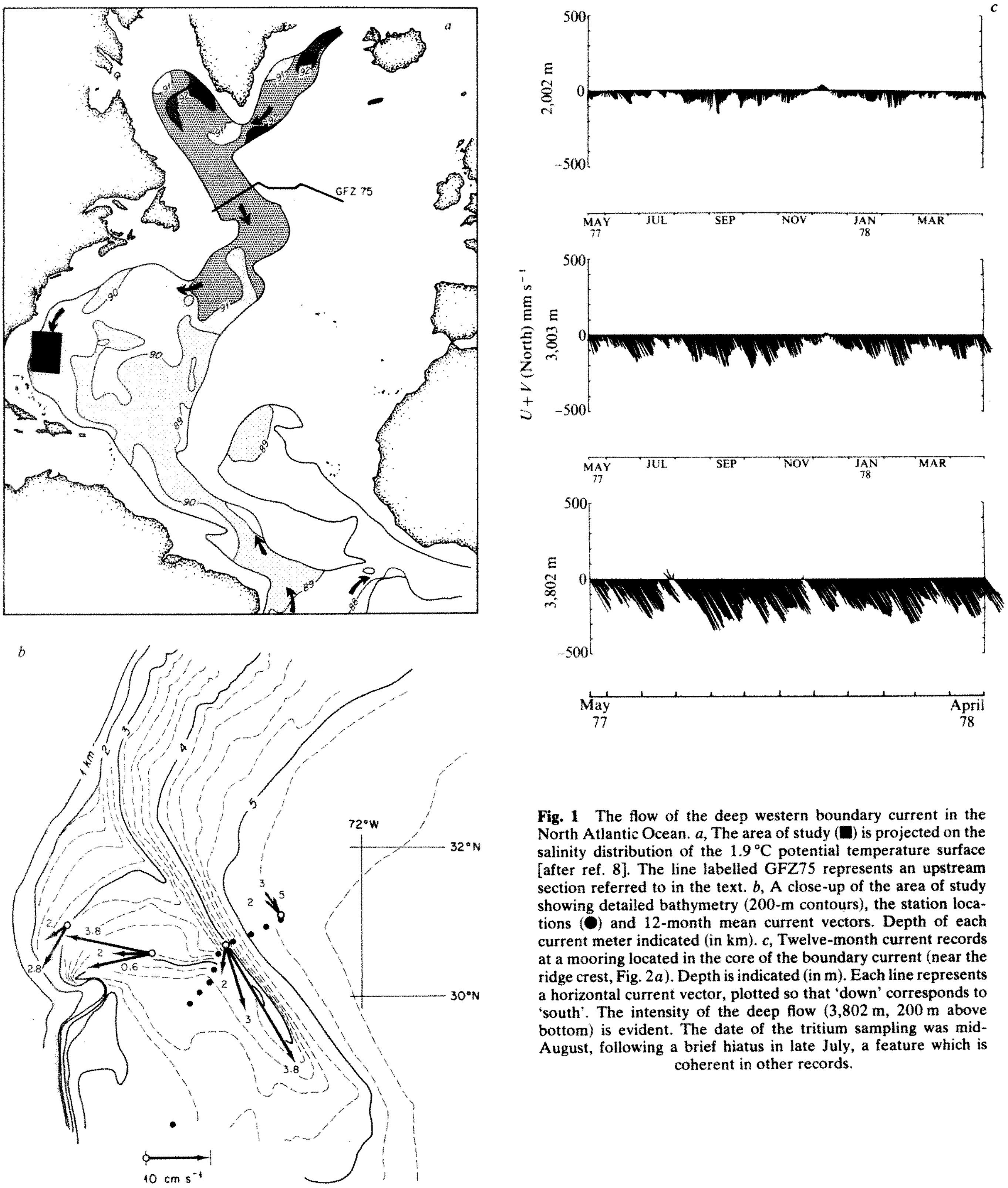

Fig. 1 The flow of the deep western boundary current in the North Atlantic Ocean. *a*, The area of study (■) is projected on the salinity distribution of the 1.9 °C potential temperature surface [after ref. 8]. The line labelled GFZ75 represents an upstream section referred to in the text. *b*, A close-up of the area of study showing detailed bathymetry (200-m contours), the station locations (●) and 12-month mean current vectors. Depth of each current meter indicated (in km). *c*, Twelve-month current records at a mooring located in the core of the boundary current (near the ridge crest, Fig. 2*a*). Depth is indicated (in m). Each line represents a horizontal current vector, plotted so that 'down' corresponds to 'south'. The intensity of the deep flow (3,802 m, 200 m above bottom) is evident. The date of the tritium sampling was mid-August, following a brief hiatus in late July, a feature which is coherent in other records.

As a part of the geochemical programme, 280 samples were taken for tritium analysis. Being part of the water molecule, tritium represents an ideally passive tracer. There are no known chemical or biological processes in the deep sea that alter or scavenge it. Tritium has well-defined but time-dependent boundary conditions and its lifetime (12.26 yr half life) is comparable to the circulation time scale of the western deep North Atlantic. Unlike the relatively steady-state nature of other geochemicals, the natural inventory of tritium has been dwarfed by massive production by recent nuclear weapons testing[10]. This tritium 'spike' entered the surface oceans primarily at high northern latitudes[11,12] in the form of tritiated water. Natural surface water tritium concentrations were about 0.2 TU. Present subtropical surface water concentrations are of the order of 5 TU, and were higher than this in 1964–65, soon after the peak in weapons testing. Östlund *et al.*[13] reported tritium measurements from the 1972 GEOSECS expedition which clearly showed the sinking and southward penetration of tritium. South of 40 °N, however, the North Atlantic GEOSECS track left the western boundary, and no further abyssal tritium was apparently recorded. At shallower depths other studies have documented the downward penetration of tritium into the main thermocline[14,15].

In the present experiment we sought to determine how much water flows equatorwards at the mid-latitude western boundary, and how much of this water is of far-northern origin. The observations were sited near the Blake–Bahama Outer Ridge at 30 °N latitude. This prominent sedimentary ridge acts as the western boundary of the ocean at levels deeper than ~3,500 m. The 12-month average currents seen at four moorings show clearly the boundary current winding along contours of constant depth (Fig. 1*b*). The easternmost mooring exhibits a weak flow counter to the jet (northwestward), thus establishing the width of the jet at ~50 km.

A sample current record[9] (Fig. 1*c*) shows the increase in intensity of the jet with depth, on the eastern flank of the ridge. Despite surges of 40 cm s^{-1} and occasional periods with no southward flow, the mean velocity, 21 cm s^{-1}, is quite representative. The time of tritium sampling, 4–8 August 1977, occurred shortly after a hiatus, but is characterized by velocity typical of mean conditions.

Samples were taken using a 24-bottle, 1.2-l Niskin rosette sampler mounted on the CTD frame. The samples were transferred to GEOSECS-type clamped copper tubes[16]. Tritium was determined by the ^{3}He regrowth technique[17] to an accuracy of 1.5% and a detection limit of 0.04 TU.

The deep western boundary current is distinctly outlined by a high concentration of tritium, Fig. 2*a*. The core overlies the ridge at ~4 km depth. Tritium levels decrease dramatically both above and to the east of the jet, but with some evidence of activity in the westernmost part of the section. The potential isotherms (dashed) superimposed on Fig. 2 are banked up on both sides of the ridge, consistent with the strong southward flow on the eastern side, and northward flow on the western side.

The most intense (highest tritium level) part of the core is noticeably smaller than the region of banked isotherms. The tritium isopleths extend over the ridge-crest, more or less along potential isotherms. If this were an ideal flow directly parallel to the depth contours, the currents on the western and eastern sides of the crest would be effectively 400 km apart, in the downstream sense. The continuity of the tritium core, however, suggests that some cross-ridge flow is taking place. This flow is verified both in current-meter and drifting float data (note the veering with depth of the mean current vectors, Fig. 1*b*). The eastward turn in the depth contours is apparently too sharp to be negotiated by the jet, which rides over the crest.

The tritium data are plotted against potential temperature in Fig. 2*b*. For reference we have also plotted the mean data for the *Panulirus* station off Bermuda (32° N, 64.5° W)[15], and for a section across 53° N[18]. This section is labelled GFZ-75 on Fig. 1*a*. The *Panulirus* data were taken at essentially the same time as the present section, whereas the 53° N section occurred 2 yr

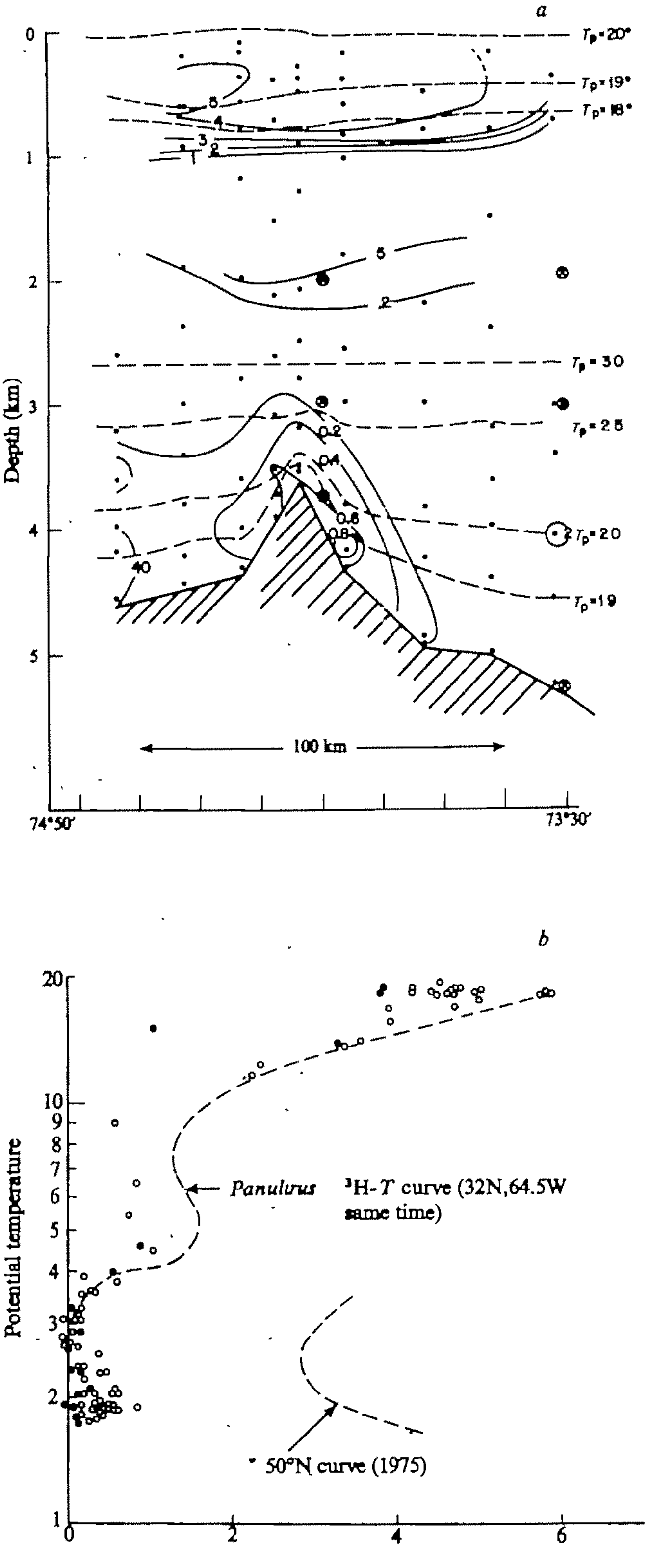

Fig. 2 The tritium results for the section. *a*, The tritium isopleths (solid lines) for the undercurrent hug the ridge, and extend over the ridge in a manner parallel to the isotherms (dashed lines). The far-northern water, marked in this way, occupies only a small part of the broader southward flow at this time. Note also the westward enhancement of the shallow (350 m) tritium maximum, and the associated thermal structure (that is, the dip in the 18 and 19 °C isotherms). ⊗, Current meter positions. *b*, The temperature–tritium relation for the stations. ●, Stations outside of the current; ○, corresponds to undercurrent stations. For comparison, the T_P–^{3}H curves for a central Sargasso Sea station (*Panulirus*) and an upstream section (see Fig. 1*a*) are shown.

earlier. The principal source for the deepest levels is the Denmark Strait overflow of waters from the Greenland–Norwegian Sea, with lesser contributions from the Iceland–Scotland overflow farther to the east. If the far northern section indeed represents the upstream boundary conditions for the deep flow at the Blake–Bahama Outer Ridge, then we are observing an effective dilution of those waters by a factor of 5–10.

Above the tritium core the concentrations decrease essentially to zero at $\sim$2.8 °C or 3,000 m depth (0.01 ± 0.03 TU, seven analyses). It is remarkable that this zero layer occurs at these temperatures, for a persistent southward flow is observed at 2,000 m and below (Fig. 1*b*), and the penetration of North Atlantic Deep Water at these levels throughout the world ocean requires southward transport at this latitude. At the time of this section, the water in the 'zero layer' had apparently been entrained from subtropical mid-ocean, rather than having flowed simply from the far north. SOFAR float data of Rossby exhibit several chance occurrences of this kind of entrainment at 1,900 m depth. An upper limit to the amount of 'northern component water' at this depth is found by comparing the <0.07 TU (95% confidence limit) in this water with the >2 TU found in the corresponding source waters, giving a maximum contribution of a few per cent. The dynamics of the mean circulation changes greatly with depth, as shown by this cut-off of tritium. The role of mesoscale eddies may be important, both in determining the time-mean circulation[19] and in causing sampling problems in sections like this one.

Above the 'zero layer', at temperature >3.4 °C, the tritium increases to a slight maximum in the range 4–6 °C. This feature corresponds closely to the feature observed in the *Panulirus* data[15], but it is less intense. The two data sets merge below this maximum (3–4 °C) and also within the main thermocline (10–15 °C). In the upper thermocline the mean gyre is larger in extent, and eddy stirring more intense, than in the deep water. One expects tritium to be more broadly distributed, therefore, at upper levels, just as Fig. 2*b* suggests. Above 18 °C the present data tend to drop to lower tritium concentrations. The subsurface maximum is evidence of southward penetration of freshly ventilated 18°-water away from its formation region, just south of the Gulf Stream. A westward tritium enhancement can be seen in section in Fig. 2*a*, at a depth of 300–500 m. Analysis of the current meters and XBT data[9] associates this upper pattern with a particularly large, energetic, anti-cyclonic eddy of the 18°-water. It may be that upper-level Gulf Stream rings and other thermocline eddies carry distinct tritium markings.

The detection of a substantial tritium signal in the core of the deep western boundary current at 30 °N establishes a transit time of $\leqslant 15$ yr for water from the far northern ocean surface, with from 5- to 10-fold dilution. The transit time along the deep western boundary, itself, would require only of the order of 2 yr, at speeds of the order of $10\ \mathrm{cm\ s^{-1}}$. Abyssal tritium has not, to our knowledge, been seen before equatorwards of the polar front. Because of the eddy mixing and eddy-induced deep circulation, particularly that beneath the Gulf Stream, we could not be certain that the core of northern water would occur in the boundary current. In fact, a neighbouring section, 150 km to the south, showed far weaker anomolies of dissolved silicate, implying that other markers of northern origin like tritium would, in that instance, be weak as well. Conversely, we expect tritium to appear intermittently outside of the boundary current, in mid-ocean (although none was reported at this latitude, at 50° W longitude, in the GEOSECS section[13]).

The strong differences in eddy stirring, mixing, and mean circulation, from one depth to the next, are mirrored in the tritium concentration. Further sampling may help to establish the broader patterns of penetration across the Gulf Stream front. The results reported here underline the value of combining a variety of measurement techniques (current meters, XBT and CTD transects, floats and standard geochemistry) with radiochemical measurements. It would be of great import to problems in deep-water circulation and to the related problems in climatology (through oceanic heat-flux), atmospheric chemistry and dynamics, to obtain more such data before the tritium transient expires.

This work was performed under the auspices of contract N00014-76-C-0197, NR 083-400 with the Office of Naval Research and grant nos OCE 76-81774 and OCE 76-81190 from the NSF. Contribution no. 4439 from the Woods Hole Oceanographic Institution.

Received 14 January; accepted 26 June 1980.

1. Warren, B. A. & Voorhis, A. D. *Nature* **228,** 849 (1970).
2. Swallow, J. C. & Worthington, L. V. *Nature* **179,** 1183–1184 (1957).
3. Wüst, G. *Deep-Sea Res.* Suppl. **3,** 373–397 (1955).
4. Reid, J., Stommel, H., Stroup, E. D. & Warren, B. A. *Nature* **217,** 937 (1968).
5. Amos, A. F., Gordon, A. L. & Schneider, E. D. *Deep-Sea Res.* **18,** 145–165 (1971).
6. Stommel, H. & Arons, A. B. *Deep-Sea Res.* **6,** 217–233 (1960).
7. Stommel, H. *Deep-Sea Res.* **5,** 80–82 (1958).
8. Worthington, L. V. & Wright, W. R. *Woods Hole Oceanographic Institution Atlas Ser.* **2** (1970).
9. Mills, C. A. & Rhines, P. B. *Woods Hole Oceanographic Institution Technical Rep. WHOI-79-85* (1979).
10. Eriksson, E. *Tellus* **17,** 118–125 (1965).
11. Dreisigacker, E. & Roether, W. *Earth planet. Sci. Lett.* **38,** 301–321 (1978).
12. Weiss, W. M. & Roether, W. *Earth planet. Sci. Lett.* (submitted).
13. Ostlund, H. G., Dorsey, H. G. & Rooth, C. G. *Earth planet. Sci. Lett.* **23,** 69–73 (1974).
14. Rooth, C. G. & Ostlund, H. G. *Deep-Sea Res.* **19,** 481–492 (1972).
15. Jenkins, W. J. *J. mar. Res.* **38,** 3 (in the press).
16. Jenkins, W. J. & Clarke, W. B. *Deep-Sea Res.* **23,** 481–494 (1976).
17. Clarke, W. B., Jenkins, W. J. & Top, Z. *Int. J. appl. Rad. Isotopes* **27,** 515–522 (1976).
18. Clark, W. B., Top, Z. & Jenkins, W. J. (in preparation).
19. Rhines, P. B. & Holland, W. R. *Dynamics Atmos. Oceans* **3,** 289–325 (1979).

New constraint on the maintenance of Mn nodules at the sediment surface

David Z. Piper & Bradford Fowler
US Geological Survey, Menlo Park, California 94025

Investigations into the association of manganese nodules with pelagic sediment in many areas of the deep ocean have mainly considered either (1) the source of metals in nodules, or (2) the occurrence of nodules predominantly at the sediment surface. The second problem is duscussed here. The mechanisms previously proposed have failed to consider that nodules retain their orientation at the sediment surface for several hundred-thousand years, during which time several tens of centimetres of sediment are fluxed down beneath them. Although we have no conclusive evidence, we consider the most plausible explanation for the surface occurrence of nodules to be bioturbation by infauna.

Approximately half of all nodules occurring in the upper few metres of pelagic sediment are at the sediment surface[1,2]. Radiometric and non-radiometric techniques[3–5] require that these nodules accrete at a rate of ~ 1–$10\ \mathrm{mm\ Myr^{-1}}$. The fine-grained fraction of sediment on which nodules rest, consisting mostly of lithogenic debris and biogenic SiO_2 and CaO_3, accumulates[5] at a rate of ~ 1–$10\ \mathrm{mm\ kyr^{-1}}$. Why then are nodules not buried by this 'avalanche' of fine-grained sediment?

Nodules, usually spherical to discoidal, have a diameter between $\sim$5 and 100 mm, but average[7] about 30 mm. Assuming an approximate growth rate of $5\ \mathrm{mm\ Myr^{-1}}$, which is independent of size[8], nodule ages are of the order of 1–10 Myr. In most areas, the surface sediment on which they rest is still accumulating. What is the mechanism which redistributes the continuously accumulating fine-grained fraction of sediment beneath nodules? In some exceptional areas, however, nodules rest on ancient sediment[9] where erosion may currently be occurring.

Because nodules are denser than the underlying sediment, this suggests that nodules should sink through the upper layer of unconsolidated clays, which consist[10] of 80%, or more, interstitial water. Hypotheses explaining the surface occurrence of nodules have been coupled with explanations of how nodules

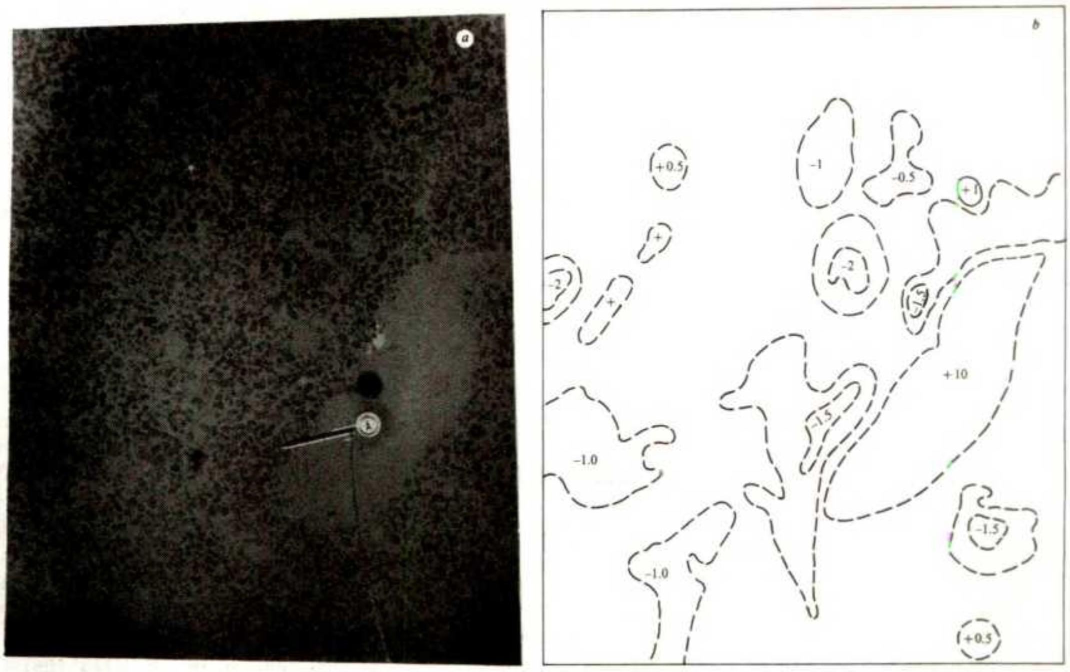

Fig. 1 *a*, Bottom photograph taken at 126°05′ W, 15°08′ N, 4,520 m depth. *b*, Relief map of the sea floor. The numbers in the enclosed contours give the approximate elevation (+) and depth (−) of these areas from the intervening area. The compass face is 7.5 cm in diameter. The compass is approximately 1 m above the bottom. Nodule coverage is often greatest in depressions; see, for example, the 2-cm depression north of the compass vane. The south-facing slope of this depression has low nodule coverage, suggesting that nodules have moved down slope into the depression. The area immediately surrounding the 10–cm mound has a nodule coverage similar to the rest of the area, suggesting that nodules have not been moved laterally during its construction.

are pushed up against this apparent tendency to sink. This approach requires active means of moving nodules upwards. There are several objections to these active mechanisms of keeping nodules on top of the sediment, but first we consider density.

According to Archimedes' principle, an object wholly or partially immersed in a fluid floats if its density is less and sinks if its density is greater than the fluid density. As the wet densities of nodules and sediment are ~2.4 and 1.3 g cm^{-3} respectively, why do nodules not sink through the upper layer of sediment? This layer, consisting of the most recently fallen sediment, is unconsolidated.

Vane shear measurements show that this sediment layer has solid- as well as fluid-like properties. Comparing these measurements with calculated loads exerted by nodules indicates that the sediment strength is much greater than that required to support surface nodules. Measurements have been made on box cores from the three Domes areas in the equatorial North Pacific[10]. Only the heaviest nodules and weakest sediment were considered. At a depth of 7 cm, the sediment has a strength 40–170-fold greater than that required to support surface nodules (Table 1). Shear strength measurements on the upper few centimetres of sediment are rare but they suggest a decrease towards the surface of ~75%. However, in the upper 7 cm of sediment, where nodules are most abundant, the critical load, the total load that sediment is capable of supporting before its failure, is six times greater than the measured shear strength, owing to the shear pattern developed during failure[11]. Thus, once nodules are positioned at the surface, the sediment strength is more than adequate to support them, that is, to prevent their sinking.

Table 1 Comparison of sediment shear strength at a depth of 7 cm in five box cores* and the load exerted by the largest nodules within each box core.

Dome cores station-box core[7]	Nodule load (p.s.i.)	Sediment strength (p.s.i.)
47–12	0.012	2.04
50–30	0.013	0.92
49–25	0.016	1.00
50–32	0.017	0.72
57–57	0.010	0.73

* The cores were collected in the equatorial North Pacific at the three Domes sites. See ref. 10 for exact locations and depths.

Previous explanations of the sea floor occurrence of nodules can be divided into two groups of mechanisms, physical and biological. The physical group considers that nodules are picked up and/or rolled over by bottom currents[12], or maintained at the surface by seismic activity[13]. Glasby[12] considered the force that bottom currents might apply to a nodule and found that it is comparable with the force necessary to maintain a nodule at the surface. However, it is not clear how a horizontally moving bottom current could move a partially buried nodule in a vertical direction without also suspending a quantity of fine sediment, which, on redeposition, would bury the nodules deeply. There are two other arguments against this mechanism.

First, if currents are responsible for rolling nodules over, large nodules are more likely to be buried than small nodules. Heath[8] has shown, however, that burial of nodules is independent of nodule size. Second, nodules retain the same orientation in the sediment for several 100,000 yr. According to Glasby, development of the different surface textures observed on the top and the bottom of nodules requires ~2.5×10^5 yr. Radiometric analysis of nodule tops and bottoms[14,15] also requires that nodules maintained a single orientation for $0.5–5\times10^5$ yr. Polynucleated nodules are frequently recovered from the sea floor. If 0.5 mm of concretion is needed to hold two nodules together, several 100,000 yr are required during which the two nodules could not have moved with respect to each other. Thus nodules are thought to turn over no more often than every 250,000–500,000 yr. The amount of sediment accumulating during this time in most nodule areas is several tens of centimetres, enough to bury nodules deeply. Thus, any dynamic process that turns nodules over cannot maintain them at the surface.

The possible effect of seismic activity[13] cannot be discounted, but nodules occur[16] in oceans in some of the World's most seismically quiet areas[17].

The role that organisms might have has been variously discussed. Menard[18] has examined bottom photographs which show organisms partially protruding from under nodule edges. He suggested that these organisms may be pushing nodules up. It has been suggested[19,24] that organisms may maintain nodules at the surface by rolling them over. This mechanism has the same difficulties as any dynamic process. Epifaunal organisms may remove sediment from nodule tops, possibly as part of their feeding activity[20]. This activity may keep the nodules free of sediment temporarily but it does not contribute to the down fluxing of sediment beneath nodules. In the absence of sediment down fluxing, the sea floor would soon develop a waffle-like pattern, with a nodule occupying the depression. No such evidence has been found in hundreds of stereophotographs taken of the seafloor in the equatorial North Pacific. Instead, sediment in internodule areas is lower than the nodule tops.

Bottom photographs indicate that organisms actually bury nodules. In many bottom photographs that show a nodule coverage of 25%, areas barren of nodules often correspond to mounds. These mounds, either circular or elongate, in plan view and a few centimetres high, often have a small caldera at the top. Mounds of this type are never surrounded by nodule concentration significantly different from that observed throughout the photograph (Fig. 1*a*). Clearly these mounds are constructed by infauna that excavate sediment from beneath and pile it on top of the nodules. This mechanism may allow nodules to drift downward, and become buried. It would also allow nodules to turn, or rotate, during any downward plunge of a few centimetres, provided that undermining was not laterally uniform.

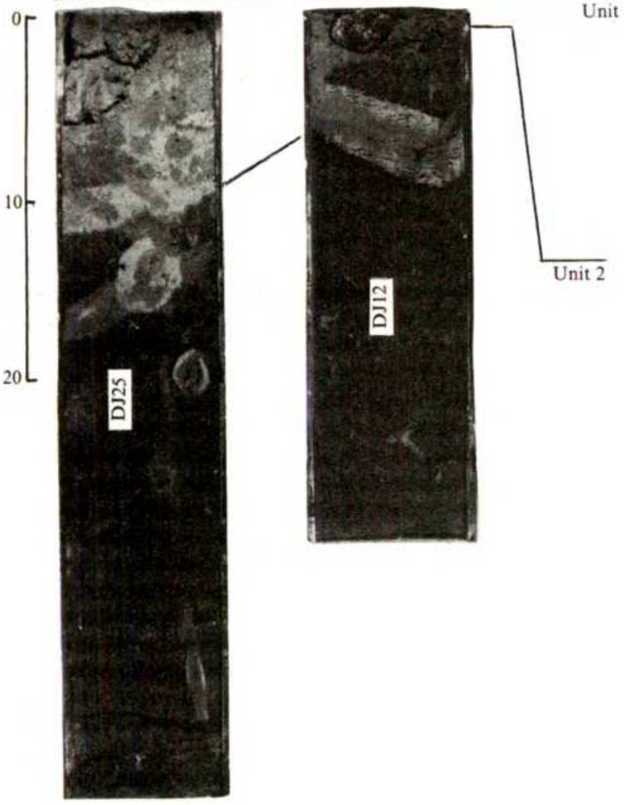

Fig. 2 Subcores from box cores DJ-25 and -12 at Domes Site A, 8°27′ N, 150°47′ W, ~5,200 m. Intersecting burrows are present in DJ-25 at a depth of 10 cm and 14 cm. The nodule in DJ-12 rests on ~0.2 cm of light-coloured surface sediment, which also fills the large burrow at 6 cm depth. Scale, 20 cm. *Unit 1*: 0.2–10 cm thick; strongly mottled; greyish-orange and pale yellowish-brown; 95% Quaternary radiolaria; surface nodules have granular texture and 2–10 cm diameter. *Unit 2*: Greyish-brown mottling with surface sediment; dominantly Miocene–Eocene radiolaria with <1–5% Quaternary radiolaria.

These mounds are superimposed on a sea floor topography consisting of ridges and depressions which have a relief of ~5 cm. These depressions, 15–25 cm across and having a relatively high nodule coverage, are usually surrounded by a ridge which slopes more steeply into than away from the depression. The steeper slope often has a relatively low nodule coverage, suggesting that nodules have drifted down slope into the depression.

How do nodules remain unburied at the sediment surface without reorientation for up to 500,000 yr and how does sediment end up beneath a relatively motionless nodule? The mechanism must transport sediment beneath the nodule at a rate fast enough to overcome sedimentation of new material as well as to overcome the activity of mound-building organisms. Bioturbation might provide the appropriate downward sediment flux which leaves the nodules exposed and undisturbed.

Bioturbation by infauna can transport sediment with two possible effects. (1) Organisms can excavate a volume of sediment at depth and fill in with an equal volume of sediment. The fill material may or may not be more compacted than the original sediment. It will probably contain a fraction of recently deposited surface sediment as this sediment should contain the greatest percentage of labile organic matter. Replacement by more compacted sediment produces a net downward flux but does not lift the sea floor. (2) Organisms can wedge through the subsurface sediment and fill in with some fraction of the uppermost surface material. This option results in lifting of the sea floor, that is, nodules and the surface veneer of sediment. At a depth as great as several millimetres below the nodules, wedging and filling might well leave surface nodules undisturbed.

Bioturbation and downfluxing of sediment through internodule areas are strongly supported by mottling (Fig. 2) and by the frequent occurrence of mixed fauna in the uppermost few tens of centimetres of sediment. Quaternary species decrease in relative abundance with depth in the sediment. Quaternary plankton often are mixed with those of Tertiary age, and the Quaternary species decrease in relative abundance with depth in the sediment[21]. Examination of 25 box cores taken at the three Domes sites supports excavation, however, as opposed to wedging. In three cores where cross-cutting burrows are well preserved (Fig. 2), the older burrow seems to be undeformed by the younger burrow.

For manganese nodules to remain at the surface of the sea floor, sediment must be transported and redistributed beneath them in a way that does not allow the nodule to move with respect to its immediate surroundings. Several tens of centimetres of sediment must be fluxed downward through internodule areas, during which time the orientation of the nodule is not changed. Active mechanisms, which require rotation of the nodules, cannot account for their occurrence at the surface of the sea floor. Wedging through the sediment by infauna such as annelid worms and pelecypods—organisms common to the abyssal environment[22]—and infilling with surface material could provide the mechanism. This type of activity within the pelagic environment, may account for the occurrence of ridges and depressions, which have a relief of a few centimetres (Fig. 1b). Wedging by earthworms has been documented by Darwin[23], but this mechanism for the deep ocean is supported more by default of other processes than by observations.

We thank J. Bischoff and H. Cook for constructive comments and the Domes office of NOAA for its support.

Received 24 April; accepted 3 July 1980.

1. Cronan, D. S. & Tooms, J. S. *Deep Sea Res.* **14,** 117 (1967).
2. Menard, H. W. & Shipek, C. J. *Nature* **182,** 1156 (1958).
3. Ku, T. L. *Marine Manganese Deposits* (ed. Glasby, G. P.) (Elsevier, Amsterdam, 1977).
4. MacDougall, J. D. in *Marine Geology and Oceanography of the Pacific Manganese Nodule Province* (eds. Bischoff, J. L. & Piper, D. Z.) 775 (Plenum, New York, 1979).

5. Kvenvolden, K. A. & Blunt, D. J. in *Marine Geology and Oceanography of the Pacific Manganese Nodule Province* (eds Bischoff, J. L. & Piper, D. Z.) 763 (Plenum, New York, 1979).
6. Ku, T. L., Broecker, W. S. & Opdyke, N. *Earth planet. Sci. Lett.* **4,** 1.
7. Mero, J. L. *The Mineral Resources of the Sea* (Elsevier, Amsterdam, 1965).
8. Heath, G. R. *Science* **205,** 904 (1979).
9. Payne, R. R. & Conolly, J. R. *Ferromanganese Deposits on the Ocean Foor* (ed. Horn, D. R.) 81 (IDOE-NSF, Washington DC, 1972).
10. Simpson, F., Wallin, C. S., Crawford, H. M. & Springer, P. C. *Deep Ocean Environmental Study: Geology and Geochemistry of DOMES Sites A, B, and C* (ed. Piper, D. Z.) 351 (USGS Open-file Rep. 77–778, 1977).
11. Terzaghi, K. *Soil Mechanics in Engineering Practice*, 219–224 (Wiley, New York, 1967).
12. Glasby, G. P. *N.Z. J. Sci.* **20,** 187 (1977).
13. Olausson, E. & Unsitalo, S. *Bull. Commn. geol. Finl.* **35,** 101 (1964).
14. Krishnaswami, S. & Cochran, J. K. *Earth planet. Sci. Lett.* **40,** 45 (1978).
15. Moore, W. S. *et al.* (in the press).
16. Cronan, D. S. *Marine Manganese Deposits* (ed. Glasby, G. P.) 11 (Elsevier, Amsterdam, 1977).
17. Tarr, A. C. *World Seismicity Map* (USGS–NOAA, 1974).
18. Menard, H. W. *Marine Geology of the Pacific* (McGraw Hill, New York, 1964).
19. Heath, G. R. *Oceanus* **21,** 60 (1978).
20. Paul, A. *Nature* **263,** 50 (1976).
21. Quinterno, P. & Theyer, F. in *Marine Geology and Oceanography of the Pacific Manganese Nodule Province* (eds Bischoff, J. L. & Piper, D. Z.) 349 (Plenum, New York, 1979).
22. Hecker, B. & Paul, A. in *Marine Geology and Oceanography of the Pacific Manganese Nodule Province* (eds Bischoff, J. L. & Piper, D. Z.) 287 (Plenum, New York, 1979).
23. Darwin, C. R. *The Formation of Vegetable Mold Through the Action of Worms with Observations on Their Habits* (Murray, London, 1881).
24. Broecker, W. S. *Chemical Oceanography* (Harcourt Brace Jovanovich, New York, 1974).

Fraction dependent variation of aspartic acid racemization age of fossil bone

Shuji Matsu'ura

Department of Anthropology, National Science Museum
(Natural History Institute), 3-23-1 Hyakunin-cho, Shinjuku-ku,
Tokyo 160, Japan

Nobuo Ueta

Department of Biochemistry, Teikyo University School of Medicine,
2-11- Kaga, Itabashi-ku, Tokyo 173, Japan

The extent of racemization of amino acids provides valuable information on the chronology of various fossil materials[1-3]. In bone, aspartic acid has received the most attention, and the D/L ratio of this amino acid has been used to estimate ages of human skeletal remains[4-9]. These estimates were, however, based on the degree of racemization determined for total remnant aspartic acid which may exist in various forms (that is, protein, peptide and free amino acid). The effect of the chemical state of amino acids on amino acid racemization rates or ages in calcareous marine sediments[10] and shells[11] has been discussed. In bones, the non-dialysable material in a heated modern sample has a lower racemization rate (isoleucine) than the total organic matrix[12]; free amino acids in fossil bone are more highly racemized than are bound (HCl-insoluble) amino acids[13]. The present investigation was designed to assess such fluctuation of aspartic acid racemization age for a given bone specimen as caused by the variability of the form in which the amino acid is present.

Bones for amino acid analysis were taken from the layers 20, 23B and 25B of the Taishaku Kannondo cave site, Taishaku Ravine, Hiroshima Prefecture in western Japan. All the specimens were long bone fragments of deer or wild boar. A radiocarbon date for a cultural horizon comparable to the layer 20 is 10,085 ± 320 yr BP (I-943)[14,15]. On the basis of stratigraphical and tephrochronological comparisons[14,16], we assume that the layer 23B is dated 16,000 yr BP. Layer 25B is of unknown age, but is overlain by the calcic layer of 24A, which was radiocarbon-dated[17] at 20,150 ± 300 yr BP. An outline of the archaeological contexts of the Taishaku Kannondo site is given elsewhere[14,15].

A small piece (~0.3 g) of transverse section of *Substantia compacta*, cut from each fossil bone, was carefully cleaned by ultrasonication in 0.1 M HCl, ether and double-distilled water. After cleansing, the bones were pulverized and mixed in layers to make an homogeneous powder weighing 1–2 g. Amino acid fractions were isolated using the procedure outlined in Fig. 1. The ratios of D to L-aspartic acid were determined by gas–liquid chromatography of the *N*-trifluoroacetyl isopropyl esters on a 30 m × 0.28 mm i.d. glass capillary coated with *N,N'*-[2,4-(6-ethoxy-s-triazine)diyl]-bis-(L-valyl-L-valine isopropyl ester)[18] (AE-402, from Gasukuro Kogyo, Inc.).

Figure 2 shows a chromatogram obtained for the Tot fraction in the sample from the layer 23B. Table 1 includes the D/L aspartic acid ratios for Ins, Sp and Tot fractions. Insufficient quantities of amino acids, except glycine, for analysis were available in any Sf fractions, and even the glycine was <0.2% relative to that in Ins fraction. This would be due to removal of free amino acids by percolation of ground water or by the ultrasonic cleansing[2].

The interconversion of aspartic acid enantiomers is a reversible first order reaction, represented by:

$$\text{L-Asp} \underset{k}{\overset{k}{\rightleftharpoons}} \text{D-Asp}$$

where k is the rate constant. Expressed in the integrated form as a function of time (t), the racemization age equation can be written as

$$\ln \alpha_t - \text{constant} = 2kt$$

where $\alpha = (1 + \text{D-Asp}/\text{L-Asp})/(1 - \text{D-Asp}/\text{L-Asp})$ at time t after the start of the reaction. The integration constant is a correction mainly due to the small amount of racemization that takes place during sample preparation procedures. For example, the value of this constant for Tot fraction, calculated from our datum (D/L = 0.063) obtained for a modern bone, is 0.126. However, where it is possible to use two bones from a single site, the dates (t_1, t_2) of which lie at a time interval suitable for 'calibration[4]', the rate constant of racemization during the interval $t_1 \sim t_2$ is given by:

$$2k = (\ln \alpha_{t_1} - \ln \alpha_{t_2})/(t_1 - t_2).$$

When $t_1 > t_2$, and t_2 is the age of the start of the Holocene (~11,000 yr), this equation yields the pre-Holocene k value. Thus the k values in Table 1, calculated with the samples from the layers 20 and 23B used for 'calibration', correspond approximately to the pre-Holocene rate constants for the respective fractions. This procedure eliminates the need of setting the enantiomeric ratio for modern bone in the aspartic

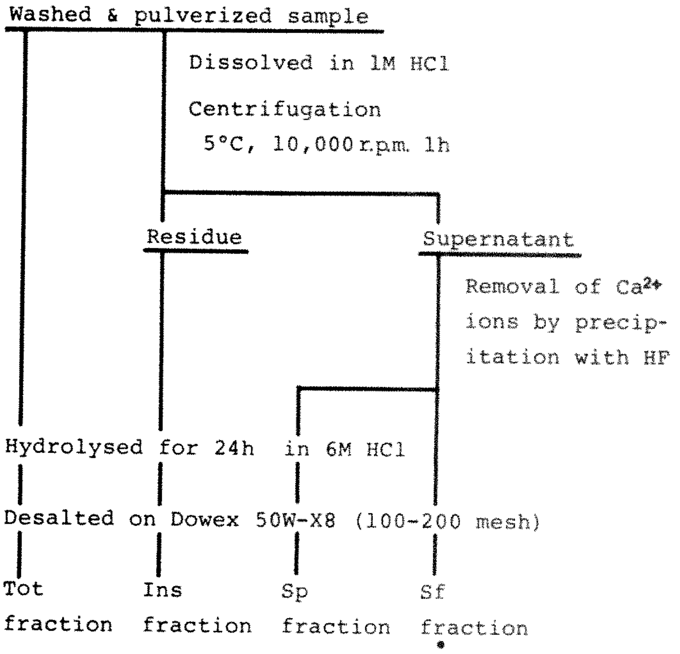
Washed & pulverized sample
Dissolved in 1M HCl
Centrifugation
5°C, 10,000 r.p.m. 1h
Residue
Supernatant
Removal of Ca²⁺ ions by precipitation with HF
Hydrolysed for 24h in 6M HCl
Desalted on Dowex 50W-X8 (100-200 mesh)
Tot fraction
Ins fraction
Sp fraction
Sf fraction

Fig. 1 Fractionation of remnant amino acids in fossil bone. Tot, Total amino acid; Ins, insoluble (protein); Sp, soluble peptide-free amino acid; Sf, free amino acid.

0028–0836/80/350883—02$01.00

acid racemization age equation, thus minimizing the errors that result from the changes in, for example, concentrations of noncollagen proteins[19,20] and metal ions in bone with the lapse of time in geological environments. Note that our k values are not directly comparable with the late Pleistocene k values presented by Bada *et al.* (see, for example, ref. 1), as we subtract out the greater part of the Holocene k value.

As Table 1 shows, the order of racemization rates is Sp fraction > Tot fraction > Ins fraction, comparing well with that observed in foraminifera[10] or in shell[11]. This result is also consistent with what Bada[12] found for the total bone organic fraction versus the non-dialysable fraction.

The racemization age of the layer 25B sample is calculated from

$$t = t_2 + (\ln \alpha_t - \ln \alpha_{t_2})/2k.$$

Substituting 10,085 for t_2, and with the other relevant data, we have 23,700 yr BP (Ins fr.), 19,900 yr BP (Sp fr.) and 22,900 yr BP (Tot fr.). The D/L Asp data in Table 1 give the proportions of aspartic acid in peptide to protein form (Sp/Ins–Asp) in bone. These values are 41, 48 and 63% for the samples from the layers 20, 23B and 25B respectively. The increase in SP/Ins–Asp value in the longer-buried bones suggests the continuous degradation of collagen. The introduction of the collagen-breakdown product (less racemized) into the Sp fraction may induce the lower age estimate for this fraction. Preliminary analyses of main components of amino acid extracts showed that these Sp fractions are collagenous in composition, although the Hypro/Pro and Ala/Pro ratios in Sp fractions are ~17% and 23% reduced relative to those in respective Ins fractions. The above findings would have a notable bearing on the radiocarbon dating of bone. The HCl-insoluble fraction, which is usually used for ^{14}C dating, becomes less and less abundant with time. Hence, it would be very interesting to radiocarbon-date the HCl-soluble fraction to which little attention has previously been paid.

The two racemization ages of the Ins and the Tot fractions are compatible with the radiocarbon date of the layer 24A. However, the age estimate based on the total aspartic acid could vary with the proportion of this amino acid in soluble to insoluble state. Variance of Sp/Ins–Asp value in the layer 25B sample, for example, from 50 to 70% should yield the racemization age of 20,000–24,000 yr BP for the Tot fraction.

Such fractional amino acid analyses provide a way of aspartic acid racemization-dating of fossil bone. Where the Sp fraction has a collagenous origin, it is useful for estimating a minimum (or maximum in the case of dating bone with an age less than that of the calibration sample) age, which because of its faster racemization rate is particularly promising for the younger fossils. The aspartic acid racemization reaction for the Ins fraction seems to be a basis to give reliable age estimates for older fossil bones with ages ranging several hundred thousand yr BP. For the Tot fraction, the degree of amino acid racemization could be depenedent on the dynamics of collagen decomposition. Provided that the ratio of partially degraded to pure collagen exhibits a steady increase with burial time (as is supposed to be the case with bones from a single site), a measurement of the extent of racemization on the total hydrolysate would still have archaeological significance. Where the same calibration is applied to fossil samples with different environmental factors involving the disintegration rate of collagen (probably mainly due to humidity in the site), assuming the effective temperature for racemization is nearly identical, then misleading age estimates would be generated.

Table 1 Aspartic acid racemization in fossil bones from the Kannondo cave site

	Layer	D/L Asp	Aspartic acid age (yr BP)
Ins fraction			
	20	0.084	$k = 1.70 \times 10^{-6}$ yr^{-1}
	23B	0.094	
	25B	0.107	23,700
Sp fraction			
	20	0.199	$k = 9.08 \times 10^{-6}$ yr^{-1}
	23B	0.250	
	25B	0.283	19,900
Tot fraction			
	20	0.115	$k = 4.30 \times 10^{-6}$ yr^{-1}
	23B	0.140	
	25B	0.169	22,900

Analysable amounts of aspartic acid have not been contained in any Sf fractions.

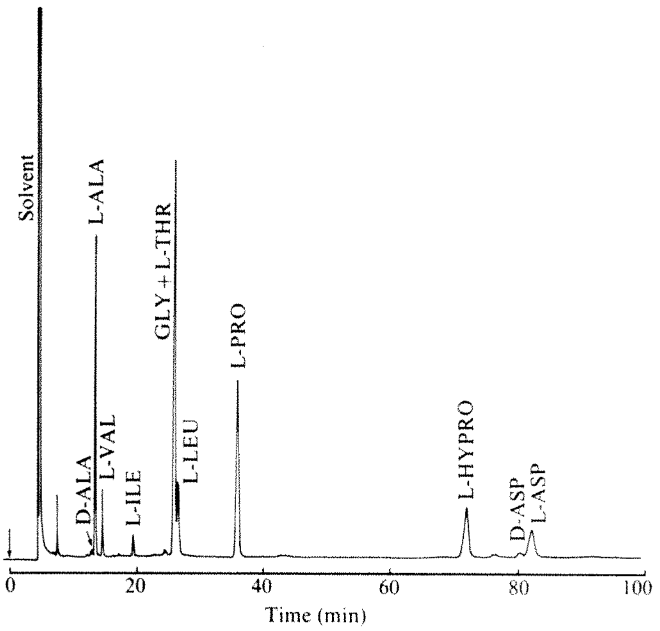

Fig. 2 Gas chromatogram of N-trifluoroacetyl isopropyl esters of amino acids recovered from the total hydrolysate of the layer 23B sample from the Kannondo cave site. Chromatography: 30 m × 0.28 mm i.d. column coated with N,N'-[2,4-(6-ethoxy-s-triazine)diyl]-bis-(L-valyl-L-valine isopropyl ester); temperature, 135 °C isothermal; He pressure, 7 p.s.i.; FID detector.

The present approach would also be useful in overcoming the obstacle caused by the difference in the 'leaching effect'[21] and in improving the reliability of the racemization dating method.

We thank Dr Y. Seyama for his interest and co-operation, Dr E. Gil-Av for advice, Dr J. L. Bada for criticisms, and Miss A. Nakatsuka for drafting help. Bone specimens were provided by the Research Group of Taishaku-kyo sites.

Received 8 April; accepted 25 June 1980.

1. Bada, J. L. & Schroeder, R. A. *Naturwissenschaften* **62,** 71–79 (1975).
2. Schroeder, R. A. & Bada, J. L. *Earth Sci. Rev.* **12,** 347–391 (1976).
3. Miller, G. H., Hollin, J. T. & Andrews, J. T. *Nature* **281,** 539–543 (1979).
4. Bada, J. L. & Protsch, R. *Proc. natn. Acad. Sci. U.S.A.* **70,** 1331–1334 (1973).
5. Bada, J. L., Schroeder, R. A., Protsch, R. & Berger, R. *Proc. natn. Acad. Sci. U.S.A.* **71,** 914–917 (1974).
6. Bada, J. L., Schroeder, R. A. & Carter, G. F. *Science* **184,** 791–793 (1974).
7. Bischoff, J. L. & Childers, W. M. *Earth planet. Sci. Lett.* **45,** 172–180 (1979).
8. Ike, D., Bada, J. L., Masters, P. M., Kennedy, G. & Vogel, J. C. *Am. Antiq.* **44,** 524–530 (1979).
9. Matsu'ura, S. in *Rep. Excavation of Nagarabarunishi Shell Mound, Iĕ Island* (Okinawa Iĕ-mura Education Committee, in the press).
10. Bada, J. L. & Schroeder, R. A. *Earth planet. Sci. Lett.* **15,** 1–11 (1972).
11. Akiyama, M. *Earth Sci.* **29,** 161–165 (1975).
12. Bada, J. L. *Earth planet. Sci. Lett.* **15,** 223–231 (1972).
13. Dungworth, G., Vincken, N. J. & Schwartz, A. W. *Comp. Biochem. Physiol.* **47B,** 391–399 (1974).
14. Shiomi, H., Fujita, H. & Kawagoe, T. in *The Sites of the Taishaku Ravine* (ed. Matsuzaki, H.) 80–103 (Akishobo, Tokyo, 1976).
15. Matsu'ura, S. *Quat. Res., Jap.* **17,** 95–104 (1978).
16. Okimura, Y., Shibata, K. & Nakatsukasa, N. in *Studies in Archaeology—in Honour of Professor Hisakazu Matsuzaki on the Occasion of His 63rd Birthday,* 1–10 (Hiroshima Prefecture, 1977).
17. Kōyama, Y., Saito, M., Shimai, Y., Totani, M. & Yamada, O. *Kyoto Sangyo Univ. Essays* **6,** 90–95 (1977).
18. Ōi, N. *J. Jap. Chem., Spec. Iss.* **120,** 39–46 (1978).
19. Ho, T. Y. *Proc. natn. Acad. Sci. U.S.A.* **54,** 26–31 (1965).
20. Hedges, R. E. M. & Wallace, C. J. A. *J. Archaeol. Sci.* **5,** 377–386 (1978).
21. Hare, P. E. *Yb. Carnegie Instn Wash.* **73,** 576–581 (1974).

Enhanced plant growth by siderophores produced by plant growth-promoting rhizobacteria

Joseph W. Kloepper*, John Leong†, Martin Teintze† & Milton N. Schroth*

*Department of Plant Pathology, University of California, Berkeley, California 94720
†Department of Chemistry, University of California, San Diego, La Jolla, California 92093

Specific strains of the *Pseudomonas fluorescens-putida* group have recently been used as seed inoculants on crop plants to promote growth and increase yields. These pseudomonads, termed plant growth-promoting rhizobacteria (PGPR), rapidly colonize plant roots of potato, sugar beet and radish, and cause statistically significant yield increases up to 144% in field tests[1-5]. These results prompted us to investigate the mechanism by which plant growth was enhanced. A previous study indicated that PGPR increase plant growth by antagonism to potentially deleterious rhizoplane fungi and bacteria, but the nature of this antagonism was not determined[6]. We now present evidence that PGPR exert their plant growth-promoting activity by depriving native microflora of iron. PGPR produce extracellular siderophores (microbial iron transport agents)[7] which efficiently complex environmental iron, making it less available to certain native microflora.

Plant growth-promoting fluorescent *Pseudomonas* strains A1, BK1, TL3B1 and B10, isolated from potato periderm or roots, exhibited *in vitro* antibiosis on King's medium B[8] agar plates (KB) against the bacterium *Erwinia carotovora*, which causes potato soft rot and seedpiece decay (Fig. 1). When KB plates were amended with 1 μM $FeCl_3$, the antibiosis against *E. carotovora* did not occur, nor was the yellow-green fluorescence of PGPR produced. The above PGPR also exhibited on KB plates *in vitro* antibiosis against *Escherichia coli* K-12 AN193, which does not produce its native siderophore, enterobactin, but not against its enterobactin-producing parent, *E. coli* K-12 AN194. These results suggested that in iron-deficient conditions, PGPR were producing fluorescent siderophores which were responsible for antibiosis against *E. carotovora* and *E. coli* K-12 AN193. Yellow-green fluorescent siderophores have previously been isolated from iron-limiting cultures of *P. fluorescens*[9-11].

We next investigated the effect of iron on plant growth-promoting activity by PGPR in soils. When potato seedpieces were dipped into PGPR suspensions (10^9 Colony-forming units (CFU) per ml) immediately before planting in field soils in a previously described greenhouse assay[5], statistically significant increases in plant growth (total plant wet weight) occurred 2 weeks after emergence. Average increases (six replications with three plants each) were 47% for strain A1, 63% for strain B10 and 74% for strain BK1. The control was an autoclaved suspension of strain A1. In contrast, when 120 ml of 100 μM ethylenediaminetetra-acetatoferrate (III) (Fe^{III} $EDTA^-$) per 600 g of soil were added on alternate days to soils planted with PGPR-inoculated potato seedpieces, PGPR did not statistically increase growth (±4%). Addition of iron alone to soils did not significantly increase plant growth over the control. The effect of iron (III) on colonization of roots by PGPR was examined with strain A1 as previously described[2,6]. Although the addition of Fe^{III} $EDTA^-$ resulted in no increase in plant growth, the bacteria, nevertheless, colonized roots at populations averaging 3.2×10^3 CFU per cm root as compared with 4.4×10^3 CFU per cm without iron.

These results suggested the intriguing proposition that a fluorescent siderophore from PGPR may mimic the biological action of PGPR. To test this, we isolated a yellow-green fluorescent pigment capable of binding iron (III) from broth cultures of strain B10 grown in an iron-deficient medium containing glycerol and proteose peptone no. 3. The pigment was purified to homogeneity by a procedure similar to that of Meyer and Abdallah[10]. This pigment exhibited properties typical of a siderophore, including complete repression of production in culture media containing micromolar amounts of iron (III). Furthermore, both the pigment and its ferric complex reversed iron starvation of strain B10 on KB plates induced by the synthetic ferric complexing agent, ethylenediamine-di-(*o*-hydroxyphenylacetic acid) (EDDA), which is not utilized by the cells[12]. As the chemical and physical properties of this siderophore seem to be different (J.L. and M.T., unpublished results) from those of others isolated earlier[10,11,13-15], we name this new siderophore, pseudobactin. When paper disks containing 20 μl of 200 μM pseudobactin were applied to KB plates previously seeded with *E. carotovora*, 3-mm radial growth inhibition zones about the disks were observed within 12–16 h. Red-brown ferric pseudobactin caused no antibiosis against *E. carotovora* up to millimolar concentrations. These results suggest that the *in vitro* antibiosis of PGPR against *E. carotovora* is caused by iron deprivation induced by the PGPR's siderophore. *E. coli* K-12 AN194 was not susceptible to PGPR because enterobactin may be able to reverse iron starvation precipitated by PGPR's siderophore.

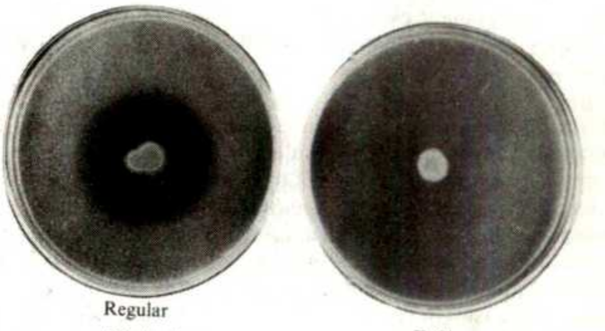

Fig. 1 Plant growth-promoting rhizobacterial antibiosis against *Erwinia carotovora* eliminated by iron (III). Both King's B agar plates were inoculated in the centre with 10 μl of a suspension of fluorescent *Pseudomonas* strain B10 (~10^6 CFU ml^{-1}), incubated for 24 h at 28 °C, and sprayed with a suspension of *E. carotovora* (~10^6 CFU ml^{-1}). The plate on the right contained 10 μM $FeCl_3$, whereas the plate on the left contained no added iron (III). The zone of growth inhibition of *E. carotovora* and the fluorescence of strain B10 were examined at 24 h. Similar results were obtained with fluorescent *Pseudomonas* strains A1, BK1 and TL3B1.

The effect of pseudobactin on plant growth and rhizoplane fungal colonization was determined in the greenhouse assay (Table 1). Both B10 suspensions and pseudobactin at 10 μM caused significant plant growth increases compared with water-treated controls. Ferric pseudobactin at 50 μM and B10 with 50 μM Fe^{III} $EDTA^-$ did not increase plant growth. In addition to increasing plant growth, pseudobactin and B10 treatments resulted in statistically significant reductions of fungal populations on the rhizoplane relative to the water-treated control. Fungal colonization of the rhizoplane, measured by the method of Huisman *et al.*[16], averaged 5.5 CFU per 10 cm root on water-treated plants compared with 2.3 CFU per 10 cm (−59%) on B10-treated plants and 1.4 CFU per 10 cm (−74%) on pseudobactin-treated plants.

Based on these results, we propose the following scenario to account for the enhancement of plant growth by PGPR.

0028–0836/80/350885—02$01.00

Following inoculation and planting of crop seeds, PGPR rapidly colonize roots of the developing plant. As a result of a limited supply of iron in the rhizoplane, PGPR produce siderophores which sequester iron in the root zone, making it unavailable to certain rhizoplane microorganisms. These microorganisms are unable to obtain essential quantities of iron for growth either because they do not produce siderophores, produce comparatively less siderophores than those of PGPR, and/or produce siderophores which have less affinity for iron than those of PGPR. The populations of these microorganisms, some of which are quasi-pathogens (T. V. Suslow and M.N.S., unpublished results), are reduced, and a more favourable environment for root growth is created. Our results with mutants of PGPR support this hypothesis. Certain mutants obtained by treatment with *N*-methyl-*N'*-nitro-nitrosoguanidine or UV light at 254 nm were non-fluorescent, did not exhibit antibiosis against *E. carotovora* and did not promote growth increase of potato in the greenhouse assay even though they were able to colonize plant roots[6]. At least five mutants derived from strains BK1, TL3B1 and TL3B2 were examined. These mutants did not produce siderophores, in contrast to their parents. An alternative hypothesis that plant growth-promoting rhizobacterial siderophores bind iron and make it directly and perhaps more readily available to the plant seems unlikely because ferric pseudobactin did not promote plant growth (Table 1).

Table 1 Enhanced plant growth of potato by pseudobactin in greenhouse assay

Treatment	Average plant weight (g)
H_2O control	1.0
50 μM Fe^{III} $EDTA^-$ control	0.9
B10	2.3*
B10 + 50 μM $Fe^{III}EDTA^-$	0.9
10 μM pseudobactin	2.5*
50 μM ferric pseudobactin control	1.1

Potato seedpieces were planted in field soil (sandy loam) from Moss Landing, California. In treatments with fluorescent *Pseudomonas* strain B10, seedpieces were dipped in approximately 10^9 CFU ml^{-1} suspension before planting. Pots were watered with 120 ml of the appropriate solution on alternate days, and a total of nine applications were made. Plants were harvested 10 days after emergence. An average of six replications with three plants per replication were obtained.

* Statistically significant increase ($P = 0.01$) compared with controls.

We thank Laurence A. Fishel and Susan M. Shoemaker for experimental assistance. This investigation was supported in part by PHS grant AI14084 from the NIH and by the California Potato Research Advisory Board.

Received 19 March; accepted 26 June 1980.

1. Kloepper, J. W. & Schroth, M. N. in *Proc 4th int. Conf. Plant Pathogenic Bacteria* Vol. 2 (ed. Station de Pathologie Végétale et Phytobactériologie) 879–882 (Gibert-Clarey, Tours, 1978).
2. Kloepper, J. W. & Schroth, M. N. *Phytopathology* (in the press).
3. Suslow, T. V. thesis, Univ. California (1980).
4. Suslow, T. V., Kloepper, J. W., Schroth, M. N. & Burr, T. J. *Calif. Agric.* **33**, 15–17 (1979).
5. Burr, T. J., Schroth, M. N. & Suslow, T. *Phytopathology* **68**, 1377–1383 (1978).
6. Kloepper, J. W. thesis, Univ. California (1979).
7. Neilands, J. B. in *Iron in Biochemistry and Medicine* (eds Jacobs, A. & Worwood, M.) (Academic, New York, in the press).
8. King, E. O., Ward, M. K. & Raney, D. E. *J. Lab. clin. Med.* **44**, 301–307 (1954).
9. Garibaldi, J. A. *J. Bact.* **105**, 1036–1038 (1971).
10. Meyer, J. M. & Abdallah, M. A. *J. gen. Microbiol.* **107**, 319–328 (1978).
11. Maurer, B., Müller, A., Keller-Schierlein, W. & Zähner, H. *Arch. Mikrobiol.* **60**, 326–339 (1968).
12. Ong, S. A., Peterson, T. & Neilands, J. B. *J. biol. Chem.* **254**, 1860–1865 (1979).
13. Cox, C. D. & Graham, R. *J. Bact.* **137**, 357–364 (1979).
14. Liu, P. V. & Shokrani, F. *Infect. Immun.* **22**, 878–890 (1978).
15. McCracken, A. R. & Swinburne, T. R. *Physiol. Pl. Path.* **15**, 331–340 (1979).
16. Huisman, O. C., Ashworth, L. J. & Harper, D. *Phytopathology* (submitted).

Antiquity of the vertebrate pattern of activity metabolism and its possible relation to vertebrate origins

John A. Ruben*

Department of Zoology, Oregon State University, Corvallis,
Oregon 97331

Albert F. Bennett

School of Biological Sciences, University of California, Irvine,
California 92717

Vertebrates generally possess well developed capacities for anaerobic metabolism, resulting in formation of lactic acid. Those capacities have traditionally been interpreted in terms of adaptation to hypoxic environments or to special situations such as diving. However, anaerobic metabolism in striated muscle tissue is frequently a major source of ATP utilized during periods of intense activity. The evolutionary significance of anaerobically supported activity has not been discussed, although the interrelationships of capacities for aerobiosis and activity have received considerable attention[1]. We present here evidence that the pattern of activity metabolism utilized by extant species probably dates back to the earliest vertebrates. It is also postulated that the evolution of extensive capacity for anaerobically supported burst activity may have been closely related to the evolution of vertebrates from invertebrate chordates.

Many animals use glycolysis, the anaerobic process by which glucose is degraded to lactic acid. Most invertebrate species resort to significant utilization of glycolysis only in the absence of sufficient environmental oxygen to maintain adequate rates of ATP generation via aerobiosis, or oxidative phosphorylation[2]. However, many vertebrate species rely on prodigious rates of glycolysis for ATP generation during periods of maximal activity[3–6]. Such a pattern of activity metabolism enables many vertebrates to reach 'burst' levels of activity otherwise unattainable if they were solely dependent on aerobic metabolism. Heavy reliance on anaerobic metabolism also has its drawbacks: it is inefficient in utilizing substrate, and is invariably associated with muscle fatigue[7]. In addition, resultant intramuscular lactic acid accumulation and subsequent diffusion of lactate into the cardiovascular system[4] disrupts maintenance of blood and tissue *p*H which may well affect enzymatic activity, protein configuration and so on[8]. This exercise-related *p*H depression may persist in lower vertebrates for several hours, or longer, following cessation of strenuous activity[9].

Although some crustaceans generate moderate quantities of lactate during exercise[10,11], most invertebrates produce little, if any, lactate during maximal activity. For example, during periods of intense activity, the insects are highly dependent on aerobiosis[12] and molluscs anaerobically generate octapene and succinate to supply themselves with sufficient ATP[13]. Hence, the vertebrate capacity for lactate generation during activity should not be considered an adaptation for anaerobiosis *per se*: it is not merely a primitive relict of the occupation of oxygen-depleted environments, but is a specific and relatively unique exploitation of glycolysis to support intense activity.

Lactic acid formation during activity has been demonstrated in many extant gnathostomes (sharks[14], teleost fish[6], amphibians[3], reptiles, mammals[5]). Those data indicate that heavy reliance on lactate formation during activity is widespread among vertebrates. However, the antiquity of this pattern of activity support is still unclear; is it a primitive characteristic dating back to, or even previous to, the origin of vertebrates? To

---

* To whom correspondence should be addressed.

0028-0836/80/350886—03$01.00

Table 1 Whole body lactic acid concentration and blood *p*H before and after activity in two species of cyclostomes and whole body lactic acid concentration before and after activity in amphioxus

	Lactic acid concentration (mg per g tissue)		Blood *p*H			
Species	Rest	Active	Rest	30 min post activity	60 min post activity	180 min post activity
Pacific hagfish (*Eptatretus stouti*)	0.14±0.01 (*n* = 4)	1.51±0.14 (*n* = 4)	8.03±0.03 (*n* = 5)	7.60±0.12 (*n* = 5)	7.48±0.14 (*n* = 5)	7.31±0.19 (*n* = 5)
Pacific brook lamprey (*Lampetrus pacifica*)	0.17±0.01 (*n* = 5)	1.65±0.18 (*n* = 7)	7.91±0.04 (*n* = 5)	7.16±0.06 (*n* = 5)	— —	— —
Amphioxus (*Branchiostoma caribaeum*)	0.14±0.03 (*n* = 4)	0.29±0.04 (*n* = 8)	—	—	—	—

Post-active depression of blood *p*H probably results from protracted diffusion of lactic acid into the cardiovascular system from striated musculature as well as slow subsequent removal of lactate from the circulatory system. Adult *Lampetra* (36) were obtained by dip net in Oak Creek, Benton County, Oregon, in May 1979. Adult *Eptatretus* (28) were caught in 'fike' traps at a depth of 150 m, 1,000 m off the coast of Coos Bay, Oregon in December 1978. Adult *Branchiostoma* (12) were collected in Tampa Bay, Florida, in December 1979. Animals were maintained in 160-l capacity tanks, situated in thermally controlled rooms set at 12 °C on an 11-h photoperiod. Tank water was kept fully aerated at all times. Experiments were performed 4–6 days after animals were captured. Twelve *Lampetra* (mean mass 6.6 g), 9 *Eptatretus* (mean mass 52.2 g) and 12 *Branchiostoma* (mean mass 0.14 g) were used to determine whole body lactate content either at rest or immediately after maximal activity. Animals were placed individually in a 1 m × 1 m × 0.25 m tank of water equilibrated to 12 °C. They were then stimulated to activity by persistent, noxious but harmless prodding. Reaction of all animals to stimulus was intense, and was assumed to represent maximal activity levels. During stimulation, both *Lampetra* and *Eptatretus* underwent an initial period of vigorous activity lasting 2.5–3.5 min. In both species, this consisted of frantic lateral undulations interspersed with frequent attempts to 'bite' the probe. During the following 1.5–2.5 min, animals appeared to tire but continued to exhibit similar types of behaviour. In addition, mucus was secreted from the slime glands of *Eptatretus* during the entire exercise period. This was removed from the tank approximately every 30 s in such a manner that movements by animals were not hindered. During the initial 10–15 s of the exercise period, *Branchiostoma* underwent intense lateral undulation. Thereafter, they appeared to tire significantly and remained essentially refractory to further stimulus. After 5 min of stimulation, animals were decapitated, homogenized in 0.6 *M* perchloric acid for 2 min in an Oster blender and total body lactate was measured spectrophotometrically by the method of Bennett and Licht[4]. Similar analyses were also made on unstimulated animals to determine lactate levels for resting individuals. Ten *Lampetra* and 20 *Eptatretus* were used to determine the effect of this activity on blood *p*H. Blood samples of 75 µl were taken in heparinized syringes from five previously undisturbed individuals of each species. Samples were withdrawn from tail incisions in *Lampetra* and from the caudal sinus in *Eptatretus*. Elapsed time between first handling and sample procurement was less than 15 s; struggling by animals was minimal during this time period. The *p*H of the sample was measured immediately with a Radiometer Copenhagen BMS3Mk2 blood micro unit connected to a Radiometer Copenhagen PHM 71 Mk 2 acid–base analyser. The temperature of the electrode was regulated at 12 °C ± 0.5 °C. This measurement was assumed to represent the *p*H of the animals' blood at rest. Different individuals of each species were then stimulated to activity for 5 min as described in the previous experiments. Blood samples were collected and analysed (as described for resting individuals) 30 min after cessation of activity in both species. Additional samples were taken 60 and 180 min after activity in *Eptatretus*

elucidate this question, we investigated patterns of activity metabolism in some living agnathans (Cyclostomata) and the protochordate, amphioxus (Cephalochordata). Morphological evidence indicates long evolutionary isolation of cyclostome and gnathostome lineages as well as independent derivation of both groups from the earliest vertebrates, the ostracoderms of the early Palaeozoic (Fig. 1)[15]. Thus, parsimony dictates that occurrence of a particular trait (burst activity supported by anaerobiosis) in both cyclostomes and gnathostomes might be the result of retention of a primitive characteristic present in the common ancestor of both groups.

Activity physiology in extant protochordates, especially cephalochordates, may well be reflective of activity metabolism in the chordate ancestors of vertebrates. Cephalochordates are thought to resemble closely protovertebrates in many aspects of their morphology and in their sedentary, microphagous filter-feeding lifestyle[16]. Consequently, their activity physiology may also be similar.

Cyclostomes investigated in this study included the Pacific brook lamprey (Petromyzontidae: *Lampetra pacifica*) and the Pacific hagfish (Myxinidae: *Eptatretus stouti*). The Pacific brook lamprey is a small, non-parasitic lamprey inhabiting streams west of the Cascade Mountains of the north-west US. These are strictly freshwater forms that never migrate to marine environments. The Pacific hagfish occurs off the west coast of North America from southern California to south-east Alaska in silty-bottom environments at depths of 18–940 m.

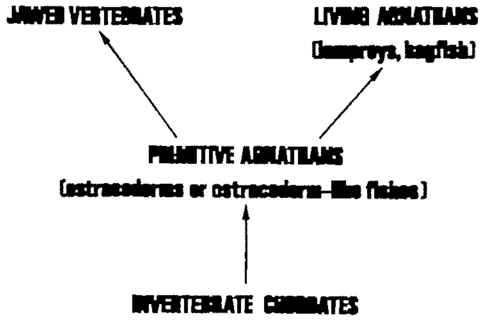

Fig. 1 Phylogenetic relationships of the vertebrates (based on refs 15, 19)

The cephalochordate investigated here was *Branchiostoma caribaeum* (Branchiostomidae). This is a small, burrowing, filter-feeding inhabitant of sandy-bottomed marine environments from Chesapeake Bay to the West Indies.

Both cyclostomes utilized glycolysis extensively during the exercise period (Table 1): lactate concentrations were approximately 10 times greater after 5 min of activity than at rest ($P < 0.05$, *t*-test). In addition, both species experienced a concomitant, protracted decline in all post-active blood *p*H measurements ($P < 0.05$, *t*-test) (Table 1). Quantities of lactate formed as a result of activity and the accompanying extended post-active decline of blood *p*H in these species closely parallel previously described modes of activity physiology among gnathostomes[7,9].

Consequently, utilization of the pattern of activity metabolism described here must be of considerable antiquity, perhaps as old as vertebrates themselves. Figure 1 illustrates the generally accepted phylogenetic relationships of the vertebrates. If these relationships are correct, we must assume the pattern of activity metabolism exhibited by living vertebrates is a result of either (1) convergent evolution between cyclostome and gnathostome lineages; or (2) retention of a primitive vertebrate characteristic. Insofar as premise (2) is the most parsimonious, it must be considered the most likely to describe the actual sequence of events.

The implications of that conclusion for the evolution of vertebrates are manifold. For example, parameters of anaerobically supported activity (such as capacity for high levels of burst activity, fatigue, extended post-active blood and tissue *p*H alteration) have probably vitally affected adaptive radiation of the morphology, physiology and behaviour of virtually all the major groups of vertebrates. In fact, only with the evolution of homeothermy in birds and mammals have aerobic potentials been expanded to the point where, for example, they can support very high levels of activity without consequent fatigue[17].

In contrast, the chordate ancestors of vertebrates may not have possessed such well developed capacities for burst activity as early vertebrates. The cephalochordate studied here was incapable of any more than 10–15 s of intense lateral undulation and generated only minimal quantities of lactate during exercise (Table 1). This pattern of activity physiology is hardly surprising:

cephalochordates, like all adult invertebrate chordates, lead a sedentary, filter-feeding existence and seldom, if ever, take any more than the briefest of forays into the water column. Thus, if current interpretations regarding vertebrate origins are correct (see above), one might reasonably postulate a similarly minimal metabolic capacity for intense activity in the chordate ancestors of vertebrates.

Those differences in capacity for activity between invertebrate chordates and the earliest vertebrates might indicate concomitant and interdependent evolution of vertebrate activity physiology and the appearance of the vertebrates themselves. Halstead[18] and others have rightly emphasized that the earliest vertebrates lacked a vertebral column, but differed from invertebrate chordates in that the latter group never exhibits a high degree of cephalization. Accordingly, as described above, all adult invertebrate chordates are at least relatively sedentary, whereas vertebrates are among the most active of the Metazoa. Thus, vertebrate cephalization may have developed in response to selection for increased sensory and locomotor control as a more active lifestyle evolved. We suggest that the expanded vertebrate capacity for burst activity contributed significantly to that active mode of existence. Consequently, evolution of the vertebrate pattern of activity metabolism may well have been a selective factor contributing to cephalization in protovertebrates and the appearance of vertebrates themselves.

We thank Drs A. Boucot and A. Blaustein for their comments on the manuscript. This research was financed by NSF grant DEB 78-10837 (to J.A.R.) and NSF grants PCM 75-10100A01 and 77-024208 and NIH grant 1 KO4 AM0 351-01 (to A.F.B.).

Received 10 December 1979; accepted 11 June 1980.

1. Martin, R. D. *Nature* **283,** 335–336 (1980).
2. Schmidt-Nielsen, K. *Animal Physiology: Adaptation and Environment* (Cambridge University Press, 1979).
3. Bennett, A. F. & Licht, P. *Comp. Biochem. Physiol.* **48A**, 319–327 (1974).
4. Bennett, A. F. & Licht, P. *J. comp. Physiol.* **81,** 177–188 (1972).
5. Ruben, J. A. & Battalia, D. E. *J. exp. Zool.* **208,** 73–76 (1979).
6. Black, E. C. *J. Fish Res. Bd Canada* **12,** 917–929 (1955).
7. Bennett, A. *Comp. Biochem. Physiol.* **46A**, 673–690 (1973).
8. Eckert, R. & Randall, D. *Animal Physiology* (Freeman, San Francisco, 1978).
9. Bennett, A. F. *A. Rev. Physiol.* **40,** 447–469 (1978).
10. Phillips, J. W., McKinney, R. J. W., Hird, F. J. R. & Macmillan, D. L. *Comp. Biochem. Physiol.* **56B**, 427–433 (1977).
11. Burke, E. M. *Biol. Bull.* **156,** 157–168 (1979).
12. Krogh, A. *Comparative Physiology of Respiratory Mechanisms* (University of Pennsylvania Press, Philadelphia, 1941).
13. de Zwan, A., Thompson, R. J. & Livingstone, D. R. *J. comp. Physiol.* B **137,** 105–114 (1980).
14. Piiper, J., Meyer, M. & Drees, F. *Respirat. Physiol.* **16,** 290–303 (1972).
15. Romer, A. S. *Vertebrate Paleontology* (University of Chicago Press, 1966).
16. Romer, A. S. & Parsons, T. S. *The Vertebrate Body* (Saunders, Philadelphia, 1977).
17. Bennett, A. F. & Ruben, J. A. *Science* **206,** 649–654 (1979).
18. Halstead, L. B. *The Pattern of Vertebrate Evolution* (Freeman, San Francisco, 1968).
19. Moy-Thomas, J. A. & Miles, R. S. *Paleozoic Fishes* (Saunders, Philadelphia, 1971).

Human cell-surface glycoprotein with unusual properties

M. Bishr Omary*, Ian S. Trowbridge* & Jun Minowada†

* Department of Cancer Biology, The Salk Institute for Biological Studies, Post Office Box 85800, San Diego, California 92138
† Cell Culture Laboratory, Department of Immunology and Immunochemistry Research, Roswell Park Memorial Institute, New York State Department of Health, 666 Elm Street, Buffalo, New York 14623

We report here the identification of human cell-surface glycoprotein with unusual and interesting properties. We initially detected this glycoprotein on the surface of cultured human haematopoietic cell lines by means of a monoclonal antibody. Although it is expressed on all cultured human haematopoietic cell lines tested, including the inducible promyelocytic tumour cell line HL-60 (ref. 1), it is not present in readily detectable amounts on most normal or leukaemic human haematopoietic cells. HL-60 cells, on exposure *in vitro* to appropriate chemical inducers, undergo morphological and functional differentiation along the granulocytic pathway or into macrophage-like cells[2–6]. One consequence of *in vitro* induction is the specific loss of the glycoprotein from the surface of HL-60 cells. The molecule does not, however, seem to be a highly tissue-specific differentiation antigen because it is also found on human tumour cell lines derived from non-haematopoietic tissues. Rather, its expression seems to be related to cell proliferation. Preliminary chemical characterization suggests that the glycoprotein may be identical to the abnormal glycoprotein previously reported by Bramwell and Harris to be associated with malignancy[7,8].

The IgG monoclonal antibody used in these studies is designated B3/25. It was obtained from fusion of BALB/c mouse spleen cells immunized against the human haematopoietic cell line K562 (ref. 9), with the non-producer myeloma cell line S194/5.XX0.BU.1, by standard procedures[10,11].

Trace antibody binding assays[12] showed that B3/25 antibody reacted with 7/7 cultured human T-leukaemic cell lines, 11/11 B-cell lines including 'normal' B-cell lines, B-cell tumours and Burkitt's lymphoma cell lines, and 10/10 non-T-, non-B-leukaemic cell lines. The antibody precipitated a labelled molecule from NP40 lysates of iodinated HL-60 cells which migrated with an apparent molecular weight of about 110,000 on SDS-polyacrylamide gels in reducing conditions (Fig. 1). Similar results were obtained in immunoprecipitation studies with other haematopoietic cell lines. This molecule, which on the basis of metabolic labelling studies and lectin affinity chromatography is a glycoprotein, seems to exist in the membrane as a disulphide-bonded dimer, as in nonreducing conditions it migrates in SDS-polyacrylamide gels with an apparent molecular weight of 200,000 (Fig. 1).

Although the glycoprotein was detected on the surface of all the human haematopoietic cell lines tested, we could not detect it on peripheral blood mononuclear cells, granulocytes or a variety of peripheral blood leukaemic cells either by fluorescence-activated cell analysis or by trace antibody binding. A more extensive survey of the distribution of the glycoprotein on normal and leukaemic haematopoietic cells was carried out by immunofluorescence microscopy. The molecule was not present in detectable amounts on a significant fraction of thymocytes, bone marrow or peripheral blood mononuclear cells, nor on leukaemic cells from patients with chronic myeloid leukaemia or chronic lymphatic leukaemia, except for apparently specific staining of a small population of cells morphologically resembling erythroblasts. The majority of blast cells from patients with acute myeloid or lymphocytic leukaemia were also negative. In some cases, however, a small fraction (0–30%) of the blast cell population was positive. In two exceptional cases, one a T-cell acute lymphocytic leukaemia, the other an erythroleukaemia, almost all the blast cells reacted strongly with B3/25 antibody.

In addition to its unusual cellular distribution, we found that the glycoprotein defined by B3/25 monoclonal antibody had another interesting property. Although the molecule is expressed on non-induced HL-60 cells, we detected a dramatic decrease in the amount of glycoprotein on cells induced to differentiate by growth in the presence of 1.25% dimethyl sulphoxide (DMSO) or 0.5 mM sodium butyrate for 5 days (Fig. 2 and ref. 1). The fact that the radioactivity bound to induced HL-60 cells incubated with B3/25 antibody in the trace antibody binding assay is barely above background indicates that the induced cells express little or no antigen. Two other low molecular weight compounds, *N*-methyl acetamide and phorbol ester, that also induce morphological and functional differentiation of HL-60 cells[2–6], cause a similar decrease in the expression of the glycoprotein on HL-60 cells.

0028–0836/80/350888—04$01.00

We studied the expression of B3/25 glycoprotein on HL-60 cells in more detail by quantitative immunofluorescence using the fluorescence-activated cell analyser. The amount of the glycoprotein found on non-induced cells varied considerably (Fig. 3*a*), and this heterogeneity was not abolished by recloning the cell line. Approximately 70% of non-induced HL-60 cells expressed sufficient antigen to be detected above nonspecific background fluorescence. After treatment with DMSO for 5 days, only 5% of the cells were scored as positive and the fluorescence profile of the specifically stained cells was indistinguishable from that of the control (Fig. 3*b*). Kinetic studies showed that the loss of B3/25 glycoprotein was detectable within 24 h and essentially complete after 48 h (Fig. 3*d*). The disappearance of the glycoprotein precedes the arrest of HL-60 cells in G1 of the cell cycle and morphological differentiation, which is not maximal until at least 5 days after induction (Fig. 3*d* and refs 2, 13). Pulse-chase metabolic labelling experiments show that the loss of the glycoprotein is due entirely to the almost complete cessation of synthesis of the molecule and not to an increased rate of degradation (M.B.O. and I.S.T., unpublished results). As shown in Fig. 3*c*, we have obtained a variant subline of HL-60 cells that continues to grow in the presence of 1.25% DMSO without undergoing terminal differentiation. In these conditions the cells express similar amounts of B3/25 glycoprotein to non-induced wild-type cells. Thus, the change in expression of the glycoprotein seems to be directly associated with the arrest of growth and differentiation of HL-60 cells *per se*.

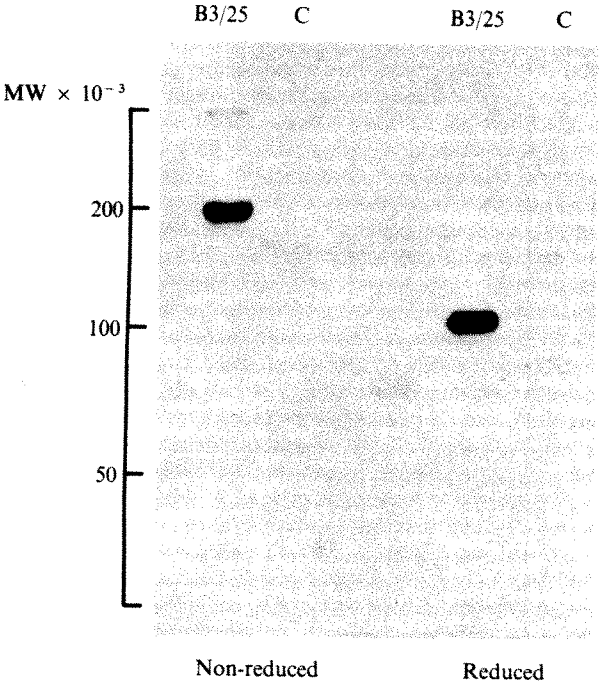

Fig. 1 SDS-polyacrylamide gel analysis of the cell-surface antigen recognized by B3/25 monoclonal antibody. HL-60 cells originally from Dr R. Gallo and recloned at the Salk Institute were iodinated by the glucose-oxidase modification of the lactoperoxidase technique as previously described[18]. Immunoprecipitates were prepared from cell lysates containing 1% NP40, 1% deoxycholate and 0.1% SDS using B3/25 antibody and adsorbing the immune complexes to *Staphylococcus aureus* essentially as described previously[19] except that goat anti-mouse IgG was used as the second antibody. Immunoprecipitates were analysed by SDS-polyacrylamide gel electrophoresis in 7.5% gels[20] after reduction with 2-mercaptoethanol or treatment with 100 mM iodoacetamide. Control immunoprecipitates from which B3/25 antibody was omitted were also prepared and analysed (gel tracks marked C). The autoradiograph shown was exposed for 1 h with the use of an intensifying screen[21] to enhance autoradiography. MW, Molecular weight.

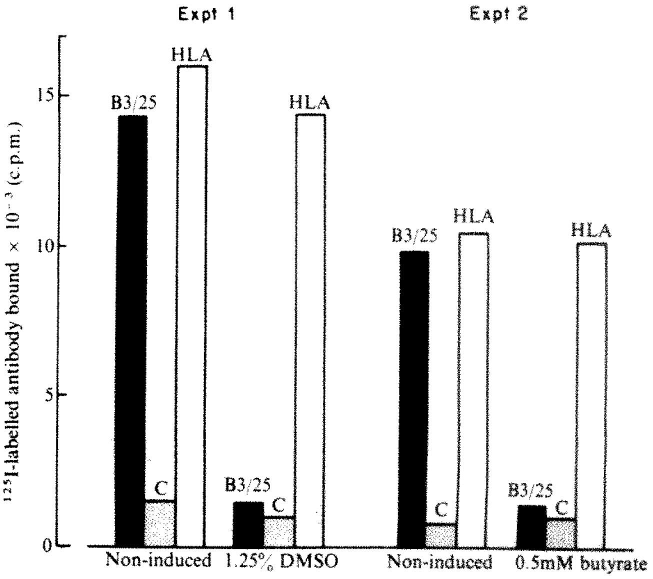

Fig. 2 Comparison of the binding of B3/25 antibody to induced and non-induced HL-60 cells. HL-60 were routinely maintained in RPM1 1640 medium supplemented with 10% fetal calf serum and 10 μM 2-mercaptoethanol. For induction experiments, cells were collected and resuspended at 2×10^5 cells per ml in fresh culture medium alone or containing either 1.25% (v/v) DMSO or 0.5 mM Na butyrate. After growth for 5 days, the cultures were collected and binding of B3/25 monoclonal antibody to non-induced and induced HL-60 cells determined by a trace antibody binding assay using ^{125}I-labelled affinity-purified rabbit F(ab′)$_2$ anti-mouse IgG antibody essentially as described by Morris and Williams[12]. In the negative control for nonspecific binding (column C), tissue culture medium was substituted for culture supernatant containing B3/25 antibody. Binding of a monoclonal antibody designated A3/10 which reacts with a common antigenic determinant on HLA molecules (M.B.O. and I.S.T., unpublished results) was used as a positive control. In expt 1, 5×10^5 cells were used per assay, in expt 2, 2×10^5 cells per assay were used and in both cases the results shown represent the average of duplicate determinations.

Although the cell-surface glycoprotein is not a cell cycle-dependent antigen in a conventional sense, as its expression on induced HL-60 cells changes before the cells arrest in G1 of the cell cycle, all the previous results are consistent with the molecule being selectively expressed on actively proliferating cells. We therefore examined whether or not the molecule was present on blast cells derived from lectin-stimulated peripheral blood lymphocytes. Trace antibody binding and quantitative immunofluorescence suggested that the glycoprotein was present on the blast cells, but in such small amounts relative to the cultured cells lines that we considered the results equivocal. However, the presence on lectin-induced blasts of a similar or identical glycoprotein to that found on cell lines could be clearly demonstrated by immunoprecipitation from lysates of iodinated cells (Fig. 4). Thus, the glycoprotein or a related molecule is clearly present on normal proliferating cells. There may, however, be quantitative differences between the expression of the glycoprotein on tumour cells and normal cells and there is no evidence that the glycoprotein on the blast cells is identical to the molecule found on the tumour cell lines. These considerations are particularly relevant because, although there has been no previous report of the presence on human haematopoietic cells of a glycoprotein with similar properties to those of the surface glycoprotein defined by B3/25 monoclonal antibody, it is probable that the molecule we are studying is related to a tumour cell-surface glycoprotein described earlier by Bramwell and Harris[7,8]. This glycoprotein seems to be expressed in greater amounts on malignant cells than on nonmalignant cells and may also be structurally modified in tumour cells.

The most compelling evidence that the two glycoproteins are closely related is that both have the same apparent molecular weight on SDS-polyacrylamide gels and share the unusual

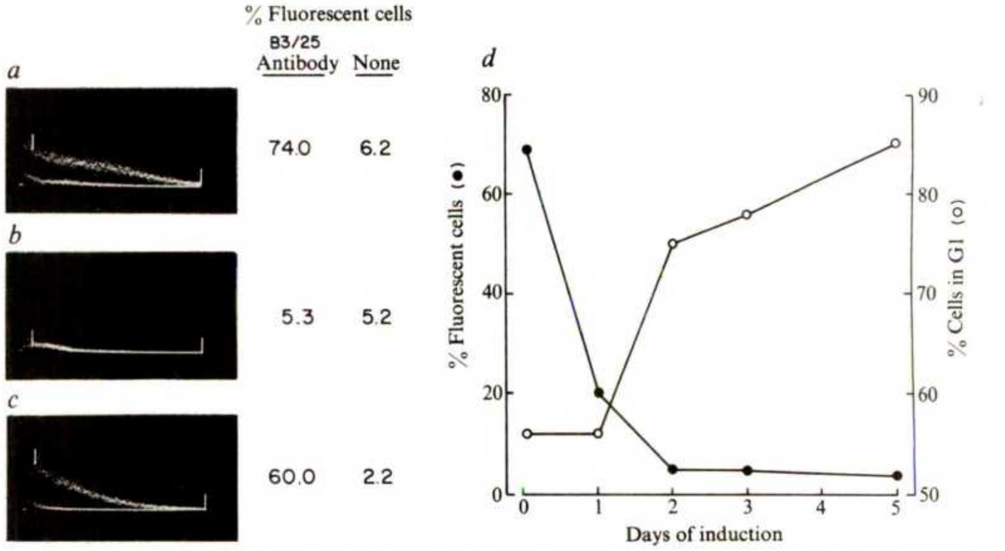

Fig. 3 Expression of B3/25 glycoprotein on induced and non-induced HL-60 cells measured by quantitative immunofluorescence. Cells were grown in the presence of 1.25% (v/v) DMSO for the period of time indicated and then stained with saturating amounts of B3/25 antibody and a fluorescein-conjugated affinity-purified goat anti-mouse IgG. Cells (50,000) were analysed on a Los Alamos-type fluorescence-activated cell analyser using a laser output of 900 mW, high voltage setting of 800 V, and a fluorescence gain of 1.0. Panels *a–c* show the histograms of non-induced HL-60 cells (*a*), HL-60 cells induced with 1.25% DMSO for 5 days (*b*), and a DMSO-resistant variant of HL-60 grown in 1.25% DMSO for 5 months (*c*) after staining with B3/25 antibody. Also shown are controls for nonspecific staining in which B3/25 antibody was omitted from the first incubation. The % of fluorescent cells within the channels indicated by the vertical bars are given. *d* Shows the % of B3/25 positive cells determined by flow microfluorimetry in the conditions just described after exposure of HL-60 cells to DMSO for various periods of time. The cell-cycle distribution of the same cells was determined from their DNA content measured by flow microfluorimetry after staining with mithramycin[22]. The % of cells in G1 is indicated.

property of existing in their native states as disulphide-bonded dimers. The glycoprotein we have studied is also similar to the molecule identified by Bramwell and Harris in other respects: it is acidic, binds to concanavalin A and wheat-germ agglutinin, and is expressed on Hela cells and other non-haematopoietic tumour cell lines (M.B.O. and I.S.T., unpublished results). Furthermore, by quantitative absorption we could not detect the glycoprotein on any normal tissue tested. Homogenates of liver, brain and kidney and red blood cells were used in the absorptions and the limit of detection was about 5% of the amount expressed on RPM1 8402, the human T-leukaemic cell line used as a positive control in these experiments.

Regardless of whether, as seems likely, the glycoprotein we have characterized is related to the one described by Bramwell and Harris, its properties warrant further investigation. Quantitative studies of the expression of the glycoprotein on normal tissues and *in vivo* tumours are required, as well as chemical characterization of the molecule isolated from both non-malignant and malignant cells. It may be possible to determine whether or not there is a causal relationship between the expression of the glycoprotein and cell proliferation by means of somatic cell genetics using HL-60 cells as a model system. It will also clearly be important to establish whether the glycoprotein is expressed on normal or leukaemic haematopoietic stem cells that can be detected by the appropriate *in vitro* assays[14–17]. The B3/25 monoclonal antibody and other monoclonal antibodies which we have obtained that react with different antigenic determinants of the same glycoprotein (I.S.T., unpublished results) will facilitate these studies.

This work was supported by grants CA 20272 and CA 14413 from the USPHS and grants from The Samuel Roberts Noble Foundation Inc. and Sigma Xi Scientific Research Society. We thank Theresa Ferson and Catherine Mazauskas for technical assistance.

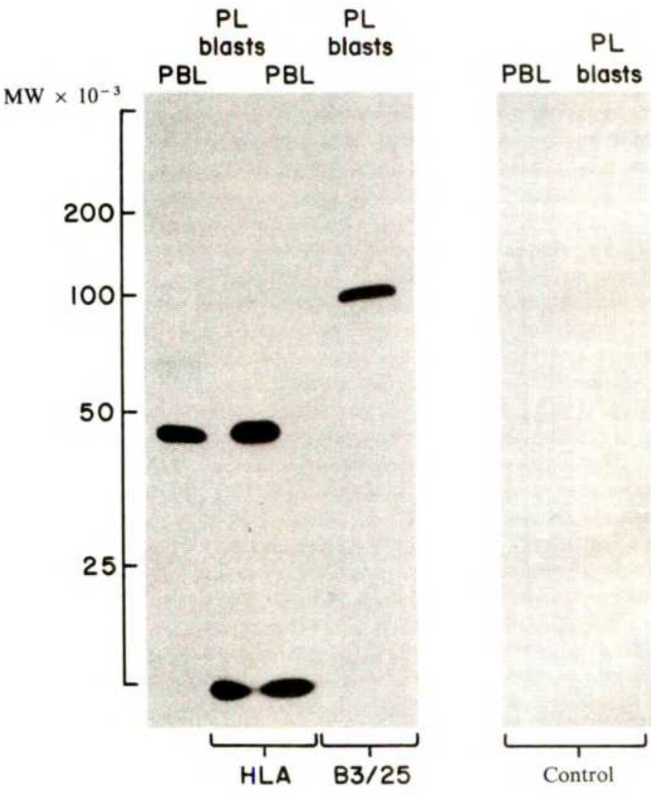

Fig. 4 Expression of B3/25 glycoprotein on lectin-stimulated peripheral blood lymphocytes (PBL). Mononuclear cells were isolated from defibrinated blood by centrifugation of Ficoll–Hypaque gradients. Fresh cells (PBL) or cells (2×10^6 per ml) stimulated for 5 days with 20 μg ml^{-1} pea lectin[23] in RPM1 1640 medium supplemented with 10% fetal calf serum (PL blasts) were iodinated and immunoprecipitates prepared and analysed as described in Fig. 1 legend except that a 10% polyacrylamide gel was used. A3/10 antibody was used to precipitate HLA as a positive control. A negative control in which B3/25 antibody was omitted from the first incubation is also shown. Exposure of the autoradiograph was 40 h.

Received 19 May; accepted 24 June 1980.

1. Gallagher, R. *et al. Blood* **54,** 713–733 (1979).
2. Collins, S. J., Ruscetti, F. W., Gallagher, R. E. & Gallo, R. C. *Proc. natn. Acad. Sci. U.S.A.* **75,** 2458–2462 (1978).
3. Collins, S. J., Ruscetti, F. W., Gallagher, R. E. & Gallo, R. C. *J. exp. Med.* **149,** 969–973 (1979).
4. Rovera, G., Santoli, D. & Damsky, C. *Proc. natn. Acad. Sci. U.S.A.* **76,** 2779–2783 (1979).
5. Huberman, E. & Callahan, M. F. *Proc. natn. Acad. Sci. U.S.A.* **76,** 1293–1297 (1979).
6. Gahmberg, C. G., Nilsson, K. & Andersson, L. C. *Proc. natn. Acad. Sci. U.S.A.* **76,** 4087–4091 (1979).

7. Bramwell, M. E. & Harris, H. *Proc. R. Soc.* **A201,** 87–106 (1978).
8. Bramwell, M. E. & Harris, H. *Proc. R. Soc.* **A203,** 93–96 (1979).
9. Lozzio, C. B. & Lozzio, B. B. *Blood* **45,** 321–334 (1975).
10. Köhler, G. & Milstein, C. *Nature* **256,** 495–497 (1975).
11. Trowbridge, I. S. *J. exp. Med.* **148,** 313–323 (1978).
12. Morris, R. J. & Williams, A. F. *Eur. J. Immun.* **5,** 274–281 (1974).
13. Rovera, G., Olashaw, N. & Meo, P. *Nature* **284,** 69–70 (1980).
14. Buick, R. N., Minden, M. D. & McCulloch, E. A. *Blood* **54,** 95–104 (1979).
15. McCulloch, E. A., Mak, T. W., Price, G. B. & Till, J. E. *Biochim. biophys. Acta* **355,** 260–299 (1974).
16. Chang, L. J. A., Till, J. E. & McCulloch, E. A. *J. cell. Physiol.* **102,** 217–222 (1980).
17. Broxmeyer, H. E. & Moore, M. A. S. *Biochim. biophys. Acta* **516,** 129–166 (1978).
18. Trowbridge, I. S., Ralph, P. & Bevan, M. J. *Proc. natn. Acad. Sci. U.S.A.* **72,** 157–161 (1975).
19. Omary, M. B. & Trowbridge, I. S. *J. biol. Chem.* **255,** 1662–1669 (1980).
20. Maizel, J. F. in *Methods in Virology* Vol. 5 (eds Maramorosch, K. & Koprowski, H.) 179–246 (Academic, New York, 1971).
21. Laskey, R. A. & Mills, A. D. *FEBS Lett.* **82,** 314–316 (1977).
22. Crissman, H. & Tobey, R. *Science* **184,** 1297–1298 (1974).
23. Trowbridge, I. S. *Proc. natn. Acad. Sci. U.S.A.* **70,** 3650–3654 (1973).

Human synovium releases a factor which stimulates chondrocyte production of PGE and plasminogen activator

J. E. Meats, M. B. McGuire & R. G. G. Russell*

Department of Human Metabolism and Clinical Biochemistry,
University of Sheffield Medical School, Beech Hill Road, Sheffield,
S10 2RX, UK

The mechanisms by which destruction of the tissues (cartilage, tendons, ligaments and bone) of joints affected by rheumatoid arthritis occurs are still poorly understood. Damage to the articular cartilage is a key event in the development of disability and deformity. Until recently it was thought that destruction of cartilage was primarily due to the release of a variety of proteolytic enzymes (collagenase and other neutral proteinases, and possibly lysosomal hydrolases) from the proliferating synovial pannus tissue[1]. Little attention has been paid to the involvement of chondrocytes themselves in the destruction of cartilage. Recently Fell and Jubb[2] have shown that when porcine synovium and cartilage are maintained in the same organ coculture system, destruction of the cartilage matrix occurs. They suggested that, in addition to inducing direct enzymatic breakdown of cartilage, synovial tissue might release a factor which activates chondrocytes to degrade their surrounding matrix. Steinberg *et al.*[3] have confirmed that synovium and cartilage interact in this way in tissue culture, with breakdown and release of proteoglycans in cartilage. The purpose of our present study was to examine whether this interaction between synovium and cartilage occurs with human tissue and to examine the mechanisms in more detail. We have, therefore, investigated the effects of normal and rheumatoid synovial tissue on chondrocytes derived from human articular cartilage. We find that the culture medium from explants of normal and rheumatoid human synovium contains a factor which stimulates the production of prostaglandin E (PGE) and plasminogen activator by chondrocytes.

Normal synovium (~1.5 g) was dissected from human knee joints obtained after surgical amputation for trauma or lower limb ischaemia. The synovial tissue was dissected into small pieces and placed in explant culture in 20 ml of Eagle's modified essential medium (MEM) with 10% (v/v) fetal calf serum (FCS) and penicillin plus streptomycin. After 1 day the medium was changed and reduced to 15 ml, with subsequent changes and collections at days 1, 6, 9, 13 and 16. Medium was stored at −20 °C. Chondrocytes were incubated with a 4% dilution of this conditioned synovial explant medium (SEM). PGE was assayed by radioimmunoassay in this medium and in the medium obtained after culture with chondrocytes. Since the antibody used detects PGB as well as PGE_1 and PGE_2, the media were subjected to silica gel microchromatography with the result that the prostaglandin produced in chondrocyte cultures was shown to be predominantly of the E-type[4].

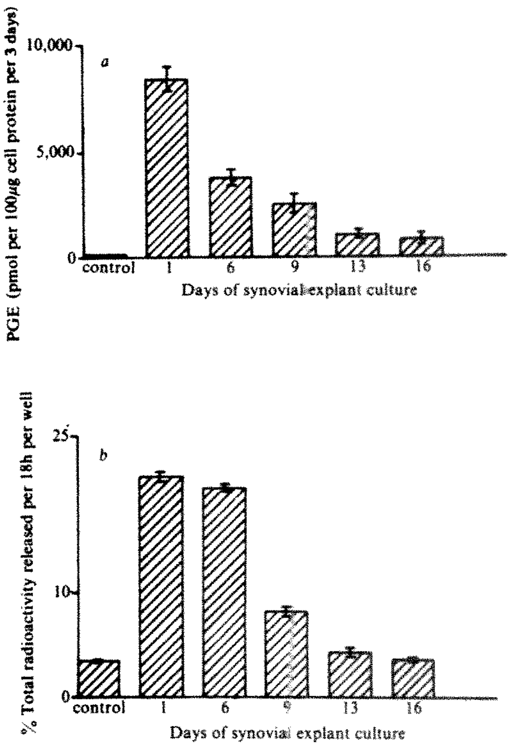

Fig. 1 *a*, Stimulation by SEM of PGE production by chondrocytes. The results represent the mean ± standard error of determinations in quadruplicate wells. A dilution of 1 : 25 (final concentration 4% v/v) of conditioned SEM in fresh MEM containing 10% FCS was added to each well containing confluent cultures of chondrocytes (second passage), derived from explants of human articular cartilage obtained from amputation specimens. Control cultures contained no SEM. Values have been corrected by subtracting the PGE present in the synovial medium (22.0% – 59.0% of total PGE measured in each well) and therefore represent the PGE produced by the chondrocytes themselves. *b*, Stimulation by SEM of production of plasminogen activator by human articular chondrocytes. Results expressed as mean ± standard error ($n = 3$ wells). Chondrocytes were grown to confluence in MEM containing 10% FCS and 20 mM HEPES buffer with 0.085% (w/v) $NaHCO_3$. Then the FCS was replaced by 10% (v/v) acid-treated FCS (acid treatment destroys the proteinase inhibitor, α_2-macroglobulin) and 4% (v/v) SEM was included in the medium. Controls did not contain SEM. Culture medium was removed after 18 h and counted for liberated ^{125}I. Residual fibrin was digested from the wells with 0.1% trypsin and this was also counted; fibrin degradation by chondrocytes was then calculated as a percentage of the total present. No significant release of ^{125}I was apparent during the preincubation of chondrocytes in normal FCS. Additional control wells containing SEM but no chondrocytes showed no significant release of ^{125}I (0.5% of the total, compared with 21.5% in the presence of chondrocytes). To demonstrate that a plasmin-like enzyme is responsible for the breakdown of fibrin, the concentration of acid-treated FCS was varied over 0–20% in the presence of a 1/25 dilution of SEM obtained after 1 day. Degradation of fibrin was shown to be dependent on the presence of serum, release of radioactivity was 0.8% ± 0.2% for cultures without serum, 5.1 ± 1.0% for those containing 5% serum and 12.9 ± 2.4% at a serum concentration of 20%. This requirement for serum to 'unmask' the fibrinolytic activity indicates that the proteinase responsible for fibrin degradation is plasmin and that the chondrocytes are releasing a plasminogen activator rather than another proteinase which directly degrades the fibrin and which would therefore act independently of the presence of serum.

To measure the release of plasminogen activator by chondrocytes, monolayer cultures were prepared using the method of Srivastava *et al.*[5], with the following modifications: fragments of cartilage were incubated in hyaluronidase (1 mg ml^{-1} in Dulbecco's Ca^{2+}- and Mg^{2+}-free phosphate-buffered saline) for 15 min, then in 0·25% trypsin for 30 min, and then digested overnight with bacterial collagenase [*Clostridium* peptidase, (Sigma type I) 3 mg ml^{-1} in MEM + 10% FCS]. Primary cultures were grown to confluence in MEM + 10% FCS, then subcultured after dislodging cells by exposure to trypsin. The cells were placed in multiwell dishes (16 mm diameter) coated with ^{125}I-fibrin[6]. Release of ^{125}I from the fibrin gel into the culture medium indicated the presence of plasminogen activator.

---

* To whom correspondence should be addressed.

0028-0836/80/350891—02$01.00

Our results indicate that a factor is produced in the synovial explant cultures which, when added to chondrocytes, stimulates the production of PGE (Fig. 1*a*). The medium obtained after one day of culture with SEM increased the production of PGE by about 50-fold and the stimulatory effect diminished with continued culture of the synovium so that after 16 days of culture the SEM produced only a five-fold elevation of PGE levels when added to chondrocytes. Figure 2 shows that the response of the chondrocytes to produce PGE is dependent on the concentration of the SEM added. Addition of dexamethasone to chondrocytes, together with SEM, suppressed this activation of prostaglandin biosynthesis (Fig. 3). Medium from explants of rheumatoid rather than normal synovium was added to chondrocytes in other experiments and exhibited similar stimulatory effects.

Figure 1*b* shows that the same SEM also markedly stimulated the production of plasminogen activator by chondrocytes. The stimulatory effect on the production of plasminogen activator also seemed to diminish the longer the synovium was kept in culture. The similarities in the profiles of activation shown in Fig. 1*a* and *b* suggest that a single stimulatory factor might be involved and that there may be a close functional relationship between the production of prostaglandin and plasminogen activator.

In addition to showing that the human synovium produces a substance(s) which stimulates chondrocytes in culture, our present experiments demonstrate the hitherto unrecognized ability of chondrocytes to produce relatively large quantities of prostaglandin in culture. Our preliminary results indicate that protein synthesis is required for production of the factor since treatment of rheumatoid synovium with cycloheximide (1 μg ml^{-1}) resulted in a 75% reduction in production of stimulatory activity (21.75 ± 2.29 as compared with 80.25 ± 5.07 ng PGE per 100 μg cell protein per 24h in the dialysed medium control. The SEM was dialysed before addition to the chondrocyte cultures to eliminate the cycloheximide).

Further work is needed to characterize the source and nature of the stimulating activity, which may be similar to the factor, named catabolin, partially characterized by Dingle *et al.*[7]. This protein, as released from porcine synovium in culture, has a molecular weight of approximately 20,000 and stimulates the breakdown of cultured bovine nasal cartilage. There is also a similarity to the mononuclear cell factor described by Dayer *et al.*[8] which stimulates production of PGE and collagenase by synovial cells and which we have found also to stimulate production of PGE by chondrocytes[9]. We have detected stimulatory activity from cultures of both normal and rheumatoid synovium which suggests that the factor is unlikely to be derived from inflammatory cells, which would only be present in appreciable numbers in pathological tissue. There are obvious similarities with a factor from rabbit macrophages which acts on rabbit chondrocytes to produce collagenase and other proteases[11,12].

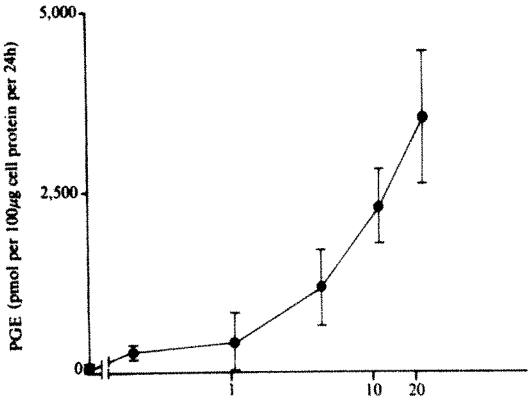

Fig. 2 The effect of SEM on PGE production by chondrocytes. The PGE originating from the SEM has been subtracted from each point. SEM collected at day 1 was incubated with chondrocytes for 24 h at dilutions between 1:250 and 1:5 (to give final concentrations of SEM in the culture fluid ranging from 0.4% and 20% as shown on the abscissa). Control cultures contained no SEM. The points shown are mean ± standard error of quadruplicate wells.

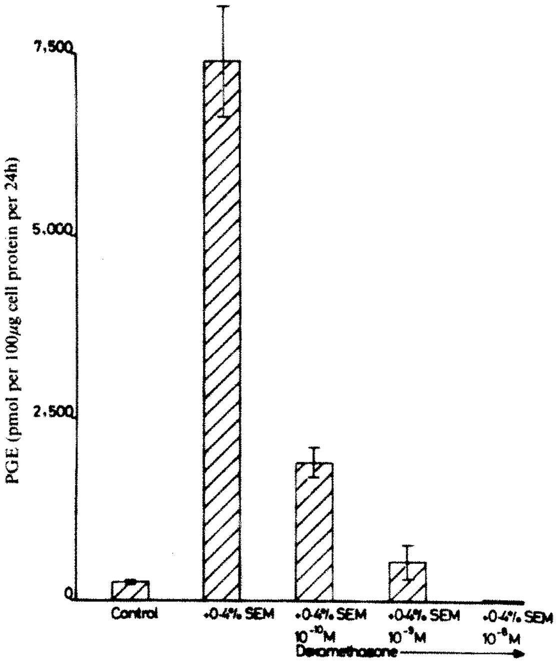

Fig. 3 Inhibition by dexamethasone of PGE production by human articular chondrocytes. Results are expressed as mean ± standard error of quadruplicate wells. Cultures did not contain FCS. SEM was collected on days 0–4 of culture and incubated with chondrocytes for 24 h. Controls did not contain SEM. PGE produced by the synovial explants has been subtracted from each point.

The release of this factor from synovium could be of considerable significance in the pathogenesis of joint disease. Enhanced production of prostaglandins by chondrocytes could contribute to the increased PGE concentration found in synovial fluids in inflammatory arthritis[10]. PGE derived from chondrocytes could alter vascular permeability in adjacent tissues and could also stimulate resorption of the subchondral bone. These prostaglandins might also influence the rate of proliferation of the synovial pannus and be involved in controlling the mobility and activity of inflammatory cells. The plasminogen activator released by chondrocytes could itself degrade cartilage matrix by direct proteolytic attack or could take part in the conversion of collagenase from latent to active form. This factor from synovial tissue could therefore be responsible for some aspects of the tissue damage seen in joints in rheumatoid arthritis. The mechanisms that prevent such a factor from acting in normal conditions and which might allow its release in pathological circumstances require further investigation. The remarkable potency of added steroid in inhibiting the action of the factor on cartilage suggest that this may be one way in which steroids exert their therapeutic action in rheumatoid arthritis.

We thank the Nuffield Foundation and the SRC for financial support for this work, Dr Hamish Humphrey (Glaxo) for the gift of ^{125}I-labelled fibrin plates and Dr L. Levine for prostaglandin antiserum.

Received 29 January; accepted 20 June 1980.

1. Harris, E. D. in *Joints and Synovial Fluid* Vol. 1 (ed. Sokoloff, L.) 243–272 (Academic, New York, 1978).
2. Fell, H. B. & Jubb, R. W. *Arthritis Rheum.* **20,** 1359–1370. (1977).
3. Steinberg, T., Sledge, C. B., Noble, J. & Stirrat, C. R. *Biochem. J.* **18,** 403–412 (1979).
4. Hillier, K. & Dilley, S. R. *Prostaglandins* **5,** 137–150 (1974).
5. Srivastava, V. M. L., Malemud, C. J., Haug, A. J., Bland, J. H. & Sokoloff, L. *Arthritis Rheum.* **19,** 165–169 (1974).
6. Unkless, J. C. *et al. J. exp. Med.* **137,** 85–111 (1973).
7. Dingle, J. T., Saklatvala, J., Hembry, R. & Tyler, J. *Biochem. J.* **184,** 177–180 (1979).
8. Dayer, J. M., Robinson, D. R. & Krane, S. M. *J. exp. Med.* **45,** 1399–1403 (1977).
9. Englis, D. J. *et al.* in *Advances in Prostaglandin and Thromboxane Research* Vol. 8 (eds Samuelsson, B., Ramwell, P. W. & Paoletti, R.) 1709–1711 (Raven, New York, 1980).
10. Robinson, D. R., McGuire, M. B. & Levine, L. *Ann. N. Y. Acad. Sci.* **256,** 318–329 (1975).
11. Deshmukh-Phadke, K., Nanda, S. & Lee, K. *Eur. J. Biochem.* **104,** 175–180 (1980).
12. Deshmukh-Phadke, K., Lawrence, M. & Nanda, S. *Biochem. biophys. Res. Commun.* **85,** 490–496 (1978).

Biosynthesis of hepatitis B virus surface antigen in *Escherichia coli*

Patrick Charnay, Monica Gervais, Anne Louise, Francis Galibert* & Pierre Tiollais

Unité de Recombinaison et Expression Génétique (INSERM U.163), Institut Pasteur, 28 rue du Dr Roux, 75724 Paris Cedex 15, France
* Laboratoire d'Hématologie Expérimentale, Centre Hayem, Hôpital Saint-Louis 2, place A. Fournier, 75010 Paris, France

Hepatitis B is a widespread viral disease[1]. In the absence of cell cultures capable of propagating the virus (HBV) an efficient vaccine has been prepared from viral envelopes isolated from the plasma of chronic carriers[2–4]. The major polypeptide of the envelope is one of molecular weight 25,000 which carries the surface antigen (HBsAg)[5–8]. Therefore, the biosynthesis of this polypeptide in *Escherichia coli* may offer an alternative procedure to produce HBsAg free from human proteins. Recently, the *HBV* genome has been cloned in *E. coli*[9–11]. Determination of its primary structure allowed the localization of the gene (called gene *S*) coding for HBsAg[12–15] and the synthesis of the core antigen in *E. coli* has been reported[9]. We have constructed a derivative of bacteriophage lambda carrying a fusion between the β-galactosidase gene (*lacZ*) and the HBsAg coding sequence (*λlacHBs-1*). Infection of *E. coli* with *λlacHBs-1* leads to the biosynthesis of a polypeptide of molecular weight 138,000 carrying antigenic determinants of HBV surface antigen.

Expression of an eukaryotic gene in *E. coli* can be obtained by fusion between the foreign gene and a bacterial gene carried by a plasmid or a phage. Thus the *lacZ* gene has already been used for hormone biosynthesis[16,17]. Sequential steps in the construction of the gene fusion between gene *S* and gene *lacZ* are illustrated in Fig. 1. By *Hha*I treatment of the previously cloned *HBV* DNA[10], we prepared a 1,084 base pair long DNA fragment which carried the entire gene *S*. Using S_1 endonuclease and *Eco*RI linkers 5'GGAATTCC, this fragment was cloned in *E. coli* using the plasmid pBR322 (ref. 20). The recombinant plasmid pBRHBs has only one *Xba*I restriction site located at the beginning of gene *S*. Digestion of this plasmid with *Eco*RI plus *Xba*I endonucleases, followed by a purification using agarose gel electrophoresis gave a DNA fragment of about 980 base pairs carrying a major part of gene *S*. After treatment with S1 endonuclease, addition of *Eco*RI linkers, and cleavage with *Eco*RI endonuclease, this 980 base pair DNA fragment was cloned in *E. coli* using the plasmid pBR322. Several clones were obtained; the DNA of three clones (p*XbaHBs-1*, p*XbaHBs-2* and p*XbaHBs-3*) was extracted and the 980-base pair *Eco*RI restriction fragment, called *HBs*-fragment, was purified in each case. Determination of the nucleotide sequence of the *Eco*RI extremity corresponding to gene *S* revealed that the nucleotide sequence was not identical in the three clones (Fig. 1*A*). The differences were possibly due to heterogeneity in the S1 endonuclease digestion. The bacteriophage λ*plac5-1UV5* genome[19] has only one *Eco*RI site located at the end of the *lacZ* gene. The reading frame of this gene at the *Eco*RI site can be deduced from the amino acid sequence of the β-galactosidase[21]. Based on the nucleotide sequence, the insertion of the *HBs* fragment from p*XbaHBs-1* into the *Eco*RI site of the *lacZ* gene of λ*plac5-1UV5* genome should lead to conservation of the reading frame of gene *S*. The recombinant bacteriophage should

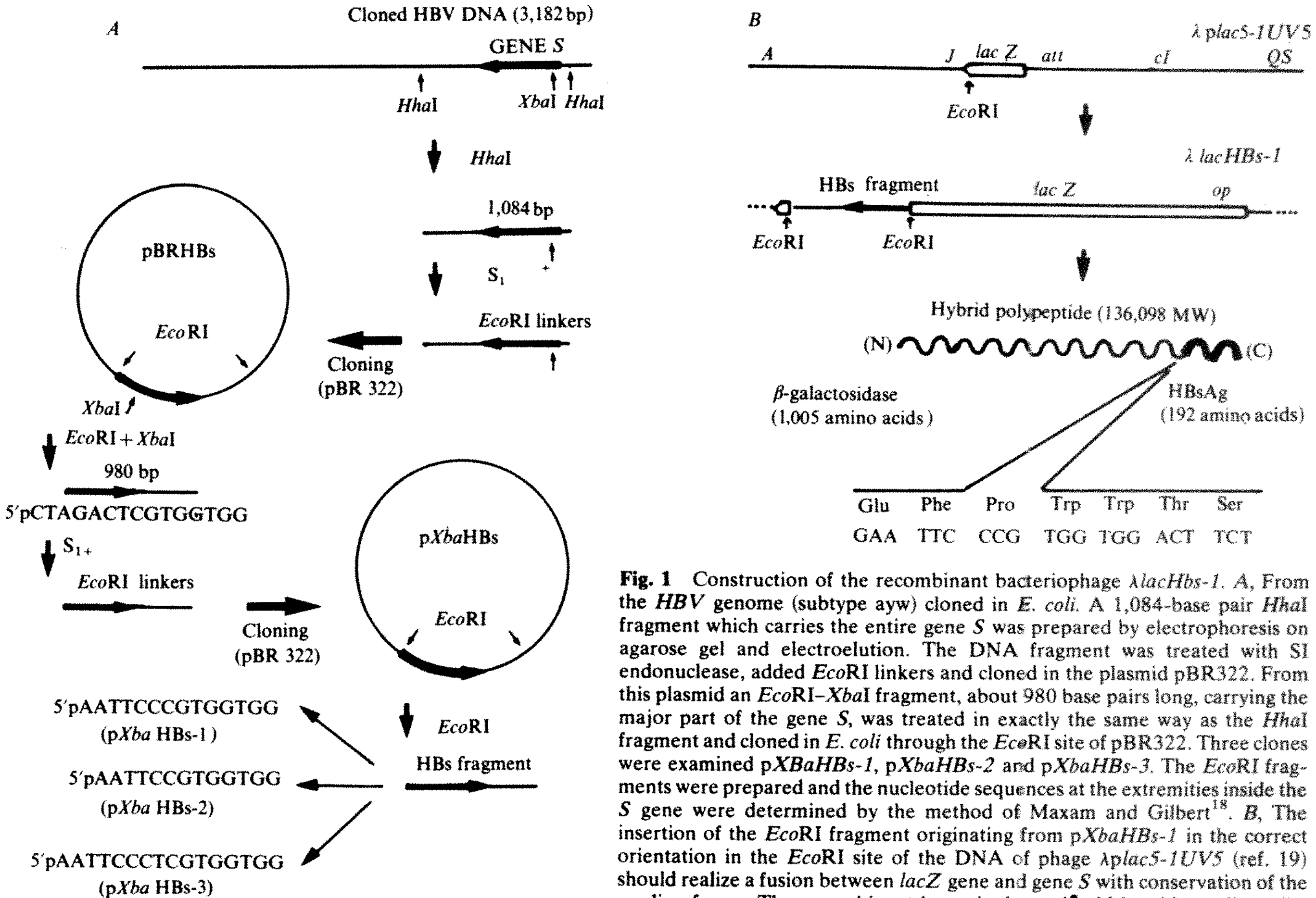

Fig. 1 Construction of the recombinant bacteriophage λ*lacHbs-1*. *A*, From the *HBV* genome (subtype ayw) cloned in *E. coli*. A 1,084-base pair *Hha*I fragment which carries the entire gene *S* was prepared by electrophoresis on agarose gel and electroelution. The DNA fragment was treated with SI endonuclease, added *Eco*RI linkers and cloned in the plasmid pBR322. From this plasmid an *Eco*RI–*Xba*I fragment, about 980 base pairs long, carrying the major part of the gene *S*, was treated in exactly the same way as the *Hha*I fragment and cloned in *E. coli* through the *Eco*RI site of pBR322. Three clones were examined p*XBaHBs-1*, p*XbaHBs-2* and p*XbaHBs-3*. The *Eco*RI fragments were prepared and the nucleotide sequences at the extremities inside the *S* gene were determined by the method of Maxam and Gilbert[18]. *B*, The insertion of the *Eco*RI fragment originating from p*XbaHBs-1* in the correct orientation in the *Eco*RI site of the DNA of phage λ*plac5-1UV5* (ref. 19) should realize a fusion between *lacZ* gene and gene *S* with conservation of the reading frame. The recombinant bacteriophage should be able to direct the synthesis of a hybrid polypeptide of molecular weight 136,098 with a NH_2 terminal portion consisting of almost the entire β-galactosidase and a COOH terminal portion consisting of a great part of the HBsAg major protein.

0028-0836/80/350893—03$01.00

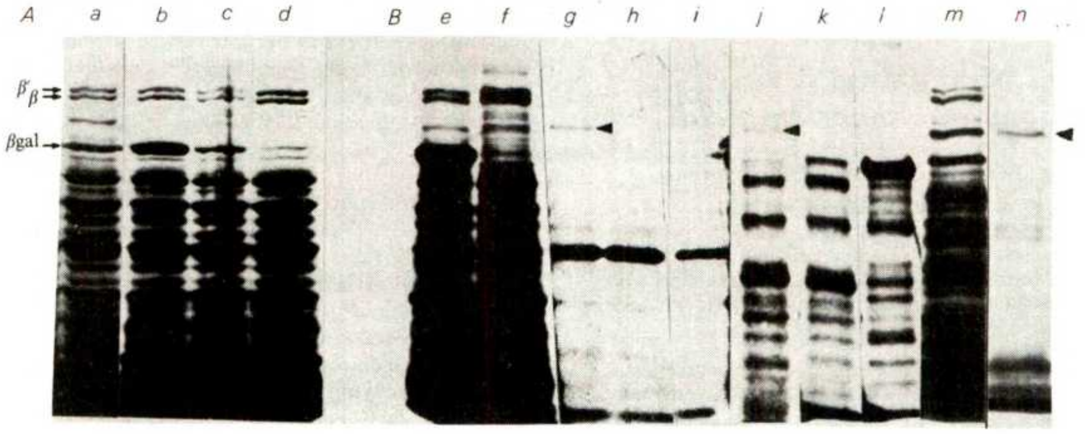

Fig. 2 Immunoprecipitation of the β-galactosidase–HBsAg hybrid protein. *A*, *E. coli* K12 3,000X74 was grown in Laemmli medium and concentrated to an absorbance of 10 units in $MgSO_4$, 10 mM. Phages were absorbed for 15 min at a multiplicity of infection of 4. Cells were diluted 10 times in Laemmli medium and incubated 25 min at 37 °C, centrifuged, resuspended in Laemmli final sample buffer[23] and boiled for 5 min. The proteins were electrophoresed on a 6% polyacrylamide–SDS gel[23] and stained with Coomassie blue. The proteins from cells infected with the following bacteriophages are shown: *a*, λ*lacHBs-1*; *b*, λp*lac5-1UV5*; *c*, λ*lacHBs-2*; *d* contains an extract of uninfected 3,000X74. The arrows show the position of size markers: β-galactosidase[21] and β,β′ subunits of RNA polymerase[24]. *B*, Infected cells were diluted 10 times in Laemmli medium (Bacto-Tryptone: 10 g, Bacto yeast extract: 5 g, NaCl: 10 g in 1 L *p*H 7.3) containing $[^{35}S]$ methionine (1050 Ci mmol^{-1}, 150 μCi ml^{-1}) and incubated for 25 min at 37 °C. Cells were centrifuged, resuspended in one-tenth volume (Tris *p*H 8 : 10 mM, EDTA : 5 mM, lysozyme : 0.5 mg ml^{-1}, PTSF : 30 μg ml^{-1}) and lysed by three freeze–thaw cycles. The suspension was then made up to 10 mM $MgCl_2$ and 20 μg ml^{-1} DNase was added; it was incubated for 15 min in ice and centrifuged. The supernatant was used for immunoprecipitation as follows: to 80 μl of this *E. coli* extract were added 120 μl TNT buffer (Tris *p*H 7.5 : 50 mM, NaCl : 150 mM, Triton X100 1%) and 2 μl antiserum and the mixture was incubated for 60 min at 37 °C. Then, 100 μl of a suspension of Protein A–Sepharose CL-4B (Pharmacia) in TNT buffer (100 mg ml^{-1}) was added and incubation was continued for 1 h at 0 °C. The beads were pelleted by a 3 min centrifugation in an Eppendorf microfuge and then washed once with 500 μl TNT buffer, three times with 500 μl LiCl buffer (LiCl 500 mM, Triton X-100 1%, SDS 0.1%) and twice with 500 μl Tris *p*H 8 : 10 mM. Finally, radioactive proteins were eluted from the beads by boiling for 5 min in 40 μl Laemmli final sample buffer[23]. They were electrophoresed on a 6% polyacrylamide-SDS gel[23] which was then treated for fluorography[25], dried and subjected to autoradiography with flash-activated Kodak Royal X-Omat films at −70 °C (ref. 26). The figure shows the proteins from cells infected with the following bacteriophages: *e*, λp*lac5-1UV5*; *f*, λ*lacHBs-1*; *g*, λ*lacHBs-1*, immunoprecipitation with human antiserum to HBsAg (subtype ayw) (generous gift from Dr J. Drouet); *h*, λ*lacHbs-1*, immunoprecipitation with the same antiserum to HBsAg in presence of HBsAg 100 μg ml^{-1}; *i*, λp*lac5-1UV5*, immunoprecipitation with the same antiserum to HBsAg; *j*, λ*lacHBs-1*, immunoprecipitation with rabbit antiserum to β-galactosidase (gift from Dr N. Guiso); *k*, λ*lacHBs-2*, immunoprecipitation with antiserum to β-galactosidase; *l*, λp*lac5-1UV5* immunoprecipitation with antiserum to β-galactosidase; *m*, λ*lacHBs-1QOS* (cells are incubated 90 min at 37 °C after infection); *n*, λ*lacHBs-1QOS*, immunoprecipitation with a sheep antiserum to purified HBs Ag of ad and ay subtypes (gift from Dr J. Pillot).

be able to direct the synthesis of a hybrid polypeptide of molecular weight 136,098 (Fig. 1*B*). The *HBs* fragment from p*XbaHBs-2* did not have a nucleotide sequence in the correct reading frame and it could be used as a control in further experiments. The *HBs* fragments from p*XbaHBs-1* and p*XbaHBs-2* were ligated with λp*lac5-1UV5* DNA previously cleaved with *Eco*RI endonuclease. The mixture was used to transfect *E. coli* strain C600*recBC rk*$^{-}$ *mk*$^{-}$. Since the insertion of a DNA fragment into the *Eco*RI site inactivates the *lacZ* gene[22], the *lac*$^{-}$ bacteriophage clones were purified on bacterial strain LA101[22]. The DNA of different bacteriophages was extracted and the orientation of the inserted DNA fragment was determined by electrophoretic analysis of the *Bam*HI restriction fragments. Two phage derivatives λ*lacHBs-1* and λ*lacHBs-2* corresponding to the plasmids p*XbaHBs-1* and p*XbaHBs-2* respectively had the *HBs* fragment in the correct orientation.

We infected strain 3,000X74 (Hfr Δ*lac*X74, Institut Pasteur Collection) with λp*lac5-1UV5*, λ*lacHBs-1* and λ*lacHBs-2*. The bacterial protein lysates were analysed by polyacrylamide–SDS gel electrophoresis[23] and Coomassie blue coloration (Fig. 2*A*). The comparison of the three electrophoretic patterns revealed two major differences: in the case of λp*lac5-1UV5*, a much more intense band was observed at a position corresponding to β-galactosidase (molecular weight 116,248) mobility[21]; in the case of λ*lacHBs-1* a new protein species (P138) of molecular weight 135,000–141,000 was detected. This protein was not present after infection with λ*lacHBs-2*.

Proteins synthesized after λ*lacHBs-1* and λp*lac5-1UV5* infection were labelled with $[^{35}S]$ methionine. Precipitation with human antiserum to HBsAg followed by autoradiography of the polyacrylamide–SDS gel revealed a band present in the case of infection with λ*lacHBs-1* and absent in the case of λp*lac5-1UV5* (Fig. 2*B*). This band disappeared specifically when the immunoprecipitation was carried out in presence of cold HBsAg. The precipitated protein co-migrated with the P138 protein. The same band was observed after immunoprecipitation with a sheep antiserum to purified HBsAg. A band was also present at the same position after immunoprecipitation with an antiserum to β-galactosidase (Fig. 2*B*).

These results demonstrate that *E. coli* infected with the bacteriophage λ*lacHBs-1* synthesizes a protein of approximate molecular weight 138,000 with antigenic determinants of both HBsAg and β-galactosidase. These characteristics are exactly those predicted for the fusion polypeptide. The quantity of hybrid polypeptide was estimated by scanning the stained gels. It represents about 10% of the quantity of β subunit of the RNA polymerase, and about 1.5% of the quantity of β-galactosidase obtained after infection with λp*lac5-1UV5*. Assuming that the β subunit represents less than 0.7% of the total cell protein[27] the quantity of the hybrid protein should account for approximately 0.05% of total cell protein. An explanation for the low amount of hybrid polypeptide obtained could be proteolysis. Indeed, when the bacteria are lysed in the absence of protease inhibitor, the amount of P138 protein is still lower. Nevertheless, the introduction of amber mutations into genes *Q* and *S*[22,28] of λp*lac HBs-1* genome, by genetic crossing with the bacteriophage λp*lac5imm434Qam501Sam7* (ref. 22) enhances the P138 polypeptide production by a factor of approximately five (Fig. 2*B*). The β-galactosidase–HBsAg hybrid polypeptide provides a model for coupling HBsAg with a carrier protein in an immunoreactive form ultimately useful in newer vaccine against HBV infection[28]. Moreover, the results presented reinforce the hypothesis that there is no intervening sequence in the HBsAg coding sequence[12,13].

Containment conditions for this study were recommended by the French National Control Committee. Growth of recombinant bacteriophages and plasmids was carried out in L3 conditions. We thank Drs P. A. Cazenave, D. Perrin, J. Thèze and G. N. Vyas for helpful discussions, J. Shapiro for reviewing the manuscript, and Drs A. Drouet and J. Drouet for critical suggestions and for providing antisera and HBsAg.

Received 10 March; accepted 6 June 1980.

1. Szmuness, W. *Am. J. Path.* **81,** 629–649 (1975).
2. Purcell, R. H. & Cerin, J. L. *Am. J. med. Sci.* **270,** 395–399 (1975).
3. Hilleman, M. R. *et al. Am. J. med. Sci.* **270,** 401–404 (1975).
4. Maupas, P., Coursaget, P., Goudeau, A. & Drucker, J. *Lancet* **i,** 1367–1370 (1976).
5. Vyas, G. N., Williams, E. W., Klaus, G. G. B. & Bond, H. E. *J. Immun.* **108,** 1114–1118 (1972).
6. Chairez, R., Steiner, S., Melnick, J. L. & Dreesman, G. R. *Intervirology* **1,** 224 (1973).
7. Chairez, R., Hollinger, F. B., Brunschwig, J. P. & Dreesman, G. R. *J. Virol.* **15,** 182 (1975).
8. Peterson, D. L., Roberts, I. M. & Vyas, G. N. *Proc. natn. Acad. Sci. U.S.A.* **74,** 1530–1534 (1977).
9. Burrel, C. J., Mackay, P., Greenaway, P. J., Hofschneider, P. H. & Murray, K. *Nature* **279,** 43–47 (1979).
10. Charnay, P., Pourcel, C., Louise, A., Fritsch, A. & Tiollais, P. *Proc. natn. Acad. Sci. U.S.A.* **76,** 2222–2226 (1979).
11. Sninsky, J. J., Siddiqui, A., Robinson, W. S. & Cohen, S. N. *Nature* **279,** 346–348 (1979).
12. Valenzuela, P. *et al. Nature* **280,** 815–819 (1979).
13. Charnay, P. *et al. Nucleic Acids Res.* **7,** 335–346 (1979).
14. Galibert, F., Mandart, E., Fitoussi, F., Tiollais, P. & Charnay, P. *Nature* **281,** 646–650 (1979).
15. Pasek, M. *et al. Nature* **282,** 575–579 (1979).
16. Itakura, K. *et al. Science* **198,** 1056–1063 (1977).
17. Goeddel, D. V. *et al. Proc. natn. Acad. Sci. U.S.A.* **76,** 106–110 (1979).
18. Maxam, A. M. & Gilbert, W. *Proc. natn. Acad. Sci. U.S.A.* **74,** 560–564 (1977).
19. Charney, P., Louise, A., Fritsch, A., Perrin, D. & Tiollais, P. *Molec. gen. Genet.* **170,** 171–178 (1979).
20. Bolivar, F. *et al. Gene* **2,** 95–113 (1977).
21. Fowler, A. V. & Zabin, I. *Proc. natn. Acad. Sci. U.S.A.* **74,** 1507–1510 (1977).
22. Pourcel, C., Marchal, C., Louise, A., Fritsch, A. & Tiollais, P. *Molec. gen. Genet.* **170,** 161–169 (1979).
23. Laemmli, U. K. *Nature* **227,** 680–685 (1970).
24. Burgess, R. R. *J. biol. Chem.* **244,** 6168–6176 (1969).
25. Bonner, W. M. & Laskey, R. A. *Eur. J. Biochem.* **46,** 83–88 (1974).
26. Laskey, R. A. & Mills, A. D. *Eur. J. Biochem.* **56,** 335–341 (1975).
27. Iwakura, Y., Ito, K. & Ishihama, A. *Molec. gen. Genet.* **133,** 1–23 (1974).
28. Moir, A. & Brammar, W. J. *Molec. gen. Genet.* **149,** 87–99 (1976).
29. Talwai, G. P. *et al. Proc. natn. Acad. Sci. U.S.A.* **73,** 218–222 (1976).

Different target antigens for T-cell subsets acting synergistically *in vivo*

Emile A. J. Wolters* & Robbert Benner†

*Erasmus University, Department of Cell Biology & Genetics, PO Box 1738, 3000 DR, Rotterdam, The Netherlands
† Basel Institute for Immunology, Basel, Switzerland

After allogenic transplantation of lymphoid cells into immunologically incompetent recipients, a graft-versus-host (GvH) reaction can occur. The original observation that the GvH reaction is mediated by two interacting types of T cell[1] has led to the proposal that T cells must be subdivided into two subpopulations according to life span and migratory properties. These consist of T_1 cells, which are short-lived, sessile cells sensitive to adult thymectomy (ATx), and T_2 cells, which are long-lived, recirculating cells sensitive to anti-thymocyte serum (ATS)[2]. T_1–T_2 cooperation has also been demonstrated *in vitro* in murine[3] and rat[4] mixed lymphocyte culture. The question arises as to whether these T-cell subpopulations are activated by different or identical parts of the major histocompatibility complex (MHC). We report here that for optimal development of the anti-host immune response in a murine GvH reaction, T_2 cells have to be amplified by T_1 cells. The former cells are activated by a set of MHC gene products that are expressed mainly on immunological cells (H–2I-coded antigens), whereas the latter recognize a different set of MHC gene products that are expressed on almost all cells of the mouse (H–2K/D-coded antigens).

A delayed type hypersensitivity (DTH) assay was used to measure the development of specific anti-host directed T-effector cells[5]. The generation of these T-effector cells is induced by the host histocompatibility (H) antigens during a GvH reaction. Therefore, spleen and lymph node cells from mice which have been irradiated and reconstituted with allogeneic lymphoid cells are transferred intravenously (i.v.) into normal secondary recipients syngeneic to the original spleen cell donor. In these secondary recipients, the anti-host DTH reactivity is assayed by challenging the animals with the specific antigen and measuring the specific DTH response 24 h later.

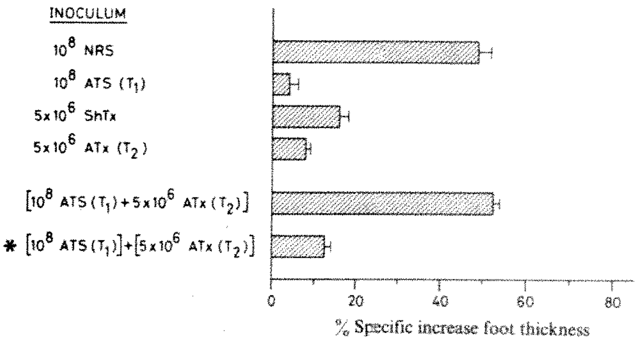

Fig. 1 GvH-related DTH responsiveness of spleen cells of lethally irradiated (C57BL/Rij × CBA/Rij)F_1 mice ($H{-}2^{b/k}$) reconstituted with T_1 and/or T_2 cells from DBA/2 mice ($H{-}2^d$). The DBA/2 donors were either treated *in vivo* with ATS (or NRS as a control) or were adult thymectomized (ATx) (or sham-thymectomized (ShTx) as a control) 6–8 weeks previously. ATS spleen cells were used as a source of T_1 cells, and ATx spleen cells as a source of T_2 cells. Five days after irradiation and reconstitution, the spleen cells of each recipient were i.v. transferred into a naive DBA/2 mouse. An asterisk means that T_1 and T_2 cells were separately injected into different lethally irradiated (C57BL × CBA)F_1 recipient mice. In that case, the spleen cells from both types of primary recipients were simultaneously transferred into the secondary DBA/2 recipients. All secondary recipients were challenged into the instep of the right hind foot with 2×10^7 (C57BL × CBA)F_1 spleen cells. These spleen cells were treated with mitomycin C (Kyowa Hakko Kogyo), 100 $\mu g\ ml^{-1}$ for 30 min at 37 °C. At 24 h after challenge, the anti-host DTH reactivity was measured as the difference in thickness of the hind feet. The relative specific increase is calculated as the relative increase in foot thickness of the immune mice minus the relative increase in foot thickness of control mice, which had only received the challenge injection. The swelling of these control mice was 12–20%. DTH responses are expressed as the specific percentage increase in foot thickness. Horizontal bars represent 1 s.e.m. ($n = 5$).

For the experiments reported here, T_1 cells were obtained by pretreatment of spleen cell donor mice with ATS *in vivo*. This pretreatment gives an enrichment of T_1 cells in the spleen by selective depletion of the pool of recirculating T_2 cells[6]. Long-lived T_2 cells were obtained either from the spleen of donors 6–8 weeks after ATx, or by isolation *in vivo* of recirculating, lymph node-seeking T_2 cells according to the method of Tigelaar and Asofsky[7].

We have previously shown that spleen cell transplantation across H-2 differences into lethally irradiated recipients did result in a transferrable anti-host DTH response[5,8]. After transplantation of as much as 10^8 ATS-treated DBA/2 spleen cells, as a source of T_1 cells, into lethally irradiated (C57BL × CBA)F_1 mice, no significant anti-host DTH-response developed (Fig. 1). In contrast, such a reactivity did appear after transplantation of 5×10^6 spleen cells from ATx DBA/2 mice as a source of T_2 cells (Fig. 1). In this combination, simultaneous transplantation of T_1 cells and T_2 cells gave a much higher anti-host DTH response than the T_2 cells only. Anti-Thy-1.2 treatment of cell suspensions containing either T_1 or T_2 cells could completely prevent amplifier and effector cell activity,

Table 1 The target H-2-subregion coded antigens for T_1 and T_2 cells

Inoculum	Recipient	H-2 subregion coding for immunizing antigen*	DTH response
10^8 C57BL NRS spleen	B10.G	K+I+D	25.9 ± 1.4
10^8 C57BL ATS spleen (T_1)	B10.G	K+I+D	−1.8 ± 3.2
1 LNS eq. C57BL (T_2)	B10.G	K+I+D	8.1 ± 1.4
10^8 C57BL ATS spleen (T_1) + 1 LNS eq. C57BL (T_2)	B10.G	K+I+D	25.2 ± 2.3
10^8 B10.AQR NRS spleen	B10.A × B10.T(6R)	K+I	33.4 ± 2.6
10^8 B10.AQR ATS spleen (T_1)	B10.A × B10.T(6R)	K+I	3.5 ± 2.5
1 LNS eq. B10.AQR (T_2)	B10.A × B10.T(6R)	K+I	11.4 ± 2.0
10^8 B10.AQR ATS spleen (T_1) + 1 LNS eq. B10.AQR (T_2)	B10.A × B10.T(6R)	K+I	26.8 ± 1.2
10^8 B10.AQR NRS spleen	B10.T(6R)	I	34.4 ± 3.3
10^8 B10.AQR ATS spleen (T_1)	B10.T(6R)	I	−0.9 ± 1.8
1 LNS eq. B10.AQR (T_2)	B10.T(6R)	I	19.6 ± 2.9
10^8 B10.AQR ATS spleen (T_1) + 1 LNS eq. B10.AQR (T_2)	B10.T(6R)	I	20.4 ± 1.6
10^8 A.TL NRS spleen	A.TH	I	31.2 ± 2.1
10^8 A.TL ATS spleen (T_1)	A.TH	I	0.1 ± 2.1
1 LNS eq. A.TL (T_2)	A.TH	I	16.5 ± 1.9
10^8 A.TL ATS spleen (T_1) + 1 LNS eq. A.TL (T_2)	A.TH	I	15.1 ± 2.0

GvH reactions were elicited by i.v. injection of the inoculum into lethally irradiated recipient mice. Recipients were lethally irradiated (700 rad) within 4 h before reconstitution. At 5 days after reconstitution a number of cells equivalent to the total cell yield obtained from spleen, inguinal, axillary and mesenteric lymph nodes of a recipient mouse were transferred i.v. to a secondary recipient syngeneic to the original spleen cell donor. Lymphoid cells from all primary recipients of a particular combination were pooled before secondary transfer. Immediately after transfer to the secondary recipients, these recipients were challenged in the right hind foot with 2×10^7 spleen cells syngeneic to the original irradiated recipients. At 24 h after challenge of the secondary recipients, DTH responses were measured. Numbers represent the arithmetic mean ± 1 s.e.m. of five mice. In view of the different donor-recipient combinations, the improvement of the T_2-cell-mediated DTH reactivity by admixing T_1 cells should be judged separately within each of the four different combinations. T_1 cells were obtained by pretreatment of donor mice subcutaneously with 0.2 ml ATS (or normal rabbit serum (NRS) as control). This amount was equally distributed over the inguinal and axillary areas. These injections were given 5 and 2 days before collecting the spleen cells. T_2 cells were isolated *in vivo*. 15×10^7 pooled spleen, peripheral and mesenteric lymph node cells of a particular donor strain were i.v. injected into syngeneic recipients which had been lethally irradiated 2 h previously. At 24 h after inoculation, only the peripheral lymph nodes were obtained from these recipients. Such peripheral lymph nodes contained about 4×10^6 more nucleated cells than lymph nodes from lethally irradiated, non-reconstituted mice. The cell yield from all peripheral lymph nodes of a single irradiated recipient is called one lymph node seeking equivalent (1 LNS eq.).

* H-2 subregion difference between inoculum donors and irradiated recipient mice. The origin of H-2 subregions (K, I-A, I-B, I-C, D) for the strains are as follows: A.TH, ssssd; A.TL, skkkd; B10.A, kkkdd; B10.AQR, qkkdd; B10.T(6R), qqqqd; C57BL, bbbbb; B10.G, qqqqq.

respectively[9]. When T_1 and T_2 cells were separately activated by H antigens and thereafter combined and simultaneously transferred into secondary recipients, no synergistic reactivity was observed (Fig. 1). This indicates that cooperation of T_1 and T_2 cells only occurs during the induction phase of the anti-host immune response and not during the inflammatory reaction in the challenged foot of the secondary recipients.

In Table 1, upper part, T_1–T_2 synergism is shown for the anti-host DTH response of C57BL lymphoid cells against B10.G mice (which differ at the K, I and D subregions of the H-2 complex), and after transplantation of B10.AQR lymphoid cells into (B10.A × B10.T(6R))F_1 mice (which differ at the K and I subregions). Also in these combinations, simultaneous transplantation of T_1 and T_2 cells gave a much higher anti-host DTH response than the T_2 cells alone. Because the anti-host DTH response after transplantation across a whole H-2 difference is directed exclusively to H-2I-coded antigens[8], and H-2K/D antigens by themselves are unable to evoke an anti-host DTH response[10], these results might suggest that T_1 cells are activated by H-2K and/or H-2D region-coded antigens, and amplify the anti-H-2I response by T_2 cells. This hypothesis was evaluated by testing the occurrence of T_1–T_2 synergism during the development of an anti-host DTH response in the case of transplantation across a H-2I difference only. This was done by transplanting T_1 and T_2 cells from B10.AQR mice into lethally irradiated B10.T(6R) mice and from A.TL mice into irradiated A.TH recipients. In both situations, no evidence for T_1–T_2 synergism could be found (Table 1, lower part). Thus, T_1 cells must be activated by H-2K/D antigens to display amplifier activity. The formal proof of this conclusion would be a positive response after transfer of mixtures of the two T-cell subpopulations after separate activation of the T_2 cells by I-coded antigens and of the T_1 cells by K/D-region coded antigens. However, such experiments are impossible because simultaneous transfer of separately activated T_1 and T_2 cells does not result in any detectable synergistic activity (Fig. 1).

The consequence of the differential specificity of receptors of T_1 (anti H-2K/D) and T_2 (anti-H-2I) cells is that both subpopulations must belong to different, parallel lines of T-cell differentiation. Recent observations[11,12] suggest that there are two separate lines of intra-thymic T-cell differentiation with regard to Lyt phenotype, one line leading to Lyt 1^+ T cells and the other to Lyt 123^+ T cells. The latter cells might further differentiate into Lyt 23^+ cells after their migration as Lyt 123^+ cells to the periphery[12,13]. A part of this post-thymic Lyt 123^+ population is ATx sensitive and may be identical to the T_1 population[14]. The data presented here indicate that post-thymic T_1 cells (probably Lyt 123^+ cells), on stimulation by K- and/or D-region coded antigens, can amplify the generation of anti-host DTH effector cells from T_2 cells (probably Lyt 1^+ cells), activated by I-region coded antigens. Such T_2-derived effector cells can release factors which lead to the expression of GvH-related DTH on transfer (in our system) or to help in humoral responses. The present results lead us to speculate that in the case of enhancement of T_2-helper cell activity by T_1-amplifier cells[15,16], both subpopulations are restricted by different H-2 subregions—T-helper cells by H-2I and T-amplifier cells by H-2K/D.

Received 24 March; accepted 2 July 1980.

1. Cantor, H. & Asofsky, R. *J. exp. Med.* **131,** 235–246 (1970).
2. Raff, M. C. & Cantor, H. in *Progress in Immunology* (ed. Amos, B.) 83–93 (Academic, New York, 1971).
3. Tittor, W., Gerbase-Delima, M. & Walford, R. L. *J. exp. Med.* **139,** 1488–1498 (1974).
4. Wright, P. W., Loop, S. M. & Bernstein, I. D. *Cell. Immun.* **43,** 245–262 (1979).
5. Wolters, E. A. J. & Benner, R. *Transplantation* **26,** 40–45 (1978).
6. Lance, E. M., Medawar, P. M. & Taub, R. N. in *Advances in Immunology* (eds Dixon, F. J. & Kunkel, H. G.) 1–92 (Academic, New York, 1973).
7. Tigelaar, R. E. & Asofsky, R. *J. exp. Med.* **137,** 239–253 (1973).
8. Wolters, E. A. J. & Benner, R. *Nature* **279,** 642–643 (1979).
9. Wolters, E. A. J. & Benner, R. *Cell. Immun.* (in the press).
10. Wolters, E. A. J., van der Kwast, Th. H., Odijk, L. M. & Benner, R. *Cell. Immun.* (in the press).
11. Mathieson, B. J., Sharrow, S. O., Campbell, P. S. & Asofsky, R. *Nature* **277,** 478–480 (1979).
12. Scollay, R., Kochen, M., Butcher, E. & Weissman, I. L. *Nature* **276,** 79–80 (1978).
13. Cantor, H. & Boyse, E. *Cold Spring Harb. Symp. quant. Biol.* **41,** 23–32 (1976).
14. Cantor, H. & Boyse, E. in *Contemporary Topics in Immunobiology* (ed. Stutman, O.) 47–67 (Plenum, New York, 1977).
15. Feldmann, M., Beverley, P. C. L., Woody, J. & McKenzie, I. F. C. *J. exp. Med.* **145,** 793–801 (1977).
16. Muirhead, D. Y. & Cudkowicz, S. *J. Immun.* **120,** 579–585 (1978).

An immunoglobulin heavy-chain gene is altered in two T-cell clones

A. Forster, M. Hobart, H. Hengartner* & T. H. Rabbitts

MRC Laboratory of Molecular Biology, Hills Road,
Cambridge CB2 2QH, UK
* Experimentelle Pathologie, Universitätspital, 8091 Zürich,
Switzerland

Thymus-derived lymphocytes (T cells) show a high degree of discrimination in their responses to various antigens, very similar to the specificity repertoire of antibody-producing B cells. The nature of the T-cell receptor which mediates antigen recognition is obscure, but the ability to discriminate between antigenic specificities implies a range of receptor specificities. Many serological and genetic data suggest that T-cell receptors use the immunoglobulin heavy (H)-chain variable (V) region genes but do not carry the antigenic determinants of the immunoglobulin H-chain constant (C) regions; they also do not seem to carry conventional light (L)-chain V- or C-region determinants[1–3]. In B cells and derivatives the expression of immunoglobulin genes is manifested, at the DNA level, by an alteration of the restriction enzyme patterns of both the H and L immunoglobulin genes[4–9]. Specifically, V-gene integration involves joining of a V gene with a J segment (in the case of the H chain probably through an intermediate D segment)[4,6,7] so that sites for restriction enzymes will undergo changes in cells in which V–J joining has occurred. Here, we describe Southern filter hybridization experiments[10] using $C\mu$ and $C\kappa$ probes on the DNA of individual T-cell clones from mice, and present evidence for alteration of sequences adjacent to the $C\mu$ gene in the cells.

The T-cell clones used in this study were two killer cell lines (AD9 and HY72)[11]. Both the cell lines were derived from stimulated splenic T cells and display an H–2-restricted cytotoxic activity against cells bearing H–Y antigen (an activity which has remained unchanged over several months of culture). The cells also express the Thy-1 surface antigen. The T cells were derived from different strains of mice and we have therefore compared the size of the restriction fragment containing the $C\mu$ gene in liver DNA from various mouse strains using a cloned $C\mu$ cDNA probe (pμ/118)[12]. Figure 1 shows the result of a Southern filter hybridization experiment between *Kpn*I digests of liver DNA and nick-translated pμ/118. Considerable polymorphism can be seen between the different strains with respect to the *Kpn*I restriction fragment containing the $C\mu$ gene. We have also found polymorphism between γH-chain genes of different mouse strains but no differences in the $C\kappa$ gene of any of the strains studied (unpublished). A separate study has shown that the intervening sequence between V and $C\gamma1$ regions of an IgG1-producing myeloma cell contains short tandemly repeated sequences which may also occur in regions adjacent to $C\mu$, to the other $C\gamma$ and to the $C\alpha$ genes[13]. It is possible, therefore, that the polymorphism in the size of restriction fragment containing the CH genes is a result of genetic instability within these tandemly repeats similar to, for example, the instability associated with the *Xenopus* rDNA tandemly repeated sequences[14].

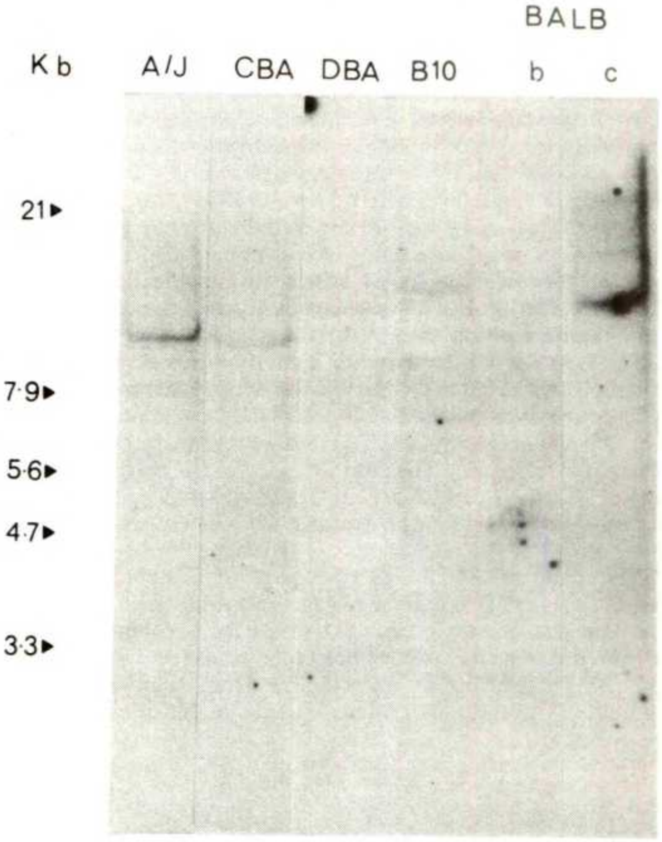

Fig. 1 Hybridization of $C\mu$ probe with liver DNA from various strains of mice. High molecular weight DNA was prepared from livers of A/J, CBA, DBA/2, B10A, BALB/c and BALB/b mice, digested to completion with *Kpn*I and 15-μg aliquots fractionated on 0.8% agarose (alongside λ phage DNA digested with *Eco*RI as size markers). The DNA was denatured and transferred to Schleicher and Schüll nitrate filters[10]. The $C\mu$ probe pμ/118 is a cDNA clone containing all of the $C\mu$ coding region plus a substantial amount of 3′ noncoding sequence[12], and was radioactively labelled by nick-translation (specific activity 4×10^7 c.p.m. per μg). The filters were hybridized as previously described[28,29] using $6\times$SSC salt conditions and 10^6 c.p.m. ml^{-1} of probe for 2 days at 65 °C. The filters were washed after hybridization in $1\times$SSC salt conditions and autoradiography was carried out for 2 weeks at −70 °C using prefogged film and an intensifying screen[30]. Fragments found in BALB/c, BALB/b and DBA are around 14 kilobases (kb), about 15 kilobases in B10A DNA, 12 kilobases in CBA and 12.5 kilobases in A/J DNA.

To detect rearrangement events around a J segment it is necessary to cleave the DNA to the 5′ side of the J segments. *Kpn*I cleaves about 1.5 kilobases to the 3′ side of the $C\mu$ gene[15]: therefore, the sizes of the *Kpn*I fragments (see Fig. 1 legend) of the different strains are all consistent with the possibility of a second cleavage site to the 5′ side of the JH region, given that JH and $C\mu$ are separated by about 8 kilobases[15]. Figure 2 compares the hybridization of pμ/118 ($C\mu$ probe) with *Kpn*I-digested T-cell DNA or liver DNA from the respective strain with a myeloma cell line (McPc 1748) which produces IgM. In each case, the liver DNAs display only a single hybridizing band which presumably reflects the presence of a single $C\mu$ gene in these mice. Compared with the liver DNA, DNA from the myeloma line (Fig. 2*a*) and the killer T-cell clones (Fig. 2*b*, *c*) display new restriction fragments hybridizing to the $C\mu$ probe. The IgM-producing myeloma shows two new hybridization bands (about 20 and 18.5 kilobases), indicating that rearrangement events have occurred on both immunoglobulin-bearing chromosomes in this cell line. Unlike the myeloma DNA, T-cell DNAs possess only single new rearranged fragments containing a $C\mu$ gene as well as a fragment approximately coincident with that found in the liver DNA. Thus, it seems likely that these cells have undergone DNA alteration at the JH cluster but that this event has occurred on only one chromosome, in contrast to the IgM-producing cell line. We have also found evidence of similar rearrangements in a Moloney virus-transformed cell line (Thy-1 positive, A. D. Lowe, personal communication), but we could find no rearrangement in a cell line such as P815 (a mouse mastocytoma).

0028–0836/80/350897—03$01.00

Furthermore, cleavage of the DNA with *Eco*RI, which cleaves between Cμ and JH[9,15], obliterates the evidence of rearrangement (unpublished data), lending support to the hypothesis that the events involve the JH region.

We have examined the possiblity of κ-chain rearrangement in the T-cell clones and in the IgM-producing clone using a similar strategy—digesting DNA with enzymes which cleave 3′ of Cκ and 5′ of Jκ (*Bst*I and *Eco*RI). McPc 1748 (Fig. 3*a*) possesses two *Eco*RI fragments hybridizing to the Cκ probe (23 and 15 kilobases) of which the latter is common to the unique Cκ-containing *Eco*RI fragment of BALB/c liver, indicating that this cell line has an integrated Vκ–Cκ gene in one chromosome. The comparative hybridization of the Cκ probe to AD9 DNA and CBA liver DNA digested with *Bst*I (Fig. 3*b*) shows only a common hybridization component (about 12.5 kilobases) which may be attributed to the unintegrated Cκ gene. Similar results were obtained with both HY72 DNA and the mastocytoma cell (P815) (unpublished). The absence of Cκ or Cμ rearrangement in P815 DNA is consistent with results recently published by Kemp *et al.*[16], who found no evidence of Cκ or Cμ transcripts in P815 RNA.

The data presented are, therefore, consistent with the conclusion that DNA changes have occurred which are associated with sequences to the 5′ end of the Cμ gene but that κ-gene rearrangements have not occurred in the T-cell clones studied. These changes around the Cμ gene, by analogy to the results in B cells, could be due to VH–JH joining or may be due to an as yet unknown DNA activity in this area. Although the T-cell and B-cell DNA may share these rearrangement features around the Cμ gene, they differ in that the T-cell DNAs show no evidence of Cκ-gene rearrangement. Although the results presented here do not necessarily imply T-cell expression of this region of the immunoglobulin locus, there is evidence that Cμ genes are expressed in thymocyte population or T-cell lymphomas[16,17]. The present study utilizes cloned T-cell lines as a source of DNA rather than tumour lines or thymus cells.

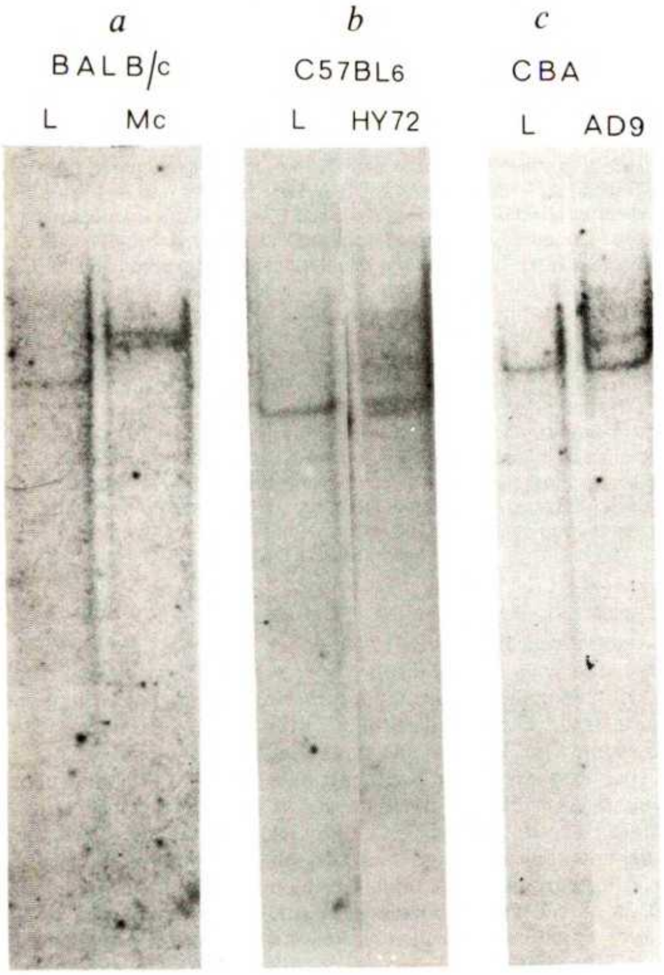

Fig. 2 Profiles of T-cell and B-cell DNA hybridization with Cμ probe. High molecular weight DNA of BALB/c liver (L) and McPc 1748 cells, C57B16 liver and HY72 cells, and CBA liver and AD9 cells were digested to completion with *Kpn*I, fractionated and hybridized as in Fig. 1 with pμ/118. *a–c* Represent separate fractionations of DNA.

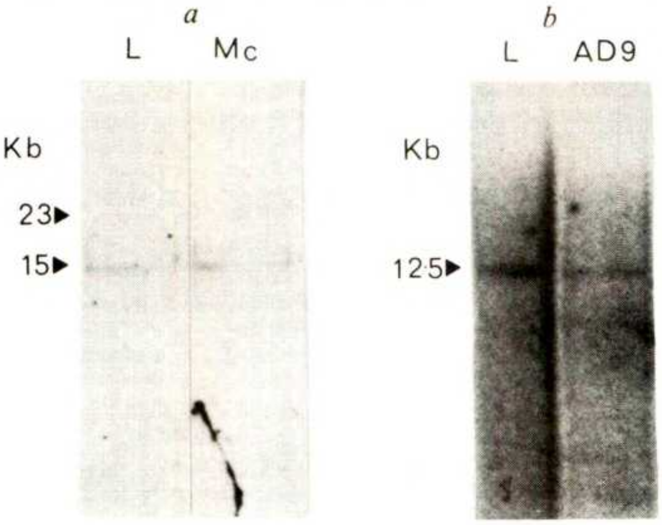

Fig. 3 Hybridization of mouse DNA to Cκ probe. The various high molecular weight DNAs were completely digested with *Eco*RI (panel *a*) and *Bst*I (panel *b*), fractionated and transferred to cellulose nitrate filters as in Fig. 1. The Cκ probe was isolated from the cloned cDNA pκ(11)[24] (ref. 31) by digestion with *Hpa*I: this enzyme cuts once in the pMB9 vector and once within the Cκ region of the insert near the V/C junction[32] to yield two fragments of which the 3.7-kilobase fragment contains the Cκ region. The fragment was isolated from a preparative agarose gel and labelled by nick-translation. The filters were hybridized and washed as in Fig. 1. *a*, L = BALB/c liver DNA; Mc = McPc 1748 DNA. *b*, L = CBA liver DNA; AD9 = AD9 killer T-cell DNA.

One can speculate on possibilities which could reconcile these results with what is known of T-cell receptors at the cellular level and H-chain genes at the molecular level. It seems that deletion of DNA between VH and CH genes occurs during the H-chain class switch[8,18–20]. Thus, as the T cells possess Cμ genes, it can be inferred that a putative constant region sequence of the T-cell receptor (C$_T$) would need to be located between the VH cluster and the Cμ gene or within the Cμ gene itself. In the mouse, JH segments and the Cμ genes are separated by about 8 kilobases of intervening sequence[15] which could easily accommodate a constant-region gene. A second possibility is that C$_T$ is generated from the Cμ gene, partly from the Cμ coding reading frame sequence and partly from new reading frames, or new combinations of coding sequences created by differential splicing, such as occurs in the formation of the SV40 and polyoma virus T antigens[21–23] or as is now known for the formation of the membrane form of μ-heavy chains[24,25]. A third possibility is that C$_T$ is located on a separate chromosome which can recombine with the immunoglobulin locus to translocate VH to C$_T$ or vice versa.

Received 30 May; accepted 11 July 1980.

1. Lindahl, K. F. & Rajewsky, K. in *Defence and Recognition*, Vol. IIA (ed. Lennox, E. S.) 221 (University Park Press, Baltimore, 1979).
2. Binny, H. & Wigzell, H. *Contemporary Topics Immunobiol.* **7**, 113–130 (1977).
3. Krawinkel, U., Cramer, M., Kindred, B. & Rajewsky, K. *Eur. J. Immun.* **9**, 815–820 (1979).
4. Sakano, H., Hüppi, K., Heinrich, G. & Tonegawa, S. *Nature* **280**, 288–294 (1979).
5. Rabbitts, T. H. & Forster, A. *Cell* **13**, 319–327 (1978).
6. Max, E. E., Seidman, J. G. & Leder, P. *Proc. natn. Acad. Sci. U.S.A.* **76**, 3450–3454 (1979).

7. Early, P., Huang, H., Davis, M., Calame, K. & Hood, L. *Cell* **19,** 981–998 (1980).
8. Rabbitts, T. H., Forster, A., Dunnick, W. & Bentley, D. L. *Nature* **283,** 351–356 (1980).
9. Gough, N. M., Kemp, D. J., Tyler, B. M., Adams, J. M. & Cory, S. *Proc. natn. Acad. Sci. U.S.A.* **77,** 554–558.
10. Southern, E. M. *J. molec. Biol.* **98,** 503–517 (1975).
11. von Boehmer, H., Hengartner, H., Nabholz, W. L., Schreirer, M. H. & Haas, W. *Eur. J. Immun.* **9,** 592–597 (1979).
12. Matthyssens, G. E. A. R. & Rabbitts, T. H. *Nucleic Acids Res.* **8,** 703–713 (1980).
13. Dunnick, W., Rabbitts, T. H. & Milstein, C. *Nature* (in the press).
14. Brown, D. D. & Dawid, I. B. *Science* **160,** 272–274 (1968).
15. Calame, K. *et al. Nature* **284,** 452–455 (1980).
16. Kemp, D. J., Harris, A. W., Cory, S. & Adams, J. M. *Proc. natn. Acad. Sci. U.S.A.* **77,** 2876–2880 (1980).
17. Storb, U., Near, R., Putnam, D. & Claggett, J. *molec. Immun.* (in the press).
18. Honjo, T. & Kataoka, T. *Proc. natn. Acad. Sci. U.S.A.* **75,** 2140–2144 (1978).
19. Cory, S. & Adams, J. M. *Cell* **19,** 37–52 (1980).
20. Coleclough, C., Cooper, D. & Perry, R. P. *Proc. natn. Acad. Sci. U.S.A.* **77,** 1422–1426 (1980).
21. Fiers, W. *et al. Nature* **273,** 113–120 (1978).
22. Reddy, V. B. *et al. Science* **200,** 494–502 (1978).
23. Soeda, E., Arrand, J. R., Smolar, N., Walsh, J. E. & Griffin, B. E. *Nature* **283,** 445–453 (1980).
24 Rogers, T. *et al. Cell* **20,** 303–312 (1980).
25 Early, P. *et al. Cell* **20,** 313–319 (1980).
26. Maniatis, T., Jeffrey, A. & Kleid, D. G. *Proc. natn. Acad. Sci. U.S.A.* **72,** 1184–1188 (1975).
27. Rigby, P. W. J., Dieckmann, M., Rhodes, C. & Berg, P. *J. molec. Biol.* **113,** 237–251 (1977).
28. Denhardt, D. T. *Biochem. biophys. Res. Commun.* **23,** 641–646 (1966).
29. Jeffreys, A. J. & Flavell, R. A. *Cell* **12,** 429–439 (1977).
30. Laskey, R. A. & Mills, A. D. *FEBS Lett.* **82,** 314–316 (1977).
31. Schibler, U., Marcu, K. B. & Perry, R. P. *Cell* **15,** 1495–1509 (1979).
32. Hamlyn, P. H., Brownlee, G. G., Cheng, C. C., Gait, M. J. & Milstein, C. *Cell* **15,** 1067–1075 (1978).

Projection patterns of single physiologically characterized optic tract fibres in cat

Douglas B. Bowling & Charles R. Michael

Department of Physiology, School of Medicine, Yale University,
New Haven, Connecticut 06510

Because the axons of retinal ganglion cells are the sole channels carrying information from the eye, the organization of their central projections is important in visual processing. However, their detailed destinations and patterns of synaptic distribution at the level of single, functionally identified cells are not known. Most anatomical studies involve populations of cells or fibres and do not examine their physiological properties; physiological studies involving intracellular recording and injection of marker substances into cell bodies[1–3] of single cells do not reveal distant axon terminals because the markers stain the fibres for only a few millimetres from the perikarya. To examine the central projections of retinal ganglion cells we have impaled single optic tract fibres near their sites of termination[4,5] and injected them iontophoretically with the marker enzyme horseradish peroxidase (HRP). We now report that this method has revealed the thalamic and midbrain ramifications of single physiologically characterized axons. The individual optic-tract fibres branch repeatedly, sending collaterals to the superior colliculus (SC), the medial interlaminar nucleus (MIN), and to one or more laminae within the dorsal lateral geniculate nucleus (LGNd). In different nuclei the single axons form arborizations of characteristically different shapes and distribute their synaptic terminals in columns (LGNd), sheets (MIN) or widely spread patches (SC).

We used standard procedures for studying visual physiology in mammals[6], for HRP histochemistry[7,8] and for morphological reconstruction. To maximize transport of the HRP out of the electrode tips we used high enzyme concentrations and large d.c. currents. The electrodes were filled by centrifugation with a pre-centrifuged solution of 200 mM potassium acetate (*p*H 6.8) and 10% HRP. The tips were broken to diameters of about 0.5 μm, giving d.c. resistances of 200–500 MΩ. To protect their tips and guide their descent to the optic tract, the electrodes were lowered from the surface of the cortex inside a stereotaxically positioned glass micropipette (Horsley–Clarke ant. 6, lat. 9; see Fig. 1*a*). The membrane potentials recorded from the axons were 10–40 mV negative with positive-going action potentials of 2–10 mV amplitude. On completing physiological testing of an impaled axon, we injected it with HRP using a current of 20–50 nA (electrode-positive) for 30–200 s. During the injection the current was periodically turned off and action potentials from the axon were observed to confirm that it remained impaled. The length of stained axon varied with the total injected charge and appeared complete in the geniculate and colliculus with 5–10 μC. At their injection sites the axons appeared swollen and were surrounded by extracellular debris (see Fig. 1*b*). Several hundred micrometres away the axons appeared normal and had diameters, including myelin, of 2–5 μm. Results reported here are based on 9 of 14 axons we recorded and injected in the optic tracts of four adult cats. All nine axons (three from ipsilateral and six from contralateral eyes) were functionally classified as Y-type based on standard criteria including high conduction velocities[9,10] (30–40 m s^{-1}) and nonlinear spatial summation in their receptive fields[11,12].

Figure 2 represents a frontal view of the left thalamus and midbrain showing the reconstruction of an on-centre optic tract axon from the contralateral eye. The axon was impaled (arrow) in the optic tract just ventral to the LGNd. The centre of the axon's receptive field was 1° in diameter and was located on the vertical midline 13° below the projection of the area centralis. The axon was spontaneously active, gave transient responses to steps of light, and responded well to rapidly moving stimuli. Based on a contrast reversal test[13], the effects of light were nonlinearly summed in its receptive field. The axon's retinal origin and its high conduction velocity (latency 0.36 ms) were demonstrated by electrical stimulation with a hook electrode placed near the head of the optic nerve.

Each of the nine axons sent collaterals to three nuclei: the LGNd, the MIN and the SC. In each nucleus the collaterals formed arborizations with characteristic patterns (see Fig. 2): converging to single loci in the LGNd, diffuse and radiating in the SC, and spread out in thin sheets in the MIN. Thus, individual ganglion cells have structurally different patterns of arborization at each of their nuclear destinations. Each axon gave rise to a total of 1,000–2,000 synaptic-like boutons which appeared in the sections as spherical or irregular swellings 0.5–3 μm in diameter. Such swellings have been identified in the LGNd as synaptic terminals[14]. The axon shown in Fig. 2 had about 1,400 of these terminals: 225 in the SC, 1,134 in the LGNd and 34 in the MIN.

In the LGNd the single axons from the contralateral eye always terminated in both laminae A and C. This is illustrated by

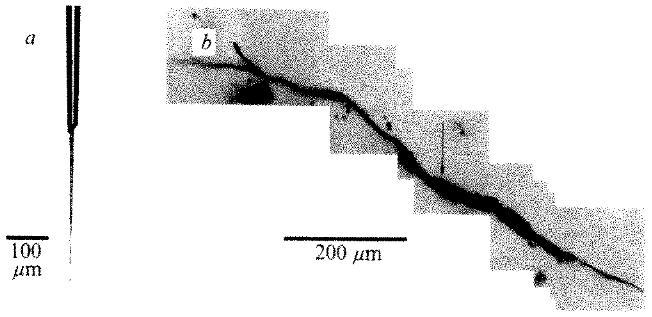

Fig. 1 *a*, Photograph of the glass micropipette used to protect and guide the tip of the electrode into the optic tract. The recording microelectrode extends out of the pipette. The micropipette was made from 1.6 mm o.d. glass pulled to a taper of 25 mm and broken to a tip diameter of about 30 μm. The electrodes were made with 30-mm tapers so that they could extend several millimetres out of the micropipette. *b*, Photographic montage showing detail of the axon of Fig. 2 at its injection site in the optic tract. The axon passes from the upper surface of the 100-μm section (lower right) to the lower surface (out of the picture at far left). It branches and sends a collateral back to the upper surface of the section (upper left). The arrow indicates the site of injection based on a line projected from the electrode track.

0028-0836/80/350899—04$01.00

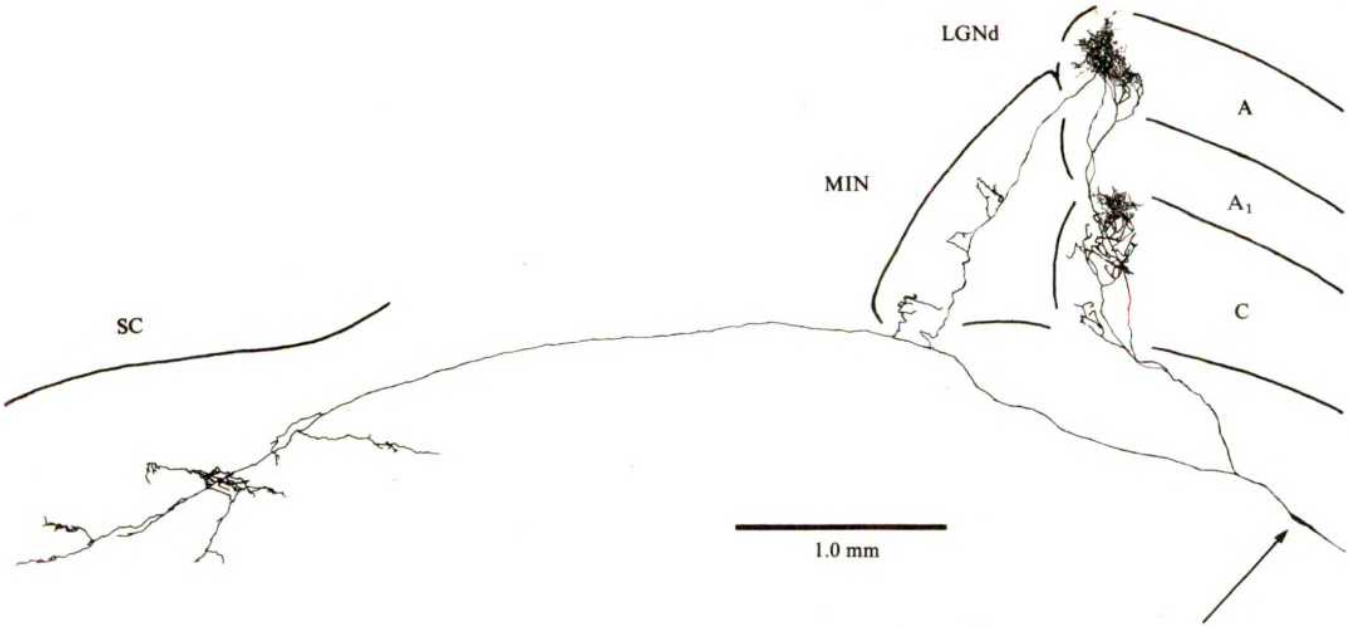

Fig. 2 Reconstruction from coronal sections of a single on-centre Y-type axon showing its terminations in the LGNd, MIN and SC. The arrow indicates the site of injection into the axon (see Fig. 1*b*). The figure represents over 3 mm of depth in the anterior–posterior axis (perpendicular to page) so that the perspective is flattened and the shapes of the nuclei and laminae are not representative of a single coronal plane. The arborization in the SC is in the anterolateral part of the nucleus.

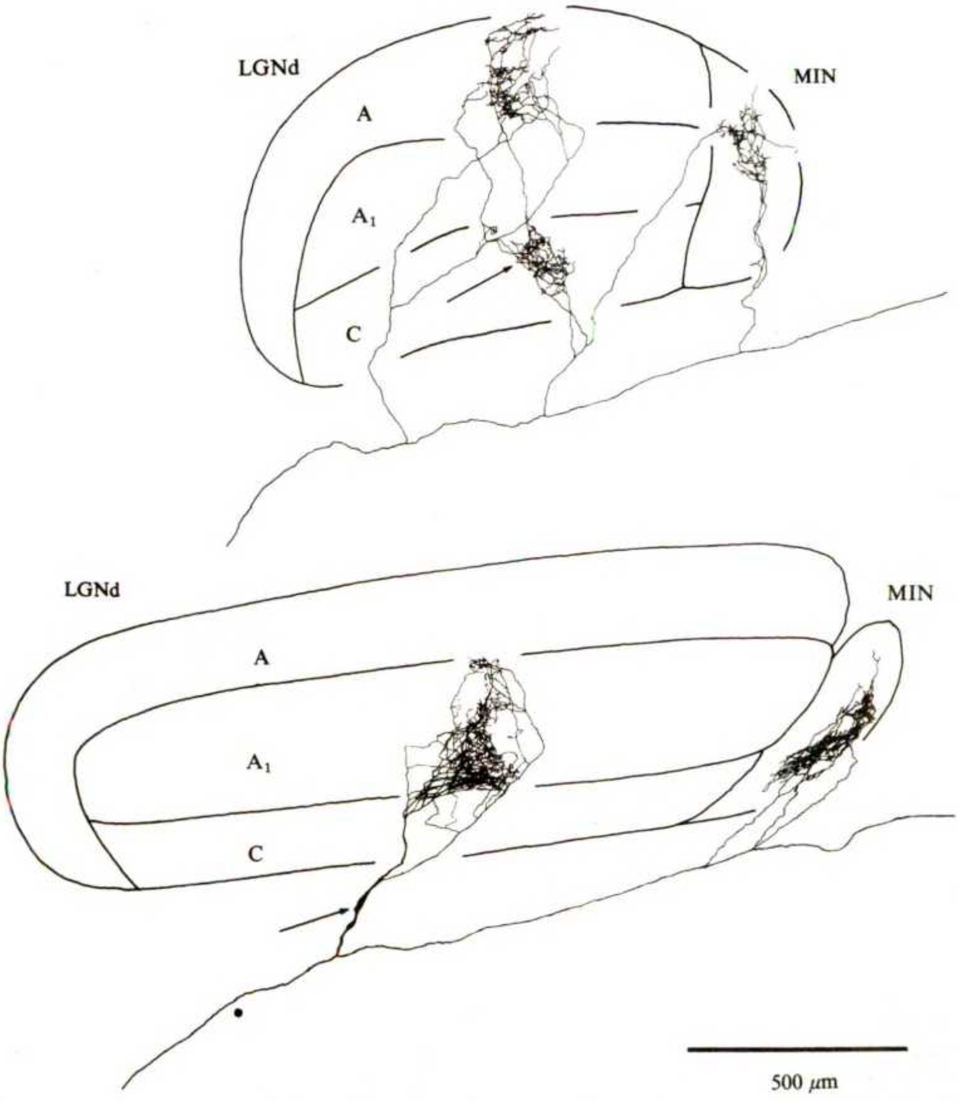

Fig. 3 Reconstructions of single axons showing their terminations in the right LGNd and MIN. The shapes of the terminal distributions in the MIN are bowl-like (concave toward the LGNd) and extend in the anterior–posterior axis about as far as they do in the plane of the figure. Arrows indicate injection sites. Upper: on-centre Y axon from the contralateral eye with a 4.5° receptive field centre located 28° below the horizontal meridian and 26° from the vertical midline. Lower: off-centre Y axon from the ipsilateral eye with a 4.5° receptive field centre located 1° above the horizontal meridian and 8.5° from the vertical midline.

the axons of Figs 2 and 3 (top). In at least two cases (for example see Fig. 2), these axons terminated in all three of the contralateral laminae (A, C, C_2). Whether this was always the case is not clear because the borders of C_2 were not always evident in our sections[15]. Axons from the ipsilateral eye terminated in only a single lamina. They arborized in A_1 but not in the other lamina (C_1) that receives ipsilateral input (see Fig. 3, bottom).

In three instances in which the sections were cut at right angles to the planes of the laminae, the synaptic terminals were seen to be distributed in broad-based columns that spanned the thickness of lamina A or A_1. Figure 4 shows one of these columns reconstructed from the axon of Fig. 3 (bottom). Each dot represents the position of a single terminal in A_1. The columns provide an anatomical basis for the physiologically observed 'projection columns'[16] which run through the nucleus. As with the projection columns at the same locations, the columns of terminals were tilted forward with respect to vertical[17]. Their broad bases, resulting in a greater density of Y terminals in the ventral portions of the laminae, may account for the apparent segregation of Y afferents that has been seen in field potential recordings[18]. The shape of the columns shows that there is an intra-laminar gradient in the spatial distribution of synaptic connections across the laminae. The functional significance of this gradient is unknown.

In the planes of the geniculate laminae, which correspond to the plane of the retinotopic map, the distributions of the terminals were basically circular. The maximum lateral spread was constant (300–400 μm) in spite of the fact that the receptive fields ranged from 1° to 4.5° in diameter and were located between 8° and 38° from the area centralis. This constancy of spread is consistent with the idea[17] that variations in geniculate receptive field sizes result from response properties of the input fibres rather than from anatomical differences within the nucleus. It also suggests uniformity and repetition in the geniculate, a plan of organization similar to that in the striate cortex, and one that may have developmental advantages[19].

In the MIN the retinotopic map is a mirror image of that in the LGNd[20]. Each axon distributed its terminals in the MIN as a sheet 300–400 μm across and about 50 μm thick. The sheets were slightly concave toward the LGNd, conforming to the general curvature of the MIN. They were orientated approximately perpendicular to the geniculate laminae. The form of the sheets can be appreciated from Fig. 3, taking into account that the perspective is distorted by projection onto a flat surface. The spread of the terminals in the plane of the MIN map (about 50 μm) was a factor of six to eight times less than the spread of the terminals in the plane of the geniculate map, a factor which is of the same order as the overall size difference between the MIN and LGNd. Thus, on the basis of the lateral spread of afferent terminals, the nuclei seem to be scaled similarly.

The synaptic terminals in the SC were in the superficial layers of the nucleus. A dorsal view of the SC arborization from Fig. 2, obtained by rotating the reconstruction graphically, revealed that the terminals were grouped into irregular patches which were distributed as an ellipse (1 × 2 mm) with its major axis orientated approximately medio-laterally. It would be interesting to know exactly how these patches are positioned relative to the columnar organization described in the SC for ipsilateral eye afferents and acetylcholinesterase activity[21]. It is clear that the major axis of distribution was approximately orthogonal to the columns and must have spanned several of them.

In the geniculate complex single axons often had two or more long branches which travelled along different paths to converge on the same retinotopic location (see especially Figs 2 and 3, top). It is not clear what functional significance, metabolic constraint, or mode of development these multiple and somewhat indirect pathways may reflect. What they do show is that in the adult there is considerable freedom in the paths that an axon may take to its target.

A second and perhaps related feature was that the forms of the arborizations in the LGNd and MIN were often only a crude guide to the spatial distribution of the axons' terminals. Some arborizations were diffuse and composed of processes that arose from branch points well outside the area of their actual terminations (compare Fig. 3, bottom, with the terminal distribution in Fig. 4). Other arborizations, such as the one in lamina A of Fig. 2, were dense and nearly congruent with the terminal distributions. The lack of close correspondence between the forms of the arborizations and the spatial distributions of the terminals was especially marked in the anterior–posterior axis of the LGNd. Here, sagittal sections showed that the arborizations were stretched out toward the posterior of the nucleus in 'cypress-like'[22] fashion. The form of the arborizations and the multiple pathways of the axons' long branches may arise during development as a result of morphological changes following synaptogenesis in the target nuclei. In the developing cat geniculate, the formation of the laminae, as well as growth and rotation of the nucleus, occurs after the arrival of the retinal afferents[23]. In the monkey geniculate similar events have been specifically shown to occur after synaptogenesis has begun[24]. If the migrating cells drag their presynaptic axons with them, then the terminals could be carried far away from the axons' branch points. In contrast to their geniculate patterns, axons in the colliculus go directly to their sites of termination by single, short paths (see Fig. 2). In this regard it would be interesting to know how the sequences of developmental events and patterns of morphogenesis differ between the cat colliculus and geniculate.

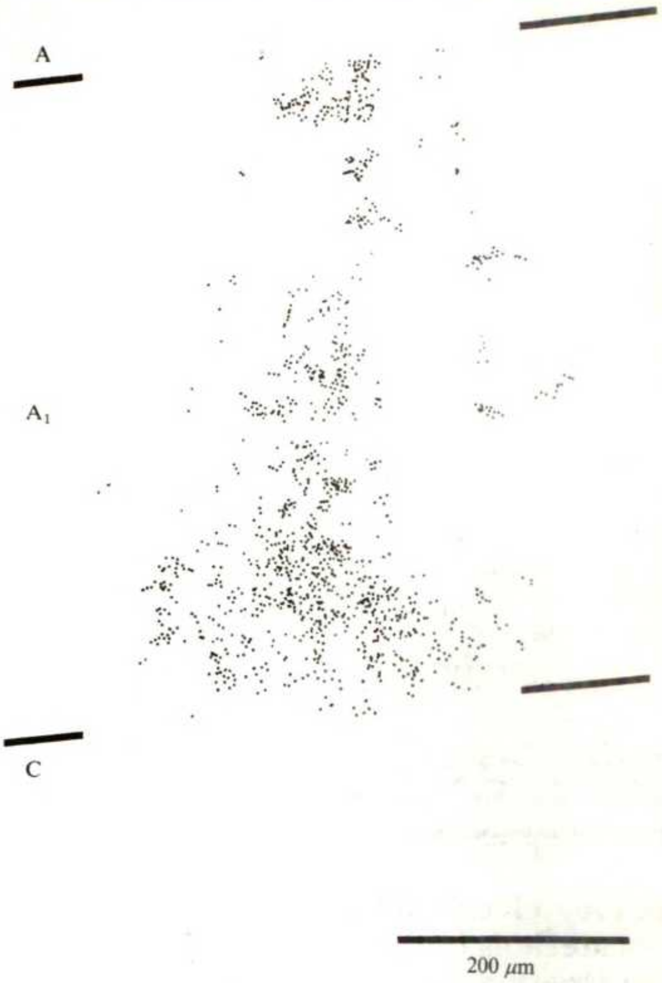

Fig. 4 Columnar distribution in lamina A_1 of terminals from the axon of Fig. 3, bottom. Reconstructed from four 100-μm serial sections. Number of terminals is about 1,200.

The results reported here are based on a sample of one physiological class of retinal axons. It will be of interest to examine single axons of other functional types, such as those from X cells[12] which have linear spatial summation and from colour cells which have opponent spectral properties. The experimental approach of staining single axons may also be useful in answering questions about axonal growth in developing preparations and in adult animals whose development has been altered by early experience, lesions or genetic factors.

We thank Drs Michael Cooper, Frederic Richards, Jonathan Stone and Mrs Winifred Craig and Faye Gomes for helpful advice and discussion and Drs Jeff Noebels, Martha Nowycky and Roger Thomas for reading the manuscript. This work was supported by NIH grant EY00568 and NIH training grant NS07102–03.

Received 1 May; accepted 7 July 1980.

1. Muller, K. J. & McMahan, U. J. *Proc. R. Soc.* B**194,** 481–499 (1976).
2. Jankowska, E., Rastad, J. & Westman, J. *Brain Res.* **105,** 562–577 (1976).
3. Snow, P. J., Rose, P. K. & Brown A. G. *Science* **191,** 312–321 (1976).
4. Brown, A. G., Rose, P. K. & Snow, P. J. *J. Physiol., Lond.* **263,** 132P–134P (1976).
5. Gilbert, C. D. & Wiesel, T. N. *Nature* **280,** 120–125 (1979).
6. Michael, C. R. *J. Neurophysiol.* **41,** 572–588 (1978).
7. Adams, J. C. *Neuroscience* **2,** 141–145 (1977).
8. Malmgren, L. & Olsson, Y. *Brain Res.* **148,** 279–294 (1978).
9. Cleland, B. G. & Levick, W. R. *J. Physiol., Lond.* **240,** 421–456 (1974).
10. Stone, J. & Fukuda, Y. *J. Neurophysiol.* **37,** 722–748 (1974).
11. Enroth-Cugell, C. & Robson, J. G. *J. Physiol., Lond.* **187,** 517–552 (1966).
12. Hochstein, S. & Shapley, R. M. *J. Physiol., Lond.* **262,** 237–264 (1976).
13. Hamasaki, D. I. & Sutija. *Expl Brain Res.* **35,** 25–36 (1979).
14. Mason, C. A. & Robson, J. A. *Neuroscience* **4,** 79–97, 99–111 (1979).
15. Guillery, R. W. *J. comp. Neurol.* **138,** 339–368 (1970).
16. Bishop, P. O., Kozak, W., Levick, W. R. & Vakkur, G. *J. Physiol., Lond.* **163,** 503–539 (1962).
17. Sanderson, K. J. *Expl Brain Res.* **13,** 159–177 (1971); *J. comp. Neurol.* **143,** 101–118 (1971).
18. Mitzdorf, J. & Singer, W. *J. Neurophysiol.* **40,** 1227–1244 (1977).
19. Hubel, D. H. & Weisel, T. N. *J. comp. Neurol.* **158,** 295–305 (1974).
20. Kinston, W. J., Vadas, M. A. & Bishop, P. O. *J. comp. Neurol.* **136,** 295–316 (1969).
21. Graybiel, A. *Brain Res.* **114,** 318–327 (1976); *Nature* **272,** 539–541 (1978).
22. Tello, F. *Lab. Invest. Biol. Univ. Madrid* **3,** 39–62 (1904).
23. Kalil, R. *Comp. Neurol.* **182,** 265–292 (1978).
24. Hendrickson, A. & Rakic, P. *Anat. Rec.* **187,** 602 (1977).

In vivo electrochemical detection of catechols in the neostriatum of anaesthetized rats: dopamine or DOPAC?

François Gonon, Michel Buda, Raymond Cespuglio*, Michel Jouvet* & Jean-François Pujol

INSERM U 171 and INSERM U 52*, Département de Médecine Expérimentale, Université Claude Bernard, 8, avenue Rockefeller, 69373 Lyon Cédex 2, France

Electroanalytical techniques for the *in vivo* measurement of neurotransmitters in brain tissue have been applied especially to the catecholamines, which are easily oxidizable[1–6]. Measurements are, however, complicated by the presence of ascorbic acid (AA) in brain tissue[1,3–6]. Lane *et al.*[7] have been able to circumvent this problem, at least in part, by the application of differential pulse voltametry (DPV) to a surface-modified platinum electrode, obtaining distinct oxidation current peaks in recordings from the rat neostriatum which are attributed to AA and to dopamine (DA), respectively, but which are also unstable. We have recently described a new type of electrode[2,8], consisting of a pyrolytic carbon fibre 8 μm thick and 0.5 mm long. We now report that the DPV method used in conjunction with an electrochemical treatment of this electrode yields stable and reproducible peaks in which catecholamines and AA are resolved from each other. Moreover, pharmacological investigations suggest that the catecholamine peak measured *in vivo* in the rat neostriatum should be attributed to 3, 4-dihydroxyphenylacetic acid (DOPAC), suggesting that our technique may be a useful means of following dopaminergic activity *in vivo*.

A classical three-electrode system was used with a conventional Ag/AgCl reference electrode. The carbon fibre electrodes were prepared as described elsewhere[8], and electrochemically treated by applying a triangular wave potential (0–3 V, frequency 70 Hz) for 20 s, with the electrode tips immersed in phosphate-buffered saline (PBS). Differential pulse (DP) voltammograms (Polarograph Tacussel PRG5; scan rate 20 mV s^{-1}, pulse modulation of 20 mV per 0.2 s) were recorded *in vitro* in PBS containing 20 μM DOPAC and 200 μM AA until the signal remained stable (~15 min). Before and after implantation each electrode was calibrated in standard solutions of DA, DOPAC, AA and dihydroxyphenylalanine (dopa). AA peaked at −50 mV and catechols, such as DOPAC, DA or dopa, peaked at +100 mV (Fig. 1). They yielded linear current responses with increasing concentrations of AA (0–1 mM), DOPAC (0–60 μM), DA or dopa (0–2 μM). These linear responses were not affected by the *in vivo* utilization of the electrode. The minimum measurable signal corresponded to about 2 μM for DOPAC and 0.2 μM for DA or dopa.

Carbon fibre electrodes were implanted in the neostriatum of anaesthetized rats (chloral hydrate 400 mg kg^{-1}). DP voltammograms recorded each 2.5 min showed two peaks: 'peak 1' appeared at the same potential as AA *in vitro* (−50 mV); and 'peak 2' appeared at the same potential as the catechols (+100 mV) (Fig. 1). We have shown that peak 1 disappeared in the striatum of guinea pigs that had been fed on a vitamin C-deficient diet and have suggested that peak 1, obtained from the striatum, is therefore due to AA[9]. Unfortunately, peak 1 was often found to be distorted, showed considerable variance from one animal to another, and appeared to be a function of the depth of anaesthesia. Thus, further work is needed to find better conditions (different parameters for the treatment of the microelectrode, use of chronic implanted rats) that will allow a more precise determination of AA *in vivo*.

In contrast, peak 2 appeared very stable and reproducible (Fig. 2). After an unilateral and selective destruction of the nigrostriatal dopaminergic pathway (performed and controlled as previously described[2]), peak 2 was suppressed in the striatum where the dopaminergic terminals degenerated, but was still present on the intact side (Fig. 1). Moreover, administration of α-methyl-*p*-tyrosine, a specific inhibitor of catecholamine synthesis[10], decreased the amplitude of peak 2 (Fig. 2). These results indicate that peak 2 represents the DP oxidation current of one or several catechol compounds, probably related to catecholaminergic nerve terminals in the striatum.

Several catechol compounds present in the striatum can be ruled out as being significant contributors to peak 2. Noradrenaline content in the striatum is about 1% that of DA[11]

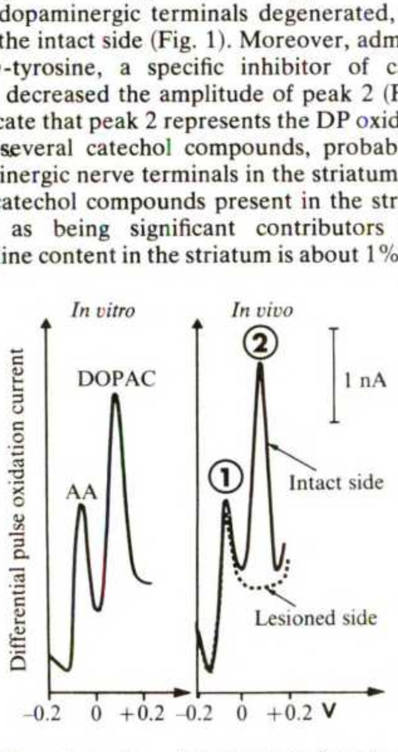

Fig. 1 Differential pulse voltammograms from *in vitro* experiments and from the neostriatum of anaesthetized rats (*in vivo*). Electrochemically treated carbon fibre electrodes were tested in PBS containing AA (200 μM) and DOPAC (20 μM). *a* Shows typical DP voltammogram. *b* Represents one typical example of DP voltammograms recorded in one rat with the same electrode implanted alternately in both striata. The lesioned side corresponds to a striatum in which the dopaminergic terminals were selectively destroyed following 6-hydroxydopamine injection in the substantia nigra[2]. Peak 2 suppression was observed with all the lesioned rats ($n = 6$).

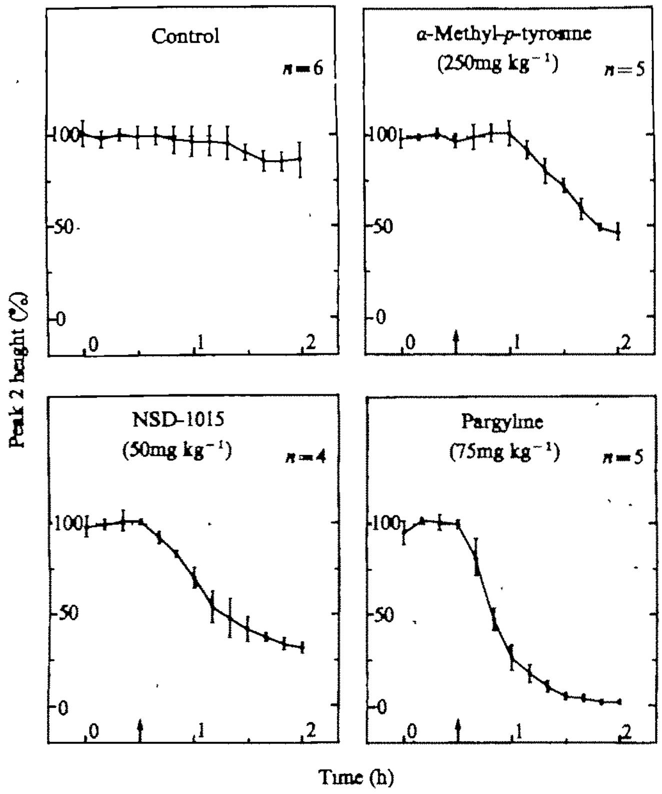

Fig. 2 Evolution of peak 2 height measured from DP voltammograms obtained from the neostriatum in control rats and rats treated with α-methyl-*p*-tyrosine (Sigma), NSD-1015 (Sandev) and pargyline (Sigma). All animals were anaesthetized with chloral hydrate (400 mg kg^{-1}, i.p.) and kept anaesthetized with additional injections as needed. Arrows indicate that i.p. drug injections were performed 30 min after the beginning of the recordings. For each animal the results were expressed as the percentage of the mean control value calculated by averaging the four initial absolute values of peak 2 height (100%). These four initial baseline responses were estimated by comparison with DOPAC calibration curves obtained after the *in vivo* experiment: the mean average value for all experiments was 22±4 μM (mean ±s.d., $n=33$). Results represent the mean ±s.d. of n rats

and the contribution of noradrenaline and its metabolites to peak 2 is thus negligible compared to that of DA and its metabolites. O-methylated metabolites of DA, such as homovanillic acid and 3-O-methyldopamine, are oxidized at more positive potentials[3,12]. dopa, DA and DOPAC are oxidized at +100 mV and consequently could contribute to peak 2 *in vivo*. They are present in the dopaminergic nerve terminals: DA is the neurotransmitter released from the nerve terminals, synthesized from dopa through dopa decarboxylase, and its major breakdown product due to monoamine oxidase activity is DOPAC. To elucidate which product was the major contributor of peak 2 the DA system was manipulated with drugs known to act at different levels of the dopaminergic metabolic pathway. Inhibition of dopa decarboxylase by NSD-1015 rapidly increases the striatal dopa concentration[13]. In our study, NSD-1015 induced a marked decrease of the peak 2 height (Fig. 2). Consequently, it is unlikely that dopa is responsible for the peak 2 recorded *in vivo*. Pargyline, which inhibits monoamine oxydase, is known to cause a rapid decrease in DOPAC[14,15] and an increase in DA concentration [16] in the striatum. Pargyline suppressed peak 2 with a half life of ~15 min, in agreement with previous observations[15,17] and this supports the notion that DOPAC is the major contributor to peak 2.

This suggestion was confirmed by the results obtained with other drugs. In fact, reserpine and haloperidol, which are known to raise striatal DOPAC levels[10,14,16,18], induced a pronounced increase in the peak 2 amplitude (Fig. 3). Amphetamine, which markedly increases DA release[10] and decreases the striatal DOPAC concentration[14,16], caused a diminution in peak 2 height. The effects of these three drugs were tested again in pargyline (75 mg kg^{-1}, intraperitoneally (i.p.)) pretreated rats (1.5 h before drugs). In these conditions, peak 2 disappeared completely and did not reappear after reserpine. After haloperidol and amphetamine (five animals each) a very small peak 2 reappeared, which reached a maximum after about 40 min. Its amplitude was in all cases found to correspond to an estimated concentration <0.2 μM DA.

These results show that peak 2 is mainly due to DOPAC oxidation. For all drugs tested alone, the variations in amplitude and time course of peak 2 were consistent with previous studies of DOPAC concentrations measured using fluorimetric or radioenzymatic methods[14–18]. In our study the concentration of DOPAC in the striatum was calculated by comparing peak 2 heights *in vivo* and *in vitro*, and was estimated to be 22±4 μM (mean ±s.d., $n=33$). This value is compatible with a global striatal tissue concentration of DOPAC under chloral hydrate anaesthesia of 7–15 μM refs 10, 14, 18).

A very slight contribution of DA to peak 2 was observed only after amphetamine or haloperidol. The very low DA levels thus measured are consistent with values found using the push–pull technique[19]. In the light of these observations and considering the size of the active part of the electrode, it can be assumed that events are recorded in the extracellular space occupying about 20% of the total tissue[20]. The presence in the striatum of a potent DA inactivating process acting through high affinity uptake by nerve terminals[21] prevents DA diffusing from the synaptic cleft to the extracellular space. thus contributing to maintaining in this space very low DA concentrations. This questions the interpretation of our previous results, suggesting that DA was responsible for the increase in the oxidation current measured in the striatum after amphetamine[2]. However, these experiments were performed using a non-selective technique (pulse amperometry and untreated carbon fibre electrodes). In the present study the decrease in peak 2 amplitude observed after amphetamine treat was always associated with a significant rise in peak 1 height, although important differences in the amplitude of this peak were observed.

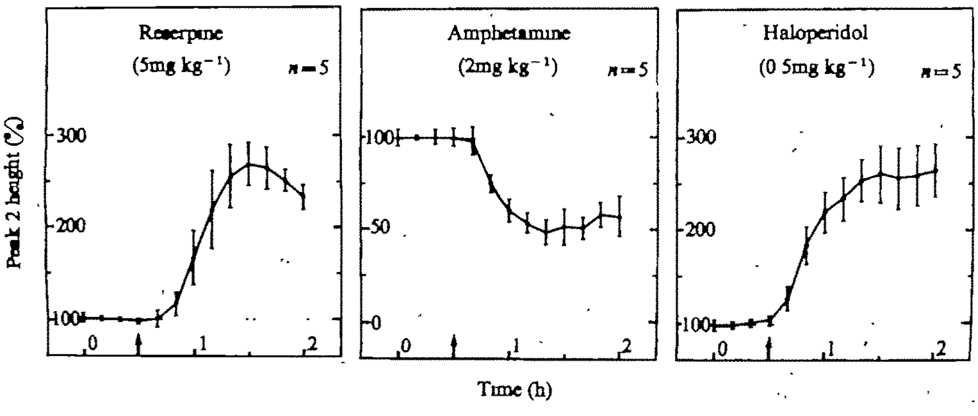

Fig. 3 Effect of reserpine (Serpasil, Ciba-Geigy), amphetamine (La Cooperation Pharmaceutique Française) and haloperidol (Haldol, Le Brun) on peak 2 height measured on DP voltammograms recorded from the neostriatum of anaesthetized rats.

The electrochemical treatment used in this study improves the selectivity, sensitivity and reproducibility of the carbon fibre electrode. In conclusion, the present investigation clearly demonstrates that the catechol oxidation current peak obtained *in vivo* from the striatum of anaesthetized rats is DOPAC and not DA.

We thank Dr T. A. Reader for reviewing this manuscript and Mr G. Verchère and Mr G. Guidon for technical assistance. This work was supported by CNRS (LA 162), INSERM (U 52 and U 171), and DGRST (grants nos 78.7.0156 and 78.7.2788).

Received 23 October 1979; accepted 26 June 1980.

1. Adams, R. N. *Analyt. Chem.* **48,** 1126A–1137A (1976).
2. Gonon, F. *et al C. r. hebd. Séanc. Acad. Sci., Paris* **286D,** 1203–1206 (1978).
3. Lane, R. F., Hubbard, A. T. & Blaha, C. D. *Bioelectrochem. Bioenergetics* **5,** 506–527 (1978).
4. Conti, J. C., Strope, E., Adams, R. N. & Marsden, C. A. *Life Sci.* **23,** 2705–2716 (1978).
5. Lane, R. F., Hubbazrd, A. T. & Blaha, C. D. *J. electroanalyt. Chem.* **95,** 117–122 (1979).
6. Huff, R., Adams, R. N. & Rutledge, C. O. *Brain Res.* **173,** 369–372 (1979).
7. Lane, R. F., Hubbard, A. T., Fukunaga, K. & Blanchard, R. J. *Brain Res.* **114,** 346–352 (1976).
8. Ponchon, J. L., Cespuglio, R., Gonon, F., Jouvet, M. & Pujol, J. L. *Analyt. Chem.* **51,** 1483–1486 (1979).
9. Buda, M., Gonon, F., Cespuglio, R., Jouvet, M. & Pujol, J. F. *C.r. hebd. Séanc. Acad. Sci., Paris* **290D,** 431–434 (1980).
10. Moore, K. E. & Kelly, P. H. in *Psychopharmacology: A generation of Progress* (eds Lipton, M. A., Dimascio, A. & Killam, K. F.) 221–234 (Raven, New York, 1978).
11. Brownstein, M., Saavedra, J. M. & Palkovits, M. *Brain Res.* **79,** 431–436 (1974).
12. Wightman, R. M., Steope, E., Plotsky, P. & Adams, R. N. *Brain Res.* **159,** 55–68 (1978).
13. Carlsson, A., Davis, J. N., Kehr, W., Lindqvist, M. & Atack, C. V. *Naunyn, Schmiedebergs Archs Pharmak* **275,** 153–168 (1972).
14. Roth, R. H., Murrin, L. C. & Walters, J. R. *Eur. J. Pharmac.* **36,** 163–171 (1976).
15. Karoum, F., Neff, N. H. & Wyatt, R. J. *Eur. J. Pharmac.* **44,** 311–318 (1977).
16. Fadda, F., Argiolas, A., Stefanini, E. & Gessa, G. L. *Life Sci.* **21,** 411–418 (1977).
17. Wilk, S., Watson, E. & Travis, B. *Eur. J. Pharmac.* **30,** 238–243 (1975).
18. Westernik, B. H. C., Lejeune, B., Korf. J. & Van Praag, H. M. *Eur. J. Pharmac.* **42,** 179–190 (1977).
19. Nieoullon, A., Cheramy, A. & Glowinski, J. *J. Neurochem.* **28,** 819–828 (1977).
20. Cragg, B. *Trends Neurosci.* **2,** 159–161 (1979).
21. Tassin, J. P., Cheramy, A., Blanc, G., Thierry, A. M. & Glowinski, J. *Brain Res.* **107,** 291–301 (1976).

Insulin triggers cyclic AMP-dependent activation and phosphorylation of a plasma membrane cyclic AMP phosphodiesterase

Robert J. Marchmont & Miles D. Houslay

Department of Biochemistry, University of Manchester Institute of Science and Technology, PO Box 88, Manchester M60 1QD, UK

Regulation of blood glucose levels by the liver is primarily achieved by the action of two peptide hormones, insulin and glucagon, which bind to specific receptors associated with the hepatocyte plasma membrane. Whilst the molecular action of glucagon at the level of the cell plasma membrane in activating adenylate cyclase is relatively well understood, we know little, if anything, of the molecular consequences of insulin occupying its receptor. We demonstrate here that insulin, at physiologically relevant concentrations, can trigger the cyclic AMP-dependent activation and phosphorylation of a low K_m cyclic AMP phosphodiesterase attached to the liver plasma membrane. Such an effect may in part explain the ability of insulin to inhibit the increase in cellular cyclic AMP content that glucagon alone produces by activation of adenylate cyclase. Our observation that basal, intracellular cyclic AMP levels are insufficient to allow insulin to activate the cyclic AMP phosphodiesterase, yet those cyclic AMP levels achieved after exposure of the cells to glucagon are sufficient, gives a molecular rationale to Butcher and Sutherland's proposal[1] that it is necessary to first elevate cellular cyclic AMP levels before they can be depressed by insulin.

The cyclic AMP phosphodiesterase activity of rat liver plasma membranes can be divided into a high K_m intrinsic enzyme exhibiting normal Michaelis kinetics and a low K_m peripheral enzyme exhibiting apparent negative cooperativity[2]. The low K_m enzyme is distinct from cytosol forms[2] and binds with high affinity to a protein site on the plasma membrane (R.J.M. and M.D.H., unpublished observations).

Treatment of purified rat liver plasma membranes with combinations of insulin, cyclic AMP and Mg^{2+}-ATP, in the conditions described in Fig. 1, resulted in a doubling of the cyclic AMP phosphodiesterase activity only when all three components were added and when native insulin was used. The activation attained maximal levels within 3 min (Fig. 1A) and was not reversed by washing the membranes with 1 mM $KHCO_3$, *p*H 7.4. The activation was entirely due to the peripheral, low K_m enzyme which could be released by high ionic strength treatment[2] in a 2.5-fold activated state when assayed at 4×10^{-7} M cyclic AMP (Fig. 1B). Relative to the native enzyme[2], the released, activated protein exhibited a slightly lower K_m, 0.59 μM, and similar V_{max}, 1,140 pmol min^{-1} mg^{-1}, but there was a significant reduction ($P<0.01$) in the Hill coefficient from 0.59 ± 0.05 (s.d., $n=4$) for the native enzyme[2] to 0.45 ± 0.03 (s.d., $n=4$) after activation.

Dose–response curves for the insulin-mediated activation of the cyclic AMP phosphodiesterase yielded a K_a of 1.4×10^{-10} M (Fig. 2), demonstrating the effectiveness of physiological concentrations. Interestingly, the cyclic AMP dependence of this phenomenon, exhibiting a K_a of 1.6×10^{-6} M, indicates that, at basal intracellular cyclic AMP levels of 0.3–0.5 μM (refs 3, 4), little if any activation would be triggered by insulin (Fig. 2). However, after exposure to glucagon, cyclic AMP levels rise to 2.0–4 μM (refs 1, 5) which would allow activation by insulin (Fig. 2).

The dependence of insulin's activation of the cyclic AMP phosphodiesterase on both Mg^{2+}-ATP and cyclic AMP indicated that a cyclic AMP-dependent phosphorylation might be involved. Because cyclic AMP-dependent protein kinases may be blocked by a specific inhibitor protein acting at the cyclic AMP regulatory subunit[6], we added such an inhibitor protein to the system and found that it prevented the activation of the cyclic AMP phosphodiesterase in a dose-dependent fashion (Fig. 1). Furthermore, polyacrylamide gel electrophoresis (PAGE) of the peripheral proteins of the liver plasma membrane after treatment with insulin, cyclic AMP and ^{32}P-ATP yielded three distinct peaks of radioactivity (Fig. 3). The major peak clearly migrated with the peripheral cyclic AMP phosphodiesterase activity. No ^{32}P from ^{32}P-ATP was incorporated into these peaks when (1) either or both cyclic AMP and insulin were absent, or (2) when a concentration of cyclic AMP protein kinase inhibitor protein just sufficient to prevent activation of the cyclic AMP phosphodiesterase was also present (Fig. 3). SDS-PAGE of the peripheral proteins obtained from liver plasma membranes pretreated with ^{32}P-ATP, insulin (10^{-9} M) and cyclic AMP (10^{-5} M) resolved three peaks of radioactivity. The major one, which is presumably the cyclic AMP phosphodiesterase, migrated with an apparent molecular weight of 52,000. From the estimates of molecular size of the enzyme in non-denaturing conditions[2], this would imply that it is a monomeric species. The two minor bands migrated with apparent molecular weights of 28,000 and 14,000. The dose–response curves for incorporation of ^{32}P into this major peak are given in Fig. 2*a*, *b*, where they demonstrate K_a's for insulin and cyclic AMP which are identical to those exhibited for the activation of the phosphodiesterase by these ligands. Indeed, a K_a of $\sim10^{-10}$ M for insulin's action is reflected in a similar affinity of insulin for specific binding to its receptor[7,21].

It is generally accepted and confirmed here (Fig. 1) that insulin alone does not activate the liver plasma membrane cyclic AMP phosphodiesterase of membrane fragments[8–11] although there is consistent evidence that such an activation can occur in intact adipocytes[8] and, in some instances, in intact hepatocytes[8,9]. Our novel observation is that for insulin to achieve such an activation then cyclic AMP and Mg^{2+}-ATP must both be present at appropriate concentrations. This may explain insulin's

0028–0836/80/350904—03$01.00

[illegible] COLLEGE [illegible] Upper Circular Road [illegible] Calcutta

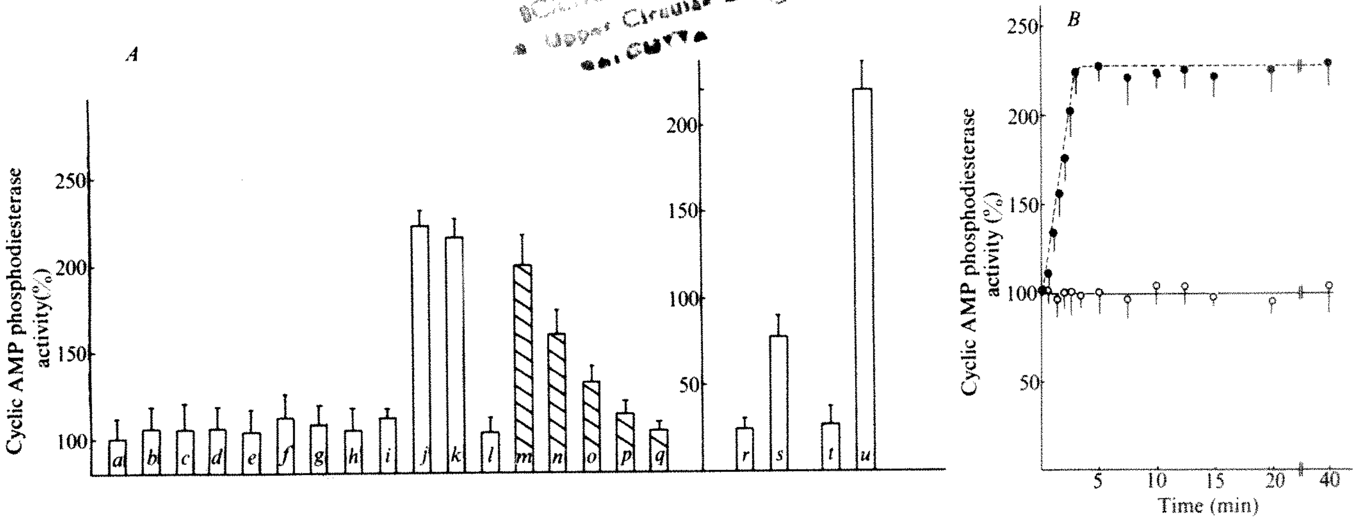

Fig. 1 *A*, Insulin requires ATP and cyclic AMP to stimulate the peripheral plasma membrane cyclic AMP phosphodiesterase activity. Purified rat liver plasma membranes[2,11] (500 μg protein ml^{-1}) were incubated for 5 min at 30 °C in a cocktail with final concentrations of 5 mM $MgCl_2$, 100 μM $CaCl_2$, 20 mM Tris HCl, *p*H 7.4, at a final volume of 250 μl. Various additions to the cocktail were made at the final concentrations stated and at a final *p*H 7.4. *a*, No additions; *b*, 3×10^{-3} M ATP; *c*, 10^{-9} M insulin; *d*, 10^{-6} M insulin; *e*, 10^{-7} M cyclic AMP; *f*, 10^{-4} M cyclic AMP; *g*, 3×10^{-3} M ATP + 10^{-6} M insulin; *h*, 3×10^{-3} M ATP + 10^{-4} M cyclic AMP; *i*, 10^{-6} M insulin + 10^{-4} M cyclic AMP; *j*, 10^{-6} M insulin + 10^{-4} M cyclic AMP + 3×10^{-3} M ATP; *k*, 10^{-9} M insulin + 4×10^{-6} M cyclic AMP + 3×10^{-3} M ATP; *l*, as in *j*, but using insulin denatured as described in ref. 13; *m–q*, as *j*, but a cyclic AMP-dependent protein kinase inhibitor, prepared as described in ref. 22, was added at final concentrations of *m*, 0.2 μg ml^{-1}; *n*, 0.4 μg ml^{-1}; *o*, 1.0 μg ml^{-1}; *p*, 1.0 μg ml^{-1}; *q*, 4.0 μg ml^{-1}. After this incubation the mixture was rapidly cooled on ice and then washed three times with 1 ml ice-cold 1 mM $KHCO_3$, *p*H 7.4, by repeated centrifugation at 14,000*g* for 10 min at 4 °C with subsequent resuspension. Aliquots (40 μg protein) of intact plasma membranes were then assayed for cyclic AMP phosphodiesterase activity as described previously[2] using 4×10^{-7} M cyclic AMP as substrate. Routinely, a modified two-step radioassay based on that described by Thompson and Appleman[23] was used as we could demonstrate negligible adenosine deaminase activity contaminating our preparations[2], although similar results were obtained using the method of Rutten *et al.*[24]. Corrections were made for adenosine bound to the resin[2]. The activity of the intrinsic enzyme was identical for both *r* (native) and *t* (treated), whereas that of the native peripheral enzyme (*s*) was increased 2.5-fold in the treated case (*u*). Separation of the peripheral and integral enzymes was carried out as in ref. 2. Similar results were obtained using plasma membrane derived from hepatocytes as isolated in ref. 2. Errors are ±s.d., $n = 6$ using six different plasma membrane preparations. *B*, Time course of the insulin-triggered, cyclic AMP-dependent activation of liver plasma membrane cyclic AMP phosphodiesterase. Liver plasma membranes were incubated in the cocktail described in legend to *A* either ●, with 10^{-9} M insulin + 4×10^{-6} M cyclic AMP + 3×10^{-3} M ATP, or ○, without such additions. Reactions were terminated as described in *A* and samples taken for assay of cyclic AMP phosphodiesterase at 4×10^{-7} M cyclic AMP. Errors are ±s.d. for three membrane preparations ($n = 3$). The initial activity of the cyclic AMP phosphodiesterase was 45 pmol min^{-1} mg^{-1} in the assay conditions used. The control enzyme was unaffected by incubation in this cocktail over a period of 40 min.

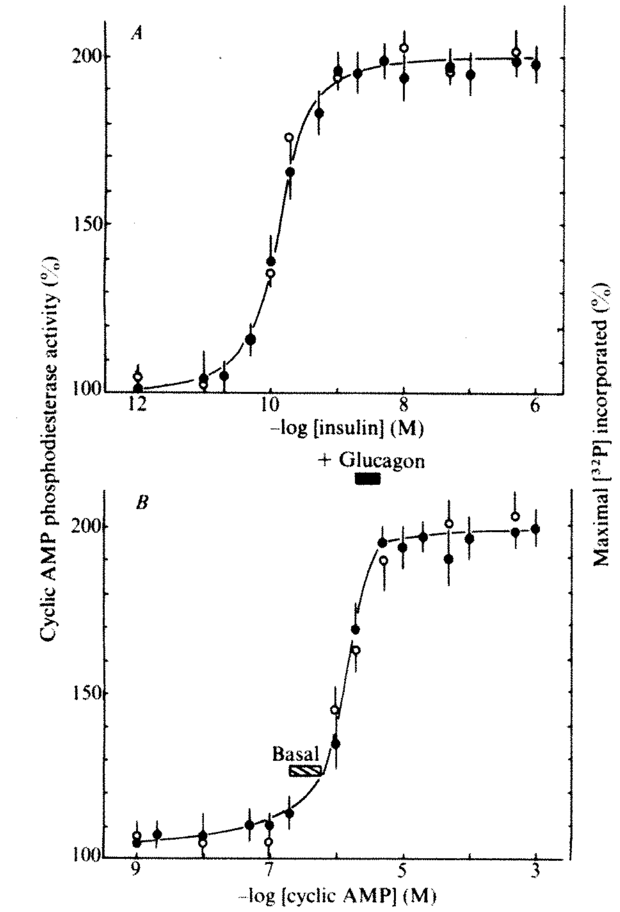

Fig. 2 Dose–response curves for the activation of the peripheral plasma membrane cyclic AMP phosphodiesterase. Incubations, assay of cyclic AMP phosphodiesterase and the release and separation of the peripheral enzyme after exposure to the stimulating ligand were carried out as described in Fig. 1*A* legend. For the assay of ^{32}P incorporation from [γ-^{32}P]ATP, the incubation mixture contained 1 mM ATP at a specific radioactivity of 200 mCi $mMol^{-1}$. The incorporation of radioactivity into the major peak found by SDS-PAGE of the peripheral proteins (see Fig. 3 legend) is plotted as a function of either insulin or cyclic AMP concentration. *A*, Dose–response curve for the activation of the peripheral cyclic AMP phosphodiesterase (●) in the presence of saturating, 10^{-6} M, bovine insulin. Similar results were obtained using 10^{-9} M insulin. The ATP concentration was 3×10^{-3} M. The dose–response curve for the incorporation of ^{32}P into the major peak obtained upon SDS-PAGE of the peripheral proteins (○) was carried out at an insulin concentration of 10^{-9} M. *B*, Dose–response curve for the activation of the peripheral cyclic AMP phosphodiesterase (●) in the presence of saturating, 10^{-4} M, cyclic AMP. Similar results were obtained using 4×10^{-6} M cyclic AMP. The ATP concentration was 3×10^{-3} M. The dose–response curve for the incorporation of ^{32}P into the major peak obtained upon SDS-PAGE of the peripheral proteins (○) was carried out at a cyclic AMP concentration of 4×10^{-6} M. Errors are ±s.d., $n = 6$ for six different plasma membrane preparations. Similar dose–response curves can be obtained when plotting ^{32}P incorporation into the two other major peaks obtained on SDS-PAGE.

apparently elusive effect on liver[9], for in the liver, cyclic AMP levels must be raised above their basal levels before insulin can trigger the cyclic AMP-dependent activation and phosphorylation of the cyclic AMP phosphodiesterase (Fig. 2).

Assayed at 1 μM cyclic AMP, the plasma membrane cyclic AMP phosphodiesterase activity of 55 pmol min^{-1} mg^{-1} represents only some 10% of the total cellular activity[2,9], which one can compare with a basal adenylate cyclase activity of 17 pmol min^{-1} mg^{-1} (refs 12, 13). Activation of the phosphodiesterase by insulin doubles its activity, to some 18% of the total, and in the presence of 1 nM glucagon, adenylate cyclase activity increases about fourfold[11,12]. It has been pointed out that small changes in phosphodiesterase activity could have a considerable effect on cyclic AMP concentration if the turnover rate was high[14] and the stimulation by insulin may take

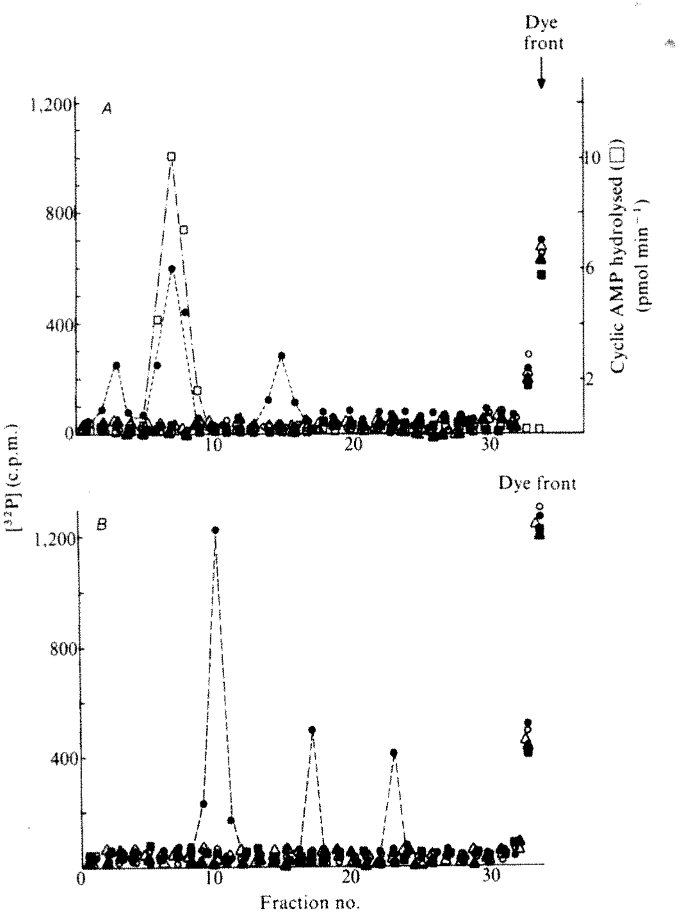

Fig. 3 Polyacrylamide gel electrophoresis of the peripheral proteins of rat liver plasma membranes. *A*, Peripheral proteins were released and subjected to PAGE in non-denaturing conditions with subsequent slicing of the gel as described in ref. 2. This figure demonstrates a typical experiment which we have now carried out over 10 times. Membranes were pretreated with various ligands in the conditions described in the Fig. 1 legend except that [γ-^{32}P]ATP was present at a final concentration of 1 mM with a specific radioactivity of 200 mCl mMol^{-1}. 100 μg of protein was loaded onto each gel. Gel slices were assayed for ^{32}P after incubation overnight in buffer[2]. △, [γ-^{32}P]ATP alone; ▲, [γ-^{32}P]ATP + 10^{-4} M cyclic AMP; ○, [γ-^{32}P]ATP + 10^{-6} M insulin; ●, [γ-^{32}P]ATP + 10^{-4} cyclic AMP + 10^{-6} M insulin; ■, [γ-^{32}P]ATP + 10^{-4} M cyclic AMP + 10^{-6} M insulin + cyclic AMP protein kinase inhibitor protein (4 μg ml^{-1}). Where [γ-^{32}P]ATP + 10^{-4} cyclic AMP + 10^{-6} M insulin were used, the eluted gel slices were also assayed for cyclic AMP phosphodiesterase activity[2]. Identical quantities of protein were loaded onto and extracted from each gel, making the results directly comparable. *B*, SDS-PAGE of the peripheral proteins. An identical experiment to that described above was set up, except that 100 μg of protein in 10 μl was mixed with 5 μl of a cocktail containing 6 mM EDTA, 0.75 M sucrose, 6% SDS, 0.03% bromothymol blue at a final *p*H 7.4. 160 mM dithiothreitol (5 μl) was added and the mixture incubated for 5 min at 100 °C. After cooling, 3 μl of 0.5 M iodoacetamide was added and this mixture incubated for 15 min at room temperature. SDS-PAGE was then carried out by the method of Laemmli[25] and gels were then sliced and incubated[2] except that 0.1% SDS was added to the buffer. This figure demonstrates a typical experiment. Similar results were obtained in both instances using 4×10^{-6} M cyclic AMP and 10^{-9} M insulin.

advantage of this. Furthermore, theoretical studies imply an importance of a low K_m phosphodiesterase bound to the plasma membrane in regulating both overall and local cyclic AMP concentrations[15]. However, we should not discount the possibility that a considerable fraction of the cyclic AMP phosphodiesterase activity is associated with intracellular membranes[2] and that the rapid internalization of insulin by endocytosis[16] may lead it to achieve a similar activation there. Furthermore, insulin may depress cyclic AMP levels in part by inhibiting adenylate cyclase in a Ca^{2+}- and adenosine-dependent fashion[17].

Occupancy of the insulin receptor in liver can lead to the cyclic AMP-dependent phosphorylation of three peripheral membrane proteins. One of these is a low K_m cyclic AMP phosphodiesterase which becomes activated. It is intriguing to speculate whether the other proteins are involved in Ca^{2+} mobilization[5,18] or in the generation of a 'mediator' of some of the other known intracellular actions of insulin[19,20] and to what extent intrinsic proteins may be affected. It would seem that, unlike the glucagon receptor where occupancy leads simply to the activation of adenylate cyclase, an occupied insulin receptor may affect several target proteins by initially triggering a membrane-bound cyclic AMP-dependent protein kinase.

We thank Dr H. G. Nimmo for advice and for a gift of the cyclic AMP-dependent protein kinase inhibitor and Professor A. A. Eddy for critical discussion of the manuscript. This work was supported by the MRC, SRC and the California Metabolic Research Foundation.

Received 13 March; accepted 9 July 1980.

1. Jefferson, L. S., Exton, J. H., Butcher, R. W., Sutherland, E. W. & Park, C. W. *J. biol. Chem.* **243,** 1031–1038 (1968).
2. Marchmont, R. J. & Houslay, M. D. *Biochem. J.* **187,** 381–392 (1980).
3. Exton, J. H., Harper, S. C., Tucker, A. L., Flagg, T. L. & Park, C. R. *Biochim. biophys. Acta* **329,** 41–57 (1973).
4. Smith, S. A., Elliott, K. R. F. & Pogson, C. I. *Biochem. J.* **176,** 817–825 (1978).
5. Blackmore, P. F., Assimacopoulos-Jeannet, F., Chan, T. M. & Exton, J. H. *J. biol. Chem.* **254,** 2828–2834 (1979).
6. Nimmo, H. G. & Cohen, P. *Adv. Cyclic Nucleotide Res.* **8,** 145–266 (1977).
7. Cuatrecasas, P. *A. Rev. Biochem.* **43,** 169–214 (1974).
8. Thompson, W. J. & Strada, S. J. in *Receptors and Hormone Action* Vol. 3 (eds Birnbaumer, L. & O'Malley, B. W.) 553–577 (Academic, New York, 1978).
9. Westwood, S. J., Luzio, J. P., Flockhart, D. A. & Siddle, K. *Biochim. biophys. Acta* **583,** 454–466 (1979).
10. Loten, E. G., Assimacopoulos-Jeannet, F. D., Exton, J. H. & Park, C. R. *J. biol. Chem.* **253,** 746–757 (1978).
11. Pilkis, S. J., Exton, J. H., Johnson, R. A. & Park, C. R. *Biochim. biophys. Acta* **343,** 250–267 (1974).
12. Desbuquois, B., Krug, F. & Cuatrecasas, P. *Biochim. biophys. Acta* **343,** 101–120 (1974).
13. Loten, E. G. & Sneyd, J. G. T. *Biochem. J.* **120,** 187–193 (1970).
14. Arch, J. R. S. & Newsholme, E. A. *Biochem. J.* **158,** 603–622 (1976).
15. Fell, D. A. *J. theor. Biol.* **84,** 361–385 (1980).
16. Desbuquois, B., Willeput, J. & Huet de Froberville, A. *FEBS Lett.* **106,** 338–344 (1979).
17. Kiss, Z. *FEBS Lett.* **92,** 29–32 (1978).
18. Severson, D. L., Denton, R. M., Pask, H. T. & Randle, P. J. *Biochem. J.* **140,** 225–237 (1974).
19. Jarrett, L. & Seals, J. R. *Science* **206,** 1407–1408 (1979).
20. Larner, J. *et al. Science* **206,** 1408–1410 (1979).
21. Czech, M. P. *A. Rev. Biochem.* **46,** 359–384 (1977).
22. Walsh, D. A. *et al. J. biol. Chem.* **246,** 1977–1985 (1971).
23. Thompson, W. J. & Appleman, M. M. *Biochemistry* **10,** 311–316 (1971).
24. Rutten, W. J., Schoot, B. M. & Dupont, J. S. H. *Biochim. biophys. Acta* **315,** 378–383 (1973).
25. Laemmli, U. K. *Nature* **222,** 680–682 (1970).

Stimulation of RNA synthesis in isolated nuclei by an insulin-induced factor in liver

Agnes Horvat*

Case Western Reserve University, Department of Medicine, Cleveland, Ohio 44106

Insulin stimulates the transport of small molecules as well as the synthesis of triglyceride, glycogen, DNA, RNA and protein. Although it is widely accepted that its differing actions are consequent to the binding to surface receptors, there is suggestive evidence that it may also act intracellularly. In 1975, we reported two well defined intracellular insulin binding sites in rat liver: the nucleus and the endoplasmic reticulum[1]. Specific binding sites for insulin on intact nuclei were shown by an immunofluorescent and autoradiographic technique, and the kinetics of insulin binding to isolated nuclear membranes were described[2,3]. Similar results have been obtained by other investigators[4–6], and the more recent reports on the internalization of insulin[7–9] give further support for an intracellular site of action of intact insulin or of its metabolic product. Investigation of the stimulatory effect of insulin on the synthesis of DNA and RNA in diabetic rats and isolated hepatocytes[10–13]

---

*Present address: University of Texas Health Science Center and Veterans Administration Medical Center, 4500 S. Lancaster Road, Dallas, Texas 75216.

suggests that the stimulation of RNA synthesis precedes that of DNA, and is likely to be an early event in the stimulation of macromolecular synthesis. I report here evidence of a low molecular weight substance in rat liver perfused with insulin which can stimulate the synthesis of RNA in isolated nuclei. These results suggest that insulin may function by binding to the cell surface, initiating or enhancing endocytosis[14] and entering the cell via a micropinocytotic route[9]. Once inside the cell, the active principle could be insulin itself, an intracellular degradation product of insulin, or a metabolic product of insulin action.

Fasted male rats were anaesthetized with Nembutal and their livers perfused with the perfusion apparatus described by Miller[15] (MRA Corporation, Clearwater, Florida). The perfusions were performed for between 5 and 30 min at 37°C. The medium was Hank's balanced salt solution 50 mM in HEPES and 3% in bovine serum albumin *p*H 7.5, with (10^{-7} and 5×10^{-8}M), and without insulin. The perfusate was equilibrated with 95% O_2 and 5% CO_2. Flow rates of 15–20 ml per min were maintained by a constant hydrostatic pressure. In these experimental conditions livers remain viable for 2–3 h without red blood cells in the perfusing medium[16]. In some instances the O_2 uptake of the liver was measured. The P_{O_2} between the inflow and outflow was lowered from 450 to 150 mm Hg. The concentration of immunoreactive insulin was determined in the perfusion medium before the onset, and after termination of the perfusion. Between 40 and 50% of the insulin was lost from the medium which is in good agreement with other reports[17,18].

After the perfusion was completed, the liver was immediately washed with ice-cold saline, homogenized in 0.25 M sucrose (20 mM in Tris-HCL *p*H 8.0) and fractionated into three subcellular fractions, nuclear, MLP (see below) and cytosol, by differential centrifugation[19]. The mixed particulate fraction, MLP (mitochondrial-lysosomal-microsomal), was obtained by centrifugation of the nuclear supernatant at 180,000 *g* for 1 h. The pellet was washed twice, suspended in 10 ml of 50 mM Tris-HCl buffer *p*H 7.8, sonicated with the MSE sonifier for 2 min and finally centrifuged again at 180,000 *g* for 90 min. Identical results were obtained when the vesicles were disrupted by multiple freezing and thawing. The soluble part, MLP soluble, was carefully separated from the pellet and the pellet suspended in 6–7 ml of 50 mM Tris-HCl *p*H 7.8 (MLP membrane). Both the MLP soluble and cytosol in subsequent steps were fractionated with the use of the Amicon ultrafiltration system. The first filtration was performed with the PM 30 membrane filter. In several experiments the fraction containing cellular components below 30,000 molecular weight was further fractionated with the UM-2 Amicon filter. The final fractions of the respective experiments (molecular weights below 30,000 or below 1,000) were lyophilized, suspended in 1 ml of water and used in the nuclear RNA synthesizing system. Nuclei from young rats (130 g) were isolated and characterized as described earlier[3] by the method of Blobel and Potter[20]. The assay conditions for RNA synthesis are described in the legend to Fig. 1.

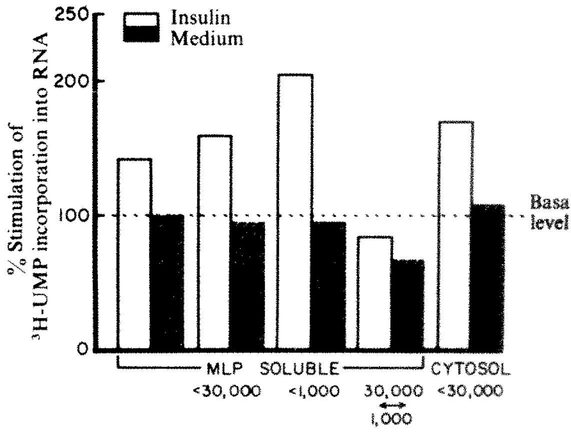

Fig. 1 Effect of insulin-induced factor on RNA synthesis in isolated rat liver nuclei. The livers were perfused with (5×10^{-8} M) or without insulin for 10 min; fractions and nuclei were isolated as described in the text. The assay for RNA synthesis was performed at 30 °C in a 250 l incubation mixture which was: ATP 400 μM, CTP, GTP 200 μM each, ^{3}H-UTP (NEN, 23.7 Ci mmol^{-1}) 330 nM, $MnCl_2$ and dithiotreitol 4 mM each, $(NH_4)_2SO_4$ 250 mM, Tris-HCl 40 mM, *p*H 7.9. The reaction was started with the addition of an aliquot of the nuclear suspension corresponding to 30–40 μg of DNA. After 5 min of incubation in a shaking water bath the reaction was stopped with 1 ml of ice-cold 10% trichloroacetic acid (TCA) and after 30 min at 0°C the precipitate was filtered on GF/C membrane filters, washed with 15 ml ice-cold 5% TCA, dried under IR lamp and counted in a scintillation counter with a 55% efficiency. The basal values (100% on the ordinate) correspond to an incorporation of 20 to 25 pmol UMP per mg DNA per 10 min. The amount of various fractions added was between 50 and 100 μg of protein as determined by the method of Miller[21] with bovine serum albumin (Armour) as standard.

Table 1 Effect of α-amanitin on the stimulation of RNA synthesis by a factor induced in liver perfused with insulin

Medium	^{3}H-UMP incorporated (d.p.m.)
Basal	21,000
+ α-amanitin	5,200
Basal + MLP soluble	29,000
+ α-amanitin	5,300

The assays were performed as described in the legend to Fig. 1. α-Amanitin concentration 0.8 μg ml^{-1}, MLP (100 μg protein) added where indicated.

Figure 1 depicts the results of a typical experiment indicating that perfusion of rat liver with 5×10^{-8} M insulin for 10 min produced a factor that directly stimulated the incorporation of ^{3}H-UMP into trichloroacetic acid insoluble material by isolated rat liver nuclei. The range of results obtained with different nuclear preparations and with fractions obtained from five insulin perfused and four non-insulin perfused liver preparations was as follows: insulin: MLP soluble, 138–200%; MLP soluble <30,000, 142–185%; MLP soluble <1,000 148–250%; cytosol <30,000, 124–200%. The corresponding values for the fractions from control livers (no insulin) were: 98–108%; 95–108%; 95–120%; 95–103%; and 96–110% of the basal levels. No stimulation was observed when intact insulin (10^{-8} – 10^{-6} M) was substituted for the perfused liver fractions in incubations with isolated nuclei (three experiments). With the MLP membrane fraction, an inhibition was noticed in two experiments. Both the basal level of RNA synthesis and the degree of stimulation depended greatly on the nuclear preparation, an observation also made by other workers[22]. Therefore, each nuclear preparation before use was checked for linearity in incorporation of ^{3}H-UMP with time and concentration of nuclei.

The results shown in Fig. 1 were all obtained in assay conditions optimal for RNA polymerase II, that is high [NH_4^+] and in the absence of α-amanitin. As shown in Table 1, when α-amanitin was added to the incubation mixture at a very low concentration (0.8 μg ml^{-1}), 75% of the basal activity was inhibited indicating that a large portion of the measured basal activity is due to RNA polymerase II[23]. All of the stimulation obtained by the MLP soluble fraction from the insulin perfused liver was completely abolished by the addition of this low concentration of α-amanitin. This could indicate that the stimulator specifically enhanced the synthesis of hnRNA in isolated nuclei[23]. The remaining activity is probably due to RNA polymerase I since the addition of 100 μg ml^{-1} α-amanitin did not affect the residual incorporation of ^{3}H-UMP into RNA[23].

In another set of experiments a dose-response effect could be demonstrated with fractions containing as much as 100 μg of protein, the latter amount not consistently exhibiting stimulation above that obtained with 50 μg. In a few experiments, the livers (insulin perfused and control) were fractionated into separate particulate subcellular fractions: nuclei, mitochondria, lysosomes, microsomes each of which was treated as described above for the MLP. Stimulation of RNA synthesis was observed with the lysosomal and to some extent with the microsomal fraction, but not with the mitochondrial or nulear fraction.

These results suggest that the vacuolar apparatus of the cell is associated with an active principle resulting from exposure of the cell to insulin. The substance is of low molecular weight, 1,000 or less, and conceivably could be a degradation product of insulin. Alternatively, it could be a compound chemically unrelated to insulin. In this regard, reports of a synthetic hexapeptide corresponding to the B_{21-26} fragment of insulin having a stimulatory effect on glucose uptake in the hind limb of rats could be pertinent to these results[24,25].

Turakulov *et al.*[26] reported the partial purification of a cytoplasmic regulator of Ca^{2+} transport by mitochondria isolated from rat liver 45 min after an intraperitoneal injection of insulin. These authors define the cytoplasm as the 30,000 *g* supernatant of the homogenate which actually contains both lysosomes and microsomes. From their results it seems that the factor is present in free and bound form supporting the suggestion presented in this paper, that is, that the primary site of formation of the active principle are membrane bound vesicles. The stimulation of RNA synthesis observed by the cytosol does not invalidate this suggestion since lysosomes are very fragile organelles and easily disrupted even with the most careful homogenization. Insulin has a delayed effect on the stimulation of RNA synthesis as compared to its very rapid effect on transport. If the formation of the active principle is indeed taking place in the vacuolar apparatus of the cell, and if it is a degradation product of insulin, the delay can be explained by the time needed for the content of the vesicles to be released into the cytoplasm. In general it is considered that the lysosomal membrane is freely permeable to small molecules, although it was also shown that 2 hours after the injection of ^{14}C-sucrose into the rat, subsequently isolated lysosomes contained both ^{14}C-glucose and ^{14}C-fructose[27]. As the factor appears to be of molecular weight below 1,000 it could reach the cytoplasm and finally the nucleus either by diffusion from the secondary lysosomes or alternatively by pyranhalysis, a process by which material entering the cell via endocytosis can be released into the cytoplasm of the cell without necessarily being completely degraded[28].

Recently, a low-molecular weight 'insulin mediator', probably a peptide, was reported to be present in insulin-treated rat muscle[29]. It mimics the action of insulin on cyclic AMP-dependent protein kinase, phosphoprotein phosphatase[29] and pyruvate dehydrogenase[30] in a cell-free system. There are several similarities between the 'mediator' and the factor detected in the present study. Both appear after a short exposure of the tssue to insulin, are of low molecular weight and have insulin-like action in a subcellular system, contrasting with previous experience where the action of insulin could be observed only in the whole animal, organ, or at least in the intact cell. There have been no previous reports of any effect of insulin or any compound derived from its action on the stimulation of RNA synthesis in a cell-free system. This report indicates the formation of a compound acting directly on the genetic material. As the insulin-induced factor enhances the synthesis of mRNA precursors it is possible that the factor affects the expression of genes known to be under the control of insulin[31-34].

I thank Drs B. R. Landau and J. Carter Jr, co-chairmen of the Division of Endocrinology, Department of Medicine, Case Western Reserve University, Cleveland, Ohio for their financial support of this investigation and many helpful discussions. I thank Susan Mann and Ed Burkett for assistance with liver perfusions and RIA assays of insulin respectively. This work was supported by the National Institutes of Health and the National Institute of Arthritis, Metabolic and Digestive Diseases.

Received 25 March; accepted 30 May 1980.

1. Horvat, A., Li, E. & Katsoyannis, P. G. *Biochim. biophys. Acta* **382,** 609–620 (1975).
2. Hollande, E. & Horvat, A. *Biol. Cell.* (submitted).
3. Horvat, A. *J. cell. Physiol.***97,** 37–47 (1978).
4. Goldfine, I. D. & Smith, G. J. *Proc natn. Acad. Sci. U.S.A.* **73,** 1427–1431 (1976).
5. Goldfine, I. D., Vigneri, R., Cohen, D. & Pliam, N. B. *Nature* **269,** 698–700 (1977).
6. Vigneri, R., Goldfine, I. D., Wong, K. Y., Smith, G. J. & Pezzino, V. *J. biol. Chem.* **253,** 2098–2103 (1978).
7. Carpentier, J. L. *et al. J. clin. Invest.* **61,** 1057–1070 (1978).
8. Schlessinger, J., Schechter, Y., Willingham, M. & Pastan, I. *Proc. natn. Acad. Sci. U.S.A.* **75,** 2659–2663 (1978).
9. Bergeron, J. J. M., Silkstrom, R., Hand, A. R. & Posner, B. I. *J. Cell Biol.* **80,** 427–443 (1979).
10. Steiner, D. F. & Williams R. H. *Biochim. Biophys. Acta* **234,** 1342–1346 (1959).
11. Younger, L. R., King, J. & Steiner, D. F. *Cancer Res.* **26,** 1408–1414 (1966).
12. Steiner, D. F. & King, J. *Biochim. biophys. Acta* **119,** 510–516 (1966).
13. Steiner, D. F., Chan, S. J., Terris, S. & Hofmann, C. *Ciba Fdn Symp.* **55,** 217–228 (1978).
14. Barnett, R. J. & Ball, E. G. *J. biophys. biochem. Cytol.* **8,** 83–101 (1960).
15. Miller, L. L. *Isolated Liver Perfusion and its Application* (eds Bartosek, I., Guartani, A. & Miller, L. L.) 11–61 (Raven, New York, 1973).
16. Friedmann, N. & Rasmussen, H. *Biochim. biophys. Acta* **222,** 41–52 (1970).
17. Terris, S. & Steiner, D. F. *J. clin. Invest.* **57,** 885–896 (1976).
18. Madison, L. L. & Kaplan, N. *J. clin. Med.* **52,** 927 (Abstract) (1958).
19. de Duve, C., Pressmann, B. C., Gianetto, R., Wattiaux, R. & Appelmans, F. *Biochem. J.* **60,** 604–617 (1955).
20. Blobel, G. & Potter, V. R. *Science* **154,** 1662–1665 (1966).
21. Miller, G. L. *Analyt. Chem.* **31,** 964 (1959).
22. Marzluff, W. F. Jr *Meth. Cell Biol.***19,** 317–332 (1978).
23. Schawartz, L. B., Sklar, V. E. F., Jaehning, J. A., Weinmann, R. & Roeder, R. G. *J. biol. Chem.* **249,** 5889–5897 (1974).
24. Weitzel, G., Bauer, F. & Eisele, K. *Hoppe Seyler's Z. Physiol. Chem.* **357,** 187–200 (1976).
25. Toyota, T., Kitahara, A. & Goto, Y. *Horm. Metab. Res.* **10,** 17–20 (1978).
26. Turakulov, Y. Kh., Gainutdinov, M. Kh., Lavina, I. I. & Akhmatov, M. S. *Dokl. Akad. Nauk SSSR* **234,** 1471–1473 (1977).
27. Horvat, A. *Biochim. biophys. Acta* **297,** 413–422 (1973).
28. Willingham, M. C. & Yamada, S. S. *J. Cell Biol.* **78,** 480–487 (1978).
29. Larner, J. *et al. Science* **206,** 1408–1410 (1979).
30. Jarett, L. & Seals, J. R. *Science* **206,** 1407–1408 (1979).
31. Reel, J. R., Lee, K. & Kenney, F. T. *J. biol. Chem.* **245,** 5800–5805 (1970).
32. Bhatena, S. J., Avigan, J. & Schreiner, M. E. *Proc. natn. Acad. Sci. U.S.A.* **71,** 2174–2178 (1974).
33. Spooner, P. M., Chernick, S. S., Garrison, M. M. & Scow, O. *J. biol. Chem.* **254,** 1305–1311 (1979).
34. Walaas, O., Walaas, E. & Grønnerød, O. *Acta endocr. Suppl.* **191,** 93–129 (1974).

Sequencing of 16S–23S spacer in a ribosomal RNA operon of *Euglena gracilis* chloroplast DNA reveals two tRNA genes

L. Graf, H. Kössel* & E. Stutz

Laboratoire de Biochimie, Université de Neuchâtel, Chantemerle 20,
CH-2000 Neuchâtel, Switzerland
* Institut für Biologie III der Universität Freiburg, Schänzlestrasse 1,
D-7800 Freiburg i. Br, FRG

Chloroplasts of the unicellular flagellate eukaryote *Euglena gracilis* contain several copies of a circular 135–140-kilobase pair DNA[1] which codes for chloroplast-specific stable RNAs (16S, 23S (refs 2, 3), 5S rRNAs[4] and tRNAs[5]) and for an unknown number of chloroplast-specific proteins. The rRNA genes are located within three tandemly repeated DNA regions of approximately 5.6 kilobase pairs each[6-8] and the arrangement of the structural genes within each repeat follows the prokaryotic pattern, being 5′-16S-23S-5S-3′ (ref. 9). Total chloroplast tRNA hybridizes to fragments of rDNA[9] and it was suggested that the 16S–23S spacer region contains tRNA coding sequences as is observed in *Escherichia coli*[10,11] and in spinach chloroplast[12] rDNA. We have therefore analysed *E. gracilis* strain Z 16S–23S spacer DNA at the nucleotide level, hoping this would allow identification of tRNA genes together with the processing sites of the respective primary transcripts. Maize chloroplast 16S rDNA shows strong sequence homology with *E. coli* 16S rRNA[13]. Sequence analysis of a total spacer in *E. gracilis* should demonstrate whether such similarities are also preserved in the chloroplast rDNA spacer region, or if this region has suffered a higher genetic drift rate. The latter is suggested from the 189 bases which have been sequenced from the 2.4-kilobase pair rDNA spacer from maize chloroplasts[14]. Flanking sequences, coding for the 3′-terminal region of 16S rRNA and for the 5′-terminal region of 23S rRNA have also been sequenced, to compare the drift rates between the spacer and its adjacent structural genes.

0028–0836/80/350908—03$01.00

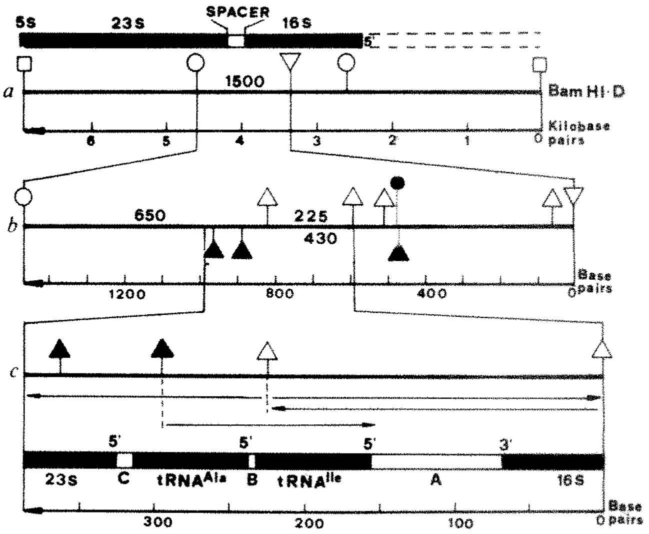

Fig. 1 *a*, Position of the *E. gracilis* rDNA region and of the spacer-containing fragment *Bgl*II–*Hpa*I$_{1,500}$ within the cloned fragment *Bam*HI·D (pEgc11)[8]. *b*, Fine mapping of fragment *Bgl*II–*Hpa*I$_{1,500}$ using the enzymes *Hae*III, *Hpa*II and *Hin*fI. *c*, Fragments used for sequence analysis of the spacer region. The arrows represent portions of 5′-terminally labelled single fragments from which unambiguous sequences could be obtained by a series of overlapping gels. Nearly all positions of fragment *Hae*III$_{225}$ have been analysed from both strands. Sequences of the right-hand portion of fragment *Bgl*II–*Hae*III$_{650}$ could be confirmed by analysing part of the complementary strand of fragment *Hin*fI$_{430}$, which also gives the necessary overlap between fragments *Bgl*II–*Hpa*I$_{650}$ and *Hae*III$_{225}$. Positions of rRNA and tRNA coding sequences and of the intergenic regions A, B and C are indicated. □, *Bam*HI; ▽, *Hpa*I; △, *Hae*III; ○, *Bgl*I; ●, *Hpa*II; ▲, *Hin*fI.

Figure 1 shows the protocol which was followed for mapping and identification of the spacer region within the restriction fragment *Bam*HI·D. This fragment, which contains one of the three rDNA repeats, has previously been cloned using the plasmid pBR322 as vector[15] and the respective clone pEgc11 (formerly pEgcKS11) was used for isolation of fragment *Bam*HI·D and its subfragments. Partial sequencing of several of the subfragments[16] revealed strong homology with regions from *E. coli*[17,18] and maize chloroplast[13] 16S rRNA (rDNA) and thereby allowed location of the 3′-terminal region of the 16S rRNA gene on the right-hand third of fragment *Hae*III$_{225}$. Since hybridization and fine-mapping data had indicated[6,7,19] that the spacer should not exceed 300 base pairs, the left-hand two-thirds of fragment *Hae*III$_{225}$ together with the neighbouring portion of fragment *Bgl*II-*Hae*III$_{650}$ should comprise the entire spacer sequence. These fragments were therefore chosen for sequence analysis according to the dimethylsulphate/hydrazine procedure[20] and the necessary overlap between the two *Hae*III fragments was obtained by sequencing the left-hand portion of fragment *Hin*fI$_{430}$.

In Fig. 2 the RNA-like strand of the *E. gracilis* spacer DNA sequence is depicted alongside the respective sequences from the *E. coli* rrnD operon. The first 63 positions comprise the 3′-terminal region of the 16S rRNA gene, the 'prokaryotic character' of which is documented by its high degree of homology with the corresponding rDNA region from *E. coli*. The reported 3′-terminal oligonucleotide AACAACUCN of *E. gracilis* 16S rRNA[21] allows exact positioning of the 3′-terminal end of the structural part of this gene. The reported T$_1$ oligonucleotide UAACAAG[21] which is highly conserved in prokaryotic 16 S rRNA[22] is found at position 22–28. The non-conserved position 59 is of particular interest, as it partly changes the recognition sequence for translational initiator regions[23,24]. This suggests that *E. gracilis* chloroplast ribosomes have a slightly altered pattern of recognition for mRNA in comparison with *E. coli* whereas in maize chloroplast ribosomes the corresponding sequence is identical to the *E. coli* 16S rRNA 3′ end[14].

A stretch of 66 nucleotides shown in the lower part of Fig. 2 represents the 5′-terminal portion of the 23S rRNA gene as evidenced by its extensive homology with the 5′-terminal region of *E. coli* 23S rDNA[10,11]. However, since the 5′-terminal oligonucleotides of *E. gracilis* 23S rRNA are not known, exact positioning of the 5′ terminus of the 23S rRNA gene is not

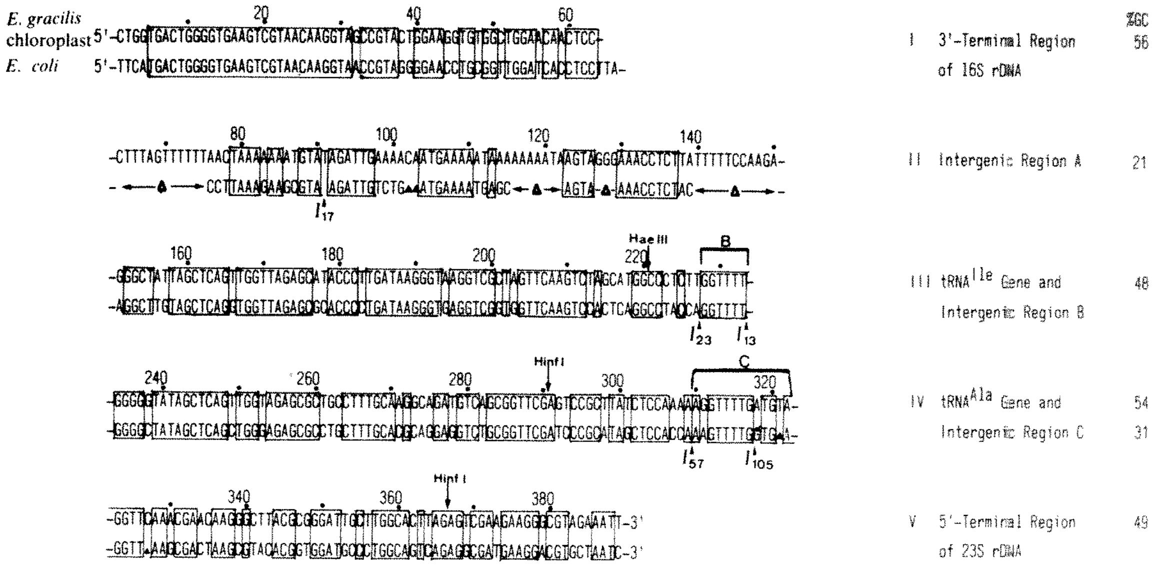

E. gracilis chloroplast
E. coli
20
40
60
80
100
120
140
160
180
200
220
240
260
280
300
320
340
360
380
I17
I23
I13
I57
I105
HaeIII
B
HinfI
C
HinfI
%GC
I 3'-Terminal Region of 16S rDNA 56
II Intergenic Region A 21
III tRNA^Ile Gene and Intergenic Region B 48
IV tRNA^Ala Gene and Intergenic Region C 54 31
V 5'-Terminal Region of 23S rDNA 49

Fig. 2 Nucleotide sequence of the 16S–23S intergenic spacer region and of the flanking region of the 16S and 23S rRNA genes from *E. gracilis* chloroplast DNA (top row) and from the rrnD operon of *E. coli*[10,11]. Only the sequences of the RNA-like strands are depicted. Homologous sequences are marked by boxing. Within the *E. coli* sequence the symbols ▲, △ and *I* indicate single point deletions, multiple deletions and insertions in respect to the *E. gracilis* sequence. The number *a* of inserted bases is indicated by I_a. Note that the *E. gracilis* sequence is depicted in the opposite orientation from that of Fig. 1. Cleavage sites for the restriction enzymes used in Fig. 1 are indicated.

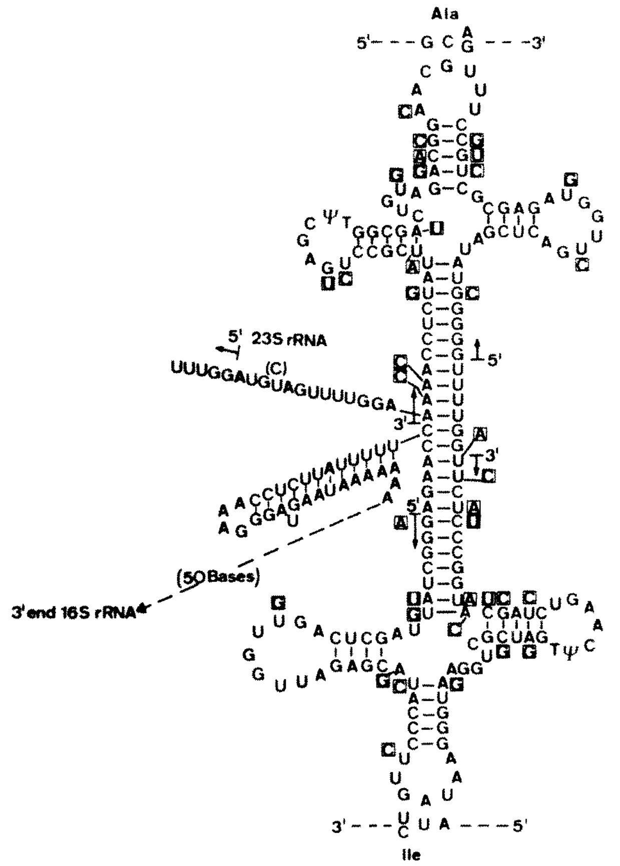

Fig. 3 Possible secondary structure of the dimeric tRNA precursor region as predicted from the corresponding DNA sequence of Fig. 2. The two tRNA cloverleaf structures are depicted without modifications of the bases except for the TΨ sequences in the T-arms. Bases different in the respective *E. coli* tRNA species[10,11] are indicated within boxes.

possible. The 16S–23S spacer DNA is thus represented by the 259 base pairs confined within positions 63 and (probably) 322. The analogous region in the *E. coli* rrnD operon is considerably larger with 437 nucleotide positions. In *E. coli* the spacer region is known to be transcribed as a part of the single transcriptional unit of the rrnD operon[10]. A large rRNA precursor containing both the 16S and 23S rRNA sequences was also observed in spinach[25,26] and *Chlamydomonas*[27] chloroplasts. A rRNA of similar large size has been observed also in *E. gracilis* chloroplasts[28] and therefore it is reasonable to assume that a similar situation exists in this case although direct experimental evidence for transcription of the intergenic spacer is lacking.

Screening for GTTC sequences, which are indicative for the GTΨC sequence present in the Ψ loop of all tRNA species[29], and for homology with the *E. coli* rDNA spacer region reveals two tRNA genes coding for an isoleucine (AU^{U}_{C})- and an alanine (GC^{A}_{G})-accepting species, respectively. The tRNA primary structures deduced from the two tRNA genes allow folding to a cloverleaf model completely consistent with all other structural criteria of tRNAs[29] (see Fig. 3). The deduced cloverleaf models contain several compensating base changes in the stem regions in addition to changes in the unpaired regions, which excludes the possibility that the two genes are derivatives of the *E. coli* genome due to a cloning or recombinational artefact. Also, the two chloroplast tRNA genes lack the CCA termini found in the respective *E. coli* tRNA genes[10,11]. The two tRNA genes are separated from each other by only six base pairs, which is reminiscent of the clustering of tRNA genes on the phage T_4 genome[30]. Within the precursor transcript, the two acceptor stems together with their neighbouring sequences can form a continuous stack of 24 base pairs (plus 2 × 5 base pairs of the two T-stems according to the tRNA tertiary model[31,32]) as drawn in Fig. 3. A possible hairpin structure directly preceding the 5′ end of the $tRNA^{Ile}$ is also depicted in Fig. 3, since its stem region could possibly also form an uninterrupted stack with the acceptor stem (and the T-stem[31,32]) of this tRNA within the precursor molecule. It is tempting to speculate that some of these possible secondary structures constitute at least part of the signal structures necessary for proper processing of the common precursor chain. Alternatively, or in addition to this, recognition of the sequence GGUUUUG, which is common to both the tRNA precursors immediately beyond the 3′ ends, may act as a signalling step during the processing events.

A comparison of the rRNA and tRNA coding sequences with the intergenic regions (Fig. 2) shows that the former are highly conserved contrary to the latter which are subject to many alterations, mainly by deletions but including some base substitutions. The short homologous stretches in the intergenic regions may have some functional significance for processing steps. Furthermore it is interesting that, similar to *E. coli* rDNA[10,11], the G + C content is high in the structural and low in the intergenic parts.

We thank Drs K. Edwards and R. Hertel for helpful criticism of the manuscript. This work was supported by grants from Fonds National Suisse de la Recherche Scientifique No. 3.452.79 to E.S. and from Deutsche Forschungsgemeinschaft (SFB 46) to H.K.

Received 30 April; accepted 20 June 1980.

1. Manning, J. E. & Richards, O. C. *Biochim. biophys. Acta* **259**, 285–296 (1972).
2. Scott, N. S. *J. molec. Biol.* **81**, 327–336 (1973).
3. Kopecka, H., Crouse, J. E. & Stutz, E. *Eur. J. Biochem.* **72**, 525–535 (1977).
4. Gray, P. W. & Hallick, R. B. *Biochemistry* **18**, 1820–1825 (1979).
5. Schwartzbach, S. D., Hecker, L. I. & Barnett, W. E. *Proc. natn. Acad. Sci. U.S.A.* **73**, 1984–1988 (1976).
6. Gray, P. W. & Hallick, R. B. *Biochemistry* **17**, 284–290 (1978).
7. Rawson, J. R. Y., Kushner, S. R., Vapnek, D., Alton, N. K. & Boerma, C. L. *Gene* **3**, 191–209 (1978).
8. Jenni, B. & Stutz, E. *Eur. J. Biochem.* **88**, 127–134 (1978).
9. Hallick, R. B., Gray, P. W., Chelm, B. K., Rushlow, K. E. & Orozco, E. M. Jr *Chloroplast Development* (eds Akoyunoglou, G. *et al.*) 619–622 (Elsevier, Amsterdam, 1978).
10. Young, R. A., Maklis, R. & Steitz, J. A. *J. biol. Chem.* **254**, 3624–3271 (1979).
11. Sekya, T. & Nishimura, S. *Nucleic Acids Res.* **6**, 575–592 (1979).
12. Bohnert, H. J. *et al. FEBS Lett.* **103**, 52–56 (1979).
13. Schwarz, Z. & Kössel, H. *Nature* **283**, 739–742 (1980).
14. Schwarz, Z. & Kössel, H. *Nature* **279**, 520–522 (1979).
15. Knopf, U. C. & Stutz, E. *Molec. gen. Genet.* **163**, 1–6 (1978).
16. Graf, L., Schwarz, Z., Kössel, H. & Stutz, E. *Experientia* **86**, 34 (1980).
17. Brosius, J., Palmer, M. L., Kennedy, P. J. & Noller, H. F. *Proc. natn. Acad. Sci. U.S.A.* **75**, 4801–4805 (1979).
18. Carbon, P., Ehresmann, C., Ehresmann, B. & Ebel, J. P. *FEBS Lett.* **94**, 152–156 (1978).
19. Jenni, B. & Stutz, E. *FEBS Lett.* **102**, 95–99 (1979).
20. Maxam, A. & Gilbert, W. *Proc. natn. Acad. Sci. U.S.A.* **74**, 560–564 (1977).
21. Zablen, L. B., Kissil, M. S., Woese, C. R. & Buetow, D. E. *Proc. natn. Acad. Sci. U.S.A.* **72**, 2418–2422 (1975).
22. Woese, C. R. *et al. Nature* **254**, 83–86 (1975).
23. Shine, J. & Dalgarno, L. *Proc. natn. Acad. Sci. U.S.A.* **71**, 1342–1346 (1974).
24. Steitz, J. A. *Biological Regulation and Control* (ed. Goldberger, R.) 349–399 (Plenum, New York, 1979).
25. Hartley, M. R., Head, C. W. & Gardiner, J. *Acides Nucléiques et Synthèse des Protéines chez les Végétaux* (eds Bogorad, L. & Weil, J. H.) 419–423 (CNRS, Paris, 1977).
26. Bohnert, H.-J., Driesel, A. J. & Herrmann, R. G. *Acides Nucléiques et Synthèse des Protéines chez les Végétaux* (eds Bogorad, L. & Weil, J. H.) 213–218 (CNRS, Paris, 1977).
27. Rochaix, J. D. & Malnoe, P. *Cell* **15**, 661–670 (1978).
28. Wollgiehn, R. & Parthier, B. *Plant Sci. Lett.* **16**, 203–210 (1979).
29. Sprinzl, M., Grueter, F., Spelzhaus, A. & Gauss, D. H. *Nucleic Acids Res.* **8**, r1–r22 (1980).
30. Abelson, J. *A. Rev. Biochem.* **48**, 1035–1069 (1979).
31. Suddath, F. L. *et al. Nature* **248**, 20–24 (1974).
32. Robertus, J. D. *et al. Nature* **250**, 546–551 (1974).

Erratum

In the letter 'Juvenile hormone mimics the photoperiodic apterization of the alate gynopara of aphid, *Aphis fabae*' by Jim Hardie, *Nature* **286**, 602–604, line 2 of paragraph 7 should read 'juvenile characters in the fifth instar. After scoring these alates' and line 5 of the same paragraph should read 'juvenilization are the second and third instars, an observation'.

MATTERS ARISING

The rhenium–osmium age of the Galaxy

LUCK, BIRCK AND ALLEGRE[1] have reported new meteoritic data on Re and Os which led to limits to the age of the Galaxy of between 13,000 and 22,400 Myr. Here I point out how these results change if one uses estimates of the s-process contribution to ^{187} Os given by Woosley and Fowler[2].

The isotope ratio used as a galactic chronometer can be written

$$R \equiv \frac{^{187}\mathrm{Os}^*}{^{187}\mathrm{Re}} = \frac{^{187}\mathrm{Os}^*}{^{186}\mathrm{Os}} \Big/ \frac{^{187}\mathrm{Re}}{^{186}\mathrm{Os}}$$

where all values are for the meteorites at formation and $^{187}\mathrm{Os}^*$ is the radiogenic component of $^{187}\mathrm{Os}$. The s-process component is written in terms of the ratio of neutron capture cross-sections and a correction factor, f, so that

$$^{187}\mathrm{Os}^*/^{186}\mathrm{Os} = (^{187}\mathrm{Os}/^{186}\mathrm{Os})_{\mathrm{total}} - (\sigma_{186}/\sigma_{187})f$$

Let us use from reference 1 the values $^{187}\mathrm{Re}/^{186}\mathrm{Os} = 3.20$ and $(^{187}\mathrm{Os}/^{186}\mathrm{Os})_{\mathrm{total}} = 0.805 \pm 0.011$ (2σ), and from ref. 2 the values $\sigma_{186}/\sigma_{187} = 0.504 \pm 0.034$ (2σ) (ref. 4) and $0.8 \leqslant f \leqslant 1.15$. These quantities give $R = 0.096 \pm 0.041$. Luck *et al*[1]. use a smaller s-process contribution, which gives $R = 0.152$.

A firm lower limit to the age of the Galaxy comes from assuming that all nucleosynthesis of Re occurred in a single burst at time $t = 0$. Then the time T of meteorite formation (4,550 Myr ago[1]) is given by $R = \exp(\lambda T) - 1$, where the decay constant $\lambda = 1.62 \times 10^{-11}$ yr^{-1} (ref.1); the age of the Galaxy is given by $t_0 > T + 4{,}550$ Myr. The value of R used by Luck *et al.* gives $t_0 > 13{,}300$ Myr, but the above revised value gives a lower limit of $10{,}200 \pm 2{,}300$ Myr.

An upper limit to t_0 cannot be obtained without a detailed model of chemical evolution, including gas flows[3]. As a simple example of an older model, the case stated by Luck *et al.* of 'steady-state nucleosynthesis' gave $t_0 = 22{,}400$ Myr with their value of R, but with the above value it gives $t_0 = 16{,}100 \pm 5{,}100$ Myr.

The main points are, as forseen by Woosley and Fowler[2], that uncertainties in the s-process seriously affect the Re–Os chronometer, and that use of the latest estimate of the s-process contribution to ^{187}Os reduces the lower limit to the age of the Galaxy by about 3,000 Myr.

BEATRICE M. TINSLEY
Yale University Observatory,
260 Whitney Ave.,
Box 6666,
New Haven, Connecticut 06511

1. Luck, J.-M., Birck, J.-L. & Allègre, C.-J. *Nature* **283**, 256 (1980).
2. Woosley, S. E. & Fowler, W. A. *Astrophys. J.* **233**, 411 (1979).
3. Tinsley, B. M. *Astrophys. J.* **216**, 548 (1977).
4. Winters, R. R., Macklin, R. L. & Halpern, J. *Phys. Rev.* C (in the press).

Accuracy of thermoluminescence dates

WE congratulate Liritzis and Thomas[1] on the first combined application of thermoluminescence dating and magnetic palaeointensity determination, particularly in view of the disadvantageous magnetic characteristics of the kiln wall material used. It is a pity, however, that the thermoluminescence age errors in their Table 1 have been quoted without qualification, as they are liable to mislead archaeologists and others into expecting a higher accuracy from the technique than it can truly give. As has been learnt with radiocarbon dating, it is important to distinguish between precision of measurement and absolute accuracy. Evidently the errors quoted in Table 1 refer to the former (because the errors quoted for the averages are substantially less than the errors quoted for the individual measurements).

The systematic errors inherent in thermoluminescence dating are of a different type from those in radiocarbon but they are, nonetheless, important if comparison is being made with archaeologists' calendar year dates. Whereas the major systematic errors in radiocarbon dates have been worldwide effects—initially, uncertainty about the value of the half life and, more recently, uncertainty about the calibration curve by which radiocarbon years are converted into calendar years—the systematic errors in thermoluminescence dating arise from more intimate effects such as differences between types of fabric measured, burial environments and laboratory techniques.

It is not appropriate here to go into detail, but on the basis of a previous assessment[2,3] and taking into account two additional interfering effects also noted[4,5] specifically in respect of quartz, it seems unlikely that tighter limits than ±5% can at present be placed on the possible systematic error for a thermoluminescence date. This is at the 67% level of confidence. Neglecting any contribution from measurement error, this 5% systematic error limit corresponds to ±200 yr for a date at around 2000 BC, falling to ± 150 yr for 1000 BC. More realistically, we would put the best overall error limit that can be achieved for the average date on a group of contemporaneous samples, except in abnormally favourable circumstances, at ±7%, that is, ±300 yr and ±200 yr, respectively.

Obviously it is to be hoped that research will lead to improvement in the accuracy of thermoluminescence dating. One notable obstacle is the uncertainty introduced by possible variation in water content during burial; although techniques have been proposed[6,7] that eliminate this interference, they have not yet reached a better accuracy than that quoted above.

M. J. AITKEN
J. HUXTABLE
Research Laboratory for Archaeology,
6 Keble Road,
Oxford OX1 3QJ, UK

1. Liritzis, Y. & Thomas, R. *Nature* **283**, 54–55 (1980).
2. Aitken, M. J. & Alldred, J. C. *Archaeometry* **14**, 257–267 (1972).
3. Aitken, M. J. *Archaeometry* **18**, 233–238 (1976).
4. Bell, W. T. & Zimmerman, D. W. *Archaeometry* **20**, 63–65 (1978).
5. Sutton, S. R. & Zimmerman, D. W. *Archaeometry* **20**, 66–70 (1978).
6. Zimmerman, D. W. *Specialist Seminar on Thermoluminescence Dating, Oxford 1978, PACT Journal* **3**, 458–465 (1979).
7. Poupeau, G., Sutton, S., Walker, R. M. & Zimmerman, D. W. *9th Congr. Un. intern. Sci. Préhist. Protohist.*, Nice 1976 (in the press).

LIRITZIS REPLIES—I would like to clarify some points. First, the systematic errors in thermoluminescence (TL) dating of well-fired kilns clays are not pronounced (as they are in most other cases), due to the kiln structure; we used the internal part of the well-fired kiln wall or internal part of a fused kiln-surface clay. Second, the dated quartz samples (15 kiln clays and 3 tiles) come from the same fabric type of the respective kiln, and all have been subjected to the same climatological factors, an 'advantage' for precise water uptake and environmental γ-radiation measurements. This mineral similarity was also found from X-ray fluorescence analysis of many samples from the same kiln, and from the TL glow curves.

Third, in general, I agree that the systematic errors of ±5% exist for TL dating, but in the favourable circumstances of studying kiln materials they are much reduced. Fourth, the quoted 67% level of confidence will ensure improved accuracy for archaeologists' estimations. Fifth, some estimated errors (many due to the operator and technique used) cancel themselves out. Therefore, an average date for many contemporaneous samples, in the same burial conditions and weathering as in kiln materials, does make sense and justifiably reduces the overall error. Finally, by taking the 'permitted' average error of many TL dates as an overall error limit of the age of a kiln, the final quoted TL accuracy, as estimated % error, of our report is valid, and the precision obviously better.

YIANNIS LIRITZIS
Physics Laboratory II,
University of Patras,
Patras, Greece

0028-0836/80/350911—01$01.00

Ignimbrite veneer deposits or pyroclastic surge deposits?

RECENTLY, Walker and others[1] applied the concept of aspect ratio[2,3] to ignimbrites and we accept this as valid reasoning. An outstanding feature of the low-aspect ratio Taupo and Rabual ignimbrites (deposits of pumiceous pyroclastic flows) they describe is a landscape-mantling deposit (ignimbrite veneer deposit) which can be traced into a more conventional topography-infilling ignimbrite (valley-ponded ignimbrite). According to Walker and others[1], recognition of these new features requires that a reappraisal be made of the emplacement mechanisms and new diagnostic criteria be drawn up for recognizing pyroclastic types. We, however, question this statement.

In the lesser Antilles, several pyroclastic flow deposits that fill valleys have been traced into finer-grained, stratified and cross-stratified deposits which mantle the interfluves between valleys. These deposits are interpreted by us as the deposits of ash-cloud pyroclastic surges. Ash-cloud surges are outwardly expanding dilute pyroclastic flows derived from an underflow or pyroclastic flow *sensu stricto*[4–6]. The flow and surge have fundamentally different transport mechanisms. Pyroclastic flows are high-concentration flows that move by laminar and/or plug flow[7,8]. Deposits are typically massive, poorly sorted and topographically controlled. Surges are flows that are turbulent and deposit beds with internal stratification and cross-stratification[4–6]. Surges are not topographically controlled and deposits can mantle landscape adhering to relatively steep slopes.

Walker and others[1] imply that the ignimbrite veneer deposit is the deposit of a high-concentration flow. The veneer is regarded by them as a 'tail deposit' left in the wake of the pyroclastic flow. From their description we contend that this tail deposit is the deposit of an ash-cloud surge derived from the main flow and is its lateral equivalent.

R. V. FISHER
Department of Geological Sciences,
University of California at Santa Barbara,
Santa Barbara, California 93106

A. L. SMITH
J. V. WRIGHT
M. J. ROOBOL
Department of Geology,
University of Puerto Rico,
Mayaguez, Puerto Rico 00708

1. Walker, G. P. L., Heming, R. F. & Wilson, C. J. N. *Nature* **283,** 286 (1980).
2. Walker, G. P. L. *Phil. Trans. R. Soc.* A**274,** 107 (1973).
3. Hulme, G. *Geophys. J. R. astr. Soc.* **39,** 361 (1974).
4. Fisher, R. V. *J. Volcanol. geotherm. Res.* **6,** 305 (1979).
5. Fisher, R. V., Smith, A. L. & Roobol, M. J. *Geology* (in the press).
6. Wright, J. V., Smith, A. L. & Self, S. *J. Volcanol. geotherm Res.* (in the press).
7. Sparks, R. S. J. *Sedimentology* **23,** 147 (1976).
8. Wright, J. V. thesis, Univ. London (1979).

WALKER ET AL. REPLY—We accept without reservation the relationships described by Fisher and others from the Lesser Antilles. We have long believed in the concept that pyroclastic flows *sensu stricto* and pyroclastic surges have fundamentally different transport mechanisms. What is in question, however, is not the basic concept but the origin of certain rocks occurring specifically at Taupo and Rabaul Volcanoes: the rocks which we have called ignimbrite veneer deposits (IVDs).

We considered very carefully the possibility that our IVDs might have been emplaced in the way that Fisher and others propose, but rejected it for the five reasons outlined below.

First, apart from having a generally smaller content of coarse pumice, the IVD is identical in its grain-size characteristics with the valley pond ignimbrite, and has identical pumice density and crystal and lithic sizes and contents. There is no laboratory test that we can apply to distinguish between the two. Moreover, the IVD is visibly in lateral continuity with, and passes gradually into, the valley pond ignimbrite.

Second, the sheer scale of the IVD at Taupo seems to us to negate the idea that it could be the deposit of a surge generated at the vent; we think it highly unlikely that any pyroclastic surge is capable of moving radially outwards against air resistance, and of remaining highly turbulent long enough, to encompass a nearly-circular area measuring more than 160 km across, or of carrying $>10^{13}$ kg of poorly sorted pyroclastic material held entrained in its gas. We note that all known far-reaching pyroclastic surges have originated on steep and high cones, and the most far-reaching one (Bezymianny 1956[1]) was strongly directional, yet it travelled no further than 29 km. The Taupo IVD is not directional, and there is no evidence that it originated on a steep or high volcanic cone.

Third, the scale again seems to us to preclude the possibility that the IVD was generated by a whole succession of pyroclastic surges jetting forwards from the advancing ash-flow, which is presumably the mechanism that Fisher and others envisage. We do not deny that such jetting may and probably does occur, but we would expect the surges to carry much less particulate material than the parent body. This relationship certainly holds at Mt Pelée (Martinique) where one of us (G.P.L.W.) has worked. At Taupo, however, the IVD constitutes about 50% of the total ignimbrite volume, and at Rabaul as much as 75%. We note that the higher the proportion of 'surge-deposited' material, the more closely in effect does the 'jetting surge' concept converge on the single 'vent-generated-surge' one.

In the 'jetting surge' model we would, moreover, expect some kind of close relationship to exist between the thickness and lateral spread of a surge deposit and the position of adjacent valley ponds, but we find no such relationship. There are many places where a normal thickness of IVD is found several kilometres laterally from, and often several hundred metres higher than, the nearest substantial valley pond.

Fourth, at Taupo we have found ponded ignimbrite in many valleys where, to reach them, the parent flow must have crossed ridges or passes standing hundreds of metres higher than the present vent position. The most extreme ignimbrite pond we know is 2–3 m deep, contains pumice fragments up to 30 cm in diameter and occurs high on Tongariro Mountain, 45 km laterally from and 1,500 m higher than its source vent. We know of no way that this valley pond could have formed other than by the passage of a high-concentration pyroclastic flow right across the mountain.

Fifth, undoubted pyroclastic surge deposits differ notably in grain size and constitution from ignimbrite. The deposits of a more or less cold (and often wet) base surge are generally well stratified, and the beds (which have a thickness commonly measured in millimetres or centimetres) associated in the same bedding set commonly vary in median diameter over a range of 5 phi units or more. In contrast, in the IVD the layers (apart from certain pumice lenses) vary typically over a range of less than 1 phi, and the presence of carbonized vegetation indicates that they were hot. The deposits of a hot pyroclastic surge (such as the dilute component of a peléean *nuée ardente*) are totally different in character from ignimbrite, typically being very strongly enriched in the denser constituents (lithic fragments, crystals) and strongly depleted in fine dust.

We are convinced from these relationships that our IVD is indeed the deposit from a high-concentration flow, a pyroclastic flow *sensu stricto*, and cannot have been produced by any surge mechanism involving a dilute 'ash cloud'. Clearly, emplacements of both the Taupo and Rabaul ignimbrites were quite exceptionally violent events, far beyond the experience of civilized man, and we believe that there is a limit to how far their products can be interpreted from the study of such relatively minor eruptions as the 1902 *nuée ardente* of Mt Pelée.

G. P. L. WALKER
R. F. HEMING
Geology Department,
University of Auckland,
New Zealand

C. J. N. WILSON
Geology Department,
Imperial College,
London SW7 2AZ, UK

1. Gorshkov, G. S. *Bull. Volcanol.* **20,** 77 (1959).

0028-0836/80/350912—01$01.00

BOOK REVIEWS

Mother science and prodigal sons: a history of haematology

William S. Beck

Blood, Pure and Eloquent: A Story of Discovery, of People, and of Ideas. Edited by M. M. Wintrobe. Pp.771. (McGraw-Hill: 1980.) $30, £18.50.

IN THE discharge of editorial duties one day, I received a critique that included the phrase "This monograph fills a much needed gap". That addled expression came to mind when I contemplated this handsome new book by Maxwell M. Wintrobe and a well chosen gallery of distinguished haematologists. There was indeed a gap — much needed if it inspired this book — in the literature of scientific history. That gap, more like a chasm, concerned haematology, a discipline that richly deserves to have its story told.

The field of haematology has several notable properties. Because blood has always fired the human imagination, it long interested philosophers and poets who contributed some of our earliest notions of it. By drawing the book's title from the emotional imagery of John Donne, Wintrobe reminds us of that fact. Because blood is readily available, it was also an early object of scientific investigation, yielding many important basic discoveries in which haematologists have taken a proper pride. Some were of such magnitude they significantly advanced whole branches of science. There can be no doubt, for example, that the discoveries of liver therapy for pernicious anaemia by Minot and Murphy in 1925 and of intrinsic factor by Castle in 1929 turned haematology from a musty descriptive discipline, dominated by blood cell morphology, into a dynamic science rooted in physiology and biochemistry. These advances launched the whole field of modern clinical investigation. For another example, the discovery that sickle cell anaemia is a 'molecular disease' opened an important new chapter in molecular biology.

These successes had interesting consequences for the mother science, which soon spawned a cluster of subdisciplines. Like prodigal sons, they achieved their own bountiful successes and left home. Those who would define haematology as the science of blood saw the perimeter breached again and again, as such subdivisions as oncohaematology, immunohaematology and haemostasis acquired their own journals, national societies, sections at the National Institutes of Health and other perquisites. This disconcerting situation is burdensome for all who teach haematology to medical students, who must take certifying examinations in medicine or pathology, who plan and fund research programmes, and who apply these disciplines in the care of patients. Still, though it has been something of a nightmare for intellectual taxonomists, haematology has been a raging success scientifically. Its opulent history is dealt with adequately for the first time in this volume. It is a grand homecoming.

Wintrobe, a widely respected academic haematologist, has collected a series of articles on the several haematological subdivisions by recognized authorities, most of whom have themselves contributed significantly to the historical record. The book begins with an essay by Wintrobe that spans the early beginnings, from the ancient roots of haematology, through the great age of microscopy, up to the modern era. Next, an interesting chapter by Hart on palaeohaematology summarizes what can be gleaned about blood in ancient times from contemporary studies of bones, bodies and ancient art — an unusual topic for a treatise on history. There follow chapters on the bone marrow by Tavassoli, stem cells by Lajtha, the spleen by Crosby, red cell metabolism by Beutler, iron and haem by London, haemolysis by Dacie, effects of altitude on blood by Erslev, the conquest of pernicious anaemia by Castle, sickle cell anaemia by Conley, the molecular basis of thalassaemia by Weatherall, phagocytosis and granulocytes by Craddock, lymphocytes by Ford, leukaemia and lymphoma by Gunz, platelets by Spaet, plasma proteins by Janeway, haemostasis by Ratnoff, and blood transfusion and blood groups by Diamond. In a rather brief final chapter, Wintrobe draws the lessons of history.

Certain of the book's features merit commendation. It has a lively literary style and a gratifying uniformity of content, level and accent. Even so, some of the authors' personalities manage to shine through discreetly. Wintrobe wisely chose to steer between the extremes of readership. It should readily appeal to intelligent readers who may lack a rigorous scientific background but who are willing to make use of the book's convenient glossary. One hopes these will include legislators and other public officials. Yet it is detailed enough to be read profitably by haematologists and serious students. Indeed I can attest that in a recent course medical students found some of the essays a better guide to complex topics than conventional textbooks. This level adjustment is more successful in some parts than in others, but on the whole it has been well done.

Why write a history of haematology — or of any branch of science? Philosophers have long debated the purposes of historical scholarship. Is it the historian's purpose to be 'descriptive', to recount past events for their own sake or for the sake of making a credit-allocating record, or is it his purpose to be 'theoretical', to interpret, to generalize and to seek wisdom that might solve contemporary problems? Or is it simply to interest and amuse?

My only criticism of this attractive book — so lovingly compiled with its fine portraits and useful bibliographies — stems from private notions on historical writing. Most of the historian's purposes are meritorious, but it is possible to pursue them in different ways. One can recount what happened — the dates, names and facts — or one can tell what *really* happened in a sort of *cinéma vérité* style of reportage that conveys the important and fascinating details, never given in ordinary literature, behind the development of scientific ideas — the accidents, personalities, conflicts and inspirations that underlie every major discovery. In my opinion, writing in the latter mode is far more likely to achieve any of the possible purposes of a historian. I am especially impressed by several recent books that reached new levels of candour in the reporting of incidents, personal characteristics and idiosyncracies — books that seemed to tell it as it was. It is a much to be admired trend in the writing of scientific history. Alas, that trend is not greatly extended by this volume, which has a somewhat conservative tone.

The book's essayists are leaders who have contributed importantly to their own specialties. The editor tells us he chose them for that reason. But the essays are filled with the works of others and barren of the kind of information that one might relish from an important actor on the stage of history, the kind of information that only he possesses. In a felicitous chapter on "blood and mountains" Erslev refers to his discovery of erythropoietin in one sentence in the third person. Why did he do this experiment? How did he do it? There is no one better qualified to tell us than Erslev himself. Beutler deserves praise for having interviewed several major figures in preparing his chapter but he omits to explain how his own work on glucose-6-phosphate dehydrogenase deficiency anticipated what is now called the Lyon hypothesis. London tells us a bit about the Schoenheimer school at Columbia but not enough about his own perceptions of it. Castle speaks interestingly of Minot's personality and antecedents but is a shadowy figure in his third person references to himself. Spaet does not mention his own work. Such modesty!

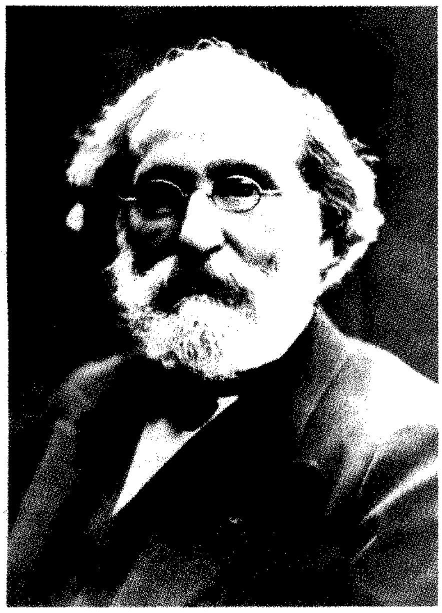

Georges Hayem (1841–1935), one of the 'fathers of haematology'.

Of course, this is probably not fair comment because it suggests that the editor and authors should have written a different book. In fact, this book is splendid and highly recommended. My only quibble is that ample room exists for more effort in this area. We all should hope that Professor Wintrobe continues to explore the many trails he has blazed with this welcome work. □

William S. Beck is Professor of Medicine at Harvard Medical School and Director of the Hematology Research Laboratory of the Massachusetts General Hospital, Boston.

Russian holography

P.W. Hawkes

Holography and Coherent Optics. By L.M. Soroko. Pp.818. (Plenum: 1980.) $59.50, £37.49.

THE decision to publish this translation, of a Russian text which first appeared in 1971, is most astonishing. At that date it was remarkably up to date, but holography is surely one branch of applied physics that has progressed out of all recognition during the 1970s. Further, the book lacks the merit of bringing early Russian work in this field to the attention of Western eyes, for there are no references at all. To cap this, it has the defect common to many Russian scientific texts: there is no index.

The book opens with some general ideas about holography, after which three chapters deal with various transforms of particular importance in optics, random signals and optical coherence. A chapter is then devoted to information theory in optics, followed by one on holography. The Russian text then concluded with a discussion of optical information processing, but for the English edition, the 'translation editor', G.W. Stroke, has included three of his own publications. Each topic is dealt with at some length, but for almost every subject much progress has been made since the book was written. In short, there really was not much point in translating this text, for in so fast-moving a subject students and research workers of the 1980s will need more recent information than that collected here. Access to a set of Professor Wolf's annual *Progress in Optics* (North-Holland) would be a great deal more useful. □

P.W. Hawkes is Maître de Recherches at the Laboratoire d'Optique Electronique du CNRS, Toulouse, France.

More of the Amboseli baboons

John M. Deag

Baboon Mothers and Infants. By Jeanne Altmann. Pp. 242. (Harvard University Press: 1980.) $17.20, £10.50.

EVER since the publication of *Baboon Ecology* by S.A. Altmann and J. Altmann (University of Chicago Press: 1970), primatologists have been waiting for further information on the social behaviour of the Amboseli baboons. *Baboon Ecology* set a new standard for primate ecological studies and Jeanne Altmann's *Baboon Mothers and Infants* will have equal influence on research into social relationships. This is no ordinary report of mother–infant behaviour and those most familiar with laboratory studies will find its scope unusual. Altmann summarizes her aims as follows: " . . . to assess the nature and extent of external influences on baboon mothers and their young infants. My general goal was to identify and measure factors affecting survival and behavior during motherhood and infancy, and to identify likely ontogenetic origins of differences in adult behaviour and life history patterns". The book therefore represents one of the first serious attempts to portray the total behavioural and ecological relationships among mothers, infants and the social group of which they form such a fundamental part.

It starts with an introduction to baboons and their habitat, and a short but important section on demography. During the first two years of life there was a per annum mortality of 0.3. Several infants were ill, wounded or suffering from possible nutritional deficiencies or poor mothering, and the author uses such cases when considering the costs and benefits of different sorts of behaviour. Mothers with young are themselves vulnerable, and older females with dependent young were found to be particularly at risk of dying when compared with younger females or those in other stages of the reproductive cycle. The effects of infants on their mothers' feeding patterns and time budgets are described and formalized in a theoretical model. It seems that if a mother had to provide all her infant's nutrition, severe time-budget problems would occur with infants more than 6–8 months old, even at slow rates of infant growth. A mother simply cannot gather enough food to maintain her body weight and to feed her infant; weaning is consequently forced upon the pair. Later sections of the book deal more directly with behavioural topics such as maternal care, infant development, spatial relationships, weaning and independence, and with how a mother's social relationships are affected by her infant's age.

The study group has been under observation since 1971 and a great deal of background information is available. The quantitative results on mothers and infants in the present study are drawn from 15 months of field work and 18 infants. Sound quantitative methods are used to provide an extremely detailed picture of the infants and their mothers. The major strength of this book lies in the detailed analyses attempted; but this is paradoxically also its main weakness, since it may make much of the book of little interest, except to the specialist prepared to wade through all the intimate details. The necessity of referring to individuals is a problem faced by all who deal in complex social relationships and yet who, except the author and her co-workers, can find it easy to follow a text studded with names which need constant back-reference to determine age, social rank and sometimes even sex? Such diversions are distracting but it is merely the presentation which is at fault — the philosophy of looking at individuals in detail is sound. No proper understanding of primate social behaviour and its evolution will be developed unless we have robust information on individual differences: on this count the book makes an important contribution. Although the sample of 18 infants may sound small it is in fact large by field (and even some laboratory) standards.

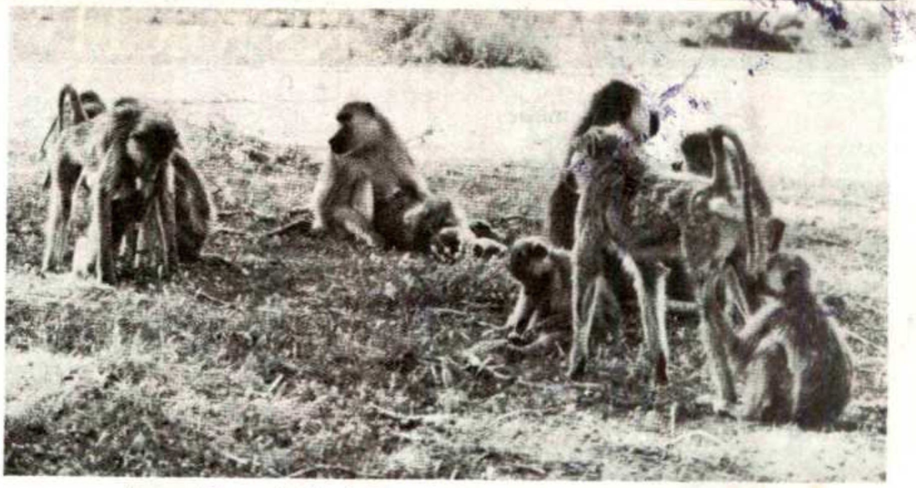

Jeanne Altmann's 'Alto's Group' of baboons, resting and grooming in Amboseli National Park, Kenya.

One of the major challenges of primatology is to see through the tangle of individual differences to reveal valid generalizations and thereby derive an understanding of the basic principles governing individual behaviour. As students of human personality will no doubt point out, this is not a straightforward task. Altmann searches for such generalizations wherever her sample size permits, and finds, for example, some interesting relationships between a mother's rank and her interaction with her infant and other group members. As would have been expected, low-ranking mothers gave more distress responses (submissive behaviour patterns) during social interactions and their infants were particularly prone to being interfered with by other members of the group. Mothers of different social rank also tended to show different styles of mothering: high rankers tended to be *'laissez-faire'* mothers (mothers tolerating separation from their infants); low rankers tended to be 'restrictive' mothers (mothers maintaining close contact with their infants). These differences in mothering appear to have consequences for infant maturation — infants of *laissez-faire* mothers became independent more rapidly. However it is much easier to describe such behavioural differences than to assess the costs and benefits (in terms of genetic fitness) with which the individual differences in behaviour are associated. The author recognizes this when considering the costs and benefits of mothering styles. Both forms have advantages and disadvantages but it is concluded that the styles adopted by mothers of different rank are adaptive because of the contrasting social pressures to which they are subjected by other group members. Arguments like this can only be speculative; they will become more convincing when larger samples of data are available.

The whole book is firmly based in modern evolutionary theory and those familiar with the parent–offspring conflict models of R. Trivers will find considerable interest in Altmann's analysis of weaning and independence. It has been proposed that the behavioural conflict during weaning between a mother and her infant is a reflection of an underlying conflict of interest — the infant attempting to secure more maternal care than the mother has been selected to provide. With her extensive field data behind her, Altmann helps to shift this argument from a theoretical to a practical plane and concludes that "parent–offspring genetic conflict of interest may arise infrequently as a relevant variable in many real-life situations".

In conclusion this book offers much to all those interested in social behaviour. Its holistic approach is attractive since it clearly acknowledges the undeniable complexity of primate social relationships but it does, however, leave one anxious for the day when sample sizes will be larger and selection pressures better understood. ☐

John M. Deag is a Lecturer in Zoology at The University of Edinburgh.

Magnetic resonance for biochemists and biophysicists

Karl-Erik Falk

ESR and NMR of Paramagnetic Species in Biological and Related Systems. Edited by I. Bertini and R.S. Drago. Pp.434. (Reidel: 1980.) Dfl.95, $50.

THIS volume comprises the papers given at a NATO Advanced Study Institute meeting held in June 1979, the subject of which was the magnetic resonance of paramagnetic species of biological importance. Twenty-four expert authors have contributed chapters covering various aspects of this large and important area of research.

The first part of the book is devoted to NMR and to the effects of paramagnetism on the NMR parameters, with chapters on the basic theory of relaxation and pulse techniques, paramagnetic effects in NMR, and a number of short reviews of current research. The applications for obtaining structural and dynamic information on various paramagnetic biological systems, ranging from purified small proteins to cell suspensions, are also discussed. The section on ESR contains a thorough consideration of theoretical aspects, focused on the 3d metal ions, followed by a discussion of the various classes of metalloproteins and, especially, the role of the metal ions. Throughout the book emphasis is put on the coupling between the unpaired electron and the nucleus, and about half of the volume deals with the complex effects of this interaction.

As a whole, the book is well balanced. NMR and ESR are given equal prominence, with theoretical descriptions, educational examples and reviews of current research results. Several of the chapters contain useful tables concerning, for example, the interpretation and description of the abbreviations used in multipulse NMR, and the network of equations and assumptions that form the basis for understanding paramagnetic relaxation. The discussion of the various metalloproteins clearly reveals the importance and applicability of magnetic resonance techniques in unravelling the biological role of the metal ions.

The collected writings are generally interesting and well prepared, although there is some duplication of material, perhaps inevitable in a multiauthor publication. Overall, then, a good book which will be of value to biochemists and biophysicists with an interest in the biological application of magnetic resonance. ☐

Karl-Erik Falk is Docent in Biophysics at the Department of Biochemistry and Biophysics, Chalmers Institute of Technology and University of Gothenburg, Gothenburg.

BOOKS RECEIVED

Mathematics

ARIS, R. and VARMA, A. (ed) The Mathematical Understanding of Chemical Engineering Systems. Selected Papers of Neal R. Amundson. Pp. x + 829. ISBN 0-08-023836-X. (Pergamon: 1980.) US $100.00, £50.00.

AVRIEL, M. (ed.) Advances in Geometric Programming. Mathematical Concepts and Methods in Science and Engineering. 21. Pp.x + 460. ISBN 0-306-40381-1. (Plenum: 1980.) $39.50.

HARRIS, C. F. Mathematical Modelling of Turbulent Diffusion in the Environment. The Institute of Mathematics and its Applications Conference Series. Pp. 500. ISBN 0-12-328350-7. (Academic: 1980.) $41, £18.

Astronomy

PAL, Y. (ed.). Space and Development. Vol. 6. Advances in Space Exploration. COSPAR Symposium Series. Pp. 97. ISBN 0-08-024441-6. (Pergamon: 1980.) $18, £8.

Physics

ATKIN, R. J. and FOX, N. An Introduction to the theory of Elasticity. Longman Mathematical Texts. Pp. 245. Flexi ISBN 0-582-44283-4. (Longman: 1980.) £6.25.

BABISTER, A. W. Aircraft Dynamic Stability and Response. Pp. 220. Hbk ISBN 0-08-024768-8 (Pergamon: 1980.) Hbk$35, £15; Flexi $15, £7.

KURJAK, A. (ed.). Recent Advances in Ultrasound Diagnosis 2. Proceedings of the International Symposium on Recent Advances in Ultrasound Diagnosis, Dubrovnik, October, 1979. Pp. 560. ISBN 90-219-0427-6. (Excerpta Medica: 1980.) $97.50, Dfl.200.

KINGSLAKE, R. and THOMPSON, B. J. (eds). Applied Optics and Optical Engineering. Vol. VI. Pp. 511. ISBN 0-12-408606-3. (Academic: 1980.) $49.50.

MARION, J. B. and HEALD, M. A. Classical Electromagnetic Radiation. 2nd Edn. Pp. 488. ISBN 0-12-472257-1. (Academic: 1980.) $22.50.

MORGAN, B. L. and McMULLAN, D. (eds). Photo-Electronic Image Devices. Advances in Electronics and Electron Physics Vol. 52. Pp. 532. ISBN 0-12-014652. (Academic: 1980.) £32.60, $75.

RÜHL, W. (ed.). Field Theoretical Methods in Particle Physics. NATA Advanced Study Institutes Vol. 55. Pp. 598. ISBN 0-306-40444-3. (Plenum: 1980.) $69.50.

SPENCER, A. J. M. Continuum Mechanics. Longman Mathematical Texts. Pp. 183. Flexi ISBN 0-582-44282-6. (Longman: 1980.) £5.50.

CROW, J.E., GUERTIN, R.P. and MIHALISIN, T.W. Crystalline. Electric Field and Structural Effects in f-Electron Systems. Pp.xii + 638. ISBN 0-306-40443-5. (Plenum: 1980.) $69.50.

DALVEN, R. Introduction to Applied Solid State Physics. Topics in the Applications of Semiconductors, Superconductors, and the Nonlinear Optical Properties of Solids. Pp.xiv + 330. ISBN 0-306-40385-4. (Plenum: 1980.) £27.50.

HELD, A. (ed.) General Relativity and Gravitation. One Hundred Years After the Birth of Albert Einstein. Volume 1. Pp.xix + 598. ISBN 0-306-40265-3. (v.1.) (Plenum: 1980.) $49.75.

HELD, A. (ed.) General Relativity and Gravitation. One Hundred Years After the Birth of Albert Einstein. Volume 2. Pp.xviii + 540. ISBN 0-306-40266-1 (v.2.) (Plenum 1980.) $49.75.

HÖHLER, G. (ed.) Springer Tracts in Modern Physics Vol.87. Point Defects in Metals II Dynamical Properties and Diffusion Controlled Reactions. Pp.x + 262. ISBN 3-540-09623-X. (Springer-Verlag, 1980.) DM 72 approx. US $40.40.

JALURIA, Y. Natural Convection; Heat and Mass Transfer. The Science and Applications of Heat and Mass Transfer Volume 5. Pp.x + 326. ISBN 0-08-025432-2. (Pergamon Press, Oxford and New York, 1980.) £22.50, $51.00.

McCALL, J.L. and FRENCH, P.M. (ed.) Metallography as a Quality Control Tool. Pp.ciii + 337. ISBN 0-306-40423-0. (Plenum: 1980.) $39.50.

MARIS, H.J. (ed.) Photon Scattering in Condensed Matter. Proceedings of the Third International Conference on Photon Scattering in Condensed Matter, held at Brown University, Providence, Rhode Island, August, 1979. Pp. xix + 481. ISBN 0-306-40355-2. (Plenum 1980.) $52.50.

RYBICKI, G.B. and LIGHTMAN, A.P. Radiative Processes in Astrophysics. A Wiley-Interscience Publication. Pp.xv + 382. ISBN 0-471-04815-1. (John Wiley and Sons 1980.) £19.00.

ANDRE, J.M. (eds) Recent Advances in Quantum Theory of Polymers: Proceedings, Namur, 1979. Lecture Notes in Physics: Series Editors Ehlers et al. 113. Pp.306. ISBN 3-540-09731-7. (Springer: Berlin, Heidelberg and New York, 1980.) DM 37.60; US $22.20.

BECKER, P. (ed.) Electron and Magnetization Densities in Molecules and Crystals. NATO Advanced Study Institutes Series. Series B. Physics. Pp.904. ISBN 0-396-40300-5 (Plenum: New York and Oxford, 1980.) $75.00.

COWSIK, R. and WILLS R.D. (eds) Non-Solar Gamma Rays. Pp.276. ISBN 0-08-024440-8 (Pergamon: Oxford and New York, 1980.) £22.00, $50.00.

DASH, J.G. and RUVALDS, J. (eds) Phase Transitions in Surface Films: Nato Advanced Study Institutes Series Physics 8. Pp.367. ISBN 0-306-40348-X. (Plenum: New York, 1980.) $42.00.

DAY, H. The Hidden Power of Vibrations. Pp.208. ISBN 0-7221-28347. (Sphere: London, 1980.) £1.10. Pbk.

DYNKIN, E.B. and YUSHKEVICH, A.A. Controlled Markov Processes. Pp.289. ISBN 3-540-90387-9. (Springer: Berlin, Heidelberg and New York, 1980.) DM 79.50; US $46.90.

FOWLER, R.H. Statistical Mechanics: The Theory of the Properties of Matter in Equilibrium. PP.864. ISBN 0-521-08377-5. (Cambridge University Press: Cambridge, 1980.) £12.50.

FRANCOIS, H. et al (eds) Solid State Nuclear Track Detectors. Pp.1090. ISBN 0-08-025029-7. (Pergamon: Oxford and New York, 1980.) £90.00, $203.00.

GRAY, D.F. and LINSKY, J.L. (eds) Lecture Notes in Physics: Stellar Turbulence 114. Pp.306. ISBN 3-540-09737-6. (Springer: Berlin, Heidelberg and New York, 1980.)

HANSSON, C.B. Prepare for Science. An introduction to Physical and Engineering Sciences. Pp.160. ISBN 0-08-024262-6. (Pergamon: Oxford and New York, 1980.) £2.00; $4.00 Pbk; $10.00; £5.00 Board

KRANEENDONK, J.V. (ed.) Intermolecular Spectroscopy and Dynamical Properties of Dense Systems: Proceedings of the International School of Physics "Enrico Fermi" Course LXXV, Varenna, Italy. Pp.xii + 473. ISBN 0-444-85 60-6. (North-Holland: Amsterdam and New York, 1980.) US $72.50; D[illegible].148.75.

LIFSHITZ, E.M. and PITAEVSKII, L.P. Statistical Physics 3rd Edition Part 1. Course of Theoretical Physics Vol. 5. Pp.544. ISBN 0-08-023038-5. $20.00; £10.00 pbk $50.00; £25.00 Board.

MAHANTHAPPA, K.T. and RANDA, J. (eds) Quantum Flavordynamics, Quantum Chromodynams and Unicsfied Theories: Nato Advanced Study Institutes Series. Physics B. Pp.494. (Plenum: New York, 1980.) 0-306-40436-2. $59.50.

POLKINGHORNE J.C. Models of High Energy Processes. Cambridge Monographs on Mathematical Physics. 5. Pp.131. ISBN 0-521-22369-5. (Cambridge University Press: Cambridge, 1980.) £11.00.

RAETHER, H. Excitation of Plasmons and Interband Transitions by Electrons. Springer Tracts in Modern Physics Vol.88. Pp.196. ISBN 3-540-09677-9. (Springer: Berlin, Heidelberg and New York, 1980.) US $34.90; DM 59.00.

SOROKO, L.M. Holography and Coherent Optics. Pp.818. ISBN 0-306-40101-0. (Plenum: New York, 1980.) $59.50.

TAMM, I.E. Fundamentals of the Theory of Electricity. Pp.672. ISBN 7147-1454-2 (MIR Publishers: Central Books: London, 1980.) £6.95.

VERMA, R.K. Master Tables for Electromagnetic Depth Sounding Interpretation. Pp.473. ISBN 0-306-65188-2 (Plenum: New York, 1980.) $75.00.

Chemistry

PERRIN, D.D., AR MAREGO, W.L.F. and PERRIN, D.R. Purification of Laboratory Chemicals. Second Edition. Pp.x + 568. ISBN 0-08-022961-1. (Pergamon Press 1980.) £32.00, $72.00.

SATCHLER, G.R. Introduction to Nuclear Reactions. Pp.316. ISBN 0-333-25907-6 (Macmillan: London and Basingstoke, 1980.) £25.00.

BOURDON, J. (ed.). Growth and Properties of Metal Cluster. Applications to Catalysis and the Phototgraphic Process. Studies in Surface Science and Catalysis 4. Pp. 549. ISBN 0-444-41877-6. (Elsevier: 1980.) $97.50, Dfl.200.

BRATOS, S. and PICK, R. M. (eds). Vibrational Spectroscopy of Molecular Liquids and Solids. NATO Advanced Study Institutes Series Vol. 56. Pp. 464. ISBN 0-306-40445-1. (Plenum: 180.) $49.50.

REINHOLD, F., HARBORNE, F. B. and SWAIN, T. (eds). Progress in Phytochemistry Vol. 6. Pp. 294. ISBN 0-08-024946-9. (Pergamon: 1980) $70, £31.

VARMAVUORI, A. 27th International Congress of Pure and Applied Chemistry. Plenery and Invited Lectures Presented at the 27th IUPAC Congress, Helsinki, Finland, August, 1979. IUPAC Symposium Series. Pp. 386. ISBN 0-08-023936-6. (Pergamon: 1980.) $100, £44.50.

BROWN, R. F. C. Pyrolytic Methods in Organic Chemistry. Organic Chemistry Vol. 41. Pp. 347. ISBN 0-12-138050-5. (Academic: 1980.) $38.50.

COOPER, J. W. Spectroscopic Techniques for Organic Chemists. Pp. 376. ISBN 0-471-05166-7. (Wiley: 1980.) £11.50.

DOYLE, M. P. and MUNGALL, W. S. Experimental Organic Chemistry. Pp. 490. ISBN 0-471-03383-9. (Wiley: 1980.) £9.50.

FITCH, R. M. (ed.). Polymer Colloids II. Proceedings of the Symposium on the Physical Chemical Properties of Colloidial Particles, held in Miami, Florida, September, 1978. Pp. 684. ISBN 0-306-40350-1. (Plenum: 1980.) $69.50.

HSIEN LIN, S. (ed.). Radiationless Transitions. Pp. 425. ISBN 0-12-450650. (Academic: 1980.) $48.50.

JENNINGS, W. Gas Chromatography with Glass Capillary Columns. 2nd Edn. Pp. 319. ISBN 0-12-384360-X. (Academic: 1980.) $25.

JONES, W. H. (ed.). Catalysis in Organic Syntheses. Proceedings of the Seventh Conference on Catalysis in Organic Syntheses held in Chicago, June, 1978. Pp. 314. ISBN 00197-534X. (Academic: 1980.) $29.50.

McDOWELL, M. R. C. and FERENDECI, A. M. (eds). Atomic and Molecular Process in Controlled Thermonuclear Fusion. NATO Advanced Study Institutes Series Vol. 53. Pp. 493. ISBN 0-306-40424-9. (Plenum: 1980.) $55.

MANN, W. B., AYRES, R. G. and GARFINKEL, S. B. Radioactivity and Its Measurement. 2nd Edn. Pergamon International Library. Pp. 282. Flexi ISBN 0-08-025027-0; hbk ISBN 0-08-025028-9. (Pergamon: 1980.) Flexi $12.50, £6; hbk $26, £13.

MARTIN, J. W. Micromechanisms in Particle-hardened Alloys. Cambridge Solid State Science Series. Pp. 201. Hbk ISBN 0-521-22623-6; pbk ISBN 0-521-29580-7. (Cambridge University Press: 1980.) Hbk £21; pbk £6.95.

MELANDER, L. and SAUNDERS, W. H. Jr. Reaction Rates of Isotopic Molecules. Pp. 331. ISBN 0-471-04396-6. (Wiley: 1980.) £16.30.

RAISWELL, R. W., BRIMBLECOMBE, P., DENT, D. L. and LISS, P. S. Environmental Chemistry. Resource and Environmental Sciences Series. Pp. 184. Flexi ISBN 0-7131-2790-2. (Edward Arnold: 1980.) £4.95.

SCOTT, G. (ed.). Developments in Polymer Stabilisation–2. The Developments Series. Pp. 244. ISBN 0-85334-885-5. (Applied Science: Barking, UK, 1980.) £18.

DeKOCK and GRAY, H.B. Chemical Structure and Bonding. Pp.xi + 491. ISBN 0-8053-2310-4. (The Benjamin/Cummings Publishing Company: California 94025, 1980.) $21.95.

DUNITZ, J.D. X-Ray Analysis and the Structure of Organic Molecules. Pp.514. ISBN 0-8014-1115-7. (Cornell University Press: Ithaca and London, 1980.) £33.00.

GERRARD, W. Gas Solubilities Widespread Applications. Pp.xxi + 497. ISBN 0-08-025248-6. (Pergamon Press: Oxford and New York, 1980.) $67.50 £30.00.

KEMP, D.S. and VBELLACCIO, F. Organic Chemistry. Pp.xiii + 1421. ISBN 0-87901-123-8. (Worth Publishers, Inc. New York, 1980.) $21.95.

PAMPLIN, B.R. (ed.) Progress in Crystal Growth and Characterization Volume 1. Pp.vi + 441. ISBN 0-08-026013-6. (Pergamon Press: 1980.) £43.00.

SCROSATI, B., and VINCENT, C.A. (eds) Solubility Data Series volume 11. Alkali Metal, Alkaline-Earth Metal and Ammonium Halides. Amine Solvents. Pp.xx + 354. ISBN 0-08-023917-X. (Pergamon Press: Oxford and New York, 1980.) £50.00, $100.00.

WEISS, U. and EDWARDS. J.M. The Biosynthesis of Aromatic Compounds. A Wiley-Interscience Publication. Pp.xiii + 727. ISBN-0-471-92690. (John Wiley & Sons: New York and Chichester, UK, 1980.) £18.50.

Technology

ESCAP National Papers for the UNCSTD. Volume 2, Volume 3 and Summary. (Regional Centre for Technology Transfer: Bangalore, India.) np flexi.

LEFEBVRE, A.H. (ed.). Gas Turbine Combustor Design Problems. Pp.xvi + 431. ISBN 0-89116-177-5. (Hemisphere Publishing Corporation: Washington, 1980.) $45.00.

VACCA, R. Modest Technologies for a Complicated World. Pp.xiv + 172. ISBN 0-08-024067-4. (Pergamon: 1980.) US $22.50 £10.00.

RYCROFT, M.J. (ed.) COSPAR Space Research volume XX. Proceedings of the Open Meetings of the Working Groups on Physical Sciences of the Twenty-second Plenary Meeting of

COSPAR, Bangalore, India, May, 1979. Pp.xiv + 285. ISBN 0-08-024437-8. (Pergamon: 1980.) £22.20 $50.00.

SALOMONSON, V.V. and BHAVSAR, P.D. (eds). The Contribution of Space Observations to Water Resources Management. Advances in Space Exploration COSPAR Symposium Series. Volume 9. Pp.ix + 280. ISBN 0-08 024473-4. (Pergamon: 1980.) £26.60 $60.00.

SIMEONS, C. Hydro-Power. The Use of Water as an Alternative Source of Energy. Pp.vii + 548. ISBN 0-08-023269-8. (Pergamon: 1980.) $75.00 £34.00.

LEE, L-H, (ed.) Adhesion and Adsorption of Polymers. Polymer Science and Technology Vol.12B. Pp.897. ISBN 0-306-40428-1. (Plenum: New York, 1980.) $39.75.

SMITH, H.T. and GREEN, T.R.G. (eds) Human Interaction with Computers. Pp.369. ISBN 0-12-652852-7. (Academic: London and New York, 1980.) £6.40; $15.00 pbk.

McCARTHY, G. J., RHYNE, J. J. and SILBER, H. B. (eds). The Rare Earths in Modern Science and Technology Vol. 2. Pp. 647. ISBN 0-306-40347-1. (Plenum: 1980.) $59.50.

WILLISON, J. H. M. and ROWE, A. J. Replica Shadowing and Freeze-Etching Techniques. Practical Methods in Electron Microscopy Vol. 8. Pp. 300. ISBN 0-444-80165-0. (Elsevier/North-Holland: 1980.) Pbk $27.25, Dfl. 56.

Computer Science

HARRISON, H.B. Structural Analysis & Design: Some Minicomputer Applications (in two parts) Pp.532. ISBN 0-080-23240. (Pergamon: 1980.) $25.00; £12.50 Pbk, $60.00; $30.00 Board

HAWKES, P.W. Computer Processing of Electron Microscope Images: Topics in Current Physics. Pp.296. ISBN 3-540-09622. (Springer/Verlag: Berlin Heidelberg and New York, 1980.) DM 65.00; US $36.40.

Earth Sciences

CORLISS, W. R. (compiled by). Unknown Earth: A Handbook of Geological Enignas. Pp. 833. ISBN 0-91554-06-2. (The Sourcebook Project: Glen Arm, Maryland, 1980.) $19.95.

DOLEZALEK, H. (ed.) The Application of Atmospheric Electricity Concepts and Methods to other Parts of Meteorology. Technical Note No. 162. Pp. 130. Flexi ISBN 92-63-10507-3. (World Meteorological Organization: Geneva, 1978.) Np.

HAYEDN, C. M., HUBERT, L. F., McCLAIN, E. P. and SEAMAN, R. S. Quantative Meteorological Data from Satellites. Technical Note No. 166. Pp. 102. Flexi ISBN 92-63-10531-6. (World Meteorological Organization: Geneva, 1979.) Np.

McBEAN, G. A. *et al.* The Planetary Boundary Layer. Technical Note No. 165. Pp. 201. Flexi ISBN 92-63-10530-8. (World Meteorological Organization: Geneva, 1979.) Np.

OKE, T. R. Review of Urban Climatology 1973–1976. Technical Note No. 169. Pp. 100. Flexi ISBN 92-63-10539-1. (World Meteorological Organization: Geneva, 1979.) Np.

YI, CHIA-SHUN. Stratified Flows. 2nd Edn. Pp. 418. ISBN 0-12-771050-7. (Academic Press: 1980.) $29.50.

BRUNN, J. H. Découverte des Sciences de la Terre. Pp. 279. ISBN 2-13-036378-4. (Presses Universitaires de France: Paris, 1980.) Np.

CARTER, W. D., ROWAN, L. C. and HUNTINGDON, J. F. (eds). Remote Sensing and Mineral Exploration. Vol. 10. Advances in Space Exploration COSPAR Symposium Series. Pp. 171. ISBN 0-08-024438-6. (Pergamon: 1980.) $32, £14.10.

HANWELL, J. D. Atmospheric Processes. Processes in Physical Geography Vol. 3. Pp. 96. Flexi ISBN 0-04-551032-6. (Allen & Unwin: London, 1980.) £3.50.

KENNETT, J. P. (ed.). Magnetic Stratigraphy of Sediments. Benchmark Papers in Geology/54. Pp. 438. ISBN 0-87933-354-5. (Academic: 1980.) $39.50.

NIHOUL, J. C. J. (ed.). Marine Turbulence. Proceedings of the 11th International Liège Colloquium on Ocean Hydrodynamics. Elsevier Oceanography Series, 28. Pp. 378. ISBN 0-444-41881-4. (Elsevier: 1980.) $58.50, Dfl. 120.

LAMBECK, K. The Earth's Variable Rotation: Geophysical Causes and Consequences. Cambridge Monographs on Mechanics and Applied Mathematics. Pp.xi + 449. ISBN 0-521-22769-0. (Cambridge University Press; Cambridge, 1980.) £35.00.

DENNIS, A. S. Weather Modification by Cloud Seeding, International Geophysics Series. Vol. 24. Pp.xv + 267. ISBN-0-12-210650-4. (Academic New York – London 1980.) np.

KING, A. The State of the Planet. A Report prepared by the International Federation of Institutes for Advanced Study. Pp. xi + 130. ISBN 0-08-024717-2 Hbk ISBN-0-08-024716-4 flexi. (Pergamon Press, Oxford – New York, 1980) $22.00 £10.00 hardback $11.00 £5.00 flexi.

NIHOUL, J. C. J. Marine Turbulence. Proceedings of the 11th International Liège Colloquium on Ocean Hydrodynamics. Elsevier Oceanography Series, 28. Pp. xii + 378. ISBN 0-444-41881-4. (Elsevier 1980.) US$58.50 Dfl.120.00.

PEARSON, R. C. Mineral Resources of the Indian Peaks Study Area, Boulder and Grand Counties, Colorado. Geological Survey Bulletin 1463. Pp. vii + 109 (United States Government Printing Office; Washington, 1980.) np. flexi.

TATSCH, J. H. Coal Deposits: Origin, Evolution, and Present Characteristics. Pp. viii + 590. ISBN 0-912890-13-4. (Tatsch Assoc, Sudbury, Mass, 1980) $156.000.

Biological Sciences

BRINKHURST, R.O. and COOK, D.G. (eds) Aquatic Oligochaete Biology. Pp.ix + 529. ISBN 0-306-40338-2. (Plenum Press 1980.) $55.00.

de SERRES, F.J. and HOLLAENDER, A. (eds) Chemical Mutagens; Principles and Methods for Their Detection, Volume 6. Sponsored by the Environmental Mutagen Society. Pp.xix + 485. ISBN 0-306-40364-1. (Plenum Press 1980.) $49.50.

FLANNAGAN, J.F. and MARSHALL, K.E. (eds) Advances in Ephemeroptera Biology. Pp.552. ISBN 0-306-40357-9. (Plenum 1980.) $49.50.

HERMAN, R.H., COHN, R.M. and McNAMARA, P.D. (eds) Principles of Metabolic Control in Mammalian Systems. Pp.xix + 669. ISBN 0-306-40261-0. (Plenum 1980.) $35.00.

JARRETT, A. (ed.). The Physiology and Pathophysiology of the Skin. Vol.6. Pp.1871-2155. ISBN 0-12-380606-2. (Academic: London and New York, 1980.) £27.20; $63.00.

LEWIS, W.M. Jr. Zooplankton Community Analysis. Studies on a Tropical System. Pp.ix + 163. ISBN 3-540-90434-4. (Springer-Verlag: Berlin, Heidelberg and New York, 1979.) DM 49 approx. US $27.50.

McLAUGHLIN, P.A. Comparative Morphology of Recent Crustacea. Pp.xii + 177. ISBN 0-7167-1121-4. (W.H. Freeman and Company: San Francisco, 1980.) £12.70.

PAOLETTI, R. and KRITCHEVSKY, D. (eds). Advances in Lipid Research Vol. 17. Pp. 308. ISBN 0-12-02-024917-0. (Academic: 1980.) $31.

RZOSKA, F. Euphrates and Tigris, Mesopotamian Econolgy and Destiny. Monographiae Biologicae Vol. 38. Pp. 122. ISBN 90-6193-090-1. (W. Junk: The Hugue, 1980.) Dutch Guilders 60, $31.50.

TURK, F. L. Delayed Hypersensivity. 3rd Revised Edn. Research Monographs in Immunology Vol. 1. Pp. 308. ISBN 0-80163-4. (Elsevier/North-Holland Biomedical: 1980.) $85.75, Dfl.135.

WILSON, B. W. (introductions by). Readings from Scientific American: Birds. Pp. 276. Hbk ISBN 0-7167-1206-7; pbk ISBN 0-7167-1207-5. (W. H. Freeman: 1980.) Hbk £10.60; pbk £4.90.

HARDING, K. A. and WELCH, K. R. G. Venomous Snakes of the World: A Checklist. Pp. 188. ISBN 0-08-025495-0. (Pergamon: 1980.) $38, £17.

HODGSON, E., BEND, J. R. and PHILPOT, R. M. (eds). Reviews in Biochemical Toxicology Vol. 2. Pp. 299. ISBN 0-444-00386-X. (Elsevier/North Holland: 1980.) $35.

HUDSON, H. J. Fungal Saprophytism. 2nd Edn. The Institute of Biology's Studies in Biology No. 32. Pp. 75. Flexi ISBN 0-7131-2792-9. (Edward Arnold: 1980.) £2.75.

HUI-LIN LI *(et al.)* Flora of Taiwan. Vol. 3. Pp. 1000. (Epoch Publishing: Taipei, Taiwan, 1980.) Np.

KANIZA, G. Organisation in Vision. Essays on Gestalt Perception. Pp. 267. ISBN 03-049071-5. (Holt-Saunders: 1979.) £16.75.

McCORMICK, D. B. and WRIGHT, L. D. (eds). Vitamins and Coenzymes Part E. Methods in Enzymology Vol. 66. Pp. 755. ISBN 0-12-181966-3. (Academic: 1980.) $55.

McCORMICK, D. B. and WRIGHT, L. D. (eds). Vitamins and Coenzymes Part F. Methods in Enzymology Vol. 67. Pp. 579. ISBN 0-12-181967-1. (Academic: 1980.) $49.50.

MACDONALD, D. W. Rabies and Wildlife: a Biologist's Perspective. Pp. 151. Hbk ISBN 0-19-857567-X; pbk ISBN 0-19-857576-9. (Oxford University Press: 1980.) Hbk £10; pbk £3.95.

MACLEOD, R. M. and SCAPAGNINI, U. (eds). Central and Peripheral Regulation of Prolactin Function. Pp. 394. ISBN 0-89004-489-9. (Raven: 1980.) $36.

MENNEMA, J., QUENÉ-BOTERENBROOD, A. J. and PLATE, C. L. (eds). Atlas of the Netherlands FLora. 1.Extinct and very rare species. Pp. 226. ISBN 90-6193-605-5. (W. Junk: 1980.) Dutch guilders 125, $65.

NOVER, L., LYNEN, F. and MOTHES, K. (eds). Cell Compartmentation and Metabolic Channeling. A Leopoldina symposium on the structural and functional organization of cells as a prerequisite of life. Pp. 523. ISBN 0-444-80150-2. (Elsevier/North-Holland Biomedical: 1980.) $65, Dfl. 133.

PUNT, W. and CLARKE, G. C. S. The Northwest European Pollen Flora, II. Parts 8–20. Pp. 265. ISBN 0-444-41880-6. (Elsevier: 1980.) $63.50, Dfl. 130.

DARNALL, D. W. and WILKINS, R. G. (eds). Methods for Determining Metal Ion Environments in Proteins: Structure and Function of Metalloproteins. Advances in Inorganic Biochemistry Vol. 2. Pp. 324. ISBN 0-444-00349-5. (Elsevier/North Holland: 1980.) $29.50.

EISEN, M. Mathematical Models in Cell Biology and Cancer Chemotherapy. Lecture Notes in Biomathematics Vol. 30. Pp. 431. Flexi ISBN 3-540-09709-0. (Springer: 1979.) DM 39, $21.50.

GROSS, E. and MEIENHOFER, J. (eds). The Peptides; Analysis, Synthesis, Biology. Vol. 2, Special Methods in Peptide Synthesis, Part A. Pp. 596. ISBN 0-12-304202-X. (Academic: 1980.) $55.

BEACHEY, E. H. (ed.). Bacterial Adherence. Receptors and Recognition Series B Volume 6. Pp. xii + 466. ISBN 0-412-21730-9. (Chapman & Hall: — Andover, 1980.) £27.50.

COKELET, G. R., MEISELMAN, H. J. and BROOKS, D. E. (eds). Erythrocyte Mechanics and Blood Flow. The KROC Foundation Series Volume 13. Pp. xiii + 285. ISBN 0-8451-0303-2. (Alan R. Liss: — New York, 1980.) $30.00 (Available in Europe, United Kingdom and the Middle East exclusively from European Book Service, Flevelaan, 36-38, P.O.B. 124, 1380 AC Weesp, Holland.) Dfl.90.00

EDWARDS, N. A. and HASSAL, K. A. Biochemistry and Physiology of the Cell. An introductory text. Second edition. Pp. xv + 448. ISBN 0-07-084097-0. (McGraw-Hill Book Company (UK) Limited: Maidenhead, 1980.) £7.95 flexi.

GRIFFITHS, D. J. Urodynamics. The Mechanics and Hydrodynamics of the Lower Urinary Tract. Medical Physics Handbooks 4. Pp. ix + 139. ISBN 0-85274-507-9. (Adam Hilger Ltd: Bristol. 1980) £11.95.

MURRAY, D. A. (ed.). Chironomidae; Ecology, Systemics, Cytology and Physiology. Proceedings of the 7th International Symposium on Chironomidae, Dublin, August, 1979. Pp. xx + 354. ISBN 0-08-025889-1. (Pergamon: 1980) $60.00 £26.50.

PRIMROSE, S. B., DIMMOCK, N. J. Introduction to modern virology. Basic microbiology volume 2. Second edition. (1980.) £5.25.

TOOZE, J. (ed.). DNA Tumer Viruses. Molecular Biology of Tumor Viruses; Second edition, Part 2. Cold Spring Harbor Monograph Series. Pp. ix + 958. ISBN 0-87969-126-3. (Cold Spring Harbor Laboratory: New York, 1980.) $55.00 USA, $66.00 elsewhere.

ANDREOLI, T. E., HOFFMAN, J. F. and FANESTIL, D. D. (eds). Membrane Physiology. Pp. 468. Flexi ISBN 0-306-40432-X. (Plenum Medical: 1980.) $19.95.

BEEFTINK, W. G. (ed.). Vegetation Dynamics. Proceedings of the Second Symposium of the Working Group on Succession Research on Permanent Plots, held at the Delta Institute for Hydrobiological Research, Yerseke, October, 1975. Pp. 134. Flexi ISBN 90-6193-606-3. (W. Junk: 1980.) Dutch guilders 60, $31.50.

BELLINGER, Dr E. G. A Key to the Common British Algae. Pp. 94. Flexi ISBN 0-901427-09-8. (The Institution of Water Engineers and Scientists: London, 1980.) Flexi £3.30.

BROMHALL, D. Devil Birds; The Life of the Swift. Pp. 96. Hbk ISBN 0-09-141730-9; pbk ISBN 0-09-141731-7. (Hutchinson: 1980.) Hbk £8.95; pbk £5.95.

CANTOR, C. R. and SCHIMMEL, P. R. Biophysical Chemistry Part 1. The Conformation of Biological Macromolecules. Pp. 341. (Hbk ISBN 0-7167-1042-0; pbk ISBN 0-7167-1188-5. (W. H. Freeman: 1980.) Hbk £17.70; pbk £9.20.

CAVALLINI, D., GAULL, G. E. and ZAPPIA, V. (eds). Natural Sulfur Compounds. Novel Biochemical and Structural Aspects. Proceedings of the Third International Meeting on Low Molecular Weight Sulfur-Containing Natural Products, held in Rome, June 1979. Pp. 552. ISBN 0-306-40335-8. (Plenum: 1980.) $49.50.

COOK, C. B., PAPPAS, P. W. and RUDOLPH, E. D. (eds). Cellular Interactions in Symbiosis and Parasitism. Pp. 305. ISBN 0-8142-0315-9. (Ohio State University Press: 1980.) $25.

MASSRY, S.G. and FLEISCH, H. (eds). Renal Handling of Phosphate. Pp.xxii + 375. ISBN 0-306-40368-4. (Plenum Medical Book Company: New York and London, 1980.) $37.50.

NICHOLLS, J. and MILLER, P. Collins Handguide to the Fishes of Britain and Europe. Pp.96. ISBN 0-00-219756-1 hardback ISBN 0-00-219751-0 paperback. (Collins: 1980.) £2.25 pbk £4.95 Hbk.

OCKLEFORD, C.D. and WHYTE, A. (eds). Coated Vesicles. Pp.xiii + 344. ISBN 0-521-22785-2. (Cambridge University Press: 1980.)

SETLOW, J.K. and HOLLAENDER, A. (eds). Genetic Engineering: Principles and Methods. Volume 2. Pp.289. ISBN 0-306-40447-8. (Plenum: 1980.) $32.50.

STEPHAN, H., BARON, G. and SCHWERDTFEGER, W.K. The Brain of the Common Marmoset (*Callithrix jaccus*) A Stereotaxic Atlas. Pp.v + 91. ISBN 3-540-09782-1. (Springer-Verlag: 1980.) DM 168 approx. US $94.10.

TANFORD, C. The Hydrophobic Effect: Formation of Micelles and Biological Membranes. Second edition. A Wiley-Interscience Publication. Pp.ix + 233. ISBN 0-471-04893-3. (John Wiley and Sons: New York and Chichester, UK, 1980.) £11.75.

SALT, B. Cassell's Rural Science Series. Rural Science 1. Pp. [illegible]52. Flexi ISBN 304-30410-7. (Cassell: 1980.) £2.50.

SCHLESSINGER, D. (ed.). Microbiology — 1980. Pp. 400. ISBN 0-914826-23-9. (American Society for Microbiology: Washington, D.C., 1980.) $22.

BES, A. and GERAUD, G. (eds). Cerebral Circulation and Neurotransmitters. Proceedings of the International Congress on Cerebral Circulation, Toulouse, September, 1979. Pp. 268. ISBN 0-444-90129-9. (Excerpta Medica: 1980.) $48.75, Dfl.100.

BOULPAEP, E. L. (guest ed.). Cellular Mechanisms of Renal Tubular Ion Transport. Current Topics in Membranes and Transport Vol. 13. Pp. 433. ISBN 0-12-153313-1. (Academic: 1980.) $45.

BOURNE, G. H. and DANIELLI, J. F. (eds). International Review of Cytology. Vol. 64. Pp. 388. ISBN 0-12-364464-X. (Academic: 1980.) $36.50.

BRADY, N. C. (ed.) Advances in Agronomy Vol. 31. Pp. 315. ISBN 0-12-000731-2. (Academic: 1980.) $32.50.

DUNCAN, T. A Taxonomic Study of the Ranunculus Hispidus Michaux Complex in the Western Hemisphere. University of California Publications: Botany, Vol. 77. Pp. 125. Flexi ISBN 0-520-09617-7. (University of California: 1980.) $7.

FRENKEL, R. A. and McGARRY, J. D. Carnitine Biosynthesis, Metabolism, and Functions. Proceedings of the Virginia Lazenby O'Hara Biochemistry Symposium held March, 1979. Pp. 356. ISBN 0-12-267060-4. (Academic: 1980.) $27.50.

GROSSMAN, L. and MOLDAVE, K. (eds). Nucleic Acids Part I. Methods in Enzymology Vol. 65. Pp. 968. ISBN 0-12-181965-5. (Academic: 1980.) $57.50.

KARE, M. R., FREGLY, M. J. and BERNARD, R. A. (eds). Biological and Behavioral Aspects of Salt Intake. The Nutrition Foundation. A Monograph Series. Pp. 426. ISBN 0-12-397750-9. (Academic: 1980.) $25.

KEATINGE, W. R. and HARMAN, M. C. Local Mechanisms Controlling Blood Vessels. Monographs of the Physiological Society No. 37. Pp. 142. ISBN 0-12-402850-0. (Academic: 1980.) $27, £11.80.

LEGRAIN, M. (ed.). Continuous Ambulatory Peritoneal Dialysis. Proceedings of an International Symposium Paris, November, 1979. Pp. 360. ISBN 0-90-219-9436-7. (Excerpta Medica: 1980.) $63.50, *Dfl.*130.

MIYOSHI, A. (ed.) Gut Peptides; Secretion, Function and Clinical Aspects. Proceedings of the Hiroshima Symposium on Gut Hormones, held at Hiroshima, July, 1979. Pp. 440. ISBN 0-444-80208-8. (Elsevier/North Holland Biomedical: 1980.) $73.25, Dfl.150.

MOSNAIM, A. D. and WOLF, M. E. (eds). Noncatecholic Phenylethylamines. Part 2 Phenylethanolamine, Tyramines, and Octopamine. Modern Pharmacology–Toxicology Series of Monographs and Textbooks. Pp. 365. ISBN 0-8247-6721-7. (Dekker: 1980.) Sw.fr.114.

WINGARD, L. B. Jr, BEREZIN, I. V. and KLYOSOV, A. A. (eds). Enzyme Engineering: Future Directions. Based on the Proceedings of the Conference on the Future of Enzyme Engineering Development, held in Tbilisi, Georgian S.S.R., June 1978. Pp. 521. ISBN 0-306-40442-7. (Plenum: 1980.) $59.50.

ZADRAZIL, S. and SPONAR, J. (eds). DNA-Recombination Interactions and Repair. Federation of European Biochemical Societies Vol. 63. Proceedings of the FEBS Symposium on DNA, Liblice, 1979. Pp. 600. ISBN 0-08-025494-2. (Pergamon: 1980.) $80, £36.

ZBINDEN, G. (ed.). Fine-Needle Aspiration Biopsy of the Rat Liver. Cytological, Cytochemical and Biochemical Methods. Proceedings of a Workshop on Technique and Application of Fine-Needle Aspiration Biopsy (FNAB) in Experimental Toxicology, Swiss Federal Institute of Technolog y and University of Zurich, May, 1979. Pp. 68. ISBN 0-08-025508-6. (Pergamon: 1980.) $25, £11.25.

Applied Biological Sciences

AEBI, H. and WHITEHEAD, R. (eds). Maternal Nutrition during Pregnancy and Lactation. Nestlé Foundation Series. Pp. 354. ISBN 3-456-80945-X. (Hans Huber: Bern, Stuttgart, Vienna, 1980.) Fr.45, DM49.

BING, R. F. New Drug Therapy with a Calcium Antagonist. Diltiazem Hakone Symposium '78. Pp. 257. ISBN 90-219-0407-1. (Excerpta medica: 1979.) $46.25, Dfl.95.

BOERINGA, R. (ed.). Alternative Methods of Agriculture. Description, Evaluation and Recommendations for Research. Developments in Agricultural and Managed-Forest Ecology, 10. Pp. 200. ISBN 0-444-41893-8. (Elsevier: 1980.) $48.75, Dfl.100.

IARC WORKING GROUP. IARC Monographs on the Evaluation of the Carcinogenic Risk of Chemicals to Humans. Sex Hormones (II). Vol. 21. Pp. 583. Flexi ISBN 92-832-1221-5. (International Agency for Research on Cancer: 1979.) Sw.Fr.60, $35. Distributed by WHO.

IARC WORKING GROUP. EARC Monographs on the Evaluation of the Carcinogenic Risk of Chemicals to Humans. Some Non-Nutritive Sweetening Agents. Vol. 22. Pp. 208. Flexi ISBN 92-832-1222-3. (International Agency for Research on Cancer: Lyon, France, 1980.) Sw.Fr.25, $15. Distributed by WHO.

INGLETT, G. E. and MUNCK, L. (eds). Cereals for Food and Beverages. Recent Progress in Cereal Chemistry and Technology. Proceedings of an International Conference on Cereals for Food and Beverages held in Copenhagen, Augest, 1979. Pp. 557. ISBN 0-12-370960-1. (Academic: 1980.) $39.50.

LUZZATTI, G., SALVADORI, B. and TAVANI, E. La Xeromammografia Xeromammography. Pp. 240. ISBN 90-129-04020. (Excerpta Medica: 1980.) $146.25, Dfl.300.

MONTESANO, R. *et al.* (eds). Handling Chemical Carcinogens in the Laboratory; Problems of Safety. Pp. 32. Flexi ISBN 92-8-321133-2. (International Agency for Research on Cancer: Lyon, France, 1979.) Sw.Fr.12, $8. Distributed by WHO.

ROBERTSON, G. W. The Role of Agrometeorology in Agricultural Development and Investment Projects. Technical Note No. 168. Pp. 85. Flexi ISBN 92-63-10536-7. (World Meteorological Organization: Geneva, 1980.)

ZOETEMAN, B. C. J. Sensory Assessment of Water Quality. Pergamon Series on Environmental Science Vol. 2. Pp. 160. ISBN 0-08-023848-3. (Pergamon: 1980.) '$27.50, £12.50.

DRILL, V. A. and LAZAR, P. (eds). Cutaneous Toxicity. Pp. ix + 277. ISBN 0-12-222050-1. (Academic: 1977) $23.00.

FITZPATRICK, E. A. Soils; their formation, classification and distribution. Pp. xix + 353. ISBN 0-652-44188-9. (Longman: 1980.) £25.00.

GORI, G. B. and BOCK, F. G. (eds). A Safe Cigarette? Banbury Report 3. Pp. xi + 364. ISBN 0-87969-202-2. (Cold Spring Harbor Laboratory: 1980.) $45. ($54 outside US.).

HADDAD, H. M. (ed.). Metabolic-Padiatric Eye Disease. Proceedings of the Third Symposium of the International Society on Metabolic Eye Disease and The First Symposium of the International Society of Pediatric Ophthalmology, Kyoto, Japan, May, 1978. Pp. vi + 234. ISBN 0-08-024-95-07. (Pergamon: 1980.) $45.00 £20.00.

NOTARI, R. E. Biopharmaceutics and Clinical Pharmacokinetics: An Introduction. Third Edition, Revised and Expanded. Pp. xii + 388. ISBN 0-8247-6928-7. (Dekker: 1980) S. Fr. 40.00.

RATHI, M. and KUMAR, S. (eds). Perinatal Medicine; Clinical and Biochemical Aspects Volume I. Pp. xi + 207. ISBN 0-89116-180-5. (Hemisphere: 1980.) $35.00.

REGNAULT, F., HOCKWIN, O. and COURTOIS, Y. (eds). Ageing of the Lens. Proceedings of the Symposium on Ageing of the Lens held in Paris, September, 1979. Pp. viii + 315. ISBN 0-444-80127-7. (Elsevier/North-Holland: 1980.) US$56.00 Dfl.115.00.

SADÉE, W. and BEELEN, G. C. M. Drug Level Monitoring. Analytical Techniques, Metabolism, and Pharmacokinetics. A Wiley-Interscience Publication. Pp. xii + 495. ISBN 0-471-048891-X. (John Wiley: 1980.) £22.00.

SODA, T. (ed.). Drug-Induced Sufferings. Medical, Pharmaceutical and Legal Aspects. Proceedings of the Kyoto International Conference Against Drug-Induced Sufferings, April 1979, Kyoto, Japan. Pp. xxii + 515. ISBN 90-219-0441-1. (Excerpta Medica: 1980.) US$97.50 Dfl.200.00.

BREKHMAN, I.I. Man and Biologically Active Substances. The Effect of Drugs, Diet, and Pollution on Health. Pp.xi + 89. ISBN 0-08-023169-1 hardback ISBN 0-08-025524-8 flexi. (Pergamon: 1980.) $15.75, £7.00 Hbk, $5.95, £1.95 flexi.

CARTER, S.K. and SAKURAI, Y. (eds). Recent Results in Cancer Research Volume 70. New Anticancer Drugs. Pp.xi + 229. ISBN 3-540-09682-5. (Springer-Verlag: 1980.) DM 86 approx. US $50.80.

ELLIS, R. (ed.). Inborn Errors of Metabolism. Croom Helm Biology in Medicine Series. Pp. 105. Hbk ISBN 0-7099-0026-0; pbk ISBN 0-7099-0027-9. (Croom Helm: 1980.) Hbk £8.95, pbk £3.50.

HAREL, S. (ed.). The At Risk Infant. A Practical Interdisciplinary Approach to the Prevention, Discovery, Assessment and Management of Developmental Disabilities. Pp. 459. ISBN 90219-0422-5. (Excerpta Medica: 1980.) $80.50, Dfl. 165.

HEAD, K. H. Manual of Soil Laboratory Testing. Vol. 1. Pp. 352. Pbk ISBN 0-7273-1304-5; hbk ISBN 0-7273-1302-9. (Pentech: London, 1980.) Hbk £14.

HUTTON, R. Bio-Revolution; DNA and the Ethics of Man-Made Life. Pp. 246. (New American Library: New York and Scarborough, Ontario/New English Library: London, 1980.) Flexi. Np.

INTERNATIONAL RICE RESEARCH INSTITUTE. Nitrogen and Rice. Pp. 499. (International Rice Research Institute, Philippines: 1979.) $11.2[illegible].

JOSLING, T. Developed-Country Agricultural Policies and Developing-Country Food Supplies: The Case of Wheat. Research Report 14. Pp. 67. Flexi ISBN 0-89629-015-8. (International Food Policy Research Institute: Washington, 1980.) Np.

KLEIN, G. and Weinhouse, S. (eds). Advances in Cancer Research Vol. 31. Pp. 331. ISB 0-12-006631-9. (Academic: 1980.) $35.

KOIVISTOINEN, P. and HYVÖNEN, L. (eds). Carbohydrate Sweeteners in Foods a Nutrition. NJF Symposium held November, 1978, Helsinki-Espoo, Finland. Pp. 289. ISB 0-12-417050-1. (Academic: 1980.) $40.50, £17.60.

KURJAK, A. (ed.). Progress in Medical Ultrasound. Reviews and comments. Vol. 1/1980. Pp. 333. Flexi ISBN 90-219-3046-3. (Excerpta Medica: 1980.) $61, Dfl. 125.

MYERS, N. (Prepared by). Conversion of Tropical Moist Forests. A Report for the Committee on Research Priorities in Tropical Biology of the National Research Council. Pp. 205. Flexi ISBN 0-309-02945-7. (Castle House: Tunbridge Wells, Kent, 1980.) £8.10.

PAWLOWSKI, L. (ed.). Physicochemical Methods for Water and Wastewater Treatment. Proceedings of the Second International Conference, Lublin, June 1979. Pp. 327. ISBN 0-08-024013-5. (Pergamon: 1980.) $50, £22.50.

PEARSON, P. B. and GREENWELL, J. R. (eds). Nutrition, Food, and Man. An Interdisciplinary Perspective. Pp. 159. Hbk ISBN 0-8165-0691-4; pbk ISBN 0-8165-0706-6. (University of Arizona Press: 1980.) Hbk $11.50; pbk $5.95.

PINDBORG, J. J. Atlas of Diseases of the Oral Mucosa. 3rd Edn. Pp. 317. ISBN 87-16-02952-6. (Munksgaard International: Copenhagen, 1980.) D.Kr. 4000.

Psychology

ALTROCCHI, J. Abnormal Behaviour. Pp. xxi + 755. ISBN 0-15-500370-4. (Harcourt Brace Jovanovich: London, 1980.) £12.95.

COLTHEART, M., PATTERSON, K. and MARSHALL, J. C. (eds). Deep dyslexia. International Library of Psychology. Pp.xi-444. ISBN 0-7100-0456-7. (Routledge & Kegan Paul: 1980.) £17.50.

COSTA, E. and TRABUCCHI, M. Advances in Biochemical Psychopharmacology. Neural Peptides and Neuronal Communication. Volume 22. Pp. xxvi + 651. ISBN 0-89004-375-2. (Raven: 1980.) $57.00.

HERSOV, L. A., BERGER, M. and NICOL, A. R. (eds). language and Language Disorders in Childhood. Book Supplement to the Journal of Child Psychology and Psychiatry, No. 2 x + 183. ISBN 0-08-02526-0 Hbk — ISBN 0-08-025205-2 flexi. (Pergamon: 1980.) $18.00 £8.00 hardback $8.80 £4.00. flexi.

LAHEY, B.B. and KAZDIN, A.E. (eds) Advances in Clinical Child Psychology Volume 3. Pp.xvii + 476. ISBN 0-306-40374-9. (Plenum: 1990.) $29.50.

RIEBER, R.W. (ed.) Psychology of Language and Thought. Essays on the Theory and History of Psycholinguistics. Studies in Applied Psycholinguistics series. Pp.x + 270. ISBN 0-306-403361-7. (Plenum: 1980.) $27.50.

SMELSER, N.J. and ERIKSON, E.H. (eds). Themes of Work and Love in Adulthood. Pp.x + 297. ISBN 0-86216-008-1. (Grant McIntyre Limited: 1980.) £9.95.

CORSON, S.A., CORSON, E.O'L. and ALEXANDER, J.A. Ethology and Nonverbal Communication in Mental Health. An Inter disciplinary Biopsychosocial Exploration. Pp.272. ISBN 0-08-023728-2. (Pergamon: 1980.) £18, $41.

KANFER, F.H. and GOLDSTEIN, A.P. (eds). Helping People Change. A Textbook c Methods. 2nd Edn. Pergamon General Psychology Series, Vol. 52. Pp.600. Flexi ISB 0-08-025097-1. (Pergamon: 1980.) £6.30.

LAWSON, B. How Designers Think. Pp.216. ISBN 0-85139-289-X. (Architectural Press: London, 1980.) £9.75.

VAN PRAAG, H.M. (ed.). Handbook of Biological Psychiatry Part II. Brain Mechanisms an Abnormal Behavior–Psychophysiology. Pp.491. ISBN 0-8247-6892-2. (Dekker: 1980.) Sw.F 93.

VICTOR, J.S. Human Sexuality. A Social Psychological Approach. Pp.396. Flexi ISB 0-13-447474-0. (Prentice/Hall: 1980.) £8.40.

WHALEN, C.K. and HENKER, B. (eds). Hyperactive Children. The Social Ecology c Identification and Treatment. Pp.407. ISBN 0-12-745950-2. (Academic: 1980.) $25.

Sociology

BEAUGRANDE, R. de. Text, Discourse, and Process Toward a Multidisciplinary Science Texts. Advances in Discourse Processes Vol. IV. Pp.351. ISBN 0-89391-033-3. (Ablex: Norwo New Jersey, 1980.) $27.50.

NEWMEYER, F.J. Linguistic Theory in America. The First Quarter-Century Transformational Generative Grammar. Pp.287. ISBN 0-12-517150-1. (Academic: 1980.) $2

OSKARSSON, M. (Prepared by). Approaches to Self-assessment in Foreign Langu learning. Pergamon Institute of English (Oxford). Pp.47. Flexi ISBN 0-08-024594-3. (Pergam 1980.) £1.95.

WEINSTEIN, M.S. Health in the City. Environmental and Behavioral Influences. Pp.9 ISBN 0-08-023375-9. (Pergamon: 1980.) £5, $10.